Special points for Brillouin-zone integrations

Physical Review B

13, 5188-5192

DOI: 10.1103/physrevb.13.5188

Citation Report

#	Article	IF	Citations
1	Self-consistent numerical-basis-set linear-combination-of-atomic-orbitals model for the study of solids in the local density formalism. Physical Review B, 1977, 15, 4716-4737.	1.1	137
2	Ground- and excited-state properties of LiF in the local-density formalism. Physical Review B, 1977, 16, 2901-2926.	1.1	188
3	Special points for Brillouin-zone integrations. Physical Review B, 1977, 16, 1746-1747.	1.1	648
4	"Special points for Brillouin-zone integrations"â€"a reply. Physical Review B, 1977, 16, 1748-1749.	1.1	2,372
5	Pseudopotential theory of the dielectric function of Al-the volume plasmon dispersion. Journal of Physics F: Metal Physics, 1978, 8, 2631-2649.	1.6	44
6	Comment on special points for Brillouin-zone integrations. Physical Review B, 1978, 18, 5897-5899.	1.1	140
7	Regular phases of atomic hydrogen chemisorbed on graphite. Surface Science, 1978, 72, 140-156.	0.8	20
8	Theory of the Thermodynamics of Simple Liquid Metals. Solid State Physics, 1978, 33, 1-81.	1.3	236
9	Dynamical effective charges in semiconductors: A pseudopotential approach. Journal of Physics C: Solid State Physics, 1978, 11, 251-262.	1.5	133
10	Charge Density and Structural Properties of Covalent Semiconductors. Physical Review Letters, 1978, 40, 950-953.	2.9	145
11	Mean-value point and dielectric properties of semiconductors and insulators. Physical Review B, 1978, 17, 4710-4717.	1.1	87
12	First-principles theoretical study on the electronic properties of theB32intermetallic compound LiAl. Physical Review B, 1978, 17, 2582-2594.	1.1	71
13	Approach to the embedding problem in chemisorption in a self-consistent-field-molecular-orbital formalism. Physical Review B, 1978, 17, 3143-3153.	1.1	77
14	Hartree-Fock density of states for extended systems. Physical Review B, 1979, 20, 1504-1513.	1.1	119
15	Theory of structural properties of covalent semiconductors. Physical Review B, 1979, 19, 5251-5264.	1.1	203
16	Theoretical study of the Raman cross section and its pressure dependence in silicon. Solid State Communications, 1979, 31, 423-426.	0.9	16
17	Lithium crystal properties from high-quality Hartree-Fock wave functions. Solid State Communications, 1979, 29, 723-725.	0.9	35
18	Semiconductor Charge Densities with Hard-Core and Soft-Core Pseudopotentials. Physical Review Letters, 1979, 42, 662-665.	2.9	333

#	Article	IF	Citations
19	First-principles nonlocal-pseudopotential approach in the density-functional formalism. II. Application to electronic and structural properties of solids. Physical Review B, 1979, 20, 4082-4108.	1.1	185
20	Exact-exchange Hartree-Fock calculations for periodic systems. I. Illustration of the method. International Journal of Quantum Chemistry, 1980, 17, 501-516.	1.0	214
21	Use of the Large Unit Cell Approach for Generating Special Points of the Brillouin Zone. Physica Status Solidi (B): Basic Research, 1980, 99, 463-470.	0.7	14
22	Ab initioHartree-Fock calculations of crystalline systems using full-symmetry analysis of basis-set expansions. Physical Review B, 1980, 22, 1534-1549.	1.1	11
23	Special directions for Brillouin-zone integration: Application to density-of-states calculations. Physical Review B, 1980, 21, 496-503.	1.1	64
24	Dependence of the phonon spectrum of InP on hydrostatic pressure. Physical Review B, 1980, 21, 4869-4878.	1.1	211
25	Initial-state screening effects in metal Auger spectra: Be. Physical Review B, 1980, 21, 430-435.	1.1	77
26	Finite-sum approximations to cubic Brillouin-zone integrals. Physical Review B, 1980, 22, 3669-3677.	1.1	6
27	Microscopic Theory of the Phase Transformation and Lattice Dynamics of Si. Physical Review Letters, 1980, 45, 1004-1007.	2.9	496
28	Structural phase transitions in malononitrile. Faraday Discussions of the Chemical Society, 1980, 69, 98.	2.2	21
29	Na chemisorption on the Al(001) surface. Surface Science, 1981, 104, 599-608.	0.8	17
30	Ground-state properties of diamond. Physical Review B, 1981, 24, 6121-6124.	1.1	137
31	On efficient integration techniques for oscillatory integrals in periodic system calculations. Journal of Computational Chemistry, 1981, 2, 376-383.	1.5	13
32	Self-ConsistentAPW-k Â· p method. I. Theory. International Journal of Quantum Chemistry, 1981, 19, 681-691.	1.0	3
33	Smooth energy-band interpolation with gradient utilization. Physical Review B, 1981, 24, 6870-6879.	1.1	5
34	Star interpolation and high-energy expansion for evaluating solid-state Green's functions. Physical Review B, 1981, 23, 4256-4259.	1.1	5
35	Cl chemisorption on the Ag(001) surface: Geometry and electronic structure. Physical Review B, 1981, 23, 4879-4887.	1.1	25
36	Comparative LCAO-LAPW study of C1 chemisorption on the Ag(001) surface. Physical Review B, 1981, 24, 6151-6155.	1.1	49

#	Article	IF	Citations
37	Self-consistent charge densities, band structures, and staging energies of graphite intercalation compounds. Physical Review B, 1981, 23, 565-574.	1.1	60
38	Dielectric matrices and local fields in polar semiconductors. Physical Review B, 1981, 23, 6615-6624.	1.1	61
39	Electronic band structure of a perfect crystal. I. A new method for extending the calculations to the whole Brillouin zone. Physical Review B, 1982, 26, 4312-4316.	1.1	1
40	Interpolation of singular energy bands. Physical Review B, 1982, 25, 7834-7835.	1.1	1
41	Electronic band structure of a perfect crystal. II. The quasi-free-electron case. Physical Review B, 1982, 26, 4317-4320.	1.1	0
42	Total-energy calculations for Si with a first-principles linear-combination-of-atomic-orbitals method. Physical Review B, 1982, 25, 1109-1115.	1.1	154
43	Pressure dependence of the optical phonons and transverse effective charge in3C-SiC. Physical Review B, 1982, 25, 3878-3888.	1.1	201
44	Phonon thermal baths: A treatment in terms of reduced models. Physical Review B, 1982, 25, 5180-5187.	1.1	31
45	Photoemission and band-structure results for NiSi2. Physical Review B, 1982, 25, 7598-7602.	1.1	93
46	Finite sum approximations to Brillouin zone integrals with symmetrized plane waves. Journal of Mathematical Physics, 1982, 23, 1538-1546.	0.5	3
47	Band structure calculation of the momentum density and Compton profile of copper. Journal of Physics F: Metal Physics, 1982, 12, 2249-2266.	1.6	24
48	Theory of static structural properties, crystal stability, and phase transformations: Application to Si and Ge. Physical Review B, 1982, 26, 5668-5687.	1.1	861
49	Ab initiostudy of metallic beryllium. Physical Review B, 1982, 25, 3731-3739.	1.1	99
50	Theory of lattice-dynamical properties of solids: Application to Si and Ge. Physical Review B, 1982, 26, 3259-3272.	1.1	297
51	Local-density-functional methods in two-dimensionally periodic systems. Hydrogen and beryllium monolayers. Physical Review B, 1982, 26, 1743-1753.	1.1	175
52	An Expansion Technique for Evaluating Densities of States and Related Integrals. Physica Status Solidi (B): Basic Research, 1982, 109, 353-360.	0.7	5
53	Spectral Point Schemes for Evaluating the Expansion Coefficients of State Densities into Orthogonal Functions. Physica Status Solidi (B): Basic Research, 1982, 112, 251-259.	0.7	6
54	Interpolation of functions in the Brillouin zone and special-point method. Soviet Physics Journal (English Translation of Izvestiia Vysshykh Uchebnykh Zavedenii, Fizika), 1983, 26, 488-491.	0.0	0

#	Article	IF	Citations
55	Application of Specialâ€Directions Method to the Optical Properties of Copper and Silver. Physica Status Solidi (B): Basic Research, 1983, 118, 575-586.	0.7	8
56	Special points of the brillouin zone and their use in the solid state theory. Physica Status Solidi (B): Basic Research, 1983, 119, 9-40.	0.7	176
57	Local force variations caused by isoelectric impurities: Method of determination from first principles. Physica B: Physics of Condensed Matter & C: Atomic, Molecular and Plasma Physics, Optics, 1983, 116, 52-57.	0.9	2
58	Electronic structure of metal overlayers on rhodium. Physical Review B, 1983, 28, 3092-3099.	1.1	38
59	Convergence of momentum space, pseudopotential calculations for Si. Physical Review B, 1983, 28, 7346-7348.	1.1	24
60	Density-functional theory of a two-dimensional charge-density-wave state in a strong magnetic field. Physical Review B, 1983, 28, 4284-4287.	1.1	8
61	Electronic structure ofBaPb1â^'xBixO3. Physical Review B, 1983, 28, 4227-4241.	1.1	396
62	Pseudopotential calculation of the ground-state properties of ferromagnetic bcc iron. Physical Review B, 1983, 27, 3111-3114.	1.1	31
63	Si-III (BC-8) crystal phase of Si and C: Structural properties, phase stabilities, and phase transitions. Physical Review B, 1984, 30, 1773-1776.	1.1	235
64	Bulk and surface electronic structure of hexagonal WC. Physical Review B, 1984, 30, 1731-1738.	1.1	94
65	"Direct" evaluation of the inverse dielectric matrix in semiconductors. Physical Review B, 1984, 29, 7045-7047.	1.1	33
66	Band model for the electronic structure of expanded liquid cesium. Physical Review B, 1984, 30, 3103-3112.	1.1	31
67	Applicability of the special-point method in lattice dynamics. Physical Review B, 1984, 30, 6917-6920.	1.1	3
68	Electronic structure of the tungsten (001) surface. Physical Review B, 1984, 29, 5372-5381.	1.1	132
69	Anomalously high metallization pressure of solid neon. Physics Letters, Section A: General, Atomic and Solid State Physics, 1984, 105, 303-306.	0.9	34
70	A New Technique for the Evaluation of Densities of States in ab initio Calculations of Periodic Systems. Physica Status Solidi (B): Basic Research, 1984, 122, 211-220.	0.7	8
71	Electronic-structure calculations, photoelectron spectra, optical spectra, and MÃ¶ssbauer parameters for the pyritesMS2(M=Fe,Co,Ni,Cu,Zn). Physical Review B, 1984, 29, 6774-6783.	1.1	60
72	Structural theory of graphite and graphitic silicon. Physical Review B, 1984, 29, 6996-6998.	1.1	236

#	Article	IF	Citations
73	Microscopic electronic screening in semiconductors. , 1985, , 183-194.		3
74	High temperature superconductivity for MoN?: A theoretical study of the relative stability of hexagonal and cubic MoN. Physica B: Physics of Condensed Matter & C: Atomic, Molecular and Plasma Physics, Optics, 1985, 135, 252-256.	0.9	6
75	Ground state properties of the group IV ionic compound silicon carbide. Solid State Communications, 1985, 56, 177-180.	0.9	37
76	Energetics of Silicide Interface Formation. Physical Review Letters, 1985, 54, 2517-2520.	2.9	52
77	Dielectric matrices in semiconductors: A direct approach. Physical Review B, 1985, 31, 5305-5310.	1.1	30
78	Linear augmented-Slater-type-orbital method for electronic-structure calculations. II. bcc, fcc, and hcp W. Physical Review B, 1985, 32, 4876-4882.	1.1	34
79	Relativistic and core-relaxation effects on the energy bands of gallium arsenide and germanium. Physical Review B, 1985, 31, 879-887.	1.1	363
80	Linear augmented-Slater-type-orbital method for electronic-structure calculations. III. Structural and cohesive energies of the 5delements Luâ€“Au. Physical Review B, 1985, 32, 4883-4891.	1.1	46
81	Ab initiorelativistic pseudopotential study of the zero-temperature structural properties of SnTe and PbTe. Physical Review B, 1985, 32, 2302-2314.	1.1	98
82	Stresses in semiconductors:Ab initiocalculations on Si, Ge, and GaAs. Physical Review B, 1985, 32, 3792-3805.	1.1	624
83	Self-consistent theory of electronic states and dielectric response in semiconductors. Physical Review B, 1986, 34, 7146-7157.	1.1	150
84	Theoretical calculations of heterojunction discontinuities in the Si/Ge system. Physical Review B, 1986, 34, 5621-5634.	1.1	1,282
85	Historical biography. Robert Boyle (1627â€“1691): a foundation stone of Analytical Chemistry in the British Isles. Part IV. Robert Boyle's determination of iron in Tunbridge water: the earliest quantitative colorimetric reaction?. Analytical Proceedings, 1986, 23, 75-77.	0.4	5
86	Ab initiocalculation of the macroscopic dielectric constant in silicon. Physical Review B, 1986, 33, 7017-7021.	1.1	499
87	Stress theorem in the determination of static equilibrium by the density functional method. Journal of Physics C: Solid State Physics, 1986, 19, 3163-3172.	1.5	73
88	Theoretical Investigation of Twist Boundaries in Germanium. Materials Research Society Symposia Proceedings, 1986, 77, 205.	0.1	1
89	On energy differences between structurally different crystals. Solid State Communications, 1986, 59, 829-832.	0.9	14
90	Simple geometric generation of special points in brillouin-zone integrations. Two-dimensional bravais lattices. International Journal of Quantum Chemistry, 1986, 30, 391-411.	1.0	107

#	Article	IF	Citations
91	Calculated ground-state properties of silicon carbide. Journal of Physics C: Solid State Physics, 1986, 19, 4413-4426.	1.5	74
92	Accelerating the convergence of self-consistent linearized augmented-plane-wave calculations. Physical Review B, 1986, 34, 8391-8393.	1.1	124
93	Recursion method in thek-space representation. Physical Review B, 1986, 34, 2336-2345.	1.1	21
94	Linear augmented-Slater-type-orbital method for electronic-structure calculations. IV.5d-5dalloys. Physical Review B, 1986, 34, 8421-8429.	1.1	23
95	Optical phonons and elasticity of diamond at megabar stresses. Physical Review B, 1986, 34, 5808-5819.	1.1	204
96	Instability of the ideal tungsten (001) surface. Physical Review Letters, 1986, 57, 3292-3295.	2.9	63
97	CrystallineAs2Se3: Optical properties. Physical Review B, 1986, 34, 8718-8727.	1.1	9
98	New layer method for the investigation of the electronic properties of two-dimensional periodic spatial structures: First applications to copper and aluminum. Physical Review B, 1986, 34, 8512-8527.	1.1	51
99	Real-space force constants for lattice dynamics in silicon and germanium in the adiabatic bond-charge model. Physical Review B, 1986, 34, 7140-7145.	1.1	49
100	Ab initiocalculation of the low-frequency Raman cross section in silicon. Physical Review B, 1986, 33, 5969-5971.	1.1	67
101	Linear augmented-plane-wave calculation of the structural properties of bulk Cr, Mo, and W. Physical Review B, 1986, 33, 823-840.	1.1	285
102	Structural calculations for bulk As. Physical Review B, 1986, 34, 2190-2198.	1.1	62
103	Numerical-Basis-Set LCAO Method Using Gaussian-Fitting of Orbitals Potential. Journal of the Physical Society of Japan, 1987, 56, 4442-4454.	0.7	5
104	Confirmation of an ANNNI-Like Model for Polytypism in SiC. Europhysics Letters, 1987, 3, 475-479.	0.7	61
105	Abinitiodetermination of the structure of a grain boundary by simulated quenching. Physical Review Letters, 1987, 58, 1348-1351.	2.9	106
106	Structural properties of GeTe atT=0. Physical Review B, 1987, 36, 3319-3324.	1.1	44
107	Theory of the structural phase transition of GeTe. Physical Review B, 1987, 36, 6631-6639.	1.1	120
108	Pressure-induced structural instability of cesium halides fromab initiopseudopotential techniques. Physical Review B, 1987, 35, 765-769.	1.1	12

#	Article	IF	Citations
109	Structural properties of the Ru(0001) surface. Physical Review B, 1987, 35, 2124-2127.	1.1	21
110	Equilibrium properties of hcp titanium and zirconium. Physical Review B, 1987, 36, 7335-7341.	1.1	42
111	Ab initiomolecular dynamics on the Ge(100) surface. Physical Review Letters, 1987, 58, 1765-1768.	2.9	155
112	Ab initiotheory of polar semiconductor surfaces. I. Methodology and the (22) reconstructions of GaAs(111). Physical Review B, 1987, 35, 9625-9635.	1.1	215
113	Recursive computation of many-phonon densities of states. Physical Review Letters, 1987, 59, 2196-2198.	2.9	8
114	The theory of the cohesive energies of solids. Advances in Physics, 1987, 36, 463-517.	35.9	157
115	Greenâ€™s-function approach to linear response in solids. Physical Review Letters, 1987, 58, 1861-1864.	2.9	1,807
116	Simple model for structural properties and crystal stability ofsp-bonded solids. Physical Review B, 1987, 35, 9666-9682.	1.1	162
117	Screening of shallow impurities in germanium within the local-density approximation. Physical Review B, 1987, 36, 5925-5932.	1.1	5
118	Brillouin zone treatment in total energy calculations of Peierls distorted chains. International Journal of Quantum Chemistry, 1987, 32, 131-136.	1.0	7
119	Beyond the LUCâ€CNDO k = 0 approximation. Physica Status Solidi (B): Basic Research, 1987, 140, 491-500.	0.7	5
120	Electronic structure of intercalated transition-metal dichalcogenides: MxTiS2(M=Fe,Cr). Journal of Physics C: Solid State Physics, 1987, 20, 395-404.	1.5	80
121	The effect of frenkel defects on the electronic structure of 1T?TiSe2. European Physical Journal B, 1987, 66, 31-37.	0.6	15
122	Theoretical study of band offsets at semiconductor interfaces. Physical Review B, 1987, 35, 8154-8165.	1.1	606
123	On the interpretation of polyoxymethylene valence XPS spectra using band calculations. Chemical Physics Letters, 1988, 143, 361-365.	1.2	15
124	Behaviour of the complex dielectric function and energy loss spectrum of copper in the [110] direction in the energy range 2 < ?? ? 4 Rydberg. Journal of Materials Science, 1988, 23, 1841-1850.	1.7	1
125	A Crystal Orbital approach for two- and three-dimensional solids on the basis ofCNDO/INDOHamiltonians. Basis equations. International Journal of Quantum Chemistry, 1988, 34, 47-71.	1.0	31
126	The use of symmetry in reciprocal space integrations. Asymmetric units and weighting factors for numerical integration procedures in any crystal symmetry. International Journal of Quantum Chemistry, 1988, 34, 571-594.	1.0	92

#	Article	IF	Citations
127	The Periodic LUCâ€MINDO Method and its Application to Diamond. Physica Status Solidi (B): Basic Research, 1988, 146, 149-160.	0.7	21
128	A unifying approach to lattice dynamical and electronic properties of solids. Physics Reports, 1988, 164, 1-117.	10.3	53
129	Electronic band structure of monolayer thin semiconductor superlattices. Vacuum, 1988, 38, 233-236.	1.6	1
130	A novel method of calculating the RPA dielectric function for a semiconductor at real energies. Solid State Communications, 1988, 67, 7-11.	0.9	5
131	GWapproach to the calculation of electron self-energies in semiconductors. Physical Review B, 1988, 38, 7530-7534.	1.1	25
132	Elastic constants of NbC and MoN: Instability ofB1-MoN. Physical Review B, 1988, 37, 3295-3298.	1.1	72
133	Microscopic atomic structure and stability of Si-Ge solid solutions. Physical Review B, 1988, 37, 1308-1314.	1.1	57
134	Linearized augmented plane wave electronic structure calculations for MgO and CaO. Journal of Geophysical Research, 1988, 93, 8009-8022.	3.3	156
135	Band Offsets in Lattice-Matched Heterojunctions: A Model and First-Principles Calculations for GaAs/AlAs. Physical Review Letters, 1988, 61, 734-737.	2.9	507
136	Self-energy operators and exchange-correlation potentials in semiconductors. Physical Review B, 1988, 37, 10159-10175.	1.1	1,246
137	Bonding and reconstruction of the W(001) surface. Physical Review B, 1988, 37, 3999-4006.	1.1	76
138	New procedure for evaluating a large number of continued-fraction parameters in periodic structures. Physical Review B, 1988, 38, 2154-2157.	1.1	10
139	Special points for superlattices and strained bulk semiconductors. Physical Review B, 1988, 38, 1999-2001.	1.1	12
140	Hydrogenation of semiconductor surfaces: Si and Ge (111). Physical Review B, 1988, 37, 8842-8848.	1.1	72
141	Usefulness of the specialqpoints in the study of rare-gas monolayers. Physical Review B, 1988, 37, 8401-8406.	1.1	1
142	Structural and electronic properties of spinel semiconductors: Anab initiopseudopotential study ofMgIn2S4. Physical Review B, 1988, 38, 8258-8263.	1.1	41
143	ndependence of the valence-band offset in (GaAs)n(AlAs)n: Role of charge redistribution, interface dipoles, and cation 3dstates. Physical Review B, 1988, 38, 1291-1295.	1.1	14
144	Local-density-approximation study of LaS and SmS. Physical Review B, 1988, 37, 10045-10049.	1.1	25

#	Article	IF	Citations
145	Local-density description of antiferromagnetic Cr. Physical Review B, 1988, 38, 12834-12836.	1.1	34
146	The coated inclusion effect on the mode of fracture of encapsulated particulates. Journal of Adhesion Science and Technology, 1988, 2, 427-448.	1.4	1
147	Longitudinal phonons in gallium phosphide at high pressures. Journal of Physics C: Solid State Physics, 1988, 21, 5933-5941.	1.5	12
148	Inter-layer interactions and the origin of SiC polytypes. Journal of Physics C: Solid State Physics, 1988, 21, 1049-1063.	1.5	191
149	Phonon dispersion in the (110) direction: a testing ground for phenomenological models of germanium. Journal of Physics C: Solid State Physics, 1988, 21, 5087-5106.	1.5	16
150	Ab initiocalculations of bismuth properties, including spinâ€“orbit coupling. Physica Scripta, 1988, 37, 785-789.	1.2	46
151	Ab Initio Determination of Li Diffusion Path in Î³-InSe. Europhysics Letters, 1988, 7, 611-616.	0.7	20
152	Solid Solutions of AB2C4 Defect Semiconductors. Materials Research Society Symposia Proceedings, 1988, 141, 195.	0.1	1
153	Effect of relaxation of the second-nearest neighbors on the thermodynamic properties of semiconducting alloys: Application toGaAsySb1â^'y. Physical Review B, 1989, 39, 5987-5997.	1.1	21
154	Theoretical study of hydrogen adsorption on Ru(0001): Possible surface and subsurface occupation sites. Physical Review B, 1989, 39, 5623-5631.	1.1	48
155	Ground-state properties of fcc and bcc lanthanum. Physical Review B, 1989, 39, 4921-4925.	1.1	22
156	Efficient direct calculation method for dielectric response in semiconductors. Physical Review B, 1989, 40, 7793-7801.	1.1	17
157	Mechanisms of dopant impurity diffusion in silicon. Physical Review B, 1989, 40, 5484-5496.	1.1	148
158	First-principles calculation of the elastic constants of AlAs. Physical Review B, 1989, 40, 11934-11936.	1.1	53
159	Simultaneous solution of diagonalization and self-consistency problems for transition-metal systems. Physical Review B, 1989, 40, 5428-5431.	1.1	24
160	Mixing enthalpy of the GaAs-AlAs random alloy: 64-atom supercell calculations. Physical Review B, 1989, 40, 8399-8403.	1.1	11
161	Shell-model interpolation of frozen phonons in cubic silicon carbide. Physical Review B, 1989, 39, 5892-5898.	1.1	28
162	Total-energy study of the equation of state of HgTe and HgSe. Physical Review B, 1989, 39, 10154-10161.	1.1	39

#	Article	IF	Citations
163	Fast diagonalisation of nonlocal pseudopotential Hamiltonians. Journal of Physics Condensed Matter, 1989, 1, 525-540.	0.7	9
164	Electronic Band Structures and Bond Orders of M1/3TiS2(M=Mn, Fe, Co, Ni). Journal of the Physical Society of Japan, 1989, 58, 3280-3289.	0.7	27
165	Predicting the structure and energy of a grain boundary in germanium. Journal of Physics Condensed Matter, 1989, 1, 327-333.	0.7	10
166	Theory of hydrogen diffusion and reactions in crystalline silicon. Physical Review B, 1989, 39, 10791-10808.	1.1	494
167	Structural, electronic and magnetic properties of metal/semiconductor superlattices: Fe/ZnSe(001). Journal of Magnetism and Magnetic Materials, 1989, 78, 195-202.	1.0	10
168	Pseudopotential methods in condensed matter applications. Computer Physics Reports, 1989, 9, 115-197.	2.3	758
169	Equation of state and metallization in compressed solid krypton. Physics Letters, Section A: General, Atomic and Solid State Physics, 1989, 140, 117-121.	0.9	9
170	A total-energy study of proton diffusion in crystalline silicon. Solid State Communications, 1989, 69, 305-309.	0.9	10
171	Modeling of chemical interactions at Cr/Cu interfaces. Journal of Physics and Chemistry of Solids, 1989, 50, 87-93.	1.9	14
172	Band gaps and spin-orbit splitting of ordered and disorderedAlxGa1â^'xAsandGaAsxSb1â^'xalloys. Physical Review B, 1989, 39, 3279-3304.	1.1	231
173	Generalized norm-conserving pseudopotentials. Physical Review B, 1989, 40, 2980-2987.	1.1	1,078
174	Linear optical response in silicon and germanium including self-energy effects. Physical Review Letters, 1989, 63, 1719-1722.	2.9	355
175	Calculations of the surface stress tensor and surface energy of the (111) surfaces of iridium, platinum and gold. Journal of Physics Condensed Matter, 1989, 1, 7555-7563.	0.7	120
176	Electronic structure and bonding of the Cu/W(001) surface alloy. Surface Science, 1989, 216, 303-310.	0.8	29
177	Brillouin-zone integration by Fourier quadrature: Special points for superlattice and supercell calculations. Physical Review B, 1989, 39, 3168-3172.	1.1	387
178	Microscopic structure of the hydrogen-boron complex in crystalline silicon. Physical Review B, 1989, 39, 10809-10824.	1.1	152
179	Method for the calculation of scanning tunneling microscope images and spectra. Physical Review B, 1989, 40, 11990-11993.	1.1	49
180	Extended norm-conserving pseudopotentials. Physical Review B, 1989, 40, 3652-3660.	1.1	128

#	Article	IF	Citations
181	Theoretical study of cubic versus tetragonal structures of defect zinc-blende semiconductors:CdIn2Se4. Physical Review B, 1989, 40, 1725-1731.	1.1	50
182	First-principles pseudopotential and full-potential linear muffin-tin-orbital calculation of anharmonic effects on the lattice-dynamical properties of AlP. Physical Review B, 1989, 40, 3975-3978.	1.1	17
183	Energy Barrier for â€˜Magic-Strainâ€™ Transformations in Crystals with Fcc Lattices. Materials Research Society Symposia Proceedings, 1990, 205, 447.	0.1	2
184	LMTO/CVM and LAPW/CVM Calculations of the Nial-Niti Pseudobinary Phase Diagram. Materials Research Society Symposia Proceedings, 1990, 213, 107.	0.1	6
185	Local Density Approximation Total Energy Calculations for Silica and Titania Structure and Defects. Journal of the American Ceramic Society, 1990, 73, 3247-3250.	1.9	114
186	Theoretical studies on structureâ€property relationships of cellulose and nitrocellulose: I. Conformation, stability and conductivity. Chinese Journal of Chemistry, 1990, 8, 390-395.	2.6	4
187	Molecular dynamics without effective potentials via the Car-Parrinello approach. Molecular Physics, 1990, 70, 921-966.	0.8	552
188	k-point sampling and the k.p method in pseudopotential total energy calculations. Journal of Physics Condensed Matter, 1990, 2, 9837-9852.	0.7	18
189	Atomic relaxation in silicon carbide polytypes. Journal of Physics Condensed Matter, 1990, 2, 5115-5134.	0.7	54
190	Density matrix of crystalline systems. I. Long-range behavior and related computational problems. International Journal of Quantum Chemistry, 1990, 38, 395-417.	1.0	27
191	LCAO Recursion Approach in kâ€Space Representations for the Treatment of Bulk and Surface Problems. Physica Status Solidi (B): Basic Research, 1990, 161, 667-676.	0.7	6
192	Theoretical calculation of electron-positron momentum density in YBa2Cu3O7â^Î´. Physica C: Superconductivity and Its Applications, 1990, 169, 137-145.	0.6	33
193	Instabilities in cubic BaBiO3 from total-energy calculations. Solid State Communications, 1990, 74, 805-808.	0.9	7
194	A pseudopotential total energy study of impurity-promoted intergranular embrittlement. Journal of Physics Condensed Matter, 1990, 2, 351-365.	0.7	87
195	Local field corrections and the influence of exchange and correlation on the microscopic longitudinal dielectric function of copper. Journal of Physics Condensed Matter, 1990, 2, 3919-3939.	0.7	9
196	Silicon carbide polytypes are equilibrium structures. Journal of Physics Condensed Matter, 1990, 2, 5097-5113.	0.7	46
197	Tailoring materials for quantum wells: band offsets at (001)-oriented GaAs/(AlAs)n(GaAs)minterfaces. Journal of Physics Condensed Matter, 1990, 2, 5265-5269.	0.7	1
198	Molecular-dynamics simulations of amorphous Si. Physical Review B, 1990, 42, 5135-5141.	1.1	88

#	Article	IF	Citations
199	Equilibrium properties of zinc. Physical Review B, 1990, 42, 8885-8889.	1.1	26
200	First-principles pseudopotential calculations of the elastic properties of diamond, Si, and Ge. Physical Review B, 1990, 42, 7462-7469.	1.1	47
201	Total-energy calculations of solid H, Li, Na, K, Rb, and Cs. Physical Review B, 1990, 42, 11637-11643.	1.1	56
202	Self-consistent dipole theory of heterojunction band offsets. Physical Review B, 1990, 41, 2813-2831.	1.1	148
203	Total energy, lattice dynamics, and structural phase transitions in silicon by the orthogonalized linear combination of atomic orbitals method. Physical Review B, 1990, 41, 12162-12179.	1.1	49
204	Vibrational frequencies of Si-P-H complexes in crystalline silicon: A theoretical study. Physical Review B, 1990, 42, 3175-3178.	1.1	23
205	Structural and electronic properties of the liquid polyvalent elements: The group-IV elements Si, Ge, Sn, and Pb. Physical Review B, 1990, 41, 1497-1515.	1.1	142
206	Electronic spectra of crystals with a subzone resummation technique. Physical Review B, 1990, 41, 3545-3550.	1.1	3
207	Local-density theory of band offsets in strained superlattices: (InAs)n/(InP)n(001). Physical Review B, 1990, 42, 3469-3477.	1.1	17
208	Absence of volume metastability in bcc copper. Physical Review B, 1990, 41, 2699-2703.	1.1	39
209	First-principles calculations of the three-dimensional structure and intrinsic defects intrans-polyacetylene. Physical Review B, 1990, 41, 12797-12817.	1.1	129
210	Stability and electronic properties of InAs/InP strained superlattices. Physical Review B, 1990, 41, 12013-12020.	1.1	8
211	Convergence of force calculations for noncrystalline Si. Physical Review B, 1990, 42, 5345-5348.	1.1	29
212	Possiblity ofLiPdHxas a new ionic superconductor. Physical Review B, 1990, 41, 861-864.	1.1	9
213	Augmented-plane-wave forces. Physical Review B, 1990, 42, 9728-9731.	1.1	153
214	Calculations of the electronic structure of highly strained GaAs/GaSb/GaAs heterostructures. Physical Review B, 1990, 42, 3044-3051.	1.1	20
215	Interplanar forces and phonon spectra of strained Si and Ge:Ab initiocalculations and applications to Si/Ge superlattices. Physical Review B, 1990, 42, 7090-7096.	1.1	32
216	Structural and electronic properties of the liquid polyvalent elements. II. The divalent elements. Physical Review B, 1990, 42, 6926-6938.	1.1	71

#	Article	IF	Citations
217	A numerical investigation of properties of the electronic self-energy potential for metallic systems. Journal of Physics Condensed Matter, 1990, 2, 1537-1548.	0.7	5
218	Correctly weighted tetrahedron method for k-space integration. Journal of Physics Condensed Matter, 1990, 2, 7445-7452.	0.7	24
219	Structural identification of hydrogen and muonium centers in silicon: First-principles calculations of hyperfine parameters. Physical Review Letters, 1990, 64, 669-672.	2.9	62
220	Formulas for the Chadi-Cohen process. Physical Review B, 1990, 41, 4469-4474.	1.1	10
221	Surface stress of aluminum and jellium. Physical Review B, 1990, 42, 10933-10939.	1.1	66
222	Optimized pseudopotentials. Physical Review B, 1990, 41, 1227-1230.	1.1	2,139
223	Total energy calculations on zinc sulphide polytypes. Journal of Physics Condensed Matter, 1990, 2, 367-376.	0.7	35
224	A new and efficient scheme for first-principles calculations of phonon spectra. Journal of Physics Condensed Matter, 1990, 2, 3431-3444.	0.7	26
225	Lattice dynamics and origin of ferroelectricity inBaTiO3: Linearized-augmented-plane-wave total-energy calculations. Physical Review B, 1990, 42, 6416-6423.	1.1	567
226	Calculations of the structural properties of cubic zinc sulfide. Physical Review B, 1990, 41, 7876-7878.	1.1	46
227	High-pressure metallic phases of boron. Physical Review B, 1990, 42, 9033-9039.	1.1	64
228	Finite basis set corrections to total energy pseudopotential calculations. Journal of Physics Condensed Matter, 1990, 2, 4395-4404.	0.7	319
229	Structural properties of ordered high-melting-temperature intermetallic alloys from first-principles total-energy calculations. Physical Review B, 1990, 41, 10311-10323.	1.1	386
230	First-principles study of As, Sb, and Bi electronic properties. Physical Review B, 1990, 41, 11827-11836.	1.1	144
231	How formaldehyde interacts and reacts with chromium and chromium oxide surfaces: A model for chromium-polyimide binding. Surface Science, 1990, 232, 209-218.	0.8	8
232	Total energy calculations of dimer reconstructions on the silicon (001) surface. Surface Science, 1990, 236, 112-121.	0.8	233
233	Optical second-harmonic generation in III-V semiconductors: Detailed formulation and computational results. Physical Review B, 1991, 44, 12781-12793.	1.1	67
234	Calculation of the nonlinear susceptibility for optical second-harmonic generation in III-V semiconductors. Physical Review Letters, 1991, 66, 41-44.	2.9	112

#	Article	IF	Citations
235	Theory of surface stress and surface reconstruction. Surface Science, 1991, 242, 215-221.	0.8	164
236	The influence of internal surfaces on the (2 Ã— 1) shuffle and glide cleavage reconstructions for Si(111). Surface Science, 1991, 256, 344-353.	0.8	28
237	Surface energy and stress of lead (111) and (110) surfaces. Physical Review B, 1991, 43, 8829-8833.	1.1	73
238	Pseudopotential calculations of the valence-band offsets at the ZnSe/Ge, ZnSe/GaAs, and GaAs/Ge (110) interfaces: Effects of the Ga and Zn 3delectrons. Physical Review B, 1991, 43, 4229-4235.	1.1	35
239	Calculated atomic structures and electronic properties of GaP, InP, GaAs, and InAs (110) surfaces. Physical Review B, 1991, 44, 6188-6198.	1.1	219
240	Atmospheric-pressure stability of energetic phases of carbon. Physical Review B, 1991, 44, 11578-11591.	1.1	85
241	Calculating the Properties of Materials from Scratch. , 1991, , 257-281.		15
242	The ab initio calculation of defect energetics in aluminium. Journal of Physics Condensed Matter, 1991, 3, 6225-6237.	0.7	87
243	Valence-band offsets at strained Si/Ge interfaces. Physical Review B, 1991, 44, 5572-5579.	1.1	177
244	Analysis of separable potentials. Physical Review B, 1991, 44, 8503-8513.	1.1	508
245	Ground-state properties of lanthanum: Treatment of extended-core states. Physical Review B, 1991, 43, 6388-6392.	1.1	530
246	First-principles study of the electronic properties of graphite. Physical Review B, 1991, 43, 4579-4589.	1.1	306
247	Self-Consistent Electronic Structure of Ni x Zr 1- x Glasses. Europhysics Letters, 1991, 16, 473-478.	0.7	25
248	First-principles statistical mechanics of structural stability of intermetallic compounds. Physical Review B, 1991, 44, 512-544.	1.1	286
249	Electronic structure of Ba(Sn,Sb)O3: Absence of superconductivity. Physical Review B, 1991, 44, 9519-9523.	1.1	57
250	A Full-Potential KKR-GREEN's Function Method to Calculate the Electronic Structure of Surfaces. Materials Research Society Symposia Proceedings, 1991, 253, 357.	0.1	10
251	Energetics of point and planar defects in aluminium from first-principles calculations. Solid State Communications, 1991, 78, 857-861.	0.9	32
252	All-electron first-principles supercell total-energy calculation of the vacancy formation energy in aluminium. Physica B: Condensed Matter, 1991, 172, 211-215.	1.3	44

#	Article	IF	Citations
253	Electronic structure of doped Sr2VO4. Physica C: Superconductivity and Its Applications, 1991, 175, 329-334.	0.6	10
254	Giant magnetooptic rotations: the role of orbital polarization and explicit correlation effects. IEEE Transactions on Magnetics, 1991, 27, 3648-3654.	1.2	33
255	Equilibrium properties of the layer Î±-ZnIn2S4. Nuovo Cimento Della Societa Italiana Di Fisica D - Condensed Matter, Atomic, Molecular and Chemical Physics, Biophysics, 1991, 13, 291-299.	0.4	3
256	Multi-Atom Bonding in Aluminium over a Wide Range of Coordination Number. Europhysics Letters, 1991, 15, 301-306.	0.7	38
257	Self-consistency in total energy calculations: implications for empirical and semi-empirical schemes. Journal of Physics Condensed Matter, 1991, 3, 8351-8367.	0.7	12
258	The k.p method in pseudopotential total energy calculations: error reduction and absolute energies. Journal of Physics Condensed Matter, 1991, 3, 8841-8853.	0.7	4
259	On the valence band offset controversy in HgTe/CdTe superlattices. Journal of Physics Condensed Matter, 1991, 3, 617-621.	0.7	8
260	Defect energetics in aluminium. Journal of Physics Condensed Matter, 1991, 3, 8777-8792.	0.7	26
261	Electronic structure of the liquid 3d and 4d transition metals. Journal of Physics Condensed Matter, 1991, 3, 4477-4490.	0.7	46
262	GW-approximation energies and Hartree-Fock bands of semiconductors. Physical Review B, 1991, 44, 1057-1065.	1.1	66
263	First-principles electronic structure and optical properties ofCrSi2. Physical Review B, 1991, 44, 9042-9044.	1.1	32
264	Gradient-corrected density functionals: Full-potential calculations for iron. Physical Review B, 1991, 43, 11628-11634.	1.1	166
265	Theory of high-pressure phases of Pb. Physical Review B, 1991, 43, 1795-1798.	1.1	37
266	Electronic structure of randomAg0.5Pd0.5andAg0.5Au0.5alloys. Physical Review B, 1991, 44, 10470-10484.	1.1	62
267	Electronic structure of antimony from density-functional calculations and angle-resolved photoemission. Physical Review B, 1991, 44, 11023-11028.	1.1	6
268	First-principles calculation of the elastic moduli ofNi3Al. Physical Review B, 1991, 43, 1805-1807.	1.1	31
269	Interband transition rate in GaAs. Physical Review B, 1991, 44, 11105-11110.	1.1	17
270	Gradient-corrected density-functional studies ofCaCuO2. Physical Review B, 1991, 44, 7715-7717.	1.1	35

#	Article	IF	Citations
271	Influence of the local-spin-density correlation functional on the stability of bcc ferromagnetic iron. Physical Review B, 1991, 44, 7701-7703.	1.1	23
272	High-pressure phase of gallium nitride. Physical Review B, 1991, 44, 10372-10373.	1.1	97
273	Structural and vibrational properties of the Si-H-Al complex in crystalline silicon. Physical Review B, 1991, 44, 3399-3402.	1.1	4
274	Adequacy of the local-spin-density approximation for Gd. Physical Review B, 1991, 44, 7451-7454.	1.1	73
275	H-point phonon in molybdenum: Superlinearized augmented-plane-wave calculations. Physical Review B, 1991, 43, 1441-1445.	1.1	24
276	All-electron and pseudopotential force calculations using the linearized-augmented-plane-wave method. Physical Review B, 1991, 43, 6411-6422.	1.1	329
277	Quasiparticle calculation of the dielectric response of silicon and germanium. Physical Review B, 1991, 43, 4187-4207.	1.1	207
278	Surface strain of tungsten (001). Physical Review B, 1991, 43, 2398-2400.	1.1	6
279	Atomic and electronic structure ofCaSi2/Si interfaces. Physical Review B, 1991, 43, 11913-11919.	1.1	12
280	Structural and electronic properties of Î±-Sn, CdTe, and their [001] monolayer superlattices. Physical Review B, 1991, 43, 8951-8961.	1.1	13
281	Atomic and electronic structures of GaAs(110) and their alkali-adsorption-induced changes. Physical Review Letters, 1991, 67, 1031-1034.	2.9	92
282	Efficientab initiomolecular-dynamics simulations of carbon. Physical Review B, 1991, 43, 5132-5134.	1.1	36
283	Electronic, structural, and mechanical properties of possible metastable phases of beryllium hydride. High Pressure Research, 1991, 6, 291-299.	0.4	0
284	The Energetics of Frenkel Defects in Li ₂ O from First Principles. Europhysics Letters, 1992, 19, 605-610.	0.7	43
285	The energetics of hydrogen in aluminium calculated from first principles. Journal of Physics Condensed Matter, 1992, 4, 599-611.	0.7	11
286	First-principles pseudopotential calculations for hydrogen in 4d transition metals. I. Mixed-basis method for total energies and forces. Journal of Physics Condensed Matter, 1992, 4, 5189-5206.	0.7	95
287	General formulae for the special points and their weighting factors in k-space integration. Journal of Physics Condensed Matter, 1992, 4, 4583-4594.	0.7	10
288	Stacking fault energies in aluminium. Journal of Physics Condensed Matter, 1992, 4, 10453-10460.	0.7	54

#	Article	IF	Citations
289	First-principles calculation of the magnetocrystalline anisotropy energy of the pnictide MnSb. Journal of Physics Condensed Matter, 1992, 4, 10469-10478.	0.7	6
290	Theoretical investigation of (111) stacking faults in aluminium. Philosophical Magazine A: Physics of Condensed Matter, Structure, Defects and Mechanical Properties, 1992, 66, 387-404.	0.8	26
291	Self-consistent pseudopotential calculations for sodium adsorption on GaAs(110). Physical Review B, 1992, 46, 10134-10145.	1.1	49
292	Calculation of the dielectric properties of semiconductors. Physical Review B, 1992, 46, 15812-15827.	1.1	39
293	Silicon-hydrogen-acceptor complexes in crystalline silicon. Physical Review B, 1992, 45, 11744-11748.	1.1	7
294	Electronic aspects of the optical-absorption spectrum of theEL2 defect in GaAs. Physical Review B, 1992, 45, 8300-8309.	1.1	20
295	Electronic structure of the layered nitrideLiMoN2. Physical Review B, 1992, 46, 9332-9335.	1.1	17
296	Elastic constants of a Si/Ge superlattice and of bulk Si and Ge. Physical Review B, 1992, 46, 12411-12420.	1.1	36
297	Theoretical calculations of the NiAl-NiTi phase diagram based on first-principles linear-muffin-tin-orbital and full-potential linearly-augmented plane-wave cohesive-energy calculations. Physical Review B, 1992, 45, 7677-7683.	1.1	31
298	Magnetism with generalized-gradient-approximation density functionals. Physical Review B, 1992, 46, 11570-11577.	1.1	107
299	Electronic structure, lattice stability, and superconductivity of CrC. Physical Review B, 1992, 46, 14969-14974.	1.1	28
300	Polymeric nitrogen. Physical Review B, 1992, 46, 14419-14435.	1.1	430
301	Calculation of phonon-phonon interactions and two-phonon bound states on the Si(111):H surface. Physical Review Letters, 1992, 69, 2543-2546.	2.9	58
302	Electric-field gradients inYBa2Cu3O7: Discrepancy between experimental and local-density-approximation charge distributions. Physical Review B, 1992, 46, 5849-5852.	1.1	32
303	Energies of atoms and solids within the local-density approximation. Physical Review B, 1992, 45, 1067-1073.	1.1	24
304	Polarization, band lineups, and stability of SiC polytypes. Physical Review B, 1992, 45, 6534-6542.	1.1	132
305	First-principles energy density and its applications to selected polar surfaces. Physical Review B, 1992, 45, 6074-6088.	1.1	174
306	Electronic structure, magnetism, and stability of Co-doped NiAl. Physical Review B, 1992, 46, 14392-14397.	1.1	19

#	Article	IF	Citations
307	Supercell calculations on the substitutional and vacancy-interstitial pair geometries of chalcogen defects in Si. Physical Review B, 1992, 46, 3839-3848.	1.1	18
308	Defect energetics in MgO treated by first-principles methods. Physical Review B, 1992, 46, 12964-12973.	1.1	120
309	Analysis of acceptor chemical shifts in Ge. Physical Review B, 1992, 45, 5944-5952.	1.1	8
310	Electronic structure ofBeCN2: A proposed nearly direct wide-band-gap semiconductor. Physical Review B, 1992, 45, 1485-1487.	1.1	27
311	Band lineup and electric fields in (Î±-Sn)m/(CdTe)n[001] and [110] superlattices. Physical Review B, 1992, 45, 5953-5960.	1.1	5
312	Strained silicon: A dielectric-response calculation. Physical Review B, 1992, 45, 4131-4140.	1.1	48
313	A first-principles pseudopotential investigation of ferroelectricity in barium titanate. Ferroelectrics, 1992, 136, 85-94.	0.3	67
314	Chemistry, interface features and strain: how do they affect the valence band offset at Si/Ge interfaces?. Physica Scripta, 1992, T45, 181-185.	1.2	0
315	Origins of the Gap States in Polycrystalline Silicon: Tight-Binding Calculations of Twist Boundaries. Materials Research Society Symposia Proceedings, 1992, 262, 567.	0.1	2
316	A Method for the Determination of Real-Space Interatomic Force-Constants.. Materials Research Society Symposia Proceedings, 1992, 291, 43.	0.1	1
317	Optimized norm-conserving pseudopotentials. Journal of Physics Condensed Matter, 1992, 4, 7451-7468.	0.7	106
318	General-potential study of the electronic and magnetic structure of FeCo. Physical Review B, 1992, 46, 11145-11148.	1.1	36
319	Self-consistent-screening calculation of interatomic force constants and phonon dispersion curves from first principles. Physical Review B, 1992, 46, 10734-10737.	1.1	116
320	Ab initio calculations of electronic structure and elastic constants in AlP. Semiconductor Science and Technology, 1992, 7, 1437-1440.	1.0	44
321	Energetics of interplanar binding in graphite. Physical Review B, 1992, 46, 7185-7188.	1.1	195
322	Adsorbate-substrate and adsorbate-adsorbate interactions of Na and K adlayers on Al(111). Physical Review B, 1992, 46, 16067-16080.	1.1	2,339
323	Dielectric tensor, effective charges, and phonons in Î±-quartz by variational density-functional perturbation theory. Physical Review Letters, 1992, 68, 3603-3606.	2.9	436
324	Ab Initio Statistical Mechanics of Structural Phase Transitions. Modern Problems in Condensed Matter Sciences, 1992, , 135-175.	0.1	2

#	Article	IF	Citations
325	Elastic instability in Î±-quartz under pressure. Physical Review Letters, 1992, 69, 2220-2223.	2.9	134
326	Band-structure methods. Topics in Applied Physics, 1992, , 25-49.	0.4	3
327	Zinc-blendeâ€“wurtzite polytypism in semiconductors. Physical Review B, 1992, 46, 10086-10097.	1.1	977
328	Field-ion microscope tunnelling calculations for the aluminium (111) and (110) surfaces. Surface Science, 1992, 277, 173-183.	0.8	15
329	Optimal meshes for integrals in real- and reciprocal-space unit cells. Physical Review B, 1992, 45, 13891-13898.	1.1	275
330	Structural and electronic properties of narrow-gapABC2chalcopyrite semiconductors. Physical Review B, 1992, 46, 10070-10077.	1.1	38
331	Electronic structure studies of the differences in ferroelectric behavior of batio₃and PbTiO₃. Ferroelectrics, 1992, 136, 65-83.	0.3	367
332	Structural and electronic properties of Y-based metallic glasses. Journal of Physics Condensed Matter, 1992, 4, 9557-9572.	0.7	18
333	Electronic structure of ordered and disorderedCu3Au andCu3Pd. Physical Review B, 1992, 45, 10314-10330.	1.1	89
334	Magnetism in bcc cobalt. Physical Review B, 1992, 45, 2258-2261.	1.1	38
335	Defect energetics in oxide materials from first principles. Physical Review Letters, 1992, 68, 3319-3322.	2.9	83
336	Periodic ab initio determination of interatomic potentials for alumina. Modelling and Simulation in Materials Science and Engineering, 1992, 1, 73-81.	0.8	106
337	Valence band x-ray photoelectron spectroscopy of poly(ether ketone) and poly(ether-ether ketone). Journal of Polymer Science, Part B: Polymer Physics, 1992, 30, 275-279.	2.4	4
338	Energetics of negatively curved graphitic carbon. Nature, 1992, 355, 333-335.	13.7	391
339	Electronic characteristics of Tl2Ba2CuO6. Physica C: Superconductivity and Its Applications, 1992, 203, 193-202.	0.6	60
340	Bonding at Cu-Al interfaces: Relevance to microcircuit packaging. Journal of Physics and Chemistry of Solids, 1992, 53, 253-260.	1.9	3
341	Charge iterated parameters for extended HÃ¼ckel calculations on polytetrafluoroethylene: relevance to X-ray photoelectron spectroscopy. Journal of Electron Spectroscopy and Related Phenomena, 1992, 58, 365-373.	0.8	6
342	Iterative minimization techniques forab initiototal-energy calculations: molecular dynamics and conjugate gradients. Reviews of Modern Physics, 1992, 64, 1045-1097.	16.4	8,643

#	Article	IF	Citations
343	Large-scale ab initio total energy calculations on parallel computers. Computer Physics Communications, 1992, 72, 14-28.	3.0	184
344	Temperature dependence of band gaps in Si and Ge in the quasi-ion model. Annalen Der Physik, 1992, 504, 34-38.	0.9	3
345	Dissociative adsorption of H2 on Cu (100). Chemical Physics Letters, 1993, 213, 422-426.	1.2	54
346	LDA calculation of the surface states on the (001), (110), and (111) surfaces of aluminum. Surface Science Letters, 1993, 285, A311.	0.1	0
347	Structure of the (0001) surface of Î±-Al2O3 from first principles calculations. Surface Science Letters, 1993, 285, L517-L521.	0.1	14
348	Theory of electronic properties of amorphous silicon-carbon alloys: Effects of short-range disorder. Solid State Communications, 1993, 87, 851-855.	0.9	21
349	Calculated electric field gradients of ferroelectric KNbO3. Solid State Communications, 1993, 88, 323-325.	0.9	0
350	Calculated atomic structures of ZnS, ZnSe and ZnTe (110) surfaces. Solid State Communications, 1993, 87, 1001-1004.	0.9	8
351	Doping limits in ZnSe. Physica B: Condensed Matter, 1993, 185, 118-127.	1.3	28
352	High-pressure structural phase transition and electronic properties of the group-III nitrides. Physica B: Condensed Matter, 1993, 185, 422-425.	1.3	15
353	Electronic structure of HgBa2CuO4. Physica C: Superconductivity and Its Applications, 1993, 212, 228-232.	0.6	49
354	Computing the total energy and the electronic structure of crystalline zirconium dioxide. Powder Metallurgy and Metal Ceramics, 1993, 32, 453-456.	0.4	0
355	On the Efficiency of Different Schemes for the Evaluation of the Density of States and Related Properties in Solids. Physica Status Solidi (B): Basic Research, 1993, 179, 429-439.	0.7	13
356	To(?) phonons in GaAs under uniaxial strain. International Journal of Quantum Chemistry, 1993, 45, 43-49.	1.0	1
357	Energetics of multilayered carbon tubules. Physical Review Letters, 1993, 70, 1858-1861.	2.9	259
358	First-principles study of the electronic structure of Î³-InSe and Î²-InSe. Physical Review B, 1993, 48, 14135-14141.	1.1	98
359	How aluminum bonds to a copper 100 surface. Journal of Physics and Chemistry of Solids, 1993, 54, 937-945.	1.9	0
360	A molecular dynamics study and the electronic properties of amorphous carbon using the Tersoff potential. Journal of Physics Condensed Matter, 1993, 5, 9157-9168.	0.7	23

#	Article	IF	Citations
361	Stability, reconstruction, and electronic properties of diamond (100) and (111) surfaces. Physical Review B, 1993, 48, 18189-18202.	1.1	118
362	Optimized and transferable nonlocal separableab initiopseudopotentials. Physical Review B, 1993, 47, 4174-4180.	1.1	1,016
363	Structure of the (0001) surface of Î±-Al2O3 from first principles calculations. Surface Science, 1993, 285, L517-L521.	0.8	123
364	LDA calculation of the surface states on the (001), (110), and (111) surfaces of aluminum. Surface Science, 1993, 285, 129-141.	0.8	28
365	Electron correlations on a potassium-covered GaAs(110) surface: ab-initio calculations of the Hubbard correlation energy. Surface Science, 1993, 287-288, 584-587.	0.8	10
366	Theory of polarization of crystalline solids. Physical Review B, 1993, 47, 1651-1654.	1.1	3,373
367	Bound bipolaron at the surface: The negative-Ubehavior of GaAs(110) with adsorbed alkali metals. Physical Review Letters, 1993, 71, 2797-2800.	2.9	44
368	Electronic and structural properties of GaN by the full-potential linear muffin-tin orbitals method: The role of thedelectrons. Physical Review B, 1993, 47, 13353-13362.	1.1	188
369	Chemical softness and impurity segregation at grain boundaries. Journal of Chemical Physics, 1993, 98, 1606-1610.	1.2	30
370	Hubbard correlations and charge transfer at the GaAs(110) surface with alkali adsorbates. Physical Review Letters, 1993, 70, 351-354.	2.9	70
371	First-principles calculations of hyperfine parameters. Physical Review B, 1993, 47, 4244-4255.	1.1	231
372	Pressure dependence of the elastic moduli in aluminum-rich Al-Li compounds. Physical Review B, 1993, 47, 2493-2500.	1.1	397
373	Ab initioHartree-Fock calculations of CaO, VO, MnO and NiO. Philosophical Magazine A: Physics of Condensed Matter, Structure, Defects and Mechanical Properties, 1993, 68, 653-666.	0.8	95
374	Structure and static properties of indium nitride at low and moderate pressures. Journal of Physics Condensed Matter, 1993, 5, 6015-6022.	0.7	52
375	Energetics and electronic structure of the hypothetical cubic zincblende form of GeC. Modelling and Simulation in Materials Science and Engineering, 1993, 1, 741-754.	0.8	47
376	Intervalley Gamma -X deformation potentials for top valence bands in III-V zincblende semiconductors by ab initio pseudopotential calculations. Journal of Physics Condensed Matter, 1993, 5, 647-662.	0.7	1
377	Ab initiocalculation of the band offset at strained GaAs/InAs (001) heterojunctions. Physical Review B, 1993, 48, 17607-17610.	1.1	37
378	First-principles calculation of the three-dimensional band structure of poly(phenylene vinylene). Physical Review B, 1993, 47, 1800-1810.	1.1	109

#	Article	IF	Citations
379	Electronic structure and equilibrium properties ofGaxAl1â^'xN alloys. Physical Review B, 1993, 48, 17841-17847.	1.1	103
380	Phase stability of wÃ¼stite at high pressure from first-principles linearized augmented plane-wave calculations. Physical Review B, 1993, 47, 7720-7731.	1.1	56
381	Weighted-density-approximation ground-state studies of solids. Physical Review B, 1993, 48, 14099-14103.	1.1	27
382	Electronic structure ofHgBa2Ca2Cu3O8: The role of mercury. Physical Review B, 1993, 48, 3571-3574.	1.1	34
383	Structural and electronic properties of InSb under pressure. Physical Review B, 1993, 47, 4841-4848.	1.1	26
384	Large local-field effects in the second-harmonic susceptibility of crystalline urea. Physical Review B, 1993, 48, 7783-7789.	1.1	23
385	Valence-band-offset transitivity at HgTe/CdTe, HgTe/InSb, and CdTe/InSb interfaces. Physical Review B, 1993, 47, 3714-3717.	1.1	15
386	First-principles calculations of the structural properties, stability, and band structure of complex tetrahedral phases of germanium: ST12 and BC8. Physical Review B, 1993, 48, 17010-17017.	1.1	61
387	Optical properties of silicon nanostructures. Physical Review B, 1993, 48, 10978-10982.	1.1	42
388	Electronic charge distribution in crystalline diamond, silicon, and germanium. Physical Review B, 1993, 47, 9385-9410.	1.1	134
389	Crystals from metallic clusters: A first-principles calculation. Physical Review B, 1993, 48, 1981-1983.	1.1	39
390	Elastic instability of bcc cobalt. Physical Review B, 1993, 47, 8515-8519.	1.1	68
391	Augmented-plane-wave calculations on small molecules. Physical Review B, 1993, 48, 2046-2056.	1.1	24
392	First Principles Study of Polymer-Metalâ€"Metal-Oxide Adhesion. Journal of Adhesion, 1993, 42, 55-63.	1.8	9
393	First-principles evaluation of dynamical response and plasmon dispersion in metals. Physical Review Letters, 1993, 70, 3955-3958.	2.9	100
394	First-principles calculation of the structural, electronic, and vibrational properties of gallium nitride and aluminum nitride. Physical Review B, 1993, 48, 7897-7902.	1.1	240
395	Self-consistent spline augmented-plane-wave calculation: Ground-state properties of Cu. Physical Review B, 1993, 48, 17703-17714.	1.1	20
396	Elastic properties ofNiSi2,CoSi2, andFeSi2by tight-binding calculations. Physical Review B, 1993, 48, 9223-9230.	1.1	38

#	Article	IF	Citations
397	Large zero-point fluctuations of the K(110) surface. Physical Review Letters, 1993, 70, 1964-1967.	2.9	11
398	Evidence for site-sensitive screening of core holes at the Si and Ge (001) surface. Physical Review Letters, 1993, 71, 2338-2341.	2.9	377
399	Structural properties of Î±-quartz under high pressure and amorphization effects. Physical Review B, 1993, 48, 12558-12565.	1.1	16
400	Periodic-cluster calculations of the valence states and native defects in diamond, silicon, germanium, ZnS, ZnSe, and SiC. Physical Review B, 1993, 47, 13219-13232.	1.1	16
401	First-principles study of graphite monofluoride (CF)n. Physical Review B, 1993, 47, 16162-16168.	1.1	125
402	Effect of Ga 3dstates on the structural properties of GaAs and GaP. Physical Review B, 1993, 47, 6751-6754.	1.1	48
403	On the structural properties of NaCl: an ab initio study of the B1-B2 phase transition. Journal of Physics Condensed Matter, 1993, 5, 2969-2976.	0.7	90
404	An ab initio pseudopotential calculation of ground-state and excited-state properties of gallium nitride. Journal of Physics Condensed Matter, 1994, 6, 8781-8794.	0.7	22
405	First-principles calculation of the elastic stiffness tensor of aluminium nitride under high pressure. Journal of Physics Condensed Matter, 1994, 6, 7617-7632.	0.7	37
406	First-principles model hamiltonians for ferroelectric phase transitions. Ferroelectrics, 1994, 151, 59-68.	0.3	9
407	The effect of impurities on the ideal tensile strength of silicon. Philosophical Magazine A: Physics of Condensed Matter, Structure, Defects and Mechanical Properties, 1994, 70, 53-62.	0.8	16
408	Bandstructure Effects in the Dynamic Response of Aluminium. Europhysics Letters, 1994, 27, 681-686.	0.7	41
409	Dissociative chemisorption of hydrogen molecules on the Si(111) (1*1) surface: first-principles calculations. Journal of Physics Condensed Matter, 1994, 6, L687-L692.	0.7	5
410	Adsorption of hydrogen atoms on the silicon(111) (1*1) surface: first-principles calculations. Journal of Physics Condensed Matter, 1994, 6, 1113-1124.	0.7	13
411	Graphite Interplanar Bonding: Electronic Delocalization and van der Waals Interaction. Europhysics Letters, 1994, 28, 403-408.	0.7	192
412	Tight-binding study of grain boundaries in Si: Energies and atomic structures of twist grain boundaries. Physical Review B, 1994, 49, 17102-17117.	1.1	72
413	Electronic properties of Î±-quartz under high pressure and the transition to the amorphous phase. Physical Review B, 1994, 50, 5950-5956.	1.1	12
414	Tetrahedral structures and phase transitions in III-V semiconductors. Physical Review B, 1994, 50, 8389-8401.	1.1	55

#	Article	IF	Citations
415	Electronic structure of Sn/Ge superlattices. Physical Review B, 1994, 49, 11238-11247.	1.1	8
416	First-principles simulated-annealing study of phase transitions and short-range order in transition-metal and semiconductor alloys. Physical Review B, 1994, 50, 6642-6661.	1.1	79
417	Ab initiostudies of hydrocarbon adsorption on stepped diamond surfaces. Physical Review B, 1994, 50, 15369-15380.	1.1	24
418	Magnetic and electronic structure of CoH. Physical Review B, 1994, 49, 12801-12804.	1.1	6
419	Charge transfer in Rb-intercalated graphites. Physical Review B, 1994, 49, 7786-7789.	1.1	9
420	Possibility of Li-Mg and Al-Mg hydrides being metallic. Physical Review B, 1994, 50, 5089-5093.	1.1	28
421	Ab initiopseudopotential calculations for aluminum-rich cobalt compounds. Physical Review B, 1994, 50, 2075-2084.	1.1	17
422	Pressure-induced amorphization, elastic instability, and soft modes in Î±-quartz. Physical Review B, 1994, 49, 3075-3081.	1.1	87
423	Linear and nonlinear optical properties of four polytypes of SiC. Physical Review B, 1994, 50, 11514-11519.	1.1	40
424	Effective-medium tight-binding model for silicon. Physical Review B, 1994, 50, 10727-10741.	1.1	27
425	Ab initiocalculations of the dynamic response of beryllium. Physical Review B, 1994, 49, 8502-8505.	1.1	36
426	Density-functional calculations for grain boundaries in aluminum. Physical Review B, 1994, 50, 15248-15260.	1.1	60
427	Self-energy effects on the surface-state energies of H-Si(111)1Ã—1. Physical Review B, 1994, 49, 4973-4980.	1.1	89
428	Theoretical study of grain boundaries in Si: Effects of structural disorder on the local electronic structure and the origin of band tails. Physical Review B, 1994, 50, 8502-8522.	1.1	59
429	Electronic structure ofPrBa2Cu3O7. Physical Review B, 1994, 50, 4106-4111.	1.1	26
430	First-principles determination of the interatomic-force-constant tensor of Au. Physical Review B, 1994, 49, 3226-3229.	1.1	26
431	Theoretical study of high-density phases of covalent semiconductors. I.Ab initiotreatment. Physical Review B, 1994, 49, 5329-5340.	1.1	74
432	First principles linear response calculations of lattice dynamics for CuCl. Physical Review Letters, 1994, 72, 368-371.	2.9	50

#	Article	IF	Citations
433	LaPt2B2C: A conventional borocarbide superconductor. Physical Review B, 1994, 50, 6486-6488.	1.1	25
434	Theoretical studies of the stability of orderedA8Bcompounds. Physical Review B, 1994, 50, 5962-5970.	1.1	11
435	Electron transport properties inRuO2rutile. Physical Review B, 1994, 49, 7107-7114.	1.1	52
436	Ground-state properties ofCoSi2determined by a total-energy pseudopotential method. Physical Review B, 1994, 49, 16300-16308.	1.1	33
437	Structural and bonding properties of solid tellurium from first-principles calculations. Physical Review B, 1994, 50, 9063-9071.	1.1	42
438	Unequal wave vectors in short- versus long-range ordering in intermetallic compounds. Physical Review B, 1994, 50, 6626-6636.	1.1	37
439	Band-Offsets Between Group-III-Nitrides. Materials Research Society Symposia Proceedings, 1994, 339, 607.	0.1	14
440	Atomic and electronic structure of the GaAs/ZnSe(001) interface. Physical Review B, 1994, 50, 8616-8628.	1.1	84
441	Electron trapping and impurity segregation without defects:Ab initiostudy of perfectly rebonded grain boundaries. Physical Review B, 1994, 49, 4525-4531.	1.1	50
442	Linearized-augmented-plane-wave method with Car-Parrinello scaling. Physical Review B, 1994, 49, 17424-17427.	1.1	3
443	Electronic properties and valence-band offset of strained ZnTe/CdTe (001) superlattices. Physical Review B, 1994, 50, 11949-11954.	1.1	16
444	Magnetism in metastable bcc and fcc ironâ€copper alloys. Journal of Applied Physics, 1994, 75, 6580-6582.	1.1	2
445	Quantum chemical simulations of hole self-trapping in semi-ionic crystals. International Journal of Quantum Chemistry, 1994, 52, 1177-1198.	1.0	26
446	Chargeâ€Density Transfer of H Adsorption on the Si(111) (1 Ã— 1) Surface. Physica Status Solidi (B): Basic Research, 1994, 186, 143-157.	0.7	1
447	First-principles study of the stacking effect on the electronic properties of graphite(s). Carbon, 1994, 32, 289-299.	5.4	193
448	Lattice strain from valence-band holes in SiGa alloys. Solid State Communications, 1994, 90, 253-256.	0.9	1
449	Third-order density-functional perturbation theory: A practical implementation with applications to anharmonic couplings in Si. Solid State Communications, 1994, 91, 813-816.	0.9	48
450	Ab initio calculation of electronic structure and structural properties of ZnSexTe1â^'x. Journal of Crystal Growth, 1994, 138, 499-503.	0.7	6

#	Article	IF	Citations
451	Ab initiomolecular-dynamics simulation of the liquid-metalâ€“amorphous-semiconductor transition in germanium. Physical Review B, 1994, 49, 14251-14269.	1.1	17,829
452	Title is missing!. Journal of Physics Condensed Matter, 1994, 6, 8149-8166.	0.7	20
453	Theory of diamondlike amorphous carbon. Physical Review B, 1994, 49, 16415-16422.	1.1	182
454	Structure and Energetics of Alumina Surfaces Calculated from First Principles. Journal of the American Ceramic Society, 1994, 77, 335-338.	1.9	203
455	First-Principles Calculations for Niobium Atoms on a Sapphire Surface. Journal of the American Ceramic Society, 1994, 77, 431-436.	1.9	64
456	First-principles investigation of ferroelectricity in perovskite compounds. Physical Review B, 1994, 49, 5828-5844.	1.1	629
457	Interatomic force constants from first principles: The case of Î±-quartz. Physical Review B, 1994, 50, 13035-13038.	1.1	229
458	Lattice dynamics and dielectric properties ofSiO2stishovite. Physical Review Letters, 1994, 72, 1686-1689.	2.9	55
459	Ab initiocalculation of the structural and electronic properties of carbon and boron nitride using ultrasoft pseudopotentials. Physical Review B, 1994, 50, 15606-15622.	1.1	370
460	Explicit treatment of the gallium 3delectrons in GaN using the plane-wave pseudopotential method. Physical Review B, 1994, 50, 2159-2165.	1.1	169
461	Derivation of interatomic potentials for microporous aluminophosphates from the structure and properties of berlinite. Journal of the Chemical Society, Faraday Transactions, 1994, 90, 3175.	1.7	124
462	Energetics and electronic structure of silver chloride. Physical Review B, 1994, 49, 17420-17423.	1.1	41
463	Improved tetrahedron method for Brillouin-zone integrations. Physical Review B, 1994, 49, 16223-16233.	1.1	5,977
464	Influence of atomic relaxations on the structural properties of SiC polytypes fromab initiocalculations. Physical Review B, 1994, 50, 17037-17046.	1.1	136
465	Impact ionization rate in GaAs. Physical Review B, 1994, 49, 4494-4500.	1.1	62
466	Ï€ bonding versus electronic-defect generation: An examination of band-gap properties in amorphous carbon. Physical Review B, 1994, 50, 1489-1501.	1.1	103
467	The energetics of NH3 adsorption at the MgO(001) surface. Surface Science, 1994, 320, 331-343.	0.8	66
468	Mechanisms of self-diffusion on flat and stepped Al surfaces. Surface Science, 1994, 307-309, 501-506.	0.8	15

#	Article	IF	Citations
469	The energetics and dynamics of H2 dissociation on Al(110). Surface Science, 1994, 304, 131-144.	0.8	48
470	First-principles calculation of the Mg(0001) surface relaxation. Surface Science, 1994, 302, 215-222.	0.8	48
471	Surface electronic properties of ZnS, ZnSe and ZnTe(110). Surface Science, 1994, 307-309, 959-962.	0.8	6
472	Surface polarons and bipolarons at GaAs(110) with adsorbed alkali metals. Surface Science, 1994, 307-309, 1001-1006.	0.8	6
473	Norm-conserving and ultrasoft pseudopotentials for first-row and transition elements. Journal of Physics Condensed Matter, 1994, 6, 8245-8257.	0.7	2,947
474	Ab initiostudy of MnO and NiO. Physical Review B, 1994, 50, 5041-5054.	1.1	441
475	Ab-initio pseudopotential calculations of the valence band offset at HgTe/CdTe, HgTe/InSb and CdTe/InSb interfaces: transitivity and orientation dependence. Computational Materials Science, 1994, 2, 395-399.	1.4	1
476	New phases and physical properties of the semiconducting nitrides: AlN, GaN, InN. Computational Materials Science, 1994, 2, 400-412.	1.4	17
477	Polarization, structural and electronic properties of SiC polytypes. Computational Materials Science, 1994, 2, 389-394.	1.4	0
478	Dielectric constants and Born effective charges ofTiO2rutile. Physical Review B, 1994, 49, 14730-14731.	1.1	30
479	Electronic structure of wide-band-gap ternary pnictides with the chalcopyrite structure. Physical Review B, 1994, 49, 4549-4558.	1.1	61
480	Electronic structure ofNaCuO2. Physical Review B, 1994, 49, 1580-1585.	1.1	13
481	Thick sodium overlayers on GaAs(110). Physical Review B, 1994, 49, 5516-5521.	1.1	4
482	Stability of carbon nitride solids. Physical Review B, 1994, 50, 10362-10365.	1.1	368
483	Electronic and magnetic properties of the spinel semiconductorCdCr2Se4. Physical Review B, 1994, 49, 2503-2508.	1.1	18
484	All-electron local-density and generalized-gradient calculations of the structural properties of semiconductors. Physical Review B, 1994, 50, 14947-14951.	1.1	172
485	Quantum Monte Carlo Calculations for Solids Using SpecialkPoints Methods. Physical Review Letters, 1994, 73, 1959-1962.	2.9	72
486	Iron at high pressure: Linearized-augmented-plane-wave computations in the generalized-gradient approximation. Physical Review B, 1994, 50, 6442-6445.	1.1	225

#	Article	IF	Citations
487	Native Defects and Impurities in Cubic and Wurtzite Gan. Materials Research Society Symposia Proceedings, 1994, 339, 687.	0.1	29
488	Density functional approach to moderately large cluster embedding for infinite metal substrates. Journal of Electron Spectroscopy and Related Phenomena, 1994, 69, 31-42.	0.8	7
489	Phase Stability and Electronic Structure of GaAs_{1â€“x}N_x Alloys. Materials Research Society Symposia Proceedings, 1995, 379, 3.	0.1	3
490	Atomic Hydrogen in GaN. Materials Research Society Symposia Proceedings, 1995, 378, 503.	0.1	7
491	Hydrogen, Acceptors, and H-Acceptor Complexes in GaN. Materials Research Society Symposia Proceedings, 1995, 395, 503.	0.1	20
492	An Ab Initio Investigation of a Grain Boundary in a Transition Metal Oxide. Materials Research Society Symposia Proceedings, 1995, 408, 271.	0.1	1
493	Valence-Band Offset at the Zn-P Interface Between ZnSe and III-V Wide Gap Semiconductor Alloys: A First-Principles Investigation. Materials Research Society Symposia Proceedings, 1995, 408, 539.	0.1	0
494	Atomistic Study of Boron-Doped Silicon. Materials Research Society Symposia Proceedings, 1995, 408, 551.	0.1	0
495	Chapter 6 Electronic screening in metals: from phonons to plasmons. Dynamical Properties of Solids, 1995, , 425-507.	0.0	0
496	Ab initio total energy study of brucite, diaspore and hypothetical hydrous wadsleyite. Physics and Chemistry of Minerals, 1995, 22, 461.	0.3	44
497	High Pressure Properties of the Alkalineâ€Earth Sulphides. Physica Status Solidi (B): Basic Research, 1995, 190, 193-197.	0.7	25
498	Study of the Electronic Structure and the Role of Gallium 3d Electrons in Gallium Nitride. Physica Status Solidi (B): Basic Research, 1995, 191, 387-394.	0.7	11
499	Atomic structure of surfactant monolayers and its role in epitaxial growth. Materials Science and Engineering B: Solid-State Materials for Advanced Technology, 1995, 30, 175-186.	1.7	37
500	Role of the InAs monomolecular plane inserted in bulk GaAs. Materials Science and Engineering B: Solid-State Materials for Advanced Technology, 1995, 35, 386-390.	1.7	0
501	Average bond energy and deformation potentials: Application to Siî—¸Ge heterointerfaces. Physica B: Condensed Matter, 1995, 215, 389-396.	1.3	4
502	Electronic structure and stability of periodically repeated Cu(Ca0.3Sr0.7)2(Ca0.3Sr0.7)nâ^'1CunO2n+2Î´ â€œdefect layersâ€•in infinite-layer superconductors. Physica C: Superconductivity and Its Applications, 1995, 251, 389-398.	0.6	1
503	A theoretical study of pressure effects on selenium-I. Journal of Physics and Chemistry of Solids, 1995, 56, 329-334.	1.9	8
504	Trade-off between increased size and increased broadening of magneto-optic effects in cerium and uranium systems. Journal of Physics and Chemistry of Solids, 1995, 56, 1509-1516.	1.9	19

#	Article	IF	Citations
505	Structural and electronic properties of nitrogen doped fourfold amorphous carbon. Solid State Communications, 1995, 93, 617-621.	0.9	17
506	High pressure phase transitions in aluminum phosphide. Solid State Communications, 1995, 95, 173-175.	0.9	15
507	Projection of plane-wave calculations into atomic orbitals. Solid State Communications, 1995, 95, 685-690.	0.9	415
508	Magnetic properties of URu2Si2. Journal of Magnetism and Magnetic Materials, 1995, 140-144, 1401-1402.	1.0	5
509	On the ab initio evaluation of dynamical electronic response in metals and its comparison with experiment. Nuclear Instruments & Methods in Physics Research B, 1995, 96, 550-564.	0.6	22
510	Ordering tendencies in Pd-Pt, Rh-Pt, and Ag-Au alloys. Journal of Phase Equilibria and Diffusion, 1995, 16, 36-45.	0.3	58
511	Theoretical study of the Si(100) surface reconstruction. Physical Review B, 1995, 51, 14504-14523.	1.1	381
512	Ab initio total energy studies of minerals using density functional theory and the local density approximation. Mineralogical Magazine, 1995, 59, 589-596.	0.6	18
513	Theory of structural, electronic, vibrational, and superconducting properties of high-pressure phases of sulfur. Physical Review B, 1995, 52, 12572-12578.	1.1	42
514	Electronic structure of GaAs with an InAs (001) monolayer. Physical Review B, 1995, 52, 10776-10779.	1.1	12
515	Interaction of hydrogen with the Be(0001) surface. Physical Review B, 1995, 51, 13748-13759.	1.1	37
516	Symmetric stress tensor in the local-density-functional framework using a separable nonlocal pseudopotential. Physical Review B, 1995, 51, 14697-14700.	1.1	9
517	Properties ofB2O: An unsymmetrical analog of carbon. Physical Review B, 1995, 52, 15807-15811.	1.1	26
518	Theory of hydrogen-decorated gallium vacancies in GaAs and of their radiative complexes. Physical Review B, 1995, 52, 11044-11051.	1.1	6
519	Calculated structural and electronic properties of CdSe under pressure. Physical Review B, 1995, 51, 4926-4930.	1.1	50
520	Pressure-induced phase transformations in AlAs: Comparison betweenab initiotheory and experiment. Physical Review B, 1995, 51, 5678-5681.	1.1	17
521	All-electron study of gradient corrections to the local-density functional in metallic systems. Physical Review B, 1995, 51, 4105-4109.	1.1	202
522	Microscopic structures of Sb-H, Te-H, and Sn-H complexes in silicon. Physical Review B, 1995, 52, 8864-8876.	1.1	8

#	Article	IF	Citations
523	Ab initioatomistic simulation of the strength of defective aluminum and tests of empirical force models. Physical Review B, 1995, 52, 15191-15207.	1.1	66
524	Spin-Polarization-Induced Structural Selectivity inPd3XandPt3X(X=3d) Compounds. Physical Review Letters, 1995, 75, 1320-1323.	2.9	37
525	Variational and diffusion quantum Monte Carlo calculations at nonzero wave vectors: Theory and application to diamond-structure germanium. Physical Review B, 1995, 51, 10591-10600.	1.1	79
526	Ab initiototal-energy pseudopotential calculations for polymorphicB2O3crystals. Physical Review B, 1995, 51, 1447-1455.	1.1	35
527	Band structure in adaptive curvilinear coordinates. Physical Review B, 1995, 51, 9508-9514.	1.1	33
528	Hydrogen passivation ofEL2 defects andH2*-like complex formation in gallium arsenide. Physical Review B, 1995, 51, 4172-4175.	1.1	12
529	Theoretical study of Ti adsorption on Si(001) surfaces. Physical Review B, 1995, 52, 14748-14754.	1.1	20
530	Extension of a local-orbital density-functional method to transition metals: Application to Pt(110) surface relaxation. Physical Review B, 1995, 52, 16420-16427.	1.1	8
531	Thermoelastic properties of perfect crystals with nonprimitive lattices. I. General theory. Physical Review B, 1995, 51, 3520-3534.	1.1	44
532	Phonon modes of diamond (100) surfaces fromab initiocalculations. Physical Review B, 1995, 51, 1989-1992.	1.1	63
533	Effects of epitaxial strain and ordering direction on the electronic properties of GaSb/InSb and InAs/InSb superlattices. Physical Review B, 1995, 52, 5247-5255.	1.1	11
534	Embedded-atom model of glass-forming Si-metal alloys. Physical Review B, 1995, 51, 14962-14975.	1.1	23
535	Scaling hypothesis for corrections to total energy and stress in plane-wave-basedab initiocalculations. Physical Review B, 1995, 52, 8160-8178.	1.1	18
536	Overlayer growth and electronic properties of the Bi/GaSb(110) interface. Physical Review B, 1995, 51, 16822-16831.	1.1	10
537	Ab initiopseudopotential calculations of the atomic and electronic structure of the Ta (100) and (110) surfaces. Physical Review B, 1995, 52, 11784-11792.	1.1	14
538	Vacancies and impurities in aluminum and magnesium. Physical Review B, 1995, 52, 6313-6326.	1.1	112
539	Theory of Adsorption and Desorption ofH2/Si(001). Physical Review Letters, 1995, 74, 952-955.	2.9	94
540	Theoretical study of H-P and H-B complexes in silicon. Physical Review B, 1995, 51, 4166-4171.	1.1	20

#	Article	IF	Citations
541	Thermoelastic properties of perfect crystals with nonprimitive lattices. II. Application to KCl and NaCl. Physical Review B, 1995, 51, 3535-3548.	1.1	17
542	First-principles theory of short-range order, electronic excitations, and spin polarization in Ni-V and Pd-V alloys. Physical Review B, 1995, 52, 8813-8828.	1.1	100
543	High-pressure low-symmetry phases of cesium halides. Physical Review B, 1995, 51, 8060-8068.	1.1	23
544	Ab initiopseudopotential calculations of the band lineups at strained ZnS/ZnSe interfaces: Including the 3delectrons of Zn as valence states. Physical Review B, 1995, 52, 1830-1838.	1.1	21
545	First-principles pseudopotential study of the structural phases of silicon. Physical Review B, 1995, 51, 9652-9660.	1.1	105
546	Application of adaptive curvilinear coordinates to the electronic structure of solids. Physical Review B, 1995, 51, 7337-7340.	1.1	109
547	Theoretical study of cubic structures based on fullerene carbon clusters:C28C and (C28)2. Physical Review B, 1995, 52, 2125-2130.	1.1	9
548	Electronic structure, surface states, surface energy, and work function of the Cu(100) surface. Physical Review B, 1995, 51, 17135-17150.	1.1	27
549	Anomalies in the pressure dependence of the effective charge in cubic semiconductors. Physical Review B, 1995, 52, R8613-R8616.	1.1	35
550	Energetics of diffusion on the (100) and (111) surfaces of Ag, Au, and Ir from first principles. Physical Review B, 1995, 52, 9078-9085.	1.1	94
551	Conjugate-gradient methods for metallic systems and band-structure calculations. Physical Review B, 1995, 52, 14497-14504.	1.1	6
552	Structure and stability of several high-pressure crystalline polymorphs of silica. Physical Review B, 1995, 51, 16392-16395.	1.1	27
553	Polymorphism and metastability in NbN: Structural predictions from first principles. Physical Review B, 1995, 52, R8585-R8588.	1.1	16
554	Ab initio calculations of the band offset at a ZnSe/ZnTe (100) interface. Semiconductor Science and Technology, 1995, 10, 270-273.	1.0	4
555	A microscopic study of barium titanate. Ferroelectrics, 1995, 164, 113-121.	0.3	20
556	Band Structure of Layered SemiconductorÎ±-In2Se3by the Numerical-Basis-Set LCAO Method. Journal of the Physical Society of Japan, 1995, 64, 1622-1628.	0.7	3
557	Coulomb interaction and ferroelectric phase transitions in perovskite compounds. Ferroelectrics, 1995, 164, 291-301.	0.3	16
558	Local density and generalized gradient approximation studies of KNbO3 and BaTiO3. Ferroelectrics, 1995, 164, 143-152.	0.3	58

#	Article	IF	Citations
559	Atomic short-range order and alloy ordering tendency in the Ag-Au system. Modelling and Simulation in Materials Science and Engineering, 1995, 3, 753-770.	0.8	16
560	Calculated structural and electronic properties of boron phosphide under pressure. Semiconductor Science and Technology, 1995, 10, 1452-1457.	1.0	27
561	The pressure-induced ferroelastic phase transition of SiO2stishovite. Journal of Physics Condensed Matter, 1995, 7, 3693-3698.	0.7	33
562	Breakdown of Rigid-Unit Vibrations in Layered Semiconductors under Pressure: Application to Germanium Sulfide. Europhysics Letters, 1995, 31, 151-155.	0.7	8
563	Ab initio study of tritium defects in lithium oxide. Journal of Physics Condensed Matter, 1995, 7, 6981-6992.	0.7	21
564	Physics and Control of Conduction Type in $f CuInS_{2}$ with Defect Chalcopyrite Structure. Japanese Journal of Applied Physics, 1995, 34, L1584-L1587.	0.8	15
565	Electronic structure and phase stability ofGaAs1â^'xNxalloys. Physical Review B, 1995, 51, 10568-10571.	1.1	273
566	Strain-induced birefringence in GaAs. Physical Review B, 1995, 51, 10477-10488.	1.1	17
567	First-principles theory of ferroelectric phase transitions for perovskites: The case ofBaTiO3. Physical Review B, 1995, 52, 6301-6312.	1.1	649
568	The structure of the stoichiometric and reduced SnO2(110) surface. Surface Science, 1995, 339, 258-271.	0.8	142
569	The energetics and electronic structure of defective and irregular surfaces on MgO. Surface Science, 1995, 343, 221-239.	0.8	186
570	Structure and properties of silicon XII: A complex tetrahedrally bonded phase. Physical Review B, 1995, 52, 4072-4085.	1.1	230
571	First-principles studies of the structural and optical properties of crystalline poly(para-phenylene). Physical Review B, 1995, 51, 9668-9676.	1.1	231
572	Quasiparticle band structure of bulk hexagonal boron nitride and related systems. Physical Review B, 1995, 51, 6868-6875.	1.1	583
573	Electronic structure of crystalline and amorphous NbxMo1-xalloys: Rigid versus rectangular bands. Journal of Physics Condensed Matter, 1995, 7, 5843-5856.	0.7	4
574	Ferroelectric phase transitions: A first-principles approach. Ferroelectrics, 1995, 164, 15-32.	0.3	35
575	Fermi-Dirac distribution inab initioGreenâ€™s-function calculations. Physical Review B, 1995, 52, 11502-11508.	1.1	104
576	Local norm-conserving pseudo-Hamiltonians. Physical Review A, 1995, 52, 236-257.	1.0	71

#	Article	IF	Citations
577	Consistent structural properties for AlN, GaN, and InN. Physical Review B, 1995, 51, 7866-7869.	1.1	266
578	Exotic structures of tetrahedral semiconductors. Reports on Progress in Physics, 1995, 58, 705-754.	8.1	41
579	Band gap and stability in the ternary intermetallic compounds NiSnM(M=Ti,Zr,Hf): A first-principles study. Physical Review B, 1995, 51, 10443-10453.	1.1	312
580	High-pressure effects in the layered semiconductor germanium selenide. Physical Review B, 1995, 51, 16750-16760.	1.1	41
581	Lattice dynamics of ferroelectrics using the lapw linear response method: Application to KNbO3. Ferroelectrics, 1995, 164, 161-167.	0.3	10
582	First-Principles Study of Carbon Nanotube Solid-State Packings. Europhysics Letters, 1995, 29, 43-48.	0.7	109
583	First-principles pseudopotential study of the phase stability of the III-V semiconductors GaAs and AlAs. Physical Review B, 1995, 52, 8881-8892.	1.1	90
584	Application of generalized gradient approximations: The diamondâ€“Î²-tin phase transition in Si and Ge. Physical Review B, 1995, 52, 2550-2556.	1.1	153
585	Dominant density parameters and local pseudopotentials for simple metals. Physical Review B, 1995, 51, 14001-14011.	1.1	175
586	Ab initiocalculation of the thermodynamic properties and atomic temperature factors ofSiO2Î±-quartz and stishovite. Physical Review B, 1995, 51, 8610-8613.	1.1	287
587	First-principles study of several hypothetical silica framework structures. Physical Review B, 1995, 52, 8064-8073.	1.1	113
588	Structural, electronic, and vibrational properties of diamond (100), (111), and (110) surfaces fromab initiocalculations. Physical Review B, 1995, 51, 14669-14685.	1.1	70
589	First-Principles Determination of Chain-Structure Instability in KNbO3. Physical Review Letters, 1995, 74, 4067-4070.	2.9	153
590	Generalized-gradient approximations to density-functional theory: A comparative study for atoms and solids. Physical Review B, 1996, 53, 1180-1185.	1.1	228
591	Dimer reconstruction and electronic surface states on clean and hydrogenated diamond (100) surfaces. Physical Review B, 1996, 53, 7334-7351.	1.1	240
592	Abinitiopseudopotential study of the structural phase transformations of ZnS under high pressure. Physical Review B, 1996, 53, 8262-8266.	1.1	44
593	Periodic boundary conditions inab initiocalculations. II. Brillouin-zone sampling for aperiodic systems. Physical Review B, 1996, 53, 15513-15517.	1.1	100
594	Generalized Kohn-Sham schemes and the band-gap problem. Physical Review B, 1996, 53, 3764-3774.	1.1	1,075

#	Article	IF	Citations
595	Anab InitioHartreeâ^'Fock Study of the Cubic and Tetragonal Phases of Bulk Tungsten Trioxide. Journal of the American Chemical Society, 1996, 118, 12174-12182.	6.6	120
596	Polarization dependence of Born effective charge and dielectric constant inKNbO3. Physical Review B, 1996, 54, 11161-11168.	1.1	54
597	Influence of gradient corrections on the bulk and surface properties ofTiO2andSnO2. Physical Review B, 1996, 53, 957-960.	1.1	166
598	Empirical potential derivation for ionic materials. The Philosophical Magazine: Physics of Condensed Matter B, Statistical Mechanics, Electronic, Optical and Magnetic Properties, 1996, 73, 3-19.	0.6	314
599	Electron-phonon interactions and related physical properties of metals from linear-response theory. Physical Review B, 1996, 54, 16487-16501.	1.1	491
600	Structural and electronic properties of rhodium surfaces: an ab initio approach. Surface Science, 1996, 346, 300-321.	0.8	118
601	Atomic and electronic structures of Te adsorbed on GaAs(100) and InAs(100). Surface Science, 1996, 352-354, 379-382.	0.8	6
602	The adsorption of H2O on TiO2 and SnO2(110) studied by first-principles calculations. Surface Science, 1996, 350, 145-158.	0.8	242
603	Arsenic adatom structures for Ge(111) and Si(111) surfaces: first-principles calculations. Surface Science, 1996, 365, 383-393.	0.8	6
604	Atomic and electronic structure of diamond (111) surfaces II. (2 Ã— 1) and (âˆš3 Ã— âˆš3) reconstructions of the clean and hydrogen-covered three dangling-bond surfaces. Surface Science, 1996, 366, 464-482.	0.8	40
605	Atomic and electronic structure of diamond (111) surfaces I. Reconstruction and hydrogen-induced de-reconstruction of the one dangling-bond surface. Surface Science, 1996, 366, 445-463.	0.8	117
606	Studies on AB2-type intermetallic compounds, I. Mg2Ge and Mg2Sn: single-crystal structure refinement and ab initio calculations. Journal of Alloys and Compounds, 1996, 235, 250-255.	2.8	65
607	Chemical trends in gold alkali alloys: A density functional theory study on stability and charge transfer Part I: Gold alkali alloys of the formula MAu. Journal of Alloys and Compounds, 1996, 233, 30-38.	2.8	19
608	Efficiency of ab-initio total energy calculations for metals and semiconductors using a plane-wave basis set. Computational Materials Science, 1996, 6, 15-50.	1.4	54,900
609	The calculation of STM images, STS spectra, and XPS peak shifts for galena: New tools for understanding mineral surface chemistry. Geochimica Et Cosmochimica Acta, 1996, 60, 2413-2426.	1.6	87
610	First-principles study of stability and vibrational properties of tetragonalPbTiO3. Physical Review B, 1996, 54, 3817-3824.	1.1	93
611	Chemisorption of H on Pd(111): Anabinitioapproach with ultrasoft pseudopotentials. Physical Review B, 1996, 54, 2157-2166.	1.1	135
612	Ab initio studies of structural instabilities in magnesium silicate perovskite. Physics and Chemistry of Minerals, 1996, 23, 107.	0.3	45

#	Article	IF	Citations
613	The energetics of adsorption of HCOOH on the MgO(100) surface. Surface Science, 1996, 367, 135-148.	0.8	36
614	Abinitiocalculations of energies and self-diffusion on flat and stepped surfaces of Al and their implications on crystal growth. Physical Review B, 1996, 53, 4958-4973.	1.1	212
615	Linear-response theory and lattice dynamics: A muffin-tin-orbital approach. Physical Review B, 1996, 54, 16470-16486.	1.1	613
616	Theory of the Anomalous Rayleigh Dispersion at H/W(110) Surfaces. Physical Review Letters, 1996, 77, 2491-2494.	2.9	51
617	Dopant Segregation at Semiconductor Grain Boundaries through Cooperative Chemical Rebonding. Physical Review Letters, 1996, 77, 1306-1309.	2.9	73
618	Ground-state properties and high-pressure phase of beryllium chalcogenides BeSe, BeTe, and BeS. Physical Review B, 1996, 54, 11861-11864.	1.1	66
619	Isotopic effects on the lattice constant in compound semiconductors by perturbation theory: Anab initiocalculation. Physical Review B, 1996, 54, 11305-11310.	1.1	93
620	Thermal properties of iron at high pressures and temperatures. Physical Review B, 1996, 53, 8296-8309.	1.1	163
621	Adsorption of atomic oxygen on the MgO (100) surface. Journal of the Chemical Society, Faraday Transactions, 1996, 92, 2075.	1.7	25
622	Cation valence charge states of MnFe2O4: an ab initio Hartreeâ€“Fock study. Journal of the Chemical Society, Faraday Transactions, 1996, 92, 2043-2047.	1.7	9
623	Ab-initio molecular dynamics calculations: a parallel implementation of the Car-Parrinello method. , 0, , .		0
624	Ground-state properties and structural phase transformation of beryllium oxide. Journal of Physics Condensed Matter, 1996, 8, 3385-3390.	0.7	44
625	Bandgap Variation at the Isostructural Phase Transformation of Wurtzite InN. MRS Internet Journal of Nitride Semiconductor Research, 1996, 1, 1.	1.0	4
626	An ab initio study of the compressional behavior of forsterite. American Mineralogist, 1996, 81, 257-260.	0.9	26
627	Electronic Structures of P-Type Doped CuInS₂. Materials Research Society Symposia Proceedings, 1996, 426, 201.	0.1	7
628	Ab Initio Pseudopotential Calculations of Carbon Impurities in SI. Materials Research Society Symposia Proceedings, 1996, 438, 33.	0.1	0
629	Ab Initio Pseudopotential Calculations of Carbon Impurities In SI. Materials Research Society Symposia Proceedings, 1996, 439, 59.	0.1	7
630	Cooperative Chemical Rebonding In The Segregation Of Impurities In Silicon Grain Boundaries. Materials Research Society Symposia Proceedings, 1996, 442, 213.	0.1	0

#	Article	IF	Citations
631	Long-Range Order Effects in Ferroelectric Pb(Zr1/2Ti1/2)O3. Materials Research Society Symposia Proceedings, 1996, 453, 191.	0.1	1
632	A Theoretical and Experimental Study of the Chemical Bonding in AgGaS2. Materials Research Society Symposia Proceedings, 1996, 453, 215.	0.1	0
633	Efficient iterative schemes forab initiototal-energy calculations using a plane-wave basis set. Physical Review B, 1996, 54, 11169-11186.	1.1	88,250
634	Relaxation in the (001) surface of MoS2: Band structure calculations. Computational and Theoretical Chemistry, 1996, 363, 303-309.	1.5	2
635	Atomistic aspects of diffusion and growth on the Si and Ge (111) surfaces. Thin Solid Films, 1996, 272, 386-398.	0.8	27
636	Density functional theory in periodic systems using local Gaussian basis sets. Computer Physics Communications, 1996, 98, 181-205.	3.0	249
637	Donor-hydrogen complexes in crystalline silicon. Nuovo Cimento Della Societa Italiana Di Fisica D - Condensed Matter, Atomic, Molecular and Chemical Physics, Biophysics, 1996, 18, 181-198.	0.4	0
638	Hydrogen interaction with shallow and deep centers in GaAs. International Journal of Quantum Chemistry, 1996, 57, 823-841.	1.0	9
639	Ground state properties and structural phase transformation of berylliumsulphide. Solid State Communications, 1996, 98, 741-743.	0.9	47
640	Ab-initio electronic structure calculation of the InAs multiple quantum wells in bulk GaAs. Applied Surface Science, 1996, 104-105, 656-660.	3.1	2
641	Electronic Structure and Pressure Dependence for Some Ternary Calcium Nitrides. Physica Status Solidi (B): Basic Research, 1996, 198, 87-91.	0.7	7
642	Electronic and Structural Properties of BeSe, BeTe, and BeS: Comparison between abâ€initio Theory and Experiments. Physica Status Solidi (B): Basic Research, 1996, 198, 439-446.	0.7	54
643	High Pressure Phases of AlSb from abâ€initio Theory. Physica Status Solidi (B): Basic Research, 1996, 198, 455-459.	0.7	19
644	Local interface dipoles and the tuning of the Al/GaAs(100) Schottky-barrier height with ultrathin Si interlayers. Europhysics Letters, 1996, 36, 67-72.	0.7	26
645	Analysis of atomic orbital basis sets from the projection of plane-wave results. Journal of Physics Condensed Matter, 1996, 8, 3859-3880.	0.7	161
646	GaAs equilibrium crystal shape from first principles. Physical Review B, 1996, 54, 8844-8855.	1.1	383
647	Electronic structure of heazlewooditeNi3S2. Physical Review B, 1996, 54, 13542-13545.	1.1	21
648	Ab initiocalculations of interaction energies of magnetic layers in noble metals: Co/Cu(100). Physical Review B, 1996, 53, 9092-9107.	1.1	58

#	Article	IF	Citations
649	Ab initiocalculations of the cohesive, elastic, and dynamical properties ofCoSi2by pseudopotential and all-electron techniques. Physical Review B, 1996, 54, 1729-1734.	1.1	120
650	Pressure and alloy-composition dependence ofAl/Ga1â^'xAlxAs(100)Schottky barriers. Physical Review B, 1996, 54, R11102-R11105.	1.1	20
651	Contribution of quantum and thermal fluctuations to the elastic moduli and dielectric constants of covalent semiconductors. Physical Review B, 1996, 53, 7259-7266.	1.1	36
652	All-electron study of the electronic properties of quartz with Al substitutional impurity. Physical Review B, 1996, 54, 13687-13693.	1.1	25
653	Anomalous effective charges and far-IR optical absorption ofAl2Ru from first principles. Physical Review B, 1996, 54, R8297-R8300.	1.1	19
654	Plane waves basis sets in the description of diatomic anions and valence charge density. Journal of Chemical Physics, 1996, 105, 8231-8236.	1.2	8
655	Isostructural phase transition in InN wurtzite. Physical Review B, 1996, 54, 8945-8949.	1.1	32
656	Structure, dynamics, and electronic structure of liquid Ag-Se alloys investigated byab initiosimulation. Physical Review B, 1996, 54, 190-202.	1.1	63
657	Local aspects of the As-stabilized 2Ã—3 reconstructed (001) surface of strainedInxGa1â^'xAs alloys: A first-principles study. Physical Review B, 1996, 53, 7417-7420.	1.1	5
658	Generalized Gradient Theory for Silica Phase Transitions. Physical Review Letters, 1996, 76, 660-663.	2.9	313
659	Adhesive energy and charge transfer for MgO/Cu heterophase interfaces. Physical Review B, 1996, 54, 7697-7700.	1.1	90
660	Pressure dependence of Born effective charges, dielectric constant, and lattice dynamics in SiC. Physical Review B, 1996, 53, 5430-5437.	1.1	59
661	Investigation of density functionals to predict both ground-state properties and band structures. Physical Review B, 1996, 54, 8420-8429.	1.1	23
662	Detailed theoretical photoelectron angular distributions for LiF(100). Physical Review B, 1996, 53, 10296-10309.	1.1	61
663	Electronic structure of defects and impurities in III-V nitrides: Vacancies in cubic boron nitride. Physical Review B, 1996, 53, 4377-4385.	1.1	58
664	Linear-response calculation of the Coulomb pseudopotentialÎ¼*for Nb. Physical Review B, 1996, 54, 1419-1422.	1.1	19
665	Stability and charge transfer ofC3B ordered structures. Physical Review B, 1996, 54, R2271-R2275.	1.1	86
666	Metastable defect complexes in GaAs. Physical Review B, 1996, 54, 7909-7916.	1.1	33

#	Article	IF	Citations
667	Compositional dependence of the luminescence ofIn0.49(AlyGa1â^'y)0.51P alloys near the directâ€"indirect band-gap crossover. Physical Review B, 1996, 53, 15893-15901.	1.1	14
668	Structural and vibrational properties of complexes formed by hydrogen and As antisites in gallium arsenide. Physical Review B, 1996, 54, 7618-7621.	1.1	1
669	Geometric structure of Be(101Â¯0). Physical Review B, 1996, 53, 13715-13719.	1.1	34
670	Weighted-density approximation in metals and semiconductors. Physical Review B, 1996, 53, 12666-12673.	1.1	19
671	Electronic structure ofCuV2S4. Physical Review B, 1996, 53, 9626-9633.	1.1	28
672	Ab initiopseudopotential calculations of B diffusion and pairing in Si. Physical Review B, 1996, 54, 4741-4747.	1.1	202
673	Transverse interplanar forces and phonon spectra of strained Si, Ge, and Si/Ge superlattices. Physical Review B, 1996, 53, 5372-5378.	1.1	3
674	First-principles study of a tilt grain boundary in rutile. Physical Review B, 1996, 54, 13727-13733.	1.1	59
675	Self-consistent relativistic full-potential Korringa-Kohn-Rostoker total-energy method and applications. Physical Review B, 1996, 54, 11187-11198.	1.1	49
676	Influence of polytypism on thermal properties of silicon carbide. Physical Review B, 1996, 54, 1791-1798.	1.1	82
677	Chemical and structural contributions to the valence-band offset at GaP/GaAs heterojunctions. Physical Review B, 1996, 54, 5691-5695.	1.1	12
678	Large atomic displacements associated with the nitrogen antisite in GaN. Physical Review B, 1996, 54, 1474-1477.	1.1	76
679	Gaussian basis density functional theory for systems periodic in two or three dimensions: Energy and forces. Journal of Chemical Physics, 1996, 105, 10983-10998.	1.2	59
680	Energetics of AlN thin films and the implications for epitaxial growth on SiC. Physical Review B, 1996, 54, R17351-R17354.	1.1	23
681	Analyses of theab initioharmonic interatomic force constants of stishovite. Physical Review B, 1996, 54, 8973-8976.	1.1	4
682	Diffusion Monte Carlo study of jellium surfaces: Electronic densities and pair correlation functions. Physical Review B, 1996, 54, 17199-17207.	1.1	43
683	Band structure of CdS and CdSe at high pressure. Physical Review B, 1996, 54, 17585-17590.	1.1	35
684	Abinitiostudy of oxygen point defects in GaAs, GaN, and AlN. Physical Review B, 1996, 54, 16676-16682.	1.1	268

#	Article	IF	Citations
685	Optimal basis sets for detailed Brillouin-zone integrations. Physical Review B, 1996, 54, 16464-16469.	1.1	66
686	Hydrogen adsorption on the (100) surfaces of rhodium and palladium: the influence of non-local exchange - correlation interactions. Journal of Physics Condensed Matter, 1996, 8, 7659-7675.	0.7	52
687	Ab initiocalculations for SiC - Al interfaces: tests of electronic-minimization techniques. Modelling and Simulation in Materials Science and Engineering, 1996, 4, 397-408.	0.8	48
688	Tight-binding parameters for silicon-boron interactions with application to boron-defect pairs in crystalline silicon. The Philosophical Magazine: Physics of Condensed Matter B, Statistical Mechanics, Electronic, Optical and Magnetic Properties, 1996, 73, 71-84.	0.6	7
689	Pressure-dependent dynamical and dielectric properties of cubic SiC. Journal of Physics Condensed Matter, 1996, 8, 2945-2955.	0.7	31
690	Modelling of adsorption of iron impurities at the surface of graphite. The Philosophical Magazine: Physics of Condensed Matter B, Statistical Mechanics, Electronic, Optical and Magnetic Properties, 1996, 73, 611-617.	0.6	16
691	Generalized stacking fault energy surfaces and dislocation properties of silicon: A first-principles theoretical study. Philosophical Magazine A: Physics of Condensed Matter, Structure, Defects and Mechanical Properties, 1996, 74, 1367-1384.	0.8	96
692	Vibrational properties of the layered semiconductor germanium sulfide under hydrostatic pressure: Theory and experiment. Physical Review B, 1996, 53, 14806-14817.	1.1	59
693	Structural properties and reorientation of the complex in gallium arsenide: a theoretical study. Journal of Physics Condensed Matter, 1996, 8, 11069-11082.	0.7	0
694	P-Type Doping of the Group V Elements in CuInS$_{f 2}$. Japanese Journal of Applied Physics, 1996, 35, L1562-L1565.	0.8	17
695	Interactions of hydrogen molecules with the Si(111) surface: first-principles calculations. Journal of Physics Condensed Matter, 1996, 8, 5857-5870.	0.7	4
696	Ab initiocalculation of the high-pressure behaviour of hydrogen cyanide. Journal of Physics Condensed Matter, 1996, 8, 9049-9057.	0.7	11
697	Anab initioapproach to determining the parameters of the model Hamiltonian. Journal of Physics Condensed Matter, 1996, 8, 2539-2548.	0.7	6
698	Electronic Structures and Effects of S Substitutions in $f CuIn(S_{0.875}X_{0.125})_{2}~(X=O,,N,,P,,C,,Si,or,B)$. Japanese Journal of Applied Physics, 1996, 35, L370-L373.	0.8	5
699	Approximating infinite-krepresentations: surface relaxations and work functions of Al(001) and Be(0001). Journal of Physics Condensed Matter, 1997, 9, 8359-8368.	0.7	5
700	First-principles calculations of band offsets of heterostructures. Journal of Physics Condensed Matter, 1997, 9, L279-L283.	0.7	6
701	Intermittent diffusion on the reconstructed Si(111) surface. Europhysics Letters, 1997, 39, 287-292.	0.7	65
702	First-principles Hartree - Fock description of the electronic structure and magnetism of hole and electron states in MnO. Journal of Physics Condensed Matter, 1997, 9, 6591-6606.	0.7	11

#	Article	IF	Citations
703	First-principles studies of the thermodynamic properties of bulk Li. Journal of Physics Condensed Matter, 1997, 9, 2135-2148.	0.7	19
704	Polymorphism of CsI. Journal of Physics Condensed Matter, 1997, 9, 9811-9817.	0.7	5
705	Ab initiostudy of the anomalies in the He-atom-scattering spectra of H/Mo(110) and H/W(110). Physical Review B, 1997, 56, 13503-13518.	1.1	34
706	Halogen adsorption on transition-metal surfaces: A case study of Cl on Ta(110). Physical Review B, 1997, 55, 10848-10853.	1.1	15
707	Carbon nitride compounds with 1:1 stoichiometry. Physical Review B, 1997, 55, 5684-5688.	1.1	32
708	Ordering of As impurities in a Si dislocation core. Applied Physics Letters, 1997, 70, 336-338.	1.5	16
709	Valence-band offsets at theAlxGa0.5â^'xIn0.5P-ZnSe(001) lattice-matched interface. Physical Review B, 1997, 55, 1718-1723.	1.1	2
710	Structure, dissociation, and the vibrational signatures of hydrogen clusters in amorphous silicon. Physical Review B, 1997, 56, 4565-4572.	1.1	18
711	Nanocontacts: Probing Electronic Structure under Extreme Uniaxial Strains. Physical Review Letters, 1997, 79, 4198-4201.	2.9	35
712	Ionic solids at elevated temperatures and high pressures: MgF2. Journal of Chemical Physics, 1997, 107, 4337-4344.	1.2	41
713	Microscopic Theory of the Shape Memory Effect in TiNi. Physical Review Letters, 1997, 78, 4789-4792.	2.9	29
714	Theoretical investigations of As overlayers on InP(110) surfaces. Physical Review B, 1997, 56, 15847-15852.	1.1	15
715	Free-energy derivatives and structure optimization within quasiharmonic lattice dynamics. Physical Review B, 1997, 56, 14380-14390.	1.1	83
716	Ab initio calculation of the quasiparticle spectrum and excitonic effects inLi2O. Physical Review B, 1997, 55, 10278-10281.	1.1	99
717	Spin- and orbital-polarized multiple-scattering theory of magneto-x-ray effects in Fe, Co, and Ni. Physical Review B, 1997, 55, 11619-11628.	1.1	36
718	Relativistic spin-polarized theory of magnetoelastic coupling and magnetic anisotropy strain dependence: Application to Co/Cu(001). Physical Review B, 1997, 56, R14259-R14262.	1.1	112
719	Effects of interface morphology on Schottky-barrier heights: A case study on Al/GaAs(001). Physical Review B, 1997, 56, 14921-14924.	1.1	19
720	Adaptive-coordinate electronic structure of3dbands:â€,TiO2. Physical Review B, 1997, 56, 14979-14984.	1.1	15

#	Article	IF	Citations
721	SiO2stishovite under high pressure:â€ƒDielectric and dynamical properties and the ferroelastic phase transition. Physical Review B, 1997, 56, 7321-7330.	1.1	31
722	Elastic instabilities in crystals fromab initiostress - strain relations. Journal of Physics Condensed Matter, 1997, 9, 8579-8589.	0.7	282
723	Aluminum break-point contacts. Physical Review B, 1997, 55, 9375-9378.	1.1	2
724	Ab initiocalculations of the atomic and electronic structure of clean and hydrogenated diamond (110) surfaces. Physical Review B, 1997, 56, 4203-4210.	1.1	71
725	Solid Molecular Hydrogen: The Broken Symmetry Phase. Physical Review Letters, 1997, 78, 2783-2786.	2.9	94
726	Metastability of the antistructure pair in GaAs. Physical Review B, 1997, 55, 6914-6917.	1.1	6
727	Screened KKR-Green's-function method for layered systems. Physical Review B, 1997, 55, 10074-10080.	1.1	64
728	Theoretical study of a five-coordinated silica polymorph. Physical Review B, 1997, 56, 5797-5806.	1.1	68
729	Energies of strained silica rings. Physical Review B, 1997, 55, 14784-14793.	1.1	82
730	Atomic and electronic structure of the diamond (100) surface: Reconstructions and rearrangements at high hydrogen coverage. Physical Review B, 1997, 55, 5364-5375.	1.1	42
731	Stability and band offsets of polar GaN/SiC(001) and AlN/SiC(001) interfaces. Physical Review B, 1997, 56, 6911-6920.	1.1	52
732	B2O3crystals investigated by plane-wave pseudopotential calculations using the generalized-gradient approximation. Physical Review B, 1997, 55, 2824-2830.	1.1	15
733	Theoretical investigation of the structure of Î²-Al2O3. Physical Review B, 1997, 55, 8721-8725.	1.1	23
734	Ab initio calculation of formation and migration volumes for vacancies in Li and Na. Physical Review B, 1997, 55, 5772-5777.	1.1	23
735	Ab initiostudy of the ferroelectric transition in cubicPb3GeTe4. Physical Review B, 1997, 56, 7947-7961.	1.1	9
736	First-principles calculations on the atomic and electronic structure ofÎ²â˜†Al2O3. Physical Review B, 1997, 56, 8553-8558.	1.1	36
737	Core effects in lithium hydride. Physical Review B, 1997, 55, 5006-5014.	1.1	11
738	Ab initiostudy of point defects inCdF2. Physical Review B, 1997, 56, 15665-15671.	1.1	23

#	Article	IF	Citations
739	First-principles calculations of the thermal expansion of metals. Physical Review B, 1997, 56, 7767-7770.	1.1	96
740	Influence of the electronic core polarization on the electric-field gradients in solids. Physical Review B, 1997, 55, 7478-7491.	1.1	16
741	Strain dependence of surface diffusion: Ag on Ag(111) and Pt(111). Physical Review B, 1997, 55, 6750-6753.	1.1	171
742	Stacking faults in magnesium. Physical Review B, 1997, 56, 10844-10851.	1.1	93
743	Elastic constants and electronic structure of beryllium chalcogenides BeS, BeSe, and BeTefrom first-principles calculations. Physical Review B, 1997, 55, 14043-14046.	1.1	121
744	Theory of the AlN/SiC(101Â¯0) interface. Physical Review B, 1997, 56, 9213-9216.	1.1	7
745	Basal-plane stacking faults and polymorphism in AlN, GaN, and InN. Journal of Applied Physics, 1997, 82, 5259-5261.	1.1	68
746	Giant lifetimes of optically excited states and the elusive structure of sodiumnitroprusside. Journal of Chemical Physics, 1997, 107, 10067-10074.	1.2	102
748	Slip energy barriers in aluminium and implications for ductile-brittle behaviour. Philosophical Magazine A: Physics of Condensed Matter, Structure, Defects and Mechanical Properties, 1997, 75, 1117-1127.	0.8	37
749	Hillock formation on ion-irradiated graphite surfaces. Radiation Effects and Defects in Solids, 1997, 142, 459-469.	0.4	5
750	First Principles Description of the Valence States in Manganese Oxides. Zeitschrift Fur Elektrotechnik Und Elektrochemie, 1997, 101, 1215-1221.	0.9	5
751	Practical methods inab initiolattice dynamics. Journal of Physics Condensed Matter, 1997, 9, 7861-7872.	0.7	127
752	Chapter 13 Density-functional theory of epitaxial growth of metals. Chemical Physics of Solid Surfaces, 1997, 8, 490-544.	0.3	17
753	Ab initioelasticity and lattice dynamics of. Journal of Physics Condensed Matter, 1997, 9, 375-380.	0.7	27
754	Structural Characterization of Crystalline Si-C-N Films. Materials Research Society Symposia Proceedings, 1997, 498, 301.	0.1	0
755	Solid molecular phases of Hydrogen via constant-pressure first-principles Molecular Dynamics. Materials Research Society Symposia Proceedings, 1997, 499, 329.	0.1	1
756	AB Initio Pseudopotential Calculations of Dopant Diffusion in SI. Materials Research Society Symposia Proceedings, 1997, 469, 151.	0.1	13
757	Theoretical Investigation Of Extended Defects In Group-III Nitrides. Materials Research Society Symposia Proceedings, 1997, 482, 808.	0.1	2

#	Article	IF	Citations
758	Structural And Electronic Properties of GaN/AL Interfaces. Materials Research Society Symposia Proceedings, 1997, 482, 845.	0.1	0
759	Ab initio calculation of structural properties ofC3B andC5B compounds. Physical Review B, 1997, 55, 8-10.	1.1	23
760	Semi-empirical methods as a tool in solid-state chemistry. Faraday Discussions, 1997, 106, 219-232.	1.6	27
761	First-principles description of the valence charge states in rutile MnO2. Journal of the Chemical Society, Faraday Transactions, 1997, 93, 3295-3300.	1.7	17
762	Anab initio Hartreeâ€“Fock study of Î±-MoO3. Journal of Materials Chemistry, 1997, 7, 959-967.	6.7	96
763	High-pressure phases of magnesium selenide and magnesium telluride. Physical Review B, 1997, 55, 775-779.	1.1	60
764	Electrical-conductivity calculation in ab initio simulations of metals:Application to liquid sodium. Physical Review B, 1997, 55, 15515-15522.	1.1	44
765	Multidimensional Energy Barrier Surface Study for the Dissociative Adsorption of H2Impinging on a Si(111)(1Ã—1) Surface:Â First-Principles Calculationsâ€. Journal of Physical Chemistry A, 1997, 101, 6545-6548.	1.1	1
766	Polarization-Based Calculation of the Dielectric Tensor of Polar Crystals. Physical Review Letters, 1997, 79, 3958-3961.	2.9	236
767	Ab initio calculations for solid molecular hydrogen. Physical Review B, 1997, 55, 11330-11341.	1.1	25
768	Theoretical study of boron nitride modifications at hydrostatic pressures. Physical Review B, 1997, 55, 6203-6210.	1.1	131
769	Diamond Nucleation on Hexagonal Boron Nitride:Â A Theoretical Investigation of the Influence of Nearest Substituents. Journal of Physical Chemistry A, 1997, 101, 9445-9448.	1.1	8
770	First-principles spin-polarized calculations on the reduced and reconstructedTiO2(110) surface. Physical Review B, 1997, 55, 15919-15927.	1.1	191
771	Ab initiostudy of silicon in theR8phase. Physical Review B, 1997, 56, 6662-6668.	1.1	103
772	Basis functions for linear-scaling first-principles calculations. Physical Review B, 1997, 55, 13485-13493.	1.1	88
773	Ab initiostudy of BaTiO3surfaces. Physical Review B, 1997, 56, 1625-1631.	1.1	268
774	Theory of semiconductor surface reconstruction. Reports on Progress in Physics, 1997, 60, 561-613.	8.1	134
775	Polar Kerr effect in Heusler alloys. Journal of Applied Physics, 1997, 81, 5429-5431.	1.1	11

#	Article	IF	Citations
776	Ab initio elasticity of three high-pressure polymorphs of silica. Geophysical Research Letters, 1997, 24, 3269-3272.	1.5	134
777	Point-defect complexes and broadband luminescence in GaN and AlN. Physical Review B, 1997, 55, 9571-9576.	1.1	428
778	Ab initio statistical mechanics of the ferroelectric phase transition inPbTiO3. Physical Review B, 1997, 55, 6161-6173.	1.1	308
779	H2dissociative adsorption on Pd(111). Physical Review B, 1997, 56, 15396-15403.	1.1	151
780	Valence-band spectra and electronic structure ofCuFeO2. Physical Review B, 1997, 56, 4584-4591.	1.1	105
781	Lattice instabilities, anharmonicity and phase transitions in PbZrO3from first principles. Ferroelectrics, 1997, 194, 135-147.	0.3	39
782	Theoretical predictions of expanded-volume phases of GaAs. Physical Review B, 1997, 55, 6904-6913.	1.1	22
783	Long-range order effects in Pb(Zr1/2Ti1/2)O3. Ferroelectrics, 1997, 194, 287-298.	0.3	20
784	Born effective charges, dielectric constants, and lattice dynamics of KNbO3. Ferroelectrics, 1997, 194, 97-107.	0.3	5
785	Lattice dynamics and ferroelectric instability of barium titanate. Ferroelectrics, 1997, 194, 39-54.	0.3	38
786	Linear phonon-strain coupling in structural phase transitions: Stability of tetragonal PbTiO3. Ferroelectrics, 1997, 194, 29-38.	0.3	0
787	Phonon Instabilities in fcc and bcc Tungsten. Physical Review Letters, 1997, 79, 2073-2076.	2.9	107
788	Prediction of hexagonalTa2O5structure by first-principles calculations. Physical Review B, 1997, 55, 11155-11160.	1.1	82
789	Dynamical matrices, Born effective charges, dielectric permittivity tensors, and interatomic force constants from density-functional perturbation theory. Physical Review B, 1997, 55, 10355-10368.	1.1	2,534
790	Maximally localized generalized Wannier functions for composite energy bands. Physical Review B, 1997, 56, 12847-12865.	1.1	3,642
791	Anab initioapproach to phonon spectrum oftrans-polyacetylene. Journal of Physics Condensed Matter, 1997, 9, L351-L354.	0.7	5
792	Lithium site preference and electronic structure ofLi4V3O8. Physical Review B, 1997, 56, 10707-10710.	1.1	21
793	Ultrasoft pseudopotentials applied to magnetic Fe, Co, and Ni: From atoms to solids. Physical Review B, 1997, 56, 15629-15646.	1.1	324

#	Article	IF	Citations
794	First-principles responses of solids to atomic displacements and homogeneous electric fields: Implementation of a conjugate-gradient algorithm. Physical Review B, 1997, 55, 10337-10354.	1.1	920
795	Ab-initio analysis of aluminum â˜ = 5 grain boundaries â€" fundamental structures and effects of silicon impurity. Computational Materials Science, 1997, 7, 271-278.	1.4	23
796	The influence of generalized gradient corrections on the structural and electronic properties of tellurium. Computational Materials Science, 1997, 8, 335-340.	1.4	14
797	Layered tantalum-rich chalcogenides. Journal of Alloys and Compounds, 1997, 246, 37-50.	2.8	18
798	The surface chemistry of metal-oxygen interactions: a first-principles study of O:Rh(110). Surface Science, 1997, 370, 166-178.	0.8	35
799	First-principles calculations of the adsorbate-induced surface stress of. Surface Science, 1997, 372, 179-184.	0.8	9
800	Adsorption of atomic and molecular oxygen on the MgO (001) surface. Surface Science, 1997, 374, 373-386.	0.8	79
801	The energetics of N2O dissociation on CaO(001). Surface Science, 1997, 376, 169-176.	0.8	24
802	Electronic properties of (2 Ã— n)-Bi reconstructions on Si(100). Surface Science, 1997, 377-379, 215-219.	0.8	7
803	The structure and phase stability of CO adsorbates on Rh(110). Surface Science, 1997, 382, L666-L671.	0.8	8
804	An ab initio Hartree-Fock study of the electron-excess gap states in oxygen-deficient rutile TiO2. Surface Science, 1997, 384, 192-200.	0.8	74
805	A systematic study of the surface energetics and structure of TiO2(110) by first-principles calculations. Surface Science, 1997, 385, 386-394.	0.8	224
806	Ab initio studies of high-pressure structural transformations in silica. Physical Review B, 1997, 55, 3465-3471.	1.1	154
807	Electronic structure and structural stability ofTiCxN1âˆ'xalloys. Physical Review B, 1997, 56, 13826-13829.	1.1	87
808	First-Principles Determination of the Soft Mode in CubicZrO2. Physical Review Letters, 1997, 78, 4063-4066.	2.9	2,341
809	Spontaneous polarization and piezoelectric constants of III-V nitrides. Physical Review B, 1997, 56, R10024-R10027.	1.1	2,662
810	Theoretical study of the high-pressure phase stability of GaP, InP, and InAs. Physical Review B, 1997, 55, 9659-9670.	1.1	101
811	Symmetrical transformation of basic translation vectors in the supercell model of imperfect crystals and in the theory of special points of the Brillouin zone. Journal of Physics Condensed Matter, 1997, 9, 3023-3031.	0.7	19

#	Article	IF	Citations
812	A theoretical study of the H-induced reconstructions of the Pd(110) surface. Surface Science, 1997, 377-379, 56-61.	0.8	20
813	Elastic properties of orthorhombic MgSiO₃perovskite at lower mantle pressures. American Mineralogist, 1997, 82, 635-638.	0.9	143
814	Ab initio calculations on point defects in forsterite (Mg₂SiO₄) and implications for diffusion and creep. American Mineralogist, 1997, 82, 1049-1053.	0.9	75
815	Structure and dynamics of protonated Mg₂SiO₄; an ab-initio molecular dynamics study. American Mineralogist, 1997, 82, 913-922.	0.9	47
816	All-atom ab initio energy minimization of the kaolinite crystal structure. American Mineralogist, 1997, 82, 657-662.	0.9	82
817	Elastic properties of zinc-blende and wurtzite AlN, GaN, and InN. Journal of Applied Physics, 1997, 82, 2833-2839.	1.1	997
818	Tight-binding modelling of materials. Reports on Progress in Physics, 1997, 60, 1447-1512.	8.1	489
819	The nature of valence band holes in pure and Feâ€doped NiO: An ab initio Hartreeâ€Fock study. Zeitschrift Fur Elektrotechnik Und Elektrochemie, 1997, 101, 169-175.	0.9	16
820	Nitrogen doping in ZnSe. Materials Science and Engineering B: Solid-State Materials for Advanced Technology, 1997, 43, 1-4.	1.7	4
821	Zinc-blende GaN: ab initio calculations. Materials Science and Engineering B: Solid-State Materials for Advanced Technology, 1997, 50, 57-60.	1.7	3
822	Dissociative adsorption of H2 on the Pd(111) surface. Journal of Molecular Catalysis A, 1997, 119, 69-76.	4.8	43
823	All-electron calculations with plane waves in solid lithium hydride. International Journal of Quantum Chemistry, 1997, 61, 647-656.	1.0	9
824	Relaxation of Crystals with the Quasi-Newton Method. Journal of Computational Physics, 1997, 131, 233-240.	1.9	2,389
825	Density-functional theory calculations for poly-atomic systems: electronic structure, static and elastic properties and ab initio molecular dynamics. Computer Physics Communications, 1997, 107, 187-222.	3.0	660
826	First principles calculations of Si(2 1 1) surface reconstructions. Journal of Crystal Growth, 1997, 180, 54-60.	0.7	20
827	Structure and properties of supercubane from density functional calculations. Chemical Physics Letters, 1998, 293, 284-288.	1.2	22
828	Antisites in silicon carbide. Physical Review B, 1998, 57, 6243-6246.	1.1	59
829	Multiscale modeling approach for calculating grain-boundary energies from first principles. Physical Review B, 1998, 57, R3181-R3184.	1.1	46

#	Article	IF	Citations
830	Modeling the structure of zircon (ZrSiO4): empirical potentials, ab initio electronic structure. Journal of Nuclear Materials, 1998, 257, 282-286.	1.3	55
831	Electronic stopping power of periodic crystals. Nuclear Instruments & Methods in Physics Research B, 1998, 135, 103-106.	0.6	19
832	Local density calculation of structural properties and cohesive energy for ScPO4, YPO4 and the apatite Ca10(PO4)6F2. Computational and Theoretical Chemistry, 1998, 426, 217-224.	1.5	5
833	Total energy pseudopotential calculation in local density approximation for BPO4. Computational and Theoretical Chemistry, 1998, 426, 241-247.	1.5	0
834	Theory of the spin dynamics of bulk Fe and ultrathin Fe(100) films. Journal of Magnetism and Magnetic Materials, 1998, 187, 23-46.	1.0	66
835	Ab-Initio Calculation of the Optical Properties of Surfaces. Physica Status Solidi A, 1998, 170, 365-375.	1.7	6
836	The Triangle Method: Reflectance Anisotropy of As-Covered InP(110) Surfaces. Physica Status Solidi A, 1998, 170, 423-429.	1.7	2
837	Density functional crystal vs. cluster models as applied to zeolites. International Journal of Quantum Chemistry, 1998, 68, 135-144.	1.0	135
838	The application of approximate density functionals to complex systems. International Journal of Quantum Chemistry, 1998, 69, 327-340.	1.0	46
839	Dependence of phonon linewidths in semiconductors on temperature and isotopic composition. Nuovo Cimento Della Societa Italiana Di Fisica D - Condensed Matter, Atomic, Molecular and Chemical Physics, Biophysics, 1998, 20, 923-930.	0.4	8
840	Electronic structure of silver halides. Solid State Communications, 1998, 105, 377-380.	0.9	23
841	A first-principles pseudopotential study of the compressibility of Ïµ-FeSi. Solid State Communications, 1998, 108, 11-15.	0.9	9
842	Theoretical study of the role of natural intralayers in the band offsets of InAs/GaSb heterojunction. Applied Surface Science, 1998, 123-124, 571-574.	3.1	1
843	First principles calculations of the band offset of the ZnSe/BeTe heterojunctions. Applied Surface Science, 1998, 123-124, 445-448.	3.1	2
844	Evaluating the minimum thickness of gate oxide on silicon using first-principles method. Applied Surface Science, 1998, 135, 137-142.	3.1	61
845	Atomic layer epitaxy of copper: an ab initio investigation of the CuCl/H2 process. Applied Surface Science, 1998, 136, 137-146.	3.1	16
846	Adsorption of CO on the TiO2(110) Surface:â€‰ A Theoretical Study. Journal of Physical Chemistry B, 1998, 102, 4556-4565.	1.2	87
847	Ab initiomolecular-dynamics studies of the graphitization of flat and stepped diamond (111) surfaces. Physical Review B, 1998, 58, 13167-13175.	1.1	52

#	Article	IF	Citations
848	Electronic structure of tin monochalcogenides from SnO to SnTe. Physical Review B, 1998, 58, 1896-1906.	1.1	286
849	Convergence of supercell calculations for point defects in semiconductors: Vacancy in silicon. Physical Review B, 1998, 58, 1318-1325.	1.1	233
850	AsNCa3 at high pressure. Computational Materials Science, 1998, 10, 298-301.	1.4	7
851	Possible n-type dopants in diamond and amorphous carbon. Computational Materials Science, 1998, 10, 351-355.	1.4	17
852	Ab initio calculation of excitonic effects in realistic materials. Computational Materials Science, 1998, 10, 356-361.	1.4	2
853	Ab initio pseudopotential calculations of dopant diffusion in Si. Computational Materials Science, 1998, 12, 309-318.	1.4	45
854	Diffusion of adsorbate atoms on the reconstructed Si(111) surface. Surface Science, 1998, 396, L261-L266.	0.8	101
855	Ab-initio dynamical properties of the Be(0001) surface. Surface Science, 1998, 402-404, 715-718.	0.8	26
856	The reconstruction of Rh(001) upon oxygen adsorption. Surface Science, 1998, 410, 151-157.	0.8	41
857	Hydrogen adsorption on palladium: a comparative theoretical study of different surfaces. Surface Science, 1998, 411, 123-136.	0.8	198
858	Ab initio study of the dissociative adsorption of H2 on the Pd(110) surface. Surface Science, 1998, 412-413, 518-526.	0.8	44
859	First principles calculation of oxygen adsorption and reconstruction of Cu(110) surface. Surface Science, 1998, 415, 194-211.	0.8	80
860	Ab initio study of SrTiO3 surfaces. Surface Science, 1998, 418, 64-70.	0.8	251
861	First principles calculation of the energy and structure of two solid surface phases on Ir{100}. Surface Science, 1998, 418, 529-535.	0.8	36
862	The electronic structure of Si(100) 2 Ã— 1î—¸Cl: reinterpreting ARP measurements. Surface Science, 1998, 398, 301-307.	0.8	8
863	High pressure elastic anisotropy of MgSiO3 perovskite and geophysical implications. Earth and Planetary Science Letters, 1998, 164, 371-378.	1.8	88
864	Valence and atomic size dependent exchange barriers in vacancy-mediated dopant diffusion. Applied Physics Letters, 1998, 73, 247-249.	1.5	63
865	Band offsets at the InAlGaAs/InAlAs (001) heterostructures lattice matched to an InP substrate. Journal of Applied Physics, 1998, 83, 5852-5854.	1.1	5

#	Article	IF	Citations
866	Theoretical examination of stress fields in Pb(Zr0.5Ti0.5)O3. Ferroelectrics, 1998, 206, 31-46.	0.3	15
867	Diamond Nucleation on Hexagonal Boron Nitride:â€‰ A Theoretical Investigation of the Influence of CH3 and Na Substituents. Journal of Physical Chemistry B, 1998, 102, 5866-5869.	1.2	5
868	Generalized stacking-fault energies for TiAl: Mechanical instability of the (111) antiphase boundary. Philosophical Magazine A: Physics of Condensed Matter, Structure, Defects and Mechanical Properties, 1998, 77, 701-714.	0.8	44
869	A Periodic Density Functional Theory and Hartreeâ"Fock Study of Alkali Halides with Gaussian Orbitals. Journal of Physical Chemistry A, 1998, 102, 10310-10317.	1.1	9
870	Compression mechanisms in quasimolecularXI3â€,(X=As,Sb,Bi)solids. Physical Review B, 1998, 58, 14812-14822.	1.1	36
871	Theoretical Study of Electronic Properties of Zintl Phase KSi. Chemistry of Materials, 1998, 10, 4025-4029.	3.2	8
872	First-principles study of piezoelectricity in tetragonal PbTiO3. Ferroelectrics, 1998, 206, 1-10.	0.3	2
873	Pressure-induced phase transitions in silver halides. Physical Review B, 1998, 57, 5098-5105.	1.1	53
874	Extension of the Fenskeâ"Hall Molecular Orbital Approach to Tight-Binding Band Structure Calculations:Â Bulk and Surface Electronic Structure of MoS2. Inorganic Chemistry, 1998, 37, 2205-2214.	1.9	14
875	First-principles calculations of bulk and interfacial thermodynamic properties for fcc-based Al-Sc alloys. Physical Review B, 1998, 57, 11265-11275.	1.1	101
876	BrÃ¸nsted Acid Sites in HSAPO-34 and Chabazite:â€‰ An Ab Initio Structural Study. Journal of Physical Chemistry B, 1998, 102, 5573-5580.	1.2	166
877	Deep electronic gap levels induced by isovalent P and As impurities in GaN. Physical Review B, 1998, 58, 1367-1373.	1.1	157
878	Phonon linewidth in III-V semiconductors from density-functional perturbation theory. Physical Review B, 1998, 57, 12847-12858.	1.1	164
879	Band engineering at interfaces: theory and numerical experiments. Journal Physics D: Applied Physics, 1998, 31, 1273-1299.	1.3	265
880	Variable-cell-shape-based structural optimization applied to calcium nitrides. Physical Review B, 1998, 57, 7615-7620.	1.1	32
881	Analytical Free Energy Minimization of Silica Polymorphs. Journal of Physical Chemistry B, 1998, 102, 5423-5431.	1.2	97
882	Theoretical investigation of edge dislocations in AlN. Applied Physics Letters, 1998, 72, 3467-3469.	1.5	42
883	First-principles study on electronic and elastic properties of BN, AlN, and GaN. Journal of Applied Physics, 1998, 84, 4951-4958.	1.1	332

#	Article	IF	Citations
884	AB initio phonon dispersion curves and interatomic force constants of barium titanate. Ferroelectrics, 1998, 206, 205-217.	0.3	82
885	Intercalation Compounds of Transition-Metal Dichalcogenides. Springer Series in Materials Science, 1998, , 107-140.	0.4	0
886	Structure and elasticity of CaO at high pressure. Journal of Geophysical Research, 1998, 103, 12405-12411.	3.3	46
887	First-principles determination of elastic properties of CaSiO3perovskite at lower mantle pressures. Geophysical Research Letters, 1998, 25, 2741-2744.	1.5	65
888	Electronic structure of possible 3d `heavy-fermion' compound. Journal of Physics Condensed Matter, 1998, 10, L119-L126.	0.7	108
889	Peierls barriers and stresses for edge dislocations in Pd and Al calculated from first principles. Physical Review B, 1998, 58, 2487-2496.	1.1	162
890	Elastic constants and anisotropy of MgSiO3 perovskite, periclase, and SiO2 at high pressure. Geodynamic Series, 1998, , 83-96.	0.1	30
891	Ab initiostudy of iron and iron hydride: I. Cohesion, magnetism and electronic structure of cubic Fe and FeH. Journal of Physics Condensed Matter, 1998, 10, 5081-5111.	0.7	40
892	First-principles investigation of phase stability inLixCoO2. Physical Review B, 1998, 58, 2975-2987.	1.1	632
893	Ab initiocalculation of the stoichiometry and structure of the (0001) surfaces of GaN and AlN. Physical Review B, 1998, 57, 15360-15371.	1.1	85
894	First-order phase transitions by first-principles free-energy calculations: The melting of Al. Physical Review B, 1998, 57, 8223-8234.	1.1	124
895	Electric-field-gradient calculations using the projector augmented wave method. Physical Review B, 1998, 57, 14690-14697.	1.1	187
896	Ab initiocalculation of the reflectance anisotropy of surfaces: The triangle method. Physical Review B, 1998, 58, 4721-4727.	1.1	11
897	Pressure-induced change of the stereochemical activity of a lone electron pair. Journal of Chemical Physics, 1998, 108, 5506-5509.	1.2	19
898	Structure and electronic properties ofFeSi2. Physical Review B, 1998, 58, 10389-10393.	1.1	110
899	Ab InitioCalculation of Excitonic Effects in the Optical Spectra of Semiconductors. Physical Review Letters, 1998, 80, 4510-4513.	2.9	803
900	Influence of surface stress on the equilibrium shape of strained quantum dots. Physical Review B, 1998, 58, 4566-4571.	1.1	192
901	Dynamical atomic charges: The case ofABO3compounds. Physical Review B, 1998, 58, 6224-6240.	1.1	482

#	Article	IF	Citations
902	Pseudopotential study of binding properties of solids within generalized gradient approximations: The role of core-valence exchange correlation. Physical Review B, 1998, 57, 2134-2145.	1.1	197
903	Comparison betweenab initiotheory and scanning tunneling microscopy for (110) surfaces of III-V semiconductors. Physical Review B, 1998, 58, 7799-7815.	1.1	71
904	Theoretical study of a three-dimensional all-sp2structure. Physical Review B, 1998, 58, 664-668.	1.1	47
905	Adsorption of Methanol on TiO2(110):Â A First-Principles Investigation. Journal of Physical Chemistry B, 1998, 102, 2017-2026.	1.2	127
906	Vacancy self-diffusion parameters in tungsten: Finite electron-temperature LDA calculations. Physical Review B, 1998, 57, 11184-11192.	1.1	74
907	Total energy differences between SiC polytypes revisited. Physical Review B, 1998, 57, 12017-12022.	1.1	106
908	The Role of Hydrogen In The Structure of Î³-Alumina. Materials Research Society Symposia Proceedings, 1998, 549, 165.	0.1	3
909	Ab-Initio MD Studies of the Structure of C(111): nH Surfaces. Surface Review and Letters, 1998, 05, 49-54.	0.5	2
910	Ab initio pseudopotentials for orbital-free density functionals. Europhysics Letters, 1998, 41, 37-42.	0.7	42
911	d-to-s bonding in GaN. Journal of Physics Condensed Matter, 1998, 10, 7155-7162.	0.7	4
912	Ab initiocalculations of the energetics of the neutral Si vacancy defect. Modelling and Simulation in Materials Science and Engineering, 1998, 6, 1-8.	0.8	41
913	Ab initiostudy of iron and iron hydride: II. Structural and magnetic properties of close-packed Fe and FeH. Journal of Physics Condensed Matter, 1998, 10, 5113-5129.	0.7	33
914	The effect of Cl coverage on Si(100) surface reactivity: implications for Cl etching of Si. Journal of Physics Condensed Matter, 1998, 10, 4515-4522.	0.7	2
915	Miniband structures and effective masses of n-type -doping superlattices in GaN. Semiconductor Science and Technology, 1998, 13, 981-988.	1.0	7
916	First-principles calculations of band offsets. Journal of Physics Condensed Matter, 1998, 10, 577-580.	0.7	6
917	Anomalous hydrogen adsorption sites found for the c(2Ã—2)-3H phases formed on the Re(101Ì„0) and Ru(101Ì„0) surfaces. Journal of Chemical Physics, 1998, 108, 8671-8679.	1.2	34
918	Relaxations of nonpolar zinc blende (110) surface of GaN, AlN, and BN. Journal of Applied Physics, 1998, 84, 1977-1980.	1.1	6
919	Influence of the exchange reaction on the electronic structure of GaN/Al junctions. Physical Review B, 1998, 58, 7906-7912.	1.1	11

#	Article	IF	Citations
920	Ab initiolocal-orbital density-functional method for transition metals and semiconductors. Physical Review B, 1998, 58, 1832-1838.	1.1	5
921	Ab initiocalculations of the atomic and electronic structure of diamond (111) surfaces with steps. Physical Review B, 1998, 58, 2161-2169.	1.1	24
922	Stability and electronic structure of the cinnabar phase in GaAs. Physical Review B, 1998, 57, R2029-R2032.	1.1	25
923	Thermodynamics and mechanism of theB1-B2phase transition in group-I halides and group-II oxides. Physical Review B, 1998, 57, 11164-11172.	1.1	87
924	Anomaly in the anisotropy of the aluminum work function. Physical Review B, 1998, 58, R7544-R7547.	1.1	52
925	Prediction of structural parameters and physical properties ofCsHSO3up to 60 GPa. Physical Review B, 1998, 57, 4321-4326.	1.1	5
926	Compton profiles of Si: Pseudopotential calculation and reconstruction effects. Physical Review B, 1998, 58, 4320-4324.	1.1	6
927	Many-body effects on bandwidths in ionic, noble gas, and molecular solids. Physical Review B, 1998, 58, 9579-9583.	1.1	76
928	Electronic dielectric constants of insulators calculated by the polarization method. Physical Review B, 1998, 58, 15292-15295.	1.1	84
929	Formation energy, lattice relaxation, and electronic structure ofAl/Si/GaAs(100)junctions. Physical Review B, 1998, 57, 9757-9762.	1.1	16
930	Electronic and structural properties of vacancies on and below the GaP(110) surface. Physical Review B, 1998, 58, 1392-1400.	1.1	43
931	Correlation Effects in the Compton Profile of Silicon. Physical Review Letters, 1998, 80, 4253-4256.	2.9	31
932	Role of Electronic Correlation on the Equation of State of Lithium Hydrides. Physical Review Letters, 1998, 80, 5576-5579.	2.9	11
933	Electronic stopping power of aluminum crystal. Physical Review B, 1998, 58, 10307-10314.	1.1	43
934	Connections between the electron-energy-loss spectra, the local electronic structure, and the physical properties of a material: A study of nickel aluminum alloys. Physical Review B, 1998, 57, 8181-8202.	1.1	185
935	Comparison of theoretical and experimental magnetization densities of Ni,Pt3Cr,andPd3Cr. Physical Review B, 1998, 58, 9252-9263.	1.1	7
936	Site preferences and formation energies of substitutional Si, Nb, Mo, Ta, and W solid solutions inL10Ti-Al. Physical Review B, 1998, 57, 13459-13470.	1.1	74
937	Nonlocal density-functional calculations of the surface electronic structure of metals: Application to aluminum and palladium. Physical Review B, 1998, 57, 14974-14982.	1.1	39

#	Article	IF	Citations
938	Ab initiostudies of the (111) and (1Â¯ 1Â¯ 1Â¯) surfaces of cubic BN: Structure and energetics. Physical Review B, 1998, 58, 15636-15646.	1.1	25
939	Thermal expansion of polymers: Mechanisms in orthorhombic polyethylene. Physical Review B, 1998, 58, 8416-8427.	1.1	44
940	Total energy calculations of the lattice properties of cubic and hexagonal diamond. Physical Review B, 1998, 57, 13355-13358.	1.1	33
941	Impurity-Induced Structural Transformation of a MgO Grain Boundary. Physical Review Letters, 1998, 81, 3675-3678.	2.9	108
942	Anomalous Isostructural Transformation in Ice VIII. Physical Review Letters, 1998, 81, 2466-2469.	2.9	25
943	Ab initiostudies of the (100), (110), and (111) surfaces ofCoSi2. Physical Review B, 1998, 57, 4088-4098.	1.1	27
944	Stabilizing Role of Itinerant Ferromagnetism in Intergranular Cohesion in Iron. Physical Review Letters, 1998, 81, 2998-3001.	2.9	19
945	Band offsets at GaInP/AlGaInP(001) heterostructures lattice matched to GaAs. Applied Physics Letters, 1998, 73, 1098-1100.	1.5	19
946	High-pressure semiconductor-semimetal transition inTiS2. Physical Review B, 1998, 57, 5106-5110.	1.1	78
947	Spin-density study of the silicon divacancy. Physical Review B, 1998, 58, 1106-1109.	1.1	41
948	Structural transformation in the90Â°partial dislocation in Si due to Ga impurities. Physical Review B, 1998, 58, 12865-12867.	1.1	3
949	Evidence of the negative-Ubehavior of H in GaAs from an investigation of H and As antisites. Physical Review B, 1998, 58, 10378-10382.	1.1	11
950	Reevaluating electron-phonon coupling strengths: Indium as a test case forab initioand many-body theory methods. Physical Review B, 1998, 58, 14511-14517.	1.1	11
951	Structural and electronic properties of ideal nitride/Al interfaces. Physical Review B, 1998, 57, 4849-4856.	1.1	20
952	Lack of atrans-cisoidphase incis-polyacetylene. Physical Review B, 1998, 57, 6-9.	1.1	15
953	H-induced reconstructions on Pd(110). Physical Review B, 1998, 57, 12482-12491.	1.1	45
954	Oxygen adsorption on the Ru(101Â¯0) surface: Anomalous coverage dependence. Physical Review B, 1998, 57, 15487-15495.	1.1	68
955	Electronic structure of black sodalite. Physical Review B, 1998, 57, 15129-15139.	1.1	33

#	Article	IF	Citations
956	Chlorine-impurity-related defects in ZnSe. Physical Review B, 1998, 57, 12164-12168.	1.1	14
957	First-principles local-orbital study of the boron-induced reconstruction of Si(001). Physical Review B, 1998, 57, 9745-9756.	1.1	19
958	Density-functional study of the magnetic and metal-insulator transition of bcc hydrogen. Physical Review B, 1998, 58, 12680-12683.	1.1	11
959	Errors in Hellmann-Feynman forces due to occupation-number broadening and how they can be corrected. Physical Review B, 1998, 57, 2102-2107.	1.1	40
960	Consistent methodology for calculating surface and interface energies. Physical Review B, 1998, 57, 7281-7291.	1.1	161
961	Structure, kinetics, and passivation of hydrogen-acceptor complexes in gallium arsenide: A theoretical study. Physical Review B, 1998, 57, 12923-12931.	1.1	10
962	First principles calculations of structural properties of Î²-Si3â^'nCnN4 (n=0, 1, 2, 3). Journal of Applied Physics, 1998, 83, 1975-1978.	1.1	36
963	Cation and vacancy ordering inLixCoO2. Physical Review B, 1998, 57, 2242-2252.	1.1	128
964	Band structures of CsCl-structured BaS and CaSe at high pressure: Implications for metallization pressures of the alkaline earth chalcogenides. Physical Review B, 1998, 58, 9793-9800.	1.1	37
965	Relaxations ofTiO2- and SrO-terminatedSrTiO3(001) surfaces. Physical Review B, 1998, 58, 8075-8078.	1.1	61
966	The effect of doping and growth stoichiometry on the core structure of a threading edge dislocation in GaN. Applied Physics Letters, 1998, 73, 2751-2753.	1.5	199
967	Analytical evaluation of energy derivatives in extended systems. I. Formalism. Journal of Chemical Physics, 1998, 109, 4209-4223.	1.2	23
968	Spin polarization and the energetics of chlorine adsorption on the GaAs(110) surface. Journal of Chemical Physics, 1998, 109, 6911-6915.	1.2	1
969	Near-band-edge resonant states of AlAs monolayers embedded in bulk GaAs: The role ofdsymmetries. Physical Review B, 1998, 57, 3733-3736.	1.1	6
970	Momentum distributions of electron-positron pairs annihilating at vacancy clusters in Si. Physical Review B, 1998, 57, 7621-7627.	1.1	124
971	Clean and As-Covered Zinc-Blende GaN (001) Surfaces: Novel Surface Structures and Surfactant Behavior. Physical Review Letters, 1998, 80, 3097-3100.	2.9	99
972	Ab initiocalculation of electron affinities of diamond surfaces. Physical Review B, 1998, 57, 9241-9245.	1.1	151
973	First-Principles Study on Piezoelectric Constants in Strained BN, AlN, and GaN. Japanese Journal of Applied Physics, 1998, 37, L1421-L1423.	0.8	68

#	Article	IF	Citations
974	First-principles theory of structural phase transitions for perovskites: Competing instabilities. Ferroelectrics, 1998, 206, 181-204.	0.3	68
975	Carbon vacancy in SiC: A negative- U system. Europhysics Letters, 1998, 44, 309-314.	0.7	17
976	First Principles Methodsversus(Semi) Empirical Methods: Modeling the Hierarchy of Length Scales in Material Systems. Molecular Simulation, 1998, 21, 173-181.	0.9	0
977	A first-principles Hartree-Fock description of MnO at high pressures. The Philosophical Magazine: Physics of Condensed Matter B, Statistical Mechanics, Electronic, Optical and Magnetic Properties, 1998, 77, 1063-1075.	0.6	3
978	First-principles Hartree-Fock description of the electronic structure of monoclinic C2/m LixMnO₂ (1 â‰¥ x â‰¥ 0). The Philosophical Magazine: Physics of Condensed Matter B, Statistical Mechanics, Electronic, Optical and Magnetic Properties, 1998, 77, 1077-1092.	0.6	19
979	<title>Internally consistent predictions of surface structural relaxations</title>. , 1998, , .		0
980	Coadsorption of CO and O on Ru(0001): A Structural Analysis by Density Functional Theory. Israel Journal of Chemistry, 1998, 38, 409-414.	1.0	10
981	Surface Structures, Surfactants and Diffusion at Cubic and Wurtzite GaN. MRS Internet Journal of Nitride Semiconductor Research, 1998, 3, 1.	1.0	38
982	A first-principles Hartree-Fock interpretation of the X-ray oxygen K-edge spectrum of haematite (Î±-Fe2O3). The Philosophical Magazine: Physics of Condensed Matter B, Statistical Mechanics, Electronic, Optical and Magnetic Properties, 1999, 79, 25-36.	0.6	10
983	STRUCTURE AND DYNAMICS OF Al TRIMER ON Al(111) SURFACE. Surface Review and Letters, 1999, 06, 787-792.	0.5	0
984	Momentum-density effects upon the electronic stopping of elemental solids. Journal of Physics Condensed Matter, 1999, 11, 3973-3985.	0.7	6
985	Theoretical study of graphitic analogues of simple semiconductors. Modelling and Simulation in Materials Science and Engineering, 1999, 7, 929-938.	0.8	13
986	Density functional study of the structure, thermodynamics and electronic properties of CdGeAs2. Journal of Physics Condensed Matter, 1999, 11, 4517-4526.	0.7	13
987	Local vibrational modes of H2and H2*complexes in crystalline Si. Semiconductor Science and Technology, 1999, 14, 1042-1047.	1.0	10
988	A first principles investigation of stacking fault energies and bonding in wurtzite materials. Journal of Physics Condensed Matter, 1999, 11, 5057-5063.	0.7	20
989	Simulation of microscopic strain in semiconducting heterojunctions. Modelling and Simulation in Materials Science and Engineering, 1999, 7, 311-320.	0.8	1
990	Photonic band gaps of three-dimensional face-centred cubic lattices. Journal of Physics Condensed Matter, 1999, 11, 997-1008.	0.7	93
991	Deliberately designed interfaces for monolithic integration in optoelectronics. Journal of Vacuum Science & Technology an Official Journal of the American Vacuum Society B, Microelectronics Processing and Phenomena, 1999, 17, 1612.	1.6	0

#	Article	IF	Citations
992	ELECTRONIC STRUCTURE OF SIX PHASES OF C3N4: A THEORETICAL APPROACH. Modern Physics Letters B, 1999, 13, 193-201.	1.0	58
993	First-principles calculations of self-interstitial defect structures and diffusion paths in silicon. Journal of Physics Condensed Matter, 1999, 11, 10437-10450.	0.7	56
994	Thermodynamic properties and lattice dynamics of silver at high pressure: A first-principles study. The Philosophical Magazine: Physics of Condensed Matter B, Statistical Mechanics, Electronic, Optical and Magnetic Properties, 1999, 79, 911-919.	0.6	20
995	Microscopic structure of oxygen defects in gallium arsenide. Physical Review B, 1999, 60, R16267-R16270.	1.1	12
996	Electronic structure of the (111) and(1Â¯1Â¯1Â¯)surfaces of cubic BN: A local-density-functionalab initiostudy. Physical Review B, 1999, 60, 8719-8726.	1.1	9
997	Maximally localized Wannier functions for simulations with supercells of general symmetry. Physical Review B, 1999, 59, 9703-9706.	1.1	105
998	Adsorption of ammonia on the rhodium (111), (100), and stepped (100) surfaces: An ab initio and experimental study. Journal of Chemical Physics, 1999, 111, 8124-8130.	1.2	45
999	Structural and electronic properties of germanium clathratesGe46andK8Ge46. Physical Review B, 1999, 60, 14177-14181.	1.1	19
1000	Atomic and electronic structure and interatomic potentials at a polar ceramic/metal interface:{222}MgO/Cu. Physical Review B, 1999, 60, 16094-16102.	1.1	48
1001	Anomalous behavior of the semiconducting gap inWO3from first-principles calculations. Physical Review B, 1999, 59, 2684-2693.	1.1	121
1002	Albrechtet al.Reply:. Physical Review Letters, 1999, 83, 3971-3971.	2.9	21
1003	Electronic and optical properties ofSi1âˆ’yCyalloys. Physical Review B, 1999, 60, 11494-11502.	1.1	11
1004	Atomic structure and electrochemical potential ofLi1+xV3O8. Physical Review B, 1999, 60, 6335-6342.	1.1	18
1005	P-P and As-As isovalent impurity pairs in GaN: Interaction of deept2levels. Physical Review B, 1999, 59, 9943-9953.	1.1	22
1006	Magnetic destabilization ofNi7Al. Physical Review B, 1999, 59, 12165-12168.	1.1	15
1007	Mechanisms of self-diffusion on Pt(110). Physical Review B, 1999, 60, R5149-R5152.	1.1	45
1008	Magnetism and anisotropy of ultrathin Ni films on Cu(001). Physical Review B, 1999, 59, 9332-9341.	1.1	22
1009	First-principles simulation of Se and Te adsorbed on GaAs(001). Physical Review B, 1999, 59, 5602-5611.	1.1	19

#	Article	IF	Citations
1010	Heterovalent andA-atom effects inA(Bâ€²Bâ€³)O3perovskite alloys. Physical Review B, 1999, 59, 1834-1839.	1.1	57
1011	Hydrogen-induced states near the GaAs band edges. Physical Review B, 1999, 59, 4869-4880.	1.1	3
1012	Calculated lifetimes of hot electrons in aluminum and copper using a plane-wave basis set. Physical Review B, 1999, 60, 8616-8623.	1.1	63
1013	First-principles calculation of uniaxial magnetic anisotropy and magnetostriction in strained colossal magnetoresistance films. Physical Review B, 1999, 60, 6254-6257.	1.1	22
1014	Nonlocal density scheme for electronic-structure calculations. Physical Review B, 1999, 60, 11329-11335.	1.1	16
1015	Surface migration during diamond growth studied by molecular orbital calculations. Physical Review B, 1999, 59, 8315-8322.	1.1	26
1017	F center in sodium electrosodalite as a physical manifestation of a non-nuclear attractor in the electron density. Physical Review B, 1999, 59, 12359-12369.	1.1	57
1018	Multilayer relaxations and stresses on Mg surfaces. Physical Review B, 1999, 60, 15613-15616.	1.1	26
1019	Theoretical study of the(3Ã—2)reconstruction ofÎ²-SiC(001). Physical Review B, 1999, 60, R5129-R5132.	1.1	22
1020	Theoretical determination of the adsorption geometry of Na on the Si(001) surface. Physical Review B, 1999, 59, 2449-2453.	1.1	5
1021	Ab initiostudy of theCoSi2(111)/Si(111)interface. Physical Review B, 1999, 60, 17112-17122.	1.1	17
1022	Atomistic simulations of structures and mechanical properties of polycrystalline diamond: Symmetrical ã€ˆ001ã€‰ tilt grain boundaries. Physical Review B, 1999, 60, 7043-7052.	1.1	38
1023	Structural stability of some possible phases ofSiC2N4. Physical Review B, 1999, 60, 11943-11946.	1.1	28
1024	Cation-rich (100) surface reconstructions of InP and GaP. Physical Review B, 1999, 60, 13283-13286.	1.1	33
1025	Muonium as a hydrogen analogue in silicon and germanium: Quantum effects and hyperfine parameters. Physical Review B, 1999, 60, 13534-13546.	1.1	42
1026	Computational study of interstitial oxygen and vacancy-oxygen complexes in silicon. Physical Review B, 1999, 60, 11449-11463.	1.1	103
1027	Finite-size errors in quantum many-body simulations of extended systems. Physical Review B, 1999, 59, 1917-1929.	1.1	98
1028	Change from sixfold to fivefold coordination of silicate polyhedra: Insights from first-principles calculations ofCaSi2O5. Physical Review B, 1999, 59, 9149-9154.	1.1	15

#	Article	IF	Citations
1029	Dynamical and thermodynamical instabilities in the disorderedRexW1â^'xsystem. Physical Review B, 1999, 60, 9999-10007.	1.1	33
1030	Extrapolative approaches to Brillouin-zone integration. Physical Review B, 1999, 59, 4685-4693.	1.1	54
1031	Raman linewidths of optical phonons in3Câ^'SiCunder pressure: First-principles calculations and experimental results. Physical Review B, 1999, 59, 6774-6783.	1.1	65
1032	Electronic structure ofZnGeP2:A detailed study of the band structure near the fundamental gap and its associated parameters. Physical Review B, 1999, 60, 8087-8096.	1.1	37
1033	Polyanionic and octet phases in the K-Sb system. I. Crystalline intermetallic compounds. Physical Review B, 1999, 59, 829-842.	1.1	17
1034	Influence of crystal structure on the lattice sites and formation energies of hydrogen in wurtzite and zinc-blende GaN. Physical Review B, 1999, 60, R5101-R5104.	1.1	39
1035	Ab initio calculation of elastic constants of SiO2 stishovite and Î±-quartz. Journal of Chemical Physics, 1999, 111, 2071-2074.	1.2	45
1036	Nitrogen Doping of Amorphous Carbon Surfaces. Physical Review Letters, 1999, 83, 5346-5349.	2.9	36
1037	Comparison of atomistic simulations and pseudopotential calculations of the MgO{100}/Ag{100} and MgO{110}/Ag{110} interfaces. Journal of Chemical Physics, 1999, 110, 8090-8097.	1.2	29
1038	Atomic-Scale Mechanisms of Oxygen Precipitation and Thin-Film Oxidation of SiC. Physical Review Letters, 1999, 83, 1624-1627.	2.9	98
1039	Ab InitioMolecular Dynamics Studies of Off-Center Displacements in CuCl. Physical Review Letters, 1999, 83, 568-571.	2.9	18
1040	Dipolar Defect Model for Fatigue in Ferroelectric Perovskites. Physical Review Letters, 1999, 83, 1231-1234.	2.9	119
1041	Dipole-Quadrupole Interactions and the Nature of Phase III of Compressed Hydrogen. Physical Review Letters, 1999, 83, 4097-4100.	2.9	46
1042	Silylated carbodiimides in molecular and extended structures. Physical Review B, 1999, 60, 3126-3139.	1.1	38
1043	Quantum Monte Carlo calculation of Compton profiles of solid lithium. Physical Review B, 1999, 59, 7907-7916.	1.1	38
1044	Surface diffusion potential energy surfaces from first principles: CO chemisorbed on Pt{110}. Journal of Chemical Physics, 1999, 111, 9461-9464.	1.2	46
1045	Zone-center modes of cubic and hexagonal diamond under high pressure: A first-principles study. Physical Review B, 1999, 60, 2964-2967.	1.1	14
1046	Ab initiocalculations of the dynamical response of copper. Physical Review B, 1999, 59, 12188-12191.	1.1	31

#	Article	IF	Citations
1047	Self-energy corrections inVO2within a modelGWscheme. Physical Review B, 1999, 60, 15699-15704.	1.1	71
1048	Scanning-tunneling-microscopy images:â€ƒA fullyab initioapproach. Physical Review B, 1999, 59, R5320-R5323.	1.1	21
1049	Exchange and correlation effects beyond the LDA on the dielectric function of silicon. Physical Review B, 1999, 60, 14224-14233.	1.1	42
1050	Ab initiopseudopotential calculations of the transverse and longitudinal phonon spectra of Ge, Î±-Sn, and Î±-Sn/Ge superlattices. Physical Review B, 1999, 60, 6452-6458.	1.1	6
1051	Density-functional study of hydrogen chemisorption on vicinal Si(001) surfaces. Physical Review B, 1999, 59, 2790-2800.	1.1	34
1052	Orbital-free kinetic-energy density functionals with a density-dependent kernel. Physical Review B, 1999, 60, 16350-16358.	1.1	212
1053	NO monomer and (NO)x polymeric chain chemisorption on Pt{110}: Structure and energetics. Journal of Chemical Physics, 1999, 110, 12082-12088.	1.2	25
1054	Polyanionic and octet phases in the K-Sb system. II. Liquid alloys. Physical Review B, 1999, 59, 843-854.	1.1	20
1055	AB-INITIO STUDY OF THE STRUCTURE OF Pd(110)-c(4Ã—2)-BENZENE. Surface Review and Letters, 1999, 06, 903-906.	0.5	0
1056	Surface reconstructions and bonding via the electron localization function: the case of Si(001). Solid State Communications, 1999, 111, 583-588.	0.9	21
1057	Anharmonic effects in the phonons of IIIâ€“V semiconductors: first principles calculations. Solid State Communications, 1999, 113, 1-10.	0.9	90
1058	Wannier function analysis of InP nanocrystals under pressure. Solid State Communications, 1999, 113, 189-193.	0.9	7
1059	Model structures and properties of the electron density distribution for low quartz at pressure: a study of the SiO bond. Journal of Molecular Structure, 1999, 485-486, 13-25.	1.8	36
1060	Transition metal defect behavior and Si density of states in the processing temperature regime. Physica B: Condensed Matter, 1999, 273-274, 358-362.	1.3	2
1061	Theoretical studies of interstitial boron defects in silicon. Physica B: Condensed Matter, 1999, 273-274, 268-270.	1.3	1
1062	Theoretical LEED parameters for the zinc-blende GaN (110) surface. Materials Science and Engineering B: Solid-State Materials for Advanced Technology, 1999, 59, 258-260.	1.7	3
1063	Semiconductor alloys for monolithic integration with Si microelectronics. Materials Science and Engineering B: Solid-State Materials for Advanced Technology, 1999, 67, 17-22.	1.7	0
1064	Density functional calculation of semiconductor surface phonons. Physics Reports, 1999, 309, 209-331.	10.3	49

#	Article	IF	Citations
1065	Existence of direct bandgap transitions in superlattices. Physics Letters, Section A: General, Atomic and Solid State Physics, 1999, 254, 233-238.	0.9	13
1066	Atomic layer epitaxy of copper: an ab initio investigation of the CuCl/H2 process. Applied Surface Science, 1999, 148, 9-16.	3.1	16
1067	Cluster and thin layer of compound semiconductor growth on hexagonal and vicinal cubic surface and the simulation of atom behavior. Microelectronics Journal, 1999, 30, 335-340.	1.1	4
1068	Cu underpotential deposition on Au(111) and Au(100). Can this be explained in terms of the energetics of the Cu/Au system?. Electrochimica Acta, 1999, 45, 691-697.	2.6	31
1069	The chemisorption of spin polarised NO on Ag{111}. Chemical Physics Letters, 1999, 300, 639-644.	1.2	53
1070	First-principles theoretical studies of the structural, electronic and magnetic properties of Co{1010}-A. Chemical Physics Letters, 1999, 309, 434-440.	1.2	12
1071	Vacancies in SiC: Influence of Jahn-Teller distortions, spin effects, and crystal structure. Physical Review B, 1999, 59, 15166-15180.	1.1	225
1072	Cohesive, structural, and electronic properties of Fe-Si compounds. Physical Review B, 1999, 59, 12860-12871.	1.1	215
1073	Accurate structure factors from pseudopotential methods. Physical Review B, 1999, 60, 7875-7880.	1.1	5
1074	First Principles Hartreeâ€“Fock Description of Lithium Insertion in Oxides. Journal of Solid State Chemistry, 1999, 142, 428-439.	1.4	43
1075	A theory of special points in two-dimensional solid-state calculations. International Journal of Quantum Chemistry, 1999, 74, 601-615.	1.0	0
1076	Approaching bulk limit for three-dimensional solids via the cyclic cluster approximation: Semiempirical INDO study. Journal of Computational Chemistry, 1999, 20, 253-261.	1.5	32
1077	Theoretical Aspects of the Optical Response of Semiconductor Surfaces. Physica Status Solidi A, 1999, 175, 5-16.	1.7	8
1078	Ab initiocalculation of the lattice dynamics and phase diagram of boron nitride. Physical Review B, 1999, 59, 8551-8559.	1.1	359
1079	First-principles study of vacancy formation and migration energies in tantalum. Physical Review B, 1999, 60, 7001-7005.	1.1	36
1080	Structure and electronic properties of amorphousWO3. Physical Review B, 1999, 60, 16463-16474.	1.1	88
1081	First-principles calculations for phonons in AgGaX2(X = Se,Te) chalcopyrite crystals. Journal of Physics Condensed Matter, 1999, 11, 9673-9678.	0.7	16
1082	Electronic-structure calculations by first-principles density-based embedding of explicitly correlated systems. Journal of Chemical Physics, 1999, 110, 7677-7688.	1.2	216

#	Article	IF	Citations
1083	High-pressure thermal expansion, bulk modulus, and phonon structure of diamond. Physical Review B, 1999, 60, 9444-9449.	1.1	84
1084	Interatomic potentials for monoatomic metals from experimental data andab initiocalculations. Physical Review B, 1999, 59, 3393-3407.	1.1	1,231
1085	Theoretical study of the vibrational modes and their pressure dependence in the pure clathrate-II silicon framework. Physical Review B, 1999, 60, 950-958.	1.1	88
1086	First-principles characterization of the four phases of barium titanate. Ferroelectrics, 1999, 220, 1-15.	0.3	50
1087	Optical properties and electronic structures of semiconductors with screened-exchange LDA. Physical Review B, 1999, 59, 7486-7492.	1.1	161
1088	Multiresolution analysis of electronic structure: semicardinal and wavelet bases. Reviews of Modern Physics, 1999, 71, 267-311.	16.4	217
1089	Ab initiostudy of structural and electronic properties of yttria-stabilized cubic zirconia. Physical Review B, 1999, 59, 797-810.	1.1	271
1090	Inelastic Lifetimes of Hot Electrons in Real Metals. Physical Review Letters, 1999, 83, 2230-2233.	2.9	116
1091	Anharmonic line shift and linewidth of the Raman mode in covalent semiconductors. Physical Review B, 1999, 59, 6182-6188.	1.1	89
1092	Retardation of O diffusion through polycrystalline Pt by Be doping. Physical Review B, 1999, 59, 16047-16052.	1.1	12
1093	Relative stability of some possible phases of graphitic carbon nitride. Physical Review B, 1999, 59, 11683-11686.	1.1	118
1094	Polytypic transformations in SiC: Anab initiostudy. Physical Review B, 1999, 60, 13261-13264.	1.1	23
1095	Plasmon Lifetime in K: A Case Study of Correlated Electrons in Solids Amenable toAb InitioTheory. Physical Review Letters, 1999, 82, 2350-2353.	2.9	48
1096	Theory of PbTiO3, BaTiO3, and SrTiO3 surfaces. Faraday Discussions, 1999, 114, 395-405.	1.6	190
1097	Elastic and optical properties ofÎ±- andÎºâ^'Al2O3. Physical Review B, 1999, 59, 12777-12787.	1.1	152
1098	Hydrogen and the Structure of the Transition Aluminas. Journal of the American Chemical Society, 1999, 121, 7493-7499.	6.6	179
1099	The adsorption of oxygen at GaN surfaces. Applied Physics Letters, 1999, 74, 1695-1697.	1.5	219
1100	Theory of electronic and optical properties of 3C-SiC. Journal of Applied Physics, 1999, 85, 2179-2184.	1.1	40

#	Article	IF	Citations
1101	Stability of ultrathin semiconductor layers. Applied Physics Letters, 1999, 74, 1722-1724.	1.5	2
1102	Periodic DFT Study of the Pt(111):â€‰ A p(1Ã—1) Atomic Oxygen Interaction with the Surface. Journal of Physical Chemistry B, 1999, 103, 7222-7232.	1.2	32
1103	Relative stabilities, bulk moduli and electronic structure properties of different ultraâ€hard materials investigated within the local spin density functional approximation. Journal of Materials Chemistry, 1999, 9, 3151-3158.	6.7	36
1104	Effects of Local and Gradient-Corrected Density Approximations on the Prediction of the Intralayer Lattice Distancec, in Graphite and LiC₆. Molecular Simulation, 1999, 22, 39-49.	0.9	19
1105	No evidence of a metal-insulator transition in dense hot aluminum: A first-principles study. Physical Review B, 1999, 60, 16382-16388.	1.1	47
1106	Impeded Dimer Formation in the High-Pressure Crystal Structure of Formic Acid. Physical Review Letters, 1999, 82, 3464-3467.	2.9	67
1107	An efficient preconditioning scheme for plane-wave-based electronic structure calculations. Computational Materials Science, 1999, 14, 4-7.	1.4	11
1108	Lattice dynamics of Ga1â^'xAlxAs studied by ab initio calculations. Computational Materials Science, 1999, 13, 232-238.	1.4	10
1109	Ab initio tensile testing simulation of aluminum and aluminum nitride ceramics based on density functional theory. Computational Materials Science, 1999, 15, 435-440.	1.4	22
1110	First-principles determination of possible geometries in cis-polyacetylene. Synthetic Metals, 1999, 101, 507-508.	2.1	0
1111	Coherent phase stability in Al-Zn and Al-Cu fcc alloys: The role of the instability of fcc Zn. Physical Review B, 1999, 60, 16448-16462.	1.1	55
1112	Unrelaxed vacancy formation energies in group-IV elements calculated by the full-potential linear muffin-tin orbital method: Invariance with crystal structure. Physical Review B, 1999, 59, 8508-8515.	1.1	66
1113	First-principles elastic constants for the hcp transition metals Fe, Co, and Re at high pressure. Physical Review B, 1999, 60, 791-799.	1.1	355
1114	First-principles calculations of phonon dispersion and lattice dynamics inLa2CuO4. Physical Review B, 1999, 59, 9278-9284.	1.1	37
1115	Electronic structure, chemical bonding, and optical properties of ferroelectric and antiferroelectricNaNO2. Physical Review B, 1999, 59, 1776-1785.	1.1	160
1116	Surface relaxation of the (110) face of rutile SnO2. Surface Science, 1999, 420, 103-109.	0.8	60
1117	A general rule for surface reconstructions of IIIâ€“V semiconductors. Surface Science, 1999, 422, L177-L182.	0.8	22
1118	Structural, electronic and magnetic properties of nickel surfaces. Surface Science, 1999, 423, 1-11.	0.8	116

#	Article	IF	Citations
1119	Hydrogen, sulphur and chlorine coadsorption on Pd(111): a theoretical study of poisoning and promotion. Surface Science, 1999, 430, 176-191.	0.8	70
1120	Ethylene, sulphur, and chlorine coadsorption on Pd(111): a theoretical study of poisoning and promotion. Surface Science, 1999, 430, 192-198.	0.8	24
1121	A theoretical analysis of adsorption and dissociation of CH3OH on the stoichiometric SnO2(110) surface. Surface Science, 1999, 430, 213-222.	0.8	70
1122	Quantum-size effect in thin Al(110) slabs. Surface Science, 1999, 432, 54-60.	0.8	52
1123	The reconstruction of nickel and rhodium (001) surfaces upon carbon, nitrogen or oxygen adsorptions. Surface Science, 1999, 437, 18-28.	0.8	36
1124	Methyl chemisorption on Ni(111) and C H M multicentre bonding: a density functional theory study. Surface Science, 1999, 437, 362-376.	0.8	84
1125	Structures of pure and Ca-segregated MgO (001) surfaces. Surface Science, 1999, 442, 251-255.	0.8	11
1126	Oxygen in the Earth's core: a first-principles study. Physics of the Earth and Planetary Interiors, 1999, 110, 191-210.	0.7	51
1127	Transition metals and their carbides and nitrides: â€ƒTrends in electronic and structural properties. Physical Review B, 1999, 60, 6343-6347.	1.1	236
1128	Ab Initio Methods. Springer Series in Solid-state Sciences, 1999, , 7-138.	0.3	5
1129	Magnetism and magneto-structural effects in transition-metal sulphides. Journal of Physics Condensed Matter, 1999, 11, 8197-8222.	0.7	60
1130	Polymorphism in silica studied in the local density and generalized-gradient approximations. Journal of Physics Condensed Matter, 1999, 11, 3833-3874.	0.7	174
1131	Comparison of the Bulk and Surface Properties of Ceria and Zirconia by ab Initio Investigations. Journal of Physical Chemistry B, 1999, 103, 10158-10170.	1.2	145
1132	Competition between the ionic and covalent character in the series of boron compounds BP, BAs, and BSb. Journal of Physics Condensed Matter, 1999, 11, 5781-5796.	0.7	53
1133	Deriving accurate work functions from thin-slab calculations. Journal of Physics Condensed Matter, 1999, 11, 2689-2696.	0.7	156
1134	Periodic density functional theory study of Pt(111): surface features of slabs of different thicknesses. Journal of Physics Condensed Matter, 1999, 11, 7463-7480.	0.7	40
1135	First-principles calculation of the thermal properties of silver. Physical Review B, 1999, 59, 965-969.	1.1	124
1136	Classical and Quantum Mechanical Studies of Crystalline Ammonium Dinitramide. Journal of Physical Chemistry B, 1999, 103, 6774-6782.	1.2	25

#	Article	IF	Citations
1137	Atomic and electronic structure of the CdTe(001) surface: LDA andGWcalculations. Physical Review B, 1999, 59, 15261-15269.	1.1	37
1138	Stability and electronic structure of GaN nanotubes from density-functional calculations. Physical Review B, 1999, 60, 7788-7791.	1.1	231
1139	Explanation of the Observed Dearth of Three-Coordinated Al on Î³-Alumina Surfaces. Journal of the American Chemical Society, 1999, 121, 10999-11001.	6.6	70
1140	Implementation of the LDA+U method using the full-potential linearized augmented plane-wave basis. Physical Review B, 1999, 60, 10763-10769.	1.1	259
1141	Electronic Structures and Optical Properties of ZnO, SnO2and In2O3. Japanese Journal of Applied Physics, 1999, 38, 3453-3458.	0.8	83
1142	Ab initiocalculation of the origin of the distortion of Î±-PbO. Physical Review B, 1999, 59, 8481-8486.	1.1	160
1143	First-principles calculations of the lattice dynamics of CuInSe2. Journal of Physics Condensed Matter, 1999, 11, 9665-9671.	0.7	28
1144	First-principles investigation of ferromagnetism and ferroelectricity in bismuth manganite. Physical Review B, 1999, 59, 8759-8769.	1.1	324
1145	Ab initio study of 180Â° domain wall energy and structure in PbTiO3. Applied Physics Letters, 1999, 75, 2830-2832.	1.5	64
1146	Phonons in GaP quantum dots. Physical Review B, 1999, 59, 2881-2887.	1.1	72
1147	Vibrations of the Interstitial Oxygen Pairs in Silicon. Physical Review Letters, 1999, 82, 4022-4025.	2.9	36
1148	Theoretical Tracing of a Novel Route from Molecular Precursors through Polymers to Dense, Hard C3N4 Solids. Journal of the American Chemical Society, 1999, 121, 4696-4703.	6.6	49
1149	Origin of the Lone Pair of Î±-PbO from Density Functional Theory Calculations. Journal of Physical Chemistry B, 1999, 103, 1258-1262.	1.2	157
1150	Intrinsic Piezoelectric Response in Perovskite Alloys: PMN-PT versus PZT. Physical Review Letters, 1999, 83, 1347-1350.	2.9	161
1151	A study of the electronic, magnetic, structural and dynamic properties of low-dimensional NiO on MgO(100) surfaces. Faraday Discussions, 1999, 114, 105-127.	1.6	15
1152	Lattice dynamics ofBaTiO3,PbTiO3, andPbZrO3:â€ƒA comparative first-principles study. Physical Review B, 1999, 60, 836-843.	1.1	416
1153	An introduction to â€œComputational Crystallographyâ€• Zeitschrift Fur Kristallographie - Crystalline Materials, 1999, 214, 506-527.	0.4	27
1154	Ab-Initio Pseudopotential Calculations of Boron Diffusion in Silicon. Materials Research Society Symposia Proceedings, 1999, 568, 91.	0.1	5

#	Article	IF	Citations
1155	First Principles Calculation of the Hot Electron Lifetime in Simple and Noble Metals. Materials Research Society Symposia Proceedings, 1999, 579, 33.	0.1	0
1156	Ab Initio Calculations of Response Properties Including the Electron-Hole Interaction. Materials Research Society Symposia Proceedings, 1999, 579, 9.	0.1	0
1157	ARC Discharge for the Synthesis of Monoclinic Ga2O3 Nanowires. Materials Research Society Symposia Proceedings, 1999, 581, 239.	0.1	0
1158	Z-Contrast STEM Imaging and Ab-Initio Calculations of Grain Boundaries in SrTiO3. Materials Research Society Symposia Proceedings, 1999, 586, 37.	0.1	1
1159	Theoretical Explanation of Pt Trimers Observed by Z-Contrast STEM. Materials Research Society Symposia Proceedings, 1999, 589, 241.	0.1	0
1160	Effect of Lattice Coherency on Solution Energies of Impurities: Stability of an Epitaxial InAs Monolayer Deposited on GaAs. Materials Transactions, JIM, 1999, 40, 1295-1300.	0.9	0
1161	Prediction of the Effect of Ti on the (111) and (100) Antiphase Boundary Energy in Ni₃Al. Materials Transactions, JIM, 1999, 40, 1301-1305.	0.9	5
1162	Total Energy Calculations for Silane Dissociative Chemisorption onto Si(100) and Si(111) Surfaces. Journal of the Chinese Chemical Society, 2000, 47, 887-894.	0.8	2
1163	The Origin of Electrical Activity at Grain Boundaries in Perovskites and Related Materials. Materials Research Society Symposia Proceedings, 2000, 654, 131.	0.1	0
1164	Lattice Trapping of Cracks in Fe Using an Interatomic Potential Derived from Experimental Data and Ab Initio Calculations. Materials Research Society Symposia Proceedings, 2000, 653, .	0.1	1
1165	Electronic structure calculations of vacancy parameters in transition metals: Impact on the bcc self-diffusion anomaly. International Journal of Quantum Chemistry, 2000, 77, 927-939.	1.0	30
1166	Electronic structure of minerals: The apatite group as a relevant example. International Journal of Quantum Chemistry, 2000, 77, 991-1006.	1.0	13
1167	Effect of spin polarization for hydrogen adsorbed on Si(111)(1ï¿½21) surface: First-principles calculations. International Journal of Quantum Chemistry, 2000, 79, 47-55.	1.0	1
1168	Electronic structure of Ge3N4 possible structures. International Journal of Quantum Chemistry, 2000, 80, 249-257.	1.0	39
1169	Implementation of the Cyclic Cluster Model in Hartree-Fock LCAO Calculations of Crystalline Systems. Physica Status Solidi (B): Basic Research, 2000, 222, 495-516.	0.7	39
1170	Pentaprismane and hypostrophene from first-principles, with plane waves. Chemical Physics Letters, 2000, 317, 381-387.	1.2	23
1171	On the origin of topological differences between experimental and theoretical crystal charge densities. Acta Crystallographica Section A: Foundations and Advances, 2000, 56, 332-339.	0.3	157
1172	The experimental charge-density approach in the evaluation of intermolecular interactions. Application of a new module of theXDprogramming package to several solids including a pentapeptide. Acta Crystallographica Section A: Foundations and Advances, 2000, 56, 585-591.	0.3	40

#	Article	IF	Citations
1173	Aplanarity of CO3 groups: a theoretical investigation. Acta Crystallographica Section B: Structural Science, 2000, 56, 648-653.	1.8	17
1174	Structure of Cu6PbO8. Acta Crystallographica Section B: Structural Science, 2000, 56, 22-26.	1.8	12
1175	Multilayer relaxations at the (0001) surface of Be and Mg. Solid State Communications, 2000, 116, 17-20.	0.9	12
1176	FP-LAPW and pseudopotential calculations of the structural phase transformations of GaN under high-pressure. Solid State Communications, 2000, 116, 389-393.	0.9	27
1177	Ab initio study of dipolar defects and 180Â° domain walls in PbTiO3. Journal of Physics and Chemistry of Solids, 2000, 61, 291-294.	1.9	24
1178	Density functional study of silane adsorption onto Si(100) surface. Thin Solid Films, 2000, 370, 192-198.	0.8	23
1179	Band-gap bowing in SixGe1âˆ'x alloy. Physica B: Condensed Matter, 2000, 293, 183-186.	1.3	11
1180	Development of glue-type potentials for the Alâ€“Pb system: phase diagram calculation. Acta Materialia, 2000, 48, 1753-1761.	3.8	77
1181	An ab initio study of the cleavage anisotropy in silicon. Acta Materialia, 2000, 48, 4517-4530.	3.8	229
1182	Electronic structure of SnO2 (110) surface. Materials Science in Semiconductor Processing, 2000, 3, 103-107.	1.9	53
1183	Computational studies for the interpretation of gas response of SnO2(110) surface. Sensors and Actuators B: Chemical, 2000, 65, 375-378.	4.0	23
1184	Atomic layer epitaxy of copper: an ab initio investigation of the CuCl/H2 process. Applied Surface Science, 2000, 157, 92-100.	3.1	14
1185	Structure and dynamics from combined neutron scattering and first-principles studies. Chemical Physics, 2000, 261, 205-216.	0.9	52
1186	The linewidth of surface states of simple metals. Physics of the Solid State, 2000, 42, 1373-1379.	0.2	3
1187	Band gap estimation for a triaminotrinitrobenzene molecular crystal by the density-functional method. Semiconductors, 2000, 34, 1161-1162.	0.2	5
1188	Localisation of adsorbate-induced demagnetisation: CO chemisorbed on Ni{110}. Chemical Physics Letters, 2000, 327, 125-130.	1.2	102
1189	Interaction of NO and NO2 with MgO(1 0 0): photoemission and density-functional studies. Chemical Physics Letters, 2000, 330, 475-483.	1.2	51
1190	Adsorbate/substrate bonding in Co{10 0}/K-c(2Ã—2) elucidated through first-principles theory. Chemical Physics Letters, 2000, 317, 372-380.	1.2	21

#	Article	IF	Citations
1191	Application of a new virtual crystal approach for the study of disordered perovskites. Journal of Physics and Chemistry of Solids, 2000, 61, 315-320.	1.9	73
1192	Band structure effects on the interaction of charged particles with solids. Nuclear Instruments & Methods in Physics Research B, 2000, 164-165, 147-160.	0.6	33
1193	Induced polarization by charged particles in real solids. Nuclear Instruments & Methods in Physics Research B, 2000, 164-165, 161-167.	0.6	3
1194	Anisotropic atomâ€“atom potentials from X-ray charge densities: application to intermolecular interactions and lattice energies in some biological and nonlinear optical materials. Computational and Theoretical Chemistry, 2000, 529, 27-35.	1.5	12
1195	Density functional study of structural and electronic properties of silane adsorbed Si(100) surface. Computational and Theoretical Chemistry, 2000, 496, 163-173.	1.5	10
1196	Free Energy of a d-Wave Superconductor in the Nearly Antiferromagnetic Fermi Liquid Model. Journal of Low Temperature Physics, 2000, 120, 65-88.	0.6	0
1197	Growth and structure of ultrathin vanadium oxide layers on Pd(111). Physical Review B, 2000, 61, 13945-13954.	1.1	124
1198	From molecules to solids with the DMol3 approach. Journal of Chemical Physics, 2000, 113, 7756-7764.	1.2	9,082
1199	Electronic structure and mechanical stability of the graphitic honeycomb lattice. Physical Review B, 2000, 62, 7614-7618.	1.1	47
1200	Structure and dynamics of liquid iron under Earthâ€™s core conditions. Physical Review B, 2000, 61, 132-142.	1.1	245
1201	Reaction of NO2 with Zn and ZnO:â€‰ Photoemission, XANES, and Density Functional Studies on the Formation of NO3. Journal of Physical Chemistry B, 2000, 104, 319-328.	1.2	371
1202	Oxygen stability, diffusion, and precipitation in SiC: Implications for thin-film oxidation. Journal of Electronic Materials, 2000, 29, 353-358.	1.0	26
1203	High-pressure phases in the Al 2 SiO 5 system and the problem of aluminous phase in the Earth's lower mantle: ab initio calculations. Physics and Chemistry of Minerals, 2000, 27, 430-439.	0.3	48
1204	Trends in band-gap pressure coefficients in boron compounds BP, BAs, and BSb. Journal of Physics Condensed Matter, 2000, 12, 5655-5668.	0.7	89
1205	Schottky barrier tuning with heterovalent interlayers: Al/Ge/GaAs versus Al/Si/GaAs. Journal of Vacuum Science & Technology an Official Journal of the American Vacuum Society B, Microelectronics Processing and Phenomena, 2000, 18, 2114.	1.6	3
1206	Ab initiostudy of ground and excited states of NiO(100) monolayer. Journal of Physics Condensed Matter, 2000, 12, 2163-2181.	0.7	29
1207	Non-spiky density of states of an icosahedral quasicrystal. Europhysics Letters, 2000, 52, 578-583.	0.7	46
1208	Electronic structure of the layered ternary carbides Ti2SnC and Ti2GeC. Journal of Physics Condensed Matter, 2000, 12, 9617-9627.	0.7	30

#	Article	IF	Citations
1209	Computational analysis of the high-pressure structures of InSb. Journal of Physics Condensed Matter, 2000, 12, 7161-7173.	0.7	14
1210	Adsorption geometry of benzene on Pd(110): Results of first-principles calculations. Europhysics Letters, 2000, 52, 698-704.	0.7	11
1211	High-pressure thermodynamic, electronic and magnetic properties of Ni. Journal of Physics Condensed Matter, 2000, 12, 8953-8962.	0.7	20
1212	A high-pressure structural study of propionic acid and the application of CCD detectors in high-pressure single-crystal x-ray diffraction. Journal of Physics Condensed Matter, 2000, 12, L613-L618.	0.7	17
1213	Dislocation core reconstruction in zinc-blende semiconductors. Journal of Physics Condensed Matter, 2000, 12, 10039-10044.	0.7	16
1214	Small aggregates of interstitials and models for platelets in diamond. Journal of Physics Condensed Matter, 2000, 12, 10257-10261.	0.7	3
1215	Prediction of solution enthalpies of substitutional impurities in aluminium. Modelling and Simulation in Materials Science and Engineering, 2000, 8, 221-232.	0.8	12
1216	Stable and metastable structures of Co on Cu(001): Anab initiostudy. Physical Review B, 2000, 61, 2211-2220.	1.1	71
1217	Interaction of sulfur with Pt(111) and Sn/Pt(111): Effects of coverage and metalâ€“metal bonding on reactivity toward sulfur. Journal of Chemical Physics, 2000, 113, 11284-11292.	1.2	50
1218	Phenomenological approximations to the self-energy operator by a generalizedXÎ± method. Physical Review B, 2000, 61, 1912-1917.	1.1	2
1219	Opposite rumpling of the MgO and CaO (100) surfaces: A density-functional theory study. Physical Review B, 2000, 62, 8318-8322.	1.1	38
1220	First-principles investigation of the quantum-well system Na on Cu(111). Physical Review B, 2000, 61, 13973-13982.	1.1	87
1221	High-pressure phases and structural bonding ofGe3N4. Physical Review B, 2000, 62, 5-8.	1.1	35
1222	Structural properties and energetics of oxygen impurities in GaAs. Physical Review B, 2000, 61, 5326-5331.	1.1	12
1223	Ab initiocalculations of the Î²-SiC(001)/Ti interface. Physical Review B, 2000, 61, 2672-2679.	1.1	65
1224	Work-function anisotropy in noble metals: Contributions fromdstates and effects of the surface atomic structure. Physical Review B, 2000, 61, 8489-8495.	1.1	57
1225	Ab initiocalculations of the phase-transition mechanism in potassium thiocyanate. Physical Review B, 2000, 62, 3083-3085.	1.1	2
1226	Electronic structure and magnetic coupling in sodium electro sodalite: All-electron density functional calculations. Journal of Chemical Physics, 2000, 113, 5466.	1.2	11

#	Article	IF	Citations
1227	First-principles calculations of hot-electron lifetimes in metals. Physical Review B, 2000, 61, 13484-13492.	1.1	81
1228	Lowest-energy site for hydrogen in diamond. Physical Review B, 2000, 61, 10711-10715.	1.1	35
1229	Pressure-induced interlinking of carbon nanotubes. Physical Review B, 2000, 62, 12648-12651.	1.1	116
1230	Theoretical investigations of bond properties in graphite and graphitic silicon. Physical Review B, 2000, 61, 12864-12870.	1.1	52
1231	Electronic excitations in beryllium chalcogenides from theab initioGWapproach. Physical Review B, 2000, 62, 2466-2474.	1.1	66
1232	Surface lattice dynamics of Mg(0001). Physical Review B, 2000, 62, 17012-17019.	1.1	16
1233	Microscopic structure of the substitutional Al defect in Î± quartz. Physical Review B, 2000, 61, 2621-2625.	1.1	33
1234	Existence of localized interface states in metal/GaAs(100) junctions: Au versus Al contacts. Physical Review B, 2000, 61, 5416-5422.	1.1	4
1235	Plasmonic excitations in noble metals: The case of Ag. Physical Review B, 2000, 61, 8033-8042.	1.1	61
1236	Surface reconstructions for InAs(001) studied with density-functional theory and STM. Physical Review B, 2000, 62, R7719-R7722.	1.1	82
1237	A density functional theory study of CH2 and H adsorption on Ni(111). Journal of Chemical Physics, 2000, 112, 6006-6014.	1.2	52
1238	C incorporation in epitaxialGe1â^'yCylayers grown on Ge(001):â€ƒAnab initiostudy. Physical Review B, 2000, 62, R7723-R7726.	1.1	20
1239	High-pressure bct to fcc structural transformation in Ga. Physical Review B, 2000, 62, 9900-9902.	1.1	18
1240	Scattering of electromagnetic waves by nearly periodic structures. Physical Review B, 2000, 61, 8099-8107.	1.1	39
1241	Optimal basis set for electronic structure calculations in periodic systems. Physical Review B, 2000, 62, 15499-15504.	1.1	4
1242	Electronic structure and total energy of SrBi/sub 2/Ta/sub 2/O/sub 9/ by first-principles calculations. IEEE Transactions on Ultrasonics, Ferroelectrics, and Frequency Control, 2000, 47, 929-939.	1.7	7
1243	First-principles study on the high-pressure behavior of the zone-center modes of lonsdaleite silicon. Physical Review B, 2000, 61, 5-8.	1.1	35
1244	Oxygen and dioxygen centers in Si and Ge: Density-functional calculations. Physical Review B, 2000, 62, 10824-10840.	1.1	232

#	Article	IF	Citations
1245	Multiscale recursion in dense hydrogen plasmas. Physical Review E, 2000, 61, 6999-7008.	0.8	4
1246	First-principles calculations of the thermodynamic and structural properties of strainedInxGa1â^'xNandAlxGa1â^'xNalloys. Physical Review B, 2000, 62, 2475-2485.	1.1	187
1247	Dissociation and sticking ofH2on the Ni(111), (100), and (110) substrate. Physical Review B, 2000, 62, 8295-8305.	1.1	191
1248	Stability and structural properties of the SC16 phase of ZnS under high pressure. Physical Review B, 2000, 61, 6521-6524.	1.1	26
1249	Intravacancy transition energies in3Câ^'and4Hâ^'SiC. Physical Review B, 2000, 61, 13655-13658.	1.1	15
1250	Far-infrared vibrational properties of high-pressure high-temperatureC60polymers and theC60dimer. Physical Review B, 2000, 61, 13191-13201.	1.1	21
1251	Self-Diffusion of Small Clusters on fcc Metal (111) Surfaces. Physical Review Letters, 2000, 85, 1044-1047.	2.9	66
1252	Theoretical and Computational Study of High-Pressure Structures in Barium. Physical Review Letters, 2000, 84, 5580-5583.	2.9	45
1253	Ab initiocalculations of rigid-body displacements at the Î£5 (210) tilt grain boundary inTiO2. Physical Review B, 2000, 61, 15645-15648.	1.1	23
1254	Structural and electronic properties ofHg1â^'yMoyBa2CuO4+Î´. Physical Review B, 2000, 62, 9163-9171.	1.1	2
1255	Lithium trapping by excess oxygen inWO3:A first-principles study. Physical Review B, 2000, 62, 1508-1511.	1.1	6
1256	Nature of Metal-Ceramic Adhesion: Computational Experiments with Co on TiC. Physical Review Letters, 2000, 85, 1898-1901.	2.9	77
1257	Interface energy and electron structure for Fe/VN. Physical Review B, 2000, 61, 2221-2229.	1.1	77
1258	Theoretical atomic volumes of the light actinides. Physical Review B, 2000, 61, 4644-4650.	1.1	104
1259	Structure, optical absorption, and luminescence energy calculations ofCe3+defects inLiBaF3. Physical Review B, 2000, 61, 16477-16490.	1.1	49
1260	Band-gap modifications ofÎ²â^'FeSi2with lattice distortions corresponding to the epitaxial relationships on Si(111). Physical Review B, 2000, 62, 11063-11070.	1.1	73
1261	Screened-exchange LDA methods for films and superlattices with applications to theSi(100)2Ã—1surface and InAs/InSb superlattices. Physical Review B, 2000, 62, 2552-2561.	1.1	24
1262	Surface structure and core-level shifts in lead chalcogenide (001) surfaces. Physical Review B, 2000, 63, .	1.1	26

#	Article	IF	Citations
1263	Ab initiostudies of theCoSi2(100)/Si(100)interface. Physical Review B, 2000, 62, 2209-2219.	1.1	14
1264	First-principles study of ferroelectric and antiferrodistortive instabilities in tetragonalSrTiO3. Physical Review B, 2000, 62, 13942-13950.	1.1	123
1265	Structural and thermoelastic properties of crystalline and amorphousTiSi2phases by tight-binding molecular dynamics. Physical Review B, 2000, 61, 14405-14413.	1.1	16
1266	Role of tight-binding parameters and scaling laws on effective charges in semiconductors. Physical Review B, 2000, 61, 4667-4671.	1.1	2
1267	Generalized-stacking-fault energy surface and dislocation properties of aluminum. Physical Review B, 2000, 62, 3099-3108.	1.1	277
1268	Investigation of chemisorbed molecular states for oxygen on rhodium (111). Journal of Chemical Physics, 2000, 113, 4388-4391.	1.2	9
1269	Unusual bridged site for adsorbed oxygen adatoms: Theory and experiment for Ir{100}â€“(1Ã—2)â€“O. Journal of Chemical Physics, 2000, 112, 10460-10466.	1.2	65
1270	Structural Properties of Lanthanide and Actinide Compounds within the Plane Wave Pseudopotential Approach. Physical Review Letters, 2000, 85, 5122-5125.	2.9	92
1271	Charge transfer and hybridization effects in Ni3Al and Ni3Ga studies by x-ray-absorption spectroscopy and theoretical calculations. Journal of Applied Physics, 2000, 87, 1312-1317.	1.1	35
1272	Phonon Anomaly in High-Pressure Zn. Physical Review Letters, 2000, 85, 5130-5133.	2.9	42
1273	Effects of Strain and Local Charge on the Formation of Deep Defects in III-V Ternary Alloys. Physical Review Letters, 2000, 84, 3923-3926.	2.9	28
1274	First principles study of Pb vacancies in PbTiO3. Applied Physics Letters, 2000, 76, 499-501.	1.5	64
1275	Spin state of vacancies: From magnetic Jahn-Teller distortions to multiplets. Physical Review B, 2000, 62, 6854-6857.	1.1	63
1276	Toward control of surface reactions with a scanning tunneling microscope. Structure and dynamics of benzene desorption from a silicon surface. Journal of Chemical Physics, 2000, 113, 4412-4423.	1.2	44
1277	Extreme softening of Vanderbilt pseudopotentials: General rules and case studies of first-row andd-electron elements. Physical Review B, 2000, 61, 4576-4587.	1.1	102
1278	A first principles study of CH3 dehydrogenation on Ni(111). Journal of Chemical Physics, 2000, 112, 8120-8125.	1.2	53
1279	Self-interaction-corrected local density approximation pseudopotential calculations of the structural phase transformations of ZnO and ZnS under high pressure. Journal of Physics Condensed Matter, 2000, 12, 5639-5653.	0.7	36
1280	Metal-induced gap states and Schottky barrier heights at nonreactive GaN/noble-metal interfaces. Physical Review B, 2000, 61, 16736-16742.	1.1	50

#	Article	IF	Citations
1281	Computational design of compounds for monolithic integration in optoelectronics. Physical Review B, 2000, 63, .	1.1	6
1282	Structure, kinetics, and vibrational properties of complexes formed by hydrogen and gallium vacancies in GaAs: A theoretical study. Physical Review B, 2000, 61, 8180-8186.	1.1	12
1283	Role of NiAs phase in pressure-induced structural phase transitions in IIA-VI chalcogenides. Physical Review B, 2000, 62, 1806-1814.	1.1	53
1284	Role of occupieddstates in the relaxation of hot electrons in Au. Physical Review B, 2000, 62, 1500-1503.	1.1	31
1285	Phonon instabilities in bcc Sc, Ti, La, and Hf. Physical Review B, 2000, 61, 11221-11224.	1.1	52
1286	First-principles calculations of interstitial boron in silicon. Physical Review B, 2000, 61, 8155-8161.	1.1	83
1287	Structural and electronic properties of theSn/Si(111)3Ã—3R30Â°surface. Physical Review B, 2000, 62, 1556-1559.	1.1	26
1288	Structural, electronic, and magnetic properties of thin Mn/Cu(100) films. Physical Review B, 2000, 61, 11492-11505.	1.1	64
1289	Elastic properties of potential superhard phases ofRuO2. Physical Review B, 2000, 61, 10029-10034.	1.1	72
1290	Phonon instabilities in high-pressure bcc-fcc and the isostructural fcc-fcc phase transitions of Cs. Physical Review B, 2000, 62, 3624-3629.	1.1	23
1291	Optimized local modes for lattice-dynamical applications. Physical Review B, 2000, 61, 3127-3130.	1.1	10
1292	Structural relaxation and longitudinal dipole moment ofSrTiO3(001)(1Ã—1)surfaces. Physical Review B, 2000, 62, 10409-10418.	1.1	87
1293	First-principles investigation of structural and electronic properties of solid cubane and its doped derivatives. Physical Review B, 2000, 62, 7625-7633.	1.1	23
1294	Theoretical investigation of the initial reaction of the NO decomposition on the Si (100) (2Ã—1) reconstructed surface. Journal of Chemical Physics, 2000, 113, 8237-8248.	1.2	10
1295	Structural properties and quasiparticle energies of cubic SrO, MgO and SrTiO3. Journal of Physics Condensed Matter, 2000, 12, 3671-3688.	0.7	67
1296	Experimental and theoretical high pressure study of Î²-Cs2SO4. Zeitschrift Fur Kristallographie - Crystalline Materials, 2000, 215, 17-22.	0.4	0
1297	Exact-exchange-based quasiparticle calculations. Physical Review B, 2000, 62, 7121-7132.	1.1	85
1298	Size, shape, and stability of InAs quantum dots on the GaAs(001) substrate. Physical Review B, 2000, 62, 1897-1904.	1.1	96

#	Article	IF	Citations
1299	Finding transition structures in extended systems: A strategy based on a combined quantum mechanicsâ€“empirical valence bond approach. Journal of Chemical Physics, 2000, 112, 6983-6996.	1.2	142
1300	Photonic bandgap optimization in inverted fcc photonic crystals. Journal of the Optical Society of America B: Optical Physics, 2000, 17, 600.	0.9	48
1301	Dissociation pathways of oxygen on copper (110) surface: a first principles study. Computational Materials Science, 2000, 17, 133-140.	1.4	23
1302	Comparison of density of states of transition metal disilicides and their related compounds systematically calculated by a first-principle pseudopotential method using plane-wave basis. Intermetallics, 2000, 8, 381-390.	1.8	49
1303	Ab initio pseudopotential calculations on the effect of Mn doped on lattice parameters of L10 TiAl. Intermetallics, 2000, 8, 637-641.	1.8	19
1304	Electronic and structural properties of BaTe. Computational Materials Science, 2000, 17, 81-87.	1.4	28
1305	Comparative study of quasiharmonic lattice dynamics, molecular dynamics and Debye model applied to MgSiO3 perovskite. Physics of the Earth and Planetary Interiors, 2000, 122, 277-288.	0.7	108
1306	Electron localization at metal surfaces. Surface Science, 2000, 450, 126-132.	0.8	59
1307	Ab initio study of Be surface dynamical properties. Surface Science, 2000, 454-456, 442-446.	0.8	17
1308	Atomic and electronic structure of the (111) surface of cubic BN: an LDF ab initio study. Surface Science, 2000, 454-456, 494-497.	0.8	8
1309	Density functional theory calculations of adsorption of water at calcium oxide and calcium fluoride surfaces. Surface Science, 2000, 452, 9-19.	0.8	83
1310	First-principles studies of adsorption of CO on the Na(100) surface. Surface Science, 2000, 453, 130-136.	0.8	4
1311	Ï€ adsorption of ethene on to the {111} surface of copper. Surface Science, 2000, 459, 93-103.	0.8	18
1312	Pathways to dissociation of O2 on Cu (110) surface: first principles simulations. Surface Science, 2000, 459, 104-114.	0.8	46
1313	First-principles study of the adsorption of atomic H on Ni (111), (100) and (110). Surface Science, 2000, 459, 287-302.	0.8	294
1314	Energetics and structure of stoichiometric SnO2 surfaces studied by first-principles calculations. Surface Science, 2000, 463, 93-101.	0.8	269
1315	Structural and dynamical behavior of Al trimer on Al(111) surface. Surface Science, 2000, 465, 65-75.	0.8	15
1316	Surface reconstructions on the (100) CoSi2 surface. Surface Science, 2000, 465, 259-265.	0.8	5

#	Article	IF	Citations
1317	High-coverage adsorption of alkali metals at the CaO and MgO (100) surfaces. Surface Science, 2000, 466, 111-118.	0.8	16
1318	A channel for dimer flipping on the Si(001) surface. Surface Science, 2000, 465, L789-L793.	0.8	27
1319	The energetics and structure of oxygen vacancies on the SnO2(110) surface. Surface Science, 2000, 467, 35-48.	0.8	87
1320	Spin and orbital polarizations around oxygen vacancies on the (001) surfaces of SrTiO3. Surface Science, 2000, 470, L75-L80.	0.8	20
1321	Theoretical proposal: a tunable heterogeneous catalyst. Surface Science, 2000, 470, L88-L92.	0.8	6
1322	Why Are There so Few Magnetic Ferroelectrics?. Journal of Physical Chemistry B, 2000, 104, 6694-6709.	1.2	3,289
1323	Electronic and optical properties of anataseTiO2. Physical Review B, 2000, 61, 7459-7465.	1.1	677
1324	Virtual crystal approximation revisited: Application to dielectric and piezoelectric properties of perovskites. Physical Review B, 2000, 61, 7877-7882.	1.1	632
1325	Studies on the Behavior of Mixed-Metal Oxides and Desulfurization:Â Reaction of H2S and SO2with Cr2O3(0001), MgO(100), and CrxMg1-xO(100). Journal of the American Chemical Society, 2000, 122, 12362-12370.	6.6	75
1326	An ab initio study of hydrogen in forsterite and a possible mechanism for hydrolytic weakening. Journal of Geophysical Research, 2000, 105, 18977-18982.	3.3	87
1327	Ab initiocalculations for a hypothetical material: Silicon nanotubes. Physical Review B, 2000, 61, 9994-9996.	1.1	240
1328	A computer simulation study of domain walls in NH4Cl. Journal of Physics Condensed Matter, 2000, 12, 2093-2101.	0.7	1
1329	Monte Carlo simulation of electron transport in simple orthorhombically strained silicon. Journal of Applied Physics, 2000, 88, 4717.	1.1	8
1330	Electronic Structure Calculation of the Structures and Energies of the Three Pure Polymorphic Forms of Crystalline HMX. Journal of Physical Chemistry B, 2000, 104, 1009-1013.	1.2	52
1331	Clathrates as effectivep-type andn-type tetrahedral carbon semiconductors. Physical Review B, 2000, 61, 12689-12692.	1.1	31
1332	Studies on the Behavior of Mixed-Metal Oxides:Â Structural, Electronic, and Chemical Properties of Î²-FeMoO4. Journal of Physical Chemistry B, 2000, 104, 8145-8152.	1.2	49
1333	Ab initiostudies on the vibrational and thermal properties ofAl3Li. Physical Review B, 2000, 61, 14531-14536.	1.1	49
1334	Virtual-crystal approximation that works: Locating a compositional phase boundary inPb(Zr1â^'xTix)O3. Physical Review B, 2000, 62, R743-R746.	1.1	136

#	Article	IF	Citations
1335	First-principles study of strain-electronic interplay in ZnO: Stress and temperature dependence of the piezoelectric constants. Physical Review B, 2000, 62, 8802-8810.	1.1	89
1336	All-electron projector-augmented-waveGWapproximation: Application to the electronic properties of semiconductors. Physical Review B, 2000, 62, 4464-4476.	1.1	90
1337	Electron correlation effects and magnetic ordering at the Gd(0001) surface. Physical Review B, 2000, 61, R9213-R9216.	1.1	47
1338	Overcoordinated Hydrogens in the Carbon Vacancy: Donor Centers of SiC. Physical Review Letters, 2000, 84, 4926-4929.	2.9	39
1339	Two-Membered Silicon Rings on the Dehydroxylated Surface of Silica. Physical Review Letters, 2000, 84, 3887-3890.	2.9	150
1340	Structure stability and carrier localization inCdX(X=S,Se,Te)semiconductors. Physical Review B, 2000, 62, 6944-6947.	1.1	212
1341	Volume and composition dependence of direct and indirect band gaps in ordered ternary III-V semiconductor compounds: A screened-exchange LDA study. Physical Review B, 2000, 61, 4677-4684.	1.1	13
1342	Lattice dynamics and thermodynamic properties of theÎ²-Sn phase in Si. Physical Review B, 2000, 62, 14784-14789.	1.1	18
1343	Diffusion of Ge below the Si(100) Surface: Theory and Experiment. Physical Review Letters, 2000, 84, 2441-2444.	2.9	78
1344	Chemistry of NO2 on CeO2 and MgO: Experimental and theoretical studies on the formation of NO3. Journal of Chemical Physics, 2000, 112, 9929-9939.	1.2	104
1345	Energetics of hydrogen chemisorbed on Cu(110): A first principles calculations study. Journal of Chemical Physics, 2000, 113, 6926-6932.	1.2	32
1346	Energetics of InAs Thin Films and Islands on the GaAs(001) Substrate. Japanese Journal of Applied Physics, 2000, 39, 4298-4301.	0.8	17
1347	Ab initio simulation of the interaction of hydrogen with the {111} surfaces of platinum, palladium and nickel. A possible explanation for their difference in hydrogenation activity. Chemical Communications, 2000, , 705-706.	2.2	33
1348	First-Principles Studies on Pd Intercalated Graphite. Molecular Crystals and Liquid Crystals, 2000, 340, 283-288.	0.3	1
1349	The coloring problem in Ba2Cu3VS6â€Šâ€. Dalton Transactions RSC, 2000, , 1009-1011.	2.3	0
1350	Stability and electronic property investigations of the graphitic C3N4 system showing an orthorhombic unit cell. Journal of Materials Chemistry, 2000, 10, 709-713.	6.7	51
1351	Heterogeneous Catalysis through Subsurface Sites. Journal of the American Chemical Society, 2000, 122, 1796-1801.	6.6	94
1352	Ionic solids at elevated temperatures and/or high pressures: lattice dynamics, molecular dynamics, Monte Carlo and ab initio studies. Physical Chemistry Chemical Physics, 2000, 2, 1099-1111.	1.3	26

#	Article	IF	Citations
1353	First-principles study of the structural instabilities in hexagonal barium titanate: Coupling between the soft optical and the acoustic Modes. Ferroelectrics, 2000, 237, 25-32.	0.3	2
1354	Electronic structure of BAs and boride III-V alloys. Physical Review B, 2000, 62, 13522-13537.	1.1	104
1355	A Novel Method to Correlate Layer Charge and the Catalytic Activity of 2:1 Dioctahedral Smectite Clays in Terms of Binding the Interlayer Cation Surrounded by Monohydrate. Journal of Physical Chemistry A, 2000, 104, 8216-8223.	1.1	42
1356	O/N Ordering in Y2Si3O3N4 with the Melilite-type Structure from First-Principles Calculations. Chemistry of Materials, 2000, 12, 1071-1075.	3.2	27
1357	Energetics of silicon suboxides. Physical Review B, 2000, 61, 9899-9901.	1.1	65
1358	A Role for Induced Molecular Polarization in Catalytic Promotion:Â CO Coadsorbed with K on Co{101ì„0}. Journal of the American Chemical Society, 2000, 122, 10610-10614.	6.6	73
1359	CO Adsorption on Molybdenum Nitride's Î³-Mo2N(100) Surface:â€‰ Formation of NCO Species? A Density Functional Study. Journal of Physical Chemistry B, 2000, 104, 11972-11976.	1.2	29
1360	Phase transformations and electronic properties in mixed-metal oxides: Experimental and theoretical studies on the behavior of NiMoO4 and MgMoO4. Journal of Chemical Physics, 2000, 112, 935-945.	1.2	111
1361	Interaction of SO2with MgO(100) and Cu/MgO(100):Â Decomposition Reactions and the Formation of SO3and SO4. Journal of Physical Chemistry B, 2000, 104, 7439-7448.	1.2	77
1362	Periodic Hartree-Fock linear combination of crystalline orbitals calculation of the structure, equation of state and elastic properties of titanium diboride. Journal of Physics Condensed Matter, 2000, 12, 7205-7222.	0.7	46
1363	Simple refinements of Brillouin zone integration. Journal of Physics Condensed Matter, 2000, 12, 549-558.	0.7	28
1364	Compression mechanisms in the anisotropically bonded elements Se and Te. Physical Review B, 2000, 61, 3851-3856.	1.1	29
1365	Linear-scaling density-functional theory with Gaussian orbitals and periodic boundary conditions: Efficient evaluation of energy and forces via the fast multipole method. Physical Review B, 2000, 61, 16440-16453.	1.1	329
1366	Adsorption and Decomposition of H2S on MgO(100), NiMgO(100), and ZnO(0001) Surfaces:Â A First-Principles Density Functional Study. Journal of Physical Chemistry B, 2000, 104, 3630-3638.	1.2	159
1367	Effect of Interstitial Hydrogen Impurities on Ferroelectric Polarization inPbTiO3. Physical Review Letters, 2000, 84, 4717-4720.	2.9	66
1368	Ab initiostudy of the phase transformations of ZnSe under high pressure: stability of the cinnabar and SC16 phases. Journal of Physics Condensed Matter, 2000, 12, 1705-1713.	0.7	29
1369	Density Functional Theory Calculations on the Interaction of Ethene with the {111} Surface of Platinum. Journal of Physical Chemistry B, 2000, 104, 6439-6446.	1.2	49
1370	Integrated Experimental and Computational Methods for Structure Determination and Characterization of a New, Highly Stable Cesium Silicotitanate Phase, Cs2TiSi6O15(SNL-A). Chemistry of Materials, 2000, 12, 3449-3458.	3.2	50

#	Article	IF	Citations
1371	First-Principles Study of Titanium Dioxide: Rutile and Anatase. Japanese Journal of Applied Physics, 2000, 39, L847-L850.	0.8	90
1372	The Role of Orbital Interactions in Determining the Interlayer Spacing in Graphite Slabs. Journal of the American Chemical Society, 2000, 122, 11871-11875.	6.6	31
1373	Use of X-ray Charge Densities in the Calculation of Intermolecular Interactions and Lattice Energies:Â Application to Glycylglycine,dl-Histidine, anddl-Proline and Comparison with Theory. Journal of Physical Chemistry B, 2000, 104, 2183-2188.	1.2	57
1374	Quasiparticle Calculations in Solids. Solid State Physics, 2000, 54, 1-218.	1.3	514
1375	Ab Initio Study of Magnetic Structure and Chemical Reactivity of Cr2O3 and Its (0001) Surface. Journal of Physical Chemistry B, 2000, 104, 6195-6201.	1.2	28
1376	Sulfur: A potential donor in diamond. Applied Physics Letters, 2000, 77, 878-879.	1.5	89
1377	Adsorption of NO on the TiO2(110) Surface:Â An Experimental and Theoretical Study. Journal of Physical Chemistry B, 2000, 104, 4408-4417.	1.2	118
1378	Band structure and optical parameters of theSnO2(110)surface. Physical Review B, 2001, 64, .	1.1	115
1379	Hop, skip or jump? Proton transport in the CaZrO3 perovskite oxide. Chemical Communications, 2001, , 661-662.	2.2	23
1380	Relevance of Heterometallic Binding Energy for Metal Underpotential Deposition. Langmuir, 2001, 17, 2219-2227.	1.6	24
1381	Smearing scheme for finite-temperature electronic-structure calculations. Physical Review B, 2001, 65, .	1.1	32
1382	Microscopic structure of hydrogen impurity in LiNbO3. Applied Physics Letters, 2001, 78, 3812-3814.	1.5	20
1383	Ab initiodensity-functional supercell calculations of hydrogen defects in cubic SiC. Physical Review B, 2001, 63, .	1.1	109
1384	Electronic structure and thermodynamics of defects inNiAl3. Physical Review B, 2001, 64, .	1.1	22
1385	Ab initiostudy ofBaTiO3andPbTiO3surfaces in external electric fields. Physical Review B, 2001, 63, .	1.1	304
1386	First-principles calculation of elastic properties of solid argon at high pressures. Physical Review B, 2001, 65, .	1.1	52
1387	Electronic and structural properties of superconductingMgB2,CaSi2,and related compounds. Physical Review B, 2001, 64, .	1.1	135
1388	MgB2andBeB2:â€ƒA comparative study of their electronic and superconducting properties. Physical Review B, 2001, 65, .	1.1	18

#	Article	IF	Citations
1389	Search for ultra-hard materials: theoretical characterisation of novel orthorhombic BC2N crystals. Solid State Sciences, 2001, 3, 943-957.	0.8	66
1390	All-electron magnetic response with pseudopotentials: NMR chemical shifts. Physical Review B, 2001, 63, .	1.1	1,502
1391	Proton Migration and Defect Interactions in the CaZrO3Orthorhombic Perovskite:Â A Quantum Mechanical Study. Chemistry of Materials, 2001, 13, 2049-2055.	3.2	142
1392	Interaction of vacancies with a grain boundary in aluminum: A first-principles study. Physical Review B, 2001, 64, .	1.1	42
1393	Theoretical investigation of carbon defects and diffusion in Î±-quartz. Physical Review B, 2001, 64, .	1.1	75
1394	Ab initiostudy of model guanine assemblies: The role ofÏ€âˆ—Ï€coupling and band transport. Physical Review B, 2001, 65, .	1.1	78
1395	Theoretical Study of Oxygen Adsorption on Graphite and the (8,0) Single-walled Carbon Nanotube. Journal of Physical Chemistry B, 2001, 105, 11227-11232.	1.2	258
1396	Density Functional Theory Calculations of Hydrogen-Containing Defects in Forsterite, Periclase, and Î±-Quartz. Journal of Physical Chemistry B, 2001, 105, 9747-9754.	1.2	53
1397	Simulating the Crystal Structures and Properties of Ionic Materials From Interatomic Potentials. Reviews in Mineralogy and Geochemistry, 2001, 42, 37-62.	2.2	10
1398	Dehydroxylation and Silanization of the Surfaces of Î²-Cristobalite Silica:Â An ab Initio Simulation. Journal of Physical Chemistry B, 2001, 105, 8007-8013.	1.2	95
1399	Theoretical maps of work-function anisotropies. Physical Review B, 2001, 65, .	1.1	32
1400	Excitonic Effects on the Silicon Plasmon Resonance. Physical Review Letters, 2001, 86, 5962-5965.	2.9	95
1401	Classical and Quantum-Mechanical Studies of Crystalline FOX-7 (1,1-Diamino-2,2-dinitroethylene). Journal of Physical Chemistry A, 2001, 105, 5010-5021.	1.1	121
1402	Experimental and theoretical study of band structure of InSe andIn1âˆ’xGaxSe(x<0.2)under high pressure:â€,Direct to indirect crossovers. Physical Review B, 2001, 63, .	1.1	73
1403	Coordination and chemical effects on the structural, electronic, and magnetic properties in Mn pnictides. Physical Review B, 2001, 64, .	1.1	156
1404	First-principles study of structural, electronic, dynamical, and dielectric properties of zircon. Physical Review B, 2001, 63, .	1.1	87
1405	An ab Initio Study of the Structure and Properties of Aluminum Hydroxide:Â Gibbsite and Bayerite. Journal of Physical Chemistry B, 2001, 105, 10236-10242.	1.2	86
1406	Chemistry of NO2on Oxide Surfaces:Â Formation of NO3on TiO2(110) and NO2â†"O Vacancy Interactions. Journal of the American Chemical Society, 2001, 123, 9597-9605.	6.6	226

#	Article	IF	Citations
1407	Structural and electronic structure properties of FeSi: the driving force behind the stability of the B20 phase. Journal of Physics Condensed Matter, 2001, 13, 2807-2815.	0.7	21
1408	I6nterstitial carbon-oxygen center and hydrogen related shallow thermal donors in Si. Physical Review B, 2001, 65, .	1.1	75
1409	Lattice dynamics and elastic properties of zinc-blende MgS. Physical Review B, 2001, 64, .	1.1	50
1410	Ab initiostudy of the vibrational and electronic properties of CdGa2S4and CdGa2Se4under pressure. Journal of Physics Condensed Matter, 2001, 13, 10117-10124.	0.7	23
1411	Light-Atom Location in Adsorbed Benzene by Experiment and Theory. Physical Review Letters, 2001, 87, 216102.	2.9	47
1412	A density functional theory study of hydroxyl and the intermediate in the water formation reaction on Pt. Journal of Chemical Physics, 2001, 114, 513.	1.2	173
1413	Catalytic Water Formation on Platinum:â€‰ A First-Principles Study. Journal of the American Chemical Society, 2001, 123, 4235-4242.	6.6	314
1414	Mg-H and Be-H complexes in cubic boron nitride. Journal of Physics Condensed Matter, 2001, 13, 8951-8956.	0.7	3
1415	Elasticity of hexagonal BeO. Journal of Physics Condensed Matter, 2001, 13, 241-251.	0.7	254
1416	Ab initiocalculations of defects in Fe and dilute Fe-Cu alloys. Physical Review B, 2001, 65, .	1.1	376
1417	Insight into electron-mediated reaction mechanisms: Catalytic CO oxidation on a ruthenium surface. Journal of Chemical Physics, 2001, 114, 8113-8118.	1.2	8
1418	Ab initiomolecular-dynamics study of highly nonideal structural and thermodynamic properties of liquid Ni-Al alloys. Physical Review B, 2001, 64, .	1.1	23
1419	Giant Anharmonicity and Nonlinear Electron-Phonon Coupling inMgB2: A Combined First-Principles Calculation and Neutron Scattering Study. Physical Review Letters, 2001, 87, 037001.	2.9	381
1420	Polarization properties of ZnO and BeO:â€ƒAnab initiostudy through the Berry phase and Wannier functions approaches. Physical Review B, 2001, 65, .	1.1	213
1421	The origin of the electron distribution in SnO. Journal of Chemical Physics, 2001, 114, 758.	1.2	96
1422	Lattice dynamics and elasticity of silver thiogallate (AgGaS2) from ab initio calculations. Journal of Chemical Physics, 2001, 114, 6734-6738.	1.2	17
1423	Tunable Adsorption on Carbon Nanotubes. Physical Review Letters, 2001, 87, 116802.	2.9	184
1424	First-principles study of the stability of BN and C. Physical Review B, 2001, 64, .	1.1	105

#	Article	IF	Citations
1425	Exohydrogenated single-wall carbon nanotubes. Physical Review B, 2001, 64, .	1.1	103
1426	Ab initio molecular dynamics simulation of liquid water and waterâ€“vapor interface. Journal of Chemical Physics, 2001, 115, 9815-9820.	1.2	71
1427	Ab initiothermodynamics of metals: Al and W. Physical Review B, 2001, 63, .	1.1	91
1428	Role of defects in the electronic properties of amorphous/crystalline Si interface. Physical Review B, 2001, 64, .	1.1	11
1429	Role of the core-valence interaction for pseudopotential calculations with exact exchange. Physical Review B, 2001, 64, .	1.1	113
1430	Electronic densities of states of Silicon-Boron system. , 0, , .		0
1431	Defect states of substitutional oxygen in diamond. Journal of Physics Condensed Matter, 2001, 13, 11607-11613.	0.7	28
1432	CO Oxidation on Pd(100) and Pd(111):Â A Comparative Study of Reaction Pathways and Reactivity at Low and Medium Coverages. Journal of the American Chemical Society, 2001, 123, 1166-1172.	6.6	226
1433	Studies on the behavior of mixed-metal oxides: Adsorption of CO and NO on MgO(100), NixMg1â^'xO(100), and CrxMg1â^'xO(100). Journal of Chemical Physics, 2001, 114, 4186-4195.	1.2	45
1434	High-pressure elastic properties of major materials of Earth's mantle from first principles. Reviews of Geophysics, 2001, 39, 507-534.	9.0	240
1435	Numerical atomic orbitals for linear-scaling calculations. Physical Review B, 2001, 64, .	1.1	992
1436	Interactions of Hydrogen with CeO2. Journal of the American Chemical Society, 2001, 123, 6609-6611.	6.6	167
1437	Structure and bonding in crystalline and molten Li-Sn alloys: A first-principles density-functional study. Physical Review B, 2001, 63, .	1.1	23
1438	Quantum Monte Carlo simulations of solids. Reviews of Modern Physics, 2001, 73, 33-83.	16.4	1,813
1439	First-principles study of dynamical and dielectric properties of tetragonal zirconia. Physical Review B, 2001, 64, .	1.1	129
1440	A Comparison of the Adsorption and Diffusion of Hydrogen on the {111} Surfaces of Ni, Pd, and Pt from Density Functional Theory Calculations. Journal of Physical Chemistry B, 2001, 105, 4889-4894.	1.2	184
1441	Plane-wave pseudopotential study of point defects in uranium dioxide. Physical Review B, 2001, 64, .	1.1	167
1442	Plane-wave DFT-LDA calculation of the electronic structure and absorption spectrum of copper. Physical Review B, 2001, 64, .	1.1	57

#	Article	IF	Citations
1443	Size or polarisability effects?. Journal of Alloys and Compounds, 2001, 314, 114-123.	2.8	4
1444	Dynamical properties of pnictide ZnSnP2 from ab initio calculations. Journal of Alloys and Compounds, 2001, 328, 162-165.	2.8	8
1445	First-principles characterisation of new ternary heterodiamond BC2N phases. Computational Materials Science, 2001, 20, 107-119.	1.4	68
1446	A comparison of orthogonal sp-based tight-binding models for silicon. Computational Materials Science, 2001, 21, 135-148.	1.4	5
1447	Electronic structure of twist grain-boundaries in ZnO and the effect of Sb doping. Computational Materials Science, 2001, 22, 38-43.	1.4	18
1448	Ab initio study of the high-pressure phase transition from the cubic-diamond to the Î²-tin structure of Si. Computational Materials Science, 2001, 22, 49-55.	1.4	26
1449	Dynamic structure factor of gold. Computational Materials Science, 2001, 22, 123-128.	1.4	13
1450	Calculation of the density of states of transition metal monosilicides by a first-principle pseudopotential method using plane-wave basis. Intermetallics, 2001, 9, 261-268.	1.8	33
1451	Screening of the possible boron-based n-type thermoelectric conversion materials on the basis of the calculated densities of states of metal borides and doped Î²-boron. Intermetallics, 2001, 9, 721-734.	1.8	40
1452	Density-functional study of the adsorption of benzene on the (111), (100) and (110) surfaces of nickel. Surface Science, 2001, 472, 133-153.	0.8	124
1453	Electron correlation in the Si(1 0 0) surface. Surface Science, 2001, 482-485, 458-463.	0.8	15
1454	Surface electronic structure of metastable FeSi(CsCl)(1 1 1). Surface Science, 2001, 482-485, 625-631.	0.8	7
1455	A molecular orbital study of surfaceâ€“adsorbate interactions during the oxidation of CO on the Pt(111) surface. Surface Science, 2001, 475, 47-60.	0.8	17
1456	Adsorption sites and STM images of C2H2 on Si(100): a first-principles study. Surface Science, 2001, 475, 83-88.	0.8	38
1457	The structure of carbon adsorbed on Ir{100}: LEED Iâ€“V analysis and benchmarking of DFT. Surface Science, 2001, 478, 49-56.	0.8	13
1458	Stability, electronic properties and chemical reactivity of palladiumâ€“vanadium(1 1 1) surface alloys. Surface Science, 2001, 482-485, 712-717.	0.8	12
1459	Si(001)/In-4Ã—3 surface: a first principles total energy calculation. Surface Science, 2001, 482-485, 1468-1473.	0.8	5
1460	Coadsorption of sodium and SO2 on MgO(100): alkali promoted Sâ€“O bond cleavage. Surface Science, 2001, 477, L279-L288.	0.8	19

#	Article	IF	Citations
1461	Substrate reconstruction and electronic surface states: Ag(001). Surface Science, 2001, 486, 65-72.	0.8	20
1462	Disproportionation of dimethylalane on aluminum surfaces. Part II. Quantum chemistry studies. Surface Science, 2001, 488, 303-324.	0.8	3
1463	The first-principle study of the iodine-modified silver surfaces. Surface Science, 2001, 487, 77-86.	0.8	21
1464	Density-functional bridge between surfaces and interfaces. Surface Science, 2001, 493, 253-270.	0.8	31
1465	Atom bridge made from magnetic materials: atomic configuration and magnetic properties. Surface Science, 2001, 493, 757-762.	0.8	16
1466	Structural and electronic properties of silver surfaces: ab initio pseudopotential density functional study. Surface Science, 2001, 490, 125-132.	0.8	48
1467	A first principles survey of stoichiometric (1Ã—2) reconstructions on the rutile surface. Surface Science, 2001, 495, 211-233.	0.8	23
1468	First-principles study of the interaction of oxygen with the SnO2(110) surface. Surface Science, 2001, 490, 221-236.	0.8	98
1469	Investigation of vinyl phosphonic acid/hydroxylated Î±-Al2O3() reaction enthalpies. Surface Science, 2001, 494, 1-20.	0.8	48
1470	A DFT study of the adsorption of thiophene on Ni(100). Surface Science, 2001, 492, 27-33.	0.8	35
1471	Comparative theory of missing-row reconstructions: Pt{110}, Pt{211} and Pt{311}. Surface Science, 2001, 494, 159-165.	0.8	39
1472	First principles study of carbon monoxide adsorption on zirconia-supported copper. Surface Science, 2001, 495, 44-50.	0.8	43
1473	Stability of sulfur induced reconstructions on InP() surfaces. Surface Science, 2001, 495, 55-67.	0.8	5
1474	Minority metallic surface states of a half-metallic ferrimagnet. Surface Science, 2001, 494, L793-L798.	0.8	53
1475	Electronic and Chemical Properties of Ce0.8Zr0.2O2(111) Surfaces:Â Photoemission, XANES, Density-Functional, and NO2Adsorption Studies. Journal of Physical Chemistry B, 2001, 105, 7762-7770.	1.2	118
1476	First-principles studies of the stability of Zintl ions in alkali-tin alloys: I. Crystalline intermetallic compounds. Journal of Physics Condensed Matter, 2001, 13, 959-980.	0.7	10
1477	Oxidative corrosion of adhesive interlayers. Physical Chemistry Chemical Physics, 2001, 3, 5140-5144.	1.3	3
1478	Covalent origin of adsorbate-induced demagnetization at ferromagnetic surfaces. Physical Review B, 2001, 64, .	1.1	23

#	Article	IF	Citations
1479	Elastic properties of TiB2and MgB2. Journal of Physics Condensed Matter, 2001, 13, 5585-5595.	0.7	122
1480	A first principles study of methanol decomposition on Pd(111): Mechanisms for Oâ€“H bond scission and Câ€“O bond scission. Journal of Chemical Physics, 2001, 115, 7182-7186.	1.2	77
1481	A density functional theory study of the reaction of C+O, C+N, and C+H on close packed metal surfaces. Journal of Chemical Physics, 2001, 114, 5792-5795.	1.2	35
1482	Metric-tensor flexible-cell algorithm for isothermalâ€“isobaric molecular dynamics simulations. Journal of Chemical Physics, 2001, 115, 10282.	1.2	74
1483	Ab initiomolecular dynamics study of the pressure-induced phase transformations in cristobalite. Physical Review B, 2001, 63, .	1.1	25
1484	The electronic structure of tantalum (oxy)nitrides TaON and Ta3N5. Journal of Materials Chemistry, 2001, 11, 1248-1252.	6.7	178
1485	Interaction between Metallic p Orbitals and the Ï€ Orbitals of Organic Molecules:â€‰ The Binding between Ethylene and Aluminum. Journal of Physical Chemistry B, 2001, 105, 641-645.	1.2	14
1486	Ab initiostudy of the electronic and structural properties of the ferroelectric transition inKH2PO4. Physical Review B, 2001, 65, .	1.1	65
1487	LDA, GW, and exact-exchange Kohn-Sham scheme calculations of the electronic structure of sp semiconductors. Physical Review B, 2001, 64, .	1.1	65
1488	Unique structural topologies involving metalâ€“metal and metalâ€“sulfur interactions: salts of [Ni(C3S5)2]xâ^' with cis-anti-cis-dicyclohexyl-18-crown-6 complexed counter ions. Dalton Transactions RSC, 2001, , 1347-1351.	2.3	17
1489	Electronic and structural properties of the layered ternary carbide Ti3AlC2. Journal of Materials Chemistry, 2001, 11, 2335-2339.	6.7	167
1490	CO Adsorption on Ptâ^'Ru Surface Alloys and on the Surface of Ptâ^'Ru Bulk Alloy. Journal of Physical Chemistry B, 2001, 105, 9533-9536.	1.2	90
1491	Quantum Mechanical Studies of Pressure Effects in Crystalline Ammonium Dinitramide. Journal of Physical Chemistry A, 2001, 105, 7413-7422.	1.1	8
1492	DeNOxReactions on MgO(100), ZnxMg1-xO(100), CrxMg1-xO(100), and Cr2O3(0001):Â Correlation between Electronic and Chemical Properties of Mixed-Metal Oxides. Journal of Physical Chemistry B, 2001, 105, 5497-5505.	1.2	41
1493	Chemical Interaction of H2, Br2, and HBr with Î±-Boron Surfaces. Journal of Physical Chemistry B, 2001, 105, 12797-12802.	1.2	6
1494	Band-offset trends in nitride heterojunctions. Physical Review B, 2001, 63, .	1.1	51
1495	First-principles structural stability study of nonstoichiometry-related planar defects in SrTiO3 and BaTiO3. Journal of Applied Physics, 2001, 89, 5622-5629.	1.1	29
1496	Density of constitutional and thermal point defects inL12Al3Sc. Physical Review B, 2001, 63, .	1.1	60

#	Article	IF	Citations
1497	Influence of Adsorbed Species on the Reconstruction of 4Hâ^'SiC(0001) Surfaces. Journal of Physical Chemistry B, 2001, 105, 7619-7623.	1.2	25
1498	First Principle Study to Correlate Location and Activity of Ruthenium Oxide Incorporated in Alkali-Metal Hexatitanates. Journal of Physical Chemistry B, 2001, 105, 3463-3469.	1.2	5
1499	Twist-averaged boundary conditions in continuum quantum Monte Carlo algorithms. Physical Review E, 2001, 64, 016702.	0.8	285
1500	DFT Study on Ferroelectricity of BaTiO3. Journal of Physical Chemistry B, 2001, 105, 5766-5771.	1.2	70
1501	A Comparative Study of the p(2 Ã— 2)-CO/M(111), M=Pt,Cu,Al Chemisorption Systems. Journal of Physical Chemistry B, 2001, 105, 3245-3260.	1.2	22
1502	Thermal equation of state of tantalum. Physical Review B, 2001, 63, .	1.1	87
1503	First-Principles Pseudo-Potential Study of the Pd(110)-c(2Ã—2)-Ethylene Adsorption System. Journal of Physical Chemistry B, 2001, 105, 8149-8154.	1.2	9
1504	Classical and Quantum Mechanical Studies of Crystalline Ammonium Nitrate. Journal of Physical Chemistry A, 2001, 105, 720-733.	1.1	50
1505	Density functional theory calculations of proton-containing defects in forsterite. Radiation Effects and Defects in Solids, 2001, 154, 255-259.	0.4	3
1506	Bulk and surface properties of hexagonal-close-packed Be and Mg. Journal of Physics Condensed Matter, 2001, 13, 10767-10776.	0.7	89
1507	Variational finite-difference representation of the kinetic energy operator. Physical Review B, 2001, 64, .	1.1	18
1508	First-principles density-functional study of metal-carbonitride interface adhesion: Co/TiC(001) and Co/TiN(001). Physical Review B, 2001, 64, .	1.1	112
1509	Theoretical study of the ordered-vacancy semiconducting compound CdAl2Se4. Journal of Physics Condensed Matter, 2001, 13, 1669-1684.	0.7	26
1510	First-principles electronic structure and its relation to thermoelectric properties ofBi2Te3. Physical Review B, 2001, 63, .	1.1	106
1511	Sb-terminated InAs(001)-(2Ã—4) and (2Ã—8) studied using scanning tunneling microscopy and ab initio density functional theory. Materials Research Society Symposia Proceedings, 2001, 692, 1.	0.1	1
1512	Modeling Boron and Indium Electrical Activities in Silicon in the Presence of Nitrogen. Materials Research Society Symposia Proceedings, 2001, 669, 1.	0.1	0
1513	Critical Currents at Grain Boundaries in High Temperature Superconductors. Materials Research Society Symposia Proceedings, 2001, 689, 1.	0.1	0
1514	Structure and elasticity of wadsleyite at high pressures. American Mineralogist, 2001, 86, 1387-1395.	0.9	49

#	Article	IF	Citations
1515	Compression mechanism of cubic silica sodalite [Si12O24]: a first principles study of the Im3Ì…m to I4Ì…3m phase transition. Zeitschrift Fur Kristallographie - Crystalline Materials, 2001, 216, 495-500.	0.4	6
1516	Prediction of hydrogen positions in complex structures. Zeitschrift Fur Kristallographie - Crystalline Materials, 2001, 216, 99-104.	0.4	18
1517	Interfacial Segregation of Early Transition Metals in Nickel Aluminide. Materials Transactions, 2001, 42, 407-410.	0.4	1
1518	Bondlengths and Phase Stability of Silicon-Germanium Alloys under Pressure. Materials Transactions, 2001, 42, 2201-2205.	0.4	17
1519	Strain Dependence of Solute Atom Energy in Aluminum-Rich Alloys. Materials Transactions, 2001, 42, 429-431.	0.4	2
1520	<I>Ab Initio</I> Calculation on the Structure and Elastic Properties of a Magnesium-Lithium Alloy. Materials Transactions, 2001, 42, 1167-1171.	0.4	18
1521	Geometry and Conduction of an Infinite Single-Row Gold Wire. Materials Transactions, 2001, 42, 2257-2260.	0.4	14
1522	Theoretical investigation of bonding in diaspore. European Journal of Mineralogy, 2001, 13, 343-349.	0.4	45
1523	Ab initio study of MgSiO3 low-clinoenstatite at high pressure. American Mineralogist, 2001, 86, 762-766.	0.9	7
1524	Pressure-induced structural change of the tetrafluoro-p-benzoquinone (p-fluoranil) crystal from ab initio total energy calculations. Chemical Physics, 2001, 264, 9-19.	0.9	3
1525	Density-functional modelling of core-hole effects in electron energy-loss near-edge spectra. Ultramicroscopy, 2001, 86, 325-337.	0.8	57
1526	Critical examination of the radial functions in the Hansenâ€“Coppens multipole model through topological analysis of primary and refined theoretical densities. Acta Crystallographica Section A: Foundations and Advances, 2001, 57, 395-405.	0.3	84
1527	Theoretical investigation of metastable Al2SiO5polymorphs. Acta Crystallographica Section A: Foundations and Advances, 2001, 57, 548-557.	0.3	29
1528	Ab initio determination of the valence electron distribution in the average structure of the incommensurately modulated calaverite AuTe2. Acta Crystallographica Section B: Structural Science, 2001, 57, 633-637.	1.8	6
1529	Electronic structure effects from hydrogen bonding in the liquid phase and in chemisorption: an integrated theory and experimental effort. Journal of Synchrotron Radiation, 2001, 8, 136-140.	1.0	7
1530	Calculation of electronic energy and density of state of iron-disilicides using a total-energy pseudopotential method, CASTEP. Thin Solid Films, 2001, 381, 176-182.	0.8	42
1531	Dislocation core properties in semiconductors. Solid State Communications, 2001, 118, 651-655.	0.9	23
1532	Pressure effect on phonon modes in gallium nitride: a molecular dynamics study. Solid State Communications, 2001, 120, 413-418.	0.9	27

#	Article	IF	Citations
1533	Lattice dynamics of Mg2SiO4. Journal of Molecular Structure, 2001, 596, 3-6.	1.8	13
1534	Calculation of debye temperature for crystalline structuresâ€"a case study on Ti, Zr, and Hf. Acta Materialia, 2001, 49, 947-961.	3.8	138
1535	Electronic structure of GaAs1â^'xNx alloys. Materials Science in Semiconductor Processing, 2001, 4, 577-580.	1.9	3
1536	The energetics of dislocation cores in semiconductors and their role on dislocation mobility. Physica B: Condensed Matter, 2001, 302-303, 398-402.	1.3	3
1537	Structural, electronic, and magnetic properties of thin V/Cu film. Physica B: Condensed Matter, 2001, 304, 67-74.	1.3	9
1538	Erbium in Si and GaN: extended versus point defects. Physica B: Condensed Matter, 2001, 308-310, 369-373.	1.3	5
1539	Evidence for trapped by carbon impurities in silicon. Physica B: Condensed Matter, 2001, 308-310, 197-201.	1.3	23
1540	Theoretical study of pressure-induced negative effective U of a tungsten atom in crystalline silicon. Physica B: Condensed Matter, 2001, 308-310, 424-426.	1.3	1
1541	Electrically active centers in partial dislocations in semiconductors. Physica B: Condensed Matter, 2001, 308-310, 489-492.	1.3	4
1542	Mgâ€"H and Beâ€"H complexes in c-BN. Physica B: Condensed Matter, 2001, 308-310, 1027-1030.	1.3	2
1543	Defect engineering in IIIâ€"V ternary alloys: effects of strain and local charge on the formation of substitutional and interstitial native defects. Physica B: Condensed Matter, 2001, 308-310, 846-849.	1.3	1
1544	Ab initio investigation of elastic constants of superconducting MgB2. Physica C: Superconductivity and Its Applications, 2001, 363, 189-193.	0.6	37
1545	Ab initio search of carbon nitrides, isoelectronic with diamond, likely to lead to new ultra hard materials. Comptes Rendus De L'Academie Des Sciences - Series IIc: Chemistry, 2001, 4, 255-272.	0.1	6
1546	Band-gap bowing calculation of SixSn1â^'x alloy. Infrared Physics and Technology, 2001, 42, 81-85.	1.3	39
1547	Computer Simulations of Thermal Expansion in Lanthanum-Based Perovskites. Journal of Solid State Chemistry, 2001, 156, 394-399.	1.4	7
1549	TlF and PbO under High Pressure: Unexpected Persistence of the Stereochemically Active Electron Pair. Angewandte Chemie - International Edition, 2001, 40, 4624-4629.	7.2	29
1550	Luminescent FeSi2/Si(111) Structures Induced by Heteroepitaxial Stress. Physica Status Solidi (B): Basic Research, 2001, 223, 253-257.	0.7	8
1551	Theoretical Study of the Elastic Properties of III-P Compounds. Physica Status Solidi (B): Basic Research, 2001, 223, 411-415.	0.7	47

#	Article	IF	Citations
1552	The High Pressure Behaviour of SnS2: X-Ray Powder Diffraction and Quantum Mechanical Calculations up to 10 GPa. Physica Status Solidi (B): Basic Research, 2001, 223, 435-440.	0.7	19
1553	Theoretical Studies of Raman Spectra for Planar Polymerized C60. Physica Status Solidi (B): Basic Research, 2001, 226, 95-106.	0.7	16
1554	First Principles Study of the Self-Interstitial Defect in Diamond. Physica Status Solidi A, 2001, 186, 215-220.	1.7	17
1555	First Principles Studies of H in Diamond. Physica Status Solidi A, 2001, 186, 263-268.	1.7	11
1556	Incorporation of C into Growth Steps of Diamond (111). Physica Status Solidi A, 2001, 186, 319-330.	1.7	9
1557	Self-consistent finite-difference electronic structure calculations. Computer Physics Communications, 2001, 136, 64-76.	3.0	7
1558	HARES: an efficient method for first-principles electronic structure calculations of complex systems. Computer Physics Communications, 2001, 137, 341-360.	3.0	37
1559	Geometry, electrons, phonons and reactions on Si(001) surfaces. Computer Physics Communications, 2001, 137, 143-162.	3.0	8
1560	Amorphous WO3: a first-principles approach. Electrochimica Acta, 2001, 46, 1989-1993.	2.6	52
1561	Systematic prediction of crystal structures. Chemical Physics Letters, 2001, 337, 36-42.	1.2	52
1562	Ab initio study of ammonia adsorption states on an ice surface I: structures, adsorption energies and linear dependences on coverage ratio. Chemical Physics Letters, 2001, 348, 107-114.	1.2	12
1563	Model for the defect-related electrical conductivity in ion-damaged diamond. Physical Review B, 2001, 64, .	1.1	40
1564	A general method to obtain well localized Wannier functions for composite energy bands in linear combination of atomic orbital periodic calculations. Journal of Chemical Physics, 2001, 115, 9708-9719.	1.2	191
1565	Surface Reconstruction and the Difference in Surface Acidity between Î³- and Î·-Alumina. Journal of the American Chemical Society, 2001, 123, 26-29.	6.6	90
1566	Thermodynamics of hexagonal-close-packed iron under Earthâ€™s core conditions. Physical Review B, 2001, 64, .	1.1	252
1567	Electronic structures of Ba1-xCaxTiO3studied by x-ray absorption spectroscopy and theoretical calculation. Journal of Physics Condensed Matter, 2001, 13, 11087-11095.	0.7	37
1568	Electronic structure and physical properties of early transition metal mononitrides: Density-functional theory LDA, GGA, and screened-exchange LDA FLAPW calculations. Physical Review B, 2001, 63, .	1.1	454
1569	Segregation Effects at a High-Angle Twist Boundary in ZnO. Journal of Materials Science, 2001, 9, 231-235.	1.2	2

#	Article	IF	Citations
1570	The phase diagram and electronic structure of Pd-V alloys:ab initiodensity functional calculations. Journal of Physics Condensed Matter, 2001, 13, 3545-3572.	0.7	22
1571	Structural, vibrational, and thermodynamic properties of Al-Sc alloys and intermetallic compounds. Physical Review B, 2001, 64, .	1.1	87
1572	Dislocation core properties of aluminum: a first-principles study. Materials Science & Engineering A: Structural Materials: Properties, Microstructure and Processing, 2001, 309-310, 142-147.	2.6	26
1573	Crystal structure and stability of complex precipitate phases in Alâ€“Cuâ€“Mgâ€“(Si) and Alâ€“Znâ€“Mg alloys. Acta Materialia, 2001, 49, 3129-3142.	3.8	394
1574	Interaction of sulfur with TiO2(1 1 0): photoemission and density-functional studies. Chemical Physics Letters, 2001, 336, 377-384.	1.2	46
1575	Structure Models for Î³â€Aluminum Oxynitride from Ab Initio Calculations. Journal of the American Ceramic Society, 2001, 84, 2633-2637.	1.9	47
1576	Stability investigation and thermal behavior of a hypothetical silicon nanotube. Computational and Theoretical Chemistry, 2001, 539, 101-106.	1.5	93
1577	First principles study of structural, electronic and magnetic interplay in ferroelectromagnetic yttrium manganite. Journal of Magnetism and Magnetic Materials, 2001, 236, 176-189.	1.0	56
1578	Self-diffusion of adatoms on Ni(100) surfaces. Journal of Physics Condensed Matter, 2001, 13, L321-L328.	0.7	18
1579	First Principles Study on Li Deintercalation Effect in Orthorhombic LiMnO2. Japanese Journal of Applied Physics, 2001, 40, 6878-6883.	0.8	1
1580	Ab initioinvestigation of mechanical behaviour of MgB2superconductor under pressure. Journal of Physics Condensed Matter, 2001, 13, L641-L645.	0.7	28
1581	Determining the range of forces in empirical many-body potentials using first-principles calculations. Philosophical Magazine A: Physics of Condensed Matter, Structure, Defects and Mechanical Properties, 2001, 81, 991-1008.	0.8	26
1582	Ab initiostudy of the structural and optical properties of orthorhombic ternary nitride crystals. Journal of Physics Condensed Matter, 2001, 13, 10417-10431.	0.7	31
1583	Interpretation ofab initiototal energy results in a chemical language: II. Stability of TiAl3and ScAl3. Journal of Physics Condensed Matter, 2001, 13, 11551-11565.	0.7	19
1584	Electronic structure and electric field gradient in MgB2under pressure: anab initiostudy. Journal of Physics Condensed Matter, 2001, 13, 11661-11667.	0.7	15
1585	Reaction Paths in Concurrence: The Electrochemical Hydrogen Reaction on GaAs(111)A- and GaAs(110)-Surfaces A Quantumchemical Approach. Zeitschrift Fur Physikalische Chemie, 2001, 215, .	1.4	2
1586	Structures and energies of AlOOH and FeOOH polymorphs from plane wave pseudopotential calculations. American Mineralogist, 2001, 86, 312-317.	0.9	45
1587	The Valency Effect on Reaction Pathways in Heterogeneous Catalysis: Insight from Density Functional Theory Calculations. Progress in Theoretical Chemistry and Physics, 2001, , 199-215.	0.2	4

#	Article	IF	Citations
1588	Electronic properties of a grain boundary in Sb-doped ZnO. Journal of Physics Condensed Matter, 2001, 13, 9937-9943.	0.7	26
1589	Does density-functional theory predict a spin-density-wave ground state for Cr?. Journal of Physics Condensed Matter, 2001, 13, L239-L247.	0.7	20
1590	Theoretical study on the phase stability, site preference, and lattice parameters for Gd(Fe, T)12. Journal of Physics Condensed Matter, 2001, 13, 2727-2736.	0.7	68
1591	Graphitization at diamond dislocation cores. Journal of Physics Condensed Matter, 2001, 13, 8965-8972.	0.7	18
1592	Theory of zeolite supralattices: Se in zeolite Linde type A. Journal of Physics Condensed Matter, 2001, 13, 10433-10457.	0.7	14
1593	A numerically improved computational scheme for the optical conductivity tensor in layered systems. Journal of Physics Condensed Matter, 2001, 13, 1529-1538.	0.7	13
1594	First-principles modeling of the infrared spectrum of kaolinite. American Mineralogist, 2001, 86, 1321-1330.	0.9	201
1595	Calculation of the elastic constants of the Al2SiO5 polymorphs andalusite, sillimanite and kyanite. Zeitschrift Fur Kristallographie - Crystalline Materials, 2001, 216, 67-70.	0.4	56
1596	Ab initiogeometry optimization and ground state properties of layered ternary carbides Ti3MC2(M = Al,) Tj ETQq0 0 0 rgBT /Overlock 10	0.7	121
1597	Tin-vacancy complexes in silicon. Physical Review B, 2001, 64, .	1.1	18
1598	Reconstruction and electronic structure of the vacancy-free N- and B-terminatedc-BN (100) surfaces. Physical Review B, 2001, 63, .	1.1	9
1599	Vibrational modes in epitaxialTi1âˆ’xScxN(001)layers: Anab initiocalculation and Raman spectroscopy study. Physical Review B, 2001, 64, .	1.1	50
1600	One-Dimensional Metallic Edge States inMoS2. Physical Review Letters, 2001, 87, 196803.	2.9	563
1601	First-principles study ofCa2+andMn2+substituents inKTaO3. Physical Review B, 2001, 63, .	1.1	22
1602	Effects of biaxial strain and chemical ordering on the band gap of InGaN. Applied Physics Letters, 2001, 78, 189-191.	1.5	25
1603	Role of Boronp-Electrons and Holes in SuperconductingMgB2, and Other Diborides: A Fully Relaxed, Full-Potential Electronic Structure Study. Physical Review Letters, 2001, 87, 087004.	2.9	66
1604	Energetics and bonding properties of the Ni /Î²-SiC (001) interface: Anabinitiostudy. Physical Review B, 2001, 64, .	1.1	13
1605	Periodic Hartreeâ€“Fock study of the adsorption of molecular oxygen on a reduced TiO2 (110) surface. Journal of Chemical Physics, 2001, 115, 4798-4810.	1.2	46

#	Article	IF	Citations
1606	Comparison of structural transformations and superconductivity in compressed sulfur and selenium. Physical Review B, 2001, 63, .	1.1	20
1607	Influence of surface morphology on the Si(100) and (111) ionization potentials. Physical Review B, 2001, 64, .	1.1	26
1608	Magnetic4dmonoatomic rows on Ag vicinal surfaces. Physical Review B, 2001, 64, .	1.1	33
1609	Density-functional calculation of van der Waals forces for free-electron-like surfaces. Physical Review B, 2001, 64, .	1.1	49
1610	Density-functional theory calculations of the interaction of protons and water with low-coordinated surface sites of calcium oxide. Physical Review B, 2001, 63, .	1.1	37
1611	Native defects and complexes in SiC. Journal of Physics Condensed Matter, 2001, 13, 9027-9037.	0.7	18
1612	Direct comparisons of rates for low temperature diffusion of hydrogen and deuterium on Cu(001) from quantum mechanical calculations and scanning tunneling microscopy experiments. Journal of Chemical Physics, 2001, 115, 5620-5624.	1.2	47
1613	Electronic Structure Analyses of Sn-doped In2O3. Japanese Journal of Applied Physics, 2001, 40, 3231-3235.	0.8	67
1614	Accuracy and limitations of localized Greenâ€™s function methods for materials science applications. Physical Review B, 2001, 64, .	1.1	16
1615	Integration over two-dimensional Brillouin zones by adaptive mesh refinement. Physical Review B, 2001, 64, .	1.1	18
1616	Structure of aluminum atomic chains. Physical Review B, 2001, 64, .	1.1	61
1617	First-principles studies of beryllium doping of GaN. Physical Review B, 2001, 63, .	1.1	133
1618	Ideal unreactive metal/semiconductor interfaces:â€ƒThe case ofZn/ZnSe(001). Physical Review B, 2001, 63, .	1.1	8
1619	Quantum treatment of H adsorbed on a Pt(111) surface. Physical Review B, 2001, 65, .	1.1	62
1620	Calculation of optical properties and density of states for systems with huge unit cells. Physical Review B, 2001, 64, .	1.1	12
1621	Spin-other-orbit interaction and magnetocrystalline anisotropy. Physical Review B, 2001, 64, .	1.1	33
1622	Patterning of Si(001) with halogens: Surface structure as a function of the halogen chemical potential. Physical Review B, 2001, 64, .	1.1	23
1623	Pseudopotential description of rare earths in oxides: The case ofEr2Si2O7. Physical Review B, 2001, 63, .	1.1	9

#	Article	IF	Citations
1624	Cd hyperfine fields at the bcc Fe/Co interface. Physical Review B, 2001, 64, .	1.1	4
1625	Adsorbate-induced demagnetization and restructuring of ultrathin magnetic films: CO chemisorbed onÎ³-Fe/Cu(100). Physical Review B, 2001, 64, .	1.1	18
1626	Photoelasticity ofÎ±-quartz from first principles. Physical Review B, 2001, 63, .	1.1	22
1627	Absence of lattice strain anomalies at the electronic topological transition in zinc at high pressure. Physical Review B, 2001, 63, .	1.1	52
1628	Termination effects at metal/ceramic junctions: Schottky barrier heights and interface properties of the Î²-SiC(001)/Ni systems. Physical Review B, 2001, 64, .	1.1	7
1629	Reconstruction defects on partial dislocations in semiconductors. Applied Physics Letters, 2001, 79, 3630-3632.	1.5	4
1630	Fast through-bond diffusion of nitrogen in silicon. Applied Physics Letters, 2001, 78, 736-738.	1.5	28
1631	Adhesion of ultrathin ZrO2(111) films on Ni(111) from first principles. Journal of Chemical Physics, 2001, 114, 5816-5831.	1.2	112
1632	Reaction of SO2 with pure and metal-doped MgO: Basic principles for the cleavage of Sâ€“O bonds. Journal of Chemical Physics, 2001, 115, 10914-10926.	1.2	47
1633	Dynamics of interstitial hydrogen molecules in crystalline silicon. Journal of Physics Condensed Matter, 2001, 13, 6271-6283.	0.7	38
1634	Synthesis and characterization of transparent conducting oxide cobaltâ€“nickel spinel films. Journal of Vacuum Science and Technology A: Vacuum, Surfaces and Films, 2001, 19, 1647-1651.	0.9	83
1635	Te covered Si(001): A variable surface reconstruction. Physical Review B, 2001, 64, .	1.1	6
1636	Ab initiostudy of CO adsorption on Ni(110): Effects on surface magnetism at low coverage. Physical Review B, 2001, 63, .	1.1	17
1637	Series of(nÃ—2)Si-rich reconstructions of Î²-SiC(001):â€, A prospective atomic wire. Physical Review B, 2001, 63, .	1.1	16
1638	Carbon-tin defects in silicon. Physical Review B, 2001, 64, .	1.1	19
1639	Nucleation ofcâ^'BNon hexagonal boron nitride. Physical Review B, 2001, 64, .	1.1	13
1640	Self-interstitialâ€“hydrogen complexes in Si. Physical Review B, 2001, 64, .	1.1	11
1641	X-ray diffraction and theoretical studies of the high-pressure structures and phase transitions in magnesium fluoride. Physical Review B, 2001, 64, .	1.1	109

#	Article	IF	Citations
1642	Ab initiodetermination of the atomistic structure ofSixGe1â^'xalloy. Physical Review B, 2001, 64, .	1.1	57
1643	Efficientkâ‹…pmethod for the calculation of total energy and electronic density of states. Physical Review B, 2001, 64, .	1.1	8
1644	Well localized crystalline orbitals obtained from Bloch functions:â€ƒThe case ofKNbO3. Physical Review B, 2001, 64, .	1.1	50
1646	Probing theYD3structure by2HNMR electric-field gradients: A comparison with first-principles calculations. Physical Review B, 2001, 64, .	1.1	31
1647	A density functional theory study of carbon monoxide oxidation on the Cu3Pt(111) alloy surface: Comparison with the reactions on Pt(111) and Cu(111). Journal of Chemical Physics, 2001, 115, 5272-5277.	1.2	72
1648	Soft tetragonal distortions in ferromagneticNi2MnGaand related materials from first principles. Physical Review B, 2001, 63, .	1.1	127
1649	Towards 100% spin-polarized charge-injection: The half-metallic NiMnSb/CdS interface. Physical Review B, 2001, 64, .	1.1	184
1650	Ab initio simulation of ammonia monohydrate (NH3â‹…H2O) and ammonium hydroxide (NH4OH). Journal of Chemical Physics, 2001, 115, 7006-7014.	1.2	44
1651	Unconstrained and constrained minimization, localization, and the Grassmann manifold: Theory and application to electronic structure. Physical Review B, 2001, 64, .	1.1	11
1652	CO adsorbed on Cu(001): A comparison between local density approximation and Perdew, Burke, and Ernezerhof generalized gradient approximation. Journal of Chemical Physics, 2001, 114, 483.	1.2	39
1653	Self-interstitial aggregation in diamond. Physical Review B, 2001, 63, .	1.1	72
1654	Electronic structure and spin polarization of Mn-containing dilute magnetic III-V semiconductors. Physical Review B, 2001, 64, .	1.1	83
1655	Density functional studies on the adsorption and decomposition of SO2 on Cu(100). Journal of Chemical Physics, 2001, 115, 454-465.	1.2	51
1656	Structural and electronic properties ofZnGeAs2. Physical Review B, 2001, 63, .	1.1	25
1657	Stability, reconstruction, and surface electronic states of group-III atoms on SiC(111). Physical Review B, 2001, 64, .	1.1	12
1658	Symmetry and site selectivity in molecular chemisorption: Benzene on Ni{111}. Journal of Chemical Physics, 2001, 114, 5765-5773.	1.2	72
1659	Multilayer relaxation of Cu(331). Physical Review B, 2001, 64, .	1.1	18
1660	Elastic properties and phase stability of AgBr under pressure. Physical Review B, 2001, 65, .	1.1	34

#	Article	IF	Citations
1661	First-principles study on structural, dielectric, and dynamical properties for three BN polytypes. Physical Review B, 2001, 63, .	1.1	143
1662	Density-functional calculations of carbon doping in III-V compound semiconductors. Physical Review B, 2001, 63, .	1.1	4
1663	Surface Structure ofSrTiO3(100)â^'(5Ã—5)â^'R26.6Â°. Physical Review Letters, 2001, 86, 1801-1804.	2.9	114
1664	Electronic structure and small polaron hole transport of copper aluminate. Physical Review B, 2001, 64, .	1.1	144
1665	First-principle theoretical study on reliability SiO/sub 2/ thin films under external electric field. , 0, , .		2
1666	Quantum size effects in metal films:â€ƒEnergies and charge densities of Pb(111) grown on Cu(111). Physical Review B, 2001, 63, .	1.1	43
1667	Strain-induced change of surface reconstructions for InAs(001). Physical Review B, 2001, 63, .	1.1	23
1668	Hydrogen in jellium: First-principles pair interactions. Physical Review B, 2001, 64, .	1.1	22
1669	Growth of face-centered-cubic Fe films on Cu(100): Interdiffusion, surfactant effects, and island formation. Physical Review B, 2001, 64, .	1.1	29
1670	First-principles equations of state for simulations of shock waves in silicon. Physical Review B, 2001, 64, .	1.1	38
1671	Density-functional calculations of semiconductor properties using a semiempirical exchange-correlation functional. Physical Review B, 2001, 63, .	1.1	38
1672	Thermodynamics of uniaxial phase transition:Ab initiostudy of the diamond-to-Î²-tin transition in Si and Ge. Physical Review B, 2001, 63, .	1.1	23
1673	Theory of metastable group-IV alloys formed from CVD precursors. Physical Review B, 2001, 64, .	1.1	12
1674	Towards a first-principles simulation and current-voltage characteristic of atomistic metal-oxideâ€“semiconductor structures. Physical Review B, 2001, 64, .	1.1	41
1675	Limits and accuracy of valence force field models forInxGa1â^'xNalloys. Physical Review B, 2001, 63, .	1.1	50
1676	Structural, electronic, and magnetic properties of MnO. Physical Review B, 2001, 64, .	1.1	73
1677	Epitaxial Sc1â^'xTixN(001): Optical and electronic transport properties. Journal of Applied Physics, 2001, 89, 401-409.	1.1	84
1678	Luminescent FeSi2 Crystal Structures Induced by Heteroepitaxial Stress on Si(111). Physical Review Letters, 2001, 86, 6006-6009.	2.9	83

#	Article	IF	Citations
1679	Tailoring Band Gap and Hardness by Intercalation: Anab initioStudy ofI8@Siâˆ'46and Related Doped Clathrates. Physical Review Letters, 2001, 87, 206405.	2.9	64
1680	Anomalous Quasiparticle Lifetime in Graphite: Band Structure Effects. Physical Review Letters, 2001, 87, 246405.	2.9	62
1681	Ab initio study of substitutional nitrogen in GaAs. Applied Physics Letters, 2001, 78, 1231-1233.	1.5	13
1682	Surface Relaxations, Current Enhancements, and Absolute Distances in High Resolution Scanning Tunneling Microscopy. Physical Review Letters, 2001, 87, 236104.	2.9	134
1683	First-principle electronic properties of ZrO/sub 2/ and HfO/sub 2/ crystals under external electric field. , 0, , .		2
1684	Hydrogenation of S to H2S on Pt(111): A first-principles study. Journal of Chemical Physics, 2001, 115, 8570-8574.	1.2	46
1685	Piezoelectricity of ordered (Ga0.5In0.5)N alloys. Applied Physics Letters, 2001, 79, 2166-2168.	1.5	24
1686	Role of water and oxygen in wet and dry oxidation of diamond. Journal of Applied Physics, 2001, 90, 1026-1034.	1.1	33
1687	Nonstoichiometry and the Electrical Activity of Grain Boundaries inSrTiO3. Physical Review Letters, 2001, 86, 4056-4059.	2.9	176
1688	Vibrational Recognition of Hydrogen-Bonded Water Networks on a Metal Surface. Physical Review Letters, 2002, 89, 176104.	2.9	229
1689	Work Functions at Facet Edges. Physical Review Letters, 2002, 88, 156802.	2.9	40
1690	Cohesive properties of group-III nitrides: A comparative study of all-electron and pseudopotential calculations using the generalized gradient approximation. Physical Review B, 2002, 65, .	1.1	126
1691	Electronic and structural properties of II-VI ternary alloys and superlattices. Physical Review B, 2002, 65, .	1.1	19
1692	Role of hydrogen for the elastic properties of alumina thin films. Applied Physics Letters, 2002, 80, 1144-1146.	1.5	68
1693	Improved triangle method for two-dimensional Brillouin zone integrations to determine physical properties. Physical Review B, 2002, 66, .	1.1	27
1694	First-principles study of the adsorption of sulfur on Pt(111): S core-level shifts and the nature of the Pt-S bond. Physical Review B, 2002, 65, .	1.1	48
1695	Energetics of hydrogen impurities in aluminum and their effect on mechanical properties. Physical Review B, 2002, 65, .	1.1	75
1696	First-principles investigations forYH3(YD3):â€ƒEnergetics, electric-field gradients, and optical properties. Physical Review B, 2002, 66, .	1.1	19

#	Article	IF	Citations
1697	Impact ionization in GaAs: A screened exchange density-functional approach. Physical Review B, 2002, 65, .	1.1	13
1698	Magnetism and mechanical stability ofÎ±-iron. Physical Review B, 2002, 66, .	1.1	35
1699	Surface structure of GaAs(2 5 11). Physical Review B, 2002, 65, .	1.1	24
1700	Adiabatic potential-energy surfaces for oxygen on Al(111). Physical Review B, 2002, 65, .	1.1	93
1701	Lattice dynamics and dielectric properties of yttrium oxysulfide. Physical Review B, 2002, 65, .	1.1	18
1702	Raman tensor calculated from the2n+1theorem in density-functional theory. Physical Review B, 2002, 66, .	1.1	36
1703	Initial adsorption of Co on Cu(001):â€,â€A first-principles investigation. Physical Review B, 2002, 65, .	1.1	34
1704	Structural, electronic and magnetic properties of chalcopyrite magnetic semiconductors: A first-principles study. Journal of Vacuum Science and Technology A: Vacuum, Surfaces and Films, 2002, 20, 2023.	0.9	3
1705	Band structure ofCdGeAs2near the fundamental gap. Physical Review B, 2002, 65, .	1.1	26
1706	Nondissociative adsorption ofO2on theSi(111)â"7Ã—7surface. Physical Review B, 2002, 66, .	1.1	10
1707	Ab initiostudies of structural and electronic properties of solid indium selenide under pressure. Physical Review B, 2002, 66, .	1.1	25
1708	The Co/sub 2/MnGe Heusler compound: a first principles study of the bulk phase and of the interface with GaAs. IEEE Transactions on Magnetics, 2002, 38, 2895-2897.	1.2	14
1709	Growth of Precursors in Silicon Using Pseudopotential Calculations. Physical Review Letters, 2002, 88, 085501.	2.9	23
1710	Isolated oxygen defects in3C- and4H-SiC:â€,A theoretical study. Physical Review B, 2002, 66, .	1.1	47
1711	Hydrogen adsorption on an open metal surface:H2/Pd(210). Physical Review B, 2002, 65, .	1.1	86
1712	First-principles study ofMgB2(0001) surfaces. Physical Review B, 2002, 65, .	1.1	31
1713	Spontaneous Roughening: Fundamental Limits in Si(100) Halogen Etch Processing. Physical Review Letters, 2002, 89, 096102.	2.9	32
1714	Density-functional investigation of magnetism inÎ´-Pu. Physical Review B, 2002, 66, .	1.1	127

#	Article	IF	Citations
1715	Ab initiocalculations of multilayer relaxations of stepped Cu surfaces. Physical Review B, 2002, 65, .	1.1	36
1716	Alphabet luminescence lines in4Hâ˜SiC. Physical Review B, 2002, 65, .	1.1	72
1717	First-principles calculations of the adsorption, diffusion, and dissociation of a CO molecule on the Fe(100) surface. Physical Review B, 2002, 66, .	1.1	121
1718	Hydrogen defects in Forsterite: A test case for the embedded cluster method. Journal of Chemical Physics, 2002, 116, 2628-2635.	1.2	38
1719	Ab initiopseudopotential study of a model tetracene/ZnSe organicâ€“inorganic superlattice: Its electronic structure and optical responses. Journal of Applied Physics, 2002, 92, 5779-5784.	1.1	0
1720	Energetics and Vibrational States for Hydrogen on Pt(111). Physical Review Letters, 2002, 88, 136101.	2.9	105
1721	Broadband Fivefold Reduction of Vacuum Fluctuations Probed by Dyes in Photonic Crystals. Physical Review Letters, 2002, 88, 143903.	2.9	112
1722	Energy barriers and chemical properties in the coadsorption of carbon monoxide and oxygen on Ru(0001). Physical Review B, 2002, 65, .	1.1	38
1723	Nonconstant electronic density of states tunneling inversion for A15 superconductors:Nb3Sn. Physical Review B, 2002, 65, .	1.1	17
1724	Pressure-induced metallization in solid boron. Physical Review B, 2002, 66, .	1.1	50
1725	First-principles study of the blue bronzeK0.3MoO3. Physical Review B, 2002, 65, .	1.1	39
1726	Electronic and dynamical properties of theMgB2surface: Implications for the superconducting properties. Physical Review B, 2002, 66, .	1.1	10
1727	Atomic and electronic properties of anion vacancies on the (110) surfaces of InP, InAs, and InSb. Physical Review B, 2002, 66, .	1.1	20
1728	First-principles study of the ferroelastic phase transition inCaCl2. Physical Review B, 2002, 65, .	1.1	15
1729	Effects ofd-band hole doping on electronic structure, magnetism, and superconductivity in Fe- and Co-dopedMgCNi3. Physical Review B, 2002, 65, .	1.1	28
1730	Electronic states of prototype supertetrahedral framework materials. Physical Review B, 2002, 66, .	1.1	3
1731	First principles study of Pt adhesion and growth on SrO- and TiO2-terminated SrTiO3(100). Journal of Chemical Physics, 2002, 116, 9914-9925.	1.2	74
1732	SrTiO3/MgO(001)andMgO/SrTiO3(001)systems:â€ƒEnergetics and stresses. Physical Review B, 2002, 66, .	1.1	15

#	Article	IF	Citations
1733	Substitutional carbon in group-III nitrides:Ab initiodescription of shallow and deep levels. Physical Review B, 2002, 66, .	1.1	38
1734	Molecular effects in solidNaNO3observed by x-ray absorption and resonant Auger spectroscopy. Physical Review B, 2002, 65, .	1.1	23
1735	Long-range ordering of methylidyne on Pt{110}(1Ã—2). Journal of Chemical Physics, 2002, 117, 3951-3955.	1.2	3
1736	Stability and electronic structure of hydrogenâ€“nitrogen complexes in GaAs. Applied Physics Letters, 2002, 81, 3816-3818.	1.5	9
1737	Dynamics of self-interstitial cluster formation in silicon. Physical Review B, 2002, 66, .	1.1	13
1738	CO on Pt(111) puzzle: A possible solution. Journal of Chemical Physics, 2002, 117, 2264-2270.	1.2	102
1739	Spontaneous dissociation of a conjugated molecule on the Si(100) surface. Journal of Chemical Physics, 2002, 117, 321-330.	1.2	32
1740	Electrical activity of carbon-hydrogen centers in Si. Physical Review B, 2002, 66, .	1.1	37
1741	Electronic properties of K-doped single-wall carbon nanotube bundles. Physical Review B, 2002, 65, .	1.1	48
1742	Work functions and surface charges at metallic facet edges. Physical Review B, 2002, 66, .	1.1	16
1743	Role of structural relaxations and chemical substitutions on piezoelectric fields and potential lineup inGaN/Aljunctions. Physical Review B, 2002, 65, .	1.1	17
1744	Electronic structure of misfit-layered calcium cobaltite. Physical Review B, 2002, 66, .	1.1	110
1745	Symmetry-driven phase transformations in single-wall carbon-nanotube bundles under hydrostatic pressure. Physical Review B, 2002, 65, .	1.1	48
1746	Ab initiointerionic potentials for NaCl by multiple lattice inversion. Physical Review B, 2002, 66, .	1.1	67
1747	Origin and consequences of aromatic back-bonding at a transition metal surface: Benzyne on Ir{100}. Journal of Chemical Physics, 2002, 117, 819-824.	1.2	20
1748	Theoretical investigation of the pure and Zn-dopedÎ±andÎ´phases ofBi2O3. Physical Review B, 2002, 65, .	1.1	75
1749	The possibility of single Câ€“H bond activation in CH4 on a MoO3-supported Pt catalyst: A density functional theory study. Journal of Chemical Physics, 2002, 116, 4281-4285.	1.2	33
1750	Understanding the negative vacancy in silicon without configuration interaction theory. Physical Review B, 2002, 65, .	1.1	13

#	Article	IF	Citations
1751	Atomic structures and bondings of Î²- and spinel-Si6â^'zAlzOzN8â^'zby first-principles calculations. Physical Review B, 2002, 66, .	1.1	30
1752	Evolution of Co/Cu multilayer conductivity during growth: Anab initiostudy. Physical Review B, 2002, 65, .	1.1	14
1753	Atomistic modeling of solid-state amorphization in an immiscible Cu-Ta system. Physical Review B, 2002, 66, .	1.1	56
1754	Properties of vacancy-rich ordered(A,[])Nb2O6perovskites. Physical Review B, 2002, 66, .	1.1	2
1755	Ab initiostudy of ferroelectric domain walls inPbTiO3. Physical Review B, 2002, 65, .	1.1	471
1756	First-principles calculation of Li adatom structures on the Mo(112) surface. Physical Review B, 2002, 66, .	1.1	30
1757	Density-functional theory investigation of hardness, stability, and electron-energy-loss spectra of carbon nitrides withC11N4stoichiometry. Physical Review B, 2002, 65, .	1.1	95
1758	Structural and magnetic properties of Fe/ZnSe(001) interfaces. Physical Review B, 2002, 65, .	1.1	10
1759	Pt80Fe20surface from first principles: Electronic structure and adsorption of CO and atomic H. Physical Review B, 2002, 66, .	1.1	29
1760	Self-diffusion on fcc (100) metal surfaces: Comparison of different approximations. Physical Review B, 2002, 65, .	1.1	17
1761	First-principles approach to spin-orbit coupling in dilute magnetic semiconductors. Physical Review B, 2002, 66, .	1.1	18
1762	Large anisotropy in the optical conductivity ofYNi2B2C. Physical Review B, 2002, 66, .	1.1	2
1763	Maximally localized Wannier functions in antiferromagnetic MnO within the FLAPW formalism. Physical Review B, 2002, 65, .	1.1	30
1764	Nonlocal density-functional description of exchange and correlation in silicon. Physical Review B, 2002, 65, .	1.1	44
1765	Ultrafast switching of photonic density of states in photonic crystals. Physical Review B, 2002, 66, .	1.1	99
1766	Spontaneous hot-carrier photon emission rates in silicon: Improved modeling and applications to metal oxide semiconductor devices. Physical Review B, 2002, 65, .	1.1	9
1767	Formation of an ordered Si dimer structure onHfB2(0001). Physical Review B, 2002, 66, .	1.1	9
1768	Assigning the(1Ã—2)surface reconstruction on reduced rutile by first-principles energetics. Physical Review B, 2002, 65, .	1.1	18

#	Article	IF	Citations
1769	First-principles study of the neutral molecular metalNi(tmdt)2. Physical Review B, 2002, 65, .	1.1	60
1770	Tight-binding molecular-dynamics simulations of amorphous silicon carbides. Physical Review B, 2002, 66, .	1.1	26
1771	Chemisorption-induced disruption of surface electronic structure: Hydrogen adsorption on theSi(100)â˜2Ã—1surface. Physical Review B, 2002, 65, .	1.1	32
1772	GW self-energy calculations for systems with huge supercells. Physical Review B, 2002, 66, .	1.1	54
1773	Surface-induced stacking transition at SiC(0001). Physical Review B, 2002, 66, .	1.1	47
1774	Structure and dynamics of atomic hydrogen on NiAl(110). Physical Review B, 2002, 65, .	1.1	7
1775	Far-infrared vibrational properties of tetragonalC60polymer. Physical Review B, 2002, 65, .	1.1	12
1776	First-principles study of transparentp-type conductiveSrCu2O2and related compounds. Physical Review B, 2002, 65, .	1.1	85
1777	Sensitivity of the Mott transition to noncubic splitting of the orbital degeneracy: Application toNH3K3C60. Physical Review B, 2002, 66, .	1.1	33
1778	Spontaneous magnetization of aluminum nanowires deposited on the NaCl(100) surface. Physical Review B, 2002, 66, .	1.1	31
1779	VIRTUAL LATTICE TECHNIQUE AND THE INTERATOMIC POTENTIALS OF ZINC-BLEND-TYPE BINARY COMPOUNDS. Modern Physics Letters B, 2002, 16, 187-194.	1.0	19
1780	Microscopic structure of the 90Â°and 30Â°partial dislocations in gallium arsenide. Journal of Physics Condensed Matter, 2002, 14, 12749-12754.	0.7	6
1781	Electronic structures of semiconducting alkaline-earth metal silicides. , 0, , .		0
1782	STABILITY OF HYPOTHETICAL CARBON PHOSPHIDE SOLIDS. International Journal of Modern Physics B, 2002, 16, 1101-1104.	1.0	14
1783	STRUCTURAL AND ELECTRONIC PROPERTIES OF AL NANOWIRES: AN AB INITIO PSEUDOPOTENTIAL STUDY. International Journal of Nanoscience, 2002, 01, 159-169.	0.4	13
1784	THE BAND STRUCTURE AND BULK MODULUS OF CUBIC (3C) AND HEXAGONAL (2H) POLYTYPES OF SILICON CARBIDE. Modern Physics Letters B, 2002, 16, 383-392.	1.0	2
1785	Properties of interfaces between cubic and hexagonal polytypes of silicon carbide. Journal of Physics Condensed Matter, 2002, 14, 12725-12731.	0.7	12
1786	Pressure dependence of energy band gaps for AlxGa1 -xN, InxGa1 -xN and InxAl1 -xN. New Journal of Physics, 2002, 4, 94-94.	1.2	32

#	Article	IF	Citations
1787	Effect of Pressure on the energy band gaps of InxGa1-xN and InxAl1-xN. Materials Research Society Symposia Proceedings, 2002, 743, L11.25.1.	0.1	0
1788	Structure of Hydrated Microporous Aluminophosphates:â€‰ Static and Molecular Dynamics Approaches of AlPO4-34 from First Principles Calculations. Journal of Physical Chemistry B, 2002, 106, 8599-8608.	1.2	34
1789	Activation of group III combinations in silicon and modifications introduced by nitrogen. Journal of Vacuum Science & Technology an Official Journal of the American Vacuum Society B, Microelectronics Processing and Phenomena, 2002, 20, 230.	1.6	8
1790	Role of hydrogen in surface reconstructions and growth of GaN. Journal of Vacuum Science & Technology an Official Journal of the American Vacuum Society B, Microelectronics Processing and Phenomena, 2002, 20, 1640.	1.6	31
1791	First-principles calculations of an oxygen deficient $Sigma$ $equal$ 3(111)[10] grain boundary in strontium titanate. Journal of Physics Condensed Matter, 2002, 14, 6455-6467.	0.7	19
1792	Analytic quadratic integration over the two-dimensional Brillouin zone. Journal of Physics Condensed Matter, 2002, 14, 621-630.	0.7	7
1793	Magnetic properties of 3d impurities substituted in GaAs. Journal of Physics Condensed Matter, 2002, 14, 3295-3302.	0.7	13
1794	New evidence of the displacive feature of the ferroelectric transition in KDP-type crystals. Journal of Physics Condensed Matter, 2002, 14, L89-L93.	0.7	7
1795	Magnetic Properties of Fe Thin Films on Cu(111). Journal of the Physical Society of Japan, 2002, 71, 2983-2985.	0.7	11
1796	Electronic Structural Properties and Superconductivity of Diborides in the MgB 2 Structure. Chinese Physics Letters, 2002, 19, 1336-1339.	1.3	17
1797	First principles calculations of niobium substitution in strontium titanate. Journal of Physics Condensed Matter, 2002, 14, L149-L156.	0.7	12
1798	Structure of Bi nanolines: using tight binding to search parameter space. Journal of Physics Condensed Matter, 2002, 14, 6761-6769.	0.7	23
1799	Phase stability and pressure-induced semiconductor to metal transition in crystalline GeSe2. Journal of Physics Condensed Matter, 2002, 14, 9589-9600.	0.7	13
1800	Planar interstitial aggregates in Si. Journal of Physics Condensed Matter, 2002, 14, 12843-12853.	0.7	18
1801	Comparative study of nonequilibrium phase of A3B and AB3 types in the Niâ€“Mo system by first principles and thermodynamic calculations. Journal of Materials Research, 2002, 17, 2720-2726.	1.2	2
1802	Orbital-Free Kinetic-Energy Density Functional Theory. , 2002, , 117-184.		61
1803	Migration of Aluminum Atoms in the Transformation of Î³â€“to Î¸â€“Alumina. Materials Research Society Symposia Proceedings, 2002, 731, 361.	0.1	0
1804	Formation and Properties of Three Copper Pairs in Silicon. Materials Research Society Symposia Proceedings, 2002, 719, 1391.	0.1	6

#	Article	IF	Citations
1805	Ab initio Calculation to Predict Possible Non-Equilibrium Solid Phases in an Immiscible Yâ€“Nb System. Journal of the Physical Society of Japan, 2002, 71, 141-143.	0.7	14
1806	Nanoscale Structure/Property Correlation Through Aberration-Corrected Stem And Theory. Materials Research Society Symposia Proceedings, 2002, 738, 111.	0.1	1
1807	The Properties of a Na-Doped Twist Boundary in SrTiO3 from First Principles. Materials Research Society Symposia Proceedings, 2002, 751, 1.	0.1	2
1808	Oxides, Silicides, and Silicates of Zirconium and Hafnium; Density Functional Theory Study. Materials Research Society Symposia Proceedings, 2002, 716, 651.	0.1	0
1809	Comparative Study of the High-Pressure Behavior of As, Sb, and Bi. Journal of the American Chemical Society, 2002, 124, 15359-15367.	6.6	63
1810	A Theoretical Study of the Electronic and Optical Properties of the Graphite Intercalation Compound K(NH3)4C24. Journal of Physical Chemistry B, 2002, 106, 12916-12928.	1.2	1
1811	Efficient algorithm for band connectivity resolution. Physical Review B, 2002, 65, .	1.1	26
1812	Periodic Density Functional Theory Study of the Dissociative Adsorption of Molecular Oxygen over La2O3. Journal of Physical Chemistry B, 2002, 106, 6543-6547.	1.2	46
1813	Oxygen Adsorption on (111)-Oriented Diamond:Â A Study with Ultraviolet Photoelectron Spectroscopy, Temperature-Programmed Desorption, and Periodic Density Functional Theory. Journal of Physical Chemistry B, 2002, 106, 5230-5240.	1.2	65
1814	GWstudy of the metal-insulator transition of bcc hydrogen. Physical Review B, 2002, 66, .	1.1	35
1815	Adsorption of Methanethiol on Stoichiometric and Defective TiO2(110) Surfaces:Â A Combined Experimental and Theoretical Study. Journal of Physical Chemistry B, 2002, 106, 9883-9891.	1.2	41
1816	A First Principles Study of Carbonâ^'Carbon Coupling over the {0001} Surfaces of Co and Ru. Journal of Physical Chemistry B, 2002, 106, 2826-2829.	1.2	67
1817	First-principles calculation of coincidence Doppler broadening of positron annihilation radiation. Physical Review B, 2002, 65, .	1.1	30
1818	Density functional study on metastable bcc copper: Electronic structure and momentum density of positron-electron pairs. Physical Review B, 2002, 65, .	1.1	52
1819	Density Functional Theory Calculations of Solid Solutions of Fluor- and Chlorapatites. Chemistry of Materials, 2002, 14, 435-441.	3.2	23
1820	Dislocations in diamond: Core structures and energies. Physical Review B, 2002, 65, .	1.1	114
1821	First Principles Calculations of the Adsorption Properties of CO and NO on the Defective TiO2(110) Surface. Journal of Physical Chemistry B, 2002, 106, 6184-6199.	1.2	66
1822	A DFT Study of CHxChemisorption and Transition States for Câ^'H Activation on the Ru(112Ì„0) Surface. Journal of Physical Chemistry B, 2002, 106, 6200-6205.	1.2	68

#	Article	IF	Citations
1823	Adhesion, atomic structure, and bonding at theAl(111)/Î±â^'Al2O3(0001)interface: A first principles study. Physical Review B, 2002, 65, .	1.1	212
1824	Interpreting Molecular Crystal Disorder in Plumbocene, Pb(C5H5)2:Â Insight from Theory. Journal of the American Chemical Society, 2002, 124, 6775-6780.	6.6	17
1825	From Local Adsorption Stresses to Chiral Surfaces:â€‰ (R,R)-Tartaric Acid on Ni(110). Journal of the American Chemical Society, 2002, 124, 503-510.	6.6	193
1826	Theoretical study of oxygen-deficientSnO2(110)surfaces. Physical Review B, 2002, 65, .	1.1	84
1827	Angle-resolved photoemission study and first-principles calculation of the electronic structure of GaTe. Physical Review B, 2002, 65, .	1.1	38
1828	O/Ag(100) Surface:â€‰ A Density Functional Study with Slab Model. Journal of Physical Chemistry B, 2002, 106, 3662-3667.	1.2	30
1829	Hydrogenation of Benzene on Ni(111)A DFT Study. Journal of Physical Chemistry B, 2002, 106, 13299-13305.	1.2	57
1830	Symmetry-general least-squares extraction of elastic data for strained materials fromab initiocalculations of stress. Physical Review B, 2002, 65, .	1.1	1,021
1831	Electronic band structure of isolated and bundled carbon nanotubes. Physical Review B, 2002, 65, .	1.1	327
1832	Dissociation of CH3I on the Al(111) Surface â^' An STM and Density Functional Theory Study. Journal of the American Chemical Society, 2002, 124, 14202-14209.	6.6	13
1833	Ab initiocalculations of the cohesive energy and the bulk modulus of aluminium. Journal of Physics Condensed Matter, 2002, 14, 8787-8793.	0.7	53
1834	The electronic structure of wurtzite and zincblende AlN: anab initiocomparative study. New Journal of Physics, 2002, 4, 64-64.	1.2	78
1835	Semi-empirical and ab initio studies of low-temperature adsorption of oxygen and CO at [110] face of SnO/sub 2/. IEEE Sensors Journal, 2002, 2, 416-421.	2.4	12
1836	Work functions of pristine and alkali-metal intercalated carbon nanotubes and bundles. Physical Review B, 2002, 65, .	1.1	183
1837	Embedded-atom potential forB2â^'NiAl. Physical Review B, 2002, 65, .	1.1	288
1838	Tight-binding description of graphene. Physical Review B, 2002, 66, .	1.1	904
1839	High-pressure thermoelasticity of body-centered-cubic tantalum. Physical Review B, 2002, 65, .	1.1	122
1840	Computational design of a material for high-efficiency spin-polarized electron source. Applied Physics Letters, 2002, 81, 3957-3959.	1.5	17

#	Article	IF	Citations
1841	Sodium monolayers on thermionic cathodes. Journal Physics D: Applied Physics, 2002, 35, 1751-1756.	1.3	28
1842	Experimental and Theoretical Studies on the Reaction of H2 with NiO:â€‰ Role of O Vacancies and Mechanism for Oxide Reduction. Journal of the American Chemical Society, 2002, 124, 346-354.	6.6	322
1843	Modeling of hP3 intermetallics in space group P-3m1: Calculated powder patterns from CRYSTMETÂ® X-ray cell data and ab initio coordinates. Powder Diffraction, 2002, 17, 165-172.	0.4	2
1844	First Principles Search for Multiferroism in BiCrO3. Journal of Physical Chemistry B, 2002, 106, 3383-3388.	1.2	95
1845	Broken symmetries in the crystalline and magnetic structures ofÎ³-iron. Physical Review B, 2002, 66, .	1.1	136
1846	Surface Structures and Crystal Morphology of ZnS:â€‰ Computational Study. Journal of Physical Chemistry B, 2002, 106, 11002-11008.	1.2	116
1847	Structure, Properties, and Dynamics of Oxygen Vacancies in AmorphousSiO2. Physical Review Letters, 2002, 89, 285505.	2.9	167
1848	Role of carbon in GaN. Journal of Applied Physics, 2002, 92, 6553-6560.	1.1	227
1849	Origins of Coexistence of Conductivity and Transparency inSnO2. Physical Review Letters, 2002, 88, 095501.	2.9	809
1850	Electrical conductivity for warm, dense aluminum plasmas and liquids. Physical Review E, 2002, 66, 025401.	0.8	426
1851	First-principles simulations of metal-ceramic interface adhesion: Co/WC versus Co/TiC. Physical Review B, 2002, 65, .	1.1	160
1852	First-principles calculation of the piezoelectric tensor dâ‡Š of IIIâ€“V nitrides. Applied Physics Letters, 2002, 80, 4145-4147.	1.5	125
1853	Effective Hamiltonian study ofPbZr0.95Ti0.05O3. Physical Review B, 2002, 65, .	1.1	25
1854	First-principles calculations of the phase stability ofTiO2. Physical Review B, 2002, 65, .	1.1	464
1855	Lattice dynamics and dielectric properties ofTiO2anatase: A first-principles study. Physical Review B, 2002, 66, .	1.1	155
1856	A computational study of twist boundary structures in strontium titanate. Journal of Physics Condensed Matter, 2002, 14, 13635-13641.	0.7	18
1857	Time-dependent density functional calculations of fully Ï€-conjugated zinc oligoporphyrins. Journal of Chemical Physics, 2002, 117, 9688-9694.	1.2	44
1858	Theory of the copper vacancy in cuprous oxide. Journal of Applied Physics, 2002, 92, 5849-5851.	1.1	75

#	Article	IF	Citations
1859	The effect of misfit on heterophase interface energies. Journal of Physics Condensed Matter, 2002, 14, 2877-2900.	0.7	54
1860	Study of Î³-Alumina Surface Reactivity:â€‰ Adsorption of Water and Hydrogen Sulfide on Octahedral Aluminum Sites. Journal of Physical Chemistry B, 2002, 106, 9359-9366.	1.2	84
1861	Talc under tension and compression: Spinodal instability, elasticity, and structure. Journal of Geophysical Research, 2002, 107, ECV 2-1-ECV 2-10.	3.3	40
1862	First-principles study ofPb2MgTeO6:â€ƒHigh-Tcubic phase and average low-Trhombohedral phase. Physical Review B, 2002, 65, .	1.1	4
1863	First-principles study of As interstitials in GaAs: Convergence, relaxation, and formation energy. Physical Review B, 2002, 66, .	1.1	53
1864	Mn-dopedCuGaS2chalcopyrites: Anab initiostudy of ferromagnetic semiconductors. Physical Review B, 2002, 66, .	1.1	38
1865	Bcc and Fcc Transition Metals and Alloys:â€‰ A Central Role for the Jahnâ^'Teller Effect in Explaining Their Ideal and Distorted Structures. Journal of the American Chemical Society, 2002, 124, 4811-4823.	6.6	33
1866	Theoretical investigation of native defects, impurities, and complexes in aluminum nitride. Physical Review B, 2002, 65, .	1.1	225
1867	Atomistic model of gallium. Physical Review B, 2002, 66, .	1.1	56
1868	First-principles study ofSn2P2Se6ferroelectrics. Physical Review B, 2002, 66, .	1.1	11
1869	Ab initioinvestigation of phonon modes in the MgAl2O4spinel. Journal of Physics Condensed Matter, 2002, 14, 3543-3552.	0.7	60
1870	Band structure, Born effective charges, and lattice dynamics of CuInS2 fromab initiocalculations. Journal of Chemical Physics, 2002, 117, 2726-2731.	1.2	47
1871	Reversible band-gap engineering in carbon nanotubes by radial deformation. Physical Review B, 2002, 65, .	1.1	121
1872	First-principles study of the dielectric and dynamical properties of lithium niobate. Physical Review B, 2002, 65, .	1.1	142
1873	First-principles calculations of vacancy effects on structural and electronic properties of TiCxand TiNx. Journal of Physics Condensed Matter, 2002, 14, 10237-10249.	0.7	65
1874	Divacancy in3Câ^'and4Hâ^'SiC:An extremely stable defect. Physical Review B, 2002, 65, .	1.1	66
1875	Density functional theory calculations of local ordering of hydroxy groups and fluoride ions in hydroxyapatite. Physical Chemistry Chemical Physics, 2002, 4, 3865-3871.	1.3	59
1876	The electronic properties of the strained CdTe/ZnTe(001) superlattices. Journal of Physics Condensed Matter, 2002, 14, 7835-7851.	0.7	19

#	Article	IF	Citations
1877	Bonding and Stability of the Hydrogen Storage Material Mg2NiH4. Inorganic Chemistry, 2002, 41, 3684-3692.	1.9	94
1878	Co2MnX(X=Si,Ge, Sn) Heusler compounds:â€ƒAnab initiostudy of their structural, electronic, and magnetic properties at zero and elevated pressure. Physical Review B, 2002, 66, .	1.1	551
1879	Hydrogen adsorption on the tetragonal ZrO2(101) surface: a theoretical study of an important catalytic reactantElectronic supplementary information (ESI) available: data for geometrical and charge differences in detail. See http://www.rsc.org/suppdata/cp/b2/b202330j/. Physical Chemistry Chemical Physics, 2002, 4, 3500-3508.	1.3	77
1880	First-principles calculation of the structure and elastic properties of a 3D-polymerized fullerite. Physical Review B, 2002, 65, .	1.1	19
1881	Screened Coulomb interactions in metallic alloys. â€,â€,II.â€ƒScreening beyond the single-site and atomic-sphere approximations. Physical Review B, 2002, 66, .	1.1	121
1882	NOx Storage on BaO(100) Surface from First Principles:â€‰ a Two Channel Scenario. Journal of Physical Chemistry B, 2002, 106, 137-145.	1.2	108
1883	Prediction of the mixing enthalpy of alloys. Europhysics Letters, 2002, 57, 526-532.	0.7	52
1884	Activation of Gold on Titania:Â Adsorption and Reaction of SO2on Au/TiO2(110). Journal of the American Chemical Society, 2002, 124, 5242-5250.	6.6	242
1885	The Interaction of Ethylene with Perfect and Defective Ag(001) Surfaces. Journal of Physical Chemistry B, 2002, 106, 9839-9846.	1.2	45
1886	Properties of hexagonal ScN versus wurtzite GaN and InN. Physical Review B, 2002, 66, .	1.1	111
1887	Oxygen and vacancies in silver: A density-functional study in the local density and generalized gradient approximations. Physical Review B, 2002, 66, .	1.1	21
1888	Properties of hexagonal polytypes of group-IV elements from first-principles calculations. Physical Review B, 2002, 66, .	1.1	134
1889	X-ray absorption near-edge structure calculations with the pseudopotentials: Application to theKedge in diamond andÎ±-quartz. Physical Review B, 2002, 66, .	1.1	281
1890	Energetically favourable sites of iodine atoms in zirconium: An ab initio approach. The Philosophical Magazine: Physics of Condensed Matter B, Statistical Mechanics, Electronic, Optical and Magnetic Properties, 2002, 82, 73-83.	0.6	2
1891	Importance of O vacancies in the behavior of oxide surfaces: Adsorption of sulfur onTiO2(110). Physical Review B, 2002, 65, .	1.1	54
1892	Structural and electronic properties of PbTiO3, PbZrO3, and PbZr0.5Ti0.5O3: First-principles density-functional studies. Journal of Chemical Physics, 2002, 117, 2699-2709.	1.2	63
1893	Structure and Short Timescale Ion Dynamics of Potassium-Ammonia Graphite Intercalation Compounds. Journal of Physical Chemistry B, 2002, 106, 1161-1172.	1.2	4
1894	Crystal structure and chemical bonding of the high-pressure phase of MgAl₂O₄from first-principles calculations. Philosophical Magazine A: Physics of Condensed Matter, Structure, Defects and Mechanical Properties, 2002, 82, 2885-2894.	0.8	2

#	Article	IF	Citations
1895	Thermodynamic stability of high-K dielectric metal oxides ZrO2 and HfO2 in contact with Si and SiO2. Applied Physics Letters, 2002, 80, 1897-1899.	1.5	346
1896	Electron localization: Band-by-band decomposition and application to oxides. Physical Review B, 2002, 66, .	1.1	24
1897	Density functional theory study on the origins of the gap bowing in Zn1-xMgxSe. Journal of Physics Condensed Matter, 2002, 14, 4025-4033.	0.7	32
1898	Structure and energetics of alkanethiol adsorption on the Au(111) surface. Journal of Chemical Physics, 2002, 117, 825-833.	1.2	227
1899	Electronic Structure and Structural Properties of Ti4AlN3Investigated byAb initioCalculations. Journal of the Physical Society of Japan, 2002, 71, 1313-1317.	0.7	22
1900	Methane transformation to carbon and hydrogen on Pd(100): Pathways and energetics from density functional theory calculations. Journal of Chemical Physics, 2002, 116, 322.	1.2	80
1901	Structure, bonding, and anharmonic librational motion of CO on Ir{100}. Journal of Chemical Physics, 2002, 116, 8097-8105.	1.2	16
1902	Carbon cage-like materials as potential low work function metallic compounds: Case of clathrates. Applied Physics Letters, 2002, 80, 1385-1387.	1.5	25
1903	First-principles study of the structural and energetic properties of H atoms on a graphite () surface. Surface Science, 2002, 496, 318-330.	0.8	301
1904	A density functional theory study of stepwise addition reactions in ammonia synthesis on Ru(). Surface Science, 2002, 496, 221-230.	0.8	61
1905	Atomic scale structure of InAs(001)-(2Ã—4) steady-state surfaces determined by scanning tunneling microscopy and density functional theory. Surface Science, 2002, 499, L129-L134.	0.8	30
1906	Effects of Co magnetism on Co/TiC() interface adhesion: a first-principles study. Surface Science, 2002, 497, 171-182.	0.8	27
1907	First-principles study of Pdâ€“V surface alloys I. Electronic structure of clean surfaces. Surface Science, 2002, 498, 21-36.	0.8	23
1908	Tip effects in scanning tunneling microscopy of atomic-scale magnetic structures. Surface Science, 2002, 498, L65-L70.	0.8	11
1909	First-principles study of metallic iron interfaces. Surface Science, 2002, 501, 261-269.	0.8	64
1910	Adhesion, stability, and bonding at metal/metal-carbide interfaces: Al/WC. Surface Science, 2002, 498, 321-336.	0.8	224
1911	Formation of interface states on a half-metal surface. Surface Science, 2002, 501, L185-L190.	0.8	35
1912	Adsorption of atomic oxygen on Ag(): a study based on density-functional theory. Surface Science, 2002, 501, 182-190.	0.8	47

#	Article	IF	Citations
1913	Theory of CO adsorption on Co{}. Surface Science, 2002, 504, 138-144.	0.8	18
1914	Synthesis, Structure Determination, and Quantum-Chemical Characterization of an Alternate HgNCN Polymorph. Inorganic Chemistry, 2002, 41, 4259-4265.	1.9	62
1915	Iron under Earthâ€™s core conditions: Liquid-state thermodynamics and high-pressure melting curve fromab initiocalculations. Physical Review B, 2002, 65, .	1.1	277
1916	Coexistence of magnetism and ferroelectricity in perovskites. Physical Review B, 2002, 65, .	1.1	173
1917	Systematic generation of finite-range atomic basis sets for linear-scaling calculations. Physical Review B, 2002, 66, .	1.1	251
1918	Absorption and diffusion of hydrogen in palladium-silver alloys by density functional theory. Physical Review B, 2002, 66, .	1.1	57
1919	Bipolar Doping and Band-Gap Anomalies in Delafossite Transparent Conductive Oxides. Physical Review Letters, 2002, 88, 066405.	2.9	314
1920	Chemistry of Sulfur Oxides on Transition Metals I:Â Configurations, Energetics, Orbital Analyses, and Surface Coverage Effects of SO2on Pt(111). Journal of Physical Chemistry B, 2002, 106, 12575-12583.	1.2	60
1921	First-principles electronic structure calculations of BaSi7N10 with both corner- and edge-sharing SiN4 tetrahedra. Journal of Alloys and Compounds, 2002, 336, 1-4.	2.8	15
1922	Band-calculation of the electronic densities of states and the total energies of boronâ€“silicon system. Journal of Alloys and Compounds, 2002, 347, 244-251.	2.8	24
1923	Energetics of alkaline-earth metal silicides calculated using a first-principle pseudopotential method. Intermetallics, 2002, 10, 333-341.	1.8	70
1924	Atomic processes at bonded Si-interfaces studied by molecular dynamics: tayloring densities and bandgaps?. Computational Materials Science, 2002, 24, 33-41.	1.4	4
1925	Density-functional study of impurity-related DX centers in CdF2. Computational Materials Science, 2002, 25, 404-412.	1.4	1
1926	Optimization of interatomic potential for Si/SiO2 system based on force matching. Computational Materials Science, 2002, 25, 447-456.	1.4	24
1927	First-principles computation of material properties: the ABINIT software project. Computational Materials Science, 2002, 25, 478-492.	1.4	2,789
1928	Phase stability of the Hf-Nb system: From first-principles to CALPHAD. Calphad: Computer Coupling of Phase Diagrams and Thermochemistry, 2002, 26, 491-511.	0.7	35
1929	Phonons and lattice dielectric properties of zirconia. Physical Review B, 2002, 65, .	1.1	440
1930	A facile route to poly[1-(2,4,6-trichlorophenyl)-1H-1,2,4-triazol-5-yl]alkane derivatives. Journal of the Chemical Society, Perkin Transactions 1, 2002, , 991-995.	1.3	2

#	Article	IF	Citations
1931	Ab initiostudy of linear and nonlinear optical responses of Si(111) surfaces. Physical Review B, 2002, 66, .	1.1	17
1932	Origin and properties of the gap in the half-ferromagnetic Heusler alloys. Physical Review B, 2002, 66, .	1.1	593
1933	Transition from direct band gap to indirect band gap in fluorinated carbon. Physical Review B, 2002, 65, .	1.1	42
1934	Elementary energy bands inab initiocalculations of theYAlO3and SbSI crystal band structure. Physical Review B, 2002, 66, .	1.1	44
1935	Ab initio chemical potentials of solid and liquid solutions and the chemistry of the Earthâ€™s core. Journal of Chemical Physics, 2002, 116, 7127-7136.	1.2	107
1936	Comparison of the high-pressure and low-temperature structures of sulfuric acid. Dalton Transactions RSC, 2002, , 1867-1871.	2.3	11
1937	Absolute surface energies of group-IV semiconductors: Dependence on orientation and reconstruction. Physical Review B, 2002, 65, .	1.1	366
1938	Cubic boron nitride growth from NH3 and BBr3 precursors: a theoretical study. Diamond and Related Materials, 2002, 11, 1286-1289.	1.8	19
1939	A spectroscopic study of the negative electron affinity of cesium oxide-coated diamond (111) and theoretical calculation of the surface density-of-states on oxygenated diamond (111). Diamond and Related Materials, 2002, 11, 1379-1384.	1.8	27
1940	Dislocations in diamond: Electron energy-loss spectroscopy. Physical Review B, 2002, 65, .	1.1	47
1941	The effect of lattice vibrations on substitutional alloy thermodynamics. Reviews of Modern Physics, 2002, 74, 11-45.	16.4	632
1942	Possible Nonactivated Conductivity of the Low-Dimensional Ternary Nitride Ca2GeN2. Inorganic Chemistry, 2002, 41, 4630-4632.	1.9	3
1943	Defect engineering in IIIâ€“V ternary alloys: Effects of strain and local charge on the formation of native deep defects. Nuclear Instruments & Methods in Physics Research B, 2002, 186, 229-233.	0.6	0
1944	Effects from hydrogen bonds on water structure in (H3O)2[Mo6Cl8X6]Â·yH2O X=Cl (y=7), Br (y=6), or I (y=6). Solid State Sciences, 2002, 4, 1017-1022.	1.5	17
1945	Ab initio Stiffness for Low Quartz and Calcite. Physica Status Solidi (B): Basic Research, 2002, 229, 1155-1161.	0.7	23
1946	Investigation of Some Ground State Properties of Lithium with the All Electron MAPW Method. Physica Status Solidi (B): Basic Research, 2002, 229, 1359-1370.	0.7	6
1947	Theoretical Studies of Self-Diffusion and Dopant Clustering in Semiconductors. Physica Status Solidi (B): Basic Research, 2002, 233, 24-30.	0.7	21
1948	Quasiparticle Calculations for Point Defects on Semiconductor Surfaces. Physica Status Solidi (B): Basic Research, 2002, 234, 346-353.	0.7	8

#	Article	IF	Citations
1949	FeGa3 and RuGa3: Semiconducting Intermetallic Compounds. Journal of Solid State Chemistry, 2002, 165, 94-99.	1.4	105
1950	Polymorphism of IrSn4. Journal of Solid State Chemistry, 2002, 168, 34-40.	1.4	23
1951	Periodic DFT approaches to crystalline alkali metal azides. Science Bulletin, 2002, 47, 1180-1183.	1.7	7
1952	Charge density distribution with pressure in Y-123. Physica B: Condensed Matter, 2002, 321, 360-364.	1.3	13
1953	Possible ultra-hard materials based upon boron icosahedra. Physica B: Condensed Matter, 2002, 322, 173-178.	1.3	27
1954	Investigation of the interfacial interdiffusion and magnetic properties of. Physica B: Condensed Matter, 2002, 324, 279-285.	1.3	7
1955	Electronic and structural properties of Î²-Be3N2. Physica B: Condensed Matter, 2002, 324, 305-311.	1.3	57
1956	Structural and electronic properties of YBa2Cu3O7 under high pressures. Physica C: Superconductivity and Its Applications, 2002, 370, 85-93.	0.6	21
1957	Fermi-surface induced variation in Tc in MgB2 alloys. Physica C: Superconductivity and Its Applications, 2002, 382, 381-385.	0.6	9
1958	Ab initio simulation on ideal shear strength of silicon. Materials Science and Engineering B: Solid-State Materials for Advanced Technology, 2002, 88, 79-84.	1.7	46
1959	Incorporating first-principles energetics in computational thermodynamics approaches. Acta Materialia, 2002, 50, 2187-2197.	3.8	91
1960	Structure and stability of hcp bulk and nano-precipitated Ag2Al. Acta Materialia, 2002, 50, 2443-2459.	3.8	31
1961	Abinitiomodelling of intermetallics with CuAl2structure type: computed powder patterns from cell-and-type CRYSTMET entries. Journal of Applied Crystallography, 2002, 35, 364-367.	1.9	0
1962	Klockmannite, CuSe: structure, properties and phase stability from ab initio modeling. Acta Crystallographica Section B: Structural Science, 2002, 58, 437-447.	1.8	40
1963	Pressure-induced polymorphism in phenol. Acta Crystallographica Section B: Structural Science, 2002, 58, 1018-1024.	1.8	47
1964	First-principles calculations for understanding high conductivity and optical transparency in InxCd1â^'xO films. Thin Solid Films, 2002, 411, 101-105.	0.8	50
1965	Anisotropy of UV-reflectivity in wurtzite crystals: a comparison between GaN and CdSe. Solid State Communications, 2002, 121, 549-554.	0.9	11
1966	Metastable states in an equilibrium immiscible Niâ€“Ru system studied by ab initio calculation and ion mixing experiment. Solid State Communications, 2002, 121, 375-379.	0.9	2

#	Article	IF	Citations
1967	Quasiparticle calculations of band offsets at AlNâ€“GaN interfaces. Solid State Communications, 2002, 124, 63-66.	0.9	33
1968	Lattice dynamics of solid cubane within the quasi-harmonic approximation. Solid State Communications, 2002, 124, 449-455.	0.9	6
1969	Adsorption and reaction of thiophene on Î±-Mo 2 C(0001). Surface Science, 2002, 511, 294-302.	0.8	46
1970	Surface relaxation and surface stress of Au(111). Surface Science, 2002, 513, 263-271.	0.8	60
1971	Applicability of the broken-bond rule to the surface energy of the fcc metals. Surface Science, 2002, 511, 1-12.	0.8	167
1972	Magnetic properties of Feâ€“Ni alloy atom bridges. Surface Science, 2002, 514, 156-160.	0.8	19
1973	STM-tip induced magnetic state change of Fe atom bridge. Surface Science, 2002, 514, 161-166.	0.8	14
1974	Reconstructions of strongly reduced SnO2(110) studied by first-principles methods. Surface Science, 2002, 513, 26-36.	0.8	52
1975	Density functional theory study of the relaxation and energy of iron surfaces. Surface Science, 2002, 513, 389-398.	0.8	154
1976	A first principles study of sub-monolayer Ge on Si(). Surface Science, 2002, 515, 483-490.	0.8	23
1977	Further studies of iron adhesion: () surfaces. Surface Science, 2002, 515, L464-L468.	0.8	19
1978	Structure determination of Cu()â€“O using X-ray diffraction and DFT calculations. Surface Science, 2002, 516, 16-32.	0.8	25
1979	Finite temperature studies of Te adsorption on. Surface Science, 2002, 519, 79-89.	0.8	18
1980	Band structure calculations on the layered compounds FeGa 2 S 4 and NiGa 2 S 4. Journal of Physics and Chemistry of Solids, 2002, 63, 2019-2028.	1.9	13
1981	A simple theory of 40K superconductivity in MgB2: first-principles calculations of Tc, its dependence on boron mass and pressure. Journal of Physics and Chemistry of Solids, 2002, 63, 2201-2206.	1.9	14
1982	Electronic structure of Î²-Fe(Si2â^'xGex) ternaries. Journal of Solid State Chemistry, 2002, 169, 19-23.	1.4	5
1983	Ab Initio Calculations of Pristine and Doped Zirconia Î£5 (310)/[001] Tilt Grain Boundaries. Journal of the American Ceramic Society, 2002, 85, 1594-1600.	1.9	34
1984	First-principles study of illiteâ€“smectite and implications for clay mineral systems. Nature, 2002, 420, 165-168.	13.7	95

#	Article	IF	Citations
1985	The hartree-fock method and density-functional theory as applied to an infinite crystal and to a cyclic cluster. Physics of the Solid State, 2002, 44, 1656-1670.	0.2	17
1986	First-principles study of metalâ€“carbide/nitride adhesion: Al/VC vs. Al/VN. Acta Materialia, 2002, 50, 619-631.	3.8	127
1987	Atomic-scale Ab-initio study of the Zr-H system: I. Bulk properties. Acta Materialia, 2002, 50, 3513-3526.	3.8	156
1988	Theoretical studies of silicon carbide surfaces. Progress in Surface Science, 2002, 69, 101-124.	3.8	45
1989	Tuning in on single molecular states: adsorption sites and STM images of maleic anhydride on Si(100). Chemical Physics Letters, 2002, 355, 347-354.	1.2	22
1990	Correlation of adsorption energy with surface structure: ethylene adsorption on Pd surfaces. Chemical Physics Letters, 2002, 358, 377-382.	1.2	63
1991	Applicability of a quantum mechanical `virtual crystal approximation' to study Al/Si-disorder. Chemical Physics Letters, 2002, 362, 266-270.	1.2	72
1992	Topotactic valence manipulation to design strontium manganate: a first principle study. Chemical Physics Letters, 2002, 362, 151-158.	1.2	0
1993	Electronic structure and STM images of self-assembled styrene lines on a Si(100) surface. Chemical Physics Letters, 2002, 365, 129-134.	1.2	34
1994	Electronic and chemical properties of mixed-metal oxides: adsorption of SO2 on SrTiO3(001). Chemical Physics Letters, 2002, 365, 380-386.	1.2	16
1995	A DFT Study on CO Oxidation over Co3O4. Journal of Catalysis, 2002, 210, 198-206.	3.1	166
1996	Mechanisms for Chain Growth in Fischerâ€“Tropsch Synthesis over Ru(0001). Journal of Catalysis, 2002, 212, 136-144.	3.1	119
1997	Electrical conductivity of hot expanded aluminum: Experimental measurements andab initiocalculations. Physical Review E, 2002, 66, 056412.	0.8	58
1998	The SIESTA method forab initioorder-Nmaterials simulation. Journal of Physics Condensed Matter, 2002, 14, 2745-2779.	0.7	9,150
1999	Periodic Density Functional Theory Study of Methane Activation over La2O3:Â Activity of O2-, O-, O22-, Oxygen Point Defect, and Sr2+-Doped Surface Sites. Journal of the American Chemical Society, 2002, 124, 8452-8461.	6.6	202
2000	Ab initiomelting curve of the fcc phase of aluminum. Physical Review B, 2002, 65, .	1.1	124
2001	Atomic Scale Mechanism of the Transformation ofÎ³-Alumina toÎ¸-Alumina. Physical Review Letters, 2002, 89, 235501.	2.9	45
2002	Pentagonal nanowires:â€ƒA first-principles study of the atomic and electronic structure. Physical Review B, 2002, 65, .	1.1	75

#	Article	IF	Citations
2003	PiezoelectricPb(Zr0.5Ti0.5)O3:â€ƒInterplay of atomic ordering, ferroelectric soft modes, and pressure. Physical Review B, 2002, 66, .	1.1	26
2004	Magnetic ground state of Cr in density-functional theory. Physical Review B, 2002, 65, .	1.1	129
2005	The microscopic origin of the doping limits in semiconductors and wide-gap materials and recent developments in overcoming these limits: a review. Journal of Physics Condensed Matter, 2002, 14, R881-R903.	0.7	169
2006	Phosphorus and sulphur doping of diamond. Physical Review B, 2002, 66, .	1.1	98
2007	Tri-s-triazine derivatives. Part I. From trichloro-tri-s-triazine to graphitic C3N4 structuresPart II: Alkalicyamelurates M3[C6N7O3], Mâ€‰=â€‰Li, Na, K, Rb, Cs, manuscript in preparation.. New Journal of Chemistry, 2002, 26, 508-512.	1.4	614
2008	First Principle Calculation of the Geometrical and Electronic Structure of Impurity-Doped Î²-FeSi2 Semiconductors. Journal of Solid State Chemistry, 2002, 163, 248-252.	1.4	25
2009	Spin-polarization in half-metals (invited). Journal of Applied Physics, 2002, 91, 8340.	1.1	201
2010	Characterization of the electronic structure of crystalline compounds through their localized Wannier functions. Journal of Chemical Physics, 2002, 116, 1120-1127.	1.2	87
2011	Ab initio phonon dispersion relations of $mathsf{alpha}$ -Ga. European Physical Journal B, 2003, 36, 87-90.	0.6	4
2012	Vibrational properties of C $mathsf{_{20}}$ -based solids. European Physical Journal B, 2003, 37, 143-148.	0.6	2
2013	LDA and GGA investigations of some ground state properties of aluminium with the all electron MAPW method. European Physical Journal B, 2003, 37, 405-411.	0.6	11
2014	Lattice dynamics of CuAu-orderedCuInSe2. Physical Review B, 2003, 68, .	1.1	31
2015	First Principles Calculations of Auger Recombination and Impact Ionization Rates in Semiconductors. Journal of Computational Electronics, 2003, 2, 197-202.	1.3	5
2016	Title is missing!. Journal of Materials Science: Materials in Electronics, 2003, 14, 149-156.	1.1	54
2017	Phase transformation mechanism between Î³- and Î¸-alumina. Physical Review B, 2003, 67, .	1.1	81
2018	Electrical conductivity of a strongly correlated aluminium plasma. Journal of Physics A, 2003, 36, 6033-6039.	1.6	22
2019	Quasiparticle band structure and screening in silicon and carbon clathrates. Physical Review B, 2003, 67, .	1.1	50
2020	Pathways of atomistic processes on TiN(001) and (111) surfaces during film growth: anab initiostudy. Journal of Applied Physics, 2003, 93, 9086-9094.	1.1	318

#	Article	IF	Citations
2021	Surface properties of metastable alumina:â€ƒA comparative study of Î²- andÎ±â^'Al2O3. Physical Review B, 2003, 67, .	1.1	104
2022	Systematic study of adsorption of single atoms on a carbon nanotube. Physical Review B, 2003, 67, .	1.1	305
2023	Undissociated screw dislocations in silicon: Calculations of core structure and energy. Philosophical Magazine, 2003, 83, 1191-1204.	0.7	50
2024	Formation Mechanism ofH2Ti3O7Nanotubes. Physical Review Letters, 2003, 91, 256103.	2.9	331
2025	First-principles calculation of the electronic, dielectric, and dynamical properties ofCaF2. Physical Review B, 2003, 68, .	1.1	62
2026	Collapsing Cristobalitelike Structures in Silica Analogues at High Pressure. Physical Review Letters, 2003, 91, 015503.	2.9	58
2027	NO2 and CO gas adsorption on carbon nanotubes: Experiment and theory. Journal of Chemical Physics, 2003, 119, 10904-10910.	1.2	221
2028	First-Principles Calculations of Carbon Nanotubes Adsorbed on Si(001). Physical Review Letters, 2003, 91, 166802.	2.9	54
2029	An ab initio investigation on nickel impurities in diamond. Physica B: Condensed Matter, 2003, 340-342, 84-88.	1.3	9
2030	First principles calculation of zero-field splitting tensors. Physica B: Condensed Matter, 2003, 340-342, 673-676.	1.3	10
2031	The formation, dissociation and electrical activity of divacancy-oxygen complexes in Si. Physica B: Condensed Matter, 2003, 340-342, 523-527.	1.3	17
2032	Electronic properties of vacancyâ€“oxygen complexes in SiGe alloys. Physica B: Condensed Matter, 2003, 340-342, 790-794.	1.3	5
2033	Density functional theory studies of sulfur binding on Pd, Cu and Ag and their alloys. Surface Science, 2003, 546, 12-26.	0.8	104
2034	Structural and electronic properties of NiMnSb Heusler compound and its interface with GaAs. Materials Science and Engineering C, 2003, 23, 743-746.	3.8	34
2035	Magnetic phase transition in strained MnAs compound. Materials Science and Engineering C, 2003, 23, 1059-1062.	3.8	3
2036	Hydrogen bonding in mixed ligand copper organophosphonates. Chemical Physics Letters, 2003, 378, 400-405.	1.2	4
2037	Theoretical study of superconductivity in MgB2 and its alloys. Bulletin of Materials Science, 2003, 26, 131-135.	0.8	9
2038	Theory of interface properties for carbide precipitates in TiAl. Metallurgical and Materials Transactions A: Physical Metallurgy and Materials Science, 2003, 34, 2097-2101.	1.1	0

#	Article	IF	Citations
2039	The electron localization function: a tool for locating favorable proton docking sites in the silica polymorphs. Physics and Chemistry of Minerals, 2003, 30, 305-316.	0.3	70
2040	Charge-density analysis of spodumene (LiAlSi2O6), from ab initio Hartree?Fock calculations. Physics and Chemistry of Minerals, 2003, 30, 606-614.	0.3	19
2041	Perspectives on the first principles elucidation and the design of active sites. Journal of Catalysis, 2003, 216, 73-88.	3.1	157
2042	Initial steps in the desulfurization of thiophene/Ni(100)â€"A DFT study. Journal of Catalysis, 2003, 214, 234-241.	3.1	27
2043	Adsorption and bonding of 2-butenal on Sn/Pt surface alloys. Journal of Catalysis, 2003, 215, 245-253.	3.1	29
2044	Adsorption of unsaturated aldehydes on the (111) surface of a Ptâ€"Fe alloy catalyst from first principles. Journal of Catalysis, 2003, 217, 354-366.	3.1	73
2045	Lattice relaxation around impurity atoms in semiconductors â€" arsenic in silicon â€" a comparison between experiment and theory. Nuclear Instruments & Methods in Physics Research B, 2003, 200, 60-65.	0.6	23
2046	Ab initio study of electronic properties of zincblende AlN and deformation potentials under hydrostatic stress. Materials Chemistry and Physics, 2003, 82, 471-477.	2.0	18
2047	Equation of state and electrical conductivity of strongly correlated aluminum and copper plasmas. Contributions To Plasma Physics, 2003, 43, 269-272.	0.5	5
2048	Determining the Strengths of Hydrogen Bonds in Solid-State Ammonia and Urea: Insight from Periodic DFT Calculations. Chemistry - A European Journal, 2003, 9, 628-634.	1.7	40
2049	High-Pressure Structural Trends of Group 15 Elements: Simple Packed Structures versus Complex Hostâ€"Guest Arrangements. Chemistry - A European Journal, 2003, 9, 1471-1478.	1.7	29
2050	Ab initio study of neutral vacancies in InP using supercells and finite size scaling. Physica B: Condensed Matter, 2003, 340-342, 407-411.	1.3	10
2051	Basal plane partial dislocations in silicon carbide. Physica B: Condensed Matter, 2003, 340-342, 160-164.	1.3	12
2052	Ab initio modeling of Nâ€"H, Pâ€"H and Asâ€"H defects in ZnSe. Physica B: Condensed Matter, 2003, 340-342, 272-274.	1.3	1
2053	Interaction between oxygen and single self-interstitials in silicon. Physica B: Condensed Matter, 2003, 340-342, 575-577.	1.3	5
2054	Interstitial boron defects in Si. Physica B: Condensed Matter, 2003, 340-342, 505-508.	1.3	12
2055	A comparative study of precipitation behavior of Heusler phase (Ni2TiAl) from B2-TiNi in Niâ€"Tiâ€"Al and Niâ€"Tiâ€"Alâ€"X (X=Hf, Pd, Pt, Zr) alloys. Acta Materialia, 2003, 51, 6341-6357.	3.8	57
2056	A comparative study of O2 adsorbed carbon nanotubes. Chemical Physics Letters, 2003, 380, 1-5.	1.2	30

#	Article	IF	Citations
2057	A periodic DFT approach to octanitrocubane crystal. Chemical Physics Letters, 2003, 382, 12-18.	1.2	14
2058	Thermal excitation of COâ€“Pt on the (2Ã—1) Pt {110} surface: a theoretical simulation of a variable-temperature STM contrast. Chemical Physics Letters, 2003, 382, 41-47.	1.2	0
2059	A tilt-dependent diffusional potential energy landscape: benzyne on Ir{100}. Chemical Physics Letters, 2003, 367, 116-122.	1.2	9
2060	The isotypism of BeH2 and SiO2: an ab initio study. Chemical Physics Letters, 2003, 378, 343-348.	1.2	14
2061	The structure, ordering and equation of state of ammonia dihydrate (nh3 Â· 2h2o). Icarus, 2003, 162, 59-73.	1.1	30
2062	Local reactivity of thin Pd overlayers on Au single crystals. Journal of Electroanalytical Chemistry, 2003, 548, 121-130.	1.9	129
2063	First principles studies of chemisorbed O on Ni{111}. Surface Science, 2003, 543, 12-18.	0.8	41
2064	Adsorption of water molecules on the CdTe surface. Surface Science, 2003, 545, 34-40.	0.8	5
2065	Reconstruction and de-reconstruction of the Ir(100) surface and ultrathin Fe/Ir(100) films. Surface Science, 2003, 546, 27-38.	0.8	22
2066	Structure of Fe() studied by quantitative LEED analysis and pseudopotential DFT calculations. Surface Science, 2003, 546, L808-L812.	0.8	4
2067	Re-evaluation of the adsorption mode of ethene on the {111} surface of palladium using density functional theory. Surface Science, 2003, 547, L853-L858.	0.8	6
2068	Adsorption and diffusion energetics of hydrogen atoms on Fe(110) from first principles. Surface Science, 2003, 547, 85-98.	0.8	161
2069	A DFT periodic study of the vanadyl pyrophosphate (100) surface. Surface Science, 2003, 547, 438-451.	0.8	11
2070	Transition metal impurities in 3C-SiC and 2H-SiC. Physica B: Condensed Matter, 2003, 340-342, 116-120.	1.3	6
2071	Ab initio modeling of Beâ€“H and Znâ€“H complexes in Si. Physica B: Condensed Matter, 2003, 340-342, 664-667.	1.3	2
2072	First-principles thermodynamics of defects in semiconductors. Physica B: Condensed Matter, 2003, 340-342, 630-636.	1.3	6
2073	Defects in mercuric iodide: an APW investigation. Physica B: Condensed Matter, 2003, 340-342, 918-922.	1.3	11
2074	Lattice vibration of Ce1â^'xScxFe4Al8. Journal of Physics and Chemistry of Solids, 2003, 64, 433-441.	1.9	2

#	Article	IF	Citations
2075	Fabrication of bipolar CuInO2 with delafossite structure. Journal of Physics and Chemistry of Solids, 2003, 64, 1675-1679.	1.9	48
2076	Epitaxially stabilized AgGaSe2 for high-efficiency spin-polarized electron source. Journal of Physics and Chemistry of Solids, 2003, 64, 1881-1885.	1.9	1
2077	On the mechanism of the interaction between oxygen and close-packed single-crystal aluminum surfaces. Journal of Physics and Chemistry of Solids, 2003, 64, 1317-1331.	1.9	35
2078	First-principles energy band calculation for undoped and N-doped InTaO4 with layered wolframite-type structure. Journal of Physics and Chemistry of Solids, 2003, 64, 2417-2421.	1.9	26
2079	Tinâ€“magnesium substitution in Ir3Sn7â€”structure and chemical bonding in MgxIr3Sn7â€“x (x=0â€“1.67). Journal of Solid State Chemistry, 2003, 173, 418-424.	1.4	27
2080	NaPdPS4 and RbPdPS4: systems with infinite straight [PdPS4]â^' chains soluble in polar solvents and the structure of cubic RbPdPS4{Rb0.33P0.4S2.23Ox}. Journal of Solid State Chemistry, 2003, 175, 133-145.	1.4	14
2081	Quantitative vs. qualitative approaches to the electronic structure of solids. Journal of Solid State Chemistry, 2003, 176, 375-389.	1.4	8
2082	Synergetic theoretical and experimental structure determination of nanocrystalline materials: study of LiMoS2. Journal of Solid State Chemistry, 2003, 175, 380-383.	1.4	12
2083	A DFT study of lithium battery materials: application to the Î²-VOXO4 systems (X=P, As, S). Journal of Solid State Chemistry, 2003, 176, 556-566.	1.4	19
2084	Theoretical investigation of TiB2 nanotubes. Microelectronics Journal, 2003, 34, 495-497.	1.1	17
2085	Electronâ€“phonon interaction in NbB2: a comparison with MgB2. Solid State Communications, 2003, 125, 323-326.	0.9	22
2086	The effect of cation doping on spinel LiMn2O4: a first-principles investigation. Solid State Communications, 2003, 126, 531-534.	0.9	52
2087	Ab initio Hartree-Fock calculations of LaMnO3 (110) surfaces. Solid State Communications, 2003, 127, 367-371.	0.9	29
2088	Electronic structure studies of Ni() surface reconstructions resulting from carbon, nitrogen, or oxygen atom adsorption. Surface Science, 2003, 522, 125-142.	0.8	27
2089	Compressibility of CO adsorbed on Ni from 10â^'6 mbar to 1.2 bar ambient CO pressures investigated with X-ray diffraction. Surface Science, 2003, 522, 161-166.	0.8	27
2090	A density functional study of Br on Cu() at low coverages. Surface Science, 2003, 524, 141-147.	0.8	10
2091	The GaAs()-c(4Ã—4) surface: a new perspective from energy loss spectra. Surface Science, 2003, 524, L71-L76.	0.8	12
2092	Coverage dependence of the work function of Li adsorbed on Ru(): ab initio studies within DFT. Surface Science, 2003, 525, 119-125.	0.8	14

#	Article	IF	Citations
2093	CO bonding on tin modified Pt()-(1Ã—2). Surface Science, 2003, 526, 184-192.	0.8	14
2094	Tight binding studies of strained Ge/Si() growth. Surface Science, 2003, 526, 356-366.	0.8	15
2095	The effects of doping a grain boundary in ZnO with various concentrations of Bi. Surface Science, 2003, 532-535, 351-358.	0.8	9
2096	Characteristics of S adsorption on Pd vicinal surfaces. Surface Science, 2003, 532-535, 154-159.	0.8	5
2097	Structure and reactivity of Pd doped Ag surfaces. Surface Science, 2003, 529, 403-409.	0.8	8
2098	Site preference of CO chemisorbed on Pt(111) from density functional calculations. Surface Science, 2003, 530, 71-87.	0.8	155
2099	Theory of NO/K phase mixing, separation and catalytic promoter action on Co{1 0 1Ì„ 0}. Surface Science, 2003, 529, 312-318.	0.8	4
2100	A combined ab initio and atomistic simulation study of the surface and interfacial structures and energies of hydrated scheelite: introducing a CaWO4 potential model. Surface Science, 2003, 531, 159-176.	0.8	58
2101	Oxygen vibrations in Oâ€“Ag(001). Surface Science, 2003, 530, 26-36.	0.8	17
2102	A spin-polarised first principles study of short dangling bond wires on Si. Surface Science, 2003, 531, L351-L355.	0.8	24
2103	Effects of the kinetic energy on the hydrogen abstraction dynamics on Cu(). Surface Science, 2003, 532-535, 148-153.	0.8	2
2104	Co-adsorption of ethylene and oxygen on the Ag(001) surface. Surface Science, 2003, 532-535, 191-197.	0.8	14
2105	Ab initio study of the one-monolayer Sb/Si(001) interface. Surface Science, 2003, 532-535, 661-665.	0.8	5
2106	N2O interaction with Pd(110): cluster vs. slab model. Surface Science, 2003, 532-535, 213-220.	0.8	5
2107	Calculation of magnetic and structural properties of small Coâ€“Rh clusters. Surface Science, 2003, 532-535, 334-340.	0.8	37
2108	Thin Pt films on the polar SrTiO3(111) surface: an experimental and theoretical study. Surface Science, 2003, 537, 134-152.	0.8	60
2109	Density functional study of Pd adsorbates at SnO2(110) surfaces. Surface Science, 2003, 537, 168-178.	0.8	17
2110	First-principles theory and microcalorimetry of CO adsorption on the { 211 } surfaces of Pt and Ni. Surface Science, 2003, 538, 171-183.	0.8	52

#	Article	IF	Citations
2111	Density functional study of alkali metals adsorption on the MgO(111) surface. Surface Science, 2003, 538, 240-248.	0.8	11
2112	Sulfur adsorption on Fe(110): a DFT study. Surface Science, 2003, 540, 420-430.	0.8	42
2113	DFT study of adsorption and dissociation of thiophene molecules on Ni(110). Surface Science, 2003, 540, 474-490.	0.8	37
2114	Surface structure of SrTiO3(100). Surface Science, 2003, 542, 177-191.	0.8	138
2115	Local techniques for the ab initio quantum-mechanical description of the chemical properties of crystalline materials. Computational and Theoretical Chemistry, 2003, 621, 141-147.	1.5	14
2116	Full potential calculations on the electron bandstructures of Sphalerite, Pyrite and Chalcopyrite. Applied Surface Science, 2003, 206, 300-313.	3.1	69
2117	Site preference and vibrational properties of ScFexAl12â^'x. Journal of Magnetism and Magnetic Materials, 2003, 256, 381-389.	1.0	12
2118	Energies and stabilities of sodium chloride clusters based on inversion pair potentials. Physica B: Condensed Matter, 2003, 325, 172-183.	1.3	24
2119	Interesting electronic and structural properties of C3P4. Materials Science and Engineering B: Solid-State Materials for Advanced Technology, 2003, 99, 527-530.	1.7	14
2120	Computational and experimental study of phase stability, cohesive properties, magnetism and electronic structure of TiMn2. Acta Materialia, 2003, 51, 1239-1247.	3.8	55
2121	Atomistic simulations of B1â€"B2 phase transition in KCl based on inversion pair potentials. Acta Materialia, 2003, 51, 6151-6161.	3.8	8
2122	Interaction of thiophene with stoichiometric and reduced rutile TiO2(1 1 0) surfaces: role of Ti3+ sites in desulfurization activity. Journal of Molecular Catalysis A, 2003, 202, 215-227.	4.8	48
2123	A computational and experimental study of anhydrous phosphotungstic acid and its interaction with water molecules. Applied Catalysis A: General, 2003, 256, 51-68.	2.2	100
2124	Structure and stability of Î±- and Î²-Ti2Se. Electron diffractionversusdensity-functional theory calculations. Acta Crystallographica Section A: Foundations and Advances, 2003, 59, 18-21.	0.3	10
2125	Theoretical analysis of d electron effects on the electronic properties of wurtzite and zincblende GaN. Physica Status Solidi (B): Basic Research, 2003, 236, 61-81.	0.7	26
2126	Shallow donor activity of Sâ€"H, Seâ€"H, and Teâ€"H complexes in silicon. Physica Status Solidi (B): Basic Research, 2003, 235, 107-110.	0.7	2
2127	Ab initio study of BAs under pressure. Physica Status Solidi (B): Basic Research, 2003, 235, 446-451.	0.7	4
2128	Theoretical study of ZnS under high pressure. Physica Status Solidi (B): Basic Research, 2003, 235, 452-455.	0.7	8

#	Article	IF	Citations
2129	Pressure induced phase transitions of BNs. Physica Status Solidi (B): Basic Research, 2003, 235, 526-530.	0.7	12
2130	Electronic structure calculationsof magnesium chalcogenides MgS and MgSe. Physica Status Solidi (B): Basic Research, 2003, 240, 565-573.	0.7	56
2131	A theoretical investigation of dislocations in cubic and hexagonal gallium nitride. Physica Status Solidi C: Current Topics in Solid State Physics, 2003, 0, 1684-1709.	0.8	33
2132	Electronic and vibrational properties of group-III nitrides:Ab initio studies. Physica Status Solidi C: Current Topics in Solid State Physics, 2003, 0, 1732-1749.	0.8	8
2133	First-Principles Calculation of Structural and Electronic Properties of Wurtzite AlxGa1â€”xN, InxGa1â€”xN, and InxAl1â€”xN Random Alloys. Physica Status Solidi C: Current Topics in Solid State Physics, 2003, 0, 315-319.	0.8	3
2134	Adsorption of Ga, In and N over GaAs(110) Surfaces. Physica Status Solidi C: Current Topics in Solid State Physics, 2003, 0, 417-420.	0.8	2
2135	First-principles elastic properties of BAs. International Journal of Quantum Chemistry, 2003, 91, 191-196.	1.0	10
2136	Properties of simple metals beyond the local density approximation of density functional theory. International Journal of Quantum Chemistry, 2003, 91, 224-229.	1.0	7
2137	DFT study of methanol conversion to hydrocarbons in a zeolite catalyst. International Journal of Quantum Chemistry, 2003, 91, 467-473.	1.0	46
2138	First-principles study of metal/nitride polar interfaces: Ti/TiN. Surface and Interface Analysis, 2003, 35, 835-841.	0.8	35
2139	Study of the electronic and atomic structure of thermally treated SrTiO3(110) surfaces. Surface and Interface Analysis, 2003, 35, 998-1003.	0.8	23
2140	Theoretical Investigation of the Solid State Reaction of Silicon Nitride and Silicon Dioxide forming Silicon Oxynitride (Si2N2O) under Pressure. Zeitschrift Fur Anorganische Und Allgemeine Chemie, 2003, 629, 1737-1750.	0.6	48
2141	Charge Transfer and Chemical Hardness along a Substitution Path in Metastable Au-Sb Alloys. Zeitschrift Fur Anorganische Und Allgemeine Chemie, 2003, 629, 1812-1824.	0.6	3
2142	The Electronic Structure of Tantalum Oxynitride and the Falsification ofÎ±-TaON. Zeitschrift Fur Anorganische Und Allgemeine Chemie, 2003, 629, 2173-2179.	0.6	47
2145	Exploiting Covalency to Enhance Metalâ€“Oxide and Oxideâ€“Oxide Adhesion at Heterogeneous Interfaces. Journal of the American Ceramic Society, 2003, 86, 373-386.	1.9	35
2146	First-Principles Calculations of Microdomain Models for Î²-Sialon Si5AlON7. Journal of the American Ceramic Society, 2003, 86, 1956-1958.	1.9	10
2147	Full inclusion of symmetry in constructing Wannier functions: Chemical bonding in MgO and TiO2 crystals. Physics of the Solid State, 2003, 45, 2072-2082.	0.2	16
2148	Density-Functional Study of Methanol Adsorption on the Al(100) Surface. Physics of the Solid State, 2003, 45, 2218.	0.2	3

#	Article	IF	Citations
2149	Local structure and electronic properties of BaTaO2N with perovskite-type structure. Journal of Physics and Chemistry of Solids, 2003, 64, 281-286.	1.9	67
2150	First principles study of electronic and magnetic properties of Co2MnGe/GaAs interfaces. Journal of Physics and Chemistry of Solids, 2003, 64, 1697-1701.	1.9	53
2151	In search of new candidates for ultra-hard materials: the ternary BC3N3 stoichiometry. Journal of Physics and Chemistry of Solids, 2003, 64, 1539-1545.	1.9	15
2152	Numerical method of Brillouin zone integrals of vectorial fields in photonic crystals. Physics Letters, Section A: General, Atomic and Solid State Physics, 2003, 308, 116-119.	0.9	6
2153	Mechanical behaviour of AgB2 in comparison to MgB2â€“â€“a first principle study. Physica C: Superconductivity and Its Applications, 2003, 390, 16-20.	0.6	12
2154	Metastable phase formation in an immiscible Cu-Ta system studied by ion-beam mixing, ab initio calculation, and molecular dynamics simulation. Acta Materialia, 2003, 51, 3885-3893.	3.8	17
2155	Enhancement of magnetocrystalline anisotropy in ferromagnetic Fe films by intra-atomic noncollinear magnetism. Physical Review B, 2003, 67, .	1.1	65
2156	Reduction of CuO and Cu2O with H2: H Embedding and Kinetic Effects in the Formation of Suboxides. Journal of the American Chemical Society, 2003, 125, 10684-10692.	6.6	490
2157	Theoretical study of native defects in BN nanotubes. Physical Review B, 2003, 67, .	1.1	151
2158	Magnetic Properties and Diffusion of Adatoms on a Graphene Sheet. Physical Review Letters, 2003, 91, 017202.	2.9	419
2159	Gallium adsorption on (0001) GaN surfaces. Physical Review B, 2003, 67, .	1.1	131
2160	Effective Pathway for Hydrogen Atom Adsorption on Graphene. Journal of the Physical Society of Japan, 2003, 72, 995-997.	0.7	69
2161	Dynamic structure factor of liquid and amorphous Ge fromab initiosimulations. Physical Review B, 2003, 67, .	1.1	37
2162	First-Principles Study of Two-Dimensional Titanium Dioxides. Journal of Physical Chemistry B, 2003, 107, 9824-9828.	1.2	152
2163	Properties of CeO2and Ce1-xZrxO2Nanoparticles:Â X-ray Absorption Near-Edge Spectroscopy, Density Functional, and Time-Resolved X-ray Diffraction Studies. Journal of Physical Chemistry B, 2003, 107, 3535-3543.	1.2	199
2164	First principles studies for the dissociative adsorption of H2 on graphene. Journal of Applied Physics, 2003, 93, 3395-3400.	1.1	145
2165	Computational quantum chemistry: A primer. Handbook of Numerical Analysis, 2003, 10, 3-270.	0.9	57
2166	Electronic structure characterization of six semiconductors through their localized Wannier functions. Physical Chemistry Chemical Physics, 2003, 5, 5319.	1.3	6

#	Article	IF	Citations
2167	Electronic and chemical properties of mixed-metal oxides: Adsorption and reaction of NO on SrTiO3(100). Journal of Chemical Physics, 2003, 118, 6562-6571.	1.2	39
2168	Adhesion of metalâ€“carbide/nitride interfaces: Al/TiC and Al/TiN. Journal of Physics Condensed Matter, 2003, 15, 8103-8114.	0.7	60
2169	Pt and Pt2 on MgO(100) and BaO(100): structure, bonding, and chemical properties. Journal of Chemical Physics, 2003, 119, 3896-3904.	1.2	41
2170	The behavior of mixed-metal oxides: Structural and electronic properties of Ce1â^'xCaxO2 and Ce1â^'xCaxO2â^'x. Journal of Chemical Physics, 2003, 119, 5659-5669.	1.2	112
2171	First-principles study on structures and energetics of intrinsic vacancies inSrTiO3. Physical Review B, 2003, 68, .	1.1	194
2172	Structural and Electronic Properties of the Layered LiNi0.5Mn0.5O2Lithium Battery Material. Chemistry of Materials, 2003, 15, 4280-4286.	3.2	84
2173	Effect of stress on the energy levels of the vacancy-oxygen-hydrogen complex in Si. Physical Review B, 2003, 68, .	1.1	27
2174	Theoretical Study of the Adsorption of Acetylene on the (111) Surfaces of Pd, Pt, Ni, and Rh. Journal of Physical Chemistry B, 2003, 107, 217-223.	1.2	107
2175	Adsorption of Unsaturated Hydrocarbons on Pd(111) and Pt(111): A DFT Study. Journal of Physical Chemistry B, 2003, 107, 12287-12295.	1.2	148
2176	Structure of the P vacancy on the InP(110) surface from first principles. Physical Review B, 2003, 67, .	1.1	8
2177	Ab initio simulation of the ice II structure. Journal of Chemical Physics, 2003, 119, 4567-4572.	1.2	28
2178	Ab initiocalculation of the ideal tensile and shear strength of cubic silicon nitride. Physical Review B, 2003, 67, .	1.1	41
2179	Ab initioelasticity of chalcopyrites. Journal of Applied Physics, 2003, 93, 3789-3795.	1.1	34
2180	Coverage Effects and the Nature of the Metalâ^'Sulfur Bond in S/Au(111):Â High-Resolution Photoemission and Density-Functional Studies. Journal of the American Chemical Society, 2003, 125, 276-285.	6.6	179
2181	Ab initiostudy of the migration of intrinsic defects in3Câ^'SiC. Physical Review B, 2003, 68, .	1.1	241
2182	CubicHf3N4andZr3N4:A class of hard materials. Physical Review B, 2003, 68, .	1.1	294
2183	Force-based many-body interatomic potential for ZrC. Journal of Applied Physics, 2003, 93, 9072-9085.	1.1	49
2184	Arsenic deactivation in Si:â€ƒElectronic structure and charge states of vacancy-impurity clusters. Physical Review B, 2003, 68, .	1.1	76

#	Article	IF	Citations
2185	Different Surface Chemistries of Water on Ru{0001}:Â From Monomer Adsorption to Partially Dissociated Bilayers. Journal of the American Chemical Society, 2003, 125, 2746-2755.	6.6	228
2186	Structure of the icosahedral Ti-Zr-Ni quasicrystal. Physical Review B, 2003, 67, .	1.1	46
2187	Electronic structure and ferromagnetism of Mn-doped group-IV semiconductors. Physical Review B, 2003, 68, .	1.1	195
2188	First-principles calculations of intrinsic defects inAl2O3. Physical Review B, 2003, 68, .	1.1	270
2189	Spontaneous Cross Linking of Small-Diameter Single-Walled Carbon Nanotubes. Nano Letters, 2003, 3, 585-587.	4.5	30
2190	A theoretical study of the energetics and IR frequencies of hydroxyl defects in forsterite. Journal of Geophysical Research, 2003, 108, .	3.3	47
2191	The catalytic role of water in CO oxidation. Journal of Chemical Physics, 2003, 119, 6324-6334.	1.2	119
2192	First-principles simulations of direct coexistence of solid and liquid aluminum. Physical Review B, 2003, 68, .	1.1	93
2193	CO-Induced Modification of the Metal/MgO(100) Interaction. Journal of Physical Chemistry B, 2003, 107, 12239-12243.	1.2	36
2194	Surface diffusion and growth of patterned nanostructures on strained surfaces. Physical Review B, 2003, 67, .	1.1	48
2195	High Temperature Microelectrophoresis Studies of the Rutile/Aqueous Solution Interface. Langmuir, 2003, 19, 3797-3804.	1.6	52
2196	Self-interaction-corrected pseudopotential scheme for magnetic and strongly-correlated systems. Physical Review B, 2003, 67, .	1.1	242
2197	Density-Functional Study of the Adsorption and Vibration Spectra of Benzene Molecules on Pt(111). Journal of Physical Chemistry B, 2003, 107, 2995-3002.	1.2	118
2198	Stability, diffusivity, and vibrational properties of monatomic and molecular hydrogen in wurtzite GaN. Physical Review B, 2003, 68, .	1.1	37
2199	Chemical termination of the CsCl-structure FeSi/Si(111) film surface and its multilayer relaxation. Physical Review B, 2003, 67, .	1.1	24
2200	Chemisorption of C2Biradical and Acetylene on Reconstructed Diamond(111)-(2 Ã— 1). Journal of Physical Chemistry B, 2003, 107, 985-993.	1.2	8
2201	First-principles study of lattice instabilities in ferromagneticNi2MnGa. Physical Review B, 2003, 68, .	1.1	179
2202	Implementation of an all-electron GW approximation based on the projector augmented wave method without plasmon pole approximation: Application to Si, SiC, AlAs, InAs, NaH, and KH. Physical Review B, 2003, 67, .	1.1	199

#	Article	IF	Citations
2203	Study of Î³-Alumina-Supported Hydrotreating Catalyst:Â I. Adsorption of Bare MoS2Sheets on Î³-Alumina Surfaces. Journal of Physical Chemistry B, 2003, 107, 8490-8497.	1.2	32
2204	Adsorption of HCl on Single-Crystal Î±-Al2O3(0001) Surface:Â A DFT Study. Journal of Physical Chemistry B, 2003, 107, 186-195.	1.2	36
2205	Laves-Phase Structural Changes in the System CaAl2-xMgx. Inorganic Chemistry, 2003, 42, 1467-1474.	1.9	70
2206	Atomic and electronic structure ofMoS2nanoparticles. Physical Review B, 2003, 67, .	1.1	352
2207	Structural and dielectric properties ofSr2TiO4from first principles. Physical Review B, 2003, 68, .	1.1	64
2208	Hydrogen bonding between adsorbed deprotonated glycine molecules on Cu(110). Journal of Chemical Physics, 2003, 119, 12577-12585.	1.2	103
2209	Structural and electronic properties of lithium intercalated graphiteLiC6. Physical Review B, 2003, 68, .	1.1	135
2210	Crystal Structures of (Pyrene)10(I3-)4(I2)10and [1,3,6,8-Tetrakis(methylthio)pyrene]3(I3-)3(I2)7:Â Structural Trends in Fused Aromatic Polyiodides. Chemistry of Materials, 2003, 15, 1420-1433.	3.2	26
2211	The layering effect of water on the structure of scheelite. Physical Chemistry Chemical Physics, 2003, 5, 433-436.	1.3	10
2212	Localized versus Delocalized Bonding in the K5Bi4Metallic Saltâ€. Inorganic Chemistry, 2003, 42, 2759-2763.	1.9	19
2213	CRYSTALLOGRAPHIC STRUCTURES OF PbWO4. High Pressure Research, 2003, 23, 343-347.	0.4	13
2214	Polymorphism in the Crystal Structures of the Group 13 Trimethyls. Organometallics, 2003, 22, 2450-2457.	1.1	33
2215	A Tutorial on Density Functional Theory. Lecture Notes in Physics, 2003, , 218-256.	0.3	40
2216	Identification of hydrogen configurations inp-type GaN through first-principles calculations of vibrational frequencies. Physical Review B, 2003, 68, .	1.1	55
2217	A DFT Study of the Structures of N2O Adsorbed on the Pd(110) Surface. Journal of Physical Chemistry B, 2003, 107, 2741-2747.	1.2	58
2218	Ozone reactivity with carbon nanotubes: experimental and theoretical studies. , 0, , .		2
2219	Theoretical studies of iridium under pressure. Journal of Physics Condensed Matter, 2003, 15, 4127-4134.	0.7	14
2220	Structure and Bonding of Sr3In11:Â How Size and Electronic Effects Determine Structural Stability of Polar Intermetallic Compounds. Inorganic Chemistry, 2003, 42, 7782-7788.	1.9	30

#	Article	IF	Citations
2221	Density Functional Theory Studies of Chemisorption and Diffusion Properties of Ni and Niâ^'Thiophene Complexes on the MoS2 Basal Plane. Journal of Physical Chemistry B, 2003, 107, 1988-2000.	1.2	16
2222	SnO2 Nanoribbons as NO2 Sensors:â€‰ Insights from First Principles Calculations. Nano Letters, 2003, 3, 1025-1028.	4.5	186
2223	All-electron and pseudopotential study of MgO: Equation of state, anharmonicity, and stability. Physical Review B, 2003, 67, .	1.1	151
2224	Chemisorption of NO2on Carbon Nanotubes. Journal of Physical Chemistry B, 2003, 107, 9363-9369.	1.2	104
2225	Electronic correlation effects in transition-metal sulfides. Journal of Physics Condensed Matter, 2003, 15, 979-996.	0.7	231
2226	Ab initio lattice dynamics and structural stability of MgO. Journal of Chemical Physics, 2003, 118, 10174-10182.	1.2	144
2227	First-Principles Calculations of the Adsorption of Nitromethane and 1,1-Diamino-2,2-dinitroethylene (FOX-7) Molecules on the Al(111) Surface. Journal of Physical Chemistry B, 2003, 107, 8953-8964.	1.2	40
2228	Electronic and structural properties of a4dperovskite: Cubic phase ofSrZrO3. Physical Review B, 2003, 68, .	1.1	96
2229	The particle-in-cell model for ab initio thermodynamics: implications for the elastic anisotropy of the Earthâ€™s inner core. Physics of the Earth and Planetary Interiors, 2003, 139, 243-253.	0.7	36
2230	Ab initiodetermination of the ground-state properties ofCa2MgSi2O7Ã¥kermanite. Physical Review B, 2003, 68, .	1.1	18
2231	The General Utility Lattice Program (GULP). Molecular Simulation, 2003, 29, 291-341.	0.9	1,921
2232	Carbon dissolution and diffusion in ferrite and austenite from first principles. Physical Review B, 2003, 67, .	1.1	398
2233	An ab initio study of the ideal tensile and shear strength of single-crystal Î²â€“Si₃N₄. Journal of Materials Research, 2003, 18, 1168-1172.	1.2	25
2234	Cluster expansion method for adsorption: Application to hydrogen chemisorption on graphene. Physical Review B, 2003, 68, .	1.1	256
2235	Ab initiomolecular dynamics simulation of femtosecond laser-induced structural modification in vitreous silica. Physical Review B, 2003, 68, .	1.1	20
2236	First-principles investigation of lattice constants and bowing parameters in wurtzite AlxGa1ÂxN, InxGa1ÂxN and InxAl1ÂxN alloys. Semiconductor Science and Technology, 2003, 18, 850-856.	1.0	109
2237	Theoretical characterization of several models of nanoporous carbon. New Journal of Physics, 2003, 5, 123-123.	1.2	32
2238	Signature of intrinsic defects in SiC:Ab initiocalculations of hyperfine tensors. Physical Review B, 2003, 67, .	1.1	66

#	Article	IF	Citations
2239	Theoretical study about adsorption of atomic oxygen on unmodified and I-modified Ag(100) surface. Journal of Chemical Physics, 2003, 118, 11210-11216.	1.2	6
2240	Derivation of Force Field Parameters for TiO2â"H2O Systems from ab Initio Calculations. Journal of Physical Chemistry B, 2003, 107, 11072-11081.	1.2	196
2241	A Computer Modeling Study of Perfect and Defective Silver (111) Surfaces. Journal of Physical Chemistry B, 2003, 107, 3528-3534.	1.2	23
2242	First-principles prediction of half-metallic ferromagnetic semiconductors: V- and Cr-doped BeTe. Physical Review B, 2003, 67, .	1.1	51
2243	Stability and electronic structure of the(1Ã—1)SrTiO3(110)polar surfaces by first-principles calculations. Physical Review B, 2003, 68, .	1.1	158
2244	Structural, electronic, and magnetic properties ofFe2SiO4fayalite: Comparison of LDA and GGA results. Physical Review B, 2003, 67, .	1.1	75
2245	Phonon Instabilities and the Ideal Strength of Aluminum. Physical Review Letters, 2003, 91, 135501.	2.9	218
2246	The structure of hematite (Î±-Fe2O3) (001) surfaces in aqueous media: scanning tunneling microscopy and resonant tunneling calculations of coexisting O and Fe terminations. Geochimica Et Cosmochimica Acta, 2003, 67, 985-1000.	1.6	125
2247	Substitution mechanism of Al ions in MgSiO3 perovskite under high pressure conditions from first-principles calculations. Earth and Planetary Science Letters, 2003, 206, 617-625.	1.8	44
2248	Anisotropy of the mobility of pentacene from frustration. Synthetic Metals, 2003, 139, 109-114.	2.1	125
2249	Magnetism of ultrathin wires suspended in free space and adsorbed on vicinal surfaces. Physical Review B, 2003, 67, .	1.1	47
2250	Adatom Kinetics On and Below the Surface: The Existence of a New Diffusion Channel. Physical Review Letters, 2003, 90, 056101.	2.9	293
2251	A modified empirical potential for energetic calculations of planar defects in GaN. Computational Materials Science, 2003, 27, 43-49.	1.4	42
2252	Electronic properties of Mn compounds under strain. Computational Materials Science, 2003, 27, 175-180.	1.4	8
2253	Trocadero: a multiple-algorithm multiple-model atomistic simulation program. Computational Materials Science, 2003, 28, 85-106.	1.4	75
2254	Prediction of the structure of LaF3 at high pressures. Journal of Alloys and Compounds, 2003, 349, 111-113.	2.8	21
2255	Ab initio interatomic potentials of cubic boron nitride. Journal of Alloys and Compounds, 2003, 349, 17-22.	2.8	9
2256	Site preference and vibrational properties of ScCuxAl12â"x. Journal of Alloys and Compounds, 2003, 349, 41-48.	2.8	12

#	Article	IF	Citations
2257	Electronic structure of magnesium nitride-fluorides from first-principles calculations. Journal of Alloys and Compounds, 2003, 351, 72-76.	2.8	23
2258	Ab initio calculation of the crystal structure of the lanthanide Ln2O3 sesquioxides. Journal of Alloys and Compounds, 2003, 351, 31-34.	2.8	137
2259	Atomistic simulation of the lattice constants and lattice vibrations in RT4Al8 (R=Nd, Sm; T=Cr, Mn, Cu,) Tj ETQq0 0 0 rgBT /Overlock 10	2.8	20
2260	Electronic structure calculations for LaNi5 and LaNi5H7: energetics and elastic properties. Journal of Alloys and Compounds, 2003, 353, 74-85.	2.8	103
2261	Electronic structures of semiconducting alkaline-earth metal silicides. Journal of Alloys and Compounds, 2003, 358, 257-263.	2.8	109
2262	First principles study of sodiumâ€“aluminumâ€“hydrogen phases. Journal of Alloys and Compounds, 2003, 356-357, 486-489.	2.8	41
2263	Electronic structures of PbBi4Te7 and GeBi4Te7 calculated by a first-principle pseudopotential method. Intermetallics, 2003, 11, 451-458.	1.8	11
2264	An ab initio model of electron transport in hematite (Î±-Fe2O3) basal planes. Journal of Chemical Physics, 2003, 118, 6455-6466.	1.2	274
2265	An Interfacial Complex in ZnO and Its Influence on Charge Transport. Physical Review Letters, 2003, 91, 165506.	2.9	45
2266	Spin injection at Heusler/semiconductor interfaces: First-principles determination of potential discontinuity and half-metallicity. Journal of Applied Physics, 2003, 94, 4723-4725.	1.1	63
2267	DFT Study of Cysteine Adsorption on Au(111). Journal of Physical Chemistry B, 2003, 107, 1151-1156.	1.2	200
2268	Hydrogen-induced unzipping of single-walled carbon nanotubes. Physical Review B, 2003, 68, .	1.1	47
2269	Ab initioapproach for high-pressure systems with application to high-pressure phases of boron:â€,â€,Perturbative momentum-space potentials. Physical Review B, 2003, 67, .	1.1	21
2270	Superconductivity in Dopedsp3Semiconductors: The Case of the Clathrates. Physical Review Letters, 2003, 91, 247001.	2.9	136
2271	Extended defects in diamond:â€ƒThe interstitial platelet. Physical Review B, 2003, 67, .	1.1	78
2272	Co-phase penetration ofWC(101Â¯0)/WC(101Â¯0)grain boundaries from first principles. Physical Review B, 2003, 67, .	1.1	85
2273	Density-functional calculations of the liquid deuterium Hugoniot, reshock, and reverberation timing. Physical Review B, 2003, 68, .	1.1	166
2274	Physical and Chemical Properties of MoP, Ni2P, and MoNiP Hydrodesulfurization Catalysts:Â Time-Resolved X-ray Diffraction, Density Functional, and Hydrodesulfurization Activity Studies. Journal of Physical Chemistry B, 2003, 107, 6276-6285.	1.2	198

#	Article	IF	Citations
2275	Electronic structure and magnetism of Mn-doped GaN. Physical Review B, 2003, 68, .	1.1	132
2276	ReaxFFSiO Reactive Force Field for Silicon and Silicon Oxide Systems. Journal of Physical Chemistry A, 2003, 107, 3803-3811.	1.1	821
2277	The vacancyâ€“nitrogenâ€“hydrogen complex in diamond: a potential deep centre in chemical vapour deposited material. Journal of Physics Condensed Matter, 2003, 15, S2903-S2911.	0.7	34
2278	Stability and electronic properties of carbon phosphide compounds with 1:1 stoichiometry. Physical Review B, 2003, 67, .	1.1	24
2279	Density functional theory studies of screw dislocation core structures in bcc metals. Philosophical Magazine, 2003, 83, 365-375.	0.7	197
2280	Validity of effective medium theory for aluminium under tension. Modelling and Simulation in Materials Science and Engineering, 2003, 11, 127-136.	0.8	17
2281	Metastable Frenkel Pair Defect in Graphite: Source of Wigner Energy?. Physical Review Letters, 2003, 91, 025505.	2.9	131
2282	Theory of hydrogen in diamond. Journal of Physics Condensed Matter, 2003, 15, R551-R580.	0.7	153
2283	Configurations, energies, and thermodynamics of the neutral MgH complex in GaN. Journal of Applied Physics, 2003, 94, 4918.	1.1	16
2284	Structure and bulk modulus of M2AlC (M=Ti, V, and Cr). Applied Physics Letters, 2003, 83, 899-901.	1.5	189
2285	Tight-binding-molecular-dynamics investigation of the atomic and electronic structure properties of a-C, a-Si and a-SiC. Diamond and Related Materials, 2003, 12, 993-997.	1.8	1
2286	Vacancy concentration in Al from combined first-principles and model potential calculations. Physical Review B, 2003, 67, .	1.1	73
2287	Crystal and electronic structure of the novel nitrides MYSi4N7 (M = Sr, Ba) with peculiar NSi4 coordination. Journal of Materials Chemistry, 2003, 13, 1480.	6.7	28
2288	Photoelastic and elastic properties of the fluorite structure materials, LiF, and Si. Physical Review B, 2003, 68, .	1.1	22
2289	Energetics, vibrational spectrum, and scanning tunneling microscopy images for the intermediate in water production reaction on Pt(111) from density functional calculations. Journal of Chemical Physics, 2003, 119, 4865-4872.	1.2	68
2290	Accurate First Principles Prediction of17O NMR Parameters in SiO2:Â Assignment of the Zeolite Ferrierite Spectrum. Journal of the American Chemical Society, 2003, 125, 541-548.	6.6	389
2291	Equation of state and phonon frequency calculations of diamond at high pressures. Physical Review B, 2003, 68, .	1.1	82
2292	Melem (2,5,8-Triamino-tri-s-triazine), an Important Intermediate during Condensation of Melamine Rings to Graphitic Carbon Nitride:Â Synthesis, Structure Determination by X-ray Powder Diffractometry, Solid-State NMR, and Theoretical Studies. Journal of the American Chemical Society, 2003, 125, 10288-10300.	6.6	954

#	Article	IF	Citations
2293	Theoretical evaluation of hydrogen storage capacity in pure carbon nanostructures. Journal of Chemical Physics, 2003, 119, 2376-2385.	1.2	263
2294	Vibrational and quasiharmonic thermal properties of CaO under pressure. Physical Review B, 2003, 68, .	1.1	73
2295	Improving the convergence of defect calculations in supercells: Anab initiostudy of the neutral silicon vacancy. Physical Review B, 2003, 67, .	1.1	163
2296	Understanding the complex metallic element Mn. I.â€,Crystalline and noncollinear magnetic structure of Î±-Mn. Physical Review B, 2003, 68, .	1.1	236
2297	Mixed-oxide formation during preparation of alumina-supported zirconia: an EXAFS and DFT study. Physical Chemistry Chemical Physics, 2003, 5, 3811-3817.	1.3	20
2298	Ideal tensile strength and band gap of single-walled carbon nanotubes. Physical Review B, 2003, 68, .	1.1	179
2299	Ab initiocalculation of the linewidth of various phonon modes in germanium and silicon. Physical Review B, 2003, 67, .	1.1	125
2300	First-principles calculations of the adsorption of nitromethane and 1,1-diamino 2,2-dinitroethylene (FOX-7) molecules on the Al[111]surface. , 0, , .		1
2301	Nucleation of Single-Walled Carbon Nanotubes. Physical Review Letters, 2003, 90, 145501.	2.9	127
2302	Hydrogen passivation of nitrogen in SiC. Applied Physics Letters, 2003, 83, 1385-1387.	1.5	16
2303	Lattice inversion for interionic pair potentials. Journal of Chemical Physics, 2003, 118, 3974-3982.	1.2	17
2304	Formation of BiOi, BiCs, and BiBsHi defects in e-irradiated or ion-implanted silicon containing boron. Applied Physics Letters, 2003, 83, 665-667.	1.5	25
2305	Interstitial H and H2 in SiC. Applied Physics Letters, 2003, 83, 923-925.	1.5	23
2306	Free-energy calculations of intrinsic point defects in silicon. Physical Review B, 2003, 68, .	1.1	77
2307	Computational chemistry models leading to mediation of gun tube erosion. , 0, , .		0
2308	Site preferences in Î²-sialon from first-principles calculations. Journal of Materials Chemistry, 2003, 13, 335-337.	6.7	13
2309	Ab-initio study on the Î³-Al₂O₃ surfaces and interfaces.. Materials Research Society Symposia Proceedings, 2003, 786, 521.	0.1	2
2310	Density Functional Theory Study of the Interaction of Cl[sup â^'] with Passivated Nickel Surfaces. Electrochemical and Solid-State Letters, 2003, 6, B47.	2.2	36

#	Article	IF	Citations
2311	ab-initio modelling of Mg:H interstitial solid solutions. Materials Research Society Symposia Proceedings, 2003, 801, 120.	0.1	0
2313	Stable Hydrogen Pair Trapped at Carbon Impurities in Silicon. Defect and Diffusion Forum, 2003, 221-223, 1-10.	0.4	2
2314	First-principles study of equilibrium properties and electronic structure of Ti3Si0.75Al0.25C2solid solution. Journal of Physics Condensed Matter, 2003, 15, 5959-5968.	0.7	47
2315	Strong dependence of the fundamental band gap on the alloy composition in cubic InxGa1-xN and InxAl1-xN alloys. Materials Research Society Symposia Proceedings, 2003, 798, 640.	0.1	0
2316	Prediction of metastable phase formation in an immiscible Cuâ€“Cr system from interatomic potential and ab initio calculation. Journal of Materials Research, 2003, 18, 2300-2303.	1.2	3
2317	The crystal structure of CaSiO3-walstromite, a special isomorph of wollastonite-II. Zeitschrift Fur Kristallographie - Crystalline Materials, 2003, 218, 811-818.	0.4	25
2318	Electronic structure of divacancyâ€“hydrogen complexes in silicon. Journal of Physics Condensed Matter, 2003, 15, S2809-S2814.	0.7	11
2319	First-principles calculation of the band offset atBaO/BaTiO3andSrO/SrTiO3interfaces. Physical Review B, 2003, 67, .	1.1	121
2320	Initial and final state effects in the x-ray absorption process ofLa1â^'xSrxMnO3. Physical Review B, 2003, 68, .	1.1	21
2321	Orbital rehybridization in n-octane adsorbed on Cu(110). Journal of Chemical Physics, 2003, 118, 3782-3789.	1.2	41
2322	Oxidation of the 3Ã—3 6H-SiC (0001) adatom cluster: A periodic density functional theory and dynamic rocking beam analysis. Journal of Chemical Physics, 2003, 119, 4905-4915.	1.2	16
2323	Cu doping effects inMgB2. Physical Review B, 2003, 67, .	1.1	5
2324	Schottky barrier height at an organic/metal junction: A first-principles study of PTCDA/X(X=Al,Ag)contacts. Physical Review B, 2003, 68, .	1.1	43
2325	Ab initiostudy on divacancy binding energies in aluminum and magnesium. Physical Review B, 2003, 68, .	1.1	62
2326	Calculated properties of nitrogen-vacancy complexes in beryllium- and magnesium-doped GaN. Physical Review B, 2003, 68, .	1.1	13
2327	Bi incorporation in GaN andAlxGa1â^'xNalloys. Physical Review B, 2003, 68, .	1.1	5
2328	Conductance calculations with a wavelet basis set. Physical Review B, 2003, 67, .	1.1	74
2329	Site occupation in the Ni-NbÎ¼phase. Physical Review B, 2003, 67, .	1.1	30

#	Article	IF	Citations
2330	Electrical activity of chalcogen-hydrogen defects in silicon. Physical Review B, 2003, 67, .	1.1	82
2331	First-principles studies of cation-doped spinelLiMn2O4for lithium ion batteries. Physical Review B, 2003, 67, .	1.1	51
2332	Glass-forming ability determined by ann-body potential in a highly immiscible Cu-W system through molecular dynamics simulations. Physical Review B, 2003, 68, .	1.1	20
2333	Metallic to insulating nature ofTaNx:â€‚Role of Ta and N vacancies. Physical Review B, 2003, 67, .	1.1	98
2334	Schottky barrier heights at polar metal/semiconductor interfaces. Physical Review B, 2003, 68, .	1.1	43
2335	Oxygenation of carbon nanotubes:â€ƒAtomic structure, energetics, and electronic structure. Physical Review B, 2003, 67, .	1.1	109
2336	Cluster-assembled materials based onNa6Pb. Physical Review B, 2003, 68, .	1.1	28
2337	Hydrogen configurations, formation energies, and migration barriers in GaN. Journal of Applied Physics, 2003, 94, 2311-2318.	1.1	46
2338	Aggregation of carbon interstitials in silicon carbide: A theoretical study. Physical Review B, 2003, 68, .	1.1	103
2339	Covalent and Reversible Short-Range Electrostatic Imaging in Noncontact Atomic Force Microscopy. Physical Review Letters, 2003, 91, 216401.	2.9	25
2340	The crystalline surfaces of Î²-PdH{111}: Ideal surface terminations of a stoichiometric bulk compound relevant to heterogeneous catalysis. Journal of Chemical Physics, 2003, 118, 5623-5634.	1.2	21
2341	NO adsorption on Rh(100). I. Structural characterization of the adlayers. Journal of Chemical Physics, 2003, 119, 12525-12533.	1.2	16
2342	Effect of Impurities in the Large Au-Au Distances in Gold Nanowires. Physical Review Letters, 2003, 90, 036101.	2.9	76
2343	First-Principles Calculations of Pseudolocal Vibrational Modes: The Case of Cu and Cu Pairs in Si. Physical Review Letters, 2003, 90, 035504.	2.9	59
2344	Electronic structure and energetics of RCo5H4 and RCo5 (R=La,Pr). Applied Physics Letters, 2003, 82, 1042-1044.	1.5	10
2345	Eleyâ€“Rideal reactions of H atoms with Cl adsorbed on Au(111): Quantum and quasiclassical studies. Journal of Chemical Physics, 2003, 118, 2357-2366.	1.2	27
2346	Catalytic role of boron atoms in self-interstitial clustering in Si. Applied Physics Letters, 2003, 83, 1047-1049.	1.5	12
2347	Physics and chemistry of hydrogen in the vacancies of semiconductors. Physical Review B, 2003, 68, .	1.1	30

#	Article	IF	Citations
2348	First-principles determination of the relative stability of theÎ±andCmcmstructures ofAlPO4. Physical Review B, 2003, 68, .	1.1	5
2349	Nanotube bundles from calcium disilicide:â€,â€,A density functional theory study. Physical Review B, 2003, 68, .	1.1	19
2350	Structure of the[ZnInâ^'VP]defect complex in Zn-doped InP. Physical Review B, 2003, 68, .	1.1	12
2351	Surface structure and stability of PdZn and PtZn alloys:â€ƒDensity-functional slab model studies. Physical Review B, 2003, 68, .	1.1	108
2352	Interaction of CO, O, and S with metal nanoparticles on Au(111): A theoretical study. Physical Review B, 2003, 67, .	1.1	37
2353	Photoelasticity of crystalline and amorphous silica from first principles. Physical Review B, 2003, 68, .	1.1	31
2354	Acoustic-mode-driven electron-phonon coupling in transition-metal diborides. Physical Review B, 2003, 67, .	1.1	8
2355	Methane hydrate under high pressure. Physical Review B, 2003, 68, .	1.1	37
2356	First-principle dynamical electronic characteristics of Al electromigration in the bulk, surface, and grain boundary. Physical Review B, 2003, 67, .	1.1	8
2357	n-type doping and passivation ofCuInSe2andCuGaSe2by hydrogen. Physical Review B, 2003, 68, .	1.1	28
2358	Determination of the B1-B2 transition path in RbCl by MÃ¶bius pair potentials. Philosophical Magazine, 2003, 83, 1451-1461.	0.7	8
2359	Copper interactions with H, O, and the self-interstitial in silicon. Physical Review B, 2003, 68, .	1.1	39
2360	Adsorption of N-containing species onto SiC(0001) surfaces: A theoretical study. Physical Review B, 2003, 67, .	1.1	9
2361	Multilayer relaxation of Cu(210) studied by layer-doubling LEED analysis and pseudopotential density functional theory calculations. Physical Review B, 2003, 68, .	1.1	18
2362	Cation substitution effects on structural, electronic and optical properties of nonlinear optical AgGa(SxSe1Âx)2crystals. Journal of Physics Condensed Matter, 2003, 15, 6043-6055.	0.7	19
2363	Characterization of the unoccupied and partially occupied states of TTF-TCNQ by XANES and first-principles calculations. Physical Review B, 2003, 68, .	1.1	54
2364	Ab initiostudy of Al-ceramic interfacial adhesion. Physical Review B, 2003, 67, .	1.1	127
2365	Formation of quantum structures on a single nanotube by modulating hydrogen adsorption. Physical Review B, 2003, 68, .	1.1	29

#	Article	IF	Citations
2366	Density-functional theory applied to Rh(111) and CO/Rh(111) systems:â€ƒGeometries, energies, and chemical shifts. Physical Review B, 2003, 67, .	1.1	46
2367	Lattice dynamics of HgSe: Neutron scattering measurements andab initiostudies. Physical Review B, 2003, 67, .	1.1	21
2368	Doping of chalcopyrites by hydrogen. Applied Physics Letters, 2003, 83, 2007-2009.	1.5	16
2369	First-principles study on the energetics and vibrational properties of theS2â^'impurity in alkali-halide crystals. Physical Review B, 2003, 68, .	1.1	6
2370	Initial growth of hexagonal and cubic boron nitride:â€ƒA theoretical study. Physical Review B, 2003, 68, .	1.1	24
2371	First-principles study of the solubility, diffusion, and clustering of C in Ni. Physical Review B, 2003, 68, .	1.1	71
2372	Deep hydrogen traps in heavily B-doped diamond. Physical Review B, 2003, 68, .	1.1	44
2373	Ab-initio investigation of the early stage of nano-scale thin film growth: Co and Al adatoms on Co (111) surface. , 0, , .		0
2374	Ab initiostudies of stepped Pd surfaces with and without S. Physical Review B, 2003, 67, .	1.1	22
2375	Exchange-correlation energy and the phase diagram of Si. Physical Review B, 2003, 68, .	1.1	38
2376	Density-functional study of nonmolecular phases of nitrogen: Metastable phase at low pressure. Physical Review B, 2003, 68, .	1.1	98
2377	Calculated properties of point defects in Be-doped GaN. Physical Review B, 2003, 67, .	1.1	23
2378	Electronic structure of solid 1,3,5-triamino-2,4,6-trinitrobenzene under uniaxial compression: Possible role of pressure-induced metallization in energetic materials. Physical Review B, 2003, 67, .	1.1	77
2379	Intermetallic bonds and midgap interface states at epitaxial Al/GaAs(001) junctions. Physical Review B, 2003, 67, .	1.1	4
2380	First-principles characterization of the electronic structure of the molecular superconductorÎ²â^'(BEDTâ^'TTF)2IBr2. Physical Review B, 2003, 67, .	1.1	18
2381	Hydrogen bonding in solid ammonia fromab initiocalculations. Journal of Chemical Physics, 2003, 118, 5987-5994.	1.2	47
2382	Diffusion and vibration of CO molecules adsorbed on a Cu(100) surface: A periodic density functional theory study. Journal of Chemical Physics, 2003, 119, 509-514.	1.2	30
2383	Effect of composition on vacancy mediated diffusion in random binary alloys: First principles study of the Si1â^'xGex system. Journal of Applied Physics, 2003, 94, 174-185.	1.1	40

#	Article	IF	Citations
2384	Vibrational modes and electronic properties of nitrogen defects in silicon. Physical Review B, 2003, 67, .	1.1	83
2385	Phase stability and intrinsic stacking faults in aluminum under pressure. Physical Review B, 2003, 67, .	1.1	12
2386	Design of Shallow Donor Levels in Diamond by Isovalent-Donor Coupling. Physical Review Letters, 2003, 91, 126406.	2.9	79
2387	RobustAb InitioCalculation of Condensed Matter: Transparent Convergence through Semicardinal Multiresolution Analysis. Physical Review Letters, 2003, 90, 216402.	2.9	11
2388	A computational study of the surface structure and reactivity of calcium fluoride. Journal of Materials Chemistry, 2003, 13, 93-101.	6.7	96
2389	Formation of thec(1Ã—1)Cu monolayer on CaO(100):â€ƒA theoretical study. Physical Review B, 2003, 68, .	1.1	6
2390	Ferromagnetic materials in the zinc-blende structure. Physical Review B, 2003, 68, .	1.1	128
2391	Electronic structure calculations of intrinsic and extrinsic hydrogen point defects inKH2PO4. Physical Review B, 2003, 68, .	1.1	43
2392	Electron- or Hole-Assisted Reactions of H Defects in Hydrogen-Bonded KDP. Physical Review Letters, 2003, 91, 015505.	2.9	106
2393	First-principles calculations of Fe on GaAs(100). Physical Review B, 2003, 67, .	1.1	65
2394	Ruderman-Kittel-Kasuya-Yosidaâ€“like Ferromagnetism inMnxGe1âˆ’x. Physical Review Letters, 2003, 90, 047204.	2.9	148
2395	Layer Spacings in Coherently Strained Epitaxial Metal Films. Physical Review Letters, 2003, 90, 216105.	2.9	35
2396	Linear monatomic wires stabilized by alloying:Ab initiodensity functional calculations. Physical Review B, 2003, 67, .	1.1	34
2397	Theoretical investigation of the solubility in(MxM2âˆ’xâ€²)AlC(MandMâ€²=Ti,V,Cr). Physical Review B, 2003, 68, .	1.1	87
2398	Single adatom adsorption and diffusion onSi(111)âˆ’(7Ã—7)surfaces:â€ƒScanning tunneling microscopy and first-principles calculations. Physical Review B, 2003, 67, .	1.1	78
2399	Structure and motion of basal dislocations in silicon carbide. Physical Review B, 2003, 68, .	1.1	92
2400	Intra-atomic noncollinear magnetism and the magnetic structures of antiferromagnetic FeMn. Physical Review B, 2003, 67, .	1.1	35
2401	Cubic polytype inclusions in 4Hâ€“SiC. Journal of Applied Physics, 2003, 93, 1577-1585.	1.1	86

#	Article	IF	Citations
2402	Identification of boron clusters and boron-interstitial clusters in silicon. Physical Review B, 2003, 67, .	1.1	38
2403	Displacement of surface arsenic atoms by insertion of oxygen atoms into Asâ€“Ga backbonds. Journal of Chemical Physics, 2003, 119, 9191-9198.	1.2	10
2404	Atomic ordering inInxGa1â^'xAsalloy thin films:â€, Action of surfactants. Physical Review B, 2003, 68, .	1.1	9
2405	Why Do Grain Boundaries Exhibit Finite Facet Lengths?. Physical Review Letters, 2003, 90, 246102.	2.9	34
2406	A density functional theory investigation of 1,1-diamino-2,2-dinitroethylene dimers and crystal. Journal of Chemical Physics, 2003, 119, 10247-10255.	1.2	53
2407	Single impurities in insulators:â€ƒAb initiostudy of Fe-dopedSrTiO3. Physical Review B, 2003, 67, .	1.1	67
2408	Uniaxial phase transition in Si:Ab initiocalculations. Physical Review B, 2003, 67, .	1.1	16
2409	Voltage profile, structural prediction, and electronic calculations forMgxMo6S8. Physical Review B, 2003, 67, .	1.1	22
2410	Ab initiostudies of quasi-one-dimensional pentagon and hexagon ice nanotubes. Journal of Chemical Physics, 2003, 118, 3913-3916.	1.2	55
2411	Local lattice relaxations in random metallic alloys: Effective tetrahedron model and supercell approach. Physical Review B, 2003, 67, .	1.1	97
2412	Soliton effects in dangling-bond wires on Si(001). Physical Review B, 2003, 68, .	1.1	12
2413	Embedded-atom-method tantalum potential developed by the force-matching method. Physical Review B, 2003, 67, .	1.1	93
2414	Local density of states in three-dimensional photonic crystals: Calculation and enhancement effects. Physical Review B, 2003, 67, .	1.1	52
2415	Electromechanical effects in carbon nanotubes:Ab initioand analytical tight-binding calculations. Physical Review B, 2003, 67, .	1.1	64
2416	Trapping with anisotropic diffusion in an applied field: H+ in Mg-doped GaN. Journal of Applied Physics, 2003, 93, 2608-2617.	1.1	9
2417	Substitutional oxygen-nitrogen pair in diamond. Physical Review B, 2003, 67, .	1.1	15
2418	Overlayer and superlattice studies of metal/ceramic interfaces: Fe/TiC. Journal of Applied Physics, 2003, 93, 6876-6878.	1.1	19
2419	First-principles study of the interaction of hydrogen with GaAs(001). Physical Review B, 2003, 68, .	1.1	5

#	Article	IF	Citations
2420	Decay Kinetic Properties of Atoms in Photonic Crystals with Absolute Gaps. Physical Review Letters, 2003, 91, 113904.	2.9	82
2421	Polarizability and dielectric constant in density-functional supercell calculations with discretek-point samplings. Physical Review B, 2003, 68, .	1.1	34
2422	Reconstruction and magnetic structure of ultrathinÎ³-Fe films on Cu(111). Physical Review B, 2003, 67, .	1.1	17
2423	Theoretical analysis of clock-reconstructed PdCu surface alloy. Physical Review B, 2003, 67, .	1.1	10
2424	Electronic and magnetic properties of MnN versus MnAs. Applied Physics Letters, 2003, 82, 766-768.	1.5	44
2425	Vibrational modes of sulfur defects in GaP. Physical Review B, 2003, 68, .	1.1	1
2426	Stacking faults in3Câ^',â€,4Hâ^',and6Hâ^'SiCpolytypes investigated by anab initiosupercell method. Physical Review B, 2003, 67, .	1.1	148
2427	Quantum Mechanical Study of Clean and H-Covered Î±-MoO3(100) Surface. Journal of Theoretical and Computational Chemistry, 2003, 02, 245-256.	1.8	2
2428	Ab initioinvestigation of the electronic structure and bonding properties of the layered ternary compound Ti3SiC2at high pressure. Journal of Physics Condensed Matter, 2003, 15, 1983-1991.	0.7	35
2429	Iron Surfaces: Pathways to Interfaces. Surface Review and Letters, 2003, 10, 169-174.	0.5	9
2430	Optical and electrical activity of boron interstitial defects in Si. Journal of Physics Condensed Matter, 2003, 15, S2851-S2858.	0.7	10
2431	Elastic constants and chemical bonding of LaNi5and LaNi5H7by first principles calculations. Journal of Physics Condensed Matter, 2003, 15, 6549-6561.	0.7	23
2432	Interface structure and stabilization of metastable B2-FeSi/Si(111) studied with low-energy electron diffraction and density functional theory. Journal of Physics Condensed Matter, 2003, 15, 5207-5221.	0.7	22
2433	First Principles Studies on the Interaction of a Hydrogen Atom with a Single-Walled Carbon Nanotube. Japanese Journal of Applied Physics, 2003, 42, 4626-4629.	0.8	14
2434	An introduction to first-principles simulations of extended systems. Handbook of Numerical Analysis, 2003, 10, 377-451.	0.9	0
2435	Studies of boronâ€“interstitial clusters in Si. Journal of Physics Condensed Matter, 2003, 15, 4967-4977.	0.7	17
2436	Vacancy formation enthalpy at high pressures in tantalum. Journal of Physics Condensed Matter, 2003, 15, 855-861.	0.7	24
2437	A comparative theoretical study of the Peierls distortion in type-II alkaline-doped clathrates. Europhysics Letters, 2003, 64, 757-762.	0.7	18

#	Article	IF	Citations
2438	Structural relaxations, vibrational dynamics and thermodynamics of vicinal surfaces. Journal of Physics Condensed Matter, 2003, 15, S3197-S3226.	0.7	27
2439	Comparison of density functional theory methods as applied to compound semiconductor-oxide interfaces: Slab versus cluster models. Journal of Vacuum Science & Technology an Official Journal of the American Vacuum Society B, Microelectronics Processing and Phenomena, 2003, 21, 1908.	1.6	10
2440	On the stability of Met-Car analogue clusters in the solid state. Journal of Physics Condensed Matter, 2003, 15, 4341-4348.	0.7	2
2441	A coherent relation between structure and conduction of infinite atomic wires. Nanotechnology, 2003, 14, 299-303.	1.3	7
2442	Germaniumâ€“hydrogen pairs in silicon. Journal of Physics Condensed Matter, 2003, 15, S2803-S2807.	0.7	7
2443	Comparison between classical potentials andab initiomethods for silicon under large shear. Journal of Physics Condensed Matter, 2003, 15, 6943-6953.	0.7	41
2444	Co-existence of ferroelectricity and ferromagnetism in 1.4 nm SrBi2Ta2O11film. Journal of Physics Condensed Matter, 2003, 15, 7901-7915.	0.7	7
2445	Small self-interstitial clusters in GaAs. Journal of Physics Condensed Matter, 2003, 15, 843-853.	0.7	27
2446	Electronic states of Si nanostructures in a strong electric field: bandgap ionization and Stark ladders. Semiconductor Science and Technology, 2003, 18, 330-333.	1.0	2
2447	First-principles molecular dynamics study of the stretching frequencies of hydrogen molecules in carbon nanotubes. New Journal of Physics, 2003, 5, 124-124.	1.2	12
2448	Ab initio study of the site ordering in the GaSb Î²-Sn phase. Europhysics Letters, 2003, 63, 545-548.	0.7	1
2449	The effect of radiation damage on local structure in the crystalline fraction of ZrSiO₄: Investigating the²⁹Si NMR response to pressure in zircon and reidite. American Mineralogist, 2003, 88, 1663-1667.	0.9	61
2450	Density Functional Study of the Effect of SiH₄/GeH₄ and Si(001)/Ge(001) on Gasâ€Surface Reactivity during Initial Dissociative Adsorption. Journal of the Chinese Chemical Society, 2003, 50, 611-620.	0.8	1
2451	Stable Hydrogen Configurations between Graphite Layers. Journal of the Physical Society of Japan, 2003, 72, 1867-1870.	0.7	22
2452	Structure, metal-insulator transitions, and magnetic properties of FeO at high pressures. American Mineralogist, 2003, 88, 257-261.	0.9	68
2453	First-Principles Band Calculation of TiO₂ with Brookite Structure. Electrochemistry, 2004, 72, 694-696.	0.6	4
2454	First-principles studies of the structural and electronic properties of poly-para-phenylene vinylene. Journal of Physics Condensed Matter, 2004, 16, 8609-8620.	0.7	33
2455	First principles force field for metallic tantalum. Modelling and Simulation in Materials Science and Engineering, 2004, 12, S445-S459.	0.8	34

#	Article	IF	Citations
2456	Structural Stability and the Correlation of Lattice Constant versus Tantalum Concentration of the Ag-Based Fcc Solid Solutions Studied by Molecular Dynamics Simulation. Japanese Journal of Applied Physics, 2004, 43, 2589-2593.	0.8	3
2457	Reliability of analytical potentials for point-defect simulation in GaAs. Journal of Physics Condensed Matter, 2004, 16, 3923-3932.	0.7	15
2458	Ab Initio Calculations for the BaTiO 3 (001) Surface Structure. Chinese Physics Letters, 2004, 21, 825-828.	1.3	3
2459	First-principles study of binary transition-metal clusters and alloys. Journal of Physics Condensed Matter, 2004, 16, S2263-S2272.	0.7	24
2460	Comparative study of metastable phase formation in the immiscible Cuâ€“W system byab initiocalculation andn-body potential. Journal of Physics Condensed Matter, 2004, 16, 5251-5258.	0.7	18
2461	Selenium passivation of GaAs(001): a combined experimental and theoretical study. Journal of Physics Condensed Matter, 2004, 16, 2187-2206.	0.7	20
2462	The interstitial CiOi defect in bulk Si and Si1ÂxGex. Journal of Physics Condensed Matter, 2004, 16, 8545-8555.	0.7	5
2463	Atomic and Electronic Structures of Zr Atomic Chains. Chinese Physics Letters, 2004, 21, 1791-1794.	1.3	8
2464	Electron density of periodic systems derived from non-orthogonal localized orbitals. Journal of Physics Condensed Matter, 2004, 16, 2575-2584.	0.7	9
2465	Properties of intrinsic di-interstitials in GaAs. Journal of Physics Condensed Matter, 2004, 16, 8991-9000.	0.7	20
2466	Enhanced dopant solubility in strained silicon. Journal of Physics Condensed Matter, 2004, 16, 9117-9126.	0.7	4
2467	Reversible short-range electrostatic imaging in frequency modulation atomic force microscopy on metallic surfaces. Nanotechnology, 2004, 15, S55-S59.	1.3	6
2468	Electromechanical and Chemical Sensing at the Nanoscale: Molecular Modeling Applications. Molecular Simulation, 2004, 30, 191-198.	0.9	6
2469	First-principle study of polytype structures of 1:1 dioctahedral phyllosilicates. American Mineralogist, 2004, 89, 1581-1585.	0.9	34
2470	Ab initiomelting curve of copper by the phase coexistence approach. Journal of Chemical Physics, 2004, 120, 2872-2878.	1.2	68
2471	An ab initio study of the relative stabilities and equations of state of Fe3S polymorphs. Mineralogical Magazine, 2004, 68, 813-817.	0.6	6
2472	First-principles investigation of the multilayer relaxation of stepped Cu surfaces. Physical Review B, 2004, 69, .	1.1	35
2473	Comparison of predicted ferromagnetic tendencies of Mn substituting the Ga site in IIIâ€“Vâ€™s and in Iâ€“IIIâ€“VI2 chalcopyrite semiconductors. Applied Physics Letters, 2004, 84, 3753-3755.	1.5	32

#	Article	IF	Citations
2474	First-principles study of the origin of retarded diffusion of boron in silicon in the presence of germanium. Physical Review B, 2004, 70, .	1.1	17
2475	Stability of reducedV2O5(001)surfaces. Physical Review B, 2004, 70, .	1.1	119
2476	Adsorption of sulfur onTiC(001):â€ƒPhotoemission and first-principles studies. Physical Review B, 2004, 69, .	1.1	30
2477	Rotation, translation, charge transfer, and electronic structure ofC60on Cu(111) surface. Physical Review B, 2004, 69, .	1.1	89
2478	Ab initiocalculation of optical second harmonic generation at the rutileTiO2(110)surface. Physical Review B, 2004, 70, .	1.1	10
2479	Electronic structures of rocksalt, litharge, and herzenbergite SnO by density functional theory. Physical Review B, 2004, 70, .	1.1	114
2480	Structural and vibrational properties of {N,N} pairs and {N,H} complexes in Si. Physical Review B, 2004, 69, .	1.1	7
2481	Carrier-mediated ferromagnetism in N codoped (Zn,Mn)O(101Â¯0)thin films. Physical Review B, 2004, 70, .	1.1	112
2482	Ferromagnetism and carrier confinement inMnâ•Gedigital alloys. Physical Review B, 2004, 70, .	1.1	24
2483	Self-energy of zone-boundary phonons in germanium:â€,â€,Ab initiocalculations versus neutron spin-echo measurements. Physical Review B, 2004, 69, .	1.1	20
2484	Electronic structure and ferromagnetism of Mn-substitutedCuAlS2,CuGaS2,CuInS2,CuGaSe2,andCuGaTe2. Physical Review B, 2004, 69, .	1.1	50
2485	Electronic and structural properties of germanium self-interstitials. Physical Review B, 2004, 70, .	1.1	55
2486	Nested Fermi surfaces, optical peaks, and laser-induced structural transition in Al. Physical Review B, 2004, 69, .	1.1	5
2487	SrTiO3(001) thin films on MgO(001): A theoretical study. Physical Review B, 2004, 69, .	1.1	18
2488	Potential-energy surfaces for excited states in extended systems. Journal of Chemical Physics, 2004, 120, 4593-4602.	1.2	103
2489	Effects of alloying, ordering, and strain on the exchange parameters of II-VI dilute magnetic semiconductors. Physical Review B, 2004, 70, .	1.1	7
2490	Structural evolution of theCuGaO2delafossite under high pressure. Physical Review B, 2004, 69, .	1.1	64
2491	First-principles simulations of STM images:â€,From tunneling to the contact regime. Physical Review B, 2004, 70, .	1.1	87

#	Article	IF	Citations
2492	Reversible scaling simulations of the melting transition in silicon. Physical Review B, 2004, 69, .	1.1	19
2493	Magnetism ofFeâˆ'Conanostructures on flat and steppedW(110)surfaces: Effects of dimensionality and substrate. Physical Review B, 2004, 70, .	1.1	22
2494	Surface energetics and structure of the Ge wetting layer on Si(100). Physical Review B, 2004, 70, .	1.1	58
2495	Self-trapping and diffusion of hydrogen in Nb and Ta from first principles. Physical Review B, 2004, 70, .	1.1	45
2496	Sample dependence of the structural, vibrational, and electronic properties ofaâˆ'Si:H:â€ƒA density-functional-based tight-binding study. Physical Review B, 2004, 70, .	1.1	20
2497	Optical and electrical properties of vanadium and erbium in4H-SiC. Physical Review B, 2004, 69, .	1.1	17
2498	Highlyn-doped silicon: Deactivating defects of donors. Physical Review B, 2004, 70, .	1.1	34
2499	Thermodynamics of impurities in semiconductors. Physical Review B, 2004, 70, .	1.1	62
2500	Lateral interactions between oxygen atoms adsorbed on platinum (111) by first principles. Molecular Physics, 2004, 102, 273-279.	0.8	33
2501	Atomic structure of B-related defects and B diffusion in Si predoped with P impurities. Physical Review B, 2004, 69, .	1.1	5
2502	Molecular Chemisorption as the Theoretically Preferred Pathway for Water Adsorption on Ideal RutileTiO2(110). Physical Review Letters, 2004, 93, 086105.	2.9	156
2503	When Langmuir Is Too Simple:H2Dissociation on Pd(111) at High Coverage. Physical Review Letters, 2004, 93, 146103.	2.9	81
2504	Changes in the Lattice Constants of Thin-Film LiCoO[sub 2] Cathodes at the 4.2 V Charged State. Journal of the Electrochemical Society, 2004, 151, A1063.	1.3	30
2505	A finite temperature linear tetrahedron method for electronic structure calculations of periodic systems. Journal of Chemical Physics, 2004, 121, 2466.	1.2	4
2506	Antiferromagnetic Coupling Driven by Bond Length Contraction near theGa1âˆ'xMnxNFilm Surface. Physical Review Letters, 2004, 93, 155501.	2.9	56
2507	Fluctuating Lattice Constants of Indium under High Pressure. Physical Review Letters, 2004, 92, 195501.	2.9	22
2508	Isolated nickel impurities in diamond: A microscopic model for the electrically active centers. Applied Physics Letters, 2004, 84, 720-722.	1.5	28
2509	New spintronic superlattices composed of half-metallic compounds with zinc-blende structure. Journal of Physics Condensed Matter, 2004, 16, S5669-S5676.	0.7	10

#	Article	IF	Citations
2510	Structure and vibrational spectra of carbon clusters in SiC. Physical Review B, 2004, 70, .	1.1	50
2511	The interaction of oxygen with TiC(001): Photoemission and first-principles studies. Journal of Chemical Physics, 2004, 121, 465.	1.2	58
2512	N vacancy diffusion and trapping in Mg-doped wurtzite GaN. Journal of Applied Physics, 2004, 96, 2015-2022.	1.1	22
2513	Electronic structure of crystalline copper phthalocyanine. Journal of Chemical Physics, 2004, 121, 1883-1889.	1.2	97
2514	Electronic structures ofA- andB-type DNA crystals. Physical Review E, 2004, 70, 011913.	0.8	41
2515	First Principles Calculation of Anomalous Hall Conductivity in Ferromagnetic bcc Fe. Physical Review Letters, 2004, 92, 037204.	2.9	715
2516	Adatom Ascending at Step Edges and Faceting on fcc Metal (110) Surfaces. Physical Review Letters, 2004, 92, 106102.	2.9	52
2517	Transferable local pseudopotentials derived via inversion of the Kohn-Sham equations in a bulk environment. Physical Review B, 2004, 69, .	1.1	77
2518	Electronic properties of metal-induced gap states at insulator/metal interfaces: Dependence on the alkali halide and the possibility of excitonic mechanism of superconductivity. Physical Review B, 2004, 69, .	1.1	13
2519	Vibrational properties of hydrogen atom adsorbed on Cu(111) and on Ir(111) surfaces. Journal of Applied Physics, 2004, 96, 5020-5025.	1.1	20
2520	Coexistence of localized magnetic moment and opposite-spin itinerant electrons in MnC. Physical Review B, 2004, 70, .	1.1	23
2521	Electronic properties and bonding configuration at the TiN/MgO(001) interface. Physical Review B, 2004, 69, .	1.1	20
2522	Interaction of neutral vacancies and interstitials with theSi(001)surface. Physical Review B, 2004, 70, .	1.1	13
2523	Carbon antisite clusters in SiC: A possible pathway to theDIIcenter. Physical Review B, 2004, 69, .	1.1	39
2524	Structural and electronic properties ofSi3P4. Physical Review B, 2004, 69, .	1.1	31
2525	Guest displacement in silicon clathrates. Physical Review B, 2004, 69, .	1.1	36
2526	Finite-size scaling as a cure for supercell approximation errors in calculations of neutral native defects inInP. Physical Review B, 2004, 70, .	1.1	62
2527	Diffusion of Fe atoms on W surfaces andFeâˆ•Wfilms and along surface steps. Physical Review B, 2004, 70, .	1.1	41

#	Article	IF	Citations
2528	Hydrogen-bridge bonding on semiconductor surfaces:â€ƒDensity-functional calculations. Physical Review B, 2004, 70, .	1.1	13
2529	Energetics ofSradatom interactions on theMo(112)surface. Physical Review B, 2004, 69, .	1.1	22
2530	Effect of semicore orbitals on the electronic band gaps of Si, Ge, and GaAs within the GW approximation. Physical Review B, 2004, 69, .	1.1	125
2531	Electronic structure of the transition-metal dicyanamidesM[N(CN)2]2(M=Mn,Fe,Co,Ni,Cu). Physical Review B, 2004, 69, .	1.1	10
2532	Calculation of deep states in SiGe alloys:â€ƒInterstitial carbon-oxygen complexes. Physical Review B, 2004, 70, .	1.1	19
2533	Density functional theory study of H and H2 interacting with NiAl(110). Journal of Chemical Physics, 2004, 121, 751-760.	1.2	44
2534	Ozone adsorption on carbon nanotubes: The role of Stoneâ€“Wales defects. Journal of Chemical Physics, 2004, 120, 7147-7152.	1.2	91
2535	Mixed-basis cluster expansion for thermodynamics of bcc alloys. Physical Review B, 2004, 70, .	1.1	95
2536	Metastability of an immiscible Cu-Mo system calculated from first-principles and a derivedn-body potential. Physical Review B, 2004, 69, .	1.1	18
2537	Magnetic properties of polymerizedC60: The influence of defects and hydrogen. Physical Review B, 2004, 70, .	1.1	71
2538	Lattice dynamics and thermal properties ofCaWO4. Physical Review B, 2004, 70, .	1.1	51
2539	Periodic density functional study on structural and vibrational properties of vanadium oxide aggregates. Physical Review B, 2004, 69, .	1.1	76
2540	Two-phonon infrared absorption spectra of germanium and silicon calculated from first principles. Physical Review B, 2004, 69, .	1.1	18
2541	Atomistic modeling and thermodynamic interpretation of the bridging phenomenon observed in the Co-Au system. Physical Review B, 2004, 70, .	1.1	7
2542	First-principles study of low-index surfaces of lead. Physical Review B, 2004, 70, .	1.1	57
2543	Microchemical inhomogeneity of multicomponent systems and its evaluation from interatomic potentials. Physical Review B, 2004, 69, .	1.1	7
2544	Trend for the multilayer relaxation sequence of stepped Cu surfaces. Physical Review B, 2004, 70, .	1.1	19
2545	Dielectric-screening properties and Coulomb pseudopotentialÎ¼*forMgB2. Physical Review B, 2004, 70, .	1.1	24

#	Article	IF	Citations
2546	Oxygen adsorption on Cu(100):â€ƒFirst-principles pseudopotential calculations. Physical Review B, 2004, 70, .	1.1	52
2547	Mg adsorption on Si(001) surface from first principles. Physical Review B, 2004, 69, .	1.1	11
2548	Chiral symmetry of double-walled carbon nanotubes detected in first-principles optical absorption spectra. Physical Review B, 2004, 69, .	1.1	17
2549	Calculation of phonon spectra to predict the high-pressure metastable phase in an equilibrium immiscible Cuâ€“Ta system. Applied Physics Letters, 2004, 85, 1517-1519.	1.5	7
2550	First-principles study of B2CN crystals deduced from the diamond structure. Journal of Physics Condensed Matter, 2004, 16, 8131-8138.	0.7	22
2551	First-principles study of magnetism in (112Ì„0)â€‰Zn1â^'xMnxO thin film. Applied Physics Letters, 2004, 84, 4170-4172.	1.5	27
2552	Energetic stabilities and the bonding mechanism of ZnO{0001}/Pd(111) interfaces. Physical Review B, 2004, 69, .	1.1	23
2553	Hole-Mediated Stabilization of Cubic GaN. Physical Review Letters, 2004, 93, 216401.	2.9	32
2554	Theoretical study of the formation, evolution, and breaking of gold nanowires. Physical Review B, 2004, 69, .	1.1	110
2555	Tantalum-fullerene clusters:â€ƒA first-principles study of static properties and dynamical behavior. Physical Review B, 2004, 70, .	1.1	16
2556	Theoretical study of strain-induced ordering in cubicInxGa1â^'xNepitaxial layers. Physical Review B, 2004, 69, .	1.1	13
2557	Structure, electronic density of states and electric field gradients of icosahedral AlCuFe: Anab initiostudy of the original and a modified Cockayne model. Physical Review B, 2004, 69, .	1.1	15
2558	Ternary half-metallics and related binary compounds:â€ƒStoichiometry, surface states, and spin. Physical Review B, 2004, 70, .	1.1	41
2559	Molecular adsorption on the surface of strongly correlated transition-metal oxides: A case study for CO/NiO(100). Physical Review B, 2004, 69, .	1.1	216
2560	Initial growth of Ba on Si(001). Physical Review B, 2004, 69, .	1.1	12
2561	Structure and diffusion of interstitial boron pairs in silicon. Physical Review B, 2004, 69, .	1.1	3
2562	First-principles study ofNaAlH4andNa3AlH6complex hydrides. Physical Review B, 2004, 70, .	1.1	80
2563	Contrasting Growth Modes of Mn on Ge(100) and Ge(111) Surfaces: Subsurface Segregation versus Intermixing. Physical Review Letters, 2004, 93, 126102.	2.9	60

#	Article	IF	Citations
2564	The effect of Cr doping on Li ion diffusion in LiFePO4from first principles investigations and Monte Carlo simulations. Journal of Physics Condensed Matter, 2004, 16, 2265-2272.	0.7	79
2565	Dimer-Anticorrelation-Induced Stabilization of Adsorbate Clustering on theSi(100)â˜'(2Ã—1)Surface. Physical Review Letters, 2004, 92, 096103.	2.9	25
2566	Bonding and classification of nanolayered ternary carbides. Physical Review B, 2004, 70, .	1.1	212
2567	First-principles equation of state and phase stability for theNiâ˜'Alsystem under high pressures. Physical Review B, 2004, 70, .	1.1	20
2568	Experimental and theoretical electronic structure determination of theÎ²â˜'SiC(001)c(4Ã—2)surface reconstruction. Physical Review B, 2004, 69, .	1.1	14
2569	Evidence from first principles calculations for a bent CO2 intermediate in the oxidation of carbon monoxide on the Cu (110) surface. Journal of Chemical Physics, 2004, 121, 4339-4345.	1.2	8
2570	Wetting of TiC and TiN by metals. Physical Review B, 2004, 69, .	1.1	98
2571	Anomalous transformations in ice VIII. Physical Review B, 2004, 70, .	1.1	21
2572	Electron delocalization at the hybrid aromatic-thiolâ•Cu(100)interface. Physical Review B, 2004, 70, .	1.1	13
2573	Hydrogen-related photoluminescent centers in SiC. Physical Review B, 2004, 70, .	1.1	2
2574	Carbon inSixGe1â˜'x:Anab initioinvestigation. Physical Review B, 2004, 69, .	1.1	8
2575	Structural stability and magnetic properties of metastable Fe-Cu alloys studied byab initiocalculations and molecular dynamics simulations. Physical Review B, 2004, 69, .	1.1	17
2576	First-principles calculation of the structure and magnetic phases of hematite. Physical Review B, 2004, 69, .	1.1	402
2577	First-principles extrapolation method for accurate CO adsorption energies on metal surfaces. Physical Review B, 2004, 69, .	1.1	204
2578	Electronic structure ofGa84cluster compounds. Physical Review B, 2004, 70, .	1.1	15
2579	Structure and dynamics of oxygen adsorbed on Ag(100) vicinal surfaces. Physical Review B, 2004, 69, .	1.1	32
2580	Diffusivity of native defects in GaN. Physical Review B, 2004, 69, .	1.1	265
2581	Site selectivity in chemisorption of C on Pd(211). Physical Review B, 2004, 70, .	1.1	16

#	Article	IF	Citations
2582	Theoretical prediction of the structure and properties of Sn3N4. Journal of Applied Physics, 2004, 96, 4015-4017.	1.1	16
2583	Initial stages ofPtgrowth onGe(001)studied by scanning tunneling microscopy and density functional theory. Physical Review B, 2004, 70, .	1.1	26
2584	A density-functional theory investigation of 3-nitro-1,2,4-triazole-5-one dimers and crystal. Journal of Chemical Physics, 2004, 121, 12523.	1.2	24
2585	Theoretical study ofGa-based nanowires and the interaction ofGawith single-wall carbon nanotubes. Physical Review B, 2004, 70, .	1.1	12
2586	Ab initiocalculation of band-gap renormalization in highly excited GaAs. Physical Review B, 2004, 69, .	1.1	45
2587	SrTiO3âˆ•Si(001)epitaxial interface: A density functional theory study. Physical Review B, 2004, 70, .	1.1	32
2588	Correlation of magnetic moment versus spacing distance of metastable fcc structured iron. Applied Physics Letters, 2004, 84, 3627-3629.	1.5	46
2589	Bi1â^'xSbxunder high pressure: Effect of alloying on the incommensurate Bi-III type composite structure. Physical Review B, 2004, 69, .	1.1	18
2590	Resistivity of hydrogen-loaded Fe/V and Mo/V (100) superlattices: The role of vanadium expansion. Physical Review B, 2004, 69, .	1.1	12
2591	Calculations of electronic structure ofGe44Mn2Ba8andGe42Mn4Ba8clathrates. Physical Review B, 2004, 70, .	1.1	5
2592	Surface morphology and ionization potentials of polar semiconductors: The case of GaAs. Physical Review B, 2004, 69, .	1.1	14
2593	Quasiparticle band structures and optical spectra of$\hat{1}^2$-cristobaliteSiO2. Physical Review B, 2004, 69, .	1.1	38
2594	Phase diagram of oxygen adsorbed on platinum (111) by first-principles investigation. Physical Review B, 2004, 70, .	1.1	103
2595	Interstitial nitrogen and its complexes in diamond. Physical Review B, 2004, 70, .	1.1	36
2596	Structure and morphology of the As-rich and the stoichiometric GaAs(114)A surface. Journal of Applied Physics, 2004, 95, 7645-7654.	1.1	11
2597	Structure and stability of rare-earth and transition-metal oxides. Physical Review B, 2004, 69, .	1.1	114
2598	First-principles study of adsorption of methanethiol onCo(0001). Physical Review B, 2004, 70, .	1.1	19
2599	Density-functional theory calculations of the adsorption of Cl at perfect and defective Ag(111) surfaces. Physical Review B, 2004, 69, .	1.1	25

#	Article	IF	Citations
2600	Structural and electronic properties of3dtransition metal impurities in silicon carbide. Physical Review B, 2004, 69, .	1.1	52
2601	Origin of vacancy and interstitial stabilization at the amorphous-crystalline Si interface. Journal of Applied Physics, 2004, 96, 3334-3338.	1.1	6
2602	Orbital ordering, Jahn-Teller distortion, and resonant x-ray scattering in KCuF3. Physical Review B, 2004, 70, .	1.1	56
2603	Ferromagnetism and stability of half-metallic MnSb and MnBi in the strained zinc-blende structure:â€ƒPredictions from full potential and pseudopotential calculations. Physical Review B, 2004, 69, .	1.1	57
2604	Supersoft silicides:Ab initiostudy of (001)TSi surfaces and (001) Si/TSi (T=Fe, Co, and Ni) interfaces. Physical Review B, 2004, 70, .	1.1	14
2605	The influence of bond flexibility and molecular size on the chemically selective bonding of In2O and Ga2O on GaAs(001)-c(2Ã—8)/(2Ã—4). Journal of Chemical Physics, 2004, 120, 5745-5754.	1.2	16
2606	Interaction between interstitials and arsenic-vacancy complexes in crystalline silicon. Applied Physics Letters, 2004, 85, 4935-4937.	1.5	15
2607	Low work function of the (1000) Ca2N surface. Journal of Applied Physics, 2004, 96, 1751-1753.	1.1	21
2608	â€œMigration energyâ€•for impurity diffusion in crystalline solids: A closer look. Journal of Applied Physics, 2004, 96, 7095-7107.	1.1	10
2609	Transformation strain by chemical disordering in silicon carbide. Journal of Applied Physics, 2004, 95, 6466-6469.	1.1	14
2610	Crystalline silicon oxycarbide: Is there a native oxide for silicon carbide?. Applied Physics Letters, 2004, 84, 4845-4847.	1.5	18
2611	The lattice location of Ni in diamond: a theoretical study. Journal of Physics Condensed Matter, 2004, 16, 4567-4578.	0.7	26
2612	Quantum mechanical study of Al/Si disorder in leucite and bicchulite. Mineralogical Magazine, 2004, 68, 819-824.	0.6	9
2613	Anisotropically Nanostructured Silicon: A First-Principle Approach.. Materials Research Society Symposia Proceedings, 2004, 832, 93.	0.1	0
2614	Density-of-states of crystalline 2,-bithiophene:ab initioanalysis and comparison with inelastic neutron scattering response. Journal of Physics Condensed Matter, 2004, 16, 7385-7396.	0.7	16
2615	Anharmonicity in the Vibrational Modes Associated with H-H, N-H, O-H, and C-H bonds. Materials Research Society Symposia Proceedings, 2004, 813, 361.	0.1	3
2616	Theory for the Potential Shift for OH[sub ads] Formation on the Pt Skin on Pt[sub 3]Cr(111) in Acid. Journal of the Electrochemical Society, 2004, 151, E85.	1.3	57
2617	The viability of 0.3 nm diameter carbon nanotubes. Nanotechnology, 2004, 15, 1000-1003.	1.3	34

#	Article	IF	Citations
2618	Carbon allotropes and strong nanotube bundles. Journal of Physics Condensed Matter, 2004, 16, 9083-9091.	0.7	19
2619	Density Functional Based Modelling of 30Â° Partial Dislocations in SiC. Materials Science Forum, 2004, 457-460, 453-456.	0.3	1
2620	Behavior of Si Interstitials and Boron-Interstitial Pairs at the Si/SiO2 Interface. Materials Research Society Symposia Proceedings, 2004, 810, 398.	0.1	0
2621	The thermodynamic stability of three near-degenerate phases of platinum dioxide. Materials Research Society Symposia Proceedings, 2004, 848, 377.	0.1	1
2622	Vibrational Spectra of Nitrogen-Oxygen Defects in Nitrogen Doped Silicon using Density Functional Theory. Materials Research Society Symposia Proceedings, 2004, 810, 380.	0.1	0
2623	Electrode Potential-Dependent Stages in OH[sub ads] Formation on the Pt[sub 3]Cr Alloy (111) Surface. Journal of the Electrochemical Society, 2004, 151, E340.	1.3	35
2624	Crystallographic properties of the calcium phosphate mineral, brushite, by means of First Principles calculations. American Mineralogist, 2004, 89, 307-313.	0.9	32
2625	Atomic and electronic structures of the lattice mismatched metalâ€“ceramic interface. Journal of Physics Condensed Matter, 2004, 16, 5781-5790.	0.7	13
2626	Convergence problems of Coulomb and multipole sums in crystals. Physics-Uspekhi, 2004, 47, 965-990.	0.8	11
2627	Ab initiocalculations of doping mechanisms in SrTiO3. Modelling and Simulation in Materials Science and Engineering, 2004, 12, 79-90.	0.8	21
2628	The local density approximation limit of the momentum density and the Compton profiles of Al. Journal of Physics Condensed Matter, 2004, 16, 7363-7378.	0.7	9
2629	Calculated properties of a {113} planar vacancy aggregate in Si. Journal of Physics Condensed Matter, 2004, 16, 3311-3318.	0.7	3
2630	Ab initiostudies of strained wurtzite GaN surfaces. Journal of Physics Condensed Matter, 2004, 16, 531-542.	0.7	7
2631	Analysis of shear deformations in Al and Cu: empirical potentials versus density functional theory. Modelling and Simulation in Materials Science and Engineering, 2004, 12, 1017-1029.	0.8	36
2632	COMPLEX DONORS IN NITROGEN-DOPED DIAMOND. International Journal of Nanoscience, 2004, 03, 455-461.	0.4	1
2633	A DENSITY FUNCTIONAL THEORY INVESTIGATION ON THE TAUTOMERS AND CRYSTAL OF 2-DIAZO-4,6-DINITROPHENOL. Journal of Theoretical and Computational Chemistry, 2004, 03, 599-607.	1.8	4
2634	Study of the Peierls distortion in Na8@Si-34 under pressure. High Pressure Research, 2004, 24, 139-147.	0.4	3
2635	The Pressure Dependence of Solid Boron. Molecular Simulation, 2004, 30, 935-939.	0.9	5

#	Article	IF	Citations
2636	Donor and acceptor states in diamond. Diamond and Related Materials, 2004, 13, 684-690.	1.8	129
2637	First-principles calculations of the stability and local structure of Â-sialon ceramics on the line Si3N4â€“Â½Ca3N2:3AlN. Journal of Physics Condensed Matter, 2004, 16, 2931-2939.	0.7	7
2638	First-principles calculations of the atomistic behaviors in Ni/Al [001] and Al/Ni [001] system. , 2004, , .		0
2639	Building a better unit cell: application to the Ag(111)/GaAs(110) system. Journal of Physics Condensed Matter, 2004, 16, 4661-4676.	0.7	2
2640	Grain Boundary Sliding of Æ©5(001) Twist Grain Boundary in Aluminium Bicrystal from First-Principles Calculations. Materials Science Forum, 2004, 447-448, 27-32.	0.3	11
2641	The elasticity of the MgSiO3 post-perovskite phase in the Earth's lowermost mantle. Nature, 2004, 430, 442-445.	13.7	248
2642	Theoretical Structure Determination of a Complex Material: Î²â€Al₂O₃. Journal of the American Ceramic Society, 1999, 82, 1365-1380.	1.9	82
2643	The influence of hydrostatic pressure on the static and dynamic properties of an InSe crystal: A first-principles study. Physics of the Solid State, 2004, 46, 179-187.	0.2	12
2644	Phonon spectra of L12 Ni3Al and B2 NiAl: Ab initio calculations. Physics of the Solid State, 2004, 46, 1188-1194.	0.2	4
2645	Special points for calculating integrals over the primitive cell of a periodic system. Physics of the Solid State, 2004, 46, 1213-1224.	0.2	0
2646	Ab initio study of novel crystals based on fullerene C60 and carbynes. Physics of the Solid State, 2004, 46, 2317-2322.	0.2	2
2647	Structural relationships, phase stability and bonding of compounds PdSnn (n=2, 3, 4). Solid State Sciences, 2004, 6, 147-155.	1.5	101
2648	DFT calculations on the electronic structure of CuTe2 and Cu7Te4. Solid State Sciences, 2004, 6, 15-20.	1.5	29
2649	First principles search of hard materials within the Sîî—¸Cî—¸N ternary system. Solid State Sciences, 2004, 6, 315-323.	1.5	18
2650	Ferromagnetism of 3d-impurities substituted in Ge. Journal of Magnetism and Magnetic Materials, 2004, 284, 253-259.	1.0	8
2651	Lattice dynamics behavior in GaN doped with Mg, As, Si, and C. Materials Chemistry and Physics, 2004, 83, 48-53.	2.0	5
2652	Hydrogenation of ethylene and formaldehyde on Pt (111) and Pt80Fe20 (111): a density-functional study. Journal of Catalysis, 2004, 226, 273-282.	3.1	43
2653	Theoretical study of Si impurities in BN nanotubes. European Physical Journal B, 2004, 38, 515-518.	0.6	22

#	Article	IF	Citations
2654	Electronic structures and bonding of oxygen on plutonium layers. European Physical Journal B, 2004, 40, 337-346.	0.6	31
2655	Oxidation of Zigzag Carbon Nanotubes by Singlet O2:â€‰ Dependence on the Tube Diameter and the Electronic Structure. Journal of Physical Chemistry B, 2004, 108, 11435-11441.	1.2	58
2656	Density Functional Study of the Aluminumâ€”Graphite Interface. Journal of Computational Electronics, 2004, 3, 51-56.	1.3	5
2657	Comparison of electronic structures of doped ZnO by various impurity elements calculated by a first-principle pseudopotential method. Journal of Materials Science: Materials in Electronics, 2004, 15, 743-749.	1.1	53
2658	Effects of Antimony Doping on Electronic Structure of SnO2. Russian Physics Journal, 2004, 47, 701-704.	0.2	7
2659	Density-functional study of charge doping inWO3. Physical Review B, 2004, 70, .	1.1	84
2660	Hydrogen in aluminum: First-principles calculations of structure and thermodynamics. Physical Review B, 2004, 69, .	1.1	300
2661	Crystal structure and thermodynamic stability of the lithium alanatesLiAlH4andLi3AlH6. Physical Review B, 2004, 69, .	1.1	114
2662	Effects of additives in Î±- and Î¸-alumina: an ab initio study. Journal of Physics Condensed Matter, 2004, 16, 8971-8980.	0.7	32
2663	Different roles of carbon and silicon interstitials in the interstitial-mediated boron diffusion inSiC. Physical Review B, 2004, 70, .	1.1	48
2664	Defect Migration and Annealing Mechanisms. Advanced Texts in Physics, 2004, , 27-55.	0.5	7
2665	Zero- and Two-Dimensional Native Defects. Advanced Texts in Physics, 2004, , 3-25.	0.5	7
2666	Theoretical study of ZnO adsorption and bonding on Al2O3 (0001) surface. Science in China Series G: Physics, Mechanics and Astronomy, 2004, 47, 664-675.	0.2	0
2667	Chromic acid evaporation upon exposure of Cr2O3(s) to H2O(g) and O2(g) â€“ mechanism from first principles. Chemical Physics Letters, 2004, 383, 549-554.	1.2	28
2668	Competitive CN and N2 formation on Rh(1 1 1): a case of entropic stabilization. Chemical Physics Letters, 2004, 385, 52-54.	1.2	16
2669	Potential new candidates for hard materials within the ternary XC3N3 (XÂ=ÂB, Al, Ga) stoichiometry. Comptes Rendus Chimie, 2004, 7, 529-535.	0.2	6
2670	Ab initio study of the tensile behavior of single polyimide molecular chain. Polymer, 2004, 45, 9023-9028.	1.8	5
2671	Ab initio phonon calculations for L12 Ni3Al and B2 NiAl. Solid State Communications, 2004, 129, 809-814.	0.9	24

#	Article	IF	Citations
2672	Interplay of local structure and magnetism in Co-doped TiO2 anatase. Solid State Communications, 2004, 129, 741-746.	0.9	44
2673	Calculated elastic properties of M2AlC (M=Ti, V, Cr, Nb and Ta). Solid State Communications, 2004, 129, 589-592.	0.9	397
2674	Electronic structure and 89Y spin-lattice relaxation for YH2. Solid State Communications, 2004, 130, 215-218.	0.9	1
2675	Lithium intercalation effects on the V2O5 (001) surface. Solid State Ionics, 2004, 166, 175-181.	1.3	5
2676	Coadsorption of methyl radicals and oxygen on Rh(111). Surface Science, 2004, 549, 265-272.	0.8	21
2677	Theoretical study of segregation of Zn and Pd in Pdâ€“Zn alloys. Surface Science, 2004, 548, 291-300.	0.8	54
2678	Adhesion and bonding of the Al/TiC interface. Surface Science, 2004, 550, 46-56.	0.8	69
2679	Ab initio study of BN nanoarches' surfaces. Surface Science, 2004, 555, 179-186.	0.8	4
2680	Structure and bonding mechanism of cyanide adsorbed on Pt(111). Surface Science, 2004, 558, 111-121.	0.8	34
2681	Effect of the electronic structure on CO oxidation on Pd doped Ag(111). Surface Science, 2004, 566-568, 1063-1066.	0.8	8
2682	Magnetic properties of supersoft transition metal silicides. Journal of Magnetism and Magnetic Materials, 2004, 272-276, E233-E234.	1.0	4
2683	Pt thin films on stepped SrTiO3 surfaces: SrTiO3(620) and SrTiO3(622). Journal of Molecular Catalysis A, 2004, 216, 233-245.	4.8	11
2684	Modelling the Deposition of High-k Dielectric Films by First Principles. Journal of Electroceramics, 2004, 13, 117-120.	0.8	20
2685	Ab initio Study of the Si Adsorption on Mo(110). Journal of Electroceramics, 2004, 13, 327-330.	0.8	2
2686	Electronic structure of heavy-metal azides. Russian Physics Journal, 2004, 47, 1056-1061.	0.2	7
2687	High-pressure phases of MgSiN 2 from first-principles calculations. Applied Physics A: Materials Science and Processing, 2004, 78, 717-719.	1.1	16
2688	A modeling of the structure and favorable H-docking sites and defects for the high-pressure silica polymorph stishovite. Physics and Chemistry of Minerals, 2004, 31, 232-239.	0.3	22
2689	High-pressure isosymmetrical phase transition in calaverite. Physics and Chemistry of Minerals, 2004, 31, 553-558.	0.3	0

#	Article	IF	Citations
2690	The vibrational spectrum of calcite (CaCO3): an ab initio quantum-mechanical calculation. Physics and Chemistry of Minerals, 2004, 31, 559-564.	0.3	182
2691	Concentrations of native and gold defects in HgCdTe from first principles calculations. Journal of Electronic Materials, 2004, 33, 737-741.	1.0	11
2692	Ab Initio High Pressure Investigations of InI. Zeitschrift Fur Anorganische Und Allgemeine Chemie, 2004, 630, 41-50.	0.6	7
2693	High Pressure Study of NH4Pb2Br5 Type Compounds. I Structural Parameters and Their Evolution under High Pressure. Zeitschrift Fur Anorganische Und Allgemeine Chemie, 2004, 630, 1924-1932.	0.6	23
2694	Interplay of Electronic Structure and Bulk Properties in 2D and 3D Ternary Carbonitrides from First Principles. Zeitschrift Fur Anorganische Und Allgemeine Chemie, 2004, 630, 2587-2598.	0.6	9
2695	First-principles periodic and semiempirical cyclic cluster calculations for single oxygen vacancies in crystalline Al2O3. Physica Status Solidi (B): Basic Research, 2004, 241, 1032-1040.	0.7	25
2696	Structural, electronic and optical calculations of Cu(In,Ga)Se2 ternary chalcopyrites. Physica Status Solidi (B): Basic Research, 2004, 241, 2516-2528.	0.7	47
2697	Surface chemistry effects on vacancy and interstitial annihilation on Si(001). Physica Status Solidi (B): Basic Research, 2004, 241, 2303-2312.	0.7	9
2698	Hydrostatic pressure effects on the structural and electronic properties of carbon nanotubes. Physica Status Solidi (B): Basic Research, 2004, 241, 3352-3359.	0.7	88
2699	Use of Wannier-type atomic orbitals in LCAO and plane wave calculations: Chemical bonding in MgO crystal. Physica Status Solidi (B): Basic Research, 2004, 241, R35-R37.	0.7	3
2700	Quantum chemical calculation of crystalline model of biomembrane. International Journal of Quantum Chemistry, 2004, 96, 106-115.	1.0	0
2701	Chemical bonding in crystalline silver halides: Wannier-type atomic functions approach. International Journal of Quantum Chemistry, 2004, 96, 95-105.	1.0	7
2702	Hartree-Fock calculations of electronic structure of (110)-surface of rutile TiO2: Comparison of single (2D) and periodic (3D) slab models. International Journal of Quantum Chemistry, 2004, 96, 282-291.	1.0	15
2703	Density functional study of XH4 (X=Si and Ge) reactivity upon dissociative adsorption onto the Si(100) surface. International Journal of Quantum Chemistry, 2004, 97, 736-746.	1.0	10
2704	Density functional theory study of point defects in the Si?SiO2 system and in substoichiometric titanium dioxide TiO2?x. International Journal of Quantum Chemistry, 2004, 99, 677-684.	1.0	12
2705	An investigation of H-atom positions in sulfuric acid crystal structures. Acta Crystallographica Section B: Structural Science, 2004, 60, 179-183.	1.8	11
2706	Effect of the Composition on the Structure of Cr-Al-C Investigated by Combinatorial Thin Film Synthesis and ab Initio Calculations. Advanced Engineering Materials, 2004, 6, 903-907.	1.6	94
2707	Quantum-Chemical Studies on the Geometric and Electronic Structures of Bertholloide Cobalt Oxynitrides. Advanced Functional Materials, 2004, 14, 371-376.	7.8	5

#	Article	IF	Citations
2708	Origin of Anomalous Pt-Pt Distances in the Pt/Alumina Catalytic System. ChemPhysChem, 2004, 5, 1893-1897.	1.0	68
2709	The calculation of the vibrational frequencies of crystalline compounds and its implementation in the CRYSTAL code. Journal of Computational Chemistry, 2004, 25, 888-897.	1.5	796
2710	Models for the treatment of crystalline solids and surfaces. Journal of Computational Chemistry, 2004, 25, 1551-1567.	1.5	56
2711	Combinedab initio computational and experimental multinuclear solid-state magnetic resonance study of phenylphosphonic acid. Magnetic Resonance in Chemistry, 2004, 42, 445-452.	1.1	88
2712	Synthesis, Characterization, and Electronic Structure of Ba5In4Bi5: An Acentric and One-Electron Deficient Phase. Chemistry - A European Journal, 2004, 10, 3615-3621.	1.7	29
2713	Molybdenum Phosphide as ano-Propylaniline Hydrodenitrogenation Catalyst: A First Principles Study. Chemistry - A European Journal, 2004, 10, 6279-6284.	1.7	10
2714	First-principles theory of copper in silicon. Materials Science in Semiconductor Processing, 2004, 7, 101-111.	1.9	22
2715	Vegard's law deviation in lattice constant and band gap bowing parameter of zincblende InxGa1â^'xN. Optics Communications, 2004, 237, 363-369.	1.0	91
2716	Full potential calculation of structural, electronic and elastic properties of alkaline earth oxides MgO, CaO and SrO. Physica B: Condensed Matter, 2004, 344, 334-342.	1.3	115
2717	Density functional approach to study structural properties and electric field gradients in rare earth materials. Physica B: Condensed Matter, 2004, 349, 76-83.	1.3	23
2718	Electronic structure and optical properties of barium strontium titanate (BaxSr1â^'xTiO3) using first-principles method. Physica B: Condensed Matter, 2004, 351, 158-162.	1.3	54
2719	A density functional study of atomic hydrogen adsorption on plutonium layers. Physica B: Condensed Matter, 2004, 352, 5-17.	1.3	39
2720	Reactivity of Pd doped Ag surfaces. Vacuum, 2004, 74, 169-172.	1.6	1
2721	Calculation of surface properties of bcc iron. Vacuum, 2004, 74, 179-183.	1.6	69
2722	An ab initio study of 4Hâ€“SiC(0001) and (0001Ì„) surface processes at experimental temperatures. Thin Solid Films, 2004, 458, 191-196.	0.8	8
2723	Ab initio calculations and experimental determination of the structure of Cr2AlC. Solid State Communications, 2004, 130, 445-449.	0.9	179
2724	H2 dissociative adsorption at the armchair edges of graphite. Solid State Communications, 2004, 132, 713-718.	0.9	37
2725	Prediction study of elastic properties under pressure effect for zincblende BN, AlN, GaN and InN. Solid-State Electronics, 2004, 48, 1601-1606.	0.8	61

#	Article	IF	Citations
2726	Revisit to the Ising model for orderâ€“disorder phase transition on Si(001). Surface Science, 2004, 554, 150-158.	0.8	7
2727	Assessment of competing mechanisms of the abstraction of hydrogen from CH4 on Li/MgO(001). Surface Science, 2004, 549, 217-226.	0.8	18
2728	Multilayer relaxations of (311), (331) and (210) fcc transition metal surfaces studied by pseudopotential DFT calculations. Surface Science, 2004, 548, 309-316.	0.8	18
2729	Alkali metals adsorption on the Mg() surface. Surface Science, 2004, 548, 22-28.	0.8	19
2730	The geometric and electronic properties of the PbS, PbSe and PbTe (001) surfaces. Surface Science, 2004, 551, 91-98.	0.8	36
2731	The atomic and electronic structure of the TiO2- and BaO-terminated BaTiO3(001) surfaces in a paraelectric phase. Surface Science, 2004, 550, 73-80.	0.8	29
2732	MEAM molecular dynamics study of a gold thin film on a silicon substrate. Surface Science, 2004, 551, 39-58.	0.8	47
2733	Electronic structure studies of adsorbate-induced surface reconstructions: oxygen on Rh(100). Surface Science, 2004, 553, 82-94.	0.8	11
2734	Sum frequency generation and density functional studies of COâ€“H interaction and hydrogen bulk dissolution on Pd(111). Surface Science, 2004, 554, 43-59.	0.8	72
2735	Surface properties of alkaline earth metal oxides. Surface Science, 2004, 554, 262-271.	0.8	90
2736	Mechanisms of monovacancy annihilation and type-A defect creation on Si(001)â€“2Ã—1. Surface Science, 2004, 555, 187-192.	0.8	7
2737	Chemisorption sites and reaction pathways for acetylene on Si(111)-(7Ã—7). Surface Science, 2004, 557, 80-90.	0.8	13
2738	CO bonded to platinum: effects of semi-core polarization. Surface Science, 2004, 559, 214-222.	0.8	11
2739	Ethylene on Cu(110) and Ni(110): electronic structure and bonding derived from X-ray spectroscopy and theory. Surface Science, 2004, 559, 85-99.	0.8	30
2740	An ab-initio study of pentacene on aluminum (100) surface. Surface Science, 2004, 562, 43-52.	0.8	33
2741	H2 dissociative adsorption on Mg, Ti, Ni, Pd and La Surfaces. Surface Science, 2004, 566-568, 703-707.	0.8	74
2742	Stability and electronic properties of carbon nanotubes adsorbed on Si(001). Surface Science, 2004, 566-568, 728-732.	0.8	17
2743	Ab initio study of the one-monolayer Sb/Ge interface. Surface Science, 2004, 566-568, 956-960.	0.8	3

#	Article	IF	Citations
2744	DFT plane-wave calculations of the Rh/MgO(001) interface. Surface Science, 2004, 566-568, 977-982.	0.8	10
2745	Low-coverage K adsorption on Mg(0001) surface. Surface Science, 2004, 566-568, 983-988.	0.8	6
2746	Adsorption of ethylene on stepped Ag() surfaces. Surface Science, 2004, 566-568, 1018-1023.	0.8	16
2747	On-surface and subsurface adsorption of oxygen on stepped Ag(210) and Ag(410) surfaces. Surface Science, 2004, 566-568, 1107-1111.	0.8	15
2748	S and O adsorption on pure and Ge doped Ag(111). Surface Science, 2004, 566-568, 1067-1070.	0.8	1
2749	Organic molecular crystals in electric fields. Surface Science, 2004, 566-568, 644-649.	0.8	13
2750	Adsorption and dissociation of CO on Fe(110) from first principles. Surface Science, 2004, 570, 167-177.	0.8	118
2751	CO and hydrogen adsorption on Pd(210). Surface Science, 2004, 570, 227-236.	0.8	27
2752	Calculation of electronic structure at bonding interface between vanadium and oxide ceramics for insulator coating applications. Journal of Nuclear Materials, 2004, 329-333, 1571-1574.	1.3	3
2753	High potential positive materials for lithium-ion batteries: transition metal phosphates. Journal of Physics and Chemistry of Solids, 2004, 65, 229-233.	1.9	85
2754	The melting curve of iron from quantum mechanics calculations. Journal of Physics and Chemistry of Solids, 2004, 65, 1573-1580.	1.9	28
2755	Atomistic modeling of polar LaMnO3 surfaces. Sensors and Actuators B: Chemical, 2004, 100, 81-87.	4.0	10
2756	The BrÃ¸nstedâ€“Evansâ€“Polanyi relation and the volcano curve in heterogeneous catalysis. Journal of Catalysis, 2004, 224, 206-217.	3.1	1,348
2757	Optical properties of the semiconductor carbon nanotube intramolecular junctions. Physics Letters, Section A: General, Atomic and Solid State Physics, 2004, 323, 122-131.	0.9	32
2758	Electronic structures of high-k transition metal silicates: first-principles calculations. Microelectronics Journal, 2004, 35, 655-658.	1.1	6
2759	Electronic levels of interstitial carbon and carbonâ€“oxygen centers in SiGe alloys. Materials Science and Engineering B: Solid-State Materials for Advanced Technology, 2004, 114-115, 304-306.	1.7	2
2760	On the ordering in new low gap semiconductors: PtSnS, PtSnSe, PtSnTe. Experimental and DFT studies. Journal of Solid State Chemistry, 2004, 177, 2591-2599.	1.4	18
2761	Investigation of the relative stabilities of various allotropic phases of elemental tellurium under pressure and their interconversion paths by electronic structure calculations and crystal structure analyses. Journal of Solid State Chemistry, 2004, 177, 4724-4731.	1.4	7

#	Article	IF	Citations
2762	A comparative ab initio study of the â€˜idealâ€™ strength of single crystal Î±- and Î²-Si3N4. Acta Materialia, 2004, 52, 233-238.	3.8	67
2763	Effects of cobalt intergranular segregation on interface energetics in WCâ€“Co. Acta Materialia, 2004, 52, 2199-2207.	3.8	91
2764	A combined CALPHAD/first-principles remodeling of the thermodynamics of Alâ€“Sr: unsuspected ground state energies by â€œrounding up the (un)usual suspectsâ€• Acta Materialia, 2004, 52, 2739-2754.	3.8	72
2765	First-principles study of polar Al/TiN(1 1 1) interfaces. Acta Materialia, 2004, 52, 3681-3688.	3.8	191
2766	First-principles study of crystal structure and stability of Al?Mg?Si?(Cu) precipitates. Acta Materialia, 2004, 52, 4213-4227.	3.8	317
2767	Simulations of intergranular fracture in nanocrystalline molybdenum. Acta Materialia, 2004, 52, 5019-5029.	3.8	69
2768	Ab initio calculations of the LaMnO3 surface properties. Applied Surface Science, 2004, 238, 457-463.	3.1	27
2769	A periodic first principle study to design microporous crystal 12MO, 7Al2O3 for selective and active Oâ˙ radicals encaging. Chemical Physics Letters, 2004, 390, 335-339.	1.2	4
2770	Metalâ€“nanotube interactions â€“ binding energies and wetting properties. Chemical Physics Letters, 2004, 395, 7-11.	1.2	147
2771	Strong and weak adsorption of CO on CeO2 surfaces from first principles calculations. Chemical Physics Letters, 2004, 396, 384-392.	1.2	108
2772	Efficient calculation of the structural and electronic properties of mixed valence materials: application to Prussian Blue analogues. Chemical Physics Letters, 2004, 397, 154-159.	1.2	23
2773	Theoretical study of propene adsorbed on sulphated Pt(111). Chemical Physics Letters, 2004, 399, 295-299.	1.2	4
2774	Effect of external stress on the patterning of nanostructures: a kinetic Monte Carlo simulation of Ta deposited on anistropically compressed Ta(100) surfaces. Chemical Physics Letters, 2004, 400, 74-77.	1.2	1
2775	First principles study of structural, electronic, elastic and optical properties of MgS, MgSe and MgTe. Catalysis Today, 2004, 89, 343-355.	2.2	137
2776	Electronic structure of the extended vanadyl pyrophosphate (1 0 0) surface. Catalysis Today, 2004, 91-92, 177-180.	2.2	9
2777	NOx storage on BaO: theory and experiment. Catalysis Today, 2004, 96, 71-78.	2.2	91
2778	Electronic and superconducting properties of silicon and carbon clathrates. Applied Surface Science, 2004, 226, 289-297.	3.1	20
2779	Density functional study of methoxide decomposition on PdZn(100). Physical Chemistry Chemical Physics, 2004, 6, 4499-4504.	1.3	29

#	Article	IF	Citations
2780	Effects of Ag and Ni Additives on Zn Diffusion in Steel Hot-Dip Galvanizing:Â An ab Initio Molecular Dynamics Simulation. Chemistry of Materials, 2004, 16, 5567-5573.	3.2	7
2781	Ab initio study of 2H-MoS2using Hay and Wadt effective core pseudo-potentials for modelling the (101Ì„0) surface structure. Physical Chemistry Chemical Physics, 2004, 6, 3023-3030.	1.3	24
2782	Doping and defect association in AZrO3(A = Ca, Ba) and LaMO3(M = Sc, Ga) perovskite-type ionic conductors. Dalton Transactions, 2004, , 3061.	1.6	106
2783	Ozone adsorption on carbon nanotubes:Ab initiocalculations and experiments. Journal of Vacuum Science and Technology A: Vacuum, Surfaces and Films, 2004, 22, 1466-1470.	0.9	40
2784	Metallic single-walled silicon nanotubes. Proceedings of the National Academy of Sciences of the United States of America, 2004, 101, 2664-2668.	3.3	124
2785	Ab initiostudy of OH-functionalized single-wall carbon nanotubes. Physical Review B, 2004, 70, .	1.1	51
2786	An Approach to Developing a Force Field for Molecular Simulation of Martensitic Phase Transitions between Phases with Subtle Differences in Energy and Structure. Journal of the American Chemical Society, 2004, 126, 396-405.	6.6	66
2787	First-principles study on thermal vibration effects ofMgH2. Physical Review B, 2004, 70, .	1.1	21
2788	Density Functional Theory Study of Silica Zeolite Structures:Â Stabilities and Mechanical Properties of SOD, LTA, CHA, MOR, and MFI. Journal of Physical Chemistry B, 2004, 108, 9208-9215.	1.2	89
2789	Oxygen vacancies on TiO2 (110) from first principles calculations. Journal of Chemical Physics, 2004, 121, 7427-7433.	1.2	75
2790	Proposed Definition of Microchemical Inhomogeneity and Application To Characterize Some Selected Miscible/Immiscible Binary Metal Systems. Journal of Physical Chemistry B, 2004, 108, 16071-16076.	1.2	20
2791	First principles calculations of the chemisorption properties of nitro-containing molecules on the Al/sub 2/O/sub 3/(0001) surface. , 2004, , .		0
2792	Systematic Research on Insertion Materials Based on Superlattice Models in a Phase Triangle of LiCoO[sub 2]-LiNiO[sub 2]-LiMnO[sub 2]. Journal of the Electrochemical Society, 2004, 151, A1499.	1.3	101
2793	Comparative study ofab initioand tight-binding electronic structure calculations applied to platinum surfaces. Physical Review B, 2004, 70, .	1.1	40
2794	Theoretical tensile strength of an Al grain boundary. Physical Review B, 2004, 69, .	1.1	116
2795	The influence of electronic structure on hydrogen absorption in palladium alloys. Journal of Physics Condensed Matter, 2004, 16, 6267-6277.	0.7	75
2796	Adhesion and adhesive transfer at aluminum/diamond interfaces:â€,A first-principles study. Physical Review B, 2004, 69, .	1.1	118
2797	Energy Partitioning Studies of CO and NO Chemisorption on the Pd(111) Surface. Journal of Physical Chemistry B, 2004, 108, 5967-5979.	1.2	2

#	Article	IF	Citations
2798	Boron alloying in GaN. Applied Physics Letters, 2004, 84, 705-707.	1.5	28
2799	Density Functional Theory Study of CO Adsorption on Fe5C2(001), -(100), and -(110) Surfaces. Journal of Physical Chemistry B, 2004, 108, 9094-9104.	1.2	62
2800	Metal-to-Semimetal Transition in Supercooled Liquid Silicon. Physical Review Letters, 2004, 92, 175701.	2.9	43
2801	Structures of Carbon Nanocrystals. Chemistry of Materials, 2004, 16, 4905-4911.	3.2	27
2802	Ab initiostudy of the Î²-tinâ†'Immaâ†'sh phase transitions in silicon and germanium. Physical Review B, 2004, 69, .	1.1	26
2803	Simulating the atomic layer deposition of alumina from first principles. Journal of Materials Chemistry, 2004, 14, 3246.	6.7	134
2804	First Principles Calculation of Defect Formation Energies in Sr- and Mg-Doped LaGaO3. Journal of Physical Chemistry B, 2004, 108, 9168-9172.	1.2	38
2805	Adsorption of CO2on Model Surfaces of Cesium Oxides Determined from First Principles. Journal of Physical Chemistry B, 2004, 108, 16798-16805.	1.2	25
2806	CH3O Decomposition on PdZn(111), Pd(111), and Cu(111). A Theoretical Study. Langmuir, 2004, 20, 8068-8077.	1.6	133
2807	A First Principles Analysis of the Location and Affinity of Protons in the Secondary Structure of Phosphotungstic Acid. Journal of Physical Chemistry B, 2004, 108, 12292-12300.	1.2	36
2808	Vibrational behavior of adsorbed CO2 on single-walled carbon nanotubes. Journal of Chemical Physics, 2004, 120, 5377-5386.	1.2	73
2809	Ice Tessellation on a Hydroxylated Silica Surface. Physical Review Letters, 2004, 92, 146102.	2.9	87
2810	Are surfaces elastically softer or stiffer?. Applied Physics Letters, 2004, 84, 1940-1942.	1.5	325
2811	Hollowing Mechanism of Zinc Sulfide Nanowires in Vacuum Induced by an Atomic Oxygen Beam. Journal of Physical Chemistry B, 2004, 108, 9631-9637.	1.2	18
2812	Effect of Sulfur Impurity on Fe(110) Adhesion:Â A DFT Study. Journal of Physical Chemistry B, 2004, 108, 10965-10972.	1.2	13
2813	Trends in the Chemisorption of Aromatic Molecules on a Pt(111) Surface:â€‰ Benzene, Naphthalene, and Anthracene from First Principles Calculations. Journal of Physical Chemistry B, 2004, 108, 12084-12091.	1.2	104
2814	First-Principles Calculation of 17O, 29Si, and 23Na NMR Spectra of Sodium Silicate Crystals and Glasses. Journal of Physical Chemistry B, 2004, 108, 4147-4161.	1.2	174
2815	Atomistic mechanism of proton conduction in solidCsHSO4by a first-principles study. Physical Review B, 2004, 69, .	1.1	22

#	Article	IF	Citations
2816	Driving Forces for Self-Organized Coadsorption:Â C6H6/2O and C6H6/2CO on Ni{111}. Journal of the American Chemical Society, 2004, 126, 10962-10971.	6.6	12
2817	Experimental determination of valence band maxima for SrTiO[sub 3], TiO[sub 2], and SrO and the associated valence band offsets with Si(001). Journal of Vacuum Science & Technology an Official Journal of the American Vacuum Society B, Microelectronics Processing and Phenomena, 2004, 22, 2205.	1.6	251
2818	Theory of Methane Dehydrogenation on Pt{110}(1 Ã— 2). Part I:â€‰ Chemisorption of CHx (x = 0 â^'3). Journal of Physical Chemistry B, 2004, 108, 5909-5919.	1.2	61
2819	Electronic, thermal, and elastic properties ofTi3Si1â^'xGexC2solid solutions. Physical Review B, 2004, 70, .	1.1	88
2820	Phase Stability in the Systems AeAl2-xMgx(Ae = Ca, Sr, Ba):Â Electron Concentration and Size Controlled Variations on the Laves Phase Structural Theme. Inorganic Chemistry, 2004, 43, 4751-4760.	1.9	28
2821	Ethylene Decomposition on Rh(100):Â Theory and Experimentâ€. Journal of Physical Chemistry B, 2004, 108, 14541-14548.	1.2	23
2822	Ab Initio Calculations of NMR Parameters of Highly Coordinated Oxygen Sites in Aluminosilicates. Journal of Physical Chemistry B, 2004, 108, 13249-13253.	1.2	57
2823	Theory of Methane Dehydrogenation on Pt{110}(1 Ã— 2). Part II:â€‰ Microscopic Reaction Pathways for CHx â†' CHx-1 (x = 1â^'3). Journal of Physical Chemistry B, 2004, 108, 5920-5929.	1.2	26
2824	Structural and Spectroelectrochemical Study of Carbonate and Bicarbonate Adsorbed on Pt(111) and Pd/Pt(111) Electrodes. Journal of Physical Chemistry B, 2004, 108, 17928-17939.	1.2	39
2825	Ab initioInvestigation of the Early Stage of Nano-scale Thin Film Growth: Al and Co Adatoms on Co (111) Surface. Japanese Journal of Applied Physics, 2004, 43, 3815-3817.	0.8	6
2826	Chemisorption of Benzene on Pt(111), Pd(111), and Rh(111) Metal Surfaces:â€‰ A Structural and Vibrational Comparison from First Principles. Journal of Physical Chemistry B, 2004, 108, 5653-5665.	1.2	158
2827	First-principles study of salicylideneaniline molecular crystals: Tautomerization reaction involving intermolecular hydrogen bonds. Physical Review B, 2004, 69, .	1.1	16
2828	The Cyclopropylmethylâ^'3-Butenyl Rearrangement on Mo(110):Â A Radical Clock on a Surface?â€. Journal of Physical Chemistry A, 2004, 108, 2972-2981.	1.1	11
2829	DFT Investigation of Product Distribution Following Reaction of 1,3-Cyclohexadiene on the Si(100)-2Ã—1 Surface. Journal of Physical Chemistry B, 2004, 108, 7827-7830.	1.2	16
2830	Antifluorite-Type Lithium Chromium Oxide Nitrides:Â Synthesis, Structure, Order, and Electrochemical Properties. Inorganic Chemistry, 2004, 43, 7050-7060.	1.9	43
2831	Conformational Analysis with Both Experimental and Computational Data for Both Gaseous and Crystalline Phases:â€‰ Unexpected Interactions in N-Methyldichloroacetamide. Journal of Physical Chemistry A, 2004, 108, 185-193.	1.1	4
2832	High-pressure behaviour of selenium-based spinels and related structuresâ€”an experimental and theoretical study. Journal of Physics Condensed Matter, 2004, 16, 53-63.	0.7	20
2833	Planar Tetracoordinate Carbon in Extended Systems. Journal of the American Chemical Society, 2004, 126, 15309-15315.	6.6	126

#	Article	IF	Citations
2834	Ab initiostudy of high-pressure behavior of a low compressibility metal and a hard material:â€ƒOsmium and diamond. Physical Review B, 2004, 70, .	1.1	71
2835	Boron-hydrogen complexes in diamond. Physical Review B, 2004, 69, .	1.1	50
2836	Density-functional study ofCuatoms, monolayers, films, and coadsorbates on polarZnOsurfaces. Physical Review B, 2004, 69, .	1.1	85
2837	Equation of state and elasticity of FeSi. Geophysical Research Letters, 2004, 31, .	1.5	52
2838	First-principles study ofH2Odiffusion on a metal surface:â€ƒH2Oon Al{100}. Physical Review B, 2004, 69, .	1.1	39
2839	Structural and electronic properties ofYBa2Cu3O7andYSr2Cu3O7under mechanical and strontium chemical pressures. Physical Review B, 2004, 70, .	1.1	17
2840	Theoretical study of crossed and parallel carbon nanotube junctions and three-dimensional grid structures. Physical Review B, 2004, 70, .	1.1	34
2841	Atomic-scale model ofcâ^'Si/a-Si:H interfaces. Physical Review B, 2004, 69, .	1.1	17
2842	Ab initiostudy of the (0001) surfaces of hematite and chromia: Influence of strong electronic correlations. Physical Review B, 2004, 70, .	1.1	357
2843	Surface Structure of Hydroxylated and Sulfated Zirconia. A Periodic Density-Functional Studyâ€. Journal of Physical Chemistry B, 2004, 108, 14652-14662.	1.2	82
2844	Thin Film Growth Related Adsorption Study of Al and O Ions on an Î±-Al2O3Surface. Journal of Physical Chemistry B, 2004, 108, 19320-19324.	1.2	10
2845	First-principles calculations for defects and impurities: Applications to III-nitrides. Journal of Applied Physics, 2004, 95, 3851-3879.	1.1	2,695
2846	Generalized-stacking-fault energy and dislocation properties inbccFe:â€ƒ A first-principles study. Physical Review B, 2004, 70, .	1.1	111
2847	Ab initiostudy of the annealing of vacancies and interstitials in cubic SiC: Vacancy-interstitial recombination and aggregation of carbon interstitials. Physical Review B, 2004, 69, .	1.1	172
2848	Ab initiostudy of structural and electronic properties of planar defects in Si and SiC. Physical Review B, 2004, 70, .	1.1	10
2849	Superhard CubicBC2NCompared to Diamond. Physical Review Letters, 2004, 93, 195504.	2.9	214
2850	First-principles study of the polar O-terminated ZnO surface in thermodynamic equilibrium with oxygen and hydrogen. Physical Review B, 2004, 69, .	1.1	245
2851	AB INITIO CALCULATION OF THE ELECTRONIC AND MECHANICAL PROPERTIES OF TRANSITION METALS AND THEIR NITRIDES. Modern Physics Letters B, 2004, 18, 281-289.	1.0	12

#	Article	IF	Citations
2852	Theoretical prediction of electronic structures of fully Ï€-conjugated zinc oligoporphyrins with curved surface structures. Journal of Chemical Physics, 2004, 120, 7963-7970.	1.2	24
2853	Electric fields with ultrasoft pseudo-potentials: Applications to benzene and anthracene. Journal of Chemical Physics, 2004, 120, 9934-9941.	1.2	42
2854	Ideal tensile strength ofB2transition-metal aluminides. Physical Review B, 2004, 70, .	1.1	52
2855	Structure and magnetic properties of adatoms on carbon nanotubes. Physical Review B, 2004, 69, .	1.1	82
2856	EPR and theoretical studies of positively charged carbon vacancy in 4H-SiC. Physical Review B, 2004, 70, .	1.1	50
2857	Locating the rate-limiting step for the interaction of hydrogen withMg(0001)using density-functional theory calculations and rate theory. Physical Review B, 2004, 70, .	1.1	154
2858	Structure and Energetics of LiBH4and Its Surfaces:Â A First-Principles Studyâ€. Journal of Physical Chemistry A, 2004, 108, 8682-8690.	1.1	66
2859	Strong affinity of hydrogen for the GaN(000-1) surface: Implications for molecular beam epitaxy and metalorganic chemical vapor deposition. Applied Physics Letters, 2004, 85, 3429-3431.	1.5	81
2860	Atomic and magnetic configurational energetics by the generalized perturbation method. Physical Review B, 2004, 70, .	1.1	128
2861	First-Principles Calculation of the17O NMR Parameters in Ca Oxide and Ca Aluminosilicates:Â the Partially Covalent Nature of the Caâ^'O Bond, a Challenge for Density Functional Theory. Journal of the American Chemical Society, 2004, 126, 12628-12635.	6.6	103
2862	Water adsorption on metal surfaces: A general picture from density functional theory studies. Physical Review B, 2004, 69, .	1.1	448
2863	First-principles study of binary bcc alloys using special quasirandom structures. Physical Review B, 2004, 69, .	1.1	266
2864	Deformation-induced site selectivity for hydrogen adsorption on boron nitride nanotubes. Physical Review B, 2004, 69, .	1.1	75
2865	Halogen-Substituted Thiophenol Molecules on Cu(111). Langmuir, 2004, 20, 10928-10934.	1.6	29
2866	Electronic structure of cross-linked carbon nanotubes doped with alkali metals. Journal of Materials Chemistry, 2004, 14, 715.	6.7	8
2867	Ab initiostudy ofÎ³â^'Al2O3surfaces. Physical Review B, 2004, 70, .	1.1	197
2868	Transistors and Atoms. Springer Series in Materials Science, 2004, , 1-38.	0.4	1
2869	Density functional theory study of the interaction of monomeric water with the Ag{111} surface. Physical Review B, 2004, 69, .	1.1	53

#	Article	IF	Citations
2870	First-principles characterization of ferromagneticMn5Ge3for spintronic applications. Physical Review B, 2004, 70, .	1.1	102
2871	Stabilization of half metallicity in Mn-doped silicon upon Ge alloying. Physical Review B, 2004, 70, .	1.1	38
2872	Site preference for Mn substitution in spintronicCuMIIIX2VIchalcopyrite semiconductors. Physical Review B, 2004, 69, .	1.1	45
2873	Adsorption of Water on the TiO2(Rutile) (110) Surface:Â A Comparison of Periodic and Embedded Cluster Calculations. Journal of Physical Chemistry B, 2004, 108, 7844-7853.	1.2	126
2874	Energetics and Electronic Structures of Individual Atoms Adsorbed on Carbon Nanotubes. Journal of Physical Chemistry B, 2004, 108, 575-582.	1.2	116
2875	Band gap modification of single-walled carbon nanotube and boron nitride nanotube under a transverse electric field. Nanotechnology, 2004, 15, 1837-1843.	1.3	159
2876	Zinc-blende AlN and GaN under pressure: structural, electronic, elastic and piezoelectric properties. Semiconductor Science and Technology, 2004, 19, 1220-1231.	1.0	68
2877	Adsorption, Diffusion, and Dissociation of H2S on Fe(100) from First Principles. Journal of Physical Chemistry B, 2004, 108, 19140-19145.	1.2	101
2878	Ab Initio Investigation of the Structural and Electronic Properties of the Molecules and Crystals of Tetraphenyl Derivatives of Group IVA Elements. Journal of Physical Chemistry B, 2004, 108, 17361-17368.	1.2	11
2879	Structure and electrical activity of rare-earth dopants in GaN. Applied Physics Letters, 2004, 84, 2841-2843.	1.5	100
2880	A computer modelling study of the uptake and segregation of fluoride ions at the hydrated hydroxyapatite (0001) surface: introducing a Ca10(PO4)6(OH)2potential model. Physical Chemistry Chemical Physics, 2004, 6, 1860-1866.	1.3	94
2881	Calculation of uniaxial magnetic anisotropy energy of tetragonal and trigonal Fe, Co, and Ni. Physical Review B, 2004, 69, .	1.1	83
2882	Adsorption, diffusion, and recombination of hydrogen on pure and boron-doped graphite surfaces. Journal of Chemical Physics, 2004, 120, 11882-11888.	1.2	58
2883	Electronic and Magnetic Properties of 3 d Transition-Metal-Doped IIIâ€“V Magnetic Semiconductor. Chinese Physics Letters, 2004, 21, 1632-1635.	1.3	12
2884	Structural and electronic properties of wide band gap silicon carbon nitride materialsâ€”a first-principles study. Diamond and Related Materials, 2004, 13, 1158-1165.	1.8	30
2885	Ab initiostudy of the hygroscopic properties of borate crystals. Physical Review B, 2004, 70, .	1.1	26
2886	Single-Component Magnetic Conductors Based on Mo3S7Trinuclear Clusters with Outer Dithiolate Ligands. Journal of the American Chemical Society, 2004, 126, 12076-12083.	6.6	88
2887	Electric Dichroism Studies on an Aqueous Dispersion of Unilamellar Titanium Oxides:â€‰ Optical Anisotropy near the Absorption Edge. Journal of Physical Chemistry B, 2004, 108, 17306-17312.	1.2	8

#	Article	IF	Citations
2888	First-principles study of hydrogen diffusion inÎ±â^'Al2O3and liquid alumina. Physical Review B, 2004, 69, .	1.1	71
2889	Structure and properties of vacancy-oxygen complexes inSi1â^'xGexalloys. Physical Review B, 2004, 69, .	1.1	42
2890	The behavior of mixed-metal oxides: Physical and chemical properties of bulk Ce1â^'xTbxO2 and nanoparticles of Ce1â^'xTbxOy. Journal of Chemical Physics, 2004, 121, 5434-5444.	1.2	113
2891	Magnetism and energetics ofMn-DopedZnO(101Â¯0)thin films. Physical Review B, 2004, 69, .	1.1	56
2892	Ab initiomolecular dynamics of metal surfaces. Journal of Physics Condensed Matter, 2004, 16, S2575-S2596.	0.7	18
2893	Ab initiostudy of the phase diagram of epitaxialBaTiO3. Physical Review B, 2004, 69, .	1.1	217
2894	High-Pressure Melting of Molybdenum. Physical Review Letters, 2004, 92, 195701.	2.9	86
2895	Properties ofLaB6elucidated by density functional theory. Physical Review B, 2004, 70, .	1.1	37
2896	Sodium atoms and clusters on graphite by density functional theory. Physical Review B, 2004, 69, .	1.1	32
2897	Role of the Dopant in the Superconductivity of Diamond. Physical Review Letters, 2004, 93, 237004.	2.9	164
2898	Ab initio investigations of TlI-type compounds under high pressure. Zeitschrift Fur Kristallographie - Crystalline Materials, 2004, 219, .	0.4	18
2899	Electronic structure and electron energy-loss spectroscopy ofZrO2zirconia. Physical Review B, 2004, 70, .	1.1	145
2900	Detecting surface resonance states ofSi(111)â^'3Ã—3â^'Agwith a scanning tunneling microscope. Physical Review B, 2004, 70, .	1.1	20
2901	High-coverage stable structures of potassium adsorbed on single-walled carbon nanotubes. Physical Review B, 2004, 69, .	1.1	16
2902	Electron-phonon coupling in a boron-doped diamond superconductor. Physical Review B, 2004, 70, .	1.1	126
2903	Hydrogen adsorption on zigzag (8,0) boron nitride nanotubes. Journal of Chemical Physics, 2004, 121, 8481.	1.2	97
2904	Water Dimer Diffusion on Pd{111} Assisted by an H-Bond Donor-Acceptor Tunneling Exchange. Physical Review Letters, 2004, 92, 136104.	2.9	114
2905	Indium versus hydrogen-terminated GaN(0001) surfaces: Surfactant effect of indium in a chemical vapor deposition environment. Applied Physics Letters, 2004, 84, 4322-4324.	1.5	60

#	Article	IF	Citations
2906	Monovacancy and divacancy formation and migration in copper: A first-principles theory. Physical Review B, 2004, 70, .	1.1	38
2907	Ab initiotransport properties of nanostructures from maximally localized Wannier functions. Physical Review B, 2004, 69, .	1.1	247
2908	Filled ice structure of gas hydratesâ€"a density functional study. Journal of Physics Condensed Matter, 2004, 16, S1171-S1176.	0.7	3
2909	The Formation and Stability of Adsorbed Formyl as a Possible Intermediate in Fischerâ^'Tropsch Chemistry on Ruthenium. Journal of Physical Chemistry B, 2004, 108, 3614-3624.	1.2	49
2910	Systematic prediction of crystal structures: An application tosp3-hybridized carbon polymorphs. Physical Review B, 2004, 70, .	1.1	70
2911	Possible structures of nonstoichiometric tin oxide: the composition Sn2O3. Modelling and Simulation in Materials Science and Engineering, 2004, 12, 33-41.	0.8	57
2912	Calculated spin-orbit splitting of all diamondlike and zinc-blende semiconductors: Effects ofp1â^•2local orbitals and chemical trends. Physical Review B, 2004, 70, .	1.1	152
2913	Ion Adsorption at the Rutileâ^'Water Interface:Â Linking Molecular and Macroscopic Properties. Langmuir, 2004, 20, 4954-4969.	1.6	298
2914	Modification of the Monkhorst-Pack special points meshes in the Brillouin zone for density functional theory and Hartree-Fock calculations. Physical Review B, 2004, 70, .	1.1	103
2915	Doping effects on the electronic and structural properties ofCoO2: AnLSDA+Ustudy. Physical Review B, 2004, 70, .	1.1	77
2916	Density functional study of the adsorption of aC60monolayer on Ag(111) and Au(111) surfaces. Physical Review B, 2004, 69, .	1.1	160
2917	Electronic and magnetic properties of zinc blende half-metal superlattices. Applied Physics Letters, 2004, 84, 239-241.	1.5	43
2918	First-principles elastic constants and phonons ofÎ´â€Pu. Physical Review B, 2004, 70, .	1.1	36
2919	First-principles study of structural, dynamical, and dielectric properties of Î²-Al2O3. Computational Materials Science, 2004, 29, 138-144.	1.4	11
2920	Bulk properties and electronic structure of SrTiO3, BaTiO3, PbTiO3 perovskites: an ab initio HF/DFT study. Computational Materials Science, 2004, 29, 165-178.	1.4	705
2921	Ab initio study on the lattice instability of silicon and aluminum under [001] tension. Computational Materials Science, 2004, 29, 397-406.	1.4	15
2922	Elastic tensor of the forsterite (Mg2SiO4) under pressure. Computational Materials Science, 2004, 29, 414-418.	1.4	30
2923	Ab initio study of the enthalpy barriers of the high-pressure phase transition from the cubic-diamond to the Î²-tin structure of silicon and germanium. Computational Materials Science, 2004, 30, 1-7.	1.4	14

#	Article	IF	Citations
2924	Ab-initio study of the Imma phase in silicon. Computational Materials Science, 2004, 30, 8-15.	1.4	7
2925	Metals at finite temperature: a modified smearing scheme. Computational Materials Science, 2004, 30, 27-33.	1.4	3
2926	Structural and electronic properties of Ti impurities in SiC: an ab initio investigation. Computational Materials Science, 2004, 30, 57-61.	1.4	4
2927	Nickel impurities in diamond: a FP-LAPW investigation. Computational Materials Science, 2004, 30, 62-66.	1.4	4
2928	Ab initio investigations on the dislocation core properties in zinc-blende semiconductors. Computational Materials Science, 2004, 30, 67-72.	1.4	4
2929	First-principles study of structural, dynamical, and dielectric properties of A-La2O3. Computational Materials Science, 2004, 31, 125-130.	1.4	28
2930	Overcoming the doping bottleneck in semiconductors. Computational Materials Science, 2004, 30, 337-348.	1.4	462
2931	Further study on structural and electronic properties of silicon phosphide compounds with 3:4 stoichiometry. Computational Materials Science, 2004, 30, 371-375.	1.4	5
2932	Structural and electronic properties of C3N4â^'nPn (n=0,1,2,3,4). Computational Materials Science, 2004, 30, 364-370.	1.4	13
2933	Propertiesofstrainedzinc-blendeGaN:first-principlesstudy. Journal of Alloys and Compounds, 2004, 366, 86-93.	2.8	44
2934	Electronic structure and Rietveld refinement parameters of Ti-doped sodium alanates. Journal of Alloys and Compounds, 2004, 375, 1-10.	2.8	81
2935	First-principles calculations of the elastic properties of ZrC and ZrN. Journal of Alloys and Compounds, 2004, 377, 221-224.	2.8	65
2936	Electronic and elastic properties of RCo5 and RCo5H (R = La, Ce, Pr). Journal of Alloys and Compounds, 2004, 379, 41-53.	2.8	23
2937	A theoretical search for intermetallic compounds and solution phases in the binary system Sn/Zn. Journal of Alloys and Compounds, 2004, 379, 110-116.	2.8	9
2938	Thermal expansion of the perovskite-type NdGaO3. Journal of Alloys and Compounds, 2004, 382, 84-91.	2.8	28
2939	Comment on â€œEnthalpies of formation of binary Laves phasesâ€•[Intermetallics, 10 (2002) 579â€“595]. Intermetallics, 2004, 12, 59-62.	1.8	23
2940	Photoelasticity of sodium silicate glass from first principles. Physical Review B, 2004, 70, .	1.1	39
2941	Direct Observation of Charge Transfer at a MgO(111) Surface. Physical Review Letters, 2004, 92, 026101.	2.9	36

#	Article	IF	Citations
2942	Magnetic properties of vacancies in graphene and single-walled carbon nanotubes. New Journal of Physics, 2004, 6, 68-68.	1.2	370
2943	Ab Initio Study of Chemisorption Reactions for Carboxylic Acids on Hydrogenated Silicon Surfaces. Journal of Physical Chemistry B, 2004, 108, 17278-17280.	1.2	21
2944	Effect of exchangeable cation on the swelling property of 2:1 dioctahedral smectiteâ€"A periodic first principle study. Journal of Chemical Physics, 2004, 120, 3414-3424.	1.2	61
2945	Resonant diffraction inFeS2:Determination of the x-ray polarization anisotropy of iron atoms. Physical Review B, 2004, 69, .	1.1	26
2946	Strain Induced Deep Electronic States around Threading Dislocations in GaN. Physical Review Letters, 2004, 93, 196401.	2.9	107
2947	Unoccupied electronic states inCaB6studied by density functional theory and EELS measurements. Physical Review B, 2004, 69, .	1.1	19
2948	Melting curve of materials: theory versus experiments. Journal of Physics Condensed Matter, 2004, 16, S973-S982.	0.7	59
2949	First-principles calculation of the electronic structure of the stoichiometric pyrite FeS2(100) surface (No. 03-11). Computational Materials Science, 2004, 29, 89-94.	1.4	21
2950	Structural phase transitions in the Cu-based Cuâ€"V solid solutions studied by molecular dynamics simulation. Journal of Alloys and Compounds, 2004, 366, 205-212.	2.8	6
2951	Hydrogen storage in LiAlH4: Predictions of the crystal structures and reaction mechanisms of intermediate phases from quantum mechanics. Journal of Chemical Physics, 2004, 121, 10623-10633.	1.2	47
2952	Alternative Low-Symmetry Structure for 13-Atom Metal Clusters. Physical Review Letters, 2004, 93, 133401.	2.9	195
2953	Role of structural defects on the half-metallic character ofCo2MnGeandCo2MnSiHeusler alloys. Physical Review B, 2004, 69, .	1.1	409
2954	Structural, electronic, and dynamical properties of calaveriteAuTe2under pressure. Physical Review B, 2004, 69, .	1.1	7
2955	Adsorption modes of cysteine on Au(111): Thiolate, amino-thiolate, disulfide. Journal of Chemical Physics, 2004, 120, 4906-4914.	1.2	190
2956	Stability and electronic properties ofSn3P4. Physical Review B, 2004, 70, .	1.1	16
2957	Sampling the diffusion paths of a neutral vacancy in silicon with quantum mechanical calculations. Physical Review B, 2004, 70, .	1.1	80
2958	Quasiharmonic approach to a second-order phase transition. Physical Review B, 2004, 70, .	1.1	17
2959	Degradation of Boron-Doped Czochralski-Grown Silicon Solar Cells. Physical Review Letters, 2004, 93, 055504.	2.9	80

#	Article	IF	Citations
2960	Electronic structure of the chainlike compound TlSe. Physical Review B, 2004, 70, .	1.1	31
2961	Solid-State Chemistry and Electrochemistry of LiCo[sub 1/3]Ni[sub 1/3]Mn[sub 1/3]O[sub 2] for Advanced Lithium-Ion Batteries. Journal of the Electrochemical Society, 2004, 151, A1545.	1.3	154
2962	Atomic and electronic structure of unreduced and reduced CeO2 surfaces: A first-principles study. Journal of Chemical Physics, 2004, 120, 7741-7749.	1.2	338
2963	Ab initiostudy of foreign interstitial atom (C, N) interactions with intrinsic point defects inÎ±-Fe. Physical Review B, 2004, 69, .	1.1	351
2964	Strain effects and anomalous x-ray scattering in tetragonal manganites. New Journal of Physics, 2004, 6, 165-165.	1.2	2
2965	Atomic configuration of boron pile-up at the Si/SiO2 interface. IEICE Electronics Express, 2004, 1, 126-130.	0.3	7
2966	Structural Stability of the Metastable Solid Solution in the Equilibrium Immiscible Agâ€“Mo System Predicted by anab InitioDerived Potential. Journal of the Physical Society of Japan, 2004, 73, 1222-1227.	0.7	5
2967	Atomistic Modeling of Metastable Phase Selection of a Highly Immiscible Agâ€“W System. Journal of the Physical Society of Japan, 2004, 73, 2023-2027.	0.7	6
2968	Periodic solids and electron bands. , 2004, , 73-99.		1
2969	The Kohnâ€“Sham auxiliary system. , 2004, , 135-151.		1
2970	Functionals for exchange and correlation. , 2004, , 152-171.		3
2971	Plane waves and grids: basics. , 2004, , 236-253.		0
2972	Localized orbitals: tight-binding. , 2004, , 272-297.		0
2973	Localized orbitals: full calculations. , 2004, , 298-312.		0
2974	Augmented functions: APW, KKR, MTO. , 2004, , 313-344.		0
2975	Quantum molecular dynamics (QMD). , 2004, , 371-386.		0
2976	Excitation spectra and optical properties. , 2004, , 406-417.		0
2982	Augmented functions: linear methods. , 2004, , 345-368.		0

#	Article	IF	Citations
2985	Calculation of boron segregation at the Si(100)/SiO2interface. EPJ Applied Physics, 2004, 27, 163-166.	0.3	4
2986	Electronic States of Sulfur Doped TiO₂ by First Principles Calculations. Materials Transactions, 2004, 45, 1987-1990.	0.4	36
2987	Ab initio Modeling of the Stress-Strain Response of SiAlON (Si_{6-z}Al_zO_zN_{8-z},) Tj ETQq0 0 0 rgBT /Overlock 10	0.4	
2988	Vibrational Contribution on Nucleation Free Energy of Cu Precipitates in Fe-Cu System. Materials Transactions, 2004, 45, 1473-1477.	0.4	7
2989	Density functional theory: foundations. , 2004, , 119-134.		6
2990	First-principles study of C60 and C60F36 as transfer dopants for p-type diamond. Journal of Physics Condensed Matter, 2005, 17, L21-L26.	0.7	18
2991	GW Method for Extended, Periodic Systems with a Mixed Slater-Orbital/Plane-Wave Basis and Fourier Transform Techniques. Advances in Quantum Chemistry, 2005, , 35-45.	0.4	2
2992	Structural Stability and Homogeneity of the Nonequilibrium Coâ€“Ag Alloys. Journal of the Physical Society of Japan, 2005, 74, 375-381.	0.7	6
2994	Elastic Constants of AlLi from First Principles. Materials Transactions, 2005, 46, 1117-1121.	0.4	32
2995	First-Principles-Calculation Method for Optimizing Strain to Reduce Gate Leakage Current in MOS Transistors with Silicon Oxynitride Gate Dielectrics. JSME International Journal Series A-Solid Mechanics and Material Engineering, 2005, 48, 14-19.	0.4	1
2996	High-Pressure Elasticity and Auxetic Property of α-Cristobalite. Materials Transactions, 2005, 46, 1161-1166.	0.4	18
2997	Band structures of rare-gas solids within theGWapproximation. Physical Review B, 2005, 71, .	1.1	16
2998	FAVORABLE SILICA MONOLAYER STRUCTURES ON THE Mo(112) SURFACE. Surface Review and Letters, 2005, 12, 449-456.	0.5	17
2999	Surface diffusion and incorporation of adatom in Co/Al (001) system. Journal of Solid State Chemistry, 2005, 178, 47-51.	1.4	6
3000	Band structure calculations on the monoclinic bulk and nano-SrAl2O4 crystals. Journal of Solid State Chemistry, 2005, 178, 230-233.	1.4	35
3001	Transition metal intermetallics: Structure maps based on quantum mechanical stability. Journal of Solid State Chemistry, 2005, 178, 1269-1283.	1.4	21
3002	Full potential linearized augmented plane wave calculations of positronic and electronic charge densities of zinc-blende AlN, InN and their alloy Al0.5In0.5N. Journal of Solid State Chemistry, 2005, 178, 2117-2127.	1.4	15
3003	Hydrides with the perovskite structure: General bonding and stability considerations and the new representative CaNiH3. Journal of Solid State Chemistry, 2005, 178, 3381-3388.	1.4	52

#	Article	IF	Citations
3004	Structure and property correlation for Ag deposition on Î±-Al2O3â€"a first principle study. Journal of Molecular Graphics and Modelling, 2005, 23, 447-456.	1.3	24
3005	Structural and magnetic properties of clean and methylthiolate-adsorbed Co(0001) surfaces: a first-principles study. Journal of Magnetism and Magnetic Materials, 2005, 286, 119-123.	1.0	7
3006	Point defects in uranium dioxide: Ab initio pseudopotential approach in the generalized gradient approximation. Journal of Nuclear Materials, 2005, 347, 44-51.	1.3	127
3007	Structure instability of A2Al2B2O7 (A=K, Na) crystals. Journal of Physics and Chemistry of Solids, 2005, 66, 1655-1659.	1.9	18
3008	First-principles calculation of defect formation energy in chalcopyrite-type CuInSe2, CuGaSe2 and CuAlSe2. Journal of Physics and Chemistry of Solids, 2005, 66, 1924-1927.	1.9	47
3009	The electronic and atomic structure of SrTiO3, BaTiO3, and PbTiO3(001) surfaces: Ab initio DFT/HF hybrid calculations. Microelectronic Engineering, 2005, 81, 472-477.	1.1	16
3010	The electronic structures and optical properties of BaTiO3 and SrTiO3 using first-principles calculations. Microelectronics Journal, 2005, 36, 725-728.	1.1	67
3011	Structural and optical properties of CaO. Microelectronics Journal, 2005, 36, 1058-1061.	1.1	19
3012	Ab initio calculation of the structural and electronic properties of the SiC (100) Surfaces. Microelectronics Journal, 2005, 36, 998-1001.	1.1	0
3013	Ab initio calculation of the SiC (100) surfaces phonon dispersion. Microelectronics Journal, 2005, 36, 1026-1028.	1.1	2
3014	Predictive study of electronic properties of siliconâ€"carbon alloys. Materials Science and Engineering B: Solid-State Materials for Advanced Technology, 2005, 122, 145-151.	1.7	4
3015	Annealing of vacancy complexes in P-doped silicon. Nuclear Instruments & Methods in Physics Research B, 2005, 228, 218-225.	0.6	25
3016	An ab initio study of H2 interaction with the Pu (100) surface. Physica B: Condensed Matter, 2005, 366, 95-109.	1.3	20
3017	First-principles calculations of the structural, electronic and optical properties of and. Physica B: Condensed Matter, 2005, 367, 142-151.	1.3	36
3018	GaN growth process using GaP(111)A and (111)B surfaces as an initial substrate. Journal of Crystal Growth, 2005, 275, e1631-e1636.	0.7	1
3019	Surfactant effect of Sb on GaN growth. Journal of Crystal Growth, 2005, 285, 146-155.	0.7	23
3020	Structural stabilities and electronic structures of Ti atomic chains. Physica E: Low-Dimensional Systems and Nanostructures, 2005, 30, 138-142.	1.3	14
3021	First-principle calculation of two-photon absorption in BaTiO3. Physics Letters, Section A: General, Atomic and Solid State Physics, 2005, 335, 499-504.	0.9	0

#	Article	IF	Citations
3022	First principles study of wurtzite and zinc blende GaN: a comparison of the electronic and optical properties. Physics Letters, Section A: General, Atomic and Solid State Physics, 2005, 336, 145-151.	0.9	30
3023	Ab initio investigation of the surface properties of Cu(111) and Li diffusion in Cu thin film. Physics Letters, Section A: General, Atomic and Solid State Physics, 2005, 337, 247-255.	0.9	45
3024	Full-potential calculations of structural, elastic and electronic properties of MgAl2O4 and ZnAl2O4 compounds. Physics Letters, Section A: General, Atomic and Solid State Physics, 2005, 344, 271-279.	0.9	73
3025	Structure and Born effective charge determination for planar-zigzag Î²-poly(vinylidene fluoride) using density-functional theory. Polymer, 2005, 46, 10431-10436.	1.8	27
3026	First-principles calculations of optical properties of GeC, SnC and GeSn under hydrostatic pressure. Physica B: Condensed Matter, 2005, 355, 392-400.	1.3	35
3027	First-principles study of bonding mechanisms in the series of Ti, V, Cr, Mo, and their carbides and nitrides. Physica B: Condensed Matter, 2005, 358, 63-71.	1.3	38
3028	First-principles study of structural, elastic and high-pressure properties of cerium chalcogenides. Physica B: Condensed Matter, 2005, 363, 255-261.	1.3	37
3029	Structural and electronic properties of BAs and BxGa1â^'xAs, BxIn1â^'xAs alloys. Physica B: Condensed Matter, 2005, 364, 263-272.	1.3	63
3030	Optical properties of BP, BAs and BSb compounds under hydrostatic pressure. Physica B: Condensed Matter, 2005, 367, 195-204.	1.3	51
3031	Occurrence of superconductivity in diboride of Zr. Physica C: Superconductivity and Its Applications, 2005, 426-431, 464-468.	0.6	2
3032	Local vibrations on hydrogen dimers in dilute SiGe crystalline solutions. Materials Science and Engineering B: Solid-State Materials for Advanced Technology, 2005, 124-125, 363-367.	1.7	3
3033	Ab initio calculations of the interaction between native point defects in silicon. Materials Science and Engineering B: Solid-State Materials for Advanced Technology, 2005, 124-125, 368-371.	1.7	7
3034	Modeling rhenium metallization of a silicon-rich (001) 6H-SiC surface. Materials Science in Semiconductor Processing, 2005, 8, 497-501.	1.9	0
3035	First-principles calculation for bowing parameter of wurtzite InxGa1â^'xN. Optics Communications, 2005, 249, 217-223.	1.0	33
3036	Theoretical studies on band structure and optical properties of 3Câ€“SiC by FPLAPW. Journal of Electron Spectroscopy and Related Phenomena, 2005, 144-147, 593-596.	0.8	9
3037	The first principle study on the atomic and electronic structure of GaN() surface. Journal of Electron Spectroscopy and Related Phenomena, 2005, 144-147, 597-600.	0.8	2
3038	First-principles calculations on the surface electronic and reactive properties of M/SnO2 (M=Ge, Mn) (110). Computational and Theoretical Chemistry, 2005, 714, 221-233.	1.5	17
3039	Quantum mechanics calculations on the diastereomeric salts of cyclic phosphoric acids with ephedrine. Computational and Theoretical Chemistry, 2005, 717, 205-214.	1.5	0

#	Article	IF	Citations
3040	Half-metallic ferromagnetism of zinc-blende CrS and CrP: a first-principles pseudopotential study. Solid State Communications, 2005, 133, 301-304.	0.9	203
3041	Electronic structure of Sc2AC (A=Al, Ga, In, Tl). Solid State Communications, 2005, 133, 381-383.	0.9	25
3042	Ab initio molecular dynamics study of ion-surface interactions. Solid State Communications, 2005, 134, 333-336.	0.9	6
3043	Ab initio studies of adsorption and migration surface processes on an Î±-Al2O3 surface. Solid State Communications, 2005, 135, 90-94.	0.9	10
3044	Structural and electronic properties of 9R diamond polytype. Solid State Communications, 2005, 136, 41-44.	0.9	9
3045	Electronic structures of V-doped anatase TiO2. Solid State Communications, 2005, 136, 142-146.	0.9	66
3046	Spontaneous emission and lame shift in photonic crystals. Science and Technology of Advanced Materials, 2005, 6, 814-822.	2.8	8
3047	Hydrogen adsorption energies on bimetallic overlayer systems at the solidâ€“vacuum and the solidâ€“liquid interface. Surface Science, 2005, 597, 42-50.	0.8	50
3048	Facetting and (nÃ—1) reconstructions of SrTiO3(110) surfaces. Surface Science, 2005, 574, 65-76.	0.8	26
3049	Ab initio studies of the cubic boron nitride (110) surface. Surface Science, 2005, 574, 269-286.	0.8	33
3050	Computational study of charge accumulation at SnO2(110) surface. Surface Science, 2005, 577, 127-138.	0.8	36
3051	DFT study of oxygen adsorption on W(112) surface. Surface Science, 2005, 577, 229-235.	0.8	17
3052	DFT study of Pt adsorption on low index SrTiO3 surfaces: SrTiO3(100), SrTiO3(111) and SrTiO3(110). Surface Science, 2005, 581, 66-87.	0.8	41
3053	Cobalt concentration effect in Pt1â^'xCox on the reversible potential for forming OHads from H2Oads in acid solution. Surface Science, 2005, 581, 105-117.	0.8	41
3054	A first principles study of adhesion and adhesive transfer at Al(111)/graphite(0001). Surface Science, 2005, 581, 155-168.	0.8	47
3055	On-surface and sub-surface oxygen on ideal and reconstructed Cu(100). Surface Science, 2005, 584, 62-69.	0.8	36
3056	First principles study of H2S adsorption and dissociation on Fe(110). Surface Science, 2005, 583, 60-68.	0.8	75
3057	On-surface and sub-surface oxygen adsorption on Ag(210): Vibrational properties. Surface Science, 2005, 587, 50-54.	0.8	12

#	Article	IF	Citations
3058	Relative stability of Si surfaces: A first-principles study. Surface Science, 2005, 588, 61-70.	0.8	62
3059	Band structure and electron gas of In chains on Si(111). Surface Science, 2005, 589, 77-90.	0.8	12
3060	Catalyst-induced changes in a substituted aromatic: A combined approach via experiment and theory. Surface Science, 2005, 589, 173-183.	0.8	23
3061	Theoretical study of oxygen adsorption at the Fe(110) and (100) surfaces. Surface Science, 2005, 590, 88-100.	0.8	138
3062	Effect of S contamination on properties of Fe(100) surfaces. Surface Science, 2005, 590, 63-75.	0.8	20
3063	A simple chemical view of relaxations at stoichiometric (110) surfaces of rutile-structure type oxides: A first-principles study of stishovite, SiO2. Surface Science, 2005, 594, 70-82.	0.8	10
3064	Effects of hydrogen on electronic properties of doped diamond. Carbon, 2005, 43, 1009-1014.	5.4	16
3065	Adsorption and decomposition of H2S on Pd(111) surface: a first-principles study. Catalysis Today, 2005, 99, 315-322.	2.2	89
3066	First principles calculations of the adsorption and diffusion of hydrogen on Fe(100) surface and in the bulk. Catalysis Today, 2005, 105, 44-65.	2.2	90
3067	A density functional theory study of the adsorption of acetone to the (111) surface of Pt: Implications for hydrogenation catalysis. Catalysis Today, 2005, 105, 85-92.	2.2	43
3068	Computational study of carbon segregation and diffusion within a nickel grain boundary. Acta Materialia, 2005, 53, 87-96.	3.8	36
3069	A combined first-principles and experimental study of the lattice site preference of Pt in B2 NiAl. Acta Materialia, 2005, 53, 2101-2109.	3.8	71
3070	First-principles study of constitutional point defects in B2 NiAl using special quasirandom structures. Acta Materialia, 2005, 53, 2643-2652.	3.8	42
3071	Grain boundary impurities in iron. Acta Materialia, 2005, 53, 2715-2726.	3.8	86
3072	Atomistic study on the structure and thermodynamic properties of Cr7C3, Mn7C3, Fe7C3. Acta Materialia, 2005, 53, 2727-2732.	3.8	83
3073	First-principles calculation of structural energetics of Alâ€“TM (TM=Ti, Zr, Hf) intermetallics. Acta Materialia, 2005, 53, 3225-3252.	3.8	202
3074	Predicting yield-stress anomalies in L12 alloys: Ni3Geâ€“Fe3Ge pseudo-binaries. Acta Materialia, 2005, 53, 3601-3612.	3.8	28
3075	Atomistic study on the site preference and thermodynamic properties for CrFeC. Acta Materialia, 2005, 53, 5305-5312.	3.8	59

#	Article	IF	Citations
3076	Density functional calculations of elastic properties of portlandite, Ca(OH)2. Cement and Concrete Research, 2005, 35, 199-202.	4.6	56
3077	Lattice inversion for interatomic potentials in AlN, GaN and InN. Chemical Physics, 2005, 309, 309-321.	0.9	22
3078	Consistent picture for the wetting structure of water/Ru(0001). Chemical Physics Letters, 2005, 402, 384-388.	1.2	57
3079	Theoretical calculation of the energy of formation of LiBH4. Chemical Physics Letters, 2005, 405, 73-78.	1.2	85
3080	Simulating temperature programmed desorption directly from density functional calculations: How adsorbate configurations relate to desorption features. Chemical Physics Letters, 2005, 407, 227-231.	1.2	9
3081	Water bilayer on the Pd/Au(111) overlayer system: Coadsorption and electric field effects. Chemical Physics Letters, 2005, 409, 157-162.	1.2	110
3082	First principles calculations of thermodynamics for semiconductor alloys. Chemical Physics Letters, 2005, 412, 92-96.	1.2	0
3083	Ab initio comparative study of montmorillonite structural models. Applied Surface Science, 2005, 242, 21-28.	3.1	19
3084	Carbon nanotube adsorbed on hydrogenated Si(001) surfaces. Applied Surface Science, 2005, 244, 124-128.	3.1	7
3085	First-principles study of electronic structure and optical properties of barium strontium titanates (Ba x Sr 1â^'x TiO 3). Applied Surface Science, 2005, 250, 146-151.	3.1	25
3086	A density functional study of molecular oxygen adsorption and reaction barrier on Pu (100) surface. European Physical Journal B, 2005, 43, 131-141.	0.6	21
3087	Relaxation of the Mo(112) and W(112) surfaces. European Physical Journal B, 2005, 44, 551-555.	0.6	15
3088	Quantum dynamics of the dissociation of H2 on Rh(111). European Physical Journal B, 2005, 45, 425-432.	0.6	9
3089	Structural, electronic and optical properties of fluorite-type compounds. European Physical Journal B, 2005, 47, 63-70.	0.6	31
3090	Structural properties of AlN from first principles calculations. European Physical Journal B, 2005, 47, 379-383.	0.6	50
3091	Effect of spin fluctuations on Tc from density-functional theory for superconductors. European Physical Journal B, 2005, 48, 207-217.	0.6	6
3092	Atomistic Deformation Modes in Strong Covalent Solids. Physical Review Letters, 2005, 94, 145505.	2.9	119
3093	Potential super-hard phases and the stability of diamond-like boronâ€“carbon structures. Journal of Physics Condensed Matter, 2005, 17, 3221-3229.	0.7	60

#	Article	IF	Citations
3094	Electronic properties of single-walled silicon nanotubes compared to carbon nanotubes. Physical Review B, 2005, 72, .	1.1	145
3095	Crystal structure of the Chevrel phaseSnMo6S8at high pressure. Physical Review B, 2005, 72, .	1.1	3
3096	Computational DFT Study of ZrSiO4 Polymorphs: Microelectronic, Nuclear Safety and Geological Implications. Materials Research Society Symposia Proceedings, 2005, 894, 1.	0.1	1
3097	Theory of Li in ZnO: A limitation for Li-basedp-type doping. Physical Review B, 2005, 71, .	1.1	323
3098	Structure and Bonding of Li1.42(5)Pd2Sn5.58(5):â€‰ A Lithium Intercalated Palladium Stannide. Chemistry of Materials, 2005, 17, 911-915.	3.2	9
3099	Titanium-Decorated Carbon Nanotubes as a Potential High-Capacity Hydrogen Storage Medium. Physical Review Letters, 2005, 94, 175501.	2.9	888
3100	An Investigation of Weak CHÂ·Â·Â·O Hydrogen Bonds in Maltose Anomers by a Combination of Calculation and Experimental Solid-State NMR Spectroscopy. Journal of the American Chemical Society, 2005, 127, 10216-10220.	6.6	185
3101	New class of non-carbon AlP nanotubes: Structure and electronic properties. JETP Letters, 2005, 81, 185-189.	0.4	18
3102	Nonchiral BN Haeckelite nanotubes. JETP Letters, 2005, 81, 346-350.	0.4	5
3103	Highly controlled acetylene accommodation in a metalâ€“organic microporous material. Nature, 2005, 436, 238-241.	13.7	1,386
3104	Geometry of {001} Surfaces of Spinel (MgAl2O4): First-Principles Simulations and Experimental Measurements. Journal of the American Ceramic Society, 2005, 88, 1544-1548.	1.9	34
3105	Structure and catalytic processes of N-containing species on Rh(111) from first principles. Journal of Catalysis, 2005, 232, 179-185.	3.1	33
3106	Full-potential investigation of the electronic and optical properties of stressed CdTe and ZnTe. Materials Chemistry and Physics, 2005, 92, 333-339.	2.0	68
3107	Full potential calculation of structural, electronic and optical properties of KMgF3. Materials Chemistry and Physics, 2005, 91, 185-191.	2.0	65
3108	Density-functional theory calculations on the magneto-optical Kerr effects in Co2TiSn and Co2ZrSn. Journal of Magnetism and Magnetic Materials, 2005, 292, 476-482.	1.0	10
3109	Phase stabilities, electronic and electrochemical properties of compounds in the LiAlSi system. Solid State Sciences, 2005, 7, 1125-1134.	1.5	27
3110	Magnetic and half-metallic properties of Cr-doped /spl beta/-SiC. IEEE Transactions on Magnetics, 2005, 41, 2733-2735.	1.2	15
3111	Magnetic property calculations for B2-Co/sub x/Al/sub 1-x/ structures at the interface of Co-Al multilayer. IEEE Transactions on Magnetics, 2005, 41, 3343-3345.	1.2	1

#	Article	IF	Citations
3112	Electronic structures, magnetism, and half-metallicities of full-Heusler Fe/sub 2-x/Co/sub x/CrAl (x=0,1,2) alloys. IEEE Transactions on Magnetics, 2005, 41, 3437-3439.	1.2	5
3113	The relationship between adsorption energies of methyl on metals and the metallic electronic properties: A first-principles DFT study. Journal of Computational Chemistry, 2005, 26, 871-878.	1.5	31
3114	A theoretical study on the structures and energetics of hypothetical TiM(NCN)3compounds of the 3dtransition metals. Journal of Computational Chemistry, 2005, 26, 1180-1188.	1.5	0
3115	Testing the Pairwise Additive Potential Approximation Using DFT: Coadsorption of CO and N on Rh(100). ChemPhysChem, 2005, 6, 473-480.	1.0	14
3116	A DFT Study of the Adsorption and Dissociation of CO on Fe(100): Influence of Surface Coverage on the Nature of Accessible Adsorption States. ChemPhysChem, 2005, 6, 254-260.	1.0	106
3117	Engineering the Electronic Structure of Single-Walled Carbon Nanotubes by Chemical Functionalization. ChemPhysChem, 2005, 6, 598-601.	1.0	71
3118	An Effective Pseudopotential for Modeling Gold Surface Slabs for Ab Initio Simulations. ChemPhysChem, 2005, 6, 1756-1760.	1.0	6
3119	The Influence of Promoters and Poisons on Carbon Monoxide Adsorption on Rh(100): A DFT Study. ChemPhysChem, 2005, 6, 1293-1298.	1.0	15
3120	Phase Stability and Broken-Symmetry Transition of Elemental Lithium up to 140 GPa. ChemPhysChem, 2005, 6, 1703-1706.	1.0	39
3121	Influence of Coadsorbates on the NO Dissociation on a Rhodium(311) Surface. ChemPhysChem, 2005, 6, 2513-2521.	1.0	15
3122	Density functional calculations of the reflectivity of shocked xenon with ionization based gap corrections. Contributions To Plasma Physics, 2005, 45, 300-304.	0.5	40
3123	Predicting New Ferromagnetic Nitrides from Electronic Structure Theory: IrFe3N and RhFe3N. Angewandte Chemie - International Edition, 2005, 44, 1205-1210.	7.2	59
3124	SrAlSiH: A Polyanionic Semiconductor Hydride. Angewandte Chemie - International Edition, 2005, 44, 7269-7273.	7.2	46
3127	Structure and Bonding of Zinc Antimonides: Complex Frameworks and Narrow Band Gaps. Chemistry - A European Journal, 2005, 11, 4912-4920.	1.7	88
3128	Structural and thermodynamic properties of water related defects in Î±-quartz. Physics and Chemistry of Minerals, 2005, 32, 323-331.	0.3	20
3129	Quantum-mechanical modeling of minerals at high pressures. The role of the Hamiltonian in a case study: the beryl (Al4Be6Si12O36). Physics and Chemistry of Minerals, 2005, 32, 471-479.	0.3	22
3130	Ab initio elasticity of FeS2 pyrite from 0 to 135ÂGPa. Physics and Chemistry of Minerals, 2005, 32, 564-567.	0.3	12
3131	Ab initio study of the high-pressure behavior of CaSiO3 perovskite. Physics and Chemistry of Minerals, 2005, 32, 146-153.	0.3	65

#	Article	IF	Citations
3132	A mapping of the electron localization function for earth materials. Physics and Chemistry of Minerals, 2005, 32, 208-221.	0.3	19
3133	Electron density distribution and bond critical point properties for forsterite, Mg2 SiO4, determined with synchrotron single crystal X-ray diffraction data. Physics and Chemistry of Minerals, 2005, 32, 301-313.	0.3	64
3134	First-principles study of the electronic properties of A2B3 minerals, with A=Bi,Sb and B=S,Se. Physics and Chemistry of Minerals, 2005, 32, 295-300.	0.3	109
3135	Vegardâ€™s law deviation in band gap and bowing parameter of AlxIn1-xN. Applied Physics A: Materials Science and Processing, 2005, 81, 651-655.	1.1	48
3136	First-principles calculation for bowing parameter of wurtzite AlxGa1-xN. Applied Physics A: Materials Science and Processing, 2005, 81, 1459-1463.	1.1	20
3137	Computer simulations in the study of gold nanowires: the effect of impurities. Applied Physics A: Materials Science and Processing, 2005, 81, 1551-1558.	1.1	15
3138	Valence basis sets for lanthanide 4f-in-core pseudopotentials adapted for crystal orbital ab initio calculations. Theoretical Chemistry Accounts, 2005, 113, 212-224.	0.5	121
3139	Wannier-type atomic orbitals for periodic systems. Theoretical Chemistry Accounts, 2005, 114, 19-28.	0.5	7
3140	Nonorthogonal ultralocalized functions and fitted Wannier functions for local electron correlation methods for solids. Theoretical Chemistry Accounts, 2005, 114, 276-282.	0.5	11
3141	Atomistic behaviors of Co adatom on Al (001) surface: first-principle approach. Journal of Magnetism and Magnetic Materials, 2005, 286, 399-404.	1.0	6
3142	Multiple lattice inversion approach to interatomic potentials for compound semiconductors. Journal of Physics and Chemistry of Solids, 2005, 66, 1256-1263.	1.9	25
3143	Second-order and third-order elastic properties of diamond: An ab initio study. Journal of Physics and Chemistry of Solids, 2005, 66, 1589-1597.	1.9	13
3144	The relationship between adsorption and solid acidity of heteropolyacids. Catalysis Today, 2005, 105, 134-143.	2.2	34
3145	Wavelet approach to quasi two-dimensional extended many-particle systems. I. Supercell Hartreeâ€“Fock method. Journal of Computational Physics, 2005, 205, 540-566.	1.9	9
3146	Electronic structure, lattice constant, optical and mechanical properties for NaCl-structured Tiâ€“Alâ€“N by density functional theory. Physica B: Condensed Matter, 2005, 358, 77-85.	1.3	6
3147	Half-metallic ferromagnetic semiconductors of V- and Cr-doped CdTe studied from first-principles pseudopotential calculations. Physica B: Condensed Matter, 2005, 366, 62-66.	1.3	110
3148	Experimental and theoretical studies of indium oxide gas sensors fabricated by spray pyrolysis. Sensors and Actuators B: Chemical, 2005, 106, 563-571.	4.0	94
3149	Elastic properties of tantalum carbide (TaC). Solid State Communications, 2005, 134, 245-250.	0.9	101

#	Article	IF	Citations
3150	First-principle calculations of structural, electronic and optical properties of BaTiO3 and BaZrO3 under hydrostatic pressure. Solid State Communications, 2005, 136, 120-125.	0.9	104
3151	First-principles study of protonic conduction in In-doped AZrO3 (A=Ca, Sr, Ba). Solid State Ionics, 2005, 176, 1091-1096.	1.3	70
3152	Progressive changes in atomic structure and gap states on Si(001) by Bi adsorption. Surface Science, 2005, 574, 43-51.	0.8	0
3153	Hybrid DFT calculations of the atomic and electronic structure for ABO3 perovskite (001) surfaces. Surface Science, 2005, 575, 75-88.	0.8	177
3154	The effect of surface symmetry on the adsorption energetics of SCH3 on gold surfaces studied using Density Functional Theory. Surface Science, 2005, 580, 19-29.	0.8	36
3155	Growth and hydrogenation of ultra-thin Mg films on Mo(111). Surface Science, 2005, 584, 17-26.	0.8	19
3156	DFT study of Rb/Si(100)-2Ã—1 system. Surface Science, 2005, 583, 119-125.	0.8	3
3157	Methane activation on Ni(111): Effects of poisons and step defects. Surface Science, 2005, 590, 127-137.	0.8	228
3158	The chemisorption of SO2 on the Cu/Au(111) surface: Interplay between ensemble and electronic effects. Surface Science, 2005, 592, 25-36.	0.8	29
3159	Energy scaling and surface patterning of halogen-terminated Si(001) surfaces. Surface Science, 2005, 591, L292-L298.	0.8	8
3160	Surface structure and energetics of oxygen and CO adsorption on Î±-Mo2C(0001). Surface Science, 2005, 596, 212-221.	0.8	60
3161	First-principles study of sulfur overlayers on Pd(111) surface. Surface Science, 2005, 596, 229-241.	0.8	38
3162	Surface atomic structure and energetics of tantalum. Surface Science, 2005, 598, 276-284.	0.8	29
3163	LEED and DFT investigation on the (2Ã—2)-S overlayer on Co(0001). Surface Science, 2005, 599, 113-121.	0.8	22
3164	Ab initio studies of hydrogen and oxygen chemisorptions on the cubic BN(111) surface. Surface Science, 2005, 599, 128-140.	0.8	4
3165	First-principles study of dielectric properties of cerium oxide. Thin Solid Films, 2005, 486, 136-140.	0.8	84
3166	From cluster calculations to molecular materials: a mixed pseudopotential approach to modeling mixed-valence systems. Journal of Molecular Modeling, 2005, 11, 288-292.	0.8	6
3167	Application of localized reactivity index in combination with periodic DFT calculation to rationalize the swelling mechanism of clay type inorganic material. Journal of Chemical Sciences, 2005, 117, 533-539.	0.7	18

#	Article	IF	Citations
3168	Linking first-principles energetics to CALPHAD: An application to thermodynamic modeling of the Al-Ca binary system. Metallurgical and Materials Transactions A: Physical Metallurgy and Materials Science, 2005, 36, 5-13.	1.1	41
3169	Diffusion of gold and native defects in mercury cadmium telluride. Journal of Electronic Materials, 2005, 34, 868-872.	1.0	5
3170	Crystal quality of InN thin films grown on ZnO substrate by radio-frequency molecular beam epitaxy. Journal of Electronic Materials, 2005, 34, 424-429.	1.0	8
3171	Atomic structure and electronic properties of the GaN/ZnO (0001) interface. Journal of Materials Science, 2005, 40, 3051-3057.	1.7	32
3172	Atomic and electronic structure of [0001]/($$ar{1}ar{2}30$$) Î£7 symmetric tilt grain boundary in ZnO bicrystal with linear current-voltage characteristic. Journal of Materials Science, 2005, 40, 3059-3066.	1.7	32
3173	Electronic Structure of Triple Phosphides MgSiP2, ZnSiP2, and CdSiP2. Russian Physics Journal, 2005, 48, 78-83.	0.2	9
3174	Electronic structure of Î±-Al2O3 in the bulk and on the surface. Russian Physics Journal, 2005, 48, 1127-1133.	0.2	4
3175	Geometrical parameterization of the crystal chemistry of P63/m apatites: comparison with experimental data and ab initio results. Acta Crystallographica Section B: Structural Science, 2005, 61, 635-655.	1.8	38
3176	L-Cysteine-I at 30 K. Acta Crystallographica Section E: Structure Reports Online, 2005, 61, o2739-o2742.	0.2	51
3177	Quantum software interfaced with crystal-structure databases: tools, results and perspectives. Journal of Applied Crystallography, 2005, 38, 697-705.	1.9	38
3178	A High Pressure Study on NH4Pb2Br5 Type Compounds Part II: Electronic Structure and Changes under High Pressure. Zeitschrift Fur Anorganische Und Allgemeine Chemie, 2005, 631, 141-147.	0.6	2
3179	Halbantiperowskite: Zur Struktur der Shandite M3/2AS (M = Co, Ni; A = In, Sn) und ihren Typ-Antitypbeziehungen. Zeitschrift Fur Anorganische Und Allgemeine Chemie, 2005, 631, 1463-1470.	0.6	66
3180	Structural and Electronic Properties of Bulk Gibbsite and Gibbsite Surfaces. Zeitschrift Fur Anorganische Und Allgemeine Chemie, 2005, 631, 1267-1271.	0.6	63
3181	Surface energies of simple metals from slabs: Comparison of exchange-correlation density functionals. International Journal of Quantum Chemistry, 2005, 101, 645-650.	1.0	10
3182	Theoretical study of the pressure-induced structural phase transition of ScSb and YSb. International Journal of Quantum Chemistry, 2005, 101, 770-773.	1.0	29
3183	Titanium oxides and silicates as high-Î² dielectrics: A first-principles investigation. International Journal of Quantum Chemistry, 2005, 101, 793-801.	1.0	19
3184	Periodic DFT approach to benzotrifuroxan crystal. International Journal of Quantum Chemistry, 2005, 102, 224-229.	1.0	13
3185	Density functional study of O2 adsorption on (100) surface of ?-uranium. International Journal of Quantum Chemistry, 2005, 102, 98-105.	1.0	33

#	Article	IF	Citations
3186	Wannier functions and chemical bonding in a slab model: MgO (001) and TiO2 (110) surfaces. International Journal of Quantum Chemistry, 2005, 104, 102-109.	1.0	1
3187	Local characteristics of the electronic structure of MgO: LCAO and plane-wave calculations. International Journal of Quantum Chemistry, 2005, 104, 110-113.	1.0	3
3188	Ab initio density functional study of MgO (001) surface with topological defects. International Journal of Quantum Chemistry, 2005, 104, 919-928.	1.0	5
3189	Ab initio study of molecular oxygen adsorption on Pu (111) surface. International Journal of Quantum Chemistry, 2005, 105, 280-291.	1.0	19
3190	Adsorption of 1-propanol on the Si(100) surface. International Journal of Quantum Chemistry, 2005, 105, 359-367.	1.0	8
3191	Trends in calculation of point and extended defects in wide-gap solids: periodic models of aperiodic systems. Physica Status Solidi A, 2005, 202, 235-242.	1.7	9
3192	Structural and electronic properties of thin fluorite-structure NiSi2, CoSi2and FeSi2interfaces and precipitates in Si. Physica Status Solidi (A) Applications and Materials Science, 2005, 202, 883-888.	0.8	14
3193	Hydrogenation and oxygenation of the (100) diamond surface and the consequences for transfer doping. Physica Status Solidi A, 2005, 202, 2091-2097.	1.7	24
3194	DFT LCAO and plane wave calculations of SrZrO3. Physica Status Solidi (B): Basic Research, 2005, 242, R11-R13.	0.7	29
3195	How do electronic properties of conventional III-V semiconductors hold for the III-V boron bismuth BBi compound?. Physica Status Solidi (B): Basic Research, 2005, 242, 2856-2863.	0.7	30
3196	Li2O at high pressures: structural properties, phase-transition, and phonons. Physica Status Solidi (B): Basic Research, 2005, 242, 1857-1863.	0.7	44
3197	First-principles calculations of the structural, electronic and optical properties of IIA-IV antifluorite compounds. Physica Status Solidi (B): Basic Research, 2005, 242, 2022-2032.	0.7	32
3198	Quasiparticle and excitonic effects in the optical spectra of diamond, SiC, Si, GaP, GaAs, InP, and AlN. Physica Status Solidi (B): Basic Research, 2005, 242, 2720-2728.	0.7	22
3199	First Principles Studies for the Interaction of Hydrogen with a Li(100) Surface. Journal of the Physical Society of Japan, 2005, 74, 478-482.	0.7	13
3200	Investigation of Structures and Properties of C3P4 Alloy Using First-Principles Electronic Structure Calculation. , 2005, , 419-425.		0
3201	Ab initiocalculation of the local vibrational modes of the interstitial boronâ€“interstitial oxygen defect in Si. Journal of Physics Condensed Matter, 2005, 17, L155-L159.	0.7	10
3202	Energetically Driven Reorganization of a Modified Catalytic Surface under Reaction Conditions. Journal of the American Chemical Society, 2005, 127, 2351-2357.	6.6	37
3203	Ab initioinvestigation of the lattice dynamics of fluoride scheelite LiYF4. Journal of Physics Condensed Matter, 2005, 17, 4953-4962.	0.7	10

#	Article	IF	Citations
3204	Composition Dependence of the Energy Barrier for Lithium Diffusion in Amorphous WO[sub 3]. Electrochemical and Solid-State Letters, 2005, 8, J21.	2.2	13
3205	Evaluations of Phases and Vacancy Formation Energies in KNbO3by First-Principles Calculation. Japanese Journal of Applied Physics, 2005, 44, 8048-8054.	0.8	51
3206	Manganese Impurity in Boron Nitride and Gallium Nitride. Materials Science Forum, 2005, 483-485, 1047-1050.	0.3	1
3207	Formation of Vacancies and Divacancies in Plane-Stressed Silicon. Solid State Phenomena, 2005, 108-109, 433-438.	0.3	3
3208	DFT Analysis of the Indium-Antimony-Vacancy Cluster in Silicon. Defect and Diffusion Forum, 2005, 245-246, 29-38.	0.4	2
3209	Metastable VO₂ Complexes in Silicon: Experimental and Theoretical Modeling Studies. Solid State Phenomena, 2005, 108-109, 223-228.	0.3	13
3210	The Effect of Compound Composition and Strain on Vacancies in Si/SiGe Heterostructures. Solid State Phenomena, 2005, 108-109, 457-462.	0.3	3
3211	IVb Transition Metal Oxides and Silicates: An Ab Initio Study. , 2005, , 249-290.		2
3212	Mechanisms of Diffusion and Dissociation of E-Centers in Silicon. Defect and Diffusion Forum, 2005, 237-240, 1129-1134.	0.4	0
3213	Segregation Effects on the Metal-Carbide Interface. Materials Science Forum, 2005, 475-479, 4251-4254.	0.3	2
3214	Theoretical study of protactinium at high pressure. Materials Research Society Symposia Proceedings, 2005, 893, 1.	0.1	0
3215	Half-metallic ferromagnetism in transition-metal encapsulated boron nitride nanotubes. New Journal of Physics, 2005, 7, 39-39.	1.2	54
3216	First-principles study of the effect of hydrogen on the metalâ€“ceramic interface. Journal of Physics Condensed Matter, 2005, 17, 5335-5348.	0.7	29
3217	Ab Initio Studies of Local Vibrations of Small Self-Interstitials Aggregates in Silicon. Solid State Phenomena, 2005, 108-109, 175-180.	0.3	0
3218	First-principles Studies of Phase Stability and the Neutral Atomic Vacancies in LiNbO3, NaNbO3 and KNbO3. Materials Research Society Symposia Proceedings, 2005, 902, 1.	0.1	2
3219	Electronic Properties and Structure of a Complex Incorporating a Self-Interstitial and two Oxygen Atoms in Silicon. Solid State Phenomena, 2005, 108-109, 273-278.	0.3	10
3220	Barrier to Migration of the Intrinsic Defects in Silicon in Different Charged System Using First-principles Calculations. Materials Research Society Symposia Proceedings, 2005, 864, 9171.	0.1	2
3221	Orientation and Composition Dependences of the Surface Energy and Work Function Observed by First-Principles Calculation for the Moâ€“Hf System. Journal of the Physical Society of Japan, 2005, 74, 1766-1771.	0.7	9

#	Article	IF	Citations
3222	First-Principles Calculations of Atomistic Behaviors in Ni/Al (001) and Al/Ni (001) System. Japanese Journal of Applied Physics, 2005, 44, 5700-5702.	0.8	14
3223	Structural relaxations around Ti, Cr and Fe impurities in Î±-Al2O3probed by x-ray absorption near-edge structure combined with first-principles calculations. Journal of Physics Condensed Matter, 2005, 17, 5467-5480.	0.7	46
3224	Vibrational properties of elemental hydrogen centres in Si, Ge and dilute SiGe alloys. Journal of Physics Condensed Matter, 2005, 17, S2155-S2164.	0.7	13
3225	Nonlinear algorithm for the solution of the Kohnâ€“Sham equations in solids. Journal of Physics Condensed Matter, 2005, 17, 3701-3715.	0.7	6
3226	The equilibrium structures of the 90Â° partial dislocation in silicon. Journal of Physics Condensed Matter, 2005, 17, 7547-7559.	0.7	9
3227	Theory of persistent, p-type, metallic conduction in c-GeTe. Journal of Physics Condensed Matter, 2005, 17, L329-L335.	0.7	55
3228	Atomic and electronic structure of carbon strings. Journal of Physics Condensed Matter, 2005, 17, 3823-3836.	0.7	30
3229	Chirality Dependence of Mechanical Properties of Single-Walled Carbon Nanotubes under Axial Tensile Strain. Japanese Journal of Applied Physics, 2005, 44, L1307-L1309.	0.8	30
3230	Ab initioelectronic and structural properties of clean and hydrogen saturated Î²-SiC(100)(3 Ã— 2) surfaces. Journal of Physics Condensed Matter, 2005, 17, 4739-4746.	0.7	10
3231	Theory of Jahnâ€“Teller distortions of the P donor in diamond. Journal of Physics Condensed Matter, 2005, 17, 5831-5837.	0.7	12
3232	Anion variations at semiconductor interfaces: ZnSe(100)/GaAs(100) superlattices. Journal of Vacuum Science & Technology an Official Journal of the American Vacuum Society B, Microelectronics Processing and Phenomena, 2005, 23, 406.	1.6	3
3233	Recent developments in surface studies of GaN and AlN. Journal of Vacuum Science & Technology an Official Journal of the American Vacuum Society B, Microelectronics Processing and Phenomena, 2005, 23, 1174.	1.6	65
3234	Stability of the Metastable Phases in the Coâ€“Ta System Studied byab initioand Thermodynamic Calculations Together with Ion-Beam-Mixing Experiment. Journal of the Physical Society of Japan, 2005, 74, 2501-2505.	0.7	11
3235	Theoretical adlayer surface morphology of wurtzite 2 Ã— 2 reconstructions of the GaN(0001) surface. Journal of Physics Condensed Matter, 2005, 17, 17-26.	0.7	10
3236	Investigation of the electronic structure in La1â^'xCaxCoO3(x= 0, 0.5) using full potential calculations. Journal of Physics Condensed Matter, 2005, 17, 7995-8003.	0.7	19
3237	Stability and properties of the cluster assembled solid phases of X8C12and YX7C12. Journal of Physics Condensed Matter, 2005, 17, 2571-2584.	0.7	4
3238	Electronic origin of shearing in M2AC (M = Ti,V,Cr,A = Al,Ga). Journal of Physics Condensed Matter, 2005, 17, 7169-7176.	0.7	51
3239	Methanol adsorption on the Si(100)-2 Ã— 1 surface: a first-principles calculation. Journal of Physics Condensed Matter, 2005, 17, 1289-1300.	0.7	19

#	Article	IF	Citations
3240	Hysteretic behaviour of the tipâ€“sample interaction on an InAs(110) surface: anab initiostudy. Nanotechnology, 2005, 16, S59-S62.	1.3	10
3241	H enhancement of N vacancy migration in GaN. Applied Physics Letters, 2005, 87, 201901.	1.5	6
3242	Thermodynamically complete equations of state for nickel-titanium alloy. Journal of Applied Physics, 2005, 98, 093512.	1.1	12
3243	Shallow electronic states induced by prismatic stacking faults in AlN and GaN. Applied Physics Letters, 2005, 86, 071901.	1.5	7
3244	Improving the orbital-free density functional theory description of covalent materials. Journal of Chemical Physics, 2005, 122, 044103.	1.2	85
3245	Activation of shallow boron acceptor in Câˆ•B coimplanted silicon carbide: A theoretical study. Applied Physics Letters, 2005, 86, 102108.	1.5	17
3246	Polarization enhancement in two- and three-component ferroelectric superlattices. Applied Physics Letters, 2005, 87, 102906.	1.5	106
3247	Molecular dissociation of group-V hydrides onSi(001). Physical Review B, 2005, 72, .	1.1	16
3248	Coverage and strain dependent magnetization of titanium-coated carbon nanotubes. Physical Review B, 2005, 71, .	1.1	14
3249	Electronic properties of the binary noble metal nitride PtN: First-principles calculations. Physical Review B, 2005, 72, .	1.1	51
3250	First-principles study of interstitial oxygen in potassium dihydrogen phosphate crystals. Physical Review B, 2005, 72, .	1.1	30
3251	Surface stress of partially H-covered Si(001) surfaces. Physical Review B, 2005, 72, .	1.1	10
3252	Electrical activity of Er and Er-O centers in silicon. Physical Review B, 2005, 71, .	1.1	9
3253	Magnetic coupling between Cr atoms doped at bulk and surface sites of ZnO. Applied Physics Letters, 2005, 87, 162509.	1.5	57
3254	Sb-induced reconstructions on Si(113): Adatoms as the key elements. Physical Review B, 2005, 72, .	1.1	5
3255	Normal mode approach for predicting the mechanical properties of solids from first principles: Application to compressibility and thermal expansion of zeolites. Physical Review B, 2005, 71, .	1.1	21
3256	Ab initiothermodynamics ofBacSr(1âˆ’c)TiO3solid solutions. Physical Review B, 2005, 71, .	1.1	56
3257	MgO addimer diffusion on MgO(100): A comparison ofab initioand empirical models. Physical Review B, 2005, 72, .	1.1	64

#	Article	IF	Citations
3258	First-principles study of a hydrogen storage material CaSi. Physical Review B, 2005, 72, .	1.1	22
3259	Role of spatial valence charge density on the metastability of an immiscible binary metal system at equilibrium. Physical Review B, 2005, 72, .	1.1	12
3260	Interpretation of the Hume-Rothery electron concentration rule in theT2Zn11(T=Ni, Pd, Co, and) Tj ETQq0 0 0 rgBT /Overlock 10 Tf 50 6	1.1	32
3261	Temperature and sample dependence of the binding free energies of complexes in crystals: The case of acceptor-oxygen complexes in Si. Physical Review B, 2005, 72, .	1.1	30
3262	Molecular-dynamics simulations of non-adiabatic processes at surfaces. Phase Transitions, 2005, 78, 773-786.	0.6	16
3263	Supported metal electronic structure: Implications for molecular adsorption. Physical Review B, 2005, 72, .	1.1	26
3264	Tunability of the dielectric response of epitaxially strainedSrTiO3from first principles. Physical Review B, 2005, 71, .	1.1	178
3265	Binding of the N interstitial with neutral MgH inp-type GaN investigated with density functional theory. Physical Review B, 2005, 72, .	1.1	4
3266	Thermal stability of the Rh(110) missing-row reconstruction: Combination of real-time core-level spectroscopy andab initiomodeling. Physical Review B, 2005, 72, .	1.1	17
3267	Verification of Hume-Rothery electron concentration rule inCu5Zn8andCu9Al4Î³brasses byab initioFLAPW band calculations. Physical Review B, 2005, 71, .	1.1	49
3268	Ab initiocharacterization of the mechanical and electronic properties ofÎ²-SiAlON (Si6â^'zAlzOzN8â^'z;z=0â€“5). Physical Review B, 2005, 71, .	1.1	16
3269	Hydrogen-induced magnetism in carbon nanotubes. Physical Review B, 2005, 72, .	1.1	53
3270	Structural model and electronic structure of the icosahedralAlâ^'Gaâ^'Pdâ^'Mnquasicrystal. Physical Review B, 2005, 72, .	1.1	6
3271	First-principles study of the (2,2) carbon nanotube. Physical Review B, 2005, 71, .	1.1	37
3272	Partitioning of solutes in multiphaseTiâ€“Alalloys. Physical Review B, 2005, 71, .	1.1	39
3273	Cluster expansion of electronic excitations: Application to fcc Niâ€“Al alloys. Journal of Chemical Physics, 2005, 122, 214706.	1.2	16
3274	Diffusion of nitrogen in silicon. Applied Physics Letters, 2005, 87, 021902.	1.5	24
3275	Metal-induced gap states in epitaxial organic-insulator/metal interfaces. Physical Review B, 2005, 72, .	1.1	19

#	Article	IF	Citations
3276	Electronic structure of Li with emphasis on the momentum density and the Compton profile. Physical Review B, 2005, 72, .	1.1	14
3277	Electronic structure and bonding ofÎ²-rhombohedral boron using cluster fragment approach. Physical Review B, 2005, 72, .	1.1	54
3278	All-electron first-principles calculations of clean surface properties of low-Miller-index Al surfaces. Physical Review B, 2005, 71, .	1.1	57
3279	Anharmonicity and lattice coupling of bond-centered hydrogen and interstitial oxygen defects in monoisotopic silicon crystals. Physical Review B, 2005, 72, .	1.1	5
3280	Vacancy-assisted arsenic diffusion and time-dependent clustering effects in silicon. Physical Review B, 2005, 71, .	1.1	6
3281	Silicon interstitials atSiâˆ•SiO2interfaces: Density functional calculations. Physical Review B, 2005, 72, .	1.1	24
3282	Electronic properties of barium chalcogenides from first-principles calculations: Tailoring wide-band-gap II-VI semiconductors. Physical Review B, 2005, 71, .	1.1	55
3283	Observation of substitutional and interstitial phosphorus on cleanSi(100)â^'(2Ã—1)with scanning tunneling microscopy. Physical Review B, 2005, 72, .	1.1	11
3284	Quasiparticle bands and optical spectra of highly ionic crystals: AlN and NaCl. Physical Review B, 2005, 72, .	1.1	65
3285	Structural, thermal, and electronic properties ofFe2VSi1â^'xAlx. Physical Review B, 2005, 71, .	1.1	22
3286	Ab initioinvestigation of noncontact atomic force microscopy tip-surface instability in InAs(110) surface. Physical Review B, 2005, 72, .	1.1	11
3287	Coverage dependence of oxygen decomposition and surface diffusion on rhodium (111): A DFT study. Journal of Chemical Physics, 2005, 122, 034710.	1.2	56
3288	Electronic properties ofFeCl3-adsorbed single-wall carbon nanotubes. Physical Review B, 2005, 72, .	1.1	11
3289	Ab initiostudy of the vibrational properties ofMg(AlH4)2. Physical Review B, 2005, 71, .	1.1	14
3290	On the convergence of isolated neutral oxygen vacancy and divacancy properties in metal oxides using supercell models. Journal of Chemical Physics, 2005, 122, 224705.	1.2	27
3291	In situpressure study ofRb4C60insulator to metal transition by Compton scattering. Physical Review B, 2005, 72, .	1.1	8
3292	Superhard hexagonal transition metal and its carbide and nitride: Os, OsC, and OsN. Physical Review B, 2005, 72, .	1.1	120
3293	Xe adsorption on metal surfaces: First-principles investigations. Physical Review B, 2005, 72, .	1.1	94

#	Article	IF	Citations
3294	Molecular hydrogen confined within nanoporous framework materials: Comparison of density functional and classical force-field descriptions. Physical Review B, 2005, 72, .	1.1	22
3295	Anomalously enhanced superconductivity andab initiolattice dynamics in transition metal carbides and nitrides. Physical Review B, 2005, 72, .	1.1	84
3296	Decomposition reactions forNaAlH4,Na3AlH6, and NaH: First-principles study. Physical Review B, 2005, 71, .	1.1	97
3297	First-principles study of the(112Â¯0)hBNâˆ•(112Â¯)cBNinterface. Physical Review B, 2005, 71, .	1.1	6
3298	Electron-phonon interaction in hole-dopedMgB2C2. Physical Review B, 2005, 72, .	1.1	14
3299	Theory of boron-vacancy complexes in silicon. Physical Review B, 2005, 71, .	1.1	19
3300	Theoretical study of nitrogen vacancies in Ti4AlN3. Applied Physics Letters, 2005, 86, 031911.	1.5	37
3301	Rotation of ad-dimers in the initial stages of Bi and Si deposition on the Si(001) surface. Physical Review B, 2005, 71, .	1.1	5
3302	BiferroicYCrO3. Physical Review B, 2005, 72, .	1.1	209
3303	First-principles study of the effect of lattice vibrations on Cu nucleation free energy in Fe-Cu alloys. Physical Review B, 2005, 72, .	1.1	32
3304	Trapping hydrogen with a bimetallic interface. Physical Review B, 2005, 71, .	1.1	17
3305	Hplacement inCr(Mo,Fe)âˆ•Vsupercells: The origin of the dead layers. Physical Review B, 2005, 71, .	1.1	9
3306	Possibility for the electrical activation of the carbon antisite by hydrogen inSiC. Physical Review B, 2005, 71, .	1.1	9
3307	Pressure induced complexity in a lithium monolayer:Ab initiocalculations. Physical Review B, 2005, 72, .	1.1	23
3308	B and N ion implantation into carbon nanotubes: Insight from atomistic simulations. Physical Review B, 2005, 71, .	1.1	88
3309	Order-disorder effects on the equation of state for fccNiâˆ’Alalloys. Physical Review B, 2005, 72, .	1.1	10
3310	Effect of magnesium on the structure and growth of GaN(0001). Applied Physics Letters, 2005, 86, 122108.	1.5	18
3311	Atomic Structure of a Thin Silica Film on a Mo(112) Substrate: A Two-Dimensional Network ofSiO4Tetrahedra. Physical Review Letters, 2005, 95, 076103.	2.9	201

#	Article	IF	Citations
3312	Fullerene in a Metal-Organic Matrix: Design of the Electronic Structure. Physical Review Letters, 2005, 95, 146403.	2.9	15
3313	Positron localization effects on the Doppler broadening of the annihilation line: Aluminum as a case study. Physical Review B, 2005, 72, .	1.1	44
3314	Role of semicore states in the electronic structure of group-III nitrides: An exact-exchange study. Physical Review B, 2005, 72, .	1.1	39
3315	van der Waals interaction of simple, parallel polymers. Journal of Chemical Physics, 2005, 122, 164902.	1.2	24
3316	Ab initio studies of a water layer at transition metal surfaces. Journal of Chemical Physics, 2005, 122, 054701.	1.2	89
3317	First-principles study of ferromagnetic coupling in Zn1â^'xCrxTe thin film. Journal of Applied Physics, 2005, 97, 043904.	1.1	16
3318	Manipulating the electronic structures of silicon carbide nanotubes by selected hydrogenation. Journal of Chemical Physics, 2005, 122, 214707.	1.2	72
3319	Initial Stages of Ti Growth on Diamond (100) Surfaces: From Single Adatom Diffusion to Quantum Wire Formation. Physical Review Letters, 2005, 94, 086101.	2.9	20
3320	Melting Curve of MgO from First-Principles Simulations. Physical Review Letters, 2005, 94, 235701.	2.9	158
3321	Influence of initial oxygen coverage and magnetic moment on the NO decomposition on rhodium (111). Journal of Chemical Physics, 2005, 122, 154702.	1.2	29
3322	N interstitial and its interaction with substitutional Mg in p-type GaN. Journal of Applied Physics, 2005, 98, 033704.	1.1	3
3323	AbÂInitioTheory of Dynamical Core-Hole Screening in Graphite from X-Ray Absorption Spectra. Physical Review Letters, 2005, 94, 167401.	2.9	51
3324	First-principles study of phonon modes inPuCoGa5superconductor. Physical Review B, 2005, 72, .	1.1	39
3325	Spin-polarized ballistic transport in a thin superlattice of zinc blende half-metallic compounds. Physical Review B, 2005, 71, .	1.1	16
3326	First-principles study of phase stability in pseudobinary(Ni1â^'xPtx)3Alalloys. Physical Review B, 2005, 72, .	1.1	38
3327	Density-functional study of oxygen adsorption on Mo(112). Journal of Chemical Physics, 2005, 122, 044712.	1.2	26
3328	Atomic and electronic structure of the(4Ã—1)and(8Ã—2)Inâ•Si(111)surfaces. Physical Review B, 2005, 71, .	1.1	25
3329	Cubic and orthorhombic structures of aluminum hydrideAlH3predicted by a first-principles study. Physical Review B, 2005, 71, .	1.1	67

#	Article	IF	Citations
3330	Origin of the C-inducedp4greconstruction of Ni(001). Physical Review B, 2005, 72, .	1.1	25
3331	Hexagonal close-packed Ni nanostructures grown on the (001) surface of MgO. Applied Physics Letters, 2005, 86, 131915.	1.5	76
3332	Structure and dynamics of the diarsenic complex in crystalline silicon. Physical Review B, 2005, 72, .	1.1	9
3333	Supported nanoclusters: Preadsorbates tuning catalytic activity. Physical Review B, 2005, 71, .	1.1	5
3334	Cu0*: A metastable configuration of the{Cus,Cui}pair in Si. Physical Review B, 2005, 72, .	1.1	21
3335	Structure and vibrational properties ofNâˆ’H2complexes in GaAs:N. Physical Review B, 2005, 72, .	1.1	21
3336	Oxygen-induced atomic desorptions in oxynitrides: Density functional calculations. Physical Review B, 2005, 72, .	1.1	5
3337	Interaction of doping impurities with the 30Â° partial dislocations in SiC: Anab initioinvestigation. Physical Review B, 2005, 72, .	1.1	16
3338	X-ray absorption spectroscopy in MnxGe1âˆ’x diluted magnetic semiconductor: Experiment and theory. Applied Physics Letters, 2005, 86, 062501.	1.5	48
3339	Theory ofMnGaâˆ’Hand other acceptor-H complexes in GaAs. Physical Review B, 2005, 72, .	1.1	7
3340	Nonadiabaticity in the initial oxidation of Mg(0001): First-principles density-functional calculations. Physical Review B, 2005, 72, .	1.1	22
3341	Substrate-dependent electronic properties of an armchair carbon nanotube adsorbed on Hâˆ•Si(001). Applied Physics Letters, 2005, 86, 213111.	1.5	34
3342	Magnetic doping of4dtransition-metal surfaces: A first-principles study. Physical Review B, 2005, 71, .	1.1	19
3343	Electron-induced stabilization of ferromagnetism inGa1âˆ’xGdxN. Physical Review B, 2005, 72, .	1.1	120
3344	Carbon monoxide reaction with UO2(111) single crystal surfaces: A theoretical and experimental study. Journal of Vacuum Science and Technology A: Vacuum, Surfaces and Films, 2005, 23, 1078-1084.	0.9	18
3345	Ab initiostudy of ferromagnetism inGa1âˆ’xCrxNthin films. Physical Review B, 2005, 72, .	1.1	21
3346	Structure and bonding ofM2SbP(M=Ti,Zr,Hf). Physical Review B, 2005, 71, .	1.1	29
3347	Ab initiocalculation of impurity effects in copper oxide materials. Physical Review B, 2005, 72, .	1.1	25

#	Article	IF	Citations
3348	A candidate LiBH4 for hydrogen storage: Crystal structures and reaction mechanisms of intermediate phases. Applied Physics Letters, 2005, 87, 111904.	1.5	65
3349	Atomic structure of theTeâˆ•Si(100)â€(2Ã—1)surface. Physical Review B, 2005, 72, .	1.1	1
3350	Density-functional study of small interstitial clusters in Si: Comparison with experiments. Physical Review B, 2005, 72, .	1.1	41
3351	Dependence of oxygen dissociative adsorption on platinum surface structures. Physical Review B, 2005, 72, .	1.1	23
3352	First-principles study of Sb-stabilized GaSb(001) surface reconstructions. Physical Review B, 2005, 71, .	1.1	26
3353	Tailoring the electronic properties of silicon with cysteine: A first-principles study. Physical Review B, 2005, 72, .	1.1	5
3354	Crossover energetics for halogenated Si(100): Vacancy line defects, dimer vacancy lines, and atom vacancy lines. Physical Review B, 2005, 71, .	1.1	12
3355	Transition from theRh2O3(II)-to-CaIrO3structure and the high-pressure-temperature phase diagram of alumina. Physical Review B, 2005, 72, .	1.1	64
3356	Relative concentration and structure of native defects in GaP. Physical Review B, 2005, 72, .	1.1	29
3357	Molecular hydrogen adsorption and dissociation on the plutonium (111) surface. Physical Review B, 2005, 72, .	1.1	32
3358	First-principles study of Mn-induced local magnetic moments in host semiconductors. Physical Review B, 2005, 71, .	1.1	23
3359	Fully relativistic two-component-spinor approach in the ultrasoft-pseudopotential plane-wave method. Physical Review B, 2005, 72, .	1.1	25
3360	Ab initiostudies on the stability and electronic structure ofLiCoO2(003) surfaces. Physical Review B, 2005, 71, .	1.1	29
3361	Transition from ferromagnetism to antiferromagnetism in Ga1â^'xMnxN. Journal of Applied Physics, 2005, 98, 083905.	1.1	18
3362	A density-functional theory study of the interaction of N2O with Rh(110). Journal of Chemical Physics, 2005, 122, 034708.	1.2	33
3363	Theoretical study of the mechanism of dry oxidation of4H-SiC. Physical Review B, 2005, 71, .	1.1	133
3364	First-principles investigation of the role of registry relaxations on stepped Cu(100) surfaces. Physical Review B, 2005, 72, .	1.1	12
3365	Ab initiostudy ofMg(AlH4)2. Physical Review B, 2005, 72, .	1.1	49

#	Article	IF	Citations
3366	Systematic, multisite short-range-order corrections to the electronic structure of disordered alloys from first principles: The KKR nonlocal CPA from the dynamical cluster approximation. Physical Review B, 2005, 72, .	1.1	39
3367	Cs adsorption on Si(001) surface: Anab initiostudy. Physical Review B, 2005, 72, .	1.1	12
3368	Isostructural phase transitions inGaNâˆ•ScNandInNâˆ•ScNsuperlattices. Physical Review B, 2005, 71, .	1.1	23
3369	Quasiparticle energy bands of NiO in theGWapproximation. Physical Review B, 2005, 71, .	1.1	61
3370	Symmetry analysis for localized function generation and chemical bonding in crystals:SrZrO3and MgO as examples. Physical Review B, 2005, 72, .	1.1	5
3371	Reduction of amplitude and wavelength of Friedel oscillation on Na(111) surface. Physical Review B, 2005, 72, .	1.1	6
3372	Effects of fluorination on electronic and excited states of fused zinc oligoporphyrins. Journal of Chemical Physics, 2005, 122, 184702.	1.2	15
3373	Ab initio dynamics study of poly-para-phenylene vinylene. Journal of Chemical Physics, 2005, 123, 024904.	1.2	15
3374	InterstitialH2in germanium by Raman scattering andab initiocalculations. Physical Review B, 2005, 72, .	1.1	19
3375	Coexistence of antiferrodistortive and ferroelectric distortions at thePbTiO3(001)surface. Physical Review B, 2005, 71, .	1.1	59
3376	First-principles study of the atomic and electronic structure of theSi(111)â˜'(5Ã—2)â˜'Ausurface reconstruction. Physical Review B, 2005, 71, .	1.1	43
3377	AbÂInitioIdentification of the Nitrogen Diffusion Mechanism in Silicon. Physical Review Letters, 2005, 95, 025901.	2.9	28
3378	Effect of the Mn clustering in (GaMn)N on the magnetic transition temperature. Physical Review B, 2005, 71, .	1.1	24
3379	Deactivation mechanism of In atoms doped in a Si crystal and reactivation due to codoping with B and C. Physical Review B, 2005, 71, .	1.1	14
3380	Physical Origin of Hydrogen-Adsorption-Induced Metallization of the SiC Surface:n-Type Doping via Formation of Hydrogen Bridge Bond. Physical Review Letters, 2005, 95, 196803.	2.9	30
3381	First-principles investigations of nitrogen-doping effects on defect aggregation processes in Czochralski Si. Journal of Applied Physics, 2005, 97, 053514.	1.1	18
3382	Electronic behavior of rare-earth dopants in AlN: A density-functional study. Physical Review B, 2005, 72, .	1.1	36
3383	Schottky defect formation energy in MgO calculated by diffusion Monte Carlo. Physical Review B, 2005, 71, .	1.1	69

#	Article	IF	Citations
3384	Heterovalent interlayers and interface states: Anab initiostudy ofGaAsâˆ•Siâˆ•GaAs(110) and (100) heterostructures. Physical Review B, 2005, 71, .	1.1	7
3385	First-principles study of ultrathin magnetic Mn films on W surfaces.. Physical Review B, 2005, 72, .	1.1	19
3386	Properties ofGaNâˆ•ScNandInNâˆ•ScNsuperlattices from first principles. Physical Review B, 2005, 72, .	1.1	37
3387	Localization of Wannier functions for entangled energy bands. Physical Review B, 2005, 71, .	1.1	15
3388	Point defect geometries in inverted opal photonic crystals. Physical Review E, 2005, 71, 056602.	0.8	11
3389	The effect of octahedral tilting on proton binding sites and transition states in pseudo-cubic perovskite oxides. Journal of Chemical Physics, 2005, 123, 094703.	1.2	89
3390	Six-dimensional quantum dynamics of dissociative chemisorption of H2 on Ru(0001). Journal of Chemical Physics, 2005, 122, 044701.	1.2	60
3391	Density-functional calculations of defect formation energies using the supercell method: Brillouin-zone sampling. Physical Review B, 2005, 71, .	1.1	26
3392	EPR and theoretical studies of negatively charged carbon vacancy in4Hâˆ’SiC. Physical Review B, 2005, 71, .	1.1	55
3393	Band-gap modification of defective carbon nanotubes under a transverse electric field. Physical Review B, 2005, 72, .	1.1	33
3394	First principles local pseudopotential for silver: Towards orbital-free density-functional theory for transition metals. Journal of Chemical Physics, 2005, 122, 184108.	1.2	35
3395	Ab initiostudy of ground-state properties of the Laves-phase compoundZrMn2. Physical Review B, 2005, 72, .	1.1	40
3396	Water adsorption at metal surfaces: A first-principles study of thep(3Ã—3)R30Â°H2Obilayer on Ru(0001). Physical Review B, 2005, 71, .	1.1	60
3397	FIRST-PRINCIPLES STUDY OF DOPED SINGLE WALL CARBON NANOTUBES. International Journal of Modern Physics C, 2005, 16, 1363-1369.	0.8	1
3398	Surface Bonding and Dynamical Behavior of the CH3SH Molecule on Au(111). Journal of Physical Chemistry B, 2005, 109, 22463-22468.	1.2	82
3399	Theoretical electron energy-loss spectroscopy and its application in materials research. Microscopy (Oxford, England), 2005, 54, 293-298.	0.7	5
3400	Electronic structure of boron-interstitial clusters in silicon. Journal of Physics Condensed Matter, 2005, 17, S2141-S2153.	0.7	38
3401	Iron-rich silicates in the Earth's D'' layer. Proceedings of the National Academy of Sciences of the United States of America, 2005, 102, 9751-9753.	3.3	100

#	Article	IF	Citations
3402	A theoretical approach to the energetic stability and geometry of hydrogen and oxygen terminated diamond (100) surfaces. Materials Research Society Symposia Proceedings, 2005, 890, 1.	0.1	1
3403	Effect of exchangeable cation and hydration layer on the swelling property of 2:1 dioctahedral smectite clayâ€"a periodic density functional study. Studies in Surface Science and Catalysis, 2005, 156, 335-342.	1.5	7
3404	Formation energy of native defects in BN nanotubes: anab initiostudy. Nanotechnology, 2005, 16, 827-831.	1.3	74
3405	First-principles study of hydrogen bond symmetrization of phase D under high pressure. American Mineralogist, 2005, 90, 44-49.	0.9	83
3406	Diffusion of Fluorine-Silicon Interstitial Complex in Crystalline Silicon. Materials Research Society Symposia Proceedings, 2005, 864, 911.	0.1	0
3407	Role of Interstitials in As TED and Clustering in Crystalline Silicon. Materials Research Society Symposia Proceedings, 2005, 864, 851.	0.1	0
3408	Revised prediction of B1 to B2 phase transition pressures in YbN, YbP and YbAs. Zeitschrift Fur Kristallographie - Crystalline Materials, 2005, 220, 700-703.	0.4	4
3409	Adsorption of atomic and molecular oxygen on the SrTiO3(001) surfaces: Computer simulations by means of hybrid density functional calculations and ab initio thermodynamics. Materials Research Society Symposia Proceedings, 2005, 894, 1.	0.1	4
3410	Vegard's law deviation in band gaps and bowing parameters of the wurtzite III-nitride ternary alloys. , 2005, 5628, 296.		14
3411	Pt 3 Cr (111) Alloy Effect on the Reversible Potential of OOH(ads) Formation from O2(ads) relative to Pt(111). Journal of Fuel Cell Science and Technology, 2005, 2, 86-93.	0.8	24
3412	First-principles equations of state and elastic properties of seven metals. Physical Review B, 2005, 72, .	1.1	112
3413	An ab Initio Study of Observed and Hypothetical Polymorphs of Glycine. Crystal Growth and Design, 2005, 5, 1437-1442.	1.4	36
3414	Deep inelastic neutron scattering from orthorhombic ordered HCl: Short-time proton dynamics and anomalous neutron cross sections. Physical Review B, 2005, 72, .	1.1	38
3415	First Principles Investigation of Mineral Component of Bone:Â CO3Substitutions in Hydroxyapatite. Chemistry of Materials, 2005, 17, 4125-4133.	3.2	142
3416	Optimization and Application of Lithium Parameters for the Reactive Force Field, ReaxFF. Journal of Physical Chemistry A, 2005, 109, 4575-4582.	1.1	92
3417	Theoretical investigations of misfit dislocations in Pd/MgO(001) interfaces. Journal of Physics Condensed Matter, 2005, 17, 6149-6172.	0.7	24
3418	Theory of sodium ordering inNaxCoO2. Physical Review B, 2005, 71, .	1.1	102
3419	Theoretical investigation of the bonding and solubility in Nb2â˜'xWxAlC. Journal of Physics Condensed Matter, 2005, 17, 6047-6056.	0.7	9

#	Article	IF	Citations
3420	Spin-orbit coupling with ultrasoft pseudopotentials: Application to Au and Pt. Physical Review B, 2005, 71, .	1.1	238
3421	Ab initiolattice dynamics and phase transformations ofZrO2. Physical Review B, 2005, 71, .	1.1	109
3422	Fe-dopedCuInSe2: Anab initiostudy of magnetic defects in a photovoltaic material. Physical Review B, 2005, 71, .	1.1	28
3423	First-principles study of OH-stretching modes in kaolinite, dickite, and nacrite. American Mineralogist, 2005, 90, 50-60.	0.9	83
3424	Surface energy, stress and structure of well-relaxed amorphous silicon: A combination approach of ab initio and classical molecular dynamics. Surface Science, 2005, 585, 17-24.	0.8	60
3425	Predicting lattice parameter as a function of cation disorder in MgAl2O4spinel. Journal of Physics Condensed Matter, 2005, 17, 7621-7631.	0.7	46
3426	Ab initioinvestigation of the nitrofluoride SiNF. Physical Review B, 2005, 72, .	1.1	7
3427	Band structures and optical spectra of InN polymorphs: Influence of quasiparticle and excitonic effects. Physical Review B, 2005, 72, .	1.1	108
3428	A Comparative Study of Unrelaxed Surfaces on Quartz and Kaolinite, Using the Periodic Density Functional Theory. Journal of Physical Chemistry B, 2005, 109, 10835-10841.	1.2	32
3429	Rational design of new inorganic compounds with the ZrSiCuAs structure type using 2D building blocks. Journal of Materials Chemistry, 2005, 15, 3525.	6.7	55
3430	Theoretical Study of the Stability of Lithium Atoms in Î±-Rhombohedral Boron. Journal of Physical Chemistry A, 2005, 109, 11975-11979.	1.1	19
3431	New infrared nonlinear optical crystal CsGeBr3: synthesis, structure and powder second-harmonic generation properties. Journal of Physics Condensed Matter, 2005, 17, 7275-7286.	0.7	57
3432	Structure and stability of hydroxyapatite: Density functional calculation and Rietveld analysis. Physical Review B, 2005, 71, .	1.1	133
3433	Photoinduced cation interstitial diffusion in IIâ€“VI semiconductors. Physical Review B, 2005, 72, .	1.1	14
3434	The Role of Ti as a Catalyst for the Dissociation of Hydrogen on a Mg(0001) Surface. Journal of Physical Chemistry B, 2005, 109, 18037-18041.	1.2	113
3435	NO Chemisorption on Pt(111), Rh/Pt(111), and Pd/Pt(111). Journal of Physical Chemistry B, 2005, 109, 17630-17634.	1.2	48
3436	A reflection absorption infrared spectroscopy and density-functional theory investigation of methanol dehydrogenation on Rh(111)âˆ•V alloy surfaces. Journal of Chemical Physics, 2005, 122, 244720.	1.2	10
3437	Calculation of ferromagnetic states in metastable bcc and hcp Ni by projector-augmented wave method. Journal of Applied Physics, 2005, 97, 106107.	1.1	27

#	Article	IF	Citations
3438	Effect of the valence electron concentration on the bulk modulus and chemical bonding in Ta2AC and Zr2AC (A=Al, Si, and P). Journal of Applied Physics, 2005, 97, 066105.	1.1	24
3439	Ab initiothermodynamics of MgSiO3 perovskite at high pressures and temperatures. Journal of Chemical Physics, 2005, 122, 124501.	1.2	22
3440	Structure, stability, and diffusion of arsenic-silicon interstitial pairs. Applied Physics Letters, 2005, 87, 231905.	1.5	26
3441	High-pressure calculations of the elastic properties of ZnSxSe1âˆ’xalloy in the virtual-crystal approximation. High Pressure Research, 2005, 25, 217-225.	0.4	15
3442	Magnetic anisotropy ofL10FePt andFe1âˆ’xMnxPt. Physical Review B, 2005, 71, .	1.1	113
3443	The structural and electronic properties of nanostructured Ce1âˆ’xâˆ’yZrxTbyO2 ternary oxides: Unusual concentration of Tb3+ and metalâ†”oxygenâ†”metal interactions. Journal of Chemical Physics, 2005, 122, 154711.	1.2	32
3444	DFT plane wave calculations of the atomic and electronic structure of LaMnO3(001) surface. Physical Chemistry Chemical Physics, 2005, 7, 2346.	1.3	54
3445	Ab initiomany-body calculation of excitons in solid Ne and Ar. Physical Review B, 2005, 72, .	1.1	13
3446	Hydrogen sites occupation in Î±-LaNi4Al hydride. Molecular Simulation, 2005, 31, 1101-1106.	0.9	1
3447	Ab-initiosimulations of magnetic iron sulphides. Molecular Simulation, 2005, 31, 379-384.	0.9	12
3448	Ab initioGreenâ€™s function formalism for band structures. Physical Review B, 2005, 72, .	1.1	19
3449	Band structure and bulk modulus calculations of germanium carbide. Journal of Materials Research, 2005, 20, 1101-1106.	1.2	28
3450	Gold Atoms and Dimers on Amorphous SiO2:Â Calculation of Optical Properties and Cavity Ringdown Spectroscopy Measurements. Journal of Physical Chemistry B, 2005, 109, 19876-19884.	1.2	47
3451	Formation of Amorphous Alloys by Ion Beam Mixing and Its Multiscale Theoretical Modeling in the Equilibrium Immiscible Scâˆ’W System. Journal of Physical Chemistry B, 2005, 109, 4391-4397.	1.2	13
3452	Ab initiostudy of electronic and optical properties of multiwall carbon nanotube structures made up of a single rolled-up graphite sheet. Physical Review B, 2005, 72, .	1.1	84
3453	Polymorphism of Crystalline Î±-Quaterthiophene and Î±-Sexithiophene:Â Ab Initio Analysis and Comparison with Inelastic Neutron Scattering Response. Journal of Physical Chemistry A, 2005, 109, 4202-4207.	1.1	36
3454	Stability of Two-Dimensional Tessellation Ice on the Hydroxylated Î²-Cristobalite (100) Surface. Journal of Physical Chemistry B, 2005, 109, 5678-5683.	1.2	20
3455	Charge-Doped and Heteroatom-Substituted Polysilane, Poly(vinylenedisilanylene), and Poly(butadienylenedisilanylene):Â Electronic Structures and Band Gaps. Journal of Physical Chemistry B, 2005, 109, 13499-13509.	1.2	20

#	Article	IF	Citations
3456	Strong interface adhesion in Fe/TiC. Philosophical Magazine, 2005, 85, 3683-3697.	0.7	41
3457	Ab Initio and Microcalorimetric Investigations of Alkene Adsorption on Phosphotungstic Acid. Langmuir, 2005, 21, 4738-4745.	1.6	25
3458	Effect of electron correlations in Pd, Ni, and Co monowires. Physical Review B, 2005, 72, .	1.1	32
3459	Vacancy Formation Process in Carbon Nanotubes:Â First-Principles Approach. Nano Letters, 2005, 5, 197-200.	4.5	76
3460	Concerning the Structure of Hydrogen Molybdenum Bronze Phase III. A Combined Theoreticalâ˜Experimental Study. Chemistry of Materials, 2005, 17, 5957-5969.	3.2	51
3461	Effects of Alloying on the Chemistry of CO and H2S on Fe Surfaces. Journal of Physical Chemistry B, 2005, 109, 20469-20478.	1.2	24
3462	Reduction of the (001) Surface of Î³-V2O5Compared to Î±-V2O5. Journal of Physical Chemistry B, 2005, 109, 374-380.	1.2	19
3463	Toward a Realistic Description of NOxStorage in BaO:Â The Aspect of BaCO3. Journal of Physical Chemistry B, 2005, 109, 9613-9621.	1.2	30
3464	Prediction of a Phase Transition to a Hydrogen Bond Ordered Form of Ice VI. Journal of Physical Chemistry B, 2005, 109, 21040-21046.	1.2	41
3465	First-principles investigation of the structural, magnetic, and electronic properties of olivineLiFePO4. Physical Review B, 2005, 71, .	1.1	57
3466	Structure, energetics, and mechanical stability of Fe-Cu bcc alloys from first-principles calculations. Physical Review B, 2005, 72, .	1.1	120
3467	Low-temperature polymorphs ofZrO2andHfO2: A density-functional theory study. Physical Review B, 2005, 72, .	1.1	194
3468	Chemisorption of CO2 on Nickel Surfaces. Journal of Physical Chemistry B, 2005, 109, 18956-18963.	1.2	186
3469	Adsorption and dissociation of hydrogen molecules on bare and functionalized carbon nanotubes. Physical Review B, 2005, 72, .	1.1	255
3470	Effect of chemical bonding on the magnetic stability and magnetic moment in Mn-based binary compounds. Physical Review B, 2005, 72, .	1.1	30
3471	Electron-Transfer Doping on a (001) Surface of Diamond:Â Quantum Mechanical Study. Journal of Physical Chemistry B, 2005, 109, 22426-22431.	1.2	17
3472	Reactions of Hydrazoic Acid on TiO2 Nanoparticles:â€‰ an Experimental and Computational Study. Journal of Physical Chemistry B, 2005, 109, 5133-5142.	1.2	14
3473	Interrelation of Work Function and Surface Stability: The Case of BaAl4. Chemistry of Materials, 2005, 17, 3879-3882.	3.2	9

#	Article	IF	Citations
3474	First-Principles Analyses and Predictions on the Reactivity of Barrier Layers of Ta and TaN toward Organometallic Precursors for Deposition of Copper Films. Langmuir, 2005, 21, 7608-7614.	1.6	31
3475	Electronic Compositionâ^'Property Relationship Applied to SO2Chemisorption on Pt(111) Surfaces, Alloys, and Overlayers. Journal of Physical Chemistry B, 2005, 109, 6948-6951.	1.2	13
3476	Effect of Sulfur Coverage on Fe(110) Adhesion:Â A DFT Study. Journal of Physical Chemistry B, 2005, 109, 10204-10212.	1.2	7
3477	Vanadium Oxides on Aluminum Oxide Supports. 2. Structure, Vibrational Properties, and Reducibility of V2O5 Clusters on Î±-Al2O3(0001). Journal of Physical Chemistry B, 2005, 109, 23532-23542.	1.2	27
3478	Catalysts for Hydrogen Evolution from the [NiFe] Hydrogenase to the Ni2P(001) Surface:Â The Importance of Ensemble Effect. Journal of the American Chemical Society, 2005, 127, 14871-14878.	6.6	1,029
3479	Diamond Surface Conductivity under Atmospheric Conditions:Â Theoretical Approach. Journal of Physical Chemistry B, 2005, 109, 10304-10311.	1.2	31
3480	Coverage-Dependent Adsorption of Atomic Sulfur on Fe(110):Â A DFT Study. Journal of Physical Chemistry B, 2005, 109, 9604-9612.	1.2	25
3481	Structures and Energies of Coadsorbed CO and H2on Fe5C2(001), Fe5C2(110), and Fe5C2(100). Journal of Physical Chemistry B, 2005, 109, 10922-10935.	1.2	46
3482	Vanadium Oxides on Aluminum Oxide Supports. 1. Surface Termination and Reducibility of Vanadia Films on Î±-Al2O3(0001). Journal of Physical Chemistry B, 2005, 109, 23523-23531.	1.2	42
3483	First-Principles Calculations of the Adsorption of Nitromethane and 1,1-Diamino-2,2-dinitroethylene (FOX-7) Molecules on the Î±-Al2O3(0001) Surface. Journal of Physical Chemistry B, 2005, 109, 1451-1463.	1.2	48
3484	Density Functional Theory Study of Pyrrole Adsorption on Mo(110). Journal of Physical Chemistry B, 2005, 109, 10863-10870.	1.2	11
3485	Location, Acid Strength, and Mobility of the Acidic Protons in Keggin 12-H3PW12O40:â€‰ A Combined Solid-State NMR Spectroscopy and DFT Quantum Chemical Calculation Study. Journal of the American Chemical Society, 2005, 127, 18274-18280.	6.6	130
3486	Pair potentials for a metalâ€“ceramic interface by inversion of adhesive energy. Journal of Physics Condensed Matter, 2005, 17, 2045-2058.	0.7	41
3487	Reactions of Trimethylindium on TiO2Nanoparticles:Â Experimental and Computational Study. Journal of Physical Chemistry B, 2005, 109, 20858-20867.	1.2	15
3488	Nonequilibrium Solid Phase Formation Studied by Lattice Dynamics Calculation and Ion Beam Mixing in an Immiscible Coâ^'Ag System. Journal of Physical Chemistry B, 2005, 109, 9362-9367.	1.2	5
3489	Potential Shift for OH(ads) Formation on the Pt Skin on Pt[sub 3]Co(111) Electrodes in Acid. Journal of the Electrochemical Society, 2005, 152, E193.	1.3	58
3490	Far- and Mid-Infrared of Crystalline 2,2â€˜-Bithiophene:â€‰ Ab Initio Analysis and Comparison with Infrared Response. Journal of Physical Chemistry A, 2005, 109, 1684-1691.	1.1	33
3491	Properties of Ternary Insulating Systems:Â The Electronic Structure of MgSO4Â·H2O. Journal of Physical Chemistry A, 2005, 109, 4118-4124.	1.1	16

#	Article	IF	Citations
3492	Effect of Steps on the Decomposition of CH3O at PdZn Alloy Surfaces. Journal of Physical Chemistry B, 2005, 109, 4568-4574.	1.2	48
3493	Effects of Water on the Structure and Bonding of Resorcinol in the Interlayer of Montmorillonite Nanocomposite:Â A Periodic First Principle Study. Journal of Physical Chemistry B, 2005, 109, 7306-7313.	1.2	14
3494	Orbital-Free Density Functional Theory Applied to NaAlH4. Journal of Physical Chemistry B, 2005, 109, 16554-16562.	1.2	12
3495	The Structure of the Chiral Pt{531} Surface:Â A Combined LEED and DFT Study. Journal of Physical Chemistry B, 2005, 109, 22456-22462.	1.2	24
3496	Phenanthrenequinone Adsorbed on Si(001):Â Geometries, Electronic Properties, and Optical Response. Journal of Physical Chemistry B, 2005, 109, 7928-7933.	1.2	24
3497	Electronic Structure of Li2Ga and Li9Al4, Two Solids Containing Infinite and Uniform Zigzag Chains. Inorganic Chemistry, 2005, 44, 374-381.	1.9	7
3498	First-Principles Study of CO Adsorption and Vibration on Au Surfaces. Journal of Physical Chemistry B, 2005, 109, 9596-9603.	1.2	28
3499	First-principles investigation of electronic structure and magnetic properties in ferromagnetic GaxMn1â^'xN and AlxMn1â^'xN. Journal Physics D: Applied Physics, 2005, 38, 1853-1859.	1.3	32
3500	Theoretical study of the structure and optical properties of carbon-doped rutile and anatase titanium oxides. Journal of Chemical Physics, 2005, 123, 084704.	1.2	140
3501	Calculated pressure dependence of the localized vibrational mode of nitrogen inGaNxAs1â^'x. Physical Review B, 2005, 72, .	1.1	20
3502	ReaxFFMgHReactive Force Field for Magnesium Hydride Systems. Journal of Physical Chemistry A, 2005, 109, 851-859.	1.1	234
3503	Conformation Dependence of Electronic Structures of Poly(ethylene oxide). Journal of Physical Chemistry B, 2005, 109, 7907-7914.	1.2	16
3504	Thermal equation of state for Pt. Physical Review B, 2005, 72, .	1.1	21
3505	N2O Decomposition on TiO2 (110) from Dynamic First-Principles Calculations. Journal of Physical Chemistry B, 2005, 109, 16223-16226.	1.2	38
3506	Comparison of the Electron Localization Function and Deformation Electron Density Maps for Selected Earth Materials. Journal of Physical Chemistry A, 2005, 109, 10022-10027.	1.1	20
3507	Ca Doping of Nanosize Ceâ^'Zr and Ceâ^'Tb Solid Solutions:Â Structural and Electronic Effects. Chemistry of Materials, 2005, 17, 4181-4193.	3.2	49
3508	Density Functional Theory Study of Hydrogen Adsorption on Fe5C2(001), Fe5C2(110), and Fe5C2(100). Journal of Physical Chemistry B, 2005, 109, 833-844.	1.2	43
3509	Electronic Structure of the K3Bi2Metallic Phase. Inorganic Chemistry, 2005, 44, 1644-1646.	1.9	8

#	Article	IF	Citations
3510	Anhydrous and Water-Assisted Proton Mobility in Phosphotungstic Acid. Journal of the American Chemical Society, 2005, 127, 5238-5245.	6.6	99
3511	Crystal Structure and Vibrational Spectra of AlVO4. A DFT Study. Journal of Physical Chemistry B, 2005, 109, 394-400.	1.2	39
3512	Reconstruction of Pristine and Hydrolyzed Quartz Surfaces. Journal of Physical Chemistry B, 2005, 109, 4144-4151.	1.2	72
3513	Simulations of the optical properties of warm dense aluminum. Physical Review E, 2005, 71, 016409.	0.8	145
3514	Ab initiocalculations on the effects of additives on alumina phase stability. Physical Review B, 2005, 71, .	1.1	25
3515	Atomic chains of group-IV elements and III-V and II-VI binary compounds studied by a first-principles pseudopotential method. Physical Review B, 2005, 72, .	1.1	70
3516	Structure and formation ofH2Ti3O7nanotubes in an alkali environment. Physical Review B, 2005, 71, .	1.1	145
3517	Strength, elasticity, and equation of state of the nanocrystalline cubic silicon nitridel³â^'Si3N4to68GPa. Physical Review B, 2005, 72, .	1.1	43
3518	The theoretical study on interaction of hydrogen with single-walled boron nitride nanotubes. I. The reactive force field ReaxFFHBN development. Journal of Chemical Physics, 2005, 123, 114703.	1.2	54
3519	First-principles determination of the dynamical properties ofPb2MgTeO6. Physical Review B, 2005, 71, .	1.1	3
3520	Water adsorption on hydroxylated silica surfaces studied using the density functional theory. Physical Review B, 2005, 71, .	1.1	105
3521	Trends in hydride formation energies for magnesium-3d transition metal alloys. Journal of Alloys and Compounds, 2005, 386, 1-7.	2.8	85
3522	Electronic densities of states of several intermetallic compounds with large coordination numbers calculated within the framework of band theory. Journal of Alloys and Compounds, 2005, 389, 220-228.	2.8	10
3523	Ab initio interionic potentials for CaO by multiple lattice inversion. Journal of Alloys and Compounds, 2005, 388, 195-207.	2.8	15
3524	Atom relaxations around hydrogen defects in lanthanum hydride. Journal of Alloys and Compounds, 2005, 404-406, 55-59.	2.8	16
3525	State of the art simulations in electronic structure and total energy for the high temperature superconductor YBa2Cu3O7. Journal of Alloys and Compounds, 2005, 403, 1-14.	2.8	8
3526	Consideration of the validity of the 14 valence electron rule for semiconducting chimney-ladder phase compounds. Intermetallics, 2005, 13, 233-241.	1.8	50
3527	O interstitial energetics in Ti from ab initio calculations. Computational Materials Science, 2005, 32, 13-19.	1.4	3

#	Article	IF	Citations
3528	First principles study of the stability of SiNF. Computational Materials Science, 2005, 34, 22-34.	1.4	4
3529	First-principles study of cubic AlxGa1â^'xN alloys. Computational Materials Science, 2005, 33, 136-140.	1.4	21
3530	Predictive process design: a theoretical model of atomic layer deposition. Computational Materials Science, 2005, 33, 20-25.	1.4	29
3531	Spin polarization and band alignments at NiMnSb/GaAs interface. Computational Materials Science, 2005, 33, 263-268.	1.4	15
3532	Local vibrational modes of Znâ€"Hâ€"As defects in GaAs, ZnSe and ZnTe. Computational Materials Science, 2005, 33, 145-147.	1.4	2
3533	Accuracy of ab initio methods in predicting the crystal structures of metals: A review of 80 binary alloys. Calphad: Computer Coupling of Phase Diagrams and Thermochemistry, 2005, 29, 163-211.	0.7	313
3534	A critical test of ab initio and CALPHAD methods: The structural energy difference between bcc and hcp molybdenum. Calphad: Computer Coupling of Phase Diagrams and Thermochemistry, 2005, 29, 17-23.	0.7	23
3535	High-throughput ab initio analysis of the Biâ€"In, Biâ€"Mg, Biâ€"Sb, Inâ€"Mg, Inâ€"Sb, and Mgâ€"Sb systems. Calphad: Computer Coupling of Phase Diagrams and Thermochemistry, 2005, 29, 155-161.	0.7	40
3536	Modification of the thermodynamic model for the Mgâ€"Zr system. Calphad: Computer Coupling of Phase Diagrams and Thermochemistry, 2005, 29, 230-238.	0.7	33
3537	The effect of temperature on the seismic anisotropy of the perovskite and post-perovskite polymorphs of MgSiO3. Earth and Planetary Science Letters, 2005, 230, 1-10.	1.8	137
3538	Elasticity of (Mg, Fe)(Si, Al)O3-perovskite at high pressure. Earth and Planetary Science Letters, 2005, 240, 529-536.	1.8	42
3539	First-principles study of spontaneous polarization in multiferroicBiFeO3. Physical Review B, 2005, 71, .	1.1	1,225
3540	Influence of strain and oxygen vacancies on the magnetoelectric properties of multiferroic bismuth ferrite. Physical Review B, 2005, 71, .	1.1	339
3541	Linear response approach to the calculation of the effective interaction parameters in theLDA+Umethod. Physical Review B, 2005, 71, .	1.1	2,754
3542	Diffusion and dissociation mechanisms of vacancy-oxygen complex in silicon. Applied Physics Letters, 2005, 86, 142107.	1.5	16
3543	Crystal symmetry and pressure effects on the valence band structure ofÎ³-InSe andÎµ-GaSe: Transport measurements and electronic structure calculations. Physical Review B, 2005, 71, .	1.1	65
3544	Theory of Fe, Co, Ni, Cu, and their complexes with hydrogen in ZnO. Physical Review B, 2005, 72, .	1.1	107
3545	Electron-concentration and pressure-induced structural changes in the alloysIn1â^'xXx(X=Cd,Sn). Physical Review B, 2005, 72, .	1.1	17

#	Article	IF	Citations
3546	Designing meaningful density functional theory calculations in materials scienceâ€"a primer. Modelling and Simulation in Materials Science and Engineering, 2005, 13, R1-R31.	0.8	342
3547	Weak ferromagnetism and magnetoelectric coupling in bismuth ferrite. Physical Review B, 2005, 71, .	1.1	1,235
3548	Structural and Electronic Properties of Li2B4O7. Journal of Physical Chemistry B, 2005, 109, 13597-13604.	1.2	61
3549	Raman study of optical phonons in ultrathinInAsâ^•InPsingle strained quantum wells. Physical Review B, 2005, 72, .	1.1	3
3550	Adsorption and nonadiabatic processes in the photodesorption of molecular oxygen from the reduced TiO2(110) surface. Israel Journal of Chemistry, 2005, 45, 59-76.	1.0	27
3551	Diffusion of phosphorus inÎ±â^'Fe: Anab initiostudy. Physical Review B, 2005, 71, .	1.1	81
3552	A density functional theory study of adsorbate-induced work function change and binding energy: Olefins on Ag(111). Molecular Physics, 2005, 103, 883-890.	0.8	39
3553	Monte Carlo simulations applied toAlxGayIn1â^'xâ^'yXquaternary alloys(X=As,P,N): A comparative study. Physical Review B, 2005, 71, .	1.1	4
3554	Phase Diagram of Silicon from Atomistic Simulations. Physical Review Letters, 2005, 94, 095701.	2.9	58
3555	Electronic and Atomistic Structures of Clean and Reduced Ceria Surfaces. Journal of Physical Chemistry B, 2005, 109, 22860-22867.	1.2	358
3556	Sphaleriteâ^'Chalcopyrite Polymorphism in Semimetallic ZnSnSb2. Chemistry of Materials, 2005, 17, 6080-6085.	3.2	21
3557	Vacancy-impurity complexes and limitations for implantation doping of diamond. Physical Review B, 2005, 72, .	1.1	132
3558	Development of atomistic MEAM potentials for the siliconâ€"oxygenâ€"gold ternary system. Modelling and Simulation in Materials Science and Engineering, 2005, 13, 1309-1329.	0.8	28
3559	A Density Functional Study of the Chemical Differences between Type I and Type II MoS2-Based Structures in Hydrotreating Catalystsâ€. Journal of Physical Chemistry B, 2005, 109, 2245-2253.	1.2	170
3560	Impact of the size 4 cluster on low temperature indium diffusion in silicon. Journal of Physics Condensed Matter, 2005, 17, S2165-S2170.	0.7	0
3561	Passivation of copper in silicon by hydrogen. Physical Review B, 2005, 72, .	1.1	26
3562	CaSiO3perovskite at lower mantle pressures. Geophysical Research Letters, 2005, 32, .	1.5	57
3563	Prediction of a new phase transition in Al2O3at high pressures. Geophysical Research Letters, 2005, 32, .	1.5	50

#	Article	IF	Citations
3564	Vibrational and thermodynamic properties of MgSiO3postperovskite. Journal of Geophysical Research, 2005, 110, .	3.3	105
3565	Electronic spin state of ferric iron in Al-bearing perovskite in the lower mantle. Geophysical Research Letters, 2005, 32, .	1.5	47
3566	High temperature elastic anisotropy of the perovskite and post-perovskite polymorphs of Al2O3. Geophysical Research Letters, 2005, 32, .	1.5	37
3567	Effect of chemistry on the stability and elasticity of the perovskite and post-perovskite phases in the MgSiO3-FeSiO3-Al2O3system and implications for the lowermost mantle. Geophysical Research Letters, 2005, 32, .	1.5	100
3568	Effect of Al on the sharpness of the MgSiO3perovskite to post-perovskite phase transition. Geophysical Research Letters, 2005, 32, n/a-n/a.	1.5	71
3569	Surfactant-favored disorder in (001)-oriented CuPt-orderedAIII(BV,CV)alloy thin films: Action of Sb and Bi. Physical Review B, 2005, 72, .	1.1	2
3570	Phase Stability, Phase Transformations, and Elastic Properties of Cu6Sn5: Ab initio Calculations and Experimental Results. Journal of Materials Research, 2005, 20, 3102-3117.	1.2	129
3571	New Insights into the Origin of Visible Light Photocatalytic Activity of Nitrogen-Doped and Oxygen-Deficient Anatase TiO2. Journal of Physical Chemistry B, 2005, 109, 20948-20952.	1.2	422
3572	Properties of the CdSe(0001), (0001Ì„), and (112Ì„0) Single Crystal Surfaces:Â Relaxation, Reconstruction, and Adatom and Admolecule Adsorption. Journal of Physical Chemistry B, 2005, 109, 19320-19328.	1.2	71
3573	Computational study of LnGaO3(Ln = Laâ€“Gd) perovskites. Journal of Physics Condensed Matter, 2005, 17, 6217-6234.	0.7	27
3574	Effect of pressure on the structural properties and Raman modes ofLiCoO2. Physical Review B, 2005, 72, .	1.1	48
3575	Geometrical, electronic, and magnetic properties ofNa0.5CoO2from first principles. Physical Review B, 2005, 71, .	1.1	18
3576	Electronic structure calculations of an oxygen vacancy inKH2PO4. Physical Review B, 2005, 72, .	1.1	50
3577	Structure and magnetic properties of theFe3O4(001)surface:â€ƒAb initiostudies. Physical Review B, 2005, 71, .	1.1	47
3578	Theoretical Prediction of New High-Performance Lead-Free Piezoelectrics. Chemistry of Materials, 2005, 17, 1376-1380.	3.2	333
3579	Adsorption of Atomic Oxygen and Nitrogen at Î²-Cristobalite (100):Â A Density Functional Theory Study. Journal of Physical Chemistry B, 2005, 109, 14954-14964.	1.2	49
3580	Structure and electronic properties of zirconium and hafnium nitrides and oxynitrides. Journal of Applied Physics, 2005, 97, 044108.	1.1	78
3581	Theoretical study of the adsorption ofH2on (3,3) carbon nanotubes. Physical Review B, 2005, 72, .	1.1	40

#	Article	IF	Citations
3582	Pressure-induced phase transition in ZnO andZnOâ^'MgOpseudobinary system: A first-principles lattice dynamics study. Physical Review B, 2005, 72, .	1.1	98
3583	Thermodynamics of structural vacancies in titanium monoxide from first-principles calculations. Physical Review B, 2005, 71, .	1.1	44
3584	Simulations on the Thermal Decomposition of a Poly(dimethylsiloxane) Polymer Using the ReaxFF Reactive Force Field. Journal of the American Chemical Society, 2005, 127, 7192-7202.	6.6	395
3585	First-principles calculations of2Ã—2reconstructions of GaN(0001) surfaces involving N, Al, Ga, In, and As atoms. Physical Review B, 2005, 72, .	1.1	28
3586	First-principles study of transition-metal-doped single-walled carbon nanotubes. Nanotechnology, 2005, 16, 3092-3096.	1.3	44
3587	Self-vacancies in gallium arsenide: Anab initiocalculation. Physical Review B, 2005, 71, .	1.1	68
3588	Ab initio study of structural parameters and gap bowing in zinc-blende AlxGa1â^'xN and AlxIn1â^'xN alloys. Journal of Applied Physics, 2005, 98, 063710.	1.1	25
3589	Ab initiostudy of the surface properties and ideal strength of (100) silicon thin films. Physical Review B, 2005, 72, .	1.1	59
3590	Mechanisms of Methanol Decomposition on Platinum:â€‰ A Combined Experimental and ab Initio Approach. Journal of Physical Chemistry B, 2005, 109, 11622-11633.	1.2	248
3591	Surface passivation method for semiconductor nanostructures. Physical Review B, 2005, 71, .	1.1	170
3592	Growth of ZnO thin filmsâ€"experiment and theory. Journal of Materials Chemistry, 2005, 15, 139-148.	6.7	364
3593	Molecular dynamics study of a low energy carbon ion moving in a single-wall carbon nanotube. Nanotechnology, 2005, 16, 2681-2684.	1.3	15
3594	A combined first principles computational and solid-state NMR study of a molecular crystal: flurbiprofen. Physical Chemistry Chemical Physics, 2005, 7, 1402.	1.3	136
3595	Electronic Structure Study of the High-pressure Vibrational Spectrum of FeS2Pyrite. Journal of Physical Chemistry B, 2005, 109, 22067-22073.	1.2	36
3596	First-principles studies of Au(100)-hex reconstruction in an electrochemical environment. Physical Review B, 2005, 72, .	1.1	28
3597	Magnetism in BN nanotubes induced by carbon doping. Applied Physics Letters, 2005, 86, 122510.	1.5	146
3598	Why Copper Is Intrinsically More Selective than Silver in Alkene Epoxidation:Â Ethylene Oxidation on Cu(111) versus Ag(111). Journal of the American Chemical Society, 2005, 127, 10774-10775.	6.6	124
3599	Substitutional and interstitial oxygen in wurtzite GaN. Journal of Applied Physics, 2005, 98, 103531.	1.1	71

#	Article	IF	Citations
3600	Unusual Physical and Chemical Properties of Cu in Ce1-xCuxO2Oxides. Journal of Physical Chemistry B, 2005, 109, 19595-19603.	1.2	262
3601	Energetics of lithium ion adsorption on defective carbon nanotubes. Physical Review B, 2005, 71, .	1.1	116
3602	Adsorption and diffusion of Ga and N adatoms on GaN surfaces: Comparing the effects of Ga coverage and electronic excitation. Physical Review B, 2005, 72, .	1.1	42
3603	First-principles study of some factors controlling the rate of ammonia decomposition on Ni and Pd surfaces. Journal of Chemical Physics, 2005, 123, 204716.	1.2	56
3604	Fully first-principles screened-exchange LDA calculations of excited states and optical properties of III-V semiconductors. Physical Review B, 2005, 71, .	1.1	45
3605	Electronic structure ofIIBâˆ’VIsemiconductors in theGWapproximation. Physical Review B, 2005, 71, .	1.1	138
3606	Structure and diffusion of excess Si atoms inSiO2. Physical Review B, 2005, 72, .	1.1	18
3607	Structure-derived electronic and optical properties of transparent conducting oxides. Physical Review B, 2005, 71, .	1.1	123
3608	Half-metallic properties of atomic chains of carbonâ€“transition-metal compounds. Physical Review B, 2005, 72, .	1.1	35
3609	Characterization of cathodic arc deposited titanium aluminium nitride films prepared using plasma immersion ion implantation. Journal of Physics Condensed Matter, 2005, 17, 2791-2800.	0.7	6
3610	First-principles calculations of small silicon clusters adsorbed on a graphite surface. Physical Review B, 2005, 72, .	1.1	6
3611	Ab initiostudy of ground-state properties of the Laves phase compoundsTiCr2,ZrCr2, andHfCr2. Physical Review B, 2005, 71, .	1.1	64
3612	Ab initiocalculations of the electronic structure and bonding characteristics ofLaB6. Physical Review B, 2005, 72, .	1.1	58
3613	Strain energy and electronic structures of silicon carbide nanotubes: Density functional calculations. Physical Review B, 2005, 71, .	1.1	239
3614	Combined theoretical and experimental study of the low-temperature properties ofBaZrO3. Physical Review B, 2005, 72, .	1.1	123
3615	Electrons and phonons in the ternary alloyCaAl2âˆ’xSixas a function of composition. Physical Review B, 2005, 72, .	1.1	54
3616	Ab initiocalculations in the virtual-crystal approximation of the structural and the elastic properties of BeSxSe1âˆ’xalloys under high pressure. Modelling and Simulation in Materials Science and Engineering, 2005, 13, 1153-1162.	0.8	24
3617	Dopant-induced stabilization of rhombohedralLiMnO2against Jahn-Teller distortion. Physical Review B, 2005, 71, .	1.1	40

#	Article	IF	Citations
3618	The (010) surface of Î±-MoO3, a DFT + U study. Physical Chemistry Chemical Physics, 2005, 7, 3819.	1.3	146
3619	On the Spectral Similarity of Bridging and Nonbridging Oxygen in Tellurites. Journal of Physical Chemistry A, 2005, 109, 7636-7641.	1.1	17
3620	Structural Studies of the Polymorphs of Carbamazepine, Its Dihydrate, and Two Solvates. Organic Process Research and Development, 2005, 9, 902-910.	1.3	117
3621	Electronic structure and properties of isoreticular metal-organic frameworks: The case of M-IRMOF1 (M=Zn, Cd, Be, Mg, and Ca). Journal of Chemical Physics, 2005, 123, 124713.	1.2	147
3622	Density Functional Theory Study of the Adsorption of Alkanethiols on Cu(111), Ag(111), and Au(111) in the Low and High Coverage Regimes. Journal of Physical Chemistry B, 2005, 109, 21737-21748.	1.2	173
3623	Carbon string structures: First-principles calculations of quantum conductance. Physical Review B, 2005, 71, .	1.1	17
3624	Nitrogen in graphite and carbon nanotubes: Magnetism and mobility. Physical Review B, 2005, 72, .	1.1	117
3625	Stiffness and thermal expansion of ZrB2: anab initiostudy. Journal of Physics Condensed Matter, 2005, 17, 2233-2241.	0.7	85
3626	Silicon and III-V compound nanotubes: Structural and electronic properties. Physical Review B, 2005, 72, .	1.1	250
3627	Registry-dependent interlayer potential for graphitic systems. Physical Review B, 2005, 71, .	1.1	413
3628	Dielectric properties of crystalline and amorphous transition metal oxides and silicates as potential high-Î¹º candidates: the contribution of density-functional theory. Journal of Physics Condensed Matter, 2005, 17, R357-R379.	0.7	91
3629	Desulfurization Reactions on Ni2P(001) and Î±-Mo2C(001) Surfaces:Â Complex Role of P and C Sites. Journal of Physical Chemistry B, 2005, 109, 4575-4583.	1.2	290
3630	Adsorption of Water Molecules on Flat and Stepped Nickel Surfaces from First Principles. Journal of Chemical Theory and Computation, 2005, 1, 78-82.	2.3	64
3631	First-principles study of epitaxial strain in perovskites. Physical Review B, 2005, 72, .	1.1	261
3632	Density Functional Study of H-Induced Defects as Nucleation Sites in Hybrid Carbon Nanomaterials. Chemistry of Materials, 2005, 17, 527-535.	3.2	31
3633	Simulating nano-carbon materials. Molecular Simulation, 2005, 31, 495-504.	0.9	5
3634	Electronic structure calculations of potassium-intercalated single-walled carbon nanotubes. Physical Review B, 2005, 72, .	1.1	11
3635	High coverage of hydrogen on a (10,0) single-walled boron nitride nanotube. Physical Review B, 2005, 72, .	1.1	42

#	Article	IF	Citations
3636	Ethene Epoxidation Selectivity Inhibited by Twisted Oxametallacycle:Â A DFT Study on Ag Surface-Oxide. Journal of the American Chemical Society, 2005, 127, 17207-17215.	6.6	62
3637	Combined First-Principles Computational and Experimental Multinuclear Solid-State NMR Investigation of Amino Acids. Journal of Physical Chemistry A, 2005, 109, 6960-6969.	1.1	169
3638	Geometric and electronic structures of the boron-doped photocatalyst TiO2. Journal of Physics Condensed Matter, 2006, 18, 87-96.	0.7	60
3639	Nonequivalence of the generalized gradient approximations PBE and PW91. Physical Review B, 2006, 73, .	1.1	129
3640	Effects of Zr doping on stoichiometric and reduced ceria: A first-principles study. Journal of Chemical Physics, 2006, 124, 224704.	1.2	131
3641	Adsorption of hydrogen molecules on the platinum-doped boron nitride nanotubes. Journal of Chemical Physics, 2006, 125, 044704.	1.2	111
3642	Adsorption and Activation of CO over Flat and Stepped Co Surfaces:Â A First Principles Analysis. Journal of Physical Chemistry B, 2006, 110, 15368-15380.	1.2	147
3643	Universal Behavior of Nearly Free Electron States in Carbon Nanotubes. Physical Review Letters, 2006, 96, 196803.	2.9	63
3644	Structure, Metastability, and Electron Density of Al Lattices in Light of the Model of Anions in Metallic Matrices. Journal of Physical Chemistry B, 2006, 110, 18609-18618.	1.2	11
3645	Atom order and thermodynamic properties of the ternary Laves phase Ti(TiyNixAl1â€“xâ€“y)2. Zeitschrift Fur Kristallographie - Crystalline Materials, 2006, 221, .	0.4	16
3646	Ionic Polarizability of Conductive Metal Oxides and Critical Thickness for Ferroelectricity inBaTiO3. Physical Review Letters, 2006, 96, 107603.	2.9	215
3647	First-principles study of the adsorption of methanol at the Î±-Al2O3(0001) surface. Journal of Physics Condensed Matter, 2006, 18, 1-12.	0.7	65
3648	Interaction of Glycine with Isolated Hydroxyl Groups at the Silica Surface:â€‰ First Principles B3LYP Periodic Simulation. Langmuir, 2006, 22, 6593-6604.	1.6	83
3649	First principles reaction modeling of the electrochemical interface: Consideration and calculation of a tunable surface potential from atomic and electronic structure. Physical Review B, 2006, 73, .	1.1	394
3650	Methanethiolate Adsorption Site on Au(111):Â A Combined STM/DFT Study at the Single-Molecule Level. Journal of Physical Chemistry B, 2006, 110, 21161-21167.	1.2	75
3651	First-Principles Study of the Diffusion of Hydrogen in ZnO. Physical Review Letters, 2006, 96, 205504.	2.9	190
3652	First-Principles Electronic Structure Study of the Monoclinic Crystal Bismuth Triborate BiB3O6. Journal of Physical Chemistry B, 2006, 110, 19254-19263.	1.2	38
3653	Oxadiazoleâ˜Metal Interface:â€‰ from Isolated Molecules to Ï€-Stacking. Langmuir, 2006, 22, 857-859.	1.6	13

#	Article	IF	Citations
3654	Lattice dynamics of polyaniline and poly(p-pyridyl vinyline): First-principles determination. Physical Review B, 2006, 74, .	1.1	14
3655	Effect of Model Potential of Adsorptive Bond on the Thermodynamic Properties of Adsorbed CO Molecules on Ni(111) Surface. Journal of Physical Chemistry B, 2006, 110, 20435-20444.	1.2	3
3656	Assigning carbon-13 NMR spectra to crystal structures by the INADEQUATE pulse sequence and first principles computation: a case study of two forms of testosterone. Physical Chemistry Chemical Physics, 2006, 8, 137-143.	1.3	142
3657	Influence of the Al distribution on the structure, elastic properties, and phase stability of supersaturated Ti1â^'xAlxN. Journal of Applied Physics, 2006, 100, 094906.	1.1	202
3658	Genuine converging solution of self-consistent field equations for extended many-electron systems. Journal of Physics: Conference Series, 2006, 35, 163-174.	0.3	3
3659	Ab Initio Simulation of Si-Doped Hydroxyapatite. Chemistry of Materials, 2006, 18, 413-422.	3.2	58
3660	Computational study of Met-Car analogue heterofullerenes. Modelling and Simulation in Materials Science and Engineering, 2006, 14, 637-646.	0.8	2
3661	Energetic and magnetic properties of transition-metal nanowire encapsulated BxCyNz composite nanotubes. Applied Physics Letters, 2006, 88, 193117.	1.5	17
3662	Magnetic and Electronic Properties of Transition Metal Doped Î²-SiC - A Diluted Magnetic Semiconductor. Key Engineering Materials, 2006, 317-318, 889-892.	0.4	1
3663	Adsorption and dimerisation of thiol molecules on Au(111) using aZ-matrix approach in density functional theory. Molecular Simulation, 2006, 32, 1219-1225.	0.9	20
3664	DFT study of the interactions of Clâ^' with passivated Nickel surfaces: energetic and structural aspects. , 2006, , 659-665.		1
3665	High-pressure synthesis and physical properties of an orthorhombic phase of chromium dioxide. Journal of Applied Physics, 2006, 99, 053909.	1.1	21
3666	Characterization and Theory of Electrocatalysts Based on Scanning Electrochemical Microscopy Screening Methods. Langmuir, 2006, 22, 10426-10431.	1.6	74
3667	A model study for the breaking of cyanogen out of CNx within DFT. Diamond and Related Materials, 2006, 15, 1609-1613.	1.8	9
3668	New high-pressure phase relations in CaSnO3. American Mineralogist, 2006, 91, 1879-1887.	0.9	21
3669	Energetics of cubic and hexagonal phases in Mn-dopedGaN: First-principles pseudopotential calculations. Physical Review B, 2006, 74, .	1.1	9
3670	The rutile TiO2 (110) surface: Obtaining converged structural properties from first-principles calculations. Journal of Chemical Physics, 2006, 124, 024708.	1.2	92
3671	Adsorption and Dissociation of H2O2on Pt and Ptâ^'Alloy Clusters and Surfaces. Journal of Physical Chemistry B, 2006, 110, 17452-17459.	1.2	76

#	Article	IF	Citations
3672	Ab initiopressure-dependent vibrational and dielectric properties ofCeO2. Physical Review B, 2006, 74, .	1.1	49
3673	Gold-Adatom-Mediated Bonding in Self-Assembled Short-Chain Alkanethiolate Species on the Au(111) Surface. Physical Review Letters, 2006, 97, 146103.	2.9	425
3674	Theoretical assessment of the elastic constants and hydrogen storage capacity of some metal-organic framework materials. Journal of Chemical Physics, 2006, 125, 084714.	1.2	94
3675	Schottky barrier formation at a carbon nanotubeâ€"metal junction. Applied Physics Letters, 2006, 89, 243107.	1.5	41
3676	Structural and electronic properties of III-V bismuth compounds. Physical Review B, 2006, 73, .	1.1	148
3677	Do all III-V compounds have the zinc-blende or wurtzite ground state structure?. Applied Physics Letters, 2006, 88, 161902.	1.5	54
3678	Tuning the structural, electronic, and optical properties of BexZn1âˆ'xTe alloys. Applied Physics Letters, 2006, 89, 061913.	1.5	42
3679	Donor levels for selectedn-type dopants in diamond: A computational study of the effect of supercell size. Physical Review B, 2006, 74, .	1.1	25
3680	Prediction of ground-state structures and order-disorder phase transitions in II-III spinel oxides: A combined cluster-expansion method and first-principles study. Physical Review B, 2006, 73, .	1.1	91
3681	Mechanisms for catalytic carbon nanofiber growth studied byab initiodensity functional theory calculations. Physical Review B, 2006, 73, .	1.1	248
3682	Density functional study of gold atoms and clusters on a graphite (0001) surface with defects. Physical Review B, 2006, 74, .	1.1	41
3683	Bond ionicities and hardness ofB13C2-like structuredByXcrystals(X=C,N,O,P,As). Physical Review B, 2006, 73, .	1.1	42
3684	Electronic and optical properties ofRuO2andIrO2. Physical Review B, 2006, 73, .	1.1	131
3685	Ab Initio and Molecular Dynamics Studies of Crystalline TNAD (trans-1,4,5,8-Tetranitro-1,4,5,8-tetraazadecalin). Journal of Physical Chemistry B, 2006, 110, 10651-10661.	1.2	52
3686	Density Functional Theory Calculations of the Dissociation of H2 on (100) 2H-MoS2 Surfaces: A Key Step in the Hydroprocessing of Crude Oil. Bulletin of Science, Technology and Society, 2006, 26, 314-322.	1.1	4
3687	Charge Carriers in Few-Layer Graphene Films. Physical Review Letters, 2006, 97, 036803.	2.9	582
3688	CO2Reforming of CH4on Ni(111):Â A Density Functional Theory Calculation. Journal of Physical Chemistry B, 2006, 110, 9976-9983.	1.2	124
3689	Computational design ofSiâ•SiO2interfaces: Stress and strain on the atomic scale. Physical Review B, 2006, 73, .	1.1	36

#	Article	IF	Citations
3690	Statistical model applied toAxByC1âˆ’xâˆ’yDquaternary alloys: Bond lengths and energy gaps ofAlxGayIn1âˆ’xâˆ’yX(X=As, P, or N) systems. Physical Review B, 2006, 73, .	1.1	16
3691	Quantum Chemical Study of Mechanisms for Oxidative Dehydrogenation of Propane on Vanadium Oxide. Journal of Physical Chemistry B, 2006, 110, 8363-8371.	1.2	54
3692	Density functional investigation of the adsorption of a methane monolayer on an MgO(100) surface. Physical Review B, 2006, 73, .	1.1	16
3693	Variational density-functional perturbation theory for dielectrics and lattice dynamics. Physical Review B, 2006, 73, .	1.1	735
3694	Density-functional electronic structure calculations for native defects and Cu impurities in CdS. Physical Review B, 2006, 74, .	1.1	58
3695	Spectroscopic and Ab Initio Characterization of the [ReH9]2-Ion. Inorganic Chemistry, 2006, 45, 10951-10957.	1.9	25
3696	Magneto-optical properties of Heusler compounds from a first-principles approach. Journal Physics D: Applied Physics, 2006, 39, 851-855.	1.3	20
3697	Pressure dependence of vibrational, thermal, and elastic properties ofZnSe: Anab initiostudy. Physical Review B, 2006, 73, .	1.1	39
3698	Structural stability, electronic properties, and quantum conductivity of small-diameter silicon nanowires. Physical Review B, 2006, 74, .	1.1	30
3699	Ab initiostructural identification of high density cubicBC2N. Physical Review B, 2006, 73, .	1.1	17
3700	First principles study on the structural, electronic and optical properties of diluted magnetic semiconductors Zn 1âˆ’ x Co x X (X =S, Se, Te). Chinese Physics B, 2006, 15, 1585-1590.	1.3	18
3701	Structural and electronic properties of single-walled AlN nanotubes of different chiralities and sizes. Journal of Physics Condensed Matter, 2006, 18, S2045-S2054.	0.7	37
3702	Structural studies of phosphorus induced dimers on Si(001). Physical Review B, 2006, 73, .	1.1	11
3703	Origins of Fermi-level pinning on GaN and InN polar and nonpolar surfaces. Europhysics Letters, 2006, 76, 305-311.	0.7	183
3704	Charge Redistribution and Phonon Entropy of Vanadium Alloys. Physical Review Letters, 2006, 97, 245701.	2.9	15
3705	Predictive models for co-doping effects between combinations of donors (P/As/Sb) and acceptors (B/Ga/In). , 2006, , .		1
3706	First-principles calculations of the structural stability and magnetic property of the metastable phases in the equilibrium immiscible Coâ€“Au system. Journal of Physics Condensed Matter, 2006, 18, 4345-4353.	0.7	7
3707	Ab initiostudy of ferromagnetic semiconductor Ge1âˆ’xMnxTe. Journal of Physics Condensed Matter, 2006, 18, 7171-7178.	0.7	8

#	Article	IF	Citations
3708	Electronic structure of cubic BaTbO3 from first-principles pseudopotential calculations. Canadian Journal of Physics, 2006, 84, 115-120.	0.4	4
3709	Local-property analysis for modeling of gate insulator materials. , 2006, , .		1
3710	Equilibrium structure and Ti-catalyzed H2 desorption in NaAlH4 nanoparticles from density functional theory. Physical Chemistry Chemical Physics, 2006, 8, 4853.	1.3	83
3711	Ab initio calculation of As-vacancy deactivation and interstitial-mediated As diffusion in strained Si. , 2006, , .		0
3712	The influence of carbon on the adsorption of CO on a Rh(100) single crystal. Physical Chemistry Chemical Physics, 2006, 8, 624-632.	1.3	23
3713	Theoretical properties of the N vacancy in p-type GaN(Mg,H) at elevated temperatures. Journal of Applied Physics, 2006, 99, 113506.	1.1	15
3714	Thermodynamic evaluation of the Alâ€“Crâ€“C system. International Journal of Materials Research, 2006, 97, 539-542.	0.8	26
3715	Pressure and temperature dependence of the lattice dynamics ofCuAlO2investigated by Raman scattering experiments andab initiocalculations. Physical Review B, 2006, 74, .	1.1	93
3716	Optical properties of cubic Ti3N4, Zr3N4, and Hf3N4. Applied Physics Letters, 2006, 89, 151908.	1.5	103
3717	Effect of electron beam treatment on adhesion of Ta/polymeric low-k interface. Applied Physics Letters, 2006, 88, 233510.	1.5	5
3718	Comparative studies of CO and H2O interactions with Pd(111) surface: A theoretical study of poisoning. Applied Physics Letters, 2006, 88, 051908.	1.5	16
3719	Phonon spectra of diamond, Si, Ge, andÎ±â˜Sn: Calculations with real-space interatomic force constants. Physical Review B, 2006, 74, .	1.1	25
3720	Local Electronic Structure around a Single Kondo Impurity. Nano Letters, 2006, 6, 1146-1150.	4.5	30
3721	Interwall interaction and elastic properties of carbon nanotubes. Physical Review B, 2006, 73, .	1.1	59
3722	Mechanism for NO2Charging on Metal Supported MgO. Journal of Physical Chemistry B, 2006, 110, 11977-11981.	1.2	91
3723	Charge transfers at metal/oxide interfaces: a DFT study of formation of KÎ´+and AuÎ´â˜species on MgO/Ag(100) ultra-thin films from deposition of neutral atoms. Physical Chemistry Chemical Physics, 2006, 8, 3335-3341.	1.3	82
3724	Multiscale Simulations of Quantum Structures. , 2006, , .		1
3725	First-Principles Calculations for Co-Doped LiMn[sub 1.5]Ni[sub 0.5]O[sub 4] and LiMn[sub 2]O[sub 4] Battery Electrodes. Electrochemical and Solid-State Letters, 2006, 9, A289.	2.2	5

#	Article	IF	Citations
3726	Fermi surfaces and electronic structure of the Heusler alloy Co2TiSn. Journal of Physics Condensed Matter, 2006, 18, 2897-2903.	0.7	16
3727	First-principles study ofNi2P(0001) surfaces. Physical Review B, 2006, 74, .	1.1	52
3728	Structural Phase Transition and Photo-Charge Carrier Transport in SrTiO3. Ferroelectrics, 2006, 337, 179-188.	0.3	8
3729	Density Functional Theory Study of Ligand Binding on CdSe (0001), (000Ì„), and (112Ì„0) Single Crystal Relaxed and Reconstructed Surfaces:Á Implications for Nanocrystalline Growth. Journal of Physical Chemistry B, 2006, 110, 18007-18016.	1.2	152
3730	Molecular dynamics calculations of the thermal expansion properties and melting points of Si and Ge. Journal of Physics Condensed Matter, 2006, 18, 3489-3498.	0.7	1
3731	Electronic structure of M2AlC(0001) surfaces (M = Ti,V,Cr). Journal of Physics Condensed Matter, 2006, 18, 8877-8881.	0.7	20
3732	First-principles study on structural stability of 3d transition metal alloying magnesium hydride. Transactions of Nonferrous Metals Society of China, 2006, 16, 23-32.	1.7	12
3733	Phase stability and structural distortion of NiO under high pressure. Transactions of Nonferrous Metals Society of China, 2006, 16, s52-s58.	1.7	2
3734	First-principle investigation of bismuth segregation at Î£5 (012) grain-boundaries in nickel. Transactions of Nonferrous Metals Society of China, 2006, 16, s813-s819.	1.7	6
3735	Influence of crystal structure and formation energies of impurities (Mg, Zn and Ca) in zinc blende GaN. Transactions of Nonferrous Metals Society of China, 2006, 16, s854-s857.	1.7	6
3736	Donor-vacancy complexes in Ge: Cluster and supercell calculations. Physical Review B, 2006, 73, .	1.1	61
3737	Transition pressures and enthalpy barriers for the cubic diamondâ†'Î²-tin transition in Si and Ge under nonhydrostatic conditions. Physical Review B, 2006, 73, .	1.1	26
3738	Ab initiostudy of the vibrational properties of crystallineTeO2: TheÎ±,Î², andÎ³phases. Physical Review B, 2006, 73, .	1.1	138
3739	Dynamical core-hole screening in the x-ray absorption spectra of graphite,C60, and carbon nanotubes: A first-principles electronic structure study. Physical Review B, 2006, 73, .	1.1	28
3740	Electronic structure of theÎ±andÎ´phases ofBi2O3: A combinedab initioand x-ray spectroscopy study. Physical Review B, 2006, 73, .	1.1	187
3741	A theoretical and experimental study of lead substitution in calcium hydroxyapatite. Physical Chemistry Chemical Physics, 2006, 8, 967.	1.3	73
3742	Graphitic Nanofilms as Precursors to Wurtzite Films: Theory. Physical Review Letters, 2006, 96, 066102.	2.9	514
3743	Density functionals from many-body perturbation theory: The band gap for semiconductors and insulators. Journal of Chemical Physics, 2006, 124, 154108.	1.2	166

#	Article	IF	Citations
3744	A periodic genetic algorithm with real-space representation for crystal structure and polymorph prediction. Physical Review B, 2006, 73, .	1.1	145
3745	First-principles study of bulk ordering and surface segregation in Pt-Rh binary alloys. Physical Review B, 2006, 74, .	1.1	67
3746	Influence of the Hydroxylation of Î³-Al2O3Surfaces on the Stability and Diffusion of Single Pd Atoms:Â A DFT Study. Journal of Physical Chemistry B, 2006, 110, 1759-1767.	1.2	103
3747	Semiempirical van der Waals correction to the density functional description of solids and molecular structures. Physical Review B, 2006, 73, .	1.1	707
3748	High-pressure melting of lead. Physical Review B, 2006, 73, .	1.1	30
3749	First-principles study ofPbSiO3alamosite. Physical Review B, 2006, 73, .	1.1	5
3750	Catalytic Oxidation Activity of Pt3O4Surfaces and Thin Films. Journal of Physical Chemistry B, 2006, 110, 14860-14869.	1.2	133
3751	Dynamical properties of guest ions in the type-I clathrate compoundsX8Ga16Ge30(X=Eu,Sr,Ba)investigated by Raman scattering. Physical Review B, 2006, 74, .	1.1	108
3752	Static ionic displacements in Feâ€“Ni alloys from first principles. Journal of Applied Physics, 2006, 99, 08P906.	1.1	7
3753	Water adsorption on hydroxylatedÎ±-quartz (0001) surfaces: From monomer to flat bilayer. Physical Review B, 2006, 73, .	1.1	117
3754	Dynamical Matrices and Free Energies. , 0, , 95-114.		1
3755	Formation and Segregation Energies of B and P Doped and BP Codoped Silicon Nanowires. Nano Letters, 2006, 6, 2781-2784.	4.5	97
3756	Origin of brown coloration in diamond. Physical Review B, 2006, 73, .	1.1	87
3757	A first-principles model of birefringent porous silicon. Journal of Applied Physics, 2006, 100, 044319.	1.1	16
3758	First-principles study of ground- and excited-state properties ofMgO,ZnO, andCdOpolymorphs. Physical Review B, 2006, 73, .	1.1	361
3759	Convergence of the formation energies of intrinsic point defects in wurtzite ZnO: first-principles study by projector augmented wave method. Journal of Physics Condensed Matter, 2006, 18, 1495-1508.	0.7	56
3760	Theoretical studies on doubly and triply linked polymers of Ge9 clusters. Inorganica Chimica Acta, 2006, 359, 3776-3784.	1.2	9
3761	First Principles Density Functional Study of the Adsorption and Dissociation of Carbonyl Compounds on Magnesium Oxide Nanosurfaces. Journal of Physical Chemistry B, 2006, 110, 25941-25949.	1.2	37

#	Article	IF	Citations
3762	Ab initiostudy of metal-organic framework-5Zn4O(1,4â^'benzenedicarboxylate)3: An assessment of mechanical and spectroscopic properties. Physical Review B, 2006, 73, .	1.1	83
3763	Phonon dispersion curves of stable and metastableBC3honeycomb epitaxial sheets and their chemical bonding: Experiment and theory. Physical Review B, 2006, 73, .	1.1	70
3764	Cu4Mo6Se8:Â Synthesis, Crystal Structure, and Electronic Structure of a New Chevrel Phase Structure Type. Inorganic Chemistry, 2006, 45, 2718-2726.	1.9	7
3765	Water adsorption on a NaCl (001) surface: A density functional theory study. Physical Review B, 2006, 74, .	1.1	43
3766	Water-Gas-Shift Reaction on Molybdenum Carbide Surfaces:â€‰ Essential Role of the Oxycarbide. Journal of Physical Chemistry B, 2006, 110, 19418-19425.	1.2	202
3767	Defect properties andp-type doping efficiency in phosphorus-doped ZnO. Physical Review B, 2006, 73, .	1.1	182
3768	Site preference, thermodynamic, and magnetic properties of the ternary Laves phase Ti(Fe_{1â€“x}Al_x)₂ with the crystal structure of the MgZn₂-type. International Journal of Materials Research, 2006, 97, 450-460.	0.8	24
3769	First-principles calculations of native defects in tin monoxide. Physical Review B, 2006, 74, .	1.1	276
3770	Structure, electronics, and interaction of hydrogen and oxygen on diamond surfaces. Physical Review B, 2006, 73, .	1.1	221
3771	First-Principle Study of Adsorption of Hydrogen on Ti-Doped Mg(0001) Surface. Journal of Physical Chemistry B, 2006, 110, 21747-21750.	1.2	52
3772	Ab initio energetic study of oxide ceramics with rare-earth elements. Rare Metals, 2006, 25, 549-555.	3.6	12
3773	Elastic anisotropy of FeSiO3end-members of the perovskite and post-perovskite phases. Geophysical Research Letters, 2006, 33, n/a-n/a.	1.5	59
3774	Electronic spin transitions and the seismic properties of ferrous iron-bearing MgSiO3post-perovskite. Geophysical Research Letters, 2006, 33, .	1.5	50
3775	Ab initiostudy of the composition dependence of the pressure-induced spin transition in the (Mg1â^'x,Fex)O system. Geophysical Research Letters, 2006, 33, .	1.5	76
3776	Density functional study of vibrational and thermodynamic properties of ringwoodite. Journal of Geophysical Research, 2006, 111, n/a-n/a.	3.3	37
3777	Magnetically induced variations in phonon frequencies. Physical Review B, 2006, 73, .	1.1	11
3778	First-principles calculations of the atomic and electronic structure ofFcenters in the bulk and on the (001) surface ofSrTiO3. Physical Review B, 2006, 73, .	1.1	152
3779	Ferroelectric Phase Transition in Individual Single-Crystalline BaTiO3 Nanowires. Nano Letters, 2006, 6, 735-739.	4.5	371

#	Article	IF	Citations
3780	Influence of pressure on the structural, dynamical, and electronic properties of theSnP2S6layered crystal. Physical Review B, 2006, 73, .	1.1	23
3781	Elasticity and piezoelectricity of zinc oxide crystals, single layers, and possible single-walled nanotubes. Physical Review B, 2006, 74, .	1.1	211
3782	Band-gap bowing coefficients in large size-mismatched II-VI alloys: first-principles calculations. Physical Review B, 2006, 74, .	1.1	78
3783	First-Principles Calculations for Insulators at Constant Polarization. Physical Review Letters, 2006, 96, 056401.	2.9	36
3784	Empirical tight-binding model for titanium phase transformations. Physical Review B, 2006, 73, .	1.1	30
3785	Adsorption of transition-metal atoms on boron nitride nanotube: A density-functional study. Journal of Chemical Physics, 2006, 125, 044711.	1.2	104
3786	Thermal stability, atomic vibrational dynamics, and superheating of confined interfacial Sn layers inSnâˆ•Simultilayers. Physical Review B, 2006, 73, .	1.1	8
3787	Structural characterization of fully coordinated ultrathin silica nanotubes by first-principles calculations. Physical Review B, 2006, 73, .	1.1	21
3788	Theoretical investigation of magnetoelectric behavior inBiFeO3. Physical Review B, 2006, 74, .	1.1	582
3789	Density Functional Theory and DFT+U Study of Transition Metal Porphines Adsorbed on Au(111) Surfaces and Effects of Applied Electric Fields. Journal of the American Chemical Society, 2006, 128, 3659-3668.	6.6	100
3790	Adsorbateâˆ’Adsorbate Interactions and Chemisorption at Different Coverages Studied by Accurate ab initio Calculations:Â CO on Transition Metal Surfacesâ€. Journal of Physical Chemistry B, 2006, 110, 3816-3822.	1.2	41
3791	Hexagon-preserving carbon foams: Properties of hypothetical carbon allotropes. Physical Review B, 2006, 74, .	1.1	92
3792	Electronic origin of the anomalous stability of Fe-rich bcc Fe-Cr alloys. Physical Review B, 2006, 73, .	1.1	175
3793	Origin of Enhanced Reducibility/Oxygen Storage Capacity of Ce1-xTixO2Compared to CeO2or TiO2. Chemistry of Materials, 2006, 18, 3249-3256.	3.2	173
3794	LSDA+Ustudy of cupric oxide: Electronic structure and native point defects. Physical Review B, 2006, 73, .	1.1	213
3795	Strained Si, Ge, andSi1âˆ’xGexalloys modeled with a first-principles-optimized full-zonekâˆ™pmethod. Physical Review B, 2006, 74, .	1.1	129
3796	Ab initiomolecular dynamics study of pressure-induced phase transition in ZnS. Journal of Physics Condensed Matter, 2006, 18, 9483-9491.	0.7	14
3797	Volume-dependent exchange interactions and noncollinear magnetism in zinc-blende MnAs. Physical Review B, 2006, 74, .	1.1	11

#	Article	IF	Citations
3798	Hydrogen Adsorption on Carbon-Doped Boron Nitride Nanotube. Journal of Physical Chemistry B, 2006, 110, 21184-21188.	1.2	105
3799	Defects-enhanced dissociation of H2 on boron nitride nanotubes. Journal of Chemical Physics, 2006, 124, 054706.	1.2	60
3800	Local cation environments in the pyropeâ€“grossularMg3Al2Si3O12â€“Ca3Al2Si3O12garnet solid solution. Physical Review B, 2006, 74, .	1.1	30
3801	EFFECT OF RELAXATION ON THE ENERGETICS AND STRUCTURE OF ANATASE TiO2 (101) SURFACE. Surface Review and Letters, 2006, 13, 825-831.	0.5	7
3802	First-principles study of optical spectra of single-wallBC2Nnanotubes. Physical Review B, 2006, 73, .	1.1	30
3803	Ideal strength of silicon: Anab initiostudy. Physical Review B, 2006, 74, .	1.1	93
3804	Adsorption of phenol on graphite(0001) andÎ±â^'Al2O3(0001): Nature of van der Waals bonds from first-principles calculations. Physical Review B, 2006, 74, .	1.1	89
3805	Systematically exact integrated density-of-states Lloydâ€™s formula for disordered alloys with short-range order. Physical Review B, 2006, 73, .	1.1	12
3806	Hydrostatic-pressure-induced porous gallium nitride from nanotube bundles: An ab initio study. Journal of Chemical Physics, 2006, 125, 174711.	1.2	2
3807	Potential superhard osmium dinitride with fluorite and pyrite structure: First-principles calculations. Physical Review B, 2006, 74, .	1.1	130
3808	Calculated Phase Diagrams for the Electrochemical Oxidation and Reduction of Water over Pt(111). Journal of Physical Chemistry B, 2006, 110, 21833-21839.	1.2	388
3809	First-principles studies of structural and electronic properties of hexagonalBC5. Physical Review B, 2006, 73, .	1.1	75
3810	Co9S8as a Catalyst for Electroreduction of O2:Â Quantum Chemistry Predictions. Journal of Physical Chemistry B, 2006, 110, 936-941.	1.2	177
3811	Ab initiocalculations of the BaF2bulk and surface F centres. Journal of Physics Condensed Matter, 2006, 18, 8367-8381.	0.7	44
3812	Catalytic Effects of Subsurface Carbon in the Chemisorption of Hydrogen on a Mg(0001) Surface:Â an Ab-initio Study. Journal of Physical Chemistry B, 2006, 110, 1814-1819.	1.2	55
3813	Ab initiocalculations of the alloy resistivities of lattice-matched and lattice-mismatched metal pairs: Influence of local-impurity-induced distortions. Physical Review B, 2006, 74, .	1.1	7
3814	Identification of an OH-Li center in ZnO: Infrared absorption spectroscopy and density functional theory. Physical Review B, 2006, 73, .	1.1	46
3815	Ab initiostudy of the critical thickness for ferroelectricity in ultrathinPtâˆ•PbTiO3âˆ•Ptfilms. Physical Review B, 2006, 74, .	1.1	66

#	Article	IF	Citations
3816	Structure and activity of oxidized Pt(110) and Î±-PtO2. Physical Chemistry Chemical Physics, 2006, 8, 1566.	1.3	71
3817	Ab initiostudy of native defects in SiC nanotubes. Physical Review B, 2006, 74, .	1.1	59
3818	Structural, electronic and magnetic properties of Gd investigated by DFT+Umethods: bulk, clean and H-covered (0001) surfaces. Journal of Physics Condensed Matter, 2006, 18, 7021-7043.	0.7	64
3819	Electron-phonon coupling in halogen-doped carbon clathrates from first principles. Physical Review B, 2006, 74, .	1.1	30
3820	Lattice Dynamics of Molybdenum at High Pressure. Physical Review Letters, 2006, 96, 115502.	2.9	38
3821	Ab initio calculated binodal and spinodal of cubic Ti1â^'xAlxN. Applied Physics Letters, 2006, 88, 071922.	1.5	130
3822	Understanding Si adsorption on GaN(0001) surfaces using first-principles calculations. Physical Review B, 2006, 73, .	1.1	43
3823	Chemical Functionalization of Boronâ^'Nitride Nanotubes with NH3and Amino Functional Groups. Journal of the American Chemical Society, 2006, 128, 12001-12006.	6.6	165
3824	Assigning powders to crystal structures by high-resolution1Hâ€“1H double quantum and1Hâ€“13C J-INEPT solid-state NMR spectroscopy and first principles computation. A case study of penicillin G. Physical Chemistry Chemical Physics, 2006, 8, 3418-3422.	1.3	79
3825	Theoretical Study of N-Doped TiO2Rutile Crystals. Journal of Physical Chemistry B, 2006, 110, 24011-24014.	1.2	140
3826	P-type transparent conductors Sr1â^'xNaxFCuS and SrF1â^'xOxCuS: design, synthesis and physical properties. Journal of Materials Chemistry, 2006, 16, 4165-4169.	6.7	22
3827	Migration Energy of He in W Revisited byAbÂInitioCalculations. Physical Review Letters, 2006, 97, 196402.	2.9	283
3828	Derivation of Force Field Parameters for SnO2â^'H2O Surface Systems from Plane-Wave Density Functional Theory Calculations. Journal of Physical Chemistry B, 2006, 110, 8386-8397.	1.2	53
3829	Analysis of scanning tunneling microscopy images of the charge-density-wave phase in quasi-one-dimensionalRb0.3MoO3. Physical Review B, 2006, 74, .	1.1	7
3830	Adsorption and Solar Light Decomposition of Acetone on Anatase TiO2 and Niobium Doped TiO2 Thin Films. Journal of Physical Chemistry B, 2006, 110, 1210-1220.	1.2	159
3831	A First-Principles Analysis of Hydrogen Interaction in Ti-Doped NaAlH4Surfaces:Â Structure and Energetics. Journal of Physical Chemistry B, 2006, 110, 25863-25868.	1.2	45
3832	Competitive Adsorption of NO, NO2, CO2, and H2O on BaO(100):Â A Quantum Chemical Study. Journal of Physical Chemistry B, 2006, 110, 17484-17492.	1.2	63
3833	Influence of Mnâ^'Oâ^'Mn Bond Angle on the Magnetic and Electronic Properties in YBaMn2O5. Journal of Physical Chemistry B, 2006, 110, 2606-2610.	1.2	8

#	Article	IF	Citations
3834	Ab initiostudy of F- and Cl-functionalized single wall carbon nanotubes. Journal of Physics Condensed Matter, 2006, 18, 5175-5184.	0.7	15
3835	One-Dimensional Transition Metalâ^'Benzene Sandwich Polymers:Â Possible Ideal Conductors for Spin Transport. Journal of the American Chemical Society, 2006, 128, 2310-2314.	6.6	202
3836	Reaction of Hydrogen with Ag(111):â€‰ Binding States, Minimum Energy Paths, and Kinetics. Journal of Physical Chemistry B, 2006, 110, 17145-17154.	1.2	51
3837	Band Gap Variation in Prussian Blue via Cation-Induced Structural Distortion. Journal of Physical Chemistry B, 2006, 110, 24294-24298.	1.2	37
3838	Theoretical Analysis of Structural, Energetic, Electronic, and Defect Properties of Li2O. Journal of Physical Chemistry B, 2006, 110, 9413-9420.	1.2	66
3839	Noncovalent interactions between organometallic metallocene complexes and single-walled carbon nanotubes. Journal of Chemical Physics, 2006, 125, 154704.	1.2	43
3840	Design of a New Family of Inorganic Compounds Ae2F2SnX3(Ae = Sr, Ba; X = S, Se) Using Rock Salt and Fluorite 2D Building Blocks. Inorganic Chemistry, 2006, 45, 917-922.	1.9	33
3841	Anisotropic and Passivation-Dependent Quantum Confinement Effects in Germanium Nanowires:Â A Comparison with Silicon Nanowires. Journal of Physical Chemistry B, 2006, 110, 18332-18337.	1.2	28
3842	Ab Initio and Work Function and Surface Energy Anisotropy of LaB6. Journal of Physical Chemistry B, 2006, 110, 18459-18465.	1.2	74
3843	Fundamental Studies of P(GeH3)3, As(GeH3)3, and Sb(GeH3)3:â€‰ Practical n-Dopants for New Group IV Semiconductors. Chemistry of Materials, 2006, 18, 6266-6277.	3.2	51
3844	Density functional calculations of the formation and migration enthalpies of monovacancies in Ni: Comparison of local and nonlocal approaches. Physical Review B, 2006, 74, .	1.1	45
3845	First-Principles Calculations of AlN Nanowires and Nanotubes:Â Atomic Structures, Energetics, and Surface States. Journal of Physical Chemistry B, 2006, 110, 8764-8768.	1.2	72
3846	First-Principles Calculations within Periodic Boundary Conditions of the NMR Shielding Tensor for a Transition Metal Nucleus in a Solid State System:Â The Example of51V in AlVO4. Journal of Physical Chemistry B, 2006, 110, 21403-21407.	1.2	27
3847	First-principles calculations of the structural, dynamical, and electronic properties of liquid MgO. Physical Review B, 2006, 73, .	1.1	68
3848	Magic Silica Clusters as Nanoscale Building Units for Super-(Tris)tetrahedral Materials. Chemistry of Materials, 2006, 18, 1464-1469.	3.2	27
3849	Quasiparticle band structures of BaO and BaS. Journal of Applied Physics, 2006, 100, 086103.	1.1	20
3850	Defect compensation, clustering, and magnetism in Cr-doped anataseTiO2. Physical Review B, 2006, 73, .	1.1	82
3851	Reactions of Hydrazoic Acid and Trimethylindium on TiO2Rutile (110) Surface:Â A Computational Study on the Formation of the First Monolayer InN. Journal of Physical Chemistry B, 2006, 110, 2263-2270.	1.2	13

#	Article	IF	Citations
3852	On the Performance of Au(111) for Ethylene Epoxidation:â€‰ A Density Functional Study. Journal of Physical Chemistry B, 2006, 110, 13310-13313.	1.2	48
3853	Ab initioinvestigation on the phase stability of Ti3SiC2, Ti3Si0.5Ge0.5C2, and Ti3GeC2at high pressures. High Pressure Research, 2006, 26, 127-130.	0.4	4
3854	Study of Phase Selectivity of Organicâ"Inorganic Hybrid Semiconductors. Chemistry of Materials, 2006, 18, 2805-2809.	3.2	35
3855	Interaction of Hydrogen with Cerium Oxide Surfaces:â€‰ a Quantum Mechanical Computational Study. Journal of Physical Chemistry B, 2006, 110, 19380-19385.	1.2	85
3856	First-Principles Study of K and Cs Adsorbed on Pd(111). Journal of Physical Chemistry B, 2006, 110, 23904-23910.	1.2	10
3857	Molecular Understanding of Alumina Supported Single-Site Catalysts by a Combination of Experiment and Theory. Journal of the American Chemical Society, 2006, 128, 9157-9169.	6.6	125
3858	Debye temperature and stiffness of carbon and boron nitride polymorphs from first principles calculations. Physical Review B, 2006, 73, .	1.1	218
3859	Interfacial Electrostatics of Self-Assembled Monolayers of Alkane Thiolates on Au(111):Â Work Function Modification and Molecular Level Alignments. Journal of Physical Chemistry B, 2006, 110, 10862-10872.	1.2	57
3860	Polyanionic Hydrides from Polar Intermetallics AeE2(Ae = Ca, Sr, Ba; E = Al, Ga, In). Journal of the American Chemical Society, 2006, 128, 817-824.	6.6	33
3861	Ridge-Bridge Adsorption of Molecular Oxygen on Pt{110}(1 Ã— 2) from First Principles. Journal of Physical Chemistry B, 2006, 110, 11962-11970.	1.2	13
3862	Characterization of the Structural and Electronic Properties of Crystalline Lithium Silicates. Journal of Physical Chemistry B, 2006, 110, 22346-22352.	1.2	56
3863	Simulating Temperature Programmed Desorption of Water on Hydrated Î³-Alumina from First-Principles Calculations. Journal of Physical Chemistry B, 2006, 110, 7392-7395.	1.2	27
3864	Toward the Comparison of Rare Earth Element and Actinide Behavior in Materials:â€‰ A Computational Study of Ce- and U-Bearing Britholites. Journal of Physical Chemistry B, 2006, 110, 19226-19232.	1.2	7
3865	Truncation of periodic image interactions for confined systems. Physical Review B, 2006, 73, .	1.1	273
3866	Periodic Density Functional Theory Study of Propane Oxidative Dehydrogenation over V2O5(001) Surface. Journal of the American Chemical Society, 2006, 128, 11114-11123.	6.6	134
3867	First Principles Study of Adsorption and Dissociation of CO on W(111). Journal of Physical Chemistry B, 2006, 110, 1344-1349.	1.2	21
3868	Mixed Aromaticâ"Alkyne System on a Pd Surface:Â A First-Principles Studyâ€. Journal of Physical Chemistry B, 2006, 110, 3499-3503.	1.2	17
3869	Electronic and magnetic properties of V-doped anataseTiO2from first principles. Physical Review B, 2006, 74, .	1.1	80

#	Article	IF	Citations
3870	Stability of the body-centered-tetragonal phase of Fe at high pressure: Ground-state energies, phonon spectra, and molecular dynamics simulations. Physical Review B, 2006, 74, .	1.1	21
3871	Ab initiostudy of nitrogen and boron substitutional impurities in single-wall SiC nanotubes. Physical Review B, 2006, 73, .	1.1	131
3872	Structure and properties ofTiN(111)â^•SixNyâ^•TiN(111)interfaces in superhard nanocomposites: First-principles investigations. Physical Review B, 2006, 74, .	1.1	69
3873	Symmetrized-basis LASTO calculations of defects in CdTe and ZnTe. Physical Review B, 2006, 73, .	1.1	41
3874	Density functional theory study on the geometrical and electronic structures of a new thinnest boron nanotube. Journal of Materials Chemistry, 2006, 16, 2429.	6.7	13
3875	Periodic Density Functional Theory Investigation of the Uranyl Ion Sorption on the TiO2Rutile (110) Face. Inorganic Chemistry, 2006, 45, 6568-6570.	1.9	29
3876	Electronic and Structural Properties of Oxygen-Doped BN Nanotubes. IEEE Nanotechnology Magazine, 2006, 5, 517-522.	1.1	54
3877	DFT Study of a Weakly Ï€-Bonded C2H4on Oxygen-Covered Ag(100). Journal of Physical Chemistry B, 2006, 110, 367-376.	1.2	20
3878	Structure and stability ofZrSiO4under hydrostatic pressure. Physical Review B, 2006, 74, .	1.1	40
3879	Effect of symmetry lowering on the dielectric response ofBaZrO3. Physical Review B, 2006, 73, .	1.1	80
3880	Interactions of Hydrogen with Pd and Pd/Ni Alloy Chain-Functionalized Single Walled Carbon Nanotubes from Density Functional Theory. Journal of Physical Chemistry B, 2006, 110, 22415-22425.	1.2	23
3881	A density-functional theory study of the adsorption of CO molecules on Au/Ni(111). Journal of Physics Condensed Matter, 2006, 18, 10825-10835.	0.7	8
3882	Raman Scattering in Crystalline Oligothiophenes:Â A Comparison between Density Functional Theory and Bond Polarizability Model. Journal of Physical Chemistry B, 2006, 110, 24869-24875.	1.2	34
3883	Small-radius clean and metal-doped boron carbide nanotubes: A density functional study. Physical Review B, 2006, 74, .	1.1	18
3884	Thickness-Dependent Phase Transition of AlxGa1-xN Thin Films on Strained GaN. Journal of Physical Chemistry B, 2006, 110, 10396-10400.	1.2	7
3885	Monitoring Two-Dimensional Coordination Reactions:Â Directed Assembly of Coâ^'Terephthalate Nanosystems on Au(111). Journal of Physical Chemistry B, 2006, 110, 5627-5632.	1.2	74
3886	Theoretical prediction of low-energy crystal structures and hydrogen storage energetics inLi2NH. Physical Review B, 2006, 73, .	1.1	67
3887	Application of the statistical moment method to thermodynamic quantities of silicon. Journal of Physics Condensed Matter, 2006, 18, 283-293.	0.7	18

#	Article	IF	Citations
3888	A theoretical and experimental study of the distorted pyrochlore Bi2Sn2O7. Journal of Materials Chemistry, 2006, 16, 3452.	6.7	30
3889	Coordination Preference of Ga in Hydrides. Inorganic Chemistry, 2006, 45, 10698-10701.	1.9	3
3890	Structure Determination of the 4d Metal Diborides:Â A Quantum Mechanical Study. Journal of Physical Chemistry B, 2006, 110, 5367-5371.	1.2	19
3891	A Neutron Scattering and Nuclear Magnetic Resonance Study of the Structure of GeO2â^'P2O5Glasses. Journal of Physical Chemistry B, 2006, 110, 20123-20128.	1.2	30
3892	The Crystal Structure and Surface Energy of NaAlH4:Â A Comparison of DFT Methodologies. Journal of Physical Chemistry B, 2006, 110, 622-630.	1.2	43
3893	Carbon Nanotubes Functionalized by NO2:Â Coexistence of Charge Transfer and Radical Transfer. Journal of Physical Chemistry B, 2006, 110, 22462-22470.	1.2	28
3894	A Systematic Density Functional Theory Study of the Câ^'N Bond Cleavage of Methylamine on Metals. Journal of Physical Chemistry B, 2006, 110, 14300-14303.	1.2	12
3895	Structures and Potential Superconductivity inSiH4at High Pressure: En Route to â€œMetallic Hydrogenâ€• Physical Review Letters, 2006, 96, 017006.	2.9	187
3896	Filling fraction limits for rare-earth atoms inCoSb3: Anab initioapproach. Physical Review B, 2006, 74, .	1.1	53
3897	Chemical Bonding, Electronâ^'Phonon Coupling, and Structural Transformations in High-Pressure Phases of Siâ€. Journal of Physical Chemistry B, 2006, 110, 3721-3726.	1.2	14
3898	Mechanistic Study of the Electrochemical Oxygen Reduction Reaction on Pt(111) Using Density Functional Theory. Journal of Physical Chemistry B, 2006, 110, 15338-15344.	1.2	91
3899	Effect of S Arrangement on Fe(110) Properties at 1/3 Monolayer Coverage:Â A DFT Study. Journal of Physical Chemistry B, 2006, 110, 956-962.	1.2	18
3900	A Quantum Chemical Study of the Decomposition of Keggin-Structured Heteropolyacids. Journal of Physical Chemistry B, 2006, 110, 4170-4178.	1.2	37
3901	Rational Design of Selective, Sulfur-Resistant Oxidation Emissions Catalysts. Journal of Physical Chemistry B, 2006, 110, 6856-6863.	1.2	6
3902	Thiophene Adsorption and Activation on MoP(001), Î³-Mo2N(100), and Ni2P(001):Â Density Functional Theory Studies. Journal of Physical Chemistry B, 2006, 110, 22563-22569.	1.2	38
3903	Structural properties ofPbTeâ^•CdTeinterfaces from first principles. Physical Review B, 2006, 74, .	1.1	51
3904	Do Methanethiol Adsorbates on the Au(111) Surface Dissociate?. Physical Review Letters, 2006, 97, 045505.	2.9	57
3905	Structure Sensitivity in the Oxidation of CO on Ir Surfaces. Langmuir, 2006, 22, 3166-3173.	1.6	32

#	Article	IF	Citations
3906	Electronic Structure and Charge Transfer in the Ternary Intercalated Graphite Î²-KS0.25C3. Inorganic Chemistry, 2006, 45, 9387-9393.	1.9	0
3907	Density Functional Study of the Interfacial Electron Transfer Pathway for Monolayer-Adsorbed InN on the TiO2Anatase (101) Surface. Journal of Physical Chemistry B, 2006, 110, 23460-23466.	1.2	19
3908	Ae2Sb2X4F2(Ae = Sr, Ba):Â New Members of the Homologous Series Ae2M1+nX3+nF2Designed from Rock Salt and Fluorite 2D Building Blocks. Inorganic Chemistry, 2006, 45, 2713-2717.	1.9	32
3909	Perturbation of Adsorbed CO by Amine Derivatives Coadsorbed on the Î³-Al2O3Surface:Â FTIR and First Principles Studies. Journal of Physical Chemistry B, 2006, 110, 4742-4750.	1.2	13
3910	Structure and Bonding of Alkanethiols on Cu(111) and Cu(100). Journal of Physical Chemistry B, 2006, 110, 17050-17062.	1.2	40
3911	Comparative Theoretical Study of Formaldehyde Decomposition on PdZn, Cu, and Pd Surfaces. Journal of Physical Chemistry B, 2006, 110, 14890-14897.	1.2	96
3912	Rebonding at coherent interfaces between rocksalt-PbTe/zinc-blende-CdTe. New Journal of Physics, 2006, 8, 317-317.	1.2	32
3913	Hydrogen adsorption and diffusion on Pt {111} and PtSn {111}. Journal of Materials Chemistry, 2006, 16, 1989.	6.7	43
3914	Effect of Double Bonds on the Conducting Properties of Ciguatoxin 3C and Tetrahydropyrane-Based Polymers:â€‰ A Theoretical Study. Journal of Physical Chemistry B, 2006, 110, 1172-1178.	1.2	3
3915	Nature of the Bottom t2g-Block Bands of Layered Perovskites. Implications for the Transport Properties of Phases Where These Bands Are Partially Filled. Journal of the American Chemical Society, 2006, 128, 4318-4329.	6.6	12
3916	First Principles Calculation of the Mechanical Compression of Two Organic Molecular Crystals. Journal of Physical Chemistry A, 2006, 110, 5173-5179.	1.1	46
3917	Concerning the Different Roles of Cations in Metallic Zintl Phases:â€‰ Ba7Ga4Sb9 as a Test Case. Inorganic Chemistry, 2006, 45, 7235-7241.	1.9	21
3918	Half-metallic ferromagnetism in Cu-doped ZnO: Density functional calculations. Physical Review B, 2006, 73, .	1.1	309
3919	A DFT Study of the Adsorption and Dissociation of CO on Sulfur-Precovered Fe(100). Journal of Physical Chemistry B, 2006, 110, 13897-13904.	1.2	46
3920	The Nature of Contact between Pd Leads and Semiconducting Carbon Nanotubes. Nano Letters, 2006, 6, 1415-1419.	4.5	48
3921	An ab initio study of nickel substitution into iron. Earth and Planetary Science Letters, 2006, 248, 147-152.	1.8	18
3922	Relative stability and electronic properties of group IV phosphides and nitrides. Computational Materials Science, 2006, 36, 65-72.	1.4	5
3923	Total energy calculations for systems with magnetic and chemical disorder. Computational Materials Science, 2006, 35, 1-5.	1.4	44

#	Article	IF	Citations
3924	A density functional theory study of CO adsorption on Ptâ€“Au nanoparticles. Computational Materials Science, 2006, 35, 247-253.	1.4	56
3925	Electronic, dynamical, and dielectric properties of lanthanum oxysulfide. Computational Materials Science, 2006, 37, 300-305.	1.4	20
3926	Murnaghanâ€™s equation of state for the electronic ground state energy. Computational Materials Science, 2006, 38, 350-353.	1.4	179
3927	Energetics of phase transitions in BaO through DFT calculations with norm-conserving pseudopotentials: LDA vs. GGA results. Computational Materials Science, 2006, 37, 349-354.	1.4	24
3928	Low energy models from scratch: Application to SiNF. Computational Materials Science, 2006, 37, 537-542.	1.4	4
3929	Electronic properties of GaN at high-pressure from local density and generalized gradient approximations. Computational Materials Science, 2006, 37, 613-617.	1.4	10
3930	First-principles calculations of the structural, electronic and optical properties of CuGaS2 and AgGaS2. Computational Materials Science, 2006, 38, 223-230.	1.4	127
3931	Elastic, electronic and optical properties of ZnS, ZnSe and ZnTe under pressure. Computational Materials Science, 2006, 38, 29-38.	1.4	278
3932	Ab initio study of structural, electronic, elastic and high pressure properties of barium chalcogenides. Computational Materials Science, 2006, 38, 263-270.	1.4	106
3933	Structure of hydrated Zn2+ at the rutile TiO2 (110)-aqueous solution interface: Comparison of X-ray standing wave, X-ray absorption spectroscopy, and density functional theory results. Geochimica Et Cosmochimica Acta, 2006, 70, 4039-4056.	1.6	52
3934	Thermodynamic modelling of the Znâ€“Zr system. Calphad: Computer Coupling of Phase Diagrams and Thermochemistry, 2006, 30, 1-13.	0.7	57
3935	First principles study of electronic and mechanical properties of molybdenum selenide type nanowires. Physical Review B, 2006, 74, .	1.1	26
3936	Spontaneous emission rates of dipoles in photonic crystal membranes. Journal of the Optical Society of America B: Optical Physics, 2006, 23, 1196.	0.9	58
3937	Sulfate may play an important role in the wavelength dependence of laser induced damage. Optics Express, 2006, 14, 12196.	1.7	9
3938	First-principles modelling of Earth and planetary materials at high pressures and temperatures. Reports on Progress in Physics, 2006, 69, 2365-2441.	8.1	152
3939	First-principles aluminum database: Energetics of binary Al alloys and compounds. Physical Review B, 2006, 73, .	1.1	110
3940	Effect of transition metal additives on electronic structure and elastic properties of TiAl andTi3Al. Physical Review B, 2006, 74, .	1.1	58
3941	Periodic ab initio study of structural and vibrational features of hexagonal hydroxyapatite Ca10(PO4)6(OH)2. Physical Chemistry Chemical Physics, 2006, 8, 2464.	1.3	153

#	Article	IF	Citations
3942	Vibrational modes and diffusion of self-interstitial atoms in body-centered-cubic transition metals: A tight-binding molecular-dynamics study. Physical Review B, 2006, 74, .	1.1	28
3943	Prediction of a Highly Activated State of CO Adsorbed on an Al/Fe(100) Bimetallic Surfaceâ€. Journal of Physical Chemistry B, 2006, 110, 22213-22219.	1.2	15
3944	Screened hybrid density functionals applied to solids. Journal of Chemical Physics, 2006, 124, 154709.	1.2	1,915
3945	Crystal stability ofÎ±- andÎ²-boron. Physical Review B, 2006, 73, .	1.1	124
3946	Adsorption of Benzene-1,4-dithiol on the Au(111) Surface and Its Possible Role in Molecular Conductance. Journal of the American Chemical Society, 2006, 128, 8996-8997.	6.6	66
3947	Electronic structure of rare-earth sesquioxides and oxysulfides. Journal of Alloys and Compounds, 2006, 408-412, 687-692.	2.8	67
3948	Electronic structures of platinum group elements silicides calculated by a first-principle pseudopotential method using plane-wave basis. Journal of Alloys and Compounds, 2006, 417, 173-179.	2.8	23
3949	Distinct magnetic states of metastable fcc structured Fe and Feâ€“Cu alloys studied by ab initio calculations. Journal of Alloys and Compounds, 2006, 414, 36-41.	2.8	25
3950	Atomistic simulation on the structural properties and phase stability for Cr23C6 and Mn23C6. Journal of Alloys and Compounds, 2006, 420, 269-272.	2.8	21
3951	Contribution of first-principles energetics to the Caâ€“Mg thermodynamic modeling. Journal of Alloys and Compounds, 2006, 420, 98-106.	2.8	36
3952	Small step graphs of cell data versus composition for ccp solid-solution binary alloys: Application to the (Pt,Ir), (Pt,Re) and (Pt,Ru) systems. Journal of Alloys and Compounds, 2006, 422, 164-172.	2.8	17
3953	Structure and thermodynamic properties of Li8Al3Si5. Journal of Alloys and Compounds, 2006, 426, 57-63.	2.8	4
3954	First-principles study of constitutional and thermal point defects in B2 PdIn. Intermetallics, 2006, 14, 248-254.	1.8	10
3955	Lattice stability of Ca, Sr and Yb disilicides. Intermetallics, 2006, 14, 1472-1486.	1.8	34
3956	Ab initio modeling of interstitial oxygen in crystalline SiGe alloys. Journal of Non-Crystalline Solids, 2006, 352, 1279-1281.	1.5	6
3957	Endohedral terthiophene in zigzag carbon nanotubes: Density functional calculations. Physical Review B, 2006, 74, .	1.1	22
3958	Electronic structure of intrinsic defects in crystalline germanium telluride. Physical Review B, 2006, 73, .	1.1	212
3959	Structures and stability of ABO3 orthorhombic perovskites at the Earth's mantle conditions from first-principles theory. Physics of the Earth and Planetary Interiors, 2006, 157, 1-7.	0.7	37

#	Article	IF	Citations
3960	Structural geomimetism: A conceptual framework for devising new materials from first principlesâˆ†. Progress in Solid State Chemistry, 2006, 34, 21-66.	3.9	8
3961	Dynamical charge tensors and infrared spectra of the crystalline Î±-quaterthiophene polymorph phases from first-principles calculations. Synthetic Metals, 2006, 156, 519-524.	2.1	9
3962	Ab-initio electronic and structural properties of the clean and hydrogen saturated Î²-SiC(100)(3Ã—2) surfaces. Journal of Physics Condensed Matter, 2006, 18, 7505-7506.	0.7	3
3963	Structural and magnetic properties of CoâˆšÎ±â€Al2O3âˆšFe magnetic tunneling junction system: Ab initio investigations. Journal of Applied Physics, 2006, 99, 08T302.	1.1	3
3964	Development of Interatomic Potential for Pb(Zr,Ti)O3 Based on Shell Model. Nihon Kikai Gakkai Ronbunshu, A Hen/Transactions of the Japan Society of Mechanical Engineers, Part A, 2006, 72, 817-822.	0.2	2
3965	Growth of intact water ice onRu(0001)between 140 and160K: Experiment and density-functional theory calculations. Physical Review B, 2006, 73, .	1.1	125
3966	Exact-exchange-based quasiparticle energy calculations for the band gap, effective masses, and deformation potentials of ScN. Physical Review B, 2006, 74, .	1.1	89
3967	Ferromagnetism in Defective Polymerised C 60. , 2006, , 523-540.		0
3968	Detritiation of Plasma-Facing Carbon Materials in Fusion Devices: The Role of Atomic Oxygen from a Quantum Molecular Dynamics Viewpoint. Fusion Science and Technology, 2006, 50, 33-42.	0.6	1
3969	Slip systems and plastic shear anisotropy in Mg2SiO4 ringwoodite: insights from numerical modelling. European Journal of Mineralogy, 2006, 18, 149-160.	0.4	49
3970	The thermoelastic properties of MgSO47D2O (epsomite) from powder neutron diffraction and ab initio calculation. European Journal of Mineralogy, 2006, 18, 449-462.	0.4	50
3971	Role of Structural Defects on the Half-Metallic Character of Heusler Alloys and Their Junctions with Ge and GaAs. Lecture Notes in Physics, 2006, , 41-66.	0.3	5
3972	Electronic structure calculations for substitutional copper and monovacancies in silicon. Physica Scripta, 2006, T126, 61-64.	1.2	6
3973	Ab-Initio Lattice Instability Analysis on Ni and Ni3Al Single Crystals. JSME International Journal Series A-Solid Mechanics and Material Engineering, 2006, 49, 100-106.	0.4	6
3974	First-Principles Calculation of Point Defects in Uranium Dioxide. Materials Transactions, 2006, 47, 2651-2657.	0.4	104
3975	Halbantiperowskite II: zur Kristallstruktur des Pd3Bi2S2. Zeitschrift Fur Anorganische Und Allgemeine Chemie, 2006, 632, 335-342.	0.6	48
3976	Half Antiperovskites. III. Crystallographic and Electronic Structure Effects in Sn2âˆ'xInxCo3S2. Zeitschrift Fur Anorganische Und Allgemeine Chemie, 2006, 632, 1531-1537.	0.6	78
3977	High-pressure polymorphism in L-cysteine: the crystal structures of L-cysteine-III and L-cysteine-IV. Acta Crystallographica Section B: Structural Science, 2006, 62, 296-309.	1.8	103

#	Article	IF	Citations
3978	Hexamer formation in tertiary butyl alcohol (2-methyl-2-propanol, C4H10O). Acta Crystallographica Section B: Structural Science, 2006, 62, 599-605.	1.8	39
3979	Theoretical determination of the structures of CaSiO3 perovskites. Acta Crystallographica Section B: Structural Science, 2006, 62, 1025-1030.	1.8	20
3980	Atomic structure of dislocations in nitride semiconductors. Physica Status Solidi C: Current Topics in Solid State Physics, 2006, 3, 1771-1774.	0.8	0
3981	Metal (Ni, Au)-vacancy complexes in GaN. Physica Status Solidi C: Current Topics in Solid State Physics, 2006, 3, 1783-1786.	0.8	0
3982	Simulation of YBa2Cu3O7/MgO surface growth. Physica Status Solidi C: Current Topics in Solid State Physics, 2006, 3, 3118-3121.	0.8	1
3983	Coupling of the electronic band structure with Ag phonon modes in Y123 and Y124 systems. Physica Status Solidi C: Current Topics in Solid State Physics, 2006, 3, 3140-3143.	0.8	1
3984	Spin polarized transport of iron nitride Fe4N: Analysis using a combination of first principles calculation and model calculation. Physica Status Solidi C: Current Topics in Solid State Physics, 2006, 3, 3303-3306.	0.8	6
3985	First-principles studies of various crystallographic phases and neutral atomic vacancies in KNbO3 and KTaO3. Physica Status Solidi C: Current Topics in Solid State Physics, 2006, 3, 2862-2866.	0.8	10
3986	DFT study of a singleF center in cubic SrTiO3 perovskite. International Journal of Quantum Chemistry, 2006, 106, 2173-2183.	1.0	30
3987	Ab initio calculations and analysis of chemical bonding in SrTiO3 and SrZrO3 cubic crystals. International Journal of Quantum Chemistry, 2006, 106, 2191-2200.	1.0	10
3988	Computational Investigation on 2,4,6-Trinitrochlorobenzene Crystal. Propellants, Explosives, Pyrotechnics, 2006, 31, 38-41.	1.0	0
3989	Computational Study on Potassium Picrate Crystal. Propellants, Explosives, Pyrotechnics, 2006, 31, 290-293.	1.0	4
3990	A First Principles Density Functional Study of Crystalline FOX-7 Chemical Decomposition Process under External Pressure. Propellants, Explosives, Pyrotechnics, 2006, 31, 355-360.	1.0	32
3991	First-principles study of nitridoaluminosilicate CaAlSiN3. Physica Status Solidi (A) Applications and Materials Science, 2006, 203, 2705-2711.	0.8	50
3992	Electronic structure and exchange constants in magnetic semiconductor digital alloys: chemical and band-gap effects. Physica Status Solidi (A) Applications and Materials Science, 2006, 203, 2738-2745.	0.8	14
3993	Theoretical studies on â€©100â€ª dislocations in single crystal CVD diamond. Physica Status Solidi (A) Applications and Materials Science, 2006, 203, 3070-3075.	0.8	29
3994	Theoretical study on the adsorption of armchair carbon nanotubes on the hydrogenated surface of diamond. Physica Status Solidi (A) Applications and Materials Science, 2006, 203, 3107-3113.	0.8	6
3995	Photoelastic constants in diamond and silicon. Physica Status Solidi (A) Applications and Materials Science, 2006, 203, 3088-3093.	0.8	26

#	Article	IF	Citations
3996	Electronic structure of Sb monolayers on the Mo(110) surface. Physica Status Solidi (B): Basic Research, 2006, 243, 584-591.	0.7	9
3997	Special directions for surface integrals in cubic lattices with application to the evaluation of the COMPTON profile of copper. Physica Status Solidi (B): Basic Research, 2006, 243, 653-665.	0.7	9
3998	First-principles study of carrier-mediated ferromagnetism in ZnTe-based thin film. Physica Status Solidi (B): Basic Research, 2006, 243, 1375-1382.	0.7	5
3999	Plain DFT and hybrid HF-DFT LCAO calculations of SnO2 (110) and (100) bare and hydroxylated surfaces. Physica Status Solidi (B): Basic Research, 2006, 243, 1823-1834.	0.7	30
4000	Ab initio modeling of small diameter silicon nanowires. Physica Status Solidi (B): Basic Research, 2006, 243, R7-R9.	0.7	14
4001	Electronic and mechanical properties of wurtzite type SiC nanowires. Physica Status Solidi (B): Basic Research, 2006, 243, R37-R39.	0.7	17
4002	Hybrid HF-DFT comparative study of SrZrO3 and SrTiO3(001) surface properties. Physica Status Solidi (B): Basic Research, 2006, 243, 2756-2763.	0.7	27
4003	Spin-polarized electronic structure of Mnâ€“IVâ€“V2 chalcopyrites. Physica Status Solidi (B): Basic Research, 2006, 243, 2159-2163.	0.7	7
4004	Carrier-mediated stabilization of ferromagnetism in semiconductors: holes and electrons. Physica Status Solidi (B): Basic Research, 2006, 243, 2170-2187.	0.7	46
4005	Tuning the Schottky barrier height in metalâ€“alkaline earth oxide interfaces. Physica Status Solidi (B): Basic Research, 2006, 243, 2081-2084.	0.7	3
4006	Electronic structure of Pd-covered (10,0) carbon nanotube. Physica Status Solidi (B): Basic Research, 2006, 243, 2164-2169.	0.7	6
4007	Predicting crystal structure by merging data mining with quantum mechanics. Nature Materials, 2006, 5, 641-646.	13.3	394
4008	Pressure induced reactivity change on the side-wall of a carbon nanotube: A case study on the addition of singlet O2. Carbon, 2006, 44, 928-938.	5.4	10
4009	A density functional study of inhibition of the HDS hydrogenation pathway by pyridine, benzene, and H2S on MoS2-based catalysts. Catalysis Today, 2006, 111, 44-51.	2.2	93
4010	First-principles calculations of the Znâ€“Zr system. Acta Materialia, 2006, 54, 473-482.	3.8	65
4011	Site preference of ternary alloying elements in Ni3Al: A first-principles study. Acta Materialia, 2006, 54, 1147-1154.	3.8	130
4012	Effects of Pt on the elastic properties of B2 NiAl: A combined first-principles and experimental study. Acta Materialia, 2006, 54, 2361-2369.	3.8	30
4013	Effect of nitrogen on generalized stacking fault energy and stacking fault widths in high nitrogen steels. Acta Materialia, 2006, 54, 2991-3001.	3.8	153

#	Article	IF	Citations
4014	Structure stability and magnetic properties of the Niâ€“Ru system studied by ab initio and molecular dynamics calculations together with ion beam mixing. Acta Materialia, 2006, 54, 3375-3381.	3.8	22
4015	A combined first-principles/CALPHAD modeling of the Alâ€“Ir system. Acta Materialia, 2006, 54, 4101-4110.	3.8	21
4016	Phase stability and cohesive properties of Tiâ€“Zn intermetallics: First-principles calculations and experimental results. Acta Materialia, 2006, 54, 4977-4997.	3.8	91
4017	Angular-dependent interatomic potential for tantalum. Acta Materialia, 2006, 54, 5013-5026.	3.8	70
4018	Nonequilibrium solid phases studied by thermodynamic calculation, molecular dynamics simulation, ab initio calculation and ion-beam manipulation in an immiscible Auâ€“Co system at equilibrium. Acta Materialia, 2006, 54, 5293-5304.	3.8	11
4019	Theoretical calculations on atomistic behaviors in transition metals (Fe, Co, Ni)â€“Al multilayer system: ab initio approach. Applied Surface Science, 2006, 252, 8380-8383.	3.1	8
4020	Adsorption of acrolein on single-crystal surfaces of silver: Density functional studies. Chemical Physics Letters, 2006, 420, 60-64.	1.2	25
4021	Nanotube-based gas sensors â€“ Role of structural defects. Chemical Physics Letters, 2006, 421, 58-62.	1.2	137
4022	A mechanistic study of H2S decomposition on Ni- and Cu-based anode surfaces in a solid oxide fuel cell. Chemical Physics Letters, 2006, 421, 179-183.	1.2	67
4023	Ion deposition induced modification of carbon nanopeapods: A computational study. Chemical Physics Letters, 2006, 422, 137-141.	1.2	7
4024	Adsorption and oxidation of NO on Au(111) surface: Density functional studies. Chemical Physics Letters, 2006, 422, 412-416.	1.2	45
4025	Structural and electronic properties of CaSiO3 triclinic. Chemical Physics Letters, 2006, 427, 113-116.	1.2	26
4026	Oxygen atoms on the (111) surface of coinage metals: On the chemical state of the adsorbate. Chemical Physics Letters, 2006, 429, 86-90.	1.2	30
4027	Prediction of increased tunneling current by bond length stretch in molecular break junctions. Chemical Physics Letters, 2006, 429, 503-506.	1.2	13
4028	Structural, electronic, and optical properties of CaCO3 aragonite. Chemical Physics Letters, 2006, 430, 293-296.	1.2	38
4029	Destabilization of adsorbed CO on the Pd(111) surface by subsurface carbon: Density functional studies. Chemical Physics Letters, 2006, 432, 184-189.	1.2	18
4030	Electronic structures of Pt clusters adsorbed on (5,5) single wall carbon nanotube. Chemical Physics Letters, 2006, 432, 213-217.	1.2	71
4031	3D-magnetic ordering of Co4+ dimers in a new Co3+,4+ oxychloride: Neutron diffraction analysis and DFT calculations. Chemical Physics Letters, 2006, 432, 88-93.	1.2	14

#	Article	IF	Citations
4032	Mechanical alloying and electronic simulations of 2Mgâ€“Fe mixture powders for hydrogen storage. Materials Science & Engineering A: Structural Materials: Properties, Microstructure and Processing, 2006, 427, 306-315.	2.6	38
4033	Structural, electronic, elastic and high-pressure properties of some alkaline-earth chalcogenides: An ab initio study. Physica B: Condensed Matter, 2006, 371, 12-19.	1.3	69
4034	D, H, and Mu in GaN: Theoretical predictions at finite temperatures. Physica B: Condensed Matter, 2006, 374-375, 363-367.	1.3	5
4035	Platinum dioxide phases: Relative thermodynamic stability and kinetics of inter-conversion from first-principles. Physica B: Condensed Matter, 2006, 381, 12-19.	1.3	10
4036	Local modes of hydrogen defects in Si:Ge and Ge:Si. Physica B: Condensed Matter, 2006, 376-377, 22-27.	1.3	2
4037	Hydrogen molecules and platelets in germanium. Physica B: Condensed Matter, 2006, 376-377, 105-108.	1.3	8
4038	Theory of anharmonicity on bond-centered hydrogen oscillators in silicon. Physica B: Condensed Matter, 2006, 376-377, 126-129.	1.3	2
4039	Boronâ€“oxygen complexes in Si. Physica B: Condensed Matter, 2006, 376-377, 133-136.	1.3	9
4040	Transfer doping of diamond: The use of and to effect p-type surface conductivity. Physica B: Condensed Matter, 2006, 376-377, 268-271.	1.3	7
4041	Instability of graphite structure induced by excited holes. Physica B: Condensed Matter, 2006, 376-377, 296-299.	1.3	2
4042	Electronic structure and half-metallic property of Mn-doped Î²-SiC diluted magnetic semiconductor. Materials Science and Engineering B: Solid-State Materials for Advanced Technology, 2006, 126, 194-196.	1.7	34
4043	Ab initio studies of intrinsic point defects, interstitial oxygen and vacancy or oxygen clustering in germanium crystals. Materials Science in Semiconductor Processing, 2006, 9, 494-497.	1.9	32
4044	Vacancy-dioxygen centers in Si-rich SiGe alloys. Materials Science in Semiconductor Processing, 2006, 9, 520-524.	1.9	0
4045	Local vibrations of interstitial carbon in SiGe alloys. Materials Science in Semiconductor Processing, 2006, 9, 514-519.	1.9	2
4046	Ab initio modeling of defect levels in Ge clusters and supercells. Materials Science in Semiconductor Processing, 2006, 9, 477-483.	1.9	7
4047	Supercell and cluster density functional calculations of the thermal stability of the divacancy in germanium. Materials Science in Semiconductor Processing, 2006, 9, 484-488.	1.9	2
4048	Formation energy and migration barrier of a Ge vacancy from ab initio studies. Materials Science in Semiconductor Processing, 2006, 9, 498-502.	1.9	42
4049	Structural and vibrational properties of high-dielectric oxides, HfO2 and TiO2: A comparative study. Materials Science in Semiconductor Processing, 2006, 9, 1014-1019.	1.9	11

#	Article	IF	Citations
4050	Distribution of BrÃ¸nsted acid sites on beta zeolite H-BEA: A periodic density functional theory calculation. Applied Catalysis A: General, 2006, 313, 160-166.	2.2	51
4051	NbB2: a density functional study. Physics Letters, Section A: General, Atomic and Solid State Physics, 2006, 350, 288-292.	0.9	39
4052	First-principles studies on the adsorption of molecular oxygen on Ba(110) surface. Physics Letters, Section A: General, Atomic and Solid State Physics, 2006, 352, 526-530.	0.9	8
4053	Electronic structure and lattice dynamics of CaPd3B studied by first-principles methods. Physics Letters, Section A: General, Atomic and Solid State Physics, 2006, 356, 251-254.	0.9	4
4054	Theoretical study of hydrogen atom adsorbed on carbon-doped BN nanotubes. Physics Letters, Section A: General, Atomic and Solid State Physics, 2006, 357, 369-373.	0.9	56
4055	Pseudo-potential calculations of structural and elastic properties of spinel oxides ZnX2O4 (, Ga, In) under pressure effect. Physics Letters, Section A: General, Atomic and Solid State Physics, 2006, 360, 339-343.	0.9	69
4056	The thermodynamic properties of lithium peroxide, Li2O2. Physics Letters, Section A: General, Atomic and Solid State Physics, 2006, 360, 352-356.	0.9	18
4057	Vibrational frequency and LOâ€“TO splitting determination for planarâ€“zigzag Î²-poly(vinylidene fluoride) using density-functional theory. Polymer, 2006, 47, 424-428.	1.8	17
4058	Quantum mechanics based multiscale modeling of stress-induced phase transformations in iron. Journal of the Mechanics and Physics of Solids, 2006, 54, 1276-1303.	2.3	30
4059	Ab initio modelling of defect properties with substitutional and interstitials elements in steels and Zr alloys. Journal of Nuclear Materials, 2006, 351, 1-19.	1.3	95
4060	Ab initio modeling of the behavior of helium and xenon in actinide dioxide nuclear fuels. Journal of Nuclear Materials, 2006, 352, 144-150.	1.3	106
4061	Elastic properties and high-pressure behavior of from ab initio calculations. Journal of Physics and Chemistry of Solids, 2006, 67, 1477-1483.	1.9	44
4062	Electronic properties and elastic constants of wurtzite, zinc-blende and rocksalt AlN. Journal of Physics and Chemistry of Solids, 2006, 67, 1888-1892.	1.9	49
4063	The role of orthorhombic distortions in gallium under high hydrostatic pressure. Journal of Physics and Chemistry of Solids, 2006, 67, 2132-2135.	1.9	11
4064	First-principles investigation of Mg(AlH4)2 complex hydride. Journal of Power Sources, 2006, 159, 111-115.	4.0	30
4065	Stability of lithium in Î±-rhombohedral boron. Journal of Solid State Chemistry, 2006, 179, 2827-2833.	1.4	6
4066	Lattice dynamics and electrical properties of wurtzite ZnO determined by a density functional theory method. Journal of Crystal Growth, 2006, 287, 199-203.	0.7	37
4067	Thin films of wÃ¼rtzite materialsâ€”AlN vs. AlP. Journal of Crystal Growth, 2006, 294, 111-117.	0.7	6

#	Article	IF	Citations
4068	A combined first-principles calculation and thermodynamic modeling of the Fâ€“Kâ€“Na system. Materials Science & Engineering A: Structural Materials: Properties, Microstructure and Processing, 2006, 418, 161-171.	2.6	13
4069	Kinetic excitation of solids: The concept of electronic friction. Nuclear Instruments & Methods in Physics Research B, 2006, 246, 333-339.	0.6	45
4070	Energetics and electronic structure of acetylene molecules encapsulated inside a carbon nanotube: A density functional theory study. Optical Materials, 2006, 29, 150-152.	1.7	2
4071	Electronic and structural properties of cementite-type M3X (M=Fe, Co, Ni; X=C or B) by first principles calculations. Physica B: Condensed Matter, 2006, 371, 126-132.	1.3	130
4072	Formation of and in p-type GaN(Mg,H). Physica B: Condensed Matter, 2006, 376-377, 477-481.	1.3	1
4073	Minor component ordering in wurtzite and. Physica B: Condensed Matter, 2006, 376-377, 502-506.	1.3	5
4074	Ab-initio modeling of acceptorâ€“hydrogen complexes in CdTe. Physica B: Condensed Matter, 2006, 376-377, 775-777.	1.3	1
4075	Energetics of native defects in. Physica B: Condensed Matter, 2006, 376-377, 808-811.	1.3	56
4076	First-principles calculation of elastic and thermodynamic properties of MgO and SrO under high pressure. Physica B: Condensed Matter, 2006, 373, 334-340.	1.3	32
4077	The elastic and optical properties of the high-pressure hydrous phase Î´-AlOOH. Solid State Communications, 2006, 137, 101-106.	0.9	35
4078	Electronic structure and optical absorption spectra of CdSe covered with ZnSe and ZnS epilayers. Solid State Communications, 2006, 137, 332-337.	0.9	9
4079	Superconducting NbB2: An ab initio study of elastic constants. Solid State Communications, 2006, 137, 253-256.	0.9	17
4080	Ab initio study of Nb2SC and Nb2S2C: Differences in coupling between the S and Nbâ€“C layers. Solid State Communications, 2006, 137, 306-309.	0.9	19
4081	Phenomenological band structure model of magnetic coupling in semiconductors. Solid State Communications, 2006, 138, 353-358.	0.9	134
4082	Ab initio pseudopotential studies of the pressure dependences of structural, electronic and optical properties for GaN. Solid State Communications, 2006, 138, 494-497.	0.9	23
4083	Elastic and electronic properties of BeB2 in comparison to superconducting MgB2 and NbB2. Solid State Communications, 2006, 139, 315-320.	0.9	16
4084	Strain induced ferroelectricity in the SrZrO3 / SrTiO3 superlattice: First principles study. Solid State Communications, 2006, 139, 144-147.	0.9	10
4085	Electronic structure and shearing in nanolaminated ternary carbides. Solid State Communications, 2006, 139, 139-143.	0.9	47

#	Article	IF	Citations
4086	Full-relativistic calculation of electronic structure of Zr2AlC and Zr2AlN. Solid State Communications, 2006, 139, 485-489.	0.9	30
4087	Ab initio â€“ phase diagram of NaBH4. Solid State Communications, 2006, 139, 516-521.	0.9	23
4088	Ab initio calculation of the properties and pressure induced transition of Sn. Solid State Communications, 2006, 140, 538-543.	0.9	37
4089	High-pressure band parameters for GaAs: first principles calculations. Solid-State Electronics, 2006, 50, 763-768.	0.8	54
4090	Elastic and optical properties of BeS, BeSe and BeTe under pressure. Solid-State Electronics, 2006, 50, 1382-1388.	0.8	73
4091	First-principle study of ferroelectricity in PbTiO3/SrTiO3 superlattices. Solid-State Electronics, 2006, 50, 1756-1760.	0.8	11
4092	Thermodynamic analysis and experimental research on Li intercalation reactions of the intermetallic compound Al2Cu. Solid State Ionics, 2006, 177, 507-513.	1.3	18
4093	Oxygen reduction reactions in the SOFC cathode of Ag/CeO2. Solid State Ionics, 2006, 177, 939-947.	1.3	101
4094	Stress, strain, and NMR. Solid State Nuclear Magnetic Resonance, 2006, 29, 113-118.	1.5	13
4095	Energy partitioning studies of adsorbate repulsion: Chemisorption and coadsorption of CO and NO on the Pd(111) surface. Surface Science, 2006, 600, 173-194.	0.8	7
4096	Surface energies of several ceramics with NaCl structure. Surface Science, 2006, 600, 257-264.	0.8	60
4097	First-principles study on the half-metallicity of zinc-blende CrP(110) surface. Surface Science, 2006, 600, 1608-1611.	0.8	24
4098	Thermodynamic separability of ultra-thin film surfaces and interfaces. Surface Science, 2006, 600, 1012-1016.	0.8	1
4099	Dissociative adsorption and adsorbate-induced reconstruction on Fe{211}. Surface Science, 2006, 600, 1431-1438.	0.8	27
4100	Molecular dynamics of nonadiabatic processes at surfaces: Chemisorption of H/Al(111). Surface Science, 2006, 600, 3624-3628.	0.8	34
4101	Vibration of small molecules on Pt(111) surface. Surface Science, 2006, 600, 3809-3814.	0.8	20
4102	First-principles investigation of functionalization-defects on silicon surfaces. Surface Science, 2006, 600, 3892-3897.	0.8	6
4103	Oxygen induced segregation of copper to Ag/Cu(100) surface. Surface Science, 2006, 600, 4103-4107.	0.8	9

#	Article	IF	Citations
4104	Structural, electronic and magnetic properties of vacancies in single-walled carbon nanotubes. Surface Science, 2006, 600, 4305-4309.	0.8	58
4105	The local adsorption geometry and electronic structure of alanine on Cu{110}. Surface Science, 2006, 600, 1924-1935.	0.8	94
4106	Comparison of S, Pt, and Hf adsorption on NiAl(110). Surface Science, 2006, 600, 2079-2090.	0.8	26
4107	Atomic and electronic structure of Sr/Si(001)-(2Ã—2). Surface Science, 2006, 600, 3614-3618.	0.8	5
4108	NO adsorption and diffusion on unreconstructed Pt{100} surface. A density functional theory investigation. Surface Science, 2006, 600, 2663-2669.	0.8	12
4109	Generalised coexistence of a low work function and a stable surface: CaAl4 and BaAuIn3. Surface Science, 2006, 600, 2495-2500.	0.8	7
4110	Microscopic model of CO oxidation on Pt(111). Surface Science, 2006, 600, 2600-2607.	0.8	13
4111	Experimental and theoretical studies of adsorption of on Î±-Fe2O3 (0001) surfaces. Surface Science, 2006, 600, 2874-2885.	0.8	17
4112	Hydrogen bonds at metal surfaces: Universal scaling and quantification of substrate effects. Surface Science, 2006, 600, 224-228.	0.8	51
4113	Density functional theory study of hydrogen sulfide dissociation on bi-metallic Niâ€“Mo catalysts. Surface Science, 2006, 600, 3202-3216.	0.8	28
4114	CH4 dissociation on Ni surfaces: Density functional theory study. Surface Science, 2006, 600, 3226-3234.	0.8	59
4115	A density-functional study on the atomic geometry and adsorption of the Cu(100) c(2Ã—2)/N Surface. Surface Science, 2006, 600, 3419-3426.	0.8	16
4116	STM study of the Mo(112) and Mo(111) surfaces. Surface Science, 2006, 600, 240-244.	0.8	14
4117	Theoretical studies on the adsorption and decomposition of H2O on Pd(111) surface. Surface Science, 2006, 600, 4572-4583.	0.8	85
4118	Initial incorporation of sulfur into the Pd(111) surface: A theoretical study. Surface Science, 2006, 600, 4508-4516.	0.8	13
4119	Adsorption of NO on unreduced and reduced CeO2 surfaces: A plane-wave DFT study. Surface Science, 2006, 600, 4953-4960.	0.8	55
4120	Structure and dynamics of the missing-row reconstruction on O/Cu(001) and O/Ag(001). Surface Science, 2006, 600, 5074-5079.	0.8	15
4121	Time-dependent density-functional molecular-dynamics study of the isotope effect in chemicurrents. Surface Science, 2006, 600, 5068-5073.	0.8	21

#	Article	IF	Citations
4122	Boron and MgB2 analogs of fullerenes and carbon nanotubes: A density functional theory study. Computational and Theoretical Chemistry, 2006, 771, 111-115.	1.5	15
4123	Structural phase stability and elastic properties of lanthanum monochalcogenides at high pressure. Computational and Theoretical Chemistry, 2006, 777, 5-10.	1.5	61
4124	Glycine adsorption on single-walled carbon nanotubes. Thin Solid Films, 2006, 509, 218-222.	0.8	35
4125	Electron spectroscopy of carbon materials: experiment and theory. Journal of Physics: Conference Series, 2006, 26, 149-152.	0.3	26
4126	Magnetic properties ofFeâˆ•Co(001)superlattices from first-principles theory. Physical Review B, 2006, 74, .	1.1	6
4127	Structural and electronic properties of4Ã…carbon nanotubes onSi(001)surfaces. Physical Review B, 2006, 74, .	1.1	23
4128	Ab initio study of semiconducting carbon nanotubes adsorbed on the Si(100) surface: Diameter- and registration-dependent atomic configurations and electronic properties. Journal of Applied Physics, 2006, 100, 124304.	1.1	20
4129	Quasiharmonic approximation applied toLiBH4and its decomposition products. Physical Review B, 2006, 73, .	1.1	51
4130	Fundamental state quantities and high-pressure phase transition in beryllium chalcogenides. Journal of Physics Condensed Matter, 2006, 18, 10365-10375.	0.7	34
4131	Heterolytic Splitting of H2and CH4on Î³-Alumina as a Structural Probe for Defect Sites. Journal of Physical Chemistry B, 2006, 110, 23944-23950.	1.2	141
4132	Linear optical properties in the projector-augmented wave methodology. Physical Review B, 2006, 73, .	1.1	2,450
4133	Ab initiocalculation of the phase stability in Au-Pd and Ag-Pt alloys. Physical Review B, 2006, 73, .	1.1	116
4134	Geometric structure and electronic properties of planar and nanotubular BN structures of the Haeckelite type. Physics of the Solid State, 2006, 48, 192-198.	0.2	6
4135	Electronic structure of CuN3(I). Physics of the Solid State, 2006, 48, 1844-1847.	0.2	8
4136	Energy and electronic properties of non-carbon nanotubes based on silicon dioxide. Physics of the Solid State, 2006, 48, 2021-2027.	0.2	8
4137	Piezoelectricity of ordered (ScxGa1-xN) alloys from first principles. European Physical Journal B, 2006, 54, 151-156.	0.6	32
4138	Geometry and electronic properties of single vacancies in achiral carbon nanotubes. European Physical Journal B, 2006, 54, 243-247.	0.6	13
4139	Amino acid adsorption on single-walled carbon nanotubes. European Physical Journal D, 2006, 38, 117-120.	0.6	62

#	Article	IF	Citations
4140	Structural deformation, strength, and instability of cubic BN compared to diamond: A first-principles study. Physical Review B, 2006, 73, .	1.1	125
4141	Theory of boron aggregates in diamond: First-principles calculations. Physical Review B, 2006, 73, .	1.1	84
4142	Prediction of a sandwichlike conducting superhard boron carbide: First-principles calculations. Physical Review B, 2006, 73, .	1.1	48
4144	Reducibility of Ce1-xZrxO2: Origin of Enhanced Oxygen Storage Capacity. Catalysis Letters, 2006, 108, 165-172.	1.4	102
4145	Computational Design of Silicon Suboxides: Chemical and Mechanical Forces on the Atomic Scale. Journal of Computer-Aided Materials Design, 2006, 13, 185-200.	0.7	4
4146	The electronic structure of Ni doped rutile TiO2. Journal of Electroceramics, 2006, 17, 951-953.	0.8	14
4147	Electronic structures of Mg3Pn2 (Pn=N, P, As, Sb and Bi) and Ca3N2 calculated by a first-principle pseudopotential method. Journal of Materials Science, 2006, 41, 2435-2441.	1.7	56
4148	Transfer doping of diamond: Buckminsterfullerene on hydrogenated, hydroxylated, and oxygenated diamond surfaces. Journal of Materials Science: Materials in Electronics, 2006, 17, 459-465.	1.1	6
4149	The seminal literature of nanotechnology research. Journal of Nanoparticle Research, 2006, 8, 193-213.	0.8	71
4150	Ab initio quantum-mechanical modeling of pyrophyllite [Al2Si4O10(OH)2] and talc [Mg3Si4O10(OH)2] surfaces. Physics and Chemistry of Minerals, 2006, 33, 63-71.	0.3	18
4151	ELF isosurface maps for the Al2SiO5 polymorphs. Physics and Chemistry of Minerals, 2006, 33, 138-144.	0.3	6
4152	Quantum-mechanical calculation of the vibrational spectrum of beryl (Al4Be6Si12O36) at the Î“ point. Physics and Chemistry of Minerals, 2006, 33, 519-532.	0.3	24
4153	Minerals at high pressure. Mechanics of compression from quantum mechanical calculations in a case study: the beryl (Al4Be6Si12O36). Physics and Chemistry of Minerals, 2006, 34, 37-52.	0.3	14
4154	Early SiO2 precipitates in Si: Vacancy-oxygen versus interstitial-oxygen clusters. Physica B: Condensed Matter, 2006, 376-377, 109-112.	1.3	15
4155	Local vibrational modes of hydrogen in GaN: Observation and theory. Physica B: Condensed Matter, 2006, 376-377, 464-467.	1.3	8
4156	Theory of Mnâ€“H co-doping for GaAs and related magnetic semiconductors. Physica B: Condensed Matter, 2006, 376-377, 654-657.	1.3	4
4157	Transition-metal and hydrogen in ZnO: A source of shallow donors. Physica B: Condensed Matter, 2006, 376-377, 731-734.	1.3	6
4158	Predicting the energetics of defects at T>0K. Physica B: Condensed Matter, 2006, 376-377, 940-944.	1.3	2

#	Article	IF	Citations
4159	First-principles study on the structural, elastic and electronic properties of platinum carbide. Physica B: Condensed Matter, 2006, 381, 174-178.	1.3	27
4160	Half-metallic ferromagnetism of Cr-doped rutile TiO2: A first-principles pseudopotential study. Physica B: Condensed Matter, 2006, 382, 14-16.	1.3	34
4161	Structure and vibrational frequency determination for Î±-poly(vinylidene fluoride) using density-functional theory. Polymer, 2006, 47, 7160-7165.	1.8	55
4162	Mn-doped GaN/AlN heterojunction for spintronic devices. Superlattices and Microstructures, 2006, 40, 530-532.	1.4	6
4163	Thermodynamic stability and disordering in La Sr1â^'MnO3 solid solutions. Solid State Ionics, 2006, 177, 217-222.	1.3	31
4164	Converged properties of clean metal surfaces by all-electron first-principles calculations. Surface Science, 2006, 600, 703-715.	0.8	252
4165	Ab initio study of atomic geometry and electronic states of GaSb(001) reconstructions. Surface Science, 2006, 600, 3803-3808.	0.8	7
4166	Intermediates in the hydrogenation of benzene to cyclohexene on Pt(111) and Pd(111): A comparison from DFT calculations. Surface Science, 2006, 600, 1339-1350.	0.8	79
4167	A theoretical investigation on Pt3Sn(102) surface alloy and COâ€“Pt3Sn(102) system. Surface Science, 2006, 600, 2026-2039.	0.8	8
4168	Energetics of the growth mode transition in InAs/GaAs(001) small quantum dot formation: A first-principles study. Surface Science, 2006, 600, 2007-2010.	0.8	9
4169	Linear scaling of the interlayer relaxations of the vicinal Cu(p,p,pâ^'2) surfaces with the number of atom-rows in the terraces. Surface Science, 2006, 600, 3008-3014.	0.8	7
4170	Organic/metal interfaces in self-assembled monolayers of conjugated thiols: A first-principles benchmark study. Surface Science, 2006, 600, 4548-4562.	0.8	128
4171	First principles study of vacancies and Al substitutional impurities in Î´-TiN. Thin Solid Films, 2006, 515, 2730-2733.	0.8	11
4172	Theoretical investigations on electronic and optical properties of rock-salt gallium nitride. Thin Solid Films, 2006, 515, 2433-2436.	0.8	7
4173	Local screening of a core hole: A real-space approach applied to hafnium oxide. Ultramicroscopy, 2006, 106, 986-993.	0.8	29
4174	Nanoscale coatings of AuAlx and PtAlx and their mesoporous elemental derivatives. Current Applied Physics, 2006, 6, 440-443.	1.1	20
4175	A reactivity index study to rationalize the effect of dopants on BrÃ¶nsted and Lewis acidity occurring in MeAlPOs. Journal of Molecular Graphics and Modelling, 2006, 24, 262-270.	1.3	11
4176	Ab initio study of Ti3Si0.5Ge0.5C2 under pressure. Journal of Physics and Chemistry of Solids, 2006, 67, 2149-2153.	1.9	5

#	Article	IF	Citations
4177	Origin of stability of the high-temperature, low-pressure Rh2O3 III form of rhodium sesquioxide. Journal of Solid State Chemistry, 2006, 179, 2126-2132.	1.4	5
4178	First-principles calculation of dehydrogenating properties of MgH2-V systems. Science in China Series D: Earth Sciences, 2006, 49, 129-136.	0.9	42
4179	Influence of impurity hydrogen on the structure and properties of bulk Li and pressure effects. Science in China Series G: Physics, Mechanics and Astronomy, 2006, 49, 740-747.	0.2	0
4180	Ab Initio calculations of phase stabilities in the Feâ^'Alâ^'C system and CALPHAD-Type assessment of the iron-rich corner. Metallurgical and Materials Transactions A: Physical Metallurgy and Materials Science, 2006, 37, 3397-3401.	1.1	34
4181	Gold nanowires and the effect of impurities. Nanoscale Research Letters, 2006, 1, 91-98.	3.1	17
4182	Ab initio investigation of a hypothetical hcp-Ï‰ phase transition in osmium. International Journal of Refractory Metals and Hard Materials, 2006, 24, 6-10.	1.7	2
4183	Theoretical investigation of 1,3-butanediol adsorption on an oxygen-defected CeO2(111) surface. Journal of Catalysis, 2006, 239, 13-22.	3.1	57
4184	Toward computational screening in heterogeneous catalysis: Pareto-optimal methanation catalysts. Journal of Catalysis, 2006, 239, 501-506.	3.1	314
4185	Energetics of methane dissociative adsorption on Rh{111} from DFT calculations. Journal of Catalysis, 2006, 242, 309-318.	3.1	90
4186	A theoretical study of coverage effects for ethylene epoxidation on Cu(111) under low oxygen pressure. Journal of Catalysis, 2006, 243, 404-409.	3.1	41
4187	A density functional theory study of the alkylation of isobutane with butene over phosphotungstic acid. Journal of Catalysis, 2006, 244, 65-77.	3.1	51
4188	First-Principles Study on Atomistic Behaviors and Magnetism of Physisorpted Co and Fe Atoms on MgO. IEEE Transactions on Magnetics, 2006, 42, 3174-3176.	1.2	5
4189	Phase stability of Ti3SiC2 at elevated temperatures. Scripta Materialia, 2006, 54, 105-107.	2.6	43
4190	A first-principles study of the site preference of Cr in B2 NiAl. Scripta Materialia, 2006, 54, 405-410.	2.6	25
4191	Quenched-in vacancies in a Î² Tiâ€“Nbâ€“Sn alloy studied by positron lifetime spectroscopy. Scripta Materialia, 2006, 54, 1751-1753.	2.6	15
4192	The strength and hardness of cubic spinel SiAlON (c-Si6â^'zAlzOzN8â^'z, z=1). Scripta Materialia, 2006, 55, 391-394.	2.6	3
4193	Site preference of transition metal elements in Ni3Al. Scripta Materialia, 2006, 55, 433-436.	2.6	133
4194	Effects of Cr on the elastic properties of B2 NiAl: A first-principles study. Scripta Materialia, 2006, 55, 759-762.	2.6	18

#	Article	IF	Citations
4195	Synthesis, crystal and electronic structure of Li8Zn2Ge3, a compound displaying an open layered anionic network. Solid State Sciences, 2006, 8, 208-215.	1.5	12
4196	A periodic density functional study of the location of titanium within TS-1. Solid State Sciences, 2006, 8, 234-240.	1.5	27
4197	Elastic properties of InAs under pressure up to 18ÂGPa. Materials Letters, 2006, 60, 3269-3271.	1.3	9
4198	Ab initio study of electronic structures and magnetism in ZnMnTe and CdMnTe diluted magnetic semiconductors. Journal of Magnetism and Magnetic Materials, 2006, 302, 536-542.	1.0	45
4199	A Simple Rule of Thumb for Diffusion on Transition-Metal Surfaces. Angewandte Chemie - International Edition, 2006, 45, 7046-7049.	7.2	109
4200	Synthesis and Structure of Ultrathin Aluminosilicate Films. Angewandte Chemie - International Edition, 2006, 45, 7636-7639.	7.2	45
4201	Doping effects on proton incorporation and conduction in SrZrO3. Journal of Computational Chemistry, 2006, 27, 711-718.	1.5	21
4202	Migration of Carbon into Subsurface Layers of Rh(100): A DFT Study. ChemPhysChem, 2006, 7, 1022-1025.	1.0	10
4203	Acetylene Decomposition on Rh(100): Theory and Experiment. ChemPhysChem, 2006, 7, 1068-1074.	1.0	6
4204	Vibrational Frequencies of Water Adsorbed on (111) and (221) Nickel Surfaces from First Principle Calculations. ChemPhysChem, 2006, 7, 1215-1219.	1.0	27
4205	Atomâ€“Molecule Interactions on Transition Metal Surfaces: A DFT Study of CO and Several Atoms on Rh(100), Pd(100) and Ir(100). ChemPhysChem, 2006, 7, 1075-1080.	1.0	7
4206	Asymmetry Induction by Cooperative Intermolecular Hydrogen Bonds in Surface-Anchored Layers of Achiral Molecules. ChemPhysChem, 2006, 7, 2197-2204.	1.0	46
4207	Surface Composition of Materials Used as Catalysts for Methanol Steam Reforming: A Theoretical Study. ChemPhysChem, 2006, 7, 1802-1812.	1.0	26
4209	Magnus' Green Salt Revisited: Impact of Platinumâ€“Platinum Interactions on Electronic Structure and Carrier Mobilities. Advanced Materials, 2006, 18, 2039-2043.	11.1	24
4210	Defect Formation Energies in Chalcopyrite-Type AgInSe2 and the Rerated Chalcopyrite Compounds by First Principles Calculations. , 2006, , .		4
4211	Properties of VAs/GaAs interface from first principles study. Journal of Physics: Conference Series, 2006, 29, 150-154.	0.3	7
4212	C and S induce changes in the electronic and geometric structure of Pd(533) and Pd(320). Journal of Physics Condensed Matter, 2006, 18, 8015-8027.	0.7	1
4213	Cationâ€“oxygen interaction and oxygen stability in CaCu3Ti4O12 and CdCu3Ti4O12 lattices. Journal of Physics Condensed Matter, 2006, 18, 1793-1803.	0.7	16

#	Article	IF	Citations
4214	TiNi Monatomic Chains Stabilized by Alloying: a First-Principles Study. Chinese Physics Letters, 2006, 23, 182-185.	1.3	6
4215	Electronic structure and elastic properties of Yn+1Co3n+5B2n(). Journal of Physics Condensed Matter, 2006, 18, 4071-4076.	0.7	5
4216	Thermodynamic modeling of the sodium alanates and the Naâ€“Alâ€“H system. International Journal of Materials Research, 2006, 97, 1484-1494.	0.1	26
4217	Electronic Structure and Magnetic Property of Mn-Incorporated Î²-SiC(100). Japanese Journal of Applied Physics, 2006, 45, 5560-5562.	0.8	4
4218	Quasiparticle Band Structure of BaS. Chinese Physics Letters, 2006, 23, 943-945.	1.3	2
4219	Ab initiostudy of basal slip in Nb2AlC. Journal of Physics Condensed Matter, 2006, 18, 4389-4395.	0.7	15
4220	Electronâ€“phonon contribution to the phonon and excited electron (hole) linewidths in bulk Pd. Journal of Physics Condensed Matter, 2006, 18, 7923-7935.	0.7	31
4221	First-principles study of osmium under high pressure. Journal of Physics Condensed Matter, 2006, 18, 8749-8759.	0.7	26
4222	Density functional study of a typical thiol tethered on a gold surface: ruptures under normal or parallel stretch. Nanotechnology, 2006, 17, 4819-4824.	1.3	19
4223	Theoretical investigation of BN armchair and zigzag nanoarch surfaces. Nanotechnology, 2006, 17, 556-560.	1.3	4
4224	Large configuration-induced band-gap fluctuations in GaNxAs1â^'xalloys. Journal Physics D: Applied Physics, 2006, 39, 2514-2521.	1.3	10
4225	Electronic Structures of the Filled Tetrahedral Semiconductor Li 3 AlN 2. Chinese Physics Letters, 2006, 23, 186-188.	1.3	3
4226	Electronic properties of silica nanowires. Journal of Physics Condensed Matter, 2006, 18, 3829-3836.	0.7	12
4227	First principles study of Asâ€“vacancy interaction and the ring mechanism of diffusion in the presence of Ge in Si. Journal of Physics Condensed Matter, 2006, 18, 4879-4886.	0.7	7
4228	Formation and structural transformation of the nonequilibrium phases in the Ruâ€“Ta system induced by ion beam mixing. Journal of Physics Condensed Matter, 2006, 18, 9911-9916.	0.7	5
4229	Adsorption of methanol and methoxy on the Î±-Cr2O3(0001) surface. Journal of Physics Condensed Matter, 2006, 18, 10751-10763.	0.7	19
4230	A density functional study of the pressure induced phase transition in LiYF4. Journal of Physics Condensed Matter, 2006, 18, 2429-2441.	0.7	12
4231	Calculations of effect of anisotropic stress/strain on dopant diffusion in silicon under equilibrium and nonequilibrium conditions. Journal of Vacuum Science & Technology B, 2006, 24, 456.	1.3	21

#	Article	IF	Citations
4232	First principles calculations of dopant solubility based on strain compensation and direct binding between dopants and group IV impurities. Journal of Vacuum Science & Technology B, 2006, 24, 700.	1.3	12
4233	A reexamination of the ice III/IX hydrogen bond ordering phase transition. Journal of Chemical Physics, 2006, 125, 064506.	1.2	33
4234	Coverage dependence and hydroperoxyl-mediated pathway of catalytic water formation on Pt (111) surface. Journal of Chemical Physics, 2006, 125, 054701.	1.2	61
4235	Relaxed core projector-augmented-wave method. Journal of Chemical Physics, 2006, 125, 104101.	1.2	112
4236	Density functional theory study of water adsorption at reduced and stoichiometric ceria (111) surfaces. Journal of Chemical Physics, 2006, 125, 204704.	1.2	61
4237	Self-diffusion constants in silicon: Ab initio calculations in combination with classical rate theory. Journal of Chemical Physics, 2006, 125, 226101.	1.2	8
4238	Orbital-corrected orbital-free density functional theory. Journal of Chemical Physics, 2006, 124, 081107.	1.2	20
4239	Constrained dynamics and extraction of normal modes fromab initiomolecular dynamics: Application to ammonia. Journal of Chemical Physics, 2006, 125, 064707.	1.2	7
4240	Analysis of methane-to-methanol conversion on clean and defective Rh surfaces. Journal of Chemical Physics, 2006, 125, 044701.	1.2	31
4241	Self-consistent embedding theory for locally correlated configuration interaction wave functions in condensed matter. Journal of Chemical Physics, 2006, 125, 084102.	1.2	126
4242	Thiol and thiolate bond formation of ferrocene-1,1-dithiol to a Ag(111) surface. Journal of Chemical Physics, 2006, 125, 194705.	1.2	7
4243	Structural and electronic properties of diazonium functionalized (4, 4) single walled carbon nanotube: anab initiostudy. Molecular Simulation, 2006, 32, 1213-1217.	0.9	4
4244	First Principles Study on Na x Li 1âˆ’ x FePO 4 As Cathode Material for Rechargeable Lithium Batteries. Chinese Physics Letters, 2006, 23, 61-64.	1.3	49
4245	Ab initio study of high-pressure phases of gallium nitride. IEE Proceedings: Optoelectronics, 2006, 153, 179-182.	0.8	9
4246	Energies of conservative and non-conservative antiphase boundaries in Ti3Al: a first principles study. Philosophical Magazine, 2006, 86, 1243-1259.	0.7	17
4247	Influence of Chemical Dopant Technique to Reduce Schottky Barriers of Pd-Contacted CNTFETs. Materials Research Society Symposia Proceedings, 2006, 963, 1.	0.1	0
4248	First-Principles Calculations of the Electrochemical Reactions of Water at an Immersed Ni(111)âˆ•H[sub 2]O Interface. Journal of the Electrochemical Society, 2006, 153, E207.	1.3	66
4249	A Computational Study of Oxygen Contamination in Sb2Te3. Materials Research Society Symposia Proceedings, 2006, 918, 11.	0.1	1

#	Article	IF	Citations
4250	Experimental and Ab-initio Investigations of Osmium Diboride. Materials Research Society Symposia Proceedings, 2006, 929, 1.	0.1	0
4251	Interstitial-Mediated Arsenic Clustering in Ultrashallow Junction Formation. Electrochemical and Solid-State Letters, 2006, 9, G354.	2.2	21
4252	Surface Diffusion and Incorporation Process of Adatom in Fe-Al Multilayer System. Key Engineering Materials, 2006, 317-318, 411-414.	0.4	3
4253	Embedded atom method potentials employing a faithful density representation. Modelling and Simulation in Materials Science and Engineering, 2006, 14, 721-731.	0.8	9
4254	Calculations for antiferrodistortive phase of SrTiO3perovskite: hybrid density functional study. Journal of Physics Condensed Matter, 2006, 18, 4845-4851.	0.7	51
4255	Molecular dynamics study of the ternary compound Li 3 AlB 2 O 6. Chinese Physics B, 2006, 15, 428-431.	1.3	2
4256	Ideal strength of a Cu multi-shell nano-wire. Modelling and Simulation in Materials Science and Engineering, 2006, 14, 1031-1039.	0.8	8
4257	Computer simulation and visualization of vacancy defects in MgSiO3perovskite. Modelling and Simulation in Materials Science and Engineering, 2006, 14, 1041-1052.	0.8	10
4258	Ab initioelectronic and magnetic structure in La0.66Sr0.33MnO3: strain and correlation effects. Journal of Physics Condensed Matter, 2006, 18, 7717-7728.	0.7	69
4259	Density functional study of antiferromagnetic copper oxide. Modelling and Simulation in Materials Science and Engineering, 2006, 14, 207-216.	0.8	17
4260	Multiscale Modeling of Growth and Structure of Silicon Nanoparticles in an Oxide Matrix. Materials Research Society Symposia Proceedings, 2006, 978, .	0.1	0
4261	Adsorption of Methane on the (100) Surface of MgO: Insight into Surface-Adsorbate and Adsorbate-Adsorbate Interactions from First-Principles Calculations. Materials Research Society Symposia Proceedings, 2006, 928, 1.	0.1	1
4262	Mechanisms for Interstitial-Mediated Transient Enhanced Diffusion of N-type Dopants. Materials Research Society Symposia Proceedings, 2006, 912, 1.	0.1	0
4263	High-pressure proton disorder in brucite. American Mineralogist, 2006, 91, 127-134.	0.9	75
4264	First-Principles Study of Orthorhombic Perovskites MgSiO 3 up to 120 GPa and Its Geophysical Implications. Chinese Physics Letters, 2006, 23, 2334-2337.	1.3	5
4265	Defective aluminium nitride nanotubes: a new way for spintronics? A density functional study. Nanotechnology, 2006, 17, 3166-3174.	1.3	34
4266	Stability and electronic structure of InN nanotubes from first-principles study. Chinese Physics B, 2006, 15, 798-801.	1.3	6
4267	Deformation Mechanism of Nanocrystalline Al-Fe Alloys by Analysis from Ab-Initio Calculations. Materials Science Forum, 2006, 503-504, 209-214.	0.3	10

#	Article	IF	Citations
4268	Effect of hydrostatic pressure on the crystal structure of sodium oxalate: X-ray diffraction study and ab initio simulations. Zeitschrift Fur Kristallographie - Crystalline Materials, 2006, 221, .	0.4	22
4269	Spin transitions in theFexMn1âˆ'xS2system. Physical Review B, 2006, 73, .	1.1	22
4270	First-principles perturbative computation of phonon properties of insulators in finite electric fields. Physical Review B, 2006, 74, .	1.1	15
4271	Half-Metallic Digital Ferromagnetic Heterostructure Composed of aÎ´-Doped Layer of Mn in Si. Physical Review Letters, 2006, 96, 027211.	2.9	56
4272	Ab initiostudy of the ideal shear strength and elastic deformation behaviors of B2FeAlandNiAl. Physical Review B, 2006, 73, .	1.1	20
4273	Prediction of different crystal structure phases in metal borides: A lithium monoboride analog toMgB2. Physical Review B, 2006, 73, .	1.1	77
4274	Bonding nature of metal/oxide incoherent interfaces by first-principles calculations. Physical Review B, 2006, 74, .	1.1	55
4275	Electronic structure and equation of state data of warm dense gold. Physical Review E, 2006, 73, 056403.	0.8	28
4276	Strain dependent bonding in solidC3N4: High elastic moduli but low strength. Physical Review B, 2006, 73, .	1.1	52
4277	First-principles calculations of the adsorption and hydrogenation reactions ofCHx(x=0,4)species on aFe(100)surface. Physical Review B, 2006, 73, .	1.1	88
4278	Solute/defect-mediated pathway for rapid nanoprecipitation in solid solutions:Î³surface analysis in fcc Al-Ag. Physical Review B, 2006, 73, .	1.1	46
4279	Magnetic properties ofGaNâ•MnxGa1âˆ'xNdigital heterostructures: First-principles and Monte Carlo calculations. Physical Review B, 2006, 73, .	1.1	15
4280	Magneto-optics in pure and defectiveGa1âˆ'xMnxAsfrom first principles. Physical Review B, 2006, 73, .	1.1	18
4281	Giant and composition-dependent optical band gap bowing in dilute GaSb1âˆ'xNx alloys. Applied Physics Letters, 2006, 88, 152109.	1.5	49
4282	Model of annealing-induced short-range order effects in (GaIn)(NP) alloys. Physical Review B, 2006, 74, .	1.1	8
4283	Anisotropic elasticity ofIVBtransition-metal mononitrides determined byab initiocalculations. Physical Review B, 2006, 73, .	1.1	43
4284	Managing the supercell approximation for charged defects in semiconductors: Finite-size scaling, charge correction factors, the band-gap problem, and theab initiodielectric constant. Physical Review B, 2006, 73, .	1.1	180
4285	Ballistic conductance and magnetism in short tip suspended Ni nanowires. Physical Review B, 2006, 73, .	1.1	37

#	Article	IF	Citations
4286	Coverage dependence of the 1-propanol adsorption on theSi(001)surface and fragmentation dynamics. Physical Review B, 2006, 73, .	1.1	14
4287	Quantum Size Effect on the Diffusion Barriers and Growth Morphology ofPb/Si(111). Physical Review Letters, 2006, 96, 226102.	2.9	68
4288	Adsorption, diffusion, and site exchange for Ge ad-dimers on Sb-coveredSi(001)from first-principles total-energy calculations. Physical Review B, 2006, 74, .	1.1	7
4289	Modeling the momentum distributions of annihilating electron-positron pairs in solids. Physical Review B, 2006, 73, .	1.1	113
4290	Symmetry-mediatedH2Odiffusion on Al{100}. Physical Review B, 2006, 74, .	1.1	11
4291	Coexistence of Gapless Excitations and Commensurate Charge-Density Wave in the2HTransition Metal Dichalcogenides. Physical Review Letters, 2006, 96, 026406.	2.9	36
4292	Computational study of ZrSiO4 polymorphs. Applied Physics Letters, 2006, 88, 181913.	1.5	10
4293	Interaction of manganese with single-wallB2Onanotubes: Anab initiostudy. Physical Review B, 2006, 73, .	1.1	2
4294	Influence of interface structure on electronic properties and Schottky barriers inFeâˆ•GaAsmagnetic junctions. Physical Review B, 2006, 73, .	1.1	33
4295	Reconstruction of quasi-one-dimensionalInâˆ•Si(111)systems: Charge- and spin-density waves versus bonding. Physical Review B, 2006, 73, .	1.1	34
4296	Ab initiostudy of the electronic properties and Fermi surface of the uranium dipnictides. Physical Review B, 2006, 73, .	1.1	23
4297	First-principles calculations of Ag-Sb nanodot formation in thermoelectricAgPbmSbTe2+m(m=6,14,30). Physical Review B, 2006, 73, .	1.1	37
4298	Short-circuit boundary conditions in ferroelectricPbTiO3thin films. Physical Review B, 2006, 74, .	1.1	30
4299	Transition state theory of the preexponential factors for self-diffusion on Cu, Ag, and Ni surfaces. Physical Review B, 2006, 74, .	1.1	44
4300	Point defects on the (110) surfaces ofInP,InAs, andInSb: A comparison with bulk. Physical Review B, 2006, 74, .	1.1	48
4301	The constrained space orbital variation analysis for periodic ab initio calculations. Journal of Chemical Physics, 2006, 124, 194105.	1.2	7
4302	Electronic structure and lattice distortions inPbMg1âˆ•3Nb2âˆ•3O3studied with density functional theory using the linearized augmented plane-wave method. Physical Review B, 2006, 73, .	1.1	28
4303	First-principles investigation of a bistable boron-oxygen interstitial pair in Si. Physical Review B, 2006, 73, .	1.1	21

#	Article	IF	Citations
4304	Ab initio calculations for properties of MAX phases Ti2TlC, Zr2TlC, and Hf2TlC. Applied Physics Letters, 2006, 88, 101911.	1.5	43
4305	Thermal properties ofCaMoO4: Lattice dynamics and synchrotron powder diffraction studies. Physical Review B, 2006, 73, .	1.1	45
4306	Adsorption and diffusion of Co on the Si(001) surface. Physical Review B, 2006, 74, .	1.1	16
4307	Comparative study of boundary conditions for molecular dynamics simulations of solids at low temperature. Physical Review B, 2006, 73, .	1.1	15
4308	Surface reconstructions and atomic ordering inInxGa1â^'xAs(001)films: A density-functional theory study. Physical Review B, 2006, 74, .	1.1	9
4309	Theoretical study of the molecular and electronic structure of one-dimensional crystals of potassium iodide and composites formed upon intercalation in single-walled carbon nanotubes. Physical Review B, 2006, 73, .	1.1	39
4310	Nitrogen incorporation and lattice constant of strained diluteGaAs1â^'xNxlayers on GaAs (001): Anab initiostudy. Physical Review B, 2006, 74, .	1.1	11
4311	First-principles study of structural and electronic properties of group IV arsenides with 3:4 stoichiometry. Physical Review B, 2006, 74, .	1.1	6
4312	Nanopores in carbon nitride nanotubes: Reversible hydrogen storage sites. Applied Physics Letters, 2006, 89, 253119.	1.5	15
4313	Composition and strain dependence of the piezoelectric coefficients inInxGa1â^'xAsalloys. Physical Review B, 2006, 74, .	1.1	40
4314	Dimer rotation on the carbon-inducedSi(001)â^'c(4Ã—4)structure. Physical Review B, 2006, 74, .	1.1	5
4315	Energetics ofCOon stepped and kinked Cu surfaces: A comparative theoretical study. Physical Review B, 2006, 74, .	1.1	29
4316	Theoretical study of metal borides stability. Physical Review B, 2006, 74, .	1.1	79
4317	Hydrogen and muonium in diamond: A path-integral molecular dynamics simulation. Physical Review B, 2006, 73, .	1.1	30
4318	Phonons in theÎ²-tin,Imma, and sh phases of silicon fromab initiocalculations. Physical Review B, 2006, 73, .	1.1	10
4319	First-principles calculations of the structural and electronic properties of cleanGaN(0001)surfaces. Physical Review B, 2006, 73, .	1.1	107
4320	Influence of valence electron concentration on elastic properties of RRh3B (R=Y, Zr, and Nb). Applied Physics Letters, 2006, 89, 121914.	1.5	31
4321	Silver-filled single-walled carbon nanotubes: Atomic and electronic structures from first-principles calculations. Physical Review B, 2006, 74, .	1.1	14

#	Article	IF	Citations
4322	Enhancement of ferromagnetic coupling in Mnâˆ•GaAs digital ferromagnetic heterostructure by free-hole injection. Journal of Applied Physics, 2006, 99, 08D517.	1.1	9
4323	Hydrogen self-trapping near silicon atoms in Ge-rich SiGe alloys. Applied Physics Letters, 2006, 88, 142112.	1.5	6
4324	Generalized planar fault energies and twinning in Cuâ€“Al alloys. Applied Physics Letters, 2006, 89, 191911.	1.5	91
4325	Toward uniform nanotubular compounds: Synthetic approach and ab initio calculations. Journal of Chemical Physics, 2006, 124, 121102.	1.2	6
4326	First-principles calculations on magnetic properties of interface-rippled Coâˆ•Î±-Al2O3âˆ•Co. Applied Physics Letters, 2006, 88, 132512.	1.5	5
4327	Effects of radial strain on the desorption of hydrogen from the surface of palladium-doped carbon nanotubes. Applied Physics Letters, 2006, 89, 083104.	1.5	5
4328	Effects of Ge content on the diffusion of group-V dopants in SiGe alloys. Applied Physics Letters, 2006, 88, 173502.	1.5	16
4329	Geometric and electronic structure of theNâˆ•Rh(100)system by core-level photoelectron spectroscopy: Experiment and theory. Physical Review B, 2006, 74, .	1.1	29
4330	Revisiting the (110) surface structure ofTiO2: A theoretical analysis. Physical Review B, 2006, 73, .	1.1	75
4331	Theoretical analysis of highly spin-polarized transport in the iron nitrideFe4N. Physical Review B, 2006, 73, .	1.1	186
4332	A new class of self-assembled monolayers on gold using an alkynyl group as a linker. , 2006, , .		1
4333	Effect of spatial nonlocality on the density functional band gap. Physical Review B, 2006, 74, .	1.1	68
4334	Carbon nanotube adsorbed on a hydrogenated Si-richÎ²â€™SiC(100)(3Ã—2)surface: First-principles pseudopotential calculations. Physical Review B, 2006, 74, .	1.1	8
4335	Interaction between a single Pt atom and a carbon nanotube studied by density functional theory. Physical Review B, 2006, 73, .	1.1	38
4336	Mechanical stability of possible structures of PtN investigated using first-principles calculations. Physical Review B, 2006, 73, .	1.1	168
4337	Ab initiostructural and electronic properties of dangling-bond-freeSiOxNy. Physical Review B, 2006, 73, .	1.1	5
4338	Theoretical study of potential high-pressure phases of TaON and a quaternaryZrTaO3N. Physical Review B, 2006, 73, .	1.1	27
4339	Exact-exchange Kohn-Sham formalism applied to one-dimensional periodic electronic systems. Physical Review B, 2006, 74, .	1.1	17

#	Article	IF	Citations
4340	Spin-dependent electronic structure of transition-metal atomic chains adsorbed on single-wall carbon nanotubes. Physical Review B, 2006, 74, .	1.1	41
4341	Atomic structure and spin magnetism of self-assembled Co nanowires onPt(332). Physical Review B, 2006, 74, .	1.1	3
4342	Improved hybrid algorithm with Gaussian basis sets and plane waves: First-principles calculations of ethylene adsorption onÎ²â^'SiC(001)â^'(3Ã—2). Physical Review B, 2006, 74, .	1.1	27
4343	Platelets and theâŸ¨110âŸ©a0â^•4{001} stacking fault in diamond. Physical Review B, 2006, 73, .	1.1	6
4344	Time-dependent density functional theory with ultrasoft pseudopotentials: Real-time electron propagation across a molecular junction. Physical Review B, 2006, 73, .	1.1	74
4345	First-principles study of electronic properties of hydrogenated graphite. Physical Review B, 2006, 74, .	1.1	13
4346	Electronic structure of theNa16Rb8Si136andK16Rb8Si136clathrates. Physical Review B, 2006, 74, .	1.1	18
4347	Relative stabilities of Ag multilayers on GaAs and GaSb determined fromab initiocalculations. Physical Review B, 2006, 74, .	1.1	1
4348	Calculations of hydrogen coverage on single-walled carbon nanotubes: Dependence on nanotube size, temperature, and pressure. Physical Review B, 2006, 74, .	1.1	28
4349	Many-body density matrices on a two-dimensional square lattice: Noninteracting and strongly interacting spinless fermions. Physical Review B, 2006, 74, .	1.1	3
4350	First-principles study on half-metallicity at surface and interface of zinc-blende CrSâ^•GaAs(001). Journal of Applied Physics, 2006, 99, 08J101.	1.1	6
4351	Comparative study of Ag, Au, Pd, and Pt adsorption on Mo andTa(112)surfaces. Physical Review B, 2006, 74, .	1.1	10
4352	Site-selective adsorption of naphthalene-tetracarboxylic-dianhydride onAg(110): First-principles calculations. Physical Review B, 2006, 73, .	1.1	32
4353	Influence of local electron interactions on phonon spectrum in iron. Physical Review B, 2006, 74, .	1.1	13
4354	Ab initiostudy ofÎ“â^'Xintervalley scattering in GaAs under pressure. Physical Review B, 2006, 74, .	1.1	28
4355	First-principles study of lattice dynamics and diffusion inDO3-typeFe3Si. Physical Review B, 2006, 73, .	1.1	34
4356	Transition metal impurities in Ge: Chemical trends and codoping studied by electronic structure calculations. Physical Review B, 2006, 73, .	1.1	52
4357	Adsorption, desorption, and dissociation of benzene onTiO2(110)andPdâ^•TiO2(110): Experimental characterization and first-principles calculations. Physical Review B, 2006, 74, .	1.1	20

#	Article	IF	Citations
4358	Electron transport in aPtâ^'COâ^'Ptnanocontact: Density functional theory calculations. Physical Review B, 2006, 73, .	1.1	28
4359	STM andab initiostudy of holmium nanowires on a Ge(111) surface. Physical Review B, 2006, 74, .	1.1	6
4360	N doping of TiO2(110): Photoemission and density-functional studies. Journal of Chemical Physics, 2006, 125, 094706.	1.2	127
4361	Atomic-Scale Mechanisms for Low-NIEL Dopant-Type Dependent Damage in Si. IEEE Transactions on Nuclear Science, 2006, 53, 3621-3628.	1.2	14
4362	The energetics and structure of rutile TiO2(110). Journal of Physics Condensed Matter, 2006, 18, 4207-4217.	0.7	69
4363	First-principles study of low compressibility osmium borides. Applied Physics Letters, 2006, 88, 221904.	1.5	113
4364	Formation energies, binding energies, structure, and electronic transitions of Si divacancies studied by density functional calculations. Physical Review B, 2006, 74, .	1.1	19
4365	Density-functional-theory calculations for the silicon vacancy. Physical Review B, 2006, 74, .	1.1	63
4366	Vacancy clustering and diffusion in silicon: Kinetic lattice Monte Carlo simulations. Physical Review B, 2006, 74, .	1.1	14
4367	Structural Stabilities and Electronic Structures of Ga Atomic Chains. Chinese Journal of Chemical Physics, 2006, 19, 219-222.	0.6	2
4368	Electronic structure of Nb2N and NbN thin films. Journal of Applied Physics, 2006, 99, 044911.	1.1	34
4369	Thermally stable carbon-related centers in 6H-SiC: Photoluminescence spectra and microscopic models. Physical Review B, 2006, 73, .	1.1	14
4370	Modulating transmission properties of nanoscale transistors by dipoles near contacts. Applied Physics Letters, 2006, 89, 243106.	1.5	0
4371	Momentum-Resolved Electron-Phonon Interaction in Lead Determined by Neutron Resonance Spin-Echo Spectroscopy. Physical Review Letters, 2006, 96, 225501.	2.9	15
4372	Comment on â€œStructural Stability of Complex Hydrides:LiBH4Revisitedâ€• Physical Review Letters, 2006, 97, 119601; author reply 119602.	2.9	16
4373	Bottom-Up Assembly of Single-Domain Titania Nanosheets on(1Ã—2)â^'Pt(110). Physical Review Letters, 2006, 97, 156101.	2.9	79
4374	Experimental and theoretical studies of theE+optical transition inGaAsNalloys. Physical Review B, 2006, 74, .	1.1	13
4375	ECenter in Silicon Has a Donor Level in the Band Gap. Physical Review Letters, 2006, 97, 106402.	2.9	37

#	Article	IF	Citations
4376	Surface Reactivity and Quantum-Size Effects on the Electronic Density Decay Length of Ultrathin Metal Films. Physical Review Letters, 2006, 96, 036805.	2.9	40
4377	Formation kinetics of the Mo(100)-Agc(2Ã—2)surface alloy. Physical Review B, 2006, 74, .	1.1	7
4378	Local electronic structure in aLiAlO2single crystal studied withLi7NMR spectroscopy and comparison with quantum chemical calculations. Physical Review B, 2006, 74, .	1.1	21
4379	Interstitial-mediated mechanisms of As and P diffusion in Si: Gradient-corrected density-functional calculations. Physical Review B, 2006, 74, .	1.1	13
4380	Oxygen-richGaN(101Â¯0)surfaces: First-principles total energy calculations. Physical Review B, 2006, 73, .	1.1	21
4381	Theoretical hardness of PtN2 with pyrite structure. Applied Physics Letters, 2006, 89, 141910.	1.5	52
4382	Understanding mixed valent materials: Effects of dynamical core-hole screening in high-pressure x-ray spectroscopy. Physical Review B, 2006, 74, .	1.1	16
4383	Ab initiostudy of CsI and its surface. Physical Review B, 2006, 74, .	1.1	15
4384	All-electron first-principles investigations of the energetics of vicinal Cu surfaces. Physical Review B, 2006, 73, .	1.1	52
4385	Dislocation formation from a surface step in semiconductors: Anab initiostudy. Physical Review B, 2006, 73, .	1.1	45
4386	Pt thin films on the polarLaAlO3(100)surface: A first-principles study. Physical Review B, 2006, 73, .	1.1	22
4387	Manganese impurities in boron nitride. Applied Physics Letters, 2006, 89, 072102.	1.5	18
4388	Ferromagnetism inAl1â^'xCrxNthin films by density functional calculations. Physical Review B, 2006, 73, .	1.1	25
4389	First-principles calculations for the structural stabilities of orderedNb4clusters on theCu(111)surface. Physical Review B, 2006, 73, .	1.1	16
4390	First-principlesLDA+Ucalculations of the Co-dopedZnOmagnetic semiconductor. Physical Review B, 2006, 73, .	1.1	81
4391	Dynamics of elemental lithium at megabar pressures. Physical Review B, 2006, 73, .	1.1	5
4392	Residual internal stress in partially crystallized photothermorefractive glass: Evaluation by nuclear magnetic resonance spectroscopy and first principles calculations. Journal of Applied Physics, 2006, 99, 083511.	1.1	21
4393	Quantum size effects in Pb films from first principles: The role of the substrate. Physical Review B, 2006, 74, .	1.1	72

#	Article	IF	Citations
4394	First-principles study of vibrational and dielectric properties ofÎ²â˜Si3N4. Physical Review B, 2006, 74, .	1.1	35
4395	Atomic structure of a thin silica film on aMo(112)substrate: A combined experimental and theoretical study. Physical Review B, 2006, 73, .	1.1	61
4396	Comparative NMR study of hybridization effect and structural stability inD022-typeNbAl3andNbGa3. Physical Review B, 2006, 74, .	1.1	31
4397	Coupling in nanolaminated ternary carbides studied by theoretical means: The influence of electronic potential approximations. Physical Review B, 2006, 73, .	1.1	50
4398	Adsorption of platinum on the stoichiometric RuO2(110) surface. Journal of Chemical Physics, 2006, 124, 141101.	1.2	10
4399	Ab initiostudy of the structural, electronic, and optical properties of ultrathin lead nanowires. Physical Review B, 2006, 74, .	1.1	26
4400	Codoping as a measure against donor deactivation in Si:Ab initiocalculations. Physical Review B, 2006, 73, .	1.1	6
4401	Generalized reconstruction model ofSiC(001)â˜(nÃ—2)surfaces and Si ad-dimer strings. Physical Review B, 2006, 73, .	1.1	12
4402	Double-resonant Raman processes in germanium: Group theory andab initiocalculations. Physical Review B, 2006, 73, .	1.1	7
4403	Pressure dependence of exchange interactions inNiO. Physical Review B, 2006, 74, .	1.1	39
4404	Density functional theory investigation of N interstitial migration in GaN. Journal of Applied Physics, 2006, 100, 123108.	1.1	3
4405	First principles study on the interface of CrSbâ•GaSb heterojunction. Journal of Applied Physics, 2006, 99, 093703.	1.1	7
4406	Ab initiodensity functional theory study of strain effects on ferroelectricity atPbTiO3surfaces. Physical Review B, 2006, 74, .	1.1	42
4407	Relationship between binding site and pressure dependence for defect-hydrogen complexes in ZnO. Applied Physics Letters, 2006, 88, 261906.	1.5	13
4408	CO adsorption and CO and O coadsorption on Rh(111) studied by reflection absorption infrared spectroscopy and density functional theory. Journal of Chemical Physics, 2006, 124, 144703.	1.2	62
4409	Importance of the embedding environment on the strain within small rings in siliceous materials. Physical Review B, 2006, 73, .	1.1	19
4410	Local and long-range order of carbon impurities on Fe(100): Analysis of self-organization at a nanometer scale. Physical Review B, 2006, 73, .	1.1	15
4411	Global and local structures of the Ge-Sb-Te ternary alloy system for a phase-change memory device. Physical Review B, 2006, 73, .	1.1	35

#	Article	IF	Citations
4412	Effect of pressure on the Raman modes of antimony. Physical Review B, 2006, 74, .	1.1	79
4413	Effective interactions between theNâ^'Hbond orientations in lithium imide and a proposed ground-state structure. Physical Review B, 2006, 74, .	1.1	60
4414	Searching for a higher superconducting transition temperature in strainedMgB2. Physical Review B, 2006, 73, .	1.1	45
4415	Complex adsorbate-substrate interplay of H onIr(100)â^'(5Ã—1)-hex: Density functional calculations. Physical Review B, 2006, 74, .	1.1	10
4416	Fcc breathing instability inBaBiO3from first principles. Physical Review B, 2006, 73, .	1.1	31
4417	Ab initiocalculation of the anomalous Hall conductivity by Wannier interpolation. Physical Review B, 2006, 74, .	1.1	397
4418	Role of intrinsic defects in the electronic and optical properties of Î±-HgI2. Applied Physics Letters, 2006, 88, 011918.	1.5	22
4419	Effect of indium-nitrogen bonding on the localized vibrational mode inInyGa1â^'yNxAs1â^'x. Physical Review B, 2006, 73, .	1.1	18
4420	Electron-mediated ferromagnetism and negativesâ^'dexchange splitting in semiconductors. Physical Review B, 2006, 73, .	1.1	23
4421	Interface reconstruction ofMSi2â^•Si(001)(M=Co,Ni)from first principles. Physical Review B, 2006, 74, .	1.1	10
4422	Comparison of two methods for circumventing the Coulomb divergence in supercell calculations for charged point defects. Physical Review B, 2006, 74, .	1.1	41
4423	First-principles study of cation disordering inMgAl2O4spinel with cluster expansion and Monte Carlo simulation. Physical Review B, 2006, 73, .	1.1	47
4424	Theoretical investigation on the stability and properties of a (10,0) BNâ€“AlN nanotube junction. Nanotechnology, 2006, 17, 1637-1641.	1.3	18
4425	Comparative behavior of Pd and Ag deposition phenomenon on clean Î±-Al2O3(001) surfaceâ€”A first principle study. Molecular Simulation, 2006, 32, 155-162.	0.9	6
4426	STRUCTURAL AND ELECTRONIC PROPERTIES OF c-BN(110) SURFACE AND SURFACE POINT DEFECTS. International Journal of Modern Physics C, 2006, 17, 795-803.	0.8	6
4427	A Performance Analysis of ABINIT on a Cluster System. , 2006, , 37-51.		1
4428	Tuning the electronic structures of semiconducting SiC nanotubes by N and NHx (x=1,2) groups. Journal of Chemical Physics, 2006, 125, 194710.	1.2	30
4429	High-pressure, high-temperature phase diagram of InSe: A comprehensive study of the electronic and structural properties of the monoclinic phase of InSe under high pressure. Physical Review B, 2006, 73, .	1.1	37

#	Article	IF	Citations
4430	MICROSCOPIC MODEL OF ASSOCIATIVE DESORPTION FOR HYDROGEN ON Mo(110). Surface Review and Letters, 2006, 13, 375-386.	0.5	11
4431	Optimization of ionic conductivity in doped ceria. Proceedings of the National Academy of Sciences of the United States of America, 2006, 103, 3518-3521.	3.3	464
4432	A pseudopotential density functional theory study of native defects and boron impurities in FeAl. Journal of Physics Condensed Matter, 2006, 18, 8859-8876.	0.7	8
4433	FIRST-PRINCIPLES STUDY OF THE ELECTRONIC PROPERTIES OF GaAs(114)A (2Ã—1) SURFACE. Modern Physics Letters B, 2006, 20, 1275-1285.	1.0	1
4434	Accurate and efficient method for the treatment of exchange in a plane-wave basis. Journal of Chemical Physics, 2006, 124, 064105.	1.2	87
4435	Ab Initio Study of Structural and Electronic Properties of Hexagonal BC 2 N. Chinese Physics Letters, 2006, 23, 2175-2178.	1.3	12
4436	FIRST PRINCIPLES SLAB RELAXATION STUDY OF THE TiFe(001) SURFACE. Surface Review and Letters, 2006, 13, 495-501.	0.5	1
4437	Realizing a Carbon-Based Hydrogen Storage Material. Japanese Journal of Applied Physics, 2006, 45, 1765-1767.	0.8	23
4438	First-principles study of silicon-doped (5,5) BN nanotubes. Europhysics Letters, 2006, 76, 664-669.	0.7	44
4439	Structural distortion and electronic properties of NiO under high pressure: anab initioGGA+Ustudy. Journal of Physics Condensed Matter, 2006, 18, 9691-9701.	0.7	8
4440	Alternative search strategy for minimal energy nanocluster structures: The case of rhodium, palladium, and silver. Journal of Chemical Physics, 2006, 125, 214708.	1.2	37
4441	Dynamical behaviour in the boron IIIâ€“V group: a first-principles study. Journal of Physics Condensed Matter, 2006, 18, 3647-3654.	0.7	55
4442	LSDA+U APPROXIMATION-BASED ANALYSIS OF THE ELECTRONIC STRUCTURE OF CeFeGe3. International Journal of Modern Physics B, 2006, 20, 287-301.	1.0	2
4443	First-Principles Determination of Piezoelectric Stress and Strain Constants of Wurtzite III-V Nitrides. Japanese Journal of Applied Physics, 2006, 45, L358-L360.	0.8	86
4444	The ferroelectric and cubic phases in BaTiO3 ferroelectrics are also antiferroelectric. Proceedings of the National Academy of Sciences of the United States of America, 2006, 103, 14695-14700.	3.3	119
4445	ELECTRONIC STRUCTURES OF S-DOPED ANATASE AND RUTILE TiO2. Journal of Theoretical and Computational Chemistry, 2007, 06, 23-32.	1.8	7
4446	First-Principles Investigations of Electrochemical Oxidation of Hydrogen at Solid Oxide Fuel Cell Operating Conditions. Journal of the Electrochemical Society, 2007, 154, B919.	1.3	43
4447	SILICON-BASED HALF-METAL: METAL-ENCAPSULATED SILICON NANOTUBE. Nano, 2007, 02, 109-114.	0.5	9

#	Article	IF	Citations
4448	Calculated structural, elastic and electronic properties of SiX2O4(X = Mg, Zn, Cd) compounds under pressure. Modelling and Simulation in Materials Science and Engineering, 2007, 15, 787-798.	0.8	12
4449	Ab initiocalculations of structural, elastic and electronic properties of Li₂O₂. Philosophical Magazine, 2007, 87, 3373-3383.	0.7	17
4450	Anomalous pre-melting volume expansion in AgBrâ€"ab initioapproach. Molecular Simulation, 2007, 33, 1129-1133.	0.9	4
4451	First-principles study of the elastic and thermodynamic properties of CaSiO3perovskite. Journal of Physics Condensed Matter, 2007, 19, 246103.	0.7	7
4452	Raman spectra and lattice dynamics of cubic gauche nitrogen. Journal of Chemical Physics, 2007, 127, 144510.	1.2	40
4453	Ab initiocalculation of the lattice dynamics of the Boron group-V compounds under high pressure. High Pressure Research, 2007, 27, 269-277.	0.4	17
4454	Experimental observation of quantum oscillation of surface chemical reactivities. Proceedings of the National Academy of Sciences of the United States of America, 2007, 104, 9204-9208.	3.3	123
4455	Adhesion of the Î³-Ni(Al)/Î±-Al₂O₃ interface: a first-principles assessment. International Journal of Materials Research, 2007, 98, 1214-1221.	0.1	40
4456	Ab initio molecular dynamics of hydrogen dissociation on metal surfaces using neural networks and novelty sampling. Journal of Chemical Physics, 2007, 127, 154716.	1.2	75
4457	Effects of coverage on the structures, energetics, and electronics of oxygen adsorption on RuO2(110). Journal of Chemical Physics, 2007, 127, 064706.	1.2	42
4458	Modifications of cubic SiC surfaces studied byab initiosimulations: from gas adsorption to organic functionalization. Journal Physics D: Applied Physics, 2007, 40, 6215-6224.	1.3	19
4459	Polynitrogen/Nanoaluminum Surface Interactions. , 2007, , .		0
4460	Theoretical Aspects on the Formation of the Tri-Interstitial Nitrogen Defect in Silicon. Solid State Phenomena, 2008, 131-133, 265-270.	0.3	0
4461	Interatomic bonds and the tensile anisotropy of trialuminides in the elastic limit: a density functional study for Al3(Sc,â€‰Ti,â€‰V,â€‰Cr). Philosophical Magazine, 2007, 87, 1769-1794.	0.7	24
4462	First-principles study of hydrogen-passivated single-crystalline silicon nanotubes: electronic and optical properties. Nanotechnology, 2007, 18, 505707.	1.3	17
4463	Prediction of MAX phases, VN+1SiCN (N=1,2), from first-principles theory. Journal of Applied Physics, 2007, 101, 013511.	1.1	16
4464	Comparison of proton conduction in KTaO3 and SrZrO3. Journal of Chemical Physics, 2007, 126, 194701.	1.2	21
4465	Oxygen adsorption on Mo(112) surface studied by ab initio genetic algorithm and experiment. Journal of Chemical Physics, 2007, 126, 234710.	1.2	37

#	Article	IF	Citations
4466	Si-SiO2-Si and Si-CaCO3-Si coreâ€“double-shell nanoparticles: Tuning light emission from infrared to ultraviolet. Journal of Applied Physics, 2007, 102, 023712.	1.1	0
4467	First-principles study of interaction between H2 molecules and BN nanotubes with BN divacancies. Journal of Chemical Physics, 2007, 127, 164718.	1.2	19
4468	The (1Ã—1)â†'hexagonal structural transition on Pt(100) studied by high-energy resolution core level photoemission. Journal of Chemical Physics, 2007, 127, 164702.	1.2	12
4469	Study on the interaction between tetracene and Cu(110) surface. Journal of Chemical Physics, 2007, 127, 224709.	1.2	21
4470	First-principles study of filled and unfilled antimony skutterudites. Journal of Physics Condensed Matter, 2007, 19, 096002.	0.7	39
4471	Highly under-coordinated atoms at Rh surfaces: interplay of strain and coordination effects on core level shift. New Journal of Physics, 2007, 9, 143-143.	1.2	45
4472	First-principles calculations of the nonlinear optical susceptibilities and Raman scattering spectra of lithium niobate. Journal of Physics Condensed Matter, 2007, 19, 456202.	0.7	54
4473	Magnetic Properties and Electronic Structure of Transition Metal Adsorbed Polar-ZnO Surfaces:Ab initioCalculations. Japanese Journal of Applied Physics, 2007, 46, 6312-6314.	0.8	6
4474	Linear and Nonlinear Optical Properties of SbSI: First-Principle Calculation. Ferroelectrics, 2007, 352, 148-152.	0.3	7
4475	Identifying Hydrogen Atoms on Graphite. Journal of the Physical Society of Japan, 2007, 76, 114703.	0.7	11
4476	Electronic structure and ferromagnetism of Cu-doped ZnO. Physica Scripta, 2007, T129, 358-361.	1.2	9
4477	First-principles calculation of electronic structure and magnetic properties of copper adsorbed polar-ZnO surface. Journal of Vacuum Science & Technology B, 2007, 25, 2616.	1.3	1
4478	Direct and indirect causes of Fermi level pinning at the SiOâˆ•GaAs interface. Journal of Chemical Physics, 2007, 126, 084703.	1.2	25
4479	Ab initio studies of crystalline nitromethane under high pressure. Journal of Chemical Physics, 2007, 126, 114701.	1.2	28
4480	Lifting of Ir{100} reconstruction by CO adsorption: An ab initio study. Journal of Chemical Physics, 2007, 126, 244701.	1.2	10
4481	Range separated hybrid density functional with long-range Hartree-Fock exchange applied to solids. Journal of Chemical Physics, 2007, 127, 054101.	1.2	89
4482	Observable consequences of formation of Au anions from deposition of Au atoms on ultrathin oxide films. Journal of Chemical Physics, 2007, 127, 144713.	1.2	29
4483	Ellipsometry andab initioapproaches to the refractive index of porous silicon. Journal of Physics Condensed Matter, 2007, 19, 395010.	0.7	11

#	Article	IF	Citations
4484	Oxygen adsorption on the clean and O-precovered Fe (110) and (100) surfaces. Journal of Physics Condensed Matter, 2007, 19, 096011.	0.7	23
4485	Potential Energy of H2Dissociation and Adsorption on Pt(111) Surface: First-Principles Calculation. Japanese Journal of Applied Physics, 2007, 46, 4233-4237.	0.8	36
4486	First-Principles Calculations for In-Terminated (000ar1) Surface of InN with Defects and Impurities. Japanese Journal of Applied Physics, 2007, 46, 6205-6207.	0.8	2
4487	Electrical activity and migration of 90Â° partial dislocations in SiC. New Journal of Physics, 2007, 9, 6-6.	1.2	17
4488	Quantum states of hydrogen atom motion on the Pd(111) surface and in the subsurface. Journal of Physics Condensed Matter, 2007, 19, 365214.	0.7	18
4489	Metastable phase formation in the immiscible Cuâ€“Co system studied by thermodynamic, molecular dynamics andab initiocalculations together with ion beam mixing. Journal of Physics Condensed Matter, 2007, 19, 026219.	0.7	8
4490	Potential energy surface for rare gases adsorbed on Cu(111): parameterization of the gas/metal interaction potential. Journal of Physics Condensed Matter, 2007, 19, 305008.	0.7	18
4491	Elastic properties of superconducting NbB_{2+x}obtained from first-principles calculations. Journal of Physics Condensed Matter, 2007, 19, 376209.	0.7	17
4492	Vibrational spectra of lead tetraborate: experimental and theoretical analysis. Journal of Physics Condensed Matter, 2007, 19, 436207.	0.7	5
4493	Theoretical study of the recombination of Frenkel pairs in irradiated silicon carbide. Journal of Physics Condensed Matter, 2007, 19, 086208.	0.7	20
4494	Evolution of a symmetry gap and synergetic quantum well states in ultrathin Ag films on Au(111) substrates. Europhysics Letters, 2007, 78, 57003.	0.7	14
4495	Structural Stabilities of Ordered Nb 4 Clusters on the Cu(111) and Cu(100) Surfaces. Chinese Physics Letters, 2007, 24, 172-175.	1.3	2
4496	Non-Local Density Functional Description of Poly- Para -Phenylene Vinylene. Chinese Physics Letters, 2007, 24, 807-810.	1.3	6
4497	Density-functional investigation of Na₁₆A₈Ge₁₃₆(A = Rb,Cs) clathrates. Journal of Physics Condensed Matter, 2007, 19, 466206.	0.7	6
4498	Maximally localized Wannier functions constructed from projector-augmented waves or ultrasoft pseudopotentials. Journal of Physics Condensed Matter, 2007, 19, 036215.	0.7	32
4499	The water adsorption on the surfaces of SrMO₃(M= Ti, Zr, and Hf) crystalline oxides: quantum and classical modelling. Journal of Physics: Conference Series, 2007, 93, 012001.	0.3	22
4500	Ab initio study of surface stress response to charging. Europhysics Letters, 2007, 78, 13001.	0.7	73
4501	First-principles study of Ï‰-phase formation in the Ti₃Al₂V system. Journal of Physics Condensed Matter, 2007, 19, 386221.	0.7	5

#	Article	IF	Citations
4502	Theoretical Study of the Stability of X@B6and X@B12Clusters: X=Hâ€“Br in Crystalline Silicon. Japanese Journal of Applied Physics, 2007, 46, 467-473.	0.8	2
4503	Theoretical prediction for the (AlN)₁₂fullerene-like cage-based nanomaterials. Journal of Physics Condensed Matter, 2007, 19, 346228.	0.7	17
4504	First-principles calculations of BaZrO3(001) and (011) surfaces. Journal of Physics Condensed Matter, 2007, 19, 356004.	0.7	34
4505	Pathways for SO₂dissociation on Cu(100): density functional theory. Journal of Physics Condensed Matter, 2007, 19, 365244.	0.7	2
4506	First-principles study of defect equilibria in lithium zinc nitride. Journal of Physics Condensed Matter, 2007, 19, 046201.	0.7	6
4507	Lattice mismatch consequences for the intrinsic characteristics in the dilute (Zn, Se)O alloys. Journal of Physics Condensed Matter, 2007, 19, 456212.	0.7	10
4508	A first-principles investigation into the ferroelectric and antiferrodistortive instabilities of cubic SrTiO₃. Journal of Physics Condensed Matter, 2007, 19, 506213.	0.7	6
4509	Ab initioand empirical studies on the asymmetry of molecular currentâ€“voltage characteristics. Journal of Physics Condensed Matter, 2007, 19, 215206.	0.7	12
4510	The effects of Zn and Mg on the mechanical properties of the Al/TiN interface: a first-principles study. Journal of Physics Condensed Matter, 2007, 19, 226003.	0.7	4
4511	A density functional study of atomic oxygen and carbon adsorptions on (100) surface of Î³-Uranium. Physica Scripta, 2007, 75, 506-514.	1.2	9
4512	Surfactant Effects of Au on Polar ZnO Surfaces. Chinese Physics Letters, 2007, 24, 800-802.	1.3	4
4513	Hindered rotation of an OH-Li center in MgO: Infrared absorption experiments and theory. Physical Review B, 2007, 75, .	1.1	4
4514	Mechanism of the electro-optic effect in the perovskite-type ferroelectric KNbO3 and LiNbO3. Journal of Applied Physics, 2007, 101, 103506.	1.1	17
4515	Distinct atomic structures of the Ni-Nb metallic glasses formed by ion beam mixing. Journal of Applied Physics, 2007, 102, .	1.1	9
4516	Structure, stability, and electronic properties of<mml:math xmlns:mml="http://www.w3.org/1998/Math/MathML" display="inline"><mml:mrow><mml:mi mathvariant="normal">Sr</mml:mi><mml:mi mathvariant="normal">Ti</mml:mi><mml:msub><mml:mi mathvariant="normal">O</mml:mi><mml:mn>3</mml:mn></mml:msub><mml:mo>â^•</mml:mo><mml:mi mathvariant="normal">La</mml:mi><mml:mi mathvariant="normal">Al</mml:mi><mml:msub><mml:mi mathvariant="normal">O</mml:mi><mml:mn>3</mml:mn></mml:msub></mml:mrow></mml:math>and<mml:math	1.1	76
4517	Ab initiostudy of the structural, electronic, and magnetic properties ofMnO(100)andMnO(110). Physical Review B, 2007, 75, .	1.1	41
4518	Bulk and surface electronic structures of alkaline-earth metal oxides: Bound surface and image-potential states from first principles. Physical Review B, 2007, 76, .	1.1	38
4519	Crystal structure of<mml:math xmlns:mml="http://www.w3.org/1998/Math/MathML" display="inline"><mml:mrow><mml:mi mathvariant="normal">Si</mml:mi><mml:msub><mml:mi mathvariant="normal">H</mml:mi><mml:mn>4</mml:mn></mml:msub></mml:mrow></mml:math>at high pressure. Physical Review B, 2007, 76, .	1.1	63

#	Article	IF	Citations
4520	Spin-polarization study ofCOmolecules adsorbed onFe(110)using metastable-atom deexcitation spectroscopy and first-principles calculations. Physical Review B, 2007, 75, .	1.1	15
4521	Mechanical and electronic properties of superhard<mml:math xmlns:mml="http://www.w3.org/1998/Math/MathML" display="inline"><mml:mrow><mml:mi mathvariant="normal">Re</mml:mi><mml:msub><mml:mi mathvariant="normal">B</mml:mi><mml:mn>2</mml:mn></mml:msub></mml:mrow></mml:math>. Physical Review B, 2007, 76, .	1.1	122
4522	Linear response separation of a solid into atomic constituents: Li, Al, and their evolution under pressure. Physical Review B, 2007, 75, .	1.1	3
4523	Determining the site preference of trivalent dopants in bixbyite sesquioxides by atomic-scale simulations. Physical Review B, 2007, 75, .	1.1	61
4524	First-principles calculations of the elastic, electronic, and optical properties of the filled skutteruditesCeFe4P12andThFe4P12. Physical Review B, 2007, 75, .	1.1	66
4525	Epitaxial phase of hafnium dioxide for ultrascaled electronics. Physical Review B, 2007, 76, .	1.1	12
4526	Pressure-induced amorphization of<mml:math xmlns:mml="http://www.w3.org/1998/Math/MathML" display="inline"><mml:mrow><mml:mi mathvariant="normal">Cu</mml:mi><mml:mi mathvariant="normal">Fe</mml:mi><mml:msub><mml:mi mathvariant="normal">S</mml:mi><mml:mn>2</mml:mn></mml:msub></mml:mrow></mml:math>studied by<mml:math xmlns:mml="http://www.w3.org/1998/Math/MathML" display="inline"><mml:mmultiscripts><mml:mi mathvariant="normal">Fe</mml:mi><mml:mprescripts />	1.1	10
4527	Effect of nitrogen on the magnetic moment of Î±-Fe and FeCo alloys from first-principle calculations. Journal of Applied Physics, 2007, 101, 033912.	1.1	9
4528	Mixing of the fully symmetric vibrational modes in carbon nanotubes. Physical Review B, 2007, 75, .	1.1	10
4529	Charge transfer of alkanethiolate adsorbed on Au(111) surface : First-principles calculations. , 2007, , .		0
4530	Calcium deposition on poly(para-phenylene vinylene): Molecular dynamics simulations. Physical Review B, 2007, 76, .	1.1	6
4531	Electronic structure of Fe-doped In2O3 magnetic semiconductor with oxygen vacancies: Evidence for F-center mediated exchange interaction. Applied Physics Letters, 2007, 91, 262514.	1.5	43
4532	Doping effects on metallic and semiconductor single-wall carbon nanotubes. Philosophical Magazine, 2007, 87, 1097-1105.	0.7	19
4533	First-principles study of oxygen vacancies in Lu₂SiO₅. Journal of Physics Condensed Matter, 2007, 19, 436215.	0.7	34
4534	Theoretical study of size-dependent properties of BN nanotubes with intrinsic defects. Physical Review B, 2007, 76, .	1.1	42
4535	Elastic constants and tensile properties ofAl2OCby density functional calculations. Physical Review B, 2007, 75, .	1.1	19
4536	Variational boundary conditions for molecular dynamics simulations of crystalline solids at finite temperature: Treatment of the thermal bath. Physical Review B, 2007, 76, .	1.1	44
4537	Polygonization and anomalous graphene interlayer spacing of multi-walled carbon nanofibers. Physical Review B, 2007, 75, .	1.1	26

#	Article	IF	Citations
4538	First-principles study of magnetic properties in V-doped ZnO. Applied Physics Letters, 2007, 91, 063116.	1.5	38
4539	First-principles prediction of phase-segregating alloy phase diagrams and a rapid design estimate of their transition temperatures. Physical Review B, 2007, 75, .	1.1	95
4540	Ab initiostudy of point defects in magnesium oxide. Physical Review B, 2007, 76, .	1.1	37
4541	Nature of Xenon adsorption on graphite: On-top versus hollow site preference. Physical Review B, 2007, 76, .	1.1	28
4542	Microstructure and mechanical properties of sputtered intermetallic Alâ€“Au coatings. Journal of Applied Physics, 2007, 102, 023523.	1.1	9
4543	Headgroup dimerization in methanethiol monolayers on the Au(111) surface: A density functional theory study. Physical Review B, 2007, 76, .	1.1	11
4544	Ferromagnetic to ferrimagnetic crossover in Cr-doped GaN nanohole arrays. Physical Review B, 2007, 75, .	1.1	11
4545	First-principles calculation of mechanical properties of SiâŸ¨001âŸ© nanowires and comparison to nanomechanical theory. Physical Review B, 2007, 75, .	1.1	113
4546	First-principles study of wurtzite<mml:math xmlns:mml="http://www.w3.org/1998/Math/MathML" display="inline"><mml:mrow><mml:mi mathvariant="normal">B</mml:mi><mml:msub><mml:mi mathvariant="normal">C</mml:mi><mml:mn>2</mml:mn></mml:msub><mml:mi mathvariant="normal">N</mml:mi></mml:mrow></mml:math>. Physical Review B, 2007, 76, .	1.1	43
4547	Electronic structure, elastic properties, surface energies, and work functions ofNiGeandPtGewithin the framework of density-functional theory for various surface terminations. Physical Review B, 2007, 75, .	1.1	23
4548	Lattice dynamics ofRuO2: Theory and experiment. Physical Review B, 2007, 75, .	1.1	15
4549	Atomic and electronic structures, elastic properties, and optical conductivity of bulk Te and Te nanowires: A first-principles study. Physical Review B, 2007, 75, .	1.1	32
4550	Theoretical study of Li and Na asn-type dopants for diamond. Physical Review B, 2007, 75, .	1.1	35
4551	Interface effects at a half-metal/ferroelectric junction. Applied Physics Letters, 2007, 91, .	1.5	100
4552	Ab initiocalculations of<mml:math xmlns:mml="http://www.w3.org/1998/Math/MathML" display="inline"><mml:mrow><mml:mi mathvariant="normal">Ba</mml:mi><mml:mi mathvariant="normal">Ti</mml:mi><mml:msub><mml:mi mathvariant="normal">O</mml:mi><mml:mn>3</mml:mn></mml:msub></mml:mrow></mml:math>and<mml:math xmlns:mml="http://www.w3.org/1998/Math/MathML" display="inline"><mml:mrow><mml:mi mathvariant="normal">Pb</mml:mi><mml:mi mathvariant="normal">Ti</mml:mi><mml:msub><mml:mi m	1.1	149
4553	Metastable Frenkel pairs and the W11â€“W14 electron paramagnetic resonance centers in diamond. Physical Review B, 2007, 76, .	1.1	6
4554	Magnetically induced dynamical stability of a Fe monolayer on W(110). Physical Review B, 2007, 76, .	1.1	11
4555	Post-<mml:math xmlns:mml="http://www.w3.org/1998/Math/MathML" display="inline"><mml:mrow><mml:msub><mml:mi mathvariant="normal">Rh</mml:mi><mml:mn>2</mml:mn></mml:msub><mml:msub><mml:mi mathvariant="normal">O</mml:mi><mml:mn>3</mml:mn></mml:msub><mml:mrow><mml:mo>(</mml:mo><mml:mn>II</mml:mn> and the high pressure-temperature phase diagram of gallia: A first-principles and x-ray diffraction study. Physical Review B, 2007, 76, .	1.1	23

#	Article	IF	Citations
4556	First-principles study of the pressure dependence of the structural and vibrational properties of the ternary metal hydrideCa2RuH6. Physical Review B, 2007, 76, .	1.1	12
4557	Magnetic properties of CrSb: A first-principle study. Journal of Applied Physics, 2007, 101, 093912.	1.1	29
4558	Phonons of (100) and (110) iron surfaces from first-principles calculations. Physical Review B, 2007, 75, .	1.1	18
4559	Ab initiostudy of small vacancy complexes in beryllium. Physical Review B, 2007, 75, .	1.1	31
4560	Size dependence of thermal properties of armchair carbon nanotubes: A first-principles study. Applied Physics Letters, 2007, 91, .	1.5	17
4561	High-pressure behavior of phosphorus from first principles calculations. Physical Review B, 2007, 76, .	1.1	11
4562	Calculations of codoping effects between combinations of donors (P/As/Sb) and acceptors (B/Ga/In) in Si. Journal of Applied Physics, 2007, 102, 123709.	1.1	3
4563	Ab initiostudies of structural, vibrational, and electronic properties of durene crystals and molecules. Physical Review B, 2007, 75, .	1.1	23
4564	Formation of electron traps in amorphous silica. Physical Review B, 2007, 76, .	1.1	12
4565	Ab initiosimulations of the structural phase transformation of2Hâ€SiCat high pressure. Physical Review B, 2007, 75, .	1.1	36
4566	Response of trialuminides to [110] uniaxial loading: Anab initiostudy for<mml:math xmlns:mml="http://www.w3.org/1998/Math/MathML" display="inline"><mml:mrow><mml:msub><mml:mi mathvariant="normal">Al</mml:mi><mml:mn>3</mml:mn></mml:msub><mml:mrow><mml:mo>(</mml:mo><mml:mi) Tj ETQq0 0 0 rg	1.1	22
4567	Phys Ab initio investigations on atomistic behaviors and magnetic properties in Feâ€“Cu multilayer system. Journal of Applied Physics, 2007, 101, 09D119.	1.1	2
4568	Hydrogen adsorption by tungsten carbide nanotube. Applied Physics Letters, 2007, 90, 223104.	1.5	34
4569	Surface influence on stability and structure of hexagon-shaped III-V semiconductor nanorods. Journal of Applied Physics, 2007, 102, 063528.	1.1	66
4570	First principle study of Co2MnSi/GaAs(001) heterostructures. Journal of Applied Physics, 2007, 102, .	1.1	38
4571	Thermoelectric Properties of P-doped Mg2Si Semiconductors. Japanese Journal of Applied Physics, 2007, 46, 3309-3314.	0.8	38
4572	The effect of reciprocal-space sampling and basis set quality on the calculated conductance of a molecular junction. Molecular Simulation, 2007, 33, 897-904.	0.9	8
4573	Ab-initio Atomic Scale Study of Nearly Frictionless Surfaces. , 2007, , 57-77.		2

#	Article	IF	Citations
4574	Vacancy-arsenic clusters in germanium. Applied Physics Letters, 2007, 91, .	1.5	75
4575	THE PROBLEM OF THE BAND GAP IN LDA CALCULATIONS. Surface Review and Letters, 2007, 14, 481-487.	0.5	69
4576	Compositional Correlation and Anticorrelation in Quaternary Alloys: Competition Between Bulk Thermodynamics and Surface Kinetics. Physical Review Letters, 2007, 99, 206103.	2.9	16
4577	Quantum Mechanical Description of Displacement Damage Formation. IEEE Transactions on Nuclear Science, 2007, 54, 1906-1912.	1.2	18
4578	First-principles study of the structure, electronic, and optical properties of orthorhombic BiInO3. Applied Physics Letters, 2007, 91, 071902.	1.5	23
4579	Structural and magnetic properties of (Ga,Mn)N from first principles. Physical Review B, 2007, 75, .	1.1	29
4580	Dimer-breaking-assisted exchange mechanism in surfactant-mediated epitaxial growth of Ge on Si(001):Ab initiototal energy calculations. Physical Review B, 2007, 76, .	1.1	3
4581	Comparison of localized basis and plane-wave basis for density-functional calculations of organic molecules on metals. Physical Review B, 2007, 75, .	1.1	64
4582	Pressure-induced structural phase transition inNaAlH4. Physical Review B, 2007, 75, .	1.1	23
4583	Elastic Property of Cu<inf>3</inf>Sn Determined by a First-Principles Calculation on the Basis of its Crystal Substructure. , 2007, , .		0
4584	Structural and electronic properties ofp-doped silicon clathrates. Physical Review B, 2007, 75, .	1.1	34
4585	Theoretical study of the chemical gap tuning in silicon nanowires. Physical Review B, 2007, 76, .	1.1	65
4586	Chemical bonding and many-body effects in site-specific x-ray photoelectron spectra of corundum<mml:math xmlns:mml="http://www.w3.org/1998/Math/MathML" display="inline"><mml:mrow><mml:msub><mml:mi mathvariant="normal">V</mml:mi><mml:mn>2</mml:mn></mml:msub><mml:msub><mml:mi mathvariant="normal">O</mml:mi><mml:mn>3</mml:mn></mml:msub></mml:mrow></mml:math>. Physical Review B, 2007, 76, .	1.1	18
4587	<mml:math xmlns:mml="http://www.w3.org/1998/Math/MathML" display="inline"><mml:mrow><mml:mi mathvariant="normal">Sr</mml:mi><mml:mi mathvariant="normal">Ti</mml:mi><mml:msub><mml:mi mathvariant="normal">O</mml:mi><mml:mn>3</mml:mn></mml:msub></mml:mrow></mml:math>substrates capped with a GaAs monolayer: Anab initiostudy. Physical Review B, 2007, 76, .	1.1	10
4588	Surface structure determination of Pd ultrathin films on Ru(0001): Possible magnetic behavior. Physical Review B, 2007, 76, .	1.1	12
4589	Density functional theory investigation of3dtransition metal NMR shielding tensors in diamagnetic systems using the gauge-including projector augmented-wave method. Physical Review B, 2007, 76, .	1.1	27
4590	Domain Sensitive Contrast in Photoelectron Emission Microscopy. Physical Review Letters, 2007, 99, 196102.	2.9	8
4591	From four- to six-coordinated silica: Transformation pathways from metadynamics. Physical Review B, 2007, 76, .	1.1	45

#	Article	IF	Citations
4592	Post-perovskite phase in selected sesquioxides from density-functional calculations. Physical Review B, 2007, 76, .	1.1	27
4593	Theoretical study of pressure-induced phase transition inAlAs: From zinc-blende toNiAsstructure. Physical Review B, 2007, 75, .	1.1	22
4594	Theoretical study of deep-defect states in bulk PbTe and in thin films. Physical Review B, 2007, 76, .	1.1	57
4595	Stability and Dynamics of Frenkel Pairs in Si. Physical Review Letters, 2007, 99, 215503.	2.9	9
4596	Large band-gap bowing in<mml:math xmlns:mml="http://www.w3.org/1998/Math/MathML" display="inline"><mml:mrow><mml:msub><mml:mi mathvariant="normal">Cu</mml:mi><mml:mrow><mml:mn>1</mml:mn><mml:mo>â^'</mml:mo><mml:mi>x</mml:mi></mml:mrow><mml:mi mathvariant="normal">Ag</mml:mi><mml:mi>x</mml:mi></mml:msub><mml:mi mathvariant="normal">Ga</mml:mi><mml:msub><mml:mi mathvariant="normal">S</mml:mi><mml:mn>2</mml:mn></mml:msub></mml:mrow></mml:math>chalcopyrite	1.1	4
4597	Surface modification of oxides by electron-stimulated desorption for growth-mode control of metal films: Experiment and density-functional calculations. Physical Review B, 2007, 76, .	1.1	21
4598	Oxygen-ion arrangements and concerted motion inÎ²â^'La2Mo2O9. Physical Review B, 2007, 76, .	1.1	25
4599	First-principles calculations of the electronic and magnetic properties of<mml:math xmlns:mml="http://www.w3.org/1998/Math/MathML" display="inline"><mml:mrow><mml:msub><mml:mi mathvariant="normal">Cs</mml:mi><mml:mn>2</mml:mn></mml:msub><mml:mi mathvariant="normal">Ag</mml:mi><mml:msub><mml:mi mathvariant="normal">F</mml:mi><mml:mn>4</mml:mn></mml:msub></mml:mrow></mml:math>. Physical Review B, 2007, 76, .	1.1	14
4600	Ab initiostudies of solid bromine under high pressure. Physical Review B, 2007, 76, .	1.1	35
4601	Ideal tensile and shear strength of<mml:math xmlns:mml="http://www.w3.org/1998/Math/MathML" display="inline"><mml:mrow><mml:mi>Î²</mml:mi><mml:mtext>â^'</mml:mtext><mml:msub><mml:mi mathvariant="normal">C</mml:mi><mml:mn>3</mml:mn></mml:msub><mml:msub><mml:mi mathvariant="normal">N</mml:mi><mml:mn>4</mml:mn></mml:msub></mml:mrow></mml:math>from Theoretical study of small silicon clusters in<mml:math xmlns:mml="http://www.w3.org/1998/Math/MathML" display="inline"><mml:mrow><mml:mn>4</mml:mn><mml:mi>H</mml:mi><mml:mtext>â^'</mml:mtext><mml:mi mathvariant="normal">Si</mml:mi><mml:mi mathvariant="normal">C</mml:mi></mml:mrow></mml:math>. Physical Review B, 2007, 76, .	1.1	29
4602		1.1	16
4603	Limits of the scaled shift correction to levels of interstitial defects in semiconductors. Physical Review B, 2007, 75, .	1.1	16
4604	Electronic and vibrational properties of framework-substituted type-II silicon clathrates. Physical Review B, 2007, 75, .	1.1	42
4605	Structural and electronic properties of fluorinated double-walled boron nitride nanotubes: Effect of interwall interaction. Physical Review B, 2007, 75, .	1.1	22
4606	Structural phase transition of gold under uniaxial, tensile, and triaxial stresses: Anab initiostudy. Physical Review B, 2007, 76, .	1.1	15
4607	Structure and stability of the low-index surfaces ofFe3Si:Ab initiodensity functional investigations. Physical Review B, 2007, 75, .	1.1	22
4608	Interactions between Al atoms on Al(110) from first-principles calculations. Physical Review B, 2007, 75, .	1.1	15
4609	Association of oxygen vacancies with impurity metal ions in lead titanate. Physical Review B, 2007, 76, .	1.1	94

#	Article	IF	Citations
4610	First-principles calculations of the effects of Cu and Ag additions on the electromigration of Sn-based solder. Journal of Applied Physics, 2007, 102, .	1.1	10
4611	Suppressed Dependence of Polarization on Epitaxial Strain in Highly Polar Ferroelectrics. Physical Review Letters, 2007, 98, 217602.	2.9	146
4612	Conductance and Kondo Effect in a Controlled Single-Atom Contact. Physical Review Letters, 2007, 98, 016801.	2.9	161
4613	Modified mean-field potential approach to thermodynamic properties of a low-symmetry crystal: Beryllium as a prototype. Physical Review B, 2007, 75, .	1.1	18
4614	Cubic phases ofBC2N: A first-principles study. Physical Review B, 2007, 75, .	1.1	43
4615	Ab initiostudy of structural stability, elastic, vibrational, and electronic properties of<mml:math xmlns:mml="http://www.w3.org/1998/Math/MathML" display="inline"><mml:mrow><mml:mi mathvariant="normal">Ti</mml:mi><mml:msub><mml:mi mathvariant="normal">Pd</mml:mi><mml:mn>2</mml:mn></mml:msub></mml:mrow></mml:math>. Physical Review B, 2007, 76, .	1.1	13
4616	Dynamical core-hole screening in the x-ray absorption spectra of hydrogenated carbon nanotubes and graphene. Physical Review B, 2007, 76, .	1.1	19
4617	Electronic structure, phase stability, and chemical ordering of theÏ‰phase in aTi3Al2X(X=Nb,V)alloy. Physical Review B, 2007, 76, .	1.1	7
4618	Adsorption and diffusion of hydrogen on Pd(211) and Pd(111): Results from first-principles electronic structure calculations. Physical Review B, 2007, 75, .	1.1	50
4619	Combinedab initioand LEED<mml:math xmlns:mml="http://www.w3.org/1998/Math/MathML" display="inline"><mml:mrow><mml:mi>I</mml:mi><mml:mo>â^•</mml:mo><mml:mi>V</mml:mi></mml:mrow></mml:math>study of submonolayer adsorption of In on W(110). Physical Review B, 2007, 76, .	1.1	6
4620	First-principles study of the interfacial structures ofAuâ^•MgO(001). Physical Review B, 2007, 75, .	1.1	16
4621	First-principles calculations of Cu adsorption on an H-terminated Si surface. Physical Review B, 2007, 76, .	1.1	18
4622	First-principles investigation of terephthalic acid on Cu(110). Physical Review B, 2007, 76, .	1.1	16
4623	Germanium diffusion mechanisms in silicon from first principles. Physical Review B, 2007, 75, .	1.1	33
4624	Stability of high-pressure phases in II-VI semiconductors by a density functional lattice dynamics approach. Physical Review B, 2007, 75, .	1.1	30
4625	Density-functional investigation of the<mml:math xmlns:mml="http://www.w3.org/1998/Math/MathML" display="inline"><mml:mrow><mml:mrow><mml:mo>(</mml:mo><mml:mn>113</mml:mn><mml:mo>)</mml:mo></mml:mrow><mml grain boundary in Co-doped anatase<mml:math xmlns:mml="http://www.w3.org/1998/Math/MathML" display="inline"><mml:mrow><mml:mi mathvariant="normal">Ti</mml:mi><mml:msub><mml:mi mathvariant="normal">O</mml:mi><mml:mn>2</mml:mn></mml:msub></mml:mrow></mml:math>. Physical Review B, 2007, 76, .	1.1	15
4626	Ab initiomodeling ofCaTiO3(110) polar surfaces. Physical Review B, 2007, 76, .	1.1	27
4627	Confined states in multiple quantum well structures of<mml:math xmlns:mml="http://www.w3.org/1998/Math/MathML" display="inline"><mml:mrow><mml:msub><mml:mi mathvariant="normal">Si</mml:mi><mml:mi>n</mml:mi></mml:msub><mml:msub><mml:mi mathvariant="normal">Ge</mml:mi><mml:mi>n</mml:mi></mml:msub></mml:mrow></mml:math>nanowire superlattices. Physical Review B, 2007, 76, .	1.1	18

#	Article	IF	Citations
4628	Interstitial Fe in Si and its interactions with hydrogen and shallow dopants. Physical Review B, 2007, 76, .	1.1	50
4629	Water adsorption on Pd {100} from first principles. Physical Review B, 2007, 76, .	1.1	37
4630	Energy decomposition analysis of metal silicide nanowires from first principles. Physical Review B, 2007, 75, .	1.1	12
4631	Adsorption and diffusion dynamics of atomic and molecular oxygen on reconstructed Cu(100). Physical Review B, 2007, 75, .	1.1	31
4632	Quantitative LEEDIâˆ'Vandab initiostudy of theSi(111)âˆ'3Ã—2âˆ'Smsurface structure and the missing half-order spots in the3Ã—1diffraction pattern. Physical Review B, 2007, 75, .	1.1	8
4633	Mechanism of Li+ diffusion in crystalline<mml:math xmlns:mml="http://www.w3.org/1998/Math/MathML" display="inline"><mml:msup><mml:mi mathvariant="normal">Li</mml:mi><mml:mo>+</mml:mo></mml:msup></mml:math>diffusion in crystalline<mml:math xmlns:mml="http://www.w3.org/1998/Math/MathML" display="inline"><mml:msup><mml:mi mathvariant="normal">Li</mml:mi><mml:mo>+</mml:mo></mml:msup></mml:math> Compression mechanism and pressure-induced amorphization of<mml:math xmlns:mml="http://www.w3.org/1998/Math/MathML" display="inline"><mml:mrow><mml:mi>Î³</mml:mi><mml:mtext>â€'</mml:mtext><mml:mi mathvariant="normal">Zr</mml:mi><mml:msub><mml:mi mathvariant="normal">W</mml:mi><mml:mn>2</mml:mn></mml:msub><mml:msub><mml:mi mathvariant="normal">O</mml:mi><mml:mn>8</mml:mn></mml:msub></mml:mrow></mml:math>. Physi	1.1	93
4634	Ionicity scale based on the centers of maximally localized Wannier functions. Physical Review B, 2007, 75, .	1.1	15
4635	Energetics of interlayer binding in graphite: The semiempirical approach revisited. Physical Review B, 2007, 76, .	1.1	36
4636	Density functional study of alkali-metal atoms and monolayers on graphite (0001). Physical Review B, 2007, 75, .	1.1	63
4637	First principles study of Mn impurities in PbTiO3 and PbZrO3. Journal of Applied Physics, 2007, 101, 043521.	1.1	99
4638	Structural and polarization properties of short-periodSrZrO3âˆ•SrTiO3superlattices. Physical Review B, 2007, 75, .	1.1	18
4639	Hydrogen-helium mixtures in the interiors of giant planets. Physical Review B, 2007, 75, .	1.1	11
4640	Probing zone-boundary optical phonons in doped graphene. Physical Review B, 2007, 76, .	1.1	176
4641	Self-consistent band-gap corrections in density functional theory using modified pseudopotentials. Physical Review B, 2007, 75, .	1.1	18
4642	Electronic structure and thermodynamic stability of double-layeredSrTiO3(001)surfaces:Ab initiosimulations. Physical Review B, 2007, 75, .	1.1	66
4643	First-principles study of the energy-gap composition dependence ofZn1âˆ'xBexSeternary alloys. Physical Review B, 2007, 75, .	1.1	92
4644	Interpretation of STM images of graphite with an atomic vacancy via density-functional calculations of electronic structure. Physical Review B, 2007, 75, .	1.1	23
4645		1.1	21

#	Article	IF	Citations
4646	Anomalous strain dependent effective masses in (111) Si nanowires. Applied Physics Letters, 2007, 91, 083116.	1.5	11
4647	Electronic structure of germanium nitride considered for gate dielectrics. Journal of Applied Physics, 2007, 102, 013507.	1.1	33
4648	First-Principles Simulations of Boron Diffusion in Graphite. Physical Review Letters, 2007, 98, 015501.	2.9	24
4649	Three-Dimensional Tomography of the Beryllium Fermi Surface: Surface Charge Redistribution. Physical Review Letters, 2007, 99, 166403.	2.9	9
4650	Half-Metallic Silicon Nanowires: First-Principles Calculations. Physical Review Letters, 2007, 99, 256806.	2.9	70
4651	Nonvolatile Memory Elements Based on the Intercalation of Organic Molecules Inside Carbon Nanotubes. Physical Review Letters, 2007, 98, 056401.	2.9	24
4652	Effect of Carbon Adsorption on the Isomer Stability of<mml:math xmlns:mml="http://www.w3.org/1998/Math/MathML" display="inline"><mml:msub><mml:mi>Ir</mml:mi><mml:mn>4</mml:mn></mml:msub></mml:math>Clusters. Physical Review Letters, 2007, 99, 165501.	2.9	16
4653	Reciprocal Space Constraints Create Real-Space Anomalies in Doped Carbon Nanotubes. Physical Review Letters, 2007, 99, 196803.	2.9	6
4654	Surface electronic structure and magnetism of NiAs structured MnAs(0001) and MnSb(0001). Journal of Applied Physics, 2007, 101, 09G502.	1.1	3
4655	First principles calculations for dilute InAs1âˆ’xNx alloys. Journal of Applied Physics, 2007, 102, .	1.1	23
4656	Energetics of positron states trapped at vacancies in solids. Physical Review B, 2007, 76, .	1.1	38
4657	AgRaman modes and ion-position dependence of the electronic structures ofYBa2Cu3O7andYBa2Cu4O8from first principles. Physical Review B, 2007, 76, .	1.1	1
4658	First-principles study of thermodynamical and mechanical stabilities of thin copper film on tantalum. Physical Review B, 2007, 76, .	1.1	51
4659	Transferable force-constant modeling of vibrational thermodynamic properties in fcc-basedAlâˆ’TM(TM=Ti, Zr, Hf) alloys. Physical Review B, 2007, 75, .	1.1	44
4660	Prediction of Bâ€“Siiâ€“F complex formation and its role in B transient enhanced diffusion suppression and deactivation. Journal of Applied Physics, 2007, 101, 066102.	1.1	1
4661	Growing extremely thin bulklike metal film on a semiconductor surface: Monolayer Al(111) on Si(111). Applied Physics Letters, 2007, 91, .	1.5	6
4662	Hydrogen interaction with native defects in<mml:math xmlns:mml="http://www.w3.org/1998/Math/MathML" display="inline"><mml:mrow><mml:mi>SiC</mml:mi></mml:mrow></mml:math>nanotubes. Physical Review B, 2007, 76, .	1.1	39
4663	Bonding characteristics and site occupancies of alloying elements in differentNb5Si3phases from first principles. Physical Review B, 2007, 76, .	1.1	39

#	Article	IF	Citations
4664	Ab initiocalculations of the optical properties of theSi(113)3Ã—2adatom-dimer-interstitial surface. Physical Review B, 2007, 75, .	1.1	6
4665	Chemical bonding effect of Ge atoms on B diffusion in Si. Physical Review B, 2007, 76, .	1.1	10
4666	Mechanisms of silicon diffusion in erbium silicide. Physical Review B, 2007, 75, .	1.1	4
4667	Band-gap bowing in<mml:math xmlns:mml="http://www.w3.org/1998/Math/MathML" display="inline"><mml:mrow><mml:mi mathvariant="normal">Ag</mml:mi><mml:mi mathvariant="normal">Ga</mml:mi><mml:msub><mml:mrow><mml:mo>(</mml:mo><mml:msub><mml:mi) Tj ETQq1 1 0.784314 rgBT	1.1	6
4668	Body-centered superhard<mml:math xmlns:mml="http://www.w3.org/1998/Math/MathML" display="inline"><mml:mrow><mml:mi mathvariant="normal">B</mml:mi><mml:msub><mml:mi mathvariant="normal">C</mml:mi><mml:mn>2</mml:mn></mml:msub><mml:mi mathvariant="normal">N</mml:mi></mml:mrow></mml:math>phases from first principles. Physical Review B, 2007, 76, .	1.1	32
4669	A prioriWannier functions from modified Hartree-Fock and Kohn-Sham equations. Physical Review B, 2007, 75, .	1.1	1
4670	Atomic and electronic structure of the cleaved6Hâ^'SiC(112Â¯0)surface. Physical Review B, 2007, 75, .	1.1	6
4671	B3LYP density functional calculations on the ground-state structure, elastic properties, and compression mechanism ofÎ±â^'ZrW2O8. Physical Review B, 2007, 75, .	1.1	16
4672	Calculations of spin-induced transport in ferromagnets. Physical Review B, 2007, 75, .	1.1	12
4673	Systematic study on the pressure dependence of<mml:math xmlns:mml="http://www.w3.org/1998/Math/MathML" display="inline"><mml:mrow><mml:msub><mml:mi>M</mml:mi><mml:mn>2</mml:mn></mml:msub><mml:mi mathvariant="normal">Al</mml:mi><mml:mi mathvariant="normal">C</mml:mi></mml:mrow></mml:math>phases<mml:math xmlns:mml="http://www.w3.org/1998/Math/MathML"		

#	Article	IF	Citations
4682	Ab initiostudy of ductility inM2AlC(M=Ti, V, Cr). Physical Review B, 2007, 75, .	1.1	125
4683	CO adsorption on metal surfaces: A hybrid functional study with plane-wave basis set. Physical Review B, 2007, 76, .	1.1	133
4684	Electron-phonon coupling in the high-pressure hcp phase of xenon: A first-principles study. Physical Review B, 2007, 75, .	1.1	20
4685	Density functional study of the electronic and vibrational properties of TiOCl. Physical Review B, 2007, 76, .	1.1	10
4686	Electronic-structure calculations for polar lattice-structure-mismatched interfaces:<mml:math xmlns:mml="http://www.w3.org/1998/Math/MathML" display="inline"><mml:mrow><mml:mi mathvariant="normal">Pb</mml:mi><mml:mi mathvariant="normal">Te</mml:mi><mml:mo>â^•</mml:mo><mml:mi mathvariant="normal">Cd</mml:mi><mml:mi mathvariant="normal">Te</mml:mi><mml:mrow><mml:mo>(</mml:mo><mml:mn>100</mml:mn><mml:mo>)</mml:mo></mml:mrow>	1.1	22
4687	Structural properties and magic structures in hydrogenated finite and infinite silicon nanowires. Applied Physics Letters, 2007, 91, 203112.	1.5	16
4688	Deep multilayer relaxations on the Al(001) surface:Ab initioall-electron calculations. Physical Review B, 2007, 76, .	1.1	13
4689	Fermi-surface calculation of the anomalous Hall conductivity. Physical Review B, 2007, 76, .	1.1	123
4690	Reaction energetics and crystal structure ofLi4BN3H10from first principles. Physical Review B, 2007, 75, .	1.1	70
4691	Ab initiostudy of the effects of transition metal doping of <mml:math xmlns:mml="http://www.w3.org/1998/Math/MathML" display="inline"><mml:mrow><mml:msub><mml:mi mathvariant="normal">Mg</mml:mi><mml:mn>2</mml:mn></mml:msub><mml:mi mathvariant="normal">Ni</mml:mi><mml:msub><mml:mi mathvariant="normal">H</mml:mi><mml:mn>4</mml:mn></mml:msub></mml:mrow></mml:math>. Physical Review B, 2007, 76,	1.1	61
4692	Quantum mechanics/molecular mechanics methodology for metals based on orbital-free density functional theory. Physical Review B, 2007, 76, .	1.1	26
4693	First-principles study of the electronic structure of cubicGaS: Metallic versus insulating polymorphs. Physical Review B, 2007, 75, .	1.1	4
4694	Electronic and magnetic structure ofLa0.875Sr0.125MnO3calculated by means of hybrid density-functional theory. Physical Review B, 2007, 76, .	1.1	26
4695	Theoretical investigation of bulk ordering and surface segregation in Ag-Pd and other isoelectornic alloys. Physical Review B, 2007, 75, .	1.1	26
4696	Theoretical calculations of mobility enhancement in strained silicon. Physical Review B, 2007, 75, .	1.1	21
4697	Electronic and structural properties of MgB2 by the linear combination of atomic orbitals method. Journal of Applied Physics, 2007, 102, 103713.	1.1	2
4698	Ab initiostudy of structural, magnetic, vibrational, and thermodynamic properties of the Laves-phase compoundHfMn2. Physical Review B, 2007, 76, .	1.1	11
4699	Ordering and segregation of aCu75Pt25(111)surface: A first-principles cluster expansion study. Physical Review B, 2007, 76, .	1.1	31

#	Article	IF	Citations
4700	Relaxations around the substitutional chromium site in emerald: X-ray absorption experiments and density functional calculations. Physical Review B, 2007, 76, .	1.1	39
4701	Initial interactions between water molecules and Ti-adsorbed carbon nanotubes. Applied Physics Letters, 2007, 91, 161906.	1.5	11
4702	Thermoelasticity of MgO at High Pressures. Chinese Journal of Chemical Physics, 2007, 20, 65-70.	0.6	8
4703	Nitrogen related shallow thermal donors in silicon. Applied Physics Letters, 2007, 91, .	1.5	12
4704	Thermoelasticity of CaO from first principles. Chinese Physics B, 2007, 16, 499-505.	1.3	14
4705	First-principles investigation on the geometry and electronic structure of the three-dimensional cuboidal C60 polymer. Journal of Chemical Physics, 2007, 127, 134906.	1.2	16
4706	First-Principles Studies on Grain Boundary Energies of [110] Tilt Grain Boundaries in Aluminum. Materials Science Forum, 2007, 561-565, 1837-1840.	0.3	11
4707	First Principles Study of Al(100) Twisted Interfaces. Solid State Phenomena, 2007, 129, 131-136.	0.3	1
4708	First-Principles Study on Elastic Anomalies in Ag/Al Multilayers. Key Engineering Materials, 2007, 345-346, 959-962.	0.4	0
4709	First-principles calculations of structural and thermodynamic properties of BeB 2 compound. Chinese Physics B, 2007, 16, 3046-3051.	1.3	2
4710	Magnetic anisotropies of iron on the Pt(111) surface. Journal of Physics Condensed Matter, 2007, 19, 365208.	0.7	16
4711	The first-principles study of ferroelectric behaviours of PbTiO 3 /SrTiO 3 and BaTiO 3 /SrTiO 3 superlattices. Chinese Physics B, 2007, 16, 1780-1785.	1.3	12
4712	Electronic Structure and Magnetic Properties of Cr-Doped AlN. Communications in Theoretical Physics, 2007, 48, 749-753.	1.1	3
4713	The Phase Boundary Between Î²-Si3N4 and Î³-Si3N4 at Elevated Temperatures and Pressures. Materials Research Society Symposia Proceedings, 2007, 1040, 1.	0.1	0
4714	Raman frequency shift in oxygen-functionalized carbon nanotubes. Nanotechnology, 2007, 18, 465706.	1.3	10
4715	Density functional calculations of the binding energies and adatom diffusion on strained AlN (0001) and GaN (0001) surfaces. Materials Research Society Symposia Proceedings, 2007, 1040, 1.	0.1	1
4716	Determination of symmetry reduced structures by a soft-phonon analysis in Ni₂MnGa. Materials Research Society Symposia Proceedings, 2007, 1050, 1.	0.1	3
4717	Structural and electronic properties of Fe-doped BaTiO 3 and SrTiO 3. Chinese Physics B, 2007, 16, 1422-1428.	1.3	40

#	Article	IF	Citations
4718	Atomistic Studies of Deformation Mechanism of Nanocrystalline Al-Ti and Al-Fe Alloys from First-Principles. Materials Science Forum, 2007, 561-565, 977-980.	0.3	4
4719	A Theoretical Study of Ultra-Thin Films with the Wurtzite and Zinc Blende Structures. Materials Research Society Symposia Proceedings, 2007, 1035, 1.	0.1	0
4720	Local Vibrational Modes of Zn-H-P in GaP, InP and ZnTe. Defect and Diffusion Forum, 2007, 261-262, 31-36.	0.4	0
4721	Oxygen at high pressures: a theoretical approach to monoatomic phases. Journal of Physics Condensed Matter, 2007, 19, 365211.	0.7	5
4722	Interstitial Carbon-Related Defects in Si_{1-x}Ge_x Alloys. Solid State Phenomena, 2008, 131-133, 59-64.	0.3	0
4723	A First-Principles Analysis for Sulfur Tolerance of CeO₂in Solid Oxide Fuel Cells. Journal of Physical Chemistry C, 2007, 111, 11117-11122.	1.5	63
4724	Electronic Structure and Defect States of Transition Metal Doped Rutile TiO₂. Solid State Phenomena, 2007, 124-126, 787-790.	0.3	0
4725	Electronic properties of adsorbates on GaAs(001)-c(2Ã—8)âˆ•(2Ã—4). Journal of Chemical Physics, 2007, 127, 134705.	1.2	41
4726	Ab Initio Study with Transition State Theory (TST) for the Calculation of the Barrier Height of Migration Energy of Neutral Indium in Silicon. Solid State Phenomena, 2007, 124-126, 1681-1684.	0.3	0
4727	First Principles Study on Ideal Strength of Cu Multi-Shell Nano-Wire. Key Engineering Materials, 2007, 345-346, 919-924.	0.4	0
4728	First principles studies on the electronic structures of Li M x Fe 1-x PO 4 (M = Co, Ni and Rh). Chinese Physics B, 2007, 16, 3042-3045.	1.3	6
4729	Fundamental Interactions of Fe in Silicon: First-Principles Theory. Solid State Phenomena, 2008, 131-133, 233-240.	0.3	8
4730	Surface states and surface stability in half-metallic systems: the cases of zinc-blende-structure MnSb {111}A, {111}B and {001}. Journal of Physics Condensed Matter, 2007, 19, 315214.	0.7	5
4731	Electronic and optical properties of CaCO₃calcite, and excitons in Si@CaCO₃and CaCO₃@SiO₂core-shell quantum dots. Journal Physics D: Applied Physics, 2007, 40, 5747-5752.	1.3	36
4732	Structural and Thermodynamic Properties of Wurtzitic Boron Nitride from First-Principle Calculations. Communications in Theoretical Physics, 2007, 48, 925-929.	1.1	9
4733	Composition and Strain Dependence of the Piezoelectric Coefficients in Semiconductor Alloys. Materials Research Society Symposia Proceedings, 2007, 1017, 32.	0.1	0
4734	First-Principles Calculations of Grain Boundary-Surface for Various Grain Boundaries with Different Energies in Aluminum. Materials Science Forum, 2007, 551-552, 331-336.	0.3	3
4735	Reactivity of ideal and defected rutile TiO2(110) surface with oxygen. Advances in Applied Ceramics, 2007, 106, 95-100.	0.6	10

#	Article	IF	Citations
4736	Shear deformation in TiAl: Atomic dynamic and static simulations. Journal of Materials Research, 2007, 22, 1685-1693.	1.2	5
4737	Effect of cation ordering and pressure on spinel elasticity by ab initio simulation. American Mineralogist, 2007, 92, 174-178.	0.9	27
4738	First principles molecular dynamics of molten NaCl. Journal of Chemical Physics, 2007, 126, 124502.	1.2	44
4739	Dynamical stability of Fe-H in the Earth's mantle and core regions. Proceedings of the National Academy of Sciences of the United States of America, 2007, 104, 9168-9171.	3.3	49
4740	Atomic Structure of Faceted Σ3 CSL Grain Boundary in Silicon: HRTEM and <I>Ab-initio</I> Calculation. Materials Transactions, 2007, 48, 2585-2589.	0.4	36
4741	Application of the Reactivity Index to Propose Intra and Intermolecular Reactivity in Metal Cluster Interaction over Oxide Surface. Materials Transactions, 2007, 48, 2152-2158.	0.4	6
4742	Development of Interatomic Potential for Zr-Ni Amorphous Systems. Materials Transactions, 2007, 48, 1313-1321.	0.4	9
4743	First-Principles Calculation on the Stable Structure and Adhesive Strength of Ni/Fe(100) or Cu/Fe(100) Interfaces. Nippon Kinzoku Gakkaishi/Journal of the Japan Institute of Metals, 2007, 71, 1024-1031.	0.2	5
4744	First Principles Calculation of the Mechanism of Oxygen Precipitation in Czochralski Silicon Crystals (Effects of Heavy Boron Doping). Journal of Solid Mechanics and Materials Engineering, 2007, 1, 1165-1174.	0.5	3
4745	Native defects and impurities in Zn₃N₂: first-principle studies using gradient-correction approximation. Physica Scripta, 2007, T129, 340-344.	1.2	3
4746	CO oxidation reaction on Pt(111) studied by the dynamic Monte Carlo method including lateral interactions of adsorbates. Journal of Chemical Physics, 2007, 126, 044704.	1.2	44
4747	Investigation of the Impact of Simple Carbon Interstitial Formations on Thermal Neutron Scattering in Graphite. Nuclear Science and Engineering, 2007, 155, 449-462.	0.5	9
4748	Structural dependence of electric field gradients in<mml:math xmlns:mml="http://www.w3.org/1998/Math/MathML" display="inline"><mml:mrow><mml:mi mathvariant="normal">Pb</mml:mi><mml:mrow><mml:mo>(</mml:mo><mml:msub><mml:mi) Tj ETQq0 0 0 rgBT /Overlock 10 Tf 50 2 mathvariant="normal">O</mml:mi><mml:mn>3</mml:. Physical Review B, 2007, 76.	1.1	11
4749	First Principles Analysis of Formation Energy of Point Defects and Voids in Silicon Crystals during the Cooling Process of Czochralski Method (Dopant Type and Concentration Dependence). Journal of Solid Mechanics and Materials Engineering, 2007, 1, 1175-1185.	0.5	0
4750	Development of Interatomic Potential for Pb(Zr, Ti)O3 Based on Shell model. Journal of Solid Mechanics and Materials Engineering, 2007, 1, 1423-1431.	0.5	13
4751	Magnetism induced by single-atom defects in nanographites. Journal of Physics: Conference Series, 2007, 61, 1294-1298.	0.3	6
4752	Methanol and Methoxide Decomposition on Silver. Journal of Physical Chemistry C, 2007, 111, 9867-9876.	1.5	29
4753	Inhomogenities of the CDW vector at the (-201) surface of Quasi-1D blue bronze Rb0.3MoO3. Journal of Physics: Conference Series, 2007, 61, 140-146.	0.3	2

#	Article	IF	Citations
4754	Theoretical simulations of regular and defective aluminium nitride nanotubes. Journal of Physics: Conference Series, 2007, 93, 012005.	0.3	1
4755	Structure, ordering, and bonding of half antiperovskites: PbNi3/2S and BiPd3/2S. Progress in Solid State Chemistry, 2007, 35, 309-327.	3.9	47
4756	Atomic scale DFT simulations of point defects in uranium nitride. Journal of Physics Condensed Matter, 2007, 19, 106208.	0.7	44
4757	DFT Studies on the Four Polymorphs of Crystalline CL-20 and the Influences of Hydrostatic Pressure on Îµ-CL-20 Crystal. Journal of Physical Chemistry B, 2007, 111, 2090-2097.	1.2	147
4758	Structural transition of PETN-I to ferroelastic orthorhombic phase PETN-III at elevated pressures. Journal of Chemical Physics, 2007, 127, 094502.	1.2	18
4759	Intrinsic lattice thermal conductivity of semiconductors from first principles. Applied Physics Letters, 2007, 91, .	1.5	756
4760	First-Principles Simulations on the Nature of the Melting Line of Sodium. Physical Review Letters, 2007, 98, 055501.	2.9	35
4761	Electronic spin transitions in iron-bearing MgSiO3 perovskite. Earth and Planetary Science Letters, 2007, 253, 282-290.	1.8	93
4762	The effect of cation-ordering on the elastic properties of majorite: An ab initio study. Earth and Planetary Science Letters, 2007, 256, 28-35.	1.8	13
4763	Predicted elastic properties of the hydrous D phase at mantle pressures: Implications for the anisotropy of subducted slabs near 670-km discontinuity and in the lower mantle. Earth and Planetary Science Letters, 2007, 259, 283-296.	1.8	32
4764	The 10ÂÃ... phase at high pressure by first principles calculations and implications for the petrology of subduction zones. Earth and Planetary Science Letters, 2007, 260, 212-226.	1.8	28
4765	A computational study of ionic vacancies and diffusion in MgSiO3 perovskite and post-perovskite. Earth and Planetary Science Letters, 2007, 260, 201-211.	1.8	29
4766	Electronic excitations: Ab initio calculations of electronic spectra and application to zirconia ZrO2, titania TiO2 and cuprous oxide Cu2O. Computational Materials Science, 2007, 38, 482-493.	1.4	22
4767	First-principles elastic constants and electronic structure of beryllium chalcogenides BeS, BeSe and BeTe. Computational Materials Science, 2007, 38, 609-617.	1.4	89
4768	First-principles study of the tensile and fracture of the Al/TiN interface. Computational Materials Science, 2007, 38, 800-806.	1.4	35
4769	First-principles investigation of lattice constants and bowing parameter in ZnSxSe1â^'x alloys. Computational Materials Science, 2007, 39, 453-456.	1.4	19
4770	Development of bond-order potentials that can reproduce the elastic constants and melting point of silicon for classical molecular dynamics simulation. Computational Materials Science, 2007, 39, 457-464.	1.4	151
4771	Ab initio calculations of the oxygenâ€“vacancy dipoles and M centers in CaF2. Computational Materials Science, 2007, 39, 430-436.	1.4	11

#	Article	IF	Citations
4772	Prediction study of structural and elastic properties under pressure effect of CdX2O4 (X=Al,Ga,In) spinel oxides. Computational Materials Science, 2007, 39, 709-712.	1.4	50
4773	Ab initio study of the structural, elastic, electronic and optical properties of the antiperovskite SbNMg3. Computational Materials Science, 2007, 39, 803-807.	1.4	102
4774	Atomistic modeling of an Fe system with a small concentration of C. Computational Materials Science, 2007, 40, 119-129.	1.4	165
4775	Atomistic-continuum and ab initio estimation of the elastic moduli of single-walled carbon nanotubes. Computational Materials Science, 2007, 40, 147-158.	1.4	53
4776	Ab initio calculations of mechanical and thermodynamic properties for the B2-based AlRE. Computational Materials Science, 2007, 40, 226-233.	1.4	38
4777	First-principles investigation of structural, electronic and dynamical properties in ScAuSn alloy. Computational Materials Science, 2007, 41, 134-137.	1.4	1
4778	Atomic and electronic structure of perfect and defective PbZrO3 perovskite: Hybrid DFT calculations of cubic and orthorhombic phases. Computational Materials Science, 2007, 41, 195-201.	1.4	37
4779	Equilibrium isotopic fractionation in the kaolinite, quartz, water system: Prediction from first-principles density-functional theory. Geochimica Et Cosmochimica Acta, 2007, 71, 3170-3181.	1.6	180
4780	Ab initiomodeling of Li-B-H boron-chain alloys for hydrogen storage applications. Physical Review B, 2007, 76, .	1.1	13
4781	Model GW band structure ofInAsandGaAsin the wurtzite phase. Physical Review B, 2007, 75, .	1.1	136
4782	Ab initio analysis of sulfur tolerance of Ni, Cu, and Niâ€“Cu alloys for solid oxide fuel cells. Journal of Alloys and Compounds, 2007, 427, 25-29.	2.8	56
4783	Ab initio studies of the electronic structure of the quaternary system LiBC4N4. Journal of Alloys and Compounds, 2007, 427, 61-66.	2.8	6
4784	Electronic structure and stability of Mgâ€“Ce intermetallic compounds from first-principles calculations. Journal of Alloys and Compounds, 2007, 428, 316-321.	2.8	45
4785	On the ternary Laves phases {Sc,Ti}2M3Si (M=Cr, Mn, Fe, Co, Ni) with MgZn2-type. Journal of Alloys and Compounds, 2007, 429, 10-18.	2.8	18
4786	Thermodynamic modeling of the Baâ€“Niâ€“Ti system. Journal of Alloys and Compounds, 2007, 430, 188-193.	2.8	9
4787	Two polymorphs of Ba3Sn2P4: Single crystal and electronic structures. Journal of Alloys and Compounds, 2007, 430, 54-59.	2.8	7
4788	Structural phase transition in the Hfâ€“Ni system studied by ab initio calculation and ion beam mixing. Journal of Alloys and Compounds, 2007, 430, 142-148.	2.8	1
4789	Energetic evaluation of possible stacking structures of Li-intercalation in graphite using a first-principle pseudopotential calculation. Journal of Alloys and Compounds, 2007, 439, 258-267.	2.8	60

#	Article	IF	Citations
4790	A density functional study of carbon monoxide adsorption on (100) surface of Î³-uranium. Journal of Alloys and Compounds, 2007, 444-445, 356-362.	2.8	23
4791	In situ observation of the formation of TiC from the elements by neutron diffraction. Journal of Alloys and Compounds, 2007, 441, 374-380.	2.8	22
4792	Hydrogen-related defects in sodium alanate. Journal of Alloys and Compounds, 2007, 446-447, 459-461.	2.8	10
4793	Experimental and theoretical investigation of the cycle durability against CO and degradation mechanism of the LaNi5 hydrogen storage alloy. Journal of Alloys and Compounds, 2007, 446-447, 208-211.	2.8	18
4794	The importance of vibrations in modelling complex metal hydrides. Journal of Alloys and Compounds, 2007, 446-447, 455-458.	2.8	16
4795	A first-principles study of Sc-doped NaAlH4 for reversible hydrogen storage. Journal of Alloys and Compounds, 2007, 446-447, 267-270.	2.8	17
4796	Electronic structure and momentum density distribution of titanium dioxide. Journal of Alloys and Compounds, 2007, 440, 51-56.	2.8	4
4797	Stability and elastic properties of L12-(Al,Cu)3(Ti,Zr) phases: Ab initio calculations and experiments. Intermetallics, 2007, 15, 44-54.	1.8	75
4798	Moisture-induced embrittlement mechanism for (Ni,Fe)Ti alloys. Intermetallics, 2007, 15, 288-293.	1.8	3
4799	Thermoelectric properties of Sb-doped Mg2Si semiconductors. Intermetallics, 2007, 15, 1202-1207.	1.8	217
4800	Energetic and the electronic structural consideration of the 13th Group element (Ga and In) impurity doping to control the conductivity of BaSi2. Intermetallics, 2007, 15, 1291-1296.	1.8	29
4801	Reassessment of the Ceâ€“Ni binary system supported by key experiments and ab initio calculations. Intermetallics, 2007, 15, 1401-1408.	1.8	24
4802	First-principles investigation of the structural and electronic properties of Cu6â^'xNixSn5 (x=0, 1, 2) intermetallic compounds. Intermetallics, 2007, 15, 1471-1478.	1.8	103
4803	The establishment of the statistical-thermodynamic model of D81-structure and its application to Î±-Nb5Si3. Intermetallics, 2007, 15, 1558-1563.	1.8	12
4804	Structural distortion of -structured MnO and FeO. Solid State Communications, 2007, 142, 6-9.	0.9	19
4805	Correlation between composition and structure in boracites. Journal of Physics Condensed Matter, 2007, 19, 275207.	0.7	6
4806	Physisorption of nucleobases on graphene: Density-functional calculations. Physical Review B, 2007, 76, .	1.1	296
4807	The nature of ferroelectricity under pressure. Phase Transitions, 2007, 80, 385-413.	0.6	43

#	Article	IF	Citations
4808	Phase stability and elastic properties of Tan+1AlCn(n= 1â€“3) at high pressure and elevated temperature. Journal of Physics Condensed Matter, 2007, 19, 136207.	0.7	39
4809	Ensemble effects on ethylene dehydrogenation on PdAu(001) surfaces investigated with first-principles calculations and nudged-elastic-band simulations. Physical Review B, 2007, 75, .	1.1	38
4810	Structural stability of intermetallic compounds of Mg-Al-Ca alloy. Transactions of Nonferrous Metals Society of China, 2007, 17, 250-256.	1.7	25
4811	Ab initio study of magnetic interaction of Fe doped ZnO with intrinsic vacancies. Applied Physics Letters, 2007, 90, 212510.	1.5	43
4812	<I>Ab initio</I> calculations of relative stabilities of different structural arrangements in dioctahedral phyllosilicates. Clays and Clay Minerals, 2007, 55, 220-232.	0.6	24
4813	Atomistic mechanism of interfacial reaction and asymmetric growth kinetics in an immiscibleCuâ^'Rusystem at equilibrium. Physical Review B, 2007, 75, .	1.1	22
4814	Tuning LDA+U for electron localization and structure at oxygen vacancies in ceria. Journal of Chemical Physics, 2007, 127, 244704.	1.2	313
4815	Electron Transfer from a Diamond (100) Surface to an Atmospheric Water Adlayer:â€‰ A Quantum Mechanical Study. Journal of Physical Chemistry C, 2007, 111, 13804-13812.	1.5	30
4816	Effects of the wave function localization in AlInGaN quaternary alloys. Applied Physics Letters, 2007, 91, 061125.	1.5	38
4817	Magnetic state, magnetovolume effects, and atomic order in<mml:math xmlns:mml="http://www.w3.org/1998/Math/MathML" display="inline"><mml:mrow><mml:msub><mml:mi mathvariant="normal">Fe</mml:mi><mml:mn>65</mml:mn></mml:msub><mml:msub><mml:mi mathvariant="normal">Ni</mml:mi><mml:mn>35</mml:mn></mml:msub></mml:mrow></mml:math>Invar alloy: A first principles study. Physical Review B, 2007, 76, .	1.1	71
4818	Electronic and structural properties of oligophenylene ethynylenes on Au(111) surfaces. Journal of Chemical Physics, 2007, 126, 184706.	1.2	8
4819	A direct first principles study on the structure and electronic properties of BexZn1â^'xO. Applied Physics Letters, 2007, 91, 121121.	1.5	64
4820	Density functional perturbation theory for lattice dynamics with fully relativistic ultrasoft pseudopotentials: Application to fcc-Pt and fcc-Au. Physical Review B, 2007, 76, .	1.1	37
4821	Structure and Stability of Small Boron and Boron Oxide Clusters. Journal of Physical Chemistry A, 2007, 111, 6539-6551.	1.1	65
4822	Hybrid functionals applied to rare-earth oxides: The example of ceria. Physical Review B, 2007, 75, .	1.1	502
4823	First-principles study of thePtâ•CeO2(111)interface. Physical Review B, 2007, 76, .	1.1	82
4824	First-principles calculations of second- and third-order elastic constants for single crystals of arbitrary symmetry. Physical Review B, 2007, 75, .	1.1	210
4825	Ferroelectricity in Asymmetric Metal-Ferroelectric-Metal Heterostructures: A Combined First-Principlesâ€“Phenomenological Approach. Physical Review Letters, 2007, 98, 207601.	2.9	93

#	Article	IF	Citations
4826	Absorption of Atomic Oxygen into Subsurfaces of Pt(100) and Pt(111):â€‰ Density Functional Theory Study. Journal of Physical Chemistry C, 2007, 111, 9877-9883.	1.5	95
4827	Chemical Environment Effects on the Atomic Oxygen Absorption into Pt(111) Subsurfaces. Journal of Physical Chemistry C, 2007, 111, 17388-17396.	1.5	50
4828	Understanding the Dehydrogenation Mechanism of Tetrahydrocarbazole over Palladium Using a Combined Experimental and Density Functional Theory Approach. Journal of Physical Chemistry C, 2007, 111, 6434-6439.	1.5	30
4829	Ab initiosupercell calculations on aluminum-related defects in SiC. Physical Review B, 2007, 75, .	1.1	24
4830	Oxygen Reduction on LaMnO3-Based Cathode Materials in Solid Oxide Fuel Cells. Chemistry of Materials, 2007, 19, 1690-1699.	3.2	126
4831	First-principles calculations of hydrogen diffusion on rutile TiO2(110) surfaces. Journal of Chemical Physics, 2007, 127, 104709.	1.2	41
4832	Electronic Effects in CO Chemisorption on Ptâ^'Pb Intermetallic Surfaces:â€‰ A Theoretical Study. Journal of Physical Chemistry C, 2007, 111, 17357-17369.	1.5	19
4833	Bi-isonicotinic Acid on Anatase (101):â€‰ Insights from Theory. Journal of Physical Chemistry C, 2007, 111, 15034-15042.	1.5	42
4834	First-principles study of the dependence of ground-state structural properties on the dimensionality and size of ZnO nanostructures. Physical Review B, 2007, 76, .	1.1	55
4835	Spin and orbital magnetic response in metals: Susceptibility and NMR shifts. Physical Review B, 2007, 76, .	1.1	51
4836	Single-Walled MoTe2Nanotubes. Nano Letters, 2007, 7, 2987-2992.	4.5	37
4837	Effect of an Electric Field on the Adsorption of Metal Clusters on Boron-Doped Carbon Surfaces. Journal of Physical Chemistry C, 2007, 111, 14804-14812.	1.5	27
4838	Adsorption of Amine Compounds on the Au(111) Surface:â€‰ A Density Functional Study. Journal of Physical Chemistry C, 2007, 111, 13886-13891.	1.5	131
4839	A computational investigation of stoichiometric and calcium-deficient oxy- and hydroxy-apatites. Faraday Discussions, 2007, 134, 195-214.	1.6	65
4840	New Solids Based on B₁₂N₁₂ Fullerenes. Journal of Physical Chemistry C, 2007, 111, 13354-13360.	1.5	72
4841	Structure and bonding in boron carbide: The invincibility of imperfections. New Journal of Chemistry, 2007, 31, 473.	1.4	118
4842	Simulating ice nucleation, one molecule at a time, with the â€˜DFT microscopeâ€™. Faraday Discussions, 2007, 136, 287.	1.6	42
4843	Structural and vibrational properties of the 6H diamond: First-principles study. Diamond and Related Materials, 2007, 16, 21-28.	1.8	18

#	Article	IF	Citations
4844	Potassium intercalation in graphite: A van der Waals density-functional study. Physical Review B, 2007, 76, .	1.1	155
4845	Hydrogen Spillover on CeO₂/Pt: Enhanced Storage of Active Hydrogen. Chemistry of Materials, 2007, 19, 6430-6436.	3.2	97
4846	First-principles study of lattice dynamics and thermodynamic properties of<mml:math xmlns:mml="http://www.w3.org/1998/Math/MathML" display="inline"><mml:mrow><mml:mi mathvariant="normal">La</mml:mi><mml:msub><mml:mi mathvariant="normal">Cl</mml:mi><mml:mn>3</mml:mn></mml:msub></mml:mrow></mml:math>and<mml:math xmlns:mml="http://www.w3.org/1998/Math/MathML" display="inline"><mml:mrow><mml:mi mathvariant="normal">La</mml:mi><mml:msub><mml:mi mathvariant="normal">Br</mml:mi><mml:mn>	1.1	15
4847	Phonon band structure and interatomic force constants for bismuth: Crucial role of spin-orbit interaction. Physical Review B, 2007, 76, .	1.1	51
4848	Synthesis, Characterization, and Catalytic Properties of Î³-Al2O3-Supported Zirconium Hydrides through a Combined Use of Surface Organometallic Chemistry and Periodic Calculations. Organometallics, 2007, 26, 3329-3335.	1.1	33
4849	Lattice dynamics of CoO from first principles. Physical Review B, 2007, 75, .	1.1	65
4850	New Forcefields for Modeling Biomineralization Processes. Journal of Physical Chemistry C, 2007, 111, 11943-11951.	1.5	119
4851	First-principles calculation ofp-type alloy scattering inSi1âˆ’xGex. Physical Review B, 2007, 75, .	1.1	17
4852	Elastic and electronic properties of CoFe3N, RhFe3N, and IrFe3N from first principles. Applied Physics Letters, 2007, 90, 241901.	1.5	29
4853	Density functional theory study of flat and stepped NaCl(001). Physical Review B, 2007, 76, .	1.1	40
4854	Theoretical Analysis of the Nature of Hydrogen at the Electrochemical Interface Between Water and a Ni(111) Single-Crystal Electrode. Journal of the Electrochemical Society, 2007, 154, F55.	1.3	41
4855	Colossal Shear-Strength Enhancement of Low-Density CubicBC2Nby Nanoindentation. Physical Review Letters, 2007, 98, 135505.	2.9	72
4856	Elastic response of cubic crystals to biaxial strain: Analytic results and comparison to density functional theory for InAs. Physical Review B, 2007, 75, .	1.1	35
4857	The mechanism of chemical disordering in Cu3Au nanometre-sized systems. Nanotechnology, 2007, 18, 235706.	1.3	19
4858	Ab initiocalculations of third-order elastic constants and related properties for selected semiconductors. Physical Review B, 2007, 76, .	1.1	109
4859	Electronic structures and superconductivity of endohedrally doped<mml:math xmlns:mml="http://www.w3.org/1998/Math/MathML" display="inline"><mml:msub><mml:mi mathvariant="normal">C</mml:mi><mml:mn>28</mml:mn></mml:msub></mml:math>solids from first principles. Physical Review B, 2007, 76, .	1.1	12
4860	Clean and metal-doped bundles of boron-carbide nanotubes: A density functional study. Physical Review B, 2007, 76, .	1.1	4
4861	Identification of positively charged carbon antisite-vacancy pairs in4Hâˆ’SiC. Physical Review B, 2007, 75, .	1.1	39

#	Article	IF	Citations
4862	First-principles study of the wurtzite-to-rocksalt phase transition in zinc oxide. Journal of Physics Condensed Matter, 2007, 19, 266207.	0.7	25
4863	Optical properties of real surfaces: Local-field effects at oxidizedSi(100)(2Ã—2)computed with an efficient numerical scheme. Physical Review B, 2007, 75, .	1.1	10
4864	Ab Initio Equation of State of an Organic Molecular Crystal:Â 1,1-Diamino-2,2-dinitroethylene. Journal of Physical Chemistry A, 2007, 111, 1721-1725.	1.1	54
4865	Electronic and vibrational properties of nickel sulfides from first principles. Journal of Chemical Physics, 2007, 127, 214705.	1.2	98
4866	Phonon dispersion and GrÃ¼neisen parameters of zinc dicyanide and cadmium dicyanide from first principles: Origin of negative thermal expansion. Physical Review B, 2007, 76, .	1.1	62
4867	Surface functionalization through adsorption of organic molecules. Journal of Physics Condensed Matter, 2007, 19, 305018.	0.7	6
4868	Density functional studies of small silicon clusters adsorbed on graphite (0001) and diamond (100). Physical Review B, 2007, 76, .	1.1	12
4869	Adsorption of As(OH)₃ on the (001) Surface of FeS₂ Pyrite:â€‰ A Quantum-mechanical DFT Study. Journal of Physical Chemistry C, 2007, 111, 11390-11396.	1.5	47
4870	Influence of aggregation, defects, and contaminant oxygen on water dissociation at Cu(110) surface: A theoretical study. Journal of Chemical Physics, 2007, 127, 104707.	1.2	35
4871	First-Principles Study of Equilibrium Properties and Electronic Structures of GeTeâ€“Sb2Te3Pseudobinary Crystalline Films. Japanese Journal of Applied Physics, 2007, 46, 4215-4219.	0.8	3
4872	Accurate heat of formation for fully hydrided<b />LaNi5 via the all-electron full-potential linearized augmented plane wave approach. Journal of Applied Physics, 2007, 102, .	1.1	8
4873	Ground-state properties of multivalent manganese oxides: Density functional and hybrid density functional calculations. Physical Review B, 2007, 75, .	1.1	288
4874	Modeling ofCeO2,Ce2O3, andCeO2â^'xin theLDA+Uformalism. Physical Review B, 2007, 75, .	1.1	333
4875	On the Promoting Role of Ag in Selective Hydrogenation Reactions over Pdâ^'Ag Bimetallic Catalysts:â€‰ A Theoretical Study. Journal of Physical Chemistry C, 2007, 111, 6852-6856.	1.5	121
4876	Ab initiostudy of electronic and magnetic properties of the C-codopedGa1â^'xMnxN(101Â¯0)surface. Physical Review B, 2007, 75, .	1.1	20
4877	Spatial distribution and magnetism in poly-Cr-doped GaN from first principles. Physical Review B, 2007, 75, .	1.1	38
4878	Ab initiosimulations of the electrochemical activation of water. Molecular Simulation, 2007, 33, 429-436.	0.9	21
4879	High-pressure phase transition observed in barium hydride. Journal of Applied Physics, 2007, 102, 043520.	1.1	32

#	Article	IF	Citations
4880	First-principles calculations of phonon and thermodynamic properties in the boron-alkaline earth metal binary systems: B-Ca, B-Sr, and B-Ba. Physical Review B, 2007, 75, .	1.1	72
4881	Ab Initiocalculations of phonon splitting in antiferromagneticZnCr2O4. Physical Review B, 2007, 75, .	1.1	15
4882	Ab initiolattice dynamics of zinc-blende Ga_xIn_{1â^'x}N alloys. Journal of Physics Condensed Matter, 2007, 19, 486209.	0.7	22
4883	Synthesis of Molecular Adducts of Beryllium, Boron, and Gallium Cyanides: Theoretical and Experimental Correlations between Solid-State and Molecular Analogues. Chemistry of Materials, 2007, 19, 5890-5901.	3.2	24
4884	Diamond-like BC₃as a superhard conductor identified by ideal strength calculations. Journal of Physics Condensed Matter, 2007, 19, 346223.	0.7	10
4885	Theoretical approaches in adsorption: alkali adatom investigations. Journal of Physics Condensed Matter, 2007, 19, 305005.	0.7	16
4886	First-Principles Prediction of High-Pressure Phase of CaC 6. Chinese Physics Letters, 2007, 24, 1668-1670.	1.3	6
4887	Theoretical hardness of the cubic BC2N. Diamond and Related Materials, 2007, 16, 526-530.	1.8	36
4888	Dopant position in Ti-doped high-temperature phase Ta2O5: First principles study. Applied Physics Letters, 2007, 91, .	1.5	9
4889	First-principles calculations of elastic properties of Cu-Sn crystalline phases. , 2007, , .		0
4890	Ab InitioStudy for Site Symmetry of Phosphorus-Doped Diamond. Japanese Journal of Applied Physics, 2007, 46, 315-317.	0.8	9
4891	Effect of structure, surface passivation, and doping on the electronic properties of Ge nanowires: A first-principles study. Physical Review B, 2007, 76, .	1.1	40
4892	Supercell and cluster density functional calculations of the thermal stability of the divacancy in germanium. Physical Review B, 2007, 75, .	1.1	15
4893	Structural, electronic and optical properties of spinel oxides: cadmium gallate and cadmium indate. EPJ Applied Physics, 2007, 38, 203-210.	0.3	18
4894	Potential energy of hydrogen atom motion on Pd(111) surface and in subsurface: A first principles calculation. Journal of Applied Physics, 2007, 101, 123530.	1.1	48
4895	Redox properties of CeO2â€“MO2 (M=Ti, Zr, Hf, or Th) solid solutions from first principles calculations. Applied Physics Letters, 2007, 90, 031909.	1.5	87
4896	Multiscale Simulations of High Performance Capacitors and Nanoelectronic Devices. , 2007, , .		1
4897	Route to a correct description of the fundamental properties of cubic InN. Applied Physics Letters, 2007, 91, .	1.5	13

#	Article	IF	Citations
4898	Impact of Structure Relaxation on the Ultimate Performance of a Small Diameter, n-Type $langle 110 angle$ Si-Nanowire MOSFET. IEEE Nanotechnology Magazine, 2007, 6, 225-229.	1.1	6
4899	Pair potential approach for metal/Al2O3interface. Journal of Physics Condensed Matter, 2007, 19, 196216.	0.7	13
4900	First-principles approach to the electronic structure in the pentacene thin film polymorph. Journal of Physics Condensed Matter, 2007, 19, 106209.	0.7	17
4901	First Principles Calculations of the Formation Energy of the Neutral Vacancy in Germanium. Solid State Phenomena, 0, 131-133, 241-246.	0.3	9
4902	Core structures and kink migrations of partial dislocations in 4Hâ€“SiC. Faraday Discussions, 2007, 134, 353-367.	1.6	28
4903	Density functional theory study of the clean and hydrated hematite(11Â¯02)surfaces. Physical Review B, 2007, 75, .	1.1	60
4904	Microscopic models of PdZn alloy catalysts: structure and reactivity in methanol decomposition. Physical Chemistry Chemical Physics, 2007, 9, 3470-3482.	1.3	96
4905	Density Functional Theory Study of CO Adsorption and Dissociation on Molybdenum(100). Journal of Physical Chemistry C, 2007, 111, 13473-13480.	1.5	16
4906	Melting curve of tantalum from first principles. Physical Review B, 2007, 75, .	1.1	99
4907	Surface Energy Estimation of Catalytically Relevant fcc Transition Metals Using DFT Calculations on Nanorods. Journal of Physical Chemistry C, 2007, 111, 4998-5005.	1.5	36
4908	A computational study of H2dissociation on silver surfaces: The effect of oxygen in the added row structure of Ag(110). Physical Chemistry Chemical Physics, 2007, 9, 1247-1254.	1.3	43
4909	CaCl2-type high-pressure phase of magnesium hydride predicted byab initiophonon calculations. Physical Review B, 2007, 75, .	1.1	33
4910	Density functional simulations of silicon-containing point defects in diamond. Physical Review B, 2007, 76, .	1.1	58
4911	Ab Initiothermodynamic and elastic properties of alkaline-earth metals and their hydrides. Physical Review B, 2007, 76, .	1.1	99
4912	Raman study of oxygen reduced and re-oxidized strontium titanate. Physical Review B, 2007, 76, .	1.1	82
4913	Atomic configurations of Pd atoms in PdAu(111) bimetallic surfaces investigated using the first-principles pseudopotential plane wave approach. Physical Review B, 2007, 75, .	1.1	72
4914	First-principles calculations of solid-state17O and29Si NMR spectra of Mg2SiO4polymorphs. Physical Chemistry Chemical Physics, 2007, 9, 1587-1598.	1.3	65
4915	Electronic structure and ferromagnetic properties of Cu-doped AlN from first principles. Journal of Applied Physics, 2007, 101, 113918.	1.1	42

#	Article	IF	Citations
4916	The broken-symmetry phase of solid hydrogen: evidence from infrared and Raman active vibrons. Journal of Physics Condensed Matter, 2007, 19, 425237.	0.7	6
4917	A first-principles study of electronâ€“phonon coupling in electron-doped LiH. Journal of Physics Condensed Matter, 2007, 19, 425218.	0.7	14
4918	Energetics and kinetics of vacancy diffusion and aggregation in shocked aluminium via orbital-free density functional theory. Physical Chemistry Chemical Physics, 2007, 9, 4951.	1.3	65
4919	Density Functional Theory and Kinetic Studies of Methanation on Iron Surface. Journal of Physical Chemistry C, 2007, 111, 11012-11025.	1.5	50
4920	Determination of the Cd-Bearing Phases in Municipal Solid Waste and Biomass Single Fly Ash Particles Using SR-Î¼XRF Spectroscopy. Analytical Chemistry, 2007, 79, 6496-6506.	3.2	16
4921	Facet Stability in Oxygen-Induced Nanofaceting of Re(123Ì…1). ACS Nano, 2007, 1, 449-455.	7.3	30
4922	Studying Reduction in Solid Oxide Fuel Cell Activity with Density Functional Theoryâˆ’ Effects of Hydrogen Sulfide Adsorption on Nickel Anode Surface. Journal of Physical Chemistry C, 2007, 111, 14457-14468.	1.5	30
4923	Chemisorption of Pentacene on Si(111)-7 Ã— 7 Studied via Scanning Tunneling Microscopy and Density Functional Theory. Journal of Physical Chemistry C, 2007, 111, 4285-4293.	1.5	12
4924	Structure of Mixed Carboxylic Acid Terminated Self-Assembled Monolayers:â€‰ Experimental and Theoretical Investigation. Journal of Physical Chemistry C, 2007, 111, 4294-4304.	1.5	41
4925	Crystal Structure and Electron Density of Tantalum Oxynitride, a Visible Light Responsive Photocatalyst. Chemistry of Materials, 2007, 19, 588-593.	3.2	90
4926	Ab initiostudy of electron affinity variation induced by organic molecule adsorption on the silicon (001) surface. Physical Review B, 2007, 76, .	1.1	32
4927	Surface Energy and Growth Mechanism of Î²-Tetragonal Boron Crystal. Journal of Physical Chemistry C, 2007, 111, 10394-10397.	1.5	19
4928	Charge Transport Parameters of the Pentathienoacene Crystal. Journal of the American Chemical Society, 2007, 129, 13072-13081.	6.6	153
4929	Nature of adsorption on TiC(111) investigated with density-functional calculations. Physical Review B, 2007, 75, .	1.1	59
4930	TUNABLE ELECTRIC CONDUCTIVITIES OF Au-DOPED BORON NITRIDE NANOTUBES. Nano, 2007, 02, 367-372.	0.5	3
4931	Experimental and Theoretical Surface Core Level Shift Study of the S-Rh(100) Local Environment. Journal of Physical Chemistry C, 2007, 111, 4003-4013.	1.5	7
4932	The Role of Surface Energy in the Growth of Boron Crystals. Journal of Physical Chemistry C, 2007, 111, 688-692.	1.5	35
4933	Comparison between in situ Total Internal Reflection Vibrational Spectroscopy of an Adsorbed Collector and Spectra Calculated by Ab Initio Density Functional Theory Methods. Journal of Physical Chemistry C, 2007, 111, 9299-9304.	1.5	9

#	Article	IF	Citations
4934	Hydrogen Storage Property on Nickel-Atom-Dispersed Organosilica Nanotubes. Chemistry of Materials, 2007, 19, 135-137.	3.2	8
4935	Polymerization at the Alkylthiolateâ"Au(111) Interface. Journal of Physical Chemistry B, 2007, 111, 3325-3327.	1.2	73
4936	Electronic structures of CuPc on a Ag(110) surface. Journal of Physics Condensed Matter, 2007, 19, 136002.	0.7	21
4937	Universal Phenomena of CO Adsorption on Gold Surfaces with Low-Coordinated Sites. Journal of Physical Chemistry C, 2007, 111, 445-451.	1.5	116
4938	Structural, Electronic, and Optical Properties of Oxygen Defects in Zn3N2. Journal of Physical Chemistry B, 2007, 111, 3379-3383.	1.2	27
4939	Ab initiostudy of oxygen adsorption on the Ti(0001) surface. Journal of Physics Condensed Matter, 2007, 19, 226004.	0.7	21
4940	Origin of the photoactivity in boron-doped anatase and rutile<mml:math xmlns:mml="http://www.w3.org/1998/Math/MathML" display="inline"><mml:mrow><mml:mi mathvariant="normal">Ti</mml:mi><mml:msub><mml:mi mathvariant="normal">O</mml:mi><mml:mn>2</mml:mn></mml:msub></mml:mrow></mml:math>calculated from first principles. Physical Review B, 2007, 76, .	1.1	107
4941	Thermodynamic Stability of Boron:Â The Role of Defects and Zero Point Motion. Journal of the American Chemical Society, 2007, 129, 2458-2465.	6.6	169
4942	Spin Polarization Study of Benzene Molecule Adsorbed on Fe(100) Surface with Metastable-Atom Deexcitation Spectroscopy and Density Functional Calculations. Journal of Physical Chemistry C, 2007, 111, 15289-15298.	1.5	20
4943	Static and Optical Transverse and Longitudinal Screened Polarizabilities of Boron Nitride Nanotubes. Journal of Physical Chemistry C, 2007, 111, 3285-3289.	1.5	17
4944	Vanadium Oxides on Aluminum Oxide Supports. 3. Metastable Î⁹-Al2O3(001) Compared to Î±-Al2O3(0001). Journal of Physical Chemistry C, 2007, 111, 5141-5153.	1.5	27
4945	Infrared Spectroscopic Study of the Adsorption of HCN by Î³-Al2O3:â€‰ Competition with Triethylenediamine for Adsorption Sites. Journal of Physical Chemistry C, 2007, 111, 5416-5425.	1.5	24
4946	17O and29Si NMR Parameters of MgSiO3Phases from High-Resolution Solid-State NMR Spectroscopy and First-Principles Calculations. Journal of the American Chemical Society, 2007, 129, 13213-13224.	6.6	104
4947	Pair-Hopping Characteristic of Lithium Diffusive Motion in Li-Doped Î²-Phase Manganese Phthalocyanine. Journal of Physical Chemistry B, 2007, 111, 10064-10068.	1.2	3
4948	Structural Transformation of (110) Ultrathin Films of Tetragonal Zirconia Induced by Polarity. Journal of Physical Chemistry C, 2007, 111, 8314-8320.	1.5	3
4949	Disorder-induced Raman scattering in rhenium trioxide (ReO3). Journal of Physics Condensed Matter, 2007, 19, 226206.	0.7	21
4950	A First-Principles Study of the Electronic and Structural Properties of Î³-TaON. Journal of Physical Chemistry A, 2007, 111, 2745-2749.	1.1	25
4951	An Efficient LDA+UBased Tight Binding Approachâ€. Journal of Physical Chemistry A, 2007, 111, 5665-5670.	1.1	15

#	Article	IF	Citations
4952	Structure and dynamics oflâ˜'Ge: Neutron scattering experiments andab initiomolecular dynamics simulations. Physical Review B, 2007, 75, .	1.1	21
4953	Density Functional Theory Study of CO and Hydrogen Co-adsorption on the Fe(111) Surface. Journal of Physical Chemistry C, 2007, 111, 4305-4314.	1.5	26
4954	Highly localized quasiatomic minimal basis orbitals for Mo fromab initiocalculations. Physical Review B, 2007, 76, .	1.1	41
4955	Interaction of NO with RuO₂(110) Surface:â€‰ A First Principles Study. Journal of Physical Chemistry C, 2007, 111, 12361-12368.	1.5	17
4956	Formation enthalpies of monovacancies in aluminum and gold under the condition of intense laser irradiation. Physical Review B, 2007, 75, .	1.1	31
4957	First-principles calculations of Cs adsorbed on Cu(001): Quantum size effect in surface energetics and surface chemical reactivities. Physical Review B, 2007, 75, .	1.1	17
4958	Crystal Structure and Electron Density of Î±-Silicon Nitride:â€‰ Experimental and Theoretical Evidence for the Covalent Bonding and Charge Transfer. Journal of Physical Chemistry B, 2007, 111, 3609-3613.	1.2	33
4959	Ab Initio Molecular Dynamics Study of H₂S Dissociation on the Fe(110) Surface. Journal of Physical Chemistry C, 2007, 111, 16372-16378.	1.5	24
4960	An Unexpected Pathway for the Catalytic Oxidation of Methylidyne on Rh{111} as a Route to Syngas. Journal of the American Chemical Society, 2007, 129, 1751-1759.	6.6	56
4961	First-Principles Study of C Adsorption and Diffusion on the Surfaces and in the Subsurfaces of Nonreconstructed and Reconstructed Ni(100). Journal of Physical Chemistry C, 2007, 111, 3447-3453.	1.5	14
4962	Integrated Experimentalâ˜'Theoretical Investigation of the Naâ˜'Liâ˜'Alâ˜'H System. Inorganic Chemistry, 2007, 46, 1401-1409.	1.9	16
4963	Structural distortions inAlF3: A test for density-functional methods. Physical Review B, 2007, 75, .	1.1	3
4964	Enantiospecific Adsorption of Alanine on the Chiral Cu{531} Surface. Journal of Physical Chemistry C, 2007, 111, 8331-8336.	1.5	63
4965	Photoinduced Formation of N2Molecules in Ammonium Compounds. Journal of Physical Chemistry A, 2007, 111, 9662-9669.	1.1	11
4966	Mechanisms of Dye Incorporation into Potassium Sulfate: Computational and Experimental Studies. Journal of Physical Chemistry C, 2007, 111, 9283-9289.	1.5	8
4967	Organic Bonding to Silicon via a Carbonyl Group:Â New Insights from Atomic-Scale Images. Journal of the American Chemical Society, 2007, 129, 11402-11407.	6.6	26
4968	Electrodeposition of Pt onto RuO₂(110) Single-Crystal Surface. Journal of Physical Chemistry C, 2007, 111, 15306-15311.	1.5	13
4969	First-principles study of cation and hydrogen arrangements in the Li-Mg-N-H hydrogen storage system. Physical Review B, 2007, 76, .	1.1	23

#	Article	IF	Citations
4970	Optical Absorption Spectra and Polarizabilities of Silicon Carbide Nanotubes:â€‰ A First Principles Study. Journal of Physical Chemistry C, 2007, 111, 18864-18870.	1.5	11
4971	Geometric and Electronic Structures of Hydrogen-Stabilized Silicon Nitride Nanosheets and Nanotubes. Journal of Physical Chemistry C, 2007, 111, 16840-16845.	1.5	10
4972	First-principles calculations of structure and high pressure phase transition in gallium nitride. Chinese Physics B, 2007, 16, 3772-3776.	1.3	6
4973	Theoretical Studies of the Formation and Reactivity of C2Hydrocarbon Species on the Fe(100) Surface. Journal of Physical Chemistry C, 2007, 111, 13149-13162.	1.5	41
4974	A Systematic Density Functional Study of Molecular Oxygen Adsorption and Dissociation on the (001) Surface of Group IVâ^'VI Transition Metal Carbides. Journal of Physical Chemistry C, 2007, 111, 16982-16989.	1.5	60
4975	Novel Superconductivity in MetallicSnH4under High Pressure. Physical Review Letters, 2007, 98, 117004.	2.9	195
4976	Equation of state of solid nickel aluminide. Physical Review B, 2007, 76, .	1.1	8
4977	First-Principles Prediction of Equilibrium Potentials for Water Activation by a Series of Metals. Journal of the Electrochemical Society, 2007, 154, F217.	1.3	30
4978	Binding Formation of 12-Hydroxydodecanoic Acid on Si(001)-(2 Ã— 2). Journal of Physical Chemistry C, 2007, 111, 4375-4378.	1.5	3
4979	First-Principles Study of Electronic Structures of MnX(X=As, Sb, or Bi): Fully Relativistic Full-Potential Calculations. Japanese Journal of Applied Physics, 2007, 46, 3455-3462.	0.8	13
4980	Reactions of Hydroxyl on the Topmost Layer of Ag(111):â€‰ A Density Functional Theory Study. Journal of Physical Chemistry C, 2007, 111, 1333-1341.	1.5	7
4981	Influence of F centres on structural and electronic properties of AlN single-walled nanotubes. Journal of Physics Condensed Matter, 2007, 19, 395021.	0.7	29
4982	Possible Dual-Charge-Carrier Mechanism of Surface Conduction on Î³-Alumina. Journal of Physical Chemistry C, 2007, 111, 5506-5513.	1.5	11
4983	First-principles calculations of the band gap ofHfxSi1â^'xO2andZrxSi1â^'xO2alloys. Physical Review B, 2007, 75, .	1.1	7
4984	Elementary energy bands concept for IVâ€“VI crystals with phase transitions. Phase Transitions, 2007, 80, 39-46.	0.6	1
4985	First-Principles Design of Well-Ordered Silica Nanotubes from Silica Monolayers and Nanorings. Journal of Physical Chemistry C, 2007, 111, 9652-9657.	1.5	10
4986	Methanol Adsorption and Dissociation on TiO2(110) from First Principles Calculations. Journal of Physical Chemistry C, 2007, 111, 10023-10028.	1.5	106
4987	Reassessment of the Alâ€“Mn system and a thermodynamic description of the Alâ€“Mgâ€“Mn system. International Journal of Materials Research, 2007, 98, 855-871.	0.1	106

#	Article	IF	Citations
4988	Adsorption and Decomposition Pathways of Vinyl Phosphonic and Ethanoic Acids on the Al(111) Surface:â€‰ a Density Functional Analysis. Journal of Physical Chemistry C, 2007, 111, 7366-7375.	1.5	14
4989	Polymorphism in Bismuth Stannate:â€‰ A First-Principles Study. Chemistry of Materials, 2007, 19, 5158-5164.	3.2	48
4990	Adsorption and Dissociation of H₂O on a W(111) Surface:â€‰ A Computational Study. Journal of Physical Chemistry C, 2007, 111, 17333-17339.	1.5	29
4991	Adsorption of Al, O, Hf, Y, Pt, and S Atoms on Î±-Al2O3(0001). Journal of Physical Chemistry C, 2007, 111, 7105-7126.	1.5	101
4992	Structural stability of thalliumâ€“V compounds. Journal of Physics Condensed Matter, 2007, 19, 106221.	0.7	34
4993	Chemisorption of 3-Aminopropyltrimethoxysilane on Si(001)-(2 Ã— 2). Journal of Physical Chemistry C, 2007, 111, 15020-15025.	1.5	10
4994	First-principles investigations of Co- and Fe-doped SnO2. Journal of Applied Physics, 2007, 101, 09H104.	1.1	35
4995	Theoretical investigations of phonon intrinsic mean-free path in zinc-blende and wurtzite AlN. Physical Review B, 2007, 76, .	1.1	26
4996	Theoretical study of<mml:math xmlns:mml="http://www.w3.org/1998/Math/MathML" display="inline"><mml:mrow><mml:mi mathvariant="normal">Ce</mml:mi><mml:msub><mml:mi mathvariant="normal">O</mml:mi><mml:mn>2</mml:mn></mml:msub></mml:mrow></mml:math>doped with tetravalent ions. Physical Review B, 2007, 76, .	1.1	61
4997	Electron-phonon interaction in graphite intercalation compounds. Physical Review B, 2007, 76, .	1.1	59
4998	Elastic Properties of Rutile TiO ₂ at High Temperature. Chinese Physics Letters, 2007, 24, 2642-2645.	1.3	14
4999	First-Principle Study of Sulfur Adsorption on Ir(100) Surface. Materials Science Forum, 2007, 561-565, 2435-2438.	0.3	1
5000	Band-structure anomalies of the chalcopyrite semiconductorsCuGaX2versusAgGaX2(X=Sand Se) and their alloys. Physical Review B, 2007, 75, .	1.1	132
5001	Electrochemical Reduction of Oxygen on Gold Surfaces:â€‰ A Density Functional Theory Study of Intermediates and Reaction Paths. Journal of Physical Chemistry C, 2007, 111, 2607-2613.	1.5	79
5002	Ab initiocalculations of the electronic structure and linear optical properties, including self-energy effects, for paraelectric SbSI. Journal of Physics Condensed Matter, 2007, 19, 116207.	0.7	14
5003	Adsorption of gold on TiC(001): Auâ€“C interactions and charge polarization. Journal of Chemical Physics, 2007, 127, 211102.	1.2	66
5004	On the structural and energetic properties of the hydrogen absorber Li2Mg(NH)2. Applied Physics Letters, 2007, 91, 091924.	1.5	14
5005	Density functional calculations on the intricacies of MoirÃ© patterns on graphite. Physical Review B, 2007, 75, .	1.1	125

#	Article	IF	Citations
5006	Adsorption Configurations and Energetics of BClx(x= 0â^'3) on TiO2Anatase (101) and Rutile (110) Surfacesâ€. Journal of Physical Chemistry A, 2007, 111, 6746-6754.	1.1	23
5007	First-Principles Study of NO[sub x] and SO[sub 2] Adsorption onto SnO[sub 2](110). Journal of the Electrochemical Society, 2007, 154, H675.	1.3	45
5008	Direct Methane-to-Methanol Conversion:â€‰ Insight from First-Principles Calculations. Journal of Physical Chemistry C, 2007, 111, 17015-17019.	1.5	9
5009	Effects Due to Interadsorbate Interactions on the Dipeptide/TiO2Surface Binding Mechanism Investigated by Molecular Dynamics Simulations. Journal of Physical Chemistry C, 2007, 111, 7765-7771.	1.5	38
5010	Structural and optical properties of single crystal Zn1â^'xMgxO nanorodsâ€"Experimental and theoretical studies. Journal of Applied Physics, 2007, 101, 033502.	1.1	39
5011	Existence of the Naâ^'HÎ´-Â·Â·Â·HÎ´â€˜+â^'O Dihydrogen Bond in the Hydrogenation Process by Na2O:â€‰ A First-Principles Identification. Journal of Physical Chemistry C, 2007, 111, 5064-5068.	1.5	5
5012	Properties of B and P doped Ge nanowires. Applied Physics Letters, 2007, 90, 263103.	1.5	35
5013	Factors Controlling the Interaction of CO₂ with Transition Metal Surfaces. Journal of Physical Chemistry C, 2007, 111, 16934-16940.	1.5	152
5014	Structural Characterization of Aldehyde-Terminated Self-Assembled Monolayers. Journal of Physical Chemistry A, 2007, 111, 12727-12739.	1.1	16
5015	Comparison of the electronic structures of four crystalline phases of<mml:math xmlns:mml="http://www.w3.org/1998/Math/MathML" display="inline"><mml:mrow><mml:mi mathvariant="normal">Fe</mml:mi><mml:mi mathvariant="normal">P</mml:mi><mml:msub><mml:mi mathvariant="normal">O</mml:mi><mml:mn>4</mml:mn></mml:msub></mml:mrow></mml:math>. Physical Review B, 2007, 76, .	1.1	13
5016	First-Principles Investigation of Stability and Structural Properties of the BaTiO3(110) Polar Surface. Journal of Physical Chemistry C, 2007, 111, 6343-6349.	1.5	32
5017	Structural, Energetic, and Vibrational Properties of NOxAdsorption on Agn,n= 1â^'8. Journal of Physical Chemistry A, 2007, 111, 6062-6067.	1.1	43
5018	Electronic Structure Investigation of Surfaceâ^'Adsorbate and Adsorbateâ^'Adsorbate Interactions in Multilayers of CH4on MgO(100). Journal of Physical Chemistry C, 2007, 111, 966-976.	1.5	14
5019	Ab initiostudy of dihydrogen binding in metal-decorated polyacetylene for hydrogen storage. Physical Review B, 2007, 76, .	1.1	104
5020	Accurate single-particle determination of the band gap in silicon nanowires. Physical Review B, 2007, 76, .	1.1	39
5021	Theoretical Investigations of Oxygen-17 NMR Chemical Shifts to Discriminate among Helical Forms. Journal of Physical Chemistry A, 2007, 111, 13099-13105.	1.1	6
5022	Beyond One-Electron Reaction in Li Cathode Materials: Â Designing Li2MnxFe1-xSiO4. Chemistry of Materials, 2007, 19, 3633-3640.	3.2	245
5023	Structural and Electronic Properties of Oxygen-Adsorbed Diamond (100) Surface. Journal of Physical Chemistry C, 2007, 111, 855-859.	1.5	13

#	Article	IF	Citations
5024	Surface reactivities of (111), (100), and (110) planes of c-BN: A quantum mechanical approach. Diamond and Related Materials, 2007, 16, 118-123.	1.8	22
5025	Magnetic properties of vacancies in a graphitic boron nitride sheet by first-principles pseudopotential calculations. Physical Review B, 2007, 75, .	1.1	184
5026	Structural, elastic, and electronic properties of SiC, BN, and BeO nanotubes. Physical Review B, 2007, 76, .	1.1	211
5027	Equation of state and optical properties of warm dense helium. Physical Review B, 2007, 76, .	1.1	62
5028	Self-Interaction and Strong Correlation in DFTBâ€. Journal of Physical Chemistry A, 2007, 111, 5671-5677.	1.1	52
5029	Effect of boron on the superconducting transition of heavily doped diamond. Diamond and Related Materials, 2007, 16, 353-358.	1.8	11
5030	Formation of lithium clusters and their effects on conductivity in diamond: A density functional theory study. Diamond and Related Materials, 2007, 16, 840-844.	1.8	5
5031	Transition-metal doping of semiconducting chalcopyrites: half-metallicity and magnetism. Journal of Physics Condensed Matter, 2007, 19, 016210.	0.7	7
5032	First-principles study of the lattice dynamics, thermodynamic properties and electron-phonon coupling of<mml:math xmlns:mml="http://www.w3.org/1998/Math/MathML" display="inline"><mml:mrow><mml:mi mathvariant="normal">Y</mml:mi><mml:msub><mml:mi mathvariant="normal">B</mml:mi><mml:mn>6</mml:mn></mml:msub></mml:mrow></mml:math>. Physical Review B, 2007, 76, .	1.1	42
5033	High-pressure–temperature phase relations of<mml:math xmlns:mml="http://www.w3.org/1998/Math/MathML" display="inline"><mml:mrow><mml:mi mathvariant="normal">Mg</mml:mi><mml:mi mathvariant="normal">Ge</mml:mi><mml:msub><mml:mi mathvariant="normal">O</mml:mi><mml:mn>3</mml:mn></mml:msub></mml:mrow></mml:math>: First-principles calculations. Physical Review B, 2007, 76, .	1.1	15
5034	Electronic structure and properties of the Fermi surface of the superconductor LaOFeP. Physical Review B, 2007, 75, .	1.1	249
5035	Computational investigation of the Bi lone-pairs in monoclinic bismuth triborate BiB3O6. Physical Chemistry Chemical Physics, 2007, 9, 2094.	1.3	20
5036	Optical and magneto-optical properties of ferromagnetic full-Heusler films: Experiments and first-principles calculations. Physical Review B, 2007, 76, .	1.1	18
5037	Oxygen vacancies and induced changes in the electronic and magnetic structures ofLa0.66Sr0.33MnO3: A combinedab initioand photoemission study. Physical Review B, 2007, 75, .	1.1	78
5038	Competition between magnetic structures in the Fe rich fcc FeNi alloys. Physical Review B, 2007, 76, .	1.1	119
5039	OxygenK-edge XANES of germanates investigated using first-principles calculations. Physical Review B, 2007, 75, .	1.1	43
5040	First-principles study of vacancy formation in hydroxyapatite. Physical Review B, 2007, 75, .	1.1	119
5041	Ab initiostudy of the thermodynamic properties of nonmagnetic elementary fcc metals: Exchange-correlation-related error bars and chemical trends. Physical Review B, 2007, 76, .	1.1	218

#	Article	IF	Citations
5042	Polarization reduction in half-metallic Heusler alloys: the effect of point defects and interfaces with semiconductors. Journal of Physics Condensed Matter, 2007, 19, 315215.	0.7	61
5043	Structure and elasticity of<mml:math xmlns:mml="http://www.w3.org/1998/Math/MathML" display="inline"><mml:mrow><mml:mi>C</mml:mi><mml:mi>m</mml:mi><mml:mi>c</mml:mi><mml:mi>m</mml:mi></mml:mrow></mml:math>-<mml:math xmlns:mml="http://www.w3.org/1998/Math/MathML" display="inline"><mml:mrow><mml:mi mathvariant="normal">Ca</mml:mi><mml:mi mathvariant="normal">Ir</mml:mi><mml:msub><mml:mi mathvariant="normal">O</mml:mi><mml:mn>3</mml:mn></mml:msub></mml:mrow></mml:math>and their pressure dependences:<i>Ab Initio. Physical Review B, 2007, 76, .	1.1	33
5044	Microscopic origins of surface states on nitride surfaces. Journal of Applied Physics, 2007, 101, 081704.	1.1	248
5045	Structural and electronic properties of ZnO nanotubes from density functional calculations. Nanotechnology, 2007, 18, 485713.	1.3	72
5046	The stability and electronic structure of single-walled ZnO nanotubes by density functional theory. Nanotechnology, 2007, 18, 345706.	1.3	64
5047	Adsorption of molecular oxygen on the walls of pristine and carbon-doped (5,5) boron nitride nanotubes: Spin-polarized density functional study. Physical Review B, 2007, 75, .	1.1	53
5048	Ab initiostudy of Cr interactions with point defects in bcc Fe. Physical Review B, 2007, 75, .	1.1	269
5049	Experimental and Theoretical Study of Cobalt Selenide as a Catalyst for O2Electroreduction. Journal of Physical Chemistry C, 2007, 111, 10508-10513.	1.5	88
5050	First-principles calculation of vibrational frequencies for monoclinic tribismuth borate BiB3O6. Zeitschrift FÃ¼r Kristallographie, 2007, 222, .	1.1	2
5051	Electronic structures and doping of SnO2, CuAlO2, and CuInO2. Journal of Applied Physics, 2007, 102, 123703.	1.1	47
5052	Electronic and optical properties of rock-salt aluminum nitride obtained from first principles. Journal of Physics Condensed Matter, 2007, 19, 425231.	0.7	9
5053	Density Functional Theory Study of ZnO Nanostructures for NO and NO2 Sensing. , 2007, , .		4
5054	Structural, electronic, and optical absorption properties of orthorhombic CaSnO3throughab initiocalculations. Journal of Physics Condensed Matter, 2007, 19, 106214.	0.7	29
5055	Elasticity of serpentines and extensive serpentinization in subduction zones. Geophysical Research Letters, 2007, 34, .	1.5	42
5056	Stability and electronic properties of vacancies and antisites inBC2Nnanotubes. Physical Review B, 2007, 75, .	1.1	51
5057	Superhard PseudocubicBC2NSuperlattices. Physical Review Letters, 2007, 98, 015502.	2.9	71
5058	Oxide-Supported Metal Thin-Film Catalysts: The How and Why. , 2007, , 13-21.		6
5059	Study of the Nitrogen Concentration Influence on N-Doped TiO₂ Anatase from First-Principles Calculations. Journal of Physical Chemistry C, 2007, 111, 12086-12090.	1.5	220

#	Article	IF	Citations
5060	Phonon and elastic instabilities in rocksalt alkali hydrides under pressure: First-principles study. Physical Review B, 2007, 75, .	1.1	39
5061	Structural behavior of uranium dioxide under pressure byLSDA+Ucalculations. Physical Review B, 2007, 75, .	1.1	97
5062	Zero-Stress Optic Glass without Lead. Chemistry of Materials, 2007, 19, 286-290.	3.2	67
5063	First-Principles Calculation of the Structural, Magnetic, and Electronic Properties of the CoxCu1-x Solid Solutions Using Special Quasirandom Structures. Journal of the Physical Society of Japan, 2007, 76, 024605.	0.7	12
5064	Scanning tunneling microscopy fingerprints of point defects in graphene: A theoretical prediction. Physical Review B, 2007, 76, .	1.1	164
5065	Understanding Photocatalytic Activity of S- and P-Doped TiO₂ under Visible Light from First-Principles. Journal of Physical Chemistry C, 2007, 111, 18985-18994.	1.5	236
5066	DFT-Based Characterization of the Multiple Adsorption Modes of Nitrogen Oxides on Pt(111). Journal of Physical Chemistry C, 2007, 111, 389-397.	1.5	84
5067	Ab initioDFT simulation of ideal shear deformation of SiC polytypes. Modelling and Simulation in Materials Science and Engineering, 2007, 15, 27-37.	0.8	31
5068	A Theoretical Study of the Energetic Stability and Geometry of Hydrogen- and Oxygen-Terminated Diamond (100) Surfaces. Journal of Physical Chemistry C, 2007, 111, 795-801.	1.5	61
5069	Structures and elastic properties ofOsN2investigated via first-principles density functional calculations. Physical Review B, 2007, 75, .	1.1	103
5070	Why does the B3LYP hybrid functional fail for metals?. Journal of Chemical Physics, 2007, 127, 024103.	1.2	481
5071	BaCe1-xPdxO3-Î´(0 â‰¤xâ‰¤ 0.1):Â Redox Controlled Ingress and Egress of Palladium in a Perovskite. Chemistry of Materials, 2007, 19, 1418-1426.	3.2	46
5072	Structural phase transition inCaH2at high pressures. Physical Review B, 2007, 75, .	1.1	47
5073	Electronic structure and magnetic properties ofFe0.125Sn0.875O2. Physical Review B, 2007, 75, .	1.1	27
5074	Sublimation of Ammonium Salts:â€‰ A Mechanism Revealed by a First-Principles Study of the NH₄Cl System. Journal of Physical Chemistry C, 2007, 111, 13831-13838.	1.5	38
5075	Electronic and magnetic properties of Mn and Fe impurities in III-nitride semiconductors. Diamond and Related Materials, 2007, 16, 1429-1432.	1.8	4
5076	Crystal and electronic structures of pentacene thin films from grazing-incidence x-ray diffraction and first-principles calculations. Physical Review B, 2007, 76, .	1.1	147
5077	Electronic structure and electric-field gradient analysis inCeIn3. Physical Review B, 2007, 75, .	1.1	26

#	Article	IF	Citations
5078	Structural Requirements and Reaction Pathways in Dimethyl Ether Combustion Catalyzed by Supported Pt Clusters. Journal of the American Chemical Society, 2007, 129, 13201-13212.	6.6	49
5079	xmlns:mml="http://www.w3.org/1998/Math/MathML" display="inline"><mml:mrow><mml:mi mathvariant="normal">Ir</mml:mi><mml:msub><mml:mi mathvariant="normal">N</mml:mi><mml:mn>2</mml:mn></mml:msub></mml:mrow></mml:math>and<mml:math xmlns:mml="http://www.w3.org/1998/Math/MathML" display="inline"><mml:mrow><mml:mi mathvariant="normal">Ir</mml:mi><mml:msub><mml:mi mathvariant="normal">N</mml:mi><mml:mn>3</mml:mn></mml:msub></mml:mrow></mml:math>	1.1	1,399
5080	The Structure and Energy of Oxygen Vacancy Formation in Clean and Doped, Very Thin Films of ZnO. Journal of Physical Chemistry C, 2007, 111, 12715-12722.	1.5	30
5081	Structure and stability of the (001) Î±-quartz surface. Physical Chemistry Chemical Physics, 2007, 9, 2146-2152.	1.3	189
5082	First-Principles Investigation of Dense B₄C₃. Journal of Physical Chemistry C, 2007, 111, 13679-13683.	1.5	11
5083	Room-Temperature Ferromagnetism in Carbon-Doped ZnO. Physical Review Letters, 2007, 99, 127201.	2.9	775
5084	Ab initiotheoretical study of hydrogen and its interaction with boron acceptors and nitrogen donors in single-wall silicon carbide nanotubes. Physical Review B, 2007, 75, .	1.1	42
5085	Periodic DFT Studies of AlPO-11:â€‰ The Role of Hydration on Structural Properties. Journal of Physical Chemistry C, 2007, 111, 9664-9670.	1.5	9
5086	Proton-Transfer Mechanism in LaPO4. Journal of Physical Chemistry C, 2007, 111, 11003-11007.	1.5	71
5087	Prediction study of structural and elastic properties under the pressure effect of M2GaCâ€ˆ(M=Ti,V,Nb,Ta). Journal of Applied Physics, 2007, 102, .	1.1	69
5088	On the origin of Si nanocrystal formation in a Si suboxide matrix. Journal of Applied Physics, 2007, 102, .	1.1	41
5089	Infrared Spectroscopic Study of ClCN Adsorption on Clean and Triethylenediamine-Precovered Î³-Al₂O₃. Journal of Physical Chemistry C, 2007, 111, 18226-18235.	1.5	12
5090	Origin of the Verwey transition in magnetite: Group theory, electronic structure, and lattice dynamics study. Physical Review B, 2007, 76, .	1.1	93
5091	Nonlocal exchange correlation in screened-exchange density functional methods. Physical Review B, 2007, 76, .	1.1	25
5092	STRUCTURAL AND ELECTRONIC PROPERTIES OF Sr(N₃)₂ UNDER PRESSURE. Journal of Theoretical and Computational Chemistry, 2007, 06, 487-494.	1.8	2
5093	Ab-Initio Modeling of Defects in Germanium. , 2007, , 187-210.		1
5094	Pd0.213Cd0.787 and Pd0.235Cd0.765 Structures: Their Longc Axis and Composite Crystals, Chemical Twinning, and Atomic Site Preferences. Chemistry - A European Journal, 2007, 13, 1394-1410.	1.7	34
5095	A Quantum Mechanically Guided View of Mg₄₄Rh₇. Chemistry - A European Journal, 2007, 13, 7852-7863.	1.7	20

#	Article	IF	Citations
5096	Interpenetrating Polar and Nonpolar Sublattices in Intermetallics: The NaCd2 Structure. Angewandte Chemie - International Edition, 2007, 46, 1958-1976.	7.2	70
5097	Low-Basicity Oxygen Atoms: A Key in the Search for Propylene Epoxidation Catalysts. Angewandte Chemie - International Edition, 2007, 46, 2055-2058.	7.2	134
5098	Computational Study on the Catalytic Mechanism of Oxygen Reduction on La_{0.5}Sr_{0.5}MnO₃ in Solid Oxide Fuel Cells. Angewandte Chemie - International Edition, 2007, 46, 7214-7219.	7.2	101
5099	Structural and Electronic Properties of Pristine and Baâ€Doped Clathrateâ€Like Carbon Fullerenes. Angewandte Chemie - International Edition, 2007, 46, 6275-6277.	7.2	9
5104	Firstâ€Principles Determination of Multicomponent Hydride Phase Diagrams: Application to the Liâ€Mgâ€Nâ€H System. Advanced Materials, 2007, 19, 3233-3239.	11.1	217
5105	Conformational Analysis of One-Dimensional Coordination Polymers Based on [Cp2Cr2(CO)4(Î¼,Î·2-P2)] by Solid-State Multinuclear NMR Spectroscopy and Density Functional Calculations. European Journal of Inorganic Chemistry, 2007, 2007, 2775-2782.	1.0	35
5106	A Theoretical Study of Surface Reduction Mechanisms of CeO2(111) and (110) by H2. ChemPhysChem, 2007, 8, 849-855.	1.0	142
5107	Adsorption, Diffusion and Desorption of Chlorine on and from Rutile TiO2{110}: A Theoretical Investigation. ChemPhysChem, 2007, 8, 444-451.	1.0	28
5108	Pitfalls in Interpreting Temperature Programmed Desorption Spectra of Alloys: The CO/CoPt Puzzle. ChemPhysChem, 2007, 8, 654-656.	1.0	12
5109	Dehydrogenation Reaction for Naï£¿Oï£¿H System: A Firstâ€Principles Study. ChemPhysChem, 2007, 8, 1979-1987.	1.0	2
5110	Prediction study of elastic properties under pressure effect for filled tetrahedral semiconductors LiZnN, LiZnP and LiZnAs. Solid State Communications, 2007, 141, 288-291.	0.9	23
5111	Infrared reflectance spectrum of BN calculated from first principles. Solid State Communications, 2007, 141, 262-266.	0.9	106
5112	Ground state structures in the polonium based IIâ€“VI compounds. Solid State Communications, 2007, 141, 523-528.	0.9	9
5113	High-pressure Raman and infrared study of ZrV 2O7. Solid State Communications, 2007, 141, 680-684.	0.9	34
5114	Adsorption of CO and NO molecules on carbon doped boron nitride nanotubes. Solid State Communications, 2007, 142, 49-53.	0.9	112
5115	Dependence of band structures on stacking and field in layered graphene. Solid State Communications, 2007, 142, 123-127.	0.9	306
5116	First-principles investigation of pressure-induced changes in structural and electronic properties of Y 2C3 superconductor. Solid State Communications, 2007, 142, 536-540.	0.9	4
5117	Structure of the Geâ€“Sbâ€“Te phase-change materials studied by theory and experiment. Solid State Communications, 2007, 143, 240-244.	0.9	57

#	Article	IF	Citations
5118	First-principles calculation on phase stability and metallization in GeH4 under pressure. Solid State Communications, 2007, 143, 353-357.	0.9	28
5119	Ab initio study on the structural and elastic properties of MAlSi (M=Ca, Sr, and Ba). Solid State Communications, 2007, 143, 425-428.	0.9	63
5120	Effects of single oxygen vacancy on electronic structure and ferromagnetism for V-doped TiO2. Solid State Communications, 2007, 144, 54-57.	0.9	21
5121	First-principles study of electron doping and disorder effects on electronic and magnetic properties in Sr2â˜xNdxFeMoO6 double perovskites. Solid State Communications, 2007, 144, 230-235.	0.9	19
5122	First-principles studies on the electronic and optical properties of CeCl3 and CeBr3. Solid State Communications, 2007, 144, 220-224.	0.9	11
5123	Energetics of oxygen vacancies at rutile TiO2(110) surface. Solid State Communications, 2007, 144, 324-328.	0.9	32
5124	Ab initio electronic structure calculation of oxygen vacancies in rutile titanium dioxide. Solid State Ionics, 2007, 178, 319-325.	1.3	34
5125	Thermal stability of superhard Tiâ€“Bâ€“N coatings. Surface and Coatings Technology, 2007, 201, 6148-6153.	2.2	59
5126	Structural, electronic, and magnetic properties of bcc iron surfaces. Surface Science, 2007, 601, 123-133.	0.8	197
5127	Segregation of Pt at clean surfaces of (Pt, Ni)3Al. Surface Science, 2007, 601, 376-380.	0.8	14
5128	Combined investigation of water sorption on TiO2 rutile (110) single crystal face: XPS vs. periodic DFT. Surface Science, 2007, 601, 518-527.	0.8	150
5129	Surface diffraction study of the hydrated hematite surface. Surface Science, 2007, 601, 460-474.	0.8	97
5130	Carbide induced reconstruction of monatomic steps on Ni(111) â€“ A density functional study. Surface Science, 2007, 601, 649-655.	0.8	12
5131	Interactions of H with tungsten carbide surfaces: An ab initio study. Surface Science, 2007, 601, 578-587.	0.8	19
5132	Ab initio study of S dynamics on iron surfaces. Surface Science, 2007, 601, 665-671.	0.8	19
5133	Density functional slab model studies of water adsorption on flat and stepped Cu surfaces. Surface Science, 2007, 601, 954-964.	0.8	89
5134	Density of states and the problem of Sm valence. Surface Science, 2007, 601, 1001-1007.	0.8	15
5135	Surface reconstructions on InN and GaN polar and nonpolar surfaces. Surface Science, 2007, 601, L15-L18.	0.8	85

#	Article	IF	Citations
5136	Kinetic aspect of CO2 reforming of CH4 on Ni(111): A density functional theory calculation. Surface Science, 2007, 601, 1271-1284.	0.8	140
5137	First-principles study of C chemisorption and diffusion on the surface and in the subsurfaces of Ni(111) during the growth of carbon nanofibers. Surface Science, 2007, 601, 1319-1325.	0.8	26
5138	The adsorption of 1,3-butadiene on Ag(111): A TPD/IRAS study and importance of lateral interactions. Surface Science, 2007, 601, 1409-1418.	0.8	6
5139	Driving force for the WO3(001) surface relaxation. Surface Science, 2007, 601, 1481-1488.	0.8	40
5140	Surface segregation in Pt25Rh75 alloys studied by Monte Carlo simulations and the modified embedded atom method. Surface Science, 2007, 601, 1668-1676.	0.8	13
5141	CO adsorption energies on metals with correction for high coordination adsorption sites â€“ A density functional study. Surface Science, 2007, 601, 1747-1753.	0.8	259
5142	Adsorption of water on (001) surface of SrTiO3 and SrZrO3 cubic perovskites: Hybrid HF-DFT LCAO calculations. Surface Science, 2007, 601, 1844-1856.	0.8	77
5143	The bonding geometry of alkylsilanes on gold: Relation to surface pattern development and STM image contrast. Surface Science, 2007, 601, 1937-1943.	0.8	5
5144	Study of Si(001)4Ã—2-Ga structure by scanning tunneling microscopy and ab initio calculation. Surface Science, 2007, 601, 2415-2419.	0.8	4
5145	An ab initio study of 3-aminopropyltrimethoxysilane molecule on Si(111)-() surface. Surface Science, 2007, 601, 3740-3744.	0.8	10
5146	Chemisorption of 4-(4-amino-phenylazo) benzoic acid molecule on the Si(001)-(4Ã—2) surface. Surface Science, 2007, 601, 3760-3764.	0.8	4
5147	NH3 on Si(001): Can Gaussian cluster and planewave slab models agree on energetics?. Surface Science, 2007, 601, 3020-3033.	0.8	14
5148	First-principles study of adsorption and diffusion on Ge/Si(001)-(2Ã—8) and Ge/Si(105)-(1Ã—2) surfaces. Surface Science, 2007, 601, 3067-3072.	0.8	9
5149	Adsorption of V on a hematite (0001) surface and its oxidation: Submonolayer coverage. Surface Science, 2007, 601, 3082-3098.	0.8	27
5150	Comparison of the adsorption of N2 on Ru(109) and Ru(001) â€“ A detailed look at the role of atomic step and terrace sites. Surface Science, 2007, 601, 3533-3547.	0.8	9
5151	Vibrational entropy-driven dealloying of Mo(100) and W(100) surface alloys. Surface Science, 2007, 601, L95-L101.	0.8	9
5152	When adding an unreactive metal enhances catalytic activity: NOx decomposition over silverâ€“rhodium bimetallic surfaces. Surface Science, 2007, 601, L103-L108.	0.8	55
5153	Surface, interface and stacking fault energies of magnesium from first principles calculations. Surface Science, 2007, 601, 5762-5765.	0.8	81

#	Article	IF	Citations
5154	Nano-faceting of fcc(1 1 0) surfaces controlled by adsorbates and atom deposition or removal. Surface Science, 2007, 601, L115-L119.	0.8	5
5155	Theoretical analysis of reactivity on Pt(111) and Ptâ€“Pd(111) alloys. Surface Science, 2007, 601, 4786-4792.	0.8	45
5156	Stress development and impurity segregation during oxidation of the Si(100) surface. Surface Science, 2007, 601, 4888-4898.	0.8	9
5157	First-principles studies of the structure of sulfur on the Pd(111) surface. Surface Science, 2007, 601, 4899-4909.	0.8	12
5158	Segregation at the surface of an Au/Pd alloy exposed to CO. Surface Science, 2007, 601, 5332-5339.	0.8	84
5159	A density functional theory study of H2S decomposition on the (111) surfaces of model Pd-alloys. Surface Science, 2007, 601, 5382-5393.	0.8	65
5160	Ice formation on kaolinite: Lattice match or amphoterism?. Surface Science, 2007, 601, 5378-5381.	0.8	101
5161	Chemical identification in the (100) surface using scanning tunneling microscopy and first-principles calculations. Surface Science, 2007, 601, 5540-5545.	0.8	16
5162	Experiments and theory on pentacene in the thin film phase: structural, electronic, transport properties, and gas response to oxygen, nitrogen, and ambient air. Thin Solid Films, 2007, 515, 8316-8321.	0.8	12
5163	First-principles study of oxygenated diamond (001) surfaces with and without hydrogen. Applied Surface Science, 2007, 253, 4260-4266.	3.1	11
5164	First principle study of SrTiO3 (001) surface and adsorption of NO on SrTiO3 (001). Applied Surface Science, 2007, 253, 8345-8351.	3.1	27
5165	Adsorption structure of germanium on the Ru(0001) surface. Applied Surface Science, 2007, 254, 431-435.	3.1	3
5166	First-principles calculations of structural, electronic, and optical absorption properties of CaCO3 Vaterite. Chemical Physics Letters, 2007, 435, 59-64.	1.2	60
5167	First-principles calculations of N2O adsorption and decomposition on GaN (0001) surface. Chemical Physics Letters, 2007, 438, 213-217.	1.2	10
5168	Designing carbon nanoframeworks tailored for hydrogen storage. Chemical Physics Letters, 2007, 439, 354-359.	1.2	19
5169	Hydrogen catalysis and scavenging action of Pd-POSS nanoparticles. Chemical Physics Letters, 2007, 440, 244-248.	1.2	18
5170	Adsorption of S on Ir(100) surface from first-principles calculations. Chemical Physics Letters, 2007, 441, 53-57.	1.2	8
5171	New structures of dense nitrogen: Pathways to the polymeric phase. Chemical Physics Letters, 2007, 442, 65-70.	1.2	31

#	Article	IF	Citations
5172	From a fullerene-like cage (SiC)12 to novel silicon carbide nanowires: An ab initio study. Chemical Physics Letters, 2007, 442, 384-389.	1.2	12
5173	First-principles study of single-crystal uranium mono- and dinitride. Chemical Physics Letters, 2007, 443, 82-86.	1.2	46
5174	Structural and electronic properties of a trimetallic nanoparticle catalyst: Ru5PtSn. Chemical Physics Letters, 2007, 443, 337-341.	1.2	10
5175	Terahertz spectroscopy of the crystalline Î±-quaterthiophene: A combined experimental and density functional theory study. Chemical Physics Letters, 2007, 445, 47-50.	1.2	14
5176	Modeling metal adsorption at amorphous silica: Gold atoms and dimers as example. Chemical Physics Letters, 2007, 444, 280-286.	1.2	22
5177	Theoretical study of O2 adsorption and reactivity on single-walled boron nitride nanotubes. Chemical Physics Letters, 2007, 449, 149-154.	1.2	39
5178	An ab initio analysis of adsorption and diffusion of silver atoms on partially hydroxylated Î±-Al2O3(0001) surfaces. Chemical Physics Letters, 2007, 449, 155-159.	1.2	12
5179	Structure and stability of Fe4C bulk and surfaces: A density functional theory study. Chemical Physics Letters, 2007, 448, 83-87.	1.2	33
5180	First-principles investigation on the elastic, magnetic and electronic properties of MFe3N (M=Fe, Ru,) Tj ETQq0 0 0 rgBT /Overlock 10 Tf	1.2	36
5181	Structural and electronic properties of the Li-ion battery cathode material LixCoSiO4. Current Applied Physics, 2007, 7, 611-616.	1.1	37
5182	First-principles study of carbon diffusion in bulk nickel during the growth of fishbone-type carbon nanofibers. Carbon, 2007, 45, 21-27.	5.4	45
5183	Hydrogen pairing on graphene. Carbon, 2007, 45, 218-220.	5.4	60
5184	A first principles study of the optical properties of BxCy single wall nanotubes. Carbon, 2007, 45, 1482-1491.	5.4	41
5185	Ab initio studies of structural and electronic properties of Li4Ti5O12 spinel. Electrochemistry Communications, 2007, 9, 1107-1112.	2.3	265
5186	Computational study of sulfurâ€“nickel interactions: A new Sâ€“Ni phase diagram. Electrochemistry Communications, 2007, 9, 2212-2217.	2.3	121
5187	TiO2 nanopowders doped with boron and nitrogen for photocatalytic applications. Chemical Physics, 2007, 339, 111-123.	0.9	194
5188	Energetic balance and kinetics for the decomposition of supersaturated Ti1â^'xAlxN. Acta Materialia, 2007, 55, 1441-1446.	3.8	106
5189	Thermal stability of Ti3SiC2 thin films. Acta Materialia, 2007, 55, 1479-1488.	3.8	198

#	Article	IF	Citations
5190	Site preference of early transition metal elements in C15 NbCr2. Acta Materialia, 2007, 55, 1599-1605.	3.8	47
5191	Surface segregation of Pt in Î³â€²-Ni3Al: A first-principles study. Acta Materialia, 2007, 55, 1641-1647.	3.8	20
5192	Effects of segregating elements on the adhesive strength and structure of the Î±-Al2O3/Î²-NiAl interface. Acta Materialia, 2007, 55, 2791-2803.	3.8	100
5193	Integrated design of Nb-based superalloys: Ab initio calculations, computational thermodynamics and kinetics, and experimental results. Acta Materialia, 2007, 55, 3281-3303.	3.8	78
5194	First-principles calculations of structural energetics of Cuâ€“TM (TM=Ti, Zr, Hf) intermetallics. Acta Materialia, 2007, 55, 3347-3374.	3.8	109
5195	Full-potential electronic structure of Hf2AlC and Hf2AlN. Acta Materialia, 2007, 55, 4161-4165.	3.8	29
5196	Phase stabilities and spinodal decomposition in the Cr1â^'xAlxN system studied by ab initio LDA and thermodynamic modeling: Comparison with the Ti1â^'xAlxN and TiN/Si3N4 systems. Acta Materialia, 2007, 55, 4615-4624.	3.8	76
5197	First-principles study of Ti3AC2 (A=Si, Al) (001) surfaces. Acta Materialia, 2007, 55, 4645-4655.	3.8	82
5198	Site preference of transition-metal elements in B2 NiAl: A comprehensive study. Acta Materialia, 2007, 55, 4799-4806.	3.8	78
5199	Anomalous diffusion in dilute solid solutions. Acta Materialia, 2007, 55, 5289-5296.	3.8	4
5200	Dipole formation due to ion-exchange processes at the metal-ceramic Al/MgAl2O4 (001) interface. Acta Materialia, 2007, 55, 5813-5821.	3.8	6
5201	Elastic anisotropy of Î³â€²-Fe4N and elastic grain interaction in Î³â€²-Fe4N1â^'y layers on Î±-Fe: First-principles calculations and diffraction stress measurements. Acta Materialia, 2007, 55, 5833-5843.	3.8	78
5202	Theoretical and experimental studies of devitrification pathways in the Zr2Cu1â^'xPdx metallic glass system. Acta Materialia, 2007, 55, 5901-5909.	3.8	13
5203	First-principles calculation of defect energetics in cubic-BaTiO3 and a comparison with SrTiO3. Acta Materialia, 2007, 55, 6535-6540.	3.8	65
5204	Predicting twinning stress in fcc metals: Linking twin-energy pathways to twin nucleation. Acta Materialia, 2007, 55, 6843-6851.	3.8	370
5205	Comparative study of H2 adsorption on W(100)-c(2Ã—2)Cu and W(100): Surface alloying effects. Applied Surface Science, 2007, 254, 82-86.	3.1	4
5206	Modeling adsorption of CO2 on Ni(110) surface. Materials Science and Engineering C, 2007, 27, 1355-1359.	3.8	26
5207	Electronic and structural properties of zincblende AlxIn1â^'xN. Optics Communications, 2007, 274, 361-365.	1.0	12

#	Article	IF	Citations
5208	Bowing parameter of zincblende InxGa1â^'xN. Optics Communications, 2007, 280, 153-156.	1.0	14
5209	A first principles analysis of the electro-oxidation of CO over Pt(111). Electrochimica Acta, 2007, 52, 5517-5528.	2.6	61
5210	Ab initio study of high permittivity phase stabilization in HfSiO. Microelectronic Engineering, 2007, 84, 2039-2042.	1.1	14
5211	First-principles calculations of CH4 dissociation on Ni(100) surface along different reaction pathways. Journal of Molecular Catalysis A, 2007, 264, 299-308.	4.8	33
5212	Density functional theory study of CO adsorption on the (100), (001) and (010) surfaces of Fe3C. Journal of Molecular Catalysis A, 2007, 269, 169-178.	4.8	60
5213	Metastable phases and spinodal decomposition in Ti1â^'xAlxN system studied by ab initio and thermodynamic modeling, a comparison with the TiNâ€“Si3N4 system. Materials Science & Engineering A: Structural Materials: Properties, Microstructure and Processing, 2007, 448, 111-119.	2.6	91
5214	Ab initio study of structural, electronic and optical properties of MnHg(SCN)4 and FeHg(SCN)4. Physica B: Condensed Matter, 2007, 390, 231-235.	1.3	5
5215	First-principles calculation of Mg(0001) thin films: Quantum size effect and adsorption of atomic hydrogen. Physica B: Condensed Matter, 2007, 390, 225-230.	1.3	16
5216	Structural and electronic properties of CaS Crystal: A density functional theory investigation. Physica B: Condensed Matter, 2007, 391, 193-198.	1.3	32
5217	Ab initio calculations of structural and electronic properties of Y2Ti2O7 and Cd2Nb2O7. Physica B: Condensed Matter, 2007, 392, 341-347.	1.3	30
5218	First-principles study of A7 to simple cubic phase transformation in As. Physica B: Condensed Matter, 2007, 400, 22-25.	1.3	7
5219	First-principles study of iron and iron pairs in Si. Physica B: Condensed Matter, 2007, 401-402, 105-108.	1.3	7
5220	First-principles study on the local vibrational modes of nitrogenâ€“oxygen defects in silicon. Physica B: Condensed Matter, 2007, 401-402, 159-162.	1.3	8
5221	Theoretical study of the CiOi and IsiCiOi defects in Si. Physica B: Condensed Matter, 2007, 401-402, 163-166.	1.3	13
5222	First-principles investigations of Feâ€“H interactions in silicon. Physica B: Condensed Matter, 2007, 401-402, 171-174.	1.3	3
5223	Strong compensation of n-type Ge via formation of donorâ€“vacancy complexes. Physica B: Condensed Matter, 2007, 401-402, 179-183.	1.3	9
5224	Interstitial carbon-related defects in Si1â^'xGex alloys. Physica B: Condensed Matter, 2007, 401-402, 200-204.	1.3	2
5225	Ab initio calculation of the formation energy of charged vacancies in germanium. Physica B: Condensed Matter, 2007, 401-402, 205-209.	1.3	21

#	Article	IF	Citations
5226	Ab-initio modeling of carbon and carbonâ€“hydrogen defects in InAs. Physica B: Condensed Matter, 2007, 401-402, 275-277.	1.3	4
5227	Stability of the cubic phase in GaN doped with 3d-transition metal ions. Physica B: Condensed Matter, 2007, 401-402, 319-322.	1.3	3
5228	What is the product of ketene hydrogenation on Fe5C2(001): Oxygenates or hydrocarbons?. Journal of Molecular Catalysis A, 2007, 272, 275-287.	4.8	24
5229	Ab initio calculations about intrinsic point defects and He in W. Nuclear Instruments & Methods in Physics Research B, 2007, 255, 23-26.	0.6	197
5230	Ab-initio modelling of defects in MgO. Nuclear Instruments & Methods in Physics Research B, 2007, 255, 166-171.	0.6	8
5231	Structural, electronic and energetic properties of silicon carbon alloys. Physica B: Condensed Matter, 2007, 388, 167-173.	1.3	4
5232	First-principle calculations of electronic and positronic properties of AlGaAs2. Physica B: Condensed Matter, 2007, 396, 169-176.	1.3	13
5233	Calculation of the thermodynamic properties of B2 AlRE (RE=Sc, Y, La, Ceâ€“Lu). Physica B: Condensed Matter, 2007, 399, 27-32.	1.3	43
5234	First-principles studies of di-arsenic interstitial and its implications for arsenic-interstitial diffusion in crystalline silicon. Physica B: Condensed Matter, 2007, 401-402, 144-147.	1.3	3
5235	Effect of Mg-doping on the structural and electronic properties of LiCoO2: A first-principles investigation. Journal of Power Sources, 2007, 171, 908-912.	4.0	79
5236	Titanium vacancy defects in solâ€“gel prepared anatase. Journal of Solid State Chemistry, 2007, 180, 670-678.	1.4	87
5237	Crystal chemistry of the G-phases in the {Ti, Zr, Hf}â€“Niâ€“Si systems. Journal of Solid State Chemistry, 2007, 180, 733-741.	1.4	12
5238	Structural arrangements of the ternary metal boride carbide compounds MB2C4 (M=Mg, Ca, La and Ce) from first-principles theory. Journal of Solid State Chemistry, 2007, 180, 2465-2470.	1.4	8
5239	Ab initio study on structure and phase transition of A- and B-type rare-earth sesquioxides Ln2O3 (Ln=Laâ€“Lu, Y, and Sc) based on density function theory. Journal of Solid State Chemistry, 2007, 180, 3280-3287.	1.4	109
5240	Investigation of structural stability and electronic properties of CuN, AgN and AuN by first principles calculations. Physics Letters, Section A: General, Atomic and Solid State Physics, 2007, 362, 73-83.	0.9	25
5241	First-principles studies on the Au surfactant on polar ZnO surfaces. Physics Letters, Section A: General, Atomic and Solid State Physics, 2007, 363, 327-331.	0.9	13
5242	Atomic relaxation and electronic redistribution of LaAlO3(001) surfaces. Physics Letters, Section A: General, Atomic and Solid State Physics, 2007, 365, 149-155.	0.9	18
5243	First-principles calculations of structural, elastic, electronic and optical properties of the antiperovskite AsNMg3. Physics Letters, Section A: General, Atomic and Solid State Physics, 2007, 371, 337-343.	0.9	80

#	Article	IF	Citations
5244	First principles simulations of kink defects on the SP 90Â° partial dislocation in silicon. Progress in Materials Science, 2007, 52, 421-463.	16.0	4
5245	First principles investigation of the electronic structure of La2MnNiO6: An insulating ferromagnet. Journal of Magnetism and Magnetic Materials, 2007, 308, 116-119.	1.0	30
5246	Characterization of dislocation loops and chromium-rich precipitates in ferritic ironâ€“chromium alloys as means of void swelling suppression. Journal of Nuclear Materials, 2007, 362, 167-173.	1.3	57
5247	First-principles energy band calculation for undoped and S-doped TiO2 with anatase structure. Journal of Physics and Chemistry of Solids, 2007, 68, 206-210.	1.9	42
5248	Atomistic study of the pressure-induced phase-transition mechanism in GaAs by MÃ¶bius inversion potentials. Journal of Physics and Chemistry of Solids, 2007, 68, 445-457.	1.9	14
5249	First principles study of the vibrational properties of. Journal of Physics and Chemistry of Solids, 2007, 68, 438-444.	1.9	6
5250	First-principles studies of pressure dependence of elastic and electronic properties in filled tetrahedral semiconductors LiMgX (, P, and As). Journal of Physics and Chemistry of Solids, 2007, 68, 549-555.	1.9	23
5251	Ab initio structural and energetic study of (, Ga) perovskites. Journal of Physics and Chemistry of Solids, 2007, 68, 570-575.	1.9	34
5252	First-principles study of electronic structure and ferromagnetism in Ti-doped ZnO. Journal of Physics and Chemistry of Solids, 2007, 68, 1500-1503.	1.9	26
5253	Vibrational, dielectric and scintillation properties of YAlO3. Journal of Luminescence, 2007, 127, 727-730.	1.5	13
5254	Slab calculations and Greenâ€™s function recursive methods combined to study the electronic structure of surfaces: application to Cu(111)â€“(4Ã—4)-Na. Progress in Surface Science, 2007, 82, 313-335.	3.8	13
5255	Influence of hydrogen coverage on Si(111) substrate on the growth of GaN buffer layer. Journal of Crystal Growth, 2007, 300, 66-69.	0.7	6
5256	Electronic structure of nitride surfaces. Journal of Crystal Growth, 2007, 300, 199-203.	0.7	54
5257	A theoretical comparative study of the surfactant effect of Sb and Bi on GaN growth. Journal of Crystal Growth, 2007, 303, 493-499.	0.7	14
5258	Density functional theory study on crystal nickel phosphides. Journal of Fuel Chemistry and Technology, 2007, 35, 458-464.	0.9	48
5259	Pair distribution functions calculated from interatomic potential models using theGeneral Utility Lattice Program. Journal of Applied Crystallography, 2007, 40, 589-594.	1.9	24
5260	Ab initio constrained crystal-chemical Rietveld refinement of Ca10(V x P1â€…â^’â€…x O4)6F2 apatites. Acta Crystallographica Section B: Structural Science, 2007, 63, 37-48.	1.8	20
5261	Structure and hydrogen bonding in 2,4-dihydroxybenzoic acid at 90, 100, 110 and 150â€…K; a theoretical and single-crystal X-ray diffraction study. Acta Crystallographica Section B: Structural Science, 2007, 63, 303-308.	1.8	26

#	Article	IF	Citations
5262	LiNaSiB3O7(OH) â€“ novel structure of the new borosilicate mineral jadarite determined from laboratory powder diffraction data. Acta Crystallographica Section B: Structural Science, 2007, 63, 396-401.	1.8	13
5263	M₂B₅ or M₂B₄? A Reinvestigation of the Mo/B and W/B System. Zeitschrift Fur Anorganische Und Allgemeine Chemie, 2007, 633, 2626-2630.	0.6	95
5264	Magnetic and electronic properties of transition metal nitride strained layers. Physica Status Solidi C: Current Topics in Solid State Physics, 2007, 4, 269-271.	0.8	0
5265	First-principles modelling of defects in advanced nuclear fuels. Physica Status Solidi C: Current Topics in Solid State Physics, 2007, 4, 1193-1196.	0.8	26
5266	Theory of partial dislocations in SiC. Physica Status Solidi C: Current Topics in Solid State Physics, 2007, 4, 2883-2887.	0.8	11
5267	Structure and energy of partial dislocations in wurtzite-GaN. Physica Status Solidi C: Current Topics in Solid State Physics, 2007, 4, 2945-2949.	0.8	14
5268	Electronic structure of zinc-blende MnTe within the GW approximation. Physica Status Solidi C: Current Topics in Solid State Physics, 2007, 4, 3270-3279.	0.8	11
5269	Optimizing the formula of rare earth-bearing materials: A computational chemistry investigation. International Journal of Quantum Chemistry, 2007, 107, 712-721.	1.0	4
5270	An accurate total energy density functional. International Journal of Quantum Chemistry, 2007, 107, 2995-3000.	1.0	4
5271	Periodic models in quantum chemical simulations of F centers in crystalline metal oxides. International Journal of Quantum Chemistry, 2007, 107, 2956-2985.	1.0	69
5272	Mercury telluride crystals encapsulated within single walled carbon nanotubes: A density functional study. International Journal of Quantum Chemistry, 2008, 108, 797-807.	1.0	13
5273	Largeâ€Scale Synthesis of Titanate and Anatase Tubular Hierarchitectures. Small, 2007, 3, 1518-1522.	5.2	69
5274	Ab-initio modeling of spintronic materials. Physica Status Solidi (A) Applications and Materials Science, 2007, 204, 33-43.	0.8	2
5275	Core reconstructions of the â©100âª edge dislocation in single crystal CVD diamond. Physica Status Solidi (A) Applications and Materials Science, 2007, 204, 2211-2215.	0.8	19
5276	Modelling the effect of doping metallic carbon nanotubes on their ability to transferâ€dope diamond. Physica Status Solidi (A) Applications and Materials Science, 2007, 204, 2898-2902.	0.8	6
5277	A theoretical study of Li as nâ€type dopants for diamond: the role of aggregation. Physica Status Solidi (A) Applications and Materials Science, 2007, 204, 2978-2984.	0.8	5
5278	Multiâ€impurity complexes for nâ€type diamond: a computational study. Physica Status Solidi (A) Applications and Materials Science, 2007, 204, 2971-2977.	0.8	11
5279	Transfer doping of diamond via 2,3â€dichloroâ€5,6â€dicyanoâ€1,4â€benzoquinone (DDQ). Physica Status Solidi (A) Applications and Materials Science, 2007, 204, 2903-2908.	0.8	3

#	Article	IF	Citations
5280	The transfer doping of graphite and graphene. Physica Status Solidi (A) Applications and Materials Science, 2007, 204, 3078-3084.	0.8	89
5281	Atomistic characterization of structural and elastic properties of auxetic crystalline SiO2. Physica Status Solidi (B): Basic Research, 2007, 244, 900-909.	0.7	30
5282	Structural and electronic properties of chalcopyrite semiconductors AgXY2 (X = In, Ga; Y = S, Se, Te) under pressure. Physica Status Solidi (B): Basic Research, 2007, 244, 629-634.	0.7	18
5283	Elementary energy bands in isovalent IVâ€“VI orthorhombic and cubic crystals and their solid solutions. Physica Status Solidi (B): Basic Research, 2007, 244, 650-668.	0.7	16
5284	Elementary energy bands in the band structure of AIV, AIIIBV crystals and superlattices built upon them. Physica Status Solidi (B): Basic Research, 2007, 244, 1318-1336.	0.7	7
5285	Structural parameters and transition pressures of ZnO: ab-initio calculations. Physica Status Solidi (B): Basic Research, 2007, 244, 1063-1069.	0.7	62
5286	Band structure and optical properties of SbSeI: densityâ€functional calculation. Physica Status Solidi (B): Basic Research, 2007, 244, 3673-3683.	0.7	15
5287	Lattice dynamics of CuAlO2 under high pressure fromab initio calculations. Physica Status Solidi (B): Basic Research, 2007, 244, 342-346.	0.7	13
5288	Effect of pressure on the structural properties and electronic band structure of GaSe. Physica Status Solidi (B): Basic Research, 2007, 244, 244-255.	0.7	33
5289	Energetic and electronic properties of BN nanotube bundle under pressure. Physica Status Solidi (B): Basic Research, 2007, 244, 110-115.	0.7	11
5290	Structural properties of ZnO polymorphs. Physica Status Solidi (B): Basic Research, 2007, 244, 1538-1543.	0.7	19
5291	Magnetism of linear Fe, Co, and Ni nanowires encapsulated in zigzag (n,0) carbon nanotubes (CNT) with n = 5 to 9: A firstâ€principles study. Physica Status Solidi (B): Basic Research, 2007, 244, 4407-4410.	0.7	8
5292	Influence of Oxygen Addition on the Structural and Elastic Properties of TiC Thin Films. Plasma Processes and Polymers, 2007, 4, S195-S199.	1.6	16
5293	Cooperative mechanisms of fast-ion conduction in gallium-based oxides with tetrahedral moieties. Nature Materials, 2007, 6, 871-875.	13.3	185
5294	Sulphate adsorption at the Fe (hydr)oxide?H2O interface: comparison of cluster and periodic slab DFT predictions. European Journal of Soil Science, 2007, 58, 978-988.	1.8	49
5295	Atomic Structures and Electrical Properties of ZnO Grain Boundaries. Journal of the American Ceramic Society, 2007, 90, 337-357.	1.9	96
5296	Ab Initio Calculation of Elastic Constants of Ceramic Crystals. Journal of the American Ceramic Society, 2007, 90, 3194-3204.	1.9	281
5297	A density functional theory study of HCN hydrogenation to methylamine on Ni(111). Journal of Catalysis, 2007, 245, 436-445.	3.1	27

#	Article	IF	Citations
5298	Density functional theory studies of methane dissociation on anode catalysts in solid-oxide fuel cells: Suggestions for coke reduction. Journal of Catalysis, 2007, 247, 20-33.	3.1	101
5299	Origin of the superior hydrogenation selectivity of gold nanoparticles in alkyne + alkene mixtures: Triple- versus double-bond activation. Journal of Catalysis, 2007, 247, 383-386.	3.1	167
5300	The hydrogenation and direct desulfurization reaction pathway in thiophene hydrodesulfurization over MoS2 catalysts at realistic conditions: A density functional study. Journal of Catalysis, 2007, 248, 188-203.	3.1	253
5301	Location and coordination of promoter atoms in Co- and Ni-promoted MoS2-based hydrotreating catalysts. Journal of Catalysis, 2007, 249, 220-233.	3.1	428
5302	A Pd-doped perovskite catalyst, BaCe1â^'xPdxO3â^'Î´BaCe1â^'xPdxO3â^'Î´, for CO oxidation. Journal of Catalysis, 2007, 249, 349-358.	3.1	91
5303	Methane oxidation over alumina supported platinum investigated by time-resolved in situ XANES spectroscopy. Journal of Catalysis, 2007, 252, 11-17.	3.1	65
5304	Dependence of structural properties of ZnO on high pressure. Materials Chemistry and Physics, 2007, 106, 11-15.	2.0	28
5305	First-principles study of the effect of hydrogen on the Ti self-diffusion characteristics in the alpha Tiâ€“H system. Scripta Materialia, 2007, 56, 77-80.	2.6	47
5306	Single adatom site exchange during the Ge growth on group V element covered Si(001). Scripta Materialia, 2007, 56, 113-116.	2.6	1
5307	Lattice and elastic constants of titaniumâ€“niobium monoborides containing aluminum and vanadium. Scripta Materialia, 2007, 56, 273-276.	2.6	14
5308	Positive correlation between the magnetic moment of Fe and atomic volume in the binary Feâ€“(Cu, Ag,) Tj ETQq0 0 0 rgBT /Overlock 1	2.6	8
5309	Thermodynamic modelling of the partially ordered solid solution Hf5â^'xNbxGe4 supported by ab initio calculations. Solid State Sciences, 2007, 9, 159-165.	1.5	8
5310	Atomic structure of preâ€Guinierâ€“Preston zones in Al alloys. Physica Status Solidi - Rapid Research Letters, 2007, 1, 172-174.	1.2	8
5311	Exploring the molecular mechanisms of reactions at surfaces. Russian Journal of Physical Chemistry B, 2007, 1, 292-306.	0.2	6
5312	Ab-initio calculation of band structure and linear optical properties of SbSI in para- and ferroelectric phases. Open Physics, 2007, 5, .	0.8	7
5313	Ab initiocalculations of the hydrogen centres in CaF2and BaF2. Journal of Physics Condensed Matter, 2007, 19, 056007.	0.7	10
5314	Ab initioheat capacity and atomic temperature factors of chalcopyrites. Physical Review B, 2007, 75, .	1.1	17
5315	Formation of the cerium orthovanadateCeVO4:DFT+Ustudy. Physical Review B, 2007, 76, .	1.1	61

#	Article	IF	Citations
5316	Thermodynamic functions and pressure-temperature phase diagram of lithium alanates byab initiocalculations. Physical Review B, 2007, 76, .	1.1	34
5317	First-Principles Studies of Ferroelectric Oxides. , 2007, , 117-174.		57
5318	Structure of Feâ€“Co/Pt(001) superlattices: a realization of tetragonal Feâ€“Co alloys. Journal of Physics Condensed Matter, 2007, 19, 016008.	0.7	13
5319	Structures and energetics of Ga₂O₃polymorphs. Journal of Physics Condensed Matter, 2007, 19, 346211.	0.7	253
5320	First-principles investigation of metal-hydride phase stability: The Ti-H system. Physical Review B, 2007, 76, .	1.1	71
5321	Pressure-Induced Cubic to Monoclinic Phase Transformation in Erbium Sesquioxide Er2O3. Inorganic Chemistry, 2007, 46, 6164-6169.	1.9	71
5322	Two-dimensional semiconducting nanostructures based on single graphene sheets with lines of adsorbed hydrogen atoms. Applied Physics Letters, 2007, 91, 183103.	1.5	65
5323	Structural investigation and electronic properties of the nickel ferrite NiFe2O4: a periodic density functional theory approach. Journal of Physics Condensed Matter, 2007, 19, 346219.	0.7	85
5324	First-principles calculations of the diffusion of atomic oxygen in nickel: thermal expansion contribution. Journal of Physics Condensed Matter, 2007, 19, 296201.	0.7	20
5325	Formation of Carbon Species on Ni(111):â€‰ Structure and Stability. Journal of Physical Chemistry C, 2007, 111, 10894-10903.	1.5	38
5326	Pressure-Driven Phase Transitions in NaBH4:Â Theory and Experiments. Journal of Physical Chemistry B, 2007, 111, 13873-13876.	1.2	37
5327	Density functional theory analysis of the structural and electronic properties of TiO2 rutile and anatase polytypes: Performances of different exchange-correlation functionals. Journal of Chemical Physics, 2007, 126, 154703.	1.2	307
5328	Defect-induced magnetism in graphene. Physical Review B, 2007, 75, .	1.1	1,268
5329	Crystal Chemistry and Electronic Structure of the Metallic Lithium Ion Conductor, LiNiN. Journal of the American Chemical Society, 2007, 129, 1912-1920.	6.6	21
5330	Structural and thermodynamic properties of hexagonal BeO at high pressures and temperatures. Journal of Physics Condensed Matter, 2007, 19, 456209.	0.7	11
5331	Density functional theory study of platinum oxides: From infinite crystals to nanoscopic particles. Physical Review B, 2007, 76, .	1.1	77
5332	Theoretical study of the thermal behavior of free and alumina-supported Fe-C nanoparticles. Physical Review B, 2007, 75, .	1.1	73
5333	Electronic properties of oxygen-deficient and aluminum-doped rutile<mml:math xmlns:mml="http://www.w3.org/1998/Math/MathML" display="inline"><mml:mrow><mml:mi mathvariant="normal">Ti</mml:mi><mml:msub><mml:mi mathvariant="normal">O</mml:mi><mml:mn>2</mml:mn></mml:msub></mml:mrow></mml:math>from first principles. Physical Review B, 2007, 76, .	1.1	119

#	Article	IF	Citations
5334	Charged Fullerenes as High-Capacity Hydrogen Storage Media. Nano Letters, 2007, 7, 2578-2583.	4.5	220
5335	Hydrogen storage capacity of Ti-doped boron-nitride and<mml:math xmlns:mml="http://www.w3.org/1998/Math/MathML" display="inline"><mml:mrow><mml:mi mathvariant="normal">B</mml:mi><mml:mo>â^•</mml:mo><mml:mi mathvariant="normal">Be</mml:mi></mml:mrow></mml:math>-substituted carbon nanotubes. Physical Review B, 2007, 76, .	1.1	86
5336	Quantum Molecular Dynamics Simulations for the Nonmetal-to-Metal Transition in Fluid Helium. Physical Review Letters, 2007, 98, 190602.	2.9	63
5337	Carbon nanotubes and their interaction with the surface of diamond. Physical Review B, 2007, 75, .	1.1	19
5338	Effects of nitrogenation on single-walled carbon nanotubes within density functional theory. Physical Review B, 2007, 76, .	1.1	93
5339	Phonon related properties of transition metals, their carbides, and nitrides: A first-principles study. Journal of Applied Physics, 2007, 101, 123519.	1.1	312
5340	Theoretical study of alloys. Physica B: Condensed Matter, 2007, 394, 127-131.	1.3	47
5341	Ab initio study of the structural and elastic properties of spinels MgX2O4(XÂ=ÂAl, Ga, In) under pressure. European Physical Journal B, 2007, 56, 1-5.	0.6	45
5342	Structural and elastic properties of Zr2AlX and Ti2AlX (X = C and N) under pressure effect. European Physical Journal B, 2007, 56, 209-215.	0.6	73
5343	Ab-initio simulation of elastic constants for some ceramic materials. European Physical Journal B, 2007, 58, 127-133.	0.6	91
5344	Mechanism of associative oxygen desorption from Pt(111) surface. European Physical Journal B, 2007, 58, 257-262.	0.6	12
5345	Structural properties of zinc-blende GaxIn1-xN: ab initio calculations. European Physical Journal B, 2007, 60, 435-438.	0.6	7
5346	Embedding atom-jellium model for metal surface. European Physical Journal D, 2007, 43, 247-250.	0.6	1
5347	Mechanistic Study on Hydrogen Spillover onto Graphitic Carbon Materials. Journal of Physical Chemistry C, 2007, 111, 18995-19000.	1.5	174
5348	Subsurface Oxygen Stabilization by a Third Species:â€‰ Carbonates on Ag(210). Journal of Physical Chemistry C, 2007, 111, 10923-10930.	1.5	16
5349	Optimisation of accurate rutile TiO2 (110), (100), (101) and (001) surface models from periodic DFT calculations. Theoretical Chemistry Accounts, 2007, 117, 565-574.	0.5	213
5350	A computational multiscale strategy to the study of amorphous materials. Theoretical Chemistry Accounts, 2007, 117, 933-942.	0.5	32
5351	Intervalley scattering in GaAs: ab initio calculation of the effective parameters for Monte Carlo simulations. Applied Physics A: Materials Science and Processing, 2007, 86, 301-307.	1.1	19

#	Article	IF	Citations
5352	Electronic and structural properties of zincblende AlxGa1-xN. Applied Physics A: Materials Science and Processing, 2007, 86, 539-543.	1.1	8
5353	High-pressure properties of diaspore, AlO(OH). Physics and Chemistry of Minerals, 2007, 34, 145-157.	0.3	45
5354	Anharmonicity of inner-OH stretching modes in hydrous phyllosilicates: assessment from first-principles frozen-phonon calculations. Physics and Chemistry of Minerals, 2007, 34, 621-625.	0.3	62
5355	Continuum and Quantum-Chemical Modeling of Oxygen Reduction on the Cathode in a Solid Oxide Fuel Cell. Topics in Catalysis, 2007, 46, 386-401.	1.3	30
5357	Theoretical study of the insulating oxides and nitrides: SiO2, GeO2, Al2O3, Si3N4, and Ge3N4. Journal of Materials Science, 2007, 42, 6555-6565.	1.7	81
5358	An investigation on the thermodynamic stability of V6Si5. Journal of Materials Science, 2007, 42, 7046-7048.	1.7	23
5359	Ab initio investigation of boron diffusion paths in germanium. Journal of Materials Science: Materials in Electronics, 2007, 18, 775-780.	1.1	20
5360	Local vibrational modes of N2â^'O n defects in Cz-Silicon. Journal of Materials Science: Materials in Electronics, 2007, 18, 683-687.	1.1	7
5361	Ab initio investigation of charge transfer technique for control of Schottky contacts in CNTs. Journal of Materials Science: Materials in Electronics, 2007, 18, 729-734.	1.1	1
5362	Density functional calculations of the properties of silicon-substituted hydroxyapatite. Journal of Materials Science: Materials in Medicine, 2007, 18, 829-837.	1.7	21
5363	Soft-Mode Behavior in Ternary Silicides MAlSi (M=Ca, Sr, Ba). Journal of Low Temperature Physics, 2007, 147, 375-386.	0.6	17
5364	Superconductivity in Lithium Under Pressure. Journal of Low Temperature Physics, 2007, 147, 549-557.	0.6	6
5365	Calcium Phosphates and Hydroxyapatite: Solid-State NMR Experiments and First-Principles Calculations. Applied Magnetic Resonance, 2007, 32, 435-457.	0.6	82
5366	First-principle investigation on stability of Co-doped spinel Î»-Mn4â^'xCoxO8. Central South University, 2007, 14, 186-190.	0.5	2
5367	The correlation between the electronic structure and elastic properties of nanolaminates. Jom, 2007, 59, 60-64.	0.9	71
5368	Structural phase transitions and piezoelectric anomalies in ordered Sc0Â·5Ga0Â·5N alloys. Bulletin of Materials Science, 2007, 30, 407-413.	0.8	2
5369	Selective Growth of CdTe on Si(211): First-Principle Calculations. Journal of Electronic Materials, 2007, 36, 925-930.	1.0	6
5370	Tuning catalytic properties of bimetallic surfaces: Oxygen adsorption on pseudomorphic Pt/Ru overlayers. Electrochimica Acta, 2007, 52, 2219-2228.	2.6	93

#	Article	IF	Citations
5371	Study of the effects of an adatom Sn on the Cu surface electromigration using a first principles method. Applied Surface Science, 2007, 253, 8652-8656.	3.1	9
5372	Structural phase transformations of GaN and InN under high pressure. Physica B: Condensed Matter, 2007, 387, 377-382.	1.3	58
5373	Phase transition and elastic constants of CaO from first-principle calculations. Physica B: Condensed Matter, 2007, 392, 229-232.	1.3	41
5374	Electronic structures and shape-memory behavior of Ti50Ni50â^'xCux (x=0, 6.25, 12.5, 18.75 and 25.0at%) by density functional theory. Physica B: Condensed Matter, 2007, 393, 18-23.	1.3	17
5375	Ab initio study of structural phase stability and elastic properties of ScSb and YSb under pressure effect. Physics Letters, Section A: General, Atomic and Solid State Physics, 2007, 362, 476-479.	0.9	59
5376	An ab initio analysis of adsorption and diffusion of silver atoms on alumina surfaces. Surface Science, 2007, 601, 134-145.	0.8	55
5377	Surface energy of M2AC(0001) determined by density functional theory (M=Ti,V,Cr; A=Al,Ga,Ge). Surface Science, 2007, 601, 896-899.	0.8	27
5378	Correlations between magnetic properties and bond formation in Rhâ€“MgO(001). Surface Science, 2007, 601, 1218-1230.	0.8	4
5379	Effect of hydrogenation on P/Si(001)-(1Ã—2). Surface Science, 2007, 601, 1489-1493.	0.8	3
5380	A multi-scale Monte Carlo study of oxide structures on the Cu(100) surface. Surface Science, 2007, 601, 1813-1821.	0.8	6
5381	Effect of hydrogenation on B/Si(001)-(1Ã—2). Surface Science, 2007, 601, 3711-3716.	0.8	2
5382	Local reactivity of ultrathin platinum overlayers and surface alloys on a gold surface. Surface Science, 2007, 601, 3702-3706.	0.8	23
5383	A theoretical study of hydrogen adsorption and diffusion on a W(110) surface. Surface Science, 2007, 601, 3003-3011.	0.8	45
5384	The surface stress of the (110) and (100) surfaces of rutile and the effect of water adsorbents. Surface Science, 2007, 601, 4824-4836.	0.8	36
5385	Consideration of the band-gap tunability of BaSi2 by alloying with Ca or Sr based on the electronic structure calculations. Thin Solid Films, 2007, 515, 8219-8225.	0.8	40
5386	A first-principles analysis of the chemisorption of hydroxide on copper under electrochemical conditions: A probe of the electronic interactions that control chemisorption at the electrochemical interface. Journal of Electroanalytical Chemistry, 2007, 607, 167-174.	1.9	29
5387	Ab initio structural, electronic and optical properties of orthorhombic. Journal of Solid State Chemistry, 2007, 180, 974-980.	1.4	20
5388	Phase stabilities of monoclinic oxoborates LaB3O6 and GdB3O6 in C121 and I12/a1 phaseâ€"Energetics and chemical bonds derived from first-principles calculations. Journal of Solid State Chemistry, 2007, 180, 2763-2774.	1.4	3

#	Article	IF	Citations
5389	Structures and crystal chemistry of the double perovskites Ba2LnBâ€²O6 (Ln=lanthanide Bâ€²=Nb5+ and) Tj ETQq0 0 0 rgBT /Overlock Journal of Solid State Chemistry, 2007, 180, 2991-3000.	1.4	50
5390	Alloying effect in the III-Asâ€“Sb ternary systems. Materials Science and Engineering B: Solid-State Materials for Advanced Technology, 2007, 137, 210-212.	1.7	11
5391	Optical properties of anatase and rutile titanium dioxide: Ab initio calculations for pure and anion-doped material. Journal of Physics and Chemistry of Solids, 2008, 69, 1820-1828.	1.9	100
5392	Free standing double walled boron nanotubes. Journal of Physics and Chemistry of Solids, 2008, 69, 2004-2012.	1.9	16
5393	Structural stability and electronic properties of Co2N, Rh2N and Ir2N. Journal of Physics and Chemistry of Solids, 2008, 69, 2723-2727.	1.9	16
5394	Li1+xFePO4 (0â‰xâ‰3) as anode material for lithium ion batteries: From ab initio studies. Journal of Power Sources, 2008, 175, 891-896.	4.0	17
5395	High-pressure modifications of CaZn2, SrZn2, SrAl2, and BaAl2: Implications for Laves phase structural trends. Journal of Solid State Chemistry, 2008, 181, 3016-3023.	1.4	22
5396	Phosphorous clustering in germanium-rich silicon germanium. Materials Science and Engineering B: Solid-State Materials for Advanced Technology, 2008, 154-155, 72-75.	1.7	51
5397	Efficient channel of the associative oxygen desorption from Pt(111). Applied Surface Science, 2008, 254, 4258-4262.	3.1	3
5398	Early precipitation stages of aluminum alloysâ€”The role of quenched-in vacancies. Applied Surface Science, 2008, 255, 132-135.	3.1	26
5399	Initial stages of hydration and Zn substitution/occupation on hydroxyapatite (0001) surfaces. Biomaterials, 2008, 29, 257-265.	5.7	73
5400	Calcium phosphates: First-principles calculations vs. solid-state NMR experiments. Comptes Rendus Chimie, 2008, 11, 398-406.	0.2	12
5401	Ab initio study on the Li deintercalation in ternary lithium nitridocuprate Li2.5Cu0.5N. Electrochimica Acta, 2008, 53, 7915-7920.	2.6	4
5402	Hexagonal silicon nanotube confined inside a carbon nanotube: A first-principles study. Physics Letters, Section A: General, Atomic and Solid State Physics, 2008, 372, 1308-1312.	0.9	8
5403	First-principle study of extrinsic defects in CuScO2 and CuYO2. Physics Letters, Section A: General, Atomic and Solid State Physics, 2008, 372, 3759-3762.	0.9	14
5404	Mechanical stability and deformation potential in beryllium chalcogenides. Superlattices and Microstructures, 2008, 44, 112-120.	1.4	24
5405	Electronic structure studies of a clock-reconstructed Al/Pd(100) surface alloy. Surface Science, 2008, 602, 943-951.	0.8	4
5406	A reactive force field (ReaxFF) for zinc oxide. Surface Science, 2008, 602, 1020-1031.	0.8	134

#	Article	IF	Citations
5407	H2S dissociation on the Fe(100) surface: An ab initio molecular dynamics study. Surface Science, 2008, 602, 1547-1553.	0.8	32
5408	2-Chlorophenol adsorption on Cu(100): First-principles density functional study. Surface Science, 2008, 602, 1554-1562.	0.8	14
5409	Effect of hydrocarbon chain length and cyclization on the adsorption strength of unsaturated hydrocarbons on Pt/3d bimetallic surfaces. Surface Science, 2008, 602, 2513-2523.	0.8	18
5410	Adsorption and diffusion of adatoms on Ru(0001): A first-principles study. Surface Science, 2008, 602, 2502-2507.	0.8	14
5411	First-principles studies of H2S adsorption and dissociation on metal surfaces. Surface Science, 2008, 602, 2758-2768.	0.8	161
5412	Atomic and electronic properties of furan on the Si(001)-(2Ã—2) surface. Surface Science, 2008, 602, 2845-2848.	0.8	5
5413	Investigation of submonolayer SiOX species formed from oxidation of silane on Pt(111). Surface Science, 2008, 602, 3225-3231.	0.8	7
5414	Interaction of acetone with the Si(001) surface. Surface Science, 2008, 602, 3484-3498.	0.8	11
5415	Uranyl interaction with the hydrated (111) nickel face: A periodic density functional theory investigation. Surface Science, 2008, 602, 3331-3337.	0.8	8
5416	CO oxidation with Pt(111) supported on pure and boron-doped carbon: A DFT investigation. Surface Science, 2008, 602, 3595-3602.	0.8	35
5417	Density functional theory studies of submonolayer oxidized silicon structures on Pd(111) and Pt(111). Surface Science, 2008, 602, 3603-3610.	0.8	4
5418	Pd(110) surface oxide structures investigated by STM and DFT. Surface Science, 2008, 602, 3706-3713.	0.8	14
5419	Ab-initio vibrational properties of SiGe alloys. Thin Solid Films, 2008, 517, 395-397.	0.8	9
5420	The charge neutrality level and the fermi level pinning in A3N (BN, AlN, GaN, InN) nitrides. Russian Physics Journal, 2008, 51, 1270-1278.	0.2	18
5421	Electronic structure and hydrogen bond in the crystal of paracetamol drugs. Structural Chemistry, 2008, 19, 613-617.	1.0	14
5422	AbÂinitio calculations of the structural and elastic properties of CoSi2. Structural Chemistry, 2008, 19, 689-692.	1.0	2
5423	A DFT study on the electronic structure for iridium nitride under high pressure. Structural Chemistry, 2008, 19, 997-1001.	1.0	4
5424	Hydrocarbon Selective Oxidation on Vanadium Phosphorus Oxide Catalysts: Insights from Electronic Structure Calculations. Topics in Catalysis, 2008, 50, 116-123.	1.3	7

#	Article	IF	Citations
5425	Dissolution and re-crystallization processes in multiphase silicon stabilized tricalcium phosphate. Journal of Materials Science: Materials in Medicine, 2008, 19, 917-927.	1.7	13
5426	Energetics of the adsorption and diffusion of hydrogen molecules in a (001) plate of nanocrystalline aluminum. Journal of Engineering Physics and Thermophysics, 2008, 81, 167-175.	0.2	2
5427	First principle study of stress effects on indium diffusion inÂuniaxially and biaxially strained silicon. Journal of Computational Electronics, 2008, 7, 411-414.	1.3	0
5428	Atomistic study of the effect of B addition in the FeAl compound. Journal of Materials Science, 2008, 43, 3867-3872.	1.7	19
5429	Electronic structures of ZnO(0001)-Zn and (000âˆ'1)-O polar surfaces. Journal of Materials Science: Materials in Electronics, 2008, 19, 229-233.	1.1	13
5430	A model study of dickite intercalated with formamide and N-methylformamide. Physics and Chemistry of Minerals, 2008, 35, 299-309.	0.3	22
5431	The compressibility and high pressure structure of diopside from first principles simulation. Physics and Chemistry of Minerals, 2008, 35, 359-366.	0.3	22
5432	Effect of different types of pseudopotentials on study of electronic dispersion for graphene and a (5,5) SWCNT. Applied Physics A: Materials Science and Processing, 2008, 92, 371-374.	1.1	10
5433	Study on H atoms diffusion and adsorption properties of MgH2-V systems. Science in China Series D: Earth Sciences, 2008, 51, 979-988.	0.9	3
5434	Sawtooth-like graphene nanoribbon. Nano Research, 2008, 1, 40-45.	5.8	41
5435	The Mechanism of Zr and Hf in Reducing Radiation-Induced Segregation in 316 Stainless Steel. Metallurgical and Materials Transactions A: Physical Metallurgy and Materials Science, 2008, 39, 218-224.	1.1	13
5436	Phase Stability and Transformations in the Zr2Ni x Cu1âˆ'x Amorphous System. Metallurgical and Materials Transactions A: Physical Metallurgy and Materials Science, 2008, 39, 1847-1856.	1.1	16
5437	Practical Surface Treatments and Surface Chemistry of n-Type and p-Type GaN. Journal of Electronic Materials, 2008, 37, 439-447.	1.0	25
5438	Determination of the Elastic Properties of Cu3Sn Through First-Principles Calculations. Journal of Electronic Materials, 2008, 37, 477-482.	1.0	38
5439	Determination of the Elastic Properties of Au5Sn and AuSn from Ab Initio Calculations. Journal of Electronic Materials, 2008, 37, 968-974.	1.0	16
5440	Effect of curvature on structures and vibrations of zigzag carbon nanotubes: A first-principles study. Bulletin of Materials Science, 2008, 31, 335-341.	0.8	19
5441	Effect of coordination on bond properties: A first principles study. Bulletin of Materials Science, 2008, 31, 569-572.	0.8	9
5442	Compton profile study of V3Ge and Cr3Ge. Pramana - Journal of Physics, 2008, 70, 323-337.	0.9	2

#	Article	IF	Citations
5443	Adsorption and reaction of organic molecules on solid surfaces â€“ ab-initio density functional investigations. Monatshefte FÃ¼r Chemie, 2008, 139, 373-387.	0.9	14
5444	Phase stability in ferroelectric bismuth titanate: a first-principles study. Acta Crystallographica Section A: Foundations and Advances, 2008, 64, 368-375.	0.3	33
5445	Molecular and crystalline structure of cycloheptanespiro-3â€²(4â€²H)-6â€²,7â€²,8â€²,9â€²-tetrahydrocyclohexa[b][1,4]thiazole-2â€²(5â€²H)-thione from powder synchrotron X-ray diffraction data. Acta Crystallographica Section B: Structural Science, 2008, 64, 217-222.	1.8	8
5446	Kaolin polytypes revisited ab initio. Acta Crystallographica Section B: Structural Science, 2008, 64, 131-143.	1.8	27
5447	Structures of 6H perovskites Ba₃CaSb₂O₉ and Ba₃SrSb₂O₉ determined by synchrotron X-ray diffraction, neutron powder diffraction and ab initio calculations. Acta Crystallographica Section B: Structural Science, 2008, 64, 154-159.	1.8	8
5448	Structure and electron density of oxysulfide Sm₂Ti₂S₂O_{4.9}, a visible-light-responsive photocatalyst. Acta Crystallographica Section B: Structural Science, 2008, 64, 291-298.	1.8	32
5449	Periodic density functional theory calculations of bulk and the (010) surface of goethite. Geochemical Transactions, 2008, 9, 4.	1.8	72
5450	Understanding the properties of interfaces between organic selfâ€assembled monolayers and noble metalsâ€”a theoretical perspective. Surface and Interface Analysis, 2008, 40, 371-378.	0.8	41
5451	Potential energy surfaces for H₂ dissociative adsorption on Pt(111) surfaceâ€”effects of vacancies. Surface and Interface Analysis, 2008, 40, 1103-1107.	0.8	11
5452	Adsorption and diffusion property of a hydrogen atom on a Pd₃Ag(111) surface. Surface and Interface Analysis, 2008, 40, 1108-1112.	0.8	17
5453	DFT study on the adsorption of NO on iron tapeâ€porphyrin. Surface and Interface Analysis, 2008, 40, 1082-1084.	0.8	9
5454	Firstâ€principles study of the (001) surface of cubic PbTiO₃. Surface and Interface Analysis, 2008, 40, 1382-1387.	0.8	18
5455	Unstable Singleâ€Layered Colloidal TiS₂ Nanodisks. Small, 2008, 4, 945-950.	5.2	85
5456	Carbon Nanotubes with an Extended Line Defect. Small, 2008, 4, 2209-2213.	5.2	19
5457	Electronicâ€Typeâ€and Diameterâ€Dependent Reduction of Singleâ€Walled Carbon Nanotubes Induced by Adsorption of Electronâ€Donor Molecules. Small, 2009, 5, 244-255.	5.2	14
5458	Filling the green gap: A firstâ€principles study of the LiMg_{1â€x}Zn_xN alloy. Physica Status Solidi C: Current Topics in Solid State Physics, 2008, 5, 2326-2328.	0.8	1
5459	First principles study of the decomposition processes of AlN in a hydrogen atmosphere. Physica Status Solidi C: Current Topics in Solid State Physics, 2008, 5, 3042-3044.	0.8	2
5460	Novel effects in finiteâ€length silicon nanowires. Physica Status Solidi (A) Applications and Materials Science, 2008, 205, 2625-2629.	0.8	2

#	Article	IF	Citations
5461	DFT studies on the thermodynamic properties of Na₂Ti₃O₇ under high temperature and high pressure. Physica Status Solidi (B): Basic Research, 2008, 245, 37-43.	0.7	13
5462	Structure and energetics for an additional H absorbed into superionic phase of CsHSO₄ by a firstâ€principles study. Physica Status Solidi (B): Basic Research, 2008, 245, 657-665.	0.7	3
5463	Firstâ€principles study of phase transition of tin and lead under high pressure. Physica Status Solidi (B): Basic Research, 2008, 245, 53-57.	0.7	17
5464	Firstâ€principles calculations of the mechanical properties of boronâ€rich compounds B₁₂N₂X (X = Be, Zn, Cd). Physica Status Solidi (B): Basic Research, 2008, 245, 58-61.	0.7	9
5465	Electronic structure of crystalline uranium nitride: LCAO DFT calculations. Physica Status Solidi (B): Basic Research, 2008, 245, 114-122.	0.7	22
5466	Atomistic study of magnetism effect on structural stability in Fe₃Al and Fe₃AlX (X = H, B, C, N, O) alloys. Physica Status Solidi (B): Basic Research, 2008, 245, 750-755.	0.7	27
5467	Electronic properties of durene crystals: Implications for charge transport. Physica Status Solidi (B): Basic Research, 2008, 245, 825-829.	0.7	4
5468	Quantum transport through nanowires: Ab initio studies using plane waves and supercells. Physica Status Solidi (B): Basic Research, 2008, 245, 854-858.	0.7	8
5469	Firstâ€principles calculations of transition phase and thermodynamic properties of CdO. Physica Status Solidi (B): Basic Research, 2008, 245, 1113-1117.	0.7	9
5470	Firstâ€principles study of the structural stability and electronic structures of TaN. Physica Status Solidi (B): Basic Research, 2008, 245, 1580-1585.	0.7	21
5471	Effects of Na, Mg and Al substitution in hypothetical superconducting Be₂B. Physica Status Solidi (B): Basic Research, 2008, 245, 2779-2785.	0.7	6
5472	Ab initio study of hydrogen chemical adsorption on platinum surface/carbon nanotube join system. Physica Status Solidi (B): Basic Research, 2008, 245, 1546-1551.	0.7	7
5473	Electronic superlattices and waveguides based on graphene: structures, properties and applications. Physica Status Solidi (B): Basic Research, 2008, 245, 2086-2089.	0.7	12
5474	New phase of polymeric C₆₀: double chains via [2+2] cycloaddition. Physica Status Solidi (B): Basic Research, 2008, 245, 2022-2024.	0.7	2
5475	Effects of a ZnSâ€shell on the structural and electronic properties of CdSeâ€nanorods. Physica Status Solidi (B): Basic Research, 2008, 245, 2111-2114.	0.7	7
5476	Understanding the Reactivity and Basicity of Zeolites: A Periodic DFT Study of the Disproportionation of N₂O₄ on Alkaliâ€Cationâ€Exchanged Zeolite Y. Chemistry - A European Journal, 2008, 14, 5168-5177.	1.7	30
5477	HPâ€Ca₂Si₅N₈â€”A New Highâ€Pressure Nitridosilicate: Synthesis, Structure, Luminescence, and DFT Calculations. Chemistry - A European Journal, 2008, 14, 7892-7902.	1.7	35
5478	Ab initio Study of Electronic Structure and Properties in Crystalline 1,1,3,3,5,5â€Hexaazidocyclotriphosphazene. Chinese Journal of Chemistry, 2008, 26, 854-858.	2.6	2

#	Article	IF	Citations
5479	Unique Reactivity of Confined Metal Atoms on a Silicon Substrate. ChemPhysChem, 2008, 9, 975-979.	1.0	24
5480	Density Functional Investigations of Electronic Structure and Dehydrogenation Reactions of Alâ€•and Siâ€Substituted Magnesium Hydride. ChemPhysChem, 2008, 9, 928-934.	1.0	32
5481	CO Adsorption on a LaNi₅ Hydrogen Storage Alloy Surface: A Theoretical Investigation. ChemPhysChem, 2008, 9, 1564-1569.	1.0	5
5482	Spatial Effect of Cï£¿H Dipoles on the Electron Affinity of Diamondâ€‰(100)â€²Ã—1 Adsorbed with Organic Molecules. ChemPhysChem, 2008, 9, 1338-1344.	1.0	3
5483	Electronic structure, chemical bonding, and geometry of pure and Srâ€doped CaCO₃. Journal of Computational Chemistry, 2008, 29, 343-349.	1.5	12
5484	Roles of cations, electronegativity difference, and anionic interlayer interactions in the metallic versus nonmetallic character of Zintl phases related to arsenic. Journal of Computational Chemistry, 2008, 29, 2144-2153.	1.5	29
5485	A firstâ€principles DFT study of UN bulk and (001) surface: Comparative LCAO and PW calculations. Journal of Computational Chemistry, 2008, 29, 2079-2087.	1.5	40
5486	DFT calculations of quadrupolar solidâ€state NMR properties: Some examples in solidâ€state inorganic chemistry. Journal of Computational Chemistry, 2008, 29, 2279-2287.	1.5	52
5487	Application of semiempirical longâ€range dispersion corrections to periodic systems in density functional theory. Journal of Computational Chemistry, 2008, 29, 2088-2097.	1.5	294
5488	Understanding Palladium Hydrogenation Catalysts: When the Nature of the Reactive Molecule Controls the Nature of the Catalyst Active Phase. Angewandte Chemie - International Edition, 2008, 47, 9274-9278.	7.2	185
5489	A Surface Coordination Network Based on Substrateâ€Derived Metal Adatoms with Local Charge Excess. Angewandte Chemie - International Edition, 2008, 47, 8442-8445.	7.2	110
5490	On the Role of Surface Modifications of Palladium Catalysts in the Selective Hydrogenation of Acetylene. Angewandte Chemie - International Edition, 2008, 47, 9299-9302.	7.2	222
5491	Evaluation of Halfâ€Heusler Compounds as Thermoelectric Materials Based on the Calculated Electrical Transport Properties. Advanced Functional Materials, 2008, 18, 2880-2888.	7.8	486
5492	Ferromagnetism in ZnO Nanowires Derived from Electroâ€deposition on AAO Template and Subsequent Oxidation. Advanced Materials, 2008, 20, 1170-1174.	11.1	135
5496	Thermodynamic modeling of the system Asâ€“Fe combined with first-principles total energy calculations. Journal of Crystal Growth, 2008, 310, 2751-2759.	0.7	6
5497	Boron phosphide as the buffer-layer for the epitaxial III-nitride growth: A theoretical study. Journal of Crystal Growth, 2008, 310, 3973-3978.	0.7	23
5498	Thickness-dependent electronic and optical properties of faceted hexagonal aluminum nitride nanotubes. Physica E: Low-Dimensional Systems and Nanostructures, 2008, 41, 254-257.	1.3	10
5499	First-principles study of native defects in rutile TiO2. Physics Letters, Section A: General, Atomic and Solid State Physics, 2008, 372, 1527-1530.	0.9	52

#	Article	IF	Citations
5500	Structural, electronic and optical properties of AgI under pressure. Physics Letters, Section A: General, Atomic and Solid State Physics, 2008, 372, 2502-2508.	0.9	19
5501	First principles study of structural, elastic, electronic and optical properties of the cubic perovskite BaHfO3. Physics Letters, Section A: General, Atomic and Solid State Physics, 2008, 372, 4527-4531.	0.9	59
5502	Structural, electronic and elastic properties of M2SC (M=Ti, Zr, Hf) compounds. Physics Letters, Section A: General, Atomic and Solid State Physics, 2008, 372, 6448-6452.	0.9	46
5503	First principles study of Eu doped carbon nanotubes. Physics Letters, Section A: General, Atomic and Solid State Physics, 2008, 372, 6677-6680.	0.9	19
5504	Interatomic potentials of the binary transition metal systems and some applications in materials physics. Physics Reports, 2008, 455, 1-134.	10.3	112
5505	Ab-initio study on parameter extraction for kinetic Monte Carlo simulation of neutral indium diffusion in uniaxially- and biaxially-strained silicon. Microelectronic Engineering, 2008, 85, 1182-1185.	1.1	0
5506	Density-functional theory study of interstitial iron and its complexes with B and Al in dilute SiGe alloys. Materials Science in Semiconductor Processing, 2008, 11, 332-335.	1.9	3
5507	Ab-initio simulation of self-interstitial in germanium. Materials Science in Semiconductor Processing, 2008, 11, 328-331.	1.9	17
5508	Electronic structure of cubic ErxGa1â˜'xN using the LSDA+U approach. Physica B: Condensed Matter, 2008, 403, 2702-2706.	1.3	8
5509	Prediction study of structural and elastic properties under pressure effect of M2SnC (M=Ti, Zr, Nb,) Tj ETQq1 1 0.784314 rgBT /Overlock	1.3	55
5510	First-principles investigation of Mg2THy (T=Ni, Co, Fe) complex hydrides. Physica B: Condensed Matter, 2008, 403, 4217-4223.	1.3	15
5511	First-principles calculations of zone-center phonons in CsB3O5: Comparison with experiment. Physica B: Condensed Matter, 2008, 403, 4189-4195.	1.3	7
5512	The phase transition and the elastic and thermodynamic properties of AlN: First principles. Physica B: Condensed Matter, 2008, 403, 4259-4263.	1.3	39
5513	Thermal stabilities of nanoporous metallic electrodes at elevated temperatures. Journal of Power Sources, 2008, 175, 75-81.	4.0	92
5514	Surface regeneration of sulfur-poisoned Ni surfaces under SOFC operation conditions predicted by first-principles-based thermodynamic calculations. Journal of Power Sources, 2008, 176, 23-30.	4.0	67
5515	First-principles investigation of R2O3(ZnO)3 (R=Al, Ga, and In) in homologous series of compounds. Journal of Solid State Chemistry, 2008, 181, 137-142.	1.4	14
5516	Density functional study on electronic properties of P-doped spinel silicon carbon nitride. Journal of Solid State Chemistry, 2008, 181, 2113-2116.	1.4	1
5517	Crystal structure and high-pressure studies of WAl2, an aluminide crystallizing with the CrSi2 structure type. Journal of Solid State Chemistry, 2008, 181, 2719-2724.	1.4	8

#	Article	IF	Citations
5518	Electronic and mechanical properties of 5d transition metal mononitrides via first principles. Journal of Solid State Chemistry, 2008, 181, 2814-2827.	1.4	90
5519	An ab initio study of possible pathways in the thermal decomposition of NaAlH4. Journal of Solid State Chemistry, 2008, 181, 3037-3043.	1.4	10
5520	Predicted energies and structures associated with the mixed calcium strontium fluorapatites. Journal of Solid State Chemistry, 2008, 181, 3287-3293.	1.4	18
5521	Reaction dynamics of H2 on Si. Ab initio supported model calculations. Progress in Surface Science, 2008, 83, 263-336.	3.8	36
5522	Electronic structure and magnetic properties of the compound. Journal of Magnetism and Magnetic Materials, 2008, 320, 36-42.	1.0	5
5523	Ab initio study of Mn adsorption on w-BN(0001) surface. Journal of Magnetism and Magnetic Materials, 2008, 320, e249-e252.	1.0	2
5524	Influence of addition of Si in FeAl alloys: Theory. Journal of Magnetism and Magnetic Materials, 2008, 320, e692-e695.	1.0	9
5525	First principles modelling of oxygen impurities in UN nuclear fuels. Journal of Nuclear Materials, 2008, 377, 492-495.	1.3	27
5526	First-principles study of the anisotropic thermal expansion of hcp metals Be and Y. Journal of Physics and Chemistry of Solids, 2008, 69, 852-858.	1.9	5
5527	Lattice dynamics of cubic SrZrO3. Journal of Physics and Chemistry of Solids, 2008, 69, 876-879.	1.9	25
5528	First-principle study of electronic properties of Ti3Si1â^'xAlxC2 solid solutions. Journal of Physics and Chemistry of Solids, 2008, 69, 1356-1361.	1.9	17
5529	Structural, electronic and phonon propertiesâ€™ investigation of YP and YAs compounds. Journal of Physics and Chemistry of Solids, 2008, 69, 791-798.	1.9	21
5530	CoO under pressure from first principles. Journal of Physics and Chemistry of Solids, 2008, 69, 1698-1703.	1.9	18
5531	Virtual crystal approximation study of nitridosilicates and oxonitridoaluminosilicates. Journal of Physics and Chemistry of Solids, 2008, 69, 1861-1868.	1.9	12
5532	Lindemann criterion and the anomalous melting curve of sodium. Journal of Physics and Chemistry of Solids, 2008, 69, 2151-2154.	1.9	23
5533	First-principles investigations of iridium low index surfaces. Journal of Physics and Chemistry of Solids, 2008, 69, 2457-2464.	1.9	7
5534	Synthesis and enhanced photocatalytic activity of NaNbO3 prepared by hydrothermal and polymerized complex methods. Journal of Physics and Chemistry of Solids, 2008, 69, 2487-2491.	1.9	91
5535	Pressure-induced phase transition of zinc-blende AlN: An ab initio molecular dynamics study. Journal of Physics and Chemistry of Solids, 2008, 69, 2894-2897.	1.9	22

#	Article	IF	Citations
5536	First principles study of barium chalcogenides. Journal of Physics and Chemistry of Solids, 2008, 69, 2924-2927.	1.9	37
5537	Characterization of diamond (100) surface with oxygen termination. Applied Surface Science, 2008, 254, 2851-2855.	3.1	13
5538	Study of vacancy on diamond (100) (2Ã—1) surface from first-principles. Applied Surface Science, 2008, 254, 6478-6482.	3.1	13
5539	wannier90: A tool for obtaining maximally-localised Wannier functions. Computer Physics Communications, 2008, 178, 685-699.	3.0	2,947
5540	Automated determination of chemical functionalisation addition routes based on magnetic susceptibility and nucleus independent chemical shifts. Computer Physics Communications, 2008, 179, 165-170.	3.0	2
5541	Sharing electronic structure and crystallographic data with ETSF_IO. Computer Physics Communications, 2008, 179, 748-758.	3.0	9
5542	Thermodynamically tuning LiBH4 by fluorine anion doping for hydrogen storage: A density functional study. Chemical Physics Letters, 2008, 450, 318-321.	1.2	101
5543	Electronic and crystal structures of nanolaminate yttrium aluminum carbide YAl3C3. Chemical Physics Letters, 2008, 451, 48-52.	1.2	13
5544	The adsorption with chiral structure of fluorene-1-carboxylic acid molecules on Cu(110) surface. Chemical Physics Letters, 2008, 452, 275-280.	1.2	6
5545	The mechanism of the displacive phase transition in vanadium dioxide. Chemical Physics Letters, 2008, 453, 167-172.	1.2	29
5546	Surface segregation of core atoms in coreâ€“shell structures. Chemical Physics Letters, 2008, 456, 64-67.	1.2	43
5547	First-principles calculations for geometrical structures and electronic properties of Si-doped TiO2. Chemical Physics Letters, 2008, 456, 71-75.	1.2	89
5548	Adsorption dynamics of O2 on Cu(1 0 0): The role of vacancies, steps and adatims in dissociative chemisorption of O2. Chemical Physics Letters, 2008, 456, 211-214.	1.2	16
5549	Effects of novel and stable intermolecular connections in the mechanical and electronic properties of C60 polymerized structures. Chemical Physics Letters, 2008, 458, 128-133.	1.2	11
5550	Ab initio simulation of the fundamental vibrational frequencies of selected pyrite-type pnictides. Chemical Physics Letters, 2008, 461, 38-41.	1.2	19
5551	First principles study on the electronic structures and stability of Cr7C3 type multi-component carbides. Chemical Physics Letters, 2008, 459, 129-132.	1.2	25
5552	Effect of pressure and temperature on structural stability of potential hydrogen storage compound Li3AlH6. Chemical Physics Letters, 2008, 460, 442-446.	1.2	8
5553	Structural transitions and electronic properties of the ultrathin SiC nanotubes under uniaxial compression. Chemical Physics Letters, 2008, 461, 280-284.	1.2	21

#	Article	IF	Citations
5554	Clusters of hafnium, Hfn= 2â€“8. Chemical Physics Letters, 2008, 462, 183-187.	1.2	9
5555	Ab initio study of the hydrogen chemisorption of single-walled aluminum nitride nanotubes. Chemical Physics Letters, 2008, 466, 197-204.	1.2	39
5556	Adsorption of formaldehyde molecule on the pristine and silicon-doped boron nitride nanotubes. Chemical Physics Letters, 2008, 467, 131-135.	1.2	117
5557	Quantum chemical study of the reactivity of boron-doped graphite layers towards water formation. Carbon, 2008, 46, 631-643.	5.4	4
5558	Phase stabilities and thermal decomposition in the Zr1â˜'Al N system studied by ab initio calculation and thermodynamic modeling. Acta Materialia, 2008, 56, 968-976.	3.8	77
5559	Structure, elastic properties and phase stability of Cr1â€“xAlxN. Acta Materialia, 2008, 56, 2469-2475.	3.8	109
5560	Modeling of phase stability of the fcc phases in the Niâ€“Irâ€“Al system using the cluster/site approximation method coupling with first-principles calculations. Acta Materialia, 2008, 56, 2576-2584.	3.8	16
5561	Cubic MgH2 stabilized by alloying with transition metals: A density functional theory study. Acta Materialia, 2008, 56, 2948-2954.	3.8	41
5562	First-principles calculations of the structural and thermodynamic properties of bcc, fcc and hcp solid solutions in the Alâ€“TM (TM=Ti, Zr and Hf) systems: A comparison of cluster expansion and supercell methods. Acta Materialia, 2008, 56, 3202-3221.	3.8	132
5563	Point defect thermodynamics and diffusion in Fe3C: A first-principles study. Acta Materialia, 2008, 56, 3236-3244.	3.8	26
5564	Theoretical investigation of typical fcc precipitates in Mg-based alloys. Acta Materialia, 2008, 56, 3353-3357.	3.8	43
5565	The effect of platinum on defect formation energies in Î²-NiAl. Acta Materialia, 2008, 56, 3502-3510.	3.8	37
5566	Atomic mobilities, diffusivities and simulation of diffusion growth in the Coâ€“Si system. Acta Materialia, 2008, 56, 3940-3950.	3.8	69
5567	Stability of Tiâ€“Bâ€“N solid solutions and the formation of nc-TiN/a-BN nanocomposites studied by combined ab initio and thermodynamic calculations. Acta Materialia, 2008, 56, 4440-4449.	3.8	40
5568	Influence of Pb segregation on the deformation of nanocrystalline Al: Insights from molecular simulations. Acta Materialia, 2008, 56, 4750-4761.	3.8	33
5569	First-principles density functional theory study of phase transformations in NbCr2 and TaCr2. Acta Materialia, 2008, 56, 4984-4992.	3.8	34
5570	A model for evolution of shape changing precipitates in multicomponent systems. Acta Materialia, 2008, 56, 4896-4904.	3.8	24
5571	Thermodynamic modeling of the Crâ€“Pt binary system using the cluster/site approximation coupling with first-principles energetics calculation. Acta Materialia, 2008, 56, 5796-5803.	3.8	10

#	Article	IF	Citations
5572	Lattice stability, elastic constants and macroscopic moduli of NiTi martensites from first principles. Acta Materialia, 2008, 56, 6232-6245.	3.8	200
5573	First-principles study of site occupancy of dilute 3d, 4d and 5d transition metal solutes in L10 TiAl. Acta Materialia, 2008, 56, 6224-6231.	3.8	49
5574	A DFT study of pseudomorphic monolayer Pt and Pd catalysts for NOx storage reduction applications. Catalysis Today, 2008, 136, 76-83.	2.2	24
5575	Coupled theoretical and experimental analysis of surface coverage effects in Pt-catalyzed NO and O2 reaction to NO2 on Pt(111). Catalysis Today, 2008, 136, 84-92.	2.2	79
5576	Structure of the hydrogen bonds and silica defects in the tetrahedral double chain of xonotlite. Cement and Concrete Research, 2008, 38, 300-311.	4.6	41
5577	Atomistic simulation of Siâ€“Ge clathrate alloys. Chemical Physics, 2008, 344, 299-308.	0.9	9
5578	Transition phase and thermodynamic properties of PtC from first-principles calculations. Solid State Communications, 2008, 145, 91-94.	0.9	71
5579	A comparative study of the electronic band structures of hydrogen-terminated silicon chains by density functional theory with and without GW correction. Solid State Communications, 2008, 145, 275-278.	0.9	19
5580	Phase transformation in Sm2O3 at high pressure: In situ synchrotron X-ray diffraction study and ab initio DFT calculation. Solid State Communications, 2008, 145, 250-254.	0.9	59
5581	Band structure and dielectric properties of orthorhombic SrZrO3. Solid State Communications, 2008, 145, 497-501.	0.9	35
5582	First-principles study of structural and elastic properties of Sc2AC (A=Al, Ga, In, Tl). Solid State Communications, 2008, 146, 175-180.	0.9	36
5583	On the structural stability of ZnO phases. Solid State Communications, 2008, 146, 324-329.	0.9	43
5584	Ferromagnetism in polycrystalline Cr-doped ZnO films: Experiment and theory. Solid State Communications, 2008, 146, 420-424.	0.9	28
5585	Atomic ordering recognized by convergence characteristics of the radial distribution function. Solid State Communications, 2008, 146, 468-471.	0.9	4
5586	Electronic structure and mechanical properties of osmium borides, carbides and nitrides from first principles. Solid State Communications, 2008, 146, 450-453.	0.9	45
5587	Lattice dynamics and electronic properties of the scintillator host material: Barium hafnate. Solid State Communications, 2008, 147, 1-3.	0.9	24
5588	Lattice dynamics and elastic properties of lanthanum monopnictides. Solid State Communications, 2008, 147, 221-225.	0.9	27
5589	First principles linear response calculations of phonons for ScP and ScAs. Solid State Communications, 2008, 147, 198-200.	0.9	11

#	Article	IF	Citations
5590	First principles study of the elastic properties in X2S (X=Li, Na, K and Rb) compounds under pressure effect. Solid State Communications, 2008, 147, 178-182.	0.9	26
5591	Theoretical models of ZnS nanoclusters and nanotubes: First-principles calculations. Solid State Communications, 2008, 147, 165-168.	0.9	20
5592	N dopant induced antiferromagnetism in anatase TiO2 : First principle study. Solid State Communications, 2008, 147, 169-171.	0.9	24
5593	Half-metallic ferromagnetism in Ca-doped AlN from first-principles study. Solid State Communications, 2008, 147, 254-257.	0.9	20
5594	Structural phases of SrHfO3. Solid State Communications, 2008, 148, 29-31.	0.9	44
5595	First-principles calculations on phase transition and elasticity of CdO under pressure. Solid State Communications, 2008, 148, 6-9.	0.9	29
5596	Effect of dopants on the structure and properties of Ge2Sb2Te5 studied by Ab initio calculations. Solid State Communications, 2008, 148, 113-116.	0.9	23
5597	Studies of the mechanism of electrical conduction in As-doped ZnO by structural and chemical-bonding analyses and first principle calculations. Solid State Communications, 2008, 148, 301-304.	0.9	15
5598	Elastic constants of B2-MgRE (REÂ= ÂSc, Y, Laâ€“Lu) calculated with first-principles. Solid State Communications, 2008, 148, 314-318.	0.9	54
5599	Structural and electronic properties of M2InC (M = Ti, Zr, and Hf). Solid State Communications, 2008, 148, 459-463.	0.9	27
5600	Elastic and electronic properties of oxygen and carbon incorporated into Zr3N4 and Hf3 N4. Solid State Communications, 2008, 148, 563-565.	0.9	9
5601	Optical investigations using ultra-soft pseudopotential calculations of Si0.5Ge0.5 alloy. Solid State Communications, 2008, 148, 521-524.	0.9	59
5602	First-principles study of the size-dependent structural and electronic properties of thick-walled ZnO nanotubes. Solid State Communications, 2008, 148, 534-537.	0.9	20
5603	Ab initio calculation of Ag monolayer adhesion on BaTiO3 (100) surfaces. Surface and Coatings Technology, 2008, 202, 3284-3289.	2.2	11
5604	First-principles study of atomic oxygen adsorption on boron-substituted graphite. Surface Science, 2008, 602, 37-45.	0.8	22
5605	Atomistic study of metal clusters supported on oxide surface. Surface Science, 2008, 602, 46-53.	0.8	10
5606	Adsorbate induced reconstruction of cobalt surfaces. Surface Science, 2008, 602, 17-27.	0.8	97
5607	Adsorption and dissociation of methanol on the fully oxidized and partially reduced (111) cerium oxide surface: Dependence on the configuration of the cerium 4f electrons. Surface Science, 2008, 602, 162-175.	0.8	61

#	Article	IF	Citations
5608	Density functional study of surface properties of chromium. Surface Science, 2008, 602, 517-524.	0.8	27
5609	First principles study of hydrogen atom adsorption and diffusion on Pd3Ag(1 1 1) surface and in its subsurface. Surface Science, 2008, 602, 859-863.	0.8	29
5610	Ab initio study of element segregation and oxygen adsorption on PtPd and CoCr binary alloy surfaces. Surface Science, 2008, 602, 876-884.	0.8	31
5611	Spin-orbit modifications and splittings of deep surface states on clean Au(111). Surface Science, 2008, 602, 893-905.	0.8	34
5612	Water on the hydroxylated (001) surface of kaolinite: From monomer adsorption to a flat 2D wetting layer. Surface Science, 2008, 602, 960-974.	0.8	155
5613	Ab initio study of pentacene on the Fe(100) surface. Surface Science, 2008, 602, 1191-1198.	0.8	10
5614	Facilitated vacancy formation at Zr-doped ceria(111) surfaces. Surface Science, 2008, 602, 1199-1206.	0.8	68
5615	Atomic and electronic structures of Tl/Si(111)-. Surface Science, 2008, 602, 1376-1380.	0.8	12
5616	Adsorption of phosphonic and ethylphosphonic acid on aluminum oxide surfaces. Surface Science, 2008, 602, 1347-1359.	0.8	97
5617	CO and O coadsorption on Pt3Sn studied by DFT: Changes in the adsorptive properties of the surface with alloying and coverage. Surface Science, 2008, 602, 1636-1642.	0.8	18
5618	Oxygen adsorption on Zr(0001) surfaces: Density functional calculations and a multiple-layer adsorption model. Surface Science, 2008, 602, 2212-2216.	0.8	23
5619	The structure and reactivity of 2-butanol on Pd(111). Surface Science, 2008, 602, 2264-2270.	0.8	18
5620	Facile dissociation of CO on Fe{211}: Evidence from microcalorimetry and first-principles theory. Surface Science, 2008, 602, 2325-2332.	0.8	42
5621	Lateral electronic confinement in unidimensional noble metal (Au, Pt) nanowires. Surface Science, 2008, 602, L104-L107.	0.8	4
5622	Zigzag chain structures of Gd on the Mo(110) surface. Surface Science, 2008, 602, 2610-2616.	0.8	16
5623	Theoretical structure and surface energy of the reconstructed {01.2} form of calcite (CaCO3) crystal. Surface Science, 2008, 602, 2774-2782.	0.8	35
5624	Theoretical investigation of Mn adsorbates aside self-organised Bi nanolines on hydrogenated Si(001) surface. Surface Science, 2008, 602, 2789-2795.	0.8	6
5625	Formation of one-dimensional molybdenum oxide on Mo(112). Surface Science, 2008, 602, 3338-3342.	0.8	23

#	Article	IF	Citations
5626	Bonding of Pt/Fe overlayer and its effects on atomic oxygen chemisorption from density functional theory study. Surface Science, 2008, 602, 3415-3423.	0.8	15
5627	The role of preadsorbed sulphur and oxygen in O2 dissociation on Pd(100). Surface Science, 2008, 602, 3660-3666.	0.8	3
5628	Surface relaxation and tilting in SrHfO3 orthorhombic perovskite: Hybrid HF-DFT LCAO calculations. Surface Science, 2008, 602, 3674-3682.	0.8	15
5629	Analysis of defects on BN nano-structures using high-resolution electron microscopy and density-functional calculations. Ultramicroscopy, 2008, 108, 1484-1489.	0.8	4
5630	Structural and electronic properties of 2,4,6-trinitrophenol (TNP). Computational and Theoretical Chemistry, 2008, 857, 33-37.	1.5	14
5631	Characterization of methanethiolate on some transition metals: A first-principle density functional theory study. Computational and Theoretical Chemistry, 2008, 862, 80-84.	1.5	5
5632	A first-principles investigation on the hydrogen bond interaction in DATB. Computational and Theoretical Chemistry, 2008, 864, 89-92.	1.5	7
5633	Adsorption of cyclohexene on nAu/Pt(100) (n=0, 1, 2): A DFT study. Computational and Theoretical Chemistry, 2008, 869, 47-52.	1.5	8
5634	Atomic geometry and electronic structure of defects in Zn3N2. Thin Solid Films, 2008, 516, 1297-1301.	0.8	34
5635	Phase stabilities of self-organized nc-TiN/a-Si3N4 nanocomposites and of Ti1â^'xSixNy solid solutions studied by ab initio calculation and thermodynamic modeling. Thin Solid Films, 2008, 516, 2264-2275.	0.8	73
5636	First-principles study of the electronic and optical properties of lanthanide bromide. Thin Solid Films, 2008, 516, 7894-7898.	0.8	5
5637	Super hard cubic phases of period VI transition metal nitrides: First principles investigation. Thin Solid Films, 2008, 517, 824-827.	0.8	72
5638	Electronic and geometric investigations of the Ca/Si(111)-() surface. Applied Surface Science, 2008, 254, 8083-8088.	3.1	1
5639	Nanostructure formation aided by self-organised Bi nanolines on Si(001). Applied Surface Science, 2008, 254, 8075-8082.	3.1	3
5640	First-principles study of structural, elastic, electronic, and optical properties of hexagonal BiAlO3. Physica B: Condensed Matter, 2008, 403, 539-543.	1.3	73
5641	First-principles calculation of electronic structures and optical properties of wurtzite InxAl1â^'xN alloys. Physica B: Condensed Matter, 2008, 403, 1666-1672.	1.3	23
5642	Stability, electronic and mechanical properties of Fe2B. Physica B: Condensed Matter, 2008, 403, 1723-1730.	1.3	78
5643	First-principles study of the structural and electronic properties of III-phosphides. Physica B: Condensed Matter, 2008, 403, 1876-1881.	1.3	108

#	Article	IF	Citations
5644	Theoretical study on the stability and mechanical property of Cr7C3. Physica B: Condensed Matter, 2008, 403, 2273-2281.	1.3	53
5645	Ab initio calculations of elastic modulus and electronic structures of cubic. Physica B: Condensed Matter, 2008, 403, 2624-2628.	1.3	38
5646	Structural and dynamical properties of iridium surfaces: First principles and molecular dynamics investigations. Physica B: Condensed Matter, 2008, 403, 2748-2753.	1.3	0
5647	Ab initio study of phase transition and thermodynamic properties of PtN. Physica B: Condensed Matter, 2008, 403, 2851-2855.	1.3	92
5648	Systematic trends in boron icosahedral structured materials. Physica B: Condensed Matter, 2008, 403, 2760-2767.	1.3	36
5649	Ab initio calculation of neutral and singly charged Mgn (nâ©½11) clusters. Physica B: Condensed Matter, 2008, 403, 3119-3124.	1.3	16
5650	First-principles study of pressure-induced phase transition in silicon carbide. Physica B: Condensed Matter, 2008, 403, 3543-3546.	1.3	41
5651	A first-principles-derived method for computing the piezoelectric coefficients of complex semiconductor Sc1â^'xGaxN alloys. Physica B: Condensed Matter, 2008, 403, 4174-4181.	1.3	10
5652	The electronic structure and ferromagnetism of TM (TM=V, Cr, and Mn)-doped BN(5,5) nanotube: A first-principles study. Physica B: Condensed Matter, 2008, 403, 4213-4216.	1.3	26
5653	Electronic structure and magnetic state of. Physica B: Condensed Matter, 2008, 403, 4232-4235.	1.3	11
5654	Vibrational Stark tuning rates from periodic DFT calculations: CO/Pt(111). Electrochimica Acta, 2008, 53, 2897-2906.	2.6	13
5655	A methodology to optimize the quantification of sp2 carbon fraction from K edge EELS spectra. Journal of Electron Spectroscopy and Related Phenomena, 2008, 164, 34-43.	0.8	44
5656	Challenges for ab initio defect modeling. Materials Science and Engineering B: Solid-State Materials for Advanced Technology, 2008, 154-155, 187-192.	1.7	18
5657	Computer simulation study of defect formation and migration energy in calcium fluoride. Nuclear Instruments & Methods in Physics Research B, 2008, 266, 2698-2701.	0.6	8
5658	First-principles modelling of radiation defects in advanced nuclear fuels. Nuclear Instruments & Methods in Physics Research B, 2008, 266, 2671-2675.	0.6	14
5659	Density Functional Theory studies of dehydrogenated and zwitterionic glycine and alanine on Pd and Cu surfaces. Journal of Molecular Catalysis A, 2008, 281, 44-48.	4.8	21
5660	Density functional theory study of H2 adsorption on the (100), (001) and (010) surfaces of Fe3C. Journal of Molecular Catalysis A, 2008, 292, 14-20.	4.8	20
5661	The structural peculiarities and chemical bonding in three organogermanes Cl3GeCH2OC(O)R with rigid coordination centre. Journal of Molecular Structure, 2008, 875, 135-142.	1.8	15

#	Article	IF	Citations
5662	First-principles study of the electronic structure and mechanical properties of CaMg2 Laves phase. Materials Science & Engineering A: Structural Materials: Properties, Microstructure and Processing, 2008, 489, 444-450.	2.6	37
5663	New generation of Ni-based superalloys designed on the basis of first-principles calculations. Materials Science & Engineering A: Structural Materials: Properties, Microstructure and Processing, 2008, 497, 18-24.	2.6	38
5664	Structural, electronic and optical properties of SrCl2 under hydrostatic stress. European Physical Journal B, 2008, 61, 165-171.	0.6	8
5665	First-principles study of high pressure phase transformations in Li3N. European Physical Journal B, 2008, 61, 397-403.	0.6	24
5666	First-principles investigation of electronic and optical properties in wurtzite Zn1-xMgxO. European Physical Journal B, 2008, 62, 417-421.	0.6	36
5667	Hydrogen associative desorption from Ru(1010). European Physical Journal B, 2008, 63, 17-24.	0.6	14
5668	Interfacial properties of Ce0.75Zr0.25O2 supported noble metals (Pd, Pt) from first principles. European Physical Journal B, 2008, 63, 455-460.	0.6	4
5669	Electronic and optical properties under pressure effect of alkali metal oxides. European Physical Journal B, 2008, 64, 35-42.	0.6	33
5670	Ab initio study of the diffusion mechanisms of gallium in a silicon matrix. European Physical Journal B, 2008, 64, 165-172.	0.6	11
5671	Stability and magnetism of vacancy in NiO: A GGA+U study. European Physical Journal B, 2008, 64, 153-158.	0.6	57
5672	Optical and piezoelectric anomalies of ordered (Sc, Ga) N and (Sc, In) N ternaries. European Physical Journal B, 2008, 65, 65-77.	0.6	12
5673	Construction and solution of a Wannier-functions based Hamiltonian in the pseudopotential plane-wave framework for strongly correlated materials. European Physical Journal B, 2008, 65, 91-98.	0.6	96
5674	Band-gap bowing and p-type doping of (Zn, Mg, Be)O wide-gap semiconductor alloys: a first-principles study. European Physical Journal B, 2008, 66, 439-444.	0.6	63
5675	Size- and Surface-dependent Stability, Electronic Properties, and Potential as Chemical Sensors: Computational Studies on One-dimensional ZnO Nanostructures. Journal of Physical Chemistry C, 2008, 112, 18926-18931.	1.5	67
5676	Adsorption of <mml:math xmlns:mml="http://www.w3.org/1998/Math/MathML" display="inline"><mml:mrow><mml:msub><mml:mi mathvariant="normal">H</mml:mi><mml:mn>2</mml:mn></mml:msub><mml:mi mathvariant="normal">O</mml:mi></mml:mrow></mml:math>,<mml:math xmlns:mml="http://www.w3.org/1998/Math/MathML" display="inline"><mml:mrow><mml:mi mathvariant="normal">N</mml:mi><mml:msub><mml:mi mathvariant="normal">H</mml:mi><mml:mn>3</mml:mn>	1.1	1,490
5677	Hydrogen spillover in the context of hydrogen storage using solid-state materials. Energy and Environmental Science, 2008, 1, 338.	15.6	133
5678	Structural properties and enthalpy of formation of magnesium hydride from quantum Monte Carlo calculations. Physical Review B, 2008, 77, .	1.1	72
5679	Inducing energy gaps in monolayer and bilayer graphene: Local density approximation calculations. Physical Review B, 2008, 78, .	1.1	117

#	Article	IF	Citations
5680	Hydrogen vacancies facilitate hydrogen transport kinetics in sodium hydride nanocrystallites. Physical Review B, 2008, 78, .	1.1	26
5681	Electron-phonon coupling and electron heat capacity of metals under conditions of strong electron-phonon nonequilibrium. Physical Review B, 2008, 77, .	1.1	1,073
5682	A first-principles study of molecular oxygen dissociation at an electrode surface: a comparison of potential variation and coadsorption effects. Physical Chemistry Chemical Physics, 2008, 10, 3613.	1.3	76
5683	Functionalization of carbon-based nanostructures with light transition-metal atoms for hydrogen storage. Physical Review B, 2008, 77, .	1.1	315
5684	Microscopic mechanisms for improper ferroelectricity in multiferroic perovskites: a theoretical review. Journal of Physics Condensed Matter, 2008, 20, 434208.	0.7	52
5685	Helical [110] Gold Nanowires Make Longer Linear Atomic Chains. Physical Review Letters, 2008, 101, 125502.	2.9	22
5686	Energy level structure of4f5dstates and the Stokes shift inLaPO4:Pr3+: A theoretical study. Physical Review B, 2008, 78, .	1.1	20
5687	Work function changes induced by deposition of ultrathin dielectric films on metals: A theoretical analysis. Physical Review B, 2008, 78, .	1.1	180
5688	¹H, ¹³C, and ¹⁵N Solid-State NMR Studies of Imidazole- and Morpholine-Based Model Compounds Possessing Halogen and Hydrogen Bonding Capabilities. Crystal Growth and Design, 2008, 8, 3941-3950.	1.4	37
5689	First-principles calculations of carbon nanotubes adsorbed on diamond (100) surfaces. Journal of Physics Condensed Matter, 2008, 20, 225016.	0.7	7
5690	First-principles studies of phonon instabilities in AgI under high pressure. Journal of Physics Condensed Matter, 2008, 20, 195218.	0.7	14
5691	Shear deformation in Ti₃Al: atomic, dynamic and static simulations. Modelling and Simulation in Materials Science and Engineering, 2008, 16, 085008.	0.8	2
5692	Interplay between magnetism and structure in atomic-size Pd contacts:Ab initiostudies. Physical Review B, 2008, 77, .	1.1	16
5693	Thermal stability of graphene edge structure and graphene nanoflakes. Journal of Chemical Physics, 2008, 128, 094707.	1.2	82
5694	Density functional study of<mml:math xmlns:mml="http://www.w3.org/1998/Math/MathML" display="inline"><mml:mrow><mml:mrow><mml:mo>âŸ¨</mml:mo><mml:mrow><mml:mn>110</mml:mn></mml:mrow><mml:mo>âŸ© thin silicon nanowires. Physical Review B, 2008, 77, .	1.1	27
5695	Molybdenum at High Pressure and Temperature: Melting from Another Solid Phase. Physical Review Letters, 2008, 100, 135701.	2.9	127
5696	Quantum molecular dynamics simulations of uranium at high pressure and temperature. Physical Review B, 2008, 78, .	1.1	32
5697	First-principles study of physisorption of nucleic acid bases on small-diameter carbon nanotubes. Nanotechnology, 2008, 19, 125701.	1.3	160

#	Article	IF	Citations
5698	Raman scattering in<mml:math xmlns:mml="http://www.w3.org/1998/Math/MathML" display="inline"><mml:mrow><mml:mi mathvariant="normal">K</mml:mi><mml:msub><mml:mi mathvariant="normal">Os</mml:mi><mml:mn>2</mml:mn></mml:msub><mml:msub><mml:mi mathvariant="normal">O</mml:mi><mml:mn>6</mml:mn></mml:msub></mml:mrow></mml:math>. Physical Review B, 2008, 77, .	1.1	57
5699	First principle study of the cation vacancy in anatase TiO₂. Physica Status Solidi - Rapid Research Letters, 2008, 2, 25-27.	1.2	39
5700	Ab initio calculations of electronic and optical properties in O-doped LiF crystal. Open Physics, 2008, 6, .	0.8	1
5701	Band structure and optical properties of antimony-sulfobromide: density functional calculation. Open Physics, 2008, 6, 64-75.	0.8	4
5702	Theoretical study of NO3â^' interacting with carbon nanotube. Open Physics, 2008, 6, 105-108.	0.8	1
5703	Theoretical analysis of the alloying system and design of new nickel-base superalloys. Doklady Physics, 2008, 53, 438-441.	0.2	11
5704	Ab initio calculations of phonon spectra of (GaP) n (AlP) m superlattices. Semiconductors, 2008, 42, 1208-1213.	0.2	7
5705	Ab initio calculations of the vibrational spectra of 1/1 approximant of i-AlCuFe quasicrystal. Physics of the Solid State, 2008, 50, 1326-1332.	0.2	2
5706	Improper ferroelectricity in perovskite oxide artificial superlattices. Nature, 2008, 452, 732-736.	13.7	791
5707	Carrier-mediated magnetoelectricity in complex oxide heterostructures. Nature Nanotechnology, 2008, 3, 46-50.	15.6	306
5708	Promoting O2 activation on noble metal surfaces. Journal of Catalysis, 2008, 254, 349-354.	3.1	23
5709	Mechanism of HCl oxidation (Deacon process) over RuO2. Journal of Catalysis, 2008, 255, 29-39.	3.1	169
5710	Non-localized charge compensation in zeolites: A periodic DFT study of cationic gallium-oxide clusters in mordenite. Journal of Catalysis, 2008, 255, 139-143.	3.1	34
5711	First principles calculations and experimental insight into methane steam reforming over transition metal catalysts. Journal of Catalysis, 2008, 259, 147-160.	3.1	559
5712	Towards an understanding of promoter action in heterogeneously catalyzed ethene epoxidation: Why chlorine is the best halogen. Journal of Catalysis, 2008, 260, 380-383.	3.1	44
5713	Crystal structure and theoretical elastic property of two new ternary ceramics Hf3Al4C6 and Hf2Al4C5. Scripta Materialia, 2008, 58, 679-682.	2.6	46
5714	Ab initio study of electronic and thermodynamic properties of NdNi4Mg and NdNi4MgH4. Scripta Materialia, 2008, 59, 147-150.	2.6	5
5715	Substitutional position and insulator-to-metal transition in Nb-doped SrTiO3. Materials Chemistry and Physics, 2008, 107, 215-219.	2.0	48

#	Article	IF	Citations
5716	The first-principles study on the LaN. Materials Chemistry and Physics, 2008, 108, 120-123.	2.0	95
5717	Theoretical study of the interactions of carbon monoxide with Rh-decorated (8,0) single-walled carbon nanotubes. Materials Chemistry and Physics, 2008, 110, 411-416.	2.0	52
5718	A first-principles study on the structural stability of Al2Ca Al4Ca and Mg2Ca phases. Materials Letters, 2008, 62, 206-210.	1.3	50
5719	Theoretical investigation of atomic-scale (001) twinned martensite in the NiTi alloy. Materials Letters, 2008, 62, 964-966.	1.3	8
5720	Two novel Zintl compounds Na12Ge8Sn and Na15Ge8SnP: Single crystal and electronic structures. Solid State Sciences, 2008, 10, 525-532.	1.5	1
5721	Effects of Cu, N, and Li intercalation on the structural stability and electronic structure of cubic Cu3N. Solid State Sciences, 2008, 10, 1651-1657.	1.5	32
5722	Half metallicity along the edge of zigzag boron nitride nanoribbons. Physical Review B, 2008, 78, .	1.1	226
5723	Modeling the compositional instability in wurtzite<mml:math xmlns:mml="http://www.w3.org/1998/Math/MathML" display="inline"><mml:mrow><mml:msub><mml:mi mathvariant="normal">Ga</mml:mi><mml:mrow><mml:mn>1</mml:mn><mml:mo>â^'</mml:mo><mml:mi>x</mml:mi></mml:mrow></mml:msub><mml:mi mathvariant="normal">In</mml:mi><mml:mi>x</mml:mi></mml:msub><mml:mi mathvariant="normal">N</mml:mi></mml:mrow></mml:math>. Physical Review B, 2008, 77, .	1.1	16
5724	Carburization of the Fe3O4(111) Surface. Journal of Physical Chemistry C, 2008, 112, 6372-6379.	1.5	17
5725	Hydrogen and magnesium incorporation onc-plane andm-plane GaN surfaces. Physical Review B, 2008, 77, .	1.1	24
5726	Generalized valence-force-field model of (Ga,In)(N,P) ternary alloys. Physical Review B, 2008, 78, .	1.1	19
5727	Long-range antiferromagnetic interactions in<mml:math xmlns:mml="http://www.w3.org/1998/Math/MathML" display="inline"><mml:mrow><mml:msub><mml:mrow><mml:mtext>ZnFe</mml:mtext></mml:mrow><mml:mn>2</mml:mn></mml:m xmlns:mml="http://www.w3.org/1998/Math/MathML" display="inline"><mml:mrow><mml:msub><mml:mrow><mml:mtext>CdFe</mml:mtext></mml:mrow><mml:mn>2</mml:mn></mml:m Physical Review B, 2008, 78, .	1.1	46
5728	Marcasite vs. arsenopyrite structural choice in MN2 (M = Ir, Os and Rh) transition metal nitrides. Journal of Materials Chemistry, 2008, 18, 2090.	6.7	21
5729	Density Functional Study of 2D Semiconductor CdSeÂ·hda_{0.5} (hda =) Tj ETQq1 1 0.784314 rgBT /Overloc	3.2	20
5730	Influence of vacancy defect density on electrical properties of armchair single wall carbon nanotube. Diamond and Related Materials, 2008, 17, 563-566.	1.8	12
5731	Template Effects in Vinyl Acetate Synthesis on PdAu Surface Alloys: A Density Functional Theory Study. Journal of the American Chemical Society, 2008, 130, 14406-14407.	6.6	44
5732	Characterizing the Interaction of Pt and PtRu Clusters with Boron-Doped, Nitrogen-Doped, and Activated Carbon: Density Functional Theory Calculations and Parameterization. Journal of Physical Chemistry C, 2008, 112, 13607-13622.	1.5	60
5733	Bulk moduli of wurtzite, zinc-blende, and rocksalt phases of ZnO from chemical bond method and density functional theory. Applied Physics Letters, 2008, 92, .	1.5	28

#	Article	IF	Citations
5734	Hybrid DFT calculations of theFcenters in cubic ABO₃perovskites. Journal of Physics: Conference Series, 2008, 117, 012019.	0.3	9
5735	First-principles supercell studies of the substitutional carbon in c-BN. Diamond and Related Materials, 2008, 17, 2025-2028.	1.8	3
5736	Binding between Carbon and the Au(111) Surface and What Makes It Different from the Sâ^'Au(111) Bond. Journal of Physical Chemistry C, 2008, 112, 17611-17617.	1.5	35
5737	Experimental and Theoretical Studies Suggesting the Possibility of Metallic Boron Nitride Edges in Porous Nanourchins. Nano Letters, 2008, 8, 1026-1032.	4.5	88
5738	O 2 evolution on a clean partially reduced rutile TiO2(110) surface and on the same surface precovered with Au1 and Au2: The importance of spin conservation. Journal of Chemical Physics, 2008, 129, 074705.	1.2	113
5739	Dimer-induced stabilization of H adsorbate cluster on BN(0001) surface. Physical Chemistry Chemical Physics, 2008, 10, 5184.	1.3	12
5740	Semiconductor Nanowires and Nanotubes: Effects of Size and Surface-to-Volume Ratio. ACS Nano, 2008, 2, 2410-2414.	7.3	125
5741	First-Principles Study on Rutile TiO2 Quantum Dots. Journal of Physical Chemistry C, 2008, 112, 13964-13969.	1.5	48
5742	Chemisorption and Reactivity of CH_x (x = 0â^'4) on Feâ^'Co Alloy Surfaces. Journal of Physical Chemistry C, 2008, 112, 13642-13649.	1.5	13
5743	Plane-Wave DFT Investigations of the Adsorption, Diffusion, and Activation of CO on Kinked Fe(710) and Fe(310) Surfaces. Journal of Physical Chemistry C, 2008, 112, 10472-10489.	1.5	48
5744	Role of Semiconducting and Metallic Tubes in P3HT/Carbon-Nanotube Photovoltaic Heterojunctions: Density Functional Theory Calculations. Nano Letters, 2008, 8, 908-912.	4.5	145
5745	Theory of the Sr-induced reconstruction of the Si (001) surface. Journal of Applied Physics, 2008, 103, 103710.	1.1	28
5746	Lattice dynamics investigation of different transition behaviors of cubic BaTiO₃and SrTiO₃by first-principles calculations. Journal of Physics Condensed Matter, 2008, 20, 215215.	0.7	25
5747	Water-Enhanced Low-Temperature CO Oxidation and Isotope Effects on Atomic Oxygen-Covered Au(111). Journal of the American Chemical Society, 2008, 130, 6801-6812.	6.6	171
5748	A first-principles study of NO adsorption and oxidation on Au(111) surface. Journal of Chemical Physics, 2008, 129, 134708.	1.2	48
5749	Computational Studies of the Adsorption and Diffusion of Hydrogen on Feâ^'Co Alloy Surfaces. Journal of Physical Chemistry C, 2008, 112, 3667-3678.	1.5	8
5750	Adsorption and Dissociation of CO on a Feâ^'Co Alloy (110) Surface:â€‰ A Theoretical Study. Journal of Physical Chemistry C, 2008, 112, 3679-3691.	1.5	13
5751	Phonons in few-layer graphene and interplanar interaction: A first-principles study. Physical Review B, 2008, 78, .	1.1	64

#	Article	IF	Citations
5752	Tuning the band structures of single walled silicon carbide nanotubes with uniaxial strain: A first principles study. Applied Physics Letters, 2008, 92, 183116.	1.5	28
5753	Hydrogen Activation on Silver:â€‰ A Computational Study on Surface and Subsurface Oxygen Species. Journal of Physical Chemistry C, 2008, 112, 1628-1635.	1.5	44
5754	Bulk and surface analysis of HÃgg Fe carbide (Fe₅C₂): a density functional theory study. Journal of Physics Condensed Matter, 2008, 20, 064238.	0.7	38
5755	DFT and RAIRS Investigations of Methanol on Cu(110) and on Oxygen-Modified Cu(110). Journal of Physical Chemistry C, 2008, 112, 14034-14040.	1.5	29
5756	No Cage, No Tube: Relative Stabilities of Nanostructures. Journal of Physical Chemistry C, 2008, 112, 13200-13203.	1.5	11
5757	The AM05 density functional applied to solids. Journal of Chemical Physics, 2008, 128, 084714.	1.2	220
5758	First-Principles Study of a Carbon Nanobud. ACS Nano, 2008, 2, 1459-1465.	7.3	59
5759	Electronic and optical properties of Ti1â^'xCdxO2: A first-principles prediction. Applied Physics Letters, 2008, 93, .	1.5	31
5761	Adsorption of atomic and molecular oxygen on the LaMnO3(001) surface: ab initio supercell calculations and thermodynamics. Physical Chemistry Chemical Physics, 2008, 10, 4644.	1.3	115
5762	Systematic investigation of the structure of the Si(553)-Au surface from first principles. Physical Review B, 2008, 77, .	1.1	27
5763	Structural, Electronic, and Optical Properties of N-doped SnO₂. Journal of Physical Chemistry C, 2008, 112, 9861-9864.	1.5	53
5764	The Origin of Stability of Helical Structure of Tellurium. Journal of Physical Chemistry C, 2008, 112, 983-989.	1.5	24
5765	Synergetic Effects of the Cu/Pt{110} Surface Alloy:â€‰ Enhanced Reactivity of Water and Carbon Monoxide. Journal of Physical Chemistry C, 2008, 112, 6422-6429.	1.5	20
5766	Magneto-optical properties of (Ga,Mn)As: Anab initiodetermination. Physical Review B, 2008, 77, .	1.1	24
5767	Electronic structure and magnetism of EuX (X = O, S, Se and Te): A first-principles investigation. Europhysics Letters, 2008, 83, 69001.	0.7	17
5768	Atomic and Electronic Structure of Cerium Oxide Stepped Model Surfaces. Journal of Physical Chemistry C, 2008, 112, 17643-17651.	1.5	40
5769	Phase transition and elastic constants of zirconium from first-principles calculations. Journal of Physics Condensed Matter, 2008, 20, 235230.	0.7	35
5770	High-Pressure Studies of 1,3,5,7-Cyclooctatetraene: Experiment and Theory. Journal of Physical Chemistry A, 2008, 112, 11501-11507.	1.1	12

#	Article	IF	Citations
5771	Edge-functionalized and substitutionally doped graphene nanoribbons: Electronic and spin properties. Physical Review B, 2008, 77, .	1.1	503
5772	Ab initiosupercell calculations on nitrogen-vacancy center in diamond: Electronic structure and hyperfine tensors. Physical Review B, 2008, 77, .	1.1	238
5773	Origin of incommensurate modulations in the high-pressure phosphorus IV phase. Physical Review B, 2008, 78, .	1.1	24
5774	Proximity of antiferromagnetism and superconductivity in<mml:math xmlns:mml="http://www.w3.org/1998/Math/MathML" display="inline"><mml:mrow><mml:msub><mml:mrow><mml:mtext>LaFeAsO</mml:mtext></mml:mrow><mml:mrow><mml:mn>1</mml:mn> Effective Hamiltonian fromab initiostudies. Physical Review B, 2008, 77, .	1.1	245
5775	Stability of MgO(111) Polar Surface:â€‰ Effect of the Environment. Journal of Physical Chemistry C, 2008, 112, 3327-3333.	1.5	26
5776	Lattice dynamics and thermal equation of state of platinum. Physical Review B, 2008, 78, .	1.1	47
5777	First-Principle Calculations of the Adsorption, Dissociation and Diffusion of Hydrogen on the Mg(0001) Surface. Acta Physico-chimica Sinica, 2008, 24, 55-60.	0.6	34
5778	Ab Initio Study of Temperature and Pressure Dependence of Energy and Phonon-Induced Dephasing of Electronic Excitations in CdSe and PbSe Quantum Dots. Journal of Physical Chemistry C, 2008, 112, 7800-7808.	1.5	89
5779	Scattering potentials at Si-Ge and Sn-Ge impurity dimers on Ge(001) studied by scanning tunneling microscopy andab initiocalculations. Physical Review B, 2008, 78, .	1.1	3
5780	Electronic structure and phase stability of MgO, ZnO, CdO, and related ternary alloys. Physical Review B, 2008, 77, .	1.1	186
5781	Platinum-group and noble metals under oxidizing conditions. Journal of Physics Condensed Matter, 2008, 20, 184023.	0.7	52
5782	Trends in adsorption of noble gases He, Ne, Ar, Kr, and Xe on<mml:math xmlns:mml="http://www.w3.org/1998/Math/MathML" display="inline"><mml:mrow><mml:mi mathvariant="normal">Pd</mml:mi><mml:mrow><mml:mo>(</mml:mo><mml:mn>111</mml:mn><mml:mo>)</mml:mo></mml:mrow> All-electron d. Physical Review B, 2008, 77, .	1.1	59
5783	DFT study of urea interaction with potassium chloride surfaces. Molecular Simulation, 2008, 34, 973-979.	0.9	25
5784	Optical properties of rocksalt and zinc blende AlN phases: First-principles calculations. Journal of Applied Physics, 2008, 103, .	1.1	61
5785	Electronic, Energetic, and Chemical Effects of Intrinsic Defects and Fe-Doping of CoAl₂O₄: A DFT+UStudy. Journal of Physical Chemistry C, 2008, 112, 12044-12050.	1.5	75
5786	A first-principles study of linear and nonlinear optical properties of 4-nitro-4[sup Ê¹]-methylbenzylidene aniline. Journal of Chemical Physics, 2008, 129, 094705.	1.2	5
5787	Electronic structure of alkali-metal fluorides, oxides, and nitrides: Density-functional calculations including self-interaction corrections. Physical Review B, 2008, 78, .	1.1	27
5788	Magnetoelectric effect at the<mml:math xmlns:mml="http://www.w3.org/1998/Math/MathML" display="inline"><mml:mrow><mml:msub><mml:mrow><mml:mtext>Fe</mml:mtext></mml:mrow><mml:mrow><mml:mn>3</mml:mn> interface: A first-principles study. Physical Review B, 2008, 78, .	1.1	155

#	Article	IF	Citations
5789	A Computational Study on Adsorption Configurations and Dissociative Reactions of the HN3 Molecule on the TiO2 Anatase (101) Surface. Journal of Physical Chemistry C, 2008, 112, 18017-18027.	1.5	7
5790	Bi₅FeTi₃O₁₅ Hierarchical Microflowers: Hydrothermal Synthesis, Growth Mechanism, and Associated Visible-Light-Driven Photocatalysis. Journal of Physical Chemistry C, 2008, 112, 17835-17843.	1.5	85
5791	Determination of the structure of the high-pressure phase of AuAl₂with the help of first-principles calculations. Journal of Physics Condensed Matter, 2008, 20, 325215.	0.7	5
5792	Probing the surface structure of hydroxyapatite using NMR spectroscopy and first principles calculations. Physical Chemistry Chemical Physics, 2008, 10, 600-606.	1.3	39
5793	First principles calculations of the formation energy and deep levels associated with the neutral and charged vacancy in germanium. Journal of Applied Physics, 2008, 103, .	1.1	25
5794	Electrocatalytic Properties of PtBi and PtPb Intermetallic Line Compounds via DFT: CO and H Adsorption. Journal of Physical Chemistry C, 2008, 112, 8266-8275.	1.5	31
5795	Magnetic properties of carbon doped CdS: A first-principles and Monte Carlo study. Physical Review B, 2008, 77, .	1.1	147
5796	Magneto-elastic effects in compressed cobalt from first-principles. Physical Review B, 2008, 77, .	1.1	21
5797	Density functional calculation of transition metal adatom adsorption on graphene. Journal of Physics Condensed Matter, 2008, 20, 115209.	0.7	210
5798	Sources of Electrical Conductivity in<mml:math xmlns:mml="http://www.w3.org/1998/Math/MathML" display="inline"><mml:msub><mml:mi>SnO</mml:mi><mml:mn>2</mml:mn></mml:msub></mml:math>. Physical Review Letters, 2008, 101, 055502.	2.9	352
5799	A Combined Experimental and Theoretical Charge Density Study of the Chemical Bonding and Magnetism in 3-Amino-propanolato Cu(II) Complexes Containing Weakly Coordinated Anions. Journal of Physical Chemistry A, 2008, 112, 9050-9067.	1.1	50
5800	Electronic structure and optical properties of Li X H ₃ and X LiH ₃ (X = Be, B or C). Chinese Physics B, 2008, 17, 2222-2228.	0.7	8
5801	Ab initio studies of structural and electronic properties. , 2008, , 17-54.		2
5802	A Periodic DFT Study of N₂O₄ Disproportionation on Alkali-Exchanged Zeolites X. Journal of Physical Chemistry C, 2008, 112, 5510-5519.	1.5	37
5803	Dynamics of Hydrogen Spillover on Carbon-Based Materials. Journal of Physical Chemistry C, 2008, 112, 17465-17470.	1.5	62
5804	Universal band gap modulation by radial deformation in semiconductor single-walled carbon nanotubes. Physical Review B, 2008, 78, .	1.1	27
5805	Interplay between External Strain and Oxygen Vacancies on a RutileTiO2(110)Surface. Physical Review Letters, 2008, 101, 116102.	2.9	67
5806	Graphene: A perfect nanoballoon. Applied Physics Letters, 2008, 93, .	1.5	346

#	Article	IF	Citations
5807	Ab initioinvestigation of phonon dispersion and anomalies in palladium. New Journal of Physics, 2008, 10, 043025.	1.2	20
5808	Phase stability and cohesive properties of Auâ€“Sn intermetallics: A first-principles study. Journal of Materials Research, 2008, 23, 1398-1416.	1.2	15
5809	Methane Activation and Oxygen Vacancy Formation over CeO₂ and Zr, Pd Substituted CeO₂ Surfaces. Journal of Physical Chemistry C, 2008, 112, 14955-14964.	1.5	180
5810	Modeling of Graphite Oxide. Journal of the American Chemical Society, 2008, 130, 10697-10701.	6.6	736
5811	High-pressure phase transitions in MgSiO3 orthoenstatite studied by atomistic computer simulation. American Mineralogist, 2008, 93, 528-532.	0.9	27
5812	First-principles calculations for elastic properties of rutile TiO ₂ under pressure. Chinese Physics B, 2008, 17, 2216-2221.	0.7	47
5813	Migration of Ag in low-temperature Ag2S from first principles. Journal of Chemical Physics, 2008, 128, 014704.	1.2	26
5814	Origin of the hot phonon effect in group-III nitrides. Physical Review B, 2008, 77, .	1.1	25
5815	The Role of Surface Oxygen Vacancies in the NO₂ Sensing Properties of SnO₂ Nanocrystals. Journal of Physical Chemistry C, 2008, 112, 19540-19546.	1.5	181
5816	Chemical doping-induced gap opening and spin polarization in graphene. Physical Review B, 2008, 77, .	1.1	128
5817	First-principles simulations of dissociated and molecular<mml:math xmlns:mml="http://www.w3.org/1998/Math/MathML" display="inline"><mml:msub><mml:mi mathvariant="normal">H</mml:mi><mml:mn>2</mml:mn></mml:msub></mml:math>adsorption on<mml:math xmlns:mml="http://www.w3.org/1998/Math/MathML" display="inline"><mml:msub><mml:mi mathvariant="normal">Pd</mml:mi><mml:mn>4</mml:mn></mml:msub></mml:math>-cluster-functionalized	1.1	8
5818	Structural, electronic and magnetic properties of manganese doping in the upper layer of bilayer graphene. Nanotechnology, 2008, 19, 205708.	1.3	55
5819	Ab initioinvestigation of boron diffusion paths in germanium. Physical Review B, 2008, 77, .	1.1	14
5820	First-principles calculations of boron-rich compounds of B13N2and B12C2X (X = Si, Ge). Journal of Physics Condensed Matter, 2008, 20, 505211.	0.7	9
5821	Concentration of intrinsic defects and self-diffusion in GaSb. Journal of Applied Physics, 2008, 104, 093714.	1.1	25
5822	Methanol and Water Dissociation on TiO2 (110): The Role of Surface Oxygen. Journal of Physical Chemistry C, 2008, 112, 17737-17740.	1.5	92
5823	Boron nitride and carbon double-wall hetero-nanotubes: first-principles calculation of electronic properties. Nanotechnology, 2008, 19, 095707.	1.3	12
5824	Adsorption of diatomic molecules on iron tape-porphyrin: A comparative study. Physical Review B, 2008, 77, .	1.1	26

#	Article	IF	Citations
5825	Semiconductor to metal transition in SWNTs caused by interaction with gold and platinum nanoparticles. Journal of Physics Condensed Matter, 2008, 20, 215211.	0.7	31
5826	First-principles study of native defects and lanthanum impurities in<mml:math xmlns:mml="http://www.w3.org/1998/Math/MathML" display="inline"><mml:mrow><mml:msub><mml:mrow><mml:mtext>NaTaO</mml:mtext></mml:mrow><mml:mn>3</mml:mn></mml:msub></mml:mrow></mml:math>. Physical Review B, 2008, 78, .	1.1	58
5827	Quantum Confinement and Electronic Properties of Rutile TiO₂ Nanowires. Journal of Physical Chemistry C, 2008, 112, 20241-20245.	1.5	50
5828	Chemical Functionalization of Single-Walled Carbon Nanotubes (SWNTs) by Aryl Groups: A Density Functional Theory Study. Journal of Physical Chemistry C, 2008, 112, 13141-13149.	1.5	29
5829	First-principles study of ZnS nanostructures: nanotubes, nanowires and nanosheets. Nanotechnology, 2008, 19, 305708.	1.3	36
5830	Stability and magnetism of hydrogen dimers on graphene. Physical Review B, 2008, 78, .	1.1	103
5831	On the Mechanisms of Hydrogen Spillover in MoO₃. Journal of Physical Chemistry C, 2008, 112, 1755-1758.	1.5	98
5832	Characterization of Layered Î³-Titanium Phosphate (C2H5NH3)[Ti(H1.5PO4)(PO4)]2Â·H2O Intercalate: A Combined NMR, Synchrotron XRD, and DFT Calculations Study. Chemistry of Materials, 2008, 20, 3944-3953.	3.2	27
5833	Electronic structure, bonding and phonon modes in the negative thermal expansion materials of Cd(CN)₂and Zn(CN)₂. Journal of Physics Condensed Matter, 2008, 20, 275224.	0.7	36
5834	Thermodynamic stabilities of ternary metal borides: Anab initioguide for synthesizing layered superconductors. Physical Review B, 2008, 78, .	1.1	29
5835	Ab initiostudy of boron-hydrogen complexes in diamond and their effect on electronic properties. Physical Review B, 2008, 78, .	1.1	14
5836	Direct measurements andab initiosimulations for expanded fluid aluminum in the metal-nonmetal transition range. Physical Review B, 2008, 78, .	1.1	59
5837	Experiments and simulations on hot expanded boron. Physical Review E, 2008, 77, 026409.	0.8	19
5838	Structures and superconducting properties of the high-pressure IV and V phases of calcium from first principles. Physical Review B, 2008, 78, .	1.1	33
5839	Fermi surface nesting and phonon instabilities in simple cubic calcium. High Pressure Research, 2008, 28, 443-448.	0.4	30
5840	First-principles calculations of structural, electronic and optical properties of orthorhombic CaPbO₃. Journal Physics D: Applied Physics, 2008, 41, 065405.	1.3	10
5841	Ab initioinvestigation of hybrid organic-inorganic perovskites based on tin halides. Physical Review B, 2008, 77, .	1.1	398
5842	Evaluation of first-principles techniques for obtaining materials parameters of<mml:math xmlns:mml="http://www.w3.org/1998/Math/MathML" display="inline"><mml:mi>Î±</mml:mi></mml:math>-uranium and the (001)<mml:math xmlns:mml="http://www.w3.org/1998/Math/MathML" display="inline"><mml:mi>Î±</mml:mi></mml:math>-uranium surface. Physical Review B, 2008, 77, .	1.1	93

#	Article	IF	Citations
5843	Silicon Carbide Nanotubes As Potential Gas Sensors for CO and HCN Detection. Journal of Physical Chemistry C, 2008, 112, 15985-15988.	1.5	133
5844	Novel One-Dimensional Organometallic Half Metals: Vanadium-Cyclopentadienyl, Vanadium-Cyclopentadienyl-Benzene, and Vanadium-Anthracene Wires. Nano Letters, 2008, 8, 3640-3644.	4.5	131
5845	Theoretical study of crystal and electronic structures of BiI₃. Journal of Physics Condensed Matter, 2008, 20, 325220.	0.7	23
5846	Magneto-mechanical coupling behavior of defective single-walled carbon nanotubes. Nanotechnology, 2008, 19, 325701.	1.3	5
5847	Nonmonotonic Composition Dependence of the Dielectric Response of Ba_{1â^'x}Ca_xZrO₃. Chemistry of Materials, 2008, 20, 5134-5138.	3.2	12
5848	First-Principles Calculations for Elastic Properties of ZnS under Pressure. Chinese Physics Letters, 2008, 25, 1064-1067.	1.3	22
5849	Hydroxyl Chain Formation on the Cu(110) Surface: Watching Water Dissociation. Journal of Physical Chemistry C, 2008, 112, 17672-17677.	1.5	52
5850	Wetting of mixed OHâ^•H2O layers on Pt(111). Journal of Chemical Physics, 2008, 128, 074701.	1.2	37
5851	Short-range and long-range contributions to the size effect in metal-ferroelectric-metal heterostructures. Physical Review B, 2008, 77, .	1.1	108
5852	Ab Initio Study of the Hydroxylated Surface of Amorphous Silica: A Representative Model. Chemistry of Materials, 2008, 20, 3336-3344.	3.2	222
5853	Neutral vs Zwitterionic Glycine Forms at the Water/Silica Interface: Structure, Energies, and Vibrational Features from B3LYP Periodic Simulations. Langmuir, 2008, 24, 14027-14034.	1.6	47
5854	First-principles study of Schottky barrier formation of a semiconducting carbon nanotube-metal contact. , 2008, , .		0
5855	Ab initio study of Pb antisite defects in <mml:math xmlns:mml="http://www.w3.org/1998/Math/MathML" display="inline"><mml:mrow><mml:msub><mml:mrow><mml:mtext>PbZrO</mml:mtext></mml:mrow><mml:mn>3</mml:mn></mml:r xmlns:mml="http://www.w3.org/1998/Math/MathML" display="inline"><mml:mrow><mml:mtext>Pb</mml:mtext><mml:mrow><mml:mo>(</mml:mo><mml:mrow><mml:mtext>Zr</mml:mt Physical Review B, 2008, 78, .	1.1	12
5856	Hypothetical three-dimensional all-<mml:math xmlns:mml="http://www.w3.org/1998/Math/MathML" display="inline"><mml:mrow><mml:mi>s</mml:mi><mml:msup><mml:mi>p</mml:mi><mml:mn>2</mml:mn></mml:msup></mml:mr phase. Physical Review B, 2008, 78, .	1.1	46
5857	First-principles calculations for electronic, optical and thermodynamic properties of ZnS. Chinese Physics B, 2008, 17, 3867-3874.	0.7	44
5858	CO Adsorption and Oxidation on Ceria Surfaces from DFT+U Calculations. Journal of Physical Chemistry C, 2008, 112, 8643-8648.	1.5	264
5859	Combined experimental and theoretical investigation of optical, structural, and electronic properties of <mml:math xmlns:mml="http://www.w3.org/1998/Math/MathML" display="inline"><mml:mrow><mml:mi mathvariant="normal">C</mml:mi><mml:msub><mml:mi mathvariant="normal">H</mml:mi><mml:mn>3</mml:mn></mml:msub><mml:mi mathvariant="normal">N</mml:mi><mml:msub><mml:mi mathvariant="normal">H</mml:mi><mml:mn>3</mml:mn></mml:msub><mml:mi mathvariant="normal">	1.1	128
5860	Surface Pourbaix diagrams and oxygen reduction activity of Pt, Ag and Ni(111) surfaces studied by DFT. Physical Chemistry Chemical Physics, 2008, 10, 3722.	1.3	480

#	Article	IF	Citations
5861	Electron-phonon interactions and high-temperature thermodynamics of vanadium and its alloys. Physical Review B, 2008, 77, .	1.1	36
5862	The effect of stretching thiylâ€“ and ethynylâ€“Au molecular junctions. Journal of Physics Condensed Matter, 2008, 20, 025207.	0.7	14
5863	Electronic Evolution of Poly(3,4-ethylenedioxythiophene) (PEDOT): From the Isolated Chain to the Pristine and Heavily Doped Crystals. Journal of the American Chemical Society, 2008, 130, 16880-16889.	6.6	150
5864	Electronic structure and magnetism of Eu-doped GaN: first-principles study based on LDA+U. Journal Physics D: Applied Physics, 2008, 41, 035004.	1.3	31
5865	<mml:math xmlns:mml="http://www.w3.org/1998/Math/MathML" display="inline"><mml:mrow><mml:mi>G</mml:mi><mml:mi>W</mml:mi></mml:mrow></mml:math>quasiparticle corrections to the<mml:math xmlns:mml="http://www.w3.org/1998/Math/MathML" display="inline"><mml:mrow><mml:mi>LDA</mml:mi><mml:mo>+</mml:mo><mml:mi>U</mml:mi><mml:mo>â^•</mml:mo><mml:mi> structure of bcc hydrogen. Physical Review B, 2008, 77, .	1.1	34
5866	Band structure engineering of graphene by strain: First-principles calculations. Physical Review B, 2008, 78, .	1.1	537
5867	Hydrogen in<mml:math xmlns:mml="http://www.w3.org/1998/Math/MathML" display="inline"><mml:mi>Î±</mml:mi></mml:math>-iron: Stress and diffusion. Physical Review B, 2008, 78, .	1.1	67
5868	Electronic Structures of AlGaN2 Nanotubes and AlN-GaN Nanotube Superlattice. Journal of Chemical Theory and Computation, 2008, 4, 703-707.	2.3	23
5869	<mml:math xmlns:mml="http://www.w3.org/1998/Math/MathML" display="inline"><mml:mrow><mml:msub><mml:mrow><mml:mtext>SrTiO</mml:mtext></mml:mrow><mml:mn>3</mml:mn></mml:m <mml:math xmlns:mml="http://www.w3.org/1998/Math/MathML" display="inline"><mml:mrow><mml:msub><mml:mrow><mml:mtext>BaTiO</mml:mtext></mml:mrow><mml:mn>3</mml:mn></mml:m using the projector augmented wave method: Performance of hybrid and semilocal functionals. Physical Review B, 2008, 78, .	1.1	219
5870	Theory of core-hole effects in<mml:math xmlns:mml="http://www.w3.org/1998/Math/MathML" display="inline"><mml:mrow><mml:mn>1</mml:mn><mml:mi>s</mml:mi></mml:mrow></mml:math>core-level spectroscopy of the first-row elements. Physical Review B, 2008, 77, .	1.1	102
5871	First-principles modeling of the magneto-optical response in inhomogeneous systems. Physical Review B, 2008, 78, .	1.1	5
5872	LDA+DMFT implemented with the pseudopotential plane-wave approach. Journal of Physics Condensed Matter, 2008, 20, 135227.	0.7	40
5873	Modeling bulk and surface Pt using the â€œGaussian and plane waveâ€•density functional theory formalism: Validation and comparison to k-point plane wave calculations. Journal of Chemical Physics, 2008, 129, 234703.	1.2	36
5874	The electronic properties of an oxygen vacancy at ZrO2-terminated (001) surfaces of a cubic PbZrO3: computer simulations from the first principles. Physical Chemistry Chemical Physics, 2008, 10, 4258.	1.3	28
5875	FFSiOH: a New Force Field for Silica Polymorphs and Their Hydroxylated Surfaces Based on Periodic B3LYP Calculations. Chemistry of Materials, 2008, 20, 2522-2531.	3.2	68
5876	Atomic and molecular adsorption on RhMn alloy surface: A first principles study. Journal of Chemical Physics, 2008, 129, 244711.	1.2	13
5877	Bowing of the band gap pressure coefficient in InxGa1â^'xN alloys. Journal of Applied Physics, 2008, 103, 033514.	1.1	53
5878	Stability of intrinsic defects and defect clusters in<mml:math xmlns:mml="http://www.w3.org/1998/Math/MathML" display="inline"><mml:mrow><mml:mi mathvariant="normal">Li</mml:mi><mml:mi mathvariant="normal">Nb</mml:mi><mml:msub><mml:mi mathvariant="normal">O</mml:mi><mml:mn>3</mml:mn></mml:msub></mml:mrow></mml:math>from density functional theory calculations. Physical Review B, 2008, 78, .	1.1	109

#	Article	IF	Citations
5879	Theoretical Study of the Adsorption of Carbon Monoxide on Pristine and Silicon-Doped Boron Nitride Nanotubes. Australian Journal of Chemistry, 2008, 61, 941.	0.5	46
5880	Structural, elastic, and electronic properties of Fe3C from first principles. Journal of Applied Physics, 2008, 103, .	1.1	134
5881	Phonons in aluminum at high temperatures studied by inelastic neutron scattering. Physical Review B, 2008, 77, .	1.1	96
5882	From pure C60 to silicon carbon fullerene-based nanotube: An ab initio study. Journal of Chemical Physics, 2008, 128, 154719.	1.2	10
5883	First-principles calculations of spin-dependent conductance of graphene flakes. Physical Review B, 2008, 78, .	1.1	93
5884	Optical absorption and electronic band structure first-principles calculations of<mml:math xmlns:mml="http://www.w3.org/1998/Math/MathML" display="inline"><mml:mi>Î±</mml:mi></mml:math>-glycine crystals. Physical Review B, 2008, 77, .	1.1	37
5885	Al5O4: A Superatom with Potential for New Materials Design. Journal of Chemical Theory and Computation, 2008, 4, 2011-2019.	2.3	14
5886	Approximation to density functional theory for the calculation of band gaps of semiconductors. Physical Review B, 2008, 78, .	1.1	381
5887	Vacancy-induced magnetism in ZnO thin films and nanowires. Physical Review B, 2008, 77, .	1.1	409
5888	First-principles study of the adsorption of atomic and molecular hydrogen on<mml:math xmlns:mml="http://www.w3.org/1998/Math/MathML" display="inline"><mml:mrow><mml:mi mathvariant="normal">B</mml:mi><mml:msub><mml:mi mathvariant="normal">C</mml:mi><mml:mn>2</mml:mn></mml:msub><mml:mi mathvariant="normal">N</mml:mi></mml:mrow></mml:math>nanotubes. Physical Review B, 2008, 77, .	1.1	30
5889	Ab initiotheory of excitons and optical properties for spin-polarized systems: Application to antiferromagnetic MnO. Physical Review B, 2008, 77, .	1.1	79
5890	Electronic Band Structure of Tetraceneâ"TCNQ and Peryleneâ"TCNQ Compounds. Journal of Physical Chemistry A, 2008, 112, 2497-2502.	1.1	46
5891	Theoretical study of the structural, elastic and electronic properties of the GeX₂O₄(X= Mg, Zn, Cd) compounds under pressure. Modelling and Simulation in Materials Science and Engineering, 2008, 16, 055007.	0.8	30
5892	Free Energy for Protonation Reaction in Lithium-Ion Battery Cathode Materials. Chemistry of Materials, 2008, 20, 5485-5490.	3.2	58
5893	Ïƒ- and Ï€-Defects at Graphene Nanoribbon Edges: Building Spin Filters. Nano Letters, 2008, 8, 2293-2298.	4.5	101
5894	â€‡Stability of wurtzite, unbuckled wurtzite, and rocksalt phases of SiC, GaN, InN, ZnO, and CdSe under loading of different triaxialities. Physical Review B, 2008, 77, .	1.1	62
5895	H₂ Chemisorption on W(100) and W(110) Surfaces. Journal of Physical Chemistry C, 2008, 112, 5579-5588.	1.5	41
5896	DFT Study of Dissociative Adsorption of Hydrogen Sulfide on Cu(111) and Au(111). Langmuir, 2008, 24, 14022-14026.	1.6	56

#	Article	IF	Citations
5897	Adsorption and dissociation of hydrogen molecules on a Pt atom on defective carbon nanotubes. Applied Physics Letters, 2008, 92, 083108.	1.5	19
5898	Phonon softening and the phase transition in VN. Physical Review B, 2008, 78, .	1.1	28
5899	Adsorption and Protonation of CO₂ on Partially Hydroxylated Î³-Al₂O₃ Surfaces: A Density Functional Theory Study. Langmuir, 2008, 24, 12410-12419.	1.6	120
5900	On the prediction of the crystal and electronic structure of mixed-valence materials by periodic density functional calculations: The case of Prussian Blue. Journal of Chemical Physics, 2008, 128, 044713.	1.2	35
5901	Electronic structure and zone-center phonon modes in multiferroic bulk BiFeO3. Journal of Applied Physics, 2008, 103, 083712.	1.1	35
5902	Electronic structures of SiC nanoribbons. Journal of Chemical Physics, 2008, 129, 174114.	1.2	222
5903	Connector model for describing many-body interactions at surfaces. Physical Review B, 2008, 78, .	1.1	13
5904	Switching on magnetism in Ni-doped graphene: Density functional calculations. Physical Review B, 2008, 78, .	1.1	83
5905	First-principles investigation on electronics characteristics of benzene derivatives with different side groups. Journal of Chemical Physics, 2008, 129, 094702.	1.2	52
5906	Density functional calculation of band-parameters for boron nitride at normal and high pressures. Journal of Alloys and Compounds, 2008, 448, 11-16.	2.8	17
5907	First-principles investigations of isotope effects in thermodynamic properties of TiX2 (X=H, D, and T) system. Journal of Alloys and Compounds, 2008, 450, 369-374.	2.8	27
5908	Lattice stability of intermediate phases of the Srâ€“Si system. Journal of Alloys and Compounds, 2008, 457, 29-35.	2.8	16
5909	Molecular dynamics study on planar clustering of xenon in UO2. Journal of Alloys and Compounds, 2008, 457, 465-471.	2.8	54
5910	Structure and optical properties of - and -cerium sesquisulfide. Journal of Alloys and Compounds, 2008, 459, 438-446.	2.8	16
5911	Energetic evaluation of possible insertion sites of Li into La3Ni2Sn7 using a first principle calculation. Journal of Alloys and Compounds, 2008, 462, 284-288.	2.8	3
5912	Thermodynamic modeling of Mgâ€“Caâ€“Ce system by combining first-principles and CALPHAD method. Journal of Alloys and Compounds, 2008, 463, 294-301.	2.8	21
5913	Thermoelectric properties of Al-doped Mg2Si1â^'xSnx (xâ‰¦0.1). Journal of Alloys and Compounds, 2008, 466, 335-340.	2.8	102
5914	First principles calculation of elastic and lattice constants of orthorhombic Cu3Sn crystal. Journal of Alloys and Compounds, 2008, 466, 517-520.	2.8	36

#	Article	IF	Citations
5915	Prediction of the ordering behaviours of the orthorhombic phase based on Ti2AlNb alloys by combining thermodynamic model with ab initio calculation. Intermetallics, 2008, 16, 42-51.	1.8	37
5916	First-principles calculations of the elastic constants of Feâ€“Pt alloys. Intermetallics, 2008, 16, 113-118.	1.8	34
5917	First principle calculations of the Î¹-Fe3AlC perovskite and ironâ€“aluminium intermetallics. Intermetallics, 2008, 16, 345-352.	1.8	72
5918	Phase equilibria, thermodynamics and solidification microstructures of Mgâ€“Snâ€“Ca alloys, Part 1: Experimental investigation and thermodynamic modeling of the ternary Mgâ€“Snâ€“Ca system. Intermetallics, 2008, 16, 299-315.	1.8	86
5919	First-principles and experimental studies of impurity doping into Mg2Si. Intermetallics, 2008, 16, 418-423.	1.8	97
5920	Crystal structure, phase stability and elastic properties of the Laves phase ZrTiCu2. Intermetallics, 2008, 16, 651-657.	1.8	19
5921	Energetic evaluation of the semiconducting mono-, sesqui-, and di-silicides of the 8th group elements (Fe, Ru and Os) using first-principle calculations. Intermetallics, 2008, 16, 769-773.	1.8	6
5922	Ab initio calculations of elastic properties of Ptâ€“Sc alloys. Intermetallics, 2008, 16, 982-986.	1.8	23
5923	Thermodynamic properties of barium silicides from vapor pressure measurements and density functional calculations. Intermetallics, 2008, 16, 1006-1012.	1.8	13
5924	Elastic properties of phase D (MgSi2O6H2) under pressure: Ab initio investigation. Physics of the Earth and Planetary Interiors, 2008, 170, 215-220.	0.7	24
5925	Ferrous iron in post-perovskite from first-principles calculations. Physics of the Earth and Planetary Interiors, 2008, 168, 147-152.	0.7	40
5926	Elastic properties of the post-perovskite phase of Fe2O3 and implications for ultra-low velocity zones. Physics of the Earth and Planetary Interiors, 2008, 170, 260-266.	0.7	15
5927	Hydrogen insertion effects on the magnetic properties and chemical bonding within C14 Laves phases. Progress in Solid State Chemistry, 2008, 36, 192-212.	3.9	7
5928	A First-Principle Study of Chain Propagation Steps in the Fischerâ€“Tropsch Synthesis on Fe(100). Journal of Physical Chemistry C, 2008, 112, 13681-13691.	1.5	17
5929	First-principles calculations of the ferroelastic transition between rutile-type and<mml:math xmlns:mml="http://www.w3.org/1998/Math/MathML" display="inline"><mml:mrow><mml:msub><mml:mrow><mml:mtext>CaCl</mml:mtext></mml:mrow><mml:mn>2</mml:mn></mml:ms xmlns:mml="http://www.w3.org/1998/Math/MathML" display="inline"><mml:mrow><mml:msub><mml:mrow><mml:mtext>SiO</mml:mtext></mml:mrow><mml:mn>2</mml:mn></mml:msu high pressures. Physical Review B, 2008, 78, .	1.1	4,498
5930	Adsorption and Dissociation of the HCl and Cl₂Molecules on W(111) Surface: A Computational Study. Journal of Physical Chemistry C, 2008, 112, 12342-12348.	1.5	10
5931	Adsorption and Dissociation of CO_x (x = 1, 2) on W(111) Surface :â€‰ A Computational Study. Journal of Physical Chemistry C, 2008, 112, 3341-3348.	1.5	21
5932	Unconventional Pairing Originating from the Disconnected Fermi Surfaces of Superconducting<mml:math xmlns:mml="http://www.w3.org/1998/Math/MathML" display="inline"><mml:msub><mml:mi>LaFeAsO</mml:mi><mml:mrow><mml:mn>1</mml:mn><mml:mo>â^’</mml:mo><mml:mi>x</mml:mi></mml:mrow></mml:msub><mml:mi mathvariant="normal">F</mml:mi><mml:msub><mml:mi>x</mml:mi></mml:msub></mml:math>. Physical Review Letters, 2008, 101, 087004.	2.9	1,552

#	Article	IF	Citations
5933	Hardness of covalent compounds: Roles of metallic component and d valence electrons. Journal of Applied Physics, 2008, 104, .	1.1	166
5934	Melting tungsten nanoparticles: a molecular dynamics study. Journal Physics D: Applied Physics, 2008, 41, 185406.	1.3	37
5935	Density Functional Characterization of the Band Edges, the Band Gap States, and the Preferred Doping Sites of Halogen-Doped TiO₂. Chemistry of Materials, 2008, 20, 6528-6534.	3.2	165
5936	Density-functional theory study of the effects of atomic impurity on the band edges of monoclinic<mml:math xmlns:mml="http://www.w3.org/1998/Math/MathML" display="inline"><mml:mrow><mml:msub><mml:mrow><mml:mtext>WO</mml:mtext></mml:mrow><mml:mn>3</mml:mn></mml:ms Physical Review B, 2008, 77, .	1.1	93
5937	Hydrogen dissociation and diffusion on Ni- and Ti-doped Mg(0001) surfaces. Journal of Chemical Physics, 2008, 128, 094703.	1.2	65
5938	Effect of the local environment on the mobility of dislocations in refractory bcc metals: Concurrent multiscale approach. Physical Review B, 2008, 78, .	1.1	4
5939	First-principles study of the H2 interaction with transition metal (Ti, V, Ni) doped Mg(0001) surface: Implications for H-storage materials. Journal of Chemical Physics, 2008, 129, 174703.	1.2	34
5940	B3LYP Simulation of the Full Vibrational Spectrum of 45S5 Bioactive Silicate Glass Compared to v-Silica. Chemistry of Materials, 2008, 20, 5610-5621.	3.2	42
5941	Molecular dynamics of hydrogen dissociation on an oxygen covered Pt(111) surface. Journal of Chemical Physics, 2008, 128, 154708.	1.2	11
5942	Analysis of semi-empirical interatomic potentials appropriate for simulation of crystalline and liquid Al and Cu. Philosophical Magazine, 2008, 88, 1723-1750.	0.7	374
5943	Structural, electronic, and magnetic properties of<mml:math xmlns:mml="http://www.w3.org/1998/Math/MathML" display="inline"><mml:mrow><mml:mn>3</mml:mn><mml:mi>d</mml:mi></mml:mrow></mml:math>transition metal monatomic chains: First-principles calculations. Physical Review B, 2008, 77, .	1.1	63
5944	Theoretical study of the Moâ€“Ru sigma phase. Calphad: Computer Coupling of Phase Diagrams and Thermochemistry, 2008, 32, 171-176.	0.7	18
5945	A Calphad assessment of Alâ€“Câ€“Fe system with the carbide modelled as an ordered form of the fcc phase. Calphad: Computer Coupling of Phase Diagrams and Thermochemistry, 2008, 32, 361-370.	0.7	60
5946	First-principles based calculation of binary and multicomponent phase diagrams for titanium carbonitride. Calphad: Computer Coupling of Phase Diagrams and Thermochemistry, 2008, 32, 543-565.	0.7	31
5947	Combined ab-initio and experimental assessment of mixed carbides. Calphad: Computer Coupling of Phase Diagrams and Thermochemistry, 2008, 32, 615-623.	0.7	29
5948	Thermodynamic re-assessment of the Alâ€“Ir system. Calphad: Computer Coupling of Phase Diagrams and Thermochemistry, 2008, 32, 686-692.	0.7	16
5949	Predicted glide systems and crystal preferred orientations of polycrystalline silicate Mg-Perovskite at high pressure: Implications for the seismic anisotropy in the lower mantle. Earth and Planetary Science Letters, 2008, 271, 135-144.	1.8	66
5950	Î±â€“Î²â€“Î³ transformations in Mg2SiO4 in Earth's transition zone. Earth and Planetary Science Letters, 2008, 273, 115-122.	1.8	62

#	Article	IF	Citations
5951	Ab initio elastic properties of talc from 0 to 12ÂGPa: Interpretation of seismic velocities at mantle pressures and prediction of auxetic behaviour at low pressure. Earth and Planetary Science Letters, 2008, 274, 327-338.	1.8	60
5952	Thermodynamics, structure, dynamics, and freezing of Mg2SiO4 liquid at high pressure. Geochimica Et Cosmochimica Acta, 2008, 72, 1427-1441.	1.6	127
5953	Characterization of calcium isotopes in natural and synthetic barite. Geochimica Et Cosmochimica Acta, 2008, 72, 5641-5658.	1.6	57
5954	First-principles study of structural and elastic properties of MgSe under hydrostatic pressure. Computational Materials Science, 2008, 41, 538-541.	1.4	15
5955	First-principles study of heavily B-doped silicon. Computational Materials Science, 2008, 42, 161-167.	1.4	8
5956	Implementation of the projector augmented-wave method in the ABINIT code: Application to the study of iron under pressure. Computational Materials Science, 2008, 42, 337-351.	1.4	484
5957	Theoretical study of acetylene adsorption on armchair nanotubes. Computational Materials Science, 2008, 42, 322-328.	1.4	7
5958	Atomistic simulation of misfit dislocation in metal/oxide interfaces. Computational Materials Science, 2008, 42, 426-433.	1.4	12
5959	First principles calculations of thermal equations of state and thermodynamical properties of MgH2 at finite temperatures. Computational Materials Science, 2008, 42, 510-516.	1.4	22
5960	Lattice dynamics of Mg2Si and Mg2Ge compounds from first-principles calculations. Computational Materials Science, 2008, 42, 531-536.	1.4	103
5961	First-principles study of structural, elastic, electronic, and optical properties of orthorhombic BiGaO3. Computational Materials Science, 2008, 42, 614-618.	1.4	38
5962	First-principles study on the structural stability, electronic and magnetic properties of Fe2C. Computational Materials Science, 2008, 42, 692-697.	1.4	55
5963	Theoretical investigations of structural, elastic, electronic and thermal properties of Damiaoite PtIn2. Computational Materials Science, 2008, 43, 243-250.	1.4	35
5964	Ab initio study on the physical properties of CoN3 and RhN3 with skutterudite structure. Computational Materials Science, 2008, 43, 495-500.	1.4	14
5965	Theoretical study of linear monoatomic nanowires, dimer and bulk of Cu, Ag, Au, Ni, Pd and Pt. Computational Materials Science, 2008, 43, 522-530.	1.4	51
5966	Electronic structures of wurtzite ZnO, BeO, MgO and p-type doping in Zn1â^'xYxO (Y=Mg, Be). Computational Materials Science, 2008, 44, 72-78.	1.4	25
5967	Structural and electronic properties of cubic HfO2 surfaces. Computational Materials Science, 2008, 44, 46-52.	1.4	61
5968	Bismuth alloying in GaAs: a first-principles study. Computational Materials Science, 2008, 43, 818-822.	1.4	58

#	Article	IF	Citations
5969	Effect of impurities on grain boundary cohesion in bcc iron. Computational Materials Science, 2008, 43, 736-743.	1.4	62
5970	Interactions between transition metals and defective carbon nanotubes. Computational Materials Science, 2008, 43, 823-828.	1.4	64
5971	Zirconium and hafnium oxide interface with silicon: Computational study of stress and strain effects. Computational Materials Science, 2008, 43, 930-937.	1.4	11
5972	Ab initio calculations for <mml:math xmlns:mml="http://www.w3.org/1998/Math/MathML" altimg="si86.gif" overflow="scroll"><mml:mrow><mml:msub><mml:mrow><mml:mtext>SrF</mml:mtext></mml:mrow><mml:mrow><mml:mn>2</mml:mn> with F- and M-centers. Computational Materials Science, 2008, 43, 980-988.	1.4	13
5973	Electronic structures of relaxed BiOX (X=F, Cl, Br, I) photocatalysts. Computational Materials Science, 2008, 43, 1101-1108.	1.4	164
5974	On the migration and trapping of single self-interstitial atoms in dilute and concentrated Feâ€“Cr alloys: Atomistic study and comparison with resistivity recovery experiments. Computational Materials Science, 2008, 43, 1183-1192.	1.4	63
5975	Formation and stability of di-transition-metal carbides TixZr1â^'xC, TixHf1â^'xC and HfxZr1â^'xC. Computational Materials Science, 2008, 44, 347-350.	1.4	18
5976	Ab initio calculation of the total energy and elastic properties of Laves phase C15 Al2RE (RE=Sc, Y, La,) Tj ETQq1 1 0.784314 rgBT /Over	1.4	48
5977	Electronic structure, elasticity and hardness of diborides of zirconium and hafnium: First principles calculations. Computational Materials Science, 2008, 44, 411-421.	1.4	134
5978	Structural, electronic and mechanical properties of ReN2 from first principles. Computational Materials Science, 2008, 44, 531-535.	1.4	26
5979	First-principles study on the mechanical, electronic and magnetic properties of Fe3C. Computational Materials Science, 2008, 44, 690-694.	1.4	74
5980	Mechanical, electronic and optical properties of antifluorites semiconductors X2C (X=Mg, Be). Computational Materials Science, 2008, 44, 664-669.	1.4	19
5981	Ab initio calculations of elastic constants and thermodynamic properties of NiAl under high pressures. Computational Materials Science, 2008, 44, 774-778.	1.4	319
5982	Phonons and heat capacity of LaAlO3. Computational Materials Science, 2008, 44, 779-782.	1.4	21
5983	Spontaneously Formed Sulfur Adlayers on Gold in Electrolyte Solutions: Adsorbed Sulfur or Gold Sulfide?. Journal of Physical Chemistry C, 2008, 112, 11394-11402.	1.5	87
5984	Atomic and electronic structure of silicon nanocrystals embedded in a silica matrix. Journal of Physics Condensed Matter, 2008, 20, 455209.	0.7	9
5985	Ab initioequation of state for the body-centered-cubic phase of iron at high pressure and temperature. Physical Review B, 2008, 78, .	1.1	34
5986	Pressure effect on the structural and elastic properties of ternary compounds M₂AlC (M) Tj ETQq1 1 0.784314 rgBT /Over	0.3	6

#	Article	IF	Citations
5987	Adsorption of O₂, H₂, CO, NH₃, and NO₂ on ZnO Nanotube:â€‰ A Density Functional Theory Study. Journal of Physical Chemistry C, 2008, 112, 5747-5755.	1.5	280
5988	Structural and Electronic Properties of Selected Rutile and Anatase TiO₂Surfaces:â€‰ An ab Initio Investigation. Journal of Chemical Theory and Computation, 2008, 4, 341-352.	2.3	204
5989	First-principles study of interphase Ni 3 Sn in Snâ€”Ni alloy for anode of lithium ion battery. Chinese Physics B, 2008, 17, 3422-3427.	0.7	20
5990	Strong covalent bonding between two graphene layers. Physical Review B, 2008, 77, .	1.1	147
5991	First-principles study of the electronic structures and magnetic properties of 3d transition metal-doped anatase TiO₂. Journal of Physics Condensed Matter, 2008, 20, 125207.	0.7	60
5992	Interaction of Iron Atoms with Pristine and Defective (8, 0) Boron Nitride Nanotubes. Journal of Physical Chemistry C, 2008, 112, 13571-13578.	1.5	17
5993	Generation of vacancy-interstitial pairs as a possible origin of resistivity switching and ferroelectric properties in<mml:math xmlns:mml="http://www.w3.org/1998/Math/MathML" display="inline"><mml:mrow><mml:msub><mml:mrow><mml:mtext>Cd</mml:mtext></mml:mrow><mml:mrow><mml:mn>1</mml:mn></mml:mr Physical Review B, 2008, 77, .	1.1	25
5994	Electron paramagnetic resonance of sulfur at a split-vacancy site in diamond. Physical Review B, 2008, 78, .	1.1	13
5995	Chemical Functionalization of Graphene with Defects. Nano Letters, 2008, 8, 4373-4379.	4.5	607
5996	Crystalline SiN x Ultrathin Films Grown on AlGaN/GaN Using In Situ Metalorganic Chemical Vapor Deposition. Journal of Electronic Materials, 2008, 37, 628-634.	1.0	23
5997	Adsorption of chlorine on Ag(111): No subsurface Cl at low coverage. Physical Review B, 2008, 78, .	1.1	37
5998	Prompted hydrogenation of carbon nanotubes by doping light metals. Applied Physics Letters, 2008, 93, .	1.5	13
5999	Silicon Carbide Nanotubes Functionalized by Transition Metal Atoms:â€‰ A Density-Functional Study. Journal of Physical Chemistry C, 2008, 112, 2558-2564.	1.5	107
6000	The influence of pressure on the structure and dynamics of hydrogen bonds in zoisite and clinozoisite. Physics and Chemistry of Minerals, 2008, 35, 25-35.	0.3	15
6001	Theory: Periodic Electronic Structure Calculations. , 0, , 323-389.		1
6002	Ground state, phonon spectrum, and superconducting properties of the nonoxide perovskite<mml:math xmlns:mml="http://www.w3.org/1998/Math/MathML" display="inline"><mml:mrow><mml:msub><mml:mrow><mml:mtext>CdCNi</mml:mtext></mml:mrow><mml:mn>3</mml:mn></mml:mr Physical Review B, 2008, 78, .	1.1	23
6003	n-Type Behavior of Graphene Supported on Si/SiO₂ Substrates. ACS Nano, 2008, 2, 2037-2044.	7.3	241
6004	Ab initiocalculations of the thermodynamics and phase diagram of zirconium. Physical Review B, 2008, 78, .	1.1	25

#	Article	IF	Citations
6005	Surface Protonation at the Rutile (110) Interface: Explicit Incorporation of Solvation Structure within the Refined MUSIC Model Framework. Langmuir, 2008, 24, 12331-12339.	1.6	88
6006	Structures and Surface Energies of (100) and Octopolar (111) Faces of Halite (NaCl): an Ab initio Quantum-Mechanical and Thermodynamical Study. Crystal Growth and Design, 2008, 8, 2163-2170.	1.4	46
6007	Electronic structure and lattice dynamical properties of different tetragonal phases of<mml:math xmlns:mml="http://www.w3.org/1998/Math/MathML" display="inline"><mml:mrow><mml:msub><mml:mrow><mml:mtext>BiFeO</mml:mtext></mml:mrow><mml:mn>3</mml:mn></mml:n Physical Review B, 2008, 78, .	1.1	67
6008	First-principles study of hydroxyapatite surfaces and water adsorption. Physical Review B, 2008, 78, .	1.1	100
6009	Prototype electrostatic ground state approach to predicting crystal structures of ionic compounds: Application to hydrogen storage materials. Physical Review B, 2008, 77, .	1.1	61
6010	Theoretical Study of the Thermodynamic and Kinetic Aspects of Terminated (111) Diamond Surfaces. Journal of Physical Chemistry C, 2008, 112, 3018-3026.	1.5	47
6011	First-principles calculation of the effect of stress on the chemical activity of graphene. Applied Physics Letters, 2008, 93, .	1.5	50
6012	Theoretical study of the vibrational edge modes in graphene nanoribbons. Physical Review B, 2008, 78, .	1.1	86
6013	Charge-induced formation of linear Au clusters on thin MgO films: Scanning tunneling microscopy and density-functional theory study. Physical Review B, 2008, 78, .	1.1	64
6014	Phonon spectra of the high-frequency modes in dilute nitride randomGaNxAs1â^'xalloy. Physical Review B, 2008, 77, .	1.1	6
6015	Bonded interactions and the crystal chemistry of minerals: a review. Zeitschrift Fur Kristallographie - Crystalline Materials, 2008, 223, 01-40.	0.4	43
6016	Optimization methods for finding minimum energy paths. Journal of Chemical Physics, 2008, 128, 134106.	1.2	1,360
6017	Density functional perturbation theory with spin-orbit coupling: Phonon band structure of lead. Physical Review B, 2008, 78, .	1.1	66
6018	Low Dimensional Nanomaterials for Spintronics. , 2008, , 247-271.		0
6019	Effect of B-complexes on lattice structure and electronic properties in heavily boron-doped diamond. Diamond and Related Materials, 2008, 17, 234-239.	1.8	18
6020	Phase stability of cation-doped LiMnO₂within the GGA+U approximation. Modelling and Simulation in Materials Science and Engineering, 2008, 16, 055008.	0.8	9
6021	Theoretical investigation on the interaction of nitrogen with dislocations in single crystal CVD diamond. Diamond and Related Materials, 2008, 17, 123-126.	1.8	3
6022	Modeling of Nanoscale Morphology of Regioregular Poly(3-hexylthiophene) on a ZnO (101Ì...0) Surface. Nano Letters, 2008, 8, 4185-4190.	4.5	33

#	Article	IF	Citations
6023	Syntheses, Structures, Physical Properties, and Electronic Properties of Some AMUQ₃ Compounds (A = Alkali Metal, M = Cu or Ag, Q = S or Se). Inorganic Chemistry, 2008, 47, 6873-6879.	1.9	30
6024			

#	Article	IF	Citations
6041	Lattice dynamics study of bismuth IIIâ€“V compounds. Journal of Physics Condensed Matter, 2008, 20, 415221.	0.7	28
6042	Electronic Band Structure of Transparent Conductor: Nb-Doped Anatase TiO2. Applied Physics Express, 2008, 1, 111203.	1.1	134
6043	A first-principle analysis on the phase stabilities, chemical bonds and band gaps of wurtzite structure A_xZn_{1â^'x}O alloys (A = Ca, Cd, Mg). Journal of Physics Condensed Matter, 2008, 20, 235221.	0.7	67
6044	Fundamental influence of segregated Bi on the mechanical properties of interconnect of bismuth-containing solder and copper. , 2008, , .		0
6045	Origin of the colossal positive and negative thermal expansion in Ag3[Co(CN)6]: anab initiodensity functional theory study. Journal of Physics Condensed Matter, 2008, 20, 255226.	0.7	23
6046	First principles site occupation and migration of hydrogen, helium, and oxygen in Î²-phase erbium hydride. Journal of Applied Physics, 2008, 103, .	1.1	34
6047	Magnetic phase stability and spin-dependent transport in<mml:math xmlns:mml="http://www.w3.org/1998/Math/MathML" display="inline"><mml:mrow><mml:msub><mml:mi>CeNi</mml:mi><mml:mn>4</mml:mn></mml:msub><mml:mi>M</mml:mi></mml:	1.1	7
6048	Size dependence of structural, electronic, elastic, and optical properties of selenium nanowires: A first-principles study. Journal of Chemical Physics, 2008, 128, 044718.	1.2	22
6049	Uranyl interaction with the hydrated (001) basal face of gibbsite: A combined theoretical and spectroscopic study. Journal of Chemical Physics, 2008, 129, 244704.	1.2	30
6050	The effect of dopants on the dielectric constant of HfO2 and ZrO2 from first principles. Applied Physics Letters, 2008, 92, .	1.5	159
6051	First-principles study on the elastic anisotropy of Au-Sn intermetallic compounds. , 2008, , .		0
6052	Surface dipole induced by alkanethiolate adsorbated on Au(111). , 2008, , .		0
6053	Elastic properties of the high-pressure rock-salt phase of ZnO. Philosophical Magazine Letters, 2008, 88, 181-190.	0.5	8
6054	Stability of singly hydrated silanone on silicon quantum dot surfaces: density functional simulations. Physical Chemistry Chemical Physics, 2008, 10, 4495.	1.3	7
6055	Size- and Strain-Dependent Electronic Structures in H-Passivated Si [112] Nanowires. Journal of Physical Chemistry C, 2008, 112, 15680-15683.	1.5	25
6056	Atomic and Electronic Structure at Au/CdSe Interfaces. ACS Nano, 2008, 2, 2225-2236.	7.3	21
6057	On the possibility of ferromagnetism in carbon-doped anatase TiO2. Applied Physics Letters, 2008, 93, 132507.	1.5	125
6058	Alkali-metal-filled<mml:math xmlns:mml="http://www.w3.org/1998/Math/MathML" display="inline"><mml:mrow><mml:mi mathvariant="normal">Co</mml:mi><mml:msub><mml:mi mathvariant="normal">Sb</mml:mi><mml:mn>3</mml:mn></mml:msub></mml:mrow></mml:math>skutterudites as thermoelectric materials: Theoretical study. Physical Review B, 2008, 77, .	1.1	52

#	Article	IF	Citations
6059	Theoretical Investigation of the Uranyl Ion Sorption on the Rutile TiO₂(110) Face. Inorganic Chemistry, 2008, 47, 10991-10997.	1.9	35
6060	Microscopic Characterization of the Interface between Aromatic Isocyanides and Au(111):â€‰ A First-Principles Investigation. Journal of Physical Chemistry C, 2008, 112, 6413-6421.	1.5	37
6061	Electronic Structures of Defective Boron Nitride Nanotubes under Transverse Electric Fields. Journal of Physical Chemistry C, 2008, 112, 8424-8428.	1.5	30
6062	Ab initiosimulation of photoemission spectroscopy in solids: Plane-wave pseudopotential approach with applications to normal-emission spectra of Cu(001) and Cu(111). Physical Review B, 2008, 77, .	1.1	9
6063	Ultrathin TiO₂ Films on (1Ã—2)-Pt(110): a LEED, Photoemission, STM, and Theoretical Investigation. Journal of Physical Chemistry C, 2008, 112, 20038-20049.	1.5	20
6064	NH₃ Oxidation on Oxygen-Precovered Au(111):â€‰ A Density Functional Theory Study on Selectivity. Journal of Physical Chemistry C, 2008, 112, 247-252.	1.5	32
6065	Thermophysical properties of warm dense hydrogen using quantum molecular dynamics simulations. Physical Review B, 2008, 77, .	1.1	204
6066	Hydrogen Storage in Pillared Li-Dispersed Boron Carbide Nanotubes. Journal of Physical Chemistry C, 2008, 112, 8458-8463.	1.5	105
6067	Hydrogen Storage in Ti-Decorated BC₄N Nanotube. Journal of Physical Chemistry C, 2008, 112, 17487-17491.	1.5	37
6068	Diamond to Î²-Sn phase transition of silicon under hydrostatic and nonhydrostatic compressions. Journal of Physics Condensed Matter, 2008, 20, 325232.	0.7	11
6069	First-principles study of cubic Bi pyrochlores. Physical Review B, 2008, 77, .	1.1	61
6070	Adsorption and Decomposition of CO on Stepped Fe(310) Surfaces. Journal of Physical Chemistry C, 2008, 112, 3692-3700.	1.5	17
6071	Effect of Codoping in Î±-Rhombohedral Boron. Journal of Physical Chemistry C, 2008, 112, 2711-2715.	1.5	12
6072	First-Principles Calculation of ¹³C NMR Chemical Shifts of Infinite Single-Walled Carbon Nanotubes: New Data for Large-Diameter and Four-Helical Nanotubes. Journal of Physical Chemistry C, 2008, 112, 16417-16421.	1.5	18
6073	(Ba,K,La)<mml:math xmlns:mml="http://www.w3.org/1998/Math/MathML" display="inline"><mml:mrow><mml:msub><mml:mrow><mml:mtext>ZrO</mml:mtext></mml:mrow><mml:mn>3</mml:mn></mml:msub></mml:mrow></mml:math> a possible lead-free ferroelectric: Density functional calculations. Physical Review B, 2008, 78, .	1.1	11
6074	Asymmetric Spin Gap Opening of Graphene on Cubic Boron Nitride (111) Substrate. Journal of Physical Chemistry C, 2008, 112, 12683-12686.	1.5	23
6075	Lithium Calcium Imide [Li2Ca(NH)2] for Hydrogen Storage: Structural and Thermodynamic Properties. Journal of Physical Chemistry B, 2008, 112, 11381-11384.	1.2	21
6076	How Electron Localization Function Quantifies and Pictures Chemical Changes in a Solid: The B3 â†' B1 Pressure Induced Phase Transition in BeO. Journal of Physical Chemistry B, 2008, 112, 9787-9794.	1.2	26

#	Article	IF	Citations
6077	Electronic structure ofÎ¼-oxygen at high pressure: GW calculations. Physical Review B, 2008, 78, .	1.1	8
6078	Insight into the Reduction of Pyruvic Acid to Lactic Acid over Cu{110}: The Crucial Role of Intramolecular Tunneling in Direct Hydrogenation. Journal of the American Chemical Society, 2008, 130, 14483-14492.	6.6	12
6079	Formation of Dopant-Pair Defects and Doping Efficiency in B- and P-Doped Silicon Nanowires. Nano Letters, 2008, 8, 3086-3091.	4.5	33
6080	The Displacive Phase Transition of Vanadium Dioxide and the Effect of Doping with Tungsten. Chemistry of Materials, 2008, 20, 1764-1772.	3.2	68
6081	Krylov subspace method for evaluating the self-energy matrices in electron transport calculations. Physical Review B, 2008, 77, .	1.1	37
6082	First-principles calculations of atomic and electronic structure of<mml:math xmlns:mml="http://www.w3.org/1998/Math/MathML" display="inline"><mml:mrow><mml:msub><mml:mrow><mml:mtext>SrTiO</mml:mtext></mml:mrow><mml:mn>3</mml:mn></mml:msub></mml:mrow></mml:math> and (011) surfaces. Physical Review B, 2008, 77, .	1.1	132
6083	Dynamical, dielectric, and elastic properties of GeTe investigated with first-principles density functional theory. Physical Review B, 2008, 78, .	1.1	56
6084	Understanding Trichloroethylene Chemisorption to Iron Surfaces Using Density Functional Theory. Environmental Science & Technology, 2008, 42, 2015-2020.	4.6	21
6085	The Reaction Pathways for HSCH₃Adsorption on Au(111):â€‰ A Density Functional Theory Study. Langmuir, 2008, 24, 3274-3279.	1.6	38
6086	Enhanced Ferromagnetism and Tunable Saturation Magnetization of Mn/C-Codoped GaN Nanostructures Synthesized by Carbothermal Nitridation. Journal of the American Chemical Society, 2008, 130, 16366-16373.	6.6	36
6087	CO Adsorption on Fe₄C (100), (110), and (111) Surfaces in Fischerâ˜Tropsch Synthesis. Journal of Physical Chemistry C, 2008, 112, 19018-19029.	1.5	25
6088	Electronic properties of bulk and thin film<mml:math xmlns:mml="http://www.w3.org/1998/Math/MathML" display="inline"><mml:mrow><mml:msub><mml:mrow><mml:mtext>SrRuO</mml:mtext></mml:mrow><mml:mn>3</mml:mn></mml:msub></mml:mrow></mml:math> Search for the metal-insulator transition. Physical Review B, 2008, 78, .	1.1	143
6089	Intrinsic Diffusion of Hydrogen on Rutile TiO₂(110). Journal of the American Chemical Society, 2008, 130, 9080-9088.	6.6	124
6090	Influence of Surface Reactions on Complex Hydride Reversibility. Journal of Physical Chemistry C, 2008, 112, 18270-18279.	1.5	4
6091	A Density Functional Study on Transition-Metal-Coated Single-Walled Carbon Nanotubes. Journal of Physical Chemistry C, 2008, 112, 9128-9132.	1.5	15
6092	Water Adsorption on a NiO(100) Surface:â€‰ A GGA+U Study. Journal of Physical Chemistry C, 2008, 112, 452-457.	1.5	43
6093	An inverse adhesion problem for extracting interfacial pair potentials for the Al(0â€‰0â€‰1)/3Câ€“SiC(0â€‰0â€‰1) interface. Inverse Problems, 2008, 24, 035019.	1.0	36
6094	Ab initioprediction of stable boron sheets and boron nanotubes: Structure, stability, and electronic properties. Physical Review B, 2008, 77, .	1.1	315

#	Article	IF	Citations
6095	Effect of the surface polarization in polar perovskites studied from first principles. Physical Review B, 2008, 77, .	1.1	77
6096	First-Principles Study of the Structural Stability and Electronic Properties of ZnS Nanowires. Journal of Physical Chemistry C, 2008, 112, 20291-20294.	1.5	11
6097	Combined Density Functional Theory and Interatomic Potential Study of the Bulk and Surface Structures and Properties of the Iron Sulfide Mackinawite (FeS). Journal of Physical Chemistry C, 2008, 112, 10960-10967.	1.5	70
6098	On the Thermodynamic Stability of (âˆš3 Ã— âˆš3)R30Â° Methanethiolate Lattice on Reconstructed Au(111) Surface Models. Journal of Physical Chemistry C, 2008, 112, 19121-19124.	1.5	20
6099	Prediction of Chemical Anisotropy on Sidewall of Boron Nitride Nanotubes: A New Application of Directional Curvature Theory. Journal of Physical Chemistry C, 2008, 112, 18787-18792.	1.5	5
6100	Vibrational Spectra of Î±-Amino Acids in the Zwitterionic State in Aqueous Solution and the Solid State: DFT Calculations and the Influence of Hydrogen Bonding. Journal of Physical Chemistry A, 2008, 112, 10333-10347.	1.1	63
6101	Superconducting High Pressure Phase of Germane. Physical Review Letters, 2008, 101, 107002.	2.9	224
6102	Effect of Ag Adatoms on High-Coverage Alkanethiolate Adsorption on Au(111). Journal of Physical Chemistry C, 2008, 112, 4557-4563.	1.5	8
6103	Theoretical strength and charge redistribution of fcc Ni in tension and shear. Journal of Physics Condensed Matter, 2008, 20, 335216.	0.7	36
6104	Structural stability and lattice dynamics of<mml:math xmlns:mml="http://www.w3.org/1998/Math/MathML" display="inline"><mml:mrow><mml:msub><mml:mrow><mml:mtext>SiO</mml:mtext></mml:mrow><mml:mn>2</mml:mn></mml:msub></mml:mrow></mml:math> Physical Review B, 2008, 78, .	1.1	33
6105	A comparative investigation of H2 adsorption strength in Cd- and Zn-based metal organic framework-5. Journal of Chemical Physics, 2008, 129, 164104.	1.2	31
6106	Calcium Adsorption on MgO(100):â€‰ Energetics, Structure, and Role of Defects. Journal of the American Chemical Society, 2008, 130, 2314-2322.	6.6	45
6107	Electronic Structure of Ternary Ruthenium-Based Hydrides. Journal of Physical Chemistry C, 2008, 112, 15586-15594.	1.5	21
6108	Search for ferromagnetism in SnO₂doped with transition metals (V, Mn, Fe, and Co). Journal of Physics Condensed Matter, 2008, 20, 045214.	0.7	63
6109	Oddâ^'Even Effects in Self-Assembled Monolayers of Ï‰-(Biphenyl-4-yl)alkanethiols:â€‰ A First-Principles Study. Langmuir, 2008, 24, 474-482.	1.6	75
6110	Influence of Subsurface Oxidation on the Structure, Stability, and Reactivity of Grafted Si(111) Surfaces. Journal of Physical Chemistry C, 2008, 112, 14867-14877.	1.5	16
6111	Theoretical Models of Silica Nanorings: First-Principles Calculations. Journal of Physical Chemistry C, 2008, 112, 17071-17075.	1.5	3
6112	Ab Initio Study of Surface Acidâ^'Base Reactions. The Case of Molecular and Dissociative Adsorption of Ammonia on the (011) Surface of Rutile TiO2. Langmuir, 2008, 24, 97-104.	1.6	22

#	Article	IF	Citations
6113	Hydrogen/silicon complexes in silicon from computational searches. Physical Review B, 2008, 78, .	1.1	46
6114	CO Oxidation Catalyzed by Single-Walled Helical Gold Nanotube. Nano Letters, 2008, 8, 195-202.	4.5	113
6115	One-Dimensional Ironâ^'Cyclopentadienyl Sandwich Molecular Wire with Half Metallic, Negative Differential Resistance and High-Spin Filter Efficiency Properties. Journal of the American Chemical Society, 2008, 130, 4023-4027.	6.6	185
6116	Effect of BaO Morphology on NO_x Abatement: NO₂ Interaction with Unsupported and Î³-Al₂O₃-Supported BaO. Journal of Physical Chemistry C, 2008, 112, 16924-16931.	1.5	22
6117	Contrast in the Electronic and Magnetic Properties of Doped Carbon and Boron Nitride Nanotubes:â€‰ A First-Principles Study. Journal of Physical Chemistry C, 2008, 112, 3464-3472.	1.5	17
6118	Energetics of Mg and B adsorption on polar zinc oxide surfaces from first principles. Physical Review B, 2008, 77, .	1.1	43
6119	Comparisons of Multilayer H₂O Adsorption onto the (110) Surfaces of Î±-TiO₂ and SnO₂ as Calculated with Density Functional Theory. Journal of Physical Chemistry B, 2008, 112, 11616-11624.	1.2	81
6120	Adsorption, Desorption, and Dissociation of CO on Tungsten(100), a DFT Study. Journal of Physical Chemistry C, 2008, 112, 7436-7444.	1.5	10
6121	Study of Lattice Constant and Bulk Modulus in Zincblende InGaN Using Local Density Approximation and Generalized Gradient Approximation. Japanese Journal of Applied Physics, 2008, 47, 3350-3353.	0.8	12
6122	Adsorption Configurations and Reactions of Boric Acid on a TiO₂ Anatase (101) Surface. Journal of Physical Chemistry C, 2008, 112, 8276-8287.	1.5	44
6123	First-principles investigations of elastic properties and energetics of antiferroelectric and ferroelectric phases of<mml:math xmlns:mml="http://www.w3.org/1998/Math/MathML" display="inline"><mml:mrow><mml:msub><mml:mrow><mml:mtext>PbZrO</mml:mtext></mml:mrow><mml:mn>3</mml:mn></mml:r Physical Review B, 2008, 77, .	1.1	27
6124	Effect of Coadsorbed Dopants on Diamond Initial Growth Processes: CH₃ Adsorption. Journal of Physical Chemistry A, 2008, 112, 5429-5435.	1.1	19
6125	Competitive Chemisorption of Bifunctional Carboxylic Acids on H:Si(100): A First-Principles Study. Journal of Physical Chemistry C, 2008, 112, 10167-10175.	1.5	4
6126	Lattice properties of<mml:math xmlns:mml="http://www.w3.org/1998/Math/MathML" display="inline"><mml:mrow><mml:mtext>Pb</mml:mtext><mml:mi>X</mml:mi></mml:mrow></mml:math><mml:math xmlns:mml="http://www.w3.org/1998/Math/MathML"		

#	Article	IF	Citations
6131	Scanning Tunneling Microscopy Images of Alkane Derivatives on Graphite: Role of Electronic Effects. Nano Letters, 2008, 8, 3160-3165.	4.5	86
6132	Chemisorption-Induced Polarization of Boron Nitride Nanotube. Journal of Physical Chemistry C, 2008, 112, 10279-10286.	1.5	9
6133	Benzene and Its Dissociation Products on Ir{100}. Journal of Physical Chemistry C, 2008, 112, 14417-14427.	1.5	4
6134	Comparative Behavior of Britholites and Monazite/Brabantite Solid Solutions during Leaching Tests: A Combined Experimental and DFT Approach. Inorganic Chemistry, 2008, 47, 10971-10979.	1.9	56
6135	New Data on the Structure of Uranium Monocarbide. Chemistry of Materials, 2008, 20, 3199-3204.	3.2	25
6136	Density-functional study of edge stress in graphene. Physical Review B, 2008, 78, .	1.1	75
6137	Coadsorption of CO and H on Fe(100). Journal of Physical Chemistry C, 2008, 112, 16505-16513.	1.5	24
6138	Polyanionic Gallium Hydrides from AlB2-Type Precursors AeGaE (Ae = Ca, Sr, Ba; E = Si, Ge, Sn). Journal of the American Chemical Society, 2008, 130, 12139-12147.	6.6	36
6139	Functionalization of Single-Walled Carbon Nanotubes with Metalloporphyrin Complexes: A Theoretical Study. Journal of Physical Chemistry C, 2008, 112, 11130-11134.	1.5	24
6140	Methane Dissociation on the Ceria (111) Surface. Journal of Physical Chemistry C, 2008, 112, 17311-17318.	1.5	62
6141	Elastic, electronic and optical properties of the filled tetrahedral semiconductor LiCdP. Semiconductor Science and Technology, 2008, 23, 105024.	1.0	6
6142	Adsorption and Reaction of Surface Carbon Species on Fe₅C₂(001). Journal of Physical Chemistry C, 2008, 112, 14883-14890.	1.5	22
6143	Oxidation of Ir(111): From Oâ^'Irâ^'O Trilayer to Bulk Oxide Formation. Journal of Physical Chemistry C, 2008, 112, 11946-11953.	1.5	77
6144	Orbital-Specific Analysis of CO Chemisorption on Transition-Metal Surfaces. Journal of Physical Chemistry C, 2008, 112, 1963-1966.	1.5	27
6145	Mercury Species and SO₂ Adsorption on CaO(100). Journal of Physical Chemistry C, 2008, 112, 16484-16490.	1.5	73
6146	DFT Study of the Thermodynamic Stability of Pdâ^'Pt Bulk Oxide Phases. Journal of Physical Chemistry C, 2008, 112, 13623-13628.	1.5	28
6147	Formation and Dissociation of a Cuâ^'H Complex in ZnO. Journal of Physical Chemistry C, 2008, 112, 19142-19146.	1.5	8
6148	Ab initio study of stress-induced domain switching in<mml:math xmlns:mml="http://www.w3.org/1998/Math/MathML" display="inline"><mml:mrow><mml:mi mathvariant="normal">Pb</mml:mi><mml:mi mathvariant="normal">Ti</mml:mi><mml:msub><mml:mi mathvariant="normal">O</mml:mi><mml:mn>3</mml:mn></mml:msub></mml:mrow></mml:math>. Physical Review B, 2008, 77, .	1.1	50

#	Article	IF	Citations
6149	Ab initiocalculations of the atomic and electronic structure of<mml:math xmlns:mml="http://www.w3.org/1998/Math/MathML" display="inline"><mml:mrow><mml:msub><mml:mrow><mml:mtext>CaTiO</mml:mtext></mml:mrow><mml:mn>3</mml:mn></mml:r and (011) surfaces. Physical Review B, 2008, 78, .	1.1	65
6150	Structural and Energetic Analysis of Mg_xM_{1â^'x}(OH)₂ (M = Zn, Cu or Ca) Brucite-Like Compounds by DFT Calculations. Journal of Physical Chemistry C, 2008, 112, 10681-10687.	1.5	28
6151	Reactions of Water Molecules in Silica-Based Network Glasses. Physical Review Letters, 2008, 100, 105503.	2.9	38
6152	First-Principles Studies on Oxygen-Induced Faceting of Ir(210). ACS Nano, 2008, 2, 1280-1288.	7.3	32
6153	Theoretical Study of Early Steps in Corrosion of Pt and Pt/Co Alloy Electrodes. Journal of Physical Chemistry C, 2008, 112, 18566-18571.	1.5	22
6154	Effect of the exchange-correlation energy and temperature on the generalized phase diagram of the 4dtransition metals. High Pressure Research, 2008, 28, 449-453.	0.4	2
6155	Structure Sensitivity in Adsorption and Decomposition of NO on Ir. Journal of Physical Chemistry C, 2008, 112, 19113-19120.	1.5	21
6156	Coupling between magnetic ordering and structural instabilities in perovskite biferroics: A first-principles study. Physical Review B, 2008, 77, .	1.1	62
6157	Au â† N Synergy and N-Doping of Metal Oxide-Based Photocatalysts. Journal of the American Chemical Society, 2008, 130, 12056-12063.	6.6	115
6158	Intermediates in the Formation of Graphitic Carbon on a Flat FCC-Co(111) Surface. Journal of Physical Chemistry C, 2008, 112, 12899-12904.	1.5	48
6159	Pressure-induced structural transformation in solid xenon studied by Raman spectroscopy. Physical Review B, 2008, 77, .	1.1	8
6160	The Mechanism Responsible for Extraordinary Cs Ion Selectivity in Crystalline Silicotitanate. Journal of the American Chemical Society, 2008, 130, 11689-11694.	6.6	132
6161	First-principles study of rare earth adsorption at<mml:math xmlns:mml="http://www.w3.org/1998/Math/MathML" display="inline"><mml:mrow><mml:mi>Î²</mml:mi><mml:msub><mml:mrow><mml:mtext>-Si</mml:mtext></mml:mrow><mml:mn>3 Physical Review B, 2008, 78, .	1.1	37
6162	Lattice dynamics and thermodynamical properties of silicon nitride polymorphs. Physical Review B, 2008, 78, .	1.1	79
6163	Small-Angle Rotation in Individual Colloidal CdSe Quantum Rods. ACS Nano, 2008, 2, 1179-1188.	7.3	19
6164	Systematics of elastic and thermodynamic properties of super-hardness cubic boron nitride under high pressure. Diamond and Related Materials, 2008, 17, 1-6.	1.8	15
6165	Dynamic Interplay between Diffusion and Reaction:â€‰ Nitrogen Recombination on Rh{211} in Car Exhaust Catalysis. Journal of the American Chemical Society, 2008, 130, 2213-2220.	6.6	24
6166	Tuning the gap in bilayer graphene using chemical functionalization: Density functional calculations. Physical Review B, 2008, 78, .	1.1	183

#	Article	IF	Citations
6167	First-principles calculation of the infrared spectrum of hematite. American Mineralogist, 2008, 93, 1019-1027.	0.9	61
6168	Structural Phase Transitions in the Potential Hydrogen Storage Compound KBH₄ under Compression. Journal of Physical Chemistry C, 2008, 112, 8452-8457.	1.5	34
6169	The di-interstitial in graphite. Journal of Physics Condensed Matter, 2008, 20, 395220.	0.7	32
6170	An ab initio constant-pressure study of pressure-induced phase transition of MgSe. Europhysics Letters, 2008, 84, 56001.	0.7	4
6171	Activated Adsorption of Ethylene on Atomic-Oxygen-Covered Ag(100) and Ag(210):â€‰ Formation of an Oxametallacycle. Journal of Physical Chemistry C, 2008, 112, 1019-1027.	1.5	21
6172	Thermodynamic analysis of hydrogen sorption reactions in Liâ€“Mgâ€“Nâ€“H systems. Applied Physics Letters, 2008, 92, 021907.	1.5	22
6173	Electronic properties and stabilities of bulk and low-index surfaces of SnO in comparison with<mml:math xmlns:mml="http://www.w3.org/1998/Math/MathML" display="inline"><mml:mrow><mml:mi mathvariant="normal">Sn</mml:mi><mml:msub><mml:mi mathvariant="normal">O</mml:mi><mml:mn>2</mml:mn></mml:msub></mml:mrow></mml:math>: A first-principles density functional approach with an empirical correction of van der Waals interactions. Physical Review B, 2008, 77, .	1.1	115
6174	Cubic metallic phase of aluminum hydride showing improved hydrogen desorption. Applied Physics Letters, 2008, 92, .	1.5	18
6175	Structural and elastic properties under pressure effect of Hf₂AlN and Hf₂AlC. High Pressure Research, 2008, 28, 45-53.	0.4	14
6176	Reducing the Metal Work Function beyond Pauli Pushback: A Computational Investigation of Tetrathiafulvalene and Viologen on Coinage Metal Surfaces. Journal of Physical Chemistry C, 2008, 112, 20357-20365.	1.5	43
6177	Structure and Optoelectronics of Electrodeposited Cadmium Ditelluride (CdTe₂). Chemistry of Materials, 2008, 20, 6550-6555.	3.2	15
6178	Mechanical Properties and Electronic Structures of Cotunnite TiO ₂. Chinese Physics Letters, 2008, 25, 4356-4359.	1.3	20
6179	Discriminating Reasons for Selectivity Enhancement of CO in Alkyne Hydrogenation on Palladium. Journal of Physical Chemistry C, 2008, 112, 9346-9350.	1.5	38
6180	Electronic Structures and Vibrational Properties of a Carbon Nanotube with Adsorption of Small Hydrocarbon Radicals. Journal of Physical Chemistry C, 2008, 112, 18876-18881.	1.5	10
6181	Refined Crystal Structure and Mechanical Properties of Superhard BC₄N Crystal: First-Principles Calculations. Journal of Physical Chemistry C, 2008, 112, 9516-9519.	1.5	38
6182	First-principles study of anatase and rutile<mml:math xmlns:mml="http://www.w3.org/1998/Math/MathML" display="inline"><mml:mrow><mml:msub><mml:mrow><mml:mtext>TiO</mml:mtext></mml:mrow><mml:mn>2</mml:mn></mml:msub></mml:mrow></mml:math> with Eu ions: A comparison of GGA and<mml:math xmlns:mml="http://www.w3.org/1998/Math/MathML" display="inline"><mml:mrow><mml:mtext>LDA</mml:mtext><mml:mo>+</mml:mo><mml:mtext>U</mml:mtext></mml:mrow></mml:math> Physical Review B, 2008, 78, .	1.1	55
6183	Origin of the Reactivity on the Nonterminated (100), (110), and (111) Diamond Surfaces: An Electronic Structure DFT Study. Journal of Physical Chemistry C, 2008, 112, 14367-14376.	1.5	31
6184	Novel Self-Organized Structure of a Agâ^'S Complex on the Ag(111) Surface below Room Temperature. Journal of Physical Chemistry C, 2008, 112, 4281-4290.	1.5	24

#	Article	IF	Citations
6185	Origin of the Visible Light Absorption of GaN-Rich Ga1â^'x ZnxN1â^'xOx (x = 0.125) Solid Solution. Journal of Physical Chemistry C, 2008, 112, 15915-15919.	1.5	51
6186	Embedded Configuration Interaction Description of CO on Cu(111):â€‰ Resolution of the Site Preference Conundrum. Journal of Physical Chemistry C, 2008, 112, 4649-4657.	1.5	47
6187	d-Alaninol Adsorption on Cu(100):â€‰ Photoelectron Spectroscopy and First-Principles Calculations. Journal of Physical Chemistry B, 2008, 112, 3963-3970.	1.2	18
6188	First-principles investigation of anisotropic constitutive relationships in pentaerythritol tetranitrate. Physical Review B, 2008, 77, .	1.1	46
6189	First-principles local density approximation+U and generalized gradient approximation+U study of plutonium oxides. Journal of Chemical Physics, 2008, 128, 084705.	1.2	106
6190	Theoretical Studies of Solid Bicyclo-HMX:â€‰ Effects of Hydrostatic Pressure and Temperature. Journal of Physical Chemistry B, 2008, 112, 3882-3893.	1.2	40
6191	Mercury adsorption on PdAu, PdAg and PdCu alloys. Main Group Chemistry, 2008, 7, 205-215.	0.4	65
6192	Structural Features of Boron-Doped Si(113) Surfaces Simulated by ab initio Calculations. Chinese Physics Letters, 2008, 25, 2177-2180.	1.3	1
6193	Ab-initiostudy of exchange constants and electronic structure in diluted magnetic group-IV semiconductors. New Journal of Physics, 2008, 10, 055017.	1.2	8
6194	Characterization of Ag adsorption on TiC(001) substrate: an ab initio study. Chinese Physics B, 2008, 17, 3856-3866.	0.7	7
6195	Theoretical Calculations for Structural, Elastic and Thermodynamic Properties of Î³TiAl Under High Pressure. Communications in Theoretical Physics, 2008, 50, 1427-1434.	1.1	7
6196	Origin of bcc to fcc phase transition under pressure in alkali metals. New Journal of Physics, 2008, 10, 063022.	1.2	26
6197	Role of Ge Switch in Phase Transition: Approach using Atomically Controlled GeTe/Sb₂Te₃ Superlattice. Japanese Journal of Applied Physics, 2008, 47, 5763.	0.8	68
6198	Electronic and magnetic structures of 4f in Ga_{1â^'x}Gd_xN. Journal of Physics Condensed Matter, 2008, 20, 295221.	0.7	11
6199	Surface rumples and band gap reductions of cubic BaZrO₃(001) surface studied by means of first-principles calculations. Chinese Physics B, 2008, 17, 274-280.	0.7	2
6200	Lattice Dynamics and Superconductivity of RuB 2 : A First-Principles Study. Chinese Physics Letters, 2008, 25, 3036-3039.	1.3	10
6201	First-principle study of native defects in CuScO ₂ and CuYO ₂. Chinese Physics B, 2008, 17, 4279-4284.	0.7	13
6202	First-Principles Calculations of Structures and Electronic Properties of Solid Pentaerythritol under Pressure. Chinese Physics Letters, 2008, 25, 3368-3371.	1.3	1

#	Article	IF	Citations
6203	First-Principles Study of Defects in CuGaO 2. Chinese Physics Letters, 2008, 25, 2997-3000.	1.3	16
6204	First-principles study of Co-doped single-walled silicon nanotubes. Nanotechnology, 2008, 19, 205707.	1.3	12
6205	Calculations for displacive ï‰-phase transformations in Tiâ€“Al alloys with Nb additions at finite temperature. Journal of Physics Condensed Matter, 2008, 20, 465206.	0.7	7
6206	Quantum molecular dynamics study of water on TiO2(110) surface. Journal of Chemical Physics, 2008, 129, 064703.	1.2	30
6207	Possible structural polymorphism in Al-bearing magnesiumsilicate post-perovskite. American Mineralogist, 2008, 93, 533-539.	0.9	18
6208	Construction of the Alâ€“Niâ€“Si phase diagram over the whole composition and temperature ranges: thermodynamic modeling supported by key experiments and first-principles calculations. International Journal of Materials Research, 2008, 99, 598-612.	0.1	21
6209	Structure and Dynamics of Ge in the Siâ€“SiO[sub 2] System: Implications for Oxide-Embedded Ge Nanoparticle Formation. Electrochemical and Solid-State Letters, 2008, 11, P17.	2.2	12
6210	Computational designing of gradient type catalytic membrane: application to the conversion of methanol to ethylene. Molecular Simulation, 2008, 34, 1091-1097.	0.9	2
6211	Structural, Elastic, and Electronic Properties of ReB₂: A First-Principles Calculation. Research Letters in Physics, 2008, 2008, 1-5.	0.2	7
6212	Shell model potential for PbTiO3and its applicability to surfaces and domain walls. Journal of Physics Condensed Matter, 2008, 20, 325225.	0.7	44
6213	Vibrational properties of Â-AlOOH under pressure. American Mineralogist, 2008, 93, 477-482.	0.9	46
6214	Reactive molecular dynamics force field for the dissociation of light hydrocarbons on Ni(111). Molecular Simulation, 2008, 34, 967-972.	0.9	11
6215	Origin of the flat-band voltage (V<inf>fb</inf>) roll-off phenomenon in metal/high-k gate stacks. , 2008, , .		2
6216	AN EFFICIENT CRITERION FOR THE FORMATION ENERGIES AND REACTIVITIES OF DEFECTS IN CNTs AND BNNTs. Journal of Theoretical and Computational Chemistry, 2008, 07, 681-695.	1.8	2
6217	Elastic and Thermodynamic Properties of CdSe from First-Principles Calculations. Communications in Theoretical Physics, 2008, 50, 220-226.	1.1	24
6218	POLARIZABILITY AND SHIELDING OF COAXIAL HYBRID DOUBLE-WALLED NANOTUBES: A FIRST-PRINCIPLES STUDY. Journal of Theoretical and Computational Chemistry, 2008, 07, 793-803.	1.8	1
6219	Electronic structures of defects in ZnO: Hybrid density functional studies. Journal of Chemical Physics, 2008, 129, 154706.	1.2	57
6220	AB INITIO CALCULATIONS OF STRUCTURAL AND ELECTRONIC PROPERTIES OF THE COMPOUND Li3AlB2O6. Modern Physics Letters B, 2008, 22, 343-352.	1.0	1

#	Article	IF	Citations
6221	Study of ZrO₂ phase structure and electronic properties. Molecular Simulation, 2008, 34, 1099-1103.	0.9	17
6222	First-Principles Investigation of the Fundamental Corrosion Properties of a Model Cu[sub 38] Nanoparticle and the (111), (113) Surfaces. Journal of the Electrochemical Society, 2008, 155, C407.	1.3	68
6223	A theoretical study of a spin polarized transport and giant magnetoresistance: The effect of the number of layers in a magnetic multilayer. Journal of Applied Physics, 2008, 103, 083903.	1.1	0
6224	Ferrocene-1,1â€²-dithiol as molecular wire between Ag electrodes: The role of surface defects. Journal of Chemical Physics, 2008, 128, 064704.	1.2	11
6225	CALCULATED STRUCTURAL AND ELASTIC PROPERTIES OF M₂InC(M=Sc, Ti,) Tj ETQq0 0 0 rgBT /Overlock 10 T Physics Letters B, 2008, 22, 2063-2076.	1.0	42
6226	First-principles local density approximation (LDA) +Uand generalized gradient approximation (GGA) +Ustudies of plutonium oxides. Chinese Physics B, 2008, 17, 1364-1370.	0.7	26
6227	FIRST PRINCIPLES STUDY OF THE ELECTRONIC STRUCTURE AND FERROMAGNETISM OF THE V-DOPED BN(5, 5) NANOTUBE. Modern Physics Letters B, 2008, 22, 1749-1756.	1.0	6
6228	FIRST-PRINCIPLES STUDY OF THE EFFECTS OF GOLD ADSORPTION ON THE Al(001) SURFACE PROPERTIES. International Journal of Modern Physics C, 2008, 19, 1563-1579.	0.8	3
6229	Transverse Pressure Induced Phase Transitions in Boron Nitride Nanotube Bundles and the Lightest Boron Nitride Crystal. Journal of the American Chemical Society, 2008, 130, 5257-5261.	6.6	33
6230	Linearized Augmented Plane Wave Band Structure Calculations and Dielectric Function of Layered TlGaSe₂. Japanese Journal of Applied Physics, 2008, 47, 8182.	0.8	9
6231	NO2 dissociation on Ag(111) revisited by theory. Journal of Chemical Physics, 2008, 128, 104704.	1.2	16
6232	The energetics of tetrahydrocarbazole aromatization over Pd(111): A computational analysis. Journal of Chemical Physics, 2008, 128, 105104.	1.2	10
6233	First-principles study of the mechanical properties of NiAl microalloyed byM(Y,â€‰Zr,â€‰Nb,â€‰Mo,â€‰Tc,â€‰Ru,â€‰Rh,â€‰Pd,â€‰Ag,â€‰Cd). Journal Physics D: Applied Physics, 2008, 41,	1.3	19
6234	First-principles study of the electronic and magnetic properties of Sr2Fe1+xMo1â^'xO6. Journal of Physics Condensed Matter, 2008, 20, 075218.	0.7	4
6235	First-principles calculations of the thermodynamic and elastic properties of the L1₂-based Al₃RE (RE = Sc, Y, Laâ€“Lu). International Journal of Materials Research, 2008, 99, 582-588.	0.1	35
6236	Vacancy-mediated dehydrogenation of sodium alanate. Proceedings of the National Academy of Sciences of the United States of America, 2008, 105, 3673-3677.	3.3	101
6237	Adhesive metal transfer at the Al(1â€‰1â€‰1)/Î±-Fe₂O₃(0â€‰0â€‰0â€‰1) interface: a study withab initiomolecular dynamics. Modelling and Simulation in Materials Science and Engineering, 2008, 16, 085001.	0.8	6
6238	NANOLAYERED MAX PHASES FROM ab initio CALCULATIONS. International Journal of Modern Physics B, 2008, 22, 4495-4499.	1.0	7

#	Article	IF	Citations
6239	First-Principles Calculations of Elastic Properties of LaNi_{4.75}Sn_{0.25}Alloys under Pressure. Chinese Physics Letters, 2008, 25, 2592-2595.	1.3	2
6240	Pressure effects on CrCl63â˜ embedded in cubic Cs2NaMCl6 (M=Sc,Y) lattices: Study through periodic and cluster calculations. Journal of Chemical Physics, 2008, 128, 144708.	1.2	21
6241	Ab-initiostudy on indium diffusion in silicon substrate under hydrostatic stress. Molecular Simulation, 2008, 34, 47-50.	0.9	0
6242	Accelerating the convergence of the total energy evaluation in density functional theory calculations. Journal of Chemical Physics, 2008, 128, 084101.	1.2	6
6243	Theoretical Evidences for Enhanced Superconducting Transition Temperature of CaSi₂ in a High-Pressure AlB₂ Phase. Journal of the Physical Society of Japan, 2008, 77, 104712.	0.7	5
6244	Core level shifts of undercoordinated Pt atoms. Journal of Chemical Physics, 2008, 128, 114706.	1.2	41
6245	First principles studies for formation mechanism and properties of ethylene molecule adsorbing on diamond (100) surface. Journal of Chemical Physics, 2008, 128, 114710.	1.2	2
6246	Thermodynamics and kinetics of oxygen-induced segregation of 3d metals in Ptâ€“3dâ€“Pt(111) and Ptâ€“3dâ€“Pt(100) bimetallic structures. Journal of Chemical Physics, 2008, 128, 164703.	1.2	85
6247	The adsorption of O2 on Pb films and the effect of quantum modulation: A first-principles prediction. Journal of Chemical Physics, 2008, 128, 164705.	1.2	19
6248	Stability of suspended gold and silver alloy monatomic chains. Journal of Chemical Physics, 2008, 128, 244703.	1.2	15
6249	First-principles study of substitutional magnesium and zinc in hydroxyapatite and octacalcium phosphate. Journal of Chemical Physics, 2008, 128, 245101.	1.2	101
6250	Structure and thermal fluctuation of one-dimensional AgO chains on Ag(110) surfaces studied with density functional theory and Monte Carlo simulations. Journal of Chemical Physics, 2008, 129, 154709.	1.2	4
6251	Nonuniform temperature dependence of the reactivity of disordered VOx/Î²-Al2O3(001) surfaces: A density functional theory based Monte Carlo study. Journal of Chemical Physics, 2008, 129, 224710.	1.2	5
6252	Predictions of melting, crystallization, and local atomic arrangements of aluminum clusters using a reactive force field. Journal of Chemical Physics, 2008, 129, 244506.	1.2	47
6253	First-Principles Study of Structural, Electronic, Magnetic, Optical, and Magneto-Optical Properties of NpN. Journal of the Physical Society of Japan, 2008, 77, 074703.	0.7	7
6254	Ab initio modeling of spin and charge ordering and lattice dynamics in CaFeO3 crystals. Journal of Chemical Physics, 2008, 129, 214704.	1.2	7
6255	Crystallographic phase stabilities and electronic structures in AgNbO3by first-principles calculation. Molecular Simulation, 2008, 34, 1105-1114.	0.9	20
6256	Reaction of rhenium and carbon at high pressures and temperatures. Zeitschrift Fur Kristallographie - Crystalline Materials, 2008, 223, 492-501.	0.4	40

#	Article	IF	Citations
6257	Phase transformation of 6H-SiC at high pressure: An ab initio constant-pressure study. Europhysics Letters, 2008, 84, 26003.	0.7	8
6258	First principles calculations of the structural, electronic and vibrational properties of the clathrates Ba8Al16Ge30and Ba8Al16Si30. Journal of Physics Condensed Matter, 2008, 20, 415214.	0.7	14
6259	Coupling of surface relaxation and polarization in PbTiO₃from atomistic simulation. Journal of Physics Condensed Matter, 2008, 20, 395004.	0.7	12
6260	Efficient evaluation of the Fourier transform over products of Slater-type orbitals on different centers. Journal of Physics A: Mathematical and Theoretical, 2008, 41, 485205.	0.7	8
6261	Density functional calculations of the electronic structure and optical properties of aluminosilicate polymorphs (Al2SiO5). American Mineralogist, 2008, 93, 114-123.	0.9	35
6262	Electronic structure of crystalline uranium nitrides UN, U₂N₃and UN₂: LCAO calculations with the basis set optimization. Journal of Physics: Conference Series, 2008, 117, 012015.	0.3	23
6263	First-principles study of a double-cation alkali metal borohydride LiK(BH₄)₂. Journal of Physics Condensed Matter, 2008, 20, 445210.	0.7	15
6264	Stability of the polar NiO(111) surface. Journal of Chemical Physics, 2008, 128, 124703.	1.2	41
6265	Phonon Spectra of Chain TlSe and TlInSe₂: Density Functional Theory Based Study. Japanese Journal of Applied Physics, 2008, 47, 8193.	0.8	10
6266	First-Principles Calculations of Elastic Properties of LaNi 5 Compound. Chinese Physics Letters, 2008, 25, 2950-2953.	1.3	4
6267	Theoretical Study of Compressibility and Thermoelasticity of LaNi _{5â˜' x} Al _x , (x = 0.3, 0.5 and 1.0). Chinese Physics Letters, 2008, 25, 4352-4355.	1.3	1
6268	Investigation of low-resistivity from hydrogenated lightly B-doped diamond by ion implantation. Science and Technology of Advanced Materials, 2008, 9, 025014.	2.8	2
6269	Theoretical study of highly strained InAs material from first-principles modelling: application to an ideal QD. Journal Physics D: Applied Physics, 2008, 41, 165505.	1.3	13
6270	Theoretical Hardness of Wurtzite-Structured Semiconductors. Chinese Physics Letters, 2008, 25, 2158-2161.	1.3	9
6271	Crystal Structure of Î²-La ₂ Mo ₂ O ₉ from First Principles Calculation. Chinese Physics Letters, 2008, 25, 3342-3345.	1.3	12
6272	Structural and electronic properties of NM-doped ceria (NM = Pt, Rh): a first-principles study. Journal of Physics Condensed Matter, 2008, 20, 035210.	0.7	39
6273	Zinc Substituted Hydroxyapatite â€“ A Comparison of Modelling and Experimental Data. Key Engineering Materials, 0, 396-398, 729-732.	0.4	9
6274	Stability and electronic properties of native defects and substitutional impurities in GaN nanotubes. Journal of Applied Physics, 2008, 104, 033712.	1.1	23

#	Article	IF	Citations
6275	Density functional characterization of B doping at rutile TiO₂(1â€‰1â€‰0) surface. Journal Physics D: Applied Physics, 2008, 41, 195411.	1.3	12
6276	Structural and mechanical properties of Mg₁₇Al₁₂and Mg₂₄Y₅from first-principles calculations. Journal Physics D: Applied Physics, 2008, 41, 195408.	1.3	65
6277	Polymerization of Silicon-Doped Heterofullerenes: an Ab Initio Study. Chinese Physics Letters, 2008, 25, 246-249.	1.3	3
6278	Pressure and Temperature Induced Phase Transition of ZnS from First-Principles Calculations. Chinese Physics Letters, 2008, 25, 675-678.	1.3	19
6279	Zero-temperature equation of state of solid⁴He at low and high pressures. Journal of Physics Condensed Matter, 2008, 20, 015223.	0.7	34
6280	Adsorbate induced changes in surface stress and phonon dispersion curves of chemisorbed systems. Journal of Physics Condensed Matter, 2008, 20, 224005.	0.7	2
6281	Formation of Ga dimer linear chains on Si(001): a first-principles study. Journal of Physics Condensed Matter, 2008, 20, 445002.	0.7	3
6282	Elastic properties of Sr_{n+1}Ti_nO_{3n+1}phases (n= 1â€“3, infty). Journal of Physics Condensed Matter, 2008, 20, 055224.	0.7	21
6283	Ab-initio melting curve and principal Hugoniot of tantalum. Journal of Physics: Conference Series, 2008, 121, 012010.	0.3	4
6284	Electron transport in open systems from finite-size calculations: Examination of the principal layer method applied to linear gold chains. Journal of Chemical Physics, 2008, 128, 154713.	1.2	4
6285	Density-functional-theory calculations for silicon vacancy migration. Journal of Applied Physics, 2008, 103, 083517.	1.1	6
6286	Coverage dependence of the structure of tetracene on Ag(110). Journal of Physics Condensed Matter, 2008, 20, 315010.	0.7	9
6287	Size-dependent momentum smearing effect of positron annihilation radiation in embedded nano Cu clusters. Journal of Physics Condensed Matter, 2008, 20, 445203.	0.7	9
6288	Elastic Constants of Co/Pt Superlattice Studied by Acoustic Measurements andAb initioCalculations. Japanese Journal of Applied Physics, 2008, 47, 3847-3850.	0.8	15
6289	Pressure-induced phase transformation in CdO: An ab initio constant-pressure study. Europhysics Letters, 2008, 84, 66003.	0.7	9
6290	Interaction between gallium atoms and the inner walls of single-walled carbon nanotubes. Nanotechnology, 2008, 19, 075706.	1.3	5
6291	Reliable lateral and vertical manipulations of a single Cu adatom on a Cu(111) surface with multi-atom apex tip: semiempirical and first-principles simulations. Nanotechnology, 2008, 19, 335710.	1.3	12
6292	Hydrogen interstitials-mediated ferromagnetism in Mn_xGe_{1â^’x} magnetic semiconductors. New Journal of Physics, 2008, 10, 055015.	1.2	6

#	Article	IF	Citations
6293	Electronic Properties of Nitrogen-Doped Carbon Nanotubes with Strain:Ab initioMethod Approach. Japanese Journal of Applied Physics, 2008, 47, 5062-5065.	0.8	4
6294	First-principles calculations of elastic constants of DO₃-Mg₃RE (RE = Sc, Y, La,) Tj ETQq1 1 0.784314 rgBT /	1.2	13
6295	The electronic structure of a single-walled aluminosilicate nanotube. Nanotechnology, 2008, 19, 175702.	1.3	17
6296	Structural, electronic and magnetic properties of the surfaces of tetragonal and cubic HfO₂. New Journal of Physics, 2008, 10, 063031.	1.2	34
6297	Electronic Structures and Atomic Surface Diffusion in Cr/Fe(001) and Fe/Cr(001) Systems: First-Principles Study. Japanese Journal of Applied Physics, 2008, 47, 5076-5078.	0.8	9
6298	Coupling ofab initiodensity functional theory and molecular dynamics for the multiscale modeling of carbon nanotubes. Nanotechnology, 2008, 19, 055702.	1.3	8
6299	The power of joint application of LEED and DFT in quantitative surface structure determination. Journal of Physics Condensed Matter, 2008, 20, 304204.	0.7	5
6300	Stacking Fault Duplication in 6H-SiC Single Crystal. Japanese Journal of Applied Physics, 2008, 47, 4491-4493.	0.8	2
6301	Bound substitutional impurity pairs in diamond: a density functional study. Journal of Physics Condensed Matter, 2008, 20, 085217.	0.7	4
6302	Atomic and electronic structure of Bi/GaAs(001)-Î±2(2 Ã— 4). Journal of Physics Condensed Matter, 2008, 20, 265003.	0.7	6
6303	The Ni₃Al(111) surface structure: experiment and theory. Journal of Physics Condensed Matter, 2008, 20, 195223.	0.7	15
6304	Vibrational effects on SrTiO₃Ti 1s absorption spectra studied using first-principles methods. Journal of Physics Condensed Matter, 2008, 20, 365221.	0.7	15
6305	Ab initiocalculation of lattice dynamics in BeO. Journal of Physics Condensed Matter, 2008, 20, 395201.	0.7	11
6306	Bond-Counting Rule for Carbon and its Application to the Roughness of Diamond (001). Physical Review Letters, 2008, 100, 026101.	2.9	8
6307	Dissociation Chemistry of Gas Molecules on Carbon Nanotubesâ€"Applications to Chemical Sensing. IEEE Sensors Journal, 2008, 8, 837-841.	2.4	15
6308	Acceleratingab initiocalculation of phonon dispersion curves:q-point convergence. Physical Review B, 2008, 77, .	1.1	11
6309	Charge carrier induced lattice strain and stress effects on As activation in Si. Applied Physics Letters, 2008, 93, .	1.5	10
6310	Structural effect of junction interface on magnetic properties in a Co/MgO/Co system: First-principles calculations. Journal of Applied Physics, 2008, 103, .	1.1	8

#	Article	IF	Citations
6311	A route to tunable direct band-gap diamond devices: Electronic structures of nanodiamond crystals. Journal of Applied Physics, 2008, 104, .	1.1	32
6312	Ferromagnetic states in<mml:math xmlns:mml="http://www.w3.org/1998/Math/MathML" display="inline"><mml:mrow><mml:mi>Fe</mml:mi><mml:mtext>â^'</mml:mtext><mml:mi>Ru</mml:mi></mml:mrow></mml:math> studied byab initiocalculation and ion-beam mixing. Physical Review B, 2008, 77, .	1.1	44
6313	Bridge structure for the graphene/Ni(111) system: A first principles study. Physical Review B, 2008, 77, .	1.1	158
6314	Electronic and vibrational properties of$\hat{}$3â^'AlH3. Physical Review B, 2008, 77, .	1.1	25
6315	High-pressure phases of calcium and their finite-temperature phase boundaries. Physical Review B, 2008, 78, .	1.1	41
6316	Disorder-Recrystallization Effects in Low-Energy Beam-Solid Interactions. Physical Review Letters, 2008, 100, 185502.	2.9	20
6317	Zero-temperature generalized phase diagram of the<mml:math xmlns:mml="http://www.w3.org/1998/Math/MathML" display="inline"><mml:mrow><mml:mn>4</mml:mn><mml:mi>d</mml:mi></mml:mrow></mml:math>transition metals under pressure. Physical Review B, 2008, 77, .	1.1	26
6318	Quantum Size Effects on Dielectric Constants and Optical Absorption of Ultrathin Silicon Films. IEEE Electron Device Letters, 2008, 29, 1302-1305.	2.2	20
6319	Large electromechanical response in silicon nanowires predicted from first-principles electronic structure calculations. Physical Review B, 2008, 77, .	1.1	4
6320	Formation of Pt islets on facets of Ru nanoparticles: First-principles study. Physical Review B, 2008, 78, .	1.1	6
6321	Calculated interband optical transition spectra of GdN. Physical Review B, 2008, 78, .	1.1	22
6322	Lattice Green function for extended defect calculations: Computation and error estimation with long-range forces. Physical Review B, 2008, 78, .	1.1	45
6323	Effects of deformation on the electronic structure of a single-walled carbon nanotube bundle. Physical Review B, 2008, 77, .	1.1	17
6324	Phase stability and elastic properties of<mml:math xmlns:mml="http://www.w3.org/1998/Math/MathML" display="inline"><mml:mrow><mml:mi>X</mml:mi><mml:msub><mml:mrow><mml:mtext>MgB</mml:mtext></mml:mrow><mml:mn>2</mml:mn></mml:msub></mml:mrow></mml:math>byab initiocalculations<mml:math xmlns:mml="http://www.w3.org/1998/Math/MathML"		

#	Article	IF	Citations
6329	Binding-energy relations and equations of state for the<mml:math xmlns:mml="http://www.w3.org/1998/Math/MathML" display="inline"><mml:mrow><mml:mn>4</mml:mn><mml:mi>d</mml:mi></mml:mrow></mml:math>and<mml:math xmlns:mml="http://www.w3.org/1998/Math/MathML" display="inline"><mml:mrow><mml:mn>5</mml:mn><mml:mi>d</mml:mi></mml:mrow></mml:math>transition metals. Physical Review B, 2008, 78, .	1.1	17
6330	Iron in silicon: Interactions with radiation defects, carbon, and oxygen. Physical Review B, 2008, 77, .	1.1	58
6331	Highly destabilized Mg-Ti-Ni-H system investigated by density functional theory and hydrogenography. Physical Review B, 2008, 77, .	1.1	39
6332	Quantum capacitance extraction for carbon nanotube interconnects. , 2008, , .		1
6333	Revealing latent structural instabilities in perovskite ferroelectrics by layering and epitaxial strain: A first-principles study of Ruddlesden-Popper superlattices. Physical Review B, 2008, 78, .	1.1	14
6334	Emergence and Visualization of an Interface State during Contact Formation with a Single Molecule. Physical Review Letters, 2008, 101, 096801.	2.9	3
6335	Ab initiosimulations of the liquid alloy Au-Cs. Physical Review B, 2008, 78, .	1.1	5
6336	Ab initiostudy of superconducting hexagonalBe2Liunder pressure. Physical Review B, 2008, 78, .	1.1	16
6337	Electronic structure investigation of the cubic inverse perovskite<mml:math xmlns:mml="http://www.w3.org/1998/Math/MathML" display="inline"><mml:mrow><mml:msub><mml:mrow><mml:mtext>Sc</mml:mtext></mml:mrow><mml:mn>3</mml:mn></mml:msub> Physical Review B, 2008, 78, .	1.1	29
6338	Hierarchical structure and phase transition of(GeTe)n(Sb2Te3)mused for phase-change memory. Physical Review B, 2008, 78, .	1.1	6
6339	First-principles Investigation of the Structural and Electronic Properties of Cu Based Intermetallics. , 2008, , .		0
6340	First-principles investigation of the atomic and electronic structure of the<mml:math xmlns:mml="http://www.w3.org/1998/Math/MathML"		

#	Article	IF	Citations
6347	First-principles investigation of Ag-Cu alloy surfaces in an oxidizing environment. Physical Review B, 2008, 77, .	1.1	43
6348	Effects of aluminum incorporation on band alignment at the<mml:math xmlns:mml="http://www.w3.org/1998/Math/MathML" display="inline"><mml:mrow><mml:mi mathvariant="normal">Si</mml:mi><mml:msub><mml:mi mathvariant="normal">O</mml:mi><mml:mn>2</mml:mn></mml:msub><mml:mo>â^•</mml:mo><mml:mi mathvariant="normal">Hf</mml:mi><mml:msub><mml:mi mathvariant="normal">O</mml:mi><mml:mn>2</mml:mn></mml:msub></mml:mrow></mml:math>interface.	1.1	38
6349	First-principles study of electronic and optical properties in wurtzite Zn1â^'xCdxO. Journal of Applied Physics, 2008, 103, .	1.1	111
6350	Atomic structure model of the reconstructed Si(557) surface with a triple step structure: Adatom-parallel dimer model. Physical Review B, 2008, 77, .	1.1	23
6351	Novel semiconducting materials for optoelectronic applications: Al1â^'xTlxN alloys. Applied Physics Letters, 2008, 92, .	1.5	29
6352	Wavevector-dependent quantum-size effect in electron decay length at Pb thin film surfaces. Applied Physics Letters, 2008, 93, 093105.	1.5	18
6353	Adsorption of oxygen atoms on the Mg3Nd(001) surface. Journal of Applied Physics, 2008, 104, 033516.	1.1	0
6354	Fluorination-induced magnetism in boron nitride nanotubes from ab initio calculations. Applied Physics Letters, 2008, 92, 102515.	1.5	52
6355	Theoretical study of the structural and electronic properties of strained ErAs. Physical Review B, 2008, 77, .	1.1	11
6356	Hydrostatic compression and high-pressure elastic constants of coesite silica. Journal of Applied Physics, 2008, 103, 053506.	1.1	23
6357	Cobalt-dopedÎ²-peptide nanotubes: A class of spintronic materials. Physical Review B, 2008, 77, .	1.1	6
6358	Electronic surface error in the Si interstitial formation energy. Physical Review B, 2008, 77, .	1.1	30
6359	Carbides in stainless steels: Results from ab initio investigations. Applied Physics Letters, 2008, 93, .	1.5	82
6360	Carrier-induced disordering dynamics in InSb studied with density functional perturbation theory. Physical Review B, 2008, 77, .	1.1	20
6361	Pressure effects on the superconducting transition in<mml:math xmlns:mml="http://www.w3.org/1998/Math/MathML" display="inline"><mml:mrow><mml:mi>n</mml:mi><mml:mi>H</mml:mi><mml:mtext>-CaAlSi</mml:mtext></mml:mrow></mml:math>: Physical Review B, 2008, 77, .	1.1	10
6362	Electronic origin of void formation in fcc metals. Physical Review B, 2008, 77, .	1.1	17
6363	Geometry and diameter dependence of the electronic and physical properties of GaN nanowires from first principles. Physical Review B, 2008, 77, .	1.1	88
6364	¹⁷O quadrupole coupling and the origin of ferroelectricity in isotopically enriched BaTiO₃and SrTiO₃. Journal of Physics Condensed Matter, 2008, 20, 085204.	0.7	12

#	Article	IF	Citations
6365	Structural, mechanical, and electronic properties of ultrathin ZnO nanowires. Applied Physics Letters, 2008, 93, 021918.	1.5	39
6366	Structure and mechanical properties of osmium carbide: First-principles calculations. Applied Physics Letters, 2008, 93, .	1.5	38
6367	Anomalies in transition metal conductivity: Strong evidence for Fermi-velocity dominance. Physical Review B, 2008, 77, .	1.1	0
6368	Vacancy-mediated dopant diffusion activation enthalpies for germanium. Applied Physics Letters, 2008, 92, .	1.5	132
6369	Ca-induced intermediate reconstructions on the Si(111) surface. Physical Review B, 2008, 77, .	1.1	8
6370	Indium-oxide polymorphs from first principles: Quasiparticle electronic states. Physical Review B, 2008, 77, .	1.1	219
6371	Nature and strength of bonding in a crystal of semiconducting nanotubes: van der Waals density functional calculations and analytical results. Physical Review B, 2008, 77, .	1.1	53
6372	Effect of atomic hydrogen on boron-doped germanium: An ab initio study. Applied Physics Letters, 2008, 93, 082107.	1.5	1
6373	Theoretical study of the surface reactivity of alkaline earth oxides: Local density of states evaluation of the local softness. Journal of Chemical Physics, 2008, 128, 034708.	1.2	31
6374	Low-energy antiphase boundaries, degenerate superstructures, and phase stability in frustrated fcc Ising model and Ag-Au alloys. Physical Review B, 2008, 77, .	1.1	32
6375	Modeling the sorption dynamics of NaH using a reactive force field. Journal of Chemical Physics, 2008, 128, 164714.	1.2	29
6376	Hydrogen diffusion behavior in N doped ZnO: First-principles study. Journal of Applied Physics, 2008, 103, .	1.1	26
6377	First-principles modeling of strain in perovskite ferroelectric thin films. Phase Transitions, 2008, 81, 607-622.	0.6	14
6378	Numerical characterization of the Ga interstitial self-diffusion mechanisms in GaAs. Journal of Applied Physics, 2008, 103, 113502.	1.1	10
6379	Monolayer structure of tetracene on Cu (100) surface: Parallel geometry. Journal of Chemical Physics, 2008, 128, 244706.	1.2	14
6380	Stabilization of the high-k tetragonal phase in HfO2: The influence of dopants and temperature fromab initiosimulations. Journal of Applied Physics, 2008, 104, .	1.1	42
6381	Pressure-induced incompressibility of ReC and effect of metallic bonding on its hardness. Applied Physics Letters, 2008, 92, .	1.5	135
6382	Optical property and electronic band structure of a piezoelectric compound Ga3PO7 studied by the first-principles calculation. Applied Physics Letters, 2008, 92, .	1.5	6

#	Article	IF	Citations
6383	Metastable phase formation and magnetic properties of the Feâ€“Nb system studied by atomistic modeling and ion beam mixing. Journal of Applied Physics, 2008, 104, 014914.	1.1	7
6384	Mechanism of the linear electro-optic effect in potassium dihydrogen phosphate crystals. Journal of Applied Physics, 2008, 104, 073116.	1.1	7
6385	First-principles calculations on solid nitrogen: A comparative study of high-pressure phases. Physical Review B, 2008, 77, .	1.1	45
6386	Compression of<mml:math xmlns:mml="http://www.w3.org/1998/Math/MathML" display="inline"><mml:mrow><mml:msub><mml:mtext>H</mml:mtext><mml:mn>2</mml:mn></mml:msub><mml:mtext>O</mml:mtext> to 126 GPa and implications for hydrogen-bond symmetrization: Synchrotron x-ray diffraction measurements and density-functional calculations. Physical Review B, 2008, 77, .	1.1	72
6387	Equivalence of dipole correction and Coulomb cutoff techniques in supercell calculations. Physical Review B, 2008, 77, .	1.1	34
6388	First principles calculations of the electronic and geometric structure ofAg27Cu7nanoalloy. Physical Review B, 2008, 77, .	1.1	35
6389	Analytic many-body potential for InAs/GaAs surfaces and nanostructures: Formation energy of InAs quantum dots. Physical Review B, 2008, 77, .	1.1	57
6390	Lattice dynamics of wurtzite and rocksalt AlN under high pressure: Effect of compression on the crystal anisotropy of wurtzite-type semiconductors. Physical Review B, 2008, 77, .	1.1	61
6391	Diffusion and defect reactions between donors, C, and vacancies in Ge. II. Atomistic calculations of related complexes. Physical Review B, 2008, 77, .	1.1	81
6392	Hydrogen-induced metallization of zinc oxide<mml:math xmlns:mml="http://www.w3.org/1998/Math/MathML" display="inline"><mml:mrow><mml:mrow><mml:mo>(</mml:mo><mml:mrow><mml:mn>2</mml:mn><mml:mover) Tj ETQq1 1 0.784	1.1	43
6393	Direct and defect-assisted electron tunneling through ultrathin<mml:math xmlns:mml="http://www.w3.org/1998/Math/MathML" display="inline"><mml:mrow><mml:msub><mml:mrow><mml:mtext>SiO</mml:mtext></mml:mrow><mml:mn>2</mml:mn></mml:msu from first principles. Physical Review B, 2008, 77, .	1.1	35
6394	Electronic structure and Fermi surface character of LaNiPO from first principles. Physical Review B, 2008, 77, .	1.1	19
6395	Effect of strain on the band gap and effective mass of zigzag single-wall carbon nanotubes: First-principles density-functional calculations. Physical Review B, 2008, 77, .	1.1	42
6396	Dissociative adsorption of<mml:math xmlns:mml="http://www.w3.org/1998/Math/MathML" display="inline"><mml:msub><mml:mi mathvariant="normal">O</mml:mi><mml:mn>2</mml:mn></mml:msub></mml:math>molecules on O-precovered Fe(110) and Fe(100): Density-functional calculations. Physical Review B, 2008, 77, .	1.1	34
6397	Engineering the free vacancy and active donor concentrations in phosphorus and arsenic double donor-doped germanium. Journal of Applied Physics, 2008, 104, .	1.1	29
6398	Hydrogen-induced magnetization and tunable hydrogen storage in graphitic structures. Physical Review B, 2008, 77, .	1.1	33
6399	Ab initiostudy of oxygen-vacancy LaAlO₃(001) surface. Chinese Physics B, 2008, 17, 655-661.	0.7	15
6400	Dissociative adsorption of<mml:math xmlns:mml="http://www.w3.org/1998/Math/MathML" display="inline"><mml:msub><mml:mi mathvariant="normal">O</mml:mi><mml:mn>2</mml:mn></mml:msub></mml:math>on Pt and Au surfaces: Potential-energy surfaces and electronic states. Physical Review B, 2008, 77, .	1.1	23

#	Article	IF	Citations
6401	Surface Modification of Ni-YSZ Using Niobium Oxide for Sulfur-Tolerant Anodes in Solid Oxide Fuel Cells. Journal of the Electrochemical Society, 2008, 155, B449.	1.3	45
6402	Lock and key behaviours of an aromatic carboxylic acid molecule with differing conformations on an Au (111) surface. Molecular Physics, 2008, 106, 2371-2380.	0.8	1
6403	Dynamical stability of the cubic metallic phase of<mml:math xmlns:mml="http://www.w3.org/1998/Math/MathML" display="inline"><mml:mrow><mml:msub><mml:mrow><mml:mtext>AlH</mml:mtext></mml:mrow><mml:mn>3</mml:mn></mml:msub> ambient pressure: Density functional calculations. Physical Review B, 2008, 78, .	1.1	26
6404	Pt-induced nanowires on Ge(001):Ab initiostudy. Physical Review B, 2008, 78, .	1.1	22
6405	First-principles study of correlation effects in<mml:math xmlns:mml="http://www.w3.org/1998/Math/MathML" display="inline"><mml:mrow><mml:msub><mml:mrow><mml:mtext>VO</mml:mtext></mml:mrow><mml:mn>2</mml:mn></mml:msub> Physical Review B, 2008, 78, .	1.1	52
6406	Enhanced spin-density wave in LaFeSbO from first principles. Physical Review B, 2008, 78, .	1.1	10
6407	Formation of interstitial carbonâ€“interstitial oxygen complexes in silicon: Local vibrational mode spectroscopy and density functional theory. Physical Review B, 2008, 78, .	1.1	23
6408	Electronic structure and thermodynamic stability of<mml:math xmlns:mml="http://www.w3.org/1998/Math/MathML" display="inline"><mml:mrow><mml:msub><mml:mrow><mml:mtext>LaMnO</mml:mtext></mml:mrow><mml:mn>3</mml:mn></mml:msub> xmlns:mml="http://www.w3.org/1998/Math/MathML" display="inline"><mml:mrow><mml:msub><mml:mrow><mml:mtext>La</mml:mtext></mml:mrow><mml:mrow><mml:mn>1</mml:mn> Physical Review B, 2008, 78, .	1.1	85
6409	Dissociation of Bâ€“H pairs in diamond as enhanced by electronic excitation and electron capture: Computational modeling. Physical Review B, 2008, 77, .	1.1	18
6410	Ab initiostudy of<mml:math xmlns:mml="http://www.w3.org/1998/Math/MathML" display="inline"><mml:mrow><mml:mi mathvariant="normal">Sr</mml:mi><mml:msub><mml:mi mathvariant="normal">Fe</mml:mi><mml:mi>x</mml:mi></mml:msub><mml:msub><mml:mi mathvariant="normal">Ti</mml:mi><mml:mrow><mml:mn>1</mml:mn><mml:mo>â^’</mml:mo><mml:mi>x</mml:mi></mml:mrow></mml:msub><mml:msub><mml:mi mathvariant="normal">O</mml:mi><mml:mn>3</mml:mn></mml:msub></mml:mrow></mml:math>:	1.1	38
6411	Efficient<mml:math xmlns:mml="http://www.w3.org/1998/Math/MathML" display="inline"><mml:mrow><mml:mi mathvariant="script">O</mml:mi><mml:mrow><mml:mo>(</mml:mo><mml:mrow><mml:msup><mml:mi>N</mml:mi><mml:mn>2</mml:mn> to solve the Bethe-Salpeter equation for excitonic bound states. Physical Review B, 2008, 78, .	1.1	117
6412	Properties of Pt-supported Co nanomagnets from relativistic density functional theory calculations. Physical Review B, 2008, 78, .	1.1	26
6413	Defect-Dipole Formation in Copper-Doped<mml:math xmlns:mml="http://www.w3.org/1998/Math/MathML" display="inline"><mml:msub><mml:mi>PbTiO</mml:mi><mml:mn>3</mml:mn></mml:msub></mml:math>Ferroelectrics. Physical Review Letters, 2008, 100, 095504.	2.9	118
6414	Density functional theory study of mercury adsorption on metal surfaces. Physical Review B, 2008, 77, .	1.1	65
6415	<mml:math xmlns:mml="http://www.w3.org/1998/Math/MathML" display="inline"><mml:mrow><mml:msub><mml:mtext>H</mml:mtext><mml:mn>2</mml:mn></mml:msub></mml:mrow></mml:math> on strained pseudomorphic monolayers of Cu and Pd on Ru(0001). Physical Review B, 2008, 77, .	1.1	34
6416	First principles calculations of the structural and electronic properties of the type-I semiconductor clathrate alloysBa8Ga16SixGe30â^’xandSr8Ga16SixGe30â^’x. Physical Review B, 2008, 77, .	1.1	23
6417	Hard-Sphere variational approach using anab initiomolecular dynamics code. Physical Review B, 2008, 77, .	1.1	9
6418	Vibrational properties of the H-N-H complex in dilute III-N-V alloys: Infrared spectroscopy and density functional theory. Physical Review B, 2008, 77, .	1.1	23

#	Article	IF	Citations
6419	Pressure-Induced Hydrogen-Dominant Metallic State in Aluminum Hydride. Physical Review Letters, 2008, 100, 045504.	2.9	136
6420	Mg acceptor energy levels in<mml:math xmlns:mml="http://www.w3.org/1998/Math/MathML" display="inline"><mml:mrow><mml:msub><mml:mi mathvariant="normal">Al</mml:mi><mml:mi>x</mml:mi></mml:msub><mml:msub><mml:mi mathvariant="normal">In</mml:mi><mml:mi>y</mml:mi></mml:msub><mml:msub><mml:mi<mml:math xmlns:mml="http://www.w3.org/1998/Math/MathML" display="inline"><mml:mrow><mml:msub><mml:mi>Rh</mml:mi><mml:mn>2</mml:mn></mml:msub><mml:msub><mml:mi mathvariant="normal">O</mml:mi><mml:mn>3</mml:mn></mml:msub><mml:mo>(</mml:mo><mml:mi>II</mml:mi><mml:mo>)</mm	1.1	15
6421	structures in<mml:math xmlns:mml="http://www.w3.org/1998/Math/MathML" display="inline"><mml:mrow><mml:msub><mml:mi>Ga</mml:mi><mml:mn>2</mml:mn></mml:msub><mml:msub><mml:mi mathvariant="normal">O</mml:mi><mml:mi><mml:. Physical Review B, 2008, 77, .	1.1	62
6422	Ground-State Properties of Crystalline Ice from Periodic Hartree-Fock Calculations and a Coupled-Cluster-Based Many-Body Decomposition of the Correlation Energy. Physical Review Letters, 2008, 101, 183005.	2.9	80
6423	Atomic-scale study of low-temperature equilibria in iron-rich Al-C-Fe. Physical Review B, 2008, 78, .	1.1	11
6424	Lubricant effect of copper nanoclusters on the dislocation core inÎ±â^'Fe. Physical Review B, 2008, 77, .	1.1	12
6425	Second-nearest-neighbor modified embedded-atom potential for binary Ta-W alloys based on first-principles calculations. Physical Review B, 2008, 77, .	1.1	8
6426	Ab initio investigation of interfacial layer formation in the Moâ^•Si boundary for extreme ultraviolet lithography. Journal of Applied Physics, 2008, 103, 124310.	1.1	0
6427	Crystal structures and mechanical properties of superhard<mml:math xmlns:mml="http://www.w3.org/1998/Math/MathML" display="inline"><mml:mrow><mml:mi mathvariant="normal">B</mml:mi><mml:msub><mml:mi mathvariant="normal">C</mml:mi><mml:mn>2</mml:mn></mml:msub><mml:mi mathvariant="normal">N</mml:mi></mml:mrow></mml:math>and<mml:math xmlns:mml="http://www.w3.org/1998/Math/MathML" display="inline"><mml:mrow><mml:mi mathvarian	1.1	35
6428	First-principles study of water on copper and noble metal (110) surfaces. Physical Review B, 2008, 77, .	1.1	99
6429	Ground-state structure of coherent lattice-mismatched zinc-blendeA1â^'xBxCsemiconductor alloys (x=0.25and 0.75). Physical Review B, 2008, 77, .	1.1	10
6430	Structure of theGaP(001)â^'4Ã—2-Insurface investigated with LEED, STM, photoelectron spectroscopy, andab initiocalculations. Physical Review B, 2008, 78, .	1.1	2
6431	Magnetic anisotropy ofFeâ^•Pt(001)andPtâ^•Feâ^•Pt(001)using a first-principles approach. Physical Review B, 2008, 77, .	1.1	38
6432	Gold work function reduction by 2.2eV with an air-stable molecular donor layer. Applied Physics Letters, 2008, 93, .	1.5	75
6433	Half-metallic NiO in zinc-blende structure from ab initio calculations. Journal of Applied Physics, 2008, 104, 046103.	1.1	4
6434	THE MULTISCALE MODEL COMBINING ELASTIC THEORY WITH AB INITIO CALCULATIONS FOR METALâ€“CERAMIC INTERFACES. Modern Physics Letters B, 2008, 22, 3135-3143.	1.0	7
6435	Ab initioinvestigation of phosphorus diffusion paths in germanium. Physical Review B, 2008, 77, .	1.1	16
6436	C4 defect and its precursors in Si: First-principles theory. Physical Review B, 2008, 77, .	1.1	20

#	Article	IF	Citations
6437	Electronic structure of Ga-, In-, and Tl-doped PbTe: A supercell study of the impurity bands. Physical Review B, 2008, 78, .	1.1	62
6438	Crystal structures and relative stabilities of the spinel oxynitrides<mml:math xmlns:mml="http://www.w3.org/1998/Math/MathML" display="inline"><mml:mrow><mml:msub><mml:mi>M</mml:mi><mml:mn>3</mml:mn></mml:msub><mml:mi mathvariant="normal">N</mml:mi><mml:msub><mml:mi mathvariant="normal">O</mml:mi><mml:mn>3</mml:mn></mml:msub></mml:mrow></mml:math><mml:math xmlns:mml="http://www.w3.org/1998/Math/MathML"		

#	Article	IF	Citations
6455	Nonlinear stability of<mml:math xmlns:mml="http://www.w3.org/1998/Math/MathML" display="inline"><mml:mi>E</mml:mi></mml:math>centers in<mml:math xmlns:mml="http://www.w3.org/1998/Math/MathML" display="inline"><mml:mrow><mml:msub><mml:mrow><mml:mtext>Si</mml:mtext></mml:mrow><mml:mrow><mml:mn>1</mml:mn> Electronic structure calculations. Physical Review B, 2008, 78, .	1.1	63
6456	Interplay of shape, interface structure, and electrostatic fields of ionic nanodots embedded in a polar semiconductor matrix. Physical Review B, 2008, 78, .	1.1	12
6457	First-principles theory of the energetics of He defects in bcc transition metals. Physical Review B, 2008, 78, .	1.1	130
6458	Generic guiding principle for the prediction of metal-induced reconstructions of compound semiconductor surfaces. Physical Review B, 2008, 78, .	1.1	17
6459	Lattice dynamics of cobalt-deficient CoO from first principles. Physical Review B, 2008, 78, .	1.1	25
6460	Doping of graphene: Density functional calculations of charge transfer between GaAs and carbon nanostructures. Physical Review B, 2008, 78, .	1.1	17
6461	Atomic oxygen adsorption and incipient oxidation of the Pb(111) surface: A density-functional theory study. Physical Review B, 2008, 78, .	1.1	25
6462	Quasiatomic orbitals forab initiotight-binding analysis. Physical Review B, 2008, 78, .	1.1	90
6463	Modeling the compositional dependence of electron diffraction in dilute GaAs- and GaP-based compound semiconductors. Physical Review B, 2008, 78, .	1.1	10
6464	Crystal structure, electronic structure, and vibrational properties of<mml:math xmlns:mml="http://www.w3.org/1998/Math/MathML" display="inline"><mml:mrow><mml:mi>M</mml:mi><mml:mtext>AlSiH</mml:mtext></mml:mrow></mml:math><mml:math xmlns:mml="http://www.w3.org/1998/Math/MathML" display="inline"><mml:mrow><mml:mo>(</mml:mo><mml:mrow><mml:mi>M</mml:mi><mml:mo>=</mml:mo><mml:mtext>Ca</mml:m Physical Review B, 2008, 78, .	1.1	24
6465	Functionalization of silicon nanowires with transition metal atoms. Physical Review B, 2008, 78, .	1.1	26
6466	First-principles study of Fe and FeAl defects in SiGe alloys. Physical Review B, 2008, 78, .	1.1	10
6467	Photoemission and quantum chemical study of<mml:math xmlns:mml="http://www.w3.org/1998/Math/MathML" display="inline"><mml:mrow><mml:msub><mml:mrow><mml:mtext>SrTiO</mml:mtext></mml:mrow><mml:mn>3</mml:mn></mml:m and their interaction with<mml:math xmlns:mml="http://www.w3.org/1998/Math/MathML" display="inline"><mml:mrow><mml:msub><mml:mrow><mml:mtext>CO</mml:mtext></mml:mrow><m. Physical Review B, 2008, 78, .	1.1	54
6468	High-pressure structural behavior of large-void CoSn-type intermetallics: Experiments and first-principles calculations. Physical Review B, 2008, 77, .	1.1	15
6469	Segregation of Cr impurities at bcc iron surfaces: First-principles calculations. Physical Review B, 2008, 78, .	1.1	44
6470	<mml:math xmlns:mml="http://www.w3.org/1998/Math/MathML" display="inline"><mml:mrow><mml:mi mathvariant="normal">C</mml:mi><mml:msub><mml:mi mathvariant="normal">H</mml:mi><mml:mn>3</mml:mn></mml:msub><mml:mi mathvariant="normal">S</mml:mi><mml:mi mathvariant="normal">H</mml:mi></mml:mrow></mml:math>molecules deposited on Cu(111) and deprotonation. Physical Review B, 2008, 77, .	1.1	8
6471	Vacancy ordering in<mml:math xmlns:mml="http://www.w3.org/1998/Math/MathML" display="inline"><mml:mrow><mml:msub><mml:mrow><mml:mtext>Co</mml:mtext></mml:mrow><mml:mn>3</mml:mn></mml:m A first-principles study. Physical Review B, 2008, 78, .	1.1	6
6472	Two FeH pairs in<mml:math xmlns:mml="http://www.w3.org/1998/Math/MathML" display="inline"><mml:mi>n</mml:mi></mml:math>-type Si and their implications: A theoretical study. Physical Review B, 2008, 78, .	1.1	8

#	Article	IF	Citations
6473	First-principles calculations of oxygen-vacancy dipoles and hydrogen impurities in<mml:math xmlns:mml="http://www.w3.org/1998/Math/MathML" display="inline"><mml:mrow><mml:msub><mml:mrow><mml:mtext>SrF</mml:mtext></mml:mrow><mml:mn>2</mml:mn></mml:msu Physical Review B, 2008, 78, .	1.1	14
6474	First-principles-based phase diagram of the cubic BNC ternary system. Physical Review B, 2008, 77, .	1.1	36
6475	First-principles study of electronic properties of biaxially strained silicon: Effects on charge carrier mobility. Physical Review B, 2008, 78, .	1.1	93
6476	Structural, thermodynamic, and electronic properties of plutonium oxides from first principles. Physical Review B, 2008, 78, .	1.1	215
6477	Tuning field-induced energy gap of bilayer graphene via interlayer spacing. Applied Physics Letters, 2008, 92, .	1.5	96
6478	A lattice dynamical study of the aragonite and post-aragonite phases of calcium carbonate rock. American Mineralogist, 2008, 93, 1608-1612.	0.9	16
6479	Intrinsic point defects in aluminum antimonide. Physical Review B, 2008, 77, .	1.1	40
6480	Density Functional Model Studies of Uranyl Adsorption on (001) Surfaces of Kaolinite. Langmuir, 2008, 24, 9515-9524.	1.6	90
6481	First principles method for the calculation of zero-field splitting tensors in periodic systems. Physical Review B, 2008, 77, .	1.1	27
6482	Fe-induced spin-polarized electronic states in a realistic semiconductor tunnel barrier. Physical Review B, 2008, 77, .	1.1	5
6483	Interaction and concerted diffusion of lithium in a (5,5) carbon nanotube. Physical Review B, 2008, 78, .	1.1	58
6484	Electronic properties of <mml:math xmlns:mml="http://www.w3.org/1998/Math/MathML" display="inline"><mml:mrow><mml:msub><mml:mi mathvariant="normal">Sc</mml:mi><mml:mn>5</mml:mn></mml:msub><mml:msub><mml:mi>M</mml:mi><mml:mn>4</mml:mn><mml:mathvariant="normal">Si</mml:mi><mml:mn>10</mml:mn></mml:msub></mml:mrow></mml:math><mml:math xmlns:mml="http://www.w3.org/1998/Math/MathML"		

#	Article	IF	Citations
6491	Electronic structure at the<mml:math xmlns:mml="http://www.w3.org/1998/Math/MathML" display="inline"><mml:msub><mml:mi mathvariant="normal">C</mml:mi><mml:mn>60</mml:mn></mml:msub></mml:math>/metal interface: An angle-resolved photoemission and first-principles study. Physical Review B, 2008, 77, .	1.1	59
6492	Structurally induced insulator-metal transition in solid oxygen: A quasiparticle investigation. Physical Review B, 2008, 77, .	1.1	17
6493	Electronic structure of cation-deficient CoO from first principles. Physical Review B, 2008, 77, .	1.1	25
6494	Electronic structure of thiol-bonded self-assembled monolayers: Impact of coverage. Physical Review B, 2008, 77, .	1.1	80
6495	High-pressure electronic structure and phase transitions in monoclinic InSe: X-ray diffraction, Raman spectroscopy, and density functional theory. Physical Review B, 2008, 77, .	1.1	40
6496	Dynamical Instabilities of Ice X. Physical Review Letters, 2008, 101, 085502.	2.9	72
6497	Influence of carbon content on the strength of cubic<mml:math xmlns:mml="http://www.w3.org/1998/Math/MathML" display="inline"><mml:mrow><mml:msub><mml:mrow><mml:mtext>BC</mml:mtext></mml:mrow><mml:mi>x</mml:mi></mml:msub></mml:math>: A first-principles study. Physical Review B, 2008, 77, .	1.1	12
6498	Local field effects at Li K edges in electron energy-loss spectra of Li,Li2Oand LiF. Physical Review B, 2008, 77, .	1.1	14
6499	Atomistic molecular dynamics study of interface formation: Al on poly(p-phenylene vinylene). Physical Review B, 2008, 78, .	1.1	12
6500	Mn-doped silicon nanowires: First-principles calculations. Physical Review B, 2008, 78, .	1.1	14
6501	First-Principles Theory of Hydrogen Diffusion in Aluminum. Physical Review Letters, 2008, 101, 075901.	2.9	32
6502	Metastable high-pressure single-bonded phases of nitrogen predicted via genetic algorithm. Physical Review B, 2008, 77, .	1.1	65
6503	Noncontact atomic force microscopy imaging mechanism on Ag(110): Experiment and first-principles theory. Physical Review B, 2008, 77, .	1.1	21
6504	Defect-Induced Photoconductivity in Layered Manganese Oxides: A Density Functional Theory Study. Physical Review Letters, 2008, 100, 146601.	2.9	98
6505	Electrical activity of hydrogen impurities in GaSb: First-principles calculations. Physical Review B, 2008, 78, .	1.1	16
6506	First-principles calculations of the vibrational and thermal properties of the type-I clathratesBa8Ga16SixGe30â^'xandSr8Ga16SixGe30â^'x. Physical Review B, 2008, 78, .	1.1	20
6507	Adsorbate cluster expansion for an arbitrary number of inequivalent sites. Physical Review B, 2008, 78, .	1.1	39
6508	Ab initio structure determination of the low-temperature phase of succinonitrile from laboratory X-ray powder diffraction dataâ€"Coping with potential poor powder quality using DFT ab initio methods. Powder Diffraction, 2008, 23, 292-299.	0.4	15

#	Article	IF	Citations
6509	Structure of and ion segregation to an alumina grain boundary: Implications for growth and creep. Journal of Materials Research, 2008, 23, 1494-1508.	1.2	25
6510	Electron Transfer from Hydrogen Molecule to Au(111) During Dissociative Adsorption: A First-Principles Study. Journal of the Physical Society of Japan, 2008, 77, 054705.	0.7	8
6511	Atomic and electronic structures of the group-IV elements on Si(111)-(âˆš3 Ã— âˆš3) surface. Journal of Physics: Conference Series, 2008, 100, 072025.	0.3	2
6512	Ab initiostudy of bulk and surface iron defects in SrTiO₃. Journal of Physics: Conference Series, 2008, 117, 012001.	0.3	3
6513	Stability and geometry of free-standing III-V nanorods. Journal of Physics: Conference Series, 2008, 100, 052053.	0.3	0
6514	Atomic and Electronic Structures of Boron Clusters in Crystalline Silicon: The Case of X@B6 and X@B12, X=Hâ€“Br. Advances in Quantum Chemistry, 2008, , 89-102.	0.4	0
6515	First-principles study of p-type transparent conductive oxides CuXO2 (X=Y, Sc, and Al). Journal of Applied Physics, 2008, 104, .	1.1	34
6516	Ab Initio Analysis of Point Defects in Plane-Stressed Si Single Crystal. Journal of Computational Science and Technology, 2008, 2, 478-487.	0.4	1
6517	Ab Initio Study of Ideal Strength of Covalent Crystals: Effect of Multiaxial Stress and Structure. Journal of Solid Mechanics and Materials Engineering, 2008, 2, 1360-1368.	0.5	0
6518	Atomic Structure of Faceted Î£3 CSL Grain Boundary in Silicon: HRTEM and Ab-Initio Calculation. Nippon Kinzoku Gakkaishi/Journal of the Japan Institute of Metals, 2008, 72, 886-891.	0.2	1
6519	First Principles Calculation of CO and H₂ Adsorption on Strained Pt Surface. Materials Transactions, 2008, 49, 2484-2490.	0.4	6
6520	<I>Ab Initio</I> Electronic Structure Study of α-Zirconium and Hydrogen. Materials Transactions, 2008, 49, 2765-2769.	0.4	5
6521	Structural, Electronic and Optical Properties of the Al₂O₃ Doped SiO₂: First Principles Calculations. Materials Transactions, 2008, 49, 2474-2479.	0.4	7
6522	Dependence of Magnetism on Doping Concentration in V-Doped Bulk ZnO. Materials Transactions, 2008, 49, 2469-2473.	0.4	6
6523	The vacancy in silicon: A critical evaluation of experimental and theoretical results. Journal of Applied Physics, 2008, 104, 076108.	1.1	58
6524	Atomic structures of supersaturated ZnOâ€“Al2O3 solid solutions. Journal of Applied Physics, 2008, 103, 014309.	1.1	68
6525	Charge transfer and adhesion in Rh/MgO(001). Journal of Physics: Conference Series, 2008, 100, 082027.	0.3	3
6526	Ferromagnetism in (Mn,Li) co-doped CdSe. Europhysics Letters, 2008, 84, 57012.	0.7	4

#	Article	IF	Citations
6527	Origin of enhanced superconducting transition temperature through structural transformation in CaSi₂. Journal of Physics: Conference Series, 2008, 121, 052010.	0.3	4
6528	Two points of view to look at symmetry. Journal of Physics: Conference Series, 2008, 117, 012030.	0.3	4
6529	New Pt-based Superalloy System Designed from First Principles. Materials Research Society Symposia Proceedings, 2008, 1128, 52801.	0.1	0
6530	Thermal properties of guest-free Si136 and Ge136 clathrates: A first-principles study. Journal of Applied Physics, 2008, 104, 033535.	1.1	16
6531	First-Principles Calculation of Lattice Dynamics of Skutterudite Compounds. Journal of the Physical Society of Japan, 2008, 77, 248-250.	0.7	8
6532	Nucleation and growth of cobalt disilicide precipitates during in situ transmission electron microscopy implantation. Journal of Applied Physics, 2008, 104, 033527.	1.1	10
6533	Ab initio investigations of the phonon anomaly and superconductivity in fcc La. Journal of Applied Physics, 2008, 104, 063916.	1.1	5
6534	First principles prediction of new high-pressure phase of InOOH. Journal of Mineralogical and Petrological Sciences, 2008, 103, 116-120.	0.4	13
6535	Interfacial electronic states of tetracene deposited on Si(111). Journal of Chemical Physics, 2009, 130, 174712.	1.2	7
6536	Electronic Structure of a Collapsed Armchair Single-Walled Carbon Nanotube. E-Journal of Surface Science and Nanotechnology, 2009, 7, 541-545.	0.1	7
6537	Equation of state and phase diagram of water at ultrahigh pressures as in planetary interiors. Physical Review B, 2009, 79, .	1.1	212
6538	Density functional study of the magnetic coupling in<mml:math xmlns:mml="http://www.w3.org/1998/Math/MathML" display="inline"><mml:mrow><mml:mtext>V</mml:mtext><mml:msub><mml:mrow><mml:mrow><mml:mo>(</mml:mo><mml:mrow> Physical Review B, 2009, 79, .	1.1	34
6539	High-pressure phase transformations, pressure-induced amorphization, and polyamorphic transition of the clathrate<mml:math xmlns:mml="http://www.w3.org/1998/Math/MathML" display="inline"><mml:mrow><mml:msub><mml:mrow><mml:mtext>Rb</mml:mtext></mml:mrow><mml:mrow><mml:mn>6.15</mml:mn> Physical Review B, 2009, 79, .	1.1	34
6540	Enhancing nitrogen solubility in GaAs and InAs by surface kinetics: Anab initiostudy. Physical Review B, 2009, 79, .	1.1	19
6541	Ab initiostudy of ferroelectricity in edgedPbTiO3nanowires under axial tension. Physical Review B, 2009, 79, .	1.1	53
6542	Elastic properties and electrostructural correlations in ternary scandium-based cubic inverse perovskites: A first-principles study. Physical Review B, 2009, 79, .	1.1	87
6543	Ab initiocalculation of phonons for bulk TiC and<mml:math xmlns:mml="http://www.w3.org/1998/Math/MathML" display="inline"><mml:mrow><mml:mtext>TiC</mml:mtext><mml:mrow><mml:mo>(</mml:mo><mml:mrow><mml:mn>001</mml:mn> Physical Review B, 2009, 80, .	1.1	16
6544	Structure and stability of Au rods on<mml:math xmlns:mml="http://www.w3.org/1998/Math/MathML" display="inline"><mml:mrow><mml:msub><mml:mrow><mml:mtext>TiO</mml:mtext></mml:mrow><mml:mrow><mml:mn>2</mml:mn> by first-principles calculations. Physical Review B, 2009, 80, .	1.1	25

#	Article	IF	Citations
6545	Surface geometry of Cu{531}. Physical Review B, 2009, 79, .	1.1	16
6546	High-pressure behavior of<mml:math xmlns:mml="http://www.w3.org/1998/Math/MathML" display="inline"><mml:mrow><mml:msub><mml:mrow><mml:mtext>TiO</mml:mtext></mml:mrow><mml:mn>2</mml:mn></mml:msub></mml:mrow></mml:math> determined by experiment and theory. Physical Review B, 2009, 79, .	1.1	86
6547	First-principles prediction of low-energy structures for<mml:math xmlns:mml="http://www.w3.org/1998/Math/MathML" display="inline"><mml:mrow><mml:msub><mml:mrow><mml:mtext>AlH</mml:mtext></mml:mrow><mml:mn>3</mml:mn></mml:msub></mml:mrow></mml:math> Physical Review B, 2009, 79, .	1.1	9
6548	Curvature effect on the interaction between folded graphitic surface and silver clusters. Physical Review B, 2009, 79, .	1.1	7
6549	First-principles study of silicon bulk and nanowire (111) surfaces terminated with trihydrides: Symmetric, rotated, and tilted. Physical Review B, 2009, 80, .	1.1	1
6550	Surface electronic structure of two- and three-dimensional holmium silicide on Si(111). Physical Review B, 2009, 79, .	1.1	6
6551	Superconducting high-pressure phase of cesium iodide. Physical Review B, 2009, 79, .	1.1	27
6552	Crystal structure, hydrogen bonds, and lattice dynamics in kanemite from first-principles calculations. Physical Review B, 2009, 79, .	1.1	3
6553	Cooperativity among defect sites in<mml:math xmlns:mml="http://www.w3.org/1998/Math/MathML" display="inline"><mml:mrow><mml:mi>A</mml:mi><mml:msub><mml:mtext>O</mml:mtext><mml:mrow><mml:mn>2</mml:mn></mml:mrow></mml:msub></mml:mrow></mml:math> xmlns:mml="http://www.w3.org/1998/Math/MathML" display="inline"><mml:mrow><mml:msub><mml:mi>A</mml:mi><mml:mn>4</mml:mn></mml:msub><mml:msub><mml:mtext>O</mml:mtext> Physical Review B, 2009, 79, .	1.1	142
6554	Formation of an anataselike phase in silica under anisotropic stress: Anab initioconstant-pressure study. Physical Review B, 2009, 80, .	1.1	7
6555	Atomic-resolution three-dimensional imaging of germanium self-interstitials near a surface: Aberration-corrected transmission electron microscopy. Physical Review B, 2009, 80, .	1.1	32
6556	Dominant role of local-moment interactions in the magnetic ordering of iron pnictide superconductors: A comparative study of arsenides and antimonides from first principles. Physical Review B, 2009, 80, .	1.1	13
6557	Quantitative prediction of twinning stress in fcc alloys: Application to Cu-Al. Physical Review B, 2009, 79, .	1.1	72
6558	Chemically selective modification of spin polarization in ultrathin ferromagnetic films: Microscopic theory and macroscopic experiment. Physical Review B, 2009, 80, .	1.1	7
6559	Instability of the body-centered tetragonal phase of iron under extreme conditions. Physical Review B, 2009, 79, .	1.1	8
6560	Electronic structure of Ni and Mo silicides investigated by x-ray emission spectroscopy and density functional theory. Physical Review B, 2009, 79, .	1.1	16
6561	Effective coordination as a predictor of adsorption energies: A model study of NO on Rh(100) and Rh/MgO(100) surfaces. Physical Review B, 2009, 79, .	1.1	10
6562	Giant perpendicular magnetic anisotropy of an Ir monolayer on a NiAl(001) surface. Physical Review B, 2009, 80, .	1.1	2

#	Article	IF	Citations
6563	Valence-band electronic structure of<mml:math xmlns:mml="http://www.w3.org/1998/Math/MathML" display="inline"><mml:mrow><mml:msub><mml:mtext>V</mml:mtext><mml:mn>2</mml:mn></mml:msub><mml:msub><mml:mtext> Identification of V and O bands. Physical Review B, 2009, 80, .	1.1	25
6564	Optimal site-centered electronic structure basis set from a displaced-center expansion: Improved results viaa prioriestimates of saddle points in the density. Physical Review B, 2009, 80, .	1.1	25
6565	Donor levels in Si nanowires determined by hybrid-functional calculations. Physical Review B, 2009, 79, .	1.1	28
6566	Density functional theory study of the initial oxidation of the Pt(111) surface. Physical Review B, 2009, 79, .	1.1	96
6567	Atomic-scale segregation behavior of Pr at a ZnO [0001]<mml:math xmlns:mml="http://www.w3.org/1998/Math/MathML" display="inline"><mml:mrow><mml:mi>Î£</mml:mi><mml:mn>49</mml:mn></mml:mrow></mml:math>tilt grain boundary. Physical Review B, 2009, 80, .	1.1	23
6568	Crucial role of surface in stability and mobility of vacancy clusters in metals. Physical Review B, 2009, 79, .	1.1	14
6569	Dye adsorbates BrPDI, BrGly, and BrAsp on anataseTiO2(001)for dye-sensitized solar cell applications. Physical Review B, 2009, 80, .	1.1	25
6570	First-principles investigation of technetium carbides and nitrides. Physical Review B, 2009, 79, .	1.1	56
6571	First-principles study of the iron pnictide superconductorBaFe2As2. Physical Review B, 2009, 79, .	1.1	43
6572	First-principles simulations of native point defects and ionic diffusion in high-pressure polymorphs of silica. Physical Review B, 2009, 79, .	1.1	13
6573	First-principles investigation of the highly tetragonal ferroelectric material<mml:math xmlns:mml="http://www.w3.org/1998/Math/MathML"		

#	Article	IF	Citations
6581	Stoichiometry and Bravais lattice diversity: Anab initiostudy of the GaSb(001) surface. Physical Review B, 2009, 79, .	1.1	21
6582	Interstitials in tetrahedrally close-packed phases: C, N, O, and F in<mml:math xmlns:mml="http://www.w3.org/1998/Math/MathML" display="inline"><mml:mi>Î²</mml:mi></mml:math>-tungsten from first principles. Physical Review B, 2009, 80, .	1.1	16
6583	Ab initiocalculations of ferroelectric instability in<mml:math xmlns:mml="http://www.w3.org/1998/Math/MathML" display="inline"><mml:mrow><mml:msub><mml:mrow><mml:mtext>PbTiO</mml:mtext></mml:mrow><mml:mn>3</mml:mn></mml:n with symmetric and asymmetric electrode layers. Physical Review B, 2009, 80, .	1.1	35
6584	Ultrafast electron and lattice dynamics at potassium-covered Cu(111) surfaces. Physical Review B, 2009, 80, .	1.1	14
6585	Indium on Cu(100) from first principles: Energetics, complex formation, and diffusion of adsorbates and vacancies on terraces and at steps. Physical Review B, 2009, 79, .	1.1	2
6586	Connection between magnetism and structure in Fe double chains on the Ir(100) surface. Physical Review B, 2009, 79, .	1.1	21
6587	Chemisorption of small fullerenes<mml:math xmlns:mml="http://www.w3.org/1998/Math/MathML" display="inline"><mml:mrow><mml:msub><mml:mtext>C</mml:mtext><mml:mi>n</mml:mi></mml:msub></mml:mrow></mml:math> xmlns:mml="http://www.w3.org/1998/Math/MathML"		

#	Article	IF	Citations
6599	Extended Frenkel pairs and band alignment at metal-oxide interfaces. Physical Review B, 2009, 79, .	1.1	31
6600	Surface dynamics and friction of K/Cu(001) characterized by helium-3 spin-echo and density functional theory. Physical Review B, 2009, 80, .	1.1	20
6601	The effect of impurities on hydrogen bonding site and local vibrational frequency in ZnO. Journal of Applied Physics, 2009, 106, 053522.	1.1	7
6602	Effect of surface energy on the growth of boron nanocrystals. Journal of Physics: Conference Series, 2009, 176, 012017.	0.3	6
6603	Ab initio study of EMIM-BF4 crystal interaction with a Li (100) surface as a model for ionic liquid/Li interfaces in Li-ion batteries. Journal of Chemical Physics, 2009, 131, 244705.	1.2	40
6604	Stoneâ€“Wales defects created by low energy recoils in single-walled silicon carbide nanotubes. Journal of Applied Physics, 2009, 106, .	1.1	15
6605	Energetics and electronic structure of aluminum point defects in HfO2: A first-principles study. Journal of Applied Physics, 2009, 106, 014104.	1.1	21
6606	Efficient First-Principles Simulation of Noncontact Atomic Force Microscopy for Structural Analysis. Physical Review Letters, 2009, 102, 176101.	2.9	18
6607	Strain effects on work functions of pristine and potassium-decorated carbon nanotubes. Journal of Chemical Physics, 2009, 131, 224701.	1.2	34
6608	Fluorine codoping in germanium to suppress donor diffusion and deactivation. Journal of Applied Physics, 2009, 106, .	1.1	61
6609	Structures of Insulating Phases of Dense Lithium. Physical Review Letters, 2009, 102, 115503.	2.9	70
6610	Electronic and optical properties of mixed anion layered oxychalcogenide semiconductors: An ab initio study. Journal of Applied Physics, 2009, 106, .	1.1	5
6611	Origin of large moments in MnxSi1â^'x at small x. Applied Physics Letters, 2009, 95, .	1.5	9
6612	Ab initio molecular dynamics study of the hydrogen-deuterium exchange in bulk lithiumborohydride (LiBH4). Applied Physics Letters, 2009, 94, 141903.	1.5	13
6613	Computation of MÃ¶ssbauer isomer shifts from first principles. Journal of Physics Condensed Matter, 2009, 21, 195501.	0.7	13
6614	Defect states in carbon nanotubes and related band structure engineering: A first-principles study. Journal of Applied Physics, 2009, 105, .	1.1	11
6615	Half-metallic properties of perovskite BaCrO3 and BaCr0.5Ti0.5O3 superlattice: LSDA+U calculations. Journal of Applied Physics, 2009, 106, .	1.1	40
6616	Mechanisms of nonstoichiometry in HfN1â^'x. Journal of Applied Physics, 2009, 106, 083502.	1.1	9

#	Article	IF	Citations
6617	Magnetic and half-metallic properties of MPo (M=Ti, V, Cr, Mn, Fe) compounds. Journal of Applied Physics, 2009, 105, 063905.	1.1	21
6618	An energetic stability predictor of hydrogen-terminated Si nanostructures. Applied Physics Letters, 2009, 95, .	1.5	14
6619	Vibrational properties of impurities in semiconductors. Modelling and Simulation in Materials Science and Engineering, 2009, 17, 084006.	0.8	9
6620	Destruction of graphene by metal adatoms. Applied Physics Letters, 2009, 95, .	1.5	101
6621	Effects of boron and arsenic doping in Î²-FeSi2. Journal of Applied Physics, 2009, 106, 023712.	1.1	12
6622	The effects of local disorder on the electronic structures of amorphous semiconductor GaAs. , 2009, , .		0
6623	The chemisorption of tetracene on Si(100)-2Ã—1 surface. Journal of Chemical Physics, 2009, 131, 044703.	1.2	8
6624	Ab initiostudy of subsurface diffusion of Cu on the H-passivated Si(001) surface. Physical Review B, 2009, 80, .	1.1	8
6625	Optical and energy-loss spectra of MgO, ZnO, and CdO fromab initiomany-body calculations. Physical Review B, 2009, 80, .	1.1	142
6626	Structure and energetics of Er defects in<mml:math xmlns:mml="http://www.w3.org/1998/Math/MathML" display="inline"><mml:mrow><mml:msub><mml:mrow><mml:mtext>LiNbO</mml:mtext></mml:mrow><mml:mn>3</mml:mn></mml:mr first-principles and thermodynamic calculations. Physical Review B, 2009, 80, .	1.1	35
6627	Ohmic contacts on silicon carbide: The first monolayer and its electronic effect. Physical Review B, 2009, 80, .	1.1	63
6628	Ab initiomethod for locating characteristic potential-energy minima of liquids. Physical Review E, 2009, 80, 051111.	0.8	20
6629	Theory of the color change of<mml:math xmlns:mml="http://www.w3.org/1998/Math/MathML" display="inline"><mml:mrow><mml:msub><mml:mrow><mml:mtext>Na</mml:mtext></mml:mrow><mml:mi>x</mml:mi></mml:msub> a function of Na-charge doping. Physical Review B, 2009, 79, .	1.1	21
6630	Nitrogen fixation at passivated Fe nanoclusters supported by an oxide surface: Identification of viable reaction routes using density functional calculations. Physical Review B, 2009, 80, .	1.1	2
6631	First-principles study of thin<mml:math xmlns:mml="http://www.w3.org/1998/Math/MathML" display="inline"><mml:mrow><mml:msub><mml:mrow><mml:mtext>TiO</mml:mtext></mml:mrow><mml:mi>x</mml:mi></mml:msub> bulklike rutile nanowires. Physical Review B, 2009, 80, .	1.1	21
6632	First-principles studies of a two-dimensional electron gas at the interface in ferroelectric oxide heterostructures. Physical Review B, 2009, 80, .	1.1	34
6633	Stability and structure of rare-earth metal and Ba-induced reconstructions on a Si(100) surface. Physical Review B, 2009, 80, .	1.1	9
6634	Crystal and electronic structure of superhard<mml:math xmlns:mml="http://www.w3.org/1998/Math/MathML" display="inline"><mml:mrow><mml:msub><mml:mrow><mml:mtext>BC</mml:mtext></mml:mrow><mml:mn>5</mml:mn></mml:msub> First-principles structural optimizations. Physical Review B, 2009, 80, .	1.1	39

#	Article	IF	Citations
6635	Fundamental interaction process between pure edge dislocation and energetically stable grain boundary. Physical Review B, 2009, 79, .	1.1	33
6636	First-principles modeling of ferroelectric capacitors via constrained displacement field calculations. Physical Review B, 2009, 80, .	1.1	60
6637	F4TCNQ on Cu, Ag, and Au as prototypical example for a strong organic acceptor on coinage metals. Physical Review B, 2009, 79, .	1.1	116
6638	Modeling charge-imbalanced<mml:math xmlns:mml="http://www.w3.org/1998/Math/MathML" display="inline"><mml:mrow><mml:msub><mml:mrow><mml:mtext>NaNbO</mml:mtext></mml:mrow><mml:mn>3</mml:mn></mml:msub></mml:mrow></mml:math> Lattice relaxation and metallicity. Physical Review B, 2009, 80, .	1.1	12
6639	Analysis of diamond nanocrystal formation from multiwalled carbon nanotubes. Physical Review B, 2009, 80, .	1.1	18
6640	Ideal barriers to polarization reversal and domain-wall motion in strained ferroelectric thin films. Physical Review B, 2009, 79, .	1.1	75
6641	Band structures and native defects of ammonia borane. Physical Review B, 2009, 80, .	1.1	20
6642	Computational study of boron nitride nanotube synthesis: How catalyst morphology stabilizes the boron nitride bond. Physical Review B, 2009, 80, .	1.1	16
6643	Fast second-order many-body perturbation method for extended systems. Physical Review B, 2009, 80, .	1.1	38
6644	Non-<mml:math xmlns:mml="http://www.w3.org/1998/Math/MathML" display="inline"><mml:mrow><mml:msup><mml:mi>d</mml:mi><mml:mn>0</mml:mn></mml:msup></mml:mrow></mml:math>Mn ferroelectricity in antiferromagnetic<mml:math xmlns:mml="http://www.w3.org/1998/Math/MathML" display="inline"><mml:mrow><mml:msub><mml:mrow><mml:mtext>BaMnO</mml:mtext></mml:mrow><mml:mn>3</mml:mn></mml:msub></mml:mrow></mml:math>	1.1	162
6645	Comparative study of clean and Bi-induced<mml:math xmlns:mml="http://www.w3.org/1998/Math/MathML" display="inline"><mml:mrow><mml:mrow><mml:mo>(</mml:mo><mml:mrow><mml:mn>2</mml:mn><mml:mo>×</mml:mo></mml:mrow> on the InP(001) surface. Physical Review B, 2009, 79, .	1.1	4
6646	First-principles calculations of clean Au(110) surfaces and chemisorption of atomic oxygen. Physical Review B, 2009, 79, .	1.1	31
6647	Activated molecular adsorption of CO on the Be(0001) surface: A density-functional theory study. Physical Review B, 2009, 80, .	1.1	7
6648	Diffusion pathways of phosphorus atoms on silicon (001). Physical Review B, 2009, 79, .	1.1	19
6649	Density functional theory studies of the hydrogenation properties of Mg and Ti. Physical Review B, 2009, 79, .	1.1	35
6650	Ab initiomodels of amorphous InN. Physical Review B, 2009, 79, .	1.1	11
6651	Near Kohn anomalies in the phonon dispersion relations of lead chalcogenides. Physical Review B, 2009, 80, .	1.1	36
6652	Interface energies of<mml:math xmlns:mml="http://www.w3.org/1998/Math/MathML" display="inline"><mml:mrow><mml:msub><mml:mrow><mml:mrow><mml:mo>(</mml:mo><mml:mrow><mml:mn>100</mml:mn> xmlns:mml="http://www.w3.org/1998/Math/MathML" display="inline"><mml:mrow><mml:msub><mml:mrow><mml:mrow><mml:mo>(</mml:mo><mml:mrow><mml:mn>111</mml:mn>	1.1	11

#	Article	IF	Citations
6653	Superhardness, stability, and metallicity of diamondlike<mml:math xmlns:mml="http://www.w3.org/1998/Math/MathML" display="inline"><mml:mrow><mml:msub><mml:mrow><mml:mtext>BC</mml:mtext></mml:mrow><mml:mn>5</mml:mn></mml:msu Density functional calculations. Physical Review B, 2009, 80, .	1.1	33
6654	Structure and stability of the<mml:math xmlns:mml="http://www.w3.org/1998/Math/MathML" display="inline"><mml:mrow><mml:mtext>Si</mml:mtext><mml:mrow><mml:mo>(</mml:mo><mml:mrow><mml:mn>331</mml:mn></mml:m reconstruction investigated with first-principles density functional theory. Physical Review B, 2009, 80, .	1.1	11
6655	Method to construct transferable minimal basis sets forab initiocalculations. Physical Review B, 2009, 80, .	1.1	1
6656	Indenter-angle-sensitive fracture modes and stress response at incipient plasticity. Physical Review B, 2009, 79, .	1.1	20
6657	Model for the electrocatalysis of hydrogen evolution. Physical Review B, 2009, 79, .	1.1	142
6658	Relevance of core-valence interaction for electronic structure calculations with exact exchange. Physical Review B, 2009, 80, .	1.1	35
6659	Stability of the ternary perovskites<mml:math xmlns:mml="http://www.w3.org/1998/Math/MathML" display="inline"><mml:mrow><mml:msub><mml:mrow><mml:mtext>Sc</mml:mtext></mml:mrow><mml:mn>3</mml:mn></mml:msub xmlns:mml="http://www.w3.org/1998/Math/MathML"		

#	Article	IF	Citations
6671	Density functional simulations of noble-gas impurities in diamond. Physical Review B, 2009, 80, .	1.1	17
6672	Density functional study of elastic and vibrational properties of the Heusler-type alloys<mml:math xmlns:mml="http://www.w3.org/1998/Math/MathML" display="inline"><mml:mrow><mml:msub><mml:mrow><mml:mtext>Fe</mml:mtext></mml:mrow><mml:mn>2</mml:mn></mml:msub>	1.1	77
6673	Hydrogen-related defects and the role of metal additives in the kinetics of complex hydrides: A first-principles study. Physical Review B, 2009, 80, .	1.1	35
6674	Superconductivity in lithium under high pressure investigated with density functional and Eliashberg theory. Physical Review B, 2009, 79, .	1.1	48
6675	High-pressure phases, vibrational properties, and electronic structure of<mml:math xmlns:mml="http://www.w3.org/1998/Math/MathML" display="inline"><mml:mrow><mml:mtext>Ne</mml:mtext><mml:msub><mml:mrow><mml:mrow><mml:mo>(</mml:mo>	1.1	59
6676	Physical Review B, 2009, 80, . Local structure of the Ag(100) surface reacting with molecular iodine: Experimental and theoretical study. Physical Review B, 2009, 80, .	1.1	22
6677	A-site ordering in colossal magnetoresistance manganite La[sub 1â^'x]Sr[sub x]MnO[sub 3]? Molecular dynamics simulations and quantum mechanics calculations. Journal of Chemical Physics, 2009, 131, 094503.	1.2	4
6678	Predicted High-Temperature Superconducting State in the Hydrogen-Dense Transition-Metal Hydride<mml:math xmlns:mml="http://www.w3.org/1998/Math/MathML" display="inline"><mml:msub><mml:mi>YH</mml:mi><mml:mn>3</mml:mn></mml:msub></mml:math>at 40ÂK and 17.7ÂGPa. Physical Review Letters, 2009, 103, 077002.	2.9	79
6679	A comparative study on the LDA + U and hybrid functional methods on the description of the electronic structure of YTiO3 under high pressure. Canadian Journal of Chemistry, 2009, 87, 1374-1382.	0.6	3
6680	Effect of oxidation of the ultrathin Fe electrode material on the strength of magnetoelectric coupling in composite multiferroics. Physical Review B, 2009, 80, .	1.1	22
6681	Theory of Spin-Conserving Excitation of the<mml:math xmlns:mml="http://www.w3.org/1998/Math/MathML" display="inline"><mml:mi>N</mml:mi><mml:mo>â^'</mml:mo><mml:msup><mml:mi>V</mml:mi><mml:mo>â^'</mml:mo></mml:msup> in Diamond. Physical Review Letters, 2009, 103, 186404.	2.9	206
6682	Manganese-hydrogen complexes in<mml:math xmlns:mml="http://www.w3.org/1998/Math/MathML" display="inline"><mml:mrow><mml:msub><mml:mrow><mml:mtext>Ga</mml:mtext></mml:mrow><mml:mrow><mml:mn>1</mml:mn> Physical Review B, 2009, 80, .	1.1	8
6683	Electronic structure of amorphous indium oxide transparent conductors. Physical Review B, 2009, 80, .	1.1	49
6684	Nonsubstitutional single-atom defects in the<mml:math xmlns:mml="http://www.w3.org/1998/Math/MathML" display="inline"><mml:mrow><mml:msub><mml:mrow><mml:mtext>Ge</mml:mtext></mml:mrow><mml:mrow><mml:mn>1</mml:mn> Physical Review B, 2009, 79, .	1.1	18
6685	Band-gap tunability of a (6,0) BN nanotube bundle under pressure:Ab initiocalculations. Physical Review B, 2009, 80, .	1.1	9
6686	Hydrogen adsorption and etching on the Si-rich 3C-SiC(001)3Ã—2surface: First-principles molecular dynamics calculations. Physical Review B, 2009, 79, .	1.1	14
6687	Structural properties and superconductivity in the ternary intermetallic compoundsMAB(M=Ca, Sr,) Tj ETQq0 0 0 rgBT /Overlock 10 Tf 5	1.1	56
6688	Density functional study of<mml:math xmlns:mml="http://www.w3.org/1998/Math/MathML" display="inline"><mml:mrow><mml:msub><mml:mrow><mml:mtext>Pt</mml:mtext></mml:mrow><mml:mrow><mml:mn>4</mml:mn> adsorbed on a carbon nanotube support. Physical Review B, 2009, 79, .	1.1	39

#	Article	IF	Citations
6689	Electronic structure and magnetic properties of monoclinic<mml:math xmlns:mml="http://www.w3.org/1998/Math/MathML" display="inline"><mml:mrow><mml:mi>Î²</mml:mi><mml:msub><mml:mrow><mml:mtext>-Cu</mml:mtext></mml:mrow><mml:mrow><mml:mtext>2</mml:mtext></mml:mrow></mml:msub><mml:mtext>O</mml:mtext></mml:mrow></mml:math>A<mml:math xmlns:mml="http://www.w3.org/1998/Math/MathML" display="inline"><mml:mrow><mml:mtext>GGA</mml:mtext><mml:. Physical Review B, 2009, 79, .	1.1	28
6690	Post-cotunnite phase ofTeO2obtained from first-principles density-functional theory methods with random-structure searching. Physical Review B, 2009, 80, .	1.1	10
6691	First-principles studies of small arsenic interstitial complexes in crystalline silicon. Physical Review B, 2009, 79, .	1.1	7
6692	First-principles model study of the phase stabilities of dilute Fe-Cu alloys: Role of vibrational free energy. Physical Review B, 2009, 80, .	1.1	23
6693	Spin-polarized electronic structure for the layered two-dimensional[FeII(TCNE)(NCMe)2][FeIIICl4]organic-based magnet. Physical Review B, 2009, 80, .	1.1	7
6694	Self-assembly of methanethiol on the reconstructed Au(111) surface. Physical Review B, 2009, 80, .	1.1	36
6695	Electric-field control of magnetic states, charge transfer, and patterning of adatoms on graphene: First-principles density functional theory calculations. Physical Review B, 2009, 80, .	1.1	25
6696	Hexagon-on-cube versus cube-on-cube epitaxy: The case of ZnSe(111) onSrTiO3(001). Physical Review B, 2009, 79, .	1.1	10
6697	Distortion of the perfect lattice structure in bilayer graphene. Physical Review B, 2009, 79, .	1.1	11
6698	Fermi-surface pockets in<mml:math xmlns:mml="http://www.w3.org/1998/Math/MathML" display="inline"><mml:mrow><mml:msub><mml:mrow><mml:mtext>YBa</mml:mtext></mml:mrow><mml:mn>2</mml:mn></mml:msub></mml:mrow></mml:math>Comparison ofab initiotechniques. Physical Review B, 2009, 79, .	1.1	11
6699	Nonequilibrium Greenâ€™s function study of<mml:math xmlns:mml="http://www.w3.org/1998/Math/MathML" display="inline"><mml:mrow><mml:msub><mml:mrow><mml:mtext>Pd</mml:mtext></mml:mrow><mml:mn>4</mml:mn></mml:msub></mml:mrow></mml:math>carbon nanotubes as hydrogen sensors. Physical Review B, 2009, 79, .	1.1	19
6700	Ab initiostudy of early stages of III-V epitaxy on high-index surfaces of group-IV semiconductors: In adsorption on Si(112). Physical Review B, 2009, 80, .	1.1	5
6701	Lattice dynamics and specific heat of<mml:math xmlns:mml="http://www.w3.org/1998/Math/MathML" display="inline"><mml:mrow><mml:mi>Î±</mml:mi><mml:mtext>-GeTe</mml:mtext></mml:mrow></mml:math>: Theoretical and experimental study. Physical Review B, 2009, 79, .	1.1	43
6702	First-principles study of Au nanostructures on rutile<mml:math xmlns:mml="http://www.w3.org/1998/Math/MathML" display="inline"><mml:mrow><mml:msub><mml:mrow><mml:mtext>TiO</mml:mtext></mml:mrow><mml:mn>2</mml:mn></mml:msub></mml:mrow></mml:math>Physical Review B, 2009, 79, .	1.1	32
6703	Electronic properties of zircon and hafnon from many-body perturbation theory. Physical Review B, 2009, 79, .	1.1	12
6704	Ab initiostudy on the surface chemistry and nanotribological properties of passivated diamond surfaces. Physical Review B, 2009, 79, .	1.1	91
6705	Nitrogen-pair paramagnetic defects in diamond: A density functional study. Physical Review B, 2009, 79, .	1.1	20
6706	Effect of germanium substrate loss and nitrogen on dopant diffusion in germanium. Journal of Applied Physics, 2009, 105, .	1.1	59

#	Article	IF	Citations
6707	Ab initio molecular dynamics study of the hydrogen diffusion in sodium and lithium hydrides. Journal of Applied Physics, 2009, 106, .	1.1	11
6708	Defect-induced chemisorption of nitrogen oxides on (10,0) single-walled carbon nanotubes: Insights from density functional calculations. Journal of Chemical Physics, 2009, 131, 114706.	1.2	20
6709	Electronic structure and vacancy formation of Li3N. Applied Physics Letters, 2009, 94, .	1.5	15
6710	Ni@B80: A single molecular magnetic switch. Applied Physics Letters, 2009, 95, 133115.	1.5	19
6711	Prediction of graphitelike BC4N from first-principles calculations. Journal of Applied Physics, 2009, 105, .	1.1	8
6712	Hydrostatic pressure induced structural instability and dielectric property of cubic BaZrO3. Journal of Applied Physics, 2009, 105, 044110.	1.1	10
6713	Magnetic properties of (ZnO)1/(CuO)1 (001) superlattice. Applied Physics Letters, 2009, 94, .	1.5	19
6714	Tunability of the piezoelectric fields in strained III-V semiconductors. Applied Physics Letters, 2009, 95, 041912.	1.5	18
6715	First-principles study of structural, thermodynamic, elastic, and magnetic properties of Cr2GeC under pressure and temperature. Journal of Applied Physics, 2009, 106, .	1.1	37
6716	Schottky barrier formation at metal electrodes and semiconducting carbon nanotubes. Applied Physics Letters, 2009, 94, 093107.	1.5	26
6717	Anomalous strength anisotropy of Î³â€²-Fe4N identified by first-principles calculations. Applied Physics Letters, 2009, 94, 151914.	1.5	9
6718	Short- and long-range orders in Feâ€“Cr: A Monte Carlo study. Journal of Applied Physics, 2009, 106, .	1.1	27
6719	Contribution of d-band electrons to ballistic transport and scattering during electron-phonon nonequilibrium in nanoscale Au films using an ab initio density of states. Journal of Applied Physics, 2009, 106, 053512.	1.1	16
6720	Bulk Modulus and Electronic Band Structure of ZnGa 2 X 4 (X = S,Se): a First-Principles Study. Chinese Physics Letters, 2009, 26, 077102.	1.3	11
6721	Modeling ZnO phases using a periodic approach: From bulk to surface and beyond. Journal of Chemical Physics, 2009, 131, 044708.	1.2	43
6722	Observation of Î“-point phonon frequency in ultrathin metallic films confirmed byab initiocalculation and lattice dynamics. Applied Physics Letters, 2009, 95, 011902.	1.5	8
6723	Chemisorption of water and carbon dioxide on nanostructured BaTiO3â€“SrTiO3(001) surfaces. Journal of Applied Physics, 2009, 106, .	1.1	69
6724	Surface Stress of Stepped Chiral Metal Surfaces. Physical Review Letters, 2009, 102, 026102.	2.9	9

#	Article	IF	Citations
6725	On the dynamical stability and metallic behavior of YH3 under pressure. Applied Physics Letters, 2009, 94, .	1.5	10
6726	Atomic hydrogen adsorption and incipient hydrogenation of the Mg(0001) surface: A density-functional theory study. Journal of Chemical Physics, 2009, 131, 034706.	1.2	17
6727	Structural Prediction and Phase Transformation Mechanisms in Calcium at High Pressure. Physical Review Letters, 2009, 103, 055503.	2.9	65
6728	Site preference of Re in NiAl and valence band structure of NiAl containing Re: First-principles study and photoelectron spectrum. Applied Physics Letters, 2009, 94, 233104.	1.5	9
6729	Nb effects on the structural and mechanical properties of TiAl alloy: Density-functional theory study. Journal of Materials Research, 2009, 24, 3165-3173.	1.2	18
6730	Anharmonic Lifetime of Phonons in Nanophononic Semiconductors. Materials Research Society Symposia Proceedings, 2009, 1172, 26.	0.1	0
6731	First-Principles Analysis of the Initial Electroreduction Steps of Oxygen over Pt(111). Journal of the Electrochemical Society, 2009, 156, B126.	1.3	207
6732	Ab Initio Study on Structural and Magnetic Properties of Ni-Pd and Ni-Pt Linear and Zigzag Nanowires. Communications in Theoretical Physics, 2009, 52, 123-127.	1.1	4
6733	Reduced Bloch mode expansion for periodic media band structure calculations. Proceedings of the Royal Society A: Mathematical, Physical and Engineering Sciences, 2009, 465, 2825-2848.	1.0	163
6734	STUDY OF HYDROGEN STORAGE IN ALUMINUM HYDRIDE COATED SINGLE-WALLED CARBON NANOTUBE. International Journal of Nanoscience, 2009, 08, 43-47.	0.4	0
6735	Element Lines: Bonding in the Ternary Gold Polyphosphides, Au2MP2 with M = Pb, Tl, or Hg. Journal of the American Chemical Society, 2009, 131, 2199-2207.	6.6	22
6736	Polarization effects on quantum levels in InN/GaN quantum wells. Nanotechnology, 2009, 20, 485204.	1.3	3
6737	Calculation of the vibrational properties of LiMgAs. Journal of Physics Condensed Matter, 2009, 21, 305402.	0.7	4
6738	FIRST PRINCIPLE CALCULATION OF ELECTRONIC BAND STRUCTURE AND OPTICAL PROPERTIES OF KIO3. International Journal of Modern Physics B, 2009, 23, 2405-2412.	1.0	1
6739	Raman scattering intensities in BaTiO₃and PbTiO₃prototypical ferroelectrics from density functional theory. Journal of Physics Condensed Matter, 2009, 21, 215901.	0.7	45
6740	p-type doping of graphene with F4-TCNQ. Journal of Physics Condensed Matter, 2009, 21, 402001.	0.7	83
6741	Bonding characteristics in NiAl intermetallics with O impurity: a first-principles computational tensile test. Journal of Physics Condensed Matter, 2009, 21, 025402.	0.7	12
6742	Effects of cation distribution in ZnFe₂O₄and CdFe₂O₄:ab initiostudies. Journal of Physics: Conference Series, 2009, 145, 012028.	0.3	14

#	Article	IF	Citations
6743	Ab initiocalculations of the wolframite MnWO₄under high pressure. High Pressure Research, 2009, 29, 578-581.	0.4	11
6744	Physical Properties of III-Antiminodes â€" a First Principles Study. Communications in Theoretical Physics, 2009, 52, 527-533.	1.1	36
6745	Electronic structures of siderite (FeCO3) and rhodochrosite (MnCO3): Oxygen K-edge spectroscopy and hybrid density functional theory. American Mineralogist, 2009, 94, 166-171.	0.9	21
6746	HYBRID HF-DFT MODELLING OF WATER ADSORPTION ON (001) SURFACE OF ORTHORHOMBIC AND CUBIC SrHfO₃. Integrated Ferroelectrics, 2009, 108, 37-45.	0.3	16
6747	From molecular to polymeric CO2: bonding transformations under pressure. High Pressure Research, 2009, 29, 113-117.	0.4	1
6748	The Lattice Stabilities and Electronic Structure of Ba_xSr_{1 â^'x}TiO₃Solid Solutions by First-Principles Calculations. Ferroelectrics, 2009, 388, 172-179.	0.3	6
6749	BINDING ENERGIES FOR OXYGEN ON TRANSITION METAL SURFACES. Surface Review and Letters, 2009, 16, 291-296.	0.5	8
6750	Atomic and electronic structure of the YBa2Cu3O7/SrTiO3 interface from first principles. Journal of Applied Physics, 2009, 106, 093714.	1.1	13
6751	DENSITY FUNCTIONAL CALCULATION OF THE ELECTRONIC STRUCTURES OF SOME A5B6C7-TYPE CRYSTALS. International Journal of Modern Physics B, 2009, 23, 97-104.	1.0	9
6752	General trend for adsorbate-induced segregation of subsurface metal atoms in bimetallic surfaces. Journal of Chemical Physics, 2009, 130, 174709.	1.2	108
6753	Atomic and electronic structures of montmorillonite in soft rock. Chinese Physics B, 2009, 18, 2933-2937.	0.7	20
6754	Electronic structure calculations of high pressure phases of metal oxynitrides. High Pressure Research, 2009, 29, 212-218.	0.4	1
6755	Dislocation modeling in calcium silicate perovskite based on the Peierls-Nabarro model. American Mineralogist, 2009, 94, 135-142.	0.9	20
6756	PRESSURE-RELATED PHASE STABILITY OF MgSiO3and(Mg0.75, Fe0.25)SiO3 AT LOWER MANTLE CONDITION. International Journal of Modern Physics B, 2009, 23, 3323-3329.	1.0	2
6757	ELECTRONIC STRUCTURE AND OPTICAL ABSORPTION OF N-DOPED ZnO. Modern Physics Letters B, 2009, 23, 3243-3251.	1.0	2
6758	ELECTRONIC AND ELASTIC PROPERTIES OF MgAl₂O₄ SPINEL AT HIGH ISOSTATIC PRESSURE: FIRST PRINCIPLE STUDY. International Journal of Modern Physics B, 2009, 23, 1695-1700.	1.0	3
6759	First-Principles Calculations of Elastic and Thermal Properties of Molybdenum Disilicide. Chinese Physics Letters, 2009, 26, 086203.	1.3	1
6760	CALCULATIONS OF HYDROGEN DIFFUSION IN THE Ti(0001)â€"(1 Ã— 1) SURFACE BY FIRST PRINCIPLES. Surface Review and Letters, 2009, 16, 905-908.	0.5	2

#	Article	IF	Citations
6761	First principles calculations of structural, electronic, thermodynamic and optical properties of BAs_{1 -x}P_xalloy. Physica Scripta, 2009, 79, 045002.	1.2	12
6762	High-pressure phases and transitions of the layered alkaline earth nitridosilicates SrSiN₂and BaSiN₂. Journal of Physics Condensed Matter, 2009, 21, 275408.	0.7	12
6763	STRUCTURAL PROPERTIES OF III-NITRIDE BINARY COMPOUNDS: A COMPREHENSIVE STUDY. Modern Physics Letters B, 2009, 23, 1111-1127.	1.0	1
6764	First-principles study of electronic structure, mechanical and optical properties of V₄AlC₃. Journal Physics D: Applied Physics, 2009, 42, 065407.	1.3	35
6765	First-principles study of phase equilibria in Cuâ€“Ptâ€“Rh disordered alloys. Journal of Physics Condensed Matter, 2009, 21, 415401.	0.7	6
6766	Effect of nucleated Cu phase on magnetic properties and electronic structures in bcc Fe: Ab initio study. Journal of Applied Physics, 2009, 106, 083910.	1.1	9
6767	Long-range empirical potential model: extension to hexagonal close-packed metals. Journal of Physics Condensed Matter, 2009, 21, 385402.	0.7	23
6768	ELECTRONIC AND OPTICAL PROPERTIES OF BaO, BaS, BaSe, BaTe AND BaPo COMPOUNDS UNDER HYDROSTATIC PRESSURE. Modern Physics Letters B, 2009, 23, 3065-3079.	1.0	19
6769	Theoretical Study of Elastic Properties of Tungsten Disilicide. Chinese Physics Letters, 2009, 26, 046302.	1.3	9
6770	Pseudo-potential investigations of structural, elastic and thermal properties of tungsten disilicide. Chinese Physics B, 2009, 18, 3495-3499.	0.7	4
6771	Tuning linear and nonlinear optical properties of wurtzite GaN byc-axial stress. Journal Physics D: Applied Physics, 2009, 42, 185107.	1.3	19
6772	DESIGNING SUPERHARD MATERIALS BY INCORPORATING BORON INTO HEAVY TRANSITION METALS. Modern Physics Letters B, 2009, 23, 1281-1290.	1.0	14
6773	Proton Transfer in Monoclinic Zirconia: A Theoretical Study. Materials Research Society Symposia Proceedings, 2009, 1177, 7.	0.1	0
6774	Structures and Solid-Liquid Phase Transition of High-Density Hydrogen Confined in Single-Walled Carbon Nanotubes. Advanced Materials Research, 2009, 79-82, 67-70.	0.3	1
6775	First-principles study of structrural and corrected band properties of wurtzite Zn _{1-x} Cd _x O and Zn _{1-x} Mg _x O systems. Chinese Physics B, 2009, 18, 2992-2997.	0.7	16
6776	Hydrogen diffusion in bulk and nanoclusters of MgH2 and the role of catalysts on the basis of ab initio molecular dynamics. Applied Physics Letters, 2009, 94, .	1.5	15
6777	Theoretical Studies on Defects of Kaolinite in Clays. Chinese Physics Letters, 2009, 26, 059101.	1.3	11
6778	Incorporation of water in iron-free ringwoodite: A first-principles study. American Mineralogist, 2009, 94, 83-89.	0.9	44

#	Article	IF	Citations
6779	Phase Transition and Thermodynamics of Ruthenium Diboride via First-Principles Calculations. Chinese Physics Letters, 2009, 26, 097101.	1.3	5
6780	First-principles calculations of elasticity and thermodynamic properties of LaNi 5 crystal under pressure. Chinese Physics B, 2009, 18, 738-743.	0.7	16
6781	Schottky Barrier Formation at a Carbon Nanotubeâ€“Scandium Junction. Chinese Physics Letters, 2009, 26, 027302.	1.3	6
6782	First-Principles Calculations of Elastic Properties of Cubic Ni 2 MnGa. Chinese Physics Letters, 2009, 26, 016201.	1.3	5
6783	A first-principles density functional study of chlorophenol adsorption on Cu2O(110):CuO. Journal of Chemical Physics, 2009, 130, 184505.	1.2	30
6784	How silylene defects at (100) Si surfaces can account for the anomalous features observed via x-ray photoelectron spectroscopy. Journal of Chemical Physics, 2009, 130, 184702.	1.2	6
6785	Amorphous Semiconductors Studied by First-principles Simulations: Structure and Electronic Properties. Materials Research Society Symposia Proceedings, 2009, 1153, 1.	0.1	1
6786	First-principles energetics and structural relaxation of antigorite. American Mineralogist, 2009, 94, 1271-1278.	0.9	14
6787	Studies of LaSn[sub 3] as a Negative Electrode for Lithium-Ion Batteries. Journal of the Electrochemical Society, 2009, 156, A536.	1.3	17
6788	Hafnia surface and high-k gate stacks. Materials Research Society Symposia Proceedings, 2009, 1155, 1.	0.1	0
6789	Phase behavior of protoenstatite at high pressure studied by atomistic simulations. American Mineralogist, 2009, 94, 950-956.	0.9	14
6790	Integrated Experimental, Atomistic, and Microstructurally Based Finite Element Investigation of the Dynamic Compressive Behavior of 2139 Aluminum. Journal of Applied Mechanics, Transactions ASME, 2009, 76, .	1.1	21
6791	Semi-Empirical Potential Methods for Atomistic Simulations of Metals and Their Construction Procedures. Journal of Engineering Materials and Technology, Transactions of the ASME, 2009, 131, .	0.8	16
6792	Origin of tunneling lineshape trends for Kondo states of Co adatoms on coinage metal surfaces. Journal of Physics Condensed Matter, 2009, 21, 355501.	0.7	9
6793	The elastic constants for Fe₃AlX (X=B, C and N) with anti-perovskite structure. Physica Scripta, 2009, 80, 055603.	1.2	7
6794	The Adsorption of NO on Various Metal Tape-Porphyrins: A First-Principles Study. Journal of the Physical Society of Japan, 2009, 78, 014706.	0.7	10
6795	Characterization of Vacancy Defect Interaction on the Electric Properties of Zigzag Single-Walled Carbon Nanotubes. Journal of the Physical Society of Japan, 2009, 78, 094715.	0.7	0
6796	Impact of germanium on vacancy clustering in germanium-doped silicon. Journal of Applied Physics, 2009, 105, .	1.1	56

#	Article	IF	Citations
6797	Comprehensive study of sodium, copper, and silver clusters over a wide range of sizes 2â‰Nâ‰75. Journal of Chemical Physics, 2009, 131, 174510.	1.2	87
6798	Mechanisms for chemical transformations of (R,R)-tartaric acid on Cu(110): A first principles study. Journal of Chemical Physics, 2009, 131, 144703.	1.2	6
6799	Model Hamiltonian for the interaction of NO with the Au(111) surface. Journal of Chemical Physics, 2009, 130, 174716.	1.2	64
6800	Surface segregation of Si and its effect on oxygen adsorption on a Î³-TiAl(111) surface from first principles. Journal of Physics Condensed Matter, 2009, 21, 225005.	0.7	33
6801	Ozonolysis of diamond. Journal of Physics Condensed Matter, 2009, 21, 264010.	0.7	2
6802	X-ray absorption near-edge structure of GaN with high Mn concentration grown on SiC. Journal of Physics Condensed Matter, 2009, 21, 295801.	0.7	9
6803	First principles calculations of the optical properties of CxNysingle walled nanotubes. Nanotechnology, 2009, 20, 175701.	1.3	41
6804	Controlling electronic structures by irradiation in single-walled SiC nanotubes: a first-principles molecular dynamics study. Nanotechnology, 2009, 20, 075708.	1.3	21
6805	Metallic properties of magnesium point contacts. New Journal of Physics, 2009, 11, 073043.	1.2	7
6806	Ab initiocalculations of structural and magnetic properties of Fe(0â€‰0â€‰1)/MgO(0â€‰0â€‰1)/Fe(0â€‰0â€‰1) magnetic tunnel junction with interfacial Mg vacancy. Journal Physics D: Applied Physics, 2009, 42, 015003.	1.3	2
6807	Synthesis and elastic properties of V₂AlC thin films by magnetron sputtering from elemental targets. Journal Physics D: Applied Physics, 2009, 42, 185408.	1.3	30
6808	First principles calculation of the effects of solute atom on electromigration resistance of Al interconnects. Journal Physics D: Applied Physics, 2009, 42, 125501.	1.3	5
6809	The structural phase transition of ZnSe under hydrostatic and nonhydrostatic compressions: anab initiomolecular dynamics study. Journal of Physics Condensed Matter, 2009, 21, 125403.	0.7	11
6810	Adsorption of benzene, phenol, propane and carbonic acid molecules on oxidized Al(111) and Î±-Al₂O₃(0001) surfaces: a first-principles study. Journal of Physics Condensed Matter, 2009, 21, 225001.	0.7	13
6811	Study of the electronic structure at the interface between fluorene-1-carboxylic acid molecules and Cu(110). Journal of Physics Condensed Matter, 2009, 21, 355005.	0.7	1
6812	Anab initiostudy of electronic and structural properties of Mn in a GaAs environment. Journal of Physics Condensed Matter, 2009, 21, 485504.	0.7	5
6813	Gradual changes in electronic properties from graphene to graphite: first-principles calculations. Journal of Physics Condensed Matter, 2009, 21, 495503.	0.7	7
6814	Accelerated molecular dynamics simulation of thin-film growth with the bond-boost method. Journal of Physics Condensed Matter, 2009, 21, 084212.	0.7	26

#	Article	IF	Citations
6815	Ab initiophase diagram of oxygen adsorption on W(110). Journal of Physics Condensed Matter, 2009, 21, 134017.	0.7	18
6816	Density functional studies of muonium in nitrogen aggregate containing diamond: the Mu_Xcentre. Journal of Physics Condensed Matter, 2009, 21, 364211.	0.7	2
6817	Instability of CaLi ₂ at high pressure: Theoretical prediction and experimental results. Europhysics Letters, 2009, 86, 56001.	0.7	13
6818	Effects of hydrogen impurities on Ge _{1â^' x} Mn _x semiconductors. Europhysics Letters, 2009, 87, 47001.	0.7	4
6819	Nanorod Calculations on Body-Centered Cubic Iron: A Method for Estimation of Size-Dependent Surface Energies of Metal Nanocrystals. Journal of Physical Chemistry C, 2009, 113, 644-649.	1.5	5
6820	Ab-initiostudy of the electronic structure and optical properties of KNO3in the ferroelectric phase. Physica Scripta, 2009, 79, 025601.	1.2	4
6821	First-Principles Analysis of Indirect-to-Direct Band Gap Transition of Ge under Tensile Strain. Japanese Journal of Applied Physics, 2009, 48, 04C125.	0.8	22
6822	Point defects in the NiAl(100) surface. Journal of Physics Condensed Matter, 2009, 21, 134007.	0.7	1
6823	Role of hydrogen adsorption on the carbon terminated Î²-SiC(100)-c(2 Ã— 2) surface structure: a theoretical approach. Journal of Physics Condensed Matter, 2009, 21, 055004.	0.7	2
6824	Vibrational properties of hexagonal Ge₂Sb₂Te₅from first principles. Journal of Physics Condensed Matter, 2009, 21, 245401.	0.7	55
6825	Effect of iron additions on intergranular cohesion in chromium. Journal of Physics Condensed Matter, 2009, 21, 485002.	0.7	12
6826	Ideal strengths, structure transitions, and bonding properties of a ZnO single crystal under tension. Journal of Physics Condensed Matter, 2009, 21, 495402.	0.7	5
6827	Electronâ€“phonon coupling in the surface electronic states on Pd(111). New Journal of Physics, 2009, 11, 103038.	1.2	12
6828	Theoretical calculations of [AlO₄/M⁺]⁰ defects in quartz and crystal-chemical controls on the uptake of Al. Mineralogical Magazine, 2009, 73, 537-550.	0.6	28
6829	Evaluation of Thermal Expansion Coefficients UsingAb-initioMolecular Dynamics with Small Cell Sizes for Materials Design. Japanese Journal of Applied Physics, 2009, 48, 111405.	0.8	3
6830	Characterization of platinum nitride from first-principles calculations. Journal of Physics Condensed Matter, 2009, 21, 485403.	0.7	10
6831	The computational design of junctions by carbon nanotube insertion into a graphene matrix. New Journal of Physics, 2009, 11, 093002.	1.2	24
6832	Scanning Tunneling Microscopy Observation of Sulfur Adsorbates on Au(111) at Liquid Nitrogen Temperature. Japanese Journal of Applied Physics, 2009, 48, 08JB12.	0.8	8

#	Article	IF	Citations
6833	Low-pressure clino- to high-pressure clinoenstatite phase transition: A phonon-related mechanism. American Mineralogist, 2009, 94, 461-466.	0.9	8
6834	New transformation mechanism for a zinc-blende to rocksalt phase transformation in MgS. Journal of Physics Condensed Matter, 2009, 21, 452204.	0.7	8
6835	First-Principles Analysis of the Activity of Transition and Noble Metals in the Direct Utilization of Hydrocarbon Fuels at Solid Oxide Fuel Cell Operating Conditions. Journal of the Electrochemical Society, 2009, 156, B1457.	1.3	43
6836	Review of Stress Effects on Dopant Solubility in Silicon and Silicon-Germanium Layers. Solid State Phenomena, 0, 156-158, 173-180.	0.3	1
6837	Electronic Structure and Electrical Resistivity of Î±-Boron under High Pressure. Journal of the Physical Society of Japan, 2009, 78, 084714.	0.7	24
6838	Methane dissociation and methyl diffusion on PdO{100}. Journal of Chemical Physics, 2009, 130, 014705.	1.2	21
6839	Preserving the half metallicity at the interface of zinc-blende CrSb/Ga0.87In0.13As heterojunction: A density functional theory study. Journal of Applied Physics, 2009, 105, 023701.	1.1	9
6840	Density functional theory, molecular dynamics, and differential scanning calorimetry study of the RbFâ€“CsF phase diagram. Journal of Chemical Physics, 2009, 130, 134716.	1.2	13
6841	Interplay between magnetic, electronic, and vibrational effects in monolayer Mn3O4 grown on Pd(100). Journal of Chemical Physics, 2009, 130, 124707.	1.2	32
6842	Surface structure of strontium titanate. Journal of Applied Physics, 2009, 105, 083526.	1.1	33
6843	Shape prediction of two-dimensional adatom islands on crystal surfaces during homoepitaxial growth. Applied Physics Letters, 2009, 94, 183107.	1.5	13
6844	Reversible atomic modification of nanostructures on surfaces using direction-depended tip-surface interaction with a trimer-apex tip. Applied Physics Letters, 2009, 95, 073105.	1.5	7
6845	Carbonyl mediated attachment to silicon: Acetaldehyde on Si(001). Journal of Chemical Physics, 2009, 131, 104707.	1.2	8
6846	Efficient organometallic spin filter based on Europium-cyclooctatetraene wire. Journal of Chemical Physics, 2009, 131, .	1.2	43
6847	Methane combustion on Pd-based model catalysts: Structure sensitive or insensitive?. Journal of Chemical Physics, 2009, 131, 144704.	1.2	36
6848	Ab initio-derived correlations for defect-dopant interactions in electronic materials. Applied Physics Letters, 2009, 95, 172104.	1.5	0
6849	Interaction potential for indium phosphide: a molecular dynamics and first-principles study of the elastic constants, generalized stacking fault and surface energies. Journal of Physics Condensed Matter, 2009, 21, 095002.	0.7	25
6850	First Principles Calculations of Linear and Second-Order Optical Responses in Rhombohedrally Distorted Perovskite Ternary Halides, CsGeX₃(X = Cl, Br, and I). Japanese Journal of Applied Physics, 2009, 48, 112402.	0.8	72

#	Article	IF	Citations
6851	High pressure investigations on hydrous magnesium silicate-phase A using first principles calculations: H---H repulsion and changes in hydrogen bond geometry with compression. High Pressure Research, 2009, 29, 405-413.	0.4	4
6852	First-Principles Study of NaFeAs, NaCoAs, and NaNiAs. Journal of the Physical Society of Japan, 2009, 78, 124712.	0.7	18
6853	Pressure-induced phase transformation of 4H-SiC: An ab initio constant-pressure study. Europhysics Letters, 2009, 87, 36001.	0.7	11
6854	Oxygen Reduction on Pt(111) Cathode of Fuel Cells. Journal of the Physical Society of Japan, 2009, 78, 114601.	0.7	7
6855	Phase stabilities and mechanical properties of two new carbon crystals. Europhysics Letters, 2009, 87, 56003.	0.7	33
6856	Effect of Substitutional or Chemisorbed Nitrogen on the Diamond (100) Growth Process. Materials Research Society Symposia Proceedings, 2009, 1203, 1.	0.1	0
6857	Halogen-Assisted Copper Atom Abstraction: A Computational Perspective. Japanese Journal of Applied Physics, 2009, 48, 095501.	0.8	2
6858	First-principles Investigation of Edged Ferroelectric PbTiO3 Nanowires and the Role of Axial Strain. Materials Research Society Symposia Proceedings, 2009, 1199, 147.	0.1	0
6859	Energetics and electronic structure of a single copper atomic chain wrapped in a carbon nanotube: a first-principles study. Chinese Physics B, 2009, 18, 5468-5473.	0.7	5
6860	Study of the theoretical tensile strength of Fe by a first-principles computational tensile test. Chinese Physics B, 2009, 18, 1923-1930.	0.7	32
6861	First-Principles Studies on Properties of Boron-Related Impurities in c-BN. Chinese Physics Letters, 2009, 26, 037105.	1.3	1
6862	Ab initiocalculations of the structure and mechanical properties of vanadium oxides. Journal of Physics Condensed Matter, 2009, 21, 145404.	0.7	45
6863	Electronic, thermodynamic and elastic properties of pyrite RuO 2. Chinese Physics B, 2009, 18, 4981-4987.	0.7	4
6864	First-principles investigation of the electronic structure and magnetism of eskolaite. Chinese Physics B, 2009, 18, 2551-2556.	0.7	3
6865	Density functional theory calculations of tetracene on low index surfaces of copper crystal. Chinese Physics B, 2009, 18, 344-348.	0.7	3
6866	Structural Stabilities of Ordered Arrays of Nb 4 Clusters on NaCl(100) Surface. Chinese Physics Letters, 2009, 26, 016802.	1.3	2
6867	Electronic Structure and Magnetic Properties of Ti-doped ZnO. Materials Research Society Symposia Proceedings, 2009, 1183, 75.	0.1	1
6868	Expanded phase of ZrO ₂ : An ab initio constant-pressure study. Europhysics Letters, 2009, 88, 66001.	0.7	7

#	Article	IF	Citations
6869	Could Porosity Induce Gaps in the Vibrational Density of States of Nanoporous Silicon?. Materials Research Society Symposia Proceedings, 2009, 1221, 7111.	0.1	0
6870	Theoretical studies of defect states in GaTe. Journal of Physics Condensed Matter, 2009, 21, 015504.	0.7	14
6871	Effects of O and N impurities on the nanostructural evolution during growth of Cr/Sc multilayers. Journal of Materials Research, 2009, 24, 79-95.	1.2	10
6872	First-Principles Study of Lithium Absorption in Boron- or Silicon-Doped Single-Walled Carbon Nanotubes. Advanced Materials Research, 2009, 79-82, 613-616.	0.3	1
6873	First-Principles Calculations of Elastic and Thermal Properties of Lanthanum Hexaboride. Chinese Physics Letters, 2009, 26, 056201.	1.3	13
6874	Density functional theory study on stacking faults and twinning in Ni nanofilms. Scripta Materialia, 2009, 60, 124-127.	2.6	33
6875	Elastic anisotropy of Ni4Ti3 from first principles. Scripta Materialia, 2009, 60, 207-210.	2.6	61
6876	Ab initio investigation of diamond coatings on steel. Scripta Materialia, 2009, 60, 504-507.	2.6	6
6877	Influence of shear strain on the hydrogen trapped in bcc-Fe: A first-principles-based study. Scripta Materialia, 2009, 60, 555-558.	2.6	43
6878	Stress-induced phase transformation in nanocrystalline UO2. Scripta Materialia, 2009, 60, 878-881.	2.6	23
6879	Role of the alloying element in suppressing the negative effect of O in NiAl: Cr as an example. Scripta Materialia, 2009, 61, 189-192.	2.6	11
6880	Electronic structure and magnetic interactions in Ni-doped Î²-Ga2O3 from first-principles calculations. Scripta Materialia, 2009, 61, 477-480.	2.6	16
6881	Hexagonal Ti2SC with high hardness and brittleness: a first-principles study. Scripta Materialia, 2009, 61, 576-579.	2.6	38
6882	Elastic properties and electronic structures of CdCNi3: A comparative study with MgCNi3. Solid State Sciences, 2009, 11, 251-258.	1.5	36
6883	High-pressure synthesis and characterization of the alkaline earth borate Î²-BaB4O7. Solid State Sciences, 2009, 11, 336-342.	1.5	21
6884	Structural, elastic, electronic and optical properties of the cubic perovskite BiAlO3. Solid State Sciences, 2009, 11, 556-561.	1.5	31
6885	Chemical bonding and MÃ¶ssbauer spectroscopic investigations on ternary polyphosphides AgSbP14, [Ag3Sn]P7 and [Au3Sn]P7. Solid State Sciences, 2009, 11, 519-527.	1.5	14
6886	Investigation of changes in crystal and electronic structures by hydrogen within LaNi5 from first-principles. Solid State Sciences, 2009, 11, 1098-1106.	1.5	17

#	Article	IF	Citations
6887	Electronic structure and chemical bonding properties of UO2F2 from first principles. Solid State Sciences, 2009, 11, 1380-1385.	1.5	5
6888	First-principles investigation of the binary AB2 type Laves phase in Mgâ€“Alâ€“Ca alloy: Electronic structure and elastic properties. Solid State Sciences, 2009, 11, 1400-1407.	1.5	100
6889	Structural and electronic properties of lithium ion battery anode material LiMN (M=Ni, Co, Cu). Solid State Sciences, 2009, 11, 1898-1902.	1.5	3
6890	Structural, electronic and elastic properties of MAX phases M2GaN (M=Ti, V and Cr). Solid State Sciences, 2009, 11, 1875-1881.	1.5	34
6891	Structural and dynamic properties of the polyanionic hydrides SrAlGeH and BaAlGeH. Solid State Sciences, 2009, 11, 1847-1853.	1.5	14
6892	Structural, elastic and electronic properties of Î²â€² phase precipitate in Mgâ€“Gd alloy system investigated via first-principles calculation. Solid State Sciences, 2009, 11, 2156-2161.	1.5	37
6893	Theoretical studies of chemical functionalization of the (8,0) boron nitride nanotube with various metalloporphyrin MP (M = Fe, Co, Ni, Cu, and Zn) complexes. Materials Chemistry and Physics, 2009, 116, 21-27.	2.0	14
6894	Structural and elastic properties of ZrC under high pressure. Materials Chemistry and Physics, 2009, 115, 789-794.	2.0	62
6895	Electronic properties of the PtxMe1â^'x/Pt(111) (Me=Au, Bi, In, Pb, Pd, Sn and Cu) surface alloys: DFT study. Materials Chemistry and Physics, 2009, 116, 94-101.	2.0	34
6896	A density functional study of structural and elastic properties of LaN under high pressure. Materials Chemistry and Physics, 2009, 118, 427-431.	2.0	17
6897	A DFT study on the removal of adsorbed sulfur from a nickel(111) surface: Reducing anode poisoning. Journal of Catalysis, 2009, 263, 380-389.	3.1	41
6898	Influence of step sites in the molecular mechanism of the water gas shift reaction catalyzed by copper. Journal of Catalysis, 2009, 268, 131-141.	3.1	96
6899	The effect of Co-promotion on MoS2 catalysts for hydrodesulfurization of thiophene: A density functional study. Journal of Catalysis, 2009, 268, 201-208.	3.1	136
6900	Electronic Structure of Selfâ€Assembled Monolayers on Au(111) Surfaces: The Impact of Backbone Polarizability. Advanced Functional Materials, 2009, 19, 3766-3775.	7.8	37
6901	Research on Advanced Materials for Liâ€ion Batteries. Advanced Materials, 2009, 21, 4593-4607.	11.1	1,633
6903	Effect of Doped Transition Metal on Reversible Hydrogen Release/Uptake from NaAlH₄. Chemistry - A European Journal, 2009, 15, 1685-1695.	1.7	36
6904	Electronic Structure and Redox Properties of Metal Nitride Endohedral Fullerenes M₃N@C_{2n} (M=Sc, Y, La, and Gd; 2n=80, 84, 88, 92, 96). Chemistry - A European Journal, 2009, 15, 10997-11009.	1.7	84
6905	The Effect of Platinum on Diffusion Kinetics in Î²â€²NiAl: Implications for Thermal Barrier Coating Lifetimes. ChemPhysChem, 2009, 10, 226-235.	1.0	12

#	Article	IF	Citations
6906	Critical Size for O₂ Dissociation by Au Nanoparticles. ChemPhysChem, 2009, 10, 348-351.	1.0	108
6907	A Comparative Study of the Structural, Electronic, and Vibrational Properties of NH₃BH₃ and LiNH₂BH₃: Theory and Experiment. ChemPhysChem, 2009, 10, 1825-1833.	1.0	38
6908	Density Functional Theory Calculations of ⁹⁵Mo NMR Parameters in Solidâ€State Compounds. ChemPhysChem, 2009, 10, 3320-3329.	1.0	21
6909	A New Class of Boron Nanotube. ChemPhysChem, 2009, 10, 3119-3121.	1.0	19
6910	Strain accommodation and interfacial structure of AlN interlayers in GaN. Crystal Research and Technology, 2009, 44, 1170-1180.	0.6	6
6911	Assembly of Novel 2D and 3D Heterometallic Sb^{III}â€“Cu^I Polymers Based on Antimony(III) Thiolates as Metallothiolato Ligands. European Journal of Inorganic Chemistry, 2009, 2009, 752-759.	1.0	3
6912	¹³C shielding tensors of crystalline amino acids and peptides: Theoretical predictions based on periodic structure models. Journal of Computational Chemistry, 2009, 30, 222-235.	1.5	29
6913	A combinatorial study of full Heusler alloys by firstâ€principles computational methods. Journal of Computational Chemistry, 2009, 30, 1290-1299.	1.5	101
6914	Investigations of an Oï£¿H Â· Â· Â· S hydrogen bond via Carâ€Parrinello and path integral molecular dynamics. Journal of Computational Chemistry, 2009, 30, 1241-1250.	1.5	13
6915	Firstâ€principles calculations of the stability and electronic properties of the PbTiO₃ (110) polar surface. Journal of Computational Chemistry, 2009, 30, 1785-1798.	1.5	18
6916	First principles investigation on the ultraâ€incompressible and hard TaN. Journal of Computational Chemistry, 2009, 30, 2358-2363.	1.5	33
6917	Allâ€electron LCAO calculations of the LiF crystal phonon spectrum: Influence of the basis set, the exchangeâ€correlation functional, and the supercell size. Journal of Computational Chemistry, 2009, 30, 2645-2655.	1.5	23
6918	Firstâ€principles calculations on the energetics, electronic structures and magnetism of SrFeO₂. Journal of Computational Chemistry, 2009, 30, 2684-2693.	1.5	5
6919	Selective oxidation of styrene on an oxygenâ€adsorbed Cu(111): A comparison with Au(111). Journal of Computational Chemistry, 2010, 31, 1618-1624.	1.5	5
6920	How Much Water Does Calcined Gypsum Contain?. Angewandte Chemie - International Edition, 2009, 48, 3520-3524.	7.2	50
6921	Structureâ€sensitivity of CH₃ dissociation on Ni(100)from firstâ€principles calculations. Asia-Pacific Journal of Chemical Engineering, 2009, 4, 511-517.	0.8	3
6922	First principles calculations on the influence of water-filled cavities on the electronic structure of Prussian Blue. Journal of Molecular Modeling, 2009, 15, 567-572.	0.8	18
6923	Hydrogen evolution and oxidationâ€”a prototype for an electrocatalytic reaction. Journal of Solid State Electrochemistry, 2009, 13, 1101-1109.	1.2	25

#	Article	IF	Citations
6924	Structural stability and magnetic properties of Co-doped or adsorbed polar-ZnO surface. Physics Letters, Section A: General, Atomic and Solid State Physics, 2009, 373, 391-395.	0.9	12
6925	First-principles study of structural, elastic, electronic, and thermal properties of SrTiO3 perovskite cubic. Physics Letters, Section A: General, Atomic and Solid State Physics, 2009, 373, 879-884.	0.9	35
6926	Structural and elastic properties under pressure effect of the cubic antiperovskite compounds ANCa3 (A=P, As, Sb, and Bi). Physics Letters, Section A: General, Atomic and Solid State Physics, 2009, 373, 1777-1781.	0.9	31
6927	First principles study of structural, electronic and vibrational properties of heavily boron-doped diamond. Physics Letters, Section A: General, Atomic and Solid State Physics, 2009, 373, 2494-2500.	0.9	31
6928	Density functional theory description of the mechanism of ferromagnetism in nitrogen-doped SnO2. Physics Letters, Section A: General, Atomic and Solid State Physics, 2009, 374, 319-322.	0.9	36
6929	Relativistic effects on the structural and transport properties of IIIâ€“V compounds: A first-principles study. Superlattices and Microstructures, 2009, 45, 80-90.	1.4	48
6930	Ab initio investigation of the CdTe (001) surface. Superlattices and Microstructures, 2009, 46, 733-744.	1.4	7
6931	First principle study of structural, phase stabilization and oxygen-ion diffusion properties of Î²-La2â^'xLxMo2O9 (L=Gd, Sm, Nd and Bi) and Î²-La2Mo2â^'yMyO9 (M=Cr, W). Solid State Ionics, 2009, 180, 946-951.	1.3	12
6932	Reactions of vinyl groups on a model chromia surface: Vinyl chloride on stoichiometric Î±-Cr2O3. Surface Science, 2009, 603, 265-272.	0.8	3
6933	Relating the coverage dependence of oxygen adsorption on Au and Pt fcc(111) surfaces through adsorbate-induced surface electronic structure effects. Surface Science, 2009, 603, 794-801.	0.8	97
6934	Surface atomic distribution and water adsorption on Ptâ€“Co alloys. Surface Science, 2009, 603, 912-920.	0.8	20
6935	SiO adsorption on a p(2Ã—2) reconstructed Si(100) surface. Surface Science, 2009, 603, 901-906.	0.8	4
6936	First-principles studies of the oxygen adsorption on unreconstructed and reconstructed Ni(110) surfaces. Surface Science, 2009, 603, 1002-1009.	0.8	12
6937	STM study of Si(113) 3Ã—2-Ga surface. Surface Science, 2009, 603, 1197-1202.	0.8	4
6938	First principles investigation on the stabilization mechanisms of the polar copper terminated Cu2O(111) surface. Surface Science, 2009, 603, 2087-2095.	0.8	49
6939	Effect of hydrogenation on the electronic structure of the P/Si(0 0 1)-(1 Ã— 2) surface. Surface Science, 2009, 603, 2271-2275.	0.8	1
6940	Stabilization of the (110) tetragonal zirconia surface by hydroxyl chemical transformation. Surface Science, 2009, 603, 2526-2531.	0.8	21
6941	Adsorption of methanol and methoxy on NiAl(110) and Ni3Al(111): A DFT study. Surface Science, 2009, 603, 2378-2386.	0.8	17

#	Article	IF	Citations
6942	Density functional study of the adsorption of aspirin on the hydroxylated (001) -quartz surface. Surface Science, 2009, 603, 2502-2506.	0.8	29
6943	CO2 dissociation on Ni(211). Surface Science, 2009, 603, 2991-2998.	0.8	47
6944	Adsorption and decomposition of NO on O-covered planar and faceted Ir(2 1 0). Surface Science, 2009, 603, 3136-3144.	0.8	20
6945	Adsorption of pairs of NOx molecules on single-walled carbon nanotubes and formation of NO+NO3 from NO2. Surface Science, 2009, 603, 3234-3238.	0.8	70
6946	DFT study on H2O activation by stepped and planar Rh surfaces. Surface Science, 2009, 603, 3275-3281.	0.8	31
6947	Adsorption of NO and NO2 on the ZnO() surface: A DFT study. Surface Science, 2009, 603, 3389-3399.	0.8	49
6948	First-principles study of ternary bcc alloys using special quasi-random structures. Acta Materialia, 2009, 57, 4716-4726.	3.8	66
6949	Ruthenium adsorption and diffusion on the GaN(0001) surface. Applied Surface Science, 2009, 255, 3837-3842.	3.1	11
6950	Theoretical characterization of carrier compensation in P-doped diamond. Applied Surface Science, 2009, 255, 3994-4000.	3.1	4
6951	Density functional theory study of hydrogenation mechanism in Fe-doped Mg(0001) surface. Applied Surface Science, 2009, 255, 6338-6344.	3.1	17
6952	Structural, electronic properties and stability of the (1Ã—1) PbTiO3 (111) polar surfaces by first-principles calculations. Applied Surface Science, 2009, 255, 8145-8152.	3.1	20
6953	Magnesium adsorption and incorporation in InN (0001) and surfaces: A first-principles study. Applied Surface Science, 2009, 255, 8475-8482.	3.1	3
6954	Mixing and magnetic properties of surface alloys: The role of the substrate. Applied Surface Science, 2009, 256, 449-454.	3.1	2
6955	Zinc incorporation into hydroxylapatite. Biomaterials, 2009, 30, 2864-2872.	5.7	215
6956	First principles studies of SnTiO3 perovskite as potential environmentally benign ferroelectric material. Chemical Physics, 2009, 355, 43-49.	0.9	74
6957	Surface structure for Au on (001) SrTiO3. Chemical Physics, 2009, 360, 79-84.	0.9	4
6958	Gas sensing properties of platinum derivatives of single-walled carbon nanotubes: A DFT analysis. Journal of Molecular Graphics and Modelling, 2009, 28, 62-69.	1.3	93
6959	An object Kinetic Monte Carlo Simulation of the dynamics of helium and point defects in tungsten. Journal of Nuclear Materials, 2009, 385, 223-227.	1.3	157

#	Article	IF	Citations
6960	Point defect properties in hcp and bcc Zr with trace solute Nb revealed by ab initio calculations. Journal of Nuclear Materials, 2009, 393, 197-202.	1.3	25
6961	Implementing first principles calculations of defect migration in a fuel performance code for UN simulations. Journal of Nuclear Materials, 2009, 393, 292-299.	1.3	25
6962	Effect of excess hydrogen on the electronic properties of passivated diamond. Journal of Physics and Chemistry of Solids, 2009, 70, 307-311.	1.9	3
6963	Solvothermal synthesis of MnF2 nanocrystals and the first-principle study of its electronic structure. Journal of Physics and Chemistry of Solids, 2009, 70, 609-615.	1.9	16
6964	Suppression of Jahnâ€“Teller distortion by chromium and magnesium doping in spinel LiMn2O4: A first-principles study using GGA and GGA+U. Journal of Physics and Chemistry of Solids, 2009, 70, 1200-1206.	1.9	35
6965	Vibrational properties of the gallium monohydrides SrGaGeH, BaGaSiH, BaGaGeH, and BaGaSnH. Journal of Solid State Chemistry, 2009, 182, 2068-2073.	1.4	14
6966	Density functional study on electronic and optical properties of C (or N)-doped cubic cerium dioxide. Journal of Solid State Chemistry, 2009, 182, 3207-3210.	1.4	6
6967	Electronic structure and photoluminescence properties of Eu2+-activated Ca2BN2F. Journal of Solid State Chemistry, 2009, 182, 3299-3304.	1.4	8
6968	Theoretical study of the phonon properties of SrS. Materials Science and Engineering B: Solid-State Materials for Advanced Technology, 2009, 162, 116-119.	1.7	21
6969	First principles study of point defects in titanium oxycarbide. Materials Science and Engineering B: Solid-State Materials for Advanced Technology, 2009, 165, 194-197.	1.7	18
6970	First-principles study of helium effect in a ferromagnetic iron grain boundary: Energetics, site preference and segregation. Nuclear Instruments & Methods in Physics Research B, 2009, 267, 3200-3203.	0.6	28
6971	A web-deployed interface for performing ab initio molecular dynamics, optimization, and electronic structure in Fireball. Computer Physics Communications, 2009, 180, 418-426.	3.0	3
6972	PHON: A program to calculate phonons using the small displacement method. Computer Physics Communications, 2009, 180, 2622-2633.	3.0	664
6973	<mml:math xmlns:mml="http://www.w3.org/1998/Math/MathML" altimg="si24.gif" display="inline" overflow="scroll"><mml:mrow><mml:msub><mml:mrow><mml:mtext>CdXO</mml:mtext></mml:mrow><mml:mrow><mml:mn>3</mml:mn> (X = C, Si, Ge, Sn, Pb) electronic band structures. Chemical Physics Letters, 2009, 480, 273-277.	2.2	22
6974	Electrical conductivity of a boron plasma through the OCP crystallization. High Energy Density Physics, 2009, 5, 31-34.	0.4	0
6975	Pt effects in Î³-Ni(Al)/Î±-Al2O3 adhesion. Journal of Materials Science, 2009, 44, 1734-1740.	1.7	23
6976	The energetics of helium and hydrogen atoms in Î²-SiC: an abÂinitio approach. Journal of Materials Science, 2009, 44, 1828-1833.	1.7	18
6977	Effect of dopants on alumina grain boundary sliding: implications for creep inhibition. Journal of Materials Science, 2009, 44, 1741-1749.	1.7	12

#	Article	IF	Citations
6978	Ab initio study of antiferroelectric PbZrO3 (001) surfaces. Journal of Materials Science, 2009, 44, 5249-5255.	1.7	19
6979	Charge compensation in an irradiation-induced phase of Î´-Sc4Zr3O12. Journal of Materials Science, 2009, 44, 4754-4757.	1.7	9
6980	Density Functional Study of the Effects of Strains on the Adsorption of Methoxide and its Decomposed Intermediates on Cu(100) Surface. Catalysis Letters, 2009, 127, 113-118.	1.4	11
6981	Potassium Promotion of Cobalt Spinel Catalyst for N2O Decompositionâ€"Accounted by Work Function Measurements and DFT Modelling. Catalysis Letters, 2009, 127, 126-131.	1.4	83
6982	Adsorption of Formic Acid and its Decomposed Intermediates on (100) Surfaces of Pt and Pd: A Density Functional Study. Catalysis Letters, 2009, 128, 221-226.	1.4	29
6983	Steam Reforming of Formaldehyde on Cu(100) Surface: A Density Functional Study. Catalysis Letters, 2009, 129, 444-448.	1.4	27
6984	Mars-van Krevelen-like Mechanism of CO Hydrogenation on an Iron Carbide Surface. Catalysis Letters, 2009, 133, 257-261.	1.4	116
6985	Electronic structure of Î³ -Li3N. Russian Physics Journal, 2009, 52, 978-983.	0.2	3
6986	An investigation into adsorption of simple organic and inorganic molecules on a silica gel surface. Russian Physics Journal, 2009, 52, 1164-1169.	0.2	9
6987	Bond covalency and electronic structure of CaB2O4(III) crystal. Structural Chemistry, 2009, 20, 221-226.	1.0	5
6988	Role of sublattices in the formation of the chemical bond in ion-covalent crystals. Journal of Structural Chemistry, 2009, 50, 1177-1180.	0.3	11
6989	3d Transition metal decorated B-C-N composite nanostructures for efficient hydrogen storage: A first-principles study. Bulletin of Materials Science, 2009, 32, 353-360.	0.8	3
6990	Structural stability and magnetism of metastable Ni-Pt intermetallic compounds studied by ab initio calculation. Science in China Series D: Earth Sciences, 2009, 52, 2681-2687.	0.9	7
6991	First-principles study on the electronic structure and optical properties of CrSi2. Science in China Series G: Physics, Mechanics and Astronomy, 2009, 52, 46-51.	0.2	10
6992	First-principle study on the electronic structure of stressed CrSi2. Science in China Series G: Physics, Mechanics and Astronomy, 2009, 52, 76-81.	0.2	4
6993	First-principles calculations on the electronic structure and optical properties of BaSi2. Science in China Series G: Physics, Mechanics and Astronomy, 2009, 52, 580-586.	0.2	8
6994	Electronic structure, chemical bond and thermal stability of hydrogen absorber Li2MgN2H2. Science Bulletin, 2009, 54, 497-503.	4.3	2
6995	Chemically decorated boron-nitride nanoribbons. Frontiers of Physics in China, 2009, 4, 367-372.	1.0	59

#	Article	IF	Citations
6996	A first-principles study on the electronic structure of one-dimensional [TM(Bz)]âˆž polymer (TM= Y, Zr,) Tj ETQq0 0 0 rgBT /Overlock 10 T	1.0	3
6997	Electronic structure of SiC (310) twin boundary doped with B, N, Al and Ti. Journal Wuhan University of Technology, Materials Science Edition, 2009, 24, 599-602.	0.4	0
6998	First-Principles Calculation of Phase Stability and Cohesive Properties of Ni-Sn Intermetallics. Metallurgical and Materials Transactions A: Physical Metallurgy and Materials Science, 2009, 40, 4-23.	1.1	41
6999	Structural, Elastic, and Electronic Properties of Al-Cu Intermetallics from First-Principles Calculations. Journal of Electronic Materials, 2009, 38, 356-364.	1.0	88
7000	Thermodynamic Assessment of the Au-Co-Sn Ternary System. Journal of Electronic Materials, 2009, 38, 2158-2169.	1.0	17
7001	Thermodynamic Assessment of the Cu-B System Supported by Key Experiment and First-Principles Calculations. Journal of Phase Equilibria and Diffusion, 2009, 30, 480-486.	0.5	7
7002	Magnetism in carbon nanoscrolls: Quasi-half-metals and half-metals in pristine hydrocarbons. Nano Research, 2009, 2, 844-850.	5.8	11
7003	Predictions on atomic structures of Ti1âˆ’xMoxC using combined approach of first-principles calculation and the cluster expansion method. Metals and Materials International, 2009, 15, 797-801.	1.8	5
7004	Investigation of indium diffusion in strained silicon by ab initio calculation. International Journal of Precision Engineering and Manufacturing, 2009, 10, 99-102.	1.1	0
7005	Interaction of biomolecular systems with titanium-based materials: computational investigations. Theoretical Chemistry Accounts, 2009, 123, 299-309.	0.5	13
7006	Uniform linear chains of group 11 atoms: do they have a bias towards a Peierls distortion?. Theoretical Chemistry Accounts, 2009, 123, 85-92.	0.5	3
7007	Influence of the exchangeâ€“correlation potential on the description of the molecular mechanism of oxygen dissociation by Au nanoparticles. Theoretical Chemistry Accounts, 2009, 123, 119-126.	0.5	47
7008	Structural and electronic structure differences due to the Oâ€“HÂ·Â·Â·O and Oâ€“HÂ·Â·Â·S bond formation in selected benzamide derivatives: a first-principles molecular dynamics study. Theoretical Chemistry Accounts, 2009, 124, 319-330.	0.5	15
7009	Calculated structural, electronic and elastic properties of M2GeC (M=Ti, V, Cr, Zr, Nb, Mo, Hf, Ta and) Tj ETQq1 1 0.784314 rgBT /Overlo	1.1	66
7010	Ab initio calculations on the O2 3âˆ’-Y3+ center in CaF2 and SrF2: its electronic structure and hyperfine constants. Physics and Chemistry of Minerals, 2009, 36, 1-7.	0.3	9
7011	Experimental and theoretical study of the structural environment of magnesium in minerals and silicate glasses using X-ray absorption near-edge structure. Physics and Chemistry of Minerals, 2009, 36, 241-257.	0.3	81
7012	Highâ€pressure Phase Transition and Properties of Cu₃N: An Experimental and Theoretical StudyÂ. Zeitschrift Fur Anorganische Und Allgemeine Chemie, 2009, 635, 1959-1968.	0.6	20
7013	Structure and stability of the crystal Fe2C and low index surfaces. Journal of Fuel Chemistry and Technology, 2009, 37, 104-108.	0.9	20

#	Article	IF	Citations
7014	Structures and energetics of H2O adsorption on the Fe3O4 (111) surface. Journal of Fuel Chemistry and Technology, 2009, 37, 506-512.	0.9	19
7015	Firstâ€principles study of the structural and electronic properties of the Î± modification of zinc diphosphide. Physica Status Solidi (B): Basic Research, 2009, 246, 77-81.	0.7	6
7016	Firstâ€principles study on the boron antimony compound. Physica Status Solidi (B): Basic Research, 2009, 246, 119-123.	0.7	23
7017	Electron momentum density in zinc oxide. Physica Status Solidi (B): Basic Research, 2009, 246, 124-128.	0.7	4
7018	Simulation of electronic density of states and optical properties of PbB₄O₇ by firstâ€principles DFT method. Physica Status Solidi (B): Basic Research, 2009, 246, 437-443.	0.7	27
7019	Elasticity, electronic structure, and dielectric property of cubic SrHfO₃ from firstâ€principles. Physica Status Solidi (B): Basic Research, 2009, 246, 135-139.	0.7	27
7020	Oxygen vacancy configuration of Î´â€Bi₂O₃: an ab initio study. Physica Status Solidi (B): Basic Research, 2009, 246, 97-101.	0.7	19
7021	Lattice dynamics of chalcopyrite semiconductors LiAlTe₂, LiGaTe₂ and LiInTe₂. Physica Status Solidi (B): Basic Research, 2009, 246, 364-371.	0.7	46
7022	Phase transition and elasticity of CdO under pressure. Physica Status Solidi (B): Basic Research, 2009, 246, 71-76.	0.7	35
7023	Vacancies in magnesium silicide â€“ stoichiometric vacancies preferred?. Physica Status Solidi (B): Basic Research, 2009, 246, 1587-1589.	0.7	11
7024	Adsorption and dissociation of water on the (0001) surface of double hexagonal close packed americium. Physica Status Solidi (B): Basic Research, 2009, 246, 1225-1237.	0.7	1
7025	Group II element nitrides M₃N₂ under pressure: a comparative density functional study. Physica Status Solidi (B): Basic Research, 2009, 246, 1604-1613.	0.7	25
7026	Firstâ€principles study of NaCdF₃. Physica Status Solidi (B): Basic Research, 2009, 246, 1334-1339.	0.7	5
7027	Firstâ€principles calculations on elasticity and the thermodynamic properties of TaC under pressure. Physica Status Solidi (B): Basic Research, 2009, 246, 1590-1596.	0.7	28
7028	Electronic structure and magnetic properties of Cuâ€doped SnO₂ from firstâ€principles study. Physica Status Solidi (B): Basic Research, 2009, 246, 1652-1655.	0.7	14
7029	Lattice dynamics and thermal properties of SrHfO₃ by firstâ€principles calculations. Physica Status Solidi (B): Basic Research, 2009, 246, 1628-1633.	0.7	11
7030	Electron momentum distribution in SnS. Physica Status Solidi (B): Basic Research, 2009, 246, 2263-2269.	0.7	8
7031	Abâ€initio theory of semiconductor band structures: New developments and progress. Physica Status Solidi (B): Basic Research, 2009, 246, 1877-1892.	0.7	120

#	Article	IF	Citations
7032	Clustering of functional molecules on a singleâ€walled carbonâ€nanotube surface and its effect on hydrogen storage. Physica Status Solidi (B): Basic Research, 2009, 246, 2248-2256.	0.7	6
7033	Pt adsorption on the PbTiO₃(110) polar surface: a density functional theory study. Surface and Interface Analysis, 2009, 41, 785-793.	0.8	0
7034	Ab initio study of ATiO₃ (001) surfaces. Surface and Interface Analysis, 2009, 41, 918-923.	0.8	12
7035	Convergence of the binding energy of oxygen on Cu(100): A cautionary tale for computational chemists using periodic bound conditions. International Journal of Quantum Chemistry, 2009, 109, 357-361.	1.0	0
7036	1D lead iodide crystals encapsulated within single walled carbon nanotubes. International Journal of Quantum Chemistry, 2009, 109, 171-175.	1.0	4
7037	First principles study on the structure and electronic properties of 2â€nitriminoâ€1â€nitroimidazolidine. International Journal of Quantum Chemistry, 2009, 109, 720-725.	1.0	6
7038	Periodic DFT investigation on the structure and properties of TNAD crystal. International Journal of Quantum Chemistry, 2009, 109, 1598-1608.	1.0	1
7039	Band gaps and the possible effect on impact sensitivity for some nitro aromatic explosive materials. International Journal of Quantum Chemistry, 2009, 109, 1547-1552.	1.0	57
7040	Theoretical study of twoâ€dimensionally fused zinc porphyrins: DFT calculations. International Journal of Quantum Chemistry, 2009, 109, 1584-1597.	1.0	13
7041	The role of gold adatoms in selfâ€assembled monolayers of thiol on Au(111). International Journal of Quantum Chemistry, 2009, 109, 3466-3472.	1.0	16
7042	My association with Frank Harris: An arc of fortyâ€four years. International Journal of Quantum Chemistry, 2009, 109, 2821-2825.	1.0	0
7043	On the Brillouinâ€zone integrations in secondâ€order manyâ€body perturbation calculations for extended systems of oneâ€dimensional periodicity. International Journal of Quantum Chemistry, 2009, 109, 2953-2959.	1.0	24
7044	Estimation of effective exchange integral value of polyradical systems based on the band calculation. International Journal of Quantum Chemistry, 2009, 109, 3632-3640.	1.0	5
7045	Temperature-dependent Debyeâ€“Waller factors for semiconductors with the wurtzite-type structure. Acta Crystallographica Section A: Foundations and Advances, 2009, 65, 227-231.	0.3	40
7046	Large, larger, largest â€“ a family of cluster-based tantalum copper aluminides with giant unit cells. II. The cluster structure. Acta Crystallographica Section B: Structural Science, 2009, 65, 318-325.	1.8	55
7047	Structure and conformational analysis of a bidentate pro-ligand, C₂₁H₃₄N₂S₂, from powder synchrotron diffraction data and solid-state DFTB calculations. Acta Crystallographica Section B: Structural Science, 2009, 65, 639-646.	1.8	8
7048	Molecular and crystalline structures of three (S)-4-alkoxycarbonyl-2-azetidinones containing long alkyl side chains from synchrotron X-ray powder diffraction data. Acta Crystallographica Section B: Structural Science, 2009, 65, 724-730.	1.8	5
7049	Shear-induced anisotropic plastic flow from body-centred-cubic tantalum before melting. Nature Materials, 2009, 8, 223-228.	13.3	70

#	Article	IF	Citations
7050	An electric current spike linked to nanoscale plasticity. Nature Nanotechnology, 2009, 4, 287-291.	15.6	66
7051	Electric displacement as the fundamental variable in electronic-structure calculations. Nature Physics, 2009, 5, 304-308.	6.5	143
7052	Diamond-like C2H nanolayer, diamane: Simulation of the structure and properties. JETP Letters, 2009, 90, 134-138.	0.4	169
7053	Firstâ€Principles Study of Elastic Constants and Interlayer Interactions of Complex Hydrated Oxides: Case Study of Tobermorite and Jennite. Journal of the American Ceramic Society, 2009, 92, 2323-2330.	1.9	190
7054	Vacancies and E-centers in silicon as multi-symmetry defects. Materials Science and Engineering B: Solid-State Materials for Advanced Technology, 2009, 159-160, 107-111.	1.7	14
7055	Ab initio study of the fundamental properties of novel IIIâ€“V nitride alloys Ga1â^'xTlxN. Materials Science and Engineering B: Solid-State Materials for Advanced Technology, 2009, 162, 26-31.	1.7	27
7056	Pressure effects on the electronic and magnetic properties of GaxV1â^'xN compounds: Ab-initio study. Materials Science and Engineering B: Solid-State Materials for Advanced Technology, 2009, 163, 190-193.	1.7	7
7057	Ab initio study of Kr in hcp Ti: Diffusion, formation and stability of small Krâ€“vacancy clusters. Nuclear Instruments & Methods in Physics Research B, 2009, 267, 2991-2994.	0.6	6
7058	First-principles approach to the properties of point defects and small helium-vacancy clusters in palladium. Nuclear Instruments & Methods in Physics Research B, 2009, 267, 3037-3040.	0.6	12
7059	Effect of He on the structure and bonding properties of W: A first-principles computational tensile test. Nuclear Instruments & Methods in Physics Research B, 2009, 267, 3193-3196.	0.6	26
7060	First-principles investigation of energetics and site preference of He in a W grain boundary. Nuclear Instruments & Methods in Physics Research B, 2009, 267, 3189-3192.	0.6	52
7061	The ideal tensile strength and deformation behavior of a tungsten single crystal. Nuclear Instruments & Methods in Physics Research B, 2009, 267, 3282-3285.	0.6	38
7062	Vibrational contributions to the stability of point defects in bcc iron: A first-principles study. Nuclear Instruments & Methods in Physics Research B, 2009, 267, 3009-3012.	0.6	50
7063	Studies of the electronic and optical properties of BaMxO1â^'x (M=S, Se, Te) using first-principle calculations. Optics Communications, 2009, 282, 48-52.	1.0	3
7064	Electronic structure of the pentaceneâ€“gold interface: A density-functional theory study. Organic Electronics, 2009, 10, 1571-1578.	1.4	25
7065	Atomic structure, electronic and optical properties of Si nanocrystals embedded in <mml:math altimg="si1.gif" display="inline" overflow="scroll" xmlns:xocs="http://www.elsevier.com/xml/xocs/dtd" xmlns:xs="http://www.w3.org/2001/XMLSchema" xmlns:xsi="http://www.w3.org/2001/XMLSchema-instance" xmlns="http://www.elsevier.com/xml/ja/dtd" xmlns:ja="http://www.elsevier.com/xml/ja/dtd" xmlns:mml="http://www.w3.org/1998/Math/MathML" xmlns:tb="http://www.elsevier.com/xml/common/table/dtd" xmlns:sb="http://www.elsevier.com/xml/common/struct-bib/dtd" xmlns:ce="http://www.elsevier.com/xml/common/dtd" xmlns:xlink="http://www.w3.org/1999/xlink" xmlns:cals="http://www.elsevier.com/xml/common/cals/dtd" xmlns:dc="http://purl.org/dc/elements/1.1/" xmlns:dcterms="http://purl.org/dc/terms/" xmlns:xsd="http://www.w3.org/2001/XMLSchema" xmlns:prism="http://prismstandard.org/namespaces/basic/2.0/" xmlns:ce="http://www.elsevier.com/xml/common/dtd" xmlns:xlink="http://www.w3.org/1999/xlink" xmlns:cals="http://www.elsevier.com/xml/common/cals/dtd" xmlns:dc="http://purl.org/dc/elements/1.1/" xmlns:dcterms="http://purl.org/dc/terms/" xmlns:xsd="http://www.w3.org/2001/XMLSchema" xmlns:prism="http://prismstandard.org/namespaces/basic/2.0/"	1.2	0
7066	Theoretical investigations of structural, elastic and thermodynamic properties for PtN2 under high pressure. Physica B: Condensed Matter, 2009, 404, 41-46.	1.3	18
7067	Structure of Geâ€“O complexes in Czochralski silicon. Physica B: Condensed Matter, 2009, 404, 58-60.	1.3	10

#	Article	IF	Citations
7068	Atomic and electronic structure of hydrogen-related centers in hydrogen storage materials. Physica B: Condensed Matter, 2009, 404, 793-797.	1.3	4
7069	The elastic properties of hexagonal osmium under pressure: The first-principles investigations. Physica B: Condensed Matter, 2009, 404, 1218-1221.	1.3	22
7070	First-principles study of structural, electronic and elastic properties of diboride of vanadium. Physica B: Condensed Matter, 2009, 404, 1527-1531.	1.3	22
7071	Phase transition and elastic properties of BeO under pressure from first-principles calculations. Physica B: Condensed Matter, 2009, 404, 1940-1946.	1.3	27
7072	Structural, elastic, and electronic properties of cubic perovskite obtained from first principles. Physica B: Condensed Matter, 2009, 404, 2192-2196.	1.3	38
7073	Energetics and electronic properties of Mg7TMH16 (TM=Sc, Ti, V, Y, Zr, Nb): An ab initio study. Physica B: Condensed Matter, 2009, 404, 2234-2240.	1.3	42
7074	Elasticity and thermodynamic properties of RuB2 under pressure. Physica B: Condensed Matter, 2009, 404, 3363-3367.	1.3	25
7075	The adsorption of In on the surface of (001) CdTe. Physica B: Condensed Matter, 2009, 404, 3530-3533.	1.3	2
7076	First principles calculations of structural phase transformation in CaTe at high pressure. Physica B: Condensed Matter, 2009, 404, 3671-3673.	1.3	5
7077	Phase transition, elastic, thermodynamic properties of zinc-blend BeSe from first-principles. Physica B: Condensed Matter, 2009, 404, 3935-3940.	1.3	25
7078	First-principles study of palladium atom adsorption on the boron- or nitrogen-doped carbon nanotubes. Physica B: Condensed Matter, 2009, 404, 4173-4177.	1.3	20
7079	Structural, elastic and thermal properties of the compound LaNi4.5Sn0.5. Physica B: Condensed Matter, 2009, 404, 4162-4167.	1.3	0
7080	Boronâ€“hydrogen complexes in diamond: Energy levels and metastable states. Physica B: Condensed Matter, 2009, 404, 4525-4528.	1.3	1
7081	Ab initio study of the magnetic interaction of Co and Ni doped ZnO with intrinsic vacancies. Physica B: Condensed Matter, 2009, 404, 4791-4793.	1.3	6
7082	The electronic properties of the interface structure between ZnO and amorphous HfO2. Physica B: Condensed Matter, 2009, 404, 4823-4826.	1.3	7
7083	Structural and electronic properties of carbon-doped c-BN(110) surface. Physica B: Condensed Matter, 2009, 404, 4937-4938.	1.3	1
7084	Study of O2 and OH adsorption energies on Pdâ€“Cu alloys surface with a quantum chemistry approach. Electrochimica Acta, 2009, 54, 1769-1776.	2.6	57
7085	Finite-temperature exchange-correlation functional in an ab initio molecular dynamics code. High Energy Density Physics, 2009, 5, 74-79.	0.4	11

#	Article	IF	Citations
7086	Freeâ€“free opacity in warm dense aluminum. High Energy Density Physics, 2009, 5, 124-131.	0.4	32
7087	Aluminum hydride coated single-walled carbon nanotube as a hydrogen storage medium. International Journal of Hydrogen Energy, 2009, 34, 370-375.	3.8	64
7088	Hydrogen solid storage: First-principles study of ZrNiH3. International Journal of Hydrogen Energy, 2009, 34, 4997-5002.	3.8	30
7089	First-principles study of hydrogen diffusion in alpha Ti. International Journal of Hydrogen Energy, 2009, 34, 3983-3987.	3.8	48
7090	Bulk and surface properties of Cu2O: A first-principles investigation. Computational and Theoretical Chemistry, 2009, 903, 41-48.	1.5	67
7091	Molecular DFT structure and packing effect of thiodipropionic and dithiodiglycolic acids and salts. Computational and Theoretical Chemistry, 2009, 911, 52-57.	1.5	0
7092	First-principles study of a new type nanojunction: Finite length carbon chain inserted into half of a carbon nanotube. Computational and Theoretical Chemistry, 2009, 915, 63-68.	1.5	3
7093	Structures and electronic properties of thin-films of polycyclic aromatic hydrocarbons. Thin Solid Films, 2009, 517, 3005-3010.	0.8	6
7094	Structural and electronic properties of Pt monolayer adsorption on PbTiO3(100) surface. Thin Solid Films, 2009, 517, 6817-6823.	0.8	1
7095	Theoretical and spectroscopic investigations on the structure and bonding in Bâ€“Câ€“N thin films. Thin Solid Films, 2009, 518, 1459-1464.	0.8	18
7096	First-principles study of O2 adsorption on the LaFeO3 (0 1 0) surface. Sensors and Actuators B: Chemical, 2009, 139, 520-526.	4.0	83
7097	Electronic structure of new RENiAsO (RE = Rare Earth Elements) compounds: Ab initio spin-density functional theory. Superlattices and Microstructures, 2009, 46, 533-540.	1.4	1
7098	Electronic and thermodynamic properties of under high pressure and temperature. Solid State Communications, 2009, 149, 56-59.	0.9	26
7099	Electronic transport properties of pheny1 based molecular devices. Solid State Communications, 2009, 149, 60-63.	0.9	11
7100	Multiferroic properties of nanocrystalline BaTiO3. Solid State Communications, 2009, 149, 1-5.	0.9	160
7101	Magnetism and vibrations in the phase of oxygen. Solid State Communications, 2009, 149, 160-162.	0.9	4
7102	Unifying description of the optical properties of InN from first principles. Solid State Communications, 2009, 149, 329-333.	0.9	6
7103	Ab initio studies on the structural and magnetic properties of RhH. Solid State Communications, 2009, 149, 322-324.	0.9	10

#	Article	IF	Citations
7104	Synthesis, crystal and electronic structures of La3Cr2N6. Solid State Communications, 2009, 149, 273-276.	0.9	8
7105	Monovacancy and substitutional defects in hexagonal silicon nanotubes. Solid State Communications, 2009, 149, 408-411.	0.9	4
7106	Pressure-induced phase transition of BeO. Solid State Communications, 2009, 149, 345-348.	0.9	17
7107	Tuning the magnetic and transport properties of boron-nitride nanotubes via oxygen-doping. Solid State Communications, 2009, 149, 486-490.	0.9	40
7108	First-principles investigations on elastic properties of - and - Ta4AlC3. Solid State Communications, 2009, 149, 441-444.	0.9	23
7109	Electronic structure of LiGaS2. Solid State Communications, 2009, 149, 572-575.	0.9	28
7110	Ab initio study of the electronic and atomic structure of the wolframite-type ZnWO4. Solid State Communications, 2009, 149, 425-428.	0.9	54
7111	First principle study on the electronic structure of fluorine-doped SnO2. Solid State Communications, 2009, 149, 527-531.	0.9	62
7112	Structural transition of Li3N under high pressure: A first-principles study. Solid State Communications, 2009, 149, 612-615.	0.9	14
7113	Structural, elastic and electronic properties of XNCa3 (X = Ge, Sn and Pb) compounds. Solid State Communications, 2009, 149, 619-624.	0.9	28
7114	First-principles study of magnetism driven by intrinsic defects in MgO. Solid State Communications, 2009, 149, 855-858.	0.9	80
7115	High-density strontium hydride: An experimental and theoretical study. Solid State Communications, 2009, 149, 830-834.	0.9	31
7116	Structural, elastic and electronic properties of ACTi3 (A=Al, In and Tl) antiperovskite. Solid State Communications, 2009, 149, 919-922.	0.9	9
7117	Theoretical study of the properties of with pyrite and marcasite structures. Solid State Communications, 2009, 149, 1021-1024.	0.9	6
7118	Structural and electronic properties of Zn on a CdTe(001) surface. Solid State Communications, 2009, 149, 982-985.	0.9	9
7119	Electronic and optical properties of doped crystals: First-principles calculations. Solid State Communications, 2009, 149, 1188-1192.	0.9	8
7120	Electronic, optical and bonding properties of CaCO3 calcite. Solid State Communications, 2009, 149, 1201-1203.	0.9	58
7121	A comparative ab initio study of bulk and surface oxygen vacancies in PbTiO3, PbZrO3 and SrTiO3 perovskites. Solid State Communications, 2009, 149, 1359-1362.	0.9	55

#	Article	IF	Citations
7122	First-principles study of crystal structures of under pressure. Solid State Communications, 2009, 149, 1342-1346.	0.9	1
7123	First-principles lattice dynamical study of ScAs and ScSb at zero and high pressure. Solid State Communications, 2009, 149, 1326-1329.	0.9	6
7124	Relaxation and electronic states of Au(100), (110) and (111) surfaces. Solid State Communications, 2009, 149, 1561-1564.	0.9	14
7125	Structural studies on Na0.75CoO2 thermoelectric material at high pressures. Solid State Communications, 2009, 149, 1712-1716.	0.9	5
7126	Remarkable effects of surface dihydride configurations in electronic properties of ã€ˆ 110 ã€‰ silicon nanowires. Solid State Communications, 2009, 149, 1666-1669.	0.9	2
7127	Elastic properties of mono- and polycrystalline (and Lu) under pressure effect. Solid State Communications, 2009, 149, 1658-1662.	0.9	10
7128	A first-principles study on the structural, elastic and electronic properties of AlCSc3 and AlNSc3. Solid State Communications, 2009, 149, 1840-1842.	0.9	8
7129	Ab initio study on magnetism at GaN (100) and (101) surfaces. Solid State Communications, 2009, 149, 1836-1839.	0.9	0
7130	Structure and electronic properties of at high pressure. Solid State Communications, 2009, 149, 1944-1946.	0.9	26
7131	Static compressibility, thermal expansion and elastic anisotropy of single crystals. Solid State Communications, 2009, 149, 2110-2114.	0.9	12
7132	Ab initio calculations of the (111) polar surfaces. Solid State Communications, 2009, 149, 1871-1876.	0.9	25
7133	First-principles study of structural, elastic, electronic and optical properties of SrMO3 (M=Ti and Sn). Solid State Communications, 2009, 149, 2244-2249.	0.9	21
7134	Lattice dynamics and phase transition of NiTi alloy. Solid State Communications, 2009, 149, 2164-2168.	0.9	12
7135	First-principles calculations on elasticity of under pressure. Solid State Communications, 2009, 149, 2135-2138.	0.9	38
7136	The structure, dynamical and thermodynamic properties of : A first-principles study. Solid State Communications, 2009, 149, 2130-2134.	0.9	11
7137	First-principles study of pressure effects on and. Solid State Communications, 2009, 149, 2125-2129.	0.9	12
7138	Compositionâ€“constitutionâ€“morphology relationship of Al2O3 thin films deposited by plasma assisted chemical vapor deposition. Surface and Coatings Technology, 2009, 204, 215-221.	2.2	21
7139	First principles calculations of oxygen adsorption on the UN(001) surface. Surface Science, 2009, 603, 50-53.	0.8	22

#	Article	IF	Citations
7140	Interaction of alkali metals with the Fe3O4(111) Surface. Surface Science, 2009, 603, 78-83.	0.8	25
7141	Initial adsorption of O2 on Si(100): Non-adiabaticity originating both from a discrete and a continuous set of electronic excitations. Surface Science, 2009, 603, 173-177.	0.8	6
7142	Agâ€“Cu alloy surfaces in an oxidizing environment: A first-principles study. Surface Science, 2009, 603, 1467-1475.	0.8	37
7143	Adsorption of molecular oxygen on the reconstructed Î²2(2Ã—4)-GaAs(001) surface: A first-principles study. Surface Science, 2009, 603, 203-208.	0.8	33
7144	Effectiveness of in situ NH3 annealing treatments for the removal of oxygen from GaN surfaces. Surface Science, 2009, 603, 387-399.	0.8	29
7145	Reactivity of the Cu2O(1 0 0) surface: Insights from first principles calculations. Surface Science, 2009, 603, 1637-1645.	0.8	70
7146	Theoretical and experimental studies of Agâ€“Pt interactions for supported Agâ€“Pt bimetallic catalysts. Surface Science, 2009, 603, 690-696.	0.8	40
7147	Flip motion of heterogeneous buckled dimers on Ge(001) by electron injection from STM tip. Surface Science, 2009, 603, 781-787.	0.8	2
7148	First-principles investigations of the Ni3Sn alloy at steam reforming conditions. Surface Science, 2009, 603, 762-770.	0.8	39
7149	Adsorbate influence on the coercive field of ultrathin Co/Cu{110}. Surface Science, 2009, 603, L45-L48.	0.8	7
7150	Structure and stability of Î²-Mo2C bulk and surfaces: A density functional theory study. Surface Science, 2009, 603, 852-859.	0.8	61
7151	A theoretical study of the water gas shift reaction mechanism on Cu(111) model system. Surface Science, 2009, 603, 2138-2144.	0.8	82
7152	The properties of the Pt6/BaO(100) interface and NO adsorption at the interface. Surface Science, 2009, 603, 2413-2421.	0.8	1
7153	Adsorption of methanol on Ni3Al(111) and NiAl(110): A high resolution PES study. Surface Science, 2009, 603, 2370-2377.	0.8	12
7154	Boron and indium incorporation in GaP(001) surfaces by vapour deposition: Density-functional supercell calculations of the surface stability. Surface Science, 2009, 603, 2520-2525.	0.8	4
7155	Reactivity of surface OH in CH4 reforming reactions on Ni(111): A density functional theory calculation. Surface Science, 2009, 603, 2600-2606.	0.8	41
7156	Atomic and electronic structure of group-IV adsorbates on the GaAs(001)-(1Ã—2) surface. Surface Science, 2009, 603, 2683-2687.	0.8	3
7157	DFT study of CO and NO adsorption on low index and stepped surfaces of gold. Surface Science, 2009, 603, 2734-2741.	0.8	77

#	Article	IF	Citations
7158	Ammonia on Ni(111) surface studied by first principles: Bonding, multilayers structure and comparison with experimental IR and XPS data. Surface Science, 2009, 603, 3025-3034.	0.8	26
7159	Stable hydroxyl network on diamond (001) via first-principles and MD investigation. Surface Science, 2009, 603, 3035-3040.	0.8	1
7160	Effects of water and electric field on atomic oxygen adsorption on Ptâ€“Co alloys. Surface Science, 2009, 603, 3239-3248.	0.8	22
7161	Energetics of oxygen embedment into unreconstructed and reconstructed Cu(1 0 0) surfaces: Density functional theory calculations. Surface Science, 2009, 603, 3404-3409.	0.8	26
7162	A systematic approach to choosing parameters for modelling fine structure in electron energy-loss spectroscopy. Ultramicroscopy, 2009, 109, 1374-1388.	0.8	23
7163	ab-initio Study of the properties of Ti1â^'xâ^'ySixAlyN solid solution. Vacuum, 2009, 83, 1240-1243.	1.6	21
7164	Energetics of point defects in TiC. Journal of the European Ceramic Society, 2009, 29, 773-777.	2.8	25
7165	Intercalation of Al into MC (M= Ti, V, Cr). Journal of the European Ceramic Society, 2009, 29, 2885-2891.	2.8	11
7166	First principles study of substoichiometric germanium oxides. Microelectronic Engineering, 2009, 86, 1760-1762.	1.1	15
7167	Modeling complexity of a complex gate oxide. Microelectronic Engineering, 2009, 86, 1763-1766.	1.1	3
7168	Strain dependence of piezoelectric coefficients for pseudomorphically grown semiconductors. Microelectronics Journal, 2009, 40, 601-603.	1.1	5
7169	First-principles study of metal atom adsorption on the boron-doped carbon nanotubes. Microelectronics Journal, 2009, 40, 863-866.	1.1	19
7170	Adsorption of small molecules on graphene. Microelectronics Journal, 2009, 40, 860-862.	1.1	121
7171	Structure and energetics of hydrogen adsorption on Fe3O4(111). Journal of Molecular Catalysis A, 2009, 302, 129-136.	4.8	57
7172	On the effectiveness of partial oxidation of propylene by gold: A density functional theory study. Journal of Molecular Catalysis A, 2009, 306, 6-10.	4.8	31
7173	Experimental and theoretical characterization of NOx species on Ag/Î±-Al2O3. Journal of Molecular Catalysis A, 2009, 314, 102-109.	4.8	22
7174	The Z-phase in 9â€“12% Cr ferritic steels: A phase stability analysis. Materials Science & Engineering A: Structural Materials: Properties, Microstructure and Processing, 2009, 505, 1-5.	2.6	31
7175	Density functional calculations of the strain effects on binding energies and adatom diffusion on (0001) GaN surfaces. Materials Science and Engineering B: Solid-State Materials for Advanced Technology, 2009, 158, 13-18.	1.7	12

#	Article	IF	Citations
7176	Elastic, electronic and optical properties of the filled tetrahedral semiconductor Î±-LiCdAs. Materials Science in Semiconductor Processing, 2009, 12, 198-205.	1.9	5
7177	First-principles calculations of elastic and thermo-physical properties of Al, Mg and rare earth lanthanide elements. Physica B: Condensed Matter, 2009, 404, 2299-2304.	1.3	11
7178	Nonlinear optical response of wurtzite ZnO from first principles. Physica B: Condensed Matter, 2009, 404, 2340-2344.	1.3	27
7179	Structural and thermodynamic properties of the cubic perovskite BiAlO3. Physica B: Condensed Matter, 2009, 404, 3534-3538.	1.3	24
7180	Preferential orientation of Te particles in melt-grown CZT. Journal of Crystal Growth, 2009, 311, 2641-2647.	0.7	16
7181	Functionalization of single-walled carbon nanotube with borane for hydrogen storage. Physica E: Low-Dimensional Systems and Nanostructures, 2009, 41, 1340-1346.	1.3	31
7182	Structural stability and electronic properties of GaSb nanowires. Physica E: Low-Dimensional Systems and Nanostructures, 2009, 42, 46-50.	1.3	7
7183	Density functional theory study of Ir atom deposited on Î³-Al2O3 (001) surface. Physics Letters, Section A: General, Atomic and Solid State Physics, 2009, 373, 277-281.	0.9	21
7184	Elastic, electronic and optical properties of SiGe2N4 under pressure: An ab initio study. Physics Letters, Section A: General, Atomic and Solid State Physics, 2009, 373, 2393-2398.	0.9	12
7185	Hydrogen adsorption on N-decorated single wall carbon nanotubes. Physics Letters, Section A: General, Atomic and Solid State Physics, 2009, 373, 2588-2591.	0.9	17
7186	Oxygen vacancy pairs on CeO2(110): A DFT+U study. Physics Letters, Section A: General, Atomic and Solid State Physics, 2009, 373, 2786-2792.	0.9	44
7187	Small polaron migration in LixMn2O4: From first principles calculations. Physics Letters, Section A: General, Atomic and Solid State Physics, 2009, 373, 2796-2799.	0.9	43
7188	Electronic structures and mechanical properties of uranium monocarbide from first-principles and calculations. Physics Letters, Section A: General, Atomic and Solid State Physics, 2009, 373, 3577-3581.	0.9	46
7189	First-principles study of lattice dynamics of LiFePO4. Physics Letters, Section A: General, Atomic and Solid State Physics, 2009, 373, 4096-4100.	0.9	48
7190	Band structure calculations for Heusler phase Co2YBi and half-Heusler phase CoYBi (Y=Mn, Cr). Journal of Magnetism and Magnetic Materials, 2009, 321, 365-372.	1.0	41
7191	Electronic and magnetic behavior of ultrathin Ti nanowires. Journal of Magnetism and Magnetic Materials, 2009, 321, 1856-1862.	1.0	8
7192	Electronic structure and magnetism in : An ab initio study. Journal of Magnetism and Magnetic Materials, 2009, 321, 2547-2549.	1.0	16
7193	Electronic and magnetic properties of Pd-Ni multilayers: Study using density functional theory. Journal of Magnetism and Magnetic Materials, 2009, 321, 3478-3482.	1.0	9

#	Article	IF	Citations
7194	Energetics of He and H atoms with vacancies in tungsten: First-principles approach. Journal of Nuclear Materials, 2009, 383, 244-246.	1.3	64
7195	Energetics of intrinsic point defects in uranium dioxide from electronic-structure calculations. Journal of Nuclear Materials, 2009, 384, 61-69.	1.3	127
7196	Vacancies, interstitials and gas atoms in beryllium. Journal of Nuclear Materials, 2009, 386-388, 79-81.	1.3	38
7197	Ab initio study of interstitial migration in Feâ€“Cr alloys. Journal of Nuclear Materials, 2009, 386-388, 86-89.	1.3	55
7198	A density functional theory assessment of the clustering behaviour of He and H in tungsten. Journal of Nuclear Materials, 2009, 386-388, 109-111.	1.3	136
7199	Multiscale modeling of point defect interactions in Feâ€“Cr alloys. Journal of Nuclear Materials, 2009, 386-388, 227-230.	1.3	25
7200	Radiation damage effects in the uranium-bearing Î´-phase oxide Y6U1O12. Journal of Nuclear Materials, 2009, 389, 497-499.	1.3	7
7201	First-principles study on cerium ion behavior in irradiated cerium dioxide. Journal of Nuclear Materials, 2009, 393, 321-327.	1.3	23
7202	Chemisorption of a molecular oxygen on the UN(001) surface: Ab initio calculations. Journal of Nuclear Materials, 2009, 393, 504-507.	1.3	25
7203	Helium atoms in chromium-rich Feâ€“Cr alloys â€“ Ab initio results. Journal of Nuclear Materials, 2009, 395, 45-49.	1.3	5
7204	Compression behaviour of nitridocarbidosilicates studied with X-ray diffraction and ab initio calculations. Journal of Physics and Chemistry of Solids, 2009, 70, 97-106.	1.9	7
7205	Ab-initio pseudopotential study of electronic structure and chemisorption of oxygen on aluminium surface. Journal of Physics and Chemistry of Solids, 2009, 70, 298-302.	1.9	9
7206	Pressure-induced phase transition in wurtzite ZnS: An ab initio constant pressure study. Journal of Physics and Chemistry of Solids, 2009, 70, 645-649.	1.9	31
7207	Ab initio simulations on the atomic and electronic structure of single-walled BN nanotubes and nanoarches. Journal of Physics and Chemistry of Solids, 2009, 70, 796-803.	1.9	27
7208	First-principles study on lithium removal from Li2MnO3. Journal of Power Sources, 2009, 189, 798-801.	4.0	158
7209	First-principles investigation of the bonding, optical and lattice dynamical properties of CeO2. Journal of Power Sources, 2009, 194, 830-834.	4.0	54
7210	The crystal structure of Hf1.5+Î´Nb1.5âˆ’Î´As and structureâ€“composition relations in the section Hf3Asâ€“Nb3As. Journal of Solid State Chemistry, 2009, 182, 896-904.	1.4	6
7211	Ab initio study on the electronic and mechanical properties of ReB and ReC. Journal of Solid State Chemistry, 2009, 182, 960-965.	1.4	20

#	Article	IF	Citations
7212	First-principles study of the electronic structures of Î±-rhombohedral boron codoped with lithium and oxygen. Journal of Solid State Chemistry, 2009, 182, 1856-1860.	1.4	6
7213	Slaterâ€“Pauling behavior within quaternary intermetallic borides of the Ti3Co5B2 structure-type. Journal of Solid State Chemistry, 2009, 182, 2613-2619.	1.4	5
7214	Electronic band structure of from first principles. Journal of Solid State Chemistry, 2009, 182, 2678-2684.	1.4	11
7215	Oxidation of methane on nanoparticulate Au/TiO2 at low temperature: A combined microreactor and DFT study. Catalysis Today, 2009, 142, 24-29.	2.2	12
7216	CO2 adsorption and activation over Î³-Al2O3-supported transition metal dimers: A density functional study. Catalysis Today, 2009, 147, 68-76.	2.2	91
7217	DFT studies of dry reforming of methane on Ni catalyst. Catalysis Today, 2009, 148, 260-267.	2.2	320
7218	Electronic structures of the Si(001) thin film under ã€ˆ110ã€‰- and ã€ˆ010ã€‰-direction uniaxial tensile strains. Computer Physics Communications, 2009, 180, 659-663.	3.0	5
7219	yambo: An ab initio tool for excited state calculations. Computer Physics Communications, 2009, 180, 1392-1403.	3.0	927
7220	Adaptive logarithmic discretization for numerical renormalization group methods. Computer Physics Communications, 2009, 180, 1271-1276.	3.0	34
7221	Terahertz optical properties of the high explosive <mml:math xmlns:mml="http://www.w3.org/1998/Math/MathML" altimg="si16.gif" display="inline" overflow="scroll"><mml:mrow><mml:mi>Î²</mml:mi></mml:mrow></mml:math>-HMX. Chemical Physics Letters, 2009, 467, 309-312.	1.2	47
7222	Preparation, characterization and visible-light-driven photocatalytic activity of Fe-doped titania nanorods and first-principles study for electronic structures. Applied Catalysis B: Environmental, 2009, 90, 595-602.	10.8	700
7223	Plasticity and ab initio characterizations on Fe4N produced on the surface of nanocrystallized 18Ni-maraging steel plasma nitrided at lower temperature. Applied Surface Science, 2009, 255, 8902-8906.	3.1	23
7224	First-principles study of the B- or N-doping effects on chemical bonding characteristics between magnesium and single-walled carbon nanotubes. Chemical Physics Letters, 2009, 469, 145-148.	1.2	13
7225	First principle studies of zigzag AlN nanoribbon. Chemical Physics Letters, 2009, 469, 183-185.	1.2	86
7226	Aggregation of organic molecules on silver surface with the balance between moleculeâ€“substrate interaction and intermolecular interaction. Chemical Physics Letters, 2009, 470, 126-130.	1.2	8
7227	All-electron embedded correlated wavefunction theory for condensed matter electronic structure. Chemical Physics Letters, 2009, 470, 347-352.	1.2	40
7228	Ti 3p electrons: Core or valence?. Chemical Physics Letters, 2009, 471, 75-79.	1.2	9
7229	Possible ferromagnetism in s- and sp-electron element nanowires. Chemical Physics Letters, 2009, 472, 99-103.	1.2	11

#	Article	IF	Citations
7230	First principles studies of ZrNi and ZrNiH3. Chemical Physics Letters, 2009, 473, 61-65.	1.2	24
7231	Helical and linear [K(As11)]2â^' chains: Role of solvent on the conformation of chains formed by Zintl anions. Chemical Physics Letters, 2009, 473, 305-311.	1.2	11
7232	Kinetics of hydrogen uptake by scavenger molecules â€“ Insights from molecular modeling. Chemical Physics Letters, 2009, 475, 223-226.	1.2	16
7233	Electronic structure and lattice anisotropy of <mml:math xmlns:mml="http://www.w3.org/1998/Math/MathML" altimg="si18.gif" display="inline" overflow="scroll"><mml:mrow><mml:mtext>Cd</mml:mtext><mml:mo stretchy="false">(</mml:mo><mml:msub><mml:mrow><mml:mtext>UO</mml:mtext></mml:mrow><mml:mrow><mml:mn>2</mml:m Chemical Physics Letters, 2009, 476, 213-217.	1.2	3
7234	Evidence of hydrogenated hexamers on graphite. Chemical Physics Letters, 2009, 478, 42-44.	1.2	14
7235	Hydrogenation of ultrasmall carbon nanotubes: A first principle study. Chemical Physics Letters, 2009, 480, 215-219.	1.2	10
7236	Adsorption and electronic structure of single C60F18 molecule on Si(111)-7Ã—7 surface. Chemical Physics Letters, 2009, 482, 307-311.	1.2	20
7237	Electrochemical reactivity and fractional conductance of nanowires. Electrochemistry Communications, 2009, 11, 1764-1767.	2.3	23
7238	Electronic structure of self-assembled (fluoro)methylthiol monolayers on the Au(111) surface: Impact of fluorination and coverage density. Journal of Electron Spectroscopy and Related Phenomena, 2009, 174, 70-77.	0.8	12
7239	First principles study of the structure and stability of carbynes. Carbon, 2009, 47, 367-383.	5.4	39
7240	Water molecule adsorption on a titaniumâ€“graphene system with high metal coverage. Carbon, 2009, 47, 531-533.	5.4	28
7241	Adsorption of carbon dioxide and methane on graphene with a high titanium coverage. Carbon, 2009, 47, 2758-2760.	5.4	43
7242	Elastic properties and electronic structure of vanadium silicides-a density functional investigation. Acta Materialia, 2009, 57, 50-55.	3.8	19
7243	First-principles study of vacancy formation and migration in clean and Re-doped Î³â€²-Ni3Al. Acta Materialia, 2009, 57, 224-231.	3.8	27
7244	Experimental investigation and thermodynamic modeling of the Niâ€“Alâ€“Ru ternary system. Acta Materialia, 2009, 57, 202-212.	3.8	18
7245	Surface modelling on heavy atom crystalline compounds: HfO2 and UO2 fluorite structures. Acta Materialia, 2009, 57, 600-606.	3.8	23
7246	Local structure variations in Al89La6Ni5 metallic glass. Acta Materialia, 2009, 57, 804-811.	3.8	32
7247	Energy landscape for martensitic phase transformation in shape memory NiTi. Acta Materialia, 2009, 57, 1624-1629.	3.8	62

#	Article	IF	Citations
7248	Influence of vibrational entropy on structural stability of Nbâ€“Si and Moâ€“Si systems at elevated temperatures. Acta Materialia, 2009, 57, 2657-2664.	3.8	57
7249	Do substitutional solutes soften or embrittle cracktips in Î±-Fe?. Acta Materialia, 2009, 57, 3091-3100.	3.8	15
7250	First-principles investigation of the structure and synergistic chemical bonding of Ag and Mg at the Al|Î© interface in a Alâ€“Cuâ€“Mgâ€“Ag alloy. Acta Materialia, 2009, 57, 3522-3528.	3.8	26
7251	Ab-initio calculations of the hydrogenâ€“uranium system: Surface phenomena, absorption, transport and trapping. Acta Materialia, 2009, 57, 4707-4715.	3.8	43
7252	Thermodynamic properties of the Alâ€“Feâ€“Ni system acquired via a hybrid approach combining calorimetry, first-principles and CALPHAD. Acta Materialia, 2009, 57, 5324-5341.	3.8	90
7253		3.8	325
7254	The effect of alloying elements on the dislocation climbing velocity in Ni: A first-principles study. Acta Materialia, 2009, 57, 5914-5920.	3.8	81
7255	Optical properties of titanium oxycarbide thin films. Applied Surface Science, 2009, 255, 5615-5619.	3.1	9
7256	First-principles calculations of hydrogen molecule adsorption on Ti (0001)-(2Ã—1) surface. Applied Surface Science, 2009, 255, 7512-7516.	3.1	6
7257	Experimental deduction of In/Si(111) 2D phase diagram and ab initio DFT modeling of 2âˆš3 phase. Applied Surface Science, 2009, 256, 348-352.	3.1	7
7258	Electronic structure of superconducting galliumâ€doped germanium from abâ€initio calculations. Physica Status Solidi - Rapid Research Letters, 2009, 3, 224-226.	1.2	8
7259	Band gap engineering of (N,Ta)-codoped TiO2: A first-principles calculation. Chemical Physics Letters, 2009, 478, 175-179.	1.2	95
7260	QUANTUM ESPRESSO: a modular and open-source software project for quantum simulations of materials. Journal of Physics Condensed Matter, 2009, 21, 395502.	0.7	18,183
7261	DFT study of halogen impurity in diamond. Journal Physics D: Applied Physics, 2009, 42, 145407.	1.3	14
7262	Evidence of the Ge nonreactivity during the initial stage of SiGe oxidation. Applied Physics Letters, 2009, 94, 041912.	1.5	10
7263	Activated dissociation ofO2on Pb(111) surfaces by Pb adatoms. Physical Review B, 2009, 80, .	1.1	7
7264	Adsorption and dissociation of<mml:math xmlns:mml="http://www.w3.org/1998/Math/MathML" display="inline"><mml:mrow><mml:msub><mml:mtext>O</mml:mtext><mml:mn>2</mml:mn></mml:msub></mml:mrow></mml:math Be(0001): First-principles prediction of an energy barrier on the adiabatic potential energy surface. Physical Review B, 2009, 79, .	1.1	16
7265	Hydrogen evolution on nano-particulate transition metal sulfides. Faraday Discussions, 2008, 140, 219-231.	1.6	732

#	Article	IF	Citations
7266	Interatomic potentials for the Beâ€“Câ€“H system. Journal of Physics Condensed Matter, 2009, 21, 445002.	0.7	56
7267	Adsorption of O and CO on Ir(100) from first principles. European Physical Journal B, 2009, 67, 35-41.	0.6	26
7268	Atomic and electronic structure of single-walled BN nanotubes containing N vacancies as well as C and O substitutes of N atoms. European Physical Journal B, 2009, 67, 519-525.	0.6	23
7269	AbÂinitio study of structural, electronic, and elastic properties of M2SbP (MÂ=ÂTi, Zr, and Hf). European Physical Journal B, 2009, 68, 193-196.	0.6	5
7270	Defect-induced ferromagnetism in fullerenes. European Physical Journal B, 2009, 68, 529-535.	0.6	38
7271	GGA+U study of the incorporation of iodine in uranium dioxide. European Physical Journal B, 2009, 69, 203-209.	0.6	61
7272	Far IR spectra of Ag2CdI4 at temperature range 10â€“420ÂK: complementary experimental and first-principle theoretical study. European Physical Journal B, 2009, 70, 443-447.	0.6	12
7273	Structural, elastic, electronic, optical and thermal properties of c-SiGe2N4. European Physical Journal B, 2009, 71, 185-194.	0.6	11
7274	First-principles study of bulk and surface oxygen vacancies in SrTiO3 crystal. European Physical Journal B, 2009, 72, 53-57.	0.6	94
7275	Fcc-to-bct phase transformation of aluminum under triaxial stresses: an ab initio constant pressure study. European Physical Journal B, 2009, 72, 241-245.	0.6	3
7276	A systematic investigation of stacking faults in magnesium via first-principles calculation. European Physical Journal B, 2009, 72, 397-403.	0.6	74
7277	Accelerated coarsening of Ag adatom islands on Ag(111) due to trace amounts of S: Mass-transport mediated by Agâ€“S complexes. Journal of Chemical Physics, 2009, 130, 094701.	1.2	26
7278	<mml:math xmlns:mml="http://www.w3.org/1998/Math/MathML" display="inline"><mml:mrow><mml:msub><mml:mrow><mml:mtext>Cu</mml:mtext></mml:mrow><mml:mn>2</mml:mn></mml:msu a potential photovoltaic material: A hybrid Hartree-Fock density functional theory study. Physical Review B, 2009, 79, .	1.1	402
7279	Evaluation of aluminum critical point using anab initiovariational approach. Physical Review B, 2009, 79, .	1.1	23
7280	Electronic structure and stability of quaternary chalcogenide semiconductors derived from cation cross-substitution of II-VI and<mml:math xmlns:mml="http://www.w3.org/1998/Math/MathML" display="inline"><mml:mrow><mml:msub><mml:mrow><mml:mtext>I-III-VI</mml:mtext></mml:mrow><mml:mn>2</mml:mn></mml:m Physical Review B, 2009, 79, .	1.1	413
7281	First-Principles Characterization of Bi-based Photocatalysts: Bi₁₂TiO₂₀, Bi₂Ti₂O₇, and Bi₄Ti₃O₁₂. Journal of Physical Chemistry C, 2009, 113, 5658-5663.	1.5	209
7282	Chemical functionalization of graphene. Journal of Physics Condensed Matter, 2009, 21, 344205.	0.7	331
7283	Ab initiotheory of the lattice thermal conductivity in diamond. Physical Review B, 2009, 80, .	1.1	507

#	Article	IF	Citations
7284	Ab initioenergetics of<mml:math xmlns:mml="http://www.w3.org/1998/Math/MathML"		

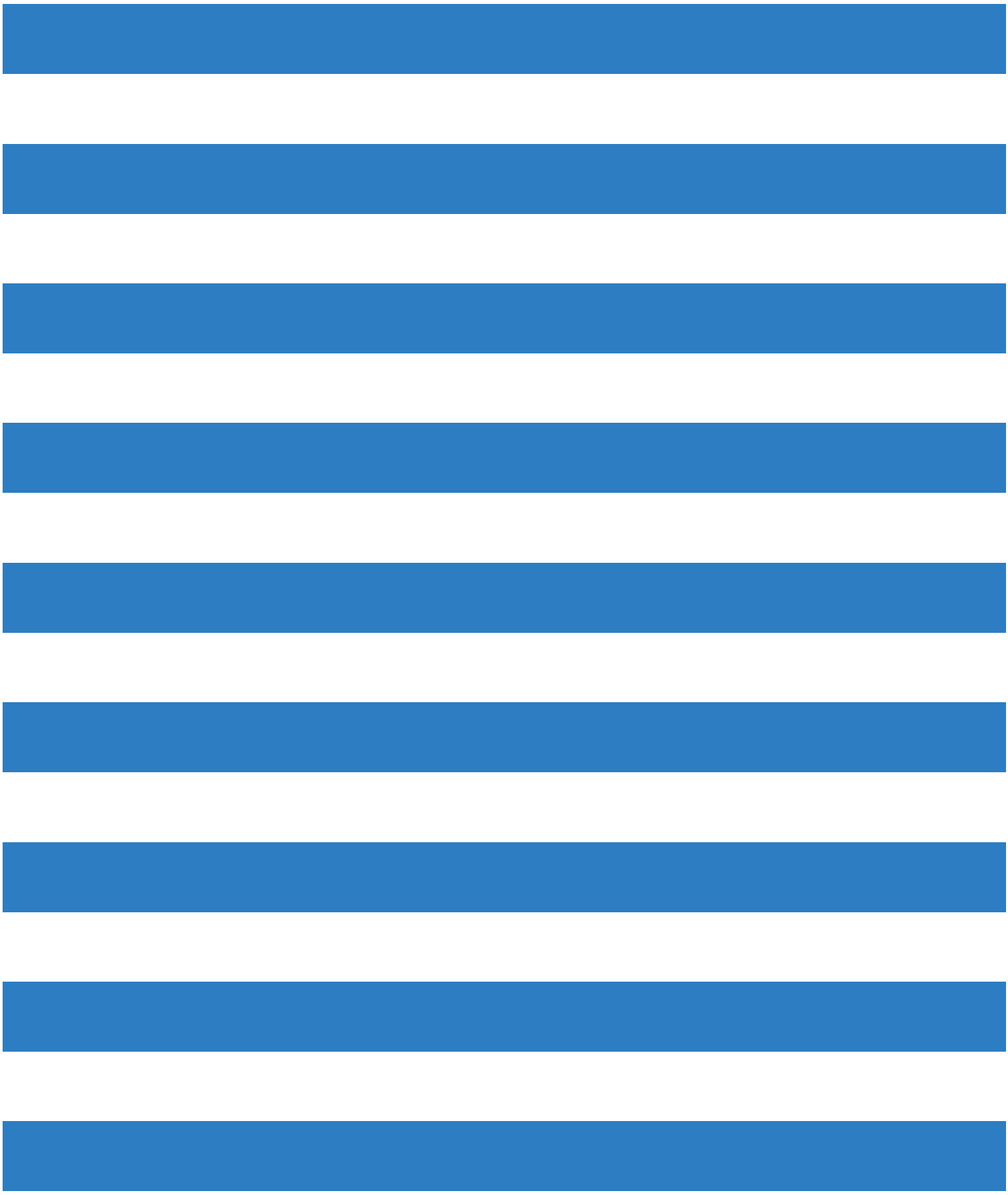

#	Article	IF	Citations
7302	Lithium Insertion and Transport in the TiO₂â^'B Anode Material: A Computational Study. Chemistry of Materials, 2009, 21, 4778-4783.	3.2	169
7303	Ab initiostudy of high-pressure structural properties of the LuVO₄and ScVO₄zircon-type orthovanadates. High Pressure Research, 2009, 29, 582-586.	0.4	12
7304	Surface Properties of LiCoO₂ Investigated by XPS Analyses and Theoretical Calculations. Journal of Physical Chemistry C, 2009, 113, 5843-5852.	1.5	132
7305	3DÂImaging of the Fermi Surface by Thermal Diffuse Scattering. Physical Review Letters, 2009, 103, 076403.	2.9	14
7306	A grid-based Bader analysis algorithm without lattice bias. Journal of Physics Condensed Matter, 2009, 21, 084204.	0.7	4,245
7307	Modeling of an ultrahigh-frequency resonator based on the relative vibrations of carbon nanotubes. Physical Review B, 2009, 80, .	1.1	24
7308	Potential of AlN Nanostructures as Hydrogen Storage Materials. ACS Nano, 2009, 3, 621-626.	7.3	201
7309	Structural, electronic and elastic properties of Ti2TlC, Zr2TlC and Hf2TlC. Open Physics, 2009, 7, .	0.8	5
7310	Modification of electronic properties of Pt(111) surface by means of alloyed and adsorbed metals: DFT study. Russian Journal of Physical Chemistry A, 2009, 83, 1531-1536.	0.1	3
7311	Nanomechanical properties and phase transitions in a double-walled (5,5)@(10,10) carbon nanotube: ab initio calculations. Journal of Experimental and Theoretical Physics, 2009, 108, 621-628.	0.2	24
7312	Specific features of electronic and vibrational properties of I-V-V2 crystals. Semiconductors, 2009, 43, 735-739.	0.2	2
7313	The level of local charge-neutrality and pinning of the Fermi level in irradiated nitrides wz-III-N (BN,) Tj ETQq1 1 0.784314 rgBT /Overlo	0.2	19
7314	Ab initio calculations of phonon spectra in ATiO3 perovskite crystals (A = Ca, Sr, Ba, Ra, Cd, Zn, Mg, Ge,) Tj ETQq0 0 0 rgBT /Overlock 10	0.2	106
7315	Ab initio calculation of the deformation potentials for intervalley phonons in silicon. Physics of the Solid State, 2009, 51, 1110-1113.	0.2	6
7316	Hydrogen adsorption on low-index surfaces of B2 titanium alloys. Physics of the Solid State, 2009, 51, 1281-1289.	0.2	18
7317	Electronic States in Zinc Magnesium Oxide Alloy Semiconductors: Hard X-ray Photoemission Spectroscopy and Density Functional Theory Calculations. Chemistry of Materials, 2009, 21, 144-150.	3.2	15
7318	Can the Localization Regime of [GaNNW/BNNT] Nanocables Change from Type II to Type I? First-Principles Studies. Journal of Physical Chemistry C, 2009, 113, 4321-4326.	1.5	1
7319	Lattice dynamics and elastic properties of LiPN2and NaPN2. Journal of Physics Condensed Matter, 2009, 21, 405404.	0.7	4

#	Article	IF	Citations
7320	Electronic Structure and Magnetic Properties of Potassium Ozonide KO3. Inorganic Chemistry, 2009, 48, 5938-5945.	1.9	9
7321	Energetic and Electronic Properties of P Doping at the Rutile TiO₂ (110) Surface from First Principles. Journal of Physical Chemistry C, 2009, 113, 9423-9430.	1.5	18
7322	First-Principles Study of the Relaxed Structures and Electronic Properties of Au Nanowires. Journal of Physical Chemistry C, 2009, 113, 17678-17684.	1.5	3
7323	Characteristic Energies and Shifts in Optical Spectra of Colloidal IVâ^'VI Semiconductor Nanocrystals. ACS Nano, 2009, 3, 3505-3512.	7.3	37
7324	Plane-Wave Density Functional Theory Investigations of the Adsorption and Activation of CO on Fe₅C₂Surfaces. Journal of Physical Chemistry C, 2009, 113, 9256-9274.	1.5	58
7325	Effects of Confinement on Oxygen Adsorbed between Pt(111) Surfaces. Journal of Physical Chemistry C, 2009, 113, 7851-7856.	1.5	14
7326	Density Functional Studies of the Adsorption and Dissociation of NO_x (x = 1,) Tj ETQq0 0 0 rgBT /Overlock 10	1.5	10
7327	Elasticity of the B2 phase and the effect of the B1â€“B2 phase transition on the elasticity of MgO. Phase Transitions, 2009, 82, 87-97.	0.6	6
7328	Mechanisms for H₂ Reduction on the PdO{101} Surface and the Pd{100}-(âˆš5 Ã—) Tj ETQq0 0 0 rgBT /Overlock 10 Tf 50	1.5	19
7329	Structural and Thermodynamic Properties of Cerium via First-Principles Plane Wave Method with a Relativistic Analytic Pseudopotential. Chinese Physics Letters, 2009, 26, 017101.	1.3	6
7330	Prediction of O2 Dissociation Kinetics on LaMnO3-Based Cathode Materials for Solid Oxide Fuel Cells. Journal of Physical Chemistry C, 2009, 113, 7290-7297.	1.5	57
7331	Modeling Hydrogen Sulfide Adsorption on Mo-Edge MoS2 Surfaces under Solid Oxide Fuel Cell Conditions. Journal of Physical Chemistry C, 2009, 113, 193-203.	1.5	25
7332	Effect of Preadsorbed S on the Adsorption of CO on Co(0001). Journal of Physical Chemistry C, 2009, 113, 16210-16215.	1.5	7
7333	Hydrogen Absorption and Diffusion in Bulk Î±-MoO₃. Journal of Physical Chemistry C, 2009, 113, 11399-11407.	1.5	126
7334	Density Functional Study of the Reaction of SO₂ on Ir(111). Journal of Physical Chemistry C, 2009, 113, 18223-18232.	1.5	20
7335	Study of Gallium Fragments Encapsulated in Single-Walled Carbon Nanotubes. Journal of Physical Chemistry C, 2009, 113, 567-570.	1.5	8
7336	Relative stability of low-index V₂O₅surfaces: a density functional investigation. Journal of Physics Condensed Matter, 2009, 21, 095008.	0.7	27
7337	Ab initiolattice dynamics and thermal expansion of<mml:math xmlns:mml="http://www.w3.org/1998/Math/MathML" display="inline"><mml:mrow><mml:msub><mml:mrow><mml:mtext>Cu</mml:mtext></mml:mrow><mml:mn>2</mml:mn></mml:m Physical Review B, 2009, 80, .	1.1	43

#	Article	IF	Citations
7338	Origin of activation of Lattice Oxygen and Synergistic Interaction in Bimetal-Ionic Ce_{0.89}Fe_{0.1}Pd_{0.01}O_{2â˜Î´} Catalyst. Chemistry of Materials, 2009, 21, 4880-4891.	3.2	91
7339	Dehydrogenation of Ethanol on a 2Ru/ZrO₂(111) Surface: Density Functional Computations. Journal of Physical Chemistry C, 2009, 113, 6132-6139.	1.5	9
7340	Vanadium Oxides Supported on a Thin Silica Film Grown on Mo(112): Insights from Density Functional Theory. Journal of Physical Chemistry C, 2009, 113, 8336-8342.	1.5	17
7341	Phase stability, electronic structure and mechanical properties of molybdenum disilicide: a first-principles investigation. Journal Physics D: Applied Physics, 2009, 42, 105413.	1.3	27
7342	Crystal Structures of the Tetragonal Ceriaâ˜Zirconia Solid Solutions Ce_xZr_{1â˜x}O₂ through First Principles Calculations (0 â‰¤ x â‰¤ 1). Journal of Physical Chemistry C, 2009, 113, 12658-12662.	1.5	30
7343	THE CO-ADSORPTION OF BENZENE ANDCOONCo(0001). Surface Review and Letters, 2009, 16, 749-755.	0.5	5
7344	First-principles investigation of pentagonal and hexagonal core-shell silicon nanowires with various core compositions. Physical Review B, 2009, 80, .	1.1	22
7345	Ab initio calculations on the borate nonlinear optical crystal BaAlBO3F2. Journal of Applied Physics, 2009, 106, .	1.1	25
7346	Orderâ˜Disorder Transition and Phase Separation in the MgB2 Metallic Sublattice Induced by Al Doping. Journal of Chemical Theory and Computation, 2009, 5, 1858-1864.	2.3	3
7347	Density Functional Theory Studies of Chloroethene Adsorption on Zerovalent Iron. Environmental Science & Technology, 2009, 43, 1192-1198.	4.6	26
7348	The Nature of Radiative Transitions in O-Doped Boron Nitride Nanotubes. Journal of the American Chemical Society, 2009, 131, 4839-4845.	6.6	42
7349	Effect of Substitutional N on Important Chemical Vapor Deposition Diamond Growth Steps. Journal of Physical Chemistry A, 2009, 113, 3274-3284.	1.1	14
7350	Hg Binding on Pd Binary Alloys and Overlays. Journal of Physical Chemistry C, 2009, 113, 7813-7820.	1.5	49
7351	Effect of the Support on the Electronic Structure of Au Nanoparticles Supported on Transition Metal Carbides: Choice of the Best Substrate for Au Activation. Journal of Physical Chemistry C, 2009, 113, 19994-20001.	1.5	28
7352	Moâ˜Sâ˜I Nanowires: A Promising Anode Material for Lithium-Ion Batteries. A First-Principles Study. Journal of Physical Chemistry C, 2009, 113, 18436-18440.	1.5	14
7353	Potential energy surface of alkali atoms adsorbed on Cu(001). Physical Review B, 2009, 80, .	1.1	16
7354	Aminoxyl Radicals on the Silicon (001) Surface. Journal of Physical Chemistry C, 2009, 113, 1020-1027.	1.5	2
7355	Attractionâ˜Repulsion Mechanism for Carbon Monoxide Adsorption on Platinum and Platinumâ˜Ruthenium Alloys. Journal of Physical Chemistry C, 2009, 113, 18730-18739.	1.5	47

#	Article	IF	Citations
7356	Strained graphene: tight-binding and density functional calculations. New Journal of Physics, 2009, 11, 115002.	1.2	197
7357	Temperature- and Pressure-Induced Proton Transfer in the 1:1 Adduct Formed between Squaric Acid and 4,4â€²-Bipyridine. Journal of the American Chemical Society, 2009, 131, 3884-3893.	6.6	82
7358	Prediction of a spin-polarized two-dimensional electron gas at theLaAlO3/EuO(001)interface. Physical Review B, 2009, 79, .	1.1	44
7359	Technetium(IV) Halides Predicted from First-Principles. Inorganic Chemistry, 2009, 48, 6555-6558.	1.9	27
7360	High-pressure phases ofZrO2: Anab initioconstant-pressure study. Physical Review B, 2009, 79, .	1.1	39
7361	Norbornadiene-Based Molecules for Functionalizing The Si(001) Surface. Journal of Physical Chemistry C, 2009, 113, 16094-16103.	1.5	4
7362	IR Spectroscopic Measurement of Diffusion Kinetics of Chemisorbed Pyridine through Nanocrystalline MgO Particles. The Involvement of Surface Defect Sites in Slow Diffusion. Journal of Physical Chemistry C, 2009, 113, 2219-2227.	1.5	19
7363	Quantum-Mechanical and Thermodynamical Study on the (100) Face of LiF Crystals. Crystal Growth and Design, 2009, 9, 404-408.	1.4	8
7364	On the Dissociative Chemisorption of Tris(dimethylamino)silane on Hydroxylated SiO₂(001) Surface. Journal of Physical Chemistry C, 2009, 113, 9731-9736.	1.5	42
7365	Elastic constants of NaBH ₄ and LiBH ₄ : Instability of Î²-LiBH ₄. Europhysics Letters, 2009, 88, 36005.	0.7	3
7366	Growth of N,Nâ€²-Bis(1-ethylpropyl)perylene-3,4,9,10-tetracarboxdiimide Films on Ag (111). Journal of Physical Chemistry C, 2009, 113, 17866-17875.	1.5	29
7367	Carbon Adsorption and Absorption in the (111) L12 Fe3Al Surface. Journal of Physical Chemistry C, 2009, 113, 18321-18330.	1.5	2
7368	Theory of the structure of electronic polarization and its strain dependence in ferroelectric perovskites. Physical Review B, 2009, 79, .	1.1	10
7369	Electronic Structure and Spin Exchange Interactions in Na2V3O7: a Vanadium(IV) Oxide Nanotubular Phase. Inorganic Chemistry, 2009, 48, 5779-5789.	1.9	7
7370	Electronic Structure of the A₈Tr₁₁ (A = K, Rb, Cs; Tr = Ga, In, Tl) Zintl Phases: Possible Chemical Reasons Behind Their Activated versus Non Activated Conductivity. Inorganic Chemistry, 2009, 48, 9792-9799.	1.9	6
7371	Adsorption and Diffusion of Light Gases in ZIF-68 and ZIF-70: A Simulation Study. Journal of Physical Chemistry C, 2009, 113, 16906-16914.	1.5	126
7372	Understanding the Electronic Structure of Metal/SAM/Organicâ^'Semiconductor Heterojunctions. ACS Nano, 2009, 3, 3513-3520.	7.3	48
7373	Ti-Decorated BC₄N Sheet: A planar Nanostructure for High-Capacity Hydrogen Storage. Journal of Physical Chemistry C, 2009, 113, 15783-15787.	1.5	31

#	Article	IF	Citations
7374	Adsorption-Induced Surface Electronic Reconstruction of Pt and Ptâ^'Sn Alloys during CO Adsorption. Journal of Physical Chemistry C, 2009, 113, 14329-14334.	1.5	7
7375	Proposed Long-Range Empirical Potential To Study the Metallic Glasses in the Niâ^'Nbâ^'Ta System. Journal of Physical Chemistry B, 2009, 113, 7282-7290.	1.2	17
7376	Theory of NH_x Â± H Reactions on Fe{211}. Journal of Physical Chemistry C, 2009, 113, 15274-15287.	1.5	24
7377	Pb(II) Adsorption on Isostructural Hydrated Alumina and Hematite (0001) Surfaces: A DFT Study. Journal of Physical Chemistry C, 2009, 113, 2159-2170.	1.5	88
7378	First-Principles Study of Chemisorption of Oxygen and Aziridine on Graphitic Nanostructures. Journal of Physical Chemistry C, 2009, 113, 14721-14726.	1.5	21
7379	Adsorption Configurations and Decomposition Pathways of Boric Acid on TiO2 Rutile (110) Surface: A Computational Study. Journal of Physical Chemistry C, 2009, 113, 3751-3762.	1.5	11
7380	Influence of vanadium spin-polarization on the dissolution of hydrogen in vanadium. Physical Review B, 2009, 79, .	1.1	2
7381	²⁷Al NMR Chemical Shifts in Oxide Crystals: A First-Principles Study. Journal of Physical Chemistry C, 2009, 113, 3869-3873.	1.5	53
7382	Density Functional Investigation of Methanol Dehydrogenation on Pd(111). Journal of Physical Chemistry C, 2009, 113, 4188-4197.	1.5	91
7383	Orientation-Dependent Stability and Quantum-Confinement Effects of Silicon Carbide Nanowires. Journal of Physical Chemistry C, 2009, 113, 12731-12735.	1.5	27
7384	How Potentials of Zero Charge and Potentials for Water Oxidation to OH(ads) on Pt(111) Electrodes Vary With Coverage. Journal of Physical Chemistry C, 2009, 113, 17484-17492.	1.5	55
7385	Polyhedral Oligomeric Silsesquioxane (POSS)-Stabilized Pd Nanoparticles: Factors Governing Crystallite Morphology and Secondary Aggregate Structure. Journal of Physical Chemistry C, 2009, 113, 19424-19431.	1.5	19
7386	Magnetic Properties of Fully Bare and Half-Bare Boron Nitride Nanoribbons. Journal of Physical Chemistry C, 2009, 113, 2273-2276.	1.5	102
7387	Adsorption Configuration and Dissociative Reaction of NH₃ on Anatase (101) Surface with and without Hydroxyl Groups. Journal of Physical Chemistry C, 2009, 113, 6663-6672.	1.5	20
7388	Adsorption and Dissociation of CO on Body-Centered Cubic Transition Metals and Alloys: Effect of Coverage and Scaling Relations. Journal of Physical Chemistry C, 2009, 113, 11041-11049.	1.5	33
7389	Effect of a NH Coadsorbate on the CH₃ (or CH₂) Adsorption to a Surface Step on Diamond (100). Journal of Physical Chemistry C, 2009, 113, 19891-19896.	1.5	11
7390	Band Engineering in Strained GaN/ultrathin InN/GaN Quantum Wells. Crystal Growth and Design, 2009, 9, 1698-1701.	1.4	12
7391	Structures and Energetics of SrFeO2.875 Calculated within the GGA + U Framework. Journal of Chemical Theory and Computation, 2009, 5, 2787-2797.	2.3	6

#	Article	IF	Citations
7392	Theoretical Study of the Adsorption of RNA/DNA Bases on the External Surfaces of Na⁺-Montmorillonite. Journal of Physical Chemistry C, 2009, 113, 13741-13749.	1.5	72
7393	Borohydride Oxidation over Au(111): A First-Principles Mechanistic Study Relevant to Direct Borohydride Fuel Cells. Journal of the Electrochemical Society, 2009, 156, B86.	1.3	70
7394	Hydrogen Interaction in Ti-Doped LiBH₄ for Hydrogen Storage: A Density Functional Analysis. Journal of Chemical Theory and Computation, 2009, 5, 3079-3087.	2.3	20
7395	Uncertainty and figure selection for DFT based cluster expansions for oxygen adsorption on Au and Pt (111) surfaces. Molecular Simulation, 2009, 35, 920-927.	0.9	35
7396	Structure and Electronic Properties of Saturated and Unsaturated Gallium Nitride Nanotubes. Journal of Physical Chemistry C, 2009, 113, 19281-19285.	1.5	14
7397	Direct Spectroscopic Observation of the Role of Humidity in Surface Diffusion through an Ionic Adsorbent Powder. The Behavior of Adsorbed Pyridine on Nanocrystalline MgO. Journal of Physical Chemistry C, 2009, 113, 2228-2234.	1.5	19
7398	Hydrogen occupancy in theRNi4Mg(R=Y, La, Ce, and Nd) intermetallic compounds and hydrides. Physical Review B, 2009, 80, .	1.1	6
7399	Transition-Metal Strings Templated on Boron-Doped Carbon Nanotubes: A DFT Investigation. Journal of Physical Chemistry C, 2009, 113, 15346-15354.	1.5	12
7400	Chainlike Auâˆ’O Structures on Au(110)-(1 Ã— r) Surfaces Calculated from First Principles. Journal of Physical Chemistry C, 2009, 113, 5690-5699.	1.5	16
7401	Semiconducting single-walled carbon nanotubes synthesized by S-doping. Nano-Micro Letters, 2009, 1, 9-13.	14.4	35
7402	Electronic Structures and Raman Features of a Carbon Nanobud. Journal of Physical Chemistry C, 2009, 113, 20822-20826.	1.5	30
7403	Chemisorption of Transition-Metal Atoms on Boron- and Nitrogen-Doped Carbon Nanotubes: Energetics and Geometric and Electronic Structures. Journal of Physical Chemistry C, 2009, 113, 7069-7078.	1.5	71
7404	A Theoretical Study of H₂ Reacting on Ti/Al(100) Surfaces. Journal of Physical Chemistry C, 2009, 113, 11027-11034.	1.5	17
7405	Triclinic CdSiO₃structural, electronic, and optical properties from first principles calculations. Journal Physics D: Applied Physics, 2009, 42, 155406.	1.3	22
7406	Geometric and Electronic Properties of Sn-Doped TiO₂ from First-Principles Calculations. Journal of Physical Chemistry C, 2009, 113, 650-653.	1.5	62
7407	Adsorption and diffusion of Au atoms on the (001) surface of Ti, Zr, Hf, V, Nb, Ta, and Mo carbides. Journal of Chemical Physics, 2009, 130, 244706.	1.2	17
7408	Surface Core Level Shift: High Sensitive Probe to Oxygen-Induced Reconstruction of Rh(100). Journal of Physical Chemistry C, 2009, 113, 13192-13198.	1.5	12
7409	First-Principles Studies of NO_xChemistry on Ag_n/Î±-Al₂O₃. Journal of Physical Chemistry C, 2009, 113, 3674-3682.	1.5	35

#	Article	IF	Citations
7410	Hostâ^'Guest Interactions, Uniform vs Fragmented Linear Atom Chains and Likeliness of Peierls Distortions in the (Ca7N4)[Mx] (M = Ag, Ga, In) Phases. Inorganic Chemistry, 2009, 48, 2919-2931.	1.9	2
7411	Ozone Oxidation of Single Walled Carbon Nanotubes from Density Functional Theory. Journal of Physical Chemistry C, 2009, 113, 17636-17642.	1.5	45
7412	Dissociative Adsorption of Methane on Surface Oxide Structures of Pdâ^'Pt Alloys. Journal of Physical Chemistry C, 2009, 113, 21097-21105.	1.5	18
7413	Growth of Carbon Structures on Stepped (211)Co Surfaces. Journal of Physical Chemistry C, 2009, 113, 15658-15666.	1.5	19
7414	On the Reversibility of Hydrogen-Storage Reactions in Ca(BH₄)₂: Characterization via Experiment and Theory. Journal of Physical Chemistry C, 2009, 113, 20088-20096.	1.5	59
7415	DFT Study of Planar Boron Sheets: A New Template for Hydrogen Storage. Journal of Physical Chemistry C, 2009, 113, 18962-18967.	1.5	130
7416	Stabilizing a molecular switch at solid surfaces: A density functional theory study of azobenzene on Cu(111), Ag(111), and Au(111). Physical Review B, 2009, 80, .	1.1	48
7417	Concerning the Possibility of Hidden One-Dimensional Fermi Surfaces for the K0.25WO3 Hexagonal Bronze. Inorganic Chemistry, 2009, 48, 11492-11494.	1.9	3
7418	Ground-state properties of simple elements from GW calculations. Physical Review B, 2009, 80, .	1.1	61
7419	Influence of Nickel Catalyst Geometry on the Dissociation Barriers of H₂ and CH₄: Ni₁₃ versus Ni(111). Journal of Physical Chemistry C, 2009, 113, 13715-13722.	1.5	42
7420	Density Functional Theory Study of Ferrihydrite and Related Fe-Oxyhydroxides. Chemistry of Materials, 2009, 21, 5727-5742.	3.2	81
7421	Manganese Borohydride As a Hydrogen-Storage Candidate: First-Principles Crystal Structure and Thermodynamic Properties. Journal of Physical Chemistry C, 2009, 113, 13416-13424.	1.5	19
7422	Vacancy trapping mechanism for hydrogen bubble formation in metal. Physical Review B, 2009, 79, .	1.1	268
7423	Size Independence and Doping Dependence of Bending Modulus in ZnO Nanowires. Crystal Growth and Design, 2009, 9, 1640-1642.	1.4	11
7424	Improving Levine model for dielectric constants of transition metal compounds. Journal of Applied Physics, 2009, 106, 094102.	1.1	7
7425	An Investigation of Distortions of the Dionâ^'Jacobson Phase RbSr₂Nb₃O₁₀ and Its Acid-Exchanged Form with ⁹³Nb Solid State NMR and DFT Calculations. Journal of Physical Chemistry C, 2009, 113, 17548-17559.	1.5	21
7426	Structural Stability and Elastic and Electronic Properties of Rhenium Borides: First Principle Investigations. Inorganic Chemistry, 2009, 48, 581-587.	1.9	33
7427	Structural Characterization of a Nanocrystalline Inorganicâ^'Organic Hybrid with Fiberlike Morphology and One-Dimensional Antiferromagnetic Properties. Chemistry of Materials, 2009, 21, 3356-3369.	3.2	36

#	Article	IF	Citations
7428	Edge-passivation induced half-metallicity of zigzag zinc oxide nanoribbons. Applied Physics Letters, 2009, 95, .	1.5	39
7429	Mechanism of Selective Hydrogenation of Î±,Î²-Unsaturated Aldehydes on Silver Catalysts: A Density Functional Study. Journal of Physical Chemistry C, 2009, 113, 13231-13240.	1.5	47
7430	Effect of oxygen on single-wall silicon carbide nanotubes studied by first-principles calculations. Physical Review B, 2009, 80, .	1.1	31
7431	SiC/Ti3SiC2interface: Atomic structure, energetics, and bonding. Physical Review B, 2009, 79, .	1.1	53
7432	Periodic density functional theory study of spin crossover in the cesium iron hexacyanochromate prussian blue analog. Journal of Chemical Physics, 2009, 130, 014702.	1.2	13
7433	Density functional theory study of hexagonal carbon phases. Journal of Physics Condensed Matter, 2009, 21, 235401.	0.7	5
7434	Phase stability and physical properties of<mml:math xmlns:mml="http://www.w3.org/1998/Math/MathML" display="inline"><mml:mrow><mml:msub><mml:mrow><mml:mtext>Ta</mml:mtext></mml:mrow><mml:mn>5</mml:mn></mml:msub from first-principles calculations. Physical Review B, 2009, 80, .	1.1	77
7435	A theoretical study of thermal stability and electronic properties of wurtzite and zincblende ZnO_xS_{1â^'x}. New Journal of Physics, 2009, 11, 093008.	1.2	42
7436	Interaction of hydrogen molecules on Ni-doped single-walled carbon nanotube. Chinese Physics B, 2009, 18, 357-362.	0.7	26
7437	First-principles study of the structural and elastic properties of zirconia. Physical Review B, 2009, 79, .	1.1	79
7438	First-principles calculations on the electronic and vibrational properties of Î²-V ₂ O ₅. Chinese Physics B, 2009, 18, 4988-4994.	0.7	20
7439	Adsorption of Late Transition Metal Atoms on MgO/Mo(100) and MgO/Ag(100) Ultrathin Films: A Comparative DFT Study. Journal of Physical Chemistry C, 2009, 113, 16694-16701.	1.5	37
7440	A theoretical study of silicon-doped boron nitride nanotubes serving as a potential chemical sensor for hydrogen cyanide. Nanotechnology, 2009, 20, 505704.	1.3	40
7441	First-principles characterization of the structure and electronic structure of<mml:math xmlns:mml="http://www.w3.org/1998/Math/MathML" display="inline"><mml:mrow><mml:mi>Î±</mml:mi><mml:mo>â^'</mml:mo><mml:mtext>S</mml:mtext></mml:mrow></mml:math ar Rh-S chalcogenides. Physical Review B, 2009, 80, .	1.1	23
7442	Ab initio study of the interaction of chlorides with defect-free hydroxylated NiO surfaces. Corrosion Science, 2009, 51, 941-948.	3.0	60
7443	Ab initio modelling of localized corrosion: Study of the role of surface steps in the interaction of chlorides with passivated nickel surfaces. Corrosion Science, 2009, 51, 2174-2182.	3.0	75
7444	FP-APW+lo study of the elastic, electronic and optical properties of the filled skutterudites CeFe4As12 and CeFe4Sb12. Current Opinion in Solid State and Materials Science, 2009, 13, 105-111.	5.6	51
7445	Electronic, electrical and thermodynamic properties of Ca5Si3 by first principles calculations and low temperature experimental techniques. Calphad: Computer Coupling of Phase Diagrams and Thermochemistry, 2009, 33, 260-264.	0.7	6

#	Article	IF	Citations
7446	Structural stability of intermetallic phases in the Snâ€“Ti system. Calphad: Computer Coupling of Phase Diagrams and Thermochemistry, 2009, 33, 250-259.	0.7	41
7447	Construction of modified embedded atom method potentials for the study of the bulk phase behaviour in binary Ptâ€“Rh, Ptâ€“Pd, Pdâ€“Rh and ternary Ptâ€“Pdâ€“Rh alloys. Calphad: Computer Coupling of Phase Diagrams and Thermochemistry, 2009, 33, 370-376.	0.7	28
7448	Thermodynamic modeling of the Crâ€“Ir binary system using the cluster/site approximation (CSA) coupling with first-principles energetic calculation. Calphad: Computer Coupling of Phase Diagrams and Thermochemistry, 2009, 33, 420-424.	0.7	10
7449	Thermodynamic investigation of the galvanizing systems, I: Refinement of the thermodynamic description for the Feâ€“Zn system. Calphad: Computer Coupling of Phase Diagrams and Thermochemistry, 2009, 33, 433-440.	0.7	44
7450	First-principles study of ground-state properties and phase stability of vanadium nitrides. Calphad: Computer Coupling of Phase Diagrams and Thermochemistry, 2009, 33, 469-477.	0.7	19
7451	Thermodynamic modeling of the Snâ€“V binary system. Calphad: Computer Coupling of Phase Diagrams and Thermochemistry, 2009, 33, 539-544.	0.7	12
7452	Thermodynamic and ab initio investigation of the Cuâ€“Dy system. Calphad: Computer Coupling of Phase Diagrams and Thermochemistry, 2009, 33, 511-516.	0.7	8
7453	Thermodynamic modeling of the Siâ€“Sr system. Calphad: Computer Coupling of Phase Diagrams and Thermochemistry, 2009, 33, 550-556.	0.7	10
7454	Thermodynamic modeling of the Mgâ€“Si system with the Kaptay equation for the excess Gibbs energy of the liquid phase. Calphad: Computer Coupling of Phase Diagrams and Thermochemistry, 2009, 33, 673-678.	0.7	42
7455	A thermodynamic description of the Geâ€“Sr system acquired via a hybrid approach of CALPHAD and first-principles calculations. Calphad: Computer Coupling of Phase Diagrams and Thermochemistry, 2009, 33, 719-722.	0.7	7
7456	First-principles study of binary special quasirandom structures for the Alâ€“Cu, Alâ€“Si, Cuâ€“Si, and Mgâ€“Si systems. Calphad: Computer Coupling of Phase Diagrams and Thermochemistry, 2009, 33, 769-773.	0.7	17
7457	Structure and elasticity of serpentine at high-pressure. Earth and Planetary Science Letters, 2009, 279, 11-19.	1.8	86
7458	Structural control over equilibrium silicon and oxygen isotopic fractionation: A first-principles density-functional theory study. Chemical Geology, 2009, 258, 28-37.	1.4	128
7459	D/H isotopic fractionation between brucite Mg(OH)2 and water from first-principles vibrational modeling. Chemical Geology, 2009, 262, 159-168.	1.4	37
7460	Vibrational properties of the filled tetrahedral compounds LiCdP and LiCdAs. Computational Materials Science, 2009, 44, 876-880.	1.4	5
7461	Ab initio modeling of electronic and optical properties of hafnium silicates. Computational Materials Science, 2009, 44, 929-932.	1.4	4
7462	DFT calculation of the stability and mobility of noble gas atoms in silicon. Computational Materials Science, 2009, 44, 1030-1033.	1.4	13
7463	First principles study on the structural properties and electronic structure of X2B (X=Cr, Mn, Fe, Co,) Tj ETQq1 1 0.784314 rgBT /Over	1.4	109

#	Article	IF	Citations
7464	Structural stabilities, electronic structures and lithium deintercalation in LixMSiO4 (M=Mn, Fe, Co,) Tj ETQq0 0 0 rgBT /Overlock 10 Tf 50	1.4	106
7465	Shallow donors in diamond: Be and Mg. Computational Materials Science, 2009, 44, 1286-1290.	1.4	8
7466	Substitutional solution of silicon in cementite: A first-principles study. Computational Materials Science, 2009, 44, 1319-1326.	1.4	78
7467	First-principles study of the (110) polar surface of cubic PbTiO3. Computational Materials Science, 2009, 44, 1360-1365.	1.4	18
7468	The first-principles study of LaSe and LaTe in B1 and B2 structures. Computational Materials Science, 2009, 44, 1371-1378.	1.4	15
7469	First-principles study of zinc-blende to rocksalt phase transition in BP and BAs. Computational Materials Science, 2009, 44, 1386-1389.	1.4	24
7470	Structural and electronic properties of iodine-doped anatase and rutile TiO2. Computational Materials Science, 2009, 45, 223-228.	1.4	46
7471	Atomistic simulation of Feâ€“C austenite. Computational Materials Science, 2009, 45, 235-239.	1.4	23
7472	Ab initio calculations of the relationship between the alpha alumina toughness and its electronic structure under pressure. Computational Materials Science, 2009, 45, 310-314.	1.4	5
7473	Ab initio study of confinement and surface effects in hexagonal AlN nanotubes. Computational Materials Science, 2009, 45, 305-309.	1.4	21
7474	FP-APW+lo calculations of the elastic properties in zinc-blende III-P compounds under pressure effects. Computational Materials Science, 2009, 45, 474-479.	1.4	137
7475	First principles calculations of the electronic, dynamical, and thermodynamic properties of the rocksalt ScX (X=N, P, As, Sb). Computational Materials Science, 2009, 45, 1025-1030.	1.4	25
7476	First-principles study of structural, elastic, electronic, and thermal properties of LaAlO3 perovskite. Computational Materials Science, 2009, 45, 1068-1072.	1.4	29
7477	Structure and bonding features of ZrB2(0001) surface. Computational Materials Science, 2009, 46, 1-6.	1.4	37
7478	First-principles study on the structural, elastic, and electronic properties of Î³-LiAlO2. Computational Materials Science, 2009, 46, 221-224.	1.4	26
7479	Local modes of vibration at the vacancy and vacancy models of defects in diamond. Computational Materials Science, 2009, 46, 520-523.	1.4	2
7480	Prediction study of the structural, elastic and electronic properties of ANSr3 (A=As, Sb and Bi). Computational Materials Science, 2009, 46, 881-886.	1.4	22
7481	Structural, elastic and electronic properties of intermetallics in the Ptâ€“Sn system: A density functional investigation. Computational Materials Science, 2009, 46, 921-931.	1.4	93

#	Article	IF	Citations
7482	Elastic, electronic and optical properties of cubic antiperovskites SbNCa3 and BiNCa3. Computational Materials Science, 2009, 46, 1051-1057.	1.4	64
7483	Structural and electronic properties of BiOX (X=F, Cl, Br, I) considering Bi 5f states. Computational Materials Science, 2009, 46, 1076-1084.	1.4	36
7484	First principles investigation on the structural, mechanical and electronic properties of OsC2. Computational Materials Science, 2009, 46, 1098-1101.	1.4	16
7485	First-principles calculations of structural, electronic and elastic properties of Ca2MgSi2O7. Computational Materials Science, 2009, 47, 35-40.	1.4	5
7486	Structural stabilities, electronic and optical properties of CaF2 under high pressure: A first-principles study. Computational Materials Science, 2009, 47, 41-45.	1.4	18
7487	NO adsorption effects on various functional molecular nanowires. Computational Materials Science, 2009, 47, 111-120.	1.4	8
7488	Density-functional tight-binding for beginners. Computational Materials Science, 2009, 47, 237-253.	1.4	324
7489	Effects of alloying elements on elastic properties of Ni by first-principles calculations. Computational Materials Science, 2009, 47, 254-260.	1.4	78
7490	First-principles calculations of mechanical and thermodynamic properties of the Laves C15-Mg2RE (RE=La, Ce, Pr, Nd, Pm, Sm, Gd). Computational Materials Science, 2009, 47, 297-301.	1.4	23
7491	Ab initio calculation of the elastic properties and the lattice dynamics of the AgBr1â^'xClx alloy. Computational Materials Science, 2009, 47, 308-313.	1.4	12
7492	First-principles study of Ni/Ni3Al interface strengthening by alloying elements. Computational Materials Science, 2009, 47, 320-325.	1.4	43
7493	Theoretical study of mechanical, electronic, chemical bonding and optical properties of Ti2SnC, Zr2SnC, Hf2SnC and Nb2SnC. Computational Materials Science, 2009, 47, 491-500.	1.4	95
7494	Comparison of interaction between Cu precipitate and vacancy in Fe using first-principle calculations and empirical N-body potential calculations. Computational Materials Science, 2009, 47, 521-525.	1.4	6
7495	First principles study of structural phase stability of wide-gap semiconductors MgTe, MgS and MgSe. Computational Materials Science, 2009, 47, 593-598.	1.4	71
7496	Zinc surface complexes on birnessite: A density functional theory study. Geochimica Et Cosmochimica Acta, 2009, 73, 1273-1284.	1.6	63
7497	On the role of Mn(IV) vacancies in the photoreductive dissolution of hexagonal birnessite. Geochimica Et Cosmochimica Acta, 2009, 73, 4142-4150.	1.6	87
7498	Iron isotope fractionation between pyrite (FeS2), hematite (Fe2O3) and siderite (FeCO3): A first-principles density functional theory study. Geochimica Et Cosmochimica Acta, 2009, 73, 6565-6578.	1.6	173
7499	Elasticity and Raman and infrared spectra of MgAl2O4 spinel from density functional perturbation theory. Physics of the Earth and Planetary Interiors, 2009, 174, 113-121.	0.7	46

#	Article	IF	Citations
7500	Elastic properties of Î´-AlOOH under pressure: First principles investigation. Physics of the Earth and Planetary Interiors, 2009, 174, 122-127.	0.7	58
7501	Theory and computer simulation of perfect and defective solids. Progress in Solid State Chemistry, 2009, 37, 70-80.	3.9	4
7502	Elastic constants of binary Mg compounds from first-principles calculations. Intermetallics, 2009, 17, 313-318.	1.8	212
7503	First-principles investigation of migration barriers and point defect complexes in B2â€“NiAl. Intermetallics, 2009, 17, 319-329.	1.8	35
7504	Effect of O impurity on structure and mechanical properties of NiAl intermetallics: A first-principles study. Intermetallics, 2009, 17, 358-364.	1.8	36
7505	First-principles study of the ideal cleavage fracture of Cr2Nb microalloyed by X (Al, Ni, Co, Ti). Intermetallics, 2009, 17, 394-399.	1.8	15
7506	First-principles calculations on the electronic structure and cohesive properties of titanium stannides. Intermetallics, 2009, 17, 768-773.	1.8	20
7507	Enthalpies of formation of magnesium compounds from first-principles calculations. Intermetallics, 2009, 17, 878-885.	1.8	159
7508	A concerted rational crystallization/amorphization mechanism of Ge2Sb2Te5. Journal of Non-Crystalline Solids, 2009, 355, 2122-2126.	1.5	10
7509	Structural stability of high-pressure phase in the immiscible Cuâ€“Nb system studied by lattice dynamics calculation. Journal of Alloys and Compounds, 2009, 468, 299-302.	2.8	1
7510	Pressure-induced phase transition and metallization of solid ZnSe. Journal of Alloys and Compounds, 2009, 472, 294-298.	2.8	22
7511	Ab initio study of the phase stability and mechanical properties of 5d transition metal nitrides MN2. Journal of Alloys and Compounds, 2009, 472, 425-428.	2.8	17
7512	Structural and elastic properties of Î³TiAl under high pressure from electronic structure calculations. Journal of Alloys and Compounds, 2009, 473, 255-261.	2.8	29
7513	Jahnâ€“Teller distortion and electronic structure of LiMn2O4. Journal of Alloys and Compounds, 2009, 474, 370-374.	2.8	169
7514	Thermodynamic and electronic properties of quaternary hydrides LixNa1â^'xMgH3. Journal of Alloys and Compounds, 2009, 474, 522-526.	2.8	23
7515	First-principles study of Be content on the structural and mechanical properties of TiAl alloy. Journal of Alloys and Compounds, 2009, 475, 401-407.	2.8	11
7516	Enthalpies of formation of the Laâ€“Zn compounds between 298K and 910K. Journal of Alloys and Compounds, 2009, 475, 79-85.	2.8	18
7517	Strong composition-dependent disorder in InAs1â^'xNx alloys. Journal of Alloys and Compounds, 2009, 475, 592-594.	2.8	3

#	Article	IF	Citations
7518	First-principles calculations on structure and elasticity of wurtzite-type indium nitride under pressure. Journal of Alloys and Compounds, 2009, 475, 885-888.	2.8	10
7519	Structural and electronic properties of ZnO under high pressure. Journal of Alloys and Compounds, 2009, 476, 306-310.	2.8	42
7520	A first-principles study of the Laâ€“H system. Journal of Alloys and Compounds, 2009, 480, 111-113.	2.8	10
7521	Volume dependent vibrational properties of cerium hydrides from first principles. Journal of Alloys and Compounds, 2009, 477, 478-483.	2.8	11
7522	Theoretical investigation of zincblende AlSb and GaSb compounds. Journal of Alloys and Compounds, 2009, 478, 653-656.	2.8	14
7523	Theoretical investigation of the electronic and optical properties of Zn2OX (X=S, Se, Te) in chalcopyrite phase by full potential methods. Journal of Alloys and Compounds, 2009, 479, 414-419.	2.8	5
7524	Phase transition and thermodynamic properties of MgTe under high pressure. Journal of Alloys and Compounds, 2009, 480, 587-591.	2.8	8
7525	Adsorption and dissociation of hydrogen on MgO surface: A first-principles study. Journal of Alloys and Compounds, 2009, 480, 788-793.	2.8	61
7526	Absence of the bowing character in the common-anion IIâ€“VI ternary alloys. Journal of Alloys and Compounds, 2009, 481, 340-344.	2.8	12
7527	Stability field of the high-(P, T) Re2C phase and properties of an analogous osmium carbide phase. Journal of Alloys and Compounds, 2009, 481, 577-581.	2.8	50
7528	The strengthening effect of Al atoms into Mgâ€“Al alloy: A first-principles study. Journal of Alloys and Compounds, 2009, 482, 540-543.	2.8	19
7529	Elastic properties and pressure induced transitions of ZnO polymorphs from first-principle calculations. Journal of Alloys and Compounds, 2009, 484, 431-438.	2.8	85
7530	High-pressure structural, electronic and optical properties of KMgF3: A first-principles study. Journal of Alloys and Compounds, 2009, 484, 597-600.	2.8	21
7531	Thermodynamics, lattice stability and defect structure of strontium silicides via first-principles calculations. Journal of Alloys and Compounds, 2009, 484, 822-831.	2.8	11
7532	Thermal conductivity of ZnTe investigated by molecular dynamics. Journal of Alloys and Compounds, 2009, 485, 488-492.	2.8	14
7533	First-principles calculations of mechanical properties of TiC and TiN. Journal of Alloys and Compounds, 2009, 485, 542-547.	2.8	225
7534	Microstructure and electronic characteristics of the 6H-type ABACAB LPSO structure in Mg97Zn1Y2 alloy. Journal of Alloys and Compounds, 2009, 485, 672-676.	2.8	24
7535	Electronic structure and optical properties of In doped SrTiO3/MgO(001). Journal of Alloys and Compounds, 2009, 485, 598-603.	2.8	2

#	Article	IF	Citations
7536	First-principles calculation of impurity doping into Mg2Ge. Journal of Alloys and Compounds, 2009, 485, 764-768.	2.8	22
7537	Ab initio investigation of the surface properties of dispenser B-type and scandate thermionic emission cathodes. Applied Physics Letters, 2009, 94, .	1.5	33
7538	Insight from first principles into the nature of the bonding between water molecules and 4d metal surfaces. Journal of Chemical Physics, 2009, 130, 184707.	1.2	94
7539	Ab initiocalculation of the elastic properties and the lattice dynamics of the ZnxCd1âˆ'xSe alloy. Semiconductor Science and Technology, 2009, 24, 045005.	1.0	25
7540	Electronic structure and phase stability of MgTe, ZnTe, CdTe, and their alloys in theB3,B4, andB8 structures. Physical Review B, 2009, 79, .	1.1	55
7541	Crystal Structures of Calcium Borohydride: Theory and Experiment. Journal of Physical Chemistry C, 2009, 113, 3352-3358.	1.5	54
7542	High-pressure structures and vibrational spectra of barium fluoride: Results obtained under nearly hydrostatic conditions. Physical Review B, 2009, 79, .	1.1	13
7543	Ab initio equation of state of<mml:math xmlns:mml="http://www.w3.org/1998/Math/MathML" display="inline"><mml:mi>Î±</mml:mi></mml:math>- and<mml:math xmlns:mml="http://www.w3.org/1998/Math/MathML" display="inline"><mml:mi>Î²</mml:mi></mml:math>-boron: Possible amorphization of<mml:math xmlns:mml="http://www.w3.org/1998/Math/MathML" display="inline"><mml:mi>Î²</mml:mi></mml:math>-boron under high pressure. Physical Review B, 2009,	1.1	19
7544	FP-APW+lo calculations of the electronic and optical properties of alkali metal sulfides under pressure. Journal of Physics Condensed Matter, 2009, 21, 095404.	0.7	32
7545	Interactions of Organic Molecules with Calcite and Magnesite Surfaces. Journal of Physical Chemistry C, 2009, 113, 3666-3673.	1.5	55
7546	Intrinsic ferromagnetism in CeO₂: dispelling the myth of vacancy site localization mediated superexchange. Journal of Physics Condensed Matter, 2009, 21, 405502.	0.7	35
7547	First-principles investigation of mechanical and electronic properties of MNNi3 (M=Zn, Mg, or Cd). Journal of Applied Physics, 2009, 105, 123921.	1.1	26
7548	Vinyl Acetate Synthesis on Homogeneous and Heterogeneous Pd-Based Catalysts: A Theoretical Analysis on the Reaction Mechanisms. Journal of Physical Chemistry A, 2009, 113, 11758-11762.	1.1	13
7549	Density functional theory for transition metals and transition metal chemistry. Physical Chemistry Chemical Physics, 2009, 11, 10757.	1.3	1,431
7550	First-principles study of the electronic, optical, and lattice dynamics properties of LiInSe2 polymorph. Journal of Applied Physics, 2009, 106, .	1.1	23
7551	Weak ferromagnetism in Mn nanochains on the CuN surface. Physical Review B, 2009, 79, .	1.1	47
7552	Accurate calculation of the local density of optical states in inverse-opal photonic crystals. Journal of the Optical Society of America B: Optical Physics, 2009, 26, 987.	0.9	39
7553	Bulk and key surface structures of hematite, magnetite, and goethite: A density functional theory study. American Mineralogist, 2009, 94, 1341-1350.	0.9	47

#	Article	IF	Citations
7554	Calculations of ZnO properties using the Heyd-Scuseria-Ernzerhof screened hybrid density functional. Physical Review B, 2009, 80, .	1.1	101
7555	Pt-incorporated anatase<mml:math xmlns:mml="http://www.w3.org/1998/Math/MathML" display="inline"><mml:mrow><mml:msub><mml:mrow><mml:mtext>TiO</mml:mtext></mml:mrow><mml:mn>2</mml:mn></mml:msub></mml:mrow></mml:math> for solar cell applications: First-principles density functional theory calculations. Physical Review B, 2009, 79, .	1.1	28
7556	Iron Endohedral-Doped Boron Fullerene: A Potential Single Molecular Device with Tunable Electronic and Magnetic Properties. Journal of Physical Chemistry C, 2009, 113, 18292-18295.	1.5	26
7557	Hydrogen in beryllium: Solubility, transport, and trapping. Physical Review B, 2009, 79, .	1.1	51
7558	Metal-Embedded Graphene: A Possible Catalyst with High Activity. Journal of Physical Chemistry C, 2009, 113, 20156-20160.	1.5	407
7559	Density functional characterization of the electronic structure and optical properties of Cr-doped SrTiO₃. Journal Physics D: Applied Physics, 2009, 42, 055401.	1.3	61
7560	Quantum dynamics of hydrogen interacting with single-walled carbon nanotubes. Journal of Chemical Physics, 2009, 130, 064701.	1.2	13
7561	Hydrogenation of bilayer graphene and the formation of bilayer graphane from first principles. Physical Review B, 2009, 80, .	1.1	120
7562	Site occupation in the Cr-Ru and Cr-Os<mml:math xmlns:mml="http://www.w3.org/1998/Math/MathML" display="inline"><mml:mi>Ïf</mml:mi></mml:math>phases. Physical Review B, 2009, 80, .	1.1	19
7563	First-principles study on ferromagnetism in Mg-doped SnO2. Applied Physics Letters, 2009, 95, .	1.5	109
7564	DFT Analysis of the Reaction Paths of Formaldehyde Decomposition on Silver. Journal of Physical Chemistry A, 2009, 113, 8125-8131.	1.1	28
7565	Structural Investigation of Activated Lattice Oxygen in Ce_{1âˆ’x}Sn_xO₂ and Ce_{1âˆ’xâˆ’y}Sn_xPd_yO_{2âˆ’Î´} by EXAFS and DFT calculation. Chemistry of Materials, 2009, 21, 5836-5847.	3.2	63
7566	B₂C Graphene, Nanotubes, and Nanoribbons. Nano Letters, 2009, 9, 1577-1582.	4.5	154
7567	Comparison of Electronic and Magnetic Properties of Fe, Co, and Ni Nanowires Encapsulated in Boron Nitride Nanotubes. Journal of Physical Chemistry C, 2009, 113, 17745-17750.	1.5	23
7568	Interaction of graphene with FCCâ€“Co(111). Physical Chemistry Chemical Physics, 2009, 11, 803-807.	1.3	53
7569	Magnetic properties of first-row element-doped ZnS semiconductors: A density functional theory investigation. Physical Review B, 2009, 80, .	1.1	79
7570	First Principles Calculations of Electronic Band Structure and Optical Properties of Cr-Doped ZnO. Journal of Physical Chemistry C, 2009, 113, 8460-8464.	1.5	229
7571	¹⁹F Chemical Shift of Crystalline Metal Fluorides: Theoretical Predictions Based on Periodic Structure Models. Journal of Physical Chemistry C, 2009, 113, 15018-15023.	1.5	61

#	Article	IF	Citations
7572	The importance of chargeâ€“quadrupole interactions for H2adsorption and diffusion in CuBTC. Molecular Simulation, 2009, 35, 60-69.	0.9	39
7573	Enhancement of Chemical Activity in Corrugated Graphene. Journal of Physical Chemistry C, 2009, 113, 14176-14178.	1.5	216
7574	The role of the Pb2+ 6s lone pair in the structure of the double perovskite Pb2ScSbO6. Dalton Transactions, 2009, , 5453.	1.6	22
7575	Band Structures of Narrow Zigzag Silicon Carbon Nanoribbons. Journal of Physical Chemistry C, 2009, 113, 12637-12640.	1.5	87
7576	Methanol to Olefin Conversion on HSAPO-34 Zeolite from Periodic Density Functional Theory Calculations: A Complete Cycle of Side Chain Hydrocarbon Pool Mechanism. Journal of Physical Chemistry C, 2009, 113, 4584-4591.	1.5	102
7577	Structural, electronic and magnetic properties of V2O5âˆ’x: An ab initio study. Journal of Chemical Physics, 2009, 130, 214704.	1.2	36
7578	bcc-to-hcp transformation pathways for iron versus hydrostatic pressure: Coupled shuffle and shear modes. Physical Review B, 2009, 79, .	1.1	44
7579	Ab initio Study on the Structural Stability and Magnetism of Metastable A3B Phases in Niâ€“Au (Cu, Zn,) Tj ETQq1 1 0.784314 rgBT /O	0.7	1
7580	Electronic structure of two-dimensional crystals fromab initiotheory. Physical Review B, 2009, 79, .	1.1	941
7581	Reaction Mechanisms for the CO Oxidation on Au/CeO₂ Catalysts: Activity of Substitutional Au³⁺/Au⁺ Cations and Deactivation of Supported Au⁺ Adatoms. Journal of the American Chemical Society, 2009, 131, 10473-10483.	6.6	304
7582	THEORETICAL STUDIES ON THE EXTRINSIC DEFECTS OF MONTMORILLONITE IN SOFT ROCK. Modern Physics Letters B, 2009, 23, 2933-2941.	1.0	11
7583	Visible Light-Induced Photocatalytic Oxidation of Phenol and Aqueous Ammonia in Flowerlike Bi₂Fe₄O₉ Suspensions. Journal of Physical Chemistry C, 2009, 113, 12826-12831.	1.5	131
7584	Ab Initio Study of Stability and Site-Specific Oxygen Adsorption Energies of Pt Nanoparticles. Journal of Physical Chemistry C, 2009, 113, 17989-17996.	1.5	75
7585	Calculation of NMR chemical shifts in organic solids: Accounting for motional effects. Journal of Chemical Physics, 2009, 130, 104701.	1.2	93
7586	Band-to-Band Visible-Light Photon Excitation and Photoactivity Induced by Homogeneous Nitrogen Doping in Layered Titanates. Chemistry of Materials, 2009, 21, 1266-1274.	3.2	284
7587	Identification of a Frenkel-pair defect in electron-irradiated 3<mml:math xmlns:mml="http://www.w3.org/1998/Math/MathML" display="inline"><mml:mrow><mml:mi>C</mml:mi></mml:mrow></mml:math>SiC. Physical Review B, 2009, 80, .	1.1	10
7588	Development of interatomic potentials appropriate for simulation of solidâ€“liquid interface properties in Alâ€“Mg alloys. Philosophical Magazine, 2009, 89, 3269-3285.	0.7	120
7589	Water on graphene: Hydrophobicity and dipole moment using density functional theory. Physical Review B, 2009, 79, .	1.1	312

#	Article	IF	Citations
7590	Point defects in CaF2 and CeO2 investigated by the periodic electrostatic embedded cluster method. Journal of Chemical Physics, 2009, 130, 174710.	1.2	88
7591	Spin Channels in Functionalized Graphene Nanoribbons. Nano Letters, 2009, 9, 3425-3429.	4.5	103
7592	Effects of uniaxial strain on the band structure of boron nitride nanotubes: a first principles study. EPJ Applied Physics, 2009, 46, 20601.	0.3	8
7593	Surface energies, work functions, and surface relaxations of low-index metallic surfaces from first principles. Physical Review B, 2009, 80, .	1.1	407
7594	First-principles calculation of nitrogen-tungsten codoping effects on the band structure of anatase-titania. Applied Physics Letters, 2009, 94, .	1.5	113
7595	Correlation-induced anomalies and extreme sensitivity in fcc Pu. Philosophical Magazine, 2009, 89, 1813-1822.	0.7	12
7596	High CO tolerance of Pt/Ru nanocatalyst: Insight from first principles calculations. Journal of Chemical Physics, 2009, 130, 124714.	1.2	27
7597	Application of density functional theory to CO tolerance in fuel cells: a brief review. Journal of Physics Condensed Matter, 2009, 21, 474226.	0.7	8
7598	Ab Initio Study of Hydrogen Adsorption in MOF-5. Journal of the American Chemical Society, 2009, 131, 4143-4150.	6.6	225
7599	H-Bond Features of Fully Hydroxylated Surfaces of Crystalline Silica Polymorphs: A Periodic B3LYP Study. Journal of Physical Chemistry C, 2009, 113, 17876-17884.	1.5	54
7600	Local environment analysis of dopants in ceramics by x-ray absorption near-edge structure with the aid of first-principles calculations. Journal of Physics Condensed Matter, 2009, 21, 104211.	0.7	12
7601	Structural, electronic, and magnetic properties of iron carbide<mml:math xmlns:mml="http://www.w3.org/1998/Math/MathML" display="inline"><mml:mrow><mml:msub><mml:mrow><mml:mtext>Fe</mml:mtext></mml:mrow><mml:mn>7</mml:mn></mml:msub> from first-principles theory. Physical Review B, 2009, 80, .	1.1	82
7602	Density functional theory study of Fe(II) adsorption and oxidation on goethite surfaces. Physical Review B, 2009, 79, .	1.1	59
7603	Influence of indium clustering on the band structure of semiconducting ternary and quaternary nitride alloys. Physical Review B, 2009, 80, .	1.1	132
7604	A proposal for an unusually stiff and moderately ductile hard coating material: Mo₂BC. Journal Physics D: Applied Physics, 2009, 42, 185406.	1.3	75
7605	Hydrogen doping in indium oxide: Anab initiostudy. Physical Review B, 2009, 80, .	1.1	167
7606	Density functional theory studies of the structural, electronic, and phonon properties of<mml:math xmlns:mml="http://www.w3.org/1998/Math/MathML" display="inline"><mml:mrow><mml:msub><mml:mrow><mml:mtext>Li</mml:mtext></mml:mrow><mml:mn>2</mml:mn></mml:msub> xmlns:mml="http://www.w3.org/1998/Math/MathML" display="inline"><mml:mrow><mml:msub><mml:mrow><mml:mtext>Li</mml:mtext></mml:mrow><mml:mn>2</mml:mn></mml:msub> Physical Review B, 2009, 79, .	1.1	92
7607	The effect of Fe doping on adsorption of CO₂/N₂within carbon nanotubes: a density functional theory study with dispersion corrections. Nanotechnology, 2009, 20, 375701.	1.3	22

#	Article	IF	Citations
7608	The vibrational spectrum of lizardite-1T [Mg3Si2O5(OH)4] at the Â point: A contribution from an ab initio periodic B3LYP calculation. American Mineralogist, 2009, 94, 986-994.	0.9	41
7609	Lattice dielectric and thermodynamic properties of yttria stabilized zirconia solids. Journal of Physics Condensed Matter, 2009, 21, 145402.	0.7	14
7610	Density Functional Theory Study of CO Hydrogenation on a MoS₂ Surface. Journal of Physical Chemistry C, 2009, 113, 5238-5243.	1.5	83
7611	Density Functional Theory Study of the Adsorption of Au Atom on Cerium Oxide: Effect of Low-Coordinated Surface Sites. Journal of Physical Chemistry C, 2009, 113, 4948-4954.	1.5	54
7612	Magnetic Properties and Vapochromic Reversible Guest-Induced Transformation in a Bispyrazolato Copper(II) Polymer: an Experimental and Dispersion-Corrected Density Functional Theory Study. Inorganic Chemistry, 2009, 48, 4044-4051.	1.9	44
7613	Effect of magnetic state on the<mml:math xmlns:mml="http://www.w3.org/1998/Math/MathML" display="inline"><mml:mrow><mml:mi>Î³</mml:mi><mml:mtext>â^'</mml:mtext><mml:mi>Î±</mml:mi></mml:mrow></mml:math>tra in iron: First-principles calculations of the Bain transformation path. Physical Review B, 2009, 79, .	1.1	61
7614	Energetic and Electronic Structure Analysis of Intrinsic Defects in SnO₂. Journal of Physical Chemistry C, 2009, 113, 439-448.	1.5	287
7615	Structural, electronic and vibrational properties of tetragonal zirconia under pressure: a density functional theory study. Journal of Physics Condensed Matter, 2009, 21, 485404.	0.7	97
7616	Ab initio thermodynamic evaluation of Pd atom interaction with CeO2 surfaces. Journal of Chemical Physics, 2009, 131, 084701.	1.2	51
7617	The anharmonic phonon decay rate in group-III nitrides. Journal of Physics Condensed Matter, 2009, 21, 174205.	0.7	19
7618	First principles study of Si-doped BC2N nanotubes. Journal of Chemical Physics, 2009, 130, 114710.	1.2	18
7619	Density functional theory study of graphite oxide for different oxidation levels. Physical Review B, 2009, 79, .	1.1	224
7620	Heyd-Scuseria-Ernzerhof hybrid functional for calculating the lattice dynamics of semiconductors. Physical Review B, 2009, 80, .	1.1	164
7621	Electronic and magnetic structure of<mml:math xmlns:mml="http://www.w3.org/1998/Math/MathML" display="inline"><mml:mrow><mml:msub><mml:mrow><mml:mtext>Fe</mml:mtext></mml:mrow><mml:mn>3</mml:mn></mml:msub> xmlns:mml="http://www.w3.org/1998/Math/MathML" display="inline"><mml:mrow><mml:mtext>GGA</mml:mtext><mml:mo>+</mml:mo><mml:mtext>U</mml:mtext></mml:mrow></mml:math> Physical Review B, 2009, 79, .	1.1	61
7622	Molecular Dynamics Simulations of Au Penetration through Alkanethiol Monolayers on the Au(111) Surface. Journal of Physical Chemistry C, 2009, 113, 6360-6366.	1.5	7
7623	Atomistic Origins of Molecular Memristors. Journal of Physical Chemistry C, 2009, 113, 20713-20718.	1.5	20
7624	Structure Sensitivity of Methanol Electrooxidation on Transition Metals. Journal of the American Chemical Society, 2009, 131, 14381-14389.	6.6	203
7625	Charge redistribution in core-shell nanoparticles to promote oxygen reduction. Journal of Chemical Physics, 2009, 130, 194504.	1.2	141

#	Article	IF	Citations
7626	First principles determination of structural, electronic and lattice dynamical properties of a model dipeptide molecular crystal. Molecular Physics, 2009, 107, 2201-2212.	0.8	6
7627	Molecular dynamics simulation of the effect of pH on the adsorption of rhodamine laser dyes on TiO₂hydroxylated surfaces. Molecular Simulation, 2009, 35, 1140-1151.	0.9	15
7628	Hybrid functional study of prototypical multiferroic bismuth ferrite. Physical Review B, 2009, 79, .	1.1	63
7629	Influence of Formamide on the Crystal Habit of LiF, NaCl, and KI: A DFT and Aqueous Solvent Model Study. Crystal Growth and Design, 2009, 9, 77-81.	1.4	24
7630	Ab initiorefinement of the thermal equation of state for bcc tantalum: the effect of bonding on anharmonicity. Journal of Physics Condensed Matter, 2009, 21, 095408.	0.7	29
7631	Structural and Electronic Properties of Finite Carbon Chains Encapsulated into Carbon Nanotubes. Journal of Physical Chemistry C, 2009, 113, 21314-21318.	1.5	8
7632	Formation entropies of intrinsic point defects in cubic In2O3 from first-principles density functional theory calculations. Physical Chemistry Chemical Physics, 2009, 11, 3226.	1.3	41
7633	First-principles approaches to intrinsic strength and deformation of materials: perfect crystals, nano-structures, surfaces and interfaces. Modelling and Simulation in Materials Science and Engineering, 2009, 17, 013001.	0.8	106
7634	First principles studies of silicon as a negative electrode material for lithium-ion batteries. Canadian Journal of Physics, 2009, 87, 625-632.	0.4	53
7635	Carbon nanotubes randomly decorated with gold clusters: from nano²hybrid atomic structures to gas sensing prototypes. Nanotechnology, 2009, 20, 375501.	1.3	109
7636	Updated references for the structural, electronic, and vibrational properties of TiO2(B) bulk using first-principles density functional theory calculations. Journal of Chemical Physics, 2009, 130, 204501.	1.2	99
7637	Pnictogen height as a possible switch between high-<mml:math xmlns:mml="http://www.w3.org/1998/Math/MathML" display="inline"><mml:mrow><mml:msub><mml:mi>T</mml:mi><mml:mi>c</mml:mi></mml:msub></mml:mrow></mml:math>nodes and low-<mml:math xmlns:mml="http://www.w3.org/1998/Math/MathML" display="inline"><mml:mrow><mml:msub><mml:mi>T</mml:mi><mml:mi>c</mml:mi></mml:msub></mml:mrow></mml:math>nodal pnictogen in iron-based superconductors. Physical Review B, 2009, 79, .	1.1	615
7638	Influence of Si and N additions on structure and phase stability of Ge₂Sb₂Te₅thin films. Journal of Physics Condensed Matter, 2009, 21, 435501.	0.7	16
7639	Mechanisms of molecular doping of graphene: A first-principles study. Physical Review B, 2009, 80, .	1.1	40
7640	First-principles study of elastic and phonon properties of the heavy fermion compound CeMg. Journal of Physics Condensed Matter, 2009, 21, 246001.	0.7	24
7641	Density Functional Characterization of the Electronic Structure and Optical Properties of N-Doped, La-Doped, and N/La-Codoped SrTiO₃. Journal of Physical Chemistry C, 2009, 113, 15046-15050.	1.5	88
7642	Quantum-mechanical calculations of zircon to scheelite transition pathways inZrSiO4. Physical Review B, 2009, 79, .	1.1	27
7643	Evolving properties of two-dimensional materials: from graphene to graphite. Journal of Physics Condensed Matter, 2009, 21, 335502.	0.7	74

#	Article	IF	Citations
7644	Phonon Dispersion and Thermodynamics Properties of CaF 2 via Shell Model Molecular Dynamics Simulations. Communications in Theoretical Physics, 2009, 51, 904-908.	1.1	3
7645	First-principles study of the atomic and electronic structures of crystalline and amorphousB4C. Physical Review B, 2009, 80, .	1.1	38
7646	Impact of Perfluorination on the Charge-Transport Parameters of Oligoacene Crystals. Journal of the American Chemical Society, 2009, 131, 1502-1512.	6.6	174
7647	Atomic and electronic structure of single and multiple vacancies in GaN nanowires from first-principles. Physical Review B, 2009, 79, .	1.1	32
7648	Synergistic Effects of Bi/S Codoping on Visible Light-Activated Anatase TiO₂ Photocatalysts from First Principles. Journal of Physical Chemistry C, 2009, 113, 8373-8377.	1.5	49
7649	Adsorption of selected ions on the anatase TiO₂(101) surface: a density-functional study. Molecular Simulation, 2009, 35, 567-576.	0.9	10
7650	Calculation of the effective interaction parameter in the<mml:math xmlns:mml="http://www.w3.org/1998/Math/MathML" display="inline"><mml:mrow><mml:mtext>LDA</mml:mtext><mml:mo>+</mml:mo><mml:mi>U</mml:mi></mml:mrow></mml:math>r by a linear response approach for<mml:math xmlns:mml="http://www.w3.org/1998/Math/MathML" display="inline"><mml:mrow><mml:mtext>Fe</mml:mtext><mml:msub><mml:mrow><mml:mrow><mml:mo>(</mml:mo><mml:mrow> Physical Review B, 2009, 80, .	1.1	1
7651	Electronic structure and spectral properties of Am, Cm, and Bk: Charge-density self-consistentLDA+HIAcalculations in the FP-LAPW basis. Physical Review B, 2009, 80, .	1.1	35
7653	Band gap engineering of GaN nanowires by surface functionalization. Applied Physics Letters, 2009, 94, .	1.5	27
7654	Ab initiostudy of the interface properties of Fe/GaAs(110). Physical Review B, 2009, 80, .	1.1	7
7655	Theoretical investigation of the divacancies in boron nitride nanotubes: Properties and surface reactivity toward various adsorbates. Journal of Chemical Physics, 2009, 131, 014706.	1.2	22
7656	Magnetism and band gap narrowing in Cu-doped ZnO. Applied Physics Letters, 2009, 94, .	1.5	195
7657	Impurity diffusion activation energies in Al from first principles. Physical Review B, 2009, 79, .	1.1	126
7658	Non-transition-metal doped diluted magnetic semiconductors. Applied Physics Letters, 2009, 94, .	1.5	64
7659	Phase-Dependent Photocatalytic Ability of TiO₂: A First-Principles Study. Journal of Chemical Theory and Computation, 2009, 5, 3074-3078.	2.3	68
7660	First-principles calculation of the 6.1 Ã... family bowing parameters and band offsets. Journal of Applied Physics, 2009, 105, .	1.1	6
7661	Hydrogen Dissociation on Pd4S Surfaces. Journal of Physical Chemistry C, 2009, 113, 18800-18806.	1.5	34
7662	Enhanced Stability of Thiolate Self-Assembled Monolayers (SAMs) on Nanostructured Gold Substrates. Langmuir, 2009, 25, 5661-5666.	1.6	70

#	Article	IF	Citations
7663	Mechanical properties of graphene nanoribbons. Journal of Physics Condensed Matter, 2009, 21, 285304.	0.7	158
7664	Ab initiopseudopotential study of vacancies and self-interstitials in hcp titanium. Philosophical Magazine, 2009, 89, 1629-1645.	0.7	50
7665	E centers in ternary Si1â^'xâ^'yGexSny random alloys. Applied Physics Letters, 2009, 95, .	1.5	64
7666	Efficient Promotion of Anatase TiO2 Photocatalysis via Bifunctional Surface-Terminating Tiâ^'Oâ^'Bâ^'N Structures. Journal of Physical Chemistry C, 2009, 113, 12317-12324.	1.5	115
7667	Mechanism for phase transitions and vacancy island formation in alkylthiol/Au(111) self-assembled monolayers based on adatom and vacancy-induced reconstructions. Physical Review B, 2009, 79, .	1.1	37
7668	Density functional theory based first-principle calculation of Nb-doped anatase TiO2 and its interactions with oxygen vacancies and interstitial oxygen. Journal of Chemical Physics, 2009, 131, 034702.	1.2	86
7669	Stable calcium adsorbates on carbon nanostructures: Applications for high-capacity hydrogen storage. Physical Review B, 2009, 79, .	1.1	74
7670	Structural and energetic analysis of the hydrogen storage materials<mml:math xmlns:mml="http://www.w3.org/1998/Math/MathML" display="inline"><mml:mrow><mml:msub><mml:mrow><mml:mtext>LiNH</mml:mtext></mml:mrow><mml:mn>2</mml:mn></mml:msub></mml:mrow></mml:math><mml:math xmlns:mml="http://www.w3.org/1998/Math/MathML"	1.1	69
7671	Chemical effects on the optical band gap of heavily doped<mml:math xmlns:mml="http://www.w3.org/1998/Math/MathML" display="inline"><mml:mrow><mml:mtext>ZnO</mml:mtext><mml:mo>:</mml:mo><mml:msub><mml:mi>M</mml:mi><mml:mrow><mml:mo xmlns:mml="http://www.w3.org/1998/Math/MathML"		

#	Article	IF	Citations
7681	High-Pressure Structural Transitions of Sc₂O₃ by X-ray Diffraction, Raman Spectra, and Ab Initio Calculations. Inorganic Chemistry, 2009, 48, 8251-8256.	1.9	49
7682	Thermodynamics of fission products in UO_{2 Â±x}. Journal of Physics Condensed Matter, 2009, 21, 435602.	0.7	52
7683	Accurate band structures and effective masses for InP, InAs, and InSb using hybrid functionals. Physical Review B, 2009, 80, .	1.1	177
7684	Optical properties of LiGaS₂: anab initiostudy and spectroscopic ellipsometry measurement. Journal of Physics Condensed Matter, 2009, 21, 455502.	0.7	18
7685	Optical properties of intermetallic compounds from first principles calculations: a search for the ideal plasmonic material. Journal of Physics Condensed Matter, 2009, 21, 144211.	0.7	51
7686	Electronic band structure and linear optical properties of paraelectric KIO₃. Journal of Physics Condensed Matter, 2009, 21, 125503.	0.7	1
7687	Electronic band structure of Cu₂O by spin density functional theory. Journal of Physics Condensed Matter, 2009, 21, 015502.	0.7	27
7688	Half-metallicity at the Heusler alloy Co₂Cr_{0.5}Fe_{0.5}Al(001) surface and its interface with GaAs(001). Journal of Physics Condensed Matter, 2009, 21, 055002.	0.7	17
7689	Mechanism of Ethanol Synthesis from Syngas on Rh(111). Journal of the American Chemical Society, 2009, 131, 13054-13061.	6.6	312
7690	First-principles study of structural and bonding properties of vanadium carbide and niobium carbide. Physica Scripta, 2009, 80, 055601.	1.2	13
7691	A first-principle study on the structure, stability and hardness of cubic BC2N. Diamond and Related Materials, 2009, 18, 1278-1282.	1.8	21
7692	Defect interactions in Sn1â^'xGex random alloys. Applied Physics Letters, 2009, 94, 252104.	1.5	65
7693	Ab initio DFT+U study of He atom incorporation into UO2 crystals. Physical Chemistry Chemical Physics, 2009, 11, 7241.	1.3	72
7694	Copper Deposition and Growth over ZnO Nonpolar (101Ì…0) and (112Ì…0) Surfaces: A Density Functional Theory Study. Journal of Physical Chemistry C, 2009, 113, 7227-7235.	1.5	33
7695	A first principles comparison of the mechanism and site requirements for the electrocatalytic oxidation of methanol and formic acid over Pt. Faraday Discussions, 2008, 140, 363-378.	1.6	400
7696	High-Pressure Phase Transition to the Gd₂S₃ Structure in Sc₂O₃: A New Trend in Dense Structures in Sesquioxides. Inorganic Chemistry, 2009, 48, 7537-7543.	1.9	38
7697	Formation Energies of Antiphase Boundaries in GaAs and GaP: An ab Initio Study. International Journal of Molecular Sciences, 2009, 10, 5104-5114.	1.8	45
7698	Ethylene Conversion to Ethylidyne over Pd(111): Revisiting the Mechanism with First-Principles Calculations. Journal of Physical Chemistry C, 2009, 113, 2512-2520.	1.5	56

#	Article	IF	Citations
7699	Ferromagnetism in Semihydrogenated Graphene Sheet. Nano Letters, 2009, 9, 3867-3870.	4.5	771
7700	Energetic Minimum Structures of Imogolite Nanotubes: A First-Principles Prediction. Journal of Physical Chemistry C, 2009, 113, 14834-14837.	1.5	28
7701	Short-range order and Fe clustering in<mml:math xmlns:mml="http://www.w3.org/1998/Math/MathML" display="inline"><mml:mrow><mml:msub><mml:mrow><mml:mtext>Mg</mml:mtext></mml:mrow><mml:mrow><mml:mn>1</mml:mn></mml:m high pressure. Physical Review B, 2009, 80, .	1.1	41
7702	Phase stability of AlYB₁₄sputtered thin films. Journal of Physics Condensed Matter, 2009, 21, 355006.	0.7	8
7703	Monoclinic to tetragonal transformations in hafnia and zirconia: A combined calorimetric and density functional study. Physical Review B, 2009, 80, .	1.1	109
7704	The Effect of Oxygen Vacancies on the Atomic and Electronic Structure of Cubic ABO₃Perovskite Bulk and the (001) Surface:Abinitio Calculations. Ferroelectrics, 2009, 379, 191-198.	0.3	12
7705	Structure and diffusion of intrinsic defects, adsorbed hydrogen, and water molecules at the surface of alkali-earth fluorides calculated using density functional theory. Physical Review B, 2009, 80, .	1.1	32
7706	N-doped ZnO thin films and nanowires: energetics, impurity distribution and magnetism. New Journal of Physics, 2009, 11, 063035.	1.2	25
7707	Ab initiostudy of the temperature-dependent structural properties of Al(110). Physical Review B, 2009, 80, .	1.1	3
7708	From bare Ge nanowire to Ge/Si core/shell nanowires: A first-principles study. Physical Review B, 2009, 80, .	1.1	39
7709	Water Adsorption on the Stoichiometric (001) and (010) Surfaces of Hydroxyapatite: A Periodic B3LYP Study. Langmuir, 2009, 25, 2188-2198.	1.6	80
7710	The delicate electronic and magnetic structure of the LaFePnO system (Pnâ€‰=â€‰pnicogen). New Journal of Physics, 2009, 11, 025004.	1.2	47
7711	Unravelling the Nature of Gold Surface Sites by Combining IR Spectroscopy and DFT Calculations. Implications in Catalysis. Journal of Physical Chemistry C, 2009, 113, 16772-16784.	1.5	136
7712	Powder NMR crystallography of thymol. Physical Chemistry Chemical Physics, 2009, 11, 2610.	1.3	180
7713	Growth of boehmite particles in the presence of xylitol: morphology oriented by the nest effect of hydrogen bonding. Physical Chemistry Chemical Physics, 2009, 11, 11310.	1.3	53
7714	Characterizing Slight Structural Disorder in Solids by Combined Solid-State NMR and First Principles Calculations. Journal of Physical Chemistry A, 2009, 113, 902-911.	1.1	47
7715	Adsorption Isotherm and Orientation of Alcohols on Hydrophilic SiO₂ under Ambient Conditions. Journal of Physical Chemistry C, 2009, 113, 10632-10641.	1.5	49
7716	First-principles study of elastic and stability properties of ZrCâ€“ZrN and ZrCâ€“TiC alloys. Journal of Physics Condensed Matter, 2009, 21, 395503.	0.7	49

#	Article	IF	Citations
7717	Accurate prediction of theSi/SiO2interface band offset using the self-consistentab initioDFT/LDA-1/2 method. Physical Review B, 2009, 79, .	1.1	73
7718	Magnetism in undoped MgO studied by density functional theory. Physical Review B, 2009, 80, .	1.1	106
7719	Effect of substituting of S for O: The sulfide perovskite<mml:math xmlns:mml="http://www.w3.org/1998/Math/MathML" display="inline"><mml:mrow><mml:msub><mml:mrow><mml:mtext>BaZrS</mml:mtext></mml:mrow><mml:mn>3</mml:mn></mml:m with density functional theory. Physical Review B, 2009, 79, .	1.1	74
7720	Order and disorder in the wetting layer on Ru(0001). Faraday Discussions, 2009, 141, 231-249.	1.6	39
7721	Tunneling dynamics of a hydroxyl group adsorbed on Cu(110). Physical Review B, 2009, 79, .	1.1	65
7722	The structural and electronic properties of amine-functionalized boron nitride nanotubes via ammonia plasmas: a density functional theory study. Nanotechnology, 2009, 20, 145703.	1.3	20
7723	Impact of hydrogen on indium incorporation at<mml:math xmlns:mml="http://www.w3.org/1998/Math/MathML" display="inline"><mml:mi>m</mml:mi></mml:math>-plane and<mml:math xmlns:mml="http://www.w3.org/1998/Math/MathML" display="inline"><mml:mi>c</mml:mi></mml:math>-plane<mml:math xmlns:mml="http://www.w3.org/1998/Math/MathML" display="inline"><mml:mrow><mml:msub><mml:m	1.1	24
7724	Structure and elastic properties of boron suboxide at 240 GPa. Journal of Applied Physics, 2009, 105, 083540.	1.1	15
7725	First-principles determination of crystal structures, phase stability, and reaction thermodynamics in the Li-Mg-Al-H hydrogen storage system. Physical Review B, 2009, 79, .	1.1	50
7726	Effects of pressure on the electronic and structural properties of LaOFeAs. Journal of Applied Physics, 2009, 106, 073910.	1.1	9
7727	Comparative Studies on the Phase Stability, Electronic Structure, and Topology of the Charge Density in the Li3XO4 (X = P, As, V) Lithium Orthosalt Polymorphs. Chemistry of Materials, 2009, 21, 1861-1874.	3.2	18
7728	Role of Coverage and Surface Oxidation Degree in the Adsorption of Acetone on TiO₂(110). A Density Functional Study. Journal of Physical Chemistry C, 2009, 113, 19973-19980.	1.5	24
7729	Calculated properties of fully hydrogenated single layers of BN,<mml:math xmlns:mml="http://www.w3.org/1998/Math/MathML" display="inline"><mml:mrow><mml:msub><mml:mrow><mml:mtext>BC</mml:mtext></mml:mrow><mml:mn>2</mml:mn></mml:msu and graphene: Graphane and its BN-containing analogues. Physical Review B, 2009, 80, .	1.1	55
7730	Conductance of Conjugated Molecular Wires: Length Dependence, Anchoring Groups, and Band Alignment. Journal of Physical Chemistry C, 2009, 113, 20967-20973.	1.5	52
7731	Interaction of CO with OH on Au(111): HCOO, CO₃, and HOCO as Key Intermediates in the Water-Gas Shift Reaction. Journal of Physical Chemistry C, 2009, 113, 19536-19544.	1.5	93
7732	Origins of bandgap bowing in compound-semiconductor common-cation ternary alloys. Journal of Physics Condensed Matter, 2009, 21, 075802.	0.7	41
7733	Theoretical study of PTCDA adsorbed on the coinage metal surfaces, Ag(111), Au(111) and Cu(111). New Journal of Physics, 2009, 11, 053010.	1.2	182
7734	Structural transformations in carbon under extreme pressure: Beyond diamond. Journal of Chemical Physics, 2009, 130, 194512.	1.2	56

#	Article	IF	Citations
7735	Tuning electronic and magnetic properties of graphene by surface modification. Applied Physics Letters, 2009, 95, .	1.5	199
7736	Adsorption and diffusion ofSCH3radicals andAu(SCH3)2complexes on the unreconstructed Au(111) surface in the submonolayer coverage regime. Physical Review B, 2009, 79, .	1.1	18
7737	Double Metallocene Nanowires. Journal of the American Chemical Society, 2009, 131, 14246-14248.	6.6	61
7738	Magnetism of C Adatoms on BN Nanostructures: Implications for Functional Nanodevices. Journal of the American Chemical Society, 2009, 131, 1796-1801.	6.6	80
7739	Magnetic properties of transition-metal-doped<mml:math xmlns:mml="http://www.w3.org/1998/Math/MathML"		

#	Article	IF	Citations
7753	Implementing and testing the AM05 spin density functional. Physical Review B, 2009, 79, .	1.1	108
7754	Theoretical study of carbon species on Pd(111): competition between migration of C atoms to the subsurface interlayer and formation of Cn clusters on the surface. Physical Chemistry Chemical Physics, 2009, 11, 10955.	1.3	27
7755	Density functional study of the adsorption and van der Waals binding of aromatic and conjugated compounds on the basal plane of MoS2. Journal of Chemical Physics, 2009, 130, 104709.	1.2	108
7756	Structure and stability of high pressure synthesized Mgâ€“TM hydrides (TM = Ti, Zr, Hf, V, Nb and Ta) as possible new hydrogen rich hydrides for hydrogen storage. Journal of Materials Chemistry, 2009, 19, 8150.	6.7	77
7757	On the difficulties of present theoretical models to predict the oxidation state of atomic Au adsorbed on regular sites of CeO[sub 2](111). Journal of Chemical Physics, 2009, 131, 094702.	1.2	64
7758	First-principles study of vacancy-hydrogen interaction in Pd. Physical Review B, 2009, 80, .	1.1	54
7759	Theoretical Prediction of the Nâˆ’H and Oâˆ’H Bonds Cleavage Catalyzed by the Single-Walled Silicon Carbide Nanotube. Journal of Physical Chemistry C, 2009, 113, 16736-16740.	1.5	39
7760	Structural, elastic, electronic, and phonon properties of zinc-blende and wurtzite BeO. Journal of Applied Physics, 2009, 105, .	1.1	66
7761	Density Functional Characterization of the Visible-Light Absorption in Substitutional C-Anion- and C-Cation-Doped TiO₂. Journal of Physical Chemistry C, 2009, 113, 2624-2629.	1.5	166
7762	Elastic and chemical contributions to the stability of magnetic surface alloys on Ru(0001). Physical Review B, 2009, 79, .	1.1	12
7763	The bulk modulus of cubic spinel selenides: an experimental and theoretical study. High Pressure Research, 2009, 29, 72-75.	0.4	8
7764	Vibrational properties of crystalline Sb₂Te₃from first principles. Journal of Physics Condensed Matter, 2009, 21, 095410.	0.7	100
7765	Chemical Bonding and Schottky Barrier for Metal-Carbon Nanotube Contacts. , 2009, , .		1
7766	Hydrogen-induced mitigation of O on Ru(101Ì„0): a density-functional study. Physical Chemistry Chemical Physics, 2009, 11, 5695.	1.3	2
7767	Synthesis, characterization and computational simulation of visible-light irradiated fluorine-doped titanium oxide thin films. Journal of Materials Chemistry, 2009, 19, 6907.	6.7	38
7768	Growth and Desorption Kinetics of Ultrathin Zn Layers on Pd(111). Journal of Physical Chemistry C, 2009, 113, 9788-9796.	1.5	36
7769	First-principles study of the<mml:math xmlns:mml="http://www.w3.org/1998/Math/MathML" display="inline"><mml:mrow><mml:msub><mml:mrow><mml:mtext>Co</mml:mtext></mml:mrow><mml:mn>2</mml:mn></mml:msu and<mml:math xmlns:mml="http://www.w3.org/1998/Math/MathML" display="inline"><mml:mrow><mml:msub><mml:mrow><mml:mtext>Co</mml:mtext></mml:mrow><mml:mn>2</mml:mn></mml:m. Physical Review B, 2009, 79, .	1.1	87
7770	First-Principles Study of S Doping at the Rutile TiO₂ (110) Surface. Journal of Physical Chemistry C, 2009, 113, 17464-17470.	1.5	19

#	Article	IF	Citations
7771	First-Principles Investigations of the Physical Properties of Magnesium Nitridoboride. Journal of Physical Chemistry C, 2009, 113, 4997-5003.	1.5	22
7772	Frontier Orbital Description of the Si(100) Surface: A Route to Symmetry-Allowed and Concerted [2 + 2] Cycloadditions. Journal of the American Chemical Society, 2009, 131, 6768-6774.	6.6	10
7773	First-principles study of the structural, electronic, vibrational, and elastic properties of orthorhombic NiSi. Physical Review B, 2009, 79, .	1.1	202
7774	DFT study of adsorption of hydrogen and carbon monoxide on PtxBi1âˆ'x/Pt(111) bimetallic overlayers: correlation to surface electronic properties. Physical Chemistry Chemical Physics, 2009, 11, 6225.	1.3	20
7775	Ferromagnetism induced by Zn vacancy defect and lattice distortion in ZnO. Journal of Applied Physics, 2009, 106, .	1.1	88
7776	First-principles calculation of elastic and thermodynamic properties of Ni ₂ MnGa Heusler alloy. Chinese Physics B, 2009, 18, 744-748.	0.7	19
7777	Ethylidyne Formation from Ethylene over Pd(111): Alternative Routes from a Density Functional Study. Journal of Physical Chemistry C, 2009, 113, 15373-15379.	1.5	29
7778	Boron fullerenes B32+8k with four-membered rings and B32 solid phases: geometrical structures and electronic properties. Physical Chemistry Chemical Physics, 2009, 11, 9696.	1.3	36
7779	Energetic and electronic properties of X- (Si, Ge, Sn, Pb) doped TiO2 from first-principles. Physical Chemistry Chemical Physics, 2009, 11, 8165.	1.3	78
7780	First-principles study of the ground state stability of IIIâ€“V bismuth compounds. Philosophical Magazine Letters, 2009, 89, 807-813.	0.5	17
7781	Electronic structure and optical properties of Nb-doped Sr ₂ TiO ₄ by density function theory calculation. Chinese Physics B, 2009, 18, 2945-2952.	0.7	12
7782	Polynitrogen/Nanoaluminum Surface Interactions. , 2009, , .		0
7783	Probing local structures of siliceous zeolite frameworks by solid-state NMR and first-principles calculations of 29Siâ€“Oâ€“29Si scalar couplings. Physical Chemistry Chemical Physics, 2009, 11, 1825.	1.3	76
7784	Ab initiostudy of structural, elastic, and high-pressure properties of rubidium halides RbX (X =) Tj ETQq1 1 0.784314 rgBT /Ove	0.6	8
7785	Chemoresistive sensing of light alkanes with SnO2 nanocrystals: a DFT-based insight. Physical Chemistry Chemical Physics, 2009, 11, 3634.	1.3	10
7786	Ensemble vs. electronic effects on the reactivity of two-dimensional Pd alloys: a comparison of CO and CH3OH adsorption on Zn/Pd(111) and Cu/Pd(111). Physical Chemistry Chemical Physics, 2009, 11, 10457.	1.3	20
7787	A computational study of electronic structure, thermodynamics and kinetics of hydrogen desorption from Al- and Si-doped Î±-, Î³-, and Î²-MgH2. Journal of Materials Chemistry, 2009, 19, 4348.	6.7	32
7788	Computational identification of a metal organic framework for high selectivity membrane-based CO2/CH4 separations: Cu(hfipbb)(H2hfipbb)0.5. Physical Chemistry Chemical Physics, 2009, 11, 11389.	1.3	83

#	Article	IF	Citations
7789	Local condensation around oxygen vacancies in t-LaNbO4 from first principles calculations. Physical Chemistry Chemical Physics, 2009, 11, 5550.	1.3	24
7790	Synthesis, structure and spectroscopic properties of a new class of polymerisable nickel dithiolenes. Journal of Materials Chemistry, 2009, 19, 6194.	6.7	8
7791	Ferromagnetism of undoped GaN mediated by through-bond spin polarization between nitrogen dangling bonds. Applied Physics Letters, 2009, 94, 162505.	1.5	112
7792	Suitability of III-V<mml:math xmlns:mml="http://www.w3.org/1998/Math/MathML" display="inline"><mml:mrow><mml:mrow><mml:mo>[</mml:mo><mml:mrow><mml:mi>X</mml:mi><mml:msub><mml:mtext>H</mml:mtext> for hydrogen storage: A density functional study. Physical Review B, 2009, 79, .	3.1	0
7793	Study on the Electronic Structure and Optical Properties for BaSi2. , 2009, , .		0
7794	A density functional study of the high-pressure chemistry of MSiN₂ (M = Be, Mg, Ca): prediction of high-pressure phases and examination of pressure-induced decomposition. Journal of Physics Condensed Matter, 2009, 21, 275407.	0.7	19
7795	Depiction of the elastic anisotropy of AuSn<inf>4</inf> and AuSn<inf>2</inf> from first-principles calculations. , 2009, , .		0
7796	Multinuclear gallium-oxide cations in high-silica zeolites. Physical Chemistry Chemical Physics, 2009, 11, 2893.	1.3	50
7797	Structural evolution and properties of subnanometer Tcn (n = 2â€“15) clusters. Physical Chemistry Chemical Physics, 2009, 11, 10003.	1.3	15
7798	Fischer-Tropsch synthesis of liquid fuels: learning lessons from homogeneous catalysis. Physical Chemistry Chemical Physics, 2009, 11, 11110.	1.3	24
7799	Theoretical study of hydrogen dissociative adsorption on strained pseudomorphic monolayers of Cu and Pd deposited onto a Ru(0001) substrate. Physical Chemistry Chemical Physics, 2009, 11, 7303.	1.3	27
7800	Density functional study of Ag in Ge₂Se₃. , 2009, , .		0
7801	Adsorption of cyanodiacetylene on ice: a periodic approach. Physical Chemistry Chemical Physics, 2009, 11, 5833.	1.3	6
7802	The optical and vibrational properties of dominant defects in undoped ZnO: A first-principles study. Journal of Applied Physics, 2009, 105, 083710.	1.1	17
7803	Barrier-free substitutional doping of graphene sheets with boron atoms:Ab initiocalculations. Physical Review B, 2009, 79, .	1.1	63
7804	Potential barrier modification and interface states formation in metal-oxide-metal tunnel junctions. Physical Review B, 2009, 80, .	1.1	23
7805	First-principles investigation of organic semiconductors for thermoelectric applications. Journal of Chemical Physics, 2009, 131, 224704.	1.2	68
7806	Nature and stability of ice X. High Pressure Research, 2009, 29, 208-211.	0.4	11

#	Article	IF	Citations
7807	First-Principles Calculations of Elastic Properties of Cu$_{3}$Sn and Cu$_{6}$Sn$_{5}$ Intermetallics. IEEE Transactions on Advanced Packaging, 2009, 32, 754-757.	1.7	6
7808	Equilibrium structure of Î´-Bi₂O₃from first principles. Journal of Physics Condensed Matter, 2009, 21, 175403.	0.7	18
7809	Thermodynamic properties of PbTe, PbSe, and PbS: First-principles study. Physical Review B, 2009, 80, .	1.1	231
7810	Energy gap opening in submonolayer lithium on graphene: Local density functional and tight-binding calculations. Physical Review B, 2009, 79, .	1.1	69
7811	First principles investigation of the structural and elastic properties of hydrous wadsleyite under pressure. Journal of Geophysical Research, 2009, 114, .	3.3	41
7812	Toward an Accurate Density-Functional Tight-Binding Description of Zinc-Containing Compounds. Journal of Chemical Theory and Computation, 2009, 5, 605-614.	2.3	113
7813	Theory of doping properties of Ag acceptors in ZnO. Physical Review B, 2009, 80, .	1.1	84
7814	Density Functional Theory Study of Finite Carbon Chains. ACS Nano, 2009, 3, 3788-3794.	7.3	56
7815	R₅Pn₃-type Phases of the Heavier Trivalent Rare-Earth-Metal Pnictides (Pn = Sb,) Tj ETQq0 0 0 rgBT /Overlock Inorganic Chemistry, 2009, 48, 4362-4371.	1.9	11
7816	First-principles studies of the electronic and dynamical properties of monosilicides MSi (M = Fe, Ru,) Tj ETQq1 1 0.784314 rgBT /Overl	0.7	28
7817	Formation of a coplanar Oâ€“Al bonding cluster: the effect of O impurity on a Î£ = 5 NiAl grain boundary from first-principles. Journal of Physics Condensed Matter, 2009, 21, 015002.	0.7	10
7818	Changing the physical and chemical properties of titanium oxynitrides<mml:math xmlns:mml="http://www.w3.org/1998/Math/MathML" display="inline"><mml:mrow><mml:msub><mml:mrow><mml:mtext>TiN</mml:mtext></mml:mrow><mml:mrow><mml:mn>1</mml:mn> changing the composition. Physical Review B, 2009, 80, .	1.1	48
7819	Interactions between co-adsorbed CO and H on a Rh(100) single crystal surface. Physical Chemistry Chemical Physics, 2009, 11, 10009.	1.3	21
7820	Accurate electronic band gap of pure and functionalized graphane from GW calculations. Physical Review B, 2009, 79, .	1.1	279
7821	High-pressure phase transition and thermodynamic properties of MgSe: Ab initio study. Canadian Journal of Physics, 2009, 87, 169-174.	0.4	6
7822	Magnetism of chromia from first-principles calculations. Physical Review B, 2009, 79, .	1.1	74
7823	Acceptor level of nitrogen in diamond and the 270-nm absorption band. Physical Review B, 2009, 80, .	1.1	49
7824	Effects of Na-substitution on structural and electronic properties of Li2CoSiO4 cathode material. Transactions of Nonferrous Metals Society of China, 2009, 19, 182-186.	1.7	24

#	Article	IF	Citations
7825	Density functional theory study on hydrogenation mechanism in catalyst-activated Mg(0001) surface. Transactions of Nonferrous Metals Society of China, 2009, 19, 383-388.	1.7	14
7826	Theoretical study of the elastic properties of titanium nitride. Acta Metallurgica Sinica (English) Tj ETQq1 1 0.784314 rgBT /Overlock 10	1.5	15
7827	First-principles calculations of LaNi5â^'xSnxHy intermetallics and intermediate phase. Acta Metallurgica Sinica (English Letters), 2009, 22, 330-338.	1.5	5
7828	A New Polymorph of N,Nâ€²-Dimethylurea Characterized by X-ray Diffraction and First-Principles Lattice Dynamics Calculations. Journal of Physical Chemistry A, 2009, 113, 5998-6003.	1.1	10
7829	Phase stability of the rare-earth sesquioxides under pressure. Physical Review B, 2009, 80, .	1.1	32
7830	Noble metal ionic catalysts: correlation of increase in CO oxidation activity with increasing effective charge on Pd ion in Pd ion substituted Ce_{1â^'x}M_xO_{2â^'Î´}(M = Ti, Zr and) Tj ETQq1 1 0.784314 rgBT	1.1	76
7831	A Computational Study on the Adsorption Configurations and Reactions of Phosphorous Acid on TiO₂ Anatase (101) and Rutile (110) Surfaces. Journal of Physical Chemistry C, 2009, 113, 8394-8406.	1.5	12
7832	A first-principles study of bulk oxide formation on Pd(100). Journal of Chemical Physics, 2009, 131, 054701.	1.2	53
7833	A Combined Experimental and Computational Investigation of Anthracene Based Sensitizers for DSSC: Comparison of Cyanoacrylic and Malonic Acid Electron Withdrawing Groups Binding onto the TiO₂ Anatase (101) Surface. Journal of Physical Chemistry C, 2009, 113, 20117-20126.	1.5	190
7834	Gas adsorption on graphene doped with B, N, Al, and S: A theoretical study. Applied Physics Letters, 2009, 95, .	1.5	643
7835	Origin of Nanoscale Phase Stability Reversals in Titanium Oxide Polymorphs. Journal of Physical Chemistry C, 2009, 113, 4240-4245.	1.5	62
7836	First-Principles Study of Faceted Single-Crystalline Silicon Carbide Nanowires and Nanotubes. Journal of Physical Chemistry C, 2009, 113, 856-861.	1.5	17
7837	Ethene stabilization on Cu(111) by surface roughness. Journal of Chemical Physics, 2009, 131, 024701.	1.2	17
7838	Structure and electronic properties of iron oxide clusters: A first-principles study. Physical Review B, 2009, 80, .	1.1	40
7839	Boronâ€“hydrogen complexes in diamond and their vibrational properties. Diamond and Related Materials, 2009, 18, 835-838.	1.8	7
7840	An ab-initio approach to the optical properties of CxNy single wall nanotubes. Diamond and Related Materials, 2009, 18, 1002-1005.	1.8	9
7841	Large spherical vacancy clusters in diamond â€“ Origin of the brown colouration?. Diamond and Related Materials, 2009, 18, 843-845.	1.8	22
7842	Effect of co-adsorbed dopants on initial diamond growth steps: H abstraction from an adsorbed CH3. Diamond and Related Materials, 2009, 18, 1152-1156.	1.8	8

#	Article	IF	Citations
7843	Hybrid density functional theory applied to magnetite: Crystal structure, charge order, and phonons. Physical Review B, 2009, 79, .	1.1	65
7844	Unconventional pairing originating from disconnected Fermi surfaces in the iron-based superconductor. New Journal of Physics, 2009, 11, 025017.	1.2	16
7845	Dissociation and Diffusion of Hydrogen on the Mg(0001) Surface: Catalytic Effect of V and Ni Double Substitution. Journal of Physical Chemistry C, 2009, 113, 10574-10579.	1.5	26
7846	Density Functional Study of Calcium Nitride: Refined Geometries and Prediction of High-Pressure Phases. Journal of Physical Chemistry C, 2009, 113, 2943-2949.	1.5	13
7847	Experimental and Density Functional Theory Study of the Tribochemical Wear Behavior of SiO₂ in Humid and Alcohol Vapor Environments. Langmuir, 2009, 25, 13052-13061.	1.6	89
7848	Assessing the performance of recent density functionals for bulk solids. Physical Review B, 2009, 79, .	1.1	740
7849	Interface Structures of Gold Nanoparticles on<mml:math xmlns:mml="http://www.w3.org/1998/Math/MathML" display="inline"><mml:msub><mml:mi>TiO</mml:mi><mml:mn>2</mml:mn></mml:msub></mml:math>(110). Physical Review Letters, 2009, 102, 136105.	2.9	76
7850	Anab initiostudy of the interaction between an iron atom and graphene containing a single Stoneâ€“Wales defect. Journal of Physics Condensed Matter, 2009, 21, 485506.	0.7	16
7851	Origin of p-Type Doping in Zinc Oxide Nanowires Induced by Phosphorus Doping: A First Principles Study. Journal of Physical Chemistry C, 2009, 113, 9541-9545.	1.5	26
7852	Adsorption of atomic nitrogen and oxygen on mathrm {ZnO(2ar {1} ar {1}0)} surface: a density functional theory study. Journal of Physics Condensed Matter, 2009, 21, 144208.	0.7	13
7853	Pressure-Induced Metallization of a Single-Component Molecular Crystal. Journal of Physical Chemistry C, 2009, 113, 19310-19316.	1.5	11
7854	Structural Characterization Combined with the First Principles Simulations of Barium/Strontium Cobaltite/Ferrite as Promising Material for Solid Oxide Fuel Cells Cathodes and High-Temperature Oxygen Permeation Membranes. ACS Applied Materials & Interfaces, 2009, 1, 1512-1519.	4.0	50
7855	Boron nitride nanotubes functionalized by a series of carbenes. Physical Chemistry Chemical Physics, 2009, 11, 6256.	1.3	15
7856	First Principles Model of Amorphous Silicon Lithiation. Journal of the Electrochemical Society, 2009, 156, A454.	1.3	177
7857	Metallization of Î±-boron by hydrogen doping. Journal of Physics: Conference Series, 2009, 176, 012005.	0.3	4
7858	First-Principles Study of the Stability and Interfacial Bonding of Tilt and Twist Grain Boundaries in Al and Cu. Nippon Kinzoku Gakkaishi/Journal of the Japan Institute of Metals, 2009, 73, 559-565.	0.2	0
7859	Local Electronic and Atomic Structure of Ce³⁺-Containing Fluoride/Oxide Determined by TEM-EELS and First-Principles Calculations. Materials Transactions, 2009, 50, 952-958.	0.4	7
7860	First-Principles Study of the Stability and Interfacial Bonding of Tilt and Twist Grain Boundaries in Al and Cu. Materials Transactions, 2009, 50, 11-18.	0.4	17

#	Article	IF	Citations
7861	Conduction-Band Structures of Wurtzite ZnO Solid Solutions by First Principles Calculations. Materials Transactions, 2009, 50, 1067-1070.	0.4	6
7862	First Principles Lattice Dynamics Calculations of Ag⁺ Doped KX (X=Cl, Br and I). Materials Transactions, 2009, 50, 999-1003.	0.4	0
7863	Influence of Hydrogen on Growth of Carbon Nanotubes. Materials Research Society Symposia Proceedings, 2009, 1204, 1.	0.1	0
7864	Stability of ferromagnetic phase in Fe-doped AlH ₃. Europhysics Letters, 2009, 85, 67006.	0.7	3
7865	Minimal model for study on Superconductivity in LaFeAsO1-xFxbased onab-initiodownfolding. Journal of Physics: Conference Series, 2009, 150, 052010.	0.3	4
7866	Single and multiple scattering XAFS Debye-Waller factors for crystalline materials using periodic Density Functional Theory. Journal of Physics: Conference Series, 2009, 190, 012011.	0.3	6
7867	Stable structure and effects of the substrate Ti pre-treatment on the epitaxial growth of SrTiO ₃ on GaAs. Europhysics Letters, 2009, 86, 46008.	0.7	15
7868	Density-Functional-Theory-Based Finite-Element Analysis of Diamond Single Crystal. Journal of Solid Mechanics and Materials Engineering, 2009, 3, 541-551.	0.5	3
7869	Absence of CO dissociation on Mo(112). Journal of Chemical Physics, 2009, 130, 174714.	1.2	10
7870	EFFECT OF DEFECTS ON INITIATION OF CHEMISTRY IN HMX. , 2009, , .		0
7871	Spontaneous Formation of Dipolar Metal Nanoclusters. Journal of Physical Chemistry A, 2009, 113, 4134-4137.	1.1	9
7872	A Periodic Density Functional Theory Analysis of CO Chemisorption on Pt(111) in the Presence of Uniform Electric Fields. Journal of Physical Chemistry A, 2009, 113, 4125-4133.	1.1	51
7873	Silylene Defect at the Dihydrogen Terminated (100) Si Surface. Journal of Physical Chemistry A, 2009, 113, 14375-14388.	1.1	4
7874	In Silico Characterization of a Fourfold Magnesium Organometallic Compound in PTCDA Thin Films. Journal of Physical Chemistry A, 2009, 113, 14813-14817.	1.1	2
7875	Possibility of imperfections in Î±-boron. Journal of Physics: Conference Series, 2009, 176, 012004.	0.3	3
7876	Finite-temperature atomic structure of 180Â° ferroelectric domain walls in PbTiO ₃. Europhysics Letters, 2010, 90, 27007.	0.7	6
7877	Electronic work function of the Cu (100) surface under different strain states. Europhysics Letters, 2010, 89, 66004.	0.7	19
7878	Minimum Energy Motion and Core Structure of Pure Edge and Screw Dislocations in Aluminum. Journal of Computational Science and Technology, 2010, 4, 185-193.	0.4	5

#	Article	IF	Citations
7879	First-Principles Study on Stability and Electronic Structures of Pt-Rh Bimetallic Nanoparticles. Materials Transactions, 2010, 51, 321-324.	0.4	12
7880	Local Atomic Configuration of Dislocation-Accumulated Grain Boundary and Energetics of Gradual Transition from Low Angle to High Angle Grain Boundary in Pure Aluminum by First-Principles Calculations. Materials Transactions, 2010, 51, 51-57.	0.4	7
7881	Effect of Zn on the adsorption of CO on Pd(111). Journal of Chemical Physics, 2010, 133, 214702.	1.2	12
7882	Communication: Emergence of localized magnetic moment at adsorbed beryllium dimer on graphene. Journal of Chemical Physics, 2010, 133, 231104.	1.2	9
7883	Theoretical studies on electronic and magnetic properties of ultrathin Mo nanowires. Journal of Applied Physics, 2010, 107, 024307.	1.1	3
7884	Oxygen-doped c-BN(110) surface: DFT calculations. IOP Conference Series: Materials Science and Engineering, 2010, 15, 012075.	0.3	1
7885	Increased Cathodic Kinetics on Platinum in IT-SOFCs by Inserting Highly Ionic-Conducting Nanocrystalline Materials. Journal of Fuel Cell Science and Technology, 2010, 7, .	0.8	14
7886	Ab initio study on pressure-induced change of effective Coulomb interaction in superconducting yttrium. Applied Physics Letters, 2010, 96, .	1.5	5
7887	First Principles Calculation on the Surface Energy of Metal Nitride with NaCl Structure. Hyomen Gijutsu/Journal of the Surface Finishing Society of Japan, 2010, 61, 535-540.	0.1	6
7888	Energetics of Pb heterostructures formation on the Cu (111) in the early stage of the deposition process. Journal of Applied Physics, 2010, 107, 114315.	1.1	3
7889	Estimation of linear thermal expansion coefficient from cohesive energy obtained by ab-initio calculation of metals and ceramics. Journal of the Ceramic Society of Japan, 2010, 118, 241-245.	0.5	17
7890	Interactions of Hydrogen with Solid Surfaces. Journal of the Vacuum Society of Japan, 2010, 53, 592-601.	0.3	2
7891	Ab initio investigation of the clustering of carbon adatoms on Fe(001) and Fe(111) surfaces. Journal of Experimental and Theoretical Physics, 2010, 110, 81-87.	0.2	1
7892	Effect of hydrogen impurity atoms and molecules on the atomic structure of palladium nanocontacts. Physics of the Solid State, 2010, 52, 641-648.	0.2	9
7893	Ground state and properties of ferroelectric superlattices based on crystals of the perovskite family. Physics of the Solid State, 2010, 52, 1448-1462.	0.2	25
7894	Digital magnetic heterostructures based on Si and Fe. Physics of the Solid State, 2010, 52, 1680-1687.	0.2	5
7895	Structural features and atomic dynamics in Si/SiO2 superlattices: First-principles calculations. Physics of the Solid State, 2010, 52, 2409-2414.	0.2	1
7896	Ab initio simulation of the influence of zirconium impurity ions on the atomic and electronic structure of BaTiO3. Technical Physics, 2010, 55, 1443-1446.	0.2	4

#	Article	IF	Citations
7897	Symmetry and stability of nanotubes based on titanium dioxide. Russian Journal of General Chemistry, 2010, 80, 1152-1167.	0.3	13
7898	First-principles investigation of the electron work function for the (001) surface of indium oxide In2O3 and indium tin oxide (ITO) as a function of the surface oxidation level. Nanotechnologies in Russia, 2010, 5, 185-190.	0.7	11
7899	First-principles investigation of the structure and electronic properties of CdS/CdSe/CdS and CdS/CdTe/CdS quantum wells using a slab approximation. Nanotechnologies in Russia, 2010, 5, 191-197.	0.7	8
7900	Tungsten carbide on the subnanoscale level: Atomic structure, electronic states, and mechanical properties. Nanotechnologies in Russia, 2010, 5, 837-843.	0.7	4
7901	First-principles study of zinc-blende to rocksalt phase transition in BN. Open Physics, 2010, 8, 628-633.	0.8	6
7902	B and N-doped double walled carbon nanotube: a theoretical study. Central European Journal of Physics, 2010, 8, 811-818.	0.3	5
7903	Piezoelastic properties of retgersite determined by ultrasonic measurements. European Physical Journal B, 2010, 73, 167-175.	0.6	15
7904	The effect of hydrogen and oxygen atoms on the adsorbed gallium inside defective carbon nanotubes. European Physical Journal B, 2010, 73, 413-416.	0.6	0
7905	Electronic transport calculation of adsorbate NO2 and NO molecules on graphene using Maximally Localized Wannier functions. European Physical Journal B, 2010, 74, 135-138.	0.6	7
7906	Mechanical and chemical bonding properties of ground state BeH2. European Physical Journal B, 2010, 74, 303-308.	0.6	25
7907	Density functional study of K and Na adsorbed on Co(0001). European Physical Journal B, 2010, 75, 469-474.	0.6	5
7908	Electronic structure of half-metallic ferromagnet Co2MnSi at high-pressure. European Physical Journal B, 2010, 76, 321-326.	0.6	19
7909	Atomic and electronic properties of tert-butanol on the Si(001)-(2Ã—1) surface. European Physical Journal B, 2010, 76, 359-363.	0.6	2
7910	ElectronicÂexcitationÂenergiesÂinÂTiO2 in the fluorite phase. European Physical Journal B, 2010, 76, 365-371.	0.6	10
7911	Structural, electronic and magnetic properties of the 3d transition metal atoms adsorbed on boron nitride nanotubes. European Physical Journal B, 2010, 76, 289-299.	0.6	19
7912	Electronic structure and magnetic coupling properties of Gd-doped AlN: first-principles calculations. European Physical Journal B, 2010, 77, 345-349.	0.6	7
7913	Thermal expansion and elasticity of PdFe3N within the quasiharmonic approximation. European Physical Journal B, 2010, 77, 401-406.	0.6	21
7914	The main factors influencing the O vacancy formation on the Ir doped ceria surface: A DFT+U study. European Physical Journal B, 2010, 77, 373-380.	0.6	20

#	Article	IF	Citations
7915	The axial compressibility, thermal expansion and elastic anisotropy of Hf2SC under pressure. European Physical Journal B, 2010, 78, 37-42.	0.6	6
7916	Diffusion of the Cu monomer and dimer on Ag(111): Molecular dynamics simulations and density functional theory calculations. Physical Review B, 2010, 82, .	1.1	28
7917	On the Role of Metal Step-Edges in Graphene Growth. Journal of Physical Chemistry C, 2010, 114, 11221-11227.	1.5	110
7918	Crystal structure prediction via particle-swarm optimization. Physical Review B, 2010, 82, .	1.1	1,870
7919	Wurtzite-derived polytypes of kesterite and stannite quaternary chalcogenide semiconductors. Physical Review B, 2010, 82, .	1.1	259
7920	Structural, magnetic, and defect properties of Co-Pt-type magnetic-storage alloys: Density-functional theory study of thermal processing effects. Physical Review B, 2010, 82, .	1.1	54
7921	Theoretical analysis of the chemical bonding and electronic structure of graphene interacting with Group IA and Group VIIA elements. Physical Review B, 2010, 81, .	1.1	130
7922	ScVO₄: Explorations of Novel Crystalline Inorganic Optical Materials in Rare-Earth Orthovanadate Systems. Crystal Growth and Design, 2010, 10, 4389-4400.	1.4	39
7923	Finding Natureâ€™s Missing Ternary Oxide Compounds Using Machine Learning and Density Functional Theory. Chemistry of Materials, 2010, 22, 3762-3767.	3.2	479
7924	Controlling Band Gap Energies in Cluster-Assembled Ionic Solids through Internal Electric Fields. ACS Nano, 2010, 4, 5813-5818.	7.3	72
7925	Defect formation energy and magnetic structure of shape memory alloys Niâ€“Xâ€“Ga (X=Mn, Fe, Co) by first principle calculation. Journal of Applied Physics, 2010, 108, .	1.1	36
7926	Prediction of a conducting hard ductile cubic IrC. Physica Status Solidi - Rapid Research Letters, 2010, 4, 230-232.	1.2	8
7927	First-order liquid-liquid phase transition in dense hydrogen. Physical Review B, 2010, 82, .	1.1	121
7928	Crystal and Electronic Structure of FeSe at High Pressure and Low Temperature. Journal of Physical Chemistry B, 2010, 114, 12597-12606.	1.2	79
7929	Statistical model of defects in Al-H system. Physical Review B, 2010, 81, .	1.1	35
7930	Theoretical investigation on synthesizing BC₅crystal. Journal of Physics: Conference Series, 2010, 215, 012116.	0.3	5
7931	Magnesium Boride Nanotubes: Relative Stability and Atomic and Electronic Structure. Journal of Physical Chemistry C, 2010, 114, 4852-4856.	1.5	8
7932	Packing Structure of Poly(3-hexylthiophene) Crystal: Ab Initio and Molecular Dynamics Studies. Journal of Physical Chemistry B, 2010, 114, 5997-6000.	1.2	84

#	Article	IF	Citations
7933	Electronic and optical properties of aluminium-doped anatase and rutile<mml:math xmlns:mml="http://www.w3.org/1998/Math/MathML" display="inline"><mml:mrow><mml:msub><mml:mrow><mml:mtext>TiO</mml:mtext></mml:mrow><mml:mn>2</mml:mn></mml:msu initiocalculations. Physical Review B, 2010, 81, .	1.1	121
7934	First-principles elastic and thermal properties of TiO₂: a phonon approach. Journal of Physics Condensed Matter, 2010, 22, 015401.	0.7	71
7935	Volcano Relation for the Deacon Process over Transitionâ€Metal Oxides. ChemCatChem, 2010, 2, 98-102.	1.8	49
7936	The Role of Surface Oxides in NO_x Storage Reduction Catalysts. ChemCatChem, 2010, 2, 658-660.	1.8	13
7937	Investigation of Acid Centers in MILâ€53(Al, Ga) for BrÃ¸nstedâ€Type Catalysis: Inâ€…Situ FTIR and Abâ€…Initio Molecular Modeling. ChemCatChem, 2010, 2, 1235-1238.	1.8	72
7938	Revisiting the Structure of Methyltrioxorhenium Chemisorbed on Alumina. ChemCatChem, 2010, 2, 812-815.	1.8	19
7939	DFTâ€Based Coverageâ€Dependent Model of Ptâ€Catalyzed NO Oxidation. ChemCatChem, 2010, 2, 1450-1460.	1.8	91
7940	Self-energy and excitonic effects in the electronic and optical properties of<mml:math xmlns:mml="http://www.w3.org/1998/Math/MathML" display="inline"><mml:mrow><mml:msub><mml:mrow><mml:mtext>TiO</mml:mtext></mml:mrow><mml:mn>2</mml:mn></mml:msu phases. Physical Review B, 2010, 82, .	1.1	236
7941	Pressure-induced isostructural phase transformation inÎ³-B28. Physical Review B, 2010, 82, .	1.1	27
7942	Atomistic models of hydrogenated amorphous silicon nitride from first principles. Physical Review B, 2010, 82, .	1.1	22
7943	Electronic and magnetic structure of bulk cobalt: The Î±, Î², and Îµ-phases from density functional theory calculations. Journal of Chemical Physics, 2010, 133, 024701.	1.2	83
7944	Nanoengineering Structures on Graphene with Adsorbed Hydrogen â€œLinesâ€• Journal of Physical Chemistry C, 2010, 114, 3225-3229.	1.5	51
7945	Carbon Nanotube Doping Mechanism in a Salt Solution and Hygroscopic Effect: Density Functional Theory. ACS Nano, 2010, 4, 5430-5436.	7.3	32
7946	Efficient Spin Filtering through Cobalt-Based Extended Metal Atom Chains. Inorganic Chemistry, 2010, 49, 5591-5597.	1.9	35
7947	Submonolayers of carbon on<mml:math xmlns:mml="http://www.w3.org/1998/Math/MathML" display="inline"><mml:mrow><mml:mi>Î±</mml:mi><mml:mtext>-Fe</mml:mtext></mml:mrow></mml:math>facets: Anab initiostudy. Physical Review B, 2010, 82, .	1.1	17
7948	Theoretical and experimental evidence of the role of electromagnetic resonance in the cleaning of nanotubes. Physical Review B, 2010, 81, .	1.1	4
7949	First principles calculations of vacancyâ€“vacancy interactions in nickel: thermal expansion effects. Journal of Physics Condensed Matter, 2010, 22, 485502.	0.7	18
7950	Adsorption of molecular oxygen on doped graphene: Atomic, electronic, and magnetic properties. Physical Review B, 2010, 81, .	1.1	232

#	Article	IF	Citations
7951	Intermetallic hydrides: A review with ab initio aspects. Progress in Solid State Chemistry, 2010, 38, 1-37.	3.9	80
7952	EPR of a defect in CVD diamond involving both silicon and hydrogen that shows preferential alignment. Physical Review B, 2010, 82, .	1.1	35
7953	Structure and Bonding of Î³-B₂₈: Is the High Pressure Form of Elemental Boron Ionic?. Inorganic Chemistry, 2010, 49, 11270-11275.	1.9	20
7954	The quasiparticle band structure of zincblende and rocksalt ZnO. Journal of Physics Condensed Matter, 2010, 22, 125505.	0.7	50
7955	Structural, Electronic, and Mechanical Properties of Single-Walled Halloysite Nanotube Models. Journal of Physical Chemistry C, 2010, 114, 11358-11363.	1.5	231
7956	Deformation and transfer doping of a single-walled carbon nanotube adsorbed on metallic substrates. Physical Review B, 2010, 81, .	1.1	13
7957	Theoretical modeling of the Al paramagnetic center and its precursors in stishovite. Physics and Chemistry of Minerals, 2010, 37, 119-127.	0.3	9
7958	Equation of state and pressure-induced structural changes in mirabilite (Na2SO4Â·10H2O) determined from ab initio density functional theory calculations. Physics and Chemistry of Minerals, 2010, 37, 265-282.	0.3	17
7959	Structure and bonding of ethoxy species adsorbed on transition metal surfaces. Theoretical Chemistry Accounts, 2010, 126, 223-229.	0.5	8
7960	Adsorption of tetralin and hydrogenated intermediates and products on the (100) surfaces of Ir, Pt and Pd: a DFT study. Theoretical Chemistry Accounts, 2010, 127, 401-409.	0.5	11
7961	Chemical functionalization of pyridine-like and porphyrin-like nitrogen-doped carbon (CN x) nanotubes with transition metal (TM) atoms: a theoretical study. Theoretical Chemistry Accounts, 2010, 127, 727-733.	0.5	53
7962	A critical consideration of magnetism and composition ofÂ(bcc)ÂCuÂprecipitates in (bcc) Fe. Applied Physics A: Materials Science and Processing, 2010, 99, 697-704.	1.1	32
7963	Effects of carbon on the weak ferromagnetism in doped GaN. Chemical Physics Letters, 2010, 487, 251-255.	1.2	24
7964	Oxygen dissociation on nitrogen-doped single wall nanotube: A first-principles study. Chemical Physics Letters, 2010, 492, 131-136.	1.2	62
7965	The influence of electron correlation and spinâ€“orbit coupling on the half metallic properties of LaSrMoReO6, LaSrMoTcO6 and LaSrVOsO6. Chemical Physics Letters, 2010, 492, 241-245.	1.2	1
7966	Elastic constants of oxynitride aluminum spinel phases. Chemical Physics Letters, 2010, 494, 323-325.	1.2	11
7967	Investigation of ferromagnetism in Al-doped 4Hâ€“SiC by density functional theory. Chemical Physics Letters, 2010, 496, 276-279.	1.2	29
7968	Evolution of a Pt (111) surface at high oxygen coverage in acid medium. Chemical Physics Letters, 2010, 498, 328-333.	1.2	15

#	Article	IF	Citations
7969	Electronic properties of F/Zr co-doped anatase TiO2 photocatalysts from GGA +U calculations. Chemical Physics Letters, 2010, 498, 338-344.	1.2	23
7970	The adsorption, diffusion and dissociation of O2 on Pt-skin Pt3Ni(111): A density functional theory study. Chemical Physics Letters, 2010, 499, 83-88.	1.2	38
7971	Initial stages of the growth of Al on GaN(0001). Journal of Crystal Growth, 2010, 312, 2419-2422.	0.7	7
7972	Hydrogenography of Mg Ni1â^'H gradient thin films: Interplay between the thermodynamics and kinetics of hydrogenation. Acta Materialia, 2010, 58, 658-668.	3.8	29
7973	Stability, structure and electronic properties of Î³-Fe23C6 from first-principles theory. Acta Materialia, 2010, 58, 2968-2977.	3.8	85
7974	Investigation on sintering mechanism of nanoscale tungsten powder based on atomistic simulation. Acta Materialia, 2010, 58, 3939-3951.	3.8	75
7975	Pressure-induced phase transformation of BaS: An ab initio constant pressure study. Chemical Physics, 2010, 367, 80-82.	0.9	12
7976	Vibrational spectra and structures of urazole and 4-methylurazole: DFT calculations of the normal modes in aqueous solution and in the solid state, and the influence of hydrogen bonding. Chemical Physics, 2010, 373, 219-227.	0.9	7
7977	Ferromagnetism in phosphorus-doped ZnO: First-principles calculation. Physics Letters, Section A: General, Atomic and Solid State Physics, 2010, 374, 628-631.	0.9	14
7978	First-principles prediction of the magnetism of 3d transition-metal-doped Rocksalt MgO. Physics Letters, Section A: General, Atomic and Solid State Physics, 2010, 374, 1292-1296.	0.9	26
7979	First-principles study on ferromagnetism in nitrogen-doped CdO. Physics Letters, Section A: General, Atomic and Solid State Physics, 2010, 374, 1889-1892.	0.9	10
7980	Ab-initio investigations of the electronic properties of bulk wurtzite Beryllia and its derived nanofilms. Physics Letters, Section A: General, Atomic and Solid State Physics, 2010, 374, 3977-3981.	0.9	5
7981	Dissociation of H2 molecule on the Î²-Ga2O3 (100)B surface: The critical role of oxygen vacancy. Physics Letters, Section A: General, Atomic and Solid State Physics, 2010, 374, 4169-4173.	0.9	27
7982	Indium distribution and light emission in wurtzite InGaN alloys: Several-atom In-N clusters. Physics Letters, Section A: General, Atomic and Solid State Physics, 2010, 374, 4767-4773.	0.9	13
7983	First-principles calculations of C diffusion through the surface and subsurface of Ag/Ni(100) and reconstructed Ag/Ni(100). Surface Science, 2010, 604, 186-195.	0.8	8
7984	Strained c(4Ã—2) CoO(100)-like monolayer on Pd(100): Experiment and theory. Surface Science, 2010, 604, 529-534.	0.8	27
7985	First-principles study of hydrogen interaction with carbon-doped GaN nanotube. Computational and Theoretical Chemistry, 2010, 956, 77-82.	1.5	8
7986	Structure and electronic properties of Na-doped adamantane crystals. Computational and Theoretical Chemistry, 2010, 961, 48-54.	1.5	2

#	Article	IF	Citations
7987	An atomistic approach to self-diffusion in uranium dioxide. Journal of Nuclear Materials, 2010, 400, 103-106.	1.3	26
7988	Structural, mechanical, thermodynamic, and electronic properties of thorium hydrides from first-principles. Journal of Nuclear Materials, 2010, 401, 124-129.	1.3	24
7989	The role of minor alloying elements on the stability and dispersion of yttria nanoclusters in nanostructured ferritic alloys: An ab initio study. Journal of Nuclear Materials, 2010, 403, 113-116.	1.3	82
7990	Ab initio interionic potentials for UN by multiple lattice inversion. Journal of Nuclear Materials, 2010, 404, 6-8.	1.3	7
7991	Development of a pair potential for Feâ€“He by lattice inversion. Journal of Nuclear Materials, 2010, 405, 156-159.	1.3	21
7992	Structural, electronic, and thermodynamic properties of UN: Systematic density functional calculations. Journal of Nuclear Materials, 2010, 406, 218-222.	1.3	34
7993	First principles study of intrinsic defects in hexagonal tungsten carbide. Journal of Nuclear Materials, 2010, 406, 323-329.	1.3	22
7994	Vacancy formation and solid solubility in the Uâ€“Zrâ€“N system. Journal of Nuclear Materials, 2010, 406, 351-355.	1.3	9
7995	First-principles investigation of the surface structures of Cu(n, nâˆ’1, 0) (n=2, 3 and 4) stepped surfaces. Journal of Physics and Chemistry of Solids, 2010, 71, 764-769.	1.9	5
7996	Structural, electronic, elastic and thermal properties of Mg2Si. Journal of Physics and Chemistry of Solids, 2010, 71, 758-763.	1.9	51
7997	First principles study of electronic structure and optical properties of LiMTe2 (M=Al, Ga, In) crystals. Journal of Physics and Chemistry of Solids, 2010, 71, 854-861.	1.9	30
7998	Ab initio electronic, dynamic, and thermodynamic properties of isotopic lithium hydrides (6LiH, 6LiD,) Tj ETQq1 1 0.784314 rgBT /Ove	1.9	12
7999	Zero point corrections and entropy effect on ab-initio equation-of-state: A case study on bulk titanium. Journal of Physics and Chemistry of Solids, 2010, 71, 1206-1212.	1.9	1
8000	First-principles study of the crystal and electronic structures of Î±-tetragonal boron. Journal of Solid State Chemistry, 2010, 183, 1521-1528.	1.4	25
8001	Nitrogen vacancy and ferromagnetism in Cr-doped GaN: First-principles calculations. Journal of Solid State Chemistry, 2010, 183, 2662-2668.	1.4	30
8002	Phase stability comparison by first principle calculation and experimental observation of microstructure evolution in a Mgâ€“6Gdâ€“2Zn(wt%) alloy. Materials Science & Engineering A: Structural Materials: Properties, Microstructure and Processing, 2010, 527, 2643-2648.	2.6	8
8003	Electronic structure analysis of Sb-doped BaSnO3. Materials Science and Engineering B: Solid-State Materials for Advanced Technology, 2010, 173, 33-36.	1.7	12
8004	Graphene-like bilayer hexagonal silicon polymorph. Nano Research, 2010, 3, 694-700.	5.8	46

#	Article	IF	Citations
8005	Electronic structure and properties of LaNi5 compound from first principles. Rare Metals, 2010, 29, 351-354.	3.6	4
8006	A multi-stage hierarchical approach to alloy design. Jom, 2010, 62, 25-29.	0.9	14
8007	Formation of an Face-Centered Cubic Ta-Rich Solid Solution by Ion Beam Mixing in the Immiscible Ag-Ta System. Metallurgical and Materials Transactions A: Physical Metallurgy and Materials Science, 2010, 41, 2480-2484.	1.1	2
8008	Comparison of Bowing Behaviors Between IIIâ€“V and IIâ€“VI Common-Cation Semiconductor Ternary Alloys. Journal of Electronic Materials, 2010, 39, 178-186.	1.0	7
8009	Weakening of the Cu/Cu3Sn(100) Interface by Bi Impurities. Journal of Electronic Materials, 2010, 39, 1277-1282.	1.0	11
8010	A First-Principles Study of the Role of Na Vacancies in the Thermoelectricity of Na x CoO2. Journal of Electronic Materials, 2010, 39, 1681-1686.	1.0	12
8011	Electronic Structures of S-Doped Capped C-SWNT from First Principles Study. Nanoscale Research Letters, 2010, 5, 1027-1031.	3.1	9
8012	Theoretical Investigations into Self-Organized Ordered Metallic Semi-Clusters Arrays on Metallic Substrate. Nanoscale Research Letters, 2010, 5, 1020-1026.	3.1	2
8013	Quantum Capacitance Extraction for Carbon Nanotube Interconnects. Nanoscale Research Letters, 2010, 5, 1424-1430.	3.1	12
8014	The effects of hydroxyl groups on Ca adsorption on rutile surfaces: a first-principles study. Journal of Materials Science: Materials in Medicine, 2010, 21, 1-10.	1.7	25
8015	Energy band genesis from sublattice states in MgSiN2 and MgGeN2 crystals. Journal of Structural Chemistry, 2010, 51, 1191-1194.	0.3	14
8016	Superconductivity in Hydrogen-rich Material: GeH4. Journal of Superconductivity and Novel Magnetism, 2010, 23, 717-719.	0.8	22
8017	First-principles study on electronic properties of SiC nanoribbon. Journal of Materials Science, 2010, 45, 3259-3265.	1.7	56
8018	First principles computational study of wurtzite CdTe nanowires. Journal of Materials Science, 2010, 45, 5463-5467.	1.7	7
8019	Chemical vapor synthesis of fluorine-doped SnO2 (FTO) nanoparticles. Journal of Nanoparticle Research, 2010, 12, 2579-2588.	0.8	33
8020	Computational investigation on 2,6-diamino-3,5-dinitropyridine-1-oxide crystal. Structural Chemistry, 2010, 21, 651-656.	1.0	6
8021	RPBE-vdW Description of Benzene Adsorption on Au(111). Topics in Catalysis, 2010, 53, 378-383.	1.3	57
8022	Hydrogen on and in Selected Overlayer Near-Surface Alloys and the Effect of Subsurface Hydrogen on the Reactivity of Alloy Surfaces. Topics in Catalysis, 2010, 53, 384-392.	1.3	27

#	Article	IF	Citations
8023	Self Blocking of CO Dissociation on a Stepped Ruthenium Surface. Topics in Catalysis, 2010, 53, 357-364.	1.3	44
8024	Theoretical Prediction and Experimental Verification of Stability of Ptâ€“3dâ€“Pt Subsurface Bimetallic Structures: From Single Crystal Surfaces to Polycrystalline Films. Topics in Catalysis, 2010, 53, 338-347.	1.3	19
8025	Establishing Relationships Between the Geometric Structure and Chemical Reactivity of Alloy Catalysts Based on Their Measured Electronic Structure. Topics in Catalysis, 2010, 53, 348-356.	1.3	60
8026	Understanding Trends in Catalytic Activity: The Effect of Adsorbateâ€“Adsorbate Interactions for CO Oxidation Over Transition Metals. Topics in Catalysis, 2010, 53, 298-310.	1.3	204
8027	Origin of the Flatband-Voltage Roll-Off Phenomenon in Metal/High- k Gate Stacks. IEEE Transactions on Electron Devices, 2010, 57, 2047-2056.	1.6	39
8028	The first-principle study of the effect of lattice impurity on adsorption of CN on sphalerite surface. Minerals Engineering, 2010, 23, 676-684.	1.8	36
8029	A DFT study on the effect of lattice impurities on the electronic structures and floatability of sphalerite. Minerals Engineering, 2010, 23, 1120-1130.	1.8	78
8030	Density functional theory modelling of and surfaces: Structure, properties and adsorption of N2O. Materials Chemistry and Physics, 2010, 119, 505-514.	2.0	34
8031	First-principles energy band calculation for CaBi2O4 with monoclinic structure. Materials Chemistry and Physics, 2010, 121, 385-389.	2.0	16
8032	Pressure effects on the phonon modes in beryllium chalcogenides. Materials Chemistry and Physics, 2010, 123, 343-346.	2.0	37
8033	Adsorption of CO, H2, N2O, NH3 and CH4 on the anatase TiO2 (0 0 1) and (1 0 1) surfaces and their competitive adsorption predicted by periodic DFT calculations. Materials Chemistry and Physics, 2010, 124, 720-725.	2.0	65
8034	High-pressure meta-stable phase of BeO: A first principle study. Materials Chemistry and Physics, 2010, 124, 768-772.	2.0	7
8035	Adsorption of Ge nanowire with 3d transition metals: A density-functional theory study. Materials Chemistry and Physics, 2010, 124, 1113-1120.	2.0	7
8036	Lattice dynamics of layered ferroelectric semiconductor compound TlGaSe2. Materials Research Bulletin, 2010, 45, 1438-1442.	2.7	6
8037	Solid-state transformation in nanocrystalline Ti induced by ball milling. Materials Letters, 2010, 64, 1215-1218.	1.3	41
8038	The ideal strength of transition metal diborides TMB2 (TM=Ti, Zr, Hf): Plastic anisotropy and the role of prismatic slip. Scripta Materialia, 2010, 62, 625-628.	2.6	62
8039	Îµ-Carbide in alloy steels: First-principles assessment. Scripta Materialia, 2010, 63, 121-123.	2.6	57
8040	First-principles understanding of environmental embrittlement of the Ni/Ni3Al interface. Scripta Materialia, 2010, 63, 391-394.	2.6	27

#	Article	IF	Citations
8041	Formation of stacking defects at surfaces: From atomistic simulations to density functional theory calculations. Solid State Sciences, 2010, 12, 172-178.	1.5	1
8042	Structural investigation of the Zn1â^'xCdxSb solid solution by density-functional theory approach. Solid State Sciences, 2010, 12, 26-32.	1.5	6
8043	DFT study of hydrogen instability and magnetovolume effects in CeNi. Solid State Sciences, 2010, 12, 59-64.	1.5	9
8044	Structural, electronic and magnetic properties of cementite-type Fe3X (X=B, C, N) by first-principles calculations. Solid State Sciences, 2010, 12, 404-408.	1.5	23
8045	First-principles study of structural, elastic, electronic and optical properties of perovskites XCaH3 (X=Cs and Rb) under pressure. Solid State Sciences, 2010, 12, 587-596.	1.5	22
8046	Structural, elastic, electronic and thermal properties of the cubic perovskite-type BaSnO3. Solid State Sciences, 2010, 12, 630-636.	1.5	49
8047	First-principles comparative study of multiferroic compound PbVO3. Solid State Sciences, 2010, 12, 938-945.	1.5	21
8048	Determining Seebeck coefficient of heavily doped La:SrTiO3 from density functional calculations. Solid State Sciences, 2010, 12, 1168-1172.	1.5	17
8049	Ab initio study on the structural and electronic properties of Li3GaP2 compared with Li3GaN2. Solid State Sciences, 2010, 12, 1080-1083.	1.5	1
8050	First-principles study of high pressure structure phase transition and elastic properties of titanium. Solid State Sciences, 2010, 12, 1473-1479.	1.5	37
8051	First-principles study of structural and electronic properties of zincblende AlxIn1â^'xN. Solid State Sciences, 2010, 12, 1641-1644.	1.5	7
8052	AMoO4 (AÂ=ÂMg, Ni) molybdates: Phase stabilities, electronic structures and chemical bonding properties from first principles. Solid State Sciences, 2010, 12, 1779-1785.	1.5	37
8053	X-ray photoelectron spectroscopic investigation on the elemental chemical shifts in multiferroic BiFeO3 and its valence band structure. Solid State Sciences, 2010, 12, 1803-1808.	1.5	39
8054	Ground state properties of perovskite and post-perovskite CaRuO3: Ferromagnetism reduction. Solid State Sciences, 2010, 12, 2003-2009.	1.5	3
8055	In situ synchrotron X-ray diffraction study of the formation of TaB2 from the elements in a laser heated diamond anvil cell. Solid State Sciences, 2010, 12, 2059-2064.	1.5	15
8056	Effects of Ta content on the phase stability and elastic properties of Î² Tiâ€“Ta alloys from first-principles calculations. Solid State Sciences, 2010, 12, 2120-2124.	1.5	25
8057	Effect of C and milling parameters on the synthesis of WC powders by mechanical alloying. International Journal of Refractory Metals and Hard Materials, 2010, 28, 211-216.	1.7	60
8058	Small tungsten carbide nanoparticles: Simulation of structure, energetics, and tensile strength. International Journal of Refractory Metals and Hard Materials, 2010, 28, 446-450.	1.7	23

#	Article	IF	Citations
8059	Partial hydrogenation of propyne over copper-based catalysts and comparison with nickel-based analogues. Journal of Catalysis, 2010, 269, 80-92.	3.1	155
8060	Atomic-scale insight into the origin of pyridine inhibition of MoS2-based hydrotreating catalysts. Journal of Catalysis, 2010, 271, 280-289.	3.1	67
8061	Catalytic activity and selectivity of methylbenzenes in HSAPO-34 catalyst for the methanol-to-olefins conversion from first principles. Journal of Catalysis, 2010, 271, 386-391.	3.1	62
8062	A density functional theory study of water gas shift over pseudomorphic monolayer alloy catalysts: Comparison with NO oxidation. Journal of Catalysis, 2010, 272, 151-157.	3.1	8
8063	Effect of surface hydroxyls on selective CO2 hydrogenation over Ni4/Î³-Al2O3: A density functional theory study. Journal of Catalysis, 2010, 272, 227-234.	3.1	159
8064	CO activation pathways and the mechanism of Fischerâ€“Tropsch synthesis. Journal of Catalysis, 2010, 272, 287-297.	3.1	487
8065	Interplay between carbon monoxide, hydrides, and carbides in selective alkyne hydrogenation on palladium. Journal of Catalysis, 2010, 273, 92-102.	3.1	182
8066	Descriptors controlling the catalytic activity of metallic surfaces toward water splitting. Journal of Catalysis, 2010, 276, 92-100.	3.1	86
8067	Selective oxidation of ammonia on RuO2(110): A combined DFT and KMC study. Journal of Catalysis, 2010, 276, 371-381.	3.1	52
8068	Hydrogen Evolution on Singleâ€Crystal Copper and Silver: A Theoretical Study. ChemPhysChem, 2010, 11, 1491-1495.	1.0	25
8069	Stability of TiO₂ Polymorphs: Exploring the Extreme Frontier of the Nanoscale. ChemPhysChem, 2010, 11, 1550-1557.	1.0	31
8070	Adsorption of Proline and Glycine on the TiO₂(110) Surface: A Density Functional Theory Study. ChemPhysChem, 2010, 11, 1053-1061.	1.0	59
8071	Chemistry of Oâ€•and Hâ€Containing Species on the (001) Surface of Anatase TiO₂: A DFT Study. ChemPhysChem, 2010, 11, 2375-2382.	1.0	33
8072	Stability of Gold and Platinum Nanowires on Graphite Edges. ChemPhysChem, 2010, 11, 2361-2366.	1.0	7
8073	Reduction of NO by CO on Unsupported Ir: Bridging the Materials Gap. ChemPhysChem, 2010, 11, 2515-2520.	1.0	20
8074	Theoretical Investigations of the Oxygen Reduction Reaction on Pt(111). ChemPhysChem, 2010, 11, 2779-2794.	1.0	200
8075	Photostimulated Reduction Processes in a Titania Hybrid Metalâ€“Organic Framework. ChemPhysChem, 2010, 11, 2341-2344.	1.0	48
8076	Firstâ€principles calculation of electronic structure of Vâ€doped anatase TiO₂. ChemPhysChem, 2010, 11, 2606-2611.	1.0	28

#	Article	IF	Citations
8077	Segregation into Layers: A General Problem for Structural Instability under Pressure, Exemplified by SnH₄. ChemPhysChem, 2010, 11, 3105-3112.	1.0	14
8078	Phase stability and mechanical properties of rhenium borides by firstâ€principles calculations. Journal of Computational Chemistry, 2010, 31, 1904-1910.	1.5	29
8079	Structural stability and phase transition in OsC and RuC. Journal of Computational Chemistry, 2010, 31, 2883-2888.	1.5	17
8080	Bandgap characters in GaAsâ€based ternary alloys. Crystal Research and Technology, 2010, 45, 59-69.	0.6	11
8081	Progress in the Theory of Dense Strongly Coupled Plasmas. Contributions To Plasma Physics, 2010, 50, 970-985.	0.5	39
8082	On the Design of Highâ€Efficiency Thermoelectric Clathrates through a Systematic Crossâ€Substitution of Framework Elements. Advanced Functional Materials, 2010, 20, 755-763.	7.8	195
8083	Universal Behavior and Electricâ€Fieldâ€Induced Structural Transition in Rareâ€Earthâ€Substituted BiFeO₃. Advanced Functional Materials, 2010, 20, 1108-1115.	7.8	364
8084	Large Spaceâ€Charge Effects in a Nanostructured Proton Conductor. Advanced Functional Materials, 2010, 20, 4107-4116.	7.8	18
8086	BCN: A Graphene Analogue with Remarkable Adsorptive Properties. Chemistry - A European Journal, 2010, 16, 149-157.	1.7	194
8087	Dynamic Supramolecular Polymers Based on Benzeneâ€1,3,5â€tricarboxamides: The Influence of Amide Connectivity on Aggregate Stability and Amplification of Chirality. Chemistry - A European Journal, 2010, 16, 810-821.	1.7	93
8088	Dynamic Vapochromic Behaviors of Organic Crystals Based on the Openâ€“Close Motions of Sâ€Shaped Donorâ€“Acceptor Folding Units. Chemistry - A European Journal, 2010, 16, 4793-4802.	1.7	73
8089	Phenakiteâ€Type BeP₂N₄â€”A Possible Precursor for a New Hard Spinelâ€Type Material. Chemistry - A European Journal, 2010, 16, 7208-7214.	1.7	34
8090	Modular, Homochiral, Porous Coordination Polymers: Rational Design, Enantioselective Guest Exchange Sorption and Ab Initio Calculations of Hostâ€“Guest Interactions. Chemistry - A European Journal, 2010, 16, 10348-10356.	1.7	67
8091	Al₃Li₄(BH₄)₁₃: A Complex Doubleâ€Cation Borohydride with a New Structure. Chemistry - A European Journal, 2010, 16, 8707-8712.	1.7	66
8092	Detection of Carbocationic Species in Zeolites: Large Crystals Pave the Way. Chemistry - A European Journal, 2010, 16, 9340-9348.	1.7	26
8093	Dynamic Calcium Metalâ€“Organic Framework Acts as a Selective Organic Solvent Sponge. Chemistry - A European Journal, 2010, 16, 11632-11640.	1.7	53
8094	A Neutral Zwitterionic Molecular Solid. Chemistry - A European Journal, 2010, 16, 14051-14059.	1.7	36
8098	Firstâ€Principles Simulations of Conditions of Enhanced Adhesion Between Copper and TaN(111) Surfaces Using a Variety of Metallic Glue Materials. Angewandte Chemie - International Edition, 2010, 49, 148-152.	7.2	16

#	Article	IF	Citations
8099	Scandiumâ€Doped AlN 1D Hexagonal Nanoprisms: A Class of Roomâ€Temperature Ferromagnetic Materials. Angewandte Chemie - International Edition, 2010, 49, 173-176.	7.2	36
8100	Ab Initio Thermochemistry of Solidâ€State Materials. Angewandte Chemie - International Edition, 2010, 49, 5242-5266.	7.2	158
8101	Electric field gradient calculations in paramagnetic compounds using the PAW approach. Application to 23Na NMR in layered vanadium phosphates. Magnetic Resonance in Chemistry, 2010, 48, S171-S175.	1.1	7
8102	Hydrogen bonds and local symmetry in the crystal structure of gibbsite. Magnetic Resonance in Chemistry, 2010, 48, 877-881.	1.1	38
8103	Structural and electronic properties of H-passivated graphene. Applied Surface Science, 2010, 256, 5783-5788.	3.1	34
8104	Ab initio calculations of generalized-stacking-fault energy surfaces and surface energies for FCC metals. Applied Surface Science, 2010, 256, 6345-6349.	3.1	89
8105	Theoretical study of Ni adsorption on the GaN(0001) surface. Applied Surface Science, 2010, 256, 6495-6498.	3.1	16
8106	Spatial and electronic structure of the Ni3P surface. Applied Surface Science, 2010, 256, 7692-7695.	3.1	11
8107	Preparation, electronic structure, and photocatalytic properties of Bi2O2CO3 nanosheet. Applied Surface Science, 2010, 257, 172-175.	3.1	171
8108	First-principles study on the structural and electronic properties of graphene upon benzene and naphthalene adsorption. Applied Surface Science, 2010, 257, 807-810.	3.1	73
8109	Substrate effects on the ordering nanostructure for La2/3Ca1/3MnO3 ultrathin films. Journal of Crystal Growth, 2010, 312, 1617-1621.	0.7	12
8110	Hydrogen evolution on a pseudomorphic Cu-layer on Ni(111) â€“ A theoretical study. Journal of Electroanalytical Chemistry, 2010, 649, 149-152.	1.9	8
8111	Origins of visible-light emissions in hydrogen-coated silicon nanocrystals: Role of passivating coating. Journal of Luminescence, 2010, 130, 2226-2237.	1.5	3
8112	The influence of Mg on the C adsorption on Ni(100): A DFT study. Journal of Molecular Catalysis A, 2010, 315, 171-177.	4.8	7
8113	Investigation the active site of methane dissociation on Ni-based catalysts: A first-principles analysis. Journal of Molecular Catalysis A, 2010, 315, 187-196.	4.8	29
8114	First principles calculation of electronic structure, bonding and chemical stability of TiB2, NbB2 and their ternary alloy Ti0.5Nb0.5B2. Physica B: Condensed Matter, 2010, 405, 540-546.	1.3	17
8115	The structure and thermodynamic properties of zinc oxide with wurtzite and rocksalt structure under high pressures. Physica B: Condensed Matter, 2010, 405, 606-612.	1.3	26
8116	Adsorption geometry of tetracene on SiO2/Si (111) substrate with the balance of moleculeâ€“substrate and intermolecular interaction. Physica B: Condensed Matter, 2010, 405, 990-995.	1.3	5

#	Article	IF	Citations
8117	First-principles study on the stability and mechanical property of eta M3W3C (M=Fe, Co, Ni) compounds. Physica B: Condensed Matter, 2010, 405, 1011-1017.	1.3	50
8118	Structural, electronic and magnetic properties of Fe nanowires encapsulated in boron nitride nanotubes. Physica B: Condensed Matter, 2010, 405, 1035-1039.	1.3	17
8119	FP-LAPW study of the elastic properties of Al2X (X=Sc,Y,La,Lu). Physica B: Condensed Matter, 2010, 405, 1817-1820.	1.3	71
8120	FP-APW+lo study of the elastic, electronic and optical properties for the cubic antiperovskite ANSr3 (A=As, Sb and Bi) under pressure effect. Physica B: Condensed Matter, 2010, 405, 1894-1900.	1.3	21
8121	Ab initio calculations of MgF2 (001) and (011) surface structure. Physica B: Condensed Matter, 2010, 405, 2125-2127.	1.3	27
8122	Full potential linear augmented plane wave study of the elastic properties of XPt3 (X=V, Cr, Mn, Fe, Co,) Tj ETQq1 1 0.784314 rgBT /Ove	1.3	12
8123	Structural and electronic properties of amorphous InSb from first principles study. Physica B: Condensed Matter, 2010, 405, 2481-2484.	1.3	5
8124	Electronic structure and properties of (Fe1â^'xNix)4N (0â‰¤xâ‰¤1.0). Physica B: Condensed Matter, 2010, 405, 2700-2705.	1.3	10
8125	Elastic properties of cubic perovskite BaRuO3 from first-principles calculations. Physica B: Condensed Matter, 2010, 405, 3117-3119.	1.3	14
8126	First principles study on the new sp3 bonded metallic carbon crystal. Physica B: Condensed Matter, 2010, 405, 3324-3327.	1.3	4
8127	First-principles study of the perfect and vacancy defect AlN nanoribbon. Physica B: Condensed Matter, 2010, 405, 3775-3781.	1.3	65
8128	Adsorption of S, O, and H on the NiAl(110)-(2Ã—2) surface. Physica B: Condensed Matter, 2010, 405, 4059-4063.	1.3	12
8129	Structural, elastic, electronic, and thermodynamic properties of PrN from first principles calculations. Physica B: Condensed Matter, 2010, 405, 4139-4144.	1.3	15
8130	Lattice dynamics and elastic properties of Mg3As2 and Mg3Sb2 compounds from first-principles calculations. Physica B: Condensed Matter, 2010, 405, 4219-4225.	1.3	41
8131	First-principles study on electronic structure and elastic properties of hexagonal Zr2Sc. Physica B: Condensed Matter, 2010, 405, 4294-4298.	1.3	45
8132	First-principle study of solid neon under high compression. Physica B: Condensed Matter, 2010, 405, 4335-4338.	1.3	17
8133	First-principles study of phase transition and thermodynamic properties of InP. Physica B: Condensed Matter, 2010, 405, 4536-4540.	1.3	11
8134	Rational design of novel cathode materials in solid oxide fuel cells using first-principles simulations. Journal of Power Sources, 2010, 195, 1441-1445.	4.0	77

#	Article	IF	Citations
8135	UTa2O(S2)3Cl6: A ribbon structure containing a heterobimetallic 5dâ€“5f M3 cluster. Journal of Solid State Chemistry, 2010, 183, 285-290.	1.4	11
8136	The influence of sulfur substitution on the atomic displacement in Bi2Ti2O7. Journal of Solid State Chemistry, 2010, 183, 262-269.	1.4	3
8137	Structural, electronic and optical properties of orthorhombic <mml:math xmlns:mml="http://www.w3.org/1998/Math/MathML" altimg="si0047.gif" overflow="scroll"><mml:msub><mml:mrow><mml:mi>CdGeO</mml:mi></mml:mrow><mml:mrow><mml:mn>3</mml:mn></mml:mrow></mml:msub></mml:math> from first principles calculations. Journal of Solid State Chemistry, 2010, 183, 437-443.	1.4	7
8138	Structural phase transition and 5f-electrons localization of PuSe explored by ab initio calculations. Journal of Solid State Chemistry, 2010, 183, 895-900.	1.4	0
8139	Formation of scandium carbides and scandium oxycarbide from the elements at high-(P, T) conditions. Journal of Solid State Chemistry, 2010, 183, 975-983.	1.4	15
8140	Synthesis of Li2PtH6 using high pressure: Completion of the homologous series A2PtH6 (A=alkali) Tj ETQq1 1 0.784314 rgBT /Overlock	1.4	21
8141	Full potential study of the elastic, electronic, and optical properties of spinels MgIn2S4 and CdIn2S4 under pressure effect. Journal of Solid State Chemistry, 2010, 183, 2818-2825.	1.4	31
8142	Origin of the improved photo-catalytic activity of F-doped ZnWO4: A quantum mechanical study. Journal of Solid State Chemistry, 2010, 183, 3052-3057.	1.4	17
8143	The adsorption of 1,3-butadiene on Pd/Ni multilayers: The interplay between spin polarization and chemisorption strength. Journal of Solid State Chemistry, 2010, 183, 3086-3092.	1.4	10
8144	Neutral vacancy-defect-induced magnetism in SiC monolayer. Physica E: Low-Dimensional Systems and Nanostructures, 2010, 42, 2451-2454.	1.3	26
8145	The chemical modification of graphene antidot lattices. Physica E: Low-Dimensional Systems and Nanostructures, 2010, 43, 33-39.	1.3	3
8146	First-principles study of transition-metal atoms adsorption on GaN nanotube. Physica E: Low-Dimensional Systems and Nanostructures, 2010, 43, 22-27.	1.3	14
8147	Stable antiferromagnetic graphone. Physica E: Low-Dimensional Systems and Nanostructures, 2010, 43, 199-201.	1.3	39
8148	AlN, GaN, Al Ga1â^'N nanotubes and GaN/Al Ga1â^'N nanotube heterojunctions. Physics Letters, Section A: General, Atomic and Solid State Physics, 2010, 374, 877-881.	0.9	18
8149	Influences of Al doping on the electronic structure of Mg(0001) and dissociation properties of H2. Physics Letters, Section A: General, Atomic and Solid State Physics, 2010, 374, 975-980.	0.9	7
8150	Electronic structures of N- and C-doped NiO from first-principles calculations. Physics Letters, Section A: General, Atomic and Solid State Physics, 2010, 374, 1184-1187.	0.9	27
8151	Hydrogen depassivation of the magnesium acceptor by beryllium in p-type GaN. Physics Letters, Section A: General, Atomic and Solid State Physics, 2010, 374, 2374-2378.	0.9	0
8152	Role of point defects on conductivity, magnetism and optical properties in In2O3. Physics Letters, Section A: General, Atomic and Solid State Physics, 2010, 374, 2879-2885.	0.9	12

#	Article	IF	Citations
8153	Stability and electronic properties of the O-terminated Cu2O(111) surfaces: First-principles investigation. Physics Letters, Section A: General, Atomic and Solid State Physics, 2010, 374, 2994-2998.	0.9	36
8154	Glassy ferromagnetism in Al-doped 4H-SiC: AlSiâ€“ complexes. Physics Letters, Section A: General, Atomic and Solid State Physics, 2010, 374, 3230-3233.	0.9	9
8155	Half-metallic ferromagnetism in transition-metal doped germanium nitride: A first-principles study. Physics Letters, Section A: General, Atomic and Solid State Physics, 2010, 374, 3234-3237.	0.9	8
8156	Ab initio study of the stability and electronic properties of wurtzite and zinc-blende BeS nanowires. Physics Letters, Section A: General, Atomic and Solid State Physics, 2010, 374, 3348-3353.	0.9	9
8157	Lattice dynamic properties of BaSi2 and BaGe2 from first principle calculations. Physics Letters, Section A: General, Atomic and Solid State Physics, 2010, 374, 3797-3800.	0.9	29
8158	A comparative first-principles study of the adsorption of a carbon atom on copper and nickel surfaces. Physics Letters, Section A: General, Atomic and Solid State Physics, 2010, 374, 4563-4567.	0.9	11
8159	Density functional theory studies on the adsorption, diffusion and dissociation of O2 on Pt(111). Physics Letters, Section A: General, Atomic and Solid State Physics, 2010, 374, 4713-4717.	0.9	31
8160	Boron carbon nanotube superlattices: Geometry, electronic structure and quantum conductance. Physics Letters, Section A: General, Atomic and Solid State Physics, 2010, 375, 63-66.	0.9	2
8161	First principle study towards the influence of Cd2+ on the morphology of sodium chloride. Journal of Molecular Graphics and Modelling, 2010, 28, 413-419.	1.3	13
8162	Stability of Ferromagnetism in Fe, Co, and Ni Metals under High Pressure with GGA and GGA+U. Journal of Magnetism and Magnetic Materials, 2010, 322, 653-657.	1.0	42
8163	Electronic structure and magnetic properties of RCo5â^'xMx (R=Y, Pr and M=Al, Si) system. Journal of Magnetism and Magnetic Materials, 2010, 322, 1052-1055.	1.0	6
8164	Relations of electronic energies and magnetic moments of tetra-3d metal (Mn, Fe, Co and Ni) nitrides calculated using a plane-wave basis method. Journal of Magnetism and Magnetic Materials, 2010, 322, 2665-2669.	1.0	45
8165	A study of electronic structure and lattice dynamics of CoSb3 skutterudite. Journal of Magnetism and Magnetic Materials, 2010, 322, 3080-3083.	1.0	24
8166	Improving sensitivity and resolution of MQMAS spectra: A 45 Sc-NMR case study of scandium sulphate pentahydrate. Journal of Magnetic Resonance, 2010, 203, 226-235.	1.2	20
8167	First-principles study of UC2 and U2C3. Journal of Nuclear Materials, 2010, 396, 218-222.	1.3	23
8168	First-principles study of ground-state properties and high pressure behavior of ThO2. Journal of Nuclear Materials, 2010, 399, 181-188.	1.3	68
8169	First principles study on elastic properties and phase transition of NpN. Journal of Nuclear Materials, 2010, 401, 113-117.	1.3	11
8170	Microstructural evolution of irradiated tungsten: Ab initio parameterisation of an OKMC model. Journal of Nuclear Materials, 2010, 403, 75-88.	1.3	177

#	Article	IF	Citations
8171	First-principles study on dissolution and diffusion properties of hydrogen in molybdenum. Journal of Nuclear Materials, 2010, 404, 109-115.	1.3	49
8172	O-vacancy and surface on CeO2: A first-principles study. Journal of Physics and Chemistry of Solids, 2010, 71, 788-796.	1.9	29
8173	High pressure and temperature study of hydrogen storage material BH3NH3 from ab initio calculations. Journal of Physics and Chemistry of Solids, 2010, 71, 1137-1139.	1.9	14
8174	Kohn anomalies and enhanced superconductivity in simple systems under pressure: Insights from the nearly free electron model. Journal of Physics and Chemistry of Solids, 2010, 71, 1159-1164.	1.9	5
8175	First principles vibrational dynamics of magnesium telluride. Journal of Physics and Chemistry of Solids, 2010, 71, 1388-1392.	1.9	10
8176	Transparent visible light activated Câ€“Nâ€“F-codoped TiO2 films for self-cleaning applications. Journal of Photochemistry and Photobiology A: Chemistry, 2010, 210, 181-187.	2.0	86
8177	Valence band of catalyst doped sodium alanate by X-ray photoelectron spectroscopy using synchrotron radiation. International Journal of Hydrogen Energy, 2010, 35, 1213-1218.	3.8	2
8178	The adsorption and dissociation of H2O on TiO2(110) and M/TiO2(110) (MÂ=ÂPt, Au) surfacesâ€“A computational investigation. International Journal of Hydrogen Energy, 2010, 35, 1530-1536.	3.8	14
8179	The role of Li and Ni metals in the adsorbate complex and their effect on the hydrogen storage capacity of single walled carbon nanotubes coated with metal hydrides, LiH and NiH2. International Journal of Hydrogen Energy, 2010, 35, 2368-2376.	3.8	38
8180	Synthesis of (CuIn)xCd2(1â^'x)S2 photocatalysts for H2 evolution under visible light by using a low-temperature hydrothermal method. International Journal of Hydrogen Energy, 2010, 35, 3297-3305.	3.8	45
8181	Hydrogen storage in Li-doped charged single-walled carbon nanotubes. International Journal of Hydrogen Energy, 2010, 35, 3546-3549.	3.8	75
8182	First principles study to identify the reversible reaction step of a multinary hydrogen storage â€œLiâ€“Mgâ€“Bâ€“Nâ€“Hâ€•system. International Journal of Hydrogen Energy, 2010, 35, 9002-9011.	3.8	5
8183	First-principles studies of the structures and properties of Al- and Ag-substituted Mg2Ni alloys and their hydrides. International Journal of Hydrogen Energy, 2010, 35, 10349-10358.	3.8	23
8184	DFT-based FEM analysis of nonlinear effects on indentation process in diamond crystal. International Journal of Mechanical Sciences, 2010, 52, 303-308.	3.6	6
8185	Molecular-level understanding of environmental interfaces using density functional theory modeling. Physics Procedia, 2010, 4, 67-83.	1.2	6
8186	Effects of doping on the electronic properties of LiFePO4: A first-principles investigation. Physica B: Condensed Matter, 2010, 405, 803-807.	1.3	63
8187	Theoretical studies of low strain n-type GaN co-doped by Si and Sn. Physica B: Condensed Matter, 2010, 405, 145-147.	1.3	9
8188	High pressure phase transition and elastic properties of Lutetium chalcogenide. Physica B: Condensed Matter, 2010, 405, 394-399.	1.3	21

#	Article	IF	Citations
8189	Structural stability and optical properties of AlN explored by ab initio calculations. Physica B: Condensed Matter, 2010, 405, 555-558.	1.3	14
8190	Effect of uniaxial strain on the band gap of zigzag carbon nanotubes. Physica B: Condensed Matter, 2010, 405, 1329-1334.	1.3	12
8191	The effect of hydrostatic pressure on the physical properties of magnesium arsenide in cubic and hexagonal phases. Physica B: Condensed Matter, 2010, 405, 1715-1720.	1.3	8
8192	A comparison study on the electronic structure of the thermoelectric materials CoSb3 and LaFe3CoSb12. Physica B: Condensed Matter, 2010, 405, 1740-1744.	1.3	18
8193	Electronic structures of silicon doped ZnO. Physica B: Condensed Matter, 2010, 405, 1980-1985.	1.3	25
8194	First-principles study of the electronic transport properties of the carbon nanobuds. Physica B: Condensed Matter, 2010, 405, 2097-2101.	1.3	16
8195	First principles electronic structure calculations of Co2CrBi Heusler system. Physica B: Condensed Matter, 2010, 405, 2162-2165.	1.3	6
8196	Lattice dynamics of Î²-FeSi2 from first-principles calculations. Physica B: Condensed Matter, 2010, 405, 2200-2204.	1.3	18
8197	The structural, electronic and optical properties of InxGa1â^'xP alloys. Physica B: Condensed Matter, 2010, 405, 2357-2361.	1.3	23
8198	Adsorption of oxygen atom on the pristine and antisite defected SiC nanotubes. Physica B: Condensed Matter, 2010, 405, 2673-2679.	1.3	14
8199	First-principles study on the relaxed structures and electronic properties of Fe nanowires. Physica B: Condensed Matter, 2010, 405, 2726-2732.	1.3	1
8200	Ab initio study of the structural, elastic, vibrational and thermodynamic properties of the hexagonal boron nitride: Performance of LDA and GGA. Physica B: Condensed Matter, 2010, 405, 2785-2794.	1.3	37
8201	Thermal stability and elastic properties of Mg3Sb2 and Mg3Bi2 phases from first-principles calculations. Physica B: Condensed Matter, 2010, 405, 2863-2868.	1.3	60
8202	Ab initio calculations of Nb doped SrTiO3. Physica B: Condensed Matter, 2010, 405, 3164-3166.	1.3	13
8203	First-principles calculations on third-order elastic constants and internal relaxation for monolayer graphene. Physica B: Condensed Matter, 2010, 405, 3501-3506.	1.3	32
8204	First-principles prediction of structural and electronic properties of RTAsO (R=La, Gd and T=Co, Ni) compounds by LSDA+U calculations. Physica B: Condensed Matter, 2010, 405, 3525-3531.	1.3	3
8205	GGA and GGA+U calculations of the ground state of SrMnO3. Physica B: Condensed Matter, 2010, 405, 3638-3641.	1.3	5
8206	First-principles determination of the structure, elastic constant, phase diagram and thermodynamics of NiTi alloy. Physica B: Condensed Matter, 2010, 405, 3665-3672.	1.3	32

#	Article	IF	Citations
8207	Calculation of structural, elastic, electronic, and thermal properties of orthorhombic CaTiO3. Physica B: Condensed Matter, 2010, 405, 3879-3884.	1.3	20
8208	The structural, electronic, elastic, vibrational, and thermodynamic properties of HoX (X=Sb, Bi). Physica B: Condensed Matter, 2010, 405, 3977-3985.	1.3	9
8209	Ab initio study of structural, elastic, electronic and optical properties of spinel SnMg2O4. Physica B: Condensed Matter, 2010, 405, 4079-4085.	1.3	24
8210	Density functional calculations for manganese impurity in bulk silicon material. Physica B: Condensed Matter, 2010, 405, 4195-4200.	1.3	3
8211	First-principles study on the lattice dynamics and thermodynamics properties of CaFe2As2. Physica B: Condensed Matter, 2010, 405, 4226-4230.	1.3	1
8212	Theoretical analysis of the spin effect on the electronic and magnetic properties of the calcium manganese oxide CaMnO3: GGA+U calculation. Physica B: Condensed Matter, 2010, 405, 4595-4606.	1.3	16
8213	Ab initio calculations for properties of Ti2AlN and Cr2AlC. Physica B: Condensed Matter, 2010, 405, 4561-4564.	1.3	38
8214	Pressure and temperature effects on NaCl-type transition metal carbide from first-principles calculations. Physica B: Condensed Matter, 2010, 405, 4620-4626.	1.3	6
8215	Electronic structures, phase stability and hardness of technetium boride: First-principles calculation. Physica B: Condensed Matter, 2010, 405, 4659-4663.	1.3	13
8216	First-principles study of the (001) surface of cubic BiAlO3. Physica B: Condensed Matter, 2010, 405, 4687-4690.	1.3	15
8217	Optical properties of silicon doped ZnO. Physica B: Condensed Matter, 2010, 405, 4763-4767.	1.3	51
8218	First principles studies on the structural and electronic properties of Srn+1TinO3n+1 (n=1, 2, 3, â^ž). Physica B: Condensed Matter, 2010, 405, 4780-4784.	1.3	1
8219	Elastic and electronic properties of ScMn2 from first-principles calculations. Physica B: Condensed Matter, 2010, 405, 4812-4817.	1.3	10
8220	Magnetic properties in nitrogen-doped CeO2 from first-principles calculations. Physica B: Condensed Matter, 2010, 405, 4858-4862.	1.3	7
8221	Synergistic effect of different phase on the photocatalytic activity of visible light sensitive silver antimonates. Journal of Molecular Catalysis A, 2010, 320, 79-84.	4.8	21
8222	Investigation of rutheniumâ€“copper bimetallic catalysts for direct epoxidation of propylene: A DFT study. Journal of Molecular Catalysis A, 2010, 330, 107-111.	4.8	26
8223	Effects of the period vacancy on the structure, electronic and magnetic properties of the zigzag BN nanoribbon. Journal of Molecular Structure, 2010, 984, 344-349.	1.8	14
8224	Computational study of the impurity induced reduction of grain boundary energies in nano- and bi-crystalline Alâ€“Pb alloys. Materials Science & Engineering A: Structural Materials: Properties, Microstructure and Processing, 2010, 527, 1769-1775.	2.6	21

#	Article	IF	Citations
8225	Interface atomic structure of LaCuOSe:Mg epitaxial thin film and MgO substrate. Materials Science and Engineering B: Solid-State Materials for Advanced Technology, 2010, 173, 229-233.	1.7	3
8226	Theoretical and experimental study of La/Ni co-doped SrTiO3 photocatalyst. Materials Science and Engineering B: Solid-State Materials for Advanced Technology, 2010, 172, 136-141.	1.7	69
8227	Aggregation of interstitial copper atoms in silicon. Materials Science in Semiconductor Processing, 2010, 13, 29-33.	1.9	2
8228	First-principles calculations of structural, elastic, electronic and optical properties of XO (X=Ca, Sr) Tj ETQq1 1 0.784314 rgBT /Overlo 92-101.	1.9	27
8229	Helium behavior in oxide nuclear fuels: First principles modeling. Nuclear Instruments & Methods in Physics Research B, 2010, 268, 3090-3094.	0.6	30
8230	First-principles study on the electronic and optical properties of SnxGe1â^'x. Optics Communications, 2010, 283, 4307-4309.	1.0	20
8231	Density-functional study for the NOx (x=1, 2) dissociation mechanism on the Cu(111) surface. Chemical Physics, 2010, 373, 300-306.	0.9	36
8232	Halogen adsorption on crystallographic (111) planes of Pt, Pd, Cu and Au, and on Pd-monolayer catalyst surfaces: First-principles study. Electrochimica Acta, 2010, 55, 1995-2003.	2.6	45
8233	On the electrocatalysis of nanostructures: Monolayers of a foreign atom (Pd) on different substrates M(111). Electrochimica Acta, 2010, 55, 4346-4352.	2.6	45
8234	The oxygen reduction reaction mechanism on Pt(111) from density functional theory calculations. Electrochimica Acta, 2010, 55, 7975-7981.	2.6	491
8235	Quantum chemical study of adsorption of Ag2, Ag4 and Ag8 on stoichiometric TiO2 (110) surface. Computational and Theoretical Chemistry, 2010, 942, 47-54.	1.5	20
8236	Structural, electronic and optical properties of smallest (2,2) carbon nanotube: A plane-wave pseudopotential total energy calculation. Computational and Theoretical Chemistry, 2010, 942, 88-92.	1.5	12
8237	Magnetic and electronic properties of a single iron atomic chain encapsulated in carbon nanotubes: A first-principles study. Computational and Theoretical Chemistry, 2010, 962, 108-112.	1.5	8
8238	Au8 cluster adsorption on Si(100):2Ã—1 asymmetric surface studied by a first principles calculation. Thin Solid Films, 2010, 518, 3234-3239.	0.8	1
8239	First principles study of native defects in a graphitic BC2N monolayer. Thin Solid Films, 2010, 518, 4356-4362.	0.8	23
8240	Superconductivity of p-type diamond (001) and (111) thin films: Ab initio calculations. Thin Solid Films, 2010, 518, 4989-4996.	0.8	4
8241	First-principles study on the formation of a vacancy in Ge under biaxial compressive strain. Thin Solid Films, 2010, 518, 6373-6377.	0.8	4
8242	Ab initio study of the binding of collagen amino acids to graphene and A-doped (A=H, Ca) graphene. Thin Solid Films, 2010, 518, 6951-6961.	0.8	64

#	Article	IF	Citations
8243	First-principles study of lattice dynamics in thallium-V compounds. Superlattices and Microstructures, 2010, 48, 560-568.	1.4	15
8244	Crystalline and random â€œdiamond-likeâ€•boronâ€“carbon structures. Solid State Communications, 2010, 150, 133-136.	0.9	20
8245	Elastic and electronic properties of a new MAX compound from first-principles calculations. Solid State Communications, 2010, 150, 49-53.	0.9	18
8246	First principles study of Jahnâ€“Teller effects in LixMnPO4. Solid State Communications, 2010, 150, 40-44.	0.9	95
8247	Ab initio investigation of oxygen adsorption on the stability of carbon nanotube field effect transistors (CNTFETs). Solid State Communications, 2010, 150, 258-261.	0.9	3
8248	First-principles study of the dielectric properties and infrared reflectance spectrum of. Solid State Communications, 2010, 150, 360-363.	0.9	16
8249	Synergistic effect of V/N-codoped anatase photocatalysts. Solid State Communications, 2010, 150, 689-692.	0.9	41
8250	Structural stability and electronic properties of LiNiN. Solid State Communications, 2010, 150, 669-674.	0.9	8
8251	First-principles investigations of the band structure and optical properties of -boron. Solid State Communications, 2010, 150, 605-608.	0.9	21
8252	First principles study on the electronic structure and effect of vanadium doping of BN nanowires. Solid State Communications, 2010, 150, 701-706.	0.9	11
8253	Bandgaps and band bowing in semiconductor alloys. Solid State Communications, 2010, 150, 888-892.	0.9	8
8254	Formation of a Cmcm phase in SnS at high pressure; an ab initio constant pressure study. Solid State Communications, 2010, 150, 870-874.	0.9	24
8255	Electronic structure and magnetic properties in Nitrogen-doped from density functional calculations. Solid State Communications, 2010, 150, 852-856.	0.9	11
8256	Electronic, optical and bonding properties of MgCO3. Solid State Communications, 2010, 150, 848-851.	0.9	37
8257	Theoretical investigations of the physical properties of tetragonal CaSiO3 perovskite. Solid State Communications, 2010, 150, 943-948.	0.9	21
8258	Ab initio investigation of the structural, elastic and electronic properties of the anti-perovskite TlNCa3. Solid State Communications, 2010, 150, 932-937.	0.9	11
8259	Ab initio studies of half-metallic ferromagnetism in carbon-doped. Solid State Communications, 2010, 150, 923-927.	0.9	13
8260	Origin of incompressibility and hardness from electronic and mechanical properties of hard material ruthenium diboride. Solid State Communications, 2010, 150, 1095-1098.	0.9	11

#	Article	IF	Citations
8261	First-principles investigation on the phase stability and chemical bonding of phase-change random alloys. Solid State Communications, 2010, 150, 1375-1377.	0.9	10
8262	Surface properties of titanium nitride: A first-principles study. Solid State Communications, 2010, 150, 1370-1374.	0.9	31
8263	Electronic structure and decomposition pathways of monoammoniate of lithium borohydride : A first-principles investigation. Solid State Communications, 2010, 150, 1552-1555.	0.9	2
8264	First-principles lattice dynamical study of the cubic antiperovskite compounds <mml:math xmlns:mml="http://www.w3.org/1998/Math/MathML" altimg="si20.gif" display="inline" overflow="scroll"><mml:msub><mml:mrow><mml:mstyle mathvariant="normal"><mml:mi>AsNBa</mml:mi></mml:mstyle></mml:mrow><mml:mrow><mml:mn>3</mml:mn></mml:mrow></mml:msub></mml:math> and <mml:math xmlns:mml="http://www.w3.org/1998/Math/MathML" altimg="si21.gif" display="inline" overflow="scroll"><mml:msub><mml:mrow><mml:mstyle mathvariant="normal">. Solid State	0.9	10
8265	Revisiting the Phillips ionicity of conductors and the quantitative determination of the hardness of carbides and nitrides of transition metals using the LDAÂÂU technique. Solid State Communications, 2010, 150, 1818-1821.	0.9	7
8266	The high-pressure melting curve of CaO. Solid State Communications, 2010, 150, 1785-1788.	0.9	12
8267	First-principles study of the structural, elastic, electronic, optical and thermodynamic properties of the cubic perovskite CsCdCl3 under high pressure. Solid State Communications, 2010, 150, 1896-1901.	0.9	47
8268	Elastic properties and electronic structures of antiperovskite-type InNCo3 and InNNi3. Solid State Communications, 2010, 150, 1874-1879.	0.9	22
8269	Prediction study of the structural and elastic properties for the cubic skutterudites LaFe4A12 (AÂ= ÂP,) Tj ETQq0 0 0 rgBT /Overlock 10 T	0.9	29
8270	Elastic and thermodynamical properties of A15 Nb3X (XÂ= ÂAl, Ga, In, Sn and Sb) compounds â€" First principles DFT study. Solid State Communications, 2010, 150, 2057-2060.	0.9	47
8271	Effects of Zr and Ti doping on the dielectric response of : A comparative first-principles study. Solid State Communications, 2010, 150, 2020-2022.	0.9	17
8272	Electronic structure and optical properties of LaNiO3: First-principles calculations. Solid State Communications, 2010, 150, 2011-2014.	0.9	30
8273	Inverse-perovskite oxides with , Ge, Sn, Pb: Structural, elastic and thermal properties. Solid State Communications, 2010, 150, 1995-2000.	0.9	12
8274	Vibrational signature of the Siâ€"N defect in Si-doped GaNxAs1âˆ'x. Solid State Communications, 2010, 150, 1967-1970.	0.9	5
8275	Band gap and chemically ordered domain structure of a graphene analogue. Solid State Communications, 2010, 150, 2262-2265.	0.9	7
8276	First-principles investigation of the concentration-dependent phase transition of alloys. Solid State Communications, 2010, 150, 2362-2365.	0.9	1
8277	Strong phonon anomalies and Fermi surface nesting of simple cubic Polonium. Solid State Communications, 2010, 150, 2337-2340.	0.9	5
8278	Size- and shape-dependent energetics of transition-metal nanocrystals. Solid State Communications, 2010, 150, 2333-2336.	0.9	4

#	Article	IF	Citations
8279	Density-functional theory study of long-range ferromagnetic properties in Mg-doped SiC. Solid State Communications, 2010, 150, 2310-2313.	0.9	7
8280	Mechanism of the linear and nonlinear optical effects of and crystals. Solid State Communications, 2010, 150, 2318-2321.	0.9	12
8281	First principles calculation of structural phase transformation in Mg2Si at high pressure. Solid State Communications, 2010, 150, 2299-2302.	0.9	16
8282	A combined conductivity and DFT study of protons in PbZrO3 and alkaline earth zirconate perovskites. Solid State Ionics, 2010, 181, 130-137.	1.3	57
8283	Atomic modification of stepped metal surfaces using vertical single-atom manipulation with a trimer-apex tip: First-principles and semiempirical simulations. Surface and Coatings Technology, 2010, 204, 3254-3257.	2.2	1
8284	Methanol adsorption on Pd(110) and Ag/Pd(110) studied by high-resolution photoelectron spectroscopy. Surface Science, 2010, 604, 89-97.	0.8	4
8285	A density functional theory study of formaldehyde adsorption and oxidation on CeO2(111) surface. Surface Science, 2010, 604, 68-78.	0.8	64
8286	The kaolinite (001) polar basal plane. Surface Science, 2010, 604, 111-117.	0.8	30
8287	Hydrazine (N2H4) adsorption on Ni(100) â€“ Density functional theory investigation. Surface Science, 2010, 604, 245-251.	0.8	48
8288	Oxygen adatoms at SrTiO3(001): A density-functional theory study. Surface Science, 2010, 604, 372-376.	0.8	20
8289	Unsaturated hydrocarbons adsorbed on low coordinated Pd surface: A periodic DFT study. Surface Science, 2010, 604, 386-395.	0.8	12
8290	Chemisorption of isocyanate (NCO) on the Pd(100) surface at different coverages. Surface Science, 2010, 604, 442-450.	0.8	10
8291	A model for the dissociative adsorption of N2O on Cu(100) using a continuous potential energy surface. Surface Science, 2010, 604, 555-561.	0.8	43
8292	Adsorption of small molecules on a (2Ã—1) PdZn surface alloy on Pd(111). Surface Science, 2010, 604, 596-608.	0.8	11
8293	Structural, electronic and energetic properties of water adsorbed on Î²-Si3N4 (0001) surface: First-principles calculations. Surface Science, 2010, 604, 617-622.	0.8	12
8294	Adsorption of molecular SiO2 on a clean Si(1 0 0) surface. Surface Science, 2010, 604, L21-L25.	0.8	2
8295	Methylamine decomposition on nickel surfaces: A density functional theory study. Surface Science, 2010, 604, 779-787.	0.8	21
8296	Sulphur adsorption on Au{110}: DFT and LEED study. Surface Science, 2010, 604, 797-803.	0.8	8

#	Article	IF	Citations
8297	Coverage effects on the adsorption of sulfur on Co(0001): A DFT study. Surface Science, 2010, 604, 817-823.	0.8	22
8298	A theoretical study of Zn adsorption and desorption on a Pd(111) substrate. Surface Science, 2010, 604, 926-931.	0.8	16
8299	Structure determination of the p3Ã—3R30â˜ Biâ€“Ag(111) surface alloy using LEED Iâ€“V and DFT analyses. Surface Science, 2010, 604, 1395-1399.	0.8	14
8300	Role of sub-surface oxygen in Cu(100) oxidation. Surface Science, 2010, 604, 1425-1431.	0.8	25
8301	A reactive force-field (ReaxFF) Monte Carlo study of surface enrichment and step structure on yttria-stabilized zirconia. Surface Science, 2010, 604, 1438-1444.	0.8	24
8302	Surface reconstruction modes of Cu2O(001) surface: A first principles study. Surface Science, 2010, 604, 1516-1523.	0.8	20
8303	A Density Functional Theory study on gold cyanide interactions: The fundamentals of ore cleaning. Surface Science, 2010, 604, 1552-1557.	0.8	18
8304	Hybrid HFâ€“DFT modeling of monolayer water adsorption on (001) surface of cubic BaHfO3 and BaZrO3 crystals. Surface Science, 2010, 604, 1591-1597.	0.8	40
8305	Near-degenerate stereomorphs of the doubly-chiral hcp-{213Ì…1} surface. Surface Science, 2010, 604, 1688-1693.	0.8	1
8306	Reaction intermediates of methanol synthesis and the waterâ€“gas-shift reaction on the ZnO(0001) surface. Surface Science, 2010, 604, 1742-1751.	0.8	29
8307	Effects of bimetallic modification on the decomposition of CH3OH and H2O on Pt/W(110) bimetallic surfaces. Surface Science, 2010, 604, 1845-1853.	0.8	13
8308	Theoretical studies of chemisorption of NO2 molecules on SiC nanotube. Surface Science, 2010, 604, 1882-1888.	0.8	21
8309	Adsorption of atomic oxygen on cubic PbTiO3 and LaMnO3 (001) surfaces: A density functional theory study. Surface Science, 2010, 604, 1889-1893.	0.8	36
8310	Ab initio study of Yb on the Ge(111)â€“(3Ã—2) and Si(111)â€“(3Ã—2) surfaces. Surface Science, 2010, 604, 1899-1905.	0.8	2
8311	Ab initio study of water adsorption on TiO2-terminated (100) surface of SrTiO3 with and without Cr doping. Surface Science, 2010, 604, 1987-1995.	0.8	16
8312	Relaxation and thermal vibrations at the NaF(100) surface. Surface Science, 2010, 604, 1996-2001.	0.8	6
8313	Role of vacancy and metal doping on combustive oxidation of Zr/ZrO2 core-shell particles. Surface Science, 2010, 604, 2116-2128.	0.8	6
8314	Tuneable molecular doping of corrugated graphene. Surface Science, 2010, 604, 2190-2193.	0.8	16

#	Article	IF	Citations
8315	Enthalpy of formation of the Laâ€“Mg intermediate phases. Thermochimica Acta, 2010, 499, 65-70.	1.2	18
8316	Long-range correlations in <mml:math xmlns:mml="http://www.w3.org/1998/Math/MathML" altimg="si0055.gif" overflow="scroll"><mml:msub><mml:mrow><mml:mi>In</mml:mi></mml:mrow><mml:mrow><mml:mn>2</mml:mn></mml:mrow></mml:msub><mml:msub><mml:mrow><mml:mi mathvariant="normal">O</mml:mi></mml:mrow><mml:mrow><mml:mn>3</mml:mn></mml:mrow></mml:msub><mml:mo stretchy="false">(</mml:mo><mml:mi>ZnO</mml:mi><mml:msub><mml:mrow><mml:mo) Ti ETQq1 1 0.784314 rgBT /Overlock 10 Tf 50	0.8	6
8317	First-principles study of soluteâ€“vacancy binding in magnesium. Acta Materialia, 2010, 58, 531-540.	3.8	113
8318	Ab initio calculations of the uraniumâ€“hydrogen system: Thermodynamics, hydrogen saturation of Î±-U and phase-transformation to UH3. Acta Materialia, 2010, 58, 1045-1055.	3.8	60
8319	The effect of platinum on Al diffusion kinetics in Î²-NiAl: Implications for thermal barrier coating lifetime. Acta Materialia, 2010, 58, 2726-2737.	3.8	41
8320	Analysis of deformation twins and the partially dehydrogenated microstructure in nanocrystalline magnesium hydride (MgH2) powder. Acta Materialia, 2010, 58, 3162-3172.	3.8	67
8321	First-principles calculations of the elastic, phonon and thermodynamic properties of Al12Mg17. Acta Materialia, 2010, 58, 4012-4018.	3.8	103
8322	Fundamental studies on stress-corrosion cracking in iron and underlying mechanisms. Acta Materialia, 2010, 58, 5142-5149.	3.8	19
8323	Atomistic mechanism of hydrogen trapping in bcc Feâ€“Y solid solution: A first principles study. Acta Materialia, 2010, 58, 5363-5369.	3.8	13
8324	Theoretical investigation of {110} generalized stacking faults and their relation to dislocation behavior in perovskite oxides. Acta Materialia, 2010, 58, 6072-6079.	3.8	40
8325	Mechanism of incorporation of zinc into hydroxyapatite. Acta Biomaterialia, 2010, 6, 2289-2293.	4.1	122
8326	Inhibition of coking and CO poisoning of Pt catalysts by the formation of Au/Pt bimetallic surfaces. Applied Catalysis A: General, 2010, 375, 303-309.	2.2	61
8327	Generalized-stacking-fault energy and surface properties for HCP metals: A first-principles study. Applied Surface Science, 2010, 256, 3409-3412.	3.1	91
8328	Molecular assembly of tetracene on the (2Ã—1)O reconstructed Cu(110) surface. Applied Surface Science, 2010, 256, 3598-3602.	3.1	1
8329	Study of ammonia molecule adsorbing on diamond (100) surface. Applied Surface Science, 2010, 256, 4136-4141.	3.1	7
8330	Valence of â€œdivalentâ€•rare earth metals. Applied Surface Science, 2010, 256, 4845-4849.	3.1	5
8331	Effects of N adsorption on the structural and electronic properties of SrTiO3(001) surface. Applied Surface Science, 2010, 256, 6262-6268.	3.1	8
8332	Density functional theory prediction for oxidation and exfoliation of graphite to graphene. Applied Surface Science, 2010, 256, 7596-7599.	3.1	15

#	Article	IF	Citations
8333	Adsorption of oxygen molecular on pristine and defected SiC nanotubes. Applied Surface Science, 2010, 257, 282-289.	3.1	11
8334	Disulphide and metal sulphide formation on the reconstructed (0 0 1) surface of chalcopyrite: A DFT study. Applied Surface Science, 2010, 257, 1319-1324.	3.1	67
8335	Density functional theory simulation of titanium migration and reaction with oxygen in the early stages of oxidation of equiatomic NiTi alloy. Biomaterials, 2010, 31, 3439-3448.	5.7	55
8336	Density functional theory study on adsorption of thiophene on TiO2 anatase (001) surfaces. Catalysis Today, 2010, 149, 218-223.	2.2	48
8337	Orthorhombic intermediate phases for the wurtzite-to-rocksalt phase transformation of CdSe: An ab initio constant pressure study. Chemical Physics, 2010, 369, 55-58.	0.9	9
8338	Lattice anisotropy, electronic and chemical structures of uranyl carbonate, UO2CO3, from first principles. Chemical Physics, 2010, 372, 46-50.	0.9	6
8339	Density-functional studies of the adsorption and reaction of HCl and H2O molecules over the W(111) surface. Chemical Physics, 2010, 374, 22-29.	0.9	0
8340	A first-principle study of the effect of vacancy defects and impurities on the adsorption of O2 on sphalerite surfaces. Colloids and Surfaces A: Physicochemical and Engineering Aspects, 2010, 363, 56-63.	2.3	56
8341	Calculations of single-crystal elastic constants made simple. Computer Physics Communications, 2010, 181, 671-675.	3.0	182
8342	Density functional theory evidence for an electron hopping process in single-walled carbon nanotube-mediated redox reactions. Carbon, 2010, 48, 1524-1530.	5.4	5
8343	In situ observations of the nucleation and growth of atomically sharp graphene bilayer edges. Carbon, 2010, 48, 2354-2360.	5.4	33
8344	A theoretical study of possible shape and phase changes of carbon nanotube crystals during contraction and expansion. Carbon, 2010, 48, 2948-2952.	5.4	1
8345	Density functional study of the metallization of a linear carbon chain inside single wall carbon nanotubes. Carbon, 2010, 48, 4057-4062.	5.4	21
8346	Vacancyâ€“indium clusters in implanted germanium. Chemical Physics Letters, 2010, 490, 38-40.	1.2	14
8347	Special quasirandom structures for binary/ternary group IV random alloys. Chemical Physics Letters, 2010, 493, 97-102.	1.2	15
8348	Role of hydroxyl groups for the O2 adsorption on CeO2 surface: A DFT+U study. Chemical Physics Letters, 2010, 493, 269-272.	1.2	18
8349	Pressure induced structural changes in the potential hydrogen storage compound ammonia borane: A combined X-ray, neutron and theoretical investigation. Chemical Physics Letters, 2010, 495, 203-207.	1.2	28
8350	Density-functional theory study on ferromagnetism in N:ZnS. Chemical Physics Letters, 2010, 496, 46-49.	1.2	19

#	Article	IF	Citations
8351	First-principles calculations of phase transition and bulk modulus of PtC. Chemical Physics Letters, 2010, 496, 64-67.	1.2	14
8352	Distinguishing hydrogen bonding networks in Î±-d-galactose using NMR experiments and first principles calculations. Chemical Physics Letters, 2010, 498, 270-276.	1.2	33
8353	Core-level shifts of the c(8Ã—2)-reconstructed InAs(100) and InSb(100) surfaces. Journal of Electron Spectroscopy and Related Phenomena, 2010, 177, 52-57.	0.8	13
8354	Structure of defective crystals at finite temperatures: A quasi-harmonic lattice dynamics approach. International Journal of Solids and Structures, 2010, 47, 1807-1821.	1.3	5
8355	Polarization effects and phase equilibria in high-energy-density polyvinylidene-fluoride-based polymers. Acta Crystallographica Section A: Foundations and Advances, 2010, 66, 553-557.	0.3	3
8356	Integral modeling approach to study the phase behavior of complex solids: application to phase transitions in MgSiO₃pyroxenes. Acta Crystallographica Section A: Foundations and Advances, 2010, 66, 535-541.	0.3	6
8357	Synthesis, Structure, and Properties of Mesoporous B/C/N MicrospheresÂ. Zeitschrift Fur Anorganische Und Allgemeine Chemie, 2010, 636, 30-35.	0.6	20
8358	Zigzag Chains of Alternating Atoms in A₂AuBi (A = Na, K) and K₂AuSb. Synthesis, Structure, and BondingÂ. Zeitschrift Fur Anorganische Und Allgemeine Chemie, 2010, 636, 67-73.	0.6	18
8359	A First-Principle Study of Oxonium Ylide Mechanism over HSAPO-34 Zeolite. Chinese Journal of Catalysis, 2010, 31, 33-37.	6.9	6
8360	Surface structures of Fe3O4 (111), (110), and (001): A density functional theory study. Journal of Fuel Chemistry and Technology, 2010, 38, 121-128.	0.9	48
8361	Theoretical Study on Thermodynamic Hydrogen Isotope Effect of VQ2 (Q=H, D and T). Rare Metal Materials and Engineering, 2010, 39, 204-208.	0.8	0
8362	Electronic and transport properties of graphene nanoribbons. Physica Status Solidi (A) Applications and Materials Science, 2010, 207, 304-308.	0.8	31
8363	Structural models of aâ€Si:H with a low defect concentration: A firstâ€principles molecular dynamics study. Physica Status Solidi (A) Applications and Materials Science, 2010, 207, 605-608.	0.8	2
8364	Spectral properties of InN and its native oxide from first principles. Physica Status Solidi (A) Applications and Materials Science, 2010, 207, 1041-1053.	0.8	11
8365	Mechanisms of doping graphene. Physica Status Solidi (A) Applications and Materials Science, 2010, 207, 2131-2136.	0.8	60
8366	Optically active point defects in high quality single crystal diamond. Physica Status Solidi (A) Applications and Materials Science, 2010, 207, 2049-2053.	0.8	8
8367	Atomistic simulation of MgS polymorphs. Physica Status Solidi (B): Basic Research, 2010, 247, 48-53.	0.7	6
8368	Elastic and electronic properties of fluorite-like boride Be₂B and its ternary compounds XBeB (XÃ¢Â€Â‰=Ã¢Â€Â‰Na, Mg, Al) from first principles. Physica Status Solidi (B): Basic Research, 2010, 247, 41-47.	0.7	3

#	Article	IF	Citations
8369	Density functional calculations of the electronic structure and optical properties of magnesium oxide. Physica Status Solidi (B): Basic Research, 2010, 247, 157-162.	0.7	11
8370	Stability and band gaps of InGaP, BGaP, and BInGaP alloys: Density-functional supercell calculations. Physica Status Solidi (B): Basic Research, 2010, 247, 59-66.	0.7	10
8371	Do the atoms at second layer block the path of vacancies in the bulk? - The DFT study of vacancies below the Mg (0001) surface. Physica Status Solidi (B): Basic Research, 2010, 247, 259-264.	0.7	0
8372	First-principles study of W, WN, WN₂, and WN₃. Physica Status Solidi (B): Basic Research, 2010, 247, 54-58.	0.7	19
8373	Elastic and thermodynamic properties of IrN₂ under pressure. Physica Status Solidi (B): Basic Research, 2010, 247, 921-926.	0.7	14
8374	Density functional study of stability of high pressure phases in InP and InAs crystals. Physica Status Solidi (B): Basic Research, 2010, 247, 273-277.	0.7	5
8375	Effect of Nb doping on electronic and magnetic properties of halfâ€metallic CoMnSb semiâ€Heusler compound from firstâ€principles calculations. Physica Status Solidi (B): Basic Research, 2010, 247, 945-949.	0.7	23
8376	Ab initio study of magnetoelectricity in composite multiferroics. Physica Status Solidi (B): Basic Research, 2010, 247, 1600-1607.	0.7	24
8377	Elementary energy bands concept, band structure, and peculiarities of bonding in Î²-InSe crystal. Physica Status Solidi (B): Basic Research, 2010, 247, 318-324.	0.7	7
8378	The effects of concentration on the electronic and optical properties in Cd_xZn_{1â^'x}S ternary alloys. Physica Status Solidi (B): Basic Research, 2010, 247, 1214-1219.	0.7	19
8379	Mobility enhancement of p-type SnO₂by In-Ga co-doping. Physica Status Solidi (B): Basic Research, 2010, 247, 299-302.	0.7	34
8380	Displacive phase transition, structural stability, and mechanical properties of the ultraâ€incompressible and hard MoN by first principles. Physica Status Solidi (B): Basic Research, 2010, 247, 1207-1213.	0.7	25
8381	First-principles study on the half-metallic ferromagnetism of zinc-blende structural ScX (Xâ€‰=â€‰C, Si, Ge,) Tj ETQq0 0 0 rgBT /Overl	0.7	13
8382	Reflectance anisotropy spectra of CdTe(001) surfaces. Physica Status Solidi (B): Basic Research, 2010, 247, 1979-1983.	0.7	2
8383	The screenedâ€exchange approximation as alternative method for DFT calculations on graphene structures. Physica Status Solidi (B): Basic Research, 2010, 247, 2945-2948.	0.7	8
8384	Structural evolution of double perovskite Sr2MgWO6 under high pressure. Physica Status Solidi (B): Basic Research, 2010, 247, 1773-1777.	0.7	13
8385	Structural stabilities and electronic and elastic properties of CdO: A first-principles study. Physica Status Solidi (B): Basic Research, 2010, 247, 2202-2206.	0.7	10
8386	(Meta-)stable phases and pre-Guinier-Preston zones in AlCu alloys constructed from ab initio relaxed atomic positions - Comparison to experimental methods. Physica Status Solidi (B): Basic Research, 2010, 247, 2168-2178.	0.7	9

#	Article	IF	Citations
8387	First principles theoretical study of complex magnetic order in transitionâ€metal nanowires. Physica Status Solidi (B): Basic Research, 2010, 247, 2610-2620.	0.7	13
8388	Calculation of Oxygen and Sulfur Average Velocity on the Iron Surface: A Twoâ€dimensional Gas Model Study. Steel Research International, 2010, 81, 949-952.	1.0	5
8389	Chemical surface passivation of 3Câ€SiC nanocrystals: A firstâ€principle study. International Journal of Quantum Chemistry, 2010, 110, 2455-2461.	1.0	15
8390	Firstâ€principle investigation of the relaxed structure and electronic properties of the Cu(110) vicinal surface. Surface and Interface Analysis, 2010, 42, 53-58.	0.8	0
8391	Firstâ€principle studies of dissociative adsorption of H₂O on NiAl(110)â€(2 Ã— 2) surface. Surface and Interface Analysis, 2010, 42, 1326-1329.	0.8	3
8392	Theoretical Defect Energetics in Calcium Phosphate Bioceramics. Journal of the American Ceramic Society, 2010, 93, 1-14.	1.9	49
8393	Crystal Structure and Theoretical Elastic Property of a New Ternary Ceramic HfAl₄C₄. Journal of the American Ceramic Society, 2010, 93, 1164-1168.	1.9	9
8394	Formation of Anatase Phase in HfO₂ in Tensile Stress: An Ab Initio Study. Journal of the American Ceramic Society, 2010, 93, 1467-1469.	1.9	0
8395	Simulation of Thermoelectric Performance of Bulk SrTiO₃ with Twoâ€Dimensional Electron Gas Grain Boundaries. Journal of the American Ceramic Society, 2010, 93, 1677-1681.	1.9	36
8396	Exploring Structures and Phase Relationships of Ceramics from First Principles. Journal of the American Ceramic Society, 2010, 93, 1201-1214.	1.9	16
8397	Firstâ€Principles Thermochemistry and Thermodynamic Modeling of the Al₂O₃â€“Nd₂O₃â€“SiO₂â€“Y₂O₃ Pseudoquaternary System. Journal of the American Ceramic Society, 2010, 93, 4158-4167.	1.9	12
8398	Deformation phase transition in vanadium under high pressure. JETP Letters, 2010, 91, 611-613.	0.4	4
8399	Metallic beta-phase silicon nanowires: Structure and electronic properties. JETP Letters, 2010, 92, 352-355.	0.4	3
8400	Using first principles to predict bimetallic catalysts for the ammonia decomposition reaction. Nature Chemistry, 2010, 2, 484-489.	6.6	381
8401	Quantitative prediction of solute strengthening in aluminium alloys. Nature Materials, 2010, 9, 750-755.	13.3	256
8402	Magnetoelectric coupling at metal surfaces. Nature Nanotechnology, 2010, 5, 792-797.	15.6	95
8403	A Theoretical Investigation of the Structural Properties of Chemically Modified Mo-S-I Nanowires. Chinese Journal of Catalysis, 2010, 31, 739-746.	6.9	1
8404	Ab initio study of structural, vibrational and dielectric properties of high-Î² HfO₂as a function of doping. IOP Conference Series: Materials Science and Engineering, 2010, 8, 012021.	0.3	4

#	Article	IF	Citations
8405	First-Principles Estimation of Hydrogen Occupancy around Lattice Defects in Al. Zairyo/Journal of the Society of Materials Science, Japan, 2010, 59, 596-603.	0.1	22
8406	On the reticular construction concept of covalent organic frameworks. Beilstein Journal of Nanotechnology, 2010, 1, 60-70.	1.5	139
8407	Multi-Physics Properties in Ferroelectric Nanowires and Related Structures from First-Principles. , 2010, , .		0
8408	Size-dependent structural and electronic properties of ZnS nanofilms: An ab initio study. Journal of Applied Physics, 2010, 108, 064317.	1.1	13
8409	First Principles Study of Oxygen Incorporation Reactions in Oxides. Transactions of the Materials Research Society of Japan, 2010, 35, 59-68.	0.2	2
8410	Deformation-Induced Electronic Structure Changes in Boron Nitride Nanotubes. Zairyo/Journal of the Society of Materials Science, Japan, 2010, 59, 604-609.	0.1	1
8411	Evaluation of domain models for Î²-cristobalite from the pair distribution function. Journal of Physics Condensed Matter, 2010, 22, 125401.	0.7	12
8412	Cubic gauche-CN: A superhard metallic compound predicted via first-principles calculations. Journal of Chemical Physics, 2010, 133, 044512.	1.2	40
8413	Surface relaxation and oxygen adsorption behavior of different SiC polytypes: a first-principles study. Journal of Physics Condensed Matter, 2010, 22, 265003.	0.7	22
8414	A Systematic Study on Iron Carbides from First-Principles. Materials Science Forum, 0, 654-656, 47-50.	0.3	4
8415	First-Principles Calculation of Water Molecules with Adsorbed Ions on the Fe(001) Surface. Materials Science Forum, 2010, 654-656, 1662-1665.	0.3	0
8416	First Principles Calculation of Adhesion at Fe/WC Interface. Advanced Materials Research, 0, 129-131, 808-813.	0.3	1
8417	First principles study of vacancy and tungsten diffusion in fcc cobalt. Modelling and Simulation in Materials Science and Engineering, 2010, 18, 015008.	0.8	13
8418	Ab initio study of structural properties for zincblende AlInN: comparison of LDA and GGA. Proceedings of SPIE, 2010, , .	0.8	0
8419	Tuning Bandgap of Si-C Heterofullerene-Based Aanotubes by H Adsorption. Chinese Physics Letters, 2010, 27, 097101.	1.3	0
8420	First Principles Study of Adsorption and Reaction of CO on SrTiO ₃ (100) Surface: the Role of Surface Oxygen Vacancies. Chinese Physics Letters, 2010, 27, 017101.	1.3	10
8421	Effect of S Substitution for P Point Defects in KDP Crystals: First-Principles Study. Chinese Physics Letters, 2010, 27, 073101.	1.3	7
8422	Electron-phonon Coupling in Gallium-Doped Germanium. Chinese Physics Letters, 2010, 27, 086102.	1.3	4

#	Article	IF	Citations
8423	Electronic, Vibrational, and Superconducting Properties of High-Pressure Metallic SiH ₄ : ab initio Calculations. Chinese Physics Letters, 2010, 27, 017401.	1.3	8
8424	First-principles study of electronic and optical properties in wurtzite Zn_{1â€“x}Cu_xO. Chinese Physics B, 2010, 19, 056104.	0.7	13
8425	A Density Functional Study of Atomic Carbon Adsorption on Î´-Pu(111) Surface. Chinese Physics Letters, 2010, 27, 097102.	1.3	4
8426	Rotation of hydrogen molecules during the dissociative adsorption on the Mg(0001) surface: a first-principles study. Chinese Physics B, 2010, 19, 058201.	0.7	3
8427	Copper mobility in CuFeS2, a layered trigonal phase obtained from LiCuFeS2. Zeitschrift FÃ¼r Kristallographie, 2010, 225, .	1.1	2
8428	Mechanical and Magnetic Properties of Rh and RhH: First-Principles Calculations. Chinese Physics Letters, 2010, 27, 027101.	1.3	6
8429	First-principles investigation of site preference and bonding properties of alloying element in TiAl with O impurity. Modelling and Simulation in Materials Science and Engineering, 2010, 18, 015007.	0.8	11
8430	Characterisation of the high-pressure structural transition and elastic properties in boron arsenic. Chinese Physics B, 2010, 19, 076201.	0.7	12
8431	Electronic Structure and Characteristics of Chemical Bonds in CuInSe2, CuGaSe2, and CuAlSe2. Japanese Journal of Applied Physics, 2010, 49, 04DP07.	0.8	25
8432	Transparency of modified vinyl-silsesquioxane films and its validation by computing energy-band structure. Journal of Materials Research, 2010, 25, 76-81.	1.2	3
8433	Structural transitions of solid germane under pressure. Europhysics Letters, 2010, 90, 66006.	0.7	22
8434	First-principles studies of liquid lithium under pressure. Journal of Physics Condensed Matter, 2010, 22, 095503.	0.7	9
8435	Pressure-induced structural transition and thermodynamic properties of NbN and effect of metallic bonding on its hardness. Europhysics Letters, 2010, 92, 56002.	0.7	22
8436	Melting of Single-Walled Silicon Carbide Nanotubes: Density Functional Molecular Dynamics Simulation. Chinese Physics Letters, 2010, 27, 106101.	1.3	10
8437	Trends in the band-gap pressure coefficients and bulk moduli in different structures of ZnGa₂S₄, ZnGa₂Se₄and ZnGa₂Te₄. Chinese Physics B, 2010, 19, 107104.	0.7	19
8438	Influence of Pb adatom on adsorption of oxygen molecules on Pb(111) surface: a first-principles study. Chinese Physics B, 2010, 19, 108201.	0.7	4
8439	First-principles study of lattice dynamics and thermodynamics of osmium under pressure. Chinese Physics B, 2010, 19, 026301.	0.7	7
8440	A first-principles study of the catalytic mechanism of the dehydriding reaction of LiNH₂through adding Ti catalysts. Chinese Physics B, 2010, 19, 048601.	0.7	5

#	Article	IF	Citations
8441	First-principles study of the structural and magnetic properties of graphene on a Fe/Ni(1â€‰1â€‰1) surface. Journal Physics D: Applied Physics, 2010, 43, 385002.	1.3	14
8442	Silane plus molecular hydrogen as a possible pathway to metallic hydrogen. Proceedings of the National Academy of Sciences of the United States of America, 2010, 107, 20893-20898.	3.3	38
8443	Impact of the Formation of Dimer Structures at the Surface on the Internal Atoms of Si Thin Film. Journal of the Electrochemical Society, 2010, 157, H323.	1.3	6
8444	Structural Stability and Elastic Properties of Wurtzite TIN under Hydrostatic Pressure. Chinese Physics Letters, 2010, 27, 080505.	1.3	8
8445	Analysis of Local Environment of Fe Ions in Hexagonal BaTiO₃. Japanese Journal of Applied Physics, 2010, 49, 091502.	0.8	19
8446	Effects of H on Electronic Structure and Ideal Tensile Strength of W: A First-Principles Calculation. Chinese Physics Letters, 2010, 27, 127101.	1.3	13
8447	First-principles investigations of the magnetic properties of graphite boron nitride sheet induced by Fe doping. Journal of Physics Condensed Matter, 2010, 22, 205501.	0.7	3
8448	Electronic band transformation from indirect gap to direct gap in Siâ€“H compound. Chinese Physics B, 2010, 19, 077103.	0.7	1
8449	Hydrogen storage on calcium-decorated BC3 sheet: A first principles study. Applied Physics Letters, 2010, 97, .	1.5	29
8450	First-principles investigation of Ge doping effects on the structural, electronic and magnetic properties in antiperovskite Mn₃CuN. Journal of Physics Condensed Matter, 2010, 22, 206003.	0.7	16
8451	Shape-Dependent Magnetic Moment and Formation Energy of Fe Heterostructures on Cu(111): An Ab initio Study. Japanese Journal of Applied Physics, 2010, 49, 06GH14.	0.8	7
8452	Characterizing electronic structure motifs in<mml:math xmlns:mml="http://www.w3.org/1998/Math/MathML" display="inline"><mml:mrow><mml:mi>Î²</mml:mi><mml:msub><mml:mrow><mml:mtext>-UH</mml:mtext></mml:mrow><mml:mr Physical Review B, 2010, 82, .	1.1	14
8453	Modulating the electronic structures and optical absorption spectra of BeO nanotubes by uniaxial strain. Applied Physics Letters, 2010, 97, 051901.	1.5	9
8454	Inhibiting Adatom Diffusion through Surface Alloying. Physical Review Letters, 2010, 105, 015703.	2.9	11
8455	Tuning electronic structure of graphene via tailoring structure: Theoretical study. Journal of Applied Physics, 2010, 107, .	1.1	20
8456	Improving the Electrochemical Activity of LiMnPO[sub 4] Via Mn-Site Substitution. Journal of the Electrochemical Society, 2010, 157, A225.	1.3	112
8457	Optimizing photoelectrochemical properties of<mml:math xmlns:mml="http://www.w3.org/1998/Math/MathML" display="inline"><mml:mrow><mml:msub><mml:mrow><mml:mtext>TiO</mml:mtext></mml:mrow><mml:mn>2</mml:mn></mml:msu chemical codoping. Physical Review B, 2010, 82, .	1.1	62
8458	Surface- and edge-states in ultrathin Biâ€“Sb films. New Journal of Physics, 2010, 12, 065006.	1.2	12

#	Article	IF	Citations
8459	Molecular adsorption of small alkanes on a PdO(101) thin film: Evidence of Ïƒ-complex formation. Journal of Chemical Physics, 2010, 132, 024709.	1.2	71
8460	Mechanism of ultrahigh Mn concentration in epitaxially grown wurtzite Ga1âˆ’xMnxN. Applied Physics Letters, 2010, 97, 222108.	1.5	1
8461	Gap opening by asymmetric doping in graphene bilayers. Physical Review B, 2010, 82, .	1.1	27
8462	Cu adhesion on tantalum and ruthenium surface: Density functional theory study. Journal of Applied Physics, 2010, 107, 103534.	1.1	23
8463	Double-diamond NaAl via pressure: Understanding structure through Jones zone activation. Journal of Chemical Physics, 2010, 132, 114106.	1.2	8
8464	An ab initio study of the elastic behavior of single crystal group (IV) diborides at elevated temperatures. Applied Physics Letters, 2010, 97, .	1.5	9
8465	Defects of the crystal structure and Jahn-Teller distortion inBiMnO3. Physical Review B, 2010, 82, .	1.1	18
8466	Phase Stability and Electronic Structure of In-Free Photovoltaic Materials: Cu₂ZnSiSe₄, Cu₂ZnGeSe₄, and Cu₂ZnSnSe₄. Japanese Journal of Applied Physics, 2010, 49, 121203.	0.8	73
8467	First-principles study of substitutional metal impurities in graphene: structural, electronic and magnetic properties. New Journal of Physics, 2010, 12, 053012.	1.2	214
8468	Vibrational properties ofRe3Nfrom experiment and theory. Physical Review B, 2010, 82, .	1.1	24
8469	Dopant-vacancy cluster formation in germanium. Journal of Applied Physics, 2010, 107, .	1.1	62
8470	Atomic and electronic structure of S-terminated GaAs(001) surface. Journal of Applied Physics, 2010, 108, 063713.	1.1	3
8471	Ferromagnetic ordering of silicon vacancies in N-doped silicon carbide. Applied Physics Letters, 2010, 96, .	1.5	44
8472	Exciton: a code for excitations in materials. Molecular Physics, 2010, 108, 3181-3188.	0.8	16
8473	ELECTRONEGATIVITY EFFECTS ON THE BANDGAP BOWING CHARACTERS IN COMPOUND-SEMICONDUCTOR TERNARY ALLOYS. International Journal of Nanoscience, 2010, 09, 609-617.	0.4	1
8474	Fluorite transition metal hydride induced destabilization of the<mml:math xmlns:mml="http://www.w3.org/1998/Math/MathML" display="inline"><mml:mrow><mml:msub><mml:mrow><mml:mtext>MgH</mml:mtext></mml:mrow><mml:mn>2</mml:mn></mml:m in<mml:math xmlns:mml="http://www.w3.org/1998/Math/MathML"	1.1	37
8475	Electronic mechanism for toughness enhancement in<mml:math xmlns:mml="http://www.w3.org/1998/Math/MathML"		

#	Article	IF	Citations
8477	Effect of adsorbed H atoms on magnetism in monoatomic Fe wires at Ir(100). Physical Review B, 2010, 81, .	1.1	5
8478	Ab initiothermodynamics of deposition growth: Surface terminations of TiC(111) and TiN(111) grown by chemical vapor deposition. Physical Review B, 2010, 82, .	1.1	8
8479	Ab initiostudy of magnetism at iron surfaces under epitaxial in-plane strain. Physical Review B, 2010, 81, .	1.1	27
8480	Atomic corrugation in scanning tunneling microscopy images of the<mml:math xmlns:mml="http://www.w3.org/1998/Math/MathML" display="inline"><mml:mrow><mml:mtext>Fe</mml:mtext><mml:mrow><mml:mo>(</mml:mo><mml:mrow><mml:mn>001</mml:mn> Physical Review B, 2010, 81, .	1.1	33
8481	Magnetocrystalline anisotropy energy of Co and Fe adatoms on the (111) surfaces of Pd and Rh. Physical Review B, 2010, 81, .	1.1	82
8482	Nonlocal orbital-free kinetic energy density functional for semiconductors. Physical Review B, 2010, 81, .	1.1	128
8483	Structure of chlorine on Ag(111): Evidence of the(3Ã—3)reconstruction. Physical Review B, 2010, 81, .	1.1	18
8484	Ab initiolattice dynamics and thermodynamics of<mml:math xmlns:mml="http://www.w3.org/1998/Math/MathML" display="inline"><mml:mrow><mml:msub><mml:mrow><mml:mtext>RuO</mml:mtext></mml:mrow><mml:mn>2</mml:mn></mml: Physical Review B, 2010, 81, .	1.1	4
8485	Asymmetric relief of surface stress induced by a chiral adsorbate: Alaninate adsorption on Cu(110). Physical Review B, 2010, 81, .	1.1	12
8486	Phase stability of<mml:math xmlns:mml="http://www.w3.org/1998/Math/MathML" display="inline"><mml:mrow><mml:msub><mml:mrow><mml:mtext>Ti</mml:mtext></mml:mrow><mml:mn>2</mml:mn></mml:msub> oxygen incorporation: A first-principles investigation. Physical Review B, 2010, 81, .	1.1	101
8487	Pressure-dependent elastic constants and sound velocities of wurtzite SiC, GaN, InN, ZnO, and CdSe, and their relation to the high-pressure phase transition: A first-principles study. Physical Review B, 2010, 82, .	1.1	87
8488	First-principles and experimental analysis of<mml:math xmlns:mml="http://www.w3.org/1998/Math/MathML" display="inline"><mml:mrow><mml:msup><mml:mi>f</mml:mi><mml:mi>n</mml:mi></mml:msup><mml:mtext>â€“k</mml:mtext><mml:mn spectra and multiplet energy levels of<mml:math xmlns:mml="http://www.w3.org/1998/Math/MathM. Physical Review B, 2010, 81, .	1.1	17
8489	Eliminating ultraviolet optical absorption through Fe-impurity engineering:Ab initiostudy of the nonlinear optical crystalK2Al2B2O7. Physical Review B, 2010, 82, .	1.1	11
8490	Incipient plasticity of twin and stable/unstable grain boundaries during nanoindentation in copper. Physical Review B, 2010, 82, .	1.1	36
8491	Density functional theory study of the relative stability of the iron disulfide polymorphs pyrite and marcasite. Physical Review B, 2010, 81, .	1.1	35
8492	Quasiparticle calculations of the electronic properties of<mml:math xmlns:mml="http://www.w3.org/1998/Math/MathML" display="inline"><mml:mrow><mml:msub><mml:mrow><mml:mtext>ZrO</mml:mtext></mml:mrow><mml:mn>2</mml:mn></mml: xmlns:mml="http://www.w3.org/1998/Math/MathML" display="inline"><mml:mrow><mml:msub><mml:mrow><mml:mtext>HfO</mml:mtext></mml:mrow><mml:mn>2</mml:mn></mml: and their interface with Si. Physical Review B, 2010, 81, .	1.1	35
8493	Electron-phonon interaction and superconductivity in metallic molecular hydrogen. I. Electronic and dynamical properties under pressure. Physical Review B, 2010, 81, .	1.1	47
8494	Mn-doped cubic BN as an atomiclike memory device: A density functional study. Physical Review B, 2010, 81, .	1.1	2

#	Article	IF	Citations
8495	Graphenelike surface boron layer: Structural phases on transition-metal diborides (0001). Physical Review B, 2010, 81, .	1.1	31
8496	Theoretical study of Schottky-barrier formation at epitaxial rare-earth-metal/semiconductor interfaces. Physical Review B, 2010, 81, .	1.1	37
8497	Accurate defect levels obtained from the HSE06 range-separated hybrid functional. Physical Review B, 2010, 81, .	1.1	297
8498	Competing strain effects in reactivity of<mml:math xmlns:mml="http://www.w3.org/1998/Math/MathML" display="inline"><mml:mrow><mml:msub><mml:mrow><mml:mtext>LaCoO</mml:mtext></mml:mrow><mml:mn>3</mml:mn></mml:mrow></mml:msub></mml:mrow></mml:math> oxygen. Physical Review B, 2010, 82, .	1.1	110
8499	Transport and band structure studies of crystalline<mml:math xmlns:mml="http://www.w3.org/1998/Math/MathML" display="inline"><mml:mrow><mml:msub><mml:mrow><mml:mtext>ZnRh</mml:mtext></mml:mrow><mml:mn>2</mml:mn></mml:msub></mml:mrow></mml:math> Physical Review B, 2010, 81, .	1.1	33
8500	Strongly correlated metal interfaces in the Gutzwiller approximation. Physical Review B, 2010, 81, .	1.1	19
8501	Signatures of oxygen on<mml:math xmlns:mml="http://www.w3.org/1998/Math/MathML" display="inline"><mml:mrow><mml:msub><mml:mrow><mml:mtext>Cu</mml:mtext></mml:mrow><mml:mn>3</mml:mn></mml:msub></mml:mrow></mml:math> From isolated impurity to oxide regimes. Physical Review B, 2010, 82, .	1.1	9
8502	<mml:math xmlns:mml="http://www.w3.org/1998/Math/MathML" display="inline"><mml:mrow><mml:msub><mml:mrow><mml:mtext>Li</mml:mtext></mml:mrow><mml:mn>2</mml:mn></mml:msub></mml:mrow></mml:math> <mml:math xmlns:mml="http://www.w3.org/1998/Math/MathML" display="inline"><mml:mrow><mml:msub><mml:mrow><mml:mtext>LiNH</mml:mtext></mml:mrow><mml:mn>2</mml:mn></mml:msub></mml:mrow></mml:math>	1.1	5
8503	Strain-field effects on the formation and migration energies of self interstitials in<mml:math xmlns:mml="http://www.w3.org/1998/Math/MathML" display="inline"><mml:mrow><mml:mi>Î±</mml:mi><mml:mtext>-Fe</mml:mtext></mml:mrow></mml:math> from first principles. Physical Review B, 2010, 81, .	1.1	50
8504	Structural assignments of NMR chemical shifts in<mml:math xmlns:mml="http://www.w3.org/1998/Math/MathML" display="inline"><mml:mrow><mml:msub><mml:mrow><mml:mtext>Ge</mml:mtext></mml:mrow><mml:mi>x</mml:mi></mml:msub></mml:mrow></mml:math> via first-principles calculations for<mml:math xmlns:mml="http://www.w3.org/1998/Math/MathML"	1.1	40
8505	Experimental and theoretical investigation of the stability of the monoclinic<mml:math xmlns:mml="http://www.w3.org/1998/Math/MathML" display="inline"><mml:mrow><mml:msub><mml:mrow><mml:mtext>BaWO</mml:mtext></mml:mrow><mml:mn>4</mml:mn></mml:msub></mml:mrow></mml:math> phase at high pressure and high temperature. Physical Review B, 2010, 81, .	1.1	19
8506	Simple descriptors for proton-conducting perovskites from density functional theory. Physical Review B, 2010, 82, .	1.1	37
8507	Low hole effective mass in thin InAs nanowires. Applied Physics Letters, 2010, 96, .	1.5	9
8508	A Density Functional Investigation on C Atom Adsorbed on Ni (111) Surface in the Steam Reforming of Acetic Acid. , 2010, , .		0
8509	Ferroelectric dead layer driven by a polar interface. Physical Review B, 2010, 82, .	1.1	51
8510	Detailed structure of the H-N-H center in<mml:math xmlns:mml="http://www.w3.org/1998/Math/MathML" display="inline"><mml:mrow><mml:msub><mml:mrow><mml:mtext>GaAs</mml:mtext></mml:mrow><mml:mi>y</mml:mi></mml:msub></mml:mrow></mml:math> by vibrational spectroscopy under uniaxial stress. Physical Review B, 2010, 81, .	1.1	19
8511	High-pressure structural phase transitions in<mml:math xmlns:mml="http://www.w3.org/1998/Math/MathML" display="inline"><mml:mrow><mml:msub><mml:mrow><mml:mtext>CuWO</mml:mtext></mml:mrow><mml:mn>4</mml:mn></mml:msub></mml:mrow></mml:math> Physical Review B, 2010, 81, .	1.1	67
8512	Magnetic quantum oscillations for the surface states of topological insulator<mml:math xmlns:mml="http://www.w3.org/1998/Math/MathML" display="inline"><mml:mrow><mml:msub><mml:mrow><mml:mtext>Bi</mml:mtext></mml:mrow><mml:mn>2</mml:mn></mml:msub></mml:mrow></mml:math> Physical Review B, 2010, 82, .	1.1	31

#	Article	IF	Citations
8513	<mml:math xmlns:mml="http://www.w3.org/1998/Math/MathML" display="inline"><mml:mrow><mml:mi>P</mml:mi><mml:mrow><mml:mo>(</mml:mo><mml:mi>V</mml:mi><mml:mo>)</mml:mo></ of state of solids: Density functional theory calculations and LDA versus GGA scaling. Physical Review B, 2010, 81, .	1.1	23
8514	Phase relations and hardness trends ofZrO2phases at high pressure. Physical Review B, 2010, 81, .	1.1	61
8515	Amorphous defect clusters of pure Si and type inversion in Si detectors. Physical Review B, 2010, 82, .	1.1	12
8516	Origin of ferromagnetism in molybdenum dioxide fromab initiocalculations. Physical Review B, 2010, 81, .	1.1	18
8517	Design of three-dimensional solid-state boron oxide networks:Ab initiocalculations using density functional theory. Physical Review B, 2010, 82, .	1.1	13
8518	Near-surface microstructure ofNi-23â€‚at.â€‰%â€‚Pt: Grazing incidence diffraction and first-principles calculations. Physical Review B, 2010, 81, .	1.1	4
8519	Asymmetric diffusion as a key mechanism in Ni/Al energetic multilayer processing: A first principles study. Journal of Vacuum Science and Technology A: Vacuum, Surfaces and Films, 2010, 28, L15-L17.	0.9	16
8520	Ab initioinvestigation of lithium on the diamond C(100) surface. Physical Review B, 2010, 82, .	1.1	49
8521	Density functional theory study of clean, hydrated, and defective alumina<mml:math xmlns:mml="http://www.w3.org/1998/Math/MathML" display="inline"><mml:mrow><mml:mrow><mml:mo>(</mml:mo><mml:mrow><mml:mn>1</mml:mn><mml:mover) Tj ETQq0 0 0 rgBT	1.1	46
8522	Physical Review B, 2010, 81, . Mechanisms of atomic diffusion on the flat, stepped, and faceted surfaces of Al(110). Physical Review B, 2010, 81, .	1.1	22
8523	Metal-terminated graphene nanoribbons. Physical Review B, 2010, 82, .	1.1	58
8524	Ab initio calculations and synthesis of the off-stoichiometric half-Heusler phase Ni1â^'xMn1+xSb. Journal of Applied Physics, 2010, 108, 093712.	1.1	10
8525	Near-ultraviolet light emitting diodes using strained ultrathin InN/GaN quantum well grown by metal organic vapor phase epitaxy. Applied Physics Letters, 2010, 96, .	1.5	23
8526	Ordered Surface Alloy of Bulk-Immiscible Components Stabilized by Magnetism. Physical Review Letters, 2010, 105, 056101.	2.9	21
8527	First-principles study of structural stability and electronic structure of La-doped Sr1.9375La0.0625TiO3.968â€‰75. Journal of Applied Physics, 2010, 107, .	1.1	12
8528	Formation, structure, and bonding of boron-vacancy pairs in graphene: A first-principles study. Physical Review B, 2010, 82, .	1.1	8
8529	Theoretical analysis of structural stability of<mml:math xmlns:mml="http://www.w3.org/1998/Math/MathML" display="inline"><mml:mrow><mml:msub><mml:mtext>TM</mml:mtext><mml:mn>5</mml:mn></mml:msub><mml:msub><mml:mrow metal silicides. Physical Review B, 2010, 82, .	1.1	17
8530	In SituThin Film Growth Stresses during Chemical Ordering. Physical Review Letters, 2010, 105, 096101.	2.9	20

#	Article	IF	Citations
8531	Band crossing in isovalent semiconductor alloys with large size mismatch: First-principles calculations of the electronic structure of Bi and N incorporated GaAs. Physical Review B, 2010, 82, .	1.1	54
8532	Oxidation of pure and potassium-doped NiTi shape memory surface: A density functional theory investigation. Physical Review B, 2010, 82, .	1.1	10
8533	Ab initiostudy of the low-temperature phases of lithium imide. Physical Review B, 2010, 82, .	1.1	18
8534	Enhanced electron-mediated ferromagnetism in Co-doped ZnO nanowires. Journal of Applied Physics, 2010, 108, .	1.1	11
8535	Theory of a three-dimensional nanoporous silicon lattice with unsaturated bonding. Applied Physics Letters, 2010, 97, 121906.	1.5	3
8536	Soft Bond-Deformation Paths in Superhard<mml:math xmlns:mml="http://www.w3.org/1998/Math/MathML" display="inline"><mml:mi>Î³</mml:mi></mml:math>-Boron. Physical Review Letters, 2010, 105, 215503.	2.9	55
8537	Magnetism in Co-doped tris-8-hydroxyquinoline aluminum studied by first-principles calculations. Applied Physics Letters, 2010, 96, 053304.	1.5	16
8538	Electronic Structure of Crystalline<mml:math xmlns:mml="http://www.w3.org/1998/Math/MathML" display="inline"><mml:mmultiscripts><mml:mi>He</mml:mi><mml:mprescripts /><mml:none /><mml:mn>4</mml:mn></mml:mmultiscripts></mml:math>at High Pressures. Physical Review Letters, 2010, 105, 186404.	2.9	26
8539	Atomic structure and<mml:math xmlns:mml="http://www.w3.org/1998/Math/MathML" display="inline"><mml:mrow><mml:msub><mml:mrow><mml:mtext>SiH</mml:mtext></mml:mrow><mml:mn>4</mml:mn></mml:msu of<mml:math xmlns:mml="http://www.w3.org/1998/Math/MathML" display="inline"><mml:mrow><mml:msub><mml:mrow><mml:mtext>SiH</mml:mtext></mml:mrow><mml:mn>4</mml:mn></mml:msu Physical Review B, 2010, 82, .	1.1	13
8540	Electronic and optical properties of the<mml:math xmlns:mml="http://www.w3.org/1998/Math/MathML" display="inline"><mml:mrow><mml:msub><mml:mrow><mml:mtext>Mg</mml:mtext></mml:mrow><mml:mrow><mml:mn>2</mml:mn From band insulator to Mott insulator. Physical Review B, 2010, 82, .	1.1	4
8541	Effects of composition, strain, and atomic disorder on optical phonon frequencies in Si1âˆ’xGex. Journal of Applied Physics, 2010, 107, 073515.	1.1	13
8542	Structure and stability of thin water films on quartz surfaces. Applied Physics Letters, 2010, 97, .	1.5	17
8543	Electronic property and bonding configuration at the TiN(111)/VN(111) interface. Journal of Applied Physics, 2010, 108, .	1.1	56
8544	First-principles study of structural, electronic, and mechanical properties of the nanolaminate compound Ti4GeC3 under pressure. Journal of Applied Physics, 2010, 107, .	1.1	30
8545	Long-ranged and high temperature ferromagnetism in (Mn,C)-codoped ZnO studied by first-principles calculations. Journal of Applied Physics, 2010, 107, 033903.	1.1	20
8546	Vacancy clustering and diffusion in heavily P doped Si. Applied Physics Letters, 2010, 97, 251909.	1.5	6
8547	A density functional theory study of the CH2I2 reaction on Ag(111): Thermodynamics, kinetics, and electronic structures. Journal of Chemical Physics, 2010, 132, 024715.	1.2	6
8548	Molecular simulation on interfacial structure and gettering efficiency of direct silicon bonded (110)/(100) substrates. Journal of Applied Physics, 2010, 107, 113509.	1.1	4

#	Article	IF	Citations
8549	Ab initioand molecular dynamics studies of solid Î²-HMX: effects of hydrostatic pressure and high temperature. Molecular Simulation, 2010, 36, 670-681.	0.9	11
8550	Nonempirical prediction of impurity segregation in Î±-Fe from first principles. Journal of Applied Physics, 2010, 107, .	1.1	9
8551	Tuning electronic and magnetic properties of endohedral Co@B80 and exohedral Co-B80 metallofullerenes by positioning Co atom. Journal of Applied Physics, 2010, 107, .	1.1	10
8552	The electronic and magnetic properties of (Mn,N)-codoped ZnO from first principles. Journal of Applied Physics, 2010, 108, .	1.1	44
8553	Interaction of A-centers with isovalent impurities in silicon. Journal of Applied Physics, 2010, 107, 093518.	1.1	59
8554	Ab initio thermodynamic model to assess stability of heterostructure nanocrystals. Applied Physics Letters, 2010, 96, 101906.	1.5	7
8555	Spin-polarized current generated by carbon chain and finite nanotube. Journal of Applied Physics, 2010, 108, 104309.	1.1	9
8556	Stability of oxygen point defects in<mml:math xmlns:mml="http://www.w3.org/1998/Math/MathML" display="inline"><mml:mrow><mml:msub><mml:mrow><mml:mtext>UO</mml:mtext></mml:mrow><mml:mn>2</mml:mn></mml:m first-principles<mml:math xmlns:mml="http://www.w3.org/1998/Math/MathML"	1.1	185
8557	Lithium-niobate<mml:math xmlns:mml="http://www.w3.org/1998/Math/MathML" display="inline"><mml:mi>X</mml:mi></mml:math>-cut,<mml:math xmlns:mml="http://www.w3.org/1998/Math/MathML" display="inline"><mml:mi>Y</mml:mi></mml:math>-cut, and<mml:math xmlns:mml="http://www.w3.org/1998/Math/MathML" display="inline"><mml:mi>Z</mml:mi></mml:math>-cut surfaces fromab initiotheory. Physical Re	1.1	117
8558	and charge inhomogeneity at the surface of superconducting<mml:math xmlns:mml="http://www.w3.org/1998/Math/MathML" display="inline"><mml:mrow><mml:msub><mml:mrow><mml:mtext>BaFe</mml:mtext></mml:mrow><mml:mrow><mml:mn>2</mml:mn> Physical Review B, 2010, 81, .	1.1	34
8559	Structural and magnetic properties of single dopants of Mn and Fe for Si-based spintronic materials. Physical Review B, 2010, 82, .	1.1	19
8560	Vibrational dynamics of a<mml:math xmlns:mml="http://www.w3.org/1998/Math/MathML" display="inline"><mml:mrow><mml:mi>c</mml:mi><mml:mrow><mml:mo>(</mml:mo><mml:mrow><mml:mn>2 induced by nitrogen adsorption on Cu(001). Physical Review B, 2010, 81, .	1.1	4
8561	Undamped low-energy plasmon in<mml:math xmlns:mml="http://www.w3.org/1998/Math/MathML" display="inline"><mml:mrow><mml:msub><mml:mrow><mml:mtext>AlH</mml:mtext></mml:mrow><mml:mn>3</mml:mn> high pressure. Physical Review B, 2010, 82, .	1.1	5
8562	Temperature and pressure effects in CO titration of ensembles in PdAu(111) alloys using first principles. Physical Review B, 2010, 82, .	1.1	29
8563	Coating geometries of metals on single-walled carbon nanotubes. Applied Physics Letters, 2010, 96, .	1.5	37
8564	Magnetism in two-dimensional<mml:math xmlns:mml="http://www.w3.org/1998/Math/MathML" display="inline"><mml:mrow><mml:msub><mml:mrow><mml:mtext>BN</mml:mtext></mml:mrow><mml:mrow><mml:mn>1</mml:m xmlns:mml="http://www.w3.org/1998/Math/MathML" display="inline"><mml:mrow><mml:msub><mml:mtext>B</mml:mtext><mml:mrow><mml:mn>1</mml:mn><mml:mo>â^ Physical Review B, 2010, 81, .	1.1	7
8565	Curvature effect on the electronic properties of BN nanoribbons. Molecular Physics, 2010, 108, 3365-3371.	0.8	6
8566	Electronic damping of anharmonic adsorbate vibrations at metallic surfaces. Physical Review B, 2010, 81, .	1.1	37

#	Article	IF	Citations
8567	Reversal of chloride-induced Cu(001) subsurface buckling in the electrochemical environment: Anin situsurface x-ray diffraction and density functional theory study. Physical Review B, 2010, 81, .	1.1	43
8568	Ab initiostudy of compressed<mml:math xmlns:mml="http://www.w3.org/1998/Math/MathML" display="inline"><mml:mrow><mml:mtext>Ar</mml:mtext><mml:msub><mml:mrow><mml:mrow><mml:mo>(</mml:mo><mml:mrow><mml:mn Structural stability and anomalous melting. Physical Review B, 2010, 81, .	1.1	20
8569	Doping of cobalt oxide with transition metal impurities:Ab initiostudy. Physical Review B, 2010, 81, .	1.1	19
8570	Diffraction of fast atoms during grazing scattering from the surface of an ultrathin silica film on Mo(112). Physical Review B, 2010, 82, .	1.1	59
8571	Theory of nitride oxide adsorption on transition metal (111) surfaces: a first-principles investigation. Physical Chemistry Chemical Physics, 2010, 12, 2459.	1.3	63
8572	Electronic and spectroscopic properties of the hydrogen-terminated Si(111) surface fromab initiocalculations. Physical Review B, 2010, 82, .	1.1	24
8573	Water adsorption and dissociation on<mml:math xmlns:mml="http://www.w3.org/1998/Math/MathML" display="inline"><mml:mrow><mml:msub><mml:mrow><mml:mtext>SrTiO</mml:mtext></mml:mrow><mml:mn>3</mml:mn A density functional theory study. Physical Review B, 2010, 81, .	3.1	67
8574	xmlns:mml="http://www.w3.org/1998/Math/MathML" display="inline"><mml:mrow><mml:msub><mml:mrow><mml:mtext>Ni</mml:mtext></mml:mrow><mml:mi>n</mml:mi></mml:msub> xmlns:mml="http://www.w3.org/1998/Math/MathML" display="inline"><mml:mrow><mml:msub><mml:mrow><mml:mtext>Fe</mml:mtext></mml:mrow><mml:mi>n</mml:mi></mml:msub>	1.1	44
8575	High-Pressureâ€"High-Temperature Polymorphism in Ta: Resolving an Ongoing Experimental Controversy. Physical Review Letters, 2010, 104, 255702.	2.9	78
8576	Chemical control of polar behavior in bicomponent short-period superlattices. Physical Review B, 2010, 81, .	1.1	14
8577	Si-compatible candidates for high-<mml:math xmlns:mml="http://www.w3.org/1998/Math/MathML" display="inline"><mml:mi>Î°</mml:mi></mml:math>dielectrics with the<mml:math xmlns:mml="http://www.w3.org/1998/Math/MathML" display="inline"><mml:mrow><mml:mi>P</mml:mi><mml:mi>b</mml:mi><mml:mi>n</mml:mi><mml:mi>m</mml:mi></mml:mrow> structure. Physical Review B, 2010, 82, .	1.1	59
8578	Stability of simple cubic calcium at high pressure: A first-principles study. Physical Review B, 2010, 82, .	1.1	23
8579	Diffusion of 1,4-butanedithiol onAu(100)â^'(1Ã—1): A DFT-based master-equation approach. Physical Review B, 2010, 82, .	1.1	4
8580	Local electronic and magnetic structure of mixed ferrite multilayer materials. Physical Review B, 2010, 81, .	1.1	9
8581	Activated<mml:math xmlns:mml="http://www.w3.org/1998/Math/MathML" display="inline"><mml:mrow><mml:msub><mml:mtext>O</mml:mtext><mml:mn>2</mml:mn></mml:msub></mml:mrow> and formation of oxide islands on Be(0001): An atomistic model for metal oxidation. Physical Review B, 2010, 82, .	1.1	7
8582	First-principles computational study of defect clustering in solid solutions of<mml:math xmlns:mml="http://www.w3.org/1998/Math/MathML" display="inline"><mml:mrow><mml:msub><mml:mrow><mml:mtext>ThO</mml:mtext></mml:mrow><mml:mn>2</mml:mn trivalent oxides. Physical Review B, 2010, 82, .	1.1	20
8583	CO adsorption on Pt-induced Ge nanowires. Physical Review B, 2010, 81, .	1.1	8
8584	Ab initioand scanning tunneling microscopy study of an indium-terminated GaAs(100) surface: An indium-induced surface reconstruction change in the<mml:math xmlns:mml="http://www.w3.org/1998/Math/MathML" display="inline"><mml:mrow><mml:mi>c</mml:mi><mml:mrow><mml:mo>(</mml:mo><mml:mrow><mml:mn>8	1.1	18

#	Article	IF	Citations
8585	First-principles study of 1,4-butanedithiol molecules and radicals adsorbed on unreconstructed Au(111) and Au(100). Physical Review B, 2010, 81, .	1.1	9
8586	Pathways for thermal phosphorus desorption from the silicon (001) surface. Physical Review B, 2010, 82, .	1.1	4
8587	Off-center rattling modes and glasslike thermal conductivity in the type-I clathrate<mml:math xmlns:mml="http://www.w3.org/1998/Math/MathML" display="inline"><mml:mrow><mml:msub><mml:mrow><mml:mtext>Ba</mml:mtext></mml:mrow><mml:mn>8</mml:mn></mml:msub> Physical Review B, 2010, 81, .	1.1	39
8588	Defect States Induced by Oxygen Vacancies in Cubic SrTiO3: First-Principles Calculations. Journal of the Physical Society of Japan, 2010, 79, 114704.	0.7	57
8589	Strong dependence of band-gap opening at the Dirac point of graphene upon hydrogen adsorption periodicity. Physical Review B, 2010, 82, .	1.1	41
8590	Origin of Rh and Pd agglomeration on the<mml:math xmlns:mml="http://www.w3.org/1998/Math/MathML" display="inline"><mml:mrow><mml:msub><mml:mrow><mml:mtext>CeO</mml:mtext></mml:mrow><mml:mn>2</mml:mn></mml:msub> Physical Review B, 2010, 82, .	1.1	18
8591	Structural changes during the formation of gold single-atom chains: Stability criteria and electronic structure. Physical Review B, 2010, 81, .	1.1	29
8592	Hydrogen interaction with point defects in tungsten. Physical Review B, 2010, 82, .	1.1	216
8593	Extrinsic point defects in aluminum antimonide. Physical Review B, 2010, 81, .	1.1	21
8594	Kinetic Monte Carlo simulations of temperature programed desorption of O/Rh(111). Journal of Chemical Physics, 2010, 132, 194701.	1.2	9
8595	Vibrational properties of ferroelectricÎ²-vinylidene fluoride polymers and oligomers. Physical Review B, 2010, 81, .	1.1	30
8596	Ab initio study of shock compressed oxygen. Journal of Chemical Physics, 2010, 132, 154307.	1.2	10
8597	Density functional study of<mml:math xmlns:mml="http://www.w3.org/1998/Math/MathML" display="inline"><mml:mrow><mml:msub><mml:mrow><mml:mtext>Li</mml:mtext></mml:mrow><mml:mn>4</mml:mn></mml:msub> xmlns:mml="http://www.w3.org/1998/Math/MathML" display="inline"><mml:mrow><mml:msub><mml:mrow><mml:mtext>Li</mml:mtext></mml:mrow><mml:mrow><mml:mn>1.5</mml:mn> Physical Review B, 2010, 81, .	1.1	16
8598	On the phase formation of sputtered hafnium oxide and oxynitride films. Journal of Applied Physics, 2010, 108, .	1.1	35
8599	Pseudopotential study of barium chalcogenides under hydrostatic pressure. High Pressure Research, 2010, 30, 207-218.	0.4	24
8600	Role of electronic friction during the scattering of vibrationally excited nitric oxide molecules from Au(111). Physical Review B, 2010, 82, .	1.1	67
8601	Density functional theory screened-exchange approach for investigating electronical properties of graphene-related materials. Physical Review B, 2010, 82, .	1.1	22
8602	H- and O-induced compressive surface stress on Pt(111): Experiments and density functional theory calculations. Physical Review B, 2010, 81, .	1.1	11

#	Article	IF	Citations
8603	Predicting order-disorder phase transitions of O/Pd(111) fromab initioWang-Landau Monte Carlo calculations. Physical Review B, 2010, 81, .	1.1	15
8604	First-principles method for impurities in quantum fluids: Positron in an electron gas. Physical Review B, 2010, 82, .	1.1	15
8605	Effect of interfacial Cr on magnetoelectricity ofFe2/CrO2/BaTiO3(001). Physical Review B, 2010, 81, .	1.1	4
8606	Single cysteine adsorption on Au(110): A first-principles study. Physical Review B, 2010, 81, .	1.1	45
8607	Anomalies in the response of V, Nb, and Ta to tensile and shear loading:Ab initiodensity functional theory calculations. Physical Review B, 2010, 81, .	1.1	59
8608	Consecutive Peierls distortions and high-pressure phase transitions in<mml:math xmlns:mml="http://www.w3.org/1998/Math/MathML" display="inline"><mml:mrow><mml:msub><mml:mrow><mml:mtext>YH</mml:mtext></mml:mrow><mml:mn>3</mml:mn></mml:msu Physical Review B, 2010, 81, .	1.1	23
8609	Density functional theory study of Pt-induced Ge(001) reconstructions. Physical Review B, 2010, 81, .	1.1	13
8610	First-principles studies of Au-induced nanowires on Ge(001). Physical Review B, 2010, 81, .	1.1	34
8611	Quasiparticle electronic structure of bismuth telluride in the<mml:math xmlns:mml="http://www.w3.org/1998/Math/MathML" display="inline"><mml:mi>G</mml:mi><mml:mi>W</mml:mi></mml:math>approximation. Physical Review B, 2010, 82, .	1.1	59
8612	Magnetostructural Effect in the Multiferroic<mml:math xmlns:mml="http://www.w3.org/1998/Math/MathML" display="inline"><mml:msub><mml:mi>BiFeO</mml:mi><mml:mn>3</mml:mn></mml:msub><mml:mtext mathvariant="normal">â^'</mml:mtext><mml:msub><mml:mi>BiMnO</mml:mi><mml:mn>3</mml:mn></mml:msub></mml:math>C from First Principles. Physical Review Letters, 2010, 104, 037202.	2.9	25
8613	Assisted self-healing in ripped graphene. Physical Review B, 2010, 82, .	1.1	7
8614	Calculation of near K edge x-ray absorption spectra and hydrogen bond network in ice XIII under compression. Journal of Chemical Physics, 2010, 132, 184506.	1.2	7
8615	First-principles investigation ofBaFe2As2(001). Physical Review B, 2010, 82, .	1.1	7
8616	First-principles study of high-field piezoelectricity in tetragonalPbTiO3. Physical Review B, 2010, 81, .	1.1	11
8617	First-principles study of quantum size effects in ultrathin Pb-Bi metal alloy films. Physical Review B, 2010, 81, .	1.1	10
8618	Multiferroic<mml:math xmlns:mml="http://www.w3.org/1998/Math/MathML" display="inline"><mml:mrow><mml:msub><mml:mrow><mml:mtext>BiFeO</mml:mtext></mml:mrow><mml:mn>3</mml:mn></mml:msub></mml:mrow></mml:math>checkerboard from first principles. Physical Review B, 2010, 82, .	3.1	16
8619	Cohesive and magnetic properties of grain boundaries in bcc Fe with Cr additions. Physical Review B, 2010, 81, .	1.1	79
8620	Ab initio study on noncompensated CrO codoping of GaN for enhanced solar energy conversion. Journal of Chemical Physics, 2010, 132, 104501.	1.2	38

#	Article	IF	Citations
8621	Goldstone-like States in a Layered Perovskite with Frustrated Polarization: A First-Principles Investigation ofPbSr2Ti2O7. Physical Review Letters, 2010, 104, 097601.	2.9	31
8622	Structure and stability of phases within the NbNâ€“AlN system. Journal Physics D: Applied Physics, 2010, 43, 145403.	1.3	49
8623	Component-specific electromechanical response in a ferroelectric/dielectric superlattice. Physical Review B, 2010, 82, .	1.1	10
8624	A theoretical study of H2 dissociation on (3Ã—3)R30Â°CO/Ru(0001). Journal of Chemical Physics, 2010, 132, 144704.	1.2	4
8625	Influence of exchange correlation on the symmetry and properties of siderite according to density-functional theory. Physical Review B, 2010, 82, .	1.1	16
8626	Magnetic trends in GaxMn1â^'xN, AlxMn1â^'xN, and InxMn1â^'xN ternary systems: A first-principles study. Journal of Applied Physics, 2010, 108, .	1.1	15
8627	Theoretical analysis of small Pt particles on rutileTiO2(110)surfaces. Physical Review B, 2010, 82, .	1.1	38
8628	Ti, Fe, and Ni in Si and their interactions with the vacancy and theAcenter: A theoretical study. Physical Review B, 2010, 81, .	1.1	46
8629	Chemical anisotropy in diamondlike<mml:math xmlns:mml="http://www.w3.org/1998/Math/MathML" display="inline"><mml:mrow><mml:msub><mml:mrow><mml:mtext>BC</mml:mtext></mml:mrow><mml:mn>2</mml:mn></mml:msub></mml:mrow></mml:math>: First-principles calculations. Physical Review B, 2010, 81, .	1.1	4
8630	Trapping of electrons near chemisorbed hydrogen on graphene. Physical Review B, 2010, 81, .	1.1	18
8631	First-principles description of atomic gold chains on Ge(001). Physical Review B, 2010, 81, .	1.1	17
8632	Bismuth-stabilized<mml:math xmlns:mml="http://www.w3.org/1998/Math/MathML" display="inline"><mml:mrow><mml:mi>c</mml:mi><mml:mrow><mml:mo>(</mml:mo><mml:mrow><mml:mn>2</mml:mn> on a InSb(100) substrate: Violation of the electron counting model. Physical Review B, 2010, 81, .	1.1	19
8633	Phonons and superconductivity in fcc and dhcp lanthanum. Physical Review B, 2010, 81, .	1.1	32
8634	Si atom adsorption and diffusion on Si(110)-(1Ã—1)and(2Ã—1). Physical Review B, 2010, 81, .	1.1	8
8635	Ultrafast thermoelectric properties of gold under conditions of strong electron-phonon nonequilibrium. Journal of Applied Physics, 2010, 108, .	1.1	4
8636	Structure and Phase Stability of NiMnGa Ferromagnetic Shape Memory Alloys by Experimental and Ab Initio Techniques. Materials Science Forum, 2010, 638-642, 2040-2045.	0.3	1
8637	Influence of pressure and transition metal<mml:math xmlns:mml="http://www.w3.org/1998/Math/MathML" display="inline"><mml:mrow><mml:mrow><mml:mo>(</mml:mo><mml:mrow><mml:mi>T</mml:mi><mml:mo>=</mml:mo><mml:mte the lanthanum bare frequency in<mml:math xmlns:mml="http://www.w3.org/1998/Math/MathML" display="inline"><mml:mrow><mml:mtext>La</mml:mtext><mml:msub><mml:mi>T</mml:mi><mml:mn>4</mml:mn>. Physical Review B, 2010, 81, .	1.1	4
8638	Pt-induced nanowires on Ge(001): A density functional theory study. Physical Review B, 2010, 81, .	1.1	30

#	Article	IF	Citations
8639	Electronic and structural properties of ununquadium from first principles. Physical Review B, 2010, 81, .	1.1	6
8640	Cobalt multilayers on diamond surfaces: Anab initiostudy. Physical Review B, 2010, 81, .	1.1	9
8641	Cluster expansion Monte Carlo study of phase stability of vanadium nitrides. Physical Review B, 2010, 81, .	1.1	23
8642	Dynamics of quantum tunneling: Effects on the rate and transition path of OH on Cu(110). Physical Review B, 2010, 81, .	1.1	14
8643	Simulating thermal motion in crystalline phase-I ammonia. Journal of Chemical Physics, 2010, 132, 134511.	1.2	15
8644	DEFECT STRUCTURE OF COPPER DOPED POTASSIUM NIOBATE CERAMICS. Functional Materials Letters, 2010, 03, 19-24.	0.7	26
8645	High-pressure phase transitions and compressibility of wolframite-type tungstates. Journal of Applied Physics, 2010, 107, .	1.1	66
8646	A comparative DFT study of electronic properties of 2H-, 4H- and 6H-SiC(0001) and SiC(000 ar{1}) clean surfaces: significance of the surface Stark effect. New Journal of Physics, 2010, 12, 043024.	1.2	30
8647	First-principles study of phase transition and elastic properties of ScSb and YSb compounds. Phase Transitions, 2010, 83, 450-456.	0.6	3
8648	First-principles study of CN carbon nitride nanotubes. Nanotechnology, 2010, 21, 195702.	1.3	19
8649	General trend for pressurized superconducting hydrogen-dense materials. Proceedings of the National Academy of Sciences of the United States of America, 2010, 107, 2793-2796.	3.3	81
8650	Ti-H and Ni-H interactions in Si: first principles theory. Materials Research Society Symposia Proceedings, 2010, 1268, 1.	0.1	0
8651	ADSORPTION PROPERTIES OF N2 ON Be(0001) SURFACE: A FIRST-PRINCIPLES CALCULATION. Modern Physics Letters B, 2010, 24, 859-865.	1.0	5
8652	First Principles Studies of Disordered Lithiated Silicon. Journal of the Electrochemical Society, 2010, 157, A392.	1.3	90
8653	Crystal engineering using functionalized adamantane. Journal of Physics Condensed Matter, 2010, 22, 315303.	0.7	2
8654	Dynamical stability and phase transition of BeO under pressure. Journal of Applied Physics, 2010, 107, .	1.1	18
8655	Quantum States and Diffusion of Lithium Atom Motion on a Graphene. Journal of the Physical Society of Japan, 2010, 79, 014601.	0.7	20
8656	First Principles Investigation of Geometrical and Electronic Structure of Semiconductor Fe_{1-X}Co_xSi₂. Materials Science Forum, 0, 663-665, 592-595.	0.3	0

#	Article	IF	Citations
8657	ABSENCE OF CO DISSOCIATION ON Mo(110): TPD AND DFT STUDY. Surface Review and Letters, 2010, 17, 469-475.	0.5	3
8658	FIRST-PRINCIPLES STUDY OF MAGNETISM AND DEFECT STATE PROPERTIES OF ANTIPEROVSKITE GaC_{1-x}Mn₃. Modern Physics Letters B, 2010, 24, 953-962.	1.0	2
8660	Impact of strain on the surface properties of transition metal carbide films: First-principles study. Journal of Applied Physics, 2010, 107, 083521.	1.1	18
8661	SITE PREFERENCE AND ELASTIC PROPERTIES OF A₂-Ti₃Al WITH OXYGEN IMPURITY: A FIRST-PRINCIPLES STUDY. International Journal of Modern Physics B, 2010, 24, 2749-2755.	1.0	14
8662	A Beâ€“W interatomic potential. Journal of Physics Condensed Matter, 2010, 22, 352206.	0.7	26
8663	First-principles study of He effects in a bcc Fe grain boundary: site preference, segregation and theoretical tensile strength. Journal of Physics Condensed Matter, 2010, 22, 375401.	0.7	43
8664	STRUCTURAL PHASE TRANSITIONS AND MECHANICAL PROPERTIES OF OsO2 UNDER HIGH PRESSURE. International Journal of Modern Physics B, 2010, 24, 4269-4279.	1.0	4
8665	PLANE-WAVE PSEUDOPOTENTIAL DENSITY FUNCTIONAL THEORY PERIODIC SLAB CALCULATIONS OF NO ADSORPTION ON Ag(001) SURFACE. Journal of Theoretical and Computational Chemistry, 2010, 09, 701-709.	1.8	0
8666	Magnetic ordering and magnetodielectric phenomena in CoSeO₄. Journal of Physics Condensed Matter, 2010, 22, 506003.	0.7	7
8667	Comparison of bond scission sequence of methanol on tungsten monocarbide and Pt-modified tungsten monocarbide. Journal of Chemical Physics, 2010, 133, 104702.	1.2	26
8668	THERMODYNAMIC PROPERTIES OF MgSiO₃ POST-PEROVSKITE. Modern Physics Letters B, 2010, 24, 315-324.	1.0	0
8669	Valence band structure of the NiAlâ€“Mo alloy from the photoelectron spectrum. Philosophical Magazine Letters, 2010, 90, 299-311.	0.5	0
8670	Kinetics versus thermodynamics in materials modeling: The case of the di-vacancy in iron. Philosophical Magazine, 2010, 90, 2585-2595.	0.7	24
8671	First-principle study of V-Si-N nanocomposite thin film structure. , 2010, , .		1
8672	First-Principles Study of Ni Adatom Adsorption on Graphene for Ni-Catalyzed Carbonization of Wood as Electromagnetic Shielding (EMS) Materials. , 2010, , .		1
8673	The interaction of Cu with Bi nanolines on H-passivated Si(001): anab initioanalysis. Journal of Physics Condensed Matter, 2010, 22, 345001.	0.7	1
8674	Interaction of small gold clusters with carbon nanotube bundles: formation of gold atomic chains. Journal of Physics Condensed Matter, 2010, 22, 125301.	0.7	3
8675	First-principles analysis of electron correlation, spin ordering and phonons in the normal state of FeSe_{1 â^’x}. Journal of Physics Condensed Matter, 2010, 22, 385701.	0.7	16

#	Article	IF	Citations
8676	A Simple Theoretical Method to Predict the Hardness of Pure Metal Crystals. Chinese Physics Letters, 2010, 27, 076201.	1.3	1
8677	Atomistic investigations of misfit dislocation for Pt/SiC(111) interface fracture. Modelling and Simulation in Materials Science and Engineering, 2010, 18, 065012.	0.8	4
8678	Ab initiostructure modelling of complex thin-film oxides: thermodynamical stability of TiC/thin-film alumina. Journal of Physics Condensed Matter, 2010, 22, 015004.	0.7	4
8679	Electronic structure of the thermoelectric materials PbTe and AgPb18SbTe20 from first-principles calculations. Journal of Materials Research, 2010, 25, 1030-1036.	1.2	6
8680	Interaction of diamond (111)-(1 Ã— 1) and (2 Ã— 1) surfaces with OH: a first principles study. Journal of Physics Condensed Matter, 2010, 22, 475005.	0.7	9
8681	Theoretical analysis of initial adsorption of high-Î° metal oxides on InxGa1â^'xAs(0â€,0â€,1)-(4Ã—2) surfaces. Journal of Chemical Physics, 2010, 133, 194702.	1.2	4
8682	The influence of hydrogen contamination on the structural stability of CoSn under compression. Journal of Physics Condensed Matter, 2010, 22, 435501.	0.7	3
8683	Computational and Experimental Design of Novel High Temperature Alloys. Advances in Science and Technology, 2010, 72, 31-39.	0.2	0
8684	A New Approach to the Computer Modeling of Amorphous Nanoporous Structures of Semiconducting and Metallic Materials: A Review. Materials, 2010, 3, 467-502.	1.3	15
8685	First-Principles Calculations of Transition Metal Nitrides TiN and NbN. Advanced Materials Research, 2010, 150-151, 174-177.	0.3	1
8686	p H -dependence of conduction type in cuprous oxide synthesized from solution. Journal of Applied Physics, 2010, 107, .	1.1	61
8687	High-pressure behavior of 2M1 muscovite. American Mineralogist, 2010, 95, 249-259.	0.9	18
8688	Density-functional study of the crystallographic structure of chromium nitride films. Journal of Physics: Conference Series, 2010, 223, 012043.	0.3	6
8689	Investigation of osmium carbides with various stoichiometries: First-principles calculations. Journal of Applied Physics, 2010, 107, .	1.1	26
8690	Dynamical effects in ab initio NMR calculations: Classical force fields fitted to quantum forces. Journal of Chemical Physics, 2010, 133, 084109.	1.2	39
8691	Shell-anchor-core structures for enhanced stability and catalytic oxygen reduction activity. Journal of Chemical Physics, 2010, 133, 134705.	1.2	18
8692	Defects responsible for the Fermi level pinning in n+ poly-Si/HfO2 gate stacks. Applied Physics Letters, 2010, 97, .	1.5	7
8693	Predicting the melting temperatures of bulk materials. Europhysics Letters, 2010, 91, 46001.	0.7	2

#	Article	IF	Citations
8694	Surface Electronic/Atomic Structure and Activation Energy on Pt(111), Pt₃Cu(111), and PtCu(111) for PEFC Cathode. Nanoscale and Microscale Thermophysical Engineering, 2010, 14, 110-122.	1.4	13
8695	Impact of oxygen on the diffusion of silicon in germanium: density functional theory calculations. Semiconductor Science and Technology, 2010, 25, 045002.	1.0	7
8696	Nanostructural interpretation for elastic softening of amorphous carbon induced by the incorporation of silicon and hydrogen atoms. Journal of Applied Physics, 2010, 107, .	1.1	9
8697	Ab initio superconducting temperature of BaSi₂at ambient pressure. Journal of Physics: Conference Series, 2010, 215, 012109.	0.3	2
8698	Reassessment of the Mgâ€“Ge binary system using CALPHAD supported by first-principles calculation. International Journal of Materials Research, 2010, 101, 1489-1496.	0.1	8
8699	Theoretical study of electronic and transport properties of PPyâ€“Pt(111) and PPyâ€“C(111):H interfaces. Journal of Physics Condensed Matter, 2010, 22, 045003.	0.7	9
8700	First-principles determination of dislocation properties in magnesium based on the improved Peierlsâ€“Nabarro equation. Physica Scripta, 2010, 81, 065601.	1.2	20
8701	Surface stress in d-band metal surfaces. Journal of Physics Condensed Matter, 2010, 22, 135007.	0.7	12
8702	Threshold defect production in germanium determined by density functional theory molecular dynamics simulations. Physica Scripta, 2010, 81, 035601.	1.2	30
8703	Trends in bulk electron-structural features of rocksalt early transition-metal carbides. Journal of Physics Condensed Matter, 2010, 22, 375501.	0.7	30
8704	Phase relationships and structures of inorganic crystals by a combination of the cluster expansion method and first principles calculations. Journal of Physics Condensed Matter, 2010, 22, 384207.	0.7	1
8705	A density functional theory study of models for the N3 and OK1 EPR centres in diamond. Journal of Physics Condensed Matter, 2010, 22, 385502.	0.7	11
8706	The atomic and electronic structure of CaF₂and BaF₂crystals with H centers: a hybrid DFT calculation study. Journal of Physics Condensed Matter, 2010, 22, 055501.	0.7	6
8707	Electronic and transport properties of a molecular junction with asymmetric contacts. Nanotechnology, 2010, 21, 065203.	1.3	5
8708	Phonon spectra of barium halide nanocrystals in fluorozirconate glasses. IOP Conference Series: Materials Science and Engineering, 2010, 15, 012021.	0.3	3
8709	First-principles analysis of the Câ€“N bond scission of methylamine on Mo-based model catalysts. Journal of Chemical Physics, 2010, 132, 044111.	1.2	13
8710	Thioglycolic acid on the gold (111) surface and Raman vibrational spectra. Journal of Chemical Physics, 2010, 132, 064702.	1.2	6
8711	The equation of state and nonmetalâ€“metal transition of benzene under shock compression. Journal of Applied Physics, 2010, 107, 083502.	1.1	10

#	Article	IF	Citations
8712	Ni endohedral-doped C60 with duality of magnetic moments. Applied Physics Letters, 2010, 96, 233103.	1.5	9
8713	Hydrogen bond symmetrization and superconducting phase of HBr and HCl under high pressure: An ab initio study. Journal of Chemical Physics, 2010, 133, 074509.	1.2	41
8714	In situ electron energy loss spectroscopy study of metallic Co and Co oxides. Journal of Applied Physics, 2010, 108, .	1.1	84
8715	Structure of the B2 phase in the Tiâ€“25Alâ€“25Zr alloy: a density functional study. Journal of Physics Condensed Matter, 2010, 22, 345502.	0.7	3
8716	Electronic structure and transport properties of hydrogenated graphene and graphene nanoribbons. New Journal of Physics, 2010, 12, 125005.	1.2	23
8717	First-principles investigation of the relation between structural and NMR parameters in vitreous GeO2. Journal of Physics Condensed Matter, 2010, 22, 145501.	0.7	11
8718	A model bismuth oxide intergranular thin film in a ZnO twist grain boundary. Journal of Physics Condensed Matter, 2010, 22, 145503.	0.7	3
8719	First principles calculations of the Ïƒ and Ï‡ phases in the Moâ€“Re and Wâ€“Re systems. Journal of Physics Condensed Matter, 2010, 22, 035402.	0.7	31
8720	Temperature-dependent Raman study of a CeFeAsO_{0.9}F_{0.1}superconductor: crystal field excitations, phonons and their coupling. Journal of Physics Condensed Matter, 2010, 22, 255402.	0.7	9
8721	Efficacy of surface error corrections to density functional theory calculations of vacancy formation energy in transition metals. Journal of Physics Condensed Matter, 2010, 22, 345501.	0.7	17
8722	Density-functional study of the methoxy intermediates at Cu(111), Cu(110) and Cu(001) surfaces. Journal of Physics Condensed Matter, 2010, 22, 395002.	0.7	5
8723	Systematically improvable optimized atomic basis sets forab initiocalculations. Journal of Physics Condensed Matter, 2010, 22, 445501.	0.7	46
8724	DFT study of structure stability and elasticity of wadsleyite II. Journal of Physics Condensed Matter, 2010, 22, 145402.	0.7	6
8725	A relation between kinetic-energy density and the band gap in alkali and alkaline-earth oxides. Journal of Physics Condensed Matter, 2010, 22, 255502.	0.7	9
8726	A density functional study of the adsorption of methane-thiol on the (111) surfaces of the Ni-group metals: I. Molecular and dissociative adsorption. Journal of Physics Condensed Matter, 2010, 22, 265005.	0.7	19
8727	Unusual titanium diffusion on a diamond(100) 2Ã—1 surface at submonolayer coverage. Europhysics Letters, 2010, 92, 46005.	0.7	0
8728	Design of type-II MgxZn1â^'xO:N/ZnO superlattices for UV photodetector applications. Semiconductor Science and Technology, 2010, 25, 045012.	1.0	1
8729	Predicting the segregation profile of the Pt₂₅Rh₇₅(100) surface from first-principles. Journal of Physics Condensed Matter, 2010, 22, 384203.	0.7	10

#	Article	IF	Citations
8730	Structure and elastic properties of Mg(OH)2from density functional theory. Journal of Physics Condensed Matter, 2010, 22, 445403.	0.7	17
8731	Computational Investigation of FeS₂ Surfaces and Prediction of Effects of Sulfur Environment on Stabilities. Journal of Physical Chemistry C, 2010, 114, 8971-8980.	1.5	75
8732	Jahn-Teller distortion and magnetic structure in<mml:math xmlns:mml="http://www.w3.org/1998/Math/MathML" display="inline"><mml:mrow><mml:msub><mml:mrow><mml:mtext>LaMnO</mml:mtext></mml:mrow><mml:mn>3</mml:mn></mml: A first-principles theoretical study with full structure optimizations. Physical Review B, 2010, 82, .	1.1	53
8733	First-principles<mml:math xmlns:mml="http://www.w3.org/1998/Math/MathML" display="inline"><mml:mrow><mml:mtext>LDA</mml:mtext><mml:mo>+</mml:mo><mml:mi>U</mml:mi></mml:mrow></mml:math> xmlns:mml="http://www.w3.org/1998/Math/MathML" display="inline"><mml:mrow><mml:mtext>GGA</mml:mtext><mml:mo>+</mml:mo><mml:mi>U</mml:mi></mml:mrow></mml:mat of neptunium dioxide. Physical Review B, 2010, 81, .	1.1	63
8734	Atomistic Oxidation Mechanism of a Carbon Nanotube in Nitric Acid. Physical Review Letters, 2010, 104, 066401.	2.9	52
8735	Defects Responsible for the Hole Gas in Ge/Si Coreâ^'Shell Nanowires. Nano Letters, 2010, 10, 116-121.	4.5	49
8736	Lone-pair states as a key to understanding impact ionization in chalcogenide semiconductors. Journal of Physics Condensed Matter, 2010, 22, 355803.	0.7	6
8737	Density Functional Theory Study of Catechol Adhesion on Silica Surfaces. Journal of Physical Chemistry C, 2010, 114, 20793-20800.	1.5	123
8738	Experimental and computational study on the phase stability of Al-containing cubic transition metal nitrides. Journal Physics D: Applied Physics, 2010, 43, 035302.	1.3	85
8739	Native and hydrogen-containing point defects in<mml:math xmlns:mml="http://www.w3.org/1998/Math/MathML" display="inline"><mml:mrow><mml:msub><mml:mrow><mml:mtext>Mg</mml:mtext></mml:mrow><mml:mn>3</mml:mn></mml:m A density functional theory study. Physical Review B, 2010, 81, .	1.1	24
8740	Migration of gold atoms in graphene ribbons: Role of the edges. Physical Review B, 2010, 81, .	1.1	41
8741	Mechanically Robust Tri-Wing Graphene Nanoribbons with Tunable Electronic and Magnetic Properties. Nano Letters, 2010, 10, 494-498.	4.5	71
8742	Structure Stability and Magnetic Properties of Ni₂XGa (X = Mn, Fe, Co) Ferromagnetic Shape Memory Alloys by DFT Approach. Solid State Phenomena, 0, 160, 69-74.	0.3	4
8743	Ab initioinvestigation of barium-scandium-oxygen coatings on tungsten for electron emitting cathodes. Physical Review B, 2010, 81, .	1.1	57
8744	A density functional theory study of the atomic structure, formation energy, and vibrational properties of nitrogen-vacancy-oxygen defects in silicon. Journal of Applied Physics, 2010, 108, .	1.1	18
8745	Boron and nitrogen functionalized diamondoids: A first principles investigation. Diamond and Related Materials, 2010, 19, 837-840.	1.8	7
8746	The metallicity of B-doped diamond surface by first-principles study. Diamond and Related Materials, 2010, 19, 824-828.	1.8	6
8747	Theoretical study of noncovalent functionalization of BN nanotubes by various aromatic molecules. Diamond and Related Materials, 2010, 19, 1073-1077.	1.8	33

#	Article	IF	Citations
8748	Atomic structure and mechanical properties of BC2N superlattice. Diamond and Related Materials, 2010, 19, 1341-1347.	1.8	5
8749	Density Functional Calculations on the Hydrogenation of Carbon Dioxide on Fe(111) and W(111) Surfaces. Journal of Physical Chemistry C, 2010, 114, 1194-1200.	1.5	27
8750	First-principles study of structural, elastic, electronic and optical properties of perovskites hydrides XLiH₃(X = Ba and Sr) under pressure. EPJ Applied Physics, 2010, 51, 20302.	0.3	13
8751	Coulomb-potential-dependent decohesion of MagnÃ©li phases. Journal of Physics Condensed Matter, 2010, 22, 292203.	0.7	20
8752	Electronic Structures and Optical Properties of Ga-Rich In_xGa_{1â^'x}N Nanotubes. Journal of Physical Chemistry C, 2010, 114, 21943-21947.	1.5	3
8753	Electronic and dynamical properties of Si/Ge core-shell nanowires. Physical Review B, 2010, 82, .	1.1	14
8754	Structure-Induced Ferromagnetic Stabilization in Free-Standing Hexagonal Fe1.3Ge Nanowires. Journal of the American Chemical Society, 2010, 132, 17447-17451.	6.6	23
8755	Effect of Waters of Crystallization on Terahertz Spectra: Anhydrous Oxalic Acid and Its Dihydrate. Journal of Physical Chemistry A, 2010, 114, 7127-7138.	1.1	60
8756	Studies of Perovskite Materials for High-Performance Storage Media, Piezoelectric, and Solar Energy Conversion Devices. , 2010, , .		3
8757	Identification of the dinitrogen<mml:math xmlns:mml="http://www.w3.org/1998/Math/MathML" display="inline"><mml:mrow><mml:mrow><mml:mo>âŸ¨</mml:mo><mml:mrow><mml:mn>001</mml:mn></mml:mrow><mml:mo>âŸ© interstitial H1a in diamond. Physical Review B, 2010, 81, .	1.1	26
8758	Codoping synergistic effects in N-doped SrTiO3 for higher energy conversion efficiency. Physical Chemistry Chemical Physics, 2010, 12, 7612.	1.3	52
8759	Confinement effects on alloy reactivity. Physical Chemistry Chemical Physics, 2010, 12, 12466.	1.3	8
8760	Synergistic effect of crystal and electronic structures on the visible-light-driven photocatalytic performances of Bi2O3 polymorphs. Physical Chemistry Chemical Physics, 2010, 12, 15468.	1.3	261
8761	DFT-Based Theoretical Calculations of Nb- and W-Doped Anatase TiO₂: Complex Formation between W Dopants and Oxygen Vacancies. Journal of Physical Chemistry C, 2010, 114, 12777-12783.	1.5	32
8762	Oxidative Decomposition of Methanol on Subnanometer Palladium Clusters: The Effect of Catalyst Size and Support Composition. Journal of Physical Chemistry C, 2010, 114, 10342-10348.	1.5	76
8763	Structured Polymer Brushes on Silicon Carbide. Chemistry of Materials, 2010, 22, 272-278.	3.2	58
8764	Visible light responsive bismuth niobate photocatalyst: enhanced contaminant degradation and hydrogen generation. Journal of Materials Chemistry, 2010, 20, 8405.	6.7	60
8765	Unconventional magnetism in semiconductors: Role of localized acceptor states. Physical Review B, 2010, 81, .	1.1	67

#	Article	IF	Citations
8766	Density functional theory calculations on magnetic properties of actinide compounds. Physical Chemistry Chemical Physics, 2010, 12, 12273.	1.3	58
8767	Solid-State ^{79/81}Br NMR and Gauge-Including Projector-Augmented Wave Study of Structure, Symmetry, and Hydration State in Alkaline Earth Metal Bromides. Journal of Physical Chemistry A, 2010, 114, 2102-2116.	1.1	43
8768	Adsorption of diatomic halogen molecules on graphene: A van der Waals density functional study. Physical Review B, 2010, 82, .	1.1	66
8769	Ternary Nitride GaFe₃N: An Experimental and Quantum-Theoretical Study. Inorganic Chemistry, 2010, 49, 10148-10155.	1.9	32
8770	Quantum dynamics of dissociative chemisorption of CH4 on Ni(111): Influence of the bending vibration. Journal of Chemical Physics, 2010, 133, 144308.	1.2	65
8771	Electronic Structure and Chemical Modification of Graphene Antidot Lattices. Journal of Physical Chemistry C, 2010, 114, 15578-15583.	1.5	31
8772	Determining the anisotropic exchange coupling of<mml:math xmlns:mml="http://www.w3.org/1998/Math/MathML" display="inline"><mml:mrow><mml:msub><mml:mrow><mml:mtext>CrO</mml:mtext></mml:mrow><mml:mn>2</mml:mn></mml:ms first-principles density functional theory calculations. Physical Review B, 2010, 81, .	1.1	28
8773	<mml:math xmlns:mml="http://www.w3.org/1998/Math/MathML" display="inline"><mml:mrow><mml:mn>3</mml:mn><mml:mi>d</mml:mi><mml:mtext>â^'</mml:mtext><mml:mn>4</mml:mn><mml: mixing in La-doped<mml:math xmlns:mml="http://www.w3.org/1998/Math/MathML" display="inline"><mml:mrow><mml:msub><mml:mrow><mml:mtext>BiFeO</mml:mtext></mml:mrow><mml:mn>3</mml:mn></mml:m Physical Review B, 2010, 82, .	1.1	74
8774	Electronic collective excitations in compressed lithium fromab initiocalculations: Importance and anisotropy of local-field effects at large momenta. Physical Review B, 2010, 81, .	1.1	15
8775	Quantifying octahedral rotations in strained perovskite oxide films. Physical Review B, 2010, 82, .	1.1	293
8776	Understanding of Adsorption and Catalytic Properties of Bimetallic Ptâ^'Co Alloy Surfaces from First Principles: Insight from Disordered Alloy Surfaces. Journal of Physical Chemistry C, 2010, 114, 7141-7152.	1.5	16
8777	Structural compression and vibrational properties of Bi₁₂SiO₂₀sillenite from experiment and theory. Journal of Physics Condensed Matter, 2010, 22, 505401.	0.7	33
8778	Magnetic properties of nonmetal atoms absorbed MoS2 monolayers. Applied Physics Letters, 2010, 96, .	1.5	199
8779	First-Principles Calculations for the H Center in SrF₂ Crystals. Journal of Physical Chemistry A, 2010, 114, 8444-8449.	1.1	9
8780	First-principles study of the effect of pressure on the five zirconia polymorphs. I. Structural, vibrational, and thermoelastic properties. Physical Review B, 2010, 82, .	1.1	30
8781	Room-Temperature Ferromagnetism in Co-Doped In₂O₃ Nanocrystals. Journal of Physical Chemistry C, 2010, 114, 17569-17573.	1.5	55
8782	Color centers in NaCl by hybrid functionals. Physical Review B, 2010, 82, .	1.1	33
8783	First-Principles Calculation of Elastic Properties of TiB₂ and ZrB₂. Advanced Materials Research, 0, 150-151, 40-43.	0.3	7

#	Article	IF	Citations
8784	A density functional study of defect migration in gadolinium doped ceria. Physical Chemistry Chemical Physics, 2010, 12, 7904.	1.3	71
8785	Conductive junctions with parallel graphene sheets. Journal of Chemical Physics, 2010, 132, 114703.	1.2	11
8786	Theoretical calculations of the thermodynamic stability of ionic substitutions in hydroxyapatite under an aqueous solution environment. Journal of Physics Condensed Matter, 2010, 22, 384210.	0.7	7
8787	Comparative Density Functional Study of Methanol Decomposition on Cu₄ and Co₄ Clusters. Journal of Physical Chemistry B, 2010, 114, 14458-14466.	1.2	35
8788	Prediction of high-pressure polymorphism in NiS₂at megabar pressures. Journal of Physics Condensed Matter, 2010, 22, 235401.	0.7	5
8789	Enhanced Oxygen Buffering by Substitutional and Interstitial Ni Point Defects in Ceria: A First-Principles DFT+U Study. Journal of Physical Chemistry C, 2010, 114, 10221-10228.	1.5	52
8790	First Principles Calculations on Site-Dependent Dissolution Potentials of Supported and Unsupported Pt Particles. Journal of Physical Chemistry C, 2010, 114, 17557-17568.	1.5	105
8791	Electron spin resonance parameters of bulk oxygen vacancy in semiconducting tin dioxide. Physical Review B, 2010, 81, .	1.1	21
8792	First-principles prediction of half-metallic ferromagnetism in Cu-doped ZnS. Journal of Applied Physics, 2010, 107, .	1.1	67
8793	Hydrostatic and uniaxial compression studies of 1,3,5-triamino- 2,4,6-trinitrobenzene using density functional theory with van der Waals correction. Journal of Applied Physics, 2010, 107, .	1.1	39
8794	Ab initiostudy of linear atomic chains in copper nanowires. Physical Review B, 2010, 81, .	1.1	14
8795	Elastic and Vibration Properties of Boronâ€“Carbon Ultra Hard Materials. NATO Science for Peace and Security Series B: Physics and Biophysics, 2010, , 131-145.	0.2	0
8796	Selectivity of Cobalt-Based Non-Platinum Oxygen Reduction Catalysts in the Presence of Methanol and Formic Acid. Journal of Physical Chemistry C, 2010, 114, 15190-15195.	1.5	19
8797	Engineering the band gap of SiC nanotubes with a transverse electric field. Applied Physics Letters, 2010, 97, .	1.5	27
8798	A systematic study of ideal and double layer reconstructions of ABO₃(001) surfaces (A =) Tj ETQq0 0 0 rgBT /Overlock 10 T	0.7	19
8799	Structural and electronic trends in rare-earth technetate pyrochlores. Dalton Transactions, 2010, 39, 7207.	1.6	13
8800	Benzonitrile Adsorption on Fe-Doped Carbon Nanostructures. Journal of Physical Chemistry C, 2010, 114, 10790-10795.	1.5	18
8801	Pressure-induced phase transition in the electronic structure of palladium nitride. Physical Review B, 2010, 82, .	1.1	27

#	Article	IF	Citations
8802	Characterization and Identification of the most Refractory Nitrogen Compounds in Hydroprocessed Vacuum Gas Oil. Industrial & Engineering Chemistry Research, 2010, 49, 3184-3193.	1.8	33
8803	DFT Study on Anatase TiO₂ Nanowires: Structure and Electronic Properties As Functions of Size, Surface Termination, and Morphology. Journal of Physical Chemistry C, 2010, 114, 12389-12400.	1.5	48
8804	Origin of the Visible Photocatalytic Activity of N-Doped In2O3: A Quantum Mechanical Study. Journal of Physical Chemistry C, 2010, 114, 3028-3036.	1.5	21
8805	Charge-injection induced magnetism and half metallicity in single-layer hexagonal group III/V (BN, BP,) Tj ETQq1 1 0.784314 rgBT /Ove	1.5	41
8806	Electronic and magnetic properties of a BN sheet decorated with hydrogen and fluorine. Physical Review B, 2010, 81, .	1.1	278
8807	Functionalization of BN honeycomb structure by adsorption and substitution of foreign atoms. Physical Review B, 2010, 82, .	1.1	92
8808	A New High-Pressure Polar Phase of Crystalline Bromoform: A First-Principles Study. Journal of Physical Chemistry B, 2010, 114, 13933-13939.	1.2	7
8809	A Surface Effect Allows HNO/NO Discrimination by a Cobalt Porphyrin Bound to Gold. Inorganic Chemistry, 2010, 49, 6955-6966.	1.9	63
8810	Molecular understanding of alkyne hydrogenation for the design of selective catalysts. Dalton Transactions, 2010, 39, 8412.	1.6	133
8811	Deviations from Vegardâ€™s law in ternary III-V alloys. Physical Review B, 2010, 82, .	1.1	89
8812	Electronic and Defect Structures of CuSCN. Journal of Physical Chemistry C, 2010, 114, 9111-9117.	1.5	155
8813	On the Thermodynamic Stability of Î±,Ï‰-Alkanedithiols Self-Assembled Monolayers on Unreconstructed and Reconstructed Au(111). Langmuir, 2010, 26, 9589-9595.	1.6	12
8814	Defects in gallium nitride nanowires: First principles calculations. Journal of Applied Physics, 2010, 108, 044305.	1.1	29
8815	Far infrared spectra of solid state aliphatic amino acids in different protonation states. Journal of Chemical Physics, 2010, 132, 115105.	1.2	23
8816	Electronic Structures and Magnetic Properties of GaN Sheets and Nanoribbons. Journal of Physical Chemistry C, 2010, 114, 11390-11394.	1.5	115
8817	Fundamental studies of methanol synthesis from CO2 hydrogenation on Cu(111), Cu clusters, and Cu/ZnO(0001Ì„). Physical Chemistry Chemical Physics, 2010, 12, 9909.	1.3	442
8818	Phase Transition and Phonon Spectrum of Zinc-Blende Structure ZnX (X = S, Se, Te). Communications in Theoretical Physics, 2010, 53, 1160-1166.	1.1	45
8819	Interphase energies of hcp precipitates in fcc metals: A density-functional theory study in Al-Ag. Physical Review B, 2010, 81, .	1.1	16

#	Article	IF	Citations
8820	Electronic Structure of Bi Nanoribbon: Greatly Influenced by Edge Chirality and Edge Reconstruction. Journal of Physical Chemistry C, 2010, 114, 19289-19293.	1.5	12
8821	Thiol with an Unusual Adsorptionâ^'Desorption Behavior: 6-Mercaptopurine on Au(111). Langmuir, 2010, 26, 17068-17074.	1.6	34
8822	DFTB⁺and lanthanides. Journal of Physics: Conference Series, 2010, 242, 012005.	0.3	9
8823	Vacancy-mediated diffusion of carbon in cobalt and its influence on CO activation. Physical Chemistry Chemical Physics, 2010, 12, 7848.	1.3	37
8824	Lithium Insertion In Silicon Nanowires: An ab Initio Study. Nano Letters, 2010, 10, 3243-3249.	4.5	201
8825	Effects of Au nanoparticles on the magnetic and transport properties of<mml:math xmlns:mml="http://www.w3.org/1998/Math/MathML" display="inline"><mml:mrow><mml:msub><mml:mrow><mml:mtext>La</mml:mtext></mml:mrow><mml:mrow><mml:mn>0.67</mml:mn></mml:mrow></mml:msub></mml:mrow></mml:math>layers. Physical Review B, 2010, 81, .	1.1	39
8826	First-principles analysis of electron-phonon interactions in graphene. Physical Review B, 2010, 81, .	1.1	189
8827	Revisiting Hydrogen Storage in Bulk BC₃. Journal of Physical Chemistry C, 2010, 114, 3260-3264.	1.5	23
8828	Mechanical properties of graphene cantilever from atomic force microscopy and density functional theory. Nanotechnology, 2010, 21, 185503.	1.3	63
8829	Transition from Mn4+ to Mn3+ induced by surface reconstruction at Î»-MnO2(001). Journal of Chemical Physics, 2010, 133, 204701.	1.2	21
8830	Theoretical Exploration of the Structural, Electronic, and Magnetic Properties of ZnO Nanotubes with Vacancies, Antisites, and Nitrogen Substitutional Defects. Journal of Physical Chemistry C, 2010, 114, 5760-5766.	1.5	39
8831	Enhancement of room temperature ferromagnetism in N-doped TiO2â^'x rutile: Correlation with the local electronic properties. Applied Physics Letters, 2010, 97, 012506.	1.5	37
8832	An investigation of the electronic properties of MgO doped with group III, IV, and V elements: trends with varying dopant atomic number. Journal of Physics Condensed Matter, 2010, 22, 046002.	0.7	24
8833	Semiconducting Superhard Ruthenium Monocarbide. Journal of Physical Chemistry C, 2010, 114, 9961-9964.	1.5	40
8834	Strain-Induced Band Gap Modification in Coherent Core/Shell Nanostructures. Nano Letters, 2010, 10, 3156-3162.	4.5	101
8835	First-principles study on ferroelectricity at PbTiO3surface steps. Journal of Physics Condensed Matter, 2010, 22, 355901.	0.7	21
8836	Ab initiostudy of ferroelectric closure domains in ultrathin<mml:math xmlns:mml="http://www.w3.org/1998/Math/MathML" display="inline"><mml:mrow><mml:msub><mml:mrow><mml:mtext>PbTiO</mml:mtext></mml:mrow><mml:mrow><mml:mn>3</mml:mn></mml:mrow></mml:msub></mml:mrow></mml:math>Physical Review B, 2010, 81, .	1.1	54
8837	Structural and electronic properties ofPbTiO3/SrTiO3superlattices from first principles. Physical Review B, 2010, 82, .	1.1	14

#	Article	IF	Citations
8838	Vibrational dynamics of anatase<mml:math xmlns:mml="http://www.w3.org/1998/Math/MathML" display="inline"><mml:mrow><mml:msub><mml:mrow><mml:mtext>TiO</mml:mtext></mml:mrow><mml:mn>2</mml:mn></mml:msub></mml:mrow></mml:math>: Polarized Raman spectroscopy andab initiocalculations. Physical Review B, 2010, 81, .	1.1	96
8839	Band structure engineering of semiconductors for enhanced photoelectrochemical water splitting: The case of<mml:math xmlns:mml="http://www.w3.org/1998/Math/MathML" display="inline"><mml:mrow><mml:msub><mml:mrow><mml:mtext>TiO</mml:mtext></mml:mrow><mml:mn>2</mml:mn></mml:msub></mml:mrow></mml:math>. Physical Review B, 2010, 82, .	1.1	300
8840	Effects on Electronic Properties of Molecule Adsorption on CuO Surfaces and Nanowires. Journal of Physical Chemistry C, 2010, 114, 17120-17126.	1.5	115
8841	Systematic Study of the Multiple-Element Filling in Caged Skutterudite CoSb₃. Chemistry of Materials, 2010, 22, 2384-2394.	3.2	40
8842	Quantum Confinement Effects and Electronic Properties of SnO₂ Quantum Wires and Dots. Journal of Physical Chemistry C, 2010, 114, 4841-4845.	1.5	56
8843	Tuning the Charge-Transport Parameters of Perylene Diimide Single Crystals via End and/or Core Functionalization: A Density Functional Theory Investigation. Journal of the American Chemical Society, 2010, 132, 3375-3387.	6.6	320
8844	Fluorination induced half metallicity in two-dimensional few zinc oxide layers. Journal of Chemical Physics, 2010, 132, 204703.	1.2	32
8845	Electronic structure and metalization of a silane-hydrogen system under high pressure investigated using density functional and GW calculations. Physical Review B, 2010, 81, .	1.1	13
8846	Experimental and theoretical analysis of magnetic moment enhancement in oxygen-deficient EuO. Physical Review B, 2010, 81, .	1.1	38
8847	Energetics of Polar and Nonpolar Facets of PbSe Nanocrystals from Theory and Experiment. ACS Nano, 2010, 4, 211-218.	7.3	93
8848	Classification of spinel structures based on first-principles cluster expansion analysis. Physical Review B, 2010, 81, .	1.1	38
8849	Impurity clustering and impurity-induced bands in PbTe-, SnTe-, and GeTe-based bulk thermoelectrics. Physical Review B, 2010, 81, .	1.1	86
8850	Structural Model Proposition and Thermodynamic and Vibrational Analysis of Hydrotalcite-Like Compounds by DFT Calculations. Journal of Physical Chemistry C, 2010, 114, 14133-14140.	1.5	78
8851	Soft-mode spectroscopy of epitaxial<mml:math xmlns:mml="http://www.w3.org/1998/Math/MathML" display="inline"><mml:mrow><mml:msub><mml:mrow><mml:mtext>BaTiO</mml:mtext></mml:mrow><mml:mn>3</mml:mn></mml:msub></mml:mrow></mml:math>. Physical Review B, 2010, 82, .	1.1	113
8852	Electron-lattice instabilities suppress cuprate-like electronic structures in<mml:math xmlns:mml="http://www.w3.org/1998/Math/MathML" display="inline"><mml:mrow><mml:msub><mml:mrow><mml:mtext>SrFeO</mml:mtext></mml:mrow><mml:mn>3</mml:mn></mml:msub></mml:mrow></mml:math>. Physical Review B, 2010, 81, .	1.1	22
8853	Oxidation functional groups on graphene: Structural and electronic properties. Physical Review B, 2010, 82, .	1.1	328
8854	Dissolution and diffusion properties of carbon in tungsten. Journal of Physics Condensed Matter, 2010, 22, 445504.	0.7	29
8855	Origin of coexisting large Seebeck coefficient and metallic conductivity in the electron dopedSrTiO3andKTaO3. Physical Review B, 2010, 81, .	1.1	34

#	Article	IF	Citations
8856	LiMSO4F (M = Fe, Co and Ni): promising new positive electrode materials through the DFT microscope. Physical Chemistry Chemical Physics, 2010, 12, 15512.	1.3	65
8857	EuAgxAl11â^'x with the BaHg11-Type Structure: Composition, Coloring, and Competition with the BaCd11-Type Structure. Chemistry of Materials, 2010, 22, 1798-1806.	3.2	13
8858	Ab initiodescription of heterostructural alloys: Thermodynamic and structural properties of<mml:math xmlns:mml="http://www.w3.org/1998/Math/MathML" display="inline"><mml:mrow><mml:msub><mml:mrow><mml:mtext>Mg</mml:mtext></mml:mrow><mml:mi>x</mml:mi></mml:msub xmlns:mml="http://www.w3.org/1998/Math/MathM. Physical Review B, 2010, 81, .	1.1	49
8859	First-principles study of Fe/MgO based magnetic tunnel junctions with Mg interlayers. Physical Review B, 2010, 82, .	1.1	28
8860	Charge carrier scattering by defects in semiconductors. Physical Review B, 2010, 81, .	1.1	47
8861	Surface segregation and stability of coreâ€"shell alloy catalysts for oxygen reduction in acid medium. Physical Chemistry Chemical Physics, 2010, 12, 2209.	1.3	114
8862	Quasiparticle self-consistent GW calculation of the work functions of Al(111), Al(100), and Al(110). Physical Review B, 2010, 81, .	1.1	9
8863	Diffusion and electrical conductivity in water at ultrahigh pressures. Physical Review B, 2010, 82, .	1.1	73
8864	Structural phase transitions in Ruddlesden-Popper phases of strontium titanate:Ab initioand modulated Ginzburg-Landau approaches. Physical Review B, 2010, 82, .	1.1	2
8865	Pressure and electrical resistivity measurements on hot expanded nickel: Comparisons with quantum molecular dynamics simulations and average atom approaches. Physical Review E, 2010, 82, 046402.	0.8	30
8866	Phonon Mechanism of the Magnetostructural Phase Transition in MnAs. Physical Review Letters, 2010, 104, 147205.	2.9	25
8867	The structural behaviour of LaF3 at high pressures. Dalton Transactions, 2010, 39, 4302.	1.6	27
8868	Structural, electronic and optical properties of ilmenite and perovskite CdSnO₃from DFT calculations. Journal of Physics Condensed Matter, 2010, 22, 435801.	0.7	20
8869	First-principles study of the stability of calcium-decorated carbon nanostructures. Physical Review B, 2010, 82, .	1.1	53
8870	Magnetically induced ferroelectricity in<mml:math xmlns:mml="http://www.w3.org/1998/Math/MathML" display="inline"><mml:mrow><mml:msub><mml:mrow><mml:mtext>Cu</mml:mtext></mml:mrow><mml:mn>2</mml:mn></mml:msu xmlns:mml="http://www.w3.org/1998/Math/MathML" display="inline"><mml:mrow><mml:msub><mml:mrow><mml:mtext>Cu</mml:mtext></mml:mrow><mml:mn>2</mml:mn></mml:msub></mml:msu Physical Review B, 2010, 82, .	1.1	20
8871	Ab Initio Study of CO Hydrogenation to Oxygenates on Reduced Rh Terraces and Stepped Surfaces. Journal of Physical Chemistry C, 2010, 114, 10171-10182.	1.5	99
8872	First principles study of thermodynamics and phase transition in lowâ€pressure (P2₁/c) and highâ€pressure (C2/c) clinoenstatite MgSiO₃. Journal of Geophysical Research, 2010, 115, .	3.3	17
8873	Elastic, vibrational, and thermodynamic properties of MgGeO₃ postperovskite investigated by first principles simulation. Journal of Geophysical Research, 2010, 115, .	3.3	5

#	Article	IF	Citations
8874	Is the spin transition in Fe²⁺â€bearing perovskite visible in seismology?. Geophysical Research Letters, 2010, 37, .	1.5	18
8875	Ab initio investigation of highâ€pressure phase relation and elasticity in the NaAlSi₂O₆ system. Geophysical Research Letters, 2010, 37, .	1.5	20
8876	Elasticity of AlFeO₃ and FeAlO₃ perovskite and postâ€perovskite from firstâ€principles calculations. Geophysical Research Letters, 2010, 37, .	1.5	9
8877	Elasticity of SrTiO₃ perovskite under high pressure in cubic, tetragonal and orthorhombic phases. Physica Scripta, 2010, 82, 025602.	1.2	37
8878	First-Principles Study on the Origin of the Different Selectivities for Methanol Steam Reforming on Cu(111) and Pd(111). Journal of Physical Chemistry C, 2010, 114, 21539-21547.	1.5	137
8879	Influence of ZnS and MgO Shell on the Photoluminescence Properties of ZnO Core/Shell Nanowires. Journal of Physical Chemistry C, 2010, 114, 1467-1471.	1.5	69
8880	Defect-induced magnetism in nitride and oxide nanowires: Surface effects and quantum confinement. Physical Review B, 2010, 82, .	1.1	44
8881	MN+1AXN(M=Ti,A=Al,X=H) phase class materials with hydrogen: Ti4AlH3 and Ti3AlH2. Applied Physics Letters, 2010, 96, 261906.	1.5	6
8882	Intrinsic electrostatic effects in nanostructured ceramics. Physical Review B, 2010, 81, .	1.1	22
8883	Embedded ribbons of graphene allotropes: an extended defect perspective. New Journal of Physics, 2010, 12, 125006.	1.2	68
8884	Elastic constants and thermophysical properties of Alâ€“Mgâ€“Si alloys from first-principles calculations. International Journal of Materials Research, 2010, 101, 1392-1397.	0.1	3
8885	Unusual Selectivity of Gold Catalysts for Hydrogenation of 1,3-Butadiene toward cis-2-Butene: A Joint Experimental and Theoretical Investigation. Journal of Physical Chemistry C, 2010, 114, 3131-3139.	1.5	65
8886	On the Nature and Behavior of Li Atoms in Si: A First Principles Study. Journal of Physical Chemistry C, 2010, 114, 17942-17946.	1.5	82
8887	Strain effect on quantum conductance of graphene nanoribbons from maximally localized Wannier functions. Physical Review B, 2010, 81, .	1.1	34
8888	Molecular Doping and Subsurface Dopant Reactivation in Si Nanowires. Nano Letters, 2010, 10, 3590-3595.	4.5	39
8889	Transformations of Ethylene on the Pd(111) Surface: A Density Functional Study. Journal of Physical Chemistry C, 2010, 114, 17683-17692.	1.5	47
8890	A DFT Study of Hydrogen Dissociation on CO- and C-Precovered Fe(100) Surfaces. Journal of Physical Chemistry C, 2010, 114, 5932-5940.	1.5	33
8891	Ab-initio Study of Transition-Metal Dimers on MgO(001) Surfaces: Comparison of Atomic and Electronic Properties. Journal of the Physical Society of Japan, 2010, 79, 074718.	0.7	20

#	Article	IF	Citations
8892	Atomic and Electronic Structure Investigation and Luminescence Property of Eu2+-Doped Î²-SiAlON Green Phosphor:Ab initioCalculations. Japanese Journal of Applied Physics, 2010, 49, 06GJ07.	0.8	5
8893	Density Functional Investigations of Methanol Dehydrogenation on Pdâ^'Zn Surface Alloy. Langmuir, 2010, 26, 10796-10802.	1.6	30
8894	Structure of the (0001) basal twin boundary in Bi2Te3. Journal of Applied Physics, 2010, 108, .	1.1	68
8895	Phase stability and mechanical properties of niobium nitrides. Physical Review B, 2010, 82, .	1.1	54
8896	Theoretical Study on Adsorption and Dissociation of NO₂Molecule on Fe(111) Surface. Langmuir, 2010, 26, 7157-7164.	1.6	27
8897	New Insights into the Atomic Structure of 45S5 Bioglass by Means of Solid-State NMR Spectroscopy and Accurate First-Principles Simulations. Chemistry of Materials, 2010, 22, 5644-5652.	3.2	131
8898	Structure of Ce1â^'xSnxO2 and its relation to oxygen storage property from first-principles analysis. Journal of Chemical Physics, 2010, 132, 194702.	1.2	32
8899	Stabilization of semiconductor surface reconstructions by configurational entropy. Physical Review B, 2010, 82, .	1.1	15
8900	Solvation and Zero-Point-Energy Effects on OH(ads) Reduction on Pt(111) Electrodes. Journal of Physical Chemistry C, 2010, 114, 14946-14952.	1.5	29
8901	Ab Initio Study of Confinement and Surface Effects in AlN Nanowires. Journal of Physical Chemistry C, 2010, 114, 11352-11357.	1.5	12
8902	Initial Growth of BN on Diamond Substrates: A Theoretical Approach. Journal of Physical Chemistry C, 2010, 114, 11448-11455.	1.5	3
8903	Chemical Trend of Pressure-Induced Metallization in Alkaline Earth Hydrides. Journal of Physical Chemistry C, 2010, 114, 14614-14617.	1.5	20
8904	Density Functional Studies of the Adsorption and Dissociation of CO₂Molecule on Fe(111) Surface. Langmuir, 2010, 26, 775-781.	1.6	23
8905	Structural and Electronic Properties of the Methyl-Terminated Si(111) Surface. Journal of Physical Chemistry C, 2010, 114, 11898-11902.	1.5	14
8906	Theoretical Study of O₂ Molecular Adsorption and Dissociation on Silicon Carbide Nanotubes. Journal of Physical Chemistry C, 2010, 114, 970-976.	1.5	37
8907	Lattice Dynamics and Thermodynamics of Molybdenum from First-Principles Calculations. Journal of Physical Chemistry B, 2010, 114, 298-310.	1.2	39
8908	CO₂ Activation and Total Reduction on Titanium(0001) Surface. Journal of Physical Chemistry C, 2010, 114, 11456-11459.	1.5	34
8909	Half-Metallic Sandwich Molecular Wires with Negative Differential Resistance and Sign-Reversible High Spin-Filter Efficiency. Journal of Physical Chemistry C, 2010, 114, 21893-21899.	1.5	32

#	Article	IF	Citations
8910	Patterned Hydrogenation of Graphene: Magnetic Quantum Dot Array. Journal of Physical Chemistry C, 2010, 114, 139-142.	1.5	35
8911	Thickness-Dependent Hydroxylation of MgO(001) Thin Films. Journal of Physical Chemistry C, 2010, 114, 18207-18214.	1.5	57
8912	Electrochemical chlorine evolution at rutile oxide (110) surfaces. Physical Chemistry Chemical Physics, 2010, 12, 283-290.	1.3	317
8913	Structural, Electronic, and Electrochemical Properties of Cathode Materials Li₂MSiO₄ (M = Mn, Fe, and Co): Density Functional Calculations. Journal of Physical Chemistry C, 2010, 114, 3693-3700.	1.5	92
8914	Hydration of Rutile TiO₂: Thermodynamics and Effects on n- and p-Type Electronic Conduction. Journal of Physical Chemistry C, 2010, 114, 9139-9145.	1.5	25
8915	Quantum Mechanically Guided Design of Transition Metal Alloyed RuO₂ Nanorods. Crystal Growth and Design, 2010, 10, 4531-4536.	1.4	16
8916	Discrimination of Chiral Solids: A Terahertz Spectroscopic Investigation of <scp>l</scp>- and <scp>dl</scp>-Serine. Journal of Physical Chemistry A, 2010, 114, 2945-2953.	1.1	74
8917	Periodic and Molecular Modeling Study of Donorâ^'Acceptor Interactions in (dbbpy)Pt(tdt)Â·TENF and [Pt(dbbpy)(tdt)]₂Â·TENF. Organometallics, 2010, 29, 795-800.	1.1	12
8918	Low O2 dissociation barrier on Pt(111) due to adsorbateâ€“adsorbate interactions. Journal of Chemical Physics, 2010, 133, 224701.	1.2	49
8919	ZnO Nanostructures for Gas Sensing: Interaction of NO₂, NO, O, and N with the ZnO(101Ì…0) Surface. Journal of Physical Chemistry C, 2010, 114, 10881-10893.	1.5	101
8920	Thiolate Induced Reconstruction of Au(111) and Cu(111) Investigated by Density Functional Theory Calculations. Journal of Physical Chemistry C, 2010, 114, 15973-15978.	1.5	38
8921	Structural Design and Two-Dimensional Conductivity of Sheet-Tube Frameworks. Journal of Physical Chemistry C, 2010, 114, 19673-19677.	1.5	11
8922	Ground-state properties and high-pressure behavior of plutonium dioxide: Density functional theory calculations. Physical Review B, 2010, 82, .	1.1	121
8923	Temperature dependence of surface stress across an order-disorder transition:p(1Ã—2)O/W(110). Physical Review B, 2010, 81, .	1.1	8
8924	The Self-Consistent Charge Density Functional Tight Binding Method Applied to Liquid Water and the Hydrated Excess Proton: Benchmark Simulations. Journal of Physical Chemistry B, 2010, 114, 6922-6931.	1.2	67
8925	The Electronic Structure of Mixed Self-Assembled Monolayers. ACS Nano, 2010, 4, 6735-6746.	7.3	43
8926	Exploration of Half Metallicity in Edge-Modified Graphene Nanoribbons. Journal of Physical Chemistry C, 2010, 114, 3937-3944.	1.5	105
8927	Complex polarization ordering in<mml:math xmlns:mml="http://www.w3.org/1998/Math/MathML" display="inline"><mml:mrow><mml:msub><mml:mrow><mml:mtext>PbTiO</mml:mtext></mml:mrow><mml:mn>3</mml:mn></mml:msub></mml:mrow></mml:math> A first-principles computational study. Physical Review B, 2010, 82, .	1.1	87

#	Article	IF	Citations
8928	Role of Hydroxyl Groups in the NH_x (x = 1â^'3) Adsorption on the TiO₂ Anatase (101) Surface Determined by a First-Principles Study. Langmuir, 2010, 26, 4813-4821.	1.6	28
8929	Ab Initio Elasticity of Poly(lactic acid) Crystals. Journal of Physical Chemistry B, 2010, 114, 3133-3139.	1.2	28
8930	Ionic layered BaFCl and<mml:math xmlns:mml="http://www.w3.org/1998/Math/MathML" display="inline"><mml:mrow><mml:msub><mml:mrow><mml:mtext>Ba</mml:mtext></mml:mrow><mml:mrow><mml:mn>1</mml:mn> Physical- and chemical-pressure effects. Physical Review B, 2010, 82, .	1.1	17
8931	Prediction for room-temperature half-metallic ferromagnetism in the half-fluorinated single layers of BN and ZnO. Applied Physics Letters, 2010, 97, .	1.5	54
8932	First-Principles Calculations of Hydrogen Generation Due to Water Splitting on Polar GaN Surfaces. Journal of Physical Chemistry C, 2010, 114, 18228-18232.	1.5	41
8933	The CO Formation Reaction Pathway in Steam Methane Reforming by Rhodium. Langmuir, 2010, 26, 16339-16348.	1.6	29
8934	Applications of electron reduced density function analysis to the study of amorphous materials: An example of Zr_{64.13}Cu_{15.75}Ni_{10.12}Al_{10.0}and Zr₅₅Cu₃₀Ni₅Al₁₀metallic glasses. Philosophical Magazine, 2010, 90, 4679-4689.	0.7	2
8935	Experimental and Theoretical Studies on the Enhanced Photocatalytic Activity of ZnWO₄ Nanorods by Fluorine Doping. Journal of Physical Chemistry C, 2010, 114, 7680-7688.	1.5	69
8936	Coverage Dependence of the Structure of Acrolein Adsorbed on Ag(111). Journal of Physical Chemistry Letters, 2010, 1, 2546-2549.	2.1	17
8937	The Fermi Level Dependent Electronic Properties of the Smallest (2,2) Carbon Nanotube. Nano Letters, 2010, 10, 3290-3296.	4.5	9
8938	Pressure and Materials Effects on the Selectivity of RuO₂ in NH₃ Oxidation. Journal of Physical Chemistry C, 2010, 114, 16660-16668.	1.5	19
8939	Site Switching from Di-Ïƒ Ethylene to Ï€-Bonded Ethylene in the Presence of Coadsorbed Nitrogen on Pt(111). Journal of Physical Chemistry C, 2010, 114, 12230-12233.	1.5	5
8940	Protonated Forms of Monoclinic Zirconia: A Theoretical Study. Journal of Physical Chemistry C, 2010, 114, 8014-8025.	1.5	17
8941	Mechanism of the Ethylene Conversion to Ethylidyne on Rh(111): A Density Functional Investigation. Journal of Physical Chemistry C, 2010, 114, 8440-8448.	1.5	31
8942	Thermodynamic and Kinetic Control on the Formation of Two Novel Metal-Organic Frameworks Based on the Er(III) Ion and the Asymmetric Dimethylsuccinate Ligand. Inorganic Chemistry, 2010, 49, 5063-5071.	1.9	30
8943	Ferromagnetic Properties of Y-Doped AlN Nanorods. Journal of Physical Chemistry C, 2010, 114, 15574-15577.	1.5	38
8944	Structural and Magnetic Characteristics of Gd₅Ga_xSi_{4â^'x}. Inorganic Chemistry, 2010, 49, 4586-4593.	1.9	17
8945	Hydrogen Adsorption on Eu/SWCNT Systems: A DFT Study. Journal of Physical Chemistry C, 2010, 114, 7733-7737.	1.5	36

#	Article	IF	Citations
8946	Decomposition of Methanthiol on Pt(111): A Density Functional Investigation. Langmuir, 2010, 26, 12017-12025.	1.6	20
8947	Periodic Density Functional Theory and Atomistic Thermodynamic Studies of Cobalt Spinel Nanocrystals in Wet Environment: Molecular Interpretation of Water Adsorption Equilibria. Journal of Physical Chemistry C, 2010, 114, 22245-22253.	1.5	103
8948	Coverage and charge-state dependent adsorption of carbon monoxide on the zinc oxide (0001) surface. Physical Review B, 2010, 82, .	1.1	13
8949	First-Principles Study of Defective and Nonstoichiometric Sr₂FeMoO₆. Chemistry of Materials, 2010, 22, 6092-6102.	3.2	37
8950	Interaction of Surfactants Containing a Sulfuric Group with a (5,5) Carbon Nanotube. Journal of Physical Chemistry C, 2010, 114, 17249-17256.	1.5	11
8951	First-principles investigation on redox properties of<mml:math xmlns:mml="http://www.w3.org/1998/Math/MathML" display="inline"><mml:mi>M</mml:mi></mml:math>-doped<mml:math xmlns:mml="http://www.w3.org/1998/Math/MathML" display="inline"><mml:mrow><mml:msub><mml:mrow><mml:mtext>CeO</mml:mtext></mml:mrow><mml:mn>2</mml:mn></mml:msub></mml:mrow></mml:math>	1.1	112
8952	Core/Shell CdSe/CdTe Heterostructure Nanowires Under Axial Strain. Journal of Physical Chemistry C, 2010, 114, 1773-1781.	1.5	41
8953	Atomistic study of misfit dislocation in metal/SiC(111) interfaces. Journal of Physics Condensed Matter, 2010, 22, 135009.	0.7	5
8954	Theoretical Analysis of the Adsorption of Late Transition-Metal Atoms on the (001) Surface of Early Transition-Metal Carbides. Journal of Physical Chemistry C, 2010, 114, 1622-1626.	1.5	25
8955	Structural Modifications and Mechanical Properties of Molybdenum Borides from First Principles. Journal of Physical Chemistry C, 2010, 114, 6722-6725.	1.5	142
8956	Ab-initioStudy of Transition-Metal Dimers on Defective MgO(001) Surfaces: Atomic and Electronic Structures. Journal of the Physical Society of Japan, 2010, 79, 124703.	0.7	11
8957	First-Principles Study of the Electronic Structure, Optical Properties, and Lattice Dynamics of BC2N. Journal of Physical Chemistry C, 2010, 114, 2783-2791.	1.5	18
8958	Simultaneously Understanding the Geometric and Electronic Structure of Anthraceneselenolate on Au(111): A Combined Theoretical and Experimental Study. Journal of Physical Chemistry C, 2010, 114, 2677-2684.	1.5	34
8959	Catalytically Active Structure of Bi Deposited on a Au(111) Electrode for the Hydrogen Peroxide Reduction Reaction. Langmuir, 2010, 26, 4590-4593.	1.6	20
8960	Ethylidyne Formation from Ethylene over Pt(111): A Mechanistic Study from First-Principle Calculations. Journal of Physical Chemistry C, 2010, 114, 12190-12201.	1.5	77
8961	Accurate projected augmented wave datasets for BaFe₂As₂. New Journal of Physics, 2010, 12, 123029.	1.2	3
8962	Calcium Borohydride for Hydrogen Storage: A Computational Study of Ca(BH₄)₂ Crystal Structures and the CaB₂H_x Intermediate. Journal of Physical Chemistry C, 2010, 114, 9503-9509.	1.5	26
8963	Proton transfer in adsorbed water dimers. Physical Chemistry Chemical Physics, 2010, 12, 3953.	1.3	28

#	Article	IF	Citations
8964	Structural, elastic, electronic and thermal properties of M2SbP (M = Ti, Zr and Hf). Philosophical Magazine, 2010, 90, 1623-1638.	0.7	0
8965	Water Dissociation on MgO/Ag(100): Support Induced Stabilization or Electron Pairing?. Journal of Physical Chemistry C, 2010, 114, 7070-7075.	1.5	34
8966	Analysis of Bonding between Conjugated Organic Molecules and Noble Metal Surfaces Using Orbital Overlap Populations. Journal of Chemical Theory and Computation, 2010, 6, 3481-3489.	2.3	12
8967	Band Gap Narrowing versus Formation of Electronic States in the Gap in Nâ^'TiO₂ Thin Films. Journal of Physical Chemistry C, 2010, 114, 22546-22557.	1.5	34
8968	On the Mechanism of Low-Temperature CO Oxidation on Ni(111) and NiO(111) Surfaces. Journal of Physical Chemistry C, 2010, 114, 21579-21584.	1.5	71
8969	Vanadia Aggregates on an Ultrathin Aluminum Oxide Film on NiAl(110). Journal of Physical Chemistry C, 2010, 114, 4983-4994.	1.5	20
8970	Adsorption, Oxidation State, and Diffusion of Pt Atoms on the CeO₂(111) Surface. Journal of Physical Chemistry C, 2010, 114, 14202-14207.	1.5	71
8971	First-Principles Calculation of Synergistic (N, P)-Codoping Effects on the Visible-Light Photocatalytic Activity of Anatase TiO₂. Journal of Physical Chemistry C, 2010, 114, 11984-11990.	1.5	55
8972	Atomic and molecular adsorption on transition-metal carbide (111) surfaces from density-functional theory: a trend study of surface electronic factors. Journal of Physics Condensed Matter, 2010, 22, 375504.	0.7	23
8973	Mechanism of F^{â^'} Elimination from Zeolitic D4R Units: A Periodic B3LYP Study on the Octadecasil Zeolite. Journal of Physical Chemistry C, 2010, 114, 2989-2995.	1.5	16
8974	Theoretical Study of the Effect of (001) TiO₂Anatase Support on V₂O₅. Journal of Physical Chemistry C, 2010, 114, 3115-3130.	1.5	41
8975	Nitric Oxide Adsorption Effects on Metal Phthalocyanines. Journal of Physical Chemistry B, 2010, 114, 10017-10021.	1.2	52
8976	Identification of the Active Cu Phase in the Waterâ^'Gas Shift Reaction over Cu/ZrO₂ from First Principles. Journal of Physical Chemistry C, 2010, 114, 8423-8430.	1.5	61
8977	Synergistic Effects on Band Gap-Narrowing in Titania by Codoping from First-Principles Calculations. Chemistry of Materials, 2010, 22, 1616-1623.	3.2	134
8978	Structure Sensitivity for Forward and Reverse Water-Gas Shift Reactions on Copper Surfaces: A DFT Study. Journal of Physical Chemistry Letters, 2010, 1, 3053-3057.	2.1	120
8979	Role of Step Sites and Surface Vacancies in the Adsorption and Activation of CO on Ï‡-Fe₅C₂ Surfaces. Journal of Physical Chemistry C, 2010, 114, 7863-7879.	1.5	43
8980	Scaling Dopant States in a Semiconducting Nanostructure by Chemically Resolved Electron Energy-Loss Spectroscopy: A Case Study on Co-Doped ZnO. Journal of the American Chemical Society, 2010, 132, 6492-6497.	6.6	41
8981	Prediction of a Three-Dimensional Conductive Superhard Material: Diamond-like BC₂. Journal of Physical Chemistry C, 2010, 114, 22688-22690.	1.5	33

#	Article	IF	Citations
8982	Diameter dependence of mechanical, electronic, and structural properties of InAs and InP nanowires: A first-principles study. Physical Review B, 2010, 81, .	1.1	64
8983	Noncovalent Functionalization of BN Nanotubes with Perylene Derivative Molecules: An ab Initio Study. ACS Nano, 2010, 4, 1313-1320.	7.3	37
8984	One-dimensional polymeric carbon structure based on five-membered rings in alkaline earth metal dicarbides<mml:math xmlns:mml="http://www.w3.org/1998/Math/MathML" display="inline"><mml:mrow><mml:msub><mml:mrow><mml:mtext>BeC</mml:mtext></mml:mrow><mml:mn>2</mml:mn></mml:ms xmlns:mml="http://www.w3.org/1998/Math/MathML" display="inline"><mml:mrow><mml:msub><mml:mrow><mml:mtext>MgC</mml:mtext></mml:mrow><mml:mn>2</mml:mn></mml:ms Physical Review B, 2010, 82, .	1.1	27
8985	Potential-Dependent Chemisorption of Carbon Monoxide at a Gold Coreâ"Platinum Shell Nanoparticle Electrode: A Combined Study by Electrochemical in Situ Surface-Enhanced Raman Spectroscopy and Density Functional Theory. Journal of Physical Chemistry C, 2010, 114, 403-411.	1.5	34
8986	Electronic Structure and Origin of Visible-Light Activity of C-Doped Cubic In₂O₃ from First-Principles Calculations. Journal of Physical Chemistry C, 2010, 114, 13942-13946.	1.5	8
8987	How Surface Reactivity Depends on the Configuration of Coadsorbed Reactants: CO Oxidation on Rh(100). Journal of Physical Chemistry C, 2010, 114, 17127-17135.	1.5	15
8988	Hydrogen-Induced De/Reconstruction of the c-BN(100) Surface. Journal of Physical Chemistry C, 2010, 114, 3516-3521.	1.5	18
8989	Structural Investigation of Solid Methane at High Pressure. Chinese Physics Letters, 2010, 27, 066101.	1.3	1
8990	First-Principles Study of High-Pressure Behavior of Solid Î²-HMX. Journal of Physical Chemistry A, 2010, 114, 1082-1092.	1.1	53
8991	Alumina as a Simultaneous Support and Co Catalyst: Cationic Hafnium Complex Evidenced by Experimental and DFT Analyses. Journal of Physical Chemistry C, 2010, 114, 18516-18528.	1.5	23
8992	Investigating the Anharmonicity of Lattice Vibrations in Water-Containing Molecular Crystals through the Terahertz Spectroscopy of <scp>l</scp>-Serine Monohydrate. Journal of Physical Chemistry A, 2010, 114, 9570-9578.	1.1	55
8993	DFT-NMR Investigation and ⁵¹V 3QMAS Experiments for Probing Surface OH Ligands and the Hydrogen-Bond Network in a Polyoxovanadate Cluster: The Case of Cs₄[H₂V₁₀O₂₈]Â·4H₂O. Journal of the American Chemical Society, 2010, 132, 4653-4668.	6.6	32
8994	Manipulating Iâ"V Characteristics of a Molecular Switch with Chemical Modifications. Journal of Physical Chemistry C, 2010, 114, 1655-1662.	1.5	13
8995	Autocatalytic Reduction of a Cu₂O/Cu(111) Surface by CO: STM, XPS, and DFT Studies. Journal of Physical Chemistry C, 2010, 114, 17042-17050.	1.5	84
8996	Stability of Pt Monolayers on Irâ"Co Cores with and without a Pd Interlayer. Journal of Physical Chemistry C, 2010, 114, 13055-13060.	1.5	19
8997	IR Spectroscopic Measurement of Diffusion Kinetics of Chemisorbed Pyridine through TiO₂Particles. Journal of Physical Chemistry C, 2010, 114, 16649-16659.	1.5	20
8998	Electronic Structureâ"Transport Property Relationships of Polyferrocenylene, Polyferrocenylacetylene, and Polyferrocenylsilane. Journal of Physical Chemistry C, 2010, 114, 9469-9477.	1.5	17
8999	High Photocatalytic Activity of Rutile TiO₂ Induced by Iodine Doping. Journal of Physical Chemistry C, 2010, 114, 6035-6038.	1.5	34

#	Article	IF	Citations
9000	A Density Functional Theory Study of the Charge State of Hydrogen in Metal Hydrides. Journal of Physical Chemistry C, 2010, 114, 10978-10985.	1.5	53
9001	First-principles study of structural, electronic, and magnetic properties of double perovskite<mml:math xmlns:mml="http://www.w3.org/1998/Math/MathML" display="inline"><mml:mrow><mml:msub><mml:mrow><mml:mtext>Ho</mml:mtext></mml:mrow><mml:mn>2</mml:mn></mml:msu Physical Review B, 2010, 82, .	1.1	15
9002	Density Functional Model Study of Uranyl Adsorption on the Solvated (001) Surface of Kaolinite. Journal of Physical Chemistry C, 2010, 114, 13287-13294.	1.5	58
9003	First-principles study of the dynamical and nonlinear optical properties of urea single crystals. Physical Chemistry Chemical Physics, 2010, 12, 835-843.	1.3	19
9004	Electronic structures of boron nitride nanotubes subjected to tension, torsion, and flattening: A first-principles DFT study. Physical Review B, 2010, 82, .	1.1	22
9005	Dopant-Induced Electronic Structure Modification of HOPG Surfaces: Implications for High Activity Fuel Cell Catalysts. Journal of Physical Chemistry C, 2010, 114, 506-515.	1.5	100
9006	The Effect of Environment on the Reaction of Water on the Ceria(111) Surface: A DFT+U Study. Journal of Physical Chemistry C, 2010, 114, 14891-14899.	1.5	105
9007	Origin of magnetism in undoped<mml:math xmlns:mml="http://www.w3.org/1998/Math/MathML" display="inline"><mml:mrow><mml:msub><mml:mrow><mml:mtext>MoO</mml:mtext></mml:mrow><mml:mn>3</mml:mn></mml:mrow><mml:mrow><mml:mtext> by first-principles calculations. Physical Review B, 2010, 81, .	1.1	22
9008	Molecular Property Investigations of anortho-Hydroxy Schiff Base Type Compound with the First-Principle Molecular Dynamics Approach. Journal of Physical Chemistry B, 2010, 114, 242-253.	1.2	27
9009	Structural Studies of Technetiumâ"Zirconium Alloys by X-ray Diffraction, High-Resolution Electron Microscopy, and First-Principles Calculations. Inorganic Chemistry, 2010, 49, 1433-1438.	1.9	14
9010	A Direct Relation between Adsorbate Interactions, Configurations, and Reactivity: CO Oxidation on Rh(100) and Rh(111). Journal of Physical Chemistry C, 2010, 114, 21672-21680.	1.5	15
9011	Magnetic Properties of Cu_mO_n Clusters: A First Principles Study. Journal of Physical Chemistry A, 2010, 114, 8417-8422.	1.1	17
9012	Grafting of Lanthanide Complexes on Silica Surfaces: A Theoretical Investigation. Journal of Physical Chemistry A, 2010, 114, 6322-6330.	1.1	29
9013	Breaking AB stacking order in graphite oxide: ab initio approach. Physical Chemistry Chemical Physics, 2010, 12, 1595.	1.3	21
9014	Ab initiothermodynamic and elastic properties ofAGaH4hydrides (A=Li, Na, K, Rb, and Cs). Physical Review B, 2010, 82, .	1.1	12
9015	High-pressure crystal structures and superconductivity of Stannane (SnH ₄). Proceedings of the National Academy of Sciences of the United States of America, 2010, 107, 1317-1320.	3.3	168
9016	Pressure-induced elemental dissociation in zinc chalcogenides. New Journal of Physics, 2010, 12, 043058.	1.2	12
9017	First-principles study on mechanical and magnetic properties of the perovskite and post-perovskite polymorphs of pure end-member FeSiO₃at the coreâ€"mantle boundary. High Pressure Research, 2010, 30, 292-300.	0.4	2

#	Article	IF	Citations
9018	First-principles study of La and Sb-doping effects on electronic structure and optical properties of SrTiO₃. Chinese Physics B, 2010, 19, 017101-8.	0.7	11
9019	Does the MgO(100)-Support Facilitate the Reaction of Nitrogen and Hydrogen Molecules Catalyzed by Zr2Pd2 Clusters? A Computational Study. Inorganic Chemistry, 2010, 49, 2557-2567.	1.9	0
9020	Implementation of Exact Exchange with Numerical Atomic Orbitals. Journal of Physical Chemistry A, 2010, 114, 1039-1043.	1.1	19
9021	Adsorption of NO₂ on Oxygen Deficient ZnO(21Ì...1Ì...0) for Gas Sensing Applications: A DFT Study. Journal of Physical Chemistry C, 2010, 114, 16603-16610.	1.5	67
9022	Pathways for Oxygen Incorporation in Mixed Conducting Perovskites: A DFT-Based Mechanistic Analysis for (La, Sr)MnO_{3â^'Î'}. Journal of Physical Chemistry C, 2010, 114, 3017-3027.	1.5	160
9023	Thermoelectric transport properties of PbTe under pressure. Physical Review B, 2010, 82, .	1.1	96
9024	Theoretical and experimental study of the structural stability of<mml:math xmlns:mml="http://www.w3.org/1998/Math/MathML" display="inline"><mml:mrow><mml:msub><mml:mrow><mml:mtext>TbPO</mml:mtext></mml:mrow><mml:mn>4</mml:mn></mml:m high pressures. Physical Review B, 2010, 81, .	1.1	46
9025	Theoretical prediction of different decomposition paths for<mml:math xmlns:mml="http://www.w3.org/1998/Math/MathML" display="inline"><mml:mrow><mml:mtext>Ca</mml:mtext><mml:msub><mml:mrow><mml:mrow><mml:mo>(</mml:mo><mml:mrow xmlns:mml="http://www.w3.org/1998/Math/MathML" display="inline"><mml:mrow><mml:mtext>M. Physical Review B, 2010, 82, .	1.1	43
9026	Hexagon Preserving Carbon Nanofoams. Carbon Materials, 2010, , 57-77.	0.2	2
9027	Oxygen vacancy migration in ceria and Pr-doped ceria: A DFT+U study. Journal of Chemical Physics, 2010, 132, 094104.	1.2	128
9028	Effects of silicon and germanium adsorbed on graphene. Applied Physics Letters, 2010, 96, .	1.5	63
9029	Dense Yttria Phase Eclipsing the A-Type Sesquioxide Structure: High-Pressure Experiments and ab initio Calculations. Inorganic Chemistry, 2010, 49, 4478-4485.	1.9	42
9030	First-principles calculations of carbon clathrates: Comparison to silicon and germanium clathrates. Physical Review B, 2010, 82, .	1.1	34
9031	Scanning Tunneling Microscopy Simulations of Nitrogen- and Boron-Doped Graphene and Single-Walled Carbon Nanotubes. ACS Nano, 2010, 4, 4165-4173.	7.3	123
9032	Exotic behavior and crystal structures of calcium under pressure. Proceedings of the National Academy of Sciences of the United States of America, 2010, 107, 7646-7651.	3.3	86
9033	Towards efficient band structure and effective mass calculations for III-V direct band-gap semiconductors. Physical Review B, 2010, 82, .	1.1	279
9034	Transition-Metal Decoration Enhanced Room-Temperature Hydrogen Storage in a Defect-Modulated Graphene Sheet. Journal of Physical Chemistry C, 2010, 114, 10297-10301.	1.5	135
9035	Trends in the Adsorption of 3d Transition Metal Atoms onto Graphene and Nanotube Surfaces: A DFT Study and Molecular Orbital Analysis. Journal of Physical Chemistry C, 2010, 114, 14141-14153.	1.5	184

#	Article	IF	Citations
9036	Prediction of Isothermal Equation of State of an Explosive Nitrate Ester by van der Waals Density Functional Theory. Journal of Physical Chemistry Letters, 2010, 1, 346-348.	2.1	5
9037	In situ observation of thermal expansion of tetragonal C11b phase in Zr2Cu(1â˜'x)Pdx alloys. Intermetallics, 2010, 18, 8-13.	1.8	6
9038	Effects of X (V, W, Mo, Hf, Ta, Zr) additions on the ideal cleavage fracture of Cr2Nb: First-principles determination. Intermetallics, 2010, 18, 65-69.	1.8	21
9039	Consideration on the possibility of band gap widening of BaSi2 by incorporation of alkali metal elements (Na, K, and Cs) using electronic energy and structure calculation. Intermetallics, 2010, 18, 348-352.	1.8	9
9040	Theoretical investigation of the Pt3Al ground state. Intermetallics, 2010, 18, 417-421.	1.8	36
9041	Point defects and chemical potentials in D88â€“Sn3Ti5. Intermetallics, 2010, 18, 459-471.	1.8	8
9042	Energetic evaluation of Baâ€“ and Srâ€“Si clathrate formation at high pressures by first-principle pseudopotential calculations. Intermetallics, 2010, 18, 542-547.	1.8	13
9043	First-principles calculation aided thermodynamic modeling of the Moâ€“Re system. Intermetallics, 2010, 18, 574-581.	1.8	11
9044	First-principles study of the structural, electronic and elastic properties of W5Si3. Intermetallics, 2010, 18, 688-693.	1.8	41
9045	Ab initio calculations of elastic constants and thermodynamic properties of Î³TiAl under high pressures. Intermetallics, 2010, 18, 761-766.	1.8	25
9046	Correlation between thermodynamics and glass forming ability in the Alâ€“Ceâ€“Ni system. Intermetallics, 2010, 18, 900-906.	1.8	24
9047	The electronic, elastic, and structural properties of Tiâ€“Pd intermetallics and associated hydrides from first principles calculations. Intermetallics, 2010, 18, 998-1006.	1.8	40
9048	Monte-Carlo simulation of atom kinetics in intermetallics: Correcting the jump rates in Ni3Al. Intermetallics, 2010, 18, 1091-1098.	1.8	8
9049	Effects of alloying elements on elastic properties of Ni3Al by first-principles calculations. Intermetallics, 2010, 18, 1163-1171.	1.8	86
9050	The Feâ€“Ni system: Thermodynamic modelling assisted by atomistic calculations. Intermetallics, 2010, 18, 1148-1162.	1.8	149
9051	Assessment of the possibility of band gap widening of BaSi2 by incorporation of carbon. Intermetallics, 2010, 18, 1432-1436.	1.8	22
9052	First-principles calculations of the structural and elastic properties of Î²-FeSi2 at high-pressure. Intermetallics, 2010, 18, 1222-1227.	1.8	12
9053	Structural stability of intermetallic phases in the Siâ€“Ti system. Point defects and chemical potentials in D88-Si3Ti5 phase. Intermetallics, 2010, 18, 1444-1454.	1.8	47

#	Article	IF	Citations
9054	Prediction of the site occupations of the ThMn12-type intermetallics YFe12â˜'Mo by combining thermodynamic model with ab-initio calculations. Intermetallics, 2010, 18, 1465-1469.	1.8	8
9055	Ni and Al diffusion in Ni-rich NiAl and the effect of Pt additions. Intermetallics, 2010, 18, 1470-1479.	1.8	17
9056	On third-order elastic constants for ductile rare-earth intermetallic compounds: AÂfirst-principles study. Intermetallics, 2010, 18, 1653-1658.	1.8	11
9057	Link between structural and mechanical stability of fcc- and bcc-based ordered Mgâ€“Li alloys. Intermetallics, 2010, 18, 2083-2089.	1.8	59
9058	Ab initio calculations on the third-order elastic constants for selected B2â€“MgRE (REÂ=ÂY, Tb, Dy, Nd) intermetallics. Intermetallics, 2010, 18, 2472-2476.	1.8	20
9059	First-principles study on the site preference of Dy in B2 NiAl. Journal of Alloys and Compounds, 2010, 492, 295-299.	2.8	15
9060	The standard enthalpies of formation of binary intermetallic compounds of some late 4d and 5d transition metals by high temperature direct synthesis calorimetry. Journal of Alloys and Compounds, 2010, 492, 105-115.	2.8	36
9061	First-principles investigation of the structural and mechanical properties of Î²â€³ phase in Mgâ€“Gd alloy system. Journal of Alloys and Compounds, 2010, 492, 416-420.	2.8	25
9062	Ab-initio investigation of structural, electronic and optical properties of InxGa1â˜'xAs, GaAs1â˜'yPy ternary and InxGa1â˜'xAs1â˜'yPy quaternary semiconductor alloys. Journal of Alloys and Compounds, 2010, 496, 226-233.	2.8	35
9063	Thermodynamic properties of Mg2Si and Mg2Ge investigated by first principles method. Journal of Alloys and Compounds, 2010, 499, 68-74.	2.8	52
9064	First principles study of adsorption of metals on Pt(111) surface. Journal of Alloys and Compounds, 2010, 497, 38-45.	2.8	21
9065	Temperature dependent elastic coefficients of Mg2X (X=Si, Ge, Sn, Pb) compounds from first-principles calculations. Journal of Alloys and Compounds, 2010, 498, 191-198.	2.8	53
9066	-Al13Co4, a new quasicrystal approximant. Journal of Alloys and Compounds, 2010, 500, 153-160.	2.8	34
9067	Studies of covalent amides for hydrogen storage systems: Structures and bonding of the MAl(NH2)4 phases with M=Li, Na and K. Journal of Alloys and Compounds, 2010, 503, 194-203.	2.8	18
9068	In situ observation of the reaction of tantalum with nitrogen in a laser heated diamond anvil cell. Journal of Alloys and Compounds, 2010, 502, 5-12.	2.8	48
9069	Theoretical study on the stability, elasticity, hardness and electronic structures of Wâ€“C binary compounds. Journal of Alloys and Compounds, 2010, 502, 28-37.	2.8	182
9070	Nitrogen-electronegativity-induced bowing character in ternary zincblende Ga1â˜'xInxN alloys. Journal of Alloys and Compounds, 2010, 503, 529-537.	2.8	10
9071	A series of BaAl2â˜'xSixH2â˜'x (0.4<x<1.6) hydrides with compositions and structures in between BaSi2 and BaAl2H2. Journal of Alloys and Compounds, 2010, 505, 1-5.	2.8	13

#	Article	IF	Citations
9072	First-principles study of the structural, elastic and electronic properties of the anti-perovskites SnBSc3 and PbBSc3. Journal of Alloys and Compounds, 2010, 504, 296-302.	2.8	15
9073	Charge disproportionation in AlV2O4: A first-principles study. Journal of Alloys and Compounds, 2010, 505, L23-L26.	2.8	8
9074	Prediction study of the axial compressibility, anisotropy and dynamic properties for single crystal Ti2GeC. Journal of Alloys and Compounds, 2010, 506, 22-26.	2.8	16
9075	First-principles study of elastic and electronic properties of MgZn2 and ScZn2 phases in Mgâ€“Scâ€“Zn alloy. Journal of Alloys and Compounds, 2010, 506, 412-417.	2.8	135
9076	First-principles study of structural, elastic, electronic and lattice dynamic properties of AsxPyN1â^'xâ^'yAl quaternary alloys. Journal of Alloys and Compounds, 2010, 507, 120-125.	2.8	10
9077	High-pressure behavior of otavite (CdCO3). Journal of Alloys and Compounds, 2010, 508, 251-257.	2.8	28
9078	Structure, thermodynamics, and diffusion in CaAl2Si2O8 liquid from first-principles molecular dynamics. Geochimica Et Cosmochimica Acta, 2010, 74, 5657-5671.	1.6	59
9079	Mechanisms of nickel sorption by a bacteriogenic birnessite. Geochimica Et Cosmochimica Acta, 2010, 74, 3076-3089.	1.6	117
9080	First-principles study of the structural and isotopic properties of Al- and OH-bearing hematite. Geochimica Et Cosmochimica Acta, 2010, 74, 3948-3962.	1.6	32
9081	Surface complexation of Pb(II) by hexagonal birnessite nanoparticles. Geochimica Et Cosmochimica Acta, 2010, 74, 6731-6740.	1.6	73
9082	Solvus boundaries of (meta)stable phases in the Alâ€“Mgâ€“Si system: First-principles phonon calculations and thermodynamic modeling. Calphad: Computer Coupling of Phase Diagrams and Thermochemistry, 2010, 34, 20-25.	0.7	34
9083	Thermodynamic assessment of the Vâ€“Zn system supported by key experiments and first-principles calculations. Calphad: Computer Coupling of Phase Diagrams and Thermochemistry, 2010, 34, 75-80.	0.7	13
9084	Thermodynamic remodeling of the Coâ€“Ga system. Calphad: Computer Coupling of Phase Diagrams and Thermochemistry, 2010, 34, 189-195.	0.7	14
9085	Elastic and thermodynamic properties of the Niâ€“B system studied by first-principles calculations and experimental measurements. Calphad: Computer Coupling of Phase Diagrams and Thermochemistry, 2010, 34, 245-251.	0.7	15
9086	Thermodynamic assessment of the Mnâ€“C system. Calphad: Computer Coupling of Phase Diagrams and Thermochemistry, 2010, 34, 279-285.	0.7	49
9087	Thermodynamic modeling of the Pdâ€“S system supported by first-principles calculations. Calphad: Computer Coupling of Phase Diagrams and Thermochemistry, 2010, 34, 324-331.	0.7	8
9088	Ab initio ternary -phase diagram: The Crâ€“Moâ€“Re system. Calphad: Computer Coupling of Phase Diagrams and Thermochemistry, 2010, 34, 487-494.	0.7	21
9089	Ab initio and thermodynamic study of the Crâ€“Re system. Calphad: Computer Coupling of Phase Diagrams and Thermochemistry, 2010, 34, 495-503.	0.7	20

#	Article	IF	Citations
9090	Insight of DFT and atomistic thermodynamics on the adsorption and insertion of halides onto the hydroxylated NiO(111) surface. Corrosion Science, 2010, 52, 2643-2652.	3.0	69
9091	Determination of the high-pressure properties of fayalite from first-principles calculations. Earth and Planetary Science Letters, 2010, 289, 449-456.	1.8	33
9092	Thermal conductivity of MgO periclase at high pressure: Implications for the Dâ€³ region. Earth and Planetary Science Letters, 2010, 292, 392-398.	1.8	90
9093	Thermodynamics of mixing in MgSiO3â€“Al2O3 perovskite and ilmenite from ab initio calculations. Earth and Planetary Science Letters, 2010, 295, 477-486.	1.8	15
9094	Structure behavior and equation of state (EOS) of Ni2P and (Fe1â^' Ni)2P (allabogdanite) from First-principles calculations. Earth and Planetary Science Letters, 2010, 295, 578-582.	1.8	3
9095	High-pressure phase relations in the composition of albite NaAlSi3O8 constrained by an ab initio and quasi-harmonic Debye model, and their implications. Earth and Planetary Science Letters, 2010, 298, 427-433.	1.8	18
9096	First-principles analysis of the adsorption of aluminum and chromium atoms on the HfC (001) surface. Computational Materials Science, 2010, 47, 625-629.	1.4	11
9097	Structural and electrochemical aspects of Mn substitution into Li2FeSiO4 from DFT calculations. Computational Materials Science, 2010, 47, 678-684.	1.4	36
9098	Atomic structures and behaviors of a fcc Cu(111) surface with submonolayer Pb coverage. Computational Materials Science, 2010, 47, 693-697.	1.4	3
9099	The structural, electronic, elastic, phonon, and thermodynamical properties of the SmX (X=P, Sb, Bi) compounds. Computational Materials Science, 2010, 47, 758-768.	1.4	5
9100	First principles studies of phase stability, electronic and elastic properties in BBi compound. Computational Materials Science, 2010, 47, 968-972.	1.4	27
9101	First principles study of structural, elastic and electronic properties of ACY3 (A=Al, In and Tl). Computational Materials Science, 2010, 47, 973-976.	1.4	8
9102	First-principles thermodynamics from phonon and Debye model: Application to Ni and Ni3Al. Computational Materials Science, 2010, 47, 1040-1048.	1.4	357
9103	First-principles study of structural, elastic, electronic and lattice dynamic properties of AsxPyN1â^'xâ^'yB quaternary alloys. Computational Materials Science, 2010, 48, 94-100.	1.4	0
9104	Structural, mechanical and electronic properties of 4d transition metal mononitrides by first-principles. Computational Materials Science, 2010, 47, 1064-1071.	1.4	72
9105	First-principles calculation and luminescence property of Eux:Si5Al1â^'xO1+xN7â^'x green phosphor. Computational Materials Science, 2010, 49, S359-S363.	1.4	4
9106	Vibrational signatures of OTe and OTeâ€“VCd in CdTe: A first-principles study. Computational Materials Science, 2010, 49, S242-S245.	1.4	11
9107	The role of structural variations in the magnetism of Fe/Cu(111): First-principles calculations. Computational Materials Science, 2010, 49, S291-S296.	1.4	5

#	Article	IF	Citations
9108	X-ray absorption spectroscopy of indium nitride, indium oxide, and their alloys. Computational Materials Science, 2010, 49, S37-S42.	1.4	5
9109	Theoretical study of stabilities and electronic properties of the vacancy and carbon-doping defects in zigzag boron nitride nanoribbons. Computational Materials Science, 2010, 48, 648-654.	1.4	34
9110	Ab initio molecular dynamics study of pressure-induced phase transformation in KCl. Computational Materials Science, 2010, 48, 672-676.	1.4	4
9111	First principles study of the physisorption of hydrogen molecule on graphene and carbon nanotube surfaces adhered by Pt atom. Computational Materials Science, 2010, 49, S15-S20.	1.4	17
9112	Dehydrogenation kinetics of magnesium hydride investigated by DFT and experiment. Computational Materials Science, 2010, 49, S144-S149.	1.4	26
9113	Ab initio study of basic material properties of Fe, Co, and Ni ferromagnetic crystals. Computational Materials Science, 2010, 48, 700-704.	1.4	5
9114	Structural, elastic and electronic properties of the hexagonal anti-perovskites SbNBa3 and BiNBa3. Computational Materials Science, 2010, 48, 711-718.	1.4	22
9115	Electronic structure and magnetism of cubic Ga1â^'xEuxN and Al1â^'xEuxN using the LSDA+U approach. Computational Materials Science, 2010, 48, 743-748.	1.4	16
9116	First-principles calculations of pressure-induced phase transformation in AlN and GaN. Computational Materials Science, 2010, 48, 768-772.	1.4	39
9117	The high-pressure phase transitions and vibrational properties of zinc-blende XTe (X=Zn, Cd, Hg): Performance of local-density-approximation density functional theory. Computational Materials Science, 2010, 48, 796-801.	1.4	37
9118	The natural valence band offset of dilute GaAs1â^'xNx and GaAs: The first-principles approach. Computational Materials Science, 2010, 49, S150-S152.	1.4	1
9119	First-principles calculations of pure elements: Equations of state and elastic stiffness constants. Computational Materials Science, 2010, 48, 813-826.	1.4	259
9120	Predicting the hydrogen bond ordered structures of ice Ih, II, III, VI and ice VII: DFT methods with localized based set. Computational Materials Science, 2010, 49, S170-S175.	1.4	28
9121	Electronic and optical properties of anatase TiO2 nanotubes. Computational Materials Science, 2010, 48, 854-858.	1.4	40
9122	Thermo-elastic and lattice dynamical properties of Rh3Hf compound. Computational Materials Science, 2010, 48, 859-865.	1.4	19
9123	Theoretical prediction of the elastic, electronic and optical properties of the filled tetrahedral semiconductor Î±-LiMgSb. Computational Materials Science, 2010, 49, 64-69.	1.4	19
9124	DFT study on elastic and piezoelectric properties of tetragonal BaTiO3. Computational Materials Science, 2010, 49, S372-S377.	1.4	34
9125	High-throughput electronic band structure calculations: Challenges and tools. Computational Materials Science, 2010, 49, 299-312.	1.4	1,140

#	Article	IF	Citations
9126	Prediction study of the structural, elastic and high pressure properties of Yttrium chalcogenide. Computational Materials Science, 2010, 49, 372-377.	1.4	29
9127	Properties of the bare, passivated and doped germanium nanowire: A density-functional theory study. Computational Materials Science, 2010, 49, 682-690.	1.4	7
9128	Ab initio studies of staggered Li adatoms on graphene. Computational Materials Science, 2010, 49, 787-791.	1.4	28
9129	Crystal structure and elastic properties of ZrB compared with ZrB2: A first-principles study. Computational Materials Science, 2010, 49, 814-819.	1.4	79
9130	Vacancy defects in strontium titanate: Ab initio calculation. Computational Materials Science, 2010, 49, 904-909.	1.4	28
9131	The energy band gap of ScN in the rocksalt phase obtained with LDA/GGA+USIC approximations in FP-LAPW method. Computational Materials Science, 2010, 50, 269-273.	1.4	19
9132	First principles study of interface structure and electronic property of Au/SrTiO3(001). Computational Materials Science, 2010, 50, 98-104.	1.4	10
9133	First-principles study on the structural stabilities, electronic and elastic properties for zirconium under pressure. Computational Materials Science, 2010, 50, 179-183.	1.4	20
9134	A DFT study of polyanion substitution into the Li-ion battery cathode material Li2FeSiO4. Computational Materials Science, 2010, 50, 191-197.	1.4	25
9135	Structural phase transition, electronic and elastic properties in TlX (X=N, P, As) compounds: Pressure-induced effects. Computational Materials Science, 2010, 50, 203-210.	1.4	34
9136	Electronic structure and magnetic properties of the ThxY1â^'xCo4B solid solution. Computational Materials Science, 2010, 50, 295-300.	1.4	0
9137	First-principles study of electronic and optical properties of Pbnm orthorhombic SrHfO3. Computational Materials Science, 2010, 50, 454-458.	1.4	8
9138	First principles study of structural, electronic and elastic properties of lutatium mono-pnictides. Computational Materials Science, 2010, 50, 538-544.	1.4	20
9139	Implementation of techniques for computing optical properties in 0â€“3 dimensions, including a real-space cutoff, in ABINIT. Computational Materials Science, 2010, 50, 698-703.	1.4	13
9140	Comparison of electronic property and structural stability of LiMn2O4 and LiNi0.5Mn1.5O4 as cathode materials for lithium-ion batteries. Computational Materials Science, 2010, 50, 776-779.	1.4	39
9141	Elasticity of (K,Na)AlSi3O8 hollandite from lattice dynamics calculations. Physics of the Earth and Planetary Interiors, 2010, 181, 21-26.	0.7	24
9142	Spin and structural transitions in AlFeO3 and FeAlO3 perovskite and post-perovskite. Physics of the Earth and Planetary Interiors, 2010, 182, 10-17.	0.7	24
9143	Equation of state (EOS) and collapse of magnetism in iron-rich meteorites at high pressure by first-principles calculations. Physics of the Earth and Planetary Interiors, 2010, 182, 175-178.	0.7	5

#	Article	IF	Citations
9144	A particularly strong organic acceptor for tuning the hole-injection barriers in modern organic devices. Synthetic Metals, 2010, 160, 1456-1462.	2.1	8
9145	First-principles investigation of graphene fluoride and graphane. Physical Review B, 2010, 82, .	1.1	397
9146	Molecular, Electronic, and Crystal Structures of Self-Assembled Hydrothermally Synthesized Zn(II)â^'Mercaptonicotinate: A Combined Spectroscopic and Theoretical Approach. Inorganic Chemistry, 2010, 49, 4099-4108.	1.9	13
9147	Enhanced static approximation to the electron self-energy operator for efficient calculation of quasiparticle energies. Physical Review B, 2010, 82, .	1.1	42
9148	Quasiparticle and optical properties of rutile and anatase<mml:math xmlns:mml="http://www.w3.org/1998/Math/MathML" display="inline"><mml:mrow><mml:msub><mml:mrow><mml:mtext>TiO</mml:mtext></mml:mrow><mml:mn>2</mml:mn></mml:msu Physical Review B, 2010, 82, .	1.1	192
9149	Density Functional Theory Calculations of Ultrathin Epitaxial Au Overlayers on CdS(0001) and CdS(0001Ì…). Journal of Physical Chemistry C, 2010, 114, 3998-4007.	1.5	9
9150	Graphene-like silicon nanoribbons on Ag(110): A possible formation of silicene. Applied Physics Letters, 2010, 96, .	1.5	874
9151	First-principles calculation of the linear and nonlinear optical properties of LiTaO₃. Physica Scripta, 2010, 81, 055703.	1.2	8
9152	Oxygen activation on gold nanoparticles: separating the influence of particle size, particle shape and support interaction. Dalton Transactions, 2010, 39, 8538.	1.6	134
9153	Water Adsorption on Native and Hydrogenated Diamond (001) Surfaces. Journal of Physical Chemistry C, 2010, 114, 7045-7053.	1.5	47
9154	Step-by-step growth of epitaxially aligned polythiophene by surface-confined reaction. Proceedings of the National Academy of Sciences of the United States of America, 2010, 107, 11200-11204.	3.3	117
9155	Structural, electronic, and optical properties of Î±, Î², and Î³-TeO2. Journal of Applied Physics, 2010, 107, .	1.1	39
9156	Functionalized Metallic Single-Walled Carbon Nanotubes as a High-Performance Single-Molecule Organic Field Effect Transistor: An ab Initio Study. Journal of Physical Chemistry C, 2010, 114, 15816-15822.	1.5	13
9157	Search and Characterization of Transition State Structures in Crystalline Systems Using Valence Coordinates. Journal of Chemical Theory and Computation, 2010, 6, 1341-1350.	2.3	19
9158	Distortions and stabilization of simple-cubic calcium at high pressure and low temperature. Proceedings of the National Academy of Sciences of the United States of America, 2010, 107, 9965-9968.	3.3	38
9159	Native Defects in ZnO Nanowires: Atomic Relaxations, Relative Stability, and Defect Healing with Organic Acids. Journal of Physical Chemistry C, 2010, 114, 18860-18865.	1.5	18
9160	Evaluation of Linear Thermal Expansion Coefficients of Perovskite Oxides Using Ab-initio Molecular Dynamics with Small Cell Sizes for Materials Design. Japanese Journal of Applied Physics, 2010, 49, 045701.	0.8	11
9161	Correlation of Oxygen Storage Capacity and Structural Distortion in Transition-Metal-, Noble-Metal-, and Rare-Earth-Ion-Substituted CeO₂ from First Principles Calculation. Chemistry of Materials, 2010, 22, 5184-5198.	3.2	190

#	Article	IF	Citations
9162	Mixed Low-Dimensional Nanomaterial: 2D Ultranarrow MoS₂ Inorganic Nanoribbons Encapsulated in Quasi-1D Carbon Nanotubes. Journal of the American Chemical Society, 2010, 132, 13840-13847.	6.6	218
9163	Bulk and Surface Properties of Rutile TiO₂ from Self-Consistent-Charge Density Functional Tight Binding. Journal of Chemical Theory and Computation, 2010, 6, 499-507.	2.3	34
9164	Gold adatoms and clusters on PPV: Anab initioinvestigation. Journal of Chemical Physics, 2010, 133, 204703.	1.2	2
9165	Ab initiolattice dynamics and thermodynamics of rare-earth hexaborides<mml:math xmlns:mml="http://www.w3.org/1998/Math/MathML" display="inline"><mml:mrow><mml:msub><mml:mrow><mml:mtext>LaB</mml:mtext></mml:mrow><mml:mn>6</mml:mn></mml: xmlns:mml="http://www.w3.org/1998/Math/MathML" display="inline"><mml:mrow><mml:msub><mml:mrow><mml:mtext>CeB</mml:mtext></mml:mrow><mml:mn>6</mml:mn></mml: Physical Review B, 2010, 82, .	1.1	38
9166	Ab initiocalculations to determine the formation enthalpy of Cu₃Au phases. Philosophical Magazine Letters, 2010, 90, 801-807.	0.5	3
9167	Theoretical Studies of the Magnetism of the First-Row Adatom on the Silicon Carbide (SiC) Nanotube. Journal of Physical Chemistry C, 2010, 114, 3825-3829.	1.5	19
9168	First principles prediction of the third conformer of hydrogenated BN sheet. Physica Status Solidi - Rapid Research Letters, 2010, 4, 368-370.	1.2	32
9169	Second-generation charge-optimized many-body potential for<mml:math xmlns:mml="http://www.w3.org/1998/Math/MathML" display="inline"><mml:mrow><mml:mtext>Si</mml:mtext><mml:mo>/</mml:mo><mml:msub><mml:mrow><mml:mtext>SiO</mml: amorphous silica. Physical Review B, 2010, 82, .	1.1	80
9170	Extended DFT +U+Vmethod with on-site and inter-site electronic interactions. Journal of Physics Condensed Matter, 2010, 22, 055602.	0.7	119
9171	Embedded-atom-method interatomic potentials from lattice inversion. Journal of Physics Condensed Matter, 2010, 22, 375503.	0.7	17
9172	Effect of magnetic disorder and strong electron correlations on the thermodynamics of CrN. Physical Review B, 2010, 82, .	1.1	129
9173	Geometric and electronic structures of graphitic-like and tubular silicon carbides:Ab-initiostudies. Physical Review B, 2010, 82, .	1.1	54
9174	Band engineering of bilayer graphene by metal atoms: First-principles calculations. Applied Physics Letters, 2010, 96, 231916.	1.5	11
9175	First-principles prediction of partitioning of alloying elements between cementite and ferrite. Acta Materialia, 2010, 58, 6276-6281.	3.8	84
9176	Structural, Electronic and Elastic Properties of Cubic Perovskites SrSnO ₃ and SrZrO ₃ under Hydrostatic Pressure Effect. Chinese Physics Letters, 2010, 27, 096201.	1.3	10
9177	A DFT study of PtAu bimetallic clusters adsorbed on MgO/Ag(100) ultrathin films. Physical Chemistry Chemical Physics, 2010, 12, 6352.	1.3	12
9178	Density Functional Theory Study of ATA, BTAH, and BTAOH as Copper Corrosion Inhibitors: Adsorption onto Cu(111) from Gas Phase. Langmuir, 2010, 26, 14582-14593.	1.6	126
9179	Electron-poor antimonides: complex framework structures with narrow band gaps and low thermal conductivity. Dalton Transactions, 2010, 39, 1036-1045.	1.6	27

#	Article	IF	Citations
9180	High-pressure studies of melamine. High Pressure Research, 2010, 30, 65-71.	0.4	11
9181	Comparison of valence-band structures of NiAl alloy containing Cr and Ti: Photoelectron spectrum and first-principles calculations. Intermetallics, 2010, 18, 1062-1066.	1.8	6
9182	First-principles calculations of surface<mml:math xmlns:mml="http://www.w3.org/1998/Math/MathML" display="inline"><mml:mi>H</mml:mi></mml:math>centers in<mml:math xmlns:mml="http://www.w3.org/1998/Math/MathML" display="inline"><mml:mrow><mml:msub><mml:mrow><mml:mtext>BaF</mml:mtext></mml:mrow><mml:mn>2</mml:mn></mml:msu Physical Review B, 2010, 81, .	1.1	16
9183	Decomposition of Methylthiolate Monolayers on Au(111) Prepared from Dimethyl Disulfide in Solution Phase. Journal of Physical Chemistry C, 2010, 114, 10183-10194.	1.5	38
9184	Predicting transition pressures for obtaining nanoporous semiconductor polymorphs: oxides and chalcogenides of Zn, Cd and Mg. Physical Chemistry Chemical Physics, 2010, 12, 8513.	1.3	26
9185	Structural and Electronic Properties of Li-Ion Battery Cathode Material FeF₃. Journal of Physical Chemistry C, 2010, 114, 16813-16817.	1.5	59
9186	Stability trends of<mml:math xmlns:mml="http://www.w3.org/1998/Math/MathML" display="inline"><mml:mrow><mml:mi>M</mml:mi><mml:mi>A</mml:mi><mml:mi>X</mml:mi></mml:mrow></mml:math>phases from first principles. Physical Review B, 2010, 81, .	1.1	98
9187	Effect of vacancy defects on electronic properties and activation of sphalerite (110) surface by first-principles. Transactions of Nonferrous Metals Society of China, 2010, 20, 502-506.	1.7	33
9188	First principles study on electronic structure and optical properties of novel Na-hP4 high pressure phase. Transactions of Nonferrous Metals Society of China, 2010, 20, 1092-1096.	1.7	0
9189	Quantum-mechanical study of effect of lattice defects on surface properties and copper activation of sphalerite surface. Transactions of Nonferrous Metals Society of China, 2010, 20, 1121-1130.	1.7	26
9190	First-principles Investigation of Bi Segregation at the Solder Interface of Cu/Cu3Sn(010). Journal of Materials Science and Technology, 2010, 26, 1057-1062.	5.6	13
9191	Optical Properties of the High-Pressure Phases of SnO₂: First-Principles Calculation. Journal of Physical Chemistry A, 2010, 114, 1052-1059.	1.1	41
9192	Origin of Predominance of Cementite among Iron Carbides in Steel at Elevated Temperature. Physical Review Letters, 2010, 105, 055503.	2.9	83
9193	Effects of alkali metal adsorption on the structural and field emission properties of graphene. Diamond and Related Materials, 2010, 19, 1377-1381.	1.8	27
9194	First-principles calculations of the atomic and electronic structure of SrZrO3and PbZrO3(001) and (011) surfaces. Journal of Physics Condensed Matter, 2010, 22, 415901.	0.7	40
9195	Decomposition of Ethanol on Pd(111): A Density Functional Theory Study. Langmuir, 2010, 26, 1879-1888.	1.6	103
9196	Electronic structure of<mml:math xmlns:mml="http://www.w3.org/1998/Math/MathML" display="inline"><mml:mrow><mml:msub><mml:mrow><mml:mtext>In</mml:mtext></mml:mrow><mml:mn>2</mml:mn></mml:msub Sn-doped<mml:math xmlns:mml="http://www.w3.org/1998/Math/MathML" display="inline"><mml:mrow><mml:msub><mml:mrow><mml:mtext>In</mml:mtext></mml:mrow><mml:mn>2</mml:mn></mml:msub Physical Review B, 2010, 81, .	1.1	114
9197	First-principles prediction of the negatively-charged nitrogen-silicon-vacancy center in cubic silicon carbide. Journal of Applied Physics, 2010, 108, .	1.1	15

#	Article	IF	Citations
9198	Metallicity of boron carbides at high pressure. Journal of Physics: Conference Series, 2010, 215, 012117.	0.3	16
9199	First-principles calculations of Znâ€“K XANES in Ca-deficient hydroxyapatite. Journal of Physics Condensed Matter, 2010, 22, 384213.	0.7	11
9200	Theoretical Confirmation of the Enhanced Facility to Increase Oxygen Vacancy Concentration in TiO₂by Iron Doping. Journal of Physical Chemistry C, 2010, 114, 6511-6517.	1.5	78
9201	Silicon nano-ribbons on Ag(110): a computational investigation. Journal of Physics Condensed Matter, 2010, 22, 045004.	0.7	65
9202	Oxygen and nitrogen interstitial ordering in hcp Ti, Zr, and Hf: Anab initiostudy. Physical Review B, 2010, 82, .	1.1	42
9203	First-Principles Prediction on the High-Pressure Structures of Transition Metal Diborides (TMB₂, TM = Sc, Ti, Y, Zr). Inorganic Chemistry, 2010, 49, 6859-6864.	1.9	41
9204	Simple Point-Ion Electrostatic Model Explains the Cation Distribution in Spinel Oxides. Physical Review Letters, 2010, 105, 075501.	2.9	48
9205	Adsorption and Electronic Structure of Single C60F18Molecule on Si(111)-7Ã—7 Surface. Fullerenes Nanotubes and Carbon Nanostructures, 2010, 18, 369-375.	1.0	2
9206	Adsorption of methylamine on Ni₃Al(111) and NiAl(110)â€”a high resolution photoelectron spectroscopy and density functional theory study. Journal of Physics Condensed Matter, 2010, 22, 395004.	0.7	3
9207	Magnetic anisotropy of Fe and Co ultrathin films deposited on Rh(111) and Pt(111) substrates: An experimental and first-principles investigation. Physical Review B, 2010, 82, .	1.1	106
9208	Cluster-Assembled Materials: Toward Nanomaterials with Precise Control over Properties. ACS Nano, 2010, 4, 235-240.	7.3	127
9209	Trends of Water Gas Shift Reaction on Close-Packed Transition Metal Surfaces. Journal of Physical Chemistry C, 2010, 114, 9826-9834.	1.5	98
9210	Towards suppressing H blistering by investigating the physical origin of the Hâ€“He interaction in W. Nuclear Fusion, 2010, 50, 115010.	1.6	137
9211	An Improved Self-Consistent-Charge Density-Functional Tight-Binding (SCC-DFTB) Set of Parameters for Simulation of Bulk and Molecular Systems Involving Titanium. Journal of Chemical Theory and Computation, 2010, 6, 266-278.	2.3	177
9212	Elastic constants and anisotropy of RuB₂under pressure. Chinese Physics B, 2010, 19, 027101.	0.7	6
9213	Structure and diffusion of intrinsic defect complexes in LiNbO₃from density functional theory calculations. Journal of Physics Condensed Matter, 2010, 22, 135002.	0.7	39
9214	Deep hole traps in boron-doped diamond. Physical Review B, 2010, 81, .	1.1	23
9215	Theoretical Study of Two-Dimensional Silica Films. Journal of Physical Chemistry C, 2010, 114, 9678-9684.	1.5	9

#	Article	IF	Citations
9216	Electronic structure of substitutionally Mn-doped graphene. New Journal of Physics, 2010, 12, 063020.	1.2	83
9217	First-principles theoretical studies of half-metallic ferromagnetism in CrTe. Physical Review B, 2010, 82, .	1.1	43
9218	Ab initiostudy of structural and magnetic properties of Si-doped<mml:math xmlns:mml="http://www.w3.org/1998/Math/MathML" display="inline"><mml:mrow><mml:msub><mml:mrow><mml:mtext>Fe</mml:mtext></mml:mrow><mml:mn>2</mml:mn></mml:msub> Physical Review B, 2010, 82, .	1.1	30
9219	Computational study of structural and elastic properties of random Al_xGa_yIn_{1 â^'xâ^'y}N alloys. Journal of Physics Condensed Matter, 2010, 22, 205801.	0.7	9
9220	Efficient implementation of the nonequilibrium Green function method for electronic transport calculations. Physical Review B, 2010, 81, .	1.1	160
9221	First-principles study of hydrogen absorption on Mg(0001) and formation of magnesium hydride. Physical Review B, 2010, 81, .	1.1	33
9222	First Principles Study of the LiNH₂/Li₂NH Transformation. Journal of Physical Chemistry C, 2010, 114, 15174-15183.	1.5	33
9223	Group-V impurities in<mml:math xmlns:mml="http://www.w3.org/1998/Math/MathML" display="inline"><mml:mrow><mml:msub><mml:mrow><mml:mtext>SnO</mml:mtext></mml:mrow><mml:mn>2</mml:mn></mml:msub> first-principles calculations. Physical Review B, 2010, 81, .	1.1	52
9224	Ab initiothermodynamics beyond the quasiharmonic approximation: W as a prototype. Physical Review B, 2010, 81, .	1.1	20
9225	Unexpected change in the electronic properties of the Au-graphene interface caused by toluene. Physical Review B, 2010, 82, .	1.1	20
9226	Rhodium atoms confined in boron nitride nanotubes: Density functional calculations. Europhysics Letters, 2010, 90, 47003.	0.7	2
9227	Electronic structure and optical properties of rutile RuO₂from first principles. Chinese Physics B, 2010, 19, 077102.	0.7	20
9228	Dissolution-Resistant Coreâ^'Shell Materials for Acid Medium Oxygen Reduction Electrocatalysts. Journal of Physical Chemistry Letters, 2010, 1, 724-728.	2.1	19
9229	Methanol Synthesis from H₂and CO₂on a Mo₆S₈Cluster: A Density Functional Study. Journal of Physical Chemistry A, 2010, 114, 3888-3895.	1.1	83
9230	Density functional theory studies of doping in titania. Molecular Simulation, 2010, 36, 618-632.	0.9	12
9231	Understanding from First-Principles Why LiNH2BH3Â·NH3BH3 Shows Improved Dehydrogenation over LiNH2BH3 and NH3BH3. Journal of Physical Chemistry C, 2010, 114, 19089-19095.	1.5	27
9232	Optical properties of strained graphene. Europhysics Letters, 2010, 92, 67001.	0.7	112
9233	Effective method to identify the vacancies in crystalline GeTe. Applied Physics Letters, 2010, 97, .	1.5	30

#	Article	IF	Citations
9234	Stability and charge transfer levels of extrinsic defects in<mml:math xmlns:mml="http://www.w3.org/1998/Math/MathML" display="inline"><mml:mrow><mml:msub><mml:mrow><mml:mtext>LiNbO</mml:mtext></mml:mrow><mml:mn>3</mml:mn></mml:r Physical Review B, 2010, 82, .	1.1	41
9235	Ab initio studies on atomic and electronic structures of black phosphorus. Journal of Applied Physics, 2010, 107, .	1.1	235
9236	Theoretical Predictions of Energetic Molecular Crystals at Ambient and Hydrostatic Compression Conditions Using Dispersion Corrections to Conventional Density Functionals (DFT-D). Journal of Physical Chemistry C, 2010, 114, 6734-6748.	1.5	136
9237	Theoretical determination of the Raman spectra of single-crystal forsterite (Mg2SiO4). American Mineralogist, 2010, 95, 980-986.	0.9	38
9238	Phase transition in twinned nanolayered silicon structures under uniaxial compression: Molecular dynamics simulations and first-principles total-energy calculations. Physical Review B, 2010, 81, .	1.1	2
9239	First-principles study of structural, elastic, lattice dynamical and thermodynamical properties of GdX (X = Bi, Sb). Philosophical Magazine, 2010, 90, 1833-1852.	0.7	9
9240	Comparing efficiencies of genetic and minima hopping algorithms for crystal structure prediction. Physical Chemistry Chemical Physics, 2010, 12, 11617.	1.3	30
9241	First-Principle Study of Hydroxyl Functional Groups on Pristine, Defected Graphene, and Graphene Epoxide. Journal of Physical Chemistry C, 2010, 114, 21625-21630.	1.5	218
9242	Ab initiomolecular dynamics simulation of hydrogen diffusion in<mml:math xmlns:mml="http://www.w3.org/1998/Math/MathML" display="inline"><mml:mi>Î±</mml:mi></mml:math>-iron. Physical Review B, 2010, 81, .	1.1	46
9243	Role of Auâ^'C Interactions on the Catalytic Activity of Au Nanoparticles Supported on TiC(001) toward Molecular Oxygen Dissociation. Journal of the American Chemical Society, 2010, 132, 3177-3186.	6.6	88
9244	First-principles study of the interaction between paramagnetic<mml:math xmlns:mml="http://www.w3.org/1998/Math/MathML" display="inline"><mml:mrow><mml:msup><mml:mtext>V</mml:mtext><mml:mrow><mml:mn>4</mml:mn><mml:mo>+</mml:mo></r through formally magnetically inactive<mml:math xmlns:mml="http://www.w3.org/1998/Math/MathML" display="inline"><mml:mrow><mml:msub><mml:mrow><mml:mtext>VO</mml:mtext></mml:mrow><mml:mn>4</mml:mn></mml:msu	1.1	6
9245	Density Functional Theory Study of the Interaction of Cu, Ag, and Au Atoms with the Regular CeO₂(111) Surface. Journal of Physical Chemistry C, 2010, 114, 1934-1941.	1.5	108
9246	Electronic structure, phonons, and thermal properties of ScN, ZrN, and HfN: A first-principles study. Journal of Applied Physics, 2010, 107, .	1.1	125
9247	Electronic Structure of an XUV Photogenerated Solid-Density Aluminum Plasma. Physical Review Letters, 2010, 104, 225001.	2.9	62
9248	Ab initio molecular dynamics study of the hydration of Li+, Na+ and K+ in a montmorillonite model. Influence of isomorphic substitution. Physical Chemistry Chemical Physics, 2010, 12, 688-697.	1.3	90
9249	Water-gas shift reaction on oxide/Cu(111): Rational catalyst screening from density functional theory. Journal of Chemical Physics, 2010, 133, 204705.	1.2	34
9250	Structure maps for hcp metals from first-principles calculations. Physical Review B, 2010, 81, .	1.1	40
9251	Dehydrogenation of methanol on Pd(100): comparison with the results of Pd(111). Physical Chemistry Chemical Physics, 2010, 12, 7794.	1.3	30

#	Article	IF	Citations
9252	Origins of magnetism in transition metal doped CuI. Journal of Applied Physics, 2010, 108, 043713.	1.1	8
9253	Stability and cooperativity of hydrogen bonds in dihydroxybenzoic acids. New Journal of Chemistry, 2010, 34, 85-91.	1.4	28
9254	Pb-free semiconductor ferroelectrics: A theoretical study of Pd-substituted<mml:math xmlns:mml="http://www.w3.org/1998/Math/MathML" display="inline"><mml:mrow><mml:mtext>Ba</mml:mtext><mml:mrow><mml:mo>(</mml:mo><mml:mrow><mml:msub><mml:mrow> Physical Review B, 2010, 82, .	1.1	48
9255	First-principles modelling of complex perovskite (Ba1-xSrx)(Co1-yFey)O3-Î´ for solid oxide fuel cell and gas separation membrane applications. Energy and Environmental Science, 2010, 3, 1544.	15.6	75
9256	First-principles calculations of Born effective charges and spontaneous polarization of ferroelectric bismuth titanate. Journal of Physics Condensed Matter, 2010, 22, 165902.	0.7	27
9257	Influencing range of vacancy defects in zigzag single-walled carbon nanotubes. Chinese Physics B, 2010, 19, 027102.	0.7	3
9258	Lattice dynamics in<mml:math xmlns:mml="http://www.w3.org/1998/Math/MathML" display="inline"><mml:mrow><mml:msub><mml:mrow><mml:mtext>ZrB</mml:mtext></mml:mrow><mml:mrow><mml:mn>12</mml:mn> <mml:math xmlns:mml="http://www.w3.org/1998/Math/MathML" display="inline"><mml:mrow><mml:msub><mml:mrow><mml:mtext>LuB</mml:mtext></mml:mrow><mml:mrow><mml:mn>12</mml:mn> initiocalculations and inelastic neutron scattering. Physical Review B, 2010, 82, .	1.1	39
9259	First-Principles Study on Native Defect Complexes in InN. Communications in Theoretical Physics, 2010, 53, 145-148.	1.1	1
9260	A Comparative Study of Hydrogen Spillover on Pd and Pt Decorated MoO₃(010) Surfaces from First Principles. Journal of Physical Chemistry C, 2010, 114, 3052-3058.	1.5	26
9261	Electronic properties of BN/C nanotube heterostructures. Journal of Applied Physics, 2010, 107, .	1.1	34
9262	New Superconducting and Semiconducting Fe-B Compounds Predicted with anAbÂInitioEvolutionary Search. Physical Review Letters, 2010, 105, 217003.	2.9	182
9263	Periodic DFT Study of Radical Species on Crystalline Silica Surfaces. Journal of Physical Chemistry C, 2010, 114, 16430-16438.	1.5	27
9264	Lithium Coordination Sites in Li_xTiO₂(B): A Structural and Computational Study. Chemistry of Materials, 2010, 22, 6426-6432.	3.2	104
9265	Equation of state of TiH2 up to 90 GPa: A synchrotron x-ray diffraction study and ab initio calculations. Journal of Applied Physics, 2010, 108, 043511.	1.1	26
9266	Bismuth doping of graphene. Applied Physics Letters, 2010, 96, .	1.5	30
9267	First-principles study of the dipole layer formation at metal-organic interfaces. Physical Review B, 2010, 81, .	1.1	48
9268	Electronic Structure of the Thiophene/Au(111) Interface Probed by Two-Photon Photoemission. Journal of Physical Chemistry C, 2010, 114, 13670-13677.	1.5	21
9269	Modulation of electronic properties of hexagonal boron nitride bilayers by an electric field: A first principles study. Journal of Applied Physics, 2010, 107, .	1.1	47

#	Article	IF	Citations
9270	Limits for n-type doping in In2O3 and SnO2: A theoretical approach by first-principles calculations using hybrid-functional methodology. Journal of Applied Physics, 2010, 108, .	1.1	57
9271	Novel Rhenium Nitrides. Physical Review Letters, 2010, 105, 085504.	2.9	148
9272	Compressing the Most Hydrogen-Rich Inorganic Ion. Journal of the American Chemical Society, 2010, 132, 748-755.	6.6	25
9273	First-principles study of uranium carbide: Accommodation of point defects and of helium, xenon, and oxygen impurities. Physical Review B, 2010, 81, .	1.1	71
9274	Computer simulations of structures and properties of the biomaterial hydroxyapatite. Journal of Materials Chemistry, 2010, 20, 5376.	6.7	72
9275	Vanadium adsorption and incorporation at the GaN(0001) surface: A first-principles study. Physical Review B, 2010, 81, .	1.1	25
9276	Diffusion of hydrogen in bcc tungsten studied with first principle calculations. Journal of Applied Physics, 2010, 107, .	1.1	174
9277	Ab initiostudy of lattice vibration and polaron properties in zinc-blende AlxGa1â^'xN alloys. Journal of Applied Physics, 2010, 108, 113710.	1.1	30
9278	Origin of antiferromagnetism in CoO: A density functional theory study. Applied Physics Letters, 2010, 96, .	1.5	56
9279	Adsorption of Catechol on TiO₂ Rutile (100): A Density Functional Theory Investigation. Journal of Physical Chemistry C, 2010, 114, 6491-6495.	1.5	39
9280	First-principles study of the effect of vacancies on magnetic properties of Zn_{1 â^'x}Co_xO thin films. Journal of Physics Condensed Matter, 2010, 22, 076002.	0.7	4
9281	Theoretical study of physisorption of nucleobases on boron nitride nanotubes: a new class of hybrid nano-biomaterials. Nanotechnology, 2010, 21, 165703.	1.3	127
9282	FIRST-PRINCIPLES STUDY OF THE EFFECTS OF THE OXYGEN VACANCY ON ELECTRONIC STRUCTURE AND FERROMAGNETISM OF Sn₂ Co₂O_{8-Î´}. International Journal of Modern Physics B, 2010, 24, 2229-2235.	1.0	1
9283	Role of Adsorbed H, C, O, and CO on the Atomic Structure of Free and MgO(100)-Supported Ir₄Clusters: An ab Initio Study. Journal of Physical Chemistry C, 2010, 114, 15653-15660.	1.5	7
9284	Investigating behaviours of hydrogen in a tungsten grain boundary by first principles: from dissolution and diffusion to a trapping mechanism. Nuclear Fusion, 2010, 50, 025016.	1.6	182
9285	CO 2 capture properties of alkaline earth metal oxides and hydroxides: A combined density functional theory and lattice phonon dynamics study. Journal of Chemical Physics, 2010, 133, 074508.	1.2	122
9286	Soft modes in strained and unstrained rutileTiO2. Physical Review B, 2010, 81, .	1.1	44
9287	B3LYP calculations of cerium oxides. Journal of Chemical Physics, 2010, 132, 054110.	1.2	65

#	Article	IF	Citations
9288	High-pressure phase transitions of solid HF, HCl, and HBr: Anab initioevolutionary study. Physical Review B, 2010, 82, .	1.1	27
9289	Boron K4 crystal: a stable chiral three-dimensional sp2 network. Physical Chemistry Chemical Physics, 2010, 12, 12420.	1.3	25
9290	Understanding conductivity in SrCu₂O₂: stability, geometry and electronic structure of intrinsic defects from first principles. Journal of Materials Chemistry, 2010, 20, 1086-1096.	6.7	42
9291	Pt promotion and spill-over processes during deposition and desorption of upd-Had and OHad on PtxRu1â^'x/Ru(0001) surface alloys. Physical Chemistry Chemical Physics, 2010, 12, 10388.	1.3	29
9292	Azobenzene versus 3,3â€²,5,5â€²-tetra-tert-butyl-azobenzene (TBA) at Au(111): characterizing the role of spacer groups. Physical Chemistry Chemical Physics, 2010, 12, 6404.	1.3	48
9293	Experimental visualization of covalent bonds and structural disorder in a gallium zinc oxynitride photocatalyst (Ga1â^'xZnx)(N1â^'xOx): origin of visible light absorption. Chemical Communications, 2010, 46, 2379.	2.2	55
9294	Rules for selectivity in oxidation processes on RuO2(110). Physical Chemistry Chemical Physics, 2010, 12, 12217.	1.3	20
9295	The effect of pressure on the crystal structure of l-alanine. CrystEngComm, 2010, 12, 2573.	1.3	65
9296	Ab initio studies of hydrogen and acceptor defects in rutile TiO2. Physical Chemistry Chemical Physics, 2010, 12, 6817.	1.3	30
9297	First-principles study of the ferroelectric and nonlinear optical properties of the LiNbO3-type ZnSnO3. Physical Chemistry Chemical Physics, 2010, 12, 9197.	1.3	61
9298	The atomic level structure of the TiO2â€“NiTi interface. Physical Chemistry Chemical Physics, 2010, 12, 9742.	1.3	18
9299	Physisorption of aromatic organic contaminants at the surface of hydrophobic/hydrophilic silica geosorbents: a B3LYP-D modeling study. Physical Chemistry Chemical Physics, 2010, 12, 6357.	1.3	60
9300	Styrene oligomerization as a molecular probe reaction for zeolite acidity: a UV-Vis spectroscopy and DFT study. Physical Chemistry Chemical Physics, 2010, 12, 7032.	1.3	42
9301	Structure, stability and work functions of the low index surfaces of pure indium oxide and Sn-doped indium oxide (ITO) from density functional theory. Journal of Materials Chemistry, 2010, 20, 10438.	6.7	177
9302	Multinuclear NMR of CaSiO3 glass: simulation from first-principles. Physical Chemistry Chemical Physics, 2010, 12, 6054.	1.3	71
9303	Modeling of hydrogen and hydroxyl group migration on graphene. Physical Chemistry Chemical Physics, 2010, 12, 15367.	1.3	54
9304	Monitoring the interaction of adsorbates on metal surfaces by surface site engineering: the case of ethoxy on Cu, Pd, Ag and Au regular and stepped surfaces. Physical Chemistry Chemical Physics, 2010, 12, 6492.	1.3	11
9305	Li+ ion conductivity and diffusion mechanism in Î±-Li3N and Î²-Li3N. Energy and Environmental Science, 2010, 3, 1524.	15.6	149

#	Article	IF	Citations
9306	The effects of different coverage of Nitrogen adsorbed on wurtzite ZnO(0001) surface. , 2010, , .		0
9307	Electronic structure and optical properties of Co doped AlN from First-principles Study. , 2010, , .		0
9308	Phase stability and mechanical properties of tungsten borides from first principles calculations. Physical Chemistry Chemical Physics, 2010, 12, 13158.	1.3	126
9309	Topography and work function measurements of thin MgO(001) films on Ag(001) by nc-AFM and KPFM. Physical Chemistry Chemical Physics, 2010, 12, 3203.	1.3	75
9310	Bidimensional versus tridimensional oxygen vacancy diffusion in SnO2â^'x under different gas environments. Physical Chemistry Chemical Physics, 2010, 12, 2401.	1.3	29
9311	Ab Initio Simulations of Li/Pyrite-MS[sub 2] (M=Fe,â€,Ni) Battery Cells. Journal of the Electrochemical Society, 2010, 157, A630.	1.3	31
9312	Theoretical Study of H₂S Dissociation and Sulfur Oxidation on a W(111) Surface. Journal of Physical Chemistry C, 2010, 114, 19489-19495.	1.5	23
9313	Ab Initio Equation of State of the Organic Molecular Crystal: Î²-Octahydro-1,3,5,7-tetranitro-1,3,5,7-tetrazocine. Journal of Physical Chemistry A, 2010, 114, 5372-5376.	1.1	23
9314	Change of Structural Behaviors of Organo-Silane Exposed Graphene Nanoflakes. Journal of Physical Chemistry C, 2010, 114, 8161-8166.	1.5	14
9315	Selenium-Based Self-Assembled Monolayers: The Nature of Adsorbateâ^'Surface Interactions. Langmuir, 2010, 26, 173-178.	1.6	40
9316	Interaction of Chlorine and Oxygen with the Cu(100) Surface. Journal of Physical Chemistry C, 2010, 114, 19048-19054.	1.5	19
9317	Interaction of Oxidized Copper Surfaces with Alkanethiols in Organic and Aqueous Solvents. The Mechanism of Cu₂O Reduction. Journal of Physical Chemistry C, 2010, 114, 3945-3957.	1.5	27
9318	Nearly Free Electron Superatom States of Carbon and Boron Nitride Nanotubes. Nano Letters, 2010, 10, 4830-4838.	4.5	45
9319	Density Functional Study of Ethanol Decomposition on Rh(111). Journal of Physical Chemistry C, 2010, 114, 21493-21503.	1.5	66
9320	Trapping of multiple hydrogen atoms in a tungsten monovacancy from first principles. Physical Review B, 2010, 82, .	1.1	124
9321	Density functional theory study of the high- and low-temperature phases of cubic iron sulfide. Physical Review B, 2010, 82, .	1.1	13
9322	Two bonding configurations for individually adsorbed<mml:math xmlns:mml="http://www.w3.org/1998/Math/MathML" display="inline"><mml:mrow><mml:msub><mml:mtext>C</mml:mtext><mml:mrow><mml:mn>60</mml:mn></mml:mrow></mml:msu on Au(111). Physical Review B, 2010, 82, .	1.1	42
9323	Effects of substitutional impurity Au and Si atoms on antiphase boundary energies in Ti3Al: A first principles study. Philosophical Magazine, 2010, 90, 3919-3934.	0.7	3

#	Article	IF	Citations
9324	Adsorption of CO on<mml:math xmlns:mml="http://www.w3.org/1998/Math/MathML" display="inline"><mml:mrow><mml:msub><mml:mrow><mml:mtext>Ni</mml:mtext></mml:mrow><mml:mn>3</mml:mn></mml:msub> using high-resolution photoemission spectroscopy and density functional theory. Physical Review B, 2010, 81, .	1.1	1
9325	Modulating the electronic and magnetic structures of P-doped graphene by molecule doping. Journal of Physics Condensed Matter, 2010, 22, 225501.	0.7	75
9326	Theoretical study on the variation of ordering vector in<mml:math xmlns:mml="http://www.w3.org/1998/Math/MathML" display="inline"><mml:mrow><mml:mtext>Ce</mml:mtext><mml:msub><mml:mrow><mml:mrow><mml:mo>(</mml:mo><mml:mrow> Physical Review B, 2010, 82, .	1.1	2
9327	Structural transformation and vibrational properties of<mml:math xmlns:mml="http://www.w3.org/1998/Math/MathML" display="inline"><mml:mrow><mml:msub><mml:mrow><mml:mtext>BaO</mml:mtext></mml:mrow><mml:mn>2</mml:mn></mml: high pressures. Physical Review B, 2010, 82, .	1.1	18
9328	Self-consistent embedding quantum mechanics/molecular mechanics method with applications to metals. Physical Review B, 2010, 82, .	1.1	15
9329	Density-wave instability in<mml:math xmlns:mml="http://www.w3.org/1998/Math/MathML" display="inline"><mml:mrow><mml:mi>Î±</mml:mi><mml:mtext>â^'</mml:mtext><mml:msub><mml:mrow><mml:mrow><mml:mo>(Physical Review B, 2010, 82, .	1.1	24
9330	Static equation of state of bcc iron. Physical Review B, 2010, 82, .	1.1	35
9331	Quantum oscillations in adsorption energetics of atomic oxygen on Pb(111) ultrathin films: A density-functional theory study. Journal of Chemical Physics, 2010, 132, 024703.	1.2	7
9332	Characterization of thin silicon overlayers on rutile<mml:math xmlns:mml="http://www.w3.org/1998/Math/MathML" display="inline"><mml:mrow><mml:msub><mml:mrow><mml:mtext>TiO</mml:mtext></mml:mrow><mml:mn>2</mml:mn></mml:msu Physical Review B, 2010, 82, .	1.1	22
9333	Binding sites and diffusion barriers of a Ga adatom on the<mml:math xmlns:mml="http://www.w3.org/1998/Math/MathML" display="inline"><mml:mrow><mml:mtext>GaAs</mml:mtext><mml:mrow><mml:mo>(</mml:mo><mml:mrow><mml:mn>001</mml:mn></mml: from first-principles computations. Physical Review B, 2010, 82, .	1.1	25
9334	Diffusion of oxygen vacancies on a strained rutile<mml:math xmlns:mml="http://www.w3.org/1998/Math/MathML" display="inline"><mml:mrow><mml:msub><mml:mrow><mml:mtext>TiO</mml:mtext></mml:mrow><mml:mn>2</mml:mn></mml:msu Physical Review B, 2010, 82, .	1.1	27
9335	Electronic structure ofLaNiO3â^'xthin films studied by x-ray photoelectron spectroscopy and density functional theory. Physical Review B, 2010, 82, .	1.1	16
9336	Synthesis and thermoelectric properties of RuO2 nanorods. Journal of Applied Physics, 2010, 108, 013707.	1.1	26
9337	Structural, electrical, and vibrational properties of Ti-H and Ni-H complexes in Si. Physical Review B, 2010, 82, .	1.1	24
9338	First-principles study of electronic and vibrational properties of<mml:math xmlns:mml="http://www.w3.org/1998/Math/MathML" display="inline"><mml:mrow><mml:msub><mml:mrow><mml:mtext>BaHfN</mml:mtext></mml:mrow><mml:mn>2</mml:mn></mml: Physical Review B, 2010, 82, .	1.1	26
9339	Spin-orbit effects in structural and electronic properties for the solid state of the group-14 elements from carbon to superheavy element 114. Physical Review B, 2010, 82, .	1.1	61
9340	First-principles calculation of the structure and dielectric properties ofBi2Ti2O7. Physical Review B, 2010, 82, .	1.1	18
9341	Absence of rippling in graphene under biaxial tensile strain. Physical Review B, 2010, 82, .	1.1	35

#	Article	IF	Citations
9342	Mechanochemistry in Cu nanowires: N and<mml:math xmlns:mml="http://www.w3.org/1998/Math/MathML" display="inline"><mml:mrow><mml:msub><mml:mtext>N</mml:mtext><mml:mn>2</mml:mn></mml:msub></mml:mrow></mml:math the atomic chain formation. Physical Review B, 2010, 82, .	1.1	10
9343	First-principles study of charge-density waves on Cu surfaces covered by In, Pb, and Bi atoms: Analysis of electronic structure and surface phonons. Physical Review B, 2010, 82, .	1.1	1
9344	Interaction of<mml:math xmlns:mml="http://www.w3.org/1998/Math/MathML" display="inline"><mml:mrow><mml:msub><mml:mtext>O</mml:mtext><mml:mn>2</mml:mn></mml:msub></mml:mrow></mml:math xmlns:mml="http://www.w3.org/1998/Math/MathML" display="inline"><mml:mrow><mml:msub><mml:mtext>H</mml:mtext><mml:mn>2</mml:mn></mml:msub><mml:mtext>O</mml:mte xmlns:mml="http://www.w3.org/1998/Math/MathML" display="inline"><mml:mrow><mml:msub><mml:mtext>N</mml:mtext><mml:mn>2</mml:m. Physical Revi	1.1	24
9345	Density functional study ofPbTiO3nanocapacitors with Pt and Au electrodes. Physical Review B, 2010, 82, .	1.1	31
9346	Liquid-state properties from first-principles density functional theory calculations: Static properties. Physical Review B, 2010, 82, .	1.1	16
9347	Phase diagram up to 105 GPa and mechanical strength of<mml:math xmlns:mml="http://www.w3.org/1998/Math/MathML" display="inline"><mml:mrow><mml:msub><mml:mrow><mml:mtext>HfO</mml:mtext></mml:mrow><mml:mn>2</mml:mn></mml:msub></mml:mrow></mml:math Elastic and structural instability of cubic<mml:math xmlns:mml="http://www.w3.org/1998/Math/MathML" display="inline"><mml:mrow><mml:msub><mml:mrow><mml:mtext>Sn</mml:mtext></mml:mrow><mml:mn>3</mml:mn></mml:msub></mml:mrow></mml:math xmlns:mml="http://www.w3.org/1998/Math/MathML" display="inline"><mml:mrow><mml:msub><mml:mtext>C</mml:mtext><mml:mn>3</mml:mn></mml:msub><mml:msub><mml:mtext> Physical Review B, 2010, 82, .	1.1	55
9348		1.1	26
9349	Theory of interface scattering of phonons in superlattices. Physical Review B, 2010, 82, .	1.1	31
9350	Effects of composition, temperature, and magnetism on phonons in bcc Fe-V alloys. Physical Review B, 2010, 82, .	1.1	19
9351	Gas adsorption and high-emission current induced degradation of field emission characteristics in solution-processed ZnO nanoneedles. Journal of Applied Physics, 2010, 108, 124318.	1.1	9
9352	Morphology and strain of self-assembled semipolar GaN quantum dots in (112Â¯2) AlN. Journal of Applied Physics, 2010, 108, .	1.1	20
9353	Shape memory effects and pseudoelasticity in bcc metallic nanowires. Journal of Applied Physics, 2010, 108, .	1.1	45
9354	The first-order structural phase transition of YSb. Canadian Journal of Physics, 2010, 88, 591-596.	0.4	1
9355	Electronic structures and ferroelectric instabilities of cubic AV O₃(A = Sr, Ba, and Pb) perovskites by first-principles calculations. Journal of Physics Condensed Matter, 2010, 22, 125501.	0.7	14
9356	Segregation of Pt₂₈Rh₂₇bimetallic nanoparticles: a first-principles study. Journal of Physics Condensed Matter, 2010, 22, 245401.	0.7	21
9357	Magnetic effects of defect pair formation in ZnO. Journal of Physics Condensed Matter, 2010, 22, 436002.	0.7	52
9358	A first-principles study of H2O adsorption and dissociation on the SrTiO3(100) surface. Molecular Simulation, 2010, 36, 604-617.	0.9	21
9359	The crucial role of chemistry on mobile properties of dislocation. Philosophical Magazine, 2010, 90, 3757-3765.	0.7	0

#	Article	IF	Citations
9360	Investigation of structure and hydrogen bonding of superhydrous phase B (HT) under pressure using first-principles density functional calculations. High Pressure Research, 2010, 30, 198-206.	0.4	12
9361	Study the dielectric and optic properties of Ti<inf>2</inf>XC (X=In, Sn, Al, Cd and Pb) by density function theory. , 2010, , .		0
9362	Bridging quantum chemistry and solid-state physics. Molecular Physics, 2010, 108, 3113-3124.	0.8	6
9363	Persistence of magic cluster stability in ultra-thin semiconductor nanorods. Nanoscale, 2010, 2, 72-77.	2.8	23
9364	Solvation of carbon nanotubes by aniline calculated with density functional tight binding. Physical Chemistry Chemical Physics, 2010, 12, 9893.	1.3	10
9365	First principles study of doped carbon supports for enhanced platinum catalysts. Physical Chemistry Chemical Physics, 2010, 12, 9461.	1.3	110
9366	Probing the influence of electronic effects of organic additives on the morphology of sodium chloride crystals: a combined experimental and computational study. CrystEngComm, 2010, 12, 4168.	1.3	1
9367	51V NMR parameters of VOCl₃: static and dynamic density functional study from the gas phase to the bulk. Physical Chemistry Chemical Physics, 2011, 13, 619-627.	1.3	19
9368	Origin of improved visible photocatalytic activity of nitrogen/hydrogen codoped cubic In₂O₃: first-principles calculations. Physical Chemistry Chemical Physics, 2011, 13, 1379-1385.	1.3	23
9369	Ferroelectric phase transition in LiNbO<inf>3</inf>: Insights from molecular dynamics. , 2011, , .		0
9370	Confinement effects for ionic carriers in SrTiO₃ultrathin films: first-principles calculations of oxygen vacancies. Physical Chemistry Chemical Physics, 2011, 13, 923-926.	1.3	17
9371	First-principles study of the excited-state properties of coumarin-derived dyes in dye-sensitized solar cells. Journal of Materials Chemistry, 2011, 21, 11101.	6.7	53
9372	H atom adsorption and diffusion on Si(110)-(1Ã—1) and (2Ã—1) surfaces. Physical Chemistry Chemical Physics, 2011, 13, 11367.	1.3	8
9373	Alanine at 13.6 GPa and its pressure-induced amorphisation at 15 GPa. CrystEngComm, 2011, 13, 5841.	1.3	48
9374	Band gap engineering of double-cation-impurity-doped anatase-titania for visible-light photocatalysts: a hybrid density functional theory approach. Physical Chemistry Chemical Physics, 2011, 13, 13698.	1.3	39
9375	High temperature Raman spectroscopic study of the micro-structure of a caesium triborate crystal and its liquid. CrystEngComm, 2011, 13, 3030.	1.3	13
9376	Nitrogen/gold codoping of the TiO2(101) anatase surface. A theoretical study based on DFT calculations. Physical Chemistry Chemical Physics, 2011, 13, 11340.	1.3	38
9377	CdS:Co diluted magnetic semiconductor nanocrystals: synthesis and ferromagnetism study. CrystEngComm, 2011, 13, 5646.	1.3	40

#	Article	IF	Citations
9378	Silica hollow nanospheres as new nanoscaffold materials to enhance hydrogen releasing from ammonia borane. Physical Chemistry Chemical Physics, 2011, 13, 18592.	1.3	37
9379	Properties of self-assembled Bi nanolines on InAs(100) studied by core-level and valence-band photoemission, and first-principles calculations. Physical Review B, 2011, 83, .	1.1	9
9380	Ab initiocalculation of the elastic properties and the lattice dynamics of the AlAsxSb1â^'xalloy under pressure. High Pressure Research, 2011, 31, 310-324.	0.4	5
9381	Raman evidence for the superconducting gap and spinâ€“phonon coupling in the superconductor Ca(Fe_{0.95}Co_{0.05})₂As₂. Journal of Physics Condensed Matter, 2011, 23, 255403.	0.7	9
9382	Molecular-Scale Structure of a Nitrobenzene Monolayer on Si(001). Journal of Physical Chemistry C, 2011, 115, 3011-3017.	1.5	6
9383	Role of Long-Range Intermolecular Forces in the Formation of Inorganic Nanoparticle Clusters. Journal of Physical Chemistry A, 2011, 115, 12933-12940.	1.1	20
9384	Surface Structure and Environment-Dependent Hydroxylation of the Nonpolar Hematite (100) from Density Functional Theory Modeling. Journal of Physical Chemistry C, 2011, 115, 23023-23029.	1.5	21
9385	Mechanisms of Ion-Beam Modification of Terthiophene Oligomers from Atomistic Simulations. Journal of Physical Chemistry C, 2011, 115, 23936-23945.	1.5	6
9386	First principles study on electronic structure and optical properties of pure and Au or Ag doped zinc blende ZnS. , 2011, , .		0
9387	Perpendicular growth of carbon chains on graphene from first-principles. Physical Review B, 2011, 83, .	1.1	44
9388	Intrinsic defects and dopants in LiNH2: a first-principles study. Physical Chemistry Chemical Physics, 2011, 13, 6043.	1.3	15
9389	Altering the spin state of transition metal centers in metalâ€“organic frameworks by molecular hydrogen adsorption: a first-principles study. Physical Chemistry Chemical Physics, 2011, 13, 5042.	1.3	10
9390	Thermodynamic and kinetic properties of hydrogen defect pairs in SrTiO3 from density functional theory. Physical Chemistry Chemical Physics, 2011, 13, 15256.	1.3	18
9391	Physical Properties of Thalliumâ€“Tellurium Based Thermoelectric Compounds Using First-Principles Simulations. Journal of Physical Chemistry A, 2011, 115, 8761-8766.	1.1	25
9392	Interplay between structure, stoichiometry and properties of technetium nitrides. Dalton Transactions, 2011, 40, 6738.	1.6	20
9393	Tunable electrical and magnetic properties of half-metallic ZnxFe3â^'xO4 from first principles. Physical Chemistry Chemical Physics, 2011, 13, 21243.	1.3	21
9394	Interlayer interaction and relative vibrations of bilayer graphene. Physical Chemistry Chemical Physics, 2011, 13, 5687.	1.3	149
9395	Role of Disorder and Anharmonicity in the Thermal Conductivity of Silicon-Germanium Alloys: A First-Principles Study. Physical Review Letters, 2011, 106, 045901.	2.9	404

#	Article	IF	Citations
9396	Interface-Dependent Spin-Reorientation Energy Barrier in Fe/MgO(001) Thin Film. IEEE Electron Device Letters, 2011, 32, 1287-1289.	2.2	8
9397	95Mo nuclear magnetic resonance parameters of molybdenum hexacarbonyl from density functional theory: appraisal of computational and geometrical parameters. Physical Chemistry Chemical Physics, 2011, 13, 19471.	1.3	12
9398	The role of long-lived oxygen precursors on AuM alloys (M = Ni, Pd, Pt) in CO oxidation. Physical Chemistry Chemical Physics, 2011, 13, 5790.	1.3	23
9399	Theoretical studies on the structural, electronic, and optical properties of Ag ₂ HgSnSe ₄. Chinese Physics B, 2011, 20, 126102.	0.7	2
9400	Trends in water monomer adsorption and dissociation on flat insulating surfaces. Physical Chemistry Chemical Physics, 2011, 13, 12447.	1.3	40
9401	Electronic structure of pyridine-based SAMs on flat Au(111) surfaces: extended charge rearrangements and Fermi level pinning. Physical Chemistry Chemical Physics, 2011, 13, 9747.	1.3	26
9402	One-pot synthesis of BiSbO4 nanophotocatalyst with enhanced visible-light performance. CrystEngComm, 2011, 13, 3920.	1.3	20
9403	Effect of transition metal (M = Co, Ni, Cu) substitution on electronic structure and vacancy formation of Li₃N. Journal of Materials Chemistry, 2011, 21, 165-170.	6.7	11
9404	Charge, orbital and spin ordering in multiferroic BiMn2O5: density functional theory calculations. Physical Chemistry Chemical Physics, 2011, 13, 9418.	1.3	12
9405	The mechanism of the water-gas shift reaction on Cu/TiO2(110) elucidated from application of density-functional theory. Physical Chemistry Chemical Physics, 2011, 13, 20393.	1.3	20
9406	The role of hydrogen bonding in waterâ€“metal interactions. Physical Chemistry Chemical Physics, 2011, 13, 3375-3384.	1.3	36
9407	Dynamics of scattering and dissociative adsorption on a surface alloy: H2/W(100)-c(2 Ã— 2)Cu. Physical Chemistry Chemical Physics, 2011, 13, 4614.	1.3	7
9408	A new photocatalyst: Bi2TiO4F2 nanoflakes synthesized by a hydrothermal method. Dalton Transactions, 2011, 40, 12670.	1.6	25
9409	Towards the computational modelling of polyoxoanions on metal surfaces: IR spectrum characterisation of [SiW12O40]4â^' on Ag(111). Physical Chemistry Chemical Physics, 2011, 13, 15143.	1.3	21
9410	Effective increasing of optical absorption and energy conversion efficiency of anatase TiO2 nanocrystals by hydrogenation. Physical Chemistry Chemical Physics, 2011, 13, 18063.	1.3	92
9411	Structural, electronic, elastic and thermodynamical properties of Ba_xSr_{1â^'x}LiH₃. Physica Scripta, 2011, 84, 065705.	1.2	5
9412	Theoretical Investigation of the Adsorption of Nh₃ on B-Doped Graphene. Key Engineering Materials, 0, 474-476, 720-724.	0.4	0
9413	Charge transition levels of boron and silicon impurities in GaAs. , 2011, , .		0

#	Article	IF	Citations
9414	Alkali Metal and Alkaline Earth Encapsulated Silicene-Like Nanotubes. Advanced Materials Research, 2011, 320, 410-414.	0.3	3
9415	Design of ferromagnetism in Cu-doped ZnO nanowires: First-principles prediction. Europhysics Letters, 2011, 95, 47011.	0.7	17
9416	LCAO Calculations of (001) Surface Oxygen Vacancy Structure in Y-Doped BaZrO3. Integrated Ferroelectrics, 2011, 123, 1-9.	0.3	4
9417	First-principles study of the interplay between grain boundaries and domain walls in ferroelectric PbTiO<mml:math xmlns:mml="http://www.w3.org/1998/Math/MathML" display="inline"><mml:mrow><mml:msub><mml:mrow /><mml:mrow><mml:mn>3</mml:mn></mml:mrow></mml:msub></mml:mrow></mml:math>. Physical <mml:math xmlns:mml="http://www.w3.org/1998/Math/MathML"	1.1	30
9418	display="inline"><mml:mi>c</mml:mi><mml:mo stretchy="false">(</mml:mo><mml:mn>2</mml:mn><mml:mo>Ã—</mml:mo><mml:mn>2</mml:mn><mml:mo) TjETQq0 0 0 rgBT /Ov	1.1	65
9419	Intrinsic stoichiometry and oxygen-induced <mml:math xmlns:mml="http://www.w3.org/1998/Math/MathML" display="inline"><mml:mi>p</mml:mi></mml:math>-type conductivity of pyrite FeS<mml:math xmlns:mml="http://www.w3.org/1998/Math/MathML" display="inline"><mml:msub><mml:mrow /><mml:mrow><mml:mn>2</mml:mn></mml:mrow></mml:msub></mml:math>. Physical Review B, 2011, 84, .	1.1	65
9420	Energetic effects of dopants on the eutectoid decomposition of Nbâ€“Siin situcomposites. Philosophical Magazine Letters, 2011, 91, 640-647.	0.5	5
9421	Study on the electronic structure and the optical performance of YB6 by the first-principles calculations. AIP Advances, 2011, 1, .	0.6	12
9422	DFT study on the clamped linear electro-optic effect in KH<inf>2</inf>PO<inf>4</inf>. , 2011, , .		0
9423	First principles study of the electric field effect on magnetization and magnetic anisotropy of FeCo/MgO(001) thin film. Applied Physics Letters, 2011, 99, .	1.5	57
9424	Diffusion of tin in germanium: A GGA+U approach. Applied Physics Letters, 2011, 99, .	1.5	28
9425	The effect of electronegative difference on the electronic structure and visible light photocatalytic activity of N-doped anatase TiO2 by first-principles calculations. Applied Physics Letters, 2011, 98, 162107.	1.5	34
9426	Pseudo-Potential Calculations of Structural, Elastic and Thermal Properties of Si₃N₄. Advanced Materials Research, 2011, 217-218, 1619-1624.	0.3	0
9427	First-Principles Study on Ga-N Co-Doped P-Type ZnO. Advanced Materials Research, 2011, 299-300, 498-502.	0.3	1
9428	First-principles study of structural and elastic properties of CrO2at high pressure. High Pressure Research, 2011, 31, 454-461.	0.4	4
9429	Promotion of water-mediated carbon removal by nanostructured barium oxide/nickel interfaces in solid oxide fuel cells. Nature Communications, 2011, 2, 357.	5.8	280
9430	Hyperfine interactions in silicon quantum dots. Physical Review B, 2011, 83, .	1.1	87
9431	Ab Initio Study on the Size and Chirality Effects on the Encapsulation of Tetrafluorotetracyano-p-quinodimethane inside Carbon Nanotubes. Journal of Physical Chemistry C, 2011, 115, 5280-5285.	1.5	4

#	Article	IF	Citations
9432	First-Principles Study of Isomorphic (â€˜Dual-Defectâ€™) Substitution in Kaolinite. Clays and Clay Minerals, 2011, 59, 501-506.	0.6	11
9433	Formation, Morphology, and Effect of Complex Defects in Boron Nitride Nanotubes: An ab initio Calculation. Journal of Physical Chemistry C, 2011, 115, 12782-12788.	1.5	7
9434	Role of Backbone Charge Rearrangement in the Bond-Dipole and Work Function of Molecular Monolayers. Journal of Physical Chemistry C, 2011, 115, 24888-24892.	1.5	31
9435	Metastable De-excitation Spectroscopy and Density Functional Theory Study of the Selective Oxidation of Crotyl Alcohol over Pd(111). Journal of Physical Chemistry C, 2011, 115, 25290-25297.	1.5	11
9436	Valence force field-based Monte Carlo bond-rotation method for the determination of sp2-bonded carbon structures. Journal of Applied Physics, 2011, 110, .	1.1	11
9437	On the Mechanism of Silicon Activation by Halogen Atoms. Langmuir, 2011, 27, 2613-2624.	1.6	12
9438	Large-Scale Patterning of Zwitterionic Molecules on a Si(111)-7â€‰Ã—â€‰7 Surface. ACS Nano, 2011, 5, 424-428.	8.3	12
9439	Photochemical Properties, Composition, and Structure in Molecular Beam Epitaxy Grown Fe â€œDopedâ€• and (Fe,N) Codoped Rutile TiO₂(110). Journal of Physical Chemistry C, 2011, 115, 15416-15424.	1.5	28
9440	Confinement-Induced Polymerization of Ethylene. Journal of Physical Chemistry C, 2011, 115, 2134-2139.	1.5	8
9441	Periodic DFT and HR-STEM Studies of Surface Structure and Morphology of Cobalt Spinel Nanocrystals. Retrieving 3D Shapes from 2D Images. Journal of Physical Chemistry C, 2011, 115, 6423-6432.	1.5	70
9442	Structural, Elastic Constant, and Vibrational Properties of Wurtzite Gallium Nitride: A First-Principles Approach. Journal of Physical Chemistry A, 2011, 115, 14502-14509.	1.1	13
9443	BH3under Pressure: Leaving the Molecular Diborane Motif. Journal of the American Chemical Society, 2011, 133, 21002-21009.	6.6	31
9444	Heterogeneous Mercury Reaction Chemistry on Activated Carbon. Journal of the Air and Waste Management Association, 2011, 61, 418-426.	0.9	80
9445	DFT Study of the Adsorption of Aspartic Acid on Pure, N-Doped, and Ca-Doped Rutile (110) Surfaces. Journal of Physical Chemistry C, 2011, 115, 18572-18581.	1.5	53
9446	Density Functional Theory Study of Cu Adhesion on Rh, Ir, Pd, Ta, Mo, Ru, Co, and Os Surfaces. Japanese Journal of Applied Physics, 2011, 50, 105701.	0.8	5
9447	Structural and thermodynamic properties of liquid Na-Li and Ca-Li alloys at high pressure. Physical Review B, 2011, 83, .	1.1	18
9448	Tunable band gap Cu2ZnSnS4xSe4(1â^'x) nanocrystals: experimental and first-principles calculations. CrystEngComm, 2011, 13, 2222.	1.3	75
9449	A First-Principles Modeling of Ni Interactions on CeO₂â^'ZrO₂Mixed Oxide Solid Solutions. Journal of Physical Chemistry C, 2011, 115, 7456-7465.	1.5	28

#	Article	IF	Citations
9450	Study of the electronic properties of Li-intercalated nitrogen doped graphite. Molecular Physics, 2011, 109, 687-694.	0.8	80
9451	Excitonic effects in the optical properties of a SiC sheet and nanotubes. Physical Review B, 2011, 84, .	1.1	136
9452	First-principles study of electronic structure and charge transport at PTCDA molecular layers on Ag(111) and Al(111) electrodes. Physical Review B, 2011, 84, .	1.1	7
9453	Antiferromagnetic superexchange via<mml:math xmlns:mml="http://www.w3.org/1998/Math/MathML" display="inline"><mml:mrow><mml:mn>3</mml:mn><mml:mi>d</mml:mi></mml:mrow></mml:math>states of titanium in EuTiO<mml:math xmlns:mml="http://www.w3.org/1998/Math/MathML" display="inline"><mml:mrow><mml:msub><mml:mrow /><mml:mrow><mml:mn>3</mml:mn></mml:mrow></mml:msub></mml:mrow></mml:math>as seen from hybrid Hartree-Fock density functional calculations. Physical Review B, 2011, 83, .	1.1	104
9454	Effect of lattice strain on hydrogen diffusion in Pd: A density functional theory study. Physical Review B, 2011, 84, .	1.1	35
9455	First-principles study of electronic and structural properties of CuO. Physical Review B, 2011, 84, .	1.1	106
9456	Novel High-Pressure Phase of RhB: First-Principles Calculations. Journal of Physical Chemistry C, 2011, 115, 19910-19915.	1.5	16
9457	Mechanical Properties and Low Elastic Anisotropy of Semiconducting Group 14 Clathrate Frameworks. Journal of Physical Chemistry C, 2011, 115, 19925-19930.	1.5	10
9458	Self-Consistent-Charge Density-Functional Tight-Binding Parameters for Cdâ€“X (X = S, Se, Te) Compounds and Their Interaction with H, O, C, and N. Journal of Chemical Theory and Computation, 2011, 7, 2262-2276.	2.3	45
9459	Nonlinear optical properties of TeO<mml:math xmlns:mml="http://www.w3.org/1998/Math/MathML" display="inline"><mml:mrow><mml:msub><mml:mrow /><mml:mrow><mml:mn>2</mml:mn></mml:mrow></mml:msub></mml:mrow></mml:math>crystalline phases from first principles. Physical Review B, 2011, 83, .	1.1	22
9460	Influence of exchange and correlation on structural and electronic properties of AlN, GaN, and InN polytypes. Physical Review B, 2011, 84, .	1.1	97
9461	Ab initiostudy of IIâ€“(VI)₂dichalcogenides. Journal of Physics Condensed Matter, 2011, 23, 405801.	0.7	13
9462	Theory of prospective perovskite ferroelectrics with double rocksalt order. Physical Review B, 2011, 83, .	1.1	22
9463	Electronic structure and transport properties of doped PbSe. Physical Review B, 2011, 84, .	1.1	53
9464	Stability of Intermediate States for Ethylene Epoxidation on Agâ€“Cu Alloy Catalyst: A First-Principles Investigation. Journal of Physical Chemistry C, 2011, 115, 10073-10079.	1.5	15
9465	Adatoms in graphene as a source of current polarization: Role of the local magnetic moment. Physical Review B, 2011, 84, .	1.1	27
9466	Ab initiostudy of<mml:math xmlns:mml="http://www.w3.org/1998/Math/MathML" display="inline"><mml:mrow><mml:mn>3</mml:mn><mml:mi>d</mml:mi></mml:mrow></mml:math>,<mml:math xmlns:mml="http://www.w3.org/1998/Math/MathML" display="inline"><mml:mrow><mml:mn>4</mml:mn><mml:mi>d</mml:mi></mml:mrow></mml:math>, and<mml:math xmlns:mml="http://www.w3.org/1998/Math/MathML" display="inline"><mml:mrow><mml:mn>5</mml:mn><mml:mi>d</mml:mi></mml:mrow></mml:math>transition	1.1	49
9467	Stability and Properties of Two-Dimensional Graphene Hydroxide. Journal of Physical Chemistry Letters, 2011, 2, 1310-1314.	2.1	14

#	Article	IF	Citations
9468	DFT Study of Interaction of Azoles with Cu(111) and Al(111) Surfaces: Role of Azole Nitrogen Atoms and Dipoleâ€“Dipole Interactions. Journal of Physical Chemistry C, 2011, 115, 24189-24197.	1.5	159
9469	Ordered phases in ruthenium binary alloys from high-throughput first-principles calculations. Physical Review B, 2011, 84, .	1.1	50
9470	Local defects enhanced dehydrogenation kinetics of the NaBH4-added Liâ€“Mgâ€“Nâ€“H system. Physical Chemistry Chemical Physics, 2011, 13, 314-321.	1.3	34
9471	Density Functional Calculations to Study the Mechanism of the Fischerâ€“Tropsch Reaction on Fe(111) and W(111) Surfaces. Journal of Physical Chemistry C, 2011, 115, 11045-11055.	1.5	36
9472	Energetics and Interactions of Mixed Halogen Adsorbates on the Si(100) Surface. Journal of Physical Chemistry C, 2011, 115, 13268-13274.	1.5	8
9473	Why Silver Nanoparticles Are Effective for Olefin/Paraffin Separations. Journal of Physical Chemistry C, 2011, 115, 1811-1818.	1.5	35
9474	First-principles simulation of cyanogen under high pressure: Formation of paracyanogen and an insulating carbon nitride solid. Physical Review B, 2011, 83, .	1.1	16
9475	High-pressure Raman spectroscopy and lattice-dynamics calculations on scintillating MgWO<mml:math xmlns:mml="http://www.w3.org/1998/Math/MathML" display="inline"><mml:mrow><mml:msub><mml:mrow /><mml:mrow><mml:mn>4</mml:mn></mml:mrow></mml:msub></mml:mrow></mml:math>: Comparison with isomorphic compounds. Physical Review B, 2011, 83, .	1.1	78
9476	Terahertz Spectroscopy and Solid-State Density Functional Theory Simulations of the Improvised Explosive Oxidizers Potassium Nitrate and Ammonium Nitrate. Journal of Physical Chemistry A, 2011, 115, 12410-12418.	1.1	26
9477	Theoretical study of structural, mechanical and spectroscopic properties of boehmite (Î³-AlOOH). Journal of Physics Condensed Matter, 2011, 23, 404201.	0.7	18
9478	Ab-initio study of Al1â€“xGaxSb compound. Zeitschrift FÃ¼r Kristallographie, 2011, 226, 83-88.	1.1	3
9479	Theoretical Fingerprints of Transition Metal L_{2,3} XANES and ELNES for Lithium Transition Metal Oxides by ab Initio Multiplet Calculations. Journal of Physical Chemistry C, 2011, 115, 11871-11879.	1.5	34
9480	Hybridization-reactivity relationship in Pb(II) adsorption on Î±-Al₂O₃-water interfaces: A DFT Study. Journal of Physical Chemistry C, 2011, 115, 4008-4021.	1.5	34
9481	CO Oxidation by Lattice Oxygen on V₂O₅ Nanotubes. Journal of Physical Chemistry C, 2011, 115, 14806-14811.	1.5	19
9482	Water Adsorption on the Reconstructed (001) Chalcopyrite Surfaces. Journal of Physical Chemistry C, 2011, 115, 10709-10717.	1.5	50
9483	Synthesis and Characterization of Crystalline Structures Based on Phenylboronate Ligands Bound to Alkaline Earth Cations. Inorganic Chemistry, 2011, 50, 7802-7810.	1.9	35
9484	Tuning Magnetism in Transition-Metal-Doped 3C Silicon Carbide Polytype. Journal of Physical Chemistry C, 2011, 115, 253-256.	1.5	28
9485	Complete Structural Characterization of Ni₃Si₂O₅(OH)₄ Nanotubes: Theoretical and Experimental Comparison. Journal of Physical Chemistry C, 2011, 115, 11442-11446.	1.5	35

#	Article	IF	Citations
9486	Are Azafullerene Encapsulated Single-Walled Carbon Nanotubes n-Type Semiconductors?. Journal of Physical Chemistry C, 2011, 115, 12760-12762.	1.5	12
9487	Sulfur-Induced Reconstruction of Ag(111) Surfaces Studied by DFT. Journal of Physical Chemistry C, 2011, 115, 9587-9592.	1.5	9
9488	Electronic Structure of the Two-Leg Spin Ladder (C5H12N)2CuBr4. Inorganic Chemistry, 2011, 50, 6399-6401.	1.9	2
9489	Density Functional Theory Study of the Adsorption and Desulfurization of Thiophene and Its Hydrogenated Derivatives on Pt(111): Implication for the Mechanism of Hydrodesulfurization over Noble Metal Catalysts. ACS Catalysis, 2011, 1, 1498-1510.	5.5	45
9490	Effects of Chlorine on Aluminum Refining: A Review and an <i>Ab Initio</i> Molecular Dynamics Study. Key Engineering Materials, 0, 467-469, 1404-1409.	0.4	1
9491	Geometric and Electronic Confinement Effects on Catalysis. Journal of Physical Chemistry C, 2011, 115, 21324-21333.	1.5	42
9492	Origin of the Strain Energy Minimum in Imogolite Nanotubes. Journal of Physical Chemistry C, 2011, 115, 5226-5231.	1.5	30
9493	Impurity Concentration Dependence of Optical Absorption for Phosphorus-Doped Anatase TiO₂. Journal of Physical Chemistry C, 2011, 115, 8184-8188.	1.5	56
9494	Role of an Aluminum Atom on Graphene for Hydrogen Adsorption. Journal of the Physical Society of Japan, 2011, 80, 074705.	0.7	24
9495	Rhodium dihydride (RhH₂) with high volumetric hydrogen density. Proceedings of the National Academy of Sciences of the United States of America, 2011, 108, 18618-18621.	3.3	78
9496	Electronic structure of cation-codoped TiO2 for visible-light photocatalyst applications from hybrid density functional theory calculations. Applied Physics Letters, 2011, 98, 142103.	1.5	38
9497	Effective Reversible Potential, Energy Loss, and Overpotential on Platinum Fuel Cell Cathodes. Journal of Physical Chemistry C, 2011, 115, 4076-4088.	1.5	60
9498	Electric Polarization Field of Phonon Modes Induced by Pressure and Maximally-Localized Wannier Functions in Beryllium Chalcogenides: Theoretical Study. Journal of Physical Chemistry C, 2011, 115, 12604-12610.	1.5	12
9499	Ab Initio Calculations of Structural Evolution and Conductance of Benzene-1,4-dithiol on Gold Leads. ACS Nano, 2011, 5, 795-804.	7.3	89
9500	Noncovalent Interactions between Modified Cytosine and Guanine DNA Base Pair Mimics Investigated by Terahertz Spectroscopy and Solid-State Density Functional Theory. Journal of Physical Chemistry A, 2011, 115, 14391-14396.	1.1	23
9501	Mechanistic Switch between Oxidative (Andrussow) and Nonoxidative (Degussa) Formation of HCN on Pt(111) by Density Functional Theory. Journal of Physical Chemistry C, 2011, 115, 5667-5674.	1.5	24
9502	Fe, Mn, and Cr doped BiCoO₃for magnetoelectric application: a first-principles study. Journal of Physics Condensed Matter, 2011, 23, 326005.	0.7	12
9503	Vacancy and Oxygen Substitution for Nitrogen-Induced Structural Stability of Ta₂N₃. Journal of Physical Chemistry C, 2011, 115, 3129-3135.	1.5	12

#	Article	IF	Citations
9504	Low Frequency Vibrational Modes of Room Temperature Ionic Liquids. Journal of Physical Chemistry B, 2011, 115, 1874-1880.	1.2	44
9505	Gold Cluster Diffusion Kinetics on Stoichiometric and Reduced Surfaces of Rutile TiO₂(110). Journal of Physical Chemistry C, 2011, 115, 11611-11617.	1.5	17
9506	Structures of the Ordered Water Monolayer on MgO(001). Journal of Physical Chemistry C, 2011, 115, 6764-6774.	1.5	88
9507	Structural Stability of Boron Clusters with Octahedral and Tetrahedral Symmetries. Journal of Physical Chemistry A, 2011, 115, 8204-8207.	1.1	30
9508	Electronic Structure and Optical Properties of Ca(NH₂BH₃)₂ Studied from GW Calculations. Journal of Physical Chemistry C, 2011, 115, 18795-18801.	1.5	13
9509	Computational Studies of Experimentally Observed Structures of Sulfur on Metal Surfaces. Journal of Physical Chemistry C, 2011, 115, 17077-17091.	1.5	24
9510	An equilibrium ab initio atomistic thermodynamics study of chlorine adsorption on the Cu(001) surface. Physical Chemistry Chemical Physics, 2011, 13, 10306.	1.3	25
9511	Structural and Vibrational Properties of Arsenic Sulfides: Alacranite (As8S9). Journal of Physical Chemistry A, 2011, 115, 4558-4562.	1.1	15
9512	A Comparative First-Principles Study of the Structure, Energetics, and Properties of Liâ€“M (M = Si, Ge,) Tj ETQq0 0 0 rgBT /Overlock 10	1.5	125
9513	Double-Hole-Mediated Coupling of Dopants and Its Impact on Band Gap Engineering in<mml:math xmlns:mml="http://www.w3.org/1998/Math/MathML" display="inline"><mml:msub><mml:mi>TiO</mml:mi><mml:mn>2</mml:mn></mml:msub></mml:math>. Physical Review Letters, 2011, 106, 066801.	2.9	134
9514	Mechanistic Studies of Waterâ€“Gas-Shift Reaction on Transition Metals. Journal of Physical Chemistry C, 2011, 115, 18582-18588.	1.5	125
9515	Vibrational Origin of the Thermal Stability in the High-Performance Piezoelectric Material GaAsO4. Journal of the American Chemical Society, 2011, 133, 8048-8056.	6.6	16
9516	The photonic Wannier function approach to photonic crystal simulations: status and perspectives. Journal of Modern Optics, 2011, 58, 365-383.	0.6	18
9517	Experimental and theoretical studies of ammonia decomposition activity on Fe-Pt, Co-Pt, and Cu-Pt bimetallic surfaces. Journal of Chemical Physics, 2011, 134, 184701.	1.2	34
9518	Edge dislocation core structures in FCC metals determined fromab initiocalculations combined with the improved Peierlsâ€“Nabarro equation. Physica Scripta, 2011, 83, 045604.	1.2	23
9519	Density Functional Theory Study of Arsenic and Selenium Adsorption on the CaO (001) Surface. Energy & Fuels, 2011, 25, 2932-2938.	2.5	31
9520	Crystal Chemistry and Electronic Structure of the Photovoltaic Buffer Layer, (In1-xAlx)2S3. Chemistry of Materials, 2011, 23, 5168-5176.	3.2	15
9521	Adsorption and Reaction of Furfural and Furfuryl Alcohol on Pd(111): Unique Reaction Pathways for Multifunctional Reagents. ACS Catalysis, 2011, 1, 1272-1283.	5.5	145

#	Article	IF	Citations
9522	Enhanced visible-light photocatalytic activity of anatase TiO2 through N and S codoping. Applied Physics Letters, 2011, 98, .	1.5	57
9523	Structural Stability of AB_y Phases in the (La,Mg)â€“Ni System Obtained by Density Functional Theory Calculations. Journal of Physical Chemistry C, 2011, 115, 25470-25478.	1.5	75
9524	Dissociation of O2 Molecules on Strained Pb(111) Surfaces. Journal of Physical Chemistry C, 2011, 115, 17378-17383.	1.5	2
9525	Transfer doping of a metallic carbon nanotube and graphene on metal surfaces. Physical Review B, 2011, 83, .	1.1	17
9526	Healing of a Vacancy Defect in a Single-Walled Carbon Nanotube by Carbon Monoxide Disproportionation. Journal of Physical Chemistry C, 2011, 115, 4649-4655.	1.5	26
9527	Self-consistent meta-generalized gradient approximation within the projector-augmented-wave method. Physical Review B, 2011, 84, .	1.1	180
9528	Electronic Structure and Bonding of an Ionic Molecular Adsorbate: c-C5H5 on Cu{111}. Journal of Physical Chemistry C, 2011, 115, 16134-16141.	1.5	9
9529	Role of Geometric Relaxation in Oxygen Binding to Metal Nanoparticles. Journal of Physical Chemistry Letters, 2011, 2, 1237-1240.	2.1	21
9530	Boron Environments in B-Doped and (B, N)-Codoped TiO₂ Photocatalysts: A Combined Solid-State NMR and Theoretical Calculation Study. Journal of Physical Chemistry C, 2011, 115, 2709-2719.	1.5	164
9531	Alkanethiol Adsorption on Platinum: Chain Length Effects on the Quality of Self-Assembled Monolayers. Journal of Physical Chemistry C, 2011, 115, 17788-17798.	1.5	34
9532	Dissociative Chemisorption of Hydrazine on an Fe{211} Surface. Journal of Physical Chemistry C, 2011, 115, 17812-17828.	1.5	30
9533	First-Principles Calculations on the LiMSO4F/MSO4F (M = Fe, Co, and Ni) Systems. Journal of Physical Chemistry C, 2011, 115, 7032-7037.	1.5	32
9534	Origin of the High Activity of the Ceria-Supported Copper Catalyst for H₂O Dissociation. Journal of Physical Chemistry C, 2011, 115, 6730-6740.	1.5	52
9535	Application of London-Type Dispersion Corrections in Solid-State Density Functional Theory for Predicting the Temperature-Dependence of Crystal Structures and Terahertz Spectra. Crystal Growth and Design, 2011, 11, 2006-2010.	1.4	19
9536	First-principles study of magnetic properties in Mo-doped graphene. Journal of Physics Condensed Matter, 2011, 23, 346001.	0.7	28
9537	High Thermal Conductivity in Short-Period Superlattices. Nano Letters, 2011, 11, 5135-5141.	4.5	81
9538	Surfactant effect of sulfuric acid on the exfoliation of bilayer graphene. Physical Review B, 2011, 84, .	1.1	15
9539	Structure and Properties of Liâ^'Si Alloys: A First-Principles Study. Journal of Physical Chemistry C, 2011, 115, 2514-2521.	1.5	187

#	Article	IF	Citations
9540	Relative Stabilities of Low Index and Stepped CeO₂ Surfaces from Hybrid and GGA + U Implementations of Density Functional Theory. Journal of Physical Chemistry C, 2011, 115, 3716-3721.	1.5	58
9541	Si₂H₆ Dissociative Chemisorption and Dissociation on Si(100)-(2Ã—1) and Ge(100)-(2Ã—1). Journal of Physical Chemistry C, 2011, 115, 24534-24548.	1.5	9
9542	Reactivity of Câ€“C Scission on Ni-Based Core/Shell Bimetallic Surfaces Investigated with Quantum-Chemical Calculations. Journal of Physical Chemistry C, 2011, 115, 19231-19238.	1.5	2
9543	VOPO4Â·H2O: A Stacking Faults Structure Studied by X-ray Powder Diffraction and DFT-D Calculations. Inorganic Chemistry, 2011, 50, 4378-4383.	1.9	12
9544	Complete Titanium Substitution by Boron in a Tetragonal Prism: Exploring the Complex Boride Series Ti_{3â^’x}Ru_{5â^’y}Ir_yB_{2+x} (0 â‰¤ Tj ET Q q 0 0 0 rgBT /Overlo	1.9	28
9545	Weak d0 magnetism in C and N doped ZnO. Journal of Applied Physics, 2011, 110, 123917.	1.1	24
9546	Halogen-Induced Reconstruction of the c-BN(100) Surface. Journal of Physical Chemistry C, 2011, 115, 22910-22916.	1.5	4
9547	sâ€“d Electronic Interaction Induced H₂ Dissociation on the Î³-U(100) Surface and Influences of Niobium Doping. Journal of Physical Chemistry C, 2011, 115, 23381-23386.	1.5	15
9548	Methane Dissociation on High and Low Indices Rh Surfaces. Journal of Physical Chemistry C, 2011, 115, 13027-13034.	1.5	35
9549	Heat-to-Connect: Surface Commensurability Directs Organometallic One-Dimensional Self-Assembly. ACS Nano, 2011, 5, 9093-9103.	7.3	64
9550	Au/TiO₂(110) Interfacial Reconstruction Stability from ab Initio. Journal of Physical Chemistry C, 2011, 115, 17799-17805.	1.5	16
9551	The Influence of Antisite Defects on the Half-Metallic Properties in Disordered LaSrVMoO₆. Journal of Physical Chemistry C, 2011, 115, 13907-13910.	1.5	3
9552	Rh-Decorated Cu Alloy Catalyst for Improved C₂Oxygenate Formation from Syngas. Journal of Physical Chemistry C, 2011, 115, 18247-18256.	1.5	62
9553	Physisorption Structure of Water on the GaN Polar Surface: Force Field Development and Molecular Dynamics Simulations. Journal of Physical Chemistry C, 2011, 115, 11684-11693.	1.5	13
9554	Reactivity of Transition Metals (Pd, Pt, Cu, Ag, Au) toward Molecular Hydrogen Dissociation: Extended Surfaces versus Particles Supported on TiC(001) or Small Is Not Always Better and Large Is Not Always Bad. Journal of Physical Chemistry C, 2011, 115, 11666-11672.	1.5	82
9555	Interaction of CO with Oxygen Adatoms on TiO₂(110). Journal of Physical Chemistry C, 2011, 115, 4163-4167.	1.5	22
9556	A Finite Cluster Approach to an Extended Transition Metal Oxide: A Wave Function Based Study. Journal of Physical Chemistry C, 2011, 115, 17540-17557.	1.5	11
9557	Pathways of Methanol Steam Reforming on PdZn and Comparison with Cu. Journal of Physical Chemistry C, 2011, 115, 20583-20589.	1.5	60

#	Article	IF	Citations
9558	First Principles Calculations of Oxygen Vacancy Formation and Migration in Ba_{1â^'x}Sr_xCo_{1â^'y}Fe_yO_{3â^'Î´}Perovskites. Journal of the Electrochemical Society, 2011, 159, B219-B226.	1.3	84
9559	Structural, electronic, and magnetic properties of C-doped GaN nanoribbon. Journal of Applied Physics, 2011, 109, .	1.1	13
9560	First-Principles Calculations of SrZrO3 (001) Surfaces. Integrated Ferroelectrics, 2011, 123, 26-31.	0.3	4
9561	Origin of the Enhanced Visible Photocatalytic Activity in (N, C)-Codoped ZnS Studied from Density Functional Theory. Journal of Physical Chemistry C, 2011, 115, 2218-2227.	1.5	31
9562	Unexpected Magnetism in Alkaline Earth Monosilicides. Journal of Physical Chemistry C, 2011, 115, 1090-1095.	1.5	18
9563	K₃B₆O₁₀Cl: A New Structure Analogous to Perovskite with a Large Second Harmonic Generation Response and Deep UV Absorption Edge. Journal of the American Chemical Society, 2011, 133, 7786-7790.	6.6	617
9564	Thermodynamic Stability of Buta-1,3-diene and But-1-ene on Pd(111) and (100) Surfaces under H₂ Pressure: A DFT Study. Journal of Physical Chemistry C, 2011, 115, 12135-12149.	1.5	40
9565	Structure Determination and Compositional Modification of Body-Centered Tetragonal PX-Phase Lead Titanate. Chemistry of Materials, 2011, 23, 2529-2535.	3.2	18
9566	First-Principle Electronic, Elastic, and Optical Study of Cubic Gallium Nitride. Journal of Physical Chemistry A, 2011, 115, 6622-6628.	1.1	15
9567	Chlorination of the Cu(110) Surface and Copper Nanoparticles: A Density Functional Theory Study. Journal of Physical Chemistry C, 2011, 115, 13412-13419.	1.5	25
9568	Structure phase transition and elastic properties of hafnium: First-principles study. Philosophical Magazine Letters, 2011, 91, 61-69.	0.5	20
9569	Theoretical Study of the Interaction of CO on TiC(001) and Au Nanoparticles Supported on TiC(001): Probing the Nature of the Au/TiC Interface. Journal of Physical Chemistry C, 2011, 115, 22495-22504.	1.5	17
9570	Compensation-doped silicon for photovoltaic applications. Physical Review B, 2011, 84, .	1.1	6
9571	Hybrid density functional theory band structure engineering in hematite. Journal of Chemical Physics, 2011, 134, 224706.	1.2	152
9572	Câ€“H versus Oâ€“H Bond Dissociation for Alcohols on a Rh(111) Surface: A Strong Assistance from Hydrogen Bonded Neighbors. ACS Catalysis, 2011, 1, 1430-1440.	5.5	85
9573	Periodic DFT and Atomistic Thermodynamic Modeling of the Surface Hydration Equilibria and Morphology of Monoclinic ZrO₂ Nanocrystals. Journal of Physical Chemistry C, 2011, 115, 24274-24286.	1.5	67
9574	Elasticity and anisotropy of Fe3C at high pressures. American Mineralogist, 2011, 96, 1530-1536.	0.9	44
9575	First-Principles Study of Water Dissociation on PdZn near Surface Alloys. Journal of Physical Chemistry C, 2011, 115, 18752-18760.	1.5	21

#	Article	IF	Citations
9576	A Comparative Hybrid DFT Study of Phonons in Several SrTiO₃ Phases. Integrated Ferroelectrics, 2011, 123, 18-25.	0.3	4
9577	Catalytic activity of Pd ensembles over Au(111) surface for CO oxidation: A first-principles study. Journal of Chemical Physics, 2011, 134, 054704.	1.2	25
9578	Ideal Strengths and Bonding Properties of PuO₂under Tension. Chinese Physics Letters, 2011, 28, 047101.	1.3	4
9579	Syntheses, Crystal Structures, Transport Properties and First-Principles Electronic Structure Study of the (tTTF)₂X (X = Br, I) Low-Dimensional Antiferromagnets. Inorganic Chemistry, 2011, 50, 4171-4181.	1.9	11
9580	Adsorption of NO Molecule on Spinel-Type CuFe₂O₄ Surface: A First-Principles Study. Journal of Physical Chemistry C, 2011, 115, 13035-13040.	1.5	54
9581	Revisiting the Zintlâ€“Klemm Concept: Alkali Metal Trielides. Inorganic Chemistry, 2011, 50, 7625-7636.	1.9	38
9582	Magnetic Response of Single-Walled Carbon Nanotubes Induced by an External Magnetic Field. ACS Nano, 2011, 5, 537-545.	7.3	46
9583	Transport Properties of Double Quantum Dots Formed by Ferrocene Units. Journal of Physical Chemistry C, 2011, 115, 5257-5264.	1.5	7
9584	Density Functional Theory Study of Sn Adsorption on the CeO₂Surface. Journal of Physical Chemistry C, 2011, 115, 16461-16466.	1.5	30
9585	The Effect of Spinâ€“Orbit Coupling on the Surface Dynamical Properties and Electronâ€“Phonon Interaction of Tl(0001). Journal of Physical Chemistry A, 2011, 115, 7352-7355.	1.1	10
9586	Strain Induced Band Dispersion Engineering in Si Nanosheets. Journal of Physical Chemistry C, 2011, 115, 23682-23687.	1.5	54
9587	Raman spectra of cubic and amorphous Ge<mml:math xmlns:mml="http://www.w3.org/1998/Math/MathML" display="inline"><mml:mrow><mml:msub><mml:mrow /><mml:mrow><mml:mn>2</mml:mn></mml:mrow></mml:msub></mml:mrow></mml:math>Sb<mml:math xmlns:mml="http://www.w3.org/1998/Math/MathML" display="inline"><mml:mrow><mml:msub><mml:mrow />	1.1	106
9588	Enhanced Photoelectrochemical Response of BaTiO₃ with Fe Doping: Experiments and First-Principles Analysis. Journal of Physical Chemistry C, 2011, 115, 24373-24380.	1.5	75
9589	Atomic Layer Deposition of Pt on Tungsten Monocarbide (WC) for the Oxygen Reduction Reaction. Journal of Physical Chemistry C, 2011, 115, 3709-3715.	1.5	94
9590	SrTiO3 Nanotubes with Negative Strain Energy Predicted from First Principles. Journal of Physical Chemistry Letters, 2011, 2, 2566-2570.	2.1	19
9591	Enhanced Chemical Reactivity of Under-Coordinated Atoms at Ptâ^'Rh Bimetallic Surfaces: A Spectroscopic Characterization. Journal of Physical Chemistry C, 2011, 115, 3378-3384.	1.5	24
9592	Chemical Functionalization of the TiO₂(110)-(1 Ã— 1) Surface by Deposition of Terephthalic Acid Molecules. A Density Functional Theory and Scanning Tunneling Microscopy Study. Journal of Physical Chemistry C, 2011, 115, 4134-4144.	1.5	28
9593	Ferromagnetism in IV main group element (C) and transition metal (Mn) doped MgO: A density functional perspective. AIP Advances, 2011, 1, 032129.	0.6	19

#	Article	IF	Citations
9594	First-principles prediction of a high-pressure hydrous phase of AlOOH. Physical Review B, 2011, 83, .	1.1	26
9595	Adsorption of Growth Species on the c-BN(100) Surface. Journal of Physical Chemistry C, 2011, 115, 16977-16983.	1.5	4
9596	Structural Composition of First-Neighbor Shells in GeSe₂ and GeSe₄ Glasses from a First-Principles Analysis of NMR Chemical Shifts. Journal of Physical Chemistry C, 2011, 115, 7755-7759.	1.5	36
9597	Density Functional Theory Study of Pyrophyllite and M-Montmorillonites (M = Li, Na, K, Mg, and Ca): Role of Dispersion Interactions. Journal of Physical Chemistry A, 2011, 115, 9695-9703.	1.1	75
9598	First-Principles Modeling of Oxygen Interaction with SrTiO₃(001) Surface: Comparative Density-Functional LCAO and Plane-Wave Study. Integrated Ferroelectrics, 2011, 123, 10-17.	0.3	11
9599	Ab initiostudy of Heusler alloys Co₂XY (Xâ€‰=â€‰Cr, Mn, Fe; Yâ€‰=â€‰Al,â€‰Ga) under high pressure. Philosophical Magazine Letters, 2011, 91, 545-553.	0.5	44
9600	Anisotropic Lithium Insertion Behavior in Silicon Nanowires: Binding Energy, Diffusion Barrier, and Strain Effect. Journal of Physical Chemistry C, 2011, 115, 9376-9381.	1.5	61
9601	First-Principles Calculations of Clean, Oxidized, and Reduced Î²-MnO₂ Surfaces. Journal of Physical Chemistry C, 2011, 115, 16992-17008.	1.5	55
9602	Germanium Adsorption and Initial Growth on SrTiO₃(001) Surface: A First-Principles Investigation. Journal of Physical Chemistry C, 2011, 115, 22893-22900.	1.5	7
9603	Chirality Transfer from a Single Chiral Molecule to 2D Superstructures in Alaninol on the Cu(100) Surface. Langmuir, 2011, 27, 7410-7418.	1.6	28
9604	Band-gap engineering via local environment in complex oxides. Physical Review B, 2011, 83, .	1.1	77
9605	Density-Functional Theory Studies of Step-Kinked Carbon Nanotubes. Journal of Physical Chemistry C, 2011, 115, 4235-4239.	1.5	11
9606	Stability of Donor-Pair Defects in Si_{1â€“x}Ge_x Alloy Nanowires. Journal of Physical Chemistry C, 2011, 115, 10345-10350.	1.5	7
9607	A COMPARATIVE STUDY OF OPTICAL PROPERTIES OF C3N AND CN3 SYSTEMS THROUGH DENSITY FUNCTIONAL THEORY (DFT). International Journal of Nanoscience, 2011, 10, 361-365.	0.4	2
9608	Density Functional Theory Study of Alkane-Alkoxide Hydride Transfer in Zeolites. ACS Catalysis, 2011, 1, 105-115.	5.5	42
9609	Chemisorption of CO and Mechanism of CO Oxidation on Supported Platinum Nanoclusters. Journal of the American Chemical Society, 2011, 133, 4498-4517.	6.6	448
9610	Effect of impurities on the mechanical and electronic properties of Au, Ag, and Cu monatomic chain nanowires. Physical Review B, 2011, 84, .	1.1	30
9611	Bistable N2â€“H complexes: The first proposed structure of a H-related colour-causing defect in diamond. Diamond and Related Materials, 2011, 20, 896-901.	1.8	9

#	Article	IF	Citations
9612	Role of metal oxide support in redox reactions of iron oxide for chemical looping applications: experiments and density functional theory calculations. Energy and Environmental Science, 2011, 4, 3661.	15.6	138
9613	Doping effects of C, Si and Ge in wurtzite [0001] GaN, AlN, and InN nanowires. Journal of Applied Physics, 2011, 110, .	1.1	18
9615	CO adsorption, CO dissociation, and C-C coupling on Cu monolayer-covered Fe(100). Journal of Fuel Chemistry and Technology, 2011, 39, 956-960.	0.9	20
9616	High-pressure behavior of iron carbide (Fe₇C₃) at inner core conditions. Journal of Geophysical Research, 2011, 116, .	3.3	75
9617	Thermodynamic properties of MgSiO₃majorite and phase transitions near 660 km depth in MgSiO₃and Mg₂SiO₄: A first principles study. Journal of Geophysical Research, 2011, 116, .	3.3	41
9618	Lattice dynamics and thermodynamic properties of (Mg,Fe²⁺)SiO₃postperovskite. Journal of Geophysical Research, 2011, 116, .	3.3	21
9619	Trench parallel anisotropy and large delay times: Elasticity and anisotropy of antigorite at high pressures. Geophysical Research Letters, 2011, 38, .	1.5	65
9620	Bond breaking electron transfer across a conducting nanowire(nanotube)/electrolyte solution interface: The role of electrical double layer effects. Journal of Electroanalytical Chemistry, 2011, 660, 309-313.	1.9	8
9621	Parameter estimation by Density Functional Theory for a lattice-gas model of Br and Cl chemisorption on Ag (100). Journal of Electroanalytical Chemistry, 2011, 662, 130-136.	1.9	8
9622	Theoretical study on the effective methanol decomposition on Pd(111) surface facilitated in alkaline medium. Journal of Electroanalytical Chemistry, 2011, 662, 251-256.	1.9	15
9623	First-principles study on thermodynamic properties and phase transitions in TiS2. Journal of Physics Condensed Matter, 2011, 23, 055401.	0.7	19
9624	Induced magnetism in transition metal intercalated graphitic systems. Journal of Materials Chemistry, 2011, 21, 18681.	6.7	46
9625	Comparative Study on the Performance of Hybrid DFT Functionals in Highly Correlated Oxides: The Case of CeO₂and Ce₂O₃. Journal of Chemical Theory and Computation, 2011, 7, 56-65.	2.3	125
9626	Interaction of hydrogen with zinc oxide nanorods: why the spacing is important. Nanotechnology, 2011, 22, 135704.	1.3	7
9627	Li Ion Diffusion Mechanisms in LiFePO₄: An ab Initio Molecular Dynamics Study. Journal of Physical Chemistry A, 2011, 115, 13045-13049.	1.1	107
9628	Atomistic simulations of the implantation of low-energy boron and nitrogen ions into graphene. Physical Review B, 2011, 83, .	1.1	127
9629	Theoretical studies of the CNx nanotube with four-nitrogen divacancy (4ND) defects. Diamond and Related Materials, 2011, 20, 36-41.	1.8	13
9630	Electronic structure, optical properties and lattice dynamics of MgSO3â‹…6H2O. Journal of Physics Condensed Matter, 2011, 23, 485401.	0.7	0

#	Article	IF	Citations
9631	Strain-induced negative differential resistance in armchair-edge graphene nanoribbons. Applied Physics Letters, 2011, 98, .	1.5	43
9632	Molecular Imaging of Reductive Coupling Reactions: Interstitial-Mediated Coupling of Benzaldehyde on Reduced TiO₂(110). ACS Nano, 2011, 5, 834-843.	7.3	35
9633	Thermoelectric Properties of Ultrasmall Single-Wall Carbon Nanotubes. Journal of Physical Chemistry C, 2011, 115, 21996-22001.	1.5	21
9634	Ideal shear strength under compression and tension in C, Si, Ge, and cubic SiC: anab initiodensity functional theory study. Journal of Physics Condensed Matter, 2011, 23, 385401.	0.7	17
9635	Characterization of Surface Hydride Hafnium Complexes on Alumina by a Combination of Experiments and DFT Calculations. Journal of Physical Chemistry C, 2011, 115, 6757-6763.	1.5	15
9636	Electronic structure and chemical bond in naphthalene and anthracene. Physical Chemistry Chemical Physics, 2011, 13, 5679.	1.3	48
9637	Graphene adhesion on MoS2 monolayer: An ab initio study. Nanoscale, 2011, 3, 3883.	2.8	346
9638	Site-Preferential Design of Itinerant Ferromagnetic Borides: Experimental and Theoretical Investigation of MRh6B3(M = Fe, Co). Inorganic Chemistry, 2011, 50, 10303-10309.	1.9	16
9639	Effect of Metal Doping on Electronic Structure and Visible Light Absorption of SrTiO₃ and NaTaO₃ (Metal = Mn, Fe, and Co). Journal of Physical Chemistry C, 2011, 115, 8305-8311.	1.5	181
9640	Adsorption of nitrogen oxides on graphene and graphene oxides: Insights from density functional calculations. Journal of Chemical Physics, 2011, 134, 044710.	1.2	172
9641	Prediction of a superconductive superhard material: Diamond-like BC7. Journal of Applied Physics, 2011, 110, 013501.	1.1	21
9642	A computational investigation of H2 adsorption and dissociation on Au nanoparticles supported on TiO2 surface. Faraday Discussions, 2011, 152, 185.	1.6	54
9643	High-Throughput Combinatorial Database of Electronic Band Structures for Inorganic Scintillator Materials. ACS Combinatorial Science, 2011, 13, 382-390.	3.8	211
9644	Assessing the Thermoelectric Properties of Sintered Compounds via High-ThroughputAb-InitioCalculations. Physical Review X, 2011, 1, .	2.8	92
9645	Magnetic ordering in tetragonal FeS: Evidence for strong itinerant spin fluctuations. Physical Review B, 2011, 83, .	1.1	57
9646	First-principles study of Cu₂ZnSnS₄and the related band offsets for photovoltaic applications. Journal of Physics Condensed Matter, 2011, 23, 404203.	0.7	90
9647	System-size convergence of point defect properties: The case of the silicon vacancy. Physical Review B, 2011, 84, .	1.1	62
9648	Phase Stability and Electronic Structure of In-Free Photovoltaic Materials Cu₂IISnSe₄ (II: Zn, Cd, Hg). Japanese Journal of Applied Physics, 2011, 50, 05FF01.	0.8	17

#	Article	IF	Citations
9649	Functionalized Graphene for High-Performance Two-Dimensional Spintronics Devices. ACS Nano, 2011, 5, 2601-2610.	7.3	116
9650	Electronic structure and bonding properties of cobalt oxide in the spinel structure. Physical Review B, 2011, 83, .	1.1	258
9651	Investigation of the structure and photoluminescence properties of Eu3+ ion-activated Y6WxMo(1) Tj ETQq0 0 0 rgBT /Overlock 10 Tf 5	6.7	57
9652	Adsorption of carbon adatoms to graphene and its nanoribbons. Journal of Applied Physics, 2011, 109, 013704.	1.1	59
9653	First-principle calculation of stacking fault energies in Ni and Ni-Co alloy. Journal of Applied Physics, 2011, 109, .	1.1	69
9654	Theoretical modeling of the electronic structure and exchange interactions in a Cu(II)Pc one-dimensional chain. Physical Review B, 2011, 84, .	1.1	22
9655	Graphene adhesion on mica: Role of surface morphology. Physical Review B, 2011, 83, .	1.1	59
9656	Density functional theory study of the structural, electronic, lattice dynamical, and thermodynamic properties of Li<mml:math xmlns:mml="http://www.w3.org/1998/Math/MathML" display="inline"><mml:msub><mml:mrow /><mml:mn>4</mml:mn></mml:msub></mml:math>SiO<mml:math xmlns:mml="http://www.w3.org/1998/Math/MathML" display="inline"><mml:msub><mml:mrow /><mml:mn>4</mml:mn></mml:msub></mml:math>and its capability for CO<mml:math xmlns:mml="http:	1.1	61
9657	Computational study of the structural phases of ZnO. Physical Review B, 2011, 84, .	1.1	40
9658	First-principles approach to phase stability for a ternary<mml:math xmlns:mml="http://www.w3.org/1998/Math/MathML" display="inline"><mml:mrow><mml:mi>Ïƒ</mml:mi></mml:mrow></mml:math>phase: Application to Cr-Ni-Re. Physical Review B, 2011, 83, .	1.1	19
9659	Effects of H-, N-, and (H, N)-Doping on the Photocatalytic Activity of TiO₂. Journal of Physical Chemistry C, 2011, 115, 12224-12231.	1.5	144
9660	Gate-Voltage Control of Oxygen Diffusion on Graphene. Physical Review Letters, 2011, 106, 146802.	2.9	99
9661	Ab initiostudy of magnetic properties of complexes formed by an Fe impurity and an intrinsic interstitial defect in ZnO. Physical Review B, 2011, 84, .	1.1	11
9662	Functionalization of Single-Layer MoS₂ Honeycomb Structures. Journal of Physical Chemistry C, 2011, 115, 13303-13311.	1.5	484
9663	Enhanced role of Al or Ga-doped graphene on the adsorption and dissociation of N2O under electric field. Physical Chemistry Chemical Physics, 2011, 13, 12472.	1.3	87
9664	On the mechanism of enhanced oxygen reduction reaction in nitrogen-doped graphene nanoribbons. Physical Chemistry Chemical Physics, 2011, 13, 17505.	1.3	646
9665	Vibrational properties of graphene fluoride and graphane. Applied Physics Letters, 2011, 98, .	1.5	68
9666	Pathways for methanol steam reforming involving adsorbed formaldehyde and hydroxyl intermediates on Cu(111): density functional theory studies. Physical Chemistry Chemical Physics, 2011, 13, 9622.	1.3	61

#	Article	IF	Citations
9667	Investigating the Quartz (101Ì…0)/Water Interface using Classical and Ab Initio Molecular Dynamics. Langmuir, 2011, 27, 8700-8709.	1.6	72
9668	Ab Initio Calculation of the Adhesion and Ideal Shear Strength of Planar Diamond Interfaces with Different Atomic Structure and Hydrogen Coverage. Langmuir, 2011, 27, 6862-6867.	1.6	83
9669	Mechanism of Î³-Al₂O₃ Support in CO₂ Reforming of CH₄â€"A Density Functional Theory Study. Journal of Physical Chemistry C, 2011, 115, 225-233.	1.5	23
9670	Electronic structure and thermoelectric properties of Sb-based semiconducting half-Heusler compounds. Physical Review B, 2011, 83, .	1.1	106
9671	DFT Study of Hydrogen Storage by Spillover on Graphene with Boron Substitution. Journal of Physical Chemistry C, 2011, 115, 9241-9249.	1.5	129
9672	First-principles calculation of the nonadiabatic spin transfer torque in Ni and Fe. Physical Review B, 2011, 84, .	1.1	25
9673	Screening for high-performance piezoelectrics using high-throughput density functional theory. Physical Review B, 2011, 84, .	1.1	125
9674	Three Dimensional Carbon-Nanotube Polymers. ACS Nano, 2011, 5, 7226-7234.	7.3	110
9675	First-Principles Study of the Graphene@MoSe₂ Heterobilayers. Journal of Physical Chemistry C, 2011, 115, 20237-20241.	1.5	121
9676	Description of Quasi Particle Bands of Ce Compounds Using the Wannier Representation. Journal of the Physical Society of Japan, 2011, 80, 114702.	0.7	2
9677	Ferromagnetism Study in ZnO Codoped with Al and Co from First-Principles Calculations. Journal of Physical Chemistry C, 2011, 115, 24478-24484.	1.5	6
9678	Third conformer of graphane: A first-principles density functional theory study. Physical Review B, 2011, 83, .	1.1	57
9679	Electrical and Lithium Ion Dynamics in Three Main Components of Solid Electrolyte Interphase from Density Functional Theory Study. Journal of Physical Chemistry C, 2011, 115, 7044-7049.	1.5	179
9680	Nanocrystals of CeVO₄ Doped by Metallic Heteroions. Inorganic Chemistry, 2011, 50, 6189-6194.	1.9	28
9681	Origin of Photocatalytic Activation of Silver Orthophosphate from First-Principles. Journal of Physical Chemistry C, 2011, 115, 4680-4687.	1.5	259
9682			

#	Article	IF	Citations
9685	Strain-induced magnetic transitions in half-fluorinated single layers of BN, GaN and graphene. Nanoscale, 2011, 3, 2301.	2.8	124
9686	Computational and Experimental Investigations into N₂O Decomposition over MgO Nanocrystals from Thorough Molecular Mechanism to ab initio Microkinetics. Journal of Physical Chemistry C, 2011, 115, 22451-22460.	1.5	41
9687	The role of the organic layer functionalization in the formation of silicon/organic layer/metal junctions with coinage metals. Physical Chemistry Chemical Physics, 2011, 13, 21411.	1.3	4
9688	Band gap engineering of bulk ZrO2 by Ti doping. Physical Chemistry Chemical Physics, 2011, 13, 17667.	1.3	58
9689	Structural characterization of amorphous alumina and its polymorphs from first-principles XPS and NMR calculations. Physical Review B, 2011, 83, .	1.1	90
9690	Quantum dynamics of hydrogen interacting with single-walled carbon nanotubes: Multiple H-atom adsorbates. Journal of Chemical Physics, 2011, 134, 074308.	1.2	10
9691	Nitrogen and sulfur co-doped TiO₂nanosheets with exposed {001} facets: synthesis, characterization and visible-light photocatalytic activity. Physical Chemistry Chemical Physics, 2011, 13, 4853-4861.	1.3	282
9692	<mml:math xmlns:mml="http://www.w3.org/1998/Math/MathML" display="inline"><mml:mi>Î²</mml:mi><mml:mtext mathvariant="normal">â^'</mml:mtext><mml:mi>tin</mml:mi><mml:mo>â†'</mml:mo><mml:mi>I</mml:mi><mml:mi>m</mml:mi> Transitions of Germanium. Physical Review Letters, 2011, 106, 135502.	2.9	38
9693	Electronic and magnetic properties of pristine and chemically functionalized germanene nanoribbons. Nanoscale, 2011, 3, 4330.	2.8	93
9694	Effect of Compensated Codoping on the Photoelectrochemical Properties of Anatase TiO₂ Photocatalyst. Journal of Physical Chemistry C, 2011, 115, 16963-16969.	1.5	135
9695	Electromechanical Response of a SiC Nanotube under Local Torsional Deformation. Journal of Physical Chemistry C, 2011, 115, 24347-24352.	1.5	6
9696	Improved visible-light photocatalytic activity of porous carbon self-doped ZnO nanosheet-assembled flowers. CrystEngComm, 2011, 13, 2533.	1.3	328
9697	Width- and Edge-Dependent Stability, Electronic Structures, and Magnetic Properties of Graphene-Like and Wurtzite ZnS Nanoribbons. Journal of Physical Chemistry C, 2011, 115, 4466-4475.	1.5	17
9698	Molecular dynamics study of the adhesion of Cu/SiO<mml:math xmlns:mml="http://www.w3.org/1998/Math/MathML" display="inline"><mml:mrow><mml:msub><mml:mrow /><mml:mrow><mml:mn>2</mml:mn></mml:mrow></mml:msub></mml:mrow></mml:math>interfaces using a variable-charge interatomic potential. Physical Review B, 2011, 83, .	1.1	47
9699	High-field multinuclear solid-state nuclear magnetic resonance (NMR) and first principle calculations in MgSO4 polymorphs. Canadian Journal of Chemistry, 2011, 89, 1076-1086.	0.6	11
9700	Structure, Properties, and Theoretical Electronic Structure of UCuOP and NpCuOP. Inorganic Chemistry, 2011, 50, 576-589.	1.9	8
9701	Oxidation of monovacancies in graphene by oxygen molecules. Journal of Materials Chemistry, 2011, 21, 18284.	6.7	50
9702	Energetics and Mechanism for H₂S Adsorption by Ceria-Lanthanide Mixed Oxides: Implications for the Desulfurization of Biomass Gasifier Effluents. Journal of Physical Chemistry C, 2011, 115, 24178-24188.	1.5	24

#	Article	IF	Citations
9703	Hydrogen Atom Adsorption on Aluminum Clusters: An Electronic Structures Density Functional Study. Materials Research Society Symposia Proceedings, 2011, 1309, 45.	0.1	1
9704	Ab Initio Studies of Cellulose I: Crystal Structure, Intermolecular Forces, and Interactions with Water. Journal of Physical Chemistry C, 2011, 115, 11533-11539.	1.5	80
9705	Band alignment at metal/ferroelectric interfaces: Insights and artifacts from first principles. Physical Review B, 2011, 83, .	1.1	114
9706	A theoretical study of a ZnO graphene analogue: adsorption on Ag(111) and hydrogen transport. Journal of Physics Condensed Matter, 2011, 23, 334215.	0.7	5
9707	Importance of Accurate Spectral Simulations for the Analysis of Terahertz Spectra: Citric Acid Anhydrate and Monohydrate. Journal of Physical Chemistry A, 2011, 115, 11039-11044.	1.1	25
9708	Relativistic effects and fully spin-polarized Fermi surface at the Tl/Si(111) surface. Physical Review B, 2011, 84, .	1.1	50
9709	Structural and Electronic Properties of (Al₂O₃)_n Clusters with n = 1â€“10 from First Principles Calculations. Journal of Physical Chemistry C, 2011, 115, 18111-18121.	1.5	60
9710	A Density Functional Theory Study of Spectroscopic and Thermodynamic Properties of Surfacic Hydrides on Ru (0001) Model Surface: The Influence of the Coordination Modes and the Coverage. Journal of Physical Chemistry C, 2011, 115, 2169-2178.	1.5	30
9711	Tin dioxide from first principles: Quasiparticle electronic states and optical properties. Physical Review B, 2011, 83, .	1.1	145
9712	Hexagonal hydroxyapatite formation on TiO2 nanotubes under urea modulation. CrystEngComm, 2011, 13, 3741.	1.3	29
9713	Half metallicity in BC2N nanoribbons: stability, electronic structures, and magnetism. Nanoscale, 2011, 3, 2583.	2.8	33
9714	Nature and Location of Cationic Lanthanum Species in High Alumina Containing Faujasite Type Zeolites. Journal of Physical Chemistry C, 2011, 115, 21763-21776.	1.5	105
9715	First-principles calculations of phase transition, elastic modulus, and superconductivity under pressure for zirconium. Journal of Applied Physics, 2011, 109, .	1.1	66
9716	Magnetism of substitutional Fe impurities in graphene nanoribbons. Journal of Chemical Physics, 2011, 134, 024704.	1.2	29
9717	Bi₂Ti₂O₇: It Is Not What You Have Read. Chemistry of Materials, 2011, 23, 4965-4974.	3.2	126
9718	Molecular dynamics study of thermal transport in GaAs-self-assembly monolayer-GaAs junctions with ab initio characterization of thiol-GaAs bonds. Journal of Applied Physics, 2011, 109, .	1.1	33
9719	Computational Investigation on Adsorption and Dissociation of the NH₃Molecule on the Fe(111) Surface. Journal of Physical Chemistry C, 2011, 115, 521-528.	1.5	32
9720	Electric Charge of Single Au Atoms Adsorbed on TiO₂(110) and Associated Band Bending. Journal of Physical Chemistry C, 2011, 115, 23848-23853.	1.5	38

#	Article	IF	Citations
9721	A density functional theory approach to mushroom-like platinum clusters on palladium-shell over Au core nanoparticles for high electrocatalytic activity. Physical Chemistry Chemical Physics, 2011, 13, 5441.	1.3	28
9722	Cluster-assembled materials based on M12N12 (M = Al, Ga) fullerene-like clusters. Physical Chemistry Chemical Physics, 2011, 13, 16182.	1.3	33
9723	CeO₂ â†" CuO_x Interactions and the Controlled Assembly of CeO₂(111) and CeO₂(100) Nanoparticles on an Oxidized Cu(111) Substrate. Journal of Physical Chemistry C, 2011, 115, 23062-23066.	1.5	44
9724	Selective Hydrogenolysis of Polyols and Cyclic Ethers over Bifunctional Surface Sites on Rhodiumâ€"Rhenium Catalysts. Journal of the American Chemical Society, 2011, 133, 12675-12689.	6.6	439
9725	First-principles characterization of an AlSiVC center in cubic silicon carbide. Journal of Applied Physics, 2011, 110, 033711.	1.1	9
9726	Electronic Structure and Optical Properties of La or In Doped SnO₂: First-Principles Calculations. Advanced Materials Research, 2011, 393-395, 80-83.	0.3	0
9727	First Principles Calculations of Electronic and Optical Properties of Al_{1-x}La_xN. Advanced Materials Research, 0, 393-395, 110-113.	0.3	2
9728	Bromination of graphene and graphite. Physical Review B, 2011, 83, .	1.1	40
9729	Ab initio<mml:math xmlns:mml="http://www.w3.org/1998/Math/MathML" display="inline"><mml:msup><mml:mrow /><mml:mn>27</mml:mn></mml:msup></mml:math>Al NMR chemical shifts and quadrupolar parameters for Al<mml:math xmlns:mml="http://www.w3.org/1998/Math/MathML" display="inline"><mml:msub><mml:mrow /><mml:mn>2</mml:mn></mml:msub></mml:math>O<mml:math xmlns:mml="http://www.w3.org/1998/Math/MathML" display="inline"><mml:msub><mml:mrow /><mml:mn>3</mml:mn></mml:msub></mml:math> polymorphs. Physical Review B, 2011, 83, .	1.1	48
9730	Ab initio<mml:math xmlns:mml="http://www.w3.org/1998/Math/MathML" display="inline"><mml:mi>p</mml:mi></mml:math>hybridization as the origin of hexagonal ferroelectricity in multiferroic HoMnO<mml:math xmlns:mml="http://www.w3.org/1998/Math/MathML" display="inline"><mml:msub><mml:mrow /><mml:mn>3</mml:mn></mml:msub></mml:math>. Physical Review B, 2011, 83, .	1.1	18
9731	Theoretical investigations into the enantiomeric and racemic forms of Î±-(trifluoromethyl)lactic acid. Physical Chemistry Chemical Physics, 2011, 13, 811-817.	1.3	17
9732	Energy density in density functional theory: Application to crystalline defects and surfaces. Physical Review B, 2011, 83, .	1.1	58
9733	Mechanism of Li Adsorption on Carbon Nanotube-Fullerene Hybrid System: A First-Principles Study. ACS Applied Materials & Interfaces, 2011, 3, 1186-1194.	4.0	29
9734	Influence of water on the properties of an Au/Mpy/Pd metal/molecule/metal junction. Beilstein Journal of Nanotechnology, 2011, 2, 384-393.	1.5	5
9735	Atomistic Simulation of the Structural, Thermodynamic, and Elastic Properties of Li₂TiO₃. Journal of Physical Chemistry C, 2011, 115, 21874-21881.	1.5	37
9736	Hydrogen adsorption on Ce/SWCNT systems: a DFT study. Physical Chemistry Chemical Physics, 2011, 13, 9483.	1.3	18
9737	Electronic structure of bismuth telluride quasi-two-dimensional crystal: A first principles study. Applied Physics Letters, 2011, 98, .	1.5	19
9738	Vibrational properties of the LiNbO3 z-surfaces. IEEE Transactions on Ultrasonics, Ferroelectrics, and Frequency Control, 2011, 58, 1751-1756.	1.7	9

#	Article	IF	Citations
9739	Ab initiostudy of the early stages of gas-phase water oxidation of the Si(100)<mml:math xmlns:mml="http://www.w3.org/1998/Math/MathML" display="inline"><mml:mrow><mml:mo>(</mml:mo><mml:mn>2</mml:mn><mml:mo>Ã—</mml:mo><mml:mn>1</mml:mn><mml:mo surface. Physical Review B, 2011, 84, .	1.1	4
9740	Ab Initio Study on a Novel Photocatalyst: Functionalized Graphitic Carbon Nitride Nanotube. ACS Catalysis, 2011, 1, 99-104.	5.5	118
9741	Pseudopotential calculation of the bulk modulus and phonon dispersion of the bcc and hcp structures of titanium. Physica Scripta, 2011, 83, 065603.	1.2	11
9742	Strain-induced band-gap deformation of H/F passivated graphene and<mml:math xmlns:mml="http://www.w3.org/1998/Math/MathML" display="inline"><mml:mrow><mml:mi>h</mml:mi></mml:mrow></mml:math>-BN sheet. Physical Review B, 2011, 84, .	1.1	45
9743	Band Gap Tuning of Hydrogenated Graphene: H Coverage and Configuration Dependence. Journal of Physical Chemistry C, 2011, 115, 3236-3242.	1.5	167
9744	Ab initiorandom structure searching. Journal of Physics Condensed Matter, 2011, 23, 053201.	0.7	832
9745	Dispersion of edge states and quantum confinement of electrons in graphene channels drawn on graphene fluoride. Physical Review B, 2011, 83, .	1.1	14
9746	Influence of Low-Symmetry Distortions on Electron Transport through Metal Atom Chains: When Is a Molecular Wire Really â€œBrokenâ€?. Journal of the American Chemical Society, 2011, 133, 12590-12599.	6.6	49
9747	Phase transitions and thermodynamic properties of yttria, Y<mml:math xmlns:mml="http://www.w3.org/1998/Math/MathML" display="inline"><mml:msub><mml:mrow /><mml:mn>2</mml:mn></mml:msub></mml:math>O<mml:math xmlns:mml="http://www.w3.org/1998/Math/MathML" display="inline"><mml:msub><mml:mrow /><mml:mn>3</mml:mn></mml:msub></mml:math>: Inelastic neutron scattering shell model and first-principles calculations. Physical Review B, 2011, 84, .	1.1	35
9748	Graphene/graphane interface energy and implications for defects. Physical Review B, 2011, 84, .	1.1	11
9749	Graphitic GaNâ€“ZnO and corresponding nanotubes. Journal of Materials Chemistry, 2011, 21, 17071.	6.7	5
9750	Growth Pattern and Electronic Properties of Cluster-Assembled Material Based on Zn₁₂O₁₂: A Density-Functional Study. Journal of Physical Chemistry C, 2011, 115, 6455-6461.	1.5	44
9751	Bonding Changes Along Solid-Solid Phase Transitions Using the Electron Localization Function Approach. , 2011, , 625-658.		3
9752	Interplay between geometrical structure and electronic properties in rippled free-standing graphene. Physical Review B, 2011, 83, .	1.1	35
9753	Role of Symmetry in the Stability and Electronic Structure of Titanium Dioxide Nanowires. Journal of Physical Chemistry C, 2011, 115, 18494-18499.	1.5	19
9754	Antiferromagnet topological insulators withAB2CHeusler structure. Physical Review B, 2011, 83, .	1.1	25
9755	Effect of Layer Stacking on the Electronic Structure of Graphene Nanoribbons. ACS Nano, 2011, 5, 6096-6101.	7.3	32
9756	Color of TiN and ZrN from first-principles calculations. Journal of Applied Physics, 2011, 110, .	1.1	28

#	Article	IF	Citations
9757	Identification and Quantification of Defects in the Cation Ordering in Mg/Al Layered Double Hydroxides. Chemistry of Materials, 2011, 23, 2821-2831.	3.2	114
9758	Mechanism of the phase transitions in MnAs. Physical Review B, 2011, 83, .	1.1	27
9759	Investigation of Gas Permeability in Carbon Nanotube (CNT)â^'Polymer Matrix Membranes via Modifying CNTs with Functional Groups/Metals and Controlling Modification Location. Journal of Physical Chemistry C, 2011, 115, 6661-6670.	1.5	83
9760	Decomposition Pathways of Glycerol via Câ€“H, Oâ€“H, and Câ€“C Bond Scission on Pt(111): A Density Functional Theory Study. Journal of Physical Chemistry C, 2011, 115, 19702-19709.	1.5	151
9761	Bi₂(IO₄)(IO₃)₃: A New Potential Infrared Nonlinear Optical Material Containing [IO₄]^{3â€“} Anion. Inorganic Chemistry, 2011, 50, 12818-12822.	1.9	102
9762	Large Isosymmetric Reorientation of Oxygen Octahedra Rotation Axes in Epitaxially Strained Perovskites. Physical Review Letters, 2011, 106, 235502.	2.9	45
9763	Structural and Electronic Properties, and Pressure-Induced Phase Transition of Layered C 5 N: A First-Principles Investigation. Chinese Physics Letters, 2011, 28, 126101.	1.3	3
9764	First-principles prediction of post-pyrite phase transitions in germanium dioxide. Physical Review B, 2011, 83, .	1.1	23
9765	Auger recombination in Si and GaAs semiconductors:Ab initioresults. Physical Review B, 2011, 84, .	1.1	36
9766	Nearly Free Electron State in Graphane Nanoribbon Superlattice. Chinese Journal of Chemical Physics, 2011, 24, 22-24.	0.6	15
9767	Electronic structures and bonding of graphyne sheet and its BN analog. Journal of Chemical Physics, 2011, 134, 174701.	1.2	182
9768	Synthesis, Characterization, and Structureâ€“Property Relationships in Two New Polar Oxides: Zn₂(MoO₄)(SeO₃) and Zn₂(MoO₄)(TeO₃). Inorganic Chemistry, 2011, 50, 5215-5222.	1.9	73
9769	Cr in diamond: A first-principles study. Physical Review B, 2011, 84, .	1.1	12
9770	Size effect of Pd clusters on hydrogen adsorption. Journal of Physics Condensed Matter, 2011, 23, 045503.	0.7	14
9771	Ab initiostudy of the magnetic ordering in Si/Mn digital alloys. Physical Review B, 2011, 84, .	1.1	12
9772	First-principles study of the structural, mechanical and electronic properties of ZnX₂O₄(X=Al, Cr and Ga). Chinese Physics B, 2011, 20, 047102.	0.7	23
9773	Vibrational properties of RbNd(WO₄)₂: high pressure Raman study, structural and phonon calculations. Journal of Physics Condensed Matter, 2011, 23, 405901.	0.7	4
9774	EELS and <I>Ab-Initio</I> Study of Faceted CSL Boundary in Silicon. Materials Transactions, 2011, 52, 276-279.	0.4	7

#	Article	IF	Citations
9775	CO₂Adsorption on Carbon Models of Organic Constituents of Gas Shale and Coal. Environmental Science & Technology, 2011, 45, 809-814.	4.6	163
9776	Water thin film-silica interaction on<mml:math xmlns:mml="http://www.w3.org/1998/Math/MathML" display="inline"><mml:mi>Î±</mml:mi></mml:math>-quartz (0001) surfaces. Physical Review B, 2011, 84, .	1.1	32
9777	Study on the Energy Band Structure of La Doped ZnO. Advanced Materials Research, 0, 233-235, 2119-2124.	0.3	1
9778	Impact of stress on band-to-band tunneling current in SOI MOSFET based on first-principles calculation. , 2011, , .		0
9779	Electronic properties of edge-functionalized zigzag graphene nanoribbons on SiO₂substrate. Nanotechnology, 2011, 22, 265702.	1.3	7
9780	Structural Principles of Semiconducting Group 14 Clathrate Frameworks. Inorganic Chemistry, 2011, 50, 1733-1742.	1.9	122
9781	Adsorption and diffusion of 3d transition metal atoms on the GaN(0001) surface. Journal of Applied Physics, 2011, 110, 083712.	1.1	19
9782	Methyl Formate Pathway in Methanol Steam Reforming on Copper: Density Functional Calculations. ACS Catalysis, 2011, 1, 1263-1271.	5.5	47
9783	Magnetic and electronic structure properties of Co-doped SnO2 nanoparticles synthesized by the sol-gel-hydrothermal technique. Journal of Applied Physics, 2011, 109, 083930.	1.1	32
9784	A first principles study of oxygen reduction reaction on a Pt(111) surface modified by a subsurface transition metal M (M = Ni, Co, or Fe). Physical Chemistry Chemical Physics, 2011, 13, 20178.	1.3	236
9785	Contribution of molecular dynamics simulations andab initiocalculations to the interpretation of Mg K-edge experimental XANES in K₂Oâ€“MgOâ€“3SiO₂glass. Journal of Physics Condensed Matter, 2011, 23, 255401.	0.7	20
9786	Theoretical Study of Electrochemical Processes on Ptâ€“Ni Alloys. Journal of Physical Chemistry C, 2011, 115, 10640-10650.	1.5	79
9787	Stoichiometry of the<mml:math xmlns:mml="http://www.w3.org/1998/Math/MathML" display="inline"><mml:mrow><mml:msub><mml:mi mathvariant="normal">LaFeO</mml:mi><mml:mrow><mml:mn>3</mml:mn></mml:mrow></mml:msub></mml:mrow></mml:math>(01 surface determined from first-principles and thermodynamic calculations. Physical Review B, 2011, 83, .	1.1	33
9788	Structural Secrets of Multiferroic Interfaces. Physical Review Letters, 2011, 106, 087203.	2.9	85
9789	Theoretical investigation of the evolution of the topological phase of Bi<mml:math xmlns:mml="http://www.w3.org/1998/Math/MathML" display="inline"><mml:msub><mml:mrow /><mml:mn>2</mml:mn></mml:msub></mml:math>Se<mml:math xmlns:mml="http://www.w3.org/1998/Math/MathML" display="inline"><mml:msub><mml:mrow /><mml:mn>3</mml:mn></mml:msub></mml:math>under mechanical strain. Physical Review B, 2011, 84, .	1.1	115
9790	Nonharmonic phonons in MgB2at elevated temperatures. Physical Review B, 2011, 83, .	1.1	4
9791	First-principles study on the electronic and magnetic properties of hydrogenated CdS nanosheets. Journal of Applied Physics, 2011, 109, .	1.1	28
9792	Lattice normal modes and electronic properties of the correlated metal LaNiO<mml:math xmlns:mml="http://www.w3.org/1998/Math/MathML" display="inline"><mml:msub><mml:mrow /><mml:mn>3</mml:mn></mml:msub></mml:math>. Physical Review B, 2011, 84, .	1.1	110

#	Article	IF	Citations
9793	Intrinsic and external strains modulated electronic properties of GaN/InN core/shell nanowires. Journal of Applied Physics, 2011, 110, .	1.1	3
9794	First-principle calculations of the bulk properties of 4d transition metal carbides and nitrides in the rocksalt, zincblende and wurtzite structures. Diamond and Related Materials, 2011, 20, 157-164.	1.8	66
9795	CO2 adsorption on TiO2(110) rutile: Insight from dispersion-corrected density functional theory calculations and scanning tunneling microscopy experiments. Journal of Chemical Physics, 2011, 134, 104707.	1.2	91
9796	Structural, magnetic, and transport properties of substitutionally doped graphene nanoribbons from first principles. Physical Review B, 2011, 83, .	1.1	124
9797	Photoinduced work function changes by isomerization of a densely packed azobenzene-based SAM on Au: a joint experimental and theoretical study. Physical Chemistry Chemical Physics, 2011, 13, 14302.	1.3	61
9798	Feasibility of band gap engineering of pyrite FeS<mml:math xmlns:mml="http://www.w3.org/1998/Math/MathML" display="inline"><mml:msub><mml:mrow /><mml:mn>2</mml:mn></mml:msub></mml:math>. Physical Review B, 2011, 84, .	1.1	48
9799	U and Xe transport in UO<mml:math xmlns:mml="http://www.w3.org/1998/Math/MathML" display="inline"><mml:msub><mml:mrow /><mml:mrow><mml:mn>2</mml:mn><mml:mo>Â±</mml:mo><mml:mi>x</mml:mi></mml:mrow></mml:msub></mml:math>: Density functional theory calculations. Physical Review B, 2011, 84, .	1.1	110
9800	Syntheses, structures and properties of coordination polymers of cadmium(ii) with 4-methyl-1,2,4-triazole-3-thiol ligand. CrystEngComm, 2011, 13, 1697.	1.3	30
9801	Exploration of optical and electronic parameters of lithium thiogallate (LiGaS<inf>2</inf>). , 2011, , .		0
9802	Theoretical study of the structure of self-assembled monolayers of short alkylthiolates on Au(111) and Ag(111): the role of induced substrate reconstruction and chainâ€“chain interactions. Physical Chemistry Chemical Physics, 2011, 13, 9353.	1.3	24
9803	Computational insight into the effect of monovalent cations on the electronic, optical, and lattice dynamic properties of XInSe2 (Xâ€‰=â€‰Cu, Ag, Li). Journal of Applied Physics, 2011, 109, .	1.1	16
9804	Hybrid density functional theory description of N- and C-doping of NiO. Journal of Chemical Physics, 2011, 134, 224703.	1.2	34
9806	Combined Experimental and Computational Hydrostatic Compression Study of Crystalline Ammonium Perchlorate. Journal of Physical Chemistry C, 2011, 115, 18782-18788.	1.5	29
9807	Bias in bonding behavior among boron, carbon, and nitrogen atoms in ion implanted a-BN, a-BC, and diamond like carbon films. Journal of Applied Physics, 2011, 110, .	1.1	20
9808	Origin of the low thermal conductivity of the thermoelectric material Î²-Zn4Sb3: An ab initio theoretical study. Applied Physics Letters, 2011, 98, .	1.5	20
9809	Interplay of epitaxial strain and rotations in PbTiO<mml:math xmlns:mml="http://www.w3.org/1998/Math/MathML" display="inline"><mml:mrow><mml:msub><mml:mrow /><mml:mn>3</mml:mn></mml:msub><mml:mo>/</mml:mo></mml:mrow></mml:math>PbZrO<mml:math xmlns:mml="http://www.w3.org/1998/Math/MathML" display="inline"><mml:msub><mml:mrow /><mml:mn>3</mml:mn></mml:msub></mml:math> superlattices from first principles. Physical Review B,	1.1	27
9810	Formation of Self-Assembled Chains of Tetrathiafulvalene on a Cu(100) Surface. Journal of Physical Chemistry A, 2011, 115, 13080-13087.	1.1	6
9811	Magnetoelastic coupling in<mml:math xmlns:mml="http://www.w3.org/1998/Math/MathML" display="inline"><mml:mi>Î³</mml:mi></mml:math>-iron investigated within anab initiospin spiral approach. Physical Review B, 2011, 84, .	1.1	39

#	Article	IF	Citations
9812	First-principles study on the interaction of H interstitials with grain boundaries in<mml:math xmlns:mml="http://www.w3.org/1998/Math/MathML" display="inline"><mml:mi>Î±</mml:mi></mml:math>-and<mml:math xmlns:mml="http://www.w3.org/1998/Math/MathML" display="inline"><mml:mi>Î³</mml:mi></mml:math>-Fe. Physical Review B, 2011, 84, .	1.1	211
9813	Optical properties of water at high temperature. Physics of Plasmas, 2011, 18, .	0.7	20
9814	Hydrogen impurities and native defects in CdO. Journal of Applied Physics, 2011, 110, .	1.1	14
9815	A model for the Heyrovsky reaction as the second step in hydrogen evolution. Physical Chemistry Chemical Physics, 2011, 13, 6992.	1.3	34
9816	Ab initiostudy of ferromagnetic single-wall nickel nanotubes. Physical Review B, 2011, 84, .	1.1	17
9817	Ab initiostudy of palladium and silicon carbide. Philosophical Magazine, 2011, 91, 458-467.	0.7	4
9818	Electronic properties of Fe clusters on a Au(111) surface. Physical Review B, 2011, 84, .	1.1	19
9819	<i>Ab Initio</i> Investigation of the Influence of Single Intrinsic Defect on the Structure, Bulk Moduli and Electronic Properties of V-Doped ZnO. Advanced Materials Research, 0, 393-395, 15-19.	0.3	0
9820	Atomic-scale investigation on lithium storage mechanism in TiNb2O7,. Energy and Environmental Science, 2011, 4, 2638.	15.6	256
9821	Electronic structure and band gap of zinc spinel oxides beyond LDA: ZnAl₂O₄, ZnGa₂O₄and ZnIn₂O₄. New Journal of Physics, 2011, 13, 063002.	1.2	105
9822	Calculated strain response of vibrational modes for H-containing point defects in diamond. Physical Chemistry Chemical Physics, 2011, 13, 11488.	1.3	6
9823	Interatomic potential for the Al-Cu system. Physical Review B, 2011, 83, .	1.1	123
9824	Boron and Nitrogen Doping Induced Half-Metallicity in Zigzag Triwing Graphene Nanoribbons. Journal of Physical Chemistry C, 2011, 115, 6195-6199.	1.5	60
9825	Applying a rigid band model to the XYB14crystal family. IOP Conference Series: Materials Science and Engineering, 2011, 18, 082024.	0.3	6
9826	First-Principles Study of the Local Magnetic Moment on a N-Doped Cu ₂ O (111) Surface. Chinese Physics Letters, 2011, 28, 127102.	1.3	1
9827	Electronic and optical properties of Mg_xZn_{1â^'x}O and Cd_xZn_{1â^'x}O fromab initiocalculations. New Journal of Physics, 2011, 13, 085012.	1.2	60
9828	Cubic inclusions in hexagonal AlN, GaN, and InN: Electronic states. Physical Review B, 2011, 84, .	1.1	50
9829	Adsorption and (photo-) electrochemical splitting of water on rutile ruthenium dioxide. Europhysics Letters, 2011, 93, 68001.	0.7	11

#	Article	IF	Citations
9830	A First-Principles Model for Hydrogen Uptake Promoted by Sulfur on Ni(111). Journal of the Electrochemical Society, 2011, 158, F36.	1.3	17
9831	Understanding and correcting the spurious interactions in charged supercells. Physical Review B, 2011, 84, .	1.1	89
9832	First-Principles Modeling of the Polycyclic Aromatic Hydrocarbons Reduction. Journal of Physical Chemistry C, 2011, 115, 16001-16005.	1.5	14
9833	First-principles study of stability of the bcc and Ï‰ phases of a low Al concentration Nb_{1 â^'x}Al_xalloy. Journal of Physics Condensed Matter, 2011, 23, 295501.	0.7	3
9834	Single substitutional nitrogen defects revealed as electron acceptor states in diamond using ultrafast spectroscopy. Physical Review B, 2011, 84, .	1.1	36
9835	Glycine Adsorption on (101Ì…0) ZnO Surfaces. Journal of Physical Chemistry C, 2011, 115, 6491-6495.	1.5	22
9836	Ab initio investigation on the magnetic ordering in Gd doped ZnO. Journal of Applied Physics, 2011, 109, 083929.	1.1	37
9837	<mml:math xmlns:mml="http://www.w3.org/1998/Math/MathML" display="inline"><mml:mrow><mml:msup><mml:mi>G</mml:mi><mml:mn>0</mml:mn></mml:msup><mml:msup><mml:mi>W</mml:mi><mml:mn>0</mml:mn></mml:msup></mml:mrow></mml:math> gap of ZnO: Effects of plasmon-pole models. Physical Review B, 2011, 84, .	1.1	102
9838	Classification of the critical resolved shear stress in the hexagonal-close-packed materials by atomic simulation: Application to Î±-zirconium and Î±-titanium. Journal of Applied Physics, 2011, 110, .	1.1	67
9839	Family-Dependent Rectification Characteristics in Ultra-Short Graphene Nanoribbon pâ€“n Junctions. Journal of Physical Chemistry C, 2011, 115, 8547-8554.	1.5	28
9841	Hybrid Density Functional Calculations and Molecular Dynamics Study of Lithium Fluorosulphate, A Cathode Material for Lithium-Ion Batteries. Journal of Physical Chemistry C, 2011, 115, 2600-2603.	1.5	26
9842	Wetting of Intact and Partially Dissociated Water Layer on Ru(0001): a Density Functional Study. Journal of Physical Chemistry C, 2011, 115, 5834-5840.	1.5	10
9843	First-principles calculations of lattice dynamics in CdTiO<mml:math xmlns:mml="http://www.w3.org/1998/Math/MathML" display="inline"><mml:msub><mml:mrow /><mml:mn>3</mml:mn></mml:msub></mml:math>and CaTiO<mml:math xmlns:mml="http://www.w3.org/1998/Math/MathML" display="inline"><mml:msub><mml:mrow /><mml:mn>3</mml:mn></mml:msub></mml:math>: Phase stability and ferroelectricity. Physical Review B, 2011, 84, .	1.1	58
9844	Surface Effect and Band-Gap Oscillation of TiO₂ Nanowires and Nanotubes. Journal of Physical Chemistry C, 2011, 115, 13837-13843.	1.5	21
9845	Switching of a substitutional-iron/oxygen-vacancy defect complex in ferroelectric PbTiO<mml:math xmlns:mml="http://www.w3.org/1998/Math/MathML" display="inline"><mml:mrow><mml:msub><mml:mrow /><mml:mrow><mml:mn>3</mml:mn></mml:mrow></mml:msub></mml:mrow></mml:math>from first principles. Physical Review B, 2011, 83, .	1.1	16
9846	On the dissociation of molecular hydrogen by Au supported on transition metal carbides: choice of the most active support. Physical Chemistry Chemical Physics, 2011, 13, 6865.	1.3	31
9847	Temperature-induced martensitic phase transitions in gum-metal approximants: First-principles investigations for Ti<mml:math xmlns:mml="http://www.w3.org/1998/Math/MathML" display="inline"><mml:msub><mml:mrow /><mml:mn>3</mml:mn></mml:msub></mml:math>Nb. Physical Review B, 2011, 84, .	1.1	41
9848	Phase stability of Ti-<mml:math xmlns:mml="http://www.w3.org/1998/Math/MathML" display="inline"><mml:mrow><mml:msub><mml:mrow /><mml:mrow><mml:mn>2</mml:mn></mml:mrow></mml:msub></mml:mrow></mml:math>O<mml:math xmlns:mml="http://www.w3.org/1998/Math/MathML" display="inline"><mml:mrow><mml:msub><mml:mrow /><mml:mrow><mml:mn>5</mml:mn></mml:mrow></mml:msub></mml:mrow></mml:math>polymorphs.	1.1	57

#	Article	IF	Citations
9849	First-principles study of the influence of (110)-oriented strain on the ferroelectric properties of rutile TiO2. Physical Review B, 2011, 84, .	1.1	20
9850	Prediction of Raman spectra with ultrasoft pseudopotentials. Physical Review B, 2011, 84, .	1.1	50
9851	Tin Monoxide: Structural Prediction from First Principles Calculations with van der Waals Corrections. Journal of Physical Chemistry C, 2011, 115, 19916-19924.	1.5	95
9852	Effects of rhenium alloying on adhesion of Mo/HfC and Mo/ZrC interfaces: A first-principles study. Journal of Applied Physics, 2011, 110, .	1.1	14
9853	Defects in SiC for quantum computing. Journal of Applied Physics, 2011, 109, .	1.1	66
9854	Hydrogen interaction with fullerenes: From C<mml:math xmlns:mml="http://www.w3.org/1998/Math/MathML" display="inline"><mml:msub><mml:mrow /><mml:mn>20</mml:mn></mml:msub></mml:math>to graphene. Physical Review B, 2011, 84, .	1.1	24
9855	Diffusion of Al, O, Pt, Hf, and Y atoms on Î±-Al₂O₃(0001): implications for the role of alloying elements in thermal barrier coatings. Journal of Materials Chemistry, 2011, 21, 1447-1456.	6.7	41
9856	Sensitivity of Boron Nitride Nanotubes toward Biomolecules of Different Polarities. Journal of Physical Chemistry Letters, 2011, 2, 2442-2447.	2.1	149
9857	Investigation of the Interface in Silica-Encapsulated Liposomes by Combining Solid State NMR and First Principles Calculations. Journal of the American Chemical Society, 2011, 133, 16815-16827.	6.6	69
9858	The influence of the stacking orientation of C and BN stripes in the structure, energetics, and electronic properties of BC₂N nanotubes. Nanotechnology, 2011, 22, 205706.	1.3	31
9859	Magnetism of Phthalocyanine-Based Organometallic Single Porous Sheet. Journal of the American Chemical Society, 2011, 133, 15113-15119.	6.6	350
9860	Improved visible-light photocatalysis of nano-Bi2Sn2O7 with dispersed s-bands. Journal of Materials Chemistry, 2011, 21, 3872.	6.7	92
9861	Trends in electrical transport of<mml:math xmlns:mml="http://www.w3.org/1998/Math/MathML" display="inline"><mml:mi>p</mml:mi></mml:math>-type skutterudites<mml:math xmlns:mml="http://www.w3.org/1998/Math/MathML" display="inline"><mml:mi>R</mml:mi></mml:math>Fe<mml:math xmlns:mml="http://www.w3.org/1998/Math/MathML" display="inline"><mml:msub><mml:mrow /><mml:mn>4</mml:mn></mml:msub></mml:math>Sb<mml:math xmlns:mml="http://www.w3.org/1998/M	1.1	76
9862	Manganese Triazacyclononane Oxidation Catalysts Grafted under Reaction Conditions on Solid Cocatalytic Supports. Journal of the American Chemical Society, 2011, 133, 18684-18695.	6.6	44
9863	Hydrothermal Carbon from Biomass: Structural Differences between Hydrothermal and Pyrolyzed Carbons via ¹³C Solid State NMR. Langmuir, 2011, 27, 14460-14471.	1.6	248
9864	First-principles study of misfit strain-stabilized ferroelectric SnTiO<mml:math xmlns:mml="http://www.w3.org/1998/Math/MathML" display="inline"><mml:msub><mml:mrow /><mml:mn>3</mml:mn></mml:msub></mml:math>. Physical Review B, 2011, 84, .	1.1	49
9865	Ethanol photo-oxidation on a rutile TiO2(110) single crystal surface. Physical Chemistry Chemical Physics, 2011, 13, 7637.	1.3	58
9867	First-principles calculation of the AlAs/GaAs interface band structure using a self-energyâ€“corrected local density approximation. Europhysics Letters, 2011, 94, 27001.	0.7	28

#	Article	IF	Citations
9868	Silver residues as a possible key to a remarkable oxidative catalytic activity of nanoporous gold. Physical Chemistry Chemical Physics, 2011, 13, 4529.	1.3	121
9869	High-Pressure Study of Lithium Azide from Density-Functional Calculations. Journal of Physical Chemistry A, 2011, 115, 4521-4529.	1.1	32
9870	DFT Studies on the Interaction of Defective Graphene-Supported Fe and Al Nanoparticles. Journal of Physical Chemistry C, 2011, 115, 8961-8970.	1.5	175
9871	Carbon Nanotube Superarchitectures: An Ab Initio Study. Journal of Physical Chemistry C, 2011, 115, 18174-18185.	1.5	25
9872	Thermodynamic modelling of nanomorphologies of hematite and goethite. Journal of Materials Chemistry, 2011, 21, 11566.	6.7	114
9873	Fe-free ferroelectrics investigated with density functional theory: SnAl<mml:math xmlns:mml="http://www.w3.org/1998/Math/MathML" display="inline"><mml:mrow><mml:msub><mml:mrow /><mml:mrow><mml:mn>1</mml:mn><mml:mo>/</mml:mo><mml:mn>2</mml:mn></mml:mrow></mml:msub></mml:mrow></mml:math>In<mml:math xmlns:mml="http://www.w3.org/1998/Math/MathML" display="inline"><mml:mrow><mml:msub><mml:mrow /><mml:mrow><mml:mn>1</mml:mn><mml:mo>/</mml:mo><mml:mn>2</mml:mn></mml:mrow></mml:msub></mml:mrow></mml:math>	1.1	19
9874	Influence of Oxygen Vacancy on Electronic and Magnetic Properties in Cr Doped SnO2 Superlattice. Journal of the Physical Society of Japan, 2011, 80, 124709.	0.7	1
9875	Energy gaps in nitrogen delta-doping graphene: A first-principles study. Applied Physics Letters, 2011, 99, 012107.	1.5	25
9876	Enhanced Hydrogen Storage on Li Functionalized BC₃ Nanotube. Journal of Physical Chemistry C, 2011, 115, 6136-6140.	1.5	38
9877	Water clusters on Cu(110): Chain versus cyclic structures. Journal of Chemical Physics, 2011, 134, 024703.	1.2	36
9878	Structural and magnetic properties of CaFe<mml:math xmlns:mml="http://www.w3.org/1998/Math/MathML" display="inline"><mml:mrow><mml:msub><mml:mrow /><mml:mrow><mml:mn>2</mml:mn></mml:mrow></mml:msub></mml:mrow></mml:math>As<mml:math xmlns:mml="http://www.w3.org/1998/Math/MathML" display="inline"><mml:mrow><mml:msub><mml:mrow /><mml:mrow><mml:mn>2</mml:mn></mml:mrow></mml:msub></mml:mrow></mml:math>	1.1	44
9879	The d-Band Structure of Pt Nanoclusters Correlated with the Catalytic Activity for an Oxygen Reduction Reaction. Journal of Physical Chemistry C, 2011, 115, 21236-21240.	1.5	129
9880	Electronic and Structural Properties of WO₃: A Systematic Hybrid DFT Study. Journal of Physical Chemistry C, 2011, 115, 8345-8353.	1.5	250
9881	Ab initiostudy of edge smoothing, atom attraction, and downward funneling in Ag/Ag(100). Physical Review B, 2011, 83, .	1.1	7
9882	Universal Phase Transitions of B1-Structured Stoichiometric Transition Metal Carbides. Inorganic Chemistry, 2011, 50, 9266-9272.	1.9	11
9883	Interfacial interactions between local defects in amorphous SiO<mml:math xmlns:mml="http://www.w3.org/1998/Math/MathML" display="inline"><mml:msub><mml:mrow /><mml:mrow><mml:mn>2</mml:mn></mml:mrow></mml:msub></mml:math>and supported graphene. Physical Review B, 2011, 84, .	1.1	38
9884	Evaluating the C, N, and F Pairwise Codoping Effect on the Enhanced Photoactivity of ZnWO4: The Charge Compensation Mechanism in Donorâ€“Acceptor Pairs. Journal of Physical Chemistry C, 2011, 115, 15516-15524.	1.5	20
9885	Polytypism of GaAs, InP, InAs, and InSb: Anab initiostudy. Physical Review B, 2011, 84, .	1.1	47

#	Article	IF	Citations
9886	Improving the Carbon Resistance of Ni-Based Steam Reforming Catalyst by Alloying with Rh: A Computational Study Coupled with Reforming Experiments and EXAFS Characterization. ACS Catalysis, 2011, 1, 574-582.	5.5	67
9887	Stability of boron nitride bilayers: Ground-state energies, interlayer distances, and tight-binding description. Physical Review B, 2011, 83, .	1.1	151
9888	Second-order piezoelectricity in wurtzite III-N semiconductors. Physical Review B, 2011, 84, .	1.1	88
9889	Multiple Dirac particles in AA-stacked graphite and multilayers of graphene. Physical Review B, 2011, 83, .	1.1	75
9890	Chemical Pressure and Rare-Earth Orbital Contributions in Mixed Rare-Earth Silicides La_{5â€“x}Y_xSi₄ (0 â‰¤ x â‰¤ 5). Inorganic Chemistry, 2011, 50, 12714-12723.	1.9	14
9891	Investigation of Counterion Influence on an Octahedral IrH6-Complex in the Solid State Hydrides AAeIrH6(A = Na, K and Ae = Ca, Sr, Ba, and Eu) with a New Structure Type. Inorganic Chemistry, 2011, 50, 11890-11895.	1.9	8
9892	RbCN₃H₄: The First Structurally Characterized Salt of a New Class of Guanidinate Compounds. Inorganic Chemistry, 2011, 50, 3799-3803.	1.9	28
9893	Energy-Level Alignment in 4â€²-Substituted Stilbene-4-thiolate Self-Assembled Monolayers on Gold. Journal of Physical Chemistry C, 2011, 115, 7487-7495.	1.5	4
9894	Structural, elastic, and thermal properties of Laves phase ZrV2 under pressure. Journal of Applied Physics, 2011, 109, .	1.1	59
9895	Noncovalent Interactions in Paired DNA Nucleobases Investigated by Terahertz Spectroscopy and Solid-State Density Functional Theory. Journal of Physical Chemistry A, 2011, 115, 9467-9478.	1.1	49
9896	Boron-Silicon complex defects in GaAs: An ab initio study. Journal of Applied Physics, 2011, 109, .	1.1	9
9897	Half-Metallicity in Hybrid Graphene/Boron Nitride Nanoribbons with Dihydrogenated Edges. Journal of Physical Chemistry C, 2011, 115, 9442-9450.	1.5	96
9898	Elastic properties of edges in BN and SiC nanoribbons and of boundaries in C-BN superlattices: A density functional theory study. Physical Review B, 2011, 83, .	1.1	39
9899	Boron and nitrogen impurities in SiC nanoribbons: anab initioinvestigation. Journal of Physics Condensed Matter, 2011, 23, 205504.	0.7	22
9900	Ab initiostudy of electron paramagnetic resonance hyperfine structure of the silicon dangling bond: Role of the local environment. Physical Review B, 2011, 83, .	1.1	7
9901	Enhanced Oxygen Reduction Activity of Platinum Monolayer on Gold Nanoparticles. Journal of Physical Chemistry Letters, 2011, 2, 67-72.	2.1	80
9902	Enantioselective Hydrogenation of Î±-Ketoesters: An in Situ Surface-Enhanced Raman Spectroscopy (SERS) Study. Journal of Physical Chemistry C, 2011, 115, 21363-21372.	1.5	9
9903	Direct correlation of crystal structure and optical properties in wurtzite/zinc-blende GaAs nanowire heterostructures. Physical Review B, 2011, 83, .	1.1	193

#	Article	IF	Citations
9904	Positive Vibrational Entropy of Chemical Ordering in FeV. Physical Review Letters, 2011, 107, 115501.	2.9	35
9905	Collectively Induced Quantum-Confined Stark Effect in Monolayers of Molecules Consisting of Polar Repeating Units. Journal of the American Chemical Society, 2011, 133, 18634-18645.	6.6	33
9906	Defect-induced magnetism in undoped wide band gap oxides: Zinc vacancies in ZnO as an example. AIP Advances, 2011, 1, .	0.6	179
9907	First-principles investigation of electronic, vibrational, elastic, and structural properties of ThN and UN up to 100 GPa. Physical Review B, 2011, 84, .	1.1	46
9908	A first-principles study of C+O reaction on NiCo(111) surface. Applied Surface Science, 2011, 257, 9455-9460.	3.1	15
9909	Energy barriers for trimethylaluminum reaction with varying surface hydroxyl density. Applied Surface Science, 2011, 258, 225-229.	3.1	28
9910	Lithium and antimony adsorbed on graphene studied by first-principles calculations. Applied Surface Science, 2011, 258, 800-805.	3.1	9
9911	Diffusion of Li+ ion on graphene: A DFT study. Applied Surface Science, 2011, 258, 1651-1655.	3.1	111
9912	Theoretical studies of arsenite adsorption and its oxidation mechanism on a perfect TiO2 anatase (101) surface. Applied Surface Science, 2011, 258, 1192-1198.	3.1	31
9913	Quantifying adhesion energy of mechanical coatings at atomistic scale. Applied Surface Science, 2011, 258, 1451-1455.	3.1	9
9914	The location of atomic hydrogen in NiTi alloy: A first principles study. Computational Materials Science, 2011, 50, 820-823.	1.4	19
9915	Electronic properties of the Mg2Si thermoelectric material investigated by linear-response density-functional theory. Computational Materials Science, 2011, 50, 847-851.	1.4	46
9916	Ab initio investigation of Al/Mo2B interfacial adhesion. Computational Materials Science, 2011, 50, 880-885.	1.4	40
9917	Theoretical study on the electronic properties and stabilities of low-index surfaces of WC polymorphs. Computational Materials Science, 2011, 50, 939-948.	1.4	55
9918	First-principles study of the electronic, optical and bonding properties in dolomite. Computational Materials Science, 2011, 50, 1037-1042.	1.4	31
9919	Structural and lattice dynamical properties of Zintl NaIn and NaTl compounds. Computational Materials Science, 2011, 50, 1070-1076.	1.4	25
9920	Efficient supercell design for surface and interface calculations of hexagonal phases: Î±-Al2O3 case study. Computational Materials Science, 2011, 50, 1197-1201.	1.4	33
9921	Electronic structure and surface properties of cubic perovskite oxide BaMnO3. Computational Materials Science, 2011, 50, 1212-1216.	1.4	15

#	Article	IF	Citations
9922	Superconducting ultraincompressible hard cubic Re4C. Computational Materials Science, 2011, 50, 1592-1596.	1.4	13
9923	First-principles studies of typical long-period superstructures Al5Ti3, h-Al2Ti and r-Al2Ti in Al-rich TiAl alloys. Computational Materials Science, 2011, 50, 1467-1476.	1.4	28
9924	Theoretical investigation on the transition-metal borides with Ta3B4-type structure: A class of hard and refractory materials. Computational Materials Science, 2011, 50, 1559-1566.	1.4	169
9925	First-principles investigations on structural, elastic and electronic properties of SnO2 under pressure. Computational Materials Science, 2011, 50, 1571-1577.	1.4	42
9926	Magnetism in non-transition-metal doped CdS studied by density functional theory. Computational Materials Science, 2011, 50, 1661-1666.	1.4	41
9927	Ab initio calculation of vibrational and thermodynamic properties of SrX (S, Se, Te) in the B1 (NaCl) and B2 (CsCl) structures. Computational Materials Science, 2011, 50, 1701-1710.	1.4	36
9928	Functionalization of low-dimensional honeycomb germanium with 3d transition-metal atoms. Computational Materials Science, 2011, 50, 1717-1724.	1.4	10
9929	Ab-initio electronic structure, optical, dielectric and bonding properties of lizardite-1T. Computational Materials Science, 2011, 50, 1725-1730.	1.4	15
9930	Oxygen-vacancy formation in LaMO3 (M= Ti, V, Cr, Mn, Fe, Co, Ni) calculated at both GGA and GGA +U levels. Computational Materials Science, 2011, 50, 1800-1805.	1.4	31
9931	Elastic properties and lattice dynamics of alkali chalcogenide compounds Na2S, Na2Se and Na2Te. Computational Materials Science, 2011, 50, 1806-1810.	1.4	17
9932	Full-potential study of structural and electronic properties of MB2-type metal diborides (M= Be, Mg) Tj ETQq0 0 0 rgBT /Overlock 10 Tf 5	1.4	5
9933	Ab initio study of structural, elastic and vibrational properties of praseodymium chalcogenides. Computational Materials Science, 2011, 50, 1958-1964.	1.4	5
9934	First-principles calculations of the structural and elastic properties of OsSi2 at high pressure. Computational Materials Science, 2011, 50, 2009-2013.	1.4	8
9935	Atomic diffusion in the Fe [001] â˜=5 (310) and (210) symmetric tilt grain boundary. Computational Materials Science, 2011, 50, 2087-2095.	1.4	4
9936	Ferromagnetic properties, electronic structures, and formation energies of Zn vacancy monodoping and (Zn vacancy, Li) codoped ZnO by first principles study. Computational Materials Science, 2011, 50, 2157-2161.	1.4	14
9937	A high-throughput infrastructure for density functional theory calculations. Computational Materials Science, 2011, 50, 2295-2310.	1.4	787
9938	Adsorption and penetration of hydrogen in W: A first principles study. Computational Materials Science, 2011, 50, 2291-2294.	1.4	29
9939	High-pressure structural and electronic behaviors of superhard BC5: Density functional calculations. Computational Materials Science, 2011, 50, 2249-2252.	1.4	3

#	Article	IF	Citations
9940	Dependence of pressure on elastic, electronic and optical properties of CeO2 and ThO2: A first principles study. Computational Materials Science, 2011, 50, 2280-2286.	1.4	36
9941	Potassium influence in the adsorption of hydrogen on graphene: A density functional theory study. Computational Materials Science, 2011, 50, 2427-2432.	1.4	28
9942	Atomic oxygen adsorption on the silicon-doped hafnium carbide (001) surface from first principles. Computational Materials Science, 2011, 50, 2530-2534.	1.4	8
9943	B3LYP investigation of response properties of alkali halides on external static electric fields. Computational Materials Science, 2011, 50, 2628-2635.	1.4	6
9944	FP-LAPW study of the structural, elastic and thermodynamic properties of spinel oxides ZnX2O4 (X=Al,) Tj ETQq0 0 0 rgBT /Overlock 10	1.4	21
9945	Study of the hydrostatic pressure on orthorhombic IVâ€“VI compounds including many-body effects. Computational Materials Science, 2011, 50, 2872-2879.	1.4	40
9946	Sign-changeable spin-filter efficiency and giant magnetoresistance in seamless graphene nanoribbon junctions. Computational Materials Science, 2011, 50, 2886-2890.	1.4	6
9947	Ab initio study of AlCu2M (M=Sc, Ti and Cr) ternary compounds under pressures. Computational Materials Science, 2011, 50, 2930-2937.	1.4	21
9948	Dehydrogenation properties of epitaxial (100) MgH2/TiH2 multilayers â€“ A DFT study. Computational Materials Science, 2011, 50, 2960-2966.	1.4	13
9949	Electronic and optical properties of ultrathin single walled boron nanotubes â€“ An ab initio study. Computational Materials Science, 2011, 50, 3038-3042.	1.4	18
9950	First-principles calculations of mechanical and thermodynamic properties of YAlO3. Computational Materials Science, 2011, 50, 3056-3062.	1.4	38
9951	Ab initio calculations of the hydroxyl impurities in BaF2. Computational Materials Science, 2011, 50, 3101-3104.	1.4	3
9952	First-principles investigation on metal tantalum under conditions of electronic excitation. Computational Materials Science, 2011, 50, 3110-3113.	1.4	6
9953	First-principle study of the effects of Nb and Ti doping on the dehydrogenation properties of Ca(BH4)2. Computational Materials Science, 2011, 50, 3114-3118.	1.4	3
9954	Structural stabilities, elastic and thermodynamic properties of Scandium Chalcogenides via first-principles calculations. Computational Materials Science, 2011, 50, 3123-3130.	1.4	61
9955	Stacking faults in B2-structured magnesium alloys from first principles calculations. Computational Materials Science, 2011, 50, 3198-3207.	1.4	11
9956	The structural and mechanical properties of CdN compound: A first principles study. Computational Materials Science, 2011, 50, 3208-3212.	1.4	31
9957	Interaction of C with vacancy in W: A first-principles study. Computational Materials Science, 2011, 50, 3213-3217.	1.4	39

#	Article	IF	Citations
9958	First-principles study of ground state properties of ZrH2. Computational Materials Science, 2011, 50, 3297-3302.	1.4	56
9959	Structural, electronic, elastic and thermodynamic properties of AlSi2RE (RE=La, Ce, Pr and Nd) from first-principle calculations. Computational Materials Science, 2011, 50, 3303-3310.	1.4	11
9960	Adsorption and dissociation of N2O molecule on Fe(1 1 1) surface: A DFT study. Computational Materials Science, 2011, 50, 3311-3314.	1.4	16
9961	Surface effects on stacking fault and twin formation in fcc nanofilms: A first-principles study. Computational Materials Science, 2011, 50, 3342-3345.	1.4	20
9962	Structural and electronic properties of a single C chain doped zigzag AlN nanoribbon. Computational and Theoretical Chemistry, 2011, 974, 151-158.	1.1	14
9963	The stability and electronic structures of B or/and N doped SiC nanotubes: A first-principles study. Computational and Theoretical Chemistry, 2011, 977, 92-96.	1.1	28
9964	Ab initio study of structural, bonding, and vibrational properties of AGaO2 (A=Ag,Cu) delafossites. Computational and Theoretical Chemistry, 2011, 977, 78-85.	1.1	14
9965	DFT study of the interactions of 2-chlorophenol/2-chlorophenoxy radical with the (6,0) single-walled ZnO nanotubes with and without an oxygen vacancy. Computational and Theoretical Chemistry, 2011, 978, 98-103.	1.1	11
9966	Adsorption of hydrogen, chlorine, and sulfur atoms on Î±-Cr2O3(0 0 0 1) surfaces: A density functional theory investigation. Corrosion Science, 2011, 53, 3612-3622.	3.0	17
9967	Uranyl adsorption at (010) edge surfaces of kaolinite: A density functional study. Geochimica Et Cosmochimica Acta, 2011, 75, 706-718.	1.6	64
9968	First-principles calculations and thermodynamic modeling of the Alâ€“Pt binary system. Calphad: Computer Coupling of Phase Diagrams and Thermochemistry, 2011, 35, 20-29.	0.7	41
9969	Structural stability of intermetallic phases in the Gaâ€“Ti system. Calphad: Computer Coupling of Phase Diagrams and Thermochemistry, 2011, 35, 133-141.	0.7	7
9970	Structural and thermal properties of calcium using an MEAM potential. Calphad: Computer Coupling of Phase Diagrams and Thermochemistry, 2011, 35, 262-268.	0.7	6
9971	Structure, elastic and thermodynamic properties of the Niâ€“P system from first-principles calculations. Calphad: Computer Coupling of Phase Diagrams and Thermochemistry, 2011, 35, 284-291.	0.7	25
9972	Electronic properties of Zn1â^'xCdxSb solid solution investigated by density-functional theory. Calphad: Computer Coupling of Phase Diagrams and Thermochemistry, 2011, 35, 639-642.	0.7	0
9973	Thermodynamic modeling of fcc order/disorder transformations in the Coâ€“Pt system. Calphad: Computer Coupling of Phase Diagrams and Thermochemistry, 2011, 35, 323-330.	0.7	25
9974	Structural stability of the <mml:math xmlns:mml="http://www.w3.org/1998/Math/MathML" altimg="si103.gif" display="inline" overflow="scroll"><mml:mi>D</mml:mi><mml:msub><mml:mrow><mml:mn>8</mml:mn></mml:mrow><mml:mrow><mml:mi>m</mml:mi></mml:mrow></mml:msub></mml:math> Ti5Sn2Si compound. Calphad: Computer Coupling of Phase Diagrams and Thermochemistry, 2011, 35, 643-647.	0.7	4
9975	Thermodynamic assessment of the Feâ€“Mnâ€“C system. Calphad: Computer Coupling of Phase Diagrams and Thermochemistry, 2011, 35, 479-491.	0.7	86

#	Article	IF	Citations
9976	Thermodynamic description of the Alâ€“Cuâ€“Y ternary system. Calphad: Computer Coupling of Phase Diagrams and Thermochemistry, 2011, 35, 574-579.	0.7	28
9977	First-principles calculations of binary Al compounds: Enthalpies of formation and elastic properties. Calphad: Computer Coupling of Phase Diagrams and Thermochemistry, 2011, 35, 562-573.	0.7	81
9978	Structural and electronic properties of ZnO nanowires: a theoretical study. Energy Procedia, 2011, 10, 128-137.	1.8	27
9979	T-Carbon: A Novel Carbon Allotrope. Physical Review Letters, 2011, 106, 155703.	2.9	421
9980	Band-gap engineering for removing shallow traps in rare-earth Lu<mml:math xmlns:mml="http://www.w3.org/1998/Math/MathML" display="inline"><mml:msub><mml:mrow /><mml:mn>3</mml:mn></mml:msub></mml:math>Al<mml:math xmlns:mml="http://www.w3.org/1998/Math/MathML" display="inline"><mml:msub><mml:mrow /><mml:mn>5</mml:mn></mml:msub></mml:math>O<mml:math xmlns:mml="http://www.w3.org/1998/Math/MathML" display="inline"><mml:msub><mml:mrow /><mml:	1.1	288
9981	Crystal Orbital Hamilton Population (COHP) Analysis As Projected from Plane-Wave Basis Sets. Journal of Physical Chemistry A, 2011, 115, 5461-5466.	1.1	1,823
9982	Hydrogen electrocatalysis on overlayers of rhodium over gold and palladium substratesâ€”more active than platinum?. Physical Chemistry Chemical Physics, 2011, 13, 16437.	1.3	29
9983	Factors in the Metal Doping of BiVO₄ for Improved Photoelectrocatalytic Activity as Studied by Scanning Electrochemical Microscopy and First-Principles Density-Functional Calculation. Journal of Physical Chemistry C, 2011, 115, 17870-17879.	1.5	409
9984	Tailoring the electronic structure of TiO<mml:math xmlns:mml="http://www.w3.org/1998/Math/MathML" display="inline"><mml:mrow><mml:msub><mml:mrow /><mml:mn>2</mml:mn></mml:msub></mml:mrow></mml:math>by cation [illegible] Physical Review B, 2011, 83, .	1.1	52
9985	display="inline"><mml:mrow><mml:msub><mml:mrow /><mml:mn>2</mml:mn></mml:msub></mml:mrow></mml:math>calculated by the HSE06 hybrid functional: Dopant passivation by carrier self-trapping. Physical Review B, 2011, 83, .	1.1	176
9986	Calculation of carrier-concentration-dependent effective mass in Nb-doped anatase crystals of TiO2. Physical Review B, 2011, 83, .	1.1	45
9987	First-principles electronic structure and relative stability of pyrite and marcasite: Implications for photovoltaic performance. Physical Review B, 2011, 83, .	1.1	122
9988	Optical gap and native point defects in kaolinite studied by the GGA-PBE, HSE functional, and GW approaches. Physical Review B, 2011, 84, .	1.1	40
9989	Metallization in hydrogen-helium mixtures. Physical Review B, 2011, 84, .	1.1	78
9990	Modeling Thermal Decomposition Mechanisms in Gaseous and Crystalline Molecular Materials: Application to Î²-HMX. Journal of Physical Chemistry B, 2011, 115, 12677-12686.	1.2	66
9991	Applications of quantum Monte Carlo methods in condensed systems. Reports on Progress in Physics, 2011, 74, 026502.	8.1	169
9992	Universal transition state scaling relations for (de)hydrogenation over transition metals. Physical Chemistry Chemical Physics, 2011, 13, 20760.	1.3	363
9993	High-spin states of cation vacancies in GaP, GaN, AlN, BN, ZnO, and BeO: A first-principles study. Physical Review B, 2011, 83, .	1.1	41

#	Article	IF	Citations
9994	First-principles investigations of electronic and magnetic properties of SrTiO3(001) surfaces with adsorbed ethanol and acetone molecules. Physical Review B, 2011, 83, .	1.1	18
9995	Role of the Support Effects on the Catalytic Activity of Gold Clusters: A Density Functional Theory Study. Catalysts, 2011, 1, 18-39.	1.6	38
9996	DFT Studies of the Interactions of a Graphene Layer with Small Water Aggregates. Journal of Physical Chemistry A, 2011, 115, 12348-12356.	1.1	73
9997	Phase stability of intermetallic PtIn2 under pressure: An in-situ transport, structural and first principles investigations. Journal of Applied Physics, 2011, 109, 083531.	1.1	4
9998	Electron Densities and Related Properties from the ab-initio Simulation of Crystalline Solids. , 2011, , 79-132.		3
9999	Stability of intermediates in the glycerol hydrogenolysis on transition metal catalysts from first principles. Physical Chemistry Chemical Physics, 2011, 13, 1448-1456.	1.3	72
10000	First-principles density functional theory study of native point defects in Bi<mml:math xmlns:mml="http://www.w3.org/1998/Math/MathML" display="inline"><mml:msub><mml:mrow /><mml:mn>2</mml:mn></mml:msub></mml:math>Te<mml:math xmlns:mml="http://www.w3.org/1998/Math/MathML" display="inline"><mml:msub><mml:mrow /><mml:mn>3</mml:mn></mml:msub></mml:math>. Physical Review B, 2011, 84, .	1.1	130
10001	High-pressure crystal structure prediction of calcium borohydride using density functional theory. Physical Review B, 2011, 83, .	1.1	20
10002	A multifaceted approach to hydrogen storage. Physical Chemistry Chemical Physics, 2011, 13, 16955.	1.3	64
10003	Lifetime distribution of spontaneous emission from emitter(s) in three-dimensional woodpile photonic crystals. Optics Express, 2011, 19, 11623.	1.7	8
10004	Engineering a Robust Quantum Spin Hall State in Graphene via Adatom Deposition. Physical Review X, 2011, 1, .	2.8	284
10005	DFT studies of hydrogen storage properties of Mg0.75Ti0.25. Journal of Alloys and Compounds, 2011, 509, 210-216.	2.8	20
10006	Crystal structure of the mirror symmetry 10H-type long-period stacking order phase in Mgâ€“Yâ€“Zn alloy. Journal of Alloys and Compounds, 2011, 509, 669-674.	2.8	24
10007	Aerosol synthesis and Rietveld analysis of tetragonal (Î²1) PdZn. Journal of Alloys and Compounds, 2011, 509, 1463-1470.	2.8	19
10008	Ab initio lattice dynamics of CoH and NiH. Journal of Alloys and Compounds, 2011, 509, S857-S859.	2.8	6
10009	Hydrogen atom adsorption on aluminum icosahedral clusters: A DFT study. Journal of Alloys and Compounds, 2011, 509, S675-S678.	2.8	5
10010	Structural, electronic, optical and thermodynamic properties of SrxCa1â^'xO, BaxSr1â^'xO and BaxCa1â^'xO alloys. Journal of Alloys and Compounds, 2011, 509, 1440-1447.	2.8	34
10011	Structural, elastic and electronic properties of Mg(Cu1â^'xZnx)2 alloys calculated by first-principles. Journal of Alloys and Compounds, 2011, 509, 2885-2890.	2.8	22

#	Article	IF	Citations
10012	Thermodynamic optimization of the Cuâ€“Nd system. Journal of Alloys and Compounds, 2011, 509, 2679-2683.	2.8	20
10013	Ab initio study of the structural, thermodynamic and electronic properties of the Cu10In7 intermetallic phase. Journal of Alloys and Compounds, 2011, 509, 3238-3245.	2.8	29
10014	Chemical trends of the band gaps of idealized crystal of semiconducting silicon clathrates, M8Si38A8 (M = Na, K, Rb, Cs; A = Ga, Al, In), predicted by first-principle pseudopotential calculations. Journal of Alloys and Compounds, 2011, 509, 3924-3930.	2.8	20
10015	Theoretical study of structural, electronic, lattice dynamical and dielectric properties of SrAl2O4. Journal of Alloys and Compounds, 2011, 509, 4300-4303.	2.8	17
10016	Thermodynamic assessment of Auâ€“La and Auâ€“Er binary systems. Journal of Alloys and Compounds, 2011, 509, 4439-4444.	2.8	9
10017	First-principles study of the ferroelectric and optical properties of BaTeMo2O9. Journal of Alloys and Compounds, 2011, 509, 4929-4934.	2.8	9
10018	The electronic, mechanical properties and theoretical hardness of chromium carbides by first-principles calculations. Journal of Alloys and Compounds, 2011, 509, 5242-5249.	2.8	233
10019	Theoretical study on the electronic and optical properties of (N, Fe)-codoped anatase TiO2 photocatalyst. Journal of Alloys and Compounds, 2011, 509, 6067-6071.	2.8	83
10020	Structural stability, electronic and optical properties of Ni-doped 3Câ€“SiC by first principles calculation. Journal of Alloys and Compounds, 2011, 509, 6117-6122.	2.8	46
10021	Investigating behaviors of H in a W single crystal by first-principles: From solubility to interaction with vacancy. Journal of Alloys and Compounds, 2011, 509, 8277-8282.	2.8	42
10022	Phase stability of magnesium-rare earth binary systems from first-principles calculations. Journal of Alloys and Compounds, 2011, 509, 6899-6907.	2.8	59
10023	Energetics of compounds related to Mg2Si as an anode material for lithium-ion batteries using first principle calculations. Journal of Alloys and Compounds, 2011, 509, 7877-7880.	2.8	12
10024	Electronic structure of antiferromagnetic PbCrO3 (001) surfaces. Journal of Alloys and Compounds, 2011, 509, 9284-9288.	2.8	5
10025	First-principles study on the electronic and optical properties of F- and Nb-doped anatase TiO2. Journal of Alloys and Compounds, 2011, 509, 9178-9182.	2.8	36
10026	Hydrogen solution in tetrahedral or octahedral interstitial sites in Al. Journal of Alloys and Compounds, 2011, 509, 9214-9217.	2.8	11
10027	Thermodynamic functions from lattice dynamic of KMgH3 for hydrogen storage applications. Journal of Alloys and Compounds, 2011, 509, 8994-8998.	2.8	12
10028	Density functional study of the structural, electronic, elastic and thermodynamic properties of ACRu3 (AÂ=ÂV, Nb and Ta) compounds. Intermetallics, 2011, 19, 476-485.	1.8	24
10029	Ab initio study of phase transformations in transition-metal disilicides. Intermetallics, 2011, 19, 919-926.	1.8	17

#	Article	IF	Citations
10030	Energetic evaluation of possible insertion sites of Cu into BaSi2 using first principle calculations. Intermetallics, 2011, 19, 1102-1106.	1.8	16
10031	Diffusion mechanisms of vacancy and doped Si in Al3Ti from first-principles calculations. Intermetallics, 2011, 19, 1036-1040.	1.8	15
10032	First-principle study on structural, elastic and electronic properties of rare-earth intermetallic compounds: TbCu and TbZn. Intermetallics, 2011, 19, 1359-1366.	1.8	13
10033	Electronic structure and transport properties of SrAl2Si2: Effect of yttrium substitution. Intermetallics, 2011, 19, 1448-1454.	1.8	10
10034	Electronic and dynamical properties of NiAl studied from first principles. Intermetallics, 2011, 19, 1959-1967.	1.8	62
10035	First-principles phonon calculations of thermodynamic properties for ductile rare-earth intermetallic compounds. Intermetallics, 2011, 19, 1599-1604.	1.8	17
10036	Density functional theory study of TiO<mml:math xmlns:mml="http://www.w3.org/1998/Math/MathML" display="inline"><mml:mrow><mml:msub><mml:mrow /><mml:mrow><mml:mn>2</mml:mn></mml:mrow></mml:msub></mml:mrow></mml:math>/Ag interfaces and their role in memristor devices. Physical Review B, 2011, 83, .	1.1	43
10037	<mml:math xmlns:mml="http://www.w3.org/1998/Math/MathML" display="inline"><mml:mrow><mml:mo>+</mml:mo></mml:mrow></mml:math><mml:math xmlns:mml="http://www.w3.org/1998/Math/MathML" display="inline"><mml:mrow><mml:mi>U</mml:mi></mml:mrow></mml:math>calculations. Physical Review B, 2011, 84, .	1.1	853
10038	Intralayer magnetic ordering in Ge/Mn digital alloys. Physical Review B, 2011, 83, .	1.1	7
10039	Phonons of the anomalous element cerium. Proceedings of the National Academy of Sciences of the United States of America, 2011, 108, 9342-9345.	3.3	47
10040	Surface structure determination of Pd on W(100) using X-ray photoelectron diffraction. Surface Science, 2011, 605, 1900-1905.	0.8	0
10041	Ammonia decomposition activity on monolayer Ni supported on Ru, Pt and WC substrates. Surface Science, 2011, 605, 2055-2060.	0.8	22
10042	D-Ï€-A organic dyes with carbazole as donor for dye-sensitized solar cells. Synthetic Metals, 2011, 161, 96-105.	2.1	100
10043	Elasticity of subducted basaltic crust at the lower mantle pressures: Insights on the nature of deep mantle heterogeneity. Physics of the Earth and Planetary Interiors, 2011, 188, 142-149.	0.7	63
10044	Structural and elastic properties of CaGeO3 perovskite at high pressures. Physics of the Earth and Planetary Interiors, 2011, 189, 151-156.	0.7	15
10045	Microstructure of 18R-type long period ordered structure phase in Mg97Y2Zn1 alloy. Transactions of Nonferrous Metals Society of China, 2011, 21, 801-806.	1.7	11
10046	A first-principle calculation of structural, mechanical and electronic properties of titanium borides. Transactions of Nonferrous Metals Society of China, 2011, 21, 1627-1633.	1.7	48
10047	Density functional theory study of influence of impurity on electronic properties and reactivity of pyrite. Transactions of Nonferrous Metals Society of China, 2011, 21, 1887-1895.	1.7	53

#	Article	IF	Citations
10048	First-principles study of phase stability and electronic properties of RhZr. Transactions of Nonferrous Metals Society of China, 2011, 21, 2301-2305.	1.7	4
10049	A first-principles study on electronic structure and elastic properties of Al4Sr, Mg2Sr and Mg23Sr6 phases. Transactions of Nonferrous Metals Society of China, 2011, 21, 2677-2683.	1.7	10
10050	Hybrid Graphene/Titania Nanocomposite: Interface Charge Transfer, Hole Doping, and Sensitization for Visible Light Response. Journal of Physical Chemistry Letters, 2011, 2, 894-899.	2.1	252
10051	First-principles investigation on optical properties of GaN and InGaN alloys. Journal Physics D: Applied Physics, 2011, 44, 495304.	1.3	17
10052	The origin of p-type conduction in Li-N codoped ZnO: An ab initio calculation study. Journal of Applied Physics, 2011, 110, 013711.	1.1	20
10053	Simulations of the Quartz(101Ì...1)/Water Interface: A Comparison of Classical Force Fields, Ab Initio Molecular Dynamics, and X-ray Reflectivity Experiments. Journal of Physical Chemistry C, 2011, 115, 2076-2088.	1.5	183
10054	Periodic Density Functional Theory Study of Water Adsorption on the Î±-Quartz (101) Surface. Journal of Physical Chemistry C, 2011, 115, 5756-5766.	1.5	73
10055	Atomic structure of Ag(111) saturated with chlorine: Formation of Ag3Cl7clusters. Physical Review B, 2011, 84, .	1.1	10
10056	Hexagonal TiO₂ for Photoelectrochemical Applications. Journal of Physical Chemistry C, 2011, 115, 18042-18045.	1.5	17
10057	Spontaneous polarization and band gap bowing in YxAlyGa1-x-yN alloys lattice-matched to GaN. Journal of Applied Physics, 2011, 110, 074114.	1.1	9
10058	Theoretical Study of the Interstitial Oxygen Atom in Anatase and Rutile TiO₂: Electron Trapping and Elongation of the r(Oâ^'O) Bond. Journal of Physical Chemistry C, 2011, 115, 8265-8273.	1.5	44
10059	Interaction between water and defective silica surfaces. Journal of Chemical Physics, 2011, 134, 114703.	1.2	20
10060	Computational Investigation of CO Adsorption and Oxidation on Iron-Modified Cerium Oxide. Journal of Physical Chemistry C, 2011, 115, 14745-14753.	1.5	63
10061	Fabrication and enhanced visible-light photocatalytic activity of carbon self-doped TiO₂sheets with exposed {001} facets. Journal of Materials Chemistry, 2011, 21, 1049-1057.	6.7	390
10062	Phonon calculations in cubic and tetragonal phases of SrTiO<mml:math xmlns:mml="http://www.w3.org/1998/Math/MathML" display="inline"><mml:mrow><mml:msub><mml:mrow /><mml:mrow><mml:mn>3</mml:mn></mml:mrow></mml:msub></mml:mrow></mml:math>: A comparative LCAO and plane-wave study. Physical Review B, 2011, 83, .	1.1	81
10063	DFT-Based Study on Oxygen Adsorption on Defective Graphene-Supported Pt Nanoparticles. Journal of Physical Chemistry C, 2011, 115, 22742-22747.	1.5	200
10064	Hydride-Assisted Hydrogenation of Ti-Doped NaH/Al: A Density Functional Theory Study. Journal of Physical Chemistry C, 2011, 115, 2522-2528.	1.5	11
10065	First-principles generalized gradient approximation + U study of cubic CuAl2O4. Applied Physics Letters, 2011, 99, 091902.	1.5	14

#	Article	IF	Citations
10066	Universal Electrostatic Origin of Cation Ordering in A₂BO₄ Spinel Oxides. Journal of the American Chemical Society, 2011, 133, 11649-11654.	6.6	71
10067	First principles study of oxygen adsorption and dissociation on the Pd/Au surface alloys. Physical Chemistry Chemical Physics, 2011, 13, 7112.	1.3	11
10068	First-principles study of the biomineral hydroxyapatite. Physical Review B, 2011, 84, .	1.1	91
10069	Hydrogen Adsorption on Rh, Ni, and Pd Functionalized Single-Walled Boron Nitride Nanotubes. Journal of Physical Chemistry C, 2011, 115, 4289-4296.	1.5	62
10070	Elastic constants, phonon density of states, and thermal properties of UO<mml:math xmlns:mml="http://www.w3.org/1998/Math/MathML" display="inline"><mml:msub><mml:mrow /><mml:mn>2</mml:mn></mml:msub></mml:math>. Physical Review B, 2011, 84, .	1.1	82
10071	Orientational ordering of interstitial atoms and martensite formation in dilute Fe-based solid solutions. Physical Review B, 2011, 83, .	1.1	36
10072	Inverse design approach to hole doping in ternary oxides: Enhancing<mml:math xmlns:mml="http://www.w3.org/1998/Math/MathML" display="inline"><mml:mi>p</mml:mi></mml:math>-type conductivity in cobalt oxide spinels. Physical Review B, 2011, 84, .	1.1	81
10073	Quantum confinement and spin-orbit interactions in PbSe and PbTe nanowires: First-principles calculation. Physical Review B, 2011, 84, .	1.1	10
10074	Formation and Mobility of Li Point Defects in LiBO₂: A First-Principles Investigation. Journal of Physical Chemistry C, 2011, 115, 12343-12349.	1.5	15
10075	Nonprecious Metal Catalysts for Low Temperature Solid Oxide Fuel Cells. Journal of Physical Chemistry C, 2011, 115, 11641-11648.	1.5	7
10076	Enhanced iron magnetic moment in the ThFe11C2 intermetallic compound. Journal of Applied Physics, 2011, 109, 083909.	1.1	3
10077	A Comparative Study of Lattice Dynamics of Three- and Two-Dimensional MoS₂. Journal of Physical Chemistry C, 2011, 115, 16354-16361.	1.5	298
10078	First-principles study of liquid gallium at ambient and high pressure. Journal of Chemical Physics, 2011, 135, 044507.	1.2	28
10079	Electronic transport coefficients fromab initiosimulations and application to dense liquid hydrogen. Physical Review B, 2011, 83, .	1.1	148
10080	Electrical and thermal conductivity of liquid sodium from first-principles calculations. Physical Review B, 2011, 84, .	1.1	64
10081	Chemical bonding and elastic properties of quaternary arsenide oxides YZnAsO and LaZnAsO investigated by first principles. Transactions of Nonferrous Metals Society of China, 2011, 21, 1378-1382.	1.7	6
10082	Compositional dependence of structural and electronic properties of Cu<mml:math xmlns:mml="http://www.w3.org/1998/Math/MathML" display="inline"><mml:mrow><mml:msub><mml:mrow /><mml:mrow><mml:mn>2</mml:mn></mml:mrow></mml:msub></mml:mrow></mml:math>ZnSn(S,Se)<mml:math xmlns:mml="http://www.w3.org/1998/Math/MathML" display="inline"><mml:mrow><mml:msub><mml:mrow /><mml:mrow><mml:mn>4</mml:mn></mml:mro	11	399
10083	First-Principles Investigation of Ag-Doped Gold Nanoclusters. International Journal of Molecular Sciences, 2011, 12, 2972-2981.	1.8	29

#	Article	IF	Citations
10084	Raman spectra of barium halides in orthorhombic and hexagonal symmetry: Anab initiostudy. Physical Review B, 2011, 83, .	1.1	9
10085	Theoretical Study of Adsorption of Ag Clusters on the Anatase TiO₂(100) Surface. Journal of Physical Chemistry C, 2011, 115, 17368-17377.	1.5	52
10086	Hydrogen Bonding and Molecular Rearrangement in 1,3,5-Triamino-2,4,6-trinitrobenzene under Compression. Journal of Physical Chemistry B, 2011, 115, 12085-12093.	1.2	31
10087	Bilayer graphene dual-gate nanodevice: Anab initiosimulation. Physical Review B, 2011, 84, .	1.1	36
10088	From Point Defects in Graphene to Two-Dimensional Amorphous Carbon. Physical Review Letters, 2011, 106, 105505.	2.9	675
10089	Bond-Order Potential for Erbium-Hydride System. Journal of Physical Chemistry C, 2011, 115, 25097-25104.	1.5	9
10090	Water induced electrical hysteresis in germanium nanowires: a theoretical study. Physical Chemistry Chemical Physics, 2011, 13, 11663.	1.3	12
10091	Electrochemistry of Os(2,2â€²-bpy)2ClPyCH2NHCOPh tethered to Au electrodes by Sâ€“Au and Câ€“Au junctions. Physical Chemistry Chemical Physics, 2011, 13, 5336.	1.3	17
10092	sp-Electron Magnetic Clusters with a Large Spin in Graphene. ACS Nano, 2011, 5, 2440-2446.	7.3	80
10093	First-principles predictions of potential hydrogen storage materials: Nanosized Ti(core)/Mg(shell) hydrides. Physical Review B, 2011, 83, .	1.1	21
10094	Electronic structure and chemical bonding of the electron-poor II-V semiconductors ZnSb and ZnAs. Physical Review B, 2011, 84, .	1.1	34
10095	First-principles analysis of ZrN/ScN metal/semiconductor superlattices for thermoelectric energy conversion. Journal of Applied Physics, 2011, 109, .	1.1	28
10096	Bandgap Opening in Graphene Antidot Lattices: The Missing Half. ACS Nano, 2011, 5, 4023-4030.	7.3	154
10097	Detailed investigation of thermodynamic properties of hexagonal osmium using the ab-initio technique. Physica B: Condensed Matter, 2011, 406, 656-662.	1.3	4
10098	Calculation of physical properties of the cubic perovskite-type oxide using the PP-PW method based on the DFT theory. Solid State Communications, 2011, 151, 908-915.	0.9	11
10099	On the Importance of Gradient-Corrected Correlation for van der Waals Density Functionals. Topics in Catalysis, 2011, 54, 1143-1150.	1.3	23
10100	Confinement-induced changes in magnetic behavior of a Ti monolayer on Pt. Chemical Physics Letters, 2011, 507, 117-121.	1.2	7
10101	Incorporation of iron on the clean and gallium-bilayer GaN(0001) surface. Journal of Applied Physics, 2011, 109, 07C102.	1.1	6

#	Article	IF	Citations
10102	Pt(111)-Alloy Surfaces for Non-Activated OOH Dissociation. E-Journal of Surface Science and Nanotechnology, 2011, 9, 352-356.	0.1	11
10103	Formation of nanoscale gold chain on a Si(110) surface: A density functional investigation. Journal of Applied Physics, 2011, 110, .	1.1	1
10104	Mechanical and Electronic Properties of Graphene Nanostructures. , 2011, , .		3
10105	Adsorbate-localized states at water-covered (100) SrTiO3 surfaces. Applied Physics Letters, 2011, 98, 012106.	1.5	8
10106	Structural and Electronic Properties of Graphene upon Molecular Adsorption: DFT Comparative Analysis. , 0, , .		2
10107	First Principles Study on the Adsorption and Dehydrogenation of Borohydride on Mn(111). E-Journal of Surface Science and Nanotechnology, 2011, 9, 257-264.	0.1	6
10108	Thermodynamics of ABO3-Type Perovskite Surfaces. , 0, , .		4
10109	Cohesive Relations for Surface Atoms in the Iron-Technetium Binary System. Journal of Metallurgy, 2011, 2011, 1-8.	1.1	12
10110	First-Principles Calculation on Initial Stage of Oxidation of Si (110)-(1 Ã— 1) Surface. Advances in Condensed Matter Physics, 2011, 2011, 1-5.	0.4	1
10111	The Beneficial Effect of Hydrogen on CO Oxidation over Au Catalysts. A Computational Study. Molecules, 2011, 16, 9582-9599.	1.7	13
10112	Bader's analysis of the electron density in the Pbca enstatite - Pbcn protoenstatite phase transition. European Journal of Mineralogy, 2011, 23, 197-205.	0.4	9
10113	Ab initio study on the lithiation mechanism of Mg<inf>2</inf>Si electrode. , 2011, , .		1
10114	Self-Interaction Corrected Electronic Structure and Energy Gap of CuAlO₂ beyond Local Density Approximation. Journal of the Physical Society of Japan, 2011, 80, 053706.	0.7	7
10115	Density Functional Theory Calculations On Magnetic Properties Of Actinide Compounds. Materials Research Society Symposia Proceedings, 2011, 1298, 103.	0.1	0
10116	Energy-distance relation for fcc transition metal nanocrystals. Europhysics Letters, 2011, 93, 26004.	0.7	2
10117	Clustering and Octet Rule Violation Impact on Band Gap Bowing: Ab Initio Calculation of the Electronic Properties of (GaAs)1â^'x(Ge2)x Alloys. Chemistry Letters, 2011, 40, 770-772.	0.7	1
10118	Investigation of Cu precipitation in bcc-Fe â€“ Comparison of numerical analysis with experiment. International Journal of Materials Research, 2011, 102, 709-716.	0.1	8
10119	Implementation of GPU-FFT into Planewave Based First Principles Calculation Method. Journal of Computational Science and Technology, 2011, 5, 89-105.	0.4	1

#	Article	IF	Citations
10121	Powder diffraction and solid state DFT study of thetrans-bis(5-methylsalicylato)-bis(N,N-diethylnicotinamide)-diaquacopper(II) complex structure. Zeitschrift FÃ¼r Kristallographie, 2011, 226, 756-761.	1.1	1
10122	Structural, elastic, electronic, optical and thermal properties of cubic perovskite CsCdF₃under pressure effect. EPJ Applied Physics, 2011, 53, 30101.	0.3	6
10123	Surface structures and magnetic anisotropies of a Fe/Pt (001) surface: An ab initio study. Journal of Applied Physics, 2011, 109, 07B764.	1.1	7
10124	Tilting angle and water slippage over hydrophobic coatings. Philosophical Transactions Series A, Mathematical, Physical, and Engineering Sciences, 2011, 369, 2537-2545.	1.6	12
10125	First Principles Calculations of the Electronic Structure of ZrN Allotropes. Journal of the Physical Society of Japan, 2011, 80, 114707.	0.7	3
10126	Modulating magnetism of ZnO:C with vacancy and substitution. Journal of Applied Physics, 2011, 110, .	1.1	10
10127	Half-metallicity of wurtzite NiO and w-NiOâˆ•ZnO (0001) interface: First principles simulation. AIP Advances, 2011, 1, 022124.	0.6	1
10128	Chemical speciation of adsorbed glycine on metal surfaces. Journal of Chemical Physics, 2011, 135, 034703.	1.2	20
10129	Gallium interstitial contributions to diffusion in gallium arsenide. AIP Advances, 2011, 1, .	0.6	8
10130	Manipulating absorption and diffusion of H atom on graphene by mechanical strain. AIP Advances, 2011, 1, 032109.	0.6	26
10131	Atomic and electronic properties of P/Si(1Â1Â1)-(2ÂÃ—Â1) surface. EPJ Applied Physics, 2011, 56, 31302.	0.3	1
10132	Thermodynamic factors limiting the preservation of aromaticity of adsorbed organic compounds on Si(100): Example of the pyridine. Journal of Chemical Physics, 2011, 134, 234708.	1.2	12
10133	Work function engineering in silicides: Chlorine doping in NiSi. Journal of Applied Physics, 2011, 109, 083703.	1.1	7
10134	Calculation of the electronic structure of delafossite AgTaN2 from first principles. Journal of the Ceramic Society of Japan, 2011, 119, 663-666.	0.5	6
10135	Computer simulation of coherent BaZrO3/MgO interfaces. Journal of the Ceramic Society of Japan, 2011, 119, 861-866.	0.5	1
10136	First-Principles Calculation for Interfacial Energy of Void Defect in CZ Silicon Crystal. Nippon Kinzoku Gakkaishi/Journal of the Japan Institute of Metals, 2011, 75, 640-644.	0.2	2
10137	Solid Solution Softening Mechanisms in Mg-Ca Alloy. Materials Transactions, 2011, 52, 1840-1843.	0.4	11
10138	Electronic Structure and Solid Solution Softening in Iron Alloys. Materials Transactions, 2011, 52, 1324-1326.	0.4	4

#	Article	IF	Citations
10139	Stability and Electronic Structures of Pt-Rh Icosahedral Nanoparticles. Materials Transactions, 2011, 52, 1339-1343.	0.4	4
10141	First-Principles Study of Water Adsorption on Î±-Al2O3(0001): Influence of Hydrogen Isotope. Fusion Science and Technology, 2011, 60, 1155-1158.	0.6	0
10142	Interface-dependent magnetic anisotropy of Fe/BaTiO3: A first principles study. Journal of Applied Physics, 2011, 109, 07D909.	1.1	8
10143	Structural stability and electronic properties of M2TaN3,Îµ-TaN and MTa2N3(M = Ti, Zr, Hf) compounds. EPJ Applied Physics, 2011, 55, 20101.	0.3	1
10144	Formation of Cotunnite Phase in ZrO₂ under Uniaxial Stress: A First Principles Study. Journal of the American Ceramic Society, 2011, 94, 932-937.	1.9	6
10145	Grain Boundaries in Uranium Dioxide: Scanning Electron Microscopy Experiments and Atomistic Simulations. Journal of the American Ceramic Society, 2011, 94, 1893-1900.	1.9	78
10146	Stabilization Mechanisms of LaFeO3 (010) Surfaces Determined with First Principles Calculations. Journal of the American Ceramic Society, 2011, 94, 1931-1939.	1.9	18
10147	Phase Stability, Electronic Structure, Compressibility, Elastic and Optical Properties of a Newly Discovered <scp>Ti₃SnC₂</scp>: A Firstâ€Principle Study. Journal of the American Ceramic Society, 2011, 94, 3907-3914.	1.9	27
10148	Atomic and electronic structure of mixed Au-Co nanowires: Ab initio molecular dynamics study. JETP Letters, 2011, 93, 129-132.	0.4	11
10149	Theoretical study of vacancies and adatoms in white graphene. JETP Letters, 2011, 93, 335-338.	0.4	10
10150	Effect of hydrogen on the formation of the atomic structure of linear carbon chains: An ab initio approach. JETP Letters, 2011, 93, 652-656.	0.4	7
10151	Effect of stretching-contraction deformations on the magnetic ordering state of mixed Pd-Fe nanowires. JETP Letters, 2011, 94, 228-232.	0.4	13
10152	Ferromagnetism driven by vacancies and C/N substitution at SrO (100) surface. Solid State Sciences, 2011, 13, 126-130.	1.5	5
10153	Pressure-induced phase transformation and magnetism transition in BaRuO3: A first-principles study. Solid State Sciences, 2011, 13, 350-355.	1.5	9
10154	Study on interactions between Cadmium and defects in Cd-doped ZnO by first-principle calculations. Solid State Sciences, 2011, 13, 384-387.	1.5	33
10155	Structural, elastic, electronic, optical and thermodynamic properties of KMgH3. Solid State Sciences, 2011, 13, 647-652.	1.5	12
10156	Ferromagnetic ordering of carbon doped GaN semiconductor: First-principles prediction. Solid State Sciences, 2011, 13, 480-483.	1.5	14
10157	The first principles study on the TmSb compound. Solid State Sciences, 2011, 13, 1291-1298.	1.5	5

#	Article	IF	Citations
10158	Ab initio investigations of the Ca2IrO4-type structure as a â€œpost-K2NiF4â€• Case study of Na2OsO4. Solid State Sciences, 2011, 13, 1396-1400.	1.5	8
10159	Theoretical prediction of the structural, elastic, electronic and optical properties of Zr3N4 and Hf3N4 compounds. Solid State Sciences, 2011, 13, 1414-1419.	1.5	16
10160	Electronic properties, magnetic properties and phase stability of alloyed cementite (Fe,M)3C (M=Co,Ni) from density-functional theory calculations. Solid State Sciences, 2011, 13, 1658-1663.	1.5	23
10161	First-principles study on surface magnetism in Co-doped (110) SnO2 thin film. Solid State Sciences, 2011, 13, 1608-1611.	1.5	19
10162	Structural, electronic and optical properties of spinel oxides ZnAl2O4, ZnGa2O4 and ZnIn2O4. Solid State Sciences, 2011, 13, 1638-1648.	1.5	86
10163	First-principles calculation of structural, electronic, and optical properties of zinc-blende AlxGa1â^'xN alloys. Solid State Sciences, 2011, 13, 1731-1734.	1.5	10
10164	Band parameters of Î±-LiBeN semiconductor from density functional calculations. Superlattices and Microstructures, 2011, 50, 319-330.	1.4	2
10165	Study on mechanical behavior and electronic structures of Alâ€“Cu intermetallic compounds based on first-principles calculations. Solid State Communications, 2011, 151, 1270-1274.	0.9	22
10166	Orbital ordering in Mott-insulators La2O3Fe2Se2 and La2O3Co2Se2. Solid State Communications, 2011, 151, 1231-1235.	0.9	4
10167	Thermoelectric properties and electronic structure of Te-doped CoSb3 compounds. Solid State Communications, 2011, 151, 1388-1393.	0.9	17
10168	Electronic and elastic properties of a double perovskite slabâ€“rocksalt layer of Eu2SrAl2O7 investigated by LSDA+U. Solid State Communications, 2011, 151, 1326-1330.	0.9	5
10169	Structural stability and electronic properties of Ni-doped armchair graphene nanoribbons. Solid State Communications, 2011, 151, 1490-1495.	0.9	29
10170	A first-principles study of vibrational modes in Cu2O and Ag2O crystals. Solid State Communications, 2011, 151, 1452-1454.	0.9	21
10171	First-principles study of martensitic transformation of IrTi alloy. Solid State Communications, 2011, 151, 1433-1436.	0.9	6
10172	First-principles studies on Ti3Si0.5Ge0.5C2 under pressure. Solid State Communications, 2011, 151, 1564-1567.	0.9	2
10173	High-pressure and high-temperature bulk modulus of cubic fluorite-type MgF2 from quasi-harmonic Debye model. Solid State Communications, 2011, 151, 1507-1510.	0.9	7
10174	First-principles study on electronic and magnetic properties of Cu-doped CdS. Solid State Communications, 2011, 151, 1712-1715.	0.9	25
10175	Theoretical investigations on the structural, lattice dynamical and thermodynamic properties of XC (X=Si, Ge, Sn). Solid State Communications, 2011, 151, 1545-1549.	0.9	22

#	Article	IF	Citations
10176	First-principles calculations of structural and thermodynamic properties of Y 3Al5O12. Solid State Communications, 2011, 151, 1559-1563.	0.9	13
10177	Structural stability and electronic properties of XyTa1â^'yTa2N3, (X=B, C, N, O, F) compounds. Solid State Communications, 2011, 151, 1672-1676.	0.9	2
10178	Mechanical properties and electronic structure of the incompressible rhenium carbides and nitrides: A first-principles study. Solid State Communications, 2011, 151, 1842-1845.	0.9	20
10179	Lattice stability and thermal equation of state of -La from first-principles calculations. Solid State Communications, 2011, 151, 1802-1805.	0.9	2
10180	Theoretical study of magnetic ordering and electronic properties of Ag Al1â^' N compounds. Solid State Communications, 2011, 151, 1794-1797.	0.9	10
10181	First-principles study of the structural, electronic, and magnetic properties of InCCo3 and InNCo3. Solid State Communications, 2011, 151, 1916-1919.	0.9	7
10182	Magnetism of Mg atomic chains on the NaCl(100) surface. Solid State Communications, 2011, 151, 1912-1915.	0.9	1
10183	Pressure dependence of electronic structure and magnetic properties in Fe16N2. Solid State Communications, 2011, 151, 1903-1906.	0.9	2
10184	Prediction of a bccâ€“hcp phase transition for Sn: A first-principles study. Solid State Communications, 2011, 151, 1873-1873.	0.9	9
10185	A theoretical study of the influence of dopant concentration on the hydration properties of yttrium-doped barium cerate. Solid State Ionics, 2011, 204-205, 27-34.	1.3	23
10186	Crystallization kinetics of amorphous Cr2AlC thin films. Surface and Coatings Technology, 2011, 206, 599-603.	2.2	78
10187	Surface morphological response of crystalline solids to mechanical stresses and electric fields. Surface Science Reports, 2011, 66, 299-346.	3.8	31
10188	First-principles calculations of vacancy formation in In-free photovoltaic semiconductor Cu2ZnSnSe4. Thin Solid Films, 2011, 519, 7513-7516.	0.8	38
10189	The structure of Tiâ€“Siâ€“N superhard nanocomposite coatings: ab initio study. Thin Solid Films, 2011, 520, 876-880.	0.8	13
10190	Effects of Bi segregation on the tensile properties of Cu/Cu3Sn(100) interface. Microelectronics Reliability, 2011, 51, 2330-2335.	0.9	7
10191	Chain growth mechanism of Fischerâ€“Tropsch synthesis on Fe5C2(001). Journal of Molecular Catalysis A, 2011, 346, 55-69.	4.8	62
10192	Band structure and photocatalytic properties of N/Zr co-doped anatase TiO2 from first-principles study. Journal of Molecular Catalysis A, 2011, 351, 11-16.	4.8	45
10193	Theoretical investigation on the structure and electronic properties of barium titanate. Journal of Molecular Structure, 2011, 1003, 75-81.	1.8	29

#	Article	IF	Citations
10194	Alâ€“Pd interatomic potential and its application to nanoscale multilayer thin films. Materials Science & Engineering A: Structural Materials: Properties, Microstructure and Processing, 2011, 530, 73-86.	2.6	13
10195	Ni/boride interfaces and environmental embrittlement in Ni-based superalloys: A first-principles study. Materials Science & Engineering A: Structural Materials: Properties, Microstructure and Processing, 2011, 530, 373-377.	2.6	10
10196	Crystal habits of LiMn2O4 and their influence on the electrochemical performance. Materials Science and Engineering B: Solid-State Materials for Advanced Technology, 2011, 176, 1257-1263.	1.7	20
10197	Molecular dynamics simulation on ionic conduction process of oxygen in Ce1â^'xMxO2â^'x/2. Journal of the European Ceramic Society, 2011, 31, 3159-3169.	2.8	20
10198	Modulation effects of Cu doping on magnetic properties of Zn(Ni)O: First-principle calculations. Journal of Magnetism and Magnetic Materials, 2011, 323, 3117-3120.	1.0	3
10199	First-principles investigation on the effect of carbon on hydrogen trapping in tungsten. Journal of Nuclear Materials, 2011, 415, S709-S712.	1.3	40
10200	Ab initio modeling of oxygen impurity atom incorporation into uranium mononitride surface and sub-surface vacancies. Journal of Nuclear Materials, 2011, 416, 200-204.	1.3	33
10201	Theoretical study on segregation of Cu, Mo and W impurities and stability of impurityâ€“vacancy pairs in bcc Fe. Journal of Nuclear Materials, 2011, 417, 1054-1057.	1.3	1
10202	Diffusion of Y and Ti/Zr in bcc iron: A first principles study. Journal of Nuclear Materials, 2011, 419, 208-212.	1.3	52
10203	First-principles study of the incorporation and diffusion of helium in cubic zirconia. Journal of Nuclear Materials, 2011, 418, 143-151.	1.3	16
10204	Ideal mechanical properties of vanadium by a first-principles computational tensile test. Journal of Nuclear Materials, 2011, 416, 345-349.	1.3	11
10205	First-principles study of H2 adsorption and dissociation on Zr(0001). Journal of Nuclear Materials, 2011, 418, 159-164.	1.3	16
10206	Ab initio study of hydrogen related defect in ZrO2: Consequences on dry and aqueous oxidation. Journal of Nuclear Materials, 2011, 416, 362-368.	1.3	12
10207	First principles study of hydrogen behaviors in hexagonal tungsten carbide. Journal of Nuclear Materials, 2011, 418, 233-238.	1.3	12
10208	Ab initio study of influence of 3d alloying elements on corrosion properties of non-passivated nickel-base alloys. Journal of Nuclear Materials, 2011, 418, 286-291.	1.3	12
10209	Stability and dissolution of heliumâ€“vacancy complexes in vanadium solid. Journal of Nuclear Materials, 2011, 419, 1-8.	1.3	51
10210	First-principles calculations on electronic, chemical bonding and optical properties of tetragonal SrHfO3. Journal of Computational Science, 2011, 2, 299-303.	1.5	3
10211	Pressure-induced phase transitions in multiferroic RbFe(MoO4)2â€”Raman scattering study. Journal of Solid State Chemistry, 2011, 184, 2812-2817.	1.4	21

#	Article	IF	Citations
10212	Studies of the defect structure for V3+ ions in wurtzite structure ZnO. Spectrochimica Acta - Part A: Molecular and Biomolecular Spectroscopy, 2011, 82, 137-139.	2.0	3
10213	Stability and structures of the Îµ-phases of iron nitrides and iron carbides from first principles. Scripta Materialia, 2011, 64, 296-299.	2.6	35
10214	Dehydrogenation behavior of ball-milled ammonia borane and lithium hydride mixtures. Scripta Materialia, 2011, 64, 737-740.	2.6	4
10215	Ab initio calculations of the generalized stacking fault energy in aluminium alloys. Scripta Materialia, 2011, 64, 916-918.	2.6	110
10216	First-principles study of long-period stacking ordered-like multi-stacking fault structures in pure magnesium. Scripta Materialia, 2011, 64, 942-945.	2.6	47
10217	Lonsdaleite â€“ A material stronger and stiffer than diamond. Scripta Materialia, 2011, 65, 229-232.	2.6	56
10218	Î³â€²-ZnFe3N thin films: A proposal for a moderately ductile, corrosion-protective coating on steel. Scripta Materialia, 2011, 65, 380-383.	2.6	8
10219	First-principles study of the generalized stacking fault energy in Mgâ€“3Alâ€“3Sn alloy. Scripta Materialia, 2011, 65, 723-726.	2.6	89
10220	Extending the rule of mixture to the sub unit-cell level. Scripta Materialia, 2011, 65, 735-738.	2.6	12
10221	Strain-induced changes in electronic structures and work function for (001), (110) and (111) of AlCu3. Physica B: Condensed Matter, 2011, 406, 4046-4051.	1.3	9
10222	The stability and the nonlinear elasticity of 2D hexagonal structures of Si and Ge from first-principles calculations. Physica B: Condensed Matter, 2011, 406, 4080-4084.	1.3	50
10223	Electronic and optical properties of BAs under pressure. Physica B: Condensed Matter, 2011, 406, 4272-4277.	1.3	24
10224	Ab-initio investigations of structural, electronic, magnetic and optical properties of ferromagnetic Cd1â€“xMnxTe. Physica B: Condensed Matter, 2011, 406, 4547-4553.	1.3	11
10225	Effect of hydrogen-doping on bonding properties of Ti3SiC2. Physica B: Condensed Matter, 2011, 406, 4460-4465.	1.3	12
10226	Elastic and thermodynamic properties of CaB6 under pressure from first principles. Physica B: Condensed Matter, 2011, 406, 4476-4482.	1.3	26
10227	Elastic, electronic, and optical properties of hypothetical SnNNi3 and CuNNi3 in comparison with superconducting ZnNNi3. Physica B: Condensed Matter, 2011, 406, 4564-4568.	1.3	26
10228	Phase transition and thermodynamic properties of Sr under high pressure. Physica B: Condensed Matter, 2011, 406, 4518-4522.	1.3	4
10229	First principle study on generalized-stacking-fault energy surfaces of B2-AlRE intermetallic compounds. Physica B: Condensed Matter, 2011, 406, 4529-4534.	1.3	8

#	Article	IF	Citations
10230	First-principles study of elastic and thermo-physical properties of kesterite-type Cu2ZnSnS4. Physica B: Condensed Matter, 2011, 406, 4604-4607.	1.3	34
10231	A first-principles study on the structural, lattice dynamical and thermodynamic properties of beryllium chalcogenides. Physica B: Condensed Matter, 2011, 406, 4666-4670.	1.3	19
10232	Electronic structure and magnetic coupling properties of EuFe2P2: First-principles calculations. Physica B: Condensed Matter, 2011, 406, 4687-4690.	1.3	5
10233	Energetics and structural properties of carbon and oxygen doped hexagonal boron nitride sheets. Physica E: Low-Dimensional Systems and Nanostructures, 2011, 44, 215-217.	1.3	15
10234	First-principles study on structural, electronic and magnetic properties of ZnO nanotube filled with Fe, Co and Ni nanowires. Physica E: Low-Dimensional Systems and Nanostructures, 2011, 44, 405-410.	1.3	9
10235	The improvement of the adsorption abilities of some gas molecules on g-BN sheet by carbon doping. Physica E: Low-Dimensional Systems and Nanostructures, 2011, 44, 495-500.	1.3	45
10236	Tuning electronic and magnetic properties of AlN nanosheets with hydrogen and fluorine: First-principles prediction. Physics Letters, Section A: General, Atomic and Solid State Physics, 2011, 375, 3583-3587.	0.9	31
10237	Electronic structure tuning and band gap opening of graphene by hole/electron codoping. Physics Letters, Section A: General, Atomic and Solid State Physics, 2011, 375, 3890-3894.	0.9	71
10238	First principles predictions on mechanical and physical properties of HoX (X=As, P). Materials Chemistry and Physics, 2011, 125, 887-894.	2.0	10
10239	High-pressure phases of lead chalcogenides. Materials Chemistry and Physics, 2011, 126, 707-710.	2.0	35
10240	Theoretical investigations of physical properties of AlxScyB1â^'xâ^'yN quaternary alloys. Materials Chemistry and Physics, 2011, 128, 195-201.	2.0	7
10241	Stable structure of platinum carbides: A first principles investigation on the structure, elastic, electronic and phonon properties. Materials Chemistry and Physics, 2011, 129, 816-822.	2.0	59
10242	Electronic and magnetic properties of perfect and defected germanium nanoribbons. Materials Chemistry and Physics, 2011, 130, 140-146.	2.0	12
10243	Spark plasma sintering of the nonstoichiometric ultrafine-grained titanium carbides with nano superstructural domains of the ordered carbon vacancies. Materials Chemistry and Physics, 2011, 130, 352-360.	2.0	28
10244	FP-LAPW study of the fundamental properties of the cubic spinel CdAl2O4. Materials Research Bulletin, 2011, 46, 2252-2260.	2.7	27
10245	Non-equilibrium phases in the Feâ€“Rh system studied by ion beam mixing and ab initio calculation. Materials Letters, 2011, 65, 1805-1807.	1.3	1
10246	Effects of hydrogen on a tungsten grain boundary: A first-principles computational tensile test. Progress in Natural Science: Materials International, 2011, 21, 240-245.	1.8	35
10247	Adsorption of cyclohexene and its dehydrogenation intermediates on nAu/Pt(100)(n = 0, 1, 2) surfaces: A DFT study. Journal of Natural Gas Chemistry, 2011, 20, 34-40.	1.8	3

#	Article	IF	Citations
10248	Why is metallic Pt the best catalyst for methoxy decomposition?. Journal of Natural Gas Chemistry, 2011, 20, 90-98.	1.8	11
10249	Adsorption and dissociation of H2O on Cu2O(100): A computational study. Journal of Natural Gas Chemistry, 2011, 20, 155-161.	1.8	33
10250	A DFT theoretical study of CH4 dissociation on gold-alloyed Ni(111) surface. Journal of Natural Gas Chemistry, 2011, 20, 611-617.	1.8	37
10251	Wear and corrosion of silicon nitride rolling tools in copper rolling. Wear, 2011, 271, 2531-2541.	1.5	15
10252	Diffusion behavior of W in the WCu/Ni interface. International Journal of Refractory Metals and Hard Materials, 2011, 29, 153-157.	1.7	6
10253	Cobalt layers crystallized on the WC(100) surface: Spin-polarized ab initio study. International Journal of Refractory Metals and Hard Materials, 2011, 29, 184-187.	1.7	15
10254	Mechanism of selective alcohol oxidation to aldehydes on gold catalysts: Influence of surface roughness on reactivity. Journal of Catalysis, 2011, 278, 50-58.	3.1	110
10255	Spectroscopy, microscopy and theoretical study of NO adsorption on MoS2 and Coâ€“Moâ€“S hydrotreating catalysts. Journal of Catalysis, 2011, 279, 337-351.	3.1	64
10256	Interaction of SO2 with Cu/TiC(001) and Au/TiC(001): Toward a new family of DeSOx catalysts. Journal of Catalysis, 2011, 279, 352-360.	3.1	28
10257	Free-energy profiles along reduction pathways of MoS2 M-edge and S-edge by dihydrogen: A first-principles study. Journal of Catalysis, 2011, 280, 178-195.	3.1	117
10258	An atomic-scale investigation of carbon in MoS2 hydrotreating catalysts sulfided by organosulfur compounds. Journal of Catalysis, 2011, 281, 345-351.	3.1	30
10259	Câ€“H bond activation of methane on clean and oxygen pre-covered metals: A systematic theoretical study. Journal of Catalysis, 2011, 282, 74-82.	3.1	101
10260	Experimental and computational investigations of sulfur-resistant bimetallic catalysts for reforming of biomass gasification products. Journal of Catalysis, 2011, 282, 249-257.	3.1	19
10261	Selectivity of chemisorbed oxygen in Câ€“H bond activation and CO oxidation and kinetic consequences for CH4â€“O2 catalysis on Pt and Rh clusters. Journal of Catalysis, 2011, 283, 10-24.	3.1	81
10262	Oxygen reduction reaction mechanism on nitrogen-doped graphene: A density functional theory study. Journal of Catalysis, 2011, 282, 183-190.	3.1	545
10263	Mechanism for the waterâ€“gas shift reaction on monofunctional platinum and cause of catalyst deactivation. Journal of Catalysis, 2011, 282, 278-288.	3.1	58
10264	Stability and reactivity of active sites for direct benzene oxidation to phenol in Fe/ZSM-5: A comprehensive periodic DFT study. Journal of Catalysis, 2011, 284, 194-206.	3.1	69
10265	Theoretical insights into the surface growth of rutile TiO2. Combustion and Flame, 2011, 158, 1868-1876.	2.8	22

#	Article	IF	Citations
10266	Interaction of valine and valine radicals with single-walled carbon nanotube (5,0). Chemical Physics Letters, 2011, 511, 299-303.	1.2	11
10267	DFT study of influences of As, Co and Ni impurities on pyrite (100) surface oxidation by O2 molecule. Chemical Physics Letters, 2011, 511, 389-392.	1.2	30
10268	The structural, energetic and electronic properties of doped carbon nanotubes by encapsulation of MCp2 (M=Fe, Co, Ni): A theoretical investigation. Chemical Physics Letters, 2011, 512, 81-86.	1.2	13
10269	The geometric and electronic structure of Xe-adsorbed Fe(001) surface by first-principles calculations. Chemical Physics Letters, 2011, 512, 99-103.	1.2	1
10270	Effects of surface modifications on band gaps and electronic states of GaN/InN core/shell nanowires. Chemical Physics Letters, 2011, 512, 251-254.	1.2	5
10271	First-principles study on absolute band edge positions for IIâ€“VI semiconductors at (110) surface. Chemical Physics Letters, 2011, 513, 72-76.	1.2	9
10272	Improved oxygen reduction activity on the Ih Cu@Pt coreâ€“shell nanoparticles. Chemical Physics Letters, 2011, 513, 118-123.	1.2	9
10273	Analysis of band gap formation in graphene by Si impurities: Local bonding interaction rules. Chemical Physics Letters, 2011, 515, 85-90.	1.2	13
10274	Work function modulation of AuCl4â^' molecule adsorbed on graphene: A first-principles simulation. Chemical Physics Letters, 2011, 516, 88-91.	1.2	3
10275	High-temperature and high-pressure thermal expansivity of cubic PtC from quasi-harmonic Debye model. Chemical Physics Letters, 2011, 516, 158-161.	1.2	7
10276	The effects of an explicit water environment on the interaction of a single wall carbon nanotube with amino acids: A theoretical study. Chemical Physics Letters, 2011, 518, 81-86.	1.2	6
10277	The effect of humidity on the adsorption of the hydrazine on single-wall carbon nanotubes: First-principles electronic structure calculations. Chemical Physics Letters, 2011, 518, 93-98.	1.2	10
10278	Exploration of magnetism in armchair graphene nanoribbons with radical groups. Chemical Physics Letters, 2011, 518, 104-108.	1.2	14
10279	A multiscale theoretical methodology for the calculation of electrochemical observables from ab initio data: Application to the oxygen reduction reaction in a Pt(111)-based polymer electrolyte membrane fuel cell. Electrochimica Acta, 2011, 56, 10842-10856.	2.6	68
10280	New crystalline NaAsF6â€“PEO8 complex: A Density Functional Theory study. Electrochimica Acta, 2011, 57, 244-249.	2.6	8
10281	Density functional theory (DFT) investigation on the structure and electronic properties of the cubic perovskite PbTiO3. Applied Catalysis A: General, 2011, 404, 54-54.	2.2	6
10282	Mechanistic analysis of direct N2O decomposition and reduction with H2 or NH3 over RuO2. Applied Catalysis B: Environmental, 2011, 110, 33-39.	10.8	8
10283	Ab initio and periodic DFT investigation of hydrogen storage on light metal-decorated MOF-5. International Journal of Hydrogen Energy, 2011, 36, 10816-10827.	3.8	61

#	Article	IF	Citations
10284	First principle study of hydrogen diffusion in equilibrium rutile, rutile with deformation twins and fluorite polymorph of Mg hydride. International Journal of Hydrogen Energy, 2011, 36, 11802-11809.	3.8	29
10285	Hydrogenation properties of the TiBx structures. International Journal of Hydrogen Energy, 2011, 36, 12268-12278.	3.8	5
10286	Intrinsic mechanisms on enhancement of hydrogen desorption from MgH2 by (001) surface doping. International Journal of Hydrogen Energy, 2011, 36, 12939-12949.	3.8	51
10287	First principles study on desorption of chemisorbed hydrogen atoms from single-walled carbon nanotubes under external electric field. International Journal of Hydrogen Energy, 2011, 36, 13645-13656.	3.8	11
10288	Ab initio calculations on energetics and electronic structures of cubic Mg3MNi2 (MÂ=ÂAl, Ti, Mn) hydrogen storage alloys. International Journal of Hydrogen Energy, 2011, 36, 14477-14483.	3.8	19
10289	Ab initio and thermodynamic investigation on the Caâ€“H system. International Journal of Hydrogen Energy, 2011, 36, 13632-13639.	3.8	8
10290	Hydrogen adsorption around lithium atoms anchored on graphene vacancies. International Journal of Hydrogen Energy, 2011, 36, 13657-13662.	3.8	40
10291	Theoretical studies on hydrogen adsorption properties of lithium decorated diborene (B2H4Li2) and diboryne (B2H2Li2). International Journal of Hydrogen Energy, 2011, 36, 15681-15688.	3.8	17
10292	Local structures of cobalt in Co-doped TiO2 by synchrotron x-ray absorption near edge structures. Current Applied Physics, 2011, 11, S279-S284.	1.1	13
10293	Surface diffusion coefficient determination by uniaxial tensile strain in Pb/Cu(111) surface systems. Current Applied Physics, 2011, 11, S400-S403.	1.1	4
10294	Guidelines for optimization of catalytic activity of 3d transition metal oxide catalysts in N2O decomposition by potassium promotion. Catalysis Today, 2011, 176, 369-372.	2.2	50
10295	Formation of oxygen active species in Ag-modified CeO2 catalyst for soot oxidation: A DFT study. Catalysis Today, 2011, 177, 31-38.	2.2	61
10296	Theory meets experiment: Electrocatalysis of hydrogen oxidation/evolution at Pdâ€“Au nanostructures. Catalysis Today, 2011, 177, 55-63.	2.2	62
10297	Synergy between iono-covalent bonds and van der Waals interactions in SAMs formation: A first-principles study of adsorption of carboxylic acids on the Znâ€“ZnO(0001) surface. Catalysis Today, 2011, 177, 39-49.	2.2	34
10298	Scaling relationships for adsorption energies of C2 hydrocarbons on transition metal surfaces. Chemical Engineering Science, 2011, 66, 6318-6323.	1.9	108
10299	Physical properties of the junction of scandium and carbon nanotubes. Journal of Zhejiang University: Science A, 2011, 12, 255-259.	1.3	1
10300	Crystal Structure, Electronic Structure, and Optical and Photoluminescence Properties of Eu(III) Ion-Doped Lu₆Mo(W)O₁₂. Inorganic Chemistry, 2011, 50, 12522-12530.	1.9	80
10301	Calculated electron affinity and stability of halogen-terminated diamond. Physical Review B, 2011, 84, .	1.1	64

#	Article	IF	Citations
10302	Calcium-Decorated Carbyne Networks as Hydrogen Storage Media. Nano Letters, 2011, 11, 2660-2665.	4.5	98
10303	The Pt(111)/Electrolyte Interface under Oxygen Reduction Reaction Conditions: An Electrochemical Impedance Spectroscopy Study. Langmuir, 2011, 27, 2058-2066.	1.6	170
10304	Electronic, optical and lattice dynamic properties of the novel diamond-like semiconductors Li₂CdGeS₄and Li₂CdSnS₄. Journal of Physics Condensed Matter, 2011, 23, 225401.	0.7	23
10305	Elastic, Electronic, and Optical Properties of Two-Dimensional Graphyne Sheet. Journal of Physical Chemistry C, 2011, 115, 20466-20470.	1.5	380
10306	High Capacity Hydrogen Storage in Ca Decorated Graphyne: A First-Principles Study. Journal of Physical Chemistry C, 2011, 115, 23221-23225.	1.5	210
10307	Temperature dependence of the band gap of perovskite semiconductor compound CsSnI3. Journal of Applied Physics, 2011, 110, .	1.1	170
10308	Influence of quantum confinement on the electronic structure of the transition metal sulfide<mml:math xmlns:mml="http://www.w3.org/1998/Math/MathML" display="inline"><mml:mrow><mml:mi>T</mml:mi></mml:mrow></mml:math>S<mml:math xmlns:mml="http://www.w3.org/1998/Math/MathML" display="inline"><mml:mrow><mml:msub><mml:mrow /><mml:mrow><mml:mn>2</mml:mn></mml:mrow></mml:msub></mml:mrow></mml:math>. Physical Re	1.1	1,474
10309	Influence of Size Effect on the Electronic and Elastic Properties of Diamond Films with Nanometer Thickness. Journal of Physical Chemistry C, 2011, 115, 132-136.	1.5	82
10310	Trends in Metal Oxide Stability for Nanorods, Nanotubes, and Surfaces. Journal of Physical Chemistry C, 2011, 115, 2244-2252.	1.5	52
10311	Electronic Structure of Partially Reduced Rutile TiO₂(110) Surface: Where Are the Unpaired Electrons Located?. Journal of Physical Chemistry C, 2011, 115, 4696-4705.	1.5	153
10312	Prediction of semiconductor band edge positions in aqueous environments from first principles. Physical Review B, 2011, 83, .	1.1	101
10313	Accelerated Materials Design for Hydrogen Separation Membranes. ACS Symposium Series, 2011, , 27-38.	0.5	4
10314	Reactivity of Chemisorbed Oxygen Atoms and Their Catalytic Consequences during CH₄â€“O₂ Catalysis on Supported Pt Clusters. Journal of the American Chemical Society, 2011, 133, 15958-15978.	6.6	184
10315	Highly optimized embedded-atom-method potentials for fourteen fcc metals. Physical Review B, 2011, 83, .	1.1	422
10316	Effect of Antisite Defects on the Formation of Oxygen Vacancies in Sr₂FeMoO₆: Implications for Ion and Electron Transport. Chemistry of Materials, 2011, 23, 4525-4536.	3.2	108
10317	Lattice dynamics and thermal properties of phononic semiconductors. Physical Review B, 2011, 84, .	1.1	20
10318	Do H-Bond Features of Silica Surfaces Affect the H₂O and NH₃ Adsorption? Insights from Periodic B3LYP Calculations. Journal of Physical Chemistry A, 2011, 115, 11221-11228.	1.1	25
10319	Band Lineup and Charge Carrier Separation in Mixed Rutile-Anatase Systems. Journal of Physical Chemistry C, 2011, 115, 3443-3446.	1.5	162

#	Article	IF	Citations
10320	V-doped SnS2: a new intermediate band material for a better use of the solar spectrum. Physical Chemistry Chemical Physics, 2011, 13, 20401.	1.3	80
10321	Structural, Mechanical Stability, and Physical Properties of Iridium Carbides with Various Stoichiometries: First-Principles Investigations. Journal of Physical Chemistry C, 2011, 115, 6948-6953.	1.5	9
10322	Surface properties of 3dtransition metals. Philosophical Magazine, 2011, 91, 3627-3640.	0.7	45
10323	Electrical Transport Properties of SnO under High Pressure. Journal of Physical Chemistry C, 2011, 115, 20710-20715.	1.5	26
10324	Prediction of the chemical trends of oxygen vacancy levels in binary metal oxides. Applied Physics Letters, 2011, 99, .	1.5	42
10325	Forces and atomic relaxation in density functional theory with the pseudopotential self-interaction correction. Physical Review B, 2011, 84, .	1.1	16
10326	Ab initiostudy of the thermodynamic properties of rare-earth-magnesium intermetallics MgRE (RE=Y, Dy, Pr, Tb). Physica Scripta, 2011, 83, 065707.	1.2	13
10327	Ab initiostudy on band-gap narrowing in SrTiO<mml:math xmlns:mml="http://www.w3.org/1998/Math/MathML" display="inline"><mml:msub><mml:mrow /><mml:mn>3</mml:mn></mml:msub></mml:math>with Nb-C-Nb codoping. Physical Review B, 2011, 84, .	1.1	54
10328	Discovery of the recoverable high-pressure iron oxide Fe₄O₅. Proceedings of the National Academy of Sciences of the United States of America, 2011, 108, 17281-17285.	3.3	120
10329	Density Functional Characterization of Pure and Alkaline Earth Metalâ€Doped Bi₁₂GeO₂₀, Bi₁₂SiO₂₀, and Bi₁₂TiO₂₀ Photocatalysts. ChemCatChem, 2011, 3, 378-385.	1.8	21
10330	Tailoring the Activity for Oxygen Evolution Electrocatalysis on Rutile TiO₂(110) by Transitionâ€Metal Substitution. ChemCatChem, 2011, 3, 1607-1611.	1.8	169
10331	Zircon to monazite phase transition in CeVO<mml:math xmlns:mml="http://www.w3.org/1998/Math/MathML" display="inline"><mml:mrow><mml:msub><mml:mrow /><mml:mrow><mml:mn>4</mml:mn></mml:mrow></mml:msub></mml:mrow></mml:math>: X-ray diffraction and Raman-scattering measurements. Physical Review B, 2011, 84, .	1.1	83
10332	Structure and electronic properties of cerium orthophosphate: Theory and experiment. Physical Review B, 2011, 83, .	1.1	36
10333	Structural and electronic bistability in ZnS single sheets and single-walled nanotubes. Physical Review B, 2011, 83, .	1.1	41
10334	Stone-Wales-type transformations in carbon nanostructures driven by electron irradiation. Physical Review B, 2011, 83, .	1.1	226
10335	Mechanical and Electronic Properties of MoS₂ Nanoribbons and Their Defects. Journal of Physical Chemistry C, 2011, 115, 3934-3941.	1.5	427
10336	Gap opening in graphene by simple periodic inhomogeneous strain. Physical Review B, 2011, 84, .	1.1	77
10337	Three-dimensional network model of carbon containing only sp2-carbon bonds and boron nitride analogues. Chemical Communications, 2011, 47, 4406.	2.2	45

#	Article	IF	Citations
10338	Group IV Graphene- and Graphane-Like Nanosheets. Journal of Physical Chemistry C, 2011, 115, 13242-13246.	1.5	288
10339	Electronic and magnetic properties of perfect, vacancy-doped, and nonmetal adsorbed MoSe2, MoTe2 and WS2 monolayers. Physical Chemistry Chemical Physics, 2011, 13, 15546.	1.3	428
10340	Ultra-narrow WS₂nanoribbons encapsulated in carbon nanotubes. Journal of Materials Chemistry, 2011, 21, 171-180.	6.7	74
10341	Electronic properties of the partially hydrogenated armchair carbon nanotubes. Physical Review B, 2011, 84, .	1.1	16
10342	Ab initioinvestigation of Ti<mml:math xmlns:mml="http://www.w3.org/1998/Math/MathML" display="inline"><mml:msub><mml:mrow /><mml:mn>2</mml:mn></mml:msub></mml:math>Al(C,N) solid solutions. Physical Review B, 2011, 84, .	1.1	19
10343	Prediction of the Unknown Crystal Structure of Creatine Using Fully Quantum Mechanical Methods. Crystal Growth and Design, 2011, 11, 5733-5740.	1.4	36
10344	Spin texture and magnetic anisotropy of Co impurities in Bi<mml:math xmlns:mml="http://www.w3.org/1998/Math/MathML" display="inline"><mml:msub><mml:mrow /><mml:mn>2</mml:mn></mml:msub></mml:math>Se<mml:math xmlns:mml="http://www.w3.org/1998/Math/MathML" display="inline"><mml:msub><mml:mrow /><mml:mn>3</mml:mn></mml:msub></mml:math>topological insulators. Physical Review B, 2011, 84, .	1.1	47
10345	Effects of Alkali Adatoms on CO and H₂S Adsorptions on the Fe(100) Surface: A Density Functional Theory Study. Journal of Physical Chemistry C, 2011, 115, 23893-23901.	1.5	19
10346	DFT study of gas-phase adsorption of benzotriazole on Cu(111), Cu(100), Cu(110), and low coordinated defects thereon. Physical Chemistry Chemical Physics, 2011, 13, 20408.	1.3	69
10347	Effect of fluorine additions on the stability of Mg3Si4O10(OH)2: Computer simulation. Glass Physics and Chemistry, 2011, 37, 441-444.	0.2	3
10348	Quantum-mechanical calculations of the Ti and Zr substitution effect on the electronic structure of the nanoporous silicate matrix. Nanotechnologies in Russia, 2011, 6, 166-170.	0.7	2
10349	Advanced materials for hydrogen storage based on iron-palladium intermetallic alloys. Inorganic Materials: Applied Research, 2011, 2, 172-175.	0.1	2
10350	A DFT study on the interaction between europium, uranium and SWCNT. Open Physics, 2011, 9, .	0.8	1
10351	Structural stability, elastic constants, bonding characteristics and thermal properties of zincblende, rocksalt and fluorite phases in copper nitrides: plane-wave pseudo-potential ab initio calculations. Open Physics, 2011, 9, .	0.8	9
10352	Simulations on the mechanism of CNT bundle growth upon smooth and nanostructured Ni as well as Î¸-Al2O3 catalysts. Open Physics, 2011, 9, 530-541.	0.8	3
10353	First-principles LCAO study of phonons in NiWO4. Open Physics, 2011, 9, .	0.8	23
10354	Ab initio calculations of the atomic and electronic structure of MgF2 (011) and (111) surfaces. Open Physics, 2011, 9, .	0.8	5
10355	First-principles investigation of structural, electronic, optical and dynamical properties in CsAu. Open Physics, 2011, 9, .	0.8	3

#	Article	IF	Citations
10356	Systematic DFT-GGA study of hydrogen adsorption on transition metals. Russian Journal of Physical Chemistry A, 2011, 85, 2373-2379.	0.1	25
10357	Theory of elastic phase transitions in metals at high pressures. Application to vanadium. Journal of Experimental and Theoretical Physics, 2011, 112, 240-245.	0.2	10
10358	Magnetic ordering in digital alloys of group-IV semiconductors with 3d-transition metals. Journal of Experimental and Theoretical Physics, 2011, 112, 625-636.	0.2	8
10359	Theoretical study of the influence of vacancies on the electronic structure of a hexagonal boron nitride monolayer. Journal of Experimental and Theoretical Physics, 2011, 112, 664-667.	0.2	6
10360	Mobility of vacancies under deformation and their effect on the elastic properties of graphene. Journal of Experimental and Theoretical Physics, 2011, 112, 820-824.	0.2	17
10361	Chlorine adsorption on the InAs (001) surface. Semiconductors, 2011, 45, 21-29.	0.2	9
10362	Effect of coverage by carbon on the possibility of forming an interstitial solid solution in Fe(001) and Fe(111) subsurface layers. Physics of the Solid State, 2011, 53, 599-605.	0.2	3
10363	Effect of alloying elements and impurities on interface properties in aluminum alloys. Physics of the Solid State, 2011, 53, 2189-2193.	0.2	12
10364	Contribution of phonons to the line width of surface electronic states on Pd(111). Physics of the Solid State, 2011, 53, 2508-2514.	0.2	4
10365	Simulation of the atomic and electronic structures of mesoporous SiO2 containing Ti4+ and Zr4+ ions. Technical Physics, 2011, 56, 567-569.	0.2	4
10366	Computational investigation of elastic properties of bulk and defective ultrahard B6O. Journal of Superhard Materials, 2011, 33, 19-28.	0.5	8
10367	Crystal structures, mechanical and electronic properties of tantalum monocarbide and mononitride. Journal of Superhard Materials, 2011, 33, 173-178.	0.5	23
10368	Effect of N doping and Stone-Wales defects on the electronic properties of graphene nanoribbons. European Physical Journal B, 2011, 79, 335-340.	0.6	42
10369	Electronic structure of fluorides: general trends for ground and excited state properties. European Physical Journal B, 2011, 81, 115-120.	0.6	25
10370	Structural, electronic and magnetic properties of hcp Fe, Co and Ni nanowires encapsulated in zigzag carbon nanotubes. European Physical Journal B, 2011, 81, 459-465.	0.6	24
10371	Ferromagnetism in Rh-doped SnO2 from first-principles calculation. European Physical Journal B, 2011, 80, 337-341.	0.6	17
10372	First-principles study of elastic and vibrational properties of Ni2MnIn magnetic shape memory alloys. European Physical Journal B, 2011, 79, 509-514.	0.6	15
10373	Structural phase transition and the related electronic and optical properties of MgZnO nanowires. European Physical Journal B, 2011, 80, 395-400.	0.6	6

#	Article	IF	Citations
10374	Structural and electronic properties of Y2CrS4 from first-principles study. European Physical Journal B, 2011, 80, 307-310.	0.6	1
10375	Spin-polarized first-principles study of ferromagnetism in zinc-blende In1â^'xMnxSb. European Physical Journal B, 2011, 81, 381-386.	0.6	8
10376	An ab initio study on gas sensing properties of graphene and Si-doped graphene. European Physical Journal B, 2011, 81, 475-479.	0.6	143
10377	Sulphur overlayers on Ir(100) and its effect on the adsorption of CO: a DFT study. European Physical Journal B, 2011, 83, 437-443.	0.6	6
10378	Hydrogen-induced interactions in vanadium from first-principles calculations. Physical Review B, 2011, 83, .	1.1	45
10379	First-principles study of band gap engineering via oxygen vacancy doping in perovskite<mml:math xmlns:mml="http://www.w3.org/1998/Math/MathML" display="inline"><mml:mrow><mml:mi>A</mml:mi><mml:mi>B</mml:mi><mml:msup><mml:mi>B</mml:mi><mml:mo>â€²</mml:mo></mml:msup><mml:msub><mml:mi>O</mml:mi><mml:mn>3</mml:mn></mml:msub></mml:mrow></mml:math> solid solutions. Physical Review B, 2011, 84, .	1.1	25
10380	Defect states of complexes involving a vacancy on the boron site in boronitrene. Physical Review B, 2011, 84, .	1.1	36
10381	Structural, Electronic, and Optical Properties of Ag-Doped ZnO Nanowires: First Principles Study. Journal of Physical Chemistry C, 2011, 115, 3552-3557.	1.5	164
10382	Density Functional Theory Simulations of Structures and Properties for Ag-Doped ZnO Nanotubes. Journal of Physical Chemistry C, 2011, 115, 2907-2913.	1.5	37
10383	High pressure partially ionic phase of water ice. Nature Communications, 2011, 2, 563.	5.8	208
10384	Predicted Novel High-Pressure Phases of Lithium. Physical Review Letters, 2011, 106, 015503.	2.9	499
10385	Spectroscopic Observation of Dual Catalytic Sites During Oxidation of CO on a Au/TiO ₂ Catalyst. Science, 2011, 333, 736-739.	6.0	907
10386	Tailoring Native Defects in LiFePO₄: Insights from First-Principles Calculations. Chemistry of Materials, 2011, 23, 3003-3013.	3.2	155
10387	Formation and electronic properties of hydrogenated few layer graphene. Nanotechnology, 2011, 22, 185202.	1.3	74
10388	Confinement Effects and Hyperfine Structure in Se Doped Silicon Nanowires. Nano Letters, 2011, 11, 4509-4514.	4.5	7
10389	One-dimensional uraniumâ€“organic coordination polymers: crystal and electronic structures of uranyl-diacetohydroxamate. Dalton Transactions, 2011, 40, 6007.	1.6	17
10390	First-Principles Study of Photoinduced Water-Splitting on Fe₂O₃. Journal of Physical Chemistry C, 2011, 115, 12901-12907.	1.5	96
10391	Splitting Water on Metal Oxide Surfaces. Journal of Physical Chemistry C, 2011, 115, 19710-19715.	1.5	45

#	Article	IF	Citations
10392	Hydrogen effect on shearing and cleavage of Al: A first-principles study. Physical Review B, 2011, 84, .	1.1	15
10393	Zigzag graphene nanoribbon edge reconstruction with Stone-Wales defects. Physical Review B, 2011, 84, .	1.1	65
10394	Hydrogen transport on graphene: Competition of mobility and desorption. Physical Review B, 2011, 84, .	1.1	36
10395	First-principle calculation of APB energy in Ni-based binary and ternary alloys. Modelling and Simulation in Materials Science and Engineering, 2011, 19, 025008.	0.8	70
10396	Prediction of stabilities, mechanical properties and electronic structures of tetragonal 3d transition metal disilicides: A first-principles investigation. Acta Materialia, 2011, 59, 5584-5592.	3.8	33
10397	Local electronic structure of LiFePO4 nanoparticles in aged Li-ion batteries. Acta Materialia, 2011, 59, 6917-6926.	3.8	19
10398	First-principles-based mesoscale modeling of the solute-induced stabilization of â€˜100â€‰ tilt grain boundaries in an Alâ€“Pb alloy. Acta Materialia, 2011, 59, 7022-7028.	3.8	7
10399	The structure and the properties of S-phase in AlCuMg alloys. Acta Materialia, 2011, 59, 7396-7405.	3.8	93
10400	Characterization of NbC and (Nb,Ti)N nanoprecipitates in TRIP assisted multiphase steels. Acta Materialia, 2011, 59, 7406-7415.	3.8	78
10401	Diffusion kinetics in aluminiumâ€“gold bond contacts from first-principles density functional calculations. Acta Materialia, 2011, 59, 7634-7644.	3.8	21
10402	Quasiparticle band structure and optical properties of NH₃BH₃. Physica Status Solidi - Rapid Research Letters, 2011, 5, 10-12.	1.2	11
10403	Firstâ€principles study of CrB₄ as a high shear modulus compound. Physica Status Solidi - Rapid Research Letters, 2011, 5, 13-15.	1.2	25
10404	Simulation of fracture in heterogeneous elastic materials with cohesive zone models. International Journal of Fracture, 2011, 168, 15-29.	1.1	34
10405	Three-scale analysis of BaTiO3 piezoelectric thin films fabrication process and its experimental validation. Journal of Materials Science, 2011, 46, 1380-1387.	1.7	7
10406	Phase equilibria and thermodynamic modeling in the Geâ€“Zr binary system. Journal of Materials Science, 2011, 46, 1405-1413.	1.7	3
10407	First-principles calculation of grain boundary energy and grain boundary excess free volume in aluminum: role of grain boundary elastic energy. Journal of Materials Science, 2011, 46, 4199-4205.	1.7	47
10408	Atomistic structure and energetics of interface between Mn-doped Î³-Ga2O3 and MgAl2O4. Journal of Materials Science, 2011, 46, 4169-4175.	1.7	12
10409	First-principles study of structure, vacancy formation, and strength of bcc Fe/V4C3 interface. Journal of Materials Science, 2011, 46, 4206-4215.	1.7	7

#	Article	IF	Citations
10410	Structure and thermodynamics of the key precipitated phases in the Alâ€“Mgâ€“Si alloys from first-principles calculations. Journal of Materials Science, 2011, 46, 7839-7849.	1.7	26
10411	Investigation of the adsorption and diffusion interaction of atomic hydrogen with low-index surfaces of crystal aluminum nanoplates. Journal of Engineering Physics and Thermophysics, 2011, 84, 554-566.	0.2	0
10412	Optical Spectra Properties of Neutral Zn-Doped Au20 Nanoclusters by First-Principles Calculations. Journal of Inorganic and Organometallic Polymers and Materials, 2011, 21, 758-765.	1.9	7
10413	Ab Initio Study of Hydrogen Interaction with Defective BC2N Nanotubes. Journal of Low Temperature Physics, 2011, 164, 41-53.	0.6	3
10414	Direct CO Oxidation by Lattice Oxygen on Zr-Doped Ceria Surfaces. Catalysis Letters, 2011, 141, 78-82.	1.4	39
10415	A DFT Study on the Adsorption of Formic Acid and Its Oxidized Intermediates on (100) Facets of Pt, Au, Monolayer and Decorated Pt@Au Surfaces. Catalysis Letters, 2011, 141, 1872-1882.	1.4	25
10416	Special features of the electronic structure of Ga2AsSb crystals. Russian Physics Journal, 2011, 53, 1216-1218.	0.2	4
10417	Fabrication and modification of the supported Al nanoparticles on the Al(001) and (110) surfaces using the reversible vertical single-atom manipulation with the Cu and Pt trimer-apex tips: a first-principles study. Journal of Nanoparticle Research, 2011, 13, 1191-1196.	0.8	1
10418	Density functional study of super cell N-doped (10,0) zigzag single-walled carbon nanotubes as CO sensor. Structural Chemistry, 2011, 22, 1205-1211.	1.0	31
10419	Gold Nanoparticles on Yttrium Modified Titania: Support Properties and Catalytic Activity. Topics in Catalysis, 2011, 54, 219-228.	1.3	25
10420	Effect of Particle Size and Adsorbates on the L3, L2 and L1 X-ray Absorption Near Edge Structure of Supported Pt Nanoparticles. Topics in Catalysis, 2011, 54, 334-348.	1.3	101
10421	Two Gold Surfaces and a Cluster with Remarkable Reactivity for CO Oxidation, a Density Functional Theory Study. Topics in Catalysis, 2011, 54, 415-423.	1.3	18
10422	Adsorption mechanism of single guanine and thymine on single-walled carbon nanotubes. Journal of Molecular Modeling, 2011, 17, 2773-2780.	0.8	12
10423	Structural phase transition of SnSe under uniaxial stress and hydrostatic pressure: an ab initio study. Journal of Molecular Modeling, 2011, 17, 2989-2994.	0.8	33
10424	Microscopic indium distribution and electron localization in zinc blende InGaN alloys and InGaN/GaN strained quantum wells. Applied Physics B: Lasers and Optics, 2011, 104, 105-111.	1.1	5
10425	High-pressure thermo-elastic properties of beryl (Al4Be6Si12O36) from ab initio calculations, and observations about the source of thermal expansion. Physics and Chemistry of Minerals, 2011, 38, 223-239.	0.3	52
10426	Vibrational and thermodynamic properties of Ni3S2 polymorphs from first-principles calculations. Physics and Chemistry of Minerals, 2011, 38, 241-249.	0.3	6
10427	Solid solution behaviour of CaSiO3 and MgSiO3 perovskites. Physics and Chemistry of Minerals, 2011, 38, 311-319.	0.3	16

#	Article	IF	Citations
10428	The enigma of post-perovskite anisotropy: deformation versus transformation textures. Physics and Chemistry of Minerals, 2011, 38, 665-678.	0.3	33
10429	Multiscale modeling for ferroelectric materials: a transition from the atomic level to phase-field modeling. Continuum Mechanics and Thermodynamics, 2011, 23, 435-451.	1.4	53
10430	DFT and kinetics study of O/O2 mixtures reacting over a graphite (0001) basal surface. Theoretical Chemistry Accounts, 2011, 128, 683-694.	0.5	34
10431	A density functional theory study of the â€˜mythicâ€™ Lindlar hydrogenation catalyst. Theoretical Chemistry Accounts, 2011, 128, 663-673.	0.5	130
10432	Charge transport and electronic properties of N-heteroquinones: quadruple weak hydrogen bonds and strong Ï€â€“Ï€ stacking interactions. Theoretical Chemistry Accounts, 2011, 128, 257-264.	0.5	20
10433	Theoretical study of phenol adsorption on the (8, 0) silicon carbide nanotube. Theoretical Chemistry Accounts, 2011, 129, 85-92.	0.5	10
10434	Attractive interaction between transition-metal atom impurities and vacancies in graphene: a first-principles study. Theoretical Chemistry Accounts, 2011, 129, 625-630.	0.5	97
10435	Adsorption of catechol on a wet silica surface: density functional theory study. Theoretical Chemistry Accounts, 2011, 130, 333-339.	0.5	49
10436	Negative rectification and negative differential resistance in nanoscale single-walled carbon nanotube p-n junctions. Theoretical Chemistry Accounts, 2011, 130, 353-359.	0.5	10
10437	Structural and electronic properties of tungsten trioxides: from cluster to solid surface. Theoretical Chemistry Accounts, 2011, 130, 103-114.	0.5	28
10438	High-pressure transitions in bulk mercury: a density functional study. Theoretical Chemistry Accounts, 2011, 130, 455-462.	0.5	12
10439	Tuning graphene nanoribbon field effect transistors via controlling doping level. Theoretical Chemistry Accounts, 2011, 130, 483-489.	0.5	5
10440	XAS study on copper red in ancient glass beads from Thailand. Analytical and Bioanalytical Chemistry, 2011, 399, 3033-3040.	1.9	35
10441	Electronic structures, mechanical and thermodynamic properties of ThN from first-principles calculations. Journal of Nuclear Materials, 2011, 408, 136-141.	1.3	37
10442	Stability and mobility of Cuâ€“vacancy clusters in Feâ€“Cu alloys: A computational study based on the use of artificial neural networks for energy barrier calculations. Journal of Nuclear Materials, 2011, 412, 106-115.	1.3	27
10443	First principles calculation of the elastic constants and phonon modes of UO2 using GGA + U with orbital occupancy control. Journal of Nuclear Materials, 2011, 412, 301-307.	1.3	31
10444	Structural and vibrational properties of Ca2FeH6 and Sr2RuH6. Journal of Physics and Chemistry of Solids, 2011, 72, 286-289.	1.9	15
10445	Ab initio study of ultra-incompressible ternary BeCN2 polymorph. Journal of Physics and Chemistry of Solids, 2011, 72, 667-672.	1.9	12

#	Article	IF	Citations
10446	H2O chemisorption and H2 oxidation on yttria-stabilized zirconia: Density functional theory and temperature-programmed desorption studies. Journal of Power Sources, 2011, 196, 7188-7194.	4.0	25
10447	Direct comparison between two structural models by DFT calculations. Journal of Solid State Chemistry, 2011, 184, 1105-1111.	1.4	66
10448	A DFT study of the effect of natural impurities on the electronic structure of galena. International Journal of Mineral Processing, 2011, 98, 132-136.	2.6	40
10449	Microstructure investigation and first-principle analysis of die-cast AZ91 alloy with calcium addition. Materials Science & Engineering A: Structural Materials: Properties, Microstructure and Processing, 2011, 528, 5283-5288.	2.6	18
10450	A-centers and isovalent impurities in germanium: Density functional theory calculations. Materials Science and Engineering B: Solid-State Materials for Advanced Technology, 2011, 176, 453-457.	1.7	25
10451	Structural analogues of graphyne family: New types of boron nitride sheets with wide band gap and strong UV absorption. Chemical Physics Letters, 2011, 502, 217-221.	1.2	39
10452	The structure of FePc on Cu(100). Chemical Physics Letters, 2011, 503, 53-56.	1.2	7
10453	Cu-doped ceria: Oxygen vacancy formation made easy. Chemical Physics Letters, 2011, 510, 60-66.	1.2	53
10454	Influence of chemical composition and magnetic effects on the elastic properties of fcc Feâ€“Mn alloys. Acta Materialia, 2011, 59, 1493-1501.	3.8	36
10455	Supertoughening in B1 transition metal nitride alloys by increased valence electron concentration. Acta Materialia, 2011, 59, 2121-2134.	3.8	166
10456	Hole doping effect on ferromagnetism in Mn-doped ZnO nanowires. Current Applied Physics, 2011, 11, 236-240.	1.1	8
10457	Lateral interaction and structures in Cl adlayers on the Ag(111) surface. Chemical Physics, 2011, 383, 35-40.	0.9	6
10458	A density functional study on adsorption and dissociation of O2 on Ir(1 0 0) surface. Chemical Physics, 2011, 385, 35-40.	0.9	22
10459	Oxygen vacancy in LiTiPO5 and LiTi2(PO4)3: A first-principles study. Physics Letters, Section A: General, Atomic and Solid State Physics, 2011, 375, 934-938.	0.9	25
10460	Interplay between lattice dynamics and the low-pressure phase of simple cubic polonium. Physics Letters, Section A: General, Atomic and Solid State Physics, 2011, 375, 1695-1697.	0.9	8
10461	Dissociation of hydrogen molecules on the clean and hydrogen-preadsorbed Be(0001) surface. Physics Letters, Section A: General, Atomic and Solid State Physics, 2011, 375, 2430-2436.	0.9	9
10462	Adsorption and diffusion of H2O molecule on the Be(0001) surface: A density-functional theory study. Physics Letters, Section A: General, Atomic and Solid State Physics, 2011, 375, 3208-3212.	0.9	8
10463	LCAO calculation of water adsorption on (001) surface of Y-doped BaZrO3. Solid State Ionics, 2011, 188, 25-30.	1.3	8

#	Article	IF	Citations
10464	First principles calculations of oxygen vacancy formation and migration in mixed conducting Ba0.5Sr0.5Co1â^'yFeyO3â^'Î´ perovskites. Solid State Ionics, 2011, 188, 1-5.	1.3	98
10465	First-principles simulations on the aggregation of F centers in BaF2: R centers. Solid State Ionics, 2011, 187, 1-7.	1.3	12
10466	CO adsorption on ionic Pt, Pd and Cu sites in Ce1-xMxO2â€‰â^'â€‰Î´ (M = Pt2+, Pd2+, Cu2+). Journal of Chemical Sciences, 2011, 123, 509-516.	0.7	25
10467	Monte Carlo simulation of B2-L21 ordering transitions in Au-Cu-Al alloy systems. Journal of Shanghai Jiaotong University (Science), 2011, 16, 186-189.	0.5	1
10468	Properties and electronic structure of iron under pressure up to 30GPa. Journal of Shanghai Jiaotong University (Science), 2011, 16, 257-261.	0.5	2
10469	Inorganic nanoribbons with unpassivated zigzag edges: Half metallicity and edge reconstruction. Nano Research, 2011, 4, 233-239.	5.8	62
10470	DFT calculations on structural and electronic properties of Bi2MO6 (M = Cr, Mo, W). Rare Metals, 2011, 30, 166-172.	3.6	60
10471	Effect of Fe ternary addition on ductility of NiAl intermetallic alloy. Rare Metals, 2011, 30, 316-319.	3.6	4
10472	Revisiting H/Pt(111) by a combined experimental study of the H-D exchange reaction and first-principles calculations. Science China Chemistry, 2011, 54, 745-755.	4.2	14
10473	Electric-field control of the activity of the graphene-based catalyst. Science China: Physics, Mechanics and Astronomy, 2011, 54, 804-808.	2.0	9
10474	First-principles investigation of the effects of B impurities on the mechanical properties of NiAl intermetallics. Science China: Physics, Mechanics and Astronomy, 2011, 54, 809-814.	2.0	4
10475	Negative differential resistance in molecular devices: the role of molecule-electrode coupling. Science China: Physics, Mechanics and Astronomy, 2011, 54, 1455-1460.	2.0	6
10476	Electronic structure and optical property of boron doped semiconducting graphene nanoribbons. Science China: Physics, Mechanics and Astronomy, 2011, 54, 1438-1442.	2.0	5
10477	First-principles study of carbon effects in a tungsten grain boundary: site preference, segregation and strengthening. Science China: Physics, Mechanics and Astronomy, 2011, 54, 2164-2169.	2.0	32
10478	Electronic origin of the anomalous solid solution hardening of Y and Gd in Mg: A first-principles study. Science Bulletin, 2011, 56, 1038-1042.	1.7	20
10479	First-principles calculations of the Î²â€²-Mg7Gd precipitate in Mg-Gd binary alloys. Science Bulletin, 2011, 56, 1142-1146.	1.7	25
10480	Mechanism and kinetics for methanol synthesis from CO2/H2 over Cu and Cu/oxide surfaces: Recent investigations by first-principles-based simulation. Frontiers of Chemistry in China: Selected Publications From Chinese Universities, 2011, 6, 164-172.	0.4	10
10481	Tripyrrylmethane based 2D porous structure for hydrogen storage. Frontiers of Physics, 2011, 6, 220-223.	2.4	6

#	Article	IF	Citations
10482	Effects of Additives and Impurity on the Adhesive Behavior of the NiAl(110)/Al2O3 (0001) Interface: An Ab Initio Study. Metallurgical and Materials Transactions A: Physical Metallurgy and Materials Science, 2011, 42, 4126-4136.	1.1	22
10483	Electronic and Lattice Vibrational Properties of BaSi2 from Density Functional Theory Calculations. Journal of Electronic Materials, 2011, 40, 620-623.	1.0	14
10484	Structural and Electronic Properties of TypeÂI Clathrates M8Ga16Ge30 (MÂ=ÂBa, Sr, Yb) from First-Principles Calculations. Journal of Electronic Materials, 2011, 40, 1298-1303.	1.0	9
10485	Density-Functional Study of the Electronic Structure and Optical Properties of Transparent Conducting Oxides In4Sn3O12 and In4Ge3O12. Journal of Electronic Materials, 2011, 40, 1501-1505.	1.0	4
10486	Self-Diffusion Coefficient of fcc Mg: First-Principles Calculations and Semi-Empirical Predictions. Journal of Phase Equilibria and Diffusion, 2011, 32, 128-137.	0.5	13
10487	First principles study on electronic structure and optical properties of quaternary arsenide oxides YZnAsO and LaZnAsO. Central South University, 2011, 18, 998-1003.	0.5	5
10488	Phase transition and thermodynamic properties of BaS: An Ab initio study. Wuhan University Journal of Natural Sciences, 2011, 16, 33-37.	0.2	3
10489	The Ternary Nitrides In_xFe_{4â€“x}N (0 â‰¤ x â‰¤ 0.8): Synthesis, Magnetic Properties, and Theoretical Considerations. Zeitschrift Fur Anorganische Und Allgemeine Chemie, 2011, 637, 935-939.	0.6	16
10490	The Complex Amide K₂[Zr(NH₂)₆]. Zeitschrift Fur Anorganische Und Allgemeine Chemie, 2011, 637, 1122-1130.	0.6	4
10491	In Search of Chemical Frustration in the Caâ€Cuâ€Cd System: Chemical Pressure Relief in the Crystal Structures of ÂCa₅Cu₂Cd and Ca₂Cu₂Cd₉. Zeitschrift Fur Anorganische Und Allgemeine Chemie, 2011, 637, 1961-1974.	0.6	19
10492	From covalent bonding to coalescence of metallic nanorods. Nanoscale Research Letters, 2011, 6, 559.	3.1	6
10493	A one-dimensional extremely covalent material: monatomic carbon linear chain. Nanoscale Research Letters, 2011, 6, 577.	3.1	24
10494	Metal-functionalized single-walled graphitic carbon nitride nanotubes: a first-principles study on magnetic property. Nanoscale Research Letters, 2011, 6, 97.	3.1	18
10495	Special directions in momentum space. I. Cubic symmetries. Journal of Applied Crystallography, 2011, 44, 1246-1254.	1.9	6
10496	The effect of pressure on the crystal structure of bianthrone. Acta Crystallographica Section B: Structural Science, 2011, 67, 226-237.	1.8	12
10497	Structural building principles of complex face-centered cubic intermetallics. Acta Crystallographica Section B: Structural Science, 2011, 67, 269-292.	1.8	50
10498	Firstâ€principles study on structural, electronic and magnetic properties of iron nanowire encapsulated in carbon nanotube. Physica Status Solidi (A) Applications and Materials Science, 2011, 208, 97-103.	0.8	8
10499	Theory of the surface effects on the luminescence of the NV^{â^’} defect in nanodiamond. Physica Status Solidi (A) Applications and Materials Science, 2011, 208, 2045-2050.	0.8	9

#	Article	IF	Citations
10500	Firstâ€principles study on the structural, phonon, and thermodynamic properties of the ternary carbides in Tiâ€“Alâ€“C system. Physica Status Solidi (A) Applications and Materials Science, 2011, 208, 1879-1884.	0.8	23
10501	Ab initio study on the electronic transport properties of carbon nanotube intramolecular junctions. Physica Status Solidi (A) Applications and Materials Science, 2011, 208, 2803-2808.	0.8	4
10502	Highâ€pressure phase transitions in NaBH₄ from firstâ€principles calculations. Physica Status Solidi (B): Basic Research, 2011, 248, 1139-1142.	0.7	3
10503	Adsorption of Sn on the Ge(111)â€(3â€‰Ã—â€‰3) surface studied by ab initio density functional theory. Physica Status Solidi (B): Basic Research, 2011, 248, 2142-2146.	0.7	1
10504	FPâ€LAPW calculations of structural and elastic properties of tantalum under high pressure. Physica Status Solidi (B): Basic Research, 2011, 248, 175-180.	0.7	5
10505	Accurate Kohnâ€“Sham DFT with the speed of tight binding: Current techniques and future directions in materials modelling. Physica Status Solidi (B): Basic Research, 2011, 248, 1309-1318.	0.7	57
10506	Ab initio study of structural, electronic, elastic, and phonon properties of ScN and ScP at ambient and high pressure. Physica Status Solidi (B): Basic Research, 2011, 248, 921-927.	0.7	7
10507	Calculations for the linear and nonlinear optical coefficients of ZCTC crystals. Physica Status Solidi (B): Basic Research, 2011, 248, 1483-1489.	0.7	4
10508	Lattice dynamics of layered semiconducting compound TlGaS₂. Physica Status Solidi (B): Basic Research, 2011, 248, 181-186.	0.7	4
10509	Firstâ€principles calculation of vibrational properties of B₁₂As₂ crystal. Physica Status Solidi (B): Basic Research, 2011, 248, 1242-1247.	0.7	7
10510	Nonâ€standard anisotropy of the energy spectrum of a layered TlGaSe₂ crystal. Physica Status Solidi (B): Basic Research, 2011, 248, 1446-1452.	0.7	2
10511	Variation of hydrogen adsorption with increasing Li doping on carbon nanotubes. Physica Status Solidi (B): Basic Research, 2011, 248, 1420-1424.	0.7	14
10512	Firstâ€principles modeling of the interactions of iron impurities with graphene and graphite. Physica Status Solidi (B): Basic Research, 2011, 248, 1347-1351.	0.7	16
10513	Ferromagnetic and metallic properties of the semihydrogenated GaN sheet. Physica Status Solidi (B): Basic Research, 2011, 248, 1442-1445.	0.7	27
10514	Highâ€pressure lattice dynamics and thermodynamics in BaO. Physica Status Solidi (B): Basic Research, 2011, 248, 1405-1411.	0.7	10
10515	Single walled carbon nanotubes functionalized with hydrides as potential hydrogen storage media: A survey of intermolecular interactions. Physica Status Solidi (B): Basic Research, 2011, 248, 2147-2158.	0.7	12
10516	Electronic and magnetic structure of carbides RRh₃C. Physica Status Solidi (B): Basic Research, 2011, 248, 1925-1932.	0.7	2
10517	First principles prediction of structural and mechanical properties of the nanolaminate compound M₄AlN₃ (Mâ€‰=â€‰V, Nb, and Ta). Physica Status Solidi (B): Basic Research, 2011, 248, 1639-1644.	0.7	7

#	Article	IF	Citations
10518	Effect of chirality and curvature of singleâ€walled carbon nanotubes on the adsorption of uracil. Physica Status Solidi (B): Basic Research, 2011, 248, 1431-1436.	0.7	13
10519	Substrate induced bandgap in multilayer epitaxial graphene on the 4Hâ€SiC ($000{ar {1}}$) surface. Physica Status Solidi (B): Basic Research, 2011, 248, 1690-1695.	0.7	6
10520	Firstâ€principles study of magnetic properties in Agâ€doped SnO₂. Physica Status Solidi (B): Basic Research, 2011, 248, 1961-1966.	0.7	26
10521	Elastic properties and electronic structures of Mgï£¿Ce intermetallic compounds from firstâ€principles calculations. Physica Status Solidi (B): Basic Research, 2011, 248, 2097-2102.	0.7	7
10522	Catalytic oxidation of CO on Ir(100). Physica Status Solidi (B): Basic Research, 2011, 248, 1425-1430.	0.7	13
10523	Firstâ€principles study of structural and elastic properties of the tetragonal ferroelectric perovskite Pb(Zr_{0.50}Ti_{0.50})O₃. Physica Status Solidi (B): Basic Research, 2011, 248, 2222-2228.	0.7	13
10524	Bundle and chirality influences on properties of carbon nanotubes studied with van der Waals density functional theory. Physica Status Solidi (B): Basic Research, 2011, 248, 2589-2592.	0.7	20
10525	Bandgap modulations of silicon carbon nanoribbons by transverse electric fields: A theoretical study. Physica Status Solidi (B): Basic Research, 2011, 248, 1676-1681.	0.7	26
10526	First principles study of structural, elastic, electronic and optical properties of Nb₂N and Ta₂N compounds. Physica Status Solidi (B): Basic Research, 2011, 248, 2787-2792.	0.7	13
10527	From electrons to materials. Physica Status Solidi (B): Basic Research, 2011, 248, 2213-2221.	0.7	4
10528	Failure of potassium dimer formation on the Î²â€SiC(100)â€c(4â€‰Ã—â€‰2) surface. Physica Status Solidi (B): Basic Research, 2011, 248, 2072-2075.	0.7	1
10529	Valence band localized states in double quantum wells from first principles. Physica Status Solidi (B): Basic Research, 2011, 248, 2877-2883.	0.7	0
10530	Oxygen adsorption on Al (111) surface interstitial site calculated by density functional theory. Surface and Interface Analysis, 2011, 43, 940-944.	0.8	7
10531	Evidence for Fe²⁺ in Wurtzite Coordination: Iron Doping Stabilizes ZnO Nanoparticles. Small, 2011, 7, 2879-2886.	5.2	44
10532	Carbonâ€Induced Ordering in Manganeseâ€Rich Austenite â€" A Densityâ€Functional Totalâ€Energy and Chemicalâ€Bonding Study. Steel Research International, 2011, 82, 101-107.	1.0	46
10533	First Principles Calculation of the Thermal Volume Expansion Coefficient of Tetragonal Zircon Dioxide. Steel Research International, 2011, 82, 1129-1132.	1.0	2
10534	A densityâ€functional theory approach to the separation of K₂ZrF₆ and K₂HfF₆ via fractional crystallization. International Journal of Quantum Chemistry, 2011, 111, 682-693.	1.0	0
10535	Adaptive smearing for Brillouin zone integration. International Journal of Quantum Chemistry, 2011, 111, 1025-1030.	1.0	13

#	Article	IF	Citations
10536	IxV curves of boron and nitrogen doping zigzag graphene nanoribbons. International Journal of Quantum Chemistry, 2011, 111, 1379-1386.	1.0	17
10537	Transport properties of twoâ€dimensionally fused zinc porphyrins from linearâ€response approach. International Journal of Quantum Chemistry, 2011, 111, 3230-3238.	1.0	5
10538	First-Principles Study on the Stabilities of the Intermetallic Compounds in Mg-Nd Alloys. Rare Metal Materials and Engineering, 2011, 40, 590-594.	0.8	8
10539	Vibrational spectra of rhombohedral TeO₃ compared to those of ReO₃â€like protoâ€phase and Î±â€TeO₂ (paratellurite): lattice dynamic and crystal chemistry aspects. Journal of Raman Spectroscopy, 2011, 42, 758-764.	1.2	14
10540	A singleâ€crystal Raman and infrared study of the nonlinear optical crystal MBANP. Journal of Raman Spectroscopy, 2011, 42, 1174-1184.	1.2	12
10541	Understanding the Terahertz Spectra of Crystalline Pharmaceuticals: Terahertz Spectroscopy and Solid-State Density Functional Theory Study of (S)-(+)-Ibuprofen and (RS)-Ibuprofen. Journal of Pharmaceutical Sciences, 2011, 100, 1116-1129.	1.6	65
10542	Tuning of Charge Densities in Graphene by Molecule Doping. Advanced Functional Materials, 2011, 21, 2687-2692.	7.8	99
10543	Surfaceâ€Modified Lowâ€Temperature Solid Oxide Fuel Cell. Advanced Functional Materials, 2011, 21, 4684-4690.	7.8	67
10544	Batteryless Chemical Detection with Semiconductor Nanowires. Advanced Materials, 2011, 23, 117-121.	11.1	22
10545	Lattice dynamics of ZnAl₂O₄ and ZnGa₂O₄ under high pressure. Annalen Der Physik, 2011, 523, 157-167.	0.9	47
10546	Li2Sr4[Si2N5]N - A Layered Lithium Nitridosilicate Nitride. European Journal of Inorganic Chemistry, 2011, 2011, 2118-2123.	1.0	8
10547	Revisiting the Zintlâ€“Klemm Concept: A₂AuBi (A = Li or Na). European Journal of Inorganic Chemistry, 2011, 2011, 3989-3998.	1.0	14
10548	Tautomerism and the Protonation/Deprotonation of Isocytosine in Liquidâ€and Solidâ€States Studied by NMR Spectroscopy and Theoretical Calculations. European Journal of Organic Chemistry, 2011, 2011, 1544-1551.	1.2	37
10549	Calcium-Decorated, Hydroxylated Single-Walled Carbon Nanotubes for Hydrogen Storage: A First-Principles Study. ChemPhysChem, 2011, 12, 777-780.	1.0	5
10550	Steric and Chain Length Effects in the (${sqrt {(3)} }$Ã—${sqrt {(3)} }$)R30Â° Structures of Alkanethiol Selfâ€Assembled Monolayers on Au(111). ChemPhysChem, 2011, 12, 999-1009.	1.0	35
10551	Outer Helmholtz Plane of the Electrical Double Layer Formed at the Solid Electrodeâ€“Liquid Interface. ChemPhysChem, 2011, 12, 1430-1434.	1.0	85
10552	Defectâ€Assisted Covalent Binding of Graphene to an Amorphous Silica Surface: A Theoretical Prediction. ChemPhysChem, 2011, 12, 2155-2159.	1.0	2
10553	New Insights into the Bandâ€Gap Narrowing of (N, P)â€Codoped TiO₂ from Hybrid Density Functional Theory Calculations. ChemPhysChem, 2011, 12, 2604-2608.	1.0	29

#	Article	IF	Citations
10554	A DFT Study of Carbon in the Subsurface Layer of Cobalt Surfaces. ChemPhysChem, 2011, 12, 2925-2928.	1.0	18
10555	Triazole, Benzotriazole, and Naphthotriazole as Copper Corrosion Inhibitors: I. Molecular Electronic and Adsorption Properties. ChemPhysChem, 2011, 12, 3547-3555.	1.0	53
10556	Electronic Properties of Vanadiumâ€Doped TiO₂. ChemPhysChem, 2011, 12, 3467-3473.	1.0	25
10557	Role of oxygen vacancies in the origin of ferromagnetism in Mnâ€doped ZnO. Crystal Research and Technology, 2011, 46, 1250-1256.	0.6	8
10558	Remarkable Uptake of CO₂ and CH₄ by Grapheneâ€Like Borocarbonitrides, B_xC_yN_z. ChemSusChem, 2011, 4, 1662-1670.	3.6	58
10559	Understanding of bonding and mechanical characteristics of cementitious mineral tobermorite from first principles. Journal of Computational Chemistry, 2011, 32, 306-314.	1.5	33
10560	Adsorption and dissociation of NH₃ on clean and hydroxylated TiO₂ rutile (110) surfaces: A computational study. Journal of Computational Chemistry, 2011, 32, 1101-1112.	1.5	13
10561	Sensitivity analysis and uncertainty calculation for dispersion corrected density functional theory. Journal of Computational Chemistry, 2011, 32, 1424-1430.	1.5	41
10562	Structural, electronic, bonding, and elastic properties of NH₃BH₃: A density functional study. Journal of Computational Chemistry, 2011, 32, 1734-1742.	1.5	37
10563	Firstâ€principles prediction on electronic and magnetic properties of hydrogenated AlN nanosheets. Journal of Computational Chemistry, 2011, 32, 3122-3128.	1.5	42
10564	Density functional theoryâ€based electrochemical models for the oxygen reduction reaction: Comparison of modeling approaches for electric field and solvent effects. Journal of Computational Chemistry, 2011, 32, 3399-3408.	1.5	61
10565	Theoretical insights on the electron doping and Curie temperature in Laâ€doped Sr₂CrWO₆. Journal of Computational Chemistry, 2011, 32, 3313-3318.	1.5	9
10571	Semiempirical Rate Constants for Complex Chemical Kinetics: Firstâ€Principles Assessment and Rational Refinement. Angewandte Chemie - International Edition, 2011, 50, 1194-1197.	7.2	42
10572	Activation Energies for Diffusion of Defects in Silicon: The Role of the Exchangeâ€Correlation Functional. Angewandte Chemie - International Edition, 2011, 50, 10221-10225.	7.2	31
10573	Carbon Chain Growth by Formyl Insertion on Rhodium and Cobalt Catalysts in Syngas Conversion. Angewandte Chemie - International Edition, 2011, 50, 5335-5338.	7.2	105
10574	The Particleâ€Size Dependence of the Activation Energy for Decomposition of Lithium Amide. Angewandte Chemie - International Edition, 2011, 50, 10170-10173.	7.2	19
10575	NaSr₃Be₃B₃O₉F₄: A Promising Deepâ€Ultraviolet Nonlinear Optical Material Resulting from the Cooperative Alignment of the [Be₃B₃O₁₂F]^{10â^'} Anionic Group. Angewandte Chemie - International Edition, 2011, 50, 9141-9144.	7.2	342
10576	The Role of Surface and Subsurface Point Defects for Chemical Model Studies on TiO₂: A Firstâ€Principles Theoretical Study of Formaldehyde Bonding on Rutile TiO₂(110). Chemistry - A European Journal, 2011, 17, 4496-4506.	1.7	72

#	Article	IF	Citations
10577	Unravelling the Mechanism of Glycerol Hydrogenolysis over Rhodium Catalyst through Combined Experimentalâ€“Theoretical Investigations. Chemistry - A European Journal, 2011, 17, 14288-14299.	1.7	99
10578	Hierarchical TiO₂ Microspheres: Synergetic Effect of {001} and {101} Facets for Enhanced Photocatalytic Activity. Chemistry - A European Journal, 2011, 17, 15032-15038.	1.7	180
10579	Lattice dynamics study of lead chalcogenides. Infrared Physics and Technology, 2011, 54, 39-43.	1.3	32
10580	Catalytic hydrogenation of benzene to cyclohexene on Ru(0001) from density functional theory investigationsâ˜†. Catalysis Today, 2011, 160, 234-241.	2.2	46
10581	Carbon monoxide adsorption and dissociation on Mn-decorated Rh(111) and Rh(553) surfaces: A first-principles study. Catalysis Today, 2011, 160, 228-233.	2.2	26
10582	A comparative density functional theory study of the direct synthesis of H2O2 on Pd, Pt and Au surfaces. Catalysis Today, 2011, 160, 242-248.	2.2	62
10583	Understanding of ethanol decomposition on Rh(111) from density functional theory and kinetic Monte Carlo simulations. Catalysis Today, 2011, 165, 64-70.	2.2	82
10584	Adsorption and activation of CO2 over the Cuâ€“Co catalyst supported on partially hydroxylated Î³-Al2O3. Catalysis Today, 2011, 165, 10-18.	2.2	35
10585	Reactivity of hydrogen and methanol on (001) surfaces of WO3, ReO3, WO3/ReO3 and ReO3/WO3. Catalysis Today, 2011, 165, 41-48.	2.2	31
10586	Density functional theory study of the effect of subsurface H, C, and Ag on C2H2 hydrogenation on Pd(111). Catalysis Today, 2011, 165, 106-111.	2.2	21
10587	First-principles study of Li adsorption in a carbon nanotube-fullerene hybrid system. Carbon, 2011, 49, 286-293.	5.4	51
10588	An experimental and theoretical examination of the effect of sulfur on the pyrolytically grown carbon nanotubes from sucrose-based solid state precursors. Carbon, 2011, 49, 508-517.	5.4	20
10589	A first-principles study of calcium-decorated, boron-doped graphene for high capacity hydrogen storage. Carbon, 2011, 49, 1561-1567.	5.4	201
10590	First-principles based kinetic modeling of effect of hydrogen on growth of carbon nanotubes. Carbon, 2011, 49, 2508-2521.	5.4	28
10591	Fermi level dependent optical transition energy in metallic single-walled carbon nanotubes. Carbon, 2011, 49, 4774-4780.	5.4	14
10592	Structural, electronic and magnetic properties of GaN nanotubes filled with nickel nanowires. Computational and Theoretical Chemistry, 2011, 963, 18-23.	1.1	9
10593	A theoretical study for the influence of coverage on Li, Na and K adsorption on Co(0001). Computational and Theoretical Chemistry, 2011, 963, 125-129.	1.1	7
10594	Comparison of electronic and magnetic properties of Fe, Co and Ni nanowires encapsulated in beryllium oxygen nanotubes. Computational and Theoretical Chemistry, 2011, 963, 273-278.	1.1	18

#	Article	IF	Citations
10595	Quantum chemical studies on beryllium hydride oligomers. Computational and Theoretical Chemistry, 2011, 963, 371-377.	1.1	16
10596	Mechanism of the phase transition in GaN under pressure up to 100GPa. Computational and Theoretical Chemistry, 2011, 964, 65-71.	1.1	10
10597	Substitutional doping of BN nanotube by transition metal: A density functional theory simulation. Computational and Theoretical Chemistry, 2011, 964, 199-206.	1.1	39
10598	Theoretical study on electronic properties and pressure-induced phase transition in Î²-CdP2. Computational and Theoretical Chemistry, 2011, 966, 149-153.	1.1	7
10599	The effects of the dangling bond on the electronic and magnetic properties of AlN nanoribbon. Computational and Theoretical Chemistry, 2011, 967, 113-119.	1.1	18
10600	First-principle investigations of CaO (100) surface and adsorption of H2O on CaO (100). Computational and Theoretical Chemistry, 2011, 967, 185-190.	1.1	16
10601	Ab initio calculation of adhesion and potential corrugation of diamond (001) interfaces. Computer Physics Communications, 2011, 182, 1796-1799.	3.0	6
10602	Accurate pseudopotential description of the GW bandstructure of ZnO. Computer Physics Communications, 2011, 182, 2029-2031.	3.0	17
10603	Phase stabilities and decomposition mechanism in the Zrâ€“Siâ€“N system studied by combined ab initio DFT and thermodynamic calculation. Acta Materialia, 2011, 59, 297-307.	3.8	37
10604	Light emission from several-atom Inâ€“N clusters in wurtzite Ga-rich InGaN alloys and InGaN/GaN strained quantum wells. Acta Materialia, 2011, 59, 2773-2782.	3.8	14
10605	Hydrogen-enhanced local plasticity at dilute bulk H concentrations: The role of Hâ€“H interactions and the formation of local hydrides. Acta Materialia, 2011, 59, 2969-2980.	3.8	132
10606	Improving the wettability of aluminum on carbon nanotubes. Acta Materialia, 2011, 59, 3313-3320.	3.8	66
10607	Thermoelastic properties of ScB2, TiB2, YB4 and HoB4: Experimental and theoretical studies. Acta Materialia, 2011, 59, 4886-4894.	3.8	63
10608	A first-principles calculation on the electronic properties of Si/N-codoped TiO2. Applied Surface Science, 2011, 257, 3000-3006.	3.1	32
10609	Ab initio study of the fcc-WC(100) surface and its interaction with cobalt monolayers. Applied Surface Science, 2011, 257, 3581-3585.	3.1	8
10610	Study on the interface between the organic and inorganic semiconductors. Applied Surface Science, 2011, 257, 4994-4999.	3.1	4
10611	Interactions between tri-methylaluminum molecules and their effect on the reaction of tri-methylaluminum with an OH-terminated Si (0 0 1) surface. Applied Surface Science, 2011, 257, 6326-6331.	3.1	13
10612	Theoretical calculations on the adhesion, stability, electronic structure, and bonding of Fe/WC interface. Applied Surface Science, 2011, 257, 5671-5678.	3.1	94

#	Article	IF	Citations
10613	Adsorption of water on TiN (1 0 0), (1 1 0) and (1 1 1) surfaces: A first-principles study. Applied Surface Science, 2011, 257, 6462-6467.	3.1	18
10614	Density functional theory prediction for diffusion of lithium on boron-doped graphene surface. Applied Surface Science, 2011, 257, 7443-7446.	3.1	40
10615	Density functional theory study of selenium adsorption on Fe(110). Applied Surface Science, 2011, 257, 6878-6883.	3.1	5
10616	Density functional theory study of the chemisorption of CO on Ir/MgO(100). Applied Surface Science, 2011, 257, 6986-6990.	3.1	2
10617	First-principles calculations on Al/AlB2 interfaces. Applied Surface Science, 2011, 257, 7831-7836.	3.1	103
10618	Magnetic properties of the semifluorinated and semihydrogenated 2D sheets of group-IV and III-V binary compounds. Applied Surface Science, 2011, 257, 7845-7850.	3.1	75
10619	Density functional theory study on activity of Î±-Fe2O3 in chemical-looping combustion system. Applied Surface Science, 2011, 257, 8647-8652.	3.1	53
10620	CH4 dissociation on NiCo (111) surface: A first-principles study. Applied Surface Science, 2011, 257, 8955-8964.	3.1	66
10621	Repair of magnetism in oxidized graphene nanoribbons. Chemical Physics Letters, 2011, 501, 396-399.	1.2	10
10622	The role of Ru atoms toward the dehydrogenation of ethanol on Ru/ZrO2(111) surface. Chemical Physics Letters, 2011, 501, 315-318.	1.2	2
10623	First principles investigations on the half metallic properties of Sr2MOsO6 (M=V, Mn, Fe, Co). Chemical Physics Letters, 2011, 501, 324-329.	1.2	32
10624	First-principles comparison of the cubic and tetragonal phases of. Chemical Physics Letters, 2011, 504, 148-152.	1.2	3
10625	Energetic stability of hydrogen-chemisorbed carbon nanotube structures. Chemical Physics Letters, 2011, 508, 107-110.	1.2	9
10626	Electronic structure and equation of state of PdO2 from ab initio. Chemical Physics Letters, 2011, 508, 215-218.	1.2	21
10627	Theoretical study of ZnO(1 0<mml:math xmlns:mml="http://www.w3.org/1998/Math/MathML") Tj ETQq0 0 0 rgBT /Overlock 10 Tf 50 20		

#	Article	IF	Citations
10631	A model for the electrical double layer combining integral equation techniques with quantum density functional theory. Electrochimica Acta, 2011, 56, 7298-7302.	2.6	10
10632	The first-principle studies of the crystal phase transitions: Fd3m-MgAl2O4â†'F4-3m-MgAl2O4. Physica B: Condensed Matter, 2011, 406, 335-338.	1.3	6
10633	Ab-initio study of electronic and elastic properties of B2-type ductile YM (M=Cu, Zn and Ag) intermetallics. Physica B: Condensed Matter, 2011, 406, 339-344.	1.3	21
10634	Electronic and thermodynamic properties of B2-FeSi from first principles. Physica B: Condensed Matter, 2011, 406, 363-367.	1.3	16
10635	Structural, elastic, electronic and optical properties of a new layered-ternary Ta4SiC3 compound. Physica B: Condensed Matter, 2011, 406, 275-279.	1.3	23
10636	Effects of pressure and temperature on the isothermal bulk modulus of CaO. Physica B: Condensed Matter, 2011, 406, 293-296.	1.3	10
10637	Comparative study of the empirical interatomic potentials and density-functional simulations of divacancy and hexavacancy in silicon. Physica B: Condensed Matter, 2011, 406, 467-470.	1.3	4
10638	First principles studies of elastic and thermodynamic properties of fcc-VH2 with pressure and temperature. Physica B: Condensed Matter, 2011, 406, 737-741.	1.3	12
10639	First principles investigation of optical properties of zinc-blende AlxGa1â^'xAs1â^'yNy materials. Physica B: Condensed Matter, 2011, 406, 930-935.	1.3	8
10640	Generalized-stacking-fault energy surfaces for B2-MgRE (RE=Y, Dy, Pr, Tb) intermetallic compounds: Ab initio calculations. Physica B: Condensed Matter, 2011, 406, 967-971.	1.3	10
10641	First-principles study on alloying stability, electronic structure, and mechanical properties of Al-based intermetallics. Physica B: Condensed Matter, 2011, 406, 1149-1153.	1.3	26
10642	Atomic and electronic structures of Mg-doped perfect SrTiO3 and crystals containing oxygen vacancies from first principles. Physica B: Condensed Matter, 2011, 406, 1420-1428.	1.3	13
10643	Periodic DFT calculation of the pressure-induced phase transition and thermodynamical properties of magnesium silicide polymorphs. Physica B: Condensed Matter, 2011, 406, 2070-2076.	1.3	3
10644	Ab initio calculations of surface structure and electronic properties caused by adsorption of Ca atoms on a Si(110) surface. Physica B: Condensed Matter, 2011, 406, 1909-1914.	1.3	0
10645	Structural and elastic properties of LaTiO3 under pressure. Physica B: Condensed Matter, 2011, 406, 1926-1931.	1.3	13
10646	Structural and thermodynamic properties of Os from first-principles calculations. Physica B: Condensed Matter, 2011, 406, 2110-2115.	1.3	11
10647	First-principles study of the structural, elastic, electronic and optical properties of the monoclinic BiScO3. Physica B: Condensed Matter, 2011, 406, 2028-2032.	1.3	14
10648	Elastic properties of MBH4 (M=Na, K, Rb, Cs). Physica B: Condensed Matter, 2011, 406, 2196-2199.	1.3	24

#	Article	IF	Citations
10649	Theoretical studies of structural, elastic, electronic and lattice dynamic properties of AlxYyB1â^'xâ^'yN quaternary alloys. Physica B: Condensed Matter, 2011, 406, 2521-2527.	1.3	13
10650	First-principles study of Friedel oscillations normal to the low index surfaces of Al. Physica B: Condensed Matter, 2011, 406, 2767-2771.	1.3	3
10651	Structural parameters, electronic structures, elastic stiffness and thermal properties of M2PC (M=V,) Tj ETQq0 0 0 rgBT /Overlock 10 Tf	1.3	15
10652	Density functional calculations for Ni adsorption on Al(110). Physica B: Condensed Matter, 2011, 406, 2994-2998.	1.3	2
10653	First-principle study on the electronic and optical properties of Mn-doped SnO2. Physica B: Condensed Matter, 2011, 406, 3137-3141.	1.3	24
10654	First principles investigation of magnesium antimonite semiconductor compound in two different phases under hydrostatic pressure. Physica B: Condensed Matter, 2011, 406, 3149-3153.	1.3	6
10655	Thermodynamic properties of OsB under high temperature and high pressure. Physica B: Condensed Matter, 2011, 406, 3338-3341.	1.3	6
10656	Uranium at high pressure from first principles. Physica B: Condensed Matter, 2011, 406, 3342-3347.	1.3	25
10657	Ab initio total energy calculation of the dynamical stability of noble metal carbides. Physica B: Condensed Matter, 2011, 406, 3556-3561.	1.3	18
10658	First-principles study on structural and electronic properties of copper nanowire encapsulated into GaN nanotube. Physica B: Condensed Matter, 2011, 406, 3502-3507.	1.3	8
10659	First principles lattice dynamical calculation of semiboride Be2B and its ternary alloys XBeB (X=Na,) Tj ETQq0 0 0 rgBT /Overlock 10 Tf 5	1.3	1
10660	Electronic structure and elastic constants of TiCxN1â^'x, ZrxNb1â^'xC and HfCxN1â^'x alloys: A first-principles study. Physica B: Condensed Matter, 2011, 406, 3631-3635.	1.3	56
10661	First-principles calculations of the structural, electronic, and optical properties of LiF up to 300GPa. Physica B: Condensed Matter, 2011, 406, 3660-3665.	1.3	11
10662	The structural stability, elastic constants and electronic structure of Alâ€“Sr intermetallics by first-principles calculations. Physica B: Condensed Matter, 2011, 406, 3681-3686.	1.3	18
10663	Effect of codoping with C or N on electronic structures and magnetic properties of ZnO:Cu. Physica B: Condensed Matter, 2011, 406, 3901-3905.	1.3	10
10664	Effects of aluminum vacancies on electronic structure and optical properties of Ta4AlC3: A first principles study. Physica B: Condensed Matter, 2011, 406, 3906-3910.	1.3	7
10665	First-principles calculations on temperature-dependent elastic constants of rare-earth intermetallic compounds: YAg and YCu. Physica B: Condensed Matter, 2011, 406, 3951-3955.	1.3	13
10666	The phase diagram of water and the magnetic fields of Uranus and Neptune. Icarus, 2011, 211, 798-803.	1.1	195

#	Article	IF	Citations
10667	Dynamic stability of palladium hydride: An ab initio study. International Journal of Hydrogen Energy, 2011, 36, 1254-1258.	3.8	23
10668	Different possible hydrogenation in narrow SWCNTs and their electronic characteristics. International Journal of Hydrogen Energy, 2011, 36, 1053-1058.	3.8	6
10669	First-principles study on the dehydrogenation properties and mechanism of Al-doped Mg2NiH4. International Journal of Hydrogen Energy, 2011, 36, 5375-5382.	3.8	24
10670	Decomposition of ethylene on transition metal surfaces M(111). A comparative DFT study of model reactions for M=Pd, Pt, Rh, Ni. Journal of Molecular Catalysis A, 2011, 344, 37-46.	4.8	52
10671	Methanol dehydrogenation on Rh(111): A density functional and microkinetic modeling study. Journal of Molecular Catalysis A, 2011, 344, 99-110.	4.8	41
10672	From the interface energy to the solubility limit of aluminium in nickel from first-principles and Kinetic Monte Carlo calculations. Materials Science and Engineering B: Solid-State Materials for Advanced Technology, 2011, 176, 767-771.	1.7	5
10673	Classical and quantum mechanical rainbow-scattering of fast He atoms from a KCl(001) surface. Nuclear Instruments & Methods in Physics Research B, 2011, 269, 799-803.	0.6	12
10674	The structural, electronic and optical properties of CdxZn1â^'xSe ternary alloys. Optics Communications, 2011, 284, 1863-1867.	1.0	61
10675	Electronic structure of MoO2. DFT periodic and cluster model studies. Applied Catalysis A: General, 2011, 391, 137-143.	2.2	30
10676	Structural and electronic properties of atomic oxygen adsorption on Pt(111): A density-functional theory study. Applied Surface Science, 2011, 257, 3047-3054.	3.1	23
10677	Structural stability and electronic structure of iron adsorption on the GaN(0001) surface. Applied Surface Science, 2011, 257, 6016-6020.	3.1	6
10678	Robustness and optimal use of design principles of arthropod exoskeletons studied by ab initio-based multiscale simulations. Journal of the Mechanical Behavior of Biomedical Materials, 2011, 4, 129-145.	1.5	91
10679	A better ferrimagnetic half-metal LuCu3Mn4O12: Predicted from first-principles investigation. Journal of Magnetism and Magnetic Materials, 2011, 323, 416-421.	1.0	53
10680	First-principles study on the electronic structure, magnetic properties and phase stability of alloyed cementite with Cr or Mn. Journal of Magnetism and Magnetic Materials, 2011, 323, 915-919.	1.0	37
10681	Half-metallic magnetism of Co2CrX (X=As, Sb) Heusler compounds: An ab initio study. Journal of Magnetism and Magnetic Materials, 2011, 323, 1156-1160.	1.0	22
10682	First-principles study of electronic structure and magnetism of cubic Al1â^'xErxN using the LSDA+U approach. Journal of Magnetism and Magnetic Materials, 2011, 323, 1174-1178.	1.0	10
10683	Origin of the multiferroicity in BiMn2O5 from first-principles calculations. Journal of Magnetism and Magnetic Materials, 2011, 323, 1599-1605.	1.0	22
10684	Magnetism of surface alloys of the type MxN1â^'x/Rh(111). Journal of Magnetism and Magnetic Materials, 2011, 323, 1873-1881.	1.0	1

#	Article	IF	Citations
10685	A comparative study of fracture in Al: Quantum mechanical vs. empirical atomistic description. Journal of the Mechanics and Physics of Solids, 2011, 59, 775-786.	2.3	11
10686	Thermodynamic study of the Npâ€“Zr system. Journal of Nuclear Materials, 2011, 409, 1-8.	1.3	8
10687	Ab-initio based modeling of diffusion in dilute bcc Feâ€“Ni and Feâ€“Cr alloys and implications for radiation induced segregation. Journal of Nuclear Materials, 2011, 411, 1-14.	1.3	101
10688	Structural, electronic, mechanical, and thermodynamic properties of UN2: Systematic density functional calculations. Journal of Nuclear Materials, 2011, 410, 46-51.	1.3	24
10689	Stability and migration property of helium and self defects in vanadium and Vâ€“4Crâ€“4Ti alloy by first-principles. Journal of Nuclear Materials, 2011, 413, 90-94.	1.3	38
10690	Buckle, ruck and tuck: A proposed new model for the response of graphite to neutron irradiation. Journal of Nuclear Materials, 2011, 413, 150-155.	1.3	63
10691	Gas-sensing properties of perovskite La0.875Ba0.125FeO3 nanocrystalline powders. Journal of Physics and Chemistry of Solids, 2011, 72, 29-33.	1.9	23
10692	Effect of the dangling bond on the electronic and magnetic properties of BN nanoribbon. Journal of Physics and Chemistry of Solids, 2011, 72, 256-262.	1.9	35
10693	Structural transition of Ti3SiC2 under high hydrostatic pressure: A first-principles study. Journal of Physics and Chemistry of Solids, 2011, 72, 740-743.	1.9	3
10694	CO adsorption on oxygen-modified molybdenum surfaces. Journal of Physics and Chemistry of Solids, 2011, 72, 744-748.	1.9	1
10695	Structural, high pressure and elastic properties of transition metal monocarbides: A FP-LAPW study. Journal of Physics and Chemistry of Solids, 2011, 72, 810-816.	1.9	34
10696	Ground state and lattice dynamical study of ionic conductors CaF2, SrF2 and BaF2 using density functional theory. Journal of Physics and Chemistry of Solids, 2011, 72, 934-939.	1.9	20
10697	First-principle study of structural and electronic properties of ternary layered Ta2AlC. Journal of Physics and Chemistry of Solids, 2011, 72, 954-956.	1.9	13
10698	Structure, thermal stability and properties of Li3Sc(BO3)2. Journal of Solid State Chemistry, 2011, 184, 115-122.	1.4	9
10699	Structural, thermodynamic and optical properties of MgF2 studied from first-principles theory. Journal of Solid State Chemistry, 2011, 184, 343-350.	1.4	75
10700	Infrared, visible and ultraviolet absorptions of transition metal doped ZnS crystals with spin-polarized bands. Journal of Solid State Chemistry, 2011, 184, 477-480.	1.4	14
10701	CO2 capture properties of Mâ€“Câ€“Oâ€“H (M=Li, Na, K) systems: A combined density functional theory and lattice phonon dynamics study. Journal of Solid State Chemistry, 2011, 184, 304-311.	1.4	74
10702	Ab initio study of phase transition and bulk modulus of NaH. Journal of Solid State Chemistry, 2011, 184, 427-431.	1.4	8

#	Article	IF	Citations
10703	Effect of high hydrostatic pressure on structural stability of Ti3GeC2: A first-principles investigation. Journal of Solid State Chemistry, 2011, 184, 786-789.	1.4	8
10704	Structural, optoelectronic, infrared and Raman spectra of orthorhombic SrSnO3 from DFT calculations. Journal of Solid State Chemistry, 2011, 184, 921-928.	1.4	85
10705	First-principles study of the electronic and magnetic properties of oxygen-deficient rutile TiO2(110) surface. Journal of Solid State Chemistry, 2011, 184, 1148-1152.	1.4	23
10706	Chemical order and local structure of the lead-free relaxor ferroelectric. Journal of Solid State Chemistry, 2011, 184, 2041-2046.	1.4	84
10707	Strain-induced ferromagnetism in LaCoO3: Theory and growth on Si (100). Microelectronic Engineering, 2011, 88, 1444-1447.	1.1	15
10708	Atomistic theory for predicting the binary metallic glass formation. Materials Science and Engineering Reports, 2011, 72, 1-28.	14.8	80
10709	Vacancy formation and clustering behavior in Y2O3 by first principles. Nuclear Instruments & Methods in Physics Research B, 2011, 269, 1720-1723.	0.6	17
10710	Study on the electronic structure and optical properties of the environmentally friendly semiconductor Ca3Si4. Physics Procedia, 2011, 11, 99-102.	1.2	3
10711	Ground state analysis of XCNi3 (X=Mg, Zn, and Ga) from first-principles. Physica B: Condensed Matter, 2011, 406, 265-269.	1.3	6
10712	First principles calculations of the vibrational properties of icosahedral solid boron oxygen B12O2. Physica B: Condensed Matter, 2011, 406, 297-303.	1.3	18
10713	Ab initio study of PrAg intermetallic compound. Physica B: Condensed Matter, 2011, 406, 388-392.	1.3	2
10714	Structural, electronic and magnetic properties of negative thermal expansion material Mn3Cu1â^'xSnxN. Physica B: Condensed Matter, 2011, 406, 1222-1225.	1.3	2
10715	Structural, electronic and thermodynamic properties of cubic Zn3N2 under high pressure from first-principles calculations. Physica B: Condensed Matter, 2011, 406, 1182-1186.	1.3	15
10716	Theoretical investigation of new type of ternary magnesium alloys AMgNi4 (A=Y, La, Ce, Pr and Nd). Physica B: Condensed Matter, 2011, 406, 1330-1335.	1.3	20
10717	Theoretical investigations on structural, elastic and electronic properties of thallium halides. Physica B: Condensed Matter, 2011, 406, 1717-1721.	1.3	4
10718	Plane-wave pseudopotential study for the structural stability of Hf: The role of spinâ€“orbit interaction. Physica B: Condensed Matter, 2011, 406, 1744-1748.	1.3	16
10719	First-principles calculations on structural, elastic, electronic, optical and thermal properties of CsPbCl3 perovskite. Physica B: Condensed Matter, 2011, 406, 1837-1843.	1.3	64
10720	Density functional theoretical study of the structural, electronic and lattice dynamical properties of platinum pernitride. Physica B: Condensed Matter, 2011, 406, 2143-2147.	1.3	16

#	Article	IF	Citations
10721	First-principles study on the structural and electronic properties of LiB and its hydrides (Li2BnHn,) Tj ETQq0 0 0 rgBT /Overlock 10 Tf 50	1.3	6
10722	First-principle study of electronic structure and optical properties of 3C-BC4N. Physica B: Condensed Matter, 2011, 406, 3154-3159.	1.3	10
10723	First-principles study of structural and thermodynamic properties of osmium. Physica B: Condensed Matter, 2011, 406, 3065-3069.	1.3	11
10724	Atomic structure and diffusivity in liquid Al80Ni20 by ab initio molecular dynamics simulations. Physica B: Condensed Matter, 2011, 406, 3089-3097.	1.3	38
10725	Theoretical studies on the structural, electronic, and optical properties of Cu2CdGeSe4. Physica B: Condensed Matter, 2011, 406, 3299-3302.	1.3	22
10726	Concentration-dependent electronic structure and optical absorption properties of B-doped anatase TiO2. Physica B: Condensed Matter, 2011, 406, 3354-3358.	1.3	18
10727	First-principles study of structural, electronic and elastic properties of single crystal CuZr. Physica B: Condensed Matter, 2011, 406, 3389-3391.	1.3	8
10728	High pressure lattice dynamics, dielectric and thermodynamic properties of SrO. Physica B: Condensed Matter, 2011, 406, 3410-3416.	1.3	12
10729	Structures, phase transition, elastic properties of SnO2 from first-principles analysis. Physica B: Condensed Matter, 2011, 406, 3508-3513.	1.3	34
10730	Structural, elastic and electronic properties of a new ternary-layered Ti2SiN. Physica B: Condensed Matter, 2011, 406, 3847-3850.	1.3	12
10731	Electronic and magnetic properties of metal atom adsorption on SWNT. Physica E: Low-Dimensional Systems and Nanostructures, 2011, 43, 889-892.	1.3	6
10732	Nonlinear elasticity of monolayer zinc oxide honeycomb structures: A first-principles study. Physica E: Low-Dimensional Systems and Nanostructures, 2011, 43, 914-918.	1.3	7
10733	Structural, electronic and magnetic properties of the 3d transition-metal-doped AlN nanotubes. Physica E: Low-Dimensional Systems and Nanostructures, 2011, 43, 1249-1254.	1.3	28
10734	Ferromagnetic and antiferromagnetic properties of the fluorinated bilayer SiC sheets. Physica E: Low-Dimensional Systems and Nanostructures, 2011, 43, 1394-1397.	1.3	6
10735	Molecular and electronic structures of Mn-doped tris-8-hydroxyquinolinate gallium: DFT calculation and experiment. Physica E: Low-Dimensional Systems and Nanostructures, 2011, 43, 1470-1474.	1.3	10
10736	Structural and electronic properties of ZnS/ZnO heteronanotubes. Physica E: Low-Dimensional Systems and Nanostructures, 2011, 43, 1522-1527.	1.3	7
10737	Transport properties of an armchair boron-nitride nanoribbon embedded between two graphene electrodes. Physica E: Low-Dimensional Systems and Nanostructures, 2011, 43, 1751-1754.	1.3	36
10738	Possible origin of ferromagnetism in un-doped ZnO: First-principles calculations. Physics Letters, Section A: General, Atomic and Solid State Physics, 2011, 375, 638-641.	0.9	13

#	Article	IF	Citations
10739	Strain-induced metal to semiconductor transition in ultra-small diameter single-wall carbon nanotubes. Physics Letters, Section A: General, Atomic and Solid State Physics, 2011, 375, 1200-1204.	0.9	10
10740	Ab initio studies of superconductivity in monatomic metallic hydrogen under high pressure. Physics Letters, Section A: General, Atomic and Solid State Physics, 2011, 375, 1264-1268.	0.9	21
10741	Comparison of confinement characters between porous silicon and silicon nanowires. Physics Letters, Section A: General, Atomic and Solid State Physics, 2011, 375, 2422-2429.	0.9	1
10742	First-principles study on the Ni@Pt12 Ih coreâ€“shell nanoparticles: A good catalyst for oxygen reduction reaction. Physics Letters, Section A: General, Atomic and Solid State Physics, 2011, 375, 3142-3148.	0.9	17
10743	Towards a quantal dynamical simulation of the neutron starâ€™s crust. Progress in Particle and Nuclear Physics, 2011, 66, 271-275.	5.6	7
10744	Effect of Mo addition on microstructure and vacuum arc characteristics of CuCr50 alloy. Vacuum, 2011, 85, 943-948.	1.6	50
10745	First-principles study of the structural, vibrational, phonon and thermodynamic properties of transition metal carbides TMC (, Zr and Hf). Solid State Communications, 2011, 151, 61-66.	0.9	36
10746	Structural, electronic and magnetic properties of the 3d transition metal-doped GaN nanotubes. Solid State Communications, 2011, 151, 139-143.	0.9	16
10747	First-principles study of the elastic properties of and alloys. Solid State Communications, 2011, 151, 238-241.	0.9	25
10748	Cobalt suppressed Jahnâ€“Teller effect in for lithium ion batteries. Solid State Communications, 2011, 151, 234-237.	0.9	23
10749	First-principles studies of the electronic and elastic properties of Ti2GeC. Solid State Communications, 2011, 151, 491-494.	0.9	7
10750	The structural, elastic and thermodynamic properties of thorium tetraboride. Solid State Communications, 2011, 151, 628-633.	0.9	4
10751	Electronic structure and magnetic properties of the N monodoping and (Li, N)-codoped ZnO. Solid State Communications, 2011, 151, 619-623.	0.9	13
10752	Structural, elastic and electronic properties of transition metal carbides TMC (TM=Ti, Zr, Hf and Ta) from first-principles calculations. Solid State Communications, 2011, 151, 602-606.	0.9	92
10753	Prediction of the phase transition from ferromagnetic perovskite to non-magnetic post-perovskite in SrRuO3 : A first-principles study. Solid State Communications, 2011, 151, 798-801.	0.9	5
10754	A first-principles study of ferromagnetism in Pd-doped ZnO. Solid State Communications, 2011, 151, 864-866.	0.9	14
10755	First-principles study on the structural and electronic properties of AlNCx nanosheet. Solid State Communications, 2011, 151, 834-837.	0.9	17
10756	Dynamical stability and high pressure phases of platinum carbide. Solid State Communications, 2011, 151, 867-869.	0.9	12

#	Article	IF	Citations
10757	The third-order elastic moduli and pressure derivatives for AlRE (RE=Y, Pr, Nd, Tb, Dy, Ce) intermetallics with B2-structure: A first-principles study. Solid State Communications, 2011, 151, 996-1000.	0.9	16
10758	Prediction study of the elastic and thermodynamic properties of the newly discovered tetragonal SrPd2Ge2 phase. Solid State Communications, 2011, 151, 976-981.	0.9	2
10759	First-principles study on the crystal, electronic structure and mechanical properties of hexagonal Al3RE (RE = La, Ce, Pr, Nd, Sm, Gd) intermetallic compounds. Solid State Communications, 2011, 151, 1135-1140.	0.9	17
10760	Electronic and magnetic properties of silicon adsorption on graphene. Solid State Communications, 2011, 151, 1128-1130.	0.9	16
10761	Structure and mechanical properties of TiAlNâ€“WNx thin films. Surface and Coatings Technology, 2011, 205, 4821-4827.	2.2	47
10762	Adsorption of Ag and Au atoms on wurtzite ZnO (0001) surface. Surface Science, 2011, 605, 40-45.	0.8	14
10763	First-principles investigations of low-coverage Ca-induced reconstructions on the Si(001) surface. Surface Science, 2011, 605, 101-106.	0.8	6
10764	Electronic structures of Ga-induced incommensurate and commensurate overlayers on the Si(111) surface. Surface Science, 2011, 605, 146-152.	0.8	6
10765	A DFT and Monte Carlo study of lateral interactions in Be layers on W(112). Surface Science, 2011, 605, 306-313.	0.8	8
10766	Density functional study of copper segregation in aluminum. Surface Science, 2011, 605, 341-350.	0.8	24
10767	The effect of Zr-doping on the interaction of water molecules with the ceria (111) surface. Surface Science, 2011, 605, 351-360.	0.8	8
10768	DFT calculations of point defects on UN(001) surface. Surface Science, 2011, 605, 396-400.	0.8	26
10769	Adsorption and activation of CO coadsorbed with K on Fe(100) surface: A plane-wave DFT study. Surface Science, 2011, 605, 401-414.	0.8	44
10770	First-principles investigations of Ni3Al(111) and NiAl(110) surfaces at metal dusting conditions. Surface Science, 2011, 605, 582-592.	0.8	11
10771	Electronic and structural properties of armchair SWCNT/TiO2(110)-(1Ã—2) system. Surface Science, 2011, 605, 593-596.	0.8	2
10772	Calculating anharmonic vibrational frequencies of molecules adsorbed on surfaces directly from ab initio energies with a molecule-independent method: H2O on Pt(111). Surface Science, 2011, 605, 616-622.	0.8	23
10773	A theoretical study of CO adsorption on FeCo(100) and the effect of alloying. Surface Science, 2011, 605, 681-688.	0.8	34
10774	Ab initio determination of atomic structure and energy of surface states of bare and hydrogen covered GaN (0001) surface â€" Existence of the Surface States Stark Effect (SSSE). Surface Science, 2011, 605, 695-713.	0.8	36

#	Article	IF	Citations
10775	Properties of rutile TiO2 surfaces from a Tight-Binding Variable-Charge model. Comparison with ab initio calculations. Surface Science, 2011, 605, 738-745.	0.8	20
10776	Initial steps in methanol steam reforming on PdZn and ZnO surfaces: Density functional theory studies. Surface Science, 2011, 605, 750-759.	0.8	58
10777	Decomposition of NH3 on Ir(110): A first-principle study. Surface Science, 2011, 605, 802-807.	0.8	20
10778	Driving forces for the adsorption of cyclopentene on InP(001). Surface Science, 2011, 605, 824-830.	0.8	0
10779	Tin-stabilized (1Ã—2) and (1Ã—4) reconstructions on GaAs(100) and InAs(100) studied by scanning tunneling microscopy, photoelectron spectroscopy, and ab initio calculations. Surface Science, 2011, 605, 883-888.	0.8	2
10780	The structure of Cu{100}-p(2Ã—6)-2mg-Sn studied by DFT and LEED. Surface Science, 2011, 605, 1000-1004.	0.8	1
10781	Understanding 4-bromostyrene Adsorption on the Si(001)-(1Ã—2) surface: A density functional theory study. Surface Science, 2011, 605, 1056-1061.	0.8	1
10782	First-principles study of atomic hydrogen adsorption on Fe3O4(100). Surface Science, 2011, 605, 1067-1073.	0.8	32
10783	DFT study of isocyanate chemisorption on Cu(100). Surface Science, 2011, 605, 1202-1208.	0.8	10
10784	Investigation of hydrogen bonds and temperature effects on the water monolayer adsorption on rutile TiO2 (110) by first-principles molecular dynamics simulations. Surface Science, 2011, 605, 1275-1280.	0.8	24
10785	Theoretical study of hydrazine adsorption on Pt(111): Anti or cis?. Surface Science, 2011, 605, 1347-1353.	0.8	27
10786	A first-principles study of oxygen adsorption and interaction with Al adatoms on Al(110). Surface Science, 2011, 605, 1391-1396.	0.8	6
10787	Structural dependence of intermediate species for the hydrogen evolution reaction on single crystal electrodes of Pt. Surface Science, 2011, 605, 1462-1465.	0.8	31
10788	DFT study of carbon monoxide adsorption on Î±-Al2O3(0001). Surface Science, 2011, 605, 1694-1703.	0.8	28
10789	Thermodynamic description of the Alâ€“Cuâ€“Mgâ€“Mnâ€“Si quinary system and its application to solidification simulation. Thermochimica Acta, 2011, 512, 258-267.	1.2	35
10790	Atomic and electronic structure of both perfect and nanostructured Ni(111) surfaces: First-principles calculations. Thin Solid Films, 2011, 519, 3745-3751.	0.8	9
10791	Structural and electronic properties of Î²-In2X3 (X=O, S, Se, Te) using ab initio calculations. Thin Solid Films, 2011, 519, 5679-5683.	0.8	9
10792	Theoretical investigation of atomic structure and electronic properties of Ca/Si(110)-(2Ã—1) reconstruction. Thin Solid Films, 2011, 519, 5467-5472.	0.8	0

#	Article	IF	Citations
10793	The metallic transport of (TMTSF)₂X organic conductors close to the superconducting phase. Journal of Physics Condensed Matter, 2011, 23, 345702.	0.7	12
10794	Ferromagnetism Induced by Vacancies in Bulk and the (1010) Surfaces of ZnO: Density Functional Theory Calculations. Japanese Journal of Applied Physics, 2011, 50, 01BE05.	0.8	3
10795	Electronic Structures and Magnetism of Al/Fe(001) Thin-Film Systems: First-Principles Calculations. Japanese Journal of Applied Physics, 2011, 50, 01BF03.	0.8	0
10796	Theoretical Calculations for Magnetic Property of FeRh Inter-Metallic Compound with Site-Exchange Defects. Japanese Journal of Applied Physics, 2011, 50, 105803.	0.8	5
10797	Elastic Tensor and Thermodynamic Property of Magnesium Silicate Perovskite from First-principles Calculations. Chinese Journal of Chemical Physics, 2011, 24, 703-710.	0.6	11
10798	Theoretical insights into the built-in electric field and band offsets of BN/C heterostructured zigzag nanotubes. Journal Physics D: Applied Physics, 2011, 44, 095405.	1.3	19
10799	Energy Stabilities, Magnetic Properties, and Electronic Structures of Diluted Magnetic Semiconductor Zn1â^'xMnxS(001) Thin Films. Chinese Journal of Chemical Physics, 2011, 24, 47-54.	0.6	1
10800	Investigation of the electronic and geometric structures of the (110) surfaces of arsenopyrite (FeAsS) and enargite (Cu₃AsS₄). Mineralogical Magazine, 2011, 75, 45-63.	0.6	14
10801	Changes in work function from stacking faults in fcc metals. Europhysics Letters, 2011, 96, 56004.	0.7	2
10802	Ab initiostudy of magnetoelectricity in Fe/BaTiO₃: the effects of n-doped perovskite interfaces. Journal of Physics Condensed Matter, 2011, 23, 455902.	0.7	3
10803	Vacancy or not: An insight on the intrinsic vacancies in rocksalt-structured GeSbTe alloys from ab initio calculations. Europhysics Letters, 2011, 95, 27002.	0.7	23
10804	Atomic-Scale Investigation on the Ti/Fe(001) Interface Structure: Molecular Dynamics Simulations andAb initioCalculations. Japanese Journal of Applied Physics, 2011, 50, 01BE07.	0.8	1
10805	Study of the structural, elastic and electronic properties of ordered Ca(Mg1â^'xLix)2alloys from first-principles calculations. Physica Scripta, 2011, 84, 055603.	1.2	4
10806	Structural and electronic properties of hydrogen adsorptions on BC₃sheet and graphene: a comparative study. Nanotechnology, 2011, 22, 135703.	1.3	24
10807	Ab initioPhonons in Magnetic Ni2MnAl. Japanese Journal of Applied Physics, 2011, 50, 05FE07.	0.8	1
10808	Electron Accumulation in LaAlO$_{3}$/SrTiO$_{3}$ Interfaces by the Broken Symmetry of Crystal Field. Japanese Journal of Applied Physics, 2011, 50, 10PF03.	0.8	0
10809	Accurate Electronic Structures of Eu-Doped SiAlON Green Phosphor with a Semilocal Exchangeâ€“Correlation Potential. Japanese Journal of Applied Physics, 2011, 50, 06GH10.	0.8	4
10810	Adsorption of halogen atom (F, Cl, I) on cation-rich GaAs(001) surface. IOP Conference Series: Materials Science and Engineering, 2011, 23, 012015.	0.3	7

#	Article	IF	Citations
10811	Stress tensor: A quantitative indicator of effective volume and stability of helium in metals. Europhysics Letters, 2011, 96, 66001.	0.7	26
10812	Influence of Molecular Structure on the Optical Property of POSS: a DFT Calculation Based Quantum Chemistry Calculation. Materials Science Forum, 0, 689, 58-63.	0.3	3
10813	First-principles investigation of the early stages of Pd adsorption on Au(111). Journal of Physics Condensed Matter, 2011, 23, 015001.	0.7	8
10814	LEEDIâ€“Vand DFT structure determination of the (surd 3imes surd 3)mathrm {R}30^{circ } Pbâ€“Ag(111) surface alloy. Journal of Physics Condensed Matter, 2011, 23, 265006.	0.7	2
10815	Surface magnetism in O₂dissociationâ€”from basics to application. Journal of Physics Condensed Matter, 2011, 23, 394207.	0.7	7
10816	Ab initiostudy of isolated chlorine defects in cubic SiC. Journal of Physics Condensed Matter, 2011, 23, 415802.	0.7	5
10817	Structural phase transition path-following and stable phase scouting through a coupled DFTâ€“BFB algorithm. Modelling and Simulation in Materials Science and Engineering, 2011, 19, 085007.	0.8	1
10818	Structure and energetics of 180Â° domain walls in PbTiO₃by density functional theory. Journal of Physics Condensed Matter, 2011, 23, 175902.	0.7	48
10819	Carbon release by selective alloying of transition metal carbides. Journal of Physics Condensed Matter, 2011, 23, 355401.	0.7	15
10820	High-pressure phases of hydrogen cyanide: formation of hydrogenated carbon nitride polymers and layers and their electronic properties. Journal of Physics Condensed Matter, 2011, 23, 405403.	0.7	11
10821	Electronic structure of HgBa2Canâ^'1CunO2n+2 (n = 1, 2, 3) superconductor parent compounds from periodic hybrid density functional theory. Journal of Chemical Physics, 2011, 134, 074709.	1.2	12
10822	Six-dimensional quasiclassical and quantum dynamics of H2 dissociation on the c(2 Ã— 2)-Ti/Al(100) surface. Journal of Chemical Physics, 2011, 134, 114708.	1.2	13
10823	The initial growth behavior of perylene on Cu(100). Journal of Chemical Physics, 2011, 134, 194702.	1.2	6
10824	Communication: Strong excitonic and vibronic effects determine the optical properties of Li2O2. Journal of Chemical Physics, 2011, 135, 121101.	1.2	45
10825	On the adsorption and formation of Pt dimers on the CeO2(111) surface. Journal of Chemical Physics, 2011, 135, 244708.	1.2	14
10826	Potential-functional embedding theory for molecules and materials. Journal of Chemical Physics, 2011, 135, 194104.	1.2	108
10827	Electronic structures of dynamically stable As<mml:math xmlns:mml="http://www.w3.org/1998/Math/MathML" display="inline"><mml:mrow><mml:msub><mml:mrow /><mml:mrow><mml:mn>2</mml:mn></mml:mrow></mml:msub></mml:mrow></mml:math>O<mml:math xmlns:mml="http://www.w3.org/1998/Math/MathML" display="inline"><mml:mrow><mml:msub><mml:mrow /><mml:mrow><mml:mn>3</mml:mn></mml:mro	1.1	38
10828	Density functional study of narrow cubic MnSe nanowires: Role of MnSe chains. Physical Review B, 2011, 83, .	1.1	12

#	Article	IF	Citations
10829	Pressure-induced electron topological transitions in Ba-doped Si clathrate. Physical Review B, 2011, 84, .	1.1	17
10830	Quantum molecular dynamics simulations for the nonmetal-metal transition in shocked methane. Physical Review B, 2011, 84, .	1.1	15
10831	Maximizing the Fermi-surface multiplicity optimizes the superconducting state of iron pnictide compounds. Physical Review B, 2011, 84, .	1.1	46
10832	Nanoscale hydride formation at dislocations in palladium:Ab initiotheory and inelastic neutron scattering measurements. Physical Review B, 2011, 83, .	1.1	8
10833	First-principles study of polar LaAlO (001) surface stabilization by point defects. Physical Review B, 2011, 84, .	1.1	34
10834	Chern-Simons orbital magnetoelectric coupling in generic insulators. Physical Review B, 2011, 83, .	1.1	89
10835	Standard hydrogen electrode and potential of zero charge in density functional calculations. Physical Review B, 2011, 84, .	1.1	118
10836	Metallic and superconducting gallane under high pressure. Physical Review B, 2011, 84, .	1.1	65
10837	Simulation of spin-polarized scanning tunneling microscopy on complex magnetic surfaces: Case of a Cr monolayer on Ag(111). Physical Review B, 2011, 84, .	1.1	16
10838	Intrinsic ferromagnetism in two-dimensional carbon structures: Triangular graphene nanoflakes linked by carbon chains. Physical Review B, 2011, 84, .	1.1	40
10839	Quantum mechanically guided design of transition metal doped SrCo0.875M0.125O3â^'Î´ (Mâ€‰=â€‰Sc, Ti, V, Cr,) Tj ETQq0 0 0 rgBT	1.5	2
10840	Structural and magnetic ground-state properties of<mml:math xmlns:mml="http://www.w3.org/1998/Math/MathML" display="inline"><mml:mi>Î³</mml:mi></mml:math>-FeMn alloys fromab initiocalculations. Physical Review B, 2011, 84, .	1.1	56
10841	Influence of hydrogen impurities on atomic and electronic structure of palladium nanowires and nanocontacts. Physical Review B, 2011, 84, .	1.1	9
10842	Local field effects in half-metals: A<mml:math xmlns:mml="http://www.w3.org/1998/Math/MathML" display="inline"><mml:mrow><mml:mi mathvariant="italic">GW</mml:mi></mml:mrow></mml:math>study of zincblende CrAs, MnAs, and MnC. Physical Review B, 2011, 83, .	1.1	18
10843	Influences of twist boundaries on optical effects: Ab initio studies of the deep ultraviolet nonlinear optical crystal KBe₂BO₃F₂. Journal of Applied Physics, 2011, 109, 073721.	1.1	8
10844	Dielectric, magnetic, and phonon properties of nickel hydroxide. Physical Review B, 2011, 84, .	1.1	99
10845	Density functional theory study of the<mml:math xmlns:mml="http://www.w3.org/1998/Math/MathML" display="inline"><mml:mrow><mml:mi>Î³</mml:mi></mml:mrow></mml:math>-MnOOH (010) surface: Response to oxygen and water partial pressures and temperature. Physical Review B, 2011, 84, .	1.1	8
10846	Adsorption and abstraction reactions of HCl on a single Si(100) dangling bond. Physical Review B, 2011, 83, .	1.1	10

#	Article	IF	Citations
10847	Construction and performance of fully numerical optimum atomic basis sets. Physical Review B, 2011, 84, .	1.1	2
10848	Organic-inorganic compounds with strong nonlinear optical properties based on 2,4,6-trimethylpyridinium and tetrahedral BF<mml:math xmlns:mml="http://www.w3.org/1998/Math/MathML" display="inline"><mml:mrow><mml:msub><mml:mrow /><mml:mrow><mml:mn>4</mml:mn></mml:mrow></mml:msub></mml:mrow></mml:math><mml:math xmlns:mml="http://www.w3.org/1998/Math/MathML" display="inline"><mml:mrow><mml:msup><mml:m	1.1	5
10849	Thermodynamic and mechanical stabilities of Î³â€²-Ir3(Al,W). Journal of Applied Physics, 2011, 109, 023504.	1.1	14
10850	First-principles calculations of 17O nuclear magnetic resonance chemical shielding in Pb(Zr1/2Ti1/2)O3 and Pb(Mg1/3Nb2/3)O3: Linear dependence on transition-metal/oxygen bond lengths. Journal of Chemical Physics, 2011, 135, 114507.	1.2	5
10851	Electronic structure and Mott localization of iron-deficient TlFe<mml:math xmlns:mml="http://www.w3.org/1998/Math/MathML" display="inline"><mml:mrow><mml:msub><mml:mrow /><mml:mrow><mml:mn>1</mml:mn><mml:mo>.</mml:mo><mml:mn>5</mml:mn></mml:mrow></mml:msub></mml:mrow></mml:m xmlns:mml="http://www.w3.org/1998/Math/MathML" display="inline">[illegible]ow>2</mml:mn></mml:msub></mml:math	1.1	27
10852	Asymmetric cation nonstoichiometry in spinels: Site occupancy in Co<mml:math xmlns:mml="http://www.w3.org/1998/Math/MathML" display="inline"><mml:msub><mml:mrow /><mml:mn>2</mml:mn></mml:msub></mml:math>ZnO<mml:math xmlns:mml="http://www.w3.org/1998/Math/MathML" display="inline"><mml:msub><mml:mrow /><mml:mn>4</mml:mn></mml:msub></mml:math>and Rh<mml:math xmlns:mml="http://www.w3.org/1998/Math/MathML" display="inline"><mml:msub><mml:mrow /><mml:	1.1	25
10853	Particle-hole symmetry breaking in the pseudogap state ofPb0.55Bi1.5Sr1.6La0.4CuO6+Î´: A quantum chemical perspective. Physical Review B, 2011, 83, .	1.1	5
10854	High pressure, mechanical, and optical properties of ZrW2O8. Journal of Applied Physics, 2011, 109, .	1.1	8
10855	Tuning the band gap and magnetic properties of BN sheets impregnated with graphene flakes. Physical Review B, 2011, 84, .	1.1	81
10856	Doubly periodic structure for the study of inhomogeneous bulk fermion matter with spatial localizations. Physical Review C, 2011, 84, .	1.1	4
10857	A multinuclear solid-state magnetic resonance and GIPAW DFT study of anhydrous calcium chloride and its hydrates. Canadian Journal of Chemistry, 2011, 89, 754-763.	0.6	20
10858	Efficient isoparametric integration over arbitrary space-filling Voronoi polyhedra for electronic structure calculations. Physical Review B, 2011, 84, .	1.1	20
10859	Structural, vibrational, and thermodynamic properties of ordered and disordered Ni<mml:math xmlns:mml="http://www.w3.org/1998/Math/MathML" display="inline"><mml:mrow><mml:msub><mml:mrow /><mml:mrow><mml:mn>1</mml:mn><mml:mo>â^'</mml:mo><mml:mi>x</mml:mi></mml:mrow></mml:msub></mml:mrow></mml:m xmlns:mml="http://www.w3.org/1998/Math/MathML" display="inline"><mml:mrow><mml:msub><mml:mrow /><mml:mrow><mml:mi>x</mml:mi></mml:mrow	1.1	49
10860	Stabilizing and activating dopants in âŸ¨112âŸ© silicon nanowires by alkene adsorptions: A first-principles study. Applied Physics Letters, 2011, 98, 073115.	1.5	8
10861	<i>Ab initio</i>study of the adsorption, migration, clustering, and reaction of palladium on the surface of silicon carbide. Physical Review B, 2011, 83, .	1.1	16
10862	The half-metallic properties and geometrical structures of cubic BaMnO3 and BaTiO3/BaMnO3 superlattice. Journal of Applied Physics, 2011, 109, .	1.1	11
10863	Crystallographic, magnetic, and electronic structures of ferromagnetic shape memory alloys Ni2XGa (X=Mn,Fe,Co) from first-principles calculations. Journal of Applied Physics, 2011, 109, 014908.	1.1	54
10864	Compressive Surface Stress in Magnetic Transition Metals. Physical Review Letters, 2011, 106, 057202.	2.9	34

#	Article	IF	Citations
10865	Local-field and excitonic effects in the optical response of<mml:math xmlns:mml="http://www.w3.org/1998/Math/MathML" display="inline"><mml:mrow><mml:mi>Î±</mml:mi></mml:mrow></mml:math>-alumina. Physical Review B, 2011, 83, .	1.1	12
10866	First-principles study of phase stability of stoichiometric vanadium nitrides. Physical Review B, 2011, 84, .	1.1	22
10867	Size effects on formation energies and electronic structures of oxygen and zinc vacancies in ZnO nanowires: A first-principles study. Journal of Applied Physics, 2011, 109, 044306-044306-5.	1.1	17
10868	Enhanced photoelectrochemical performance of rutile TiO2 by Sb-N donor-acceptor coincorporation from first principles calculations. Applied Physics Letters, 2011, 99, .	1.5	41
10869	Electronic structure, Born effective charges and spontaneous polarization in magnetoelectric gallium ferrite. Journal of Physics Condensed Matter, 2011, 23, 325902.	0.7	39
10870	Thermal conductivity of half-Heusler compounds from first-principles calculations. Physical Review B, 2011, 84, .	1.1	187
10871	Possible routes for synthesis of new boron-rich Feâ€“B and Fe1â^'xCrxB4 compounds. Applied Physics Letters, 2011, 98, .	1.5	46
10872	Ab initio study of acoustic velocities in molybdenum under high pressure and high temperature. Applied Physics Letters, 2011, 99, 191906.	1.5	6
10873	Phase stability and the arsenic vacancy defect in In<mml:math xmlns:mml="http://www.w3.org/1998/Math/MathML" display="inline"><mml:msub><mml:mrow /><mml:mi>x</mml:mi></mml:msub></mml:math>Ga<mml:math xmlns:mml="http://www.w3.org/1998/Math/MathML" display="inline"><mml:msub><mml:mrow /><mml:mrow><mml:mn>1</mml:mn><mml:mo>â^'</mml:mo><mml:mi>x</mml:mi></mml:mrow></mml:msub></mml:math>As. Physical Review B, 2011, 84, .	1.1	26
10874	Formation and diffusion of vacancy-polaron complex in olivine-type LiMnPO<mml:math xmlns:mml="http://www.w3.org/1998/Math/MathML" display="inline"><mml:msub><mml:mrow /><mml:mn>4</mml:mn></mml:msub></mml:math>and LiFePO<mml:math xmlns:mml="http://www.w3.org/1998/Math/MathML" display="inline"><mml:msub><mml:mrow /><mml:mn>4</mml:mn></mml:msub></mml:math>. Physical Review B, 2011, 84, .	1.1	40
10875	Solar radiation shielding material for windows TiN studied from first-principles theory. Applied Physics Letters, 2011, 99, 061906.	1.5	10
10876	Transition-metal-molecular sandwich nanowires as magnetic on/off switch. Applied Physics Letters, 2011, 99, .	1.5	18
10877	Hydrogen impurity in paratellurite<mml:math xmlns:mml="http://www.w3.org/1998/Math/MathML" display="inline"><mml:mrow><mml:mi>Î±</mml:mi></mml:mrow></mml:math>-TeO<mml:math xmlns:mml="http://www.w3.org/1998/Math/MathML" display="inline"><mml:mrow><mml:msub><mml:mrow /><mml:mrow><mml:mn>2</mml:mn></mml:mrow></mml:msub></mml:mrow></mml:math>: Muon-spin rotation andab initiostudies. Physical Review B, 2011, 84, .	1.1	24
10878	Mechanical properties and chemical bonding characteristics of Cr7C3 type multicomponent carbides. Journal of Applied Physics, 2011, 109, .	1.1	136
10879	Quantum mechanical embedding theory based on a unique embedding potential. Journal of Chemical Physics, 2011, 134, 154110.	1.2	236
10880	Effects of nonhydrostatic pressure on the structural and magnetic properties of BaFe<mml:math xmlns:mml="http://www.w3.org/1998/Math/MathML" display="inline"><mml:mrow><mml:msub><mml:mrow /><mml:mrow><mml:mn>2</mml:mn></mml:mrow></mml:msub></mml:mrow></mml:math>As<mml:math xmlns:mml="http://www.w3.org/1998/Math/MathML"	1.1	16
10881	Band alignment at the SiO<mml:math xmlns:mml="http://www.w3.org/1998/Math/MathML" display="inline"><mml:msub><mml:mrow /><mml:mn>2</mml:mn></mml:msub></mml:math>/HfO<mml:math xmlns:mml="http://www.w3.org/1998/Math/MathML" display="inline"><mml:msub><mml:mrow /><mml:mn>2</mml:mn></mml:msub></mml:math>interface: Group IIIA versus group IIIB metal dopants. Physical Review B, 2011, 84, .	1.1	19
10882	Electronic and transport properties of a nanometer-scale Au/AlN(0001)/Au junction from first-principles. Applied Physics Letters, 2011, 98, .	1.5	1

#		IF	Citations
10883	Experimental and theoretical study of structural properties and phase transitions in YAsO<mml:math xmlns:mml="http://www.w3.org/1998/Math/MathML" display="inline"><mml:mrow><mml:msub><mml:mrow /><mml:mrow><mml:mn>4</mml:mn></mml:mrow></mml:msub></mml:mrow></mml:math>and YCrO<mml:math xmlns:mml="http://www.w3.org/1998/Math/MathML" display="inline"><mml:mrow><mml:msub><mml:mrow /><mml:mrow><mml:mn>4</mml:mn></mml:mrow></mml:msub></mml:mrow></mml:math>.	1.1	43
10884	First-principles calculations of electronic, vibrational, and structural properties of scheelite EuWO<mml:math xmlns:mml="http://www.w3.org/1998/Math/MathML" display="inline"><mml:msub><mml:mrow /><mml:mn>4</mml:mn></mml:msub></mml:math>under pressure. Physical Review B, 2011, 84, .	1.1	24
10885	Structural and thermodynamic properties of compressed palladium:Ab initioand molecular dynamics study. Physical Review B, 2011, 83, .	1.1	38
10886	Influence of Ge content on the optical properties ofXandWcenters in dilute Si-Ge alloys. Physical Review B, 2011, 84, .	1.1	16
10887	Calculations show improved photoelectrochemical performance for N, Ce, and Ceâ€‰+â€‰N doped anatase TiO2. Journal of Applied Physics, 2011, 110, 033519.	1.1	22
10888	Electronic structure of elemental curium studied by photoemission. Physical Review B, 2011, 83, .	1.1	14
10889	Density functional theory calculations for a single Re impurity in silicon. Physical Review B, 2011, 83, .	1.1	10
10890	Low-temperature structure ofÎ¾â€²-Al-Pd-Mn optimized byab initiomethods. Physical Review B, 2011, 84, .	1.1	14
10891	Ab initio charge analysis of pure and hydrogenated perovskites. Journal of Applied Physics, 2011, 109, .	1.1	16
10892	Effect of carbon/hydrogen species incorporation on electronic structure of anatase-TiO2. Journal of Applied Physics, 2011, 110, .	1.1	18
10893	Thermodynamic stability of PuO2surfaces: Influence of electronic correlations. Physical Review B, 2011, 84, .	1.1	30
10894	Elastic anisotropy of<mml:math xmlns:mml="http://www.w3.org/1998/Math/MathML" display="inline"><mml:mrow><mml:mi>É</mml:mi></mml:mrow></mml:math>-Fe under conditions at the Earth's inner core. Physical Review B, 2011, 83, .	1.1	26
10895	Ab initiostudy of ferromagnetism in edged iron nanowires under axial strain. Physical Review B, 2011, 84, .	1.1	13
10896	Magnetic state effect upon the order-disorder phase transition in Fe-Co alloys: A first-principles study. Physical Review B, 2011, 83, .	1.1	25
10897	Vibrational dynamics of YPO<mml:math xmlns:mml="http://www.w3.org/1998/Math/MathML" display="inline"><mml:mrow><mml:msub><mml:mrow /><mml:mrow><mml:mn>4</mml:mn></mml:mrow></mml:msub></mml:mrow></mml:math>and ScPO<mml:math xmlns:mml="http://www.w3.org/1998/Math/MathML" display="inline"><mml:mrow><mml:msub><mml:mrow /><mml:mrow><mml:mn>4</mml:mn></mml:mrow></mml:msub></mml:mrow></mml:math>single crysta	1.1	28
10898	Ag-induced Si(100) reconstruction: Si(100)-(22Ã—22)R45â˜…-Ag. Physical Review B, 2011, 84, .	1.1	3
10899	Oxidized In-containing III-V(100) surfaces: Formation of crystalline oxide films and semiconductor-oxide interfaces. Physical Review B, 2011, 83, .	1.1	32
10900	Diffusion of E centers in germanium predicted using GGA+U approach. Applied Physics Letters, 2011, 99, 072112.	1.5	77

#	Article	IF	Citations
10901	Impact of local lattice distortions on the structural stability of Fe-Pd magnetic shape-memory alloys. Physical Review B, 2011, 83, .	1.1	30
10902	<i>Ab initio</i>energetics and kinetics study of H<mml:math xmlns:mml="http://www.w3.org/1998/Math/MathML" display="inline"><mml:msub><mml:mrow /><mml:mn>2</mml:mn></mml:msub></mml:math>and CH<mml:math xmlns:mml="http://www.w3.org/1998/Math/MathML" display="inline"><mml:msub><mml:mrow /><mml:mn>4</mml:mn></mml:msub></mml:math>in the SI clathrate hydrate. Physical Review B, 2011, 84, .	1.1	30
10904	Epitaxial strain and interfacial electronic topological transition in O-rich MgO/FeO/Fe(001) interfaces. Physical Review B, 2011, 83, .	1.1	24
10905	Boundary conditions in periodic density functional calculations of insulating materials. Physical Review B, 2011, 83, .	1.1	4
10906	The catalytic potential of high-Îº dielectrics for graphene formation. Applied Physics Letters, 2011, 98, .	1.5	63
10907	Electronic structure of Si(110)-(<mml:math xmlns:mml="http://www.w3.org/1998/Math/MathML") Tj ETQq1 1 0.784314 rgBT /Overlock studied by scanning tunneling spectroscopy and density functional theory. Physical Review B, 2011, 84, .	1.1	22
10908	Effect of onsite Coulomb repulsion on thermoelectric properties of full-Heusler compounds with pseudogaps. Physical Review B, 2011, 84, .	1.1	52
10909	Orbital tomography: Deconvoluting photoemission spectra of organic molecules. Physical Review B, 2011, 84, .	1.1	99
10910	<mml:math xmlns:mml="http://www.w3.org/1998/Math/MathML" display="inline"><mml:mrow><mml:mi>P</mml:mi><mml:msub><mml:mn>6</mml:mn><mml:mn>2</mml:mn></mml:msub><mml:mn of yttrium above 206 GPa from first principles. Physical Review B, 2011, 84, .	1.1	11
10911	A First Principles Study of O₂/Ag(111) â€"Adsorption and Magnetic Propertiesâ€". Journal of the Physical Society of Japan, 2011, 80, 084605.	0.7	10
10912	Endotaxial Si nanolines in Si(001):H. Physical Review B, 2011, 84, .	1.1	11
10913	Ab initiostudy of the electronic, mechanical, and vibrational properties of different Al2Si2Sr crystalline phases. Physical Review B, 2011, 83, .	1.1	4
10914	Surface reactivity of<mml:math xmlns:mml="http://www.w3.org/1998/Math/MathML" display="inline"><mml:mrow><mml:msub><mml:mi mathvariant="normal">V</mml:mi><mml:mrow><mml:mn>2</mml:mn></mml:mrow></mml:msub></mml:mrow></mml:math>O<mml: xmlns:mml="http://www.w3.org/1998/Math/MathML" display="inline"><mml:mrow><mml:msub><mml:mrow /><mml:mrow><mml:mn>5</mml:mn></mml:mrow></mml:msub></mml:mrow></mml:math>(001): Effects	1.1	29
10915	First-principles study of the adsorption of Au atoms and Au<mml:math xmlns:mml="http://www.w3.org/1998/Math/MathML" display="inline"><mml:msub><mml:mrow /><mml:mn>2</mml:mn></mml:msub></mml:math>and Au<mml:math xmlns:mml="http://www.w3.org/1998/Math/MathML" display="inline"><mml:msub><mml:mrow /><mml:mn>4</mml:mn></mml:msub></mml:math>clusters on FeO/Pt(111). Physical Review B, 2011, 84, .	1.1	20
10916	First-Principles Study on Electronic and Thermal Properties of Zinc-Blende Metal Telluride. Advanced Materials Research, 0, 335-336, 1056-1060.	0.3	0
10917	First-Principles Calculations of the Atomic and Electronic Structure of CaTiO₃(111) Surfaces. Ferroelectrics, 2011, 424, 1-6.	0.3	10
10918	On the solubility of yttrium in RuO2. Journal of Applied Physics, 2011, 110, 054317.	1.1	5
10919	Progressive changes in surface structure and electronic properties on Si(001) surface by CaF2adsorption. Journal of Applied Physics, 2011, 109, 123708.	1.1	5

#	Article	IF	Citations
10920	Effect of vacancy on the sliding of an iron grain boundary. Journal of Applied Physics, 2011, 109, 113512.	1.1	11
10921	Prediction of a Ca(BH<mml:math xmlns:mml="http://www.w3.org/1998/Math/MathML"> Tj ETQq1 1 0.784314 rgBT /Overlock 10 Tf 50 7	1.1	16
10922	first-principles calculations. Physical Review B, 2011, 84, . Ab initiostudy of the cubic-to-hexagonal phase transition promoted by interstitial hydrogen in iron. Physical Review B, 2011, 84, .	1.1	15
10923	First-principles study of elastic properties of Cr- and Fe-rich Fe-Cr alloys. Physical Review B, 2011, 84, .	1.1	49
10924	Band offsets in cubic GaN/AlN superlattices. Physical Review B, 2011, 83, .	1.1	54
10925	Charge redistribution and interlayer coupling in twisted bilayer graphene under electric fields. Physical Review B, 2011, 84, .	1.1	55
10926	Barium titanate ground- and excited-state properties from first-principles calculations. Physical Review B, 2011, 83, .	1.1	85
10927	Structural, electronic, and optical properties of crystalline iodoform under high pressure: A first-principles study. Journal of Chemical Physics, 2011, 134, 034508.	1.2	6
10928	Development of orthogonal tight-binding models for Ti-C and Ti-N systems. Physical Review B, 2011, 84, .	1.1	23
10929	Optical and electronic properties of dense sodium. Physical Review B, 2011, 83, .	1.1	48
10930	Effect of oxygen adsorption on magnetic properties of graphite. Physical Review B, 2011, 83, .	1.1	21
10931	Terminating Surface Electromigration at the Source. Physical Review Letters, 2011, 106, 156404.	2.9	15
10932	Doping of fluorographene by surface adsorbates. Physical Review B, 2011, 84, .	1.1	28
10933	Rainbow scattering under axial surface channeling from a KCl(001) surface. Physical Review B, 2011, 84, .	1.1	16
10934	Modulated Na$_{2}$Ti$_{4}$O$_{9}$:Zr Nanobelt via Site-Specific Zr Doping. Applied Physics Express, 2011, 4, 085003.	1.1	3
10935	Mo- and N-doped BiNbO4 for photocatalysis applications. Applied Physics Letters, 2011, 99, .	1.5	47
10936	The effects of alloying element Co on Niâ€“Mnâ€“Ga ferromagnetic shape memory alloys from first-principles calculations. Applied Physics Letters, 2011, 98, .	1.5	47
10937	Thermoelectric properties of<mml:math xmlns:mml="http://www.w3.org/1998/Math/MathML" display="inline"><mml:mi>p</mml:mi></mml:math>-type CuInSe<mml:math xmlns:mml="http://www.w3.org/1998/Math/MathML" display="inline"><mml:msub><mml:mrow /><mml:mn>2</mml:mn></mml:msub></mml:math>chalcopyrites enhanced by introduction of manganese. Physical Review B, 2011, 84, .	1.1	57

#	Article	IF	Citations
10938	Microscopic modeling of the dielectric properties of silicon nitride. Physical Review B, 2011, 84, .	1.1	14
10939	Density functional theory investigation of the interaction of water with<mml:math xmlns:mml="http://www.w3.org/1998/Math/MathML" display="inline"><mml:mrow><mml:mi>Î±</mml:mi><mml:mo>â^'</mml:mo><mml:msub><mml:mi mathvariant="normal">Al</mml:mi><mml:mrow><mml:mn>2</mml:mn></mml:mrow></mml:msub><mml:msub><mml:mi	1.1	26
10940	Density functional theory study on the electronic structure of<mml:math xmlns:mml="http://www.w3.org/1998/Math/MathML" display="inline"><mml:mi>n</mml:mi></mml:math>- and<mml:math xmlns:mml="http://www.w3.org/1998/Math/MathML" display="inline"><mml:mi>p</mml:mi></mml:math>-type doped SrTiO<mml:math xmlns:mml="http://www.w3.org/1998/Math/MathML" display="inline"><mml:msub><mml:mrow /><mml:mn>3</mml:mn></mml:msub></mml:math>at anodic solid oxide fuel cell conditions. Physical R	1.1	16
10941	First-principles investigations of elastic stability and electronic structure of cubic platinum carbide under pressure. Journal of Applied Physics, 2011, 110, .	1.1	22
10942	Prediction of reconstruction in heteroepitaxial systems using the Frenkel-Kontorova model. Physical Review B, 2011, 84, .	1.1	5
10943	Electronic structure and stability of layered superlattice composed of graphene and boron nitride monolayer. Physical Review B, 2011, 83, .	1.1	50
10944	Hybrid functional study of Si and O donors in wurtzite AlN. Applied Physics Letters, 2011, 99, .	1.5	51
10945	Dielectric properties and lattice dynamics of<mml:math xmlns:mml="http://www.w3.org/1998/Math/MathML" display="inline"><mml:mi>Î±</mml:mi></mml:math>-PbO<mml:math xmlns:mml="http://www.w3.org/1998/Math/MathML" display="inline"><mml:msub><mml:mrow /><mml:mn>2</mml:mn></mml:msub></mml:math>-type TiO<mml:math xmlns:mml="http://www.w3.org/1998/Math/MathML" display="inline"><mml:msub><mml:mrow />	1.1	24
10946	Electronic origin of the phase transition in ternary alloy Mo(Si1â^'x,Alx)2. Applied Physics Letters, 2011, 98, 101903.	1.5	5
10947	Magnetic anisotropy of thin Co and Ni films on diamond surfaces. Physical Review B, 2011, 84, .	1.1	22
10948	Oxygen adsorption at<mml:math xmlns:mml="http://www.w3.org/1998/Math/MathML" display="inline"><mml:mrow><mml:msub><mml:mi mathvariant="normal">La</mml:mi><mml:mrow><mml:mn>1</mml:mn><mml:mo>â^'</mml:mo><mml:mi>x</mml:mi></mml:mrow><mml:mi mathvariant="normal">Sr</mml:mi><mml:mrow><mml:mi>x</mml:mi></mml:mrow></mml:msub><mml:msub><mml:mi mathvariant="normal">MnO</mml:mi><mml:mrow><mml:mn>3</mml:mn></mml:mrow></mml:msub></mml:mrow></mml:math>(001 surfaces: Predictions from first principles. Physical Review B, 2011, 83, .	1.1	32
10949	Role of carbon and nitrogen in Fe<mml:math xmlns:mml="http://www.w3.org/1998/Math/MathML" display="inline"><mml:msub><mml:mrow /><mml:mn>2</mml:mn></mml:msub></mml:math>C and Fe<mml:math xmlns:mml="http://www.w3.org/1998/Math/MathML" display="inline"><mml:msub><mml:mrow /><mml:mn>2</mml:mn></mml:msub></mml:math>N from first-principles calculations. Physical Review B, 2011, 84, .	1.1	29
10950	Interedge magnetic coupling in transition-metal terminated graphene nanoribbons. Physical Review B, 2011, 83, .	1.1	25
10951	Observation of a surface alloying-to-dealloying transition during growth of Bi on Ag(111). Physical Review B, 2011, 83, .	1.1	33
10952	Calculation of the diameter-dependent polytypism in GaAs nanowires from an atomic motif expansion of the formation energy. Physical Review B, 2011, 84, .	1.1	53
10953	Superconductivity in layered binary silicides: A density functional theory study. Physical Review B, 2011, 84, .	1.1	21
10954	Commensurate-incommensurate phase transition in bilayer graphene. Physical Review B, 2011, 84, .	1.1	86
10955	Crystal structure and electronic states of tripotassium picene. Physical Review B, 2011, 83, .	1.1	45

#	Article	IF	Cites
	van der Waals interactions in the ground state of Mg(BH<mml:math) Tj ETQq0 0 0 rgBT /Overlock 10 Tf 50 767 Td [(xmlns:mml="http://v		
10956	xmlns:mml="http://www.w3.org/1998/Math/MathML" display="inline"><mml:mrow><mml:msub><mml:mrow /><mml:mrow><mml:mn>2</mml:mn></mml:mrow></mml:msub></mml:mrow><mml:mo>+</mml:mo><mml:mrow><mml:msub><mml:mrow /><mml:mrow><mml:mn>2</mml:mn></mml:mrow></mml:msub></mml:mrow></mml:math> dissociation: Prediction of the thermodynamic stability	1.1	47
10957	First-principles prediction of the thermodynamic stability of xenon in monoclinic, tetragonal, and yttrium-stabilized cubic ZrO<mml:math xmlns:mml="http://www.w3.org/1998/Math/MathML" display="inline"><mml:mrow><mml:msub><mml:mrow /><mml:mrow><mml:mn>2</mml:mn></mml:mrow></mml:msub></mml:mrow></mml:math>. Physical Review B, 2011, 83, .	1.1	14
10958	Modification of the band offset in boronitrene. Physical Review B, 2011, 84, .	1.1	19
10959	Free energy of defect formation: Thermodynamics of anion Frenkel pairs in indium oxide. Physical Review B, 2011, 83, .	1.1	24
10960	Alkali-metal adsorption and manipulation on a hydroxylated TiO<mml:math xmlns:mml="http://www.w3.org/1998/Math/MathML" display="inline"><mml:msub><mml:mrow /><mml:mn>2</mml:mn></mml:msub></mml:math>(110) surface using atomic force microscopy. Physical Review B, 2011, 84, .	1.1	19
10961	Fluorine effect on As diffusion in Ge. Journal of Applied Physics, 2011, 109, .	1.1	73
10962	Magnetic properties of tris(8-hydroxyquinoline)iron: Experimental and theoretical investigation. Applied Physics Letters, 2011, 99, .	1.5	12
10963	Mechanical properties of clusters in quasicrystal approximants: The example of the 1/1 Al-Cu-Fe approximant. Physical Review B, 2011, 84, .	1.1	1
10964	Four-copper complexes in Si and the Cu-photoluminescence defect: A first-principles study. Physical Review B, 2011, 84, .	1.1	33
10965	Î±-iron facet with enhanced carbon mobility. Physical Review B, 2011, 83, .	1.1	4
10966	Dense close-packed phase of tin above 157 GPa observed experimentally via angle-dispersive x-ray diffraction. Physical Review B, 2011, 84, .	1.1	30
10967	DFT… <mml:math xmlns:mml="http://www.w3.org/1998/Math/MathML" display="inline"><mml:mi>U</mml:mi></mml:math> study of magnetic order in doped La<mml:math xmlns:mml="http://www.w3.org/1998/Math/MathML" display="inline"><mml:msub><mml:mrow /><mml:mn>2</mml:mn></mml:msub></mml:math>CuO<mml:math xmlns:mml="http://www.w3.org/1998/Math/MathML" display="inline"><mml:msub><mml:mrow /><mml:mn>4</mml:mn></mml:msub></mml:math> crystals. Physical Review B, 2011, 84, .	1.1	22
10968	Mapping the energy surface of PbTiO3in multidimensional electric-displacement space. Physical Review B, 2011, 84, .	1.1	25
10969	High-pressure phase transition and metallization in Ar(H2)2. Physical Review B, 2011, 83, .	1.1	10
10970	Ultrastiffness and metallicity of rhenium nitrides. Journal of Applied Physics, 2011, 109, .	1.1	15
10971	First-principles study of the solid solution of hydrogen in lanthanum. Physical Review B, 2011, 84, .	1.1	5
10972	Cu/ZnO(0001) under oxidating and reducing conditions: A first-principles survey of surface structures. Physical Review B, 2011, 84, .	1.1	30
10973	Nanotube bundles and tube-tube orientation: A van der Waals density functional study. Physical Review B, 2011, 84, .	1.1	11

#	Article	IF	Citations
10974	Relative Isomer Abundance of Fullerenes and Carbon Nanotubes Correlates with Kinetic Stability. Physical Review Letters, 2011, 107, 175506.	2.9	18
10975	First-principles study for the adsorption of segments of BPA-PC on<mml:math xmlns:mml="http://www.w3.org/1998/Math/MathML" display="inline"><mml:mi>Î±</mml:mi></mml:math>-Al<mml:math xmlns:mml="http://www.w3.org/1998/Math/MathML" display="inline"><mml:msub><mml:mrow /><mml:mn>2</mml:mn></mml:msub></mml:math>O<mml:math xmlns:mml="http://www.w3.org/1998/Math/MathML" display="inline"><mml:msub><mml:mrow	1.1	8
10976	Local hydroxyl adsorption geometry on TiO<mml:math xmlns:mml="http://www.w3.org/1998/Math/MathML" display="inline"><mml:msub><mml:mrow /><mml:mn>2</mml:mn></mml:msub></mml:math>(110). Physical Review B, 2011, 84, .	1.1	9
10977	Diffusion of Ag alongÎ£3 grain boundaries in 3C-SiC. Physical Review B, 2011, 84, .	1.1	44
10978	Manifold electronic structure transition of BNC biribbons. Journal of Applied Physics, 2011, 110, .	1.1	30
10979	Theoretical study of the role of the tip in enhancing the sensitivity of differential conductance tunneling spectroscopy on magnetic surfaces. Physical Review B, 2011, 83, .	1.1	17
10980	Identification of post-pyrite phase transitions in SiO<mml:math xmlns:mml="http://www.w3.org/1998/Math/MathML" display="inline"><mml:mrow><mml:msub><mml:mrow /><mml:mrow><mml:mn>2</mml:mn></mml:mrow></mml:msub></mml:mrow></mml:math>by a genetic algorithm. Physical Review B, 2011, 83, .	1.1	46
10981	Energetics and kinetics of the<mml:math xmlns:mml="http://www.w3.org/1998/Math/MathML" display="inline"><mml:mrow><mml:mi>c</mml:mi></mml:mrow></mml:math>(<mml:math) Tj ETQq1 1 0.784314 rgBT /Overlock 10 Tf		

#	Article	IF	Citations
10992	Effect of tin doping on oxygen- and carbon-related defects in Czochralski silicon. Journal of Applied Physics, 2011, 110, .	1.1	58
10993	Stability and electronic structure of bilayer graphone. Applied Physics Letters, 2011, 98, .	1.5	13
10994	3<mml:math xmlns:mml="http://www.w3.org/1998/Math/MathML" display="inline"><mml:mi>d</mml:mi></mml:math>transition metal impurities in diamond: Electronic properties and chemical trends. Physical Review B, 2011, 84, .	1.1	16
10995	First-principles study of defect properties of zinc blende MgTe. Physical Review B, 2011, 83, .	1.1	24
10996	Stress balance in nanopatterned N/Cu(001) surfaces. Physical Review B, 2011, 84, .	1.1	5
10997	Functionalization of hydrogenated (111) silicon surface with hydrophobic polymer chains. Physical Review B, 2011, 84, .	1.1	7
10998	Nonlinear variations in the electronic structure of IIâ€“VI and IIIâ€“V wurtzite semiconductors with biaxial strain. Applied Physics Letters, 2011, 98, .	1.5	24
10999	Native defects in LiNH<mml:math xmlns:mml="http://www.w3.org/1998/Math/MathML" display="inline"><mml:mrow><mml:msub><mml:mrow /><mml:mrow><mml:mn>2</mml:mn></mml:mrow></mml:msub></mml:mrow></mml:math>: A first-principles study. Physical Review B, 2011, 84, .	1.1	19
11000	Modeling the iron oxides and oxyhydroxides for the prediction of environmentally sensitive phase transformations. Physical Review B, 2011, 83, .	1.1	64
11001	Magnetic nanoscale laminates with tunable exchange coupling from first principles. Physical Review B, 2011, 84, .	1.1	75
11002	Effects of nitrogen incorporation on the electronic structure of rutile-TiO2. Journal of Applied Physics, 2011, 109, .	1.1	11
11003	Water Interaction with native defects on rutile TiO2 nanowire: Ab initio calculations. Applied Physics Letters, 2011, 98, 083115.	1.5	12
11004	The trapping of N2 molecules and the reduction in its bonding length in Ge(001) due to N2+ ion implantation. Journal of Applied Physics, 2011, 109, .	1.1	4
11005	First principles study of native defects in InI. Journal of Applied Physics, 2011, 109, 113518.	1.1	17
11006	Structure of Sn1â^'xGex random alloys as obtained from the coherent potential approximation. Journal of Applied Physics, 2011, 110, 036105.	1.1	24
11007	First principles study on the switching mechanism in Resistance Random Access Memory devices. , 2011, , .		0
11008	First principles calculation of polarization induced interfacial charges in GaN/AlN heterostructures. Applied Physics Letters, 2011, 98, .	1.5	7
11009	Glass-forming ability and atomic-level structure of the ternary Agâ€“Niâ€“Zr metallic glasses studied by molecular dynamics simulations. Journal of Applied Physics, 2011, 109, 053505.	1.1	7

#	Article	IF	Citations
11010	Electronic structural and electrochemical properties of lithium zirconates and their capabilities of CO2 capture: A first-principles density-functional theory and phonon dynamics approach. Journal of Renewable and Sustainable Energy, 2011, 3, .	0.8	51
11011	Electronic structure, vibrational spectrum, and thermal properties of yttrium nitride: A first-principles study. Journal of Applied Physics, 2011, 109, 073720.	1.1	49
11012	Multiple negative differential resistance and the modulation in a nanotubelike fullerene D5h(1)-C90. Applied Physics Letters, 2011, 98, 163107.	1.5	6
11013	Size- and surface-dependent electronic structures of crystalline SiC nanotubes. Journal of Applied Physics, 2011, 109, 084318.	1.1	3
11014	Improved calculation of vacancy properties in Ge using the Heyd-Scuseria-Ernzerhof range-separated hybrid functional. Journal of Applied Physics, 2011, 110, .	1.1	19
11015	Ab initio investigation of structural, electronic, mechanical, and thermodynamic properties of AlSc2 intermetallic compound under pressure. Journal of Applied Physics, 2011, 110, 033533.	1.1	16
11016	CO2 adsorption on TiO2(101) anatase: A dispersion-corrected density functional theory study. Journal of Chemical Physics, 2011, 135, 124701.	1.2	119
11017	Electronic and thermoelectric analysis of phases in the In2O3(ZnO)k system. Journal of Applied Physics, 2011, 109, .	1.1	36
11018	Ab Inito Study of Absorption Spectra in Ultra Small Diameter Single Walled Boron Nanotubes. Advanced Materials Research, 2011, 217-218, 16-20.	0.3	0
11019	Modulation of Band Gaps of Codoping GaN: A First Principles Study. Advanced Materials Research, 2011, 287-290, 306-312.	0.3	1
11020	The decomposition of H ₂ O ₂ over the components of Au/TiO ₂ Âcatalysts. Proceedings of the Royal Society A: Mathematical, Physical and Engineering Sciences, 2011, 467, 1885-1899.	1.0	35
11021	The Configuration and Evolution of Ti-Si-N Island on TiN(<i>001</i>) Surface: <i>Ab Initio</i> Study. Advanced Materials Research, 0, 295-297, 301-306.	0.3	1
11022	The Effect of Vacancy on the Phase Stability of TiNi Shape Memory Alloy from First-Principle Calculation. Materials Science Forum, 2011, 687, 528-532.	0.3	1
11023	First Principles Calculation on Adsorption of S on Fe(100). Advanced Materials Research, 0, 337, 690-694.	0.3	3
11024	Influence of Intercalated Silicon on the Transport Properties of Graphene. Materials Science Forum, 2011, 679-680, 793-796.	0.3	1
11025	Investigation of the Structure and Photoluminescence Properties of Ln3+(Eu3+, Dy3+, Sm3+) Ion-Doped NaY(MoO4)2. Journal of the Electrochemical Society, 2011, 158, J387.	1.3	15
11026	Mechanisms of Cr and H incorporation in stishovite determined by single-crystal EPR spectroscopy and DFT calculations. American Mineralogist, 2011, 96, 1331-1342.	0.9	8
11027	The Li-adsorbed C(100)-(1x1):O Diamond Surface. Materials Research Society Symposia Proceedings, 2011, 1282, 163.	0.1	8

#	Article	IF	Citations
11028	Synergistic effects on band gap-narrowing in titania by doping from first-principles calculations: density functional theory studies. Materials Research Society Symposia Proceedings, 2011, 1352, 9.	0.1	1
11029	A First-Principles Study of Hydrogen Molecules Adsorption on Graphene. Advanced Materials Research, 2011, 213, 586-589.	0.3	0
11030	Pressure-induced structural transition of OsN ₂ and effect of metallic bonding on its hardness. Europhysics Letters, 2011, 95, 66005.	0.7	17
11031	Cu₂O behavior under pressure: anab initiostudy. Journal of Physics Condensed Matter, 2011, 23, 045502.	0.7	18
11032	Elastic and Electronic Properties of Mg₂Ca and Mg₂Y Phases. Advanced Materials Research, 0, 233-235, 2231-2238.	0.3	3
11033	First Principles Analysis of Ultra-Thin Silicon Films with Dimer Structures. Materials Research Society Symposia Proceedings, 2011, 1370, 89.	0.1	0
11034	Phonon and Elastic Instabilities in Zincblende TlN under Hydrostatic Pressure from First Principles Calculations. Chinese Physics Letters, 2011, 28, 100503.	1.3	7
11035	Solubility Products for Precipitate Phases in Steels from First-principles Calculations. Materials Research Society Symposia Proceedings, 2011, 1296, 1.	0.1	0
11036	First principle investigation of CrSi₂ with doping V. , 2011, , .		1
11037	Ab Initio Phonon Dispersion Curves Used to Check Experimentally Determined Elastic Constants of the MAX Phase Ti₃SiC₂. Advanced Materials Research, 2011, 275, 135-138.	0.3	1
11038	Electronic structure interpolation via atomic orbitals. Journal of Physics Condensed Matter, 2011, 23, 325501.	0.7	17
11039	Identification of the pressure-induced phase transition of ZnSe with the positron annihilation method. Chinese Physics B, 2011, 20, 108105.	0.7	4
11040	First-principles calculation of electronic structure of Mg x Zn 1â^' x O codoped with aluminium and nitrogen. Chinese Physics B, 2011, 20, 017101.	0.7	10
11041	Rectifying Properties of a Nitrogen/Boron-Doped Capped-Carbon-Nanotube-Based Molecular Junction. Chinese Physics Letters, 2011, 28, 047301.	1.3	4
11042	Phase transition, structural and thermodynamic properties of Mg₂Si polymorphs. Chinese Physics B, 2011, 20, 030508.	0.7	12
11043	First-Principles Study of Structural, Electronic, Elastic, Phonon, and Thermodynamical Properties of the Niobium Carbide. Solid State Phenomena, 0, 171, 67-77.	0.3	14
11044	A density functional theory study of structural, mechanical and electronic properties of crystalline phosphorus pentoxide. Journal of Chemical Physics, 2011, 135, 234513.	1.2	14
11045	Simulation approaches for studying the conductance behavior of gold nanowires during tensile deformation. Modelling and Simulation in Materials Science and Engineering, 2011, 19, 074001.	0.8	4

#	Article	IF	Citations
11046	Effects of Mg Addition on Thickness of Galvalume Coating: A First-Principles Study. Advanced Materials Research, 0, 291-294, 125-128.	0.3	1
11047	Effect of strain in LaAlO<inf>3</inf>/BaTiO<inf>3</inf> superlattice. , 2011, , .		0
11048	Surface alloy formation of noble adatoms adsorbed on Si(111)-sqrt {3}imes sqrt {3} â€“Pb surface: a first-principles study. Journal of Physics Condensed Matter, 2011, 23, 265001.	0.7	3
11049	Synergy Effect of Ce/N Co-Doping on Anatase TiO₂ Photocatalysts from First Principles Calculation. Materials Science Forum, 2011, 675-677, 1045-1048.	0.3	0
11050	Hydrogen Atom Adsorption on Î±-Al₂O₃(0001) Surface from First Principles. Advanced Materials Research, 2011, 399-401, 2261-2265.	0.3	2
11051	First Principles Calculation of Geometrical and Electronic Structure of Semiconductor Fe_{1-x}Mn_xSi₂. Advanced Materials Research, 2011, 213, 483-486.	0.3	0
11052	Wide Spectrum Absorption of CuGaS₂ with Intermediate Bands. Applied Mechanics and Materials, 0, 148-149, 1558-1561.	0.2	5
11053	Theoretical Investigation on Microstructure of the Novel 24R-Type LPSO Phase in Mg₉₇Zn₁Y₂ Alloy. Advanced Materials Research, 0, 233-235, 2359-2366.	0.3	0
11054	Density Functional Theory Calculations of Properties of the Grain Boundaries in Aluminum. Materials Research Society Symposia Proceedings, 2011, 1297, 155.	0.1	3
11055	The Electronic and Magnetic Properties of Chemically Decorated Boron Nitride Sheet. Applied Mechanics and Materials, 2011, 130-134, 1439-1443.	0.2	0
11056	A density functional theory study of the electronic structures and magnetic properties of Fe (1â^' x) Co x alloy nanowires encapsulated in (10,0) carbon nanotubes. Chinese Physics B, 2011, 20, 127302.	0.7	4
11057	Theory of phonon conductivity of semiconductor superlattices. Materials Research Society Symposia Proceedings, 2011, 1347, 1.	0.1	0
11058	First Principle Study on Hydrogen Diffusion in Degassing. Key Engineering Materials, 2011, 474-476, 1384-1387.	0.4	2
11059	Low temperature CVD growth of graphene nano-flakes directly on high K dielectrics. Materials Research Society Symposia Proceedings, 2011, 1284, 19.	0.1	2
11060	A first-principles study of the phase transition from Holl-I to Holl-II in the composition KAlSi3O8. American Mineralogist, 2011, 96, 974-982.	0.9	14
11061	Comparativeab initiostudy of lattice dynamics and thermodynamics of Fe₂SiO₄- and Mg₂SiO₄-spinels. Journal of Physics Condensed Matter, 2011, 23, 105401.	0.7	11
11062	High-pressure theoretical and experimental study of HgWO4. High Pressure Research, 2011, 31, 58-63.	0.4	1
11063	The origin of predominance of cementite among iron carbides in steel at elevated temperature. Materials Research Society Symposia Proceedings, 2011, 1296, 1.	0.1	1

#	Article	IF	Citations
11064	Hydrogen Adsorption on Palladium and Platinum Overlayers: DFT Study. Advances in Physical Chemistry, 2011, 2011, 1-8.	2.0	44
11065	Effect of biaxial strain on half-metallicity of transition metal alloyed zinc-blende ZnO and GaAs: a first-principles study. Journal Physics D: Applied Physics, 2011, 44, 205002.	1.3	5
11066	Electronic Structure of KFe ₂ Se ₂ from First-Principles Calculations. Chinese Physics Letters, 2011, 28, 057402.	1.3	46
11067	Modeling of epitaxial graphene functionalization. Nanotechnology, 2011, 22, 055708.	1.3	28
11068	Tuning of the periodicity of stable self-organized metallic templates. Chinese Physics B, 2011, 20, 020513.	0.7	0
11069	Theoretical study on the positron annihilation in Rocksalt structured magnesium oxide. Chinese Physics B, 2011, 20, 057802.	0.7	6
11070	First-principles study of CO oxidation on bismuth-promoted Pt(111) surfaces. Molecular Simulation, 2011, 37, 648-658.	0.9	8
11071	Localised Phonon Modes at LiNbO₃(0001) Surfaces. Ferroelectrics, 2011, 419, 1-8.	0.3	11
11072	Effect of Lithium Absorption at Tetrahedral Site and Isomorphic Substitution on Montmorillonite Properties: A Density Functional Theory Study. Japanese Journal of Applied Physics, 2011, 50, 055701.	0.8	5
11073	Structural stability and electronic properties of the new superconductor (Ca₄Al₂O_{6 â^'x})(Fe₂As₂) from first-principles study. Superconductor Science and Technology, 2011, 24, 105014.	1.8	4
11074	Effect of impurities on structural, cohesive and magnetic properties of grain boundaries in Î±-Fe. Modelling and Simulation in Materials Science and Engineering, 2011, 19, 025001.	0.8	56
11075	Carbon, oxygen and intrinsic defect interactions in germanium-doped silicon. Semiconductor Science and Technology, 2011, 26, 105024.	1.0	15
11076	Vacancy and H Interactions in Nb. Chinese Physics Letters, 2011, 28, 127101.	1.3	4
11077	Ab initio study of the electronic structure and elastic properties of Al 5 C 3 N. Chinese Physics B, 2011, 20, 126201.	0.7	5
11078	Electronic Structure Magnetic Properties and Optical Properties of Co-doped AlN from First Principles. Communications in Theoretical Physics, 2011, 55, 893-900.	1.1	3
11079	Ab initio studies on the mechanic and magnetic properties of PdH x. Chinese Physics B, 2011, 20, 026201.	0.7	7
11080	Electronic Density Decay Lengths of Pb Films from First Principles Calculations. Chinese Physics Letters, 2011, 28, 047302.	1.3	1
11081	The pressureâ€“temperature phase diagram of MgH₂and isotopic substitution. Journal of Physics Condensed Matter, 2011, 23, 305403.	0.7	16

#	Article	IF	Citations
11082	Effect of Doping on the Thermoelectric Properties of Thallium Tellurides Using First Principles Calculations. Solid State Phenomena, 0, 172-174, 985-989.	0.3	2
11083	Study on Electronic Structure and Optical Property of Silicon Doped with Transition Metal by First Principles. Advanced Materials Research, 0, 217-218, 930-935.	0.3	2
11084	The dielectric properties of La(Mg_{0.5}Ti_{0.5})O₃ceramics studied by Raman-scattering, infrared reflectivity spectroscopy, and first-principles calculations. Journal of Physics Condensed Matter, 2011, 23, 225901.	0.7	4
11085	First-Principles Calculations of Elastic and Thermodynamic Properties of Cubic CdTe. Advanced Materials Research, 2011, 268-270, 886-891.	0.3	0
11086	A Fast Method for Electronic Band Structure Calculations. , 2011, , .		0
11087	Influence of concentration of Ag on electron and crystallographic structure of reactively co-sputtered CFUBMS TiN/Ag nanocomposite coatings. Materials Technology, 2011, 26, 40-45.	1.5	2
11088	Dependence of the electrical properties of defective single-walled carbon nanotubes on the vacancy density. Chinese Physics B, 2011, 20, 087303.	0.7	3
11089	Pressure-Induced Structural Transition and Enhancement of Energy Gap of CuAlO₂. Journal of the Physical Society of Japan, 2011, 80, 024706.	0.7	14
11090	Nanocatalyst structure as a template to define chirality of nascent single-walled carbon nanotubes. Journal of Chemical Physics, 2011, 134, 014705.	1.2	36
11091	Boron/nitrogen pairs Co-doping in metallic carbon nanotubes: a first-principle study. Chinese Physics B, 2011, 20, 027102.	0.7	7
11092	First-principles studies for the stability of a graphene-like boron layer on CrB₂(0001) and MoB₂(0001). Journal of Physics Condensed Matter, 2011, 23, 225501.	0.7	13
11093	Energy investigation of effects of O on mechanical properties of NiAl intermetallics. Journal of Physics Condensed Matter, 2011, 23, 025501.	0.7	9
11094	Interphase Energies and Nonequilibrium Growth of Î³-precipitates in Al-Ag: A DFT Study. Materials Research Society Symposia Proceedings, 2011, 1297, 47.	0.1	0
11095	Geometric and Electronic Structures at the Interface between Iron Phthalocyanine and Si (110). Chinese Physics Letters, 2011, 28, 116804.	1.3	3
11096	Structural Study of Î±-Rhombohedral Boron at High Pressures. Journal of the Physical Society of Japan, 2011, 80, 084601.	0.7	21
11097	First principles theoretical study of the hole-assisted conversion of CO to CO2 on the anatase TiO2(101) surface. Journal of Chemical Physics, 2011, 134, 104701.	1.2	39
11098	FERROELECTRIC SWITCHING PATH IN MONODOMAIN RHOMBOHEDRAL BiFeO₃ CRYSTAL: A FIRST-PRINCIPLES STUDY. Journal of Advanced Dielectrics, 2011, 01, 179-184.	1.5	2
11099	First-principles study of Be doped CuAlS2 for p-type transparent conductive materials. Journal of Applied Physics, 2011, 109, .	1.1	10

#	Article	IF	Citations
11100	First-principles calculation of the elastic moduli of sheet silicates and their application to shale anisotropy. American Mineralogist, 2011, 96, 125-137.	0.9	92
11101	First Principles Calculations of Defect Formation in In-Free Photovoltaic Semiconductors Cu₂ZnSnS₄ and Cu₂ZnSnSe₄. Japanese Journal of Applied Physics, 2011, 50, 04DP07.	0.8	83
11102	Controllability of Electrical Conductivity by Oxygen Vacancies and Charge Carrier Trapping at Interface between CoO and Electrodes. Japanese Journal of Applied Physics, 2011, 50, 071101.	0.8	6
11103	Thermophysical properties for shock compressed polystyrene. Physics of Plasmas, 2011, 18, .	0.7	33
11104	Phonon Frequencies of Ferroelectric Semiconductor SbSBr by First Principle Calculation. Ferroelectrics, 2011, 414, 113-120.	0.3	2
11105	First-principles study of the electronic structure and optical properties of Ce-doped ZnO. Journal of Applied Physics, 2011, 109, .	1.1	55
11106	Implementation of screened hybrid density functional for periodic systems with numerical atomic orbitals: Basis function fitting and integral screening. Journal of Chemical Physics, 2011, 135, 034110.	1.2	24
11107	STRUCTURAL, ELECTRONIC AND OPTICAL PROPERTIES OF THE TETRAGONAL PHASE OFCaSiO₃PEROVSKITE UNDER PRESSURE: FIRST-PRINCIPLES CALCULATIONS. Modern Physics Letters B, 2011, 25, 41-52.	1.0	5
11108	Tailoring the electronic structure of graphene for catalytic and nanoelectronic applications. , 2011, , .		0
11109	AB INITIO STUDY OF ELECTRONIC AND MAGNETIC STRUCTURE OF INTERMETALLIC RE5Ge3 COMPOUNDS. Modern Physics Letters B, 2011, 25, 2427-2438.	1.0	4
11110	STRUCTURAL AND ELECTRONIC PROPERTIES AND PHONONS OF PLATINUM NITRIDES BY DENSITY FUNCTIONAL THEORY. International Journal of Modern Physics B, 2011, 25, 1543-1551.	1.0	5
11111	COMPARATIVE STUDY OF ELECTRONIC PROPERTIES OF GRAPHITE AND HEXAGONAL BORON NITRIDE (h-BN) USING PSEUDOPOTENTIAL PLANE WAVE METHOD. Modern Physics Letters B, 2011, 25, 1855-1866.	1.0	26
11112	First-principles study of ZnO cluster-decorated carbon nanotubes. Nanotechnology, 2011, 22, 445705.	1.3	13
11113	Theoretical prediction of the growth and surface structure of Pt and Ni nanoparticles. Europhysics Letters, 2011, 96, 66005.	0.7	10
11114	Ab-initio aprroach to the electronic, structural, elastic, and finite-temperature thermodynamic properties of Ti2AX (Aâ€‰=â€‰Al or Ga and Xâ€‰=â€‰C or N). Journal of Applied Physics, 2011, 110, .	1.1	35
11115	First-principles studies of Pb doping in graphene: stability, energy gap and spinâ€“orbit splitting. New Journal of Physics, 2011, 13, 123018.	1.2	23
11116	The mechanical, electronic structure and thermodynamic properties of B2-based AgRE studied from first-principles. Physica Scripta, 2011, 83, 045301.	1.2	12
11117	Structural transition, dielectric and bonding properties of BeCN 2. Chinese Physics B, 2011, 20, 016201.	0.7	15

#	Article	IF	Citations
11118	Electronic Structures and Thermoelectric Properties of NaCo₂O₄ Thermoelectric Material. Advanced Materials Research, 2011, 317-319, 2051-2055.	0.3	3
11119	Electronic structures of porous nanocarbons. Scientific Reports, 2011, 1, 36.	1.6	40
11120	Quantum molecular dynamic simulations of warm dense carbon monoxide. Journal of Chemical Physics, 2011, 135, 064501.	1.2	10
11121	Ab initiocharacterization of the electronic properties of PbTe quantum dots embedded in a CdTe matrix. Semiconductor Science and Technology, 2011, 26, 014005.	1.0	6
11122	Electronic structures of an epitaxial graphene monolayer on SiC(0001) after gold intercalation: a first-principles study. Nanotechnology, 2011, 22, 275704.	1.3	21
11123	Effect of impurity atoms on Î±2/Î³ lamellar interfacial misfit in Tiâ€“Al alloy: a systematic first principles study. Philosophical Magazine, 2011, 91, 3685-3704.	0.7	7
11124	Ab initio investigations on the stability of seven-fold approximants. Philosophical Magazine, 2011, 91, 2567-2578.	0.7	10
11125	Electric-field effects on magnetic anisotropy in Pd/Fe/Pd(0â€‰0â€‰1) surface. Journal Physics D: Applied Physics, 2011, 44, 064005.	1.3	23
11126	Atomic-Level Investigation of<mml:math xmlns:mml="http://www.w3.org/1998/Math/MathML"><mml:msub><mml:mtext>CH</mml:mtext><mml:mi>x</mml:mi></mml:msub><mml:mtext>-</mml:mtext><mml:mi>Î²</mml:mi></mml:math>-SiC (111) Surface for CVD Diamond Growth from DF. Journal of Nanomaterials, 2011, 2011, 1-6.	1.5	2
11127	Direct observation of the substitution effects on the hydrogen bridge dynamics in selected Schiff basesâ€”A comparative molecular dynamics study. Journal of Chemical Physics, 2011, 134, 034308.	1.2	9
11128	First-principles study of void induced stresses at a diamond (100) grain boundary. Journal of Applied Physics, 2011, 109, 033518.	1.1	6
11129	Theoretical investigations of candidate crystal structures for Î²-carbonic acid. Journal of Chemical Physics, 2011, 134, 124511.	1.2	13
11130	Toward CH₄dissociation and C diffusion during Ni/Fe-catalyzed carbon nanofiber growth: A density functional theory study. Journal of Chemical Physics, 2011, 134, 134704.	1.2	30
11131	A density-functional theory study of water on clean and hydrogen preadsorbed Rh(111) surfaces. Journal of Chemical Physics, 2011, 134, 154701.	1.2	12
11132	Intrinsic stability and hydrogen affinity of pure and bimetallic nanowires. Journal of Chemical Physics, 2011, 134, 174106.	1.2	3
11133	First-principles study towards the reactivity of the Pd(111) surface with low Zn deposition. Journal of Chemical Physics, 2011, 134, 184702.	1.2	6
11134	Rare earth chalcogenide Ce3Te4 as high efficiency high temperature thermoelectric material. Applied Physics Letters, 2011, 98, .	1.5	18
11135	C-N coupling on transition metal surfaces: A density functional theory study. Journal of Chemical Physics, 2011, 135, 124707.	1.2	4

#	Article	IF	Citations
11136	Stabilizing the defect-induced dilute magnetic semiconductors: Li-doping in GaN with Ga vacancies. Europhysics Letters, 2011, 93, 57006.	0.7	7
11137	Response of fcc metals andL1₂andD0₂₂type trialuminides to uniaxial loading along [100] and [001]:ab initioDFT calculations. Philosophical Magazine, 2011, 91, 491-516.	0.7	11
11138	The WURM project--a freely available web-based repository of computed physical data for minerals. American Mineralogist, 2011, 96, 437-443.	0.9	48
11139	Electronic and Optical Properties of Substitutional and Interstitial Si-Doped ZnO. Materials, 2012, 5, 2088-2100.	1.3	63
11140	Theoretical Investigation on Single-Wall Carbon Nanotubes Doped with Nitrogen, Pyridine-Like Nitrogen Defects, and Transition Metal Atoms. Journal of Nanomaterials, 2012, 2012, 1-14.	1.5	40
11141	The electronic and optical properties of warm dense nitrous oxide using quantum molecular dynamics simulations. Physics of Plasmas, 2012, 19, 112701.	0.7	3
11142	Al-Doped CuInSe₂: An <i>Ab Initio</i> Study of Structural and Electronic Properties of a Photovoltaic Material. Advanced Materials Research, 0, 512-515, 1543-1547.	0.3	1
11143	First Principles Calculation on Adsorption of S on Impurity Fe (100). Advanced Materials Research, 0, 472-475, 1538-1543.	0.3	0
11144	First-Principles Study on the Structural, Electronic and Elastic Properties of Alloyed Austenite with Co and Ni. Advanced Materials Research, 2012, 503-504, 684-687.	0.3	1
11145	Field Emission of Gallium-Doped Carbon Nanotubes. Advanced Materials Research, 2012, 535-537, 61-66.	0.3	0
11146	First Principles Study on Different Size of Pd-Doped CdS. Advanced Materials Research, 2012, 569, 198-201.	0.3	0
11147	Electronic and Optical Properties of RB₆ (R=La, Nd): A Computer Aided Design. Advanced Materials Research, 0, 571, 239-242.	0.3	3
11148	A Possible New Parent Compound Sr4Al2O6Fe2As2 with High-TC Superconductivity. Journal of the Physical Society of Japan, 2012, 81, 024713.	0.7	4
11149	A first-principles density functional theory study of the electronic structural and thermodynamic properties of M2ZrO3 and M2CO3 (Mâ€‰=â€‰Na, K) and their capabilities for CO2 capture. Journal of Renewable and Sustainable Energy, 2012, 4, 013109.	0.8	25
11150	Ab Initio Study on the Structural and Magnetic Properties of Co-Pd and Co-Pt Linear and Zigzag Nanowires. Integrated Ferroelectrics, 2012, 136, 132-138.	0.3	1
11151	Force and conductance during contact formation to a C₆₀molecule. New Journal of Physics, 2012, 14, 073032.	1.2	46
11152	Equation of state of dense plasmas by ab initio simulations: Bridging the gap between quantum molecular dynamics and orbital-free molecular dynamics at high temperature. Physics of Plasmas, 2012, 19, 122712.	0.7	25
11153	Optical Properties of LaB₆: A Computer Aided Simulation. Advanced Materials Research, 2012, 571, 292-295.	0.3	0

#	Article	IF	Citations
11154	Twisted ZBâ€“CdTe/RSâ€“PbTe (111) heterojunction as a metastable interface structure. New Journal of Physics, 2012, 14, 113021.	1.2	13
11155	Optical Properties of Î²-Si₃N₄ Studied from First-Principles Method. Advanced Materials Research, 0, 490-495, 3253-3256.	0.3	1
11156	First-Principles Study of Electronic Structure and Elastic Properties of Si Doping Ti₃Al_{1-x}Si_xC₂ Solid Solutions. Advanced Materials Research, 2012, 624, 122-126.	0.3	2
11157	High pressure ionic and molecular crystals of ammonia monohydrate within density functional theory. Journal of Chemical Physics, 2012, 137, 064506.	1.2	21
11158	Surface structure and phase transition of K adsorption on Au(111): By ab initio atomistic thermodynamics. Journal of Chemical Physics, 2012, 136, 044510.	1.2	7
11159	Robust surface state of intrinsic topological insulator Bi₂Te₂Se thin films: a first-principles study. Journal of Physics Condensed Matter, 2012, 24, 035502.	0.7	17
11160	Magnetic Properties of Iron on Strained Graphene: Density Functional Theory Study. Japanese Journal of Applied Physics, 2012, 51, 06FD13.	0.8	0
11161	Simultaneous measurement of lithium and fluorine momentum in⁷LiF. Journal of Physics Condensed Matter, 2012, 24, 365401.	0.7	11
11162	Effect of Electronegativity and Charge Balance on the Visible-Light-Responsive Photocatalytic Activity of Nonmetal Doped Anatase TiO₂. International Journal of Photoenergy, 2012, 2012, 1-8.	1.4	22
11163	Structures and magnetic properties of Fe and Ni monoatomic chains encapsulated by an Au nanotube. Chinese Physics B, 2012, 21, 118102.	0.7	1
11164	An unexpected softening from WB ₃ to WB ₄. Europhysics Letters, 2012, 98, 66004.	0.7	45
11165	Nitrogen pair â^' hydrogen complexes in ZnO and p-type doping.. Materials Research Society Symposia Proceedings, 2012, 1394, 27.	0.1	5
11166	First-principles transition state study of oxygen reduction reaction on Pt (111) surface modified by subsurface transition metals. Materials Research Society Symposia Proceedings, 2012, 1384, 1.	0.1	1
11167	Ultra thin transition metal oxide coatings on diamond for thermionic applications. Materials Research Society Symposia Proceedings, 2012, 1511, 1.	0.1	0
11168	Energy Band Gap Modification of Graphene Deposited on a Multilayer Hexagonal Boron Nitride Substrate. Materials Research Society Symposia Proceedings, 2012, 1407, 45.	0.1	1
11169	Strain dependence of internal displacement and effective charge in wurtzite III-N semiconductors. Journal of Physics: Conference Series, 2012, 367, 012006.	0.3	1
11170	Rare earth 4f hybridization with the GaN valence band. Semiconductor Science and Technology, 2012, 27, 115017.	1.0	22
11171	First Principles Study of Copper Sulfides (for Applications as Photoconductors). Materials Science Forum, 0, 730-732, 111-116.	0.3	3

#	Article	IF	Citations
11172	Long-Range Interaction between H and (B or P) Dopant Atoms in Silicon Crystals Investigated by First Principles Calculation. Journal of the Electrochemical Society, 2012, 159, H450-H454.	1.3	1
11173	First-Principles Study of Energy Band Gap of Graphene-Like B-C-N by Strain. Advanced Materials Research, 2012, 476-478, 1313-1317.	0.3	1
11174	Effect of C doping on the structural and electronic properties of LiFePO ₄ : A first-principles investigation. Chinese Physics B, 2012, 21, 097401.	0.7	10
11175	A theoretical study of the reactivity of Cu2O(111) surfaces: the case of NO dissociation. Journal of Physics Condensed Matter, 2012, 24, 262001.	0.7	5
11176	Predicting active slip systems in Î²-Sn from ideal shear resistance. Modelling and Simulation in Materials Science and Engineering, 2012, 20, 035003.	0.8	32
11177	Structureâ€“property relations and thermodynamic properties of monoclinic petalite, LiAlSi₄O₁₀. Journal of Physics Condensed Matter, 2012, 24, 345402.	0.7	14
11178	Experimental and theoretical study of electron-beam-induced spin-reorientation transition reversal in the CO/Co(1â€‰1â€‰0) system. Journal Physics D: Applied Physics, 2012, 45, 275003.	1.3	2
11179	Theoretical Study of the Filling Fraction Limit of Fe-Substituted Ba-Filled Skutterudite <i>Ba_yFe_{4x}Co_{4-4x}Sb₁₂</i>. Key Engineering Materials, 0, 519, 169-173.	0.4	0
11180	Electronic structures and optical properties of Zn-doped Î²-Ga ₂ O ₃ with different doping sites. Chinese Physics B, 2012, 21, 127104.	0.7	23
11181	Pressure-induced structural transition and thermodynamic properties of RhN₂and the effect of metallic bonding on its hardness. Chinese Physics B, 2012, 21, 086103.	0.7	7
11182	Ab initioinvestigation of the mechanical properties of copper. Chinese Physics B, 2012, 21, 096102.	0.7	11
11183	Mechanical and electronic properties of novel tungsten nitride. Europhysics Letters, 2012, 100, 46001.	0.7	9
11184	Electronic Structures of InGaN ₂ Nanotubes. Chinese Physics Letters, 2012, 29, 107301.	1.3	1
11185	High volumetric hydrogen density phases of magnesium borohydride at high-pressure: A first-principles study. Chinese Physics B, 2012, 21, 086104.	0.7	6
11186	First Principles Calculation on Adsorption of S on Fe(100) with Different Pressure. Applied Mechanics and Materials, 2012, 217-219, 1811-1814.	0.2	0
11187	Effect of Y and Zn Substitution on Tensile Properties of 6H-Type LPSO Phase in Mg₉₇Zn₁Y₂ Alloy. Advanced Materials Research, 0, 476-478, 2469-2475.	0.3	2
11188	A first-principle investigation of antigorite up to 30 GPa: Structural behavior under compression. American Mineralogist, 2012, 97, 1177-1186.	0.9	14
11189	Raman Scattering Study of Hydrogen Storage Material LiNH₂. Journal of the Physical Society of Japan, 2012, 81, 094603.	0.7	8

#	Article	IF	Citations
11190	Fundamental Electronic Properties and Elastic Properties of Lanthanum Hexaboride: A Computer Aided Design. Advanced Materials Research, 2012, 580, 461-464.	0.3	1
11191	Density Functional Simulations of Transition Metal Terminated (001)-Diamond Surfaces. Materials Science Forum, 2012, 717-720, 1311-1314.	0.3	0
11192	Oscillation of the magnetic moment in modulated martensites in Ni2MnGa studied by ab initio calculations. Applied Physics Letters, 2012, 100, .	1.5	26
11193	First-Principles Study of H₂O Adsorption on Oxygen-Covered Fe Surface. Materials Science Forum, 0, 706-709, 1481-1484.	0.3	5
11194	Theoretical Investigation of Migration Pathways for Li Diffusion in h-LiTiS ₂ . Zeitschrift Fur Physikalische Chemie, 2012, 226, 449-459.	1.4	8
11195	First-Principles Investigation of Hexagonal WB2 Surfaces. Journal of the Physical Society of Japan, 2012, 81, 044712.	0.7	3
11196	Comprehensive Study of the X-Ray Photoelectron Spectroscopy Peak Shift of La-Incorporated Hf Oxide for Gate Dielectrics. Japanese Journal of Applied Physics, 2012, 51, 048005.	0.8	0
11197	Ab initiostudy of Ru-terminated and Ru-doped armchair graphene nanoribbons. Molecular Physics, 2012, 110, 2295-2300.	0.8	14
11198	STRAIN INDUCED ENHANCED MIGRATION OF POLARON AND LITHIUM ION IN Î»-MnO₂. Functional Materials Letters, 2012, 05, 1250037.	0.7	23
11199	A First-Principles Study of the Ferroelectric Phase of AgNbO₃. Japanese Journal of Applied Physics, 2012, 51, 09LE02.	0.8	8
11200	Tunable Magnetic Properties of Rhombohedral Graphite Thin Films: Effects of Insulating Substrate on Magnetic Properties. Japanese Journal of Applied Physics, 2012, 51, 02BN04.	0.8	0
11201	Ab initiocalculation of strain effect on the magnetic properties of the thiogermanate [(CH₃)₄N]₂FeGe₄S₁₀. Journal of Physics Condensed Matter, 2012, 24, 245501.	0.7	4
11202	Analysis of Charge Compensation Mechanisms in Pr$_{1-x}$A$_{x}$CoO$_{3-delta}$ (A = Ca, Sr) by X-ray Absorption Near-Edge Structure. Japanese Journal of Applied Physics, 2012, 51, 073201.	0.8	2
11203	Origin of magnetic interactions and their influence on the structural properties of Ni₂MnGa and related compounds. Journal of Physics Condensed Matter, 2012, 24, 185501.	0.7	26
11204	Band gap of Î²-PtO2 from first-principles. AIP Advances, 2012, 2, 022172.	0.6	22
11205	Ab-initio Study of Interactions of Gold Atoms with Hydroxylated MgO(001) Surfaces. Journal of the Physical Society of Japan, 2012, 81, 054601.	0.7	17
11206	First-principles study on the incipient oxidization of Nb(110). Journal of Physics Condensed Matter, 2012, 24, 225005.	0.7	5
11207	Helium, neon and argon diffraction from Ru(0001). Journal of Physics Condensed Matter, 2012, 24, 354002.	0.7	16

#	Article	IF	Citations
11208	Metallization of the potassium overlayer on the Î²-SiC(100) c(4 Ã— 2) surface. Journal of Physics Condensed Matter, 2012, 24, 485001.	0.7	1
11209	First-principles study of nanometer-sharp domain walls in ferromagnetic Fe monolayers under in-plane strain. Journal of Physics Condensed Matter, 2012, 24, 095303.	0.7	3
11210	Oxygen Vacancy Chain Formation in TiO$_{2}$ under External Strain for Resistive Switching Memory. Japanese Journal of Applied Physics, 2012, 51, 06FG14.	0.8	2
11211	Density functional studies of the defect-induced electronic structure modifications in bilayer boronitrene. Journal of Physics: Conference Series, 2012, 367, 012004.	0.3	1
11212	Rare-earth-metal oxide buffer for epitaxial growth of single crystal GeSi and Ge on Si(111). Journal of Vacuum Science and Technology B:Nanotechnology and Microelectronics, 2012, 30, 02B110.	0.6	3
11213	Experimental and theoretical investigation of graphene layers on SiC(0001Â¯) in different stacking arrangements. Journal of Vacuum Science and Technology B:Nanotechnology and Microelectronics, 2012, 30, 03D117.	0.6	2
11214	First-principles calculations and XPS measurements of gold segregation at the Cu3Au(111) surface. Journal of Vacuum Science and Technology B:Nanotechnology and Microelectronics, 2012, 30, 051802.	0.6	9
11215	X-ray emission spectroscopy and density functional study of CO/Fe(100). Journal of Chemical Physics, 2012, 136, 034702.	1.2	21
11216	Ab initio calculation of lattice dynamics and thermodynamic properties of beryllium. Journal of Applied Physics, 2012, 111, .	1.1	38
11217	Structures and magnetism of multinuclear vanadium-pentacene sandwich clusters and their 1D molecular wires. Journal of Chemical Physics, 2012, 137, 164309.	1.2	8
11218	The structure of N2 adsorbed on the rumpled NaCl(100) surfaceâ€”A combined LEED and DFT-D study. Journal of Chemical Physics, 2012, 137, 174705.	1.2	10
11219	Size-dependent chemical reactivity of porous graphene for purification of exhaust gases. Journal of Chemical Physics, 2012, 137, 184309.	1.2	5
11220	Growth of a Pt film on non-reduced ceria: A density functional theory study. Journal of Chemical Physics, 2012, 136, 044705.	1.2	13
11221	Helium mediated deposition: Modeling the Heâ‹¯TiO₂(110)-(1Ã—1) interaction potential and application to the collision of a helium droplet from density functional calculations. Journal of Chemical Physics, 2012, 136, 124703.	1.2	31
11222	On the early stage of aluminum oxidation: An extraction mechanism via oxygen cooperation. Journal of Chemical Physics, 2012, 137, 094707.	1.2	42
11223	High resolution electron energy loss spectroscopy of clean and hydrogen covered Si(001) surfaces: First principles calculations. Journal of Chemical Physics, 2012, 137, 094701.	1.2	1
11224	Uranyl ion interaction at the water/NiO(100) interface: A predictive investigation by first-principles molecular dynamic simulations. Journal of Chemical Physics, 2012, 137, 164701.	1.2	7
11225	Potential energy surface of H2O on Al{111} and Rh{111} from theoretical methods. Journal of Chemical Physics, 2012, 137, 204702.	1.2	11

#	Article	IF	Citations
11226	Structural, elastic, and vibrational properties of layered titanium dichalcogenides: A van der Waals density functional study. Journal of Chemical Physics, 2012, 137, 224509.	1.2	19
11227	Inducing novel electronic properties in âŒ©112âŒª Ge nanowires by means of variations in their size, shape and strain: a first-principles computational study. Journal of Physics Condensed Matter, 2012, 24, 015301.	0.7	6
11228	Phase transitions in KIO₃. Journal of Physics Condensed Matter, 2012, 24, 325401.	0.7	12
11229	Modeling the radiation ionization energy and energy resolution of trigonal and amorphous selenium from first principles. Journal of Physics Condensed Matter, 2012, 24, 455502.	0.7	3
11230	Ab-initio modeling of metastable precipitation processes in aluminum 7xxx alloys. International Journal of Materials Research, 2012, 103, 972-979.	0.1	6
11231	Structural and optoelectronic properties, and infrared spectrum of cubic BaSnO3 from first principles calculations. Journal of Applied Physics, 2012, 112, .	1.1	54
11232	First-principles Study of Geometric and Electronic Structures of Si(111)-â^š7ÂÃ—Ââ^š3-In Surface Reconstruction. Chinese Journal of Chemical Physics, 2012, 25, 403-408.	0.6	8
11233	Electronic structures of single-layer boron pnictides. Applied Physics Letters, 2012, 101, .	1.5	114
11234	Poisoning of magnetism in silicon doped with Re, caused by a charge transfer from interstitials to substitutionals, by means of the self-interaction corrected density-functional approach. Journal of Applied Physics, 2012, 112, 013919.	1.1	3
11235	Spin-polarization of VGaON center in GaN and its application in spin qubit. Applied Physics Letters, 2012, 100, 192401.	1.5	25
11236	Quantum molecular dynamics simulations for the nonmetal-metal transition in fluid nitrogen oxide. Journal of Applied Physics, 2012, 112, 033501.	1.1	7
11237	Selection rule of preferred doping site for n-type oxides. Applied Physics Letters, 2012, 100, 262109.	1.5	10
11238	Polymorphic phases of sp3-hybridized superhard CN. Journal of Chemical Physics, 2012, 137, 184506.	1.2	40
11239	Pressure-induced phase transition and mechanical properties of molybdenum diboride: First principles calculations. Journal of Applied Physics, 2012, 112, .	1.1	11
11240	High pressure transport, structural, and first principles investigations on the fluorite structured intermetallic, PtAl2. Journal of Applied Physics, 2012, 111, .	1.1	2
11241	Low bias short channel impurity mobility in graphene from first principles. Applied Physics Letters, 2012, 101, 093102.	1.5	9
11242	Digital magnetic heterostructures based on GaN using GGA-1/2 approach. Applied Physics Letters, 2012, 101, .	1.5	18
11243	The atomic structure of protons and hydrides in Sm1.92Ca0.08Sn2O7â^'Î´ pyrochlore from DFT calculations and FTIR spectroscopy. Journal of Applied Physics, 2012, 112, .	1.1	4

#	Article	IF	Citations
11244	First-principles characterization of ferromagnetism in N-doped SrTiO3 and BaTiO3. Applied Physics Letters, 2012, 100, 062409.	1.5	44
11245	Theoretical investigation of Fe substitution for Mn in complex hydride YMn2H6. Applied Physics Letters, 2012, 100, 021908.	1.5	10
11246	Influence of doping on the photoactive properties of magnetron-sputtered titania coatings: Experimental and theoretical study. Physical Review B, 2012, 86, .	1.1	23
11247	Ab initiostudy of spin-spiral noncollinear magnetism in a free-standing Fe(110) monolayer under in-plane strain. Physical Review B, 2012, 85, .	1.1	17
11248	First-principles study of hydrogen and fluorine intercalation into graphene-SiC(0001) interface. Physical Review B, 2012, 86, .	1.1	33
11249	Optical spectra of alkali-metal fluorides. Physical Review B, 2012, 86, .	1.1	13
11250	Transport properties of oxygen vacancy filaments in metal/crystalline or amorphous HfO<mml:math xmlns:mml="http://www.w3.org/1998/Math/MathML" display="inline"><mml:msub><mml:mrow /><mml:mn>2</mml:mn></mml:msub></mml:math>/metal structures. Physical Review B, 2012, 86, .	1.1	70
11251	First-principles insight into the degeneracy of ground-state LiBH4structures. Physical Review B, 2012, 86, .	1.1	8
11252	A unique arrangement of atoms for the homologous compounds InMO3(ZnO)m (Mâ€‰=â€‰Al, Fe, Ga, and In). Journal of Applied Physics, 2012, 111, 113716.	1.1	8
11253	Simulation of spin-polarized scanning tunneling spectroscopy on complex magnetic surfaces: Case of a Cr monolayer on Ag(111). Physical Review B, 2012, 85, .	1.1	13
11254	Polymerization of cyanoacetylene under pressure: Formation of carbon nitride polymers and bulk structures. Physical Review B, 2012, 85, .	1.1	5
11255	Influence of Al concentration on the optoelectronic properties of Al-doped MgO. Physical Review B, 2012, 86, .	1.1	5
11256	Li-doped BC3 sheet for high-capacity hydrogen storage. Applied Physics Letters, 2012, 100, .	1.5	58
11257	Incorporation and migration of hydrogen in yttria-stabilized cubic zirconia: Insights from semilocal and hybrid-functional calculations. Physical Review B, 2012, 86, .	1.1	23
11258	Mass transport and thermal stability of TiN/Al2O3/InGaAs nanofilms. Journal of Applied Physics, 2012, 112, .	1.1	21
11259	Tuning the electronic structure of ultrathin crystalline silica films on Ru(0001). Physical Review B, 2012, 85, .	1.1	85
11260	Nuclear inelastic scattering studies of lattice dynamics in magnetite with a first- and second-order Verwey transition. Physical Review B, 2012, 85, .	1.1	19
11261	Mechanical properties of ZnS nanowires and thin films: Microscopic origin of the dependence on size and growth direction. Physical Review B, 2012, 86, .	1.1	17

#	Article	IF	Citations
11262	Detailed calculation of the thermoelectric figure of merit in an<mml:math xmlns:mml="http://www.w3.org/1998/Math/MathML" display="inline"><mml:mi>n</mml:mi></mml:math>-doped SiGe alloy. Physical Review B, 2012, 86, .	1.1	13
11263	Electrons, phonons and superconductivity in rocksalt and tungstenâ€“carbide phases of CrC. Journal of Physics Condensed Matter, 2012, 24, 455704.	0.7	19
11264	Transmutation in<mml:math xmlns:mml="http://www.w3.org/1998/Math/MathML" display="inline"><mml:msup><mml:mrow /><mml:mn>90</mml:mn></mml:msup></mml:math>SrF<mml:math xmlns:mml="http://www.w3.org/1998/Math/MathML" display="inline"><mml:msub><mml:mrow /><mml:mn>2</mml:mn></mml:msub></mml:math>: A density functional theory study of phase stability in ZrF<mml:math xmlns:mml="http://www.w3.org/1998/Math/MathML" display="inline"><mml:msub><mml:m	1.1	3
11265	Screened Coulomb interaction of localized electrons in solids from first principles. Physical Review B, 2012, 85, .	1.1	62
11266	Adsorption of oxygen-containing functional groups on free and supported graphene using point contact. Physical Review B, 2012, 85, .	1.1	6
11267	Toward an orbital-free density functional theory of transition metals based on an electron density decomposition. Physical Review B, 2012, 85, .	1.1	27
11268	Effect of Temperature on Young's Modulus of Graphene. Journal of Thermal Stresses, 2012, 35, 913-920.	1.1	14
11269	Ab initioelastic tensor of cubic Ti<mml:math xmlns:mml="http://www.w3.org/1998/Math/MathML" display="inline"><mml:msub><mml:mrow /><mml:mrow><mml:mn>0.5</mml:mn></mml:mrow></mml:msub></mml:math>Al<mml:math xmlns:mml="http://www.w3.org/1998/Math/MathML" display="inline"><mml:msub><mml:mrow /><mml:mrow><mml:mn>0.5</mml:mn></mml:mrow></mml:msub></mml:math>N alloys: Dependence of elastic constants on size and shape of the supercell model and their convergence. Physical Review B,	1.1	125
11270	Electronic structure of room-temperature ferromagnetic Mg_{1â^'x}Fe_xO_y thin films. Applied Physics Letters, 2012, 101, 082411.	1.5	7
11271	Effects of biaxial strains on the magnetic properties of Co-graphene heterojunctions. Journal of Applied Physics, 2012, 111, .	1.1	3
11272	Interaction Effect of Protons on Their Migration in Bulk Undoped Barium Zirconate Using Density Functional Theory. Japanese Journal of Applied Physics, 2012, 51, 09MA01.	0.8	4
11273	Investigation of nickel lattice sites in diamond: Density functional theory and x-ray absorption near-edge structure experiments. Physical Review B, 2012, 86, .	1.1	8
11274	Effect of light impurities on the electronic structure of copper nanowires. Physical Review B, 2012, 85, .	1.1	8
11275	Half-metallic ferromagnetism in (CrN)1/(GaN)1 (001) and (VN)1/(InN)1 (001) superlattices. Journal of Applied Physics, 2012, 112, 083703.	1.1	3
11276	Reflectivity of warm dense deuterium along the principal Hugoniot. Physical Review B, 2012, 85, .	1.1	13
11277	Structural phase transition below 250 K in superconducting K<mml:math xmlns:mml="http://www.w3.org/1998/Math/MathML" display="inline"><mml:msub><mml:mrow /><mml:mrow><mml:mn>0.75</mml:mn></mml:mrow></mml:msub></mml:math>Fe<mml:math xmlns:mml="http://www.w3.org/1998/Math/MathML" display="inline"><mml:msub><mml:mrow /><mml:mrow><mml:mn>1.75</mml:mn></mml:mrow></mml:msub></mml:math>Se<mml:math xmlns:mml="http://www.w3.org/1998/Math/MathML" display="inline"><mml:msub><mml:mrow	1.1	10
11278	Stabilization and growth of non-native nanocrystals at low and atmospheric pressures. Journal of Chemical Physics, 2012, 136, 044703.	1.2	11
11279	Interaction of n-type dopants with oxygen in silicon and germanium. Journal of Applied Physics, 2012, 112, .	1.1	10

#	Article	IF	Citations
11280	Room temperature ferromagnetism via unpaired dopant electrons and<mml:math xmlns:mml="http://www.w3.org/1998/Math/MathML" display="inline"><mml:mrow><mml:mi>p</mml:mi><mml:mo>â^'</mml:mo><mml:mi>p</mml:mi></mml:mrow></mml:math>coupling in carbon-doped In<mml:math xmlns:mml="http://www.w3.org/1998/Math/MathML" display="inline"><mml:msub><mml:mrow /><mml:mn>2</mml:mn></mml:msub></mml:math>O<mml:math xmlns:mml="http://www.w3.org/1998/Ma	1.1	33
11281	Structural, electronic and optical properties of titania nanotubes. Advances in Applied Ceramics, 2012, 111, 72-93.	0.6	8
11282	Stabilizing the Zigzag Edge: Graphene Nanoribbons with Sterically Constrained Terminations. Physical Review Letters, 2012, 109, 076802.	2.9	17
11283	Atomic-scale friction in graphene oxide: An interfacial interaction perspective from first-principles calculations. Physical Review B, 2012, 86, .	1.1	89
11284	Anharmonic phonons of NaZr<mml:math xmlns:mml="http://www.w3.org/1998/Math/MathML" display="inline"><mml:msub><mml:mrow /><mml:mn>2</mml:mn></mml:msub></mml:math>(PO<mml:math) Tj ETQq0 0 0 rgBT /Overlock 10 Tf 50 587 Td (xmlns:mml="http://www.w3.org/1998/Math/MathML" display="inline"><mml:msub><mml:mrow /><mml:	1.1	43
11285	Stable ordered structures of binary technetium alloys from first principles. Physical Review B, 2012, 85, .	1.1	14
11286	Microscopic origin of the structural phase transitions at the Cr<mml:math xmlns:mml="http://www.w3.org/1998/Math/MathML" display="inline"><mml:msub><mml:mrow /><mml:mn>2</mml:mn></mml:msub></mml:math>O<mml:math xmlns:mml="http://www.w3.org/1998/Math/MathML" display="inline"><mml:msub><mml:mrow /><mml:mn>3</mml:mn></mml:msub></mml:math>(0001) surface. Physical Review B, 2012, 86, .	1.1	13
11287	Quantum molecular dynamics simulations of thermophysical properties of fluid ethane. Physical Review E, 2012, 86, 061111.	0.8	5
11288	Modeling configurational energetics on multiple lattices through extended cluster expansion. Physical Review B, 2012, 85, .	1.1	12
11289	Electronic properties and lattice dynamics of the As(111) surface. Physical Review B, 2012, 86, .	1.1	7
11290	Joint density functional theory of the electrode-electrolyte interface: Application to fixed electrode potentials, interfacial capacitances, and potentials of zero charge. Physical Review B, 2012, 86, .	1.1	257
11292	Pt<mml:math xmlns:mml="http://www.w3.org/1998/Math/MathML" display="inline"><mml:msub><mml:mrow /><mml:mn>3</mml:mn></mml:msub></mml:math>Zr(0001): A substrate for growing well-ordered ultrathin zirconia films by oxidation. Physical Review B, 2012, 86, .	1.1	41
11293	Excitation, relaxation, and quantum diffusion of CO on copper. Physical Review B, 2012, 86, .	1.1	23
11294	Cluster expansion with controlled accuracy for the MgO/ZnO pseudobinary system via first-principles calculations. Physical Review B, 2012, 86, .	1.1	9
11295	Hybrid molecular dynamics and first-principles study on the work function of a Pt(111) electrode immersed in aqueous solution at room temperature. Physical Review B, 2012, 86, .	1.1	18
11296	Structural and magnetic properties of NiCr<mml:math xmlns:mml="http://www.w3.org/1998/Math/MathML" display="inline"><mml:msub><mml:mrow /><mml:mi>x</mml:mi></mml:msub></mml:math>and NiN<mml:math xmlns:mml="http://www.w3.org/1998/Math/MathML" display="inline"><mml:msub><mml:mrow />		

#	Article	IF	Citations
11299	Formation of NaCl-Type Monodeuteride LaD by the Disproportionation Reaction of<mml:math xmlns:mml="http://www.w3.org/1998/Math/MathML" display="inline"><mml:msub><mml:mi>LaD</mml:mi><mml:mn>2</mml:mn></mml:msub></mml:math>. Physical Review Letters, 2012, 108, 205501.	2.9	24
11300	xmlns:mml="http://www.w3.org/1998/Math/MathML" display="inline"><mml:mi>Î²</mml:mi></mml:math>-Li<mml:math xmlns:mml="http://www.w3.org/1998/Math/MathML" display="inline"><mml:mrow><mml:msub><mml:mrow		

#	Article	IF	Citations
11317	Intrinsic defects and conduction characteristics of Sc<mml:math xmlns:mml="http://www.w3.org/1998/Math/MathML" display="inline"><mml:msub><mml:mrow /><mml:mn>2</mml:mn></mml:msub></mml:math>O<mml:math xmlns:mml="http://www.w3.org/1998/Math/MathML" display="inline"><mml:msub><mml:mrow /><mml:mn>3</mml:mn></mml:msub></mml:math>in thermionic cathode systems. Physical Review B, 2012, 86, .	1.1	19
11318	Prediction of optical properties of<mml:math xmlns:mml="http://www.w3.org/1998/Math/MathML" display="inline"><mml:mi>F</mml:mi></mml:math>centers in oxides from quasiparticle excitations. Physical Review B, 2012, 85, .	1.1	7
11319	Influence of 3d transition metals on the stability and electronic structure of MgH2. Journal of Applied Physics, 2012, 111, .	1.1	37
11320	Indentation strength of ultraincompressible rhenium boride, carbide, and nitride from first-principles calculations. Physical Review B, 2012, 86, .	1.1	58
11321	Unexpectedly low indentation strength of WB<mml:math xmlns:mml="http://www.w3.org/1998/Math/MathML" display="inline"><mml:msub><mml:mrow /><mml:mn>3</mml:mn></mml:msub></mml:math>and MoB<mml:math xmlns:mml="http://www.w3.org/1998/Math/MathML" display="inline"><mml:msub><mml:mrow /><mml:mn>3</mml:mn></mml:msub></mml:math>from first principles. Physical Review B, 2012, 86, .	1.1	49
11322	<mml:math xmlns:mml="http://www.w3.org/1998/Math/MathML" display="inline"><mml:msup><mml:mi>d</mml:mi><mml:mn>5</mml:mn></mml:msup></mml:math>cations: Theory for MnO and Fe<mml:math xmlns:mml="http://www.w3.org/1998/Math/MathML" display="inline"><mml:msub><mml:mrow /><mml:mn>2</mml:mn></mml:msub></mml:math>O<mml:math	1.1	74
11323	Solution enthalpy of hydrogen in fourth row elements: Systematic trends derived from first principles. Physical Review B, 2012, 85, .	1.1	13
11324	Formation of nitrogen-vacancy complexes during plasma-assisted nitrogen doping of epitaxial graphene on SiC(0001). Applied Physics Letters, 2012, 100, 233119.	1.5	11
11325	Cation off-stoichiometry leads to high<mml:math xmlns:mml="http://www.w3.org/1998/Math/MathML" display="inline"><mml:mi>p</mml:mi></mml:math>-type conductivity and enhanced transparency in Co<mml:math xmlns:mml="http://www.w3.org/1998/Math/MathML" display="inline"><mml:msub><mml:mrow /><mml:mn>2</mml:mn></mml:msub></mml:math>ZnO<mml:math xmlns:mml="http://www.w3.org/1998/Math/MathML" display="inline"><mml:msub><mml:mrow /><mml:mn>	1.1	73
11326	First-principles calculations of surfactant-assisted growth of polar CaO(111) oxide film: The case of water-based surfactant. Physical Review B, 2012, 86, .	1.1	2
11327	Equation of state of paramagnetic CrN fromab initiomolecular dynamics. Physical Review B, 2012, 85, .	1.1	70
11328	Fracture Strength of<mml:math xmlns:mml="http://www.w3.org/1998/Math/MathML" display="inline"><mml:msub><mml:mi>AlLiB</mml:mi><mml:mn>14</mml:mn></mml:msub></mml:math>. Physical Review Letters, 2012, 109, 145501.	2.9	8
11329	Atomistic modeling of As diffusion in ZnO. Physical Review B, 2012, 85, .	1.1	23
11330	Diffusion of Hydrogen in Pd Assisted by Inelastic Ballistic Hot Electrons. Physical Review Letters, 2012, 108, 115902.	2.9	19
11331	Unusual rigidity and ideal strength of CrB4 and MnB4. Applied Physics Letters, 2012, 100, .	1.5	54
11332	Electronic-structure origin of the anisotropic thermopower of nanolaminated Ti<mml:math xmlns:mml="http://www.w3.org/1998/Math/MathML" display="inline"><mml:msub><mml:mrow /><mml:mn>3</mml:mn></mml:msub></mml:math>SiC<mml:math xmlns:mml="http://www.w3.org/1998/Math/MathML" display="inline"><mml:msub><mml:mrow /><mml:mn>2</mml:mn></mml:msub></mml:math>determined by polarized x-ray spectroscopy and Seebeck measurements. Physical Review B, 2012, 85, .	1.1	31
11333	Orbital-dependent electron tunneling within the atom superposition approach: Theory and application to W(110). Physical Review B, 2012, 86, .	1.1	20
11334	Modeling the role of the fluorine dopant in the magnetic phase diagram of LaFeAsO<mml:math xmlns:mml="http://www.w3.org/1998/Math/MathML" display="inline"><mml:msub><mml:mrow /><mml:mrow><mml:mn>1</mml:mn><mml:mo>â’</mml:mo><mml:mi>x</mml:mi></mml:mrow></mml:msub></mml:math>F<mml:math xmlns:mml="http://www.w3.org/1998/Math/MathML" display="inline"><mml:msub><mml:mrow /><mml:mi>x</mml:mi></mml:msub></mml:math>superconductors. Physical Review B, 2012, 85, .	1.1	1

#	Article	IF	Citations
11335	Ground-state characterizations of systems predicted to exhibit<mml:math xmlns:mml="http://www.w3.org/1998/Math/MathML" display="inline"><mml:mrow><mml:mi>L</mml:mi><mml:msub><mml:mn>1</mml:mn><mml:mn>1</mml:mn></mml:msub></mml:mr xmlns:mml="http://www.w3.org/1998/Math/MathML" display="inline"><mml:mrow><mml:mi>L</mml:mi><mml:msub><mml:mn>1</mml:mn><mml:mn>3</mml:mn></mml:msub></mml:mr structures. Physical Review B, 2012, 85, .	1.1	19
11336	Flat bands near Fermi level of topological line defects on graphite. Applied Physics Letters, 2012, 101, .	1.5	30
11337	Electron-phonon interaction in bulk Pb: Beyond the Fermi surface. Physical Review B, 2012, 85, .	1.1	20
11338	Stable interstitial dopantâ€“vacancy complexes in ZnO. Physical Review B, 2012, 85, .	1.1	26
11339	Structural transformation and vibrational properties of BaC<mml:math xmlns:mml="http://www.w3.org/1998/Math/MathML" display="inline"><mml:msub><mml:mrow /><mml:mn>2</mml:mn></mml:msub></mml:math>at high pressure. Physical Review B, 2012, 85, .	1.1	25
11340	Plane-wave transport method for low-symmetry lattices and its application. Physical Review B, 2012, 86, .	1.1	6
11341	Benzene adsorption and the encapsulation processes in SiC nanotubes. Journal of Applied Physics, 2012, 112, 023702.	1.1	3
11342	Ab initiostudies on the optical effects in the deep ultraviolet nonlinear optical crystals of the KBe₂BO₃F₂family. Journal of Physics Condensed Matter, 2012, 24, 335503.	0.7	40
11343	Quantum Monte Carlo study of pressure-induced<mml:math xmlns:mml="http://www.w3.org/1998/Math/MathML" display="inline"><mml:mrow><mml:mi>B</mml:mi><mml:mn>3</mml:mn><mml:mo>â^'</mml:mo><mml:mi>B</mml:mi><mml:mn>1< transition in GaAs. Physical Review B, 2012, 86, .	1.1	10
11344	Effect of surface hydrogen on the anomalous surface segregation behavior of Cr in Fe-rich Fe-Cr alloys. Physical Review B, 2012, 86, .	1.1	3
11345	Oxidation of the GaAs(001) surface: Insights from first-principles calculations. Physical Review B, 2012, 85, .	1.1	18
11346	Electronic and vibrational properties of vanadium-carbide nanowires. Journal of Applied Physics, 2012, 112, .	1.1	3
11347	Optical properties of the iron-pnictide analog BaMn2As2. Physical Review B, 2012, 86, .	1.1	13
11348	Electronic and transport properties of azobenzene monolayer junctions as molecular switches. Physical Review B, 2012, 86, .	1.1	22
11349	Adsorbate-induced segregation: First-principles study for C/Pt25Rh75(100). Physical Review B, 2012, 86, .	1.1	10
11350	Magnetic properties of ZnS doped with noble metals (Xâ€‰=â€‰Ru, Rh, Pd, and Ag). Journal of Applied Physics, 2012, 112, .	1.1	16
11351	Magnetic and electronic properties of Î±-graphyne nanoribbons. Journal of Chemical Physics, 2012, 136, 244702.	1.2	75
11352	Electron-phonon coupling and superconductivity in arsenic under pressure. Physical Review B, 2012, 86, .	1.1	15

#	Article	IF	Citations
11353	An unusual variation of stability and hardness in molybdenum borides. Applied Physics Letters, 2012, 101, .	1.5	36
11354	Band discontinuities at Si-TCO interfaces from quasiparticle calculations: Comparison of two alignment approaches. Physical Review B, 2012, 85, .	1.1	62
11355	Surface properties of the clean and Au/Pd covered Fe<mml:math xmlns:mml="http://www.w3.org/1998/Math/MathML" display="inline"><mml:msub><mml:mrow /><mml:mn>3</mml:mn></mml:msub></mml:math>O<mml:math xmlns:mml="http://www.w3.org/1998/Math/MathML" display="inline"><mml:msub><mml:mrow /><mml:mn>4</mml:mn></mml:msub></mml:math>(111): DFT and DFT+<mml:math xmlns:mml="http://www.w3.org/1998/Math/MathML" display="inline"><mml:mi>Î</mml:mi></mml:math>-(BEDT-TTF)<mml:math xmlns:mml="http://www.w3.org/1998/Math/MathML" display="inline"><mml:msub><mml:mrow /><mml:mn>2</mml:mn></mml:msub></mml:math>I<mml:math xmlns:mml="http://www.w3.org/1998/Math/MathML" display="inline"><mml:msub><mml:mrow />	1.1	68
11356	Electronic and optical properties of free-standing and supported vanadium nanowires. Journal of Applied Physics, 2012, 111, 093506.	1.1	77
11357	Possible magnetic behavior in oxygen-deficient<mml:math xmlns:mml="http://www.w3.org/1998/Math/MathML" display="inline"><mml:mi>Î²</mml:mi></mml:math>-PtO<mml:math xmlns:mml="http://www.w3.org/1998/Math/MathML" display="inline"><mml:msub><mml:mrow /><mml:mn>2</mml:mn></mml:msub></mml:math>. Physical Review B, 2012, 85, .	1.1	8
11358	Magnetic exchange interactions and antiferromagnetism ofATcO3(A=Ca, Sr, Ba) studied from first principles. Physical Review B, 2012, 85, .	1.1	9
11359	Structural properties and relative stability of (meta)stable ordered, partially ordered, and disordered Al-Li alloy phases. Physical Review B, 2012, 85, .	1.1	16
11360	First-principles study on phase stability of MoSi<mml:math xmlns:mml="http://www.w3.org/1998/Math/MathML" display="inline"><mml:msub><mml:mrow /><mml:mn>2</mml:mn></mml:msub></mml:math>-NbSi<mml:math xmlns:mml="http://www.w3.org/1998/Math/MathML" display="inline"><mml:msub><mml:mrow /><mml:mn>2</mml:mn></mml:msub></mml:math>pseudobinary alloys. Physical Review B, 2012, 85, .	1.1	34
11361	Validity of the rigid band approximation in the study of the thermopower of narrow band gap semiconductors. Physical Review B, 2012, 85, .	1.1	6
11362	STRUCTURAL AND ELECTRONIC PROPERTIES OF ZINCBLENDE AlInN ALLOY: A HYBRID DENSITY FUNCTIONAL STUDY. Modern Physics Letters B, 2012, 26, 1250120.	1.1	93
11363	Electronic and magnetic properties of substitutionally Fe-, Co-, and Ni-doped BC3 honeycomb structure. Journal of Applied Physics, 2012, 111, .	1.0	1
11364	First principles calculation of the electronic properties and lattice dynamics of Cu2ZnSn(S1â^'xSex)4. Journal of Applied Physics, 2012, 111, .	1.1	12
11365	Poly â€“NÂ=ÂNâ€“ linked 1,5-dihydro-1,5-diazocine, the two-dimensional polymer withDirac insulatorproperties:ab initiostudy. Molecular Simulation, 2012, 38, 886-891.	1.1	73
11366	Tuning the polarization and magnetism in BiCoO3 by strain and oxygen vacancy effect: A first-principle study. Journal of Applied Physics, 2012, 111, 013901.	0.9	3
11367	Microscopic origin of compressive strain in hydrogen-irradiated dilute GaAs<mml:math xmlns:mml="http://www.w3.org/1998/Math/MathML" display="inline"><mml:msub><mml:mrow /><mml:mrow><mml:mn>1</mml:mn><mml:mo>â^'</mml:mo><mml:mi>y</mml:mi></mml:mrow></mml:msub></mml:math>N<mml:math xmlns:mml="http://www.w3.org/1998/Math/MathML" display="inline"><mml:msub><mml:mrow /><mml:mi>y</mml:mi></mml:msub></mml:math>alloys: Role of N-H<mml:math xmlns:mml="http://www.w3.org/1998/Math/MathML" display="inline"><mml:msub><mml:mrow />	1.1	12
11368	First-principles studies of the effect of (001) surface terminations on the electronic properties of the negatively charged nitrogen-vacancy defect in diamond. Physical Review B, 2012, 86, .	1.1	15
11369	Band engineering in silicide alloys. Physical Review B, 2012, 85, .	1.1	22
11370		1.1	10

#	Article	IF	Citations
11371	Electronic origin of the anomalous segregation behavior of Cr in Fe-rich Fe-Cr alloys. Physical Review B, 2012, 85, .	1.1	25
11372	Ab initiostudy of the electrostatic dipole modulation due to cation substitution in HfO<mml:math xmlns:mml="http://www.w3.org/1998/Math/MathML" display="inline"><mml:msub><mml:mrow /><mml:mn>2</mml:mn></mml:msub></mml:math>/SiO<mml:math xmlns:mml="http://www.w3.org/1998/Math/MathML" display="inline"><mml:msub><mml:mrow /><mml:mn>2</mml:mn></mml:msub></mml:math>interfaces. Physical Review B, 2012, 86, .	1.1	11
11373	Epitaxial growth mechanisms of graphene and effects of substrates. Physical Review B, 2012, 85, .	1.1	39
11374	Virtual-crystal approach to aluminum-avoidance materials: A first-principles density-functional calculation of micas. Physical Review B, 2012, 85, .	1.1	4
11375	First-Principles Study of the Influence of (110) Strain on the Ferroelectric Trends of TiO₂. Ferroelectrics, 2012, 429, 31-42.	0.3	8
11376	Stability of Sb-Te layered structures: First-principles study. Physical Review B, 2012, 85, .	1.1	12
11377	First-principles study on superconductivity of simple cubic, modulated and simple hexagonal phases in phosphorus. High Pressure Research, 2012, 32, 3-10.	0.4	6
11378	First-principles study of Zintl aluminide SrAl2. Physical Review B, 2012, 85, .	1.1	11
11379	First-principles calculation of x-ray absorption spectra and x-ray magnetic circular dichroism of ultrathin Fe films on BaTiO<mml:math xmlns:mml="http://www.w3.org/1998/Math/MathML" display="inline"><mml:msub><mml:mrow /><mml:mn>3</mml:mn></mml:msub></mml:math>(001). Physical Review B, 2012, 85, .	1.1	16
11380	Half-metallicity induced by charge injection in hexagonal boron nitride clusters embedded in graphene. Physical Review B, 2012, 86, .	1.1	19
11381	AuCu intermetallic nanoparticles: surfactant-free synthesis and novel electrochemistry. Journal of Materials Chemistry, 2012, 22, 15769.	6.7	68
11382	Electronic structure of oxygen vacancies in<mml:math xmlns:mml="http://www.w3.org/1998/Math/MathML" display="inline"><mml:msub><mml:mrow><mml:mi mathvariant="normal">SrTiO</mml:mi></mml:mrow><mml:mn>3</mml:mn></mml:msub></mml:math>and<mml:math xmlns:mml="http://www.w3.org/1998/Math/MathML" display="inline"><mml:msub><mml:mrow><mml:mi mathvariant="normal">LaAlO</mml:mi></mml:mrow><mml:mn>3</mml:mn></mml:msub></mml:math>. Physical Review B, 2012, 86, .	1.1	146
11383	Structure of nanoscale copper precipitates in neutron-irradiated Fe-Cu-C alloys. Physical Review B, 2012, 85, .	1.1	17
11384	Al enhances the H<mml:math xmlns:mml="http://www.w3.org/1998/Math/MathML" display="inline"><mml:msub><mml:mrow /><mml:mn>2</mml:mn></mml:msub></mml:math>storage capacity of graphene at nanoribbon borders but not at central sites: A study using nonlocal van der Waals density functionals. Physical Review B, 2012, 85, .	1.1	25
11385	Ab initioatomistic thermodynamics study of the early stages of Cu(100) oxidation. Physical Review B, 2012, 86, .	1.1	42
11386	Frequencies and polarization vectors of phonons: Results from force constants which are fitted to experimental data or calculatedab initio. Physical Review B, 2012, 86, .	1.1	4
11387	FIRST-PRINCIPLES STUDY OF STRUCTURAL AND ELECTRONIC PROPERTIES OF SrLiSb UNDER HIGH PRESSURE. International Journal of Modern Physics B, 2012, 26, 1250151.	1.0	1
11388	Structural, elastic, phonon and electronic properties of a MnPd alloy. Chinese Physics B, 2012, 21, 077102.	0.7	7

#	Article	IF	Citations
11389	Water adsorption on ZnO(101Ì„0): The role of intrinsic defects. Europhysics Letters, 2012, 97, 17014.	0.7	15
11390	Effects of temperature and pressure on the thermal expansion of sodium chloride. Physica Scripta, 2012, 85, 045707.	1.2	2
11391	FIRST-PRINCIPLE STUDY ON STRUCTURAL, ELASTIC AND ELECTRONIC PROPERTIES OF BINARY RARE EARTH INTERMETALLIC COMPOUNDS: GdCu AND GdZn. International Journal of Computational Materials Science and Engineering, 2012, 01, 1250005.	0.5	3
11392	STRUCTURAL, MECHANICAL AND LATTICE DYNAMICAL STABILITY OF AgC AND AuC COMPOUNDS: A FIRST PRINCIPLES STUDY. Modern Physics Letters B, 2012, 26, 1250107.	1.0	3
11393	Adsorption, Diffusion, and Dissociation of H ₂ O on Kaolinite (001): a Density Functional Study. Chinese Physics Letters, 2012, 29, 036801.	1.3	6
11394	First-principles study of atomic and electronic structures of kaolinite in soft rock. Chinese Physics B, 2012, 21, 039101.	0.7	4
11395	AB INITIO STUDY OF STRUCTURAL PROPERTIES OF INTERMETALLIC COMPOUNDS PtX (X = Si, Ge, Sn AND Pb) UNDER HIGH PRESSURE. International Journal of Modern Physics B, 2012, 26, 1250127.	1.0	0
11396	Band gap engineering of (N, Si)-codoped TiO₂from hybrid density functional theory calculations. New Journal of Physics, 2012, 14, 053007.	1.2	26
11397	Structure and stability of weakly chemisorbed ethene adsorbed on low-index Cu surfaces: performance of density functionals with van der Waals interactions. Journal of Physics Condensed Matter, 2012, 24, 424217.	0.7	19
11398	THERMOMAGNETIC PROPERTIES OF RARE-EARTH REPLACEMENT CRITICAL MAGNETIC MATERIALS FROM DFT CALCULATION: MnBi AND MnSb. International Journal of Computational Materials Science and Engineering, 2012, 01, 1250036.	0.5	1
11399	Non-linear electro-elastic coupling in non-centrosymmetric materials. Journal of Physics: Conference Series, 2012, 367, 012005.	0.3	1
11400	Band engineering of type-II ZnO/ZnSe heterostructures for solar cell applications. Journal of Materials Research, 2012, 27, 730-733.	1.2	9
11401	H2 ADSORPTION ON LiB (001) SURFACE: A FIRST PRINCIPLES CALCULATION. Journal of Theoretical and Computational Chemistry, 2012, 11, 781-790.	1.8	3
11402	A novel potential: the interlayer potential for the fcc (111) plane family. Journal of Physics Condensed Matter, 2012, 24, 045001.	0.7	2
11403	Charge redistribution and local lattice structure of (F, Zn)-codoped LaFeAsO superconductor. New Journal of Physics, 2012, 14, 033005.	1.2	5
11404	Effect of site-disorder on magnetism and magneto-structural coupling in gallium ferrite: A first-principles study. Journal of Applied Physics, 2012, 111, .	1.1	16
11405	Melting and dissociation of ammonia at high pressure and high temperature. Journal of Chemical Physics, 2012, 137, 064507.	1.2	26
11406	Structural and Optical Properties of GaAs 0.5 Sb 0.5 and In 0.5 Ga 0.5 As 0.5 Sb 0.5 : ab initio Calculations for Pure and Doped Materials. Chinese Physics Letters, 2012, 29, 037302.	1.3	8

#	Article	IF	Citations
11407	Theoretical and experimental investigation of magnetotransport in iron chalcogenides. Science and Technology of Advanced Materials, 2012, 13, 054402.	2.8	18
11408	Interaction between impurity nitrogen and tungsten: a first-principles investigation. Chinese Physics B, 2012, 21, 016105.	0.7	18
11409	Generation of hydrogen peroxide on a pyridine-like nitrogen-nickel doped graphene surface. Materials Research Society Symposia Proceedings, 2012, 1451, 69-74.	0.1	1
11410	Construction of embedded-atom-method interatomic potentials for alkaline metals (Li, Na, and K) by lattice inversion. Chinese Physics B, 2012, 21, 053401.	0.7	1
11411	Magnetic properties of Fe-pnictides superconductors as a function of pressure and doping. Materials Research Society Symposia Proceedings, 2012, 1434, 1.	0.1	0
11412	Electrical resistivity and thermal conductivity of liquid Fe alloys at high P and T , and heat flux in Earthâ€™s core. Proceedings of the National Academy of Sciences of the United States of America, 2012, 109, 4070-4073.	3.3	268
11414	d⁰ferromagnetic surface in HfO₂. Journal of Physics: Conference Series, 2012, 400, 032008.	0.3	0
11415	First Principles Investigation of Electronic Structure, Chemical Bonding, Elastic and Optical Properties of Novel Rhenium Nitrides. Key Engineering Materials, 0, 512-515, 883-889.	0.4	0
11416	Theoretical Study on Hydrazine Chemisorption on Transition Metal Surfaces. Journal of the Physical Society of Japan, 2012, 81, 124705.	0.7	11
11417	Isothermal bulk modulus and its first pressure derivative of NaCl at high pressure and high temperature. Chinese Physics B, 2012, 21, 037103.	0.7	10
11418	Understanding the effect of the layer-to-layer distance on Li-intercalated graphite. Journal of Applied Physics, 2012, 111, .	1.1	27
11419	Predictions of Surface Electrochemistry of Saturated and Alkaline NH4Cl Solutions Interacting with Fe(110) from Ab Initio Calculations. Corrosion, 2012, 68, 591-599.	0.5	19
11420	Vibrational and thermal properties of ScN and YN: quasi-harmonic approximation calculations and anharmonic effects. Journal of Physics Condensed Matter, 2012, 24, 035401.	0.7	8
11421	AB INITIO SIMULATIONS FOR MATERIAL PROPERTIES ALONG THE JUPITER ADIABAT. Astrophysical Journal, Supplement Series, 2012, 202, 5.	3.0	170
11422	First-principles investigation of diffusion behaviours of H isotopes: From W(110) surface into bulk and in bulk W. Chinese Physics B, 2012, 21, 126103.	0.7	5
11423	FERROMAGNETIC PROPERTIES IN V-DOPED AlN FROM FIRST PRINCIPLES. Modern Physics Letters B, 2012, 26, 1250132.	1.0	0
11424	The thickness, electric field, and strain effects on the magnetic anisotropy of FeCo/MgO(001) thin films: A first principles study. Journal of Applied Physics, 2012, 111, 07C109.	1.1	25
11425	First-principles study of pressure-induced phase transitions and electronic structure of Be₃P₂polymorphs. Philosophical Magazine, 2012, 92, 1159-1169.	0.7	4

#	Article	IF	Citations
11426	First-Principles Study on the Ideal Strengths of Typical Hcp Metals. Advanced Materials Research, 2012, 476-478, 2523-2529.	0.3	5
11427	Computer Simulation of the Metal Silicide. Applied Mechanics and Materials, 2012, 170-173, 3367-3370.	0.2	1
11428	Is yne-diamond a super-hard material?. Europhysics Letters, 2012, 100, 56003.	0.7	19
11429	K-intercalated carbon systems: Effects of dimensionality and substrate. Europhysics Letters, 2012, 98, 67003.	0.7	26
11430	Phase stability and elastic properties of the NAL and CF phases in the NaMg2Al5SiO12 system from first principles. American Mineralogist, 2012, 97, 305-314.	0.9	21
11431	Theoretical Investigations of the High-Pressure Optical Properties of Î³-Si₃N₄. Advanced Materials Research, 0, 490-495, 3874-3877.	0.3	0
11432	Theory, Experiment and Computation of Half Metals for Spintronics: Recent Progress in Si-based Materials. The Nanoscale Systems: Mathematical Modelingory and Applications, 2012, 1, 1-22.	0.3	4
11433	LCAO Calculations on Uranium Nitrides. Springer Series in Solid-state Sciences, 2012, , 603-630.	0.3	0
11434	<i>Ab Initio</i> Based O-O Investigation and the Snoek Relaxation in Nb-O. Solid State Phenomena, 0, 184, 63-68.	0.3	1
11435	Ab initio studies of the crystal structure of cellulose triacetate I. Materials Research Society Symposia Proceedings, 2012, 1470, 21.	0.1	1
11436	Cerium-Doped Endohedral Fullerene: A Density-Functional Theory Study. , 2012, 2012, 1-8.		8
11437	Polymorphism, Hydrogen Bond Properties, and Vibrational Structure of 1H-Pyrrolo[3,2-h]Quinoline Dimers. Journal of Atomic, Molecular, and Optical Physics, 2012, 2012, 1-11.	0.5	3
11438	LDA and GGA Investigations of Some Ground-State Properties and the Compton Profile of Copper with the All-Electron MAPW Method. ISRN Materials Science, 2012, 2012, 1-13.	1.0	2
11439	Peculiar structure and tensile strength of WB4: nonstoichiometric origin. AIP Advances, 2012, 2, .	0.6	46
11440	Surface stress of Ni adlayers on W(110): the critical role of the surface atomic structure. Journal of Physics Condensed Matter, 2012, 24, 135001.	0.7	8
11441	First-principles study of the electronic and optical properties of the (Y, N)-codoped anatase TiO ₂ photocatalyst. Chinese Physics B, 2012, 21, 033103.	0.7	14
11442	Adsorption of Methane on Pristine and Al-Doped Graphene: A Comparative Study via First-Principles Calculation. Advanced Materials Research, 0, 602-604, 870-873.	0.3	18
11443	First Principle Study of the Electronic Properties of 3C-SiC Doped with Different Amounts of Ni. Chinese Physics Letters, 2012, 29, 077701.	1.3	15

#	Article	IF	Citations
11444	Defect properties of CuCrO₂: A density functional theory calculation. Chinese Physics B, 2012, 21, 087105.	0.7	13
11445	Predictions of pressure-induced structural transition, mechanical and thermodynamic properties of Î±- and Î²-Si ₃ N ₄ ceramics: ab initio and quasi-harmonic Debye modeling. Chinese Physics B, 2012, 21, 060508.	0.7	8
11446	First-Principles Study of Hydrogen Impact on the Formation and Migration of Helium Interstitial Defects in hcp Titanium. Chinese Physics Letters, 2012, 29, 013102.	1.3	6
11447	A density-functional theory investigation on desorption of O 2 on Sn(111) and its comparison with initial oxidation on the X (111) (X = Si, Ge, Sn, Pb) surfaces. Chinese Physics B, 2012, 21, 126803.	0.7	1
11448	Computer Simulation of the Magnesium Silicide Polymorphs. Applied Mechanics and Materials, 0, 170-173, 3312-3315.	0.2	0
11449	First Principle Study of Dynamical Properties of a New Perovskite Material Based on GeTiO₃. Advanced Materials Research, 2012, 501, 352-356.	0.3	8
11450	Hydrogen fluoride adsorption and reaction on the Î±-Al2O3(0001) surface: A density functional theory study. Journal of Chemical Physics, 2012, 136, 114701.	1.2	15
11451	Sulfur-induced embrittlement of nickel: a first-principles study. Modelling and Simulation in Materials Science and Engineering, 2012, 20, 065007.	0.8	28
11452	High-pressure structures of InBi predicted by particle swarm optimization algorithm. Chinese Physics B, 2012, 21, 026102.	0.7	4
11453	Atomic and electronic structure of N-terminated GaN(0001Ì„) (1 Ã— 1) surface. Journal of Physics: Conference Series, 2012, 398, 012013.	0.3	4
11454	First-Principles Investigation of Electronic Structural and Optical Properties of Rare Earth Doped Î²-Si₃N₄ Crystals. Key Engineering Materials, 0, 512-515, 864-868.	0.4	1
11455	Ab initiocalculations of theFcenters in MgF2bulk and on the (001) surface. Physica Scripta, 2012, 86, 035304.	1.2	9
11456	Ab initiocalculations of theHcenters in MgF2crystals. IOP Conference Series: Materials Science and Engineering, 2012, 38, 012041.	0.3	0
11457	High Superconducting Critical Temperature of Hole-Doped CuAlO2. Journal of the Physical Society of Japan, 2012, 81, SB031.	0.7	2
11458	Study on the effect of pressure on the properties of intrinsic point defects in monoclinic zirconia: Ab initio calculations. Journal of Applied Physics, 2012, 111, .	1.1	6
11459	Electronic and magnetic properties of oxygen patterned graphene superlattice. Journal of Applied Physics, 2012, 112, .	1.1	10
11460	Nitrogen induced ferromagnetism in Cobalt doped BaTiO3. AIP Advances, 2012, 2, 032148.	0.6	1
11461	A study on density functional theory of the effect of pressure on the formation and migration enthalpies of intrinsic point defects in growing single crystal Si. Journal of Applied Physics, 2012, 111, .	1.1	28

#	Article	IF	Citations
11462	High pressure study on structural and vibrational properties of NH₃BH₃. Journal of Physics: Conference Series, 2012, 377, 012088.	0.3	4
11463	Thermophysical properties of B1-LiF. Journal of Physics: Conference Series, 2012, 377, 012063.	0.3	1
11464	On Dynamic and Elastic Stability of Lanthanum Carbide. Journal of Physics: Conference Series, 2012, 377, 012087.	0.3	1
11465	Ferromagnetic nanostructures of oxygen on Ag(111). Journal of Physics: Conference Series, 2012, 379, 012013.	0.3	2
11466	The role of pressure in elastic properties of cerium. Journal of Physics: Conference Series, 2012, 377, 012090.	0.3	2
11467	Strong quantum size effects in transition metal silicide ultrathin films: Critical role of Fermi surface nesting. Journal of Applied Physics, 2012, 112, 104313.	1.1	3
11468	Effects of atmospheric species and vacancy defect on electron transfer between diamond (0 0 1) surface and adlayer. EPJ Applied Physics, 2012, 59, 11303.	0.3	2
11469	Prediction of glass-forming ability and characterization of atomic structure of the Co-Ni-Zr metallic glasses by a proposed long range empirical potential. Journal of Applied Physics, 2012, 111, 033521.	1.1	4
11470	Structure and properties of metal-exchanged zeolites studied using gradient-corrected and hybrid functionals. I. Structure and energetics. Journal of Chemical Physics, 2012, 136, 064501.	1.2	58
11471	Effects of Co Addition on Crystal Structure, Thermal Stability and Magnetic Properties of Ni-Mn-Ga Ferromagnetic Shape Memory Alloys from First-Principles Calculations . Materials Science Forum, 0, 706-709, 1990-1995.	0.3	0
11472	First-principles calculation of grain boundary excess volume and free volume in nanocrystalline and ultrafine-grained aluminum. Keikinzoku/Journal of Japan Institute of Light Metals, 2012, 62, 464-471.	0.1	2
11473	Experimental Determination and Thermodynamic Assessment of Phase Equilibria in the Co–Mo System. Materials Transactions, 2012, 53, 1425-1435.	0.4	16
11474	First-Principles Tensile Tests of Tilt and Twist Grain Boundaries in Al. Materials Transactions, 2012, 53, 140-146.	0.4	15
11475	First-principles prediction of layered antiperovskite superconductors A2CNi4 (A = Al, Ga, and Sn). AIP Advances, 2012, 2, .	0.6	5
11476	Database of atomistic reaction mechanisms with application to kinetic Monte Carlo. Journal of Chemical Physics, 2012, 137, 014105.	1.2	14
11477	Ab initioinvestigations of phonons and superconductivity in the cubic Laves structures LaAl2and YAl2. Journal of Applied Physics, 2012, 111, 033514.	1.1	10
11478	High Pressure Phase Transitions in Yttria, Y₂O₃. Journal of Physics: Conference Series, 2012, 377, 012036.	0.3	4
11479	Ab-initioinvestigation of point-like defects in AlN nanowires. Journal of Physics: Conference Series, 2012, 338, 012014.	0.3	0

#	Article	IF	Citations
11480	A first principles study of lattice dynamical and electronic properties of Yb-pnictides (YbX, X= N, P and) Tj ETQq0 0 0 rgBT /Overlock 10 T	0.3	1
11481	Oxidation of Germanium and Silicon surfaces (100): a comparative study through DFT methodology. IOP Conference Series: Materials Science and Engineering, 2012, 41, 012007.	0.3	9
11482	Enhanced grain boundary embrittlement of an Fe grain boundary segregated by hydrogen (H). Journal of Materials Research, 2012, 27, 1589-1597.	1.2	9
11483	First-principles calculations of lattice vibrations on LaT₂Zn₂₀(T = Ru and Ir). Journal of Physics: Conference Series, 2012, 391, 012016.	0.3	22
11484	Theoretical modeling of the electronic structure and exchange interactions in Cu(II)Pc. Journal of Physics: Conference Series, 2012, 391, 012119.	0.3	1
11485	Electronic properties of rippled graphene. Journal of Physics: Conference Series, 2012, 402, 012004.	0.3	10
11486	Optoelectronic performance of gallium nitride devices: the role of tilt grain boundaries and point defects. IOP Conference Series: Materials Science and Engineering, 2012, 29, 012017.	0.3	0
11487	Design and computer modeling of the supracrystals. Journal of Physics: Conference Series, 2012, 345, 012025.	0.3	4
11489	Growth and thermal stability of (V,Al)₂C_x thin films. Journal of Materials Research, 2012, 27, 2511-2519.	1.2	14
11490	Microscopic mechanism of low thermal conductivity in lead telluride. Physical Review B, 2012, 85, .	1.1	115
11491	Milling-induced polymorphic transformation in MoSi₂. International Journal of Materials Research, 2012, 103, 1130-1136.	0.1	2
11492	Electronâ€“Vibron Interaction Effects on Scanning Tunneling Microscopy Current through Melamine Adsorbed on Cu(100). Journal of the Physical Society of Japan, 2012, 81, 104711.	0.7	0
11493	Coherent Phonon Heat Conduction in Superlattices. Science, 2012, 338, 936-939.	6.0	489
11494	Structure of Iron to 1ÂGbar and 40â€‰000ÂK. Physical Review Letters, 2012, 108, 055505.	2.9	83
11495	Mechanism and Kinetics for Ammonium Dinitramide (ADN) Sublimation: A First-Principles Study. Journal of Physical Chemistry A, 2012, 116, 10836-10841.	1.1	11
11496	Computation of Charge Distribution and Electrostatic Potential in Silicates with the Use of Chemical Potential Equalization Models. Journal of Physical Chemistry C, 2012, 116, 490-504.	1.5	47
11497	Comparison of density functional approximations and the finite-temperature Hartree-Fock approximation in warm dense lithium. Physical Review E, 2012, 86, 056704.	0.8	26
11498	Obtaining mixed ionic/electronic conductivity in perovskite oxides in a reducing environment: A computational prediction for doped SrTiO3. Solid State Ionics, 2012, 228, 37-45.	1.3	19

#	Article	IF	Citations
11499	Fluorinated derivatives of sp2 graphene allotropes: Structure, stability, and electronic properties. Chemical Physics Letters, 2012, 545, 78-82.	1.2	18
11500	Quantitative Fracture Strength and Plasticity Measurements of Lithiated Silicon Nanowires by In Situ TEM Tensile Experiments. ACS Nano, 2012, 6, 9425-9432.	7.3	106
11501	Semiconducting Monolayer Materials as a Tunable Platform for Excitonic Solar Cells. ACS Nano, 2012, 6, 10082-10089.	7.3	145
11502	A versatile low temperature solid-state synthesis of vanadium nitride (VN) via a â€œguanidinium-routeâ€: experimental and theoretical studies from the key-intermediate to the final product. Dalton Transactions, 2012, 41, 14381.	1.6	17
11503	Hydrocarbon Adsorption on Carbonate Mineral Surfaces: A First-Principles Study with van der Waals Interactions. Journal of Physical Chemistry C, 2012, 116, 24538-24548.	1.5	34
11504	First-principles based thermodynamic model of phase equilibria in bcc Fe-Cr alloys. Physical Review B, 2012, 86, .	1.1	48
11505	Phonons in lanthanum manganite: Inelastic neutron scattering and density functional theory studies. Physical Review B, 2012, 86, .	1.1	2
11506	Defects in Oxygen-Depleted Titanate Nanostructures. Langmuir, 2012, 28, 7851-7858.	1.6	16
11507	A density functional study for adsorption and oxidation of NO on Ir (1 0 0) surface. Applied Catalysis A: General, 2012, 449, 9-14.	2.2	7
11508	Structure, Elastic Stiffness, and Hardness of Os_{1â€“x}Ru_xB₂ Solid Solution Transition-Metal Diborides. Journal of Physical Chemistry C, 2012, 116, 11746-11751.	1.5	10
11509	Solvent- and anion-controlled photochromism of viologen-based metalâ€“organic hybrid materials. Journal of Materials Chemistry, 2012, 22, 12212.	6.7	145
11510	The Electronic Structures, Born Effective Charges, and Interatomic Force Constants in <scp><scp>BaMO</scp></scp>₃ (MÂ=ÂTi, Zr, Hf, Sn): A Comparative Firstâ€Principles Study. Journal of the American Ceramic Society, 2012, 95, 3597-3604.	1.9	21
11511	Existence of Erbium Hexaboride Nanowires. Journal of the American Ceramic Society, 2012, 95, 3992-3996.	1.9	8
11512	Thermodynamic properties and structural stability of thorium dioxide. Journal of Physics Condensed Matter, 2012, 24, 225801.	0.7	68
11513	Structural and Thermodynamic Properties of TiAl intermetallics under High Pressure. Communications in Theoretical Physics, 2012, 57, 141-144.	1.1	5
11514	Thermodynamic properties of magnesium oxide: a comparison ofab initioand empirical models. Physica Scripta, 2012, 85, 045702.	1.2	4
11515	Ab Initio Calculations of Hydroxyl Impurities in CaF₂. Journal of Physical Chemistry C, 2012, 116, 6392-6400.	1.5	10
11516	Ab Initio Calculations of the Transfer and Aggregation of F Centers in CaF₂. Journal of Physical Chemistry C, 2012, 116, 4832-4839.	1.5	26

#	Article	IF	Citations
11517	Selectivity of Palladiumâ€“Cobalt Surface Alloy toward Oxygen Reduction Reaction. Journal of Physical Chemistry C, 2012, 116, 6200-6207.	1.5	24
11518	display="inline"><mml:mi>Î±</mml:mi></mml:math>-<mml:math xmlns:mml="http://www.w3.org/1998/Math/MathML" display="inline"><mml:mi>Î²</mml:mi></mml:math>phase transition in quartz-type FePO<mml:math xmlns:mml="http://www.w3.org/1998/Math/MathML" display="inline"><mml:msub><mml:mrow /><mml:mn>4</mml:mn></mml:msub></mml:math>at high temperature investigated by total neutron	1.1	9
11519	Structure, phase stability and elastic properties in the Ti1â€“xZrxN thin-film system: Experimental and computational studies. Acta Materialia, 2012, 60, 5601-5614.	3.8	71
11520	Ab initioinvestigation of graphene-based one-dimensional superlattices and their interfaces. Physical Review B, 2012, 86, .	1.1	13
11521	Properties of atoms under pressure: Bonded interactions of the atoms in three perovskites. Journal of Chemical Physics, 2012, 137, 164313.	1.2	12
11522	Uranyl adsorption on solvated edge surfaces of pyrophyllite: a DFT model study. Physical Chemistry Chemical Physics, 2012, 14, 5815.	1.3	46
11523	Half-metallic ferromagnetism in substitutionally doped boronitrene. Physical Review B, 2012, 86, .	1.1	10
11524	High-Pressure Phase Favored by a Symmetry-Recognized Nanoconfinement Effect. Journal of Physical Chemistry Letters, 2012, 3, 2154-2158.	2.1	2
11525	Band structure, phase transition, phonon and elastic instabilities in calcium polonide under pressure: A first-principles study. Solid State Communications, 2012, 152, 2058-2062.	0.9	10
11526	Pressure-induced phase transition and structural properties of CrO₂. Phase Transitions, 2012, 85, 708-717.	0.6	6
11527	Preparation and Photoelectrochemical Properties of p-type Cu₅Ta₁₁O₃₀ and Cu₃Ta₇O₁₉ Semiconducting Polycrystalline Films. Journal of Physical Chemistry C, 2012, 116, 10490-10497.	1.5	57
11528	Band-Gap Engineering via Tailored Line Defects in Boron-Nitride Nanoribbons, Sheets, and Nanotubes. ACS Nano, 2012, 6, 4104-4112.	7.3	121
11529	The Raman spectrum of diopside: a comparison between ab initio calculated and experimentally measured frequencies. European Journal of Mineralogy, 2012, 24, 457-464.	0.4	60
11530	Pressure-Induced Formation of Noble Metal Hydrides. Journal of Physical Chemistry C, 2012, 116, 1995-2000.	1.5	46
11531	Identification of magnetic dopants on the surfaces of topological insulators: Experiment and theory for Fe on Bi<mml:math xmlns:mml="http://www.w3.org/1998/Math/MathML" display="inline"><mml:msub><mml:mrow /><mml:mn>2</mml:mn></mml:msub></mml:math>Te<mml:math xmlns:mml="http://www.w3.org/1998/Math/MathML" display="inline"><mml:msub><mml:mrow /><mml:mn>3</mml:mn></mml:msub></mml:math>(111). Physical Review B, 2012, 85, .	1.1	49
11532	New Insights into the Molecular Structures, Compositions, and Cation Distributions in Synthetic and Natural Montmorillonite Clays. Chemistry of Materials, 2012, 24, 4376-4389.	3.2	79
11533	First-principles calculations of electronic and magnetic properties in semi-fluorinated CdS sheet. Physics Letters, Section A: General, Atomic and Solid State Physics, 2012, 376, 3402-3406.	0.9	12
11534	Dynamical stability and phase transition of ZrC under pressure. Phase Transitions, 2012, 85, 1060-1069.	0.6	14

#	Article	IF	Citations
11535	First-principle calculations to investigate the elastic and thermodynamic properties ofRBRh₃(Râ€‰=â€‰Sc, Y and La) perovskite compounds. Molecular Physics, 2012, 110, 121-128.	1.8	55
11536	Crystal and Electronic Structure and Magnetic Properties of Divalent Europium Perovskite Oxides EuMO₃ (M = Ti, Zr, and Hf): Experimental and First-Principles Approaches. Inorganic Chemistry, 2012, 51, 4560-4567.	1.9	54
11537	Cation coordination and interstitial oxygen occupancy in co-doped zirconia from first principles. Solid State Ionics, 2012, 227, 66-72.	1.3	12
11538	Quantitative theory of the oxygen vacancy and carrier self-trapping in bulk TiO<mml:math xmlns:mml="http://www.w3.org/1998/Math/MathML" display="inline"><mml:msub><mml:mrow /><mml:mn>2</mml:mn></mml:msub></mml:math>. Physical Review B, 2012, 86, .	1.1	169
11539	Atomistic Description of Electron Beam Damage in Nitrogen-Doped Graphene and Single-Walled Carbon Nanotubes. ACS Nano, 2012, 6, 8837-8846.	7.3	119
11540	Complex Surface Chemistry of 4-Mercaptopyridine Self-Assembled Monolayers on Au(111). Langmuir, 2012, 28, 6839-6847.	1.6	45
11541	Ab Initio Study of the Sodium Intercalation and Intermediate Phases in Na_{0.44}MnO₂ for Sodium-Ion Battery. Chemistry of Materials, 2012, 24, 1205-1211.	3.2	223
11542	Adsorption of Reactive Blue 4 dye from water solutions by carbon nanotubes: experiment and theory. Physical Chemistry Chemical Physics, 2012, 14, 11139.	1.3	155
11543	Influence of the surface dipole layer and Pauli repulsion on band energies and doping in graphene adsorbed on metal surfaces. Physical Review B, 2012, 86, .	1.1	35
11544	Ab initiosimulations of hot dense methane during shock experiments. Physical Review B, 2012, 86, .	1.1	31
11545	The structure, thermal properties and phase transformations of the cubic polymorph of magnesium tetrahydroborate. Physical Chemistry Chemical Physics, 2012, 14, 11800.	1.3	49
11546	Thermodynamically Stable Calcium-Decorated Graphyne as a Hydrogen Storage Medium. Journal of Physical Chemistry C, 2012, 116, 20220-20224.	1.5	147
11547	Isoelectronic Doping of Graphdiyne with Boron and Nitrogen: Stable Configurations and Band Gap Modification. Journal of Physical Chemistry A, 2012, 116, 3934-3939.	1.1	142
11548	Lattice electrical resistivity of magnetic bcc iron from first-principles calculations. Physical Review B, 2012, 85, .	1.1	42
11549	Pressure-induced group-subgroup phase transitions and post-cotunnite phases in actinide dioxides. Physical Review B, 2012, 85, .	1.1	17
11550	First-principles study of hydrogenated graphyne and its family: Stable configurations and electronic structures. Diamond and Related Materials, 2012, 29, 42-47.	1.8	71
11551	Lithium-decorated oxidized porous graphene for hydrogen storage by first principles study. Journal of Applied Physics, 2012, 112, 124312.	1.1	30
11552	Ab initioinvestigation of the electronic properties of graphene on InAs(111)A. Journal of Physics Condensed Matter, 2012, 24, 485004.	0.7	3

#	Article	IF	Citations
11553	First-Principles Characterization of Potassium Intercalation in Hexagonal 2H-MoS₂. Journal of Physical Chemistry C, 2012, 116, 1826-1832.	1.5	50
11554	Simulation of STM Images on a Flat Si (110)-(8Ã—2) Surface Using Density Functional Theory. Journal of the Electrochemical Society, 2012, 159, H201-H207.	1.3	4
11555	Molecular dynamics study of Co-Au and Ag-Au bimetallic atomic chain formation. European Physical Journal B, 2012, 85, 1.	0.6	19
11556	Theoretical analysis of the conversion mechanism of acetylene to ethylidyne on Pt(111). Physical Chemistry Chemical Physics, 2012, 14, 5642.	1.3	17
11557	First-principles study of the magnetic properties of NpN, PuN and AmN. Physica A: Statistical Mechanics and Its Applications, 2012, 391, 6587-6593.	1.2	1
11558	Environment-dependent surface structures and stabilities of SnO2 from the first principles. Journal of Applied Physics, 2012, 111, .	1.1	32
11559	Catalytic Oxygen Activation on Helical Gold Nanowires. Journal of Physical Chemistry C, 2012, 116, 11189-11194.	1.5	13
11560	The adsorption of acrolein on a Pt (1 1 1): A study of chemical bonding and electronic structure. Applied Surface Science, 2012, 263, 79-85.	3.1	9
11561	Type-I clathrate Ba8NixSi46â^'x: Phase relations, crystal chemistry and thermoelectric properties. Dalton Transactions, 2012, 41, 8839.	1.6	25
11562	First-Principles Predictions of Thermoelectric Figure of Merit for Organic Materials: Deformation Potential Approximation. Journal of Chemical Theory and Computation, 2012, 8, 3338-3347.	2.3	59
11563	Retarded oxygen diffusion in heavily phosphorus-doped Czochralski silicon: experiments and first-principles calculations. Journal of Physics Condensed Matter, 2012, 24, 495802.	0.7	2
11564	A theoretical study of structural and electronic properties of pentacene/Al(1 0 0) interface. Journal of Molecular Graphics and Modelling, 2012, 38, 334-341.	1.3	10
11565	AFLOW: An automatic framework for high-throughput materials discovery. Computational Materials Science, 2012, 58, 218-226.	1.4	898
11566	Geometric, electronic, and optical properties of the Si(111)2Ã—1 surface: Positive and negative buckling. Physical Review B, 2012, 86, .	1.1	15
11567	Quantum Modeling of Water and Oxygen Adsorption on Beryllium Surface. Journal of Physical Chemistry C, 2012, 116, 4662-4670.	1.5	10
11568	Octagraphene as a versatile carbon atomic sheet for novel nanotubes, unconventional fullerenes, and hydrogen storage. Journal of Applied Physics, 2012, 112, .	1.1	110
11569	Suppression of antiferroelectric state in NaNbO3 at high pressure from in situ neutron diffraction. Applied Physics Letters, 2012, 101, .	1.5	27
11570	Exotic Cubic Carbon Allotropes. Journal of Physical Chemistry C, 2012, 116, 24233-24238.	1.5	53

#	Article	IF	Citations
11571	Effects of Composition on Atomic Structure, Diffusivity, and Viscosity of Liquid Al-Zr Alloys. Metallurgical and Materials Transactions A: Physical Metallurgy and Materials Science, 2012, 43, 3471-3480.	1.1	21
11572	Integration of first-principles methods and crystallographic database searches for new ferroelectrics: Strategies and explorations. Journal of Solid State Chemistry, 2012, 195, 21-31.	1.4	42
11573	LiGaGe₂Se₆: A New IR Nonlinear Optical Material with Low Melting Point. Inorganic Chemistry, 2012, 51, 1035-1040.	1.9	103
11574	Strain-engineered artificial atom as a broad-spectrum solar energy funnel. Nature Photonics, 2012, 6, 866-872.	15.6	907
11575	Effects of strain on band structure and effective masses in MoS<mml:math xmlns:mml="http://www.w3.org/1998/Math/MathML" display="inline"><mml:msub><mml:mrow /><mml:mn>2</mml:mn></mml:msub></mml:math>. Physical Review B, 2012, 86, .	1.1	405
11576	Thermodynamic assessment of Crâ€“Nbâ€“C and Mnâ€“Nbâ€“C systems. Calphad: Computer Coupling of Phase Diagrams and Thermochemistry, 2012, 39, 54-61.	0.7	26
11577	Electronic structure of C2N2X (Xâ€‰=â€‰O, NH, CH2): Wide band gap semiconductors. Journal of Applied Physics, 2012, 112, .	1.1	10
11578	Stepwise Photocatalytic Dissociation of Methanol and Water on TiO₂(110). Journal of the American Chemical Society, 2012, 134, 13366-13373.	6.6	244
11579	Inelastic neutron scattering study of phonon density of states in nanostructured Si<mml:math xmlns:mml="http://www.w3.org/1998/Math/MathML" display="inline"><mml:msub><mml:mrow /><mml:mn>1</mml:mn><mml:mo>â^’</mml:mo><mml:mi>x</mml:mi></mml:mrow></mml:msub></mml:math>Ge<mml:math xmlns:mml="http://www.w3.org/1998/Math/MathML" display="inline"><mml:msub><mml:mrow /><mml:mi>x</mml:mi></mml:msub></mml:math>thermoelectrics. Physical Review B, 2012, 86, .	1.1	6
11580	Strain dependent polarization and dielectric properties of epitaxial BaTiO3from first-principles. Journal of Applied Physics, 2012, 112, 014109.	1.1	14
11581	Ab InitioCalculations of the Atomic and Electronic Structure of SrZrO3(111) Surfaces. Ferroelectrics, 2012, 436, 5-11.	0.3	6
11582	Energetic Driving Force of H Spillover between Rhodium and Titania Surfaces: A DFT View. Journal of Physical Chemistry C, 2012, 116, 25362-25367.	1.5	18
11583	An effective structure prediction method for layered materials based on 2D particle swarm optimization algorithm. Journal of Chemical Physics, 2012, 137, 224108.	1.2	275
11584	Low-energy structures of zinc borohydride Zn(BH<mml:math) Tj ETQq1 1 0.784314 rgBT /Overlock 10 Tf 50 237 Td (xmlns:mml="http://www.w3.org/1998/Math/MathML" display="inline"><mml:msub><mml:mrow /><mml:mn>2</mml:mn></mml:msub></mml:math>. Physical Review B, 2012, 86, .	1.1	27
11585	A new insight into the initial step in the Fischerâ€“Tropsch synthesis: CO dissociation on Ru surfaces. Physical Chemistry Chemical Physics, 2012, 14, 16686.	1.3	28
11586	Phononic band gap engineering in graphene. Journal of Applied Physics, 2012, 112, .	1.1	13
11587	Analysis of structural and electronic properties of Pr2NiO4through first-principles calculations. Journal of Physics Condensed Matter, 2012, 24, 405504.	0.7	13
11588	Effect of Subsurface Vacancies on Oxygen Reduction Reaction Activity of Pt-Based Alloys. Journal of Physical Chemistry C, 2012, 116, 14414-14422.	1.5	32

#	Article	IF	Citations
11589	Binding of an Oxide Layer to a Metal: The Case of Ti(101Ì...0)/TiO2(100). Journal of Physical Chemistry C, 2012, 116, 4224-4233.	1.5	8
11590	High Stability and Reactivity of Pt-Based Coreâ€“Shell Nanoparticles for Oxygen Reduction Reaction. Journal of Physical Chemistry C, 2012, 116, 13774-13780.	1.5	17
11591	Growth mode and atomic structure of MnSi thin films on Si(111). Physical Review B, 2012, 86, .	1.1	33
11592	Electronic charge redistribution in LaAlO<mml:math xmlns:mml="http://www.w3.org/1998/Math/MathML" display="inline"><mml:msub><mml:mrow /><mml:mn>3</mml:mn></mml:msub></mml:math>(001) thin films deposited at SrTiO<mml:math xmlns:mml="http://www.w3.org/1998/Math/MathML" display="inline"><mml:msub><mml:mrow /><mml:mn>3</mml:mn></mml:msub></mml:math>(001) substrate: First-principles analysis and the role	1.1	18
11593	Vibrational dynamics of single-crystal YVO<mml:math xmlns:mml="http://www.w3.org/1998/Math/MathML" display="inline"><mml:msub><mml:mrow /><mml:mn>4</mml:mn></mml:msub></mml:math>studied by polarized micro-Raman spectroscopy andab initiocalculations. Physical Review B, 2012, 86, .	1.1	21
11594	Potential energy surface for graphene on graphene:Ab initioderivation, analytical description, and microscopic interpretation. Physical Review B, 2012, 86, .	1.1	128
11595	Ab initio calculations and thermodynamic modeling for the Feâ€“Mnâ€“Nb system. Calphad: Computer Coupling of Phase Diagrams and Thermochemistry, 2012, 38, 43-58.	0.7	46
11596	Semiconducting graphene nanomeshes. Physical Review B, 2012, 85, .	1.1	7
11597	Contact-induced spin polarization in graphene/h-BN/Ni nanocomposites. Journal of Applied Physics, 2012, 112, .	1.1	20
11598	Rhombohedralâ€“orthorhombic morphotropic phase boundary in BiFeO3-based multiferroics: first-principles prediction. Journal of Materials Chemistry, 2012, 22, 1667-1672.	6.7	51
11599	Tri-Wing Graphene Nano-Paddle-Wheel with a Single-File Metal Joint: Formation of Multi-Planar Tetracoordinated-Carbon (ptC) Strips. Journal of Physical Chemistry C, 2012, 116, 11378-11385.	1.5	24
11600	Elastic and Vibrational Properties of Î±- and Î²-PbO.. Journal of Physical Chemistry C, 2012, 116, 21514-21522.	1.5	38
11601	Electron correlation and spin-orbit coupling effects in US3 and USe3. Journal of Chemical Physics, 2012, 137, 214703.	1.2	1
11602	Electronic bands of III-V semiconductor polytypes and their alignment. Physical Review B, 2012, 86, .	1.1	134
11603	Generalization of Natural Bond Orbital Analysis to Periodic Systems: Applications to Solids and Surfaces via Plane-Wave Density Functional Theory. Journal of Chemical Theory and Computation, 2012, 8, 1902-1911.	2.3	177
11604	Chemical and optical properties of carbon-doped TiO2: A density-functional study. Applied Physics Letters, 2012, 100, 102114.	1.5	54
11605	Surface Oxygen Atom as a Cooperative Ligand in Pd Nanoparticle Catalysis for Selective Hydration of Nitriles to Amides in Water: Experimental and Theoretical Studies. ACS Catalysis, 2012, 2, 2467-2474.	5.5	56
11606	Ab initioprediction of pressure-induced structural phase transitions of CrVO<mml:math xmlns:mml="http://www.w3.org/1998/Math/MathML" display="inline"><mml:msub><mml:mrow /><mml:mn>4</mml:mn></mml:msub></mml:math>-type orthophosphates. Physical Review B, 2012, 86, .	1.1	39

#	Article	IF	Citations
11607	First principles study of foreign interstitial atom (carbon, nitrogen) interactions with intrinsic defects in tungsten. Journal of Nuclear Materials, 2012, 430, 270-278.	1.3	40
11608	First-Principles Calculation of NMR Parameters Using the Gauge Including Projector Augmented Wave Method: A Chemistâ€™s Point of View. Chemical Reviews, 2012, 112, 5733-5779.	23.0	446
11609	Bonding Mechanisms of Graphene on Metal Surfaces. Journal of Physical Chemistry C, 2012, 116, 7360-7366.	1.5	133
11610	Ferromagnetism carried by highly delocalized hybrid states in Sc-doped ZnO thin films. Applied Physics Letters, 2012, 100, 222406.	1.5	16
11611	Achieving fast convergence of ab initio free energy perturbation calculations with the adaptive force-matching method. Theoretical Chemistry Accounts, 2012, 131, 1.	0.5	25
11612	Firstâ€"principles study of stacking fault energies in Ni3Al intermetallic alloys. Transactions of Nonferrous Metals Society of China, 2012, 22, 661-664.	1.7	35
11613	First principles study of electronic structure, chemical bonding and elastic properties of BiOCuS. Transactions of Nonferrous Metals Society of China, 2012, 22, 1197-1202.	1.7	24
11614	Band gap narrowing of TiO2 by compensated codoping for enhanced photocatalytic activity. Journal of Natural Gas Chemistry, 2012, 21, 302-307.	1.8	31
11615	First-Principles Calculations on Structure, Elastic and Thermodynamic Properties of Al2X (X=Sc, Y) under Pressure. Journal of Materials Science and Technology, 2012, 28, 155-163.	5.6	28
11616	Band structure of gold from many-body perturbation theory. Physical Review B, 2012, 86, .	1.1	91
11617	Many-body potential for nitrogen in Î±-iron. Philosophical Magazine Letters, 2012, 92, 656-667.	0.5	3
11619	Bistability Loss as a Key Feature in Azobenzene (Nonâ€)Switching on Metal Surfaces. Angewandte Chemie - International Edition, 2012, 51, 12009-12011.	7.2	31
11620	Effect of Platinum Incorporation on the Energetics and Oxygen Chemisorption Properties of the Ni(1â€‰1â€‰1) Surface. ChemCatChem, 2012, 4, 2005-2012.	1.8	4
11621	A 3D AgCl Hierarchical Superstructure Synthesized by a Wet Chemical Oxidation Method. Chemistry - A European Journal, 2012, 18, 16090-16096.	1.7	36
11622	Firstâ€Principles Study toward CO Adsorption on Au/Ni Surface Alloys. ChemPhysChem, 2012, 13, 3909-3915.	1.0	10
11623	The Interaction of Noble Metal With La_{1â€"}_xSr_xMnO₃ (001) Surface and Catalytic Role for Oxygen Adsorption: A Density Functional Theory Study. Fuel Cells, 2012, 12, 1048-1055.	1.5	0
11624	DFT investigation of the influence of ordered vacancies on elastic and magnetic properties of graphene and grapheneâ€like SiC and BN structures. Physica Status Solidi (B): Basic Research, 2012, 249, 2549-2552.	0.7	28
11625	Ab initio quantum-mechanical study of the effects of the inclusion of iron on thermoelastic and thermodynamic properties of periclase (MgO). Physics and Chemistry of Minerals, 2012, 39, 649-663.	0.3	16

#	Article	IF	Citations
11626	Elastic constants of La, LaH2, and LaH3. Monatshefte FÃ¼r Chemie, 2012, 143, 1325-1328.	0.9	4
11627	Selective oxidation of propylamine on oxygen-covered Au(111): a DFT study. Journal of Molecular Modeling, 2012, 18, 3793-3804.	0.8	4
11628	Interaction between an icosahedron Li13 cluster and a graphene layer doped with a hydrogen atom. Journal of Molecular Modeling, 2012, 18, 5029-5033.	0.8	7
11629	Tunable band structures of polycrystalline graphene by external and mismatch strains. Acta Mechanica Sinica/Lixue Xuebao, 2012, 28, 1539-1544.	1.5	10
11630	Modeling van der Waals Interactions in Zeolites with Periodic DFT: Physisorption of n-Alkanes in ZSM-22. Catalysis Letters, 2012, 142, 1057-1060.	1.4	61
11631	Transition metal complexes enslaved in the supercages of zeolite-Y: DFT investigation and catalytic significance. Journal of Inclusion Phenomena and Macrocyclic Chemistry, 2012, 74, 117-127.	1.6	16
11632	A blend of first-principles and kinetic lattice Monte Carlo computation to optimize samarium-doped ceria. Journal of Materials Science, 2012, 47, 7530-7541.	1.7	30
11633	Dielectric permittivity of ultrathin PbTiO3 nanowires from first principles. Journal of Materials Science, 2012, 47, 7580-7586.	1.7	23
11634	GGA+U method from first principles: application to reductionâ€“oxidation properties in ceria-based oxides. Journal of Materials Science, 2012, 47, 7542-7548.	1.7	20
11635	Properties of amorphous and crystalline titanium dioxide from first principles. Journal of Materials Science, 2012, 47, 7515-7521.	1.7	173
11636	Ab initio studies of pristine and oxidized Cu3Au(100) and (111) surfaces. Journal of Materials Science, 2012, 47, 7594-7600.	1.7	7
11637	Electron trapping at the lattice Ti atoms adjacent to the Nb dopant in Nb-doped rutile TiO2. Journal of Materials Science, 2012, 47, 7522-7529.	1.7	9
11638	Pressure-dependent electronic properties of MgO polymorphs: a first-principles study of Compton profiles and autocorrelation functions. Journal of Materials Science, 2012, 47, 7549-7557.	1.7	15
11639	Electronic structure of Li2O2 {0001} surfaces. Journal of Materials Science, 2012, 47, 7564-7570.	1.7	82
11640	Native point defects in binary InP semiconductors. Journal of Materials Science, 2012, 47, 7482-7497.	1.7	20
11641	Tracing magnetism and pairing in FeTe-based systems. Journal of Materials Science, 2012, 47, 7671-7677.	1.7	4
11642	Influences of Cd-Substitution and Intrinsic Vacancies on the Electronic Structures and Optical Properties of ZnO Nanotubes. Journal of Superconductivity and Novel Magnetism, 2012, 25, 2457-2463.	0.8	4
11643	Phase transition and thermodynamic properties of TiN under pressure via first-principles calculations. Journal of Thermal Analysis and Calorimetry, 2012, 110, 973-978.	2.0	20

#	Article	IF	Citations
11644	Electronic properties of boron- and nitrogen-doped graphene: a first principles study. Journal of Nanoparticle Research, 2012, 14, 1.	0.8	95
11645	Interaction of sodium bisulfate with mono- and bi-layer graphene. Journal of Nanoparticle Research, 2012, 14, 1.	0.8	6
11646	Theoretic insights into the Ag doping in monolayer and bilayer ZnO armchair nanoribbons: edge effect and position-dependent properties. Journal of Nanoparticle Research, 2012, 14, 1.	0.8	5
11647	Double layers of H2 adsorption on an AlN sheet induced by electric field. Journal of Nanoparticle Research, 2012, 14, 1.	0.8	1
11648	Adsorption and dissociation of molecular hydrogen on the edges of graphene nanoribbons. Journal of Nanoparticle Research, 2012, 14, 1.	0.8	15
11649	Effect of inhomogeneous deformation on the electronic structure of SnO2 and Sn x Sb1â€“x O2 phases. Powder Metallurgy and Metal Ceramics, 2012, 51, 353-362.	0.4	2
11650	Theoretical Study of Superlow Friction Between Two Single-Side Hydrogenated Graphene Sheets. Tribology Letters, 2012, 48, 255-261.	1.2	47
11651	Contribution to the Understanding of Tribological Properties of Graphite Intercalation Compounds with Metal Chloride. Tribology Letters, 2012, 47, 367-379.	1.2	4
11652	Selective CO2 hydrogenation on the Î³-Al2O3 supported bimetallic Coâ€“Cu catalyst. Catalysis Today, 2012, 194, 30-37.	2.2	18
11653	Copper ionic pairs as possible active sites in N2O decomposition on CuOx/CeO2 catalysts. Catalysis Today, 2012, 191, 129-133.	2.2	30
11654	Role of passivated Nâ€“F pairs in enhancing photoactivity of ZnWO4 (010) surface: Emphasis on correlation between codoping forms and compensation mechanisms. Chemical Engineering Journal, 2012, 211-212, 168-178.	6.6	9
11655	Physisorption to chemisorption transition of NO2 on graphene induced by the interplay of SiO2 substrate and van der Waals forces: A first principles study. Chemical Physics, 2012, 405, 161-166.	0.9	23
11656	Structural determination of stable MoOx monolayers on O/Cu3Au(100): DFT calculations. Chemical Physics, 2012, 406, 47-49.	0.9	1
11657	Electronic structure and optical properties of zinc-blende GaN. Optik, 2012, 123, 2208-2212.	1.4	40
11658	Ab-initio study of the effect of rare-earth elements on the stacking faults of Mg solid solutions. Intermetallics, 2012, 29, 21-26.	1.8	58
11659	First-principles molecular dynamics simulations to study the crystal-to-amorphous transition in the Mgâ€“Zn system. Intermetallics, 2012, 29, 75-79.	1.8	13
11660	Phase transformation and crystal structure of IrTi. Intermetallics, 2012, 31, 26-33.	1.8	11
11661	First-principles investigation of structural and electronic properties of MgCu2 Laves phase under pressure. Intermetallics, 2012, 31, 257-263.	1.8	97

#	Article	IF	Citations
11662	Systematic study of the elastic properties of Mn3AC antiperovskite with A=Zn, Al, Ga, In, Tl, Ge and Sn. Journal of Alloys and Compounds, 2012, 541, 75-78.	2.8	7
11663	Ab initio comparative study of the Cuâ€"In and Cuâ€"Sn intermetallic phases in Cuâ€"Inâ€"Sn alloys. Journal of Alloys and Compounds, 2012, 542, 280-292.	2.8	29
11664	A first principles analysis of the hydrogenation of C1C4 aldehydes and ketones over Ru(0001). Journal of Catalysis, 2012, 295, 31-44.	3.1	48
11665	Atomic-scale insight into adsorption of sterically hindered dibenzothiophenes on MoS2 and Coâ€"Moâ€"S hydrotreating catalysts. Journal of Catalysis, 2012, 295, 146-154.	3.1	116
11666	Reaction path analysis of propene selective oxidation over V2O5 and V2O5/TiO2. Journal of Catalysis, 2012, 295, 195-206.	3.1	22
11667	Highly efficient and stable nonplatinum anode catalyst with Au@Pd coreâ€"shell nanostructures for methanol electrooxidation. Journal of Catalysis, 2012, 295, 217-222.	3.1	68
11668	Atomic site preferences and its effect on magnetic structure in the intermetallic borides M2Fe(Ru0.8T0.2)5B2 (M=Sc, Ti, Zr; T=Ru, Rh, Ir). Journal of Solid State Chemistry, 2012, 196, 168-174.	1.4	8
11669	Pressure-induced phase transition on K2MoO4: A Raman scattering study and ab initio calculations. Journal of Solid State Chemistry, 2012, 196, 197-202.	1.4	9
11670	Theoretical prediction of the fundamental properties for the ternary Li2PtH6 and Na2PtH6. Journal of Solid State Chemistry, 2012, 196, 498-503.	1.4	4
11671	First-principles study of electronic structure and elasticity of UAlx (x=1,2,3) system. Physica B: Condensed Matter, 2012, 407, 748-755.	1.3	9
11672	Transition metal hydrido-complexes: Electronic structure and bonding properties. Progress in Solid State Chemistry, 2012, 40, 31-40.	3.9	8
11673	First-principles study on the structure, elastic and electronic properties of hexagonal HfPtAl under pressure. Solid State Communications, 2012, 152, 462-465.	0.9	0
11674	Pressure induced phase transition of molybdenum nitride: A first principles study. Thin Solid Films, 2012, 525, 200-207.	0.8	7
11675	First principles study of zone centre phonons in rare-earth pyrochlore titanates, RE2Ti2O7 (RE=Gd, Dy,) Tj ETQq1 1 0.784314 rgBT /Over	1.2	39
11676	Conformational behaviour of antioxidant chromones. A vibrational spectroscopy study. Vibrational Spectroscopy, 2012, 63, 325-337.	1.2	15
11677	Compositional variation of magnetic moment, magnetic anisotropy energy and coercivity in Fe(1â^'x)M x (MÂ=ÂCo/Ni) nanowires: an ab initio study. Applied Nanoscience (Switzerland), 2012, 2, 409-415.	1.6	14
11678	Structural stability of nitrogen-doped ultrathin single-walled boron nanotubes: an ab initio study. Applied Nanoscience (Switzerland), 2012, 2, 345-349.	1.6	5
11679	First principles calculation on the structure and electronic properties of BNNTs functionalized with isoniazid drug molecule. Applied Nanoscience (Switzerland), 2012, 2, 389-400.	1.6	52

#	Article	IF	Citations
11680	Azopyridine molecular conductor: A superior device for molecular switch technology. Electronic Materials Letters, 2012, 8, 565-570.	1.0	7
11681	The structural and electronic properties of silicon nanoribbons on Ag(110): A first principles study. Physica B: Condensed Matter, 2012, 407, 4695-4699.	1.3	34
11682	Struggle between inner atoms of ultra-thin silicon film and both its dimer surfaces. Results in Physics, 2012, 2, 185-189.	2.0	2
11683	Bandgap tuning in armchair MoS₂nanoribbon. Journal of Physics Condensed Matter, 2012, 24, 335501.	0.7	71
11684	Electronic Structure and Initial Dehydrogenation Mechanism of M(BH₄)₂Â·2NH₃ (M = Mg, Ca, and Zn): A First-Principles Investigation. Journal of Physical Chemistry C, 2012, 116, 11900-11906.	1.5	43
11685	Disruption of the Chemical Environment and Electronic Structure in p-Type Cu₂O Films by Alkaline Doping. Journal of Physical Chemistry C, 2012, 116, 13524-13535.	1.5	18
11686	Energy band gap engineering in borate ultraviolet nonlinear optical crystals:ab initiostudies. Journal of Physics Condensed Matter, 2012, 24, 145503.	0.7	32
11687	The high-pressure electronic structure of the [Ni(ptdt)2] organic molecular conductor. Journal of Chemical Physics, 2012, 137, 024701.	1.2	1
11688	Physical insight into reduced surface roughness scattering in strained silicon inversion layers. Applied Physics Letters, 2012, 101, 073504.	1.5	4
11689	Electronic structure of superlattices of graphene and hexagonal boron nitride. Journal of Materials Chemistry, 2012, 22, 919-922.	6.7	90
11690	Ideal strength and structural instability of aluminum at finite temperatures. Physical Review B, 2012, 86, .	1.1	24
11691	TDDFT study of time-dependent and static screening in graphene. Physical Review B, 2012, 86, .	1.1	29
11692	Density Functional Theory Study of Niâ€“N_x/C Electrocatalyst for Oxygen Reduction in Alkaline and Acidic Media. Journal of Physical Chemistry C, 2012, 116, 17378-17383.	1.5	120
11693	Theoretical study on the leaching of palladium in a CO atmosphere. Catalysis Science and Technology, 2012, 2, 2238.	2.1	18
11694	Materials Properties of Ultra-Incompressible Re₂P. Chemistry of Materials, 2012, 24, 3240-3246.	3.2	15
11695	Underpinning energetics of lithium bonding and stability in the Liâ€“Ptâ€“Sn system. Solid State Sciences, 2012, 14, 1471-1475.	1.5	4
11696	Structural and electronic properties of the Laves phase based on rare earth type BaM2 (M=Rh, Pd, Pt). Results in Physics, 2012, 2, 58-65.	2.0	89
11697	First-principles studies of structural, mechanical, electronic, optical properties and pressure-induced phase transition of CuInO2 polymorph. Physica B: Condensed Matter, 2012, 407, 4665-4670.	1.3	6

#	Article	IF	Citations
11698	Synthesis, crystal structure and properties of a new strontium cadmium diborate. Inorganica Chimica Acta, 2012, 392, 459-464.	1.2	3
11699	Structural and elastic properties of single-crystal and polycrystalline Ti1âˆ'xZrxN alloys: A computational study. Journal of Alloys and Compounds, 2012, 536, S138-S142.	2.8	13
11700	First-principles investigation of the elastic and electronic properties of the binary intermetallics in the Alâ€"La alloy system. Physica B: Condensed Matter, 2012, 407, 4706-4711.	1.3	10
11701	Phase stability, elastic, electronic, thermal and optical properties of Ti3Al1âˆ'xSixC2 (0â‰¤xâ‰¤1): First principle study. Physica B: Condensed Matter, 2012, 407, 4221-4228.	1.3	38
11702	Equation of state and elastic properties of ACrO3 (A=Pb, Ca, Sr and Ba) perovskites under high pressure. Physica B: Condensed Matter, 2012, 407, 4671-4675.	1.3	3
11703	First-principle study of the electronic and optical properties of BInGaAs quaternary alloy lattice-matched to GaAs. Physica B: Condensed Matter, 2012, 407, 4570-4573.	1.3	16
11704	First principles study of dielectric and vibrational properties of pyrochlore hafnates. Solid State Sciences, 2012, 14, 1405-1411.	1.5	30
11705	Density functional theory on the comparison of the Pd segregation behavior at LaO- and FeO2-terminated surfaces of LaFe1âˆ'xPd O3âˆ'. Current Applied Physics, 2012, 12, S105-S109.	1.1	7
11706	Investigations of meta-stable and post-spinel silicon nitrides. Physica B: Condensed Matter, 2012, 407, 4660-4664.	1.3	9
11707	The electronic structure and properties of Fe6(N1âˆ'xCx)2 carbonitrides by first-principles calculations. Physica B: Condensed Matter, 2012, 407, 4104-4107.	1.3	4
11708	DFT study on electronic structure and optical properties of N-doped, S-doped, and N/S co-doped SrTiO3. Physica B: Condensed Matter, 2012, 407, 4649-4654.	1.3	26
11709	First Principles Study of U-Al System Ground State. , 2012, 1, 514-519.		9
11710	First principles study of orthoâ€"para H2 conversion on the O2(0.25ÂML)/Ag(111) system. Current Applied Physics, 2012, 12, S115-S118.	1.1	4
11711	First-principles study on the atomic and electronic structures of graphene-protected magnetic Fe/Ni(111) thin film. Current Applied Physics, 2012, 12, S37-S40.	1.1	1
11712	Structural and thermodynamic properties of WB at high pressure and high temperature. Physica B: Condensed Matter, 2012, 407, 4760-4764.	1.3	5
11713	First-principles study on ferromagnetism in two-dimensional ZnO nanosheet. Chemical Physics Letters, 2012, 548, 60-63.	1.2	20
11714	Origins of high visible light transparency and solar heat-shielding performance in LaB₆. Applied Physics Letters, 2012, 101, 041913.	1.5	62
11715	On the determination of the glass forming ability of AlxZr1âˆ'x alloys using molecular dynamics, Monte Carlo simulations, and classical thermodynamics. Journal of Applied Physics, 2012, 112, 073508.	1.1	9

#	Article	IF	Citations
11716	Defect configurations of high-k cations in germanium. Journal of Applied Physics, 2012, 111, 023714.	1.1	15
11717	Strain-induced improvements on linear and nonlinear optical properties of SrB4O7 crystal. AIP Advances, 2012, 2, 032170.	0.6	15
11718	Hybrid functional study rationalizes the simple cubic phase of calcium at high pressures. Journal of Chemical Physics, 2012, 137, 184502.	1.2	15
11719	Influence of magnetic ordering on the elastic properties of PdFe3N. Journal of Vacuum Science and Technology A: Vacuum, Surfaces and Films, 2012, 30, .	0.9	4
11720	Amorphization and amorphous stability of Bi2Te3 chalcogenide films. Applied Physics Letters, 2012, 100, .	1.5	10
11721	New view of the occupied band structure of Mo(112). Physical Review B, 2012, 85, .	1.1	9
11722	Hydrogen impurity in yttria:Ab initioand<mml:math xmlns:mml="http://www.w3.org/1998/Math/MathML" display="inline"><mml:mi>Î¼</mml:mi></mml:math>SR perspectives. Physical Review B, 2012, 85, .	1.1	32
11723	Electronic topological transition in LaSn<mml:math xmlns:mml="http://www.w3.org/1998/Math/MathML" display="inline"><mml:msub><mml:mrow /><mml:mn>3</mml:mn></mml:msub></mml:math>under pressure. Physical Review B, 2012, 85, .	1.1	50
11724	Transition-metal dispersion on carbon-doped boron nitride nanostructures: Applications for high-capacity hydrogen storage. Physical Review B, 2012, 86, .	1.1	45
11725	Dynamics of H2 dissociation on the 1/2 ML c(2 Ã— 2)-Ti/Al(100) surface. Physical Chemistry Chemical Physics, 2012, 14, 3234.	1.3	14
11726	Charge-distribution-related regioisomerism of photoresponsive metalâ€“organic polymeric chains. Dalton Transactions, 2012, 41, 13441.	1.6	47
11727	Correlation of lithium ion distribution and X-ray absorption near-edge structure in O3- and O2-lithium cobalt oxides from first-principle calculation. Journal of Materials Chemistry, 2012, 22, 17340.	6.7	38
11728	Electronic and magnetic properties of the two-dimensional C4H-type polymer with strain effects, intrinsic defects and foreign atom substitutions. Physical Chemistry Chemical Physics, 2012, 14, 3651.	1.3	21
11729	Nitrogen and hydrogen defect equilibria in Ca12Al14O33: a combined experimental and computational study. Journal of Materials Chemistry, 2012, 22, 15828.	6.7	14
11730	Anomalous decrease in structural disorder due to charge redistribution in Cr-doped Li4Ti5O12 negative-electrode materials for high-rate Li-ion batteries. Energy and Environmental Science, 2012, 5, 9903.	15.6	143
11731	Decomposition of methylamine on nitrogen atom modified Mo(100): a density functional theory study. Physical Chemistry Chemical Physics, 2012, 14, 6869.	1.3	10
11732	First principles study of sulfuric acid anion adsorption on a Pt(111) electrode. Physical Chemistry Chemical Physics, 2012, 14, 3208.	1.3	53
11733	Computational study of ethanol adsorption and reaction over rutile TiO2 (110) surfaces. Physical Chemistry Chemical Physics, 2012, 14, 11910.	1.3	48

#	Article	IF	Citations
11734	Graphene substrate-mediated catalytic performance enhancement of Runanoparticles: a first-principles study. Dalton Transactions, 2012, 41, 1289-1296.	1.6	61
11735	Electrochemical properties of crystallized dilithium squarate: insight from dispersion-corrected density functional theory. Physical Chemistry Chemical Physics, 2012, 14, 11398.	1.3	23
11736	Reduced Pd density of states in Pd/SAM/Au junctions: the role of adsorbed hydrogen atoms. Physical Chemistry Chemical Physics, 2012, 14, 2353.	1.3	10
11737	Unraveling the Fischerâ€“Tropsch mechanism: a combined DFT and microkinetic investigation of Câ€“C bond formation on Ru. Physical Chemistry Chemical Physics, 2012, 14, 7028.	1.3	20
11738	Decomposition mechanism and the effects of metal additives on the kinetics of lithium alanate. Physical Chemistry Chemical Physics, 2012, 14, 2840.	1.3	19
11739	H₂dissociation on individual Pd atoms deposited on Cu(111). Physical Chemistry Chemical Physics, 2012, 14, 303-310.	1.3	39
11740	Stress induced half-metallicity in surface defected germanium nanowires. Physical Chemistry Chemical Physics, 2012, 14, 1166-1174.	1.3	2
11741	Hydrogen-bonded assembly of methanol on Cu(111). Physical Chemistry Chemical Physics, 2012, 14, 11846.	1.3	28
11742	Effects of Titanium-Containing Additives on the Dehydrogenation Properties of LiAlH₄: A Computational and Experimental Study. Journal of Physical Chemistry C, 2012, 116, 22327-22335.	1.5	18
11743	Study of the Initial Stage of Solid Electrolyte Interphase Formation upon Chemical Reaction of Lithium Metal and N-Methyl-N-Propyl-Pyrrolidinium-Bis(Fluorosulfonyl)Imide. Journal of Physical Chemistry C, 2012, 116, 19789-19797.	1.5	178
11744	Ca₂MnRuO₆: Magnetic Order Arising from Chemical Chaos. Chemistry of Materials, 2012, 24, 2757-2763.	3.2	11
11745	Origin of synergistic effect over Ni-based bimetallic surfaces: A density functional theory study. Journal of Chemical Physics, 2012, 137, 014703.	1.2	64
11746	Much stronger binding of metal adatoms to silicene than to graphene: A first-principles study. Physical Review B, 2012, 86, .	1.1	208
11747	Ultra-incompressible Orthorhombic Phase of Osmium Tetraboride (OsB₄) Predicted from First Principles. Journal of Physical Chemistry C, 2012, 116, 4293-4297.	1.5	41
11748	Dual Defects of Cation and Anion in Memristive Nonvolatile Memory of Metal Oxides. Journal of the American Chemical Society, 2012, 134, 2535-2538.	6.6	44
11749	Energetics and electronic structure of GaN codoped with Eu and Si. Physical Review B, 2012, 85, .	1.1	24
11750	Modelling the rheology of MgO under Earthâ€™s mantle pressure, temperature and strain rates. Nature, 2012, 481, 177-180.	13.7	96
11751	One-pot template-free synthesis, growth mechanism and enhanced photocatalytic activity of monodisperse (BiO)2CO3 hierarchical hollow microspheres self-assembled with single-crystalline nanosheets. CrystEngComm, 2012, 14, 3534.	1.3	79

#	Article	IF	Citations
11752	Structure and hydrogenstorage properties of the first rare-earth metal borohydride ammoniate: Y(BH₄)₃Â·4NH₃. Journal of Materials Chemistry, 2012, 22, 1061-1068.	6.7	55
11753	First-principles studies of proton-Ba interactions in doped LaPO4. Journal of Materials Chemistry, 2012, 22, 3758.	6.7	5
11754	Thin silica films on Ru(0001): monolayer, bilayer and three-dimensional networks of [SiO4] tetrahedra. Physical Chemistry Chemical Physics, 2012, 14, 11344.	1.3	106
11755	Electronic and optical properties of new multifunctional materials via half-substituted hematite: first principles calculations. RSC Advances, 2012, 2, 10708.	1.7	24
11756	Mode-specificity and transition state-specific energy redistribution in the chemisorption of CH4 on Ni{100}. Physical Chemistry Chemical Physics, 2012, 14, 15879.	1.3	33
11757	Theoretical Study of Properties of Goethite (Î±-FeOOH) at Ambient and High-Pressure Conditions. Journal of Physical Chemistry C, 2012, 116, 6703-6713.	1.5	46
11758	First-Principle Study on Structural and Electronic Properties of Pristine and Adsorbed LiF Nanotubes. Journal of Physical Chemistry C, 2012, 116, 1650-1657.	1.5	9
11759	Oxygen Adsorption and Diffusion on NiTi Alloy (100) Surface: A Theoretical Study. Journal of Physical Chemistry C, 2012, 116, 21771-21779.	1.5	15
11760	Hydrogen-Saturated Silicon Nanowires Heavily Doped with Interstitial and Substitutional Transition Metals. Journal of Physical Chemistry C, 2012, 116, 15713-15722.	1.5	30
11761	Investigation of Adsorption Behavior of Mercury on Au(111) from First Principles. Environmental Science & Technology, 2012, 46, 7260-7266.	4.6	51
11762	Vibrational properties of BaClF, BaBrF and BaIF under high pressure. Journal of Physics: Conference Series, 2012, 377, 012070.	0.3	3
11763	Ab initiopredictions of structural and elastic properties of struvite: contribution to urinary stone research. Computer Methods in Biomechanics and Biomedical Engineering, 2012, 15, 1329-1336.	0.9	10
11764	A possible mechanism of copper corrosion in anoxic water. Philosophical Magazine, 2012, 92, 4618-4627.	0.7	5
11765	Experimental evidence for the structural models of Re<mml:math xmlns:mml="http://www.w3.org/1998/Math/MathML" display="inline"><mml:msub><mml:mrow /><mml:mn>2</mml:mn></mml:msub></mml:math>N and Re<mml:math xmlns:mml="http://www.w3.org/1998/Math/MathML" display="inline"><mml:msub><mml:mrow /><mml:mn>2</mml:mn></mml:msub></mml:math>C from micro-Raman spectroscopy. Physical Review B, 2012, 86, .	1.1	10
11766	First-principles study of the structural and elastic properties of rhenium-based transition-metal alloys. Physical Review B, 2012, 86, .	1.1	26
11767	Oxygen molecule dissociation on carbon nanostructures with different types of nitrogen doping. Nanoscale, 2012, 4, 1184-1189.	2.8	220
11768	Penetration of alkali atoms throughout a graphene membrane: theoretical modeling. Nanoscale, 2012, 4, 1749.	2.8	18
11769	Solvothermal synthesis of two new coordination polymers: in situ heterocycle conversion and N-alkylation, network topologies and luminescence properties. CrystEngComm, 2012, 14, 4794.	1.3	9

#	Article	IF	Citations
11770	A first-principles prediction of two-dimensional superconductivity in pristine B2C single layers. Nanoscale, 2012, 4, 3032.	2.8	67
11771	Structure, bonding, vibration and ideal strength of primitive-centered tetragonal boron nitride. Physical Chemistry Chemical Physics, 2012, 14, 869-876.	1.3	55
11772	SMARTER crystallography of the fluorinated inorganicâ€“organic compound Zn3Al2F12Â·[HAmTAZ]6. Dalton Transactions, 2012, 41, 6232.	1.6	43
11773	Unusual intermediate spin Fe3+ ion in antiferromagnetic Li3FeN2. Journal of Applied Physics, 2012, 111, 063704.	1.1	4
11774	Stability, electronic and magnetic properties of embedded triangular graphene nanoflakes. Physical Chemistry Chemical Physics, 2012, 14, 1253-1261.	1.3	11
11775	Rare earth induced formation of Î´-BiB3O6 at ambient pressure with strong second harmonic generation. Journal of Materials Chemistry, 2012, 22, 17934.	6.7	27
11776	The first-principles treatment of the electron-correlation and spinâ€“orbital effects in uranium mononitride nuclear fuels. Physical Chemistry Chemical Physics, 2012, 14, 4482.	1.3	70
11777	Nitrogen defects in wide band gap oxides: defect equilibria and electronic structure from first principles calculations. Physical Chemistry Chemical Physics, 2012, 14, 11808.	1.3	15
11778	NaGe₃P₃: a new ternary germanium phosphide featuring an unusual [Ge₃P₇] ring. Dalton Transactions, 2012, 41, 484-489.	1.6	19
11779	Boratabenzene-vanadium sandwich molecular wire and its properties. Nanoscale, 2012, 4, 7557.	2.8	3
11780	Ferroelectric phase transition in LiNbO₃: Insights from molecular dynamics. IEEE Transactions on Ultrasonics, Ferroelectrics, and Frequency Control, 2012, 59, 1925-1928.	1.7	18
11781	Effects of reactive elements on the structure and diffusivity of liquid chromia: Anab initiomolecular dynamics study. Physical Review B, 2012, 85, .	1.1	19
11782	Promoters in the hydrogenation of alkynes in mixtures: insights from density functional theory. Chemical Communications, 2012, 48, 1379-1391.	2.2	183
11783	Surface phase diagram of hematite pseudocubes in hydrous environments. Journal of Materials Chemistry, 2012, 22, 161-167.	6.7	12
11784	DFT and DRIFTS studies of the oxidative carbonylation of methanol over Î³-Cu2Cl(OH)3: the influence of Cl. RSC Advances, 2012, 2, 8752.	1.7	7
11785	Interaction of oxygen vacancies in yttrium germanates. Physical Chemistry Chemical Physics, 2012, 14, 14630.	1.3	11
11786	Magnetic behavior and clustering effects in Mn-doped boron nitride sheets. Journal of Physics Condensed Matter, 2012, 24, 326003.	0.7	6
11787	Ab initiostudy on the formation of chemically ordered Zr2Al phase by coupled replaciveâ€“displacive transformation. Philosophical Magazine, 2012, 92, 4040-4055.	0.7	6

#	Article	IF	Citations
11788	Electron Properties of F, and N Doped Hematite: The Application for Photocatalysis. Advanced Materials Research, 2012, 562-564, 298-301.	0.3	5
11789	Computer Modeling of Crystalline Electrolytes: Lithium Thiophosphates and Phosphates. Journal of the Electrochemical Society, 2012, 159, A538-A547.	1.3	41
11790	First Principles Study on the Electronic Properties of Cr, Fe, Mn and Ni Doped Î²-Ga₂O₃. Advanced Materials Research, 0, 535-537, 36-41.	0.3	14
11791	Thermoelectric properties of HfN/ScN metal/semiconductor superlattices: a first-principles study. Journal of Physics Condensed Matter, 2012, 24, 415303.	0.7	21
11792	Importance of Correlation in Determining Electrocatalytic Oxygen Evolution Activity on Cobalt Oxides. Journal of Physical Chemistry C, 2012, 116, 21077-21082.	1.5	305
11793	Polymerization of Carbon Dioxide: A Chemistry View of Molecular-to-Nonmolecular Phase Transitions. Journal of Physical Chemistry C, 2012, 116, 2061-2067.	1.5	19
11794	Antisite Atom Segregation in Porous Boron Nitride Nanotubes: Formation Mechanism and Characterization. Journal of Physical Chemistry C, 2012, 116, 22051-22056.	1.5	2
11795	Chemical-State Analysis of Organic Semiconductors Using Soft X-ray Absorption Spectroscopy Combined with First-Principles Calculation. Journal of Physical Chemistry A, 2012, 116, 1527-1531.	1.1	5
11796	New Insights on Vibrational Dynamics of Corannulene. Journal of Physical Chemistry C, 2012, 116, 25089-25096.	1.5	14
11797	Non-innocent Dissociation of H₂O on GaP(110): Implications for Electrochemical Reduction of CO₂. Journal of the American Chemical Society, 2012, 134, 13600-13603.	6.6	48
11798	Boron Sheet Adsorbed on Metal Surfaces: Structures and Electronic Properties. Journal of Physical Chemistry C, 2012, 116, 18202-18206.	1.5	58
11799	Information-Theoretic Approach for the Discovery of Design Rules for Crystal Chemistry. Journal of Chemical Information and Modeling, 2012, 52, 1812-1820.	2.5	40
11800	CO₂ Hydrogenation to Formic Acid on Ni(111). Journal of Physical Chemistry C, 2012, 116, 3001-3006.	1.5	141
11801	Thermodynamic and Electrochemical Properties of the Liâ€“Coâ€“O and Liâ€“Niâ€“O Systems. Chemistry of Materials, 2012, 24, 97-105.	3.2	42
11802	Experimental and Theoretical Studies on a High Pressure Monoclinic Phase of Ammonia Borane. Journal of Physical Chemistry C, 2012, 116, 2172-2178.	1.5	40
11803	The magnetic and quantum transport properties of benzeneâ€“vanadiumâ€“borazine mixed sandwich clusters: a new kind of spin filter. Journal of Physics Condensed Matter, 2012, 24, 445501.	0.7	2
11804	Chemical Modeling of Mixed Occupations and Site Preferences in Anisotropic Crystal Structures: Case of Complex Intermetallic Borides. Inorganic Chemistry, 2012, 51, 5677-5685.	1.9	17
11805	Elastic moduli and band gap of PbTe under pressure: ab initio study. Materials Science and Technology, 2012, 28, 1308-1313.	0.8	6

#	Article	IF	Citations
11806	Surface Chemistry of 2-Iodoethanol on Pd(111): Orientation of Surface-Bound Alcohol Controls Selectivity. Journal of Physical Chemistry C, 2012, 116, 4201-4208.	1.5	13
11807	Oxidation State of Uranium in A₆Cu₁₂U₂S₁₅ (A = K, Rb,) Tj ETQq1 1 0.784314 rgB	1.9	28
11808	Role of Multivalent Pr in the Formation and Migration of Oxygen Vacancy in Pr-Doped Ceria: Experimental and First-Principles Investigations. Chemistry of Materials, 2012, 24, 4261-4267.	3.2	86
11809	Acetaldehyde Production in the Direct Ethanol Fuel Cell: Mechanistic Elucidation by Density Functional Theory. Journal of Physical Chemistry C, 2012, 116, 7185-7188.	1.5	18
11810	Structures of uranyl peroxide hydrates: a first-principles study of studtite and metastudtite. Dalton Transactions, 2012, 41, 9748.	1.6	58
11811	Reactivity and Morphology of Oxygen-Modified Au Surfaces. Journal of Physical Chemistry C, 2012, 116, 18292-18299.	1.5	13
11812	Pressure-induced amorphous-to-amorphous configuration change in Ca-Al metallic glasses. Scientific Reports, 2012, 2, 376.	1.6	47
11813	First principle calculation of electronic and optical properties of InP. , 2012, , .		0
11814	On the Mechanisms of SiO₂ Thin-Film Growth by the Full Atomic Layer Deposition Process Using Bis(t-butylamino)silane on the Hydroxylated SiO₂(001) Surface. Journal of Physical Chemistry C, 2012, 116, 947-952.	1.5	50
11815	Exploring the electronic properties of relaxed bilayer nitrogen-graphene alloy using density functional theory. , 2012, , .		0
11816	First-Principles Study on Cd Doping in Cu₂ZnSnS₄ and Cu₂ZnSnSe₄. Japanese Journal of Applied Physics, 2012, 51, 10NC11.	0.8	32
11817	Theoretical study of the adsorption of DNA bases on the acidic external surface of montmorillonite. Physical Chemistry Chemical Physics, 2012, 14, 945-954.	1.3	39
11818	Robust Electronic Properties of Sealed Graphene for Electronic Applications. Journal of Physical Chemistry C, 2012, 116, 8027-8033.	1.5	6
11819	First-principles investigations of crystallographic, magnetic, and electronic structures in Ni2XIn (Xâ€‰=â€‰Mn, Fe, and Co). Journal of Applied Physics, 2012, 112, 114901.	1.1	20
11820	Insights into Li⁺ Migration Pathways in Î±-Li₃VF₆: A First-Principles Investigation. Journal of Physical Chemistry Letters, 2012, 3, 3120-3124.	2.1	9
11821	Electronic structure, growth mechanism and photoluminescence of CaWO₄crystals. CrystEngComm, 2012, 14, 853-868.	1.3	200
11822	Synthesis, Crystal Structure, Chemical Bonding, and Physical Properties of the Ternary Na/Mg Stannide Na₂MgSn. Inorganic Chemistry, 2012, 51, 4810-4816.	1.9	19
11823	Work Function Dependence on the Adhesion Configuration of Self-Assembled Alkylsilane Coatings of a (111) Silicon Surface. Journal of Physical Chemistry C, 2012, 116, 24935-24942.	1.5	2

#	Article	IF	Citations
11824	Crystal Structures, Phase Stabilities, and Hydrogen Storage Properties of Metal Amidoboranes. Journal of Physical Chemistry C, 2012, 116, 14224-14231.	1.5	18
11825	Adsorption of Pt and Bimetallic PtAu Clusters on the Partially Reduced Rutile (110) TiO₂ Surface: A First-Principles Study. Journal of Physical Chemistry C, 2012, 116, 5735-5746.	1.5	40
11826	First-Principles Study of EMIM-FAFSA Molecule Adsorption on a Li(100) Surface as a Model for Li-Ion Battery Electrodes. Journal of Physical Chemistry C, 2012, 116, 8493-8509.	1.5	32
11827	Potential-Dependent Structural Memory Effects in Auâ€“Pd Nanoalloys. Journal of Physical Chemistry Letters, 2012, 3, 315-321.	2.1	39
11828	Graphene-diamond interface: Gap opening and electronic spin injection. Physical Review B, 2012, 85, .	1.1	95
11829	Communication: Oscillated band gaps of B/N-codoped Î±-graphyne. Journal of Chemical Physics, 2012, 137, 201101.	1.2	38
11830	Electronic transport at monolayer-bilayer junctions in epitaxial graphene on SiC. Physical Review B, 2012, 86, .	1.1	85
11831	Ab-initio study of active lone pair of Ge²⁺ cation in novel perovskite GeTiO<inf>3</inf> compound. , 2012, , .		0
11832	Phase transitions and electronâ€“phonon coupling in platinum hydride. Journal of Physics Condensed Matter, 2012, 24, 035701.	0.7	12
11833	Two-Dimensional Superstructure Formation of Fluorinated Fullerene on Au(111): A Scanning Tunneling Microscopy Study. ACS Nano, 2012, 6, 2679-2685.	7.3	18
11834	First-principles study of Î³-CuI for p-type transparent conducting materials. Journal Physics D: Applied Physics, 2012, 45, 145102.	1.3	40
11835	Ab Initio Molecular Dynamics Study of the AlOOH Boehmite/Water Interface: Role of Steps in Interfacial Grotthus Proton Transfers. Journal of Physical Chemistry C, 2012, 116, 12514-12524.	1.5	77
11836	Density functional theory studies on the electronic, structural, phonon dynamical and thermo-stability properties of bicarbonates MHCO₃, M = Li, Na, K. Journal of Physics Condensed Matter, 2012, 24, 325501.	0.7	11
11837	Silicon-Containing Multidecker Organometallic Complexes and Nanowires: A Density Functional Theory Study. Journal of Physical Chemistry Letters, 2012, 3, 151-156.	2.1	8
11838	Quasiparticle band structures and optical properties of magnesium fluoride. Journal of Physics Condensed Matter, 2012, 24, 085602.	0.7	12
11839	Strain-driven spin-state transition and superexchange interaction in LaCoO<mml:math xmlns:mml="http://www.w3.org/1998/Math/MathML" display="inline"><mml:msub><mml:mrow /><mml:mn>3</mml:mn></mml:msub></mml:math>:<mml:math xmlns:mml="http://www.w3.org/1998/Math/MathML" display="inline"><mml:mrow><mml:mi>A</mml:mi><mml:mi>b</mml:mi></mml:mrow></mml:math>initiostudy. Physical Review B, 2012, 86, .	1.1	72
11840	Single Gold Atom Adsorption on the Fe₃O₄(111) Surface. Journal of Physical Chemistry C, 2012, 116, 10632-10638.	1.5	57
11841	Anisotropic elasticity of DyScO₃substrates. Journal of Physics Condensed Matter, 2012, 24, 385404.	0.7	16

#	Article	IF	Citations
11842	Bloch-type domain walls in rhombohedral BaTiO<mml:math xmlns:mml="http://www.w3.org/1998/Math/MathML" display="inline"><mml:msub><mml:mrow /><mml:mn>3</mml:mn></mml:msub></mml:math>. Physical Review B, 2012, 86, .	1.1	53
11843	Reconstruction of the Chalcopyrite Surfacesâ€"A DFT Study. Journal of Physical Chemistry C, 2012, 116, 6357-6366.	1.5	94
11844	Intrinsic defects in multiferroic BiFeO<mml:math xmlns:mml="http://www.w3.org/1998/Math/MathML" display="inline"><mml:msub><mml:mrow /><mml:mn>3</mml:mn></mml:msub></mml:math>and their effect on magnetism. Physical Review B, 2012, 85, .	1.1	153
11845	Hydrogen Storage in Yttrium-Decorated Single Walled Carbon Nanotube. Journal of Physical Chemistry C, 2012, 116, 22502-22508.	1.5	115
11846	The study of pressure induced structural phase transition in spin-frustrated Yb2Ti2O7 pyrochlore. Journal of Applied Physics, 2012, 111, .	1.1	12
11847	Quasiparticle band structure of alkali-metal fluorides, oxides, and nitrides. Physical Review B, 2012, 85, .	1.1	21
11848	Surface orientation effects in crystallineâ€"amorphous silicon interfaces. Physical Chemistry Chemical Physics, 2012, 14, 15173.	1.3	18
11849	Cagelike Diamondoid Nitrogen at High Pressures. Physical Review Letters, 2012, 109, 175502.	2.9	176
11850	Spiral chain O ₄ form of dense oxygen. Proceedings of the National Academy of Sciences of the United States of America, 2012, 109, 751-753.	3.3	111
11851	Supramolecular Ordering of PTCDA Molecules: The Key Role of Dispersion Forces in an Unusual Transition from Physisorbed into Chemisorbed State. ACS Nano, 2012, 6, 8536-8545.	7.3	49
11852	NMR Crystallography Comparative Studies of Chiral (1R,2S,3R,5R)-3-Amino-6,6-dimethylbicyclo[3.1.1]heptan-2-ol and Its p-Toluenesulfonamide Derivative. Crystal Growth and Design, 2012, 12, 5956-5965.	1.4	4
11853	Structure and Magnetism of Hybrid Fe and Co Nanoclusters up to NÂ‰Â7 Atoms. Journal of Cluster Science, 2012, 23, 953-966.	1.7	9
11854	Impact of Fluorination on Initial Growth and Stability of Pentacene on Cu(111). Journal of Physical Chemistry C, 2012, 116, 7726-7734.	1.5	29
11855	Adsorption, Dissociation, and Hydrogenation of CO₂ on WC(0001) and WC-Co Alloy Surfaces Investigated with Theoretical Calculations. Journal of Physical Chemistry C, 2012, 116, 13202-13209.	1.5	27
11856	Charge-Transport Parameters of Acenedithiophene Crystals: Realization of One-, Two-, or Three-Dimensional Transport Channels through Alkyl and Phenyl Derivatizations. Journal of Physical Chemistry C, 2012, 116, 5215-5224.	1.5	25
11857	Unambiguous Description of the Oxygen Environment in Multicomponent Aluminosilicate Glasses from ¹⁷O Solid State NMR Computational Spectroscopy. Journal of Physical Chemistry C, 2012, 116, 14599-14609.	1.5	59
11858	Structural properties and energetics of Li2FeSiO4 polymorphs and their delithiated products from first-principles. Physical Chemistry Chemical Physics, 2012, 14, 7346.	1.3	47
11859	Synergistic Effects in La/N Codoped TiO₂ Anatase (101) Surface Correlated with Enhanced Visible-Light Photocatalytic Activity. Langmuir, 2012, 28, 5882-5891.	1.6	42

#	Article	IF	Citations
11860	First-Principles Study of Hydrogenation of Ethylene on a H_xMoO₃(010) Surface. Journal of Physical Chemistry C, 2012, 116, 24630-24638.	1.5	25
11861	First Principles Study of Electron Tunneling through Ice. Journal of Physical Chemistry C, 2012, 116, 22129-22138.	1.5	14
11862	As₂O₃ Polymorphs: Theoretical Insight into Their Stability and Ammonia Templated Claudetite II Crystallization. Crystal Growth and Design, 2012, 12, 5663-5670.	1.4	23
11863	Surface Dependence of CO₂ Adsorption on Zn₂GeO₄. Langmuir, 2012, 28, 10415-10424.	1.6	71
11864	First-Principle Study of the Electronic and Optical Properties of Ti Doped ZnS. Advanced Materials Research, 2012, 430-432, 173-176.	0.3	1
11865	First-Principles Study on the Initial Oxidization of a Nb(100) Surface. Journal of Physical Chemistry C, 2012, 116, 23371-23376.	1.5	4
11866	First-Principles Study of Biaxial Strain Effect on Hydrogen Adsorbed Mg (0001) Surface. Journal of Physical Chemistry C, 2012, 116, 14943-14949.	1.5	24
11867	Initial Hydrogenations of Pyridine on MoP(001): A Density Functional Study. Langmuir, 2012, 28, 3129-3137.	1.6	24
11868	Role of sidewall diffusion in GaAs nanowire growth: A first-principles study. Physical Review B, 2012, 86, .	1.1	25
11869	The electronic and optical properties of carbon-doped SrTiO3: Density functional characterization. AIP Advances, 2012, 2, .	0.6	34
11870	Biomimetic Carbon Nanotube for Catalytic CO₂ Hydrolysis: First-Principles Investigation on the Role of Oxidation State and Metal Substitution in Porphyrin. Journal of Physical Chemistry Letters, 2012, 3, 1369-1373.	2.1	15
11871	A meta-GGA Made Free of the Order of Limits Anomaly. Journal of Chemical Theory and Computation, 2012, 8, 2078-2087.	2.3	49
11872	Thermodynamics and elastic properties of Ta from first-principles calculations. Chinese Physics B, 2012, 21, 127102.	0.7	7
11873	High-pressure phases of lithium borohydride LiBH<mml:math xmlns:mml="http://www.w3.org/1998/Math/MathML" display="inline"><mml:msub><mml:mrow /><mml:mn>4</mml:mn></mml:msub></mml:math>: A first-principles study. Physical Review B, 2012, 86, .	1.1	16
11874	Structural, Electronic, and Mechanical Properties of Single-Walled Chrysotile Nanotube Models. Journal of Physical Chemistry C, 2012, 116, 9405-9411.	1.5	37
11875	Crystal and Electronic Structures of Neptunium Nitrides Synthesized Using a Fluoride Route. Journal of the American Chemical Society, 2012, 134, 3111-3119.	6.6	20
11876	On the Need for Spin Polarization in Heterogeneously Catalyzed Reactions on Nonmagnetic Metallic Surfaces. Journal of Chemical Theory and Computation, 2012, 8, 1737-1743.	2.3	21
11877	Electronic Structure and Properties of the Alkaline Earth Monosilicides. Journal of Physical Chemistry C, 2012, 116, 2536-2542.	1.5	11

#	Article	IF	Citations
11878	Negative Differential Resistance in a Hybrid Silicon-Molecular System: Resonance between the Intrinsic Surface-States and the Molecular Orbital. ACS Nano, 2012, 6, 7066-7076.	7.3	14
11879	Structural properties of PbVO₃perovskites under hydrostatic pressure conditions up to 10.6 GPa. Journal of Physics Condensed Matter, 2012, 24, 435403.	0.7	16
11880	Porous Alumina Protective Coatings on Palladium Nanoparticles by Self-Poisoned Atomic Layer Deposition. Chemistry of Materials, 2012, 24, 2047-2055.	3.2	110
11881	High-pressure ionic and molecular phases of ammonia within density functional theory. Physical Review B, 2012, 86, .	1.1	23
11882	Origin of Optical Excitations in Fluorine-Doped Titania from Response Function Theory: Relevance to Photocatalysis. Journal of Physical Chemistry Letters, 2012, 3, 2269-2274.	2.1	32
11883	Synthesis, Structure, and Characterization of New Li+â€“ d0â€“Lone-Pair â€“ Oxides: Noncentrosymmetric Polar Li6(Mo2O5)3(SeO3)6and Centrosymmetric Li2(MO3)(TeO3) (M = Mo6+or W6+). Inorganic Chemistry, 2012, 51, 9529-9538.	1.9	44
11884	Interface atomic structures and magnetic anisotropy of Fe and Pd/Fe monatomic films on Pd(001). Physical Review B, 2012, 85, .	1.1	6
11885	Analysis of Charge Transfer for in Situ Li Intercalated Carbon Nanotubes. Journal of Physical Chemistry C, 2012, 116, 11364-11369.	1.5	25
11886	Validation of Interstitial Iron and Consequences of Nonstoichiometry in Mackinawite (Fe_{1+x}S). Journal of Physical Chemistry A, 2012, 116, 2234-2243.	1.1	18
11887	Autocatalytic and Cooperatively Stabilized Dissociation of Water on a Stepped Platinum Surface. Journal of the American Chemical Society, 2012, 134, 19217-19222.	6.6	53
11888	Atomic and Electronic Processes during the Formation of an Ionic NaCl Monolayer on a Covalent Si(100) Surface. Journal of Physical Chemistry C, 2012, 116, 11526-11538.	1.5	7
11889	Electronic and lattice instability and its relaxation mechanism in Pt-Co interfaces. Physical Review B, 2012, 85, .	1.1	1
11890	Mechanisms of Defect Generation and Clustering in CH3S Self-Assembled Monolayers on Au(111). Journal of Physical Chemistry Letters, 2012, 3, 2159-2163.	2.1	9
11891	Comparison of the Site Occupancies Determined by Combined Rietveld Refinement and Density Functional Theory Calculations: Example of the Ternary Moâ€“Niâ€“Re Ïƒ Phase. Inorganic Chemistry, 2012, 51, 3071-3078.	1.9	30
11892	Oxygen Vacancy-Assisted Coupling and Enolization of Acetaldehyde on CeO₂(111). Journal of the American Chemical Society, 2012, 134, 18034-18045.	6.6	97
11893	Quasiclassical Trajectory Dynamics Study of Atomic Oxygen Collisions on an O-Preadsorbed Graphite (0001) Surface with a New Analytical Potential Energy Surface. Journal of Physical Chemistry C, 2012, 116, 13092-13103.	1.5	18
11894	Kinetics and Mechanisms for the Adsorption, Dissociation, and Diffusion of Hydrogen in Ni and Ni/YSZ Slabs: A DFT Study. Langmuir, 2012, 28, 5596-5605.	1.6	34
11895	NaBr Poisoning of Au/TiO₂ Catalysts: Effects on Kinetics, Poisoning Mechanism, and Estimation of the Number of Catalytic Active Sites. ACS Catalysis, 2012, 2, 684-694.	5.5	29

#	Article	IF	Citations
11896	Influence of water on the electronic structure of metal-supported graphene: Insights from van der Waals density functional theory. Physical Review B, 2012, 85, .	1.1	70
11897	DFT Study of the Electronic Properties of LaOCl Surfaces. Journal of Physical Chemistry C, 2012, 116, 681-691.	1.5	13
11898	Role of NH₃ in the Dehydrogenation of Calcium Amidoborane Ammoniate and Magnesium Amidoborane Ammoniate: A First-Principles Study. Inorganic Chemistry, 2012, 51, 76-87.	1.9	14
11899	Sulfidization of Au(111) from Thioacetic Acid: An Experimental and Theoretical Study. Langmuir, 2012, 28, 15278-15285.	1.6	16
11900	Defect energetics in LaAlO3polymorphs: A first-principles study. Physical Review B, 2012, 86, .	1.1	17
11901	Electrochemical, High-Resolution Photoemission Spectroscopy and vdW-DFT Study of the Thermal Stability of Benzenethiol and Benzeneselenol Monolayers on Au(111). Langmuir, 2012, 28, 13624-13635.	1.6	42
11902	Friction of Diamond in the Presence of Water Vapor and Hydrogen Gas. Coupling Gas-Phase Lubrication and First-Principles Studies. Journal of Physical Chemistry C, 2012, 116, 6966-6972.	1.5	90
11903	Direct Experimental Evidence of Metal-Mediated Etching of Suspended Graphene. ACS Nano, 2012, 6, 4063-4071.	7.3	141
11904	Extending the Density Functional Tight Binding Method to Carbon Under Extreme Conditions. Journal of Physical Chemistry C, 2012, 116, 2198-2204.	1.5	29
11905	pâ€“n Junction at the Interface between Metallic Systems. Journal of Physical Chemistry Letters, 2012, 3, 818-825.	2.1	5
11906	Vacancy trapping mechanism for multiple hydrogen and helium in beryllium: a first-principles study. Journal of Physics Condensed Matter, 2012, 24, 095004.	0.7	19
11907	On the possibility of a hetero-epitaxial Fe/ZrO2interface: a density-functional-theory point of view. Modelling and Simulation in Materials Science and Engineering, 2012, 20, 045011.	0.8	3
11908	Influence of the Triel Elements (M = Al, Ga, In) on the Transport Properties of Ca₅M₂Sb₆ Zintl Compounds. Chemistry of Materials, 2012, 24, 2091-2098.	3.2	90
11909	Anti-Kubas Type Interaction in Hydrogen Storage on a Li Decorated BHNH Sheet: A First-Principles Based Study. Journal of Physical Chemistry C, 2012, 116, 3840-3844.	1.5	35
11910	Dynamic structure factor in warm dense beryllium. New Journal of Physics, 2012, 14, 055020.	1.2	52
11911	First-principles study of the electronic structure and optical properties of defect chalcopyrite CdGa ₂ Te ₄. Chinese Physics B, 2012, 21, 123101.	0.7	7
11912	Ab initiostudies of hydrogen adatoms on bilayer graphene. Physical Review B, 2012, 85, .	1.1	64
11913	CO Oxidation Mechanism on Tungsten Nanoparticle. Journal of Physical Chemistry C, 2012, 116, 18803-18815.	1.5	10

#	Article	IF	Citations
11914	Strain-Induced Spin Crossover in Phthalocyanine-Based Organometallic Sheets. Journal of Physical Chemistry Letters, 2012, 3, 3109-3114.	2.1	54
11915	First-Principles Assessment of the Reactions of Boric Acid on NiO(001) and ZrO2(1Ì...11) Surfaces. Journal of Physical Chemistry C, 2012, 116, 10113-10119.	1.5	7
11916	The Role of Stable and Mobile Carbon Adspecies in Copper-Promoted Graphene Growth. Journal of Physical Chemistry C, 2012, 116, 5802-5809.	1.5	70
11917	Electronic properties of graphene nanoribbon doped by boron/nitrogen pair: a first-principles study. Chinese Physics B, 2012, 21, 027102.	0.7	16
11918	Anisotropic Strain Enhanced Hydrogen Solubility in bcc Metals: The Independence on the Sign of Strain. Physical Review Letters, 2012, 109, 135502.	2.9	101
11919	Zn-Doped CdS Nanoarchitectures Prepared by Hydrothermal Synthesis: Mechanism for Enhanced Photocatalytic Activity and Stability under Visible Light. Journal of Physical Chemistry C, 2012, 116, 9078-9084.	1.5	120
11920	Influence of Step Defects on the H2S Splitting on Copper Surfaces from First-Principles Microkinetic Modeling. Journal of Physical Chemistry C, 2012, 116, 20321-20331.	1.5	14
11921	A DFT+U study of acetylene selective hydrogenation on oxygen defective anatase (101) and rutile (110) TiO2 supported Pd4 cluster. Journal of Chemical Physics, 2012, 136, 104107.	1.2	54
11922	Mechanical properties of graphene and boronitrene. Physical Review B, 2012, 85, .	1.1	713
11923	Structure of Isolated Molybdenum(VI) and Molybdenum(IV) Oxide Species on Silica: Periodic and Cluster DFT Studies. Journal of Physical Chemistry C, 2012, 116, 5571-5584.	1.5	60
11924	Ab Initio Prediction of Adsorption Isotherms for Small Molecules in Metalâ€“Organic Frameworks: The Effect of Lateral Interactions for Methane/CPO-27-Mg. Journal of the American Chemical Society, 2012, 134, 18354-18365.	6.6	90
11925	Syntheses and Characterization of Six Quaternary Uranium Chalcogenides A₂M₄U₆Q₁₇ (A = Rb or Cs; M = Pd or Pt; Q = S or Se). Inorganic Chemistry, 2012, 51, 8873-8881.	1.9	15
11926	Strain-Induced ZnO Spinterfaces. Journal of Physical Chemistry C, 2012, 116, 610-617.	1.5	14
11927	Simulated Photoemission Spectra of Hydroxylated MgO(100) at Elevated Temperatures. Journal of Physical Chemistry C, 2012, 116, 3545-3551.	1.5	15
11928	Tuning Semiconductor Band Edge Energies for Solar Photocatalysis via Surface Ligand Passivation. Nano Letters, 2012, 12, 383-388.	4.5	124
11929	Modified Corrections for London Forces in Solid-State Density Functional Theory Calculations of Structure and Lattice Dynamics of Molecular Crystals. Journal of Physical Chemistry A, 2012, 116, 6927-6934.	1.1	24
11930	Physical Origin of General Oscillation of Structure, Surface Energy, and Electronic Property in Rutile TiO₂ Nanoslab. ACS Applied Materials & Interfaces, 2012, 4, 2192-2198.	4.0	12
11931	Bi<mml:math xmlns:mml="http://www.w3.org/1998/Math/MathML" display="inline"><mml:msub><mml:mrow /><mml:mn>2</mml:mn></mml:msub></mml:math>-based layered superconductor Bi<mml:math xmlns:mml="http://www.w3.org/1998/Math/MathML" display="inline"><mml:msub><mml:mrow /><mml:mn>4</mml:mn></mml:msub></mml:math>O<mml:math xmlns:mml="http://www.w3.org/1998/Math/MathML" display="inline"><mml:msub><mml:mrow /><mml:	1.1	373

#	Article	IF	Citations
11932	Density Functional Theory Study of Oxygen Reduction Activity on Ultrathin Platinum Nanotubes. Journal of Physical Chemistry C, 2012, 116, 16499-16510.	1.5	18
11933	Magnetic properties of phthalocyanine-based organometallic nanowire. Applied Physics Letters, 2012, 101, 062405.	1.5	24
11934	New Implicit Solvation Scheme for Solid Surfaces. Journal of Physical Chemistry C, 2012, 116, 22458-22462.	1.5	47
11935	Electronic Properties and Reactivity of Simulated Fe³⁺ and Cr³⁺ Substituted Î±-Al₂O₃ (0001) Surface. Journal of Physical Chemistry C, 2012, 116, 18847-18856.	1.5	23
11936	Bimetallic Borohydrides in the System M(BH₄)₂â€“KBH₄ (M = Mg, Mn): On the Structural Diversity. Journal of Physical Chemistry C, 2012, 116, 10829-10840.	1.5	69
11937	Formic Acid Dehydrogenation on Ni(111) and Comparison with Pd(111) and Pt(111). Journal of Physical Chemistry C, 2012, 116, 4149-4156.	1.5	115
11938	A theoretical study of the hydrogen-storage potential of (H2)4CH4in metal organic framework materials and carbon nanotubes. Journal of Physics Condensed Matter, 2012, 24, 424204.	0.7	12
11939	Comparative study of defect transition energy calculation methods: The case of oxygen vacancy in In<mml:math xmlns:mml="http://www.w3.org/1998/Math/MathML" display="inline"><mml:msub><mml:mrow /><mml:mn>2</mml:mn></mml:msub></mml:math>O<mml:math xmlns:mml="http://www.w3.org/1998/Math/MathML" display="inline"><mml:msub><mml:mrow /><mml:mn>3</mml:mn></mml:msub></mml:math> and ZnO. Physical Review B, 2012, 86, .	1.1	23
11940	Three Alkali-Metalâ€“Goldâ€“Gallium Systems. Ternary Tunnel Structures and Some Problems with Poorly Ordered Cations. Inorganic Chemistry, 2012, 51, 7711-7721.	1.9	40
11941	⁸⁷Sr Solid-State NMR as a Structurally Sensitive Tool for the Investigation of Materials: Antiosteoporotic Pharmaceuticals and Bioactive Glasses. Journal of the American Chemical Society, 2012, 134, 12611-12628.	6.6	68
11942	Phase Transition of Mg during Hydrogenation of Mgâ€“Nb₂O₅ Evaporated Composites. Journal of Physical Chemistry C, 2012, 116, 17089-17093.	1.5	2
11943	Electronic Structure, Optical Properties, and Hydrogen Adsorption Characteristics of Supercubane-Based Three-Dimensional Porous Carbon. Journal of Physical Chemistry C, 2012, 116, 25015-25021.	1.5	20
11944	Controlled Synthesis of Rh Nanoparticles on TiO₂(110) via Rh(CO)₂(acac). Journal of Physical Chemistry C, 2012, 116, 11987-11993.	1.5	13
11945	Density Functional Theory Study on the Role of Ceria Addition in TixCe1â€“xO2 Adsorbents for Thiophene Adsorption. Journal of Physical Chemistry C, 2012, 116, 3457-3466.	1.5	25
11946	The Importance of Attractive Three-Point Interaction in Enantioselective Surface Chemistry: Stereospecific Adsorption of Serine on the Intrinsically Chiral Cu{531} Surface. Journal of the American Chemical Society, 2012, 134, 9615-9621.	6.6	47
11947	Catalytic Activity of Au and Au₂ on the h-BN Surface: Adsorption and Activation of O₂. Journal of Physical Chemistry C, 2012, 116, 9054-9062.	1.5	84
11948	Half-Metallic Properties Induced by Fluorine in Aluminum Nitride Nanosheet. Journal of the Physical Society of Japan, 2012, 81, 044705.	0.7	2
11949	Atomic-Scale Study of Ambient-Pressure Redox-Induced Changes for an Oxide-Supported Submonolayer Catalyst: VO_x/Î±-TiO₂(110). Journal of Physical Chemistry Letters, 2012, 3, 2845-2850.	2.1	20

#	Article	IF	Citations
11950	Si/Ge Double-Layered Nanotube Array as a Lithium Ion Battery Anode. ACS Nano, 2012, 6, 303-309.	7.3	225
11951	Formaldehyde Decomposition and Coupling on V(100): A First-Principles Study. Journal of Physical Chemistry C, 2012, 116, 10639-10648.	1.5	7
11952	First principles calculation on thermal stability of metastable precipitates in Mgâ€“Gd binary alloys. Materials Science and Technology, 2012, 28, 794-798.	0.8	7
11953	Tuning of the Surface-Exposing and Photocatalytic Activity for AgX (X = Cl and Br): A Theoretical Study. Journal of Physical Chemistry C, 2012, 116, 19372-19378.	1.5	31
11954	Dynamics of Nitrogen Scattering off N-Covered Ag(111). Journal of Physical Chemistry C, 2012, 116, 21903-21912.	1.5	14
11955	Structural, electronic, and polarization properties of Bi2ZnTiO6 supercell from first-principles. Journal of Applied Physics, 2012, 111, 114101.	1.1	9
11956	Ab Initio Modeling of Î±-GeTe(111) Surfaces. Journal of Physical Chemistry C, 2012, 116, 15801-15811.	1.5	55
11957	Periodic DFT Study of Acidic Trace Atmospheric Gas Molecule Adsorption on Ca- and Fe-Doped MgO(001) Surface Basic Sites. Journal of Physical Chemistry A, 2012, 116, 7950-7958.	1.1	17
11958	First-Principles Prediction of Intermediate Products in the Decomposition of Metal Amidoboranes. Journal of Physical Chemistry C, 2012, 116, 26728-26734.	1.5	8
11959	Coverage-Dependent Structural Evolution in the Interaction of NO₂ with Au{111}. Journal of Physical Chemistry C, 2012, 116, 5637-5645.	1.5	5
11960	Influence of Dipoleâ€“Dipole Interactions on Coverage-Dependent Adsorption: CO and NO on Pt(111). Langmuir, 2012, 28, 8408-8417.	1.6	67
11961	Melanin films on Au(1 1 1): Adsorption and molecular conductance. Organic Electronics, 2012, 13, 1844-1852.	1.4	4
11962	The effect of pressure on the elastic properties and seismic anisotropy of diopside and jadeite from atomic scale simulation. Physics of the Earth and Planetary Interiors, 2012, 192-193, 81-89.	0.7	28
11963	The CuPL defect and the Cus1Cui3 complex. Physica B: Condensed Matter, 2012, 407, 2967-2969.	1.3	4
11964	Theoretical study of band gap in CuAlO2: Pressure dependence and self-interaction correction. Physica B: Condensed Matter, 2012, 407, 2861-2863.	1.3	2
11965	Three carbon pairs in Si. Physica B: Condensed Matter, 2012, 407, 2981-2984.	1.3	10
11966	First principles study of O defects in CdSe. Physica B: Condensed Matter, 2012, 407, 2841-2845.	1.3	9
11967	First-principles study of the segregation of boron dopants near the interface between crystalline Si and amorphous SiO2. Physica B: Condensed Matter, 2012, 407, 2989-2992.	1.3	7

#	Article	IF	Citations
11968	Electronic structure of Î±-Al2O3 slabs: A local environment study. Physica B: Condensed Matter, 2012, 407, 3093-3095.	1.3	6
11969	Ab initio study of the structural, electronic and elastic properties of AgSbTe2, AgSbSe2, Pr3AlC, Ce3AlC, Ce3AlN, La3AlC and La3AlN compounds. Physica B: Condensed Matter, 2012, 407, 3320-3327.	1.3	13
11970	Ab initio study of the structural, electronic, elastic and magnetic properties of Cu2GdIn, Ag2GdIn and Au2GdIn. Physica B: Condensed Matter, 2012, 407, 3328-3334.	1.3	8
11971	Impurity doping into Mg2Sn: A first-principles study. Physica B: Condensed Matter, 2012, 407, 3493-3498.	1.3	17
11972	High pressure structural phase transitions of PbPo. Physica B: Condensed Matter, 2012, 407, 3520-3523.	1.3	5
11973	In assisted realization of p-type C-doped ZnO: A first-principles study. Physica B: Condensed Matter, 2012, 407, 3539-3542.	1.3	17
11974	Studies of the structural, electronic and dielectric properties of Ca1â^'xSrxTiO3. Physica B: Condensed Matter, 2012, 407, 3705-3708.	1.3	4
11975	Pressure-dependent dynamical properties of Zn-based IIâ€“VI semiconductors. Physica B: Condensed Matter, 2012, 407, 3570-3574.	1.3	9
11976	Ab initio study of some fundamental properties of the M3X (M=Cr, V; X=Si, Ge) compounds. Physica B: Condensed Matter, 2012, 407, 3591-3595.	1.3	4
11977	Structural and elastic properties of TiN under high pressure. Physica B: Condensed Matter, 2012, 407, 3617-3621.	1.3	10
11978	Dependence of optical properties of monoclinic MnWO4 on the electric field of incident light. Physica B: Condensed Matter, 2012, 407, 3654-3659.	1.3	6
11979	First and second harmonic generation of the XAl2Se4 (X=Zn,Cd,Hg) defect chalcopyrite compounds. Physica B: Condensed Matter, 2012, 407, 3760-3766.	1.3	20
11980	Ga vacancy induced ferromagnetism enhancement and electronic structures of RE-doped GaN. Physica B: Condensed Matter, 2012, 407, 3818-3827.	1.3	15
11981	Structure, bonding and stability of semi-carbides M2C and sub-carbides M4C (M=V, Cr, Nb, Mo, Ta, W): A first principles investigation. Physica B: Condensed Matter, 2012, 407, 3833-3838.	1.3	28
11982	First-principles study of CaTiO3 oxygen-vacancies (001) surface. Physica B: Condensed Matter, 2012, 407, 3970-3974.	1.3	7
11983	Electronic and magnetic properties of Mn-doped ZnO: Total-energy calculations. Physica B: Condensed Matter, 2012, 407, 3975-3981.	1.3	6
11984	A systematic spectroscopic study of the FePcâ€“Si interfaces. Physica E: Low-Dimensional Systems and Nanostructures, 2012, 44, 1572-1579.	1.3	3
11985	The mechanism of spontaneous doping of boron atoms into graphene. Physica E: Low-Dimensional Systems and Nanostructures, 2012, 44, 2016-2020.	1.3	4

#	Article	IF	Citations
11986	Electromechanical switch in metallic graphene nanoribbons via twisting. Physica E: Low-Dimensional Systems and Nanostructures, 2012, 44, 2021-2026.	1.3	10
11987	The environmental dependence of redox energetics of PuO2 and Î±-Pu2O3: A quantitative solution from. Physics Letters, Section A: General, Atomic and Solid State Physics, 2012, 376, 2672-2676.	0.9	10
11988	Understanding the chiral selectivity of gold nanotubes. Physics Letters, Section A: General, Atomic and Solid State Physics, 2012, 376, 2707-2711.	0.9	6
11989	Dielectric and piezoelectric responses of nylon-7: A first-principles study. Polymer, 2012, 53, 2751-2757.	1.8	12
11990	First-principles investigation of the ternary scandium based inverse-perovskite carbides Sc3AC (AÂ=ÂAl,) Tj ETQq0 0 0 rgBT /Overlock 10	1.5	22
11991	Structure, elasticity, thermodynamics and high pressure behavior of ZnB4O7 and CdB4O7. Solid State Sciences, 2012, 14, 1080-1085.	1.5	12
11992	Synthesis, crystal structure and characterization of a new compound, Li3NaBaB6O12. Solid State Sciences, 2012, 14, 1186-1190.	1.5	22
11993	Synthesis, structure, physical properties, and electronic structure of KGaSe2. Solid State Sciences, 2012, 14, 1152-1156.	1.5	22
11994	First principles prediction of the elastic, electronic, and optical properties of Sb2S3 and Sb2Se3 compounds. Solid State Sciences, 2012, 14, 1211-1220.	1.5	124
11995	First-principles calculations of structural stability, elastic, dynamical and thermodynamic properties of SiGe, SiSn, GeSn. Superlattices and Microstructures, 2012, 52, 459-469.	1.4	70
11996	Imposing changes of band and spinâ€“orbit gaps in GaNBi. Solid State Communications, 2012, 152, 1700-1702.	0.9	15
11997	Pressure-dependent structure, mechanical and thermodynamic properties of tetragonal AsTiZr arsenide: A density functional theory study. Solid State Communications, 2012, 152, 1694-1699.	0.9	1
11998	Orbital-decomposed electronic structures of cubic zirconia. Solid State Communications, 2012, 152, 1673-1677.	0.9	8
11999	Interaction of zinc interstitial with oxygen vacancy in zinc oxide: An origin of n-type doping. Solid State Communications, 2012, 152, 1711-1714.	0.9	54
12000	First-principles studies on the structural and electronic properties of Li-ion battery cathode material CuF2. Solid State Communications, 2012, 152, 1703-1706.	0.9	20
12001	A density functional theory study on the origin of lithium-montmorillonite's conductivity at low water content: A first investigation. Solid State Communications, 2012, 152, 1862-1866.	0.9	7
12002	First principles study of the structural, elastic, electronic and optical properties of CaSrTt (Tt=Si, Ge,) Tj ETQq0 0 0 rgBT /Overlock 10 Tf	0.9	4
12003	Quintuple-period Si atomic wires with alternative double and triple modulations by metal: Mg/Si(557). Surface Science, 2012, 606, 57-61.	0.8	1

#	Article	IF	Citations
12004	Fast atom diffraction during grazing scattering from a MgO(001) surface. Surface Science, 2012, 606, 161-173.	0.8	39
12005	Strain effect on diffusion properties of oxygen vacancies in bulk and subsurface of rutile TiO2. Surface Science, 2012, 606, 186-191.	0.8	26
12006	Formation of a missing row reconstruction on a Cu(100) surface: An atom scale density functional theory based study. Surface Science, 2012, 606, 192-201.	0.8	11
12007	DFT-GGA study of NO adsorption on the LaO (001) surface of LaFeO3. Surface Science, 2012, 606, 337-343.	0.8	19
12008	Passivation effect of allylamine molecule on the electronic structure of a Si(001)â˜'(2Ã—1) surface. Surface Science, 2012, 606, 470-474.	0.8	3
12009	Relative stability of armchair, zigzag and reczag graphene edges on the Ru(0001) surface. Surface Science, 2012, 606, 485-489.	0.8	10
12010	The adsorption and reconstruction of strong electron acceptor tetracyanoethylene (TCNE) on Si(001)-(2Ã—1): A density functional theory investigation. Surface Science, 2012, 606, 523-526.	0.8	1
12011	Structural and electronic properties of cobalt carbide Co2C and its surface stability: Density functional theory study. Surface Science, 2012, 606, 598-604.	0.8	79
12012	Effect of platinum promoters on the removal of O from the surface of cobalt catalysts: A DFT study. Surface Science, 2012, 606, 634-643.	0.8	27
12013	Reactive molecular dynamic simulations of hydrocarbon dissociations on Ni(111) surfaces. Surface Science, 2012, 606, 615-623.	0.8	22
12014	Hydrogen adsorption, absorption and diffusion on and in transition metal surfaces: A DFT study. Surface Science, 2012, 606, 679-689.	0.8	380
12015	Study of the TiSi interface formed by Ti deposition on a clean Si (100) surface. Surface Science, 2012, 606, 754-761.	0.8	3
12016	Unique geometric and electronic structure of CO adsorbed on Ge(100): A DFT study. Surface Science, 2012, 606, 784-790.	0.8	6
12017	First principles investigations of hydrazine adsorption conformations on Ni(111) surface. Surface Science, 2012, 606, 766-771.	0.8	45
12018	Density functional theory-based analysis on O2 molecular interaction with the tri-s-triazine-based graphitic carbon nitride. Surface Science, 2012, 606, 892-901.	0.8	56
12019	Fe3O4 surface electronic structures and stability from GGA+U. Surface Science, 2012, 606, 872-879.	0.8	115
12020	Spin-polarized surface states on Fe-deposited Au(111) surface: A theoretical study. Surface Science, 2012, 606, 950-955.	0.8	4
12021	Polypropyleneâ€“MAlN (M=Ti, Cr) interface interactions. Surface Science, 2012, 606, 986-989.	0.8	15

#	Article	IF	Citations
12022	CO2 hydrogenation to formic acid on Ni(110). Surface Science, 2012, 606, 1050-1055.	0.8	76
12023	Structural, electronic, stability and reduction properties of perovskite surfaces: The case of rhombohedral BaCeO3. Surface Science, 2012, 606, 1078-1087.	0.8	23
12024	Surface interactions of Au(I) cyclo-trimer with Au(111) and Al(111) surfaces: A computational study. Surface Science, 2012, 606, 1100-1107.	0.8	7
12025	Theoretical study of hydrogen dissociation and diffusion on Nb and Ni co-doped Mg(0001): A synergistic effect. Surface Science, 2012, 606, L45-L49.	0.8	21
12026	A density functional theory study of CF3CH2I adsorption and reaction on Ag(111). Surface Science, 2012, 606, 1227-1232.	0.8	15
12027	Diffusion of a Ga adatom on the GaAs(001)â€¢(4Ã—4)â€heterodimer surface: A first principles study. Surface Science, 2012, 606, 1303-1307.	0.8	12
12028	Structure and properties of a model oxide-supported catalyst under redox conditions: WOx/Î±-Fe2O3 (0001). Surface Science, 2012, 606, 1367-1381.	0.8	6
12029	Ab initio study of shear strain effects on ferroelectricity at PbTiO3 thin films. Surface Science, 2012, 606, 1331-1339.	0.8	3
12030	Interfacial structure of Co porphyrins on Au(111) electrode: Interaction of porphyrin molecules with substrate. Surface Science, 2012, 606, 1560-1564.	0.8	8
12031	Mechanistic understanding of hydrogenation of acetaldehyde on Au(111): A DFT investigation. Surface Science, 2012, 606, 1608-1617.	0.8	17
12032	Surface composition of clean and oxidized Pd75Ag25(100) from photoelectron spectroscopy and density functional theory calculations. Surface Science, 2012, 606, 1777-1782.	0.8	34
12033	Adsorption behavior of iron phthalocyanine at the initial stage on Cu(100) surface. Surface Science, 2012, 606, 1749-1754.	0.8	12
12034	Structure of ordered oxide on InAs(100) surface. Surface Science, 2012, 606, 1837-1841.	0.8	5
12035	Ab-initio study of Sr-doping effects on nitric oxide adsorption on the LaO (001) surface of LaFeO3. Surface Science, 2012, 606, 1783-1789.	0.8	5
12036	A theoretical study of the structure and stability of borohydride on 3d transition metals. Surface Science, 2012, 606, 1954-1959.	0.8	23
12037	3C-SiC(001)-3 Ã— 2 reconstructed surface analyzed by high-resolution medium energy ion scattering. Surface Science, 2012, 606, 1942-1947.	0.8	4
12038	Scandium-Decorated MOF-5 as Potential Candidates for Room-Temperature Hydrogen Storage: A Solution for the Clustering Problem in MOFs. Journal of Physical Chemistry C, 2012, 116, 17336-17342.	1.5	50
12039	Ab Initio Study of Reaction Pathways Related to Initial Steps of Thermal Decomposition of the Layered Double Hydroxide Compounds. Journal of Physical Chemistry C, 2012, 116, 13679-13687.	1.5	32

#	Article	IF	Citations
12040	Strain dependence of polarization and piezoelectric response in epitaxial BiFeO₃thin films. Journal of Physics Condensed Matter, 2012, 24, 162202.	0.7	66
12041	The Intrinsic Defects, Disordering, and Structural Stability of Ba_xSr_{1â€“x}Co_yFe_{1â€“y}O_{3âˆ’Î´} Perovskite Solid Solutions. Journal of Physical Chemistry C, 2012, 116, 18605-18611.	1.5	56
12042	Phonons and electron-phonon interaction at the Sb(111) surface. Physical Review B, 2012, 86, .	1.1	26
12043	Chiral graphene nanoribbon inside a carbon nanotube: ab initio study. Nanoscale, 2012, 4, 4522.	2.8	32
12044	Calcium-based functionalization of carbon nanostructures for peptide immobilization in aqueous media. Journal of Materials Chemistry, 2012, 22, 19684.	6.7	26
12045	In situ surface coverage analysis of RuO2-catalysed HCl oxidation reveals the entropic origin of compensation in heterogeneous catalysis. Nature Chemistry, 2012, 4, 739-745.	6.6	85
12046	Physical and Chemical Nature of the Scaling Relations between Adsorption Energies of Atoms on Metal Surfaces. Physical Review Letters, 2012, 108, 116103.	2.9	233
12047	A Computational Investigation of Li₉M₃(P₂O₇)₃(PO₄)₂(M) Tj ETQq1 1 0.784	1.1	66
12048	How to fabricate a semihydrogenated graphene sheet? A promising strategy explored. Applied Physics Letters, 2012, 101, 073114.	1.5	34
12049	Anatase TiO₂ Surface Functionalization by Alkylphosphonic Acid: A DFT+D Study. Journal of Physical Chemistry C, 2012, 116, 2819-2828.	1.5	39
12050	High hydrogen-adsorption-rate material based on graphane decorated with alkali metals. Physical Review B, 2012, 86, .	1.1	52
12051	Structure determination of an amorphous compound AlB4H11. Chemical Science, 2012, 3, 3183.	3.7	13
12052	Two-Dimensional Boron Monolayer Sheets. ACS Nano, 2012, 6, 7443-7453.	7.3	690
12053	Long-range interactions between substitutional nitrogen dopants in graphene: Electronic properties calculations. Physical Review B, 2012, 86, .	1.1	91
12054	Guided Self-Assembly of Metal Atoms on Silicon Using Organic-Molecule Templating. Journal of the American Chemical Society, 2012, 134, 15312-15317.	6.6	17
12055	Native defects in second-generation topological insulators: Effect of spin-orbit interaction on Bi<mml:math xmlns:mml="http://www.w3.org/1998/Math/MathML" display="inline"><mml:msub><mml:mrow /><mml:mn>2</mml:mn></mml:msub></mml:math>Se<mml:math xmlns:mml="http://www.w3.org/1998/Math/MathML" display="inline"><mml:msub><mml:mrow /><mml:mn>3</mml:mn></mml:msub></mml:math>. Physical Review B, 2012, 86, .	1.1	117
12056	Characterization of zero-point vibration in one-component crystals. Europhysics Letters, 2012, 98, 66007.	0.7	12
12057	First-Principles Investigation of Bilayer Fluorographene. Journal of Physical Chemistry C, 2012, 116, 19240-19245.	1.5	43

#	Article	IF	Citations
12058	Electronic properties and STM images of doped bilayer graphene. Physical Review B, 2012, 85, .	1.1	30
12059	Understanding the Metal-Directed Growth of Single-Crystal M-TCNQF₄ Organic Nanowires with Time-Resolved, in Situ X-ray Diffraction and First-Principles Theoretical Studies. Journal of the American Chemical Society, 2012, 134, 14353-14361.	6.6	17
12060	Semimetallic dense hydrogen above 260ÂGPa. Proceedings of the National Academy of Sciences of the United States of America, 2012, 109, 9766-9769.	3.3	27
12061	Semiconducting allotrope of graphene. Nanotechnology, 2012, 23, 385704.	1.3	36
12062	Oxygen density dependent band gap of reduced graphene oxide. Journal of Applied Physics, 2012, 111, .	1.1	160
12063	Quantum confinement and surface relaxation effects in rutile TiO<mml:math xmlns:mml="http://www.w3.org/1998/Math/MathML" display="inline"><mml:msub><mml:mrow /><mml:mn>2</mml:mn></mml:msub></mml:math>nanowires. Physical Review B, 2012, 85, .	1.1	11
12064	Effect of hydrogen passivation on the electronic structure of ionic semiconductor nanostructures. Physical Review B, 2012, 85, .	1.1	38
12065	Effect of nitrogen impurities on the physical properties of ZnO nanowires: First-principles study. Physical Review B, 2012, 85, .	1.1	13
12066	Correcting density functional theory for accurate predictions of compound enthalpies of formation: Fitted elemental-phase reference energies. Physical Review B, 2012, 85, .	1.1	454
12067	Intrinsic Piezoelectricity in Two-Dimensional Materials. Journal of Physical Chemistry Letters, 2012, 3, 2871-2876.	2.1	871
12068	Modified embedded atom method potential for Al, Si, Mg, Cu, and Fe alloys. Physical Review B, 2012, 85, .	1.1	267
12069	Electrical properties of improper ferroelectrics from first principles. Physical Review B, 2012, 86, .	1.1	44
12070	Theoretical Insight into the Structural Stability of KZnB3O6Polymorphs with Different BOxPolyhedral Networks. Inorganic Chemistry, 2012, 51, 6762-6770.	1.9	11
12071	Stability, Electronic and Magnetic Properties of In-Plane Defects in Graphene: A First-Principles Study. Journal of Physical Chemistry C, 2012, 116, 8161-8166.	1.5	187
12072	Mn monolayer modified Rh for syngas-to-ethanol conversion: a first-principles study. Nanoscale, 2012, 4, 1123-1129.	2.8	32
12073	Influence of indium cluster on the high and constant background electron density in ternary In_xGa_{1â^'x}N alloys. Applied Physics Letters, 2012, 101, 062102.	1.5	8
12074	Half-metallicity and magnetism of GeTe doped with transition metals V, Cr, and Mn: A theoretical study from the viewpoint of application in spintronics. Journal of Applied Physics, 2012, 112, 053902.	1.1	20
12075	Density functional theory study of phase stability, vibrational, and electronic properties of Mo3Al2C. Physical Review B, 2012, 86, .	1.1	10

#	Article	IF	Citations
12076	Neural network interatomic potential for the phase change material GeTe. Physical Review B, 2012, 85, .	1.1	198
12077	Stability and Segregation of B and P Dopants in Si/SiO₂ Coreâ€“Shell Nanowires. Nano Letters, 2012, 12, 5068-5073.	4.5	19
12078	Formation and Stability of Cellular Carbon Foam Structures: AnAbÂInitioStudy. Physical Review Letters, 2012, 109, 135501.	2.9	27
12079	High pressure phase determination and electronic properties of lithiumamidoborane. Applied Physics Letters, 2012, 101, 111902.	1.5	4
12080	Tuning the band gaps and work functions via topology and carbon concentration: a first-principles investigation of Cx(BN)y compounds. Physical Chemistry Chemical Physics, 2012, 14, 4391.	1.3	24
12081	Crystal Chemistry in the Barium Fluoride Chloride System. Crystal Growth and Design, 2012, 12, 1124-1131.	1.4	22
12082	Electronic and structural properties of diamond (001) surfaces terminated by selected transition metals. Physical Review B, 2012, 86, .	1.1	26
12083	Probing graphene grain boundaries with optical microscopy. Nature, 2012, 490, 235-239.	13.7	352
12084	Computational Study of Structural, Electronic, and Optical Properties of Crystalline NH₄N₃. Journal of Physical Chemistry C, 2012, 116, 16910-16917.	1.5	29
12085	The structure of fluoride-containing bioactive glasses: new insights from first-principles calculations and solid state NMR spectroscopy. Journal of Materials Chemistry, 2012, 22, 12599.	6.7	88
12086	Pressure effects on the electronic and optical properties of<mml:math xmlns:mml="http://www.w3.org/1998/Math/MathML" display="inline"><mml:mi>A</mml:mi></mml:math>WO<mml:math xmlns:mml="http://www.w3.org/1998/Math/MathML" display="inline"><mml:msub><mml:mrow		

#	Article	IF	Citations
12094	Quasi-Molecular and Atomic Phases of Dense Solid Hydrogen. Journal of Physical Chemistry C, 2012, 116, 9221-9226.	1.5	78
12095	Stability and crystal structures of iron carbides: A comparison between the semi-empirical modified embedded atom method and quantum-mechanical DFT calculations. Physical Review B, 2012, 85, .	1.1	23
12096	A multiscale physical model for the transient analysis of PEM water electrolyzer anodes. Physical Chemistry Chemical Physics, 2012, 14, 10215.	1.3	33
12097	Passivation of CuI Quantum Dots. Journal of Physical Chemistry C, 2012, 116, 21039-21045.	1.5	3
12098	Assessment of ten DFT methods in predicting structures of sheet silicates: Importance of dispersion corrections. Journal of Chemical Physics, 2012, 137, 114105.	1.2	117
12099	Oxygen incorporation in M2AlC (M=Ti, V, Cr). Acta Materialia, 2012, 60, 4810-4818.	3.8	53
12100	Soluteâ€“vacancy binding of the rare earths in magnesium from first principles. Acta Materialia, 2012, 60, 5151-5159.	3.8	50
12101	The stability boundary of group-III transition metal diboride ScB2 (0001) surfaces. Applied Surface Science, 2012, 258, 3328-3330.	3.1	1
12102	First-principles study on the catalytic role of Ag in the oxygen adsorption of LaMnO3(001) surface. Applied Surface Science, 2012, 258, 2602-2606.	3.1	15
12103	Density functional theory study on oxygen adsorption in LaSrCoO4: An extended cathode material for solid oxide fuel cells. Applied Surface Science, 2012, 258, 3133-3138.	3.1	22
12104	A periodic DFT study on binding of Pd, Pt and Au on the anatase TiO2 (001) surface and adsorption of CO on the TiO2 surface-supported Pd, Pt and Au. Applied Surface Science, 2012, 258, 3298-3301.	3.1	43
12105	Adsorption of ammonia on vanadiumâ€“antimony mixed oxides. Applied Surface Science, 2012, 258, 3617-3623.	3.1	10
12106	Reaction mechanism for CO oxidation on Cu(311): A density functional theory study. Applied Surface Science, 2012, 258, 3980-3985.	3.1	7
12107	Nitric oxide adsorption on Nb(110) surface. Applied Surface Science, 2012, 258, 4428-4435.	3.1	10
12108	Tuning of CeO2 buffer layers for coated superconductors through doping. Applied Surface Science, 2012, 260, 32-35.	3.1	29
12109	First-principles study of the adsorption of lysine on hydroxyapatite (100) surface. Applied Surface Science, 2012, 258, 4911-4916.	3.1	38
12110	Effect of dangling bonds of ultra-thin silicon film surface on electronic states of internal atoms. Applied Surface Science, 2012, 258, 5265-5269.	3.1	7
12111	Investigation of the doped transition metal promotion effect on CO2 chemisorption on Ni (111). Applied Surface Science, 2012, 258, 6239-6245.	3.1	17

#	Article	IF	Citations
12112	Adsorption and surface reaction of bis-diethylaminosilane as a Si precursor on an OH-terminated Si (0) Tj ETQq0 0 0 rgBT /Overlock 10 T	3.1	27
12113	First-principles study on the electronic structure and optical properties for SnO2 with oxygen vacancy. Applied Surface Science, 2012, 258, 6987-6992.	3.1	32
12114	Theoretical analysis of semiconductor surface passivation by adsorption of alkaline-earth metals and chalcogens. Applied Surface Science, 2012, 258, 8377-8386.	3.1	5
12115	Ab initio studies of electronic and optical properties of graphene and grapheneâ€“BN interface. Applied Surface Science, 2012, 258, 8338-8342.	3.1	33
12116	Ab-initio modeling of oxygen on the surface passivation of 3CSiC nanostructures. Applied Surface Science, 2012, 258, 8360-8365.	3.1	14
12117	Theoretical study of Cs adsorption on GaN(0001) surface. Applied Surface Science, 2012, 258, 7425-7429.	3.1	54
12118	Insight into CH4 dissociation on NiCu catalyst: A first-principles study. Applied Surface Science, 2012, 258, 8177-8184.	3.1	59
12119	Study on adsorption of O2 on LaFe1â^'xMgxO3 (010) surface by density function theory calculation. Applied Surface Science, 2012, 258, 8678-8682.	3.1	6
12120	Effects of interactions between NiM (M=Mn, Fe, Co and Cu) bimetals with MgO (100) on the adsorption of CO2. Applied Surface Science, 2012, 258, 8831-8836.	3.1	17
12121	Effect of SO3 on elemental mercury adsorption on a carbonaceous surface. Applied Surface Science, 2012, 258, 8853-8860.	3.1	38
12122	Theoretical prediction of hydrogen storage on Li decorated planar boron sheets. Applied Surface Science, 2012, 258, 8874-8879.	3.1	29
12123	The austenite/É› martensite interface: A first-principles investigation of the fcc Fe(1 1 1)/hcp Fe(0 0 0 1) system. Applied Surface Science, 2012, 258, 9977-9981.	3.1	69
12124	Influence of Mn concentration on the electronic and magnetic properties of Mn doped <mml:math altimg="si0039.gif" overflow="scroll" xmlns:xocs="http://www.elsevier.com/xml/xocs/dtd" xmlns:xs="http://www.w3.org/2001/XMLSchema" xmlns:xsi="http://www.w3.org/2001/XMLSchema-instance" xmlns="http://www.elsevier.com/xml/ja/dtd" xmlns:ja="http://www.elsevier.com/xml/ja/dtd" xmlns:mml="http://www.w3.org/1998/Math/MathML" xmlns:tb="http://www.elsevier.com/xml/common/table/dtd" xmlns:sb="http://www.elsevier.com/xml/co	1.0	3
12125	First principle electronic structure calculations of ternary alloys Hg1â^'xMnxTe in zinc-blende structure. Journal of Magnetism and Magnetic Materials, 2012, 324, 3017-3023.	1.0	2
12126	Structural, electronic and magnetic properties of layered REB2C compounds (RE=Dy, Tm, Lu). Journal of Solid State Chemistry, 2012, 191, 121-128.	1.4	12
12127	First-principles study of the structural and elastic properties of Cr2AlX (X=N, C) compounds. Journal of Solid State Chemistry, 2012, 191, 147-152.	1.4	33
12128	First-principles study on stability, energy gaps, optical phonon and related parameters of In1â^'xâ^'yAlxGayAs alloys. Journal of Solid State Chemistry, 2012, 192, 161-167.	1.4	5
12129	The complex metal-rich boride Ti1+xRh2â^'x+yIr3â^'yB3 (x=0.68, y=1.06) with a new structure type containing B4 zigzag fragments: Synthesis, crystal chemistry and theoretical calculations. Journal of Solid State Chemistry, 2012, 192, 113-119.	1.4	23

#	Article	IF	Citations
12130	Defect and phase stability of solid solutions of Mg2X with an antifluorite structure: An ab initio study. Journal of Solid State Chemistry, 2012, 193, 133-136.	1.4	22
12131	Elastic and electronic properties of the Ti5X3 (X=Si, Ge, Sn, Pb) compounds from first-principles calculations. Journal of Solid State Chemistry, 2012, 194, 127-134.	1.4	8
12132	First-principles investigation of the thermo-physical properties of Ca3Si4. Journal of Solid State Chemistry, 2012, 194, 179-187.	1.4	13
12133	Theoretical study of the origin of the enhanced visible light photocatalytic activity of N-doped CsTaWO6: Charge compensation effects modulated by N and other defects. Journal of Solid State Chemistry, 2012, 194, 352-360.	1.4	14
12134	CdSe/CdTe interface band gaps and band offsets calculated using spinâ€“orbit and self-energy corrections. Materials Science and Engineering B: Solid-State Materials for Advanced Technology, 2012, 177, 1460-1464.	1.7	15
12135	A Density Functional Theory study of the chemical surface modification of Î²-SiC nanopores. Materials Science and Engineering B: Solid-State Materials for Advanced Technology, 2012, 177, 1482-1486.	1.7	6
12136	Theoretical study of charge trapping levels in silicon nitride using the LDA-1/2 self-energy correction scheme for excited states. Materials Science and Engineering B: Solid-State Materials for Advanced Technology, 2012, 177, 1497-1500.	1.7	7
12137	First principles calculations of structural, electronic and optical properties of zinc aluminum oxide. Materials Science in Semiconductor Processing, 2012, 15, 301-307.	1.9	40
12138	Direct octane fuel cells: A promising power for transportation. Nano Energy, 2012, 1, 448-455.	8.2	118
12139	GaN/ZnO superlattice nanowires as photocatalyst for hydrogen generation: A first-principles study on electronic and magnetic properties. Nano Energy, 2012, 1, 488-493.	8.2	60
12140	DFT study of H2 adsorption on Pd-decorated single walled carbon nanotubes with C-vacancies. International Journal of Hydrogen Energy, 2012, 37, 10156-10164.	3.8	34
12141	Nanoporous PtCo and PtNi alloy ribbons for methanol electrooxidation. International Journal of Hydrogen Energy, 2012, 37, 10489-10498.	3.8	125
12142	Band gap of C3N4 in the GW approximation. International Journal of Hydrogen Energy, 2012, 37, 11072-11080.	3.8	208
12143	Energetics of Ti and Zr transition metals in D03-Fe3Al and its Î£5 (310) [001] grain boundary. Intermetallics, 2012, 22, 251-254.	1.8	7
12144	Dimorphic LaPdSn and ErAgSn â€“ A first principles study. Intermetallics, 2012, 20, 33-38.	1.8	5
12145	Thermodynamic properties of Laves phases in the Mgâ€“Alâ€“Ca system at finite temperature from first-principles. Intermetallics, 2012, 22, 17-23.	1.8	28
12146	First-principles investigation of the Alâ€“Siâ€“Sr ternary system: Ground state determination and mechanical properties. Intermetallics, 2012, 21, 31-44.	1.8	19
12147	An alternative DFT-based model for calculating structural and elastic properties of random binary HCP, FCC and BCC alloys: Mgâ€“Li system as test case. Intermetallics, 2012, 21, 88-96.	1.8	15

#	Article	IF	Citations
12148	First-principles study of B2-like intermetallics LaMg and YMg. Intermetallics, 2012, 22, 218-225.	1.8	4
12149	Electronic structure and mechanical properties of Sc3AC (AÂ=ÂAl, Ga, In, Tl) and Sc3BN(BÂ=ÂAl, In): Ab-initio study. Intermetallics, 2012, 23, 39-48.	1.8	30
12150	Investigation of structural, electronic and thermodynamic properties of Ni6Si2B and Ni6Ge2B compounds with the Fe2P-type structure. Intermetallics, 2012, 24, 73-78.	1.8	4
12151	First-principles investigations of elastic, electronic and thermodynamic properties of Al12X (XÂ=ÂMo, W) Tj ETQq1 1 0.784314 rgBT /	1.8	17
12152	Effect of interstitial atoms on the stability and electronic structure of Re3Zn alloy: First-principles calculations. Intermetallics, 2012, 24, 95-98.	1.8	2
12153	First-principles calculations on finite temperature elastic properties of B2-AlRE (REÂ=ÂY, Tb, Pr, Nd, Dy) intermetallics. Intermetallics, 2012, 26, 57-61.	1.8	5
12154	The nature of the atomic-level structure in the Cuâ€“Zr binary metallic glasses. Intermetallics, 2012, 26, 8-10.	1.8	17
12155	First principle study of the effect of Ti and Zr transition metals located in bulk D03Fe3Al and â^5 (310)[001] grain boundary. Intermetallics, 2012, 28, 1-10.	1.8	4
12156	First-principles studies of structural stabilities and enthalpies of formation of refractory intermetallics: TM and TM3 (TÂ=ÂTi, Zr, Hf; MÂ=ÂRu, Rh, Pd, Os, Ir, Pt). Intermetallics, 2012, 28, 16-24.	1.8	70
12157	Theoretical study of structure, magnetism and lattice vibrations of intermetallics Lu2(Fe, T)17 and their hydrides. Intermetallics, 2012, 28, 77-83.	1.8	10
12158	Site occupation behavior of sulfur and phosphorus in NiAl, TiAl and FeAl. Intermetallics, 2012, 28, 156-163.	1.8	10
12159	First-principles study of pressure-induced magnetic transition in siderite FeCO3. Journal of Alloys and Compounds, 2012, 510, L1-L4.	2.8	13
12160	First-principles calculations of electronic and optical properties of Ti-doped monoclinic HfO2. Journal of Alloys and Compounds, 2012, 510, 78-82.	2.8	30
12161	Ab initio lattice dynamics of Ni2MnX (X=Sn, Sb) magnetic shape memory alloys. Journal of Alloys and Compounds, 2012, 511, 9-13.	2.8	20
12162	Structural phase transition, elastic and electronic properties of TmSb and YbSb: A LSDA + U study under pressure. Journal of Alloys and Compounds, 2012, 515, 26-31.	2.8	12
12163	First principles studies of band structure and electronic properties of ZnSe. Journal of Alloys and Compounds, 2012, 513, 294-299.	2.8	20
12164	Ferroelectric and nonlinear optical properties of the LiNbO3-type ZnGeO3 from first-principles study. Journal of Alloys and Compounds, 2012, 514, 113-119.	2.8	16
12165	Electronic, structural, and optical properties of host materials for inorganic phosphors. Journal of Alloys and Compounds, 2012, 513, 630-640.	2.8	27

#	Article	IF	Citations
12166	Magnetism-induced ductility in NiAl intermetallic alloys with Fe additions: Theory and experiment. Journal of Alloys and Compounds, 2012, 519, 101-105.	2.8	8
12167	High-pressure elasticity and lattice dynamics of Mg2La from first principles. Journal of Alloys and Compounds, 2012, 520, 93-97.	2.8	12
12168	Effects of nitrogen concentration on N-doped anatase TiO2: Density functional theory and Hubbard U analysis. Journal of Alloys and Compounds, 2012, 522, 46-50.	2.8	37
12169	A first principles calculations of structural, electronic, magnetic and dynamical properties of mononitrides FeN and CoN. Journal of Alloys and Compounds, 2012, 522, 106-113.	2.8	26
12170	First principles investigations on elastic and electronic properties of BaHfN2 under pressure. Journal of Alloys and Compounds, 2012, 526, 74-78.	2.8	14
12171	Structural, mechanical and electronic properties of ZnTe polymorphs under pressure. Journal of Alloys and Compounds, 2012, 529, 148-157.	2.8	13
12172	Elastic and thermodynamic properties of AuAl2 under pressures. Journal of Alloys and Compounds, 2012, 528, 115-120.	2.8	9
12173	Structural and elastic properties of LiBH4 for hydrogen storage applications. Journal of Alloys and Compounds, 2012, 534, 20-24.	2.8	62
12174	Effect of Nb and W substitutions on the stability of the A15 Mo3Si phase. Journal of Alloys and Compounds, 2012, 537, 65-70.	2.8	16
12175	Synergistic effect of Ti and F co-doping on dehydrogenation properties of MgH2 from first-principles calculations. Journal of Alloys and Compounds, 2012, 538, 205-211.	2.8	35
12176	Electronic, elastic and optical properties of zircon GdVO4 investigated from experiments and LSDA+U. Journal of Alloys and Compounds, 2012, 538, 56-60.	2.8	27
12177	First principles study on the p-type transparent conducting properties of rutile Ti1â^'xInxO2. Journal of Alloys and Compounds, 2012, 539, 221-225.	2.8	7
12178	First-principles study on the electronic structure of a LiFePO4 (010) surface adsorbed with carbon. Journal of Alloys and Compounds, 2012, 540, 121-126.	2.8	26
12179	CO hydrogenation to methanol on Cuâ€“Ni catalysts: Theory and experiment. Journal of Catalysis, 2012, 293, 51-60.	3.1	195
12180	Periodic trends of oxygen vacancy formation and Câ€“H bond activation over transition metal-doped CeO2 (1 1 1) surfaces. Journal of Catalysis, 2012, 293, 103-115.	3.1	139
12181	The energies of formation and mobilities of Cu surface species on Cu and ZnO in methanol and water gas shift atmospheres studied by DFT. Journal of Catalysis, 2012, 293, 205-214.	3.1	45
12182	Properties of nitrogen-doped titanium oxides. Journal of Crystal Growth, 2012, 350, 11-16.	0.7	10
12183	The structure and electronic properties of AlN/SrTiO3 (111) interfaces. Journal of Crystal Growth, 2012, 353, 134-139.	0.7	7

#	Article	IF	Citations
12184	Ab initio investigation of adsorption of atomic and molecular hydrogen at GaN(0001) surface. Journal of Crystal Growth, 2012, 358, 64-74.	0.7	19
12185	Spin states and hyperfine interactions of iron incorporated in MgSiO3 post-perovskite. Earth and Planetary Science Letters, 2012, 331-332, 1-7.	1.8	36
12186	Effect of chemistry on the compressibility of silicate perovskite in the lower mantle. Earth and Planetary Science Letters, 2012, 333-334, 181-190.	1.8	78
12187	The elasticity of lawsonite at high pressure and the origin of low velocity layers in subduction zones. Earth and Planetary Science Letters, 2012, 349-350, 116-125.	1.8	35
12188	Reversal segregation driven by lattice vibration for alloy nanoparticles. Calphad: Computer Coupling of Phase Diagrams and Thermochemistry, 2012, 36, 151-154.	0.7	1
12189	Critical assessment: Martensite-start temperature for the <mml:math xmlns:mml="http://www.w3.org/1998/Math/MathML" altimg="si20.gif" display="inline" overflow="scroll"><mml:mi>Î³</mml:mi><mml:mo>â†’</mml:mo><mml:mi>Îµ</mml:mi></mml:math> transformation. Calphad: Computer Coupling of Phase Diagrams and Thermochemistry, 2012, 36, 16-22.	0.7	55
12190	Grid-increment cluster expansion for polymorphic structures in alloys. Calphad: Computer Coupling of Phase Diagrams and Thermochemistry, 2012, 36, 23-27.	0.7	3
12191	First principles study of the structural stability of intermetallic compounds in the Siâ€“Zr system. Calphad: Computer Coupling of Phase Diagrams and Thermochemistry, 2012, 36, 118-126.	0.7	19
12192	Thermodynamic modeling of the Geâ€“Sc system supported by key experiments and first-principles calculation. Calphad: Computer Coupling of Phase Diagrams and Thermochemistry, 2012, 37, 18-24.	0.7	11
12193	Thermodynamic description of the Geâ€“Na and Geâ€“K systems using the CALPHAD approach supported by first-principles calculations. Calphad: Computer Coupling of Phase Diagrams and Thermochemistry, 2012, 37, 72-76.	0.7	11
12194	Thermodynamic assessment of Auâ€“Ho and Auâ€“Tm binary systems. Calphad: Computer Coupling of Phase Diagrams and Thermochemistry, 2012, 37, 87-93.	0.7	9
12195	Elastic, phonon and thermodynamic properties of Mgâ€“Ga compounds from first-principles calculations. Calphad: Computer Coupling of Phase Diagrams and Thermochemistry, 2012, 37, 137-144.	0.7	11
12196	Thermodynamic description of the LiNiO2â€“NiO2 pseudo-binary system and extrapolation to the Li(Co,Ni)O2â€“(Co,Ni)O2 system. Calphad: Computer Coupling of Phase Diagrams and Thermochemistry, 2012, 37, 100-107.	0.7	32
12197	First-principles thermal equation of state of tungsten carbide. Computational Materials Science, 2012, 59, 41-47.	1.4	16
12198	Ab initio study of the effect of Zr content on elastic and electronic properties of L12â€“Al3(Sc1â^'xZrx) alloys. Computational Materials Science, 2012, 59, 87-93.	1.4	22
12199	First-principle studies of the structural, electronic and optical properties of the intermetallics semiconducting compounds RuAl2, RuGa2 and OsAl2. Computational Materials Science, 2012, 61, 20-26.	1.4	15
12200	Theoretical investigation on the magnetic and electronic properties of La2NiIrO6. Computational Materials Science, 2012, 60, 149-152.	1.4	6
12201	Strategy for the optical property studies in ultraviolet nonlinear optical crystals from density functional theory. Computational Materials Science, 2012, 60, 99-104.	1.4	71

#	Article	IF	Citations
12202	Prediction study of the elastic and thermodynamic properties of the SnMg2O4, SnZn2O4 and SnCd2O4 spinel oxides. Computational Materials Science, 2012, 60, 217-223.	1.4	16
12203	Electronic structure and elastic properties of TiB2 and ZrB2. Computational Materials Science, 2012, 61, 150-157.	1.4	39
12204	First-principles investigations on elastic and thermodynamic properties of zirconium under pressure. Computational Materials Science, 2012, 61, 42-49.	1.4	32
12205	Structural, electronic and elastic properties of the new ternary alkali metal chalcogenides KLiX (X=S,) Tj ETQq1 1 0.784314 rgBT /Ove	1.4	7
12206	Point defect concentrations of impurity carbon in tungsten. Computational Materials Science, 2012, 62, 282-284.	1.4	16
12207	Interlayer potentials for fcc (111) planes of Pdâ€“Ag random alloys. Computational Materials Science, 2012, 63, 20-27.	1.4	12
12208	Adsorption and diffusion studies of an O adatom on anatase surfaces with first principles calculations. Computational Materials Science, 2012, 63, 58-65.	1.4	14
12209	Elastic, thermodynamic, electronic and optical properties of U2Ti. Computational Materials Science, 2012, 63, 256-260.	1.4	18
12210	Electronic and magnetic properties of Fe, Co and Ni atomic chains encapsulated in BN nanotube bundle. Computational and Theoretical Chemistry, 2012, 979, 10-16.	1.1	12
12211	DFT study of Sb(III) and Sb(V) adsorption and heterogeneous oxidation on hydrated oxide surfaces. Computational and Theoretical Chemistry, 2012, 987, 103-114.	1.1	24
12212	The electronic structures and magnetic properties of N-doped ZnO with and without Zn vacancy. Computational and Theoretical Chemistry, 2012, 983, 65-68.	1.1	6
12213	Classical dynamics study of atomic oxygen over graphite (0001) with new interpolated and analytical potential energy surfaces. Computational and Theoretical Chemistry, 2012, 990, 132-143.	1.1	17
12214	Orthorhombic SrHfO3 (0 0 1) surfaces: Surface structure and electronic properties with first-principles calculations. Computational and Theoretical Chemistry, 2012, 989, 59-64.	1.1	7
12215	Structural, elastic, electronic and magnetic properties of Mn3ZnC and Mn3GeC. Computational and Theoretical Chemistry, 2012, 991, 161-164.	1.1	10
12216	On the nature of inhibition performance of imidazole on iron surface. Corrosion Science, 2012, 57, 254-259.	3.0	55
12217	Impact energy dependence of defect formation in single-walled carbon nanotubes. Chemical Physics Letters, 2012, 541, 92-95.	1.2	5
12218	Electronic structure and chemical bonding of Li4Pt3Si. Chemical Physics Letters, 2012, 542, 47-51.	1.2	3
12219	Density functional theory study of heterogeneous CO oxidation over an oxygen-enriched yttria-stabilized zirconia surface. Chemical Physics Letters, 2012, 543, 213-217.	1.2	9

#	Article	IF	Citations
12220	A theoretical evaluation and comparison of M Ce1â^'O2â^' (M = Au, Pd, Pt, and Rh) catalysts. Catalysis Communications, 2012, 27, 63-68.	1.6	13
12221	The adsorption mechanism of elemental mercury on CuO (110) surface. Chemical Engineering Journal, 2012, 200-202, 91-96.	6.6	97
12222	Comparative Structural, thermodynamic and electronic analyses of ZnAlAnâ^' hydrotalcite-like compounds (Anâ^'Clâ^', Fâ^', Brâ^', OHâ^', CO32â^' or NO3â^'): An ab initio study. Applied Clay Science, 2012, 56, 16-22.	2.6	131
12223	Thermal stability and elastic properties of Mg2X (X = Si, Ge, Sn, Pb) phases from first-principle calculations. Computational Materials Science, 2012, 51, 409-414.	1.4	86
12224	Thermal properties of BeX (X = S, Se and Te) compounds from ab initio quasi-harmonic method. Computational Materials Science, 2012, 51, 135-140.	1.4	38
12225	Stability and structures of the CFCC-TmC phases: A first-principles study. Computational Materials Science, 2012, 51, 146-150.	1.4	24
12226	First-principles calculations of a corrugated anatase TiO2 surface. Computational Materials Science, 2012, 51, 78-82.	1.4	3
12227	First-principles study of structural and mechanical properties of AgB2 and AuB2 compounds under pressure. Computational Materials Science, 2012, 51, 83-90.	1.4	43
12228	Theoretical prediction of the structural, electronic and optical properties of SnB2O4 (B = Mg, Zn, Cd). Computational Materials Science, 2012, 51, 194-205.	1.4	25
12229	The electronic, elastic and structural properties of Pdâ€"Zr intermetallic. Computational Materials Science, 2012, 51, 1-6.	1.4	21
12230	First-principles calculations on the crystal, electronic structures and elastic properties of Ag-rich Î³â€² phase approximates in Alâ€"Ag alloys. Computational Materials Science, 2012, 51, 415-421.	1.4	4
12231	Structural, elastic, electronic, chemical bonding and thermodynamic properties of CaMg2N2 and SrMg2N2: First-principles calculations. Computational Materials Science, 2012, 53, 204-213.	1.4	12
12232	DFT study of the coverage effects for Al adsorption on Si(111) surfaces. Computational Materials Science, 2012, 53, 382-387.	1.4	4
12233	Origin of the rigidity in tetragonal MB (M=Cr, Mo and W) and softening of defective WB: First-principles investigations. Computational Materials Science, 2012, 53, 460-463.	1.4	15
12234	First-principles calculations on surface hydroxyl impurities in BaF2. Computational Materials Science, 2012, 53, 220-225.	1.4	2
12235	Alloying element additions to Ni3Al: Site preferences and effects on elastic properties from first-principles calculations. Computational Materials Science, 2012, 53, 436-443.	1.4	125
12236	Structural, electronic and elastic properties of V5Si3 phases from first-principles calculations. Computational Materials Science, 2012, 53, 169-174.	1.4	20
12237	Effects of pressure on the elasticity and stability of zircon (ZrSiO4): First-principle investigations. Computational Materials Science, 2012, 54, 157-164.	1.4	25

#	Article	IF	Citations
12238	First-principle study of Mn adsorption on ZnO surfaces: Structural and magnetic properties. Computational Materials Science, 2012, 54, 105-108.	1.4	9
12239	First-principle calculations of structural, electronic and optical properties of BaHfxTi1â^'xO3. Computational Materials Science, 2012, 54, 119-124.	1.4	8
12240	Electronic structure and optical transition in heavy metal doped ZnO by first-principle calculations. Computational Materials Science, 2012, 54, 75-80.	1.4	22
12241	First-principles studies of structural, electronic and optical properties of AB2 (A=Si, Ge and B=O, S) nanotubes. Computational Materials Science, 2012, 54, 84-90.	1.4	4
12242	Tailoring the band gap of GaN codoped by VO for enhanced solar energy conversion from first-principles calculations. Computational Materials Science, 2012, 54, 101-104.	1.4	2
12243	Theory study of structural parameters, elastic stiffness, electronic structures and lattice dynamics of RBRh3 (R=Sc, Y, La and Lu). Computational Materials Science, 2012, 54, 336-344.	1.4	4
12244	Structural and electronic properties of the hydrogen storage compound Ca(BH4)2Â·2NH3 from first-principles. Computational Materials Science, 2012, 54, 345-349.	1.4	3
12245	A theoretical investigation of the stability of crystalline silicon dicarbide. Computational Materials Science, 2012, 55, 186-191.	1.4	7
12246	First-principles study of (Ti5â^'xMgx)Si3 phases with the hexagonal D88 structure: Elastic properties and electronic structure. Computational Materials Science, 2012, 54, 287-292.	1.4	16
12247	First-principles investigation on diffusion and permeation behaviors of hydrogen isotopes in molybdenum. Computational Materials Science, 2012, 54, 32-36.	1.4	13
12248	The structure, elastic, electronic properties and Debye temperature of M2AlC (MV, Nb and Ta) under pressure from first-principles. Computational Materials Science, 2012, 54, 16-22.	1.4	39
12249	Electronic band structure of the Pt(111) surface: An ab initio and tight-binding study â€“ I. Computational Materials Science, 2012, 56, 141-146.	1.4	7
12250	First-principles study of grain boundary embrittlement in Feâ€“Niâ€“S alloy. Computational Materials Science, 2012, 55, 17-22.	1.4	16
12251	First-principles determination of the absolute band-edge positions of BiOX (X=F, Cl, Br, I). Computational Materials Science, 2012, 55, 166-170.	1.4	27
12252	First-principles calculations of structural, elastic and electronic properties of Nb2SnC under pressure. Computational Materials Science, 2012, 55, 142-146.	1.4	37
12253	Calcium-decorated graphene for hydrogen storage: A van der Waals density functional study. Computational Materials Science, 2012, 55, 180-185.	1.4	33
12254	Ab initio calculations of magnetic properties of Ag-doped GaN. Computational Materials Science, 2012, 55, 171-174.	1.4	13
12255	Lattice dynamics of PbTe polymorphs from first principles. Computational Materials Science, 2012, 56, 18-24.	1.4	10

#	Article	IF	Citations
12256	Computational study of super cell Al-substituted single-walled carbon nanotubes as CO sensor. Computational Materials Science, 2012, 58, 45-50.	1.4	18
12257	Structural stability, phase transition, and mechanical and electronic properties of transition metal nitrides MN (M=Tc, Re, Os, and Ir): First-principles calculations. Computational Materials Science, 2012, 56, 116-121.	1.4	20
12258	First-principles investigation of adsorption of N2O on the anatase TiO2 (101) and the CO pre-adsorbed TiO2 surfaces. Computational Materials Science, 2012, 58, 24-30.	1.4	21
12259	Formaldehyde adsorption on pristine, Al-doped and mono-vacancy defected boron nitride nanosheets: A first principles study. Computational Materials Science, 2012, 56, 122-130.	1.4	76
12260	Ab initio study of some fundamental physical properties of the cubic inverse-perovskite Mn3ZnC and Mn3GeC. Computational Materials Science, 2012, 58, 162-166.	1.4	5
12261	Atomic and electronic structures of Si[001] (130) symmetric tilt grain boundaries based on first-principles calculations. Computational Materials Science, 2012, 58, 38-44.	1.4	13
12262	Hybrid density-functional calculations of structural, elastic and electronic properties for a series of cubic perovskites CsMF3 (M=Ca, Cd, Hg, and Pb). Computational Materials Science, 2012, 58, 101-112.	1.4	28
12263	Structural, electronic, elastic and thermodynamic properties of CaAl2Zn2 compound under different pressures. Computational Materials Science, 2012, 59, 33-40.	1.4	3
12264	On the limitations of the DFT+U approach to energetics of actinides. Computational Materials Science, 2012, 59, 48-56.	1.4	6
12265	As(III) immobilization on gibbsite: Investigation of the complexation mechanism by combining EXAFS analyses and DFT calculations. Geochimica Et Cosmochimica Acta, 2012, 83, 205-216.	1.6	56
12266	Cation distribution and mixing thermodynamics in Fe/Ni thiospinels. Geochimica Et Cosmochimica Acta, 2012, 88, 275-282.	1.6	21
12267	Periodic Trends in Adsorption and Activation Energies for Heterometallic Diffusion on (100) Transition Metal Surfaces. Journal of Physical Chemistry C, 2012, 116, 22469-22475.	1.5	8
12268	First-principles study of phase stability of Ti2N under pressure. Physical Review B, 2012, 86, .	1.1	9
12269	Tuning Electronic Structure of Bilayer MoS₂ by Vertical Electric Field: A First-Principles Investigation. Journal of Physical Chemistry C, 2012, 116, 21556-21562.	1.5	297
12270	Structural and magnetic analysis of epitaxial films of Gd-doped ZnO. Physical Review B, 2012, 85, .	1.1	35
12271	Orbital ordering under reduced symmetry in transition metal perovskites: Oxygen vacancy in SrTiO<mml:math xmlns:mml="http://www.w3.org/1998/Math/MathML" display="inline"><mml:msub><mml:mrow /><mml:mn>3</mml:mn></mml:msub></mml:math>. Physical Review B, 2012, 86, .	1.1	49
12272	In- and Out-Dependent Interactions of Iron with Carbon Nanotubes. Journal of Physical Chemistry C, 2012, 116, 16461-16466.	1.5	30
12273	Hexagonal<mml:math xmlns:mml="http://www.w3.org/1998/Math/MathML" display="inline"><mml:mi>A</mml:mi><mml:mi>B</mml:mi><mml:mi>C</mml:mi></mml:math>Semiconductors as Ferroelectrics. Physical Review Letters, 2012, 109, 167602.	2.9	114

#	Article	IF	Citations
12274	Geometric Arrangement of Components in Bimetallic PdZn/Pd(111) Surfaces Modified by CO Adsorption: A Combined Study by Density Functional Calculations, Polarization-Modulated Infrared Reflection Absorption Spectroscopy, and Temperature-Programmed Desorption. Journal of Physical Chemistry C, 2012, 116, 18768-18778.	1.5	40
12275	Liâ€“Na ternary amidoborane for hydrogen storage: experimental and first-principles study. Dalton Transactions, 2012, 41, 4754.	1.6	18
12276	Predicted Lithiumâ€“Boron Compounds under High Pressure. Journal of the American Chemical Society, 2012, 134, 18599-18605.	6.6	113
12277	Mercury chemistry on brominated activated carbon. Fuel, 2012, 99, 188-196.	3.4	125
12278	Enhanced visible-light photocatalytic activity of g-C3N4â€“ZnWO4 by fabricating a heterojunction: investigation based on experimental and theoretical studies. Journal of Materials Chemistry, 2012, 22, 23428.	6.7	227
12279	Interface-driven phase separation in multifunctional materials: The case of the ferromagnetic semiconductor GeMn. Physical Review B, 2012, 85, .	1.1	22
12280	Combined ab initio, experimental, and CALPHAD approach for an improved thermodynamic evaluation of the Mgâ€“Si system. Calphad: Computer Coupling of Phase Diagrams and Thermochemistry, 2012, 37, 77-86.	0.7	19
12281	Centralâ€Atom Size Effects on the Methyl Torsions of Groupâ€…XIV Tetratolyls. Chemistry - A European Journal, 2012, 18, 13018-13024.	1.7	8
12282	Initial Decomposition of Methanol and Water on In₂O₃(110): A Periodic DFT Study. Chinese Journal of Chemistry, 2012, 30, 2036-2040.	2.6	13
12283	Synthesis and Crystallochemical Characterisation of the Intermetallic Phases La(Ag_xMg_{1â€“x})₁₂ (0.11 â‰¤ x â‰¤ 0.21), LaAg_{4+x}Mg_{2â€“x} (â€“0.15 â‰¤ x â‰¤ 1.05) and LaAg_{2+x}Mg_{2â€“x} (0 < x â‰¤ 0.45). European Journal of Inorganic Chemistry, 2012, 2012, 4811-4821.	1.0	18
12284	Accelerating VASP electronic structure calculations using graphic processing units. Journal of Computational Chemistry, 2012, 33, 2581-2589.	1.5	143
12285	Theoretical studies of the structural, electronic, and optical properties of Cu₂HgGeS₄. Physica Status Solidi (B): Basic Research, 2012, 249, 2202-2206.	0.7	13
12286	Theoretical study of the magnetic properties of ordered vacancies in 2D hexagonal structures: Graphene, 2D-SiC, and h-BN. JETP Letters, 2012, 95, 555-559.	0.4	29
12287	Chemical and deformational interactions in solid solution of carbon in nickel. Physics of Metals and Metallography, 2012, 113, 831-835.	0.3	6
12288	Electronic structure of the CuBS2 crystal. Physics of the Solid State, 2012, 54, 1764-1767.	0.2	4
12289	Half-metallicity in Rh-doped TiO2 from ab initio calculations. European Physical Journal B, 2012, 85, 1.	0.6	5
12290	Tuning Fermi level within half-metallic gap in Co-based Heusler alloys. European Physical Journal B, 2012, 85, 1.	0.6	8
12291	Electronic and optical properties of Full-Heusler alloy Fe3â^'xMnxSi. European Physical Journal B, 2012, 85, 1.	0.6	18

#	Article	IF	Citations
12292	A density functional theory study of ordered oxygen overlayers on Ir(100). European Physical Journal B, 2012, 85, 1.	0.6	6
12293	Dielectric function of graphene based quantum dot under the uniaxial stress. European Physical Journal B, 2012, 85, 1.	0.6	2
12294	Effects of plasmon pole models on the G0W0 electronic structure of various oxides. European Physical Journal B, 2012, 85, 1.	0.6	24
12295	High performance silicene nanoribbon field effect transistors with current saturation. European Physical Journal B, 2012, 85, 1.	0.6	48
12296	Electronic and transport properties of a biased multilayer hexagonal boron nitride. European Physical Journal B, 2012, 85, 1.	0.6	11
12297	Efficient calculation of the polarizability: a simplified effective-energy technique. European Physical Journal B, 2012, 85, 1.	0.6	6
12298	Model of the CO oxidation reaction on Au-covered Mo(112). European Physical Journal B, 2012, 85, 1.	0.6	3
12299	Spin dependent transport behavior in small world networks. European Physical Journal B, 2012, 85, 1.	0.6	4
12300	First-principles study of elastic and structural properties of Zr3Al3C5. European Physical Journal B, 2012, 85, 1.	0.6	5
12301	Lateral interaction in Be and Mg layers on the Mo(112) surface. European Physical Journal B, 2012, 85, 1.	0.6	8
12302	Rare earth rhodium borides RRh3B (R = Y, Zr, and Nb): mechanical, thermal and optical properties. European Physical Journal B, 2012, 85, 1.	0.6	20
12303	NH3 molecular doping of silicon nanowires grown along the [112], [110], [001], and [111] orientations. Nanoscale Research Letters, 2012, 7, 308.	3.1	24
12304	The electronic and magnetic properties of functionalized silicene: a first-principles study. Nanoscale Research Letters, 2012, 7, 422.	3.1	150
12305	Doping of vanadium to nanocrystalline diamond films by hot filament chemical vapor deposition. Nanoscale Research Letters, 2012, 7, 441.	3.1	6
12306	Spontaneous formation of graphene-like stripes on high-index diamond C(331) surface. Nanoscale Research Letters, 2012, 7, 460.	3.1	3
12307	Computational simulation of the effects of oxygen on the electronic states of hydrogenated 3C-porous SiC. Nanoscale Research Letters, 2012, 7, 471.	3.1	17
12308	Ferromagnetism and semiconducting of boron nanowires. Nanoscale Research Letters, 2012, 7, 678.	3.1	6
12309	Effects of hydrogen adsorption on mechanical properties of chiral single-walled zinc oxide nanotubes. Journal of Applied Physics, 2012, 111, .	1.1	32

#	Article	IF	Citations
12310	Accurate Hydrogen Positions in Organic Crystals: Assessing a Quantum-Chemical Aide. Crystal Growth and Design, 2012, 12, 1014-1021.	1.4	68
12311	An Extensive Theoretical Study of the Phonon Conductivity and Thermoelectric Properties of SiGe Alloys. Materials Research Society Symposia Proceedings, 2012, 1404, 19.	0.1	1
12312	Robust Room-Temperature Ferromagnetism with Giant Anisotropy in Nd-Doped ZnO Nanowire Arrays. Nano Letters, 2012, 12, 3994-4000.	4.5	157
12313	Lattice dynamics of Ferroelectric TlInS2 crystal. Canadian Journal of Physics, 2012, 90, 407-412.	0.4	6
12314	First-principles calculation of phase equilibrium of V-Nb, V-Ta, and Nb-Ta alloys. Physical Review B, 2012, 85, .	1.1	46
12315	Li⁺ionic conductivities and diffusion mechanisms in Li-based imides and lithium amide. Physical Chemistry Chemical Physics, 2012, 14, 1596-1606.	1.3	43
12316	Effect of gadolinium doping on the electronic band structure of europium oxide. Physical Review B, 2012, 85, .	1.1	25
12317	First-principles study of pressure-induced phase transition and electronic property of PbCrO3. Journal of Applied Physics, 2012, 111, 013503.	1.1	16
12318	Engineered Piezoelectricity in Graphene. ACS Nano, 2012, 6, 1387-1394.	7.3	283
12319	Electronic structure of transparent oxides with the Tranâ€“Blaha modified Beckeâ€“Johnson potential. Journal of Physics Condensed Matter, 2012, 24, 205503.	0.7	86
12320	A fresh look at dense hydrogen under pressure. I. An introduction to the problem, and an index probing equalization of Hâ€“H distances. Journal of Chemical Physics, 2012, 136, 074501.	1.2	61
12321	A fresh look at dense hydrogen under pressure. III. Two competing effects and the resulting intra-molecular H-H separation in solid hydrogen under pressure. Journal of Chemical Physics, 2012, 136, 074503.	1.2	35
12322	A fresh look at dense hydrogen under pressure. IV. Two structural models on the road from paired to monatomic hydrogen, via a possible non-crystalline phase. Journal of Chemical Physics, 2012, 136, 074504.	1.2	29
12323	Hydration of Calcium Oxide Surface Predicted by Reactive Force Field Molecular Dynamics. Langmuir, 2012, 28, 4187-4197.	1.6	190
12324	Self-Assembled Ti Quantum Wire on Zigzag Graphene Nanoribbons with One Edge Saturated. Journal of Physical Chemistry C, 2012, 116, 24824-24828.	1.5	2
12325	The STM Images of Pt (111) (<img) Tj ETQq1 1 0.784314 rgBT /Overlock 10 Tf 50 152 Td (src="http://latex.codecog Calculations. Advances in Materials Physics and Chemistry, 2012, 02, 99-109.	0.3	0
12326	Synthesis and Characterization of Sr₂Cu(W_{1â€“x}Mo_x)O₆: A Quasi-Two-Dimensional Magnetic System. Chemistry of Materials, 2012, 24, 2764-2774.	3.2	32
12327	Self-consistent supercell approach to alloys with local environment effects. Physical Review B, 2012, 85, .	1.1	56

#	Article	IF	Citations
12328	Development and Validation of a ReaxFF Reactive Force Field for Fe/Al/Ni Alloys: Molecular Dynamics Study of Elastic Constants, Diffusion, and Segregation. Journal of Physical Chemistry A, 2012, 116, 12163-12174.	1.1	61
12329	Structural behavior of the acetylide carbides Li2C2 and CaC2 at high pressure. Journal of Chemical Physics, 2012, 137, 224507.	1.2	31
12330	Structural, elastic, magnetic and electronic properties of 4d perovskite CaTcO3: a DFT+Uinvestigation. Journal of Physics Condensed Matter, 2012, 24, 185401.	0.7	3
12331	Compression of Silver Sulfide: X-ray Diffraction Measurements and Total-Energy Calculations. Inorganic Chemistry, 2012, 51, 5289-5298.	1.9	44
12332	Energetics and dynamics of a new type of extended line defects in graphene. Nanoscale, 2012, 4, 2580.	2.8	15
12333	Phononic bandgaps in graphene-based materials. Applied Physics Letters, 2012, 100, .	1.5	6
12334	First-principles study on the effective masses of zinc-blend-derived Cu2Znâ^'IVâ^'VI4 (IVâ€‰=â€‰Sn, Ge, Si) Tj ETQq0 0 0 rgBT /	1.1	74
12336	Role of<mml:math xmlns:mml="http://www.w3.org/1998/Math/MathML" display="inline"><mml:mi>p</mml:mi></mml:math>-<mml:math xmlns:mml="http://www.w3.org/1998/Math/MathML" display="inline"><mml:mi>d</mml:mi></mml:math>and<mml:math xmlns:mml="http://www.w3.org/1998/Math/MathML" display="inline"><mml:mi>s</mml:mi></mml:math>-<mml:math xmlns:mml="http://www.w3.org/1998/Math/Mat	1.1	41
12337	Confinement-dependent ferromagnetism in Mn-doped InAs quantum dots embedded in InP nanowires. Physical Review B, 2012, 86, .	1.1	3
12338	First-principles studies of the electronic properties of native and substitutional anionic defects in bulk iron pyrite. Physical Review B, 2012, 85, .	1.1	83
12339	Influence of Pressure on the Structural, Electronic and Mechanical Properties of Cubic SrHfO₃: A First-Principles Study. Chinese Physics Letters, 2012, 29, 127103.	1.3	3
12340	Design of SHG materials with mid-infrared transparency based on genetic engineering for Ba2BiInA5 (A) Tj ETQq1 1 0.784314 rgBT /O	6.7	20
12341	Influence of orbital hybridization on the atomic and electronic structures in hydrogenated monolayer graphene. Journal of the Korean Physical Society, 2012, 60, 816-820.	0.3	1
12342	First-principles study on the relaxed structures and electronic properties of Cu [110] nanowires. Journal of the Korean Physical Society, 2012, 61, 1015-1020.	0.3	2
12343	Modeling thermoelectric transport in organic materials. Physical Chemistry Chemical Physics, 2012, 14, 16505.	1.3	93
12344	Efficient computation of magnon dispersions within time-dependent density functional theory using maximally localized Wannier functions. Physical Review B, 2012, 85, .	1.1	39
12345	Spin-wave method for the total energy of paramagnetic state. Physical Review B, 2012, 85, .	1.1	57
12346	Activation mechanism of carbon monoxide on Î±-Fe₂O₃ (0001) surface studied by using first principle calculations. Applied Physics Letters, 2012, 101, 041603.	1.5	3

#	Article	IF	Citations
12347	Effects of Surface Heterogeneity on the Adsorption of CO₂ in Microporous Carbons. Environmental Science & Technology, 2012, 46, 1940-1947.	4.6	243
12348	Hole mediated coupling in Sr2Nb2O7 for visible light photocatalysis. Physical Chemistry Chemical Physics, 2012, 14, 4891.	1.3	28
12349	Optical transitions due to native defects in nonlinear optical crystals LiGaS2. Journal of Applied Physics, 2012, 111, .	1.1	22
12350	Prediction of orientational phase transition in boron carbide. Solid State Sciences, 2012, 14, 1648-1652.	1.5	31
12351	Electronic Structure and Phase Transition in Ferroelectic Sn2P2S6 Crystal. International Journal of Molecular Sciences, 2012, 13, 14356-14384.	1.8	41
12352	Electronic, magnetic and dielectric properties of multiferroic MnTiO3. Journal of Materials Research, 2012, 27, 1421-1429.	1.2	17
12353	Optical isotropy in structurally anisotropic halide scintillators:Ab initiostudy. Physical Review B, 2012, 86, .	1.1	27
12354	First principle study on generalized stacking fault energy and surface energy of B2-AgRE intermetallics. Physica B: Condensed Matter, 2012, 407, 4117-4122.	1.3	1
12355	The Chemistry of Water on Î±-Alumina: Kinetics and Nuclear Quantum Effects from First Principles. Journal of Physical Chemistry C, 2012, 116, 26829-26840.	1.5	26
12356	Enhanced optical absorption and photocatalytic activity of anatase TiO₂ through (Si,Ni) codoping. Applied Physics Letters, 2012, 101, 062106.	1.5	21
12357	B and N doping in graphene ruled by grain boundary defects. Physical Review B, 2012, 85, .	1.1	46
12358	Density functional theory study of CO2 capture with transition metal oxides and hydroxides. Journal of Chemical Physics, 2012, 136, 064516.	1.2	26
12359	Local electronic properties at organicâ€“metal interfaces: thiophene derivatives on Pt(111). Physical Chemistry Chemical Physics, 2012, 14, 15412.	1.3	9
12360	Comparative DFT study of inner-sphere As(iii) complexes on hydrated Î±-Fe2O3(0001) surface models. Journal of Environmental Monitoring, 2012, 14, 1860.	2.1	26
12361	Elastic and optical properties of Cu₂ZnSn(Se_xS<sub>1) Tj ETQq0 0 0 rgBT /Overlock 10 Tf 50 187 Td (Technology, 2012, 27, 115001.	1.0	20
12362	The Nature of Transannular Interactions in E4N4 and E82+ (E = S, Se). Journal of Chemical Theory and Computation, 2012, 8, 4249-4258.	2.3	13
12363	HALF-METALLIC SILICENE AND GERMANENE NANORIBBONS: TOWARDS HIGH-PERFORMANCE SPINTRONICS DEVICE. Nano, 2012, 07, 1250037.	0.5	105
12364	Tunable Bandgap in Silicene and Germanene. Nano Letters, 2012, 12, 113-118.	4.5	1,248

#	Article	IF	Citations
12365	Carbonophosphates: A New Family of Cathode Materials for Li-Ion Batteries Identified Computationally. Chemistry of Materials, 2012, 24, 2009-2016.	3.2	131
12366	High Thermoelectric and Reversible p-n-p Conduction Type Switching Integrated in Dimetal Chalcogenide. Journal of the American Chemical Society, 2012, 134, 18460-18466.	6.6	164
12367	Screened hybrid density functional study on Sr2Nb2O7 for visible light photocatalysis. Applied Physics Letters, 2012, 100, .	1.5	31
12368	First principles molecular dynamics study of nitrogen vacancy complexes in boronitrene. Journal of Physics Condensed Matter, 2012, 24, 265002.	0.7	8
12369	Effect of pressure on itinerant magnetism and spin disorder in cubic FeGe. Journal of Physics Condensed Matter, 2012, 24, 096003.	0.7	8
12370	First-principles description of anomalously low lattice thermal conductivity in thermoelectric Cu-Sb-Se ternary semiconductors. Physical Review B, 2012, 85, .	1.1	196
12371	Edge-dependent structural, electronic and magnetic properties of MoS2 nanoribbons. Journal of Materials Chemistry, 2012, 22, 7280.	6.7	250
12372	Crystal structure of ammonia dihydrate II. Journal of Chemical Physics, 2012, 136, 174512.	1.2	17
12373	Pressure-induced spin transitions of iron in MgSiO3perovskite: a GGA+U study. High Pressure Research, 2012, , 1-10.	0.4	0
12374	Elastic stiffness coefficients of thenardite and their pressure and temperature dependence. Zeitschrift Fur Kristallographie - Crystalline Materials, 2012, 227, 503-513.	0.4	4
12375	Carbon monoxide adsorption on a nickel iron surface: bonding and electronic structure computational study. Molecular Physics, 2012, 110, 113-120.	0.8	4
12376	Oxygen reduction reactions on pure and nitrogen-doped graphene: a first-principles modeling. Nanoscale, 2012, 4, 417-420.	2.8	103
12377	Thermodynamic and stoichiometric stability of the Cd-terminated CdTe (111) surface. Physical Review B, 2012, 85, .	1.1	9
12378	Optimal Electron Density Mechanism for Hydrogen on the Surface and at a Vacancy in Tungsten. Chinese Physics Letters, 2012, 29, 077101.	1.3	7
12379	Adsorption and Dissociation of Ammonia on Graphene Oxides: A First-Principles Study. Journal of Physical Chemistry C, 2012, 116, 8778-8791.	1.5	131
12380	Metastable C-centered orthorhombic Si₈and Ge₈. Journal of Physics Condensed Matter, 2012, 24, 405803.	0.7	4
12381	Density Functional Theory Predictions of the Nonlinear Optical Properties in Î±-Quartz-type Germanium Dioxide. Journal of Physical Chemistry C, 2012, 116, 8692-8698.	1.5	37
12382	Palladium Nanoparticles/Defective Graphene Composites as Oxygen Reduction Electrocatalysts: A First-Principles Study. Journal of Physical Chemistry C, 2012, 116, 2710-2719.	1.5	94

#	Article	IF	Citations
12383	Diamondization of chemically functionalized graphene and grapheneâ€“BN bilayers. Physical Chemistry Chemical Physics, 2012, 14, 8179.	1.3	52
12384	Surface effect on electronic and optical properties of Bi2Ti2O7 nanowires for visible light photocatalysis. Journal of Applied Physics, 2012, 111, 124306.	1.1	15
12385	Are 4-Mercaptobenzoic Acid Self Assembled Monolayers on Au(111) a Suitable System to Test Adatom Models?. Journal of Physical Chemistry C, 2012, 116, 25765-25771.	1.5	35
12386	First-Principles Study of Spontaneous Polarization in SbFeO₃. Journal of the Physical Society of Japan, 2012, 81, 074702.	0.7	5
12387	Hydrogen adsorption on and spillover from Au- and Cu-supported Pt3 and Pd3 clusters: a density functional study. Physical Chemistry Chemical Physics, 2012, 14, 16062.	1.3	28
12388	Self-assembly mechanisms of short atomic chains on single-layer graphene and boron nitride. Physical Review B, 2012, 86, .	1.1	24
12389	Electronic structure and band gap engineering of CdTe semiconductor nanowires. Journal of Materials Chemistry, 2012, 22, 10716.	6.7	32
12390	Ab Initio Thermodynamics Examination of Sulfur Species Present on Rh, Ni, and Binary Rhâ€“Ni Surfaces under Steam Reforming Reaction Conditions. Langmuir, 2012, 28, 5660-5668.	1.6	10
12391	Rapid Materials Degradation Induced by Surfaces and Voids: Ab Initio Modeling of Î²-Octatetramethylene Tetranitramine. Journal of the American Chemical Society, 2012, 134, 11815-11820.	6.6	65
12392	Precursor to the Onset of the Bulk Oxidation of Cu(100). Physical Review Letters, 2012, 108, 176101.	2.9	20
12393	Electronic and Magnetic Properties of Fluorinated Graphene with Different Coverage of Fluorine. Journal of Physical Chemistry C, 2012, 116, 18193-18201.	1.5	142
12394	Effects of Mg, Ca, and Fe(II) Doping on the Kaolinite (001) Surface with H₂O Adsorption. Clays and Clay Minerals, 2012, 60, 330-337.	0.6	16
12395	Activation of Lattice Oxygen of TiO₂ by Pd²⁺ Ion: Correlation of Low-Temperature CO and Hydrocarbon Oxidation with Structure of Ti_{1â€“x}Pd_xO_{2â€“x} (x = 0.01â€“0.03). Chemistry of Materials, 2012, 24, 4491-4502.	3.2	45
12396	Modelling amorphous silicon with hydrogenated defects: GW treatment of the ST12 phase. Journal of Physics Condensed Matter, 2012, 24, 325803.	0.7	2
12397	Structural and electronic properties of CuSbS2 and CuBiS2: potential absorber materials for thin-film solar cells. Physical Chemistry Chemical Physics, 2012, 14, 7229.	1.3	144
12398	Growth mechanism of palladium clusters on rutile TiO2(110) surface. Journal of Natural Gas Chemistry, 2012, 21, 544-555.	1.8	10
12399	Mechanistic Insights into Selective Oxidation of Ethanol on Au(111): A DFT Study. Chinese Journal of Catalysis, 2012, 33, 407-415.	6.9	29
12400	Firstâ€principles study of highâ€pressure elasticity of CFâ€•and CTâ€structure MgAl₂O₄. Geophysical Research Letters, 2012, 39, .	1.5	2

#	Article	IF	Citations
12401	First principles investigations on the elasticity and phase stability of grossular garnet. Journal of Geophysical Research, 2012, 117, .	3.3	22
12402	Is a cation ordering transition of the Mgâ€Fe olivine phase in the mantle responsible for the shallow mantle seismic discontinuity beneath the Indian Craton?. Journal of Geophysical Research, 2012, 117, .	3.3	11
12403	Elastic properties of face-centred cubic Feâ€“Mnâ€“C studied by nanoindentation and ab initio calculations. Acta Materialia, 2012, 60, 6025-6032.	3.8	43
12404	Emergence of ferromagnetism at a vacancy on a non-magnetic ferroelectric PbTiO3 surface: A first-principles study. Acta Materialia, 2012, 60, 6322-6330.	3.8	20
12405	Multi-length scale modeling of martensitic transformations in stainless steels. Acta Materialia, 2012, 60, 6508-6517.	3.8	31
12406	Double-atomic-wall-based dynamic precipitates of the early-stage S-phase in AlCuMg alloys. Acta Materialia, 2012, 60, 6573-6580.	3.8	58
12408	Oxygen vacancy formation on the Ni/Ce0.75Zr0.25O2(111) surface. A DFT+U study. International Journal of Hydrogen Energy, 2012, 37, 14937-14944.	3.8	15
12409	A first principles study of the hydrogen reaction in alkaline media: OH effect. International Journal of Hydrogen Energy, 2012, 37, 14796-14800.	3.8	6
12410	Stability of a hydrogen molecule in a vacancy of palladium hydrides. International Journal of Hydrogen Energy, 2012, 37, 12351-12357.	3.8	7
12411	Hybrid density functional study on SrTiO3 for visible light photocatalysis. International Journal of Hydrogen Energy, 2012, 37, 11611-11617.	3.8	67
12412	Computational analysis of atomic C and S adsorption on Ni, Cu, and Ni-Cu SOFC anode surfaces. International Journal of Hydrogen Energy, 2012, 37, 11941-11945.	3.8	29
12413	Mg2â^'xTixNi (xÂ=ÂO, 0.5) alloys prepared by mechanical alloying for electrochemical hydrogen storage: Experiments and first-principles calculations. International Journal of Hydrogen Energy, 2012, 37, 14248-14256.	3.8	27
12414	Hydrogen adsorption on and diffusion through MoS2 monolayer: First-principles study. International Journal of Hydrogen Energy, 2012, 37, 14323-14328.	3.8	105
12415	Hybrid functionals studies of structural and electronic properties of ZnxCd(1â^'x)S and (ZnxCd1â^'x)(SexS1â^'x) solid solution photocatalysts. International Journal of Hydrogen Energy, 2012, 37, 17870-17881.	3.8	27
12416	Resolving the stability and structure of strontium chloride amines from equilibrium pressures, XRD and DFT. International Journal of Hydrogen Energy, 2012, 37, 18927-18936.	3.8	37
12417	Neutron generation via the mechanism adsorption of pressurized deuterium on an electron deficient titanium matrix. An MDâ€“DFT combined analysis on the mechanism of the Tiâ€“D bond formation. International Journal of Hydrogen Energy, 2012, 37, 18959-18971.	3.8	2
12418	Environmentally dependent stability of low-index hematite surfaces. Journal of Colloid and Interface Science, 2012, 386, 315-324.	5.0	23
12419	Adsorption of atomic oxygen on HfC and TaC (110) surface from first principles. Applied Surface Science, 2012, 261, 214-218.	3.1	12

#	Article	IF	Citations
12420	Thermodynamic modeling of the Srâ€“X (X=H, Li, Na, Sc) systems. Calphad: Computer Coupling of Phase Diagrams and Thermochemistry, 2012, 38, 17-22.	0.7	6
12421	Thermodynamic evaluations and optimizations of binary Mg-light Rare Earth (La, Ce, Pr, Nd, Sm) systems. Calphad: Computer Coupling of Phase Diagrams and Thermochemistry, 2012, 38, 100-116.	0.7	64
12422	Ab initio study of cation disorder in dolomite. Calphad: Computer Coupling of Phase Diagrams and Thermochemistry, 2012, 38, 177-184.	0.7	12
12423	Phase stability of Vâ€“Ta alloy using cluster expansion and Monte Carlo techniques. Calphad: Computer Coupling of Phase Diagrams and Thermochemistry, 2012, 39, 33-36.	0.7	5
12424	Thermodynamic modeling of the Hfâ€“Sn and Snâ€“Y systems. Calphad: Computer Coupling of Phase Diagrams and Thermochemistry, 2012, 39, 91-96.	0.7	10
12425	B-splines and NURBS based finite element methods for Kohnâ€“Sham equations. Computer Methods in Applied Mechanics and Engineering, 2012, 241-244, 112-127.	3.4	24
12426	Molecular simulation of CO2 adsorption in micro- and mesoporous carbons with surface heterogeneity. International Journal of Coal Geology, 2012, 104, 83-95.	1.9	156
12427	Anisotropic surface energies and adsorption behaviors of scheelite crystal. Colloids and Surfaces A: Physicochemical and Engineering Aspects, 2012, 415, 439-448.	2.3	140
12428	First principles study on structural, electronic and elastic properties of AgX and AuX (X=Mg, Sc, Zn) Tj ETQq0 0 0 rgBT /Overlock 10 Tf 5	1.4	18
12429	Tunable band gap in half-fluorinated bilayer graphene under biaxial strains. Computational Materials Science, 2012, 65, 165-169.	1.4	7
12430	Investigations on the structural, elastic and electronic properties of the orthorhombic Zirconiumâ€“Nickel alloy under different pressure. Computational Materials Science, 2012, 65, 127-132.	1.4	14
12431	Modification of graphene as active hydrogen storage medium by strain engineering. Computational Materials Science, 2012, 65, 144-148.	1.4	21
12432	Structural, elastic and thermodynamic properties of anti-ReO3 type Cu3N under pressure from first principles. Computational Materials Science, 2012, 65, 247-253.	1.4	13
12433	First principles study of band gap of Cu doped ZnO single-wall nanotube modulated by impurity concentration and concentration gradient. Computational Materials Science, 2012, 65, 175-181.	1.4	19
12434	First-principles calculations of MnB4, TcB4, and ReB4 with the MnB4-type structure. Computational Materials Science, 2012, 65, 372-376.	1.4	18
12435	Structural, dynamical and thermodynamics properties of YBi. Computational Materials Science, 2012, 65, 331-334.	1.4	2
12436	Ab initio structure modeling of ZrO2 nanosheets and single-wall nanotubes. Computational Materials Science, 2012, 65, 395-405.	1.4	31
12437	MAX phases Nb2AC (A=S, Sn): An ab initio study. Computational Materials Science, 2012, 65, 365-371.	1.4	22

#	Article	IF	Citations
12438	First-principle studies of properties of ternary layered M2PbC (M=Ti, Zr and Hf). Computational Materials Science, 2012, 65, 377-382.	1.4	12
12439	Ab initio investigations of structural, elastic and electronic properties of ZnSiP2: Pressure effect. Computational Materials Science, 2012, 65, 520-527.	1.4	29
12440	Ab initio study of Tiâ€“C precipitates in hcp titanium: Formation energies, elastic moduli and theoretical diffraction patterns. Computational Materials Science, 2012, 65, 434-441.	1.4	16
12441	The electronic, mechanical and lattice dynamic properties of TiSiY from first-principles calculations. Computational Materials Science, 2012, 65, 485-489.	1.4	1
12442	First-principles calculations of Zn substitutions in Cu6Sn5. Computational Materials Science, 2012, 65, 490-493.	1.4	17
12443	Density-functional study of LixMoS2 intercalates (0â©½xâ©½1). Computational and Theoretical Chemistry, 2012, 999, 13-20.	1.1	120
12444	Density functional theory study of imidazole, benzimidazole and 2-mercaptobenzimidazole adsorption onto clean Cu(111) surface. Corrosion Science, 2012, 63, 140-147.	3.0	88
12445	Amorphous TiO2 as a Photocatalyst for Hydrogen Production: A DFT Study of Structural and Electronic Properties. Energy Procedia, 2012, 29, 291-299.	1.8	108
12446	Equation of state and phase diagram of Feâ€“16Si alloy as a candidate component of Earth's core. Earth and Planetary Science Letters, 2012, 357-358, 268-276.	1.8	55
12447	Diffusion of transition metals in periclase by experiment and first-principles, with implications for coreâ€“mantle equilibration during metal percolation. Earth and Planetary Science Letters, 2012, 357-358, 42-53.	1.8	6
12448	Theoretical prediction of the structural, elastic, electronic and thermodynamic properties of V3M (M=Si, Ge and Sn) compounds. Superlattices and Microstructures, 2012, 52, 697-703.	1.4	5
12449	First-principles studies on stabilities and electronic properties of AlN nanostructures. Superlattices and Microstructures, 2012, 52, 662-668.	1.4	9
12450	Magnetic properties of Mn doped BN compound. Superlattices and Microstructures, 2012, 52, 880-884.	1.4	12
12451	Mechanical properties of two-dimensional graphyne sheet under hydrogen adsorption. Solid State Communications, 2012, 152, 1885-1889.	0.9	54
12452	Influence of antiphase boundary period parameter Mâ€² on elastic and electronic properties of one dimensional long period structures of Al3Ti. Solid State Communications, 2012, 152, 1939-1944.	0.9	7
12453	The electronic structure of ScVO3. Solid State Communications, 2012, 152, 2049-2052.	0.9	2
12454	Chemical trend of superconducting transition temperature in hole-doped delafossite of CuAlO2, AgAlO2 and AuAlO2. Solid State Communications, 2012, 152, 2078-2081.	0.9	14
12455	Structural and electronic properties of hexagonal ZnO: A hybrid functional study. Solid State Communications, 2012, 152, 2045-2048.	0.9	8

#	Article	IF	Citations
12456	Structural, elastic and electronic properties of Î¸ (Al2Cu) and S (Al2CuMg) strengthening precipitates in Alâ€“Cuâ€“Mg series alloys: First-principles calculations. Solid State Communications, 2012, 152, 2100-2104.	0.9	105
12457	First-principle study of the electronic structure and magnetic properties of CeRu2Al2B. Solid State Communications, 2012, 152, 2105-2108.	0.9	1
12458	Intra-octahedral proton transfer in bulk orthorhombic perovskite barium cerate. Solid State Ionics, 2012, 226, 71-75.	1.3	8
12459	Lattice distortion effect on electrical properties of GDC thin films: Experimental evidence and computational simulation. Solid State Ionics, 2012, 229, 45-53.	1.3	24
12460	Effects of the orientation of the 23Naâ€“29Si dipolar vector on the dipolar mediated heteronuclear solid state NMR correlation spectrum of crystalline sodium silicates. Solid State Nuclear Magnetic Resonance, 2012, 45-46, 1-10.	1.5	11
12461	Dimensionality effects in the electronic structure of organic semiconductors consisting of polar repeat units. Organic Electronics, 2012, 13, 3165-3176.	1.4	19
12462	The low velocity layer in subduction zone: Structure and elasticity of glaucophane at high pressures. Physics of the Earth and Planetary Interiors, 2012, 208-209, 50-58.	0.7	26
12463	Electronic and magnetic properties for Co13 clusters deposited on graphene: A first-principles exploration. Physica E: Low-Dimensional Systems and Nanostructures, 2012, 46, 6-11.	1.3	27
12464	The highly active Ce4O8 nanoparticle for CO oxidation. Physics Letters, Section A: General, Atomic and Solid State Physics, 2012, 376, 3235-3240.	0.9	8
12465	Enhanced magnetism of SiC with He defects. Physics Letters, Section A: General, Atomic and Solid State Physics, 2012, 376, 3363-3367.	0.9	4
12466	Strain-induced phase transitions in multiferroic BiFeO3 <mml:math xmlns:mml="http://www.w3.org/1998/Math/MathML" altimg="si1.gif" overflow="scroll"><mml:msub><mml:mrow><mml:mo stretchy="false">(</mml:mo><mml:mn>110</mml:mn><mml:mo) Tj ETQq0 0 0 rgBT /Overlock 10 Tf 50 332 Td (stretchy="false">)</mm	0.9	7
12467	epitaxial film. Physics Letters, Section A: General, Atomic and Solid State Physics, 2012, 376, 3368-3371. Strain-tunable band parameters of ZnO monolayer in graphene-like honeycomb structure. Physics Letters, Section A: General, Atomic and Solid State Physics, 2012, 376, 3287-3289.	0.9	29
12468	First-principles investigations of O2 dissociation on low-coordinated Pd ensembles over stepped Au surfaces. Physics Letters, Section A: General, Atomic and Solid State Physics, 2012, 376, 3432-3438.	0.9	11
12469	Theoretical study of thermoelectric properties of Y-doped Mg2Si using density functional methods. Procedia Engineering, 2012, 27, 109-114.	1.2	1
12470	Phase transformation and grain refinement in hydrogenated metastable austenitic steel. Scripta Materialia, 2012, 67, 979-982.	2.6	8
12471	Interfacial electronic structure and magnetoelectric effect in M/BaTiO3 (M=Ni, Fe) superlattices. Journal of Magnetism and Magnetic Materials, 2012, 324, 3937-3943.	1.0	22
12472	First-principles calculations of adhesion, bonding and magnetism of the Fe/HfC interface. Journal of Magnetism and Magnetic Materials, 2012, 324, 4155-4160.	1.0	13
12473	Interaction of hot carriers with optical phonons in Selenium. Journal of Non-Crystalline Solids, 2012, 358, 2434-2436.	1.5	5

#	Article	IF	Citations
12474	The dangling-bond defect in amorphous silicon: Statistical random versus kinetically driven defect geometries. Journal of Non-Crystalline Solids, 2012, 358, 2063-2066.	1.5	14
12475	Interplay of ballistic and chemical effects in the formation of structural defects for Sn and Pb implanted silica. Journal of Non-Crystalline Solids, 2012, 358, 3187-3192.	1.5	4
12476	Electronic, mechanical and thermodynamic properties of Î±-UH3: A comparative study by using the LDA and LDA+U approaches. Journal of Nuclear Materials, 2012, 430, 137-141.	1.3	23
12477	Structure, elasticity and stability of reidite (ZrSiO4) under hydrostatic pressure: A density functional study. Materials Chemistry and Physics, 2012, 135, 322-329.	2.0	15
12478	Theoretical investigation of nerve agent DMMP adsorption onto Stoneâ€“Wales defected single-walled carbon nanotube. Materials Chemistry and Physics, 2012, 135, 569-574.	2.0	24
12479	Electronic structure of polycrystalline cadmium dichloride studied by X-ray spectroscopies and ab initio calculations. Materials Chemistry and Physics, 2012, 135, 1036-1043.	2.0	3
12480	Lattice dynamics and Raman spectrum of rutile TiO2: The role of soft phonon modes in pressure induced phase transition. Materials Chemistry and Physics, 2012, 137, 282-289.	2.0	65
12481	Chemistry of the interaction between azole type corrosion inhibitor molecules and metal surfaces. Materials Chemistry and Physics, 2012, 137, 331-339.	2.0	123
12482	Experimental and theoretical studies of second harmonic generation for Bi2O2[NO3(OH)]. Materials Research Bulletin, 2012, 47, 2573-2578.	2.7	39
12483	An intermediate fcc Zr state observed in the Cuâ€“Zrâ€“Ni system upon ion beam mixing. Materials Letters, 2012, 89, 90-92.	1.3	2
12484	Crystal size and direction dependence of the elastic properties of Cu3Sn through molecular dynamics simulation and nanoindentation testing. Microelectronics Reliability, 2012, 52, 1699-1710.	0.9	19
12485	Theoretical insight into the desulfurization of thiophene on Pt(110): A density functional investigation. Journal of Molecular Catalysis A, 2012, 363-364, 18-25.	4.8	15
12486	The role of van der Waals interactions in the adsorption of noble gases on metal surfaces. Journal of Physics Condensed Matter, 2012, 24, 424211.	0.7	42
12487	The structure of Mn-doped tris(8-hydroxyquinoline)gallium by extended x-ray absorption fine structure spectroscopy and first principles calculations. Journal of Applied Physics, 2012, 112, 113519.	1.1	5
12488	General Method for Determination of the Surface Composition in Bimetallic Nanoparticle Catalysts from the L Edge X-ray Absorption Near-Edge Spectra. ACS Catalysis, 2012, 2, 2433-2443.	5.5	16
12489	Synthesis of Ptâ€“Pd Coreâ€“Shell Nanostructures by Atomic Layer Deposition: Application in Propane Oxidative Dehydrogenation to Propylene. Chemistry of Materials, 2012, 24, 3525-3533.	3.2	104
12490	Synthesis and Characterization of Th₂N₂(NH) Isomorphous to Th₂N₃. Inorganic Chemistry, 2012, 51, 3332-3340.	1.9	9
12491	Electronic and magnetic properties of Ti₂O₃, Cr₂O₃, and Fe₂O₃calculated by the screened exchange hybrid density functional. Journal of Physics Condensed Matter, 2012, 24, 325504.	0.7	82

#	Article	IF	Citations
12492	Molecular Simulation for Gas Adsorption at NiO (100) Surface. ACS Applied Materials & Interfaces, 2012, 4, 5691-5697.	4.0	64
12493	Extreme Poisson's ratios and their electronic origin in B2 CsCl-type AB intermetallic compounds. Physical Review B, 2012, 85, .	1.1	42
12494	Superoxide and Peroxide Species on CeO₂(111), and Their Oxidation Roles. Journal of Physical Chemistry C, 2012, 116, 15986-15991.	1.5	94
12495	Analysis of Intrinsic Defects in CeO₂ Using a Koopmans-Like GGA+U Approach. Journal of Physical Chemistry C, 2012, 116, 2443-2452.	1.5	144
12496	Hartreeâ€“Fock LCAO Method for Periodic Systems. Springer Series in Solid-state Sciences, 2012, , 109-155.	0.3	1
12497	Bimetallic Auâ€“Pd Alloy Catalysts for N₂O Decomposition: Effects of Surface Structures on Catalytic Activity. Journal of Physical Chemistry C, 2012, 116, 6222-6232.	1.5	128
12498	ELECTRONIC AND ELASTIC PROPERTIES OF CrO₂ IN THE ORTHORHOMBIC CaCl₂-TYPE STRUCTURE. International Journal of Modern Physics B, 2012, 26, 1250091.	1.0	3
12499	On the Structure of Î²-Molybdenum Dichloride. Inorganic Chemistry, 2012, 51, 4965-4971.	1.9	3
12500	Using carbon chains to mediate magnetic coupling in zigzag graphene nanoribbons. Applied Physics Letters, 2012, 100, 173106.	1.5	17
12501	Compare Study of Electronic Structure, Chemical Bonding and Elastic Properties of Ti₃AC₂ (A=Al, Si, Sn) by First-Principles. Advanced Materials Research, 0, 624, 117-121.	0.3	2
12503	Syntheses, Structures, Physical Properties, and Electronic Structures of Ba₂MLnTe₅ (M = Ga and Ln = Sm, Gd, Dy, Er, Y; M = In and Ln = Ce, Nd, Sm, Gd, Dy,) Tj ET Q q 0 0 0 rg BT /Overl	1.0	9
12504	CO₂ Reduction on Transition Metal (Fe, Co, Ni, and Cu) Surfaces: In Comparison with Homogeneous Catalysis. Journal of Physical Chemistry C, 2012, 116, 5681-5688.	1.5	247
12505	Theoretical Study of the Electronic Properties of Silicon Nanocrystals Partially Passivated with Cl and F. Journal of Physical Chemistry C, 2012, 116, 3988-3994.	1.5	29
12506	First-principles study of electronic, vibrational, elastic, and magnetic properties of FeF<mml:math xmlns:mml="http://www.w3.org/1998/Math/MathML" display="inline"><mml:msub><mml:mrow /><mml:mn>2</mml:mn></mml:msub></mml:math>as a function of pressure. Physical Review B, 2012, 85, .	1.1	50
12507	Wannier-based calculation of the orbital magnetization in crystals. Physical Review B, 2012, 85, .	1.1	73
12508	Sulfidation of Ceria Surfaces from Sulfur and Sulfur Diffusion. Journal of Physical Chemistry C, 2012, 116, 8417-8425.	1.5	19
12509	Density functional study of gold and iron clusters on perfect and defected graphene. Physical Review B, 2012, 85, .	1.1	53
12510	Transferable pair potentials for CdS and ZnS crystals. Journal of Chemical Physics, 2012, 136, 234111.	1.2	44

#	Article	IF	Citations
12511	First-principles study of the oxygen adsorption and dissociation on graphene and nitrogen doped graphene for Li-air batteries. Journal of Applied Physics, 2012, 112, .	1.1	133
12512	display="inline"><mml:msub><mml:mrow /><mml:mi>x</mml:mi></mml:msub></mml:math>Ga<mml:math xmlns:mml="http://www.w3.org/1998/Math/MathML" display="inline"><mml:msub><mml:mrow /><mml:mrow><mml:mn>1</mml:mn><mml:mo>â^’</mml:mo><mml:mi>x</mml:mi></mml:mrow></mml:msub></mml:math>N and In<mml:math xmlns:mml="http://www.w3.org/1998/Math/MathML" display="inline"><mml:msub><mml:mrow /><mml:mi>x</mml:mi></mml:msub></mml:math>Ga<mml:math	1.1	22
12513	Crystal facet-dependent photocatalytic oxidation and reduction reactivity of monoclinic WO3 for solar energy conversion. Journal of Materials Chemistry, 2012, 22, 6746.	6.7	356
12514	Hydrogen Adsorption on PdGa(110): A DFT Study. Journal of Physical Chemistry C, 2012, 116, 17518-17524.	1.5	17
12515	Ceâ€“Mn Oxides for High-Temperature Gasifier Effluent Desulfurization. Energy & Fuels, 2012, 26, 6765-6776.	2.5	30
12516	Single-Crystal Structures, Optical Absorptions, and Electronic Distributions of Thorium Oxychalcogenides ThOQ (Q = S, Se, Te). Inorganic Chemistry, 2012, 51, 8112-8118.	1.9	20
12517	Transition levels of defects in ZnO: Total energy and Janak's theorem methods. Journal of Chemical Physics, 2012, 137, 054709.	1.2	22
12518	Optical dielectric functions of wurtzite III-V semiconductors. Physical Review B, 2012, 85, .	1.1	30
12519	Half-Heusler Semiconductors as Piezoelectrics. Physical Review Letters, 2012, 109, 037602.	2.9	180
12520	Quasiparticle band gaps of boron nitride nanoribbons. Physical Review B, 2012, 85, .	1.1	11
12521	Si₃AlP: A New Promising Material for Solar Cell Absorber. Journal of the American Chemical Society, 2012, 134, 12653-12657.	6.6	37
12522	Electronic correlations and crystal structure distortions in BaBiO₃. Journal of Physics Condensed Matter, 2012, 24, 415603.	0.7	27
12523	First principles calculation on the adsorption of water on lithiumâ€“montmorillonite (Liâ€“MMT). Journal of Physics Condensed Matter, 2012, 24, 475506.	0.7	11
12524	Metal-Supported Metal Clusters: A Density Functional Study of Pt₃ and Pd₃. Journal of Physical Chemistry C, 2012, 116, 10057-10063.	1.5	12
12525	Linking 31P Magnetic Shielding Tensors to Crystal Structures: Experimental and Theoretical Studies on Metal(II) Aminotris(methylenephosphonates). Inorganic Chemistry, 2012, 51, 11466-11477.	1.9	19
12526	Hybrid Graphene and Graphitic Carbon Nitride Nanocomposite: Gap Opening, Electronâ€“Hole Puddle, Interfacial Charge Transfer, and Enhanced Visible Light Response. Journal of the American Chemical Society, 2012, 134, 4393-4397.	6.6	565
12527	First-Principles Calculations of Potassium Amidoborane KNH₂BH₃: Structure and ³⁹K NMR Spectroscopy. Journal of Physical Chemistry C, 2012, 116, 20666-20672.	1.5	9
12528	Mechanical properties of graphene oxides. Nanoscale, 2012, 4, 5910.	2.8	239

#	Article	IF	Citations
12529	Nanocrystalline hybrid inorganicâ€“organic one-dimensional chain systems tailored with 2- and 3-phenyl ring monocarboxylic acids. Journal of Materials Chemistry, 2012, 22, 10255.	6.7	5
12530	Tailor-made ultrathin manganese oxide nanostripes: â€˜magic widthsâ€™ on Pd(1 1N) terraces. Journal of Physics Condensed Matter, 2012, 24, 042001.	0.7	7
12531	First-principles modeling of the thermoelectric properties of SrTiO<mml:math xmlns:mml="http://www.w3.org/1998/Math/MathML" display="inline"><mml:msub><mml:mrow /><mml:mn>3</mml:mn></mml:msub></mml:math>/SrRuO<mml:math xmlns:mml="http://www.w3.org/1998/Math/MathML" display="inline"><mml:msub><mml:mrow /><mml:mn>3</mml:mn></mml:msub></mml:math> heterostructures: A first-principles study. Physical Review B, 2012, 86, .	1.1	28
12532	First-principles study of the ferroelectric and multiferroic phases of bismuth ferrite. Physical Review B, 2012, 86, .	1.1	43
12533	Structural and Electronic Properties of Neutral and Ionic (Ga₂O₃)_n Clusters with n = 1â€“10. Journal of Physical Chemistry C, 2012, 116, 2691-2701.	1.5	17
12534	First-principles investigation of transition metal atom M (M = Cu, Ag, Au) adsorption on CeO2(110). Physical Chemistry Chemical Physics, 2012, 14, 1923.	1.3	52
12535	Exploration of the formation ofXLi3N2compounds (X=Sc-Zn) by means of density functional theory. Physical Review B, 2012, 85, .	1.1	7
12536	A combined first principles and analytical treatment for determination of the surface elastic constants: application to Si(001) ideal and reconstructed surfaces. Philosophical Magazine Letters, 2012, 92, 7-19.	0.5	23
12537	Ab-Initio Modeling of the Resistance Switching Mechanism in RRAM Devices: Case Study of Hafnium Oxide (HfO2). Materials Research Society Symposia Proceedings, 2012, 1430, 72.	0.1	11
12538	Mechanisms of the Oxygen Reduction Reaction on Defective Graphene-Supported Pt Nanoparticles from First-Principles. Journal of Physical Chemistry C, 2012, 116, 3653-3660.	1.5	312
12539	Effect of alloying element on dislocation cross-slip in Î³â€²-Ni₃Al: a first-principles study. Philosophical Magazine, 2012, 92, 4028-4039.	0.7	20
12540	Hybrid density functional study of the structural, bonding, and electronic properties of bismuth vanadate. Physical Review B, 2012, 86, .	1.1	55
12541	Improved oxygen surface exchange kinetics at grain boundaries in nanocrystalline yttria-stabilized zirconia. MRS Communications, 2012, 2, 107-111.	0.8	15
12542	Strain relief and disorder in commensurate water layers formed on Pd(111). Journal of Physics Condensed Matter, 2012, 24, 124102.	0.7	14
12543	Optical properties of Mg-doped VO2: Absorption measurements and hybrid functional calculations. Applied Physics Letters, 2012, 101, .	1.5	70
12544	On the entanglement of electrostriction and non-linear piezoelectricity in non-centrosymmetric materials. Applied Physics Letters, 2012, 100, .	1.5	29
12545	Theoretical study on the oxidation of zigzag silicon carbide nanotubes (SiCNTs) by singlet O2. Physica B: Condensed Matter, 2012, 407, 4238-4243.	1.3	1
12546	Effects of uniaxial strains on the magnetic properties and the electronic structures of Fe/graphene system: An ab initio study. Journal of Applied Physics, 2012, 111, 07C306.	1.1	4

#	Article	IF	Citations
12547	Optical absorption and DFT calculations in<mml:math xmlns:mml="http://www.w3.org/1998/Math/MathML" display="inline"><mml:mi>L</mml:mi></mml:math>-aspartic acid anhydrous crystals: Charge carrier effective masses point to semiconducting behavior. Physical Review B, 2012, 86, .	1.1	51
12548	Attenuation of Conductance in Cobalt Extended Metal Atom Chains. Journal of Physical Chemistry C, 2012, 116, 20163-20172.	1.5	14
12549	Possible nâ€“type carrier sources in In2O3(ZnO)k. Chemistry of Materials, 2012, 24, 106-114.	3.2	38
12550	A Density Functional Theory Study on Carbon Monoxide Adsorption on Platinumâ€“Osmium and Platinumâ€“Rutheniumâ€“Osmium Alloys. Journal of Physical Chemistry C, 2012, 116, 21447-21458.	1.5	13
12551	Vibrational properties and phase transitions in IIâ€“VI materials: lattice dynamics,ab initiostudies and inelastic neutron scattering measurements. Journal of Physics Condensed Matter, 2012, 24, 115401.	0.7	16
12552	Origin of unipolarity in carbon nanotube field effect transistors. Journal of Materials Chemistry, 2012, 22, 1994-1997.	6.7	14
12553	First-principles analysis of oxide-ion conduction mechanism in lanthanum silicate. Journal of Materials Chemistry, 2012, 22, 7265.	6.7	29
12554	Stoneâ€“Wales defects can cause a metalâ€“semiconductor transition in carbon nanotubes depending on their orientation. Journal of Physics Condensed Matter, 2012, 24, 035301.	0.7	12
12555	First-principles studies of BN sheets with absorbed transition metal single atoms or dimers: stabilities, electronic structures, and magnetic properties. Journal of Physics Condensed Matter, 2012, 24, 145501.	0.7	33
12556	Structural evolution of amino acid crystals under stress from a non-empirical density functional. Journal of Physics Condensed Matter, 2012, 24, 424209.	0.7	65
12557	First-Principles Study on Al or/and P Doped SiC Nanotubes. Advanced Materials Research, 2012, 510, 747-752.	0.3	1
12558	The Structural and Electronic Properties of Tin Oxide Nanowires: An Ab Initio Investigation. Journal of Physical Chemistry C, 2012, 116, 13382-13387.	1.5	8
12559	Controllable synthesis of brookite/anatase/rutile TiO2 nanocomposites and single-crystalline rutile nanorods array. Journal of Materials Chemistry, 2012, 22, 7937.	6.7	188
12560	THE AB INITIO CALCULATION OF THE DYNAMICAL AND THE THERMODYNAMIC PROPERTIES OF THE ZINC-BLENDE GaX (X=N, P, As AND Sb). International Journal of Computational Materials Science and Engineering, 2012, 01, 1250026.	0.5	2
12561	An ab-initio study of the structural, electronic and magnetic properties of half-metallic ferromagnetism in Cr-doped BeSe and BeTe. Solid State Sciences, 2012, 14, 1525-1535.	1.5	73
12562	The ionic conductivity in lithium-boron oxide materials and its relation to structural, electronic and defect properties: insights from theory. Journal of Physics Condensed Matter, 2012, 24, 203201.	0.7	22
12563	Benzene adsorbed on metals: Concerted effect of covalency and van der Waals bonding. Physical Review B, 2012, 86, .	1.1	243
12564	First principles and Monte Carlo study of Mn-doped CuCl/CuBr as room-temperature ferromagnetism materials. Journal of Applied Physics, 2012, 111, 063913.	1.1	3

#	Article	IF	Citations
12565	Electronic and structural properties of InAs/InP core/shell nanowires: A first principles study. Journal of Applied Physics, 2012, 111, 054315.	1.1	14
12566	First principles study of the magnetism driven by cation defects in CeO₂: the important role of O2p states. Chinese Physics B, 2012, 21, 047505.	0.7	8
12567	Ni-Assisted Transformation of Graphene Flakes to Fullerenes. Journal of Physical Chemistry C, 2012, 116, 6572-6584.	1.5	38
12568	First-principles study on the reconstruction induced by the adsorption of C60 on Pt(111). Physical Chemistry Chemical Physics, 2012, 14, 4959.	1.3	9
12569	Fragmentation of the Fluorite Type in Fe8Al17.4Si7.6: Structural Complexity in Intermetallics Dictated by the 18 Electron Rule. Inorganic Chemistry, 2012, 51, 10341-10349.	1.9	21
12570	Oxygen Vacancy Induced Band-Gap Narrowing and Enhanced Visible Light Photocatalytic Activity of ZnO. ACS Applied Materials & Interfaces, 2012, 4, 4024-4030.	4.0	1,269
12571	Ab initio electronic structure of NiCoCrGa half-metallic quaternary Heusler compound. Solid State Sciences, 2012, 14, 1273-1276.	1.5	45
12572	Mild Bromination-Assisted Density-Gradient Ultracentrifugation to Sort Single-Walled Carbon Nanotubes by Metallicity. Journal of Physical Chemistry C, 2012, 116, 23027-23035.	1.5	5
12573	Rare-earth impurities in gallium nitride: The role of the Hubbard potential. Diamond and Related Materials, 2012, 27-28, 64-67.	1.8	5
12574	Many MÂ©Bn boron wheels are local, but not global minima. Physical Chemistry Chemical Physics, 2012, 14, 14898.	1.3	29
12575	CO Adsorption Behavior on Decorated Pt@Au Nanoelectrocatalysts: A Combined Experimental and DFT Theoretical Calculation Study. Journal of Physical Chemistry C, 2012, 116, 3851-3856.	1.5	20
12576	Ab initio calculation of the CdSe/CdTe heterojunction band offset using the local-density approximation-1/2 technique with spin-orbit corrections. Journal of Applied Physics, 2012, 111, 073708.	1.1	18
12577	Enhancement of Ag cluster mobility on Ag surfaces by chloridation. Journal of Chemical Physics, 2012, 137, 184705.	1.2	3
12578	Investigation of radionuclide 60Co(II) binding to TiO2 by batch technique, surface complexation model and DFT calculations. Science China Chemistry, 2012, 55, 1752-1759.	4.2	17
12579	Non-equilibrium alloy phase formation and transformation driven by ion beam mixing in the Fe-Hf-Nb multilayers. Science China Technological Sciences, 2012, 55, 640-645.	2.0	3
12580	First-principles study of the adsorption of oxygen atoms on copper nanowires. Science China: Physics, Mechanics and Astronomy, 2012, 55, 413-418.	2.0	6
12581	The structural, electronic and magnetic properties of the 3d TM (V, Cr, Mn, Fe, Co, Ni and Cu) doped ZnO nanotubes: A first-principles study. Science China: Physics, Mechanics and Astronomy, 2012, 55, 428-435.	2.0	20
12582	Modulation of the electronic and magnetic properties of a GaN nanoribbon from dangling bonds. Science China: Physics, Mechanics and Astronomy, 2012, 55, 631-638.	2.0	6

#	Article	IF	Citations
12583	Stability and diffusion properties of self-interstitial atoms in tungsten: a first-principles investigation. Science China: Physics, Mechanics and Astronomy, 2012, 55, 614-618.	2.0	21
12584	AbÂInitio Studies of the Unreconstructed Polar CdTe (111) Surface. Journal of Electronic Materials, 2012, 41, 2745-2753.	1.0	13
12585	High-pressure physical properties of magnesium silicate post-perovskite from ab initio calculations. Bulletin of Materials Science, 2012, 35, 665-672.	0.8	4
12586	Metal azides under pressure: An emerging class of high energy densityÂmaterials. Journal of Chemical Sciences, 2012, 124, 1391-1398.	0.7	22
12587	Magnesium amidoborane monoammoniate: Plane-wave DFT calculations. Chemical Physics Letters, 2012, 545, 26-28.	1.2	1
12588	Stability and magnetism of tetracyanoethylene adsorbed on substitutionally doped graphene. Journal of Applied Physics, 2012, 111, 083713.	1.1	7
12589	On the buckling behavior of single-walled silicon carbide nanotubes. Scientia Iranica, 2012, 19, 1984-1990.	0.3	32
12590	The Active Site of Methanol Synthesis over Cu/ZnO/Al ₂ O ₃ Industrial Catalysts. Science, 2012, 336, 893-897.	6.0	2,018
12591	Coadsorption properties of CO2 and H2O on TiO2 rutile (110): A dispersion-corrected DFT study. Journal of Chemical Physics, 2012, 137, 074704.	1.2	63
12592	Band gap engineering in BiNbO4 for visible-light photocatalysis. Applied Physics Letters, 2012, 100, 182102.	1.5	54
12593	First-principles theoretical analysis of transition-metal doping of ZnSe quantum dots. Journal of Applied Physics, 2012, 112, 024301.	1.1	3
12594	Efficient<mml:math xmlns:mml="http://www.w3.org/1998/Math/MathML" display="inline"><mml:mrow><mml:mi>G</mml:mi><mml:mi>W</mml:mi></mml:mrow></mml:math>calculations for SnO<mml:math xmlns:mml="http://www.w3.org/1998/Math/MathML" display="inline"><mml:msub><mml:mrow /><mml:mn>2</mml:mn></mml:msub></mml:math>, ZnO, and rubrene: The effective-energy technique. Physical Review B, 2012, 85, .	1.1	56
12595	Electronic Structure of the CuCl₂(100) Surface: A DFT First-Principle Study. Journal of Nanomaterials, 2012, 2012, 1-7.	1.5	5
12596	Evolutionary Chlorination of Graphene: From Charge-Transfer Complex to Covalent Bonding and Nonbonding. Journal of Physical Chemistry C, 2012, 116, 844-850.	1.5	94
12597	Nanoscale mechanical surface properties of single crystalline martensitic Niâ€“Mnâ€“Ga ferromagnetic shape memory alloys. New Journal of Physics, 2012, 14, 033029.	1.2	24
12598	Phonon instability and mechanism of superionic conduction in Li<mml:math xmlns:mml="http://www.w3.org/1998/Math/MathML" display="inline"><mml:msub><mml:mrow /><mml:mn>2</mml:mn></mml:msub></mml:math>O. Physical Review B, 2012, 85, .	1.1	19
12599	Predicted Suppression of the Superconducting Transition of New High-Pressure Yttrium Phases with Increasing Pressure from First-Principles Calculations. Physical Review Letters, 2012, 109, 157004.	2.9	31
12600	Effect of van der Waals interactions on the structural and elastic properties of black phosphorus. Physical Review B, 2012, 86, .	1.1	315

#	Article	IF	Citations
12601	A comparative density functional study of the low pressure phases of solid ZnX, CdX, and HgX: Trends and relativistic effects. Journal of Chemical Physics, 2012, 136, 034504.	1.2	25
12602	Band gap engineering of silicene zigzag nanoribbons with perpendicular electric fields: a theoretical study. Journal of Physics Condensed Matter, 2012, 24, 455302.	0.7	33
12603	Solution and Solid-State Effects on NMR Chemical Shifts in Sesquiterpene Lactones: NMR, X-ray, and Theoretical Methods. Journal of Physical Chemistry A, 2012, 116, 680-688.	1.1	21
12604	Potential applications of two ultrathin Pd nanowires to the hydrogen economy. Journal of Materials Chemistry, 2012, 22, 20319.	6.7	12
12605	First-Principles Study of Ferromagnetism in Two-Dimensional Silicene with Hydrogenation. Journal of Physical Chemistry C, 2012, 116, 4163-4166.	1.5	246
12606	n-type doping in Cu2O with F, Cl, and Br: A first-principles study. Journal of Applied Physics, 2012, 111, .	1.1	31
12607	Band renormalization of a polymer physisorbed on graphene investigated by many-body perturbation theory. Physical Review B, 2012, 86, .	1.1	33
12608	The thermodynamic properties of cubic fluorite-type MgF₂: first-principles prediction. Physica Scripta, 2012, 85, 065707.	1.2	1
12609	Ab Initio Study of the Charge-Storage Mechanisms in RuO₂-Based Electrochemical Ultracapacitors. Journal of Physical Chemistry C, 2012, 116, 1450-1457.	1.5	61
12610	Tunable and sizable band gap of single-layer graphene sandwiched between hexagonal boron nitride. NPG Asia Materials, 2012, 4, e6-e6.	3.8	158
12611	Quantum Monte Carlo study of high-pressure cubic TiO2. Applied Physics Letters, 2012, 100, 261902.	1.5	26
12612	Ab Initio Study of the Phonon Frequency, Electrical and Thermal Properties of TiN. Applied Mechanics and Materials, 2012, 155-156, 291-297.	0.2	0
12613	Strength, hardness, and lattice vibrations of<mml:math xmlns:mml="http://www.w3.org/1998/Math/MathML" display="inline"><mml:mi>Z</mml:mi></mml:math>-carbon and<mml:math xmlns:mml="http://www.w3.org/1998/Math/MathML" display="inline"><mml:mi>W</mml:mi></mml:math>-carbon: First-principles calculations. Physical Review B, 2012, 85, .	1.1	51
12614	First-principles investigation on the elastic stability and thermodynamic properties of Ti₂SC. Chinese Physics B, 2012, 21, 056301.	0.7	12
12615	New Insight into the Atomic Structure of Electrochemically Delithiated O3-Li_(1â€“x)CoO₂ (0 â‰¤ x â‰¤ 0.5) Nanoparticles. Nano Letters, 2012, 12, 6192-6197.	12.5	128
12616	Analysis of Hydroxide Sorbents for CO₂ Capture from Warm Syngas. Industrial & Engineering Chemistry Research, 2012, 51, 13473-13481.	1.8	15
12617	Multiferroic Materials Based on Organic Transition-Metal Molecular Nanowires. Journal of the American Chemical Society, 2012, 134, 14423-14429.	6.6	49
12618	Speeding up the solution of the Bethe-Salpeter equation by a double-grid method and Wannier interpolation. Physical Review B, 2012, 86, .	1.1	42

#	Article	IF	Citations
12619	Ab initio investigations of the electronic structure and lithium stability in Li2UN2 and LiUN2. Monatshefte FÃ¼r Chemie, 2012, 143, 1341-1348.	0.9	2
12620	First-Principles Calculations on Stabilization of Iron Carbides (Fe3C, Fe5C2, and Î-Fe2C) in Steels by Common Alloying Elements. Metallurgical and Materials Transactions A: Physical Metallurgy and Materials Science, 2012, 43, 4436-4444.	1.1	52
12621	A first-principles investigation on the effects of magnetism on the Bain transformation of Î±-phase FeNi systems. Journal of Applied Physics, 2012, 111, 063503.	1.1	8
12622	Formation of native defects in the Î³-ray detector material Cs2Hg6S7. Applied Physics Letters, 2012, 101, .	1.5	11
12623	Chemical functionalization of BN graphene with the metal-arene group: a theoretical study. Journal of Materials Chemistry, 2012, 22, 9343.	6.7	21
12624	The force-field derivation and atomistic simulation of HMXâ€“fluoropolymer mixture explosives. Colloid and Polymer Science, 2012, 290, 1855-1866.	1.0	13
12625	Dynamic and steady control of quantum coherence in photonic crystals via the Zeeman effect. Science China: Physics, Mechanics and Astronomy, 2012, 55, 2300-2304.	2.0	3
12626	Diffusion behaviors of hydrogen isotopes in niobium from first-principles. Science China: Physics, Mechanics and Astronomy, 2012, 55, 2378-2382.	2.0	5
12627	DFT Study of Furfural Conversion to Furan, Furfuryl Alcohol, and 2-Methylfuran on Pd(111). ACS Catalysis, 2012, 2, 2496-2504.	5.5	232
12628	High-pressure structures and metallization of sodium chloride. Europhysics Letters, 2012, 100, 26005.	0.7	16
12629	Crystal and electronic structures of CuxS solar cell absorbers. Applied Physics Letters, 2012, 100, .	1.5	105
12630	Ab initio study of phase stability in doped TiO2. Computational Mechanics, 2012, 50, 185-194.	2.2	78
12631	Pressure-induced ferromagnetism in open structure alkali metals from first principles. Applied Physics Letters, 2012, 100, .	1.5	21
12632	Solubility and clustering of ruthenium fission products in uranium dioxide as determined by density functional theory. Physical Review B, 2012, 85, .	1.1	15
12633	Tailoring magnetocrystalline anisotropy of FePt by external strain. Journal of Applied Physics, 2012, 111, .	1.1	23
12634	Calculations of the thermodynamic and kinetic properties of Li<mml:math xmlns:mml="http://www.w3.org/1998/Math/MathML" display="inline"><mml:msub><mml:mrow /><mml:mrow><mml:mn>1</mml:mn><mml:mo>+</mml:mo><mml:mi>x</mml:mi></mml:mrow></mml:msub></mml:math>V<mml:math xmlns:mml="http://www.w3.org/1998/Math/MathML" display="inline"><mml:msub><mml:mrow /><mml:mn>3</mml:mn></mml:msub></mml:math>O<mml:math xmlns:mml="http://www.w3.org/1998/Math/MathML" display="inline"><mml:msub><mml:mrow /><mml:mrow /></mml:msub></mml:math>	1.1	16
12635	First-principles study of electronic structure and magnetic properties of Cu-doped CeO2. Journal of Applied Physics, 2012, 112, .	1.1	6
12636	Mechanisms for the decomposition and dehydrogenation of Li amide/imide. Physical Review B, 2012, 85, .	1.1	27

#	Article	IF	Citations
12637	Creation and Destruction of Morphotropic Phase Boundaries through Electrical Poling: A Case Study of Lead-Free <mml:math xmlns:mml="http://www.w3.org/1998/Math/MathML" display="inline"><mml:mo mathvariant="bold"		

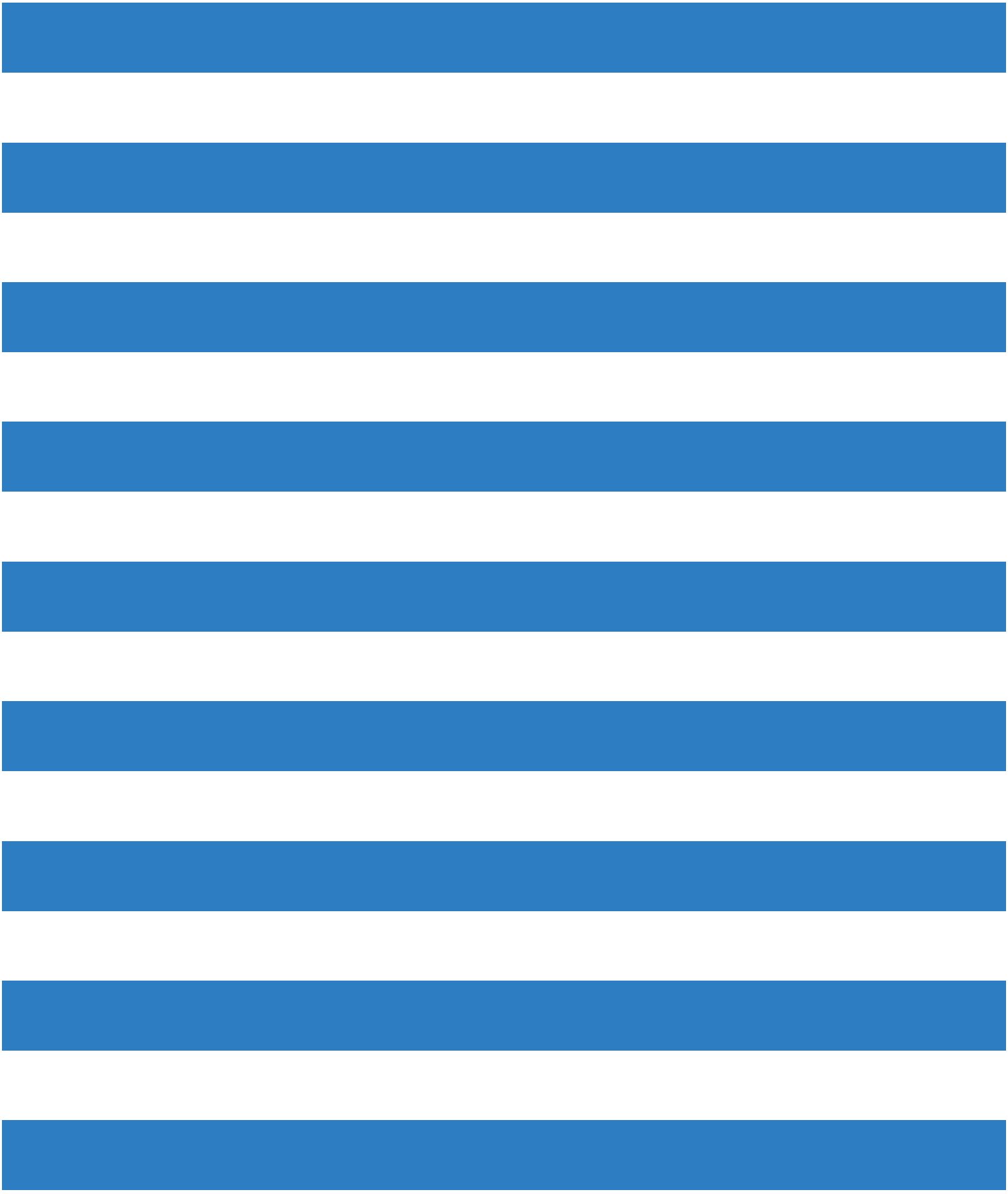

#	Article	IF	Citations
12655	Electronic and Structural Properties of BC₃ Nanotubes with Defects. Journal of Physical Chemistry C, 2012, 116, 13225-13230.	1.5	21
12656	Formation energy of dangling bonds on hydrogenated diamond surfaces: A first-principles study. Physical Review B, 2012, 85, .	1.1	5
12657	Discovery of the Ternary Nanolaminated Compound<mml:math xmlns:mml="http://www.w3.org/1998/Math/MathML" display="inline"><mml:msub><mml:mi>Nb</mml:mi><mml:mn>2</mml:mn></mml:msub><mml:mi>GeC</mml:mi></mml:math>by a Systematic Theoretical-Experimental Approach. Physical Review Letters, 2012, 109, 035502.	2.9	73
12658	Selective nucleation induced by defect nanostructures: A way to control cobalt disilicide precipitation during ion implantation. Journal of Applied Physics, 2012, 112, 123504.	1.1	6
12659	Ab initiostudy of neutral (TiO₂)_nclusters and their interactions with water and transition metal atoms. Journal of Physics Condensed Matter, 2012, 24, 305301.	0.7	27
12660	Tunable and sizable band gap in silicene by surface adsorption. Scientific Reports, 2012, 2, 853.	1.6	253
12661	New Crystal Structures of IrB and IrB₂: First-Principles Calculations. Journal of Physical Chemistry C, 2012, 116, 21961-21966.	1.5	19
12662	Band gap engineering by functionalization of BN sheet. Physical Review B, 2012, 85, .	1.1	135
12663	Physical properties of thermoelectric zinc antimonide using first-principles calculations. Physical Review B, 2012, 85, .	1.1	59
12664	Terahertz Spectroscopy of the Explosive Taggant 2,3-Dimethyl-2,3-Dinitrobutane. Journal of Physical Chemistry A, 2012, 116, 6879-6884.	1.1	15
12665	Strain-induced semimetal-metal transition in silicene. Europhysics Letters, 2012, 99, 17010.	0.7	75
12666	High-Pressure Structures of Disilane and Their Superconducting Properties. Physical Review Letters, 2012, 108, 117004.	2.9	86
12667	Quantum mechanically guided design of Co₄₃Fe₂₀Ta_{5.5}X_{31.5}(X=B, Si, P, S) metallic glasses. Journal of Physics Condensed Matter, 2012, 24, 175402.	0.7	5
12668	First-principles study of spontaneous polarization and band gap bowing in ScxAlyGa1 â^'xâ^'yN alloys lattice-matched to GaN. Semiconductor Science and Technology, 2012, 27, 105014.	1.0	4
12669	Lattice Dynamics Study of Magnesium Chalcogenides. Communications in Theoretical Physics, 2012, 57, 295-300.	1.1	5
12670	Elastic and electronic properties of tI26-type Mg₁₂RE (RE = Ce, Pr and Nd) phases. Modelling and Simulation in Materials Science and Engineering, 2012, 20, 035018.	0.8	50
12671	Large Volume Collapse during Pressure-Induced Phase Transition in Lithium Amide. Journal of Physical Chemistry C, 2012, 116, 9744-9749.	1.5	32
12672	Understanding the Origins of Conformational Disorder in the Crystalline Polymorphs of Irbesartan. Crystal Growth and Design, 2012, 12, 5017-5024.	1.4	50

#	Article	IF	Citations
12673	Nanotube-based scanning rotational microscope. Applied Physics Letters, 2012, 100, 173101.	1.5	8
12674	Y_xAl_{1â^'x}N thin films. Journal Physics D: Applied Physics, 2012, 45, 422001.	1.3	42
12675	Applying precipitateâ€“host lattice coherency for compositional determination of precipitates in Alâ€“Mgâ€“Siâ€“Cu alloys. Philosophical Magazine, 2012, 92, 3833-3856.	0.7	47
12676	Hydrogenation of Ferrimagnetic Graphene on a Co Surface: Significant Enhancement of Spin Moments by Câ€“H Functionality. Journal of Physical Chemistry Letters, 2012, 3, 2582-2587.	2.1	9
12677	Role of Si as carrier suppressor in amorphous Znâ€“Snâ€“O. Current Applied Physics, 2012, 12, S12-S16.	1.1	36
12678	First-principles study of bandgap effects in graphene due to hydrogen adsorption. Journal of Physics Condensed Matter, 2012, 24, 235304.	0.7	13
12679	Ab initiostudy of phase transition and dielectric constants of high-<mml:math xmlns:mml="http://www.w3.org/1998/Math/MathML" display="inline"><mml:mi>Î</mml:mi></mml:math>HfO<mml:math xmlns:mml="http://www.w3.org/1998/Math/MathML" display="inline"><mml:msub><mml:mrow /><mml:mn>2</mml:mn></mml:msub></mml:math>as a function of Ge alloying. Physical Review B, 2012, 85, .	1.1	11
12680	First-principles investigation of chemical and structural disorder in magnetic Ni<mml:math xmlns:mml="http://www.w3.org/1998/Math/MathML" display="inline"><mml:msub><mml:mrow /><mml:mn>2</mml:mn></mml:msub></mml:math>Mn<mml:math xmlns:mml="http://www.w3.org/1998/Math/MathML" display="inline"><mml:msub><mml:mrow /><mml:mn>1</mml:mn><mml:mo>â^'</mml:mo><mml:mi>x</mml:mi></mml:mrow></mml:msub></mml:math>Sn<mml:math xmlns:mml="http://www.w3.org/1998/Math/MathML" display="inline"><mml:msub><mml:mrow /><mml:mn>1</mml:mn><mml:mo>+</mml:mo><mml:mi>x</mml:mi></mml:mrow></mml:msub></mml:math>Heusler alloys: Spin-lattice coupling and phonon dispersion. Physical Review B, 2012, 85, .	1.1	111
12681	Pressure-induced phase transitions and structure of chemically ordered nanoregions in the lead-free relaxor ferroelectric Na<mml:math xmlns:mml="http://www.w3.org/1998/Math/MathML" display="inline"><mml:msub><mml:mrow /><mml:mn>1</mml:mn><mml:mo>/</mml:mo><mml:mn>2</mml:mn></mml:mrow></mml:msub></mml:math>Bi<mml:math xmlns:mml="http://www.w3.org/1998/Math/MathML" display="inline"><mml:msub><mml:mrow /><mml:mn>1</mml:mn><mml:mo>/</mml:mo><mml:mn>2</mml:mn></mml:mrow></mml:msub></mml:math>.	1.1	32
12682	Ab initiostudy of phase transition and dielectric constants of high-<mml:math xmlns:mml="http://www.w3.org/1998/Math/MathML" display="inline"><mml:msub><mml:mrow /><mml:mn>2</mml:mn></mml:msub></mml:math>O<mml:math xmlns:mml="http://www.w3.org/1998/Math/MathML" display="inline"><mml:msub><mml:mrow /><mml:mn>4</mml:mn></mml:msub></mml:math>from first principles. Physical Review B, 2012, 86, .	1.1	25
12683	Origin of the Ferrielectricty and Visible-Light Photocatalytic Activity of Silver Niobate AgNbO₃. Journal of Physical Chemistry C, 2012, 116, 24902-24906.	1.5	43
12684	BN-Embedded Graphene with a Ubiquitous Gap Opening. Journal of Physical Chemistry C, 2012, 116, 21098-21103.	1.5	83
12685	Concentration of point defects in wurtzite AlN: A hybrid functional study. Europhysics Letters, 2012, 98, 36003.	0.7	14
12686	Intriguing Behavior of Halogenated Two-Dimensional Tin. Journal of Physical Chemistry C, 2012, 116, 12977-12981.	1.5	54
12687	DFT+U Study of Properties of MoO₃ and Hydrogen Adsorption on MoO₃(010). Journal of Physical Chemistry C, 2012, 116, 25757-25764.	1.5	79
12688	Ideal tensile and shear strength of a gum metal approximant:Ab initiodensity functional calculations. Physical Review B, 2012, 85, .	1.1	19
12689	Pressure-induced phase transitions and structure of chemically ordered nanoregions in the lead-free relaxor ferroelectric Na<mml:math xmlns:mml="http://www.w3.org/1998/Math/MathML" display="inline"><mml:msub><mml:mrow /><mml:mn>1</mml:mn><mml:mo>/</mml:mo><mml:mn>2</mml:mn></mml:mrow></mml:msub></mml:math>Bi<mml:math xmlns:mml="http://www.w3.org/1998/Math/MathML" display="inline"><mml:msub><mml:mrow /><mml:mn>1</mml:mn><mml:mo>/</mml:mo><mml:mn>2</mml:mn></mml:mrow></mml:msub></mml:math>.	1.1	32
12690	Density functional theory studies of Nbâ€“benzene and Nbâ€“borazine sandwich clusters and molecular wires. Journal of Physics B: Atomic, Molecular and Optical Physics, 2012, 45, 025102.	0.6	6

#	Article	IF	Citations
12691	Band-Gap Engineering of Carbon Nanotubes with Grain Boundaries. Journal of Physical Chemistry C, 2012, 116, 2271-2277.	1.5	11
12692	Ab Initio Thermodynamic Study of the CO2Capture Properties of Potassium Carbonate Sesquihydrate, K2CO3Â·1.5H2O. Journal of Physical Chemistry C, 2012, 116, 14461-14470.	1.5	36
12693	First-Principles Study of Lithium Adsorption and Diffusion on Graphene with Point Defects. Journal of Physical Chemistry C, 2012, 116, 21780-21787.	1.5	256
12694	Effects of site disorder, off-stoichiometry and epitaxial strain on the optical properties of magnetoelectric gallium ferrite. Journal of Physics Condensed Matter, 2012, 24, 435501.	0.7	14
12695	Theoretical studies of elastic and thermodynamic properties of cubic B20 CoSi. Physica B: Condensed Matter, 2012, 407, 4700-4705.	1.3	13
12696	Stability of the bandgap in Cu-poor CuInSe₂. Journal of Physics Condensed Matter, 2012, 24, 455503.	0.7	10
12697	Local suppression of ferroelectricity at PbTiO₃surface steps: a density functional theory study. Journal of Physics Condensed Matter, 2012, 24, 045903.	0.7	9
12698	Periodic trends in electron transport through extended metal atom chains: comparison of Ru3(dpa)4(NCS)2 with its first-row analogues. Chemical Science, 2012, 3, 1319.	3.7	35
12699	Theoretical prediction of mechanical stability of ferromagnetic fcc Fe-Cu alloys from first principles. Journal of Applied Physics, 2012, 111, 053517.	1.1	11
12700	Bifunctional Mixed-Lanthanide Cyano-Bridged Coordination Polymers Ln0.5Lnâ€²0.5(H2O)5[W(CN)8] (Ln/Lnâ€²) Ti ETQq1 1 0.784314	1.9	41
12701	Adsorption and Cyclotrimerization Kinetics of C₂H₂ at a Cu(110) Surface. Journal of Physical Chemistry C, 2012, 116, 9550-9560.	1.5	20
12702	DFT-Based Molecular Transport Implementation in ADF/BAND. Journal of Physical Chemistry C, 2012, 116, 24393-24412.	1.5	42
12703	The electronic structure of RbTiOPO₄and the effects of the A-site cation substitution in KTiOPO₄-family crystals. Journal of Physics Condensed Matter, 2012, 24, 405503.	0.7	32
12704	Electronic Structure, Optical Properties, and Photocatalytic Activities of LaFeO₃â€“NaTaO₃ Solid Solution. Journal of Physical Chemistry C, 2012, 116, 22767-22773.	1.5	60
12705	Density Functional Theory Simulation of NEXAFS Spectra of Molecules Adsorbed on Surfaces: C₂H₄ on Si(100) Case Study. Journal of Physical Chemistry C, 2012, 116, 18910-18919.	1.5	16
12706	Structural, electronic properties and heat of formation of Mg₂FeH₆complex hydride: anab initiostudy. Physica Scripta, 2012, 86, 015701.	1.2	16
12707	Strain-induced changes to the electronic structure of germanium. Journal of Physics Condensed Matter, 2012, 24, 195802.	0.7	67
12708	Carbon allotropes with triple bond predicted by first-principle calculation: Triple bond modified diamond and<mml:math xmlns:mml="http://www.w3.org/1998/Math/MathML" display="inline"><mml:mrow><mml:mi>T</mml:mi></mml:mrow></mml:math>-carbon. Physical Review B, 2012, 86, .	1.1	72

#	Article	IF	Citations
12709	Lowest enthalpy polymorph of cold-compressed graphite phase. Physical Chemistry Chemical Physics, 2012, 14, 4347.	1.3	80
12710	Superhard F-carbon predicted byab initioparticle-swarm optimization methodology. Journal of Physics Condensed Matter, 2012, 24, 165504.	0.7	42
12711	Identifying a Structural Preference in Reduced Rare-Earth Metal Halides by Combining Experimental and Computational Techniques. Inorganic Chemistry, 2012, 51, 11356-11364.	1.9	29
12712	The interaction of iron pyrite with oxygen, nitrogen and nitrogen oxides: a first-principles study. Physical Chemistry Chemical Physics, 2012, 14, 3627.	1.3	27
12713	Structural investigation of aluminium doped ZnO nanoparticles by solid-state NMR spectroscopy. Physical Chemistry Chemical Physics, 2012, 14, 11610.	1.3	60
12714	Giant piezoelectric resistance effect of nanoscale zinc oxide tunnel junctions: first principles simulations. Physical Chemistry Chemical Physics, 2012, 14, 7051.	1.3	14
12715	Tetragonal Allotrope of Group 14 Elements. Journal of the American Chemical Society, 2012, 134, 12362-12365.	6.6	170
12716	Periodic DFT Study of the Tetragonal ZrO₂ Nanocrystals: Equilibrium Morphology Modeling and Atomistic Surface Hydration Thermodynamics. Journal of Physical Chemistry C, 2012, 116, 19307-19320.	1.5	63
12717	Phonons and superconductivity in the cubic perovskite Cr3RhN. Journal of Applied Physics, 2012, 112, .	1.1	15
12718	Oxidation of a two-dimensional hexagonal boron nitride monolayer: a first-principles study. Physical Chemistry Chemical Physics, 2012, 14, 5545.	1.3	90
12719	A database for equations of state and resistivities measurements in the warm dense matter regime. Physics of Plasmas, 2012, 19, 082702.	0.7	65
12720	Theoretical study on the possibility of using silicon carbide nanotubes as dehydrogenation catalysts for ammoniaâ€“borane. RSC Advances, 2012, 2, 7561.	1.7	15
12721	Bonding and structural changes in siderite at high pressure. American Mineralogist, 2012, 97, 1421-1426.	0.9	45
12722	DFT-BASEDAB INITIOSTUDY OF THE ELECTRONIC AND OPTICAL PROPERTIES OF CESIUM BASED FLUORO-PEROVSKITECsMF₃(M = CaANDSr). International Journal of Modern Physics B, 2012, 26, 1250199.	1.0	18
12723	First-principles study on electronic structures and magnetic properties of AlN nanosheets and nanoribbons. Journal of Applied Physics, 2012, 111, .	1.1	58
12724	Electrical and thermal conductivity of Al liquid at high pressures and temperatures fromab initiocomputations. Physical Review B, 2012, 85, .	1.1	37
12725	Stability of Graphene Edges under Electron Beam: Equilibrium Energetics versus Dynamic Effects. ACS Nano, 2012, 6, 671-676.	7.3	120
12726	Thermodynamic properties of neptunium nitride: a first principles study. Journal of Nuclear Science and Technology, 2012, 49, 328-333.	0.7	6

#	Article	IF	Citations
12727	Size Effects in Monolayer Catalysisâ€"Model Study: Pt Submonolayers on Au(111). Electrocatalysis, 2012, 3, 203-210.	1.5	38
12728	Calculation of the lattice dynamics and Raman spectra of copper zinc tin chalcogenides and comparison to experiments. Journal of Applied Physics, 2012, 111, .	1.1	221
12729	Mechanical, Electronic, and Adsorption Properties of Porous Aromatic Frameworks. Journal of Physical Chemistry C, 2012, 116, 22878-22884.	1.5	22
12730	Dislocations and Grain Boundaries in Two-Dimensional Boron Nitride. ACS Nano, 2012, 6, 7053-7058.	7.3	216
12731	Chemical bonding, conductive network, and thermoelectric performance of the ternary semiconductors Cu<mml:math xmlns:mml="http://www.w3.org/1998/Math/MathML" display="inline"><mml:msub><mml:mrow /><mml:mn>2</mml:mn></mml:msub></mml:math>Sn<mml:math xmlns:mml="http://www.w3.org/1998/Math/MathML"		

#	Article	IF	Citations
12745	Evidence of the Existence of Magnetism in Pristine VX₂ Monolayers (X = S, Se) and Their Strain-Induced Tunable Magnetic Properties. ACS Nano, 2012, 6, 1695-1701.	7.3	733
12746	Towards theoretical connection between tensile strength of a grain boundary and segregated impurity concentration: Helium in iron as an example. Europhysics Letters, 2012, 98, 17001.	0.7	28
12747	Mechanistic Insights on the Hydrogenation of Î±,Î²-Unsaturated Ketones and Aldehydes to Unsaturated Alcohols over Metal Catalysts. ACS Catalysis, 2012, 2, 671-683.	5.5	206
12748	Fe-Anchored Graphene Oxide: A Low-Cost and Easily Accessible Catalyst for Low-Temperature CO Oxidation. Journal of Physical Chemistry C, 2012, 116, 2507-2514.	1.5	189
12749	Effects of 3<mml:math xmlns:mml="http://www.w3.org/1998/Math/MathML" display="inline"><mml:mi>d</mml:mi></mml:math>and 4<mml:math xmlns:mml="http://www.w3.org/1998/Math/MathML" display="inline"><mml:mi>d</mml:mi></mml:math>transition metal substitutional impurities on the electronic properties of CrO<mml:math xmlns:mml="http://www.w3.org/1998/Math/MathML" display="inline"><mml:msub><mml:mrow /><mml:mn>2</mml:mn></mml:msub></mml:math>. Physical Re	1.1	11
12750	Dominant Factors Governing the Rate Capability of a TiO₂ Nanotube Anode for High Power Lithium Ion Batteries. ACS Nano, 2012, 6, 8308-8315.	7.3	184
12751	First Principles Calculations of 1-methoxymethyl-1-methylpyrrolidinium and 1-ethyl-3-methylimidazolium Adsorption on Graphene. Journal of the Vacuum Society of Japan, 2012, 55, 198-203.	0.3	2
12752	Guanine: A Combined Study Using Vibrational Spectroscopy and Theoretical Methods. Spectroscopy, 2012, 27, 273-292.	0.8	50
12753	Effect of Fe Concentration on Fe-Doped Anatase TiO₂from GGA +UCalculations. International Journal of Photoenergy, 2012, 2012, 1-6.	1.4	19
12754	Ab initiomodelling of UN grain boundary interfaces. IOP Conference Series: Materials Science and Engineering, 2012, 38, 012058.	0.3	0
12755	First Principles Simulations on Surface Properties and Oxidation of Nitride Nuclear Fuels. , 0, , .		5
12756	Surface Properties of Transparent Conducting Oxides from First Principles: In₂O₃, SnO₂, and ZnO. E-Journal of Surface Science and Nanotechnology, 2012, 10, 216-220.	0.1	2
12757	Experimental Study and Atomic Level Description of Adsorption Process of CO2 on Doped Alkaline Earth Oxides. ISIJ International, 2012, 52, 1233-1240.	0.6	4
12758	Plasma Sprayed Bioceramic Coatings on Ti-Based Substrates: Methods for Investigation of Their Crystallographic Structures and Mechanical Properties. , 0, , .		1
12759	Stable structure and effects of sulfur in CdTe/CdS heterojunctions. Surface and Interface Analysis, 2012, 44, 434-438.	0.8	10
12760	Magnetic ordering and electronic properties of Pdâ€doped ZnO. Physica Status Solidi (B): Basic Research, 2012, 249, 198-201.	0.7	6
12761	Boron and nitrogen substitutional impurities inducing magnetic and halfâ€metallic behavior in zigzag silicon carbon nanoribbons. Physica Status Solidi (B): Basic Research, 2012, 249, 91-98.	0.7	22
12762	Impact of shortâ€range order and clusterization on the bandgap bowing: Firstâ€principles calculations on the electronic properties of metastable (GaAs)_{1â€“x}(Ge₂)_x alloys. Physica Status Solidi (B): Basic Research, 2012, 249, 29-37.	0.7	4

#	Article	IF	Citations
12763	Firstâ€principles studies of structural and electronic properties of layered C₃N phases. Physica Status Solidi (B): Basic Research, 2012, 249, 784-788.	0.7	30
12764	CO adsorption on metalâ€oxide surfaces doped with transitionâ€metal adatoms. Physica Status Solidi (B): Basic Research, 2012, 249, 1046-1057.	0.7	11
12765	Thermodynamic stability of BaTiO₃ (110) surfaces. Physica Status Solidi (B): Basic Research, 2012, 249, 796-800.	0.7	17
12766	Role of nitrogen distribution in asymmetric Stoneâ€“Wales defects on electronic transport of graphene nanoribbons. Physica Status Solidi (B): Basic Research, 2012, 249, 128-133.	0.7	4
12767	Magnetic properties in semifluorinated GaN sheet from first principles calculations. Physica Status Solidi (B): Basic Research, 2012, 249, 1465-1469.	0.7	10
12768	Boehmite (Î³â€AlOOH) nanoparticles: Hydrothermal synthesis, characterization, pHâ€controlled morphologies, optical properties, and DFT calculations. Physica Status Solidi (B): Basic Research, 2012, 249, 1264-1270.	0.7	52
12769	Ab initio density functional theory calculation of stacking fault energy and stress in 3Câ€SiC. Physica Status Solidi (B): Basic Research, 2012, 249, 1229-1234.	0.7	23
12770	Synthesis and firstâ€principles calculations of the structural and electronic properties of typeâ€I clathrates Sr₈Ga₁₆Sn_xGe_{30â€‰â^'â€‰x}. Physica Status Solidi (B): Basic Research, 2012, 249, 1423-1430.	0.7	3
12771	Properties of crystalline coronene: Dispersion forces leading to a larger van der Waals radius for carbon. Physica Status Solidi (B): Basic Research, 2012, 249, 1438-1444.	0.7	27
12772	Controlling the Electrical Behavior of Semiconducting Carbon Nanotubes via Tube Contact. Small, 2012, 8, 220-224.	5.2	7
12773	Barium Peroxide: a Simple Test Case for Firstâ€Principles Investigations on the Temperature Dependence of Solidâ€State Vibrational Frequencies. Zeitschrift Fur Anorganische Und Allgemeine Chemie, 2012, 638, 1403-1406.	0.6	8
12774	Crystal Structure and Vibrational Properties of a Sodium Oxoferrate(II) Hydroxide, Na₅[FeO₃][OH]. Zeitschrift Fur Anorganische Und Allgemeine Chemie, 2012, 638, 2087-2092.	0.6	4
12775	Atomic and electronic structure of rigid carbon atomic chains. Physica Status Solidi (A) Applications and Materials Science, 2012, 209, 1738-1743.	0.8	2
12776	Thermodynamic stability and electronic properties of Fâ€and Clâ€terminated diamond. Physica Status Solidi (A) Applications and Materials Science, 2012, 209, 1709-1714.	0.8	8
12777	Bromine functionalisation of diamond: An ab initio study. Physica Status Solidi (A) Applications and Materials Science, 2012, 209, 1703-1708.	0.8	10
12778	Effect of different surface coverages of transition metals on the electronic and structural properties of diamond. Physica Status Solidi (A) Applications and Materials Science, 2012, 209, 1697-1702.	0.8	16
12779	Hydrogen in Câ€rich Si and the diffusion of vacancyâ€“H complexes. Physica Status Solidi (A) Applications and Materials Science, 2012, 209, 1872-1879.	0.8	24
12780	Light induced degradation in B doped Czâ€Si solar cells. Physica Status Solidi (A) Applications and Materials Science, 2012, 209, 1894-1897.	0.8	11

#	Article	IF	Citations
12781	Local structures and roles of Fe³⁺ and Cr³⁺ in pâ€type semiconductor CuAlO₂. Physica Status Solidi (B): Basic Research, 2012, 249, 1559-1565.	0.7	6
12782	Mechanical properties of L1₂ type Al₃X (Xâ€‰=â€‰Mg, Sc, Zr) from firstâ€principles study. Physica Status Solidi (B): Basic Research, 2012, 249, 1510-1516.	0.7	23
12783	Pressureâ€dependent properties of a multifunctional material: Lithium platinum boride (LiPt₃B). Physica Status Solidi (B): Basic Research, 2012, 249, 1744-1755.	0.7	3
12784	Density functional study of the TiN/Ge₂Sb₂Te₅ interface. Physica Status Solidi (B): Basic Research, 2012, 249, 2140-2144.	0.7	9
12785	Electronic structure and enhanced visibleâ€light absorption of N,Bâ€codoped TiO₂. Physica Status Solidi - Rapid Research Letters, 2012, 6, 172-174.	1.2	7
12786	Adsorption of polyfunctional 5â€fluorouracil and 2,4â€dithioâ€5â€fluorouracil on Au(111) surface: Structure, energy, and electronic transmission. International Journal of Quantum Chemistry, 2012, 112, 2287-2293.	1.0	2
12787	Hydrogenâ€“hydrogen interaction in the LaNiInH_{4/3} hydride. International Journal of Quantum Chemistry, 2012, 112, 3490-3497.	1.0	3
12788	Firstâ€principles study of oxidized BC₂N nanotubes. International Journal of Quantum Chemistry, 2012, 112, 3312-3319.	1.0	6
12789	Hydrogen site occupation and electronic structure in the La₂Ni₂In intermetallic and hydrides. International Journal of Quantum Chemistry, 2012, 112, 3606-3611.	1.0	0
12790	Adhesion, atomic structure, and bonding variation at TiN/VN interface by chemical segregation. Surface and Interface Analysis, 2012, 44, 1261-1270.	0.8	6
12791	Change in the electronic properties of an InAs (111)A surface at oxygen and fluorine adsorption. Semiconductors, 2012, 46, 49-55.	0.2	8
12792	The structural, elastic and thermodynamic properties of intermetallic compound CeGa2. Open Physics, 2012, 10, .	0.8	0
12793	The nonlinear optical susceptibility and electro-optic tensor of ferroelectrics: first-principle study. Open Physics, 2012, 10, .	0.8	15
12794	Octahedral Rotationâ€Induced Ferroelectricity in Cation Ordered Perovskites. Advanced Materials, 2012, 24, 1961-1968.	11.1	288
12795	High-pressure melting curve of platinum fromab initioZ method. Physical Review B, 2012, 85, .	1.1	50
12796	Hydrogen Adsorption on Co Surfaces: A Density Functional Theory and Temperature Programmed Desorption Study. ACS Catalysis, 2012, 2, 1097-1107.	5.5	107
12797	Structural phase transition in LiFeSi2O6fromab initiocalculations. Journal of Physics Condensed Matter, 2012, 24, 195401.	0.7	4
12798	First-Principles Investigation of NO_x and SO_x Adsorption on Anatase-Supported BaO and Pt Overlayers. Journal of Physical Chemistry C, 2012, 116, 6191-6199.	1.5	20

#	Article	IF	Citations
12799	The Fuzzy Quantum Proton in the Hydrogen Chloride Hydrates. Journal of the American Chemical Society, 2012, 134, 8557-8569.	6.6	45
12800	Mechanically tunable magnetism on graphene nanoribbon adsorbed SiO2 surface. Journal of Applied Physics, 2012, 111, 074317.	1.1	5
12801	Ionic Polymers as a New Structural Motif for High-Energy-Density Materials. Journal of the American Chemical Society, 2012, 134, 1422-1425.	6.6	233
12802	The Structure, Thermodynamics, and Solubility of Organic Crystals from Simulation with a Polarizable Force Field. Journal of Chemical Theory and Computation, 2012, 8, 1721-1736.	2.3	77
12803	Hierarchical Nanoporous PtFe Alloy with Multimodal Size Distributions and Its Catalytic Performance toward Methanol Electrooxidation. Langmuir, 2012, 28, 1886-1892.	1.6	96
12804	Surface-Enhanced Decomposition Kinetics of Molecular Materials Illustrated with Cyclotetramethylene-tetranitramine. Journal of Physical Chemistry C, 2012, 116, 11077-11081.	1.5	52
12805	Domain Structure in the Tetragonal Phase of BaTiO₃â€“ from Bulk to Nanoparticles. Ferroelectrics, 2012, 426, 21-30.	0.3	14
12806	The structural, dielectric, elastic, and piezoelectric properties of KNbO3 from first-principles methods. Journal of Applied Physics, 2012, 111, .	1.1	42
12807	Symmetrical Negative Differential Resistance Behavior of a Resistive Switching Device. ACS Nano, 2012, 6, 2517-2523.	7.3	103
12808	Room temperature ferromagnetism in Teflon due to carbon dangling bonds. Nature Communications, 2012, 3, 727.	5.8	56
12809	From layers to nanotubes: Transition metal disulfides TMS2. European Physical Journal B, 2012, 85, 1.	0.6	67
12810	Ab initioEPR parameters for dangling-bond defect complexes in silicon: Effect of Jahn-Teller distortion. Physical Review B, 2012, 85, .	1.1	14
12811	Thermoelectric properties of Ba-Cu-Si clathrates. Physical Review B, 2012, 85, .	1.1	35
12812	Silicene: Compelling Experimental Evidence for Graphenelike Two-Dimensional Silicon. Physical Review Letters, 2012, 108, 155501.	2.9	3,275
12813	Investigation of Vibrational Modes and Phonon Density of States in ZnO Quantum Dots. Journal of Physical Chemistry C, 2012, 116, 6893-6901.	1.5	37
12814	Configuration and binding energy of multiple hydrogen atoms trapped in monovacancy in bcc transition metals. Physical Review B, 2012, 85, .	1.1	100
12815	A red metallic oxide photocatalyst. Nature Materials, 2012, 11, 595-598.	13.3	430
12816	Structure and Energetics of Shuttlecock-Shaped Tin-Phthalocyanine on Ag(111): A Density Functional Study Employing Dispersion Correction. Journal of Physical Chemistry C, 2012, 116, 9487-9497.	1.5	25

#	Article	IF	Citations
12817	Band-gap engineering in chemically conjugated bilayer graphene:Ab initiocalculations. Physical Review B, 2012, 85, .	1.1	29
12818	Solution of the Bethe-Salpeter equation without empty electronic states: Application to the absorption spectra of bulk systems. Physical Review B, 2012, 85, .	1.1	49
12819	Nature of Ag Islands and Nanoparticles on the CeO₂(111) Surface. Journal of Physical Chemistry C, 2012, 116, 1122-1132.	1.5	92
12820	Novel Structural Motifs in Low Energy Phases of<mml:math xmlns:mml="http://www.w3.org/1998/Math/MathML" display="inline"><mml:msub><mml:mi>LiAlH</mml:mi><mml:mn>4</mml:mn></mml:msub></mml:math>. Physical Review Letters, 2012, 108, 205505.	2.9	43
12821	Magnetic properties of Co2C and Co3C nanoparticles and their assemblies. Applied Physics Letters, 2012, 101, .	1.5	64
12822	Interplay between nitrogen dopants and native point defects in graphene. Physical Review B, 2012, 85, .	1.1	133
12823	Study on the electronic structure and hydrogen adsorption by transition metal decorated single wall carbon nanotubes. Journal of Physics Condensed Matter, 2012, 24, 185505.	0.7	53
12824	Site-Specific Transition Metal Occupation in Multicomponent Pyrophosphate for Improved Electrochemical and Thermal Properties in Lithium Battery Cathodes: A Combined Experimental and Theoretical Study. Journal of the American Chemical Society, 2012, 134, 11740-11748.	6.6	37
12825	Stable, Single-Layer MX₂ Transition-Metal Oxides and Dichalcogenides in a Honeycomb-Like Structure. Journal of Physical Chemistry C, 2012, 116, 8983-8999.	1.5	1,196
12826	Systhesis, phase transformation and photoluminescence properties of Eu:La1â^'xGdxVO4 nanofibers by electrospinning method. Nanoscale, 2012, 4, 5065.	2.8	18
12827	Ab initioinvestigation of FeAs/GaAs heterostructures for potential spintronic and superconducting applications. Physical Review B, 2012, 85, .	1.1	6
12828	Structure-driven mixed-site borateâ€“phosphate K5Ta8BP4O34: synthesis, structural, spectroscopic and theoretical study. CrystEngComm, 2012, 14, 5071.	1.3	7
12829	Magnetism mechanism in ZnO and ZnO doped with nonmagnetic elements X (Xâ€‰=â€‰Li, Mg, and Al): A first-principles study. Applied Physics Letters, 2012, 100, .	1.5	44
12830	Dispersion-Corrected Density Functional Theory and Classical Force Field Calculations of Water Loading on a Pyrophyllite(001) Surface. Journal of Physical Chemistry C, 2012, 116, 17134-17141.	1.5	40
12831	First-principles study of lithium intercalated bilayer graphene. Science China: Physics, Mechanics and Astronomy, 2012, 55, 1376-1382.	2.0	28
12832	Effect of van der Waals interaction on energetics and transport properties of a single anthracene molecule adsorbed or confined inside a carbon nanotube. Physical Review B, 2012, 85, .	1.1	5
12833	P-type doping of lithium peroxide with carbon sheets. Applied Physics Letters, 2012, 101, .	1.5	19
12834	The roles of Ï€ electrons in the electronic structures and optical properties of graphyne. Science Bulletin, 2012, 57, 3080-3085.	1.7	15

#	Article	IF	Citations
12835	Highly entangled K0.5V2O5 superlong nanobelt membranes for flexible nonvolatile memory devices. Journal of Materials Chemistry, 2012, 22, 18214.	6.7	22
12836	Calculating the energy of vacancies and adatoms in a hexagonal SiC monolayer. Russian Journal of Physical Chemistry A, 2012, 86, 1091-1095.	0.1	3
12837	Quantum-chemical calculations on the stability and mobility of vacancies in graphene. Russian Journal of Physical Chemistry A, 2012, 86, 1088-1090.	0.1	3
12838	First-principles study of hydrogen ordering in lanthanum hydride and its effect on the metal-insulator transition. Physical Review B, 2012, 86, .	1.1	5
12839	Dangling bonds and magnetism of grain boundaries in graphene. Physical Review B, 2012, 85, .	1.1	57
12840	Electronic Structure Engineering in Heterogeneous Catalysis: Identifying Novel Alloy Catalysts Based on Rapid Screening for Materials with Desired Electronic Properties. Topics in Catalysis, 2012, 55, 376-390.	1.3	80
12841	A Comparative Density Functional Theory Study of Water Gas Shift Over PdZn(111) and NiZn(111). Topics in Catalysis, 2012, 55, 313-321.	1.3	12
12842	Electrically controlled electron transfer and resistance switching in reduced graphene oxide noncovalently functionalized with thionine. Journal of Materials Chemistry, 2012, 22, 16422.	6.7	42
12843	Firstâ€principles calculations on thermodynamic properties of BaTiO₃ rhombohedral phase. Journal of Computational Chemistry, 2012, 33, 1554-1563.	1.5	12
12844	A new massively parallel version of CRYSTAL for large systems on high performance computing architectures. Journal of Computational Chemistry, 2012, 33, 2276-2284.	1.5	43
12845	Simulation of vibrational spectra of crystals by ab initio calculations: an invaluable aid in the assignment and interpretation of the Raman signals. The case of jadeite (NaAlSi 2 O 6). Journal of Raman Spectroscopy, 2012, 43, 1567-1569.	1.2	29
12846	Computing Raman and infrared wavenumbers of nanostructures: application to silicon nanowires. Journal of Raman Spectroscopy, 2012, 43, 1214-1220.	1.2	2
12847	Firstâ€principles study on influence of alloying elements on electrochemical stability of cobaltâ€base alloys. Materials and Corrosion - Werkstoffe Und Korrosion, 2012, 63, 735-738.	0.8	9
12848	Solidâ€state ¹¹B and ¹³C NMR, IR, and Xâ€ray crystallographic characterization of selected arylboronic acids and their catechol cyclic esters. Magnetic Resonance in Chemistry, 2012, 50, 388-401.	1.1	30
12849	Firstâ€principles calculations on the four phases of BaTiO₃. Journal of Computational Chemistry, 2012, 33, 1123-1130.	1.5	89
12850	Self-consistent GW calculation of the electronic structure of co-doped ZnO. Journal of the Korean Physical Society, 2012, 60, 292-296.	0.3	1
12851	Initial oxidation structure of chlorinated Si(001). Journal of the Korean Physical Society, 2012, 60, 398-402.	0.3	0
12852	Influence of surface segregation on the elastic property of Ptâ€“Ni alloy nanowires. Computational Materials Science, 2012, 55, 81-84.	1.4	5

#	Article	IF	Citations
12853	High-capacity electrode material BC<mml:math xmlns:mml="http://www.w3.org/1998/Math/MathML" display="inline"><mml:msub><mml:mrow /><mml:mn>3</mml:mn></mml:msub></mml:math>for lithium batteries proposed byab initiosimulations. Physical Review B, 2012, 85, .	1.1	42
12854	Electron emission in three and four particle collisions<mml:math xmlns:mml="http://www.w3.org/1998/Math/MathML" display="inline"><mml:msub><mml:mrow /><mml:mrow><mml:mn>1</mml:mn><mml:mo>â^'</mml:mo><mml:mi>x</mml:mi></mml:mrow></mml:msub></mml:math>Se<mml:math xmlns:mml="http://www.w3.org/1998/Math/MathML" display="inline"><mml:msub><mml:mrow /><mml:mi>x</mml:mi></mml:msub></mml:math>from first-principles calculations. Physical Review B, 2012, 85, .	1.1	463
12855	Structural and magnetic properties of N doped ZnO thin films. Journal of Applied Physics, 2012, 111, .	1.1	34
12856	Spinel oxides: Î”1 spin-filter barrier for a class of magnetic tunnel junctions. Applied Physics Letters, 2012, 100, .	1.5	56
12857	Structural and Electronic Properties of<mml:math xmlns:mml="http://www.w3.org/1998/Math/MathML" display="inline"><mml:mi>T</mml:mi></mml:math>Graphene: A Two-Dimensional Carbon Allotrope with Tetrarings. Physical Review Letters, 2012, 108, 225505.	2.9	377
12858	Optoelectronic Properties in Monolayers of Hybridized Graphene and Hexagonal Boron Nitride. Physical Review Letters, 2012, 108, 226805.	2.9	108
12859	Graphyne and Graphdiyne: Promising Materials for Nanoelectronics and Energy Storage Applications. Journal of Physical Chemistry C, 2012, 116, 5951-5956.	1.5	430
12860	Structural and electronic properties of bilayer and trilayer graphdiyne. Nanoscale, 2012, 4, 3990.	2.8	156
12861	Elastic and thermodynamic properties of potentially superhard carbon boride materials. Journal of Superhard Materials, 2012, 34, 28-36.	0.5	6
12862	On the generalized stacking energy, core structure and Peierls stress of the $$rac{1} {2}leftlangle {110} ightangle left{ {110} ight}$$ dislocations in alkali halide. European Physical Journal B, 2012, 85, 1.	0.6	5
12863	Symmetry and Stability of the Rutile-Based TiO₂ Nanowires: Models and Comparative LCAO-Plane Wave DFT Calculations. Journal of Physical Chemistry C, 2012, 116, 13395-13402.	1.5	21
12864	Enhancement of magnetoelectric effect by combining different interfacial coupling mechanisms. Journal of Applied Physics, 2012, 111, .	1.1	24
12865	Tuning the Electronic and Magnetic Properties of MoS₂ Nanoribbons by Strain Engineering. Journal of Physical Chemistry C, 2012, 116, 11752-11757.	1.5	212
12866	CNT Arrays Grown upon Catalytic Nickel Particles as Applied in the Nanoelectronic Devices: Ab Initio Simulation of Growth Mechanism. NATO Science for Peace and Security Series B: Physics and Biophysics, 2012, , 101-114.	0.2	1
12867	Ab Initio Calculations of SrTiO3 (111) Surfaces. NATO Science for Peace and Security Series B: Physics and Biophysics, 2012, , 125-132.	0.2	3
12868	Nanodevices and Nanomaterials for Ecological Security. NATO Science for Peace and Security Series B: Physics and Biophysics, 2012, , .	0.2	7
12869	Photoelectrochemical Determination of the Absolute Band Edge Positions as a Function of Particle Size for ZnO Quantum Dots. Journal of Physical Chemistry C, 2012, 116, 15692-15701.	1.5	54
12870	Melting of cubic boron nitride at extreme pressures. Journal of Physics Condensed Matter, 2012, 24, 055401.	0.7	6

#	Article	IF	Citations
12871	An ab initio molecular dynamics study of ionic conductivity in hexagonal lithium lanthanum titanate oxide La 0.5 Li 0.5 TiO 3. Ionics, 2012, 18, 371-377.	1.2	13
12872	Halogenated two-dimensional germanium: candidate materials for being of Quantum Spin Hall state. Journal of Materials Chemistry, 2012, 22, 12587.	6.7	79
12873	About the Nitrogen Location in Nanocrystalline N-Doped TiO₂: Combined DFT and EXAFS Approach. Journal of Physical Chemistry C, 2012, 116, 1764-1771.	1.5	74
12874	First-principles calculations of phonon and thermodynamic properties of AlRE (RE = Y, Gd, Pr, Yb) intermetallic compounds. Physica Scripta, 2012, 85, 035705.	1.2	10
12875	Stability and Hydrolyzation of Metal Organic Frameworks with Paddle-Wheel SBUs upon Hydration. Chemistry of Materials, 2012, 24, 3153-3167.	3.2	368
12876	Investigating Tautomeric Polymorphism in Crystalline Anthranilic Acid Using Terahertz Spectroscopy and Solid-State Density Functional Theory. Journal of Physical Chemistry A, 2012, 116, 8051-8057.	1.1	37
12877	Influence of Surface Segregation on the Mechanical Property of Metallic Alloy Nanowires. Materials Research Society Symposia Proceedings, 2012, 1424, 127.	0.1	0
12878	Preferential sites for adsorption of methanol and methoxy on Pt and Pt-alloy surfaces. Physica Scripta, 2012, 85, 015605.	1.2	5
12879	Emergence of giant magnetic anisotropy in freestanding Au/Co nanowires. Applied Physics Letters, 2012, 101, 043108.	1.5	21
12880	A Firstâ€Principles Investigation of the Compositional Dependent Properties of Magnetic Shape Memory Heusler Alloys. Advanced Engineering Materials, 2012, 14, 530-546.	1.6	54
12881	Ab Initioâ€Based Prediction of Phase Diagrams: Application to Magnetic Shape Memory Alloys. Advanced Engineering Materials, 2012, 14, 547-561.	1.6	37
12882	Geâ€Based Spinâ€Photodiodes for Roomâ€Temperature Integrated Detection of Photon Helicity. Advanced Materials, 2012, 24, 3037-3041.	11.1	40
12883	A Novel Codoping Approach for Enhancing the Performance of LiFePO₄ Cathodes. Advanced Energy Materials, 2012, 2, 1028-1032.	10.2	72
12884	Metal Oxideâ€Supported Platinum Overlayers as Protonâ€Exchange Membrane Fuel Cell Cathodes. ChemCatChem, 2012, 4, 228-235.	1.8	44
12885	Molecular Understanding of Enyne Hydrogenation over Palladium and Copper Catalysts. ChemCatChem, 2012, 4, 1420-1427.	1.8	18
12886	DFT Study of Steam Reforming of Formaldehyde on Cu, PdZn, and Ir. ChemCatChem, 2012, 4, 1311-1320.	1.8	14
12887	Volcano Relations for Oxidation of Hydrogen Halides over Rutile Oxide Surfaces. ChemCatChem, 2012, 4, 1856-1861.	1.8	11
12888	A Computational Investigation of the Catalytic Properties of Graphene Oxide: Exploring Mechanisms by using DFT Methods. ChemCatChem, 2012, 4, 1844-1849.	1.8	129

#	Article	IF	Citations
12889	Smallâ€Sized and Contacting Ptâ€“WC Nanostructures on Graphene as Highly Efficient Anode Catalysts for Direct Methanol Fuel Cells. Chemistry - A European Journal, 2012, 18, 7443-7451.	1.7	83
12890	Highâ€Potential Reversible Li Deintercalation in a Substituted Tetrahydroxyâ€pâ€benzoquinone Dilithium Salt: An Experimental and Theoretical Study. Chemistry - A European Journal, 2012, 18, 8800-8812.	1.7	68
12891	Piezochromism in Nickel Salicylaldoximato Complexes: Tuning Crystalâ€Field Splitting with High Pressure. Chemistry - A European Journal, 2012, 18, 7738-7748.	1.7	33
12892	A DFT Study on the Structure and Properties of Cu/Cr₂O₃ Catalyst. Chinese Journal of Chemistry, 2012, 30, 771-778.	2.6	7
12893	The Surface Chemistry of Water on Fe(100): A Density Functional Theory Study. ChemPhysChem, 2012, 13, 1583-1590.	1.0	35
12894	A Density Functional Theory Study on the Effect of Zeroâ€Point Energy Corrections on the Methanation Profile on Fe(100). ChemPhysChem, 2012, 13, 1591-1596.	1.0	50
12895	Covalent Functionalization of Strained Graphene. ChemPhysChem, 2012, 13, 1463-1469.	1.0	38
12896	A DFT Study of the Structures of Au_x Clusters on a CeO₂(111) Surface. ChemPhysChem, 2012, 13, 1261-1271.	1.0	33
12897	The Influence of Defects on Moâ€Doped TiO₂ by Firstâ€Principles Studies. ChemPhysChem, 2012, 13, 1514-1521.	1.0	31
12898	The Role of Effective Mass of Carrier in the Photocatalytic Behavior of Silver Halideâ€Based Ag@AgX (X=Cl, Br, I): A Theoretical Study. ChemPhysChem, 2012, 13, 2304-2309.	1.0	99
12899	A Firstâ€Principle Calculation of Sulfur Oxidation on Metallic Ni(111) and Pt(111), and Bimetallic Ni@Pt(111) and Pt@Ni(111) Surfaces. ChemPhysChem, 2012, 13, 3194-3203.	1.0	16
12900	Mechanistic Investigation on the Formation and Dehydrogenation of Calcium Amidoborane Ammoniate. ChemSusChem, 2012, 5, 927-931.	3.6	10
12901	Ab Initio Simulation of Complex Dielectric Function for Dense Aluminum Plasma. Contributions To Plasma Physics, 2012, 52, 145-148.	0.5	19
12902	van der Waals interaction in magnetic bilayer graphene nanoribbons. Physical Review B, 2012, 85, .	1.1	41
12903	Density functional theory study of phase IV of solid hydrogen. Physical Review B, 2012, 85, .	1.1	134
12904	Modeling oxidation of Pt-based alloy surfaces for fuel cell cathode electrocatalysts. Catalysis, 0, , 323-357.	0.6	0
12905	Vibrational Davydov Splittings and Collective Mode Polarizations in Oriented Organic Semiconductor Crystals. Journal of Physical Chemistry C, 2012, 116, 14491-14503.	1.5	25
12906	Near room-temperature synthesis of transfer-free graphene films. Nature Communications, 2012, 3, 645.	5.8	205

#	Article	IF	Citations
12907	Molecular Dynamics Simulation: From â€œAb Initioâ€•to â€œCoarse Grainedâ€• , 2012, , 195-238.		11
12908	Highly efficient visible-light-driven photocatalytic activities in synthetic ordered monoclinic BiVO4 quantum tubesâ€“graphene nanocomposites. Nanoscale, 2012, 4, 3761.	2.8	121
12909	Explorative computational study of the singlet fission process. Molecular Physics, 2012, 110, 2445-2454.	0.8	83
12910	Impacts of image force on the Schottky barrier height at metal-carbon nanotube contacts. Applied Physics Letters, 2012, 100, 173104.	1.5	7
12911	Unveiling Structureâ€“Property Relationships in Sr₂Fe_{1.5}Mo_{0.5}O_{6â^'Î´}, an Electrode Material for Symmetric Solid Oxide Fuel Cells. Journal of the American Chemical Society, 2012, 134, 6826-6833.	6.6	172
12912	Origin of the nitrogen over- and understoichiometry in Ti_{0.5}Al_{0.5}N thin films. Journal of Physics Condensed Matter, 2012, 24, 155401.	0.7	45
12913	Atom-by-Atom Observation of Grain Boundary Migration in Graphene. Nano Letters, 2012, 12, 3168-3173.	4.5	178
12914	Electric Field Induced Phase Transitions in Polymers: A Novel Mechanism for High Speed Energy Storage. Physical Review Letters, 2012, 108, 087802.	2.9	43
12915	Constraints on the phase diagram of molybdenum from first-principles free-energy calculations. Physical Review B, 2012, 85, .	1.1	55
12916	Structural phase transitions in Si under hydrostatic and uniaxial compression. Physical Review B, 2012, 85, .	1.1	12
12917	Modelling of the reactivity and stability of carbon nanotubes under environmentally relevant conditions. Physical Chemistry Chemical Physics, 2012, 14, 10080.	1.3	15
12918	Electronic Structure of F-Doped Bulk Rutile, Anatase, and Brookite Polymorphs of TiO₂. Journal of Physical Chemistry C, 2012, 116, 12738-12746.	1.5	68
12919	Solvothermal Synthesis, Crystal Growth, and Structure Determination of Sodium and Potassium Guanidinate. Inorganic Chemistry, 2012, 51, 7425-7430.	1.9	23
12920	Tuning magnetic properties of graphene nanoribbons with topological line defects: From antiferromagnetic to ferromagnetic. Physical Review B, 2012, 85, .	1.1	67
12921	Giant magnetoresistance in silicene nanoribbons. Nanoscale, 2012, 4, 3111.	2.8	216
12922	Effect of Li-doping on the magnetic properties of ZnO with Zn vacancies. Journal of Applied Physics, 2012, 111, 093902.	1.1	19
12923	Electronic Excitations and Lattice Dynamics of Coordinatively â€œUnsaturatedâ€•Complex Transition Metal Compounds. Inorganic Chemistry, 2012, 51, 5822-5830.	1.9	2
12924	Engineering the work function of armchair graphene nanoribbons using strain and functional species: a first principles study. Journal of Physics Condensed Matter, 2012, 24, 075501.	0.7	61

#	Article	IF	Citations
12925	First-principles prediction of charge mobility in carbon and organic nanomaterials. Nanoscale, 2012, 4, 4348.	2.8	551
12926	NiW and NiRu Bimetallic Catalysts for Ethylene Steam Reforming: Alternative Mechanisms for Sulfur Resistance. Catalysis Letters, 2012, 142, 718-727.	1.4	16
12927	Effects of Cu and Al on the crystal structure and composition of Î· (MgZn2) phase in over-aged Alâ€“Znâ€“Mgâ€“Cu alloys. Journal of Materials Science, 2012, 47, 5419-5427.	1.7	64
12928	Fabrication and evaluation of SixNy coatings for total joint replacements. Journal of Materials Science: Materials in Medicine, 2012, 23, 1879-1889.	1.7	28
12929	Importance of non linear piezoelectric effect in Wurtzite III-N semiconductors. Optical and Quantum Electronics, 2012, 44, 195-203.	1.5	15
12930	Comprehensive study of the structure of aluminum trihalides from electron diffraction and computation. Structural Chemistry, 2012, 23, 879-893.	1.0	12
12931	Reactions of Propylene Oxide on Supported Silver Catalysts: Insights into Pathways Limiting Epoxidation Selectivity. Topics in Catalysis, 2012, 55, 3-12.	1.3	21
12932	Influence of Sulfur Poisoning on CO Adsorption on Pd(100). Topics in Catalysis, 2012, 55, 267-279.	1.3	10
12933	Enantiospecific Chemisorption of Amino Acids on Step Decorated Chiral Cu Surfaces. Topics in Catalysis, 2012, 55, 243-259.	1.3	20
12934	Density Functional Theory Study of Selectivity Considerations for Câ€“C Versus Câ€“O Bond Scission in Glycerol Decomposition on Pt(111). Topics in Catalysis, 2012, 55, 280-289.	1.3	41
12935	Selectivity of Adsorption of Thiophene and its Derivatives on Titania Anatase Surfaces: A Density Functional Theory Study. Topics in Catalysis, 2012, 55, 229-242.	1.3	9
12936	Negative differential resistance behaviors in OPE derivatives combined C60 molecular junctions modulated with side groups. Science China: Physics, Mechanics and Astronomy, 2012, 55, 1412-1416.	2.0	0
12937	First principles study on magnetic and electronic properties with rare-earth atoms doped SWCNTs. Frontiers of Physics, 2012, 7, 353-359.	2.4	7
12938	Hydrogen diffusion in aluminum melts: An ab initio molecular dynamics study. Journal Wuhan University of Technology, Materials Science Edition, 2012, 27, 560-567.	0.4	4
12939	Adsorption of croconate dyes on TiO2 anatase (101) surface: A periodic DFT study to understand the binding of diketo groups#. Journal of Chemical Sciences, 2012, 124, 301-310.	0.7	15
12940	Electronic structures of the F-terminated AlN nanoribbons. Pramana - Journal of Physics, 2012, 78, 469-474.	0.9	10
12941	The structural and electronic properties of type-I clathrates Ba8Cu x Ga16â^'x Sn30 from first-principle calculations. Indian Journal of Physics, 2012, 86, 447-453.	0.9	3
12942	Carbon monoxide adsorption on transition element-doped single wall carbon nanotube. Indian Journal of Physics, 2012, 86, 677-680.	0.9	10

#	Article	IF	Citations
12943	First-principles simulations of the 27Al and 17O solid-state NMR spectra of the CaAl2Si3O10 glass. Theoretical Chemistry Accounts, 2012, 131, 1.	0.5	34
12944	Role of step sites on water dissociation on stoichiometric ceria surfaces. Theoretical Chemistry Accounts, 2012, 131, 1.	0.5	30
12945	High-P, T phase relations in the NaAlSi2O6 system from first principles computation. Physics and Chemistry of Minerals, 2012, 39, 305-310.	0.3	7
12946	Si-doped graphene: an ideal sensor for NO- or NO2-detection and metal-free catalyst for N2O-reduction. Journal of Molecular Modeling, 2012, 18, 2043-2054.	0.8	117
12947	Chemical functionalization of graphene via aryne cycloaddition: a theoretical study. Journal of Molecular Modeling, 2012, 18, 2861-2868.	0.8	16
12948	Acetylene hydrogenation on anatase TiO2(101) supported Pd4 cluster: oxygen deficiency effect. Journal of Molecular Modeling, 2012, 18, 3329-3339.	0.8	15
12949	Stability of (Ti, M)C (M = Nb, V, Mo and W) carbide in steels using first-principles calculations. Acta Materialia, 2012, 60, 208-217.	3.8	301
12950	Effects of alloying elements on thermal expansions of Î³-Ni and Î³â€²-Ni3Al by first-principles calculations. Acta Materialia, 2012, 60, 1846-1856.	3.8	42
12951	Elastic properties of Î³â€²-Fe4N probed by nanoindentation and ab initio calculation. Acta Materialia, 2012, 60, 2054-2060.	3.8	44
12952	On the possibility of rhenium clustering in nickel-based superalloys. Acta Materialia, 2012, 60, 2866-2872.	3.8	78
12953	Tantalum-doped hydroxyapatite thin films: Synthesis and characterization. Acta Materialia, 2012, 60, 3435-3443.	3.8	25
12954	Solute strengthening from first principles and application to aluminum alloys. Acta Materialia, 2012, 60, 3873-3884.	3.8	185
12955	The structural, electronic, elastic and optical properties of AlCu(Se1â˜'Te)2 compounds from first-principle calculations. Current Applied Physics, 2012, 12, 373-379.	1.1	9
12956	Ab initio investigation into the structural, electronic and elastic properties of AlCu2TM (TMÂ=ÂTi, Zr) Tj ETQq1 1 0.784314 rgBT /Over	1.1	9
12957	Methane cracking on single-wall carbon nanotubes studied by semi-empirical tight binding simulations. Carbon, 2012, 50, 411-420.	5.4	9
12958	Atomic hydrogen adsorption on lithium-doped graphite surfaces. Carbon, 2012, 50, 510-517.	5.4	17
12959	Amorphous structural models for graphene oxides. Carbon, 2012, 50, 1690-1698.	5.4	114
12960	In situ transmission electron microscopy of electrochemical lithiation, delithiation and deformation of individual graphene nanoribbons. Carbon, 2012, 50, 3836-3844.	5.4	98

#	Article	IF	Citations
12961	The effect of surface oxidation on atomic hydrogen adsorption on lithium-doped graphite surfaces. Carbon, 2012, 50, 3882-3888.	5.4	6
12962	Insight into elastic behavior of calcium silicate hydrated oxide (Câ€“Sâ€“H) under pressure and composition effect. Cement and Concrete Research, 2012, 42, 306-312.	4.6	34
12963	Molecular-level understanding of WGS and reverse WGS reactions on Rh through hierarchical multiscale approach. Chemical Engineering Science, 2012, 74, 296-299.	1.9	35
12964	Physisorption of helium on a TiO2(110) surface: Periodic and finite cluster approaches. Chemical Physics, 2012, 399, 272-280.	0.9	10
12965	High-capacity hydrogen storage of magnesium-decorated boron fullerene. Chemical Physics, 2012, 392, 16-20.	0.9	48
12966	First principles studies of the electronic properties and catalytic activity of single-walled carbon nanotube doped with Pt clusters and chains. Chemical Physics, 2012, 393, 96-106.	0.9	13
12967	Silicene-like beryllium encapsulated nanowires. Chemical Physics, 2012, 397, 42-47.	0.9	2
12968	The structural and electronic properties of monovalent sidewall functionalized double-walled carbon nanotubes. Chemical Physics, 2012, 402, 91-95.	0.9	5
12969	The importance of London dispersion forces in crystalline magnesium nitrate hexahydrate. Inorganica Chimica Acta, 2012, 389, 176-182.	1.2	11
12970	Hydrogen storage on Ti decorated SiC nanostructures: A first principles study. International Journal of Hydrogen Energy, 2012, 37, 3733-3740.	3.8	39
12971	Stability of transition metals on Mg(0001) surfaces and their effects on hydrogen adsorption. International Journal of Hydrogen Energy, 2012, 37, 309-317.	3.8	48
12972	Band gap engineering by anion doping in the photocatalyst BiTaO4: First principle calculations. International Journal of Hydrogen Energy, 2012, 37, 3014-3018.	3.8	29
12973	Local structural arrangements around oxygen and hydrogen-related defects in proton conducting LaP3O9 investigated by first principles calculations. International Journal of Hydrogen Energy, 2012, 37, 7995-8003.	3.8	10
12974	First-principles study on hydrogen storage by graphitic carbon nitride nanotubes. International Journal of Hydrogen Energy, 2012, 37, 4170-4178.	3.8	96
12975	Stability of erbium hydrides studied by DFT calculations. International Journal of Hydrogen Energy, 2012, 37, 4246-4253.	3.8	12
12976	Density functional study of hydrogen spillover on direct Pd-doped metal-organic frameworks IRMOF-1. International Journal of Hydrogen Energy, 2012, 37, 5081-5089.	3.8	18
12977	The structural and electronic properties of Li-doped fluorinated graphene and its application to hydrogen storage. International Journal of Hydrogen Energy, 2012, 37, 5754-5761.	3.8	50
12978	Defects at the (1 1 0) surface of rutile TiO2 from ab initio calculations. International Journal of Hydrogen Energy, 2012, 37, 8110-8117.	3.8	13

#	Article	IF	Citations
12979	Mechanism for the decomposition of lithium borohydride. International Journal of Hydrogen Energy, 2012, 37, 5825-5832.	3.8	32
12980	Hydrogen adsorption on palladium dimer decorated graphene: A bonding study. International Journal of Hydrogen Energy, 2012, 37, 6653-6665.	3.8	61
12981	Atomistic study of LaNbO4; surface properties and hydrogen adsorption. International Journal of Hydrogen Energy, 2012, 37, 6674-6685.	3.8	13
12982	An atomistic-based boundary element method for the reduction of molecular statics models. Computer Methods in Applied Mechanics and Engineering, 2012, 225-228, 1-13.	3.4	7
12983	Structural stability of silicene-like nanotubes. Computer Physics Communications, 2012, 183, 30-33.	3.0	5
12984	Water wetting on representative metal surfaces: Improved description from van der Waals density functionals. Chemical Physics Letters, 2012, 521, 161-166.	1.2	18
12985	CO oxidation by co-adsorbed atomic O on the Au(321) surface with Ag impurities: A mechanistic study from first-principles calculations. Chemical Physics Letters, 2012, 525-526, 87-91.	1.2	26
12986	First-principles study of magnetic properties in V-doped GaN. Chemical Physics Letters, 2012, 529, 35-38.	1.2	16
12987	NMR and NQR parameters of ethanol crystal. Chemical Physics Letters, 2012, 531, 105-109.	1.2	3
12988	Magnetism in Sc-doped ZnO with zinc vacancies: A hybrid density functional and GGA+U approaches. Chemical Physics Letters, 2012, 532, 96-99.	1.2	43
12989	Density functional theory study of sulfur tolerance of copper: New copperâ€“sulfur phase diagram. Chemical Physics Letters, 2012, 533, 20-24.	1.2	18
12990	Charge carrier density in Li-intercalated graphene. Chemical Physics Letters, 2012, 534, 29-33.	1.2	37
12991	Ab-initio study of structural and vibrational properties of <mml:math xmlns:mml="http://www.w3.org/1998/Math/MathML" altimg="si38.gif" overflow="scroll"><mml:mrow><mml:msub><mml:mrow><mml:mtext>KN</mml:mtext></mml:mrow><mml:mrow><mml:mn>3</mml:mn></mml:r under pressure. Chemical Physics Letters, 2012, 533, 35-39.	1.2	25
12992	Ab-initio calculations of the direct and hydrogen-assisted dissociation of CO on Fe(3 1 0). Chemical Physics Letters, 2012, 534, 54-57.	1.2	16
12993	Transport spin polarization of magnetic C28 molecular junctions. Chemical Physics Letters, 2012, 535, 111-115.	1.2	15
12994	Far-infrared spectroscopy investigation of sulfurâ€“oxygen interactions in Ï€-conjugated oligomers. Chemical Physics Letters, 2012, 535, 116-119.	1.2	2
12995	Barriers to motion and rotation of graphene layers based on measurements of shear mode frequencies. Chemical Physics Letters, 2012, 536, 82-86.	1.2	43
12996	Ab initio investigation of the electronic structure of CeRh2Sb2. Chemical Physics Letters, 2012, 537, 48-52.	1.2	0

#	Article	IF	Citations
12997	The electronic properties at the iron-phthalocyanine/Ag(110) interface. Chemical Physics Letters, 2012, 537, 53-57.	1.2	7
12998	Doping and temperature dependence of thermoelectric properties of AgGaTe2: First principles investigations. Chemical Physics Letters, 2012, 537, 62-64.	1.2	25
12999	Boron nitride substrate-induced reversible hydrogen storage in bilayer solid matrix via interlayer spacing. International Journal of Hydrogen Energy, 2012, 37, 9677-9687.	3.8	13
13000	Structural, electronic and thermodynamic properties of Al- and Si-doped Î±-, Î³-, and Î²-MgH2: Density functional andÂhybrid density functional calculations. International Journal of Hydrogen Energy, 2012, 37, 9112-9122.	3.8	27
13001	Ab intio study of inhibitors influence on growth of WC crystallites in WC/Co hard alloys. International Journal of Refractory Metals and Hard Materials, 2012, 31, 263-265.	1.7	16
13002	Unprecedented selectivity to the direct desulfurization (DDS) pathway in a highly active FeNi bimetallic phosphide catalyst. Journal of Catalysis, 2012, 285, 1-5.	3.1	73
13003	Tuning the selectivity for ring-opening reactions of methylcyclopentane over Pt catalysts: A mechanistic study from first-principles calculations. Journal of Catalysis, 2012, 285, 124-133.	3.1	38
13004	Accurate coverage-dependence incorporated into first-principles kinetic models: Catalytic NO oxidation on Pt (111). Journal of Catalysis, 2012, 286, 88-94.	3.1	146
13005	Performance, structure, and mechanism of CeO2 in HCl oxidation to Cl2. Journal of Catalysis, 2012, 286, 287-297.	3.1	185
13006	Unraveling the mechanism of the NO reduction by CO on gold based catalysts. Journal of Catalysis, 2012, 289, 11-20.	3.1	36
13007	Solvent effects in the hydrogenation of 2-butanone. Journal of Catalysis, 2012, 289, 30-41.	3.1	140
13008	Reaction path analysis of propane selective oxidation over V2O5 and V2O5/TiO2. Journal of Catalysis, 2012, 289, 127-139.	3.1	71
13009	Electrochemical detection of the thermal stability of n-alkanethiolate monolayers on Au(111). Electrochimica Acta, 2012, 61, 132-139.	2.6	12
13010	The electric double layer on graphite. Electrochimica Acta, 2012, 71, 82-85.	2.6	53
13011	Decomposition of methylamine on Mo(100) surface: A DFT study. Journal of Natural Gas Chemistry, 2012, 21, 132-137.	1.8	8
13012	Thermodynamic properties of (Mg,Fe2+)SiO3 perovskite at the lower-mantle pressures and temperatures: an internally consistent LSDA+Ustudy. Geophysical Journal International, 2012, 190, 310-322.	1.0	40
13013	<scp><scp>N</scp></scp>Â+Â<scp><scp>Ni</scp></scp> Codoped Anatase <scp><scp>TiO</scp></scp>₂ Nanocrystals with Exposed {001} Facets Through Twoâ€Step Hydrothermal Route. Journal of the American Ceramic Society, 2012, 95, 2951-2956.	1.9	35
13014	Minimizing the Kohnâ€“Sham total energy for periodic systems. Linear Algebra and Its Applications, 2012, 436, 2764-2779.	0.4	0

#	Article	IF	Citations
13015	Effect of Y and Zn substitution on elastic properties of 6H-type ABCBCB LPSO structure in Mg97Zn1Y2 alloy. Materials Chemistry and Physics, 2012, 131, 634-641.	2.0	7
13016	Structural, thermodynamic, electronic, and optical properties of NaH from first-principles calculations. Materials Chemistry and Physics, 2012, 133, 346-355.	2.0	6
13017	Visible-light photocatalytic activity of Ni-doped TiO2 from ab initio calculations. Materials Chemistry and Physics, 2012, 133, 746-750.	2.0	35
13018	First principles study of structural, electronic and optical properties of Pb doped SrHfO3. Materials Chemistry and Physics, 2012, 133, 857-862.	2.0	17
13019	A new approach to establish both stable and metastable phase equilibria for fcc ordered/disordered phase transition: application to the Alâ€“Ni and Niâ€“Si systems. Materials Chemistry and Physics, 2012, 135, 94-105.	2.0	23
13020	Theoretical study of negative thermal expansion mechanism of ZnF2. Materials Research Bulletin, 2012, 47, 1113-1118.	2.7	39
13021	Chemical doping the XYB14 complex borides. Materials Letters, 2012, 74, 5-7.	1.3	11
13022	Ab initio investigation on structural, electronic and lattice dynamical properties of MgN and GdN crystals. Results in Physics, 2012, 2, 34-40.	2.0	6
13023	Generalized stacking fault energy in magnesium alloys: Density functional theory calculations. Scripta Materialia, 2012, 66, 219-222.	2.6	157
13024	Structural stability and generalized stacking fault energies in Î² Tiâ€“Nb alloys: Relation to dislocation properties. Scripta Materialia, 2012, 66, 682-685.	2.6	35
13025	Superhard solid solutions of diamond and cubic boron nitride. Scripta Materialia, 2012, 66, 781-784.	2.6	27
13026	Effects of surface structure and Agâ€“Sb nanodots on electronic properties of PbTe (100) facets from first-principles calculations. Scripta Materialia, 2012, 67, 17-20.	2.6	2
13027	First-principles study of Î±-Pu2O3. Journal of Nuclear Materials, 2012, 420, 159-163.	1.3	19
13028	First-principles calculations of phase transition, elasticity, and thermodynamic properties for TiZr alloy. Journal of Nuclear Materials, 2012, 420, 501-507.	1.3	31
13029	Ab initio modelling of volatile fission products in uranium mononitride. Journal of Nuclear Materials, 2012, 422, 137-142.	1.3	33
13030	Retention and diffusion of H, He, O, C impurities in Be. Journal of Nuclear Materials, 2012, 423, 164-169.	1.3	34
13031	Adsorption and dissociation of H2O on Zr(0001) with density-functional theory studies. Journal of Nuclear Materials, 2012, 424, 51-56.	1.3	8
13032	First-principles study of surface properties of PuO2: Effects of thickness and O-vacancy on surface stability and chemical activity. Journal of Nuclear Materials, 2012, 426, 139-147.	1.3	40

#	Article	IF	Citations
13033	First-principles study of the stability of fission products in uranium monocarbide. Journal of Nuclear Materials, 2012, 426, 189-197.	1.3	22
13034	A long-range Uâ€“Nb potential for the calculation of some chemical and physical properties of the Uâ€“Nb system. Journal of Nuclear Materials, 2012, 427, 239-244.	1.3	12
13035	Role of water on the stability of oxygen vacancies in ZrO2: An ab initio based study. Journal of Nuclear Materials, 2012, 429, 173-176.	1.3	5
13036	Trapping of multiple hydrogen atoms in a vanadium monovacancy: A first-principles study. Journal of Nuclear Materials, 2012, 429, 216-220.	1.3	34
13037	First principles calculation of noble gas atoms properties in 3Câ€“SiC. Journal of Nuclear Materials, 2012, 429, 329-334.	1.3	32
13038	Ab initio studies of Nb doping effect on the formation of oxygen vacancy in rutile TiO2. Journal of Physics and Chemistry of Solids, 2012, 73, 84-93.	1.9	15
13039	Study on the electronic structures of the reduced anatase TiO2 by the first-principle calculation. Journal of Physics and Chemistry of Solids, 2012, 73, 302-307.	1.9	14
13040	First-principles study of bonding, elasticity-relevant and acoustic properties of BaAlBO3F2. Journal of Physics and Chemistry of Solids, 2012, 73, 109-114.	1.9	9
13041	Ab initio lattice dynamics and thermodynamic properties of SrO under pressure. Journal of Physics and Chemistry of Solids, 2012, 73, 129-135.	1.9	25
13042	First-principles study of high-capacity hydrogen storage on graphene with Li atoms. Journal of Physics and Chemistry of Solids, 2012, 73, 245-251.	1.9	88
13043	Ab initio based investigation of interstitial interactions and Snoek relaxation in Nbâ€“O. Journal of Physics and Chemistry of Solids, 2012, 73, 182-187.	1.9	5
13044	First-principles studies on the electronic and optical properties of CuAlSe2 and CuAl5Se8. Journal of Physics and Chemistry of Solids, 2012, 73, 617-621.	1.9	5
13045	Structural, electronic and magnetic properties of Fe(1â^'x)Cox alloy nanowires encapsulated inside (10,0) boron nitride nanotube. Journal of Physics and Chemistry of Solids, 2012, 73, 530-534.	1.9	12
13046	Crystal structures, elastic, and lattice dynamical properties of BeB2, NaB2, and CaB2 from the first principles. Journal of Physics and Chemistry of Solids, 2012, 73, 593-598.	1.9	7
13047	Thermoelastic parameter Î±KT of sodium chloride at high pressure and high temperature. Journal of Physics and Chemistry of Solids, 2012, 73, 992-998.	1.9	0
13048	Strain-tunable band gap in graphene/h-BN hetero-bilayer. Journal of Physics and Chemistry of Solids, 2012, 73, 818-821.	1.9	42
13049	A comparative study of electronic structure and bonding in transition metal monocarbides. Journal of Physics and Chemistry of Solids, 2012, 73, 873-880.	1.9	11
13050	Ab initio calculations on the structural and lattice dynamical properties of TmX (X=As, P) compounds. Journal of Physics and Chemistry of Solids, 2012, 73, 917-924.	1.9	3

#	Article	IF	Citations
13051	Investigation of urania within LDA+U method. Journal of Physics and Chemistry of Solids, 2012, 73, 1003-1009.	1.9	12
13052	Lattice dynamics properties of XAs (X=Al, Ga and In) with zinc-blende structure from first-principle calculations. Journal of Physics and Chemistry of Solids, 2012, 73, 1034-1039.	1.9	2
13053	Effects of Fe2+ and Zn2+ substitution on the structure and high-pressure stability of MgAl2O4 spinel from DFT calculations. Journal of Physics and Chemistry of Solids, 2012, 73, 1099-1105.	1.9	4
13054	Electronic states of metal (Cu, Ag, Au) atom on CeO2(111) surface: The role of local structural distortion. Journal of Power Sources, 2012, 197, 28-37.	4.0	46
13055	Oxygen adsorption on the Ag/La1â^'xSrxMnO3(001) catalysts surfaces: A first-principles study. Journal of Power Sources, 2012, 209, 158-162.	4.0	15
13056	Electronic structure and anisotropic chemical bonding in TiNF from ab initio study. Journal of Solid State Chemistry, 2012, 185, 25-30.	1.4	6
13057	Theoretical investigations of the physical properties of zircon-type YVO4. Journal of Solid State Chemistry, 2012, 185, 42-48.	1.4	31
13058	Structural, energetic and thermodynamic analyses of Ca(BH4)2Â·2NH3 from first principles calculations. Journal of Solid State Chemistry, 2012, 185, 206-212.	1.4	10
13059	Synthesis, structure, and electronic structure of CsAgGa2Se4. Journal of Solid State Chemistry, 2012, 186, 54-57.	1.4	6
13060	Electronic structure and chemical bonding of Î±- and Î²-CeIr2Si2 intermediate valence compounds. Journal of Solid State Chemistry, 2012, 186, 81-86.	1.4	5
13061	Structural and electronic properties of SrxBa1â^'xSnO3 from first principles calculations. Journal of Solid State Chemistry, 2012, 187, 186-194.	1.4	47
13062	Exploration on anion ordering, optical properties and electronic structure in K3WO3F3 elpasolite. Journal of Solid State Chemistry, 2012, 187, 159-164.	1.4	95
13063	Effects of oxygen vacancy and N-doping on the electronic and photocatalytic properties of Bi2MO6 (M=Mo, W). Journal of Solid State Chemistry, 2012, 187, 103-108.	1.4	78
13064	Li2Sr4B12O23: A new alkali and alkaline-earth metal mixed borate with [B10O18]6â^' network and isolated [B2O5]4â^' unit. Journal of Solid State Chemistry, 2012, 190, 92-97.	1.4	21
13065	The T2 phase in the Nbâ€“Siâ€“B system studied by ab initio calculations and synchrotron X-ray diffraction. Journal of Solid State Chemistry, 2012, 190, 111-117.	1.4	11
13066	Ab initio investigations of the electronic structure and chemical bonding of Li2ZrN2. Journal of Solid State Chemistry, 2012, 190, 191-195.	1.4	6
13067	Decohesion of Ti3SiC2 induced by He impurities. Materials Letters, 2012, 83, 23-26.	1.3	22
13068	Ab initio study of boron segregation and deactivation at Si/SiO2 interface. Microelectronic Engineering, 2012, 89, 120-123.	1.1	16

#	Article	IF	Citations
13069	Phonon optical modes and electronic properties in diamond nanowires. Microelectronic Engineering, 2012, 90, 92-95.	1.1	10
13070	Phonon band structure of porous Ge from ab initio supercell calculation. Microelectronic Engineering, 2012, 90, 141-144.	1.1	3
13071	Chromium sites in zeolite framework: Chromyl or chromium hydroxyl groups?. Microporous and Mesoporous Materials, 2012, 159, 66-73.	2.2	18
13072	Theoretical insight into the minor role of paring mechanism in the methanol-to-olefins conversion within HSAPO-34 catalyst. Microporous and Mesoporous Materials, 2012, 158, 264-271.	2.2	47
13073	Depression of pyrite in alkaline medium and its subsequent activation by copper. Minerals Engineering, 2012, 26, 64-69.	1.8	58
13074	First-principles study of the methyl formate pathway of methanol steam reforming on PdZn(111) with comparison to Cu(111). Journal of Molecular Catalysis A, 2012, 356, 165-170.	4.8	30
13075	Boron adsorption induced magnetism in zigzag boron nitride nanotubes. Journal of Molecular Structure, 2012, 1020, 183-187.	1.8	4
13076	Ideal strength and deformation-induced phase transformation of hcp metals Re, Ru, and Os: A first-principles study. Materials Science & Engineering A: Structural Materials: Properties, Microstructure and Processing, 2012, 534, 353-364.	2.6	12
13077	The effects of alloying elements on generalized stacking fault energies, strength and ductility of Î³â€²-Ni3Al. Materials Science & Engineering A: Structural Materials: Properties, Microstructure and Processing, 2012, 539, 38-41.	2.6	61
13078	Mechanical properties and work function of L21 structure AlCu2X (X=Ti, Mn, Zr, or Hf) intermetallics. Materials Science & Engineering A: Structural Materials: Properties, Microstructure and Processing, 2012, 545, 13-19.	2.6	11
13079	Electronic transport signatures of common defects in irradiated graphene-based systems. Nuclear Instruments & Methods in Physics Research B, 2012, 282, 108-111.	0.6	3
13080	Methodological aspects of the GW calculation of the carbon vacancy in 3C-SiC. Nuclear Instruments & Methods in Physics Research B, 2012, 277, 77-79.	0.6	17
13081	Impeding effect of Ce on He bubble growth in bcc Fe. Nuclear Instruments & Methods in Physics Research B, 2012, 280, 22-25.	0.6	19
13082	First-principles prediction of metastable niobium and tantalium nitrides M4N5 and M5N6 stoichiometry. Solid State Sciences, 2012, 14, 80-83.	1.5	8
13083	Electronic structure and chemical bonding of LiYSi. Solid State Sciences, 2012, 14, 375-380.	1.5	7
13084	7Li and 29Si solid state NMR and chemical bonding of La2Li2Si3. Solid State Sciences, 2012, 14, 367-374.	1.5	10
13085	Structural, electronic, elastic, thermodynamic and vibration properties of TbN compound from first principles calculations. Solid State Sciences, 2012, 14, 401-408.	1.5	22
13086	Influence of nitrogen partial pressure on morphology, structure and transport properties of reactive sputtered polycrystalline TiN films. Solid State Sciences, 2012, 14, 435-439.	1.5	8

#	Article	IF	Citations
13087	Elastic properties and electronic structures of typical Alâ€“Ce structures from first-principles calculations. Solid State Sciences, 2012, 14, 555-561.	1.5	41
13088	Structural, mechanical and electronic properties of transition metal hydrides MH2 (MÂ=ÂTi, Zr, Hf, Sc, Y,) Tj ETQq1 1 0.784314 rgBT /Ov	1.5	17
13089	Electronic structure and bonding of the hydrides Mg3TH7 (TÂ=ÂMn, Re) from first principles. Solid State Sciences, 2012, 14, 639-643.	1.5	2
13090	Ab initio calculations of structural, electronic, and optical properties of Cu2HgSnSe4. Solid State Sciences, 2012, 14, 890-893.	1.5	8
13091	First principles study of structure and properties of La- and Mn-modified BiFeO3. Solid State Sciences, 2012, 14, 782-788.	1.5	19
13092	Theoretical prediction of the structural, elastic, electronic, optical and thermal properties of the cubic perovskites CsXF3 (XÂ=ÂCa, Sr and Hg) under pressure effect. Solid State Sciences, 2012, 14, 903-913.	1.5	28
13093	First principles study of structural, electronic, elastic and thermal properties of YX (XÂ=ÂCd, In, Au, Hg) Tj ETQq0 0 0 rgBT /Overlock 10 T	1.5	20
13094	First principles studies of Fe/Co superlattices and multilayers with bcc (001) and (110) orientations. Superlattices and Microstructures, 2012, 51, 92-102.	1.4	8
13095	First-principles calculations to investigate optical properties of ByAlxIn1â^'xâ^'yN alloys for optoelectronic devices. Superlattices and Microstructures, 2012, 51, 404-411.	1.4	22
13096	Electronic and magnetic properties of single-wall GeC nanotubes filled with iron nanowires. Superlattices and Microstructures, 2012, 51, 754-764.	1.4	16
13097	Superconductivity in ordered LiBe alloy under high pressure: A first-principles study. Solid State Communications, 2012, 152, 151-154.	0.9	7
13098	The magnetic phase transition in Cu-doped ZnO: From bulk to nanocluster. Solid State Communications, 2012, 152, 50-52.	0.9	11
13099	Computational materials design for superconductivity in hole-doped delafossite CuAlO2 : Transparent superconductors. Solid State Communications, 2012, 152, 24-27.	0.9	24
13100	Effects of uniaxial strain on magnetic interactions in Co-doped ZnO nanowires: First-principles calculations. Solid State Communications, 2012, 152, 19-23.	0.9	13
13101	First-principles study on the lattice dynamics of FeSb2. Solid State Communications, 2012, 152, 231-234.	0.9	7
13102	Possible approach to fabricate p-type ZnO through the Beâ€“N codoping method: First-principles calculations. Solid State Communications, 2012, 152, 1-4.	0.9	19
13103	Elastic properties, Debye temperature, density of states and electronâ€“phonon coupling of ZrB12 under pressure. Solid State Communications, 2012, 152, 249-252.	0.9	6
13104	The predominance of the rutile phase of SnO2 : First principles study. Solid State Communications, 2012, 152, 349-353.	0.9	6

#	Article	IF	Citations
13105	Unusual competition of structural phases and semi-conducting behaviour of bands in superheavy Copernicium. Solid State Communications, 2012, 152, 530-533.	0.9	4
13106	Elastic and vibrational properties of Mg2Si1â^'xSnx alloy from first principles calculations. Solid State Communications, 2012, 152, 821-824.	0.9	17
13107	Mechanical properties of graphene under molecular hydrogen physisorption: An ab initio study. Solid State Communications, 2012, 152, 842-845.	0.9	17
13108	A first principles study of constitutional and thermal defects in D8m-Si3Nb5. Solid State Communications, 2012, 152, 989-993.	0.9	3
13109	Electronic and optical properties of distorted rare-earth manganite under hydrostatic pressure. Solid State Communications, 2012, 152, 1036-1041.	0.9	4
13110	Evidence of a medium-range ordered phase and mechanical instabilities in strontium under high pressure. Solid State Communications, 2012, 152, 1172-1175.	0.9	2
13111	Theoretical investigation on electronic structure and mechanical properties of cubic crystallographic structures with point defects in Al-based alloys. Solid State Communications, 2012, 152, 1263-1269.	0.9	11
13112	Temperature-induced magnetization reversal and ultra-fast magnetic switch at low field in SmFeO3. Solid State Communications, 2012, 152, 1112-1115.	0.9	92
13113	Energy barriers for proton migration in yttrium-doped barium zirconate super cell with Î£5 (310)/[001] tilt grain boundary. Solid State Ionics, 2012, 213, 18-21.	1.3	23
13114	Formation and migration of oxygen and zirconium vacancies in cubic zirconia and zirconium oxysulfide. Solid State Ionics, 2012, 212, 117-122.	1.3	38
13115	A solid-state NMR study of C70: A model molecule for amorphous carbons. Solid State Nuclear Magnetic Resonance, 2012, 42, 81-86.	1.5	12
13116	Characterization and analysis of epitaxial silicon phosphorus alloys for use in n-channel transistors. Thin Solid Films, 2012, 520, 3158-3162.	0.8	31
13117	The adsorption of O on (001) and (111) CdTe surfaces: A first-principles study. Thin Solid Films, 2012, 520, 3960-3964.	0.8	6
13118	Toughness enhancement in TiAlN-based quarternary alloys. Thin Solid Films, 2012, 520, 4080-4088.	0.8	79
13119	First-principles analysis on V-doped GaN. Optical Materials, 2012, 34, 1593-1597.	1.7	25
13120	Theoretical characterization of the TTF/Au (111) interface: STM imaging, band alignment and charging energy. Organic Electronics, 2012, 13, 399-408.	1.4	16
13121	First principles study of native defects in BeO. Physics Procedia, 2012, 28, 79-83.	1.2	13
13122	First principles study of pressure induced structural phase transition in hydrogen storage materialâ€"MgH2. Physica B: Condensed Matter, 2012, 407, 54-59.	1.3	12

#	Article	IF	Citations
13123	The temperature-dependent elastic properties of B2-MgRE intermetallic compounds from first principles. Physica B: Condensed Matter, 2012, 407, 96-102.	1.3	13
13124	First-principle calculations of dilute nitride GaP1â^'xNx alloy in zinc-blende structures. Physica B: Condensed Matter, 2012, 407, 112-115.	1.3	4
13125	Structural, elastic, and electronic properties of orthorhombic NH3BH3: An ab initio study. Physica B: Condensed Matter, 2012, 407, 565-570.	1.3	4
13126	First principles calculation of thermodynamic properties of NaAlSi ternary. Physica B: Condensed Matter, 2012, 407, 193-197.	1.3	3
13127	Atomic and electronic structures of divacancy in graphene nanoribbons. Physica B: Condensed Matter, 2012, 407, 204-208.	1.3	7
13128	Elastic and electronic properties of YNi2B2C under pressure from first principles. Physica B: Condensed Matter, 2012, 407, 227-231.	1.3	11
13129	A first-principle study of the structural, elastic, lattice dynamical and thermodynamic properties of PrX (X=P, As). Physica B: Condensed Matter, 2012, 407, 316-323.	1.3	8
13130	Ab initio study of lattice dynamics and thermal equation of state of Ni. Physica B: Condensed Matter, 2012, 407, 330-334.	1.3	7
13131	First-principles investigations on elastic, phonon and thermodynamic properties of SrB6 under pressure. Physica B: Condensed Matter, 2012, 407, 361-367.	1.3	9
13132	Structural and electronic properties of zinc blende BxAl1â^'xNyP1â^'y quaternary alloys via ï¬rst-principle calculations. Physica B: Condensed Matter, 2012, 407, 426-432.	1.3	13
13133	Electronic structure and magnetic properties of Cr monodoped and (Cr, Al) codoped ZnO. Physica B: Condensed Matter, 2012, 407, 464-467.	1.3	7
13134	Coadsorption of CO and O on Ir(100): First principles calculations. Physica B: Condensed Matter, 2012, 407, 468-471.	1.3	7
13135	Electronic structures of zigzag AlN, GaN nanoribbons and AlxGa1â^'xN nanoribbon heterojunctions: First-principles study. Physica B: Condensed Matter, 2012, 407, 515-518.	1.3	16
13136	Volume dependence of electronic structure and magnetic properties of Fe16N2. Physica B: Condensed Matter, 2012, 407, 519-522.	1.3	6
13137	Crystal structure, electronic and elastic properties for novel Hf3AlN and Zr3AlN ceramics explored by first principles studies. Physica B: Condensed Matter, 2012, 407, 547-550.	1.3	6
13138	Molecular dynamic study of the melting temperature in MgF2 with the fluorite structure. Physica B: Condensed Matter, 2012, 407, 551-554.	1.3	5
13139	First-principles study of single intrinsic vacancy formation and its effect on the electronic density states and magnetic moment of V-doped ZnO. Physica B: Condensed Matter, 2012, 407, 719-723.	1.3	11
13140	Elastic properties and phonon dispersions of rhenium in hexagonal-close-packed structure under pressure from first principles. Physica B: Condensed Matter, 2012, 407, 778-783.	1.3	18

#	Article	IF	Citations
13141	Structural and electronic properties of copper nanowire encapsulated into BeO nanotube: First-principles study. Physica B: Condensed Matter, 2012, 407, 784-789.	1.3	3
13142	Pressure-induced structural phase transition in RbAu. Physica B: Condensed Matter, 2012, 407, 805-807.	1.3	7
13143	Effect of impurity ions configurations on the magnetic properties of Mn-doped ZnO. Physica B: Condensed Matter, 2012, 407, 883-887.	1.3	6
13144	Electronic, elastic, optical properties of rutile TiO2 under pressure: A DFT study. Physica B: Condensed Matter, 2012, 407, 958-965.	1.3	52
13145	Orbital-decomposed electronic and magnetic properties of the double perovskite Sr2FeReO6. Physica B: Condensed Matter, 2012, 407, 912-917.	1.3	16
13146	Theoretical investigation of manganese adsorption on graphene and graphane: A first-principles comparative study. Physica B: Condensed Matter, 2012, 407, 992-1002.	1.3	17
13147	Structural, electronic and vibrational properties of InN under high pressure. Physica B: Condensed Matter, 2012, 407, 1008-1013.	1.3	19
13148	Sn1â^'xBixO2 and Sn1â^'xTaxO2 (0â‰¤xâ‰¤0.75): A first-principles study. Physica B: Condensed Matter, 2012, 407, 1020-1026.	1.3	23
13149	Thermoelectric transport coefficients of n-doped CaTiO3, SrTiO3 and BaTiO3: A theoretical study. Physica B: Condensed Matter, 2012, 407, 1114-1118.	1.3	31
13150	Electronic properties of anatase TiO2 doped by lanthanides: A DFT+U study. Physica B: Condensed Matter, 2012, 407, 1038-1043.	1.3	61
13151	Ab initio calculations of band structure and thermophysical properties for SnS2 and SnSe2. Physica B: Condensed Matter, 2012, 407, 1146-1152.	1.3	41
13152	Smearing induced dynamical stability of NbN and MoN in rocksalt structure. Physica B: Condensed Matter, 2012, 407, 1978-1984.	1.3	4
13153	Structural, elastic and mechanical properties of orthorhombic SrHfO3 under pressure from first-principles calculations. Physica B: Condensed Matter, 2012, 407, 2009-2013.	1.3	13
13154	Structural relative stabilities and pressure-induced phase transitions for lanthanide trihydrides REH3 (RE=Sm, Gd, Tb, Dy, Ho, Er, Tm, and Lu). Physica B: Condensed Matter, 2012, 407, 2050-2057.	1.3	16
13155	First principles studies of a Xe atom adsorbed on Nb(110) surface. Physica B: Condensed Matter, 2012, 407, 2100-2104.	1.3	2
13156	Theoretical study on stability, mechanical properties and thermodynamic parameters of the orthorhombic-A2N2O (A=C, Si and Ge). Physica B: Condensed Matter, 2012, 407, 2190-2200.	1.3	14
13157	First-principles study of electronic and optical properties of N-doped SrHfO3. Physica B: Condensed Matter, 2012, 407, 2239-2242.	1.3	4
13158	Structural, elastic and thermodynamic properties under pressure and temperature effects of MgIn2S4 and CdIn2S4. Physica B: Condensed Matter, 2012, 407, 2295-2300.	1.3	17

#	Article	IF	Citations
13159	First-principles study on structural and electronic properties of AlNSix heterosheet. Physica B: Condensed Matter, 2012, 407, 2301-2305.	1.3	9
13160	Comparison of O adsorption on Ni3Al (001), (011), and (111) surfaces through first-principles calculations. Physica B: Condensed Matter, 2012, 407, 2321-2328.	1.3	7
13161	Origins of ferromagnetism in transition metal doped diamond. Physica B: Condensed Matter, 2012, 407, 2347-2350.	1.3	4
13162	Mechanical properties and electronic structure of TiC, Ti0.75W0.25C, Ti0.75W0.25C0.75N0.25, TiC0.75N0.25 and TiN. Physica B: Condensed Matter, 2012, 407, 2542-2548.	1.3	34
13163	First-principles study on the elastic property of hexagonal alunite. Physica B: Condensed Matter, 2012, 407, 2606-2609.	1.3	15
13164	Structural, electronic and magnetic properties of the double perovskite Pb2FeReO6. Physica B: Condensed Matter, 2012, 407, 2617-2621.	1.3	14
13165	Electronic band structure, stability, structural, and elastic properties of IrTi alloys. Physica B: Condensed Matter, 2012, 407, 2744-2748.	1.3	3
13166	Structural, electronic and elastic properties of potassium hexatitanate crystal from first-principles calculations. Physica B: Condensed Matter, 2012, 407, 2811-2815.	1.3	17
13167	Electronic structure and properties of BaAlGe and SrAlGe. Physica C: Superconductivity and Its Applications, 2012, 476, 54-58.	0.6	6
13168	Effect of contact interface configuration on electronic transport in (C20)2-based molecular junctions. Physics Letters, Section A: General, Atomic and Solid State Physics, 2012, 376, 773-778.	0.9	6
13169	Mechanical and electronic properties of monolayer MoS2 under elastic strain. Physics Letters, Section A: General, Atomic and Solid State Physics, 2012, 376, 1166-1170.	0.9	313
13170	First-principles studies of the hydrogenation effects in silicene sheets. Physics Letters, Section A: General, Atomic and Solid State Physics, 2012, 376, 1230-1233.	0.9	119
13171	A study of the size-dependent elastic properties of silicon carbide nanotubes: First-principles calculations. Physics Letters, Section A: General, Atomic and Solid State Physics, 2012, 376, 1631-1635.	0.9	9
13172	Hydrogenation of ethene catalyzed by Ir atom deposited on Î³-Al2O3(001) surface: From ab initio calculations. Physics Letters, Section A: General, Atomic and Solid State Physics, 2012, 376, 1919-1923.	0.9	5
13173	Competition between ferromagnetic and anti-ferromagnetic couplings in Co doped ZnO with vacancies and Ga co-dopants. Journal of Magnetism and Magnetic Materials, 2012, 324, 1733-1738.	1.0	6
13174	The origin of ferromagnetism in Pd-doped CdS. Journal of Magnetism and Magnetic Materials, 2012, 324, 2039-2042.	1.0	11
13175	Effect of electron and hole doping on magnetic properties of zinc-blende SrC and BaC from first principles. Journal of Magnetism and Magnetic Materials, 2012, 324, 2588-2592.	1.0	12
13176	Electronic, magnetic and elastic properties of Îµ-phases Fe3X(X=B, C, N) from density-functional theory calculations. Journal of Magnetism and Magnetic Materials, 2012, 324, 2271-2276.	1.0	32

#	Article	IF	Citations
13177	Effect of Au proximity on the LSMO surface: An ab initio study. Journal of Magnetism and Magnetic Materials, 2012, 324, 2659-2663.	1.0	5
13178	Parameters for temperature dependence of mean-square displacements for B-, Bi- and Tl-containing binary IIIâ€“V compounds. Acta Crystallographica Section A: Foundations and Advances, 2012, 68, 319-323.	0.3	3
13179	Computer simulation and experimental investigation of the crystal structure and electronic properties of InN/Si and GaN/Si thin films. Bulletin of the Russian Academy of Sciences: Physics, 2012, 76, 696-698.	0.1	0
13180	Features of the structure and properties of Î²-FeSi2 nanofilms and a Î²-FeSi2/Si interface. JETP Letters, 2012, 95, 20-24.	0.4	3
13181	Theoretical study of the diffusion of lithium in crystalline and amorphous silicon. JETP Letters, 2012, 95, 143-147.	0.4	16
13182	Nature of contrast in Ge/Si(111) layers in scanning tunneling microscopy in the presence of Bi and Sb surfactants. JETP Letters, 2012, 95, 259-265.	0.4	0
13183	Ab initio study of the structure of oriented films of linearly chain carbon. JETP Letters, 2012, 95, 462-466.	0.4	6
13184	A first-principles investigation of the effect of relaxation on the alloy formation in the aluminum-3d-transition-metal system. Physics of Metals and Metallography, 2012, 113, 427-437.	0.3	1
13185	Ab Initio calculation of elastic and electromechanical constants of langasite family crystals. Crystallography Reports, 2012, 57, 131-133.	0.1	7
13186	Adhesion at the interfaces between BCC metals and Î±-Al2O3. Journal of Experimental and Theoretical Physics, 2012, 114, 305-313.	0.2	12
13187	Theoretical investigation of the atomic and electronic structure of Li x BC3 intercalated compounds. Journal of Experimental and Theoretical Physics, 2012, 114, 1018-1021.	0.2	3
13188	First-principles investigation of the phonon spectrum of Î²-GaS. Physics of the Solid State, 2012, 54, 1092-1095.	0.2	5
13189	First-principles study of the phonon spectrum of É›-GaSe. Physics of the Solid State, 2012, 54, 1467-1470.	0.2	3
13190	Energy spectrum of electrons in multilayer graphenes doped with atoms of alkaline metals. Nanotechnologies in Russia, 2012, 7, 140-148.	0.7	1
13191	Band structure of Au layers on the Ru(0001) and graphene/Ru(0001) surfaces. European Physical Journal B, 2012, 85, 1.	0.6	12
13192	High-pressure effect on elastic constants, stacking fault energy and correlation with dislocation properties in MgO and CaO. European Physical Journal B, 2012, 85, 1.	0.6	12
13193	Self assembly and chirality transfer in D-Alaninol on the Cu(100) surface. European Physical Journal D, 2012, 66, 1.	0.6	2
13194	Epitaxial deposition of silver ultra-fine nano-clusters on defect-free surfaces of HOPG-derived few-layer graphene in a UHV multi-chamber by in situ STM, ex situ XPS, and ab initio calculations. Nanoscale Research Letters, 2012, 7, 173.	3.1	14

#	Article	IF	Citations
13195	The Mechanism of Lowâ€Temperature CO Oxidation on IB Group Metals and Metal Oxides. ChemCatChem, 2012, 4, 100-111.	1.8	25
13196	Adsorption of Uranyl Species onto the Rutile (110) Surface: A Periodic DFT Study. Chemistry - A European Journal, 2012, 18, 1458-1466.	1.7	37
13197	The effect of structure and phase transformation on the mechanical properties of Re₂N and the stability of Mn₂N. Journal of Computational Chemistry, 2012, 33, 18-24.	1.5	11
13198	Dispersive interactions in water bilayers at metallic surfaces: A comparison of the PBE and RPBE functional including semiempirical dispersion corrections. Journal of Computational Chemistry, 2012, 33, 695-701.	1.5	136
13199	Density functional study of electronic,bonding, and vibrational properties of Ca (NH₂BH₃)₂. Journal of Computational Chemistry, 2012, 33, 987-997.	1.5	7
13200	Vibrational averaging of the chemical shift in crystalline Î±â€glycine. Journal of Computational Chemistry, 2012, 33, 1080-1089.	1.5	26
13201	A complete set of selfâ€consistent charge densityâ€functional tightâ€binding parametrization of zinc chalcogenides (ZnX; X=O, S, Se, and Te). Journal of Computational Chemistry, 2012, 33, 1165-1178.	1.5	30
13202	Structure and Electronic Properties and Phase Stabilities of the Cd_{1â^'x}Zn_xS Solid Solution in the Range of 0â‰¤xâ‰¤1. ChemPhysChem, 2012, 13, 147-154.	1.0	21
13203	Structures, Energetics and Reaction Mechanisms of Nitrous Oxide on Transitionâ€Metalâ€Doped and â€Undoped Singleâ€Wall Carbon Nanotubes. ChemPhysChem, 2012, 13, 583-587.	1.0	13
13204	Direct versus Hydrogenâ€Assisted CO Dissociation on the Feâ€‰(100) Surface: a DFT Study. ChemPhysChem, 2012, 13, 89-91.	1.0	55
13205	Magnetic Contrast in Phaseâ€Change Materials Doped with Fe Impurities. Advanced Materials, 2012, 24, 1429-1433.	11.1	23
13206	Sulfur-doped zinc oxide (ZnO) Nanostars: Synthesis and simulation of growth mechanism. Nano Research, 2012, 5, 20-26.	5.8	41
13207	Layer-by-layer removal of insulating few-layer mica flakes for asymmetric ultra-thin nanopore fabrication. Nano Research, 2012, 5, 99-108.	5.8	49
13208	Effects of 3d Transition Metal Elements in the B2-FeAl Structure. Metallurgical and Materials Transactions A: Physical Metallurgy and Materials Science, 2012, 43, 757-762.	1.1	4
13209	Microstructure and Thickness of 55 pct Al-Zn-1.6 pct Si-0.2 pct RE Hot-Dip Coatings: Experiment, Thermodynamic, and First-Principles Study. Metallurgical and Materials Transactions B: Process Metallurgy and Materials Processing Science, 2012, 43, 198-205.	1.0	16
13210	Electronic and Lattice Vibrational Properties of Cubic SrHfO3 from First-Principles Calculations. Journal of Electronic Materials, 2012, 41, 535-539.	1.0	7
13211	Thermodynamic Optimization of the Sc-X (XÂ=ÂLa, Li, Ca, Cr) Systems. Journal of Phase Equilibria and Diffusion, 2012, 33, 40-45.	0.5	3
13212	Elastic, electronic and thermodynamic properties of fluoro-perovskite KZnF3 via first-principles calculations. Applied Physics A: Materials Science and Processing, 2012, 106, 645-653.	1.1	48

#	Article	IF	Citations
13213	Ab initio investigation into the elasticity of ultrahigh-pressure phases of SiO2. Physics and Chemistry of Minerals, 2012, 39, 177-187.	0.3	4
13214	Thermodynamic Properties of MgSc and AlSc from First-Principles Phonon Calculations. International Journal of Thermophysics, 2012, 33, 300-310.	1.0	16
13215	The doping effect of N substituting for different atoms in orthorhombic SrHfO3. Journal of Materials Science, 2012, 47, 3046-3051.	1.7	1
13216	Elastic properties of random L12â€“Al3(Sc0.5TM0.5) alloys from first-principle SQSs calculations. Journal of Materials Science, 2012, 47, 3793-3800.	1.7	7
13217	An ab initio study of ground state, electronic and thermodynamical properties of GaP and Ga2P. Journal of Thermal Analysis and Calorimetry, 2012, 107, 39-44.	2.0	5
13218	Density functional theoretical study of lattice-specific heat and thermal properties of magnesium nitride. Journal of Thermal Analysis and Calorimetry, 2012, 107, 45-48.	2.0	11
13219	High pressure study on the phonon spectra and thermal properties in hafnium nitride and zirconium nitride. Journal of Thermal Analysis and Calorimetry, 2012, 107, 49-53.	2.0	11
13220	Theoretical insights into the effects of the diameter and helicity on the adsorption of formic acid on silicon carbide nanotube. Journal of Nanoparticle Research, 2012, 14, 1.	0.8	10
13221	Role of cross section on the stability and electronic structure of Ag-doped ZnO nanowires. Journal of Nanoparticle Research, 2012, 14, 1.	0.8	6
13222	Structure and electronic properties of boron nitride sheet with grain boundaries. Journal of Nanoparticle Research, 2012, 14, 1.	0.8	14
13223	Theoretical study of the surface properties of poly(dimethylsiloxane) and poly(tetrafluoroethylene). Journal of Molecular Modeling, 2012, 18, 239-250.	0.8	3
13224	Noncovalent and covalent functionalization of a (5, 0) single-walled carbon nanotube with alanine and alanine radicals. Journal of Molecular Modeling, 2012, 18, 771-781.	0.8	19
13225	Pressure-induced phase transition in wurtzite ZnTe: an ab initio study. Journal of Molecular Modeling, 2012, 18, 1167-1172.	0.8	5
13226	Oxygen activation and dissociation on hâ€BN supported Au atoms. International Journal of Quantum Chemistry, 2013, 113, 443-452.	1.0	39
13227	Hydrogen sulfide adsorption on a defective graphene. International Journal of Quantum Chemistry, 2013, 113, 786-791.	1.0	50
13228	Vacancy spatial distribution causes different magnetism in graphene. International Journal of Quantum Chemistry, 2013, 113, 792-796.	1.0	5
13229	Firstâ€principles study of vanadium adsorption and diffusion on the AlN(0001) surface. International Journal of Quantum Chemistry, 2013, 113, 797-801.	1.0	3
13230	Firstâ€principles investigation of magnetic property and defect formation energy in Niâ€Mnâ€Ga ferromagnetic shape memory alloy. International Journal of Quantum Chemistry, 2013, 113, 847-851.	1.0	10

#	Article	IF	Citations
13231	A comparison of the effect of nanotube chirality and electronic properties on the Ï€â€“Ï€ interaction of singleâ€wall carbon nanotubes with pyrazinamide antitubercular drug. International Journal of Quantum Chemistry, 2013, 113, 1272-1284.	1.0	17
13232	Geometric and magnetic properties of Co adatom decorated nitrogen-doped graphene. Journal of Applied Physics, 2013, 113, .	1.1	11
13233	Absorbing a Little Water: The Structural, Thermodynamic, and Kinetic Relationship between Pyrogallol and Its Tetarto-Hydrate. Crystal Growth and Design, 2013, 13, 4071-4083.	1.4	39
13234	Tailoring the Surface Reactivity of Silicon Surfaces by Partial Halogenation. Journal of Physical Chemistry C, 2013, 117, 18021-18030.	1.5	5
13235	Observation of higher stiffness in nanopolycrystal diamond than monocrystal diamond. Nature Communications, 2013, 4, 2343.	5.8	68
13236	Firstâ€principles study of hydrogenated CdS nanowires. Physica Status Solidi (B): Basic Research, 2013, 250, 1278-1282.	0.7	4
13237	A density functional theory analysis of trends in glycerol decomposition on close-packed transition metal surfaces. Physical Chemistry Chemical Physics, 2013, 15, 6475.	1.3	72
13238	The Elastic Properties, Generalized Stacking Fault Energy and Dissociated Dislocations in MgB2 Under Different Pressure. Journal of Superconductivity and Novel Magnetism, 2013, 26, 3401-3409.	0.8	4
13239	Superconductivity in Î²-Tin Germanium. Journal of Superconductivity and Novel Magnetism, 2013, 26, 2009-2011.	0.8	0
13240	Ferric garnet matrices for immobilization of actinides. Journal of Nuclear Materials, 2013, 436, 1-7.	1.3	17
13241	An accurate molecular mechanics model for computation of size-dependent elastic properties of armchair and zigzag single-walled carbon nanotubes. Meccanica, 2013, 48, 1355-1367.	1.2	31
13242	Manipulation of half-metallicity and ferromagnetism in N-doped CdS nanowire. Journal of Nanoparticle Research, 2013, 15, 1.	0.8	6
13243	A density functional theory study of the adsorption of bimetallic Fe n Pt m clusters on defective graphene: structural, electronic, and magnetic properties. Journal of Nanoparticle Research, 2013, 15, 1.	0.8	13
13244	Thermodynamic modeling of the Uâ€“Zr system â€“ A revisit. Journal of Nuclear Materials, 2013, 443, 331-341.	1.3	60
13245	First-Principles Study of Microporous Magnets M-MOF-74 (M = Ni, Co, Fe, Mn): the Role of Metal Centers. Inorganic Chemistry, 2013, 52, 9356-9362.	1.9	94
13246	Vacancies and defect levels in IIIâ€“V semiconductors. Journal of Applied Physics, 2013, 114, .	1.1	53
13247	Electronic Structures of Antimony Oxides. Journal of Physical Chemistry C, 2013, 117, 14759-14769.	1.5	80
13248	Octahedral tilting-induced ferroelectricity in<mml:math xmlns:mml="http://www.w3.org/1998/Math/MathML" display="inline"><mml:mi>A</mml:mi></mml:math>SnO<mml:math xmlns:mml="http://www.w3.org/1998/Math/MathML" display="inline"><mml:msub><mml:mrow /><mml:mn>3</mml:mn></mml:msub></mml:math>/<mml:math xmlns:mml="http://www.w3.org/1998/Math/MathML" display="inline"><mml:msup><mml:mi>A</mml:mi>	1.1	30

#	Article	IF	Citations
13249	Theory and Modeling of Oxide Semiconductors. Semiconductors and Semimetals, 2013, 88, 1-37.	0.4	8
13250	Electronic State of Oxidized Nanographene Edge with Atomically Sharp Zigzag Boundaries. ACS Nano, 2013, 7, 6868-6874.	7.3	24
13251	On the connection between structural distortion and magnetism in graphene with a single vacancy. Solid State Communications, 2013, 175-176, 71-75.	0.9	25
13252	Ab initio calculation of transport and optical properties of aluminum: Influence of simulation parameters. Computational Materials Science, 2013, 79, 817-829.	1.4	44
13253	Two-dimensional carbon allotropes from graphene to graphyne. Journal of Materials Chemistry C, 2013, 1, 3677.	2.7	116
13254	Magnetic and electronic properties of Fe/Cu multilayered nanowires: A first-principles investigation. Physica E: Low-Dimensional Systems and Nanostructures, 2013, 50, 1-5.	1.3	24
13255	Characterization of grapheneâ€“fullerene interactions: Insights from density functional theory. Chemical Physics Letters, 2013, 582, 115-118.	1.2	26
13256	First principle and ReaxFF molecular dynamics investigations of formaldehyde dissociation on Fe(100) surface. Journal of Computational Chemistry, 2013, 34, 1982-1996.	1.5	11
13257	First-principles structural, electronic and vibrational properties of zinc-blende zirconium carbide. Solid State Communications, 2013, 169, 32-36.	0.9	4
13258	First-principles study of structure and stability in Siâ€“Câ€“O-based materials. Theoretical Chemistry Accounts, 2013, 132, 1.	0.5	8
13259	Structural stability of higher-energy phases in Cu and Cuâ€“Fe alloy revealed by ab initio calculations. Computational Materials Science, 2013, 79, 463-467.	1.4	8
13260	The Feâ€“Mn enthalpy phase diagram from first principles. Journal of Alloys and Compounds, 2013, 577, 370-375.	2.8	15
13261	Formation of CO₂ and Ethane from Propionyl over Platinum: A Density Functional Theory Study. ACS Catalysis, 2013, 3, 1730-1738.	5.5	5
13262	Theoretical study of selective hydrogenation in a mixture of acetylene and ethylene over Fe@W(111) bimetallic surfaces. Applied Catalysis A: General, 2013, 462-463, 296-301.	2.2	5
13263	A density functional theory study on the interaction mechanism between H2S and the Î±-Fe2O3(0001) surface. Fuel Processing Technology, 2013, 115, 26-33.	3.7	58
13264	First-principles insights into p magnetism in CaC and CaN ionic compounds. Journal of Magnetism and Magnetic Materials, 2013, 341, 56-59.	1.0	6
13265	The interaction of H2S with the ZnO(101Ì„0) surface. Physical Chemistry Chemical Physics, 2013, 15, 8373.	1.3	22
13266	A molecular dynamics study of the effects of fast molecular motions on solid-state NMR parameters. CrystEngComm, 2013, 15, 8705.	1.3	77

#	Article	IF	Citations
13267	Experimental and theoretical evidence of zinc structurally bound in vermiculite from naturally metal-enriched soils. Clay Minerals, 2013, 48, 529-541.	0.2	5
13268	First principles investigations of structural, electronic, elastic, and dielectric properties of KMgF3. Journal of Materials Science, 2013, 48, 7635-7641.	1.7	19
13269	Absorption and diffusion of beryllium in graphite, beryllium carbide formation investigated by density functional theory. Journal of Applied Physics, 2013, 113, 213514.	1.1	16
13270	Fluorographynes: Stability, structural and electronic properties. Superlattices and Microstructures, 2013, 55, 75-82.	1.4	26
13271	A-centers in silicon studied with hybrid density functional theory. Applied Physics Letters, 2013, 103, 052101.	1.5	40
13272	Different Crystal Growth Mechanisms of Si(001)-(2 Ã— 1):H during Plasma-Enhanced Chemical Vapor Deposition of SiH₃ and SiH₂ Radicals: Tight-Binding Quantum Chemical Molecular Dynamics Simulations. Journal of Physical Chemistry C, 2013, 117, 15602-15614.	1.5	13
13273	A combined experimental and quantum chemical study of CO2 adsorption in the metalâ€“organic framework CPO-27 with different metals. Chemical Science, 2013, 4, 3544.	3.7	172
13274	Two-step spin-switchable tetranuclear Fe(II) molecular solid:Ab initiotheory and predictions. Physical Review B, 2013, 88, .	1.1	12
13275	Orientation dependence of elastic constants and electronic properties of rhenium nitrides first-principle calculations. Journal of Materials Science, 2013, 48, 4284-4296.	1.7	6
13276	Structural and electronic properties of grapheneâ€“ZnO interfaces: dispersion-corrected density functional theory investigations. Nanotechnology, 2013, 24, 305401.	1.3	67
13277	Mechanical properties of hydrogenated bilayer graphene. Journal of Chemical Physics, 2013, 138, 244709.	1.2	4
13278	Firstâ€Principles Study of Elastic, Structural, Electronic, Thermodynamical, and Optical Properties of Yttria (<scp><scp>Y</scp></scp>₂<scp><scp>O</scp></scp>₃) Ceramic in Cubic Phase. Journal of the American Ceramic Society, 2013, 96, 1832-1840.	1.9	46
13279	Ab initio study of Li adsorption in carbon nanotubes functionalized with amine and carboxyl groups. Chemical Physics, 2013, 418, 35-41.	0.9	4
13280	PDECO: Parallel differential evolution for clusters optimization. Journal of Computational Chemistry, 2013, 34, 1046-1059.	1.5	38
13281	Mechanical and Electronic Properties of Graphyne and Its Family under Elastic Strain: Theoretical Predictions. Journal of Physical Chemistry C, 2013, 117, 14804-14811.	1.5	151
13282	Site preference, magnetism and lattice vibrations of intermetallics M7â^'xTxB3 (MÂ=ÂRh, Ru; TÂ=ÂFe, Co). Intermetallics, 2013, 42, 112-119.	1.8	8
13283	Heating of Zeolites under Microwave Irradiation: A Density Functional Theory Approach to the Ion Movements Responsible of the Dielectric Loss in Na, K, and Ca A-Zeolites. Journal of Physical Chemistry C, 2013, 117, 15659-15666.	1.5	16
13284	Synthesis, structure, optical property, and electronic structure of Ba7AgGa5Se15. Journal of Alloys and Compounds, 2013, 565, 115-119.	2.8	7

#	Article	IF	Citations
13285	Adsorption of formaldehyde and formyl intermediates on Pt, PtRu-, and PtRuMo-alloy surfaces: A density functional study. Applied Surface Science, 2013, 266, 405-409.	3.1	10
13286	Ab initio study of CO adsorption on PdGa(110). Computational Materials Science, 2013, 71, 192-196.	1.4	9
13287	Structural, electronic and magnetic properties of linear monoatomic chains adsorption on beryllium oxide nanotube: First-principle study. Journal of Magnetism and Magnetic Materials, 2013, 330, 174-180.	1.0	20
13288	Comparison of analytic and numerical bond-order potentials for W and Mo. Journal of Physics Condensed Matter, 2013, 25, 265002.	0.7	3
13289	C4 Carbon allotropes with triple-bonds predicted by first-principles calculations. Solid State Communications, 2013, 169, 50-56.	0.9	9
13290	Van der Waals density-functional study of 100% hydrogen coverage on bilayer graphene. Computational Materials Science, 2013, 78, 1-8.	1.4	1
13291	Effects of aluminum diffusion on the adhesive behavior of the Ni(111)/Cr2O3(0001) interface: First principle study. Computational Materials Science, 2013, 78, 116-122.	1.4	36
13292	Electromechanical properties of alternating AlN and SiC nanoribbon sheets. Computational Materials Science, 2013, 78, 129-133.	1.4	11
13293	Dirac Cones in Two-Dimensional Lattices: Janugraphene and Chlorographene. Journal of Physical Chemistry Letters, 2013, 4, 2471-2476.	2.1	25
13294	First-principles study of L12â€“Al3(Sc1â^'xTMx) alloys using special quasirandom structures. Computational Materials Science, 2013, 79, 136-142.	1.4	10
13295	Structural stabilities and uniaxial strain modulated electronic properties of AlN/SiC-coreâ€“shell nanowires: A first-principles study. Superlattices and Microstructures, 2013, 57, 19-26.	1.4	5
13296	Electronic and molecular behaviors of a novel ionic paramagnetic ruthenium(iii) complex. Physical Chemistry Chemical Physics, 2013, 15, 15392.	1.3	0
13297	First-principles calculations of finite-temperature elastic properties of Ti2AlX (X=C or N). Computational Materials Science, 2013, 79, 296-302.	1.4	24
13298	Unusual Magnetic Properties of Functionalized Graphene Nanoribbons. Journal of Physical Chemistry Letters, 2013, 4, 2482-2488.	2.1	22
13299	Thermodynamics of carbon solubility in ferrite and vacancy formation in cementite in strained pearlite. Acta Materialia, 2013, 61, 1773-1784.	3.8	43
13300	Theoretical Understanding of Enhanced Photoelectrochemical Catalytic Activity of Sn-Doped Hematite: Anisotropic Catalysis and Effects of Morin Transition and Sn Doping. Journal of Physical Chemistry C, 2013, 117, 3779-3784.	1.5	51
13301	First-Principles Calculation of Lithium Adsorption and Diffusion on Silicene. Chinese Physics Letters, 2013, 30, 017103.	1.3	27
13302	Edge reconstruction limited electron transport of zigzag graphene nanoribbon. European Physical Journal B, 2013, 86, 1.	0.6	7

#	Article	IF	Citations
13303	Enhancement of the solubility, thermal stability, and electronic properties of carbon nanotubes functionalized with MEH-PPV: a combined experimental and computational study. Monatshefte FÃ¼r Chemie, 2013, 144, 925-935.	0.9	9
13304	First-principles calculations of the Young's modulus of double wall boron-nitride nanotubes. Materials Chemistry and Physics, 2013, 138, 963-966.	2.0	18
13305	Defective Graphene Supported MPd₁₂ (M = Fe, Co, Ni, Cu, Zn, Pd) Nanoparticles as Potential Oxygen Reduction Electrocatalysts: A First-Principles Study. Journal of Physical Chemistry C, 2013, 117, 1350-1357.	1.5	88
13306	Single-Layer Group-III Monochalcogenide Photocatalysts for Water Splitting. Chemistry of Materials, 2013, 25, 3232-3238.	3.2	675
13307	Ferromagnetic sandwich-like wires constructed with transition metals and anthracene. Applied Physics Letters, 2013, 103, 032404.	1.5	4
13308	TiO₂-Based Gas Sensor: A Possible Application to SO₂. ACS Applied Materials & Interfaces, 2013, 5, 8516-8522.	4.0	186
13309	Ab initio calculations for the F-center transfer and R centers in SrF2. Computational Materials Science, 2013, 79, 527-533.	1.4	4
13310	Local electronic structure, optical bandgap and photoluminescence (PL) properties of Ba(Zr0.75Ti0.25)O3 powders. Materials Science in Semiconductor Processing, 2013, 16, 1035-1045.	1.9	31
13311	Interfacial Properties of Bilayer and Trilayer Graphene on Metal Substrates. Scientific Reports, 2013, 3, 2081.	1.6	86
13312	Thermodynamic stability of various phases of zinc tin oxides from ab initio calculations. Journal of Materials Chemistry C, 2013, 1, 6364.	2.7	28
13313	Ab initio electronic band structure study of IIIâ€“VI layered semiconductors. European Physical Journal B, 2013, 86, 1.	0.6	23
13314	Effects of pressure on the electronic structures of LaOFeP. Physics Letters, Section A: General, Atomic and Solid State Physics, 2013, 377, 1479-1485.	0.9	0
13315	Local deformations and chemical bonding in Fe-X (X = Si, Al, Ga, Ge) soft magnetic alloys. Physics of Metals and Metallography, 2013, 114, 469-473.	0.3	8
13316	First-principles investigations of interatomic interactions in Ni3Al alloyed by interstitial and substitutional impurities. Physics of Metals and Metallography, 2013, 114, 191-196.	0.3	4
13317	Compressibility and structural properties of jadeite, NaAlSi2O6 at high pressure. Journal of Earth Science (Wuhan, China), 2013, 24, 57-64.	1.1	4
13318	Pressure effect on structural, elastic and electronic properties of (B3) BSb compound. Indian Journal of Physics, 2013, 87, 355-362.	0.9	11
13319	High pressure iso-structural phase transition in BiMn₂O₅. Journal of Physics Condensed Matter, 2013, 25, 325401.	0.7	8
13320	Effect of zinc oxide as a sintering aid on proton migration across Î£5 (310)/[001] tilt grain boundary of barium zirconate. Journal of Electroceramics, 2013, 30, 19-23.	0.8	1

#	Article	IF	Citations
13321	Strained coherent interface energy of the Guinierâ€“Preston II phase in Alâ€“Cu during stress aging. Journal of Materials Science, 2013, 48, 7927-7934.	1.7	9
13322	Wetting and adhesion at Mg/MgO interfaces. Journal of Materials Science, 2013, 48, 6008-6017.	1.7	13
13323	Impact of the germanium concentration in the stability of E-centers and A-centers in Si1â^'xGex. Journal of Materials Science: Materials in Electronics, 2013, 24, 2772-2776.	1.1	6
13324	Newly found phase transition and mechanical stability of AuAl2: A first-principles study. Journal of Alloys and Compounds, 2013, 574, 486-489.	2.8	6
13325	Hydrogen trapping in Î´-Pu: insights from electronic structure calculations. Journal of Physics Condensed Matter, 2013, 25, 265001.	0.7	12
13326	Stability and mechanical properties of C2N2X (X=O, NH and CH2) from first-principles calculations. Physica B: Condensed Matter, 2013, 428, 97-105.	1.3	3
13327	Minimum thermal conductivity in superlattices: A first-principles formalism. Physical Review B, 2013, 87, .	1.1	126
13328	Reactivity of the ZnS(101Ì…0) Surface to Small Organic Ligands by Density Functional Theory. Journal of Physical Chemistry C, 2013, 117, 16034-16041.	1.5	6
13329	Half metallic ferromagnetism in alkaline-earth metal nitrides XN (X=Ca, Sr and Ba): A first principles study. Journal of Magnetism and Magnetic Materials, 2013, 346, 26-37.	1.0	16
13330	First principles LDA +Uand GGA +Ustudy of protactinium and protactinium oxides: dependence on the effectiveUparameter. Journal of Physics Condensed Matter, 2013, 25, 145603.	0.7	20
13331	DFT study of the chemistry of sulfur in graphite, including interactions with defects, edges and folds. Carbon, 2013, 62, 256-262.	5.4	17
13332	Temperature-driven phase transformation in Y3Co: Neutron scattering and first-principles studies. Physical Review B, 2013, 88, .	1.1	6
13333	First-Principles Investigations of Metal (Cu, Ag, Au, Pt, Rh, Pd, Fe, Co, and Ir) Doped Hexagonal Boron Nitride Nanosheets: Stability and Catalysis of CO Oxidation. Journal of Physical Chemistry C, 2013, 117, 17319-17326.	1.5	300
13334	Surface Magnetism: Relativistic Effects at Semiconductor Interfaces and Solar Cells. , 2013, , 129-143.		0
13335	Bandgap engineering of graphene by corrugation on lattice-mismatched MgO (111). Journal of Materials Chemistry C, 2013, 1, 1595.	2.7	25
13336	Half-metallicity in a chem{BiFeO_3/La_{rac{2}{3}}Sr_{rac{1}{3}}MnO_3} superlattice: A first-principles study. Europhysics Letters, 2013, 102, 67009.	0.7	9
13337	Corrugation-induced metal-semiconductor transition in single-wall carbon nanotubes with a small radius. Physical Review B, 2013, 88, .	1.1	9
13338	Electronic and Magnetic Engineering in Zigzag Graphene Nanoribbons Having a Topological Line Defect at Different Positions with or without Strain. Journal of Physical Chemistry C, 2013, 117, 4791-4799.	1.5	38

#	Article	IF	Citations
13339	Solution softening in magnesium alloys: the effect of solid solutions on the dislocation core structure and nonbasal slip. Journal of Physics Condensed Matter, 2013, 25, 022202.	0.7	54
13340	Insights into electrochemical performance of Li2FeSiO4 from first-principles calculations. Electrochimica Acta, 2013, 111, 172-178.	2.6	30
13341	Methane oxidation over Pd and Pt studied by DFT and kinetic modeling. Surface Science, 2013, 616, 206-213.	0.8	87
13342	Chemisorption of uracil on gold surfaces via density functional theory. Surface Science, 2013, 614, 20-23.	0.8	13
13343	Elastic, optoelectronic, and thermal properties of cubic CSi2N4: an ab initio study. Journal of Materials Science, 2013, 48, 8235-8243.	1.7	24
13344	The structural and electronic properties of (10,0) zigzag Single-Wall Carbon Nanotubes modified by thiophene groups. Chemical Physics Letters, 2013, 584, 177-181.	1.2	2
13345	Surface effects on the structure and lithium behavior in lithiated silicon: A first principles study. Surface Science, 2013, 612, 16-23.	0.8	30
13346	A theoretical study of CH4 dissociation on NiPd(111) surface. Surface Science, 2013, 612, 63-68.	0.8	29
13347	Band structure analysis of (1Ã—2)-H/Pd(110)-pr. Surface Science, 2013, 615, 119-124.	0.8	3
13348	Photoelectron spectroscopic study of CO and NO adsorption on Pd(100) surface under ambient pressure conditions. Surface Science, 2013, 615, 33-40.	0.8	15
13349	The study of the effect of increasing adsorbed hydrogen's atomic percentage on electronic properties of boron-nitride nanotube. Physica E: Low-Dimensional Systems and Nanostructures, 2013, 53, 168-172.	1.3	5
13350	Scanning tunneling spectroscopy and density functional calculation of silicon dangling bonds on the Si(100)-2Ã—1:H surface. Surface Science, 2013, 609, 147-151.	0.8	18
13351	Investigation of the mechanical and electronic properties of Ag-Au and Co-Au nanocontacts by the method of first-principle molecular dynamics. Moscow University Physics Bulletin (English) Tj ETQq0 0 0 rgBT /Overlock 10 Tf 50 257 Td		5
13352	First-principles study of electronic structure and optical properties of Sr(Ti,Zr)O3. Open Physics, 2013, 11, .	0.8	1
13353	Zirconium adsorption and incorporation on a reconstructed Al-T4 AlN(0001) surface. Journal of Physics and Chemistry of Solids, 2013, 74, 1387-1391.	1.9	7
13354	Nickel adsorption and incorporation on a 2Ã—2-T4 GaN(0001) surface: A DFT study. Applied Surface Science, 2013, 266, 205-208.	3.1	3
13355	Ab initioprediction of the critical thickness of a precipitate. Journal of Physics Condensed Matter, 2013, 25, 355005.	0.7	7
13356	CO Hydrogenation on Pd(111): Competition between Fischerâ€“Tropsch and Oxygenate Synthesis Pathways. Journal of Physical Chemistry C, 2013, 117, 14667-14676.	1.5	30

#	Article	IF	Citations
13357	Toward the Microscopic Identification of Anions and Cations at the Ionic Liquid|Ag(111) Interface: A Combined Experimental and Theoretical Investigation. ACS Nano, 2013, 7, 7773-7784.	7.3	100
13358	Structural phase transition and mechanical properties of TiO₂ under high pressure. Physica Status Solidi (B): Basic Research, 2013, 250, 2206-2214.	0.7	33
13359	FIRST-PRINCIPLES CALCULATION OF LEAD-FREE PEROVSKITE SnTiO₃. International Journal of Modern Physics B, 2013, 27, 1350144.	1.0	13
13360	Electronic properties of pure and p-type doped hexagonal sheets and zigzag nanoribbons of InP. Journal of Physics Condensed Matter, 2013, 25, 085506.	0.7	3
13361	A comparison of electronic transport properties of graphene with hexagonal boron nitride substrate and graphane, a first principle study. European Physical Journal B, 2013, 86, 1.	0.6	11
13362	DFT calculations of the electronic structure of SnOx layers on Pd(110). European Physical Journal B, 2013, 86, 1.	0.6	5
13363	Electronic properties of C-substituted boron nanotubes: a first principles study. European Physical Journal B, 2013, 86, 1.	0.6	1
13364	Mathematical modelling radiation impact on nanostructures. Bulletin of the Russian Academy of Sciences: Physics, 2013, 77, 814-819.	0.1	3
13365	SrTiO3 (001) surface and strained thin films: Atomic simulations using a tight-binding variable-charge model. Surface Science, 2013, 616, 19-28.	0.8	10
13366	A first-principles study of CO hydrogenation into methane on molybdenum carbides catalysts. Surface Science, 2013, 614, 53-63.	0.8	48
13367	Analysis of sulfur-induced selectivity changes for anhydrous methanol dehydrogenation on Ni(100) surfaces. Surface Science, 2013, 613, 58-62.	0.8	7
13368	Theoretical and experimental study of the interaction of CO on TiC surfaces: Regular versus low coordinated sites. Surface Science, 2013, 613, 63-73.	0.8	5
13369	Comparison of wurtzite and zinc-blende GaAs surfaces as possible nanowire side walls: DFT stability calculations. Surface Science, 2013, 613, 74-79.	0.8	14
13370	Energy band gap and optical properties of lithium niobate from ab initio calculations. Computational Materials Science, 2013, 79, 125-131.	1.4	64
13371	Monolayer Doping via Phosphonic Acid Grafting on Silicon: Microscopic Insight from Infrared Spectroscopy and Density Functional Theory Calculations. Advanced Functional Materials, 2013, 23, 3471-3477.	7.8	64
13372	The surface oxygen vacancy induced visible activity and enhanced UV activity of a ZnO1â^'x photocatalyst. Catalysis Science and Technology, 2013, 3, 3136.	2.1	167
13373	BaTiO3: Energy, geometrical and electronic structure, relationship between optical constant and density from first-principles calculations. Optical Materials, 2013, 35, 2629-2637.	1.7	69
13374	Polarized microâ€Raman spectroscopy and ab initio phonon modes calculations of LuPO₄. Journal of Raman Spectroscopy, 2013, 44, 1411-1415.	1.2	7

#	Article	IF	Citations
13375	Computational simulation of adsorption and thermodynamic study of xanthate, dithiophosphate and dithiocarbamate on galena and pyrite surfaces. Minerals Engineering, 2013, 46-47, 136-143.	1.8	63
13376	Pressure dependence of superconductivity in simple cubic phosphorus. Physical Review B, 2013, 88, .	1.1	26
13377	CO2 hydrogenation on Au/TiC, Cu/TiC, and Ni/TiC catalysts: Production of CO, methanol, and methane. Journal of Catalysis, 2013, 307, 162-169.	3.1	214
13378	Proxies from Ab Initio Calculations for Screening Efficient Ce³⁺ Phosphor Hosts. Journal of Physical Chemistry C, 2013, 117, 17955-17959.	1.5	176
13379	Novel electronic and magnetic properties in AlN nanoribbons: First-principles prediction. Europhysics Letters, 2013, 103, 37009.	0.7	4
13380	Influence of lone pair doping on the multiferroic property of orthorhombic HoMnO3:ab initioprediction. Journal of Physics Condensed Matter, 2013, 25, 385901.	0.7	0
13381	Effect of alloying elements on in-plane ordering and disordering of solute clusters in Mg-based long-period stacking ordered structures: A first-principles analysis. Scripta Materialia, 2013, 69, 594-597.	2.6	54
13382	Dramatic increase in the Raman signal of functional groups on carbon nanotube surfaces. Carbon, 2013, 56, 235-242.	5.4	9
13383	Ethanoldecomposition on a Pd(110) surface: a density functional theory investigation. Dalton Transactions, 2013, 42, 2309-2318.	1.6	25
13384	Thermodynamic modeling of Auâ€“Ceâ€“Sn ternary system. Calphad: Computer Coupling of Phase Diagrams and Thermochemistry, 2013, 42, 38-50.	0.7	20
13385	Electron Mobility via Polaron Hopping in Bulk Ceria: A First-Principles Study. Journal of Physical Chemistry C, 2013, 117, 14502-14509.	1.5	75
13386	Dynamical response and instability in ceria under lattice expansion. Physical Review B, 2013, 87, .	1.1	48
13387	Magnetic semiconductor and metalâ€“semiconductor junction by nanoparticles encapsulated in beryllium oxygen nanotube. Journal of Magnetism and Magnetic Materials, 2013, 344, 162-166.	1.0	8
13388	A density functional theory study of oxygen reduction reaction on Meâ€“N4 (Me = Fe, Co, or Ni) clusters between graphitic pores. Journal of Materials Chemistry A, 2013, 1, 10790.	5.2	253
13389	Theoretical assessment of graphene-metal contacts. Journal of Chemical Physics, 2013, 138, 244701.	1.2	58
13390	Effect of pressure on the atomic and electronic structure of enstatite MgSiO3: Ab initio calculations. Technical Physics, 2013, 58, 692-695.	0.2	1
13391	Band structure design of semiconductors for enhanced photocatalytic activity: The case of TiO2. Progress in Natural Science: Materials International, 2013, 23, 402-407.	1.8	220
13392	Structural and elastic properties of Ce2O3 under pressure from LDA+U method. Frontiers of Physics, 2013, 8, 405-411.	2.4	6

#	Article	IF	Citations
13393	Stability of Pt-Modified Cu(111) in the Presence of Oxygen and Its Implication on the Overall Electronic Structure. Journal of Physical Chemistry C, 2013, 117, 16371-16380.	1.5	5
13394	Anharmonic vibrational properties in periodic systems: energy, electron-phonon coupling, and stress. Physical Review B, 2013, 87, .	1.1	151
13395	The high conductivity of iron and thermal evolution of the Earthâ€™s core. Physics of the Earth and Planetary Interiors, 2013, 224, 88-103.	0.7	251
13396	Raman spectroscopic properties and Raman identification of CaSâ€MgSâ€MnSâ€FeSâ€Cr₂FeS₄ sulfides in meteorites and reduced sulfurâ€rich systems. Meteoritics and Planetary Science, 2013, 48, 1415-1426.	0.7	68
13397	TEM study of structural and microstructural characteristics of a precipitate phase in Ni-rich Niâ€“Tiâ€“Hf and Niâ€“Tiâ€“Zr shape memory alloys. Acta Materialia, 2013, 61, 6191-6206.	3.8	169
13398	Origin of the vanishing critical thickness for ferroelectricity in free-standing PbTiO3 ultrathin films from first principles. Journal of Applied Physics, 2013, 114, .	1.1	11
13399	Geometrical Correction for the Inter- and Intramolecular Basis Set Superposition Error in Periodic Density Functional Theory Calculations. Journal of Physical Chemistry A, 2013, 117, 9282-9292.	1.1	123
13400	Firstâ€Principles Investigations of the Structural, Vibrational and Thermochemical Properties of Barium Cerate â€“ Another Test Case for Densityâ€Functional Theory. Zeitschrift Fur Anorganische Und Allgemeine Chemie, 2013, 639, 1227-1231.	0.6	20
13401	First-Principles Study on the Synergistic Mechanism of SnO₂ and Graphene As a Lithium Ion Battery Anode. Journal of Physical Chemistry C, 2013, 117, 23-27.	1.5	53
13402	NH3/Ir(100): Electronic structure and dehydrogenation. International Journal of Hydrogen Energy, 2013, 38, 2965-2972.	3.8	16
13403	Possibility of a 2D SiC monolayer formation on Mg(0001) and MgO(111) substrates. Russian Journal of Physical Chemistry A, 2013, 87, 1332-1335.	0.1	7
13404	First principles study of electronic and optical properties of Cu2ZnSnX4 (XÂ=ÂS, Se) solar absorbers by Tranâ€“Blaha-modified Beckeâ€“Johnson potential approach. Journal of Materials Science, 2013, 48, 8259-8267.	1.7	12
13405	Physisorption vs. chemisorption of probe molecules on boron nitride nanomaterials: the effect of surface curvature. Physical Chemistry Chemical Physics, 2013, 15, 13190.	1.3	30
13406	An ab initio study of the peak tensile strength of tungsten with an account of helium point defects. International Journal of Plasticity, 2013, 48, 54-71.	4.1	19
13407	Vibrational mode analysis and heat capacity calculation of K2SiSi3O9-wadeite. Physics and Chemistry of Minerals, 2013, 40, 563-574.	0.3	8
13408	Stability and equation of state of post-aragonite BaCO3. Physics and Chemistry of Minerals, 2013, 40, 447-453.	0.3	17
13409	Effects of pressure on PbWO4-III. Physics and Chemistry of Minerals, 2013, 40, 341-348.	0.3	2
13410	Thermodynamic properties and phase stability of wadsleyite II. Physics and Chemistry of Minerals, 2013, 40, 251-257.	0.3	2

#	Article	IF	Citations
13411	Ligand-Directed Formation of Gold Tetrapod Nanostructures. Journal of Physical Chemistry C, 2013, 117, 17143-17150.	1.5	30
13412	Layered Perovskite Sr2Ta2O7 for Visible Light Photocatalysis: A First Principles Study. Journal of Physical Chemistry C, 2013, 117, 5043-5050.	1.5	47
13413	Mn-Doped CeO₂: DFT+U Study of a Catalyst for Oxidation Reactions. Journal of Physical Chemistry C, 2013, 117, 18063-18073.	1.5	68
13414	The investigation on the electronic structures of hybrid GNR-ZnO. Applied Physics A: Materials Science and Processing, 2013, 112, 357-362.	1.1	5
13415	Decomposition of Ethanol Over Ru(0001): A DFT Study. Topics in Catalysis, 2013, 56, 874-884.	1.3	36
13416	The Role of Hydrogen Bonding and Proton Transfer in the Formation of Uracil Networks on the Gold (100) Surface: A Density Functional Theory Approach. Journal of Physical Chemistry C, 2013, 117, 3949-3957.	1.5	31
13417	Ab initio calculations on the effect of Mn substitution in the Î¹-carbide Fe3AlC. Journal of the Korean Physical Society, 2013, 62, 481-485.	0.3	14
13418	Lithium metasilicate and lithium disilicate nanomaterials: optical properties and density functional theory calculations. International Nano Letters, 2013, 3, 1.	2.3	12
13419	Investigation of structural and electronic transport properties of graphene and graphane using maximally localized Wannier functions. Journal of Theoretical and Applied Physics, 2013, 7, 9.	1.4	11
13420	Completing a family: LiCN3H4, the lightest alkali metal guanidinate. Dalton Transactions, 2013, 42, 15080.	1.6	17
13421	Coupling Solid-State NMR with GIPAW ab Initio Calculations in Metal Hydrides and Borohydrides. Journal of Physical Chemistry C, 2013, 117, 9991-9998.	1.5	26
13422	A new many-body potential with the second-moment approximation of tight-binding scheme for Hafnium. Science China: Physics, Mechanics and Astronomy, 2013, 56, 2071-2080.	2.0	1
13423	Effects of hydrogen in a vanadium grain boundary: From site occupancy to mechanical properties. Science China: Physics, Mechanics and Astronomy, 2013, 56, 1389-1395.	2.0	4
13424	Lattice instability of V2AlC at high pressure. Science China: Physics, Mechanics and Astronomy, 2013, 56, 916-924.	2.0	13
13425	Elastic and thermo-physical properties of stannite-type Cu2ZnSnS4 and Cu2ZnSnSe4 from first-principles calculations. Acta Metallurgica Sinica (English Letters), 2013, 26, 285-292.	1.5	14
13426	Phase transition characters and thermodynamics modeling of the newly-discovered wII- and post-spinel Si3N4 polymorphs: A first-principles investigation. Acta Metallurgica Sinica (English) Tj ETQq1 1 0.784314 rgBT /Overlock	1.5	0
13427	Reduction of conductivity and ferromagnetism induced by Ag doping in ZnO:Co. Thin Solid Films, 2013, 545, 488-495.	0.8	2
13428	Regioselective Oxidation of Strained Graphene for Controllable Synthesis of Nanoribbons. Journal of Physical Chemistry C, 2013, 117, 19160-19166.	1.5	6

#	Article	IF	Citations
13429	Shape-controlled TiO2nanoparticles and TiO2P25 interacting with CO and H2O2molecular probes: a synergic approach for surface structure recognition and physico-chemical understanding. Physical Chemistry Chemical Physics, 2013, 15, 307-315.	1.3	65
13430	Tunable doping and band gap of graphene on functionalized hexagonal boron nitride with hydrogen and fluorine. Physical Chemistry Chemical Physics, 2013, 15, 5067.	1.3	70
13431	Nanocolumnar Germanium Thin Films as a High-Rate Sodium-Ion Battery Anode Material. Journal of Physical Chemistry C, 2013, 117, 18885-18890.	1.5	175
13432	Twin-induced one-dimensional homojunctions yield high quantum efficiency for solar hydrogen generation. Nature Communications, 2013, 4, 2278.	5.8	325
13433	Conductance of ferro- and antiferro-magnetic single-atom contacts: A first-principles study. Journal of Applied Physics, 2013, 114, 063711.	1.1	4
13434	Ab-initio study of anisotropy and nonuniaxial anisotropy coefficients in Pd nanochains. Chemical Physics Letters, 2013, 583, 109-113.	1.2	5
13435	Magnetic properties of 3d transition metals and nitrogen functionalized armchair graphene nanoribbon. RSC Advances, 2013, 3, 21110.	1.7	10
13436	Lithium Insertion into Titanium Dioxide (Anatase): A Raman Study with ^{16/18}O and ^{6/7}Li Isotope Labeling. Chemistry of Materials, 2013, 25, 3710-3717.	3.2	17
13437	First-principles investigation of the size-dependent structural stability and electronic properties of O-vacancies at the ZnO polar and non-polar surfaces. Journal of Applied Physics, 2013, 113, .	1.1	170
13438	Effect of pressure on the free ion and crystal field parameters of Sm2+ in BaFBr and SrFBr hosts. Journal of Luminescence, 2013, 134, 678-685.	1.5	15
13439	An empirical model for silver tantalate. Modelling and Simulation in Materials Science and Engineering, 2013, 21, 055002.	0.8	12
13440	Atomistic study of stress-induced switching of 90Â° ferroelectric domain walls in PbTiO3: size, temperature and structural effect. Modelling and Simulation in Materials Science and Engineering, 2013, 21, 065019.	0.8	4
13441	Physical properties of zircon and scheelite lutetium orthovanadate: Experiment and first-principles calculation. Journal of Solid State Chemistry, 2013, 205, 97-103.	1.4	11
13442	Elastic properties of an Mgâ€“Znâ€“Y alloy single crystal with a long-period stacking-ordered structure. Acta Materialia, 2013, 61, 6338-6351.	3.8	125
13443	Ab Initio Molecular Dynamics Study of the Very Short Oâ€“HÂ·Â·Â·O Hydrogen Bonds in the Condensed Phases. Journal of Chemical Theory and Computation, 2013, 9, 65-72.	2.3	11
13444	First-principles investigation of thiophene adsorption on Ni13 and Zn@Ni12 nanoclusters. Computational and Theoretical Chemistry, 2013, 1020, 136-142.	1.1	13
13445	Optical and vibrational properties of hydrogenated BN-sheet: First principles study. Applied Surface Science, 2013, 284, 638-643.	3.1	6
13446	Effect of strain on the stacking fault energy of copper: A first-principles study. Physical Review B, 2013, 88, .	1.1	60

#	Article	IF	Citations
13447	Electrochemical formation and surface characterisation of Cu2â^'xTe thin films with adjustable content of Cu. RSC Advances, 2013, 3, 21648.	1.7	8
13448	Electronic Conductivity of Solids. , 2013, , 1007-1034.		0
13449	Phosphorousâ€"vacancyâ€"oxygen defects in silicon. Journal of Materials Chemistry A, 2013, 1, 11384.	5.2	11
13450	Computational Methods for Solids. , 2013, , 59-87.		2
13451	Tunable electronic and magnetic properties of WS2 nanoribbons. Journal of Applied Physics, 2013, 114, .	1.1	48
13452	STRUCTURAL, ELASTIC AND ELECTRONIC PROPERTIES OF OXYGEN SUBSTITUTION IN CUBIC Zr₃N₄ AND Ti₃N₄. International Journal of Modern Physics B, 2013, 27, 1350095.	1.0	3
13453	Electrical Spin Switch in Hydrogenated Multilayer Graphene. Journal of Physical Chemistry C, 2013, 117, 6420-6425.	1.5	12
13454	Phase transition and thermodynamic properties of CaF2 via first principles. Physica B: Condensed Matter, 2013, 426, 13-19.	1.3	15
13455	Direct Formation of Acetate from the Partial Oxidation of Ethylene on a Au/TiO2 Catalyst. Topics in Catalysis, 2013, 56, 1512-1524.	1.3	11
13456	Why (1 0 0) Terraces Break and Make Bonds: Oxidation of Dimethyl Ether on Platinum Single-Crystal Electrodes. Journal of the American Chemical Society, 2013, 135, 14329-14338.	6.6	46
13457	Fermi level influence on the adsorption at semiconductor surfacesâ€"ab initio simulations. Journal of Applied Physics, 2013, 114, .	1.1	35
13458	Molecular hydrogen uptake by zigzag graphene nanoribbons doped with early 3d transition-metal atoms. International Journal of Hydrogen Energy, 2013, 38, 8872-8880.	3.8	22
13459	Optical properties of hexagonal boron nanotubes by first-principles calculations. Journal of Applied Physics, 2013, 114, 073514.	1.1	13
13460	O2 Adsorption and Oxidative Activity on Gold-Based Catalysts with and without a Ceria Support. Journal of Physical Chemistry C, 2013, 117, 18986-18993.	1.5	23
13461	Theoretical study of sorption and diffusion of lithium atoms on the surface of crystalline silicon and inside it. JETP Letters, 2013, 97, 634-638.	0.4	3
13462	Spin pumping and interlayer exchange coupling through palladium. Physical Review B, 2013, 88, .	1.1	14
13463	Linear infinite cadmium chains in CaAu4Cd2 and other intermetallics with YbMo2Al4-type structure. Monatshefte FÃ¼r Chemie, 2013, 144, 751-760.	0.9	19
13464	Multi-physics analysis of nano-structured ferroelectrics by first-principles simulations. Acta Mechanica, 2013, 224, 1261-1270.	1.1	2

#	Article	IF	Citations
13465	Oxygen subsurface adsorption on the Cu(110)-c(6Ã—2) surface. Surface Science, 2013, 615, 57-64.	0.8	15
13466	Electronic structure and optical properties of Cu-doping and Zn vacancy impurities in ZnTe. Journal of Molecular Modeling, 2013, 19, 3805-3812.	0.8	7
13467	Density functional theory studies of the adsorption of hydrogen sulfide on aluminum doped silicane. Journal of Molecular Modeling, 2013, 19, 2925-2934.	0.8	9
13468	Vibrational spectra of an RDX film over an aluminum substrate from molecular dynamics simulations and density functional theory. Journal of Molecular Modeling, 2013, 19, 2773-2778.	0.8	5
13469	Structural, mechanical and electronic properties of nano-fibriform silica and its organic functionalization by dimethyl silane: a SCC-DFTB approach. Journal of Molecular Modeling, 2013, 19, 1995-2005.	0.8	5
13470	Ab-initio study of anisotropic and chemical surface modifications of Î²-SiC nanowires. Journal of Molecular Modeling, 2013, 19, 2043-2048.	0.8	16
13471	Theoretical study on the encapsulation of Pd3-based transition metal clusters inside boron nitride nanotubes. Journal of Molecular Modeling, 2013, 19, 1143-1151.	0.8	23
13472	Molecular vibrational spectroscopy characterization of epoxy graphene oxide from density functional calculations. Journal of Molecular Modeling, 2013, 19, 1429-1434.	0.8	6
13473	First-principles prediction of the transition from graphdiyne to a superlattice of carbon nanotubes and graphene nanoribbons. Carbon, 2013, 65, 341-348.	5.4	52
13474	Stability and Hydrogen Affinity of Graphite-Supported Wires of Cu, Ag, Au, Ni, Pd, and Pt. Journal of Physical Chemistry C, 2013, 117, 19239-19244.	1.5	10
13475	Structural, electronic and thermodynamic properties of R3ZnH5 (R=K, Rb, Cs): A first-principle calculation. Journal of Solid State Chemistry, 2013, 198, 433-439.	1.4	6
13476	Estimation of the Youngâ€™s modulus of single-walled carbon nanotubes under electric field using tight-binding method. Superlattices and Microstructures, 2013, 59, 178-186.	1.4	7
13477	Prediction of (TiO₂)_x(Cu₂O)_yalloys for efficient photoelectrochemical water splitting. Physical Chemistry Chemical Physics, 2013, 15, 1778-1781.	1.3	17
13478	Electronic Structures and Magnetic Properties in Ti-Doped ZnO. Advanced Materials Research, 2013, 721, 308-311.	0.3	2
13479	Computational testing of trivalent dopants in CeO₂for improved high-Îº dielectric behaviour. Journal of Materials Chemistry C, 2013, 1, 1093-1098.	2.7	35
13480	First-principles study of small palladium clusters on NiAl(110) alloy surface. Physica E: Low-Dimensional Systems and Nanostructures, 2013, 53, 7-13.	1.3	9
13481	Quantum chemical studies on adsorption of CO2 on nitrogen-containing molecular segment models of coal. Surface Science, 2013, 616, 85-92.	0.8	34
13482	Localized electronic states induced by oxygen vacancies on anatase TiO2 (101) surface. Surface Science, 2013, 616, 115-119.	0.8	45

#	Article	IF	Citations
13483	Critical island size for a shape transition in strained Cu/Ni(100) islands. Surface Science, 2013, 616, 120-124.	0.8	3
13484	Interaction of O2 with reduced rutile TiO2(110) surface. Surface Science, 2013, 610, 33-41.	0.8	18
13485	First-principle modeling of gold adsorption on BeO (0001). Surface Science, 2013, 609, 39-43.	0.8	6
13486	Ab initio study of the surface properties of austenitic stainless steel alloys. Surface Science, 2013, 609, 190-194.	0.8	13
13487	Scanning tunneling microscopy investigation of electronic properties of cobalt nanoislands supported by Cuâ€“9at.%Al(111). Surface Science, 2013, 609, 172-176.	0.8	2
13488	Anisotropic effects on the radial breathing mode of silicon nanowires: An ab initio study. Physica E: Low-Dimensional Systems and Nanostructures, 2013, 51, 10-14.	1.3	10
13489	Understanding Chemical Changes across the Î±-Cristobalite to Stishovite Transition Path in Silica. Journal of Physical Chemistry C, 2013, 117, 8950-8958.	1.5	15
13490	Examination of Oxygen Vacancy Formation in Mn-Doped CeO₂ (111) Using DFT+U and the Hybrid Functional HSE06. Langmuir, 2013, 29, 10120-10131.	1.6	53
13491	New insights into the BiB₃O₆melt structure. CrystEngComm, 2013, 15, 995-1000.	1.3	14
13492	Atomic and electronic structure of molybdenum carbide phases: bulk and low Miller-index surfaces. Physical Chemistry Chemical Physics, 2013, 15, 12617.	1.3	189
13493	Cationicâ€“anionic mediated charge compensation on La2Ti2O7 for visible light photocatalysis. Physical Chemistry Chemical Physics, 2013, 15, 17150.	1.3	21
13494	Electromechanical properties of zigzag-shaped carbon nanotubes. Physical Chemistry Chemical Physics, 2013, 15, 17134.	1.3	12
13495	Spin-polarized electronic structure and magnetic properties of Ge 1â^'x TM x Te (TM=Mn, Fe). Journal of Magnetism and Magnetic Materials, 2013, 345, 222-229.	1.0	3
13496	Ab initio calculation of valley splitting in monolayer Î´-doped phosphorus in silicon. Nanoscale Research Letters, 2013, 8, 111.	3.1	28
13497	Ab initio study of the formation of structural kinks in carbon chains. Journal of Surface Investigation, 2013, 7, 479-484.	0.1	0
13498	Investigation into the adsorption of atomic nitrogen on an Al2O3 (0001) surface. Journal of Surface Investigation, 2013, 7, 76-80.	0.1	0
13499	Electronic structures and optic properties of Fe2TiO5 using LSDA+U approach. Progress in Natural Science: Materials International, 2013, 23, 413-419.	1.8	25
13500	Computational study of lattice defects in metalâ€“hydrogen systems. Journal of Alloys and Compounds, 2013, 580, S131-S134.	2.8	8

#	Article	IF	Citations
13501	First-principles investigation into the effect of Cr on the segregation of multi-H at the Fe Î£3 (111) grain boundary. Journal of Nuclear Materials, 2013, 441, 301-305.	1.3	27
13502	Preparation, characterization and electronic structures of Fe-doped TiO2 nanostructured fibers. Materials Research Bulletin, 2013, 48, 2737-2745.	2.7	17
13503	First-principle study of electronic, structural properties and stability of Sn0.5M0.5O2, M=Ti, Mn, Sb, Pb. Physica B: Condensed Matter, 2013, 421, 132-137.	1.3	7
13504	A combined LEED and DFT surface structure determination of Cu3Au(001): Evidence of a surface stacking fault. Surface Science, 2013, 618, 167-172.	0.8	2
13505	Effects of hydroxyl group on H2 dissociation on graphene: A density functional theory study. Journal of Energy Chemistry, 2013, 22, 493-497.	7.1	8
13506	The standard enthalpies of formation of some binary intermetallic compounds of lanthanideâ€“iron systems by high temperature direct synthesis calorimetry. Journal of Alloys and Compounds, 2013, 554, 232-239.	2.8	30
13507	The structural, mechanical and electronic properties of (4,4) SiC/C nanotube heterojunction: A first-principles study. Computational Materials Science, 2013, 68, 367-370.	1.4	8
13508	First-principles calculation of superconductivity in hole-doped LiBC: Through partial substitution of B or C atoms. Solid State Communications, 2013, 168, 15-18.	0.9	1
13509	Oxygen induced transformations of the Î´-Pu(111) surface. Surface Science, 2013, 618, 101-108.	0.8	9
13510	Electronâ€“phonon interaction, superconductivity and thermal conductivity of palladium carbide using ab initio calculation. Computational Materials Science, 2013, 70, 196-200.	1.4	4
13511	Sound velocities and elastic properties of PbTiO3 and PbZrO3 under pressure: First principles study. Ceramics International, 2013, 39, S277-S281.	2.3	5
13512	First-principles calculations for the surface termination of Li2TiO3(001) surfaces. Journal of Nuclear Materials, 2013, 442, S705-S709.	1.3	3
13513	Scaffolds of magnetically active 3d metals in the valence electron controlled borides Ti9â^'xM2+xRu18B8 (M=Crâ€“Ni; x=0.5â€“1): Structutral, electronic and magnetic properties. Journal of Solid State Chemistry, 2013, 204, 283-290.	1.4	5
13514	Geometry and electronic structure of the Zn-doped GaAs (100) Î²2(2Ã—4) surface: A first-principle study. Applied Surface Science, 2013, 283, 954-957.	3.1	14
13515	On the dual deuterium/deuteron nature of D charge distribution in the Ti host matrix: A DFT analysis. International Journal of Hydrogen Energy, 2013, 38, 16477-16484.	3.8	0
13516	Role of oxygen vacancies in the resistive switching of SrZrO3 for resistance random access memory. Journal of Alloys and Compounds, 2013, 580, 148-151.	2.8	44
13517	Composition-dependent ground state of martensite in Niâ€“Mnâ€“Ga alloys. Acta Materialia, 2013, 61, 3858-3865.	3.8	45
13518	Dehydrogenation mechanisms of Ca(NH2BH3)2: TheÂless the charge transfer, the lower the barrier. International Journal of Hydrogen Energy, 2013, 38, 11313-11320.	3.8	8

#	Article	IF	Citations
13519	Density functional study of elastic, mechanical and thermodynamic properties of MgCu with a CsCl-type structure. Journal of Magnesium and Alloys, 2013, 1, 128-133.	5.5	20
13520	Oxygen reduction reaction of Ptâ€“In alloy: Combined theoretical and experimental investigations. Electrochimica Acta, 2013, 114, 706-712.	2.6	17
13521	First-principles study of structural stability, elastic and electronic properties of ternary rare earth-transition metalâ€”Borides and carbides (RTxZ, R=Sc, Y, and La, T=Pt and Pd, Z=B and C, and x=2, 3,) Tj ETQq1 1 0.0 0 rgBT /Overlock	1.0	
13522	Structural and reaction pathway analyses of Mg(BH4)2Â·2NH3 for hydrogen storage : A first-principles study. International Journal of Hydrogen Energy, 2013, 38, 2836-2845.	3.8	7
13523	The crystallographic and morphological evolution of the strengthening precipitates in Cuâ€“Niâ€“Si alloys. Acta Materialia, 2013, 61, 1210-1219.	3.8	115
13524	First principles screening of B2 stabilizers in CuPd-based hydrogen separation membranes: (1) Substitution for Pd. Journal of Alloys and Compounds, 2013, 574, 368-376.	2.8	16
13525	Electronic structure and magnetism of various surfaces of the catalytic material Pt3Ni: Density-functional study. Journal of Magnetism and Magnetic Materials, 2013, 339, 89-93.	1.0	2
13526	Work-function modification of the (111) gold surface upon deposition of self-assembled monolayers based on alkanethiol derivatives. Journal of Electron Spectroscopy and Related Phenomena, 2013, 189, 32-38.	0.8	22
13527	First-principles studies of Fe atoms adsorption on hydrogen-terminated boron nitride nanoribbons. Physics Letters, Section A: General, Atomic and Solid State Physics, 2013, 377, 1016-1020.	0.9	14
13528	Behaviors of alloying element titanium in vanadium: From energetics to tensile/shear deformation. Computational Materials Science, 2013, 77, 348-354.	1.4	9
13529	Electronic and mechanical properties of ordered (Pu, U) O2 compounds: A density functional theory +U study. Journal of Nuclear Materials, 2013, 433, 345-350.	1.3	40
13530	Elastic anisotropy and phonon focusing in NiAl: Atomic study. Intermetallics, 2013, 42, 156-164.	1.8	7
13531	Study of sapphire and MgO as thermal neutron filters for the moroccan TRIGA research reactor beam. , 2013, , .		0
13532	Applying vibrational spectroscopy to the study of nucleobases â€“ adenine as a case-study. New Journal of Chemistry, 2013, 37, 2691.	1.4	36
13533	Magnetism, half-metallicity and electrical transport properties of V- and Cr-doped semiconductor SnTe: A theoretical study. Journal of Applied Physics, 2013, 114, 213704.	1.1	8
13534	Lattice dynamics of Ti-based pnictide superconductors Ba1â^'xNaxTi2Sb2O. Physical Review B, 2013, 87, .	1.1	5
13535	Insights into the phase diagram of bismuth ferrite from quasiharmonic free-energy calculations. Physical Review B, 2013, 88, .	1.1	50
13536	Fundamental constraints on the strength of transition-metal borides: The case of CrB<mml:math xmlns:mml="http://www.w3.org/1998/Math/MathML" display="inline"><mml:msub><mml:mrow /><mml:mn>4</mml:mn></mml:msub></mml:math>. Physical Review B, 2013, 87, .	1.1	46

#	Article	IF	Citations
13537	Ab initiocharacterization of a Ni-related defect in diamond: The W8 center. Physical Review B, 2013, 87, .	1.1	15
13538	Ab initiostudy of the split silicon-vacancy defect in diamond: Electronic structure and related properties. Physical Review B, 2013, 88, .	1.1	143
13539	Monolayer semiconducting transition metal dichalcogenide alloys: Stability and band bowing. Journal of Applied Physics, 2013, 113, .	1.1	214
13540	Anisotropic elastic and thermal properties of titanium borides by first-principles calculations. Journal of Alloys and Compounds, 2013, 579, 457-467.	2.8	136
13541	Evaluating London Dispersion Force Corrections in Crystalline Nitroguanidine by Terahertz Spectroscopy. IEEE Transactions on Terahertz Science and Technology, 2013, 3, 281-287.	2.0	22
13542	Stability maps to predict anomalous ductility in B2 materials. Physical Review B, 2013, 87, .	1.1	17
13543	Band offsets for mismatched interfaces: The special case of ZnO on CdTe (001). Journal of Vacuum Science and Technology A: Vacuum, Surfaces and Films, 2013, 31, 061102.	0.9	4
13544	Mechanics and Mechanically Tunable Band Gap in Single-Layer Hexagonal Boron-Nitride. Materials Research Letters, 2013, 1, 200-206.	4.1	141
13545	Unified interatomic potential and energy barrier distributions for amorphous oxides. Journal of Chemical Physics, 2013, 139, 154506.	1.2	35
13546	First principles study on surface structure and stability of alloyed cementite doped with Cr. Materials Letters, 2013, 100, 170-172.	1.3	20
13547	Density functional theory calculations on the adsorption of formaldehyde and other harmful gases on pure, Ti-doped, or N-doped graphene sheets. Applied Surface Science, 2013, 283, 559-565.	3.1	113
13548	Divacancy-assisted transition metal adsorption on the BN graphene and its interaction with hydrogen molecules: a theoretical study. Applied Surface Science, 2013, 273, 293-301.	3.1	36
13549	Tunable band gap in few-layer graphene by surface adsorption. Scientific Reports, 2013, 3, .	1.6	55
13550	Adsorption of oxygen atom on Zn-terminated (0001) surface of wurtzite ZnO: A density-functional theory investigation. Physica E: Low-Dimensional Systems and Nanostructures, 2013, 48, 7-12.	1.3	16
13551	Reaction mechanism of ethanol decomposition on Mo2C(100) investigated by the first principles study. Journal of Molecular Catalysis A, 2013, 377, 180-189.	4.8	32
13552	Structure, elastic and dynamical properties of KN3 and RbN3: A van der Waals density functional study. Solid State Sciences, 2013, 23, 17-25.	1.5	9
13553	First-principles study of the electronic and optical properties of the (Eu,N)-codoped anatase TiO2 photocatalyst. Computational Materials Science, 2013, 68, 234-237.	1.4	10
13554	Electronic and optical performances of Si and Fe-codoped TiO2 nanoparticles: A photocatalyst for the degradation of methylene blue. Applied Catalysis B: Environmental, 2013, 142-143, 38-44.	10.8	24

#	Article	IF	Citations
13555	First-principles study of electronic and magnetic properties of FeCl3-based graphite intercalation compounds. Physica B: Condensed Matter, 2013, 425, 72-77.	1.3	8
13556	First-Principles Study of Interstitial Boron and Oxygen Dimer Complex in Silicon. Applied Physics Express, 2013, 6, 041301.	1.1	10
13557	Surface diffusion on SrTiO3 (100): A temperature accelerated dynamics and first principles study. Surface Science, 2013, 617, 237-241.	0.8	10
13558	Universal infrared absorbance of two-dimensional honeycomb group-IV crystals. Physical Review B, 2013, 87, .	1.1	157
13559	Structure and stability of acrolein and allyl alcohol networks on Ag(111) from density functional theory based calculations with dispersion corrections. Surface Science, 2013, 617, 175-182.	0.8	6
13560	Pressure driven spin crossover and isostructural phase transition in LaFeO3. Journal of Applied Physics, 2013, 114, .	1.1	11
13561	The initial stage of atmospheric corrosion on interstitial free steel investigated by in situ SPM. Corrosion Science, 2013, 70, 188-193.	3.0	24
13562	Ab initio prediction of the first and second pressure derivatives of isothermal bulk modulus for the high-pressure rocksalt phase of ZnO. Chemical Physics Letters, 2013, 559, 46-49.	1.2	3
13563	Elastic and thermodynamic properties of ZnSc2S4 and CdSc2S4 compounds under pressure and temperature effects. Computational Materials Science, 2013, 70, 107-113.	1.4	18
13564	Antiphase inversion domains in lithium cobaltite thin films deposited on single-crystal sapphire substrates. Acta Materialia, 2013, 61, 7671-7678.	3.8	29
13565	Structural Behaviors of Cytosine into the Hydrated Interlayer of Na⁺-Montmorillonite Clay. An ab Initio Molecular Dynamics Study. Journal of Physical Chemistry C, 2013, 117, 26179-26189.	1.5	17
13566	Theoretical and Experimental Investigations of N2-selective Membranes. Energy Procedia, 2013, 37, 1093-1103.	1.8	1
13567	Nonwetting â€œwhite grapheneâ€•films. Acta Materialia, 2013, 61, 1266-1273.	3.8	46
13568	Single crystal growth, transport, and electronic band structure of YCoGa5. Journal of Alloys and Compounds, 2013, 578, 543-546.	2.8	2
13569	Syntheses, crystal structures, and optical properties of Pb6B3O10X (X=F, Cl, Br). Journal of Solid State Chemistry, 2013, 204, 64-69.	1.4	17
13570	Study of MgxCd1â^'xO applying density functional theory: Stability, structural phase transition and electronic properties. Journal of Solid State Chemistry, 2013, 204, 367-372.	1.4	12
13571	A DFT study of SF6 decomposed gas adsorption on an anatase (101) surface. Applied Surface Science, 2013, 286, 47-53.	3.1	42
13572	Modeling of Structural Properties of Hexagonal Semiconductors. Procedia Engineering, 2013, 53, 707-709.	1.2	2

#	Article	IF	Citations
13573	Electronic, elastic and thermal properties of SrCu2As2 via first principles calculation. Journal of Alloys and Compounds, 2013, 570, 156-161.	2.8	9
13574	BeO nanotube bundle as a gas sensor. Superlattices and Microstructures, 2013, 60, 291-299.	1.4	10
13575	Mechanical deformation modes and anisotropy of IVB transition metal nitrides. Journal of Alloys and Compounds, 2013, 575, 137-144.	2.8	17
13576	Periodic graphene nanobuds: A novel Li-storage material. Materials Chemistry and Physics, 2013, 142, 44-51.	2.0	23
13577	Performance Analysis of Strained Monolayer ${m MoS}_{2}$ MOSFET. IEEE Transactions on Electron Devices, 2013, 60, 2782-2787.	1.6	30
13578	Platinum redispersion on metal oxides in low temperature fuel cells. Physical Chemistry Chemical Physics, 2013, 15, 3279.	1.3	10
13579	Unprecedented Electronâ€Poor Octahedral Ta₆ Clusters in a Solidâ€State Compound: Synthesis, Characterisations and Theoretical Investigations of Cs₂BaTa₆Br₁₅O₃. Chemistry - A European Journal, 2013, 19, 12711-12719.	1.7	14
13580	A thermodynamic criterion for designing superhard transition-metal borides with ultimate boron content. Computational Materials Science, 2013, 68, 222-228.	1.4	47
13581	Role of ReOx in Re-modified Rh/ZrO2 and Ir/ZrO2 catalysts in glycerol hydrogenolysis: Insights from first-principles study. Chinese Journal of Catalysis, 2013, 34, 1656-1666.	6.9	18
13582	Ag-Cu catalysts for ethylene epoxidation: Selectivity and activity descriptors. Journal of Chemical Physics, 2013, 138, 184707.	1.2	25
13583	Roles of oxygen vacancy on ferromagnetism in Ni doped In2O3: A hybrid functional study. Journal of Magnetism and Magnetic Materials, 2013, 348, 55-60.	1.0	5
13584	Nitrogen-induced local spin polarization in graphene on cobalt. Journal of Magnetism and Magnetic Materials, 2013, 342, 144-148.	1.0	2
13585	Grain misorientation and grain-boundary rotation dependent mechanical properties in polycrystalline graphene. Journal of the Mechanics and Physics of Solids, 2013, 61, 1421-1432.	2.3	109
13586	Theory of magnetic enhancement in strontium hexaferrite through Znâ€“Sn pair substitution. Journal of Magnetism and Magnetic Materials, 2013, 348, 75-81.	1.0	33
13587	An atomic study of hydrogen effect on the early stage oxidation of transition metal surfaces. International Journal of Hydrogen Energy, 2013, 38, 1644-1656.	3.8	29
13588	A first-principles study of the diffusion of atomic oxygen in nickel. Corrosion Science, 2013, 75, 248-255.	3.0	21
13589	Hexagonal MIn₂S₄ (M = Mn, Fe, Co): Formation and Phase Transition. Journal of Physical Chemistry C, 2013, 117, 20054-20059.	1.5	11
13590	Improving the Adsorption of Au Atoms and Nanoparticles on Graphite via Li Intercalation. Journal of Physical Chemistry C, 2013, 117, 22683-22695.	1.5	4

#	Article	IF	Citations
13591	High thermoelectric performance of oxyselenides: intrinsically low thermal conductivity of Ca-doped BiCuSeO. NPG Asia Materials, 2013, 5, e47-e47.	3.8	349
13592	Spin Transport of Polyacetylene Chains Bridging Zigzag Graphene Nanoribbon Electrodes: A Nonequilibrium Treatment of Structural Control and Spin Filtering. Journal of Physical Chemistry C, 2013, 117, 21178-21185.	1.5	16
13593	DFT study of the adsorption of the corrosion inhibitor 2-mercaptoimidazole onto Fe(100) surface. Electrochimica Acta, 2013, 112, 577-586.	2.6	78
13594	Synthesis of nitrogen-doped single-walled carbon nanotubes and monitoring of doping by Raman spectroscopy. Chinese Physics B, 2013, 22, 086101.	0.7	7
13595	Hybrid nanotubeâ€“graphene junctions: spin degeneracy breaking and tunable electronic structure. Physical Chemistry Chemical Physics, 2013, 15, 20281.	1.3	5
13596	Photo-active and optical properties of bismuth ferrite (BiFeO3): An experimental and theoretical study. Chemical Physics Letters, 2013, 572, 78-84.	1.2	67
13597	First-principle prediction of half-metallic ferrimagnetism in Mn-based full-Heusler alloys with highly ordered structure. Journal of Magnetism and Magnetic Materials, 2013, 333, 162-168.	1.0	54
13598	The Effect of Metalâ€“Cation Vacancies on Vanadium Antimonate Surface Properties. A Theoretical Study. Journal of Physical Chemistry C, 2013, 117, 20548-20556.	1.5	4
13599	Comparison of Reaction Energetics for Oxygen Reduction Reactions on Pt(100), Pt(111), Pt/Ni(100), and Pt/Ni(111) Surfaces: A First-Principles Study. Journal of Physical Chemistry C, 2013, 117, 6284-6292.	1.5	171
13600	Theoretical examination of superconductivity in the cubic antiperovskite Cr3GaN under pressure. Journal of Applied Physics, 2013, 114, 053905.	1.1	10
13601	Shock-induced plasticity in tantalum single crystals: Interatomic potentials and large-scale molecular-dynamics simulations. Physical Review B, 2013, 88, .	1.1	216
13602	Ferromagnetism in Nd-doped ZnO nanowires and the influence of oxygen vacancies: ab initio calculations. Physical Chemistry Chemical Physics, 2013, 15, 17793.	1.3	18
13603	Water adsorption and dissociation on Ni surface: Effects of steps, dopants, coverage and self-aggregation. Physical Chemistry Chemical Physics, 2013, 15, 17804.	1.3	28
13604	Predicting a new photocatalyst and its electronic properties by density functional theory. Journal of Applied Physics, 2013, 114, .	1.1	24
13605	Ab initiostudy of the electronic and magnetic structure of the TiO<mml:math xmlns:mml="http://www.w3.org/1998/Math/MathML" display="inline"><mml:msub><mml:mrow /><mml:mn>2</mml:mn></mml:msub></mml:math>rutile (110)/Fe interface. Physical Review B, 2013, 88, .	1.1	5
13606	Softening of hydroxyapatite by vacancies: A first principles investigation. Materials Science and Engineering C, 2013, 33, 1109-1115.	3.8	35
13607	Ab initio density functional theory investigation of the structural, electronic and optical properties of Ca3Sb2 in hexagonal and cubic phases. Journal of Solid State Chemistry, 2013, 207, 140-146.	1.4	5
13608	Thermodynamic assessment of the Gaâ€“X (X=B, Ca, Sr, Ba) systems supported by first-principles calculations. Calphad: Computer Coupling of Phase Diagrams and Thermochemistry, 2013, 43, 52-60.	0.7	8

#	Article	IF	Citations
13609	Stable ferromagnetism and half-metallicity in two-dimensional polyporphyrin frameworks. RSC Advances, 2013, 3, 7016.	1.7	43
13610	Crystal Structure, Optical Properties, and Electronic Structure of Calcium Strontium Tungsten Oxynitrides Ca_xSr_{1â€“x}WO₂N. Journal of Physical Chemistry C, 2013, 117, 18529-18539.	1.5	12
13611	High-Pressure Synthesis and Characterization of Li₂Ca₃[N₂]₃â€”An Uncommon Metallic Diazenide with [N₂]^{2â€“} Ions. Journal of the American Chemical Society, 2013, 135, 16668-16679.	6.6	19
13612	Ab initio design of GaN-based photocatalyst: ZnO-codoped GaN nanotubes. Journal of Power Sources, 2013, 232, 323-331.	4.0	22
13613	Antisites and anisotropic diffusion in GaAs and GaSb. Applied Physics Letters, 2013, 103, 142107.	1.5	11
13614	First-principles study of Co concentration and interfacial resonance states in Fe<mml:math xmlns:mml="http://www.w3.org/1998/Math/MathML" display="inline"><mml:msub><mml:mrow /><mml:mrow><mml:mn>1</mml:mn><mml:mo>â”</mml:mo><mml:mi>x</mml:mi></mml:mrow></mml:msub></mml:math>Co<mml:math xmlns:mml="http://www.w3.org/1998/Math/MathML" display="inline"><mml:msub><mml:mrow /><mml:mi>x</mml:mi></mml:msub></mml:math> magnetic tunnel junctions. Physical Review B, 2013, 88, .	1.1	2
13615	Functionalization of Monolayer h-BN by a Metal Support for the Oxygen Reduction Reaction. Journal of Physical Chemistry C, 2013, 117, 21359-21370.	1.5	109
13616	Mixing and non-stoichiometry in Feâ€“Niâ€“Crâ€“Znâ€“O spinel compounds: density functional theory calculations. Physical Chemistry Chemical Physics, 2013, 15, 15550.	1.3	44
13617	Phonon spectrum, mechanical and thermophysical properties of thorium carbide. Journal of Nuclear Materials, 2013, 437, 135-138.	1.3	29
13618	Structural, elastic, electronic and optical properties of layered alkaline-earth halofluoride scintillators. Philosophical Magazine, 2013, 93, 3563-3575.	0.7	11
13619	Ligand-Field Theory-Based Analysis of the Adsorption Properties of Ruthenium Nanoparticles. ACS Nano, 2013, 7, 9823-9835.	7.3	22
13620	Promoted Ceria: A Structural, Catalytic, and Computational Study. ACS Catalysis, 2013, 3, 2256-2268.	5.5	92
13621	Large-scale first-principles determination of anisotropic mechanical properties of magnetostrictive Feâ€“Ga alloys. Acta Materialia, 2013, 61, 2919-2925.	3.8	40
13622	DFT Modeling of Reaction Mechanism and Ab Initio Microkinetics of Catalytic N₂O Decomposition over Alkaline Earth Oxides: From Molecular Orbital Picture Account to Simulation of Transient and Stationary Rate Profiles. Journal of Physical Chemistry C, 2013, 117, 18488-18501.	1.5	33
13623	Determination of the surface structure of CeO2(111) by low-energy electron diffraction. Journal of Chemical Physics, 2013, 139, 114703.	1.2	12
13624	Towards a perfect system for solar hydrogen production: an example of synergy on the atomic scale. , 2013, , .		1
13625	Ab initio study of elasticity, piezoelectricity, and nonlinear optical performance in monoclinic NaAsSe2. Journal of Alloys and Compounds, 2013, 568, 16-20.	2.8	25
13626	A computational study of the insertion of Li, Na, and Mg atoms into Si(111) nanosheets. Nano Energy, 2013, 2, 1149-1157.	8.2	76

#	Article	IF	Citations
13627	A first-principles study on the structural, elastic, electronic, optical, lattice dynamical, and thermodynamic properties of zinc-blende CdX (X= S, Se, and Te). Journal of Alloys and Compounds, 2013, 579, 583-593.	2.8	46
13628	Optical properties of impact diamonds from the Popigai astrobleme. Diamond and Related Materials, 2013, 37, 8-16.	1.8	24
13629	Bonding, stability, and electronic properties of the BC<mml:math xmlns:mml="http://www.w3.org/1998/Math/MathML" display="inline"><mml:msub><mml:mrow /><mml:mn>3</mml:mn></mml:msub></mml:math>honeycomb monolayer structure on NbB<mml:math xmlns:mml="http://www.w3.org/1998/Math/MathML" display="inline"><mml:msub><mml:mrow /><mml:mn>2</mml:mn></mml:msub></mml:math>(0001). Physical Review B, 2013, 88, .	1.1	15
13630	Lithium Chalcogenidotetrelates: LiChTâ€”Synthesis and Characterization of New Li⁺ Ion Conducting Li/Sn/Se Compounds. Chemistry of Materials, 2013, 25, 2961-2969.	3.2	32
13631	Prediction of Novel SiCN Compounds: First-Principles Calculations. Journal of Physical Chemistry C, 2013, 117, 21943-21948.	1.5	20
13632	Synthesis of Phosphorus Included Multiwalled Carbon Nanotubes by Pyrolysis of Sucrose. Journal of Physical Chemistry C, 2013, 117, 24554-24560.	1.5	3
13633	New Layered Structures of Cuprous Chalcogenides as Thin Film Solar Cell Materials:<mml:math xmlns:mml="http://www.w3.org/1998/Math/MathML" display="inline"><mml:msub><mml:mi>Cu</mml:mi><mml:mn>2</mml:mn></mml:msub><mml:mi>Te</mml:mi></mml:math>and<mm xmlns:mml="http://www.w3.org/1998/Math/MathML" display="inline"><mml:msub><mml:mi>Cu</mml:mi><mml:mn>2</mml:mn></mml:msub><mml:mi>Se</mml:mi></mml:math>. Physical Review Letters, 2013, 111, 165502.	2.9	103
13634	The increase in conductance of a gold single atom chain during elastic elongation. Journal of Applied Physics, 2013, 113, 054316.	1.1	7
13635	CH4 dissociation on NiM(111) (M=Co, Rh, Ir) surface: A first-principles study. Surface Science, 2013, 617, 149-155.	0.8	32
13636	First-principles LDA+U study of magnetism in CuxIn1âˆ’xN. Solid State Communications, 2013, 156, 64-68.	0.9	3
13637	Limitations of the hybrid functional approach to electronic structure of transition metal oxides. Physical Review B, 2013, 88, .	1.1	24
13638	Long-range ferromagnetic ordering in manganese-doped two-dimensional dichalcogenides. Physical Review B, 2013, 88, .	1.1	271
13639	Phase Stability and Thermoelectric Properties of the Mineral FeS₂: An Ab Initio Study. Journal of Physical Chemistry C, 2013, 117, 21120-21131.	1.5	65
13640	Electronic and Optical Properties of Silicon Carbide Nanostructures. Springer Series in Materials Science, 2013, , 139-159.	0.4	2
13641	Relative Photooxidation and Photoreduction Activities of the {100}, {101}, and {001} Surfaces of Anatase TiO₂. Langmuir, 2013, 29, 13647-13654.	1.6	86
13642	Accurate determination of thermodynamic properties for liquid alloys based on ab initio molecular dynamics simulation. Fluid Phase Equilibria, 2013, 360, 44-53.	1.4	10
13643	Structural models of activated Î³-alumina surfaces revisited: Thermodynamics, NMR and IR spectroscopies from ab initio calculations. Chemical Physics, 2013, 423, 62-72.	0.9	29
13644	Terahertz Vibrations of Crystalline Acyclic and Cyclic Diglycine: Benchmarks for London Force Correction Models. Journal of Physical Chemistry A, 2013, 117, 10504-10512.	1.1	19

#	Article	IF	Citations
13645	Adsorption of CO₂ at ZnO: A Surface Structure Effect from DFT+U Calculations. Journal of Physical Chemistry C, 2013, 117, 22954-22966.	1.5	107
13646	Conductivity of boron-doped polycrystalline diamond films: influence of specific boron defects. European Physical Journal B, 2013, 86, 1.	0.6	55
13647	Origin of Indirect Optical Transitions in Few-Layer MoS₂, WS₂, and WSe₂. Nano Letters, 2013, 13, 5627-5634.	4.5	435
13648	Structural Stability of La₂Ce₂O₇ as a Proton Conductor: A First-Principles Study. Journal of Physical Chemistry C, 2013, 117, 20379-20386.	1.5	26
13649	B4â”B1phase transition of GaN under isotropic and uniaxial compression. Physical Review B, 2013, 88, .	1.1	27
13650	Adsorption of gas molecules on monolayer MoS2 and effect of applied electric field. Nanoscale Research Letters, 2013, 8, 425.	3.1	581
13651	Phase stability, thermodynamic and mechanical properties of AlZr2, FeZr2 and Al2FeZr6 from first-principles calculations. Journal of Nuclear Materials, 2013, 440, 6-10.	1.3	13
13652	A comparative density functional theory study of electronic structure and optical properties of -aminobutyric acid and its cocrystals with oxalic and benzoic acid. Chemical Physics Letters, 2013, 587, 20-24.	1.2	17
13653	Spin-flip transitions and departure from the Rashba model in the Au(111) surface. Physical Review B, 2013, 88, .	1.1	12
13654	Unusual Metallic Microporous Boron Nitride Networks. Journal of Physical Chemistry Letters, 2013, 4, 3484-3488.	2.1	80
13655	Interaction between Olivine and Water Based on Density Functional Theory Calculations. Journal of Physical Chemistry C, 2013, 117, 21203-21216.	1.5	24
13656	Atomic Structure and Magnetic Properties of HfCo$_{7}$ Alloy. IEEE Transactions on Magnetics, 2013, 49, 3281-3283.	1.2	6
13657	Theoretical predictions for hexagonal BN based nanomaterials as electrocatalysts for the oxygen reduction reaction. Physical Chemistry Chemical Physics, 2013, 15, 2809.	1.3	95
13658	Density functional theory study of the impact of tin doping on oxygen diffusion in Czochralski silicon. Physica Status Solidi (A) Applications and Materials Science, 2013, 210, 2199-2203.	0.8	4
13659	The structural, electronic and magnetic properties of bi-layered MoS2 with transition-metals doped in the interlayer. RSC Advances, 2013, 3, 12939.	1.7	33
13660	Electronic properties of carbon nanotubes partially unzipped by oxygenation or fluorination. Solid State Communications, 2013, 167, 27-30.	0.9	1
13661	Palladium Nanoparticles on Graphite Oxide: A Recyclable Catalyst for the Synthesis of Biaryl Cores. ACS Catalysis, 2013, 3, 2776-2789.	5.5	91
13662	Compressed carbon nanotubes: A family of new multifunctional carbon allotropes. Scientific Reports, 2013, 3, 1331.	1.6	80

#	Article	IF	Citations
13663	Stable three-dimensional metallic carbon with interlocking hexagons. Proceedings of the National Academy of Sciences of the United States of America, 2013, 110, 18809-18813.	3.3	134
13664	Molecular adsorption study of nicotine and caffeine on single-walled carbon nanotubes from first principles. Chemical Physics Letters, 2013, 580, 57-61.	1.2	23
13665	Density functional simulations of hexagonal Ge2Sb2Te5at high pressure. Physical Review B, 2013, 87, .	1.1	5
13666	Stability and electronic structure of carbon capsules with superior gas storage properties: A theoretical study. Chemical Physics, 2013, 426, 23-30.	0.9	8
13667	Insights into the Surface Chemistry of Tin Oxide Atomic Layer Deposition from Quantum Chemical Calculations. Journal of Physical Chemistry C, 2013, 117, 19056-19062.	1.5	20
13668	Effects of catalyst surface and hydrogen bond on ethanol dehydrogenation to ethoxy on Cu catalysts. Chemical Physics Letters, 2013, 585, 89-94.	1.2	27
13669	Molecular dynamics simulation of the initial stages of He bubbles formation in silicon. Modelling and Simulation in Materials Science and Engineering, 2013, 21, 065002.	0.8	24
13670	Unraveling the Role of Metalâ€“Support Interactions in Heterogeneous Catalysis: Oxygenate Selectivity in Fischerâ€“Tropsch Synthesis. ACS Catalysis, 2013, 3, 2881-2890.	5.5	54
13671	Hyperfine coupling of point defects in semiconductors by hybrid density functional calculations: The role of core spin polarization. Physical Review B, 2013, 88, .	1.1	79
13672	h-BN Monolayer on the Ni(111) Surface: A Potential Catalyst for Oxidation. ACS Applied Materials & Interfaces, 2013, 5, 10404-10408.	4.0	46
13673	Revision of the Liâ€“Si Phase Diagram: Discovery and Single-Crystal X-ray Structure Determination of the High-Temperature Phase Li_{4.11}Si. Chemistry of Materials, 2013, 25, 4623-4632.	3.2	51
13674	Two novel derivatives of ammonia borane for hydrogen storage: synthesis, structure, and hydrogen desorption investigation. Journal of Materials Chemistry A, 2013, 1, 12263.	5.2	18
13675	The Role of Surface Oxygen in the Growth of Large Single-Crystal Graphene on Copper. Science, 2013, 342, 720-723.	6.0	977
13676	Inducing Aromaticity Patterns and Tuning the Electronic Transport of Zigzag Graphene Nanoribbons via Edge Design. Journal of Physical Chemistry C, 2013, 117, 26371-26384.	1.5	11
13677	Adsorption and diffusion of Pb(II) on the kaolinite(001) surface: A density-functional theory study. Applied Clay Science, 2013, 85, 74-79.	2.6	25
13678	Gallium arsenide thermal conductivity and optical phonon relaxation times from first-principles calculations. Europhysics Letters, 2013, 101, 16001.	0.7	100
13679	Magnetocaloric and magnetic properties of Ni2Mn1â^'xCuxGa Heusler alloys: An insight from the direct measurements and ab initio and Monte Carlo calculations. Journal of Applied Physics, 2013, 114, .	1.1	30
13680	Ab initio thermodynamic study of (Ba,Sr)(Co,Fe)O3 perovskite solid solutions for fuel cell applications. Journal of Materials Chemistry A, 2013, 1, 14320.	5.2	28

#	Article	IF	Citations
13681	Insights into the Role of Surface Distortion in Promoting the Separation and Transfer of Photogenerated Carriers in Anatase TiO₂. Journal of Physical Chemistry C, 2013, 117, 24496-24502.	1.5	32
13682	Standard enthalpies of formation of some Lanthanideâ€“Cobalt binary alloys by high temperature direct synthesis calorimetry. Journal of Alloys and Compounds, 2013, 578, 465-470.	2.8	15
13683	Substitutional C on B sites in AlLiB14. Journal of Physics Condensed Matter, 2013, 25, 225502.	0.7	2
13684	Stability, elastic properties and fracture toughness of Al_{0.75}X_{0.75}B₁₄(X=Sc, Ti, V, Cr, Y, Zr, Nb, Mo) investigated usingab initiocalculations. Journal of Physics Condensed Matter, 2013, 25, 335501.	0.7	11
13685	Electronic Structure and Spontaneous Polarization in Sc_xAl_yGa_{1-x-y}N Alloys Lattice-Matched to GaN: A First-Principles Study. Japanese Journal of Applied Physics, 2013, 52, 08JM04.	0.8	1
13686	Optical Absorption and Band Gap Reduction in (Fe1â€“xCrx)2O3 Solid Solutions: A First-Principles Study. Journal of Physical Chemistry C, 2013, 117, 25504-25512.	1.5	43
13687	Effect of ZnO Nanostructure Morphology on the Sensing of H2S Gas. Journal of Physical Chemistry C, 2013, 117, 26106-26118.	1.5	39
13688	Conformers of hydrogenated SiC honeycomb structure: A first principles study. AIP Advances, 2013, 3, 082136.	0.6	9
13689	Alignment of ferroelectric polarization and defect complexes in copper-doped potassium niobate. Physical Review B, 2013, 88, .	1.1	14
13690	Lattice-matched versus lattice-mismatched models to describe epitaxial monolayer graphene on Ru(0001). Physical Review B, 2013, 88, .	1.1	35
13691	First-principles calculation of entropy for liquid metals. Physical Review E, 2013, 88, 062145.	0.8	56
13692	First-principles and experimental characterization of the electronic and optical properties of CaS and CaO. Optical Materials, 2013, 35, 1477-1480.	1.7	13
13693	Magnetic properties in zinc-blende CdS induced by Cd vacancies. Physics Letters, Section A: General, Atomic and Solid State Physics, 2013, 377, 572-576.	0.9	23
13694	First principles study of hydroxyapatite surface. Journal of Chemical Physics, 2013, 139, 044714.	1.2	40
13695	Inter-cation interaction in partial dynamic structure factorsS_{Î¾Î·}(k,Ï‰) and electrical properties of molten Aglâ€“RbI system. Physics and Chemistry of Liquids, 2013, 51, 414-428.	0.4	6
13696	A computational investigation of CO oxidation on ruthenium-embedded hexagonal boron nitride nanosheet. Computational and Theoretical Chemistry, 2013, 1011, 5-10.	1.1	107
13697	Structure, energetics, and electronic states of IIIâ€“V compound polytypes. Journal of Physics Condensed Matter, 2013, 25, 273201.	0.7	101
13698	Atomistic modeling of the polarization of nitrogen centers in diamond due to growth surface orientation. Physical Review B, 2013, 88, .	1.1	19

#	Article	IF	Citations
13699	Structural properties of Y-doped BaZrO3 as a function of dopant concentration and position: A density functional study. Solid State Ionics, 2013, 232, 1-12.	1.3	9
13700	Investigation of the diffusion of atomic fission products in UC by density functional calculations. Journal of Nuclear Materials, 2013, 434, 240-247.	1.3	18
13701	Gold intercalation of boron-doped graphene on Ni(111): XPS and DFT study. Journal of Physics Condensed Matter, 2013, 25, 445002.	0.7	12
13702	First-principles study on stability and electronic properties of W(001), W(110) and W(111) surfaces. Surface and Coatings Technology, 2013, 229, 55-59.	2.2	8
13703	Effects of strain on the valence band structure and exciton-polariton energies in ZnO. Physical Review B, 2013, 88, .	1.1	42
13704	Investigation of new superhard carbon allotropes with promising electronic properties. Journal of Applied Physics, 2013, 114, 183708.	1.1	10
13705	Improvement in hydrogen storage characteristics of Mg-based metal hydrides by doping nonmetals with high electronegativity: A first-principle study. Computational Materials Science, 2013, 78, 83-90.	1.4	29
13706	Oxygen Reduction Activity on Perovskite Oxide Surfaces: A Comparative First-Principles Study of LaMnO₃, LaFeO₃, and LaCrO₃. Journal of Physical Chemistry C, 2013, 117, 2106-2112.	1.5	140
13707	Changes in electrodic reaction rates due to elastic stress and stress-induced surface patterns. Electrochimica Acta, 2013, 111, 814-822.	2.6	31
13708	Study of B1 (NaCl-type) to B2 (CsCl-type) pressure-induced structural phase transition in BaS, BaSe and BaTe usingab initiocomputations. Journal of Physics Condensed Matter, 2013, 25, 075401.	0.7	8
13709	An embedded atom method potential of beryllium. Modelling and Simulation in Materials Science and Engineering, 2013, 21, 085001.	0.8	18
13710	Effect of alloying elements on <111> dislocation in NiAl: A first-principles study. Physica B: Condensed Matter, 2013, 417, 9-12.	1.3	10
13711	First-principles study of the ideal strength of Fe3C cementite. Materials Science & Engineering A: Structural Materials: Properties, Microstructure and Processing, 2013, 572, 25-29.	2.6	14
13712	Grain boundary segregation of C, N and O in hexagonal close-packed titanium from first principles. Modelling and Simulation in Materials Science and Engineering, 2013, 21, 075009.	0.8	12
13713	Stone-Wales defects in silicene: Formation, stability, and reactivity of defect sites. Physical Review B, 2013, 88, .	1.1	108
13714	Reducing self-compensating Mn interstitials in (Ga, Mn)As via nanostructure engineering. Journal Physics D: Applied Physics, 2013, 46, 175005.	1.3	8
13715	Assessing the Role of Water on the Electronic Structure and Vibrational Spectra of Monohydrated <scp>l</scp>-Aspartic Acid Crystals. Crystal Growth and Design, 2013, 13, 4844-4851.	1.4	22
13716	Transition Metal Decorated Graphyne: An Efficient Catalyst for Oxygen Reduction Reaction. Journal of Physical Chemistry C, 2013, 117, 26021-26028.	1.5	82

#	Article	IF	Citations
13717	Theoretical study on the interaction of pristine, defective and strained graphene with Fen and Nin (n=13, 38, 55) clusters. Chemical Physics Letters, 2013, 588, 203-207.	1.2	32
13718	Magic Numbers in a One-Dimensional Nanosystem: ZnS Single-Walled Nanotubes. Journal of Physical Chemistry C, 2013, 117, 22908-22914.	1.5	9
13719	Study on the electron structure and optical properties of Ga0.5Al0.5As(100) Î²2(2Ã—4) reconstruction surface. Applied Surface Science, 2013, 266, 380-385.	3.1	18
13720	Massive Dirac quasiparticles in the optical absorbance of graphene, silicene, germanene, and tinene. Journal of Physics Condensed Matter, 2013, 25, 395305.	0.7	179
13721	Thermodynamic assessment of the Feâ€“Nbâ€“V system. Calphad: Computer Coupling of Phase Diagrams and Thermochemistry, 2013, 43, 143-148.	0.7	8
13722	Nuclear quantum effects and hydrogen bond fluctuations in water. Proceedings of the National Academy of Sciences of the United States of America, 2013, 110, 15591-15596.	3.3	204
13723	Electromechanics in MoS2 and WS2: nanotubes vs. monolayers. Scientific Reports, 2013, 3, 2961.	1.6	142
13724	Effect of Ligand Coordination on the Structures and Visible-Light Photocatalytic Activity of Manganese Vanadate Hybrids. Crystal Growth and Design, 2013, 13, 5282-5288.	1.4	29
13725	Self-Organization of Gold Chloride Molecules on Au(111) Surface. Journal of Physical Chemistry C, 2013, 117, 24948-24954.	1.5	16
13726	Ab initio study of magnetic coupling in CaCu<mml:math xmlns:mml="http://www.w3.org/1998/Math/MathML" display="inline"><mml:msub><mml:mrow /><mml:mn>3</mml:mn></mml:msub></mml:math><mml:math xmlns:mml="http://www.w3.org/1998/Math/MathML" display="inline"><mml:msub><mml:mi>B</mml:mi><mml:mn>4</mml:mn></mml:msub></mml:math>O<mml:math xmlns:mml="http://www.w3.org/1998/Math/MathML" display="inline"><mml:msub><mml:mrow />	1.1	31
13727	Electrically Driven Tuning of the Dielectric Constant in MoS₂ Layers. ACS Nano, 2013, 7, 10741-10746.	7.3	179
13728	Continuous Growth of Hexagonal Graphene and Boron Nitride In-Plane Heterostructures by Atmospheric Pressure Chemical Vapor Deposition. ACS Nano, 2013, 7, 10129-10138.	7.3	170
13729	An efficient method of DFT/LDA band-gap correction. Computer Physics Communications, 2013, 184, 2680-2683.	3.0	13
13730	Average and Local Structural Origins of the Optical Properties of the Nitride Phosphor La_{3â€“x}Ce_xSi₆N₁₁ (0 < x â‰¤ 3). Inorganic Chemistry, 2013, 52, 13730-13741.	1.9	103
13731	Li-Ion Adsorption and Diffusion on Two-Dimensional Silicon with Defects: A First Principles Study. ACS Applied Materials & Interfaces, 2013, 5, 10690-10695.	4.0	73
13732	Ann-body potential for a Zrâ€“Nb system based on the embedded-atom method. Journal of Physics Condensed Matter, 2013, 25, 105404.	0.7	23
13733	Ba₄Ta₂O₉ Oxide Prepared from an Oxalate-Based Molecular Precursorâ€”Characterization and Properties. Inorganic Chemistry, 2013, 52, 14299-14308.	1.9	25
13734	CO Dissociation Mechanism on Cu-Doped Fe(100) Surfaces. Journal of Physical Chemistry C, 2013, 117, 24920-24931.	1.5	38

#	Article	IF	Citations
13735	First-principles study of the mechanisms of the pressure-induced dielectric anomalies in ferroelectric perovskites. Phase Transitions, 2013, 86, 1069-1084.	0.6	57
13736	Anomalous perovskite PbRuO ₃ stabilized under high pressure. Proceedings of the National Academy of Sciences of the United States of America, 2013, 110, 20003-20007.	3.3	14
13737	Born effective charges of Cu2ZnSnS4 quaternary compound: First principles calculations. Thin Solid Films, 2013, 535, 311-313.	0.8	7
13738	Superconducting properties of barium in three phases under high pressure from first principles. Chinese Physics B, 2013, 22, 087403.	0.7	3
13739	A nanoparticle Mg-doped Li4Ti5O12 for high rate lithium-ion batteries. Electrochimica Acta, 2013, 114, 198-204.	2.6	100
13740	Antiferroelectricity and ferroelectricity in epitaxially strained PbZrO<mml:math xmlns:mml="http://www.w3.org/1998/Math/MathML" display="inline"><mml:msub><mml:mrow /><mml:mn>3</mml:mn></mml:msub></mml:math>from first principles. Physical Review B, 2013, 88, .	1.1	59
13741	De Novo Determination of the Crystal Structure of a Large Drug Molecule by Crystal Structure Prediction-Based Powder NMR Crystallography. Journal of the American Chemical Society, 2013, 135, 17501-17507.	6.6	173
13742	Properties of the thermoelectric cubic lanthanum chalcogenides La<mml:math xmlns:mml="http://www.w3.org/1998/Math/MathML" display="inline"><mml:mrow><mml:msub><mml:mrow /><mml:mrow><mml:mn>3</mml:mn><mml:mo>â^’</mml:mo><mml:mi>y</mml:mi></mml:mrow></mml:msub><mml:msub>	1.1	22
13743	Testing density functionals for structural phase transitions of solids under pressure: Si, SiO<mml:math xmlns:mml="http://www.w3.org/1998/Math/MathML" display="inline"><mml:msub><mml:mrow /><mml:mn>2</mml:mn></mml:msub></mml:math>, and Zr. Physical Review B, 2013, 88, .	1.1	87
13744	Electronic structure of topological insulators with MMâ€²X half-Heusler compounds using density functional theory. Thin Solid Films, 2013, 546, 436-438.	0.8	11
13745	Vibrational properties of 2H-PbI2 semiconductors studied via Density Functional Theory calculations. Thin Solid Films, 2013, 541, 9-11.	0.8	6
13746	Syntheses and characterizations of compounds Ba4F4XGa2S6 (X = Cr, Mn, Fe) and Ba4F4MnIn2S6 with 2D layered structures. Dalton Transactions, 2013, 42, 9938.	1.6	11
13747	First-principles study on the dilute Si in bcc Fe: Electronic and elastic properties up to 12.5at.%Si. Computational Materials Science, 2013, 70, 100-106.	1.4	19
13748	Effect of Al Electronic Configuration on the SiO₂ Thin Film Growth via Catalytic Self-Assembling Deposition. Journal of Physical Chemistry C, 2013, 117, 22705-22713.	1.5	6
13749	Effects of alloying and transmutation impurities on stability and mobility of helium in tungsten under a fusion environment. Nuclear Fusion, 2013, 53, 073049.	1.6	43
13750	Direct approach for flexoelectricity from first-principles calculations: cases for SrTiO₃and BaTiO₃. Journal of Physics Condensed Matter, 2013, 25, 415901.	0.7	33
13751	Curvature Effects on the Interfacial Capacitance of Carbon Nanotubes in an Ionic Liquid. Journal of Physical Chemistry C, 2013, 117, 23539-23546.	1.5	53
13752	Structural and electronic properties of perylene from first principles calculations. Journal of Chemical Physics, 2013, 138, 094509.	1.2	35

#	Article	IF	Citations
13753	First-principles study of hydronitrogen compounds: Molecular crystalline NH4N3 and N2H5N3. Computational and Theoretical Chemistry, 2013, 1014, 37-42.	1.1	13
13754	Correlation and relativistic effects in U metal and U-Zr alloy: Validation ofab initioapproaches. Physical Review B, 2013, 88, .	1.1	74
13755	Structural stability of ternary C22â€“Zr6X2Co (X=Al, Ga, Sn, As, Sb, Bi, Te) and C22â€“Zr6Sn2Tâ€² (Tâ€²=Fe, Co, Ni,) Tj ETQq0 0 0 rgBT	1.4	7
13756	Optical Characterization of Chemistry in Shocked Nitromethane with Time-Dependent Density Functional Theory. Journal of Physical Chemistry A, 2013, 117, 12288-12298.	1.1	14
13757	Experimental investigation and first-principle calculations coupled with thermodynamic modeling of the Mnâ€“Nd phase diagram. Calphad: Computer Coupling of Phase Diagrams and Thermochemistry, 2013, 42, 27-37.	0.7	5
13758	Prospects for Fluoride Carbonate Nonlinear Optical Crystals in the UV and Deep-UV Regions. Journal of Physical Chemistry C, 2013, 117, 25684-25692.	1.5	92
13759	CsPbCO₃F: A Strong Second-Harmonic Generation Material Derived from Enhancement via pâ^'Ï€ Interaction. Journal of the American Chemical Society, 2013, 135, 18560-18566.	6.6	242
13760	Structural and mechanical stability of rare-earth diborides. Chinese Physics B, 2013, 22, 046202.	0.7	63
13761	Phase stability, physical properties of rhenium diboride under high pressure and the effect of metallic bonding on its hardness. Journal of Alloys and Compounds, 2013, 581, 206-212.	2.8	14
13762	Synthetic Route to Metal Nitrides: High-Pressure Solid-State Metathesis Reaction. Inorganic Chemistry, 2013, 52, 13356-13362.	1.9	44
13763	Investigation on the thermoelectric properties of nanostructured. Journal of Solid State Chemistry, 2013, 199, 90-95.	1.4	30
13764	Hydrogen generation from formic acid decomposition on Ni(211), Pd(211) and Pt(211). Journal of Molecular Catalysis A, 2013, 379, 169-177.	4.8	38
13765	Atomic Scale Design of Polar Perovskite Oxides without Second-Order Jahnâ€“Teller Ions. Chemistry of Materials, 2013, 25, 4545-4550.	3.2	41
13766	Contributions of point defects, chemical disorder, and thermal vibrations to electronic properties of Cd<mml:math xmlns:mml="http://www.w3.org/1998/Math/MathML" display="inline"><mml:msub><mml:mrow /><mml:mrow><mml:mn>1</mml:mn><mml:mo>â^'</mml:mo><mml:mi>x</mml:mi></mml:mrow></mml:msub></mml:math>Zn<mml:math xmlns:mml="http://www.w3.org/1998/Math/MathML" display="inline"><mml:msub><mml:mrow /><mml:mi>x</mml:mi></mml:msub></mml:math>Te alloys. Physical Review B, 2013, 88, .	1.1	11
13767	Ab initio study of the role of niobium oxides as catalysts in magnesium hydride. Journal of Alloys and Compounds, 2013, 580, S229-S232.	2.8	6
13768	On the perfect MgH2(â€“Nb,â€“Zr) systems and the influence of vacancy-like defects on their structural properties. A self-consistent first principle calculations study of the electron and positron parameters. Journal of Alloys and Compounds, 2013, 556, 188-197.	2.8	8
13769	The transition behavior of FePc on Ag(110). Chemical Physics Letters, 2013, 582, 90-94.	1.2	5
13770	First-principles study of the behavior of O, N and C impurities in vanadium solids. Journal of Nuclear Materials, 2013, 435, 71-76.	1.3	33

#	Article	IF	Citations
13771	Study on the electronic structure and optical properties of different Al constituent Ga1â^'Al As. Optik, 2013, 124, 4402-4405.	1.4	14
13772	Layer-Resolved Study of Mg Atom Incorporation at the<mml:math xmlns:mml="http://www.w3.org/1998/Math/MathML" display="inline"><mml:mi>MgO</mml:mi><mml:mo>/</mml:mo><mml:mi>Ag</mml:mi><mml:mo stretchy="false">(</mml:mo><mml:mn>001</mml:mn><mml:mo) Tj ETQq1 1 0.784314 rgBT /Overlock 10 Tf 50 687 Td (stretchy="fals	2.9	22
13773	Projection potentials and angular momentum convergence of total energies in the full-potential Korringaâ€“Kohnâ€“Rostoker method. Journal of Physics Condensed Matter, 2013, 25, 105505.	0.7	6
13774	Magnetic properties of Co2â^'xTMxC and Co3â^'xTMxC nanoparticles. Journal of Applied Physics, 2013, 114, 243909.	1.1	7
13775	Direct observation of the oxygenated species during oxygen reduction on a platinum fuel cell cathode. Nature Communications, 2013, 4, .	5.8	325
13776	Highly efficient and robust cathode materials for low-temperature solid oxide fuel cells: PrBa0.5Sr0.5Co2â^'xFexO5+Î´. Scientific Reports, 2013, 3, 2426.	1.6	285
13777	High-Pressure Phase Transitions and Structures of Topological Insulator BiTeI. Journal of Physical Chemistry C, 2013, 117, 25677-25683.	1.5	50
13778	Role of the Siâ€“Si bond stability in the first stages of Ti diffusion on a Si(111) 2Ã—1 surface. A periodic DFT study. Applied Surface Science, 2013, 273, 496-501.	3.1	2
13779	First principles study on lattice dynamics, thermodynamics and elastic properties of Na2Te under high pressure. Physica Scripta, 2013, 88, 035602.	1.2	6
13780	Strain-induced incommensurate distortions in epitaxial Ruddlesden-Popper-type Ba2TiO4. Physical Review B, 2013, 88, .	1.1	3
13781	Pressure-induced pseudoatom bonding collapse and isosymmetric phase transition in Zr2Cu: First-principles predictions. Journal of Chemical Physics, 2013, 139, 234504.	1.2	10
13782	Temperature-dependent effective third-order interatomic force constants from first principles. Physical Review B, 2013, 88, .	1.1	266
13783	Structural and electronic properties of pentagonal and hexagonal copper nanowires: First-principles investigation. Journal of Physics and Chemistry of Solids, 2013, 74, 1115-1121.	1.9	2
13784	Microstructural study of high-temperature Crâ€“Niâ€“Alâ€“Ti alloys supported by first-principles calculations. Intermetallics, 2013, 35, 33-40.	1.8	9
13785	Dynamical Simulation of Electron Transfer Processes in Alkanethiolate Self-Assembled Monolayers at the Au(111) Surface. Journal of Physical Chemistry C, 2013, 117, 25334-25342.	1.5	15
13786	First-principles calculations of structural, electronic and optical properties of BaGaXH (X=Si, Ge, Sn). Materials Science in Semiconductor Processing, 2013, 16, 1558-1565.	1.9	3
13787	Exploring High-Pressure Lithium Beryllium Hydrides: A New Chemical Perspective. Journal of Physical Chemistry C, 2013, 117, 13879-13886.	1.5	28
13788	Hydrogen accommodation in Zr second phase particles: Implications for H pick-up and hydriding of Zircaloy-2 and Zircaloy-4. Corrosion Science, 2013, 69, 1-4.	3.0	43

#	Article	IF	Citations
13789	First-principles study of rare gas incorporation in titanium nitride. Physical Review B, 2013, 87, .	1.1	25
13790	Ab initio study of dielectric function of C-substituted single walled boron nanotubes. European Physical Journal B, 2013, 86, 1.	0.6	1
13791	Structural properties and high-temperature spin and electronic transitions in GdCoO3: Experiment and theory. Physical Review B, 2013, 88, .	1.1	33
13792	Magnetic properties in Pd doped ZnS from ab initio calculations. European Physical Journal B, 2013, 86, 1.	0.6	4
13793	Structures, Energetics, and Electronic Properties of Layered Materials and Nanotubes of Cadmium Chalcogenides. Journal of Physical Chemistry C, 2013, 117, 25817-25825.	1.5	26
13794	Effects of NaOH in Solid NaH: Solution/Segregation Phase Transition and Diffusion Acceleration. Journal of Physical Chemistry C, 2013, 117, 23575-23581.	1.5	6
13795	New Functionalized Metalâ€“Organic Frameworks MIL-47-X (X = â^'Cl, â^'Br, â^'CH₃,) Tj ETQq0 0 0 rgBT /Overlock 10 Tf 50 Adsorption Properties. Journal of Physical Chemistry C, 2013, 117, 22784-22796.	1.5	79
13796	Adsorption of CH4 on nitrogen- and boron-containing carbon models of coal predicted by density-functional theory. Applied Surface Science, 2013, 285, 190-197.	3.1	62
13797	Density functional study of the structural, electronic, and vibrational properties of<mml:math xmlns:mml="http://www.w3.org/1998/Math/MathML" display="inline"><mml:mi>Î²</mml:mi></mml:math>-Ba<mml:math xmlns:mml="http://www.w3.org/1998/Math/MathML" display="inline"><mml:msub><mml:mrow /><mml:mn>2</mml:mn></mml:msub></mml:math>TiO<mml:math xmlns:mml="http://www.w3.org/1998/Math/MathML" display="inline"><mml:msub><mml:mrow /><mml:	1.1	2
13798	Tailoring the Adsorption of Benzene on PdFe Surfaces: A Density Functional Theory Study. Journal of Physical Chemistry C, 2013, 117, 24317-24328.	1.5	45
13799	Role of magnetism in Cu precipitation in<mml:math xmlns:mml="http://www.w3.org/1998/Math/MathML" display="inline"><mml:mi>Î±</mml:mi></mml:math>-Fe. Physical Review B, 2013, 88, .	1.1	31
13800	The structural, electronic and optical properties of CuGa (SexS1-x)2 compounds from first-principle calculations. European Physical Journal B, 2013, 86, 1.	0.6	7
13801	Electronic and optical properties of the Covalent Triazine-based Framework-1: First-principles calculations. Microelectronic Engineering, 2013, 108, 192-194.	1.1	6
13802	Temperature-dependent lithium storage behavior in tetragonal boron (B50) thin film anode for Li-ion batteries. Electrochimica Acta, 2013, 87, 230-235.	2.6	8
13803	Shock-induced phase transformations in gallium single crystals by atomistic methods. Physical Review B, 2013, 88, .	1.1	15
13804	Thermal effects on electronic properties of CO/Pt(111) in water. Physical Chemistry Chemical Physics, 2013, 15, 13619.	1.3	2
13805	Hydrogenated bilayer wurtzite SiC nanofilms: a two-dimensional bipolar magnetic semiconductor material. Physical Chemistry Chemical Physics, 2013, 15, 497-503.	1.3	55
13806	Carrier-Mediated Magnetoelectric Coupling in Functionalized Graphene. ACS Nano, 2013, 7, 9927-9932.	7.3	10

#	Article	IF	Citations
13807	Stability and properties of the two-dimensional hexagonal boron nitride monolayer functionalized by hydroxyl (OH) radicals: a theoretical study. Journal of Molecular Modeling, 2013, 19, 5143-5152.	0.8	34
13808	Study of multivacancies in alpha Fe. Journal of Nuclear Materials, 2013, 441, 168-177.	1.3	20
13809	Fluorine Patterning in Room-Temperature Fluorinated Graphite Determined by Solid-State NMR and DFT. Journal of Physical Chemistry C, 2013, 117, 7940-7948.	1.5	51
13810	Structural and elastic properties of La2Mg17 from first-principles calculations. Journal of Solid State Chemistry, 2013, 206, 272-276.	1.4	3
13811	Optimization of a hybrid exchangeâ€“correlation functional for silicon carbides. Chemical Physics Letters, 2013, 579, 58-63.	1.2	9
13812	Theoretical Study of Atomic Fluorine Diffusion through Bulk TiO₂ Polymorphs. Journal of Physical Chemistry C, 2013, 117, 5855-5860.	1.5	13
13813	Independent Ordering of Two Interpenetrating Magnetic Sublattices in the Double Perovskite Sr₂CoOsO₆. Journal of the American Chemical Society, 2013, 135, 18824-18830.	6.6	92
13814	Thermal conductivity of one-, two- and three-dimensional sp²carbon. New Journal of Physics, 2013, 15, 105019.	1.2	29
13815	Understanding the defect chemistry of tin monoxide. Journal of Materials Chemistry C, 2013, 1, 8194.	2.7	75
13816	Electrooxidation of methanol in an alkaline fuel cell: determination of the nature of the initial adsorbate. Physical Chemistry Chemical Physics, 2013, 15, 20170.	1.3	9
13817	Density Functional Theory Investigation of Bi(Ga,Al)O3Solid Solution for High-Performance Lead-Free Piezoelectric Materials. Ferroelectrics, 2013, 452, 43-49.	0.3	2
13818	Band offset of the ZnO/Cu2O heterojunction from ab initio calculations. Superlattices and Microstructures, 2013, 64, 311-318.	1.4	10
13819	Behaviors and interactions of La atom with other foreign substitutional atoms (Al, Si, Ti, V, Cr, Mn,) Tj ETQq0 0 0 rgBT /Overlock 10 Tf 50 Science, 2013, 73, 120-127.	1.4	14
13820	Ab initiostudy of thermodynamic, electronic, magnetic, structural, and elastic properties of Ni<mml:math xmlns:mml="http://www.w3.org/1998/Math/MathML" display="inline"><mml:msub><mml:mrow /><mml:mn>4</mml:mn></mml:msub></mml:math>N allotropes. Physical Review B, 2013, 88, .	1.1	19
13821	Effects of hydrogen adsorption on the electronic and magnetic structures for variant terminations of NbRu (001) and M/NbRu (001) surfaces (M=Fe, Ni). Journal of Magnetism and Magnetic Materials, 2013, 335, 131-138.	1.0	8
13822	The electronic structure of organicâ€“inorganic hybrid compounds: (NH₄)₂CuCl₄, (CH₃NH₃)₂CuCl₄and (C₂H₅NH₃)₂CuCl₄. Journal of Physics Condensed Matter, 2013, 25, 295502.	0.7	39
13823	Rearrangement of Ï€-Electron Network and Switching of Edge-Localized Ï€ State in Reduced Graphene Oxide. ACS Nano, 2013, 7, 11190-11199.	7.3	18
13824	First-principles investigation of dual substitutional impurity-induced electronic structural modulation of PbTe on cationic and anionic sites. Acta Materialia, 2013, 61, 6428-6442.	3.8	6

#	Article	IF	Citations
13825	Functionalization of monolayer MoS2 by substitutional doping: A first-principles study. Physics Letters, Section A: General, Atomic and Solid State Physics, 2013, 377, 1362-1367.	0.9	285
13826	Backward Reconstructions on GaAs(001) Surface Induced by Atomic Hydrogen Reactions: Surfactant-Assisted Low-Temperature Surface Ordering. Journal of Physical Chemistry C, 2013, 117, 9723-9733.	1.5	9
13827	First principle study on electronic structure and optical phonon properties of 2H-MoS2. Physica B: Condensed Matter, 2013, 426, 103-107.	1.3	17
13828	Interface formation of scandium nitride on the GaN(0001) surface: A first-principles study. Computational Materials Science, 2013, 70, 77-81.	1.4	6
13829	Initial stages of the adsorption of Sc and ScN thin films on GaN(0001): First principles calculations. Applied Surface Science, 2013, 268, 16-21.	3.1	10
13830	HCl Oxidation on IrO₂-Based Catalysts: From Fundamentals to Scale-Up. ACS Catalysis, 2013, 3, 2813-2822.	5.5	52
13831	Negative-<mml:math xmlns:mml="http://www.w3.org/1998/Math/MathML"><mml:mi>U</mml:mi></mml:math>carbon vacancy in 4<mml:math xmlns:mml="http://www.w3.org/1998/Math/MathML"><mml:mi>H</mml:mi></mml:math>-SiC: Assessment of charge correction schemes and identification of the negative carbon vacancy at the quasicubic site. Physical Review B, 2013, 88, .	1.1	45
13832	First-principles study of excitonic effects in Raman intensities. Physical Review B, 2013, 88, .	1.1	33
13833	New theoretical model on the electronic structure and magnetic properties of the YMnO3 perovskite oxide: Implementation of the U-Hubbard Hamiltonian. Results in Physics, 2013, 3, 219-230.	2.0	15
13834	A first-principles investigation of the optical spectra of oxidized graphene. Applied Physics Letters, 2013, 102, .	1.5	28
13835	Formation of the OOH radical at steps of the boehmite surface and its inhibition by gallic acid: A theoretical study including DFT-based dynamics. Journal of Inorganic Biochemistry, 2013, 128, 164-173.	1.5	19
13836	Electronic structure, structural stability, mechanical and superconducting properties of group VB nitrides: A first principles study. Solid State Sciences, 2013, 19, 36-44.	1.5	24
13837	The first principles studies of the MgB7 compound: Hard material. Intermetallics, 2013, 39, 84-88.	1.8	29
13838	Quasiparticle electronic structure of barium-silicon oxynitrides for white-LED application. Physical Review B, 2013, 88, .	1.1	8
13839	Theoretical predictions of the two-dimensional solid-state NMR spectra: A case study of the 13Câ€“1H correlations in metergoline. Chemical Physics Letters, 2013, 586, 56-60.	1.2	18
13840	Magnetic, transport and electronic properties of SmNi4Si compound. Journal of Alloys and Compounds, 2013, 577, 19-24.	2.8	8
13841	A first-principles calculation of the elastic and vibrational anomalies of lizardite under pressure. American Mineralogist, 2013, 98, 2046-2052.	0.9	16
13842	Effect of temperature and pressure on emission lifetime of Sm2+ ion doped in MFX (M=Sr, Ba; X=Br, I) crystals. Journal of Luminescence, 2013, 142, 66-74.	1.5	25

#	Article	IF	Citations
13843	Binary nature of monolayer boron sheets from ab initio global searches. Journal of Chemical Physics, 2013, 138, 024701.	1.2	44
13844	Can CO2 molecule adsorb effectively on Al-doped boron nitride single walled nanotube?. Applied Surface Science, 2013, 285, 350-356.	3.1	47
13845	Ab initio calculation of the thermodynamic properties and phase diagram of gallium nitride. Physica B: Condensed Matter, 2013, 431, 115-119.	1.3	4
13846	Elastic and thermodynamic properties of Re2N at high pressure and high temperature. Transactions of Nonferrous Metals Society of China, 2013, 23, 3714-3721.	1.7	7
13847	Ab initio calculations on elastic properties in L12 structure Al3X and X3Al-type (X=transition or main) Tj ETQq0 0 0 rgBT /Overlock 10 Tf	0.9	59
13848	Mechanical and thermodynamic properties of Al3Sc and Al3Li precipitates in Alâ€“Liâ€“Sc alloys from first-principles calculations. Physica B: Condensed Matter, 2013, 427, 85-90.	1.3	100
13849	Proton or Deuteron Transfer in Phase IV of Solid Hydrogen and Deuterium. Physical Review Letters, 2013, 110, 025903.	2.9	59
13850	Anharmonicity of graphite from UV Raman spectroscopy to 2700K. Carbon, 2013, 54, 68-75.	5.4	18
13851	Ab initio studies of ternary semiconductor BeB2C2. Computational Materials Science, 2013, 68, 174-180.	1.4	9
13852	The structural, electronic, elastic, vibration and thermodynamic properties of GdMg. Solid State Sciences, 2013, 16, 168-174.	1.5	12
13853	Direct calculation of exciton binding energies with time-dependent density-functional theory. Physical Review B, 2013, 87, .	1.1	44
13854	Possible doping strategies for MoS<mml:math xmlns:mml="http://www.w3.org/1998/Math/MathML" display="inline"><mml:msub><mml:mrow /><mml:mn>2</mml:mn></mml:msub></mml:math>monolayers: Anab initiostudy. Physical Review B, 2013, 88, .	1.1	489
13855	Structural and electronic properties of<mml:math xmlns:mml="http://www.w3.org/1998/Math/MathML" display="inline"><mml:mi>Î±</mml:mi></mml:math>-tin nanocrystals from first principles. Physical Review B, 2013, 87, .	1.1	29
13856	Substrate-induced changes in the magnetic and electronic properties of hexagonal boron nitride. Physical Review B, 2013, 87, .	1.1	29
13857	Ab initio study of elastic properties of super hard and graphitic structures of C3N4. Computational Materials Science, 2013, 69, 299-303.	1.4	31
13858	Intrinsic Properties of Fe-Substituted $L1_{0}$ Magnets. IEEE Transactions on Magnetics, 2013, 49, 5194-5198.	1.2	23
13859	Electronic structure of silicene on Ag(111): Strong hybridization effects. Physical Review B, 2013, 88, .	1.1	186
13860	Biaxial strain effects on adatom surface diffusion on tungsten from first principles. Physical Review B, 2013, 88, .	1.1	12

#	Article	IF	Citations
13861	Pressure-induced phase-transition sequence in CoF<mml:math xmlns:mml="http://www.w3.org/1998/Math/MathML" display="inline"><mml:msub><mml:mrow /><mml:mn>2</mml:mn></mml:msub></mml:math>: An experimental and first-principles study on the crystal, vibrational, and electronic properties. Physical Review B, 2013, 88, .	1.1	29
13862	Performance limits of transition metal dichalcogenide (MX2) nanotube surround gate ballistic field effect transistors. Journal of Applied Physics, 2013, 113, 194502.	1.1	11
13863	Theoretical investigation on helium incorporation in Ti3AlC2. Nuclear Instruments & Methods in Physics Research B, 2013, 304, 27-31.	0.6	26
13864	Pressure-constrained deformation and superior strength: Compressed graphite versus diamond. Physical Review B, 2013, 88, .	1.1	4
13865	Phase transition character and thermodynamic modeling of the and hexagonal Siâ€“N system supplemented by first-principles calculations. Journal of Alloys and Compounds, 2013, 581, 747-752.	2.8	7
13866	First-principles study of hydrogen vacancies in lithium amide doped with titanium and niobium. International Journal of Hydrogen Energy, 2013, 38, 11303-11312.	3.8	9
13867	Electronic-structure modification of graphene on Ni(111) surface by the intercalation of a noble metal. Physical Review B, 2013, 87, .	1.1	23
13868	Ab initiostudy of the stabilities of and mechanism of superionic transport in lithium-rich antiperovskites. Physical Review B, 2013, 87, .	1.1	135
13869	First principles study of structural, electronic and optical properties of AgSbS2. Materials Science in Semiconductor Processing, 2013, 16, 1439-1446.	1.9	18
13870	Theoretical study on tetragonal transition metal dinitrides from first principles calculations. Journal of Alloys and Compounds, 2013, 581, 508-514.	2.8	26
13871	Adhesion of the TiN/Fe interface with point defects from first principles. Journal of Applied Physics, 2013, 113, 014905.	1.1	11
13872	First-principles phonon calculations on the lattice dynamics and thermodynamics of rare-earth intermetallics TbCu and TbZn. Intermetallics, 2013, 43, 65-70.	1.8	7
13873	Effects of Potassium Ion Substitution on Lattice Parameters and Proton Migration in Barium Phosphate. Japanese Journal of Applied Physics, 2013, 52, 117101.	0.8	4
13874	Stabilities and Reconstructions of PbTe Crystal Surfaces from Density-Functional Theory. Journal of Physical Chemistry C, 2013, 117, 24455-24461.	1.5	20
13875	First-principles study of negative thermal expansion in zinc oxide. Journal of Applied Physics, 2013, 114, .	1.1	38
13876	Optical isotropization of anisotropic wurtzite Al-rich AlGaN via asymmetric modulation with ultrathin (GaN) _m /(AlN) _n superlattices. Laser and Photonics Reviews, 2013, 7, 572-579.	4.4	17
13877	Infrared dielectric anisotropy and phonon modes of rutile TiO2. Journal of Applied Physics, 2013, 113, 164102.	1.1	35
13878	Phase transition and thermodynamic properties of ThO2 from first-principles calculations. Physica B: Condensed Matter, 2013, 423, 77-81.	1.3	5

#	Article	IF	Citations
13879	A computational analysis of graphene adhesion on amorphous silica. Journal of Applied Physics, 2013, 113, 164901.	1.1	19
13880	A GGA+U study of the optical properties of vanadium doped ZnO with and without single intrinsic vacancy. Optics Communications, 2013, 297, 79-84.	1.0	38
13881	Effect of hydrogen incorporation on the negative bias illumination stress instability in amorphous In-Ga-Zn-O thin-film-transistors. Journal of Applied Physics, 2013, 113, .	1.1	62
13882	High pressure induced structural, elastic and electronic properties of Calcium Chalcogenides CaX (X=S, Se and Te) via first-principles calculations. Computational Materials Science, 2013, 68, 325-334.	1.4	17
13883	Mechanism for adsorption, dissociation and diffusion ofÂhydrogen in hydrogen permeation barrier of Î±-Al2O3: AÂdensity functional theory study. International Journal of Hydrogen Energy, 2013, 38, 1157-1165.	3.8	78
13884	Three-Dimensional Metallic Boron Nitride. Journal of the American Chemical Society, 2013, 135, 18216-18221.	6.6	145
13885	First principles study of structural, electronic and elastic properties of group IB metal nitrides TMNx (TM=Cu, Ag and Au: x=1, 2). Journal of Alloys and Compounds, 2013, 580, 332-340.	2.8	3
13886	Density functional theory study of the structure and vibrational modes of acrylonitrile adsorbed on Cu(100). Physical Chemistry Chemical Physics, 2013, 15, 1288-1295.	1.3	11
13887	Pressure-induced phase transition for ScVO4: A first-principles study. Physica B: Condensed Matter, 2013, 426, 20-23.	1.3	3
13888	Structures and stabilities of alkaline earth metal peroxides XO2 (X = Ca, Be, Mg) studied by a genetic algorithm. RSC Advances, 2013, 3, 22135.	1.7	20
13889	Sensing of phosgene by a porous-like nanocrystalline diamond layer with buried metallic electrodes. Sensors and Actuators B: Chemical, 2013, 188, 675-680.	4.0	18
13890	Adsorption configurations of carbon monoxide on gold monolayer supported by graphene or monolayer hexagonal boron nitride: a first-principles study. European Physical Journal B, 2013, 86, 1.	0.6	6
13891	CO adsorption on a zigzag SiC nanotube: effects of concentration density and local torsion on transport. Journal of Nanoparticle Research, 2013, 15, 1.	0.8	9
13892	First-Principles Investigation of Thermophysical Properties of Cubic ZrC Under High Pressure. International Journal of Thermophysics, 2013, 34, 2019-2026.	1.0	10
13893	Oxygen Atom Adsorption on and Diffusion into Nb(110) and Nb(100) from First Principles. Jom, 2013, 65, 1473-1481.	0.9	8
13894	Calculation of thermodynamic potentials with the inclusion of fractional occupation numbers and investigation of FCC-BCC structural phase transitions in alkaline-earth metals. Physics of the Solid State, 2013, 55, 1991-2000.	0.2	2
13895	Mechanical properties of CaN, SrN, and BaN compounds by density functional theory. Journal of Theoretical and Applied Physics, 2013, 7, 16.	1.4	4
13896	First-principles investigation on the segregation of Pd at LaFe1-xPd x O3-y surfaces. Nanoscale Research Letters, 2013, 8, 203.	3.1	25

#	Article	IF	Citations
13897	FP-LAPW Calculation of Elastic, Thermal Properties and Chemical Bonding of Heavy REN (REâ€‰=â€‰Tbâ€“Lu). Journal of Low Temperature Physics, 2013, 173, 106-119.	0.6	8
13898	Carbyne bundles for a lithium-ion-battery anode. Journal of the Korean Physical Society, 2013, 63, 1014-1018.	0.3	5
13899	A novel layer-structured PtN2: First-principles calculations. Journal of Superhard Materials, 2013, 35, 339-349.	0.5	2
13900	Structural, thermodynamic and phonon properties of SbSI and SbSBr single crystals. Journal of the Korean Physical Society, 2013, 63, 2133-2137.	0.3	8
13901	Magnetic interactions between native defects in ZnO: A first-principles study. Journal of the Korean Physical Society, 2013, 63, 2170-2174.	0.3	1
13902	Effect of the local coulomb interaction of strongly correlated electrons on phonon, elastic, and electronic properties of ZnSe crystals. Physics of the Solid State, 2013, 55, 2554-2557.	0.2	1
13903	Energy investigations on the mechanical properties of magnesium alloyed by X = C, B, N, O and vacancy. Frontiers of Materials Science, 2013, 7, 405-412.	1.1	3
13904	Study of the polarizations of (Al,Ga,AlGa)N nitride compounds and the charge density of various interfaces based on them. Semiconductors, 2013, 47, 1621-1625.	0.2	9
13905	On the electronic structure and band gap of ZnSxSe1âˆ’x. European Physical Journal Plus, 2013, 128, 1.	1.2	4
13906	Method for calculating coefficients of concentrational variations in lattice constants and the distribution of impurity atoms between sublattices in intermetallic compounds. Bulletin of the Russian Academy of Sciences: Physics, 2013, 77, 1360-1362.	0.1	1
13907	Prediction Study of the Mechanical and Thermodynamic Properties of the $$hbox {RBRh}_{3}$$ RBRh 3 (R $$=$$ = Sm, Eu, Gd, and Tb) Compounds. International Journal of Thermophysics, 2013, 34, 2102-2118.	1.0	0
13908	Elastic and piezoelectric properties, sound velocity and Debye temperature of (B3) boronâ€“bismuth compound under pressure. Pramana - Journal of Physics, 2013, 81, 885-892.	0.9	8
13909	Prediction of Semimetallic Tetragonal<mml:math xmlns:mml="http://www.w3.org/1998/Math/MathML" display="inline"><mml:msub><mml:mi>Hf</mml:mi><mml:mn>2</mml:mn></mml:msub><mml:msub><mml:mi mathvariant="bold">O</mml:mi><mml:mn>3</mml:mn></mml:msub></mml:math>and<mml:math xmlns:mml="http://www.w3.org/1998/Math/MathML" display="inline"><mml:msub><mml:mi>Zr</mml:mi><mml:mn>2</mml:mn></mml:msub><mml:msub><mml:mi mathvariant="bold">O</mml:mi><mml:mn>3</mml:mn></mml:msub></mml:math>from First Principles.	2.9	77
13910	Effects of Adsorbed F, OH, and Cl Ions on Formaldehyde Adsorption Performance and Mechanism of Anatase TiO₂ Nanosheets with Exposed {001} Facets. ACS Applied Materials & Interfaces, 2013, 5, 8165-8172.	4.0	68
13911	Ab initio Studies of Structural and Electronic Properties. , 2013, , 21-73.		1
13912	Trends in Adsorption Characteristics of Benzene on Transition Metal Surfaces: Role of Surface Chemistry and van der Waals Interactions. Journal of Physical Chemistry C, 2013, 117, 20572-20583.	1.5	147
13913	Ab initiostudy of symmetrical tilt grain boundaries in bcc Fe: structural units, magnetic moments, interfacial bonding, local energy and local stress. Journal of Physics Condensed Matter, 2013, 25, 135004.	0.7	52
13914	A DFT study on CO oxidation on Pd4 and Rh4 clusters and adsorbed Pd and Rh atoms on CeO2 and Ce0.75Zr0.25O2 supports for TWC applications. Applied Surface Science, 2013, 285, 927-936.	3.1	19

#	Article	IF	Citations
13915	Catalyst-free achieving of controllable carbon doping of boron nitride nanosheets by CO molecules: a theoretical prediction. RSC Advances, 2013, 3, 4917.	1.7	19
13916	Possibility of spin-polarized electric current through Mn-, Fe-, Co-, or Ni-doped BaSi2 predicted by their calculated densities of states. Journal of Magnetism and Magnetic Materials, 2013, 344, 25-29.	1.0	3
13917	Design Principles of Heteroepitaxial Bimetallic Catalysts. ACS Catalysis, 2013, 3, 2248-2255.	5.5	31
13918	First-order versus second-order phase transformation in AuZn. Physical Review B, 2013, 88, .	1.1	9
13919	A DFT study on structural, vibrational properties, and quasiparticle band structure of solid nitromethane. Journal of Chemical Physics, 2013, 138, 184705.	1.2	54
13920	Ab Initio DFT+U Analysis of Oxygen Vacancy Formation and Migration in La_{1-x}Sr_xFeO_{3-Î´}(x= 0, 0.25, 0.50). Chemistry of Materials, 2013, 25, 3011-3019.	3.2	153
13921	Analytic projection from plane-wave and PAW wavefunctions and application to chemical-bonding analysis in solids. Journal of Computational Chemistry, 2013, 34, 2557-2567.	1.5	1,178
13922	Principal physical properties of GaN/AlN multiquantum well systems determined by density functional theory calculations. Journal of Applied Physics, 2013, 113, .	1.1	32
13923	The incorporation of water into lower-mantle perovskites: A first-principles study. Earth and Planetary Science Letters, 2013, 364, 37-43.	1.8	41
13924	First-principles study of the electronic and optical properties of Si with nanometer-sized pores. Journal Physics D: Applied Physics, 2013, 46, 315302.	1.3	1
13925	Ferroelectric mechanism of croconic acid: A first-principles and Monte Carlo study. Journal of Chemical Physics, 2013, 139, 044702.	1.2	15
13926	Insights into Degradation of Si Anodes from First-Principle Calculations. Journal of Physical Chemistry C, 2013, 117, 18796-18803.	1.5	32
13927	Light metals decorated covalent triazine-based frameworks as a high capacity hydrogen storage medium. Journal of Materials Chemistry A, 2013, 1, 11705.	5.2	47
13928	Morphology and atomic-scale structure of single-layer WS2 nanoclusters. Physical Chemistry Chemical Physics, 2013, 15, 15971.	1.3	65
13929	Self-organization in Pd/W(110): interplay between surface structure and stress. Journal of Physics Condensed Matter, 2013, 25, 355010.	0.7	4
13930	Lithiation Behavior of Silicon-Rich Oxide (SiO_{1/3}): A First-Principles Study. Chemistry of Materials, 2013, 25, 3435-3440.	3.2	80
13931	On Tetrafluorobromates(III): Crystal Structures of the Dibromate CsBr₂F₇ and the Monobromate CsBrF₄. Zeitschrift Fur Anorganische Und Allgemeine Chemie, 2013, 639, 2846-2850.	0.6	39
13932	Elasticity and lattice dynamics of enstatite at high pressure. Journal of Geophysical Research: Solid Earth, 2013, 118, 4071-4082.	1.4	29

#	Article	IF	Citations
13933	Towards a multiscale approach for assessing fission product behaviour in UN. Journal of Nuclear Materials, 2013, 442, 253-261.	1.3	18
13934	GGA+U studies of the early actinide mononitrides and dinitrides. Journal of Nuclear Materials, 2013, 442, 235-244.	1.3	33
13935	Investigation of boron antimonide as hot carrier absorber material. Solar Energy Materials and Solar Cells, 2013, 111, 123-126.	3.0	27
13936	Ab initio calculation of vibrational spectra of orthorhombic IVâ€“VI layered crystals. Physics of the Solid State, 2013, 55, 1802-1807.	0.2	9
13937	Adsorption of sulfuric acid on graphene with a high titanium coverage and on the [001] titanium surface. Surface Science, 2013, 618, 36-41.	0.8	1
13938	Origin of the Bipolar Doping Behavior of SnO from X-ray Spectroscopy and Density Functional Theory. Chemistry of Materials, 2013, 25, 3114-3123.	3.2	135
13939	Stabilization of Rocksalt CdSe at Atmospheric Pressures via Pseudomorphic Growth. Journal of Physical Chemistry C, 2013, 117, 7643-7647.	1.5	10
13940	Electronic, vibrational, superconducting and thermodynamic properties of cubic antiperovskite ZnNNi₃. Philosophical Magazine, 2013, 93, 4469-4487.	0.7	8
13941	Ab-initio molecular dynamics simulation of Î´-Bi3YO6. Solid State Ionics, 2013, 245-246, 43-48.	1.3	7
13942	Structural and electronic properties of hybrid graphene and boron nitride nanostructures on Cu. Physical Review B, 2013, 88, .	1.1	9
13943	Ordered bilayer rutheniumâ€“platinum core-shell nanoparticles as carbon monoxide-tolerant fuel cell catalysts. Nature Communications, 2013, 4, 2466.	5.8	200
13944	First-Principles Study of a Full Cycle of Atomic Layer Deposition of SiO₂Thin Films with Di(sec-butylamino)silane and Ozone. Journal of Physical Chemistry C, 0, , 130911145338002.	1.5	13
13945	Density functional theory study of Fe adatoms adsorbed monolayer and bilayer MoS2 sheets. Journal of Applied Physics, 2013, 114, .	1.1	35
13946	High pressure high-temperature behavior and magnetic properties of Fe₄N: experiment and theory. High Pressure Research, 2013, 33, 684-696.	0.4	27
13947	First-principles study of cubane-type ZnO: Another ZnO polymorph. Chemical Physics Letters, 2013, 557, 102-105.	1.2	12
13948	Thinning down of thermal conductivity in ultrashort period superlattices. Physical Review B, 2013, 88, .	1.1	11
13949	Computational study of cysteine interaction with the rutile TiO2 (110) surface. Surface Science, 2013, 617, 60-67.	0.8	33
13950	Density Functional Kinetic Monte Carlo Simulation of Waterâ€“Gas Shift Reaction on Cu/ZnO. Journal of Physical Chemistry C, 2013, 117, 3414-3425.	1.5	48

#	Article	IF	Citations
13951	Contrasting Elastic Properties of Heavily B- and N-doped Graphene with Random Impurity Distributions Including Aggregates. Journal of Physical Chemistry C, 2013, 117, 20229-20235.	1.5	28
13952	Elastic, superconducting, and thermodynamic properties of the cubic metallic phase of AlH3 via first-principles calculations. Journal of Applied Physics, 2013, 114, .	1.1	13
13953	A combined first principles and analytical determination of the modulus of cohesion, surface energy, and the additional constants in the second strain gradient elasticity. International Journal of Solids and Structures, 2013, 50, 3967-3974.	1.3	33
13954	Anomalous surface segregation behaviour of some 3d elements in ferromagnetic iron. Journal of Physics Condensed Matter, 2013, 25, 415502.	0.7	6
13955	Electronic, magnetic, optical and elastic properties of Fe2YAl (Y=Ti, V and Cr) using first principles methods. Journal of Magnetism and Magnetic Materials, 2013, 339, 142-150.	1.0	36
13956	Room-temperature spin-spiral multiferroicity in high-pressure cupric oxide. Nature Communications, 2013, 4, 2511.	5.8	76
13957	Î²-Mn-Type Co_{8+x}Zn_{12â€“x} as a Defect Cubic Laves Phase: Site Preferences, Magnetism, and Electronic Structure. Inorganic Chemistry, 2013, 52, 9399-9408.	1.9	34
13958	Modelling zirconium hydrides using the special quasirandom structure approach. Physical Chemistry Chemical Physics, 2013, 15, 7599.	1.3	24
13959	Factors affecting the magnetic coupling in Sr2V3O9 type oxides: As for V substitution in the VO4 tetrahedra and nature of the cation. Dalton Transactions, 2013, 42, 15555.	1.6	1
13960	Controllable modulation of the electronic properties of graphene and silicene by interface engineering and pressure. Journal of Materials Chemistry C, 2013, 1, 4869.	2.7	28
13961	Electronic and magnetic properties of silicene nanoflakes by first-principles calculations. Physics Letters, Section A: General, Atomic and Solid State Physics, 2013, 377, 2792-2795.	0.9	12
13962	Group III dopant segregation and semiconductor-to-metal transition in ZnO nanowires: a first principles study. RSC Advances, 2013, 3, 19793.	1.7	2
13963	Tunable band gap of AlN, GaN nanoribbons and AlN/GaN nanoribbon heterojunctions: A first-principle study. Solid State Communications, 2013, 172, 24-28.	0.9	26
13964	Understanding Photoelectrochemical Properties of Bâ€“N Codoped Anatase TiO₂ for Solar Energy Conversion. Journal of Physical Chemistry C, 2013, 117, 15911-15917.	1.5	33
13965	First-principles calculations of Pd-terminated symmetrical armchair graphene nanoribbons. Computational Materials Science, 2013, 68, 18-22.	1.4	26
13966	Impact of Local Curvature and Structural Defects on Grapheneâ€“C₆₀ Fullerene Fusion Reaction Barriers. Journal of Physical Chemistry C, 2013, 117, 19664-19671.	1.5	20
13967	LiH as a Li+ and Hâ¯ ion provider. Solid State Ionics, 2013, 253, 53-56.	1.3	7
13968	Structural and electronic properties of SiC nanotubes filled with Cu nanowires: A first-principles study. Physica E: Low-Dimensional Systems and Nanostructures, 2013, 54, 319-325.	1.3	6

#	Article	IF	Citations
13969	The Intrinsic Ferromagnetism in a MnO₂ Monolayer. Journal of Physical Chemistry Letters, 2013, 4, 3382-3386.	2.1	171
13970	A DFT+U study of CO oxidation at CeO2(110) and (111) surfaces with oxygen vacancies. Surface Science, 2013, 618, 140-147.	0.8	51
13971	The half-metallicity of zinc-blende CaC/GaAs(001) heterojunction: A density functional theory study. Journal of Magnetism and Magnetic Materials, 2013, 332, 81-84.	1.0	9
13972	First principles study on oxygen vacancy formation in rock salt-type oxides MO (M: Mg, Ca, Sr and Ba). Ceramics International, 2013, 39, S287-S292.	2.3	13
13973	First-principles calculations of the electronic structure and defects of Al2O3. Journal of Applied Physics, 2013, 114, .	1.1	28
13974	Characterization of Electronic States inside Metallic Nanopores. Journal of Physical Chemistry C, 2013, 117, 18406-18413.	1.5	3
13975	Silver Nanoparticles for Olefin Production: New Insights into the Mechanistic Description of Propyne Hydrogenation. ChemCatChem, 2013, 5, 3750-3759.	1.8	88
13976	Changes in valence, coordination and reactivity that occur upon oxidation of fresh metal surfaces. Philosophical Magazine, 2013, 93, 4286-4310.	0.7	14
13977	Na₈Lu₂(CO₃)₆F₂ and Na₃Lu(CO₃)₂F₂: Rare Earth Fluoride Carbonates as Deep-UV Nonlinear Optical Materials. Chemistry of Materials, 2013, 25, 3147-3153.	3.2	123
13978	Raman-scattering measurements and first-principles calculations of strain-induced phonon shifts in monolayer MoS<mml:math xmlns:mml="http://www.w3.org/1998/Math/MathML" display="inline"><mml:msub><mml:mrow /><mml:mn>2</mml:mn></mml:msub></mml:math>. Physical Review B, 2013, 87, .	1.1	495
13979	Carbon nanotubes dressed by aromatic molecules. Molecular Physics, 2013, 111, 2427-2438.	0.8	11
13980	STRAIN-TUNABLE BAND GAP OF BC₃ SHEET: A FIRST-PRINCIPLES INVESTIGATION. Modern Physics Letters B, 2013, 27, 1350110.	1.0	3
13981	Phonon and magnon Raman scattering in CuB<mml:math xmlns:mml="http://www.w3.org/1998/Math/MathML" display="inline"><mml:msub><mml:mrow /><mml:mn>2</mml:mn></mml:msub></mml:math>O<mml:math xmlns:mml="http://www.w3.org/1998/Math/MathML" display="inline"><mml:msub><mml:mrow /><mml:mn>4</mml:mn></mml:msub></mml:math>. Physical Review B, 2013, 88, .	1.1	10
13982	Electronics and Structural Properties of Single-Walled Carbon Nanotubes Interacting with a Glucose Molecule:ab initioCalculations. Communications in Theoretical Physics, 2013, 60, 341-347.	1.1	6
13983	The investigation of NbO₂ and Nb₂O₅ electronic structure by XPS, UPS and first principles methods. Surface and Interface Analysis, 2013, 45, 1206-1210.	0.8	112
13984	Adsorption of Î²-d-glucose and cellobiose on kaolinite surfaces: Density functional theory (DFT) approach. Applied Clay Science, 2013, 71, 73-81.	2.6	78
13985	First principles selection and design of mid-IR nonlinear optical halide crystals. Journal of Materials Chemistry C, 2013, 1, 7363.	2.7	117
13986	Comparison of Hemi-Squaraine Sensitized TiO₂ and ZnO Photoanodes for DSSC Applications. Journal of Physical Chemistry C, 2013, 117, 22778-22783.	1.5	30

#	Article	IF	Citations
13987	A first-principles investigation of the thermodynamic and mechanical properties of Niâ€“Tiâ€“Sn Heusler and half-Heusler materials. RSC Advances, 2013, 3, 22176.	1.7	40
13988	Ab initio study of the highâ€temperature phase transition in crystalline GeO₂. Journal of Computational Chemistry, 2013, 34, 2320-2326.	1.5	16
13989	Energy benchmarks for water clusters and ice structures from an embedded many-body expansion. Journal of Chemical Physics, 2013, 139, 114101.	1.2	60
13990	High-pressure structural transformations of Sn up to 138 GPa: Angle-dispersive synchrotron x-ray diffraction study. Physical Review B, 2013, 88, .	1.1	54
13991	Decomposition mechanism of Al1â^'xSixNy solid solution and possible mechanism of the formation of covalent nanocrystalline AlN/Si3N4 nanocomposites. Acta Materialia, 2013, 61, 4226-4236.	3.8	21
13992	First-principles molecular dynamics study of the thermal stability of the BN, AlN, SiC and SiN interfacial layers in TiN-based heterostructures: Comparison with experiments. Thin Solid Films, 2013, 545, 391-400.	0.8	24
13993	Organometallic Hexahapto-Functionalized Graphene: Band Gap Engineering with Minute Distortion to the Planar Structure. Journal of Physical Chemistry C, 2013, 117, 22156-22161.	1.5	31
13994	Mechanistic Study of the Oxidative Steam Reforming of EtOH on Rh(111): The Importance of the Oxygen Effect. ChemCatChem, 2013, 5, 3164-3174.	1.8	11
13995	Further Theoretical Evidence for Hydrogen-Assisted CO Dissociation on Ru(0001). Journal of Physical Chemistry C, 2013, 117, 20562-20571.	1.5	18
13996	A variational method for density functional theory calculations on metallic systems with thousands of atoms. Journal of Chemical Physics, 2013, 139, 054107.	1.2	51
13997	Defect formation energy and magnetic properties of off-stoichiometric Ni-Mn-In alloys by first-principles calculations. Journal of Applied Physics, 2013, 113, .	1.1	12
13998	Enhancement of p-type mobility in tin monoxide by native defects. Applied Physics Letters, 2013, 102, .	1.5	51
13999	Computational Search for Single-Layer Transition-Metal Dichalcogenide Photocatalysts. Journal of Physical Chemistry C, 2013, 117, 20440-20445.	1.5	468
14000	Electronic Structural MoirÃ© Pattern Effects on MoS₂/MoSe₂ 2D Heterostructures. Nano Letters, 2013, 13, 5485-5490.	4.5	296
14001	Reinterpretation of the bond-valence model with bond-order formalism: An improved bond-valence-based interatomic potential for PbTiO<mml:math xmlns:mml="http://www.w3.org/1998/Math/MathML" display="inline"><mml:msub><mml:mrow /><mml:mn>3</mml:mn></mml:msub></mml:math>. Physical Review B, 2013, 88, .	1.1	50
14002	Simulations of the elastic properties of nanomaterials using multiscale modelling methods. Mechanics of Materials, 2013, 67, 74-78.	1.7	4
14003	Heterogeneous Uptake and Adsorption of Gas-Phase Formic Acid on Oxide and Clay Particle Surfaces: The Roles of Surface Hydroxyl Groups and Adsorbed Water in Formic Acid Adsorption and the Impact of Formic Acid Adsorption on Water Uptake. Journal of Physical Chemistry A, 2013, 117, 11316-11327.	1.1	43
14004	First-Principles Study of Point Defect Formation in AgNbO₃. Japanese Journal of Applied Physics, 2013, 52, 09KF08.	0.8	22

#	Article	IF	Citations
14005	Effect of magnetism on the solution energy of 3p (Al, Si) and 4p (Ga, Ge) elements in iron. Physics of Metals and Metallography, 2013, 114, 885-892.	0.3	7
14006	DFT study of interaction of O, O2, and OH with unreconstructed Pt(hkl) (h, k, l = 0, 1) surfacesâ€"similarities, differences, and universalities. Russian Journal of Physical Chemistry A, 2013, 87, 2214-2218.	0.1	7
14007	Lithium Adsorption on Hexagonal Boron Nitride Nanosheet Using Dispersion-Corrected Density Functional Theory Calculations. Japanese Journal of Applied Physics, 2013, 52, 06GG08.	0.8	20
14008	First-principle calculations on the structural stability and electronic properties of superhard B_xC_ycompounds. Journal of Physics Condensed Matter, 2013, 25, 425502.	0.7	8
14009	Electronic and phononic properties of V2AlC via first principles. Canadian Journal of Physics, 2013, 91, 822-825.	0.4	5
14010	Design of Shallow Acceptors in GaN through Zincâ€"Magnium Codoping: First-Principles Calculation. Applied Physics Express, 2013, 6, 042104.	1.1	5
14011	Comparative study on the performance of exchange and correlation in wide-gap semiconductors: the case of BeS, BeSe, and BeTe. Journal of Materials Science, 2013, 48, 5499-5508.	1.7	6
14012	Semiconducting layered technetium dichalcogenides: insights from first-principles. Dalton Transactions, 2013, 42, 15288.	1.6	23
14013	Band structure, shape controllable synthesis and luminescence properties of the precursor and final product Lu6O5F8:Eu/Tb/Ce/Dy nano/microstructures. Journal of Materials Chemistry C, 2013, 1, 7952.	2.7	11
14014	Asymmetrical growth and dissolution along polar axis of Î±-resorcinol crystal: role of solvent and external environment. CrystEngComm, 2013, 15, 8493.	1.3	14
14015	Formamide adsorption over the TiO2 (110) surface: a theoretical study. RSC Advances, 2013, 3, 16829.	1.7	3
14016	Growth and dissolution mechanism at the opposite and hemihedral faces of polar crystals. CrystEngComm, 2013, 15, 4143.	1.3	13
14017	Strain effects on hydrogen storage in Ti decorated pyridinic N-doped graphene. Physical Chemistry Chemical Physics, 2013, 15, 12757.	1.3	14
14018	Relative contributions of quantum and double layer capacitance to the supercapacitor performance of carbon nanotubes in an ionic liquid. Physical Chemistry Chemical Physics, 2013, 15, 19741-19747.	1.3	68
14019	Room-temperature proton transport and its effect on thermopower in a solid ionic semiconductor, TTFCOONH4. Journal of Materials Chemistry A, 2013, 1, 5089.	5.2	5
14020	Dimension-dependent phase transition and magnetic properties of VS2. Journal of Materials Chemistry A, 2013, 1, 10821.	5.2	183
14021	Water and ammonia on Cu{110}: comparative structure and bonding. Physical Chemistry Chemical Physics, 2013, 15, 4785.	1.3	14
14022	First-principles structural design of superhard material of ZrB4. Physical Chemistry Chemical Physics, 2013, 15, 20894.	1.3	52

#	Article	IF	Citations
14023	First principles studies on the redox ability of (Ga1â^'xZnx)N1â^'xOx solid solutions and thermal reactions for H2 and O2 production on their surfaces. Physical Chemistry Chemical Physics, 2013, 15, 19807.	1.3	12
14024	Strain-induced Dirac cone-like electronic structures and semiconductorâ€“semimetal transition in graphdiyne. Physical Chemistry Chemical Physics, 2013, 15, 8179.	1.3	81
14025	Study of the thermal processes in molecular crystals of peptides by means of NMR crystallography. CrystEngComm, 2013, 15, 8680.	1.3	14
14026	Bilayer silicene with an electrically-tunable wide band gap. RSC Advances, 2013, 3, 21943.	1.7	32
14027	Adsorption of hydrogen on the surface and sub-surface of Cu(111). Journal of Chemical Physics, 2013, 139, 044712.	1.2	38
14028	Simulation Studies of the Phase Stability of the Ruddlesdenâ€“Popper Phases. Journal of the American Ceramic Society, 2013, 96, 2316-2321.	1.9	14
14029	A theoretical analysis of the role of defects in the adsorption of hydrogen sulfide on graphene. AIP Advances, 2013, 3, .	0.6	21
14030	Theoretical perspective of photocatalytic properties of single-layer SnS<mml:math xmlns:mml="http://www.w3.org/1998/Math/MathML" display="inline"><mml:msub><mml:mrow /><mml:mn>2</mml:mn></mml:msub></mml:math>. Physical Review B, 2013, 88, .	1.1	215
14031	Dispersion Corrected Hartreeâ€“Fock and Density Functional Theory for Organic Crystal Structure Prediction. Topics in Current Chemistry, 2013, 345, 1-23.	4.0	72
14032	Characterization of a high pressure, high temperature modification of ammonia borane (BH3NH3). Journal of Chemical Physics, 2013, 139, 054507.	1.2	14
14033	Electronic and Magnetic Properties of Li_{1.5}Mn_{0.5}As Alloys in the Cu₂Sb Structure. Advanced Materials Research, 0, 702, 231-235.	0.3	1
14034	First principle study of elastic and thermodynamic properties of FeB4 under high pressure. Journal of Applied Physics, 2013, 114, .	1.1	42
14035	Adsorption of Sulfurâ€Containing Species on LaCrO₃ (001) Surface: A Firstâ€Principles Study. Fuel Cells, 2013, 13, 1040-1047.	1.5	3
14036	First-principles calculation of intrinsic carrier mobility of silicene. Journal of Applied Physics, 2013, 114, .	1.1	211
14037	Stability and superconductivity of Ca-B phases at ambient and high pressure. Physical Review B, 2013, 88, .	1.1	32
14038	First-principles study of the structural, electronic, and optical properties of Y-doped SrSi2. Journal of Applied Physics, 2013, 113, .	1.1	3
14039	Negative differential resistance and effect of defects and deformations in MoS2 armchair nanoribbon metal-oxide-semiconductor field effect transistor. Journal of Applied Physics, 2013, 114, .	1.1	30
14040	Spatial distribution of neutral oxygen vacancies on ZnO nanowire surfaces: An investigation combining confocal microscopy and first principles calculations. Journal of Applied Physics, 2013, 114, .	1.1	227

#	Article	IF	Citations
14041	Thickness dependence of the growth of magnetron-sputtered TiO2 films studied by Raman and optical transmittance spectroscopy. Journal of Applied Physics, 2013, 114, .	1.1	22
14042	Molecular adsorption on silicon (001): A systematic evaluation of size effects in slab and cluster models. AIP Advances, 2013, 3, 042117.	0.6	13
14043	H₂S splitting on Cu(110): Insight from combined periodic density functional theory calculations and microkinetic simulation. International Journal of Quantum Chemistry, 2013, 113, 1992-2001.	1.0	26
14044	First-principles Thermodynamic Models in Heterogeneous Catalysis. RSC Catalysis Series, 2013, , 59-115.	0.1	9
14045	Predictions of the structural, electronic and thermodynamic properties of the anti-fluorite-type Mg₂Sn under pressure from first principles. Physica Scripta, 2013, 88, 045302.	1.2	24
14046	A First Principles Study of Thermal Properties of Yb-Pnictides (YbX, X= N, P and As) Compounds. Advanced Materials Research, 2013, 665, 353-358.	0.3	0
14047	Effective band gap reduction of titanium oxide semiconductors by codoping from first-principles calculations. International Journal of Quantum Chemistry, 2013, 113, 2546-2553.	1.0	14
14048	The CO oxidation mechanism and reactivity on PdZn alloys. Physical Chemistry Chemical Physics, 2013, 15, 7768.	1.3	55
14049	Structure and stress of Re(112Ì„1); chiral terraces at a racemic surface. Physical Chemistry Chemical Physics, 2013, 15, 20823.	1.3	2
14050	Theoretical study of water adsorption and dissociation on Ta3N5(100) surfaces. Physical Chemistry Chemical Physics, 2013, 15, 16054.	1.3	28
14051	Ba6Sn6Se13: a new mixed valence selenostannate with NLO property. Dalton Transactions, 2013, 42, 13635.	1.6	43
14052	Entropies of defect formation in ceria from first principles. Physical Chemistry Chemical Physics, 2013, 15, 15935.	1.3	48
14053	Local surface structure effect on reactivity of molecules confined between metallic surfaces. Physical Chemistry Chemical Physics, 2013, 15, 1647-1654.	1.3	9
14054	Engineering intriguing electronic and magnetic properties in novel one-dimensional staircase-like metallocene wires. Journal of Materials Chemistry C, 2013, 1, 941-946.	2.7	20
14055	Phonon-mediated superconductivity in silicene predicted by first-principles density functional calculations. Europhysics Letters, 2013, 104, 36001.	0.7	55
14056	CO2 capture properties of lithium silicates with different ratios of Li2O/SiO2: an ab initio thermodynamic and experimental approach. Physical Chemistry Chemical Physics, 2013, 15, 13538.	1.3	100
14057	First principles study of Fe in diamond: A diamond-based half metallic dilute magnetic semiconductor. Journal of Applied Physics, 2013, 114, 223703.	1.1	6
14058	First-principles study of the formation and migration of native defects in LiNH₂BH₃. Physical Chemistry Chemical Physics, 2013, 15, 893-900.	1.3	7

#	Article	IF	Citations
14059	Thermodynamic properties of the Î±-quartz-type and rutile-type GeO2 from first-principles calculations. Physical Chemistry Chemical Physics, 2013, 15, 15943.	1.3	15
14060	Structural and electronic properties of Li8ZrO6 and its CO2 capture capabilities: an ab initio thermodynamic approach. Physical Chemistry Chemical Physics, 2013, 15, 9752.	1.3	36
14061	Ab initio determination of the bulk modulus of the chromium nitride CrN. RSC Advances, 2013, 3, 17813.	1.7	6
14062	Computational investigation of defect segregation at the (001) surface of BaCeO3 and BaZrO3: the role of metalâ€“oxygen bond strength in controlling vacancy segregation. Journal of Materials Chemistry A, 2013, 1, 2840.	5.2	18
14063	Oxide ion transport in Sr2Fe1.5Mo0.5O6â^'Î´, a mixed ion-electron conductor: new insights from first principles modeling. Physical Chemistry Chemical Physics, 2013, 15, 6250.	1.3	59
14064	The effects of water molecules on the electronic and structural properties of peptide nanotubes. Physical Chemistry Chemical Physics, 2013, 15, 7555.	1.3	38
14065	LaBeB3O7: a new phase-matchable nonlinear optical crystal exclusively containing the tetrahedral XO4 (X = B and Be) anionic groups. Journal of Materials Chemistry C, 2013, 1, 3616.	2.7	30
14066	Mode selectivity in methane dissociative chemisorption on Ni(111). Chemical Science, 2013, 4, 3249.	3.7	115
14067	K2CaV2O7: a pyrovanadate with a new layered type of structure in the A2BV2O7family. Dalton Transactions, 2013, 42, 1057-1064.	1.6	7
14068	Modulating the electronic properties of germanium nanowires via applied strain and surface passivation. Physical Chemistry Chemical Physics, 2013, 15, 5927.	1.3	12
14069	Electronic and magnetic properties of one dimensional sandwich polymers: [(Ge5)TM]â^ž (TM = Ti, V, Cr,) Tj ETQq0 0 0 rgBT /Overlock 1	2.7	9
14070	Mechanistic insights into the partial oxidation of acetic acid by O2 at the dual perimeter sites of a Au/TiO2 catalyst. Faraday Discussions, 2013, 162, 247.	1.6	35
14071	Effects of atomic scale roughness at metal/insulator interfaces on metal work function. Physical Chemistry Chemical Physics, 2013, 15, 19615.	1.3	19
14072	Investigation of structural stability and electronic properties of group III nitrides: a first principles study. Phase Transitions, 2013, 86, 570-584.	0.6	11
14073	Theoretical calculations for structural, elastic, and thermodynamic properties of c-W₃N₄ under high pressure. Journal of Applied Physics, 2013, 114, 063512.	1.1	16
14074	Non-orthogonal tight-binding model for tellurium and selenium. Philosophical Magazine, 2013, 93, 3216-3230.	0.7	11
14075	Pressure-Induced Local Lattice Distortions in Î±-Co[N(CN)₂]₂. Inorganic Chemistry, 2013, 52, 14148-14154.	1.9	8
14076	Oxygen reduction and transport on the La1â^'xSrxCo1â^'yFeyO3â^'Î´ cathode in solid oxide fuel cells: a first-principles study. Journal of Materials Chemistry A, 2013, 1, 12932.	5.2	55

#	Article	IF	Citations
14077	Effects of graphene coating and charge injection on water adsorption of solid surfaces. Nanoscale, 2013, 5, 10414.	2.8	12
14078	Single-crystal adsorption calorimetry and density functional theory of CO chemisorption on fcc Co{110}. Physical Chemistry Chemical Physics, 2013, 15, 4059.	1.3	20
14079	Selective molecular adsorption in sub-nanometer cages of a Cu2O surface oxide. Physical Chemistry Chemical Physics, 2013, 15, 10726.	1.3	22
14080	Generalized trends in the formation energies of perovskite oxides. Physical Chemistry Chemical Physics, 2013, 15, 7526.	1.3	85
14081	Interactions of iron-oxide filled carbon nanotubes with gas molecules. Physical Chemistry Chemical Physics, 2013, 15, 14340.	1.3	2
14082	Ensemble and ligand effects on the acetylene adsorption on ordered PdxAg1â^'x/Pd(100) surface alloys investigated by periodic DFT study. Physical Chemistry Chemical Physics, 2013, 15, 20345.	1.3	18
14083	Polymerization of nitrogen in lithium azide. Journal of Chemical Physics, 2013, 139, 164710.	1.2	69
14084	Conformational change-induced switching behavior in pure-carbon systems. RSC Advances, 2013, 3, 16672.	1.7	17
14085	Quantum Monte Carlo study of the three-dimensional spin-polarized homogeneous electron gas. Physical Review B, 2013, 88, .	1.1	79
14086	Tuning the electronic and magnetic properties of zigzag silicene nanoribbons by edge hydrogenation and doping. RSC Advances, 2013, 3, 24075.	1.7	63
14087	Study the gas sensing mechanism of oxygen atom on Pd doped ZnO (0001). , 2013, , .		1
14088	Six-dimensional quantum dynamics study for the dissociative adsorption of HCl on Au(111) surface. Journal of Chemical Physics, 2013, 139, 184705.	1.2	56
14089	Simple pair-wise interactions for hybrid Monte Carloâ€“molecular dynamics simulations of titania/yttria-doped iron. Journal of Physics Condensed Matter, 2013, 25, 055402.	0.7	9
14090	Superconductivity in Fe<mml:math xmlns:mml="http://www.w3.org/1998/Math/MathML"><mml:msub><mml:mrow /><mml:mrow><mml:mn>1.05</mml:mn></mml:mrow></mml:msub></mml:math>Te:O<mml:math xmlns:mml="http://www.w3.org/1998/Math/MathML"><mml:msub><mml:mrow /><mml:mrow>x</mml:mrow></mml:msub></mml:math> single crystals. Physical Review B, 2013, 88, .	1.1	21
14091	Ab initioand cluster expansion study of surface alloys of Fe and Au on Ru(0001) and Mo(110): Importance of magnetism. Physical Review B, 2013, 88, .	1.1	4
14092	Topological phase transitions in (Bi<mml:math xmlns:mml="http://www.w3.org/1998/Math/MathML">	1.1	45
14093	Periodic ab initio bulk investigation of hydroxylapatite and type A carbonated apatite with both pseudopotential and all-electron basis sets for calcium atoms. American Mineralogist, 2013, 98, 410-416.	0.9	35
14094	Surface Coverage and SEI Induced Electrochemical Surface Stress Changes during Li Deposition in a Model System for Li-Ion Battery Anodes. Journal of the Electrochemical Society, 2013, 160, A888-A896.	1.3	55

#	Article	IF	Citations
14095	Graphene-protected Fe layers atop Ni(111): Evidence for strong Fe-graphene interaction and structural bistability. Physical Review B, 2013, 88, .	1.1	21
14096	display="inline"><mml:msub><mml:mrow /><mml:mrow><mml:mn>0.8</mml:mn></mml:mrow></mml:msub></mml:math>Fe<mml:math xmlns:mml="http://www.w3.org/1998/Math/MathML" display="inline"><mml:msub><mml:mrow /><mml:mrow><mml:mn>1.6</mml:mn></mml:mrow></mml:msub></mml:math>Se<mml:math xmlns:mml="http://www.w3.org/1998/Math/MathML" display="inline"><mml:msub><mml:mrow /><mml:mml:	1.1	17
14097	Magnetoelectric effect in functionalized few-layer graphene. Physical Review B, 2013, 87, .	1.1	8
14098	Nonempirical generalized gradient approximation free-energy functional for orbital-free simulations. Physical Review B, 2013, 88, .	1.1	106
14099	Electrical characteristics of C 36 molecular conductor and its B- and N-Doped isomers. Electronic Materials Letters, 2013, 9, 63-69.	1.0	3
14100	Partition behavior of alloying elements and phase transformation temperatures inÂCoâ€“Alâ€“W-base quaternary systems. Intermetallics, 2013, 32, 274-283.	1.8	193
14101	Thermodynamic, structural and elastic properties of Co3X (XÂ=ÂTi, Ta, W, V, Al) compounds from first-principles calculations. Intermetallics, 2013, 32, 303-311.	1.8	55
14102	Band gap calculations of the semiconductor BNxP1â^'x using modified Beckeâ€“Johnson approximation. Journal of Alloys and Compounds, 2013, 546, 151-156.	2.8	16
14103	The elastic and mechanical properties of MB12 (M=Zr, Hf, Y, Lu) as a function of pressure. Journal of Alloys and Compounds, 2013, 546, 157-164.	2.8	95
14104	Magnetic CrX and MnX (X=Si, Ge, and As) nanowires: Stability enhancement and linearization. Journal of Alloys and Compounds, 2013, 547, 138-146.	2.8	2
14105	First-principles density functional calculation of mechanical, thermodynamic and electronic properties of CuIn and Cu2In crystals. Journal of Alloys and Compounds, 2013, 546, 286-295.	2.8	59
14106	First-principles study of structural, vibrational and dielectric properties of double perovskites Ba2LnSbO6 (Ln=Sm, Gd, Dy and Y). Journal of Alloys and Compounds, 2013, 547, 81-85.	2.8	10
14107	Magnetism and large magnetocaloric effect in HoFe2â^'xAlx. Journal of Alloys and Compounds, 2013, 549, 64-69.	2.8	13
14108	Energetic consideration of the conduction type of Mg2Si doped with Cu, Ag, or Au using first-principle calculations. Journal of Alloys and Compounds, 2013, 549, 175-178.	2.8	20
14109	Structural stability, band structure and magnetic properties of ZnS and Zn0.75Cr0.25S under pressure. Journal of Alloys and Compounds, 2013, 549, 184-189.	2.8	13
14110	Structure, electronic characteristic and thermodynamic properties of K2ZnH4 hydride crystal: A first-principles study. Journal of Alloys and Compounds, 2013, 549, 30-37.	2.8	6
14111	Microkinetics of steam methane reforming on platinum and rhodium metal surfaces. Journal of Catalysis, 2013, 297, 227-235.	3.1	43
14112	A simplified approach to the band gap correction of defect formation energies: Al, Ga, and In-doped ZnO. Journal of Physics and Chemistry of Solids, 2013, 74, 45-50.	1.9	38

#	Article	IF	Citations
14113	First principles study of structural, bonding and vibrational properties of PtCoO2, PdCoO2 and PdRhO2 metallic delafossites. Journal of Physics and Chemistry of Solids, 2013, 74, 305-310.	1.9	12
14114	Reaction mechanism for methanol oxidation on Au(111): A density functional theory study. Applied Surface Science, 2013, 265, 443-451.	3.1	29
14115	Insights into the preference of CHx(x=1â€“3) formation from CO hydrogenation on Cu(111) surface. Applied Surface Science, 2013, 265, 720-730.	3.1	51
14116	The adsorption of bisulfate and sulfate anions over a Pt(111) electrode: A first principle study of adsorption configurations, vibrational frequencies and linear sweep voltammogram simulations. Catalysis Today, 2013, 202, 20-35.	2.2	60
14117	Electronic changes at the Pt(111) interface induced by the adsorption of OH species. Catalysis Today, 2013, 202, 120-127.	2.2	9
14118	Inhibition of water dissociation on a pitted Pt(111) surface: First principles study. Catalysis Today, 2013, 202, 163-167.	2.2	9
14119	Modeling of the symmetry factor of electrochemical proton discharge via the Volmer reaction. Catalysis Today, 2013, 202, 168-174.	2.2	16
14120	Hydrogen oxidation on ordered intermetallic phases of platinum and tin â€“ A combined experimental and theoretical study. Catalysis Today, 2013, 202, 191-196.	2.2	13
14121	Atomic ensemble effects on formic acid oxidation on PdAu electrode studied by first-principles calculations. Journal of Power Sources, 2013, 224, 241-249.	4.0	58
14122	Synthesis and crystal structure of Mg0.5NbO2: An ion-exchange reaction with Mg2+ between trigonal [NbO2]â^' layers. Journal of Solid State Chemistry, 2013, 197, 471-474.	1.4	4
14123	DFT+U study of the oxide-ion conductor pentalanthanum hexamolybdenum henicosaoxide. Journal of Solid State Chemistry, 2013, 197, 304-311.	1.4	16
14124	Hybrid functional calculation of electronic and phonon structure of BaSnO. Journal of Solid State Chemistry, 2013, 197, 134-138.	1.4	42
14125	On the key role of hydroxyl groups in platinum-catalysed alcohol oxidation in aqueous medium. Catalysis Science and Technology, 2013, 3, 339-350.	2.1	51
14126	Theoretical calculation on electronic excitation and compression effect in tungsten. Physica B: Condensed Matter, 2013, 413, 69-72.	1.3	2
14127	First-principle calculations of thermodynamic properties of ZrC and ZrN at high pressures and high temperatures. Physica B: Condensed Matter, 2013, 410, 57-62.	1.3	22
14128	Growth, properties and first-principles study of mid-IR nonlinear optical crystal LiInS2. Journal of Crystal Growth, 2013, 362, 271-275.	0.7	9
14129	Na-Si Clathrates Are High-Pressure Phases: A Melt-Based Route to Control Stoichiometry and Properties. Crystal Growth and Design, 2013, 13, 303-307.	1.4	75
14130	First principles calculation of mixing enthalpy of Î²-Ti with transition elements. Journal of Alloys and Compounds, 2013, 550, 501-508.	2.8	14

#	Article	IF	Citations
14131	Interactions of carbonâ€“nitrogen and carbonâ€“nitrogenâ€“vacancy in Î±-Fe from first-principles calculations. Computational Materials Science, 2013, 67, 222-228.	1.4	20
14132	Electronic Origin of the Surface Reactivity of Transition-Metal-Doped TiO₂(110). Journal of Physical Chemistry C, 2013, 117, 460-465.	1.5	87
14133	First-principles calculations of vibrational and thermodynamical properties of rare-earth diborides. Computational Materials Science, 2013, 68, 307-313.	1.4	4
14134	Exfoliated graphene-supported Pt and Pt-based alloys as electrocatalysts for direct methanol fuel cells. Carbon, 2013, 52, 595-604.	5.4	117
14135	Electronic structure of A2CrSbO6 [A=Sr, Ca]: Ab-initio study. Journal of Physics and Chemistry of Solids, 2013, 74, 250-254.	1.9	10
14136	Tuning the Catalytic Activity of Ru@Pt Coreâ€“Shell Nanoparticles for the Oxygen Reduction Reaction by Varying the Shell Thickness. Journal of Physical Chemistry C, 2013, 117, 1748-1753.	1.5	140
14137	MnO2-coated graphitic petals for supercapacitor electrodes. Journal of Power Sources, 2013, 227, 254-259.	4.0	195
14138	Ab-initio calculation of C and CO adsorption on the Co (110) surface. Surface Science, 2013, 608, 282-291.	0.8	3
14139	Indirect interaction in Ag and Pd adsorbed layers on the Mo(112) surface. Applied Surface Science, 2013, 265, 615-620.	3.1	8
14140	Theoretical design and experimental implementation of Ag/Au electrodes for the electrochemical reduction of nitrate. Physical Chemistry Chemical Physics, 2013, 15, 3196.	1.3	98
14141	Lattice, elastic properties and Debye temperatures of ATiO3 (A=Ba, Ca, Pb, Sr) from first-principles. Journal of Alloys and Compounds, 2013, 549, 336-340.	2.8	69
14142	NMR crystallography of Î±-poly(l-lactide). Physical Chemistry Chemical Physics, 2013, 15, 3137.	1.3	39
14143	Understanding CeO2 as a Deacon catalyst by probe molecule adsorption and in situ infrared characterisations. Physical Chemistry Chemical Physics, 2013, 15, 3454.	1.3	47
14144	Evolutionary search for BiInS3 crystal structure and predicting its second-order nonlinear optical property. Journal of Solid State Chemistry, 2013, 199, 78-83.	1.4	6
14145	Electronic, magnetic and elastic properties of Î³-Fe4X (X=B/C/N) from density functional theory calculations. Journal of Magnetism and Magnetic Materials, 2013, 333, 39-45.	1.0	33
14146	Hydrogen Dissociation Catalyzed by Carbonâ€Coated Nickel Nanoparticles: Experiment and Theory. ChemPhysChem, 2013, 14, 381-385.	1.0	26
14147	Band offsets and heterostructures of two-dimensional semiconductors. Applied Physics Letters, 2013, 102, .	1.5	1,361
14148	Orthorhombic<mml:math xmlns:mml="http://www.w3.org/1998/Math/MathML" display="inline"><mml:mi>A</mml:mi><mml:mi>B</mml:mi><mml:mi>C</mml:mi></mml:math>Semiconductors as Antiferroelectrics. Physical Review Letters, 2013, 110, 017603.	2.9	59

#	Article	IF	Citations
14149	⁹⁵Mo Solid-State Nuclear Magnetic Resonance Spectroscopy and Quantum Simulations: Synergetic Tools for the Study of Molybdenum Cluster Materials. Inorganic Chemistry, 2013, 52, 617-627.	1.9	12
14150	Formation and structure of inhibitive molecular film of imidazole on iron surface. Corrosion Science, 2013, 68, 195-203.	3.0	87
14151	Synthesis and Structure Determination of CaSi_{1/3}B_{2/3}O_{8/3}: A New Calcium Borosilicate. Inorganic Chemistry, 2013, 52, 4250-4258.	1.9	31
14152	Method of preparation and thermodynamic properties of transparent Y3Al5O12 nanoceramics. Journal of Thermal Analysis and Calorimetry, 2013, 111, 289-294.	2.0	5
14153	Ab initio study of edge effect on relative motion of walls in carbon nanotubes. Journal of Chemical Physics, 2013, 138, 024703.	1.2	22
14154	The role of van der Waals forces in water adsorption on metals. Journal of Chemical Physics, 2013, 138, 024708.	1.2	173
14155	Comparative studies on total energetics of nonequivalent hexagonal polytypes for group IV semiconductors and group III nitrides. Journal of Materials Research, 2013, 28, 7-16.	1.2	5
14156	Dissociation and reconstruction of O2 on Al (111) studied by First-principles. Applied Surface Science, 2013, 264, 247-254.	3.1	15
14157	Formation of n-hexane from methylcyclopentane via a metallacyclobutane intermediate at step sites of Pt surfaces: Mechanism from first-principles calculations. Journal of Catalysis, 2013, 299, 146-149.	3.1	10
14158	A density functional theory study of CO oxidation on Pd-Ni alloy with sandwich structure. Applied Catalysis A: General, 2013, 451, 79-85.	2.2	35
14159	Structural and elastic properties of ternary metal nitrides TixTa1â^'xN alloys: First-principles calculations versus experiments. Surface and Coatings Technology, 2013, 215, 199-208.	2.2	39
14160	Structure, hydrogen bond network and proton conductivity of new benzimidazole compounds with dicarboxylic acids. CrystEngComm, 2013, 15, 1950.	1.3	30
14161	The electronic and optical properties of MB₁₂(M = Zr, Hf, Y, Lu) dodecaboride compounds. Physica Scripta, 2013, 87, 015702.	1.2	6
14162	Structural, elastic and electronic properties of equiatomic PtTi as potential high-temperature shape memory alloy. Intermetallics, 2013, 33, 27-32.	1.8	37
14163	Structural, magnetic, multiferroic and electronic properties of Sr2ZrMnO6 double perovskite. Journal of Molecular Structure, 2013, 1034, 233-237.	1.8	19
14164	Trivalent Actinide and Lanthanide Complexation of 5,6-Dialkyl-2,6-bis(1,2,4-triazin-3-yl)pyridine (RBTP; R =) Tj ETQq1 1 0.784314 rgBT /O 52, 761-776.	1.9	18
14165	N- and Mo-doping Bi2WO6 in photocatalytic water splitting. Computational Materials Science, 2013, 67, 88-92.	1.4	39
14166	Graphene with line defect as a membrane for gas separation: Design via a first-principles modeling. Surface Science, 2013, 607, 153-158.	0.8	55

#	Article	IF	Citations
14167	Study of the interaction of formic acid, formaldehyde and formamide with the bulk terminated (1Ã—1) and reconstructed (2Ã—1) surfaces of rutile TiO2(011). Surface Science, 2013, 607, 187-196.	0.8	20
14168	The first principles investigation of lattice dynamical and thermodynamical properties of Al2Ca and Al2Mg compounds in the cubic Laves structure. Computational Materials Science, 2013, 68, 27-31.	1.4	32
14169	First-principles studies on lattice constants and local lattice distortions in solid solution aluminum alloys. Computational Materials Science, 2013, 67, 1-10.	1.4	121
14170	The influence of hydrostatic pressure on the electronic structure and optical properties of tin dioxide: A first-principle study. Physica B: Condensed Matter, 2013, 408, 73-78.	1.3	6
14171	Band gap change induced by defect complexes in Cu2ZnSnS4. Thin Solid Films, 2013, 535, 265-269.	0.8	91
14172	Ab initio study of ZnCoO diluted magnetic semiconductor and its magnetic properties. Journal of Alloys and Compounds, 2013, 551, 306-311.	2.8	19
14173	Electronic, elastic, thermodynamic properties and structure disorder of Î³-AlON solid solution from ab initio calculations. Journal of Alloys and Compounds, 2013, 548, 228-234.	2.8	14
14174	New type of possible high-pressure polymorphism in NiAs minerals in planetary cores. Physics and Chemistry of Minerals, 2013, 40, 183-193.	0.3	10
14175	Structural phase transition of CdTe: an ab initio study. Journal of Molecular Modeling, 2013, 19, 421-426.	0.8	3
14176	The Oxygen Reduction Reaction on Nitrogen-Doped Graphene. Catalysis Letters, 2013, 143, 58-60.	1.4	69
14177	Electronic and optical properties of (Al x Ga1â^'x)1â^'y Mn y As single crystal: a new candidate for integrated optical isolators and spintronics. Journal of Materials Science, 2013, 48, 758-764.	1.7	11
14178	The effect of the phase transition on the elasticity of cubic platinum carbide. Journal of Materials Science, 2013, 48, 1660-1668.	1.7	4
14179	P-type reduced graphene oxide membranes induced by iodine doping. Journal of Materials Science, 2013, 48, 2284-2289.	1.7	28
14180	Pb2B5O9Cl: a chloride borate with second harmonic generation effect. Journal of Materials Science, 2013, 48, 2590-2596.	1.7	33
14181	Electronic and Phonon Structures of BaFe2As2 Superconductor by Ab-initio Density Functional Theory. Journal of Superconductivity and Novel Magnetism, 2013, 26, 93-100.	0.8	10
14182	Mechanism of Alcoholâ€“Water Separation in Metalâ€“Organic Frameworks. Journal of Physical Chemistry C, 2013, 117, 4124-4130.	1.5	33
14183	Electric-Field Dependence of the Effective Dielectric Constant in Graphene. Nano Letters, 2013, 13, 898-902.	4.5	181
14184	Molecular Simulation Studies of CO₂ Adsorption by Carbon Model Compounds for Carbon Capture and Sequestration Applications. Environmental Science & Technology, 2013, 47, 95-101.	4.6	192

#	Article	IF	Citations
14185	Binding of atomic oxygen on graphene from small epoxy clusters to a fully oxidized surface. Carbon, 2013, 54, 482-488.	5.4	50
14186	Investigation of initial epitaxial growth of (Ba, Sr)TiO3 thin film on (001) SrTiO3 substrate using first-principles calculations. Journal of Alloys and Compounds, 2013, 559, 11-15.	2.8	4
14187	Four Polymorphs of Methyl Paraben: Structural Relationships and Relative Energy Differences. Crystal Growth and Design, 2013, 13, 1206-1217.	1.4	41
14188	Ab Initio Based conformational study of the crystalline Î±â€chitin. Biopolymers, 2013, 99, 22-34.	1.2	27
14189	A Highly Efficient, Cleanâ€Surface, Porous Platinum Electrocatalyst and the Inhibition Effect of Surfactants on Catalytic Activity. Chemistry - A European Journal, 2013, 19, 240-248.	1.7	71
14190	Effect of Spinâ€Crossoverâ€Induced Pore Contraction on CO₂â€“Host Interactions in the Porous Coordination Polymers [Fe(pyrazine)M(CN)₄] (M = Ni, Pt). European Journal of Inorganic Chemistry, 2013, 2013, 511-519.	1.0	15
14191	Electronic structure, chemical bonding and magnetism of the metal-rich borides MRh6B3 (MÂ=ÂCr, Mn,) Tj ETQq0 0 0 rgBT /Overlock 10 14-20.	1.5	13
14192	First principles calculation of electronic structure, chemical bonding and elastic properties of ultra-incompressible Re2P. Transactions of Nonferrous Metals Society of China, 2013, 23, 3400-3404.	1.7	2
14193	First-principles study of stacking fault energies in Mg-based binary alloys. Computational Materials Science, 2013, 79, 564-569.	1.4	107
14194	The catalytic effect of Nb, NbO and Nb2O5 with different surface planes on dehydrogenation in MgH2: Density functional theory study. Journal of Alloys and Compounds, 2013, 580, S25-S28.	2.8	22
14195	Surface morphology of MnSi thin films grown on Si(111). Surface Science, 2013, 617, 106-112.	0.8	9
14196	Hydrogen solubility in zirconium intermetallic second phase particles. Journal of Nuclear Materials, 2013, 443, 502-506.	1.3	25
14197	The detailed orbital-decomposed electronic structures of tetragonal ZrO2. Physica B: Condensed Matter, 2013, 411, 126-130.	1.3	8
14198	Energetics and diffusion of hydrogen in Î±-Al2O3 and Er2O3. Fusion Engineering and Design, 2013, 88, 2646-2649.	1.0	14
14199	First principle calculations of MAX ceramics Cr2GeC, V2GeC and their substitutional solid solutions. Computational Materials Science, 2013, 74, 40-49.	1.4	12
14200	Effect of doping Fe and Si on electronic structure and optical Properties of CdS. Physica B: Condensed Matter, 2013, 417, 17-23.	1.3	11
14201	Vacancy trapping mechanism for multiple helium in monovacancy and small void of vanadium solid. Journal of Nuclear Materials, 2013, 440, 557-561.	1.3	32
14202	Oxygen doped SiC nanowires: An ab initio study. Chemical Physics Letters, 2013, 568-569, 140-145.	1.2	10

#	Article	IF	Citations
14203	Ferroelectricity at a junction structure of a 180Â° domain wall and a (001) surface in PbTiO3: A density functional theory study. Physica B: Condensed Matter, 2013, 410, 22-27.	1.3	5
14204	Tight-binding studies of bulk properties and hydrogen vacancies in KBH4. Computational Materials Science, 2013, 79, 888-895.	1.4	3
14205	Generalized planar fault energies and mechanical twinning in gamma TiAl alloys. Scripta Materialia, 2013, 68, 759-762.	2.6	32
14206	Behaviors of helium in vanadium: Stability, diffusion, vacancy trapping and ideal tensile strength. Progress in Natural Science: Materials International, 2013, 23, 459-463.	1.8	14
14207	Investigation of the (1Ã—2)-H/Pd(110)-pr system using DFT. Chemical Physics Letters, 2013, 568-569, 117-120.	1.2	3
14208	Thermodynamic assessment of the Cdâ€“X (X= Sr, Ti, B, V) systems. Calphad: Computer Coupling of Phase Diagrams and Thermochemistry, 2013, 42, 6-12.	0.7	2
14209	The feasibility of tunable p-type Mg doping in a GaN monolayer nanosheet. Acta Materialia, 2013, 61, 7720-7725.	3.8	81
14210	Ideal strength of Mg2X (XÂ=ÂSi, Ge, Sn and Pb) from first-principles. Journal of Magnesium and Alloys, 2013, 1, 163-168.	5.5	23
14211	Oxygen adsorption on honeycomb <mml:math altimg="si0001.gif" overflow="scroll" xmlns:xocs="http://www.elsevier.com/xml/xocs/dtd" xmlns:xs="http://www.w3.org/2001/XMLSchema" xmlns:xsi="http://www.w3.org/2001/XMLSchema-instance" xmlns="http://www.elsevier.com/xml/ja/dtd" xmlns:ja="http://www.elsevier.com/xml/ja/dtd" xmlns:mml="http://www.w3.org/1998/Math/MathML" xmlns:tb="http://www.elsevier.com/xml/common/table/dtd" xmlns:sb="http://www.elsevier.com/xml/common/struct-bib/dtd" xmlns:ce="http://www.elsevier.co. Ma	1.3	5
14212	Improvement of resistive switching in ZnO film by Ti doping. Thin Solid Films, 2013, 537, 279-284.	0.8	26
14213	Energetic and structural analysis of N2H4BH3 inorganic solid and its modified material for hydrogen storage. International Journal of Hydrogen Energy, 2013, 38, 6718-6725.	3.8	7
14214	Effect of non-metal elements (B, C, N, F, P, S) mono-doping as anions on electronic structure of SrTiO3. Computational Materials Science, 2013, 79, 69-74.	1.4	56
14215	Facile NOx interconversion over preoxidized Ag(111). Surface Science, 2013, 617, 167-174.	0.8	5
14216	Hexavalent hydrogen complex in hypothetical Y2CrH6. Journal of Alloys and Compounds, 2013, 580, S274-S277.	2.8	7
14217	Universal ground state hexagonal phases and mechanical properties of stoichiometric transition metal tetraborides: TMB4 (TM=W, Tc, and Re). Computational Materials Science, 2013, 68, 371-378.	1.4	26
14218	Theoretical study of phase stability, magnetization and lattice vibrations of Fe23CB6 structure with Cr23C6 prototype. Journal of Solid State Chemistry, 2013, 199, 27-33.	1.4	8
14219	Avoiding pitfalls in the modeling of electrochemical interfaces. Chemical Physics Letters, 2013, 555, 145-148.	1.2	50
14220	Theoretical study on optoelectronic properties of Ga0.75Al0.25N (001) reconstruction surfaces. Applied Surface Science, 2013, 287, 1-7.	3.1	5

#	Article	IF	Citations
14221	Combined studies of DFT atomistic modelling and in situ FTIR spectroscopy on surface oxidants and CO oxidation at Ru electrodes. Journal of Electroanalytical Chemistry, 2013, 688, 216-223.	1.9	11
14222	Effect of dopant nature on structures and lattice dynamics of proton-conducting BaZrO3. Solid State Ionics, 2013, 253, 195-200.	1.3	16
14223	Structural stability and electronic structure study of YCu2â€“YZn2 Laves phases by first-principles calculations. Computational Materials Science, 2013, 77, 366-371.	1.4	9
14224	Ab initio investigation of structural and electronic properties of zinc blende AlN1â^'xBix alloys. Solid State Communications, 2013, 155, 12-15.	0.9	28
14225	Interfacial potentials for Ag/GaN(0001) interfaces by inversion of adhesive energy. Physica B: Condensed Matter, 2013, 431, 97-101.	1.3	5
14226	Interactions of lead with carboxyl and hydroxyl-decorated(10, 0) single-walled carbon nanotubes: First-principle calculations. Applied Surface Science, 2013, 285, 198-204.	3.1	12
14227	Using Raman spectroscopy to understand the origin of the phase transition observed in the crystalline sulfur based amino acid l-methionine. Vibrational Spectroscopy, 2013, 65, 132-141.	1.2	18
14228	Catalytic behavior and surface species investigation over Î³-Al2O3 in dimethyl ether hydrolysis. Applied Catalysis A: General, 2013, 460-461, 99-105.	2.2	13
14229	First-principles study on iron-pnictide superconductors Ca(Fe1â^'xCox)2As2. Solid State Communications, 2013, 154, 11-14.	0.9	6
14230	Prediction of elastic and electronic properties of cubic Al18Ti2Mg3 phase coexisting with Al3Ti in Alâ€“Tiâ€“Mg system. Physica B: Condensed Matter, 2013, 408, 68-72.	1.3	14
14231	Stability and migration of vacancy in Vâ€“4Crâ€“4Ti alloy: Effects of Al, Si, Y trace elements. Journal of Nuclear Materials, 2013, 442, 370-376.	1.3	21
14232	Ab-initio studies of the Sc adsorption and the ScN thin film formation on the GaN(000-1)-(2Ã—2) surface. Thin Solid Films, 2013, 548, 317-322.	0.8	8
14233	Strain modulated electronic properties of silicon nanoribbons with armchair edges. Chemical Physics Letters, 2013, 561-562, 77-81.	1.2	17
14234	The simulation of adhesion, stability, electronic structure of W/ZrB2 interface using first-principles. Surface and Coatings Technology, 2013, 228, S583-S587.	2.2	12
14235	The electronic and optical properties of Cu doped CdI2. Optik, 2013, 124, 3230-3234.	1.4	6
14236	First-principles investigation on vacancy trapping behaviors of hydrogen in vanadium. Journal of Nuclear Materials, 2013, 442, S688-S693.	1.3	27
14237	Structural, electrical, and electrochemical properties of cobalt-doped NiFe2O4 as a potential cathode material for solid oxide fuel cells. International Journal of Hydrogen Energy, 2013, 38, 14329-14336.	3.8	21
14238	Work function tuning of an ultrathin MgO film on an Ag substrate by generating oxygen impurities at the interface. Thin Solid Films, 2013, 544, 541-544.	0.8	10

#	Article	IF	Citations
14239	Effect of polar distortion on electronic structures of (001) LaGaO3/SrTiO3 interface. Physics Letters, Section A: General, Atomic and Solid State Physics, 2013, 377, 577-581.	0.9	9
14240	Local structure of Fe in Fe-doped misfit-layered calcium cobaltite: An X-ray absorption spectroscopy study. Journal of Solid State Chemistry, 2013, 204, 257-265.	1.4	20
14241	Density functional studies of selected metal dioxides. Journal of Physics and Chemistry of Solids, 2013, 74, 1632-1639.	1.9	15
14242	Density functional theory study of the vibrational properties of hydrogenated graphene. Solid State Communications, 2013, 157, 24-28.	0.9	13
14243	Theoretical study of the impact of stress on the behavior of intrinsic point defects in large-diameter defect-free Si crystals. Journal of Crystal Growth, 2013, 363, 97-104.	0.7	30
14244	Si(111) surface functionalized with H-bonded SAM: A theoretical study. Applied Surface Science, 2013, 267, 17-20.	3.1	4
14245	Effect of Co doping on the electrochemical properties ofÂSr2Fe1.5Mo0.5O6 electrode for solid oxide fuel cell. International Journal of Hydrogen Energy, 2013, 38, 4108-4115.	3.8	67
14246	Ab initio calculations of the atomic and electronic structure of BaZrO3 (111) surfaces. Solid State Ionics, 2013, 230, 43-47.	1.3	47
14247	Electronic features induced by Stoneâ€“Wales defects in zigzag and chiral carbon nanotubes. Computational Materials Science, 2013, 79, 82-86.	1.4	15
14248	The electronic and optical properties of quaternary BxGa1â^'xAs1â^'ySby alloys with low boron concentration: A first-principles study. Journal of Alloys and Compounds, 2013, 563, 18-21.	2.8	4
14249	The carbon-tolerance mechanism of Ni-based alloy with coinage metals. Physics Letters, Section A: General, Atomic and Solid State Physics, 2013, 377, 2189-2194.	0.9	16
14250	Adsorption of H atoms on cubic Er2O3 (001) surface: A DFT study. Journal of Nuclear Materials, 2013, 443, 555-561.	1.3	4
14251	Structural, elastic and electronic properties of CeVO4 via first-principles calculations. Computational Materials Science, 2013, 79, 811-816.	1.4	15
14252	First principles study of structural and vibrational properties of Sr2BWO6 (BÂ=ÂMg, Zn) in cubic and tetragonal phases. Solid State Sciences, 2013, 23, 72-78.	1.5	3
14253	Theoretical study of the adsorption and dissociation mechanism for methylamine on Pd(111). Applied Surface Science, 2013, 271, 291-298.	3.1	16
14254	Ab initio calculation of fundamental properties of CaxMg1â^'xA (A=Se and Te) alloys in the rock-salt structure. Physica E: Low-Dimensional Systems and Nanostructures, 2013, 49, 83-91.	1.3	1
14255	Ab initio study of the structural, mechanical, and dynamical properties of the rare-earth dihydrides XH2 (X=Sc, Y, and La). Physica B: Condensed Matter, 2013, 429, 119-126.	1.3	22
14256	First-principles investigation of electronic, mechanical and thermodynamic properties of L12 ordered Co3(M, W) (M = Al, Ge, Ga) phases. Acta Materialia, 2013, 61, 5437-5448.	3.8	72

#	Article	IF	Citations
14257	Theoretical study of the pressure-induced B3â€“B1 phase transition in Cd1â^'xMnxTe. Solid State Sciences, 2013, 16, 117-120.	1.5	0
14258	Alkali metal induced effects on coadsorbed carbon monoxide on Co(0001): A density functional theory study. Computational and Theoretical Chemistry, 2013, 1009, 55-59.	1.1	6
14259	Formaldehyde adsorption geometry and energies over TiO2(110) rutile surface. Chemical Physics Letters, 2013, 572, 125-129.	1.2	15
14260	Predicted ferromagnetism in hole doped armchair nanoribbons: A first principles study. Chemical Physics Letters, 2013, 555, 173-177.	1.2	4
14261	Confinement effects on structural, electronic properties and dehydrogenation thermodynamics of LiBH4. International Journal of Hydrogen Energy, 2013, 38, 8367-8375.	3.8	11
14262	The thermodynamic, electronic and magnetic properties of Ni2MnX (X=Ge, Sn, Sb) Heusler alloys: a quasi-hormonic Debye model and first principles study. Physica B: Condensed Matter, 2013, 409, 35-41.	1.3	28
14263	First-principles investigation of the elastic, electronic, and thermodynamic properties of a nitrogen-doped (Ti0.75W0.25)C solid solution. Solid State Communications, 2013, 156, 25-30.	0.9	14
14264	Energetics of interstitial oxygen in Î²-TiX (X=transition elements) alloys using first principles methods. Journal of Alloys and Compounds, 2013, 571, 107-113.	2.8	8
14265	A first-principles study on lattice dynamics, thermodynamics and elastic properties of lithium selenide under high pressure. Computational Materials Science, 2013, 79, 903-907.	1.4	5
14266	Prediction of the pressureâ€“volumeâ€“temperature equation of state for zinc-blende ZnO from quasi-harmonic Debye model. Solid State Communications, 2013, 166, 27-31.	0.9	1
14267	Ab initio study of structural, electronic and thermodynamic properties of tungstate double perovskites Ba2MWO6 (M=Mg, Ni, Zn). Computational Materials Science, 2013, 77, 316-321.	1.4	45
14268	Computational Mechanistic Study of Borohydride Electrochemical Oxidation on Au₃Ni(111). Journal of Physical Chemistry C, 2013, 117, 3818-3825.	1.5	19
14269	First-principles study on the high-pressure phase transition and elasticity of KAlSi3O8 hollandite. American Mineralogist, 2013, 98, 207-218.	0.9	16
14270	Role of Oxygen Vacancies in Catalytic SO₃ Decomposition over Cu₂V₂O₇ in Solar Thermochemical Water Splitting Cycles. Journal of Physical Chemistry C, 2013, 117, 26710-26715.	1.5	33
14271	First-principles study of the structural and electronic properties of MoS₂â€“WS₂and MoS₂â€“MoTe₂monolayer heterostructures. Journal Physics D: Applied Physics, 2013, 46, 505308.	1.3	51
14272	Catalytic activity of Coâ€“N_x/C electrocatalysts for oxygen reduction reaction: a density functional theory study. Physical Chemistry Chemical Physics, 2013, 15, 148-153.	1.3	303
14273	Surface Chemistry of 4-Mercaptobenzoic Acid Self-Assembled on Ag(111) and Ag Nanoparticles. Journal of Physical Chemistry C, 2013, 117, 24967-24974.	1.5	21
14274	Atomic-scale inversion of spin polarization at an organic-antiferromagnetic interface. Physical Review B, 2013, 88, .	1.1	30

#	Article	IF	Citations
14275	Electronic and atomic structure of Co/Ge nanoislands on the Ge(111) surface. Physical Review B, 2013, 88, .	1.1	6
14276	Correlation effects in insulating surface nanostructures. Physical Review B, 2013, 88, .	1.1	16
14277	Knock-on damage in bilayer graphene: Indications for a catalytic pathway. Physical Review B, 2013, 88, .	1.1	19
14278	Insights into the atomic and electronic structure triggered by ordered nitrogen vacancies in CrN. Physical Review B, 2013, 87, .	1.1	22
14279	Free energies of (Co, Fe, Ni, Zn)Fe₂O₄spinels and oxides in water at high temperatures and pressure from density functional theory: results for stoichiometric NiO and NiFe₂O₄surfaces. Journal of Physics Condensed Matter, 2013, 25, 445008.	0.7	47
14280	xmlns:mml="http://www.w3.org/1998/Math/MathML" display="inline"><mml:msub><mml:mrow /><mml:mn>2</mml:mn></mml:msub></mml:math>O<mml:math xmlns:mml="http://www.w3.org/1998/Math/MathML" display="inline"><mml:msub><mml:mrow /><mml:mn>3</mml:mn></mml:msub></mml:math>, Fe<mml:math	1.1	53
14281	Ab initioSternheimer-GW method for quasiparticle calculations using plane waves. Physical Review B, 2013, 88, .	1.1	36
14282	Band nesting and the optical response of two-dimensional semiconducting transition metal dichalcogenides. Physical Review B, 2013, 88, .	1.1	261
14283	Determination of the Electronic Structure and UVâ€“Vis Absorption Properties of (Na2â€“xCux)Ta4O11 from First-Principle Calculations. Journal of Physical Chemistry C, 2013, 117, 17477-17484.	1.5	32
14284	Arbitrary tip orientation in STM simulations: 3D WKB theory and application to W(110). Journal of Physics Condensed Matter, 2013, 25, 445009.	0.7	11
14285	Dependence of equilibrium stacking fault width in fcc metals on theÎ³-surface. Modelling and Simulation in Materials Science and Engineering, 2013, 21, 025015.	0.8	45
14286	Mechanistic Insight into the Au-3d Metal Alloy-Catalyzed Borohydride Electro-Oxidation: From Electronic Properties to Thermodynamics. ACS Catalysis, 2013, 3, 3031-3040.	5.5	25
14287	Atomic-Scale Engineering of the Electrostatic Landscape of Semiconductor Surfaces. Nano Letters, 2013, 13, 2418-2422.	4.5	15
14288	On the Complex Structural Picture of the Ionic Conductor Sr₆Ta₂O₁₁. Journal of Physical Chemistry C, 2013, 117, 9543-9549.	1.5	6
14289	Beneficial Effect of Cu on a Cu-Modified Au Catalytic Surface for CO Oxidation Reaction: A DFT Study. Journal of Physical Chemistry C, 2013, 117, 5084-5094.	1.5	27
14290	Structural, electronic, and magnetic properties of the period vacancy in zigzag Ga<scp>N</scp> nanoribbons. Physica Status Solidi (B): Basic Research, 2013, 250, 1510-1518.	0.7	13
14291	Ab Initio Prediction of Surface Stability of Fluorite Materials and Experimental Verification. Journal of Physical Chemistry C, 2013, 117, 6639-6650.	1.5	24
14292	Stacking in Bulk and Bilayer Hexagonal Boron Nitride. Physical Review Letters, 2013, 111, 036104.	2.9	252

#	Article	IF	Citations
14293	Strain-dependent modulation of conductivity in single-layer transition-metal dichalcogenides. Physical Review B, 2013, 87, .	1.1	255
14294	Reaction Barriers and Cooperative Effects for the Adsorption of Pyridine on Si(100). Journal of Physical Chemistry C, 2013, 117, 26644-26651.	1.5	9
14295	Ab initio study of the cohesive properties, electronic structure and thermodynamic stability of the Niâ€“In and Niâ€“Sn intermetallics. Journal of Alloys and Compounds, 2013, 576, 302-316.	2.8	22
14296	Exploration of a new compound in the Mâ€“Bâ€“Oâ€“X (M: alkali metals; X: halogen) system: Preparation, crystal and electronic structures, and optical properties of Na3B6O10Br. Inorganica Chimica Acta, 2013, 406, 205-210.	1.2	16
14297	First principles study of structural, electronic and mechanical properties of transition metal hydrides (TMH, TM=Mo, Tc, Ru). Transactions of Nonferrous Metals Society of China, 2013, 23, 2700-2707.	1.7	12
14298	Synthesis and characterization of Zn3Ta2O8 nanomaterials by hydrothermal method. Journal of Alloys and Compounds, 2013, 573, 53-57.	2.8	9
14299	Electronic, mechanical, and thermodynamic properties of americium dioxide. Journal of Nuclear Materials, 2013, 441, 411-420.	1.3	33
14300	New approach for the spin effect on the ground state properties of the cubic and hexagonal YFeO3 perovskite oxide: GGA+U based on the DFT+U description. Results in Physics, 2013, 3, 61-69.	2.0	13
14301	The optical absorption and hydrogen production by water splitting of (Si,Fe)-codoped anatase TiO2 photocatalyst. International Journal of Hydrogen Energy, 2013, 38, 5209-5214.	3.8	58
14302	Synthesis, structure, and bonding of the hexagonal form of the oxide carbide ScAlOC. Solid State Sciences, 2013, 26, 121-127.	1.5	5
14303	Synthesis, crystal structure and optical properties of a new lithium dilead pentaborate, LiPb2B5O10. Journal of Molecular Structure, 2013, 1040, 180-183.	1.8	4
14304	First-principles study of oxygen-induced copper segregation in Cu3Au(1 1 1). Chemical Physics, 2013, 410, 99-102.	0.9	9
14305	A density functional theory study on influence of 3d alloying elements on electrochemical properties of cobalt-base alloys. Computational Materials Science, 2013, 68, 206-211.	1.4	6
14306	Effect of vacancy on the dissolution and diffusion properties of hydrogen and helium in molybdenum. Journal of Nuclear Materials, 2013, 433, 167-173.	1.3	31
14307	An examination of nickel doping effect on the mechanical strength of a tungsten grain boundary. Computational Materials Science, 2013, 77, 131-138.	1.4	14
14308	C-REDOR curves of extended spin systems. Solid State Nuclear Magnetic Resonance, 2013, 49-50, 12-22.	1.5	9
14309	Study of Cs adsorption on Ga(Mg)0.75Al0.25N (0001) surface: A first principle calculation. Applied Surface Science, 2013, 282, 308-314.	3.1	31
14310	Implication of volume changes in uranium oxides: A density functional study. Solid State Sciences, 2013, 24, 44-53.	1.5	13

#	Article	IF	Citations
14311	Kinetic considerations of gas-phase abstraction of H and F from the c-BN(100) surface. Thin Solid Films, 2013, 548, 280-287.	0.8	3
14312	Site preference, magnetism and lattice vibrations of intermetallics Lu2Fe17â^'xTx (T=Cr, Mn, Ru). Journal of Solid State Chemistry, 2013, 201, 250-255.	1.4	8
14313	Enhanced photoelectrochemical performance of anatase TiO2 by metal-assisted Sâ€“O coupling for water splitting. International Journal of Hydrogen Energy, 2013, 38, 1251-1257.	3.8	27
14314	Comparative computational study of the diffusion of Li, Na, and Mg in silicon including the effect of vibrations. Solid State Ionics, 2013, 253, 157-163.	1.3	51
14315	Dissolution and diffusion behaviors of hydrogen in copper: A first-principles investigation. Computational Materials Science, 2013, 79, 923-928.	1.4	21
14316	Synthesis, structure, elastic properties, lattice dynamics and thermodynamics of YVO4 polymorphs from experiments and density functional theory calculation. Journal of Alloys and Compounds, 2013, 580, 544-549.	2.8	10
14317	Theoretical studies on the stabilities and reactivities of Ta3N5 (1 0 0) surfaces. Chemical Physics Letters, 2013, 561-562, 57-62.	1.2	20
14318	Ordering and phonons in Ba3CaNb2O9 complex perovskite. Materials Research Bulletin, 2013, 48, 3298-3303.	2.7	20
14319	Solidâ€“aqueous equilibrium in the BaSO4â€“RaSO4â€“H2O system: First-principles calculations and a thermodynamic assessment. Geochimica Et Cosmochimica Acta, 2013, 122, 398-417.	1.6	48
14320	Formation of aluminides on Ni-based superalloy 690 substrate, their characterization and first-principle Ni(111)/NiAl(110) interface simulations. Surface and Coatings Technology, 2013, 235, 741-747.	2.2	17
14321	Structural investigation of Si0.5Ge0.5 alloy for optoelectronic applications: Ab initio study. Optik, 2013, 124, 5674-5678.	1.4	8
14322	Theoretical study on the electronic structures and magnetism of Fe3Si intermetallic compound. Journal of Alloys and Compounds, 2013, 552, 324-328.	2.8	20
14323	First-principle study of optical properties of Cu-doped CdS. Optics Communications, 2013, 295, 45-52.	1.0	65
14324	Role of acetylenic bonds in the mechanical, electronic and optical properties of yne-diamonds. Diamond and Related Materials, 2013, 37, 55-63.	1.8	9
14325	First-principles thermodynamic calculations of diffusion characteristics of impurities in Î³-iron. Journal of Nuclear Materials, 2013, 442, S684-S687.	1.3	7
14326	Significant effects of graphite fragments on hydrogen storage performances of LiBH4: A first-principles approach. International Journal of Hydrogen Energy, 2013, 38, 13717-13727.	3.8	13
14327	Size-dependent and intra-band photoluminescence of NiS2 nano-alloys synthesized by microwave assisted hydrothermal technique. Journal of Alloys and Compounds, 2013, 552, 345-350.	2.8	23
14328	Magnetoelectric effect in organometallic vanadiumâ€“benzene wires. Chemical Physics Letters, 2013, 568-569, 121-124.	1.2	10

#	Article	IF	Citations
14329	The new understanding on photocatalytic mechanism of visible-light response NS codoped anatase TiO2 by first-principles. Applied Catalysis B: Environmental, 2013, 142-143, 45-53.	10.8	151
14330	First-principles prediction of ferroelastic phase transition in AlPO4. Solid State Communications, 2013, 155, 88-91.	0.9	4
14331	Structural and electronic properties of sodium azide at high pressure: A first principles study. Solid State Communications, 2013, 161, 13-18.	0.9	47
14332	Theoretical calculation of ethanol molecule adsorption on LaFeO3 (010) surface. Computational Materials Science, 2013, 68, 90-94.	1.4	9
14333	First-principles calculations on elastic, electronic and optical properties for the alkaline platinum hydrides A2PtH6 (A=K, Rb and Cs). Materials Science in Semiconductor Processing, 2013, 16, 940-946.	1.9	5
14334	Effects of Zn atoms on the basal dislocation in magnesium solution from Peierlsâ€“Nabarro model. Materials Science & Engineering A: Structural Materials: Properties, Microstructure and Processing, 2013, 582, 299-304.	2.6	8
14335	Ln3FeGaQ7: A new series of transition-metal rare-earth chalcogenides. Journal of Solid State Chemistry, 2013, 202, 269-275.	1.4	23
14336	Bonds, bands and elasticity of smithsonite rock. Solid State Communications, 2013, 166, 76-82.	0.9	15
14337	Synergetic effect of H and He with vacancy in vanadium solid from first-principles simulations. Nuclear Instruments & Methods in Physics Research B, 2013, 303, 75-80.	0.6	15
14338	Electronic and optical properties of S/I-codoped anatase TiO2 from ab initio calculations. Solid State Communications, 2013, 171, 17-21.	0.9	4
14339	Structural and electronic properties of nanoribbons: A first principles study. Solid State Communications, 2013, 175-176, 132-138.	0.9	16
14340	17O MAS NMR and first principles calculations of ZrO2 polymorphs. Chemical Physics Letters, 2013, 555, 96-100.	1.2	9
14341	Lattice dynamics and thermal properties of CaxMg1â^'xS ternary alloys. Computational Materials Science, 2013, 69, 148-152.	1.4	3
14342	First principles calculations of the agglomeration of Ti nanoparticles. Materials Letters, 2013, 104, 91-93.	1.3	4
14343	In situ study of the formation of rhenium borides from the elements atÂhigh-(p, T) conditions: Extreme incompressibility of Re7B3 and formation of new phases. Solid State Sciences, 2013, 25, 85-92.	1.5	6
14344	Electronic structure and magnetism of V-doped AlN. Journal of Magnetism and Magnetic Materials, 2013, 331, 117-121.	1.0	26
14345	Vacancies in ordered and disordered titanium monoxide: Mechanism of B1 structure stabilization. Journal of Solid State Chemistry, 2013, 204, 146-152.	1.4	32
14346	Ab initio theoretical and photoemission studies on formation of 4H-SiC(0001)/SiO2 interface. Applied Surface Science, 2013, 280, 500-503.	3.1	2

#	Article	IF	Citations
14347	Ab initio energetics of charge compensating point defects: A case study on MgO. Computational Materials Science, 2013, 73, 41-55.	1.4	10
14348	Effect of lattice anharmonicity in the structural phase transformation of Laves phase HfV2 alloy: A first-principles investigation. Acta Materialia, 2013, 61, 7473-7480.	3.8	3
14349	Dynamical stability of the lanthanum dihydride under high pressure: A density functional lattice dynamics approach. International Journal of Hydrogen Energy, 2013, 38, 4654-4663.	3.8	17
14350	Electronic, elastic and thermal properties of lutetium intermetallic compounds. Solid State Sciences, 2013, 18, 141-148.	1.5	6
14351	Density functional theory investigations of bismuth vanadate: Effect of hybrid functionals. Computational Materials Science, 2013, 74, 33-39.	1.4	28
14352	Theoretical study on the dissociative adsorption of CH4 on Pd-doped Ni surfaces. Chinese Journal of Catalysis, 2013, 34, 911-922.	6.9	32
14353	Modeling of crystal field and spin-Hamiltonian parameters for Ti3+:MgO. Physica B: Condensed Matter, 2013, 430, 64-66.	1.3	25
14354	Effect of the adsorption of ethylene carbonate on Si surfaces on the Li insertion behavior. Chemical Physics Letters, 2013, 585, 157-161.	1.2	2
14355	Rehybridization-induced defect-level of open-core edge dislocation in GaN. Scripta Materialia, 2013, 69, 537-540.	2.6	2
14356	Electronic structures and optical properties of GaN nanotubes with MgGaâ€“ON co-doping. Materials Chemistry and Physics, 2013, 138, 225-229.	2.0	10
14357	Ferromagnetism and antiferromagnetism in hydrogenated g-C3N4: A first-principles study. Physica B: Condensed Matter, 2013, 421, 46-49.	1.3	14
14358	A theoretical study of thorium titanium-based alloys. Journal of Nuclear Materials, 2013, 440, 229-235.	1.3	14
14359	First-principles thermodynamics of metal-oxide surfaces andinterfaces: A case study review. Transactions of Nonferrous Metals Society of China, 2013, 23, 180-192.	1.7	19
14360	Elastic, vibrational and thermodynamic properties of based group IV semiconductors and GeC under pressure. Journal of Physics and Chemistry of Solids, 2013, 74, 1615-1625.	1.9	16
14361	Nitrogen-tuned bonding mechanism of Li and Ti adatom embedded graphene. Journal of Solid State Chemistry, 2013, 205, 160-164.	1.4	7
14362	Comments on the paper â€œOn the nature of inhibition performance of imidazole on iron surfaceâ€•by J.O. Mendes, E.C. da Silva, A.B. Rocha. Corrosion Science, 2013, 68, 286-289.	3.0	7
14363	Investigation of thermal neutron scattering cross sections for LiH. Nuclear Engineering and Design, 2013, 262, 365-370.	0.8	14
14364	Study of structural, electronic and magnetic properties of Rh2MnX (X=Al, Ge and Sn) Heusler alloys using GGA-WC and GGA+U approaches. Physica B: Condensed Matter, 2013, 418, 58-64.	1.3	18

#	Article	IF	Citations
14365	Synergistic effects of codopants on photocatalytic O2 evolution in BiVO4. Solid State Sciences, 2013, 24, 79-84.	1.5	20
14366	Energy levels and deformation potentials for rocksalt MgO. Optik, 2013, 124, 2670-2673.	1.4	9
14367	Prediction of the site ordering behaviours of elements in C15 NbCr2-based intermetallics by combining thermodynamic model with ab-initio calculation. Intermetallics, 2013, 35, 104-109.	1.8	13
14368	First-principles study of Sc-doping effect on the stability, electronic structure and photocatalytic properties of Sr2TiO4. Thin Solid Films, 2013, 542, 276-280.	0.8	9
14369	Methanol adsorption and decomposition on <mml:math xmlns:mml="http://www.w3.org/1998/Math/MathML" altimg="si11.gif" overflow="scroll"><mml:mrow><mml:mtext>ZnO</mml:mtext><mml:mo stretchy="false">(</mml:mo><mml:mn>10</mml:mn><mml:mover) Tj ETQq0 0 0 rgBT /Overlock 10 Tf 50 577 Td (accent="true"><mml	2.1	12
14370	Vacancy trapping behaviors of oxygen in tungsten: A first-principles study. Journal of Nuclear Materials, 2013, 437, 6-10.	1.3	17
14371	Lithium storage in amorphous TiNi hydride: Electrode for rechargeable lithium-ion batteries. Materials Chemistry and Physics, 2013, 141, 348-354.	2.0	15
14372	Opening a large band gap for graphene by covalent addition. Chemical Physics Letters, 2013, 555, 1-6.	1.2	18
14373	Sr3B6O11F2: a promising polar fluoroborate with short UV absorption edge and moderate second harmonic generation response. Scripta Materialia, 2013, 69, 449-452.	2.6	25
14374	Half metal to insulator transition driven by electron doping in Ba2FeReO6. Journal of Magnetism and Magnetic Materials, 2013, 339, 163-167.	1.0	7
14375	Pd/Au(100) alloy for vinyl acetate synthesis: Effects of surface properties on reagents adsorption. Computational and Theoretical Chemistry, 2013, 1019, 33-38.	1.1	12
14376	Na adsorption on SrTiO3 (0 0 1) surface and its interaction with water: A DFT calculation. Applied Surface Science, 2013, 270, 359-363.	3.1	6
14377	Energetic prediction of Mg2Siâ€“Ca2Si pseudobinary system using first-principles calculations. Journal of Alloys and Compounds, 2013, 558, 179-187.	2.8	13
14378	Structure-sensitivity of ethane hydrogenolysis over molybdenum carbides: A density functional theory study. Applied Surface Science, 2013, 276, 369-376.	3.1	12
14379	Adsorption and dissociation of methanol on defective rutile TiO2 (110) surface with bridging oxygen-vacancy pairs. Chemical Physics Letters, 2013, 584, 98-102.	1.2	5
14380	Investigating permeation and transport of H isotopes in tungsten by first-principles. Fusion Engineering and Design, 2013, 88, 368-373.	1.0	16
14381	Investigation of bonding within ab initio models of GeAsSe glasses. Chemical Physics Letters, 2013, 575, 97-100.	1.2	3
14382	Interactions of foreign interstitial and substitutional atoms in bcc iron from ab initio calculations. Physica B: Condensed Matter, 2013, 417, 57-69.	1.3	13

#	Article	IF	Citations
14383	Structural, electronic and magnetic properties of Ï‡-carbides Fe5â^'xMnxC2 (xÂ=Â1â€“5) from density-functional theory calculations. Solid State Sciences, 2013, 26, 110-114.	1.5	5
14384	Structural transformation of sputtered o-LiMnO2 thin-film cathodes induced by electrochemical cycling. Thin Solid Films, 2013, 549, 263-267.	0.8	8
14385	Density functional theory study on configurations and electronic properties of periodic nanoridges. Computational Materials Science, 2013, 77, 312-315.	1.4	1
14386	First principle study of valence-band offsets at AlN/diamond heterojunctions. Diamond and Related Materials, 2013, 31, 25-29.	1.8	15
14387	Coronal multi-walled silicon nanotubes. Journal of Energy Chemistry, 2013, 22, 408-412.	7.1	12
14388	First principles calculations of the electronic structure and optical properties of (001), (011) and (111) Ga0.5Al0.5As surfaces. Materials Science in Semiconductor Processing, 2013, 16, 1813-1820.	1.9	11
14389	The detailed geometrical and electronic structures of monoclinic zirconia. Journal of Physics and Chemistry of Solids, 2013, 74, 518-523.	1.9	24
14390	Ab initio static and molecular dynamics studies of helium behavior in beryllium. Journal of Nuclear Materials, 2013, 442, S694-S698.	1.3	16
14391	Density functional theory studies of Yb-, Ca- and Sr-substituted Mg2NiH4 hydrides. Computational Materials Science, 2013, 74, 55-64.	1.4	15
14392	Theoretical study of the Fluorine doped anatase surfaces. Surface Science, 2013, 618, 154-158.	0.8	25
14393	Crystal growth of lead carbonates: Influence of the medium and relationship between structure and habit. Journal of Crystal Growth, 2013, 376, 1-10.	0.7	24
14394	high activation energy for proton migration at <mml:math xmlns:mml="http://www.w3.org/1998/Math/MathML" altimg="si6.gif" overflow="scroll"><mml:mstyle displaystyle="true"><mml:mo>â^'</mml:mo><mml:mrow><mml:mn>3</mml:mn><mml:mfenced open="(") Tj ETQq1 1 0.784314 rgB open="[" close="]"><mml:mrow><mml:mn>1</mml:mn><mml:mover accent="true"><mml:mn>1</mml:mn><mml:mo stretchy="true">~</mml:mo></mml:mover></mml:mrow>	1.3	14
14395	Effects of interfacial structure and polarity on charge transfer between carbonaceous nanomaterials and rutile (110) surface. Computational Materials Science, 2013, 69, 180-185.	1.4	4
14396	Elastic and electronic properties of Ce2O3 from first principles. Journal of Alloys and Compounds, 2013, 551, 672-676.	2.8	13
14397	First-principle study of amorphous SiZnSnO thin-film transistor with excellent stability. Thin Solid Films, 2013, 534, 609-613.	0.8	29
14398	Effects of Li and Na intercalation on electronic, bonding and thermoelectric transport properties of MX2 (M=Ta; X=S or Se) dichalcogenides â€“ Ab initio investigation. Journal of Alloys and Compounds, 2013, 581, 731-740.	2.8	19
14399	Ab initio study of ã€^111ã€‰ {110} superdislocation properties in B2-MgRE (RE=Laâ€“Er) intermetallics. Computational Materials Science, 2013, 69, 168-172.	1.4	5
14400	Tuning the spin dependent behavior of monatomic carbon wires between nickel electrodes. Physics Letters, Section A: General, Atomic and Solid State Physics, 2013, 377, 1766-1773.	0.9	15

#	Article	IF	Citations
14401	Magnetic ordering and electron correlation of iron-based superconductor (Ca3Al2O5â^'x)(Fe2As2) from first-principles study. Solid State Communications, 2013, 172, 41-48.	0.9	0
14402	Effect of carbon on helium trapping in tungsten: A first-principles investigation. Journal of Nuclear Materials, 2013, 440, 338-343.	1.3	16
14403	Effect of cation ordering on the electronic and lattice dynamic properties of Ag2CdGeS4 polytypes: First-principle calculation. Journal of Solid State Chemistry, 2013, 201, 48-55.	1.4	6
14404	K2FeGe3Se8: A New Antiferromagnetic Iron Selenide. Inorganic Chemistry, 2013, 52, 2022-2028.	1.9	24
14405	Synthesis, Structure, and Characterization of Two New Polar Sodium Tungsten Selenites: Na₂(WO₃)₃(SeO₃)Â·2H₂O and Na₆(W₆O₁₉)(SeO₃)₂. Inorganic Chemistry, 2013, 52, 2637-2647.	1.9	44
14406	Electrically driven octahedral rotations in SrTiO3and PbTiO3. Physical Review B, 2013, 87, .	1.1	16
14407	Topological states ruled by stacking faults in Bi2Se3 and Bi2Te3. Journal of Applied Physics, 2013, 113, 023705.	1.1	21
14408	Programming Hierarchical Supramolecular Nanostructures by Molecular Design. Journal of Physical Chemistry C, 2013, 117, 3440-3445.	1.5	20
14409	Anharmonic vibrations of the carboxyl group in acetic acid on TiO2: implications for adsorption mode assignment in dye-sensitized solar cells. Physical Chemistry Chemical Physics, 2013, 15, 10028.	1.3	24
14410	Powder crystallography of pharmaceutical materials by combined crystal structure prediction and solid-state 1H NMR spectroscopy. Physical Chemistry Chemical Physics, 2013, 15, 8069.	1.3	155
14411	Methane dehydrogenation on Au/Ni surface alloys â€“ a first-principles study. Catalysis Science and Technology, 2013, 3, 1343.	2.1	36
14412	Decomposition and Oxidation of Methanol on Ir(111): A First-Principles Study. Journal of Physical Chemistry C, 2013, 117, 4574-4584.	1.5	23
14413	Molecular Doping and Band-Gap Opening of Bilayer Graphene. ACS Nano, 2013, 7, 2790-2799.	7.3	120
14414	Structural, electronic and dynamical stability of heavy metal iron pernitride: a spin polarized first-principles study. European Physical Journal B, 2013, 86, 1.	0.6	9
14415	Structural, elastic, electronic and dynamical properties of Ba2MgWO6 double perovskite under pressure from first principles. European Physical Journal B, 2013, 86, 1.	0.6	19
14416	Spin-polarized transport in zigzag graphene nanoribbons adsorbing nonmagnetic atomic chain. European Physical Journal B, 2013, 86, 1.	0.6	6
14417	Electrochemical water splitting by gold: evidence for an oxide decomposition mechanism. Chemical Science, 2013, 4, 2334.	3.7	229
14418	Effect of chemical doping of boron and nitrogen on the electronic, optical, and electrochemical properties of carbon nanotubes. Progress in Materials Science, 2013, 58, 565-635.	16.0	276

#	Article	IF	Citations
14419	Phase transition and thermodynamic properties of BiFeO₃from first-principles calculations. Chinese Physics B, 2013, 22, 037101.	0.7	24
14420	Thermoelectric performance of MX2 (Mâ€‰=â€‰Mo,W; Xâ€‰=â€‰S,Se) monolayers. Journal of Applied Physics, 2013, 113, .	1.1	202
14421	Modelling the electronic structure and magnetic properties of LiFeAs and FeSe using hybrid-exchange density functional theory. Solid State Communications, 2013, 161, 23-28.	0.9	6
14422	Stable p- and n-type doping of few-layer graphene/graphite. Carbon, 2013, 57, 507-514.	5.4	42
14423	Tunable electronic and dielectric behavior of GaS and GaSe monolayers. Physical Chemistry Chemical Physics, 2013, 15, 7098.	1.3	182
14424	Coke-Tolerant Ni/BaCe_{1â€“x}Y_xO_{3â^Î´} Anodes for Solid Oxide Fuel Cells: DFT+U Study. Journal of Physical Chemistry C, 2013, 117, 7086-7096.	1.5	26
14425	Compensation in Al-Doped ZnO by Al-Related Acceptor Complexes: Synchrotron X-Ray Absorption Spectroscopy and Theory. Physical Review Letters, 2013, 110, 055502.	2.9	92
14426	Superlattices of Fluorinated Interlayer-Bonded Domains in Twisted Bilayer Graphene. Journal of Physical Chemistry C, 2013, 117, 7315-7325.	1.5	41
14427	Attractive forces between ions in quantum plasmas: Failure of linearized quantum hydrodynamics. Physical Review E, 2013, 87, .	0.8	53
14428	A growth mechanism for graphene deposited on polycrystalline Co film by plasma enhanced chemical vapor deposition. New Journal of Chemistry, 2013, 37, 1616.	1.4	23
14429	Structural, Spectroscopic, and Electronic Properties of Cubic G0-Rb₂KTiOF₅ Oxyfluoride. Journal of Physical Chemistry C, 2013, 117, 7269-7278.	1.5	38
14430	The stability of alloying additions in Zirconium. Journal of Nuclear Materials, 2013, 437, 122-129.	1.3	43
14431	Structural and elastic properties of orthorhombic CaGeO3 under pressure from first principles. Physica B: Condensed Matter, 2013, 411, 81-87.	1.3	7
14432	Pressure-Induced Polymorphic Transitions in Crystalline Diborane Deduced by Comparison of Simulated and Experimental Vibrational Spectra. Journal of Physical Chemistry C, 2013, 117, 2210-2215.	1.5	27
14433	Quasiparticle band structure of rocksalt-CdO determined using maximally localized Wannier functions. Journal of Physics Condensed Matter, 2013, 25, 035501.	0.7	6
14434	A combination of multiple chromophores enhances second-harmonic generation in a nonpolar noncentrosymmetric oxide: CdTeMoO6. Journal of Materials Chemistry C, 2013, 1, 2906.	2.7	67
14435	Atomistic Modeling of Warm Dense Matter in the Twoâ€Temperature State. Contributions To Plasma Physics, 2013, 53, 129-139.	0.5	52
14436	Mechanism for the<mml:math xmlns:mml="http://www.w3.org/1998/Math/MathML" display="inline"><mml:mrow><mml:mi>Î±</mml:mi><mml:mo>â†’</mml:mo><mml:mi>Îµ</mml:mi></mml:mrow></mml:math>phase transition in iron. Physical Review B, 2013, 87, .	1.1	84

#	Article	IF	Citations
14437	First-Principles Study of Electronic, Elastic, and Lattice Vibrational Properties of Pbnm Orthorhombic SrHfO3. Journal of Electronic Materials, 2013, 42, 993-998.	1.0	5
14438	Effect of tin on point defects and oxygen precipitation in Czochralski silicon: Experimental and theoretical studies. Journal of Applied Physics, 2013, 113, .	1.1	36
14439	CO oxidation on h-BN supported Au atom. Journal of Chemical Physics, 2013, 138, 034701.	1.2	71
14440	Two-Dimensional Carbon Compounds Derived from Graphyne with Chemical Properties Superior to Those of Graphene. Scientific Reports, 2013, 3, 1271.	1.6	36
14441	Effects of Ga concentration on electronic and optical properties of Ga-doped ZnO from first principles calculations. Optical Materials, 2013, 35, 509-515.	1.7	80
14442	The role of impurity oxygen in hydrogen bubble nucleation in tungsten. Journal of Nuclear Materials, 2013, 433, 357-363.	1.3	45
14443	The surface states of lithium tetraborate. Journal of Physics Condensed Matter, 2013, 25, 045014.	0.7	2
14444	Sulfur- and Oxygen-Induced Alterations of the Iron (001) Surface Magnetism and Work Function: A Theoretical Study. Journal of Physical Chemistry C, 2013, 117, 6161-6171.	1.5	17
14445	Defect-induced room temperature ferromagnetism in B-doped ZnO. Ceramics International, 2013, 39, 4609-4617.	2.3	30
14446	Phonon frequencies of tetragonally strained PbTiO₃from first principles. Phase Transitions, 2013, 86, 200-205.	0.6	4
14447	A novel BiOCl thin film prepared by electrochemical method and its application in photocatalysis. Applied Catalysis B: Environmental, 2013, 132-133, 332-341.	10.8	156
14448	Metastable Cu(I)-Niobate Semiconductor with a Low-Temperature, Nanoparticle-Mediated Synthesis. ACS Nano, 2013, 7, 1699-1708.	7.3	43
14449	A Computational Study of the Interfacial Structure and Capacitance of Graphene in [BMIM][PF₆] Ionic Liquid. Journal of the Electrochemical Society, 2013, 160, A1-A10.	1.3	229
14450	Mechanism of linear and nonlinear optical properties of bis-thiourea cadmium chloride single crystal. Physica B: Condensed Matter, 2013, 408, 175-182.	1.3	8
14451	The behavior of oxygen in liquid leadâ€“bismuth eutectic. Journal of Nuclear Materials, 2013, 437, 62-65.	1.3	16
14452	Electronic structure of Î±-SrB₄O₇: experiment and theory. Journal of Physics Condensed Matter, 2013, 25, 085503.	0.7	24
14453	Electronic and optical properties of cadmium fluoride: The role of many-body effects. Physical Review B, 2013, 87, .	1.1	20
14454	Strain-induced topological insulator phase transition in HgSe. Physical Review B, 2013, 87, .	1.1	33

#	Article	IF	Citations
14455	Hyperfine interactions at nitrogen interstitial defects in diamond. Journal of Physics Condensed Matter, 2013, 25, 065802.	0.7	3
14456	Systematic study on the electronic structure and mechanical properties of X₂BC (X = Mo,) Tj ETQq1 1 0.784314 rgBT /Ov	0.7	45
14457	Insight into the initial oxidation of 4<mml:math xmlns:mml="http://www.w3.org/1998/Math/MathML" display="inline"><mml:mi>H</mml:mi></mml:math>-SiC from first-principles thermodynamics. Physical Review B, 2013, 87, .	1.1	15
14458	[illegible] and ferromagnetism in layered<mml:math xmlns:mml="http://www.w3.org/1998/Math/MathML" display="inline"><mml:mrow><mml:mn>1</mml:mn><mml:mi>T</mml:mi></mml:mrow></mml:math>-CrSe<mml:math xmlns:mml="http://www.w3.org/1998/Math/MathML" display="inline"><mml:msub><mml:mrow [illegible] Physical Review B, 2013,	1.1	32
14459	Effect of substitutional doping on the NÃ©el temperature of<mml:math xmlns:mml="http://www.w3.org/1998/Math/MathML" display="inline"><mml:mrow><mml:msub><mml:mi mathvariant="bold">Cr</mml:mi><mml:mn mathvariant="bold">2</mml:mn></mml:msub><mml:msub><mml:mi mathvariant="bold">O</mml:mi><mml:mn mathvariant="bold">3</mml:mn></mml:msub></mml:mrow></mml:math>. Physical Review B, 2013, 87, .	1.1	51
14460	Two-dimensional carbon allotrope with strong electronic anisotropy. Physical Review B, 2013, 87, .	1.1	108
14461	H<mml:math xmlns:mml="http://www.w3.org/1998/Math/MathML" display="inline"><mml:msub><mml:mrow /><mml:mn mathvariant="bold">4</mml:mn></mml:msub></mml:math>O and other hydrogen-oxygen compounds at giant-planet core pressures. Physical Review B, 2013, 87, .	1.1	18
14462	First-principles investigation of incipient ferroelectric trends of rutile TiO2in bulk and at the (110) surface. Physical Review B, 2013, 87, .	1.1	16
14463	Solid state adaptive natural density partitioning: a tool for deciphering multi-center bonding in periodic systems. Physical Chemistry Chemical Physics, 2013, 15, 5022.	1.3	143
14464	Structural, Electronic, and Ferroelectric Properties of Compressed CdPbO₃ Polymorphs. Inorganic Chemistry, 2013, 52, 1032-1039.	1.9	14
14465	Twoâ€Đimensional CdSe Nanosheets and their Interaction with Stabilizing Ligands. Advanced Materials, 2013, 25, 261-266.	11.1	39
14466	High Surface Reactivity and Water Adsorption on NiFe₂O₄ (111) Surfaces. Journal of Physical Chemistry C, 2013, 117, 5678-5683.	1.5	52
14467	Structural and electronic properties of atomic oxygen adsorption on Cu(111) surface: A first-principles investigation. Science China: Physics, Mechanics and Astronomy, 2013, 56, 573-580.	2.0	9
14468	Chemical Expansion and Change in Lattice Constant of Yâ€Đoped <scp><scp>BaZrO</scp></scp>₃ by Hydration/Dehydration Reaction and Final Heatâ€Treating Temperature. Journal of the American Ceramic Society, 2013, 96, 879-884.	1.9	65
14470	n-Diamond: Dynamical stability of proposed structures. Diamond and Related Materials, 2013, 34, 60-64.	1.8	12
14471	Phonon softening and direct to indirect band gap crossover in strained single-layer MoSe<mml:math xmlns:mml="http://www.w3.org/1998/Math/MathML" display="inline"><mml:msub><mml:mrow /><mml:mn>2</mml:mn></mml:msub></mml:math>. Physical Review B, 2013, 87, .	1.1	200
14472	DFT-assisted structure determination of Î±1- and Î±2-VOPO4: new insights into the understanding of the catalytic performances of vanadium phosphates. Dalton Transactions, 2013, 42, 8124.	1.6	16
14473	Efficient electron and hole doping in compositionally abrupt Si/Ge nanowires. Nanoscale, 2013, 5, 3880.	2.8	1

#	Article	IF	Citations
14474	Structure and thermodynamic studies of the LaMgNi4 compound and its hydrides by density functional theory. Intermetallics, 2013, 38, 30-35.	1.8	15
14475	New insight into the structure of saturated chlorine layer on Ag(111): LT-STM and DFT study. Applied Surface Science, 2013, 267, 21-25.	3.1	10
14476	Multilayer Graphynes for Lithium Ion Battery Anode. Journal of Physical Chemistry C, 2013, 117, 6919-6923.	1.5	189
14477	Cage-Forming Compounds in the Baâ€“Rhâ€“Ge System: From Thermoelectrics to Superconductivity. Inorganic Chemistry, 2013, 52, 931-943.	1.9	20
14478	Role of Magnetism in Catalysis: RuO₂ (110) Surface. Journal of Physical Chemistry C, 2013, 117, 6353-6357.	1.5	98
14479	Ab initiostudy of boron in<mml:math xmlns:mml="http://www.w3.org/1998/Math/MathML" display="inline"><mml:mi>Î±</mml:mi></mml:math>-iron: Migration barriers and interaction with point defects. Physical Review B, 2013, 87, .	1.1	29
14480	Evolution of ac Conductivity in Nonequilibrium Warm Dense Gold. Physical Review Letters, 2013, 110, 135001.	2.9	84
14481	Investigations of Structural, Electronic, and Half-metallic Ferromagnetic Properties in (Al, Ga, In)1â^'x M x N (M = Fe, Mn) Diluted Magnetic Semiconductors. Journal of Superconductivity and Novel Magnetism, 2013, 26, 515-525.	0.8	41
14482	Density Functional Theory Study of an Oxygen Reduction Reaction on a Pt₃Ti Alloy Electrocatalyst. Journal of Physical Chemistry C, 2013, 117, 7107-7113.	1.5	61
14483	Is there a Difference in Van Der Waals Interactions between Rare Gas Atoms Adsorbed on Metallic and Semiconducting Single-Walled Carbon Nanotubes?. Physical Review Letters, 2013, 110, 135503.	2.9	19
14484	Synthesis, Crystal Structure, and Solid-State NMR Investigations of Heteronuclear Zn/Co Coordination Networks â€" A Comparative Study. Inorganic Chemistry, 2013, 52, 4431-4442.	1.9	17
14485	Crystal Chemistry, Band Engineering, and Photocatalytic Activity of the LiNb₃O₈â€“CuNb₃O₈ Solid Solution. Inorganic Chemistry, 2013, 52, 4443-4450.	1.9	62
14486	Negative differential resistance and spin polarization of metal-C6H6multidecker complexes. Journal of Applied Physics, 2013, 113, 113901.	1.1	3
14487	Ca<mml:math xmlns:mml="http://www.w3.org/1998/Math/MathML" display="inline"><mml:msub><mml:mrow /><mml:mn>2</mml:mn></mml:msub></mml:math>Zn(Sn,Ge)Se<mml:math xmlns:mml="http://www.w3.org/1998/Math/MathML" display="inline"><mml:msub><mml:mrow /><mml:mn>4</mml:mn></mml:msub></mml:math>and Cu<mml:math xmlns:mml="http://www.w3.org/1998/Math/MathML" display="inline"><mml:msub><mml:mrow	1.1	90
14488	First-principles study on the geometric and electronic structures and phase transition of PbZr_{1â^'x}Ti_xO₃solid solutions. Chinese Physics B, 2013, 22, 017702.	0.7	6
14489	Chemical trends of magnetic interaction in Mn-doped III-V semiconductors. Applied Physics Letters, 2013, 102, 122409.	1.5	10
14490	Improved multiferroic behavior in [111]-oriented BiFeO3/BiAlO3 superlattice. Journal of Applied Physics, 2013, 113, 123703.	1.1	10
14491	Structural stability of Cr-related defect complex in diamond for single photon sources: A first-principles study. Journal of Applied Physics, 2013, 113, .	1.1	6

#	Article	IF	Citations
14492	Self-organized chromium oxide monolayers on Fe(001). Physical Review B, 2013, 87, .	1.1	25
14493	First principles studies of the self trapped hole and the fluorine adsorption on the SrF2(111) surface. Computational Materials Science, 2013, 73, 9-14.	1.4	3
14494	First-principles study of structural, electronic, optical and bonding properties of celestine, SrSO4. Solid State Communications, 2013, 158, 5-8.	0.9	15
14495	Effect of nitrogen induced defects in Li dispersed graphene onÂhydrogen storage. International Journal of Hydrogen Energy, 2013, 38, 4611-4617.	3.8	59
14496	First principles calculations of (Ba,Sr)(Co,Fe)O3â^Î´ structural stability. Solid State Ionics, 2013, 230, 21-26.	1.3	18
14497	Atomistic structures and phase transition of In2Se3 nanowires studied by DFT calculations and synchrotron radiation X-ray diffraction. Solid State Communications, 2013, 162, 28-33.	0.9	4
14498	Structural and electronic properties of BaCrO4 at high-pressures. Solid State Communications, 2013, 155, 45-48.	0.9	3
14499	Hybridization of Surface Waves with Organic Adlayer Librations: A Helium Atom Scattering and Density Functional Perturbation Theory Study of Methyl-Si(111). Physical Review Letters, 2013, 110, 156102.	2.9	13
14500	An updated thermodynamic modeling of the Gaâ€“Ti system. Calphad: Computer Coupling of Phase Diagrams and Thermochemistry, 2013, 41, 140-149.	0.7	4
14501	Elastic modulus, optical phonon modes and polaron properties in Al1â^'xBxN alloys. Current Applied Physics, 2013, 13, 493-499.	1.1	13
14502	Structure of Monomeric Chromium(VI) Oxide Species Supported on Silica: Periodic and Cluster DFT Studies. Journal of Physical Chemistry C, 2013, 117, 8138-8149.	1.5	63
14503	Cesium stability in a typical mica structure in dry and wet environments from first-principles. Geochimica Et Cosmochimica Acta, 2013, 109, 62-73.	1.6	11
14504	Electronic states of intrinsic surface and bulk vacancies in FeS₂. Journal of Physics Condensed Matter, 2013, 25, 045004.	0.7	35
14505	Point defect engineering strategies to retard phosphorous diffusion in germanium. Physical Chemistry Chemical Physics, 2013, 15, 367-371.	1.3	28
14506	Electronic, Thermal, and Structural Properties of Graphene Oxide Frameworks. Journal of Physical Chemistry C, 2013, 117, 8276-8281.	1.5	26
14507	Mechanical instability and ideal strengths of layered M2SC (Mâ€‰=â€‰Ti, Zr, and Hf) compounds. Journal of Applied Physics, 2013, 113, .	1.1	10
14508	First-principles study of structure and properties of Ï‰-Ti2Zr. Computational Materials Science, 2013, 74, 129-137.	1.4	8
14509	A Beaded-String Silicon Anode. ACS Nano, 2013, 7, 2717-2724.	7.3	68

#	Article	IF	Citations
14510	Accommodation of Lattice Mismatch in a Thiol Self-Assembled Monolayer. Journal of Physical Chemistry C, 2013, 117, 4647-4656.	1.5	6
14511	Ab initioanalysis of the defect structure of ceria. Physical Review B, 2013, 87, .	1.1	125
14512	Development of a bond-valence based interatomic potential for BiFeO₃for accurate molecular dynamics simulations. Journal of Physics Condensed Matter, 2013, 25, 102202.	0.7	47
14513	The relation between adsorption bonding and corrosion inhibition of azole molecules on copper. Corrosion Science, 2013, 73, 7-17.	3.0	90
14514	Catalyzed Rehydrogenation of NaAlH₄: Ti and Friends Are Active on NaH Surfaces; Pt and Friends Are Not. Journal of Physical Chemistry C, 2013, 117, 8150-8155.	1.5	5
14515	Tunable topological electronic structures in Sb(111) bilayers: A first-principles study. Applied Physics Letters, 2013, 102, .	1.5	107
14516	Electronic and magnetic properties of double perovskite slab-rocksalt layer rare earth strontium aluminates natural superlattice structure. Journal of Applied Physics, 2013, 113, .	1.1	10
14517	Does Dispersion Dominate over H-Bonds in Drugâ€“Surface Interactions? The Case of Silica-Based Materials As Excipients and Drug-Delivery Agents. Journal of Chemical Theory and Computation, 2013, 9, 2404-2415.	2.3	72
14518	Adsorption capacity of H2O, NH3, CO, and NO2 on the pristine graphene. Journal of Applied Physics, 2013, 113, .	1.1	80
14519	Plasmonic Harvesting of Light Energy for Suzuki Coupling Reactions. Journal of the American Chemical Society, 2013, 135, 5588-5601.	6.6	597
14520	Density-functional study of perovskite-type hydride LiNiH<mml:math xmlns:mml="http://www.w3.org/1998/Math/MathML" display="inline"><mml:msub><mml:mrow /><mml:mn>3</mml:mn></mml:msub></mml:math>and its synthesis: Mechanism for formation of metallic perovskite. Physical Review B, 2013, 87, .	1.1	18
14521	Multi-scale modeling and synthesis of polyester ionomers. Physical Chemistry Chemical Physics, 2013, 15, 6128.	1.3	11
14522	Enhanced hydrogen storage properties under external electric fields of N-doped graphene with Li decoration. Physical Chemistry Chemical Physics, 2013, 15, 3243.	1.3	29
14523	Density Functional Theory study of electric field effects on CO and OH adsorption and co-adsorption on gold surfaces. Electrochimica Acta, 2013, 101, 244-253.	2.6	35
14524	Anomalous Manganese Activation of a Pyrophosphate Cathode in Sodium Ion Batteries: A Combined Experimental and Theoretical Study. Journal of the American Chemical Society, 2013, 135, 2787-2792.	6.6	165
14525	Chemisorption of hydrogen on Fe clusters through hybrid bonding mechanisms. Applied Physics Letters, 2013, 102, 113108.	1.5	22
14526	Insights into the adsorption and energy transfer of Ag clusters on the AgCl(100) surface. Physical Chemistry Chemical Physics, 2013, 15, 8722.	1.3	48
14527	Flexural Electromechanical Coupling: A Nanoscale Emergent Property of Boron Nitride Bilayers. Nano Letters, 2013, 13, 1681-1686.	4.5	75

#	Article	IF	Citations
14528	New form of polymeric nitrogen from dynamic shock simulation. Journal of Chemical Physics, 2013, 138, 054503.	1.2	9
14529	Structural, elastic, electronic and lattice dynamical properties of III-P quaternary alloys matched to AlP. Materials Science in Semiconductor Processing, 2013, 16, 718-726.	1.9	34
14530	Structural and electronic properties of ultrathin copper nanowires: A density-functional theory study. Physica B: Condensed Matter, 2013, 410, 105-111.	1.3	11
14531	First-principles study on the structural stability and electronic properties of AlN/GaN heterostructure nanoribbons. Superlattices and Microstructures, 2013, 57, 37-43.	1.4	2
14532	Structural, elastic, electronic and optical properties of beryllium chalcogenides BeX (X=S, Se, Te) with zinc-blende structure. Journal of Alloys and Compounds, 2013, 561, 16-22.	2.8	35
14533	Adsorption of beryllium atoms and clusters both on graphene and in a bilayer of graphite investigated by DFT. Journal of Physics Condensed Matter, 2013, 25, 015002.	0.7	13
14534	Electronic structure and vibrational entropies of fcc Au-Fe alloys. Physical Review B, 2013, 87, .	1.1	16
14535	Surface Defects: Possible Source of Room Temperature Ferromagnetism in Co-Doped ZnO Nanorods. Journal of Physical Chemistry C, 2013, 117, 8968-8973.	1.5	42
14536	First-principles simulations of iron with nitrogen: from surface adsorption to bulk diffusion. Modelling and Simulation in Materials Science and Engineering, 2013, 21, 045004.	0.8	14
14537	Role of Interface in the Lithiation of Silicon-Graphene Composites: A First Principles Study. Journal of Physical Chemistry C, 2013, 117, 9598-9604.	1.5	36
14538	Imogolite-like nanotubes: structure, stability, electronic and mechanical properties of the phosphorous and arsenic derivatives. Physical Chemistry Chemical Physics, 2013, 15, 4303.	1.3	25
14539	Effect of pressure on structural phase transition and elastic properties in NiSi. High Pressure Research, 2013, 33, 15-26.	0.4	4
14540	Stability and strength of covalent crystals under uniaxial and triaxial loading from first principles. Journal of Physics Condensed Matter, 2013, 25, 035401.	0.7	11
14541	Density Functional Study of the First Wetting Layer on the GaN (0001) Surface. Journal of Physical Chemistry C, 2013, 117, 8774-8783.	1.5	28
14542	Adsorption and Diffusion of Oxygen on Single-Layer Graphene with Topological Defects. Journal of Physical Chemistry C, 2013, 117, 10366-10374.	1.5	79
14543	DFT study on the reaction of O2 dissociation catalyzed by gold surfaces doped with transition metal atoms. Applied Catalysis A: General, 2013, 458, 90-102.	2.2	23
14544	Structural Stability and Electronic and Magnetic Properties of Fluorinated Bilayer Graphene. Journal of Physical Chemistry C, 2013, 117, 3572-3579.	1.5	38
14545	Novel half-metal and spin gapless semiconductor properties in N-doped silicene nanoribbons. Journal of Applied Physics, 2013, 113, .	1.1	37

#	Article	IF	Citations
14546	Ab initio study on structural stability of uranium carbide. Journal of Nuclear Materials, 2013, 437, 81-86.	1.3	21
14547	Destabilisation of hydrogen bonding and the phase stability of aniline at high pressure. CrystEngComm, 2013, 15, 1047-1060.	1.3	41
14548	He, Kr and Xe diffusion in ZrN â€“ An atomic scale study. Journal of Nuclear Materials, 2013, 438, 7-14.	1.3	12
14549	Nitrogen: unraveling the secret to stable carbon-supported Pt-alloy electrocatalysts. Energy and Environmental Science, 2013, 6, 2957.	15.6	99
14550	Interaction and electronic structures of oxygen divacancy in HfO₂. Physica Status Solidi (B): Basic Research, 2013, 250, 352-355.	0.7	16
14551	Carrier Mobility in Graphyne Should Be Even Larger than That in Graphene: A Theoretical Prediction. Journal of Physical Chemistry Letters, 2013, 4, 1443-1448.	2.1	328
14552	Understanding the Electronic Structures of Graphene Quantum Dot Physisorption and Chemisorption onto the TiO₂ (110) Surface: A Firstâ€Principles Calculation. ChemPhysChem, 2013, 14, 579-582.	1.0	36
14553	ElaStic: A tool for calculating second-order elastic constants from first principles. Computer Physics Communications, 2013, 184, 1861-1873.	3.0	362
14554	A General Protocol for Determining the Structures of Molecularly Ordered but Noncrystalline Silicate Frameworks. Journal of the American Chemical Society, 2013, 135, 5641-5655.	6.6	70
14555	Bandgap opening in Janus-type mosaic graphene. Journal of Applied Physics, 2013, 113, .	1.1	25
14556	Electronic structure of Zn doped Ga0.5Al0.5As photocathodes from first-principles. Solid State Communications, 2013, 164, 50-53.	0.9	7
14557	Electronic properties of the MoS<mml:math xmlns:mml="http://www.w3.org/1998/Math/MathML" display="inline"><mml:msub><mml:mrow /><mml:mn>2</mml:mn></mml:msub></mml:math>-WS<mml:math xmlns:mml="http://www.w3.org/1998/Math/MathML" display="inline"><mml:msub><mml:mrow /><mml:mn>2</mml:mn></mml:msub></mml:math>heterojunction. Physical Review B, 2013, 87, .	1.1	424
14558	Growth of carbon structured over Pd, Pt and Ni: A comparative DFT study. Applied Surface Science, 2013, 268, 11-15.	3.1	2
14559	A Systematic Investigation of p-Nitrophenol Reduction by Bimetallic Dendrimer Encapsulated Nanoparticles. Journal of Physical Chemistry C, 2013, 117, 7598-7604.	1.5	349
14560	Pressure-Induced Stabilization and Insulator-Superconductor Transition of BH. Physical Review Letters, 2013, 110, 165504.	2.9	76
14561	Computational discovery of single-layer III-V materials. Physical Review B, 2013, 87, .	1.1	318
14562	A study of the electronic structures and optical properties of CuXTe2 (X = Al, Ga, In) ternary semiconductors. Computational and Theoretical Chemistry, 2013, 1010, 67-72.	1.1	24
14563	Borocarbonitrides, BxCyNz. Journal of Materials Chemistry A, 2013, 1, 5806.	5.2	143

#	Article	IF	Citations
14564	Surface structure and equilibrium particle shape of the LiMn<mml:math xmlns:mml="http://www.w3.org/1998/Math/MathML" display="inline"><mml:msub><mml:mrow /><mml:mn>2</mml:mn></mml:msub></mml:math>O<mml:math xmlns:mml="http://www.w3.org/1998/Math/MathML" display="inline"><mml:msub><mml:mrow /><mml:mn>4</mml:mn></mml:msub></mml:math>spinel from first-principles calculations. Physical Review B, 2013, 87, .	1.1	116
14565	Structure, Stability, and Property Modulations of Stoichiometric Graphene Oxide. Journal of Physical Chemistry C, 2013, 117, 1064-1070.	1.5	22
14566	The contribution made by lattice vacancies to the Wigner effect in radiation-damaged graphite. Journal of Physics Condensed Matter, 2013, 25, 135403.	0.7	37
14567	Single crystalline ultrathin gold nanowires: Promising nanoscale interconnects. AIP Advances, 2013, 3, .	0.6	25
14568	Hydrogen behaviors in molybdenum and tungsten and a generic vacancy trapping mechanism for H bubble formation. Journal of Nuclear Materials, 2013, 434, 395-401.	1.3	74
14569	Structural and Electronic Properties of Carbon Nanotubes and Graphenes Functionalized with Cyclopentadienylâ€“Transition Metal Complexes: A DFT Study. Journal of Physical Chemistry C, 2013, 117, 8758-8766.	1.5	20
14570	In silicooptimization of phase-change materials for digital memories: a survey of first-row transition-metal dopants for Ge₂Sb₂Te₅. Journal of Physics Condensed Matter, 2013, 25, 205801.	0.7	21
14571	Crystal growth and electronic properties of a 3D Rashba material, BiTeI, with adjusted carrier concentrations. Journal of Physics Condensed Matter, 2013, 25, 135801.	0.7	18
14572	First-principles study of layered antiferromagnetic CuCrX₂(X = S, Se and Te). Journal of Physics Condensed Matter, 2013, 25, 105504.	0.7	15
14573	Investigations of the Very Short Hydrogen Bond in the Crystal of Nitromalonamide via Carâ€“Parrinello and Path Integral Molecular Dynamics. Journal of Physical Chemistry B, 2013, 117, 5430-5440.	1.2	23
14574	Ab initio investigation on the highâ€temperature thermodynamic properties of Fe³⁺â€bearing MgSiO₃ perovskite. Journal of Geophysical Research: Solid Earth, 2013, 118, 83-91.	1.4	29
14575	Phase equilibria of (Mg,Fe)2SiO4 at the Earthâ€™s upper mantle conditions from first-principles studies. Physics of the Earth and Planetary Interiors, 2013, 217, 36-47.	0.7	8
14576	Electronic Structure of Semiconducting and Metallic Tubes in TiO₂/Carbon Nanotube Heterojunctions: Density Functional Theory Calculations. Journal of Physical Chemistry Letters, 2013, 4, 1340-1346.	2.1	55
14577	Density functional theory study on the adsorption and decomposition of the formic acid catalyzed by highly active mushroom-like Au@Pd@Pt tri-metallic nanoparticles. Physical Chemistry Chemical Physics, 2013, 15, 4625.	1.3	22
14578	Comprehensive examination of dopants and defects in BaTiO<mml:math xmlns:mml="http://www.w3.org/1998/Math/MathML" display="inline"><mml:msub><mml:mrow /><mml:mn>3</mml:mn></mml:msub></mml:math>from first principles. Physical Review B, 2013, 87, .	1.1	43
14579	DFT+U Study of Molecular and Dissociative Water Adsorptions on the Fe₃O₄(110) Surface. Journal of Physical Chemistry C, 2013, 117, 7648-7655.	1.5	46
14580	Stability and electronic properties of 3D covalent organic frameworks. Journal of Molecular Modeling, 2013, 19, 2143-2148.	0.8	36
14581	Effect of local metal microstructure on adsorption on bimetallic surfaces: Atomic nitrogen on Ni/Pt(111). Journal of Chemical Physics, 2013, 138, 174702.	1.2	21

#	Article	IF	Citations
14582	Isomers of C12N12 as potential hydrogen storage materials and the effect of the electric field therein. RSC Advances, 2013, 3, 6991.	1.7	12
14583	Theoretical study on the reactivity of the surface of pure oxides: The Influence of the support and oxygen vacancies. Applied Surface Science, 2013, 274, 1-6.	3.1	11
14584	A new crystalline LiPON electrolyte: Synthesis, properties, and electronic structure. Solid State Ionics, 2013, 233, 95-101.	1.3	118
14585	Zn_{1â€“x}Cd_xS Solid Solutions with Controlled Bandgap and Enhanced Visible-Light Photocatalytic H₂-Production Activity. ACS Catalysis, 2013, 3, 882-889.	5.5	565
14586	Siliconâ€“doping in carbon nanotubes: formation energies, electronic structures, and chemical reactivity. Journal of Molecular Modeling, 2013, 19, 1667-1675.	0.8	29
14587	Silicon clathrates as anode materials for lithium ion batteries?. Journal of Materials Chemistry A, 2013, 1, 7782.	5.2	42
14588	Defect Thermodynamics and Diffusion Mechanisms in Li₂CO₃ and Implications for the Solid Electrolyte Interphase in Li-Ion Batteries. Journal of Physical Chemistry C, 2013, 117, 8579-8593.	1.5	228
14589	Scalable Patterning of One-Dimensional Dangling Bond Rows on Hydrogenated Si(001). ACS Nano, 2013, 7, 4422-4428.	7.3	13
14590	Modeling CO2 reduction on Pt(111). Physical Chemistry Chemical Physics, 2013, 15, 7114.	1.3	80
14591	Raman spectroscopy investigation of alpha boron at elevated pressures and temperatures. Solid State Communications, 2013, 154, 34-39.	0.9	27
14592	Strong Light-Matter Interactions in Heterostructures of Atomically Thin Films. Science, 2013, 340, 1311-1314.	6.0	2,179
14593	Xâ€ray Crystallographic and Firstâ€Principles Theoretical Studies of K₂[TcOCl₅] and UV/Vis Investigation of the [TcOCl₅]^{2â€“} and [TcOCl₄]^{â€“} Ions. European Journal of Inorganic Chemistry, 2013, 2013, 1097-1104.	1.0	3
14594	Fermi surface properties of AB₃ (A = Y, La; B = Pb, In, Tl) intermetallic compounds under pressure. Journal of Physics Condensed Matter, 2013, 25, 155501.	0.7	18
14595	Theoretical study on electronic structure and optical properties of Ga0.75Al0.25N(0001) surface. Applied Surface Science, 2013, 273, 111-117.	3.1	9
14596	Role of screening in the density functional applied to transition-metal defects in semiconductors. Physical Review B, 2013, 87, .	1.1	35
14597	Novel Electronic and Magnetic Properties of Twoâ€Dimensional Transition Metal Carbides and Nitrides. Advanced Functional Materials, 2013, 23, 2185-2192.	7.8	1,418
14598	Crystal structure analysis and first principle investigation of F doping in LiFePO4. Journal of Power Sources, 2013, 241, 70-79.	4.0	42
14599	Electronic and optical properties of ZnSc2S4 and CdSc2S4 cubic spinels by the modified Beckeâ€“Johnson density functional. Solid State Sciences, 2013, 20, 127-134.	1.5	10

#	Article	IF	Citations
14600	Ab initio study of the stable phases of 1:1 tantalum nitride. Acta Materialia, 2013, 61, 3799-3807.	3.8	28
14601	Exploration of Structures of Two-Dimensional Boronâ€“Silicon Compounds with sp² Silicon. Journal of Physical Chemistry Letters, 2013, 4, 561-567.	2.1	75
14602	First-principles study of temperature-dependent diffusion coefficients: Hydrogen, deuterium, and tritium in Î±-Ti. Journal of Applied Physics, 2013, 113, .	1.1	26
14603	Sign-changeable spin-filter efficiency in linear carbon atomic chain. Physica E: Low-Dimensional Systems and Nanostructures, 2013, 48, 101-105.	1.3	0
14604	The equation of state for hydrogen at high densities. High Energy Density Physics, 2013, 9, 448-456.	0.4	15
14605	Acrolein Hydrogenation on Ni(111). Journal of Physical Chemistry C, 2013, 117, 12715-12724.	1.5	14
14606	An experimental and first-principles study of the effect of B/N doping in TiO2 thin films for visible light photo-catalysis. Journal of Photochemistry and Photobiology A: Chemistry, 2013, 254, 25-34.	2.0	27
14607	Nanofilm versus Bulk Polymorphism in Wurtzite Materials. Physical Review Letters, 2013, 110, 245501.	2.9	24
14608	Bandgap tuning in highly c-axis oriented Zn1â^'xMgxO thin films. Applied Physics Letters, 2013, 102, .	1.5	95
14609	Ab initioinvestigations of the strontium gallium nitride ternaries Sr₃GaN₃and Sr₆GaN₅: promising materials for optoelectronic. Semiconductor Science and Technology, 2013, 28, 085005.	1.0	6
14610	The structural, elastic and thermoelectric properties of Fe2VAl at pressures. Journal of Alloys and Compounds, 2013, 565, 22-28.	2.8	37
14611	First-principles study of structural, elastic, electronic, vibrational and thermodynamic properties of UN. Journal of Nuclear Materials, 2013, 440, 63-69.	1.3	37
14612	AbÂInitio Calculations and Measurements of Thermoelectric Properties of V2O5 Films. Journal of Electronic Materials, 2013, 42, 1597-1603.	1.0	11
14613	Optical and energy-loss spectra of ZnS from ab initio molecular dynamics simulation: Temperature effect. Optik, 2013, 124, 5095-5098.	1.4	21
14614	DFT study of platinum and palladium overlayers on tungsten carbide: Structure and electrocatalytic activity toward hydrogen oxidation/evolution reaction. International Journal of Hydrogen Energy, 2013, 38, 5009-5018.	3.8	68
14615	Bandgaps in the deep ultraviolet borate crystals: Prediction and improvement. Applied Physics Letters, 2013, 102, 231904.	1.5	47
14616	Orbital Overlap Effects in Electron Transfer Reactions across a Metal Nanowire/Electrolyte Solution Interface. Journal of Physical Chemistry C, 2013, 117, 13021-13027.	1.5	11
14617	First-Principles Modeling of Mixed Halide Organometal Perovskites for Photovoltaic Applications. Journal of Physical Chemistry C, 2013, 117, 13902-13913.	1.5	861

#	Article	IF	Citations
14618	Interaction of La₂NiO₄ (100) Surface with Oxygen Molecule: A First-Principles Study. Journal of Physical Chemistry C, 2013, 117, 12991-12999.	1.5	52
14619	Impact of tensile strain on the oxygen vacancy migration in SrTiO3: Density functional theory calculations. Journal of Applied Physics, 2013, 113, .	1.1	13
14620	Ab initio study of electronic structure, elastic and optical properties of anti-perovskite type alkali metal oxyhalides. Solid State Sciences, 2013, 20, 120-126.	1.5	19
14621	A DFT +Ustudy of (Rh, Nb)-codoped rutile TiO₂. Journal of Physics Condensed Matter, 2013, 25, 085501.	0.7	23
14622	Role of Solvent and External Growth Environments to Determine Growth Morphology of Molecular Crystals. Crystal Growth and Design, 2013, 13, 2413-2425.	1.4	76
14623	Two C28 Clathrates. Carbon Materials, 2013, , 75-89.	0.2	1
14624	Antibacterial and photocatalytic activity of TiO2 and ZnO nanomaterials in phosphate buffer and saline solution. Applied Microbiology and Biotechnology, 2013, 97, 5565-5573.	1.7	38
14625	Atomic and electronic structures of single-layer FeSe on SrTiO<mml:math xmlns:mml="http://www.w3.org/1998/Math/MathML" display="inline"><mml:msub><mml:mrow /><mml:mn>3</mml:mn></mml:msub></mml:math>(001): The role of oxygen deficiency. Physical Review B, 2013, 87, .	1.1	86
14626	Explicit Roles of Au and TiO₂ in a Bifunctional Au/TiO₂ Catalyst for the Waterâ€Gas Shift Reaction: A DFT Study. ChemCatChem, 2013, 5, 2479-2488.	1.8	23
14627	Exotic Geometrical and Electronic Properties in Hydrogenated Graphyne. Journal of Physical Chemistry C, 2013, 117, 11960-11967.	1.5	41
14628	Screened Coulomb Hybrid DFT Study on Electronic Structure and Optical Properties of Anionic and Cationic Te-Doped Anatase TiO₂. Journal of Physical Chemistry C, 2013, 117, 12942-12948.	1.5	28
14629	Ab initio simulations of oxygen interaction with surfaces and interfaces in uranium mononitride. Journal of Nuclear Materials, 2013, 435, 102-106.	1.3	18
14630	Periodic Density-Functional Calculations on Work-Function Change Induced by Adsorption of Halogens on Cu(111). Physical Review Letters, 2013, 110, 156804.	2.9	81
14631	The mechanical and thermo-physical properties and electronic structures of SnS and SnSe in orthorhombic structure. Journal of Alloys and Compounds, 2013, 556, 86-93.	2.8	45
14632	Half-Metallic and Magnetic Silicon Nanowires Functionalized by Transition-Metal Atoms. Springer Series in Materials Science, 2013, , 149-169.	0.4	1
14633	Free Radical Reactions in Two Dimensions: A Case Study on Photochlorination of Graphene. Small, 2013, 9, 1388-1396.	5.2	19
14634	Intrinsic region length scaling of heavily doped carbon nanotube pâ€“iâ€“n junctions. Nanoscale, 2013, 5, 6999.	2.8	17
14635	Atomistic Modelling and Simulation of Warm Dense Matter. Conductivity and Reflectivity. Contributions To Plasma Physics, 2013, 53, 300-310.	0.5	25

#	Article	IF	Citations
14636	Two-Dimensional Hexagonal Beryllium Sulfide Crystal. Journal of Physical Chemistry Letters, 2013, 4, 1856-1860.	2.1	38
14637	Liâ€Doped Cr₂MnO₄: A New pâ€Type Transparent Conducting Oxide by Computational Materials Design. Advanced Functional Materials, 2013, 23, 5267-5276.	7.8	57
14638	Experimental and Theoretical Comparison of Gas Desorption Energies on Metallic and Semiconducting Single-Walled Carbon Nanotubes. Journal of the American Chemical Society, 2013, 135, 7768-7776.	6.6	20
14639	New insight into the enhanced visible-light photocatalytic activities of B-, C- and B/C-doped anatase TiO2 by first-principles. Physical Chemistry Chemical Physics, 2013, 15, 12040.	1.3	148
14640	Role of dopants in LiF:Mg,Cu, LiF:Mg,P and LiF:Mg,Cu,P detectors. Journal of Solid State Chemistry, 2013, 202, 282-290.	1.4	8
14641	Structure, Energetic and Tribological Properties, and Possible Applications in Nanoelectromechanical Systems of Argon-Separated Double-Layer Graphene. Journal of Physical Chemistry C, 2013, 117, 11428-11435.	1.5	7
14642	Physical properties of high-pressure scheelite YVO4 from density functional calculations. Computational Materials Science, 2013, 69, 527-532.	1.4	11
14643	Resolving Precursor Deligation, Surface Species Evolution, and Nanoparticle Nucleation during Palladium Atomic Layer Deposition. Journal of Physical Chemistry C, 2013, 117, 11141-11148.	1.5	30
14644	KAg11(VO4)4 as a candidate p-type transparent conducting oxide. Journal of Chemical Physics, 2013, 138, 194703.	1.2	6
14645	Theoretical study of structural, elastic, electronic properties, and dispersion of optical functions of hexagonal ZnTiO₃. Physica Status Solidi (B): Basic Research, 2013, 250, 1810-1815.	0.7	14
14646	First principles assessment of perovskite dopants for proton conductors with chemical stability and high conductivity. RSC Advances, 2013, 3, 3333.	1.7	28
14647	Polymorphism in Cisplatin Anticancer Drug. Journal of Physical Chemistry B, 2013, 117, 6421-6429.	1.2	34
14648	Electrocatalytic Reduction of Nitrate on a Pt Electrode Modified by pâ€Block Metal Adatoms in Acid Solution. ChemCatChem, 2013, 5, 1773-1783.	1.8	45
14649	Optical signature of hydrogen-helium demixing at extreme density-temperature conditions. Physical Review B, 2013, 87, .	1.1	24
14650	Cation and magnetic orders in MnFe2O4 from density functional calculations. Journal of Applied Physics, 2013, 113, .	1.1	46
14651	Mobile metal adatoms on single layer, bilayer, and trilayer graphene: Anab initioDFT study with van der Waals corrections correlated with electron microscopy data. Physical Review B, 2013, 87, .	1.1	84
14652	Chargeâ€Transfer Interaction between Fewâ€Layer MoS₂ and Tetrathiafulvalene. Chemistry - an Asian Journal, 2013, 8, 1780-1784.	1.7	61
14653	The Periodateâ€Based Double Perovskites M₂NaIO₆ (M = Ca, Sr, and) Tj ETQq1 1 0.784314 r	0.6	23

#	Article	IF	Citations
14654	Progressive structural and electronic properties of nano-structured carbon atomic chains. Journal of Applied Physics, 2013, 113, 193704.	1.1	5
14655	On the properties of binary rutile MO2 compounds, M = Ir, Ru, Sn, and Ti: A DFT study. Journal of Chemical Physics, 2013, 138, 194706.	1.2	50
14656	Phase Stability, Physical Properties, and Hardness of Transition-Metal Diborides MB₂ (M =) Tj ETQq0 0 0 rgBT /Overlock 10	1.5	72
14657	FIRST PRINCIPLES STUDY ON IRON PNICTIDE SUPERCONDUCTOR Ca0.88Pr0.12Fe2As2. Modern Physics Letters B, 2013, 27, 1350100.	1.0	0
14658	Formation and Properties of Selenium Double-Helices inside Double-Wall Carbon Nanotubes: Experiment and Theory. ACS Nano, 2013, 7, 5607-5613.	7.3	57
14659	Mechanistic Insight into Catalytic Oxidation of Ammonia on Clean, Oâ€•and OHâ€Assisted Ir(1â€‰1â€‰1) Surfaces. ChemCatChem, 2013, 5, 1832-1841.	1.8	17
14660	Mechanisms of Atomic Motion Through Crystalline GeTe. Chemistry of Materials, 2013, 25, 2220-2226.	3.2	38
14661	Giant Molecular Magnetocapacitance. Physical Review Letters, 2013, 110, 217205.	2.9	15
14662	Analysis of the molecular interactions governing the polymorphism of benzamide â€“ a guide to syntheses?. Physical Chemistry Chemical Physics, 2013, 15, 9219.	1.3	8
14663	Growth and electronic structure of boron-doped graphene. Physical Review B, 2013, 87, .	1.1	113
14664	Initial Growth of N,Nâ€²-Bis(1-ethylpropyl)perylene-3,4,9,10-tetracarboxdiimide Films on Cu(100). Journal of Physical Chemistry C, 2013, 117, 11679-11685.	1.5	7
14665	Defect segregation at grain boundary and its impact on photovoltaic performance of CuInSe2. Applied Physics Letters, 2013, 102, .	1.5	50
14666	Mg-doped VO2 nanoparticles: hydrothermal synthesis, enhanced visible transmittance and decreased metalâ€“insulator transition temperature. Physical Chemistry Chemical Physics, 2013, 15, 7505.	1.3	178
14667	Effects of atomic relaxation on phonon dispersion relations and thermal properties of ultrathin (Si)<mml:math xmlns:mml="http://www.w3.org/1998/Math/MathML" display="inline"><mml:msub><mml:mrow /><mml:mi mathvariant="bold">n</mml:mi></mml:msub></mml:math>(Ge)<mml:math xmlns:mml="http://www.w3.org/1998/Math/MathML" display="inline"><mml:msub><mml:mrow /><mml:mi mathvariant="bold">n</mml:mi></mml:msub></mml:math> [001] superlattices. Physical Review	1.1	3
14668	Role of high-order electromechanical coupling terms in thermodynamics of ferroelectric thin films. Physical Review B, 2013, 87, .	1.1	27
14669	Insight into the Preference Mechanism of CH_x (x = 1â€“3) and Câ€“C Chain Formation Involved in C₂ Oxygenate Formation from Syngas on the Cu(110) Surface. Journal of Physical Chemistry C, 2013, 117, 6594-6606.	1.5	59
14670	Density Functional Theory and Beyond for Band-Gap Screening: Performance for Transition-Metal Oxides and Dichalcogenides. Journal of Chemical Theory and Computation, 2013, 9, 2950-2958.	2.3	99
14671	Scanning Tunneling Microscopy and Density Functional Theory Studies of Adatom-Involved Adsorption of Methylnitrene on Copper(110) Surface. Journal of Physical Chemistry C, 2013, 117, 12111-12116.	1.5	5

#	Article	IF	Citations
14672	Oxygen vacancy-mediated room-temperature ferromagnetism in insulating cobalt-substituted SrTiO<mml:math xmlns:mml="http://www.w3.org/1998/Math/MathML" display="inline"><mml:msub><mml:mrow /><mml:mn>3</mml:mn></mml:msub></mml:math>epitaxially integrated with silicon. Physical Review B, 2013, 87, .	1.1	26
14673	Wetting at the BaTiO3/Pt interface. Journal of Applied Physics, 2013, 113, 184102.	1.1	10
14674	Ab initiocalculation of optical properties with excitonic effects in wurtzite InxGa1â^'xN and InxAl1â^'xN alloys. Physical Review B, 2013, 87, .	1.1	14
14675	Understanding the reentrant superconducting phase diagram of the iron pnictide Ca4Al2O6Fe2(As1â^'xPx)2: First-principles calculations. Physical Review B, 2013, 87, .	1.1	5
14676	Pressure-Induced Superconductivity in SnTe: A First-Principles Study. Journal of Physical Chemistry C, 2013, 117, 12266-12271.	1.5	31
14677	Charge transfer and formation of Ce3+ upon adsorption of metal atom M (MÂ=ÂCu, Ag, Au) on CeO2 (100) surface. Journal of Power Sources, 2013, 234, 69-81.	4.0	32
14678	First principles investigation of zinc-anode dissolution in zincâ€“air batteries. Physical Chemistry Chemical Physics, 2013, 15, 6416.	1.3	44
14679	The existence/absence of Dirac cones in graphynes. New Journal of Physics, 2013, 15, 023004.	1.2	112
14680	Increased Loading of Eu³⁺ Ions in Monazite LaVO₄ Nanocrystals via Pressure-Driven Phase Transitions. Crystal Growth and Design, 2013, 13, 2344-2349.	1.4	15
14681	Experimental and DFT-D Studies of the Molecular Organic Energetic Material RDX. Journal of Physical Chemistry C, 2013, 117, 8062-8071.	1.5	56
14682	First-Principles Elucidation of Atomic Size Effects Using DFT-Chemical Pressure Analysis: Origins of Ca₃₆Sn₂₃â€™s Long-Period Superstructure. Journal of Chemical Theory and Computation, 2013, 9, 3170-3180.	2.3	32
14683	Rationale for the Higher Reactivity of Interfacial Sites in Methanol Decomposition on Au₁₃/TiO₂(110). Journal of the American Chemical Society, 2013, 135, 7629-7635.	6.6	56
14684	Direct observation of lithium-ion transport under an electrical field in LixCoO2 nanograins. Scientific Reports, 2013, 3, 1084.	1.6	77
14685	Dependence on the structure and surface polarity of ZnS photocatalytic activities of water splitting: first-principles calculations. Physical Chemistry Chemical Physics, 2013, 15, 9531.	1.3	23
14686	Periodic Trends in 3d Metal Mediated CO2 Activation. ACS Symposium Series, 2013, , 67-88.	0.5	3
14687	First principles simulation of amorphous InSb. Physical Review B, 2013, 87, .	1.1	16
14688	Sodium Storage and Transport Properties in Layered Na₂Ti₃O₇ for Roomâ€Temperature Sodiumâ€ion Batteries. Advanced Energy Materials, 2013, 3, 1186-1194.	10.2	456
14689	The structural, elastic, phonon, thermal and electronic properties of MnX (X=Ni, Pd and Pt) alloys: First-principles calculations. Journal of Magnetism and Magnetic Materials, 2013, 333, 93-99.	1.0	18

#	Article	IF	Citations
14690	Atomic and electronic structure of La2CoMnO6 on SrTiO3 and LaAlO3 substrates from first principles. Journal of Applied Physics, 2013, 113, .	1.1	6
14691	First-principle prediction of single-carrier avalanche multiplication in chalcopyrite semiconductors. Journal of Applied Physics, 2013, 113, .	1.1	2
14692	The canonical work function-strain relationship of the platinum metal: A first-principles approach to metal-gate transistor optimization. Applied Physics Letters, 2013, 102, .	1.5	20
14693	Impact of rapid thermal processing on oxygen precipitation in heavily arsenic and antimony doped Czochralski silicon. Journal of Applied Physics, 2013, 113, 163510.	1.1	14
14694	Formation of linear Ni nanochains inside carbon nanotubes: Prediction from density functional theory. Chemical Physics Letters, 2013, 577, 92-95.	1.2	5
14695	K2Ta4O11 (â€œkalitantiteâ€): a wide band gap semiconductor synthesized in molybdate flux medium. CrystEngComm, 2013, 15, 5539.	1.3	5
14696	Visible and IR photoluminescence of c-FeSi@aâ€“Si coreâ€“shell nano-fibres produced by vapour transport. Journal of Luminescence, 2013, 143, 113-119.	1.5	8
14697	Comparative Theoretical Analysis of BN Nanotubes Doped with Al, P, Ga, As, In, and Sb. Journal of Physical Chemistry C, 2013, 117, 14235-14240.	1.5	27
14698	First-Principles Study of the Structural, Electronic and Optical Properties of Hexagonal LiIO ₃. Chinese Physics Letters, 2013, 30, 067101.	1.3	10
14699	Density functional calculation of activation energies for lattice and grain boundary diffusion in alumina. Physical Review B, 2013, 87, .	1.1	28
14700	Thermodynamics of Al-substitution in Fe-oxyhydroxides. Geochimica Et Cosmochimica Acta, 2013, 120, 514-530.	1.6	33
14701	The helical surface states of the S-covered topological insulator Sb₂Te₃(0001). Journal of Physics Condensed Matter, 2013, 25, 265005.	0.7	2
14702	Quaternary Diamondâ€Like Chalcogenidometalate Networks as Efficient Anode Material in Lithiumâ€Ion Batteries. Advanced Functional Materials, 2013, 23, 5693-5699.	7.8	26
14703	Mechanics and morphology of single-walled carbon nanotubes: from graphene to the elastica. Philosophical Magazine, 2013, 93, 2057-2088.	0.7	20
14704	Surface Reaction of Acetylene with H-Terminated Silicon Surfaces. A Theoretical Study from Hybrid DFT-D2 Periodic Simulations. Journal of Physical Chemistry C, 2013, 117, 15130-15138.	1.5	6
14705	Self-organisation and magnetic properties of Co nanostructures embedded in a Cu(100) surface. Surface Science, 2013, 612, 48-56.	0.8	29
14706	Site preference and phase stability of Ti doping Niâ€“Mnâ€“Ga shape memory alloys from first-principles calculations. Journal of Alloys and Compounds, 2013, 575, 297-300.	2.8	17
14707	Diaminoethane adsorption and water substitution on hydrated TiO2: a thermochemical study based on first-principles calculations. Physical Chemistry Chemical Physics, 2013, 15, 10824.	1.3	12

#	Article	IF	Citations
14708	The electronic and magnetic properties with intrinsic defects in ZnO nanosheets: First-principles prediction. Current Applied Physics, 2013, 13, 799-802.	1.1	7
14709	Temperature dependence of stacking-fault and anti-phase boundary energies in Al Sc fromab initiocalculations. Philosophical Magazine, 2013, 93, 3423-3441.	0.7	5
14710	Solvent-Exfoliated and Functionalized Graphene with Assistance of Supercritical Carbon Dioxide. ACS Sustainable Chemistry and Engineering, 2013, 1, 144-151.	3.2	80
14711	First-principles study on the mechanism of coking inhibition by the Ni(111) surface doped with IB-group metals at the anode of solid oxide fuel cells. Journal of Power Sources, 2013, 242, 762-767.	4.0	10
14712	Ab initio study of iron nanowires encapsulated inside silicon nitride nanotubes. Physica E: Low-Dimensional Systems and Nanostructures, 2013, 49, 97-104.	1.3	5
14713	Multiple Proton Diffusion and Film Densification in Atomic Layer Deposition Modeled by Density Functional Theory. Chemistry of Materials, 2013, 25, 878-889.	3.2	40
14714	Dissociative Adsorption of Hydrogen on PdO(101) Studied by HRCLS and DFT. Journal of Physical Chemistry C, 2013, 117, 13510-13519.	1.5	25
14715	Ab initiocalculations on the defect structure of<mml:math xmlns:mml="http://www.w3.org/1998/Math/MathML" display="inline"><mml:mi>Î²</mml:mi></mml:math>-Ga<mml:math xmlns:mml="http://www.w3.org/1998/Math/MathML" display="inline"><mml:msub><mml:mrow /><mml:mn>2</mml:mn></mml:msub></mml:math>O<mml:math xmlns:mml="http://www.w3.org/1998/Math/MathML" display="inline"><mml:msub><mml:mrow />	1.1	123
14716	Initial reaction of silicon precursors with a varying number of dimethylamino ligands on a hydroxyl-terminated silicon (001) surface. Applied Surface Science, 2013, 280, 207-211.	3.1	23
14717	The effect of earth metal ion on the property of peptide-based metalâ€“organic frameworks. CrystEngComm, 2013, 15, 5545.	1.3	12
14718	Two-dimensional electron gas at the metastable twisted interfaces of CdTe/PbTe (111) single heterojunctions. Physical Review B, 2013, 87, .	1.1	27
14719	First-principles study of the electronic structure of Al and Sn co-doping ZnO system. Materials Science in Semiconductor Processing, 2013, 16, 1057-1062.	1.9	17
14720	Effect of Pt and Ru promoters on deactivation of Co catalysts by C deposition during Fischerâ€“Tropsch synthesis: A DFT study. Applied Catalysis A: General, 2013, 462-463, 107-115.	2.2	20
14721	Surface Temperature Effects on Dissociative Chemisorption of H₂ on Cu(100). Journal of Physical Chemistry C, 2013, 117, 8851-8863.	1.5	33
14722	Polymerization of Tetracyanoethylene under Pressure. Journal of Physical Chemistry C, 2013, 117, 712-720.	1.5	10
14723	Fullerene Interfaced with a TiO₂(110) Surface May Not Form an Efficient Photovoltaic Heterojunction: First-Principles Investigation of Electronic Structures. Journal of Physical Chemistry Letters, 2013, 4, 2223-2229.	2.1	36
14724	First-principles study of atomic hydrogen adsorption and initial hydrogenation of Zr(0001) surface. Journal of Applied Physics, 2013, 113, .	1.1	9
14725	Thorium in tungsten: construction of interatomic EAM potentials fromab initiodata. Modelling and Simulation in Materials Science and Engineering, 2013, 21, 055019.	0.8	0

#	Article	IF	Citations
14726	Role of electronic correlation in high-low temperature phase transition of hexagonal nickel sulfide: A comparative density functional theory study with and without correction for on-site Coulomb interaction. Journal of Chemical Physics, 2013, 138, 244703.	1.2	13
14727	Magneto-electronic properties and spin-resolved Iâ€“V curves of a Co/GeSe heterojunction diode: an ab initio study. Applied Physics A: Materials Science and Processing, 2013, 111, 923-927.	1.1	1
14728	First-principles prediction of half-metallicity at the low index surfaces of rocksalt KS. Surface Science, 2013, 616, 71-75.	0.8	5
14729	First-principles investigation of magnetism and ferroelectricity in Ni-doped BiCoO₃. Physica Status Solidi (B): Basic Research, 2013, 250, 1864-1869.	0.7	6
14730	Electronic and magnetic properties of adsorbed H2 on graphene with atomic defects: Ab initio study. Physica E: Low-Dimensional Systems and Nanostructures, 2013, 52, 127-135.	1.3	11
14731	Fluxionality of Au Clusters at Ceria Surfaces during CO Oxidation: Relationships among Reactivity, Size, Cohesion, and Surface Defects from DFT Simulations. Journal of Physical Chemistry Letters, 2013, 4, 2256-2263.	2.1	76
14732	Evaluating the Roles of Conformational Strain and Cohesive Binding in Crystalline Polymorphs of Aripiprazole. Crystal Growth and Design, 2013, 13, 2943-2952.	1.4	45
14733	Synthesis, crystal structure and properties of Mg3B36Si9C and related rare earth compounds RE3â^'xB36Si9C (RE=Y, Gdâ€“Lu). Journal of Solid State Chemistry, 2013, 204, 113-122.	1.4	6
14734	Rhombohedrally Distorted Î³-Au5â€“xZn8+y Phases in the Auâ€“Zn System. Inorganic Chemistry, 2013, 52, 1328-1337.	1.9	12
14735	Anionâ€“Anion Mediated Coupling in Layered Perovskite La₂Ti₂O₇ for Visible Light Photocatalysis. Journal of Physical Chemistry C, 2013, 117, 13845-13852.	1.5	46
14736	Experimental and Theoretical Studies on the Linear and Nonlinear Optical Properties of Bi₂ZnOB₂O₆. Journal of Physical Chemistry C, 2013, 117, 14149-14157.	1.5	54
14737	A Comparative Ab Initio Thermodynamic Study of Oxygen Vacancies in ZnO and SrTiO₃: Emphasis on Phonon Contribution. Journal of Physical Chemistry C, 2013, 117, 13776-13784.	1.5	72
14738	Thermodynamic evaluation and optimization of the (Na+X) binary systems (X=Ag, Ca, In, Sn, Zn) using combined Calphad and first-principles methods of calculation. Journal of Chemical Thermodynamics, 2013, 66, 22-33.	1.0	23
14739	Equation of state and phase diagram of ammonia at high pressures from ab initio simulations. Journal of Chemical Physics, 2013, 138, 234504.	1.2	39
14740	Structural Principles and Thermoelectric Properties of Polytypic Group 14 Clathrateâ€II Frameworks. ChemPhysChem, 2013, 14, 1807-1817.	1.0	14
14741	Thermodynamic Modeling of the La-B and La-Bi Systems Supported by First-Principles Calculations. Journal of Phase Equilibria and Diffusion, 2013, 34, 297-306.	0.5	15
14742	Structural and Electronic Properties of Superlattice Composed of Graphene and Monolayer MoS₂. Journal of Physical Chemistry C, 2013, 117, 15347-15353.	1.5	99
14743	Effects of charging and electric field on graphene functionalized with titanium. Journal of Physics Condensed Matter, 2013, 25, 275302.	0.7	6

#	Article	IF	Citations
14744	Induced changes in vibrational properties of NaH and KH under hydrostatic pressure. Journal of Physics and Chemistry of Solids, 2013, 74, 698-701.	1.9	3
14745	On the thermoelectric transport properties of graphyne by the first-principles method. Journal of Chemical Physics, 2013, 138, 204704.	1.2	57
14746	Benzene adsorption on PtCo(111): A DFT study. Applied Surface Science, 2013, 282, 17-24.	3.1	7
14747	The Structural, Electronic and Elastic Properties, and the Raman Spectra of Orthorhombic CaSnO ₃ through First Principles Calculations. Chinese Physics Letters, 2013, 30, 077101.	1.3	13
14748	Thermodynamics of glycerol hydrogenolysis to propanediols over supported copper clusters: Insights from first-principles study. Science China Chemistry, 2013, 56, 763-772.	4.2	11
14749	Rigidity of the conductance of an anchored dithioazobenzene optomechanical switch. Physical Review B, 2013, 87, .	1.1	3
14750	Nucleation of Graphene Precursors on Transition Metal Surfaces: Insights from Theoretical Simulations. Journal of Physical Chemistry C, 2013, 117, 14858-14864.	1.5	39
14751	First-principles study of sulfur multi-absorption in nickel and its segregation to the Ni(100) and Ni(111) surfaces. Surface Science, 2013, 617, 15-21.	0.8	19
14752	Effects of strain on the electrical properties of silicon carbide. Journal of Applied Physics, 2013, 114, .	1.1	12
14753	Benzene adsorption on binary Pt3M alloys and surface alloys: a DFT study. Physical Chemistry Chemical Physics, 2013, 15, 12197.	1.3	28
14754	Abâ€initio calculations of the CO adsorption and dissociation on substitutional Feâ€“Cu surface alloys relevant to Fischerâ€“Tropsch Synthesis: bccâ€(Cu)Fe(100) and fccâ€(Fe)Cu(100). Surface and Interface Analysis, 2013, 45, 1081-1087.	0.8	18
14755	Electron-pinned defect-dipoles for high-performance colossal permittivity materials. Nature Materials, 2013, 12, 821-826.	13.3	784
14756	van der Waals interaction in iron-chalcogenide superconductors. Physical Review B, 2013, 87, .	1.1	23
14757	Structure and magnetism of disordered carbon. Journal of Physics Condensed Matter, 2013, 25, 255301.	0.7	0
14758	Identification of Nitrogen Dopants in Single-Walled Carbon Nanotubes by Scanning Tunneling Microscopy. ACS Nano, 2013, 7, 7219-7226.	7.3	10
14759	Tunable double Dirac cone spectrum in bilayer Î±-graphyne. Applied Physics Letters, 2013, 103, .	1.5	62
14760	Na₂FeP₂O₇ as a Promising Ironâ€Based Pyrophosphate Cathode for Sodium Rechargeable Batteries: A Combined Experimental and Theoretical Study. Advanced Functional Materials, 2013, 23, 1147-1155.	7.8	316
14761	Density Functional Calculations of the Structural and Electronic Properties of (Y2O3)n0,Â±1 Clusters with n = 1â€“10. Journal of Physical Chemistry A, 2013, 117, 5542-5550.	1.1	22

#	Article	IF	Citations
14762	Magnetic and optical properties of Cu-doped ZnO nanosheet: First-principles calculations. Physica E: Low-Dimensional Systems and Nanostructures, 2013, 53, 101-105.	1.3	40
14763	Understanding electronic and optical properties of anatase TiO2 photocatalysts co-doped with nitrogen and transition metals. Physical Chemistry Chemical Physics, 2013, 15, 9549.	1.3	93
14764	Density functional theory study on adsorption of Pt nanoparticle on graphene. International Journal of Hydrogen Energy, 2013, 38, 6283-6287.	3.8	18
14765	Density Functional Theory Study of the Interaction of Arginine-Glycine-Aspartic Acid with Graphene, Defective Graphene, and Graphene Oxide. Journal of Physical Chemistry C, 2013, 117, 5708-5717.	1.5	66
14766	Thermodynamics of a Potts-like model for a reconstructed zigzag edge in graphene nanoribbons. Physical Review B, 2013, 87, .	1.1	3
14767	Characterization of Metal Nanocatalyst State and Morphology during Simulated Single-Walled Carbon Nanotube Growth. Journal of Physical Chemistry C, 2013, 117, 12061-12070.	1.5	13
14768	Effect of interstitial carbon on the mechanical properties of electrodeposited bulk nanocrystalline Ni. Acta Materialia, 2013, 61, 3360-3369.	3.8	74
14769	Ab initio calculations of characteristic lengths of crystalline materials in first strain gradient elasticity. Mechanics of Materials, 2013, 61, 73-78.	1.7	52
14770	The Influence of Grain Boundary Scattering on Thermoelectric Properties of Mg2Si and Mg2Si0.8Sn0.2. Journal of Electronic Materials, 2013, 42, 1707-1710.	1.0	27
14771	Revision of the Geâ€“Ti phase diagram and structural stability of the new phase Ge4Ti5. Journal of Alloys and Compounds, 2013, 577, 211-216.	2.8	13
14772	Sub-10 nm Gate Length Graphene Transistors: Operating at Terahertz Frequencies with Current Saturation. Scientific Reports, 2013, 3, 1314.	1.6	98
14773	First-principle study on structural and electronic properties of CeO<mml:math xmlns:mml="http://www.w3.org/1998/Math/MathML" display="inline"><mml:msub><mml:mrow /><mml:mn>2</mml:mn></mml:msub></mml:math>and ThO<mml:math xmlns:mml="http://www.w3.org/1998/Math/MathML" display="inline"><mml:msub><mml:mrow /><mml:mn>2</mml:mn></mml:msub></mml:math>under high pressures. Physical Review B, 2013, 87, .	1.1	22
14774	The impact of edges and dopants on the work function of graphene nanostructures: The way to high electronic emission from pure carbon medium. Applied Physics Letters, 2013, 102, 183112.	1.5	43
14775	Structure change, layer sliding, and metallization in high-pressure MoS<mml:math xmlns:mml="http://www.w3.org/1998/Math/MathML" display="inline"><mml:msub><mml:mrow /><mml:mn>2</mml:mn></mml:msub></mml:math>. Physical Review B, 2013, 87, .	1.1	116
14776	Half-metallic hole-doped Mn/Si trilayers. Journal Physics D: Applied Physics, 2013, 46, 165502.	1.3	3
14777	Effects of alloying elements on structural, electronic and mechanical properties of AlSc2 by first-principles calculations. Computational Materials Science, 2013, 69, 160-167.	1.4	9
14778	Density functional theory study of the electronic structure of fluorite Cu2Se. Journal of Physics Condensed Matter, 2013, 25, 125503.	0.7	41
14779	The Effect of Hydrogen and Fluorine Coadsorption on the Piezoelectric Properties of Graphene. Journal of Physical Chemistry C, 2013, 117, 3615-3620.	1.5	96

#	Article	IF	Citations
14780	Structural Deformation of Grapheneâ€“Nanotube Contacts: First-Principles Simulations. Japanese Journal of Applied Physics, 2013, 52, 035101.	0.8	1
14781	Geometrically Controlled Nanoporous PdAu Bimetallic Catalysts with Tunable Pd/Au Ratio for Direct Ethanol Fuel Cells. ACS Catalysis, 2013, 3, 1220-1230.	5.5	152
14782	First-principle calculation of yield stress anomaly of Ni3Al-based alloys. Materials Science & Engineering A: Structural Materials: Properties, Microstructure and Processing, 2013, 565, 317-320.	2.6	11
14783	Electronic structure of SnO and SnO2 layers on Rh(111). Surface Science, 2013, 613, 48-53.	0.8	2
14784	Simple and accurate determination of Xâ€“H distances under ultra-fast MAS NMR. Journal of Magnetic Resonance, 2013, 233, 56-63.	1.2	59
14785	Flux Growth of Single-Crystal Na₂Ta₄O₁₁ Particles and their Photocatalytic Hydrogen Production. Crystal Growth and Design, 2013, 13, 2322-2326.	1.4	41
14786	Novel electronic and magnetic properties in N or B doped silicene nanoribbons. Journal of Materials Chemistry C, 2013, 1, 2735.	2.7	73
14787	One-Dimensional Ni-Based Nanostructures and Their Application as Solid Oxide Fuel Cell Anodes: A DFT Investigation. Journal of Physical Chemistry C, 2013, 117, 1315-1322.	1.5	8
14788	Pressure induced phase transitions in TiH2. Journal of Applied Physics, 2013, 113, 103512.	1.1	17
14789	Understanding the High Capacity of Li₂FeSiO₄: In Situ XRD/XANES Study Combined with First-Principles Calculations. Chemistry of Materials, 2013, 25, 2014-2020.	3.2	82
14790	Interaction between hydrogen flux and carbon monolayer on SiC(0001): graphene formation kinetics. Nanoscale, 2013, 5, 671-680.	2.8	18
14791	First-principles investigations of structural, elastic, electronic and magnetic properties of Ga1â^'x Mn x P and In1â^'x Mn x P. Journal of Materials Science, 2013, 48, 6074-6082.	1.7	16
14792	Activation Volume Tensor for Oxygen-Vacancy Migration in Strained<mml:math xmlns:mml="http://www.w3.org/1998/Math/MathML" display="inline"><mml:msub><mml:mi>CeO</mml:mi><mml:mn>2</mml:mn></mml:msub></mml:math>Electrolytes. Physical Review Letters, 2013, 110, 205901.	2.9	55
14793	CALPHAD modeling of metastable phases in the Alâ€“Mgâ€“Si system. Calphad: Computer Coupling of Phase Diagrams and Thermochemistry, 2013, 43, 94-104.	0.7	45
14794	Energetics of Câ€“N coupling reactions on Pt(111) and Ni(111) surfaces from application of density-functional theory. Physical Chemistry Chemical Physics, 2013, 15, 10395.	1.3	3
14795	How Cr changes the dislocation core structure of Î±-Fe: the role of magnetism. Journal of Physics Condensed Matter, 2013, 25, 085403.	0.7	1
14796	Anisotropy of the silicon valence band induced by strain with various orientations. Journal of Applied Physics, 2013, 113, .	1.1	4
14797	Tuning the catalytic property of TiO2 nanotube arrays for water splitting. International Journal of Hydrogen Energy, 2013, 38, 2095-2105.	3.8	13

#	Article	IF	Citations
14798	Trapping and diffusion behaviors of helium at vacancy in iron from first principles. Science China: Physics, Mechanics and Astronomy, 2013, 56, 1100-1106.	2.0	7
14799	Ultraâ€Flexible Boronâ€Oxygen 3D Solidâ€State Networks. Advanced Functional Materials, 2013, 23, 5887-5892.	7.8	7
14800	Insight into the active phase of CO oxidation on Ni/Pt and NiO1â^'x/Pt model catalysts from a first principles investigation. Surface Science, 2013, 614, 30-37.	0.8	2
14801	Electronic and Field Emission Properties of Wrinkled Graphene. Journal of Physical Chemistry C, 2013, 117, 692-696.	1.5	75
14802	First-principles calculations of structural properties and lattice dynamics in ZnSexTe1â^'x alloys. Computational Materials Science, 2013, 77, 403-407.	1.4	0
14803	Ab initio calculations for the tetragonal PbZr0.5Ti0.5O3. Computational Materials Science, 2013, 77, 399-402.	1.4	9
14804	Novel Two-Dimensional Tetragonal Monolayer: Metalâ€“TCNQ Networks. Journal of Physical Chemistry A, 2013, 117, 5171-5177.	1.1	32
14805	Theoretical study about the 5-azido-1H-tetrazole and its ion salts. Journal of Molecular Modeling, 2013, 19, 2383-2389.	0.8	1
14806	Interplay between Supramolecularity and Substrate Symmetry in the Dehydrogenation of <scp>d</scp>-Alaninol on Cu(100) and Cu(110) Surfaces. Journal of Physical Chemistry C, 2013, 117, 10545-10551.	1.5	8
14807	Electronic structure, photocatalytic properties and phonon dispersions of X-doped (XÂ=ÂN, B and Pt) rutile TiO2 from density functional theory. Solid State Sciences, 2013, 22, 8-15.	1.5	12
14808	Nickel: A very fast diffuser in silicon. Journal of Applied Physics, 2013, 113, .	1.1	81
14809	Role of Van der Waals Forces in Graphene Adsorption over Pd, Pt, and Ni. Brazilian Journal of Physics, 2013, 43, 126-129.	0.7	5
14810	Density functional theory study of the structural and electronic properties of Mg₃Bi₂in hexagonal and cubic phases. EPJ Applied Physics, 2013, 61, 10103.	0.3	12
14811	DFT based study of transition metal nano-clusters for electrochemical NH3 production. Physical Chemistry Chemical Physics, 2013, 15, 7785.	1.3	159
14812	Microspheric Na₂Ti₃O₇consisting of tiny nanotubes: an anode material for sodium-ion batteries with ultrafast chargeâ€“discharge rates. Nanoscale, 2013, 5, 594-599.	2.8	167
14813	The Oxidation of Cobalt Nanoparticles into Kirkendall-Hollowed CoO and Co₃O₄: The Diffusion Mechanisms and Atomic Structural Transformations. Journal of Physical Chemistry C, 2013, 117, 14303-14312.	1.5	128
14814	Ab-initio study of new Ga-rich GaAs(001) surface (4Ã—4) reconstruction. Surface Science, 2013, 615, 97-102.	0.8	6
14815	Adsorption of NO₂ on YSZ(111) and Oxygen-Enriched YSZ(111) Surfaces. Journal of Physical Chemistry C, 2013, 117, 12472-12482.	1.5	9

#	Article	IF	Citations
14816	Hybrid Hartree-Fock density functional study of charged point defects in ferroelectric PbTiO<mml:math xmlns:mml="http://www.w3.org/1998/Math/MathML" display="inline"><mml:msub><mml:mrow /><mml:mn>3</mml:mn></mml:msub></mml:math>. Physical Review B, 2013, 87, .	1.1	63
14817	Spin switching and magnetization reversal in single-crystal NdFeO<mml:math xmlns:mml="http://www.w3.org/1998/Math/MathML" display="inline"><mml:msub><mml:mrow /><mml:mn>3</mml:mn></mml:msub></mml:math>. Physical Review B, 2013, 87, .	1.1	166
14818	Strain effects on formation and migration energies of oxygen vacancy in perovskite ferroelectrics: A first-principles study. Journal of Applied Physics, 2013, 113, .	1.1	42
14819	Enhanced photocatalytic properties of titaniaâ€“graphene nanocomposites: a density functional theory study. Physical Chemistry Chemical Physics, 2013, 15, 6025.	1.3	72
14820	Synthesis, Crystal Structure, Magnetic Property, and Electronic Structure of Ba₂YbInSe₅. Zeitschrift Fur Anorganische Und Allgemeine Chemie, 2013, 639, 1021-1025.	0.6	5
14821	Ca-VII: A Chain Ordered Host-Guest Structure of Calcium above 210ÂGPa. Physical Review Letters, 2013, 110, 235501.	2.9	38
14822	Interstitialâ€“interstitial interactions in bcc VB group metals: Ab initiocalculations. Journal of Physics and Chemistry of Solids, 2013, 74, 716-722.	1.9	3
14823	H Atom Adsorption on a Silicate Surface: The (010) Surface of Forsterite. Journal of Physical Chemistry C, 2013, 117, 12612-12621.	1.5	27
14824	<scp>l</scp>-Serine Anhydrous Crystals: Structural, Electronic, and Optical Properties by First-Principles Calculations, and Optical Absorption Measurement. Crystal Growth and Design, 2013, 13, 2793-2802.	1.4	27
14825	A comparative DFT study of the mechanical and electronic properties of greigite Fe3S4 and magnetite Fe3O4. Journal of Chemical Physics, 2013, 138, 204712.	1.2	75
14826	Pressure impact on the structure, elasticity, and electron density distribution of CaSi<mml:math xmlns:mml="http://www.w3.org/1998/Math/MathML" display="inline"><mml:msub><mml:mrow /><mml:mn>2</mml:mn></mml:msub></mml:math>O<mml:math xmlns:mml="http://www.w3.org/1998/Math/MathML" display="inline"><mml:msub><mml:mrow /><mml:mn>5</mml:mn></mml:msub></mml:math>. Physical Review B, 2013, 87, .	1.1	8
14827	First principles study of electronic, bonding, elastic properties and intrinsic hardness of CdSiP2. Computational Materials Science, 2013, 77, 114-119.	1.4	32
14828	A first-principles study on the structural, elastic and electronic properties of the C14 Laves phase compounds TiX2 (X=Cr, Mn, Fe). Physica B: Condensed Matter, 2013, 419, 11-18.	1.3	27
14829	Newly synthesized nanolaminate Nb2GeC: Hardness, thermodynamic and optical properties by first-principles method. Computational Materials Science, 2013, 74, 119-123.	1.4	18
14830	Mechanical and optical properties of inverse-perovskites Sc3InX (X=B, C, N). Computational Materials Science, 2013, 73, 1-8.	1.4	13
14831	Electronic and lattice vibrational properties of cubic BaHfO3 from first principles calculations. Physics Letters, Section A: General, Atomic and Solid State Physics, 2013, 377, 927-931.	0.9	14
14832	Electronic, magnetic and elastic properties of Mo2FeB2: First-principles calculations. Computational Materials Science, 2013, 70, 133-139.	1.4	23
14833	Unravelling the interplay of crystal structure and electronic band structure of tantalum oxide (Ta₂O₅). Physical Chemistry Chemical Physics, 2013, 15, 1352-1357.	1.3	55

#	Article	IF	Citations
14834	Ti-doped molybdenum-based perovskites as anodes for solid oxide fuel cells. Journal of Power Sources, 2013, 241, 627-633.	4.0	45
14835	Structure determination of ultra dense magnesium borohydride: A first-principles study. Journal of Chemical Physics, 2013, 138, 214503.	1.2	3
14836	Structural and electronic properties of substitutionally doped armchair silicene nanoribbons. Physica B: Condensed Matter, 2013, 425, 66-71.	1.3	43
14837	Vibrational and Thermal Properties of Ag₃[Co(CN)₆] from First-Principles Calculations and Infrared Spectroscopy. Journal of Physical Chemistry C, 2013, 117, 12848-12857.	1.5	17
14838	A DFT study of the NO dissociation on gold surfaces doped with transition metals. Journal of Chemical Physics, 2013, 138, 074701.	1.2	9
14839	Origin of site preference of CO and NO adsorption on Pd(111) at different coverages: A density functional theory study. Computational and Theoretical Chemistry, 2013, 1004, 22-30.	1.1	12
14840	Structural and Electronic Properties and Stability of MXenes Ti₂C and Ti₃C₂ Functionalized by Methoxy Groups. Journal of Physical Chemistry C, 2013, 117, 13637-13643.	1.5	194
14841	Ab Initio Study of the Friction Mechanism of Fluorographene and Graphane. Journal of Physical Chemistry C, 2013, 117, 12520-12525.	1.5	90
14842	First-Principles Study of the Electronic Properties of B/N Atom Doped Silicene Nanoribbons. Journal of Physical Chemistry C, 2013, 117, 13620-13626.	1.5	49
14843	First principle study of the structural, electronic and magnetic properties of Fe, Co, Ni atomic nanochains encapsulated in single walled and double walled beryllium oxygen nanotubes. Physica E: Low-Dimensional Systems and Nanostructures, 2013, 47, 40-45.	1.3	19
14844	Single Crystal Growth and Thermodynamic Stability of Li₁₇Si₄. Chemistry of Materials, 2013, 25, 1960-1967.	3.2	50
14845	C/B codoping effect on band gap narrowing and optical performance of TiO2 photocatalyst: a spin-polarized DFT study. Journal of Materials Chemistry A, 2013, 1, 4516.	5.2	42
14846	Resolution of Organic Polymorphic Crystals by Raman Spectroscopy. Journal of Physical Chemistry B, 2013, 117, 7297-7307.	1.2	25
14847	Strain-induced structure transformations on Si(111) and Ge(111) surfaces: A combined density-functional and scanning tunneling microscopy study. Journal of Chemical Physics, 2013, 138, 224702.	1.2	34
14848	Effects of Dy on the adherence of Al2O3/NiAl interface: A combined first-principles and experimental studies. Corrosion Science, 2013, 66, 59-66.	3.0	39
14849	FHI-gap: A code based on the all-electron augmented plane wave method. Computer Physics Communications, 2013, 184, 348-366.	3.0	56
14850	Understanding the trends in transition metal sorption by vacancy sites in birnessite. Geochimica Et Cosmochimica Acta, 2013, 101, 222-232.	1.6	90
14851	Phase stability, mechanical properties and electronic structure of hexagonal and trigonal Ti5Al2C3: An ab initio study. Intermetallics, 2013, 33, 105-112.	1.8	12

#	Article	IF	Citations
14852	The first-principles study of martensitic transformations in MnMe (MeÂ=ÂRh, Pd) alloys at low temperatures. Intermetallics, 2013, 34, 83-88.	1.8	3
14853	A simulation study of the shape of Î²â€² precipitates in Mgâ€“Y and Mgâ€“Gd alloys. Acta Materialia, 2013, 61, 453-466.	3.8	150
14854	Ab initio LCAO study of the atomic, electronic and magnetic structures and the lattice dynamics of triclinic CuWO4. Acta Materialia, 2013, 61, 371-378.	3.8	49
14855	Substitutional adsorption mechanism and controllable magnetic properties of Mn on PbTe(111) surface. Applied Surface Science, 2013, 265, 120-123.	3.1	2
14856	First-principles investigation of structural phase transitions and electronic properties of CuGaSe2 up to 100 GPa. Computational Materials Science, 2013, 67, 21-26.	1.4	19
14857	First principle investigation into hexagonal and cubic structures of Gallium Selenide. Computational Materials Science, 2013, 67, 73-82.	1.4	34
14858	A DFT study of gas molecules adsorption on the anatase (001) nanotube arrays. Computational Materials Science, 2013, 67, 174-181.	1.4	39
14859	First-principles investigation of the mechanical, electronic and thermophysical properties of Q-phase in Alâ€“Mgâ€“Siâ€“Cu alloys. Computational Materials Science, 2013, 67, 334-340.	1.4	8
14860	Enhanced magnetization and conductive phase in NiFe2O4. Journal of Magnetism and Magnetic Materials, 2013, 325, 144-146.	1.0	18
14861	Half-metallicity and ferromagnetism of TcX (X=C, Si and Ge) in zinc blende structure. Journal of Magnetism and Magnetic Materials, 2013, 327, 177-184.	1.0	4
14862	Hydrogen storage in the manganese containing metalâ€“organic framework MOF-73. Microporous and Mesoporous Materials, 2013, 165, 205-209.	2.2	13
14863	Predicting the impact of functionalized ligands on CO2 adsorption in MOFs: A combined DFT and Grand Canonical Monte Carlo study. Microporous and Mesoporous Materials, 2013, 168, 225-238.	2.2	47
14864	Mechanical and electronic properties of Ag3Sn intermetallic compound in lead free solders using ab initio atomistic calculation. Materials Science and Engineering B: Solid-State Materials for Advanced Technology, 2013, 178, 10-21.	1.7	29
14865	Theory studies on the linear and nonlinear optical properties of MnHg(SCN)4 crystal. Optics Communications, 2013, 286, 322-328.	1.0	3
14866	First-principles prediction of an intrinsic half-metallic graphitic hydrogenated carbon nitride. Physics Letters, Section A: General, Atomic and Solid State Physics, 2013, 377, 347-350.	0.9	30
14867	Solubility of carbon in tetragonal ferrite in equilibrium with austenite. Scripta Materialia, 2013, 68, 195-198.	2.6	81
14868	Strain field of interstitial hydrogen atom in body-centered cubic iron and its effect on hydrogenâ€“dislocation interaction. Scripta Materialia, 2013, 68, 249-252.	2.6	21
14869	Manipulation of surface energy anisotropy in iron using surface segregation of phosphorus: An atomistic simulation. Scripta Materialia, 2013, 68, 329-332.	2.6	13

#	Article	IF	Citations
14870	Magnetic behavior of (MnN)1/(AlN)1, (MnN)1/(GaN)1, and (MnN)1/(InN)1 superlattices. Superlattices and Microstructures, 2013, 53, 16-23.	1.4	10
14871	Mechanical properties of multilayer boron nitride with different stacking orders. Superlattices and Microstructures, 2013, 53, 223-231.	1.4	40
14872	Oxygen-induced Y surface segregation in a CuPdY ternary alloy. Surface Science, 2013, 608, 61-66.	0.8	5
14873	Comparative study of friction properties for hydrogen- and fluorine-modified diamond surfaces: A first-principles investigation. Surface Science, 2013, 608, 74-79.	0.8	30
14874	Valence band electronic structure characterization of the rutile TiO2 (110)-(1Ã—2) reconstructed surface. Surface Science, 2013, 608, 92-96.	0.8	19
14875	Hydroxylation-induced surface stability of AnO2 (An=U, Np, Pu) from first-principles. Surface Science, 2013, 608, 180-187.	0.8	59
14876	Structural transformations of Cu(110) surface induced by adsorption of molecular chlorine. Surface Science, 2013, 608, 135-145.	0.8	23
14877	Reconstructions and surface facets of the GaAs(112)A and (112)B surfaces: First-principles DFT supercell calculations. Surface Science, 2013, 608, 204-211.	0.8	11
14878	Four-faceted nanowires generated from densely-packed TiO2 rutile surfaces: Ab initio calculations. Surface Science, 2013, 608, 226-240.	0.8	20
14879	Carbon monoxide adsorption on beryllium surfaces. Surface Science, 2013, 608, 265-274.	0.8	4
14880	Thermodynamic assessment of the Laâ€“Sb and the Hoâ€“Sb systems using the associate model. Thermochimica Acta, 2013, 551, 104-109.	1.2	0
14881	Structure and thermoelectric properties of EuTi(O,N)3â€‰Â±â€‰Î´. Journal of Applied Physics, 2013, 114,	1.1	24
14882	Influence of Step Defects on Methanol Decomposition: Periodic Density Functional Studies on Pd(211) and Kinetic Monte Carlo Simulations. Journal of Physical Chemistry C, 2013, 117, 451-459.	1.5	28
14883	Digitized Charge Transfer Magnitude Determined by Metalâ€“Organic Coordination Number. ACS Nano, 2013, 7, 2814-2819.	7.3	36
14884	Linear Compressibility and Thermal Expansion of KMn[Ag(CN)₂]₃ Studied by Raman Spectroscopy and First-Principles Calculations. Journal of Physical Chemistry C, 2013, 117, 25704-25713.	1.5	18
14885	DFT Study of Hg Oxidation across Vanadia-Titania SCR Catalyst under Flue Gas Conditions. Journal of Physical Chemistry C, 2013, 117, 1761-1772.	1.5	108
14886	Determination of a Density Functional Tight Binding Model with an Extended Basis Set and Three-Body Repulsion for Carbon Under Extreme Pressures and Temperatures. Journal of Physical Chemistry C, 2013, 117, 7885-7894.	1.5	28
14887	First Principles Study on Ta₃N₅:Ti₃O₃N₂ Solid Solution As a Water-Splitting Photocatalyst. Journal of Physical Chemistry C, 2013, 117, 24710-24715.	1.5	16

#	Article	IF	Citations
14888	Dangling-bond defect in a-Si:H: Characterization of network and strain effects by first-principles calculation of the EPR parameters. Physical Review B, 2013, 87, .	1.1	15
14889	Workâ€Function Modification of Au and Ag Surfaces upon Deposition of Selfâ€Assembled Monolayers: Influence of the Choice of the Theoretical Approach and the Thiol Decomposition Scheme. ChemPhysChem, 2013, 14, 2939-2946.	1.0	14
14890	Multiscale quantum/atomistic coupling using constrained density functional theory. Physical Review B, 2013, 87, .	1.1	32
14891	Phase-Transition Induced Elastic Softening and Band Gap Transition in Semiconducting PbS at High Pressure. Inorganic Chemistry, 2013, 52, 8638-8643.	1.9	27
14892	Consequences of Metalâ€“Oxide Interconversion for Câ€“H Bond Activation during CH₄ Reactions on Pd Catalysts. Journal of the American Chemical Society, 2013, 135, 15425-15442.	6.6	256
14893	Electrochemical ammonia production on molybdenum nitride nanoclusters. Physical Chemistry Chemical Physics, 2013, 15, 20957.	1.3	68
14894	Understanding the High Photocatalytic Activity of (B, Ag)-Codoped TiO₂ under Solar-Light Irradiation with XPS, Solid-State NMR, and DFT Calculations. Journal of the American Chemical Society, 2013, 135, 1607-1616.	6.6	230
14895	Revisiting the Dependence of the Optical and Mobility Gaps of Hydrogenated Amorphous Silicon on Hydrogen Concentration. Journal of Physical Chemistry C, 2013, 117, 23956-23963.	1.5	23
14896	Properties of Weakly Bound Molecular Oxygen on the Rutile TiO₂(110) Surface from Density Functional Theory. Journal of Physical Chemistry C, 2013, 117, 17151-17158.	1.5	2
14897	Germanium Growth Orientation on SrTiO3 (001) 2 Ã— 1 Surface: Role of Surface Reduction. Journal of Physical Chemistry C, 2013, 117, 9887-9894.	1.5	1
14898	Temperature dependence of TiN elastic constants fromab initiomolecular dynamics simulations. Physical Review B, 2013, 87, .	1.1	78
14899	Yb₅Ga₂Sb₆: A Mixed Valent and Narrow-Band Gap Material in the RE₅M₂X₆ Family. Inorganic Chemistry, 2013, 52, 13631-13638.	1.9	28
14900	Interaction of Titanium Oxide Nanostructures with Graphene and Functionalized Graphene Nanoribbons: A DFT Study. Journal of Physical Chemistry C, 2013, 117, 25424-25432.	1.5	32
14901	First-principles study of group III impurity doped PbSe: Bulk and nanowire. Physical Review B, 2013, 87, .	1.1	8
14902	Au-Decorated Silicene: Design of a High-Activity Catalyst toward CO Oxidation. Journal of Physical Chemistry C, 2013, 117, 483-488.	1.5	63
14903	DFT Simulations of Titanium Oxide Films on Titanium Metal. Journal of Physical Chemistry C, 2013, 117, 358-367.	1.5	20
14904	Theoretical Investigation of Ge(100) Nitridation by Nitric Oxide: Monomeric or Dimeric Dissociation?. Journal of Physical Chemistry C, 2013, 117, 17111-17118.	1.5	0
14905	Combined LDA and LDA-1/2 method to obtain defect formation energies in large silicon supercells. Physical Review B, 2013, 88, .	1.1	22

#	Article	IF	Citations
14906	First-Principles Study of Structural Prototypes for NaAlH4: Elevated Pressure Polymorph in Symmetry Fmm2 Leads to a Single-Step Decomposition Pathway. Journal of Physical Chemistry C, 2013, 117, 8864-8870.	1.5	3
14907	Electron Exchange and Conduction in Nontronite from First-Principles. Journal of Physical Chemistry C, 2013, 117, 2032-2040.	1.5	43
14908	Suppression of hydride precipitates in niobium superconducting radio-frequency cavities. Superconductor Science and Technology, 2013, 26, 105003.	1.8	13
14909	Unraveling the adsorption mechanism of aromatic and aliphatic diols on the TiO2 surface: a density functional theory analysis. Physical Chemistry Chemical Physics, 2013, 15, 9761.	1.3	15
14910	Experimental Investigation and Thermodynamic Modeling for the Mg-Nd-Sr System. Metallurgical and Materials Transactions A: Physical Metallurgy and Materials Science, 2013, 44, 5634-5641.	1.1	6
14911	Theoretical Study on Structural Stability of Fully Filled p-Type Skutterudites RETM4Sb12 (REÂ=ÂRare) Tj ETQq1 1 0.784314 rgBT /Ove	1.0	20
14912	Ab initio study of I2 and T2 stacking faults in C14 Laves phase MgZn2. European Physical Journal B, 2013, 86, 1.	0.6	16
14913	First principles study on magnetic properties in ZnS doped with palladium. European Physical Journal B, 2013, 86, 1.	0.6	18
14914	The mystery of abnormally large volume of PbCrO3 with a structurally consistent Hubbard U from first-principles. European Physical Journal B, 2013, 86, 1.	0.6	4
14915	Structural and electronic properties of BeO nanotubes filled with Cu nanowires. European Physical Journal B, 2013, 86, 1.	0.6	3
14916	Elucidating hydrogen assisting vacancy formation in metals: Mo and Nb as examples. European Physical Journal B, 2013, 86, 1.	0.6	15
14917	Structural, electronic, vibrational, and elastic properties of SWCNTs doped with B and N: an ab initio study. European Physical Journal D, 2013, 67, 1.	0.6	10
14918	Application of the SCC-DFTB Method to Hydroxide Water Clusters and Aqueous Hydroxide Solutions. Journal of Physical Chemistry B, 2013, 117, 5165-5179.	1.2	56
14919	Toward a Process-Based Molecular Model of SiC Membranes. 1. Development of a Reactive Force Field. Journal of Physical Chemistry C, 2013, 117, 3308-3319.	1.5	39
14920	First-principles studies of phase stability and crystal structures in Li-Zn mixed-metal borohydrides. Physical Review B, 2013, 88, .	1.1	11
14921	Linear and non-linear optical properties of AgBO<inf>3</inf>(B=Nb, Ta): First principle study. , 2013, , .		0
14922	Scattering of Nitrogen Atoms off Ag(111) Surfaces: A Theoretical Study. Journal of Physical Chemistry C, 2013, 117, 9779-9790.	1.5	20
14923	Mechanistic insight into the hydrazine decomposition on Rh(111): effect of reaction intermediate on catalytic activity. Physical Chemistry Chemical Physics, 2013, 15, 16172.	1.3	39

#	Article	IF	Citations
14924	Theoretical study of the ground-state structures and properties of niobium hydrides under pressure. Physical Review B, 2013, 88, .	1.1	63
14925	Preferential Adsorption of Zigzag Single-Walled Carbon Nanotubes on the ST-Cut Surface of Quartz. Journal of Physical Chemistry C, 2013, 117, 4639-4646.	1.5	3
14926	First-principles studies of the structural and electronic properties of the C14 Laves phase XCr2(Xâ€‰=â€‰Ti,) Tj ETQq0 0 0 rgBT /Over	0.7	10
14927	Electronic, ductile, phase transition and mechanical properties of Lu-monopnictides under high pressures. Journal of Molecular Modeling, 2013, 19, 5343-5354.	0.8	15
14928	Palladium-vacancy pairs in p-type and n-type germanium. Hyperfine Interactions, 2013, 221, 65-72.	0.2	4
14929	Theoretical Study of H₂O Adsorption on Zn₂GeO₄ Surfaces: Effects of Surface State and Structureâ€“Activity Relationships. ACS Applied Materials & Interfaces, 2013, 5, 6893-6901.	4.0	11
14930	Structure and stability of borohydride on Au(111) and Au₃M(111) (M = Cr, Mn, Fe, Co, Ni) surfaces. Dalton Transactions, 2013, 42, 770-775.	1.6	34
14931	Conformation and Hydrogen-Bond-Assisted Polymerization in Glycine Lithium Sulfate at High Pressures. Journal of Physical Chemistry A, 2013, 117, 5734-5741.	1.1	13
14932	Platinum Ion-Doped TiO₂: High Catalytic Activity of Pt²⁺ with Oxide Ion Vacancy in Ti⁴⁺_{1â€“x}Pt²⁺_xO_{2â€“x} Compared to Pt⁴⁺ without Oxide Ion Vacancy in Ti⁴⁺_{1â€“x}Pt⁴⁺_xO₂. Chemistry of Materials, 2013, 25, 3822-3833.	3.2	40
14933	First-Principles Study on a Potential Hydrogen Storage Medium of Mg/TiAl Sandwiched Films. Journal of Physical Chemistry C, 2013, 117, 25374-25380.	1.5	11
14934	Can cation vacancy defects induce room temperature ferromagnetism in GaN?. Applied Physics Letters, 2013, 102, 062411.	1.5	28
14935	New Insights into the Origin of Visible-Light Photocatalytic Activity in Se-Modified Anatase TiO₂ from Screened Coulomb Hybrid DFT Calculations. Journal of Physical Chemistry C, 2013, 117, 25229-25235.	1.5	28
14936	BaClBF4: a new noncentrosymmetric pseudo-Aurivillius type material with transparency range from deep UV to middle IR and a high laser damage threshold. Journal of Materials Chemistry C, 2013, 1, 4740.	2.7	36
14937	Formation and migration energies of the vacancy in Si calculated using the HSE06 range-separated hybrid functional. Physical Review B, 2013, 88, .	1.1	35
14938	Ferroelectric control of magnetic anisotropy of FePt/BaTiO3 magnetoelectric heterojunction: A density functional theory study. Journal of Applied Physics, 2013, 113, .	1.1	17
14939	Ab initio study of unzipping processes in carbon and boron nitride nanotubes under atomic oxygen impact. RSC Advances, 2013, 3, 15362.	1.7	9
14940	Unusual Pressure Effect on the Shear Modulus in MgAl2O4 Spinel. Journal of Physical Chemistry C, 2013, 117, 24518-24526.	1.5	18
14941	First principles study of magnetic anisotropy and magnetoelectric effect of FePd/MgO(001) ultrathin films. Journal of Applied Physics, 2013, 113, .	1.1	8

#	Article	IF	Citations
14942	Effect of doping on electronic structure and photocatalytic behavior of amorphous TiO2. Journal of Physics Condensed Matter, 2013, 25, 475501.	0.7	30
14943	First-Principles Investigation on Elastic Constants of TiN under High Pressure. Advanced Materials Research, 0, 802, 109-113.	0.3	1
14944	Ordered arrays of metalâ€“organic magnets at surfaces. Journal of Physics Condensed Matter, 2013, 25, 484007.	0.7	16
14945	Electronic and Magnetic Properties of Zigzag Boron-Nitride Nanoribbons with Even and Odd-Line Stone-Wales (5â€“7 Pair) Defects. Journal of Physical Chemistry C, 2013, 117, 3580-3594.	1.5	22
14946	High CO2 Selectivity of ZnO Powder Catalysts for Methanol Steam Reforming. Journal of Physical Chemistry C, 2013, 117, 6493-6503.	1.5	27
14947	A DFT Study of the Effect of Natural Impurities on the Electronic Structure of Sphalerite. Advanced Materials Research, 2013, 669, 39-45.	0.3	4
14948	From One-Dimensional Linear Chain to Two-Dimensional Layered Chalcogenides XBi₄S₇ (X = Mn, Fe): Syntheses, Crystal and Electronic Structures, and Physical Properties. Crystal Growth and Design, 2013, 13, 4118-4124.	1.4	13
14949	Polymorphic energy ordering of MgO, ZnO, GaN, and MnO within the random phase approximation. Physical Review B, 2013, 87, .	1.1	51
14950	Oxidation of Silanes to Silanols on Pd Nanoparticles: H₂ Desorption Accelerated by Surface Oxygen Atom. Journal of Physical Chemistry C, 2013, 117, 22967-22973.	1.5	21
14951	Study of the Formation Mechanism of Boehmite with Different Morphology upon Surface Hydroxyls and Adsorption of Chloride Ions. Journal of Physical Chemistry C, 2013, 117, 15279-15286.	1.5	47
14952	Ab Initio molecular dynamics study of ethylene adsorption onto Si(001) surface: Shortâ€time fourier transform analysis of structural coordinate autocorrelation function. Journal of Computational Chemistry, 2013, 34, 2697-2706.	1.5	9
14953	Composition-dependent elastic modulus, vibration frequency and polaron properties of ZnSexTe1â^'x system. Optical Materials, 2013, 35, 2303-2308.	1.7	17
14954	Computational study of the structural, electronic and optical properties of M2N2(NH): M=C, Si, Ge, Sn. Computational Materials Science, 2013, 79, 710-714.	1.4	9
14955	Cr segregation at C11b/C40 interface in MoSi2-based alloys: A first-principles study. Intermetallics, 2013, 42, 165-169.	1.8	14
14956	Electronic structure and optical properties of the nonlinear optical crystal Pb4O(BO3)2 by first-principles calculations. Journal of Solid State Chemistry, 2013, 198, 77-80.	1.4	9
14957	Elastic anisotropy and thermodynamic properties of tetrahedrally bonded dense C₂N₂(NH) under high pressure and high temperature. Physica Status Solidi (B): Basic Research, 2013, 250, 1293-1299.	0.7	5
14958	Chemical ordering rather than random alloying in SbAs. Physical Review B, 2013, 87, .	1.1	14
14959	Structural study and dehydrogenation mechanisms of a novel mixed metal amidoborane: Sodium magnesium amidoborane. Chemical Physics Letters, 2013, 590, 27-34.	1.2	7

#	Article	IF	Citations
14960	Elasticity, electronic properties and hardness of MoC investigated by first principles calculations. Physica B: Condensed Matter, 2013, 419, 45-50.	1.3	52
14961	First-principles calculations of structural, electronic, optical and elastic properties of LiEu2Si3. Solid State Sciences, 2013, 20, 36-39.	1.5	18
14962	Platinum-mediated healing of defective graphene produced by irradiating glassy carbon with a hydrogen ion-beam. Materials Chemistry and Physics, 2013, 141, 27-34.	2.0	11
14963	First Principle Study of the Optical Properties of Transition Metal Nitrides XN (X=Ti, Zr, Hf). Advanced Materials Research, 2013, 668, 710-714.	0.3	4
14964	Spin reorientation transition of Fe/FeCo/Cu(001) and Fe/FeCo/Co/Cu(001). Journal of Magnetism and Magnetic Materials, 2013, 343, 262-267.	1.0	5
14965	First principles study of structural and vibrational properties of Ba2YTaO6 in cubic and tetragonal phases. Journal of Alloys and Compounds, 2013, 555, 335-338.	2.8	7
14966	Atomic Structure of an Ultrathin Fe-Silicate Film Grown on a Metal: AÂMonolayer of Clay?. Journal of the American Chemical Society, 2013, 135, 19222-19228.	6.6	35
14967	Hydroxyl-decorated graphene systems as candidates for organic metal-free ferroelectrics, multiferroics, and high-performance proton battery cathode materials. Physical Review B, 2013, 87, .	1.1	100
14968	On the structural stability of CeN at high pressures: Ab initio calculations. Journal of Applied Physics, 2013, 113, .	1.1	12
14969	Effect of MgO(100) support on structure and properties of Pd and Pt nanoparticles with 49-155 atoms. Journal of Chemical Physics, 2013, 139, 084701.	1.2	41
14970	Structural and elastic properties of carbon nanotubes containing Fe atoms using first principles. Superlattices and Microstructures, 2013, 64, 220-226.	1.4	12
14971	Density functional theory calculations of hydrogen adsorption on Ti-, Zn-, Zr-, Al-, and N-doped and intrinsic graphene sheets. International Journal of Hydrogen Energy, 2013, 38, 14269-14275.	3.8	92
14972	Density functional theory (DFT) study of Zn, O2 and O adsorption on polar ZnO(0001) and ZnO (0001) surfaces. Journal of Crystal Growth, 2013, 374, 53-59.	0.7	10
14973	Lattice dynamics and electronic structure of energetic solids LiN3 and NaN3: A first principles study. Chemical Physics Letters, 2013, 586, 44-50.	1.2	17
14974	Structure and interactions in benzamide molecular crystals. Molecular Simulation, 2013, 39, 1079-1083.	0.9	6
14975	Is platinum necessary for efficient hydrogen evolution? â€“ DFT study of metal monolayers on tungsten carbide. International Journal of Hydrogen Energy, 2013, 38, 16071-16079.	3.8	59
14976	Anisotropic charge screening and supercell size convergence of defect formation energies. Physical Review B, 2013, 87, .	1.1	91
14977	Synergistic Effect of Tungsten Carbide and Palladium on Graphene for Promoted Ethanol Electrooxidation. ACS Applied Materials & Interfaces, 2013, 5, 6571-6579.	4.0	108

#	Article	IF	Citations
14978	Theoretical investigation of the electronic structure and quantum transport in the grapheneâ€“C(111) diamond surface system. Journal of Physics Condensed Matter, 2013, 25, 435302.	0.7	13
14979	Bonding trends within ternary isocoordinate chalcogenide glasses GexAsySe1âˆ’xâˆ’y. Physical Chemistry Chemical Physics, 2013, 15, 4582.	1.3	9
14980	On the role of strong electron correlations in the surface properties and chemistry of uranium dioxide. Dalton Transactions, 2013, 42, 4570.	1.6	32
14981	Molecular Dynamics Simulations of the Surface Reconstructions of Pt(557) and Au(557) under Exposure to CO. Journal of Physical Chemistry C, 2013, 117, 14579-14587.	1.5	5
14982	Role of WO₃ in the Hg Oxidation across the V₂O₅â€“WO₃â€“TiO₂ SCR Catalyst: A DFT Study. Journal of Physical Chemistry C, 2013, 117, 24397-24406.	1.5	107
14983	Adsorption behavior and electronic properties of Pd_n(nâ‰ 10) clusters on silicon carbide nanotubes: a first-principles study. Journal of Physics Condensed Matter, 2013, 25, 085302.	0.7	1
14984	Ab initio study of the distribution of point defects at grain boundaries in crystalline silicon. JETP Letters, 2013, 98, 76-79.	0.4	2
14985	The evolution of electronic configuration and magnetic characterization of Fe9Ni1, Fe8Ni2 alloy in theoretical calculation. European Physical Journal B, 2013, 86, 1.	0.6	3
14986	Exchange parameters and adiabatic magnon energies from spin-spiral calculations. Physical Review B, 2013, 88, .	1.1	30
14987	Carrier-mediated magnetism in transition metal doped Bi2Se3 topological insulator. Journal of Physics Condensed Matter, 2013, 25, 445003.	0.7	5
14988	Ring-Opening Reactions of Methylcyclopentane over Metal Catalysts, M = Pt, Rh, Ir, and Pd: A Mechanistic Study from First-Principles Calculations. ACS Catalysis, 2013, 3, 196-205.	5.5	33
14989	Ï‡ and Ïƒ Phases in Binary Rheniumâ€“Transition Metal Systems: a Systematic First-Principles Investigation. Inorganic Chemistry, 2013, 52, 3674-3686.	1.9	31
14990	Establishing the Accuracy of Broadly Used Density Functionals in Describing Bulk Properties of Transition Metals. Journal of Chemical Theory and Computation, 2013, 9, 1631-1640.	2.3	184
14991	Elaboration of Hydrogen-Bonded 2D Supramolecular Assemblies on Au(111) From Solutions: Toward Naphthalene Tetracarboxylic Diimideâ€“Melamine Nanoporous Networks. Journal of Physical Chemistry C, 2013, 117, 8737-8745.	1.5	20
14992	Ni-Doping Effects on Carbon Diffusion and Oxidation over Mo₂C Surfaces. Journal of Physical Chemistry C, 2013, 117, 18936-18946.	1.5	12
14993	Effect of Defects in the Formation of AlB₂-Type WB₂ and MoB₂. Inorganic Chemistry, 2013, 52, 7573-7577.	1.9	29
14994	Donor Wave Functions Delocalization in Silicon Nanowires: The Peculiar [011] Orientation. Nano Letters, 2013, 13, 4963-4968.	4.5	5
14995	H₂ Dissociation over NbO: The First Step toward Hydrogenation of Mg. Langmuir, 2013, 29, 12059-12065.	1.6	14

#	Article	IF	Citations
14996	Atomic and electronic structure of GaP/Si(111), GaP/Si(110), and GaP/Si(113) interfaces and superlattices studied by density functional theory. Physical Review B, 2013, 88, .	1.1	37
14997	Structural Phase Transitions on AgCuS Stromeyerite Mineral under Compression. Inorganic Chemistry, 2013, 52, 355-361.	1.9	26
14998	Two novel nonlinear optical carbonates in the deep-ultraviolet region: KBeCO3F and RbAlCO3F2. Scientific Reports, 2013, 3, 1366.	1.6	79
14999	Sr₃BeB₆O₁₃: A New Borate in the SrO/BeO/B₂O₃ System with Novel Tri-Six-Membered Ring (BeB₆O₁₅)^{10â€“} Building Block. Inorganic Chemistry, 2013, 52, 6136-6141.	1.9	21
15000	Tailoring the band gap of ZnO/MgZnO coaxial nanowires by the size and the component of Mg. Physical Chemistry Chemical Physics, 2013, 15, 2932.	1.3	6
15001	Computational Investigation of CO Adsorption and Oxidation on Mn/CeO₂(111) Surface. Journal of Physical Chemistry C, 2013, 117, 433-441.	1.5	75
15002	Heterogeneous Mercury Oxidation on Au(111) from First Principles. Environmental Science & Technology, 2013, 47, 8515-8522.	4.6	103
15003	Transport properties for liquid silicon-oxygen-iron mixtures at Earth's core conditions. Physical Review B, 2013, 87, .	1.1	131
15004	Vertex corrections to the mean-field electrical conductivity in disordered electron systems. Journal of Physics Condensed Matter, 2013, 25, 175502.	0.7	5
15005	Pressure depended elastic, vibration and optical properties of NbIrSn from first principles calculations. Materials Science and Technology, 2013, 29, 925-930.	0.8	8
15006	Oxygen segregation at coherent grain boundaries of cubic boron nitride. Applied Physics Letters, 2013, 102, 091607.	1.5	4
15007	NiO-MgO and CoO-MgO Thin-Film Solid Oxide Solutions on a Mo(100) Support: Formation, Reduction, and Influence of the Support. Journal of Physical Chemistry C, 2013, 117, 280-287.	1.5	9
15008	Connecting bulk symmetry and orbital polarization in strained RNiO<mml:math xmlns:mml="http://www.w3.org/1998/Math/MathML" display="inline"><mml:msub><mml:mrow /><mml:mn>3</mml:mn></mml:msub></mml:math>ultrathin films. Physical Review B, 2013, 88, .	1.1	40
15009	First principles study of the interface between silicone and undoped/doped BaTiO3. Journal of Applied Physics, 2013, 113, .	1.1	5
15010	Nontrivial topological electronic structures in a single Bi(111) bilayer on different substrates: A first-principles study. Physical Review B, 2013, 88, .	1.1	83
15011	Infrared signatures of OH-defects in wadsleyite: A first-principles study. American Mineralogist, 2013, 98, 2132-2143.	0.9	13
15012	Density functional study of the stability of various Î±-Bi2O3 surfaces. Journal of Chemical Physics, 2013, 138, 054703.	1.2	26
15013	Insight into Organometallic Intermediate and Its Evolution to Covalent Bonding in Surface-Confined Ullmann Polymerization. ACS Nano, 2013, 7, 8190-8198.	7.3	190

#	Article	IF	Citations
15014	Multi-Scale Characterization Studies of Aged Li-Ion Large Format Cells for Improved Performance: An Overview. Journal of the Electrochemical Society, 2013, 160, A2111-A2154.	1.3	50
15015	Atomic Layer Deposition of Ruthenium on a Titanium Nitride Surface: A Density Functional Theory Study. Journal of Physical Chemistry C, 0, , 130911130741001.	1.5	6
15016	Electronic Anisotropy at Vicinal Ag(11n) Surfaces: Work Function Changes Induced by Steps and Hydrogen Adsorption. Journal of Physical Chemistry C, 2013, 117, 4606-4618.	1.5	23
15017	DFT Studies of Pristine Hexagonal Ge₁Sb₂Te₄(0001), Ge₂Sb₂Te₅(0001), and Ge₁Sb₄Te₇(0001) Surfaces. Journal of Physical Chemistry C, 2013, 117, 15075-15089.	1.5	29
15018	NH₃â€“NO Coadsorption System on Pt(111). I. Structure of the Mixed Layer. Journal of Physical Chemistry C, 2013, 117, 21186-21195.	1.5	14
15019	First principle study of electronic structure and mechanical properties of Zr doped Al₂Cu. Materials Science and Technology, 2013, 29, 1219-1224.	0.8	6
15020	The Influence of Water and Hydroxyl on a Bimetallic (âˆš3 Ã— âˆš3)R30Â° Sn/Pt Surface Alloy. Journal of Physical Chemistry C, 2013, 117, 4032-4039.	1.5	11
15021	Reduction Mechanisms of Ethylene Carbonate on Si Anodes of Lithium-Ion Batteries: Effects of Degree of Lithiation and Nature of Exposed Surface. ACS Applied Materials & Interfaces, 2013, 5, 13457-13465.	4.0	68
15022	Site-Specific Scaling Relations for Hydrocarbon Adsorption on Hexagonal Transition Metal Surfaces. Journal of Physical Chemistry C, 2013, 117, 20078-20088.	1.5	36
15023	Controlling the Dehydrogenation Reaction toward Reversibility of the LiBH₄â€“Ca(BH₄)₂ Eutectic System. Journal of Physical Chemistry C, 2013, 117, 8878-8886.	1.5	20
15024	First-Principles Investigations on the Na₂MnPO₄F as a Cathode Material for Na-Ion Batteries. Journal of the Electrochemical Society, 2013, 160, A927-A932.	1.3	34
15025	Effects of interface bonding and defects on boron diffusion at Si/SiO2 interface. Journal of Applied Physics, 2013, 114, .	1.1	12
15026	Ferroelectric ground state and polarization-switching path of orthorhombic YMnO3with coexistingE-type and cycloidal spin phases. Physical Review B, 2013, 88, .	1.1	6
15027	A Combined Experimental and Theoretical Study on the Formation of Crystalline Vanadium Nitride (VN) in Low Temperature through a Fully Solid-State Synthesis Route. Journal of Physical Chemistry C, 2013, 117, 25659-25668.	1.5	33
15028	ELECTRONIC STRUCTURE AND LINEAR OPTICAL PROPERTIES OF MIXED ALKALI-METAL BOROPHOSPHATES (LiK2BP2O8, Li3K2BP4O14): A FIRST-PRINCIPLES STUDY. Functional Materials Letters, 2013, 06, 1350046.	0.7	0
15029	The role of water in the adsorption of oxygenated aromatics on Pt and Pd. Journal of Computational Chemistry, 2013, 34, 60-66.	1.5	18
15030	Intrinsic uncertainty on ab initio phase diagram and compound formation energy calculations: BCC Moâ€“Fe as a test case. Physica Status Solidi (B): Basic Research, 2013, 250, 77-85.	0.7	7
15031	ScPdZn and ScPtZn with YAlGe Type Structure â€“ Groupâ€“Subgroup Relation and ⁴⁵Sc Solid State NMR Spectroscopy. Zeitschrift Fur Anorganische Und Allgemeine Chemie, 2013, 639, 246-253.	0.6	6

#	Article	IF	Citations
15032	Highâ€Throughput Computational Screening of New Liâ€Ion Battery Anode Materials. Advanced Energy Materials, 2013, 3, 252-262.	10.2	150
15033	Realization of the Switching Mechanism in Resistance Random Access Memoryâ„¢ Devices: Structural and Electronic Properties Affecting Electron Conductivity in a Hafnium Oxideâ€“Electrode System Through First-Principles Calculations. Journal of Electronic Materials, 2013, 42, 143-150.	1.0	10
15034	BaTiO₃â€based nanolayers and nanotubes: Firstâ€principles calculations. Journal of Computational Chemistry, 2013, 34, 175-186.	1.5	15
15035	Firstâ€principles calculations of point defects in inorganic nanotubes. Physica Status Solidi (B): Basic Research, 2013, 250, 793-800.	0.7	15
15036	Structural and electronic properties of GeTe under pressure:ab initiostudy. Materials Technology, 2013, 28, 305-309.	1.5	3
15037	Highly Efficient and Accurate Calculation of Local Density of States in Two-Dimensional Photonic Crystals. Journal of the Physical Society of Japan, 2013, 82, 044402.	0.7	0
15038	Electronic and Oxygen Migration Properties of Monoclinic La₂GeO_{5-Î´}. Journal of the Physical Society of Japan, 2013, 82, 084702.	0.7	0
15039	Optimal finite-range atomic basis sets for liquid water and ice. Journal of Physics Condensed Matter, 2013, 25, 435504.	0.7	25
15040	Sign-inverted response of aluminum work function to tangential strain. Journal of Physics Condensed Matter, 2013, 25, 445012.	0.7	3
15041	Manifestation of long-range ordered state in layered VX₂(X = Cl, Br, I) systems. Journal of Physics Condensed Matter, 2013, 25, 476001.	0.7	7
15042	First-Principles Investigation on Trapping of Multiple Helium Atoms within a Tungsten Monovacancy. Japanese Journal of Applied Physics, 2013, 52, 01AL03.	0.8	28
15043	Structure and stability of He and Heâ€“vacancy clusters at a Î£5(310)/[001] grain boundary in bcc Fe from first-principles. Journal of Physics Condensed Matter, 2013, 25, 095001.	0.7	12
15044	Templating ultra-small manganese isomers with preference for adsorption sites and narrow distribution tuned by different moirÃ© periodicities of monolayer graphene on Ru(0001). Nanotechnology, 2013, 24, 215302.	1.3	4
15045	Structural and stable properties of ZnSe/Si core-shell nanowire heterostructures: The first principles calculation. Proceedings of SPIE, 2013, , .	0.8	0
15046	Energy ordering of grain boundaries in Cr2O3: insights from theory. Journal of Physics Condensed Matter, 2013, 25, 485005.	0.7	5
15047	Electronic structure and thermodynamic stability of uranium-doped yttrium iron garnet. Journal of Physics Condensed Matter, 2013, 25, 495502.	0.7	13
15048	Phase stability and elastic properties of Crâ€“V alloys. Journal of Physics Condensed Matter, 2013, 25, 075402.	0.7	31
15049	Size-dependent permittivity and intrinsic optical anisotropy of nanometric gold thin films: a density functional theory study. Optics Express, 2013, 21, 11827.	1.7	52

#	Article	IF	Citations
15050	Substrate dependence of Pt4 electronic properties. Journal of Physics Condensed Matter, 2013, 25, 222001.	0.7	3
15051	Magnetic anisotropy of FeO and CoO: the influence of gradient corrections on exchange and correlation. Journal of Physics Condensed Matter, 2013, 25, 486002.	0.7	6
15052	Optical absorption and emission of Î±-Sn nanocrystals from first principles. Nanotechnology, 2013, 24, 405702.	1.3	13
15053	The atomic and electronic structures of NiO(001)/Au(001) interfaces. Journal of Chemical Physics, 2013, 139, 144705.	1.2	7
15054	Non-polar p-type Zn0.94Mn0.05Na0.01O texture: Growth mechanism and codoping effect. Journal of Applied Physics, 2013, 113, 083513.	1.1	8
15055	Surface-termination-dependent Pd bonding and aggregation of nanoparticles on LaFeO3 (001). Journal of Chemical Physics, 2013, 138, 144705.	1.2	10
15056	Hydroxylation induced stabilization of near-surface rocksalt nanostructure on wurtzite ZnO structure. Journal of Chemical Physics, 2013, 138, 224701.	1.2	5
15057	Origin of the unusual reflectance and density contrasts in the phase-change material Cu₂GeTe₃. Applied Physics Letters, 2013, 102, 224105.	1.5	37
15058	Exploration on pressure-induced phase transition of cerium mononitride from first-principles calculations. Applied Physics Letters, 2013, 102, .	1.5	16
15059	Unusual sevenfold coordination of Ru in complex hydride Na3RuH7: Prospect for formation of [FeH7]3â€“ anion. Applied Physics Letters, 2013, 103, 113903.	1.5	10
15060	AA stacking, tribological and electronic properties of double-layer graphene with krypton spacer. Journal of Chemical Physics, 2013, 139, 154705.	1.2	23
15061	Low-bias electron transport properties of germanium telluride ultrathin films. Journal of Applied Physics, 2013, 113, 063711.	1.1	24
15062	Pressure induced dimer to ionic insulator and metallic structural changes in Al2Br6. Journal of Chemical Physics, 2013, 138, 094501.	1.2	2
15063	Strain-engineered A-type antiferromagnetic order in YTiO3: A first-principles calculation. Journal of Applied Physics, 2013, 113, .	1.1	18
15064	Density functional study of methanol decomposition on clean and O or OH adsorbed PdZn(111). Journal of Chemical Physics, 2013, 138, 184701.	1.2	13
15065	Surface adsorption in strontium chloride ammines. Journal of Chemical Physics, 2013, 138, 164701.	1.2	15
15066	Absorption induced modulation of magnetism in two-dimensional metal-phthalocyanine porous sheets. Journal of Chemical Physics, 2013, 138, 204706.	1.2	17
15067	Grain boundary composition and conduction in HfO2: An ab initio study. Applied Physics Letters, 2013, 102, .	1.5	54

#	Article	IF	Citations
15068	A unifying model for non-adiabatic coupling at metallic surfaces beyond the local harmonic approximation: From vibrational relaxation to scanning tunneling microscopy. Journal of Chemical Physics, 2013, 138, 244106.	1.2	16
15069	The structure of SrTiO3(001)-2â€‰Ã—â€‰1 surface analyzed by high-resolution medium energy ion scattering coupled with ab initio calculations. Journal of Chemical Physics, 2013, 138, 244705.	1.2	4
15070	A first principle study for the adsorption and absorption of carbon atom and the CO dissociation on Ir(100) surface. Journal of Chemical Physics, 2013, 139, 174703.	1.2	4
15071	Tuning patterning conditions by co-adsorption of gases: Br2 and H2 on Si(001). Journal of Chemical Physics, 2013, 139, 184713.	1.2	3
15072	Comparison between Gaussian-type orbitals and plane wave ab initio density functional theory modeling of layer silicates: Talc [Mg3Si4O10(OH)2] as model system. Journal of Chemical Physics, 2013, 139, 204101.	1.2	44
15073	Oxidation of step edges on vicinal 4H-SiC(0001) surfaces. Applied Physics Letters, 2013, 103, 211603.	1.5	7
15074	Solar-blind wurtzite MgZnO alloy films stabilized by Be doping. Journal Physics D: Applied Physics, 2013, 46, 245103.	1.3	31
15075	Mechanisms of Visible Light Photocatalysis in N-Doped Anatase TiO2with Oxygen Vacancies from GGA+U Calculations. International Journal of Photoenergy, 2013, 2013, 1-7.	1.4	15
15076	Ab Initio Investigation of Nitride in Comparison with Carbide Phase of Superconducting InX (Xâ€‰=â€‰C, N). , 2013, 2013, 1-9.		14
15077	Magnetic-field-enhanced carbon solution in proeutectoid ferrite. Journal Physics D: Applied Physics, 2013, 46, 385002.	1.3	2
15078	Reactive potential for the study of phase-change materials: GeTe. New Journal of Physics, 2013, 15, 123006.	1.2	18
15079	Unusual Bi-Containing Surface Layers of IIIâ€“V Compound Semiconductors. Springer Series in Materials Science, 2013, , 225-261.	0.4	0
15081	First-Principle Study of Electronic Structure and Stability of Ru_{1-x}Pd_xZr. Advanced Materials Research, 2013, 798-799, 151-156.	0.3	0
15082	Density Functional Theory Study of the Mechanical and Electronic Properties of Rutile TiO₂: A Computer Simulation. Applied Mechanics and Materials, 0, 333-335, 1955-1958.	0.2	0
15083	The DFT Studies on a Novel Hydrogen Storage Material Mg₁₂Ni_{6-x}Cr_x(x=0,1). Applied Mechanics and Materials, 2013, 457-458, 181-184.	0.2	1
15084	Effect of Carbon Doped in BN on Electronic Structures and Mechanical Properties. Advanced Materials Research, 0, 652-654, 1410-1415.	0.3	0
15085	First Principles Calculation on Adsorption of S on Fe(111). Advanced Materials Research, 0, 704, 120-125.	0.3	0
15086	Surface Stoichiometry and Oxidation of NiTi. Applied Mechanics and Materials, 2013, 307, 387-390.	0.2	0

#	Article	IF	Citations
15087	Modification on TiO₂-a Photosensitive Material. Key Engineering Materials, 0, 579-580, 148-152.	0.4	0
15088	Characterization of the Mechanical Properties of Monolayer Molybdenum Disulfide Nanosheets Using First Principles. Journal of Nanotechnology in Engineering and Medicine, 2013, 4, .	0.8	5
15089	Multiscale analysis of adsorption-induced surface stress of alkanethiol on microcantilever. Journal Physics D: Applied Physics, 2013, 46, 035301.	1.3	5
15090	Enhanced upper critical fields in a new quasi-one-dimensional superconductor Nb₂Pd_xSe₅. New Journal of Physics, 2013, 15, 123031.	1.2	35
15091	Ab initioand atomistic study of generalized stacking fault energies in Mg and Mgâ€“Y alloys. New Journal of Physics, 2013, 15, 043020.	1.2	97
15092	Elastic Properties, Mechanical Stability, and State Densities of Aluminnides. Acta Physica Polonica A, 2013, 123, 668-672.	0.2	5
15093	DFT simulation of the occurrences and correlation of gold and arsenic in pyrite. American Mineralogist, 2013, 98, 1765-1771.	0.9	19
15094	ELECTRONIC BAND STRUCTURE, OPTICAL, THERMAL AND BONDING PROPERTIES OF XMg₂O₄(X = Si, Ge) SPINEL COMPOUNDS. International Journal of Modern Physics B, 2013, 27, 1350082.	1.0	9
15095	Theoretical Calculation of the Gas-Sensing Properties of Pt-Decorated Carbon Nanotubes. Sensors, 2013, 13, 15159-15171.	2.1	55
15096	Optical Properties of the LaNi_{4.5}M_{0.5} (M=Al, Mn) Intermetallic Alloys. Applied Mechanics and Materials, 2013, 321-324, 491-494.	0.2	0
15097	Investigations of the Optical Properties of LaNi₅ and LaNi_{4.5}Sn_{0.5}. Applied Mechanics and Materials, 0, 321-324, 495-498.	0.2	1
15098	The Effect of Carbon Monoxide Co-Adsorption on Ni-Catalysed Water Dissociation. International Journal of Molecular Sciences, 2013, 14, 23301-23314.	1.8	10
15099	Effect of Carbon Doped in BN on Thermodynamic Properties. Advanced Materials Research, 0, 706-708, 85-89.	0.3	1
15100	Pseudopotential Calculation for the Electronic Properties of TbFeO₃ with Perovskite Structure. Applied Mechanics and Materials, 0, 483, 124-129.	0.2	0
15101	High Pressure Properties of Superconducting Material Palladium. Advanced Materials Research, 0, 813, 327-331.	0.3	0
15102	Structural and Vibrational Properties of Manganese Sulfide. Solid State Phenomena, 0, 209, 186-189.	0.3	0
15103	Improvement in the hydrogen desorption from MgH2 upon transition metals doping: A hybrid density functional calculations. AIP Advances, 2013, 3, .	0.6	11
15104	First-Principles Study on Diffusion of Cd in CuInSe2. Materials Research Society Symposia Proceedings, 2013, 1538, 21-25.	0.1	2

#	Article	IF	Citations
15105	Density Functional Theory Study on How Electron Spin Configuration of Co3+Ion Affects the Structure and Magnetism of Co-Doped Bismuth Ferrite. Japanese Journal of Applied Physics, 2013, 52, 09KB01.	0.8	2
15106	Graphene and some of its structural analogues: full-potential density functional theory calculations. World Journal of Engineering, 2013, 10, 39-48.	1.0	27
15107	Comparative study of metallic silicideâ€“germanide orthorhombic MnP systems. Journal of Physics Condensed Matter, 2013, 25, 355403.	0.7	3
15108	Hydrogenated K4 carbon: A new stable cubic gauche structure of carbon hydride. Journal of Chemical Physics, 2013, 138, 024702.	1.2	18
15109	Iron complexes with gallic acid: a computational study on coordination compounds of interest for the preservation of cultural heritage. Journal of Coordination Chemistry, 2013, 66, 1709-1719.	0.8	13
15110	First-Principles Calculation of the Electronic Properties of Single-Walled Carbon Nanotubes under Torsions. Materials Research Society Symposia Proceedings, 2013, 1505, 1.	0.1	0
15111	Theoretical Study of the Impact of Stress on the Behavior of Intrinsic Point Defects in Large-Diameter Defect-Free Si Crystals. Solid State Phenomena, 2013, 205-206, 163-168.	0.3	0
15112	Theoretical Study on Ni₂XIn (X=Mn, Fe and Co) Magnetic Shape Memory Alloys by Ab Initio Calculations. Advanced Materials Research, 2013, 712-715, 288-292.	0.3	1
15113	The Electronic Structures and Optical Properties of Substituted Rare-Earth Manganite Tb 1â^' x Yb x MnO 3. Chinese Physics Letters, 2013, 30, 053601.	1.3	1
15114	Modulation of Dirac points and band-gaps in graphene via periodic fullerene adsorption. AIP Advances, 2013, 3, .	0.6	18
15115	First Principles Prediction on the Formation and Properties of Polyanion Deficient Iron Phosphate. ECS Electrochemistry Letters, 2013, 2, A111-A113.	1.9	2
15116	Geometrical and Electronic Structure Investigations of S-Doped Graphene. Advanced Materials Research, 0, 669, 144-148.	0.3	5
15117	Ab initio studies of the structure and the interaction of cellulose IIII crystal. Materials Research Society Symposia Proceedings, 2013, 1554, 1.	0.1	0
15118	Intrinsic Brittlement of Mo₃Si by First-Principle Calculations. Materials Science Forum, 2013, 747-748, 63-68.	0.3	4
15119	Phase stability of Cr_{n+ 1}GaC_n MAX phases from first principles and Cr₂GaC thinâ€film synthesis using magnetron sputtering from elemental targets. Physica Status Solidi - Rapid Research Letters, 2013, 7, 971-974.	1.2	32
15120	First-principles study of one-dimensional sandwich wires [(P)5TM]âˆž (TM = Ti, V, Cr, Mn, Fe, Co). Journal of Physics Condensed Matter, 2013, 25, 395503.	0.7	1
15121	Effects of N Concentration on Electronic Structure and Optical Absorption Properties of N-Doped SrTiO₃ from First Principles. Materials Science Forum, 2013, 749, 561-568.	0.3	2
15122	SURFACE ENERGY ENGINEERING OF Cu SURFACE BY STRAIN: FIRST-PRINCIPLES CALCULATIONS. Surface Review and Letters, 2013, 20, 1350054.	0.5	6

#	Article	IF	Citations
15123	A first-principles study of the structural and elastic properties of orthorhombic and tetragonal Ca₃Mn₂O₇. Chinese Physics B, 2013, 22, 066201.	0.7	6
15124	Ground-state structure determination and mechanical properties of palladium seminitride. Chinese Physics B, 2013, 22, 116104.	0.7	4
15125	Research on Optical Properties of Ga_{1-x}Al_xN with Different Al Component. Applied Mechanics and Materials, 0, 423-426, 258-262.	0.2	0
15126	Formation of Titanium Nitride on the GaN(0001) Surface: A Density Functional Theory Study. Japanese Journal of Applied Physics, 2013, 52, 055601.	0.8	2
15127	Band structure, structural properties and stability of Ca_xMg_{1â^'x}S alloys. Physica Scripta, 2013, 87, 015701.	1.2	4
15128	Density Functional Theory Investigations of the Mechanical Properties of Anatase: A Computer Simulation. Applied Mechanics and Materials, 2013, 333-335, 1903-1906.	0.2	0
15129	Novel high-pressure phase with pseudo-benzene â€œN ₆ â€•molecule of LiN ₃. Europhysics Letters, 2013, 101, 26004.	0.7	55
15130	High-pressure phonon dispersion of copper by using the modified analytic embedded atom method. Chinese Physics B, 2013, 22, 096301.	0.7	6
15131	Differences in the adsorption of FePc on coinage metal surfaces. Chinese Physics B, 2013, 22, 063101.	0.7	3
15132	First-principles study on the elastic properties of Bâ€² and Q phase in Alâ€“Mgâ€“Si (â€“Cu) alloys. Physica Scripta, 2013, 87, 015601.	1.2	22
15133	Study on Electronic and Optical Properties of Al-Doped ZnS from Density Function Theory. Advanced Materials Research, 0, 734-737, 2405-2410.	0.3	1
15134	Electronic structure and optical properties of Al and Mg co-doped GaN. Chinese Physics B, 2013, 22, 117103.	0.7	11
15135	A first-principles study of B2 NiAl alloyed with rare earth elements Pr, Pm, Sm, and Eu. Chinese Physics B, 2013, 22, 027102.	0.7	4
15136	Foundations of ab initio simulations of electric charges and fields at semiconductor surfaces within slab models. Journal of Applied Physics, 2013, 114, .	1.1	32
15137	The opticalâ€”electrical properties of doped Î²-FeSi₂. Journal of Semiconductors, 2013, 34, 103003.	2.0	1
15138	Carbon Mono and Dioxide Hydrogenation over Pure and Metal Oxide Decorated Graphene Oxide Substrates: Insight from DFT. Graphene, 2013, 02, 109-114.	0.3	3
15139	Computational study of Mg insertion into amorphous silicon: advantageous energetics over crystalline silicon for Mg storage. Materials Research Society Symposia Proceedings, 2013, 1540, 3601.	0.1	3
15140	Effects of chromium on structure and mechanical properties of vanadium: A first-principles study. Chinese Physics B, 2013, 22, 106109.	0.7	2

#	Article	IF	Citations
15141	An accidental visualization of the Brillouin zone in an Niâ€“W alloyviadiffuse scattering. Journal of Applied Crystallography, 2013, 46, 1211-1215.	1.9	10
15142	The new phase of HgF ₂ at high pressure. Europhysics Letters, 2013, 102, 36002.	0.7	8
15143	First-Principles Calculations of Elastic Properties of HoBi and ErBi. Advanced Materials Research, 2013, 664, 672-676.	0.3	0
15144	First-Principles Studies on Cd Doping in CuInSe₂ and Related Compounds during Chemical Bath Deposition of CdS Buffer Layer. Japanese Journal of Applied Physics, 2013, 52, 061201.	0.8	11
15145	Theoretical Calculation of Electronic Structure and Chemical Bonding in Tetragonal Phase KNbO₃. Advanced Materials Research, 0, 709, 80-83.	0.3	2
15146	Why Clorine Is an Inefficient n-Type Dopant in CuInSe2?. Japanese Journal of Applied Physics, 2013, 52, 100208.	0.8	0
15147	Ab initioidentified design principles of solid-solution strengthening in Al. Science and Technology of Advanced Materials, 2013, 14, 025001.	2.8	11
15148	First-Principles Calculations on Electronic, Chemical Bonding and Optical Properties of Cubic Hf ₃ N ₄. Communications in Theoretical Physics, 2013, 59, 105-109.	1.1	3
15149	Electronic Structure, Lattice Dynamics and Thermoelectric Properties of PbTe from First-Principles Calculation. Chinese Physics Letters, 2013, 30, 017101.	1.3	8
15150	The structural, elastic, and electronic properties of Zr _x Nb _{1â^' x} C alloys from first principle calculations. Chinese Physics B, 2013, 22, 107105.	0.7	7
15151	Nitrogen reactivity toward beryllium: surface reactions. Journal of Physics Condensed Matter, 2013, 25, 225002.	0.7	6
15152	First-Principles Investigations on Magnetic Properties in Off-Stoichiometric Ni₂MnIn Magnetic Shape Memory Alloys. Advanced Materials Research, 2013, 750-752, 730-733.	0.3	0
15153	Role of Inter-Dopant Interactions on the Diffusion of Li and Na Atoms in Bulk Si Anodes. Materials Research Society Symposia Proceedings, 2013, 1541, 75601.	0.1	2
15154	Density functional theory study on the interactions of l-cysteine with graphene: adsorption stability and magnetism. Nanotechnology, 2013, 24, 495702.	1.3	13
15155	Polar P6 ₃ cm phase as a marginally stable ground-state structure of InMnO ₃ : First-principles study. Europhysics Letters, 2013, 104, 57001.	0.7	1
15156	Water Trapping at the Graphene/Al₂O₃ Interface. Japanese Journal of Applied Physics, 2013, 52, 06GD09.	0.8	5
15157	Pressure-induced phase transition in silicon nitride material. Chinese Physics B, 2013, 22, 023104.	0.7	3
15158	Electronic Structure and Optical Property of Phosphorus Doped Semiconducting Graphene Nanoribbons. Applied Mechanics and Materials, 2013, 328, 813-816.	0.2	0

#	Article	IF	Citations
15159	Enhanced reduction of graphene oxide by means of charging and electric fields applied to hydroxyl groups. Journal of Physics Condensed Matter, 2013, 25, 435304.	0.7	13
15160	Photoelectric Properties of the Doped Silicon with Carbon Family Elements. Advanced Materials Research, 0, 873, 793-798.	0.3	3
15161	Formation of Propane in the Aqueousâ€Phase Processing of 1â€Propanol over Platinum: A DFT Study. ChemCatChem, 2013, 5, 3299-3308.	1.8	10
15162	Airâ€Promoted Adsorptive Desulfurization over Ti_{0.9}Ce_{0.1}O₂ Mixed Oxides from Diesel Fuel under Ambient Conditions. ChemCatChem, 2013, 5, 3582-3586.	1.8	17
15163	Structural and Vibrational Properties of FeO Using First-Principles. Advanced Materials Research, 2013, 665, 49-52.	0.3	0
15164	Theoretical Study on Absorption Properties of In_xGa_{1-x}As with Different in Component. Applied Mechanics and Materials, 0, 423-426, 439-442.	0.2	2
15165	Influence of normal and shear strain on magnetic anisotropy energy of hcp cobalt: An ab initio study. Journal of Materials Research, 2013, 28, 1559-1566.	1.2	3
15166	The core structure and pseudo-magnetic field of the dislocation in graphene. Europhysics Letters, 2013, 104, 26002.	0.7	7
15167	Density Functional Study of the Structure, Stability and Oxygen Reduction Activity of Ultrathin Platinum Nanowires. Journal of the Electrochemical Society, 2013, 160, F548-F553.	1.3	7
15168	High pressure phase of pnictides yttrium YAs and YBi: first-principles studies. Physica Scripta, 2013, 88, 055601.	1.2	2
15169	First Principles Study on the Stability and Mechanical Properties of MB (M=V, Nb and Ta) Compounds. Chinese Physics Letters, 2013, 30, 117101.	1.3	11
15170	Electronic correlation effects in the Cr₂GeC M_{n+1}AX_xphase. Journal of Physics Condensed Matter, 2013, 25, 035601.	0.7	34
15171	First-Principles Study on Chemical Bonding Characteristics between Cr and Single-Walled Silicon Nanotubes. Advanced Materials Research, 0, 798-799, 30-34.	0.3	0
15172	Conductivity and transparency of TiO2from first principles. , 2013, , .		2
15173	Atomic and Electronic Structure of Multilayer Graphene on a Monolayer Hexagonal Boron Nitride. Materials Research Society Symposia Proceedings, 2013, 1549, 65-70.	0.1	0
15174	From Graphite to Graphene: The Confinement of the Fermi Surface to the Line KH. , 2013, 2013, 1-9.		0
15175	Al and Si Influences on Hydrogen Embrittlement of Carbide-Free Bainitic Steel. Advances in Materials Science and Engineering, 2013, 2013, 1-7.	1.0	3
15176	<i>Ab Initio</i> Calculations of a Refractory Ceramic (Î²-Ge₃N₄): A Computer Simulation. Advanced Materials Research, 0, 738, 18-21.	0.3	0

#	Article	IF	Citations
15177	First-Principles Study of Polarization Behavior in BaTiO₃/PbTiO₃ Ferroelectric Superlattices. Advanced Materials Research, 0, 833, 3-7.	0.3	1
15178	Structural Transformation Relationship for Hafnia Ferroelectric Phase. Advanced Materials Research, 0, 873, 865-870.	0.3	2
15179	First-Principles Study of Diffusion of Cu and In Atoms in CuInSe₂. Japanese Journal of Applied Physics, 2013, 52, 04CR01.	0.8	11
15180	Synthesis of Î³-AlOOH nanocrystals with different morphologies due to the effect of sulfate ions and the corresponding formation mechanism study. Physical Chemistry Chemical Physics, 2013, 15, 18290.	1.3	21
15181	First-principles investigation of phase stability and electronic structure of tetragonal (P4/m) Ga_{3â^'}_xAl_xTi₂(xâ€‰=â€‰0â€“3) compounds. Philosophical Magazine Letters, 2013, 93, 273-282.	0.5	1
15182	Permutation-invariant collective variable to track and drive vacancy dynamics in simulations of solids. Physical Review B, 2013, 88, .	1.1	3
15183	DNA sequencing with titanium nitride electrodes. International Journal of Quantum Chemistry, 2013, 113, 2295-2305.	1.0	6
15184	Interplay between lattice dynamics and superconductivity in Nb<mml:math xmlns:mml="http://www.w3.org/1998/Math/MathML" display="inline"><mml:msub><mml:mrow /><mml:mn>3</mml:mn></mml:msub></mml:math>Sn thin films. Physical Review B, 2013, 88, .	1.1	7
15185	Hydrogen on III-V (110) surfaces: Charge accumulation and STM signatures. Physical Review B, 2013, 88, .	1.1	11
15186	Nonlinear characteristics of structural properties and spontaneous polarization in wurtzite MgxZn1â^'xO: A first-principles study. Physical Review B, 2013, 88, .	1.1	29
15187	Magnetization of bilayer graphene with interplay between monovacancy in each layer. Journal of Applied Physics, 2013, 114, 084313.	1.1	4
15188	Ab initiostudy of low-energy collective electronic excitations in bulk Pb. Physical Review B, 2013, 87, .	1.1	13
15189	Schottky barrier at the AlN/metal junction. Journal of Applied Physics, 2013, 113, .	1.1	6
15190	Phonon spectrum, thermodynamic properties, and pressure-temperature phase diagram of uranium dioxide. Physical Review B, 2013, 88, .	1.1	75
15191	Detection of surface carbon and hydrocarbons in hot spot regions of niobium superconducting rf cavities by Raman spectroscopy. Physical Review Special Topics: Accelerators and Beams, 2013, 16, .	1.8	26
15192	The Diffusion Behaviors of Hydrogen Atoms Inside an Octahedral Pd Nanowire. Integrated Ferroelectrics, 2013, 146, 10-16.	0.3	1
15193	Size-, shape-, and orientation-dependent properties of SiC nanowires of selected bulk polytypes. Journal of Materials Research, 2013, 28, 57-67.	1.2	11
15194	Energy landscape in frustrated systems: Cation hopping in pyrochlores. Applied Physics Letters, 2013, 103, 022901.	1.5	6

#	Article	IF	Citations
15195	Comprehensive Search for New Phases and Compounds in Binary Alloy Systems Based on Platinum-Group Metals, Using a Computational First-Principles Approach. Physical Review X, 2013, 3, .	2.8	47
15196	Observation of superconductivity and anomalous electrical resistivity in single-crystal Ir<mml:math xmlns:mml="http://www.w3.org/1998/Math/MathML" display="inline"><mml:msub><mml:mrow /><mml:mn>3</mml:mn></mml:msub></mml:math>Te<mml:math xmlns:mml="http://www.w3.org/1998/Math/MathML" display="inline"><mml:msub><mml:mrow /><mml:mn>8</mml:mn></mml:msub></mml:math>. Physical Review B, 2013, 87, .	1.1	8
15197	Strain induced phase transitions in silicene bilayers: a first principles and tight-binding study. AIP Advances, 2013, 3, .	0.6	32
15198	Optimizing Electronic Structure and Quantum Transport at the Graphene-Si(111) Interface: AnAbÂInitioDensity-Functional Study. Physical Review Letters, 2013, 110, 176805.	2.9	23
15199	Lateral band formation and hybridization in molecular monolayers: NTCDA on Ag(110) and Cu(100). Physical Review B, 2013, 88, .	1.1	30
15200	Strain stabilization and thickness dependence of magnetism in epitaxial transition metal monosilicide thin films on Si(111). Physical Review B, 2013, 88, .	1.1	16
15201	XAFS analysis of indium oxynitride thin films grown on silicon substrates. X-Ray Spectrometry, 2013, 42, 87-92.	0.9	6
15202	Synthesis, characterization, electronic structure, and phonon properties of the noncentrosymmetric superconductor LaPtSi. Physical Review B, 2013, 88, .	1.1	39
15203	Ewald summation on a helix: A route to self-consistent charge density-functional based tight-binding objective molecular dynamics. Journal of Chemical Physics, 2013, 139, 094110.	1.2	9
15204	Large spin splitting in the conduction band of transition metal dichalcogenide monolayers. Physical Review B, 2013, 88, .	1.1	341
15205	Magnetic properties of copper hexadecaphthalocyanine (F16CuPc) thin films and powders. Journal of Applied Physics, 2013, 113, 013914.	1.1	17
15206	Environment-dependent noncollinear magnetic orders and spin-wave spectra of Fe chains and stripes. Physical Review B, 2013, 87, .	1.1	9
15207	Structural, elastic, and thermodynamic properties under pressure of the FeC in the martensitic phase: an ab-initio study. High Pressure Research, 2013, 33, 572-583.	0.4	1
15208	Mechanical properties, anisotropy and hardness of group IVA ternary spinel nitrides. Molecular Physics, 2013, 111, 3054-3066.	0.8	1
15209	Electronic structures and magnetic moments of Co3FeN thin films grown by molecular beam epitaxy. Applied Physics Letters, 2013, 103, .	1.5	11
15210	Characterization of plasma chemistry and ion energy in cathodic arc plasma from Ti-Si cathodes of different compositions. Journal of Applied Physics, 2013, 113, 163304.	1.1	22
15211	Electrical control of the spin polarization of a current in â€œpure-carbonâ€•systems based on partially hydrogenated graphene nanoribbon. Journal of Applied Physics, 2013, 113, .	1.1	14
15212	Carbon monoxide-induced reduction and healing of graphene oxide. Journal of Vacuum Science and Technology A: Vacuum, Surfaces and Films, 2013, 31, .	0.9	17

#	Article	IF	Citations
15213	Investigation of skutterudite MgyCo4Sb12: High pressure synthesis and thermoelectric properties. Journal of Applied Physics, 2013, 113, 113703.	1.1	35
15214	Spin-dependent resonant tunneling of multiferroic tunnel junction via head-to-head 180Â° domain wall. Journal of Applied Physics, 2013, 114, 163703.	1.1	6
15215	Theoretical study of elastic properties and phase stability of M0.5Al0.5N1â^'xOx (Mâ€‰=â€‰Sc, Ti,) Tj ETQq0 0 0 rgBT /(	1.1	14
15216	Co-doping with antimony to control phosphorous diffusion in germanium. Journal of Applied Physics, 2013, 113, .	1.1	15
15217	Importance of ligands in the electronic properties of FeTe0.6Se0.4. Journal of Applied Physics, 2013, 114, 163906.	1.1	10
15218	Adsorption configurations and scanning voltage determined STM images of small hydrogen clusters on bilayer graphene. Journal of Chemical Physics, 2013, 139, 194708.	1.2	2
15219	Structural, electronic, and optical properties of hydrogenated few-layer silicene: Size and stacking effects. Journal of Applied Physics, 2013, 114, .	1.1	26
15220	Surface-induced charge at a Ge (100) dimer surface and its interaction with vacancies and self-interstitials. Journal of Applied Physics, 2013, 113, .	1.1	8
15221	Dissolving, trapping and detrapping mechanisms of hydrogen in bcc and fcc transition metals. AIP Advances, 2013, 3, .	0.6	82
15222	A comparison of the carrier density at the surface of quantum wells for different crystal orientations of silicon, gallium arsenide, and indium arsenide. Applied Physics Letters, 2013, 103, 162107.	1.5	2
15223	Three-chain B6n+14 cages as possible precursors for the syntheses of boron fullerenes. Journal of Chemical Physics, 2013, 139, 224307.	1.2	16
15224	Chirality dependence of quantum thermal transport in carbon nanotubes at low temperatures: A first-principles study. Journal of Chemical Physics, 2013, 139, 044711.	1.2	6
15225	Quantum-size effects in hafnium-oxide resistive switching. Applied Physics Letters, 2013, 102, 183505.	1.5	151
15226	Density functional theory study on the impact of heavy doping on Si intrinsic point defect properties and implications for single crystal growth from a melt. Journal of Applied Physics, 2013, 114, .	1.1	50
15227	High-pressure synthesis and in-situ high pressure x-ray diffraction study of cadmium tetraphosphide. Journal of Applied Physics, 2013, 113, 053507.	1.1	5
15228	Shell model of BaTiO₃ derived from ab-initio total energy calculations. Journal of Applied Physics, 2013, 114, 174108.	1.1	35
15229	Ab initio atomistic thermodynamics calculations of the initial deposition of epitaxial MgO film on GaAs(001)-Î²2(2â€‰Ã—â€‰4). Journal of Applied Physics, 2013, 113, 053501.	1.1	0
15230	Can nitrogen-based cobalt pnictides exist?. Journal of Applied Physics, 2013, 114, 093701.	1.1	0

#	Article	IF	Citations
15231	Chemistry at molecular junctions: Rotation and dissociation of O2 on the Ag(110) surface induced by a scanning tunneling microscope. Journal of Chemical Physics, 2013, 139, 074702.	1.2	21
15232	Surface electronic structure for various surface preparations of Nb-doped SrTiO₃ (001). Journal of Applied Physics, 2013, 114, 103710.	1.1	33
15233	Metal to semiconductor transition in metallic transition metal dichalcogenides. Journal of Applied Physics, 2013, 114, 174307.	1.1	31
15234	First-principles study of superconductivity in the hole self-doped LiB1.1C0.9. Journal of Applied Physics, 2013, 113, 133910.	1.1	11
15235	Phase stability, mechanical properties, hardness, and possible reactive routing of chromium triboride from first-principle investigations. Journal of Chemical Physics, 2013, 139, 234503.	1.2	10
15236	Thin film bulk acoustic wave resonators tuning from first principles. Journal of Applied Physics, 2013, 113, .	1.1	5
15237	Dihydride structures of deuterium on germanium (001) surfaces. Journal of Applied Physics, 2013, 113, 023703.	1.1	1
15238	Graphdiyne as a high-capacity lithium ion battery anode material. Applied Physics Letters, 2013, 103, .	1.5	104
15239	Lead incorporation mechanism in LiF crystals. Applied Physics Letters, 2013, 102, 081107.	1.5	5
15240	A first-principles characterization of water adsorption on forsterite grains. Philosophical Transactions Series A, Mathematical, Physical, and Engineering Sciences, 2013, 371, 20110582.	1.6	23
15241	Surface and subsurface phonons of Bi(111) measured with helium atom scattering. Physical Review B, 2013, 87, .	1.1	42
15242	Regularization of the Coulomb singularity in exact exchange by Wigner-Seitz truncated interactions: Towards chemical accuracy in nontrivial systems. Physical Review B, 2013, 87, .	1.1	102
15243	Common effect of chemical and external pressures on the magnetic properties of <mml:math xmlns:mml="http://www.w3.org/1998/Math/MathML"		

#	Article	IF	Citations
15249	Mechanism of dopant-vacancy association in Î±-quartz GeO2. Journal of Applied Physics, 2013, 113, .	1.1	3
15250	First-principles insights into the structure of the incipient magnesium oxide and its instability to decomposition: Oxygen chemisorption to Mg(0001) and thermodynamic stability. Physical Review B, 2013, 87, .	1.1	39
15251	Visualization of electronic states on atomically smooth graphitic edges with different types of hydrogen termination. Physical Review B, 2013, 87, .	1.1	41
15252	Mode-selective electron-phonon coupling in laser photoemission on Cu(110). Physical Review B, 2013, 88, .	1.1	6
15253	First-principles study of temperature-dependent diffusion coefficients for helium in Î±-Ti. Journal of Applied Physics, 2013, 114, 153507.	1.1	11
15254	Simulated doping of Si from first principles using pseudoatoms. Physical Review B, 2013, 87, .	1.1	16
15255	Relative entropy as model selection tool in cluster expansions. Physical Review B, 2013, 87, .	1.1	10
15256	Epilayer thickness and strain dependence of Ge(113) surface energies. Physical Review B, 2013, 87, .	1.1	10
15257	Vacancy compensation and related donor-acceptor pair recombination in bulk AlN. Applied Physics Letters, 2013, 103, .	1.5	80
15258	Influence of monolayer contamination on electric-field-noise heating in ion traps. Physical Review A, 2013, 87, .	1.0	27
15259	Temperature Effect on Young's Modulus of Boron Nitride Sheets. Journal of Thermal Stresses, 2013, 36, 152-159.	1.1	8
15260	Theoretical prediction of high pressure phase transition in ScC and YC: Ab initio calculations. Journal of Applied Physics, 2013, 114, 053516.	1.1	5
15261	Enhancing structural transition by carrier and quantum confinement: Stabilization of cubic InN quantum dots by Mn incorporation. Applied Physics Letters, 2013, 103, .	1.5	4
15262	All-out band structure and band offset ab initio predictions for AlN/GaN and AlP/GaP interfaces. Journal of Applied Physics, 2013, 114, .	1.1	11
15263	GeSi Raman spectra vs. local clustering/anticlustering: Percolation scheme and ab initio calculations. Journal of Applied Physics, 2013, 114, .	1.1	8
15264	Stability of MnB2 with AlB2-type structure revealed by first-principles calculations and experiments. Applied Physics Letters, 2013, 102, .	1.5	14
15265	Rationalizing strain engineering effects in rare-earth nickelates. Physical Review B, 2013, 88, .	1.1	58
15266	Orbital Kondo effect in V-doped<mml:math xmlns:mml="http://www.w3.org/1998/Math/MathML" display="inline"><mml:mrow><mml:mn>1</mml:mn><mml:mi>T</mml:mi></mml:mrow></mml:math>-CrSe<mml:math xmlns:mml="http://www.w3.org/1998/Math/MathML" display="inline"><mml:msub><mml:mrow /><mml:mn>2</mml:mn></mml:msub></mml:math>. Physical Review B, 2013, 88, .	1.1	9

#	Article	IF	Citations
15267	Enhanced photoconductivity of 3C-SiC by Al/N codoping. Journal of Applied Physics, 2013, 114, 104901.	1.1	5
15268	First-principles study of band gap engineering of ZnO by alloying with LiGaO2 for ultraviolet applications. Journal of Applied Physics, 2013, 114, .	1.1	9
15269	Ferromagnetism, adatom effect, and edge reconstruction induced by Klein boundary in graphene nanoribbons. Journal of Applied Physics, 2013, 113, 194302.	1.1	8
15270	Electronic structure and exchange interactions in cobalt-phthalocyanine chains. Physical Review B, 2013, 88, .	1.1	31
15271	Electronic structure of phosphorus and arsenicÎ´-doped germanium. Physical Review B, 2013, 88, .	1.1	4
15272	Comment on â€œFirst-principles study of the influence of (110)-oriented strain on the ferroelectric properties of rutile TiO<mml:math xmlns:mml="http://www.w3.org/1998/Math/MathML" display="inline"><mml:msub><mml:mrow /><mml:mn>2</mml:mn></mml:msub></mml:math>â€• Physical Review B, 2013, 88, .	1.1	9
15273	Ab initio study on the size effect of symmetric and asymmetric ferroelectric tunnel junctions: A comprehensive picture with regard to the details of electrode/ferroelectric interfaces. Journal of Applied Physics, 2013, 114, 064105.	1.1	23
15274	Structural variants and the modified Slater-Pauling curve for transition-metal-based half-Heusler alloys. Journal of Applied Physics, 2013, 113, .	1.1	20
15275	Structure stability and electronic transport of gold nanowires on a BeO (0â€‰0â€‰0â€‰1) surface. Modelling and Simulation in Materials Science and Engineering, 2013, 21, 075003.	0.8	2
15276	Elastic and vibrational properties of group IV semiconductors in empirical potential modelling. Journal of Physics Condensed Matter, 2013, 25, 425801.	0.7	6
15277	Half-metallicity and stability of the rock salt BaC and SrC (111) surfaces: A density functional study. Journal of Applied Physics, 2013, 114, .	1.1	3
15278	Applicability of carbon and boron nitride nanotubes as biosensors: Effect of biomolecular adsorption on the transport properties of carbon and boron nitride nanotubes. Applied Physics Letters, 2013, 102, .	1.5	10
15279	Interface effect on the magnitude and stability of ferroelectric polarization in ultrathin PbTiO3 films from first-principles study. Journal of Applied Physics, 2013, 114, .	1.1	7
15280	High-throughput ab initio screening of binary solid solutions in olivine phosphates for Li-ion battery cathodes. Modelling and Simulation in Materials Science and Engineering, 2013, 21, 074004.	0.8	5
15281	Study of titanium adsorption on perfect and defected BC3nanotubes using density functional theory. Molecular Physics, 2013, 111, 888-895.	0.8	3
15282	First principles study of polarization-strain coupling in SrBi2Ta2O9. AIP Advances, 2013, 3, 052134.	0.6	13
15283	Pressure induced structural phase transition in solid oxidizer KClO3: A first-principles study. Journal of Chemical Physics, 2013, 138, 174701.	1.2	18
15284	Crystal Structure of 3Râ€ŁiTiS₂ and its Stability Compared to Other Polymorphs. Zeitschrift Fur Anorganische Und Allgemeine Chemie, 2013, 639, 2822-2825.	0.6	12

#	Article	IF	Citations
15285	Abnormal Photocurrent Response and Enhanced Photocatalytic Activity Induced by Charge Transfer between WS₂ Nanosheets and WO₃ Nanoparticles. ChemPhysChem, 2013, 14, 4069-4073.	1.0	37
15286	Interface structural stability of Zr on the <scp>AlN</scp>(0001) surface: An abâ€initio study. Physica Status Solidi (B): Basic Research, 2013, 250, 1526-1531.	0.7	3
15287	Quantum mechanical modeling of hydrogen assisted cracking in aluminum. Physical Review B, 2013, 88, .	1.1	27
15288	Spin Hall effect induced by Bi impurities in Cu: Skew scattering and side-jump. Physical Review B, 2013, 88, .	1.1	17
15289	PHASE TRANSITION, ELASTIC AND THERMODYNAMIC PROPERTIES OF BERYLLIUM VIA FIRST PRINCIPLES. International Journal of Modern Physics B, 2013, 27, 1350130.	1.0	3
15290	Role of nitrogen in AlNxMn3: A density functional theory study. Journal of Applied Physics, 2013, 113, 023905.	1.1	10
15291	Lattice screening of the polar catastrophe and hidden in-plane polarization in KNbO3/BaTiO3interfaces. Physical Review B, 2013, 87, .	1.1	10
15292	As vacancies, Ga antisites, and Au impurities in zinc blende and wurtzite GaAs nanowire segments from first principles. Physical Review B, 2013, 87, .	1.1	27
15293	Electronic, elastic, vibrational, and thermodynamic properties of type-VIII clathrates Ba8Ga16Sn30 and Ba8Al16Sn30 by first principles. Journal of Applied Physics, 2013, 114, 163509.	1.1	12
15294	Ab initiocalculations of BaTiO₃(111) surfaces. Phase Transitions, 2013, 86, 1115-1120.	0.6	10
15295	Dissimilar-electrodes-induced asymmetric characteristic and diode effect of current transport in zinc oxide tunnel junctions. Journal of Applied Physics, 2013, 114, 044111.	1.1	10
15296	The role of octahedral tilting in the structural phase transition and magnetic anisotropy in SrRuO3 thin film. Journal of Applied Physics, 2013, 113, .	1.1	40
15297	Electronic and phonon bandstructures of pristine few layer and metal doped graphene using first principles calculations. AIP Advances, 2013, 3, .	0.6	57
15298	Contribution of the electron-phonon coupling to the pairing interaction in LiFeAs. Physical Review B, 2013, 88, .	1.1	4
15299	Formation and annealing behaviors of qubit centers in 4H-SiC from first principles. Journal of Applied Physics, 2013, 114, .	1.1	18
15300	Oxygen vacancy migration in compressively strained SrTiO3. Journal of Applied Physics, 2013, 113, 024108.	1.1	25
15301	Chemical bonds and vibrational properties of ordered (U, Np, Pu) mixed oxides. Journal of Applied Physics, 2013, 113, 013501.	1.1	12
15302	Local and chemical environment dependence of the magnetic properties of CoRh core-shell nanoparticles. Physical Review B, 2013, 88, .	1.1	17

#	Article	IF	Citations
15303	Thermodynamic and mechanical stabilities of Î±- and Î²-Ta4AlC3 via first-principles investigations. Journal of Applied Physics, 2013, 114, 213517.	1.1	4
15304	k<mml:math xmlns:mml="http://www.w3.org/1998/Math/MathML" display="inline"><mml:mo>Â·</mml:mo></mml:math>p subband structure of the LaAlO<mml:math xmlns:mml="http://www.w3.org/1998/Math/MathML" display="inline"><mml:msub><mml:mrow /><mml:mn>3</mml:mn></mml:msub></mml:math>/SrTiO<mml:math xmlns:mml="http://www.w3.org/1998/Math/MathML" display="inline"><mml:msub><mml:mrow /><mml:mn>3</mml:mn></mml:msub></mml:math>interface. Physical Review B, 2013, 88, .	1.1	25
15305	Magnetism-dependent phonon anomaly in LaFeAsO observed via inelastic x-ray scattering. Physical Review B, 2013, 87, .	1.1	7
15306	Asymmetric electron transport and highest occupied molecular orbital assisted tunneling through Zn-porphyrin molecular junctions. Applied Physics Letters, 2013, 103, .	1.5	8
15307	ELECTRONIC STRUCTURES AND MAGNETISM IN Cu-DOPED ZnO MONOLAYER. Modern Physics Letters B, 2013, 27, 1350204.	1.0	4
15308	Electronic and structural properties of nitrogen adsorbed Nb(100) surfaces: An ab initio study. Journal of Applied Physics, 2013, 114, 063705.	1.1	1
15309	Negative differential resistance in electron tunneling in ultrathin films near the two-dimensional limit. Journal of Applied Physics, 2013, 113, 034308.	1.1	8
15310	First-principles study of structural phase transitions in CsSnI3. Journal of Applied Physics, 2013, 114, .	1.1	26
15311	Development of a ReaxFF potential for Pd/O and application to palladium oxide formation. Journal of Chemical Physics, 2013, 139, 044109.	1.2	83
15312	Spontaneous assembly of ordered atomic wires with a long interwire distance on a stepped atomic template. Applied Physics Letters, 2013, 102, 201611.	1.5	4
15313	Suitability of chromium phthalocyanines to test Haldane's conjecture: First-principles calculations. Physical Review B, 2013, 88, .	1.1	8
15314	Comment on â€œStructural and Electronic Properties ofTGraphene: A Two-Dimensional Carbon Allotrope with Tetraringsâ€• Physical Review Letters, 2013, 110, 029601.	2.9	22
15315	Anisotropic infrared response of vanadium dioxide microcrystals. Physical Review B, 2013, 87, .	1.1	41
15316	Decay behavior of localized states at reconstructed armchair graphene edges. Physical Review B, 2013, 88, .	1.1	15
15317	Non-hexagonal symmetry-induced functional T graphene for the detection of carbon monoxide. Journal of Chemical Physics, 2013, 139, 034704.	1.2	20
15318	Thermodynamic stability of alkali-metalâ€“zinc double-cation borohydrides at low temperatures. Physical Review B, 2013, 88, .	1.1	29
15319	Low-Energy Polymeric Phases of Alanates. Physical Review Letters, 2013, 110, 135502.	2.9	38
15320	Quantification of finite-temperature effects on adsorption geometries of<mml:math xmlns:mml="http://www.w3.org/1998/Math/MathML" display="inline"><mml:mi>Ï€</mml:mi></mml:math>-conjugated molecules: Azobenzene/Ag(111). Physical Review B, 2013, 88, .	1.1	43

#	Article	IF	Citations
15321	Epitaxial Zintl aluminide SrAl4grown on a LaAlO3substrate. Physical Review B, 2013, 88, .	1.1	3
15322	Correlation between magnetic state and bulk modulus of Cr2AlC. Journal of Applied Physics, 2013, 113, .	1.1	50
15323	Large-scale atomistic density functional theory calculations of phosphorus-doped silicon quantum bits. Physical Review B, 2013, 88, .	1.1	9
15324	ELECTRONIC AND MAGNETIC PROPERTIES OF SILICENE AND SILICANE NANORIBBONS. International Journal of Computational Materials Science and Engineering, 2013, 02, 1350011.	0.5	3
15325	STRUCTURAL AND ELECTRONIC EVOLUTION FROM SiC SHEET TO SILICENE. International Journal of Modern Physics B, 2013, 27, 1350188.	1.0	2
15326	Ab Initio Study of the Ge₃N₄ Semiconductor Materials in its Cubic Î³ Phase: A Computer Simulation. Advanced Materials Research, 2013, 738, 22-25.	0.3	0
15327	ELECTRONIC AND OPTICAL PROPERTIES OF Câ€“N-CODOPED TiO2: A FIRST-PRINCIPLES GGA+U INVESTIGATION. International Journal of Modern Physics B, 2013, 27, 1350123.	1.0	20
15328	Superior Field Emission Properties of Layered WS2-RGO Nanocomposites. Scientific Reports, 2013, 3, 3282.	1.6	218
15329	Theoretical Investigation of the Effect of Growth Orientation on Indium Incorporation Efficiency during InGaN Thin Film Growth by Metalâ€“Organic Vapor Phase Epitaxy. Japanese Journal of Applied Physics, 2013, 52, 08JC02.	0.8	21
15330	Adsorption of methylamine on mackinawite (FES) surfaces: A density functional theory study. Journal of Chemical Physics, 2013, 139, 124708.	1.2	45
15331	Importance of local force fields on lattice thermal conductivity reduction in PbTe 1â^'x Se x alloys. Europhysics Letters, 2013, 102, 46002.	0.7	39
15332	Structural, elastic, thermodynamic and lattice dynamic properties of PrX (Xâ€‰=â€‰Sb, Bi). International Journal of Materials Research, 2013, 104, 99-108.	0.1	3
15333	Multiscale simulations in face-centered cubic metals: A method coupling quantum mechanics and molecular mechanics. Chinese Physics B, 2013, 22, 027101.	0.7	1
15334	Thermodynamic properties of 3Câ€”SiC. Chinese Physics B, 2013, 22, 106401.	0.7	13
15335	Towards understanding the carbon trapping mechanism in copper by investigating the carbonâ€”vacancy interaction. Chinese Physics B, 2013, 22, 076104.	0.7	9
15336	Investigations of high-pressure and high-temperature behaviors of the newly-discovered willemite-II and post-phenacite silicon nitrides. Chinese Physics B, 2013, 22, 126301.	0.7	3
15337	Adhesion energy between mica surfaces: Implications for the frictional coefficient under dry and wet conditions. Journal of Geophysical Research: Solid Earth, 2013, 118, 6066-6075.	1.4	37
15338	Quantum molecular dynamics simulations of the thermophysical properties of shocked liquid ammonia for pressures up to 1.3 TPa. Journal of Chemical Physics, 2013, 139, 134505.	1.2	11

#	Article	IF	Citations
15339	THE FIRST-PRINCIPLES STABILITY STUDY OF PdC AND CdC COMPOUNDS. International Journal of Modern Physics B, 2013, 27, 1350016.	1.0	1
15340	FIRST-PRINCIPLE INVESTIGATION OF ELECTRIC STRUCTURES AND THERMODYNAMIC PROPERTIES FOR ZIRCONIUM NITRIDE UNDER HIGH PRESSURE. International Journal of Modern Physics B, 2013, 27, 1350040.	1.0	4
15341	Anisotropic thermal anharmonicity of CdSiP2 and ZnGeP2: Ab initio calculations. Journal of Applied Physics, 2013, 114, .	1.1	12
15342	THE ELECTRONIC AND MAGNETIC STRUCTURES OF TMAl₅H₁₂ SYSTEMS. Surface Review and Letters, 2013, 20, 1350025.	0.5	2
15343	BAND STRUCTURE, HARDNESS, THERMODYNAMIC AND OPTICAL PROPERTIES OF SUPERCONDUCTING Nb₂AsC, Nb₂InC AND Mo₂GaC. International Journal of Computational Materials Science and Engineering, 2013, 02, 1350007.	0.5	28
15344	ELECTRONIC AND ELASTIC PROPERTIES OF ZINC-BLENDE MgSe. International Journal of Modern Physics B, 2013, 27, 1350027.	1.0	5
15345	An improved density functional theory description of the Ge(100)c(4Ã—2) surface using the MBJLDA xc potential and spinâ€“orbit interactions. Journal of Physics Condensed Matter, 2013, 25, 056007.	0.7	6
15346	Ab-initio studies of some rare-earth borides: CeB₂, PrB₂, NdB₂, and PmB₂. International Journal of Materials Research, 2013, 104, 858-864.	0.1	0
15347	TUNING THE "d⁰" FERROMAGNETISM IN In₂O₃ QUANTUM DOTS BY DANGLING BONDS AND VACANCY BASED ON THE FIRST-PRINCIPLE CALCULATION. Modern Physics Letters B, 2013, 27, 1350068.	1.0	7
15348	Effects of Na Substitution on Li Ion Migration in Li₂CoSiO₄Cathode Material. Journal of the Electrochemical Society, 2013, 160, A658-A661.	1.3	15
15349	Initial reduction of the NiO(100) surface in hydrogen. Journal of Chemical Physics, 2013, 139, 024704.	1.2	9
15350	THERMAL PROPERTIES OF THE XB₂(X = Ag, Au) COMPOUNDS: A FIRST-PRINCIPLES STUDY. International Journal of Modern Physics B, 2013, 27, 1350046.	1.0	0
15351	Engineering a topological phase transition in Î²-InSe via strain. New Journal of Physics, 2013, 15, 073008.	1.2	29
15352	Site occupation of doping La³⁺cations and phase transition in Na_{0.5}Bi_{0.5}TiO₃-BaTiO₃solid solution. Chinese Physics B, 2013, 22, 036401.	0.7	4
15353	THEORETICAL STUDY OF PHASE FORMING, MAGNETIZATION AND LATTICE VIBRATIONS OF Fe23-xTxB6(T = Cr,) Tj ETQq0 0 0 rgBT /Over	1.0	1
15354	Origins of electrochemical performance of olivine phosphate as cathodes in Li-ion batteries: Charge transfer, spin-state, and structural distortion. Journal of Renewable and Sustainable Energy, 2013, 5, 053130.	0.8	7
15355	FIRST-PRINCIPLES STUDY ON Î²-SiC/BNNT CORE/SHELL NANOCABLE. Modern Physics Letters B, 2013, 27, 1350169.	1.0	0
15356	FIRST-PRINCIPLES STUDIES OF PRESSURE-INDUCED STRUCTURAL AND INSULATOR-TO-METAL TRANSITIONS IN ALKALINE-EARTH-METAL DICARBIDES MC₂ (M =) Tj ETQq1 1 0.784314 rgBT /Overlock 10 Tf 5		

#	Article	IF	Citations
15357	Mechanical properties and electronic structures of VC, V₄C₃and V₈C₇from first principles. Physica Scripta, 2013, 88, 015301.	1.2	32
15358	Disparate effects of an O2 internal impurity on the elongation and quantum transport of gold and silver nanowires. Journal of Applied Physics, 2013, 114, 074315.	1.1	1
15359	A first-principles study on defect association and oxygen ion migration of Sm³⁺and Gd³⁺co-doped ceria. Journal of Physics Condensed Matter, 2013, 25, 225401.	0.7	20
15360	FIRST PRINCIPLES DENSITY FUNCTIONAL INVESTIGATION OF SUPPORTED TUNGSTEN CLUSTER (W_n; n = 1 TO 6) ON ANCHORED GRAPHITE (0001) SURFACE. International Journal of Computational Materials Science and Engineering, 2013, 02, 1350015.	0.5	0
15361	The pressure dependences of elastic and lattice dynamic properties of AlAs fromab initiocalculations. Chinese Physics B, 2013, 22, 026201.	0.7	3
15362	Lattice stability and formation energies of intrinsic defects in Mg2Si and Mg2Ge via first principles simulations. Journal of Physics Condensed Matter, 2013, 25, 035403.	0.7	36
15363	Structural and Optoelectronic Characterization of RF Sputtered ZnSnN₂. Advanced Materials, 2013, 25, 2562-2566.	11.1	161
15364	Topologically close-packed phases in binary transition-metal compounds: matching high-throughputab initiocalculations to an empirical structure map. New Journal of Physics, 2013, 15, 115016.	1.2	40
15365	Pressure-induced changes in electronic and vibrational properties of LaS. Philosophical Magazine Letters, 2013, 93, 152-157.	0.5	1
15366	Firstâ€Principles Calculations of Lithiumâ€Ion Migration at a Coherent Grain Boundary in a Cathode Material, LiCoO₂. Advanced Materials, 2013, 25, 618-622.	11.1	149
15367	Between Scylla and Charybdis: Hydrophobic Graphene-Guided Water Diffusion on Hydrophilic Substrates. Scientific Reports, 2013, 3, 2309.	1.6	60
15368	First-principles investigations on the thermoelectric properties of Bi2Te3 doped with Se. Materials Research Society Symposia Proceedings, 2013, 1543, 23-28.	0.1	4
15369	Ferroelectricity Driven by Twisting of Silicate Tetrahedral Chains. Angewandte Chemie - International Edition, 2013, 52, 8088-8092.	7.2	62
15370	Formation Energy of Intrinsic Point Defects in Si and Ge and Implications for Ge Crystal Growth. ECS Journal of Solid State Science and Technology, 2013, 2, P104-P109.	0.9	19
15371	Mixed-mode mechanical responses of Ni(111)/Î±-Al2O3(0001) interface by first-principle calculations. Journal of Materials Research, 2013, 28, 3018-3028.	1.2	11
15372	Local environment of silicon in cubic boron nitride. Journal of Applied Physics, 2013, 114, 233502.	1.1	10
15373	FIRST-PRINCIPLES STUDY OF Ti-CATALYZED HYDROGEN ADSORPTION ON LiB (001) SURFACE. Journal of Theoretical and Computational Chemistry, 2013, 12, 1350065.	1.8	2
15374	A new cathode material for super-valent battery based on aluminium ion intercalation and deintercalation. Scientific Reports, 2013, 3, 3383.	1.6	286

#	Article	IF	Citations
15375	Electronic structure analysis of rare earth ions Ce and Nd doped gallium nitride. Journal of Applied Physics, 2013, 114, 123703.	1.1	7
15376	Magnetic behaviour of Er1â^'xZrxFe2intermetallic compounds. Journal of Physics Condensed Matter, 2013, 25, 466003.	0.7	5
15377	Intrinsic to extrinsic phonon lifetime transition in a GaAsâ€"AlAs superlattice. Journal of Physics Condensed Matter, 2013, 25, 295401.	0.7	6
15378	First-principles calculations of niobium hydride formation in superconducting radio-frequency cavities. Superconductor Science and Technology, 2013, 26, 095002.	1.8	17
15379	Structure and functionality of bromine doped graphite. Journal of Chemical Physics, 2013, 138, 164702.	1.2	8
15380	Ferromagnetism in ZnO:Co originating from a hydrogenated Coâ€"Oâ€"Co complex. Journal of Physics Condensed Matter, 2013, 25, 116002.	0.7	6
15381	Predicting Atomic Arrangement of Solute Clusters in Dilute Mg Alloys. Materials Research Letters, 2013, 1, 213-219.	4.1	44
15382	Investigation of PbTiO₃ thin films with reduced and re-oxidized treatment using Raman spectroscopy. Journal of the Ceramic Society of Japan, 2013, 121, 859-862.	0.5	5
15383	Density Function Theoretical Investigation on the Ni3PP Structure and the Hydrogen Adsorption Property of the Ni2P(0001) Surface. Chemistry Letters, 2013, 42, 1481-1483.	0.7	25
15384	Asymmetric Diarylethene as a Dual-Functional Device Combining Switch and Diode. Bulletin of the Chemical Society of Japan, 2013, 86, 947-954.	2.0	4
15385	Band gap of silicon nanowires along [111] direction doped with Al atoms. International Journal of Nanoparticles, 2013, 6, 275.	0.1	1
15386	First-principles study of H adsorption on graphene/SiC(0001). Physica Status Solidi (B): Basic Research, 2013, 250, 2523-2528.	0.7	4
15388	Effects of Hindered Rotation on H₂Nuclear Spin Conversion on Ag(111). Journal of the Physical Society of Japan, 2013, 82, 023601.	0.7	9
15389	Introduction to carbon-based nanostructures. , 0, , 1-10.		0
15390	Electronic properties of carbon-based nanostructures. , 0, , 11-90.		0
15391	Hybrid functional study on diffusion of silicate cathode material Li₂NiSiO₄. Journal of Physics: Conference Series, 2013, 454, 012061.	0.3	13
15392	First principles electronic structure of coincidence site epitaxial Ag/Si(111) interface. Physica Status Solidi (B): Basic Research, 2013, 250, 1313-1319.	0.7	17
15393	Crystal structure solution of an elusive polymorph of Dibenzylsquaramide. Powder Diffraction, 2013, 28, S470-S480.	0.4	6

#	Article	IF	Citations
15394	Magnetic ordering and structural stability of La_{2/3}Sr_{1/3}MnO₃/SrTiO₃ (001) interfaces: A densityâ€functional theory study. Physica Status Solidi (B): Basic Research, 2013, 250, 402-410.	0.7	0
15395	Low intensity conduction states in FeS₂: implications for absorption, open-circuit voltage and surface recombination. Journal of Physics Condensed Matter, 2013, 25, 465801.	0.7	38
15396	Extracting the hybrid functional mixing parameter from a GW quasiparticle approach. Physica Status Solidi (B): Basic Research, 2013, 250, 1449-1452.	0.7	2
15397	Nonâ€linear electroâ€elastic coupling in highly strained zincâ€blende compounds: InGaP/GaP [111] quantum wells. Physica Status Solidi (B): Basic Research, 2013, 250, 765-768.	0.7	0
15398	Origin of the visible light absorption of Co²⁺ and <scp>NH</scp>₄⁺ coâ€doped hydrogen titanate nanotube thin films. Physica Status Solidi (B): Basic Research, 2013, 250, 1592-1598.	0.7	6
15399	Carbon at the Ti site in strontium titanate from first principles. Journal of Physics: Conference Series, 2013, 472, 012006.	0.3	5
15401	Vacancy clustering in pure metals: some first principle calculations of positron lifetimes and momentum distributions. Journal of Physics: Conference Series, 2013, 443, 012019.	0.3	10
15402	Ab initio-aided CALPHAD thermodynamic modeling of the Sn-Pb binary system under current stressing. Scientific Reports, 2013, 3, 2731.	1.6	17
15403	First-principles study of structural and electronic properties of Laves phases structures YM2(M = Cu) Tj ETQq0 0 0 rgBT /Overlock 10 Tf 5	0.1	5
15404	Rational design of Nb-based alloys for hydrogen separation: A first principles study. AIP Advances, 2013, 3, .	0.6	2
15406	Computational Modeling of the Size Effects on the Optical Vibrational Modes of H-Terminated Ge Nanostructures. Molecules, 2013, 18, 4776-4785.	1.7	6
15407	Thermodynamic Analysis of Phase Equilibria in the Mg–Al–Ho Ternary System. Materials Transactions, 2013, 54, 647-655.	0.4	6
15408	Electronic structures of oxygen-deficient Ta2O5. AIP Advances, 2013, 3, .	0.6	26
15409	Structural, electronic and magnetic properties of Fe and Co monatomic nanochains encapsulated in BN nanotube bundle. EPJ Applied Physics, 2013, 62, 30402.	0.3	14
15410	Promising ferrimagnetic double perovskite oxides towards high spin polarization at high temperature. AIP Advances, 2013, 3, .	0.6	14
15411	Structural, elastic, electronic and magnetic properties of Fe₃AC; A = Al, Ga and In. MATEC Web of Conferences, 2013, 5, 04042.	0.1	2
15412	Empirical Prediction of Electronic Potentials of Single-Walled Carbon Nanotubes With a Specific Chirality (n,m). Scientific Reports, 2013, 3, 2959.	1.6	51
15413	Rotational Effects on the Dissociative Adsorption and Abstraction Dynamics of O₂/Al(111). Journal of the Physical Society of Japan, 2013, 82, 113602.	0.7	4

#	Article	IF	Citations
15414	First-Principles Prediction of Possible Synthesis of Li-Fe Based Complex Hydride Li4FeH6. Nippon Kinzoku Gakkaishi/Journal of the Japan Institute of Metals, 2013, 77, 604-608.	0.2	10
15415	Theoretical Calculations of Segregation Behavior of Zinc and Magnesium at Hydroxyapatite Surface in Contact with Water. Materials Transactions, 2013, 54, 1262-1267.	0.4	2
15416	First Principles Calculations of Solute Ordering in Mg–Zn–Y Alloys. Materials Transactions, 2013, 54, 656-660.	0.4	3
15417	First-Principles Investigation on the Lithium Ion Insertion/Extraction in Trirutile LixFeF3. Electrochemistry, 2013, 81, 12-15.	0.6	8
15418	Enthalpies of Solution in Ti–X (X = Mo, Nb, V and W) Alloys from First-Principles Calculations. Materials Transactions, 2013, 54, 484-492.	0.4	36
15419	First-Principles Calculation on Interaction of Dopant-Point Defect Complex and Metal Atom in Si Crystal. Nihon Kikai Gakkai Ronbunshu, A Hen/Transactions of the Japan Society of Mechanical Engineers, Part A, 2013, 79, 327-335.	0.2	0
15420	First-Principles Calculation of Grain Boundary Excess Volume and Free Volume in Nanocrystalline and Ultrafine-Grained Aluminum. Materials Transactions, 2013, 54, 1597-1604.	0.4	13
15421	Energetic Stability and Thermoelectric Property of Alkali-Metal-Encapsulated Type-I Silicon-Clathrate from First-Principles Calculation. Materials Transactions, 2013, 54, 276-285.	0.4	16
15422	Theoretical Characterizations of Spinels Containing Iron and Vanadium via ab initio Calculations. ISIJ International, 2013, 53, 245-249.	0.6	5
15423	First-Principles Elucidation of the Surface Chemistry of the C2Hx (x = 0â€“6) Adsorbate Series on Fe(100). Molecules, 2013, 18, 3806-3824.	1.7	22
15424	Density Functional Theory with Modified Dispersion Correction for Metals Applied to Self-Assembled Monolayers of Thiols on Au(111). Journal of Theoretical Chemistry, 2013, 2013, 1-9.	1.5	37
15425	Low-Resistivity p-Type Doping in Wurtzite ZnS Using Codoping Method. Advances in Condensed Matter Physics, 2013, 2013, 1-4.	0.4	2
15426	Structural, Elastic, and Electronic Properties of Antiperovskite Chromium-Based Carbides ACCr₃(A = Al and Ga). Advances in Condensed Matter Physics, 2013, 2013, 1-7.	0.4	8
15427	Effect of Intrinsic Point Defect on the Magnetic Properties of ZnO Nanowire. Scientific World Journal, The, 2013, 2013, 1-6.	0.8	5
15428	Elements Science and Technology Project: Design of Precious Metal Free Catalyst for NO Dissociation. Journal of the Japan Petroleum Institute, 2013, 56, 357-365.	0.4	4
15429	On the electronic properties of some metals using density-functional theory. International Journal of Physical Research, 2013, 1, .	0.5	0
15431	Graphene-Based Sensors for Monitoring Strain. International Journal of Chemoinformatics and Chemical Engineering, 2013, 3, 74-83.	0.1	0
15432	First-Principles Calculation of Hydrogen Effects on the Formation and Diffusion of Vacancies in Alpha Iron: Discussion of the Hydrogen-Enhanced Strain-Induced Vacancy Mechanism. Zairyo/Journal of the Society of Materials Science, Japan, 2014, 63, 182-187.	0.1	27

#	Article	IF	Citations
15433	Core level binding energies of functionalized and defective graphene. Beilstein Journal of Nanotechnology, 2014, 5, 121-132.	1.5	70
15434	The role of oxygen and water on molybdenum nanoclusters for electro catalytic ammonia production. Beilstein Journal of Nanotechnology, 2014, 5, 111-120.	1.5	25
15435	Preparation of Compensation Ions Codoped SrTiO3:Pr3+ Red Phosphor with the Sol-Gel Method and Study of Its Luminescence Enhancement Mechanism. Advances in OptoElectronics, 2014, 2014, 1-9.	0.6	1
15436	Study of Structural and Electronic Behavior of BeH2 as Hydrogen Storage Compound: An Ab Initio Approach. Conference Papers in Science, 2014, 2014, 1-5.	0.3	1
15437	Thermal Conductivity of Uranium Nitride and Carbide. International Journal of Nuclear Energy, 2014, 2014, 1-7.	0.4	30
15438	Preparation of Zirconium Oxide Powder Using Zirconium Carboxylate Precursors. Advances in Physical Chemistry, 2014, 2014, 1-8.	2.0	8
15439	Optical Properties of Al- and Zr-Doped Rutile Single Crystals Grown by Tilting-Mirror-Type Floating Zone Method and Study of Structure-Property Relationships by First Principle Calculations. Chinese Journal of Inorganic Chemistry, 2014, 2014, 1-11.	0.2	2
15440	Revisiting the Zinc-Blende/Wurtzite Heterocrystalline Structure in CdS. Advances in Condensed Matter Physics, 2014, 2014, 1-7.	0.4	5
15441	DFT Study of the Electronic Structure of Cubic-SiC Nanopores with a C-Terminated Surface. Journal of Nanomaterials, 2014, 2014, 1-7.	1.5	7
15442	Effect of Nitrogen Impurity on Electronic Properties of Boron Nanotubes. Advances in Condensed Matter Physics, 2014, 2014, 1-8.	0.4	0
15443	Effects of Vacancy Cluster Defects on Electrical and Thermodynamic Properties of Silicon Crystals. Scientific World Journal, The, 2014, 2014, 1-8.	0.8	5
15444	Noble-Metal Chalcogenide Nanotubes. Inorganics, 2014, 2, 556-564.	1.2	7
15445	The Role of Lead (Pb) in the High Temperature Formation of MoS2 Nanotubes. Inorganics, 2014, 2, 363-376.	1.2	7
15446	Ab. initio study of the structural, elastic, electronic and optical properties of Cu3N. Materials Research, 2014, 17, 303-310.	0.6	19
15447	Quasi-1D physics in metal-organic frameworks: MIL-47(V) from first principles. Beilstein Journal of Nanotechnology, 2014, 5, 1738-1748.	1.5	23
15448	A comparative study TiC/TiN and TiN/CN multilayers. DYNA (Colombia), 2014, 81, 160-165.	0.2	6
15449	Structural, electronic and magnetic properties of Fe, Co, Ni monatomic nanochains encapsulated in BeO nanotubes bundle. EPJ Applied Physics, 2014, 65, 20402.	0.3	11
15450	Advanced study of hydrogen storage by substitutional doping of Mn and Ti in Mg2Ni phase. International Journal for Simulation and Multidisciplinary Design Optimization, 2014, 5, A24.	0.6	2

#	Article	IF	Citations
15451	Ab initio parameterisation of the 14 band kÂ·p Hamiltonian: Zincblende study. Journal of Physics: Conference Series, 2014, 526, 012004.	0.3	0
15452	First-Principles Study of Ferroelectric-Ferromagnetic Coupling in Multiferroic BiFeO3. Zairyo/Journal of the Society of Materials Science, Japan, 2014, 63, 168-173.	0.1	1
15453	Structural properties of (B3) TlP under pressure. International Journal of Physical Research, 2014, 2, .	0.5	3
15454	Analysis of the Changes in Electronic Structures and Work Function Variation in Alkali Metal^|^mdash;Metal Surface Systems. Journal of the Vacuum Society of Japan, 2014, 57, 27-31.	0.3	7
15455	Theoretical Study on the High-Temperature P6Ì„ and P6Ì„â€² Phases of Si3N4: A Tool to Aid in Ceramics Development. Chinese Journal of Chemical Physics, 2014, 27, 103-108.	0.6	0
15456	Optoelectronic and thermal properties of boron-bismuth compound. International Journal of Physical Research, 2014, 2, .	0.5	5
15457	First-principles study of structural, electronic and optical properties of ZnF ₂. Chinese Physics B, 2014, 23, 077102.	0.7	6
15458	Fe₃S₄and Fe₃O₄magnetic nanocrystals: magneto-optical and MÂ¶ssbauer spectroscopy study. Materials Research Express, 2014, 1, 025033.	0.8	13
15459	Solute effect on basal and prismatic slip systems of Mg. Journal of Physics Condensed Matter, 2014, 26, 445004.	0.7	21
15460	The generalized planar fault energy, ductility, and twinnability of Al and Alâ€”RE(RE= Sc, Y,) Tj ETQq1 1 0.784314 rgBT	0.7	6
15461	Stability and mobility of rhenium and osmium in tungsten: first principles study. Modelling and Simulation in Materials Science and Engineering, 2014, 22, 075006.	0.8	81
15462	Effect of temperature on elastic constants, generalized stacking fault energy and dislocation cores in MgO and CaO. Computational Condensed Matter, 2014, 1, 38-44.	0.9	13
15463	Physical properties of RbAu compound. Computational Condensed Matter, 2014, 1, 32-37.	0.9	8
15464	Determination of the finite-temperature anisotropic elastic and thermal properties of Ge3N4: A first-principles study. Computational Condensed Matter, 2014, 1, 1-7.	0.9	9
15465	First principles study on the structural, electronic and magnetic properties of Ni4C. Computational Condensed Matter, 2014, 1, 51-57.	0.9	11
15466	First Principles Study on the Electrochemical, Thermal and Mechanical Properties of LiCoO2 for Thin Film Rechargeable Battery. Materials Today: Proceedings, 2014, 1, 82-93.	0.9	28
15467	Trends in the Adsorption and Dissociation of Water Clusters on Flat and Stepped Metallic Surfaces. Journal of Physical Chemistry C, 2014, 118, 29990-29998.	1.5	27
15468	Electrical control of spin polarization of conductance in Mn-encapsulated Si nanotube. Applied Physics Express, 2014, 7, 075001.	1.1	1

#	Article	IF	Citations
15469	DFT study on the interaction between atomic aluminum and graphene. Journal of Theoretical and Computational Chemistry, 2014, 13, 1450055.	1.8	7
15470	Theoretical investigation of thermodynamic stability and mobility of the oxygen vacancy in ThO₂â€“UO₂solid solutions. Physical Chemistry Chemical Physics, 2014, 16, 25461-25467.	1.3	22
15471	Ab initio study of the structural, electronic, elastic and thermal properties of RMn2Ge2 (R = Ca, Nd) Tj ETQq0 0 0 rgBT /Overlock 10 Tf 5	2.8	8
15472	First-principles calculations on Si (220) located 6Hâ€”SiC (101Ì„0) surface with different stacking sites. Chinese Physics B, 2014, 23, 106802.	0.7	1
15473	Effects of C impurities on the elastic properties of NiAl intermetallics. Progress in Natural Science: Materials International, 2014, 24, 637-641.	1.8	9
15474	Luminescent centers in GaN codoped with Eu and Mg: Calculation on density functional theory. Japanese Journal of Applied Physics, 2014, 53, 061001.	0.8	8
15475	Electronic structure, magnetic and thermal properties of Rh2MnZ (Z=Ge, Sn, Pb) compounds under pressure from ab-initio quasi-harmonic method. Journal of Magnetism and Magnetic Materials, 2014, 371, 130-134.	1.0	8
15476	Piezoelectricity enhancement in Dion-Jacobson RbBiNb ₂ O ₇ via negative pressure. Europhysics Letters, 2014, 108, 67006.	0.7	13
15477	THEORETICAL STUDY OF THE ADSORPTION AND DIFFUSION OF OXYGEN ATOM ON O-TERMINATED ZnO$(000ar 1)$ SURFACE. Nano, 2014, 09, 1450006.	0.5	2
15478	First principles calculations of electronic and optical properties of GaN_{1â^’x}Bi_xalloys. Journal of Semiconductors, 2014, 35, 122002.	2.0	3
15479	THE ELECTRONIC AND OPTICAL PROPERTIES OF X-DOPED SrTiO₃ (X = Rh, Pd,) Tj ETQq0 0 0 rgBT /Overlock	1.0	8
15480	DENSITY FUNCTIONAL THEORY STUDIES ON THE ADSORPTION OF 4-METHYLBENZENETHIOL AND 4-ETHYLBENZENETHIOL MOLECULES ONAu(111) SURFACE. Surface Review and Letters, 2014, 21, 1450087.	0.5	1
15481	Highly mobile segments in crystalline poly(ethylene oxide)8:NaPF6 electrolytes studied by solid-state NMR spectroscopy. Journal of Chemical Physics, 2014, 140, 074901.	1.2	10
15482	Full-wave techniques for the electromagnetic-quantum transport modeling in nano-devices. , 2014, , .		0
15483	FIRST-PRINCIPLES STUDY OF ELECTRONIC AND OPTICAL PROPERTIES OF Mn-DOPED 3C-SiC FILMS. Surface Review and Letters, 2014, 21, 1450002.	0.5	7
15484	Electronic structure, elastic and thermal properties of semiconductor GaX (X = N, P, As, Sb) with zinc blende from first-principles calculation. International Journal of Modern Physics B, 2014, 28, 1450183.	1.0	7
15485	First-principles study of the stability of silicane and germanane under strain. Modern Physics Letters B, 2014, 28, 1450138.	1.0	4
15486	Effect of Surface Dangling Bonds and Molecular Passivation on Doped GaAs Nanowires. Chinese Journal of Chemical Physics, 2014, 27, 685-689.	0.6	1

#	Article	IF	Citations
15487	The investigation of transition metal doped CuGaS₂ for promising intermediate band materials. RSC Advances, 2014, 4, 62380-62386.	1.7	49
15488	Ab initio design of nanostructures for solar energy conversion: a case study on silicon nitride nanowire. Nanoscale Research Letters, 2014, 9, 531.	3.1	2
15489	Structure, Phase Transition, and Electronic Properties of <scp><scp>K</scp></scp>_{1â^'x}<scp><scp>Na</scp></scp>_x<scp><scp>NbO</scp></scp><sul Solid Solutions from Firstâ€Principles Theory. Journal of the American Ceramic Society, 2014, 97, 4019-4023.	1.9	25
15490	Unexpected change in the electron affinity of diamond caused by the ultra-thin transition metal oxide films. Europhysics Letters, 2014, 108, 46005.	0.7	20
15491	ELASTIC, ELECTRONIC AND THERMODYNAMIC PROPERTIES OF Rh₃X(X = Zr, Nb and) Tj ETQq0 0 0 rgBT /Overlock 10 Tf 50 582 T 1450006.	1.0	6
15492	Effects of defects on the electronic properties of WTe₂armchair nanoribbons. Journal of Semiconductors, 2014, 35, 113002.	2.0	9
15493	Effect of hydrostatic pressure on the thermoelectric properties of<mml:math xmlns:mml="http://www.w3.org/1998/Math/MathML"><mml:mrow><mml:msub><mml:mi mathvariant="bold">Bi</mml:mi><mml:mn>2</mml:mn></mml:msub><mml:msub><mml:mi mathvariant="bold">Te</mml:mi><mml:mn>3</mml:mn></mml:msub></mml:mrow></mml:math>. Physical Review B, 2014, 90, .	1.1	29
15494	Pressure-Induced Enhancement of Superconductivity and Structural Transition in BiS₂-Layered LaO_{1â^'}_xF_xBiS₂. Journal of the Physical Society of Japan, 2014, 83, 063704.	0.7	111
15495	INTERLAYER INTERACTION AND SCREENING IN MoS₂. Surface Review and Letters, 2014, 21, 1450039.	0.5	13
15496	Molecular modeling of the conductivity of carbon nanotubes under different temperature and humidity. , 2014, , .		0
15497	Electronic, phononic, and thermoelectric properties of graphyne sheets. Applied Physics Letters, 2014, 105, 223108.	1.5	64
15498	DFT calculation on relaxation and electronic structure of sulfide minerals surfaces in presence of H2O molecule. Journal of Central South University, 2014, 21, 3945-3954.	1.2	35
15499	Adsorption and diffusion of oxygen atom on UN2(100) surface and subsurface: a density functional theory study (DFT and DFTÂ+ÃU). Journal of Nanostructure in Chemistry, 2014, 4, 143-151.	5.3	4
15500	Understanding the structure and electronic properties of N-doped graphene nanoribbons upon hydrogen saturation. Journal of Chemical Sciences, 2014, 126, 1737-1742.	0.7	26
15501	The Reduction-Coupled Oxo Activation (ROA) Mechanism Responsible for the Catalytic Selective Activation and Functionalization of n-Butane to Maleic Anhydride by Vanadium Phosphate Oxide. Topics in Catalysis, 2014, 57, 1171-1187.	1.3	39
15502	A DFT, X- and W-band EPR and ENDOR Study of Nitrogen-Centered Species in (Nano)Hydroxyapatite. Applied Magnetic Resonance, 2014, 45, 1189-1203.	0.6	27
15503	A DFT Study of Ethanol Adsorption and Dehydrogenation on Cu/Cr2O3 Catalyst. Catalysis Letters, 2014, 144, 1978-1986.	1.4	17
15504	Ab-initio study of the interfacial properties in ultrathin MgO films on O-rich FeO/Fe(001) surfaces. Journal of the Korean Physical Society, 2014, 65, 702-708.	0.3	4

#	Article	IF	Citations
15505	Stability of vacancy-hydrogen clusters in nickel from first-principles calculations. Acta Materialia, 2014, 78, 135-143.	3.8	70
15506	Mechanical Properties and Electronic Structure of N and Ta Doped TiC: A First-Principles Study. Communications in Theoretical Physics, 2014, 62, 895-902.	1.1	13
15507	Electronic structure and magnetic properties of (Mn, N)-codoped ZnO. Chinese Physics B, 2014, 23, 123101.	0.7	1
15508	Stability and electronic structure studies of LaAlO 3 /SrTiO 3 (110) heterostructures. Chinese Physics B, 2014, 23, 087302.	0.7	6
15509	Effect of Cr, Mo, and Nb additions on intergranular cohesion of ferritic stainless steel: First-principles determination. Chinese Physics B, 2014, 23, 037102.	0.7	10
15510	Elastic and thermodynamic properties of vanadium nitride under pressure and the effect of metallic bonding on its hardness. Chinese Physics B, 2014, 23, 026201.	0.7	9
15511	DFT study of nitrogenâ€“vacancy complexions in (fcc) Fe. Modelling and Simulation in Materials Science and Engineering, 2014, 22, 055004.	0.8	5
15512	Ab initiostudy on stacking sequences, free energy, dynamical stability and potential energy surfaces of graphite structures. Modelling and Simulation in Materials Science and Engineering, 2014, 22, 035016.	0.8	13
15513	Effects of the 3d transition metal doping on the structural, electronic, and magnetic properties of BeO nanotubes. Chinese Physics B, 2014, 23, 017103.	0.7	1
15514	A strategy of enhancing the photoactivity of TiO ₂ containing nonmetal and transition metal dopants. Chinese Physics B, 2014, 23, 027305.	0.7	4
15515	Reflectance anisotropy of the anatase Tio₂(0â€‰0â€‰1)-(4 Ã— 1) surface. Journal of Physics Condensed Matter, 2014, 26, 445006.	0.7	1
15516	Modulation of transport properties of RuO₂with 3d transition metals. Materials Research Express, 2014, 1, 045034.	0.8	8
15517	First-principles investigation of chemical modification on two-dimensional ironâ€”phthalocyanine sheet. Chinese Physics B, 2014, 23, 018103.	0.7	3
15518	Modeling of the self trapping of helium and the trap mutation in tungsten using DFT and empirical potentials based on DFT. Journal of Materials Research, 2014, 29, 2374-2386.	1.2	35
15519	Adsorptions and diffusions of carbon atoms on the surface and in the subsurface of Co (200): A first-principles density-functional study. Chinese Physics B, 2014, 23, 086802.	0.7	1
15520	Role of helium in the sliding and mechanical properties of a vanadium grain boundary: A first-principles study. Chinese Physics B, 2014, 23, 056104.	0.7	5
15521	Anisotropy of elasticity and minimum thermal conductivity of monocrystal M 4 AlC 3 (M = Ti, Zr, Hf). Chinese Physics B, 2014, 23, 096201.	0.7	7
15522	First-principles study of the Pdâ€“Si system and Pd(0 0 1)/SiC(0 0 1) hetero-structure. Journal of Nuclear Materials, 2014, 454, 308-314.	1.3	7

#	Article	IF	Citations
15523	DFT investigation of high temperature water gas shift reaction on chromiumâ€“iron mixed oxide catalyst. International Journal of Hydrogen Energy, 2014, 39, 19563-19569.	3.8	6
15524	High Pressure Phase of LiAlO2: A First Principles Study. Integrated Ferroelectrics, 2014, 156, 15-22.	0.3	5
15525	First-principles study of point defects in thorium carbide. Journal of Nuclear Materials, 2014, 454, 217-222.	1.3	18
15526	First-principles investigation of the structural, electronic and elastic properties of Al2Ca and Al4Sr phases in Mg-Al-Ca(Sr) alloy. Journal Wuhan University of Technology, Materials Science Edition, 2014, 29, 1049-1056.	0.4	7
15527	A First-principles Study of Spin-polarized Transport Properties of a Co-coordination Complex. Chinese Physics Letters, 2014, 31, 067302.	1.3	2
15528	Species fractionation in atomic chains from mechanically stretched alloys. Journal of Physics Condensed Matter, 2014, 26, 435304.	0.7	0
15529	Automated effective band structures for defective and mismatched supercells. Journal of Physics Condensed Matter, 2014, 26, 485501.	0.7	6
15530	Strain-induced improvements on piezoelectric and nonlinear optical properties of BiAlO3. Materials Research Express, 2014, 1, 036301.	0.8	2
15531	Ab initio calculation of the thermal conductivity of indium antimonide. Semiconductor Science and Technology, 2014, 29, 124002.	1.0	6
15532	Thermodynamic Properties of Copper in a Wide Range of Pressure and Temperature Within the Quasi-Harmonic Approximation. International Journal of Thermophysics, 2014, 35, 1501-1511.	1.0	7
15533	Synthesis of TaC and Ta $$_2$$ 2 C from tantalum and graphite in the laser-heated diamond anvil cell. Science Bulletin, 2014, 59, 5283-5289.	1.7	2
15534	Electronic properties of BaTiO3 (110) polar terminations. Chemical Research in Chinese Universities, 2014, 30, 794-799.	1.3	5
15535	Cation Vacancy-Induced Ferromagnetism in Nanocrystalline CaTiO₃ Plate. IEEE Transactions on Magnetics, 2014, 50, 1-4.	1.2	1
15536	Vibrational lifetimes of hydrogen on lead films: An ab initio molecular dynamics with electronic friction (AIMDEF) study. Journal of Chemical Physics, 2014, 141, 234702.	1.2	40
15537	Atomistic Origin of the Enhanced Crystallization Speed and nâ€Type Conductivity in Biâ€doped Geâ€Sbâ€Te Phaseâ€Change Materials. Advanced Functional Materials, 2014, 24, 7291-7300.	7.8	38
15538	Simple bond-order-type interatomic potential for an intermixed Fe-Cr-C system of metallic and covalent bondings in heat-resistant ferritic steels. Journal of Applied Physics, 2014, 116, 244311.	1.1	2
15539	Charging mechanism of AlGaN/GaN open-gate pH sensor and electrolyte interface. , 2014, , .		3
15540	Ab initio study of native defects in SnO under strain. Europhysics Letters, 2014, 106, 16001.	0.7	22

#	Article	IF	Citations
15541	Ab initio computation on the Fe L-edge X-ray emission spectroscopy of Fe-bearing MgSiO3 perovskite. American Mineralogist, 2014, 99, 387-392.	0.9	1
15542	Hydrogen adsorption of Be-, Zn-, and Cd-zeolitic imidazolate framework-23: A comparative study. Japanese Journal of Applied Physics, 2014, 53, 08NK03.	0.8	3
15543	Density Functional Study of Benzoic Acid Derivatives Modified SnO2 (110) Surface. Materials Research Society Symposia Proceedings, 2014, 1633, 69-74.	0.1	0
15544	Hexagonal Na0.41[Na0.125Mg0.79Al0.085]2[Al0.79Si0.21]6O12 (NAL phase): Crystal structure refinement and elasticity. American Mineralogist, 2014, 99, 1562-1569.	0.9	10
15545	NMR characterization of hydrocarbon adsorption on calcite surfaces: A first principles study. Journal of Chemical Physics, 2014, 141, 204705.	1.2	14
15546	Comparative modelling of chemical ordering in palladium-iridium nanoalloys. Journal of Chemical Physics, 2014, 141, 224307.	1.2	23
15547	Spin-coupling in dimers of 2,3-dicyano-5,6-dichlorosemiquinone radical anions in the crystalline state. Acta Crystallographica Section B: Structural Science, Crystal Engineering and Materials, 2014, 70, 181-190.	0.5	16
15548	Tritium Solubility in Li₂TiO₃ from First-Principles Simulations. Journal of Physical Chemistry C, 2014, 118, 29525-29532.	1.5	33
15549	Fluorinated graphene and hexagonal boron nitride as ALD seed layers for graphene-based van der Waals heterostructures. Nanotechnology, 2014, 25, 355202.	1.3	5
15550	Structure and Electronic and Charge-Transfer Properties of Mercaptobenzoic Acid and Mercaptobenzoic Acidâ€“Undecanethiol Mixed Monolayers on Au(111). Journal of Physical Chemistry C, 2014, 118, 30013-30022.	1.5	11
15551	Elastic constants and Debye temperature of wz-AlN and wz-GaN semiconductors under high pressure from first-principles. Pramana - Journal of Physics, 2014, 83, 413-425.	0.9	7
15552	Enhanced visible light photocatalytic activity of anatase TiO₂ through C, N, and F codoping. Canadian Journal of Physics, 2014, 92, 71-75.	0.4	7
15553	Elastic properties and lattice dynamics of ruthenium at high pressures. Journal of Physics: Conference Series, 2014, 490, 012059.	0.3	4
15555	Adsorption and activation of copper ions on chalcopyrite surfaces: A new viewpoint of self-activation. Transactions of Nonferrous Metals Society of China, 2014, 24, 3955-3963.	1.7	40
15556	Inâ€Gap States in Electronic Structure of Nonpolar Surfaces of Insulating Metal Oxides. Advanced Materials Interfaces, 2014, 1, 1300131.	1.9	11
15557	Uniform B-C-N Ternary Monolayer from Non-Metal Filled g-C3N4 Sheet. Chinese Journal of Chemical Physics, 2014, 27, 394-398.	0.6	4
15558	Comparative investigation of NbN and Nb-Si-N films: Experiment and theory. Journal of Superhard Materials, 2014, 36, 381-392.	0.5	7
15559	First-principles Study of Antisite Defects in Orthorhombic PbZrO3. Integrated Ferroelectrics, 2014, 156, 86-92.	0.3	4

#	Article	IF	Citations
15560	Electronic properties of two-dimensional ZnO atomically sheet on Cu substrate: a first-principles study. Modern Physics Letters B, 2014, 28, 1450204.	1.0	3
15561	The investigation of dependences of mechanical and electronic properties of TiB₂on pressure using the first-principles method. Physica Scripta, 2014, 89, 115702.	1.2	16
15562	Electronic and thermoelectric properties of InN studied using ab initio density functional theory and Boltzmann transport calculations. Journal of Applied Physics, 2014, 116, 223706.	1.1	8
15563	Ab initio study of point defects in PbSe and PbTe: Bulk and nanowire. Journal of Applied Physics, 2014, 116, .	1.1	10
15564	Ab initio prediction of SiC nanotubes with negative strain energy. Applied Physics Letters, 2014, 104, .	1.5	4
15565	PHASE TRANSITION AND THERMODYNAMIC PROPERTIES OF MAGNESIUM FLUORIDE BY FIRST PRINCIPLES. International Journal of Modern Physics B, 2014, 28, 1450026.	1.0	7
15566	Complex borides based on AlLiB₁₄ as high-temperature thermoelectric compounds. Physical Chemistry Chemical Physics, 2014, 16, 25337-25341.	1.3	14
15567	Band engineering of GaN/AlN quantum wells by Si dopants. Journal of Applied Physics, 2014, 115, 124305.	1.1	6
15568	Zirconium metal-based MAX phases Zr₂AC (A =) Tj ETQq0 0 0 rgBT /Overlock 10 Tf 50 427 Td International Journal of Modern Physics B, 2014, 28, 1550022.	1.0	41
15569	Insights into Elastic and Thermodynamics Properties of Binary Intermetallics in Ni-Al Alloys under Extreme Condition: Full-Electronic Quasi-Harmonic Study. Chinese Journal of Chemical Physics, 2014, 27, 399-406.	0.6	4
15570	Adsorption and Surface Diffusion of Au Monomers and Dimers on Strongly Correlated NiO(001) Surfaces. Journal of the Physical Society of Japan, 2014, 83, 113602.	0.7	6
15571	Stability and electronic properties of hexagonal boron nitride monolayer with irregular graphene domains embedded. Modern Physics Letters B, 2014, 28, 1450144.	1.0	4
15572	First-principles studies of phase transition and structural stability of SrC2 under pressure. Modern Physics Letters B, 2014, 28, 1450190.	1.0	4
15573	Ab initio investigations of structural and electronic properties of AlSc3. International Journal of Computational Materials Science and Engineering, 2014, 03, 1450019.	0.5	1
15574	First Principles Study of Structural Stability and Magnetic Property of Non-equilibrium Coâ€“Mo Alloys. Acta Metallurgica Sinica (English Letters), 2014, 27, 1057-1062.	1.5	2
15575	Structural, elastic, electronic and optical properties of various mineral phases of TiO₂from first-principles calculations. Physica Scripta, 2014, 89, 075703.	1.2	15
15576	Mechanistic Study of CO Titration on Cu_xO/Cu(1â€‰1â€‰1) (xâ‰2) Surfaces. ChemCatChem, 2014, 6, 2364-2372.	1.8	31
15577	Effect of vacancy defects on generalized stacking fault energy of fcc metals. Journal of Physics Condensed Matter, 2014, 26, 115404.	0.7	21

#	Article	IF	Citations
15578	The (√3X√3) R30° sulfur over layer on the iridium(111) surface: A DFT study. , 2014, , .		1
15579	Development of nonlinear optical materials promoted by density functional theory simulations. International Journal of Modern Physics B, 2014, 28, 1430018.	1.0	27
15580	Effects of Mg Local Structure on Mg K-edge XANES Spectra of MgxZn1-xO Alloy: A First-principles Study. Integrated Ferroelectrics, 2014, 156, 72-78.	0.3	0
15581	Charge transition levels of Mn-doped Si calculated with the GGA-1/2 method. Physical Review B, 2014, 90, .	1.1	10
15582	Strain-induced variation of electronic structure of helium in tungsten and its effects on dissolution and diffusion. Computational Materials Science, 2014, 95, 536-539.	1.4	9
15583	First-principles calculations of the structural, phonon and thermal properties of ZnX (X = S, Se,Te) chalcogenides. Physica Scripta, 2014, 89, 075704.	1.2	24
15584	First-principles Prediction for Mechanical and Optical Properties of Al ₃ BC ₃. Chinese Physics Letters, 2014, 31, 066201.	1.3	3
15585	Atomic study of fracture progress ofFe[110]/TMC[100] (TM=Ti,ZrandHf) semi-coherent interfaces. Modern Physics Letters B, 2014, 28, 1450192.	1.0	1
15586	Tunable topological electronic structure of silicene on a semiconducting Bi/Si(111)-3Ã—3substrate. Physical Review B, 2014, 90, .	1.1	11
15587	Thickness Dependence of Fe3O4/MgO Thin Film Properties: Density Functional Theory Investigation. Integrated Ferroelectrics, 2014, 155, 143-149.	0.3	1
15588	Is silicene stable in O ₂ ? â€"First-principles study of O ₂ dissociation and O ₂ -dissociationâ€"induced oxygen atoms adsorption on free-standing silicene. Europhysics Letters, 2014, 106, 47001.	0.7	31
15589	First-Principles Study on the Corrosion Mechanism of Degradable Medical Mg Alloys in the Medium Containing Cl-. Applied Mechanics and Materials, 0, 528, 132-137.	0.2	0
15590	Density Functional Study of Bulk and Surface Properties of Rhodium Hydride. Acta Physica Polonica A, 2014, 125, 29-35.	0.2	6
15591	Energetic Studies on the B Effect on the Oxidation of Î³-TiAl Alloys. Advanced Materials Research, 2014, 1052, 28-33.	0.3	3
15592	Cr, Fe - Doped Anatase TiO2 Photocatalyst: DFT+U Investigation on Band Gap. Advanced Materials Research, 2014, 893, 31-34.	0.3	3
15593	Hydrogen Storage Mechanism of Fe₃O₄: A First-Principles Study. Advanced Materials Research, 2014, 936, 515-522.	0.3	0
15594	Strain-induced phase transition of a C₅₈ solid. Physical Chemistry Chemical Physics, 2014, 16, 25176-25181.	1.3	1
15595	Effect of Ni(111) surface alloying by Pt on partial oxidation of methane to syngas: A DFT study. Surface Science, 2014, 630, 236-243.	0.8	43

#	Article	IF	Citations
15596	Adsorption of ammonia at GaN(0001) surface in the mixed ammonia/hydrogen ambient - a summary of ab initio data. AIP Advances, 2014, 4, .	0.6	23
15597	Ab-Initio Calculations of Structural, Electronic, and Optical Properties of Cd1â€“xMnxTeAb-Initio Calculations of Structural, Electronic, and Optical Properties of Cd1â€“xMnxTe. International Journal of Applied Physics and Mathematics, 2014, 4, 176-179.	0.3	6
15598	Magnetocrystalline anisotropy and its electric-field-assisted switching of Heusler-compound-based perpendicular magnetic tunnel junctions. New Journal of Physics, 2014, 16, 103033.	1.2	43
15599	The two aluminum sites in the 27Al MAS NMR spectrum of kaolinite: Accurate determination of isotropic chemical shifts and quadrupolar interaction parameters. American Mineralogist, 2014, 99, 393-400.	0.9	11
15600	Tunable Band Gap and Conductivity Type of ZnSe/Si Core-Shell Nanowire Heterostructures. Materials, 2014, 7, 7276-7288.	1.3	1
15601	Atomic Study of Semi-Coherent Interfacial Structure at Fe[110]/TMC[001] (TM=V, Nb and Ta) Interfaces. Advanced Materials Research, 2014, 1081, 232-236.	0.3	6
15602	Silicene on metal and metallized surfaces:ab initiostudies. New Journal of Physics, 2014, 16, 075004.	1.2	24
15603	Phase stability predictions of (M= Ti, Hf, Zr;A= Si,X= B). Journal Physics D: Applied Physics, 2014, 47, 065308.	1.3	17
15604	First-principles investigation of bowing parameter in zinc-blendeSc_xGa_{1â^'x}N. Philosophical Magazine Letters, 2014, 94, 724-731.	0.5	3
15605	Optical Properties of BN and BBi Compounds. Acta Physica Polonica A, 2014, 125, 574-576.	0.2	3
15606	A New Potential Superhard Phase of OsN_2. Acta Physica Polonica A, 2014, 126, 740-747.	0.2	23
15607	Bounds on the range of density-functional-theory point-defect levels in semiconductors and insulators. Computational Materials Science, 2014, 92, 431-438.	1.4	11
15608	A comparative DFT study of the structural and electronic properties of nonpolar GaN surfaces. Applied Surface Science, 2014, 314, 794-799.	3.1	12
15609	Li adsorption on a Fullereneâ€“Single wall carbon nanotube hybrid system: Density functional theory approach. Current Applied Physics, 2014, 14, 1748-1754.	1.1	17
15610	Site preference and magnetic orderings in the intermetallic boride series M 1.5 Rh 5.5 B 3 (M = Cr, Mn,) Tj ETQq0 0 0 rgBT /Overlock 10	1.4	4
15611	CuPc/Au(1 1 0): Determination of the azimuthal alignment by a combination of angle-resolved photoemission and density functional theory. Journal of Electron Spectroscopy and Related Phenomena, 2014, 195, 293-300.	0.8	25
15612	Structural, electronic, elastic and thermodynamic properties of Zr 2 Fe and Zr 2 FeH 5 : A comprehensive study using first principles approach. Journal of Alloys and Compounds, 2014, 615, 234-242.	2.8	26
15613	First-principles study of water adsorption and dissociation on the UO2 (1 1 1), (1 1 0) and (1 0 0) surfaces. Journal of Nuclear Materials, 2014, 454, 446-454.	1.3	36

#	Article	IF	Citations
15614	Catalyst Poisoning Property of Sulfonimide Acid Ionomer on Pt (111) Surface. Journal of the Electrochemical Society, 2014, 161, F649-F652.	1.3	106
15615	Magnetic exchange force microscopy from first principles: application to the antiferromagnetic NiO(001) surface. New Journal of Physics, 2014, 16, 023020.	1.2	13
15616	Electronic and magnetic states of Mn2and Mn2H on Ag(111). New Journal of Physics, 2014, 16, 063021.	1.2	7
15617	First-principles study on the geometry and electronic structures of IIIA atoms doped Î±-Al2O3:VO. Canadian Journal of Physics, 2014, 92, 1135-1140.	0.4	1
15618	Enhancement of TE polarized light extraction efficiency in nanoscale (AlN)_m/(GaN)_n(m>n) superlattice substitution for Al-rich AlGaN disorder alloy: ultra-thin GaN layer modulation. New Journal of Physics, 2014, 16, 113065.	1.2	14
15619	ALattice parameters and band structure of ternary mixed crystals Al_xGa_{1â€“x}As from first-principle calculations. Journal of Physics: Conference Series, 2014, 490, 012172.	0.3	5
15620	First-Principles Study of the Structural, Elastic, and Mechanical Properties of Ni₃Ga Compound under Pressure. Acta Physica Polonica A, 2014, 125, 54-59.	0.2	4
15621	Elemental vacancy diffusion database from high-throughput first-principles calculations for fcc and hcp structures. New Journal of Physics, 2014, 16, 015018.	1.2	67
15622	Effects of electronic modification and structural distortion on ferromagnetism in sputtered CeO₂films with isovalent Sn⁴⁺doping. RSC Advances, 2014, 4, 63228-63233.	1.7	4
15623	Engineering electronic properties of metalâ€“MoSe₂ interfaces using self-assembled monolayers. Journal of Materials Chemistry C, 2014, 2, 9842-9849.	2.7	25
15624	Electronic Structures of the High-Pressure hcp and bcc Phases of Al: A Computer Aided Design and Simulation. Applied Mechanics and Materials, 2014, 556-562, 523-526.	0.2	0
15625	First-Principles Study on Hydrogen Desorption Properties of Li₄BN₃H₁₀ Doped by Chlorine Anion. Applied Mechanics and Materials, 0, 574, 363-367.	0.2	1
15626	Depleted Uranium as Hydrogen Storage Material. Advances in Science and Technology, 2014, 94, 32-37.	0.2	0
15627	Electron-Energy-Loss Spectra of Free-Standing Silicene. Journal of Nano Research, 2014, 28, 1-7.	0.8	3
15628	Computer Simulation: A Tool for Researching the Basic Physical Properties of NiAl and Ni₃Al. Advanced Materials Research, 0, 989-994, 216-219.	0.3	0
15629	Energetics of Slip Deformation in Beta-Sn: A First-Principles Study. Key Engineering Materials, 0, 626, 46-49.	0.4	3
15630	Establishment of Structural and Elastic Properties of Titanate Compounds Based on Pb, Sn and Ge by First-Principles Calculation. Applied Mechanics and Materials, 0, 510, 57-62.	0.2	6
15631	First-Principles Study of the Mechanical Properties of ScAl Microalloyed by 4d-Transition Metals. Advanced Materials Research, 0, 852, 198-202.	0.3	1

#	Article	IF	Citations
15632	First-principles elasticity of monocarboaluminate hydrates. American Mineralogist, 2014, 99, 1360-1368.	0.9	21
15633	Density Functional Theory Simulations of Semiconductors for Photovoltaic Applications: Hybrid Organic-Inorganic Perovskites and III/V Heterostructures. International Journal of Photoenergy, 2014, 2014, 1-11.	1.4	23
15634	Adsorption and reconstruction of metal-phthalocyanine molecules on Pt(001) investigated by density functional theory. Surface Science, 2014, 630, 202-207.	0.8	5
15635	Electronic Structure and Optical Properties of N/Si-Codoped Anatase TiO2Evaluated Using First Principles Calculations. International Journal of Photoenergy, 2014, 2014, 1-7.	1.4	1
15636	Ab initio thermodynamic and thermophysical properties of sapphirine end-members in the join Mg4Al8Si2O20-Mg3Al10SiO20. American Mineralogist, 2014, 99, 1449-1461.	0.9	20
15637	Electronic Structure of Wurtzite Ga_{0.75}Al_{0.25}N: A First Principle Calculation. Applied Mechanics and Materials, 0, 556-562, 43-46.	0.2	0
15638	Atomic and electronic structure of the SrNbO3/SrNbO3.4 interface. Applied Physics Letters, 2014, 105, .	1.5	18
15639	The structure of carbon monoxide adsorbed on the NaCl(100) surfaceâ€”A combined LEED and DFT-D/vdW-DF study. Journal of Chemical Physics, 2014, 141, 214708.	1.2	14
15640	Multi-scale simulation of the stability and diffusion of lithium in the presence of a 90Â° partial dislocation in silicon. Journal of Applied Physics, 2014, 116, 213504.	1.1	5
15641	Effect of nitrogen impurity on the structural, mechanical and phonon properties of diamond from first-principle study. Journal of Physics: Conference Series, 2014, 510, 012030.	0.3	1
15642	An environment-dependent semi-empirical tight binding model suitable for electron transport in bulk metals, metal alloys, metallic interfaces, and metallic nanostructures. I. Model and validation. Journal of Applied Physics, 2014, 115, 123703.	1.1	12
15643	Temperature dependence of electronic eigenenergies in the adiabatic harmonic approximation. Physical Review B, 2014, 90, .	1.1	91
15644	Atomic scale analysis of the GaP/Si(100) heterointerface by<i>in situ</i>reflection anisotropy spectroscopy and<i>ab initio</i>density functional theory. Physical Review B, 2014, 90, .	1.1	40
15645	Six-dimensional quantum dynamics for dissociative chemisorption of H₂and D₂on Ag(111) on a permutation invariant potential energy surface. Physical Chemistry Chemical Physics, 2014, 16, 24704-24715.	1.3	59
15646	The spin-dependent transport of Co-encapsulated Si nanotubes contacted with Cu electrodes. Applied Physics Letters, 2014, 104, 063103.	1.5	2
15647	Band gap engineering strategy via polarization rotation in perovskite ferroelectrics. Applied Physics Letters, 2014, 104, .	1.5	129
15648	Formation, nature, and stability of the arsenic-silicon-oxygen alloy for plasma doping of non-planar silicon structures. Applied Physics Letters, 2014, 105, 262102.	1.5	3
15649	In search of new reconstructions of (001) Î±-quartz surface: a first principles study. RSC Advances, 2014, 4, 55599-55603.	1.7	32

#	Article	IF	Citations
15650	Exploring the behavior of molybdenum diboride (MoB2): A high pressure x-ray diffraction study. Journal of Applied Physics, 2014, 115, .	1.1	17
15651	Structural, vibrational, elastic and topological properties of PaN under pressure. Journal of Physics Condensed Matter, 2014, 26, 035403.	0.7	3
15652	Pressure effects on the electronic structure and superconducting critical temperature of Li2B2. Journal of Physics Condensed Matter, 2014, 26, 115701.	0.7	8
15653	First-Principles Study on Stability and Mechanical Properties of Cr7C3. Rare Metal Materials and Engineering, 2014, 43, 2903-2907.	0.8	12
15654	Phosphorene nanoribbons. Europhysics Letters, 2014, 108, 47005.	0.7	134
15655	Magnetic structure map for face-centered tetragonal iron: Appearance of a collinear spin structure. Physical Review B, 2014, 90, .	1.1	4
15656	Density functional theory calculations insight to the effect of anion on the nonlinear optical properties of LiInX2 (X = S, Se). Journal of Molecular Modeling, 2014, 20, 2528.	0.8	7
15657	Magnetoelectric properties of the<mml:math xmlns:mml="http://www.w3.org/1998/Math/MathML"><mml:mtext>Co</mml:mtext><mml:mo>/</mml:mo><mml:msub><mml:mtext><mml:msub><mml:mtext>Ti</mml:mtext><mml:mrow><mml:mn>1</mml:mn></mml:mrow></mml:msub><mml:msub><mml:mtext>O</mml:mtext><mml:mn>3</mml:mn></mm. Physical Review B, 2014, 90, .	1.1	20
15658	Trends in electronic structures and structural properties of MAX phases: a first-principles study on M₂AlC (M = Sc, Ti, Cr, Zr, Nb, Mo, Hf, or Ta), M₂AlN, and hypothetical M₂AlB phases. Journal of Physics Condensed Matter, 2014, 26, 505503.	0.7	116
15659	Effects of boron-nitride substrates on Stone-Wales defect formation in graphene: An ab initio molecular dynamics study. Applied Physics Letters, 2014, 104, 203106.	1.5	5
15660	Temperature effects on the energy bandgap and conductivity effective masses of charge carriers in lead telluride from first-principles calculations. Journal of Applied Physics, 2014, 116, .	1.1	7
15661	Hybrid DFT calculation of<mml:math xmlns:mml="http://www.w3.org/1998/Math/MathML"><mml:mmultiscripts><mml:mi mathvariant="normal">Fe</mml:mi><mml:mprescripts /><mml:none /><mml:mrow><mml:mn>57</mml:mn></mml:mrow></mml:mmultiscripts></mml:math>NMR resonances and orbital order in magnetite. Physical Review B, 2014, 90, .	1.1	8
15662	Structural stability and thermodynamics of CrN magnetic phases fromab initiocalculations and experiment. Physical Review B, 2014, 90, .	1.1	95
15663	Thermodynamics and Kinetics of Three<mml:math xmlns:mml="http://www.w3.org/1998/Math/MathML" display="inline"><mml:mrow><mml:mi>Mg</mml:mi><mml:mtext>â</mml:mtext><mml:mi mathvariant="normal">H</mml:mi><mml:mtext>â</mml:mtext><mml:msub><mml:mrow><mml:mi>V</mml:mi></mml:mrow><mml:mi mathvariant="normal">N</mml:mi></mml:msub></mml:mrow></mml:math>Complexes in MgSrN₂ from Combined First-Principles Calculation and Experiment. Physical Review Letters, 2014, 113, .	2.9	16
15664	Enhanced and adjustable adsorption of organo-functional groups on Li decorated carbon nanotubes: A first principle study. Journal of Applied Physics, 2014, 116, 084308.	1.1	4
15665	Microscopic origin of pressure-induced isosymmetric transitions in fluoromanganate cryolites. Physical Review B, 2014, 90, .	1.1	4
15666	Coupling between octahedral rotations and local polar displacements in<mml:math xmlns:mml="http://www.w3.org/1998/Math/MathML"><mml:mi mathvariant="normal">W</mml:mi><mml:msub><mml:mi mathvariant="normal">O</mml:mi><mml:mn>3</mml:mn></mml:msub></mml:math>/<mml:math xmlns:mml="http://www.w3.org/1998/Math/MathML"><mml:mi>Re</mml:mi><mml:msub><mml:mi mathvariant="normal">O</mml:mi><mml:mn>3</mml:mn></mml:msub></mml:math>superlattices. Physi	1.1	8
15667	Effect of tensile strain on the electronic structure of Ge: A first-principles calculation. Journal of Applied Physics, 2014, 116, 113105.	1.1	17

#	Article	IF	Citations
15668	First-principles study of HgTe/CdTe heterostructures under perturbations preserving time-reversal symmetry. Physical Review B, 2014, 90, .	1.1	14
15669	Stable path to ferromagnetic hydrogenated graphene growth. Physical Review B, 2014, 90, .	1.1	20
15670	Plasticity of hexagonal systems: Split slip modes and inverse Peierls relation in<mml:math xmlns:mml="http://www.w3.org/1998/Math/MathML"><mml:mi>Î±</mml:mi></mml:math>-Ti. Physical Review B, 2014, 89, .	1.1	35
15671	Elasticity and Thermodynamic Properties of EuS Related to Phase Transition. Chinese Journal of Chemical Physics, 2014, 27, 387-393.	0.6	2
15672	Improper ferroelectricity and piezoelectric responses in rhombohedral (<mml:math) Tj ETQq0 0 0 rgBT /Overlock 10 Tf 50 602 Td (xmlns xmlns:mml="http://www.w3.org/1998/Math/MathML"><mml:msub><mml:mi>B</mml:mi><mml:mn>2</mml:mn></mml:msub><mml:m mathvariant="normal">O</mml:mi><mml:mn>6</mml:mn></mml:msub></mml:math>perovskite oxides. Physical Review B, 2014, 89, .	1.1	20
15673	Electronic and optical properties of NbO2. Journal of Applied Physics, 2014, 116, .	1.1	67
15674	Octahedral tilting and ferroelectricity in Rb<mml:math xmlns:mml="http://www.w3.org/1998/Math/MathML"><mml:mi>A</mml:mi></mml:math>Nb<mml:math xmlns:mml="http://www.w3.org/1998/Math/MathML"><mml:msub><mml:mrow /><mml:mn>2</mml:mn></mml:msub></mml:math>O<mml:math xmlns:mml="http://www.w3.org/1998/Math/MathML"><mml:msub><mml:mrow		

#	Article	IF	Citations
15686	Antisites in III-V semiconductors: Density functional theory calculations. Journal of Applied Physics, 2014, 116, .	1.1	12
15687	Superconductivity in noncentrosymmetric<mml:math xmlns:mml="http://www.w3.org/1998/Math/MathML"><mml:mrow><mml:mi>Ba</mml:mi><mml:msub><mml:mi>Al</mml:mi></mml:msub><mml structures. Physical Review B, 2014, 90, .	1.1	32
15688	Magnetic orders of LaTiO3 under epitaxial strain: A first-principles study. Journal of Applied Physics, 2014, 115, 17E108.	1.1	14
15689	Magnetic analytic bond-order potential for modeling the different phases of Mn at zero Kelvin. Physical Review B, 2014, 89, .	1.1	11
15690	Finding Unprecedentedly Low-Thermal-Conductivity Half-Heusler Semiconductors via High-Throughput Materials Modeling. Physical Review X, 2014, 4, .	2.8	210
15691	Spin-orbit spillage as a measure of band inversion in insulators. Physical Review B, 2014, 90, .	1.1	19
15692	Ab initio calculations of elastic constants of plagioclase feldspars. American Mineralogist, 2014, 99, 2344-2352.	0.9	14
15693	Theoretical prediction of morphotropic compositions inNa1/2Bi1/2TiO3-based solid solutions from transition pressures. Physical Review B, 2014, 89, .	1.1	10
15694	Correlation between the ionic potential and thermal stability of metal borohydrides: First-principles investigations. Physical Review B, 2014, 90, .	1.1	12
15695	First-principles study of multicontrol graphene doping using light-switching molecules. Physical Review B, 2014, 89, .	1.1	9
15696	Origin of the Increased Photocatalytic Performance of TiO2Nanocrystal Composed of Pure Core and Heavily Nitrogen-Doped Shell: A Theoretical Study. ACS Applied Materials & Interfaces, 2014, 6, 22815-22822.	4.0	25
15697	Theoretical Study on the Encapsulation of Li Atoms inside Boron Nitride Nanotubes: Physical Properties and Catalytic Reactivity for the Oxygen Reduction Reaction. Journal of Physical Chemistry C, 2014, 118, 30325-30332.	1.5	11
15698	The structure, stability, and electronic properties of ultra-thin BC2N nanotubes: a first-principles study. Journal of Molecular Modeling, 2014, 20, 2536.	0.8	2
15699	Quantum molecular dynamics study on the structures and dc conductivity of warm dense silane. Physical Review E, 2014, 89, 022128.	0.8	10
15700	Spin caloritronics in graphene with Mn. Applied Physics Letters, 2014, 104, .	1.5	18
15701	Ab initiosimulations of MgO under extreme conditions. Physical Review B, 2014, 89, .	1.1	39
15702	Fermi surfaces and phase stability of Ba(Fe1â^'xMx)2As2(M=Co,Ni,Cu,Zn). Physical Review B, 2014, 89, .	1.1	9
15703	Anisotropic optical properties of Fe/GaAs(001) nanolayers from first principles. Physical Review B, 2014, 90, .	1.1	9

#	Article	IF	Citations
15704	Direct imaging of monovacancy-hydrogen complexes in a single graphitic layer. Physical Review B, 2014, 89, .	1.1	44
15705	The interaction of organic adsorbate vibrations with substrate lattice waves in methyl-Si(111)-(1â€‰Ã—â€‰1). Journal of Chemical Physics, 2014, 141, 024702.	1.2	8
15706	Interstitial Fe in MgO. Journal of Applied Physics, 2014, 115, 023508.	1.1	7
15707	Magnetic property of transition metal-Si atomic line on silicon Î£3 grain boundary: A theoretical study. Journal of Applied Physics, 2014, 115, 223906.	1.1	2
15708	Impact of excess iron on the calculated electronic and magnetic properties of Co3â^'xFexSi Heusler-compound. Journal of Applied Physics, 2014, 116, .	1.1	3
15709	Skutterudites under pressure: An ab initio study. Journal of Applied Physics, 2014, 115, 093903.	1.1	7
15710	Structure and dynamics of cadmium telluride studied by x-ray and inelastic neutron scattering. Applied Physics Letters, 2014, 105, 102101.	1.5	1
15711	Critical role of Fock exchange in characterizing dopant geometry and magnetic interaction in magnetic semiconductors. Physical Review B, 2014, 89, .	1.1	12
15712	Phase transitions in delafossite CuLaO2 at high pressures. Journal of Applied Physics, 2014, 115, .	1.1	7
15713	Topologically Protected Conduction State at Carbon Foam Surfaces: AnAb initioStudy. Physical Review Letters, 2014, 112, 026803.	2.9	32
15714	The role of the carbon-silicon complex in eliminating deep ultraviolet absorption in AlN. Applied Physics Letters, 2014, 104, .	1.5	59
15715	First-principles study of the structure of Mg/Nb multilayers. Applied Physics Letters, 2014, 105, 071602.	1.5	26
15716	Effects of non-local exchange on core level shifts for gas-phase and adsorbed molecules. Journal of Chemical Physics, 2014, 141, 034706.	1.2	29
15717	Optical anisotropy in bismuth titanate: An experimental and theoretical study. Journal of Applied Physics, 2014, 115, 133509.	1.1	3
15718	Effect of oxygen incorporation on the structure and elasticity of Ti-Al-O-N coatings synthesized by cathodic arc and high power pulsed magnetron sputtering. Journal of Applied Physics, 2014, 116, .	1.1	51
15719	High-pressure phase transition of MH3 (M: Er, Ho). Journal of Chemical Physics, 2014, 141, 054703.	1.2	6
15720	Collective Diffusion of Gold Clusters and F-Centers at MgO(100) and CaO(100) Surfaces. Journal of Physical Chemistry C, 2014, 118, 28720-28724.	1.5	1
15721	Structural and ferroelectric transitions in magnetic nickelate PbNiO₃. New Journal of Physics, 2014, 16, 015030.	1.2	23

#	Article	IF	Citations
15722	Strain engineering of Dirac cones in graphyne. Applied Physics Letters, 2014, 104, 213107.	1.5	51
15723	Ab initio calculations of B2 type RHg (R = Ce, Pr, Eu and Gd) intermetallic compounds. European Physical Journal B, 2014, 87, 1.	0.6	2
15724	Structural, elastic, and lattice dynamic stability of yttrium selenide (YSe) under pressure: A first principle study. Journal of Applied Physics, 2014, 116, 193504.	1.1	2
15725	A Model to Determine the Chemical Expansion in Non-Stoichiometric Oxides Based on the Elastic Force Dipole. Journal of the Electrochemical Society, 2014, 161, F3060-F3064.	1.3	9
15726	First-principles electronic structure and formation energies of group V and VII impurities in the Î±-Fe2O3 alloys. Journal of Applied Physics, 2014, 116, .	1.1	4
15727	Monolayers of MoS2 as an oxidation protective nanocoating material. Journal of Applied Physics, 2014, 116, .	1.1	55
15728	Band gap of epitaxial in-plane-dimerized single-phase NbO₂films. Applied Physics Letters, 2014, 104, 092901.	1.5	40
15729	Anharmonicity, mechanical instability, and thermodynamic properties of the Cr-Re Ïƒ-phase. Journal of Chemical Physics, 2014, 140, 144502.	1.2	6
15730	Half-metallicity modulation of hybrid BN-C nanotubes by external electric fields: A first-principles study. Journal of Chemical Physics, 2014, 140, 234702.	1.2	5
15731	Adaptive cluster expansion approach for predicting the structure evolution of graphene oxide. Journal of Chemical Physics, 2014, 141, 224703.	1.2	3
15732	Transition-metal and metalloid substitutions in L10-ordered FeNi. Journal of Applied Physics, 2014, 115, 17A710.	1.1	12
15733	TaON surface energetics and optical spectra. Physica Status Solidi - Rapid Research Letters, 2014, 8, 587-591.	1.2	10
15734	Structural, electronic, and optical properties of GaInO3: A hybrid density functional study. Journal of Applied Physics, 2014, 115, .	1.1	33
15735	Results for aliovalent doping of CeBr3 with Ca2+. Journal of Applied Physics, 2014, 115, .	1.1	91
15736	Oxygen and nitrogen diffusion in Î±-hafnium from first principles. Applied Physics Letters, 2014, 104, .	1.5	9
15737	Boron deactivation in heavily boron-doped Czochralski silicon during rapid thermal anneal: Atomic level understanding. Applied Physics Letters, 2014, 104, 032102.	1.5	2
15738	Modeling intrinsic defects in LiNbO₃ within the Slater-Janak transition state model. Journal of Chemical Physics, 2014, 140, 234113.	1.2	33
15739	Electronic structure and optical responses of nanocrystalline BiGaO3 films: A combination study of experiment and theory. Journal of Applied Physics, 2014, 115, .	1.1	7

#	Article	IF	Citations
15740	Non-covalent functionalization of single wall carbon nanotubes and graphene by a conjugated polymer. Applied Physics Letters, 2014, 105, .	1.5	21
15741	Effects of the Cu off-stoichiometry on transport properties of wide gap p-type semiconductor, layered oxysulfide LaCuSO. Applied Physics Letters, 2014, 105, .	1.5	24
15742	Influence of longitudinal isotope substitution on the thermal conductivity of carbon nanotubes: Results of nonequilibrium molecular dynamics and local density functional calculations. Journal of Chemical Physics, 2014, 140, 144704.	1.2	9
15743	Large theoretical thermoelectric power factor of suspended single-layer MoS2. Applied Physics Letters, 2014, 105, 193901.	1.5	73
15744	Assessing hafnium on hafnia as an oxygen getter. Journal of Applied Physics, 2014, 115, .	1.1	37
15745	Adsorption structure of water molecules on the Be(0001) surface. Journal of Applied Physics, 2014, 115, 213511.	1.1	9
15746	An ab initio study on the electronic and magnetic properties of MgO with intrinsic defects. RSC Advances, 2014, 4, 51366-51373.	1.7	24
15747	Cu-Deficiency in the p-Type Semiconductor Cu_{5â€“x}Ta₁₁O₃₀: Impact on Its Crystalline Structure, Surfaces, and Photoelectrochemical Properties. Chemistry of Materials, 2014, 26, 6711-6721.	3.2	28
15748	Electrostatics-based finite-size corrections for first-principles point defect calculations. Physical Review B, 2014, 89, .	1.1	320
15749	Tailoring Li adsorption on graphene. Physical Review B, 2014, 90, .	1.1	42
15750	L-asparagine crystals with wide gap semiconductor features: Optical absorption measurements and density functional theory computations. Journal of Chemical Physics, 2014, 140, 124511.	1.2	15
15751	Donor and acceptor levels in semiconducting transition-metal dichalcogenides. Physical Review B, 2014, 89, .	1.1	38
15752	First-principles study of octahedral tilting and ferroelectric-like transition in metallic<mml:math xmlns:mml="http://www.w3.org/1998/Math/MathML"><mml:msub><mml:mi mathvariant="normal">LiOsO</mml:mi><mml:mn>3</mml:mn></mml:msub></mml:math>. Physical Review B, 2014, 89, .	1.1	44
15753	Tunable Oxygen Vacancy Formation Energetics in the Complex Perovskite Oxide Sr_xLa_{1â€“x}Mn_yAl_{1â€“y}O_{3â€“δ}. Chemistry of Materials, 2014, 26, 6595-6602.	8.2	90
15754	Origin of the magnetostructural coupling in<mml:math xmlns:mml="http://www.w3.org/1998/Math/MathML"><mml:msub><mml:mi mathvariant="normal">FeMnP</mml:mi><mml:mrow><mml:mn>0.75</mml:mn></mml:mrow></mml:msub><mml:msub><mml:mi mathvariant="normal">Si</mml:mi><mml:mrow><mml:mn>0.25</mml:mn></mml:mrow></mml:msub></mml:math>. Physical Review B, 2014, 90, .	1.1	17
15755	Pressure-induced instability in CdO. Physica Status Solidi (B): Basic Research, 2014, 251, 1426-1430.	0.7	2
15756	Ytterbium-driven strong enhancement of electron-phonon coupling in graphene. Physical Review B, 2014, 90, .	1.1	19
15757	Strain tuning of Dirac states at the SnTe (001) surface. Physical Review B, 2014, 90, .	1.1	14

#	Article	IF	Citations
15758	Molybdenum Sulfides and Selenides as Possible Electrocatalysts for CO₂ Reduction. ChemCatChem, 2014, 6, 1899-1905.	1.8	255
15759	Prediction of Mode Specificity, Bond Selectivity, Normal Scaling, and Surface Lattice Effects in Water Dissociative Chemisorption on Several Metal Surfaces Using the Sudden Vector Projection Model. Journal of Physical Chemistry C, 2014, 118, 26851-26858.	1.5	29
15760	A DFT+UStudy of Strain-Dependent Ionic Migration in Sm-Doped Ceria. Journal of the Physical Society of Japan, 2014, 83, 094707.	0.7	15
15761	Electronic structure and optical properties of Ag-doped SnO₂ nanoribbons. RSC Advances, 2014, 4, 41819-41824.	1.7	12
15762	mBEEF: An accurate semi-local Bayesian error estimation density functional. Journal of Chemical Physics, 2014, 140, 144107.	1.2	117
15763	Superconducting properties of<mml:math xmlns:mml="http://www.w3.org/1998/Math/MathML"><mml:msub><mml:mi mathvariant="normal">K</mml:mi><mml:mrow><mml:mn>1</mml:mn><mml:mtext>â^'</mml:mtext><mml:mi>x</mml:mi></mml:mro mathvariant="normal">Na</mml:mi><mml:mi>x</mml:mi></mml:msub><mml:msub><mml:mi mathvariant="normal">Fe</mml:mi><mml:mn>2</mml:mn></mml:msub><mml:msub><mml:mi mathvariant="normal">As</mml:mi><mml:mn>2</mml:mn></mml:msub></mml:math>under pressure. Ph	1.1	13
15764	Electronic Properties of Transitionâ€Metalâ€Decorated Silicene. ChemPhysChem, 2014, 15, 4095-4099.	1.0	15
15765	Electronic and bonding analysis of hardness in pyrite-type transition-metal pernitrides. Physical Review B, 2014, 90, .	1.1	108
15766	Ethanol Synthesis from Syngas on the Stepped Rh(211) Surface: Effect of Surface Structure and Composition. Journal of Physical Chemistry C, 2014, 118, 22691-22701.	1.5	46
15767	An ab initio investigation of flexoelectric effect in ultrathin BaTiO3 nanotubes. Journal of Applied Physics, 2014, 115, .	1.1	9
15768	The electronic properties and lattice dynamics of (Na0.5Bi0.5)TiO3: From cubic to tetragonal and rhombohedral phases. Journal of Applied Physics, 2014, 115, 124107.	1.1	24
15769	Phase stability of Liâ€“Mnâ€“O oxides as cathode materials for Li-ion batteries: insights from ab initio calculations. Physical Chemistry Chemical Physics, 2014, 16, 11233-11242.	1.3	56
15770	Polymorphism and thermodynamic ground state of silver fulminate studied from van der Waals density functional calculations. Journal of Chemical Physics, 2014, 140, 224705.	1.2	3
15772	Spectroscopic and Computational Characterizations of Alkalineâ€Earthâ€and Heavyâ€Metalâ€Exchanged Natrolites. ChemPlusChem, 2014, 79, 1096-1102.	1.3	3
15773	Adsorption of a Pt₁₃ Cluster on Graphene Oxides at Varied Ratios of Oxygen to Carbon and Its Catalytic Reactions for CO Removal Investigated with Quantum-Chemical Calculations. Journal of Physical Chemistry C, 2014, 118, 26764-26771.	1.5	17
15774	Experimental assessment of the elastic properties of thin TiN/AlN superlattice and nano-multilayer coatings. Surface and Coatings Technology, 2014, 257, 87-94.	2.2	18
15775	The effect of pressure on the physical properties of Cu3N. Physica Scripta, 2014, 89, 035801.	1.2	13
15776	Universal tight binding model for chemical reactions in solution and at surfaces. III. Stoichiometric and reduced surfaces of titania and the adsorption of water. Journal of Chemical Physics, 2014, 141, 044505.	1.2	4

#	Article	IF	Citations
15777	Effect of Cu alloying on S poisoning of Ni surface viaab initiothermodynamics calculations. Physica Status Solidi (A) Applications and Materials Science, 2014, 211, 1882-1888.	0.8	4
15778	Effect of tensile strain on the negative differential resistance in the WTe₂armchair nanoribbon. Materials Research Express, 2014, 1, 025037.	0.8	1
15779	Understanding the Effects of Ion-Exchange in Titanosilicate ETS-10: A Joint Theoretical and Experimental Study. Journal of Physical Chemistry C, 2014, 118, 27281-27291.	1.5	8
15780	Clustering of H and He, and their effects on vacancy evolution in tungsten in a fusion environment. Nuclear Fusion, 2014, 54, 103007.	1.6	69
15781	Incisive Probing of Intermolecular Interactions in Molecular Crystals: Core Level Spectroscopy Combined with Density Functional Theory. Journal of Physical Chemistry B, 2014, 118, 12121-12129.	1.2	28
15782	Orbital resolution of molecules covalently attached to a clean semiconductor surface. Nature Communications, 2014, 5, 3721.	5.8	8
15783	Electronic and structural properties at the interface between iron-phthalocyanine and Cu(110). Journal of Chemical Physics, 2014, 140, 094704.	1.2	12
15784	New stable Reâ€“B phases for ultra-hard materials. Journal of Physics Condensed Matter, 2014, 26, 455401.	0.7	6
15785	Understanding the interactions between oxygen vacancies atSrTiO3(001) surfaces. Physical Review B, 2014, 90, .	1.1	26
15786	First-Principles Investigation of Câ€“H Bond Scission and Formation Reactions in Ethane, Ethene, and Ethyne Adsorbed on Ru(0001). Journal of Physical Chemistry C, 2014, 118, 26683-26694.	1.5	24
15787	A comparative study on magnetism in Zn-doped AlN and GaN from first-principles. Journal of Applied Physics, 2014, 116, .	1.1	9
15788	High-throughput computational screening of thermal conductivity, Debye temperature, and GrÃ¼neisen parameter using a quasiharmonic Debye model. Physical Review B, 2014, 90, .	1.1	230
15789	Large magneto-electric effects in hexagonal La0.7Ba0.3MnO3-BaTiO3 solid solutions and magneto-electric coupling mechanism discussion. Journal of Applied Physics, 2014, 116, 134103.	1.1	8
15790	Structural, Electronic and Elastic Properties of ZnO and CdO: A First-Principles Study. , 2014, 5, 1034-1042.		17
15791	A theoretical study of the thermodynamic properties of YMgX4 (X=Co, Ni, Cu) compounds. AIP Advances, 2014, 4, .	0.6	7
15792	Order-by-disorder degeneracy lifting of interacting bosons on the dice lattice. Physical Review A, 2014, 90, .	1.0	6
15793	Modeling time-coincident ultrafast electron transfer and solvation processes at molecule-semiconductor interfaces. Journal of Chemical Physics, 2014, 140, 234109.	1.2	5
15794	Anisotropic polaron localization and spontaneous symmetry breaking: Comparison of cation-site acceptors in GaN and ZnO. Physical Review B, 2014, 90, .	1.1	15

#	Article	IF	Citations
15795	Engineering relativistic effects in ferroelectric SnTe. Physical Review B, 2014, 90, .	1.1	64
15796	Finite-size supercell correction scheme for charged defects in one-dimensional systems. Physical Review B, 2014, 90, .	1.1	4
15797	Orientation- and passivation-dependent stability and electronic properties of Î±-Si₃N₄nanobelts. Physical Chemistry Chemical Physics, 2014, 16, 24266-24274.	1.3	7
15798	Metalized T graphene: A reversible hydrogen storage material at room temperature. Journal of Applied Physics, 2014, 116, .	1.1	31
15799	Structure, hydrogen bonding and thermal expansion of ammonium carbonate monohydrate. Acta Crystallographica Section B: Structural Science, Crystal Engineering and Materials, 2014, 70, 948-962.	0.5	14
15800	Exploration of stable compounds, crystal structures, and superconductivity in the Be-H system. AIP Advances, 2014, 4, .	0.6	25
15801	Tunable Electronic and Magnetic Properties of Graphene Flake-Doped Boron Nitride Nanotubes. Journal of Physical Chemistry C, 2014, 118, 28616-28624.	1.5	35
15802	Nuclear forward scattering and first-principles studies of the iron oxide phase<mml:math xmlns:mml="http://www.w3.org/1998/Math/MathML"><mml:msub><mml:mrow><mml:mi mathvariant="normal">Fe</mml:mi></mml:mrow><mml:mn>4</mml:mn></mml:msub><mml:msub><mml:mrow><mml:mi mathvariant="normal">O</mml:mi></mml:mrow><mml:mn>5</mml:mn></mml:msub></mml:math>. Physical Review B, 2014, 90, .	1.1	8
15803	Temperature measurements of shocked silica aerogel foam. Physical Review E, 2014, 90, 033107.	0.8	23
15804	Fermi level pinning and the charge transfer contribution to the energy of adsorption at semiconducting surfaces. Journal of Applied Physics, 2014, 115, 043529.	1.1	21
15805	Effects of Concentration, Crystal Structure, Magnetism, and Electronic Structure Method on First-Principles Oxygen Vacancy Formation Energy Trends in Perovskites. Journal of Physical Chemistry C, 2014, 118, 28776-28790.	1.5	105
15806	Sensing propensity of a defected graphane sheet towards CO, H₂O and NO₂. Nanotechnology, 2014, 25, 325501.	1.3	53
15807	Mechanical and thermal properties of Yb₂SiO₅: First-principles calculations and chemical bond theory investigations. Journal of Materials Research, 2014, 29, 1609-1619.	1.2	37
15808	Unveiling the origin of oxygen atomic impurities in Au nanowires. Physical Review B, 2014, 89, .	1.1	6
15809	Influence of U doping on the growth behavior, electronic structure and magnetic properties of Pd n (n = 1â€“12) clusters: a first principles study. European Physical Journal D, 2014, 68, 1.	0.6	10
15810	The valence band structure of AgxRh1â€“x alloy nanoparticles. Applied Physics Letters, 2014, 105, .	1.5	27
15811	Insight into the description of van der Waals forces for benzene adsorption on transition metal (111) surfaces. Journal of Chemical Physics, 2014, 140, 084704.	1.2	158
15812	Ab-initio modeling of electromechanical coupling at Si surfaces. Journal of Applied Physics, 2014, 116, 073507.	1.1	4

#	Article	IF	Citations
15813	Optimal Thickness for Charge Transfer in Multilayer Graphene Electrodes. Physical Review Applied, 2014, 1, .	1.5	9
15814	Effects of<mml:math xmlns:mml="http://www.w3.org/1998/Math/MathML"><mml:mrow><mml:mn>5</mml:mn><mml:mi>d</mml:mi></mml:mrow></mml:math> and spin-orbit interaction on the characteristics of bulk plasmons in lead. Physical Review B, 2014, 90, .	1.1	6
15815	Local curvature and stability of two-dimensional systems. Physical Review B, 2014, 90, .	1.1	24
15816	Imprint Control of Nonvolatile Shape Memory with Asymmetric Ferroelectric Multilayers. Chemistry of Materials, 2014, 26, 6911-6914.	3.2	17
15817	Extracting semiconductor band gap zero-point corrections from experimental data. Physical Review B, 2014, 90, .	1.1	20
15818	The structural diversity of ABS3 compounds with d electronic configuration for the B-cation. Journal of Chemical Physics, 2014, 140, 224703.	1.2	55
15819	Orbital tomography of hybridized and dispersing molecular overlayers. Physical Review B, 2014, 90, .	1.1	47
15820	Computed electronic and optical properties of SnO2 under compressive stress. Optical Materials, 2014, 38, 161-166.	1.7	20
15821	Systematic calculations of On (n = 1 to 6) polytypes of LiCoO₂. Physica Status Solidi - Rapid Research Letters, 2014, 8, 545-548.	1.2	4
15822	Metal to semiconductor transition and phase stability of Ti1â^'xMgxNyalloys investigated by first-principles calculations. Physical Review B, 2014, 89, .	1.1	41
15823	Sharply distinctd-band quantum-well states in palladium thin films. Physical Review B, 2014, 90, .	1.1	11
15824	Weyl semimetals from noncentrosymmetric topological insulators. Physical Review B, 2014, 90, .	1.1	194
15825	Phonon anomalies and superconductivity in the Heusler compound YPd2Sn. Journal of Applied Physics, 2014, 116, .	1.1	9
15826	Understanding the<mml:math xmlns:mml="http://www.w3.org/1998/Math/MathML"><mml:mi>Î¼</mml:mi></mml:math>SR spectra of MnSi without magnetic polarons. Physical Review B, 2014, 89, .	1.1	40
15827	Operando Characterization of an Amorphous Molybdenum Sulfide Nanoparticle Catalyst during the Hydrogen Evolution Reaction. Journal of Physical Chemistry C, 2014, 118, 29252-29259.	1.5	87
15828	Inductive crystal field control in layered metal oxides with correlated electrons. APL Materials, 2014, 2, .	2.2	12
15829	Pathways towards ferroelectricity in hafnia. Physical Review B, 2014, 90, .	1.1	351
15830	Role of Antiferromagnetic Ordering in the (1Ã—2) Surface Reconstruction ofCa(Fe1â^'xCox)2As2. Physical Review Letters, 2014, 112, 077205.	2.9	7

#	Article	IF	Citations
15831	Ab-initio study of hydrogen doping and oxygen vacancy at anatase TiO2 surface. AIP Advances, 2014, 4, 027129.	0.6	22
15832	Abâ€initio calculations and structural studies of (SiTe) 2 (Sb 2 Te 3) n (n : 1, 2, 4 and 6) phaseâ€change superlattice films. Physica Status Solidi - Rapid Research Letters, 2014, 8, 302-306.	1.2	29
15833	Three-dimensional polymeric structures of single-wall carbon nanotubes. Journal of Chemical Physics, 2014, 140, 204709.	1.2	8
15834	Elastic anisotropy and shear-induced atomistic deformation of tetragonal silicon carbon nitride. Journal of Applied Physics, 2014, 116, .	1.1	2
15835	First-Principles and Kinetic Monte Carlo Simulation Studies of the Reactivity of Tc(0001), MoTc(111) and MoTc(110) Surfaces. Journal of the Electrochemical Society, 2014, 161, C83-C88.	1.3	11
15836	Enhanced osteoconductivity of sodiumâ€substituted hydroxyapatite by system instability. Journal of Biomedical Materials Research - Part B Applied Biomaterials, 2014, 102, 1046-1062.	1.6	67
15837	Silicon-induced faceting at the Ag(110) surface. Physical Review B, 2014, 89, .	1.1	25
15838	Green's function multiple-scattering theory with a truncated basis set: An augmented-KKR formalism. Physical Review B, 2014, 90, .	1.1	10
15839	Effect of As-chain layers in<mml:math xmlns:mml="http://www.w3.org/1998/Math/MathML"><mml:msub><mml:mtext>CaFeAs</mml:mtext><mml:mn>2</mml:mn></mml:m Physical Review B, 2014, 89, .	1.1	41
15840	Thermoelectric transport properties of molybdenum from<mml:math xmlns:mml="http://www.w3.org/1998/Math/MathML"><mml:mi mathvariant="italic">ab</mml:mi><mml:mspace width="0.28em" /><mml:mi mathvariant="italic">initio</mml:mi></mml:math>simulations. Physical Review B, 2014, 90, .	1.1	27
15841	Unraveling the<mml:math xmlns:mml="http://www.w3.org/1998/Math/MathML"><mml:msub><mml:mrow><mml:mtext>LiNbO</mml:mtext></mml:mrow><mml: surface by atomic force microscopy and density functional theory. Physical Review B, 2014, 89, .	1.1	10
15842	Topological transition and edge states in HgTe quantum wells from first principles. Physical Review B, 2014, 89, .	1.1	17
15843	Concentration of Charge Carriers, Migration, and Stability in Li₃OCl Solid Electrolytes. Chemistry of Materials, 2014, 26, 7137-7144.	3.2	68
15844	Comparison of Permeation Measurements and Hybrid Density-Functional Calculations on Oxygen Vacancy Transport in Complex Perovskite Oxides. Journal of Physical Chemistry C, 2014, 118, 29542-29553.	1.5	25
15845	DFT Study of Spin States on Bare and Partially Hydrogenated Si(111) and Si(100) Surfaces. Journal of Physical Chemistry C, 2014, 118, 26926-26930.	1.5	1
15846	FP-LAPW investigation of electronic, magnetic, elastic and thermal properties of Fe-doped zirconium nitride. AIP Advances, 2014, 4, .	0.6	7
15847	Adsorption of multivalent alkylthiols on Au(111) surface: Insights from DFT. Journal of Computational Chemistry, 2014, 35, 204-213.	1.5	12
15848	Combined hybrid functional and DFT+U calculations for metal chalcogenides. Journal of Chemical Physics, 2014, 141, 044106.	1.2	37

#	Article	IF	Citations
15849	Synergistic Effect of Mo + Cu Codoping on the Photocatalytic Behavior of Metastable TiO₂ Solid Solutions. Journal of Physical Chemistry C, 2014, 118, 29788-29795.	1.5	20
15850	Thermoelectric properties of AgSbTe2 from first-principles calculations. Journal of Applied Physics, 2014, 116, .	1.1	15
15851	Configuration dependence of the properties of Cd_{1â€“x}<scp>Z</scp>n_x<scp>S</scp> solid solutions by firstâ€principles calculations. Physica Status Solidi (B): Basic Research, 2014, 251, 655-660.	0.7	5
15852	Hardness of FeB4: Density functional theory investigation. Journal of Chemical Physics, 2014, 140, 174505.	1.2	80
15853	Lattice dynamics and lattice thermal conductivity of thorium dicarbide. Journal of Nuclear Materials, 2014, 454, 142-148.	1.3	10
15854	Pressure-induced ferroelastic phase transition in SnO2 from density functional theory. Journal of Chemical Physics, 2014, 140, 164706.	1.2	2
15855	Charge Polarization at a Auâ€“TiC Interface and the Generation of Highly Active and Selective Catalysts for the Lowâ€Temperature Waterâ€“Gas Shift Reaction. Angewandte Chemie - International Edition, 2014, 53, 11270-11274.	7.2	67
15856	Phonon pressure coefficients and deformation potentials of wurtzite AlN determined by uniaxial pressure-dependent Raman measurements. Physical Review B, 2014, 90, .	1.1	16
15857	Planar fault energies of copper at large strain: A density functional theory study. Journal of Applied Physics, 2014, 116, .	1.1	3
15858	Novel structure and abnormal electronic properties of ultra-thin BC2N nanotubes from first-principles investigation. Chemical Physics Letters, 2014, 616-617, 61-66.	1.2	6
15859	Benchmarking the performance of density functional theory and point charge force fields in their description of sI methane hydrate against diffusion Monte Carlo. Journal of Chemical Physics, 2014, 140, 174703.	1.2	41
15860	Electronic and optical properties of Au-doped Cu₂O: A first principles investigation. Chinese Physics B, 2014, 23, 057104.	0.7	8
15861	Composition-dependent photoluminescence and electronic structure of 2-dimensional borocarbonitrides, BC_XN (x= 1, 5). Materials Research Express, 2014, 1, 025603.	0.8	26
15862	First-Principles Prediction of Oxygen Reduction Activity on Pdâ€“Cuâ€“Si Metallic Glasses. Journal of Physical Chemistry C, 2014, 118, 28609-28615.	1.5	11
15863	Theoretical investigation of charge accumulation layer on the Bi-induced InAs(111)-(2â€‰Ã—â€‰2) surface. Journal of Applied Physics, 2014, 115, 163702.	1.1	0
15864	Theoretical study of InN/GaN short period superlattices to mimic disordered alloys. Journal of Applied Physics, 2014, 115, .	1.1	14
15865	Polymerization of nitrogen in cesium azide under modest pressure. Journal of Chemical Physics, 2014, 141, 044717.	1.2	50
15866	Geometric Matching Principle for Adsorption Selectivity of Ionic Liquids: A Simple Method into the Fascinating World of Shapeâ€Controlled Chemistry. Chemistry - A European Journal, 2014, 20, 9012-9017.	1.7	11

#	Article	IF	Citations
15867	On the Electrochemical Deposition and Dissolution of Divalent Metal Ions. ChemPhysChem, 2014, 15, 132-138.	1.0	28
15868	High Stability of Faceted Nanotubes and Fullerenes of Multiphase Layered Phosphorus: A Computational Study. Physical Review Letters, 2014, 113, 226801.	2.9	91
15869	Tiling Phosphorene. ACS Nano, 2014, 8, 12763-12768.	7.3	122
15870	Toward tailorable surfaces: A combined theoretical and experimental study of lanthanum niobate layered perovskites. Journal of Chemical Physics, 2014, 141, 024704.	1.2	7
15871	Band structure and optical transitions in LaFeO₃: theory and experiment. Journal of Physics Condensed Matter, 2014, 26, 505502.	0.7	100
15872	Half-metallicity and tetragonal distortion in semi-Heusler alloy FeCrSe. Journal of Applied Physics, 2014, 115, 043713.	1.1	6
15873	Modeling and stabilities of Mg/MgH2 interfaces: A first-principles investigation. AIP Advances, 2014, 4, .	0.6	13
15874	First-principles predicted low-energy structures of NaSc(BH4)4. Journal of Chemical Physics, 2014, 140, 124708.	1.2	25
15875	The role of vibrations in thermodynamic properties of Cu-Ni alloys. European Physical Journal B, 2014, 87, 1.	0.6	7
15876	Elastic and phonon properties of quaternary Heusler alloys CoFeCrZ (Z = Al, Si, Ga and Ge) from density functional theory. Philosophical Magazine Letters, 2014, 94, 708-715.	0.5	25
15877	Room-temperature magnetoelectric coupling in nanocrystalline Na0.5Bi0.5TiO3. Journal of Applied Physics, 2014, 116, .	1.1	51
15878	Mechanical Properties, Electronic Structures, and Potential Applications in Lithium Ion Batteries: A First-Principles Study toward SnSe₂ Nanotubes. Journal of Physical Chemistry C, 2014, 118, 28291-28298.	1.5	37
15879	Thermodynamic stability and structures of iron chloride surfaces: A first-principles investigation. Journal of Chemical Physics, 2014, 141, 054709.	1.2	9
15880	First principles investigation of the initial stage of H-induced missing-row reconstruction of Pd(110) surface. Journal of Chemical Physics, 2014, 140, 244707.	1.2	11
15881	Spin dependent transport properties of Mn-Ga/MgO/Mn-Ga magnetic tunnel junctions with metal(Mg,) Tj ETQq0 0 0 rgBT /Overlock 10 T	1.1	8
15882	A first principles analysis of the effect of hydrogen concentration in hydrogenated amorphous silicon on the formation of strained Si-Si bonds and the optical and mobility gaps. Journal of Applied Physics, 2014, 115, .	1.1	16
15883	Periodic subsystem density-functional theory. Journal of Chemical Physics, 2014, 141, 174101.	1.2	42
15884	Theoretical study of phonon density of states, thermodynamic properties and phase transitions for HMX. Philosophical Magazine, 2014, 94, 2656-2677.	0.7	27

#	Article	IF	Citations
15885	Magnetic properties in CdS monolayer doped with first-row elements: A density functional theory investigation. Physica Status Solidi (B): Basic Research, 2014, 251, 1257-1264.	0.7	19
15886	The effects of surface polarity and dangling bonds on the electronic properties of monolayer and bilayer MoS2 on Î±-quartz. New Journal of Physics, 2014, 16, 113055.	1.2	19
15887	Attosecond band-gap dynamics in silicon. Science, 2014, 346, 1348-1352.	6.0	415
15888	Ab initio study of irradiation tolerance for different Mn+1AXn phases: Ti3SiC2 and Ti3AlC2. Journal of Applied Physics, 2014, 115, .	1.1	69
15889	Ab Initio Transport Calculations for Single-Atom Copper Junctions in the Presence of Hydrogen Chloride. Journal of Physical Chemistry C, 2014, 118, 28252-28257.	1.5	4
15890	Electronic Friction Dominates Hydrogen Hot-Atom Relaxation on Pd(100). Physical Review Letters, 2014, 112, 103203.	2.9	112
15891	Effect of atmospheric CO2 on surface segregation and phase formation in La0.6Sr0.4Co0.2Fe0.8O3â˜' thin films. Applied Surface Science, 2014, 323, 71-77.	3.1	51
15892	Formation and stability of point defects in monolayer rhenium disulfide. Physical Review B, 2014, 89, .	1.1	151
15893	Ab initio molecular dynamics calculations on scattering of hyperthermal H atoms from Cu(111) and Au(111). Journal of Chemical Physics, 2014, 141, 054705.	1.2	41
15894	Two-Dimensional Ordering of Solute Nanoclusters at a Close-Packed Stacking Fault: Modeling and Experimental Analysis. Scientific Reports, 2014, 4, 7318.	1.6	37
15895	Contact-induced spin polarization in BNNT(CNT)/TM (TM=Co, Ni) nanocomposites. Journal of Applied Physics, 2014, 116, 084309.	1.1	9
15896	Lattice dynamics, thermodynamics, and elastic properties of Na₂Se under pressure investigated by first principles method. Canadian Journal of Physics, 2014, 92, 1464-1469.	0.4	3
15897	Achieving a direct band gap in oxygen functionalized-monolayer scandium carbide by applying an electric field. Physical Chemistry Chemical Physics, 2014, 16, 26273-26278.	1.3	82
15898	First principles study on energetic, structural, and electronic properties of defective g-C3N4-zz3 nanotubes. Journal of Theoretical and Computational Chemistry, 2014, 13, 1450021.	1.8	7
15899	Wannier center sheets in topological insulators. Physical Review B, 2014, 89, .	1.1	139
15900	HYDROGEN ADSORPTION ON Î²-TiAl (001) AND Ni/TiAl (001) SURFACES. Surface Review and Letters, 2014, 21, 1450034.	0.5	4
15901	Vibrational free energy and phase stability of paramagnetic and antiferromagnetic CrN fromab initiomolecular dynamics. Physical Review B, 2014, 89, .	1.1	46
15902	First-principles calculations of energetics and electronic structure for reconstructed<mml:math xmlns:mml="http://www.w3.org/1998/Math/MathML"><mml:mrow><mml:mi>Si</mml:mi><mml:mo>(</mml:mo><mml:mn>111</mml:mn> Physical Review B, 2014, 90, .	1.1	8

#	Article	IF	Citations
15903	Strain induced modification in phonon dispersion curves of monolayer boron pnictides. Journal of Applied Physics, 2014, 115, .	1.1	42
15904	Optimizing the Magnetocaloric Effect in Niâ€“Mnâ€“Sn by Substitution: A First-Principles Study. IEEE Transactions on Magnetics, 2014, 50, 1-4.	1.2	9
15905	High-temperature Raman spectroscopy of microstructure around the growing Î²-BaB₂O₄crystal in the BaOâ€“B₂O₃â€“Na₂O system. Journal of Applied Crystallography, 2014, 47, 739-744.	1.9	4
15906	First principles study on structural and electronic properties and defect formation enthalpies of cubic Hf₃N₄ under high pressure. Canadian Journal of Physics, 2014, 92, 1581-1586.	0.4	1
15907	Electronic structure calculations of delafossite Cu-based transparent conducting oxides<mml:math xmlns:mml="http://www.w3.org/1998/Math/MathML"><mml:mrow><mml:mi>Cu</mml:mi><mml:mi>M</mml:mi><mml:msub><mml:m mathvariant="normal">O</mml:mi><mml:mn>2</mml:mn></mml:msub></mml:mrow></mml:math><mml:math		

#	Article	IF	Citations
15921	Fermi surface and effect of high magnetic fields on the metal-semimetal Peierls-like transition of (TSeT)2Cl. Low Temperature Physics, 2014, 40, 307-310.	0.2	0
15922	Mechanical and electronic properties of Ti₂AlN and Ti₄AlN₃: a first-principles study. Canadian Journal of Physics, 2014, 92, 1652-1657.	0.4	40
15923	Ferroelectricity in wurtzite structure simple chalcogenide. Applied Physics Letters, 2014, 104, .	1.5	52
15924	Electromigration of bivalent functional groups on graphene. Physical Review B, 2014, 89, .	1.1	13
15925	First-principles study of configurational disorder in<mml:math xmlns:mml="http://www.w3.org/1998/Math/MathML"><mml:msub><mml:mrow><mml:mi mathvariant="normal">B</mml:mi></mml:mrow><mml:mn>4</mml:mn></mml:msub><mml:mi mathvariant="normal">C</mml:mi></mml:math>using a superatom-special quasirandom structure method. Physical Review B, 2014, 90, .	1.1	54
15926	Theoretical studies of Ir₅Th and Ir₅Ce nanoscale precipitates in Ir. Philosophical Magazine, 2014, 94, 991-1000.	0.7	2
15927	Investigations of the electronic and magnetic structures of Co2YGa (Y=Cr, Mn) Heusler alloys and their (100) surfaces. Journal of Applied Physics, 2014, 115, 113905.	1.1	18
15928	Computational prediction and characterization of single-layer CrS₂. Applied Physics Letters, 2014, 104, 022116.	1.5	108
15929	Local structure of CuxZn2â^'xTiO4 inverse spinel. Applied Physics Letters, 2014, 105, 071911.	1.5	8
15930	Density functional theory study of hypothetical<mml:math xmlns:mml="http://www.w3.org/1998/Math/MathML"><mml:msub><mml:mtext>PbTiO</mml:mtext><mml:mn>3</mml:mn></mml:msub></mml:math> oxysulfides. Physical Review B, 2014, 89, .	1.1	30
15931	⁷⁵As NQR signature of the isoelectronic nature of ruthenium for iron substitution in LaFeRuAsO. Physica Status Solidi (B): Basic Research, 2014, 251, 974-979.	0.7	4
15932	Theoretical Investigations on the Structural, Electronic, Mechanical, and Thermal Properties of <scp><scp>MP</scp></scp>₂<scp><scp>O</scp></scp>₇ (<scp><scp>M</scp></scp>Â=Â<scp><scp>Ti</scp></scp>,<scp><scp>Hf</scp></scp>). Journal of the American Ceramic Society, 2014, 97, 2484-2490.	1.9	11
15933	Energetics of the Waterâ€“Gas-Shift Reaction on the Active Sites of the Industrially Used Cu/ZnO/Al2O3 Catalyst. Catalysis Letters, 2014, 144, 1973-1977.	1.4	29
15934	Density functional study of Cr atom adsorption on hydrogen-terminated armchair boron nitride nanoribbons. , 2014, , .		0
15935	Formation energies of carbon related defects in Cu<inf>2</inf>ZnSnS<inf>4</inf>. , 2014, , .		0
15936	Theoretical examination of electronâ€“phonon interaction and superconductivity in the hexagonal pnictide SrPtAs. Philosophical Magazine, 2014, 94, 2692-2704.	0.7	3
15937	Influences of Surface Substitutional Ti Atom on Hydrogen Adsorption, Dissociation, and Diffusion Behaviors on the Î±-U(001) Surface. Journal of Physical Chemistry C, 2014, 118, 26634-26640.	1.5	12
15938	Theoretical Study of Optical Properties of Native Point Defects in Î±-Al₂O₃. Integrated Ferroelectrics, 2014, 156, 79-85.	0.3	14

#	Article	IF	Citations
15939	Experimental and computed phase diagrams of the Feâ€“Re system. Journal of Physics Condensed Matter, 2014, 26, 485402.	0.7	6
15940	Semiconducting Clathrates Meet Gas Hydrates: Xe₂₄[Sn₁₃₆]. Chemistry - A European Journal, 2014, 20, 6693-6698.	1.7	14
15941	London Force Correction Disparity in the Modeling of Crystalline Asparagine and Glutamine. Journal of Physical Chemistry A, 2014, 118, 12221-12228.	1.1	9
15942	Exploring High-Pressure Structures of N₂CO. Journal of Physical Chemistry C, 2014, 118, 27252-27257.	1.5	16
15943	Band structure engineering of anatase TiO2 by metal-assisted P-O coupling. Journal of Chemical Physics, 2014, 140, 174705.	1.2	29
15944	Temperature effects in first-principles solid state calculations of the chemical shielding tensor made simple. Journal of Chemical Physics, 2014, 141, 134113.	1.2	28
15945	A multi-scale analysis of the impact of pressure on melting of crystalline phase change material germanium telluride. Applied Physics Letters, 2014, 105, 173509.	1.5	5
15946	Photo-induced change of dielectric response in BaCoSiO4 stuffed tridymite. Journal of Applied Physics, 2014, 115, .	1.1	19
15947	Adsorption of C₂H₄ on Stepped Cu(410) Surface: A Combined TPD, FTIR, and DFT Study. Journal of Physical Chemistry C, 2014, 118, 27436-27448.	1.5	22
15948	A first-principles study on structural stability and mechanical properties of polar intermetallic phases CaZn₂and SrZn₂. Philosophical Magazine, 2014, 94, 3945-3959.	0.7	8
15949	Elastic Anisotropy and Anisotropic Transport Properties of Cu₃SbSe₄and Cu₃SbS₄. Journal of the Physical Society of Japan, 2014, 83, 094606.	0.7	13
15950	First-principles investigation of the structural stability and electronic properties of Pd doped monoclinic Cu6Sn5 intermetallic compounds. Materials Science-Poland, 2014, 32, 592-596.	0.4	1
15951	Beneficial compressive strain for oxygen reduction reaction on Pt (111) surface. Journal of Chemical Physics, 2014, 141, 124713.	1.2	66
15952	Pressure induced phase transition in MH2 (M = V, Nb). Journal of Chemical Physics, 2014, 140, 114703.	1.2	18
15953	Study of the Mechanical and Thermodynamic Properties on NiAl and Ni₃Al. Applied Mechanics and Materials, 0, 584-586, 1256-1263.	0.2	6
15954	The nature of dielectric state and self compensation mechanisms in PbTe doped with Ga. Materials Research Express, 2014, 1, 025905.	0.8	1
15955	First-principles study of sulfur isotope fractionation in sulfides. European Journal of Mineralogy, 2014, 26, 717-725.	0.4	8
15956	Stabilization of Ferromagnetism in Co Codoped ZnO:N. Integrated Ferroelectrics, 2014, 158, 90-97.	0.3	1

#	Article	IF	Citations
15957	First principles study of metal contacts to monolayer black phosphorous. Journal of Applied Physics, 2014, 116, .	1.1	29
15958	Charge spill-out and work function of few-layer graphene on SiC(0â€‰0â€‰0â€‰1). Journal Physics D: Applied Physics, 2014, 47, 295303.	1.3	13
15959	The growth of ultra-thin zirconia films on Pd₃Zr(0â€‰0â€‰0â€‰1). Journal of Physics Condensed Matter, 2014, 26, 225003.	0.7	38
15960	Giant Birefringence in Layered Compound LaOBiS 2. Chinese Physics Letters, 2014, 31, 047802.	1.3	8
15961	Insights and challenges of applying theGWmethod to transition metal oxides. Journal of Physics Condensed Matter, 2014, 26, 475501.	0.7	16
15962	A combined experimental-computational study on nitrogen doped Cu₂O as the wide-spectrum absorption material. Journal of Semiconductors, 2014, 35, 103001.	2.0	8
15963	Efficiency analysis and electronic structures of 3C-SiC and 6H-SiC with 3d elements impurities as intermediate band photovoltaics. Journal of Photonics for Energy, 2014, 4, 042098.	0.8	16
15964	Effect of amino ligand size of Si precursors on initial reaction with an â€“OH-terminated Si(001) surface for atomic layer deposition. Japanese Journal of Applied Physics, 2014, 53, 08NE04.	0.8	8
15965	Surface correlation effects in two-band strongly correlated slabs. Journal of Physics Condensed Matter, 2014, 26, 075601.	0.7	1
15966	A Comparative Computational Study of Li, Na, and Mg Insertion in Î±-Sn. Materials Research Society Symposia Proceedings, 2014, 1678, 1.	0.1	7
15967	Electronic structure, optical and magnetic properties of Zn<inf>1−x</inf>M<inf>x</inf>Te (M = Ti, Cr and Mn) Ab initio calculations. , 2014, , .		0
15968	Theoretical Study of the Lithium Diffusion in the Crystalline and Amorphous Silicon as well as on its Surface. Solid State Phenomena, 0, 213, 29-34.	0.3	2
15969	Static corrections versus dynamic correlation effects in the valence band Compton profile spectra of Ni. Physical Review B, 2014, 90, .	1.1	6
15970	First-Principles Study on Structural, Electronic, and Magnetic Properties of 3d Transition-Metal Nanowires Encapsulated Inside GaN Nanotubes. Journal of Superconductivity and Novel Magnetism, 2014, 27, 2539-2545.	0.8	2
15971	First-principle study on the relaxation of defected titanium dioxide under electric fields and its impacts on capacitor-voltage curves. European Physical Journal B, 2014, 87, 1.	0.6	1
15972	Advanced techniques for the band structure-quantum transport modeling in graphene and 2D-materials beyond graphene. , 2014, , .		0
15973	Boron-Phosphorus Pairs in Compensated Crystalline Silicon. ECS Solid State Letters, 2014, 3, N23-N25.	1.4	0
15974	Martensitic Transformation Behaviour of Ti₅₀Pt_{50-x}Co_x Shape Memory Alloys. Advanced Materials Research, 2014, 1019, 385-390.	0.3	0

#	Article	IF	Citations
15975	First Principles Study of Electronic and Elastic Properties of AlY. Advanced Materials Research, 2014, 1047, 45-50.	0.3	0
15976	Towards a Mechanism Underlying the Stability of the Tetragonal CuO Phase: Comparison with NiO and CoO by Hybrid Density Functional Calculation. Chinese Physics Letters, 2014, 31, 027402.	1.3	6
15977	Magneto-Electric Control of Surface Anisotropy and Nucleation Modes in L1<inline-formula><tex-math> $_{0}$</tex-math></inline-formula>-CoPt Thin Films. IEEE Magnetics Letters, 2014, 5, 1-4.	0.6	2
15978	Computational nano-materials design for circularly polarized luminescence in (Eu,Mg,O)-codoped GaN. Applied Physics Express, 2014, 7, 121002.	1.1	11
15979	Adsorption and diffusion of lithium on 1T-MoS2 monolayer. Computational Materials Science, 2014, 93, 86-90.	1.4	62
15980	Zeolite-Y entrapped bivalent transition metal complexes as hybrid nanocatalysts: density functional theory investigation and catalytic aspects. Green Chemistry Letters and Reviews, 2014, 7, 278-287.	2.1	36
15981	A stable, quasi-2D modification of silver: optical, electronic, vibrational and mechanical properties, and first principles calculations. Journal of Physics Condensed Matter, 2014, 26, 025402.	0.7	31
15982	Structures and Electronic Properties of Graphene with Vacancy Defects. Materials Research Society Symposia Proceedings, 2014, 1658, 70.	0.1	0
15983	Magnetism and Magnetocrystalline Anisotropy in Low-Dimensional Rh and Ir. IEEE Transactions on Magnetics, 2014, 50, 1-4.	1.2	0
15984	Pressure-induced phase transitions in coesite. American Mineralogist, 2014, 99, 755-763.	0.9	16
15985	First principles investigation into effects of Cr on segregation of S or Cl at Î±-Fe Î£5(210) grain boundary. Materials Research Innovations, 2014, 18, S4-1012-S4-1016.	1.0	3
15986	Phases Stability of Ni-Mn-Ga Alloys Studied by <i>Ab Initio</i> Calculations. Materials Science Forum, 0, 783-786, 1646-1651.	0.3	1
15987	Spectroscopic and atomic force studies of the functionalisation of carbon surfaces: new insights into the role of the surface topography and specific chemical states. Faraday Discussions, 2014, 173, 257-272.	1.6	18
15988	Effect of Nitriding on the Hydrogen Diffusion Coefficient through AISI 4340. Journal of the Electrochemical Society, 2014, 161, C261-C267.	1.3	9
15989	Magnetic Properties of Off-Stoichiometric Ni-X-In (X=Mn, Fe and Co) Magnetic Shape Memory Alloys by First-Principles Calculations. Materials Science Forum, 0, 783-786, 2419-2422.	0.3	0
15990	Newly Determined Crystal Structure and Optical Property of the Intermetallic NiAl and Ni₃Al Alloys: A First-Principles Computer Simulated Investigation. Advanced Materials Research, 2014, 989-994, 220-223.	0.3	0
15991	A Quantum Mechanics Study on the Electronic Structure of Impurity-Bearing Sphalerite (ZnS). Advanced Materials Research, 2014, 919-921, 1282-1285.	0.3	0
15992	MECHANICAL PROPERTIES OF CHIRAL SILICON CARBIDE NANOTUBES UNDER HYDROGEN ADSORPTION: A MOLECULAR MECHANICS APPROACH. Nano, 2014, 09, 1450043.	0.5	14

#	Article	IF	Citations
15993	First-principles study of Schottky barrier behavior at Fe3Si/Ge(111) interfaces. Japanese Journal of Applied Physics, 2014, 53, 035701.	0.8	5
15994	Ab Initio Thermal Transport. Topics in Applied Physics, 2014, , 137-173.	0.4	29
15995	Computational Raman spectroscopy of organometallic reaction products in lithium and sodium-based battery systems. Physical Chemistry Chemical Physics, 2014, 16, 24549-24558.	1.3	13
15996	Pressure and tension effects on mechanical properties of ZrAl2. AIP Advances, 2014, 4, 117141.	0.6	6
15997	Theoretical Investigations on Graphite Oxide Immersed in Water or Methanol. Chinese Journal of Chemical Physics, 2014, 27, 9-14.	0.6	4
15998	Study on Electronic Structure of GaN under Pressure. Advanced Materials Research, 2014, 900, 217-221.	0.3	0
15999	First Principles Study the Stability and Mechanical Properties of M3B2(M=V, Nb and Ta) Compounds. Rare Metal Materials and Engineering, 2014, 43, 2898-2902.	0.8	10
16000	Pâ€Vâ€T equation of state of cubic CaSiO₃ perovskite from firstâ€principles computation. Journal of Geophysical Research: Solid Earth, 2014, 119, 2801-2809.	1.4	19
16001	Crystal structure prediction and hydrogen-bond symmetrization of solid hydrazine under high pressure: a first-principles study. Acta Crystallographica Section C, Structural Chemistry, 2014, 70, 112-117.	0.2	2
16002	Density Functional Theory Study of H₂O Molecules on Cr₂O₃ Surfaces. Materials Science Forum, 0, 783-786, 2172-2175.	0.3	0
16003	Hydrogen trapping under the effect of Wâ€“C mixed layers. Nuclear Fusion, 2014, 54, 033013.	1.6	7
16004	Electronic Transport of a Molecular Photoswitch with Graphene Nanoribbon Electrodes. Chinese Physics Letters, 2014, 31, 057304.	1.3	4
16005	New high-pressure phase of MgH 2 : An ab initio constant-pressure study. Europhysics Letters, 2014, 105, 46001.	0.7	3
16006	Impact of Stone-Wales and lattice vacancy defects on the electro-thermal transport of the free standing structure of metallic ZGNR. Journal of Computational Electronics, 2014, 13, 862-871.	1.3	2
16007	The nature of the structural phase transition from the hexagonal (4H) phase to the cubic (3C) phase of silver. Journal of Physics Condensed Matter, 2014, 26, 115405.	0.7	17
16008	First principles calculations of solution energies of dopants around stacking faults in Si crystal. Japanese Journal of Applied Physics, 2014, 53, 061302.	0.8	11
16009	Thermoelectric Properties of Carbon Nanotubes and Related One-Dimensional Structures. Lecture Notes in Nanoscale Science and Technology, 2014, , 363-391.	0.4	0
16010	A general group theoretical method to unfold band structures and its application. New Journal of Physics, 2014, 16, 033034.	1.2	33

#	Article	IF	Citations
16011	Adsorption Mechanism of Carbon Monoxide on PtRu and PtRuMo Surfaces in the Density Functional Theory Perspective. Advanced Materials Research, 0, 896, 537-540.	0.3	4
16012	Quantum Chemical Study of Point Defects in Tin Dioxide. Lecture Notes in Electrical Engineering, 2014, , 13-24.	0.3	6
16013	Rationalization of the Hubbard U parameter in CeOx from first principles: Unveiling the role of local structure in screening. Journal of Chemical Physics, 2014, 140, 084101.	1.2	36
16014	Analysis of two-phonon infrared spectral features of gallium arsenide and indium phosphide by first-principles calculations. Materials Research Express, 2014, 1, 045901.	0.8	4
16015	Effects of additive elements on structural and electronic properties of Sn-based intermetallics by first principles. Materials Research Express, 2014, 1, 025702.	0.8	10
16016	Ammonium azide under hydrostatic compression. Journal of Physics: Conference Series, 2014, 500, 162006.	0.3	3
16017	Hydrogenated ultra-thin tin films predicted as two-dimensional topological insulators. New Journal of Physics, 2014, 16, 115008.	1.2	56
16018	A theoretical study of the elastic and thermal properties of ScRu compound under pressure. Physica Scripta, 2014, 89, 065702.	1.2	23
16019	Study of the High-Pressure HCP Phase of Al: A Computer Aided Design and Simulation. Applied Mechanics and Materials, 2014, 556-562, 412-415.	0.2	0
16020	Phonon Deformation Potential Constants of Wurtzite ZnO: A First-Principles Study. Materials Research Society Symposia Proceedings, 2014, 1588, 1.	0.1	0
16021	Electronic Properties of Hydrogenated Graphene-Like Materials Under Strains. Materials Research Society Symposia Proceedings, 2014, 1658, 76.	0.1	0
16022	Structural, Electronic, Elastic and Mechanical Properties of ScNi, ScPd and ScPt: A FP-LAPW Study. Advanced Materials Research, 0, 1047, 27-34.	0.3	9
16023	Structural, conductivity and dielectric properties of Li₂SO₄. EPJ Applied Physics, 2014, 66, 30906.	0.3	7
16024	Density Functional Theory Study: Interactions of Lithium-Montmorillonite with Poly(Ethylene Oxide) as Preliminary Investigation of Lithium Polymer Conductivity. Advanced Materials Research, 2014, 893, 790-793.	0.3	0
16025	Can slow-diffusing solute atoms reduce vacancy diffusion in advanced high-temperature alloys?. Materials Science & Engineering A: Structural Materials: Properties, Microstructure and Processing, 2014, 617, 194-199.	2.6	11
16026	The Studies of ScB₂(0001) Surfaces from the First-Principles. Advanced Materials Research, 2014, 989-994, 688-693.	0.3	0
16027	Electronic Transport Properties of Doped C28 Fullerene. Research Letters in Physics, 2014, 2014, 1-7.	0.2	4
16028	A Density Functional Theory Study of the Adsorption of Benzene on Hematite (Î±-Fe2O3) Surfaces. Minerals (Basel, Switzerland), 2014, 4, 89-115.	0.8	105

#	Article	IF	Citations
16029	Origin of Visible Light Photocatalytic Activity of Ag₃AsO₄from First-Principles Calculation. International Journal of Photoenergy, 2014, 2014, 1-5.	1.4	10
16030	Comparison of intermolecular interactions in two phases of MeNSOF₂. Zeitschrift Fur Kristallographie - Crystalline Materials, 2014, 229, 649-660.	0.4	1
16031	Distinguishing tautomerism in the crystal structure of (Z)-N-(5-ethyl-2,3-dihydro-1,3,4-thiadiazol-2-ylidene)-4-methylbenzenesulfonamide using DFT-D calculations and¹³C solid-state NMR. Acta Crystallographica Section C, Structural Chemistry, 2014, 70, 784-789.	0.2	17
16032	CONTROL OF CONDUCTANCE AND MAGNETORESISTANCE OF MOLECULAR JUNCTIONS. Spin, 2014, 04, 1440011.	0.6	1
16033	Calculation of defect formation energies in UO2. Materials Research Society Symposia Proceedings, 2014, 1645, 1.	0.1	5
16034	First Principles Study on Adsorption for Different Concentration of H₂S on Fe(100). Advanced Materials Research, 0, 1015, 521-525.	0.3	3
16035	Study of Structural, Electronic and Elastic Properties of LuPd₃ Compound. Advanced Materials Research, 0, 1047, 61-64.	0.3	0
16036	Dynamical stability of Pmn21 phase of NH3BH3: a vdW density functional study. Philosophical Magazine Letters, 2014, 94, 278-287.	0.5	2
16037	Exact exchange plane-wave-pseudopotential calculations for slabs. Journal of Chemical Physics, 2014, 140, 18A505.	1.2	18
16038	Experimental and theoretical studies of band gap alignment in GaAs1âˆ’xBix/GaAs quantum wells. Journal of Applied Physics, 2014, 116, .	1.1	52
16039	Ab-Initio Study of Cobalt Impurity Effects on Phonon Spectra, Mechanical and Thermal Properties of Single Wall Carbon Nanotube (5,0). Chinese Physics Letters, 2014, 31, 046301.	1.3	0
16040	Spin polarization of Co(0001)/graphene junctions from first principles. Journal of Physics Condensed Matter, 2014, 26, 104204.	0.7	15
16041	A comparative first-principles study of martensitic phase transformations in TiPd₂ and TiPd intermetallics. Journal of Physics Condensed Matter, 2014, 26, 135401.	0.7	1
16042	First-principles study of hydrogen configurations at the core of a high-angle grain boundary in cubic yttria-stabilized zirconia. Journal of Physics Condensed Matter, 2014, 26, 025502.	0.7	7
16043	Density functional study of electronic structure, elastic and optical properties of MNH₂(M=Li, Na, K, Rb). Journal of Physics Condensed Matter, 2014, 26, 235503.	0.7	6
16044	Tunneling anisotropic magnetoresistance effect of single adatoms on a noncollinear magnetic surface. Journal of Physics Condensed Matter, 2014, 26, 394010.	0.7	7
16045	Modelling [1â€‰0â€‰0] and [0â€‰1â€‰0] screw dislocations in MgSiO₃perovskite based on the Peierlsâ€“Nabarroâ€“Galerkin model. Modelling and Simulation in Materials Science and Engineering, 2014, 22, 025020.	0.8	16
16046	Van der Waals interaction in a boron nitride bilayer. New Journal of Physics, 2014, 16, 113015.	1.2	37

#	Article	IF	Citations
16047	Crystallographic and Electronic Structure of the Sr₃Sb₂CoO₉ Triple Perovskite. Journal of Physics: Conference Series, 2014, 480, 012022.	0.3	2
16048	First principles study of half Heusler alloys PdFeBi and PdCoBi. , 2014, , .		1
16049	Identification of mixed bromidochloridotellurate anions in disordered crystal structures of (bdmim)2[TeX2Y4] (X, Y=Br, Cl; bdmim=1-butyl-2,3-dimethylimidazolium) by combined application of Raman spectroscopy and solid-state DFT calculations. Spectrochimica Acta - Part A: Molecular and Biomolecular Spectroscopy, 2014, 117, 728-738.	2.0	9
16050	First principles study the stability and mechanical properties of MC (M=Ti, V, Zr, Nb, Hf and Ta) compounds. Journal of Alloys and Compounds, 2014, 582, 500-504.	2.8	142
16051	Elastic properties, lattice dynamics and structural transitions in molybdenum at high pressures. Computational Materials Science, 2014, 81, 313-318.	1.4	23
16052	Method and advantages of genetic algorithms in parameterization of interatomic potentials: Metal oxides. Computational Materials Science, 2014, 81, 453-465.	1.4	13
16053	First-principles-based phase diagrams and thermodynamic properties of TCP phases in Reâ€“X systems (X=Ta, V, W). Computational Materials Science, 2014, 81, 433-445.	1.4	32
16054	Structural and electronic inhomogeneity for graphene grown on the C-face of SiC: Insights from ab initio calculations. Applied Surface Science, 2014, 291, 69-73.	3.1	6
16055	Elastic modulus and thermal properties of InN in the rocksalt phase. Computational Materials Science, 2014, 81, 374-377.	1.4	15
16056	Semi-metallic to semiconducting transition in graphene nanosheet with site specific co-doping of boron and nitrogen. Physica E: Low-Dimensional Systems and Nanostructures, 2014, 56, 64-68.	1.3	50
16057	First-principle calculations of the electronic, optical and elastic properties of ZnSiP2 semiconductor. Journal of Alloys and Compounds, 2014, 582, 101-107.	2.8	50
16058	First-principles study of point defects in Ni₃Al. Philosophical Magazine, 2014, 94, 20-34.	0.7	28
16059	Origin of Tunable Photocatalytic Selectivity of Wellâ€Defined Î±â€Fe₂O₃ Nanocrystals. Small, 2014, 10, 674-679.	5.2	88
16060	Electron transfer through solid-electrolyte-interphase layers formed on Si anodes of Li-ion batteries. Electrochimica Acta, 2014, 140, 250-257.	2.6	59
16061			

#	Article	IF	Citations
16065	Functionalization of silicon carbide nanotube by dichlorocarbene: A density functional theory study. Physica E: Low-Dimensional Systems and Nanostructures, 2014, 56, 377-385.	1.3	7
16066	Electronic and elastic properties of Sr2RuO4 with pressure effects by first principles calculation. Physica B: Condensed Matter, 2014, 441, 62-67.	1.3	8
16067	Silicon-based counterpart of alpha-graphyne. Physics Letters, Section A: General, Atomic and Solid State Physics, 2014, 378, 1313-1315.	0.9	3
16068	Radiation defects in complex perovskite solid solutions. Nuclear Instruments & Methods in Physics Research B, 2014, 326, 243-246.	0.6	1
16069	Thermophysical properties of LiFePO4 cathodes with carbonized pitch coatings and organic binders: Experiments and first-principles modeling. Journal of Power Sources, 2014, 251, 8-13.	4.0	30
16070	Effect of alloying on elastic properties of ZrN based transition metal nitride alloys. Surface and Coatings Technology, 2014, 255, 140-145.	2.2	34
16071	Thermal stability and thermal expansion studies of cubic fluorite-type MgF2 up to 135GPa. Materials Research Bulletin, 2014, 52, 151-157.	2.7	5
16072	Theoretical studies of elastic properties of orthorhombic LiBH4. Computational Materials Science, 2014, 81, 378-385.	1.4	38
16073	Structural phase transformations and new intermediate phases of MgF2 under high-pressures applied via conjugate-gradient method. Journal of Alloys and Compounds, 2014, 609, 185-191.	2.8	9
16074	Proton migration in bulk orthorhombic barium cerate using density functional theory. Solid State Ionics, 2014, 259, 1-8.	1.3	17
16075	Large magnetoelectric coupling in ferromagnetic/ferroelectric superlattices with asymetric interfaces. Journal of Magnetism and Magnetic Materials, 2014, 354, 299-302.	1.0	3
16076	Prediction of two-dimensional materials with half-metallic Dirac cones: Ni2C18H12 and Co2C18H12. Carbon, 2014, 73, 382-388.	5.4	48
16077	Hydrogen-induced metallicity and strengthening of MoS2. Chemical Physics, 2014, 434, 20-24.	0.9	19
16078	Genetic algorithm prediction of crystal structure of metastable Si-IX phase. Solid State Communications, 2014, 182, 14-16.	0.9	7
16079	O2 activation on the outer surface of carbon nanotubes modified by encapsulated iron clusters. Applied Surface Science, 2014, 300, 91-97.	3.1	11
16080	Orthorhombic martensitic phase in Tiâ€“Nb alloys: A first principles study. Computational Materials Science, 2014, 83, 222-228.	1.4	31
16081	Study on the trap site in Niâ€“Cr alloy by first principle approach. Vacuum, 2014, 101, 321-323.	1.6	1
16082	Chlorine molecule adsorbed on graphene and doped graphene: A first-principle study. Physica B: Condensed Matter, 2014, 436, 54-58.	1.3	20

#	Article	IF	Citations
16083	The influence of Ti- and Si-doping on the structure, morphology and photo-response properties of Î±-Fe2O3 for efficient water-splitting: Insights from experiment and first-principles calculations. Chemical Physics Letters, 2014, 592, 242-246.	1.2	18
16084	Elastic properties and electronic structures of CrxBy as superhard compounds. Journal of Alloys and Compounds, 2014, 610, 684-694.	2.8	49
16085	First-principles calculations of structural, elastic and electronic properties of Li2B12H12. Journal of Alloys and Compounds, 2014, 593, 169-175.	2.8	12
16086	Electronic structures, elastic properties, and minimum thermal conductivities of cermet M3AlN. Journal of Solid State Chemistry, 2014, 216, 1-8.	1.4	14
16087	First-principles study of mechanical and electronic properties of TiB compound under pressure. Intermetallics, 2014, 52, 64-71.	1.8	21
16088	Realization of controlling the band alignment via atomic substitution. Carbon, 2014, 69, 495-501.	5.4	3
16089	Effects of F and Cl on the stability of MgH2. International Journal of Hydrogen Energy, 2014, 39, 877-883.	3.8	36
16090			

#	Article	IF	Citations
16101	A DFT study of dopant (Zr, Nb) and vacancies on the dehydrogenation on MgH2 (001) surface. International Journal of Hydrogen Energy, 2014, 39, 1732-1739.	3.8	18
16102	Realizing high visible-light-induced carriers mobility in TiO2-based photoanodes. Journal of Power Sources, 2014, 251, 195-201.	4.0	3
16103	Influence of titanium and nickel dopants on the dehydrogenation properties of Mg(AlH4)2: Electronic structure mechanisms. International Journal of Hydrogen Energy, 2014, 39, 9276-9287.	3.8	8
16104	Atomistic study on phase stability and electronic structures of Z phase CrNbNx (x=1, 2, 3). Journal of Alloys and Compounds, 2014, 598, 89-94.	2.8	11
16105	Mechanical and thermodynamic properties of Î±-UH3 under pressure. Journal of Alloys and Compounds, 2014, 604, 171-174.	2.8	9
16106	Elastic properties and lattice vibration modes in ZnTe1â^'xOx. Computational Materials Science, 2014, 83, 22-26.	1.4	4
16107	Formaldehyde molecule adsorbed on doped graphene: A first-principles study. Applied Surface Science, 2014, 293, 216-219.	3.1	49
16108	Effect of oxygen vacancy concentration on the absorption spectra of Dy2Ti2O7 crystal. Journal of Alloys and Compounds, 2014, 599, 170-174.	2.8	9
16109	Theoretical study of magnetic phase transitions of cubic SrMnO3 under physical and chemical pressures. Computational Materials Science, 2014, 83, 394-397.	1.4	8
16110	Manifold electronic structure transition of hybrid silicaneâ€“silicene nanoribbons. Chemical Physics Letters, 2014, 595-596, 20-24.	1.2	9
16111	First-principles study of the dislocation core structures on basal plane in magnesium. European Journal of Mechanics, A/Solids, 2014, 45, 1-7.	2.1	3
16112	A first-principles study of methyl lactate adsorption on the chiral Cu (643) surface. Surface Science, 2014, 629, 28-34.	0.8	4
16113	First-principles study of Pt-film stability on doped graphene sheets. Surface Science, 2014, 621, 7-15.	0.8	10
16114	Ab initio investigation of the passivation effect of the acrylonitrile molecule on the Si(100)-(2Ã—1) surface. Chemical Physics, 2014, 439, 12-16.	0.9	1
16115	Comparison of optical properties between Wurtzite and zinc-blende Ga0.75Al0.25N. Optik, 2014, 125, 424-427.	1.4	29
16116	Comment on the A.B. Rochaâ€™s reply to second comment on the paper â€œOn the nature of inhibition performance of imidazole on iron surfaceâ€• Corrosion Science, 2014, 79, 215-220.	3.0	5
16117	Strongly reduced band gap in NiMn2O4 due to cation exchange. Journal of Magnetism and Magnetic Materials, 2014, 358-359, 149-152.	1.0	5
16118	Toward a microscopic understanding of the calciumâ€“silicateâ€“hydrates/water interface. Applied Surface Science, 2014, 290, 207-214.	3.1	31

#	Article	IF	Citations
16119	Ni-doping effect of Mg(0001) surface to use it as a hydrogen storage material. Journal of Alloys and Compounds, 2014, 609, 93-99.	2.8	10
16120	Physical, mechanical, thermodynamic and electronic characterization of Cu11In9 crystal using first-principles density functional theory calculation. Computational Materials Science, 2014, 81, 146-157.	1.4	22
16121	First-principles investigation of the intrinsic defects in Ti3SiC2. Journal of Physics and Chemistry of Solids, 2014, 75, 384-390.	1.9	17
16122	The states of nitrogen atoms in the processing of Niâ€“Cr alloy surface nitriding modification. Applied Surface Science, 2014, 301, 346-350.	3.1	3
16123	Lithium-doped triazine-based graphitic C3N4 sheet for hydrogen storage at ambient temperature. Computational Materials Science, 2014, 81, 275-279.	1.4	75
16124	DFT study of the adsorption and dissociation of water on Ni(111), Ni(110) and Ni(100) surfaces. Surface Science, 2014, 627, 1-10.	0.8	109
16125	Novel high pressure structures and superconductivity of niobium disulfide. Journal of Alloys and Compounds, 2014, 610, 472-477.	2.8	23
16126	Hole -character and delocalization in (Ga,Mn)As revised with pSIC and MLWF approaches â€“ Newly found spin-unpolarized gap states of s-type below 1 of Mn. Chemical Physics, 2014, 430, 7-12.	0.9	9
16127	A density functional study of vacancy formation in grain boundaries of undoped Î±-alumina. Acta Materialia, 2014, 69, 365-371.	3.8	23
16128	Interface structure of nanodiamond composite films: First-principles studies. Journal of Alloys and Compounds, 2014, 599, 183-187.	2.8	9
16129	Fluorine interaction with defects on graphite surface by a first-principles study. Applied Surface Science, 2014, 292, 488-493.	3.1	8
16130	Structural stability in Aurivillius phases based on ab initio thermodynamics. Journal of Physics and Chemistry of Solids, 2014, 75, 1088-1093.	1.9	3
16131	DFT calculations for SO4/graphene with and without a Pd atom. Computational Materials Science, 2014, 83, 418-425.	1.4	3
16132	First-principles study of the properties of Li, Al and Cd doped Mg alloys. Journal of Alloys and Compounds, 2014, 596, 63-68.	2.8	22
16133	Pressure-induced phase transitions in LiBH4: Density functional theory calculations. International Journal of Hydrogen Energy, 2014, 39, 9330-9338.	3.8	6
16134	Influence of interstitial distribution on the elastic and electronic properties of phase by first-principles calculations. Physics Letters, Section A: General, Atomic and Solid State Physics, 2014, 378, 270-275.	0.9	2
16135	Nitrogen and Boron substitutional doped zigzag silicene nanoribbons: Ab initio investigation. Physica E: Low-Dimensional Systems and Nanostructures, 2014, 60, 112-117.	1.3	21
16136	Electronic structure and bonding of small Pd clusters on stoichiometric and reduced SnO2(110) surfaces. Vacuum, 2014, 106, 86-93.	1.6	13

#	Article	IF	Citations
16137	Novel high-pressure crystal structures of boron trifluoride. Journal of Physics and Chemistry of Solids, 2014, 75, 1094-1098.	1.9	2
16138	Electronic and optical properties of C and Nb co-doped anatase TiO2. Computational Materials Science, 2014, 85, 164-171.	1.4	19
16139	Electronic and optical properties of Ga-doped ZnO. Thin Solid Films, 2014, 570, 464-470.	0.8	24
16140	Structural parameters, elastic properties and piezoelectric constants of wurtzite ZnS and ZnSe under pressure. Superlattices and Microstructures, 2014, 67, 88-96.	1.4	37
16141	He-induced vacancy formation in bcc Fe solid from first-principles simulation. Journal of Nuclear Materials, 2014, 444, 147-152.	1.3	48
16142	Worthy hydrogen storage capacity of Li-decorated BC7 sheet. Physica E: Low-Dimensional Systems and Nanostructures, 2014, 61, 9-13.	1.3	1
16143	Hydrogen atom absorption in hydrogen-covered Pd(110) (1ÂÃ—Â2) missing-row surface. International Journal of Hydrogen Energy, 2014, 39, 6598-6603.	3.8	16
16144	Structural and electronic properties of copper nanowires inside zigzag carbon nanotubes. Physica B: Condensed Matter, 2014, 447, 77-82.	1.3	2
16145	Interactions of solute (3 p , 4 p , 5 p and 6 p) with solute, vacancy and divacancy in bcc Fe. Journal of Nuclear Materials, 2014, 455, 68-72.	1.3	13
16146	The first-principles study on physical properties and phase stability of Boron-V (BN, BP, BAs, BSb and) Tj ETQq1 1 0.784314 rgBT /Over	1.4	70
16147	Structure and elasticity of phlogopite under compression: Geophysical implications. Physics of the Earth and Planetary Interiors, 2014, 233, 1-12.	0.7	36
16148	Dehydrogenation properties of La-doped NaAlH4 (001) surface: A first-principle approach. International Journal of Hydrogen Energy, 2014, 39, 9744-9751.	3.8	3
16149	Relation between reactivity and electronic structure for Î±â€²L-, Î²- and Î³-dicalcium silicate: A first-principles study. Cement and Concrete Research, 2014, 57, 28-32.	4.6	59
16150	The disproportionation reaction phase transition, mechanical, and lattice dynamical properties of the lanthanum dihydrides under highÂpressure: A first principles study. Solid State Sciences, 2014, 32, 76-82.	1.5	9
16151	Energetic stability and magnetic moment of tri-, tetra-, and octa- ferromagnetic element nitrides predicted by first-principle calculations. Journal of Alloys and Compounds, 2014, 611, 440-445.	2.8	22
16152	Lattice instability in the AlMgB14 structure. Physica B: Condensed Matter, 2014, 438, 9-12.	1.3	12
16153	Ferromagnetism in stacked bilayers of Pd/C60. Journal of Magnetism and Magnetic Materials, 2014, 349, 128-134.	1.0	9
16154	High-throughput calculations of alloyed delafossite materials: Application to CuGa1â^'xFexO2. Computational Materials Science, 2014, 86, 155-164.	1.4	10

#	Article	IF	Citations
16155	Density functional study of GaN(0001)/AlN(0001) high electron mobility transistor structures. Journal of Crystal Growth, 2014, 401, 30-32.	0.7	3
16156	Density functional study of acrolein adsorption on Pt (111). Vacuum, 2014, 99, 259-264.	1.6	11
16157	Precipitation in Î± $alpha$ -Fe based Fe-Cu-Ni-Mn-alloys: behaviour of Ni and Mn modelled by ab initio and kinetic Monte Carlo simulations. Applied Physics A: Materials Science and Processing, 2014, 115, 679-687.	1.1	11
16158	Optical properties of ZnTe doped with transition metals (Ti, Cr and Mn). Optical and Quantum Electronics, 2014, 46, 75-86.	1.5	24
16159	Lattice-strain effect on oxygen vacancy formation in gadolinium-doped ceria. Journal of Electroceramics, 2014, 32, 72-77.	0.8	24
16160	Rational design of mixed ionic and electronic conducting perovskite oxides for solid oxide fuel cell anode materials: A case study for doped SrTiO3. Journal of Power Sources, 2014, 245, 875-885.	4.0	19
16161	Engineering Grain Boundaries in Cu₂ZnSnSe₄ for Better Cell Performance: A Firstâ€Principle Study. Advanced Energy Materials, 2014, 4, 1300712.	10.2	135
16162	Three-dimensional Wentzel-Kramers-Brillouin approach for the simulation of scanning tunneling microscopy and spectroscopy. Frontiers of Physics, 2014, 9, 711-747.	2.4	14
16163	Magnetism in Cu-Doped Rutile SnO2 Semiconductor Induced by the RKKY Interaction. Journal of Superconductivity and Novel Magnetism, 2014, 27, 581-586.	0.8	11
16164	Theoretical predictions of the structural and thermodynamic properties of MgZn2 Laves phase under high pressure. Applied Physics A: Materials Science and Processing, 2014, 115, 323-331.	1.1	17
16165	First-Principles Investigation of Half-metallic Ferromagnetism in V-doped BeS, BeSe, and BeTe. Journal of Superconductivity and Novel Magnetism, 2014, 27, 293-300.	0.8	42
16166	Half-metallic behavior of Co2YZ (YÂ=ÂV, Cr; ZÂ=ÂAl, Ga) under pressure: a DFT study. Applied Physics A: Materials Science and Processing, 2014, 116, 1199-1209.	1.1	9
16167	Elastic properties of eta carbide (Î·-Fe2C) from ab initio calculations: application to cryogenically treated gear steel. Journal of Materials Science, 2014, 49, 2383-2390.	1.7	19
16168	The Electronic Structures and Magnetism in Al Doped 4H-SiC: The First-Principles Calculation. Journal of Superconductivity and Novel Magnetism, 2014, 27, 1513-1516.	0.8	16
16169	Experimental and first-principles theoretical studies on Ag-doped cuprous oxide as photocathode in photoelectrochemical splitting of water. Journal of Materials Science, 2014, 49, 868-876.	1.7	22
16170	Properties of interfaces between iron-group metals (Fe, Co, Ni) and HfC via first-principles modeling. Journal of Materials Science, 2014, 49, 407-414.	1.7	8
16171	Infrared spectroscopic properties of goethite: anharmonic broadening, long-range electrostatic effects and Al substitution. Physics and Chemistry of Minerals, 2014, 41, 289-302.	0.3	24
16172	The Elastic Constants and Anisotropy of Superconducting MgCNi3 and CdCNi3 Under Different Pressure. Journal of Superconductivity and Novel Magnetism, 2014, 27, 1187-1194.	0.8	6

#	Article	IF	Citations
16173	Modification of the electronic properties of zigzag (nÂ=Â5â€“10) and armchair (nÂ=Â3, 5) carbon nanotubes by K atom adsorption. Structural Chemistry, 2014, 25, 1005-1012.	1.0	5
16174	First-Principles Study of Pressure-Induced Structural and Magnetic Phase Transitions of Binary Ferromagnets: MnSn and MnSb. Journal of Superconductivity and Novel Magnetism, 2014, 27, 1257-1264.	0.8	4
16175	Study of structural and electronic properties of NdSb employing local spin density approximation and Hubbard correction. Indian Journal of Physics, 2014, 88, 501-504.	0.9	3
16176	Piezoelectricity Across a Strainâ€Induced Isosymmetric Ferriâ€toâ€Ferroelectric Transition. Advanced Materials Interfaces, 2014, 1, 1400042.	1.9	15
16177	Topological states in<mml:math xmlns:mml="http://www.w3.org/1998/Math/MathML"><mml:msub><mml:mtext>Bi</mml:mtext><mml:mn>2</mml:mn></mml:msub><mml:msub><mml:mtext>Se</mml:mtext><mml:mn>3</mml:mn></mml:msub></mml:math>created by cleavage within a quintuple layer: Analysis in terms of the Shockley criterion. Physical Review B, 2014, 89, .	1.1	15
16178	Momentum space anisotropy of electronic correlations in Fe and Ni: An analysis of magnetic Compton profiles. Physical Review B, 2014, 89, .	1.1	8
16179	Theoretical study of hydrogen adsorption on nitrogen doped graphene decorated with palladium clusters. International Journal of Hydrogen Energy, 2014, 39, 6558-6566.	3.8	77
16180	A Nanolaminated Magnetic Phase: Mn₂GaC. Materials Research Letters, 2014, 2, 89-93.	4.1	128
16181	Iâ€“IIâ€“V and Iâ€“IIIâ€“IV half-Heusler compounds for optoelectronic applications: Comparative ab initio study. Journal of Alloys and Compounds, 2014, 587, 451-458.	2.8	123
16182	Electronic and optical properties of the SiB2O4 (B=Mg, Zn, and Cd) spinel oxides: An ab initio study with the Tranâ€“Blaha-modified Beckeâ€“Johnson density functional. Physica B: Condensed Matter, 2014, 443, 24-34.	1.3	17
16183	Chiral selectivity of improper ferroelectricity in single-wall<mml:math xmlns:mml="http://www.w3.org/1998/Math/MathML"><mml:msub><mml:mi>PbTiO</mml:mi><mml:mn>3</mml:mn></mml:msub></m Physical Review B, 2014, 89, .	1.1	9
16184	Pressure effect on elastic, lattice dynamic and superconducting behaviour of yttrium sulfide: A first principle study. Journal of Applied Physics, 2014, 115, .	1.1	15
16185	A first-principles study on the role of hydrogen in early stage of graphene growth during the CH4 dissociation on Cu(111) and Ni(111) surfaces. Carbon, 2014, 74, 255-265.	5.4	54
16186	IntrinsicLiNbO3point defects from hybrid density functional calculations. Physical Review B, 2014, 89, .	1.1	36
16187	Structural, mechanical and electronic properties of OsTM and TMOs2 (TM=Ti, Zr and Hf): First-principles calculations. Journal of Alloys and Compounds, 2014, 589, 278-282.	2.8	22
16188	A possible superhard orthorhombic carbon. Diamond and Related Materials, 2014, 43, 49-54.	1.8	27
16189	Elastic and electronic properties of MnTi2O4 under pressure: A first-principle study. Computational Materials Science, 2014, 84, 156-162.	1.4	9
16190	Structural, electronic and elastic properties of alkali hydrides (MH: M=Li, Na, K, Rb, Cs): Ab initio study. Computational Materials Science, 2014, 84, 206-216.	1.4	20

#	Article	IF	Citations
16191	First-principles investigation of the structural, mechanical and electronic properties of the NbO-structured 3d, 4d and 5d transition metal nitrides. Computational Materials Science, 2014, 84, 365-373.	1.4	78
16192	First-principles investigation of the structural, electronic and elastic properties of MgxAl4â^'xSr (x=0,) Tj ETQq1 1 0.784314 rgBT /Ove	1.4	41
16193	Crystal and electronic structures of solid M(NH 2 BH 3) n (MÂ=ÂLi, Na, K) and the decomposition mechanisms. International Journal of Hydrogen Energy, 2014, 39, 21372-21379.	3.8	7
16194	Electronic, elastic and optical properties of ZnGeP2 semiconductor under hydrostatic pressures. Materials Science and Engineering B: Solid-State Materials for Advanced Technology, 2014, 182, 52-58.	1.7	50
16195	Improved Calculation of the Electronic and Optical Properties of Tetragonal Barium Titanate. Journal of Electronic Materials, 2014, 43, 1443-1449.	1.0	6
16196	High pressure phase transitions in SnO2 polymorphs by first-principles calculations. Journal of Alloys and Compounds, 2014, 587, 638-645.	2.8	29
16197	Structural and elastic properties of TiCxN1â^'x, TiCxO1â^'x, TiOxN1â^'x solid solutions from first-principles calculations. Computational Materials Science, 2014, 88, 86-91.	1.4	18
16198	Electric control of magnetism at the Fe/BaTiO3 interface. Nature Communications, 2014, 5, 3404.	5.8	179
16199	Mechanical properties and atomistic deformation mechanism of spinel-type BeP2N4. Computational Materials Science, 2014, 83, 457-462.	1.4	10
16200	Ab initio study of the structural, elastic, thermodynamic, electronic and vibration properties of TbMg intermetallic compound. Superlattices and Microstructures, 2014, 71, 46-61.	1.4	6
16201	First-principles investigation of the binary intermetallics in Mgâ€"Alâ€"Sr alloy: Stability, elastic properties and electronic structure. Computational Materials Science, 2014, 86, 24-29.	1.4	36
16202	First-principles study of the structural, electronic and optical properties of tetragonal LiIO3. Computational Materials Science, 2014, 84, 350-354.	1.4	4
16203	First-principle calculations of structural, elastic and thermodynamic properties of Feâ€"B compounds. Intermetallics, 2014, 46, 211-221.	1.8	72
16204	Electronic and elastic properties of Îµ-phases Cr2-xVxN (x=0, 1, 2) from density-functional calculations. Journal of Alloys and Compounds, 2014, 583, 79-84.	2.8	21
16205	Determination of the thermal properties of AlB2-type WB2. Applied Surface Science, 2014, 288, 324-330.	3.1	24
16206	First-principles calculations for point defects in solids. Reviews of Modern Physics, 2014, 86, 253-305.	16.4	1,967
16207	Synthesis, Crystal Structure, and Characterization of a ÂCongruent Melting Compound Magnesium Strontium Diborate MgSrB2O5. Zeitschrift Fur Anorganische Und Allgemeine Chemie, 2014, 640, 1805-1809.	0.6	7
16208	The optical properties of NiAs phase ZnO under pressure calculated by GGA+U method. Optics Communications, 2014, 312, 185-191.	1.0	23

#	Article	IF	Citations
16209	Work function modification of the (111) gold surface covered by long alkanethiol-based self-assembled monolayers. Physical Chemistry Chemical Physics, 2014, 16, 2866.	1.3	26
16210	Pressure effect on the structural, elastic and electronic properties of Nb2AC (A=S and In) phases; ab initio study. Computational Materials Science, 2014, 81, 184-190.	1.4	19
16211	Halfmetallic ferromagnetism in rare earth nitrides RENs (RE=Gd, Dy, and Ho): A first principles study. Ceramics International, 2014, 40, 1993-2004.	2.3	5
16212	First-principles calculations on mechanical and elastic properties of 2H- and 3R-WS2 under pressure. Solid State Communications, 2014, 187, 43-47.	0.9	23
16213	Comparative study of A-site order in the lead-free bismuth titanates M1/2Bi1/2TiO3 (M=Li, Na, K, Rb, Cs,) Tj ETQq0 0 0 rgBT /Overlock 10	1.4	18
16214	Cohesion energetics of carbon allotropes: Quantum Monte Carlo study. Journal of Chemical Physics, 2014, 140, 114702.	1.2	166
16215	Electronic and optical properties of SrTiO3 under pressure effect: Ab initio study. Solid State Communications, 2014, 189, 32-37.	0.9	14
16216	Defect engineering of graphene for effective hydrogen storage. International Journal of Hydrogen Energy, 2014, 39, 4981-4995.	3.8	96
16217	Theoretical investigation on compressibility, electronic and thermodynamic properties of single crystal PtAs2 under high pressure. Computational Materials Science, 2014, 86, 124-129.	1.4	13
16218	Noncovalent functionalization of single-walled carbon nanotubes by aromatic diisocyanate molecules: A computational study. Chemical Physics Letters, 2014, 598, 10-16.	1.2	13
16219	Ab initiocalculation of x-ray absorption of iron up to 3 Mbar and 8000 K. Physical Review B, 2014, 89, .	1.1	13
16220	Electronic structure and thermodynamic properties of millerite NiS from first principles: Complex fermi surface and large thermal expansion coefficient. Computational Materials Science, 2014, 83, 412-417.	1.4	12
16221	Anisotropic Etching of Graphite Flakes with Water Vapor to Produce Armchairâ€Edged Graphene. Small, 2014, 10, 2809-2814.	5.2	23
16222	Will a graphitic-like ZnO single-layer be an ideal substrate for graphene?. RSC Advances, 2014, 4, 17478.	1.7	16
16223	Anisotropies of elasticity and thermal conductivity in some novel superhard materials. Computational Materials Science, 2014, 88, 103-109.	1.4	7
16224	Temperature-dependent mechanical properties of alpha-/beta-Nb5Si3 phases from first-principles calculations. Intermetallics, 2014, 46, 72-79.	1.8	30
16225	Inorganic Doubleâ€Helix Nanotoroid of Simple Lithiumï£¿Phosphorus Species. Chemistry - A European Journal, 2014, 20, 2431-2435.	1.7	15
16226	First-principles studies concerning optimization of hydrogen storage in nanoporous reduced graphite oxide. International Journal of Hydrogen Energy, 2014, 39, 4396-4403.	3.8	10

#	Article	IF	Citations
16227	Dangling bond modulating the electronic and magnetic properties of zigzag SiGe nanoribbon. Physica E: Low-Dimensional Systems and Nanostructures, 2014, 58, 1-5.	1.3	4
16228	Substrate induced modulation of electronic, magnetic and chemical properties of MoSe2 monolayer. AIP Advances, 2014, 4, .	0.6	13
16229	Structural, electronic and magnetic properties of C atom doped AlN nanoribbons. Superlattices and Microstructures, 2014, 69, 10-16.	1.4	9
16230	Electronic and elastic properties of Al4Ce binary compound under pressure via first-principles. Superlattices and Microstructures, 2014, 69, 76-86.	1.4	8
16231	Effect of boron vacancies on mechanical properties of ReB2 from first-principles calculation. Computational Materials Science, 2014, 82, 12-16.	1.4	11
16232	Shear strain induced indirect to direct transition in band gap in AlN monolayer nanosheet. Computational Materials Science, 2014, 86, 206-210.	1.4	44
16233	High-pressure structural phase transitions and intermediate phases of magnesium fluoride. Journal of Alloys and Compounds, 2014, 597, 155-160.	2.8	16
16234	Electron-Phonon Coupling and the Metallization of Solid Helium at Terapascal Pressures. Physical Review Letters, 2014, 112, 055504.	2.9	64
16235	On the electrochemical properties of platinum stepped surfaces vicinal to the (100) pole. A computational study. Electrochimica Acta, 2014, 125, 666-673.	2.6	9
16236	Adsorption of hydrazine on the perfect and defective copper (111) surface: A dispersion-corrected DFT study. Surface Science, 2014, 622, 1-8.	0.8	76
16237	A first-principles study of self-diffusion coefficients of fcc Ni. Computational Materials Science, 2014, 86, 17-23.	1.4	40
16238	Chromium coordination compounds with bis(3,5-dimethylpyrazol-1-yl)acetic acid or its anion. Polyhedron, 2014, 70, 119-124.	1.0	2
16239	Lattice dynamics and superconducting properties of antiperovskite La3InZ (Z=N,O). Solid State Communications, 2014, 181, 54-59.	0.9	13
16240	Hydrogen embrittlement of Pt3Zr compound from first-principles. Journal of Alloys and Compounds, 2014, 585, 549-554.	2.8	14
16241	Tuning the MoS₂ Edge-Site Activity for Hydrogen Evolution via Support Interactions. Nano Letters, 2014, 14, 1381-1387.	4.5	660
16242	Influences of the type of dopant and substrate on ferromagnetism in ZnO:Mn. Journal of Magnetism and Magnetic Materials, 2014, 355, 51-57.	1.0	23
16243	First principles calculations in Vâ€“Si system. Defects in A15-V3Si phase. Computational Materials Science, 2014, 85, 94-101.	1.4	9
16244	Interplay between Subnanometer Ag and Pt Clusters and Anatase TiO2 (101) Surface: Implications for Catalysis and Photocatalysis. Journal of Physical Chemistry C, 2014, 118, 4702-4714.	1.5	38

#	Article	IF	Citations
16245	Centered Honeycomb NiSe₂ Nanoribbons: Structure and Electronic Properties. Journal of Physical Chemistry C, 2014, 118, 3295-3304.	1.5	27
16246	The role of dipole moment in determining the nonlinear optical behavior of materials: ab initio studies on quaternary molybdenum tellurite crystals. Journal of Materials Chemistry C, 2014, 2, 530-537.	2.7	81
16247	Band structure engineering of CdSe nanosheet by strain: A first-principles study. Chemical Physics Letters, 2014, 595-596, 91-96.	1.2	5
16248	Understanding and controlling indium incorporation and surface segregation on In<mml:math xmlns:mml="http://www.w3.org/1998/Math/MathML"><mml:msub><mml:mrow /><mml:mi>x</mml:mi></mml:msub></mml:math>Ga<mml:math xmlns:mml="http://www.w3.org/1998/Math/MathML"><mml:msub><mml:mrow /><mml:mrow><mml:mn>1</mml:mn><mml:mo>â^’</mml:mo><mml:mi>x</mml:mi></mml:mrow></mml:msub></mml:math>N surfaces: Anab initioapproach. Physical Review B, 2014, 89, .	1.1	47
16249	Structural stability and elastic properties of IrSi in B31 and B20-phase from first-principles calculations. Journal of Alloys and Compounds, 2014, 585, 491-496.	2.8	2
16250	First-principles study of atomic ordering in fcc Ni-Cr alloys. Physical Review B, 2014, 89, .	1.1	24
16251	DFT study of electronic and structural properties of Sm:GaN. Computational Materials Science, 2014, 88, 71-75.	1.4	4
16252	First-principles study on the phase transition, elastic properties and electronic structure of Pt3Al alloys under high pressure. Journal of Alloys and Compounds, 2014, 597, 200-204.	2.8	20
16253	Mechanical, electronic and thermodynamic properties of Mg2Ca Laves phase under high pressure: A first-principles calculation. Computational Materials Science, 2014, 88, 61-70.	1.4	38
16254	Phase transition and elasticity of enstatite under pressure from experiments and first-principles studies. Physics of the Earth and Planetary Interiors, 2014, 228, 63-74.	0.7	23
16255	Effect of Pd and Pt metal on sulfur adsorption on Co(0001) by surface alloying. European Physical Journal B, 2014, 87, 1.	0.6	1
16256	Mechanical, piezoelectric and some thermal properties of (B3) BP under pressure. Journal of Central South University, 2014, 21, 58-64.	1.2	10
16257	Density-Functional Theoretical Study on the Role of Lewis and BrÃ¸nsted Acid Sites on CeO2(110) Surfaces for Nitrile Hydration. Topics in Catalysis, 2014, 57, 1094-1102.	1.3	14
16258	Encapsulation of sodium radio-iodide in fullerene C60. Journal of Molecular Modeling, 2014, 20, 2130.	0.8	4
16259	Theoretical prediction of novel ultrafine nanowires formed by Si12C12 cage-like clusters. European Physical Journal D, 2014, 68, 1.	0.6	4
16260	First-principles calculations of nickel, cadmium, and lead adsorption on a single-walled (10,0) carbon nanotube. Journal of Molecular Modeling, 2014, 20, 2094.	0.8	11
16261	Theoretical study of the adsorption of pentachlorophenol on the pristine and Fe-doped boron nitride nanotubes. Journal of Molecular Modeling, 2014, 20, 2093.	0.8	9
16262	Reaction mechanism of methylamine decomposition on Ru(0001): a density functional theory study. Journal of Molecular Modeling, 2014, 20, 2137.	0.8	5

#	Article	IF	Citations
16263	Adsorption and Catalytic Activation of the Molecular Oxygen on the Metal Supported h-BN. Topics in Catalysis, 2014, 57, 1032-1041.	1.3	34
16264	Role of magnetism in the formation of a short-range order in an Fe-Ga alloy. JETP Letters, 2014, 98, 809-812.	0.4	7
16265	First-principles study of molecular NO dissociation on Ir(100) surface. European Physical Journal B, 2014, 87, 1.	0.6	2
16266	First principles calculation on electronic structure, chemical bonding, elastic and optical properties of novel tungsten triboride. Journal of Central South University, 2014, 21, 500-505.	1.2	11
16267	First-principles study of high-pressure stability, structure, and elasticity of FeS2 polymorphs. Physics and Chemistry of Minerals, 2014, 41, 189-196.	0.3	12
16268	The hydrogenation-dependent thermal expansion properties of hydrogenated graphene. European Physical Journal B, 2014, 87, 1.	0.6	3
16269	Interfacial properties in ultrathin MgO films on TiN(001) surfaces: Ab-initio calculations. Journal of the Korean Physical Society, 2014, 64, 289-294.	0.3	7
16270	Structural and electronic properties of chiral single-wall copper nanotubes. Science China: Physics, Mechanics and Astronomy, 2014, 57, 644-651.	2.0	6
16271	Theoretical investigation of the structure and properties of the VN(111) monolayer on the MgO(111) surface. Physics of the Solid State, 2014, 56, 229-234.	0.2	6
16272	Elastic Properties of Monoclinic $$hbox {ZrO}_{2}$$ ZrO 2 at Finite Temperatures Via First Principles. International Journal of Thermophysics, 2014, 35, 145-153.	1.0	3
16273	The Influence of Particle Shape and Size on the Activity of Platinum Nanoparticles for Oxygen Reduction Reaction: A Density Functional Theory Study. Catalysis Letters, 2014, 144, 380-388.	1.4	66
16274	Novel and Simple Solution-processed MIS Ultraviolet (UV) Detector Based on Coreâ€“Shell Si/SiO2 Nanocrystals. Journal of Electronic Materials, 2014, 43, 1249-1254.	1.0	5
16275	Ab initio perspective of the âŒ©110âŒª symmetrical tilt grain boundaries in bcc Fe: application of local energy and local stress. Journal of Materials Science, 2014, 49, 3980-3995.	1.7	41
16276	High Mg effective incorporation in Al-rich Al x Ga1 - xN by periodic repetition of ultimate V/III ratio conditions. Nanoscale Research Letters, 2014, 9, 40.	3.1	23
16277	Theoretical study on the adsorption mechanism of iodine molecule on platinum surface in dye-sensitized solar cells. Theoretical Chemistry Accounts, 2014, 133, 1.	0.5	13
16278	Effect of CVD diamond growth by doping with nitrogen. Theoretical Chemistry Accounts, 2014, 133, 1.	0.5	50
16279	Pb3B6O11F2: the first non-centrosymmetric lead borate fluoride with a large second harmonic generation response. Journal of Materials Chemistry C, 2014, 2, 1704.	2.7	55
16280	Novel metalâ€“organic framework linkers for light harvesting applications. Chemical Science, 2014, 5, 2081-2090.	3.7	152

#	Article	IF	Citations
16281	Temperature effects on adsorption and diffusion dynamics of CH3CH2(ads) and H3Câ€“Câ‰¡C(ads) on Ag(111) surface and their self-coupling reactions: Ab initio molecular dynamics approach. Journal of Chemical Physics, 2014, 140, 024706.	1.2	2
16282	Stability, elastic and electronic properties of the Rhâ€“Zr compounds from first-principles calculations. Intermetallics, 2014, 44, 31-36.	1.8	13
16283	Vibrational zero point energy for H-doped silicon. Chemical Physics Letters, 2014, 601, 49-53.	1.2	4
16284	Metallization and superconductivity of BeH2 under high pressure. Journal of Chemical Physics, 2014, 140, 124707.	1.2	50
16285	Site preference and alloying effect on elastic properties of ternary B2ÂRuAl-based alloys. Intermetallics, 2014, 51, 24-29.	1.8	21
16286	Structural, electronic properties and stability of AlCMn3 (1 1 1) surfaces by first-principles calculations. Applied Surface Science, 2014, 289, 351-357.	3.1	7
16287	First-principles calculations of the stability and hydrogen storage behavior of C14 Laves phase compound TiCrMn. Solid State Sciences, 2014, 32, 1-7.	1.5	19
16288	Geometrical Description of Crystals: Direct and Reciprocal Lattices. , 2014, , 67-105.		2
16289	Strain effect on the electronic and optical properties of CdSe nanosheet. Physica Status Solidi (A) Applications and Materials Science, 2014, 211, 952-957.	0.8	7
16290	Electronic bands and excited states of III-V semiconductor polytypes with screened-exchange density functional calculations. Applied Physics Letters, 2014, 104, 132101.	1.5	3
16291	Ab initio study of the structural, electronic and elastic properties of anti-fluorite Li2X (X=S and Te) compounds under pressure effect. Computational Materials Science, 2014, 86, 49-56.	1.4	12
16292	Quasi-particle energies and excitonic effects in bilayer of hexagonal boron nitride. Solid State Communications, 2014, 187, 1-4.	0.9	8
16293	Experimental and DFT study on the catalytic asymmetric hydrogenation performance of (1S,2S)-DPEN-Ru(TPP)2 encapsulated in zeolite. Journal of Molecular Catalysis A, 2014, 385, 85-90.	4.8	5
16294	DFT analysis of Li intercalation mechanisms in the Fe-phthalocyanine cathode of Li-ion batteries. Physical Chemistry Chemical Physics, 2014, 16, 743-752.	1.3	26
16295	A Theoretical Study of the Effect of Zr-, Nb-Doped and Vacancy-like Defects on H Desorption on MgH₂ (110) Surface. Journal of Physical Chemistry C, 2014, 118, 4231-4237.	1.5	22
16296	A hybrid functional study of the electronic and optical properties of tetragonal PbO-type phase of ZnO under pressure. Journal of Alloys and Compounds, 2014, 586, 611-615.	2.8	9
16297	First-principles study of high-pressure crystal structures and superconductivity of Li3Be alloy. Computational Materials Science, 2014, 88, 45-49.	1.4	0
16298	A New Route to Low Resistance Contacts for Performanceâ€Enhanced Organic Electronic Devices. Advanced Materials Interfaces, 2014, 1, 1300130.	1.9	15

#	Article	IF	Citations
16299	Formation of two-dimensional uranium silicide film and its electronic structure study. Physica B: Condensed Matter, 2014, 436, 215-219.	1.3	4
16300	Generalized BrÃ¸nstedâ€“Evansâ€“Polanyi relationships and descriptors for Oâ€“H bond cleavage of organic molecules on transition metal surfaces. Journal of Catalysis, 2014, 313, 24-33.	3.1	42
16301	Lattice dynamics of cubic AuZn from first principles. Physical Review B, 2014, 89, .	1.1	4
16302	Synthesis, structure, and characterization of a new rubidium cadmium borate: RbCdB3O6. Journal of Alloys and Compounds, 2014, 588, 514-518.	2.8	8
16303	Mechanical properties and electronic structure of anti-ReO3 structured cubic nitrides, M3N, of d block transition metals M: An ab initio study. Journal of Alloys and Compounds, 2014, 595, 80-86.	2.8	55
16304	Proton Conducting Compound of Benzimidazole with Sebacic Acid: Structure, Molecular Dynamics, and Proton Conductivity. Crystal Growth and Design, 2014, 14, 1211-1220.	1.4	23
16305	Distinct Solidâ€Electrolyteâ€Interphases on Sn (100) and (001) Electrodes Studied by Soft Xâ€Ray Spectroscopy. Advanced Materials Interfaces, 2014, 1, 1300115.	1.9	94
16306	Density functional study of the mechanical and phonon properties of Al12X (XÂ=ÂMo, Tc, Ru, W, Re, and) Tj ETQq1 1 0.784314 rgBT	1.8	13
16307	Performance analysis of boron nitride embedded armchair graphene nanoribbon metalâ€“oxideâ€“semiconductor field effect transistor with Stone Wales defects. Journal of Applied Physics, 2014, 115, .	1.1	17
16308	Hydrothermal synthesis, electronic structure and tunable luminescence of single-phase Ca₅(PO₄)₃F:Tb³⁺,Eu³⁺microrods. Dalton Transactions, 2014, 43, 2819-2827.	1.6	55
16309	Epoxy monomer adsorption on Group III (B, Al, Ga) nitride nanotubes: vdW-DF studies on mechanical and electronic properties. Superlattices and Microstructures, 2014, 67, 127-143.	1.4	9
16310	Formic acid decomposition on Au catalysts: DFT, microkinetic modeling, and reaction kinetics experiments. AIChE Journal, 2014, 60, 1303-1319.	1.8	87
16311	Hydrogen storage on calcium-decorated BC7 sheet: A first-principles study. International Journal of Hydrogen Energy, 2014, 39, 2142-2148.	3.8	25
16312	Si(111)2Ã—1 surface isomers: DFT investigations on stability and doping effects. Surface Science, 2014, 621, 123-127.	0.8	6
16313	Structural, electronic, elastic, mechanical and thermal behavior of RESn3(REÂ=ÂY, La and Ce) compounds: A first principles study. Intermetallics, 2014, 51, 1-10.	1.8	14
16314	Thermodynamic modeling and first-principles calculations of the Moâ€“O system. Calphad: Computer Coupling of Phase Diagrams and Thermochemistry, 2014, 45, 178-187.	0.7	30
16315	Bonding in intermetallics may be deceptive â€“ The case of the new type structure Au2InGa2. Intermetallics, 2014, 46, 40-44.	1.8	6
16316	Ab-initio calculation of electronic and optical properties of nitrogen and boron doped graphene nanosheet. Carbon, 2014, 73, 275-282.	5.4	165

#	Article	IF	Citations
16317	Highâ€Temperature Elastic Moduli of Fluxâ€Grown Î±â€GeO₂ Single Crystal. ChemPhysChem, 2014, 15, 118-125.	1.0	18
16318	Phase transition, dynamical and electronic properties of BeO: First-principles investigations. Physica B: Condensed Matter, 2014, 438, 60-64.	1.3	8
16319	Density functional theory study of interactions between glycine and TiO2/graphene nanocomposites. Chemical Physics Letters, 2014, 599, 86-91.	1.2	23
16320	The nitrogen vacancy and oxygen substitution of OsN2: First-principles investigation. Journal of Alloys and Compounds, 2014, 590, 27-32.	2.8	1
16321	First principles study the stability, mechanical and electronic properties of manganese carbides. Computational Materials Science, 2014, 87, 19-25.	1.4	53
16322	Understanding the Thermal and Mechanical Stabilities of Olivine-Type LiMPO₄ (M = Fe, Mn) as Cathode Materials for Rechargeable Lithium Batteries from First Principles. ACS Applied Materials & Interfaces, 2014, 6, 4033-4042.	4.0	66
16323	Quantum chemistry investigation of rigid A-IRMOF-M0 series (A=zinc, cadmium, and alkaline-earth) Tj ETQq0 0 0 rgBT /Overlock 10 Tf 50 properties. Microporous and Mesoporous Materials, 2014, 183, 218-233.	2.2	18
16324	Investigation of the adsorption of amino acids on Pd(111): A density functional theory study. Applied Surface Science, 2014, 301, 199-207.	3.1	13
16325	First-principles study of optical properties of Î±-CuSe/klockmannite: Bulk and nano-layers. Thin Solid Films, 2014, 556, 425-433.	0.8	8
16326	Structural, electronic and thermodynamic properties of britholites Ca10â^'xLax(PO4)6â^'x(SiO4)xF2 (0â‰¤xâ‰¤6): Experiment and theory. Materials Research Bulletin, 2014, 51, 210-216.	2.7	22
16327	A comparative study of experimental and theoretical results of conformations of oxovanadium(IV) complexes with 4-acyl pyrazolone ligands using DFT method. Spectrochimica Acta - Part A: Molecular and Biomolecular Spectroscopy, 2014, 128, 447-451.	2.0	5
16328	Tailoring the Electronic Band Gap of Graphyne. Journal of Physical Chemistry C, 2014, 118, 2463-2468.	1.5	34
16329	On equation of state, elastic, and lattice dynamic stability of bcc bismuth under high pressure: Ab-initio calculations. Journal of Applied Physics, 2014, 115, .	1.1	11
16330	Gap opening and tuning of the electronic instability in Au intercalated bilayer graphene. Carbon, 2014, 71, 76-86.	5.4	9
16331	Contribution of the entropy on the thermodynamic equilibrium of vacancies in nickel. Journal of Chemical Physics, 2014, 140, 104705.	1.2	37
16332	Theoretical and kinetic assessment of the mechanism of ethane hydrogenolysis on metal surfaces saturated with chemisorbed hydrogen. Journal of Catalysis, 2014, 311, 350-356.	3.1	55
16333	Theoretical investigation on the structural phase transition, elastic properties and hardness of RhSi under high pressure. Journal of Alloys and Compounds, 2014, 592, 42-47.	2.8	13
16334	Experimental investigation and thermodynamic analysis of the Scâ€“Ni system supplemented with first-principles calculations. Thermochimica Acta, 2014, 586, 30-39.	1.2	13

#	Article	IF	Citations
16335	Structural, elastic, and thermal properties of cementite (<mml:math) Tj ETQq0 0 0 rgBT /Overlock 10 Tf 50 747 Td (xmlns:mml="http://w calculated using a modified embedded atom method. Physical Review B, 2014, 89, .	1.1	81
16336	Structural and electronic properties of MnO3(4) superhalogen clusters embedded in graphene. Chemical Physics Letters, 2014, 601, 16-20.	1.2	24
16337	Hybrid density functional investigations of Li2MSiO4 (M=Mn, Fe and Co) cathode materials. Computational Materials Science, 2014, 83, 45-50.	1.4	14
16338	Homologous series of layered structures in binary and ternary Bi-Sb-Te-Se systems:Ab initiostudy. Physical Review B, 2014, 89, .	1.1	5
16339	Lifshitz Transition and Chemical Instabilities in<mml:math xmlns:mml="http://www.w3.org/1998/Math/MathML" display="inline"><mml:mrow><mml:msub><mml:mrow><mml:mi>Ba</mml:mi></mml:mrow><mml:mrow><mml:mn>2</mml:mn></mml:mrow></mml:msub><mml:mi mathvariant="normal">K</mml:mi></mml:mrow><mml:mrow><mml:mi>x</mml:mi></mml:mrow></mml:msub><mml:msub><mml:mro Physical Review Letters, 2014, 112, 156401.	2.9	45
16340	Ab initio studies of 1,3,5,7-tetranitro-1,3,5,7-tetrazocine/1,3-dimethyl-2-imidazolidinone cocrystal under high pressure using dispersion corrected density functional theory. Journal of Applied Physics, 2014, 115, .	1.1	24
16341	A First-Principles Study: Structure and Decomposition of Mono-/Bimetallic Ammine Borohydrides. Journal of Physical Chemistry C, 2014, 118, 8271-8279.	1.5	15
16342	Ultralow thermal conductivity and high thermoelectric figure of merit in SnSe crystals. Nature, 2014, 508, 373-377.	13.7	3,963
16343	First-principles Raman spectra of MoS2, WS2 and their heterostructures. Nanoscale, 2014, 6, 5394.	2.8	348
16344	Atomistic modeling of intrinsic and radiation-enhanced fission gas (Xe) diffusion in <mml:math xmlns:mml="http://www.w3.org/1998/Math/MathML" altimg="si236.gif" overflow="scroll"><mml:mrow><mml:msub><mml:mrow><mml:mi mathvariant="normal">UO</mml:mi></mml:mrow><mml:mrow><mml:mn>2</mml:mn><mml:mo>Â±</mml:mo><mml:mi>x</mml:mi> Implications for nuclear fuel performance modeling. Journal of Nuclear Materials, 2014, 451, 225-242.	1.3	83
16345	Modelling self trapping and trap mutation in tungsten using DFT and Molecular Dynamics with an empirical potential based on DFT. Journal of Nuclear Materials, 2014, 455, 10-15.	1.3	65
16346	Ab initiobased thermal property predictions at a low cost: An error analysis. Physical Review B, 2014, 89, .	1.1	23
16347	On the origin of the significant difference in lithiation behavior between silicon and germanium. Journal of Power Sources, 2014, 263, 252-258.	4.0	44
16348	First-principles calculations of electronic structures and optical properties of group-IIIA elements doped wurtzite CdS. Solid State Communications, 2014, 187, 72-76.	0.9	9
16349	Selectivity of metal oxide atomic layer deposition on hydrogen terminated and oxidized Si(001)-(2Ã—1) surface. Journal of Vacuum Science and Technology B:Nanotechnology and Microelectronics, 2014, 32, .	0.6	40
16350	Water formation via HCl oxidation on Cu(100). Applied Surface Science, 2014, 299, 156-161.	3.1	5
16351	Mechanical and electronic properties of Rh and Rh3Zr from first-principles calculation. Solid State Communications, 2014, 189, 43-46.	0.9	8
16352	Electronic structure of Eu2+-doped SrAl2O4 using modified Beckeâ€“Johnson exchange potential. Solid State Communications, 2014, 186, 46-49.	0.9	11

#	Article	IF	Citations
16353	Using the electron localization function to correct for confinement physics in semi-local density functional theory. Journal of Chemical Physics, 2014, 140, 18A536.	1.2	18
16354	Structural, energetic and elastic properties of Cu2ZnSn(SxSe1â^'x)4 (x=1, 0.75, 0.5, 0.25, 0) alloys from first-principles computations. Solar Energy, 2014, 102, 276-281.	2.9	35
16355	A DFT study of the stoichiometric and reduced anatase (001) surfaces. Applied Surface Science, 2014, 294, 42-48.	3.1	23
16356	First-principles study on armchair AlN nanoribbons with different edge terminations. Superlattices and Microstructures, 2014, 67, 40-46.	1.4	23
16357	Density functional study of XRh (X=Sc, Y, Ti and Zr) intermetallic compounds. Computational Materials Science, 2014, 89, 205-215.	1.4	17
16358	Combination of EPR Measurements and DFT Calculations To Study Nitrate Impurities in the Carbonated Nanohydroxyapatite. Journal of Physical Chemistry A, 2014, 118, 1519-1526.	1.1	41
16359	Silicene-derived phases on Ag(111) substrate versus coverage:Ab initiostudies. Physical Review B, 2014, 89, .	1.1	60
16360	First-principles study of 4d solute diffusion in nickel. Journal of Materials Science, 2014, 49, 4038-4044.	1.7	17
16361	Hybrid functional with semi-empirical van der Waals study of native defects in hexagonal BN. Solid State Communications, 2014, 177, 74-79.	0.9	19
16362	Structural, vibrational, and quasiparticle band structure of 1,1-diamino-2,2-dinitroethelene from ab initio calculations. Journal of Chemical Physics, 2014, 140, 014105.	1.2	39
16363	Systematic analysis of the structural, elastic, and electronic properties of Tiâ€“Cuâ€“Me (Me=Al, Ga and) Tj ETQq0 0 0 rgBT /Overlock 10	1.9	2
16364	Evolutionary search for new high-kdielectric materials: methodology and applications to hafnia-based oxides. Acta Crystallographica Section C, Structural Chemistry, 2014, 70, 76-84.	0.2	44
16365	The adsorption and dissociation of CO on Fe(111). Surface Science, 2014, 625, 69-83.	0.8	10
16366	Electronic transport properties in graphene oxide frameworks. Physical Review B, 2014, 89, .	1.1	10
16367	Elastic and mechanical properties of intrinsic and doped PbSe and PbTe studied by first-principles. Materials Chemistry and Physics, 2014, 146, 472-477.	2.0	19
16368	Silicon carbide-derived carbon nanocomposite as a substitute for mercury in the catalytic hydrochlorination of acetylene. Nature Communications, 2014, 5, 3688.	5.8	181
16369	Boosting sensitivity of boron nitride nanotube (BNNT) to nitrogen dioxide by Fe encapsulation. Journal of Molecular Graphics and Modelling, 2014, 51, 1-6.	1.3	23
16370	The adsorption of NO on YSZ(111) and oxygen-enriched YSZ(111) surfaces. Chemical Physics Letters, 2014, 593, 61-68.	1.2	3

#	Article	IF	Citations
16371	High-temperature antiferromagnetism in molecular semiconductor thin films and nanostructures. Nature Communications, 2014, 5, 3079.	5.8	76
16372	Structural, elastic and electronic properties of CuYO2 from first-principles study. Journal of Alloys and Compounds, 2014, 603, 183-189.	2.8	9
16373	<scp>DFT</scp> study of hydrogen adsorption on Euâ€decorated singleâ€and doubleâ€sided graphene. Physica Status Solidi (B): Basic Research, 2014, 251, 229-234.	0.7	18
16374	Electronic and magnetic properties of transition-metal atoms absorbed on Stoneâ€“Wales defected graphene sheet: A theory study. Computational Materials Science, 2014, 81, 348-352.	1.4	13
16375	Designing a robustly metallic noncenstrosymmetric ruthenate oxide with large thermopower anisotropy. Nature Communications, 2014, 5, 3432.	5.8	134
16376	Energetics and configurations of Heâ€“He pair in vacancy of transition metals. Nuclear Instruments & Methods in Physics Research B, 2014, 322, 34-40.	0.6	9
16377	Solid-state NMR/NQR and first-principles study of two niobium halide cluster compounds. Solid State Nuclear Magnetic Resonance, 2014, 59-60, 20-30.	1.5	6
16378	New Ab Initio Based Pair Potential for Accurate Simulation of Phase Transitions in ZnO. Journal of Physical Chemistry C, 2014, 118, 11050-11061.	1.5	45
16379	Understanding electronic and optical properties of Nâ€“Sn codoped anatase TiO2. Computational Materials Science, 2014, 85, 264-268.	1.4	13
16380	Synthesis, structures, optical properties and electronic structures of two mixed metal borates MBaB5O9 (M=Na, K). Journal of Alloys and Compounds, 2014, 585, 602-607.	2.8	22
16381	DFT investigation of structural and vibrational properties of type B and mixed A-B carbonated hydroxylapatite. American Mineralogist, 2014, 99, 117-127.	0.9	35
16382	A first-principle study of calcium-decorated BC2N sheet doped by boron or carbon for high hydrogen storage. International Journal of Hydrogen Energy, 2014, 39, 9307-9320.	3.8	36
16383	Hydrogen storage in TiO2 functionalized (10, 10) single walled carbon nanotube (SWCNT) â€“ First principles study. International Journal of Hydrogen Energy, 2014, 39, 4973-4980.	3.8	26
16384	Structural stability, elastic and electronic properties of zincblende (GaN)1/(ZnO)1 superlattice: Modified Beckeâ€“Johnson exchange potential. Materials Science in Semiconductor Processing, 2014, 19, 179-185.	1.9	20
16385	Magnetism of Zn-doped SnO2: Role of surfaces. Journal of Applied Physics, 2014, 115, .	1.1	11
16386	Vibrationally Promoted Dissociation of Water on Ni(111). Science, 2014, 344, 504-507.	6.0	175
16387	Identification of the structure of the 3107 cm^{â^'1}H-related defect in diamond. Journal of Physics Condensed Matter, 2014, 26, 145801.	0.7	76
16388	First-principles study of a single Fe-chain doped zigzag AlN nanoribbons. Superlattices and Microstructures, 2014, 69, 136-143.	1.4	2

#	Article	IF	Citations
16389	First-principles studies on (001) surface electronic bonding and magnetic properties of ZnCMn3 and ZnNMn3 intermetallic antiperovskites type compounds. Journal of Alloys and Compounds, 2014, 586, 230-238.	2.8	2
16390	NMR Chemical Shifts of ¹¹B in Metal Borohydrides from First-Principle Calculations. Journal of Physical Chemistry C, 2014, 118, 6594-6603.	1.5	30
16391	Direct, Nonoxidative Conversion of Methane to Ethylene, Aromatics, and Hydrogen. Science, 2014, 344, 616-619.	6.0	1,113
16392	Theoretical Study on Amino Acid-Based Ionic Pairs and Their Interaction with Carbon Nanostructures. Journal of Physical Chemistry C, 2014, 118, 9741-9757.	1.5	34
16393	Adsorption of perfluoropentacene on aluminum (100) surface: Structural and electronic properties from first principle study. Computational Materials Science, 2014, 89, 216-223.	1.4	2
16394	Novel electronic structures of superlattice composed of graphene and silicene. Materials Research Bulletin, 2014, 50, 268-272.	2.7	12
16395	Armchair graphene nanoribbons under shear strain. Physica E: Low-Dimensional Systems and Nanostructures, 2014, 60, 156-159.	1.3	7
16396	A DFT study on carbon monoxide adsorption onto hydroxylated Î±-Al₂O₃(0001) surfaces. Physical Chemistry Chemical Physics, 2014, 16, 14287-14297.	1.3	13
16397	Structural and elastic properties of hybrid bilayer graphene/h-BN with different interlayer distances using DFT. Superlattices and Microstructures, 2014, 72, 230-237.	1.4	23
16398	The wurtziteâ€“rocksalt phase transition for a BexMgyZn1â^'xâ^'yO alloy: Be content vs Mg content. Journal of Alloys and Compounds, 2014, 608, 197-201.	2.8	6
16399	A theoretical investigation of the Î±-MnO2 (110) surface. Computational and Theoretical Chemistry, 2014, 1031, 1-6.	1.1	20
16400	Structure and catalytic properties of <mml:math xmlns:mml="http://www.w3.org/1998/Math/MathML" altimg="si1.gif" overflow="scroll"><mml:msub><mml:mrow><mml:mi mathvariant="normal">Pd</mml:mi></mml:mrow><mml:mrow><mml:mi>m</mml:mi></mml:mrow></mml:msub><mml:msub><mml:mrow><mml:mi mathvariant="normal">Au</mml:mi></mml:mrow><mml:mrow><mml:mi>n</mml:mi></mml:mrow></mml:msub></mml:math>		

#	Article	IF	Citations
16407	Thermal Expansion, Anharmonicity and Temperatureâ€Dependent Raman Spectra of Singleâ€and Fewâ€Layer MoSe₂ and WSe₂. ChemPhysChem, 2014, 15, 1592-1598.	1.0	242
16408	A Firstâ€Principles Study of Carbonâ€“Oxygen Bond Scission in Multiatomic Molecules on Flat and Stepped Metal Surfaces. ChemCatChem, 2014, 6, 1755-1762.	1.8	13
16409	Reactivity of the calciteâ€“water-interface, from molecular scale processes to geochemical engineering. Applied Geochemistry, 2014, 45, 158-190.	1.4	90
16410	Chemical functionalization of graphene by carbene cycloaddition: A density functional theory study. Applied Surface Science, 2014, 311, 377-383.	3.1	31
16411	Electronic and magnetic properties of F atoms adsorbed on TiO₂:Mn(001) diluted magnetic semiconductor surfaces: First-principles calculations. International Journal of Modern Physics B, 2014, 28, 1450096.	1.0	1
16412	Graphene/MoS₂ Hybrid Technology for Large-Scale Two-Dimensional Electronics. Nano Letters, 2014, 14, 3055-3063.	4.5	554
16413	How to represent crystal structures for machine learning: Towards fast prediction of electronic properties. Physical Review B, 2014, 89, .	1.1	353
16414	Six-dimensional potential energy surface of the dissociative chemisorption of HCl on Au(111) using neural networks. Science China Chemistry, 2014, 57, 147-155.	4.2	50
16415	Carrier induced magnetic coupling transitions in phthalocyanine-based organometallic sheet. Nanoscale, 2014, 6, 328-333.	2.8	44
16416	Copper-Organic/Octamolybdates: Structures, Bandgap Sizes, and Photocatalytic Activities. Inorganic Chemistry, 2014, 53, 3464-3470.	1.9	35
16417	Potentiated Electron Transference in Î±-Ag₂WO₄ Microcrystals with Ag Nanofilaments as Microbial Agent. Journal of Physical Chemistry A, 2014, 118, 5769-5778.	1.1	99
16418	Effects of<mml:math xmlns:mml="http://www.w3.org/1998/Math/MathML"><mml:mi>d</mml:mi></mml:math>-band shape on the surface reactivity of transition-metal alloys. Physical Review B, 2014, 89, .	1.1	387
16419	Prediction of New Stable Compounds and Promising Thermoelectrics in the Cuâ€“Sbâ€“Se System. Chemistry of Materials, 2014, 26, 3427-3435.	3.2	64
16420	Density functional theory calculations of continuum lowering in strongly coupled plasmas. Nature Communications, 2014, 5, 3533.	5.8	94
16421	Enriching physisorption of H₂S and NH₃ gases on a graphane sheet by doping with Li adatoms. Physical Chemistry Chemical Physics, 2014, 16, 8100-8105.	1.3	53
16422	Substrate effects: Disappearance of adsorbate-induced magnetism in graphene. Physical Review B, 2014, 89, .	1.1	23
16423	Structural, stability and electronic properties of C15-AB2Â(A = Ti, Zr; B = Cr) intermetallic compounds and their hydrides: An ab initio study. International Journal of Modern Physics B, 2014, 28, 1450105.	1.0	3
16424	Firstâ€principles study of spâ€electron halfâ€metallic superlattices in wurtzite structure. Physica Status Solidi (B): Basic Research, 2014, 251, 1076-1082.	0.7	3

#	Article	IF	Citations
16425	Early Stages of Halogen Adsorption on Cation-Rich InAs(001): Surface Etching Mechanism. Journal of Physical Chemistry C, 2014, 118, 10097-10105.	1.5	11
16426	A Combined <italic>Ab Initio</italic> and Experimental Study on the Nature of Conductive Filaments in <inline-formula> <tex-math notation="TeX">${m Pt}/{m Hf}{m O}_{2}/{m Pt}$ </tex-math></inline-formula> Resistive Random Access Memory. IEEE Transactions on Electron Devices, 2014, 61, 1394-1402.	1.6	55
16427	Robust Diffusive Proton Motions in Phase IV of Solid Hydrogen. Journal of Physical Chemistry C, 2014, 118, 11902-11905.	1.5	7
16428	Six-dimensional quantum dynamics study for the dissociative adsorption of DCl on Au(111) surface. Journal of Chemical Physics, 2014, 140, 144701.	1.2	45
16429	InN growth on BaTiO3 (111) substrates: A first-principles study. Journal of Crystal Growth, 2014, 395, 98-103.	0.7	0
16430	Theoretical aspects of WS₂ nanotube chemical unzipping. Nanoscale, 2014, 6, 8400-8404.	2.8	5
16431	Oxygen adsorption characteristics on hybrid carbon and boronâ€nitride nanotubes. Journal of Computational Chemistry, 2014, 35, 1058-1063.	1.5	13
16432	Study of atomic and molecular oxygen chemisorption on BC3 nanotubes with Stoneâ€“Wales defects using density functional theory. Chemical Physics, 2014, 438, 16-22.	0.9	3
16433	Ab initio modeling of radiation damage in MgF2 crystals. Nuclear Instruments & Methods in Physics Research B, 2014, 326, 314-317.	0.6	15
16434	Gas adsorption on MoS2 monolayer from first-principles calculations. Chemical Physics Letters, 2014, 595-596, 35-42.	1.2	328
16435	Effects of silver adatoms on the electronic structure of silicene. Applied Surface Science, 2014, 311, 9-13.	3.1	25
16436	Surface structure and polarization of cubic and tetragonal BaTiO3: An ab initio study. Computational Materials Science, 2014, 87, 123-128.	1.4	13
16437	Surface electronic structure calculations using the MBJLDA potential: Application to Si(111)2 Ã— 1. Journal of Computational Chemistry, 2014, 35, 1248-1254.	1.5	5
16438	First-Principles Study of Structure, Vibrational, and Elastic Properties of Stoichiometric and Calcium-Deficient Hydroxyapatite. Crystal Growth and Design, 2014, 14, 3131-3141.	1.4	52
16439	Electronic and magnetic structures and bonding properties of Ce2T2X (TÂ=Ând element; XÂ=ÂMg, Cd, Pb or) Tj ETQq0 0 0 rgBT /Overlo	1.8	9
16440	Thermodynamic assessment of the Alâ€“Dy, Dyâ€“Zr and Alâ€“Dyâ€“Zr systems. Science Bulletin, 2014, 59, 1738-1746.	1.7	6
16441	Ab initio computations of electronic, mechanical, lattice dynamical and thermal properties of ZrP2O7. Journal of the European Ceramic Society, 2014, 34, 1809-1818.	2.8	39
16442	Research on electronic structure and optical properties of Mg doped Ga0.75Al0.25N. Optical Materials, 2014, 36, 787-796.	1.7	22

#	Article	IF	Citations
16443	The Effect of Surface Geometry of Copper on Adsorption of Benzotriazole and Cl. Part I. Journal of Physical Chemistry C, 2014, 118, 933-943.	1.5	42
16444	Two-dimensional pentagonal crystals and possible spin-polarized Dirac dispersion relations. Journal of Applied Physics, 2014, 115, .	1.1	15
16445	Generalized self-assembly of scalable two-dimensional transition metal oxide nanosheets. Nature Communications, 2014, 5, 3813.	5.8	741
16446	First-principles characterization of the electronic and optical properties of hexagonal <mml:math xmlns:mml="http://www.w3.org/1998/Math/MathML" altimg="si79.gif" overflow="scroll"><mml:mrow><mml:msub><mml:mrow><mml:mi mathvariant="normal">LiIO</mml:mi></mml:mrow><mml:mrow><mml:mn>3</mml:mn></mml:mrow></mml:msub></mml:mrow></mml:math> Optical Materials, 2014, 36, 1494-1501.	1.7	13
16447	First principle study of elastic and thermodynamic properties of ZrZn2 and HfZn2 under high pressure. Journal of Applied Physics, 2014, 115, .	1.1	17
16448	Structural and Relative Stabilities, Electronic Properties, and Hardness of Iron Tetraborides from First Prinicples. Inorganic Chemistry, 2014, 53, 3471-3479.	1.9	13
16449	Tailoring Exciton Dynamics by Elastic Strainâ€Gradient in Semiconductors. Advanced Materials, 2014, 26, 2572-2579.	11.1	76
16450	Qualitative link between work of adhesion and thermal conductance of metal/diamond interfaces. Journal of Applied Physics, 2014, 115, .	1.1	46
16451	Chiral Co(II) Metalâ€“Organic Framework in the Heterogeneous Catalytic Oxidation of Alkenes under Aerobic and Anaerobic Conditions. ACS Catalysis, 2014, 4, 1032-1039.	5.5	53
16452	Cation-Induced Band-Gap Tuning in Organohalide Perovskites: Interplay of Spinâ€“Orbit Coupling and Octahedra Tilting. Nano Letters, 2014, 14, 3608-3616.	4.5	1,033
16453	Ab-initio study of the structural, electronic and optical properties of BSb (110) and (100) surfaces. Surface Science, 2014, 628, 1-7.	0.8	8
16454	Half metallicity and magnetic stability of sp-electron superlattices in rock-salt structure: A first-principles study. Solid State Communications, 2014, 192, 64-70.	0.9	5
16455	Formation, Characterization, and Stability of Methaneselenolate Monolayers on Au(111): An Electrochemical High-Resolution Photoemission Spectroscopy and DFT Study. Langmuir, 2014, 30, 3754-3763.	1.6	7
16456	Cr3+ in diffusion doped Cr2+:ZnS. Ceramics International, 2014, 40, 7573-7577.	2.3	5
16457	Oxidation and hydrogen uptake in zirconium, Zircaloy-2 and Zircaloy-4: Computational thermodynamics and ab initio calculations. Journal of Nuclear Materials, 2014, 444, 65-75.	1.3	38
16458	The stability and diffusion properties of foreign impurity atoms on the surface and in the bulk of vanadium: A first-principles study. Computational Materials Science, 2014, 81, 191-198.	1.4	21
16459	Interactions of xanthate with pyrite and galena surfaces in the presence and absence of oxygen. Journal of Industrial and Engineering Chemistry, 2014, 20, 268-273.	2.9	35
16460	Width- and edge-dependent magnetic properties, electronic structures, and stability of SnSe2 nanoribbons. Physica E: Low-Dimensional Systems and Nanostructures, 2014, 59, 102-106.	1.3	13

#	Article	IF	Citations
16461	Half-metallicity in carbon-substituted CdS monolayer. Physica E: Low-Dimensional Systems and Nanostructures, 2014, 59, 230-234.	1.3	8
16462	Inversion Symmetry Breaking by Oxygen Octahedral Rotations in the Ruddlesden-Popper<mml:math xmlns:mml="http://www.w3.org/1998/Math/MathML" display="inline"><mml:mrow><mml:mi>Na</mml:mi><mml:mi>R</mml:mi><mml:msub><mml:mrow><mml:mi>TiO</mml:mi></mml:mrow> Physical Review Letters, 2014, 112, 187602.	2.9	60
16463	First-principles microscopic model of exchange-driven magnetoelectric response with application to<mml:math xmlns:mml="http://www.w3.org/1998/Math/MathML"><mml:msub><mml:mrow><mml:mtext>Cr</mml:mtext></mml:mrow> xmlns:mml="http://www.w3.org/1998/Math/MathML"><mml:msub><mml:mrow><mml:mtext>O</mml:mtext></mml:mrow><mml:mn> Physical Review B, 2014, 89, .	1.1	11
16464	Mechanism of strain-influenced quantum well thickness reduction in GaN/AlN short-period superlattices. Nanotechnology, 2014, 25, 245602.	1.3	18
16465	Competition and cooperation between antiferrodistortive and ferroelectric instabilities in the model perovskite SrTiO₃. Journal of Physics Condensed Matter, 2014, 26, 122203.	0.7	92
16466	Ballistic Transport Performance of Silicane and Germanane Transistors. IEEE Transactions on Electron Devices, 2014, 61, 1590-1598.	1.6	51
16467	COMPUTATIONAL STUDY OF PLATINUM GROUP SUPERALLOYS. International Journal of Modern Physics B, 2014, 28, 1450066.	1.0	9
16468	Following Molecules through Reactive Networks: Surface Catalyzed Decomposition of Methanol on Pd(111), Pt(111), and Ni(111). Journal of Physical Chemistry C, 2014, 118, 12364-12383.	1.5	35
16469	Carbon Monoxide Adsorption Coverage Study on Platinum and Ruthenium Surfaces. Journal of Physical Chemistry C, 2014, 118, 11711-11722.	1.5	35
16470	Prediction of Large-Gap Two-Dimensional Topological Insulators Consisting of Bilayers of Group III Elements with Bi. Nano Letters, 2014, 14, 2505-2508.	4.5	173
16471	Analysis of the Configurations of a Crystal Surface. Pyrope (Mg₃Al₂Si₃O₁₂) as a Case Study. Crystal Growth and Design, 2014, 14, 2357-2365.	1.4	7
16472	First-principles study of the structural, elastic, and optical properties for Sr _{0.5} Ca _{0.5} TiO ₃. Chinese Physics B, 2014, 23, 026301.	0.7	5
16473	Hydroxylation of the surface of PbS nanocrystals passivated with oleic acid. Science, 2014, 344, 1380-1384.	6.0	404
16474	Electronic Structure of Î²-Na_xV₂O₅ (x â‰ˆ 0.33) Polycrystalline Films: Growth, Spectroscopy, and Theory. Journal of Physical Chemistry C, 2014, 118, 1081-1094.	1.5	21
16475	Nonlocal First-Principles Calculations in Cu-Au and Other Intermetallic Alloys. Physical Review Letters, 2014, 112, 075502.	2.9	39
16476	CO₃^{2â€“} Mobility in Carbonate Apatite As Revealed by Density Functional Modeling. Journal of Physical Chemistry C, 2014, 118, 1364-1369.	1.5	20
16477	Electronic structure and optical properties of Si, Ge and diamond in the lonsdaleite phase. Journal of Physics Condensed Matter, 2014, 26, 045801.	0.7	51
16478	N incorporation and associated localized vibrational modes in GaSb. Physical Review B, 2014, 89, .	1.1	14

#	Article	IF	Citations
16479	Absolute Organic Crystal Thermodynamics: Growth of the Asymmetric Unit into a Crystal via Alchemy. Journal of Chemical Theory and Computation, 2014, 10, 2781-2791.	2.3	24
16480	Ab initioquasiparticle band structure of ABA and ABC-stacked graphene trilayers. Physical Review B, 2014, 89, .	1.1	26
16481	Visible-Wavelength Polarized-Light Emission with Small-Diameter InN Nanowires. Nano Letters, 2014, 14, 3709-3714.	4.5	32
16482	Thermal Expansion, Heat Capacity, and Thermal Conductivity of Nickel Ferrite (NiFe₂O₄). Journal of the American Ceramic Society, 2014, 97, 1559-1565.	1.9	51
16483	<mml:math xmlns:mml="http://www.w3.org/1998/Math/MathML"><mml:msup><mml:mrow><mml:mi mathvariant="italic">sp</mml:mi></mml:mrow><mml:mn>3</mml:mn></mml:msup></mml:math> -hybridized framework structure of group-14 elements discovered by genetic algorithm. Physical Review B, 2014, 89, .	1.1	23
16484	Anisotropic Mo₂â€“Phthalocyanine Sheet: A New Member of the Organometallic Family. Journal of Physical Chemistry A, 2014, 118, 304-307.	1.1	13
16485	Optimizing the Band Edges of Tungsten Trioxide for Water Oxidation: A First-Principles Study. Journal of Physical Chemistry C, 2014, 118, 6019-6028.	1.5	63
16486	First-principles study of structural, elastic and lattice dynamical properties of chalcopyrite BeSiV2 and MgSiV2 (V=P, As, Sb). Journal of Alloys and Compounds, 2014, 611, 210-218.	2.8	52
16487	Acidâ€“base concerted mechanism in the dehydration of 1,4-butanediol over bixbyite rare earth oxide catalysts. Catalysis Today, 2014, 226, 124-133.	2.2	23
16488	Some properties of intermetallic compounds of Sn with noble metals relevant for hydrogen electrocatalysis. Electrochimica Acta, 2014, 116, 39-43.	2.6	9
16489	Reduction behavior of oxidized Pd(100) and Pd75Ag25(100) surfaces using CO. Surface Science, 2014, 621, 31-39.	0.8	19
16490	Uniform size and composition tuning of PtNi octahedra for systematic studies of oxygen reduction reactions. Journal of Catalysis, 2014, 309, 343-350.	3.1	41
16491	Structure of CoO(001) surface from DFT+U calculations. Surface Science, 2014, 621, 1-6.	0.8	38
16492	Electronic properties on GaN(0001) surface â€“ ab initio investigation. Vacuum, 2014, 99, 166-174.	1.6	12
16493	Density functional theory studies of methyl dissociation on a Ni(111) surface in the presence of an external electric field. Physical Chemistry Chemical Physics, 2014, 16, 2399-2410.	1.3	31
16494	DFT study of benzene and CO co-adsorption on PtCo(111). Applied Surface Science, 2014, 289, 502-510.	3.1	8
16495	Electronic properties of 2D and 3D hybrid organic/inorganic perovskites for optoelectronic and photovoltaic applications. Optical and Quantum Electronics, 2014, 46, 1225-1232.	1.5	60
16496	Self-assembled monolayers of methylselenolate on the Au(111) surface: A combined STM and DFT study. Surface Science, 2014, 619, 67-70.	0.8	4

#	Article	IF	Citations
16497	Ab initio study of InxGa1â^'xN â€“ Performance of the alchemical mixing approximation. Computational Materials Science, 2014, 81, 358-365.	1.4	25
16498	First-principles study of the elastic, electronic and optical properties of Îµ-GaSe layered semiconductor. Physica B: Condensed Matter, 2014, 436, 188-192.	1.3	10
16499	Band-gap modulation of graphane-like SiC nanoribbons under uniaxial elastic strain. Physics Letters, Section A: General, Atomic and Solid State Physics, 2014, 378, 565-569.	0.9	17
16500	CO Adsorption on Clean and Oxidized Pd(111). Journal of Physical Chemistry C, 2014, 118, 1118-1128.	1.5	69
16501	Insight into the Effect of Sn on CO and Formic Acid Oxidation at PtSn Catalysts. Journal of Physical Chemistry C, 2014, 118, 278-289.	1.5	48
16502	Initial stages of Cu3Au(111) oxidation: oxygen induced Cu segregation and the protective Au layer profile. Physical Chemistry Chemical Physics, 2014, 16, 3815.	1.3	16
16503	Optoelectronic and thermoelectric properties of KAuX5 (XÂ=ÂS, Se): a first principles study. Journal of Materials Science, 2014, 49, 1179-1192.	1.7	9
16504	A first-principles study on the structural, elastic, electronic, and optical properties of CdRh2O4. Journal of Materials Science, 2014, 49, 1205-1214.	1.7	20
16505	Effect of trivalent dopants on local coordination and electronic structure in crystalline and amorphous ZnO. Thin Solid Films, 2014, 555, 117-121.	0.8	10
16506	Error Estimates for Solid-State Density-Functional Theory Predictions: An Overview by Means of the Ground-State Elemental Crystals. Critical Reviews in Solid State and Materials Sciences, 2014, 39, 1-24.	6.8	404
16507	Nitrogen-vacancy induced intrinsic ferromagnetism and half-metallicity in BN. Computational Materials Science, 2014, 81, 212-215.	1.4	8
16508	Oxygen vacancy formation energies in Sr-doped complex perovskites: ab initio thermodynamic study. Solid State Ionics, 2014, 254, 11-16.	1.3	26
16509	Bandgap engineering through nanoporosity. Nanoscale, 2014, 6, 1181-1187.	2.8	26
16510	First-principles study of hydrogen storage and diffusion in B2 FeTi alloy. Computational Materials Science, 2014, 81, 517-523.	1.4	23
16511	Ag (100)/MgO (100) interface: A van der Waals density functional study. Applied Surface Science, 2014, 288, 115-121.	3.1	7
16512	Synergistic effect of rhenium and ruthenium in nickel-based single-crystal superalloys. Journal of Alloys and Compounds, 2014, 582, 299-304.	2.8	44
16513	A first principles study of pristine and Al-doped boron nitride nanotubes interacting with platinum-based anticancer drugs. Physica E: Low-Dimensional Systems and Nanostructures, 2014, 57, 47-55.	1.3	39
16514	Activity and Selectivity Trends in Synthesis Gas Conversion to Higher Alcohols. Topics in Catalysis, 2014, 57, 135-142.	1.3	173

#	Article	IF	Citations
16515	Elasticity behavior, phonon spectra, and the pressureâ€“temperature phase diagram of HfTi alloy: A density-functional theory study. Computational Materials Science, 2014, 82, 5-11.	1.4	15
16516	Improved plastic anisotropy of Mgâ€“Znâ€“Ca alloys exhibiting high-stretch formability: A first-principles study. Acta Materialia, 2014, 65, 207-214.	3.8	90
16517	Phase Diagram of Quasi-Two-Dimensional Carbon, From Graphene to Diamond. Nano Letters, 2014, 14, 676-681.	4.5	154
16518	NiTiSn a material of technological interest: Ab initio calculations ofÂphase stability and defects. Intermetallics, 2014, 46, 103-110.	1.8	44
16519	Does the fcc phase exist in the Fe bccâ€“hcp transition? A conclusion from first-principles studies. Modelling and Simulation in Materials Science and Engineering, 2014, 22, 025007.	0.8	26
16520	Nanocrystal energetics via quantum similarity measures. Modelling and Simulation in Materials Science and Engineering, 2014, 22, 025009.	0.8	1
16521	Effects of different nitrogen-to-titanium atomic ratios on the evolution of Tiâ€“Siâ€“N islands on TiN(001) surfaces: First-principle studies. Journal of Alloys and Compounds, 2014, 586, 431-435.	2.8	3
16522	Modifying the electronic and magnetic properties of the boron nitride (BN) nanosheet by NHx (x=0, 1,) Tj ETQq1 1 0.784314 rgBT /Over	1.8	23
16523	First-Principles Study on the Electronic and Magnetic Properties of Zigzag AlN-SiC Nanoribbons. Journal of Superconductivity and Novel Magnetism, 2014, 27, 1079-1082.	0.8	4
16524	Theoretical Study of Li Migration in Lithiumâ€“Graphite Intercalation Compounds with Dispersion-Corrected DFT Methods. Journal of Physical Chemistry C, 2014, 118, 2273-2280.	1.5	141
16525	Can Metalâ€“Organic Framework Separate 1-Butene from Butene Isomers?. Journal of Physical Chemistry Letters, 2014, 5, 440-446.	2.1	29
16526	Modulating the atomic and electronic structures through alloying and heterostructure of single-layer MoS₂. Journal of Materials Chemistry A, 2014, 2, 2101-2109.	5.2	92
16527	Formation and magnetic properties of metastable phases observed in the Fe50(HfxTa1â^'x)50 films by ion beam mixing. Applied Surface Science, 2014, 290, 495-498.	3.1	1
16528	Effective bandgap engineering in wrinkled germanane via tiny electric field. Journal of Materials Chemistry C, 2014, 2, 1125-1130.	2.7	35
16529	Ferromagnetism in MnX2 (X = S, Se) monolayers. Physical Chemistry Chemical Physics, 2014, 16, 4990.	1.3	199
16530	Cr adsorption induced magnetism in Bi2Se3 film by proximity effects. Physica E: Low-Dimensional Systems and Nanostructures, 2014, 55, 9-12.	1.3	8
16531	The density functional study of electronic structure, electronic charge density, linear and nonlinear optical properties of single crystal alpha-LiAlTe2. Journal of Alloys and Compounds, 2014, 592, 92-99.	2.8	30
16532	Band gap engineering in huge-gap semiconductor SrZrO3 for visible-light photocatalysis. International Journal of Hydrogen Energy, 2014, 39, 2042-2048.	3.8	72

#	Article	IF	Citations
16533	First-principles studies of electronic structure and optical properties of GaN surface doped with Si. Optik, 2014, 125, 2234-2238.	1.4	6
16534	Emergence of spin-filter states in Ptâ€“Fe nanowires. Physical Chemistry Chemical Physics, 2014, 16, 8360-8366.	1.3	15
16535	The origin of p-type conductivity in ZnM2O4 (M = Co, Rh, Ir) spinels. Physical Chemistry Chemical Physics, 2014, 16, 2588.	1.3	57
16536	An assessment of finite element analysis to predict the elastic modulus and Poissonâ€™s ratio of singlewall carbon nanotubes. Computational Materials Science, 2014, 82, 257-263.	1.4	30
16537	Fluorination of BCN nanostructures: A first principles study. Thin Solid Films, 2014, 551, 136-141.	0.8	7
16538	Room-temperature ferromagnetism in hydrogenated ZnO nanoparticles. Journal of Applied Physics, 2014, 115, .	1.1	38
16539	Effect of pressure on elastic, mechanical and electronic properties of WSe2: A first-principles study. Materials Research Bulletin, 2014, 50, 503-508.	2.7	46
16540	On the mechanism of sulfur fast diffusion in 3-D transition metals. Acta Materialia, 2014, 67, 95-101.	3.8	16
16541	Characterization of Fe Substitution into La-Hexaaluminate Systems and the Effect on N₂O Catalytic Decomposition. Journal of Physical Chemistry C, 2014, 118, 1999-2010.	1.5	21
16542	Energetics and nucleation of point defects in aluminum under extreme tensile hydrostatic stresses. Physical Review B, 2014, 89, .	1.1	22
16543	Ab initiostudy of the effects of interfacial structure on the ferroelectric, magnetic, and magnetoelectric coupling properties ofFe/BaTiO3multiferroic tunnel junctions. Physical Review B, 2014, 89, .	1.1	11
16544	Towards designing La 1â^'x Sr x Co y Fe 1â^'y O 3â^'d with enhanced phase stability: Role of the defect structure. Solid State Ionics, 2014, 255, 108-112.	1.3	14
16545	First-principles study of anhydrite, polyhalite and carnallite. Chemical Physics Letters, 2014, 594, 1-5.	1.2	17
16546	Structural, elastic, electronic and optical properties of the newly synthesized monoclinic Zintl phase BaIn2P2. Solid State Sciences, 2014, 29, 12-23.	1.5	54
16547	Ab initio calculations of band structure of solid solutions of copper and silver chalcogenides. Solid State Ionics, 2014, 257, 29-31.	1.3	4
16548	Experimental investigation and thermodynamic modeling of the Gaâ€“Zr system. Journal of Alloys and Compounds, 2014, 587, 497-505.	2.8	6
16549	A metallic carbon allotrope with superhardness: a first-principles prediction. Journal of Materials Chemistry C, 2014, 2, 2751-2757.	2.7	40
16550	The orbital minimization method for electronic structure calculations with finite-range atomic basis sets. Computer Physics Communications, 2014, 185, 873-883.	3.0	20

#	Article	IF	Citations
16551	Optical conductivity of hydrogenated graphene from first principles. Physical Review B, 2014, 89, .	1.1	15
16552	An optimized interatomic potential for Cuâ€“Ni alloys with the embedded-atom method. Journal of Physics Condensed Matter, 2014, 26, 035404.	0.7	57
16553	Thermochemical Ranking and Dynamic Stability of TeO₂ Polymorphs from Ab Initio Theory. Crystal Growth and Design, 2014, 14, 871-878.	1.4	32
16554	Tailoring the structural and electronic properties of a graphene-like ZnS monolayer using biaxial strain. Journal Physics D: Applied Physics, 2014, 47, 075302.	1.3	31
16555	First principles studies on hydrogen storage in single-walled carbon nanotube functionalized with TiO2. Solid State Communications, 2014, 183, 1-7.	0.9	19
16556	Graphene/g-C3N4 bilayer: considerable band gap opening and effective band structure engineering. Physical Chemistry Chemical Physics, 2014, 16, 4230.	1.3	138
16557	A Density Functional Theory Study of the Adsorption of 2-Cyclohexenone on Rh(111). Advances in Quantum Chemistry, 2014, , 175-190.	0.4	0
16558	Lonsdaleite Films with Nanometer Thickness. Journal of Physical Chemistry Letters, 2014, 5, 541-548.	2.1	56
16559	The structural stability and magnetic properties of the ferromagnetic Heusler alloy Niâ€“Mnâ€“Sn: A first principle investigation. Journal of Magnetism and Magnetic Materials, 2014, 355, 173-179.	1.0	18
16560	A new investigation of oxygen flow influence on ITO thin films by magnetron sputtering. Solar Energy Materials and Solar Cells, 2014, 120, 157-162.	3.0	91
16561	Computational thermodynamics of the CoNiGa high temperature shape memory alloy system. Calphad: Computer Coupling of Phase Diagrams and Thermochemistry, 2014, 45, 167-177.	0.7	4
16562	Mechanism of Hydrogen Spillover on WO₃(001) and Formation of H_xWO₃ (x = 0.125, 0.25, 0.375, and 0.5). Journal of Physical Chemistry C, 2014, 118, 494-501.	1.5	89
16563	Ab initio calculations of structural, electronic, optical and thermodynamic properties of alkaline earth tellurides BaxSr1âˆ’xTe. Journal of Physics and Chemistry of Solids, 2014, 75, 307-314.	1.9	11
16564	Crystal-Chemistry Guidelines for Noncentrosymmetric A₂BO₄ Ruddlesdenâ€“Popper Oxides. Inorganic Chemistry, 2014, 53, 336-348.	1.9	73
16565	Photocatalyst AgInS2 for active overall water-splitting: A first-principles study. Chemical Physics Letters, 2014, 591, 189-192.	1.2	43
16566	Universal binding energy relation for cleaved and structurally relaxed surfaces. Journal of Physics Condensed Matter, 2014, 26, 055006.	0.7	13
16567	Strong band hybridization between silicene and Ag(111) substrate. Physica E: Low-Dimensional Systems and Nanostructures, 2014, 58, 38-42.	1.3	43
16568	N1s and C1s Near-Edge X-ray Absorption Fine Structure Spectra of Model Systems for Pyridine on Si(100): A DFT Simulation. Journal of Physical Chemistry C, 2014, 118, 1049-1061.	1.5	16

#	Article	IF	Citations
16569	Unexpected magnetic properties in carbon-doped SnO2 from first-principles calculation. Computational Materials Science, 2014, 83, 5-11.	1.4	26
16570	Physical properties of the cubic spinel LiMn2O4. Journal of Physics and Chemistry of Solids, 2014, 75, 463-469.	1.9	11
16571	Structures and Phase Transition of a MoS₂ Monolayer. Journal of Physical Chemistry C, 2014, 118, 1515-1522.	1.5	432
16572	Ground-state and spin-wave dynamics in Brownmillerite SrCoO_{2.5}â€"a combined hybrid functional and LSDA + U study. Journal of Physics Condensed Matter, 2014, 26, 036004.	0.7	13
16573	Effect of impurities on vacancy migration energy in Fe-based alloys. Journal of Nuclear Materials, 2014, 445, 224-226.	1.3	39
16574	First-principles study of structural, elastic, electronic, magnetic and thermoproperties of Ni2ZrX (X=Sn, Sb) Heusler alloys under pressure. Computational Materials Science, 2014, 82, 76-85.	1.4	26
16575	Self-Accelerating CO Sorption in a Soft Nanoporous Crystal. Science, 2014, 343, 167-170.	6.0	434
16576	Engineering the field emission properties of graphene film by gas adsorbates. Physical Chemistry Chemical Physics, 2014, 16, 1850-1855.	1.3	18
16577	Phase stability, electronic structure and optical properties of BiInO3under strain. Journal Physics D: Applied Physics, 2014, 47, 055302.	1.3	4
16578	Interfacial effects on the spin density wave in FeSe/SrTiO<mml:math xmlns:mml="http://www.w3.org/1998/Math/MathML"><mml:msub><mml:mrow /><mml:mn>3</mml:mn></mml:msub></mml:math>thin films. Physical Review B, 2014, 89, .	1.1	52
16579	Conformation versus cohesion in the relative stabilities of gabapentin polymorphs. RSC Advances, 2014, 4, 855-864.	1.7	11
16580	Verification of first-principles codes: Comparison of total energies, phonon frequencies, electronâ€"phonon coupling and zero-point motion correction to the gap between ABINIT and QE/Yambo. Computational Materials Science, 2014, 83, 341-348.	1.4	88
16581	Thermochemistry and micro-kinetic analysis of methanol synthesis on ZnO (0 0 0 1). Journal of Catalysis, 2014, 309, 397-407.	3.1	54
16582	Predicted stability, structures, and magnetism of 3d transition metal nitrides: the M4N phases. RSC Advances, 2014, 4, 7885.	1.7	36
16583	First principles analysis of graphene and its ability to maintain long-ranged interaction with H2S. Surface Science, 2014, 621, 168-174.	0.8	31
16584	The adsorption and dissociation of H2S on Cu(100) surface: A DTF study. Surface Science, 2014, 620, 51-58.	0.8	44
16585	First-principles study of the structural, electronic and elastic properties of ternary Zr2AN (A=Ga, In) Tj ETQq0 0 0 rgBT /Overlock 10 Tf 50	1.4	7
16586	Adsorption of sulfur hexafluoride on graphene and on graphene with high titanium coverage. Computational Materials Science, 2014, 84, 134-138.	1.4	0

#	Article	IF	Citations
16587	Elastic and electronic properties of Pbca-BN: First-principles calculations. Computational Materials Science, 2014, 85, 80-87.	1.4	114
16588	Concentration-dependent crystal structure, elastic constants and electronic structure of Zr x Ti1â^'x alloys under high pressure. Frontiers of Physics, 2014, 9, 219-225.	2.4	11
16589	Low-frequency Raman study of the ferroelectric phase transition in a layered<mml:math xmlns:mml="http://www.w3.org/1998/Math/MathML"><mml:msub><mml:mi mathvariant="bold">CuCl</mml:mi><mml:mn mathvariant="bold">4</mml:mn></mml:msub></mml:math>-based organic-inorganic hybrid. Physical Review B, 2014, 89, .	1.1	25
16590	Energy Level Realignment in Weakly Interacting Donorâ€“Acceptor Binary Molecular Networks. ACS Nano, 2014, 8, 1699-1707.	7.3	35
16591	Probing Hydrogen Bond Networks in Half-Sandwich Ru(II) Building Blocks by a Combined 1H DQ CRAMPS Solid-State NMR, XRPD, and DFT Approach. Inorganic Chemistry, 2014, 53, 139-146.	1.9	14
16592	Indirect-to-direct band gap transition of the ZrS2 monolayer by strain: first-principles calculations. RSC Advances, 2014, 4, 7396.	1.7	91
16593	Quasiparticle energies and optical excitations in the GaAs monolayer. Physica E: Low-Dimensional Systems and Nanostructures, 2014, 59, 107-109.	1.3	11
16594	Improved Oxygen Reduction Performance of Ptâ€“Ni Nanoparticles by Adhesion on Nitrogen-Doped Graphene. Journal of Physical Chemistry C, 2014, 118, 2804-2811.	1.5	65
16595	First-principles study on the electronic and optical properties of cubic ABX3 halide perovskites. Physics Letters, Section A: General, Atomic and Solid State Physics, 2014, 378, 290-293.	0.9	233
16596	Influence of carbonâ€“vacancy interaction on carbon and vacancy diffusivity in tungsten. Computational Materials Science, 2014, 83, 1-4.	1.4	21
16597	First-principles study on electronic structure and optical properties of Cu-doped Î²-Ga2O3. Physica B: Condensed Matter, 2014, 434, 181-184.	1.3	38
16598	BoltzWann: A code for the evaluation of thermoelectric and electronic transport properties with a maximally-localized Wannier functions basis. Computer Physics Communications, 2014, 185, 422-429.	3.0	219
16599	Theories of Phonon Transport in Bulk and Nanostructed Solids. Topics in Applied Physics, 2014, , 81-114.	0.4	0
16600	Structural analysis of Y3Ba5Cu8O19â^Î´ high-Tc superconductor by ab initio density functional theory. Physica C: Superconductivity and Its Applications, 2014, 497, 84-88.	0.6	9
16601	Gold catalyzed hydrogenations of small imines and nitriles: enhanced reactivity of Au surface toward H₂via collaboration with a Lewis base. Chemical Science, 2014, 5, 1082-1090.	3.7	91
16602	Electronic structure and ferromagnetism of Fe11NiSi4, Fe11CoSi4, Fe11CrSi4 and Fe3Si from first principles. Intermetallics, 2014, 46, 12-17.	1.8	8
16603	The germanium-doped boron nitride nanotube serving as a potential resource for the detection of carbon monoxide and nitric oxide. Computational Materials Science, 2014, 82, 361-366.	1.4	30
16604	Theoretical study of structural, elastic and thermodynamic properties of CZTX (X=S and Se) alloys. Journal of Alloys and Compounds, 2014, 589, 137-142.	2.8	19

#	Article	IF	Citations
16605	Tailoring the performance of graphene-based supercapacitors using topological defects: A theoretical assessment. Carbon, 2014, 68, 734-741.	5.4	78
16606	Mechanical and Electronic Properties of Iridium Nitride. Chinese Physics Letters, 2014, 31, 086202.	1.3	6
16607	Quasiparticle and optical properties of polythiophene-derived polymers. Physical Review B, 2014, 90, .	1.1	18
16608	Electronic structure study on 2D hydrogenated Icosagens nitride nanosheets. Superlattices and Microstructures, 2014, 76, 213-220.	1.4	8
16609	Dopant-Induced Surface Magnetism in Î²-SiC Controlled by Dopant Depth. Journal of Physical Chemistry C, 2014, 118, 25429-25433.	1.5	7
16610	The different roles of Pu-oxide overlayers in the hydrogenation of Pu-metal: An ab initio molecular dynamics study based on van der Waals density functional (vdW-DF)+U. Journal of Chemical Physics, 2014, 140, 164709.	1.2	22
16611	Angular momentum dependent orbital-free density functional theory: Formulation and implementation. Physical Review B, 2014, 89, .	1.1	21
16612	Nanostructuration of CoSi by mechanical milling and mechanical alloying. Solid State Sciences, 2014, 38, 129-137.	1.5	12
16613	Cu/ZnO nanocatalysts in response to environmental conditions: surface morphology, electronic structure, redox state and CO₂ activation. Physical Chemistry Chemical Physics, 2014, 16, 26119-26136.	1.3	17
16614	Graphene/Ni(111) surface structure probed by low-energy electron diffraction, photoelectron diffraction, and first-principles calculations. Physical Review B, 2014, 90, .	1.1	38
16615	Coupled experimental and<mml:math xmlns:mml="http://www.w3.org/1998/Math/MathML"><mml:mrow><mml:mi>DFT</mml:mi><mml:mspace width="0.16em" /><mml:mo>+</mml:mo><mml:mspace width="0.16em" /><mml:mi>U</mml:mi></mml:mrow></mml:math>investigation of positron lifetimes in<mml:math xmlns:mml="http://www.w3.org/1998/Math/MathML"><mml:msub><mml:mi>UO</mml:mi><mml:mn>2</mml:mn></mml:msub></mml	1.1	24
16616	Physical Review B, 2014, 90, . Assessing the Performances of Dispersion-Corrected Density Functional Methods for Predicting the Crystallographic Properties of High Nitrogen Energetic Salts. Journal of Chemical Theory and Computation, 2014, 10, 4982-4994.	2.3	22
16617	Native Defects in Î±-Mo₂C: Insights from First-Principles Calculations. Journal of Physical Chemistry C, 2014, 118, 25517-25524.	1.5	20
16618	Hydrodeoxygenation of Guaiacol over Ru(0001): A DFT Study. ACS Catalysis, 2014, 4, 4178-4188.	5.5	105
16619	Correlation between structural and electronic orderâ€“disorder effects and optical properties in ZnO nanocrystals. Journal of Materials Chemistry C, 2014, 2, 10164-10174.	2.7	31
16620	Magnetism in undoped ZnS studied from density functional theory. Journal of Applied Physics, 2014, 115, .	1.1	34
16621	The structures and thermodynamic stability of copper(<scp>ii</scp>) chloride surfaces. Physical Chemistry Chemical Physics, 2014, 16, 24209-24215.	1.3	13
16622	First-principles investigations of defect and phase stabilities in thermoelectric (GeTe)x(AgSbTe2)1â^'x. Japanese Journal of Applied Physics, 2014, 53, 111201.	0.8	6

#	Article	IF	Citations
16623	Study of the optical-electrical characteristics of In Ga1â^'N alloy with low in doping. Optik, 2014, 125, 6909-6913.	1.4	0
16624	A computational investigation of adsorption of organics on mineral surfaces: Implications for organics delivery in the early solar system. Earth and Planetary Science Letters, 2014, 408, 355-361.	1.8	15
16625	Electronic structure and magnetic properties of PbMO₃ (M =) Tj ETQq0 0 0 rgBT /Overlock 10 Tf 50 667 Td (International Journal of Modern Physics B, 2014, 28, 1450205.	1.0	11
16626	Third-order elastic constants of ZnO and size effect in ZnO nanowires. Journal of Applied Physics, 2014, 115, 213516.	1.1	17
16627	Selenium adsorption at different coverages on Fe(1 0 0) and Fe(1 1 1): A DFT study. Applied Surface Science, 2014, 315, 252-260.	3.1	11
16628	Interactions and phase transformations in Fe-Pd. Physical Review B, 2014, 89, .	1.1	11
16629	Elementary Surface Chemistry during CuO/Al Nanolaminate-Thermite Synthesis: Copper and Oxygen Deposition on Aluminum (111) Surfaces. ACS Applied Materials & Interfaces, 2014, 6, 15086-15097.	4.0	47
16630	An atomistic picture of the diffusion of two vacancies forming a diâ€vacancy in Si. Physica Status Solidi (B): Basic Research, 2014, 251, 2185-2188.	0.7	4
16631	Atomic structures and electronic properties of 2H-NbSe2: The impact of Ti doping. Journal of Applied Physics, 2014, 116, 103709.	1.1	11
16632	Hinge-like structure induced unusual properties of black phosphorus and new strategies to improve the thermoelectric performance. Scientific Reports, 2014, 4, 6946.	1.6	202
16633	Metallic BSi₃ Silicene and Its One-Dimensional Derivatives: Unusual Nanomaterials with Planar Aromatic D_{6h} Six-Membered Silicon Rings. Journal of Physical Chemistry C, 2014, 118, 25825-25835.	1.5	37
16634	On factors controlling activity of submonolayer bimetallic catalysts: Nitrogen desorption. Journal of Chemical Physics, 2014, 140, 014703.	1.2	6
16635	Trends in Formic Acid Decomposition on Model Transition Metal Surfaces: A Density Functional Theory study. ACS Catalysis, 2014, 4, 4434-4445.	5.5	190
16636	Predicting oxygen vacancy non-stoichiometric concentration in perovskites from first principles. Applied Surface Science, 2014, 323, 65-70.	3.1	6
16637	Spontaneous Graphitization of Ultrathin Cubic Structures: A Computational Study. Nano Letters, 2014, 14, 7126-7130.	4.5	31
16638	Tuning electronic and magnetic properties of SnSe₂ armchair nanoribbons via edge hydrogenation. Journal of Materials Chemistry C, 2014, 2, 10175-10183.	2.7	17
16639	Effect of strain on electronic and thermoelectric properties of few layers to bulk MoS₂. Nanotechnology, 2014, 25, 465701.	1.3	101
16640	Methanol synthesis on ZnO($000overline{1}$0001Â¯). IV. Reaction mechanisms and electronic structure. Journal of Chemical Physics, 2014, 141, 124710.	1.2	18

#	Article	IF	Citations
16641	DFT comparison of intrinsic WGS kinetics over Pd and Pt. Journal of Catalysis, 2014, 320, 106-117.	3.1	106
16642	First-principles studies of the structural, electronic and optical properties of dinitrides CN2, SiN2 and GeN2. Computational Materials Science, 2014, 95, 706-711.	1.4	5
16643	Structural, electronic and elastic properties of FeBO₃(B = Ti, Sn, Si, Zr) ilmenite: a density functional theory study. RSC Advances, 2014, 4, 59839-59846.	1.7	28
16644	Potential variations around grain boundaries in impurity-doped BaSi2 epitaxial films evaluated by Kelvin probe force microscopy. Journal of Applied Physics, 2014, 116, .	1.1	23
16645	Structural determination and physical properties of 4d transitional metal diborides by first-principles calculations. Modern Physics Letters B, 2014, 28, 1450213.	1.0	4
16646	Graphitic Phase of NaCl. Bulk Properties and Nanoscale Stability. Journal of Physical Chemistry Letters, 2014, 5, 4014-4019.	2.1	16
16647	A local topological view of pressure-induced polymorphs in SiO2. Theoretical Chemistry Accounts, 2014, 133, 1.	0.5	6
16648	Charge density wave and metallic state coexistence in the multiband conductor<mml:math xmlns:mml="http://www.w3.org/1998/Math/MathML"><mml:mrow><mml:msub><mml:mrow><mml:mi>TTF</mml:mi><mml:mi><mml:mo>[</mml:mo> Physical Review B, 2014, 90, .	1.1	14
16649	Spin-orbit torques in Co/Pt(111) and Mn/W(001) magnetic bilayers from first principles. Physical Review B, 2014, 90, .	1.1	164
16650	Quantum spin Hall effect in two-dimensional transition metal dichalcogenides. Science, 2014, 346, 1344-1347.	6.0	1,558
16651	The extraordinary magnetoelectric response in silicene doped with Fe and Cr atoms. Applied Physics Letters, 2014, 105, .	1.5	18
16652	Disappearance of ferroelectric critical thickness in epitaxial ultrathin<mml:math xmlns:mml="http://www.w3.org/1998/Math/MathML"><mml:mrow><mml:mi>BaZr</mml:mi><mml:msub><mml:mi mathvariant="normal">O</mml:mi><mml:mn>3</mml:mn></mml:msub></mml:mrow></mml:math>films. Physical Review B, 2014, 90, .	1.1	21
16653	The modulation of metalâ€“insulator transition temperature of vanadium dioxide: a density functional theory study. Journal of Materials Chemistry C, 2014, 2, 9283-9293.	2.7	58
16654	Lithium-decorated oxidized graphyne for hydrogen storage by first principles study. Journal of Applied Physics, 2014, 116, .	1.1	11
16655	Edge-states ferromagnetism of WS2 nanosheets. Applied Physics Letters, 2014, 104, .	1.5	42
16656	Structural, electronic, vibrational, and dielectric properties of LaBGeO5 from first principles. Journal of Applied Physics, 2014, 115, 074103.	1.1	7
16657	Permutation invariant polynomial neural network approach to fitting potential energy surfaces. III. Molecule-surface interactions. Journal of Chemical Physics, 2014, 141, 034109.	1.2	120
16658	Linker Rectifiers for Covalent Attachment of Transitionâ€Metal Catalysts to Metalâ€Oxide Surfaces. ChemPhysChem, 2014, 15, 1138-1147.	1.0	20

#	Article	IF	Citations
16659	Tetravalent Doping of <scp><scp>CeO</scp></scp>₂: The Impact of Valence Electron Character on Group IV Dopant Influence. Journal of the American Ceramic Society, 2014, 97, 258-266.	1.9	36
16660	Tuning Hydrogen Storage in Lithiumâ€Functionalized BC₂N Sheets by Doping with Boron and Carbon. ChemPhysChem, 2014, 15, 3015-3025.	1.0	11
16661	A theoretical investigation of the (0001) covellite surfaces. Journal of Chemical Physics, 2014, 141, 044702.	1.2	17
16662	Adsorption and dissociation of O₂ on MoSe₂ and MoTe₂ monolayers: ab initio study. International Journal of Modern Physics B, 2014, 28, 1450195.	1.0	10
16663	AB INITIO INVESTIGATIONS OF THE MAGNETISM IN DILUTED MAGNETIC SEMICONDUCTOR Fe-DOPED GaN. Modern Physics Letters B, 2014, 28, 1450031.	1.0	0
16664	Structural, electronic, vibrational and dielectric properties of selected high-shape K semiconductor oxides. Journal Physics D: Applied Physics, 2014, 47, 413001.	1.3	5
16665	Topological<mml:math xmlns:mml="http://www.w3.org/1998/Math/MathML"><mml:mi>Î±</mml:mi></mml:math>-Sn surface states versus film thickness and strain. Physical Review B, 2014, 90, .	1.1	26
16666	Theoretical Study of Hydrogen Adsorption on Ru-Decorated (8,0) Single-Walled Carbon Nanotube. Journal of Physical Chemistry C, 2014, 118, 27672-27680.	1.5	43
16667	Quantitative Correlation between Defect Density and Heterogeneous Electron Transfer Rate of Single Layer Graphene. Journal of the American Chemical Society, 2014, 136, 16609-16617.	6.6	206
16668	Quinoneâ€Modified Surfaces for Enhanced Enzymeâ€“Electrode Interactions in Pyrroloquinolineâ€Quinoneâ€Dependent Glucose Dehydrogenase Anodes. ChemElectroChem, 2014, 1, 2017-2028.	1.7	14
16669	Long- and Short-Range Constraints for the Structure Determination of Layered Silicates with Stacking Disorder. Chemistry of Materials, 2014, 26, 6994-7008.	3.2	24
16670	Fe adsorption on hematite (Î±-Fe2O3) (0001) and magnetite (Fe3O4) (111) surfaces. Journal of Chemical Physics, 2014, 141, 134707.	1.2	14
16671	Electronic structure and crystal phase stability of palladium hydrides. Journal of Applied Physics, 2014, 116, .	1.1	37
16672	A Theoretical Study of the Interaction of Hydrogen and Oxygen with Palladium or Gold Adsorbed on Pyridineâ€Like Nitrogenâ€Doped Graphene. ChemPhysChem, 2014, 15, 4042-4048.	1.0	17
16673	Organic molecule-functionalized Zn3P2 nanowires for photochemical H2 production: DFT and experimental analyses. International Journal of Hydrogen Energy, 2014, 39, 19887-19898.	3.8	5
16674	Effect of adsorbents on electronic transport in graphene. , 2014, , 265-291.		3
16675	Topological transport and atomic tunnellingâ€“clustering dynamics for aged Cu-doped Bi2Te3 crystals. Nature Communications, 2014, 5, 5022.	5.8	60
16676	Large-Scale B3LYP Simulations of Ibuprofen Adsorbed in MCM-41 Mesoporous Silica as Drug Delivery System. Journal of Physical Chemistry C, 2014, 118, 26737-26749.	1.5	52

#	Article	IF	Citations
16677	Kinetics and Thermodynamics of H₂O Dissociation on Reduced CeO₂(111). Journal of Physical Chemistry C, 2014, 118, 27402-27414.	1.5	91
16678	Ferromagnetism of Pd(001) substrate induced by antiferromagnetic CoO. Physics Letters, Section A: General, Atomic and Solid State Physics, 2014, 378, 3642-3644.	0.9	5
16679	First-Principles Predictions and in Situ Experimental Validation of Alumina Atomic Layer Deposition on Metal Surfaces. Chemistry of Materials, 2014, 26, 6752-6761.	3.2	68
16680	Theoretical studies of strongly correlated rare-earth intermetallics RIn3 and RSn3 (Râ€‰=â€‰Sm, Eu, and Gd). Journal of Applied Physics, 2014, 116, .	1.1	36
16681	Modelling of monovacancy diffusion in W over wide temperature range. Journal of Applied Physics, 2014, 115, 123504.	1.1	16
16682	Adsorption of formic acid on rutile TiO2 (110) revisited: An infrared reflection-absorption spectroscopy and density functional theory study. Journal of Chemical Physics, 2014, 140, 034705.	1.2	49
16683	The Local Atomic Structures of Liquid CO at 3.6â€…GPa and Polymerized CO at 0 to 30â€…GPa from Highâ€Pressure Pair Distribution Function Analysis. Chemistry - A European Journal, 2014, 20, 11531-11539.	1.7	17
16684	Inelastic Neutron Scattering and Density Functional Theoryâ€“Molecular Dynamics Study of Si Dynamics in <scp><scp>Ti</scp></scp>₃<scp><scp>SiC</scp></scp>₂. Journal of the American Ceramic Society, 2014, 97, 916-922.	1.9	2
16685	Thermodynamics and density functional theory study of potassium dichromate interaction with galena. International Journal of Minerals, Metallurgy and Materials, 2014, 21, 947-954.	2.4	6
16686	Electronic structure, optical properties, and lattice dynamics in atomically thin indium selenide flakes. Nano Research, 2014, 7, 1556-1568.	5.8	160
16687	Trends in the Hydrodeoxygenation Activity and Selectivity of Transition Metal Surfaces. Catalysis Letters, 2014, 144, 1968-1972.	1.4	15
16688	Uniaxial strain-induced mechanical and electronic property modulation of silicene. Nanoscale Research Letters, 2014, 9, 521.	3.1	61
16689	First-Principles Investigations on Structural, Phonon, and Thermodynamic Properties of Cubic $$ext {CeO}_{2}$$ CeO 2. International Journal of Thermophysics, 2014, 35, 1601-1612.	1.0	4
16690	Sulfur dimers adsorbed on Au(111) as building blocks for sulfur octomers formation: A density functional study. Journal of Chemical Physics, 2014, 141, 044713.	1.2	7
16691	Photoelectrochemical Hydrogen Production on Î±â€Fe₂O₃ (0001): Insights from Theory and Experiments. ChemSusChem, 2014, 7, 162-171.	3.6	27
16692	First-principles study for stability and binding mechanism of graphene/Ni(111) interface: Role of vdW interaction. Journal of Chemical Physics, 2014, 141, 044708.	1.2	56
16693	Role of strain on electronic and mechanical response of semiconducting transition-metal dichalcogenide monolayers: An ab-initio study. Journal of Applied Physics, 2014, 115, .	1.1	111
16694	Multi-scale quantum point contact model for filamentary conduction in resistive random access memories devices. Journal of Applied Physics, 2014, 115, .	1.1	54

#	Article	IF	Citations
16695	Semiconductor with intrinsic spin: a hybrid structure of zigzag edge graphene nanoribbon/singleâ€walled carbon nanotube. Physica Status Solidi - Rapid Research Letters, 2014, 8, 187-190.	1.2	6
16696	Li4FeH6: Iron-containing complex hydride with high gravimetric hydrogen density. APL Materials, 2014, 2, .	2.2	31
16697	Ab initio study of molecular and atomic oxygen on GeTe(111) surfaces. Journal of Applied Physics, 2014, 116, .	1.1	10
16698	Electronic structures and optical properties of SnSe2(1â^'x)O2x alloys. Computational Materials Science, 2014, 95, 712-717.	1.4	9
16699	Band engineering of ZnS by codoping for visible-light photocatalysis. Applied Physics A: Materials Science and Processing, 2014, 116, 741-750.	1.1	32
16700	Density functional theory study of adsorption of H2O, H, O, and OH on stepped platinum surfaces. Journal of Chemical Physics, 2014, 140, 134708.	1.2	83
16701	Density functional theory calculations of stability and diffusion mechanisms of impurity atoms in Ge crystals. Journal of Applied Physics, 2014, 116, .	1.1	12
16702	Improved Photoelectrochemical Water Splitting Performance of Cu₂O/SrTiO₃ Heterojunction Photoelectrode. Journal of Physical Chemistry C, 2014, 118, 25320-25329.	1.5	86
16703	High Coverage Water Aggregation and Dissociation on Fe(100): A Computational Analysis. Journal of Physical Chemistry C, 2014, 118, 26139-26154.	1.5	47
16704	New phases of binary compounds: CsCl-type RuGe and RuSn. Europhysics Letters, 2014, 107, 56003.	0.7	6
16705	Tunable Cobalt Vacancies and Related Properties in LaCo_xAs₂. Chemistry of Materials, 2014, 26, 6221-6225.	3.2	15
16706	Metallic BSi₃ Silicene: A Promising High Capacity Anode Material for Lithium-Ion Batteries. Journal of Physical Chemistry C, 2014, 118, 25836-25843.	1.5	62
16707	Structural, optical, and electrical properties of strained La-doped SrTiO3 films. Journal of Applied Physics, 2014, 116, .	1.1	53
16708	Magnetic properties of Fe and Co nanoclusters embedded in the first Cu(100) surface layer. JETP Letters, 2014, 99, 646-649.	0.4	8
16709	Ab initio study of heterojunction discontinuities in the ZnO/Cu2O system. Journal of Experimental and Theoretical Physics, 2014, 118, 945-950.	0.2	2
16710	Theoretical study of the thermodynamic stability and electronic structure of thin films of 3C, 2H, and 2D silicon carbides. Physics of the Solid State, 2014, 56, 1654-1658.	0.2	1
16711	Electronic, elastic properties and hardness of the novel tetragonal silicon. Journal of the Korean Physical Society, 2014, 65, 45-51.	0.3	8
16712	Atomic and magnetic ordering in bcc Cuâ€"Alâ€"Mn: computational study. Modelling and Simulation in Materials Science and Engineering, 2014, 22, 085007.	0.8	7

#	Article	IF	Citations
16713	Atomic structures and electronic properties of Ta-doped 2H-NbSe2. RSC Advances, 2014, 4, 57541-57546.	1.7	9
16714	Infrared Spectroscopy and Density Functional Theory Investigation of Calcite, Chalk, and Coccolithsâ€”Do We Observe the Mineral Surface?. Journal of Physical Chemistry A, 2014, 118, 10720-10729.	1.1	22
16715	Dissociative Adsorption of Molecules on Graphene and Silicene. Journal of Physical Chemistry C, 2014, 118, 27574-27582.	1.5	43
16716	Band gap engineering by lanthanide doping in the photocatalyst LaOF: First-principles study. International Journal of Modern Physics B, 2014, 28, 1450069.	1.0	6
16717	Assessing the performance of density functional theory in optimizing molecular crystal structure parameters. Acta Crystallographica Section B: Structural Science, Crystal Engineering and Materials, 2014, 70, 259-267.	0.5	28
16718	[illegible] into<mml:math xmlns:mml="http://www.w3.org/1998/Math/MathML"><mml:msup><mml:mi mathvariant="normal">Zn</mml:mi><mml:mrow><mml:mn>2</mml:mn><mml:mo>+</mml:mo></mml:mrow></mml:msup></mml:math xmlns:mml="http://www.w3.org/1998/Math/MathML"><mml:msub><mml:mi mathvariant="normal">KNbO</mml:mi><mml:mn>3</mml:mn></mml:msub></mml:math>and [illegible]	1.1	45
16719	A charge optimized many-body potential for titanium nitride (TiN). Journal of Physics Condensed Matter, 2014, 26, 265004.	0.7	10
16720	Electronic structure and magnetic properties of substitutional transition-metal atoms in GaN nanotubes. Chinese Physics B, 2014, 23, 017301.	0.7	14
16721	Efficient luminescent center by codoping (Eu,Mg,O) into GaN. Applied Physics Express, 2014, 7, 071005.	1.1	13
16722	Design of the Alkali-Metal-Doped WO₃ as a Near-Infrared Shielding Material for Smart Window. Industrial & Engineering Chemistry Research, 2014, 53, 17981-17988.	1.8	68
16723	The effect of the interlayer element on the exfoliation of layered Mo₂AC (A = Al, Si, P, Ga,) Tj ETQq0 0 0 rgBT /Overlock 10 T of Advanced Materials, 2014, 15, 014208.	2.8	78
16724	Superconductivity of Ca2InN with a layered structure embedding an anionic indium chain array. Superconductor Science and Technology, 2014, 27, 055005.	1.8	3
16725	Silicane nanoribbons: electronic structure and electric field modulation. New Journal of Physics, 2014, 16, 115006.	1.2	14
16726	Optoelectronic excitations and photovoltaic effect in strongly correlated materials. Physical Review B, 2014, 90, .	1.1	26
16727	The stabilities and electronic structures of single-layer bismuth oxyhalides for photocatalytic water splitting. Physical Chemistry Chemical Physics, 2014, 16, 25854-25861.	1.3	105
16728	Raman Spectra of Monolayer, Few-Layer, and Bulk ReSe₂: An Anisotropic Layered Semiconductor. ACS Nano, 2014, 8, 11154-11164.	7.3	296
16729	Oxidation of a Graphite Surface: The Role of Water. Journal of Physical Chemistry C, 2014, 118, 27594-27598.	1.5	20
16730	Strain-induced electronic phase transition and strong enhancement of thermopower of<mml:math xmlns:mml="http://www.w3.org/1998/Math/MathML"><mml:msub><mml:mrow><mml:mi mathvariant="normal">TiS</mml:mi></mml:mrow><mml:mn>2</mml:mn></mml:msub></mml:math>. Physical Review B, 2014, 90, .	1.1	24

#	Article	IF	Citations
16731	Electronic Bandgap and Edge Reconstruction in Phosphorene Materials. Nano Letters, 2014, 14, 6400-6406.	4.5	459
16732	The stability, electronic properties, and hardness of SiN2 under high pressure. RSC Advances, 2014, 4, 55023-55027.	1.7	9
16733	The influence of hydrogen bonding on the nonlinear optical properties of a semiorganic material NH₄B[<scp>d</scp>-(+)-C₄H₄O₅]₂Â·H₂O: a theoretical perspective. Physical Chemistry Chemical Physics, 2014, 16, 20089.	1.8	17
16734	First-principles investigations on the adsorption and diffusion of carbon atoms on the surface and in the subsurface of Co (111) related to the growth of graphene. RSC Advances, 2014, 4, 34237.	1.7	7
16735	Mode coupling between nonpolar and polar phonons as the origin of improper ferroelectricity in hexagonal LuMnO₃. Journal of Materials Chemistry C, 2014, 2, 4126-4132.	2.7	13
16736	Thermoelectric properties of marcasite and pyrite FeX2 (X = Se, Te): a first principle study. RSC Advances, 2014, 4, 9424.	1.7	37
16737	Choosing a proper exchangeâ€“correlation functional for the computational catalysis on surface. Physical Chemistry Chemical Physics, 2014, 16, 18563-18569.	1.3	21
16738	Poisoning effect of adsorbed CO during CO₂ electroreduction on late transition metals. Physical Chemistry Chemical Physics, 2014, 16, 20429-20435.	1.3	63
16739	Ab initio DFT+U analysis of oxygen transport in LaCoO₃: the effect of Co³⁺ magnetic states. Journal of Materials Chemistry A, 2014, 2, 8060-8074.	5.2	76
16740	Large polarization but small electron transfer for water around Al3+ in a highly hydrated crystal. Physical Chemistry Chemical Physics, 2014, 16, 9351.	1.3	4
16741	Designing mixed metal halide ammines for ammonia storage using density functional theory and genetic algorithms. Physical Chemistry Chemical Physics, 2014, 16, 19732-19740.	1.3	24
16742	Experimental and theoretical investigation of the magnetic and photoconductive nature of a novel two-dimensional, mixed-valence bis(2-thioxo-1,3-dithiole-4,5-dithiolato)nickelate molecular solid. Inorganic Chemistry Frontiers, 2014, 1, 426-433.	3.0	10
16743	Rectifying, giant magnetoresistance, spin-filtering, newgative differential resistance, and switching effects in single-molecule magnet Mn(dmit) 2 -based molecular device with graphene nanoribbon electrodes. Organic Electronics, 2014, 15, 3615-3623.	1.4	13
16744	First-principles calculations of finite-temperature thermodynamic properties of binary solid solutions in the Alâ€“Cuâ€“Mg system. Calphad: Computer Coupling of Phase Diagrams and Thermochemistry, 2014, 47, 196-210.	0.7	7
16745	Density Functional Theory Calculations of Pressure Effects on the Structure and Vibrations of 1,1-Diamino-2,2-dinitroethene (FOX-7). Journal of Physical Chemistry A, 2014, 118, 10002-10010.	1.1	35
16746	Effects of atomic ordering on the elastic properties of TiN- and VN-based ternary alloys. Thin Solid Films, 2014, 571, 145-153.	0.8	34
16747	First-principles calculations of electronic, optical and elastic Properties of Y8CoIn3. , 2014, , .		0
16748	Electronic and Magnetic Properties of BiFeO₃: Gd³⁺. Ferroelectrics, 2014, 461, 85-91.	0.3	6

#	Article	IF	Citations
16749	Structural characterization of slightly boron-deficient LiB, LiB_{0.9} and LiB_{0.8}, under pressure. Journal of Physics Condensed Matter, 2014, 26, 475402.	0.7	1
16750	Supramolecular self-assembled network formation containing Nâ‹¯Br halogen bonds in physisorbed overlayers. Physical Chemistry Chemical Physics, 2014, 16, 19608-19617.	1.3	10
16751	Near-infrared photocatalytic activity induced by intrinsic defects in Bi₂MO₆ (M = W, Mo). Physical Chemistry Chemical Physics, 2014, 16, 18596.	1.3	82
16752	Site-specific catalytic activity in exfoliated MoS₂ single-layer polytypes for hydrogen evolution: basal plane and edges. Journal of Materials Chemistry A, 2014, 2, 20545-20551.	5.2	150
16753	Ab initio ORTEP drawings: a case study of N-based molecular crystals with different chemical nature. CrystEngComm, 2014, 16, 10907-10915.	1.3	32
16754	Nitranilic acid hexahydrate, a novel benchmark system of the Zundel cation in an intrinsically asymmetric environment: spectroscopic features and hydrogen bond dynamics characterised by experimental and theoretical methods. Physical Chemistry Chemical Physics, 2014, 16, 998-1007.	1.3	14
16755	Structural skeleton of preferentially interpenetrated clusters and correlation with shear localization in Mgâ€“Cuâ€“Ni ternary metallic glasses. Physical Chemistry Chemical Physics, 2014, 16, 19590.	1.3	19
16756	Light-induced reversible modification of the work function of a new perfluorinated biphenyl azobenzene chemisorbed on Au (111). Nanoscale, 2014, 6, 8969-8977.	2.8	31
16757	Superior flexibility of a wrinkled carbon shell under electrochemical cycling. Journal of Materials Chemistry A, 2014, 2, 4192.	5.2	17
16758	New manifold two-dimensional single-layer structures of zinc-blende compounds. Journal of Materials Chemistry A, 2014, 2, 17971-17978.	5.2	107
16759	Carbon coated face-centered cubic Ruâ€“C nanoalloys. Nanoscale, 2014, 6, 10370-10376.	2.8	17
16760	Density functional study of the Ge(111)c(2 Ã— 8) surface using the modified Becke-Johnson exchange potential with LDA correlation and spinâ€“orbit interactions. RSC Advances, 2014, 4, 48245-48253.	1.7	2
16761	Gap openings in graphene regarding interfacial interaction from substrates. Physical Chemistry Chemical Physics, 2014, 16, 5600.	1.3	3
16762	In search of structureâ€“function relationships in transition-metal based rectifiers. Inorganic Chemistry Frontiers, 2014, 1, 468-477.	3.0	5
16763	Mechanical and electronic properties of pristine and Ni-doped Si, Ge, and Sn sheets. Physical Chemistry Chemical Physics, 2014, 16, 1667-1671.	1.3	46
16764	Irradiation induced non-equilibrium phase formation and structural transformation in the Feâ€“Tiâ€“Nb multilayered films. RSC Advances, 2014, 4, 9098-9102.	1.7	1
16765	Thermodynamics of thorium substitution in yttrium iron garnet: comparison of experimental and theoretical results. Journal of Materials Chemistry A, 2014, 2, 16945-16954.	5.2	22
16766	Enhanced adsorption of acidic gases (CO2, NO2 and SO2) on light metal decorated graphene oxide. Physical Chemistry Chemical Physics, 2014, 16, 11031.	1.3	87

#	Article	IF	Citations
16767	Direct vs. indirect pathway for nitrobenzene reduction reaction on a Ni catalyst surface: a density functional study. Physical Chemistry Chemical Physics, 2014, 16, 26365-26374.	1.3	103
16768	Decomposition of methyl species on a Ni(211) surface: investigations of the electric field influence. Catalysis Science and Technology, 2014, 4, 4020-4035.	2.1	29
16769	Further findings of X-ray absorption near-edge structure in lithium manganese spinel oxide using first-principles calculations. Journal of Materials Chemistry A, 2014, 2, 8017-8025.	5.2	18
16770	High throughput first-principles calculations of bixbyite oxides for TCO applications. Physical Chemistry Chemical Physics, 2014, 16, 17724-17733.	1.3	25
16771	A semiconductive superhard FeB₄phase from first-principles calculations. Physical Chemistry Chemical Physics, 2014, 16, 22008-22013.	1.3	15
16772	A DFT study of furan hydrogenation and ring opening on Pd(111). Green Chemistry, 2014, 16, 736-747.	4.6	80
16773	A lithium peroxide precursor on the Î±-MnO₂(100) surface. Journal of Materials Chemistry A, 2014, 2, 16538-16546.	5.2	25
16774	Fe₄[Fe(CN)₆]₃: a cathode material for sodium-ion batteries. RSC Advances, 2014, 4, 42991-42995.	1.7	30
16775	Assignment of Raman-active vibrational modes of tetragonal mackinawite: Raman investigations and ab initio calculations. RSC Advances, 2014, 4, 25827-25834.	1.7	17
16776	Halide adsorption on close-packed metal electrodes. Physical Chemistry Chemical Physics, 2014, 16, 13630-13634.	1.3	54
16777	Mechanical and metallic properties of tantalum nitrides from first-principles calculations. RSC Advances, 2014, 4, 10133.	1.7	55
16778	Improving photocatalytic properties of SrTiO₃through (Sb, N) codoping: a hybrid density functional study. RSC Advances, 2014, 4, 45703-45709.	1.7	31
16779	First-principles study of the lattice dynamics of Sb₂S₃. Physical Chemistry Chemical Physics, 2014, 16, 345-350.	1.3	72
16780	Investigations on V₂C and V₂CX₂ (X = F, OH) Monolayer as a Promising Anode Material for Li Ion Batteries from First-Principles Calculations. Journal of Physical Chemistry C, 2014, 118, 24274-24281.	1.5	301
16781	Surface stabilities and NO oxidation kinetics on hexagonal-phase LaCoO₃ facets: a first-principles study. Catalysis Science and Technology, 2014, 4, 3687-3696.	2.1	12
16782	Ethanol Gas Sensing Mechanism in ZnO Nanowires: An ab Initio Study. Journal of Physical Chemistry C, 2014, 118, 24533-24537.	1.5	34
16783	Temperature- and Pressure-Induced Changes in the Crystal Structure of Sr(NH₃)₈Cl₂. Journal of Physical Chemistry C, 2014, 118, 24349-24356.	1.5	18
16784	Anomalous Interfacial Lithium Storage in Graphene/TiO₂ for Lithium Ion Batteries. ACS Applied Materials & Interfaces, 2014, 6, 18147-18151.	4.0	65

#	Article	IF	Citations
16785	Thermodynamic study of benzene and hydrogen coadsorption on Pd(111). Physical Chemistry Chemical Physics, 2014, 16, 23754-23768.	1.3	25
16786	Screened coulomb hybrid DFT investigation of band gap and optical absorption predictions of CuVO₃, CuNbO₃ and Cu₅Ta₁₁O₃₀ materials. Physical Chemistry Chemical Physics, 2014, 16, 18198-18204.	1.3	40
16787	Role of Interchain Interaction in Determining the Band Gap of Trigonal Selenium: A Density Functional Theory Study with a Linear Combination of Bloch Orbitals. Journal of Physical Chemistry C, 2014, 118, 19294-19307.	1.5	10
16788	Competing Cationâ€“Anion Interactions and Noncentrosymmetry in Metal Oxide-Fluorides: A First-Principles Theoretical Study. Crystal Growth and Design, 2014, 14, 131-139.	1.4	8
16789	Large indentation strain-stiffening in nanotwinned cubic boron nitride. Nature Communications, 2014, 5, 4965.	5.8	105
16790	High pressure phases of different tetraboranes. High Pressure Research, 2014, 34, 59-69.	0.4	3
16791	Carâ€“Parrinello and path integral molecular dynamics study of the intramolecular hydrogen bonds in the crystals of benzoylacetone and dideuterobenzoylacetone. Physical Chemistry Chemical Physics, 2014, 16, 23026-23037.	1.3	21
16792	Elastic and electronic properties of cubic cerium oxide under pressure via first principles. International Journal of Modern Physics B, 2014, 28, 1450070.	1.0	1
16793	Effect by Doping and Surface Termination on c-BN Surface Reactivity: A Theoretical DFT Approach. Journal of Physical Chemistry C, 2014, 118, 10061-10075.	1.5	2
16794	Ab initio calculation of relative permittivity of La-doped HfO2. Physica B: Condensed Matter, 2014, 454, 184-188.	1.3	2
16795	Effects of Mg and Al doping on the electronic structure and dehydrogenation of LiBH4Â·NH3. International Journal of Hydrogen Energy, 2014, 39, 17144-17152.	3.8	8
16796	Hydrogen-Coverage-Dependent Stark Effect in Bilayer Graphene and Graphene/BN Nanofilms. Journal of Physical Chemistry C, 2014, 118, 10472-10480.	1.5	9
16797	Cooperativity Assisted Shortening of Hydrogen Bonds in Crystalline Oxalic Acid Dihydrate: DFT and NBO Model Studies. Journal of Chemical Theory and Computation, 2014, 10, 1817-1823.	2.3	17
16798	First-Principles Study of Water Reaction and H₂ Formation on UO₂ (111) and (110) Single Crystal Surfaces. Journal of Physical Chemistry C, 2014, 118, 21935-21944.	1.5	35
16799	First-Principles Calculations of Electronic Structure and Optical Properties of Si-doped Orthorhombic SrHfO3. Rare Metal Materials and Engineering, 2014, 43, 1079-1083.	0.8	4
16800	Tuning the properties of visible-light-responsive tantalum (oxy)nitride photocatalysts by non-stoichiometric compositions: a first-principles viewpoint. Physical Chemistry Chemical Physics, 2014, 16, 20548-20560.	1.3	86
16801	Phase stability and mechanical properties of ruthenium borides from first principles calculations. Computational Materials Science, 2014, 95, 377-383.	1.4	14
16802	Ca₃Be₆B₅O₁₆F: the first alkaline-earth beryllium borate with fluorine anions. Dalton Transactions, 2014, 43, 9998-10004.	1.6	10

#	Article	IF	Citations
16803	Ce-Pr mixed oxides as active supports for Water-gas Shift reaction: Experimental and density functional theory characterization. Applied Catalysis A: General, 2014, 485, 123-132.	2.2	37
16804	Layered uranium(<scp>vi</scp>) hydroxides: structural and thermodynamic properties of dehydrated schoepite Î±-UO₂(OH)₂. Dalton Transactions, 2014, 43, 17191-17199.	1.6	35
16805	Postperovskite Phase Transition of ZnGeO₃: Comparative Crystal Chemistry of Postperovskite Phase Transition from Germanate Perovskites. Inorganic Chemistry, 2014, 53, 11732-11739.	1.9	5
16806	Effects of hydrogen and impurities on void nucleation in copper: simulation point of view. Philosophical Magazine, 2014, 94, 3522-3548.	0.7	35
16807	Self-trapping of carbon atoms in<mml:math xmlns:mml="http://www.w3.org/1998/Math/MathML"><mml:msup><mml:mi>Î±</mml:mi><mml:mo>â€²</mml:mo></mml:msup></mm during the martensitic transformation: A qualitative picture fromab initiocalculations. Physical Review B, 2014, 90, .	1.1	27
16808	The interaction of beryllium with benzene and graphene: a comparative investigation based on DFT, MP2, CCSD(T), CAS-SCF and CAS-PT2. Physical Chemistry Chemical Physics, 2014, 16, 1957-1966.	1.3	11
16809	A first-principles study of Hg adsorption on Pd(111) and Pd/Î³-Al2O3(110) surfaces. Applied Surface Science, 2014, 321, 30-37.	3.1	31
16810	Ab initio study of the structural, electronic, phase diagram, and thermal properties of cadium beryllium selenide mixed crystals. Materials Science in Semiconductor Processing, 2014, 26, 642-648.	1.9	6
16811	First-principles insight into the surface magnetism of Cu-doped SnO₂(110) thin film. RSC Advances, 2014, 4, 39860.	1.7	8
16812	Magnetic phase transition of Ag₂S:Eu diluted magnetic semiconductor nanoparticles. RSC Advances, 2014, 4, 33645.	1.7	8
16813	Insulating to metallic transition of an oxidized boron nitride nanosheet coating by tuning surface oxygen adsorption. Nanoscale, 2014, 6, 3731-3736.	2.8	12
16814	Anomalous high adsorption energy of H₂O on fluorinated graphenes: a first principles study. Physical Chemistry Chemical Physics, 2014, 16, 20464-20470.	1.3	16
16815	The chemical origin and catalytic activity of coinage metals: from oxidation to dehydrogenation. Physical Chemistry Chemical Physics, 2014, 16, 7481-7490.	1.3	14
16816	With the same Clar formulas, do the two-dimensional sandwich nanostructures Xâ€“Crâ€“X (X = C4H,) Tj ETQq1 1 0.784314 rgBT /O	1.3	13
16817	Enhanced photocatalytic mechanism for the hybrid g-C₃N₄/MoS₂ nanocomposite. Journal of Materials Chemistry A, 2014, 2, 7960-7966.	5.2	347
16818	Does Bi form clusters in GaAs1 â^'xBixalloys?. Semiconductor Science and Technology, 2014, 29, 115007.	1.0	11
16819	Detecting gas molecules via atomic magnetization. Dalton Transactions, 2014, 43, 13070-13075.	1.6	5
16820	The decomposition of Î±-LiN₂H₃BH₃: an unexpected hydrogen release from a homopolar protonâ€“proton pathway. Journal of Materials Chemistry A, 2014, 2, 15627.	5.2	7

#	Article	IF	Citations
16821	An experimental and computational investigation of the oxygen storage properties of BaLnFe2O5+Î´ and BaLnCo2O5+Î´ (Ln = La, Y) perovskites. Journal of Materials Chemistry A, 2014, 2, 2397.	5.2	22
16822	Size- effect induced high thermoelectric figure of merit in PbSe and PbTe nanowires. Physical Chemistry Chemical Physics, 2014, 16, 8114-8118.	1.3	15
16823	CO₂ Adsorption on Anatase TiO₂ (101) Surfaces in the Presence of Subnanometer Ag/Pt Clusters: Implications for CO₂ Photoreduction. Journal of Physical Chemistry C, 2014, 118, 26236-26248.	1.5	57
16824	Density functional calculations of extended, periodic systems using Coulomb corrected molecular fractionation with conjugated caps method (CC-MFCC). Physical Chemistry Chemical Physics, 2014, 16, 21252-21270.	1.3	7
16825	Structural stability and compressive behavior of ZrH₂under hydrostatic pressure and nonhydrostatic pressure. RSC Advances, 2014, 4, 46780-46786.	1.7	13
16826	Interactions of adsorbed CO2 on water ice at low temperatures. Physical Chemistry Chemical Physics, 2014, 16, 15630.	1.3	25
16827	Variable-composition structural optimization and experimental verification of MnB₃and MnB₄. Physical Chemistry Chemical Physics, 2014, 16, 15866-15873.	1.3	49
16828	Control of the anisotropic shape of cobalt nanorods in the liquid phase: from experiment to theoryâ€¦ and back. Nanoscale, 2014, 6, 2682.	2.8	39
16829	Highly efficient Pd-based coreâ€“shell nanowire catalysts for O₂ dissociation. Physical Chemistry Chemical Physics, 2014, 16, 20532-20536.	1.3	5
16830	Tin-decorated ruthenium nanoparticles: a way to tune selectivity in hydrogenation reaction. Nanoscale, 2014, 6, 9806-9816.	2.8	24
16831	Emergence of electric polarity in BiTeX (X = Br and I) monolayers and the giant Rashba spin splitting. Physical Chemistry Chemical Physics, 2014, 16, 17603.	1.3	73
16832	High-pressure phase transition and lattice dynamics of rock-salt and FeSi-type phases of MgS. Philosophical Magazine Letters, 2014, 94, 198-204.	0.5	2
16833	Eu(<scp>ii</scp>) luminescence in the perovskite host lattices KMgH₃, NaMgH₃ and mixed crystals LiBa_xSr_{1â^'x}H₃. Journal of Materials Chemistry C, 2014, 2, 4799-4804.	2.7	24
16834	Adsorbate induced vacancy formation on silver surfaces. Physical Chemistry Chemical Physics, 2014, 16, 9002.	1.3	17
16835	Copper atoms embedded in hexagonal boron nitride as potential catalysts for CO oxidation: a first-principles investigation. RSC Advances, 2014, 4, 38750-38760.	1.7	57
16836	Preference for a propellane motif in pure silicon nanosheets. Physical Chemistry Chemical Physics, 2014, 16, 11186-11190.	1.3	12
16837	DFT study on the effects of defect and metal-doping on the decomposition of H₂S on the Î±-Fe₂O₃(0001) surface. RSC Advances, 2014, 4, 22411-22418.	1.7	21
16838	Ligand design for long-range magnetic order in metalâ€“organic frameworks. Chemical Communications, 2014, 50, 13990-13993.	2.2	52

#	Article	IF	Citations
16839	Novel Si Networks in the Ca/Si Phase Diagram under Pressure. Journal of Physical Chemistry C, 2014, 118, 25167-25175.	1.5	15
16840	A theoretical study of electronic and optical properties of SiC nanowires and their quantum confinement effects. Dalton Transactions, 2014, 43, 5505.	1.6	12
16841	Two-dimensional ferromagnetic iron crystals constrained by graphene edges: a first principles study. RSC Advances, 2014, 4, 17008-17014.	1.7	8
16842	An inelastic neutron scattering study of dietary phenolic acids. Physical Chemistry Chemical Physics, 2014, 16, 7491-7500.	1.3	10
16843	New Be-intercalated hexagonal boron layer structure of BeB2. RSC Advances, 2014, 4, 15061-15065.	1.7	5
16844	Widely tunable band gaps of graphdiyne: an ab initio study. Physical Chemistry Chemical Physics, 2014, 16, 8935-8939.	1.3	56
16845	Softest elastic mode governs materials hardness. Science Bulletin, 2014, 59, 1747-1754.	1.7	14
16846	Tuning of the electronic and optical properties of single-layer black phosphorus by strain. Physical Review B, 2014, 90, .	1.1	279
16847	Structural and electronic property calculations of III-As (III:Ga, In) semiconductors using PAW+U by first principles. , 2014, , .		1
16848	An Investigation into Methanol Oxidation Reactions and CO, OH Adsorption on Pt-Ru-Mo Catalysts for a Direct Methanol Fuel Cell. Journal of the Electrochemical Society, 2014, 161, F405-F414.	1.3	13
16849	Theoretical Study on Adsorption and Doping of Pd Atom on Graphene. Advanced Materials Research, 2014, 893, 15-18.	0.3	0
16850	First-Principle Studies on the Stability of AlN(0001)/NbB₂(0001) Interface. Advanced Materials Research, 2014, 1052, 18-23.	0.3	0
16851	First-Principle Study of Atomic Structures of Fe/TMC (TM=Ti, Zr and Hf) Interface. Advanced Materials Research, 2014, 852, 193-197.	0.3	0
16852	Experimental and modeling study of thermal and catalytic cracking of n-decane. Journal of Analytical and Applied Pyrolysis, 2014, 110, 463-469.	2.6	27
16853	Theoretical Study of Structural, Elastic Properties and Phase Transitions of Cu₂ZnSnS₄. Advanced Materials Research, 0, 1058, 113-117.	0.3	2
16854	Spin Hall Effects in Metallic Antiferromagnets. Physical Review Letters, 2014, 113, 196602.	2.9	313
16855	Spontaneous formation of metallic nanostructures on highly oriented pyrolytic graphite (HOPG): an ab initio and experimental study. Faraday Discussions, 2014, 172, 327-347.	1.6	14
16856	cuse-based layered compound,mml:math xmlns:mml="http://www.w3.org/1998/Math/MathML"><mml:msub><mml:mrow><mml:mi mathvariant="normal">Bi</mml:mi></mml:mrow><mml:mn>2</mml:mn></mml:msub><mml:msub><mml:mrow><mml:mi mathvariant="normal">YO</mml:mi></mml:mrow><mml:mn>4</mml:mn></mml:msub><mml:msub><mml:mrow>K<mml:mi mathvariant="normal">Cu</mml:mi></mml:mrow><mml:mn>2</mml:mn></mml:msub><mml:msub><mml:mrow><mml:mi mathvariant="normal">Se</mml:mi></mml:mrow><mml:mn>2</mml:mn></mml:msub></mml:math>as a q		15

#	Article	IF	Citations
16857	Nature of Holes, Oxidation States, and Hypervalency in Covellite (CuS). Inorganic Chemistry, 2014, 53, 12402-12406.	1.9	68
16858	Property of Mn-Doped Fe₂O₃ and its Effect on CO Adsorption. Advanced Materials Research, 0, 1008-1009, 342-345.	0.3	0
16859	Polarons and oxygen vacancies at the surface of anatase TiO₂. Physica Status Solidi - Rapid Research Letters, 2014, 8, 583-586.	1.2	46
16860	Significant variation of surface spin polarization through group IV atom (C, Si, Ge, Sn) adsorption on Fe₃O₄(100). Physical Chemistry Chemical Physics, 2014, 16, 95-102.	1.3	10
16861	Ab initio calculations of quantum transport of Auâ€“GaNâ€“Au nanoscale junctions. RSC Advances, 2014, 4, 51838-51844.	1.7	4
16862	Electro-reduction of nitrogen on molybdenum nitride: structure, energetics, and vibrational spectra from DFT. Physical Chemistry Chemical Physics, 2014, 16, 3014.	1.3	55
16863	Understanding the electronic and ionic conduction and lithium over-stoichiometry in LiMn₂O₄ spinel. Journal of Materials Chemistry A, 2014, 2, 18271-18280.	5.2	68
16864	Ideal two-dimensional systems with a gain Rashba-type spin splitting: SrFBiS₂and BiOBiS₂nanosheets. Journal of Materials Chemistry C, 2014, 2, 8539-8545.	2.7	13
16865	Mechanisms of enhanced sulfur tolerance on samarium (Sm)-doped cerium oxide (CeO₂) from first principles. Physical Chemistry Chemical Physics, 2014, 16, 10727-10733.	1.3	16
16866	Effect on the Electronic, Magnetic and Thermoelectric Properties of ${hbox{Bi}}_{2}{hbox{Te}}_{3}$ by the Cerium Substitution. IEEE Transactions on Magnetics, 2014, 50, 1-4.	1.2	9
16867	Realizing semiconductorâ€“half-metal transition in zigzag graphene nanoribbons supported on hybrid fluorographeneâ€“graphane nanoribbons. Physical Chemistry Chemical Physics, 2014, 16, 23214-23223.	1.3	23
16868	Acoustic phonons and negative thermal expansion in MOF-5. Physical Chemistry Chemical Physics, 2014, 16, 21144-21152.	1.3	61
16869	Line defects and induced doping effects in graphene, hexagonal boron nitride and hybrid BNC. Physical Chemistry Chemical Physics, 2014, 16, 21473-21485.	1.3	26
16870	Ab initio calculation of magnetic properties of p-block element doped ZnO. RSC Advances, 2014, 4, 45598-45602.	1.7	22
16871	A facile and versatile method for preparation of colored TiO₂ with enhanced solar-driven photocatalytic activity. Nanoscale, 2014, 6, 10216-10223.	2.8	382
16872	First-principles study of ground-state properties of U₂Mo. Physical Chemistry Chemical Physics, 2014, 16, 26974-26982.	1.3	26
16873	Defect chemistry in layered transition-metal oxides from screened hybrid density functional calculations. Journal of Materials Chemistry A, 2014, 2, 5224-5235.	5.2	96
16874	Oxygen Vacancy Effect on Photoluminescence Properties of Self-Activated Yttrium Tungstate. Journal of Physical Chemistry C, 2014, 118, 25633-25642.	1.5	45

#	Article	IF	Citations
16875	Origin of enhanced thermoelectric properties of doped CrSi₂. RSC Advances, 2014, 4, 3482-3486.	1.7	8
16876	Nasicon material NaZr₂(PO₄)₃: a novel storage material for sodium-ion batteries. Journal of Materials Chemistry A, 2014, 2, 1341-1345.	5.2	44
16877	Verification of the dual cycle mechanism for methanol-to-olefin conversion in HSAPO-34: a methylbenzene-based cycle from DFT calculations. Catalysis Science and Technology, 2014, 4, 2631-2638.	2.1	54
16878	The role of water co-adsorption on the modification of ZnO nanowires using acetic acid. Physical Chemistry Chemical Physics, 2014, 16, 8509-8514.	1.3	8
16879	Defect-induced semiconductor to metal transition in graphene monoxide. Physical Chemistry Chemical Physics, 2014, 16, 13477-13482.	1.3	12
16880	H₂ production through electro-oxidation of SO₂: identifying the fundamental limitations. Physical Chemistry Chemical Physics, 2014, 16, 9572-9579.	1.3	36
16881	The bending machine: CO₂ activation and hydrogenation on Î´-MoC(001) and Î²-Mo₂C(001) surfaces. Physical Chemistry Chemical Physics, 2014, 16, 14912-14921.	1.3	175
16882	Porous Graphitic Carbon Nitride: A Possible Metal-free Photocatalyst for Water Splitting. Journal of Physical Chemistry C, 2014, 118, 26479-26484.	1.5	172
16883	The characteristics of n- and p-type dopants in SnS2monolayer nanosheets. Physical Chemistry Chemical Physics, 2014, 16, 19674.	1.3	98
16884	Hybrid platforms of graphaneâ€“graphene 2D structures: prototypes for atomically precise nanoelectronics. Physical Chemistry Chemical Physics, 2014, 16, 23558-23563.	1.3	10
16885	Reduction mechanisms of additives on Si anodes of Li-ion batteries. Physical Chemistry Chemical Physics, 2014, 16, 17091-17098.	1.3	80
16886	NO oxidation catalysis on copper doped hexagonal phase LaCoO3: a combined experimental and theoretical study. Physical Chemistry Chemical Physics, 2014, 16, 5106.	1.3	59
16887	Origin of blue emission in ThO₂ nanorods: exploring it as a host for photoluminescence of Eu³⁺, Tb³⁺ and Dy³⁺. RSC Advances, 2014, 4, 51244-51255.	1.7	45
16888	Ab initio investigations of dioctahedral interlayer-deficient mica: Modeling particles of illite found within gas shale. American Mineralogist, 2014, 99, 1962-1972.	0.9	5
16889	Several different charge transfer and Ce³⁺localization scenarios for Rhâ€“CeO₂(111). Journal of Materials Chemistry A, 2014, 2, 2333-2345.	5.2	26
16890	Tuning electronic and magnetic properties of silicene with magnetic superhalogens. Physical Chemistry Chemical Physics, 2014, 16, 22979-22986.	1.3	35
16891	Electronic and optical properties of silicene nanomeshes. RSC Advances, 2014, 4, 37998-38003.	1.7	23
16892	Doping strategies to control A-centres in silicon: insights from hybrid density functional theory. Physical Chemistry Chemical Physics, 2014, 16, 8487.	1.3	16

#	Article	IF	Citations
16893	C K-edge NEXAFS spectra of graphene with physical and chemical defects: a study based on density functional theory. Physical Chemistry Chemical Physics, 2014, 16, 14083-14095.	1.3	70
16894	Effect of Bi bilayers on the topological states of<mml:math xmlns:mml="http://www.w3.org/1998/Math/MathML"><mml:mrow><mml:msub><mml:mi>Bi</mml:mi><mml:mn>21</mml:mn></mml:msub></mml:mrow></mml:math> A first-principles study. Physical Review B, 2014, 90, .	3.7	81
16895	First-principles study of nitrogen adsorption and dissociation on Î±-uranium (001) surface. RSC Advances, 2014, 4, 57308-57321.	1.7	15
16896	Charge inhomogeneity of graphene on SiO₂: dispersion-corrected density functional theory study on the effect of reactive surface sites. RSC Advances, 2014, 4, 37236-37243.	1.7	18
16897	Atomistic Structure and Ab Initio Electrochemical Properties of Li₄Ti₅O₁₂Defect Spinel for Li Ion Batteries. Journal of the Electrochemical Society, 2014, 161, A439-A444.	1.3	67
16898	Aliovalent doping of CeO₂: DFT study of oxidation state and vacancy effects. Journal of Materials Chemistry A, 2014, 2, 13723-13737.	5.2	93
16899	Tunable band gap and doping type in silicene by surface adsorption: towards tunneling transistors. Nanoscale, 2014, 6, 7609-7618.	2.8	151
16900	On the fate of hydrogen during zirconium oxidation by water: effect of oxygen dissolution in Î±-Zr. RSC Advances, 2014, 4, 11050-11058.	1.7	12
16901	Ligand-stabilized CdSe nanoplatelet hybrid structures with tailored geometric and electronic properties. New insights from theory. RSC Advances, 2014, 4, 55980-55989.	1.7	17
16902	Dynamics of water molecules and sodium ions in solid hydrates of nucleotides. CrystEngComm, 2014, 16, 6756-6764.	1.3	12
16903	Doping of rhenium disulfide monolayers: a systematic first principles study. Physical Chemistry Chemical Physics, 2014, 16, 16771-16779.	1.3	62
16904	The influence of the Hubbard U parameter in simulating the catalytic behaviour of cerium oxide. Physical Chemistry Chemical Physics, 2014, 16, 21032-21038.	1.3	26
16905	Adsorption and desulfurization reaction mechanism of thiophene and its hydrogenated derivatives over NbC(001) and NbN(001): an ab initio DFT study. Catalysis Science and Technology, 2014, 4, 2550-2563.	2.1	15
16906	Tuning the crystal shape of materials by chemical potential: a combined theoretical and experimental study for NiSe2. RSC Advances, 2014, 4, 13395-13404.	1.7	4
16907	CO oxidation catalyzed by Pt-embedded graphene: a first-principles investigation. Physical Chemistry Chemical Physics, 2014, 16, 23584-23593.	1.3	111
16908	Trends in electrochemical CO2 reduction activity for open and close-packed metal surfaces. Physical Chemistry Chemical Physics, 2014, 16, 4720.	1.3	375
16909	Decomposition mechanism of methylamine to hydrogen cyanide on Pt(111): selectivity of the Câ€“H, Nâ€“H and Câ€“N bond scissions. RSC Advances, 2014, 4, 12266.	1.7	19
16910	Stacking interactions of nickel bis(dithiolene) with graphene and beyond. RSC Advances, 2014, 4, 13361.	1.7	9

#	Article	IF	Citations
16911	Insight into the general rule for the activation of the Xâ€“H bonds (X = C, N, O, S) induced by chemisorbed oxygen atoms. Physical Chemistry Chemical Physics, 2014, 16, 2621.	1.3	40
16912	A first-principles study of the spin transport properties of a 4H-TAHDI-based multifunctional spintronic device with graphene nanoribbon electrodes. Journal of Materials Chemistry C, 2014, 2, 6648-6654.	2.7	30
16913	Theoretical predictions of the structural, mechanical and lattice dynamical properties of XW2(Xâ€‰=â€‰Zr,) Tj ETQq0 0 0 rgBT /Overl	0.7	21
16914	Modulated T carbon-like carbon allotropes: an ab initio study. RSC Advances, 2014, 4, 17364.	1.7	29
16915	Computational screening of structural and compositional factors for electrically conductive coordination polymers. Physical Chemistry Chemical Physics, 2014, 16, 14463-14472.	1.3	23
16916	Transition metal-doped BiFeO₃nanofibers: forecasting the conductivity limit. Physical Chemistry Chemical Physics, 2014, 16, 23089-23095.	1.3	15
16917	Phase stability and elastic properties of (W0.5Al0.5)C phase with a novel NiAs-type structure. RSC Advances, 2014, 4, 42585-42590.	1.7	0
16918	Polycrystalline boron nitride constructed from hexagonal boron nitride. RSC Advances, 2014, 4, 38589-38593.	1.7	7
16919	Interfacial Interactions of Semiconductor with Graphene and Reduced Graphene Oxide: CeO₂ as a Case Study. ACS Applied Materials & Interfaces, 2014, 6, 20350-20357.	4.0	71
16920	A DFT study of the structures, stabilities and redox behaviour of the major surfaces of magnetite Fe₃O₄. Physical Chemistry Chemical Physics, 2014, 16, 21082-21097.	1.3	178
16921	Formation of nickelâ€“carbon heterofullerenes under electron irradiation. Dalton Transactions, 2014, 43, 7499-7513.	1.6	12
16922	Enhancing the hydrogen storage capacity of TiFe by utilizing clusters. Physical Chemistry Chemical Physics, 2014, 16, 16765.	1.3	12
16923	Adsorption properties of nitrogen dioxide on hybrid carbon and boron-nitride nanotubes. Physical Chemistry Chemical Physics, 2014, 16, 22853-22860.	1.3	31
16924	Induced work function changes at Mg-doped MgO/Ag(001) interfaces: Combined Auger electron diffraction and density functional study. Physical Review B, 2014, 90, .	1.1	15
16925	High throughput exploration of ZrxSi1â^'xO2 dielectrics by evolutionary first-principles approaches. Physics Letters, Section A: General, Atomic and Solid State Physics, 2014, 378, 3549-3553.	0.9	7
16926	Hydrogen generation by water splitting on hematite (0001) surfaces: first-principles calculations. Physical Chemistry Chemical Physics, 2014, 16, 25442-25448.	1.3	32
16927	Ba2B10O17: a new centrosymmetric alkaline-earth metal borate with a deep-UV cut-off edge. Dalton Transactions, 2014, 43, 8905-8910.	1.6	44
16928	Novel heterostructures by stacking layered molybdenum disulfides and nitrides for solar energy conversion. Journal of Materials Chemistry A, 2014, 2, 15389-15395.	5.2	87

#	Article	IF	Citations
16929	Improved permeability and selectivity in porous graphene for hydrogen purification. Physical Chemistry Chemical Physics, 2014, 16, 25755-25759.	1.3	39
16930	Impact of bonding at multi-layer graphene/metal Interfaces on thermal boundary conductance. RSC Advances, 2014, 4, 35852-35861.	1.7	47
16931	Role of vacancies to p-type semiconducting properties of SiGe nanowires. Journal of Materials Chemistry C, 2014, 2, 6536-6546.	2.7	5
16932	Role of MoO₃ on a Rhodium Catalyst in the Selective Hydrogenolysis of Biomass-Derived Tetrahydrofurfuryl Alcohol into 1,5-Pentanediol. Journal of Physical Chemistry C, 2014, 118, 25555-25566.	1.5	63
16933	A novel model for the (âˆš3 Ã— âˆš3)R30Â° alkanethiolateâ€“Au(111) phase based on alkanethiolateâ€“Au adatom complexes. Physical Chemistry Chemical Physics, 2014, 16, 19017.	1.3	13
16935	Ab Initio Study of Water Related Defects in Cr₂O₃and the Consequences for the Stability of Passive Films of Stainless Steels. Journal of the Electrochemical Society, 2014, 161, C486-C493.	1.3	11
16936	Electron spin-polarization and spin lattices in the boron- and nitrogen-doped organic framework COF-5. Physical Chemistry Chemical Physics, 2014, 16, 23286-23291.	1.3	17
16937	Density functional theory study on the full ALD process of silicon nitride thin film deposition via BDEAS or BTBAS and NH₃. Physical Chemistry Chemical Physics, 2014, 16, 18501.	1.3	28
16938	Experimental and Theoretical Analysis of Fast Lithium Ionic Conduction in a LiBH₄â€“C₆₀ Nanocomposite. Journal of Physical Chemistry C, 2014, 118, 21755-21761.	1.5	21
16939	Thermodynamic and Kinetic Analyses of the CO₂ Chemisorption Mechanism on Na₂TiO₃: Experimental and Theoretical Evidences. Journal of Physical Chemistry C, 2014, 118, 19822-19832.	1.5	37
16940	Ab initio calculations of SrTiO₃, BaTiO₃, PbTiO₃, CaTiO₃, SrZrO₃, PbZrO₃ and BaZrO₃ (001), (011) and (111) surfaces as well as F centers, polarons, KTN solid solutions and Nb impurities therein. International Journal of Modern Physics B, 2014, 28, 1430009.	1.0	98
16941	High ZT in p-Type (PbTe)_{1â€“2x}(PbSe)_x(PbS)_x Thermoelectric Materials. Journal of the American Chemical Society, 2014, 136, 3225-3237.	6.6	228
16942	A hybrid continuum and molecular mechanics model for the axial buckling of chiral single-walled carbon nanotubes. Current Applied Physics, 2014, 14, 1360-1368.	1.1	21
16943	Electron correlation effects in diamond: A wave-function quantum-chemistry study of the quasiparticle band structure. Physical Review B, 2014, 89, .	1.1	4
16944	Hidden Thermodynamic Ground State of Calcium Diazenide. Journal of Physical Chemistry C, 2014, 118, 650-656.	1.5	8
16945	Prediction on the Surface Phase Diagram and Growth Morphology of Nanocrystal Ruthenium Dioxide. Journal of the American Ceramic Society, 2014, 97, 3702-3709.	1.9	11
16946	Low-Temperature Phase Transition in Crystalline Aripiprazole Leads to an Eighth Polymorph. Crystal Growth and Design, 2014, 14, 5004-5010.	1.4	33
16947	Meta-Positioning of Carbonitrile Functional Groups Induces Interfacial Edge-On Phase of Oligophenyl Derivatives. Journal of Physical Chemistry C, 2014, 118, 2622-2633.	1.5	6

#	Article	IF	Citations
16948	Periodic DFT and Atomistic Thermodynamic Modeling of Reactivity of H₂, O₂, and H₂O Molecules on Bare and Oxygen Modified ZrC (100) Surface. Journal of Physical Chemistry C, 2014, 118, 12952-12961.	1.5	19
16949	One- and two-particle effects in the electronic and optical spectra of barium fluoride. Journal of Physics Condensed Matter, 2014, 26, 125501.	0.7	6
16950	Density functional theory studies of the electronic and magnetic structure of GdxSr1â^'xFeO3 perovskite alloys. Materials Science in Semiconductor Processing, 2014, 27, 810-818.	1.9	1
16951	Full Color Emission in ZnGa₂O₄: Simultaneous Control of the Spherical Morphology, Luminescent, and Electric Properties via Hydrothermal Approach. Advanced Functional Materials, 2014, 24, 6581-6593.	7.8	82
16952	DFT +Uinvestigation of charged point defects and clusters in UO₂. Journal of Physics Condensed Matter, 2014, 26, 325501.	0.7	43
16953	Study of the interaction of solutes with Î£5 (013) tilt grain boundaries in iron using density-functional theory. Journal of Applied Physics, 2014, 115, .	1.1	71
16954	Real space pseudopotential calculations for size trends in Ga- and Al-doped zinc oxide nanocrystals with wurtzite and zincblende structures. Journal of Chemical Physics, 2014, 141, 094309.	1.2	7
16955	An effective method of tuning conducting properties: First-principles studies on electronic structures of graphene nanomeshes. Carbon, 2014, 79, 646-653.	5.4	18
16956	First-principles calculations of the indigo encapsulation and adsorption by MgO nanotubes. Journal of Applied Physics, 2014, 115, 213507.	1.1	2
16957	Theoretical Study of the Deposition of Pt Clusters on Defective Hexagonal Boron Nitride (h-BN) Sheets: Morphologies, Electronic Structures, and Interactions with O. Journal of Physical Chemistry C, 2014, 118, 8868-8876.	1.5	45
16958	A hybrid DFT based investigation of the photocatalytic activity of cationâ€“anion codoped SrTiO₃ for water splitting under visible light. Physical Chemistry Chemical Physics, 2014, 16, 24527-24535.	1.3	40
16959	Asymmetric Environmental Effects on the Structure and Vibrations ofcis-[Pt(NH3)2Cl2] in Condensed Phases. Journal of Physical Chemistry B, 2014, 118, 11487-11495.	1.2	9
16960	Tunable Indirect to Direct Band Gap Transition of Monolayer Sc₂CO₂ by the Strain Effect. ACS Applied Materials & Interfaces, 2014, 6, 14724-14728.	4.0	175
16961	Pressureâ€induced sp ferromagnetism in electrideâ€like elemental potassium from firstâ€principles. Physica Status Solidi (B): Basic Research, 2014, 251, 527-532.	0.7	9
16962	Electron-Deficient Telluride Cs₃Cu₂₀Te₁₃ with Sodalite-Type Network: Syntheses, Structures, and Physical Properties. Inorganic Chemistry, 2014, 53, 5575-5580.	1.9	20
16963	First Principles Calculations on Crystal and Electronic Structure of Co2P4O12. Integrated Ferroelectrics, 2014, 156, 115-121.	0.3	3
16964	CO₂ Adsorption Thermodynamics over N-Substituted/Grafted Graphanes: A DFT Study. Langmuir, 2014, 30, 1837-1844.	1.6	30
16965	Effects of enhanced electronic correlation on magnetic properties of light non-metallic element (B,) Tj ETQq1 1 0.784314 rgBT /Overlo State Physics, 2014, 378, 3001-3005.	0.9	9

#	Article	IF	Citations
16966	Pressure-induced magnetic, structural, and electronic phase transitions in LaFeO3: A density functional theory (generalized gradient approximation)â€‰+â€‰U study. Journal of Applied Physics, 2014, 116, .	1.1	17
16967	The hydrogen adsorption on Zr-decorated LiB (001): A DFT study. Vacuum, 2014, 110, 62-68.	1.6	14
16968	Tungsten Carbide Supports for Single-Atom Platinum-Based Fuel-Cell Catalysts: First-Principles Study on the Metalâ€“Support Interactions and O₂ Dissociation on W_xC Low-Index Surfaces. Journal of Physical Chemistry C, 2014, 118, 13525-13538.	1.5	54
16969	Theoretical Predictions of Freestanding Honeycomb Sheets of Cadmium Chalcogenides. Journal of Physical Chemistry C, 2014, 118, 16236-16245.	1.5	48
16970	Combination study of DFT calculation and experiment for photocatalytic properties of S-doped anatase TiO2. Applied Surface Science, 2014, 319, 50-59.	3.1	51
16971	Role of oxygen vacancies in room-temperature ferromagnetism in cobalt-substituted<mml:math xmlns:mml="http://www.w3.org/1998/Math/MathML"><mml:msub><mml:mi>SrTiO</mml:mi><mml:mn>3</mml:mn></mml:msub><m Physical Review B, 2014, 90, .	1.1	14
16972	First-principles calculations of structural, electronic, and thermodynamic properties of ZnO _{1â" x} S _x alloys. Chinese Physics B, 2014, 23, 106108.	0.7	12
16973	Identification of oxygen defects in CdTe revisited: First-principles study. Journal of Applied Physics, 2014, 115, 203511.	1.1	5
16974	Structural, bonding and elastic properties of Mg(NH2BH3)2, Ca(NH2BH3)2 and Sr(NH2BH3)2. Materials Chemistry and Physics, 2014, 148, 364-370.	2.0	4
16975	Characteristics of p-type Mg-doped GaS and GaSe nanosheets. Physical Chemistry Chemical Physics, 2014, 16, 18799.	1.3	44
16976	Excitons in anisotropic two-dimensional semiconducting crystals. Physical Review B, 2014, 90, .	1.1	136
16977	Nanograined Halfâ€Heusler Semiconductors as Advanced Thermoelectrics: An Ab Initio Highâ€Throughput Statistical Study. Advanced Functional Materials, 2014, 24, 7427-7432.	7.8	117
16978	Photocarrier relaxation pathway in two-dimensional semiconducting transition metal dichalcogenides. Nature Communications, 2014, 5, 4543.	5.8	372
16979	Structural, Magnetic, Electronic, Defect, and Diffusion Properties of Cr₂O₃: A DFT+U Study. Journal of Physical Chemistry C, 2014, 118, 18133-18145.	1.5	66
16980	Role of van der Waals Forces in Thermodynamics and Kinetics of Layered Transition Metal Oxide Electrodes: Alkali and Alkaline-Earth Ion Insertion into V₂O₅. Journal of Physical Chemistry C, 2014, 118, 19599-19607.	1.5	79
16981	Role of edge geometry and chemistry in the electronic properties of graphene nanostructures. Faraday Discussions, 2014, 173, 173-199.	1.6	58
16982	Major Difference in Visible-Light Photocatalytic Features between Perfect and Self-Defective Ta₃N₅ Materials: A Screened Coulomb Hybrid DFT Investigation. Journal of Physical Chemistry C, 2014, 118, 20784-20790.	1.5	39
16983	Initial Assessment of an Empirical Potential as a Portable Tool for Rapid Investigation of Li⁺ Diffusion in Li⁺-Battery Cathode Materials. Journal of Physical Chemistry C, 2014, 118, 11203-11214.	1.5	12

#	Article	IF	Citations
16984	First-principles studies of hydrogen behavior interacting with oxygen-enriched nanostructured particles in the ODS steels. International Journal of Hydrogen Energy, 2014, 39, 18506-18519.	3.8	7
16985	Electron-phonon couplings and carrier mobility in graphynes sheet calculated using the Wannier-interpolation approach. Journal of Chemical Physics, 2014, 141, 034704.	1.2	82
16986	Effect of Interstitial Si on Different Boron Nitride Allotropes. Journal of Physical Chemistry C, 2014, 118, 20264-20274.	1.5	1
16987	Graphene spintronics: Spin injection and proximity effects from first principles. Physical Review B, 2014, 90, .	1.1	43
16988	Impact of microscopic bonding on the thermal stability and mechanical property of CaB6: A first-principles investigation. Ceramics International, 2014, 40, 15997-16002.	2.3	12
16989	Phonons, lithium diffusion and thermodynamics of LiMPO₄(M = Mn, Fe). Journal of Materials Chemistry A, 2014, 2, 14729-14738.	5.2	13
16990	First-principles calculation on oxygen ion migration in alkaline-earth doped La₂GeO₅. Journal of Physics Condensed Matter, 2014, 26, 255503.	0.7	1
16991	Thermodynamic evaluation of the Npâ€“Zr system using CALPHAD and ab initio methods. Journal of Nuclear Materials, 2014, 452, 569-577.	1.3	9
16992	Ab initio study of the intermetallics in Nbâ€“Si binary system. Intermetallics, 2014, 54, 125-132.	1.8	69
16993	Ground state, phonon spectrum, and superconducting properties of the cubic inverse perovskite CuNNi 3. Physica C: Superconductivity and Its Applications, 2014, 507, 10-16.	0.6	8
16994	One-step synthesis of graphene/polyaniline hybrids by in situ intercalation polymerization and their electromagnetic properties. Nanoscale, 2014, 6, 8140-8148.	2.8	221
16995	New superconductor (Na 0.25 K 0.45) Ba 3 Bi 4 O 12 : A first-principles study. Physica C: Superconductivity and Its Applications, 2014, 506, 53-58.	0.6	22
16996	Improving the stability and optical properties of germanane via one-step covalent methyl-termination. Nature Communications, 2014, 5, 3389.	5.8	201
16997	Effects of Chlorine in Titanium Oxide on Palladium Atomic Layer Deposition. Journal of Physical Chemistry C, 2014, 118, 22611-22619.	1.5	24
16998	First-principles materials applications and design of nonlinear optical crystals. Journal Physics D: Applied Physics, 2014, 47, 253001.	1.3	201
16999	Single Molecule Rectification Induced by the Asymmetry of a Single Frontier Orbital. Journal of Chemical Theory and Computation, 2014, 10, 3393-3400.	2.3	36
17000	Strain-Controllable Magnetism in Co Decorated Pyridinic N-Doped Graphene. IEEE Transactions on Magnetics, 2014, 50, 1-4.	1.2	3
17001	Extended x-ray absorption fine structure spectroscopy and first-principles study of SnWO₄. Physica Scripta, 2014, 89, 044005.	1.2	9

#	Article	IF	Citations
17002	First principles investigation of the conversion of N2O and CO to N2 and CO2 on a modified N + Fe/TiO2 (101) surface. RSC Advances, 2014, 4, 17896.	1.7	2
17003	Study of Phase Stability and Hydride Diffusion Mechanism of BaTiO₃ Oxyhydride from First-Principles. Journal of Physical Chemistry C, 2014, 118, 17254-17259.	1.5	31
17004	Electrical and lithium ion dynamics in Li₂IrO₃ from density functional theory study. RSC Advances, 2014, 4, 42462-42466.	1.7	7
17005	Resistance to sulfur poisoning of the gold doped nickel/yttria-stabilized zirconia with interface oxygen vacancy. Journal of Power Sources, 2014, 271, 516-521.	4.0	13
17006	Monoethanolamine Adsorption on TiO2(110): Bonding, Structure, and Implications for Use as a Model Solid-Supported CO2 Capture Material. Journal of Physical Chemistry C, 2014, 118, 1576-1586.	1.5	15
17007	Theoretical research on optical properties and quantum efficiency of Ga1â^'Al N photocathodes. Optik, 2014, 125, 4906-4910.	1.4	0
17008	Role of oxygen in Cu(1 1 0) surface restructuring in the vicinity of step edges. Chemical Physics Letters, 2014, 613, 64-69.	1.2	15
17009	Electronic and thermodynamic properties of Î± -Pu 2 O 3. Physics Letters, Section A: General, Atomic and Solid State Physics, 2014, 378, 3060-3065.	0.9	16
17010	Ab initiostudy of structural and electronic properties of partially reduced graphene oxide. Physica Scripta, 2014, T162, 014019.	1.2	9
17011	Thermodynamic phase diagram and electronic properties of Co₂VAlâ€˜001â€‰ film: A first-principles study. International Journal of Modern Physics B, 2014, 28, 1450145.	1.0	9
17012	On the origin of anisotropic lithiation in crystalline silicon over germanium: A first principles study. Applied Surface Science, 2014, 323, 78-81.	3.1	14
17013	Catalytic propane reforming mechanism over Zr-doped CeO₂(111). Catalysis Science and Technology, 2014, 4, 3278.	2.1	12
17014	Negative thermal expansion in TiF3 from the first-principles prediction. Physics Letters, Section A: General, Atomic and Solid State Physics, 2014, 378, 2906-2909.	0.9	14
17015	Ionic Liquid Chiral Resolution: Methyl 2-Ammonium Chloride Propanoate on Al(854)^S Surface. Journal of Physical Chemistry C, 2014, 118, 1568-1575.	1.5	3
17016	Theoretical Insights on the C2Hy Formation Mechanism During CH4 Dissociation on Cu(100) Surface. Journal of Physical Chemistry C, 2014, 118, 17662-17669.	1.5	3
17017	High-Pressure Raman Scattering of CaWO₄ Up to 46.3 GPa: Evidence of a New High-Pressure Phase. Inorganic Chemistry, 2014, 53, 9729-9738.	1.9	29
17018	Ab initio study of Fermi surface and dynamical properties of Ni2XAl (X = Ti, V, Zr, Nb, Hf and Ta). Journal of Alloys and Compounds, 2014, 616, 527-534.	2.8	34
17019	A Density Functional Tight Binding Model with an Extended Basis Set and Three-Body Repulsion for Hydrogen under Extreme Thermodynamic Conditions. Journal of Physical Chemistry A, 2014, 118, 5520-5528.	1.1	18

#	Article	IF	Citations
17020	Phase transition, lattice dynamical and thermodynamic properties of yttrium antimonide with the rock salt structure under high pressure: first-principles investigations. High Pressure Research, 2014, 34, 78-88.	0.4	1
17021	Charge and magnetic states of Mn-, Fe-, and Co-doped monolayer MoS2. Journal of Applied Physics, 2014, 116, .	1.1	92
17022	Joint first-principles/continuum calculations of electromechanical properties of MoS2 monolayer. Applied Physics Letters, 2014, 105, 061910.	1.5	1
17023	First-principles calculations of electronic and optical properties of C-doped and F, C-codoped cubic ZrO 2. Journal of Alloys and Compounds, 2014, 617, 86-92.	2.8	6
17024	Density Functional Theory Calculations and Analysis of Reaction Pathways for Reduction of Nitric Oxide by Hydrogen on Pt(111). ACS Catalysis, 2014, 4, 3307-3319.	5.5	93
17025	Structural and electronic properties of the adsorbed and defected Cu nanowires: A density-functional theory study. Physica B: Condensed Matter, 2014, 454, 110-114.	1.3	4
17026	Theoretical Investigation of H₂ Oxidation on the Sr₂Fe_{1.5}Mo_{0.5}O₆ (001) Perovskite Surface under Anodic Solid Oxide Fuel Cell Conditions. Journal of the American Chemical Society, 2014, 136, 8374-8386.	6.6	68
17027	Structure of Intermediate Phase II of LiNH₂ under High Pressure. Journal of Physical Chemistry B, 2014, 118, 9991-9996.	1.2	5
17028	Nanotubes With Well-Defined Structure: Single- and Double-Walled Imogolites. Journal of Physical Chemistry C, 2014, 118, 5945-5953.	1.5	45
17029	Pressure evolution of two polymorphs of Tb2(MoO4)3. High Pressure Research, 2014, 34, 184-190.	0.4	3
17030	Temperature and composition dependence of short-range order and entropy, and statistics of bond length: the semiconductor alloy (GaN)_{1â^'x}(ZnO)_x. Journal of Physics Condensed Matter, 2014, 26, 274204.	0.7	3
17031	DFT study on effect of CO on the system of acetoxylation of ethylene to vinyl acetate. RSC Advances, 2014, 4, 17709.	1.7	7
17032	First-principles study of full a-dislocations in pure magnesium. Journal of Applied Mechanics and Technical Physics, 2014, 55, 672-681.	0.1	3
17033	Stability of the hcp Ruthenium at high pressures from first principles. Journal of Applied Physics, 2014, 116, .	1.1	15
17034	Self-Organized Overlayers Formed by Alanine on Cu{311} Surfaces. Journal of Physical Chemistry C, 2014, 118, 18589-18603.	1.5	14
17035	Hydrogen adsorption on the Î±-graphyne using ab initio calculations. Superlattices and Microstructures, 2014, 75, 340-346.	1.4	16
17036	A promising new nonlinear optical crystal with high laser damage threshold for application in the IR region: synthesis, crystal structure and properties of noncentrosymmetric CsHgBr₃. Journal of Materials Chemistry C, 2014, 2, 6796-6801.	2.7	20
17037	Spin-polarized investigation of ferromagnetism on magnetic semiconductors Mn x Ca 1â^'x S in the rock-salt phase. Materials Chemistry and Physics, 2014, 148, 1000-1007.	2.0	10

#	Article	IF	Citations
17038	Carbon-rich icosahedral boron carbide designed from first principles. Applied Physics Letters, 2014, 105, .	1.5	31
17039	Two dimensional Dirac carbon allotropes from graphene. Nanoscale, 2014, 6, 1113-1118.	2.8	198
17040	Investigation of the bulk and surface properties of CdSe: insights from theory. Physical Chemistry Chemical Physics, 2014, 16, 23251-23259.	1.3	17
17041	Spin-filtering, giant magnetoresistance, rectifying and negative differential resistance effects in planar four-coordinate Fe complex with graphene nanoribbon electrodes. Journal of Chemical Physics, 2014, 140, 044311.	1.2	27
17042	Antiferroelectricity in thin-film<mml:math xmlns:mml="http://www.w3.org/1998/Math/MathML"><mml:msub><mml:mrow><mml:mi mathvariant="normal">ZrO</mml:mi></mml:mrow><mml:mn>2</mml:mn></mml:msub></mml:math>from first principles. Physical Review B, 2014, 90, .	1.1	205
17043	Bulk ionization potentials and band alignments from three-dimensional periodic calculations as demonstrated on rocksalt oxides. Physical Review B, 2014, 90, .	1.1	33
17044	The adsorption of H 2 on Fe-coated C 5 H 5 and its application in hydrogen storage. International Journal of Hydrogen Energy, 2014, 39, 19621-19629.	3.8	5
17045	Density Functional Theory Study of the Adsorption of Hydrazine on the Perfect and Defective Copper (100), (110), and (111) Surfaces. Journal of Physical Chemistry C, 2014, 118, 26103-26114.	1.5	58
17046	First principles investigations on the electronic structure of anchor groups on ZnO nanowires and surfaces. Journal of Applied Physics, 2014, 115, .	1.1	16
17047	CO Oxidation on the Pd(111) Surface. ACS Catalysis, 2014, 4, 3435-3443.	5.5	62
17048	Adsorption of CO Molecules on Si(001) at Room Temperature. Journal of Physical Chemistry C, 2014, 118, 21463-21468.	1.5	5
17049	Optical characteristics of an epitaxial Fe3Si/Si(111) iron silicide film. JETP Letters, 2014, 99, 565-569.	0.4	9
17050	Group-IV nanosheets with vacancies: a tight-binding extended HÃ¼ckel study. Journal of Physics Condensed Matter, 2014, 26, 365501.	0.7	9
17051	Solar Energy Storage in Phase Change Materials: First-Principles Thermodynamic Modeling of Magnesium Chloride Hydrates. Journal of Physical Chemistry C, 2014, 118, 4618-4625.	1.5	44
17052	Theoretical and experimental studies of electronic band structure for GaSb1âˆ'xBix in the dilute Bi regime. Journal Physics D: Applied Physics, 2014, 47, 355107.	1.3	50
17053	New Insights into the Structure of the C-Terminated Î²-Mo₂C (001) Surface from First-Principles Calculations. Journal of Physical Chemistry C, 2014, 118, 19224-19231.	1.5	13
17054	Ab initiostudy of multiferroic<mml:math xmlns:mml="http://www.w3.org/1998/Math/MathML"><mml:mi>Bi</mml:mi><mml:mi>Fe</mml:mi><mml:msub><mml:mi mathvariant="normal">O</mml:mi><mml:mn>3</mml:mn></mml:msub></mml:math>(110) surfaces. Physical Review B, 2014, 89, .	1.1	16
17055	Oxygenâ€Terminated Diamond Electrodes in Alkaline Media: Structure and OH Generation. ChemElectroChem, 2014, 1, 933-939.	1.7	11

#	Article	IF	Citations
17056	Density functional theory study of carbon dioxide electrochemical reduction on the Fe(100) surface. Physical Chemistry Chemical Physics, 2014, 16, 13708-13717.	1.3	25
17057	Hydrogen adsorption and diffusion around Si(0â€‰0â€‰1)/Si(1â€‰1â€‰0) corners in nanostructures. Journal of Physics Condensed Matter, 2014, 26, 295301.	0.7	2
17058	Dynamical and dielectric properties of MP2O7 (M=Ti, Zr, and Hf): A first-principles investigation. Computational Materials Science, 2014, 95, 371-376.	1.4	8
17059	Alloying InAs and InP nanowires for optoelectronic applications: A first principles study. Physics Letters, Section A: General, Atomic and Solid State Physics, 2014, 378, 2872-2875.	0.9	3
17060	Fluorite TiO₂(111) Surface Phase for Enhanced Visible-Light Solar Energy Conversion. Journal of Physical Chemistry C, 2014, 118, 20107-20111.	1.5	15
17061	Optical and magnetic properties of Ba₅(BO₃)₃F single crystals. Physical Chemistry Chemical Physics, 2014, 16, 24884-24891.	1.3	9
17062	Phosphorus vacancy cluster model for phosphorus diffusion gettering of metals in Si. Journal of Applied Physics, 2014, 115, 054906.	1.1	24
17063	Visibility of Al Surface Sites of Î³-Alumina: A Combined Computational and Experimental Point of View. Journal of Physical Chemistry C, 2014, 118, 15292-15299.	1.5	97
17064	A first-principles investigation of the stabilities and electronic properties of SrZrO₃(1â€‰1â€‰0) (1â€‰Ã— â€‰1) polar terminations. Journal of Physics Condensed Matter, 2014, 26, 395002.	0.7	13
17065	High-Pressure Studies of Bi₂S₃. Journal of Physical Chemistry A, 2014, 118, 1713-1720.	1.1	81
17066	Covalent-bonded graphyne polymers with high hardness. Journal of Superhard Materials, 2014, 36, 257-269.	0.5	13
17067	A Novel Superhard Tetragonal Carbon Mononitride. Journal of Physical Chemistry C, 2014, 118, 3202-3208.	1.5	32
17068	Tweaking the magnetism of MoS2 nanoribbon with hydrogen and carbon passivation. Nanotechnology, 2014, 25, 165703.	1.3	20
17069	Electronic and Magnetic Properties of Vanadium Dichalcogenides Monolayers Tuned by Hydrogenation. Journal of Physical Chemistry C, 2014, 118, 13248-13253.	1.5	109
17070	Stability and mobility of screw dislocations in 4H, 2H and 3C silicon carbide. Acta Materialia, 2014, 78, 236-244.	3.8	47
17071	Epitaxial strain and composition-dependent magnetic properties of<mml:math xmlns:mml="http://www.w3.org/1998/Math/MathML"><mml:mrow><mml:msub><mml:mi>Mn</mml:mi><mml:mi>x</mml:mi></mml:msub></mml:mrow></mml:math> Physical Review B, 2014, 90, .	1.1	26
17072	On a new FeOF polymorph: Synthesis and stability. Solid State Sciences, 2014, 38, 55-61.	1.5	6
17073	Interplay between Oxidized Monovacancy and Nitrogen Doping in Graphene. Journal of Physical Chemistry C, 2014, 118, 19795-19805.	1.5	11

#	Article	IF	Citations
17074	Why Are Diphenylalanine-Based Peptide Nanostructures so Rigid? Insights from First Principles Calculations. Journal of the American Chemical Society, 2014, 136, 963-969.	6.6	136
17075	Contribution of interstitial solute strengthening in aluminum. Philosophical Magazine Letters, 2014, 94, 63-71.	0.5	14
17076	Transition between direct gap and indirect gap in two dimensional hydrogenated honeycomb Si x Ge1â^'x alloys. Theoretical Chemistry Accounts, 2014, 133, 1.	0.5	6
17077	The Role of Hydrogen on the Adsorption Behavior of Carboxylic Acid on TiO₂ Surfaces. Journal of Physical Chemistry C, 2014, 118, 10771-10779.	1.5	28
17078	First-Principles Comparative Study of the Electronic and Optical Properties of Tetragonal (P4mm) ATiO₃ (A = Pb,Sn,Ge). Integrated Ferroelectrics, 2014, 155, 23-32.	0.3	23
17079	The effects of alloying and segregation for the reactivity and diffusion of oxygen on Cu₃Au(111). Physical Chemistry Chemical Physics, 2014, 16, 19702.	1.3	14
17080	First-principles studies on vacancy-modified interstitial diffusion mechanism of oxygen in nickel, associated with large-scale atomic simulation techniques. Journal of Applied Physics, 2014, 115, .	1.1	33
17081	Phase transition, elastic and thermodynamical properties of TcC under high pressure from first-principles calculations. Physica Status Solidi (B): Basic Research, 2014, 251, 1372-1379.	0.7	6
17082	Syntheses, structures, optical properties, and electronic structures of KBaMSe 3 (M = As, Sb). Journal of Alloys and Compounds, 2014, 617, 287-291.	2.8	19
17083	A₂BiI₅O₁₅(A = K⁺or Rb⁺): two new promising nonlinear optical materials containing [I₃O₉]^{3â^'}bridging anionic groups. Journal of Materials Chemistry C, 2014, 2, 4057-4062.	2.7	59
17084	Nickelâ€“silver alloy electrocatalysts for hydrogen evolution and oxidation in an alkaline electrolyte. Physical Chemistry Chemical Physics, 2014, 16, 19250.	1.3	101
17085	Ab Initio Thermodynamic Model for Magnesium Carbonates and Hydrates. Journal of Physical Chemistry A, 2014, 118, 7469-7488.	1.1	56
17086	The simulated vibrational spectra of HfO₂ polymorphs. Journal Physics D: Applied Physics, 2014, 47, 115502.	1.3	44
17087	Modelling copper-phthalocyanine/cobalt-phthalocyanine chains: towards magnetic quantum metamaterials. Journal of Physics Condensed Matter, 2014, 26, 296002.	0.7	6
17088	Origin of Poor Cyclability in Li₂MnSiO₄ from First-Principles Calculations: Layer Exfoliation and Unstable Cycled Structure. Chemistry of Materials, 2014, 26, 3896-3899.	3.2	45
17089	Copper Deficiency in the p-Type Semiconductor Cu_{1â€“x}Nb₃O₈. Chemistry of Materials, 2014, 26, 2095-2104.	3.2	35
17090	Tunable band gaps in graphene/GaN van der Waals heterostructures. Journal of Physics Condensed Matter, 2014, 26, 295304.	0.7	17
17091	Ab Initio Calculations of the Main Crystal Surfaces of Forsterite (Mg₂SiO₄): A Preliminary Study to Understand the Nature of Geochemical Processes at the Olivine Interface. Journal of Physical Chemistry C, 2014, 118, 2498-2506.	1.5	48

#	Article	IF	Citations
17092	First-principles calculation of the indentation strength of<mml:math xmlns:mml="http://www.w3.org/1998/Math/MathML"><mml:msub><mml:mi mathvariant="normal">FeB</mml:mi><mml:mn>4</mml:mn></mml:msub></mml:math>. Physical Review B, 2014, 90, .	1.1	36
17093	The role of oxygen during the catalytic oxidation of ammonia on Co 3 O 4 (1 0 0). Applied Surface Science, 2014, 316, 355-365.	3.1	18
17094	First-principle calculations of the electronic, elastic and thermoelectric properties of Ag doped CuGaTe2. Intermetallics, 2014, 55, 204-209.	1.8	17
17095	Semiconducting ferroelectric perovskites with intermediate bands via<mml:math xmlns:mml="http://www.w3.org/1998/Math/MathML"><mml:mi>B</mml:mi></mml:math>-site<mml:math xmlns:mml="http://www.w3.org/1998/Math/MathML"><mml:msup><mml:mi mathvariant="normal">Bi</mml:mi><mml:mrow><mml:mn>5</mml:mn><mml:mo>+</mml:mo></mml:mrow></mml:msup></mml:m Physical Review B, 2014, 90, .	1.1	23
17096	Phase transition and thermodynamic properties of ThO 2 : Quasi-harmonic approximation calculations and anharmonic effects. Chinese Physics B, 2014, 23, 017101.	0.7	5
17097	Surface Modification of ITO Nanoparticles by Trimesic Acid: A Combined Experimental and DFT Study. Journal of Physical Chemistry C, 2014, 118, 21244-21249.	1.5	8
17098	Graphitic Carbon Nitride Nanotubes As Li-Ion Battery Materials: A First-Principles Study. Journal of Physical Chemistry C, 2014, 118, 9318-9323.	1.5	62
17099	Predicted roles of defects on band offsets and energetics at CIGS (Cu(In,Ga)Se2/CdS) solar cell interfaces and implications for improving performance. Journal of Chemical Physics, 2014, 141, 094701.	1.2	20
17100	Stability of Pt near surface alloys under electrochemical conditions: a model study. Physical Chemistry Chemical Physics, 2014, 16, 16615-16622.	1.3	20
17101	Band gap engineering of early transition-metal-doped anatase TiO₂: first principles calculations. Physical Chemistry Chemical Physics, 2014, 16, 21446-21451.	1.3	58
17102	First principles study of fluorine substitution on two-dimensional germanane. Journal of Physics Condensed Matter, 2014, 26, 335302.	0.7	14
17103	Investigation of electron transmission through Co/C/Co magnetic tunnel junctions. Physical Review B, 2014, 89, .	1.1	4
17104	Structural paradox in submonolayer chlorine coverage on Au(111). Physical Review B, 2014, 89, .	1.1	15
17105	Hydrogen-Induced Reconstruction of Cu(100): Two-Dimensional and One-Dimensional Structures of Surface Hydride. Journal of Physical Chemistry C, 2014, 118, 15773-15778.	1.5	13
17106	Synthesis, Structure, and Properties of the Electron-Poor IIâ€“V Semiconductor ZnAs. Inorganic Chemistry, 2014, 53, 8691-8699.	1.9	12
17107	Ab initiocalculation of the solution enthalpies of substitutional and interstitial impurities in paramagnetic fcc Fe. Physical Review B, 2014, 90, .	1.1	38
17108	Electrochemical Adsorption of OH on Pt(111) in Alkaline Solutions: Combining DFT and Molecular Dynamics. ChemPhysChem, 2014, 15, 2003-2009.	1.0	24
17109	Directional Control of the Electronic and Transport Properties of Graphynes. Journal of Physical Chemistry C, 2014, 118, 18793-18798.	1.5	18

#	Article	IF	Citations
17110	Effects of Quantum Nuclear Delocalisation on NMR Parameters from Path Integral Molecular Dynamics. Chemistry - A European Journal, 2014, 20, 2201-2207.	1.7	52
17111	Wide Range Bandgap Modulation Based on ZnO-based Alloys and Fabrication of Solar Blind UV Detectors with High Rejection Ratio. ACS Applied Materials & Interfaces, 2014, 6, 14152-14158.	4.0	55
17112	Defect induced magnetism in planar silicene: a first principles study. RSC Advances, 2014, 4, 32221.	1.7	44
17113	Metal-Free Magnetism and Half-Metallicity of Carbon Nitride Nanotubes: A First-Principles Study. Journal of Physical Chemistry C, 2014, 118, 22491-22498.	1.5	22
17114	Theoretical exploration of the half-metallicity of graphene nanoribbons/boron nitride bilayer system. Computational Materials Science, 2014, 95, 384-392.	1.4	4
17115	Elucidating Ionic Liquid Environments That Affect the Morphology of TiO₂ Nanocrystals: A DFT+D Study. Journal of Physical Chemistry C, 2014, 118, 23320-23327.	1.5	18
17116	Versatile Electronic and Magnetic Properties of SnSe₂ Nanostructures Induced by the Strain. Journal of Physical Chemistry C, 2014, 118, 9251-9260.	1.5	68
17117	Electronic structure of Zrâ€“Niâ€“Sn systems: role of clustering and nanostructures in half-Heusler and Heusler limits. Journal of Physics Condensed Matter, 2014, 26, 275501.	0.7	36
17118	An ab Initio Investigation of Proton Stability at BaZrO₃ Interfaces. Chemistry of Materials, 2014, 26, 4915-4924.	3.2	12
17119	Atomic Structure of <scp><scp>ZnO</scp></scp> Î£13 [0001]/{130} Symmetric Tilt Grain Boundary. Journal of the American Ceramic Society, 2014, 97, 617-621.	1.9	6
17120	How Organophosphonic Acid Promotes Silane Deposition onto Aluminum Surface: A Detailed Investigation on Adsorption Mechanism. Journal of Physical Chemistry C, 2014, 118, 17724-17736.	1.5	16
17121	The (100), (111) and (110) surfaces of diamond: anab initioB3LYP study. Molecular Physics, 2014, 112, 1030-1039.	0.8	55
17122	Novel three-dimensional boron nitride allotropes from compressed nanotube bundles. Journal of Materials Chemistry C, 2014, 2, 7022.	2.7	20
17123	Favored Composition Design and Atomic Structure Characterization for Ternary Alâ€“Cuâ€“Y Metallic Glasses via Proposed Interatomic Potential. Journal of Physical Chemistry B, 2014, 118, 4442-4449.	1.2	16
17124	First-principles-based optimization of electronic structures for bimetallic nanoparticles. Calphad: Computer Coupling of Phase Diagrams and Thermochemistry, 2014, 47, 144-147.	0.7	4
17125	Formation of Hydroxyl Groups at Calcium-Silicate-Hydrate (C-S-H): Coexistence of Caâ€“OH and Siâ€“OH on Wollastonite(001). Journal of Physical Chemistry C, 2014, 118, 8007-8013.	1.5	28
17126	Water-Induced Interactions between Boron-Doped Carbon Nanotubes. Journal of Physical Chemistry C, 2014, 118, 17838-17846.	1.5	5
17127	An ab-initio investigation of the effect of graphene on the strength-electron density correlation in SiC grain boundaries. Computational Materials Science, 2014, 92, 422-430.	1.4	3

#	Article	IF	Citations
17128	Effect of Al substitution on Ti, Al, and N adatom dynamics on TiN(001), (011), and (111) surfaces. Surface Science, 2014, 630, 28-40.	0.8	37
17129	Hydrogen-related phenomena due to decreases in lattice defect energiesâ€"Molecular dynamics simulations using the embedded atom method potential with pseudo-hydrogen effects. Computational Materials Science, 2014, 92, 362-371.	1.4	24
17130	Adsorption of alkali metal atoms on germanene: A first-principles study. Applied Surface Science, 2014, 314, 15-20.	3.1	57
17131	Polaron states and migration in F-doped Li2MnO3. Physics Letters, Section A: General, Atomic and Solid State Physics, 2014, 378, 2449-2452.	0.9	20
17132	First principles calculations of pentaheptite graphene and boronitrene derivatives. Computational Materials Science, 2014, 92, 395-400.	1.4	11
17133	Structure Stability and Elastic Properties of Î² Type Ti-X (X=Nb, Mo) Alloys from First-Principles Calculations. Rare Metal Materials and Engineering, 2014, 43, 553-558.	0.8	7
17134	First principles calculation on ternary stannide phase narrow band gap semiconductor Na2MgSn. Transactions of Nonferrous Metals Society of China, 2014, 24, 1853-1858.	1.7	4
17135	Trapping of oxide ions in Î´-Bi3YO6. Solid State Ionics, 2014, 264, 49-53.	1.3	9
17136	Crystal structure and free energy of Ti 2 Ni 3 precipitates in Tiâ€"Ni alloys from first principles. Computational Materials Science, 2014, 93, 46-49.	1.4	11
17137	Composition dependent phase stability of Niâ€"Mnâ€"Ga alloys studied by ab initio calculations. Journal of Alloys and Compounds, 2014, 614, 126-130.	2.8	13
17138	Effect of vacancies (O, Ti) on the interfacial bonding strength and magnetoelectricity in Fe/BaTiO 3 : A first-principles study. Computational Materials Science, 2014, 93, 6-10.	1.4	0
17139	Effects of strain on PdZn(100) for methoxide decomposition: A DFT study. Journal of Molecular Catalysis A, 2014, 393, 296-301.	4.8	2
17140	DFT characterization of cadmium doped zinc oxide for photovoltaic and solar cell applications. Solar Energy Materials and Solar Cells, 2014, 130, 6-14.	3.0	53
17141	Ferromagnetism in Cu-doped MgO: Density-functional calculations. Solid State Communications, 2014, 194, 1-5.	0.9	21
17142	Adsorption of Ni, Pd, Pt, Cu, Ag and Au on the Fe3O4(111) surface. Surface Science, 2014, 628, 141-147.	0.8	42
17143	A molecular dynamics simulation of hydrogen atoms collisions on an H-preadsorbed silica surface. Plasma Sources Science and Technology, 2014, 23, 045016.	1.3	19
17144	The New Phase [Tl₄Sb₆Se₁₀][Sn₅Sb₂Se₁₄]: A Naturally Formed Semiconducting Heterostructure with Two-Dimensional Conductance. Journal of the American Chemical Society, 2014, 136, 11079-11084.	6.6	14
17145	Non-Grotthuss proton diffusion mechanism in tungsten oxide dihydrate from first-principles calculations. Journal of Materials Chemistry A, 2014, 2, 12280.	5.2	52

#	Article	IF	Citations
17146	Surface-Induced Hybridization between Graphene and Titanium. ACS Nano, 2014, 8, 7704-7713.	7.3	38
17147	Diffusion on Demand to Control Precipitation Aging: Application to Al-Mg-Si Alloys. Physical Review Letters, 2014, 112, 225701.	2.9	132
17148	Electronic structures and optical properties of III A -doped wurtzite Mg 0.25 Zn 0.75 O. Chinese Physics B, 2014, 23, 087101.	0.7	5
17149	Critical Role of the Semiconductorâ€“Electrolyte Interface in Photocatalytic Performance for Water-Splitting Reactions Using Ta₃N₅ Particles. Chemistry of Materials, 2014, 26, 4812-4825.	3.2	98
17150	Polarization alignment, phase transition, and piezoelectricity development in polycrystalline<mml:math xmlns:mml="http://www.w3.org/1998/Math/MathML"><mml:mi>0.5Ba</mml:mi><mml:mo>(</mml:mo><mml:msub><mml:mi>Zr</mm Physical Review B, 2014, 90, .	3.7	78
17151	Generalized stacking fault energies, cleavage energies, ionicity and brittleness of Cu(Al/Ga/In)Se₂and CuGa(S/Se/Te)₂. Modelling and Simulation in Materials Science and Engineering, 2014, 22, 035002.	0.8	2
17152	Symbiotic CeH 2.73 /CeO 2 catalyst: A novel hydrogen pump. Nano Energy, 2014, 9, 80-87.	8.2	159
17153	Thermodynamic re-assessment of the Alâ€“Gd and Gdâ€“Zr systems. Thermochimica Acta, 2014, 591, 51-56.	1.2	11
17154	Density functional theory study of water interactions on Mn-doped CeO2(111) surface. Applied Surface Science, 2014, 313, 784-793.	3.1	16
17155	Theoretical investigation of novel phenothiazine-based Dâ€“Ï€â€“A conjugated organic dyes as dye-sensitizer in dye-sensitized solar cells. Computational and Theoretical Chemistry, 2014, 1045, 145-153.	1.1	19
17156	The effect of hydrogen on the mechanical properties of FeTi for hydrogen storage applications. International Journal of Hydrogen Energy, 2014, 39, 12667-12675.	3.8	24
17157	Atomic and electronic structure of tetrahedral amorphous carbon surfaces from density functional theory: Properties and simulation strategies. Carbon, 2014, 77, 1168-1182.	5.4	41
17158	Effect of lattice strain on the oxygen vacancy formation and hydrogen adsorption at CeO2(111) surface. Physics Letters, Section A: General, Atomic and Solid State Physics, 2014, 378, 2570-2575.	0.9	82
17159	Impact of short-range ordering on yield strength of high manganese austenitic steels. Materials Science & Engineering A: Structural Materials: Properties, Microstructure and Processing, 2014, 614, 122-128.	2.6	48
17160	Design of sustainable V-based hydrogen separation membranes based on grain boundary segregation. International Journal of Hydrogen Energy, 2014, 39, 12031-12044.	3.8	19
17161	A study of the spin reorientation with tâ€“e orbital hybridization in SmCrO 3. Solid State Communications, 2014, 195, 21-25.	0.9	25
17162	Theoretical study of SO 2 adsorption on goethite (1 1 0) surface. Applied Surface Science, 2014, 314, 558-563.	3.1	14
17163	Microstructure and mechanical properties of a Mo-toughened Mo3Si-based in situ nanocomposite. Vacuum, 2014, 109, 112-119.	1.6	13

#	Article	IF	Citations
17164	Structural and mechanical properties of GaAs under pressure up to 200 GPa. Solid State Communications, 2014, 195, 26-30.	0.9	15
17165	Carborane-wheeled nanocar moving on graphene/graphyne surfaces: van der Waals corrected density functional theory study. Materials Chemistry and Physics, 2014, 148, 435-443.	2.0	25
17166	Computational Investigation of NO₂ Adsorption and Reduction on Ceria and M-Doped CeO₂ (111) (M = Mn, Fe) Surfaces. Journal of Physical Chemistry C, 2014, 118, 10043-10052.	1.5	20
17167	Periodic DFT Study of Benzene Adsorption on Pd(100) and Pd(110) at Medium and Saturation Coverage. Journal of Physical Chemistry C, 2014, 118, 21483-21499.	1.5	16
17168	Collective Descriptors for the Adsorption of Sugar Alcohols on Pt and Pd(111). Journal of Physical Chemistry C, 2014, 118, 17531-17537.	1.5	23
17169	Applicability of density functional theory in reproducing accurate vibrational spectra of surface bound species. Journal of Computational Chemistry, 2014, 35, 1921-1929.	1.5	2
17170	High-Pressure Structural Stability and Optical Properties of Scheelite-type ZrGeO4 and HfGeO4 X-ray Phosphor Hosts. Journal of Physical Chemistry C, 2014, 118, 4325-4333.	1.5	11
17171	Site-Dependent Lewis Acidity of Î³-Al₂O₃ and Its Impact on Ethanol Dehydration and Etherification. Journal of Physical Chemistry C, 2014, 118, 12899-12907.	1.5	80
17172	Removal of Water Adsorbates on GaN Surfaces via Hopping Processes and with the Aid of a Pt₄ Cluster: An Ab Initio Study. Journal of Physical Chemistry C, 2014, 118, 20383-20392.	1.5	5
17173	Enhanced Fe₂O₃ Reducibility via Surface Modification with Pd: Characterizing the Synergy within Pd/Fe Catalysts for Hydrodeoxygenation Reactions. ACS Catalysis, 2014, 4, 3381-3392.	5.5	114
17174	Effect of Pressure on Elastic Constants, Generalized Stacking Fault Energy, and Dislocation Properties in Antiperovskite-Type Ni-Rich Nitrides ZnNNi3 and CdNNi3. Journal of Superconductivity and Novel Magnetism, 2014, 27, 2607-2615.	0.8	1
17175	Three New Silver Uranyl Diphosphonates: Structures and Properties. Inorganic Chemistry, 2014, 53, 2787-2796.	1.9	23
17176	Anharmonicity and finite-temperature effects on the structure, stability, and vibrational spectrum of phase III of solid molecular hydrogen. Physical Review B, 2014, 90, .	1.1	15
17177	Formation of an Organic/Metal Interface State from a Shockley Resonance. Journal of Physical Chemistry Letters, 2014, 5, 50-55.	2.1	41
17178	Gutzwiller electronic structure calculations applied to transition metals: Kinetic energy gain with ferromagnetic order in bcc Fe. Physical Review B, 2014, 90, .	1.1	15
17179	The study of the P doped silicene nanoribbons with first-principles. Computational Materials Science, 2014, 95, 429-434.	1.4	25
17180	Silica-Based Materials as Drug Adsorbents: First Principle Investigation on the Role of Water Microsolvation on Ibuprofen Adsorption. Journal of Physical Chemistry A, 2014, 118, 5801-5807.	1.1	47
17181	Fine Refinement of Solid-State Molecular Structures of Leu- and Met-Enkephalins by NMR Crystallography. Journal of Physical Chemistry B, 2014, 118, 3298-3309.	1.2	22

#	Article	IF	Citations
17182	Si segregation at Fe grain boundaries analyzed byab initiolocal energy and local stress. Journal of Physics Condensed Matter, 2014, 26, 355005.	0.7	37
17183	Surface design of alloy protection against CO-poisoning from first principles. Journal of Physics Condensed Matter, 2014, 26, 355006.	0.7	2
17184	Comparison of the stability of free-standing silicene and hydrogenated silicene in oxygen: a first principles investigation. Journal of Physics Condensed Matter, 2014, 26, 355007.	0.7	28
17185	A combined study of the equation of state of monazite-type lanthanum orthovanadate usingin situhigh-pressure diffraction andab initiocalculations. Acta Crystallographica Section B: Structural Science, Crystal Engineering and Materials, 2014, 70, 533-538.	0.5	16
17186	Theoretical Study on Equation of State of Porous Mo and Sn. Chinese Physics Letters, 2014, 31, 016402.	1.3	1
17187	SO_x Oxidation Kinetics on Pt(111) and Pd(111): First-Principles Computations Meet Microkinetic Modeling. Journal of Physical Chemistry C, 2014, 118, 6934-6940.	1.5	18
17188	Effect of Interfacial Octahedral Behavior in Ultrathin Manganite Films. Nano Letters, 2014, 14, 2509-2514.	4.5	121
17189	Defect Engineering of BiI₃ Single Crystals: Enhanced Electrical and Radiation Performance for Room Temperature Gamma-Ray Detection. Journal of Physical Chemistry C, 2014, 118, 3244-3250.	1.5	72
17190	Interactions between hydrogen and tungsten carbide: a first principles study. RSC Advances, 2014, 4, 39912.	1.7	17
17191	Digermane Deposition on Si(100) and Ge(100): from Adsorption Mechanism to Epitaxial Growth. Journal of Physical Chemistry C, 2014, 118, 482-493.	1.5	6
17192	Structural prediction, analysis and decomposition mechanism of solid M(NH2BH3)n (M = Mg, Ca and) Tj ETQq0 0 0 rgBT /Overlock 10 Tf	1.7	9
17193	Tuning the reactivity of Ru nanoparticles by defect engineering of the reduced graphene oxide support. RSC Advances, 2014, 4, 22230-22240.	1.7	20
17194	SnO2: A comprehensive review on structures and gas sensors. Progress in Materials Science, 2014, 66, 112-255.	16.0	933
17195	New Basic Insights into the Low Hot Electron Injection Efficiency of Gold-Nanoparticle-Photosensitized Titanium Dioxide. ACS Applied Materials & Interfaces, 2014, 6, 12388-12394.	4.0	36
17196	First-Principles Calculations and Electron Density Topological Analysis of Covellite (CuS). Journal of Physical Chemistry A, 2014, 118, 5823-5831.	1.1	111
17197	The elastic behavior of dense C3N4 under high pressure: First-principles calculations. Journal of Physics and Chemistry of Solids, 2014, 75, 1324-1333.	1.9	13
17198	Metal adatoms-decorated silicene as hydrogen storage media. International Journal of Hydrogen Energy, 2014, 39, 14027-14032.	3.8	72
17199	Atomic structure and physical properties of fused porphyrin nanoclusters. Journal of Porphyrins and Phthalocyanines, 2014, 18, 552-568.	0.4	2

#	Article	IF	Citations
17200	A simulation of Pd-doped SWCNTs used to detect SF 6 decomposition components under partial discharge. Applied Surface Science, 2014, 315, 196-202.	3.1	71
17201	Effect of electric field and Sn grain orientation on Cu consumption in Sn/Cu solder joint. Computational Materials Science, 2014, 95, 166-171.	1.4	5
17202	A density functional theory (DFT) study of CO2 adsorption on Mg-rich minerals by enhanced charge distribution. Computational Materials Science, 2014, 95, 181-186.	1.4	32
17203	Theoretical two-atom thick semiconducting carbon sheet. Physical Chemistry Chemical Physics, 2014, 16, 18118-18123.	1.3	19
17204	Numerical simulations and modeling of the stability of noble gas atoms in interaction with vacancies in silicon. Computational Materials Science, 2014, 95, 149-158.	1.4	10
17205	The thermodynamics of hydride precipitation: The importance of entropy, enthalpy and disorder. Acta Materialia, 2014, 79, 351-362.	3.8	59
17206	Extremely Slow Photoconductivity Response of CH₃NH₃PbI₃ Perovskites Suggesting Structural Changes under Working Conditions. Journal of Physical Chemistry Letters, 2014, 5, 2662-2669.	2.1	301
17207	Electronic and optical properties of Co-doped 3C-SiC from density functional calculations. Solid State Communications, 2014, 196, 28-31.	0.9	9
17208	Nitrogen and vanadium Co-doped TiO 2 mesosponge layers for enhancement in visible photocatalytic activity. Applied Surface Science, 2014, 315, 131-137.	3.1	27
17209	18-Electron rule inspired Zintl-like ions composed of all transition metals. Physical Chemistry Chemical Physics, 2014, 16, 20241-20247.	1.3	7
17210	Prediction of Superconductivity in 3d Transition-Metal Based Antiperovskites via Magnetic Phase Diagram. Journal of the Physical Society of Japan, 2014, 83, 054704.	0.7	11
17211	Modeling graphite under stress: Equations of state, vibrational modes, and interlayer friction. Physical Review B, 2014, 90, .	1.1	7
17212	A New Kind of Edge-Modified Spin Semiconductor in Graphene Nanoribbons. Journal of Physical Chemistry C, 2014, 118, 4475-4482.	1.5	12
17213	Mechanism of insulator-to-metal transition in heavily Nb doped anatase TiO₂. Materials Research Express, 2014, 1, 015911.	0.8	9
17214	First-principles investigation of ZnO sodalite-like cage binding onto TiO2 (001) surface and its ability for CO oxidation to CO2. Journal of Materials Science, 2014, 49, 7620-7624.	1.7	0
17215	Strain-Induced Gap Modification in Black Phosphorus. Physical Review Letters, 2014, 112, 176801.	2.9	1,303
17216	Hybrid Quantum Mechanics/Molecular Mechanics Solvation Scheme for Computing Free Energies of Reactions at Metalâ€“Water Interfaces. Journal of Chemical Theory and Computation, 2014, 10, 3354-3368.	2.3	42
17217	Density Functional Theory Study of Methanol Steam Reforming on Co(0001) and Co(111) Surfaces. Journal of Physical Chemistry C, 2014, 118, 15274-15285.	1.5	65

#	Article	IF	Citations
17218	Computational Simulation of Rare Earth Catalysis. Advances in Chemical Engineering, 2014, , 1-60.	0.5	6
17219	Precise Determination of the Threshold Diameter for a Single-Walled Carbon Nanotube To Collapse. ACS Nano, 2014, 8, 9657-9663.	7.3	43
17220	Density functional studies on (NCH)n azagraphane: activated surface for organocatalysis. Physical Chemistry Chemical Physics, 2014, 16, 19861-19865.	1.3	3
17221	Predicting and Comparing Câ€“M and Oâ€“M Bond Strengths for Adsorption on Transition Metal Surfaces. Journal of Physical Chemistry C, 2014, 118, 2666-2672.	1.5	36
17222	Pdâ€“Ir alloy as an anode material for borohydride oxidation. Journal of Power Sources, 2014, 269, 498-508.	4.0	45
17223	Structure and reactivity of zero-, two- and three-dimensional Pd supported on SrTiO3(001). Surface Science, 2014, 630, 46-63.	0.8	6
17224	Physical properties of Î±-Fe upon the introduction of H, He, C, and N. Solid State Communications, 2014, 195, 70-73.	0.9	8
17225	Exceptionally long-ranged lattice relaxation in oxygen-deficient Ta2O5. Solid State Communications, 2014, 195, 16-20.	0.9	10
17226	Structural, electronic and elastic properties of noble metal sub-nitrides M2N (M=Ru, Rh, Pd). International Journal of Refractory Metals and Hard Materials, 2014, 47, 113-123.	1.7	3
17227	Solute/impurity diffusivities in bcc Fe: A first-principles study. Journal of Nuclear Materials, 2014, 455, 354-359.	1.3	14
17228	Effects of intrinsic defects on electronic structure and optical properties of Ga-doped ZnO. Journal of Alloys and Compounds, 2014, 616, 122-127.	2.8	24
17229	Structure and stability of graphene edges in O2 and H2 environments from ab initio thermodynamics. Carbon, 2014, 78, 181-189.	5.4	15
17230	Selective oxidation of vinyl chloride on Ag2O(100), Cu2O(100), and Au2O(100) surfaces: A density functional theory study. Surface Science, 2014, 630, 116-124.	0.8	4
17231	Thermodynamic and mechanical properties of actinium and lanthanum dihydride. Journal of Alloys and Compounds, 2014, 616, 42-46.	2.8	2
17232	Modification of conductive properties of (10,0) zigzag single-walled carbon nanotubes (SWCNT) by alkali metals absorption. Journal of Molecular Structure, 2014, 1076, 49-54.	1.8	10
17233	First-principles study of structural stability and elastic properties of MgPd3 and its hydride. Journal of Magnesium and Alloys, 2014, 2, 165-174.	5.5	61
17234	Electronic structure and phase stability of plutonium hydrides: Role of Coulomb repulsion and spin-orbital coupling. International Journal of Hydrogen Energy, 2014, 39, 13255-13265.	3.8	23
17235	Ab initiomodel of optical properties of two-temperature warm dense matter. Physical Review B, 2014, 90, .	1.1	59

#	Article	IF	Citations
17236	Hydrogen storage in Li dispersed graphene with Stoneâ€“Wales defects: A first-principles study. International Journal of Hydrogen Energy, 2014, 39, 13189-13194.	3.8	50
17237	First-Principles Study of Chemical Stability of the Lithium Oxide Garnets Li₇La₃M₂O₁₂ (M = Zr, Sn, or Hf). Journal of Physical Chemistry C, 2014, 118, 17402-17406.	1.5	37
17238	Theoretical investigation of structural and thermo-mechanical properties of thoria up to 3300ÂK temperature. Solid State Sciences, 2014, 36, 35-40.	1.5	17
17239	The regeneration mechanisms of sulfurized Î± -Fe 2 O 3 surfaces under O 2 atmosphere: A density functional theory study. Fuel Processing Technology, 2014, 128, 238-250.	3.7	11
17240	Direct CO oxidation by lattice oxygen on the SnO₂(110) surface: a DFT study. Physical Chemistry Chemical Physics, 2014, 16, 12488-12494.	1.3	51
17241	Second-order phase transition at high-pressure in GeS crystal. Physica B: Condensed Matter, 2014, 454, 56-59.	1.3	3
17242	Electronic structures and optical properties of rutile TiO2 with different point defects from DFT+U calculations. Physics Letters, Section A: General, Atomic and Solid State Physics, 2014, 378, 2719-2724.	0.9	49
17243	Elastic properties of stishovite and the CaCl2-type silica at the mantle temperature and pressure: An ab initio investigation. Earth and Planetary Science Letters, 2014, 404, 14-21.	1.8	62
17244	Electronically driven structural transitions inA₁₀(PO₄)₆F₂apatites (A= Ca, Sr, Pb, Cd) Tj ETQq0 0 0 rgBT /Overlo 2014, 70, 612-615.	0.5	11
17245	Fermi Level Pinning and Orbital Polarization Effects in Molecular Junctions: The Role of Metal Induced Gap States. Advanced Functional Materials, 2014, 24, 6154-6165.	7.8	59
17246	Structural and electronic properties of half-Heusler alloy PdMnBi calculated from first principles. Materials Chemistry and Physics, 2014, 148, 32-38.	2.0	19
17247	The effect of the stacking fault on the diffusion of chemisorbed hydrogen atoms inside few-layered graphene. RSC Advances, 2014, 4, 9223.	1.7	6
17248	A novel three dimensional semimetallic MoS2. Journal of Applied Physics, 2014, 115, .	1.1	6
17249	Phase diagram of the CuInSe2-CuGaSe2 pseudobinary system studied by combined ab initio density functional theory and thermodynamic calculation. Journal of Applied Physics, 2014, 116, .	1.1	16
17250	A strong linear correlation between the surface charge density on Ag nanoparticles and the amount of propylene adsorbed. Journal of Materials Chemistry A, 2014, 2, 6987.	5.2	6
17251	The role of Bi vacancies in the electrical conduction of BiFeO₃: a first-principles approach. Dalton Transactions, 2014, 43, 10787-10793.	1.6	47
17252	Computational materials design of negative effectiveUsystem in hole-doped chalcopyrite CuFeS₂. Journal of Physics Condensed Matter, 2014, 26, 355502.	0.7	8
17253	HAADF-STEM and DFT investigations of the Zn-containing Î²â€³ phase in Alâ€“Mgâ€“Si alloys. Acta Materialia, 2014, 78, 245-253.	3.8	52

#	Article	IF	Citations
17254	Intercalated graphitic carbon nitride: a fascinating two-dimensional nanomaterial for an ultra-sensitive humidity nanosensor. Nanoscale, 2014, 6, 9250.	2.8	108
17255	Role of Au in Graphene Growth on a Ni Surface. ACS Catalysis, 2014, 4, 892-902.	5.5	8
17256	Formation of NV centers in diamond: A theoretical study based on calculated transitions and migration of nitrogen and vacancy related defects. Physical Review B, 2014, 89, .	1.1	149
17257	Roles of an oxygen Frenkel pair in the photoluminescence of Bi³⁺-doped Y₂O₃: computational predictions and experimental verifications. Journal of Materials Chemistry C, 2014, 2, 6017-6024.	2.7	25
17258	Impact of Surface on the <inline-formula> <tex-math notation="TeX">d^{0} </tex-math></inline-formula> Ferromagnetism of Lithium-Doped Zinc Oxide Nanowires. IEEE Transactions on Magnetics, 2014, 50, 1-7.	1.2	3
17259	Structural, elastic, and mechanical properties of germanium dioxide from first-principles calculations. Materials Science in Semiconductor Processing, 2014, 27, 765-776.	1.9	29
17260	Tunable electronic properties induced by a defect-substrate in graphene/BC₃heterobilayers. Physical Chemistry Chemical Physics, 2014, 16, 22861-22866.	1.3	30
17261	Pressure-induced spin collapse of octahedrally coordinated <mml:math xmlns:mml="http://www.w3.org/1998/Math/MathML"><mml:msup><mml:mrow><mml:mi mathvariant="normal">Fe</mml:mi></mml:mrow><mml:mrow><mml:mn>3</mml:mn><mml:mo>+</mml:mo></mml:mrow></mml:msup></mml:math> in <mml:math xmlns:mml="http://www.w3.org/1998/Math/MathML"><mml:msub><mml:mrow><mml:mi mathvariant="normal">Ca</mml:mi></mml:mrow><mml:mn>3</mml:mn></mml:msub><mml:msub><mml:mrow><mml:mi mathvariant="normal">Fe</mml:mi></mml:mrow><mml:mn>2</mml:mn></mml:msub> Physical Review B, 2014, 90, .	1.1	12
17262	Prediction and Characterization of MXene Nanosheet Anodes for Non-Lithium-Ion Batteries. ACS Nano, 2014, 8, 9606-9615.	7.3	814
17263	A first-principles study of CO oxidation by surface oxygen on Pt-incorporated perovskite catalyst (CaPt_xTi_{1â"x}O₃). RSC Advances, 2014, 4, 30530-30535.	1.7	5
17264	Impact of Graphene Edges on Enhancing the Performance of Electrochemical Double Layer Capacitors. Journal of Physical Chemistry C, 2014, 118, 21770-21777.	1.5	54
17265	DFT study of adsorption and dissociation behavior of H2S on Fe-doped graphene. Applied Surface Science, 2014, 317, 511-516.	3.1	135
17266	Testing the Jacob's ladder of density functionals for electronic structure and magnetism of rutile<mml:math xmlns:mml="http://www.w3.org/1998/Math/MathML"><mml:msub><mml:mi mathvariant="normal">VO</mml:mi><mml:mn>2</mml:mn></mml:msub></mml:math>. Physical Review B, 2014, 90, .	1.1	20
17267	Experimental and theoretical electronic structure of quinacridone. Physical Review B, 2014, 90, .	1.1	70
17268	Monolayer Nanoislands of Pt on Au and Cu: A First-Principles Computational Study. Journal of Physical Chemistry C, 2014, 118, 22102-22110.	1.5	8
17269	Phosphorene nanoribbon as a promising candidate for thermoelectric applications. Scientific Reports, 2014, 4, 6452.	1.6	308
17270	First-Principles Study of Lead Iodide Perovskite Tetragonal and Orthorhombic Phases for Photovoltaics. Journal of Physical Chemistry C, 2014, 118, 19565-19571.	1.5	220
17271	Permanent magnetism of intermetallic compounds between light and heavy transition-metal elements. Journal of Physics Condensed Matter, 2014, 26, 064209.	0.7	27

#	Article	IF	Citations
17272	Potential rare earth free permanent magnet: interstitial boron doped FeCo. Journal Physics D: Applied Physics, 2014, 47, 415002.	1.3	17
17273	Charge Transport Properties of Durene Crystals from First-Principles. Journal of Chemical Theory and Computation, 2014, 10, 4624-4632.	2.3	16
17274	Rhodium Nanoparticle Anchoring on AlPO₄ for Efficient Catalyst Sintering Suppression. Chemistry of Materials, 2014, 26, 5799-5805.	3.2	38
17275	Theoretical prediction of low-density nanoporous frameworks of zinc sulfide based on Zn_nS_n(n = 12, 16) nanocaged clusters. RSC Advances, 2014, 4, 37333-37341.	1.7	19
17276	Band Structure Tuning of TiO₂ for Enhanced Photoelectrochemical Water Splitting. Journal of Physical Chemistry C, 2014, 118, 7451-7457.	1.5	95
17277	Utilizing the Gate-Opening Mechanism in ZIF-7 for Adsorption Discrimination between N₂O and CO₂. Journal of Physical Chemistry C, 2014, 118, 17831-17837.	1.5	51
17278	Molecular Spintronics: Destructive Quantum Interference Controlled by a Gate. Journal of the American Chemical Society, 2014, 136, 15065-15071.	6.6	65
17279	EELS modelling of graphitisation. Journal of Physics: Conference Series, 2014, 522, 012014.	0.3	1
17280	First-principles study of O₂ reduction on BaZr_{1â”x}Co_xO₃ cathodes in protonic-solid oxide fuel cells. Journal of Materials Chemistry A, 2014, 2, 16707-16714.	5.2	29
17281	[illegible] xmlns:mml="http://www.w3.org/1998/Math/MathML"><mml:mrow><mml:msub><mml:mi mathvariant="bold">Cu</mml:mi><mml:mn>2</mml:mn></mml:msub><mml:msub><mml:mi mathvariant="bold">CdGeS</mml:mi><mml:mn>4</mml:mn></mml:msub></mml:mrow></mml:math>and<mml:math xmlns:mml="http://www.w3.org/1998/Math/MathML"><mml:mrow><mml:msub><mml:mi [illegible]	1.1	35
17282	Reversible potentials for steps in methanol and formic acid oxidation to CO2; adsorption energies of intermediates on the ideal electrocatalyst for methanol oxidation and CO2 reduction. Physical Chemistry Chemical Physics, 2014, 16, 10587-10599.	1.3	19
17283	Adsorption of phenol on Fe (110) and Pd (111) from first principles. Surface Science, 2014, 630, 244-253.	0.8	52
17284	First-principles high-pressure unreacted equation of state and heat of formation of crystal 2,6-diamino-3, 5-dinitropyrazine-1-oxide (LLM-105). Journal of Chemical Physics, 2014, 141, 064702.	1.2	36
17285	Coverage-Dependent Adsorption of Bifunctional Molecules: Detailed Insights into Interactions between Adsorbates. Journal of Physical Chemistry C, 2014, 118, 23811-23820.	1.5	20
17286	First-principles study on CuAlTe 2 and AgAlTe 2 for water splitting. Materials Chemistry and Physics, 2014, 148, 882-886.	2.0	13
17287	Carbon-Doped Boron Nitride Nanomesh: Stability and Electronic Properties of Adsorbed Hydrogen and Oxygen. Journal of Physical Chemistry C, 2014, 118, 23888-23896.	1.5	9
17288	In Silico Design of Three-Dimensional Porous Covalent Organic Frameworks via Known Synthesis Routes and Commercially Available Species. Journal of Physical Chemistry C, 2014, 118, 23790-23802.	1.5	40
17289	Stability and properties of 2D porous nanosheets based on tetraoxa[8]circulene analogues. Nanoscale, 2014, 6, 14962-14970.	2.8	27

#	Article	IF	Citations
17290	Charge Distribution View: Large Difference in Friction Performance Between Graphene and Hydrogenated Graphene Systems. Tribology Letters, 2014, 55, 405-412.	1.2	31
17291	Surface Band Tuning of Bi2Te3 Topological Insulator Thin Films by Gas Adsorption. Journal of Electronic Materials, 2014, 43, 3105-3109.	1.0	5
17292	Full-Potential Study of the Electronic and Optical Properties of the Transparent Oxide ZnCo2O4 by Use of PBE and TB-mBJ Potentials. Journal of Electronic Materials, 2014, 43, 3659-3665.	1.0	10
17293	Using a scale-bridging technique to determine the effect of elastic properties on stress distribution around the femoral stem of an artificial hip joint with a simplified geometry. Metals and Materials International, 2014, 20, 593-600.	1.8	1
17294	Terahertz Vibrational Modes of the Rigid Crystal Phase of Succinonitrile. Journal of Physical Chemistry A, 2014, 118, 2442-2446.	1.1	20
17295	Li decorated 6,6,12-graphyne: A new star for hydrogen storage material. International Journal of Hydrogen Energy, 2014, 39, 17112-17117.	3.8	45
17296	Modulation of the Electronic Properties of Ultrathin Black Phosphorus by Strain and Electrical Field. Journal of Physical Chemistry C, 2014, 118, 23970-23976.	1.5	252
17297	Mechanism of Sulfur Poisoning of Sr₂Fe_{1.5}Mo_{0.5}O_{6-Î´} Perovskite Anode under Solid Oxide Fuel Cell Conditions. Journal of Physical Chemistry C, 2014, 118, 23545-23552.	1.5	23
17298	Key Structureâ€“Property Relationships in CO₂ Capture by Supported Alkanolamines. Journal of Physical Chemistry C, 2014, 118, 19252-19258.	1.5	8
17299	Feasible Catalytic Strategy for Writing Conductive Nanoribbons on a Single-Layer Graphene Fluoride. Journal of Physical Chemistry C, 2014, 118, 22643-22648.	1.5	0
17300	Modeling of resistive random access memory (RRAM) switching mechanisms and memory structures. , 2014, , 262-284e.		3
17301	The Characterization, Stability, and Reactivity of Synthetic Calcium Silicate Surfaces from First Principles. Journal of Physical Chemistry C, 2014, 118, 15214-15219.	1.5	58
17302	Observation of Majorana fermions in ferromagnetic atomic chains on a superconductor. Science, 2014, 346, 602-607.	6.0	1,581
17303	Noncentrosymmetric chalcohalide NaBa₄Ge₃S₁₀Cl with large band gap and IR NLO response. Journal of Materials Chemistry C, 2014, 2, 4590-4596.	2.7	96
17304	Group Additivity for Estimating Thermochemical Properties of Furanic Compounds on Pd(111). Industrial & Engineering Chemistry Research, 2014, 53, 11929-11938.	1.8	27
17305	Unraveling the Factors That Control Soft Landing of Small Silyl Ions on Fluorinated Self-Assembled Monolayers. Journal of Physical Chemistry C, 2014, 118, 10159-10169.	1.5	5
17306	First-principles prediction of the magnetism of 4f rare-earth-metal-doped wurtzite zinc oxide. Journal of Rare Earths, 2014, 32, 715-721.	2.5	65
17307	Electronic structure and peculiar bonding properties of NdNiMg5 from first principles. Solid State Sciences, 2014, 38, 1-6.	1.5	5

#	Article	IF	Citations
17308	Indirectâ€“direct bandgap transition and gap width tuning in bilayer MoS 2 superlattices. Chemical Physics Letters, 2014, 613, 74-79.	1.2	22
17309	Nitrogen Adsorption, Dissociation, and Subsurface Diffusion on the Vanadium (110) Surface: A DFT Study for the Nitrogen-Selective Catalytic Membrane Application. Journal of Physical Chemistry C, 2014, 118, 4238-4249.	1.5	39
17310	Strong Photoluminescence Enhancement of MoS₂ through Defect Engineering and Oxygen Bonding. ACS Nano, 2014, 8, 5738-5745.	7.3	995
17311	Lead-free perovskite and hybrid improper ferroelectricity in<mml:math xmlns:mml="http://www.w3.org/1998/Math/MathML"><mml:msub><mml:mi mathvariant="normal">RbHgF</mml:mi><mml:mn>3</mml:mn></mml:msub></mml:math>perovskite and hybrid improper ferroelectricity in<mml:math xmlns:mml="http://www.w3.org/1998/Math/MathML"><mml:mo>(</mml:mo><mml:mtext>Na</mml:mtext><mml:mo>,</mml:mo><mml:mi mathvariant="normal">Hg</mml:mi><mml:mn>2</mml:mn></mml:msub><mml:msub><mml:mi	1.1	14
17312	Theoretical study of stability and electronic structure of the new type of ferroelectric materials XSnO₃ (X = Mn, Zn, Fe, Mg). International Journal of Modern Physics B, 2014, 28, 1450224.	1.0	12
17313	Phase Transformation in Titanium Nanoparticles from First Principles. Solid State Phenomena, 0, 213, 42-46.	0.3	0
17314	Structural tale of two novel (Cr, Mn)C carbides in steel. Acta Materialia, 2014, 78, 161-172.	3.8	11
17315	Crystal Structure, Electronic Structure, and Photoluminescence Properties of La₃BW_{1â€“x}Mo_xO₉:Eu³⁺ Red Phosphor. Inorganic Chemistry, 2014, 53, 9541-9547.	1.9	64
17316	Theoretical insights into the adsorption of monatomic Ag on the (2Ã—2) BiOCl (001) surfaces. Computational Materials Science, 2014, 95, 113-120.	1.4	16
17317	Ab initio study of Tl on Si(111)-(3Ã—1) surface. Physica Status Solidi (B): Basic Research, 2014, 251, 1570-1573.	0.7	4
17318	Hydrogen-dimer lines and electron waveguides in graphene. Physical Chemistry Chemical Physics, 2014, 16, 17610-17616.	1.3	4
17319	Ab initio-based prediction and TEM study of silicide precipitation in titanium. Computational Materials Science, 2014, 95, 456-463.	1.4	20
17320	Mechanical anisotropy and origin of shear plastic deformation of tetragonal B ₄ C ₄. Europhysics Letters, 2014, 108, 16001.	0.7	4
17321	Point Defects and Non-stoichiometry in Li₂TiO₃. Chemistry of Materials, 2014, 26, 1629-1638.	3.2	63
17322	BrÃ¸nstedâ€“Evansâ€“Polanyi and Transition State Scaling Relations of Furan Derivatives on Pd(111) and Their Relation to Those of Small Molecules. ACS Catalysis, 2014, 4, 604-612.	5.5	68
17323	Interaction of H with stacking fault in W(111) film: A possible formation mechanism of H bubbles. RSC Advances, 2014, 4, 7030.	1.7	8
17324	Mechanical and thermal properties of NpO2 using LSDA+U approach. Progress in Natural Science: Materials International, 2014, 24, 373-377.	1.8	3
17325	First principles prediction of structural stability, elastic, lattice dynamical and thermal properties of osmium carbides. Materials Science and Technology, 2014, 30, 842-849.	0.8	8

#	Article	IF	Citations
17326	Comparative density functional theory based study of the reactivity of Cu, Ag, and Au nanoparticles and of (111) surfaces toward CO oxidation and NO2 reduction. Journal of Molecular Modeling, 2014, 20, 2448.	0.8	12
17327	Water Adsorption and Dissociation on BaTiO₃ Single-Crystal Surfaces. Journal of Physical Chemistry C, 2014, 118, 15910-15918.	1.5	40
17328	Modeling of molar volume of the sigma phase involving transition elements. Computational Materials Science, 2014, 95, 540-550.	1.4	10
17329	Phonons, nature of bonding, and their relation to anomalous thermal expansion behavior of M2O (M) Tj ETQq1 1 0.784314 rgBT /Ove	1.1	80
17330	Li-decorated double vacancy graphene for hydrogen storage application: A first principles study. International Journal of Hydrogen Energy, 2014, 39, 11016-11026.	3.8	118
17331	Li-decorated graphyne as high-capacity hydrogen storage media: First-principles plane wave calculations. International Journal of Hydrogen Energy, 2014, 39, 17104-17111.	3.8	67
17332	Point defects and non-stoichiometry in thoria. Solid State Ionics, 2014, 267, 80-87.	1.3	39
17333	Photoelectrochemical response and electronic structure analysis of mono-dispersed cuboid-shaped Bi₂Fe₄O₉ crystals with near-infrared absorption. RSC Advances, 2014, 4, 28209-28218.	1.7	29
17334	Surface-Step-Induced Oscillatory Oxide Growth. Physical Review Letters, 2014, 113, 136104.	2.9	52
17335	Acoustic plasmons in extrinsic free-standing graphene. New Journal of Physics, 2014, 16, 083003.	1.2	53
17336	Kinetic Barriers of the Phase Transition in the Oxygen Chemisorbed Cu(110)-(2 Ã— 1)-O as a Function of Oxygen Coverage. Journal of Physical Chemistry C, 2014, 118, 20858-20866.	1.5	24
17337	Density Functional Investigation of the Adsorption of Isooctane, Ethanol, and Acetic Acid on a Water-Covered Fe(100) Surface. Journal of Physical Chemistry C, 2014, 118, 21428-21437.	1.5	17
17338	Effect of Surface Termination on Diamond (100) Surface Electrochemistry. Journal of Physical Chemistry C, 2014, 118, 22995-23002.	1.5	28
17339	Intrinsic Ligand Effect Governing the Catalytic Activity of Pd Oxide Thin Films. ACS Catalysis, 2014, 4, 3330-3334.	5.5	79
17340	Coâ€“Co₂C and Coâ€“Co₂C/AC Catalysts for Hydroformylation of 1-Hexene under Low Pressure: Experimental and Theoretical Studies. Journal of Physical Chemistry C, 2014, 118, 19114-19122.	1.5	41
17341	Surface Structure and Morphology of M[Coâ€²]O₄(M = Mg, Zn, Fe, Co and Mâ€² = Ni, Al, Mn,) Tj ETQq1 1 0.784314 r 2014, 118, 19085-19097.	1.5	77
17342	Microwave and Conventional Hydro(solvo)thermal Syntheses of Three Co(II) Coordination Polymers: Supramolecular Isomerism and Structural Transformations Accompanied by Tunable Magnetic Properties. Crystal Growth and Design, 2014, 14, 4430-4438.	1.4	26
17343	Thermal Expansion of Niâ€“Tiâ€“Sn Heusler and Half-Heusler Materials from First-Principles Calculations and Experiments. Journal of Physical Chemistry C, 2014, 118, 22405-22411.	1.5	17

#	Article	IF	Citations
17344	Theoretical Model of Oxidative Adsorption of Water on a Highly Reduced Reconstructed Oxide Surface. Journal of Physical Chemistry Letters, 2014, 5, 3408-3414.	2.1	25
17345	Oxygen Adsorption on Irreducible Oxides Doped with Higher Valence Ions: O₂ Binding to the Dopant. Journal of Physical Chemistry C, 2014, 118, 23070-23082.	1.5	5
17346	Identifying Potential BO₂ Oxide Polymorphs for Epitaxial Growth Candidates. ACS Applied Materials & Interfaces, 2014, 6, 3630-3639.	4.0	26
17347	Beryllium-free Li4Sr(BO3)2 for deep-ultraviolet nonlinear optical applications. Nature Communications, 2014, 5, 4019.	5.8	384
17348	CO Activation Pathways of Fischerâ€“Tropsch Synthesis on Ï‡-Fe5C2 (510): Direct versus Hydrogen-Assisted CO Dissociation. Journal of Physical Chemistry C, 2014, 118, 10170-10176.	1.5	104
17349	First principles calculations of electronic and optical properties of Mo and C co-doped anatase TiO2. Applied Physics A: Materials Science and Processing, 2014, 117, 831-839.	1.1	12
17350	ReaxFF molecular dynamics simulations of CO collisions on an O-preadsorbed silica surface. Journal of Molecular Modeling, 2014, 20, 2160.	0.8	5
17351	Mechanical, electronic, and optical properties of Bi2S3 and Bi2Se3 compounds: first principle investigations. Journal of Molecular Modeling, 2014, 20, 2180.	0.8	68
17352	Theoretical study of oxidation of monovacancies in hexagonal boron nitride (h-BN) sheet by oxygen molecules. Journal of Molecular Modeling, 2014, 20, 2197.	0.8	12
17353	Adsorption of 2,3,7,8-tetrochlorodibenzo-p-dioxins on intrinsic, defected, and Ti (N, Ag) doped graphene: a DFT study. Journal of Molecular Modeling, 2014, 20, 2238.	0.8	15
17354	CO, CO2 and H2 adsorption on ZnO, CeO2, and ZnO/CeO2 surfaces: DFT simulations. Journal of Molecular Modeling, 2014, 20, 2270.	0.8	40
17355	Theoretical prediction of the mechanisms for defect healing or oxygen doping in a hexagonal boron nitride (h-BN) sheet with nitrogen vacancies by NO2 molecules. Journal of Molecular Modeling, 2014, 20, 2307.	0.8	8
17356	Understanding the structural and electronic properties of the cathode material NaFeF3 in a Na-ion battery. Journal of Solid State Electrochemistry, 2014, 18, 2071-2075.	1.2	14
17357	Trends in Hydrodesulfurization Catalysis Based on Realistic Surface Models. Catalysis Letters, 2014, 144, 1425-1432.	1.4	32
17358	First-principles study of A-site substitution in ferroelectric bismuth titanate. Journal of Materials Science, 2014, 49, 6363-6372.	1.7	4
17359	First-Principle Investigations of Structural, Electronic, and Half-Metallic Ferromagnetic Properties in In1â˜’xTM x P (TM = Cr, Mn). Journal of Superconductivity and Novel Magnetism, 2014, 27, 1603-1614.	0.8	20
17360	Nonlinear Elastic Properties of Superconducting Antiperovskites MNNi3 (M =Zn, Cd, Mg, Al, Ga, and In) from First Principles. Journal of Superconductivity and Novel Magnetism, 2014, 27, 1851-1859.	0.8	7
17361	A structural investigation of tris(ethyl acetoacetate)aluminium (III). Journal of Sol-Gel Science and Technology, 2014, 71, 217-223.	1.1	4

#	Article	IF	Citations
17362	Assessing Carbon-Based Anodes for Lithium-Ion Batteries: A Universal Description of Charge-Transfer Binding. Physical Review Letters, 2014, 113, 028304.	2.9	93
17363	Semiconducting Layered Blue Phosphorus: A Computational Study. Physical Review Letters, 2014, 112, 176802.	2.9	996
17364	First-principles studies of lithium storage in reduced graphite oxide. Electrochimica Acta, 2014, 140, 232-237.	2.6	20
17365	Size-Induced Chemical and Magnetic Ordering in Individual Feâ€“Au Nanoparticles. ACS Nano, 2014, 8, 8113-8120.	7.3	36
17366	Tensile and fracture process of the TiN/VN interface from first principles. Ceramics International, 2014, 40, 14453-14462.	2.3	34
17367	Electronic and magnetic properties of armchair graphene nanoribbons with 558 grain boundary. Physical Chemistry Chemical Physics, 2014, 16, 10607.	1.3	15
17368	Electronic structure of epitaxial graphene grown on stepped Pt(997). Physical Review B, 2014, 89, .	1.1	10
17369	Na₄La₂(CO₃)₅ and CsNa₅Ca₅(CO₃)₈: Two New Carbonates as UV Nonlinear Optical Materials. Inorganic Chemistry, 2014, 53, 8098-8104.	1.9	58
17370	Unusual electronic properties and transmission in hexagonal SiB monolayers. Physical Chemistry Chemical Physics, 2014, 16, 14473.	1.3	10
17371	Al_xC Monolayer Sheets: Two-Dimensional Networks with Planar Tetracoordinate Carbon and Potential Applications as Donor Materials in Solar Cell. Journal of Physical Chemistry Letters, 2014, 5, 2058-2065.	2.1	95
17372	Electron quantum conductance of bimetallic Pt-Fe nanowires. Bulletin of the Russian Academy of Sciences: Physics, 2014, 78, 149-151.	0.1	1
17373	Effect of van der Waals interaction on the structural and cohesive properties of black phosphorus. Journal of the Korean Physical Society, 2014, 64, 547-553.	0.3	21
17374	Atomistic processes of Ni and Pd atoms on MgO(001) surfaces with surface-functional hydroxyl groups: Ab-initio calculations. Journal of the Korean Physical Society, 2014, 64, 554-560.	0.3	10
17375	Electronic structure calculations of positron lifetimes in SiC: Self-consistent schemes and relaxation effect. Nuclear Instruments & Methods in Physics Research B, 2014, 327, 63-67.	0.6	10
17376	Internal-strain effect on the valence band of strained silicon and its correlation with the bond angles. Journal of Applied Physics, 2014, 115, .	1.1	1
17377	Effect of enzymatic orientation through the use of syringaldazine molecules on multiple multi-copper oxidase enzymes. Physical Chemistry Chemical Physics, 2014, 16, 13367-13375.	1.3	39
17378	Analytic bond-order potentials for the bcc refractory metals Nb, Ta, Mo and W. Journal of Physics Condensed Matter, 2014, 26, 195501.	0.7	14
17379	Molecular modeling studies of oleate adsorption on iron oxides. Applied Surface Science, 2014, 295, 115-122.	3.1	74

#	Article	IF	Citations
17380	Tunable band gap in germanene by surface adsorption. Physica E: Low-Dimensional Systems and Nanostructures, 2014, 59, 60-65.	1.3	84
17381	Structural and electronic properties of single-side fluorinated graphene C4F under equibiaxial strains. Physica E: Low-Dimensional Systems and Nanostructures, 2014, 58, 59-62.	1.3	6
17382	Vibrational and elastic properties of 2D carbon allotropes: A first principles study. Solid State Communications, 2014, 189, 58-62.	0.9	10
17383	Vibrational and thermodynamic properties of GeSe in the quasiharmonic approximation. Physical Review B, 2014, 89, .	1.1	59
17384	Density functional theory study of chemical sensing on surfaces of single-layer MoS2 and graphene. Journal of Applied Physics, 2014, 115, .	1.1	31
17385	Augmented methane adsorption at Ca decorated carbon nanotubesâ€"a DFT study. Journal Physics D: Applied Physics, 2014, 47, 075305.	1.3	3
17386	Density functional study of Al/N co-doped (10,0) zigzag single-walled carbon nanotubes as CO sensor. Computational Materials Science, 2014, 82, 497-502.	1.4	23
17387	OptaDOS: A tool for obtaining density of states, core-level and optical spectra from electronic structure codes. Computer Physics Communications, 2014, 185, 1477-1485.	3.0	124
17388	Atomic Scale Identification of Coexisting Graphene Structures on Ni(111). Journal of Physical Chemistry Letters, 2014, 5, 467-473.	2.1	92
17389	High pressure structural, elastic, mechanical and thermal behavior of LaX3 (X=In, Sn, Tl and Pb) compounds: A FP-LAPW study. Computational Materials Science, 2014, 81, 423-432.	1.4	12
17390	First principles study of the occurrence of gold in pyrite. Computational Materials Science, 2014, 88, 1-6.	1.4	33
17391	Edge-, width- and strain-dependent semiconductorâ€"metal transition in SnSe nanoribbons. RSC Advances, 2014, 4, 6933.	1.7	23
17392	Structural, mechanical and electronic properties of 3d transition metal nitrides in cubic zincblende, rocksalt and cesium chloride structures: a first-principles investigation. Journal of Physics Condensed Matter, 2014, 26, 025404.	0.7	86
17393	Theoretical Study of the Energetic Stability and Geometry of Terminated and B-Doped Diamond (111) Surfaces. Journal of Physical Chemistry C, 2014, 118, 1944-1957.	1.5	50
17394	Half-metallic ferromagnetism in zinc-blende (CaX)1/(YX)1 (001)(Y=Al, Ga, and In; X=N, P, and As) superlattices: A first-principles study. Computational Materials Science, 2014, 84, 306-309.	1.4	6
17395	Effects of van der Waals density functional corrections on trends in furfural adsorption and hydrogenation on close-packed transition metal surfaces. Surface Science, 2014, 622, 51-59.	0.8	101
17396	Adsorption and dissociation of H2S on Mo(100) surface by first-principles study. Applied Surface Science, 2014, 292, 328-335.	3.1	36
17397	Graphdiyne as a metal-free catalyst for low-temperature CO oxidation. Physical Chemistry Chemical Physics, 2014, 16, 5640-5648.	1.3	102

#	Article	IF	Citations
17398	Long-Range Periodicity of S/Au(111) Structures at Low and Intermediate Coverages. Journal of Physical Chemistry C, 2014, 118, 290-297.	1.5	18
17399	Effects of in-plane electric field and temperature change on Youngâ€™s modulus of hexagonal boron nitride nanosheets with different chiralities. Superlattices and Microstructures, 2014, 68, 16-26.	1.4	15
17400	The structure determination of Al20Cu2Mn3 by near atomic resolution chemical mapping. Journal of Alloys and Compounds, 2014, 601, 25-30.	2.8	67
17401	Prediction of diffusivities in fcc phase of the Alâ€“Cuâ€“Mg system: First-principles calculations coupled with CALPHAD technique. Computational Materials Science, 2014, 90, 32-43.	1.4	6
17402	Mechanisms of charge transfer and redistribution in LaAlO3/SrTiO3 revealed by high-energy optical conductivity. Nature Communications, 2014, 5, 3663.	5.8	70
17403	Toward an accurate ab initio estimation of compressibility and thermal expansion of diamond in the [0, 3000 K] temperature and [0, 30 GPa] pressures ranges, at the hybrid HF/DFT theoretical level. American Mineralogist, 2014, 99, 1147-1154.	0.9	16
17404	Structural, electronic and elastic properties of AlFe 2 B 2 : First-principles study. Computational Materials Science, 2014, 92, 253-257.	1.4	32
17405	Methanol synthesis by CO and CO2 hydrogenation on Cu/Î³-Al2O3 surface in liquid paraffin solution. Applied Surface Science, 2014, 290, 398-404.	3.1	25
17406	Electronic structure and magnetic properties of diluted magnetic semiconductor K and Mn co-doped BaCd2As2 from first-principles calculations. Modern Physics Letters B, 2014, 28, 1450111.	1.0	1
17407	An energetic evaluation of dissolution corrosion capabilities of liquid metals on iron surface. Physical Chemistry Chemical Physics, 2014, 16, 16837.	1.3	29
17408	Structural stability, electronic structure and mechanical properties of 4d transition metal nitrides TMN (TM=Ru, Rh, Pd). Journal of Physics and Chemistry of Solids, 2014, 75, 888-902.	1.9	11
17409	Ab initio calculations of mechanical stability of bcc Cu under pressure. Solid State Communications, 2014, 184, 25-28.	0.9	4
17410	A DFT study of cyclopropane adsorption on Pt(111). Electronic structure and bonding. Applied Surface Science, 2014, 303, 324-330.	3.1	1
17411	Ion-exchange between Na2Ti3O7 and H2Ti3O7 nanosheets at different pH levels: An experimental and first-principles study. Physica E: Low-Dimensional Systems and Nanostructures, 2014, 60, 210-213.	1.3	10
17412	Molybdenum carbide catalysed hydrogen production from formic acid â€“ A density functional theory study. Journal of Power Sources, 2014, 246, 548-555.	4.0	45
17413	Elastic and electronic properties of LiBSi 2 under pressure from first principles. Computational Materials Science, 2014, 92, 231-237.	1.4	4
17414	Two-dimensional molybdenum carbides: potential thermoelectric materials of the MXene family. Physical Chemistry Chemical Physics, 2014, 16, 7841-7849.	1.3	395
17415	Modulating magnetic characteristics of Pt embedded graphene by gas adsorption (N2, O2, NO2, SO2). Applied Surface Science, 2014, 289, 445-449.	3.1	103

#	Article	IF	Citations
17416	ComprehensiveAb InitioStudy of Doping in Bulk ZnO with Group-V Elements. Physical Review Applied, 2014, 1, .	1.5	32
17417	Pressure stabilization of long-missing bare C6 hexagonal rings in binary sesquicarbides. Chemical Science, 2014, 5, 3936-3940.	3.7	21
17418	The electronic structure of the antimony chalcogenide series: Prospects for optoelectronic applications. Journal of Solid State Chemistry, 2014, 213, 116-125.	1.4	86
17419	AAg₂(Mâ€²_{1/3}M_{2/3})[VO₄]₂: Synthesis, Magnetic Properties, and Lattice Dynamics of Honeycomb-Type Lattices. Inorganic Chemistry, 2014, 53, 4994-5001.	1.9	14
17420	Understanding the influence of grain boundary thickness variation on the mechanical strength of a nickel-doped tungsten grain boundary. International Journal of Plasticity, 2014, 53, 135-147.	4.1	14
17421	Lithium diffusion in the spinel phase<mml:math xmlns:mml="http://www.w3.org/1998/Math/MathML"><mml:msub><mml:mtext>Li</mml:mtext><mml:mn>4</mml:mn></mml:msub><mml:msub><mml:mtext>Ti</mml:mtext><mml:mn>5</mml:mn></mml:msub><mml:msub><mml:mtext>O</mml:mtext><mml:mn>12</mml:mn></mml:msub></mml:math> in the rocksalt phase<mml:math xmlns:mml="http://www.w3.org/1998/Math/MathML. Physical Review B, 2014, 89, .	1.1	105
17422	Free-electron properties of metals under ultrafast laser-induced electron-phonon nonequilibrium: A first-principles study. Physical Review B, 2014, 89, .	1.1	89
17423	<scp>R</scp>aman scattering in orthorhombic Cu<scp>I</scp>n<scp>S</scp>₂ nanocrystals. Physica Status Solidi (A) Applications and Materials Science, 2014, 211, 195-199.	0.8	24
17424	Comparing electron-phonon coupling strength in diamond, silicon, and silicon carbide: First-principles study. Physical Review B, 2014, 89, .	1.1	77
17425	Reaction Pathway for Oxygen Reduction on FeN₄ Embedded Graphene. Journal of Physical Chemistry Letters, 2014, 5, 452-456.	2.1	307
17426	Ab initio calculation of the electronic, mechanical, and thermodynamic properties of yttrium nitride with the rocksalt structure. Physica Status Solidi (B): Basic Research, 2014, 251, 792-802.	0.7	7
17427	First principles calculations of LiNH2BH3, LiNH3BH4, and NaNH2BH3. Physica Status Solidi (B): Basic Research, 2014, 251, 898-906.	0.7	5
17428	Density functional theory study of the influence of Ti and V partitioning to cementite in ferritic steels. Physica Status Solidi (B): Basic Research, 2014, 251, 950-957.	0.7	9
17429	The Near Edge Structure of Hexagonal Boron Nitride. Microscopy and Microanalysis, 2014, 20, 1053-1059.	0.2	24
17430	Ab initio study on mechanical-bending-induced ferroelectric phase transition in ultrathin perovskite nanobelts. Acta Materialia, 2014, 76, 472-481.	3.8	11
17431	Suppression of the critical thickness threshold for conductivity at the LaAlO3/SrTiO3 interface. Nature Communications, 2014, 5, 4291.	5.8	57
17432	Theoretical Chemistry of Î±-Graphyne: Functionalization, Symmetry Breaking, and Generation of Dirac-Fermion Mass. Chemistry of Materials, 2014, 26, 3701-3708.	3.2	15
17433	Investigation of the electronic, magnetic and optical properties of ${sf Co}_{sf 2}{sf CrZ}$ (Z = Si,) Tj ETQq1 1 0.784314 rgBT /Overl	1.2	7

#	Article	IF	Citations
17434	Rapid Microwave Preparation and ab Initio Studies of the Stability of the Complex Noble Metal Oxides La₂BaPdO₅ and La₂BaPtO₅. Inorganic Chemistry, 2014, 53, 2628-2634.	1.9	10
17435	Determination of the Crystal Structure of Hexaphenyldisilane from Powder Diffraction Data and Its Thermodynamic Properties. Crystal Growth and Design, 2014, 14, 2937-2944.	1.4	7
17436	Theoretical Study of Hydrogen Permeation through Mixed NiOâ€“MgO Films Supported on Mo(100): Role of the Oxideâ€“Metal Interface. Journal of Physical Chemistry A, 2014, 118, 5756-5761.	1.1	3
17437	System-level-model development of an SWCNT based piezoresistive sensor in VHDL-AMS. , 2014, , .		2
17438	Anab initiostudy of transition metals doped with WSe₂for long-range room temperature ferromagnetism in two-dimensional transition metal dichalcogenide. Journal of Physics Condensed Matter, 2014, 26, 306004.	0.7	37
17439	Collective spin 1 singlet phase in high-pressure oxygen. Proceedings of the National Academy of Sciences of the United States of America, 2014, 111, 10427-10432.	3.3	21
17440	Smooth cubic commensurate oxides on gallium nitride. Journal of Applied Physics, 2014, 115, .	1.1	9
17441	Probing graphene interfaces with secondary electrons. Carbon, 2014, 77, 796-802.	5.4	23
17442	Effect of Strain on the Magnetism of Transition Metal-Doped ZnO: The First-Principles Calculations. Journal of Superconductivity and Novel Magnetism, 2014, 27, 2397-2400.	0.8	5
17443	Structural Modeling of Ge_{6.25}As_{32.5}Se_{61.25} Using a Combination of Reverse Monte Carlo and Ab Initio Molecular Dynamics. Journal of Physical Chemistry A, 2014, 118, 4790-4796.	1.1	8
17444	Three-dimensional Gd-doped TiO₂ fibrous photoelectrodes for efficient visible light-driven photocatalytic performance. RSC Advances, 2014, 4, 11750-11757.	1.7	31
17445	Theoretical Investigation on Mechanical and Thermal Properties of a Promising Thermal Barrier Material: Yb3Al5O12. Journal of Materials Science and Technology, 2014, 30, 631-638.	5.6	54
17446	Understanding the Mechanism of Photocatalysis Enhancements in the Graphene-like Semiconductor Sheet/TiO2 Composites. Journal of Physical Chemistry C, 2014, 118, 5954-5960.	1.5	65
17447	Adsorption and photocatalytic splitting of water on graphitic carbon nitride: a combined first principles and semiempirical study. Physical Chemistry Chemical Physics, 2014, 16, 15917-15926.	1.3	151
17448	Structural and Mechanical Properties of Platinum Carbide. Inorganic Chemistry, 2014, 53, 5797-5802.	1.9	19
17449	Electronic structure of low-pressure and high-pressure phases of silicon disulfide. Applied Physics A: Materials Science and Processing, 2014, 117, 1499-1514.	1.1	6
17450	A Density Functional Theory Study of the Reconstruction of Gold (111) Surfaces. Journal of Physical Chemistry C, 2014, 118, 15624-15629.	1.5	15
17451	DNA Base Detection Using a Single-Layer MoS₂. ACS Nano, 2014, 8, 7914-7922.	7.3	305

#	Article	IF	Citations
17452	Coexistence of superconductivity and charge-density-wave domain in 1T-FexTa1â^'xSSe. Applied Physics Letters, 2014, 104, 252601.	1.5	7
17453	Active edge sites in MoSe₂ and WSe₂ catalysts for the hydrogen evolution reaction: a density functional study. Physical Chemistry Chemical Physics, 2014, 16, 13156-13164.	1.3	426
17454	Electronic and magnetic properties of honeycomb transition metal monolayers: first-principles insights. Physical Chemistry Chemical Physics, 2014, 16, 13383-13389.	1.3	33
17455	Formation of solid solutions of gallium in Feâ€"Cr and Feâ€"Co alloys: MÃ¶ssbauer studies and first-principles calculations. Journal of Alloys and Compounds, 2014, 614, 297-304.	2.8	9
17456	Electronic and optical properties of 2D graphene-like compounds titanium carbides and nitrides: DFT calculations. Solid State Communications, 2014, 195, 61-69.	0.9	177
17457	Structural and electronic properties of organo-halide lead perovskites: a combined IR-spectroscopy and ab initio molecular dynamics investigation. Physical Chemistry Chemical Physics, 2014, 16, 16137-16144.	1.3	211
17458	Identifying the spin transition in Fe2+-rich MgSiO3 perovskite from X-ray diffraction and vibrational spectroscopy. American Mineralogist, 2014, 99, 1270-1276.	0.9	10
17459	One Hydrogen Bondâ€"Two Ways To Build a Structure. The Role of Nâ€"HÂ·Â·Â·O Hydrogen Bonds in Crystal Structures of N,N-Dimethylglycine. Crystal Growth and Design, 2014, 14, 1851-1864.	1.4	17
17460	First-Principles Analysis of Phase Stability in Layeredâ€"Layered Composite Cathodes for Lithium-Ion Batteries. Chemistry of Materials, 2014, 26, 2407-2413.	3.2	32
17461	Na⁺ and K⁺ ion selectivity by size-controlled biomimetic graphene nanopores. Nanoscale, 2014, 6, 10666-10672.	2.8	89
17462	Investigation of the vibrational behavior and stability characteristics of single-walled zinc sulfide nanotubes. Superlattices and Microstructures, 2014, 74, 85-99.	1.4	5
17463	Pressure-induced gap closing and metallization of<mml:math xmlns:mml="http://www.w3.org/1998/Math/MathML"><mml:mrow><mml:mi>Mo</mml:mi><mml:msub><mml:mi>Se</mml:mi><mml:mn>2</mml:mn></mml:msub></mml:mrow></mml:math>and<mml:math xmlns:mml="http://www.w3.org/1998/Math/MathML"><mml:mrow><mml:mi>Mo</mml:mi><mml:msub><mml:mi>Te</mml:mi><mml:mn>2</mml:mn></mml:msub></mml:mrow></mml:math>. Physical Review B, 2014, 90, .	1.5	50
17464	Silicon Carbide on Silicon (110): Surface Structure and Mechanisms of Epitaxial Growth. Russian Physics Journal, 2014, 56, 1439-1444.	0.2	6
17465	Electronic properties of bilayer and trilayer graphyne in the presence of electric field. Structural Chemistry, 2014, 25, 853-858.	1.0	18
17466	On the Structure Sensitivity of Direct NO Decomposition over Low-Index Transition Metal Facets. Topics in Catalysis, 2014, 57, 80-88.	1.3	64
17467	Ethanol Synthesis from Syngas on Transition Metal-Doped Rh(111) Surfaces: A Density Functional Kinetic Monte Carlo Study. Topics in Catalysis, 2014, 57, 125-134.	1.3	30
17468	Pt Skin Versus Pt Skeleton Structures of Pt3Sc as Electrocatalysts for Oxygen Reduction. Topics in Catalysis, 2014, 57, 245-254.	1.3	47
17469	LDA+U calculation of structural and thermodynamic properties of Ce2O3. Frontiers of Physics, 2014, 9, 483-489.	2.4	5

#	Article	IF	Citations
17470	Stress-Induced Grain Growth in an Ultra-Fine Grained Al Alloy. Metallurgical and Materials Transactions B: Process Metallurgy and Materials Processing Science, 2014, 45, 795-810.	1.0	16
17471	The Systems Tantalum (Niobium)-Cobalt-Boron. Journal of Phase Equilibria and Diffusion, 2014, 35, 43-85.	0.5	6
17472	Enthalpies of Formation and Electronic Densities of States of Vanadium Borides. Journal of Phase Equilibria and Diffusion, 2014, 35, 396-405.	0.5	7
17473	First-principles study on mechanical properties of LaMg3 and LaCuMg2. Journal of Central South University, 2014, 21, 2136-2142.	1.2	2
17474	TiO2 nanotube branched tree on a carbon nanofiber nanostructure as an anode for high energy and power lithium ion batteries. Nano Research, 2014, 7, 491-501.	5.8	42
17475	First-principle investigation on mechanism of Ca ion activating flotation of spodumene. Rare Metals, 2014, 33, 358-362.	3.6	31
17476	Ytterbium monopnictides under high pressure and high temperature: Structural and electronic properties studied using local spin density approximation and Hubbard corrections approach. Indian Journal of Physics, 2014, 88, 593-601.	0.9	2
17477	Effects of edge passivations on the electronic and magnetic properties of zigzag boron-nitride nanoribbons with even and odd-line stoneâ€“wales (5â€“7 pair) defects. Indian Journal of Physics, 2014, 88, 931-938.	0.9	3
17478	Nitrogen-containing species in the structure of the synthesized nano-hydroxyapatite. JETP Letters, 2014, 99, 196-203.	0.4	27
17479	Oxidation and magnetic states of chalcopyrite CuFeS2: A first principles calculation. Optics and Spectroscopy (English Translation of Optika I Spektroskopiya), 2014, 116, 885-888.	0.2	29
17480	First-principle study of the structural, electronic, and thermodynamic properties of cuprous oxide under pressure. Journal of Experimental and Theoretical Physics, 2014, 118, 235-241.	0.2	12
17481	Features of the band structure of (CuInSe2)1 â^' x (MeSe) x alloys (Me = Mn, Fe). Semiconductors, 2014, 48, 417-422.	0.2	3
17482	Ab initio investigation of the pressure influence on elastic properties of the GaS layered compound. Physics of the Solid State, 2014, 56, 619-625.	0.2	5
17483	Effect of pressure on phonon spectra and elastic properties of orthorhombic GeSe. Physics of the Solid State, 2014, 56, 761-764.	0.2	5
17484	Effect of Zr on the mechanical properties of BaTiO3. Glass Physics and Chemistry, 2014, 40, 256-260.	0.2	0
17485	Electronic and magnetic properties of single-layer graphene doped by nitrogen atoms. European Physical Journal B, 2014, 87, 1.	0.6	19
17486	Acoustic waves and phonon focus in Li crystal: the first principle study. European Physical Journal B, 2014, 87, 1.	0.6	3
17487	The key role of carbon in hydrogen solubility in copper. European Physical Journal B, 2014, 87, 1.	0.6	2

#	Article	IF	Citations
17488	Structure and elastic anisotropy of uranium under pressure up to 100 GPa. European Physical Journal B, 2014, 87, 1.	0.6	5
17489	Investigation of aniline by high pressure Raman scattering spectroscopy and quantum chemical calculation. European Physical Journal D, 2014, 68, 1.	0.6	4
17490	Optical properties of Eu2+/Eu3+ mixed valence, silicon nitride based materials. Journal of Solid State Chemistry, 2014, 213, 126-131.	1.4	9
17491	First-principles study on surface structural, magnetic and electronic properties of alloyed cementite with Co or Ni. Computational Materials Science, 2014, 85, 154-158.	1.4	9
17492	High-pressure behavior of Fe3P and the role of phosphorus in planetary cores. Earth and Planetary Science Letters, 2014, 390, 296-303.	1.8	34
17493	Ferromagnetic spin-order in p-type N-doped SnO2 films prepared by thermal oxidation of SnNx. Journal of Magnetism and Magnetic Materials, 2014, 362, 14-19.	1.0	24
17494	Modulation of the Band Gap Increase in Nanocrystals by Surface Passivation. Journal of Physical Chemistry C, 2014, 118, 14026-14030.	1.5	2
17495	Influence of substitutional impurities on hydrogen diffusion in B2-TiFe alloy. International Journal of Hydrogen Energy, 2014, 39, 12213-12220.	3.8	19
17496	A charge optimized many-body (comb) potential for titanium and titania. Journal of Physics Condensed Matter, 2014, 26, 315007.	0.7	21
17497	Structural phase transitions in two-dimensional Mo- and W-dichalcogenide monolayers. Nature Communications, 2014, 5, 4214.	5.8	832
17498	Superconductivity of lithium-doped hydrogen under high pressure. Acta Crystallographica Section C, Structural Chemistry, 2014, 70, 104-111.	0.2	59
17499	Structural and electronic properties of new 1D and 2D carbon allotropes with mixed sp1â^'sp3 hybridization types. Chemical Physics Letters, 2014, 609, 15-20.	1.2	4
17500	Ab initio calculation of half-metallic ferromagnetism in zinc-blende (CaN)1/(AlN)x and (CaN)x/(AlN)1 (x=2, 3) (001) superlattices. Solid State Communications, 2014, 194, 43-47.	0.9	1
17501	Ab Initio Atomistic Thermodynamics of Water Reacting with Uranium Dioxide Surfaces. Journal of Physical Chemistry C, 2014, 118, 8491-8500.	1.5	26
17502	Occupation matrix control of d- and f-electron localisations using DFT + U. Physical Chemistry Chemical Physics, 2014, 16, 21016-21031.	1.3	160
17503	Stability of the D8m-Ti5Sn2Ga compound. Experimental determinations and first principle calculations. Journal of Chemical Thermodynamics, 2014, 78, 269-277.	1.0	2
17504	Alkali cation specific adsorption onto fcc(111) transition metal electrodes. Physical Chemistry Chemical Physics, 2014, 16, 13699-13707.	1.3	93
17505	Electronic structures and magnetism of transition metal doped BiAlO3: An ab initio study. Physica B: Condensed Matter, 2014, 451, 76-79.	1.3	3

#	Article	IF	Citations
17506	Enhanced visible-light photocatalytic activity of g-C3N4/Zn2GeO4 heterojunctions with effective interfaces based on band match. Nanoscale, 2014, 6, 2649.	2.8	227
17507	Atomic Structure, Electronic Properties, and Reactivity of In-Plane Heterostructures of Graphene and Hexagonal Boron Nitride. Journal of Physical Chemistry C, 2014, 118, 16104-16112.	1.5	20
17508	Molecular and Electronic Structure of Cyclic Trinuclear Gold(I) Carbeniate Complexes: Insights for Structure/Luminescence/Conductivity Relationships. Inorganic Chemistry, 2014, 53, 7485-7499.	1.9	32
17509	Large Capacitance Enhancement Induced by Metal-Doping in Graphene-Based Supercapacitors: A First-Principles-Based Assessment. ACS Applied Materials & Interfaces, 2014, 6, 12168-12176.	4.0	40
17510	Hydrogen embrittlement of a carbon segregated <mml:math xmlns:mml="http://www.w3.org/1998/Math/MathML" altimg="si0032.gif" overflow="scroll"><mml:mi>Î£</mml:mi><mml:mn>5</mml:mn><mml:mo>(</mml:mo><mml:mn>310</mml:mn><mml:mo>)</mml:mo> symmetrical tilt grain boundary in Î±-Fe. Materials Science & Engineering A: Structural Materials: Properties, Microstructure and Processing, 2014, 612, 462-467.	2.6	19
17511	Development of a ReaxFF Reactive Force Field for Ammonium Nitrate and Application to Shock Compression and Thermal Decomposition. Journal of Physical Chemistry A, 2014, 118, 1469-1478.	1.1	29
17512	Interplay of growth mode and thermally induced spin accumulation in epitaxial<mml:math xmlns:mml="http://www.w3.org/1998/Math/MathML"><mml:msub><mml:mtext>Al/Co</mml:mtext><mml:mn>2</mml:mn></mml:msu xmlns:mml="http://www.w3.org/1998/Math/MathML"><mml:msub><mml:mtext>Al/Co</mml:mtext><mml:mn>2</mml:mn></mml:msu Physical Review B, 2014, 89, .	1.1	19
17513	Electronic structures and energy band properties of Be- and S-doped wurtzite ZnO. Chinese Physics B, 2014, 23, 066301.	0.7	7
17514	Experimental and theoretical study of the electronic properties of Cu-doped anatase TiO2. Physical Chemistry Chemical Physics, 2014, 16, 3835.	1.3	111
17515	Dynamic Effects on the Charge Transport in an Organic Near-Infrared Absorber Material. Journal of Physical Chemistry C, 2014, 118, 6537-6547.	1.5	15
17516	Morphology dependence of catalytic properties of Ni nanoparticles at the tips of carbon nanofibers for ammonia decomposition to generate hydrogen. International Journal of Hydrogen Energy, 2014, 39, 20722-20730.	3.8	16
17517	Response of MoS 2 nanosheet field effect transistor under different gas environments and its long wavelength photoresponse characteristics. Journal of Alloys and Compounds, 2014, 615, 989-993.	2.8	24
17518	Understanding the interaction of DNAâ€“RNA nucleobases with different ZnO nanomaterials. Physical Chemistry Chemical Physics, 2014, 16, 15355.	1.3	63
17519	Structural and electronic properties of Pd-decorated graphene oxides and their effects on the adsorption of nitrogen oxides: insights from density functional calculations. RSC Advances, 2014, 4, 23084-23096.	1.7	28
17520	Electron Spectroscopy and the Electronic Structure of KNbO₃: First Principle Calculations. Ferroelectrics, 2014, 461, 99-105.	0.3	13
17521	Electronic and transport properties of T-graphene nanoribbon: Symmetry-dependent multiple Dirac points, negative differential resistance and linear current-bias characteristics. Europhysics Letters, 2014, 107, 37004.	0.7	25
17522	Band gap engineering of FeS₂ under biaxial strain: a first principles study. Physical Chemistry Chemical Physics, 2014, 16, 24466-24472.	1.3	38
17523	Characterization of SiCN thin films: Experimental and theoretical investigations. Thin Solid Films, 2014, 569, 57-63.	0.8	39

#	Article	IF	Citations
17524	First Principles <I>Ab Initio</I> Study of Co₂ Adsorption On The Kaolinite (001) Surface. Clays and Clay Minerals, 2014, 62, 153-160.	0.6	12
17525	A <scp>DFT</scp> Study of Structural and Electronic Properties of <scp><scp>ZnS</scp></scp> Polymorphs and its Pressureâ€Induced Phase Transitions. Journal of the American Ceramic Society, 2014, 97, 4011-4018.	1.9	43
17526	Understanding the local environment of Sm³⁺ in doped SrZrO₃ and energy transfer mechanism using time-resolved luminescence: a combined theoretical and experimental approach. RSC Advances, 2014, 4, 29202-29215.	1.7	83
17527	High-capacity hydrogen storage using Li-decorated Li 2 P sheet. Chemical Physics Letters, 2014, 614, 129-135.	1.2	2
17528	Preparation, Crystal Structure, and Magnetotransport Properties of the New CdCu₃Mn₄O₁₂ Perovskite: A Comparison with Density Functional Theory Calculations. Journal of Physical Chemistry C, 2014, 118, 9652-9658.	1.5	9
17529	First Principles Calculation Study on Surfaces and Water Interfaces of Boron-Doped Diamond. Journal of Physical Chemistry C, 2014, 118, 22040-22052.	1.5	29
17530	Polytypism in ZnS, ZnSe, and ZnTe: First-principles study. Physical Review B, 2014, 89, .	1.1	42
17531	Strain tunable ferroelectric and dielectric properties of BaZrO3. Journal of Applied Physics, 2014, 115, 224107.	1.1	20
17532	Stability and spectroscopy of Mg sulfate minerals: Role of hydration on sulfur isotope partitioning. American Mineralogist, 2014, 99, 1216-1220.	0.9	2
17533	A metallic carbon consisting of helical carbon triangle chains. Journal of Physics Condensed Matter, 2014, 26, 235402.	0.7	10
17534	Experimental Characterization of Unimolecular Water Dissociative Adsorption on Î±-Alumina. Journal of Physical Chemistry C, 2014, 118, 13623-13630.	1.5	34
17535	Phase Coexistence and Metal-Insulator Transition in Few-Layer Phosphorene: A Computational Study. Physical Review Letters, 2014, 113, 046804.	2.9	556
17536	Linear optical and electronic properties of the polar metallic ruthenate (Sr,Ca)Ru2O6. Journal of Physics Condensed Matter, 2014, 26, 265501.	0.7	2
17537	Structural and Vibrational Properties of the Ordered Y₂CaGe₄O₁₂ Germanate: A Periodic Ab Initio Study. Journal of Physical Chemistry C, 2014, 118, 8090-8101.	1.5	18
17538	Adsorption Properties of the o-Al₁₃Co₄(100) Surface toward Molecules Involved in the Semihydrogenation of Acetylene. Journal of Physical Chemistry C, 2014, 118, 23032-23041.	1.5	12
17539	An ab initio thermodynamics study of cobalt surface phases under ethanol steam reforming conditions. Catalysis Science and Technology, 2014, 4, 3379-3389.	2.1	27
17540	Influences of Epitaxial Strain and Volume on BaTiO3: Ab Initio Total Energy Calculation. Integrated Ferroelectrics, 2014, 155, 91-99.	0.3	3
17541	Electronic structure of BSb defective monolayers and nanoribbons. Journal of Physics Condensed Matter, 2014, 26, 325303.	0.7	9

#	Article	IF	Citations
17542	Ab-initiostudy of long-period superstructures and anti-phase boundaries in Al-richÎ³-TiAl (L1₀)-based alloys. Philosophical Magazine, 2014, 94, 1202-1218.	0.7	7
17543	Roles of Plasmonic Excitation and Protonation on Photoreactions of p-Aminobenzenethiol on Ag Nanoparticles. Journal of Physical Chemistry C, 2014, 118, 6893-6902.	1.5	33
17544	Multiphase equation of state for carbon addressing high pressures and temperatures. Physical Review B, 2014, 89, .	1.1	127
17545	First-principles study of a novel superhardsp3carbon allotrope. Physics Letters, Section A: General, Atomic and Solid State Physics, 2014, 378, 3326-3330.	0.9	27
17546	Alloying-related trends in thermal properties of ternary TiN-based nitrides. International Journal of Modern Physics B, 2014, 28, 1450087.	1.0	3
17547	Similarities between Zinc Hydroxide Chloride Monohydrate and Its Dehydrated Form: A Theoretical Study of Their Structures and Anionic Exchange Properties. Journal of Physical Chemistry C, 2014, 118, 19106-19113.	1.5	24
17548	Effects of van der Waals interaction and electric field on the electronic structure of bilayer MoS₂. Journal of Physics Condensed Matter, 2014, 26, 405302.	0.7	49
17549	First-principles calculations of elastic and thermodynamic properties of the four main intermetallic phases in Alâ€“Znâ€“Mgâ€“Cu alloys. Computational Materials Science, 2014, 93, 210-220.	1.4	72
17550	First-principles studies on structural, mechanical, thermodynamic and electronic properties of Niâ€“Zr intermetallic compounds. Intermetallics, 2014, 54, 110-119.	1.8	64
17551	Ag₃Ga₃SiSe₈: a new infrared nonlinear optical material with a chalcopyrite structure. CrystEngComm, 2014, 16, 6836.	1.3	32
17552	Composition dependent intrinsic defect structures in SrTiO₃. Physical Chemistry Chemical Physics, 2014, 16, 15590-15596.	1.3	51
17553	Diffusion of Te vacancy and interstitials of Te, Cl, O, S, P and Sb in CdTe: A density functional theory study. Solar Energy Materials and Solar Cells, 2014, 128, 343-350.	3.0	9
17554	A Minimal Cluster Model of Valence Electrons in Adatom-Assisted Adsorbed Molecules: NCH₃/Cu(110) and OCH₃/Cu(110). Journal of Physical Chemistry C, 2014, 118, 9443-9449.	1.5	0
17555	Effect of temperature-induced solute distribution on stacking fault energy in Mgâ€“X(Xâ€‰=â€‰Li, Cu, Zn, Al, Y)	0.7	31
17556	Catalytic NO activation and NOâ€“H 2 reaction pathways. Journal of Catalysis, 2014, 319, 95-109.	3.1	31
17557	Atomistic mechanisms of codoping-induced p- to n-type conversion in nitrogen-doped graphene. Nanoscale, 2014, 6, 14911-14918.	2.8	30
17558	Role of magnetic degrees of freedom in a scenario of phase transformations in steel. Physical Review B, 2014, 90, .	1.1	23
17559	Anomalous properties of antiferroelectric<mml:math xmlns:mml="http://www.w3.org/1998/Math/MathML"><mml:msub><mml:mtext>PbZrO</mml:mtext><mml:mn>3</mml:mn></mml:msub></mml:math> hydrostatic pressure. Physical Review B, 2014, 89, .	1.1	11

#	Article	IF	Citations
17560	Unexpected Synergy between Magnetic Iron Chains and Stacked B₆ Rings in Nb₆Fe_{1â^'x}Ir_{6+x}B₈. Angewandte Chemie - International Edition, 2014, 53, 13174-13177.	7.2	22
17561	Influence of unlike dispersion interactions in modeling methane clathrate hydrates. Fluid Phase Equilibria, 2014, 381, 108-115.	1.4	17
17562	Large scale supercell calculations for forces around substitutional defects in NiTi. Physica Status Solidi (B): Basic Research, 2014, 251, 2048-2054.	0.7	5
17563	B3LYP Periodic Study of the Physicochemical Properties of the Nonpolar (010) Mg-Pure and Fe-Containing Olivine Surfaces. Journal of Physical Chemistry A, 2014, 118, 5866-5875.	1.1	20
17564	Equation of state of lead from high-pressure neutron diffraction up to 8.9 GPa and its implication for the NaCl pressure scale. Physical Review B, 2014, 90, .	1.1	48
17565	Ab Initio calculations of the lattice dynamics and the ferroelectric instability of the BiFeO3 multiferroic. Physics of the Solid State, 2014, 56, 1799-1805.	0.2	8
17566	DFT study of reaction processes of methane combustion on PdO(100). Chemical Physics, 2014, 443, 53-60.	0.9	25
17567	Exploring the Structural Complexity of Intermetallic Compounds by an Adaptive Genetic Algorithm. Physical Review Letters, 2014, 112, 045502.	2.9	97
17568	Reactivity of the Defective Rutile TiO₂ (110) Surfaces with Two Bridging-Oxygen Vacancies: Water Molecule as a Probe. Journal of Physical Chemistry C, 2014, 118, 20257-20263.	1.5	20
17569	Absolute surface energies of polar and nonpolar planes of GaN. Physical Review B, 2014, 89, .	1.1	89
17570	The covariance of the differences between experimental and theoretical chemical shifts as an aid for assigning two-dimensional heteronuclear correlation solid-state NMR spectra. Chemical Physics Letters, 2014, 608, 334-339.	1.2	20
17571	Ab Initio Study of H2 Associative Desorption on Ad-Dimer Reconstructed Si(001) and Ge(001)-(2Ã—1) Surfaces. Journal of Physical Chemistry C, 2014, 118, 10088-10096.	1.5	5
17572	Semimetallic molybdenum disulfide ultrathin nanosheets as an efficient electrocatalyst for hydrogen evolution. Nanoscale, 2014, 6, 8359-8367.	2.8	248
17573	Thermodynamic optimizations on the binary Liâ€“Sn system and ternary Mgâ€“Snâ€“Li system. Calphad: Computer Coupling of Phase Diagrams and Thermochemistry, 2014, 47, 100-113.	0.7	23
17574	Stabilization of the tetragonal distortion of Fe<mml:math xmlns:mml="http://www.w3.org/1998/Math/MathML"><mml:msub><mml:mrow /><mml:mi>x</mml:mi></mml:msub></mml:math>Co<mml:math xmlns:mml="http://www.w3.org/1998/Math/MathML"><mml:msub><mml:mrow /><mml:mrow><mml:mn>1</mml:mn><mml:mo>â^'</mml:mo><mml:mi>x</mml:mi></mml:mrow></mml:msub></mml:math>alloys by C impurities: A potential new permanent magnet. Physical Review B, 2014, 89, .	1.1	60
17575	Tunable electronic structures of p-type Mg doping in AlN nanosheet. Journal of Applied Physics, 2014, 116, .	1.1	33
17576	Oxide enthalpy of formation and band gap energy as accurate descriptors of oxygen vacancy formation energetics. Energy and Environmental Science, 2014, 7, 1996.	15.6	109
17577	Bulk Properties of Transition Metals: A Challenge for the Design of Universal Density Functionals. Journal of Chemical Theory and Computation, 2014, 10, 3832-3839.	2.3	245

#	Article	IF	Citations
17578	Adsorption of methanethiol on Au(1 1 1): Role of hydrogen bonds. Chemical Physics Letters, 2014, 610-611, 381-387.	1.2	2
17579	Compressibility Systematics of Calcite-Type Borates: An Experimental and Theoretical Structural Study on ABO₃ (A = Al, Sc, Fe, and In). Journal of Physical Chemistry C, 2014, 118, 4354-4361.	1.5	22
17580	Lattice dynamics, thermodynamics and elastic properties of Li₂Te under high pressure: first principles study. Materials Science and Technology, 2014, 30, 732-738.	0.8	17
17581	Novel band structures in silicene on monolayer zinc sulfide substrate. Journal of Physics Condensed Matter, 2014, 26, 395003.	0.7	13
17582	First-principles study of AlN nanosheets with chlorination. RSC Advances, 2014, 4, 7500.	1.7	17
17583	Disordered photonic crystals: a cluster coherent potential approach using photonic Wannier functions. Journal of the Optical Society of America B: Optical Physics, 2014, 31, 2246.	0.9	2
17584	Theoretical study on Si-doped hexagonal boron nitride (h -BN) sheet: Electronic, magnetic properties, and reactivity. Physics Letters, Section A: General, Atomic and Solid State Physics, 2014, 378, 2989-2994.	0.9	74
17585	Polar Cation Ordering: A Route to Introducing >10% Bond Strain Into Layered Oxide Films. Advanced Functional Materials, 2014, 24, 6884-6891.	7.8	21
17586	Simulation of Diffusion in FCC NiFe Binary Alloys Using Kinetic Monte Carlo Method. Journal of Physical Chemistry C, 2014, 118, 22221-22228.	1.5	12
17587	Oxygen and Hydroxyl Species Induce Multiple Reaction Pathways for the Partial Oxidation of Allyl Alcohol on Gold. Journal of the American Chemical Society, 2014, 136, 6489-6498.	6.6	37
17588	Exploring Hardness and the Distorted sp² Hybridization of Bâ€“B Bonds in WB₃. Chemistry of Materials, 2014, 26, 5297-5302.	3.2	80
17589	Nanocatalyst Superior to Pt for Oxygen Reduction Reactions: The Case of Core/Shell Ag(Au)/CuPd Nanoparticles. Journal of the American Chemical Society, 2014, 136, 15026-15033.	6.6	172
17590	Thermo-selective Tm_xTi_{1â^'x}O_{2â^'x/2}nanoparticles: from Tm-doped anatase TiO₂to a rutile/pyrochlore Tm₂Ti₂O₇mixture. An experimental and theoretical study with a photocatalytic application. Nanoscale, 2014, 6, 12740-12757.	2.8	32
17591	Thickness-Dependent Crossover from Charge- to Strain-Mediated Magnetoelectric Coupling in Ferromagnetic/Piezoelectric Oxide Heterostructures. ACS Nano, 2014, 8, 894-903.	7.3	61
17592	Sodiumâ€“rare earth carbonates with shorite structure and large second harmonic generation response. CrystEngComm, 2014, 16, 4414.	1.3	41
17593	Direct evidence of active and inactive phases of Fe catalyst nanoparticles for carbon nanotube formation. Journal of Catalysis, 2014, 319, 54-60.	3.1	57
17594	First-principles study on the interaction of nitrogen atom with Î±â€“uranium: From surface adsorption to bulk diffusion. Journal of Applied Physics, 2014, 115, .	1.1	12
17595	A first principles study of phase stability, bonding, electronic and lattice dynamical properties of beryllium chalcogenides at high pressure. Journal of Alloys and Compounds, 2014, 617, 905-914.	2.8	12

#	Article	IF	Citations
17596	Toward Equatorial Planarity about Uranyl: Synthesis and Structure of Tridentate Nitrogen-Donor {UO₂}²⁺ Complexes. Inorganic Chemistry, 2014, 53, 2506-2515.	1.9	17
17597	Understanding the Interface of Six-Shell Cuboctahedral and Icosahedral Palladium Clusters on Reduced Graphene Oxide: Experimental and Theoretical Study. Journal of the American Chemical Society, 2014, 136, 6626-6633.	6.6	55
17598	Electron Emission Energy Barriers and Stability of Sc₂O₃ with Adsorbed Ba and Baâ€“O. Journal of Physical Chemistry C, 2014, 118, 19742-19758.	1.5	24
17599	Bayesian uncertainty quantification in the evaluation of alloy properties with the cluster expansion method. Computer Physics Communications, 2014, 185, 2885-2892.	3.0	19
17600	Effects of van der Waals Interactions in the Adsorption of Isooctane and Ethanol on Fe(100) Surfaces. Journal of Physical Chemistry C, 2014, 118, 17608-17615.	1.5	61
17601	Revisiting the Crystal Structure of Rhombohedral Lead Metaniobate. Inorganic Chemistry, 2014, 53, 9715-9721.	1.9	10
17602	SurfKin: An ab initio kinetic code for modeling surface reactions. Journal of Computational Chemistry, 2014, 35, 1890-1899.	1.5	20
17603	Stability characteristics of single-layered zinc oxide nanosheets under uniaxial loading. Acta Mechanica Solida Sinica, 2014, 27, 429-440.	1.0	3
17604	First-principles calculations for the structural, elastic and thermodynamic properties of cubic perovskite BaHfO₃under pressure. Physica Scripta, 2014, 89, 105703.	1.2	12
17605	Convergence of an analytic bond-order potential for collinear magnetism in Fe. Modelling and Simulation in Materials Science and Engineering, 2014, 22, 034005.	0.8	16
17606	Substitution Mechanism of Mn and Fe Ions in <inline-formula> <tex-math notation="TeX">${m Bi}_{4}{m Ti}_{3}{m O}_{12}$ </tex-math></inline-formula>. IEEE Transactions on Magnetics, 2014, 50, 1-6.	1.2	1
17607	Electronic structures mechanical and thermal properties of Vâ€“C binary compounds. RSC Advances, 2014, 4, 44959-44971.	1.7	62
17608	Two-dimensional hexagonal tin: ab initio geometry, stability, electronic structure and functionalization. 2D Materials, 2014, 1, 021004.	2.0	107
17609	Correlating Growth Characteristics in Atomic Layer Deposition with Precursor Molecular Structure: The Case of Zinc Tin Oxide. Chemistry of Materials, 2014, 26, 2795-2802.	3.2	45
17610	Density functional theory study on the interaction of CO with the Fe3O4(001) surface. Applied Surface Science, 2014, 317, 752-759.	3.1	28
17611	Role of Surface Hydroxyl Groups on Zinc Adsorption Characteristics on Î±-Al₂O₃(0001) Surfaces: First-Principles Study. Journal of Physical Chemistry C, 2014, 118, 13578-13589.	1.5	33
17612	Band alignments and polarization properties of BN polymorphs. Applied Physics Express, 2014, 7, 031001.	1.1	46
17613	Optical and electronic properties of nanosized BiTaO₄ and BiNbO₄ photocatalysts: Experiment and theory. Physica Status Solidi (B): Basic Research, 2014, 251, 1034-1039.	0.7	11

#	Article	IF	Citations
17614	Periodic Quantum Chemical Studies on Anhydrous and Hydrated Acid Clinoptilolite. Journal of Physical Chemistry A, 2014, 118, 5779-5789.	1.1	11
17615	Effect of Terminating Species on the Initial Growth of BN on Diamond Substrates. Journal of Physical Chemistry C, 2014, 118, 3490-3503.	1.5	4
17616	Electronic structure and optical properties of nonpolar Ga0.75Al0.25N surfaces. Optik, 2014, 125, 6260-6265.	1.4	1
17617	A DFT study on the interaction between glycine molecules/radicals and the (8, 0) SiCNT. Physical Chemistry Chemical Physics, 2014, 16, 17988-17997.	1.3	14
17618	Optical and Acoustic Vibrations Confined in Anatase TiO2Nanoparticles under High-Pressure. Journal of Physical Chemistry C, 2014, 118, 10495-10501.	1.5	10
17619	Tunable electronic properties of ultra-thin boron-carbon-nitrogen heteronanotubes for various compositions. Journal of Molecular Modeling, 2014, 20, 2371.	0.8	2
17620	First-principles study of structural stabilities of AlH3 under high pressure. Journal of Physics and Chemistry of Solids, 2014, 75, 803-807.	1.9	6
17621	Theoretical study of elastic, mechanical and thermodynamic properties of MgRh intermetallic compound. Journal of Magnesium and Alloys, 2014, 2, 59-63.	5.5	48
17622	First-principles study of hydrogen adsorption and permeation in reconstructed cubic erbium oxide surfaces. Fusion Engineering and Design, 2014, 89, 1294-1298.	1.0	2
17623	Simulated non-contact atomic force microscopy for GaAs surfaces based on real-space pseudopotentials. Applied Surface Science, 2014, 303, 163-167.	3.1	11
17624	Structural, electronic, elastic and thermal properties of some transition metal CuX (X=Sc and Pd) intermetallics: A FP-LAPW study. Computational Materials Science, 2014, 83, 64-69.	1.4	16
17625	Phonon instabilities leading to structural phase transition in YN and YP: A first-principles study. Journal of Alloys and Compounds, 2014, 588, 133-137.	2.8	6
17626	Density functional theory calculations for Pd adsorption on SO4 adsorbed on h-BN. Computational Materials Science, 2014, 82, 231-236.	1.4	16
17627	Engineering by Mn embedment and adsorption in defective boron nitrogen sheet. Physica E: Low-Dimensional Systems and Nanostructures, 2014, 56, 24-31.	1.3	3
17628	Negatively curved cubic carbon crystals with octahedral symmetry. Carbon, 2014, 76, 266-274.	5.4	48
17629	Density functional study of NO adsorption on undefected and oxygen defective Auâ€“BaO(100) surfaces. Applied Surface Science, 2014, 307, 165-171.	3.1	3
17630	Hydrogen storage on nitrogen induced defects in palladium-decorated graphene: A first-principles study. Applied Surface Science, 2014, 292, 921-927.	3.1	53
17631	The study of the optical properties of the GaAs with point defects. Optik, 2014, 125, 419-423.	1.4	2

#	Article	IF	Citations
17632	A DFT study of SO₂ and H₂S gas adsorption on Au-doped single-walled carbon nanotubes. Physica Scripta, 2014, 89, 065803.	1.2	86
17633	Strontium, Nickel, Cadmium, and Lead Substitution into Calcite, Studied by Density Functional Theory. Langmuir, 2014, 30, 6129-6133.	1.6	33
17634	Electronâ€“Hole Pair Generation of the Visible-Light Plasmonic Photocatalyst Ag@AgCl: Enhanced Optical Transitions Involving Midgap Defect States of AgCl. Journal of Physical Chemistry C, 2014, 118, 12133-12140.	1.5	48
17635	First-principles quantum molecular dynamics study of Ti_xZr_{1â^'x}N(111)/SiN_y heterostructures and comparison with experimental results. Science and Technology of Advanced Materials, 2014, 15, 025007.	2.8	47
17636	Impact of co-adsorbed oxygen on crotonaldehyde adsorption over gold nanoclusters: a computational study. Physical Chemistry Chemical Physics, 2014, 16, 11202-11210.	1.3	3
17637	A ReaxFF Investigation of Hydride Formation in Palladium Nanoclusters via Monte Carlo and Molecular Dynamics Simulations. Journal of Physical Chemistry C, 2014, 118, 4967-4981.	1.5	53
17638	Investigation on AgGaSe 2 for water splitting from first-principles calculations. Europhysics Letters, 2014, 105, 37007.	0.7	8
17639	Microscopic origin of the<mml:math xmlns:mml="http://www.w3.org/1998/Math/MathML"><mml:mi>p</mml:mi></mml:math>-type conductivity of the topological crystalline insulator SnTe and the effect of Pb alloying. Physical Review B, 2014, 89, .	1.1	84
17640	Experimental and Firstâ€Principles Studies of the Ternary Borides Ta₃Ru₅B₂ and M_{3â€“x}Ru_{5+x}B₂ (M = Zr, Hf). European Journal of Inorganic Chemistry, 2014, 2014, 3085-3094.	1.0	10
17641	Tuning the Performance of Niâ€Based Catalyst by Doping Coinage Metal on Steam Reforming of Methane and Carbonâ€Tolerance. Fuel Cells, 2014, 14, 251-258.	1.5	26
17642	Structural and electronic properties of germanene/MoS2 monolayer and silicene/MoS2 monolayer superlattices. Nanoscale Research Letters, 2014, 9, 110.	3.1	69
17643	Electronic and Structural Properties of Highly Aluminum Ion Doped TiO₂ Nanoparticles: A Combined Experimental and Theoretical Study. ChemPhysChem, 2014, 15, 2267-2280.	1.0	29
17644	Effect of alloying of magnetic and non-magnetic low reactivity atoms into atomic chain. Physica Status Solidi (B): Basic Research, 2014, 251, 871-876.	0.7	9
17645	Effect of dispersion on surface interactions of cobalt(<scp>ii</scp>) octaethylporphyrin monolayer on Au(111) and HOPG(0001) substrates: a comparative first principles study. Physical Chemistry Chemical Physics, 2014, 16, 14096-14107.	1.3	58
17646	A Fundamental Understanding of Catechol and Water Adsorption on a Hydrophilic Silica Surface: Exploring the Underwater Adhesion Mechanism of Mussels on an Atomic Scale. Langmuir, 2014, 30, 6906-6914.	1.6	89
17647	Linear and Nonlinear Optical Properties of K₃B₆O₁₀Br Single Crystal: Experiment and Calculation. Journal of Physical Chemistry C, 2014, 118, 11849-11856.	1.5	73
17648	Crystal Structures, Phase Stability, and Decomposition Reactions in the Quaternary Mgâ€“Bâ€“Nâ€“H Hydrogen Storage System. Journal of Physical Chemistry C, 2014, 118, 11193-11202.	1.5	8
17649	Investigation of Acrylic Acid at High Pressure Using Neutron Diffraction. Journal of Physical Chemistry B, 2014, 118, 4044-4051.	1.2	14

#	Article	IF	Citations
17650	Anisotropic thermal expansion in molecular solids: Theory and experiment on<mml:math xmlns:mml="http://www.w3.org/1998/Math/MathML"><mml:msub><mml:mi>LiBH</mml:mi><mml:mn>4</mml:mn></mml:msub></mml:math> Physical Review B, 2014, 89, .	1.1	9
17651	A New UV Nonlinear Optical Material CsZn₂B₃O₇: ZnO₄ Tetrahedra Double the Efficiency of Second-Harmonic Generation. Inorganic Chemistry, 2014, 53, 2521-2527.	1.9	98
17652	Density functional study of hydrogen adsorption and diffusion on Niâ€loaded graphene and graphene oxide. International Journal of Quantum Chemistry, 2014, 114, 879-884.	1.0	8
17653	Prediction of half-metallic ferromagnetism in C-doped CdS nanowire. RSC Advances, 2014, 4, 24399.	1.7	8
17654	Role of intermediate phase for stable cycling of Na ₇ V ₄ (P ₂ O) Tj ETQq0 0 0 rgBT /Overlock 10 Academy of Sciences of the United States of America, 2014, 111, 599-604.	3.3	136
17655	Comparison of Multilayer Water Adsorption on the Hydrophobic Galena (PbS) and Hydrophilic Pyrite (FeS₂) Surfaces: A DFT Study. Journal of Physical Chemistry C, 2014, 118, 11657-11665.	1.5	108
17656	Enhanced charge ordering transition in doped<mml:math xmlns:mml="http://www.w3.org/1998/Math/MathML"><mml:msub><mml:mi mathvariant="normal">CaFeO</mml:mi><mml:mn>3</mml:mn></mml:msub></mml:math>through steric templating. Physical Review B, 2014, 89, .	1.1	9
17657	The molecular spin filter constructed from 1D organic chain. Physics Letters, Section A: General, Atomic and Solid State Physics, 2014, 378, 2020-2023.	0.9	5
17658	DFT-GGA errors in NO chemisorption energies on (111) transition metal surfaces. Surface Science, 2014, 621, 23-30.	0.8	20
17659	Full-potential study of Fe2NiZ (ZÂ=ÂAl, Si, Ga, Ge). Materials Chemistry and Physics, 2014, 146, 303-312.	2.0	50
17660	Stacking fault emission from grain boundaries: Material dependencies and grain size effects. Materials Science & Engineering A: Structural Materials: Properties, Microstructure and Processing, 2014, 600, 200-210.	2.6	37
17661	First principles study on the influence of vacancy defects on electronic structure and optical properties of Ga0.5Al0.5As photocathodes. Optik, 2014, 125, 587-592.	1.4	9
17662	LDA+U evaluation of the stability of low-index facets of LaCoO3 perovskite. Surface Science, 2014, 619, 71-76.	0.8	23
17663	Superhard and high-strength yne-diamond semimetals. Diamond and Related Materials, 2014, 46, 15-20.	1.8	18
17664	First-principles study of hydrogen dissociation and diffusion on transition metal-doped Mg(0001) surfaces. Applied Surface Science, 2014, 305, 40-45.	3.1	31
17665	Adsorption and oxidation of sulfur dioxide on the yttria-stabilized zirconia surface: ab initio atomistic thermodynamics study. Physics Letters, Section A: General, Atomic and Solid State Physics, 2014, 378, 659-666.	0.9	5
17666	A comparative computational study of the diffusion of Na and Li atoms in Sn(111) nanosheets. Solid State Ionics, 2014, 268, 273-276.	1.3	7
17667	Nitrogen-containing carbon nanostructures: A promising carrier for catalysis of ammonia borane dehydrogenation. Carbon, 2014, 68, 462-472.	5.4	27

#	Article	IF	Citations
17668	Initial adsorption of water molecule on HfC and TaC (001) surfaces from density-functional study. Applied Surface Science, 2014, 290, 35-39.	3.1	4
17669	Energetic prediction on the stability of A2Mg12Si7, A2Mg4Si3, and AMgSi in the A2Siâ€“Mg2Si system (A=Ca, Sr and Ba) and their calculated electronic structures. Journal of Alloys and Compounds, 2014, 590, 579-585.	2.8	7
17670	Diffusion of Cd vacancy and interstitials of Cd, Cu, Ag, Au and Mo in CdTe: A first principles investigation. Solar Energy, 2014, 101, 245-253.	2.9	21
17671	First-principle calculations of the elastic properties of semiconductors. Computational Materials Science, 2014, 87, 227-231.	1.4	20
17672	The influence of pre-adsorbed Pt on hydrogen adsorption on B2 FeTi(111). International Journal of Hydrogen Energy, 2014, 39, 8621-8630.	3.8	6
17673	Predicting lattice energy and structure of molecular crystals by first-principles method: Role of dispersive interactions. Journal of Crystal Growth, 2014, 396, 14-23.	0.7	17
17674	Strain-dependent diffusion behavior of H within tungsten. Physica B: Condensed Matter, 2014, 443, 76-79.	1.3	10
17675	First-principles thermodynamic description of hydrogen electroadsorption on the Pt(111) surface. Surface Science, 2014, 625, 104-111.	0.8	41
17676	Phenylacetylene hydrogenation on Fe@C and Ni@C coreâ€“shell nanoparticles: About intrinsic activity of graphene-like carbon layer in H2 activation. Carbon, 2014, 74, 291-301.	5.4	69
17677	Low formation energy and kinetic barrier of Stoneâ€“Wales defect in infinite and finite silicene. Chemical Physics Letters, 2014, 592, 52-55.	1.2	22
17678	Refined phase coexistence line between graphite and diamond from density-functional theory and van der Waals correction. Physica B: Condensed Matter, 2014, 434, 185-193.	1.3	20
17679	Effect of strain on atomic-scale friction in layered MoS2. Tribology International, 2014, 77, 211-217.	3.0	33
17680	Significant interplay effect of silicon dopants on electronic properties in graphene. Physics Letters, Section A: General, Atomic and Solid State Physics, 2014, 378, 1841-1844.	0.9	12
17681	Density function theory investigation on the thermodynamic properties of the Liâ€“Nâ€“H system. Materials Chemistry and Physics, 2014, 144, 484-490.	2.0	4
17682	Organizational chirality expression as a function of the chirality measure of simple amino alcohols on Cu(100). Surface Science, 2014, 629, 41-47.	0.8	5
17683	The photo-catalytic activities of MP (M=Ba, Ca, Cu, Sr, Ag; P=PO43â^', HPO42â^') microparticles. Applied Surface Science, 2014, 292, 570-575.	3.1	9
17684	Origin of the ferroelectricity in hydrogen-bonded ferroelectrics [MIICl3(H-MPPA)] (M=Co and Zn) from first-principles study. Solid State Communications, 2014, 185, 47-51.	0.9	3
17685	Structural, electronic and thermodynamic properties of BiF3-type Mg3Gd compound: A first-principle study. Physica B: Condensed Matter, 2014, 432, 33-39.	1.3	26

#	Article	IF	Citations
17686	Influence of a parallel electric field on the dispersion relation of graphene â€“ A new route to Dirac logics. Journal of Crystal Growth, 2014, 401, 869-873.	0.7	2
17687		3.1	12
17688	First-principles study of lattice stability of ReO3-type hypothetical TaO3. Computational Materials Science, 2014, 90, 177-181.	1.4	7
17689	Heterostructural bilayers of graphene and molybdenum disulfide: Configuration types, band opening and enhanced light response. Superlattices and Microstructures, 2014, 68, 56-65.	1.4	7
17690	Thermodynamic and kinetic properties of intrinsic defects and Mg transmutants in 3Câ€“SiC determined by density functional theory. Journal of Nuclear Materials, 2014, 448, 121-128.	1.3	11
17691	Ferromagnetism in Cu-doped polar and nonpolar GaN surfaces. Computational Materials Science, 2014, 83, 217-221.	1.4	7
17692	Dimethylsulfoxide as a modifier of platinum electrocatalytic activity toward oxygen reduction reaction in aqueous solutions: Combined theoretical and experimental study. Journal of Electroanalytical Chemistry, 2014, 714-715, 11-18.	1.9	6
17693	DFT calculations on H, OH and O adsorbate formations on Pt(111) and Pt(332) electrodes. Journal of Electroanalytical Chemistry, 2014, 716, 31-44.	1.9	85
17694	First-principles investigation of structural stability, mechanical properties and electronic structure of Ru1â^'xRexB2 and Re1â^'xRuxB2 borides. Computational Materials Science, 2014, 89, 19-23.	1.4	11
17695	Gas adsorption on silicene: A theoretical study. Computational Materials Science, 2014, 87, 218-226.	1.4	132
17696	DFT study of chlorine adsorption on bimetallic surfaces - Case study of Pd3M and Pt3M alloy surfaces. Electrochimica Acta, 2014, 130, 453-463.	2.6	13
17697	Structural stability and electronic structures of (111) twin boundaries in the rock-salt MnS. Journal of Alloys and Compounds, 2014, 582, 181-185.	2.8	20
17698	Temperature-dependent dielectric function of germanium in the UVâ€“vis spectral range: A first-principles study. Journal of Quantitative Spectroscopy and Radiative Transfer, 2014, 141, 24-30.	1.1	10
17699	First principles calculations of the stability of the T2 and D88 phases in the Vâ€“Siâ€“B system. Intermetallics, 2014, 50, 108-116.	1.8	9
17700	Electronic structure and magnetic properties of transition-metal (Y, Zr, Nb, Mo, Tc, Ru, Rh, Pd, Ag and) Tj ETQq0 0 0 rgBT /Overlock 10 T	1.4	16
17701	Surface structures and thermodynamics of low-index of rutile, brookite and anatase â€“ A comparative DFT study. Applied Surface Science, 2014, 288, 275-287.	3.1	68
17702	First-principles investigations on the electronic properties and stabilities of low-index surfaces of L12â€“Al3Sc intermetallic. Applied Surface Science, 2014, 288, 609-618.	3.1	45
17703	Adsorption of H2S on carbonaceous materials of different dimensionality. International Journal of Hydrogen Energy, 2014, 39, 6610-6619.	3.8	41

#	Article	IF	Citations
17704	CH4 dissociation on the perfect and defective MgO(001) supported Ni4. Fuel, 2014, 123, 285-292.	3.4	31
17705	First-principles study of structural and electronic properties of C14-type Laves phase Al2Zr and Al2Hf. Computational Materials Science, 2014, 83, 27-34.	1.4	198
17706	First-principles molecular dynamics study on temperature-dependent dielectric function of bulk 3C and 6H SiC in the energy range 3â€“8eV. Physica B: Condensed Matter, 2014, 436, 182-187.	1.3	11
17707	Conformational origins of polymorphism in two forms of flufenamic acid. Journal of Molecular Structure, 2014, 1078, 83-89.	1.8	26
17708	Electronic, structural and magnetic studies of niobium borides of group 8 transition metals, Nb2MB2 (M=Fe, Ru, Os) from first principles calculations. Journal of Solid State Chemistry, 2014, 211, 227-234.	1.4	17
17709	A DF-vdW study of the CH4 adsorption on different Ni surfaces. Surface Science, 2014, 625, 64-68.	0.8	27
17710	Density functional study of H2O adsorption and dissociation on WC(0001). Computational and Theoretical Chemistry, 2014, 1039, 75-80.	1.1	21
17711	Antisite defect in nonstoichiometric yttrium aluminum garnet: Experimental and first-principles calculation. Journal of the European Ceramic Society, 2014, 34, 783-790.	2.8	11
17712	Density Functional Theory study of the hydrogen storage in a vacancy zone of an ironâ€“nickel cell. International Journal of Hydrogen Energy, 2014, 39, 8744-8748.	3.8	7
17713	Electronic structure and lattice dynamics of CaxMg1â^'xS in the rock-salt phase. Materials Science in Semiconductor Processing, 2014, 18, 71-79.	1.9	3
17714	Dielectric function spectra and inter-band optical transitions in TlGaS2. Thin Solid Films, 2014, 571, 589-592.	0.8	9
17715	Effect of carbon vacancies on thermodynamic properties of TiCâ€“ZrC mixed carbides. Calphad: Computer Coupling of Phase Diagrams and Thermochemistry, 2014, 46, 87-91.	0.7	28
17716	Mechanisms for adsorption, dissociation and diffusion of hydrogen in hydrogen permeation barrier of Î±-Al2O3: The role of crystal orientation. International Journal of Hydrogen Energy, 2014, 39, 610-619.	3.8	40
17717	Can binary sp half-metallic ferromagnets maintain half-metallicity when they form superlattices? A first-principles approach. Physics Letters, Section A: General, Atomic and Solid State Physics, 2014, 378, 1208-1212.	0.9	9
17718	Theoretical insights into structuralâ€“electronic relationships and relative stability of the Cu-, Al- and O-terminated CuAlO2(0001) surfaces. Vacuum, 2014, 107, 90-98.	1.6	13
17719	Ab initio thermodynamics of zirconium hydrides and deuterides. Computational Materials Science, 2014, 86, 211-222.	1.4	64
17720	Arc characteristics and microstructure evolution of Wâ€“Cu contacts during the vacuum breakdown. Vacuum, 2014, 107, 83-89.	1.6	35
17721	Intrinsic brittleness of Mo5SiB2 and alloying effect on ductility studied by first-principles calculations. Intermetallics, 2014, 50, 79-85.	1.8	10

#	Article	IF	Citations
17722	DFT+U study on the oxygen adsorption and dissociation on CeO2-supported platinum cluster. Applied Surface Science, 2014, 288, 244-250.	3.1	26
17723	Dynamics of point defect formation, clustering and pit initiation on the pyrite surface. Electrochimica Acta, 2014, 127, 416-426.	2.6	52
17724	Compressive strain as the main origin of enhanced oxygen reduction reaction activity for Pt electrocatalysts on chromium-doped titania support. Applied Catalysis B: Environmental, 2014, 158-159, 112-118.	10.8	50
17725	First principles study of the ZrX2 (XÂ=ÂH, D and T) compounds. International Journal of Hydrogen Energy, 2014, 39, 9681-9689.	3.8	21
17726	Density functional study on ferromagnetism in (Al, Fe)-codoped 4H-SiC. Computational Materials Science, 2014, 87, 72-75.	1.4	16
17727	Can twins enhance the elastic stiffness of face-centered-cubic metals?. Computational Materials Science, 2014, 89, 24-29.	1.4	2
17728	Alloys based on Crâ€“Cr2Ta containing Si. Intermetallics, 2014, 48, 62-70.	1.8	19
17729	Hydrostatic pressure effects on structural and electronic properties of TATB from first principles calculations. Chemical Physics, 2014, 436-437, 1-7.	0.9	30
17730	Effects of native defects on the electronic structure and photocatalytic activity in anatase TiO2 by first principles calculations. Optik, 2014, 125, 3145-3149.	1.4	3
17731	First-principles calculation of electronic structure and microwave dielectric properties of Fe-doped o-Cr7C3. Computational Materials Science, 2014, 83, 298-302.	1.4	13
17732	Theoretical study on SmxSr1â^'xMnO3 as a potential solid oxide fuel cell cathode. Journal of Power Sources, 2014, 253, 138-142.	4.0	17
17733	Theoretical study of mixing energetics in homovalent fluorite-structured oxide solid solutions. Journal of Nuclear Materials, 2014, 444, 292-297.	1.3	8
17734	Single crystalline VO2 nanosheets: A cathode material for sodium-ion batteries with high rate cycling performance. Journal of Power Sources, 2014, 250, 181-187.	4.0	78
17735	First-principles study of Al/A13Ti heterogeneous nucleation interface. Applied Surface Science, 2014, 307, 593-600.	3.1	74
17736	Thermodynamic stability of oxide phases of Feâ€“Cr based ODS steels via quantum mechanical calculations. Calphad: Computer Coupling of Phase Diagrams and Thermochemistry, 2014, 45, 188-193.	0.7	32
17737	Magnetism in Ni-doped AlN with N vacancy: A first-principles study. Computational Materials Science, 2014, 91, 1-5.	1.4	6
17738	A thermodynamic adsorption/entrapment model for selenium(IV) coprecipitation with calcite. Geochimica Et Cosmochimica Acta, 2014, 134, 16-38.	1.6	46
17739	Phase equilibrium of a CuInSe2â€“CuInS2 pseudobinary system studied by combined first-principles calculations and cluster expansion Monte Carlo simulations. Materials Science in Semiconductor Processing, 2014, 25, 251-257.	1.9	20

#	Article	IF	Citations
17740	ShengBTE: A solver of the Boltzmann transport equation for phonons. Computer Physics Communications, 2014, 185, 1747-1758.	3.0	1,931
17741	Theoretical study of the adsorption of CHO radicals on hexagonal boron nitride sheet: Structural and electronic changes. Applied Surface Science, 2014, 295, 137-143.	3.1	20
17742	Theoretical study of InN growth on Mn-stabilized zirconia (111) substrates. Thin Solid Films, 2014, 551, 110-113.	0.8	0
17743	Structural, half-metallic and elastic properties of the half-Heusler compounds NiMnM (MÂ=ÂSb, As and) Tj ETQq1 1 0.784314 rgBT /O	1.8	40
17744	Effects of interfacial electron transfer on the magnetic structure of SrMnO3 in LaAlO3/SrMnO3 heterostructures. Computational Materials Science, 2014, 81, 483-487.	1.4	6
17745	Crystal structures of LaO1â^'xFxBiS2 (x~0.23, 0.46): Effect of F doping on distortion of Biâ€“S plane. Journal of Solid State Chemistry, 2014, 212, 213-217.	1.4	58
17746	Mechanical properties of doped g-C3N4 â€“ A first-principle study. Vacuum, 2014, 106, 79-85.	1.6	33
17747	Comparative computational study of the energetics of Li, Na, and Mg storage in amorphous and crystalline silicon. Computational Materials Science, 2014, 94, 214-217.	1.4	70
17748	Electronic, magnetic and ferroelectric properties of multiferroic TlNiO3: A first principles study. Computational Materials Science, 2014, 82, 191-196.	1.4	1
17749	Charge separation across P3HT/carbon nanotube interface: First-principles calculations of electronic structures. Chemical Physics Letters, 2014, 597, 45-50.	1.2	3
17750	Elastic anisotropy and thermodynamic properties of iron tetraboride under high pressure and high temperature. Solid State Communications, 2014, 187, 53-58.	0.9	14
17751	Study the high photocatalytic activity of vanadium and phosphorus co-doped TiO2 from experiment and DFT calculations. Computational Materials Science, 2014, 83, 309-317.	1.4	12
17752	Relating the electronic structure and reactivity of the 3d transition metal monoxide surfaces. Catalysis Communications, 2014, 52, 60-64.	1.6	19
17753	Effective mass and band gap of strained graphene. Current Applied Physics, 2014, 14, S136-S139.	1.1	18
17754	Computational study of structural, elastic and electronic properties of lithium disilicate (Li 2 Si 2 O 5) Tj ETQq0 0 0 rgBT /Overlock 10 Tf	1.5	52
17755	Ab initio study on the effects of dopantâ€“defect cluster on the electronic properties of TiO2-based photocatalysts. International Journal of Hydrogen Energy, 2014, 39, 2049-2055.	3.8	17
17756	Oxygen chemisorption-induced surface phase transitions on Cu(110). Surface Science, 2014, 627, 75-84.	0.8	40
17757	Stability of 41 metalâ€“boron systems at 0GPa and 30GPa from first principles. Calphad: Computer Coupling of Phase Diagrams and Thermochemistry, 2014, 46, 184-204.	0.7	89

#	Article	IF	Citations
17758	Electronic structure and point defect concentrations of C11b MoSi2 by first-principles calculations. Journal of Alloys and Compounds, 2014, 605, 45-50.	2.8	21
17759	The sulfur tolerance mechanism of the Cu/CeO2 system. International Journal of Hydrogen Energy, 2014, 39, 1957-1966.	3.8	5
17760	Anisotropic elasticity, sound velocity and thermal conductivity of TiO2 polymorphs from first principles calculations. Computational Materials Science, 2014, 82, 202-218.	1.4	41
17761	First-principles calculations of electronic and optical properties of Mn-doped cubic HfO2. Journal of Alloys and Compounds, 2014, 609, 107-110.	2.8	14
17762	STM contrast inversion of the Fe(110) surface. Applied Surface Science, 2014, 304, 65-72.	3.1	13
17763	Microscopic partition of pressure and elastic constants in CdTe polymorphs. Journal of Alloys and Compounds, 2014, 592, 150-156.	2.8	7
17764	Bonding in PdH2 and Pd2H2 systems adsorbed on carbon nanotubes: Implications for hydrogen storage. International Journal of Hydrogen Energy, 2014, 39, 8780-8790.	3.8	23
17765	Comparative study of metal atom adsorption on free-standing h-BN and h-BN/Ni (111) surfaces. Applied Surface Science, 2014, 299, 29-34.	3.1	36
17766	The structural analysis of Cu(111)-Te <mml:math xmlns:mml="http://www.w3.org/1998/Math/MathML" altimg="si18.gif" overflow="scroll"><mml:mfenced open="(") Tj ETQq0 0 0 rgBT /Overlock 10 Tf 50 437 Td (close=")"><mml:mrow><mml:mn and <mml:math xmlns:mml="http://www.w3.org/1998/Math/MathML" altimg="si19.gif" overflow="scroll"><mml:mfenced open="(") Tj ETQq0 0 0 rgBT /Overlock 10 Tf 50 407 Td (close=")"><mml:mrow><mml:mn>2</mml:mn	0.8	8
17767	Surfac Gate-induced half-metallicity in semihydrogenated silicene. Physica E: Low-Dimensional Systems and Nanostructures, 2014, 56, 43-47.	1.3	16
17768	Silicon isotope fractionation in silicate minerals: Insights from first-principles models of phyllosilicates, albite and pyrope. Geochimica Et Cosmochimica Acta, 2014, 134, 137-154.	1.6	85
17769	Electronic and magnetic properties of 3d-metal trioxides superhalogen cluster-doped monolayer MoS2: A first-principles study. Physics Letters, Section A: General, Atomic and Solid State Physics, 2014, 378, 1651-1656.	0.9	20
17770	Bimetallic two-dimensional PtAg coverage on h-BN substrate: First-principles calculations. Applied Surface Science, 2014, 303, 306-311.	3.1	20
17771	First-principles calculations of the mechanical and electronic properties of Feâ€“Wâ€“C ternary compounds. Computational Materials Science, 2014, 82, 26-32.	1.4	42
17772	Vacancy migration energy dependence on local chemical environment in Feâ€“Cr alloys: A Density Functional Theory study. Journal of Nuclear Materials, 2014, 452, 425-433.	1.3	19
17773	O H versus C H bond scission sequence in ethanol decomposition on Pd(111). Surface Science, 2014, 619, 114-118.	0.8	22
17774	Effect of N distribution on elastic and electronic properties of hexagonal Îµ-Fe6Nx by first-principles calculations. Journal of Magnetism and Magnetic Materials, 2014, 354, 200-204.	1.0	17
17775	Self diffusion anomaly in ferromagnetic metals: A density-functional-theory investigation of magnetically ordered and disordered Fe and Co. Acta Materialia, 2014, 70, 130-136.	3.8	39

#	Article	IF	Citations
17776	Alpha to omega martensitic phase transformation pathways in pure Zr. Journal of Alloys and Compounds, 2014, 586, 693-698.	2.8	24
17777	Structural and electrochemical properties of aluminium doped LiMn2O4 cathode materials for Li battery: Experimental and ab initio calculations. Sustainable Energy Technologies and Assessments, 2014, 5, 44-49.	1.7	38
17778	Investigation of the structure and interaction of cellulose triacetate I crystal using ab initio calculations. Carbohydrate Research, 2014, 388, 61-66.	1.1	5
17779	Curvature induced magnetic nanonodes in (6, 0) SiC/C nanotube heterojunction superlattice. Physica E: Low-Dimensional Systems and Nanostructures, 2014, 58, 153-156.	1.3	1
17780	Facile composition-controlled preparation and photocatalytic application of BiOCl/Bi2O2CO3 nanosheets. Applied Catalysis B: Environmental, 2014, 150-151, 486-495.	10.8	134
17781	Sintering of nickel steam reforming catalysts: Effective mass diffusion constant for Ni-OH at nickel surfaces. Catalysis Today, 2014, 228, 22-31.	2.2	33
17782	Ab initio study of stacking faults and deformation mechanism in C15 Laves phases Cr2X (XÂ=ÂNb, Zr, Hf). Materials Chemistry and Physics, 2014, 143, 702-706.	2.0	20
17783	Interactions of extrinsic interstitial atoms (H, He, O, C) with vacancies in beryllium from first-principles. Computational Materials Science, 2014, 90, 116-122.	1.4	3
17784	A study of structure, energy and electronic properties of TiB2/c-BN interface by first principles calculations. Optical Materials, 2014, 36, 1459-1462.	1.7	13
17785	First-principles study on stability and photoelectron spectroscopy of Ga As2(n= 1â€“9) clusters. Spectrochimica Acta - Part A: Molecular and Biomolecular Spectroscopy, 2014, 118, 533-537.	2.0	4
17786	Surface structure and reaction property of CuCl2-PdCl2 bimetallic catalyst in methanol oxycarbonylation: A DFT approach. Applied Surface Science, 2014, 292, 117-127.	3.1	15
17787	Comparison and stability of the low-index surfaces of c-BN by first-principles. Vacuum, 2014, 104, 92-96.	1.6	12
17788	Temperature dependent LiNbO3(0001): Surface reconstruction and surface charge. Applied Surface Science, 2014, 301, 70-78.	3.1	28
17789	Insights into structural stability and Li superionic conductivity of Li10GeP2S12 from first-principles calculations. Chemical Physics Letters, 2014, 591, 16-20.	1.2	36
17790	Structural, elastic, electronic, chemical bonding and optical properties of Cu-based oxides ACuO (A=Li, Na, K and Rb): An ab initio study. Computational Materials Science, 2014, 81, 561-574.	1.4	53
17791	Functionalization layer effect on the mechanical properties of silicon based micro-cantilever mass sensors: A theoretical study. Sensors and Actuators B: Chemical, 2014, 195, 177-180.	4.0	7
17792	Can graphynes turn into graphene at room temperature?. Carbon, 2014, 73, 283-290.	5.4	27
17793	Co-adsorption of water and glycine on Cu{110}. Physical Chemistry Chemical Physics, 2014, 16, 6101.	1.3	19

#	Article	IF	Citations
17794	In Situ Self-Assembled FeWO₄/Graphene Mesoporous Composites for Li-Ion and Na-Ion Batteries. Chemistry of Materials, 2014, 26, 3721-3730.	3.2	52
17795	Palladium Clusters Anchored on Graphene Vacancies and Their Effect on the Reversible Adsorption of Hydrogen. Journal of Physical Chemistry C, 2014, 118, 5081-5090.	1.5	73
17796	Elastic Constants and Pressure-Induced Effects in MoS₂. Journal of Physical Chemistry C, 2014, 118, 12073-12076.	1.5	60
17797	Porous Boron Nitride with Tunable Pore Size. Journal of Physical Chemistry Letters, 2014, 5, 393-398.	2.1	81
17798	Tuning the electronic properties of half- and full-hydrogenated germanene by chlorination and hydroxylation: A first-principles study. Computational Materials Science, 2014, 92, 244-252.	1.4	23
17799	First-principles study of transition-metal atoms adsorption on MoS2 monolayer. Physica E: Low-Dimensional Systems and Nanostructures, 2014, 63, 276-282.	1.3	88
17800	Pt Skin on AuCu Intermetallic Substrate: A Strategy to Maximize Pt Utilization for Fuel Cells. Journal of the American Chemical Society, 2014, 136, 9643-9649.	6.6	220
17801	Phosphorene: An Unexplored 2D Semiconductor with a High Hole Mobility. ACS Nano, 2014, 8, 4033-4041.	7.3	5,474
17802	Density Functional Theory Study of the Water Dissociation on Platinum Surfaces: General Trends. Journal of Physical Chemistry A, 2014, 118, 5832-5840.	1.1	106
17803	Dependence of the electronic and transport properties of<mml:math xmlns:mml="http://www.w3.org/1998/Math/MathML"><mml:msub><mml:mtext>metal-MoSe</mml:mtext><mml:mn>2</mml:mn></mml:msub></mml:math> on contact structures. Physical Review B, 2014, 89, .	1.1	48
17804	Oxygen-Vacancy-Induced Polar Behavior in (LaFeO3)2/(SrFeO3) Superlattices. Nano Letters, 2014, 14, 2694-2701.	4.5	53
17805	Role of the main adsorption modes in the interaction of the dye [COOHâ€“TPP-Zn(ii)] on a periodic TiO2 slab exposing a rutile (110) surface in a dye-sentized solar cell. RSC Advances, 2014, 4, 9639.	1.7	12
17806	Effect of Anharmonicity on Adsorption Thermodynamics. Journal of Chemical Theory and Computation, 2014, 10, 2479-2487.	2.3	101
17807	First-principles prediction of a promising p-type transparent conductive material CsGeCl₃. Applied Physics Express, 2014, 7, 041201.	1.1	14
17808	Mechanism of Oxygen Exchange between CO₂ and TiO₂(101) Anatase. Journal of Physical Chemistry C, 2014, 118, 1628-1639.	1.5	31
17809	Room temperature ferromagnetic ordering in 4 MeV Ar⁵⁺irradiated TiO₂. Journal Physics D: Applied Physics, 2014, 47, 025001.	1.3	27
17810	Monolithic graphene oxide sheets with controllable composition. Nature Communications, 2014, 5, 3383.	5.8	31
17811	Ab initio study of the structural and optoelectronic properties of the half-Heusler CoCrZ (Z = Al, Ga). Canadian Journal of Physics, 2014, 92, 1105-1112.	0.4	60

#	Article	IF	Citations
17812	Synthesis of Î²-Mg2C3: A Monoclinic High-Pressure Polymorph of Magnesium Sesquicarbide. Inorganic Chemistry, 2014, 53, 7020-7027.	1.9	40
17813	Accurate Modeling of Organic Molecular Crystals by Dispersion-Corrected Density Functional Tight Binding (DFTB). Journal of Physical Chemistry Letters, 2014, 5, 1785-1789.	2.1	155
17814	Structural, electronic and optical properties of novel carbonate fluorides ABCO3F (A=K, Rb, Cs; B=Ca,) Tj ETQq0 0 0 rgBT /Overlock 10 T	1.4	20
17815	Zinc inclusion to heterogeneous nickel catalysts reduces oligomerization during the semi-hydrogenation of acetylene. Journal of Catalysis, 2014, 316, 164-173.	3.1	82
17816	Role of Defects on structural and electronic properties of zigzag C3N nanotubes: A first-principle study. Physica E: Low-Dimensional Systems and Nanostructures, 2014, 56, 48-54.	1.3	18
17817	Theoretical and experimental investigations of the properties of Ge2Sb2Te5 and indium-doped Ge2Sb2Te5 phase change material. Applied Physics A: Materials Science and Processing, 2014, 117, 1307-1314.	1.1	14
17818	Surface Dipoles and Electron Transfer at the Metal Oxideâ€“Metal Interface: A 2PPE Study of Size-Selected Metal Oxide Clusters Supported on Cu(111). Journal of Physical Chemistry C, 2014, 118, 13697-13706.	1.5	30
17819	First-Principles Study of Barium and Zirconium Stability in Uranium Mononitride Nuclear Fuels. Journal of Physical Chemistry C, 2014, 118, 14579-14585.	1.5	11
17820	Electronic and optical properties of silicon based porous sheets. Physical Chemistry Chemical Physics, 2014, 16, 16832.	1.3	16
17821	A quantum chemistry study of natural gas hydrates. Journal of Molecular Modeling, 2014, 20, 2182.	0.8	18
17822	Ab initio investigation of a new boron nitride allotrope. Physica Status Solidi (B): Basic Research, 2014, 251, 1282-1285.	0.7	11
17823	Influence of Hydroxyls on Pd Atom Mobility and Clustering on Rutile TiO₂(011)-2 Ã— 1. ACS Nano, 2014, 8, 6321-6333.	7.3	49
17824	Thermal physics of the lead chalcogenides PbS, PbSe, and PbTe from first principles. Physical Review B, 2014, 89, .	1.1	212
17825	The dependence of SO3 dissociation on the diameter of single-wall carbon nanotubes based on first-principles calculations. Chemical Physics Letters, 2014, 608, 1-5.	1.2	4
17826	First-Principles Study of Lanthanum Strontium Manganite: Insights into Electronic Structure and Oxygen Vacancy Formation. Journal of Physical Chemistry C, 2014, 118, 13346-13356.	1.5	82
17827	Bandâ€Gap Manipulations of Monolayer Graphene by Phenyl Radical Adsorptions: A Density Functional Theory Study. ChemPhysChem, 2014, 15, 2610-2617.	1.0	0
17828	Computational and experimental determinations of the UV adsorption of polyvinylsilsesquioxane-silica and titanium dioxide hybrids. Bio-Medical Materials and Engineering, 2014, 24, 651-657.	0.4	3
17829	Water Splitting over Graphene-Based Catalysts: Ab Initio Calculations. ACS Catalysis, 2014, 4, 2016-2021.	5.5	55

#	Article	IF	Citations
17830	Molecular-Level Understanding of CeO₂ as a Catalyst for Partial Alkyne Hydrogenation. Journal of Physical Chemistry C, 2014, 118, 5352-5360.	1.5	112
17831	Anharmonic force constants extracted from first-principles molecular dynamics: applications to heat transfer simulations. Journal of Physics Condensed Matter, 2014, 26, 225402.	0.7	325
17832	Determination of ground-state and low-energy structures of perovskite superlattices from first principles. Physical Review B, 2014, 89, .	1.1	9
17833	Adsorption of hydrogen and hydrocarbon molecules on SiC(001). Surface Science Reports, 2014, 69, 55-104.	3.8	13
17834	New Coâ€“Pdâ€“Zn Î³-Brasses with Dilute Ferrimagnetism and Co₂Zn₁₁ Revisited: Establishing the Synergism between Theory and Experiment. Chemistry of Materials, 2014, 26, 2624-2634.	3.2	23
17835	Local Structure of Fe Impurity Atoms in ZnO: Bulk versus Surface. Journal of Physical Chemistry C, 2014, 118, 5336-5345.	1.5	15
17836	Quasiparticle spectra, absorption spectra, and excitonic properties of NaI and<mml:math xmlns:mml="http://www.w3.org/1998/Math/MathML"><mml:msub><mml:mrow><mml:mi>SrI</mml:mi></mml:mrow><mml:mn>2</mml:mn></mml:msub></mml:math> many-body perturbation theory. Physical Review B, 2014, 89, .	1.1	32
17837	Density functional theory study of the oxygen reduction reaction mechanism in a BN co-doped graphene electrocatalyst. Journal of Materials Chemistry A, 2014, 2, 10273.	5.2	88
17838	A density functional theory study of oxygen reduction reaction on non-PGM Feâ€“Nxâ€“C electrocatalysts. Physical Chemistry Chemical Physics, 2014, 16, 13800.	1.3	170
17839	Electronic structure and anion ordering in<mml:math xmlns:mml="http://www.w3.org/1998/Math/MathML"><mml:msub><mml:mrow><mml:mo>(</mml:mo><mml:mi) Tj ETQq1 1 0.784314 xmlns:mml="http://www.w3.org/1998/Math/MathML"><mml:msub><mml:mtext>ClO</mml:mtext><mml:mn>4</mml:mn></mml:msub		

#	Article	IF	Citations
17848	Multiple satellites in materials with complex plasmon spectra: From graphite to graphene. Physical Review B, 2014, 89, .	1.1	38
17849	Relaxation of atomic orbitals in a plane-wave basis. Physical Review B, 2014, 89, .	1.1	1
17850	Effect of pressure on<mml:math xmlns:mml="http://www.w3.org/1998/Math/MathML"><mml:msub><mml:mtext>La</mml:mtext><mml:mn>2</mml:mn></mml:msub><mml:mi>(</mml:mi><mml:msub><mml:mtext>WO</mml:mtext><mml:mn>4</mml:mn></mml:msub><mml:mi>)</mml:mi><mml:msub><mml:mrow /><mml:mn>3</mml:mn></mml:msub></mml:math>with a modulated scheelite-type structure. Physical Review B, 2014, 89, .	1.1	9
17851	Stress-Induced Grain Growth in an Ultra-Fine Grained Al Alloy. Metallurgical and Materials Transactions A: Physical Metallurgy and Materials Science, 2014, 45, 2673-2688.	1.1	21
17853	Ab initio calculations of structural, elastic, and thermodynamic properties of HoX (X=N, O, S and Se). Materials Science in Semiconductor Processing, 2014, 26, 205-217.	1.9	16
17854	Lattice dynamics and thermodynamical study of yttrium monochalcogenides. Computational Materials Science, 2014, 92, 69-75.	1.4	9
17855	Identification of the partitioning characteristics of refractory elements in Ïƒ and Î³ phases of Ni-based single crystal superalloys based on first principles. Materials Chemistry and Physics, 2014, 147, 483-487.	2.0	7
17856	Solute effect on the <mml:math xmlns:mml="http://www.w3.org/1998/Math/MathML" altimg="si26.gif" overflow="scroll"><mml:mrow><mml:mo stretchy="false">ã€ˆ</mml:mo><mml:mi>a</mml:mi><mml:mo>+</mml:mo><mml:mi>c</mml:mi><mml:mo stretchy="false">ã€‰</mml:mo></mml:mrow></mml:math> dislocation nucleation mechanism in magnesium. Acta Materialia, 2014, 75, 106-112.	3.8	56
17857	Two-dimensional Sc2C: A reversible and high-capacity hydrogen storage material predicted by first-principles calculations. International Journal of Hydrogen Energy, 2014, 39, 10606-10612.	3.8	163
17858	Electronic structure, phase stability and elastic properties of ruthenium based four intermetallic compounds: Ab-initio study. Intermetallics, 2014, 54, 79-85.	1.8	20
17859	Optical properties of PuO2 and Î±-Pu2O3 by GGA+U+QA studies. Journal of Nuclear Materials, 2014, 452, 414-418.	1.3	19
17860	First-principles simulations of H centers in CaF2. Computational Materials Science, 2014, 89, 247-256.	1.4	6
17861	Uniaxial loading response of one dimensional long period structures of Al3Ti. Computational Materials Science, 2014, 91, 153-158.	1.4	15
17862	Theoretical prediction of the electronic structure, bonding behavior and elastic moduli of scandium intermetallics. Intermetallics, 2014, 53, 129-139.	1.8	25
17863	Mechanisms of Zr surface corrosion determined via molecular dynamics simulations with charge-optimized many-body (COMB) potentials. Journal of Nuclear Materials, 2014, 452, 285-295.	1.3	29
17864	Microstructural characteristics of the microphase Y-Ti2SC in nickel-based superalloys. Journal of Alloys and Compounds, 2014, 611, 104-110.	2.8	8
17865	In silico CrNF, a half-metallic ferromagnetic nitrideâ€“fluoride mimicking CrO2. Journal of Magnetism and Magnetic Materials, 2014, 368, 105-110.	1.0	7
17866	d0 Ferromagnetism in oxygen-doped CuCl: First principles study. Solid State Communications, 2014, 189, 68-71.	0.9	12

#	Article	IF	Citations
17867	The sensing mechanism of Pt-doped SnO2 surface toward CO: A first-principle study. Sensors and Actuators B: Chemical, 2014, 202, 83-92.	4.0	55
17868	Effect of 3d transition elements substitution for Ni in Ni2Mn1+xSn1-x on the phase stability and magnetic properties: A first principle investigation. Journal of Magnetism and Magnetic Materials, 2014, 368, 286-294.	1.0	12
17869	CO oxidation on Ag(111): The catalytic role of H2O. Surface Science, 2014, 628, 104-110.	0.8	10
17870	Point defects in garnet-type solid electrolyte (c-Li7La3Zr2O12) for Li-ion batteries. Solid State Ionics, 2014, 261, 100-105.	1.3	34
17871	Kinetic considerations of gas-phase adsorption of growth species on the c-BN(100) surface. Thin Solid Films, 2014, 564, 246-252.	0.8	0
17872	Phase stability, elasticity, hardness and the minimum thermal conductivity of Si2N2O polymorphs from first principles calculations. Physica B: Condensed Matter, 2014, 449, 236-245.	1.3	8
17873	Spin polarization, orbital occupation and band gap opening in vanadium dioxide: The effect of screened Hartreeâ€“Fock exchange. Chemical Physics Letters, 2014, 608, 126-129.	1.2	16
17874	Energy investigations on the adhesive properties of Al/TiC interfaces: First-principles study. Physica B: Condensed Matter, 2014, 449, 269-273.	1.3	30
17875	Integrated experimental and theoretical approach for corrosion and wear evaluation of laser surface nitrided, Tiâ€“6Alâ€“4V biomaterial in physiological solution. Journal of the Mechanical Behavior of Biomedical Materials, 2014, 37, 153-164.	1.5	22
17876	Segregation of hydrogen to defects in nickel using first-principles calculations: The case of self-interstitials and cavities. Journal of Alloys and Compounds, 2014, 614, 211-220.	2.8	46
17877	Ab Initio Calculation of Proton Transport in DyPO₄. Journal of Physical Chemistry C, 2014, 118, 5073-5080.	1.5	3
17878	A DFT + U study of acetylene selective hydrogenation over anatase supported PdaAgb(a + b = 4) cluster. Physical Chemistry Chemical Physics, 2014, 16, 17541.	1.3	35
17879	First-principles prediction for the stability of LiK(BH4)2. Physica Status Solidi (B): Basic Research, 2014, 251, 1539-1544.	0.7	5
17880	Application of Diffusion Monte Carlo to Materials Dominated by van der Waals Interactions. Journal of Chemical Theory and Computation, 2014, 10, 3417-3422.	2.3	67
17881	Significant Quantum Effects in Hydrogen Activation. ACS Nano, 2014, 8, 4827-4835.	7.3	44
17882	Improving SO2 gas sensing properties of graphene by introducing dopant and defect: A first-principles study. Applied Surface Science, 2014, 313, 405-410.	3.1	102
17883	Unified mechanism for hydrogen trapping at metal vacancies. International Journal of Hydrogen Energy, 2014, 39, 11321-11327.	3.8	30
17884	Ab initio studies of Th3N4, Th2N3 and Th2N2(NH). Solid State Communications, 2014, 193, 41-44.	0.9	10

#	Article	IF	Citations
17885	The nature of oxygen states on the surfaces of CeO2 and La-doped CeO2. Chemical Physics Letters, 2014, 608, 239-243.	1.2	31
17886	Structural, elastic, electronic, and thermodynamic properties of intermetallic Zr2Cu: A first-principles study. Intermetallics, 2014, 54, 7-14.	1.8	14
17887	First-principles prediction of the glass-forming ability in Zrâ€“Ni binary metallic glasses. Intermetallics, 2014, 53, 177-182.	1.8	8
17888	First principles calculations of the pressure affection to g-C3N4. Computational Materials Science, 2014, 91, 258-265.	1.4	16
17889	Elastic, electronic, optical, and spectroscopic properties of Î² -AgMO 2 (M = Al and Ga): First-principles calculations. Computational Materials Science, 2014, 92, 92-101.	1.4	12
17890	Electronic, magnetic and multiferroic properties of magnetoelectric NiTiO3. Journal of Alloys and Compounds, 2014, 613, 401-406.	2.8	30
17891	Chemical and physical adsorption of a H2O molecule on a metal doped Zr (0001) surface. Journal of Nuclear Materials, 2014, 452, 493-499.	1.3	6
17892	First-principles study of single atom adsorption on capped single-walled carbon nanotubes. International Journal of Hydrogen Energy, 2014, 39, 10161-10168.	3.8	10
17893	Electronic structure and stability of hydrogen defects in diamond and boron doped diamond: A density functional theory study. Computational Materials Science, 2014, 89, 257-263.	1.4	5
17894	First-principles investigation of mechanical, electronic and optical properties of Al3Sc intermetallic compound under pressure. Computational Materials Science, 2014, 91, 165-172.	1.4	28
17895	Density functional theory study of tin and titanium dioxides: Structural and mechanical properties in the tetragonal rutile phase. Materials Science in Semiconductor Processing, 2014, 28, 59-65.	1.9	4
17896	Clathrate formation in the systems Srâ€“Cuâ€“Ge and {Ba,Sr}â€“Cuâ€“Ge. Journal of Solid State Chemistry, 2014, 217, 169-179.	1.4	4
17897	Spin-polarized bandgap of graphene induced by alternative chemisorption with MgO (1 1 1) substrate. Carbon, 2014, 77, 208-214.	5.4	9
17898	Structure and energetics of Ni from ab initio molecular dynamics calculations. Computational Materials Science, 2014, 89, 242-246.	1.4	16
17899	Strain tuned Li diffusion in LiCoO2 material for Li ion batteries: A first principles study. Solid State Ionics, 2014, 263, 46-48.	1.3	92
17900	First-principles molecular dynamics investigation of thermal and mechanical stability of the TiN(001)/AlN and ZrN(001)/AlN heterostructures. Thin Solid Films, 2014, 564, 284-293.	0.8	22
17901	Prediction and fabrication of Tiâ€“Zrâ€“Co ternary metallic glasses based on effective atomic radius in Ti solid solution from first-principles calculations. Journal of Non-Crystalline Solids, 2014, 400, 67-71.	1.5	9
17902	Origin of piezoelectricity in monolayer halogenated graphane piezoelectrics. Chemical Physics Letters, 2014, 603, 62-66.	1.2	30

#	Article	IF	Citations
17903	Magnetic properties in carbon-doped In2O3: A density functional theory investigation. Physica B: Condensed Matter, 2014, 450, 54-57.	1.3	4
17904	Oxygen-doped boron nitride nanosheets with excellent performance in hydrogen storage. Nano Energy, 2014, 6, 219-224.	8.2	210
17905	Thermodynamic properties of In1â^'xBxP semiconducting alloys: A first-principles study. Computational Materials Science, 2014, 91, 279-284.	1.4	5
17906	Structural and electrical properties of Sn-doped Ga1.375In0.625O3 with different doping concentrations. Physica B: Condensed Matter, 2014, 443, 125-129.	1.3	6
17907	Simulation of magnesium hydroxide surface and interface. Journal of Alloys and Compounds, 2014, 612, 315-322.	2.8	18
17908	Vectorial doping-promoting charge transfer in anatase TiO2 {001} surface. Applied Surface Science, 2014, 319, 167-172.	3.1	55
17909	An ab initio computational study of pure Zn3N2 and its native point defects and dopants Cu, Ag and Au. Thin Solid Films, 2014, 564, 331-338.	0.8	29
17910	Hydrogen concentration estimation in metals at finite temperature using first-principles calculations and vibrational analysis. Computational Materials Science, 2014, 91, 211-222.	1.4	22
17911	Mechanical and electrochemical properties of nanocrystalline (Mo1â^'xCrx)3Si coatings: Experimental and modeling studies. Journal of Alloys and Compounds, 2014, 611, 179-190.	2.8	4
17912	Hybrid Hartreeâ€"Fock-density functional theory study of V2O5 three phases: Comparison of bulk and layer stability, electron and phonon properties. Acta Materialia, 2014, 75, 246-258.	3.8	20
17913	First principle study of the physical properties of semiconducting binary antimonide compounds under hydrostatic pressures. Materials Science in Semiconductor Processing, 2014, 26, 477-490.	1.9	39
17914	Elastic and lattice dynamical properties of ternary strontium chalcogenide alloys. Materials Science in Semiconductor Processing, 2014, 26, 267-275.	1.9	7
17915	First-principles electronic functionalization of silicene and germanene by adatom chemisorption. Applied Surface Science, 2014, 291, 104-108.	3.1	69
17916	First-principles studies of oxygen chemisorption on Co(0001). Surface Science, 2014, 619, 90-97.	0.8	22
17917	Room temperature ferromagnetism in Cd-doped ZnO thin films through defect engineering. Journal of Alloys and Compounds, 2014, 598, 120-125.	2.8	16
17918	Kinetic Monte Carlo modeling of reaction-induced phase separation in Au/Ni(111) surface alloy. Surface and Coatings Technology, 2014, 255, 15-21.	2.2	4
17919	Density functional study of manganese atom adsorption on hydrogen-terminated armchair boron nitride nanoribbons. Physica B: Condensed Matter, 2014, 447, 65-69.	1.3	5
17920	Structural and phonon dynamical stability of the hypothetical RbN and CsN compounds. Computational Materials Science, 2014, 89, 1-5.	1.4	5

#	Article	IF	Citations
17921	Fe-substituted 10Al2O3Â·2B2O3 as a multifunctional support for automotive Pd catalysts. Applied Catalysis B: Environmental, 2014, 146, 50-56.	10.8	3
17922	Enhanced bioactivity and osteoconductivity of hydroxyapatite through chloride substitution. Journal of Biomedical Materials Research - Part A, 2014, 102, 455-469.	2.1	45
17923	Analysis of Atomic and Electronic Structures on CSL Boundary in Silicon. Nippon Kinzoku Gakkaishi/Journal of the Japan Institute of Metals, 2014, 78, 1-6.	0.2	1
17924	Preparation and photocatalytic properties of new calcium and lead bismuthates. Journal of the Ceramic Society of Japan, 2014, 122, 509-512.	0.5	18
17926	First-principles studies on electronic structures and mechanical properties of AlCu₃with divacancy defects. EPJ Applied Physics, 2014, 67, 10901.	0.3	0
17927	Density functional investigation of structural, electronic and magnetic properties of Cu-codoped ZnO nanotubes. EPJ Applied Physics, 2014, 67, 20403.	0.3	10
17928	Understanding the Adsorption of CuPc and ZnPc on Noble Metal Surfaces by Combining Quantum-Mechanical Modelling and Photoelectron Spectroscopy. Molecules, 2014, 19, 2969-2992.	1.7	69
17929	Gas-Phase and Microsolvated Glycine Interacting with Boron Nitride Nanotubes. A B3LYP-D2* Periodic Study. Inorganics, 2014, 2, 334-350.	1.2	15
17930	Electromechanical Properties of Small Transition-Metal Dichalcogenide Nanotubes. Inorganics, 2014, 2, 155-167.	1.2	18
17931	First principles study of hydrogen doping in anatase TiO₂. EPJ Applied Physics, 2014, 67, 30401.	0.3	20
17932	First-principle study on the effects of electric field and anisotropic oxygen vacancy on dielectric properties of rutile titanium dioxide. EPJ Applied Physics, 2014, 68, 10104.	0.3	0
17933	Unusually large shear wave anisotropy for chlorite in subduction zone settings. Geophysical Research Letters, 2014, 41, 1506-1513.	1.5	58
17934	Interfacial Nb-substitution induced anomalous enhancement of polarization and conductivity in BaTiO3 ferroelectric tunnel junctions. AIP Advances, 2014, 4, 127148.	0.6	3
17935	Fe nanochain and nanowires encapsulation in isolated finite thickness ZnO nanotube and its bundle systems. EPJ Applied Physics, 2014, 67, 20406.	0.3	4
17937	Effect of Hydrogen in a Vanadium Grain Boundary by First Principles. Fusion Science and Technology, 2014, 66, 106-111.	0.6	3
17938	Inelastic Electron-Phonon Coupling in Photoemission Process: Analysis of the Laser-Photoemission Spectrum on the Cu Surface. Hyomen Kagaku, 2014, 35, 409-414.	0.0	0
17939	Investigating individual arsenic dopant atoms in silicon using low-temperature scanning tunnelling microscopy. Journal of Physics Condensed Matter, 2014, 26, 012001.	0.7	28
17940	Energy band structures of group IV compound semiconductors for solar cells. Physica Status Solidi (B): Basic Research, 2014, 251, 2221-2224.	0.7	6

#	Article	IF	Citations
17942	Pressure-induced semimetallic behavior of calcium fromab initiocalculations. Journal of Physics: Conference Series, 2014, 510, 012028.	0.3	1
17943	A Combined Metalâ€“Halide/Metal Flux Synthetic Route towards Typeâ€Ÿ Clathrates: Crystal Structures and Thermoelectric Properties of A₈Al₈Si₃₈ (A=K, Rb, and Cs). Chemistry - A European Journal, 2014, 20, 15077-15088.	1.7	26
17944	Description of polarons in ceria using Density Functional Theory. Journal of Physics: Conference Series, 2014, 526, 012002.	0.3	13
17945	A Predictive Model to Link Molecular Structures to Carbonate Rock Wettability: Adsorption of Various Organic Molecules on Flat and Rugged Calcite Surfaces. , 2014, , .		0
17946	Effect of Ga and As vacancies on electronic properties of Ga_{0.9375}Al_{0.0625}As. Molecular Physics, 2014, 112, 2970-2978.	0.8	0
17947	Synthesis and Characterization of Barium Tetrafluoridobromate(III) Ba(BrF₄)₂. European Journal of Inorganic Chemistry, 2014, 2014, 6261-6267.	1.0	20
17948	Impact of <scp>M</scp>n on the solution enthalpy of hydrogen in austenitic <scp>F</scp>eâ€“<scp>M</scp>n alloys: A firstâ€principles study. Journal of Computational Chemistry, 2014, 35, 2239-2244.	1.5	8
17949	Crystallographic Studies of Cesium Tetrafluorobromates(III). Procedia Chemistry, 2014, 11, 35-42.	0.7	6
17950	Thermodynamic Stability of Oxide Phases of Fe-Cr Based ODS Steels via Quantum Mechanical Calculations. Procedia Engineering, 2014, 86, 788-798.	1.2	12
17951	Mechanical and chemical effects of solute elements on generalized stacking fault energy of Mg. Journal of Materials Research, 2014, 29, 2576-2586.	1.2	13
17952	Effect of Al doping on band gap of pentagonal cross section SiNWs. International Journal of Nanoparticles, 2014, 7, 49.	0.1	1
17953	Layered Grapheneâ€“Hexagonal BN Nanocomposites: Experimentally Feasible Approach to Chargeâ€Induced Switchable CO₂ Capture. ChemSusChem, 2015, 8, 2987-2993.	3.6	43
17954	Theoretical investigations on mechanical and thermal properties of MSiO₄ (M = Zr, Hf). Journal of Materials Research, 2015, 30, 2030-2039.	1.2	27
17955	Quasiparticle theoretical characterization of electronic and optical properties of the photocatalytic material Ti3â^Ï‘O4N. Journal of Materials Research, 2015, 30, 2934-2939.	1.2	3
17956	A study of the oxygen effect on the properties of magnetic anisotropy of Co nanowires on the Cu(210) surface: An ab initio approach. Physics of the Solid State, 2015, 57, 1366-1371.	0.2	3
17957	Approaching extremely low thermal conductivity by crystal structure engineering in Mg₂Al₄Si₅O₁₈. Journal of Materials Research, 2015, 30, 3729-3739.	1.2	18
17958	Nano-domains in thermoelectric Half-Heusler CoTi0.5Sc0.5Sb alloys. Materials Research Society Symposia Proceedings, 2015, 1735, 1.	0.1	0
17959	Electronic properties of monolayer molybdenum dichalcogenides under strains. Materials Research Society Symposia Proceedings, 2015, 1726, 31.	0.1	0

#	Article	IF	Citations
17960	Electronic and optical properties of Zn(Cu,V)O studied by first principles. Optik, 2015, 126, 4731-4734.	1.4	2
17961	Charge Difference Calculation in Fe/Fe3O4 Interfaces from DFT Results. , 2015, 9, 612-618.		14
17962	Data in support of crystal structures of highly-ordered long-period stacking-ordered phases with 18R, 14H and 10H-type stacking sequences in the Mgâ€“Znâ€“Y system. Data in Brief, 2015, 5, 314-320.	0.5	11
17963	Density Functional Modeling of Defects and Impurities in Silicon Materials. Lecture Notes in Physics, 2015, , 69-127.	0.3	2
17964	The AFLOW standard for high-throughput materials science calculations. Computational Materials Science, 2015, 108, 233-238.	1.4	244
17965	Band and scattering tuning for high performance thermoelectric Sn1â^'xMnxTe alloys. Journal of Materiomics, 2015, 1, 307-315.	2.8	193
17966	The study of electronic structure and absorption coefficient of ZnTe:O alloys: A GGA+U method. Computational Materials Science, 2015, 109, 225-230.	1.4	5
17967	Composition and temperature dependences of site occupation for Al, Cr, W, and Nb in MoSi ₂. Chinese Physics B, 2015, 24, 120502.	0.7	8
17968	Elastic properties and electronic structures of NaAlSi ternary obtained with first-principle calculations. Materials Research Innovations, 2015, 19, S5-343-S5-348.	1.0	1
17969	Half-Metallic Ferromagnetic Property Related to Spintronic Applications in 3d (V, Cr, and Mn)-Doped GaP DMSs. Journal of Superconductivity and Novel Magnetism, 2015, 28, 3163-3172.	0.8	18
17970	Atomic scale onset of Al adhesion on Mo2BC. Thin Solid Films, 2015, 589, 707-711.	0.8	5
17971	Ferromagnetic origin of Mn-doped Sr3La2O5Zn2As2: Ab initio study. JETP Letters, 2015, 101, 798-801.	0.4	0
17972	<i>Ab Initio</i> Study of MgSe Self-Interstitial (Mg<i>_i) Tj ETQq0 0 0 rgBT /Overlock 10 Tf 50 262	0.3	8
17973	Thermodynamic and optical properties of CuAlO2 under pressure from first principle. Journal Wuhan University of Technology, Materials Science Edition, 2015, 30, 1338-1344.	0.4	6
17974	Optical Properties of the Narrow-Band Ferroelectrics: First Principle Calculations. Ferroelectrics, 2015, 483, 43-52.	0.3	5
17975	The effect of atomic environment on Bâ€“O bonding state based on the ab initio calculations. Materials Research Innovations, 2015, 19, S283-S286.	1.0	0
17976	Elastic properties of solids at high pressure. Physics-Uspekhi, 2015, 58, 1106-1114.	0.8	8
17977	A Density Functional Study of Iron Segregation at ISFs and Î£5-(001) GBs in mc-Si. Solid State Phenomena, 0, 242, 224-229.	0.3	7

#	Article	IF	Citations
17978	Work function change of Ni, HfO₂films and Ni/HfO₂interfaces as a function of external electric field. International Journal of Modern Physics B, 2015, 29, 1550168.	1.0	3
17979	Adsorption of alkali and alkaline-earth metal atoms on the reconstructed graphene-like BN single sheet. Solid State Sciences, 2015, 50, 69-73.	1.5	17
17980	Effect of Subsurface Oxygen on Selective Catalytic Reduction of NO by H₂ on Pt(100): A First-Principles Study. Journal of Physical Chemistry C, 2015, 119, 24819-24826.	1.5	14
17981	Structure and stability of as cast AlCrFeMnNiTi high entropy alloy. Materials Science and Technology, 2015, 31, 1153-1158.	0.8	5
17982	First-principle study on energy gap of CNT superlattice structure. Journal of Semiconductors, 2015, 36, 102002.	2.0	3
17983	Spin crossovers in iron-bearing MgSiO3 and MgGeO3: Their influence on the post-perovskite transition. Physics of the Earth and Planetary Interiors, 2015, 249, 11-17.	0.7	9
17984	Red-light emission induced by Mn-doped magnesium fluorogermanate. Journal Physics D: Applied Physics, 2015, 48, 475101.	1.3	1
17985	Electronic Structures, Bonding Configurations, and Bandâ€Gapâ€Opening Properties of Graphene Binding with Lowâ€Concentration Fluorine. ChemistryOpen, 2015, 4, 642-650.	0.9	22
17986	Theoretical stability, thin film synthesis and transport properties of the Mo_{n+1}GaC_n MAX phase. Physica Status Solidi - Rapid Research Letters, 2015, 9, 197-201.	1.2	28
17987	Cu adatom charging on Mo supported ScN, MgO and NaF. RSC Advances, 2015, 5, 94436-94445.	1.7	3
17988	Hybrid functional study on the ferroelectricity of domain walls with O-vacancies in PbTiO₃. Mechanical Engineering Journal, 2015, 2, 15-00037-15-00037.	0.2	3
17989	Anisotropic thermoelectric behavior in armchair and zigzag mono- and fewlayer MoS2 in thermoelectric generator applications. Scientific Reports, 2015, 5, 13706.	1.6	61
17990	Conductive Graphitic Carbon Nitride as an Ideal Material for Electrocatalytically Switchable CO2 Capture. Scientific Reports, 2015, 5, 17636.	1.6	60
17991	Hydrogen segregation and its roles in structural stability and metallization: silane under pressure. Scientific Reports, 2015, 5, 13039.	1.6	17
17992	Ab Initio High-Pressure Simulations. , 2015, , 75-104.		0
17993	Preferential Eu Site Occupation and Its Consequences in the Ternary Luminescent Halides<mml:math xmlns:mml="http://www.w3.org/1998/Math/MathML" display="inline"><mml:mrow><mml:msub><mml:mrow><mml:mi>AB</mml:mi></mml:mrow><mml:mrow><mml:mn>2</mml:mn></mml:mrow></mml:msub><mml:mo>â¶</mml:mo><mml:msub><mml:mrow><mml:mi mathvariant="normal">I</mml:mi></mml:mrow><mml:mrow><mml:mn>5</mml:mn></mml:mrow></mml:msub><mml:mo>â¶</mml:mo><mml:msub><mml:mrow><mml:mi>Ln</mml:mi></mml:mrow><mml:mrow><mml:mn>3</mml:mn></mml:mrow></mml:msub></mml:mrow></mml:math>. Physical Review Applied, 2015, 4, .	1.5	14
17994	Construction of a thermodynamic potential for the water ices VII and X. Physical Review B, 2015, 91, .	1.1	36
17995	Heavy-impurity resonance, hybridization, and phonon spectral functions in<mml:math		

#	Article	IF	Citations
17996	Electronic structure of the heavy-fermion caged compound<mml:math xmlns:mml="http://www.w3.org/1998/Math/MathML"><mml:mrow><mml:msub><mml:mtext>Ce</mml:mtext><mml:mn>3</mml:mn> width="4pt" /><mml:mrow><mml:mo>(</mml:mo><mml:mi>X</mml:mi><mml:mo>=</mml:mo><mml:mtext>Si,</mml:mtext><mml:mspace) Tj ETQ	1.1	5
17997	B, 2015, 91, . Electronic stopping power in a narrow band gap semiconductor from first principles. Physical Review B, 2015, 91, .	1.1	57
17998	Structure of Cr monolayer on Ag(001): A buried two-dimensional<mml:math xmlns:mml="http://www.w3.org/1998/Math/MathML"><mml:mrow><mml:mi>c</mml:mi><mml:mo>(</mml:mo><mml:mn>2 Physical Review B, 2015, 91, .	1.1	20
17999	Structural, vibrational, and dielectric properties of Ruddlesden-Popper<mml:math xmlns:mml="http://www.w3.org/1998/Math/MathML"><mml:mrow><mml:msub><mml:mi>Ba</mml:mi><mml:mn>2 first principles. Physical Review B, 2015, 91, .	1.1	9
18000	Noncentrosymmetric structural transitions in ultrashort ferroelectricAGaO3/Aâ€²GaO3superlattices. Physical Review B, 2015, 91, .	1.1	6
18001	First-principles study of the phonon modes in bismuth sillenites. Physical Review B, 2015, 91, .	1.1	5
18002	Atomically thin dilute magnetism in Co-doped phosphorene. Physical Review B, 2015, 91, .	1.1	130
18003	Interface disorder probed at the atomic scale for graphene grown on the C face of SiC. Physical Review B, 2015, 91, .	1.1	20
18004	Electronic structure of<mml:math xmlns:mml="http://www.w3.org/1998/Math/MathML"><mml:mrow><mml:msub><mml:mi>Ce</mml:mi><mml:mn>2 A two-dimensional heavy-fermion system studied by angle-resolved photoemission spectroscopy. Physical Review B, 2015, 91, .	1.1	9
18005	Optical phonon production by upconversion: Heterojunction-transmitted versus native phonons. Physical Review B, 2015, 91, .	1.1	5
18006	Adhesion and material transfer between contacting Al and TiN surfaces from first principles. Physical Review B, 2015, 91, .	1.1	37
18007	Finding the stable structures of<mml:math xmlns:mml="http://www.w3.org/1998/Math/MathML"><mml:mrow><mml:msub><mml:mtext>N</mml:mtext><mml:mrow> anab initiohigh-throughput approach. Physical Review B, 2015, 91, .	1.1	54
18008	Assessing the accuracy of the van der Waals density functionals for rare-gas and small molecular systems. Physical Review B, 2015, 91, .	1.1	34
18009	Magnetic, electrical, and thermodynamic properties of NpIr: Ambient and high-pressure measurements, and electronic structure calculations. Physical Review B, 2015, 91, .	1.1	2
18010	Manipulating femtosecond spin-orbit torques with laser pulse sequences to control magnetic memory states and ringing. Physical Review B, 2015, 91, .	1.1	18
18011	Revealing the hidden correlated electronic structure of strained graphene. Physical Review B, 2015, 91, .	1.1	12
18012	Band-gap engineering with a twist: Formation of intercalant superlattices in twisted graphene bilayers. Physical Review B, 2015, 91, .	1.1	18
18013	Ferroelectric soft mode of polarZnTiO3investigated by Raman spectroscopy at high pressure. Physical Review B, 2015, 91, .	1.1	15

#	Article	IF	Citations
18014	High-pressure polymorph ofLuFe2O4with room-temperature antiferromagnetic order. Physical Review B, 2015, 91, .	1.1	5
18015	Structure classification and melting temperature prediction in octet AB solids via machine learning. Physical Review B, 2015, 91, .	1.1	65
18016	Thermal and vibrational properties of thermoelectric ZnSb: Exploring the origin of low thermal conductivity. Physical Review B, 2015, 91, .	1.1	43
18017	Heats of formation of solids with error estimation: The mBEEF functional with and without fitted reference energies. Physical Review B, 2015, 91, .	1.1	33
18018	Antiferromagnetic structures and electronic energy levels at reconstructed NiO(111) surfaces: A<mml:math xmlns:mml="http://www.w3.org/1998/Math/MathML"><mml:mrow><mml:mi>DFT</mml:mi><mml:mo>+</mml:mo><mml:mi>U</mml:mi><mml:mo>+</mml:mo><mml:mi>V</mml:mi></mml:mrow></mml:math> study. Physical Review B, 2015, 91, .	1.1	22
18019	Two-dimensional inversion-asymmetric topological insulators in functionalized III-Bi bilayers. Physical Review B, 2015, 91, .	1.1	60
18020	Single-layer crystalline phases of antimony: Antimonenes. Physical Review B, 2015, 91, .	1.1	261
18021	Ab initiostudy of the electronic properties and thermodynamic stability of supported and functionalized two-dimensional Sn films. Physical Review B, 2015, 91, .	1.1	39
18022	First-principles simulations of a graphene-based field-effect transistor. Physical Review B, 2015, 91, .	1.1	15
18023	Equilibrium segregation patterns and alloying in Cu/Ni nanoparticles: Experiments versus modeling. Physical Review B, 2015, 91, .	1.1	15
18024	Melting and metallization of silica in the cores of gas giants, ice giants, and super Earths. Physical Review B, 2015, 92, .	1.1	18
18025	Comparative study of the carbide-modified surfaces<mml:math xmlns:mml="http://www.w3.org/1998/Math/MathML"><mml:mrow><mml:mi mathvariant="normal">C</mml:mi><mml:mo>/</mml:mo><mml:mi>Mo</mml:mi><mml:mo>(</mml:mo><mml:mn>110</mml:mn><mml:mo>)</mml:mo></mml:mrow></mml:math> and <mml:math xmlns:mml="http://www.w3.org/1998/Math/MathML"><mml:mrow><mml:mi mathvariant="normal">C</mml:mi><mml:mo>/</mml:mo><mml:mi>Mo</mml:mi><mml:mo>(</mml:mo><mml:mn>100</mml:mn><mml:mo>)</mml:mo></mml:mrow></mml:math> surfaces. Physical Review B, 2015, 92, .	1.1	7
18026	Pressure-induced spin collapse of octahedrally coordinated<mml:math xmlns:mml="http://www.w3.org/1998/Math/MathML"><mml:msup><mml:mrow><mml:mi>Mn</mml:mi></mml:mrow><mml:mrow><m the tetragonal hydrogarnet henritermierite<mml:math xmlns:mml="http://www.w3.org/1998/Math/MathML"><mml:mrow><mml:msub><mml:mi>Ca</mml:mi><mml:mn>3</mml:mn></mml:msub> Physical Review B, 2015, 92, .	1.1	8
18027	Configurational order-disorder induced metal-nonmetal transition in<mml:math xmlns:mml="http://www.w3.org/1998/Math/MathML"><mml:mrow><mml:msub><mml:mtext>B</mml:mtext><mml:mn>13</mml:mn></mml:msub> with first-principles superatom-special quasirandom structure method. Physical Review B, 2015, 92, .	1.1	22
18028	Anisotropic lattice dynamics and intermediate-phase magnetism in delafossite<mml:math xmlns:mml="http://www.w3.org/1998/Math/MathML"><mml:msub><mml:mi>CuFeO</mml:mi><mml:mn>2</mml:mn></mml:msub> Physical Review B, 2015, 92, .	1.1	16
18029	Structure and dynamics of the fullerene polymer<mml:math xmlns:mml="http://www.w3.org/1998/Math/MathML"><mml:mrow><mml:msub><mml:mi>Li</mml:mi><mml:mn>4</mml:mn></mml:msub><mml:mi mathvariant="normal">C</mml:mi><mml:mn>60</mml:mn></mml:mrow></mml:math> studied Superexchange interaction in the <mml:math xmlns:mml="http://www.w3.org/1998/Math/MathML"><mml:mi>A</mml:mi></mml:math> -site ordered perovskite <mml:math xmlns:mml="http://www.w3.org/1998/Math/MathML"><mml:mrow><mml:msub><mml:mi>YMn</mml:mi><mml:mn>3</mml:mn></mml:msub><mml:msub><mml:mi mathvariant="normal">O</mml:mi><mml:mn>12</mml:mn></mml:msub></mml:mrow></mml:math>. Physical Review B, 2015, 92, .	1.1	9
18030		1.1	12
18031	Superconductivity and spin fluctuations in the actinoidâ€“platinum metal borides{Th,U}Pt3B. Physical Review B, 2015, 92, .	1.1	2

#	Article	IF	Citations
18032	Origin of tunnel electroresistance effect in<mml:math xmlns:mml="http://www.w3.org/1998/Math/MathML"><mml:mrow><mml:mi>PbTi</mml:mi><mml:msub><mml:mi mathvariant="normal">O</mml:mi><mml:mn>3</mml:mn></mml:msub></mml:mrow></mml:math>-based multiferroic tunnel junctions. Physical Review B, 2015, 92, .	1.1	29
18033	Simple screened exact-exchange approach for excitonic properties in solids. Physical Review B, 2015, 92, .	1.1	55
18034	Orbital engineering of two-dimensional materials with hydrogenation: A realization of giant gap and strongly correlated topological insulators. Physical Review B, 2015, 92, .	1.1	16
18035	Accurate band gaps of extended systems via efficient vertex corrections in<mml:math xmlns:mml="http://www.w3.org/1998/Math/MathML"><mml:mrow><mml:mi>G</mml:mi><mml:mi>W</mml:mi></mml:mrow></mml:m Physical Review B, 2015, 92, .	1.1	81
18036	Oxygen deficiency in<mml:math xmlns:mml="http://www.w3.org/1998/Math/MathML"><mml:mrow><mml:mi>Ti</mml:mi><mml:msub><mml:mi mathvariant="normal">O</mml:mi><mml:mn>2</mml:mn></mml:msub></mml:mrow></mml:math>: Similarities and differences between the Ti self-interstitial and the O vacancy in bulk rutile and anatase. Physical Review B, 2015, 92, .	1.1	57
18037	First-principles survey of the structure, formation energies, and transition levels of As-interstitial defects in InGaAs. Physical Review B, 2015, 92, .	1.1	7
18038	Beyond the Tamm-Dancoff approximation for extended systems using exact diagonalization. Physical Review B, 2015, 92, .	1.1	101
18039	Pressure-induced structural phase transition in CeNi: X-ray and neutron scattering studies and first-principles calculations. Physical Review B, 2015, 92, .	1.1	3
18040	Stability analysis of the martensitic phase transformation in<mml:math xmlns:mml="http://www.w3.org/1998/Math/MathML"><mml:mrow><mml:msub><mml:mi>Co</mml:mi><mml:mn>2</mml:mn></mml:m alloy. Physical Review B, 2015, 92, .	1.1	11
18041	Ferroelectricity ind0double perovskite fluoroscandates. Physical Review B, 2015, 92, .	1.1	1
18042	Effect of magnetism and atomic order on static atomic displacements in the Invar alloy Fe-27 at.% Pt. Physical Review B, 2015, 92, .	1.1	3
18043	Ab initioinvestigation of BCS-type superconductivity in<mml:math xmlns:mml="http://www.w3.org/1998/Math/MathML"><mml:msub><mml:mi mathvariant="normal">LuNi</mml:mi><mml:mn>2</mml:mn></mml:msub><mml:msub><mml:mi mathvariant="normal">B</mml:mi><mml:mn>2</mml:mn></mml:msub><mml:mi -type superconductors. Physical Review B, 2015, 92, .	1.1	33
18044	Structural transformations of<mml:math xmlns:mml="http://www.w3.org/1998/Math/MathML"><mml:mrow><mml:msub><mml:mi>Li</mml:mi><mml:mn>2</mml:mn></mml:m mathvariant="normal">C</mml:mi><mml:mn>2</mml:mn></mml:msub></mml:mrow></mml:math>at high pressures. Physical Review B, 2015, 92, .	1.1	8
18045	Electronic and magnetic effects of a stacking fault in cobalt nanoscale islands on the Ag(111) surface. Physical Review B, 2015, 92, .	1.1	13
18046	High-temperature superconductivity in heavily N- or B-doped graphene. Physical Review B, 2015, 92, .	1.1	45
18047	Spin-dependent transport in a multiferroic tunnel junction: Theory for<mml:math xmlns:mml="http://www.w3.org/1998/Math/MathML"><mml:mi>Co</mml:mi><mml:mo>/</mml:mo><mml:msub><mml:mi mathvariant="normal">PbTiO</mml:mi><mml:mn>3</mml:mn></mml:msub><mml:mo>/</mml:mo><mml:mi>Co</mml:mi></mml:m Physical Review B, 2015, 92, .	1.1	31
18048	First-principles embedded-cluster calculations of the neutral and charged oxygen vacancy at the rutile<mml:math xmlns:mml="http://www.w3.org/1998/Math/MathML"><mml:msub><mml:mi mathvariant="normal">TiO</mml:mi><mml:mn>2</mml:mn></mml:msub></mml:math>(110) surface. Physical Review B, 2015, 92, .	1.1	25
18049	OH-terminated two-dimensional transition metal carbides and nitrides as ultralow work function materials. Physical Review B, 2015, 92, .	1.1	342

#	Article	IF	Citations
18050	<mml:math xmlns:mml="http://www.w3.org/1998/Math/MathML"><mml:msub><mml:mi>TiS</mml:mi><mml:mn>3</mml:mn></mml:msub></mml Width-independent band gap and strain-tunable electronic properties. Physical Review B, 2015, 92, .	1.1	58
18051	Testing predictions from density functional theory at finite temperatures:<mml:math xmlns:mml="http://www.w3.org/1998/Math/MathML"><mml:msub><mml:mi>Î²</mml:mi><mml:mn>2</mml:mn></mml:msub><mml:m ground states in Co-Pt. Physical Review B, 2015, 92, .	1.1	6
18052	Crystal and electronic structures of nitridophosphate compounds as cathode materials for Na-ion batteries. Physical Review B, 2015, 92, .	1.1	10
18053	Phosphorene analogues: Isoelectronic two-dimensional group-IV monochalcogenides with orthorhombic structure. Physical Review B, 2015, 92, .	1.1	391
18054	First-principles study of surface charging in<mml:math xmlns:mml="http://www.w3.org/1998/Math/MathML"><mml:mrow><mml:msub><mml:mi>LaAlO</mml:mi><mml:mn>3</mml:mn></m Physical Review B, 2015, 92, .	1.1	16
18055	Van Hove singularity and ferromagnetic instability in phosphorene. Physical Review B, 2015, 92, .	1.1	41
18056	Interwire coupling for<mml:math xmlns:mml="http://www.w3.org/1998/Math/MathML"><mml:mi mathvariant="normal">I</mml:mi><mml:mtext>n</mml:mtext><mml:mo>(</mml:mo><mml:mrow><mml:mn>4</mml:mn> probed by surface transport. Physical Review B, 2015, 92, .	1.1	8
18057	Electronic and vibrational properties of<mml:math xmlns:mml="http://www.w3.org/1998/Math/MathML"><mml:msub><mml:mi>TiSe</mml:mi><mml:mn>2</mml:mn></mml:msub> the charge-density-wave phase from first principles. Physical Review B, 2015, 92, .	1.1	56
18058	Rashba effect in single-layer antimony telluroiodide SbTeI. Physical Review B, 2015, 92, .	1.1	60
18059	Monolayer II-VI semiconductors: A first-principles prediction. Physical Review B, 2015, 92, .	1.1	226
18060	Incorporation of Mn in<mml:math xmlns:mml="http://www.w3.org/1998/Math/MathML"><mml:mrow><mml:msub><mml:mi>Al</mml:mi><mml:mi>x</mml:mi></mml:ms mathvariant="normal">N</mml:mi></mml:mrow></mml:math>probed by x-ray absorption and emission spectroscopy, high-resolution microscopy, x-ray diffraction, and first-principles calculations. Physical Review B, 2015, 92, .	1.1	2
18061	Two-dimensional electron gas at the<mml:math xmlns:mml="http://www.w3.org/1998/Math/MathML"><mml:mrow><mml:mi>PbTi</mml:mi><mml:msub><mml:mi mathvariant="normal">O</mml:mi><mml:mn>3</mml:mn></mml:msub><mml:mo>/</mml:mo><mml:mi>SrTi</mml:mi><mml:msub> mathvariant="normal">O</mml:mi><mml:mn>3</mml:mn></mml:msub></mml:mrow></mml:math>interface: Anab initiostudy. Physical Review B, 2015, 92, .	1.1	84
18062	Unusual ferroelectricity induced by the Jahn-Teller effect: A case study on lacunar spinel compounds. Physical Review B, 2015, 92, .	1.1	33
18063	Prediction of a two-dimensional crystalline structure of nitrogen atoms. Physical Review B, 2015, 92, .	1.1	109
18064	Dynamical simulations of an electronically induced solid-solid phase transformation in tungsten. Physical Review B, 2015, 92, .	1.1	44
18065	Quasiparticle spectra of<mml:math xmlns:mml="http://www.w3.org/1998/Math/MathML"><mml:mrow><mml:mn>2</mml:mn><mml:mi>H</mml:mi><mml:mo>-</mml:mo> Two-band superconductivity and the role of tunneling selectivity. Physical Review B, 2015, 92, .	1.1	66
18066	Supercell-size convergence of formation energies and gap levels of vacancy complexes in crystalline silicon in density functional theory calculations. Physical Review B, 2015, 92, .	1.1	16
18067	Origins and implications of the ordering of oxygen vacancies and localized electrons on partially reduced<mml:math xmlns:mml="http://www.w3.org/1998/Math/MathML"><mml:msub><mml:mi>CeO</mml:mi><mml:mn>2</mml:mn></mml:msub> Physical Review B, 2015, 92, .	1.1	37

#	Article	IF	Citations
18068	Dispersion effects in<mml:math xmlns:mml="http://www.w3.org/1998/Math/MathML"><mml:msub><mml:mi>SiO</mml:mi><mml:mn>2</mml:mn></mml:msub></mml:math> Anab initiostudy. Physical Review B, 2015, 92, .	1.1	27
18069	Common effect of chemical and external pressures on the magnetic properties ofRCoPOÂ(R=La,Pr,Nd,Sm). II.. Physical Review B, 2015, 92, .	1.1	5
18070	Spincaloric properties of epitaxial<mml:math xmlns:mml="http://www.w3.org/1998/Math/MathML"><mml:mrow><mml:msub><mml:mi>Co</mml:mi><mml:mn>2</mml:mn></mml:msub></mml:mrow></mml:math> tunnel junctions. Physical Review B, 2015, 92, .	1.1	29
18071	First-principles study of the adsorption of MgO molecules on a clean Fe(001) surface. Physical Review B, 2015, 92, .	1.1	11
18072	Spin-dependent properties and images of MnO, FeO, CoO, and NiO(001) surfaces. Physical Review B, 2015, 92, .	1.1	16
18073	Calculated hybrid and semilocal functionals and<mml:math xmlns:mml="http://www.w3.org/1998/Math/MathML"><mml:mrow><mml:mi>G</mml:mi><mml:mi>W</mml:mi></mml:mrow></mml:math> structure of the metal trifluorides<mml:math xmlns:mml="http://www.w3.org/1998/Math/MathML"><mml:mrow><mml:mi>M</mml:mi><mml:msub><mml:mi		

#	Article	IF	Citations
18086	Modeling interfaces between solids: Application to Li battery materials. Physical Review B, 2015, 92, .	1.1	68
18087	Negative thermal expansion of<mml:math xmlns:mml="http://www.w3.org/1998/Math/MathML"><mml:msub><mml:mi>ScF</mml:mi><mml:mn>3</mml:mn></mml:msub></mml:math>: Insights from density-functional molecular dynamics in the isothermal-isobaric ensemble. Physical Review B, 2015, 92, .	1.1	34
18088	New class of planar ferroelectric Mott insulators via first-principles design. Physical Review B, 2015, 92, .	1.1	4
18089	Incomplete Peierls-like chain dimerization as a mechanism for intrinsic conductivity and optical transparency: A La-Cu-O-S phase with mixed-anion layers as a case study. Physical Review B, 2015, 92, .	1.1	4
18090	Li adsorption versus graphene intercalation on Ir(111): From quenching to restoration of the Ir surface state. Physical Review B, 2015, 92, .	1.1	27
18091	Transport properties of hydrogen-helium mixtures at extreme density and temperature conditions. Physical Review E, 2015, 92, 043108.	0.8	3
18092	Experimental andab initioinvestigations of microscopic properties of laser-shocked Ge-doped ablator. Physical Review E, 2015, 92, 063108.	0.8	27
18093	Quantum Monte Carlo Calculations in Solids with Downfolded Hamiltonians. Physical Review Letters, 2015, 114, 226401.	2.9	44
18094	Candidate Source of Flux Noise in SQUIDs: Adsorbed Oxygen Molecules. Physical Review Letters, 2015, 115, 077002.	2.9	43
18095	Design of a Mott Multiferroic from a Nonmagnetic Polar Metal. Physical Review Letters, 2015, 115, 087202.	2.9	64
18096	First-Principles Study of the Magnetic Structure ofNa2IrO3. Physical Review Letters, 2015, 115, 167204.	2.9	20
18097	Anomalous Stress Response of Ultrahard<mml:math xmlns:mml="http://www.w3.org/1998/Math/MathML" display="inline"><mml:mrow><mml:msub><mml:mrow><mml:mi>WB</mml:mi></mml:mrow><mml:mrow><mml:mi>n</mml:mi></mml:mrow></mml:msub></mml:mrow></mml:math>. Physical Review Letters, 2015, 115, 185502.	2.9	107
18098	Quantum Critical Origin of the Superconducting Dome in<mml:math xmlns:mml="http://www.w3.org/1998/Math/MathML" display="inline"><mml:mrow><mml:msub><mml:mrow><mml:mi>SrTiO</mml:mi></mml:mrow><mml:mrow><mml:mn>3</mml:mn></mml:mrow></mml:msub></mml:mrow></mml:math>. Physical Review Letters, 2015, 115, 247002.	2.9	148
18099	First-principles calculation of defect free energies: General aspects illustrated in the case of bcc Fe. Physical Review B, 2015, 92, .	1.1	29
18100	Electron transport properties of sub-3-nm diameter copper nanowires. Physical Review B, 2015, 92, .	1.1	28
18101	Nature of the metal-insulator transition in<mml:math xmlns:mml="http://www.w3.org/1998/Math/MathML"><mml:mrow><mml:mi>Nb</mml:mi><mml:msub><mml:mi mathvariant="normal">O</mml:mi><mml:mn>2</mml:mn></mml:msub></mml:mrow></mml:math>. Physical Review B, 2015, 91, .	1.1	47
18102	Analysis of hyperfine structure in chalcogen-doped silicon and germanium nanowires. Physical Review B, 2015, 91, .	1.1	1
18103	Phase stability and transformations in the halide perovskite<mml:math xmlns:mml="http://www.w3.org/1998/Math/MathML"><mml:msub><mml:mi>CsSnI</mml:mi><mml:mn>3</mml:mn></mml:msub></mml:math>. Physical Review B, 2015, 91, .	1.1	138

#	Article	IF	Citations
18104	High-pressure structure, decomposition, and superconductivity of<mml:math xmlns:mml="http://www.w3.org/1998/Math/MathML"><mml:msub><mml:mi mathvariant="normal">MoS</mml:mi><mml:mn>2</mml:mn></mml:msub></mml:math>. Physical Review B, 2015, 91, .	1.1	18
18105	Chen's derivative rule revisited: Role of tip-orbital interference in STM. Physical Review B, 2015, 91, .	1.1	31
18106	Atomic short-range order and incipient long-range order in high-entropy alloys. Physical Review B, 2015, 91, .	1.1	148
18107	Crystal and electronic structure of BiTeI, AuTeI, and PdTeI compounds: A dispersion-corrected density-functional study. Physical Review B, 2015, 91, .	1.1	13
18108	Modified Schottky emission to explain thickness dependence and slow depolarization in<mml:math xmlns:mml="http://www.w3.org/1998/Math/MathML"><mml:msub><mml:mi>BaTiO</mml:mi><mml:mn>3</mml:mn></mml:msub></m Physical Review B, 2015, 91, .	1.1	3
18109	Tunneling and electronic structure of the two-gap superconductor<mml:math xmlns:mml="http://www.w3.org/1998/Math/MathML"><mml:msub><mml:mi>MgB</mml:mi><mml:mn>2</mml:mn></mml:msub></ Physical Review B, 2015, 92, .	1.1	5
18110	Charge neutrality in epitaxial graphene on<mml:math xmlns:mml="http://www.w3.org/1998/Math/MathML"><mml:mrow><mml:mn>6</mml:mn><mml:mi>H</mml:mi></mml:mrow></mml: via nitrogen intercalation. Physical Review B, 2015, 92, .	1.1	29
18111	Influence of dislocation strain fields on the diffusion of interstitial iron impurities in silicon. Physical Review B, 2015, 92, .	1.1	8
18112	Interpreting core-level spectra of oxidizing phosphorene: Theory and experiment. Physical Review B, 2015, 92, .	1.1	35
18113	Giant electron-phonon interactions in molecular crystals and the importance of nonquadratic coupling. Physical Review B, 2015, 92, .	1.1	42
18114	Synthesis of a predicted layered LiB via cold compression. Physical Review B, 2015, 92, .	1.1	21
18115	Phonon effects on x-ray absorption and nuclear magnetic resonance spectroscopies. Physical Review B, 2015, 92, .	1.1	31
18116	Effects of structural relaxation, interdiffusion, and surface termination on two-dimensional electron gas formation at the<mml:math xmlns:mml="http://www.w3.org/1998/Math/MathML"><mml:mrow><mml:msub><mml:mi>LaAlO</mml:mi><mml:mn>3</mml:mn></m interface. Physical Review B, 2015, 92, .	1.1	17
18117	Layer- and strain-dependent optoelectronic properties of hexagonal AlN. Physical Review B, 2015, 92, .	1.1	53
18118	Crystal structure and electronic properties of bulk and thin film brownmillerite oxides. Physical Review B, 2015, 92, .	1.1	67
18119	Vibrational contributions to the phase stability of PbS-PbTe alloys. Physical Review B, 2015, 92, .	1.1	18
18120	Transition matrix elements for electron-phonon scattering: Phenomenological theory andab initioelectron theory. Physical Review B, 2015, 92, .	1.1	1
18121	Small polarons and point defects in barium cerate. Physical Review B, 2015, 92, .	1.1	33

#	Article	IF	Citations
18122	Collapsed armchair single-walled carbon nanotubes as an analog of closed-edged bilayer graphene nanoribbons. Physical Review B, 2015, 92, .	1.1	18
18123	Electronic Friction-Based Vibrational Lifetimes of Molecular Adsorbates: Beyond the Independent-Atom Approximation. Physical Review Letters, 2015, 115, 046102.	2.9	65
18124	Computing Equilibrium Shapes of Wurtzite Crystals: The Example of GaN. Physical Review Letters, 2015, 115, 085503.	2.9	66
18125	Light-Induced Exciton Spin Hall Effect in van der Waals Heterostructures. Physical Review Letters, 2015, 115, 166804.	2.9	48
18126	Interlayer bonding energy of layered minerals: Implication for the relationship with friction coefficient. Journal of Geophysical Research: Solid Earth, 2015, 120, 2212-2219.	1.4	33
18127	Controlling stability and electronic properties of small-diameter SiC nanowires by fluorination. International Journal of Nanotechnology, 2015, 12, 218.	0.1	5
18128	Anisotropic bias dependent transport property of defective phosphorene layer. Scientific Reports, 2015, 5, 12482.	1.6	45
18129	Atomistic Design of Favored Compositions for Synthesizing the Al-Ni-Y Metallic Glasses. Scientific Reports, 2015, 5, 16218.	1.6	6
18130	Nanostructured fuzz growth on tungsten under low-energy and high-flux He irradiation. Scientific Reports, 2015, 5, 10959.	1.6	64
18131	Stacked bilayer phosphorene: strain-induced quantum spin Hall state and optical measurement. Scientific Reports, 2015, 5, 13927.	1.6	64
18132	Predicted Growth of Two-Dimensional Topological Insulator Thin Films of III-V Compounds on Si(111) Substrate. Scientific Reports, 2015, 5, 15463.	1.6	46
18133	Generalized-stacking-fault energy and twin-boundary energy of hexagonal close-packed Au: A first-principles calculation. Scientific Reports, 2015, 5, 10213.	1.6	50
18134	Small shear modulus of cubic CaSiO₃ perovskite. Geophysical Research Letters, 2015, 42, 2718-2726.	1.5	40
18135	A New Silicon Phase with Direct Band Gap and Novel Optoelectronic Properties. Scientific Reports, 2015, 5, 14342.	1.6	74
18136	Defective Ti2Nb10O27.1: an advanced anode material for lithium-ion batteries. Scientific Reports, 2015, 5, 17836.	1.6	81
18137	Structural stability and mechanical property of Ni(111)â€“grapheneâ€“Ni(111) layered composite: A first-principles study. Japanese Journal of Applied Physics, 2015, 54, 125503.	0.8	3
18138	The origin of electronic band structure anomaly in topological crystalline insulator group-IV tellurides. Npj Computational Materials, 2015, 1, .	3.5	38
18139	Strain induced piezoelectric effect in black phosphorus and MoS2 van der Waals heterostructure. Scientific Reports, 2015, 5, 16448.	1.6	88

#	Article	IF	Citations
18140	Quantum Spin Hall States in Stanene/Ge(111). Scientific Reports, 2015, 5, 14196.	1.6	38
18141	Novel Two-Dimensional Mechano-Electric Generators and Sensors Based on Transition Metal Dichalcogenides. Scientific Reports, 2015, 5, 12854.	1.6	21
18142	Graphdiyne as a promising material for detecting amino acids. Scientific Reports, 2015, 5, 16720.	1.6	59
18143	Density Functional Theory Study Of The Interaction Of Hydroxyl Groups With Iron Surface. Archives of Metallurgy and Materials, 2015, 60, 931-933.	0.6	3
18144	The influence of hydrogen on the seismic properties of solid iron. Geophysical Research Letters, 2015, 42, 3780-3785.	1.5	40
18145	First-principle calculations of optical and phonon properties of wurtzite gallium nitride. AIP Conference Proceedings, 2015, , .	0.3	0
18146	Magnetostructural, mechanical and electronic properties of manganese tetraboride. AIP Advances, 2015, 5, 117208.	0.6	4
18147	Highly tunable magnetism in silicene doped with Cr and Fe atoms under isotropic and uniaxial tensile strain. Applied Physics Letters, 2015, 107, .	1.5	14
18148	Surface and bulk properties of chromium oxide: Implications for reduction by methane. AIP Conference Proceedings, 2015, , .	0.3	1
18149	Methane dissociation on Ni(111): A fifteen-dimensional potential energy surface using neural network method. Journal of Chemical Physics, 2015, 143, 144701.	1.2	68
18151	Atomic-scale diffractive imaging of sub-cycle electron dynamics in condensed matter. Scientific Reports, 2015, 5, 14581.	1.6	38
18152	Experimental and theoretical characterization of ordered MAX phases Mo2TiAlC2 and Mo2Ti2AlC3. Journal of Applied Physics, 2015, 118, .	1.1	217
18153	Bandgap engineering of MagnÃ©li phase TinO2nâˆ’1: Electron-hole self-compensation. Journal of Chemical Physics, 2015, 143, 054701.	1.2	10
18154	Site preference and magnetic properties of Ga/In-substituted strontium hexaferrite: An ab initio study. Journal of Applied Physics, 2015, 118, .	1.1	19
18155	Ab-initio study of dynamical properties of two dimensional MoS2 under strain. AIP Advances, 2015, 5, 107103.	0.6	22
18156	Crystal structure optimisation using an auxiliary equation of state. Journal of Chemical Physics, 2015, 143, 184101.	1.2	21
18157	Ab initiostudy of anisotropic mechanical properties of LiCoO2 during lithium intercalation and deintercalation process. Journal of Applied Physics, 2015, 118, .	1.1	56
18158	Indication of non-thermal contribution to visible femtosecond laser-induced CO oxidation on Ru(0001). Journal of Chemical Physics, 2015, 143, 074701.	1.2	14

#	Article	IF	Citations
18159	Carbon related defects in irradiated silicon revisited. Scientific Reports, 2014, 4, 4909.	1.6	38
18160	Structural, electronic and optical properties of well-known primary explosive: Mercury fulminate. Journal of Chemical Physics, 2015, 143, 204704.	1.2	6
18161	Interactions of small platinum clusters with the TiC(001) surface. Journal of Applied Physics, 2015, 118, .	1.1	15
18162	Crystal structure, equation of state and elasticity of phase H (MgSiO4H2) at Earthâ€™s lower mantle pressures. Scientific Reports, 2015, 5, 15534.	1.6	26
18163	Exchange coupling transformations in Cu (II) heterospin complexes of â€œbreathing crystalsâ€•under structural phase transitions. AIP Advances, 2015, 5, .	0.6	21
18164	Theoretical study of the thermodynamic properties, phase transition wave, and phase transition velocity for octahydro-1,3,5,7-tetranitro-1,3,5,7-tetrazocine. Journal of Applied Physics, 2015, 118, .	1.1	9
18165	The Schottky barrier modulation at PtSi/Si interface by strain and structural deformation. AIP Advances, 2015, 5, 087109.	0.6	6
18166	Quantum capacitance of graphene in contact with metal. Applied Physics Letters, 2015, 107, .	1.5	12
18167	Comparison of alpha and beta tin for lithium, sodium, and magnesium storage: Anab initiostudy including phonon contributions. Journal of Chemical Physics, 2015, 143, 204701.	1.2	19
18168	Classification of octet AB-type binary compounds using dynamical charges: A materials informatics perspective. Scientific Reports, 2015, 5, 17504.	1.6	14
18169	Electronic, Dielectric and Plasmonic Properties of Two-Dimensional Electride Materials X2N (X=Ca,) Tj ETQq0 0 0 rgBT /Overlock 10 Tf 50	1.6	73
18170	Stable Lithium Argon compounds under high pressure. Scientific Reports, 2015, 5, 16675.	1.6	34
18171	First Principles Calculation of Thermal Expansion of Carbon and Boron Nitrides Based on Quasi-Harmonic Approximation. Materials Transactions, 2015, 56, 1452-1456.	0.4	12
18172	First-Principles Based Phonon Calculation and Raman Spectroscopy Measurement of RuGa₂ and RuAl₂ with High Thermoelectric Power Factor. Nippon Kinzoku Gakkaishi/Journal of the Japan Institute of Metals, 2015, 79, 591-596.	0.2	0
18173	The electronic properties of impurities (N, C, F, Cl and S) in Ag3PO4: A hybrid functional method study. Scientific Reports, 2015, 5, 12750.	1.6	6
18174	Effects of Hydrogen Atoms on Vacancy Formation at fcc Fe(111) Surfaces. Nippon Kinzoku Gakkaishi/Journal of the Japan Institute of Metals, 2015, 79, 447-451.	0.2	2
18175	Stability of 12CaO·7Al₂O₃ Crystal under High-Pressure: Experimental and First-Principles Approaches. Materials Transactions, 2015, 56, 1350-1353.	0.4	6
18176	Yet Another Marked Difference among Impurities as Modifier Elements for Refinement of Eutectic Si in Al-Si Alloys. Materials Transactions, 2015, 56, 1475-1483.	0.4	5

#	Article	IF	Citations
18177	Study of Σ3 BaZrO₃ (210)[001] tilt grain boundaries using density functional theory and a space charge layer model. Journal of the Ceramic Society of Japan, 2015, 123, 245-249.	0.5	9
18178	Influences of carbon concentration on crystal structures and ideal strengths of B2CxO compounds in the B-C-O system. Scientific Reports, 2015, 5, 15481.	1.6	23
18179	First-principles study on electronic, optic, elastic, dynamic and thermodynamic properties of RbH compound. International Journal for Simulation and Multidisciplinary Design Optimization, 2015, 6, A6.	0.6	7
18180	Unraveling the luminescence signatures of chemical defects in polyethylene. Journal of Chemical Physics, 2015, 143, 124907.	1.2	21
18181	Fingerprints of energy dissipation for exothermic surface chemical reactions: O2 on Pd(100). Journal of Chemical Physics, 2015, 143, 034705.	1.2	19
18182	Experimental and ab initio studies on sub-lattice ordering and magnetism in Co2Fe(Ge1â^'xSix) alloys. Journal of Applied Physics, 2015, 118, 133906.	1.1	3
18183	Towards a new class of heavy ion doped magnetic semiconductors for room temperature applications. Scientific Reports, 2015, 5, 17053.	1.6	19
18184	Remarkably stable amorphous metal oxide grown on Zr-Cu-Be metallic glass. Scientific Reports, 2015, 5, 18196.	1.6	16
18185	Determination of the hyperfine magnetic field in magnetic carbon-based materials: DFT calculations and NMR experiments. Scientific Reports, 2015, 5, 14761.	1.6	20
18186	Ultra-sensitive pressure dependence of bandgap of rutile-GeO2 revealed by many body perturbation theory. Journal of Chemical Physics, 2015, 143, 064703.	1.2	9
18187	First-principles study of the stability of free-standing germanene in oxygen atmosphere. Journal of Applied Physics, 2015, 118, 124303.	1.1	19
18188	Defect calculations in semiconductors through a dielectric-dependent hybrid DFT functional: The case of oxygen vacancies in metal oxides. Journal of Chemical Physics, 2015, 143, 134702.	1.2	84
18189	Structural and electronic properties of GaN nanowires with embedded InxGa1â^'xN nanodisks. Journal of Applied Physics, 2015, 118, 034301.	1.1	11
18190	Ab initio and atomistic simulation of local structure and defect segregation on the tilt grain boundaries in silicon. Journal of Applied Physics, 2015, 118, .	1.1	17
18191	U-shaped relationship between current and pitch in helicene molecules. Scientific Reports, 2015, 5, 16731.	1.6	24
18192	First-principles study on defected titanium dioxide with the Zr substitution for improved reliability of the conduction path. EPJ Applied Physics, 2015, 70, 10103.	0.3	3
18193	First-principles study of nitric oxide oxidation on Pt(111) versus Pt overlayer on 3d transition metals. Journal of Vacuum Science and Technology A: Vacuum, Surfaces and Films, 2015, 33, 021402.	0.9	3
18194	Electronic structure and optical properties of Cs2AX2â€²X4 (A=Ge,Sn,Pb; Xâ€²,X=Cl,Br,I). AIP Advances, 2015, 5, .	0.6	28

#	Article	IF	Citations
18195	First principles design of divacancy defected graphene nanoribbon based rectifying and negative differential resistance device. AIP Advances, 2015, 5, .	0.6	23
18196	Exploration of tetrahedral structures in silicate cathodes using a motif-network scheme. Scientific Reports, 2015, 5, 15555.	1.6	27
18197	Cu diffusion in single-crystal and polycrystalline TiN barrier layers: A high-resolution experimental study supported by first-principles calculations. Journal of Applied Physics, 2015, 118, .	1.1	36
18198	Computational phase diagrams of noble gas hydrates under pressure. Journal of Chemical Physics, 2015, 143, 154507.	1.2	30
18199	A computational study of the electronic properties of one-dimensional armchair phosphorene nanotubes. Journal of Applied Physics, 2015, 118, .	1.1	45
18200	Graphene nanoribbons production from flat carbon nanotubes. Journal of Applied Physics, 2015, 118, 184301.	1.1	0
18201	Controlling the Electronic Structures and Properties of in-Plane Transition-Metal Dichalcogenides Quantum Wells. Scientific Reports, 2015, 5, 17578.	1.6	28
18202	Rise and fall of ferromagnetism in O-irradiated Al2O3 single crystals. Journal of Applied Physics, 2015, 117, 233904.	1.1	7
18203	Density functional theory studies on Cs activation mechanism between GaN (0001) and Al0.25Ga0.75N (0001) surface. Journal of Vacuum Science and Technology B:Nanotechnology and Microelectronics, 2015, 33, 051214.	0.6	3
18204	Topologically protected surface states in a centrosymmetric superconductor Î²-PdBi2. Nature Communications, 2015, 6, 8595.	5.8	113
18205	Electronic transition above room temperature in CaMn7O12 films. Applied Physics Letters, 2015, 107, 142901.	1.5	9
18206	Raman and ab initio investigation of negative thermal expansion material TaVO5: Insights into phase stability and anharmonicity. Journal of Applied Physics, 2015, 117, .	1.1	28
18207	Unconventional interplay between heterovalent dopant elements: Switch-and-modulator band-gap engineering in (Y, Co)-Codoped CeO2 nanocrystals. Scientific Reports, 2015, 5, 15415.	1.6	12
18208	Site occupancy and magnetic properties of Al-substituted M-type strontium hexaferrite. Journal of Applied Physics, 2015, 117, .	1.1	48
18209	Structural phase transitions in Bi2Se3 under high pressure. Scientific Reports, 2015, 5, 15939.	1.6	56
18210	Exotic stable cesium polynitrides at high pressure. Scientific Reports, 2015, 5, 16902.	1.6	58
18211	Spin splitting in 2D monochalcogenide semiconductors. Scientific Reports, 2015, 5, 17044.	1.6	55
18212	Electrical/thermal transport and electronic structure of the binary cobalt pnictides CoPn2 (Pn = As) Tj ETQq1 1 0.784314 rgBT /Overlo	0.6	10

#	Article	IF	Citations
18213	Site-specific dissociation dynamics of H2/D2 on Ag(111) and Co(0001) and the validity of the site-averaging model. Journal of Chemical Physics, 2015, 143, 114706.	1.2	34
18214	Diverse lattice dynamics in ternary Cu-Sb-Se compounds. Scientific Reports, 2015, 5, 13643.	1.6	51
18215	Interlayer coupling effects on Schottky barrier in the arsenene-graphene van der Waals heterostructures. Applied Physics Letters, 2015, 107, .	1.5	128
18216	Identification of nitrogen acceptor in Cu2O: First-principles study. Applied Physics Letters, 2015, 107, .	1.5	17
18217	The role of acoustic phonon anharmonicity in determining thermal conductivity of CdSiP2 and AgGaS2: First principles calculations. AIP Advances, 2015, 5, .	0.6	16
18218	Materials Prediction via Classification Learning. Scientific Reports, 2015, 5, 13285.	1.6	68
18219	An efficient molecular mechanics model for the torsional buckling analysis of multi-walled silicon carbide nanotubes. EPJ Applied Physics, 2015, 70, 10401.	0.3	3
18220	â€œTreasure mapsâ€•for magnetic high-entropy-alloys from theory and experiment. Applied Physics Letters, 2015, 107, .	1.5	84
18221	Electronic band structure, optical, dynamical and thermodynamic properties of cesium chloride (CsCl) from first-principles. International Journal for Simulation and Multidisciplinary Design Optimization, 2015, 6, A7.	0.6	4
18223	Structure, thermodynamics, and crystallization of amorphous hafnia. Journal of Applied Physics, 2015, 118, .	1.1	12
18224	Visualizing chemical states and defects induced magnetism of graphene oxide by spatially-resolved-X-ray microscopy and spectroscopy. Scientific Reports, 2015, 5, 15439.	1.6	31
18225	Application of Grid Increment Cluster Expansion to Modeling Potential Energy Surface of Cu-Based Alloys. Materials Transactions, 2015, 56, 1077-1080.	0.4	1
18226	First Principles Calculations of Solute Sweeping and Stacking Faults in Mg-Zn-Y Alloy. Materials Transactions, 2015, 56, 933-936.	0.4	4
18227	Electronic and optical properties of titanium nitride bulk and surfaces from first principles calculations. Journal of Applied Physics, 2015, 118, 195302.	1.1	14
18228	Ab-initio calculation study on the formation mechanism of boron-oxygen complexes in c-Si. AIP Advances, 2015, 5, .	0.6	6
18229	Improving p-type doping efficiency in Al0.83Ga0.17N alloy substituted by nanoscale (AlN)5/(GaN)1 superlattice with MgGa-ONâ€ˆÎ´-codoping: Role of O-atom in GaN monolayer. AIP Advances, 2015, 5, .	0.6	6
18230	Structures and magnetic properties of Co-Zr-B magnets studied by first-principles calculations. Journal of Applied Physics, 2015, 117, .	1.1	15
18231	Dopant-mediated structural and magnetic properties of TbMnO3. Applied Physics Letters, 2015, 107, .	1.5	18

#	Article	IF	Citations
18232	Lattice Distortion in In3SbTe2 Phase Change Material with Substitutional Bi. Scientific Reports, 2015, 5, 12867.	1.6	17
18233	First-principles study on structural, electronic, elastic and thermodynamic properties of the full-Heusler alloys Co₂YZ (Y=Sc, Cr and Z=Al, Ga). EPJ Applied Physics, 2015, 70, 31001.	0.3	23
18234	Electronic structure and insulating gap in epitaxial VO2 polymorphs. APL Materials, 2015, 3, .	2.2	47
18235	Ab-initio Study of Cation-rich InP(001) and GaP(001) Surface Reconstructions and Iodine Adsorption. IOP Conference Series: Materials Science and Engineering, 2015, 77, 012004.	0.3	1
18236	Effect of disorder on electronic and magnetic properties of Co2VGa Heusler alloy. AIP Conference Proceedings, 2015, , .	0.3	5
18237	Thermoelectric properties of Al doped Mg2Si material. AIP Conference Proceedings, 2015, , .	0.3	0
18238	Visualizing Non-abrupt Transition of Quantum Well States at Stepped Silver Surfaces. Scientific Reports, 2015, 5, 12847.	1.6	3
18239	Study of Pb-doped Ge2Sb2Te5 in crystalline phase using first principle calculations. AIP Conference Proceedings, 2015, , .	0.3	2
18240	Adsorption of Fe atoms on strongly-correlated NiO(001) surfaces with surface oxygen vacancies: Oxide support effects. Journal of the Korean Physical Society, 2015, 67, 1798-1803.	0.3	0
18241	Communication: Hole localization in Al-doped quartz SiO2 within ab initio hybrid-functional DFT. Journal of Chemical Physics, 2015, 143, 111103.	1.2	32
18242	Charge-transfer potentials for ionic crystals: Cauchy violation, LO-TO splitting, and the necessity of an ionic reference state. Journal of Chemical Physics, 2015, 143, 224101.	1.2	2
18243	Monte Carlo analysis of transient electron transport in wurtzite Zn1â^'xMgxO combined with first principles calculations. AIP Advances, 2015, 5, .	0.6	6
18244	First-Principles Study of Lithium and Sodium Atoms Intercalation in Fluorinated Graphite. Engineering, 2015, 1, 243-246.	3.2	16
18245	Electron-phonon interaction and scattering in Si and Ge: Implications for phonon engineering. Journal of Applied Physics, 2015, 118, .	1.1	23
18246	Adhesion Energy of the Fe(BCC)/Magnetite Interface within the DFT Approach. , 2015, 8, 1066-1072.		6
18247	High-temperature stability of Î'â€²-ZrO. Calphad: Computer Coupling of Phase Diagrams and Thermochemistry, 2015, 51, 292-298.	0.7	21
18248	Ab initio studies on the structure of and atomic interactions in cellulose IIII crystals. Carbohydrate Research, 2015, 417, 72-77.	1.1	5
18249	Modeling dislocation glide in Mg 2 SiO 4 ringwoodite: Towards rheology under transition zone conditions. Physics of the Earth and Planetary Interiors, 2015, 248, 20-29.	0.7	12

#	Article	IF	Citations
18250	Insulatorâ€“metal transition in 1Tâ€²-MoS2 under uniaxial strain. Physics Letters, Section A: General, Atomic and Solid State Physics, 2015, 379, 2883-2889.	0.9	7
18251	Active role of the support in NO x storage and reductioncatalytic systems. Applied Surface Science, 2015, 355, 1295-1305.	3.1	2
18252	Synergistic interplay between H and He in molybdenum: A first-principles study. Journal of Nuclear Materials, 2015, 466, 194-200.	1.3	11
18253	Interparticle potential of 10 nanometer titanium nanoparticles in liquid sodium: theoretical approach. Nuclear Engineering and Technology, 2015, 47, 662-668.	1.1	3
18254	Plasticity of the dense hydrous magnesium silicate phase A at subduction zones conditions. Physics of the Earth and Planetary Interiors, 2015, 248, 1-11.	0.7	1
18255	Band Gap Characters and Ferromagnetic/Antiferromagnetic Coupling in Group-IV Monolayers Tuned by Chemical Species and Hydrogen Adsorption Configurations. Nanoscale Research Letters, 2015, 10, 1040.	3.1	46
18256	Effect of Doping on Hydrogen Evolution Reaction of Vanadium Disulfide Monolayer. Nanoscale Research Letters, 2015, 10, 480.	3.1	31
18257	Features of the valence electron charge distribution in LiBIIXV crystals. Journal of Structural Chemistry, 2015, 56, 1036-1042.	0.3	1
18258	Thermodynamics of the pseudobinary GaAs1-xBix (0Ââ‰ÂxÂâ‰Â1) alloys studied by different exchange-correlation functionals, special quasi-random structures and Monte Carlo simulations. Computational Condensed Matter, 2015, 5, 7-13.	0.9	5
18259	Atomic Surface Structure of CH3-Ge(111) Characterized by Helium Atom Diffraction and Density Functional Theory. Journal of Physical Chemistry C, 2015, 119, 18458-18466.	1.5	5
18260	Magnetization dynamics of mixed Coâ€“Au chains on Cu(110) substrate: Combined ab initio and kinetic Monte Carlo study. Chinese Physics B, 2015, 24, 097302.	0.7	21
18261	Theoretical Study of Î±â€V₂O₅â€Based Doubleâ€Wall Nanotubes. ChemPhysChem, 2015, 16, 3007-3014.	1.0	8
18262	Structural, Vibrational and Electronic Properties of Defective Singleâ€Walled Carbon Nanotubes Functionalised with Carboxyl Groups: Theoretical Studies. ChemPhysChem, 2015, 16, 2775-2782.	1.0	16
18263	Band structure of the MoS₂ bilayer with adsorbed and intercalated Na. Physica Status Solidi (B): Basic Research, 2015, 252, 2693-2697.	0.7	6
18264	The Density of States and the Transport Effective Mass in a Highly Oriented Semiconducting Polymer: Electronic Delocalization in 1D. Advanced Materials, 2015, 27, 7759-7765.	11.1	52
18265	Bound electron polarons in lithium niobate. , 2015, , .		0
18266	Technetium Incorporation into Goethite (Î±-FeOOH): An Atomic-Scale Investigation. Environmental Science & Technology, 2015, 49, 13699-13707.	4.6	58
18267	Quantum mechanical ab initio calculations of the structural, electronic and optical properties of bulk gold nitrides. European Physical Journal B, 2015, 88, 1.	0.6	3

#	Article	IF	Citations
18268	Timeâ€•and Energyâ€Efficient Solution Combustion Synthesis of Binary Metal Tungstate Nanoparticles with Enhanced Photocatalytic Activity. ChemSusChem, 2015, 8, 1652-1663.	3.6	44
18269	First-principles calculation of the electronic structure, chemical bonding, and thermodynamic properties of Î² -US ₂. Chinese Physics B, 2015, 24, 127101.	0.7	1
18270	Relative stability and contrasting elastic properties of serpentine polymorphs from firstâ€principles calculations. Journal of Geophysical Research: Solid Earth, 2015, 120, 4831-4842.	1.4	16
18271	The Effects of Embedded Dipoles in Aromatic Selfâ€Assembled Monolayers. Advanced Functional Materials, 2015, 25, 3943-3957.	7.8	90
18272	Design and Synthesis of the Berylliumâ€Free Deepâ€Ultraviolet Nonlinear Optical Material Ba₃(ZnB₅O₁₀)PO₄. Advanced Materials, 2015, 27, 7380-7385.	11.1	262
18273	Identifying Different Types of Catalysts for CO₂ Reduction by Ethane through Dry Reforming and Oxidative Dehydrogenation. Angewandte Chemie - International Edition, 2015, 54, 15501-15505.	7.2	99
18274	Selective Stereochemical Catalysis Controlled by Specific Atomic Arrangement of Ordered Alloys. ChemCatChem, 2015, 7, 3472-3479.	1.8	28
18275	Theoretical Study of Cubic and Orthorhombic Nd_{1â€“}_xSr_xMnO₃ as a Potential Solid Oxide Fuel Cell Cathode. Fuel Cells, 2015, 15, 839-844.	1.5	6
18276	Pressure effects on structural and elastic properties of BeO from first-principles calculations. Physica Status Solidi (B): Basic Research, 2015, 252, 212-218.	0.7	5
18277	Ultraviolet Raman spectroscopy of graphene and transition-metal dichalcogenides. Physica Status Solidi (B): Basic Research, 2015, 252, 2363-2374.	0.7	14
18278	Prediction and theoretical investigation of new 2D and 3D periodical structures, having graphene-like bandstructures. Physica Status Solidi (B): Basic Research, 2015, 252, 2407-2411.	0.7	2
18279	Surfaceâ€Supported Robust 2D Lanthanideâ€Carboxylate Coordination Networks. Small, 2015, 11, 6358-6364.	5.2	43
18280	Ab-initio study of the segregation and electronic properties of neutral and charged B and P dopants in Si and Si/SiO2 nanowires. Journal of Applied Physics, 2015, 118, 104306.	1.1	3
18281	Theoretical Investigation on the Au-Anchor Site in Phosphate-Doped Au/Al₂O₃Catalysts. E-Journal of Surface Science and Nanotechnology, 2015, 13, 380-384.	0.1	6
18282	Pressureâ€induced phase transition in MnCO₃ and its implications on the deep carbon cycle. Journal of Geophysical Research: Solid Earth, 2015, 120, 4069-4079.	1.4	23
18283	Enhanced Stability of Carbon Doped Boron Nanotubes: An ab-initio Approach. IOP Conference Series: Materials Science and Engineering, 2015, 73, 012075.	0.3	0
18284	Density Functional Theory Study on Defect Feature of AsGaGaAsin Gallium Arsenide. Journal of Nanomaterials, 2015, 2015, 1-5.	1.5	0
18285	Influence of Carbon Nanotubes on the Structure Formation of Cement Matrix. IOP Conference Series: Materials Science and Engineering, 2015, 96, 012046.	0.3	7

#	Article	IF	Citations
18286	The photorefractive characteristics of bismuth-oxide doped lithium niobate crystals. AIP Advances, 2015, 5, 017132.	0.6	13
18287	Tuning the Electronic Structure of Graphene through Collective Electrostatic Effects. Advanced Materials Interfaces, 2015, 2, 1500323.	1.9	8
18288	Adsorption of nitrogenâ€•and sulfurâ€containing compounds on NiMoS for hydrotreating reactions: A DFT and vdWâ€corrected study. AICHE Journal, 2015, 61, 4036-4050.	1.8	39
18289	Synergic Catalysis of PdCu Alloy Nanoparticles within a Macroreticular Basic Resin for Hydrogen Production from Formic Acid. Chemistry - A European Journal, 2015, 21, 12085-12092.	1.7	102
18290	Improvement in Hydrogen Desorption from Î²â€•and Î³â€MgH₂ upon Transitionâ€Metal Doping. ChemPhysChem, 2015, 16, 2557-2561.	1.0	22
18291	RbBrF₄ Revisited. Zeitschrift Fur Anorganische Und Allgemeine Chemie, 2015, 641, 2593-2598.	0.6	22
18292	Exploiting the locality of periodic subsystem density-functional theory: efficient sampling of the Brillouin zone. Journal of Physics Condensed Matter, 2015, 27, 495501.	0.7	23
18293	Valence-lattice interaction on YbPd. Journal of Physics: Conference Series, 2015, 592, 012061.	0.3	1
18294	Reaction Energy for an Electrode Surface Atom Inserting into an R-H Bond and Its Dependence on Electrode Potential: Application to Pt(111). Journal of the Electrochemical Society, 2015, 162, H583-H589.	1.3	0
18295	Advances in the study of the deformation mechanism of stishovite. Physica Status Solidi (B): Basic Research, 2015, 252, 1486-1491.	0.7	13
18296	Phonon signature of the highâ€pressure rocksalt phase of InN. Physica Status Solidi (B): Basic Research, 2015, 252, 2104-2110.	0.7	0
18297	High hydrogen storage capacity in calciumâ€decorated silicene nanostructures. Physica Status Solidi (B): Basic Research, 2015, 252, 2072-2078.	0.7	12
18298	Structural and thermodynamic properties of Cuâ€doped Snâ€based singleâ€crystalline clathrates. Physica Status Solidi (B): Basic Research, 2015, 252, 2751-2757.	0.7	3
18299	Properties of armchair and zigzag CdS nanoribbons: A density functional study. Physica Status Solidi (B): Basic Research, 2015, 252, 2280-2289.	0.7	3
18300	Interaction of oxygen vacancy and its impact on transmission coefficient in oxygenâ€deficient titanium dioxide: Ab initio calculations. Physica Status Solidi (B): Basic Research, 2015, 252, 2735-2744.	0.7	4
18301	Effects of coverage and solvent on H₂S adsorption on the Cu(100) surface: A DFT study. Surface and Interface Analysis, 2015, 47, 565-571.	0.8	7
18302	2D-GaS as a Photocatalyst for Water Splitting to Produce H₂. Small, 2015, 11, 4723-4730.	5.2	61
18303	Supramolecular Frameworks Built up from Redâ€PhosphorÂescent transâ€Re₆ Cluster Building Blocks: One Pot Synthesis, Crystal Structures, and DFT Investigations. Zeitschrift Fur Anorganische Und Allgemeine Chemie, 2015, 641, 1156-1163.	0.6	21

#	Article	IF	Citations
18304	Study of electronic and magnetic properties and related x-ray absorption spectroscopy of ultrathin Co films on BaTiO₃. Journal of Physics Condensed Matter, 2015, 27, 426003.	0.7	2
18305	Investigation of high pressure phase transition and electronic properties of Lutetium Nitride. Journal of Physics: Conference Series, 2015, 640, 012029.	0.3	11
18306	Suppressing Manganese Dissolution from Lithium Manganese Oxide Spinel Cathodes with Singleâ€Layer Graphene. Advanced Energy Materials, 2015, 5, 1500646.	10.2	72
18307	Identifying Different Types of Catalysts for CO 2 Reduction by Ethane through Dry Reforming and Oxidative Dehydrogenation. Angewandte Chemie, 2015, 127, 15721-15725.	1.6	7
18308	A Comprehensive Study of Formic Acid Oxidation on Palladium Nanocrystals with Different Types of Facets and Twin Defects. ChemCatChem, 2015, 7, 2077-2084.	1.8	111
18309	The origin of anisotropy and high density of states in the electronic structure of Cr2GeC by means of polarized soft x-ray spectroscopy andab initiocalculations. Journal of Physics Condensed Matter, 2015, 27, 415501.	0.7	9
18310	Mechanical, electronic, and thermodynamic properties of zirconium carbide from first-principles calculations. Chinese Physics B, 2015, 24, 116301.	0.7	17
18311	First-principles study of hydrogen diffusion in transition metal Rhodium. Journal of Physics: Conference Series, 2015, 574, 012047.	0.3	2
18312	The Challenge of Electrochemical Ammonia Synthesis: A New Perspective on the Role of Nitrogen Scaling Relations. ChemSusChem, 2015, 8, 2180-2186.	3.6	1,018
18313	Flux Crystal Growth of the Ternary Polygermanide LaPtGe₂, a pâ€Type Metal. European Journal of Inorganic Chemistry, 2015, 2015, 2164-2172.	1.0	10
18314	Hard Radiation Detection from the Selenophosphate Pb₂P₂Se₆. Advanced Functional Materials, 2015, 25, 4874-4881.	7.8	33
18315	Phase stability of transition metal dichalcogenide by competing ligand field stabilization and charge density wave. 2D Materials, 2015, 2, 035019.	2.0	29
18316	Crystallization Behavior of Amorphous Si₂BC₃N Ceramic Monolith Subjected to High Pressure. Journal of the American Ceramic Society, 2015, 98, 3788-3796.	1.9	16
18318	DFT Investigation on the Competition of the Waterâ€“Gas Shift Reaction Versus Methanation on Clean and Potassiumâ€Modified Nickel(1â€‰1â€‰1) Surfaces. ChemCatChem, 2015, 7, 3928-3935.	1.8	54
18319	Ab initio molecular dynamics investigations of low-energy recoil events in Ni and NiCo. Journal of Physics Condensed Matter, 2015, 27, 435006.	0.7	14
18320	New crystal structure and physical properties of TcB from first-principles calculations. Chinese Physics B, 2015, 24, 106104.	0.7	7
18321	Significance of Surface Trivalent Manganese in the Electrocatalytic Activity of Water Oxidation in Undoped and Doped MnO₂ Nanowires. ChemCatChem, 2015, 7, 1848-1856.	1.8	44
18322	Potassiumâ€Induced Effect on the Structure and Chemical Activity of the Cu_xO/Cu(1â€‰1â€‰1) (x â‰ 2) Surface: A Combined Scanning Tunneling Microscopy and Density Functional Theory Study. ChemCatChem, 2015, 7, 3865-3872.	1.8	38

#	Article	IF	Citations
18323	Suzuki Coupling Reactions Catalyzed by PdO Dispersed on Dealuminated Y Zeolite in Air under Ambient Conditions. ChemPhysChem, 2015, 16, 1719-1726.	1.0	12
18324	A Study of Overheating of Thermostatically Controlled TiO₂ Thin Films by Using Raman Spectroscopy. ChemPhysChem, 2015, 16, 3949-3958.	1.0	0
18325	An analytical bondâ€order potential for carbon. Journal of Computational Chemistry, 2015, 36, 1719-1735.	1.5	36
18326	Structural and elastic properties of ternary silicides ScTSi (Tâ•Co, Ni, Cu, Ru, Rh, Pd, Ir, Pt) and of the equiatomic intermetallic compounds YTX (Tâ•Ni, Ir and Xâ•Si, Ge, Sn, Pb). Physica Status Solidi (B): Basic Research, 2015, 252, 2769-2777.	0.7	5
18327	Îºâ€Phase Formation in Feâ€“Mnâ€“Alâ€“C Austenitic Steels. Steel Research International, 2015, 86, 1161-1169.	1.0	61
18328	K₅Mn₃O₆ and Rb₈Mn₅O₁₀, New Charge Ordered Quasi Oneâ€Dimensional Oxomanganates (II, III). Zeitschrift Fur Anorganische Und Allgemeine Chemie, 2015, 641, 316-321.	0.6	9
18329	Ba₂In₂Q₅ (Q = S, Se): Synthesis, Crystal Structures, Electronic Structures, and Optical Properties. Zeitschrift Fur Anorganische Und Allgemeine Chemie, 2015, 641, 1329-1333.	0.6	8
18330	The Double Molybdate Rb₂Ba(MoO₄)₂: Synthesis, Crystal Structure, Optical, Thermal, Vibrational Properties, and Electronic Structure. Zeitschrift Fur Anorganische Und Allgemeine Chemie, 2015, 641, 2321-2325.	0.6	14
18331	Titanium Trisulfide Monolayer: Theoretical Prediction of a New Directâ€Gap Semiconductor with High and Anisotropic Carrier Mobility. Angewandte Chemie - International Edition, 2015, 54, 7572-7576.	7.2	239
18332	Reflectance anisotropy spectroscopy of clean and Sb covered Ge(001) surfaces and comparison with clean Si(001) surfaces. Physica Status Solidi (B): Basic Research, 2015, 252, 78-86.	0.7	6
18333	Ab initio study of the lowâ€pressure phases of TiO. Physica Status Solidi (B): Basic Research, 2015, 252, 659-662.	0.7	10
18334	Theoretical calculations on the structural, electronic, and optical properties of bulk silver nitrides. Physica Status Solidi (B): Basic Research, 2015, 252, 2840-2852.	0.7	10
18335	Comparative ab initio calculations of SrTiO₃ and CaTiO₃ polar (111) surfaces. Physica Status Solidi (B): Basic Research, 2015, 252, 635-642.	0.7	30
18337	Magneto-structural transformations via a solid-state nudged elastic band method: Application to iron under pressure. Journal of Chemical Physics, 2015, 143, 064707.	1.2	15
18338	Piezoelectric, Mechanical and Acoustic Properties of KNaNbOF5 from First-Principles Calculations. Materials, 2015, 8, 8578-8589.	1.3	5
18339	Investigations of mechanical and electronic properties for Al-based intermetallics with different Ti content. EPJ Applied Physics, 2015, 69, 10203.	0.3	4
18340	Calculations of helium separation via uniform pores of stanene-based membranes. Beilstein Journal of Nanotechnology, 2015, 6, 2470-2476.	1.5	9
18341	Physical properties of some noble metal compounds from PAW-DFT calculations. Journal of Science and Technology (Ghana), 2015, 34, 47.	0.4	2

#	Article	IF	Citations
18342	Existence of the Î²-tin structure in Sr: First evidence from computational approach. AIP Advances, 2015, 5, .	0.6	10
18343	Irregular Homogeneity Domains in Ternary Intermetallic Systems. Applied Sciences (Switzerland), 2015, 5, 1570-1589.	1.3	9
18344	Pt Monolayer Electrocatalyst for Oxygen Reduction Reaction on Pd-Cu Alloy: First-Principles Investigation. Catalysts, 2015, 5, 1193-1201.	1.6	12
18345	A Comparative Density Functional Theory and Density Functional Tight Binding Study of Phases of Nitrogen Including a High Energy Density Material N8. Computation, 2015, 3, 574-585.	1.0	6
18346	Enthalpies of Formation of Transition Metal Diborides: A First Principles Study. Crystals, 2015, 5, 562-582.	1.0	11
18347	Structure Determination of Au on Pt(111) Surface: LEED, STM and DFT Study. Materials, 2015, 8, 2935-2952.	1.3	45
18348	The Electronic Structures and Optical Properties of Alkaline-Earth Metals Doped Anatase TiO2: A Comparative Study of Screened Hybrid Functional and Generalized Gradient Approximation. Materials, 2015, 8, 5508-5525.	1.3	25
18349	Unique Reactivity of Transition Metal Atoms Embedded in Graphene to CO, NO, O2 and O Adsorption: A First-Principles Investigation. Molecules, 2015, 20, 19540-19553.	1.7	17
18350	Density functional simulation of carbon at the titanium site in perovskite barium titanate. IOP Conference Series: Materials Science and Engineering, 2015, 80, 012002.	0.3	2
18351	Effects of nitrogen-related defects on visible light photocatalytic response in N+implanted TiO2: A first-principles study. Journal of Applied Physics, 2015, 118, 115702.	1.1	7
18352	Structural and Electronic Properties of GaN (0001)/Î±-Al₂O₃(0001) Interface. Advances in Condensed Matter Physics, 2015, 2015, 1-6.	0.4	5
18353	The Electronic Structures and Optical Properties of Electron Tuned Fe-Doped SnO₂Materials. Journal of Nanomaterials, 2015, 2015, 1-6.	1.5	1
18354	Nature of the Interstitials in Titanium Dioxide and Their Impact on Transmission Coefficient:Ab InitioCalculations. Journal of Nanomaterials, 2015, 2015, 1-9.	1.5	2
18355	Effect of Dopant Compensation on the Behavior of Dissolved Iron and Iron-Boron Related Complexes in Silicon. International Journal of Photoenergy, 2015, 2015, 1-6.	1.4	1
18356	Electronic Structure, Electronic Charge Density, and Optical Properties Analysis of GdX₃ (X = In, Sn, Tl, and Pb) Compounds: DFT Calculations. Indian Journal of Materials Science, 2015, 2015, 1-11.	0.6	12
18357	Synthesis of the ZnGa₂S₄Nanocrystals and Their Visible-Light Photocatalytic Degradation Property. Journal of Nanomaterials, 2015, 2015, 1-7.	1.5	3
18358	Tuning Electronic Structures of BN and C Double-Wall Hetero-Nanotubes. Journal of Nanomaterials, 2015, 2015, 1-9.	1.5	2
18359	Two-Dimensional Metallicity with a Large Spin-Orbit Splitting: DFT Calculations of the Atomic, Electronic, and Spin Structures of the Au/Ge(111)-<mml:math xmlns:mml="http://www.w3.org/1998/Math/MathML" id="M1"><mml:mo stretchy="false">(</mml:mo><mml:msqrt><mml:mn>3</mml:mn></mml:msqrt><mml:mo>Ã—</mml:mo><mml:msqrt><mml:mn>3</mml:mn> Advances in Condensed Matter Physics, 2015, 2015, 1-10.	0.4	0

#	Article	IF	Citations
18360	Importance of Metal Cations and Water for Stability of MnO2 Crystals. Chinese Journal of Chemical Physics, 2015, 28, 711-715.	0.6	1
18361	Improvement of Anti-aging Property at Low Temperature by Cr Addition in Bake Hardenable Ultra Low Nitrogen Steels. ISIJ International, 2015, 55, 2648-2656.	0.6	2
18362	Ab initio Studies of O2 Adsorption on (110) Nickel-Rich Pentlandite (Fe4Ni5S8) Mineral Surface. Minerals (Basel, Switzerland), 2015, 5, 665-678.	0.8	23
18363	Ab-initio calculations of magnetic behavior in wurtzite AlxV1-xN compound. International Journal of Physical Sciences, 2015, 10, 520-527.	0.1	4
18364	Hydrogen influence on diffusion in nickel from first-principles calculations. Physical Review B, 2015, 91, .	1.1	19
18365	Convergence of quasiparticle self-consistent<mml:math xmlns:mml="http://www.w3.org/1998/Math/MathML"><mml:mrow><mml:mi>G</mml:mi><mml:mi>W</mml:mi></mml:mrow></mml of transition-metal monoxides. Physical Review B, 2015, 91, .	1.1	22
18366	Understanding the Effects of Point Defects on the Electronic Properties of Titania Nanoparticles: An Ab Initio Study. Spectroscopy Letters, 2015, 48, 691-694.	0.5	1
18367	Guestâ€“host interactions in gas clathrate hydrates under pressure. High Pressure Research, 2015, 35, 49-56.	0.4	9
18368	Pressure-induced zigzag phosphorus chain and superconductivity in boron monophosphide. Scientific Reports, 2015, 5, 8761.	1.6	16
18369	Effect of solute atoms on dislocation motion in Mg: An electronic structure perspective. Scientific Reports, 2015, 5, 8793.	1.6	69
18370	High-temperature Superconductivity in compressed Solid Silane. Scientific Reports, 2015, 5, 8845.	1.6	25
18371	On the mechanism of catalytic hydrogenation of thiophene on hydrogen tungsten bronze. Physical Chemistry Chemical Physics, 2015, 17, 9698-9705.	1.3	11
18372	Synthesis of palladium nanoparticles on TiO₂(110) using a beta-diketonate precursor. Physical Chemistry Chemical Physics, 2015, 17, 6470-6477.	1.3	7
18373	4d transition-metal doped hematite for enhancing photoelectrochemical activity: theoretical prediction and experimental confirmation. RSC Advances, 2015, 5, 19353-19361.	1.7	26
18374	Removal of NO with silicene: a DFT investigation. RSC Advances, 2015, 5, 22135-22147.	1.7	15
18375	The enhanced field emission properties of K and Rb doped (5,5) capped single-walled carbon nanotubes. RSC Advances, 2015, 5, 16718-16722.	1.7	4
18376	Coverage dependent water dissociative adsorption on Fe(110) from DFT computation. Physical Chemistry Chemical Physics, 2015, 17, 8811-8821.	1.3	60
18377	Pb6Ba2(BO3)5X (X = Cl, Br): new borate halides with strong predicted optical anisotropies derived from Pb2+and (BO3)3â". Dalton Transactions, 2015, 44, 7041-7047.	1.6	22

#	Article	IF	Citations
18378	The effect of the aliphatic carboxylate linkers on the electronic structures, chemical bonding and optical properties of the uranium-based metalâ€“organic frameworks. RSC Advances, 2015, 5, 26735-26748.	1.7	9
18379	Electronic properties of tin dichalcogenide monolayers and effects of hydrogenation and tension. Journal of Materials Chemistry C, 2015, 3, 3714-3721.	2.7	34
18380	Design principles of tuning oxygen vacancy diffusion in SrZrO₃ for resistance random access memory. Journal of Materials Chemistry C, 2015, 3, 4081-4085.	2.7	20
18381	Two-dimensional metalloporphyrin monolayers with intriguing electronic and spintronic properties. Journal of Materials Chemistry C, 2015, 3, 6901-6907.	2.7	22
18382	Electron-phonon interaction and thermal boundary resistance at the crystal-amorphous interface of the phase change compound GeTe. Journal of Applied Physics, 2015, 117, .	1.1	41
18383	Origin of the smaller conductances of Rh, Pb, and Co atomic junctions in hydrogen environment. Journal of Applied Physics, 2015, 117, 064310.	1.1	1
18384	Designing low thermal conductivity of RuO2 for thermoelectric applications. Applied Physics Letters, 2015, 106, .	1.5	14
18385	The origin of ferroelectricity in Hf1â^'xZrxO2: A computational investigation and a surface energy model. Journal of Applied Physics, 2015, 117, .	1.1	578
18386	A Novel Sb₂Te₃ Polymorph Stable at the Nanoscale. Chemistry of Materials, 2015, 27, 4368-4373.	3.2	13
18387	Detailed Atomistic Investigation of Fe-Doped Rutile Phases. Journal of Physical Chemistry A, 2015, 119, 5742-5748.	1.1	10
18388	Influence of Structural Defects and Oxidation onto Hole Conductivity in P3HT. Journal of Physical Chemistry B, 2015, 119, 6481-6491.	1.2	11
18389	Hydrogen Adsorption and Associated Electronic and Magnetic Properties of Rh-Decorated (8,0) Carbon Nanotubes Using Density Functional Theory. Journal of Physical Chemistry C, 2015, 119, 13238-13247.	1.5	32
18390	Exploring Furfural Catalytic Conversion on Cu(111) from Computation. ACS Catalysis, 2015, 5, 4020-4032.	5.5	109
18391	Dependence on Size of Supported Rh Nanoclusters in the Decomposition of Methanol. ACS Catalysis, 2015, 5, 4276-4287.	5.5	25
18392	Mechanistic Insights into Metal Lewis Acid-Mediated Catalytic Transfer Hydrogenation of Furfural to 2-Methylfuran. ACS Catalysis, 2015, 5, 3988-3994.	5.5	244
18393	Structural and Electrical Investigation of C₆₀â€“Graphene Vertical Heterostructures. ACS Nano, 2015, 9, 5922-5928.	7.3	151
18394	Theoretical Investigation on Incorporation and Diffusion Properties of Xe in Uranium Mononitride. Journal of Physical Chemistry C, 2015, 119, 5783-5789.	1.5	14
18395	DFT Study of the Conversion of Furfuryl Alcohol to 2-Methylfuran on RuO₂ (110). Journal of Physical Chemistry C, 2015, 119, 5938-5945.	1.5	37

#	Article	IF	Citations
18396	Shear-Induced Mechanochemistry: Pushing Molecules Around. Journal of Physical Chemistry C, 2015, 119, 7115-7123.	1.5	65
18397	GaAsO₄: A Bifunctional Material for Piezoelectricity and Second Harmonic Generation. Journal of Physical Chemistry C, 2015, 119, 8459-8464.	1.5	5
18398	Critical evaluation of the colossal Seebeck coefficient of nanostructured rutile MnO2. Journal of Physics Condensed Matter, 2015, 27, 115302.	0.7	6
18399	Transformation of electronic properties and structural phase transition from HfN to Hf₃N₄. Journal of Physics Condensed Matter, 2015, 27, 225501.	0.7	7
18400	Influence of surface stresses on indentation response. Nanotechnology, 2015, 26, 125704.	1.3	5
18401	Incorporation of water into olivine during nebular condensation: Insights from density functional theory and thermodynamics, and implications for phyllosilicate formation and terrestrial water inventory. Meteoritics and Planetary Science, 2015, 50, 578-589.	0.7	25
18402	Thermal and nonthermal melting of silicon exposed to femtosecond pulses of x-ray irradiation. Proceedings of SPIE, 2015, , .	0.8	2
18403	The structure and elastic properties of phosphorene edges. Nanotechnology, 2015, 26, 235707.	1.3	60
18404	Ab initio study of structural transition and pseudoelasticity in Cu nanowires. Surface Science, 2015, 641, 1-5.	0.8	5
18405	Fractionation of silicon isotopes in liquids: The importance of configurational disorder. Chemical Geology, 2015, 396, 239-254.	1.4	58
18406	Triggering the electrocatalytic hydrogen evolution activity of the inert two-dimensional MoS₂ surface via single-atom metal doping. Energy and Environmental Science, 2015, 8, 1594-1601.	15.6	1,109
18407	First principles study of structural, elastic and piezoelectric properties of CdSexTe1â^'x ternary alloys in the wurtzite structure. Physica Scripta, 2015, 90, 035702.	1.2	9
18408	Unusual case of desmotropy. Combined spectroscopy (1H-14N NQDR) and quantum chemistry (periodic) Tj ETQq0 0 0 rgBT /Overlock 1 State Nuclear Magnetic Resonance, 2015, 68-69, 13-24.	1.5	1
18409	First-principles study of the inversion thermodynamics and electronic structure of<mml:math xmlns:mml="http://www.w3.org/1998/Math/MathML"><mml:mrow><mml:mi>Fe</mml:mi><mml:msub><mml:mi>M</mml:mi><mml:		

#	Article	IF	Citations
18414	Ab initio models for polycrystalline diamond constructed from cold-compressed disordered graphite. Materials Research Express, 2015, 2, 045601.	0.8	1
18415	Quantum chemical investigation on the role of Li adsorbed on anatase (101) surface nano-materials on the storage of molecular hydrogen. Journal of Molecular Modeling, 2015, 21, 142.	0.8	4
18416	A first-principles study of the electronic structure and mechanical and optical properties of CaAlSiN₃. Physical Chemistry Chemical Physics, 2015, 17, 15065-15070.	1.3	33
18417	The stability of free-standing germanane in oxygen: First-principles investigation. Europhysics Letters, 2015, 110, 17007.	0.7	5
18418	Density Functional Characterization of the Electronic Structures and Band Bending of Rutile RuO₂/TiO₂(110) Heterostructures. Journal of Physical Chemistry C, 2015, 119, 12394-12399.	1.5	13
18419	Energy and dose dependence of proton-irradiation damage in graphene. RSC Advances, 2015, 5, 31861-31865.	1.7	21
18420	High carrier mobility of few-layer PbX (X = S, Se, Te). Journal of Materials Chemistry C, 2015, 3, 6284-6290.	2.7	41
18421	Direct observation and control of hydrogen-bond dynamics using low-temperature scanning tunneling microscopy. Progress in Surface Science, 2015, 90, 239-291.	3.8	46
18422	Antisite defects in nonstoichiometric Lu₃Al₅O₁₂:Ce ceramic scintillators. Physica Status Solidi (B): Basic Research, 2015, 252, 1993-1999.	0.7	24
18423	Giant dielectric permittivity and electronic structure in (Al+Sb)co-doped TiO2 ceramics. Microelectronic Engineering, 2015, 146, 32-37.	1.1	54
18424	Terahertz Spectroscopy and Computational Investigation of the Flufenamic Acid/Nicotinamide Cocrystal. Journal of Physical Chemistry A, 2015, 119, 3269-3276.	1.1	29
18425	Calculation of Half-Metal, Debye and Curie Temperatures of Co₂VAl Compound: First Principles Study*. Communications in Theoretical Physics, 2015, 63, 641-647.	1.1	42
18426	Two-dimensional metallic behavior at polar MgO/BaTiO ₃ (110) interfaces. Chinese Physics B, 2015, 24, 037301.	0.7	4
18427	Temperature dependent electron paramagnetic resonance (EPR) of SrZrO. Journal of Magnetism and Magnetic Materials, 2015, 391, 101-107.	1.0	14
18428	Spin rotation driven ferroelectric polarization with a 180Â° flop in double-perovskite Lu2CoMnO6. RSC Advances, 2015, 5, 43432-43439.	1.7	8
18429	Enhanced electrochemical performance by facile oxygen vacancies from lower valence-state doping for ramsdellite-MnO₂. Journal of Materials Chemistry A, 2015, 3, 12461-12467.	5.2	54
18430	Structures of the metallic and superconducting high pressure phases of solid CS2. Scientific Reports, 2015, 5, 10458.	1.6	18
18431	Hydrogen sulfide gas sensor based on decorated zigzag graphene nanoribbon with copper. Sensors and Actuators B: Chemical, 2015, 219, 338-345.	4.0	37

#	Article	IF	Citations
18432	Half-metallicity induced by boron adsorption on an Fe₃O₄(100) surface. Physical Chemistry Chemical Physics, 2015, 17, 15386-15391.	1.3	7
18433	Chemical modifications and stability of phosphorene with impurities: a first principles study. Physical Chemistry Chemical Physics, 2015, 17, 15209-15217.	1.3	78
18434	Methane capture at room temperature: adsorption on cubic Î´-MoC and orthorhombic Î²-Mo₂C molybdenum carbide (001) surfaces. RSC Advances, 2015, 5, 33737-33746.	1.7	18
18435	Thermodynamic and spectroscopic properties of oxygen on silver under an oxygen atmosphere. Physical Chemistry Chemical Physics, 2015, 17, 9288-9312.	1.3	103
18436	Modulating the magnetic behavior of Fe(<scp>ii</scp>)â€“MOF-74 by the high electron affinity of the guest molecule. Physical Chemistry Chemical Physics, 2015, 17, 16977-16982.	1.3	23
18437	Giant magnetocrystalline anisotropy of 5d transition metal-based phthalocyanine sheet. Physical Chemistry Chemical Physics, 2015, 17, 17182-17189.	1.3	19
18438	Pyrimidine and s-triazine as structural motifs for ordered adsorption on Si(100): a first principles study. Physical Chemistry Chemical Physics, 2015, 17, 16876-16885.	1.3	6
18439	Anisotropic relaxation of a CuO/TiO₂ surface under an electric field and its impact on visible light absorption: ab initio calculations. Physical Chemistry Chemical Physics, 2015, 17, 17880-17886.	1.3	7
18440	A first-principles study of sodium adsorption and diffusion on phosphorene. Physical Chemistry Chemical Physics, 2015, 17, 16398-16404.	1.3	75
18441	Hydroxylation of a metal-supported hexagonal boron nitride monolayer by oxygen induced water dissociation. Physical Chemistry Chemical Physics, 2015, 17, 16428-16433.	1.3	10
18442	Spin transport of dibenzotetraaza[14]annulene complexes with first row transition metals. RSC Advances, 2015, 5, 52938-52944.	1.7	16
18443	Exploration of stable stoichiometries, physical properties and hardness in the Rhâ€“Si system: a first-principles study. RSC Advances, 2015, 5, 53497-53503.	1.7	9
18444	Quasiparticle band structures and thermoelectric transport properties of p-type SnSe. Journal of Applied Physics, 2015, 117, .	1.1	135
18445	Theoretical study of electronic transport properties of a graphene-silicene bilayer. Journal of Applied Physics, 2015, 117, 225101.	1.1	11
18446	Application of a VanÂDerÂWaals Density Functional to Small Molecular Complexes and Solids. , 2015, , .		1
18447	Structural analysis of zeolite beta through periodic ab initio simulations of XRD and <mml:math xmlns:mml="http://www.w3.org/1998/Math/MathML" altimg="si26.gif" overflow="scroll"><mml:mrow><mml:msup><mml:mrow /><mml:mrow><mml:mn>29</mml:mn></mml:mrow></mml:msup><mml:mtext>Si</mml:mtext></mml:mrow></mml:math> and <mml:math xmlns:mml="http://www.w3.org/1998/Math/MathML" altimg="si27.gif" overflow="scroll"><mml:mrow><mml:msup><mml:mrow /><mml:mrow><mml:mn>17</mml:mn></mml:mrow></mml:msup><mml:mtext>O</mml:mtext></mml:mrow></mml:math>		7
18448	First-principles study on the effect of alloying elements on the elastic deformation response in Î²-titanium alloys. Journal of Applied Physics, 2015, 117, .	1.1	14
18449	Influence of hydrogen on the structure and stability of ultra-thin ZnO on metal substrates. Applied Physics Letters, 2015, 106, .	1.5	14

#	Article	IF	Citations
18450	Accelerated DFT-Based Design of Materials for Ammonia Storage. Chemistry of Materials, 2015, 27, 4552-4561.	3.2	18
18451	Phase stability, chemical bonding and mechanical properties of titanium nitrides: a first-principles study. Physical Chemistry Chemical Physics, 2015, 17, 11763-11769.	1.3	126
18452	Tuning the acidâ€“metal balance in Pd/ and Pt/zeolite catalysts for the hydroalkylation of m-cresol. Journal of Catalysis, 2015, 328, 173-185.	3.1	42
18453	Effects of vdW Interaction and Electric Field on Friction in MoS2. Tribology Letters, 2015, 59, 1.	1.2	15
18454	Defect Engineering and Phase Junction Architecture of Wide-Bandgap ZnS for Conflicting Visible Light Activity in Photocatalytic H₂ Evolution. ACS Applied Materials & Interfaces, 2015, 7, 13915-13924.	4.0	193
18455	Interactions of h-AlN monolayer with platinum, oxygen, and their clusters. Chemical Physics, 2015, 455, 73-80.	0.9	13
18456	Mechanism of CO methanation on the Ni4/Î³-Al2O3 and Ni3Fe/Î³-Al2O3 catalysts: A density functional theory study. International Journal of Hydrogen Energy, 2015, 40, 8864-8876.	3.8	34
18457	First principles studies of electronic and optical properties of helium adsorption on Sc-doped BN monolayer. Journal of the Iranian Chemical Society, 2015, 12, 1983-1990.	1.2	21
18458	A computational study on water adsorption on Cu2O(111) surfaces: The effects of coverage and oxygen defect. Applied Surface Science, 2015, 343, 33-40.	3.1	59
18459	Theoretical study of the anion exchange properties and the thermal decomposition of Zn5(OH)8(NO3)22H2O and Zn5(OH)8(NO3)22NH3. Applied Clay Science, 2015, 114, 103-111.	2.6	20
18460	Improvement in dehydrogenation performance ofÂMg(BH4)2Â·2NH3 doped with transition metal: First-principles investigation. International Journal of Hydrogen Energy, 2015, 40, 8721-8731.	3.8	15
18461	The native point defects in C14 Mg2Ca Laves phase: A first-principles study. Intermetallics, 2015, 65, 29-34.	1.8	7
18462	Electronic properties and adsorption structures of tetracene on the Ag(110) surface. Surface Science, 2015, 641, 135-140.	0.8	6
18463	Surface structure effect on the magnetic anisotropy of Co/Pd (001) thin film: A first principles study. Thin Solid Films, 2015, 589, 252-257.	0.8	2
18464	Electronic and structural characterization of InN heterostructures grown on Î²-LiGaO2 (001) substrates. Vacuum, 2015, 119, 106-111.	1.6	9
18465	First-principles calculations of structural, electronic, elastic and thermal properties of phase M2SiC (M=Ti, V, Cr, Zr, Nb, Mo, Hf, Ta and W). Transactions of Nonferrous Metals Society of China, 2015, 25, 915-925.	1.7	25
18466	Prediction of ordered omega phase formation by coupled replaciveâ€“displacive processes in Zr3Al2Nb and Zr4AlNb alloy: a first-principles study. Philosophical Magazine, 2015, 95, 1201-1220.	0.7	5
18467	Roles of Crystal Surface in Pt-Loaded Titania for Photocatalytic Conversion of Organic Pollutants: A First-Principle Theoretical Calculation. ACS Applied Materials & Interfaces, 2015, 7, 12671-12678.	4.0	25

#	Article	IF	Citations
18468	Hybrid structures of a BN nanoribbon/single-walled carbon nanotube: ab initio study. RSC Advances, 2015, 5, 55458-55467.	1.7	6
18469	A combined theoretical and experimental investigation of uranium dioxide under high static pressure. Journal of Physics Condensed Matter, 2015, 27, 265401.	0.7	9
18470	Ab Initio Comparison of Bonding Environments and Threshold Behavior in Ge_xAs₁₀Se_{90â€“x} and Ge_xSb₁₀Se_{90â€“x} Glass Models. Journal of Physical Chemistry A, 2015, 119, 6421-6427.	1.1	5
18471	turboEELSâ€”A code for the simulation of the electron energy loss and inelastic X-ray scattering spectra using the Liouvilleâ€“Lanczos approach to time-dependent density-functional perturbation theory. Computer Physics Communications, 2015, 196, 460-469.	3.0	41
18472	Hydrogen adsorption of nitrogen-doped carbon nanotubes functionalized with 3d-block transition metals. Journal of Chemical Sciences, 2015, 127, 751-759.	0.7	33
18473	Reaction Network of Methanol Synthesis over Cu/ZnO Nanocatalysts. ACS Catalysis, 2015, 5, 4201-4218.	5.5	87
18474	Surface Chemistry of Diamond. Topics in Applied Physics, 2015, , 53-83.	0.4	3
18475	Electronic structure and microscopic chargeâ€transport properties of a newâ€type diketopyrrolopyrroleâ€based material. Journal of Computational Chemistry, 2015, 36, 695-706.	1.5	14
18477	Amorphous (Glassy) Carbon, a Promising Material for Sodium Ion Battery Anodes: a Combined First-Principles and Experimental Study. Journal of Physical Chemistry C, 2015, 119, 13496-13501.	1.5	60
18478	Trade-Off between Accuracy and Universality in Linear Energy Relations for Alcohol Dehydrogenation on Transition Metals. Journal of Physical Chemistry C, 2015, 119, 12988-12998.	1.5	46
18479	Toward Controlled Growth of Helicity-Specific Carbon Nanotubes. Journal of Physical Chemistry Letters, 2015, 6, 2232-2237.	2.1	7
18480	Enhancement of photocatalytic activity of a two-dimensional GeH/graphene heterobilayer under visible light. RSC Advances, 2015, 5, 52264-52268.	1.7	18
18481	How focussing on hydrogen bonding interactions in amino acids can miss the bigger picture: a high-pressure neutron powder diffraction study of Îµ-glycine. CrystEngComm, 2015, 17, 5315-5328.	1.3	35
18482	The effect of cation order on the elasticity of omphacite from atomistic calculations. Physics and Chemistry of Minerals, 2015, 42, 677-691.	0.3	9
18483	First principle defect study of MoSe2 field effect transistor. Applied Physics B: Lasers and Optics, 2015, 119, 297-303.	1.1	8
18484	First-Principles Study of Ferromagnetic Nanowires Encapsulated Inside Silicon Carbide Nanotubes. Journal of Superconductivity and Novel Magnetism, 2015, 28, 2605-2611.	0.8	4
18485	Periodic DFT study of Ti deposition on defective Si(100) surfaces. Applied Surface Science, 2015, 335, 160-166.	3.1	1
18486	Selectivity of Ni-based surface alloys toward hydrazine adsorption: A DFT study with van der Waals interactions. Applied Surface Science, 2015, 339, 36-45.	3.1	20

#	Article	IF	Citations
18487	Adsorption properties of transition metal atoms on strongly correlated NiO(001) surfaces with surface oxygen vacancies. Current Applied Physics, 2015, 15, 679-682.	1.1	12
18488	A first-principle study of oxygen reduction reaction on monoclinic zirconia (1Â¯11), (1Â¯01) and (110) surfaces. Catalysis Communications, 2015, 69, 16-19.	1.6	12
18489	Effect of diameter and chirality on the structure and electronic properties of BC2N nanotubes. Chemical Physics, 2015, 455, 88-93.	0.9	7
18490	Investigation of thermophysical, electronic and lattice dynamic properties for CaX2Si2 (X=Ni,Zn,Cu,Ag,Au) via first-principles calculations. Computational Materials Science, 2015, 102, 167-173.	1.4	7
18491	First principle investigation of phase transition and thermodynamic properties of SiC. Computational Materials Science, 2015, 106, 76-82.	1.4	38
18492	Electrochemical specific adsorption of halides on Cu 111 , 100 , and 211 : A Density Functional Theory study. Electrochimica Acta, 2015, 173, 302-309.	2.6	82
18493	Kaolinite: Defect defined material properties â€“ A soft X-ray and first principles study of the band gap. Journal of Electron Spectroscopy and Related Phenomena, 2015, 202, 11-15.	0.8	10
18494	Theoretical investigation of new Heusler alloys Ru2VGa1â^'xAlx. Journal of Alloys and Compounds, 2015, 637, 557-563.	2.8	12
18495	First principles study of a new half-metallic ferrimagnets Mn2-based full Heusler compounds: Mn2ZrSi and Mn2ZrGe. Journal of Magnetism and Magnetic Materials, 2015, 388, 59-67.	1.0	79
18496	Molecular modelling of the decomposition of NH3 over CoO(100). Materials Chemistry and Physics, 2015, 156, 141-149.	2.0	8
18497	Interaction between vacancies and the Î±-Fe/Y 2 O 3 interface: A first-principles study. Nuclear Instruments & Methods in Physics Research B, 2015, 352, 67-71.	0.6	9
18498	Elasticity and phase stability of pyrope garnet from ab initio computation. Physics of the Earth and Planetary Interiors, 2015, 240, 125-131.	0.7	12
18499	Structural, electronic and magnetic properties of 8-hydroxyquinoline-based small molecules TMQx (TM=Cr, Mn, Fe, Co, Ni, Cu, Zn, and x=2 or 3). Physica E: Low-Dimensional Systems and Nanostructures, 2015, 70, 77-83.	1.3	5
18500	Water interaction with perfect and fluorine-doped Co3O4 (100) surface. Solid State Ionics, 2015, 277, 77-82.	1.3	24
18501	Dissociative adsorption of water on Au/MgO/Ag(001) from first principles calculations. Surface Science, 2015, 640, 10-17.	0.8	4
18502	Atomistic modeling to optimize composition and characterize structure of Niâ€“Zrâ€“Mo metallic glasses. Physical Chemistry Chemical Physics, 2015, 17, 13355-13365.	1.3	19
18503	Electron-phonon interaction and superconductivity in hexagonal BaSn5. Philosophical Magazine, 2015, 95, 2128-2137.	0.7	1
18504	Enhancement Mechanism of the Conversion Effficiency of Dye-Sensitized Solar Cells Based on Nitrogen-, Fluorine-, and Iodine-Doped TiO₂ Photoanodes. Journal of Physical Chemistry C, 2015, 119, 13425-13432.	1.5	21

#	Article	IF	Citations
18505	Structure of magnesium selenate enneahydrate, MgSeO4Â·9H2O, from 5 to 250â€…K using neutron time-of-flight Laue diffraction. Acta Crystallographica Section B: Structural Science, Crystal Engineering and Materials, 2015, 71, 313-327.	0.5	4
18506	Fock-exchange for periodic structures in the real-space formalism and the KLI approximation. Physical Chemistry Chemical Physics, 2015, 17, 31510-31515.	1.3	6
18507	Anomalous doping effect in black phosphorene using first-principles calculations. Physical Chemistry Chemical Physics, 2015, 17, 16351-16358.	1.3	109
18508	First-principles investigation of helium dissolution and clustering at a tungsten (1 1 0) surface. Journal of Nuclear Materials, 2015, 461, 230-235.	1.3	33
18509	Thermodynamics of H₂O Splitting and H₂ Formation at the Cu(110)â€“Water Interface. Journal of Physical Chemistry C, 2015, 119, 14102-14113.	1.5	31
18510	Two-Dimensional Hydrous Silica: Nanosheets and Nanotubes Predicted from First-Principles Simulations. Journal of Physical Chemistry C, 2015, 119, 14343-14350.	1.5	9
18511	Theoretical study of Î³â€²-Fe4N and É›-Fe x N iron nitrides at pressures up to 500 GPa. JETP Letters, 2015, 101, 371-375.	0.4	11
18512	Intrinsic defects in gallium sulfide monolayer: a first-principles study. RSC Advances, 2015, 5, 50883-50889.	1.7	27
18513	A density functional (PBE, PBEsol, HSE06) study of the structural, electronic and optical properties of the ternary compounds AgAlX2 (X = S, Se, Te). European Physical Journal B, 2015, 88, 1.	0.6	35
18514	The effect of temperature and pressure on the crystal structure of piperidine. Chemistry Central Journal, 2015, 9, 18.	2.6	17
18515	Hybrid-exchange density-functional theory study of the electronic structure ofMnV2O4: Exotic orbital ordering in the cubic structure. Physical Review B, 2015, 91, .	1.1	3
18516	Defect complexes in congruent<mml:math xmlns:mml="http://www.w3.org/1998/Math/MathML"><mml:msub><mml:mi mathvariant="normal">LiNbO</mml:mi><mml:mn>3</mml:mn></mml:msub></mml:math>and their optical signatures. Physical Review B, 2015, 91, .	1.1	45
18517	The corrosive influence of chloride ions preference adsorption on Î±-Al2O3 (0 0 0 1) surface. Applied Surface Science, 2015, 347, 386-391.	3.1	35
18518	Comparison of bulk material candidates for hot carrier absorber. Solar Energy Materials and Solar Cells, 2015, 140, 422-427.	3.0	16
18519	Ab initio-based fracture toughness estimates and transgranular traction-separation modelling of zirconium hydrides. Modelling and Simulation in Materials Science and Engineering, 2015, 23, 045015.	0.8	10
18520	Electronic and energetic properties of FeCl3 and CrO3 interacting with single wall BN nanotube. Applied Surface Science, 2015, 349, 948-951.	3.1	1
18521	Raman spectra of few-layer phosphorene studied from first-principles calculations. Journal of Physics Condensed Matter, 2015, 27, 185302.	0.7	38
18522	Atomic-Level Structural and Electronic Properties of Hybrid Inorganicâ€“Organic ZnO:Hydroquinone Superlattices Fabricated by ALD/MLD. Journal of Physical Chemistry C, 2015, 119, 13105-13114.	1.5	75

#	Article	IF	Citations
18523	Structures, electronic properties and stability phase diagrams for copper(<scp>i</scp>/<scp>ii</scp>) bromide surfaces. Physical Chemistry Chemical Physics, 2015, 17, 9341-9351.	1.3	14
18524	Density Functional Theory-Assisted Microkinetic Analysis of Methane Dry Reforming on Ni Catalyst. Industrial & Engineering Chemistry Research, 2015, 54, 5901-5913.	1.8	158
18525	High-Pressure Stability of Energetic Crystal of Dihydroxylammonium 5,5â€²-Bistetrazole-1,1â€²-diolate: Raman Spectroscopy and DFT Calculations. Journal of Physical Chemistry B, 2015, 119, 6836-6847.	1.2	51
18526	Insight into the mechanism and possibility of ethanol formation from syngas on Cu(100) surface. Journal of Molecular Catalysis A, 2015, 404-405, 115-130.	4.8	46
18527	Reduced spin-Hall effects from magnetic proximity. Physical Review B, 2015, 91, .	1.1	74
18528	Lattice-Directed Formation of Covalent and Organometallic Molecular Wires by Terminal Alkynes on Ag Surfaces. ACS Nano, 2015, 9, 6305-6314.	7.3	114
18529	Structural, electronic and optical properties of Ilmenite ATiO3(A=Fe, Co, Ni). Materials Science in Semiconductor Processing, 2015, 39, 6-16.	1.9	26
18530	Theoretical study of cesium and oxygen activation processes on GaN (0001) surface. Materials Science in Semiconductor Processing, 2015, 39, 61-66.	1.9	10
18531	First principles study of magnetoelectric coupling in Co2FeAl/BaTiO3 tunnel junctions. Physical Chemistry Chemical Physics, 2015, 17, 14986-14993.	1.3	16
18532	High temperature oxidation resistance in titaniumâ€“niobium alloys. Journal of Alloys and Compounds, 2015, 643, 100-105.	2.8	26
18533	Adsorption of Sulfurâ€™s Atoms on the Outer Surface of Carbon Nanotubes. Advanced Materials Research, 0, 1091, 25-29.	0.3	1
18534	Water steam effect during high CO₂ chemisorption in lithium cuprate (Li₂CuO₂) at moderate temperatures: experimental and theoretical evidence. RSC Advances, 2015, 5, 34157-34165.	1.7	29
18535	Electronic structure and magnetic properties of graphene/Co composite. Carbon, 2015, 91, 298-303.	5.4	21
18536	First-principle study of the electronic structures and optical properties of six typical hexaferrites. Computational Materials Science, 2015, 105, 27-31.	1.4	7
18537	The Structural, Dielectric, Lattice Dynamical and Thermodynamic Properties of Zinc-Blende Cd X (X=S ,) Tj ETQq0 0 0 rgBT /Overlock 10	1.3	3
18538	Phase stability and Raman vibration of the molybdenum ditelluride (MoTe₂) monolayer. Physical Chemistry Chemical Physics, 2015, 17, 14866-14871.	1.3	104
18539	Hydrogen generation by the reaction of H₂O with Al₂O₃-based materials: a computational analysis. Physical Chemistry Chemical Physics, 2015, 17, 6834-6843.	1.3	28
18540	Energetic stability, atomic and electronic structures of extended Î³-graphyne: A density functional study. Journal of Molecular Modeling, 2015, 21, 154.	0.8	7

#	Article	IF	Citations
18541	Electronic structure, structural phase stability, optical and thermoelectric properties of Sr2AlM'O6 (M'Â=ÂNb and Ta) from first principle calculations. Computational Condensed Matter, 2015, 4, 13-22.	0.9	22
18542	Adsorption of choline benzoate ionic liquid on graphene, silicene, germanene and boron-nitride nanosheets: a DFT perspective. Physical Chemistry Chemical Physics, 2015, 17, 16315-16326.	1.3	39
18543	Operational characteristics of a graphene-based electron field emitter. Journal of Vacuum Science and Technology B:Nanotechnology and Microelectronics, 2015, 33, 041801.	0.6	7
18544	The sulfur poisoning of the nickel/oxygen-enriched yttria-stabilized zirconia. Journal of Power Sources, 2015, 293, 635-641.	4.0	11
18545	Structures, stabilities and electronic properties of defects in monolayer black phosphorus. Scientific Reports, 2015, 5, 10848.	1.6	90
18546	Postadsorption Work Function Tuning via Hydrogen Pressure Control. Journal of Physical Chemistry C, 2015, 119, 27162-27172.	1.5	12
18547	Promoting Ï‡-Fe₅C₂(100)_{0.25} with copper â€“ a DFT study. Journal of Lithic Studies, 2015, 1, 11-18.	0.1	6
18548	Elastic properties of zincblende III-nitrides: A first-principles study. , 2015, , .		0
18549	Challenges in developing an accurate predictive model for electrochemical energy storage devices. , 2015, , .		0
18550	Point Defects and Defect-Induced Optical Response in Ternary LiInSe₂ Crystals: First-Principles Insight. Journal of Physical Chemistry C, 2015, 119, 29123-29131.	1.5	12
18551	Trimethyl-phosphite dissociative adsorption on iron by combined first-principle calculations and XPS experiments. RSC Advances, 2015, 5, 101162-101168.	1.7	26
18552	Influence of the â€œsurface effectâ€•on the segregation parameters of S in Fe(100): A multi-scale modelling and Auger Electron Spectroscopy study. Superlattices and Microstructures, 2015, 88, 403-416.	1.4	2
18553	Variable-Cell Double-Ended Surface Walking Method for Fast Transition State Location of Solid Phase Transitions. Journal of Chemical Theory and Computation, 2015, 11, 4885-4894.	2.3	58
18554	Exploring the Role of La Codoping beyond Charge Compensation for Enhanced Hydrogen Evolution by Rhâ€“SrTiO₃. Journal of Physical Chemistry B, 2015, 119, 11089-11098.	1.2	54
18555	Comparative First-Principles Calculations of SrTiO₃, BaTiO₃, PbTiO₃ and CaTiO₃ (001), (011) and (111) Surfaces. Ferroelectrics, 2015, 483, 53-67.	0.3	39
18556	Theoretical Modelling of the Energy Surface (001) and Topology of CaZrO3 Perovskite. Ferroelectrics, 2015, 483, 75-85.	0.3	9
18557	Effect of zinc concentration on the structural, electronic and elastic properties of ZnxCd1â^'xO dilute alloys. Physica Scripta, 2015, 90, 115701.	1.2	3
18558	Ab initiosimulations on N and S co-doped titania nanotubes for photocatalytic applications. Physica Scripta, 2015, 90, 094013.	1.2	10

#	Article	IF	Citations
18559	Thermal conductivity of biaxial-strained MoS₂: sensitive strain dependence and size-dependent reduction rate. Nanotechnology, 2015, 26, 465707.	1.3	60
18560	Evolutionary algorithm based structure search for hard ruthenium carbides. Modelling and Simulation in Materials Science and Engineering, 2015, 23, 085006.	0.8	8
18561	Structural, elastic, and electronic properties of recently discovered ternary silicide superconductor Li₂IrSi₃: Anab-initiostudy. Chinese Physics B, 2015, 24, 117401.	0.7	33
18562	Magnetic properties of Câ€“N planar structures: d0 ferromagnetism and half-metallicity. Physical Chemistry Chemical Physics, 2015, 17, 31995-31999.	1.3	4
18563	Predicting experimentally stable allotropes: Instability of penta-graphene. Proceedings of the National Academy of Sciences of the United States of America, 2015, 112, 15609-15612.	3.3	82
18564	A single iron site confined in a graphene matrix for the catalytic oxidation of benzene at room temperature. Science Advances, 2015, 1, e1500462.	4.7	719
18565	Reactions of CO, H₂O, CO₂, and H₂ on the Clean and Precovered Fe(110) Surfaces â€“ A DFT Investigation. Journal of Physical Chemistry C, 2015, 119, 28377-28388.	1.5	40
18566	Theoretical Insights to Niobium-Doped Monolayer MoS₂â€“Gold Contact. IEEE Transactions on Electron Devices, 2015, 62, 2346-2351.	1.6	14
18567	Effect of sulfation on the surface activity of CaO for N2O decomposition. Applied Surface Science, 2015, 357, 951-960.	3.1	7
18568	Development of a ReaxFF Reactive Force Field for Fe/Cr/O/S and Application to Oxidation of Butane over a Pyrite-Covered Cr₂O₃ Catalyst. ACS Catalysis, 2015, 5, 7226-7236.	5.5	98
18569	Fe and Co nanostructures embedded into the Cu(100) surface: Self-Organization and magnetic properties. Journal of Experimental and Theoretical Physics, 2015, 121, 616-622.	0.2	9
18570	First principle investigations on structural, mechanical, spin polarized electronic and magnetic properties of TmZn and TmCd. Iranian Physical Journal, 2015, 9, 273-284.	1.2	5
18571	Vibrational Spectroscopy and Phonon-Related Properties of the <scp>l</scp>-Aspartic Acid Anhydrous Monoclinic Crystal. Journal of Physical Chemistry A, 2015, 119, 11791-11803.	1.1	22
18572	Physisorption Controls the Conformation and Density of States of an Adsorbed Porphyrin. Journal of Physical Chemistry C, 2015, 119, 27982-27994.	1.5	34
18573	Adsorption and Diffusion of Lithium on Monolayer Transition Metal Dichalcogenides (MoS_{2(1â€“x)}Se_{2x}) Alloys. Journal of Physical Chemistry C, 2015, 119, 28648-28653.	1.5	76
18574	Effect of carbon content and electronic strong correlation on the mechanical and thermodynamic properties of ytterbium carbides. RSC Advances, 2015, 5, 103082-103090.	1.7	5
18575	Influence of boron vacancies on phase stability, bonding and structure ofMB₂(Mâ€‰â€‰=â€‰â€‰Ti, Zr, Hf, V, Nb, Ta, Cr, Mo, W) with AlB₂type structure. Journal of Physics Condensed Matter, 2015, 27, 435702.	2.7	33
18576	Diamond-like phases formed from fullerene-like clusters. Physics of the Solid State, 2015, 57, 2331-2341.	0.2	17

#	Article	IF	Citations
18577	First principles study of Ca in BaTiO₃and Bi_{0.5}Na_{0.5}TiO₃. Philosophical Magazine, 2015, 95, 3785-3797.	0.7	4
18578	First-principles calculation of electronic properties of isoelectronic impurity complexes in Si. Applied Physics Express, 2015, 8, 081301.	1.1	15
18579	On the Structure Sensitivity of Dimethyl Ether Electro-oxidation on Eight FCC Metals: A First-Principles Study. Topics in Catalysis, 2015, 58, 1159-1173.	1.3	13
18580	Piezoelectricity in two-dimensional group-III monochalcogenides. Nano Research, 2015, 8, 3796-3802.	5.8	219
18581	Mechanisms of Oxidase and Superoxide Dismutation-like Activities of Gold, Silver, Platinum, and Palladium, and Their Alloys: A General Way to the Activation of Molecular Oxygen. Journal of the American Chemical Society, 2015, 137, 15882-15891.	6.6	407
18582	Combined experimentalâ€“theoretical study of the optoelectronic properties of non-stoichiometric pyrochlore bismuth titanate. Journal of Materials Chemistry C, 2015, 3, 12032-12039.	2.7	29
18583	Melting curves of metals with excited electrons in the quasiharmonic approximation. Physical Review B, 2015, 92, .	1.1	58
18584	Crystal behavior of potassium bromate under compression. Acta Crystallographica Section B: Structural Science, Crystal Engineering and Materials, 2015, 71, 798-804.	0.5	3
18585	On the Nb-Ge Binary System. Metallurgical and Materials Transactions A: Physical Metallurgy and Materials Science, 2015, 46, 5526-5536.	1.1	15
18586	Effect of twin boundaries and structural polytypes on electron transport in GaAs. Computational Materials Science, 2015, 108, 258-263.	1.4	15
18587	Calculation of electronic structure and mechanical properties of DO₃â€“Fe_{75-x}Si₂₅Ni_x intermetallic compounds by first principles. International Journal of Modern Physics B, 2015, 29, 1550087.	1.0	1
18588	First principles investigation of the diffusion of interstitial Cu, Ag and Au in ZnTe. International Journal of Modern Physics B, 2015, 29, 1550130.	1.0	0
18589	Electronic Structure and Photocatalytic Water-Splitting Properties of Ag₂ZnSn(S_{1â€“x}Se_x)₄. Journal of Physical Chemistry C, 2015, 119, 27900-27908.	1.5	68
18590	Dynamic Nonlinear Optical Processes in Some Oxygen-Octahedra Ferroelectrics: First Principle Calculations. Ferroelectrics, 2015, 483, 26-42.	0.3	2
18591	Theoretical investigations of physical stability, electronic properties and hardness of transition-metal tungsten borides WBx(x=2.5, 3). Chemical Physics Letters, 2015, 635, 205-209.	1.2	21
18592	Catalytic water dehydrogenation and formation on nickel: Dual path mechanism in high electric fields. Journal of Catalysis, 2015, 332, 187-200.	3.1	52
18593	Negative differential resistance, rectifying performance and switching behaviour in carbon-chain based molecular devices. Organic Electronics, 2015, 27, 92-100.	1.4	18
18594	Ab initio study of atomic disorder on As-rich GaAs(111)A surface. Surface Science, 2015, 641, 330-335.	0.8	1

#	Article	IF	Citations
18595	Upward Shift in Conduction Band of Ta2O5 Due to Surface Dipoles Induced by N-Doping. Journal of Physical Chemistry C, 2015, 119, 26925-26936.	1.5	27
18596	First-Principles Calculation of Quantum Capacitance of Codoped Graphenes as Supercapacitor Electrodes. Journal of Physical Chemistry C, 2015, 119, 26290-26295.	1.5	118
18597	First-Principles Study on Ligand Binding and Positional Disorder in Pentlandite. Journal of Physical Chemistry C, 2015, 119, 25457-25468.	1.5	13
18598	Enhanced Luminescence with Fast Nanosecond Lifetime in In₂S₃:Tb³⁺ Nanophosphors. Journal of Physical Chemistry C, 2015, 119, 27688-27694.	1.5	21
18599	Computational Study of Cation Diffusion in Ceria. Journal of Physical Chemistry C, 2015, 119, 27307-27315.	1.5	45
18600	Migration of Single Iridium Atoms and Tri-iridium Clusters on MgO Surfaces: Aberration-Corrected STEM Imaging and Ab Initio Calculations. Journal of Physical Chemistry Letters, 2015, 6, 4675-4679.	2.1	12
18601	Nature and Catalytic Role of Extraframework Aluminum in Faujasite Zeolite: A Theoretical Perspective. ACS Catalysis, 2015, 5, 7024-7033.	5.5	92
18602	A hybrid density functional study on the visible light photocatalytic activity of (Mo,Cr)â€“N codoped KNbO₃. Physical Chemistry Chemical Physics, 2015, 17, 28743-28753.	1.3	67
18603	Realizing semiconductor to metal transition in graphitic ZnO and MoS₂ nanocomposite with external electric field. RSC Advances, 2015, 5, 99153-99163.	1.7	20
18604	First-principles study of structural and electronic properties of carbon clusters. Materials Research Innovations, 2015, 19, S8-14-S8-16.	1.0	0
18605	Switching mechanism of Al/La_{1â^'x}Sr_xMnO₃ resistance random access memory. I. Oxygen vacancy formation in perovskites. RSC Advances, 2015, 5, 102772-102779.	1.7	10
18606	From soft to hard magnetic Feâ€“Coâ€“B by spontaneous strain: a combined first principles and thin film study. Journal of Physics Condensed Matter, 2015, 27, 476002.	0.7	29
18607	DFT STUDY OF OXYGEN ADSORPTION ON THE Be-COVERED Mo (112) SURFACE. Surface Review and Letters, 2015, 22, 1550059.	0.5	2
18608	Hydrogen adsorption on nitrogen and boron doped graphene. Journal of Physics Condensed Matter, 2015, 27, 425502.	0.7	19
18609	First-Principle Calculations of the MgYA4 (AÂ=ÂCo and Ni) Phase with AuBe5-Type Structure. Acta Metallurgica Sinica (English Letters), 2015, 28, 1326-1331.	1.5	4
18610	Exploring the low-friction mechanism of CN x films in inert atmospheres by first-principles calculations. Applied Surface Science, 2015, 356, 1082-1085.	3.1	8
18611	Hindered rotational physisorption states of H2 on Ag(111) surfaces. Physical Chemistry Chemical Physics, 2015, 17, 19625-19630.	1.3	3
18612	On the energetics of cation ordering in tungsten-bronze-type oxides. Physical Chemistry Chemical Physics, 2015, 17, 30343-30351.	1.3	15

#	Article	IF	Citations
18613	Crystal structures and properties of nitrogen oxides under high pressure. RSC Advances, 2015, 5, 103373-103379.	1.7	3
18614	Determining dilute-limit solvus boundaries in multi-component systems using defect energetics: Na in PbTe and PbS. Journal of Materials Chemistry C, 2015, 3, 10630-10649.	2.7	27
18615	Silicene on metallic quantum wells: An efficient way of tuning silicene-substrate interaction. Physical Review B, 2015, 92, .	1.1	13
18616	First-Principles Investigation on Electronic Structure and Optical Properties of Wurtzite InxGa1-xN Alloys. Rare Metal Materials and Engineering, 2015, 44, 3027-3031.	0.8	7
18617	Structural and electronic properties of atomically thin germanium selenide polymorphs. Science China Materials, 2015, 58, 929-935.	3.5	54
18618	Enhanced Ab Initio Molecular Dynamics Simulation of the Temperature-Dependent Thermodynamics for the Diffusion of Carbon Monoxide on Ru(0001) Surface. Journal of Physical Chemistry C, 2015, 119, 26422-26428.	1.5	9
18619	Accelerated materials property predictions and design using motif-based fingerprints. Physical Review B, 2015, 92, .	1.1	136
18620	First-principles study on the electronic and bonding properties of PbTiO3 (110) polar terminations. Chemical Research in Chinese Universities, 2015, 31, 825-829.	1.3	1
18621	Ab initio study of the structural, vibrational and thermal properties of Ge2Sb2Te5. International Journal of Computational Materials Science and Engineering, 2015, 04, 1550009.	0.5	0
18622	Electronic structure and photocatalytic activities of (Bi2â^'Y)Sn2O7 solid solution. Applied Surface Science, 2015, 357, 2364-2371.	3.1	9
18623	H trapping and mobility in nanostructured tungsten grain boundaries: a combined experimental and theoretical approach. Nuclear Fusion, 2015, 55, 113009.	1.6	31
18624	Amorphous Ge quantum dots embedded in crystalline Si:ab initioresults. Journal of Physics Condensed Matter, 2015, 27, 405302.	0.7	12
18625	(Ti/Zr,N) codoped hematite for enhancing the photoelectrochemical activity of water splitting. Physical Chemistry Chemical Physics, 2015, 17, 22179-22186.	1.3	41
18626	Mechanisms of Pyrrole Hydrogenation on Ru(0001) and Hydrogen Molybdenum Bronze Surfaces. Journal of Physical Chemistry C, 2015, 119, 22477-22485.	1.5	7
18627	Influential Electronic and Magnetic Properties of the Gallium Sulfide Monolayer by Substitutional Doping. Journal of Physical Chemistry C, 2015, 119, 29148-29156.	1.5	40
18628	N-Carbamoyl-Piperidine-4-Carboxylic Acid: An X-ray and Density Functional Tight-Binding Studies. Molecular Crystals and Liquid Crystals, 2015, 623, 358-364.	0.4	0
18629	Structural and electronic control of the metal to insulator transition and local orderings in theÎ,-(BEDT-TTF)₂X organic conductors. Journal of Physics Condensed Matter, 2015, 27, 465702.	0.7	15
18630	Ab initiostudy of scintillating lanthanide oxyhalide host materials. Materials Research Express, 2015, 2, 105901.	0.8	12

#	Article	IF	Citations
18631	First-principles study of the structural and electronic properties of ultrathin silver nanowires. European Physical Journal B, 2015, 88, 1.	0.6	4
18632	Fermi arcs and pseudogap emerging from dimensional crossover at the Fermi surface in La 2â^'x Sr x CuO 4. Europhysics Letters, 2015, 112, 37011.	0.7	5
18633	Hydrogenation of bilayer graphene: A small twist makes a big difference. Nano Research, 2015, 8, 3887-3897.	5.8	9
18634	Robust intrinsic ferromagnetism and half semiconductivity in stable two-dimensional single-layer chromium trihalides. Journal of Materials Chemistry C, 2015, 3, 12457-12468.	2.7	569
18635	Charge Transfer Stabilization of Late Transition Metal Oxide Nanoparticles on a Layered Niobate Support. Journal of the American Chemical Society, 2015, 137, 16216-16224.	6.6	60
18636	Resistance to sulfur poisoning of Ni-based alloy with coinage (IB) metals. Applied Surface Science, 2015, 357, 1785-1791.	3.1	11
18637	First-principles study of structural, elastic and thermodynamic properties of AuIn2. Modern Physics Letters B, 2015, 29, 1550222.	1.0	1
18638	Gadolinium-Vacancy Clusters in the (111) Surface of Gadolinium-Doped Ceria: A Density Functional Theory Study. Chemistry of Materials, 2015, 27, 7910-7917.	3.2	26
18639	Defect stability in thorium monocarbide: An ab initio study. Chinese Physics B, 2015, 24, 097101.	0.7	4
18640	Theoretical calculations on structural and electronic properties of BGaAsBi alloys. European Physical Journal B, 2015, 88, 1.	0.6	2
18641	First-principles study of structural, elastic, and electronic properties of CeB6 under pressure. Frontiers of Physics, 2015, 10, 1.	2.4	4
18642	Ab initio study of thermoelectric properties of doped SnO2 superlattices. Journal of Solid State Chemistry, 2015, 231, 123-131.	1.4	5
18643	Investigating the Energetic Ordering of Stable and Metastable TiO₂ Polymorphs Using DFT+U and Hybrid Functionals. Journal of Physical Chemistry C, 2015, 119, 21060-21071.	1.5	81
18644	Theoretical Study of EMIM⁺ Adsorption on Silver Electrode Surfaces. Journal of Physical Chemistry C, 2015, 119, 20023-20029.	1.5	44
18645	Magnetic Exchange in Mn^{II}[TCNE] (TCNE = Tetracyanoethylene) Molecule-Based Magnets with Two- and Three-Dimensional Magnetic Networks. Journal of Physical Chemistry C, 2015, 119, 25036-25046.	1.5	8
18646	Kinetically Trapped Two-Component Self-Assembled Adlayer. Journal of Physical Chemistry C, 2015, 119, 25364-25376.	1.5	27
18647	Theoretical investigation of defect structure in B2 TrSc (Tr =Cd, Ru) alloys. Modern Physics Letters B, 2015, 29, 1550234.	1.0	1
18648	First-principles calculation of the structural and elastic properties of ternary metal nitrides Ta_xMo_{1-x}N and Ta_xW_{1-x}N. Journal of Physics: Conference Series, 2015, 640, 012022.	0.3	3

#	Article	IF	Citations
18649	Understanding Hematite Doping with Group IV Elements: A DFT+U Study. Journal of Physical Chemistry C, 2015, 119, 26303-26310.	1.5	66
18650	Adsorption of Water on Yttria-Stabilized Zirconia. Journal of Physical Chemistry C, 2015, 119, 22526-22533.	1.5	24
18651	Pressure-induced phase transition in CrO2. Journal of Molecular Modeling, 2015, 21, 304.	0.8	7
18652	Atomic and electronic structures of Si(1 1) Tj ETQq1 1 0.784314 rgBT /Overlock 10 Tf 50 627 Td (1)-$\left(sqrt{mathbf{3}}imessqrt{ma and (6 Ã— 6)-Au surfaces. Journal of Physics Condensed Matter, 2015, 27, 475001.	0.7	3
18653	Electronic and chemical structures of pyrite and arsenopyrite. Mineralogical Magazine, 2015, 79, 1779-1789.	0.6	20
18654	Effect of electron correlations on the<mml:math xmlns:mml="http://www.w3.org/1998/Math/MathML"><mml:msub><mml:mi mathvariant="normal">Fe</mml:mi><mml:mn>3</mml:mn></mml:msub><mml:mtext>Si</mml:mtext></mml:math>and<mml:math xmlns:mml="http://www.w3.org/1998/Math/MathML"><mml:mi>Î±</mml:mi><mml:mtext>â^'</mml:mtext><mml:msub><mml:mi mathvariant="normal">FeSi</mml:mi><mml:mn>2</mml:mn></mml:msub></mml:math>band structure and optical properties. Physical Review B, 2015, 92, .	1.1	21
18655	Elastic properties, hardness, and anisotropy in baddeleyite IVTMO2 (M=Ti, Zr, Hf). Science China Materials, 2015, 58, 893-905.	3.5	5
18656	First-Principles Investigation on Structural and Electronic Properties of Ferromagnetic Fe2P4O12. Ferroelectrics, 2015, 482, 113-120.	0.3	2
18657	First-principles study of direct and narrow band gap semiconductingÎ²-CuGaO₂. Materials Research Express, 2015, 2, 045902.	0.8	9
18658	First principles study of structural, electronic and optical properties of BiFeO3 in ferroelectric and paraelectric phases. Materials Research Innovations, 2015, 19, S5-684-S5-688.	1.0	15
18659	<i>Ab Initio</i> Study of the Oxygen Effect on Magnetic Interactions within 3d Metal Nanowires on Vicinal Rh (553) Surface. Solid State Phenomena, 0, 233-234, 546-549.	0.3	0
18660	Strain-induced asymmetric modulation of band gap in narrow armchair-edge graphene nanoribbon. Modern Physics Letters B, 2015, 29, 1550224.	1.0	2
18661	Hybrid carbon nanomaterials for electrochemical detection of biomolecules. Physica Scripta, 2015, 90, 094006.	1.2	3
18662	Theoretical investigation on the solution behaviors of Ba and Zr in uranium dinitride. Science China Chemistry, 2015, 58, 1891-1897.	4.2	3
18663	The role of magnetism in the formation of the two-phase miscibility gap in Î² Cuâ€“Alâ€“Mn. Journal of Magnetism and Magnetic Materials, 2015, 395, 234-239.	1.0	10
18664	Calculation of proton conductivity at the Î£3111/11Â¯0 tilt grain boundary of barium zirconate using density functional theory. Solid State Ionics, 2015, 279, 60-65.	1.3	15
18665	Order and disorder in quaternary atomic laminates from first-principles calculations. Physical Chemistry Chemical Physics, 2015, 17, 31810-31821.	1.3	71
18666	A study of uranium adsorption to single-crystal tungsten. Journal of Nuclear Materials, 2015, 467, 628-634.	1.3	2

#	Article	IF	Citations
18667	Effect of surface functionalization on the electronic transport properties of Ti ₃ C ₂ MXene. Europhysics Letters, 2015, 111, 67002.	0.7	106
18668	Structural, mechanical, electronic and optical properties of BBi, BP and their ternary alloys BBi_{1â^'x}P_x. Journal Physics D: Applied Physics, 2015, 48, 475304.	1.3	21
18669	Insights into SO2 and H2O co-adsorption on Cu (100) surface with calculations of density functional theory. Transactions of Nonferrous Metals Society of China, 2015, 25, 4102-4109.	1.7	7
18670	Phase transitions and optical properties of the semiconducting and metallic phases of single-layer MoS2. Nanotechnology, 2015, 26, 435705.	1.3	13
18671	Improving the Description of Nonmagnetic and Magnetic Molecular Crystals via the van der Waals Density Functional. Journal of the Physical Society of Japan, 2015, 84, 024715.	0.7	14
18672	Elastic properties and electronic structures of lanthanide hexaborides. Chinese Physics B, 2015, 24, 096201.	0.7	18
18673	Dynamics of ultrathin gold layers on vitreous silica probed by density functional theory. Physical Chemistry Chemical Physics, 2015, 17, 27488-27495.	1.3	7
18674	Reduction of the Mg acceptor activation energy in GaN, AlN, Al_{0.83}Ga_{0.17}N and Mg_{Ga}Î´-doping (AlN)₅/(GaN)₁: the strain effect. Journal Physics D: Applied Physics, 2015, 48, 475104.	1.3	6
18675	The Electronic Structure of Structurally Strained Mn₃O₄Postspinel and the Relationship with Mn₃O₄Spinel. Journal of the Physical Society of Japan, 2015, 84, 114702.	0.7	15
18676	Ab Initio and Phenomenological Modeling of the Phonon Spectrum of Superhard cp-BC2N. Russian Physics Journal, 2015, 58, 978-986.	0.2	5
18677	Methylene Blue Adsorption on the Basal Surfaces of Kaolinite: Structure and Thermodynamics from Quantum and Classical Molecular Simulation. Clays and Clay Minerals, 2015, 63, 185-198.	0.6	45
18678	DFT study of interactions between calcium hydroxyl ions and pyrite, marcasite, pyrrhotite surfaces. Applied Surface Science, 2015, 355, 577-581.	3.1	61
18679	Covalent effects in magnetic ferroelectrics MnMO₃ (Mâ€‰=â€‰Ti, Sn). Physica Status Solidi (B): Basic Research, 2015, 252, 626-634.	0.7	8
18680	Exothermic Mechanism for the Abstraction of Hydrogen from Methane on Li-Doped MgO. Journal of Physical Chemistry C, 2015, 119, 196-215.	1.5	8
18681	Structural, electronic, and elastic properties of CuFeS2: first-principles study. Applied Physics A: Materials Science and Processing, 2015, 118, 1145-1152.	1.1	29
18682	Characterization of M-O bonds in Y₂Ti₂O₇and Y₂TiO₅with EELS. Physica Status Solidi (B): Basic Research, 2015, 252, 206-211.	0.7	5
18683	Electronic and optical properties of mixed Snâ€“Pb organohalide perovskites: a first principles investigation. Journal of Materials Chemistry A, 2015, 3, 9208-9215.	5.2	170
18684	A first principles study on the mechanical properties of hexagonal zinc oxide sheets. Superlattices and Microstructures, 2015, 79, 15-20.	1.4	10

#	Article	IF	Citations
18685	Electronic structures and magnetic properties in Ti-doped ZnS. Solid State Communications, 2015, 205, 9-13.	0.9	12
18686	Phase transition of iron doped MgO under high pressure by first-principles study. International Journal of Modern Physics C, 2015, 26, 1550020.	0.8	1
18687	Structural evolution and electronic mechanism for KBH4 phase transition from first-principles calculations. Chemical Physics Letters, 2015, 620, 88-91.	1.2	0
18688	Insight into carbon formation from ethylene decomposition over Pd(100) via density functional theory calculations. Applied Surface Science, 2015, 328, 583-590.	3.1	13
18689	Structural stability, electronic structure and mechanical properties of ZnN and CdN: A first principles study. Computational Materials Science, 2015, 99, 117-124.	1.4	9
18690	Ab initio investigation of the intermetallics in the Nbâ€“Sn binary system. Acta Materialia, 2015, 86, 23-33.	3.8	39
18691	Phonon and electronic properties of Ti 2 SiC from first-principles calculations. Solid State Communications, 2015, 204, 37-40.	0.9	18
18692	Optical excitations and quasiparticle energies in the AlN monolayer honeycomb structure. Superlattices and Microstructures, 2015, 79, 38-44.	1.4	24
18693	Electronic properties of Î²-graphyne bilayers. Chemical Physics Letters, 2015, 620, 67-72.	1.2	14
18694	Theoretical investigations on the elastic wave propagation and phonon focusing in AlLi crystal. Materials Chemistry and Physics, 2015, 152, 34-40.	2.0	2
18695	Sub-10â€‰nm rutile titanium dioxide nanoparticles for efficient visible-light-driven photocatalytic hydrogen production. Nature Communications, 2015, 6, 5881.	5.8	653
18696	First principles study of structural, electronic, elastic and magnetic properties of gadolinium hydride system GdHx (x=1, 2, 3). Materials Science in Semiconductor Processing, 2015, 31, 415-430.	1.9	6
18697	Ultrafast palladium diffusion in germanium. Journal of Materials Chemistry A, 2015, 3, 3832-3838.	5.2	14
18698	Thermodynamics of hydrogen-induced superabundant vacancy in tungsten. Journal of Nuclear Materials, 2015, 458, 187-197.	1.3	30
18699	Pressure-induced phase transition of BiOF: novel two-dimensional layered structures. Physical Chemistry Chemical Physics, 2015, 17, 4434-4440.	1.3	15
18700	Mnâ€“Mn interaction induced metallic or insulating character of doped silicon: An ab initio study. Computational Materials Science, 2015, 97, 186-192.	1.4	1
18701	Fe₃W₃C/WC/Graphitic Carbon Ternary Nanojunction Hybrids for Dyeâ€Sensitized Solar Cells. ChemSusChem, 2015, 8, 726-733.	3.6	16
18702	Electronic and optical modeling of solar cell compound CuXY2 (XÂ=ÂIn, Ga, Al; YÂ=ÂS, Se, Te): first-principles study via Tranâ€“Blaha-modified Beckeâ€“Johnson exchange potential approach. Journal of Materials Science, 2015, 50, 1710-1717.	1.7	37

#	Article	IF	Citations
18703	Electronic Interaction between Nitrogen Atoms in Doped Graphene. ACS Nano, 2015, 9, 670-678.	7.3	69
18704	DFT investigations on the structure and properties of MBP dimers and crystal with strong hydrogen-bonding interactions. Structural Chemistry, 2015, 26, 845-858.	1.0	4
18705	Anisotropic intrinsic lattice thermal conductivity of phosphorene from first principles. Physical Chemistry Chemical Physics, 2015, 17, 4854-4858.	1.3	379
18706	Third Order Elastic Constants and Debye Temperature of MgB2 Under Different Pressure: First-Principles Methods. Journal of Superconductivity and Novel Magnetism, 2015, 28, 1483-1489.	0.8	7
18707	Evidence of â€œnew hot spotsâ€•from determining the nonlinear optical behavior of materials: mechanistic studies of the vanadium borate crystal, Na₃VO₂B₆O₁₁. Physical Chemistry Chemical Physics, 2015, 17, 5338-5344.	1.3	15
18708	Anab initiostudy of the structural, elastic, electronic and optical properties of the newly synthesized nitridoaluminate LiCaAlN₂. Philosophical Magazine, 2015, 95, 41-63.	0.7	4
18709	The bond force constants of graphene and benzene calculated by density functional theory. Molecular Physics, 2015, 113, 1297-1305.	0.8	10
18710	Highâ€Pressure Investigation in the System SiO₂â€“GeO₂: Mutual Solubility of Si and Ge in Quartz, Coesite and Rutile Phases. Journal of the American Ceramic Society, 2015, 98, 982-989.	1.9	8
18711	Theoretical investigations on mechanical anisotropy and intrinsic thermal conductivity of YbAlO 3. Journal of the European Ceramic Society, 2015, 35, 1549-1557.	2.8	19
18712	Insights into the mechanism of heterogeneous mercury oxidation by HCl over V2O5/TiO2 catalyst: Periodic density functional theory study. Proceedings of the Combustion Institute, 2015, 35, 2855-2865.	2.4	83
18713	The effect of in-plane strain on the electronic properties of LaAlO3/SrTiO3 interface. Computational Materials Science, 2015, 99, 57-61.	1.4	16
18714	Investigations of Electronic Structure and Half-Metallic Ferromagnets in Cr-Doped Zinc-Blende BeS Semiconductor. Journal of Superconductivity and Novel Magnetism, 2015, 28, 157-164.	0.8	22
18715	The growth of Fe clusters over graphene/Cu(111). 2D Materials, 2015, 2, 014001.	2.0	4
18716	Domain boundaries and their influence on Li migration in solid-state electrolyte (La,Li)TiO3. Journal of Power Sources, 2015, 276, 203-207.	4.0	75
18717	A Theoretical Study on the Adsorption of CO2 on CuO(110) Surface. Journal of the Physical Society of Japan, 2015, 84, 015003.	0.7	5
18718	Temperature-Driven Changes of the Graphene Edge Structure on Ni(111): Substrate vs Hydrogen Passivation. Nano Letters, 2015, 15, 56-62.	4.5	27
18719	Electronic properties and 1/3 magnetization plateau of the S=1/2 magnetism Cu3 (P2 O6 OH)2. International Journal of Quantum Chemistry, 2015, 115, 406-412.	1.0	2
18720	Strain effects in monolayer iron-chalcogenide superconductors. 2D Materials, 2015, 2, 015001.	2.0	15

#	Article	IF	Citations
18721	Syntheses, structures, and optical properties of Ba₄Ga₄SnSe₁₂and Ba₆Ga₂SnSe₁₁. Dalton Transactions, 2015, 44, 2259-2266.	1.6	18
18722	The effects of screening length in the non-local screened-exchange functional. Journal of Physics Condensed Matter, 2015, 27, 025501.	0.7	10
18723	Special directions in momentum space. III. Practical applications. Journal of Applied Crystallography, 2015, 48, 11-19.	1.9	2
18724	High sensitive and selective flexible H2S gas sensors based on Cu nanoparticle decorated SWCNTs. Sensors and Actuators B: Chemical, 2015, 210, 1-8.	4.0	114
18725	Doping properties of MoS 2 /ZnO (0001) heterojunction ruled by interfacial micro-structure: From first principles. Solid State Communications, 2015, 204, 67-71.	0.9	23
18726	Influence of Interconfigurational Electronic States on Fe, Co, Ni-Silicene Materials Selection for Spintronics. Scientific Reports, 2014, 4, 7594.	1.6	25
18727	Structural, vibrational and thermodynamic properties of <mml:math xmlns:mml="http://www.w3.org/1998/Math/MathML" altimg="si566.gif" overflow="scroll"><mml:mrow><mml:msub><mml:mrow><mml:mtext>Mg</mml:mtext></mml:mrow><mml:mrow><mml:mn>2</mml:mn></mml:mrow></mml:msub></mml:mrow></mml:math> and <mml:math xmlns:mml="http://www.w3.org/1998/Math/MathML" altimg="si567.gif" overflow="scroll"><mml:mrow><mml:msu. Physics of the Earth and Planetary Interiors, 2015, 240, 1-24.	0.7	30
18728	The elastic, electronic and thermodynamic properties of PdTe under high pressure from first-principles calculations. Physica C: Superconductivity and Its Applications, 2015, 509, 34-41.	0.6	13
18729	First-principles and Monte Carlo studies on the magnetic stability of half-metallic zinc-blende CaC and similar compounds. Journal of Magnetism and Magnetic Materials, 2015, 378, 469-477.	1.0	13
18730	Investigation of structural and magnetic properties of nanoscale Cu doped SnO2: An experimental and density functional study. Journal of Alloys and Compounds, 2015, 627, 261-267.	2.8	36
18731	Coverage-Induced Conformational Effects on Activity and Selectivity: Hydrogenation and Decarbonylation of Furfural on Pd(111). ACS Catalysis, 2015, 5, 104-112.	5.5	172
18732	Structural stability of ternary D8mâ€“Ti5Sb2X (X=Al, Ga, In, Si, Ge, Sn) compounds. Calphad: Computer Coupling of Phase Diagrams and Thermochemistry, 2015, 49, 8-18.	0.7	2
18733	Structure and bonding nature of [PbCl]+ adsorption on the kaolinite(0 0 1) surface in aqueous system. Applied Surface Science, 2015, 330, 411-417.	3.1	7
18734	Clustering of Oâ€“X, XÂ=Â(Ag, Al, Ga, Sn, Sc, Zn, Zr) point defects in hexagonal Ti: Formation mechanism and ductility variations. Materials Chemistry and Physics, 2015, 154, 137-143.	2.0	12
18735	Alkali metal â€“ yttrium borohydrides: The link between coordination of small and large rare-earth. Journal of Solid State Chemistry, 2015, 225, 231-239.	1.4	27
18736	Understanding the mechanism of H atom absorption in the Pd(1 1 0) surface. Journal of Alloys and Compounds, 2015, 645, S123-S127.	2.8	10
18737	On the influence of polarization effects in predicting the interfacial structure and capacitance of graphene-like electrodes in ionic liquids. Journal of Chemical Physics, 2015, 142, 024701.	1.2	44
18738	Non-empirical phase equilibria in the Crâ€“Mo system: A combination of first-principles calculations, cluster expansion and Monte Carlo simulations. Solid State Sciences, 2015, 41, 19-24.	1.5	11

#	Article	IF	Citations
18739	A Toolbox for Controlling the Energetics and Localization of Electronic States in Selfâ€Assembled Organic Monolayers. Advanced Science, 2015, 2, 1400016.	5.6	20
18740	Electronic structures and dehydrogenation properties of bimetallic amidoboranes. International Journal of Hydrogen Energy, 2015, 40, 2500-2508.	3.8	7
18741	First-principles calculations of structural stability and elastic properties of REB12 strengthening phases in boriding Mgâ€“RE alloys. Journal of Alloys and Compounds, 2015, 632, 68-72.	2.8	9
18742	Electronic structures and phase transition characters of Î²-, P61-, P62- and Î´-Si₃N₄under extreme conditions: A density functional theory study. Journal of Semiconductors, 2015, 36, 023003.	2.0	0
18743	Room-temperature ferromagnetism with high magnetic moment in Cu-doped AlN single crystal whiskers. Chinese Physics B, 2015, 24, 027503.	0.7	3
18744	First-principles study on electronic structure and conductivity of Sn-doped Ga1.375In0.625O3. Journal of Semiconductors, 2015, 36, 012003.	2.0	2
18745	Searching for high magnetization density in bulk Fe: the new metastable Fe6phase. Journal of Physics Condensed Matter, 2015, 27, 016001.	0.7	1
18746	First-principles study of structure and nonlinear optical properties of CdHg(SCN) 4 crystal. Chinese Physics B, 2015, 24, 024221.	0.7	2
18747	Electronic structure, phase stability and resistivity of hybrid hexagonal <mml:math xmlns:mml="http://www.w3.org/1998/Math/MathML" altimg="si0021.gif" overflow="scroll"><mml:msub><mml:mrow><mml:mi mathvariant="normal">C</mml:mi></mml:mrow><mml:mrow><mml:mi>x</mml:mi></mml:mrow></mml:msub><mml:msub><mml:mrc stretchy="false">(</mml:mo><mml:mi>BN</mml:mi><mml:mo) Tj ETQq0 0 0 rgBT /Overlock 10 Tf 50 402 Td (stretchy="false">)</mml:m	1.3	12
18748	Phase transitions and mechanical stability of TiO2 polymorphs under high pressure. Journal of Alloys and Compounds, 2015, 631, 192-201.	2.8	70
18749	Linear and nonlinear properties of ultraviolet fluorine crystal: A first-principles study. Solid State Communications, 2015, 205, 33-38.	0.9	5
18750	Graphene antidot lattices as potential electrode materials for supercapacitors. Physica E: Low-Dimensional Systems and Nanostructures, 2015, 69, 316-321.	1.3	5
18751	High pressure structural behavior of YGa2: A combined experimental and theoretical study. Journal of Solid State Chemistry, 2015, 226, 11-16.	1.4	3
18752	Surface effects on the Frenkel pair defects stability in the vicinity of the Si(001) surface. Materials Science in Semiconductor Processing, 2015, 32, 179-187.	1.9	1
18753	Study of the reaction products of SF6 and C in the laser heated diamond anvil cell by pair distribution function analysis and micro-Raman spectroscopy. Journal of Solid State Chemistry, 2015, 225, 141-148.	1.4	4
18754	Relationship between monolayer stacking faults and twins in nanocrystals. Acta Materialia, 2015, 88, 207-217.	3.8	26
18755	Band gap characterization of ternary BBi1â^'xNx (0â‰¤xâ‰¤1) alloys using modified Beckeâ€“Johnson (mBJ) potential. Physica B: Condensed Matter, 2015, 462, 64-69.	1.3	21
18756	First-principles calculation of the structural, electronic, dynamical and thermodynamic properties of Î³-LiAlO2. International Journal of Hydrogen Energy, 2015, 40, 3762-3770.	3.8	18

#	Article	IF	Citations
18757	First-principles study of H2S adsorption and dissociation on Mo(1 1 0). Computational Materials Science, 2015, 101, 47-55.	1.4	13
18758	Structural, electronic, and optical properties of ordered Si1â^'Ge C alloys: A first principles study. Journal of Alloys and Compounds, 2015, 632, 629-633.	2.8	4
18759	Thermodynamic stability and structure of cuprous chloride surfaces: a DFT investigation. Physical Chemistry Chemical Physics, 2015, 17, 7038-7045.	1.3	8
18760	An amorphous SiO2/4H-SiC(0001) interface: Band offsets and accurate charge transition levels of typical defects. Solid State Communications, 2015, 205, 28-32.	0.9	22
18761	Tailored Synthesis of a Nonlinear Optical Phosphate with a Short Absorption Edge. Angewandte Chemie - International Edition, 2015, 54, 4217-4221.	7.2	205
18762	Electronic excitation induced amorphization in titanate pyrochlores: an ab initio molecular dynamics study. Scientific Reports, 2015, 5, 8265.	1.6	20
18763	Synergistic Oxygen Evolving Activity of a TiO₂-Rich Reconstructed SrTiO₃(001) Surface. Journal of the American Chemical Society, 2015, 137, 2939-2947.	6.6	58
18764	First principles characterization of silicate sites in clay surfaces. Physical Chemistry Chemical Physics, 2015, 17, 4952-4960.	1.3	21
18765	Molecular adsorption of NO on PdO(101). Surface Science, 2015, 640, 150-158.	0.8	6
18766	The Interaction of Formic Acid with Zinc Oxide: A Combined Experimental and Theoretical Study on Single Crystal and Powder Samples. Topics in Catalysis, 2015, 58, 174-183.	1.3	32
18767	Modulating the charge injection in organic field-effect transistors: fluorinated oligophenyl self-assembled monolayers for high work function electrodes. Journal of Materials Chemistry C, 2015, 3, 3007-3015.	2.7	62
18768	Evaluating Pristine and Modified SnS₂ as a Lithium-Ion Battery Anode: A First-Principles Study. ACS Applied Materials & Interfaces, 2015, 7, 4000-4009.	4.0	75
18769	A first-principles study of n-type and p-type doping of germanium carbide sheet. Applied Surface Science, 2015, 332, 147-151.	3.1	41
18770	First-Principles Study of Redox End Members in Lithiumâ€“Sulfur Batteries. Journal of Physical Chemistry C, 2015, 119, 4675-4683.	1.5	65
18771	Identification of specific phonon contributions in BCS-type superconductivity of boride-carbide crystals with a layer-like structure. Solid State Communications, 2015, 206, 1-5.	0.9	3
18772	First principles study of structural stability, electronic structure and mechanical properties of alkali beryllium hydrides ABeH3 (A=K, Rb, Cs). Journal of Physics and Chemistry of Solids, 2015, 81, 34-39.	1.9	7
18773	Synergistic effect of C, Ag-codoped TiO2 photocatalyst within the GGAÂ+ U framework. RSC Advances, 2015, 5, 434-439.	1.7	9
18774	Correlation-induced metal-insulator transitions in d0 magnetic superlattices based on alkaline-earth monoxides: Insights from ab initio calculations. Journal of Magnetism and Magnetic Materials, 2015, 384, 33-39.	1.0	8

#	Article	IF	Citations
18775	Novel catalytic activity for oxygen reduction reaction on MnN4 embedded graphene: A dispersion-corrected density functional theory study. Carbon, 2015, 84, 500-508.	5.4	166
18776	A density-functional study on the electronic and vibrational properties of layered antimony telluride. Journal of Physics Condensed Matter, 2015, 27, 085402.	0.7	18
18777	The Core Structure and Peierls Stress of âŒ© 11 2 Â¯ 0 âŒª $langle 11overline {2}0angle $ Dislocations in MgB2 with Mg and B Vacancies. Journal of Superconductivity and Novel Magnetism, 2015, 28, 1743-1748.	0.8	1
18778	First-principles nickel database: Energetics of impurities and defects. Computational Materials Science, 2015, 101, 77-87.	1.4	40
18779	An ab initio investigation of the effect of alloying elements on the elastic properties and magnetic behavior of Ni3Al. Computational Materials Science, 2015, 101, 39-46.	1.4	31
18780	Electronic and magnetic properties of AGNRs with different edge configurations of 558 grain boundary. Chemical Physics Letters, 2015, 623, 60-67.	1.2	1
18781	Dependence of the thermal stability of the interface states of d metals (Cu, Pd, Ti, Ni) and Al with graphene on the character of sorption and diffusion mobility in a contact zone. Russian Journal of Physical Chemistry A, 2015, 89, 531-546.	0.1	15
18782	A first-principles modeling of glycerol and ammonia interactions on the cation-deficient VSbO4(110) surface. Catalysis Today, 2015, 254, 53-61.	2.2	2
18783	Enhanced ferromagnetic properties of Cu doped two-dimensional GaN monolayer. International Journal of Modern Physics C, 2015, 26, 1550009.	0.8	10
18784	First-principles study of the adsorption sensitivity of Ni-doped single-walled zigzag (n,0)CNTs (n=4,5,6) toward SO2 molecules. Applied Surface Science, 2015, 335, 17-22.	3.1	23
18785	Atomic-scale origin of piezoelectricity in wurtzite ZnO. Physical Chemistry Chemical Physics, 2015, 17, 7857-7863.	1.3	20
18786	Study of carrier mobility of tubular and planar graphdiyne. Applied Physics A: Materials Science and Processing, 2015, 119, 571-579.	1.1	36
18787	Two-Dimensional Cu₂Si Monolayer with Planar Hexacoordinate Copper and Silicon Bonding. Journal of the American Chemical Society, 2015, 137, 2757-2762.	6.6	335
18788	Oxidation of CO on a carbon-based material composed of nickel hydroxide and hydroxyl graphene oxide, (Ni4(OH)3â€“hGO) â€“ a first-principles calculation. Physical Chemistry Chemical Physics, 2015, 17, 7555-7563.	1.3	2
18789	A first-principles study of the IIIâ€“IVâ€“V semiconductor nanosheets. Physical Chemistry Chemical Physics, 2015, 17, 1039-1046.	1.3	9
18790	First-principles study on the structural and electronic properties of clean and atomic oxygen adsorbed ZrC(0 0 1) surface. Computational Materials Science, 2015, 101, 115-119.	1.4	31
18791	Phosphorene oxides: Bandgap engineering of phosphorene by oxidation. Physical Review B, 2015, 91, .	1.1	181
18792	Structural and Vibrational Properties of Silyl (SiH₃^{â€“}) Anions in KSiH₃ and RbSiH₃: New Insight into Siâ€“H Interactions. Inorganic Chemistry, 2015, 54, 2300-2309.	1.9	18

#	Article	IF	Citations
18793	Molecular bonding-based descriptors for surface adsorption and reactivity. Journal of Catalysis, 2015, 324, 50-58.	3.1	17
18794	Electrochemical performance of Zr-doped Li3V2(PO4)3/C composite cathode materials for lithium ion batteries. Journal of Applied Electrochemistry, 2015, 45, 123-130.	1.5	28
18795	Electronic properties and photoelectron circular dichroism of adsorbed chiral molecules. Physical Review B, 2015, 91, .	1.1	4
18796	The Effects of Te^{2â^'} and I^{â^'} Substitutions on the Electronic Structures, Thermoelectric Performance, and Hardness in Meltâ€Quenched Highly Dense Cu_{2â€x}Se. Advanced Electronic Materials, 2015, 1, 1400015.	2.6	51
18797	Prediction of new high pressure phase of TaB3: First-principles. Journal of Alloys and Compounds, 2015, 632, 37-43.	2.8	14
18798	PdIIâ€“PdII bonding interaction in dinuclear PdII complex with non-macrocyclic (O&N) chelates: Characterization, kinetics and DFT study. Polyhedron, 2015, 89, 101-109.	1.0	16
18799	Electrical control of carriers' spin orientation in the FeVTiSi Heusler alloy. Journal of Materials Chemistry C, 2015, 3, 2563-2567.	2.7	30
18800	Theoretical studies of the interaction of terephthalate anion in MgAl-layered double hydroxides. Applied Clay Science, 2015, 107, 131-137.	2.6	25
18801	Ab initio studies of adatom- and vacancy-induced band bending in<mml:math xmlns:mml="http://www.w3.org/1998/Math/MathML"><mml:mrow><mml:msub><mml:mi>Bi</mml:mi><mml:mn>2</mml:mn></mml:m Physical Review B, 2015, 91, .	2.1	29
18802	Anchoring and Bending of Pentacene on Aluminum (001). Journal of Physical Chemistry C, 2015, 119, 3624-3633.	1.5	21
18803	Exploring the activity of a novel Au/TiC(001) model catalyst towards CO and CO2 hydrogenation. Surface Science, 2015, 640, 141-149.	0.8	17
18804	TOMBO: All-electron mixed-basis approach to condensed matter physics. Computer Physics Communications, 2015, 189, 20-30.	3.0	28
18805	Spin asymmetric band gap opening in graphene by Fe adsorption. Surface Science, 2015, 634, 62-67.	0.8	16
18806	Doping induces large variation in the electrical properties of MoS2 monolayers. Solid-State Electronics, 2015, 106, 44-49.	0.8	17
18807	Density functional study of vibrational, thermodynamic and elastic properties of ZrCo and ZrCoX3 (X=H, D and T) compounds. Journal of Alloys and Compounds, 2015, 629, 297-304.	2.8	31
18808	Effect of skeleton conformation on the electronic structure of 50% Ti substituted polysilanes from density functional calculations. Synthetic Metals, 2015, 202, 98-102.	2.1	1
18809	Airâ€promoted adsorptive desulfurization of diesel fuel over <scp>T</scp>iâ€<scp>C</scp>e mixed metal oxides. AICHE Journal, 2015, 61, 631-639.	1.8	53
18810	Increasing the band gap of FeS2 by alloying with Zn and applying biaxial strain: A first-principles study. Journal of Alloys and Compounds, 2015, 629, 43-48.	2.8	25

#	Article	IF	Citations
18811	First-principle investigation of magnetic and electronic properties of vanadium- and chromium-doped cubic aluminum phosphide. Materials Science in Semiconductor Processing, 2015, 32, 166-171.	1.9	34
18812	Polycrystalline Mg2Si thin films: A theoretical investigation of their electronic transport properties. Journal of Solid State Chemistry, 2015, 225, 174-180.	1.4	5
18813	Ab initio calculation of fundamental properties of CdxZn1â^'xTe ternary alloys in the zinc-blende structure. Physica E: Low-Dimensional Systems and Nanostructures, 2015, 68, 184-189.	1.3	12
18814	Elastic and thermodynamic properties of Mo2C polymorphs from first principles calculations. Ceramics International, 2015, 41, 5239-5246.	2.3	26
18815	TDPAC and first-principles study of electronic and structural properties of a Pd-vacancy complex in undoped germanium. Current Applied Physics, 2015, 15, 319-325.	1.1	2
18816	Alloying effects of Ta on the mechanical properties of Î³â€™ Co3(Al, W): A first-principles study. Scripta Materialia, 2015, 100, 5-8.	2.6	27
18817	Effect of external strain on electronic structure of stanene. Computational Materials Science, 2015, 101, 164-167.	1.4	86
18818	Modulating the interactions between MgH2 and graphene using different dopants. Chemical Physics Letters, 2015, 623, 82-88.	1.2	3
18819	First-principles study of the phonon, dielectric, and piezoelectric response in Bi2ZnTiO6 supercell. Computational Materials Science, 2015, 101, 227-232.	1.4	7
18820	Crystal structure determination of incommensurate modulated martensite in Niâ€“Mnâ€“In Heusler alloys. Acta Materialia, 2015, 88, 375-388.	3.8	83
18821	Separation of the attractive and repulsive contributions to the adsorbateâ€“adsorbate interactions of polar adsorbates on Si(100). Surface Science, 2015, 641, 282-288.	0.8	7
18822	Spectral neighbor analysis method for automated generation of quantum-accurate interatomic potentials. Journal of Computational Physics, 2015, 285, 316-330.	1.9	608
18823	Electronic and optical properties of the LiCdX (X = N, P, As and Sb) filled-tetrahedral compounds with the Tranâ€“Blaha modified Beckeâ€“Johnson density functional. Materials Research Bulletin, 2015, 64, 337-346.	2.7	9
18824	Structural, anisotropic elastic and electronic properties of Srâ€“Zn binary system intermetallic compounds: A first-principles study. Computational Materials Science, 2015, 99, 381-389.	1.4	28
18825	Optical properties of transition metal atom adsorbed graphene: A density functional theoretical calculation. Physica E: Low-Dimensional Systems and Nanostructures, 2015, 69, 306-315.	1.3	19
18826	Enhancing phase stability and kinetics of lithium-rich layered oxide for an ultra-high performing cathode in Li-ion batteries. Journal of Power Sources, 2015, 281, 77-84.	4.0	39
18827	Pt atoms stabilized on hexagonal boron nitride as efficient single-atom catalysts for CO oxidation: a first-principles investigation. RSC Advances, 2015, 5, 10452-10459.	1.7	54
18828	First principles lattice dynamics study of SnO2 polymorphs. Journal of Alloys and Compounds, 2015, 633, 272-279.	2.8	7

#	Article	IF	Citations
18829	The tunable electronic structure and mechanical properties of halogenated silicene: a first-principles study. Journal of Materials Chemistry C, 2015, 3, 3087-3094.	2.7	54
18830	Effect of vacancies in monolayer MoS₂ on electronic properties of Moâ€“MoS₂ contacts. RSC Advances, 2015, 5, 20538-20544.	1.7	37
18831	Magnetic nanopantograph in the SrCu ₂ (BO ₃) ₂ Shastryâ€“Sutherland lattice. Proceedings of the National Academy of Sciences of the United States of America, 2015, 112, 1971-1976.	3.3	36
18832	Growth of an Ultrathin Zirconia Film on Pt₃Zr Examined by High-Resolution X-ray Photoelectron Spectroscopy, Temperature-Programmed Desorption, Scanning Tunneling Microscopy, and Density Functional Theory. Journal of Physical Chemistry C, 2015, 119, 2462-2470.	1.5	46
18833	Surface Dynamics of Xe(111): An Ambiguous Nobility. Journal of Physical Chemistry C, 2015, 119, 14579-14584.	1.5	7
18834	Porphyrin-based porous sheet: Optoelectronic properties and hydrogen storage. International Journal of Hydrogen Energy, 2015, 40, 3689-3696.	3.8	22
18835	Structural Stability, Electronic Structure and Mechanical Properties of Liâ€“Nâ€“H System. Acta Metallurgica Sinica (English Letters), 2015, 28, 550-558.	1.5	2
18836	Water Adsorption and Dissociation at Metal-Supported Ceria Thin Films: Thickness and Interface-Proximity Effects Studied with DFT+U Calculations. Journal of Physical Chemistry C, 2015, 119, 2537-2544.	1.5	16
18837	Theoretical Study of Phase Separation of Scandium Hydrides under High Pressure. Journal of Physical Chemistry C, 2015, 119, 5614-5625.	1.5	37
18838	Investigation of the Optical Absorbance, Electronic, and Photocatalytic Properties of (Cu1â€“xCox)2(OH)PO4 Solid Solutions. Journal of Physical Chemistry C, 2015, 119, 4684-4693.	1.5	7
18839	Ultrathin Gold Nanowires: Soft-Templating versus Liquid Phase Synthesis, a Quantitative Study. Journal of Physical Chemistry C, 2015, 119, 4422-4430.	1.5	40
18840	Efficient and Reliable Strategy for Identifying Muon Sites Based on the Double Adiabatic Approximation. Journal of Physical Chemistry C, 2015, 119, 4278-4285.	1.5	28
18841	Epitaxial Retrieval of a Disappearing Polymorph. Crystal Growth and Design, 2015, 15, 115-123.	1.4	10
18842	Adsorption and Dehydrogenation Behaviors of the NH₃ Molecule on the W(111) Surface: A First-Principles Study. Journal of Physical Chemistry C, 2015, 119, 4188-4198.	1.5	7
18843	Electronic Structures and Transport Properties of n-Type-Doped Indium Oxides. Journal of Physical Chemistry C, 2015, 119, 4789-4795.	1.5	20
18844	Propylene Adsorption On a Nonstoichiometric VSbO₄(110) Surface. Journal of Physical Chemistry C, 2015, 119, 4967-4975.	1.5	2
18845	Nitrogen(II) Oxide Charge Transfer Complexes on TiO₂: A New Source for Visible-Light Activity. Journal of Physical Chemistry C, 2015, 119, 4488-4501.	1.5	33
18846	Unveiling the Janus-Like Properties of OH^{â€“}. Journal of Physical Chemistry Letters, 2015, 6, 272-278.	2.1	17

#	Article	IF	Citations
18847	Diarylethene Molecules on a Ag(111) Surface: Stability and Electron-Induced Switching. Journal of Physical Chemistry C, 2015, 119, 4874-4883.	1.5	30
18848	Interaction of Al with O2 exposed Mo2BC. Applied Surface Science, 2015, 332, 699-703.	3.1	21
18849	Light Metals on Oxygen-Terminated Diamond (100): Structure and Electronic Properties. Chemistry of Materials, 2015, 27, 1306-1315.	3.2	26
18850	A Theoretical Study of the Effect of Dopants on Diamond (100) Surface Stabilization for Different Termination Scenarios. Journal of Physical Chemistry C, 2015, 119, 2545-2556.	1.5	10
18851	Hydrogenous Zintl Phase Ba₃Si₄H_x (x = 1â€“2): Transforming Si₄ â€œButterflyâ€•Anions into Tetrahedral Moieties. Inorganic Chemistry, 2015, 54, 756-764.	1.9	4
18852	Reaction of Trimethylaluminum with Water on Pt(111) and Pd(111) from 10^{â€“5} to 10^{â€“1} Millibar. Journal of Physical Chemistry C, 2015, 119, 2399-2411.	1.5	21
18853	A Linear Response DFT+U Study of Trends in the Oxygen Evolution Activity of Transition Metal Rutile Dioxides. Journal of Physical Chemistry C, 2015, 119, 4827-4833.	1.5	86
18854	Origins of Hydration Differences in Homochiral and Racemic Crystals of Aspartic Acid. Journal of Physical Chemistry A, 2015, 119, 1396-1403.	1.1	7
18855	Diffusion Monte Carlo Study of Para-Diiodobenzene Polymorphism Revisited. Journal of Chemical Theory and Computation, 2015, 11, 907-917.	2.3	22
18856	First-Principles Investigation of Optoelectronic and Redox Properties of (Ta_{1â€“x}Nb_x)ON Compounds for Photocatalysis. Journal of Physical Chemistry C, 2015, 119, 4565-4572.	1.5	26
18857	Convergence of Atomic Charges with the Size of the Enzymatic Environment. Journal of Chemical Information and Modeling, 2015, 55, 564-571.	2.5	17
18858	Theoretical Insight into the Reaction Mechanism of Ethanol Steam Reforming on Co(0001). Journal of Physical Chemistry C, 2015, 119, 2680-2691.	1.5	22
18859	NiAl(110) Surface as a Template for Growing Transition Metal Linear Atomic Chains: A DFT Investigation. Journal of Physical Chemistry C, 2015, 119, 2456-2461.	1.5	5
18860	Tailoring Native Defects and Zinc Impurities in Li₄Ti₅O₁₂: Insights from First-Principles Study. Journal of Physical Chemistry C, 2015, 119, 5238-5245.	1.5	23
18861	Interface-level thermodynamic stability diagram for in situ internal oxidation of Ag(SnO2)p composites. Journal of Materials Science, 2015, 50, 1646-1654.	1.7	14
18862	A DFT study of elastic and structural properties of (3,3) boron nitride nanotube under external electric field. Superlattices and Microstructures, 2015, 82, 90-102.	1.4	21
18863	Electronic and magnetic properties of an AlN monolayer doped with first-row elements: a first-principles study. RSC Advances, 2015, 5, 18352-18358.	1.7	50
18864	Defects in Silicene: Vacancy Clusters, Extended Line Defects and Di-adatoms. Scientific Reports, 2015, 5, 7881.	1.6	92

#	Article	IF	Citations
18865	Epitaxially Grown Strained Pentacene Thin Film on Graphene Membrane. Small, 2015, 11, 2037-2043.	5.2	53
18866	Massive band gap variation in layered oxides through cation ordering. Nature Communications, 2015, 6, 6191.	5.8	36
18867	Single-point kinetic energy density functionals: A pointwise kinetic energy density analysis and numerical convergence investigation. Physical Review B, 2015, 91, .	1.1	46
18868	Ferroelectric Domain Wall Induced Band Gap Reduction and Charge Separation in Organometal Halide Perovskites. Journal of Physical Chemistry Letters, 2015, 6, 693-699.	2.1	293
18869	Isocyanate (NCO) evidence in the CO+NO reaction over palladium. Applied Catalysis A: General, 2015, 494, 48-56.	2.2	12
18870	Ti-decorated zigzag graphene nanoribbons for hydrogen storage. A van der Waals-corrected density-functional study. International Journal of Hydrogen Energy, 2015, 40, 4960-4968.	3.8	65
18871	External pressure and composition effects on the atomic and electronic structure of SnWO4. Solar Energy Materials and Solar Cells, 2015, 143, 627-634.	3.0	19
18872	Betheâ€“Salpeter calculation of optical-absorption spectra of In₂O₃and Ga₂O₃. Semiconductor Science and Technology, 2015, 30, 024010.	1.0	38
18873	Computational study of interaction of alkali metals with C3N nanotubes. Journal of Molecular Modeling, 2015, 21, 20.	0.8	4
18874	First-principle and molecular dynamics calculations for physical properties of Niâ€“Sn alloy system. Computational Materials Science, 2015, 99, 274-284.	1.4	21
18875	Theoretical limits on the stability of single-phase kesterite-Cu2ZnSnS4. Journal of Applied Physics, 2015, 117, .	1.1	22
18876	Topological states in<mml:math xmlns:mml="http://www.w3.org/1998/Math/MathML"><mml:mi>Î±</mml:mi><mml:mo>â^'</mml:mo><mml:mi>Sn</mml:mi><mml:mn>1</mml:mn></mml:math>HgTe quantum wells: A comparison ofab initioresults. Physical Review B, 2015, 91, .	1.1	20
18877	Optical, electronic, and photoelectrochemical properties of the p-type Cu_{3â^'x}VO₄ semiconductor. Journal of Materials Chemistry A, 2015, 3, 4501-4509.	5.2	75
18878	Metalâ€“organic Kagome lattices M₃(2,3,6,7,10,11-hexaiminotriphenylene)₂ (M =) Tj ETQq1 1 0.784314 rgBT /Overlock 10 Tf 5 Physics, 2015, 17, 5954-5958.	1.3	108
18879	First-Principles Study of Half-Metallic and Magnetic Properties for the Heusler Alloys Fe2CrX (X = P,) Tj ETQq0 0 0 rgBT /Overlock 10 Tf 5	0.8	8
18880	First-Principles Study of Magnetic Properties and Martensitic Transformation of Pd â^' Mn â^' Sn Magnetic Shape Memory Alloys. Journal of Superconductivity and Novel Magnetism, 2015, 28, 1639-1643.	0.8	3
18881	Oxygen Defects in Phosphorene. Physical Review Letters, 2015, 114, 046801.	2.9	511
18882	Native point defects in few-layer phosphorene. Physical Review B, 2015, 91, .	1.1	104

#	Article	IF	Citations
18883	Bimetallic dimers adsorbed on a defect-free MgO(001) surface: bonding, structure and reactivity. Physical Chemistry Chemical Physics, 2015, 17, 9666-9679.	1.3	9
18884	Effect of helium and vacancies in a vanadium grain boundary by first-principles. Nuclear Instruments & Methods in Physics Research B, 2015, 352, 121-124.	0.6	8
18885	Glycerolysis of methyl oleate on MgO: Experimental and theoretical study of the reaction selectivity. Journal of Catalysis, 2015, 323, 132-144.	3.1	18
18886	Structure dependent active sites of Ni_xS_y as electrocatalysts for hydrogen evolution reaction. Nanoscale, 2015, 7, 5157-5163.	2.8	121
18887	Different mechanism of capacitance change for gas detection using semiconducting and metallic single-walled carbon nanotubes. Current Applied Physics, 2015, 15, 377-382.	1.1	1
18888	From carbon atom to graphene on Cu(111): an ab-initio study. European Physical Journal B, 2015, 88, 1.	0.6	17
18889	Ab initio study of shallow acceptors in bixbyite V2O3. Journal of Applied Physics, 2015, 117, 015703.	1.1	4
18890	Static impedance behavior of programmable metallization cells. Solid-State Electronics, 2015, 106, 27-33.	0.8	22
18891	Electric Field Changes on Au Nanoparticles on Semiconductor Supports â€“ The Molecular Voltmeter and Other Methods to Observe Adsorbate-Induced Charge-Transfer Effects in Au/TiO₂ Nanocatalysts. Journal of the American Chemical Society, 2015, 137, 1972-1982.	6.6	49
18892	Magnesium oxide nanosheets as effective catalysts for the synthesis of diethyl carbonate from ethyl carbamate and ethanol. Catalysis Science and Technology, 2015, 5, 1021-1034.	2.1	36
18893	Revealing the properties of the cubic ZrO2 (111) surface by periodic DFT calculations: reducibility and stabilization through doping with aliovalent Y2O3. RSC Advances, 2015, 5, 13941-13951.	1.7	22
18894	Crystalline structures of polymeric hydrocarbon with 3,4-fold helical chains. Scientific Reports, 2015, 5, 7723.	1.6	9
18895	B₈₄: a quasi-planar boron cluster stabilized with hexagonal holes. Nanoscale, 2015, 7, 4055-4062.	2.8	44
18896	Stabilizing graphene-based organometallic sandwich structures through defect engineering. Physical Review B, 2015, 91, .	1.1	7
18897	Enhanced Ferromagnetism in a Mn₃C₁₂N₁₂H₁₂ Sheet. ChemPhysChem, 2015, 16, 614-620.	1.0	39
18898	High-Pressure Experimental and DFT-D Structural Studies of the Energetic Material FOX-7. Journal of Physical Chemistry C, 2015, 119, 2322-2334.	1.5	69
18899	The Magnetic and Optical Properties of ErP and ErSb Nanolayers. Journal of Superconductivity and Novel Magnetism, 2015, 28, 943-947.	0.8	0
18900	Antiferromagnetic ground state with pair-checkerboard order in FeSe. Physical Review B, 2015, 91, .	1.1	59

#	Article	IF	Citations
18901	Mechanisms for Hydrolysis of Silicon Nanomembranes as Used in Bioresorbable Electronics. Advanced Materials, 2015, 27, 1857-1864.	11.1	98
18902	Hydrogen adsorption on palladium anchored defected graphene with B-doping: A theoretical study. International Journal of Hydrogen Energy, 2015, 40, 2473-2483.	3.8	32
18903	Carbon impurities in SrTiO₃from first principles. Modelling and Simulation in Materials Science and Engineering, 2015, 23, 015002.	0.8	8
18904	Investigations on Radiation Tolerance of M_{n+1}AX_n Phases: Study of Ti₃SiC₂, Ti₃AlC₂, Cr₂AlC, Cr₂GeC, Ti₂AlC, and Ti₂AlN. Journal of the American Ceramic Society, 2015, 98, 1323-1331.	1.9	83
18905	Polymorphs of CaSeO₄ under Pressure: A First-Principles Study of Structural, Electronic, and Vibrational Properties. Inorganic Chemistry, 2015, 54, 1765-1777.	1.9	31
18906	A first-principles study on uniaxial strain effects of nonplanar oxygen-functionalized armchair graphene nanoribbons. Journal of Alloys and Compounds, 2015, 631, 219-224.	2.8	7
18907	First principles investigation of the finite temperature dependence of the elastic constants of zirconium, magnesium and gold. Computational Materials Science, 2015, 99, 361-372.	1.4	15
18908	Reduced ceria nanofilms from structure prediction. Nanoscale, 2015, 7, 4361-4366.	2.8	20
18909	Effect of defects on the electronic properties of WS2armchair nanoribbon. Journal of Semiconductors, 2015, 36, 013003.	2.0	3
18910	Electronic structure and transport properties of Cu-deficient kuramite Cu_{3â^'}_xSnS₄. Japanese Journal of Applied Physics, 2015, 54, 021801.	0.8	10
18911	Organic molecules deposited on graphene: A computational investigation of self-assembly and electronic structure. Journal of Chemical Physics, 2015, 142, 044301.	1.2	23
18912	Effects of nitrogen on hydrogen retention in tungsten: First-principles calculations. Journal of Nuclear Materials, 2015, 459, 143-149.	1.3	18
18913	Mechanical Origin of the Structural Phase Transition in Methylammonium Lead Iodide CH₃NH₃PbI₃. Journal of Physical Chemistry Letters, 2015, 6, 681-685.	2.1	63
18914	Synthesis and Characterization of Melt-Spun Metastable Al6Ge5. Journal of Electronic Materials, 2015, 44, 948-952.	1.0	4
18915	Strain sensitivity of band gaps of Sn-containing semiconductors. Physical Review B, 2015, 91, .	1.1	24
18916	On-the-fly machine-learning for high-throughput experiments: search for rare-earth-free permanent magnets. Scientific Reports, 2014, 4, 6367.	1.6	212
18917	Toward Optimizing the Performance of Self-Regenerating Pt-Based Perovskite Catalysts. ACS Catalysis, 2015, 5, 1112-1118.	5.5	20
18918	Prediction of the electronic structures, thermodynamic and mechanical properties in manganese doped magnesium-based alloys and their saturated hydrides based on density functional theory. Journal of Power Sources, 2015, 280, 147-154.	4.0	7

#	Article	IF	Citations
18919	Magnetic and Electronic Evolutions of Hydrogenated VTe2 Monolayer under Tension. Scientific Reports, 2014, 4, 7524.	1.6	58
18920	Origin of dramatic oxygen solute strengthening effect in titanium. Science, 2015, 347, 635-639.	6.0	255
18921	Converting Chemically Functionalized Few-Layer Graphene to Diamond Films: A Computational Study. Journal of Physical Chemistry C, 2015, 119, 2828-2836.	1.5	50
18922	MoS2 Quantum Dot: Effects of Passivation, Additional Layer, and h-BN Substrate on Its Stability and Electronic Properties. Journal of Physical Chemistry C, 2015, 119, 1565-1574.	1.5	24
18923	Phase stability of ternary fcc and bcc Fe-Cr-Ni alloys. Physical Review B, 2015, 91, .	1.1	114
18924	Ab initio thermodynamics investigation of titanium hydrides. Computational Materials Science, 2015, 97, 263-275.	1.4	25
18925	Study of the thermodynamic properties of CeO2 from ab initio calculations: The effect of phonon-phonon interaction. Journal of Chemical Physics, 2015, 142, 014503.	1.2	9
18926	Ferromagnetism in Fe-doped Bi2Se3 topological insulators with Se vacancies. Physics Letters, Section A: General, Atomic and Solid State Physics, 2015, 379, 417-420.	0.9	15
18927	Pressure effects on structural, elastic and electronic properties of BaZnO2: first-principles study. Philosophical Magazine, 2015, 95, 64-78.	0.7	9
18928	Phase stability, structural and elastic properties of C15-type Laves transition-metal compounds MCo2 from first-principles calculations. Journal of Alloys and Compounds, 2015, 630, 202-208.	2.8	105
18929	The effective adsorption and decomposition of N₂O on Al-decorated graphene oxide under electric field. RSC Advances, 2015, 5, 18761-18766.	1.7	12
18930	Surface ReO_x Sites on Al₂O₃ and Their Molecular Structureâ€“Reactivity Relationships for Olefin Metathesis. ACS Catalysis, 2015, 5, 1432-1444.	5.5	64
18931	Penta-graphene: A new carbon allotrope. Proceedings of the National Academy of Sciences of the United States of America, 2015, 112, 2372-2377.	3.3	1,114
18932	First-principles calculation and molecular dynamics simulation of fracture behavior of VN layers under uniaxial tension. Physica E: Low-Dimensional Systems and Nanostructures, 2015, 69, 224-231.	1.3	23
18933	Role of Oxygen Vacancy on the Photoluminescence of BaMgSiO₄:Eu Phosphors: Experimental and Theoretical Analysis. Inorganic Chemistry, 2015, 54, 1556-1562.	1.9	83
18934	Conversion of CO₂ and C₂H₆ to Propanoic Acid on an Iridium-Modified Graphene Oxide Surface: Quantum-Chemical Investigation. Industrial & Engineering Chemistry Research, 2015, 54, 1539-1546.	1.8	5
18935	Controlled Surface Segregation Leads to Efficient Cokeâ€Resistant Nickel/Platinum Bimetallic Catalysts for the Dry Reforming of Methane. ChemCatChem, 2015, 7, 819-829.	1.8	78
18936	The Same at a First Glance: The Diffractogram of a New Polymorph of Anhydrous Sodium Luminolate Almost Perfectly Resembles the Diffraction Trace of an Already Known Polymorph. Zeitschrift Fur Anorganische Und Allgemeine Chemie, 2015, 641, 332-338.	0.6	6

#	Article	IF	Citations
18937	Electronic Structure of Twisted Bilayers of Graphene/MoS₂ and MoS₂/MoS₂. Journal of Physical Chemistry C, 2015, 119, 4752-4758.	1.5	131
18938	Bandâ€gap and phonon distribution in alkali halides. Physica Status Solidi (B): Basic Research, 2015, 252, 490-495.	0.7	19
18939	Contracted interlayer distance in graphene/sapphire heterostructure. Nano Research, 2015, 8, 1535-1545.	5.8	26
18940	High-pressure phases of SF6 up to 32GPa from X-ray diffraction and Raman spectroscopy. Journal of Physics and Chemistry of Solids, 2015, 80, 11-21.	1.9	4
18941	Structural, mechanical, and electronic properties of P3m1-BCN. Journal of Physics and Chemistry of Solids, 2015, 79, 89-96.	1.9	79
18942	The functionalisation of graphite surfaces with nitric acid: Identification of functional groups and their effects on gold deposition. Journal of Catalysis, 2015, 323, 10-18.	3.1	59
18943	Atomistic approach to predict the glass-forming ability in Zrâ€“Cuâ€“Al ternary metallic glasses. Journal of Alloys and Compounds, 2015, 627, 48-53.	2.8	27
18944	Roles of charge state and interatomic distance in the magnetic properties of C-doped MgO. Chemical Physics Letters, 2015, 621, 52-57.	1.2	7
18945	Vibrational mode frequencies of H2S and H2O adsorbed on Ge(001)-(2Ã—1) surfaces. Applied Surface Science, 2015, 329, 363-370.	3.1	6
18946	New template for Li and Ca decoration and hydrogen adsorption on graphene-like SiC: A first-principles study. Computational Materials Science, 2015, 99, 150-155.	1.4	12
18947	The density functional theory studies on the promoting effect of the Cu-modified Fe 3 O 4 catalysts. Physics Letters, Section A: General, Atomic and Solid State Physics, 2015, 379, 607-612.	0.9	17
18948	Strain effects on the electronic structure of ZnSnP2 via modified Beckeâ€“Johnson exchange potential. Physics Letters, Section A: General, Atomic and Solid State Physics, 2015, 379, 427-430.	0.9	9
18949	Electronic structure and lattice dynamics in the<mml:math xmlns:mml="http://www.w3.org/1998/Math/MathML"><mml:msub><mml:mi>FeSb</mml:mi><mml:mn>3</mml:mn></mml:msub></mml:math> from density functional theory. Physical Review B, 2015, 91, .	1.1	10
18950	Density functional theory calculations of atomic, electronic and thermodynamic properties of cubic LaCoO3and La1â^'xSrxCoO3surfaces. RSC Advances, 2015, 5, 760-769.	1.7	43
18951	Cluster Models for Studying CO2 Reduction on Semiconductor Photoelectrodes. Topics in Catalysis, 2015, 58, 46-56.	1.3	30
18952	Assessing the Viability of Extended Nonmetal Atom Chains in M_nF_{4n+2} (M=S and Se). Angewandte Chemie - International Edition, 2015, 54, 1476-1480.	7.2	15
18953	Estimating Bulk-Composition-Dependent H₂ Adsorption Energies on Cu_xPd_{1â€“x} Alloy (111) Surfaces. ACS Catalysis, 2015, 5, 1020-1026.	5.5	24
18954	Pressure control of magnetic clusters in strongly inhomogeneous ferromagnetic chalcopyrites. Scientific Reports, 2015, 5, 7720.	1.6	11

#	Article	IF	Citations
18955	Observation of a magnetic phase transition but absence of an electrical response in a new two-dimensional mixed-valence nickel-bis-dithiolene molecular crystal. RSC Advances, 2015, 5, 13857-13866.	1.7	7
18956	Stability of surface and subsurface hydrogen on and in Au/Ni near-surface alloys. Surface Science, 2015, 640, 190-197.	0.8	4
18957	Tuning phonon properties in thermoelectric materials. Reports on Progress in Physics, 2015, 78, 026501.	8.1	18
18958	First-principles studies of lone-pair-induced distortions in epitaxial phases of perovskite<mml:math xmlns:mml="http://www.w3.org/1998/Math/MathML"><mml:msub><mml:mi>SnTiO</mml:mi><mml:mn>3</mml:mn></mml:msub><mml:mo>/</mml:mo><mml:msub><mml:mi>PbTiO</mml:mi><mml:mn>3</mml:mn></mml:msub></mml:math>. Physical Review B, 2015, 91, .	1.1	29
18959	Silicene, a promising new 2D material. Progress in Surface Science, 2015, 90, 46-83.	3.8	221
18960	Carrier density modulation in a germanium heterostructure by ferroelectric switching. Nature Communications, 2015, 6, 6067.	5.8	75
18961	Density Functional Theory Comparison of Methanol Decomposition and Reverse Reactions on Metal Surfaces. ACS Catalysis, 2015, 5, 1027-1036.	5.5	83
18962	Confinement effects for the F center in non-stoichiometric BaZrO₃ ultrathin films. Physica Status Solidi (B): Basic Research, 2015, 252, 139-143.	0.7	6
18963	Bonding characteristics and site occupancies of alloying elements in Zr3Al2 compound from first principles. Journal of Alloys and Compounds, 2015, 622, 960-965.	2.8	5
18964	A first-principles study on hydrogen in ZnS: Structure, stability and diffusion. Physics Letters, Section A: General, Atomic and Solid State Physics, 2015, 379, 487-490.	0.9	4
18965	Electronic and structural properties at the interface between CuPc and graphene. Journal of Applied Physics, 2015, 117, 013701.	1.1	7
18966	VV and VO2 defects in silicon studied with hybrid density functional theory. Journal of Materials Science: Materials in Electronics, 2015, 26, 1568-1571.	1.1	8
18967	Reversible Hydrogenation of Graphene on Ni(111)â€”Synthesis of â€œGraphoneâ€. Chemistry - A European Journal, 2015, 21, 3347-3358.	1.7	57
18968	A First-Principles Study on Electron Donor and Acceptor Molecules Adsorbed on Phosphorene. Journal of Physical Chemistry C, 2015, 119, 2871-2878.	1.5	152
18969	Effect of alumina hydroxylation on glycerol hydrogenolysis to 1,2-propanediol over Cu/Al₂O₃: combined experiment and DFT investigation. RSC Advances, 2015, 5, 11188-11197.	1.7	42
18970	Numerical modeling of the core structure of [100] dislocations in Fe 3 C cementite. Scripta Materialia, 2015, 99, 61-64.	2.6	2
18971	High pressure structures and superconductivity of AlH₃(H₂) predicted by first principles. RSC Advances, 2015, 5, 5096-5101.	1.7	33
18972	Atomistic simulations of Â½â€ˆ1 1 0â€‰ screw dislocation core in magnesium oxide. Computational Materials Science, 2015, 103, 250-255.	1.4	22

#	Article	IF	Citations
18973	Ferroelectrically driven spatial carrier density modulation in graphene. Nature Communications, 2015, 6, 6136.	5.8	142
18974	Prediction of chirality- and size-dependent elastic properties of single-walled boron nitride nanotubes based on an accurate molecular mechanics model. Superlattices and Microstructures, 2015, 80, 196-205.	1.4	19
18975	Diffusion of Zr, Ru, Ce, Y, La, Sr and Ba fission products in UO2. Journal of Nuclear Materials, 2015, 459, 90-96.	1.3	15
18976	Diamond-like phases prepared from graphene layers. Physics of the Solid State, 2015, 57, 205-212.	0.2	26
18977	First-principles study of electronic structure of CuSbS2 and CuSbSe2 photovoltaic semiconductors. Thin Solid Films, 2015, 582, 401-407.	0.8	44
18978	Ab initio study on the adsorption of oxygen on Co(111) and its subsurface incorporation. European Physical Journal B, 2015, 88, 1.	0.6	4
18979	Electronic properties of double wall BN nanotube under hydrostatic pressure: an ab initio study. European Physical Journal B, 2015, 88, 1.	0.6	2
18980	A joint experimental and theoretical study on the electronic structure and photoluminescence properties of Al2(WO4)3 powders. Journal of Molecular Structure, 2015, 1081, 381-388.	1.8	22
18981	A new high-pressure polymeric nitrogen phase in potassium azide. RSC Advances, 2015, 5, 11825-11830.	1.7	23
18982	Systematic study on the anisotropic elastic properties of tetragonal XYSb (XÂ=ÂTi, Zr, Hf; YÂ=ÂSi, Ge) compounds. Solid State Sciences, 2015, 40, 92-100.	1.5	50
18983	Interstitial iron impurities at grain boundaries in silicon: A first-principles study. Physical Review B, 2015, 91, .	1.1	35
18984	First-principles calculations of electronic and optical properties of F, Mn-codoped cubic ZrO2. Solid State Sciences, 2015, 40, 101-104.	1.5	1
18985	Magnetoelectric coupling at the epitaxial Ni/PbTiO3 heterointerface from first principles. Physica B: Condensed Matter, 2015, 456, 383-387.	1.3	5
18986	First-principles calculations of the mechanic and vibration properties of AgRE (RE = Ho, Er, Tm) intermetallic compounds under pressure. Physica Scripta, 2015, 90, 025701.	1.2	4
18987	Electric field improved hydrogen storage of Ca-decorated monolayer MoS2. Physics Letters, Section A: General, Atomic and Solid State Physics, 2015, 379, 815-819.	0.9	25
18988	Strain-induced metal-semimetal transition of BeB₂ monolayer. RSC Advances, 2015, 5, 11392-11396.	1.7	19
18989	A density functional theory study on 3d metal/graphene for the removal of CO from H2feed gas in hydrogen fuel cells. RSC Advances, 2015, 5, 16394-16399.	1.7	9
18990	A DFT study of atomic geometry and electronic structures for oxidized Al0.25Ga0.75N (001) (2Ã—2) reconstruction surfaces. Applied Surface Science, 2015, 333, 201-206.	3.1	7

#	Article	IF	Citations
18991	Elastic and electronic properties of Imm2- and I<mml:math xmlns:mml="http://www.w3.org/1998/Math/MathML" altimg="si1.gif" overflow="scroll"><mml:mrow><mml:mover accent="true"><mml:mrow><mml:mn>4</mml:mn></mml:mrow><mml:mrow><mml:mo>Â¯</mml:mo></mml:mrow></mml:mover></m Computational Materials Science, 2015, 97, 6-13.	1.4	25
18992	Atomic bonding in the AlLiB14. Solid State Sciences, 2015, 47, 3-6.	1.5	1
18993	The heat capacities of thermomiotic ScF3 and ScF3â€“YF3 solid solutions. Journal of Materials Science, 2015, 50, 3409-3415.	1.7	24
18994	Topological phase driven by confinement effects in Bi bilayers. Physical Review B, 2015, 91, .	1.1	16
18995	Ab-initio study of structural, electronic, elastic and mechanical properties of RuAl1âˆ’xGax (x=0, 0.25,) Tj ETQq0 0 0 rgBT /Overlock 10 Tf	1.9	2
18996	Hydroxyapatite: Vibrational spectra and monoclinic to hexagonal phase transition. Journal of Applied Physics, 2015, 117, 074701.	1.1	15
18997	Ab initioelectronic structure, optical, and magneto-optical properties of MnGaAs digital ferromagnetic heterostructures. Physical Review B, 2015, 91, .	1.1	8
18998	An ab initio study of TiS₃: a promising electrode material for rechargeable Li and Na ion batteries. RSC Advances, 2015, 5, 21455-21463.	1.7	58
18999	A new evidence of first-order phase transition for hydrogen at 3000 K. Europhysics Letters, 2015, 109, 36003.	0.7	4
19000	Effect of Fe doping on electronic structure, chemical bonds and dielectric properties of o-Mn7C3. Physics Letters, Section A: General, Atomic and Solid State Physics, 2015, 379, 1219-1223.	0.9	2
19001	Hydrogen diffusion behavior and vacancy interaction behavior in OsO2 and RuO2 by ab initio calculations. Computational Materials Science, 2015, 102, 14-20.	1.4	2
19002	Hydrogen isotope in erbium oxide: Adsorption, penetration, diffusion, and vacancy trapping. Fusion Engineering and Design, 2015, 92, 35-40.	1.0	9
19003	Hydrogen centers and the conductivity of<mml:math xmlns:mml="http://www.w3.org/1998/Math/MathML"><mml:mrow><mml:mi mathvariant="normal">I</mml:mi><mml:msub><mml:mi mathvariant="normal">n</mml:mi><mml:mn>2</mml:mn></mml:msub><mml:msub><mml:mi mathvariant="normal">O</mml:mi><mml:mn>3</mml:mn></mml:msub></mml:mrow></mml:math>single crystals. Physical Review B, 2015, 91, .	1.1	34
19004	O2 dissociation on the side wall of aluminum nitride nanotube: a DFT investigation. Sensors and Actuators B: Chemical, 2015, 213, 139-149.	4.0	9
19005	Robust magnetic moments on the basal plane of the graphene sheet effectively induced by OH groups. Scientific Reports, 2015, 5, 8448.	1.6	49
19006	Graphdiyneâ€“metal contacts and graphdiyne transistors. Nanoscale, 2015, 7, 2116-2127.	2.8	94
19007	Structural and elastic properties characterization of Be and Mg doped boron nitride nanotubes using DFT calculations. Superlattices and Microstructures, 2015, 82, 113-123.	1.4	12
19008	Oxygen-assisted water partial dissociation on copper: a model study. Physical Chemistry Chemical Physics, 2015, 17, 8231-8238.	1.3	29

#	Article	IF	Citations
19009	Electronic structures and mechanical properties of Al(111)/ZrB₂(0001) heterojunctions from first-principles calculation. Molecular Physics, 2015, 113, 1794-1801.	0.8	21
19010	Adsorption and decomposition of methylamine on a Pt(100) surface: a density functional theory study. RSC Advances, 2015, 5, 20208-20217.	1.7	9
19011	Visible-light photocatalysis on C-doped ZnO derived from polymer-assisted pyrolysis. RSC Advances, 2015, 5, 27690-27698.	1.7	158
19012	The origin of the site preference of H adsorption on Pd(100). Science China Chemistry, 2015, 58, 156-161.	4.2	5
19013	Interstitial H+-Mediated Ferromagnetism in Co-Doped ZnS. Journal of Superconductivity and Novel Magnetism, 2015, 28, 1389-1393.	0.8	7
19014	Half-Metallic Ferromagnetism in Cu-Doped ZnO Nanostructures from First-Principle Prediction. Journal of Superconductivity and Novel Magnetism, 2015, 28, 2033-2038.	0.8	9
19015	Second-order phase transition in a SnS orthorhombic crystal under pressure. Physics of the Solid State, 2015, 57, 378-380.	0.2	6
19016	Theoretical study of propene oxidation on Bi2O3 surfaces. Science China Chemistry, 2015, 58, 593-600.	4.2	3
19017	Buckling of multi-walled silicon carbide nanotubes under axial compression via a molecular mechanics model. Applied Physics A: Materials Science and Processing, 2015, 118, 845-854.	1.1	1
19018	Vibrational and magnetic properties of crystalline CuTe2O5. JETP Letters, 2015, 100, 652-656.	0.4	10
19019	Experimental and theoretical investigations of structural and optical properties of copper doped ZnO nanorods. Journal of Sol-Gel Science and Technology, 2015, 74, 756-764.	1.1	40
19020	Dissecting graphene capacitance in electrochemical cell. Electrochimica Acta, 2015, 163, 296-302.	2.6	18
19021	Rutile Band-Gap States Induced by Doping with Manganese in Various Oxidation States. Journal of Physical Chemistry C, 2015, 119, 5534-5541.	1.5	16
19022	First-principles quantum molecular calculations of structural and mechanical properties of TiN/SiNx heterostructures, and the achievable hardness of the nc-TiN/SiNx nanocomposites. Thin Solid Films, 2015, 578, 83-92.	0.8	36
19023	Theoretical investigation of electronic structure and optical response in relation to the transport properties of Ga1â'xInxN (xÂ=ÂO, 0.25, 0.50, 0.75). Current Applied Physics, 2015, 15, 608-616.	1.1	4
19024	Mechanism of hydrogen treatment in KTiOPO₄ crystals at high temperature: experimental and first-principles studies. CrystEngComm, 2015, 17, 3793-3799.	1.3	12
19025	Electronic structure calculations of oxygen-doped diamond using DFT technique. Microelectronic Engineering, 2015, 146, 26-31.	1.1	14
19026	Effect of stoichiometry on the atomic and electronic structure of BaTiO₃nanoparticles: a first-principles study. Molecular Physics, 2015, 113, 3291-3295.	0.8	4

#	Article	IF	Citations
19027	Adsorption of insoluble polysulfides Li2Sx (x = 1, 2) on Li2S surfaces. Physical Chemistry Chemical Physics, 2015, 17, 9032-9039.	1.3	53
19028	Vibrational dynamics of rutile-type GeO₂from micro-Raman spectroscopy experiments and first-principles calculations. Europhysics Letters, 2015, 109, 26007.	0.7	4
19029	Interstitial impurity-induced magnetism inÎ±-PbO surface. Journal of Physics Condensed Matter, 2015, 27, 016002.	0.7	1
19030	Chemical tuning of band alignments for Cu/HfO2 interfaces. Physica Status Solidi (B): Basic Research, 2015, 252, 298-304.	0.7	3
19031	A critical evaluation of GGA +Umodeling for atomic, electronic and magnetic structure of Cr₂AlC, Cr₂GaC and Cr₂GeC. Journal of Physics Condensed Matter, 2015, 27, 095601.	0.7	23
19032	Sources ofn-type conductivity in GaInO₃. Journal Physics D: Applied Physics, 2015, 48, 015101.	1.3	13
19033	Compressive Straining of Bilayer Phosphorene Leads to Extraordinary Electron Mobility at a New Conduction Band Edge. Nano Letters, 2015, 15, 2006-2010.	4.5	40
19034	Tuning metalâ€“graphene interaction by non-metal intercalation: a case study of the graphene/oxygen/Ni (1â€‰×â€‰1) system. Journal Physics D: Applied Physics, 2015, 48, 015308.	1.3	8
19035	Structural, Electrical, and Lithium Ion Dynamics of Li ₂ MnO ₃ from Density Functional Theory. Chinese Physics Letters, 2015, 32, 017102.	1.3	11
19036	Quasi-Particle Properties in Copper Using the GW Approximation. Chinese Physics Letters, 2015, 32, 017101.	1.3	1
19037	Structural and Electronic Properties of Zigzag Graphene Nanoribbons on Si(001) Substrates. Chinese Physics Letters, 2015, 32, 027101.	1.3	0
19038	Theoretical determination of the microstructure of Cs covering of Mo in negative ion sources for nuclear fusion applications. Plasma Physics and Controlled Fusion, 2015, 57, 035005.	0.9	16
19039	First Principles Study on Mechanical Properties of Superhard Î±-Ga Boron. Chinese Physics Letters, 2015, 32, 026101.	1.3	2
19040	Li Storage Performance for the Composite Structure Of Graphene and Boron Fullerene. Chinese Physics Letters, 2015, 32, 026102.	1.3	4
19041	The mechanical and electronic properties of Al/TiC interfaces alloyed by Mg, Zn, Cu, Fe and Ti: First-principles study. Physica Scripta, 2015, 90, 035701.	1.2	13
19042	Reduced tight-binding models for elemental Si and N, and ordered binary Si-N systems. Physical Review B, 2015, 91, .	1.1	11
19043	Enhanced gas sorption properties of a new sulfone functionalized aluminum metal-organic framework: Synthesis, characterization, andÂDFT studies. Microporous and Mesoporous Materials, 2015, 216, 20-26.	2.2	17
19044	Tuning electronic and magnetic properties of GaN nanosheets by surface modifications and nanosheet thickness. Physical Chemistry Chemical Physics, 2015, 17, 8692-8698.	1.3	26

#	Article	IF	Citations
19045	Thermal expansion tensors, GrÃ¼neisen parameters and phonon velocities of bulk MT₂ (M =) Tj ETQq0 0 0 rgBT /Overlock	1.7	85
19046	Mechanical properties of chiral and achiral silicon carbide nanotubes under oxygen chemisorption. Journal of Molecular Modeling, 2015, 21, 51.	0.8	4
19047	A first-principles study of He, Xe, Kr and O incorporation in thorium carbide. Journal of Nuclear Materials, 2015, 460, 216-220.	1.3	8
19048	Microscopic structure and properties of discrete water layer in Na-exchanged montmorillonite. Journal of Colloid and Interface Science, 2015, 448, 24-31.	5.0	28
19049	A DFT perspective of potassium promotion of Ï‡-Fe5C2(100). Applied Catalysis A: General, 2015, 496, 64-72.	2.2	30
19050	Novel monolayer pyrite FeS2 with atomic-thickness for magnetic devices. Computational Materials Science, 2015, 101, 255-259.	1.4	27
19051	Ultrahardness: Measurement and Enhancement. Journal of Physical Chemistry C, 2015, 119, 5633-5638.	1.5	37
19052	A density functional theory study of hydrocarbon combustion and synthesis on Ni surfaces. Journal of Molecular Modeling, 2015, 21, 46.	0.8	7
19053	Superiority of the bi-phasic mixture of a tin-based alloy nanocomposite as the anode for lithium ion batteries. Journal of Materials Chemistry A, 2015, 3, 3794-3800.	5.2	43
19054	Multiscale approach to the electronic structure of doped semiconductor surfaces. Physical Review B, 2015, 91, .	1.1	29
19055	Palladium-defect complexes in diamond and silicon carbide. Hyperfine Interactions, 2015, 230, 115-122.	0.2	2
19056	Theoretical and experimental evidence for the post-cotunnite phase transition in zirconia at high pressure. Physics and Chemistry of Minerals, 2015, 42, 385-392.	0.3	24
19057	Adsorption of Pb(II) on the kaolinite(001) surface in aqueous system: A DFT approach. Applied Surface Science, 2015, 339, 28-35.	3.1	47
19058	Interaction of aluminum dimer with defective graphene. Computational and Theoretical Chemistry, 2015, 1059, 27-34.	1.1	11
19059	Exploring the Electronic Structure of an Organic Semiconductor Based on a Compactly Fused Electron Donorâ€“Acceptor Molecule. ChemPhysChem, 2015, 16, 1361-1365.	1.0	8
19060	Core level shifts in Cuâ€“Pd alloys as a function of bulk composition and structure. Surface Science, 2015, 640, 127-132.	0.8	11
19061	Effective atomic charges and orbital hybridization in ZnX (X = S, Se, Te) crystals from first principles. Inorganic Materials, 2015, 51, 11-14.	0.2	0
19062	Ring Activation of Furanic Compounds on Ruthenium-Based Catalysts. Journal of Physical Chemistry C, 2015, 119, 6075-6085.	1.5	29

#	Article	IF	Citations
19063	Estimation of the temperature dependent interaction between uncharged point defects in Si. AIP Advances, 2015, 5, .	0.6	5
19064	Antiferromagnetic phase of the gapless semiconductor<mml:math xmlns:mml="http://www.w3.org/1998/Math/MathML"><mml:mrow><mml:msub><mml:mi mathvariant="normal">V</mml:mi><mml:mn>3</mml:mn></mml:msub><mml:mi>Al</mml:mi></mml:mrow></mml:math>. Physical Review B, 2015, 91, .	1.1	31
19065	Influence of Electric Field on the Mechanical Properties of Hexagonal Boron-Nitride Sheets Using ab-initio Calculations. Nano, 2015, 10, 1550047.	0.5	7
19066	Intriguing electronic properties of two-dimensional MoS₂/TM₂CO₂(TM = Ti, Zr, or Hf) hetero-bilayers: type-II semiconductors with tunable band gaps. Nanotechnology, 2015, 26, 135703.	1.3	57
19067	The roles of the temperature on the structural and electronic properties of deep-level VAsVGa defects in gallium arsenide. Journal of Alloys and Compounds, 2015, 637, 16-19.	2.8	3
19068	Phase Stability and Phase Structure of Ruâ€“Tiâ€“O Complex Oxide Electrocatalyst. Journal of the American Ceramic Society, 2015, 98, 1915-1924.	1.9	15
19069	High resolution energy dispersive spectroscopy mapping of planar defects in L12-containing Co-base superalloys. Acta Materialia, 2015, 89, 423-437.	3.8	127
19070	First-principles investigation on the structural, electronic properties and diffusion barriers of Mg/Al doped NaCoO₂as the cathode material of rechargeable sodium batteries. RSC Advances, 2015, 5, 27229-27234.	1.7	33
19071	First-principle Studies of Lattice and Electronic Structure of BexZn1-xO. Journal of Physics: Conference Series, 2015, 574, 012049.	0.3	1
19072	First-principles Study of Structural Properties of MgxZn1-xO ternary alloys. Journal of Physics: Conference Series, 2015, 574, 012169.	0.3	1
19073	First-principles investigations of structural, electronic, optical and thermodynamic properties of Cd Mg1â^'S alloys. Computational Materials Science, 2015, 101, 242-247.	1.4	3
19074	Stable kagome lattices from group IV elements. Physical Review B, 2015, 91, .	1.1	13
19075	Energetic stability and photocatalytic activity of SrTiO3 nanowires: ab initio simulations. RSC Advances, 2015, 5, 24115-24125.	1.7	14
19076	Mechanical properties of jennite: A theoretical and experimental study. Cement and Concrete Research, 2015, 71, 106-114.	4.6	33
19077	Elastic properties of chiral carbon nanotubes under oxygen adsorption. Physica E: Low-Dimensional Systems and Nanostructures, 2015, 70, 129-134.	1.3	10
19078	High stability and reactivity of defective graphene-supported Fe n Pt13â^'n (nÂ=Â1, 2, and 3) nanoparticles for oxygen reduction reaction: a theoretical study. Journal of Nanoparticle Research, 2015, 17, 1.	0.8	9
19079	Synthesis and Calculation of Structural, Morphologic, Electric, and Electronic Properties of the Sr $$_{2}$$ 2 TiCrO $$_{6}$$ 6 Double Perovskite. Journal of Low Temperature Physics, 2015, 178, 229-236.	0.6	2
19080	Ab initio study of the linear and nonlinear optical properties of hexagonal CdSe. Computational Condensed Matter, 2015, 3, 41-45.	0.9	3

#	Article	IF	Citations
19081	Active Sites on Tiâ€“Ce Mixed Metal Oxides for Reactive Adsorption of Thiophene and Its Derivatives: A DFT Study. Journal of Physical Chemistry C, 2015, 119, 5903-5913.	1.5	15
19082	Friedel oscillations responsible for stacking fault of adatoms: The case of<mml:math xmlns:mml="http://www.w3.org/1998/Math/MathML"><mml:mrow><mml:mrow><mml:mi>Mg</mml:mi><mml:mo>(</mml:mo></mml:mrow><mml:mrow><mml:mi>Be</mml:mi><mml:mo>(</mml:mo><mml:mn>0001</mml:mn> Physical Review B, 2015, 91, .	1.1	5
19083	First-principles study of the relative stability of various zirconium hydrides using the special quasirandom structures approach. International Journal of Hydrogen Energy, 2015, 40, 4597-4604.	3.8	14
19084	Deformation of singleâ€walled carbon nanotubes by interaction with graphene: A firstâ€principles study. Journal of Computational Chemistry, 2015, 36, 717-722.	1.5	8
19085	Lattice-Mismatch-Induced Twinning for Seeded Growth of Anisotropic Nanostructures. ACS Nano, 2015, 9, 3307-3313.	7.3	86
19086	Influence of the van der Waals interaction in the dissociation dynamics of N2 on W(110) from first principles. Journal of Chemical Physics, 2015, 142, 074704.	1.2	23
19087	Optoelectronic properties of transition metals doped cubic Cadmium Sulfide. Materials Science in Semiconductor Processing, 2015, 36, 184-191.	1.9	8
19088	Theoretical Studies on the Synergetic Effects of Auâ€“Pd Bimetallic Catalysts in the Selective Oxidation of Methanol. Journal of Physical Chemistry C, 2015, 119, 16072-16081.	1.5	45
19089	Hydrogen storage properties of light metal adatoms (Li, Na) decorated fluorographene monolayer. Nanotechnology, 2015, 26, 275401.	1.3	28
19090	Ideal Strengths and Bonding Properties of UO ₂ under Tension. Chinese Physics Letters, 2015, 32, 037102.	1.3	3
19091	Electronic structure and magnetic properties of quaternary Heusler alloys CoRhMnZ (ZÂ=ÂAl, Ga, Ge) Tj ETQq0 0 0 rgBT /Overlock 10 Tf	2.8	101
19092	Superconductivity in an expanded phase of ZnO: anab initiostudy. New Journal of Physics, 2015, 17, 043034.	1.2	10
19093	Density Functional Theory applied to magnetic materials: Mn3O4 at different hybrid functionals. Journal of Magnetism and Magnetic Materials, 2015, 391, 166-171.	1.0	58
19094	Chemical Descriptors of Yttria-Stabilized Zirconia at Low Defect Concentration: An ab Initio Study. Journal of Physical Chemistry A, 2015, 119, 6412-6420.	1.1	16
19095	Electronic and optical properties of reduced graphene oxide. Journal of Materials Chemistry C, 2015, 3, 7632-7641.	2.7	78
19096	Band-gap tuning of graphene by Be doping and Be, B co-doping: a DFT study. RSC Advances, 2015, 5, 55762-55773.	1.7	75
19097	Unraveling the Atomistic Sodiation Mechanism of Black Phosphorus for Sodium Ion Batteries by First-Principles Calculations. Journal of Physical Chemistry C, 2015, 119, 15041-15046.	1.5	135
19098	Electric-Field Tunable Band Offsets in Black Phosphorus and MoS₂ van der Waals p-n Heterostructure. Journal of Physical Chemistry Letters, 2015, 6, 2483-2488.	2.1	193

#	Article	IF	Citations
19099	Coexistence pressure for a martensitic transformation from theory and experiment: Revisiting the bcc-hcp transition of iron under pressure. Physical Review B, 2015, 91, .	1.1	30
19100	Manipulation of Magnetic State in Armchair Black Phosphorene Nanoribbon by Charge Doping. ACS Applied Materials & Interfaces, 2015, 7, 14423-14430.	4.0	34
19101	Trends of Oxygen Reduction Reaction on Platinum Alloys: A Computational and Experimental Study. Journal of Physical Chemistry C, 2015, 119, 15224-15231.	1.5	52
19102	Pressure-driven dome-shaped superconductivity and electronic structural evolution in tungsten ditelluride. Nature Communications, 2015, 6, 7805.	5.8	324
19103	Low temperature pollutant trapping and dissociation over two-dimensional tin. Physical Chemistry Chemical Physics, 2015, 17, 21394-21396.	1.3	28
19104	Ab initioinvestigation of superconductivity in noncentrosymmetric Ca₃Ir₄Ge₄. Philosophical Magazine, 2015, 95, 2228-2239.	0.7	1
19105	First-principles calculations of properties of orthorhombic iron carbide<mml:math xmlns:mml="http://www.w3.org/1998/Math/MathML"><mml:mrow><mml:msub><mml:mi>Fe</mml:mi><mml:mn>7</mml:mn></mml:r mathvariant="normal">C</mml:mi><mml:mn>3</mml:mn></mml:msub></mml:mrow></mml:math>at the Earth's core conditions. Physical Review B, 2015, 91, .	1.1	20
19106	Computational Density Functional Theory Study of Hydrazine Adsorption on Ni(110) Surface. Advanced Materials Research, 2015, 1112, 217-220.	0.3	1
19107	First-principles study of the structural, electronic, dynamical, andÂthermodynamic properties of Li5AlO4. Journal of Nuclear Materials, 2015, 465, 170-176.	1.3	10
19108	Size effects and strain localization in atomic-scale cleavage modeling. Journal of Physics Condensed Matter, 2015, 27, 345002.	0.7	7
19109	First-principles study of structural, elastic and electronic properties of ZrIr alloy. Computational Materials Science, 2015, 105, 66-70.	1.4	9
19110	Enhanced stability of the strengthening phase Ni2(Cr,Mo) in Niâ€“Crâ€“Mo alloys by adjacent instability. Computational Materials Science, 2015, 109, 111-114.	1.4	3
19111	Thermodynamical and electronic properties of<mml:math xmlns:mml="http://www.w3.org/1998/Math/MathML" altimg="si0009.gif" overflow="scroll"><mml:mrow><mml:msub><mml:mrow><mml:mi mathvariant="normal">B</mml:mi></mml:mrow><mml:mrow><mml:mi>x</mml:mi></mml:mrow></mml:msub></mml:mrow><mml:mr mathvariant="normal">N</mml:mi></mml:math>alloys: A first principle. Journal of Physics and Chemistry of Solids, 2015, 86, 101-107.	1.9	16
19112	High-Performance WSe₂ Complementary Metal Oxide Semiconductor Technology and Integrated Circuits. Nano Letters, 2015, 15, 4928-4934.	4.5	204
19113	Understanding Polyol Decomposition on Bimetallic Ptâ€“Mo Catalystsâ€”A DFT Study of Glycerol. ACS Catalysis, 2015, 5, 4942-4950.	5.5	25
19114	Designing Isoelectronic Counterparts to Layered Group V Semiconductors. ACS Nano, 2015, 9, 8284-8290.	7.3	128
19115	Quantifying the origin of inter-adsorbate interactions on reactive surfaces for catalyst screening and design. Physical Chemistry Chemical Physics, 2015, 17, 22227-22234.	1.3	2
19116	Half-metallic and magnetic properties in nonmagnetic element embedded graphitic carbon nitride sheets. Physical Chemistry Chemical Physics, 2015, 17, 22136-22143.	1.3	25

#	Article	IF	Citations
19117	Site preference and alloying effect of Re atoms in the edge dislocation cores in Ni3Al. Philosophical Magazine Letters, 2015, 95, 253-259.	0.5	5
19118	Structural and mechanic properties of RFeO3 with R = Y, Eu and La perovskites: a first-principles calculation. European Physical Journal D, 2015, 69, 1.	0.6	10
19119	Transition metal incorporation into mackinawite (tetragonal FeS). American Mineralogist, 2015, 100, 1509-1517.	0.9	26
19120	Electronic transport properties of selected carbon Ï€-bowls with different size, curvature and solid state packing. Carbon, 2015, 94, 174-180.	5.4	19
19121	Hydrogen diffusion in Î±-Fe under an applied 3-axis strain: A quantum manifestation. International Journal of Hydrogen Energy, 2015, 40, 10340-10345.	3.8	15
19122	Ab initio study of magnetism in nonmagnetic metal substituted monolayer MoS2. Solid State Communications, 2015, 220, 67-71.	0.9	21
19123	Thermoelectric Properties of Sn-Containing Mg2Si Nanostructures. Journal of Physical Chemistry C, 2015, 119, 17515-17521.	1.5	5
19124	Energetics of Rutile TiO₂ Vicinal Surfaces with âŸ¨001âŸ© Steps from the Energy Density Method. Journal of Physical Chemistry C, 2015, 119, 18203-18209.	1.5	8
19125	Promoting ethylene epoxidation on gold nanoclusters: self and CO induced O₂ activation. Physical Chemistry Chemical Physics, 2015, 17, 22336-22341.	1.3	13
19126	High-energy, stable and recycled molecular solar thermal storage materials using AZO/graphene hybrids by optimizing hydrogen bonds. Nanoscale, 2015, 7, 16214-16221.	2.8	61
19127	First principles study of the structural, mechanical, phonon, optical, and thermodynamic properties of half-Heusler (HH) compound NbFeSb. Physica Scripta, 2015, 90, 095701.	1.2	17
19128	Electronic and structural properties of vacancies and hydrogen adsorbates on trilayer graphene. Journal of Physics Condensed Matter, 2015, 27, 335302.	0.7	6
19129	Stabilization of wurtzite Sc0.4Al0.6N in pseudomorphic epitaxial Sc Al1â^'N/In Al1â^'N superlattices. Acta Materialia, 2015, 94, 101-110.	3.8	19
19130	Synthesis and properties of crystalline thin film of antimony trioxide on the Si(1 0 0) substrate. Applied Surface Science, 2015, 349, 259-263.	3.1	13
19131	High coverage hydrogen adsorption on the Fe3O4(110) surface. Applied Surface Science, 2015, 353, 973-978.	3.1	16
19132	Density functional theory study of SO 2 -adsorbed Ni(1 1 1) and hydroxylated NiO(1 1 1) surface. Applied Surface Science, 2015, 355, 429-435.	3.1	17
19133	A density functional theory study of partial oxidation of propylene on Cu 2 O(0 0 1) and CuO(0 0 1) surfaces. Applied Surface Science, 2015, 355, 660-666.	3.1	38
19134	Assessments of molar volume of the binary C14 Laves phase. Calphad: Computer Coupling of Phase Diagrams and Thermochemistry, 2015, 50, 82-91.	0.7	6

#	Article	IF	Citations
19135	Temperature and pressure effects on the elasticity behavior, electronic and vibrational properties of Al, Li, LiAl and Li2Al: A density functional theory study. Computational Materials Science, 2015, 106, 50-58.	1.4	4
19136	YN nanostructure formation on the GaN(0001) surface: First principles studies. Computational Materials Science, 2015, 106, 155-160.	1.4	6
19137	Electronic structures and magnetic properties in nonmetallic element substituted MoS2 monolayer. Computational Materials Science, 2015, 107, 72-78.	1.4	55
19138	Multiscale ab initio simulation of Ni-based alloys: Real-space distribution of atoms in Î³ + Î³ â€² phase. Computational Materials Science, 2015, 108, 192-204.	1.4	13
19139	A theoretical study of a homologous series of zinc n-alkanoates (2 â‰¤ n â‰¤ 8): Structural analysis, evaluation of their interactions and monofilm formation. Chemical Physics Letters, 2015, 636, 154-162.	1.2	4
19140	THE INFLUENCE OF INTERCALATED IONS ON CYCLIC STABILITY OF V2O5/GRAPHITE COMPOSITE IN AQUEOUS ELECTROLYTIC SOLUTIONS: EXPERIMENTAL AND THEORETICAL APPROACH. Electrochimica Acta, 2015, 176, 130-140.	2.6	25
19141	Optical properties of Ga0.75Al0.25N with interstitial defects. Optik, 2015, 126, 3349-3352.	1.4	2
19142	Solubility and ordering of Ti, Ta, Mo and W on the Al sublattice in L12-Co3Al. Intermetallics, 2015, 64, 44-50.	1.8	27
19143	Cross over between ferro and antiferromagnetic order in Fe itinerant electron magnetism: An experimental and theoretical study of the model (Hf,Ta)Fe 2 Laves phases. Journal of Alloys and Compounds, 2015, 643, 239-246.	2.8	17
19144	Dependence of constituent elements of AB5 type metal hydrides on hydrogenation degradation by CO2 poisoning. Journal of Alloys and Compounds, 2015, 647, 198-203.	2.8	21
19145	Effects of the defects on the structural, electronic and magnetic properties of Sr2FeMoO6. Journal of Alloys and Compounds, 2015, 648, 374-381.	2.8	10
19146	Effect of atomic sites on electronic and mechanical properties of (Fe,Mo)6C carbides. Journal of Alloys and Compounds, 2015, 649, 1089-1093.	2.8	14
19147	Mechanical properties and electronic structures of M23C6 (MÂ=ÂFe, Cr, Mn)-type multicomponent carbides. Journal of Alloys and Compounds, 2015, 648, 874-880.	2.8	53
19148	High spin polarization and spin splitting in equiatomic quaternary CoFeCrAl Heusler alloy. Journal of Magnetism and Magnetic Materials, 2015, 394, 82-86.	1.0	79
19149	Novel high-pressure phase of ZrO2: An ab initio prediction. Journal of Solid State Chemistry, 2015, 230, 233-236.	1.4	10
19150	Electronic, elastic and dynamic properties of the filled tetrahedral semiconductor LiMgN under pressures. Journal of Solid State Chemistry, 2015, 231, 1-6.	1.4	13
19151	Charge carrier mobility in hybrid halide perovskites. Scientific Reports, 2015, 5, 12746.	1.6	294
19152	g-C₃N₄ and Others: Predicting New Nanoporous Carbon Nitride Planar Structures with Distinct Electronic Properties. Journal of Physical Chemistry C, 2015, 119, 19743-19751.	1.5	24

#	Article	IF	Citations
19153	DFT Investigation into Alumina ALD Growth Inhibition on Hydroxylated Amorphous Silica Surface. Journal of Physical Chemistry C, 2015, 119, 18380-18388.	1.5	28
19154	Ideal Spintronics in Molecule-Based Novel Organometallic Nanowires. Scientific Reports, 2015, 5, 12772.	1.6	11
19155	A Comparative Study of Methanol Adsorption and Dissociation over WO3(001) and ReO3(001). Topics in Catalysis, 2015, 58, 655-664.	1.3	6
19156	CO Dissociation at Vacancy Sites on HÃgg Iron Carbide: Direct Versus Hydrogen-Assisted Routes Investigated with DFT. Topics in Catalysis, 2015, 58, 665-674.	1.3	25
19157	Estimation of the activation energy for surface diffusion during metastable phase formation. Acta Materialia, 2015, 98, 135-140.	3.8	41
19158	Novel 2D RuPt core-edge nanocluster catalyst for CO electro-oxidation. Surface Science, 2015, 640, 50-58.	0.8	15
19159	Magnetite Fe₃O₄ (111) Surfaces: Impact of Defects on Structure, Stability, and Electronic Properties. Chemistry of Materials, 2015, 27, 5856-5867.	3.2	93
19160	Anomalous Stagewise Lithiation of Gold-Coated Silicon Nanowires: A Combined In Situ Characterization and First-Principles Study. ACS Applied Materials & Interfaces, 2015, 7, 16976-16983.	4.0	9
19161	A van der Waals Density Functional Investigation on the Improved Adsorption Properties of NO on the Rhn/MgO (100) Interface. ACS Applied Materials & Interfaces, 2015, 7, 17499-17509.	4.0	4
19162	DFT studies of the bonding mechanism of 8-hydroxyquinoline and derivatives on the (111) aluminum surface. Physical Chemistry Chemical Physics, 2015, 17, 22243-22258.	1.3	36
19163	The effect of impurities in ultra-thin hydrogenated silicene and germanene: a first principles study. Physical Chemistry Chemical Physics, 2015, 17, 22210-22216.	1.3	30
19164	Tuning the charge state of Ag and Au atoms and clusters deposited on oxide surfaces by doping: a DFT study of the adsorption properties of nitrogen- and niobium-doped TiO₂ and ZrO₂. Physical Chemistry Chemical Physics, 2015, 17, 22342-22360.	1.3	42
19165	K₃LaTe₂O₉: a new alkali-rare earth tellurate with face-sharing TeO₆ octahedra. Dalton Transactions, 2015, 44, 15576-15582.	1.6	10
19166	Study of formaldehyde adsorption on silicene with point defects by DFT method. RSC Advances, 2015, 5, 65255-65263.	1.7	22
19167	Stability and electronic structure of two-dimensional allotropes of group-IV materials. Physical Review B, 2015, 92, .	1.1	124
19168	Origin of Excess Irreversible Capacity in Lithium-Ion Batteries Based on Carbon Nanostructures. Journal of the Electrochemical Society, 2015, 162, A2106-A2115.	1.3	29
19169	Mechanistic insight into the water photooxidation on pure and sulfur-doped g-C3N4 photocatalysts from DFT calculations with dispersion corrections. Journal of Molecular Catalysis A, 2015, 406, 137-144.	4.8	81
19170	Vibrational spectra of Ruthenium Carbide structures yielded by the structure search employing evolutionary algorithm. Materials Science in Semiconductor Processing, 2015, 40, 484-490.	1.9	8

#	Article	IF	Citations
19171	First-principles investigation of electronic and optical properties and thermodynamic stability of Zn1â^'Be O semiconductor alloy. Materials Science in Semiconductor Processing, 2015, 40, 803-810.	1.9	12
19172	Anisotropic dielectric functions of (0001) sapphire from spectroscopic ellipsometry and first-principles study. Physica B: Condensed Matter, 2015, 473, 35-41.	1.3	7
19173	Electronic structures and magnetic properties in Cu-doped two-dimensional dichalcogenides. Physica E: Low-Dimensional Systems and Nanostructures, 2015, 73, 69-75.	1.3	33
19174	Pressure-induced structural phase transition, elastic and thermodynamic properties of ReC under high pressure. Solid State Sciences, 2015, 48, 49-55.	1.5	5
19175	First principles study on the spin unrestricted electronic structure properties of transition metal doped InN nanoribbons. Superlattices and Microstructures, 2015, 84, 170-180.	1.4	18
19176	Phase transition in crystal hydrogen under high pressure. Solid State Communications, 2015, 217, 6-12.	0.9	1
19177	Cutting a chemical bond with demon's scissors: Mode- and bond-selective reactivity of methane on metal surfaces. Surface Science, 2015, 640, 25-35.	0.8	41
19178	Screened Hybrid Exact Exchange Correction Scheme for Adsorption Energies on Perovskite Oxides. Journal of Physical Chemistry C, 2015, 119, 17662-17666.	1.5	7
19179	Observation of Surface-Bound Negatively Charged Hydride and Hydroxide on GaP(110) in H₂O Environments. Journal of Physical Chemistry C, 2015, 119, 17762-17772.	1.5	39
19180	Exploring the metallic phase of N2O under high pressure. RSC Advances, 2015, 5, 65745-65749.	1.7	5
19181	Model of two-dimensional electron gas formation at ferroelectric interfaces. Physical Review B, 2015, 92, .	1.1	30
19182	Electronic Origins of Anomalous Twin Boundary Energies in Hexagonal Close Packed Transition Metals. Physical Review Letters, 2015, 115, 065501.	2.9	23
19183	First-principles calculations of the twin boundary energies and adhesion energies of interfaces for cubic face-centered transition-metal nitrides and carbides. Applied Surface Science, 2015, 355, 1132-1135.	3.1	27
19184	An alternative approach to investigate the origin of p-type conductivity in arsenic doped ZnO. Current Applied Physics, 2015, 15, 1256-1261.	1.1	13
19185	A computational study on the effect of local curvature on the adsorption of oxygen on single-walled carbon nanotubes. Carbon, 2015, 94, 936-941.	5.4	8
19186	The phase stability, magnetic and vibrational properties of A2Ni21B6 Â(A=Th,ÂU) and Ce3Pd20Si6. Computer Physics Communications, 2015, 193, 72-77.	3.0	3
19187	High pressure stability of the monosilicides of cobalt and the platinum group elements. Journal of Alloys and Compounds, 2015, 626, 375-380.	2.8	16
19188	Structural and elastic stabilities of InN in both B4 and B1 phases under high pressure using density-functional perturbation theory. Journal of Alloys and Compounds, 2015, 650, 450-457.	2.8	1

#	Article	IF	Citations
19189	New Ag(F 1â^'x Cl x) phases for energy storage applications. Journal of Fluorine Chemistry, 2015, 174, 22-29.	0.9	10
19190	Effect of Cr on electronic and magnetic properties of Ï‡-carbide (Fe,Cr)5C2. Journal of Magnetism and Magnetic Materials, 2015, 392, 1-5.	1.0	5
19191	DFT study of the effects of interstitial impurities on the resistance of Cr-doped Î³-Fe(111) surface dissolution corrosion. Journal of Molecular Modeling, 2015, 21, 206.	0.8	6
19192	Rapid thermal processing induced vacancy-oxygen complexes in Czochralski-grown Si1â^'xGex. Journal of Materials Science: Materials in Electronics, 2015, 26, 7666-7672.	1.1	0
19193	Adsorption and oxidation of NO on various SnO2(1 1 0) surfaces: A density functional theory study. Sensors and Actuators B: Chemical, 2015, 221, 717-722.	4.0	51
19194	DFT study of Hg adsorption on M-substituted Pd(1 1 1) and PdM/Î³-Al 2 O 3 (1 1 0) (M = Au, Ag, Cu) surfaces. Applied Surface Science, 2015, 355, 902-911.	3.1	12
19195	Charge states of point defects in plutonium oxide: A first-principles study. Journal of Alloys and Compounds, 2015, 649, 544-552.	2.8	30
19196	Preparation and Instability of Nanocrystalline Cuprous Nitride. Inorganic Chemistry, 2015, 54, 6356-6362.	1.9	22
19197	Raman scattering efficiency in<mml:math xmlns:mml="http://www.w3.org/1998/Math/MathML"><mml:msub><mml:mi>LiTaO</mml:mi><mml:mn>3</mml:mn></mml:msub></m xmlns:mml="http://www.w3.org/1998/Math/MathML"><mml:msub><mml:mi>LiNbO</mml:mi><mml:mn>3</mml:mn></mml:msub></m Physical Review B, 2015, 91, .	1.1	94
19198	Elasticity and Debye temperature of defected fcc crystals (AlCu3, Al, Cu): Molecular dynamics and first-principles calculations. Computational Materials Science, 2015, 109, 194-199.	1.4	5
19199	Oxidized graphene as an electrode material for rechargeable metal-ion batteries â€“ a DFT point of view. Electrochimica Acta, 2015, 176, 1092-1099.	2.6	33
19200	High pressure phase transition in Zrâ€“Ni binary system: A first principle study. Journal of Alloys and Compounds, 2015, 648, 951-957.	2.8	4
19201	Effect of surface composition on electronic properties of methylammonium lead iodide perovskite. Journal of Materiomics, 2015, 1, 213-220.	2.8	49
19202	Colossal Ultraviolet Photoresponsivity of Few-Layer Black Phosphorus. ACS Nano, 2015, 9, 8070-8077.	7.3	204
19203	Relative stability and reducibility of CeO2 and Rh/CeO2 species on the surface and in the cavities of Î³-Al2O3: a periodic DFT study. Physical Chemistry Chemical Physics, 2015, 17, 22389-22401.	1.3	6
19204	The Birmingham parallel genetic algorithm and its application to the direct DFT global optimisation of Ir_N(N = 10â€“20) clusters. Nanoscale, 2015, 7, 14032-14038.	2.8	74
19205	Highly sensitive and fast phototransistor based on large size CVD-grown SnS₂nanosheets. Nanoscale, 2015, 7, 14093-14099.	2.8	126
19206	Electronic structure, optical and dielectric properties of BaTiO₃/CaTiO₃/SrTiO₃ ferroelectric superlattices from first-principles calculations. Journal of Materials Chemistry C, 2015, 3, 8625-8633.	2.7	96

#	Article	IF	Citations
19207	Au and Ti induced charge redistributions on monolayer WS ₂. Chinese Physics B, 2015, 24, 077301.	0.7	1
19208	Effects of alloying on oxidation and dissolution corrosion of the surface of Î³-Fe(111): a DFT study. Journal of Molecular Modeling, 2015, 21, 181.	0.8	17
19209	Study of the growth kinetics of biomimetically grown hydroxyapatite coatings in large gradient magnetic fields. Applied Surface Science, 2015, 351, 594-599.	3.1	2
19210	From determination of the fugacity coefficients to estimation of hydrogen storage capacity: A convenient theoretical method. International Journal of Hydrogen Energy, 2015, 40, 10908-10917.	3.8	11
19211	The study of structural, electronic, elastic and optical properties in Be1âˆ’xZnxTe alloys. Materials Science in Semiconductor Processing, 2015, 39, 629-635.	1.9	4
19212	Excitonic effects in GeC hybrid: Many-body Green's function calculations. Physica E: Low-Dimensional Systems and Nanostructures, 2015, 74, 377-381.	1.3	47
19213	Molecular adsorption and methanol synthesis on the oxidized Cu/ZnO(0001) surface. Surface Science, 2015, 641, 97-104.	0.8	6
19214	Hydrogen adsorption of novel N-doped carbon nanotubes functionalized with Scandium. International Journal of Hydrogen Energy, 2015, 40, 9352-9358.	3.8	38
19215	Kinetic Monte Carlo simulation of surface segregation in Pdâ€“Cu alloys. Journal of Alloys and Compounds, 2015, 648, 1090-1096.	2.8	18
19216	Uncovering the Mode of Action of Solvent and Additive Controlled Crystallization of Urea Crystal: A Molecular-Scale Study. Crystal Growth and Design, 2015, 15, 3220-3234.	1.4	26
19217	Influence of Structural Fluctuations, Proton Transfer, and Electric Field on Polarization Switching of Supported Two-Dimensional Hydrogen-Bonded Oxocarbon Monolayers. Chemistry of Materials, 2015, 27, 4839-4847.	3.2	13
19218	First-Principles Study of Carbon and Vacancy Structures in Niobium. Journal of Physical Chemistry C, 2015, 119, 14728-14736.	1.5	15
19219	DFT Study of Antimony(V) Oxyanion Adsorption on Î±-Al₂O₃(11Ì…02). Journal of Physical Chemistry C, 2015, 119, 18149-18159.	1.5	24
19220	Early Stage Hydration of Wollastonite: Kinetic Aspects of the Metal-Proton Exchange Reaction. Journal of Physical Chemistry C, 2015, 119, 10493-10499.	1.5	23
19221	Spontaneous Local Symmetry Breaking: A Conformational Study of Glycine on Cu{311}. Journal of Physical Chemistry C, 2015, 119, 13041-13049.	1.5	12
19222	First-Principles Calculation of Terahertz Absorption with Dispersion Correction of 2,2â€²-Bithiophene as Model Compound. Journal of Physical Chemistry C, 2015, 119, 12598-12607.	1.5	15
19223	Tuning the Surface Chemistry of Chiral Cu(531)^S for Enhanced Enantiospecific Adsorption of Amino Acids. Journal of Physical Chemistry C, 2015, 119, 15195-15203.	1.5	16
19224	First-Principles Calculations of Lithiation of a Hydroxylated Surface of Amorphous Silicon Dioxide. Journal of Physical Chemistry C, 2015, 119, 16424-16431.	1.5	43

#	Article	IF	Citations
19225	High-Field17O MAS NMR Reveals1J(17O-127I) with its Sign and the NMR Crystallography of the Scheelite Structures for NaIO4and KIO4. Journal of Physical Chemistry C, 2015, , 150612155518000.	1.5	9
19226	Characterization of a Hexagonal Phosphorus Adlayer on Platinum (111). Journal of Physical Chemistry C, 2015, 119, 12291-12297.	1.5	7
19227	Density functional theory calculations of the hydrazine decomposition mechanism on the planar and stepped Cu(111) surfaces. Physical Chemistry Chemical Physics, 2015, 17, 21533-21546.	1.3	39
19228	An unusual density evolution between SrCdB2O5 polymorphs. Dalton Transactions, 2015, 44, 15823-15828.	1.6	5
19229	Photocatalytic activity of ZnO/GaP_{1â^'x}N_xfor water splitting. Journal of Materials Chemistry A, 2015, 3, 18083-18089.	5.2	14
19230	C2/m-carbon: structural, mechanical, and electronic properties. Journal of Materials Science, 2015, 50, 7104-7114.	1.7	44
19231	An ab-initio study of adsorption of gaseous molecules on doped graphene structures. Physica E: Low-Dimensional Systems and Nanostructures, 2015, 74, 515-526.	1.3	10
19232	Relative stability, electronic and structural properties in the family of NH4V3O7 polymorphs from first principles calculations. Computational and Theoretical Chemistry, 2015, 1070, 9-13.	1.1	0
19233	Alkane reforming on partially sulfided CeO2 (1 1 1) surfaces. Journal of Catalysis, 2015, 330, 167-176.	3.1	17
19234	Mechanistic Insight into the Facet-Dependent Adsorption of Methanol on a Pt₃Ni Nanocatalyst. Journal of Physical Chemistry C, 2015, 119, 18352-18363.	1.5	19
19235	Thermodynamic stability and transport properties of tavorite LiFeSO₄F as a cathode material for lithium-ion batteries. Journal of Materials Chemistry A, 2015, 3, 19728-19737.	5.2	14
19236	Structural, electronic and magnetic properties of Mn3N2(0 0 1) surfaces. Applied Surface Science, 2015, 355, 623-630.	3.1	17
19237	Investigation of helium interstitials aggregation in silicon: Why bubbles formation by a self-trapping mechanism does not work. Nuclear Instruments & Methods in Physics Research B, 2015, 352, 152-155.	0.6	8
19238	Lattice thermal conductivity of LaSe. Physica B: Condensed Matter, 2015, 468-469, 21-24.	1.3	1
19239	Trends in adsorbate induced core level shifts. Surface Science, 2015, 640, 59-64.	0.8	21
19240	Structural, electronic and magnetic properties of 5d transition metal mediated benzene adsorption on graphene: A first-principles study. Synthetic Metals, 2015, 209, 225-231.	2.1	11
19241	Hardness and optical gap enhancement of germanium carbon films by nitrogen incorporation. Thin Solid Films, 2015, 584, 208-213.	0.8	5
19242	Theoretical Limits to the Anode Potential in Aqueous Mgâ€“Air Batteries. Journal of Physical Chemistry C, 2015, 119, 19660-19667.	1.5	47

#	Article	IF	Citations
19243	Room Temperature Multiferroicity of Charge Transfer Crystals. ACS Nano, 2015, 9, 9373-9379.	7.3	38
19244	Structural, mechanical, thermodynamic and electronic properties of AgIn2 and Ag3In intermetallic compounds: ab initio investigation. RSC Advances, 2015, 5, 70609-70618.	1.7	8
19245	Analysis of optical and magnetooptical spectra of Fe5Si3 and Fe3Si magnetic silicides using spectral magnetoellipsometry. Journal of Experimental and Theoretical Physics, 2015, 120, 886-893.	0.2	12
19246	A density functional theory study of adsorption and dissociation of isopropyl nitrate on an Al(111) surface. Canadian Journal of Chemistry, 2015, 93, 362-367.	0.6	12
19247	First-principles study of group V and VII impurities in SnS2. Superlattices and Microstructures, 2015, 85, 664-671.	1.4	20
19248	Metal-free ferromagnetic metal and intrinsic spin semiconductor: two different kinds of SWCNT functionalized BN nanoribbons. Physical Chemistry Chemical Physics, 2015, 17, 7949-7959.	1.3	7
19249	Effects of intrinsic defects and extrinsic doping on the electronic and photocatalytic properties of Ta₃N₅. RSC Advances, 2015, 5, 59390-59397.	1.7	33
19250	First-principles calculations of bismuth induced changes in the band structure of dilute Gaâ€“Vâ€“Bi and Inâ€“Vâ€“Bi alloys: chemical trends versus experimental data. Semiconductor Science and Technology, 2015, 30, 094001.	1.0	85
19251	Single layer of MX₃ (M = Ti, Zr; X = S, Se, Te): a new platform for nano-electronics and optics. Physical Chemistry Chemical Physics, 2015, 17, 18665-18669.	1.3	128
19252	The electronic structure of quasi-free-standing germanene on monolayer MX (M = Ga, In; X = S, Se, Te). Physical Chemistry Chemical Physics, 2015, 17, 19039-19044.	1.3	26
19253	Extended Lagrangian Density Functional Tight-Binding Molecular Dynamics for Molecules and Solids. Journal of Chemical Theory and Computation, 2015, 11, 3357-3363.	2.3	26
19254	Quantum size effects in layered VX2 (Xâ€‰=â€‰S, Se) materials: Manifestation of metal to semimetal or semiconductor transition. Journal of Applied Physics, 2015, 117, .	1.1	67
19255	Unusual spin correlations in a nanomagnet. Applied Physics Letters, 2015, 106, .	1.5	24
19256	Probing local site environments and distribution of manganese in SrZrO3:Mn; PL and EPR spectroscopy complimented by DFT calculations. RSC Advances, 2015, 5, 17501-17513.	1.7	51
19257	Fabrication and characterization of nanostructured Fe3S4, an isostructural compound of half-metallic Fe3O4. Journal of Applied Physics, 2015, 117, .	1.1	16
19258	Relative stability and local curvature analysis in carbon nanotori. Physical Review B, 2015, 91, .	1.1	9
19259	First-principles calculation of the bulk photovoltaic effect in<mml:math xmlns:mml="http://www.w3.org/1998/Math/MathML"><mml:msub><mml:mrow><mml:mi mathvariant="normal">KNbO</mml:mi></mml:mrow><mml:mn>3</mml:mn></mml:msub></mml:math>and (K,Ba)(Ni,Nb)<mml:math xmlns:mml="http://www.w3.org/1998/Math/MathML"><mml:msub><mml:mrow><mml:mi mathvariant="normal">O</mml:mi></mml:mrow><mml:mrow><mml:mn>3</mml:mn><mml:mo>â^’</mml:mo><mml:mi>Î´</mml:mi></	1.1	53
19260	First-principles study of B or Al-doping effect on the structural, electronic structure and magnetic properties of Î³ -graphyne. Computational Materials Science, 2015, 108, 147-152.	1.4	20

#	Article	IF	Citations
19261	Atomic-Scale Interfacial Magnetism in Fe/Graphene Heterojunction. Scientific Reports, 2015, 5, 11911.	1.6	30
19262	Vibrational properties and bonding nature of Sb₂Se₃and their implications for chalcogenide materials. Chemical Science, 2015, 6, 5255-5262.	3.7	89
19263	Analysis of the CO₂â€“H₂O Chemisorption in Lithium Silicates at Low Temperatures (30â€“80 Â°C). Industrial & Engineering Chemistry Research, 2015, 54, 6884-6892.	1.8	15
19264	Periodically Modulated Size-Dependent Elastic Properties of Armchair Graphene Nanoribbons. Nano Letters, 2015, 15, 4883-4888.	4.5	10
19265	The new dimension of silver. Physical Chemistry Chemical Physics, 2015, 17, 19695-19699.	1.3	52
19266	High-pressure phase transitions of TiN: anab initioconstant pressure study. Philosophical Magazine, 2015, 95, 2376-2384.	0.7	2
19267	An Investigation of Structural and Electronic Properties of Novel Cathode Material Li₂MnP₂O₇ and its Delithiated Li_{2-x}MnP₂O₇ (x=1,2): A First Principle Study. Advanced Materials Research, 2015, 1107, 485-490.	0.3	0
19268	Hydrodenitrogenation of pyridine on MoP(010): Competition between hydrogenation and denitrification. Inorganica Chimica Acta, 2015, 435, 30-37.	1.2	11
19269	Synergistic effect of co-alloying elements on site preferences and elastic properties of Ni3Al: A first-principles study. Intermetallics, 2015, 65, 75-80.	1.8	29
19270	Ab-initio study of phase stability, elastic and thermodynamic properties of AlY alloy under pressure. Journal of Alloys and Compounds, 2015, 648, 67-74.	2.8	7
19271	Electronic structure and magnetism of new ilmenite compounds for spintronic devices: FeBO3 (B = Ti,) Tj ETQq0 0 0 rgBT /Overlock 10 T	1.0	32
19272	Electro-oxidation of water on hematite: Effects of surface termination and oxygen vacancies investigated by first-principles. Surface Science, 2015, 640, 45-49.	0.8	43
19273	An atomic scale study of ultralow friction between phosphorus-doped nanocrystalline diamond films. Tribology International, 2015, 86, 85-90.	3.0	9
19274	First-principles study of B doping effect on the electronic structure and magnetic properties of Î³-graphyne. Thin Solid Films, 2015, 589, 662-668.	0.8	11
19275	Lithium Ion Conduction in LiTi₂(PO₄)₃ and Related Compounds Based on the NASICON Structure: A First-Principles Study. Chemistry of Materials, 2015, 27, 5040-5048.	3.2	186
19276	Embedded atom model for the liquid Uâ€“10Zr alloy based on density functional theory calculations. RSC Advances, 2015, 5, 61495-61501.	1.7	6
19277	Nature of defects in blue light emitting CaZrO₃: spectroscopic and theoretical study. RSC Advances, 2015, 5, 56526-56533.	1.7	58
19278	First Principles Studies of the Phonon, Polarization, Dielectric and Piezoelectric Responses of Pyrochlore Cd₂Nb₂O₇. Ferroelectrics, 2015, 478, 106-117.	0.3	4

#	Article	IF	Citations
19279	<i>Ab Initio</i> Calculations of Absolute Surface Energies of Clean and Hydrogen Covered 3C-SiC(001), (110) and (111) Surfaces. Materials Science Forum, 0, 821-823, 363-366.	0.3	8
19280	Oxygen Effect on Magnetic Anisotropy Energy of Co Nanowires on Cu(210) Surface - An <i>Ab Initio</i> Study. Solid State Phenomena, 0, 233-234, 530-533.	0.3	0
19281	First-principles investigation on structural and electrochemical properties of NaCoO2 for rechargeable Na-ion batteries. Journal of Central South University, 2015, 22, 2036-2042.	1.2	6
19282	Metallization and stiffness of the Li-intercalated MoS2 bilayer. Applied Surface Science, 2015, 353, 333-337.	3.1	12
19283	Predictions on the compositions, structures, and mechanical properties of intermediate phases in binary Mgâ€“X (X = Sn, Y, Sc, Ag) alloys. Computational Materials Science, 2015, 106, 180-187.	1.4	15
19284	Effects of the defects on the half-metallic characters and magnetic properties in double perovskite Pb2FeMoO6. Materials Chemistry and Physics, 2015, 162, 711-723.	2.0	3
19285	Magnetic transport properties of DBTAA-based nanodevices with graphene nanoribbon electrodes. Organic Electronics, 2015, 25, 308-316.	1.4	25
19286	Electronic Properties of Halogen-Adsorbed Graphene. Journal of Physical Chemistry C, 2015, 119, 17271-17277.	1.5	42
19287	Ab Initio Molecular-Dynamics Simulation of Neuromorphic Computing in Phase-Change Memory Materials. ACS Applied Materials & Interfaces, 2015, 7, 14223-14230.	4.0	28
19288	Pb₂Ba₃(BO₃)₃Cl: A Material with Large SHG Enhancement Activated by Pb-Chelated BO₃ Groups. Journal of the American Chemical Society, 2015, 137, 9417-9422.	6.6	255
19289	Hexagonal-structured Îµ-NbN: ultra-incompressibility, high shear rigidity and a possible hard superconducting material. Scientific Reports, 2015, 5, 10811.	1.6	46
19290	The Interplay of manganese and nitrate in hydroxyapatite nanoparticles as revealed by pulsed EPR and DFT. Physical Chemistry Chemical Physics, 2015, 17, 20331-20337.	1.3	30
19291	A first principles study of CO₂ adsorption on Î±-SiO₂(001) surfaces. Physical Chemistry Chemical Physics, 2015, 17, 20125-20133.	1.3	17
19292	Hydrogen-bonding-mediated structural stability and electrochemical performance of iron fluoride cathode materials. Journal of Materials Chemistry A, 2015, 3, 16222-16228.	5.2	34
19293	Synthesis and thermoelectric properties of half-Heusler alloy YNiBi. Journal of Applied Physics, 2015, 117, .	1.1	35
19294	Electronic, elastic and dynamical properties of MgSe under pressure: rocksalt and iron silicide phase. Philosophical Magazine, 2015, 95, 2240-2256.	0.7	2
19295	Density functional theory study of the thermodynamic and elastic properties of Ni-based superalloys. Journal of Physics Condensed Matter, 2015, 27, 295401.	0.7	16
19296	Computational discovery of ferromagnetic semiconducting single-layer<mml:math xmlns:mml="http://www.w3.org/1998/Math/MathML"><mml:msub><mml:mi>CrSnTe</mml:mi><mml:mn>3</mml:mn></mml:msub></mml:math> Physical Review B, 2015, 92, .	1.1	2

#	Article	IF	Citations
19297	The nontrivial electronic structure of Bi/Sb honeycombs on SiC(0001). New Journal of Physics, 2015, 17, 025005.	1.2	100
19298	Energy of interaction between carbon impurities in paramagnetic Î³-iron. Journal of Experimental and Theoretical Physics, 2015, 120, 716-724.	0.2	10
19299	First-Principles Study of Electronic Structure and Optical Properties of V-Doped CrSi₂. Advanced Materials Research, 0, 1104, 125-130.	0.3	2
19300	Hydrogen sorption in the LaNi5-xAlx-H system (0Âå‰ÂxÂå‰Â1). Intermetallics, 2015, 62, 7-16.	1.8	25
19301	Sn2SiS4, synthesis, structure, optical and electronic properties. Optical Materials, 2015, 47, 379-385.	1.7	14
19302	In Situ Electrical Conductivity of Li_xMnO₂ Nanowires as a Function of x and Size. Chemistry of Materials, 2015, 27, 3494-3504.	3.2	13
19303	A new phase from compression of carbon nanotubes with anisotropic Dirac fermions. Scientific Reports, 2015, 5, 10713.	1.6	23
19304	Covalent nitrophenyl diazonium functionalized silicene for spintronics: a first-principles study. Physical Chemistry Chemical Physics, 2015, 17, 17957-17961.	1.3	13
19305	The dynamics of adsorption and dissociation of N2 in a monolayer of iron on W(110). Physical Chemistry Chemical Physics, 2015, 17, 19432-19445.	1.3	7
19306	Ethylene formation by methane dehydrogenation and Câ€“C coupling reaction on a stoichiometric IrO₂ (110) surface â€“ a density functional theory investigation. Catalysis Science and Technology, 2015, 5, 4064-4071.	2.1	46
19307	Contrastive band gap engineering of strained graphyne nanoribbons with armchair and zigzag edges. RSC Advances, 2015, 5, 59344-59348.	1.7	11
19308	Highly crystalline, small sized, monodisperse Î±-NiS nanocrystal ink as an efficient counter electrode for dye-sensitized solar cells. Journal of Materials Chemistry A, 2015, 3, 15905-15912.	5.2	69
19309	Theoretical study of the interaction of electron donor and acceptor molecules with monolayer WS₂. Journal Physics D: Applied Physics, 2015, 48, 285303.	1.3	25
19310	Physical Origins of Thermal Properties of Cement Paste. Physical Review Applied, 2015, 3, .	1.5	86
19311	First-Principles Study of Electronic and Elastic Properties of Hexagonal Layered Crystal MoS₂ Under Pressure. Zeitschrift Fur Naturforschung - Section A Journal of Physical Sciences, 2015, 70, 529-537.	0.7	13
19312	Interatomic spacing distribution in multicomponent alloys. Acta Materialia, 2015, 97, 156-169.	3.8	92
19313	First-principles calculation of structural, thermodynamic and mechanical properties of 5d transitional metal triborides TMB3 (TM=Hfâ€“Au). Computational Condensed Matter, 2015, 3, 53-60.	0.9	8
19314	Crystallographic information of intermediate phases in binary Mgâ€“ X (X =Sn, Y, Sc, Ag) alloys. Data in Brief, 2015, 4, 190-192.	0.5	3

#	Article	IF	Citations
19315	Equation of state and electronic properties of EuVO4: A high-pressure experimental and computational study. Journal of Alloys and Compounds, 2015, 648, 1005-1016.	2.8	17
19316	First-principles study of native point defects and diffusion behaviors of helium in zirconium carbide. Journal of Nuclear Materials, 2015, 465, 161-166.	1.3	26
19317	Spin Doublet Point Defects in Graphenes: Predictions for ESR and NMR Spectral Parameters. Journal of Chemical Theory and Computation, 2015, 11, 3746-3754.	2.3	12
19318	Influence of Clusterâ€“Support Interactions on Reactivity of Size-Selected Nb_xO_y Clusters. Journal of Physical Chemistry C, 2015, 119, 14756-14768.	1.5	29
19319	N2 Emission via Intermediate N2O in a Steady-State NO + CO + D2 Reaction on Stepped Pd(211) by Angle-Resolved Desorption. Journal of Physical Chemistry C, 2015, 119, 11699-11713.	1.5	8
19320	Molecular-Level Details about Liquid H₂O Interactions with CO and Sugar Alcohol Adsorbates on Pt(111) Calculated Using Density Functional Theory and Molecular Dynamics. Journal of Physical Chemistry C, 2015, 119, 13642-13651.	1.5	44
19321	Ab Initio Investigation of Surface Chemistry of Alumina ALD on Hydroxylated Î³-Alumina Surface. Journal of Physical Chemistry C, 2015, 119, 13050-13061.	1.5	20
19322	Hydrogen Activation on the Promoted and Unpromoted ReS2 (001) Surfaces under the Sulfidation Conditions: A First-Principles Study. Journal of Physical Chemistry C, 2015, 119, 17092-17101.	1.5	12
19323	Solar Synthesis of PbSâ€“SnS₂ Superstructure Nanoparticles. ACS Nano, 2015, 9, 7831-7839.	7.3	18
19324	Express penetration of hydrogen on Mg(10Íž13) along the close-packed-planes. Scientific Reports, 2015, 5, 10776.	1.6	89
19325	Robust magnetic domains in fluorinated ReS₂ monolayer. Physical Chemistry Chemical Physics, 2015, 17, 18843-18853.	1.3	17
19326	Prediction of new high pressure structural sequence in thorium carbide: A first principles study. Journal of Applied Physics, 2015, 117, .	1.1	18
19327	Photocatalytic H2 production from spinels ZnGa2â^'Cr O4 (0â‰¤xâ‰¤2) solid solutions. Journal of Solid State Chemistry, 2015, 230, 95-101.	1.4	38
19328	Migration energy barriers of symmetric tilt grain boundaries in body-centered cubic metal Fe. Scripta Materialia, 2015, 107, 75-78.	2.6	17
19329	A Cu(111) supported h-BN nanosheet: a potential low-cost and high-performance catalyst for CO oxidation. Physical Chemistry Chemical Physics, 2015, 17, 22097-22105.	1.3	48
19330	Zr5Sb3â^'xRux, a new superconductor in the W5Si3 structure type. Journal of Materials Chemistry C, 2015, 3, 8235-8240.	2.7	13
19331	Theoretical investigation of sulfur defects on structural, electronic, and elastic properties of ZnSe semiconductor. Chinese Physics B, 2015, 24, 076106.	0.7	8
19332	Stacking fault energy, yield stress anomaly, and twinnability of Ni ₃ Al: A first principles study. Chinese Physics B, 2015, 24, 077102.	0.7	12

#	Article	IF	Citations
19333	The deformation and failure behaviour of phosphorene nanoribbons under uniaxial tensile strain. 2D Materials, 2015, 2, 035007.	2.0	39
19334	Negative thermal expansion in isostructural cubic ReO 3 and ScF 3 : A comparative study. Computational Materials Science, 2015, 107, 157-162.	1.4	33
19335	Study of the Zn0.75M0.25Te (MÂ=ÂFe, Co, Ni) diluted magnetic semiconductor system by first principles approach. Materials Chemistry and Physics, 2015, 162, 831-838.	2.0	40
19336	Ultrathin Ti-Silicate Film on a Ru(0001) Surface. Journal of Physical Chemistry C, 2015, 119, 15443-15448.	1.5	17
19337	The possibilities to lower the stacking fault energies of aluminum materials investigated by first-principles energy calculations. Computational Materials Science, 2015, 108, 136-146.	1.4	36
19338	Al3Pd2, a novel intermetallic compound: A first-principles study. Journal of Alloys and Compounds, 2015, 649, 54-61.	2.8	6
19339	Phase stability, elastic properties and electronic structures of Mgâ€“Y intermetallics from first-principles calculations. Journal of Magnesium and Alloys, 2015, 3, 127-133.	5.5	27
19340	Electronic structure, magnetic and optical properties of the Ba7(BO3)4â^'F2+3 crystal. Journal of Solid State Chemistry, 2015, 229, 358-365.	1.4	7
19341	Carbyne Fiber Synthesis within Evaporating Metallic Liquid Carbon. Journal of Physical Chemistry C, 2015, 119, 21605-21611.	1.5	32
19342	Enhancement of white-light-emission from single-phase Sr₅(PO₄)₃F:Eu²⁺,Mn²⁺ phosphors for near-UV white LEDs. Dalton Transactions, 2015, 44, 15006-15013.	1.6	35
19343	Insights into the growth of bismuth nanoparticles on 2D structured BiOCl photocatalysts: an in situ TEM investigation. Dalton Transactions, 2015, 44, 15888-15896.	1.6	27
19344	Electronic structure and optical properties of Bi,N co-doped SnO2. Journal of Materials Science, 2015, 50, 6993-6999.	1.7	15
19345	Effect of oxygen and nitrogen functionalization on the physical and electronic structure of graphene. Nano Research, 2015, 8, 2620-2635.	5.8	47
19346	Geometrical structures, and electronic and transport properties of a novel two-dimensional Î²-GaS transparent conductor. Nano Research, 2015, 8, 3177-3185.	5.8	3
19347	A theoretical view of 1,3-butadiene selective hydrogenation toward cis-2-butene on PdNi layered catalyst. Applied Surface Science, 2015, 353, 820-828.	3.1	12
19348	A density functional theory study of methanol dehydrogenation on the PtPd 3 (111) surface. International Journal of Hydrogen Energy, 2015, 40, 9656-9669.	3.8	10
19349	The synthesis and gas sensitivity of the Î²-Ti3O5 powder: Experimental and DFT study. Journal of Alloys and Compounds, 2015, 649, 939-948.	2.8	19
19350	Influence of one CO molecule on structural and electronic properties of monatomic Cu chain. Physica E: Low-Dimensional Systems and Nanostructures, 2015, 73, 89-95.	1.3	1

#	Article	IF	Citations
19351	C-, N-, S-, and Fe-Doped TiO₂ and SrTiO₃ Nanotubes for Visible-Light-Driven Photocatalytic Water Splitting: Prediction from First Principles. Journal of Physical Chemistry C, 2015, 119, 18686-18696.	1.5	104
19352	Stability, equilibrium morphology and hydration of ZrC(111) and (110) surfaces with H₂O: a combined periodic DFT and atomistic thermodynamic study. Physical Chemistry Chemical Physics, 2015, 17, 21401-21413.	1.3	17
19353	Thermodynamic modelling of the general NiAs-type structure: A study of first principle energies of formation for binary Ni-containing B8 compounds. Calphad: Computer Coupling of Phase Diagrams and Thermochemistry, 2015, 50, 174-181.	0.7	7
19354	New interatomic potentials for studying the behavior of noble gas atoms in tungsten. Journal of Nuclear Materials, 2015, 467, 398-405.	1.3	16
19355	Stable ScS2 nanostructures with tunable electronic and magnetic properties. Solid State Communications, 2015, 220, 12-16.	0.9	12
19356	The Electronic Structure and Bonding of Acetylene on PdGa(110). Journal of Physical Chemistry C, 2015, 119, 18229-18238.	1.5	15
19357	Low Barrier Carbon Induced CO Dissociation on Stepped Cu. Physical Review Letters, 2015, 114, 246101.	2.9	8
19358	Manganeseâ€“Vanadate Hybrids: Impact of Organic Ligands on Their Structures, Thermal Stabilities, Optical Properties, and Photocatalytic Activities. Inorganic Chemistry, 2015, 54, 7388-7401.	1.9	16
19359	CO Oxidation on Gold-Supported Iron Oxides: New Insights into Strong Oxideâ€“Metal Interactions. Journal of Physical Chemistry C, 2015, 119, 16614-16622.	1.5	62
19360	Relationships among the structural topology, bond strength, and mechanical properties of single-walled aluminosilicate nanotubes. Nanoscale, 2015, 7, 16222-16229.	2.8	15
19361	Three dimensional graphdiyne polymers with tunable band gaps. Carbon, 2015, 91, 518-526.	5.4	35
19362	Ab initio and empirical modeling of lithium atoms penetration into silicon. Computational Materials Science, 2015, 109, 76-83.	1.4	3
19363	Ab initio study of La 10â^'x Sr x (Si,Ge) 6 O 27â^'0.5x apatite for SOFC electrolyte. Computational Materials Science, 2015, 109, 25-33.	1.4	4
19364	Mechanistic Study of Carbon Monoxide Methanation over Pure and Rhodium- or Ruthenium-Doped Nickel Catalysts. Journal of Physical Chemistry C, 2015, 119, 16537-16551.	1.5	44
19365	Hydrogen Abstraction Energies and Ammonia Binding to BEA, ZSM-5, and Î±-Quartz Doped with Al, Sc, B, or Ga. Journal of Physical Chemistry C, 2015, 119, 16106-16114.	1.5	11
19366	Atomic-Scale View of VO_Xâ€“WO_X Coreduction on the Î±-Al₂O₃ (0001) Surface. Journal of Physical Chemistry C, 2015, 119, 16179-16187.	1.5	9
19367	Electronâ€“phonon interaction and thermal boundary resistance at the interfaces of Ge₂Sb₂Te₅with metals and dielectrics. Journal of Physics Condensed Matter, 2015, 27, 175009.	0.7	8
19368	Examination of Solid-Solution Phase Formation Rules for High Entropy Alloys from Atomistic Monte Carlo Simulations. Jom, 2015, 67, 2364-2374.	0.9	23

#	Article	IF	Citations
19369	Structural and electronic properties of cubic KNbO3 (001) surfaces: A first-principles study. Applied Surface Science, 2015, 351, 558-564.	3.1	14
19370	Greatly enhanced adsorption of platinum on periodic graphene nanobuds: A first-principles study. Applied Surface Science, 2015, 351, 1105-1115.	3.1	19
19371	CuAlTe2: A promising bulk thermoelectric material. Journal of Alloys and Compounds, 2015, 648, 958-965.	2.8	13
19372	Electronic structures and thermoelectric properties of La or Ce-doped Bi2Te3 alloys from first principles calculations. Journal of Physics and Chemistry of Solids, 2015, 85, 239-244.	1.9	11
19373	Spray pyrolytically deposited Fe-doped Cu2O thin films for solar hydrogen generation: Experiments & first-principles analysis. Materials Chemistry and Physics, 2015, 160, 32-39.	2.0	16
19374	Theoretical and Experimental Study of the Crystal Structures, Lattice Vibrations, and Band Structures of Monazite-Type PbCrO₄, PbSeO₄, SrCrO₄, and SrSeO₄. Inorganic Chemistry, 2015, 54, 7524-7535.	1.9	90
19375	Solvation Effects on OH Adsorbates on Stepped Pt Surfaces. Journal of Physical Chemistry C, 2015, 119, 16743-16753.	1.5	24
19376	Intrinsic Ladders of Affinity for Amino-Acid-Analogues on Boron Nitride Nanomaterials: A B3LYP-D2* Periodic Study. Journal of Physical Chemistry C, 2015, 119, 17707-17717.	1.5	18
19377	Density Functional Theory Study of the Oxygen Chemistry and NO Oxidation Mechanism on Low-Index Surfaces of SmMn₂O₅ Mullite. ACS Catalysis, 2015, 5, 4913-4926.	5.5	55
19378	Effect of annealing in oxygen on alloy structures of Pdâ€“Au bimetallic model catalysts. Physical Chemistry Chemical Physics, 2015, 17, 20588-20596.	1.3	23
19379	Super-saturated hydrogen effects on radiation damages in tungsten under the high-flux divertor plasma irradiation. Nuclear Fusion, 2015, 55, 083019.	1.6	35
19380	Computer simulation of biomoleculeâ€“biomaterial interactions at surfaces and interfaces. Biomedical Materials (Bristol), 2015, 10, 032001.	1.7	40
19381	First-principles investigation of the activation of CO2 molecule on TM/Cu (TM=Fe, Co and Ni) surface alloys. Applied Surface Science, 2015, 353, 902-912.	3.1	38
19382	Structural, elastic, electronic and optical properties of the quaternary nitridogallate LiCaGaN2: First-principles study. Materials Science in Semiconductor Processing, 2015, 40, 64-76.	1.9	19
19383	Density Functional Theory for Molecular and Periodic Systems Using Density Fitting and Continuous Fast Multipole Methods. Journal of Chemical Theory and Computation, 2015, 11, 3029-3041.	2.3	45
19384	First principles study on stability and hydrogen adsorption properties of Mg/Ti interface. Physical Chemistry Chemical Physics, 2015, 17, 16594-16600.	1.3	13
19385	Merging open metal sites and Lewis basic sites in a NbO-type metalâ€“organic framework for improved C₂H₂/CH₄ and CO₂/CH₄ separation. Dalton Transactions, 2015, 44, 14823-14829.	1.6	39
19386	A first principles approach to magnetic and optical properties in single-layer graphene sandwiched between boron nitride monolayers. Materials Research Express, 2015, 2, 075601.	0.8	6

#	Article	IF	Citations
19387	Investigation of electronic structure, magnetic and transport properties of half-metallic Mn2CuSi and Mn2ZnSi Heusler alloys. Journal of Magnetism and Magnetic Materials, 2015, 395, 81-88.	1.0	63
19388	Insight into structural, mechanical, electronic and thermodynamic properties of intermetallic phases in Zrâ€“Sn system from first-principles calculations. Journal of Physics and Chemistry of Solids, 2015, 86, 177-185.	1.9	21
19389	Photocatalytic Hydrogen Production over Chromium Doped Layered Perovskite Sr₂TiO₄. Inorganic Chemistry, 2015, 54, 7445-7453.	1.9	84
19390	Novel Superconducting Phases of HCl and HBr under High Pressure: An Ab Initio Study. Journal of Physical Chemistry C, 2015, 119, 17039-17043.	1.5	18
19391	Relationship between crystal structure and thermo-mechanical properties of kaolinite clay: beyond standard density functional theory. Dalton Transactions, 2015, 44, 12550-12560.	1.6	40
19392	Computational support for a pyrolitic lower mantle containing ferric iron. Nature Geoscience, 2015, 8, 556-559.	5.4	75
19393	Is mixed oxide of Sn x Ti 1â˜'x O 2 more effective for H 2 O decomposition? A first principles study. Chemical Physics Letters, 2015, 633, 175-180.	1.2	4
19394	Coverage Dependent Water Dissociative Adsorption on the Clean and O-Precovered Fe(111) Surfaces. Journal of Physical Chemistry C, 2015, 119, 11714-11724.	1.5	27
19395	Lithium Diffusion Pathways in 3R-Li_xTiS₂: A Combined Neutron Diffraction and Computational Study. Journal of Physical Chemistry C, 2015, 119, 11370-11381.	1.5	16
19396	Impact of structural differences in carcinopreventive agents indole-3-carbinol and 3,3â€²-diindolylmethane on biological activity. An X-ray, 1Hâ€“14N NQDR, 13C CP/MAS NMR, and periodic hybrid DFT study. European Journal of Pharmaceutical Sciences, 2015, 77, 141-153.	1.9	4
19397	Combining density functional and incremental post-Hartree-Fock approaches for van der Waals dominated adsorbate-surface interactions: Ag2/graphene. Journal of Chemical Physics, 2015, 143, 102804.	1.2	34
19398	Study of temperature and ligand flexibility effects on coordination polymer formation from cyclobutanetetracarboxylic acid. CrystEngComm, 2015, 17, 5921-5931.	1.3	11
19399	Prediction of torsional buckling behaviour of single-walled SiC nanotubes based on molecular mechanics. Engineering Computations, 2015, 32, 1837-1866.	0.7	5
19400	Mechanical and dynamical stability of TiAsTe compound from ab initio calculations. Philosophical Magazine, 2015, 95, 2294-2305.	0.7	17
19401	Density Functional Theory Study on the Carbon-Adhering Reaction on Fe3O4(111) Surface. Metallurgical and Materials Transactions B: Process Metallurgy and Materials Processing Science, 2015, 46, 2288-2295.	1.0	17
19402	Effects of stacking sequence and short-range ordering of solute atoms on elastic properties of Mgâ€“Znâ€“Y alloys with long-period stacking ordered structures. Acta Materialia, 2015, 96, 170-188.	3.8	42
19403	Ab initio investigation of the Nbâ€“Al system. Computational Materials Science, 2015, 107, 116-121.	1.4	33
19404	Pressure-induced structural phase transition in iron phosphide. Computational Materials Science, 2015, 107, 204-209.	1.4	7

#	Article	IF	Citations
19405	The roles of mercapto, benzene, and methyl groups in the corrosion inhibition of imidazoles on copper: II. Inhibitorâ€“copper bonding. Corrosion Science, 2015, 98, 457-470.	3.0	109
19406	Electronic band structures of binary skutterudites. Journal of Alloys and Compounds, 2015, 647, 364-369.	2.8	13
19407	Computational study of the adsorption of benzene and hydrogen onÂpalladiumâ€“iridium nanoalloys. Journal of Organometallic Chemistry, 2015, 792, 190-193.	0.8	10
19408	Octahedral and trigonal-prismatic coordination preferences in Nb-, Mo-, Ta-, and W-based ABX2 layered oxides, oxynitrides, and nitrides. Journal of Solid State Chemistry, 2015, 229, 272-277.	1.4	17
19409	Crystal structure, electronic structure, and photoluminescent properties of SrMoO4:Tb3+ phosphors. Materials Research Bulletin, 2015, 70, 403-411.	2.7	26
19410	NaLa(MoO4)2: RE3+ (RE3+=Eu3+, Sm3+, Er3+/Yb3+) microspheres: the synthesis and optical properties. Materials Research Bulletin, 2015, 70, 779-783.	2.7	14
19411	A Comparative First-Principles Study on Sodiation of Silicon, Germanium, and Tin for Sodium-Ion Batteries. Journal of Physical Chemistry C, 2015, 119, 14843-14850.	1.5	95
19412	Single-Atom Alloy Pdâ€“Ag Catalyst for Selective Hydrogenation of Acrolein. Journal of Physical Chemistry C, 2015, 119, 18140-18148.	1.5	150
19413	Preferential Adsorption of TiO₂ Nanostructures on Functionalized Single-Walled Carbon Nanotubes: A DFT Study. Journal of Physical Chemistry C, 2015, 119, 15085-15093.	1.5	18
19414	Strong N-Doped Graphene: The Case of of Physical Chemistry C, 2015, 119, 15103-15111.	1.5	14
19415	Tuning Magnetic Properties of BiFeO₃ Thin Films by Controlling Rare-Earth Doping: Experimental and First-Principles Studies. Journal of Physical Chemistry C, 2015, 119, 14351-14357.	1.5	36
19416	Gluing together metallic and covalent layers to form Ru₂C under ambient conditions. Physical Chemistry Chemical Physics, 2015, 17, 9730-9736.	1.3	9
19417	Anomalous lattice vibrations of monolayer MoS₂ probed by ultraviolet Raman scattering. Physical Chemistry Chemical Physics, 2015, 17, 14561-14568.	1.3	36
19418	Origin of enhanced visible light driven water splitting by (Rh, Sb)-SrTiO₃. Physical Chemistry Chemical Physics, 2015, 17, 15274-15283.	1.3	40
19419	Post-anti-van't Hoff-Le Bel motif in atomically thin germaniumâ€“copper alloy film. Physical Chemistry Chemical Physics, 2015, 17, 17545-17551.	1.3	81
19420	Thermodynamics of technetium: reconciling theory and experiment using density functional perturbation analysis. Dalton Transactions, 2015, 44, 12735-12742.	1.6	11
19421	Characterization of adsorbed water in MIL-53(Al) by FTIR spectroscopy and ab-initio calculations. Journal of Chemical Physics, 2015, 142, 124702.	1.2	47
19422	Impact of Oxygen Vacancy on Band Structure Engineering of n-p Codoped Anatase TiO2. Chinese Journal of Chemical Physics, 2015, 28, 155-160.	0.6	6

#	Article	IF	Citations
19423	On Theoretical Study of Magnetic Behavior of Diamond Doped with Transition Metals. Acta Physica Polonica A, 2015, 127, 823-826.	0.2	0
19424	Detection of concealed targets using spintronic microwave sensor. , 2015, , .		0
19425	First-principles study of hydrogen diffusion in transition metal palladium. Modern Physics Letters B, 2015, 29, 1550064.	1.0	2
19426	Behavior of Transition Metals Penetrating Silicon Substrate through SiO₂and Si₃N₄Films by Arsenic Ion Implantation and Annealing. ECS Journal of Solid State Science and Technology, 2015, 4, P131-P136.	0.9	18
19427	Experimental and Theoretical Investigations on Structural and Vibrational Properties of Melilite-Type Sr₂ZnGe₂O₇ at High Pressure and Delineation of a High-Pressure Monoclinic Phase. Inorganic Chemistry, 2015, 54, 6594-6605.	1.9	23
19428	Amorphous-crystalline transition in thermoelectric NbO₂. Journal Physics D: Applied Physics, 2015, 48, 275301.	1.3	15
19429	Versatile Single-Layer Sodium Phosphidostannate(II): Strain-Tunable Electronic Structure, Excellent Mechanical Flexibility, and an Ideal Gap for Photovoltaics. Journal of Physical Chemistry Letters, 2015, 6, 2682-2687.	2.1	60
19430	Palladiumâ€“platinum core-shell icosahedra with substantially enhanced activity and durability towards oxygen reduction. Nature Communications, 2015, 6, 7594.	5.8	440
19431	Vertical twinning of the Dirac cone at the interface between topological insulators and semiconductors. Nature Communications, 2015, 6, 7630.	5.8	26
19432	Insights into the mechanisms of CO2 methanation on Ni(111) surfaces by density functional theory. Applied Surface Science, 2015, 351, 504-516.	3.1	157
19433	Nitrogen doped epitaxial graphene on 4H-SiC(0001) â€“ Experimental and theoretical study. Carbon, 2015, 94, 214-223.	5.4	8
19434	Phase stability and elastic properties of CuGaSe2 under high pressure. Solid State Communications, 2015, 218, 1-5.	0.9	12
19435	Selective Crystal Growth and Structural, Optical, and Electronic Studies of Mn3Ta2O8. Inorganic Chemistry, 2015, 54, 6513-6519.	1.9	6
19436	Geometrical and Electronic Properties of Hydrated Sodium Montmorillonite and Tetracycline Montmorillonite from DFT Calculations. Journal of Physical Chemistry C, 2015, 119, 16082-16088.	1.5	19
19437	Thiolate-Bonded Self-Assembled Monolayers on Ni(111): Bonding Strength, Structure, and Stability. Journal of Physical Chemistry C, 2015, 119, 15455-15468.	1.5	21
19438	â€œZwitterionic Proton Spongeâ€•Hydrogen Bonding Investigations on the Basis of Carâ€“Parrinello Molecular Dynamics. Journal of Chemical Information and Modeling, 2015, 55, 1148-1157.	2.5	12
19439	Theoretical investigation of H₂S removal on Î³-Al₂O₃ surfaces of different hydroxyl coverage. RSC Advances, 2015, 5, 55372-55382.	1.7	11
19440	Intense red emitting monoclinic LaPO₄:Eu³⁺ nanoparticles: hostâ€“dopant energy transfer dynamics and photoluminescence properties. RSC Advances, 2015, 5, 58832-58842.	1.7	81

#	Article	IF	Citations
19441	Mechanism of charge transfer and its impacts on Fermi-level pinning for gas molecules adsorbed on monolayer WS2. Journal of Chemical Physics, 2015, 142, 214704.	1.2	124
19442	The First Principles Study of Hydrogen Adsorption on Ni-Decorated LiB (001) Surface. Chinese Physics Letters, 2015, 32, 057302.	1.3	3
19443	A new class of high strength high temperature Cobalt based Î³â€“Î³â€² Coâ€“Moâ€“Al alloys stabilized with Ta addition. Acta Materialia, 2015, 97, 29-40.	3.8	151
19444	Pressure-induced phase transition of zinc nitride chlorine. Computational Materials Science, 2015, 106, 175-179.	1.4	0
19445	Energy Bands of the 1H-MoS2 over Reduced Graphene Oxide. Materials Today: Proceedings, 2015, 2, 108-112.	0.9	0
19446	Doping strategies for increased oxygen permeability of CaTiO3 based membranes. Journal of Membrane Science, 2015, 482, 137-143.	4.1	22
19447	Framework and Channel Modifications in Mayenite (12CaOÂ·7Al2O3) Nanocages By Cationic Doping. Chemistry of Materials, 2015, 27, 4731-4741.	3.2	43
19448	Electronic Structure of Nitrogen-Doped Graphene in the Ground and Core-Excited States from First-Principles Simulations. Journal of Physical Chemistry C, 2015, 119, 16660-16666.	1.5	31
19449	Flexoelectricity in Carbon Nanostructures: Nanotubes, Fullerenes, and Nanocones. Journal of Physical Chemistry Letters, 2015, 6, 2740-2744.	2.1	68
19450	Coupling of Metals and Biominerals: Characterizing the Interface between Ferromagnetic Shape-Memory Alloys and Hydroxyapatite. ACS Applied Materials & Interfaces, 2015, 7, 15331-15338.	4.0	9
19451	Rotational Spectromicroscopy: Imaging the Orbital Interaction between Molecular Hydrogen and an Adsorbed Molecule. Physical Review Letters, 2015, 114, 206101.	2.9	27
19452	Strong Influence of Coadsorbate Interaction on CO Desorption Dynamics on Ru(0001) Probed by Ultrafast X-Ray Spectroscopy andAbÂInitioSimulations. Physical Review Letters, 2015, 114, 156101.	2.9	25
19453	Low-temperature phase transformation from nanotube to sp ³ superhard carbon phase. Chinese Physics B, 2015, 24, 066102.	0.7	0
19454	First-principles study of NO oxidation on Pt/CaTiO3 interface. Computational and Theoretical Chemistry, 2015, 1066, 88-93.	1.1	1
19455	Dynamics of Water Dissociative Chemisorption on Ni(111): Effects of Impact Sites and Incident Angles. Physical Review Letters, 2015, 114, 166101.	2.9	90
19456	Estimating Excitonic Effects in the Absorption Spectra of Solids: Problems and Insight from a Guided Iteration Scheme. Physical Review Letters, 2015, 114, 146402.	2.9	56
19457	Comparative Research on Cs Activation Mechanism for Al_{0.5}Ga_{0.5}As (001) and Al_{0.25}Ga_{0.75}N (0001) Surface. IEEE Sensors Journal, 2015, 15, 5252-5257.	2.4	2
19458	Direct observation of an abrupt insulator-to-metal transition in dense liquid deuterium. Science, 2015, 348, 1455-1460.	6.0	241

#	Article	IF	Citations
19459	Structural morphologies of high-pressure polymorphs of strontium hydrides. Physical Chemistry Chemical Physics, 2015, 17, 19379-19385.	1.3	39
19460	Donorâ€“anion interactions at the charge localization and charge ordering transitions of (TMTTF)₂AsF₆ probed by NEXAFS. Physical Chemistry Chemical Physics, 2015, 17, 19202-19214.	1.3	13
19461	Ba₇(BO₃)₃GeO₄X (XÂ= Cl, Br): borogermanate halides with rigid GeO₄tetrahedra and flexible XBa₆octahedra. RSC Advances, 2015, 5, 53448-53454.	1.7	11
19462	Emission properties of body-centered cubic elemental metal photocathodes. Journal of Applied Physics, 2015, 117, 134901.	1.1	13
19463	The evolution of polarization inside ultrathin PbTiO₃films: a theoretical study. Philosophical Magazine, 2015, 95, 2067-2077.	0.7	2
19464	Relaxation of 6H-SiC (0001) Surface and Si Adsorption on 6H-SiC (0001): an ab initio Study. Chinese Physics Letters, 2015, 32, 036801.	1.3	2
19465	Interplay between spinâ€“orbit coupling and crystal-field effect in topological insulators. Journal of Physics Condensed Matter, 2015, 27, 285801.	0.7	4
19466	Thickness dependent of phase shift between surface energy and work function in Pb ultrathin films. New Journal of Physics, 2015, 17, 053006.	1.2	4
19467	The effects of electric field and gate bias pulse on the migration and stability of ionized oxygen vacancies in amorphous Inâ€“Gaâ€“Znâ€“O thin film transistors. Science and Technology of Advanced Materials, 2015, 16, 034902.	2.8	18
19468	Linear optical properties of defective KDP with oxygen vacancy: First-principles calculations. Chinese Physics B, 2015, 24, 077802.	0.7	12
19469	Transition Metal Ions in Semiconductors: LDA, LDA+U, and Experiment. Acta Physica Polonica A, 2015, 127, 321-323.	0.2	4
19470	Study of sulfur adlayers on Au(1 1 1) from basic hydrolysis of piperazine bis(dithiocarbamate) sodium salt. Applied Surface Science, 2015, 345, 394-399.	3.1	7
19471	Enhanced ferromagnetism in N-doped BiFeO3: A first-principles prediction. Journal of Alloys and Compounds, 2015, 644, 30-39.	2.8	12
19472	Reactivity and reaction intermediates for acetic acid adsorbed on CeO2(1 1 1). Catalysis Today, 2015, 253, 65-76.	2.2	43
19473	Computational Exploration of the Mechanism of the Hydrogenation Step of the Anthraquinone Process for Hydrogen Peroxide Production. Journal of Physical Chemistry C, 2015, 119, 8748-8754.	1.5	40
19474	Study of Wetting on Chemically Soften Interfaces by Using Combined Solution Thermodynamics and DFT Calculations: Forecasting Effective Softening Elements. ACS Applied Materials & Interfaces, 2015, 7, 7576-7583.	4.0	8
19475	First-Principles Investigation of the Molecular Adsorption and Dissociation of Hydrazine on Niâ€“Fe Alloy Surfaces. Journal of Physical Chemistry C, 2015, 119, 8763-8774.	1.5	19
19476	Precipitation of CH₃NH₃PbCl₃ in CH₃NH₃PbI₃ and Its Impact on Modulated Charge Separation. Journal of Physical Chemistry C, 2015, 119, 9926-9933.	1.5	42

#	Article	IF	Citations
19477	Density Functional Theory of MHâ€“MOH Solid Solubility (M = Alkali) and Experiments in NaHâ€“NaOH. Journal of Physical Chemistry C, 2015, 119, 8062-8069.	1.5	1
19478	First-Principles Determination of the K-Conductivity Pathways in KAlO₂. Journal of Physical Chemistry C, 2015, 119, 9092-9098.	1.5	9
19479	Electronic Properties of Biphenylthiolates on Au(111): The Impact of Coverage Revisited. Journal of Physical Chemistry C, 2015, 119, 7817-7825.	1.5	20
19480	Synthesis and Characterization of Mid-Infrared Transparency Compounds: Acentric BaHgS2and Centric Ba8Hg4S5Se7. Inorganic Chemistry, 2015, 54, 2772-2779.	1.9	47
19481	Effect of compositional and antisite disorder on the electronic and magnetic properties of Niâ€“Mnâ€“In Heusler alloy. Journal of Physics Condensed Matter, 2015, 27, 175502.	0.7	10
19482	Greatly improved electrochemical performance of lithiumâ€“oxygen batteries with a bimetallic platinumâ€“copper alloy catalyst. Journal of Power Sources, 2015, 288, 296-301.	4.0	49
19483	PbGa₄S₇: a wide-gap nonlinear optical material. Journal of Materials Chemistry C, 2015, 3, 3060-3067.	2.7	80
19484	Structural and electrical properties of layered perovskite type Pr₂Ti₂O₇: experimental and theoretical investigations. Journal of Materials Chemistry C, 2015, 3, 4570-4584.	2.7	45
19485	Theoretical investigations into the electronic structures and electron transport properties of fluorine and carbonyl end-functionalized quarterthiophenes. Journal of Molecular Graphics and Modelling, 2015, 59, 50-58.	1.3	2
19486	Suppression of boron-oxygen defects in Czochralski silicon by carbon co-doping. Applied Physics Letters, 2015, 106, 102105.	1.5	7
19487	Densely Packed Perylene Layers on the Rutile TiO₂(110)-(1 Ã— 1) Surface. Journal of Physical Chemistry C, 2015, 119, 7809-7816.	1.5	11
19488	Ab initio structural and electronic bandâ€structure study of MgSe. Physica Status Solidi (B): Basic Research, 2015, 252, 663-669.	0.7	13
19489	SnGa₂GeS₆: synthesis, structure, linear and nonlinear optical properties. Dalton Transactions, 2015, 44, 7404-7410.	1.6	40
19490	Magnetic anisotropy of C and N doped bulk FeCo alloy: A first principles study. Journal of Magnetism and Magnetic Materials, 2015, 388, 101-105.	1.0	12
19491	Electronic structure and phase stability of oxide semiconductors: Performance of dielectric-dependent hybrid functional DFT, benchmarked against<mml:math xmlns:mml="http://www.w3.org/1998/Math/MathML"><mml:mrow><mml:mi>G</mml:mi><mml:mi>W</mml:mi></mml:mrow></mml:m structure calculations and experiments. Physical Review B, 2015, 91, .	1.1	140
19492	First principles investigation of cluster consisting of hydrogenâ€“helium atoms interstitially-trapped in tungsten. Journal of Nuclear Materials, 2015, 463, 355-358.	1.3	13
19493	Thermoelectric properties of IVâ€“VI-based heterostructures and superlattices. Journal of Solid State Chemistry, 2015, 227, 123-131.	1.4	8
19494	A class of rare antiferromagnetic metallic oxides: double perovskite AMn₃V₄O₁₂ (A = Na⁺, Ca²⁺, and) Tj ETQq1 1 0.784314 rgBT /Over 12717-12721.	1.3	6

#	Article	IF	Citations
19495	Optoelectronic properties of cubic BxInyGa1â^'xâ^'yN alloys matched to GaN for designing quantum well Lasers: First-principles study within mBJ exchange potential. Materials Science in Semiconductor Processing, 2015, 36, 192-203.	1.9	19
19497	Holistic quantum design of thermoelectric niobium oxynitride. Solid State Communications, 2015, 212, 5-9.	0.9	14
19498	Ab initio study of electronic structure and magnetic properties in ferromagnetic Sr1â^'x(Mn, Cr)xO alloys. Materials Science in Semiconductor Processing, 2015, 38, 101-106.	1.9	19
19499	Octahedral tilt transitions in the relaxor ferroelectric Na1/2Bi1/2TiO3. Journal of Solid State Chemistry, 2015, 227, 117-122.	1.4	20
19500	Prediction of novel hard phases of Si3N4: First-principles calculations. Journal of Solid State Chemistry, 2015, 228, 20-26.	1.4	20
19501	First principles study of structural, magnetic and electronic properties of C-doped monoclinic ZrO2. Journal of Magnetism and Magnetic Materials, 2015, 389, 90-94.	1.0	14
19502	First principles study of (Cd, Hg, In, Tl, Sn, Pb, As, Sb, Bi, Se) modified Pt(111), Pt(100) and Pt(211) electrodes as CO oxidation catalysts. Electrochimica Acta, 2015, 168, 370-378.	2.6	7
19503	Adsorption of RuSex (x=1â€“5) cluster on Se-doped graphene: First principle calculations. Applied Surface Science, 2015, 347, 808-815.	3.1	5
19504	Fine refinement of solid state structure of racemic form of phospho-tyrosine employing NMR Crystallography approach. Solid State Nuclear Magnetic Resonance, 2015, 65, 2-11.	1.5	24
19505	Energetics of native point defects in GaN: A density-functional study. Microelectronic Engineering, 2015, 147, 51-54.	1.1	46
19506	Ab initio study of the electronic structure and band gaps of Eu-doped LaSi3N5 phosphors: A role of oxygen atom. Journal of the European Ceramic Society, 2015, 35, 3249-3253.	2.8	2
19507	Theoretical study of structural, mechanical, thermal and electronic properties of Ti3B4 with Ta3B4 structure under high pressure. Computational Materials Science, 2015, 104, 29-34.	1.4	13
19508	Chlorine adsorption on Cu(111) revisited: LT-STM and DFT study. Surface Science, 2015, 639, 7-12.	0.8	13
19509	First-principles investigation of novel polymorphs of Mg₂C. Physical Chemistry Chemical Physics, 2015, 17, 12970-12977.	1.3	8
19510	First-principles study on ferromagnetism in Mn-doped tetragonal BiFeO3. Computational Materials Science, 2015, 105, 1-5.	1.4	18
19511	First principles hybrid DFT calculations of BaTiO3/SrTiO3(001) interface. Solid State Ionics, 2015, 274, 29-33.	1.3	35
19512	Effect of Impregnation on the Structure of Niobium Oxide/Alumina Catalysts Studied by Multinuclear Solid-State NMR, FTIR, and Quantum Chemical Calculations. Journal of Physical Chemistry C, 2015, 119, 10400-10411.	1.5	10
19513	Evolution behavior of C and Si atoms on diamond (001) surface: A first principle study. Applied Surface Science, 2015, 346, 464-469.	3.1	9

#	Article	IF	Citations
19514	Phase Transformations in the Pulsed Laser Deposition Grown TiO₂ Thin Films as a Consequence of O₂ Partial Pressure and Nd Doping. Journal of Physical Chemistry C, 2015, 119, 11578-11587.	1.5	12
19515	Rational Design of Organotin Polyesters. Macromolecules, 2015, 48, 2422-2428.	2.2	54
19516	A first principles study of the mechanical properties of Liâ€“Sn alloys. RSC Advances, 2015, 5, 36022-36029.	1.7	41
19517	Effect of electric field on the mechanical properties of bilayer boron nitride with AB stacking order: An ab initio study. Superlattices and Microstructures, 2015, 83, 498-506.	1.4	10
19518	Revealing the role of organic cations in hybrid halide perovskite CH3NH3PbI3. Nature Communications, 2015, 6, 7026.	5.8	564
19519	Nano-scale displacement sensing based on van der Waals interactions. Nanoscale, 2015, 7, 8962-8967.	2.8	18
19520	Functional materials integrated on IIIâ€“V semiconductors. Microelectronic Engineering, 2015, 147, 117-121.	1.1	11
19521	Adsorption of RGD tripeptide on anatase (001) surface â€“ A first principle study. Computational Materials Science, 2015, 104, 124-129.	1.4	16
19522	Extraordinary diffusion in Co/Cu grain boundaries. Scripta Materialia, 2015, 101, 52-55.	2.6	0
19523	Crystal structure, thermodynamics, magnetics and disorder properties of Beâ€“Feâ€“Al intermetallics. Journal of Alloys and Compounds, 2015, 639, 111-122.	2.8	11
19524	Group Additivity and Modified Linear Scaling Relations for Estimating Surface Thermochemistry on Transition Metal Surfaces: Application to Furanics. Journal of Physical Chemistry C, 2015, 119, 10417-10426.	1.5	28
19525	Stable porous crystalline silicon with nanotubular structure: A predicted allotrope with direct band gap. Physica B: Condensed Matter, 2015, 466-467, 59-63.	1.3	11
19526	Loss of Linear Band Dispersion and Trigonal Structure in Silicene on Ir(111). Journal of Physical Chemistry Letters, 2015, 6, 1065-1070.	2.1	20
19527	Electronâ€“phonon coupling and associated scattering rates in diamond. Diamond and Related Materials, 2015, 56, 1-5.	1.8	26
19528	Experimental study and thermodynamic assessment of the Zrâ€“Alâ€“Gd system. Thermochimica Acta, 2015, 609, 36-48.	1.2	1
19529	Density functional study of Î±-graphyne derivatives: Energetic stability, atomic and electronic structure. Physica E: Low-Dimensional Systems and Nanostructures, 2015, 70, 190-197.	1.3	13
19530	The reason why thin-film silicon grows layer by layer in plasma-enhanced chemical vapor deposition. Scientific Reports, 2015, 5, 9052.	1.6	15
19531	Electrical and structural properties of annealed ZnO:B thin films. Journal of Alloys and Compounds, 2015, 636, 102-105.	2.8	11

#	Article	IF	Citations
19532	Hydrostatic pressure effects on structural and electronic properties of pentacene from first principles calculations. IOP Conference Series: Materials Science and Engineering, 2015, 81, 012120.	0.3	2
19533	A first-principles study on gas sensing properties of graphene and Pd-doped graphene. Applied Surface Science, 2015, 343, 121-127.	3.1	217
19534	Impact of twin boundaries on bulk elastic constants: Density-functional theory data for Young×³s modulus of Ag. Data in Brief, 2015, 3, 209-215.	0.5	4
19535	Mechanical properties and electronic structures of the Hfâ€“Si system: First-principles calculations. Solid State Communications, 2015, 205, 39-45.	0.9	14
19536	First-principles investigation of site preference and diffusion behaviors of carbon in copper. Nuclear Instruments & Methods in Physics Research B, 2015, 352, 72-76.	0.6	4
19537	Effect of silicon on the elasticâ€“plastic transition of GaAs crystal. Scripta Materialia, 2015, 102, 31-34.	2.6	6
19538	Linking diffusion kinetics to defect electronic structure in metal oxides: Charge-dependent vacancy diffusion in alumina. Scripta Materialia, 2015, 101, 20-23.	2.6	15
19539	Electronic structures and optical properties induced by silicon twin boundaries: The first-principle calculation. Physics Letters, Section A: General, Atomic and Solid State Physics, 2015, 379, 1384-1390.	0.9	9
19540	Phase transitions, band structures, elastic and lattice dynamic properties of CdSnV2 (V=P, As, Sb) under pressure from first principles. Materials Science in Semiconductor Processing, 2015, 35, 149-161.	1.9	8
19541	High stability and superior catalytic reactivity of nitrogen-doped graphene supporting Pt nanoparticles as a catalyst for the oxygen reduction reaction: a density functional theory study. RSC Advances, 2015, 5, 34070-34077.	1.7	42
19542	First-principles calculations of heat capacities of ultrafast laser-excited electrons in metals. Applied Surface Science, 2015, 336, 79-84.	3.1	22
19543	Decomposition mechanisms of Cu-based oxygen carriers for chemical looping with oxygen uncoupling based on density functional theory calculations. Combustion and Flame, 2015, 162, 1265-1274.	2.8	58
19544	First principles study of structural, magnetic and electronic properties of N-doped monoclinic ZrO 2. Journal of Magnetism and Magnetic Materials, 2015, 387, 58-61.	1.0	5
19545	The reconstructed edges of the hexagonal BN. Nanoscale, 2015, 7, 9723-9730.	2.8	41
19546	Atomic geometry and electronic structures of Be-doped and Be-, O-codoped Ga0.75Al0.25N. Computational Materials Science, 2015, 99, 306-315.	1.4	8
19547	Segregation and trapping of oxygen vacancies near the SrTiO3 Σ3 (1 1 2) <mml:math xmlns:mml="http://www.w3.org/1998/Math/MathML" altimg="si1.gif" overflow="scroll"><mml:mo mathvariant="bold">[</mml:mo><mml:mover accent="true"><mml:mrow><mml:mn mathvariant="bold">1</mml:mn></mml:mrow><mml:mrow><mml:mo mathvariant="bold">Â¯</mml:mo></mml:mrow></mml:mover><mml:mspace width="0.12em" /><mml:mn mathvariant="bold">1</mml:mn><mml:mspace width="0.12em" /><mml:mn mathvariant="bold">0</mml:mn>	3.8	23
19548	A grapheneâ€“boron nitride lateral heterostructure â€“ a first-principles study of its growth, electronic properties, and chemical topology. Journal of Materials Chemistry C, 2015, 3, 5918-5932.	2.7	28
19549	Tunable Ag⁺ ion release from Ag@C for antibacterial and antifouling performances. RSC Advances, 2015, 5, 39384-39391.	1.7	13

#	Article	IF	Citations
19550	Exploring d 0 magnetism in doped SnO 2 â€“a first principles DFT study. Journal of Magnetism and Magnetic Materials, 2015, 385, 207-216.	1.0	20
19551	Metal-atom-induced charge redistributions and their effects on the electrical contacts to WS₂ monolayers. Physica Status Solidi (B): Basic Research, 2015, 252, 1783-1791.	0.7	2
19552	Polarization screening-induced magnetic phase gradients at complex oxide interfaces. Nature Communications, 2015, 6, 6735.	5.8	71
19553	The electronic properties tuned by the phase transition between the semiconducting and metallic phase of monolayer MoS₂/WS₂. Phase Transitions, 2015, 88, 726-734.	0.6	2
19554	Strong Long-Range Relaxations of Structural Defects in Graphene Simulated Using a New Semiempirical Potential. Journal of Physical Chemistry C, 2015, 119, 9646-9655.	1.5	20
19555	The oxygen reduction reaction on Pt(111) and Pt(100) surfaces substituted by subsurface Cu: a theoretical perspective. Journal of Materials Chemistry A, 2015, 3, 11444-11452.	5.2	102
19556	CO tolerance of a Pt₃Sn(111) catalyst in ethanol decomposition. Catalysis Science and Technology, 2015, 5, 3246-3258.	2.1	17
19557	The magnetic and optical properties of 3d transition metal doped SnO₂ nanosheets. RSC Advances, 2015, 5, 24306-24312.	1.7	29
19558	A DFT-based genetic algorithm search for AuCu nanoalloy electrocatalysts for CO₂ reduction. Physical Chemistry Chemical Physics, 2015, 17, 28270-28276.	1.3	65
19559	Lateral heterojunctions within monolayer h-BN/graphene: a first-principles study. RSC Advances, 2015, 5, 33037-33043.	1.7	37
19560	Enhanced visible-light photocatalytic activity of a g-C₃N₄/BiVO₄nanocomposite: a first-principles study. Physical Chemistry Chemical Physics, 2015, 17, 10218-10226.	1.3	157
19561	Mechanical stability of zinc oxide nanowires under tensile loading: is wurtzite stable at the nanoscale?. RSC Advances, 2015, 5, 43563-43570.	1.7	9
19562	Silicene nanomesh. Scientific Reports, 2015, 5, 9075.	1.6	42
19563	Interaction of cesium adatoms with free-standing graphene and graphene-veiled SiO₂ surfaces. RSC Advances, 2015, 5, 38623-38629.	1.7	2
19564	Microscopic origin of MXenes derived from layered MAX phases. RSC Advances, 2015, 5, 25403-25408.	1.7	61
19565	Flavonols on graphene: a DFT insight. Theoretical Chemistry Accounts, 2015, 134, 1.	0.5	7
19566	Density functional investigation of the thermophysical and thermochemical properties of talc [Mg3Si4O10(OH)2]. Physics and Chemistry of Minerals, 2015, 42, 151-162.	0.3	31
19567	First-principles investigation of the lattice vibrations in the alkali feldspar solid solution. Physics and Chemistry of Minerals, 2015, 42, 243-249.	0.3	9

#	Article	IF	Citations
19568	Structural, vibrational and thermophysical properties of pyrophyllite by semi-empirical density functional modelling. Physics and Chemistry of Minerals, 2015, 42, 609-627.	0.3	27
19569	First-Principles Study of Oxygen Evolution Reaction on the Oxygen-Containing Species Covered Coll-Exposing Co3O4 (100) Surface. Catalysis Letters, 2015, 145, 1169-1176.	1.4	18
19570	Pressureâ€“Temperature Dependence of Thermodynamic Properties of $$hbox {ScAlO}_{3}$$ ScAlO 3 Perovskite from First Principles. International Journal of Thermophysics, 2015, 36, 2273-2282.	1.0	2
19571	Electronic Structure and Ferromagnetic Properties of MgDoped Cubic BN from First-Principles Calculation. Journal of Superconductivity and Novel Magnetism, 2015, 28, 2425-2430.	0.8	2
19572	New semi-empirical computational analysis of catalytic reactions for automobile. Research on Chemical Intermediates, 2015, 41, 9475-9484.	1.3	0
19573	The adsorption and dissociation of multilayer CH3OH on TiO2 (110). Science China Chemistry, 2015, 58, 614-619.	4.2	7
19574	Theoretical Prediction of Structural, Elastic and Electronic Properties of M5Si3 (Mâ€‰=â€‰Ti, Zr) Compounds. Brazilian Journal of Physics, 2015, 45, 302-307.	0.7	1
19575	Mechanical properties of U-0.95Âmass fraction of Ti alloy quenching and aging treatment: a first principles study. Advances in Manufacturing, 2015, 3, 244-251.	3.2	1
19576	First-principles molecular dynamics study of water dissociation on theÎ³-U(1â€‰0â€‰0) surface. Journal of Physics Condensed Matter, 2015, 27, 175005.	0.7	8
19577	The hydrogen storage behavior of Li-decorated monolayer WS2: A first-principles study. Vacuum, 2015, 117, 63-67.	1.6	20
19578	Effects of non-metal dopants and defects on electronic properties of barium titanate as photocatalyst. International Journal of Hydrogen Energy, 2015, 40, 4766-4776.	3.8	16
19579	Presence of Gap States at Cu/TiO₂ Anatase Surfaces: Consequences for the Photocatalytic Activity. Journal of Physical Chemistry C, 2015, 119, 6696-6702.	1.5	76
19580	Thermodynamic modeling of the Coâ€“Hf system supported by key experiments and first-principles calculations. Thermochimica Acta, 2015, 608, 49-58.	1.2	10
19581	A molecular view of cisplatin's mode of action: interplay with DNA bases and acquired resistance. Physical Chemistry Chemical Physics, 2015, 17, 5155-5171.	1.3	39
19582	Insights into the hydrogenation mechanism of nitrobenzene to aniline on Pd₃/Pt(111): a density functional theory study. RSC Advances, 2015, 5, 34319-34326.	1.7	45
19583	Phase stability in nanoscale material systems: extension from bulk phase diagrams. Nanoscale, 2015, 7, 9868-9877.	2.8	66
19584	Effect of interfacial structures on spin dependent tunneling in epitaxial L1-FePt/MgO/FePt perpendicular magnetic tunnel junctions. Journal of Applied Physics, 2015, 117, .	1.1	18
19585	Analysis and Calculation of Electronic Properties and Light Absorption of Defective Sulfur-Doped Silicon and Theoretical Photoelectric Conversion Efficiency. Journal of Physical Chemistry A, 2015, 119, 3753-3761.	1.1	11

#	Article	IF	Citations
19586	Ferromagnetic Graphene Nanoribbons: Edge Termination with Organic Radicals. Journal of Physical Chemistry C, 2015, 119, 10109-10115.	1.5	25
19587	The effects of thermal and electric fields on the electronic structures of silicene. Physical Chemistry Chemical Physics, 2015, 17, 13366-13373.	1.3	13
19588	First principles study of the temperature-dependent elastic properties of W. Philosophical Magazine Letters, 2015, 95, 211-219.	0.5	8
19589	Al15Ge4Ni3: A new intergrowth structure with Cu3Au- and CaF2-type building blocks. Journal of Solid State Chemistry, 2015, 225, 240-248.	1.4	5
19590	Mechanical, electronic and thermal properties of Cu5Zr and Cu5Hf by first-principles calculations. Journal of Alloys and Compounds, 2015, 640, 455-461.	2.8	24
19591	Ab initio study of intrinsic point defects in PbTe: an insight into phase stability. Acta Materialia, 2015, 92, 72-80.	3.8	46
19592	First-principles investigation of hydrous post-perovskite. Physics of the Earth and Planetary Interiors, 2015, 244, 42-48.	0.7	15
19593	Effect of the components' interface on the synthesis of methanol over Cu/ZnO from CO₂/H₂: a microkinetic analysis based on DFT + U calculations. Physical Chemistry Chemical Physics, 2015, 17, 7317-7333.	1.3	28
19594	A robust carbon tolerant anode for solid oxide fuel cells. Science China Materials, 2015, 58, 204-212.	3.5	19
19595	Theoretical study of oxygen sorption and diffusion in the volume and on the surface of a Î³-TiAl alloy. Journal of Experimental and Theoretical Physics, 2015, 120, 257-267.	0.2	19
19596	Influence of semiempirical long-range dispersion corrections of the density functional in the study of phase transitions in molecular crystals. Physics of the Solid State, 2015, 57, 467-471.	0.2	3
19597	First-principle investigation of half-metallic ferromagnetism in octahedrally bonded Cr-doped rock-salt SrS, SrSe, and SrTe. European Physical Journal B, 2015, 88, 1.	0.6	41
19598	Catalytic activities of noble metal atoms on WO3 (001): nitric oxide adsorption. Nanoscale Research Letters, 2015, 10, 60.	3.1	8
19599	First-principles calculations of the lattice instability and the symmetry-lowering modulation of PtSi. Journal of the Korean Physical Society, 2015, 66, 612-616.	0.3	8
19600	Density-functional-theory study of monatomic and diatomic vacancies on the non-polar ZnO $$(10ar) Tj ETQq0 0 0 rgBT /Overlock 10 Tf	0.3	3
19601	Strain-induced metal-semiconductor transition in monolayers and bilayers of gray arsenic: A computational study. Physical Review B, 2015, 91, .	1.1	178
19602	Adsorption and Dissociation of H₂O on Monolayered MoS₂ Edges: Energetics and Mechanism from ab Initio Simulations. Journal of Physical Chemistry C, 2015, 119, 6518-6529.	1.5	107
19603	Ab initio study of germanium-hydride compounds under high pressure. RSC Advances, 2015, 5, 19432-19438.	1.7	13

#	Article	IF	Citations
19604	A systematic study of metal-supported boron nitride materials for the oxygen reduction reaction. Physical Chemistry Chemical Physics, 2015, 17, 12722-12727.	1.3	65
19605	Tailored upconversion emission of Eu3+ in Sr2Ca(W,Mo)O6:Yb3+,Eu3+ by a laser via an electronic polarization mechanism. Journal of Materials Chemistry C, 2015, 3, 4997-5003.	2.7	12
19606	Electrically Engineered Band Gap in Two-Dimensional Ge, Sn, and Pb: A First-Principles and Tight-Binding Approach. Journal of Physical Chemistry C, 2015, 119, 11896-11902.	1.5	41
19607	The bond ionicity in ANB8âˆ'N compounds from maximally localized Wannier functions. Journal of Physics and Chemistry of Solids, 2015, 82, 82-90.	1.9	12
19608	A first principles study of structural and mechanical properties of Ti2AlZr intermetallic. Intermetallics, 2015, 63, 37-44.	1.8	6
19609	Inelastic neutron scattering studies of phonon spectra, and simulations of pressure-induced amorphization in tungstates<mml:math xmlns:mml="http://www.w3.org/1998/Math/MathML"><mml:mrow><mml:mi>A</mml:mi><mml:mi mathvariant="normal">W</mml:mi><mml:msub><mml:mi		

#	Article	IF	Citations
19622	Low-Frequency Raman Fingerprints of Two-Dimensional Metal Dichalcogenide Layer Stacking Configurations. ACS Nano, 2015, 9, 6333-6342.	7.3	151
19623	Hole-doping of mechanically exfoliated graphene by confined hydration layers. Nano Research, 2015, 8, 3020-3026.	5.8	19
19624	Adsorption of Aun (n = 1â€“4) clusters on Fe3O4(001) B-termination. RSC Advances, 2015, 5, 45446-45453.	1.7	16
19625	Growth, structure, and optical properties of a self-activated crystal: Na2Nd2O(BO3)2. Optical Materials, 2015, 46, 461-466.	1.7	7
19626	Stabilizing and increasing the magnetic moment of half-metals: The role of Li in half-Heusler<mml:math xmlns:mml="http://www.w3.org/1998/Math/MathML"><mml:mi mathvariant="normal">LiMn</mml:mi><mml:mi>Z</mml:mi></mml:math><mml:math xmlns:mml="http://www.w3.org/1998/Math/MathML"><mml:mo>(</mml:mo><mml:mi>Z</mml:mi><mml:mo>=</mml:mo><mml:mtext Physical Review B, 2015, 91, .	1.1	35
19627	First principle investigation of electronic structure, chemical bonding and optical properties of tetrabarium gallium trinitride oxide single crystal. Materials Research Bulletin, 2015, 70, 436-441.	2.7	3
19628	Prediction of large-gap quantum spin hall insulator and Rashba-Dresselhaus effect in two-dimensional g-TlA (A = N, P, As, and Sb) monolayer films. Nano Research, 2015, 8, 2954-2962.	5.8	46
19629	Theoretical studies on the mechanism of oxygen reduction reaction on clean and O-substituted Ta₃N₅(100) surfaces. Catalysis Science and Technology, 2015, 5, 2769-2776.	2.1	34
19630	Accommodation of tin in tetragonal ZrO2. Journal of Applied Physics, 2015, 117, .	1.1	36
19631	The properties of Irn (n = 2â€“10) clusters and their nucleation on Î³-Al2O3 and MgO surfaces: from ab initio studies. Physical Chemistry Chemical Physics, 2015, 17, 1680-1687.	1.3	25
19632	Catalytic propane reforming mechanism over Mn-Doped CeO2 (111). Surface Science, 2015, 640, 119-126.	0.8	14
19633	Ba2GeS4and Mg2SnS4: synthesis, structures, optical properties and electronic structures. RSC Advances, 2015, 5, 33646-33652.	1.7	31
19634	Adsorption of Hydrogen at the GaN(0001Ì…) Surface: An Ab Initio Study. Journal of Physical Chemistry C, 2015, 119, 11563-11569.	1.5	15
19635	Structural, mechanical, electronic and magnetic properties of a new series of quaternary Heusler alloys CoFeMnZ (Z=Si, As, Sb): A first-principle study. Journal of Magnetism and Magnetic Materials, 2015, 393, 165-174.	1.0	109
19636	Comparative study between TB-mBJ and GGA+U on magnetic and optical properties of CdFe2O4. Journal of Magnetism and Magnetic Materials, 2015, 393, 183-187.	1.0	45
19637	Unbiased crystal structure prediction of NiSi under high pressure. Journal of Applied Crystallography, 2015, 48, 906-908.	1.9	3
19638	Biexciton formation and exciton coherent coupling in layered GaSe. Journal of Chemical Physics, 2015, 142, 212422.	1.2	31
19639	Hybrid functional band gap calculation of SnO6 containing perovskites and their derived structures. Journal of Solid State Chemistry, 2015, 228, 214-220.	1.4	8

#	Article	IF	Citations
19640	Ab Initio Nonequilibrium Thermodynamic and Transport Properties of Ultrafast Laser Irradiated 316L Stainless Steel. Journal of Physical Chemistry C, 2015, 119, 11438-11446.	1.5	46
19641	Stability and morphology-dependence of Sc3+ ions incorporation and substitution kinetics within ZnO host lattice. Materials Science in Semiconductor Processing, 2015, 39, 103-111.	1.9	15
19642	Two-dimensional electron gas and its electric control at the interface between ferroelectric and antiferromagnetic insulator studied from first principles. Physical Chemistry Chemical Physics, 2015, 17, 12812-12825.	1.3	10
19643	Elastic properties of perovskite ATiO3 (Aâ€‰=â€‰Be, Mg, Ca, Sr, and Ba) and PbBO3 (Bâ€‰=â€‰Ti, Zr, and Hf): First principles calculations. Journal of Applied Physics, 2015, 117, .	1.1	30
19644	Effect of BN/CC Isosterism on the Thermodynamics of Surface and Bulk Binding: 1,2-Dihydro-1,2-azaborine vs Benzene. Journal of Physical Chemistry C, 2015, 119, 14624-14631.	1.5	11
19645	Adiabatic-connection fluctuation-dissipation DFT for the structural properties of solidsâ€”The renormalized ALDA and electron gas kernels. Journal of Chemical Physics, 2015, 143, 102802.	1.2	56
19646	Diffusion of Cd and Te adatoms on CdTe(111) surfaces: A computational study using density functional theory. AIP Advances, 2015, 5, .	0.6	5
19647	Double resonance Raman modes in monolayer and few-layer<mml:math xmlns:mml="http://www.w3.org/1998/Math/MathML"><mml:msub><mml:mi mathvariant="normal">MoTe</mml:mi><mml:mn>2</mml:mn></mml:msub></mml:math>. Physical Review B, 2015, 91, .	1.1	99
19648	Insights into carbon nanotube nucleation: Cap formation governed by catalyst interfacial step flow. Scientific Reports, 2014, 4, 6510.	1.6	46
19649	First-principles investigation on the mechanical, vibrational and thermodynamics properties of AuCu3-type X3Sc (X=Al, Ga, In) intermetallic compounds. Computational Materials Science, 2015, 106, 38-44.	1.4	14
19650	Suppressing band gap of MoS2 by the incorporation of four- and eight-membered rings. Journal of Nanoparticle Research, 2015, 17, 1.	0.8	4
19651	The use of ultrasonic cavitation for near-surface structuring of robust and low-cost AlNi catalysts for hydrogen production. Green Chemistry, 2015, 17, 2745-2749.	4.6	37
19652	Phase-Field Simulation of Orowan Strengthening by Coherent Precipitate Plates in an Aluminum Alloy. Metallurgical and Materials Transactions A: Physical Metallurgy and Materials Science, 2015, 46, 3287-3301.	1.1	41
19653	The electronic and magnetic properties of transition-metal element doped three-dimensional topological Dirac semimetal in Cd₃As₂. Journal of Materials Chemistry C, 2015, 3, 3547-3551.	2.7	19
19654	Tuning the thermoelectric properties of a single-molecule junction by mechanical stretching. Physical Chemistry Chemical Physics, 2015, 17, 5386-5392.	1.3	13
19655	Flexible two-dimensional Ti_{n+1}C_n(n = 1, 2 and 3) and their functionalized MXenes predicted by density functional theories. Physical Chemistry Chemical Physics, 2015, 17, 15348-15354.	1.3	247
19656	Tuning the ferroelectric polarization in AAâ€²MnWO₆ double perovskites through A cation substitution. Dalton Transactions, 2015, 44, 10644-10653.	1.6	29
19657	From orientation disordered to ordered-Anab initiosimulation on ammonia borane phase transition within van der Waals corrections. Journal of Computational Chemistry, 2015, 36, 22-32.	1.5	4

#	Article	IF	Citations
19658	First-principles phase stability and elastic properties of Alâ€“La binary system intermetallic compounds. Intermetallics, 2015, 60, 92-97.	1.8	13
19659	Vibrational models for a crystal with 36 water molecules in the unit cell: IR spectra from experiment and calculation. Physical Chemistry Chemical Physics, 2015, 17, 10520-10531.	1.3	20
19660	Oxygen Adsorption on PdPt/Au(111) â€“ DFT Calculations. Journal of Physical Chemistry C, 2015, 119, 8213-8216.	1.5	17
19661	Nano-Scale Corrugations in Graphene: A Density Functional Theory Study of Structure, Electronic Properties and Hydrogenation. Journal of Physical Chemistry C, 2015, 119, 7900-7910.	1.5	39
19662	Effect of monolayer supports on the electronic structure of single-layer MoS2. IOP Conference Series: Materials Science and Engineering, 2015, 76, 012011.	0.3	8
19663	Magnetism, electronic structure and half-metallic property of transition metal (V, Cr, Mn, Fe, Co) substituted Zn3P2 dilute magnetic semiconductors: An ab-initio study. Computational Materials Science, 2015, 102, 85-94.	1.4	16
19664	Electronic structure and optical properties of orthorhombic and rhombohedral RAlO3 (RÂ=ÂSm, Nd). Solid State Sciences, 2015, 42, 37-44.	1.5	10
19665	Theoretical study of the structural, elastic, electronic and optical properties of XCaF3 (XÂ=ÂK and Rb). Solid State Sciences, 2015, 43, 9-14.	1.5	22
19666	Site- and bond-centered ordering driven ferroelectricity in DyNiO3. Journal of Alloys and Compounds, 2015, 639, 45-50.	2.8	1
19667	Thermal transport in free-standing silicon membranes: influence of dimensional reduction and surface nanostructures. European Physical Journal B, 2015, 88, 1.	0.6	27
19668	Insights into HÃgg Iron-Carbide-Catalyzed Fischerâ€“Tropsch Synthesis: Suppression of CH₄ Formation and Enhancement of Câ€“C Coupling on Ï‡-Fe₅C₂ (510). ACS Catalysis, 2015, 5, 2203-2208.	5.5	122
19669	Relationship between structure and cleavage behavior in the nonlinear optical crystal MnTeMoO 6. Journal of Crystal Growth, 2015, 419, 25-30.	0.7	10
19670	A DFT study of oxygen reduction reaction mechanism over O-doped graphene-supported Pt4, Pt3Fe and Pt3V alloy catalysts. International Journal of Hydrogen Energy, 2015, 40, 5126-5134.	3.8	36
19671	Line and rotational defects in boron-nitrene: Structure, energetics, and dependence on mechanical strain from first-principles calculations. Physica Status Solidi (B): Basic Research, 2015, 252, 1725-1730.	0.7	7
19672	Coverage-dependent thermodynamic analysis of the formation of water and hydrogen peroxide on a platinum model catalyst. Physical Chemistry Chemical Physics, 2015, 17, 11392-11400.	1.3	20
19673	Achieving Type I, II, and III Heterojunctions Using Functionalized MXene. ACS Applied Materials & Interfaces, 2015, 7, 7163-7169.	4.0	120
19674	Ultrabright X-ray laser scattering for dynamic warm dense matter physics. Nature Photonics, 2015, 9, 274-279.	15.6	208
19675	First principles calculations of structure parameters and transition pressures of GaN1 â^' x Bi x alloys. Semiconductors, 2015, 49, 279-284.	0.2	4

#	Article	IF	Citations
19676	Lithium and sodium storage on tetracyanoethylene (TCNE) and TCNE-(doped)-graphene complexes: A computational study. Materials Chemistry and Physics, 2015, 156, 180-187.	2.0	34
19677	Rich stoichiometries of stable Ca-Bi system: Structure prediction and superconductivity. Scientific Reports, 2015, 5, 9326.	1.6	12
19678	Improving the sintering resistance of Ni/Al 2 O 3 steam-reforming catalysts by promotion with noble metals. Applied Catalysis A: General, 2015, 498, 117-125.	2.2	62
19679	Electronic structures, mechanical and thermodynamic properties of cubic alkaline-earth hexaborides from first principles calculations. Journal of Alloys and Compounds, 2015, 635, 213-224.	2.8	87
19680	Correlated Visible-Light Absorption and Intrinsic Magnetism of SrTiO₃ Due to Oxygen Deficiency: Bulk or Surface Effect?. Inorganic Chemistry, 2015, 54, 3759-3765.	1.9	21
19681	Tuning negative differential resistance in single-atomic layer boron-silicon sheets. Journal of Applied Physics, 2015, 117, 114307.	1.1	9
19682	Ab Initio Study of the Dielectric and Electronic Properties of Multilayer GaS Films. Journal of Physical Chemistry Letters, 2015, 6, 1059-1064.	2.1	34
19683	Vacancy filling effect in thermoelectric NbO. Journal of Physics Condensed Matter, 2015, 27, 115501.	0.7	10
19684	Strain engineering the magnetic states of vacancy-doped monolayer MoSe 2. Journal of Alloys and Compounds, 2015, 635, 307-313.	2.8	35
19685	Structural, anisotropic elastic and thermal properties of MB (M=Ti, Zr and Hf) monoborides. Ceramics International, 2015, 41, 6831-6843.	2.3	92
19686	Structural, electronic, mechanical and magnetic properties of rare earth nitrides REN (RE= Pm, Eu and) Tj ETQq0 0 0 rgBT /Overlock 10 T	1.6	8
19687	Theoretical Prediction of Phosphorene and Nanoribbons As Fast-Charging Li Ion Battery Anode Materials. Journal of Physical Chemistry C, 2015, 119, 6923-6928.	1.5	96
19688	High intrinsic carrier mobility and photon absorption in the perovskite CH₃NH₃PbI₃. Physical Chemistry Chemical Physics, 2015, 17, 11516-11520.	1.3	182
19689	First principles study of structural, electronic, elastic and magnetic properties of cerium and praseodymium hydrogen system REHx (RE: Ce, Pr and x=2, 3). Journal of Rare Earths, 2015, 33, 289-303.	2.5	14
19691	Interfacial spin-filter assisted spin transfer torque effect in Co/BeO/Co magnetic tunnel junction. Journal of Applied Physics, 2015, 117, 093901.	1.1	2
19692	GGA+U study of the electronic and optical properties of hexagonal BN phase ZnO under pressure. Computational Materials Science, 2015, 102, 196-201.	1.4	20
19693	First principles calculation on the magnetic, optical properties and oxygen vacancy effect of CexY3â^'xFe5O12. Applied Physics Letters, 2015, 106, .	1.5	27
19694	Structural, electronic and mechanical properties ofCrN: A first principles study. Modern Physics Letters B, 2015, 29, 1550009.	1.0	11

#	Article	IF	Citations
19695	Investigation of Structural, Electronic and Mechanical Properties of Rubidium Metal Hydrides RbMH4 (MÂ=ÂB, Al, Ga). Acta Metallurgica Sinica (English Letters), 2015, 28, 975-983.	1.5	1
19696	Assessment of LaM0.25Mn0.75O3- (M = Fe, Co, Ni, Cu) as promising cathode materials for intermediate-temperature solid oxide fuel cells. Electrochimica Acta, 2015, 169, 264-275.	2.6	17
19697	Synergy between Pd and Au in a Pdâ€“Au(100) bimetallic surface for the water gas shift reaction: a DFT study. RSC Advances, 2015, 5, 47066-47073.	1.7	14
19698	Control of selectivity in allylic alcohol oxidation on gold surfaces: the role of oxygen adatoms and hydroxyl species. Physical Chemistry Chemical Physics, 2015, 17, 4730-4738.	1.3	22
19699	Bio-inspired design of electrocatalysts for oxalate oxidation: a combined experimental and computational study of Mnâ€“Nâ€“C catalysts. Physical Chemistry Chemical Physics, 2015, 17, 13235-13244.	1.3	26
19700	FeCoCp₃ Molecular Magnets as Spin Filters. Journal of Physical Chemistry C, 2015, 119, 12119-12129.	1.5	33
19701	Low-Frequency Interlayer Breathing Modes in Few-Layer Black Phosphorus. Nano Letters, 2015, 15, 4080-4088.	4.5	182
19702	Influence of chemical bonding and magnetism on elastic properties of the A2MB2 borides (A=Nb, Ta;) Tj ETQq1 1 0.784314 rgBT /Ove	1.4	22
19703	Electronic structures and current conductivities of B, C, N and F defects in amorphous titanium dioxide. Physical Chemistry Chemical Physics, 2015, 17, 11908-11913.	1.3	19
19704	A high energy density azobenzene/graphene hybrid: a nano-templated platform for solar thermal storage. Journal of Materials Chemistry A, 2015, 3, 11787-11795.	5.2	89
19705	Torsional buckling analysis of chiral multi-walled carbon nanotubes based on an accurate molecular mechanics model. Acta Mechanica, 2015, 226, 2955-2972.	1.1	7
19706	Electronic Structure, Phonon Dynamical Properties, andCO2Capture Capability ofNa2â^'xMxZrO3(M=Li,K): Density-Functional Calculations and Experimental Validations. Physical Review Applied, 2015, 3, .	1.5	20
19707	Enhanced Visible-Light Photocatalytic Activity of BiOI/BiOCl Heterojunctions: Key Role of Crystal Facet Combination. ACS Catalysis, 2015, 5, 3540-3551.	5.5	307
19708	Strong increase in superconducting Tc for Nb2InC under compressive strain. Journal of Applied Physics, 2015, 117, 093908.	1.1	3
19709	Ion diffusion mechanism in Pn Na_xLi_{2â^'x}MnSiO₄. CrystEngComm, 2015, 17, 2123-2128.	1.3	21
19710	Density Functional Theory Study of Adsorption of Benzotriazole on Cu₂O Surfaces. Journal of Physical Chemistry C, 2015, 119, 11625-11635.	1.5	42
19711	Electronic Structure and Magnetic Properties of CuFeS₂. Inorganic Chemistry, 2015, 54, 4840-4849.	1.9	69
19712	Conformational Stability and Thermal Pathways of Relaxation in Triclosan (Antibacterial/Excipient/Contaminant) in Solid-State: Combined Spectroscopic (¹H NMR) and Computational (Periodic DFT) Study. Journal of Physical Chemistry A, 2015, 119, 4864-4874.	1.1	21

#	Article	IF	Citations
19713	Spin-glass behavior and zero-field-cooled exchange bias in a Cr-based antiperovskite compound PdNCr₃. Journal of Materials Chemistry C, 2015, 3, 5683-5696.	2.7	53
19714	Oxygen Activation and Reaction on Pdâ€“Au Bimetallic Surfaces. Journal of Physical Chemistry C, 2015, 119, 11754-11762.	1.5	57
19715	Cluster expansion modeling and Monte Carlo simulation of alnico 5â€“7 permanent magnets. Journal of Applied Physics, 2015, 117, .	1.1	7
19716	Thermodynamic, structural and electronic, properties of SnO2: By GGA and GGA + trans-blaha-modified Beckeâ€“Johnson (TB-mBJ) calculation. Superlattices and Microstructures, 2015, 84, 80-90.	1.4	12
19717	Theoretical study on the electronic structure, mechanical property, and thermal expansion of yttrium oxysulfide. International Journal of Computational Materials Science and Engineering, 2015, 04, 1550004.	0.5	0
19718	Adsorption of C and CH_x Radicals on Anatase (001) and the Influence of Oxygen Vacancies. Journal of Physical Chemistry C, 2015, 119, 4908-4921.	1.5	19
19719	Single Layer Molybdenum Disulfide under Direct Out-of-Plane Compression: Low-Stress Band-Gap Engineering. Nano Letters, 2015, 15, 3139-3146.	4.5	75
19720	Electronic interaction between platinum nanoparticles and nitrogen-doped reduced graphene oxide: effect on the oxygen reduction reaction. Journal of Materials Chemistry A, 2015, 3, 11891-11904.	5.2	143
19721	Phonon Modes of Organic Electro-Optic Molecular Crystals for Terahertz Photonics. Journal of Physical Chemistry C, 2015, 119, 10031-10039.	1.5	20
19722	Manipulating interfacial hydrogens at palladium via STM. Physical Chemistry Chemical Physics, 2015, 17, 13973-13983.	1.3	7
19723	Thermal spin transport of a nitroxide radical-based molecule. RSC Advances, 2015, 5, 20699-20703.	1.7	5
19724	Hydriding and dehydriding energies of PuHx from ab initio calculations. Physics Letters, Section A: General, Atomic and Solid State Physics, 2015, 379, 1649-1653.	0.9	19
19725	Pseudo Jahnâ€“Teller Origin of Buckling Distortions in Two-Dimensional Triazine-Based Graphitic Carbon Nitride (g-C₃N₄) Sheets. Journal of Physical Chemistry C, 2015, 119, 12008-12015.	1.5	40
19726	Simulation of Atomic Diffusion in the Fcc NiAl System: A Kinetic Monte Carlo Study. Journal of Physical Chemistry C, 2015, 119, 11809-11817.	1.5	11
19727	Vertical/Planar Growth and Surface Orientation of Bi₂Te₃ and Bi₂Se₃ Topological Insulator Nanoplates. Nano Letters, 2015, 15, 3147-3152.	4.5	39
19728	Theoretical insight into the strain effect on the intercalation potential of Liâ€“FePO₄ materials. RSC Advances, 2015, 5, 35667-35674.	1.7	9
19729	Density functional studies of small silicon clusters adsorbed on graphene. RSC Advances, 2015, 5, 38680-38689.	1.7	3
19730	The electronic structure and luminescence properties of Ce3+ doped Sr10[(PO4)5.5(BO4)0.5]BO2 under UV/VUV and X-ray excitation. Optical Materials, 2015, 45, 13-21.	1.7	1

#	Article	IF	Citations
19731	Greatly Enhanced Electronic Conduction and Lithium Storage of Faceted TiO₂ Crystals Supported on Metallic Substrates by Tuning Crystallographic Orientation of TiO₂. Advanced Materials, 2015, 27, 3507-3512.	11.1	79
19732	Atomic-scale friction modulated by potential corrugation in multi-layered graphene materials. Journal of Applied Physics, 2015, 117, .	1.1	10
19733	Novel diffusions of interstitial atoms in IIâ€“VI compounds zinc selenide. Modern Physics Letters B, 2015, 29, 1550044.	1.0	0
19734	Enhancement of multiferroic in BiFeO3 by Co doping. Journal of Alloys and Compounds, 2015, 645, 78-84.	2.8	29
19735	Proton conduction at BaO-terminated (001) BaZrO3 surface using density functional theory. Solid State Ionics, 2015, 275, 19-22.	1.3	25
19736	Hydrazine network on Cu(111) surface: A Density Functional Theory approach. Surface Science, 2015, 637-638, 140-148.	0.8	21
19737	Ab initio strain engineering of graphene: opening bandgaps up to 1 eV. RSC Advances, 2015, 5, 43810-43814.	1.7	40
19738	Molecular Mechanisms for the Lithiation of Ruthenium Oxide Nanoplates as Lithium-Ion Battery Anode Materials: An Experimentally Motivated Computational Study. Journal of Physical Chemistry C, 2015, 119, 9705-9713.	1.5	24
19739	Phase transition and thermodynamic properties of beryllium telluride under high pressure. International Journal of Modern Physics B, 2015, 29, 1550096.	1.0	0
19740	Superhard-driven search of the covalent network in the B₃NO system. RSC Advances, 2015, 5, 35882-35887.	1.7	18
19741	Bandgap engineering of oxygen-rich TiO2+x for photocatalyst with enhanced visible-light photocatalytic ability. Journal of Materials Science, 2015, 50, 4324-4329.	1.7	20
19743	First principles study of the electronic structure and phonon dispersion of naphthalene under pressure. Journal of Physics and Chemistry of Solids, 2015, 83, 24-31.	1.9	15
19744	A metallic superhard boron carbide: first-principles calculations. Physical Chemistry Chemical Physics, 2015, 17, 9748-9751.	1.3	14
19745	The Mechanism of Slow Hot-Hole Cooling in Lead-Iodide Perovskite: First-Principles Calculation on Carrier Lifetime from Electronâ€“Phonon Interaction. Nano Letters, 2015, 15, 3103-3108.	4.5	140
19746	Effect of Ni and Mn on the formation of Cu precipitates in Î±-Fe. Scripta Materialia, 2015, 102, 11-14.	2.6	45
19747	Dissolution and diffusion of hydrogen in a molybdenum grain boundary: A first-principles investigation. Computational Materials Science, 2015, 102, 243-249.	1.4	13
19748	Growth mode and structures of silicene on the Ag(111) surface. Applied Surface Science, 2015, 354, 187-195.	3.1	12
19749	Magnetic properties of double-side partially fluorinated graphene from first principles calculations. Carbon, 2015, 89, 300-307.	5.4	30

#	Article	IF	Citations
19750	Nanoscale Magnetization Reversal Caused by Electric Field-Induced Ion Migration and Redistribution in Cobalt Ferrite Thin Films. ACS Nano, 2015, 9, 4210-4218.	7.3	60
19751	First principles investigation of the activity of thin film Pt, Pd and Au surface alloys for oxygen reduction. Physical Chemistry Chemical Physics, 2015, 17, 11647-11657.	1.3	41
19752	Anisotropic Electronâ€“Phonon Coupling in Colloidal Layered TiS₂ Nanodiscs Observed via Coherent Acoustic Phonons. Journal of Physical Chemistry C, 2015, 119, 7436-7442.	1.5	11
19753	Hybrid functional studies on the optical and electronic properties of graphane and silicane. Solid State Communications, 2015, 209-210, 59-65.	0.9	6
19754	A Strategy to Stabilize Kesterite CZTS for High-Performance Solar Cells. Chemistry of Materials, 2015, 27, 2920-2927.	3.2	63
19755	A benchmark database for adsorption bond energies to transition metal surfaces and comparison to selected DFT functionals. Surface Science, 2015, 640, 36-44.	0.8	396
19756	Structural and electronic properties of Li-ion battery cathode material MoF3 from first-principles. Journal of Solid State Chemistry, 2015, 227, 25-29.	1.4	4
19757	Does the Dirac Cone Exist in Silicene on Metal Substrates?. Scientific Reports, 2014, 4, 5476.	1.6	92
19758	First-principles study of the lattice integration of palladium defects in doped germanium and silicon. Materials Science in Semiconductor Processing, 2015, 34, 99-103.	1.9	0
19759	Vacancy formation in MoS2 supported on MgO: Electronic and energetic analysis. Chemical Physics Letters, 2015, 626, 55-62.	1.2	5
19760	Energies and Forces. Springer Series in Solid-state Sciences, 2015, , 129-161.	0.3	0
19761	Conductance and spin-filter effects of oxygen-incorporated Au, Cu, and Fe single-atom chains. Journal of Applied Physics, 2015, 117, 043902.	1.1	11
19762	The synergistic mechanism of graphene and MoS₂ for hydrogen generation: insights from density functional theory. Physical Chemistry Chemical Physics, 2015, 17, 11375-11381.	1.3	32
19763	Dielectric Properties of Self-Assembled Monolayer Coatings on a (111) Silicon Surface. Journal of Physical Chemistry C, 2015, 119, 7264-7274.	1.5	12
19764	Widely available active sites on Ni₂P for electrochemical hydrogen evolution â€“ insights from first principles calculations. Physical Chemistry Chemical Physics, 2015, 17, 10823-10829.	1.3	118
19765	Modeling thermal properties of plutonium mononitride. Journal of Nuclear Materials, 2015, 461, 51-55.	1.3	0
19766	Comparative investigations of the crystal structure and photoluminescence property of eulytite-type Ba₃Eu(PO₄)₃and Sr₃Eu(PO₄)₃. Dalton Transactions, 2015, 44, 7679-7686.	1.6	161
19767	Shape dependent magnetic and optical properties in silicene nanodisks: A first principles study. Journal of Physics and Chemistry of Solids, 2015, 83, 32-39.	1.9	17

#	Article	IF	Citations
19768	Strong spin-lattice coupling in CrSiTe3. APL Materials, 2015, 3, .	2.2	192
19769	Yttrium-dispersed B ₈₀ fullerenes: Promising materials for hydrogen storage. Europhysics Letters, 2015, 109, 56004.	0.7	11
19770	First-principle study of structural and mechanical properties of hexagonal polytypes of diamond. Crystallography Reports, 2015, 60, 257-262.	0.1	5
19771	Role of F in Improving the Photocatalytic Activity of Rh-Doped SrTiO₃. Journal of Physical Chemistry C, 2015, 119, 7215-7224.	1.5	56
19772	Theoretical investigation of magnetic, electronic and optical properties of orthorhombic YFeO3: A first-principle study. Materials Science in Semiconductor Processing, 2015, 34, 114-120.	1.9	51
19773	Understanding the low-loss mechanism of general organicâ€“inorganic perovskites from first-principles calculation. Chemical Physics Letters, 2015, 627, 13-19.	1.2	13
19774	CO₂ Capture on h-BN Sheet with High Selectivity Controlled by External Electric Field. Journal of Physical Chemistry C, 2015, 119, 6912-6917.	1.5	183
19775	First principle study of structural, electronic and magnetic properties of silicon doped zigzag boron nitride nanoribbon. European Physical Journal B, 2015, 88, 1.	0.6	4
19776	Role of hydrogen-bonding and its interplay with octahedral tilting in CH₃NH₃PbI₃. Chemical Communications, 2015, 51, 6434-6437.	2.2	173
19777	Tuning the Electronic and Magnetic Properties of Phosphorene by Vacancies and Adatoms. Journal of Physical Chemistry C, 2015, 119, 6530-6538.	1.5	125
19778	Effect of Sn-Substitution on Thermoelectric Properties of Copper-Based Sulfide, Famatinite Cu₃SbS₄. Journal of the Physical Society of Japan, 2015, 84, 044706.	0.7	47
19779	First-principles density functional calculations of physical properties of orthorhombic Au2Al crystal. Intermetallics, 2015, 62, 60-68.	1.8	19
19780	First principle study on the temperature dependent elastic constants, anisotropy, generalized stacking fault energy and dislocation core of NiAl and FeAl. Computational Materials Science, 2015, 103, 116-125.	1.4	40
19781	Nine New Phosphorene Polymorphs with Non-Honeycomb Structures: A Much Extended Family. Nano Letters, 2015, 15, 3557-3562.	4.5	275
19782	Electronic structure and magnetism on FeSiAl alloy: A DFT study. Journal of Magnetism and Magnetic Materials, 2015, 389, 73-76.	1.0	11
19783	First principles calculations of (La,Mg)2Ni7 hydrides. Journal of Alloys and Compounds, 2015, 645, S5-S8.	2.8	13
19784	Computational study of hydroxyapatite structures, properties and defects. Journal Physics D: Applied Physics, 2015, 48, 195302.	1.3	59
19785	High Pressure Effects on the Properties of âŒ©110âŒª {001} Dislocation in Superconducting ZnCNi3 and MgCNi3 Determined from First Principles Calculations Combined with an Improved Peierls-Nabarro Equation. Journal of Superconductivity and Novel Magnetism, 2015, 28, 2281-2291.	0.8	0

#	Article	IF	Citations
19786	First-principles calculation of structural stability, lattice dynamic and thermodynamic properties of BeX (X = S, Se and Te) compounds under high pressure. Philosophical Magazine, 2015, 95, 275-288.	0.7	4
19787	First-principles investigation on mechanical, electronic, and thermodynamic properties of Mg2Sr under high pressure. Journal of Applied Physics, 2015, 117, .	1.1	19
19788	Influence of coadsorbed H in CO dissociation and CHn formation on Fe(100): A DFT study. Applied Surface Science, 2015, 346, 438-442.	3.1	9
19789	Electrochemically Deposited Sb and In Doped Tin Sulfide (SnS) Photoelectrodes. Journal of Physical Chemistry C, 2015, 119, 6471-6480.	1.5	27
19790	Functionalization of a GaSe monolayer by vacancy and chemical element doping. Physical Chemistry Chemical Physics, 2015, 17, 10737-10748.	1.3	40
19791	Theoretic Insight into the Desulfurization Mechanism: Removal of H₂S by Ceria (110). Journal of Physical Chemistry C, 2015, 119, 7678-7688.	1.5	11
19792	Ab initio modeling of single wall nanotubes folded from Î±- and Î³-V2O5 monolayers: structural, electronic and vibrational properties. CrystEngComm, 2015, 17, 3277-3285.	1.3	5
19793	Ab-initio calculation of optical properties of AA-stacked bilayer graphene with tunable layer separation. Current Applied Physics, 2015, 15, 691-697.	1.1	24
19794	Complementing the adsorption energies of CO ₂ , H ₂ S and NO ₂ to h-BN sheets by doping with carbon. Europhysics Letters, 2015, 109, 57008.	0.7	24
19795	Study on key step of 1,3-butadiene formation from ethanol on MgO/SiO₂. RSC Advances, 2015, 5, 25959-25966.	1.7	41
19796	Mechanical properties and variation in SOC going from La to Nd in intermetallic RIn3 and RSn3 (RÂ= La,) Tj ETQq0 0 0 rgBT /Overlock 10	1.7	11
19797	Electrical conductivity enhancement by boron-doping in diamond using first principle calculations. Applied Surface Science, 2015, 334, 40-44.	3.1	32
19798	An ab-initio analysis of the influence of knock-on atom induced damage on the peak tensile strength of 3C-SiC grain boundaries. International Journal of Damage Mechanics, 2015, 24, 446-467.	2.4	2
19799	The physical properties of Li-doped g-C3N4 monolayer sheet investigated by the first-principles. Materials Research Bulletin, 2015, 66, 156-162.	2.7	72
19800	Synergistic Effects of Intrinsic Cation Disorder and Electron-Deficient Substitution on Ion and Electron Conductivity in La1â€“xSrxCo0.5Mn0.5O3â^'Î´ (x = 0, 0.5, and 0.75). Inorganic Chemistry, 2015, 54, 2820-2829.	1.9	9
19801	Composition-dependent structural and magnetic properties of Niâ€“Mnâ€“Ga alloys studied by ab initio calculations. Journal of Materials Science, 2015, 50, 3825-3834.	1.7	16
19802	Optical properties of a conjugated-polymer-sensitised solar cell: the effect of interfacial structure. Physical Chemistry Chemical Physics, 2015, 17, 14489-14494.	1.3	0
19803	Modeling atomic force microscopy at LiNbO 3 surfaces from first-principles. Computational Materials Science, 2015, 103, 145-150.	1.4	11

#	Article	IF	Citations
19804	Structure, chemisorption properties and electrocatalysis by Pd3Au overlayers on tungsten carbide â€“ A DFT study. International Journal of Hydrogen Energy, 2015, 40, 6085-6096.	3.8	24
19805	O^{â€“} centers in LuAG:Ce,Mg ceramics. Physica Status Solidi - Rapid Research Letters, 2015, 9, 245-249.	1.2	35
19806	Tuning Carrier Confinement in the MoS₂/WS₂ Lateral Heterostructure. Journal of Physical Chemistry C, 2015, 119, 9580-9586.	1.5	74
19807	Structural Transitions in Monolayer MoS₂by Lithium Adsorption. Journal of Physical Chemistry C, 2015, 119, 10602-10609.	1.5	109
19808	Firstâ€principles calculation of Cu₂SnS₃ and related compounds. Physica Status Solidi (B): Basic Research, 2015, 252, 1230-1234.	0.7	36
19809	Electronic band structure of compressively strained Ge1â^'xSnx with xâ€‰<â€‰0.11 studied by contactless electroreflectance. Applied Physics Letters, 2015, 106, .	1.5	33
19810	Cluster characteristics and physical properties of binary Alâ€“Zr intermetallic compounds from first principles studies. Computational Materials Science, 2015, 103, 170-178.	1.4	30
19811	Experimental and theoretical investigation of the superior contact properties of dielectrophoretically processed graphene and tantalum nitride electrodes. Physica Status Solidi (B): Basic Research, 2015, 252, 765-772.	0.7	2
19812	Nb-doped LiBH 4 (010) surface for hydrogen desorption: First-principles calculations. International Journal of Hydrogen Energy, 2015, 40, 6365-6372.	3.8	8
19813	A new phase of ThC at high pressure predicted from a first-principles study. Physics Letters, Section A: General, Atomic and Solid State Physics, 2015, 379, 1607-1611.	0.9	17
19814	Study of systematic trends in electronic and optical properties within ZnM2O4 (M=Co, Rh, Ir) family by FPLAPW method with PBE and TB-mBJ potentials. Optical Materials, 2015, 45, 141-147.	1.7	16
19815	A first principles study of hydrogen storage on lithium decorated two dimensional carbon allotropes. International Journal of Hydrogen Energy, 2015, 40, 6128-6136.	3.8	53
19816	Chemisorbed Oxygen on the Au(321) Surface Alloyed with Silver: A First-Principles Investigation. Journal of Physical Chemistry C, 2015, 119, 9215-9226.	1.5	41
19817	Density functional investigation of the thermo-physical and thermo-chemical properties of 2M1 muscovite. American Mineralogist, 2015, 100, 935-944.	0.9	34
19818	LaMgX and CeMgX (XÂ=ÂGa, In, Tl, Pd, Ag, Pt, Au) with ZrNiAl type structure â€“ A systematic view on electronic structure and chemical bonding. Solid State Sciences, 2015, 43, 28-34.	1.5	3
19819	Adsorption of carbon monoxide, carbon dioxide and methane on hexagonal boron nitride with high titanium coverage. Surface Science, 2015, 637-638, 48-52.	0.8	5
19820	Cubic C₉₆: a novel carbon allotrope with a porous nanocube network. Journal of Materials Chemistry A, 2015, 3, 10448-10452.	5.2	47
19821	Correlation of Electronic Structure with Catalytic Activity: H₂â€“D₂ Exchange across Cu_xPd_{1â€“x} Composition Space. ACS Catalysis, 2015, 5, 3137-3147.	5.5	18

#	Article	IF	Citations
19822	First-Principles Investigation of the Electronic Properties and Stabilities of the LaAlO₃ (001) and (110) (1 Ã— 1) Polar Terminations. Journal of Physical Chemistry C, 2015, 119, 9364-9374.	1.5	13
19823	Ru_{0.01}Ti_{0.99}Nb₂O₇ as an intercalation-type anode material with a large capacity and high rate performance for lithium-ion batteries. Journal of Materials Chemistry A, 2015, 3, 8627-8635.	5.2	131
19824	Porous BN for hydrogen generation and storage. Journal of Materials Chemistry A, 2015, 3, 9632-9637.	5.2	83
19825	Effects of single- and co-substitution of Ti on dehydrogenation of Mg 2 NiH 4 : A first-principles study. Computational Materials Science, 2015, 103, 45-51.	1.4	12
19826	Two-Dimensional Metal Dichalcogenides and Oxides for Hydrogen Evolution: A Computational Screening Approach. Journal of Physical Chemistry Letters, 2015, 6, 1577-1585.	2.1	75
19827	Density functional theory study on organically surface-modified silicene. RSC Advances, 2015, 5, 33831-33837.	1.7	21
19828	Highly active Nâ€“PtTe/reduced graphene oxide intermetallic catalyst for formic acid oxidation. Nano Energy, 2015, 15, 24-32.	8.2	26
19829	Special quasirandom structure method in application for advanced properties of alloys: A study on Ti 0.5 Al 0.5 N and TiN/Ti 0.5 Al 0.5 N multilayer. Computational Materials Science, 2015, 103, 194-199.	1.4	9
19830	Lattice strain at c-Si surfaces: a density functional theory calculation. Metrologia, 2015, 52, 214-221.	0.6	13
19831	High-Fidelity Hugoniots of Î± Phase RDX Solid from High-Quality Force Field with Thermal, Zero-Point Vibration, and Anharmonic Effects. Chinese Physics Letters, 2015, 32, 080501.	1.3	1
19832	Achieving a high magnetization in sub-nanostructured magnetite films by spin-flipping of tetrahedral Fe3+ cations. Nano Research, 2015, 8, 2935-2945.	5.8	21
19833	Selected properties of Pt(111) modified surfaces: A DFT study. Electrochemistry Communications, 2015, 60, 135-138.	2.3	6
19834	Superionic Phases of the 1:1 Waterâ€“Ammonia Mixture. Journal of Physical Chemistry A, 2015, 119, 10582-10588.	1.1	36
19835	Molecular Precursor Induced Surface Reconstruction at Graphene/Pt(111) Interfaces. Journal of Physical Chemistry C, 2015, 119, 22534-22541.	1.5	15
19836	Fluorographane: a promising material for bipolar doping of MoS2. Physical Chemistry Chemical Physics, 2015, 17, 27636-27641.	1.3	7
19837	Mechanical properties of monolayer sulphides: a comparative study between MoS₂, HfS₂ and TiS₃. Physical Chemistry Chemical Physics, 2015, 17, 27742-27749.	1.3	99
19838	Pd₁/BN as a promising single atom catalyst of CO oxidation: a dispersion-corrected density functional theory study. RSC Advances, 2015, 5, 84381-84388.	1.7	68
19839	Density functional studies of zirconia with different crystal phases for oxygen reduction reaction. RSC Advances, 2015, 5, 85122-85127.	1.7	11

#	Article	IF	Citations
19840	Reaction kinetics of the electrochemical oxidation of CO and syngas fuels on a Sr₂Fe_{1.5}Mo_{0.5}O_{6â^'Î´} perovskite anode. Journal of Materials Chemistry A, 2015, 3, 21618-21629.	5.2	13
19841	Low-energy electron diffraction and density functional theory study of potassium adsorbed on Pb(1â€‰0â€‰0). Journal of Physics Condensed Matter, 2015, 27, 345001.	0.7	1
19842	A first-principles study of the vibrational properties of crystalline tetracene under pressure. Journal of Physics Condensed Matter, 2015, 27, 375402.	0.7	13
19843	An ab initio study of strained two-dimensional MoSe2. Journal of Semiconductors, 2015, 36, 043001.	2.0	4
19844	Structure, energetic stability and tunable electronic properties of BxCyNz armchair nanotubes: a theoretical study on the influence of diameter and local carbon concentration. European Physical Journal B, 2015, 88, 1.	0.6	14
19845	Realization of Dirac Cones in Few Bilayer Sb(111) Films by Surface Modification. Nanoscale Research Letters, 2015, 10, 1043.	3.1	9
19846	Graphene-covered perovskites: an effective strategy to enhance light absorption and resist moisture degradation. RSC Advances, 2015, 5, 82346-82350.	1.7	43
19847	Excitonic gap formation in neutral bilayer structures. Physica Scripta, 2015, 90, 085806.	1.2	2
19848	Phonon dispersion and zero-point renormalization of LiNbO₃from density-functional perturbation theory. Journal of Physics Condensed Matter, 2015, 27, 385402.	0.7	34
19849	Interplay of coupling between strain and rotation in ferroelectric SrZrO3/SrTiO3superlattices. Journal of Physics Condensed Matter, 2015, 27, 385901.	0.7	3
19850	Dynamic process of H-controlled oxygen concentration in LBE: AÂfirst-principles study. Journal of Nuclear Materials, 2015, 467, 181-185.	1.3	3
19851	O₂â€“CO₂ Mixed Gas Production Using a Zr-Doped Cu-Based Oxygen Carrier. Industrial & Engineering Chemistry Research, 2015, 54, 9805-9812.	1.8	26
19852	Formation of Li₃O₄nano particles in the discharge products of non-aqueous lithiumâ€“oxygen batteries leads to lower charge overvoltage. Physical Chemistry Chemical Physics, 2015, 17, 29859-29866.	1.3	22
19853	Phase stability and lattice dynamics of ammonium azide under hydrostatic compression. Physical Chemistry Chemical Physics, 2015, 17, 29210-29225.	1.3	20
19854	Enhanced thermoelectric performance of n-type Cu_{0.008}Bi₂Te_{2.7}Se_{0.3} by band engineering. Journal of Materials Chemistry C, 2015, 3, 10604-10609.	2.7	34
19855	Strong interface-induced spinâ€“orbit interaction in graphene on WS2. Nature Communications, 2015, 6, 8339.	5.8	314
19856	Facts and fictions about polymorphism. Chemical Society Reviews, 2015, 44, 8619-8635.	18.7	499
19857	A nano Ag₅ cluster tip probing the vertical transfer of CO_(ads) adsorbed on Ag(110) with simulated inelastic electron tunneling spectroscopy. RSC Advances, 2015, 5, 64682-64688.	1.7	0

#	Article	IF	Citations
19858	Architectural design and phase engineering of N/B-codoped TiO₂(B)/anatase nanotube assemblies for high-rate and long-life lithium storage. Journal of Materials Chemistry A, 2015, 3, 22591-22598.	5.2	49
19859	Study on adsorption and desorption of ammonia on graphene. Nanoscale Research Letters, 2015, 10, 359.	3.1	44
19860	A DFT study of adsorption of imidazole, triazole, and tetrazole on oxidized copper surfaces: Cu₂O(111) and Cu₂O(111)-w/o-Cu^{CUS}. Physical Chemistry Chemical Physics, 2015, 17, 28602-28615.	1.3	45
19861	Photocatalytic splitting of water on s-triazine based graphitic carbon nitride: an ab initio investigation. Journal of Materials Chemistry A, 2015, 3, 23011-23016.	5.2	53
19862	Ab initio studies on the adsorption and implantation of Al and Fe to nitride materials. Journal of Applied Physics, 2015, 118, 125306.	1.1	4
19863	First-principles study of trimethylamine adsorption on anatase TiO2 nanorod surfaces. Theoretical Chemistry Accounts, 2015, 134, 1.	0.5	7
19864	Combined experimental and theoretical assessments of the lattice dynamics and optoelectronics of TaON and Ta3N5. Journal of Solid State Chemistry, 2015, 229, 219-227.	1.4	88
19865	Multifunctional pure and Eu³⁺ doped Î²-Ag₂MoO₄: photoluminescence, energy transfer dynamics and defect induced properties. Dalton Transactions, 2015, 44, 19097-19110.	1.6	62
19866	Energy transfer dynamics and luminescence properties of Eu³⁺ in CaMoO₄ and SrMoO₄. Dalton Transactions, 2015, 44, 18957-18969.	1.6	137
19867	Vibrational dynamics and band structure of methyl-terminated Ge(111). Journal of Chemical Physics, 2015, 143, 124705.	1.2	3
19868	Ternary intermetallic compounds in Auâ€“Sn soldering systemsâ€”structure and properties. Journal of Materials Science, 2015, 50, 7808-7820.	1.7	10
19869	Full elastic constants of Cu 6 Sn 5 intermetallic by Resonant Ultrasound Spectroscopy (RUS) and ab initio calculations. Scripta Materialia, 2015, 107, 26-29.	2.6	10
19870	Stress-induced phase and structural changes in KDP crystals. Computational Materials Science, 2015, 109, 359-366.	1.4	11
19871	Influence of strain on the properties of CeRuPO and CeOsPO Kondo systems. Journal of Magnetism and Magnetic Materials, 2015, 393, 175-178.	1.0	0
19872	Effects of Co Content in Pd-Skin/PdCo Alloys for Oxygen Reduction Reaction: Density Functional Theory Predictions. Journal of Physical Chemistry C, 2015, 119, 24364-24372.	1.5	20
19873	Experimental and Theoretical Insights into the Hydrogen-Efficient Direct Hydrodeoxygenation Mechanism of Phenol over Ru/TiO₂. ACS Catalysis, 2015, 5, 6509-6523.	5.5	219
19874	Formation and nitrile hydrogenation performance of Ru nanoparticles on a K-doped Al₂O₃ surface. Physical Chemistry Chemical Physics, 2015, 17, 24791-24802.	1.3	24
19875	Magnetic properties in a IIIA-nitride monolayer doped with Cu: a density functional theory investigation. RSC Advances, 2015, 5, 82357-82362.	1.7	10

#	Article	IF	Citations
19876	Ab initio calculations of polarization, piezoelectric constants, and elastic constants of InAs and InP in the wurtzite phase. Journal of Experimental and Theoretical Physics, 2015, 121, 246-249.	0.2	11
19877	The role of alloying element on the behaviors of helium in vanadium: Ti as an example. Computational Condensed Matter, 2015, 3, 1-8.	0.9	7
19878	Unravelling the interplay of dopant concentration and band structure engineering of monoclinic niobium pentoxide: AÂmodelÂphotoanode for water splitting. International Journal of Hydrogen Energy, 2015, 40, 13867-13875.	3.8	22
19879	Ab initio study of domain structures in half-metallic CoTi1âˆ'Mn Sb and thermoelectric CoTi1âˆ'Sc Sb half-Heusler alloys. Journal of Alloys and Compounds, 2015, 650, 728-740.	2.8	13
19880	First-principles calculation of Mg/MgO interfacial free energies. Journal of Alloys and Compounds, 2015, 650, 228-238.	2.8	26
19881	DFT calculations on H, OH and O adsorbate formations on Pt(322) electrode. Journal of Electroanalytical Chemistry, 2015, 757, 116-127.	1.9	15
19882	Electronâ€“phonon interaction and superconductivity in SnAs with the sodium chloride crystal structure. Solid State Communications, 2015, 221, 24-27.	0.9	19
19883	Crystal Structures and Chemical Bonding of Magnesium Carbide at High Pressure. Journal of Physical Chemistry C, 2015, 119, 23168-23174.	1.5	18
19884	Role of Site Stability in Methane Activation on Pd_xCe_{1â€“x}O_{Î´} Surfaces. ACS Catalysis, 2015, 5, 6187-6199.	5.5	69
19885	A novel crystalline SiCO compound. Physical Chemistry Chemical Physics, 2015, 17, 25055-25060.	1.3	7
19886	Surface chemistry of copper metal and copper oxide atomic layer deposition from copper(<scp>ii</scp>) acetylacetonate: a combined first-principles and reactive molecular dynamics study. Physical Chemistry Chemical Physics, 2015, 17, 26892-26902.	1.3	34
19887	Mechanical control of magnetism in oxygen deficient perovskite SrTiO3. Physical Chemistry Chemical Physics, 2015, 17, 27136-27144.	1.3	28
19888	Versatile electronic properties of atomically layered ScO₂. Journal of Materials Chemistry C, 2015, 3, 6627-6644.	2.7	5
19889	Pressure effect on electronic, elastic and optical properties of Eu:CaF₂crystal: a first-principles study. Philosophical Magazine, 2015, 95, 2974-2989.	0.7	4
19890	Functionalized single-walled carbon nanotube (5, 0) as a carrier for isoniazid â€" A tuberculosis drug. International Journal of Computational Materials Science and Engineering, 2015, 04, 1550014.	0.5	3
19891	Enhancement of Visible Light Photocatalytic Activity of SrTiO₃: A Hybrid Density Functional Study. Journal of Physical Chemistry C, 2015, 119, 23503-23514.	1.5	78
19892	Study of morphology effects on magnetic interactions and band gap variations for 3d late transition metal bi-doped ZnO nanostructures by hybrid DFT calculations. Journal of Chemical Physics, 2015, 143, 084309.	1.2	4
19893	Density functional theory for dielectric properties of warm dense matter. Molecular Physics, 2015, , 1-7.	0.8	3

#	Article	IF	Citations
19894	Electronic structure and optical properties of boron-sulfur symmetric codoping in 4 Ã— 4 graphene systems. European Physical Journal B, 2015, 88, 1.	0.6	11
19895	Ab initio study of compositional trends in solid solution strengthening in metals with low Peierls stresses. Acta Materialia, 2015, 98, 367-376.	3.8	23
19896	Ab initio study of GaAs(100) surface stability over As2, H2 and N2 as a model for vapor-phase epitaxy of <mml:math xmlns:mml="http://www.w3.org/1998/Math/MathML" altimg="si0020.gif" overflow="scroll"><mml:msub><mml:mrow><mml:mi>GaAs</mml:mi></mml:mrow><mml:mrow><mml:mn>1</mml:mn><mml:mo>â^' <mathvariant="normal">N</mml:mi></mml:mrow><mml:mrow><mml:mi>x</mml:mi></mml:mrow></mml:msub></mml:math>. Journal of Crystal Growth, 2015, 432, 6-14.	1.7	3
19897	Metal Thiophosphates with Good Mid-infrared Nonlinear Optical Performances: A First-Principles Prediction and Analysis. Journal of the American Chemical Society, 2015, 137, 13049-13059.	6.6	345
19898	A novel surface modification scheme for ITO nanocrystals by acetylene: a combined experimental and DFT study. Physical Chemistry Chemical Physics, 2015, 17, 26740-26744.	1.3	1
19899	Synthesis, structures, and properties of two magnesium silicate fluorides Mg₅(SiO₄)₂F₂and Mg₃SiO₄F₂. New Journal of Chemistry, 2015, 39, 8866-8873.	1.4	11
19900	Structural and electrical behaviour in Bi14YO22.5. RSC Advances, 2015, 5, 83471-83479.	1.7	2
19901	Structure and electronic properties of Cu nanoclusters supported on Mo2C(001) and MoC(001) surfaces. Journal of Chemical Physics, 2015, 143, 114704.	1.2	25
19902	New insight into the helium-induced damage in MAX phase Ti3AlC2 by first-principles studies. Journal of Chemical Physics, 2015, 143, 114707.	1.2	26
19903	A new C=C embedded porphyrin sheet with superior oxygen reduction performance. Nano Research, 2015, 8, 2901-2912.	5.8	35
19904	Influences of Al, Ti and Nb doping on the structure and hydrogen storage property of Mg(BH 4) 2 (001) surface â€“ A theoretical study. International Journal of Hydrogen Energy, 2015, 40, 10516-10526.	3.8	12
19905	Study of the thermodynamic stability of iron at inner core from first-principles theory combined with lattice dynamics. Physics of the Earth and Planetary Interiors, 2015, 248, 12-19.	0.7	7
19906	Phonon softening induced cubic-to-tetragonal phase transition in ReO 3. Physics Letters, Section A: General, Atomic and Solid State Physics, 2015, 379, 2756-2760.	0.9	3
19907	Electronic Structure of Pd Multilayers on Re(0001): The Role of Charge Transfer. Journal of Physical Chemistry C, 2015, 119, 23436-23444.	1.5	37
19908	In Situ Probing of the Active Site Geometry of Ultrathin Nanowires for the Oxygen Reduction Reaction. Journal of the American Chemical Society, 2015, 137, 12597-12609.	6.6	46
19909	Modulation of the electronic property of phosphorene by wrinkle and vertical electric field. Applied Physics Letters, 2015, 107, .	1.5	12
19910	Structural and electronic properties of XSi2 (X = Cr, Mo, and W). Journal of Experimental and Theoretical Physics, 2015, 121, 104-109.	0.2	9
19911	Lithium Intercalation in Graphene/MoS₂ Composites: First-Principles Insights. Journal of Physical Chemistry C, 2015, 119, 25860-25867.	1.5	78

#	Article	IF	Citations
19912	First-Principles Investigation of Mercury Adsorption on the Î±-Fe₂O₃(11Ì…02) Surface. Journal of Physical Chemistry C, 2015, 119, 26512-26518.	1.5	60
19913	A comparison between ab initio calculated and measured Raman spectrum of triclinic albite (NaAlSi₃O₈). Journal of Raman Spectroscopy, 2015, 46, 501-508.	1.2	42
19914	Crotonaldehyde adsorption on Ir(1 1 1), an interesting trans- and cis-configuration transformation. Applied Surface Science, 2015, 357, 369-375.	3.1	9
19915	Computational investigation of NH₃ adsorption and dehydrogenation on a W-modified Fe(111) surface. Physical Chemistry Chemical Physics, 2015, 17, 30598-30605.	1.3	6
19916	MoS₂ supported single platinum atoms and their superior catalytic activity for CO oxidation: a density functional theory study. Journal of Materials Chemistry A, 2015, 3, 23113-23119.	5.2	56
19917	Density-Functional Calculation of Methane Adsorption on Graphenes. IEEE Electron Device Letters, 2015, 36, 1366-1368.	2.2	49
19918	Substituent effects on the croconate dyes in dye sensitized solar cell applications: a density functional theory study. Journal of Molecular Modeling, 2015, 21, 297.	0.8	5
19919	Metal-free graphitic carbon nitride as mechano-catalyst for hydrogen evolution reaction. Journal of Catalysis, 2015, 332, 149-155.	3.1	127
19920	Metastable Ni₇B₃: A New Paramagnetic Boride from Solution Chemistry, Its Crystal Structure and Magnetic Properties. Inorganic Chemistry, 2015, 54, 10873-10877.	1.9	25
19921	Stability of dioctahedral 2:1 phyllosilicate edge structures based on pyrophyllite models. Theoretical Chemistry Accounts, 2015, 134, 1.	0.5	19
19922	Optoelectronic properties of GaN, AlN, and GaAlN alloys. Optik, 2015, 126, 3357-3361.	1.4	13
19923	Electronic, optical and thermal properties of TiCr2 and TiMn2 by ab initio simulations. International Journal of Modern Physics B, 2015, 29, 1550223.	1.0	5
19924	Understanding the adsorption behavior of surface active molecules on ZnO nanostructures by experimental and first-principles calculations. Physical Chemistry Chemical Physics, 2015, 17, 30450-30460.	1.3	15
19925	Structures and electronic properties of GaSe and GaS nanoribbons. RSC Advances, 2015, 5, 94679-94684.	1.7	15
19926	Ab-initio Study of the Structural Stability and Electronic Properties of ZnO Nanowires. , 2015, , .		0
19927	Cation-Mutation Design of Quaternary Nitride Semiconductors Lattice-Matched to GaN. Chemistry of Materials, 2015, 27, 7757-7764.	3.2	23
19928	Ba₃Pt₄Al₄â€”Structure, Properties, and Theoretical and NMR Spectroscopic Investigations of a Complex Platinide Featuring Heterocubane [Pt₄Al₄] Units. Inorganic Chemistry, 2015, 54, 10785-10793.	1.9	23
19929	Linearly Polymerized Benzene Arrays As Intermediates, Tracing Pathways to Carbon Nanothreads. Journal of the American Chemical Society, 2015, 137, 14373-14386.	6.6	86

#	Article	IF	Citations
19930	Transport properties of atomic-size aluminum chains: first principles and nonequilibrium Green's function studies. RSC Advances, 2015, 5, 91288-91294.	1.7	3
19931	Comparative analysis of the electronic structures of mono- and bi-atomic chains of IV, IIIâ€“V and IIâ€“VI group elements calculated using the DFT LCAO and LACW methods. RSC Advances, 2015, 5, 91751-91759.	1.7	6
19932	Materials Design of Visible-Light Ferroelectric Photovoltaics from First Principles. Ferroelectrics, 2015, 483, 1-12.	0.3	27
19933	Analysis of vacancy defects in hybrid graphene-boron nitride armchair nanoribbon based n-MOSFET at ballistic limit. , 2015, , .		0
19934	First-principles calculation of structural, electronic, and optical properties of wurtziteâ€“stannite Cu2MgSi(S Se1â^')4 alloys. Computational and Theoretical Chemistry, 2015, 1074, 163-167.	1.1	2
19935	A new approach to construct bulk and size-dependent continuous binary solution phase diagrams of alloys. RSC Advances, 2015, 5, 96323-96327.	1.7	5
19936	Defect-strain engineering for multiferroic and magnetoelectric properties in epitaxial (110) ferroelectric lead titanate. Physical Review B, 2015, 92, .	1.1	17
19937	Effects of different alloying additives X (X=Si, Al, V, Ti, Mo, W, Nb, Y) on the adhesive behavior of Fe/Cr2O3 interfaces: A first-principles study. Computational Materials Science, 2015, 109, 293-299.	1.4	36
19938	Computation assisted design of favored composition for ternary Mgâ€“Cuâ€“Y metallic glass formation. Physical Chemistry Chemical Physics, 2015, 17, 14879-14889.	1.3	3
19939	Stable Si-based pentagonal monolayers: high carrier mobilities and applications in photocatalytic water splitting. Journal of Materials Chemistry A, 2015, 3, 24055-24063.	5.2	132
19940	Ethylenediamine Grafting on Oxide-Free H-, 1/3 ML F-, and Cl-Terminated Si(111) Surfaces. Chemistry of Materials, 2015, 27, 6268-6281.	3.2	26
19941	Structure and properties of nanostructured NbN and Nb-Si-N films depending on the conditions of deposition: Experiment and theory. Physics of Metals and Metallography, 2015, 116, 1015-1028.	0.3	11
19942	Theoretical prediction of the structural, elastic, mechanical and phonon properties of bismuth telluride under pressure. International Journal of Modern Physics B, 2015, 29, 1550222.	1.0	11
19943	A DFT study of phenol adsorption on a low doping Mnâ€“Ce composite oxide model. Applied Surface Science, 2015, 359, 14-20.	3.1	15
19944	Diffusion in thorium carbide: A first-principles study. Journal of Nuclear Materials, 2015, 467, 572-575.	1.3	7
19945	Nitrogen Activation in a Marsâ€“van Krevelen Mechanism for Ammonia Synthesis on Co₃Mo₃N. Journal of Physical Chemistry C, 2015, 119, 28368-28376.	1.5	135
19946	Polymorphic, Porous, and Hostâ€“Guest Nanostructures Directed by Monolayerâ€“Substrate Interactions: Epitaxial Self-Assembly Study of Cyclic Trinuclear Au(I) Complexes on HOPG at the Solutionâ€“Solid Interface. Journal of Physical Chemistry C, 2015, 119, 24844-24858.	1.5	15
19947	Oxidation and Dissociation of Formyl on Ni(111), Ni(110) and Ni(100) Surfaces: A Comparative Density Functional Theory Study. Topics in Catalysis, 2015, 58, 1136-1149.	1.3	2

#	Article	IF	Citations
19948	On the role of hydrogen filled vacancies on the embrittlement of zirconium: An ab initio investigation. Journal of Nuclear Materials, 2015, 467, 311-319.	1.3	26
19949	Selective Oxidation of 1,2-Propanediol in Alkaline Anion-Exchange Membrane Electrocatalytic Flow Reactors: Experimental and DFT Investigations. ACS Catalysis, 2015, 5, 6926-6936.	5.5	29
19950	Density Functional Theory Study of Active Oxygen at the Perimeter of Au/TiO₂ Catalysts. Journal of Physical Chemistry C, 2015, 119, 25907-25916.	1.5	40
19951	Polymorphs of Theophylline Characterized by DNP Enhanced Solid-State NMR. Molecular Pharmaceutics, 2015, 12, 4146-4153.	2.3	77
19952	Mechanical properties of zirconium alloys and zirconium hydrides predicted from density functional perturbation theory. Dalton Transactions, 2015, 44, 18769-18779.	1.6	60
19953	Adsorption and Deposition of Li₂O₂ on the Pristine and Oxidized TiC Surface by First-principles Calculation. Journal of Physical Chemistry C, 2015, 119, 25684-25695.	1.5	32
19954	Synthesis, and crystal and electronic structure of sodium metal phosphate for use as a hybrid capacitor in non-aqueous electrolyte. Dalton Transactions, 2015, 44, 20108-20120.	1.6	50
19955	Trends of amino acid adsorption onto graphene and graphene oxide surfaces: a dispersion corrected DFT study. RSC Advances, 2015, 5, 92843-92857.	1.7	62
19956	Electronic properties of two-dimensional van der Waals GaS/GaSe heterostructures. Journal of Materials Chemistry C, 2015, 3, 11548-11554.	2.7	66
19957	Far infrared spectra of solid state l-serine, l-threonine, l-cysteine, and l-methionine in different protonation states. Spectrochimica Acta - Part A: Molecular and Biomolecular Spectroscopy, 2015, 150, 301-307.	2.0	22
19958	Interstitial Lithium Diffusion Pathways in Î³-LiAlO₂: A Computational Study. Journal of Physical Chemistry Letters, 2015, 6, 4622-4626.	2.1	29
19959	Enhancement of the thermoelectric properties of MnSb₂Se₄through Cu resonant doping. RSC Advances, 2015, 5, 99065-99073.	1.7	11
19960	Density functional theory study on the reaction between hematite and methane during chemical looping process. Applied Energy, 2015, 159, 132-144.	5.1	77
19961	Reconstructions and stabilities of PbTe(1 1 1) crystal surface from experiments and density-functional theory. Applied Surface Science, 2015, 356, 742-746.	3.1	6
19962	Effect of high bismuth deficiency on structure and oxide ion conductivity of a Bi_{0.55}MoO₄ single crystal. CrystEngComm, 2015, 17, 8746-8751.	1.3	3
19963	Analysis of local molecular motions of aromatic sidechains in proteins by 2D and 3D fast MAS NMR spectroscopy and quantum mechanical calculations. Physical Chemistry Chemical Physics, 2015, 17, 28789-28801.	1.3	19
19964	Magnetism in olivine-type LiCo_{1â^'x}Fe_xPO₄cathode materials: bridging theory and experiment. Physical Chemistry Chemical Physics, 2015, 17, 31202-31215.	1.3	16
19965	The atomic and electronic structure of nitrogen- and boron-doped phosphorene. Physical Chemistry Chemical Physics, 2015, 17, 27210-27216.	1.3	38

#	Article	IF	Citations
19966	An investigation of new infrared nonlinear optical material: BaCdSnSe₄, and three new related centrosymmetric compounds: Ba₂SnSe₄, Mg₂GeSe₄, and Ba₂Ge₂S₆. Dalton Transactions, 2015, 44, 19856-19864.	1.6	67
19967	Benzoic Acid and Phthalic Acid on Atomically Well-Defined MgO(100) Thin Films: Adsorption, Interface Reaction, and Thin Film Growth. Journal of Physical Chemistry C, 2015, 119, 26968-26979.	1.5	22
19968	Carbon nanodot decorated graphitic carbon nitride: new insights into the enhanced photocatalytic water splitting from ab initio studies. Physical Chemistry Chemical Physics, 2015, 17, 31140-31144.	1.3	105
19969	First-Principles Study of Structural and Vibrational Properties of Î±-SiO₂ under Pressure. Applied Mechanics and Materials, 0, 775, 191-196.	0.2	0
19970	A Comparative DFT and DFT+U Study on Magnetism in Nickel-Doped Wurtzite AlN. Journal of Superconductivity and Novel Magnetism, 2015, 28, 3185-3192.	0.8	3
19971	Atomic and electronic structure of the TiN/MgO interface from first principles. Computational Materials Science, 2015, 105, 83-89.	1.4	18
19972	Electronic and magnetic properties of second main-group and second sub-group metals substitution for Al in delafossite CuAlO2. Chemical Physics Letters, 2015, 633, 181-185.	1.2	5
19973	Controllable hydrogen adsorption and desorption by strain modulation on Ti decorated defective graphene. International Journal of Hydrogen Energy, 2015, 40, 12063-12071.	3.8	30
19974	Simulation of He embrittlement at grain boundaries in bcc transition metals. Journal of Nuclear Materials, 2015, 465, 695-701.	1.3	14
19975	Links between the Crystal and Electronic Structure in the New Family of Unconventional Superconductors A2Cr3As3 (A = K, Rb, Cs). Inorganic Chemistry, 2015, 54, 8029-8034.	1.9	18
19976	Six-dimensional quantum dynamics of dissociative chemisorption of H2 on Co(0001) on an accurate global potential energy surface. Physical Chemistry Chemical Physics, 2015, 17, 23346-23355.	1.3	23
19977	Adsorption properties of trifluoroacetic acid on anatase (101) and (001) surfaces: a density functional theory study. Physical Chemistry Chemical Physics, 2015, 17, 23627-23633.	1.3	6
19978	Photocatalytic H₂ generation over In₂TiO₅, Ni substituted In₂TiO₅ and NiTiO₃ â€“ a combined theoretical and experimental study. RSC Advances, 2015, 5, 61218-61229.	1.7	23
19979	Designing electronic anisotropy of three-dimensional carbon allotropes for the all-carbon device. Applied Physics Letters, 2015, 107, 021905.	1.5	2
19980	Ba and Sr Binary Phosphides: Synthesis, Crystal Structures, and Bonding Analysis. Inorganic Chemistry, 2015, 54, 8608-8616.	1.9	31
19981	A study on K2SbF2Cl3 as a new mid-IR nonlinear optical material: new synthesis and excellent properties. Journal of Materials Chemistry C, 2015, 3, 9588-9593.	2.7	41
19982	Optically probing Alâ€”O and Oâ€”H vibrations to characterize water adsorption and surface reconstruction on Î±-alumina: An experimental and theoretical study. Journal of Chemical Physics, 2015, 142, 054704.	1.2	52
19983	The onset of sub-surface oxidation induced by defects in a chemisorbed oxygen layer. Journal of Chemical Physics, 2015, 142, 084701.	1.2	10

#	Article	IF	Citations
19984	Structural properties of Ge on SrTiO3 (001) surface and Ge/SrTiO3 interface. Journal of Applied Physics, 2015, 117, .	1.1	3
19985	Cation ordering and effect of biaxial strain in double perovskite CsRbCaZnCl6. Journal of Applied Physics, 2015, 117, .	1.1	8
19986	Structural stability and electronic properties of InSb nanowires: A first-principles study. Journal of Applied Physics, 2015, 117, .	1.1	6
19987	Elastic anisotropy, vibrational, and thermodynamic properties of U2Ti intermetallic compound with AlB2-type structure under high pressure up to 100â€‰GPa. Journal of Applied Physics, 2015, 117, .	1.1	5
19988	Observing and tuning the density distribution of localized states of monolayer graphene oxide by using external electric field. Applied Physics Letters, 2015, 106, .	1.5	6
19989	Atomic and molecular oxygen adsorbed on (111) transition metal surfaces: Cu and Ni. Journal of Chemical Physics, 2015, 142, 154702.	1.2	52
19990	Diffusion of hydrogen interstitials in the near-surface region of Pd(111) under the influence of surface coverage and external static electric fields. Journal of Chemical Physics, 2015, 142, 154704.	1.2	7
19991	Electronic properties of substitutional impurities in InGaN monolayer quantum wells. Applied Physics Letters, 2015, 106, 192102.	1.5	3
19992	Oxygen vacancy induced magnetization switching in Fe3O4 epitaxial ultrathin films on GaAs(100). Applied Physics Letters, 2015, 106, .	1.5	17
19993	Kinetically induced irreversibility in electro-oxidation and reduction of Pt surface. Journal of Chemical Physics, 2015, 142, 184709.	1.2	21
19994	Optical phonon modes in rhombohedral boron monosulfide under high pressure. Journal of Applied Physics, 2015, 117, .	1.1	13
19995	Stabilization of Pt monolayer catalysts under harsh conditions of fuel cells. Journal of Chemical Physics, 2015, 142, 194710.	1.2	11
19996	Influence of hydrogen surface passivation on Sn segregation, aggregation, and distribution in GeSn/Ge(001) materials. Journal of Applied Physics, 2015, 117, .	1.1	13
19997	Optical properties of alkali halide crystals from all-electron hybrid TD-DFT calculations. Journal of Chemical Physics, 2015, 142, 214705.	1.2	14
19998	Brittle fracture toughnesses of GaN and AlN from first-principles surface-energy calculations. Applied Physics Letters, 2015, 106, .	1.5	21
19999	Electronic structure and transport in graphene/haeckelite hybrids: an ab initio study. 2D Materials, 2015, 2, 035001.	2.0	18
20000	Application of the bounds-analysis approach to arsenic and gallium antisite defects in gallium arsenide. Physical Review B, 2015, 91, .	1.1	8
20001	First-principles modeling of quantum nuclear effects and atomic interactions in solid<mml:math xmlns:mml="http://www.w3.org/1998/Math/MathML"><mml:mmultiscripts><mml:mi mathvariant="normal">He</mml:mi><mml:mprescripts /><mml:none /><mml:mrow><mml:mn>4</mml:mn></mml:mrow></mml:mmultiscripts></mml:math>at high pressure. Physical Review B, 2015, 91, .	1.1	18

#	Article	IF	Citations
20002	Diamond nanowires with nitrogen vacancy under a transverse electric field. Physical Review B, 2015, 91, .	1.1	11
20003	Nitrogen vacancy, self-interstitial diffusion, and Frenkel-pair formation/dissociation in<mml:math xmlns:mml="http://www.w3.org/1998/Math/MathML"><mml:mrow><mml:mi>B</mml:mi><mml:mn>1</mml:mn></mml:mrow></mml:m studied byab initioand classical molecular dynamics with optimized potentials. Physical Review B, 2015, 91, .	1.1	53
20004	Superior magnetic and mechanical property of<mml:math xmlns:mml="http://www.w3.org/1998/Math/MathML"><mml:mrow><mml:msub><mml:mtext>MnFe</mml:mtext><mml:mn by electron correlation and lattice anharmonicity. Physical Review B, 2015, 91, .	1.1	13
20005	Calculation of the graphene C<mml:math xmlns:mml="http://www.w3.org/1998/Math/MathML"><mml:mrow><mml:mn>1</mml:mn><mml:mi>s</mml:mi></mml:mrow></mm level binding energy. Physical Review B, 2015, 91, .	1.1	36
20006	Temperature-dependent lattice dynamics and electronic transitions in<mml:math xmlns:mml="http://www.w3.org/1998/Math/MathML"><mml:mn>0.93</mml:mn><mml:mi mathvariant="normal">P</mml:mi><mml:mtext>b</mml:mtext><mml:mo>(</mml:mo><mml:mrow><mml:msub><mml:mi>Zn</mml:m Physical Review B, 2015, 91, .	1.1	23
20007	Lattice-mismatched heteroepitaxy of IV-VI thin films on PbTe(001): Anab initiostudy. Physical Review B, 2015, 91, .	1.1	7
20008	Energetics of neutral Si dopants in InGaAs: Anab initioand semiempirical Tersoff model study. Physical Review B, 2015, 91, .	1.1	11
20009	Polaronic deformation at the<mml:math xmlns:mml="http://www.w3.org/1998/Math/MathML"><mml:msup><mml:mtext>Fe</mml:mtext><mml:mrow><mml:mn>2</mml:mn> site in<mml:math xmlns:mml="http://www.w3.org/1998/Math/MathML"><mml:msub><mml:mtext>Fe:LiNbO</mml:mtext><mml:mn>3</mml:mn></mml:m Physical Review B, 2015, 91, .	1.1	33
20010	Interface formation for a ferromagnetic/antiferromagnetic bilayer system studied by scanning tunneling microscopy and first-principles theory. Physical Review B, 2015, 91, .	1.1	13
20011	Switchable conductivity at the ferroelectric interface: Nonpolar oxides. Physical Review B, 2015, 91, .	1.1	78
20012	Exciton binding energies and luminescence of phosphorene under pressure. Physical Review B, 2015, 91, .	1.1	48
20013	The Effects of a Low-Level Boron, Phosphorus, and Nitrogen Doping on the Oxygen Reduction Activity of Ordered Mesoporous Carbons. Electrocatalysis, 2015, 6, 498-511.	1.5	35
20014	The electronic and magnetic properties of B-doping Stoneâ€“Wales defected graphene decorated with transition-metal atoms. Physica E: Low-Dimensional Systems and Nanostructures, 2015, 73, 257-261.	1.3	5
20015	High-Pressure Synthesis of Novel Boron Oxynitride B6N4O3 with Sphalerite Type Structure. Chemistry of Materials, 2015, 27, 5907-5914.	3.2	22
20016	First-Principles Evaluation of the Alkali and/or Alkaline Earth Beryllium Borates in Deep Ultraviolet Nonlinear Optical Applications. ACS Photonics, 2015, 2, 1183-1191.	3.2	117
20017	Self-assembled two-dimensional nanoporous molecular arrays and photoinduced polymerization of 4-bromo-4â€²-hydroxybiphenyl on Ag(111). Journal of Chemical Physics, 2015, 142, 101902.	1.2	21
20018	Sensitivity of CoSi2 precipitation in silicon to extra-low dopant concentrations. II. First-principles calculations. Journal of Applied Physics, 2015, 117, 045704.	1.1	2
20019	Electronic and magnetic properties of zigzag silicene nanoribbons with Stoneâ€“Wales defects. Journal of Applied Physics, 2015, 117, .	1.1	16

#	Article	IF	Citations
20020	Dirac points and van Hove singularities of silicene under uniaxial strain. Journal of Applied Physics, 2015, 117, 164305.	1.1	14
20021	The temperature-dependent diffusion coefficient of helium in zirconium carbide studied with first-principles calculations. Journal of Applied Physics, 2015, 117, .	1.1	13
20022	Ba2TeO as an optoelectronic material: First-principles study. Journal of Applied Physics, 2015, 117, 195705.	1.1	3
20023	Theoretical studies of the work functions of Pd-based bimetallic surfaces. Journal of Chemical Physics, 2015, 142, 214706.	1.2	17
20024	First-principles theory of field-effect doping in transition-metal dichalcogenides: Structural properties, electronic structure, Hall coefficient, and electrical conductivity. Physical Review B, 2015, 91, .	1.1	127
20025	Phonon properties, thermal expansion, and thermomechanics of silicene and germanene. Physical Review B, 2015, 91, .	1.1	96
20026	Theoretical investigation of dielectric properties of rare earth stillwellite compounds. International Journal of Modern Physics B, 2015, 29, 1550154.	1.0	0
20027	First principles study of normal and fast diffusing metallic impurities in hcp titanium. Computational Materials Science, 2015, 109, 380-387.	1.4	9
20028	Structural, energetic and electronic properties of (100) surfaces for alkaline earth metal oxides as calculated with hybrid density functional theory. Surface Science, 2015, 642, 58-65.	0.8	18
20029	Cobalt Spinel at Various Redox Conditions: DFT+U Investigations into the Structure and Surface Thermodynamics of the (100) Facet. Journal of Physical Chemistry C, 2015, 119, 19180-19191.	1.5	59
20030	Magnetization of ternary alloys based on Fe0.65Ni0.35 invar with 3d transition metal additions: An ab initio study. Journal of Applied Physics, 2015, 117, .	1.1	7
20031	Phonon scattering limited performance of monolayer MoS2 and WSe2 n-MOSFET. AIP Advances, 2015, 5, .	0.6	20
20032	Pressure effect on structural, elastic, and thermodynamic properties of tetragonal B4C4. AIP Advances, 2015, 5, .	0.6	8
20033	Ferroelectricity in high-density H2O ice. Journal of Chemical Physics, 2015, 142, 134501.	1.2	6
20034	A comparative ab initio study of superconductivity in the body centered tetragonal YC2 and LaC2. Journal of Applied Physics, 2015, 117, .	1.1	15
20035	Towards a predictive route for selection of doping elements for the thermoelectric compound PbTe from first-principles. Journal of Applied Physics, 2015, 117, 175102.	1.1	16
20036	The perturbation energy: A missing key to understand the â€œnoblenessâ€•of bulk gold. Journal of Chemical Physics, 2015, 142, 194705.	1.2	6
20037	First principles-based multiparadigm, multiscale strategy for simulating complex materials processes with applications to amorphous SiC films. Journal of Chemical Physics, 2015, 142, 174703.	1.2	10

#	Article	IF	Citations
20038	A periodic energy decomposition analysis method for the investigation of chemical bonding in extended systems. Journal of Chemical Physics, 2015, 142, 194105.	1.2	82
20039	Temperature-dependence of structural and mechanical properties of TiB2: A first principle investigation. Journal of Applied Physics, 2015, 117, .	1.1	33
20040	Theoretical investigations of the structural, electronic and optical properties of Hg_{1â^'x}Cd_xTe alloys. Philosophical Magazine, 2015, 95, 2466-2481.	0.7	11
20041	Piezoelectric coefficients and spontaneous polarization of ScAlN. Journal of Physics Condensed Matter, 2015, 27, 245901.	0.7	209
20042	Comment on â€œStructural, elastic, electronic, magnetic and optical properties of RbSrX (C, Sl, Ge) half-Heusler compoundsâ€• Journal of Magnetism and Magnetic Materials, 2015, 396, 219-221.	1.0	9
20043	A DFT+U study of A-site and B-site substitution in BaFeO_{3â^'Î´}. Physical Chemistry Chemical Physics, 2015, 17, 23511-23520.	1.3	46
20044	Chemical interaction of water molecules with framework Al in acid zeolites: a periodic ab initio study on H-clinoptilolite. Physical Chemistry Chemical Physics, 2015, 17, 23657-23666.	1.3	9
20045	The accessibility of nitrogen sites makes a difference in selective CO2 adsorption of a family of isostructural metalâ€“organic frameworks. Journal of Materials Chemistry A, 2015, 3, 19417-19426.	5.2	80
20046	Structural stability, vibrational, and bonding properties of potassium 1, 1â€²-dinitroamino-5, 5â€²-bistetrazolate: An emerging green primary explosive. Journal of Chemical Physics, 2015, 143, 064508.	1.2	8
20047	Hexagonal Boron Nitride with Designed Nanopores as a High-Efficiency Membrane for Separating Gaseous Hydrogen from Methane. Journal of Physical Chemistry C, 2015, 119, 19826-19831.	1.5	71
20048	Ab initio design of CsSn(XxY 1â^'x)3 (X and Y = Cl, Br, and I) perovskites for photovoltaics. AIP Advances, 2015, 5, .	0.6	17
20049	Electronic and optical properties of zinc-blende GeC by first principles study. Modern Physics Letters B, 2015, 29, 1550103.	1.0	0
20050	On the possibility of contact-induced spin polarization in interfaces of armchair nanotubes with transition metal substrates. Journal of Magnetism and Magnetic Materials, 2015, 396, 102-105.	1.0	2
20051	Relationship between Carbon Nitride Structure and Exciton Binding Energies: A DFT Perspective. Journal of Physical Chemistry C, 2015, 119, 25188-25196.	1.5	104
20052	SnS44â€“, SbS43â€“, and AsS33â€“ Metal Chalcogenide Surface Ligands: Couplings to Quantum Dots, Electron Transfers, and All-Inorganic Multilayered Quantum Dot Sensitized Solar Cells. Journal of the American Chemical Society, 2015, 137, 13827-13835.	6.6	32
20053	The transition metal surface passivated edges of hexagonal boron nitride (h-BN) and the mechanism of h-BN's chemical vapor deposition (CVD) growth. Physical Chemistry Chemical Physics, 2015, 17, 29327-29334.	1.3	51
20054	Periodic DFT investigation of methanol coverage on surfaces of MgCl 2 -supported Zieglerâ€“Natta catalysts. Applied Surface Science, 2015, 356, 967-971.	3.1	6
20055	Effect of lithium and sodium ion adsorption on the electronic transport properties of Ti3C2 MXene. Applied Surface Science, 2015, 359, 153-157.	3.1	50

#	Article	IF	Citations
20056	Effect of Mg doping on the structural and electrochemical performance of LiNi0.6Co0.2Mn0.2O2 cathode materials. Electrochimica Acta, 2015, 182, 795-802.	2.6	149
20057	Protons in Oxysulfides, Oxysulfates, and Sulfides: A First-Principles Study of La₂O₂S, La₂O₂SO₄, SrZrS₃, and BaZrS₃. Journal of Physical Chemistry C, 2015, 119, 23875-23882.	1.5	23
20058	Reactive Oxygen Species on the (100) Facet of Cobalt Spinel Nanocatalyst and their Relevance in ¹⁶O₂/¹⁸O₂ Isotopic Exchange, deN₂O, and deCH₄ Processesâ€"A Theoretical and Experimental Account. ACS Catalysis, 2015, 5, 6879-6892.	5.5	71
20059	Atomic Disorders Induced by Silver and Magnesium Ion Migrations Favor High Thermoelectric Performance in Î±â€²MgAgSbâ€Based Materials. Advanced Functional Materials, 2015, 25, 6478-6488.	7.8	70
20060	Charge carrier transport and separation in pristine and nitrogen-doped graphene nanowiggle heterostructures. Carbon, 2015, 95, 833-842.	5.4	16
20061	A density functional theory study of CO oxidation on CuO1-x(111). Journal of Molecular Modeling, 2015, 21, 195.	0.8	17
20062	Stabilities and mechanical and electronic properties on BN doped zigzag single-wall carbon nanotubes. Solid State Communications, 2015, 223, 28-31.	0.9	3
20063	Self-association of organic solutes in solution: a NEXAFS study of aqueous imidazole. Faraday Discussions, 2015, 179, 269-289.	1.6	35
20064	First Principles Study of Electronic Structure, Magnetic, and Mechanical Properties of Transition Metal Monoxides TMO(TM=Co and Ni). Zeitschrift Fur Naturforschung - Section A Journal of Physical Sciences, 2015, 70, 797-804.	0.7	11
20065	First-Principles Study of Electronic, Elastic, and Optical Properties of Yb:CaF₂ Crystals. Zeitschrift Fur Naturforschung - Section A Journal of Physical Sciences, 2015, 70, 889-896.	0.7	3
20066	First-principles investigation on the magnetism of low-concentration 3d (Cr, Mn, Fe Co, Ni)-doped BeTe semiconductors. Computational Condensed Matter, 2015, 5, 14-18.	0.9	3
20067	Mechanical Properties from Periodic Plane Wave Quantum Mechanical Codes: The Challenge of the Flexible Nanoporous MIL-47(V) Framework. Journal of Physical Chemistry C, 2015, 119, 23752-23766.	1.5	37
20068	Effect of Boron Modifications of Palladium Catalysts for the Production of Hydrogen from Formic Acid. ACS Catalysis, 2015, 5, 6579-6586.	5.5	88
20069	Structural, Thermodynamic, Elastic, and Electronic Properties of Î±-SnS at High Pressure from First-Principles Investigations. Zeitschrift Fur Naturforschung - Section A Journal of Physical Sciences, 2015, 70, 949-960.	0.7	2
20070	Semiconductor Behavior of a Three-Dimensional Strontium-Based Metalâ€"Organic Framework. ACS Applied Materials & Interfaces, 2015, 7, 22767-22774.	4.0	71
20071	Theoretical prediction of silicene as a new candidate for the anode of lithium-ion batteries. Physical Chemistry Chemical Physics, 2015, 17, 29689-29696.	1.3	63
20072	(Sub)surface-Promoted Disproportionation and Absolute Band Alignment in High-Power LiMn₂O₄ Cathodes. Journal of Physical Chemistry C, 2015, 119, 21358-21368.	1.5	29
20073	Investigation of stable germane structures under high-pressure. Physical Chemistry Chemical Physics, 2015, 17, 27630-27635.	1.3	16

#	Article	IF	Citations
20074	Direct versus hydrogen-assisted CO dissociation over stepped Ni and Ni₃Fe surfaces: a computational investigation. Physical Chemistry Chemical Physics, 2015, 17, 29616-29627.	1.3	17
20075	Electronic structures of in-plane two-dimensional transition-metal dichalcogenide heterostructures. Physical Chemistry Chemical Physics, 2015, 17, 29380-29386.	1.3	34
20076	Solid-state chemistry of glassy antimony oxides. Journal of Materials Chemistry C, 2015, 3, 11349-11356.	2.7	12
20077	CO₂ Electroreduction Performance of Transition Metal Dimers Supported on Graphene: A Theoretical Study. ACS Catalysis, 2015, 5, 6658-6664.	5.5	227
20078	Structural properties, phase stability, elastic properties and electronic structures of Cuâ€“Ti intermetallics. Philosophical Magazine, 2015, 95, 3535-3553.	0.7	29
20079	Vacancy effects on the electronic structure of MgO compound. Modern Physics Letters B, 2015, 29, 1550147.	1.0	5
20080	The first principle study: Electronic and optical properties in Bi2Se3. Computational Condensed Matter, 2015, 4, 59-63.	0.9	37
20081	Vacancy induced magnetism in N-doped 4Hâ€“SiC by first-principle calculations. Solid State Sciences, 2015, 49, 78-82.	1.5	12
20082	Structural and Electronic Features of Î²-Ni(OH)₂ and Î²-NiOOH from First Principles. Journal of Physical Chemistry C, 2015, 119, 24315-24322.	1.5	145
20083	New Phosphorene Allotropes Containing Ridges with 2- and 4-Coordination. Journal of Physical Chemistry C, 2015, 119, 24674-24680.	1.5	37
20084	Origin of the highly anisotropic thermal expansion of the semiconducting ZnSb and relations with its thermoelectric applications. RSC Advances, 2015, 5, 87118-87131.	1.7	10
20085	Adhesion strength and nucleation thermodynamics of four metals (Al, Cu, Ti, Zr) on AlN substrates. Applied Surface Science, 2015, 357, 8-13.	3.1	28
20086	Imaging and spectrum of monolayer graphene oxide in external electric field. Carbon, 2015, 93, 843-850.	5.4	16
20087	Band structure of graphene modulated by Ti or N dopants and applications in gas sensoring. Journal of Molecular Graphics and Modelling, 2015, 61, 224-230.	1.3	24
20088	Heâ€“He and Heâ€“metal interactions in transition metals from first-principles. Journal of Nuclear Materials, 2015, 467, 465-471.	1.3	25
20089	DFT-based ab initio MD simulation of the ionic conduction in doped ZrO₂systems under epitaxial strain. Physical Chemistry Chemical Physics, 2015, 17, 29057-29063.	1.3	21
20090	A novel theoretical design of electronic structure and half-metallic ferromagnetism in the 3d (V)-doped rock-salts SrS, SrSe, and SrTe for spintronics. RSC Advances, 2015, 5, 92328-92334.	1.7	32
20091	Superconductivity in CaSn₃ single crystals with a AuCu₃-type structure. Journal of Materials Chemistry C, 2015, 3, 11432-11438.	2.7	22

#	Article	IF	Citations
20092	Charge Modulation in Graphitic Carbon Nitride as a Switchable Approach to Highâ€Capacity Hydrogen Storage. ChemSusChem, 2015, 8, 3626-3631.	3.6	37
20093	Guaiacol Hydrodeoxygenation over Platinum Catalyst: Reaction Pathways and Kinetics. Industrial & Engineering Chemistry Research, 2015, 54, 10638-10644.	1.8	88
20094	Bâ€“N@Graphene: Highly Sensitive and Selective Gas Sensor. Journal of Physical Chemistry C, 2015, 119, 24827-24836.	1.5	112
20095	Design of a polypyrrole MIP-SAW sensor for selective detection of flumequine in aqueous media. Correlation between experimental results and DFT calculations. RSC Advances, 2015, 5, 88666-88674.	1.7	38
20096	Equation of state and elasticity of the 3.65 Ã... phase: Implications for the X-discontinuity. American Mineralogist, 2015, 100, 2199-2208.	0.9	17
20097	Adsorptions of SO2, SOF2, and SO2F2 on Pt-modified anatase (101) surface: Sensing mechanism study. Applied Surface Science, 2015, 353, 662-669.	3.1	12
20098	Adsorption of F2CCFCl on TiO2 nano-powder: Structures, energetics and vibrational properties from DRIFT spectroscopy and periodic quantum chemical calculations. Applied Surface Science, 2015, 353, 986-994.	3.1	28
20099	A first principle study on the magnetic properties of Cu2O surfaces. Current Applied Physics, 2015, 15, 1303-1311.	1.1	23
20100	Density functional theories study on the properties of Ga1â^'xCrxAs. Materials and Design, 2015, 87, 877-882.	3.3	4
20101	DFT predictions of ferromagnetism in the AlC 0.0625 N 0.9375 and AlC 0.125 N 0.875 compounds. Results in Physics, 2015, 5, 281-285.	2.0	8
20102	Highly Selective Colorimetric and Luminescence Response of a Square-Planar Platinum(II) Terpyridyl Complex to Aqueous TcO₄^{â€“}. Inorganic Chemistry, 2015, 54, 9914-9923.	1.9	39
20103	Core/Shell Face-Centered Tetragonal FePd/Pd Nanoparticles as an Efficient Non-Pt Catalyst for the Oxygen Reduction Reaction. ACS Nano, 2015, 9, 11014-11022.	7.3	165
20104	Exploring three-dimensional orbital imaging with energy-dependent photoemission tomography. Nature Communications, 2015, 6, 8287.	5.8	76
20105	Structural and electrochemical properties of Mg-doped nickel based cathode materials LiNi_{0.6}Co_{0.2}Mn_{0.2â^'x}Mg_xO₂for lithium ion batteries. RSC Advances, 2015, 5, 88773-88779.	1.7	47
20106	Study of the electronic structure of Ag, Au, Pt and Pd clusters adsorption on graphene and their effect on conductivity. European Physical Journal B, 2015, 88, 1.	0.6	27
20107	Adsorption-site dependence of electronic and magnetic properties of hydrogen impurities on bilayer graphene. International Journal of Modern Physics B, 2015, 29, 1550198.	1.0	0
20108	Elastic, lattice dynamical and thermal properties of zinc-blende CdSe x Te 1â^' x ternary alloys. Chemical Physics, 2015, 457, 147-151.	0.9	10
20109	Ab-initio calculations of physical properties of alkali chloride XCl (XÂ=ÂK, Rb and Li) under pressure. Computational Condensed Matter, 2015, 4, 6-12.	0.9	14

#	Article	IF	Citations
20110	An ab initio study of oxide ion dynamics in type-II Bi3NbO7. Journal of Materials Chemistry A, 2015, 3, 21882-21890.	5.2	4
20111	Thermodynamic Modeling of the Niâ€“H System. Journal of Physical Chemistry C, 2015, 119, 24546-24557.	1.5	6
20112	Dopants Control Electronâ€“Hole Recombination at Perovskiteâ€“TiO₂ Interfaces: Ab Initio Time-Domain Study. ACS Nano, 2015, 9, 11143-11155.	7.3	108
20113	Theoretical model of the interaction of glycine with hydrogenated amorphous carbon (HAC). Physical Chemistry Chemical Physics, 2015, 17, 28966-28976.	1.3	6
20114	Strain-induced semimetal-to-semiconductor transition and indirect-to-direct band gap transition in monolayer 1T-TiS₂. RSC Advances, 2015, 5, 83876-83879.	1.7	34
20115	An integrated cobalt disulfide (CoS₂) co-catalyst passivation layer on silicon microwires for photoelectrochemical hydrogen evolution. Journal of Materials Chemistry A, 2015, 3, 23466-23476.	5.2	68
20116	Synthesis, characterization and modelling of zinc and silicate co-substituted hydroxyapatite. Journal of the Royal Society Interface, 2015, 12, 20150190.	1.5	41
20117	Using density functional theory to engineer direct gap germanium-tin alloy. , 2015, , .		2
20118	Interaction of hydrogen with impurities in group IVB metals. Physics of the Solid State, 2015, 57, 1921-1931.	0.2	5
20119	Pressure-induced vibrational and superconducting properties of lanthanum hydrides from first principles calculations. Canadian Journal of Physics, 2015, 93, 1630-1637.	0.4	2
20120	Effects of B and Al on tensile strengths and electronic structure of CuZr: A first-principles study. Computational Condensed Matter, 2015, 5, 1-6.	0.9	1
20121	First-principles study on the structural, electronic and magnetic properties of the Ti2VZ (ZÂ=ÂSi, Ge, Sn) full-Heusler compounds. Materials Chemistry and Physics, 2015, 164, 177-182.	2.0	21
20122	Structural Evolution in Methylammonium Lead Iodide CH₃NH₃PbI₃. Journal of Physical Chemistry A, 2015, 119, 11033-11038.	1.1	66
20123	2D Electrides as Promising Anode Materials for Na-Ion Batteries from First-Principles Study. ACS Applied Materials & Interfaces, 2015, 7, 24016-24022.	4.0	181
20124	A Thermally Stable Crâ€“Cu Nanostructure Embedded in the CeO₂ Surface as a Substitute for Platinum-Group Metal Catalysts. ACS Catalysis, 2015, 5, 6738-6747.	5.5	51
20125	Electronic Structure Modification of Ion Implanted Graphene: The Spectroscopic Signatures of p- and n-Type Doping. ACS Nano, 2015, 9, 11398-11407.	7.3	75
20126	Experimental and theoretical studies of optical and nonlinear optical properties for MnTeMoO 6 crystal. Journal of Alloys and Compounds, 2015, 651, 585-589.	2.8	18
20127	Hydrogen Dissociative Adsorption on Lanthana: Polaron Formation and the Role of Acidâ€“Base Interactions. Journal of Physical Chemistry C, 2015, 119, 19876-19882.	1.5	22

#	Article	IF	Citations
20128	Flexible structural and electronic properties of a pentagonal B₂C monolayer via external strain: a computational investigation. Physical Chemistry Chemical Physics, 2015, 17, 24151-24156.	1.3	127
20129	Ab initio thermodynamics of the CoCrFeMnNi high entropy alloy: Importance of entropy contributions beyond the configurational one. Acta Materialia, 2015, 100, 90-97.	3.8	389
20130	Theoretical insights on the influence of doped Ni in the early stage of graphene growth during the CH4 dissociation on Niâ€“Cu(111) surface. Applied Catalysis A: General, 2015, 506, 1-7.	2.2	14
20131	Transition metal adatoms on graphene: A systematic density functional study. Carbon, 2015, 95, 525-534.	5.4	144
20132	Two-dimensional octagon-structure monolayer of nitrogen group elements and the related nano-structures. Computational Materials Science, 2015, 110, 109-114.	1.4	36
20133	Electronic structure and soft magnetic properties of Se/FeSiAl (110) films. Applied Surface Science, 2015, 354, 401-407.	3.1	8
20134	Mechanical and electronic properties of Ca1â^'Mg O alloys. Materials Science in Semiconductor Processing, 2015, 40, 676-684.	1.9	18
20135	Dislocation modelling in Ti₂AlN MAX phase based on the Peierlsâ€“Nabarro model. Philosophical Magazine, 2015, 95, 2539-2552.	0.7	27
20136	Structure and electronic properties of GaN tubelike clusters and single-walled GaN nanotubes. International Journal of Modern Physics B, 2015, 29, 1550116.	1.0	8
20137	Al-dopedZnONanostructured Thin Films: Density Functional Theory and Experiment. International Journal of Nanoscience, 2015, 14, 1550015.	0.4	1
20138	An ab-initio study of CuInSe2 based ordered defect compounds. Materials Chemistry and Physics, 2015, 162, 372-379.	2.0	0
20139	Novel electronic properties in silicene on MoSe2 monolayer: An excellent prediction for FET. Materials Chemistry and Physics, 2015, 164, 150-156.	2.0	23
20140	Improved Ammonolytic Synthesis, Structure Determination, Electronic Structure, and Magnetic Properties of the Solid Solution Sn_xFe_{4â€“x}N (0 â‰¤ x â‰¤ 0.9). Inorganic Chemistry, 2015, 54, 8800-8807.	1.9	20
20141	Adsorption and interaction of CO₂ on rutile TiO₂(110) surfaces: a combined UHV-FTIRS and theoretical simulation study. Physical Chemistry Chemical Physics, 2015, 17, 23994-24000.	1.3	25
20142	Revealing the local properties ofÎ²-HP₄N₇, a promising candidate for high pressure synthesis of new materials. Materials Research Express, 2015, 2, 045904.	0.8	0
20143	Structural transformations among austenite, ferrite and cementite in Feâ€“C alloys: A unified theory based on ab initio simulations. Acta Materialia, 2015, 99, 281-289.	3.8	59
20144	A first-principles study of light non-metallic atom substituted blue phosphorene. Applied Surface Science, 2015, 356, 110-114.	3.1	95
20145	Chemisorption of benzene on Pt (1 1 1) surface: A DFT study with van der Waals interaction. Chemical Physics Letters, 2015, 637, 182-188.	1.2	15

#	Article	IF	Citations
20146	Applicability of special quasi-random structure models in thermodynamic calculations using semi-empirical Debyeâ€“GrÃ¼neisen theory. Journal of Alloys and Compounds, 2015, 650, 564-571.	2.8	16
20147	Structural Transition in Layered As_{1â€“x}P_x Compounds: A Computational Study. Nano Letters, 2015, 15, 6042-6046.	4.5	74
20148	From Graphene Nanoribbons on Cu(111) to Nanographene on Cu(110): Critical Role of Substrate Structure in the Bottom-Up Fabrication Strategy. ACS Nano, 2015, 9, 8997-9011.	7.3	127
20149	A theoretical guide for fabricating a conductive molecular wire on a silicon surface via an in situ surface polymerization reaction. Nanoscale, 2015, 7, 15277-15283.	2.8	4
20150	A first-principles study of Pt thin films on SrTiO3(100): Support effects on CO adsorption. Journal of Chemical Physics, 2015, 142, 124704.	1.2	13
20151	First-Principles Calculations of the Quantum Size Effects on the Stability and Reactivity of Ultrathin Ru(0001) Films. Chinese Physics Letters, 2015, 32, 067302.	1.3	1
20152	Solution-combustion synthesized aluminium-doped spinel (LiAl x Mn2â^'x O4) as a high-performance lithium-ion battery cathode material. Applied Physics A: Materials Science and Processing, 2015, 121, 51-57.	1.1	16
20153	Ab initio hybrid DFT calculations of BaTiO3, PbTiO3, SrZrO3 and PbZrO3 (111) surfaces. Applied Surface Science, 2015, 358, 556-562.	3.1	83
20154	Spin States of 2D Nanocomposites of Ni and V Nanoclusters on Hexagonal h-BN, BC3 and Graphene. Journal of Materials Science and Technology, 2015, 31, 979-985.	5.6	1
20155	Novel <mml:math altimg="si1.gif" overflow="scroll" xmlns:xocs="http://www.elsevier.com/xml/xocs/dtd" xmlns:xs="http://www.w3.org/2001/XMLSchema" xmlns:xsi="http://www.w3.org/2001/XMLSchema-instance" xmlns="http://www.elsevier.com/xml/ja/dtd" xmlns:ja="http://www.elsevier.com/xml/ja/dtd" xmlns:mml="http://www.w3.org/1998/Math/MathML" xmlns:tb="http://www.elsevier.com/xml/common/table/dtd" xmlns:sb="http://www.elsevier.com/xml/common/struct-bib/dtd" xmlns:ce="http://www.elsevier.com/x	0.9	2
20156	Discovery of Î³-MnP₄ and the Polymorphism of Manganese Tetraphosphide. Inorganic Chemistry, 2015, 54, 8761-8768.	1.9	8
20157	Characterization of AlPO₄(110) Surface in Adsorption of Rh Dimer and Its Comparison with Î³-Al₂O₃(100) Surface: A Theoretical Study. Journal of Physical Chemistry C, 2015, 119, 19752-19762.	1.5	17
20158	Understanding Deviations in Hydrogen Solubility Predictions in Transition Metals through First-Principles Calculations. Journal of Physical Chemistry C, 2015, 119, 19642-19653.	1.5	31
20159	Trapping and Characterization of a Single Hydrogen Molecule in a Continuously Tunable Nanocavity. Journal of Physical Chemistry Letters, 2015, 6, 3453-3457.	2.1	21
20160	Antagonism between Spinâ€“Orbit Coupling and Steric Effects Causes Anomalous Band Gap Evolution in the Perovskite Photovoltaic Materials CH₃NH₃Sn_{1â€“x}Pb_xI₃. Journal of Physical Chemistry Letters, 2015, 6, 3503-3509.	2.1	202
20161	Nature of Rutile Nuclei in Anatase-to-Rutile Phase Transition. Journal of the American Chemical Society, 2015, 137, 11532-11539.	6.6	106
20162	Re-examining the Chevrel phase Mo₆S₈ cathode for Mg intercalation from an electronic structure perspective. Physical Chemistry Chemical Physics, 2015, 17, 22548-22551.	1.3	49
20163	Chirality control of nonplanar lead phthalocyanine (PbPc) and its potential application in high-density storage: a theoretical investigation. Physical Chemistry Chemical Physics, 2015, 17, 23651-23656.	1.3	9

#	Article	IF	Citations
20164	Local environments of boron heteroatoms in non-crystalline layered borosilicates. Physical Chemistry Chemical Physics, 2015, 17, 21664-21682.	1.3	11
20165	Enhanced photocatalytic H₂-evolution by immobilizing CdS nanocrystals on ultrathin Co_{0.85}Se/RGOâ€“PEI nanosheets. Journal of Materials Chemistry A, 2015, 3, 18711-18717.	5.2	51
20166	Band gap control and transformation of monolayer-MoS₂-based hetero-bilayers. Journal of Materials Chemistry C, 2015, 3, 9403-9411.	2.7	30
20167	Optical conductivity of partially oxidized graphene from first principles. Journal of Applied Physics, 2015, 118, 014304.	1.1	10
20168	First-principles study of electronic, dynamical and thermodynamic properties of Î³-Li4SiO4. International Journal of Modern Physics B, 2015, 29, 1550128.	1.0	3
20169	Insights into the Nature of Formate Species in the Decomposition and Reaction of Methanol over Cerium Oxide Surfaces: A Combined Infrared Spectroscopy and Density Functional Theory Study. Journal of Physical Chemistry C, 2015, 119, 21452-21464.	1.5	47
20170	Inserting Tin or Antimony Atoms into Mg2Si: Effect on the Electronic and Thermoelectric Properties. Journal of Electronic Materials, 2015, 44, 4452-4464.	1.0	5
20171	A first-principles study of cementite (Fe3C) and its alloyed counterparts: Structural properties, stability, and electronic structure. Computational Materials Science, 2015, 110, 169-181.	1.4	34
20172	Chemisorbed oxygen atom on the activation of Câ€“H bond in methane: a Rh model study. RSC Advances, 2015, 5, 66221-66230.	1.7	10
20173	Tunable electronic structures in the two-dimension SnX 2 (X = S and Se) nanosheets by stacking effects. Applied Surface Science, 2015, 356, 1200-1206.	3.1	17
20174	Behavior of fission gases in nuclear fuel: XAS characterization of Kr in UO2. Journal of Nuclear Materials, 2015, 466, 379-392.	1.3	22
20175	Structural Phase Stability Control of Monolayer MoTe₂ with Adsorbed Atoms and Molecules. Journal of Physical Chemistry C, 2015, 119, 21674-21680.	1.5	74
20176	Isoxazolone-based single crystals with large second harmonic generation effect. CrystEngComm, 2015, 17, 7316-7322.	1.3	18
20177	Theoretical study of hydration in Y2Mo3O12: Effects on structure and negative thermal expansion. AIP Advances, 2015, 5, .	0.6	17
20178	Chemical trends of stability and band alignment of lattice-matched II-VI/III-V semiconductor interfaces. Physical Review B, 2015, 91, .	1.1	21
20179	The effect of oxygen vacancy on holes-induced d0 magnetism in CaTiO3 and CaZrO3. Modern Physics Letters B, 2015, 29, 1550137.	1.0	3
20180	Ultrahigh-Capacity Molecular Hydrogen Storage of a Lithium-Decorated Boron Monolayer. Journal of Physical Chemistry C, 2015, 119, 19681-19688.	1.5	49
20181	The electronic structure, mechanical and thermodynamic properties of Mo2XB2 and MoX2B4 (Xâ€‰=â€‰Fe,) Tj ETQq1 1 0.784314 rg	1.1	32

#	Article	IF	Citations
20182	Ab initiostudy of Ga-GaN system: Transition from adsorbed metal atoms to a metalâ€“semiconductor junction. Journal of Vacuum Science and Technology A: Vacuum, Surfaces and Films, 2015, 33, 061101.	0.9	5
20183	Hydrogen Isotopic Effects of Uranium Hydrides: First-Principles Calculations. Materials Science Forum, 2015, 817, 675-684.	0.3	1
20184	Band gap engineering of graphenylene by hydrogenation and halogenation: a density functional theory study. RSC Advances, 2015, 5, 70766-70771.	1.7	26
20185	Systematic study of finite-size effects in quantum Monte Carlo calculations of real metallic systems. Journal of Chemical Physics, 2015, 143, 102807.	1.2	26
20186	First-principles study on the band structure, magnetic and elastic properties of half-metallic Cr2MnAl. Modern Physics Letters B, 2015, 29, 1550139.	1.0	14
20187	Uranyl Carboxyphosphonates Derived from Hydrothermal in Situ Ligand Reaction: Syntheses, Structures, and Computational Investigations. Inorganic Chemistry, 2015, 54, 8617-8624.	1.9	24
20188	Band Gap on/off Switching of Silicene Superlattice. Journal of Physical Chemistry C, 2015, 119, 20747-20754.	1.5	21
20189	O-O bonding stabilized zinc vacancy as origin of p-type doping on Î£7 ZnO grain boundary. Journal of Applied Physics, 2015, 118, 045708.	1.1	6
20190	Thermodynamic properties of neutral and charged oxygen vacancies in BaZrO₃ based on first principles phonon calculations. Physical Chemistry Chemical Physics, 2015, 17, 20765-20774.	1.3	47
20191	Structural and chemical determination of the new nanolaminated carbide Mo2Ga2C from first principles and materials analysis. Acta Materialia, 2015, 99, 157-164.	3.8	75
20192	Hydration Mechanism of Reactive and Passive Dicalcium Silicate Polymorphs from Molecular Simulations. Journal of Physical Chemistry C, 2015, 119, 19869-19875.	1.5	68
20193	Revisited phonon assignment and electro-mechanical properties of chromium disilicide. RSC Advances, 2015, 5, 19106-19116.	1.7	18
20194	Structural, electronic and optical properties of a hybrid triazine-based graphitic carbon nitride and graphene nanocomposite. Physical Chemistry Chemical Physics, 2015, 17, 23613-23618.	1.3	27
20195	Interatomic interactions and thermodynamic parameters in dilute solid solutions of the Ag-Au system. Physics of Metals and Metallography, 2015, 116, 671-675.	0.3	1
20196	Crystal structures of highly-ordered long-period stacking-ordered phases with 18R, 14H and 10H-type stacking sequences in the Mgâ€“Znâ€“Y system. Acta Materialia, 2015, 99, 228-239.	3.8	145
20197	Spectroscopic and Computational Study of Structural Changes in Î³-LiV₂O₅ Cathodic Material Induced by Lithium Intercalation. Journal of Physical Chemistry C, 2015, 119, 20801-20809.	1.5	25
20198	Janus Solidâ€“Liquid Interface Enabling Ultrahigh Charging and Discharging Rate for Advanced Lithium-Ion Batteries. Nano Letters, 2015, 15, 6102-6109.	4.5	90
20199	Predicting suitable optoelectronic properties of monoclinic VON semiconductor crystals for photovoltaics using accurate first-principles computations. Physical Chemistry Chemical Physics, 2015, 17, 25244-25249.	1.3	10

#	Article	IF	Citations
20200	Atomic-scale properties of Ni-based FCC ternary, and quaternary alloys. Acta Materialia, 2015, 99, 307-312.	3.8	159
20201	DFT-based modeling of benzene hydrogenation on Pt at industrially relevant coverage. Journal of Catalysis, 2015, 330, 406-422.	3.1	34
20202	Chemical Functionalization of GaN Monolayer by Adatom Adsorption. Journal of Physical Chemistry C, 2015, 119, 20911-20916.	1.5	65
20203	Graphyne as a promising substrate for the noble-metal single-atom catalysts. Carbon, 2015, 95, 756-765.	5.4	181
20204	Overpotential for CO₂ electroreduction lowered on strained penta-twinned Cu nanowires. Chemical Science, 2015, 6, 6829-6835.	3.7	60
20205	Defects responsible for abnormal n-type conductivity in Ag-excess doped PbTe thermoelectrics. Journal of Applied Physics, 2015, 118, .	1.1	17
20206	Activation and dissociation of CO2 on the (001), (011), and (111) surfaces of mackinawite (FeS): A dispersion-corrected DFT study. Journal of Chemical Physics, 2015, 143, 094703.	1.2	46
20207	The effect of point defects on diffusion pathway within Î±-Fe. Journal of Physics Condensed Matter, 2015, 27, 175007.	0.7	7
20208	Characterization of the PtNi(111) surface and their influence on the selectivity of CC and COOH bonds: A DFT study. Applied Surface Science, 2015, 353, 1164-1169.	3.1	3
20209	The micro-mechanism for the effect of Sn grain orientation on substrate consumption in Sn solder joints. Computational Materials Science, 2015, 108, 1-7.	1.4	5
20210	Investigation of Methacrylic Acid at High Pressure Using Neutron Diffraction. Journal of Physical Chemistry B, 2015, 119, 12147-12154.	1.2	4
20211	DFT+U studies of Cu doping and p-type compensation in crystalline and amorphous ZnS. Physical Chemistry Chemical Physics, 2015, 17, 26270-26276.	1.3	27
20212	Water adsorption induced in-plane domain switching on BaTiO3 surface. Journal of Applied Physics, 2015, 118, .	1.1	13
20213	Comparison between the Oxygen Reduction Reaction Activity of Pd₅Ce and Pt₅Ce: The Importance of Crystal Structure. ACS Catalysis, 2015, 5, 6032-6040.	5.5	21
20214	Atomic-Scale Magnetism of Cr-Doped Bi₂Se₃ Thin Film Topological Insulators. ACS Nano, 2015, 9, 10237-10243.	7.3	54
20215	The effect of the morphology of supported subnanometer Pt clusters on the first and key step of CO₂ photoreduction. Physical Chemistry Chemical Physics, 2015, 17, 25379-25392.	1.3	25
20216	Synergistically optimized electrical and thermal transport properties of SnTe via alloying high-solubility MnTe. Energy and Environmental Science, 2015, 8, 3298-3312.	15.6	268
20217	A chemical link between Geâ€“Sbâ€“Te and Inâ€“Sbâ€“Te phase-change materials. Journal of Materials Chemistry C, 2015, 3, 9519-9523.	2.7	44

#	Article	IF	Citations
20218	Ab initio quasi-particle approximation bandgaps of silicon nanowires calculated at density functional theory/local density approximation computational effort. Journal of Applied Physics, 2015, 117, .	1.1	8
20219	Many-body dispersion effects in the binding of adsorbates on metal surfaces. Journal of Chemical Physics, 2015, 143, 102808.	1.2	69
20220	Manifestation of axion electrodynamics through magnetic ordering on edges of a topological insulator. Proceedings of the National Academy of Sciences of the United States of America, 2015, 112, 11514-11518.	3.3	11
20221	Structural, Elastic, and Electronic Properties of a New Phase of Carbon. Communications in Theoretical Physics, 2015, 64, 237-243.	1.1	17
20222	Chemical Interaction, Space-Charge Layer, and Molecule Charging Energy for a TiO₂/TCNQ Interface. Journal of Physical Chemistry C, 2015, 119, 22086-22091.	1.5	9
20223	Thermo-Elastic and Lattice Dynamical Properties of Pd3X (Xâ€‰=â€‰Ti, Zr, Hf) Alloys: An Ab Initio Study. Brazilian Journal of Physics, 2015, 45, 604-614.	0.7	3
20224	Energetics of gaseous and volatile fission products in molten Uâ€“10Zr alloy: A density functional theory study. Journal of Nuclear Materials, 2015, 466, 583-587.	1.3	1
20225	Resolving the Controversy about the Band Alignment between Rutile and Anatase: The Role of OH^{â€“}/H⁺ Adsorption. Journal of Physical Chemistry C, 2015, 119, 21952-21958.	1.5	43
20226	Promising Piezoelectric Performance of Single Layer Transition-Metal Dichalcogenides and Dioxides. Journal of Physical Chemistry C, 2015, 119, 23231-23237.	1.5	164
20227	In Situ Ambient Pressure X-ray Photoelectron Spectroscopy Studies of Methanol Oxidation on Pt(111) and Ptâ€“Re Alloys. Journal of Physical Chemistry C, 2015, 119, 23082-23093.	1.5	20
20228	Tin(II) Sulfide (SnS) Nanosheets by Liquid-Phase Exfoliation of Herzenbergite: IVâ€“VI Main Group Two-Dimensional Atomic Crystals. Journal of the American Chemical Society, 2015, 137, 12689-12696.	6.6	220
20229	On the mechanical stability of uranyl peroxide hydrates: implications for nuclear fuel degradation. RSC Advances, 2015, 5, 79090-79097.	1.7	46
20230	The accurate calculation of the band gap of liquid water by means of GW corrections applied to plane-wave density functional theory molecular dynamics simulations. Physical Chemistry Chemical Physics, 2015, 17, 365-375.	1.3	54
20231	Unexpected origin of magnetism in monoclinic Nb₁₂O₂₉ from first-principles calculations. Journal of Materials Chemistry C, 2015, 3, 651-657.	2.7	9
20232	The system Ceâ€“Znâ€“Si for <33.3 at.% Ce: phase relations, crystal structures and physical properties. RSC Advances, 2015, 5, 36480-36497.	1.7	3
20233	Precise control of defects in graphene using oxygen plasma. Journal of Vacuum Science and Technology A: Vacuum, Surfaces and Films, 2015, 33, .	0.9	32
20234	Magnetic properties of one-dimensional Au-Co chains on the copper(110) surface. Physics of the Solid State, 2015, 57, 1513-1518.	0.2	13
20235	The GW electronic structure of cubic RbMF3 perovskites (M = Be, Mg, Ca, Sr, Ba). European Physical Journal B, 2015, 88, 1.	0.6	5

#	Article	IF	Citations
20236	A lattice theory of the Stone-Wales defect as dipole of dislocation and anti-dislocation. European Physical Journal B, 2015, 88, 1.	0.6	11
20237	A DFT study of electronic and magnetic properties of titanium decorating point-defective graphene. Applied Surface Science, 2015, 356, 1025-1031.	3.1	9
20238	First-principles investigations on ferromagnetic behaviour of Be1â^'xVxZ (ZÂ=ÂS, Se and Te) (xÂ=Â0.25). Superlattices and Microstructures, 2015, 88, 139-149.	1.4	24
20239	Ab Initio Study of Interaction of Water, Hydroxyl Radicals, and Hydroxide Ions with CH₃NH₃PbI₃ and CH₃NH₃PbBr₃ Surfaces. Journal of Physical Chemistry C, 2015, 119, 22370-22378.	1.5	122
20240	Li-Filled, B-Substituted Carbon Clathrates. Journal of the American Chemical Society, 2015, 137, 12639-12652.	6.6	42
20241	Bismuth and chromium co-doped strontium titanates and their photocatalytic properties under visible light irradiation. Physical Chemistry Chemical Physics, 2015, 17, 26320-26329.	1.3	57
20242	A visualized probe method for localization of surface oxygen vacancy on TiO₂: Au in situ reduction. Nanoscale, 2015, 7, 17488-17495.	2.8	14
20243	Electronic properties and lithium storage capacities of two-dimensional transition-metal nitride monolayers. Journal of Materials Chemistry A, 2015, 3, 21486-21493.	5.2	79
20244	BaGa₂SnSe₆: a new phase-matchable IR nonlinear optical material with strong second harmonic generation response. Journal of Materials Chemistry C, 2015, 3, 10998-11004.	2.7	54
20245	Graphene/ferroelectrics/graphene hybrid structure: Asymmetric doping of graphene layers. Applied Physics Letters, 2015, 106, .	1.5	13
20246	Gas adsorption on graphene with different layers: A first-principles study. , 2015, , .		2
20247	Group 14 element-based non-centrosymmetric quantum spin Hall insulators with large bulk gap. Nano Research, 2015, 8, 3412-3420.	5.8	30
20248	Sulfamerazine: Understanding the Influence of Slip Planes in the Polymorphic Phase Transformation through X-Ray Crystallographic Studies and ab Initio Lattice Dynamics. Molecular Pharmaceutics, 2015, 12, 3735-3748.	2.3	10
20249	Hydrogen binding energies and electronic structure of Niâ€“Pd particles: a clue to their special catalytic properties. Physical Chemistry Chemical Physics, 2015, 17, 26140-26148.	1.3	15
20250	Theoretical study of surface dependence of NH₃adsorption and decomposition on spinel-type MgAl₂O₄. RSC Advances, 2015, 5, 77973-77985.	1.7	4
20251	Composition dependence of the optical properties and band structure of the zinc-blende ZnS_{1-x}O_x: a first principles study. Philosophical Magazine, 2015, 95, 2627-2638.	0.7	6
20252	Migration of noble gas atoms in interaction with vacancies in silicon. Semiconductor Science and Technology, 2015, 30, 085022.	1.0	5
20253	Calculations of thermoelectric properties: Mg2Si under uniaxial [110] strains versus (110)-oriented thin film. European Physical Journal B, 2015, 88, 1.	0.6	4

#	Article	IF	Citations
20254	Theoretical investigation of elastic and phononic properties of Zn1â^'xBexO alloys. Modern Physics Letters B, 2015, 29, 1550140.	1.0	5
20255	First-principles study on alkali-metal effect of Li, Na, and K in CuInSe₂and CuGaSe₂. Japanese Journal of Applied Physics, 2015, 54, 08KC20.	0.8	38
20256	Hydrogen assisted vacancy formation in tungsten: A first-principles investigation. Journal of Nuclear Materials, 2015, 465, 135-141.	1.3	27
20257	Temperature dependence of the electronic structure of semiconductors and insulators. Journal of Chemical Physics, 2015, 143, 102813.	1.2	139
20258	Large Tunability of Physical Properties of Manganite Thin Films by Epitaxial Strain. Chinese Physics Letters, 2015, 32, 087504.	1.3	7
20259	Computer simulation of the point defect formation in MgSiO3-based ceramic materials. Journal of Structural Chemistry, 2015, 56, 454-457.	0.3	3
20260	Surface orientation dependence of the activation energy of S diffusion in bcc Fe. Applied Surface Science, 2015, 356, 213-220.	3.1	7
20261	First-principles study of Cd impurities localized at and near the (001) Î±-Al2O3 surface. Computational Materials Science, 2015, 107, 15-23.	1.4	3
20262	Real-Time Study of CVD Growth of Silicon Oxide on Rutile TiO₂(110) Using Tetraethyl Orthosilicate. Journal of Physical Chemistry C, 2015, 119, 19149-19161.	1.5	10
20263	Structure, Relative Stabilities, Physical Properties, and Hardness of Osmium Carbides with Various Stoichiometries: First-Principle Investigations. Journal of Physical Chemistry C, 2015, 119, 21639-21648.	1.5	13
20264	Coro-graphene and circumcoro-graphyne: novel two-dimensional materials with exciting electronic properties. RSC Advances, 2015, 5, 78910-78916.	1.7	26
20265	First-principles studies of p-type nitrogen-doped Î±-Fe2O3-xSx alloys. Journal of Applied Physics, 2015, 117, .	1.1	0
20266	Effect of interstitial impurities on grain boundary cohesive strength in vanadium. Computational Materials Science, 2015, 110, 163-168.	1.4	10
20267	In Situ Photoconductivity Kinetic Study of Nano-TiO₂ during the Photocatalytic Oxidation of Formic Acid: Effects of New Recombination and Current Doubling. Journal of Physical Chemistry C, 2015, 119, 21711-21722.	1.5	19
20268	A novel two-dimensional material B₂S₃and its structural implication to new carbon and boron nitride allotropes. Journal of Materials Chemistry C, 2015, 3, 9921-9927.	2.7	13
20269	CO catalytic oxidation on Al-doped graphene-like ZnO monolayer sheets: a first-principles study. Journal of Materials Chemistry C, 2015, 3, 9964-9972.	2.7	58
20270	Structural, elastic, electronic, phonon and thermal properties of Ir₃Ta and Rh₃Ta alloys. Philosophical Magazine Letters, 2015, 95, 392-400.	0.5	7
20271	Understanding the combined effects of microcrystal growth and band gap reduction for Fe(1â^')Ti F3 nanocomposites as cathode materials for lithium-ion batteries. Nano Energy, 2015, 17, 140-151.	8.2	63

#	Article	IF	Citations
20272	High temperature enthalpy increments and thermodynamic functions of ZrCo: An experimental and theoretical study. Thermochimica Acta, 2015, 614, 16-20.	1.2	9
20273	The oxidation of copper catalysts during ethylene epoxidation. Physical Chemistry Chemical Physics, 2015, 17, 25073-25089.	1.3	43
20274	The Electronic Structure and Magnetic Properties of Transition Metal Anti-sites-Doped ZnO: the First-Principles Calculations. Journal of Superconductivity and Novel Magnetism, 2015, 28, 3065-3068.	0.8	4
20275	Structural, elastic and electronic properties of Cu-X compounds from first-principles calculations. Journal of Central South University, 2015, 22, 1585-1594.	1.2	3
20276	The characterization of Co-nanoparticles supported on graphene. RSC Advances, 2015, 5, 75600-75606.	1.7	46
20277	Density functional theory analysis of hexagonal close-packed elemental metal photocathodes. Physical Review Special Topics: Accelerators and Beams, 2015, 18, .	1.8	9
20278	Structural, electronic, mechanical and superconducting properties of ReC and TcC. International Journal of Refractory Metals and Hard Materials, 2015, 52, 219-228.	1.7	6
20279	Heavy-Metal Adsorption Behavior of Two-Dimensional Alkalization-Intercalated MXene by First-Principles Calculations. Journal of Physical Chemistry C, 2015, 119, 20923-20930.	1.5	193
20280	Effect of cation substitution on structural transition: synthesis, characterization and theoretical studies of NaCa₄B₃O₉, NaCaBO₃, NaSrBO₃and Li₄CaB₂O₆. Physical Chemistry Chemical Physics, 2015, 17, 26359-26368.	1.3	16
20281	Elastic properties of magnesium with virtual long-period stacking-ordered structure: First-principles study. Computational Materials Science, 2015, 110, 191-197.	1.4	9
20282	Thermally activated surface oxygen defects at the perimeter of Au/TiO₂: a DFT+U study. Physical Chemistry Chemical Physics, 2015, 17, 25403-25410.	1.3	26
20283	Adsorption of aromatics on the (111) surface of PtM and PtM₃ (M = Fe, Ni) alloys. RSC Advances, 2015, 5, 85705-85719.	1.7	14
20284	Structural and electronic properties of the transition layer at the SiO2/4H-SiC interface. AIP Advances, 2015, 5, .	0.6	14
20285	Density functional theory calculations of NO molecule adsorption on monolayer MoS2 doped by Fe atom. Modern Physics Letters B, 2015, 29, 1550160.	1.0	3
20286	Methane Recovery from Coal Bed Gas Using Modified Activated Carbons: A Combined Method for Assessing the Role of Functional Groups. Energy & Fuels, 2015, 29, 6858-6865.	2.5	13
20287	Different Product Distributions and Mechanistic Aspects of the Hydrodeoxygenation of m-Cresol over Platinum and Ruthenium Catalysts. ACS Catalysis, 2015, 5, 6271-6283.	5.5	137
20288	Density-functional calculations of the conversion of methane to methanol on platinum-decorated sheets of graphene oxide. Physical Chemistry Chemical Physics, 2015, 17, 26191-26197.	1.3	27
20289	Glitter in a 2D monolayer. Physical Chemistry Chemical Physics, 2015, 17, 26036-26042.	1.3	68

#	Article	IF	Citations
20290	Revealing unusual chemical bonding in planar hyper-coordinate Ni₂Ge and quasi-planar Ni₂Si two-dimensional crystals. Physical Chemistry Chemical Physics, 2015, 17, 26043-26048.	1.3	95
20291	Edge State-Induced Novel Electronic Structures and Magnetic Properties of Zigzag AlN/SiC Nanoribbons. Journal of Superconductivity and Novel Magnetism, 2015, 28, 3053-3057.	0.8	0
20292	Structural and electronic properties of crystalline graphite-like BC3. Computational Materials Science, 2015, 109, 248-252.	1.4	11
20293	Electronic and magnetic properties of C-doped Î±-Al2O3 by DFT calculations. Computational Materials Science, 2015, 110, 368-374.	1.4	16
20294	Prediction on anisotropic elasticity, sound velocity, and thermodynamic properties of MoSi2 under pressure. Journal of Alloys and Compounds, 2015, 652, 106-115.	2.8	32
20295	Fabrication of One-Dimensional Zigzag [6,6]-Phenyl-C₆₁-Butyric Acid Methyl Ester Nanoribbons from Two-Dimensional Nanosheets. ACS Nano, 2015, 9, 10516-10522.	7.3	10
20296	Crystalline adducts of the Lawsone molecule (2-hydroxy-1,4-naphthaquinone): optical properties and computational modelling. CrystEngComm, 2015, 17, 7684-7692.	1.3	14
20297	The effect of surface modification by reduced graphene oxide on the electrocatalytic activity of nickel towards the hydrogen evolution reaction. Physical Chemistry Chemical Physics, 2015, 17, 26864-26874.	1.3	86
20298	Dendritic Tip-on Polytriazine-Based Carbon Nitride Photocatalyst with High Hydrogen Evolution Activity. Chemistry of Materials, 2015, 27, 8237-8247.	3.2	140
20299	Influence of Carboxylation on Structural and Mechanical Properties of Carbon Nanotubes: Composite Reinforcement and Toxicity Reduction Perspectives. Journal of Physical Chemistry C, 2015, 119, 26734-26746.	1.5	18
20300	First Principles Calculations on Cu-Doped TiO₂. Advanced Materials Research, 0, 1101, 70-74.	0.3	1
20301	Adsorption of Organic Molecules on the Hydrogenated Germanene: A DFT Study. Journal of Physical Chemistry C, 2015, 119, 27995-28004.	1.5	23
20302	Ab initiomolecular dynamics with simultaneous electron and phonon excitations: Application to the relaxation of hot atoms and molecules on metal surfaces. Physical Review B, 2015, 92, .	1.1	76
20303	Electronic structure and lattice dynamics of the Î±-Zncl2 crystal. Journal of Structural Chemistry, 2015, 56, 823-828.	0.3	2
20304	Theoretical and experimental studies on wide-band-gap p-type conductive BaCuSeF and related compounds. Japanese Journal of Applied Physics, 2015, 54, 08KC07.	0.8	10
20305	Co-Adsorbent Effect on the Sensitization of TiO₂ and ZnO Surfaces: A Theoretical Study. Journal of Physical Chemistry C, 2015, 119, 27348-27353.	1.5	11
20306	Electronic and transport properties of phosphorene nanoribbons. Physical Review B, 2015, 92, .	1.1	145
20307	Structures and stability of novel transition-metal<mml:math		

#	Article	IF	Citations
20308	A density functional theory study on the conversion of ethylene to carbon monomer on PdAu(1 0 0) surface. Applied Surface Science, 2015, 356, 1252-1261.	3.1	9
20309	Effect of binding group on hybridization across the silicon/aromatic-monolayer interface. Journal of Electron Spectroscopy and Related Phenomena, 2015, 204, 149-158.	0.8	8
20310	Pressure induced structural instability of FeV intermetallic compound with B2 ordering. Journal of Alloys and Compounds, 2015, 650, 537-541.	2.8	3
20311	Effect of alloying elements on hydrogen absorption properties of palladium-based solid solution alloys. Journal of Alloys and Compounds, 2015, 653, 444-452.	2.8	14
20312	From solid solution to cluster formation of Fe and Cr in Î± -Zr. Journal of Nuclear Materials, 2015, 467, 320-331.	1.3	23
20313	Phase stability, electronic and elastic properties of Fe6â^'xWxC (xÂ=Â0â^'6) from density functional theory. Materials Chemistry and Physics, 2015, 164, 115-121.	2.0	8
20314	Computational materials design of attractive Fermion system with large negative effective Ueff in the hole-doped Delafossite of CuAlO2, AgAlO2 and AuAlO2: Charge-excitation induced Ueff < 0. Physica C: Superconductivity and Its Applications, 2015, 519, 168-183.	0.6	4
20315	Impurity distribution and ferromagnetism in Mn-doped GaAs nanowires: A first-principle study. Physics Letters, Section A: General, Atomic and Solid State Physics, 2015, 379, 2745-2749.	0.9	23
20316	Effects of Oxygen Vacancy on the Electronic Structure of Cubic LaAlO3. Rare Metal Materials and Engineering, 2015, 44, 1099-1103.	0.8	3
20317	Formation and Growth Mechanisms of Solid-Electrolyte Interphase Layers in Rechargeable Batteries. Chemistry of Materials, 2015, 27, 7990-8000.	3.2	225
20318	Prediction of Stable Ruthenium Silicides from First-Principles Calculations: Stoichiometries, Crystal Structures, and Physical Properties. ACS Applied Materials & Interfaces, 2015, 7, 26776-26782.	4.0	42
20319	First-principles prediction of superconductivity in LiBSi_{1-x}Al_x. International Journal of Modern Physics B, 2015, 29, 1550064.	1.0	1
20320	Quantum states of hydrogen atom on Pd(1 1 0) surface. Applied Surface Science, 2015, 359, 687-691.	3.1	4
20321	Structural, electronic, and optical properties of bulk Cu2Se. Current Applied Physics, 2015, 15, 1417-1420.	1.1	13
20322	On the Raman and infrared vibrational spectra of the É› and Î¶ phases of oxygen. Systematic DFT studies with localized basis sets. Chemical Physics Letters, 2015, 638, 82-86.	1.2	7
20323	Patterning germanene into superlattices: An efficient method for tuning conducting properties. Chemical Physics Letters, 2015, 638, 187-190.	1.2	10
20324	Investigations on structures, thermal expansion and electrochemical properties of La0.75Sr0.25Cu0.5â^'xCoxMn0.5O3â^'Î´ (x=0, 0.25, and 0.5) as potential cathodes for intermediate temperature solid oxide fuel cells. Electrochimica Acta, 2015, 186, 262-270.	2.6	7
20325	Stability, phonon dispersion and specific heat of solid poly(vinylÂalcohol) using density functional theory. Polymer, 2015, 81, 45-49.	1.8	11

#	Article	IF	Citations
20326	The mechanism for the nonlinear optical properties in La₉Na₃B₈O₂₇, La₂Na₃B₃O₉and La₂CaB₁₀O₁₉:ab initiostudies. Journal of Physics Condensed Matter, 2015, 27, 485501.	0.7	7
20327	Structural and electronic properties of Cu-doped Zn5(OH)6(CO3)2 from first principles. Journal of Materials Science, 2015, 50, 6794-6807.	1.7	7
20328	Multiple Dirac Points and Hydrogenation-Induced Magnetism of Germanene Layer on Al (111) Surface. Journal of Physical Chemistry Letters, 2015, 6, 4936-4942.	2.1	41
20329	Improvement of electronic properties of carboxylated zigzag single wall carbon nanotubes by interaction with benzene derivatives. Current Applied Physics, 2015, 15, 1593-1598.	1.1	1
20330	Theoretical prediction on mechanical and thermal properties of a promising thermal barrier material: Y4Al2O9. Journal of Advanced Ceramics, 2015, 4, 83-93.	8.9	63
20331	Ab initio investigation of native point defects in Mg 24 Y 5. Materials Chemistry and Physics, 2015, 167, 70-76.	2.0	6
20332	Study of Lithium Migration Pathways in the Organic Electrode Materials of Li-Battery by Dispersion-Corrected Density Functional Theory. Journal of Physical Chemistry C, 2015, 119, 25719-25725.	1.5	24
20333	Molecular Electronic Effects on the Thermal Grafting of Aryl Iodides to TiO₂ Surfaces. Journal of Physical Chemistry C, 2015, 119, 27972-27981.	1.5	0
20334	Role of Interlayer Coupling on the Evolution of Band Edges in Few-Layer Phosphorene. Journal of Physical Chemistry Letters, 2015, 6, 4876-4883.	2.1	38
20335	Thickness-Dependent Dielectric Constant of Few-Layer In₂Se₃ Nanoflakes. Nano Letters, 2015, 15, 8136-8140.	4.5	99
20336	Capacitive Sensing of Intercalated H₂O Molecules Using Graphene. ACS Applied Materials & Interfaces, 2015, 7, 25804-25812.	4.0	30
20337	Assembling an alkyl rotor to access abrupt and reversible crystalline deformation of a cobalt(II) complex. Nature Communications, 2015, 6, 8810.	5.8	69
20338	Tuning oxide activity through modification of the crystal and electronic structure: from strain to potential polymorphs. Physical Chemistry Chemical Physics, 2015, 17, 28943-28949.	1.3	31
20339	Sn(ii,iv) steric and electronic structure effects enable self-selective doping on Fe/Si-sites of Li2FeSiO4 nanocrystals for high performance lithium ion batteries. Journal of Materials Chemistry A, 2015, 3, 24437-24445.	5.2	15
20340	Two-dimensional Ni(OH) ₂ -XS ₂ (X = Mo and W) heterostructures. 2D Materials, 2015, 2, 034014.	2.0	11
20341	Effect of oxygen on the magnetic property of Bis(8-hydroxyquinoline)copper (CuQ2): An experimental and theoretical study. International Journal of Modern Physics B, 2015, 29, 1542027.	1.0	1
20342	Reactivity at the Lithiumâ€“Metal Anode Surface of Lithiumâ€“Sulfur Batteries. Journal of Physical Chemistry C, 2015, 119, 26828-26839.	1.5	140
20343	Morphology-dependent antimicrobial activity of Cu/CuxO nanoparticles. Ecotoxicology, 2015, 24, 2067-2072.	1.1	28

#	Article	IF	Citations
20344	Selective Catalytic Hydrogenolysis of Carbonâ€“Carbon Ïƒ Bonds in Primary Aliphatic Alcohols over Supported Metals. ACS Catalysis, 2015, 5, 7199-7207.	5.5	19
20345	Optimized multi-site local orbitals in the large-scale DFT program CONQUEST. Physical Chemistry Chemical Physics, 2015, 17, 31427-31433.	1.3	25
20346	Translation Symmetry Breakdown in Low-Dimensional Lattices of Pentagonal Rings. Journal of Physical Chemistry Letters, 2015, 6, 4525-4531.	2.1	35
20347	Exploration of High-Performance Single-Atom Catalysts on Support M₁/FeO_x for CO Oxidation via Computational Study. ACS Catalysis, 2015, 5, 544-552.	5.5	217
20348	Oxygen adsorption properties on a palladium promoted La_{1â^'x}Sr_xMnO₃solid oxide fuel cell cathode. RSC Advances, 2015, 5, 7761-7765.	1.7	16
20349	Sharp variations in the electronic properties of graphene deposited on the h-BN layer. Physical Chemistry Chemical Physics, 2015, 17, 4354-4359.	1.3	10
20350	First-principles study of half-fluorinated silicene sheets. RSC Advances, 2015, 5, 6238-6245.	1.7	28
20351	Stability of iron crystal structures at 0.3â€“1.5 TPa. Earth and Planetary Science Letters, 2015, 409, 299-306.	1.8	23
20352	A Firstâ€Principles Study of Lithium Adsorption on a Grapheneâ€“Fullerene Nanohybrid System. ChemPhysChem, 2015, 16, 789-795.	1.0	29
20353	Selective Heterogeneous CO₂ Electroreduction to Methanol. ACS Catalysis, 2015, 5, 965-971.	5.5	167
20354	Access to Novel Grapheneâ€Like Sheet of Hydroboron: Firstâ€Principles Investigation. Chemistry - an Asian Journal, 2015, 10, 362-369.	1.7	2
20355	Chemical Stability toward O₂ and H₂O of Si(111) Grafted with â€”CH₃, â€”CH₂CH₂CH₃, â€”CHCHCH₃, and â€”CCCH₃. Journal of Physical Chemistry C, 2015, 119, 284-295.	1.5	11
20356	Anomalous elastic properties in stishovite. RSC Advances, 2015, 5, 8974-8980.	1.7	15
20357	Synthesis, Crystal Structure, and Optical Properties of a New Sodiumâ€Cadmium Carbonate Na₄Cd₃(CO₃)₄(OH)₂. Zeitschrift Fur Anorganische Und Allgemeine Chemie, 2015, 641, 460-463.	0.6	3
20358	First-principles study of sulfur isotope fractionation in pyrite-type disulfides. American Mineralogist, 2015, 100, 203-208.	0.9	15
20359	Platinumâ€“carbide interactions: coreâ€“shells for catalytic use. Physical Chemistry Chemical Physics, 2015, 17, 4250-4258.	1.3	23
20360	Phenol Deoxygenation Mechanisms on Fe(110) and Pd(111). ACS Catalysis, 2015, 5, 523-536.	5.5	116
20361	Atomic, electronic and magnetic structure of graphene/iron and nickel interfaces: theory and experiment. RSC Advances, 2015, 5, 9173-9179.	1.7	11

#	Article	IF	Citations
20362	Graphene monolayers on GaN(0001). Applied Surface Science, 2015, 326, 7-11.	3.1	12
20363	Structure evolution of nanoparticulate Fe₂O₃. Nanoscale, 2015, 7, 2960-2969.	2.8	47
20364	Impact of Process Conditions on the Sintering Behavior of an Alumina-Supported Cobalt Fischerâ€“Tropsch Catalyst Studied with an in Situ Magnetometer. ACS Catalysis, 2015, 5, 841-852.	5.5	83
20365	Ab initio calculations of the ideal tensile and shear strengths of uranium metal. Journal of Nuclear Materials, 2015, 458, 122-128.	1.3	7
20366	First principles study of the structural, electronic, mechanical and superconducting properties of WX (X=C, N). Journal of Physics and Chemistry of Solids, 2015, 77, 38-49.	1.9	18
20367	Ab initio calculations of structural, elastic and thermal properties of TiCr2 and (Ti,Mg)(Mg,Cr)2 Laves phases. Computational Materials Science, 2015, 96, 348-353.	1.4	14
20368	Covalent functionalization of single-walled carbon nanotubes through attachment of aromatic diisocyanate molecules from first principles. Chemical Physics Letters, 2015, 619, 103-108.	1.2	4
20369	Theoretical Predictions of Electronic Structure and Half-Metallic Ferromagnetism in Al1âˆ’x Mn x P Diluted Magnetic Semiconductors. Journal of Superconductivity and Novel Magnetism, 2015, 28, 143-150.	0.8	15
20370	Quantum molecular dynamics study of expanded beryllium: Evolution from warm dense matter to atomic fluid. Scientific Reports, 2014, 4, 5898.	1.6	19
20371	Structural, electronic and mechanical properties of alkaline earth metal oxides MO (M=Be, Mg, Ca, Sr,) Tj ETQq1 1 0.784314 rgBT /Ov	1.9	35
20372	An efficient method to enhance the stability of sulphide semiconductor photocatalysts: a case study of N-doped ZnS. Physical Chemistry Chemical Physics, 2015, 17, 1870-1876.	1.3	79
20373	Chain growth mechanism on bimetallic surfaces for higher alcohol synthesis from syngas. Catalysis Communications, 2015, 61, 57-61.	1.6	37
20374	Microstructural stability of Feâ€“Crâ€“Al alloys at 450â€“550 Â°C. Journal of Nuclear Materials, 2015, 457, 291-297.	1.3	81
20375	Structure, Superconductivity, and Magnetism of Ce(O,F)BiS2 Single Crystals. Crystal Growth and Design, 2015, 15, 39-44.	1.4	32
20376	Self-assembly of metal atoms (Na, K, Ca) on graphene. Nanoscale, 2015, 7, 2352-2359.	2.8	10
20377	Many body effects study of electronic & optical properties of siliceneâ€“graphene hybrid. Physica E: Low-Dimensional Systems and Nanostructures, 2015, 68, 38-41.	1.3	46
20378	Significant enhancement of the thermoelectric performance of phosphorene through the application of tensile strain. Applied Physics Express, 2015, 8, 015202.	1.1	20
20379	Magnesium interatomic potential for simulating plasticity and fracture phenomena. Modelling and Simulation in Materials Science and Engineering, 2015, 23, 015004.	0.8	117

#	Article	IF	Citations
20380	Interplay between Reaction Mechanism and Hydroxyl Species for Water Formation on Pt(111). ACS Catalysis, 2015, 5, 1068-1077.	5.5	24
20381	Understanding the Effect of the Adatoms in the Formic Acid Oxidation Mechanism on Pt(111) Electrodes. ACS Catalysis, 2015, 5, 645-654.	5.5	81
20382	Three structure types and intermediate cerium valence in the solid solution CeRu1â€“xNixSn. Solid State Sciences, 2015, 40, 36-43.	1.5	10
20383	Ab initio study of electronic density of state and photoabsorption of Ga1â^'xMnxAs under pressure. Solid State Communications, 2015, 202, 19-23.	0.9	5
20384	Magnetism in Oxygen-Functionalized Hexagonal Boron Nitride Nanosheet on Copper Substrate. Journal of Physical Chemistry C, 2015, 119, 873-878.	1.5	11
20385	CO catalytic oxidation on iron-embedded monolayer MoS2. Applied Surface Science, 2015, 328, 71-77.	3.1	100
20386	A Theoretical Study of Single-Atom Catalysis of CO Oxidation Using Au Embedded 2D h-BN Monolayer: A CO-Promoted O2 Activation. Scientific Reports, 2014, 4, 5441.	1.6	211
20387	Synthesis, crystal growth, and second-order nonlinear optical properties of new configurationally locked polyene derivatives. CrystEngComm, 2015, 17, 1050-1055.	1.3	19
20388	First-Principles Study of C₂ Oxygenates Synthesis Directly from Syngas over CoCu Bimetallic Catalysts. Journal of Physical Chemistry C, 2015, 119, 216-227.	1.5	47
20389	Comment on â€˜Study of electronic, magnetic, optical and elastic properties of Cu2MnAl a gapless full heusler compoundâ€™. Journal of Alloys and Compounds, 2015, 626, 277-279.	2.8	18
20390	Effects of strain on the band gap and effective mass in two-dimensional monolayer GaX (XÂ= S, Se, Te). RSC Advances, 2015, 5, 5788-5794.	1.7	75
20391	The electronic, optical and ferroelectric properties of BiFeO3 during polarization reversal: A first principle study. Journal of Alloys and Compounds, 2015, 623, 393-400.	2.8	23
20392	Electronic and Optical Properties of Nanoporous Silicon for Solar-Cell Applications. ACS Photonics, 2015, 2, 208-215.	3.2	43
20393	NO dissociation and reduction by H 2 on Pd(1 1 1): A first-principles study. Journal of Catalysis, 2015, 322, 73-83.	3.1	51
20394	First-principles study of energy and atomic solubility of twinning-associated boundaries in hexagonal metals. Acta Materialia, 2015, 85, 144-154.	3.8	97
20395	Reduced partition function ratios of iron and oxygen in goethite. Geochimica Et Cosmochimica Acta, 2015, 151, 19-33.	1.6	38
20396	First-principles study of native defects in LiTi2O4. Computational Materials Science, 2015, 96, 263-267.	1.4	6
20397	On the Cauchyâ€“Born approximation at finite temperature. Computational Materials Science, 2015, 99, 21-28.	1.4	3

#	Article	IF	Citations
20398	New insights into assessing the favorable co-doping dopants with various co-doped cases for the band gap engineering of SrTiO 3. International Journal of Hydrogen Energy, 2015, 40, 1343-1351.	3.8	17
20399	Structural, electronic, elastic and superconducting properties of noble metal nitrides MN2 (MÂ=ÂRu,) Tj ETQq1 1 0.784314 rgBT /Ove	2.0	4
20400	Structural and electronic properties of a single Si chain doped zigzag AlN nanoribbon. Physica E: Low-Dimensional Systems and Nanostructures, 2015, 68, 59-64.	1.3	1
20401	First-principles study of the phonon vibrational spectra and thermal properties of hexagonal MoS2. Solid State Sciences, 2015, 40, 1-6.	1.5	15
20402	First-principles calculations of phonon and thermodynamic properties of OsSi2. Materials Science in Semiconductor Processing, 2015, 31, 251-255.	1.9	2
20403	A first principles study of Ti 2 AlNb intermetallic. Solid State Communications, 2015, 204, 9-15.	0.9	40
20404	Fundamentals of Methanol Synthesis on Metal Carbide Based Catalysts: Activation of CO2 and H2. Topics in Catalysis, 2015, 58, 159-173.	1.3	64
20405	First-principles study on the ferrimagnetic half-metallic Mn2FeAs alloy. Journal of Solid State Chemistry, 2015, 225, 8-12.	1.4	21
20406	Mechanism of enhanced photocatalytic activities on N-doped La 2 Ti 2 O 7 : An insight from density-functional calculations. International Journal of Hydrogen Energy, 2015, 40, 980-989.	3.8	27
20407	Density functional theory study on boron- and phosphorus-doped hydrogen-passivated silicene. Physical Chemistry Chemical Physics, 2015, 17, 4146-4151.	1.3	33
20408	A computational study of platinum adsorption on defective and non-defective silicon carbide nanotubes. Monatshefte FÃ¼r Chemie, 2015, 146, 883-890.	0.9	3
20409	The nature of the Feâ€“graphene interface at the nanometer level. Nanoscale, 2015, 7, 2450-2460.	2.8	44
20410	First-principle calculations of the structural and elastic properties of titanium nanowires. Materials Letters, 2015, 141, 333-335.	1.3	4
20411	Computationally efficient and quantitatively accurate multiscale simulation of solid-solution strengthening by ab initio calculation. Acta Materialia, 2015, 85, 53-66.	3.8	47
20412	Dielectric Screening in Atomically Thin Boron Nitride Nanosheets. Nano Letters, 2015, 15, 218-223.	4.5	129
20413	Adsorbate Diffusion on Transition Metal Nanoparticles. Nano Letters, 2015, 15, 629-634.	4.5	26
20414	Modulating the phase transition between metallic and semiconducting single-layer MoS₂ and WS₂ through size effects. Physical Chemistry Chemical Physics, 2015, 17, 1099-1105.	1.3	38
20415	Band structure engineering of monolayer MoS₂: a charge compensated codoping strategy. RSC Advances, 2015, 5, 7944-7952.	1.7	26

#	Article	IF	Citations
20416	Investigation of high spin-polarization, magnetic, electronic and half-metallic properties in RuMn2Ge and RuMn2Sb Heusler alloys. Materials Science and Engineering B: Solid-State Materials for Advanced Technology, 2015, 193, 70-75.	1.7	34
20417	Influences of interfacial terminations on electronic structure and magnetoelectric coupling in Fe/KNbO 3 superlattices. Chemical Physics Letters, 2015, 619, 163-168.	1.2	10
20418	Phase stability and mechanical properties of sigma phase in Coâ€“Mo system by first principles calculations. Computational Materials Science, 2015, 98, 424-429.	1.4	10
20419	First-principles investigation of the stability and stabilization mechanism of Ni2Zn11 Î³ brasses under high pressure. Computational Materials Science, 2015, 98, 430-434.	1.4	4
20420	Responses of the topological surface states to Mn-covered on topological insulators Bi2Se3 film. Solid State Communications, 2015, 203, 46-50.	0.9	1
20421	Ab-initio study of the stability of the D8m-Nb5Sn2Ga and D8m-Ta5SnGa2 compounds. Journal of Alloys and Compounds, 2015, 625, 57-63.	2.8	3
20422	Effect of oxygen vacancy on the adsorption of O2 on anatase TiO2(001): A DFT-based study. Surface Science, 2015, 633, 38-45.	0.8	52
20423	Enhancing mechanical toughness of aluminum surfaces by nano-boron implantation: An ab initio study. Chemical Physics Letters, 2015, 620, 25-28.	1.2	3
20424	Atomic geometry and electronic structure of Al0.25Ga0.75N(0001) surfaces covered with different coverages of cesium: A first-principle research. Applied Surface Science, 2015, 326, 251-256.	3.1	15
20425	Stable interface structures of heterovalent semiconductor superlattices: The case of (GaSb) (ZnTe). Computational Materials Science, 2015, 98, 340-344.	1.4	6
20426	Theoretical Insights into the Impact of Ru Catalyst Anchors on the Efficiency of Photocatalytic CO₂ Reduction on Ta₂O₅. Journal of Physical Chemistry B, 2015, 119, 7186-7197.	1.2	20
20427	Structural phase transition, elastic and thermal properties of boron arsenide: Pressure-induced effects. Materials Science in Semiconductor Processing, 2015, 31, 124-130.	1.9	72
20428	Ultra-Flexibility and Unusual Electronic, Magnetic and Chemical Properties of Waved Graphenes and Nanoribbons. Scientific Reports, 2014, 4, 4198.	1.6	33
20429	Single adatom dynamics at monatomic steps of free-standing few-layer reduced graphene. Scientific Reports, 2014, 4, 6037.	1.6	10
20430	High-Performance Few-layer Mo-doped ReSe2 Nanosheet Photodetectors. Scientific Reports, 2014, 4, 5442.	1.6	82
20431	Strain-induced quantum spin Hall effect in methyl-substituted germanane GeCH3. Scientific Reports, 2014, 4, 7297.	1.6	68
20432	Revisiting the Al/Al2O3 Interface: Coherent Interfaces and Misfit Accommodation. Scientific Reports, 2014, 4, 4485.	1.6	78
20433	Atomic-scale configurations of synchroshear-induced deformation twins in the ionic MnS crystal. Scientific Reports, 2015, 4, 5118.	1.6	7

#	Article	IF	Citations
20434	Diamond-based electrodes for organic photovoltaic devices. Solar Energy Materials and Solar Cells, 2015, 134, 73-79.	3.0	15
20435	Na₃Ba₂(B₃O₆)₂F: Next Generation of Deep-Ultraviolet Birefringent Materials. Crystal Growth and Design, 2015, 15, 523-529.	1.4	159
20436	Unravelling Orientation Distribution and Merging Behavior of Monolayer MoS₂ Domains on Sapphire. Nano Letters, 2015, 15, 198-205.	4.5	136
20437	First principles study of structural stability, electronic structure and mechanical properties of ReN and TcN. Journal of Physics and Chemistry of Solids, 2015, 78, 118-126.	1.9	10
20438	Theoretical evaluation of the surface electrochemistry of perovskites with promising photon absorption properties for solar water splitting. Physical Chemistry Chemical Physics, 2015, 17, 2634-2640.	1.3	58
20439	Ab-initio study of structural, electronic and elastic properties of cobalt intermetallic compounds. Computational Materials Science, 2015, 98, 226-233.	1.4	8
20440	Graphyne-supported single Fe atom catalysts for CO oxidation. Physical Chemistry Chemical Physics, 2015, 17, 1441-1449.	1.3	136
20441	Solubility of zirconium and silicon in molybdenum studied by first-principles calculations. Scripta Materialia, 2015, 97, 1-4.	2.6	10
20442	Thermodynamic description of the Biâ€“Cs and Biâ€“Tm system supported by first-principles calculations. Calphad: Computer Coupling of Phase Diagrams and Thermochemistry, 2015, 48, 72-78.	0.7	10
20443	Dynamics of Pd monomers and dimers adsorbed on the (001) surfaces of strongly correlated nickel oxides. Current Applied Physics, 2015, 15, 98-102.	1.1	7
20444	Catalytic properties of Au electrodes modified by an underlayer of Pd. Surface Science, 2015, 631, 235-247.	0.8	23
20445	New diluted magnetic semiconductor (BaK)(ZnMn)2As2: Electronic structure and magnetic properties. Computational Materials Science, 2015, 98, 93-98.	1.4	6
20446	Theoretical study of electronic structure, phase transition, elastic, and thermodynamic properties of ReN. Physica B: Condensed Matter, 2015, 458, 124-131.	1.3	6
20447	Diamond polytypes under high pressure: A first-principles study. Computational Materials Science, 2015, 98, 129-135.	1.4	12
20448	Small-Molecule Activation Driven by Confinement Effects. ACS Catalysis, 2015, 5, 215-224.	5.5	8
20449	Universality in surface mixing rule of adsorption strength for small adsorbates on binary transition metal alloys. Physical Chemistry Chemical Physics, 2015, 17, 3123-3130.	1.3	27
20450	First-principles study of La2CoMnO6: a promising cathode material for intermediate-temperature solid oxide fuel cells due to intrinsic Co-Mn cation disorder. Ionics, 2015, 21, 1675-1681.	1.2	30
20451	DFT study of the cohesive and structural properties of YNi5H compounds. Journal of Alloys and Compounds, 2015, 622, 1041-1048.	2.8	5

#	Article	IF	Citations
20452	On the solid-state NMR spectra of naproxen. Chemical Physics Letters, 2015, 619, 230-235.	1.2	15
20453	Strain effects on oxygen migration in perovskites. Physical Chemistry Chemical Physics, 2015, 17, 2715-2721.	1.3	70
20454	Phase transition, effective mass and carrier mobility of MoS2 monolayer under tensile strain. Applied Surface Science, 2015, 325, 27-32.	3.1	132
20455	Guaiacol Hydrodeoxygenation Mechanism on Pt(111): Insights from Density Functional Theory and Linear Free Energy Relations. ChemSusChem, 2015, 8, 315-322.	3.6	109
20456	First principles account for large changes in electronic structure and bonding from LaCu to LaCuMg and LaCuMg4. Computational Materials Science, 2015, 97, 231-236.	1.4	0
20457	Interface of Pt with SrTiO3(001); A combined theoretical and experimental study. Surface Science, 2015, 633, 8-16.	0.8	7
20458	Catalytic effects of Zr doping ion on ceria-based catalyst. Fuel Processing Technology, 2015, 131, 1-6.	3.7	19
20459	External strain effect on the electronic and mechanical properties of the superconductor Nb2InC. Journal of Physics and Chemistry of Solids, 2015, 78, 28-34.	1.9	8
20460	Elasticity of superhydrous phase, B, Mg10Si3O14(OH)4. Physics of the Earth and Planetary Interiors, 2015, 238, 42-50.	0.7	15
20461	DFT and experimental studies of oxygen adsorption on galena surface bearing Ag, Mn, Bi and Cu impurities. Minerals Engineering, 2015, 71, 170-179.	1.8	17
20462	Theoretical characterization of quaternary iridium based hydrides NaAeIrH6 (AeÂ=ÂCa, Ba and Sr). Materials Chemistry and Physics, 2015, 149-150, 87-93.	2.0	2
20463	Elastic and thermodynamic properties of Rh and Rh3Zr under pressure from first-principles calculation. Materials Chemistry and Physics, 2015, 149-150, 553-558.	2.0	7
20464	Electronic and optical properties of BBi and AlBi: Hybrid (YS-PBE0) function. Computational Materials Science, 2015, 98, 136-141.	1.4	25
20465	First principles study of van der Waals heterobilayers. Computational Condensed Matter, 2015, 2, 1-10.	0.9	33
20466	Phase stability, magnetism, elastic properties and hardness of binary iron nitrides from first principles. Journal of Alloys and Compounds, 2015, 625, 224-230.	2.8	39
20467	A density functional theory study of the tunable structure, magnetism and metal-insulator phase transition in VS2 monolayers induced by in-plane biaxial strain. Nano Research, 2015, 8, 1348-1356.	5.8	116
20468	Spintronic properties of Li1.5Mn0.5Z (Z=As, Sb) compounds in the Cu2Sb structure. Journal of Magnetism and Magnetic Materials, 2015, 377, 411-418.	1.0	3
20469	Bilayered semiconductor graphene nanostructures with periodically arranged hexagonal holes. Nano Research, 2015, 8, 1250-1258.	5.8	25

#	Article	IF	Citations
20470	Experimental study and theoretical calculation on the conductivity and stability of praseodymium doped tin oxide electrode. Electrochimica Acta, 2015, 151, 177-185.	2.6	6
20471	Mechanisms for Ethanol Electrooxidation on Pt(111) and Adsorption Bond Strengths Defining an Ideal Catalyst. Journal of the Electrochemical Society, 2015, 162, F115-F122.	1.3	39
20472	Topological crystalline insulator nanomembrane with strain-tunable band gap. Nano Research, 2015, 8, 967-979.	5.8	56
20473	Structural and electronic properties of half-Heusler alloys PtXBi (with X=Mn, Fe, Co and Ni) calculated from first principles. Journal of Magnetism and Magnetic Materials, 2015, 377, 252-258.	1.0	42
20474	Thermoelectric, electronic, optical and chemical bonding properties of Ba2PrRuO6: At temperature 7 K and 150 K. Materials Research Bulletin, 2015, 61, 551-559.	2.7	3
20475	Electronic and magnetic properties of Fe(Mn)-doped Cd and Zn nitrides for spintronic applications: a first-principles study. Journal of Materials Science, 2015, 50, 1446-1456.	1.7	8
20476	pentahexoctite: A new two-dimensional allotrope of carbon. Scientific Reports, 2014, 4, 7164.	1.6	85
20477	BC₃ Sheet Functionalized with Lithiumâ€Rich Species Emerging as a Reversible Hydrogen Storage Material. ChemPhysChem, 2015, 16, 634-639.	1.0	9
20478	Fine precipitation scenarios of AlZnMg(Cu) alloys revealed by advanced atomic-resolution electron microscopy study Part II: Fine precipitation scenarios in AlZnMg(Cu) alloys. Materials Characterization, 2015, 99, 142-149.	1.9	50
20479	Half-metallicity, magnetism and electrical resistivity of Sn1â^'xMnxTe alloys in rock salt and zinc blende structures. Journal of Magnetism and Magnetic Materials, 2015, 375, 15-25.	1.0	7
20480	Ab initio investigations of electron correlation effect and phonon dynamics of orthorhombic uranium. Physica Status Solidi (B): Basic Research, 2015, 252, 521-531.	0.7	7
20481	Equilibrium coverage of halides on metal electrodes. Surface Science, 2015, 631, 17-22.	0.8	72
20482	Stability characteristics of single-walled boron nitride nanotubes. Archives of Civil and Mechanical Engineering, 2015, 15, 162-170.	1.9	39
20483	Adsorption of SF6 decomposed gas on anatase (101) and (001) surfaces with oxygen defect: A density functional theory study. Scientific Reports, 2014, 4, 4762.	1.6	28
20484	The role of Co atoms in spin dependent electronic properties of graphite-like ZnO structures. Journal of Magnetism and Magnetic Materials, 2015, 373, 96-102.	1.0	6
20485	Noble-metal-free plasmonic photocatalyst: hydrogen doped semiconductors. Scientific Reports, 2015, 4, 3986.	1.6	48
20486	Theoretical calculations of structural, electronic, optical, elastic, and thermal properties of YX3 (XÂ=ÂIn, Sn, Tl, and Pb) compounds based on density functional theory. Journal of Materials Science, 2015, 50, 542-554.	1.7	8
20487	Synthesis of NiGa2O4Octahedron Nanocrystal with Exposed {111} Facets and Enhanced Efficiency of Photocatalytic Water Splitting. ChemPlusChem, 2015, 80, 223-230.	1.3	18

#	Article	IF	Citations
20488	Ab-initio study of planar strain on electronic structure properties of graphene sheets with nanoholes. Indian Journal of Physics, 2015, 89, 23-29.	0.9	6
20489	Stability and diffusion properties of Ti atom on Î±-uranium surfaces: A first-principles study. Computational Materials Science, 2015, 97, 201-208.	1.4	3
20490	Mechanical properties of fully hydrogenated graphene sheets. Solid State Communications, 2015, 201, 1-4.	0.9	30
20491	Pseudo Jahnâ€“Teller origin of ferroelectric instability in BaTiO3 type perovskites: The Green's function approach and beyond. Physica B: Condensed Matter, 2015, 457, 296-309.	1.3	54
20492	Mechanical, electronic, optical, thermodynamic properties and superconductivity of ScGa. Physica B: Condensed Matter, 2015, 457, 320-325.	1.3	24
20493	Allâ€Metallic Vertical Transistors Based on Stacked Dirac Materials. Advanced Functional Materials, 2015, 25, 68-77.	7.8	59
20494	Effect of Line Defects on the Electrical Transport Properties of Monolayer MoS<inline-formula> <tex-math notation="LaTeX">$_{f 2}$</tex-math></inline-formula> Sheet. IEEE Nanotechnology Magazine, 2015, 14, 51-56.	1.1	15
20495	Abnormal drop in electrical resistivity with impurity doping of single-crystal Ag. Scientific Reports, 2014, 4, 5450.	1.6	33
20496	Exploring the ring current of carbon nanotubes by first-principles calculations. Chemical Science, 2015, 6, 902-908.	3.7	15
20497	Magnesium Hydride Doped on Single-Walled Carbon Nanotubes for Hydrogen Adsorption. Fullerenes Nanotubes and Carbon Nanostructures, 2015, 23, 175-180.	1.0	5
20498	First-principles study on the electronic and magnetic properties of InN nanosheets doped with 2p elements. Physica E: Low-Dimensional Systems and Nanostructures, 2015, 67, 1-6.	1.3	20
20499	Metal-like fluorine-doped Î²-FeOOH nanorods grown on carbon cloth for scalable high-performance supercapacitors. Nano Energy, 2015, 11, 119-128.	8.2	184
20500	Interactions of water molecule with HfB2 and TaB2 (0001) surfaces: A first-principles investigation. Computational Materials Science, 2015, 97, 116-120.	1.4	7
20501	The 3R polymorph of CaSi2. Journal of Solid State Chemistry, 2015, 222, 18-24.	1.4	27
20502	Elastic, phonon and thermodynamic properties of ZnAl2O4 and ZnAl2S4 compounds from firstâ€“principles calculations. Solid State Sciences, 2015, 40, 7-12.	1.5	4
20503	Reducing Mg Acceptor Activation-Energy in Al0.83Ga0.17N Disorder Alloy Substituted by Nanoscale (AlN)5/(GaN)1 Superlattice Using MgGa Î´-Doping: Mg Local-Structure Effect. Scientific Reports, 2015, 4, 6710.	1.6	11
20504	Comparative molecular dynamics study of fcc-Ni nanoplate stress corrosion in water. Surface Science, 2015, 633, 94-101.	0.8	30
20505	Stabilization of H3+ in the high pressure crystalline structure of HnCl (n = 2â€“7). Chemical Science, 2015, 6, 522-526.	3.7	28

#	Article	IF	Citations
20506	Hydrogenâ€“water mixtures in giant planet interiors studied with ab initio simulations. High Energy Density Physics, 2015, 17, 157-161.	0.4	7
20507	Oxygen vacancy and hole conduction in amorphous TiO₂. Physical Chemistry Chemical Physics, 2015, 17, 541-550.	1.3	194
20508	Adsorption of Glucose Molecule onto Platinum-Decorated Single-Walled Carbon Nanotubes: A Dispersion-Corrected DFT Simulation. Fullerenes Nanotubes and Carbon Nanostructures, 2015, 23, 273-282.	1.0	8
20509	Optical properties of P and Al doped silicene: a first principles study. RSC Advances, 2015, 5, 41-50.	1.7	52
20510	Substrate-Specific Heterogeneous Catalysis of CeO₂ by Entropic Effects via Multiple Interactions. ACS Catalysis, 2015, 5, 20-26.	5.5	43
20511	Simulation of Epitaxial Growth byÂMeans of Density Functional Theory, Kinetic Monte Carlo, andÂPhase Field Methods. , 2015, , 521-559.		1
20512	Electronic and structural properties of bulk arsenopyrite and its cleavage surfaces â€“ a DFT study. RSC Advances, 2015, 5, 2013-2023.	1.7	34
20513	First-principles calculations of electronic structure and optical properties of Boron-doped ZnO with intrinsic defects. Optical Materials, 2015, 39, 34-39.	1.7	18
20514	Crystal structure, stability, and electronic properties of hydrated metal sulfates MSO4(H2O)n (M=Ni,) Tj ETQq0 0 0 rgBT /Overlock 10 Tf 77-86.	1.9	13
20515	Synthesis, structures, optical properties and electronic structures of PbGa2Q4 (Q=S, Se) crystals. Journal of Molecular Structure, 2015, 1082, 174-179.	1.8	11
20516	Formation mechanism of precipitate T1 in AlCuLi alloys. Journal of Alloys and Compounds, 2015, 624, 22-26.	2.8	71
20517	Theoretical study of defects Cu3SbSe4: Search for optimum dopants for enhancing thermoelectric properties. Journal of Alloys and Compounds, 2015, 625, 346-354.	2.8	51
20518	A theoretical study of Ti nanoparticle effect on sodium water reaction: Using ab initio calculation. Nuclear Engineering and Design, 2015, 281, 15-21.	0.8	4
20519	First-principles Studies on Electronic and Magnetic Properties of I A â€“III A and I A â€“IV A Compounds with Zinc-Blende and Wurtzite Structures. Journal of Superconductivity and Novel Magnetism, 2015, 28, 1535-1541.	0.8	4
20520	High pressure synthesis of Te-doped CoSb3 with enhanced thermoelectric performance. Journal of Materials Science: Materials in Electronics, 2015, 26, 385-391.	1.1	17
20521	Enhancing Thermoelectric Performance of PbTe-Based Compounds by Substituting Elements: A First Principles Study. Journal of Electronic Materials, 2015, 44, 1460-1468.	1.0	22
20522	Density functional theory calculations on oxygen adsorption on the Cu2O surfaces. Applied Surface Science, 2015, 324, 53-60.	3.1	50
20523	First-principles calculations of electronic structure and optical properties of boronâ€“phosphorus co-doped zinc oxide. Materials Science in Semiconductor Processing, 2015, 30, 406-412.	1.9	4

#	Article	IF	Citations
20524	Electronic and magnetic properties of CdSe nanoribbon: First-principles calculations. Physics Letters, Section A: General, Atomic and Solid State Physics, 2015, 379, 41-46.	0.9	6
20525	Electronic structure, phase stability, and vibrational properties of Ir-based intermetallic compound IrX (X=Al, Sc, and Ga). Journal of Physics and Chemistry of Solids, 2015, 77, 126-132.	1.9	22
20526	Heâ€“vacancy interaction and multiple He trapping in small void of silicon carbide. Journal of Nuclear Materials, 2015, 457, 36-41.	1.3	26
20527	Ab initio study of adsorption properties of hazardous organic molecules on graphene: Phenol, phenyl azide, and phenylnitrene. Chemical Physics Letters, 2015, 618, 57-62.	1.2	26
20528	Temperature-driven stabilization of fcc-ThH2 from first-principles theory coupled with lattice dynamics. Computational Materials Science, 2015, 98, 15-17.	1.4	8
20529	Ab initio prediction of the equilibrium shape of supported Ag nanoparticles on Î±-Al 2 O 3 (0 0 0 1). Journal of Catalysis, 2015, 321, 1-6.	3.1	31
20530	Thermodynamic study of reconstructed crystal surfaces.. Surface Science, 2015, 632, 180-184.	0.8	2
20531	The interplay between interface structure, energy level alignment and chemical bonding strength at organicâ€“metal interfaces. Physical Chemistry Chemical Physics, 2015, 17, 1530-1548.	1.3	100
20532	Research on Cs activation mechanism for Ga0.5Al0.5As(001) and GaN(0001) surface. Applied Surface Science, 2015, 324, 300-303.	3.1	15
20533	Thermodynamic modeling of the Caâ€“In and Caâ€“Sb systems supported with first-principles calculations. Calphad: Computer Coupling of Phase Diagrams and Thermochemistry, 2015, 48, 35-42.	0.7	8
20534	Defect driven ferromagnetism in SnO₂: a combined study using density functional theory and positron annihilation spectroscopy. RSC Advances, 2015, 5, 1148-1152.	1.7	35
20535	Stable zinc-blende ZnO thin films: formation and physical properties. Journal of Materials Science, 2015, 50, 28-33.	1.7	13
20536	Structures and optical properties of two phases of SrMgF₄. Physical Chemistry Chemical Physics, 2015, 17, 500-508.	1.3	9
20537	Structural and transport properties of double perovskite Dy2NiMnO6. Materials Research Bulletin, 2015, 62, 153-160.	2.7	42
20538	Carbon-free and two-dimensional cathode structure based on silicene for lithiumâ€“oxygen batteries: A first-principles calculation. Journal of Power Sources, 2015, 275, 32-37.	4.0	37
20539	Novel metastable compounds in the Zrâ€“B system: an ab initio evolutionary study. Physical Chemistry Chemical Physics, 2015, 17, 1180-1188.	1.3	22
20540	Combined effects of defects and hydroxyl groups on the electronic transport properties of reduced graphene oxide. Applied Physics A: Materials Science and Processing, 2015, 118, 885-892.	1.1	12
20541	A shear localization mechanism for lubricity of amorphous carbon materials. Scientific Reports, 2014, 4, 3662.	1.6	92

#	Article	IF	Citations
20542	Interaction of H₂O and H₂S with Cu(111) and the impact of the electric field: the rotating & translating adsorbate, and the rippled surface. Physical Chemistry Chemical Physics, 2015, 17, 588-598.	1.3	9
20543	Synthesis, X-ray crystal structure, optical properties and DFT studies of a new 2D layered iodide bridged Pb(II) coordination polymer with 2,3-bis(2-pyridyl)pyrazine. Journal of Solid State Chemistry, 2015, 221, 433-440.	1.4	8
20544	Structural stability, electronic structure and mechanical properties of platinum group metal nitrides PGMN (PGM=Os, Ir, Pt). International Journal of Refractory Metals and Hard Materials, 2015, 48, 382-397.	1.7	3
20545	N2O dissociation on small Rh clusters: A density functional study. Computational Materials Science, 2015, 97, 32-35.	1.4	15
20546	The effect of Î³â€“Î³â€² interface on the tensile and shear strengths of nickel-based superalloys: A first-principles study. Computational Materials Science, 2015, 97, 26-31.	1.4	6
20547	Mechanical, spin polarized electronic and magnetic properties of TmX <font>(X = Cu,) Tj ETQq1 1 0.784314 rgBT /Over	1.0	7
20548	Effects of group II elements on the cold stretch formability of Mgâ€“Zn alloys. Acta Materialia, 2015, 83, 294-303.	3.8	120
20549	Electronic structure and magnetic properties of quaternary Heusler alloy Co2CrGa1â^'Ge (x=0â^'1). Journal of Magnetism and Magnetic Materials, 2015, 377, 70-76.	1.0	10
20550	Electronic structure and surface properties of PrMnO 3 (001): A density functional theory study. Solid State Communications, 2015, 201, 31-35.	0.9	17
20551	Vibrational and thermodynamic properties of orthorhombic CaSnO3 from DFT and DFPT calculations. Journal of Physics and Chemistry of Solids, 2015, 77, 85-91.	1.9	48
20552	Investigation of structural, elastic, and lattice-dynamical properties of Ca2Si, Ca2Ge, and Ca2Sn based on first-principles density functional theory. Computational Materials Science, 2015, 97, 36-41.	1.4	19
20553	Adsorption and diffusion of oxygen on Î³-TiAl(0 0 1) and (1 0 0) surfaces. Computational Materials Science, 2015, 97, 55-63.	1.4	32
20554	Thermoelectric and optoelectronic properties of a heterocyclic isoxazolone nucleus compound. Materials Science in Semiconductor Processing, 2015, 30, 197-207.	1.9	4
20555	Structural stability and electronic properties of Î²-tetragonal boron: A first-principles study. Journal of Solid State Chemistry, 2015, 221, 378-383.	1.4	5
20556	Influence of carbon vacancy formation on the elastic constants and hardening mechanisms in transition metal carbides. Journal of the European Ceramic Society, 2015, 35, 95-103.	2.8	134
20557	First-principles calculations of electronic and optical properties of F, C-codoped cubic HfO2. Journal of Magnetism and Magnetic Materials, 2015, 375, 61-64.	1.0	11
20558	Aluminum doping improves the energetics of lithium, sodium, and magnesium storage in silicon: A first-principles study. Journal of Power Sources, 2015, 274, 65-70.	4.0	59
20559	Effects of Stone-Wales Defect Symmetry on the Electronic Structure and Transport Properties of Narrow Armchair Graphene Nanoribbon. Journal of Physics and Chemistry of Solids, 2015, 77, 8-13.	1.9	17

#	Article	IF	Citations
20560	Volcano-like Behavior of Au-Pd Core-shell Nanoparticles in the Selective Oxidation of Alcohols. Scientific Reports, 2014, 4, 5766.	1.6	73
20561	A comprehensive DFT investigation of bulk and low-index surfaces of ZrO₂polymorphs. Journal of Computational Chemistry, 2015, 36, 9-21.	1.5	61
20562	A possible critical temperature mechanism for H blistering nucleation/dissociation in metals. Solid State Communications, 2015, 201, 43-48.	0.9	5
20563	Ab initio modeling of wall structure and shape in perovskite-based nanotubes. Computational Materials Science, 2015, 96, 124-133.	1.4	6
20564	Structural, optoelectronic, infrared and Raman spectra from first principles calculations of Î³-Cd(OH)2. Journal of Physics and Chemistry of Solids, 2015, 76, 45-50.	1.9	16
20565	Ab initio study on the electronic origin of glass-forming ability in the binary Cuâ€“Zr and the ternary Cuâ€“Zrâ€“Al(Ag) metallic glasses. Journal of Alloys and Compounds, 2015, 619, 16-19.	2.8	26
20566	Application of the GGA-1/2 excited-state correction method to p-electron defective states: the special case of nitrogen-doped TiO₂. Canadian Journal of Physics, 2015, 93, 261-266.	0.4	8
20567	Revisiting the surface properties of Mg(0001) thin films and their effect on the adatom binding energy and self-diffusion. Surface Science, 2015, 632, 14-19.	0.8	3
20568	Electronic and vibrational properties of graphene monolayers with iron adatoms: A density functional theory study. Applied Surface Science, 2015, 334, 2-6.	3.1	11
20569	Magnetic, electronic, high-spin polarization and half-metallic properties of Ru2VGe and Ru2VSb Heusler alloys: An FP-LAPW study. Journal of Magnetism and Magnetic Materials, 2015, 374, 209-213.	1.0	30
20570	Metal Dichalcogenides Monolayers: Novel Catalysts for Electrochemical Hydrogen Production. Scientific Reports, 2014, 4, 5348.	1.6	151
20571	Spin-dependent transport properties of an armchair boron-phosphide nanoribbon embedded between two graphene nanoribbon electrodes. Physica E: Low-Dimensional Systems and Nanostructures, 2015, 65, 61-67.	1.3	13
20572	Methylene migration and coupling on a non-reducible metal oxide: The reaction of dichloromethane on stoichiometric Î±-Cr2O3(0001). Surface Science, 2015, 632, 28-38.	0.8	4
20573	Elastic and mechanical properties of lanthanide monoxides. Journal of Alloys and Compounds, 2015, 618, 292-298.	2.8	32
20574	Pb₇Bi₄Se₁₃: A Lillianite Homologue with Promising Thermoelectric Properties. Inorganic Chemistry, 2015, 54, 746-755.	1.9	60
20575	SiH/TiO2 and GeH/TiO2 Heterojunctions: Promising TiO2-based Photocatalysts under Visible Light. Scientific Reports, 2014, 4, 4810.	1.6	43
20576	First-principles study of spin transition and seismic properties of ferric iron-bearing post-perovskite with oxygen vacancy. Physics and Chemistry of Minerals, 2015, 42, 163-169.	0.3	0
20577	Adsorption of nonmetallic elements on defect-free MgO(001) surface â€“ DFT study. Surface Science, 2015, 632, 39-49.	0.8	19

#	Article	IF	Citations
20578	The effects of stepped sites and ruthenium adatom decoration on methanol dehydrogenation over platinum-based catalyst surfaces. Catalysis Today, 2015, 242, 230-239.	2.2	10
20579	Sr3Bi2(SeO3)6Â·H2O: A novel anionic layer consisting of second-order Jahnâ€“Teller (SOJT) distortive cations. Journal of Solid State Chemistry, 2015, 221, 73-78.	1.4	8
20580	Structural, mechanical and thermodynamic properties of AuIn2 crystal under pressure: A first-principles density functional theory calculation. Journal of Alloys and Compounds, 2015, 619, 576-584.	2.8	18
20581	Phase boundaries and molar volumes of high-temperature and high-pressure phase V of LiBH4. Journal of Physics and Chemistry of Solids, 2015, 76, 40-44.	1.9	5
20582	The effects of vacancies in the mechanical properties of tungsten: A first-principles study. Nuclear Instruments & Methods in Physics Research B, 2015, 342, 70-75.	0.6	12
20583	Electronic and high pressure elastic properties of RECd and REHg (RE=Sc, La and Yb) intermetallic compounds. Journal of Physics and Chemistry of Solids, 2015, 76, 70-81.	1.9	4
20584	Solid solution bariumâ€“strontium chlorides with tunable ammonia desorption properties and superior storage capacity. Journal of Solid State Chemistry, 2015, 221, 32-36.	1.4	14
20585	First-principles-aided design of a new Ni-base superalloy: Influence of transition metal alloying elements on grain boundary and bulk cohesion. Acta Materialia, 2015, 82, 369-377.	3.8	119
20586	New Lightâ€Harvesting Materials Using Accurate and Efficient Bandgap Calculations. Advanced Energy Materials, 2015, 5, 1400915.	10.2	124
20587	First-principles study of magnetic properties in Co-doped BiFeO3. Physica B: Condensed Matter, 2015, 457, 1-4.	1.3	17
20588	First principles investigations on the mechanical and vibrational properties for the selected B2-AgRE (RE=Sc, Y, La, Ce) intermetallics. Physica B: Condensed Matter, 2015, 457, 22-29.	1.3	1
20589	First-principles study of Si3N2. Computational Materials Science, 2015, 96, 140-145.	1.4	6
20590	DFT investigations of silicane/graphane conformers. Computational Materials Science, 2015, 96, 165-170.	1.4	13
20591	Amorphous Wâ€“Sâ€“N thin films: The atomic structure behind ultra-low friction. Acta Materialia, 2015, 82, 84-93.	3.8	31
20592	First principles study on the spin dependent electronic behavior of Co doped ZnO structures joining the Al electrodes. Journal of Alloys and Compounds, 2015, 619, 91-97.	2.8	10
20593	Oxidation of NO on Pt/M (M = Pt, Co, Fe, Mn): a first-principles density functional theory study. Catalysis Science and Technology, 2015, 5, 882-886.	2.1	11
20594	Anomalous electrical properties in superionic (Ag x Cu1â^'x)Br (xâ€‰=â€‰0.5): ab initio study. Ionics, 2015, 21, 161-166.	1.2	6
20595	Ab Initio Study of Binary and Ternary Nb3(X,Y) A15ÂIntermetallic Phases (X,YÂ=ÂAl, Ge, Si, Sn). Metallurgical and Materials Transactions A: Physical Metallurgy and Materials Science, 2015, 46, 566-576.	1.1	29

#	Article	IF	Citations
20596	Structural, electronic and magnetic properties of the (001), (110) and (111) surfaces of rocksalt sodium sulfide: A first-principles study. Journal of Physics and Chemistry of Solids, 2015, 76, 94-99.	1.9	14
20597	Structural, electronic and magnetic properties of the Si chains doped zigzag AlN nanoribbons. Physica E: Low-Dimensional Systems and Nanostructures, 2015, 65, 114-119.	1.3	7
20598	Statistical model and first-principles simulation on concentration of He V cluster and He bubble formation in Î±-Fe and W. Journal of Nuclear Materials, 2015, 456, 162-173.	1.3	20
20599	Magnetic, elastic and optical properties of zinc peroxide (ZnO2): First principles study. Journal of Alloys and Compounds, 2015, 620, 156-163.	2.8	11
20600	Structural, elastic, thermodynamic, electronic properties and phase transition in half-Heusler alloy NiVSb at high pressures. Computational Materials Science, 2015, 96, 72-80.	1.4	28
20601	Band gap and partial density of states for ZnO: Under high pressure. Journal of Alloys and Compounds, 2015, 619, 812-819.	2.8	31
20602	Hydrogen adsorption and storage on palladium-decorated graphene with boron dopants and vacancy defects: A first-principles study. Physica E: Low-Dimensional Systems and Nanostructures, 2015, 66, 40-47.	1.3	29
20603	Study of the Influence of Transition Metal Atoms on Electronic and Magnetic Properties of Graphyne Nanotubes Using Density Functional Theory. Fullerenes Nanotubes and Carbon Nanostructures, 2015, 23, 494-499.	1.0	8
20604	Phase diagram and thermodynamic properties of AlPO4 based on first-principles calculations and the quasiharmonic approximation. Physics and Chemistry of Minerals, 2015, 42, 15-27.	0.3	4
20605	Nature of active sites in Ni2P hydrotreating catalysts as probed by iron substitution. Applied Catalysis B: Environmental, 2015, 164, 204-216.	10.8	91
20606	First-principles prediction of the structural, elastic, thermodynamic, electronic and optical properties of Li4Sr3Ge2N6 quaternary nitride. Journal of Alloys and Compounds, 2015, 618, 84-94.	2.8	22
20607	Phase competition mediated by composition and pressure in Zr2Cu1â^'Ni system. Journal of Alloys and Compounds, 2015, 618, 73-77.	2.8	5
20608	Ab initio study of the compound-energy modeling of multisublattice structures: The (hP6) Ni2In-type intermetallics of the Niâ€“Inâ€“Sn system. Journal of Alloys and Compounds, 2015, 619, 464-473.	2.8	4
20609	Theoretical calculation of half-metallic ferromagnetism in Al1-xVxN compound. International Journal of Physical Sciences, 2016, 11, 11-18.	0.1	3
20610	A Prediction for Adhesion Forces Between Resin/metal Interfaces Through the First Principles Calculation. Journal of the Adhesion Society of Japan, 2016, 52, 287-292.	0.0	0
20611	First principles study of the relative stability and electronic properties of the VN/GaN/VN interlayer. International Journal of Physical Sciences, 2016, 11, 262-268.	0.1	0
20612	Ab-Initio Modeling of Adhesive Behaviors at Material Interfaces. , 2016, , .		0
20613	Coverage-dependent structural phase transformations in the adsorption of pentacene on an aperiodically modulated Cu film. Journal of Chemical Physics, 2016, 145, 154707.	1.2	1

#	Article	IF	Citations
20614	Comment on â€œHigh-pressure synthesis of orthorhombic SrIrO3 perovskite and its positive magnetoresistanceâ€•[J. Appl. Phys. 103, 103706 (2008)]. Journal of Applied Physics, 2016, 119, 086102.	1.1	6
20615	Structural and Electronic Properties of Cation Doping on the Spinel LiMn2O4: a First-Principles Theory. International Journal of Electrochemical Science, 2016, , 9394-9401.	0.5	1
20616	Influence of Defects in Boron Nitride Nanotubes in the Adsorption of Molecules. Insights from B3LYP-D2* Periodic Simulations. Crystals, 2016, 6, 63.	1.0	22
20617	Ab-initio study on electronic and magnetic properties of (Ga,Co) co-doped ZnO. Journal of Physics: Conference Series, 2016, 743, 012002.	0.3	0
20618	Elastic Properties and the Band Gap of<mml:math xmlns:mml="http://www.w3.org/1998/Math/MathML" id="M1"><mml:msub><mml:mrow><mml:mtext mathvariant="bold">AlN</mml:mtext></mml:mrow><mml:mrow><mml:mi>x</mml:mi></mml:mrow></mml:msub><mml:msub><mml:r mathvariant="bold">P</mml:mtext></mml:mrow><mml:mrow><mml:mn fontstyle="italic">1</mml:mn><mml:mo>-</mml:mo><mml:mi>x</mml:mi></mml:mrow></mml:msub></mml:math>Semiconductor Alloy: A Comparative Study of VariousAb InitioApproaches. Advances in Materials Science and En	1.0	2
20619	Energetics, atomic structure, and magnetics of rare earth-doped GaN bulk and nanoparticles. , 2016, , 103-126.		1
20620	A New Phase of GaN. Journal of Chemistry, 2016, 2016, 1-9.	0.9	10
20621	Atomic Scale Simulations of Relationship between Macroscopic Mechanical Properties and Microscopic Defect Evolution in Ultrafine-grained Metals. Materials Transactions, 2016, 57, 1476-1481.	0.4	1
20622	Transient Changes of Optical Properties in Semiconductors in Response to Femtosecond Laser Pulses. Applied Sciences (Switzerland), 2016, 6, 238.	1.3	9
20623	Mechanical Properties and Atomic Explanation of Plastic Deformation for Diamond-Like BC2. Materials, 2016, 9, 514.	1.3	3
20624	Effects of Aluminum on Hydrogen Solubility and Diffusion in Deformed Fe-Mn Alloys. Advances in Materials Science and Engineering, 2016, 2016, 1-9.	1.0	3
20625	Ab-initio structural search in solid oxygen at high pressure: from zero to finite temperature. Journal of Physics: Conference Series, 2016, 743, 012001.	0.3	0
20626	Surface Charge Storage Properties of Selected Graphene Samples in pH-neutral Aqueous Solutions of Alkali Metal Chlorides - Particularities and Universalities. International Journal of Electrochemical Science, 2016, 11, 8662-8682.	0.5	28
20627	DFT study of the formate formation on Ni(111) surface doped by transition metals [Ni(111)-M; M=Cu, Pd, Pt, Rh]. Journal of Physics: Conference Series, 2016, 739, 012082.	0.3	1
20628	Theoretical Investigation on Structural and Electronic Properties of InN Growth on Ce-Stabilized Zirconia (111) Substrates. Advances in Condensed Matter Physics, 2016, 2016, 1-7.	0.4	1
20629	Properties of the Free-Standing Two-Dimensional Copper Monolayer. Journal of Nanomaterials, 2016, 2016, 1-6.	1.5	13
20630	Temperature-Dependent Generalized Planar Fault Energy and Twinnability of Mg Microalloyed with Er, Ho, Dy, Tb, and Gd: First-Principles Study. Advances in Materials Science and Engineering, 2016, 2016, 1-9.	1.0	3
20631	On the Electronic Effect of V, Fe, and Ni on MgO(100) and BaO(100) Surface: An Explanation from a Periodic Density Functional. Journal of Chemistry, 2016, 2016, 1-8.	0.9	1

#	Article	IF	Citations
20632	Pressure Prediction of Electronic, Anisotropic Elastic, Optical, and Thermal Properties of Quaternary (M_{2/3}Ti_{1/3})₃AlC₂(M = Cr, Mo, and Ti). Advances in Condensed Matter Physics, 2016, 2016, 1-18.	0.4	4
20633	ZnSnS3: Structure Prediction, Ferroelectricity, and Solar Cell Applications. International Journal of Photoenergy, 2016, 2016, 1-9.	1.4	4
20634	First Principle Evaluation of Photocatalytic Suitability for TiO2-Based Nanotubes. , 2016, , .		1
20635	Energetic Stabilities, Structural and Electronic Properties of Monolayer Graphene Doped with Boron and Nitrogen Atoms. Electronics (Switzerland), 2016, 5, 91.	1.8	18
20636	Rb2Na(NO3)3: A Congruently Melting UV-NLO Crystal with a Very Strong Second-Harmonic Generation Response. Crystals, 2016, 6, 42.	1.0	65
20637	Vanadium Pentoxide Nanobelt-Reduced Graphene Oxide Nanosheet Composites as High-Performance Pseudocapacitive Electrodes: ac Impedance Spectroscopy Data Modeling and Theoretical Calculations. Materials, 2016, 9, 615.	1.3	22
20638	Effects of the CO2 Guest Molecule on the sI Clathrate Hydrate Structure. Materials, 2016, 9, 777.	1.3	33
20639	First-Principles Point Defect Models for Zr7Ni10 and Zr2Ni7 Phases. Batteries, 2016, 2, 23.	2.1	3
20640	Carbon-Doped Hexagonal Boron Nitride: Analysis as Ï€-Conjugate Molecules Embedded in Two Dimensional Insulator. Journal of Carbon Research, 2016, 2, 2.	1.4	9
20641	Interaction of Hydrogen with Au Modified by Pd and Rh in View of Electrochemical Applications. Computation, 2016, 4, 26.	1.0	6
20642	Silicene Nanoribbons on Pb-Reconstructed Si(111) Surface. Condensed Matter, 2016, 1, 8.	0.8	11
20643	On the Stability and Electronic Structure of Transition-Metal Dichalcogenide Monolayer Alloys Mo1â^'xXxS2â^'ySey with X = W, Nb. Electronics (Switzerland), 2016, 5, 1.	1.8	44
20644	First-Principles Study of Mo Segregation in MoNi(111): Effects of Chemisorbed Atomic Oxygen. Materials, 2016, 9, 5.	1.3	15
20645	Electronic Structure and Optical Property Analysis of Al/Ga-Codoped ZnO through First-Principles Calculations. Materials, 2016, 9, 164.	1.3	20
20646	The Mechanical and Electronic Properties of Carbon-Rich Silicon Carbide. Materials, 2016, 9, 333.	1.3	19
20647	Two Novel C3N4 Phases: Structural, Mechanical and Electronic Properties. Materials, 2016, 9, 427.	1.3	34
20648	A Reinvestigation of a Superhard Tetragonal sp3 Carbon Allotrope. Materials, 2016, 9, 484.	1.3	18
20649	Crystal Structures and Mechanical Properties of Ca2C at High Pressure. Materials, 2016, 9, 570.	1.3	15

#	Article	IF	Citations
20650	Effects of Al-Impurity Type on Formation Energy, Crystal Structure, Electronic Structure, and Optical Properties of ZnO by Using Density Functional Theory and the Hubbard-U Method. Materials, 2016, 9, 647.	1.3	15
20651	Nitrogen-Rich Energetic Metal-Organic Framework: Synthesis, Structure, Properties, and Thermal Behaviors of Pb(II) Complex Based on N,N-Bis(1H-tetrazole-5-yl)-Amine. Materials, 2016, 9, 681.	1.3	33
20652	Effect of Guest Atom Composition on the Structural and Vibrational Properties of the Type II Clathrate-Based Materials AxSi136, AxGe136 and AxSn136 (A = Na, K, Rb, Cs; 0 â‰¤ x â‰¤ 24). Materials, 2016, 9, 691.	1.3	6
20653	Pressure-Induced Phase Transition and Mechanical Properties of Mg2Sr Intermetallics. Materials, 2016, 9, 902.	1.3	1
20654	First-Principles Study on the Structural Stability and Segregation Behavior of Î³-Fe/Cr2N Interface with Alloying Additives M (M = Mn, V, Ti, Mo, and Ni). Metals, 2016, 6, 156.	1.0	15
20655	Edge Structure of Montmorillonite from Atomistic Simulations. Minerals (Basel, Switzerland), 2016, 6, 25.	0.8	28
20656	First Principles Based Study of Ground State and Electronic Properties of TmPb₃ Intermetallic Compound. Journal of Metastable and Nanocrystalline Materials, 2016, 28, 43-46.	0.1	0
20657	A New Superhard Phase and Physical Properties of ZrB3 from First-Principles Calculations. Materials, 2016, 9, 703.	1.3	21
20658	Energetic and electronic properties in a multilayered ZnO graphene-like nanostructure. Materials Research, 2016, 19, 497-504.	0.6	6
20659	First Principles Investigation of Electronic Property and High Pressure Phase Stability of SmN. Chinese Journal of Chemical Physics, 2016, 29, 219-222.	0.6	1
20660	Adsorption and Decomposition of NH3 on Ni/Pt(111) and Ni/WC(001) Surfaces: A First-Principles Study. Chinese Journal of Chemical Physics, 2016, 29, 710-716.	0.6	3
20661	FT-IR, XPS, and DFT Study of Adsorption Mechanism of Sodium Acetohydroxamate onto Goethite or Hematite. Chinese Journal of Chemical Physics, 2016, 29, 308-318.	0.6	18
20662	Enhanced photocatalytic activity of anatase-TiO2 nanoparticles by fullerene modification: A theoretical and experimental study. Applied Surface Science, 2016, 387, 750-758.	3.1	95
20663	Effects of coordination number of Au catalyst on oxygen species and their catalytic roles. Applied Surface Science, 2016, 387, 875-881.	3.1	12
20664	Bromine as a Preferred Etchant for Si Surfaces in the Supersaturation Regime: Insights from Calculations of Atomic Scale Reaction Pathways. Journal of Physical Chemistry C, 2016, 120, 15230-15234.	1.5	5
20665	Reactivity of Hydrogen on and in Nanostructured Molybdenum Nitride: Crotonaldehyde Hydrogenation. ACS Catalysis, 2016, 6, 5797-5806.	5.5	44
20666	Comparative density functional theory and density functional tight binding study of arginine and arginine-rich cell penetrating peptide TAT adsorption on anatase TiO₂. Physical Chemistry Chemical Physics, 2016, 18, 19902-19917.	1.3	24
20667	Structural transitions and electronic properties of sodium superoxide at high pressures. RSC Advances, 2016, 6, 67910-67915.	1.7	5

#	Article	IF	Citations
20668	Multiple Dirac cones in BN co-doped Î²-graphyne. Journal of Materials Chemistry C, 2016, 4, 7339-7344.	2.7	14
20669	Global structure search and physical properties of Os2C. Journal of Physics Condensed Matter, 2016, 28, 365502.	0.7	1
20670	First-principles modeling hydrogenation of bilayered boron nitride. Chinese Physics B, 2016, 25, 057301.	0.7	0
20671	Thermal conductivity and dielectric functions of alkali chlorideXCl (X= Li, Na, K and Rb): a first-principles study. Materials Research Express, 2016, 3, 075006.	0.8	2
20672	Anisotropic elastic and vibrational properties of Ru₂B₃and Os₂B₃: a first-principles investigation. Materials Research Express, 2016, 3, 076501.	0.8	16
20673	Structural and Electrical Irregularities Caused by Selected Dopants in Black-Phosphorus. ECS Journal of Solid State Science and Technology, 2016, 5, Q3026-Q3032.	0.9	19
20674	Structural stability, electronic structure and magnetic properties of the new hypothetical half-metallic ferromagnetic full-Heusler alloy CoNiMnSi. Materials Science-Poland, 2016, 34, 85-93.	0.4	25
20675	Chemical Stability of 2D-Nanostructured WO3 in Hydrogen Sensing Under Varied Operation Temperature. Nano, 2016, 11, 1650092.	0.5	3
20676	The structural response to pressure of energetic crystal 1,3-Diamino-2,4,6-trinitrobenzene: Density functional theory calculations and Hirshfeld surfaces analysis. Computational and Theoretical Chemistry, 2016, 1091, 57-63.	1.1	5
20677	Density functional theory-based derivation of an interatomic pair potential for helium impurities in nickel. Journal of Nuclear Materials, 2016, 479, 240-248.	1.3	20
20678	A comparative first-principles study of the lithiation, sodiation, and magnesiation of black phosphorus for Li-, Na-, and Mg-ion batteries. Physical Chemistry Chemical Physics, 2016, 18, 21391-21397.	1.3	73
20679	An interatomic potential for Wâ€“N interactions. Modelling and Simulation in Materials Science and Engineering, 2016, 24, 065007.	0.8	5
20680	The role of the oxide shell on the stability and energy storage properties of MWCNT@TiO $$_2$$ 2 nanohybrid materials used in Li-ion batteries. Theoretical Chemistry Accounts, 2016, 135, 1.	0.5	9
20681	Heterogeneous reaction mechanism of gaseous HNO3 with solid NaCl: a density functional theory study. Frontiers of Environmental Science and Engineering, 2016, 10, 1.	3.3	3
20682	Unusually strong lateral interaction in the CO overlayer in phosphorene-based systems. Nano Research, 2016, 9, 2598-2605.	5.8	15
20683	Point defect induced segregation of alloying solutes in Î±-Fe. Journal of Nuclear Materials, 2016, 479, 11-18.	1.3	5
20684	The role of minor yttrium in tailoring the failure resistance of surface oxide film formed on Mg alloys. Thin Solid Films, 2016, 615, 29-37.	0.8	11
20685	Activating Catalytic Inert Basal Plane of Molybdenum Disulfide to Optimize Hydrogen Evolution Activity via Defect Doping and Strain Engineering. Journal of Physical Chemistry C, 2016, 120, 16761-16766.	1.5	138

#	Article	IF	Citations
20686	Microphase separation upon crystallization of small amphiphilic molecules: â€˜lowâ€™ temperature form II of sodium benzoate (E 211). CrystEngComm, 2016, 18, 5811-5817.	1.3	3
20688	Significant Roles of Intrinsic Point Defects in Mg₂X (X = Si, Ge, Sn) Thermoelectric Materials. Advanced Electronic Materials, 2016, 2, 1500284.	2.6	75
20689	Trends in Hydrogen Evolution Activity of Metalâ€Modified Molybdenum Carbides in Alkaline and Acid Electrolytes. ChemElectroChem, 2016, 3, 1686-1693.	1.7	19
20690	Enhanced Catalytic Activity in Liquidâ€Exfoliated FeOCl Nanosheets as a Fentonâ€Like Catalyst. Chemistry - A European Journal, 2016, 22, 9321-9329.	1.7	59
20691	Nuclear magnetic resonance study of sulfate reorientations in LiNaSO₄. Journal of Physics Condensed Matter, 2016, 28, 176003.	0.7	2
20692	Stability of concentration-related self-interstitial atoms in fusion material tungsten. Chinese Physics B, 2016, 25, 056102.	0.7	6
20693	Pressure induced phase transition and thermo-physical properties in LuX (X = N, P). Materials Research Express, 2016, 3, 046502.	0.8	3
20694	Modulating the Electronic and Optical Properties of Tetragonal ZnSe Monolayers by Chalcogen Dopants. ChemPhysChem, 2016, 17, 1993-1998.	1.0	11
20695	Electronic Structure Properties of Doped and Imperfect ZnO Sheets. IEEE Nanotechnology Magazine, 2016, 15, 775-781.	1.1	2
20696	Nitrogenâ€Rich Manganese Oxynitrides with Enhanced Catalytic Activity in the Oxygen Reduction Reaction. Angewandte Chemie, 2016, 128, 8095-8099.	1.6	8
20697	DFT Study of Synergistic Catalysis of the Waterâ€Gasâ€Shift Reaction on Cuâ€“Au Bimetallic Surfaces. ChemCatChem, 2016, 8, 1208-1217.	1.8	14
20698	First Principles Modeling of Pdâ€doped (La,Sr)(Co,Fe)O₃ Complex Perovskites. Fuel Cells, 2016, 16, 267-271.	1.5	5
20699	Magnetic properties in AlN nanosheet doped with alkali metals: A first-principles study. Physica Status Solidi (B): Basic Research, 2016, 253, 1816-1823.	0.7	12
20700	Ab initio lattice dynamics and thermochemistry of layered bismuth telluride (Bi₂Te₃). Journal of Physics Condensed Matter, 2016, 28, 115401.	0.7	17
20701	Benefits of oxygen incorporation in atomic laminates. Journal of Physics Condensed Matter, 2016, 28, 135501.	0.7	7
20702	Dumbbell silicene: a strain-induced room temperature quantum spin Hall insulator. New Journal of Physics, 2016, 18, 043001.	1.2	24
20703	A study ab-initio of relative stability and electronic properties of substitutions of C by B and N atoms in the w-BN compound. Journal of Physics: Conference Series, 2016, 687, 012054.	0.3	0
20704	Effects of substitutions of C atoms by Al and N in the w-AlN compound. Journal of Physics: Conference Series, 2016, 687, 012114.	0.3	2

#	Article	IF	Citations
20705	Effective band structure of Ru-doped BaFe₂As₂. Journal of Physics: Conference Series, 2016, 689, 012027.	0.3	6
20706	Combining Nuclear Magnetic Resonance Spectroscopy and Density Functional Theory Calculations to Characterize Carvedilol Polymorphs. Journal of Pharmaceutical Sciences, 2016, 105, 2648-2655.	1.6	3
20707	Strong excitonic effects in hydrogen-graphene-fluorine janus graphene. Physica Status Solidi (B): Basic Research, 2016, 253, 712-717.	0.7	5
20708	First principle study on alkali metals promotion of CO oxidation over Ir(100). Physica Status Solidi (B): Basic Research, 2016, 253, 983-989.	0.7	6
20709	LiTaO3 phonon dispersion and ferroelectric transition calculated from first principles. Physica Status Solidi (B): Basic Research, 2016, 253, 683-689.	0.7	22
20710	Doping behaviors of adatoms adsorbed on phosphorene. Physica Status Solidi (B): Basic Research, 2016, 253, 1156-1166.	0.7	18
20711	Halfâ€Heusler compounds with a 1â€‰eV (1.7â€‰eV) direct band gap, latticeâ€matched to GaAs (Si), for solar cell application: A firstâ€principles study. Physica Status Solidi (B): Basic Research, 2016, 253, 889-894.	0.7	16
20712	Electronic and elastic properties of BaLiF₃with pressure effects: First-principles study. Physica Status Solidi (B): Basic Research, 2016, 253, 1788-1794.	0.7	8
20713	Graphene on clean (0001) Î±-quartz: Numerical determination of a minimum energy path from metal to semiconductor. Physica Status Solidi (B): Basic Research, 2016, 253, 1799-1807.	0.7	5
20714	H2S adsorption and decomposition on the gradually reduced Î±-Fe2O3(001) surface: A DFT study. Applied Surface Science, 2016, 387, 720-731.	3.1	53
20715	Effects of Cr and W additions on the stability and migration of He in bcc Fe: A first-principles study. Computational Materials Science, 2016, 123, 85-92.	1.4	20
20716	Implementation and Validation of Fully Relativistic GW Calculations: Spinâ€“Orbit Coupling in Molecules, Nanocrystals, and Solids. Journal of Chemical Theory and Computation, 2016, 12, 3523-3544.	2.3	156
20717	CO Poisoning Effects on FeNC and CN_x ORR Catalysts: A Combined Experimentalâ€“Computational Study. Journal of Physical Chemistry C, 2016, 120, 15173-15184.	1.5	57
20718	Predicted lithiumâ€“iron compounds under high pressure. RSC Advances, 2016, 6, 66721-66728.	1.7	4
20719	An overview of first-principles calculations of NMR parameters for paramagnetic materials. Materials Science and Technology, 2016, 32, 181-194.	0.8	5
20720	Insights on the atomistic origin of X and W photoluminescence lines inc-Si fromab initiosimulations. Journal Physics D: Applied Physics, 2016, 49, 075109.	1.3	10
20721	Energetics of carbon and nitrogen impurities and their interactions with vacancy in vanadium. Chinese Physics B, 2016, 25, 036104.	0.7	8
20722	First-principles study of strain effect on the formation and electronic structures of oxygen vacancy in SrFeO ₂. Chinese Physics B, 2016, 25, 057103.	0.7	1

#	Article	IF	Citations
20723	Effect of relaxation on the energetics and electronic structure of clean Ag₃PO₄(111) surface. Journal of Semiconductors, 2016, 37, 033001.	2.0	3
20724	Electronic Structure of ABC-stacked Multilayer Graphene and Trigonal Warping:A First Principles Calculation. Journal of Physics: Conference Series, 2016, 707, 012022.	0.3	7
20725	Stability, bonding, and electronic properties of silicon and germanium arsenides. Physica Status Solidi (B): Basic Research, 2016, 253, 862-867.	0.7	28
20726	C-chain-doping induced band-state transition in armchair AlN nanoribbons. Physica Status Solidi (B): Basic Research, 2016, 253, 1643-1648.	0.7	2
20727	Effects of Na, Mg, and Al substitution on the electronic, optical, lattice dynamical, and thermodynamic properties of semiboride Be2B. Physica Status Solidi (B): Basic Research, 2016, 253, 1596-1606.	0.7	0
20728	Observation of large lowâ€field magnetoresistance in spinel cobaltite: A new halfâ€metal. Physica Status Solidi - Rapid Research Letters, 2016, 10, 190-196.	1.2	14
20729	A Firstâ€Principles Study on the Electronic, Vibrational, and Thermodynamic Properties of Jadeite and its Tentative Lowâ€Density Polymorph. Zeitschrift Fur Anorganische Und Allgemeine Chemie, 2016, 642, 590-596.	0.6	4
20730	Chloroform Hydrodechlorination over Palladiumâ€“Gold Catalysts: A Firstâ€Principles DFT Study. ChemCatChem, 2016, 8, 1739-1746.	1.8	12
20731	Origin of the Ability of Î±â€Fe₂O₃ Mesopores to Activate Câ€H Bonds in Methane. Chemistry - A European Journal, 2016, 22, 2046-2050.	1.7	7
20732	Firstâ€Principles Study on Doping of SnSe₂ Monolayers. ChemPhysChem, 2016, 17, 375-379.	1.0	30
20733	Hybrid Density Functional Study on Monoâ€and Codoped NaNbO₃ for Visibleâ€Light Photocatalysis. ChemPhysChem, 2016, 17, 489-499.	1.0	40
20734	Density Functional Theory Calculation on the Dissociation Mechanism of Nitric Oxide Catalyzed by Cu₄ Cluster in ZSMâ€5 (Cu₄â€ZSMâ€5) and Bimetal Cu₃Fe in ZSMâ€5 (Cu₃Feâ€ZSMâ€5). Journal of the Chinese Chemical Society, 2016, 63, 499-505.	0.8	6
20735	Hybrid Functional Calculation of Defects in Pseudoâ€binary Indium Oxynitride. Journal of the Chinese Chemical Society, 2016, 63, 539-544.	0.8	2
20736	First Principles Calculations of Structural and Elastic Properties of Perovskite Crystals: The Case of SrTiO₃. Journal of the Chinese Chemical Society, 2016, 63, 521-525.	0.8	2
20737	Orbital-free density functional theory study of amorphous Liâ€“Si alloys and introduction of a simple density decomposition formalism. Modelling and Simulation in Materials Science and Engineering, 2016, 24, 035014.	0.8	4
20738	Structural and magnetic properties CuAl_{1-x}Cr_xS₂alloys. Journal of Physics: Conference Series, 2016, 687, 012051.	0.3	0
20739	Extremely Weak van der Waals Coupling in Vertical ReS₂ Nanowalls for Highâ€Currentâ€Density Lithiumâ€Ion Batteries. Advanced Materials, 2016, 28, 2616-2623.	11.1	204
20740	Colloidal Gold Nanocups with Orientationâ€Dependent Plasmonic Properties. Advanced Materials, 2016, 28, 6322-6331.	11.1	74

#	Article	IF	Citations
20741	Quasi 2D Ultrahigh Carrier Density in a Complex Oxide Brokenâ€Gap Heterojunction. Advanced Materials Interfaces, 2016, 3, 1500432.	1.9	32
20742	Spatially Resolved Quantification of the Surface Reactivity of Solid Catalysts. Angewandte Chemie - International Edition, 2016, 55, 6239-6243.	7.2	87
20743	Temperature dependence of strain energy and thermodynamic properties of V₂O₅â€based singleâ€walled nanotubes: Zoneâ€folding approach. Journal of Computational Chemistry, 2016, 37, 1442-1450.	1.5	8
20744	A Theoretical Study on the Design, Structure, and Electronic Properties of Novel Forms of Graphynes. Journal of Physical Chemistry C, 2016, 120, 15153-15161.	1.5	54
20745	Phase Stability of Lanthanum Orthovanadate at High Pressure. Journal of Physical Chemistry C, 2016, 120, 13749-13762.	1.5	42
20746	Like Charges Attract?. Journal of Physical Chemistry Letters, 2016, 7, 2689-2695.	2.1	26
20747	Terahertz Conductivity within Colloidal CsPbBr₃ Perovskite Nanocrystals: Remarkably High Carrier Mobilities and Large Diffusion Lengths. Nano Letters, 2016, 16, 4838-4848.	4.5	489
20748	Core electron excitations in U⁴⁺: modelling of the nd¹⁰5f²â†' nd⁹5f³transitions with n = 3, 4 and 5 by ligand field tools and density functional theory. Physical Chemistry Chemical Physics, 2016, 18, 19020-19031.	1.3	21
20749	Does the Dirac cone of germanene exist on metal substrates?. Physical Chemistry Chemical Physics, 2016, 18, 19451-19456.	1.3	39
20750	Electronic structures of p-type impurity in ZrS₂ monolayer. RSC Advances, 2016, 6, 58325-58328.	1.7	6
20751	Investigation of the elemental partitioning behaviour and site preference in ternary model nickel-based superalloys by atom probe tomography and first-principles calculations. Philosophical Magazine, 2016, 96, 2204-2218.	0.7	27
20752	Magnetic properties in BiFeO₃ doped with nonâ€metallic element: Firstâ€principles investigation. Physica Status Solidi (B): Basic Research, 2016, 253, 279-283.	0.7	10
20753	Atomic and electronic structures of a-ZnSnO3/a-SiO2interface byab initiomolecular dynamics simulations. Physica Status Solidi (B): Basic Research, 2016, 253, 1765-1770.	0.7	3
20754	Crystal structure and vibrational properties of Cu₂ZnSiSe₄quaternary semiconductor. Physica Status Solidi (B): Basic Research, 2016, 253, 1808-1815.	0.7	22
20755	Neural network and ReaxFF comparison for Au properties. International Journal of Quantum Chemistry, 2016, 116, 979-987.	1.0	66
20756	Structural, electronic, and magnetic properties of 3d transition metal doped GaN nanosheet: A first-principles study. International Journal of Quantum Chemistry, 2016, 116, 1000-1005.	1.0	37
20757	Hexagonal FeS nanosheets with high-energy (001) facets: Counter electrode materials superior to platinum for dye-sensitized solar cells. Nano Research, 2016, 9, 2862-2874.	5.8	38
20758	Surface atomic relaxation and magnetism on hydrogen-adsorbed Fe(110) surfaces from first principles. Applied Surface Science, 2016, 387, 385-392.	3.1	9

#	Article	IF	Citations
20759	Formation mechanism of gas bubble superlattice in UMo metal fuels: Phase-field modeling investigation. Journal of Nuclear Materials, 2016, 479, 202-215.	1.3	54
20760	Electronic structures and quantum capacitance of monolayer and multilayer graphenes influenced by Al, B, N and P doping, and monovacancy: Theoretical study. Carbon, 2016, 108, 7-20.	5.4	99
20761	Interplay between propylene and H2S co-adsorption on the H2 flux characteristics of Pd-alloy membranes employed in propane dehydrogenation (PDH) processes. Chemical Engineering Journal, 2016, 304, 134-140.	6.6	17
20762	Water-adsorption effect on electrical resistivity of nanoporous gold. Scripta Materialia, 2016, 123, 30-33.	2.6	14
20763	Electric field modulated half-metallicity of semichlorinated GaN nanosheets. Solid State Communications, 2016, 245, 5-10.	0.9	6
20764	Quantum confinement induced band gaps in MgB ₂ nanosheets. 2D Materials, 2016, 3, 031003.	2.0	12
20765	Dendriteâ€Free Lithium Deposition Induced by Uniformly Distributed Lithium Ions for Efficient Lithium Metal Batteries. Advanced Materials, 2016, 28, 2888-2895.	11.1	877
20766	A DFT Study of CO₂ Hydrogenation on Faujasiteâ€Supported Ir₄ Clusters: on the Role of Water for Selectivity Control. ChemCatChem, 2016, 8, 2500-2507.	1.8	17
20767	Crystallographic and Dynamic Aspects of Solidâ€State NMR Calibration Compounds: Towards ab Initio NMR Crystallography. ChemPhysChem, 2016, 17, 2496-2502.	1.0	12
20768	Temperature-dependent Raman spectroscopic studies of microstructure present in dipotassium molybdate crystals and their melts. Journal of Raman Spectroscopy, 2016, 47, 1259-1265.	1.2	17
20769	New developments in the multiscale hybrid energy density computational method. Chinese Physics B, 2016, 25, 013105.	0.7	0
20770	Efficient Photocatalytic Hydrogen Production over Rhâ€Doped Inverse Spinel Zn₂TiO₄. ChemCatChem, 2016, 8, 2289-2295.	1.8	40
20771	Anab initiocharacterization of the electronic structure of LaCoxFe1-xO3forxâ€‰â‰€â€‰0.5. Physica Status Solidi (B): Basic Research, 2016, 253, 1673-1687.	0.7	0
20772	Relevance of semiâ€coreâ€valence interaction for exact exchange calculations for group IVA, IIIAâ€“VA, and IIBâ€“VIA semiconductors. International Journal of Quantum Chemistry, 2016, 116, 867-879.	1.0	4
20773	Phase transition, elastic and electronic properties of topological insulator Sb ₂ Te ₃ under pressure: First principle study. Chinese Physics B, 2016, 25, 026401.	0.7	13
20774	A first-principles study on the effect of phosphorus-doped palladium catalyst for formic acid dissociation. Applied Surface Science, 2016, 387, 221-227.	3.1	10
20775	Adsorption and dissociation of H2S on monometallic and monolayer bimetallic Ni/Pd(111) surfaces: A first-principles study. Applied Surface Science, 2016, 387, 301-307.	3.1	25
20776	Substrate-dependent Au cluster: A new insight into Au /CeO2. Applied Surface Science, 2016, 387, 557-568.	3.1	13

#	Article	IF	Citations
20777	First-principles investigation of structural, mechanical and electronic properties for Cuâ€“Ti intermetallics. Computational Materials Science, 2016, 123, 70-78.	1.4	98
20778	Ab-initio study of structural, vibrational and optical properties of solid oxidizers. Materials Chemistry and Physics, 2016, 181, 54-66.	2.0	13
20779	Functional Group Adsorption on Calcite: I. Oxygen Containing and Nonpolar Organic Molecules. Journal of Physical Chemistry C, 2016, 120, 16586-16596.	1.5	89
20780	Functional Group Adsorption on Calcite: II. Nitrogen and Sulfur Containing Organic Molecules. Journal of Physical Chemistry C, 2016, 120, 16597-16607.	1.5	48
20781	Insight on the Interaction of Methanol-Selective Oxidation Intermediates with Au- or/and Pd-Containing Monometallic and Bimetallic Core@Shell Catalysts. Langmuir, 2016, 32, 7493-7502.	1.6	25
20782	Quantifying Uncertainty in Activity Volcano Relationships for Oxygen Reduction Reaction. ACS Catalysis, 2016, 6, 5251-5259.	5.5	70
20783	A multi-nuclear magnetic resonance and density functional theory investigation of epitaxially grown InGaP₂. Physical Chemistry Chemical Physics, 2016, 18, 21296-21304.	1.3	3
20784	The cluster-assembled nanowires based on M₁₂N₁₂ (M = Al and Ga) clusters as potential gas sensors for CO, NO, and NO₂ detection. Physical Chemistry Chemical Physics, 2016, 18, 21431-21441.	1.3	51
20785	A first-principles study of the thermodynamic and electronic properties of Mg and MgH₂nanowires. Physical Chemistry Chemical Physics, 2016, 18, 19412-19419.	1.3	18
20786	A new hard phase and physical properties of Tc2C predicted from first principles. RSC Advances, 2016, 6, 66066-66073.	1.7	6
20787	Controlling armchair and zigzag edges in oxidative cutting of graphene. Journal of Materials Chemistry C, 2016, 4, 6539-6545.	2.7	8
20788	Optical properties of quaternary kesterite-type Cu₂Zn(Sn_{1â^'x}Ge_x)S₄crystalline alloys: Raman scattering, photoluminescence and first-principle calculations. RSC Advances, 2016, 6, 67756-67763.	1.7	25
20789	Pressure induced thermoelectric enhancement in SnSe crystals. Journal of Materials Chemistry A, 2016, 4, 12073-12079.	5.2	81
20790	Metalâ€“Oxygen Bond Ionicity as an Efficient Descriptor for Doped NiOOH Photocatalytic Activity. ChemPhysChem, 2016, 17, 1630-1636.	1.0	25
20791	Theoretical Insight into the Trends that Guide the Electrochemical Reduction of Carbon Dioxide to Formic Acid. ChemSusChem, 2016, 9, 358-363.	3.6	311
20792	Sr₂Pd₄Al₅: Synthesis, Crystal and Electronic Structures, and Chemical Bonding of a Polar Intermetallic Compound. European Journal of Inorganic Chemistry, 2016, 2016, 1108-1114.	1.0	8
20793	Understanding and Controlling the Work Function of Perovskite Oxides Using Density Functional Theory. Advanced Functional Materials, 2016, 26, 5471-5482.	7.8	127
20794	Highâ€Performance Phototransistor of Epitaxial PbS Nanoplateâ€Graphene Heterostructure with Edge Contact. Advanced Materials, 2016, 28, 6497-6503.	11.1	51

#	Article	IF	Citations
20795	First-principles investigation of superconductivity in the body-centred tetragonal. Philosophical Magazine, 2016, 96, 2059-2073.	0.7	11
20796	Rock-salt structure lithium deuteride formation in liquid lithium with high-concentrations of deuterium: a first-principles molecular dynamics study. Nuclear Fusion, 2016, 56, 016020.	1.6	10
20797	First-principles investigation of ferroelectricity in LaBGeO5. Journal of Physics Condensed Matter, 2016, 28, 165901.	0.7	3
20798	Bandgap narrowing in the layered oxysulfide semiconductor Ba₃Fe₂O₅Cu₂S₂: Role of FeO₂layer. Chinese Physics B, 2016, 25, 026101.	0.7	5
20799	Electronic and magnetic properties GaN/MnN/GaN and MnN/GaN/MnN interlayers. Journal of Physics: Conference Series, 2016, 687, 012052.	0.3	1
20800	First-principles study of electronic and optical properties of Sr₂ZnN₂ under pressure. Modern Physics Letters B, 2016, 30, 1650139.	1.0	0
20801	Resistance switching behavior of atomic layer deposited SrTiO3 film through possible formation of Sr2Ti6O13 or Sr1Ti11O20 phases. Scientific Reports, 2016, 6, 20550.	1.6	17
20802	Positron annihilation spectroscopy of vacancy-related defects in CdTe:Cl and CdZnTe:Ge at different stoichiometry deviations. Scientific Reports, 2016, 6, 20641.	1.6	22
20803	A hybrid density functional study of silicon and phosphorus doped hexagonal boron nitride monolayer. Journal of Physics: Conference Series, 2016, 759, 012042.	0.3	4
20804	Surface strain effects on the adsorption and the diffusion of Au atoms on MgO(001) surfaces. Journal of the Korean Physical Society, 2016, 69, 1776-1780.	0.3	5
20805	Azobenzene/graphene hybrid for high-density solar thermal storage by optimizing molecular structure. Science China Technological Sciences, 2016, 59, 1383-1390.	2.0	25
20806	Electronic topological transitions in Nb3X (Xâ€‰=â€‰Al, Ga, In, Ge, and Sn) under compression investigated by first principles calculations. Journal of Applied Physics, 2016, 119, .	1.1	9
20807	Mechanical properties of bimetallic one-dimensional structures. Proceedings of SPIE, 2016, , .	0.8	0
20808	Evaluation of Pt Alloys as Electrocatalysts for Oxalic Acid Oxidation: A Combined Experimental and Computational Study. Journal of the Electrochemical Society, 2016, 163, H787-H795.	1.3	4
20809	Crystal metamorphosis at stress extremes: how soft phonons turn into lattice defects. NPG Asia Materials, 2016, 8, e320-e320.	3.8	8
20810	Investigation of the interface characteristics of Y2O3/GaAs under biaxial strain, triaxial strain, and non-strain conditions. Journal of Applied Physics, 2016, 120, .	1.1	8
20811	The incorporation site of Er in nanosized CaF2. Journal of Physics Condensed Matter, 2016, 28, 485301.	0.7	2
20812	High pressure and time resolved studies of optical properties of n-type doped GaN/AlN multi-quantum wells: Experimental and theoretical analysis. Journal of Applied Physics, 2016, 120, .	1.1	14

#	Article	IF	Citations
20813	A first-principle study on the phase transition, electronic structure, and mechanical properties of three-phase ZrTi2 alloy under high pressure*. European Physical Journal B, 2016, 89, 1.	0.6	2
20814	Band Gap Insensitivity to Large Chemical Pressures in Ternary Bismuth Iodides for Photovoltaic Applications. Journal of Physical Chemistry C, 2016, 120, 28924-28932.	1.5	54
20815	Nearly-free-electron system of monolayer Na on the surface of single-crystal <mml:math xmlns:mml="http://www.w3.org/1998/Math/MathML"><mml:msub><mml:mi>HfSe</mml:mi><mml:mn>2</mml:mn></mml:msub></mml:mr Physical Review B, 2016, 94, .	1.1	13
20816	Exact special twist method for quantum Monte Carlo simulations. Physical Review B, 2016, 94, .	1.1	21
20817	Effects of Monoatomic Vacancies and Alloy Atoms on Hydrogen Diffusion at Al(111) Surfaces. Nippon Kinzoku Gakkaishi/Journal of the Japan Institute of Metals, 2016, 80, 570-574.	0.2	0
20818	Effect of Alloying Element X on Transformation Strains and Phase Stabilities between α′′ and β Ti-Nb-X (X = Al, Sn, Zr, Ta) Ternary Alloys from First-Principles Calculations. Materials Transactions, 2016, 57, 263-268.	0.4	9
20819	Controlling Factors for the Formation of Guinier-Preston Zones in Al-Cu Alloys: An Atomistic Study. Nippon Kinzoku Gakkaishi/Journal of the Japan Institute of Metals, 2016, 80, 575-584.	0.2	8
20820	Self-Trapped Charge Carriers in Defected Amorphous TiO₂. Journal of Physical Chemistry C, 2016, 120, 27910-27916.	1.5	17
20821	The Enhancement of Surface Reactivity on CeO₂ (111) Mediated by Subsurface Oxygen Vacancies. Journal of Physical Chemistry C, 2016, 120, 27917-27924.	1.5	17
20822	Origin and structure of polar domains in doped molecular crystals. Nature Communications, 2016, 7, 13351.	5.8	36
20823	Ferroelectricity and magnetism in metal-formate frameworks of [NH₄][M(HCOO)₃] (M = Sc to Zn): a first-principles study. RSC Advances, 2016, 6, 113234-113239.	1.7	8
20824	B₄CN₃and B₃CN₄monolayers as the promising candidates for metal-free spintronic materials. New Journal of Physics, 2016, 18, 093021.	1.2	27
20825	Bis(dithioline)-Based Metalâ€“Organic Frameworks with Superior Electronic and Magnetic Properties: Spin Frustration to Spintronics and Gas Sensing. Journal of Physical Chemistry C, 2016, 120, 28307-28319.	1.5	55
20826	Unusually Stable Helical Coil Allotrope of Phosphorus. Nano Letters, 2016, 16, 7865-7869.	4.5	29
20827	Structural and electronic properties of two-dimensional stanene and graphene heterostructure. Nanoscale Research Letters, 2016, 11, 525.	3.1	43
20828	Edge effects on the characteristics of uranium diffusion on graphene and graphene nanoribbons. Chinese Physics B, 2016, 25, 086301.	0.7	1
20829	Vanadium interactions in crystalline silicon. Physical Review B, 2016, 94, .	1.1	10
20830	Diffusion in Ni-Based Single Crystal Superalloys with Density Functional Theory and Kinetic Monte Carlo Method. Communications in Computational Physics, 2016, 20, 603-618.	0.7	9

#	Article	IF	Citations
20831	Resonance Raman scattering and ab initio calculation of electron energy loss spectra of MoS 2 nanosheets. Physics Letters, Section A: General, Atomic and Solid State Physics, 2016, 380, 4057-4061.	0.9	3
20832	Visible-Light-Responsive Chalcogenide Photocatalyst Ba₂ZnSe₃: Crystal and Electronic Structure, Thermal, Optical, and Photocatalytic Activity. Inorganic Chemistry, 2016, 55, 12783-12790.	1.9	40
20833	Theoretical Investigation of Molecular and Electronic Structures of Buckminsterfullerene-Silicon Quantum Dot Systems. Journal of Physical Chemistry A, 2016, 120, 9767-9775.	1.1	2
20834	Synergistic Effects of Water and Oxygen Molecule Co-adsorption on (001) Surfaces of Tetragonal CH₃NH₃PbI₃: A First-Principles Study. Journal of Physical Chemistry C, 2016, 120, 28448-28455.	1.5	47
20835	Selectivity and Reactivity of Pd-Rich PdGa Surfaces toward Selective Hydrogenation of Acetylene: Interplay of Surface Roughness and Ensemble Effect. Journal of Physical Chemistry C, 2016, 120, 28654-28663.	1.5	19
20836	High-pressure X-ray diffraction, Raman and computational studies of MgCl2 up to 1 Mbar: Extensive pressure stability of the Î²-MgCl2 layered structure. Scientific Reports, 2016, 6, 30631.	1.6	15
20837	Ultra-high electrochemical catalytic activity of MXenes. Scientific Reports, 2016, 6, 32531.	1.6	105
20838	First-principles calculations of elastic, phonon and thermodynamic properties of W. Molecular Physics, 2016, 114, 3430-3436.	0.8	9
20839	Charge doping versus impurity scattering in chemically substituted iron pnictides. Physical Review B, 2016, 94, .	1.1	9
20840	Continuum approach for long-wavelength acoustic phonons in quasi-two-dimensional structures. Physical Review B, 2016, 94, .	1.1	45
20841	Strain-induced quasi-one-dimensional rare-earth silicide structures on Si(111). Physical Review B, 2016, 94, .	1.1	9
20842	Structural, electronic, sodium diffusion and elastic properties of Naâ€“P alloy anode for Na-ion batteries: Insight from first-principles calculations. Modern Physics Letters B, 2016, 30, 1650385.	1.0	5
20843	Metallic behavior of GaAs/BaTiO ₃ heterostructure. Europhysics Letters, 2016, 115, 16001.	0.7	4
20844	All The Catalytic Active Sites of MoS₂ for Hydrogen Evolution. Journal of the American Chemical Society, 2016, 138, 16632-16638.	6.6	664
20845	Metastable Layered Cobalt Chalcogenides from Topochemical Deintercalation. Journal of the American Chemical Society, 2016, 138, 16432-16442.	6.6	61
20846	Silicene nanomeshes: bandgap opening by bond symmetry breaking and uniaxial strain. Scientific Reports, 2016, 6, 20971.	1.6	16
20847	Optimizing the Dopant and Carrier Concentration of Ca5Al2Sb6 for High Thermoelectric Efficiency. Scientific Reports, 2016, 6, 29550.	1.6	10
20848	The structural, elastic and optical properties of ScM (M = Rh, Cu, Ag, Hg) intermetallic compounds under pressure by ab initio simulations. International Journal of Computational Materials Science and Engineering, 2016, 05, 1650024.	0.5	7

#	Article	IF	Citations
20849	The impact of the dopants on the formation of conductive path in titanium dioxide: ab initio calculations. European Physical Journal B, 2016, 89, 1.	0.6	1
20850	Integrating superconducting phase and topological crystalline quantum spin Hall effect in hafnium intercalated gallium film. Applied Physics Letters, 2016, 108, 253102.	1.5	4
20851	Density and localized states' impact on amorphous carbon electron transport mechanisms. Journal of Applied Physics, 2016, 120, 214303.	1.1	3
20852	Role of Y Admixture in <mml:math xmlns:mml="http://www.w3.org/1998/Math/MathML" display="inline"><mml:mrow><mml:mo stretchy="false">(</mml:mo><mml:msub><mml:mrow><mml:mi>Lu</mml:mi></mml:mrow><mml:mrow><mml:mn>1</mml:mn><mml:mn> Physical Review Applied, 2016, 6, .	1.5	23
20853	High pressure behaviour of uranium dicarbide (UC2): Ab-initio study. Journal of Applied Physics, 2016, 120, .	1.1	10
20854	Ab-initio study of pressure effects and hydrogen impurity in HgO. Journal of the Korean Physical Society, 2016, 68, 1476-1480.	0.3	0
20855	Perspective: Methods for large-scale density functional calculations on metallic systems. Journal of Chemical Physics, 2016, 145, 220901.	1.2	106
20856	First-principles study of the pressure effects on the structural and electronic properties of crystalline organic azide C10H8N6O4. Journal of Structural Chemistry, 2016, 57, 1074-1078.	0.3	2
20857	Inherent instability by antibonding coupling in AgSbTe₂. Japanese Journal of Applied Physics, 2016, 55, 041801.	0.8	15
20858	Theoretical investigation of the electronic structure and optical properties of zinc-doped magnesium oxide. Journal of Computational Electronics, 2016, 15, 1521-1530.	1.3	20
20859	Surface-hydrogen-induced metallization and rumpling in thin <mml:math xmlns:mml="http://www.w3.org/1998/Math/MathML"><mml:mrow><mml:mi>BaTi</mml:mi><mml:msub><mml:mi mathvariant="normal">O</mml:mi><mml:mn>3</mml:mn></mml:msub></mml:mrow></mml:math> films. Physical Review B, 2016, 94, .	1.1	3
20860	Electronic structure tuning via surface modification in semimetallic nanowires. Physical Review B, 2016, 94, .	1.1	6
20861	Pressure-induced structural transition of CdxZn1â^'xO alloys. Applied Physics Letters, 2016, 108, .	1.5	10
20862	Local environment dependance of the water diffusion energy barrier onto the (101) anatase surface. AIP Conference Proceedings, 2016, , .	0.3	1
20863	The force-field derivation and application of explosive/additive interfaces. Modelling and Simulation in Materials Science and Engineering, 2016, 24, 075013.	0.8	3
20864	On the structural and electronic properties of Ir-silicide nanowires on Si(001) surface. Journal of Applied Physics, 2016, 120, .	1.1	8
20865	Origin of the performances degradation of two-dimensional-based metal-oxide-semiconductor field effect transistors in the sub-10â€‰nm regime: A first-principles study. Applied Physics Letters, 2016, 108, .	1.5	5
20866	Analysis of the structural, electronic and optic properties of Ni doped MgSiP2 semiconductor chalcopyrite compound. AIP Conference Proceedings, 2016, , .	0.3	2

#	Article	IF	Citations
20867	Nonstoichiometry and Weyl fermionic behavior in TaAs. Physical Review B, 2016, 94, .	1.1	20
20868	Magneto-electric coupling in antiferromagnet/ferroelectric Mn2Au/BaTiO3 interface. Journal of Applied Physics, 2016, 120, .	1.1	12
20869	Topological Phase in Non-centrosymmetric Material NaSnBi. Chinese Physics Letters, 2016, 33, 127301.	1.3	11
20870	First-principles study of structure, initial lattice expansion, and pressure-composition-temperature hysteresis for substituted LaNi₅and TiMn₂alloys. Modelling and Simulation in Materials Science and Engineering, 2016, 24, 085007.	0.8	8
20871	Cadmium and lithium doping in silver orthophosphate: An ab initio study. Scientific Reports, 2016, 6, 32574.	1.6	2
20872	Theoretical impurity-limited carrier mobility of monolayer black phosphorus. Applied Physics Letters, 2016, 108, .	1.5	14
20873	Effects of interlayer screening and temperature on dielectric functions of graphene by first-principles. Journal of Applied Physics, 2016, 120, .	1.1	7
20874	Density functional study of adsorptions of CO₂, NO₂and SO₂molecules on Zn(0002) surfaces. Journal of Physics: Conference Series, 2016, 739, 012080.	0.3	16
20875	Experimental and theoretical study of rotationally inelastic diffraction of H2(D2) from methyl-terminated Si(111). Journal of Chemical Physics, 2016, 145, 084705.	1.2	3
20876	Comparative Study of Electronic and Elastic Properties of Aluminum Gadolinium. Journal of Metastable and Nanocrystalline Materials, 2016, 28, 71-76.	0.1	0
20877	A perfect wetting of Mg monolayer on Ag(111) under atomic scale investigation: First principles calculations, scanning tunneling microscopy, and Auger spectroscopy. Journal of Chemical Physics, 2016, 144, 194708.	1.2	1
20878	CO2 adsorption on Fe-doped graphene nanoribbons: First principles electronic transport calculations. AIP Advances, 2016, 6, .	0.6	21
20879	Intra- and inter-atomic optical transitions of Fe, Co, and Ni ferrocyanides studied using first-principles many-electron calculations. Journal of Applied Physics, 2016, 119, .	1.1	12
20880	Novel high-pressure phases of AlP from first principles. Journal of Applied Physics, 2016, 119, .	1.1	11
20881	Toward the IIIâ€“V/Si co-integration by controlling the biatomic steps on hydrogenated Si(001). Applied Physics Letters, 2016, 109, .	1.5	46
20882	Tunable magnetic states on the zigzag edges of hydrogenated and halogenated group-IV nanoribbons. Scientific Reports, 2016, 6, 39083.	1.6	15
20883	The mechanism of the area negative thermal expansion in KBe2BO3F2 family crystals: A first-principles study. Journal of Applied Physics, 2016, 119, .	1.1	4
20884	Hydrogen bonding in the protic ionic liquid triethylammonium nitrate explored by density functional tight binding simulations. Journal of Chemical Physics, 2016, 145, 234504.	1.2	14

#	Article	IF	Citations
20885	Ab Initio Investigation of Structural and Electronic Properties of ErPb₃ in AB₃ Structure. Journal of Metastable and Nanocrystalline Materials, 2016, 28, 39-42.	0.1	1
20886	Structural, mechanical, and magnetic properties of GaFe3N thin films. Journal of Vacuum Science and Technology A: Vacuum, Surfaces and Films, 2016, 34, 040601.	0.9	3
20887	Guiding ab initio calculations by alchemical derivatives. Journal of Chemical Physics, 2016, 144, 104103.	1.2	25
20888	Structural, electronic and vibrational properties of lanthanide monophosphide at high pressure. AIP Conference Proceedings, 2016, , .	0.3	0
20889	TCNQ Grown on Cu (001): Its Atomic and Electronic Structure Determination. Journal of Physical Chemistry C, 2016, 120, 26889-26898.	1.5	5
20890	Influence of ambient gas pressure and carbon adsorption on dark current emission from a cathode. Journal of Vacuum Science and Technology B:Nanotechnology and Microelectronics, 2016, 34, .	0.6	4
20891	Strong piezoelectric response in stable TiZnN2, ZrZnN2, and HfZnN2 found by ab initio high-throughput approach. Journal of Applied Physics, 2016, 120, .	1.1	17
20892	Interaction of methanol and its dehydrogenation species with Pt-alloy surfaces. AIP Conference Proceedings, 2016, , .	0.3	1
20893	How to Fabricate a Surface-Grafted Polythiophene on H-Si(100)2Ã—1 Surface via Self-Assembling and in Situ Surface Polymerization: A Theoretical Guide. Journal of Physical Chemistry C, 2016, 120, 25612-25619.	1.5	3
20894	Mechanism of oxidation protection of the Si(001) surface by sub-monolayer Sr template. Journal of Applied Physics, 2016, 120, .	1.1	17
20895	Ab initio modelling of dielectric screening and plasmon resonances in extrinsic silicene. , 2016, , .		0
20896	Super-stretchable borophene. Europhysics Letters, 2016, 116, 36001.	0.7	22
20897	Theoretical insights into kesterite and stannite phases of Cu2(Sn1â€“XGeX)ZnSe4 based alloys: A prospective photovoltaic material. AIP Advances, 2016, 6, 125303.	0.6	5
20898	MÃ¶ssbauer parameters of Fe-related defects in group-IV semiconductors: First principles calculations. Journal of Applied Physics, 2016, 119, .	1.1	7
20899	Advances in modeling semiconductor epitaxy: Contributions of growth orientation and surface reconstruction to InN metalorganic vapor phase epitaxy. Applied Physics Express, 2016, 9, 125601.	1.1	12
20900	Effective optical constants of silver nanofilms calculated in wide frequency range. Proceedings of SPIE, 2016, , .	0.8	1
20901	The influence of Lifshitz forces and gas on premelting of ice within porous materials. Europhysics Letters, 2016, 115, 13001.	0.7	7
20902	Mechanism of polarization switching in wurtzite-structured zinc oxide thin films. Applied Physics Letters, 2016, 109, .	1.5	30

#	Article	IF	Citations
20903	First-principles investigation on solar radiation shielding performance of rutile VO2 filters for smart windows. Applied Physics Letters, 2016, 109, .	1.5	10
20904	First principles calculation of thermoelectric parameters of Monolayer- and Bilayer-Graphene and Heterostructures of Graphene andh-BN. Journal of Physics: Conference Series, 2016, 759, 012040.	0.3	3
20905	First-Principles Investigation on Electronic Structure of Bi 2 Se 3 Thin Film and the Films Doped with Pb. Rare Metal Materials and Engineering, 2016, 45, 2809-2813.	0.8	0
20906	Mechanical properties of Liâ€“Sn alloys for Li-ion battery anodes: A first-principles perspective. AIP Advances, 2016, 6, .	0.6	23
20907	Experimental and theoretical investigation of Cr1-xScxN solid solutions for thermoelectrics. Journal of Applied Physics, 2016, 120, .	1.1	33
20908	Band structure, Fermi surface, elastic, thermodynamic, and optical properties of AlZr₃, AlCu₃, and AlCu₂Zr: First-principles study. Chinese Physics B, 2016, 25, 083101.	0.7	11
20909	Donors in Ge as qubits â€"Establishing physical attributes. Europhysics Letters, 2016, 116, 20002.	0.7	1
20910	Effect of van der Waals interactions on the chemisorption and physisorption of phenol and phenoxy on metal surfaces. Journal of Chemical Physics, 2016, 145, 104701.	1.2	21
20911	A first principle study of the pressure dependent elastic properties of monazite LaPO4. AIP Conference Proceedings, 2016, , .	0.3	5
20912	First-principles studies of electronic, optical, and mechanical properties of Î³ -Bi 2 Sn 2 O 7. Chinese Physics B, 2016, 25, 067801.	0.7	6
20913	Vectorial mapping of noncollinear antiferromagnetic structure of semiconducting FeSe surface with spin-polarized scanning tunneling microscopy. Applied Physics Letters, 2016, 108, .	1.5	9
20914	Structural and configurational properties of nanoconfined monolayer ice from first principles. Scientific Reports, 2016, 6, 18651.	1.6	61
20915	Ab Initio Monte Carlo Simulations of the Acidic Dissolution of Stainless Steels: Influence of the Alloying Elements. Journal of the Electrochemical Society, 2016, 163, C807-C814.	1.3	7
20916	Electric field response in bilayer graphene: Ab initio investigation. Applied Physics Express, 2016, 9, 115104.	1.1	2
20917	First-principles determination of band-to-band electronic transition energies in cubic and hexagonal AlGaInN alloys. AIP Advances, 2016, 6, 085308.	0.6	4
20918	Tuned Magnetic Properties of L10-MnGa/Co(001) Films by Epitaxial Strain. Scientific Reports, 2016, 6, 19508.	1.6	8
20919	Understanding the Formation Mechanism of Two-Dimensional Atomic Islands on Crystal Surfaces by the Condensing Potential Model. Zeitschrift Fur Naturforschung - Section A Journal of Physical Sciences, 2016, 71, 321-324.	0.7	0
20920	CO adsorption on small Aun (n = 1â€“4) structures supported on hematite. I. Adsorption on iron terminated Î±-Fe2O3 (0001) surface. Journal of Chemical Physics, 2016, 144, 044704.	1.2	10

#	Article	IF	Citations
20921	Exotic d magnetism in partial hydrogenated silicene. Applied Physics Letters, 2016, 108, .	1.5	19
20922	Electrolyte decomposition on Li-metal surfaces from first-principles theory. Journal of Chemical Physics, 2016, 145, 204701.	1.2	30
20923	The effect of Al segregation on Schottky barrier height and effective work function in TiAl/TiN/HfO₂gate stacks. Journal Physics D: Applied Physics, 2016, 49, 275104.	1.3	3
20924	Investigation of structural, electronic, elastic and optical properties of Cd1-x-yZnxHgyTe alloys. AIP Advances, 2016, 6, 065115.	0.6	6
20925	Multiporous carbon allotropes transformed from symmetry-matched carbon nanotubes. AIP Advances, 2016, 6, .	0.6	11
20926	First-principles study of Auâ€“Cu alloy surface changes induced by gas adsorption of CO, NO, or O2. Journal of Chemical Physics, 2016, 145, 024701.	1.2	24
20927	Core properties and mobility of the basal screw dislocation in wurtzite GaN: a density functional theory study. Modelling and Simulation in Materials Science and Engineering, 2016, 24, 075001.	0.8	21
20928	The growth of zinc phthalocyanine thin films by pulsed laser deposition. Journal of Materials Research, 2016, 31, 163-172.	1.2	19
20929	Strain-engineering the anisotropic electrical conductance in ReS2 monolayer. Applied Physics Letters, 2016, 108, .	1.5	53
20930	Magnetic ordering and conduction mechanism of different electroactive regions in Lu2NiMnO6. Journal of Applied Physics, 2016, 120, .	1.1	18
20931	Spin-polarized quantum transport properties through flexible phosphorene. Applied Physics Letters, 2016, 109, 142409.	1.5	21
20932	Two-Step Phase Transition in SnSe and the Origins of its High Power Factor from First Principles. Physical Review Letters, 2016, 117, 276601.	2.9	91
20933	Temperatureâ€dependent elastic and thermodynamic properties of Fe₃Ga (DO₃,) Tj ETQq0 0 0 rgBT /Overloch (B): Basic Research, 2016, 253, 2236-2244.	0.7	5
20934	The Nature of Metastable AAâ€™ Graphite: Low Dimensional Nano- and Single-Crystalline Forms. Scientific Reports, 2016, 6, 39624.	1.6	34
20935	Structural and electronic properties of multilayer graphene on monolayer hexagonal boron nitride/nickel (111) interface system: A van der Waals density functional study. Journal of Applied Physics, 2016, 119, .	1.1	5
20936	Superhardsp2â€“sp3hybrid carbon allotropes with tunable electronic properties. AIP Advances, 2016, 6, 055020.	0.6	20
20937	Investigation of the structural, mechanical, dynamical and thermal properties of CsCaF₃and CsCdF₃. Materials Research Express, 2016, 3, 045903.	0.8	10
20939	Electronic structure of cubic ScF3 from first-principles calculations. Low Temperature Physics, 2016, 42, 556-560.	0.2	9

#	Article	IF	Citations
20940	A computational ab initio study of surface diffusion of sulfur on the CdTe (111) surface. AIP Advances, 2016, 6, 085002.	0.6	1
20941	Thermomechanical response of thermoelectrics. Applied Physics Letters, 2016, 109, 223903.	1.5	23
20942	On the tautomerisation of porphycene on copper (111): Finding the subtle balance between van der Waals interactions and hybridisation. Journal of Chemical Physics, 2016, 145, 244701.	1.2	5
20943	Structural, electronic, and magnetic properties of tris(8-hydroxyquinoline)iron(III) molecules and their magnetic coupling with ferromagnetic surface: first-principles study. Journal of Physics Condensed Matter, 2016, 28, 176004.	0.7	6
20944	Monoclinic high-pressure polymorph of AlOOH predicted from first principles. Physical Review B, 2016, 94, .	1.1	13
20945	Effects of electronic relaxation processes on vibrational linewidths of adsorbates on surfaces: The case of CO/Cu(100). Physical Review B, 2016, 94, .	1.1	31
20946	Effect of Organic Cations on Hydrogen Oxidation Reaction of Carbon Supported Platinum. Journal of the Electrochemical Society, 2016, 163, F1503-F1509.	1.3	29
20947	A Database of the Structural and Electronic Properties of Prussian Blue, Prussian White, and Berlin Green Compounds through Density Functional Theory. Inorganic Chemistry, 2016, 55, 12851-12862.	1.9	92
20948	Effects of Applied Potential and Water Intercalation on the Surface Chemistry of Ti₂C and Mo₂C MXenes. Journal of Physical Chemistry C, 2016, 120, 28432-28440.	1.5	104
20949	Enhancing Sodium Ion Battery Performance by Strongly Binding Nanostructured Sb₂S₃ on Sulfur-Doped Graphene Sheets. ACS Nano, 2016, 10, 10953-10959.	7.3	344
20950	Magnetic characteristics of Auâ€“Mn nanowires. JETP Letters, 2016, 103, 593-597.	0.4	3
20951	Ab initiocalculations on the initial stages of GaN and ZnO growth on lattice-matched ScAlMgO4(0001) substrates. Materials Research Express, 2016, 3, 125903.	0.8	1
20952	Coupling and competition between ferroelectricity, magnetism, strain, and oxygen vacancies in AMnO3 perovskites. MRS Communications, 2016, 6, 182-191.	0.8	62
20953	Ethanol Reaction on Co3O4(110) and Co(0001): A Microkinetic Model Analysis. Journal of Physical Chemistry C, 2016, 120, 28110-28124.	1.5	12
20954	Reversible switching between pressure-induced amorphization and thermal-driven recrystallization in VO2(B) nanosheets. Nature Communications, 2016, 7, 12214.	5.8	47
20955	Nonmetallization and band inversion in beryllium dicarbide at high pressure. Scientific Reports, 2016, 6, 26398.	1.6	2
20956	First-principles investigation of the structural, dynamical, and dielectric properties of kesterite, stannite, and PMCA phases of <mml:math xmlns:mml="http://www.w3.org/1998/Math/MathML"><mml:mrow><mml:msub><mml:mi>Cu</mml:mi><mml:mn>2</mml:mn></mml: Physical Review B, 2016, 94, .	1.1	23
20957	First-principles calculations of SO2 sensing with Si nanowires. European Physical Journal B, 2016, 89, 1.	0.6	4

#	Article	IF	Citations
20958	Tinselenidene: a Two-dimensional Auxetic Material with Ultralow Lattice Thermal Conductivity and Ultrahigh Hole Mobility. Scientific Reports, 2016, 6, 19830.	1.6	155
20959	Theoretical prediction of the band offsets at the ZnO/anatase TiO2 and GaN/ZnO heterojunctions using the self-consistent ab initio DFT/GGA-1/2 method. Journal of Chemical Physics, 2016, 144, 014704.	1.2	9
20960	Effect of oxygen vacancies on the electronic and optical properties of tungsten oxide from first principles calculations. Journal of Applied Physics, 2016, 120, .	1.1	34
20961	Interfacial charge rearrangement and intermolecular interactions: Density-functional theory study of free-base porphine adsorbed on Ag(111) and Cu(111). Journal of Chemical Physics, 2016, 144, 024701.	1.2	23
20962	A DFT+U study of the structural, electronic, magnetic, and mechanical properties of cubic and orthorhombic SmCoO3. Journal of Chemical Physics, 2016, 145, 224704.	1.2	15
20963	Magnetic and electronic properties of porphyrin-based molecular nanowires. AIP Advances, 2016, 6, 015216.	0.6	9
20964	Electric field dependence of optical phonon frequencies in wurtzite GaN observed in GaN high electron mobility transistors. Journal of Applied Physics, 2016, 120, .	1.1	12
20965	Hydrogen-Induced Core Structures Change of Screw and Edge Dislocations in Tungsten. , 2016, , 253-259.		0
20966	Structural, anisotropic and thermodynamic properties of Imm2-BCN. Journal Wuhan University of Technology, Materials Science Edition, 2016, 31, 1272-1279.	0.4	1
20967	Additive and Photochemical Manufacturing of Copper. Scientific Reports, 2016, 6, 39584.	1.6	28
20968	The formation of H bubbles at small-angle tilt grain boundaries in W films. Physical Chemistry Chemical Physics, 2016, 18, 33103-33108.	1.3	6
20969	High-coercivity magnetism in nanostructures with strong easy-plane anisotropy. Applied Physics Letters, 2016, 108, 152406.	1.5	25
20970	Tunable electronic and magnetic properties of Cr2Mâ€²â€‰=â€‰Ti or V; Tâ€‰=â€‰O, OH or F). Applied Physics Letters, 2016, 109, .	1.5	81
20971	Wetting layer of copper on the tantalum (001) surface. Physical Review B, 2016, 94, .	1.1	6
20972	Discharge, Relaxation, and Charge Model for the Lithium Trivanadate Electrode: Reactions, Phase Change, and Transport. Journal of the Electrochemical Society, 2016, 163, A2890-A2898.	1.3	17
20973	First-principles study of the optoelectronic properties and photovoltaic absorber layer efficiency of Cu-based chalcogenides. Journal of Applied Physics, 2016, 120, .	1.1	41
20974	First-principles calculation of the elastic dipole tensor of a point defect: Application to hydrogen inÎ±-zirconium. Physical Review B, 2016, 94, .	1.1	24
20975	First-principles investigation on elastic and thermodynamic properties of Pnnm-CN under high pressure. AIP Advances, 2016, 6, 125040.	0.6	3

#	Article	IF	Citations
20976	Electronic Structure of Iron Porphyrin Adsorbed to the Pt(111) Surface. Journal of Physical Chemistry C, 2016, 120, 29173-29181.	1.5	13
20977	Experimental and Theoretical Studies on Oxidation of Cu-Au Alloy Surfaces: Effect of Bulk Au Concentration. Scientific Reports, 2016, 6, 31101.	1.6	33
20978	Epitaxy of highly ordered organic semiconductor crystallite networks supported by hexagonal boron nitride. Scientific Reports, 2016, 6, 38519.	1.6	26
20979	Density functional theory based study of chlorine doped WS2-metal interface. Applied Physics Letters, 2016, 108, .	1.5	16
20980	First-principles study of crystalline and amorphous AlMgB14-based materials. Journal of Applied Physics, 2016, 119, .	1.1	24
20981	Density functional study on the mechanism for the highly active palladium monolayer supported on titanium carbide for the oxygen reduction reaction. Journal of Chemical Physics, 2016, 144, 204703.	1.2	18
20982	Two-dimensional boron: Lightest catalyst for hydrogen and oxygen evolution reaction. Applied Physics Letters, 2016, 109, .	1.5	86
20983	Insight into the mechanism for the methanol synthesis via the hydrogenation of CO2 over a Co-modified Cu(100) surface: A DFT study. Journal of Chemical Physics, 2016, 145, 134701.	1.2	14
20984	Mechanical and electronic coupling in few-layer graphene and hBN wrinkles: a first-principles study. Nanotechnology, 2016, 27, 505702.	1.3	12
20985	Unraveling the composition dependence of the martensitic transformation temperature: A first-principles study of Ti-Ta alloys. Physical Review B, 2016, 94, .	1.1	25
20986	High-pressure compressibility and vibrational properties of (Ca,Mn)CO₃. American Mineralogist, 2016, 101, 2723-2730.	0.9	29
20987	Mechanism for Solid-State Ion Exchange of Cu⁺ into Zeolites. Journal of Physical Chemistry C, 2016, 120, 29182-29189.	1.5	33
20988	Correlation of optical and structural properties of GaN/AlN multi-quantum wellsâ€”Ab initio and experimental study. Journal of Applied Physics, 2016, 119, 015703.	1.1	27
20989	Computational characterization of lightweight multilayer MXene Li-ion battery anodes. Applied Physics Letters, 2016, 108, .	1.5	79
20990	Electronic transport in organometallic perovskite CH₃NH₃PbI₃: The role of organic cation orientations. Applied Physics Letters, 2016, 108, 053901.	1.5	28
20991	The electric field induced ferroelectric phase transition of AgNbO3. Journal of Applied Physics, 2016, 119, .	1.1	31
20992	The influence of structural characteristics on the electronic and thermal properties of GaN/AlN core/shell nanowires. Journal of Applied Physics, 2016, 119, .	1.1	8
20993	Optimum thickness of soft magnetic phase in FePt/FeCo permanent magnet superlattices with high energy product and large magnetic anisotropy energy. AIP Advances, 2016, 6, .	0.6	5

#	Article	IF	Citations
20994	Hexagonal boron nitride and water interaction parameters. Journal of Chemical Physics, 2016, 144, 164118.	1.2	89
20995	Calculations of oxide formation on low-index Cu surfaces. Journal of Chemical Physics, 2016, 145, 044711.	1.2	25
20996	The modification of benzene adsorption on zigzag single-wall carbon nanotubes by carboxylation. Materials Research Express, 2016, 3, 125010.	0.8	5
20997	First-principles study on Al₄Sr as the heterogeneous nucleus of Mg₂Si. Materials Research Express, 2016, 3, 126503.	0.8	4
20998	Matildite versus schapbachite: First-principles investigation of the origin of photoactivity in<mml:math xmlns:mml="http://www.w3.org/1998/Math/MathML"><mml:mrow><mml:mi>AgBi</mml:mi><mml:msub><mml:mi mathvariant="normal">S</mml:mi><mml:mn>2</mml:mn></mml:msub></mml:mrow></mml:math>. Physical Review B, 2016, 94, .	1.1	39
20999	Ab Initio Thermodynamics and the Relationship between Octahedral Distortion, Lattice Structure, and Proton Substitution Defects in Malachite/Rosasite Group Endmember Pokrovskite Mg₂CO₃(OH)₂. Journal of Physical Chemistry A, 2016, 120, 10181-10195.	1.1	9
21000	Tight-binding approach to penta-graphene. Scientific Reports, 2016, 6, 22672.	1.6	41
21001	Tunable electronic and magnetism of SrTiO3/BiFeO3 (001) superlattice: For electrochemical applications. Applied Physics Letters, 2016, 108, 011602.	1.5	6
21002	Electronic structure and thermoelectric properties of half-Heusler compounds with eight electron valence countâ€”KScX (Xâ€‰=â€‰C and Ge). Journal of Applied Physics, 2016, 119, .	1.1	31
21003	Modulating the band gap of a boron nitride bilayer with an external electric field for photocatalyst. Journal of Applied Physics, 2016, 119, .	1.1	19
21004	Synchrotron-based far-infrared spectroscopy of nickel tungstate. Low Temperature Physics, 2016, 42, 552-555.	0.2	5
21005	A multi-scale study of the adsorption of lanthanum on the (110) surface of tungsten. Journal of Applied Physics, 2016, 120, .	1.1	3
21006	AZn₂BO₃X₂(A = K, Rb, NH₄; X = Cl, Br): New Members of KBBF Family Exhibiting Large SHG Response and the Enhancement of Layer Interaction by Modified Structures. Chemistry of Materials, 2016, 28, 9122-9131.	3.2	134
21007	Zr-Doped Mesoporous Ta₃N₅ Microspheres for Efficient Photocatalytic Water Oxidation. ACS Applied Materials & Interfaces, 2016, 8, 35407-35418.	4.0	57
21008	Thermodynamic origin of instability in hybrid halide perovskites. Scientific Reports, 2016, 6, 37654.	1.6	76
21009	Crystal-to-crystal photo-reversible polymerization mechanism of bis-thymine derivative. RSC Advances, 2016, 6, 107317-107322.	1.7	5
21010	First-principles prediction of solar radiation shielding performance for transparent windows of GdB6. Journal of Applied Physics, 2016, 119, .	1.1	14
21011	An ab initio investigation of vibrational, thermodynamic, and optical properties of Sc ₂ AlC MAX compound. Chinese Physics B, 2016, 25, 103102.	0.7	40

#	Article	IF	Citations
21012	Structural, elastic, electronic, and thermodynamic properties of MgAgSb investigated by density functional theory. Chinese Physics B, 2016, 25, 086302.	0.7	12
21013	Analyzing relationships between surface perturbations and local chemical reactivity of metal sites: Alkali promotion of O2 dissociation on Ag(111). Journal of Chemical Physics, 2016, 144, 234704.	1.2	13
21014	Magnetism and magnetocrystalline anisotropy in single-layer PtSe2: Interplay between strain and vacancy. Journal of Applied Physics, 2016, 120, .	1.1	51
21015	The role of the cationic Pt sites in the adsorption properties of water and ethanol on the Pt4/Pt(111) and Pt4/CeO2(111) substrates: A density functional theory investigation. Journal of Chemical Physics, 2016, 145, 124709.	1.2	10
21016	Computational prediction of the diversity of monolayer boron phosphide allotropes. Applied Physics Letters, 2016, 109, .	1.5	35
21017	The effect of spin orbit interaction for superconductivity in the noncentrosymmetric superconductor CaIrSi3. Journal of Alloys and Compounds, 2016, 681, 205-211.	2.8	13
21018	Atomic-scale observation of structural and electronic orders in the layered compound Î±-RuCl3. Nature Communications, 2016, 7, 13774.	5.8	66
21019	Bilayered graphene/h-BN with folded holes as new nanoelectronic materials: modeling of structures and electronic properties. Scientific Reports, 2016, 6, 38029.	1.6	12
21020	Structural anisotropy results in strain-tunable electronic and optical properties in monolayer GeX and SnX (X = S, Se, Te). Journal of Chemical Physics, 2016, 144, 114708.	1.2	161
21021	Room temperature d0 ferromagnetism in ZnS nanocrystals. Journal of Applied Physics, 2016, 119, 223901.	1.1	18
21022	Electronic structure and magnetism of Mn-doped GaSb for spintronic applications: A DFT study. Journal of Applied Physics, 2016, 120, .	1.1	33
21023	Stable single-layer structure of group-V elements. Physical Review B, 2016, 94, .	1.1	108
21024	Biaxially strained PtPb/Pt core/shell nanoplate boosts oxygen reduction catalysis. Science, 2016, 354, 1410-1414.	6.0	1,262
21025	Enhancement of figure of merit (ZT) by doping Bi in Mg2Si for energy harvesting applications. Progress in Natural Science: Materials International, 2016, 26, 533-539.	1.8	14
21026	Substantial bulk photovoltaic effect enhancement via nanolayering. Nature Communications, 2016, 7, 10419.	5.8	62
21027	Thermal equation of state of silicon carbide. Applied Physics Letters, 2016, 108, .	1.5	33
21028	Tuning conductivity and magnetism in isopolar oxide superlattices via compressive and tensile strain: A case study of SrVO3/SrMnO3 and SrCrO3/SrMnO3 heterostructure. Journal of Applied Physics, 2016, 119, .	1.1	5
21029	Tunable electronic structure of black phosphorus/blue phosphorus van der Waals p-n heterostructure. Applied Physics Letters, 2016, 108, .	1.5	109

#	Article	IF	Citations
21030	Effects of configurational disorder on the elastic properties of icosahedral boron-rich alloys based on B6O, B13C2, and B4C, and their mixing thermodynamics. Journal of Chemical Physics, 2016, 144, 134503.	1.2	18
21031	Extended application of Kohn-Sham first-principles molecular dynamics method with plane wave approximation at high energyâ€"From cold materials to hot dense plasmas. Physics of Plasmas, 2016, 23, .	0.7	54
21032	DFT-D2 simulations of water adsorption and dissociation on the low-index surfaces of mackinawite (FeS). Journal of Chemical Physics, 2016, 144, 174704.	1.2	33
21033	First-principles study of twin grain boundaries in epitaxial BaSi2 on Si(111). Journal of Applied Physics, 2016, 120, .	1.1	22
21034	Orthorhombic boron oxide under pressure: In situ study by X-ray diffraction and Raman scattering. Journal of Applied Physics, 2016, 120, 175901.	1.1	11
21035	Observation of an intermediate phase in tungsten doped Sb₂Te phase change thin films by temperature dependent measurements of structural, optical, and electronic properties. Journal Physics D: Applied Physics, 2016, 49, 265105.	1.3	3
21036	High pressure structural, electronic, and optical properties of polymorphic InVO4 phases. Journal of Applied Physics, 2016, 119, 085702.	1.1	17
21037	The structure and electronic properties of hexagonal Fe2Si. AIP Advances, 2016, 6, .	0.6	12
21038	Graphene grown out of diamond. Applied Physics Letters, 2016, 109, 162105.	1.5	16
21039	Preferred site occupation and magnetic properties of Ni-Fe-Ga-Co ferromagnetic shape memory alloys by first-principles calculations. AIP Advances, 2016, 6, 125007.	0.6	1
21040	Empirical relation between Pauling electronegativity and self-energy cutoffs in local-density approximation-1/2 quasi-particle approach applied to the calculation of band gaps of binary compound semiconductors. MRS Communications, 2016, 6, 99-103.	0.8	6
21041	Role of Vacancy in Trapping Impurity of Nitrogen in Molybdenum. Rare Metal Materials and Engineering, 2016, 45, 1973-1977.	0.8	1
21042	Robust Room-Temperature Quantum Spin Hall Effect in Methyl-functionalized InBi honeycomb film. Scientific Reports, 2016, 6, 23242.	1.6	25
21043	Correlative theoretical and experimental investigation of the formation of AlYB14 and competing phases. Journal of Applied Physics, 2016, 119, .	1.1	6
21044	Influence of the exchange and correlation functional on the structure of amorphous InSb and In3SbTe2 compounds. Journal of Chemical Physics, 2016, 144, 204508.	1.2	8
21045	Physisorption mechanism in graphene/noble metal (111)/Ni(111) heterostructures: An ab-initio study. Journal of Applied Physics, 2016, 120, 075301.	1.1	1
21046	Elastic anisotropy and electronic properties of Si3N4 under pressures. AIP Advances, 2016, 6, .	0.6	11
21047	First-principles calculations of high-pressure phase transition of TiO2 during decompression: From baddeleyite-type TiO2 to Î±-PbO2-type TiO2. Journal of Applied Physics, 2016, 120, 142108.	1.1	5

#	Article	IF	Citations
21048	Experimental and density functional study of Mn doped Bi2Te3 topological insulator. APL Materials, 2016, 4, .	2.2	14
21049	Mechanical characterization of nanoporous Au modified with self-assembled monolayers. Applied Physics Letters, 2016, 109, 261905.	1.5	5
21050	Calcium Silicate Phases Explained by High-Temperature-Resistant Phosphate Probe Molecules. Langmuir, 2016, 32, 13577-13584.	1.6	13
21051	Electronic structure, elasticity, bonding features and mechanical behaviour of zinc intermetallics: A DFT study. AIP Conference Proceedings, 2016, , .	0.3	1
21052	Stabilization of metastable phases in hafnia owing to surface energy effects. Applied Physics Letters, 2016, 108, .	1.5	108
21053	Interactions between Mn dopant and oxygen vacancy for insulation performance of BaTiO3. Journal of Applied Physics, 2016, 120, .	1.1	16
21054	The impact of nitrogen content and vacancies on structure and mechanical properties of Moâ€“N thin films. Journal of Applied Physics, 2016, 120, .	1.1	55
21055	Bandgap modulation in photoexcited topological insulator Bi2Te3 via atomic displacements. Journal of Chemical Physics, 2016, 145, 024504.	1.2	20
21056	A density functional theory study of the adsorption behaviour of CO2 on Cu2O surfaces. Journal of Chemical Physics, 2016, 145, 044709.	1.2	55
21057	High pressure structural, elastic and vibrational properties of green energetic oxidizer ammonium dinitramide. Journal of Chemical Physics, 2016, 145, .	1.2	18
21058	Suitable Fundamental Properties of Ta_{0.75}V_{0.25}ON Material for Visible-Light-Driven Photocatalysis: A DFT Study. ACS Omega, 2016, 1, 1041-1048.	1.6	14
21059	Spin-orbit coupling enhanced superconductivity in Bi-rich compounds ABi3 (Aâ€‰=â€‰Sr and Ba). Scientific Reports, 2016, 6, 21484.	1.6	20
21060	Catalytic Mechanisms of Methanol Oxidation to Methyl Formate on Vanadiaâ€“Titania and Vanadiaâ€“Titaniaâ€“Sulfate Catalysts. Journal of Physical Chemistry C, 2016, 120, 29290-29301.	1.5	20
21061	Establishing and Understanding Adsorptionâ€“Energy Scaling Relations with Negative Slopes. Journal of Physical Chemistry Letters, 2016, 7, 5302-5306.	2.1	43
21062	Direct evidence of interaction-induced Dirac cones in a monolayer silicene/Ag(111) system. Proceedings of the National Academy of Sciences of the United States of America, 2016, 113, 14656-14661.	3.3	76
21063	Phase transition of solid bismuth under high pressure. Chinese Physics B, 2016, 25, 108103.	0.7	10
21065	Energy band gap and spectroscopic studies in Mn1âˆ’xCuxWO4 (0 â‰¤ x â‰¤ 0.125). AIP Conference Proceedings, 2016, , .	0.3	0
21066	Theoretical modeling and experimental observations of the atomic layer deposition of SrO using a cyclopentadienyl Sr precursor. Journal of Chemical Physics, 2016, 145, 064701.	1.2	3

#	Article	IF	Citations
21067	Adsorption of oxygen on low-index surfaces of the TiAl3 alloy. Journal of Experimental and Theoretical Physics, 2016, 123, 991-1007.	0.2	13
21068	First-principles study on the formation energies of Ga₁__xCr_xAs. Journal of Physics: Conference Series, 2016, 743, 012007.	0.3	6
21069	Band structure and phonon properties of lithium fluoride at high pressure. AIP Conference Proceedings, 2016, , .	0.3	1
21070	Structural and Electronic Properties of Neptunium Sulphide: An Ab Initio Study. Journal of Metastable and Nanocrystalline Materials, 2016, 28, 23-26.	0.1	0
21071	Effect of metal-to-metal interface states on the electric-field modified magnetic anisotropy in MgO/Fe/non-magnetic metal. Journal of Applied Physics, 2016, 119, 133905.	1.1	9
21072	Lattice dynamics and elasticity of SrCO₃. Journal of Applied Crystallography, 2016, 49, 1982-1990.	1.9	21
21073	Investigating the effects of phosphorus in a binary-phase TiAl-Ti3Al alloy by first-principles: from site preference, interfacial energetics to mechanical properties. European Physical Journal B, 2016, 89, 1.	0.6	2
21074	Quasi-freestanding graphene on Ni(111) by Cs intercalation. Scientific Reports, 2016, 6, 26753.	1.6	14
21075	Prediction of structural and mechanical properties of atom-decorated porous graphene via density functional calculations. EPJ Applied Physics, 2016, 74, 10401.	0.3	11
21076	Modification of Electronic and Vibrational Properties of Doped Black-P Films. MRS Advances, 2016, 1, 2285-2290.	0.5	1
21077	Strain-induced water dissociation on supported ultrathin oxide films. Scientific Reports, 2016, 6, 22853.	1.6	19
21078	Electronic and magnetic properties of H-terminated graphene nanoribbons deposited on the topological insulator Sb2Te3. Scientific Reports, 2016, 6, 29009.	1.6	6
21079	Theoretical investigation of the electronic and structural properties of AlN thin films. Russian Microelectronics, 2016, 45, 600-602.	0.1	1
21080	Spin-polarized, orbital-selected hole gas at the EuO/Pt interface. Journal of Applied Physics, 2016, 119, .	1.1	6
21081	Near-infrared radiation absorption properties of covellite (CuS) using first-principles calculations. AIP Advances, 2016, 6, .	0.6	21
21082	The effect of tantalum (Ta) doping on mechanical properties of tungsten (W): A first-principles study. Journal of Materials Research, 2016, 31, 3401-3408.	1.2	34
21083	Electrostriction coefficient of ferroelectric materials from ab initio computation. AIP Advances, 2016, 6, 065122.	0.6	21
21084	Electronic structure and magnetism of Ge(Sn)TMXTe1â˜'X (TM = V, Cr, Mn): A first principles study. AIP Advances, 2016, 6, 125005.	0.6	4

#	Article	IF	Citations
21085	Assignment of 13C hyperfine interactions in the P1-center in diamond. Diamond and Related Materials, 2016, 70, 118-123.	1.8	13
21086	The nature of hydrogen-bonding interaction in the prototypic hybrid halide perovskite, tetragonal CH3NH3PbI3. Scientific Reports, 2016, 6, 21687.	1.6	123
21087	Magnetism in transition metal-substituted germanane: A search for room temperature spintronic devices. Journal of Applied Physics, 2016, 119, .	1.1	46
21088	Determination of the electronic, dielectric, and optical properties of sillenite Bi12TiO20 and perovskite-like Bi4Ti3O12 materials from hybrid first-principle calculations. Journal of Chemical Physics, 2016, 144, 134702.	1.2	45
21089	HRTEM low dose: the unfold of the morphed graphene, from amorphous carbon to morphed graphenes. Advanced Structural and Chemical Imaging, 2016, 2, 10.	4.0	33
21090	Magnetism and electronic phase transitions in monoclinic transition metal dichalcogenides with transition metal atoms embedded. Journal of Applied Physics, 2016, 120, 064305.	1.1	10
21091	Effect of Pressure and Temperature on the Local Structure and Lattice Dynamics of Copper(II) Oxide. Physics Procedia, 2016, 85, 27-35.	1.2	6
21092	Alloying effects of refractory elements in the dislocation of Ni-based single crystal superalloys. Progress in Natural Science: Materials International, 2016, 26, 636-642.	1.8	6
21093	A first-principles study of the SnO2 monolayer with hexagonal structure. Journal of Chemical Physics, 2016, 145, 174702.	1.2	34
21094	A Density Functional Theory Study of Codoping Characteristics of Sulfur with Alkaline Earth in Delafossite CuAlO 2. Communications in Theoretical Physics, 2016, 65, 527-530.	1.1	5
21095	Solute segregation and deviation from bulk thermodynamics at nanoscale crystalline defects. Science Advances, 2016, 2, e1601796.	4.7	56
21096	A new type of vanadium carbide V5C3 and its hardening by tuning Fermi energy. Scientific Reports, 2016, 6, 21794.	1.6	22
21097	Structure family and polymorphous phase transition in the compounds with soft sublattice: Cu2Se as an example. Journal of Chemical Physics, 2016, 144, 194502.	1.2	35
21098	Large magnetic anisotropy predicted for rare earth-free <mml:math xmlns:mml="http://www.w3.org/1998/Math/MathML"><mml:mrow><mml:mi mathvariant="normal">F</mml:mi><mml:msub><mml:mi mathvariant="normal">e</mml:mi><mml:mrow><mml:mn>16</mml:mn><mml:mo>â^'</mml:mo><mml:mi>x</mml:mi></mml:mrow></mml:msub><mml:mi mathvariant="normal">C</mml:mi><mml:msub><mml:mi mathvariant="normal">o</mml:mi><mml:mi>x</mml:mi></mml:msub><mml:mi mathvariant="normal">	1.1	46
21099	Atomic partial charges on CH3NH3PbI3 from first-principles electronic structure calculations. Journal of Applied Physics, 2016, 119, .	1.1	20
21100	Atomic, electronic, and magnetic properties of bimetallic ZrCo clusters: A first-principles study. Journal of Applied Physics, 2016, 120, .	1.1	5
21101	Migration processes of the As interstitial in GaAs. Journal of Applied Physics, 2016, 120, .	1.1	15
21102	Point defects stabilise cubic Mo-N and Ta-N. Journal Physics D: Applied Physics, 2016, 49, 375303.	1.3	64

#	Article	IF	Citations
21103	A polymer dataset for accelerated property prediction and design. Scientific Data, 2016, 3, 160012.	2.4	139
21104	Interactions between carbon species and Î²-spodumene by first principles calculation. RSC Advances, 2016, 6, 70284-70291.	1.7	0
21105	Lattice dynamics and thermal conductivity of calcium fluoride via first-principles investigation. Journal of Applied Physics, 2016, 119, .	1.1	16
21106	Molecular simulation of CO chemisorption on Co(0001) in presence of supercritical fluid solvent: A potential of mean force study. Journal of Chemical Physics, 2016, 145, 084506.	1.2	5
21107	Two-dimensional electron gas in GaAs/SrHfO3 heterostructure. Journal of Applied Physics, 2016, 119, 235304.	1.1	6
21108	Effects of domain size on x-ray absorption spectra of boron nitride doped graphenes. Applied Physics Letters, 2016, 109, .	1.5	9
21109	Hybrid crystals of cuprates and iron-based superconductors. Chinese Physics B, 2016, 25, 077402.	0.7	3
21110	First principles and molecular dynamics modeling investigation on polyethylene. , 2016, , .		0
21111	First-principles study of thermodynamic and stability properties of TiC-SiC alloys. , 2016, , .		3
21112	First-principles study of water adsorption on Î±-SiO2 [110] surface. AIP Advances, 2016, 6, 085001.	0.6	15
21113	Modeling of half-Heusler crystals with the chalcopyrite structure: Li2MgZnX 2 (X = N, P, As, Sb). Journal of Structural Chemistry, 2016, 57, 1499-1504.	0.3	1
21114	Density functional theory + U modeling of polarons in organohalide lead perovskites. AIP Advances, 2016, 6, .	0.6	25
21115	Magnetism in molybdenum disulphide monolayer with sulfur substituted by 3d transition metals. Journal of Applied Physics, 2016, 120, 144305.	1.1	11
21116	Toward Routine Gauge-Including Projector Augmented-Wave Calculations for Metallic Systems: The Case of ScT2Al (T = Ni, Pd, Pt, Cu, Ag, Au) Heusler Phases. Journal of Physical Chemistry C, 2016, 120, 25530-25540.	1.5	8
21117	Role of magnesium in ZnS structure: Experimental and theoretical investigation. AIP Advances, 2016, 6, .	0.6	16
21118	Ferroelasticity and domain physics in two-dimensional transition metal dichalcogenide monolayers. Nature Communications, 2016, 7, 10843.	5.8	125
21119	Emergence of new red-shifted carbon nanotube photoluminescence based on proximal doped-site design. Scientific Reports, 2016, 6, 28393.	1.6	73
21120	Anisotropy, band-to-band transitions, phonon modes, and oxidation properties of cobalt-oxide core-shell slanted columnar thin films. Applied Physics Letters, 2016, 108, .	1.5	12

#	Article	IF	Citations
21121	Research of the structural and electronic properties of VN/AlN/VN and AlN/VN/AlN based on DFT calculation. Journal of Physics: Conference Series, 2016, 743, 012004.	0.3	0
21122	Predicting Physical Properties of Tetragonal, Monoclinic and Orthorhombic M 3 N 4 (M =C, Si, Sn) Polymorphs via First-Principles Calculations. Chinese Physics Letters, 2016, 33, 066301.	1.3	5
21123	Intra- and inter-layer charge redistribution in biased bilayer graphene. AIP Advances, 2016, 6, .	0.6	8
21124	Ab initio study of vacancy formation in cubic LaMnO3 and SmCoO3 as cathode materials in solid oxide fuel cells. Journal of Chemical Physics, 2016, 145, 014703.	1.2	25
21125	Studying the electronic and phononic structure of penta-graphane. Science and Technology of Advanced Materials, 2016, 17, 610-617.	2.8	44
21126	First-Principles-Based Phonon Calculation and Raman Spectroscopy Measurement of RuGa₂ and RuAl₂ with High Thermoelectric Power Factors. Materials Transactions, 2016, 57, 1050-1054.	0.4	3
21127	High pressure structural changes in aluminium triiodide: A first principles study. Journal of Chemical Physics, 2016, 144, 124507.	1.2	2
21128	High-throughput exploration of thermoelectric and mechanical properties of amorphous NbO2 with transition metal additions. Journal of Applied Physics, 2016, 120, .	1.1	11
21129	A single-volume approach for vacancy formation thermodynamics calculations. Europhysics Letters, 2016, 116, 16001.	0.7	4
21130	Investigations into the slip behavior of zirconium diboride. Journal of Materials Research, 2016, 31, 2749-2756.	1.2	11
21131	Computational Analysis of Li Diffusion in NZP-Type Materials by Atomistic Simulation and Compositional Screening. , 2016, , 177-187.		0
21132	First principles prediction of the electronic structure and carrier mobilities of biaxially strained molybdenum trioxide (MoO3). Journal of Applied Physics, 2016, 120, 055105.	1.1	17
21133	First-principles calculations of the OHâ˜’ adsorption energy on perovskite oxide. AIP Conference Proceedings, 2016, , .	0.3	6
21134	Spontaneous bidirectional ordering of CH3NH3+ in lead iodide perovskites at room temperature: The origins of the tetragonal phase. Scientific Reports, 2016, 6, 24443.	1.6	37
21135	Ab initio calculations of carbon impurities in ferroelectric lead titanate. , 2016, , .		0
21136	Materials design for electrocatalytic carbon capture. APL Materials, 2016, 4, .	2.2	20
21137	Elastic properties of AlAs-like and InSb-like strained interfaces in [InAs/AlSb] heterostructures. Applied Physics Letters, 2016, 109, .	1.5	2
21138	Electronic and Thermoelectric Properties of Layered Sn- and Pb-Doped Ge2Sb2Te5 Alloys Using First Principle Calculations. Journal of Electronic Materials, 2016, 45, 2950-2956.	1.0	4

#	Article	IF	Citations
21139	Density-Functional Study of the La₂Zr₂O₇ (001) and (011) Surfaces and Bulk. Journal of Physical Chemistry C, 2016, 120, 7522-7531.	1.5	11
21140	Ab initio-based Monte Carlo and mean field studies of phase separated Î±NiSn (Î±Â=Ti1â^'Hf , Ti1â^'Zr , Hf1â^'Zr) compounds with C1 structure. Acta Materialia, 2016, 111, 157-165.	3.8	7
21141	Intimately coupled hybrid of graphitic carbon nitride nanoflakelets with reduced graphene oxide for supporting Pd nanoparticles: A stable nanocatalyst with high catalytic activity towards formic acid and methanol electrooxidation. Electrochimica Acta, 2016, 200, 131-141.	2.6	50
21142	Building compact dislocation cores in an elasto-plastic model of dislocation fields. International Journal of Plasticity, 2016, 82, 241-259.	4.1	10
21143	Interfacial effect on strengthening nanoscale metallic multilayers - a combined Hall-Petch relation and atomistic simulation study. Materials Science & Engineering A: Structural Materials: Properties, Microstructure and Processing, 2016, 663, 29-37.	2.6	9
21144	Raman light scattering, infrared absorption and neutron scattering studies of the phase transition and reorientational dynamics of H2O ligands and ClO4â†™ anions in [Ca(H2O)4](ClO4)2. Vibrational Spectroscopy, 2016, 83, 26-35.	1.2	4
21145	Carbene-mediated self-assembly of diamondoids on metal surfaces. Nanoscale, 2016, 8, 8966-8975.	2.8	20
21146	Boron diffusion in bcc-Fe studied by first-principles calculations. Chinese Physics B, 2016, 25, 036601.	0.7	8
21147	Semiconducting and optical properties of selected binary compounds by linear response DFT+U and hybrid functional methods. Theoretical Chemistry Accounts, 2016, 135, 1.	0.5	13
21148	A first-principles study of the mechanical properties of AlN with Raman verification. Computational Materials Science, 2016, 112, 342-346.	1.4	14
21149	First-principles study on the structural and electronic properties of Li4SiO4 and Al-doped Li4SiO4. Fusion Engineering and Design, 2016, 113, 331-335.	1.0	10
21150	Electronic and optical properties of (U,Th)O 2 compound from screened hybrid density functional studies. Physics Letters, Section A: General, Atomic and Solid State Physics, 2016, 380, 1481-1486.	0.9	12
21151	Metallic Intermediate Hydride Phase of LaMg₂Ni with Niâ€“H Covalent Bonding: Precursor State for Complex Hydride Formation. Journal of Physical Chemistry C, 2016, 120, 5926-5931.	1.5	16
21152	Effects of scandium composition on the structural, electronic, and thermodynamic properties of SC_xY_{1â€“x}metallic alloys. Philosophical Magazine, 2016, 96, 498-510.	0.7	4
21153	Shift of indirect to direct bandgap and thermoelectric response of the cubic BiScO3 via DFT-mBJ studies. Materials Science in Semiconductor Processing, 2016, 49, 40-47.	1.9	47
21154	Abâ€initio study of germanium di -interstitial using a hybrid functional (HSE). Physica B: Condensed Matter, 2016, 480, 191-195.	1.3	16
21155	Ammonia Adsorption and Decomposition on Co(0001) in Relation to Fischerâ€“Tropsch Synthesis. Journal of Physical Chemistry C, 2016, 120, 3834-3845.	1.5	14
21156	Nitrogen-doped carbon nanotube as a potential metal-free catalyst for CO oxidation. Physical Chemistry Chemical Physics, 2016, 18, 12093-12100.	1.3	38

#	Article	IF	Citations
21157	Tuning the activity of Pt alloy electrocatalysts by means of the lanthanide contraction. Science, 2016, 352, 73-76.	6.0	783
21158	XPS study of the electronic density of states in the superconducting Mo2B and Mo2BC compounds. Journal of Materials Science, 2016, 51, 6411-6418.	1.7	18
21159	Adsorption of sugars on Al- and Ga-doped boron nitride surfaces: A computational study. Applied Surface Science, 2016, 377, 9-16.	3.1	32
21160	Influence of the thickness and surface composition on the electronic structure of FeS 2 layers. Applied Surface Science, 2016, 377, 184-190.	3.1	10
21161	RhNi nanocatalyst: Spontaneous alloying and high activity for hydrogen generation from hydrous hydrazine. International Journal of Hydrogen Energy, 2016, 41, 6362-6368.	3.8	24
21162	Three-Parameter Crystal-Structure Prediction for sp-d-Valent Compounds. Chemistry of Materials, 2016, 28, 2550-2556.	3.2	26
21163	Electronic Structure and Bonding in Co-Based Single and Mixed Valence Oxides: A Quantum Chemical Perspective. Inorganic Chemistry, 2016, 55, 3307-3315.	1.9	40
21164	Structural Characterization, Optical Properties, and Phase Transitions of In_{1â€“x}Sn_x Alloy Thin Films. Journal of Physical Chemistry C, 2016, 120, 7822-7828.	1.5	4
21165	Oxidation and Equilibrium Morphology of Zirconium Carbide Low Index Surfaces Using DFT and Atomistic Thermodynamic Modeling. Journal of Physical Chemistry C, 2016, 120, 8759-8771.	1.5	15
21166	Lithium Diffusion Pathways in Î²-Li₂TiO₃: A Theoretical Study. Journal of Physical Chemistry C, 2016, 120, 7061-7066.	1.5	34
21167	Mechanism of Dehydration of Phenols on Noble Metals via First-Principles Microkinetic Modeling. ACS Catalysis, 2016, 6, 3047-3055.	5.5	69
21168	Dirac node arcs in PtSn4. Nature Physics, 2016, 12, 667-671.	6.5	223
21169	Chiral phosphorus nanotubes: structure, bonding, and electronic properties. Physical Chemistry Chemical Physics, 2016, 18, 12414-12418.	1.3	17
21170	The spin-dependent transport of transition metal encapsulated B₄₀fullerene. RSC Advances, 2016, 6, 40155-40161.	1.7	27
21171	Universal synthesis method for mixed phase TiO₂(B)/anatase TiO₂thin films on substrates via a modified low pressure chemical vapour deposition (LPCVD) route. Journal of Materials Chemistry A, 2016, 4, 5685-5699.	5.2	39
21172	Origin of low sodium capacity in graphite and generally weak substrate binding of Na and Mg among alkali and alkaline earth metals. Proceedings of the National Academy of Sciences of the United States of America, 2016, 113, 3735-3739.	3.3	462
21173	Theoretical study on the phase stability, elasticity, hardness and electronic structures of Niâ€“P compounds. Phase Transitions, 2016, 89, 1078-1089.	0.6	7
21174	Structural and optical properties of Ge60Te40: experimental and theoretical verification. Journal Physics D: Applied Physics, 2016, 49, 155105.	1.3	5

#	Article	IF	Citations
21175	Free energy model for solid high-pressure phases of carbon. Journal of Physics Condensed Matter, 2016, 28, 145401.	0.7	2
21176	Catalytic water dissociation by greigite Fe ₃ S ₄ surfaces: density functional theory study. Proceedings of the Royal Society A: Mathematical, Physical and Engineering Sciences, 2016, 472, 20160080.	1.0	17
21177	Chemisorption of thiolâ€functionalized metallocene molecules on Si(111)â€•Agâˆš3Ã—âˆš3 surface: A density functional theory study. International Journal of Quantum Chemistry, 2016, 116, 35-41.	1.0	0
21178	Modeling the effects of Si-X (XÂ=ÂF, Cl) bonds on the chemical and electronic properties of Si-surface terminated porous 3C-SiC. Theoretical Chemistry Accounts, 2016, 135, 1.	0.5	8
21180	Ab Initio Study of Phosphorus Anodes for Lithium- and Sodium-Ion Batteries. Chemistry of Materials, 2016, 28, 2011-2021.	3.2	182
21181	Early Oxidation Processes on the Greigite Fe₃S₄(001) Surface by Water: A Density Functional Theory Study. Journal of Physical Chemistry C, 2016, 120, 8616-8629.	1.5	32
21182	Can Ice-Like Structures Form on Non-Ice-Like Substrates? The Example of the K-feldspar Microcline. Journal of Physical Chemistry C, 2016, 120, 6704-6713.	1.5	43
21183	The Effects of the Organicâ€“Inorganic Interactions on the Thermal Transport Properties of CH₃NH₃PbI₃. Nano Letters, 2016, 16, 2749-2753.	4.5	95
21184	Niâ€“Mâ€“O (M = Sn, Ti, W) Catalysts Prepared by a Dry Mixing Method for Oxidative Dehydrogenation of Ethane. ACS Catalysis, 2016, 6, 2852-2866.	5.5	120
21185	Chemically functionalized germanene for spintronic devices: a first-principles study. Physical Chemistry Chemical Physics, 2016, 18, 9809-9815.	1.3	20
21186	Ab initio study of tungsten defects near the surface. Modelling and Simulation in Materials Science and Engineering, 2016, 24, 045006.	0.8	12
21187	Ab Initio Calculations of Phonon Dispersion in ZnGa2Se4. Semiconductors, 2016, 50, 285-288.	0.2	4
21188	Influence of the tensile strain on CH4 dissociation on Cu(1 0 0) surface: A theoretical study. Applied Surface Science, 2016, 360, 826-832.	3.1	5
21189	First-principles investigation on the interface of transition metal dichalcogenide MX2 (M = Mo, W; X =) Tj ETQq1 1 0.784314 rgBT /Over	1.4	16
21190	Effect of oxygen incorporation in the Mg2Si lattice on its conductivity type â€“ A possible reason of the p-type conductivity of postannealed Mg2Si thin film. Journal of Alloys and Compounds, 2016, 676, 91-95.	2.8	14
21191	Positron annihilation lifetime characterization of oxygen ion irradiated rutile TiO2. Nuclear Instruments & Methods in Physics Research B, 2016, 379, 215-218.	0.6	33
21192	Structural, electronic, and magnetic properties of 3D metal trioxide and tetraoxide superhalogen cluster-doped monolayer BN. Physics Letters, Section A: General, Atomic and Solid State Physics, 2016, 380, 2300-2306.	0.9	17
21193	Infrared studies of propene and propene oxide adsorption on nanoparticulate Au/TiO2. Surface Science, 2016, 652, 172-182.	0.8	23

#	Article	IF	Citations
21194	Density Functional Theory Investigation on Thiophene Hydrodesulfurization Mechanism Catalyzed by ReS₂ (001) Surface. Journal of Physical Chemistry C, 2016, 120, 12012-12021.	1.5	14
21195	Mn₂C monolayer: a 2D antiferromagnetic metal with high NÃ©el temperature and large spinâ€“orbit coupling. Nanoscale, 2016, 8, 12939-12945.	2.8	131
21196	Elastic and electronic properties of M585 carbon under pressure. Chinese Journal of Physics, 2016, 54, 398-407.	2.0	2
21197	First principles study on the electronic, elastic and vibrational properties of marcasite-type OsP2. Computational Materials Science, 2016, 121, 54-60.	1.4	3
21198	Insights into MoS2-coated LiVPO4F for lithium ion batteries: A first-principles investigation. Journal of Alloys and Compounds, 2016, 681, 253-259.	2.8	8
21199	Effect of point defects on the properties of silicene-like BSi3 sheets from first-principles. Journal of Physics and Chemistry of Solids, 2016, 95, 106-113.	1.9	3
21200	Stress induced phase transition on the medium-high carbon alloy steel hardfacing coating during the work hardening process: Experiments and first-principles calculation. Materials Science & Engineering A: Structural Materials: Properties, Microstructure and Processing, 2016, 670, 49-56.	2.6	3
21201	The role of Ti and Si in the nucleation of Î±-Al during hot dip coating of steel with Alâ€“43.4wt.%Znâ€“1.6wt.%Si alloy. Surface and Coatings Technology, 2016, 299, 56-64.	2.2	14
21202	Iodine adsorption on Ni(111): STM and DFT study. Surface Science, 2016, 651, 112-119.	0.8	9
21203	A Copperâ€“Nitroxide Adduct Exhibiting Separate Single Crystal-to-Single Crystal Polymerizationâ€“Depolymerization and Spin Crossover Transitions. Inorganic Chemistry, 2016, 55, 5853-5861.	1.9	36
21204	New Insight into the Interface Chemistry and Stability of Glutathione Self-Assembled Monolayers on Au(111). Journal of Physical Chemistry C, 2016, 120, 14597-14607.	1.5	10
21205	Disparate Strain Dependent Thermal Conductivity of Two-dimensional Penta-Structures. Nano Letters, 2016, 16, 3831-3842.	4.5	183
21206	Ab initio study of the parent (BCC) and martensitic (HCP) phases of nonferrous Ti, Zr, and Hf metals. Chinese Journal of Physics, 2016, 54, 127-134.	2.0	5
21207	On the predictions of the 11B solid state NMR parameters. Chemical Physics Letters, 2016, 655-656, 66-70.	1.2	12
21208	Investigation of the energetics of structural transformations in Co-based binary alloys. Journal of Alloys and Compounds, 2016, 663, 693-700.	2.8	5
21209	Edge effects in vertically-oriented graphene based electric double-layer capacitors. Journal of Power Sources, 2016, 324, 309-316.	4.0	75
21210	Magnetoresistance in Co/2D MoS₂/Co and Ni/2D MoS₂/Ni junctions. Physical Chemistry Chemical Physics, 2016, 18, 16367-16376.	1.3	29
21211	Accurate force fields and methods for modelling organic molecular crystals at finite temperatures. Physical Chemistry Chemical Physics, 2016, 18, 15828-15837.	1.3	81

#	Article	IF	Citations
21212	Pressure effect on the properties of magnetic moments and phase transitions in YMnO₃ from first principles. RSC Advances, 2016, 6, 54041-54048.	1.7	6
21213	Doping Effect on Edge-Terminated Ferromagnetic Graphene Nanoribbons. Journal of Physical Chemistry C, 2016, 120, 11237-11244.	1.5	22
21214	The Interplay between Homogeneous and Heterogeneous Phases of PdAu Catalysts for the Oxidation of Alcohols. ACS Catalysis, 2016, 6, 4135-4143.	5.5	30
21215	An ab initio molecular dynamics study of D2 dissociation on CO-precovered Ru(0001). Physical Chemistry Chemical Physics, 2016, 18, 21190-21201.	1.3	3
21216	Structural stability, band structure and optical properties of different BiVO4 phases under pressure. Journal of Materials Science, 2016, 51, 6662-6673.	1.7	15
21217	On the verification of solâ€“gel-derived ZnO nanoparticle properties using first-principles calculation. Journal of Sol-Gel Science and Technology, 2016, 80, 56-67.	1.1	11
21218	Structural, electronic, elastic, optical, and vibrational properties of HfXSb (XÂ=ÂCo, Rh, Ru) half-Heusler compounds: an ab initio study. Indian Journal of Physics, 2016, 90, 1233-1241.	0.9	20
21219	First-principles study on band structures and electrical transports of doped-SnTe. Journal of Materiomics, 2016, 2, 158-164.	2.8	22
21220	The structure phase transition in atom-wide Co wires on a vicinal Cu{111} surface. Materials Letters, 2016, 179, 69-72.	1.3	16
21221	Quantitative Understanding of van der Waals Interactions by Analyzing the Adsorption Structure and Low-Frequency Vibrational Modes of Single Benzene Molecules on Silver. Journal of Physical Chemistry Letters, 2016, 7, 2228-2233.	2.1	6
21222	T-ZrS nanoribbons: structure and electronic properties. Philosophical Magazine, 2016, 96, 2074-2087.	0.7	8
21223	Two-dimensional GeS with tunable electronic properties via external electric field and strain. Nanotechnology, 2016, 27, 274001.	1.3	85
21224	Modelling defects in Niâ€“Al with EAM and DFT calculations. Modelling and Simulation in Materials Science and Engineering, 2016, 24, 045012.	0.8	20
21225	First-principles studying the properties of oxygen in vanadium: Thermodynamics and tensile/shear behavior. Computational Condensed Matter, 2016, 7, 7-13.	0.9	7
21226	First principles study on defectives BN nanotubes for water splitting and hydrogen storage. Chemical Physics Letters, 2016, 653, 161-166.	1.2	8
21227	Tribochemistry of graphene on iron and its possible role in lubrication of steel. Carbon, 2016, 106, 118-124.	5.4	100
21228	Sr2SmNbO6 perovskite: Synthesis, characterization and density functional theory calculations. Materials Chemistry and Physics, 2016, 179, 55-64.	2.0	14
21229	First-Principles Study of Thermoelectric Properties of Covalent Organic Frameworks. Journal of Electronic Materials, 2016, 45, 3445-3452.	1.0	16

#	Article	IF	Citations
21230	Ammonia modification of oxide-free Si(111) surfaces. Surface Science, 2016, 650, 285-294.	0.8	10
21231	Selective Improvement of NO₂ Gas Sensing Behavior in SnO₂ Nanowires by Ion-Beam Irradiation. ACS Applied Materials & Interfaces, 2016, 8, 13646-13658.	4.0	110
21232	Hydrogen on silicene: like or unlike graphene?. Physical Chemistry Chemical Physics, 2016, 18, 15654-15666.	1.3	27
21233	Alloying Effects on the Phase Stability and Mechanical Properties of Doped Cu-Sn IMCs: A First-Principle Study. Journal of Electronic Materials, 2016, 45, 4018-4027.	1.0	15
21234	Photocatalytic reduction of CO2 with H2O over modified TiO2 nanofibers: Understanding the reduction pathway. Nano Research, 2016, 9, 1956-1968.	5.8	62
21235	Oxygen vacancies, the optical band gap (Eg) and photocatalysis of hydroxyapatite: Comparing modelling with measured data. Applied Catalysis B: Environmental, 2016, 196, 100-107.	10.8	146
21236	Ab initio thermodynamics of magnesium carbonates and hydrates in water-saturated supercritical CO2 and CO2-rich regions. Chemical Geology, 2016, 434, 1-11.	1.4	23
21237	Inconsistencies in modelling interstitials in FeCr with empirical potentials. Computational Materials Science, 2016, 121, 204-208.	1.4	6
21238	Single-layer cadmium chalcogenides: promising visible-light driven photocatalysts for water splitting. Physical Chemistry Chemical Physics, 2016, 18, 17029-17036.	1.3	75
21239	Thermodynamic reassessment of the cerium gold binary system. Journal of Alloys and Compounds, 2016, 683, 599-609.	2.8	3
21240	A first-principle study of Os-based compounds: Electronic structure and vibrational properties. Journal of Physics and Chemistry of Solids, 2016, 96-97, 121-127.	1.9	17
21241	Electric field modulation of the band gap, dielectric constant and polarizability in SnS atomically thin layers. Physics Letters, Section A: General, Atomic and Solid State Physics, 2016, 380, 2227-2232.	0.9	19
21242	The charge states of Au on gold-substituted Ce1â^'xO2(111) surfaces with multiple oxygen vacancies. Physical Chemistry Chemical Physics, 2016, 18, 15884-15893.	1.3	16
21243	First-principles investigation of carbon substitution for lead in ferroelectric lead titanate. Ferroelectrics, 2016, 498, 12-17.	0.3	2
21244	Optical and electronic properties of orthorhombic and trigonal AXO₃ (A=Cd, Zn; X=Sn,) Tj ETQq0 0 0 rgBT /Overlock 10 Tf	0.3	4
21245	Characterization of Nickel Aluminide Formed on Ni-Based Superalloy 690 Substrate, First-Principle Ni(Cr)/NiAl Interface Simulations and Stability of Aluminide in Aggressive Environment in Pre-oxidized State. Transactions of the Indian Institute of Metals, 2016, 69, 1889-1897.	0.7	2
21246	First-Principles Study on the MAX Phases Ti n+1GaN n (nÂ=Â1,2, and 3). Journal of Electronic Materials, 2016, 45, 4256-4264.	1.0	29
21247	Dopants induced structural and optical anomalies of anisotropic edges of black phosphorous thin films and crystals. Ceramics International, 2016, 42, 13113-13127.	2.3	17

#	Article	IF	Citations
21248	New insights into electrocatalytic ozone generation via splitting of water over PbO2 electrode: A DFT study. Chemical Physics Letters, 2016, 654, 46-51.	1.2	23
21249	Thermodynamic optimization of the Liâ€“Pb system aided by first-principles calculations. Journal of Nuclear Materials, 2016, 477, 95-101.	1.3	15
21250	Promotional effects of chemisorbed oxygen and hydroxide in the activation of Câ€“H and Oâ€“H bonds over transition metal surfaces. Surface Science, 2016, 650, 210-220.	0.8	57
21251	Surface-Induced Phase of Tyrian Purple (6,6â€²-Dibromoindigo): Thin Film Formation and Stability. Crystal Growth and Design, 2016, 16, 3647-3655.	1.4	15
21252	Reversed Hysteresis during CO Oxidation over Pd75Ag25(100). ACS Catalysis, 2016, 6, 4154-4161.	5.5	31
21253	Mechanisms for High Selectivity in the Hydrodeoxygenation of 5-Hydroxymethylfurfural over PtCo Nanocrystals. ACS Catalysis, 2016, 6, 4095-4104.	5.5	124
21254	Stability of solution-processed MAPbI₃ and FAPbI₃ layers. Physical Chemistry Chemical Physics, 2016, 18, 13413-13422.	1.3	208
21255	Doped penta-graphene and hydrogenation of its related structures: a structural and electronic DFT-D study. Physical Chemistry Chemical Physics, 2016, 18, 15505-15509.	1.3	37
21256	Spin friction between Co monolayer and Mn/W(110) surface: Ab Initio investigations. Tribology International, 2016, 95, 419-425.	3.0	9
21257	Heterointerface Electronic States and Charge Transport of Crystalline N,Nâ€²-1H,1Hâ€²-Perfluorobutil Dicyanoperylene Diimide in Field-Effect Transistor Configuration. Journal of Physical Chemistry C, 2016, 120, 12083-12091.	1.5	2
21258	CO Molecules on a NaCl(100) Surface: Structures, Energetics, and Vibrational Davydov Splittings at Various Coverages. Journal of Physical Chemistry C, 2016, 120, 12637-12653.	1.5	12
21259	Low-dimensional ScO₂with tunable electronic and magnetic properties: first-principles studies. Journal of Physics Condensed Matter, 2016, 28, 015004.	0.7	1
21260	Adsorption of Carbon Monoxide on Platinumâ€“Ruthenium, Platinumâ€“Osmium, Platinumâ€“Rutheniumâ€“Osmium, and Platinumâ€“Rutheniumâ€“Osmiumâ€“Iridium Alloys. Journal of Physical Chemistry C, 2016, 120, 10427-10441.	1.5	17
21261	Controlled Sculpture of Black Phosphorus Nanoribbons. ACS Nano, 2016, 10, 5687-5695.	7.3	111
21262	Synergistic Effects in Bimetallic Palladiumâ€“Copper Catalysts Improve Selectivity in Oxygenate Coupling Reactions. Journal of the American Chemical Society, 2016, 138, 6805-6812.	6.6	94
21263	First-principles study of electronic transport and optical properties of penta-graphene, penta-SiC₂ and penta-CN₂. RSC Advances, 2016, 6, 50867-50873.	1.7	62
21264	Assessment of the CSL and SU models for bcc-Fe grain boundaries from first principles. Computational Materials Science, 2016, 122, 22-29.	1.4	22
21265	Surface-Bulk Model for d⁰ Ferromagnetism in ZnS Quantum Dots and Wires. Journal of Physical Chemistry C, 2016, 120, 11253-11261.	1.5	14

#	Article	IF	Citations
21266	Understanding oxidative dehydrogenation of ethane on Co3O4 nanorods from density functional theory. Catalysis Science and Technology, 2016, 6, 6861-6869.	2.1	37
21267	Theoretical study on electronic and optical properties of Zn-doped In0.25Ga0.75As photocathodes. Optical Review, 2016, 23, 84-91.	1.2	2
21268	Adsorption of oxygen atom on MoSi 2 (110) surface. Applied Surface Science, 2016, 382, 239-248.	3.1	37
21269	High hydrogen retention in the sub-surfaces of tungsten plasma facing materials: A theoretical insight. Scripta Materialia, 2016, 122, 14-17.	2.6	18
21270	Tuning Dirac points by strain in MoX₂nanoribbons (X = S, Se, Te) with a 1Tâ€² structure. Physical Chemistry Chemical Physics, 2016, 18, 16361-16366.	1.3	5
21271	Glycerol oxidehydration to pyruvaldehyde over silver-based catalysts for improved lactic acid production. Green Chemistry, 2016, 18, 4682-4692.	4.6	32
21272	Fine tuning the band-gap of graphene by atomic and molecular doping: a density functional theory study. RSC Advances, 2016, 6, 55990-56003.	1.7	40
21273	Low-density superhard materials: computational study of Li-inserted B-substituted closo-carboranes LiBC₁₁ and Li₂B₂C₁₀. RSC Advances, 2016, 6, 52695-52699.	1.7	8
21274	Dislocation/hydrogen interaction mechanisms in hydrided nanocrystalline palladium films. Acta Materialia, 2016, 111, 253-261.	3.8	28
21275	An Efficient Strategy for Controlled Band Gap Engineering of KTaO₃. Journal of Physical Chemistry C, 2016, 120, 6920-6929.	1.5	63
21276	Synthesis, characterization and DFT studies of zinc-doped copper oxide nanocrystals for gas sensing applications. Journal of Materials Chemistry A, 2016, 4, 6527-6539.	5.2	157
21277	Mechanism of CO2 reduction by H2 on Ru(0 0 0 1) and general selectivity descriptors for late-transition metal catalysts. Journal of Catalysis, 2016, 343, 86-96.	3.1	104
21278	Structural stability and electronic properties of AgInS2 under pressure. European Physical Journal B, 2016, 89, 1.	0.6	9
21279	Hydrogen sensitive field-effect transistor based on germanene nanoribbon and optical properties of hydrogenated germanene. Journal of Computational Electronics, 2016, 15, 381-388.	1.3	16
21280	First-Principles Study the Electronic and Thermodynamic Properties for CoBi3 Superconductor. Journal of Superconductivity and Novel Magnetism, 2016, 29, 1203-1211.	0.8	1
21281	Phenomenological effets of tantalum incorporation into diamond films: Experimental and first principle studies. Applied Surface Science, 2016, 380, 83-90.	3.1	6
21282	Effect of adatoms and molecules on the physical properties of platinum-doped and -substituted silicene: A first-principles investigation. Applied Surface Science, 2016, 371, 314-321.	3.1	30
21283	Formaldehyde molecule adsorption on the doped monolayer MoS2: A first-principles study. Applied Surface Science, 2016, 371, 180-188.	3.1	129

#	Article	IF	Citations
21284	Novel high-pressure phases of AlN: A first-principles study. Computational Materials Science, 2016, 117, 496-501.	1.4	29
21285	Identification of metal s states in Sn-doped anatase by polarisation dependent hard X-ray photoelectron spectroscopy. Chemical Physics Letters, 2016, 647, 59-63.	1.2	7
21286	Ab initio investigation of superconductivity in orthorhombic MgPtSi. Journal of Alloys and Compounds, 2016, 673, 302-308.	2.8	2
21287	Intrinsic currentâ€“voltage characteristics of metal-carbon nanotube networks: A first-principles study. Organic Electronics, 2016, 31, 278-286.	1.4	5
21288	Zirconium-peroxo embedded in non-stoichiometric yttria stabilized zirconia (110) from first-principles. Solid State Ionics, 2016, 285, 215-221.	1.3	2
21289	Nature, Strength, and Cooperativity of the Hydrogen-Bonding Network in Î±-Chitin. Biomacromolecules, 2016, 17, 996-1003.	2.6	57
21290	Self-Sensitized Photocatalytic Degradation of Colorless Organic Pollutants Attached to Rutile Nanorodsâ€”Experimental and Theoretical DFT+D Studies. Journal of Physical Chemistry C, 2016, 120, 5442-5456.	1.5	53
21291	Surface-Specific DFT + U Approach Applied to Î±-Fe₂O₃(0001). Journal of Physical Chemistry C, 2016, 120, 4919-4930.	1.5	90
21292	Robust room-temperature inversion-asymmetry topological transitions in functionalized HgSe monolayer. Journal of Materials Chemistry C, 2016, 4, 2243-2251.	2.7	22
21293	Prediction of a new graphenelike<mml:math xmlns:mml="http://www.w3.org/1998/Math/MathML"><mml:mrow><mml:msub><mml:mi>Si</mml:mi><mml:mn>21</mml:mn></mml:msub></mml:mrow></mml:math> Physical Review B, 2016, 93, .	3.7	65
21294	Pressure-induced variation of structural, elastic, vibrational, electronic, thermodynamic properties and hardness of Ruthenium Carbides. Journal of Physics and Chemistry of Solids, 2016, 94, 47-58.	1.9	2
21295	Confined linear carbon chains as a route to bulkÂcarbyne. Nature Materials, 2016, 15, 634-639.	13.3	341
21296	Structural and electronic properties of the PbCrO₄ chrome yellow pigment and of its light sensitive sulfate-substituted compounds. RSC Advances, 2016, 6, 36336-36344.	1.7	21
21297	Effect of Temperature on the Desorption of Lithium from Molybdenum(110) Surfaces: Implications for Fusion Reactor First Wall Materials. Journal of Physical Chemistry B, 2016, 120, 6110-6119.	1.2	15
21298	First-Principles Study on Nitrobenzene-Doped Graphene as a Metal-Free Electrocatalyst for Oxygen Reduction Reaction. Journal of Physical Chemistry C, 2016, 120, 8804-8812.	1.5	42
21299	Graphene Monoxide Bilayer As a High-Performance on/off Switching Media for Nanoelectronics. ACS Applied Materials & Interfaces, 2016, 8, 10477-10482.	4.0	10
21300	DFT Insights into the Competitive Adsorption of Sulfur- and Nitrogen-Containing Compounds and Hydrocarbons on Co-Promoted Molybdenum Sulfide Catalysts. ACS Catalysis, 2016, 6, 2904-2917.	5.5	66
21301	Investigation of magnetic and electronic properties of transition metal doped Sc₂CT₂(T = O, OH or F) using a first principles study. Physical Chemistry Chemical Physics, 2016, 18, 12914-12919.	1.3	70

#	Article	IF	Citations
21302	The effect of calcium on nitric oxide heterogeneous adsorption on carbon: A first-principles study. Energy, 2016, 106, 212-220.	4.5	30
21303	Theoretical and experimental investigation of possible ferromagnetic ordering in wide band gap ZnO and related systems. Nuclear Instruments & Methods in Physics Research B, 2016, 379, 18-22.	0.6	7
21304	Optical and electronic properties of SO 2 molecule adsorbed on Si-doped (8, 0) boron nitride nanotube. Physica E: Low-Dimensional Systems and Nanostructures, 2016, 83, 365-371.	1.3	2
21305	Theoretical Studies of Sandwich Molecular Wires with Europium and Boratacyclooctatetraene Ligand and the Structure on a H-Ge(001)-2Ã—1 Surface. Journal of Physical Chemistry C, 2016, 120, 7088-7093.	1.5	16
21306	Adatom Interactions on GaN(0001) Surface I: Coverage-Dependent Adsorption. Journal of Physical Chemistry C, 2016, 120, 8076-8086.	1.5	9
21307	Atomic-Scale Analysis of the RuO₂/Water Interface under Electrochemical Conditions. Journal of Physical Chemistry C, 2016, 120, 8096-8103.	1.5	41
21308	Atomic and Electronic Structures of WTe₂ Probed by High Resolution Electron Microscopy and ab Initio Calculations. Journal of Physical Chemistry C, 2016, 120, 8364-8369.	1.5	37
21309	Tuning the electronic and mechanical properties of penta-graphene via hydrogenation and fluorination. Physical Chemistry Chemical Physics, 2016, 18, 14191-14197.	1.3	103
21310	Ab initio study of the pressure effect on the structural and electronic properties of crystalline hydrogen azide. Journal of Structural Chemistry, 2016, 57, 1-7.	0.3	2
21311	Transport properties through hexagonal boron nitride clusters embedded in graphene nanoribbons. Nanotechnology, 2016, 27, 185203.	1.3	7
21312	Transition from Diffusionâ€Controlled Intercalation into Extrinsically Pseudocapacitive Charge Storage of MoS₂ by Nanoscale Heterostructuring. Advanced Energy Materials, 2016, 6, 1501115.	10.2	185
21313	Strain Manipulated Magnetic Properties in ZnO and GaN Induced by Cation Vacancy. Journal of Electronic Materials, 2016, 45, 3300-3306.	1.0	1
21314	Density functional theory insights into the structural stability and Li diffusion properties of monoclinic and orthorhombic Li 2 FeSiO 4 cathodes. Journal of Power Sources, 2016, 318, 136-145.	4.0	34
21315	Structural, electronic and elastic properties of the Laves phases WFe2, MoFe2, WCr2 and MoCr2 from first-principles. Solid State Sciences, 2016, 56, 16-22.	1.5	25
21316	Structural, elastic and thermodynamic properties of tetragonal and orthorhombic polymorphs of Sr₂GeN₂: an ab initio investigation. High Pressure Research, 2016, 36, 198-219.	0.4	15
21317	Spin-polarized charge transfer induced by transition metal adsorption on graphene. Physica Scripta, 2016, 91, 053007.	1.2	7
21318	Interfacial potential approach for Ag/Si(111) interface. Modern Physics Letters B, 2016, 30, 1650104.	1.0	2
21319	Structural, Electronic, Magnetic and Optical Properties of Ni,Ti/Al-based Heusler Alloys: A First-Principles Approach. Zeitschrift Fur Naturforschung - Section A Journal of Physical Sciences, 2016, 71, 129-134.	0.7	7

#	Article	IF	Citations
21320	Generalization of first-principles thermodynamic model: Application to hexagonal close-packed <mml:math xmlns:mml="http://www.w3.org/1998/Math/MathML" altimg="si49.gif" overflow="scroll"><mml:mrow><mml:mi>Îµ</mml:mi></mml:mrow></mml:math>-Fe3N. Computational Materials Science, 2016, 117, 83-89.	1.4	4
21321	First principle study of the attachment of graphene onto non-doped and doped diamond (111). Diamond and Related Materials, 2016, 66, 52-60.	1.8	14
21322	Rietveld refinement, electronic structure and ionic conductivity of Sr4La6(SiO4)6F2 and Sr4La6(SiO4)6O ceramics. Journal of Solid State Chemistry, 2016, 239, 84-90.	1.4	11
21323	High pressure polyhydrides of molybdenum: A first-principles study. Solid State Communications, 2016, 239, 14-19.	0.9	15
21324	Nanotexturing To Enhance Photoluminescent Response of Atomically Thin Indium Selenide with Highly Tunable Band Gap. Nano Letters, 2016, 16, 3221-3229.	4.5	155
21325	The structureâ€“function relationship for alumina supported platinum during the formation of ammonia from nitrogen oxide and hydrogen in the presence of oxygen. Physical Chemistry Chemical Physics, 2016, 18, 10850-10855.	1.3	2
21326	Magnetic remanence in single atoms. Science, 2016, 352, 318-321.	6.0	259
21327	Theoretical investigations of the structural, electronic and optical properties of Hg1â^'xCdxS alloys. Modern Physics Letters B, 2016, 30, 1650173.	1.0	7
21328	Effect of charge on point defect size misfits from ab initio: Aliovalently doped <mml:math xmlns:mml="http://www.w3.org/1998/Math/MathML" altimg="si1.gif" overflow="scroll"><mml:mrow><mml:msub><mml:mrow><mml:mtext>SrTiO</mml:mtext></mml:mrow><mml:mrow><mml:mn>3</mml:mn></mml:mrow></mml:msub></mml:mrow></mml:math> Computational Materials Science, 2016, 119, 41-45.	1.4	5
21329	Synthesis, optical characterization and DFT calculations of electronic structure of Sb2O3 films obtained by thermal oxidation of Sb2S3. Journal of Alloys and Compounds, 2016, 681, 197-204.	2.8	18
21330	Molecular Origin of Properties of Organicâ€“Inorganic Hybrid Perovskites: The Big Picture from Small Clusters. Journal of Physical Chemistry Letters, 2016, 7, 1596-1603.	2.1	60
21331	Performance of polarisation functionals for linear and nonlinear optical properties of bulk zinc chalcogenides ZnX (X = S, Se, and Te). Physical Chemistry Chemical Physics, 2016, 18, 21179-21189.	1.3	13
21332	First-principles investigations of the structure and physical properties for new TcN crystal structure. Molecular Physics, 2016, 114, 1952-1959.	0.8	5
21333	Tuning band gap and optical properties of SnX₂ nanosheets: Hybrid functional studies. Modern Physics Letters B, 2016, 30, 1650120.	1.0	3
21334	COMPARISON OF ELECTRONIC AND OPTICAL PROPERTIES OF GaN MONOLAYER AND BULK STRUCTURE: A FIRST PRINCIPLE STUDY. Surface Review and Letters, 2016, 23, 1650026.	0.5	5
21335	Thermoelectric properties of nanoscale three dimensional Si phononic crystals. International Journal of Heat and Mass Transfer, 2016, 99, 102-106.	2.5	18
21336	Ruddlesdenâ€“Popper Hybrid Lead Iodide Perovskite 2D Homologous Semiconductors. Chemistry of Materials, 2016, 28, 2852-2867.	3.2	1,607
21337	Conceptual design of tetraazaporphyrin- and subtetraazaporphyrin-based functional nanocarbon materials: electronic structures, topologies, optical properties, and methane storage capacities. Physical Chemistry Chemical Physics, 2016, 18, 13503-13518.	1.3	3

#	Article	IF	Citations
21338	Mechanical Properties Evaluation of Zr Addition in L12-Al3(Sc1â^'x Zr x) Using First-Principles Calculation. Jom, 2016, 68, 1293-1300.	0.9	10
21339	Electronic structure and magnetism of doped wurtzite InSb nanowire. Journal Physics D: Applied Physics, 2016, 49, 175303.	1.3	9
21340	Solid-state NMR and thermodynamic investigations on LiBH4LiNH2 system. International Journal of Hydrogen Energy, 2016, 41, 14475-14483.	3.8	17
21341	Adsorption and dissociation of H₂O on the (001) surface of uranium mononitride: energetics and mechanism from first-principles investigation. Physical Chemistry Chemical Physics, 2016, 18, 13255-13266.	1.3	17
21342	Experimental Part. Springer Theses, 2016, , 103-114.	0.0	0
21343	High catalytic activity of oxygen-induced (200) surface of Ta2O5 nanolayer towards durable oxygen evolution reaction. Nano Energy, 2016, 25, 60-67.	8.2	36
21344	Exploring the sensitivity of ZnO nanotubes to tyrosine nitration: A DFT approach. Physics Letters, Section A: General, Atomic and Solid State Physics, 2016, 380, 2090-2097.	0.9	9
21345	The role of vdW interactions in coverage dependent adsorption energies of atomic adsorbates on Pt(111) and Pd(111). Surface Science, 2016, 650, 196-202.	0.8	5
21346	Scanning tunneling microscopy and density functional theory investigations on molecular self-assembly of graphene on Ru(0 0 0 1). Applied Surface Science, 2016, 367, 424-431.	3.1	7
21347	Interaction between single vacancies in graphene sheet: An ab initio calculation. Solid State Communications, 2016, 240, 5-9.	0.9	11
21348	Significantly enhanced oxygen reduction reaction performance of N-doped carbon by heterogeneous sulfur incorporation: synergistic effect between the two dopants in metal-free catalysts. Journal of Materials Chemistry A, 2016, 4, 7422-7429.	5.2	71
21349	Microthermokinetic study of xanthate adsorption on impurity-doped galena. Transactions of Nonferrous Metals Society of China, 2016, 26, 272-281.	1.7	23
21350	Theoretical insights on the reaction pathways for oxygen reduction reaction on phosphorus doped graphene. Carbon, 2016, 105, 214-223.	5.4	57
21351	Theoretical investigation of superconductivity in SrAuSi3 and SrAu2Si2. Journal of Physics and Chemistry of Solids, 2016, 95, 65-73.	1.9	8
21352	Cation synergies affect ammonia adsorption over VOX and (V,W)OX dispersed on Î±-Al2O3 (0001) and Î±-Fe2O3 (0001). Surface Science, 2016, 651, 41-50.	0.8	7
21353	Transition Metal Ordering Optimization for High-Reversible Capacity Positive Electrode Materials in the Liâ€“Niâ€“Coâ€“Mn Pseudoquaternary System. Journal of Physical Chemistry C, 2016, 120, 8540-8549.	1.5	24
21354	Predicting Coherency Loss of $$ gamma^{primeprime} $$ Precipitates in IN718 Superalloy. Metallurgical and Materials Transactions A: Physical Metallurgy and Materials Science, 2016, 47, 3235-3247.	1.1	46
21355	Effects of Thermal Electronic Excitations on the Diffusion of Oxygen Adatoms on Graphene. Journal of Physical Chemistry A, 2016, 120, 2607-2613.	1.1	11

#	Article	IF	Citations
21356	Probing the Electronic Structure of Heterogeneous Metal Interfaces by Transition Metal Shelled Gold Nanoparticle-Enhanced Raman Spectroscopy. Journal of Physical Chemistry C, 2016, 120, 20684-20691.	1.5	28
21357	Stabilities and Reconstructions of Clean PbS and PbSe Surfaces: DFT Results and the Role of Dispersion Forces. Journal of Physical Chemistry C, 2016, 120, 8813-8820.	1.5	18
21358	Intrinsic Ferroelasticity and/or Multiferroicity in Two-Dimensional Phosphorene and Phosphorene Analogues. Nano Letters, 2016, 16, 3236-3241.	4.5	491
21359	Polar metals by geometric design. Nature, 2016, 533, 68-72.	13.7	262
21360	Mechanistic Insight into the C₂ Hydrocarbons Formation from Syngas on fcc-Co(111) Surface: A DFT Study. Journal of Physical Chemistry C, 2016, 120, 9132-9147.	1.5	53
21361	Structural, elastic, electronic and optical properties of Cu3MTe4 (M = Nb, Ta) sulvanites â€" An abÂinitio study. International Journal of Modern Physics B, 2016, 30, 1650089.	1.0	18
21362	Theoretical insights on the catalytic activity and mechanism for oxygen reduction reaction at Fe and P codoped graphene. Physical Chemistry Chemical Physics, 2016, 18, 12675-12681.	1.3	22
21363	Superhard superstrong carbon clathrate. Carbon, 2016, 105, 151-155.	5.4	33
21364	Mechanistic insights into the Cu(I) oxide-catalyzed conversion of CO 2 to fuels and chemicals: A DFT approach. Journal of CO2 Utilization, 2016, 15, 96-106.	3.3	35
21365	Structural stabilities, surface morphologies and electronic properties of spinel LiTi2O4 as anode materials for lithium-ion battery: A first-principles investigation. Journal of Power Sources, 2016, 319, 185-194.	4.0	22
21366	Hydrogenation induced structure and property changes in GdGa. Journal of Solid State Chemistry, 2016, 239, 184-191.	1.4	7
21367	The many phases of CaC2. Journal of Solid State Chemistry, 2016, 239, 204-213.	1.4	14
21368	Kinetic Regimes in Ethylene Hydrogenation over Transition-Metal Surfaces. ACS Catalysis, 2016, 6, 3277-3286.	5.5	43
21369	Mechanism of Electrochemical Hydrogen Storage for Î±-Fe₂O₃Particles as Anode Material for Aqueous Rechargeable Batteries. Journal of the Electrochemical Society, 2016, 163, H566-H569.	1.3	14
21370	Elastic anisotropy and phonon focusing for tetragonal crystals: Application to Î³-TiAl. Computational Materials Science, 2016, 118, 117-123.	1.4	9
21371	Equation of state for technetium from Xâ€ray diffraction and first-principle calculations. Journal of Physics and Chemistry of Solids, 2016, 95, 6-11.	1.9	5
21372	Stark Effect and Nonlinear Impedance of the Asymmetric Ag-CO-Ag Junction: An Optical Rectenna. Journal of Physical Chemistry C, 2016, 120, 20914-20921.	1.5	13
21373	Dynamics and Mechanisms of Exfoliated Black Phosphorus Sublimation. Journal of Physical Chemistry Letters, 2016, 7, 1667-1674.	2.1	36

#	Article	IF	Citations
21374	Role of ligandâ€“ligand vs. coreâ€“core interactions in gold nanoclusters. Physical Chemistry Chemical Physics, 2016, 18, 12716-12724.	1.3	20
21375	Crystal growth, experimental and theoretical studies on the electronic structure of CNGS and Nd:CNGS. CrystEngComm, 2016, 18, 3481-3487.	1.3	22
21376	Absence of a stable atomic structure in fluorinated graphene. Physical Chemistry Chemical Physics, 2016, 18, 13287-13293.	1.3	11
21377	Quantum spin Hall insulators in functionalized arsenene (AsX, X = F, OH and CH₃) monolayers with pronounced light absorption. Nanoscale, 2016, 8, 9657-9666.	2.8	63
21378	Well-structured bimetallic surface capable of molecular recognition for chemoselective nitroarene hydrogenation. Chemical Science, 2016, 7, 4476-4484.	3.7	75
21379	Impurity effect of Mg on the generalized planar fault energy of Al. Journal of Materials Science, 2016, 51, 6552-6568.	1.7	46
21380	Automating impurity-enhanced antiphase boundary energy calculations from ab initio Monte Carlo. Calphad: Computer Coupling of Phase Diagrams and Thermochemistry, 2016, 53, 20-24.	0.7	13
21381	Insights into stability, electronic properties, defect properties and Li ions migration of Na, Mg and Al-doped LiVPO4F for cathode materials of lithium ion batteries: A first-principles investigation. Journal of Solid State Chemistry, 2016, 239, 228-236.	1.4	19
21382	Quantum Phase Transition in Germanene and Stanene Bilayer: From Normal Metal to Topological Insulator. Journal of Physical Chemistry Letters, 2016, 7, 1919-1924.	2.1	33
21383	Methanol Oxidation on Pt₃Sn(111) for Direct Methanol Fuel Cells: Methanol Decomposition. ACS Applied Materials & Interfaces, 2016, 8, 12194-12204.	4.0	52
21384	Markedly different adsorption behaviors of gas molecules on defective monolayer MoS₂: a first-principles study. Physical Chemistry Chemical Physics, 2016, 18, 15110-15117.	1.3	126
21385	In situ optical measurement of the rapid Li intercalation and deintercalation dynamics in colloidal 2D layered TiS₂nanodiscs. Nanoscale, 2016, 8, 11248-11255.	2.8	5
21386	Density functional theory calculations, growth, structure, and optical properties of birefringent LiNaV₂O₆. Journal of Materials Research, 2016, 31, 488-494.	1.2	6
21387	First-principles investigation of electronic properties of Al x In1â^'x P semiconductor alloy. Journal of Materials Science, 2016, 51, 7343-7354.	1.7	15
21388	Geometric and electric properties of graphitic carbon nitride sheet with embedded single manganese atom under bi-axial tensile strain. Current Applied Physics, 2016, 16, 809-815.	1.1	19
21389	First-Principles studies of silicon underpotential deposition on defective graphene and its relevance for lithium-ion battery materials. Electrochimica Acta, 2016, 208, 92-101.	2.6	14
21390	Band structures in silicene on monolayer gallium phosphide substrate. Solid State Communications, 2016, 239, 32-36.	0.9	6
21391	Density Functional Theory Investigations of Ferrocene-Terminated Self-Assembled Monolayers: Electronic State Changes Induced by Electric Dipole Field of Coadsorbed Species. Journal of Physical Chemistry C, 2016, 120, 8684-8692.	1.5	7

#	Article	IF	Citations
21392	Stationary Full Li-Ion Batteries with Interlayer-Expanded V6O13 Cathodes and Lithiated Graphite Anodes. Electrochimica Acta, 2016, 203, 171-177.	2.6	42
21393	Ab initio study of the structural and electronic properties of Nb2AlC. Computational Condensed Matter, 2016, 6, 1-4.	0.9	5
21394	Oxygen vacancy diffusion in bulk SrTiO3 from density functional theory calculations. Computational Materials Science, 2016, 118, 309-315.	1.4	48
21395	Site specific interaction of aromatic amino acids with ZnO nanotubes: A density functional approach. Computational and Theoretical Chemistry, 2016, 1086, 36-44.	1.1	7
21396	The calculated magnetic, electronic and thermodynamic properties of Ce3Co29Si4B10 compound. Journal of Solid State Chemistry, 2016, 237, 174-182.	1.4	1
21397	Chemisorption of Acetophenone on Si(111)-7 Ã— 7. Polar Aromatic Molecule on Electronically Complex Surface. Journal of Physical Chemistry C, 2016, 120, 9200-9206.	1.5	2
21398	First-Principle Framework for Total Charging Energies in Electrocatalytic Materials and Charge-Responsive Molecular Binding at Gasâ€“Surface Interfaces. ACS Applied Materials & Interfaces, 2016, 8, 10897-10903.	4.0	18
21399	First-principles study of Mn alloying into Fe3AlC: Towards the improvement of ductility. Journal of Alloys and Compounds, 2016, 681, 283-292.	2.8	6
21400	Critical analysis of the vacancy induced magnetism in Scandium Nitride (ScN): An ab-initio study. Journal of Magnetism and Magnetic Materials, 2016, 413, 19-24.	1.0	7
21401	Ferromagnetism in 4H-GaN polytype doped by non-magnetic light elements Li, Be, B, C, O, F, Ne, Na, and Mg: Ab-initio study. Journal of Magnetism and Magnetic Materials, 2016, 414, 153-157.	1.0	10
21402	First-principles investigation of stability diagram and electronic properties of SrHfO3 (110) polar terminations. Materials Chemistry and Physics, 2016, 174, 195-203.	2.0	5
21403	Pressure-induced structural and valence transition in AgO. Physical Chemistry Chemical Physics, 2016, 18, 15322-15326.	1.3	3
21404	Effect of van der Waals corrections on DFT-computed metallic surface properties. Materials Research Express, 2016, 3, 046501.	0.8	28
21405	3d transition metal embedded C2N monolayers as promising single-atom catalysts: A first-principles study. Carbon, 2016, 105, 463-473.	5.4	167
21406	Exploring high-pressure FeB2: Structural and electronic properties predictions. Journal of Alloys and Compounds, 2016, 678, 109-112.	2.8	11
21407	Impact of Short-Range Forces on Defect Production from High-Energy Collisions. Journal of Chemical Theory and Computation, 2016, 12, 2871-2879.	2.3	49
21408	Impact of Point Defects on Proton Conduction in Strontium Cerate. Journal of Physical Chemistry C, 2016, 120, 9562-9568.	1.5	11
21409	Pseudocapacitance and excellent cyclability of 2,5-dimethoxy-1,4-benzoquinone on graphene. Energy and Environmental Science, 2016, 9, 2586-2594.	15.6	129

#	Article	IF	Citations
21410	Synthesis and morphological transformation of BaWO4 crystals: Experimental and theoretical insights. Ceramics International, 2016, 42, 10913-10921.	2.3	45
21411	Hexagonal boron nitride and graphene in-plane heterostructures: An experimentally feasible approach to charge-induced switchable CO 2 capture. Chemical Physics, 2016, 478, 139-144.	0.9	25
21412	Electronic properties of Ga In1â^'P ternary alloy from first-principles. Computational Materials Science, 2016, 120, 70-76.	1.4	5
21413	Atomistic Mechanisms of Chemical Mechanical Polishing of a Cu Surface in Aqueous H₂O₂: Tight-Binding Quantum Chemical Molecular Dynamics Simulations. ACS Applied Materials & Interfaces, 2016, 8, 11830-11841.	4.0	42
21414	Role of various defects in the photoluminescence characteristics of nanocrystalline Nd₂Zr₂O₇: an investigation through spectroscopic and DFT calculations. Journal of Materials Chemistry C, 2016, 4, 4988-5000.	2.7	99
21415	First principles study of nanostructured TiS2 electrodes for Na and Mg ion storage. Journal of Power Sources, 2016, 320, 322-331.	4.0	46
21416	Tuning electronic and magnetic properties of blue phosphorene by doping Al, Si, As and Sb atom: A DFT calculation. Solid State Communications, 2016, 242, 36-40.	0.9	72
21417	Pyramidal Structure Formation at the Interface between III/V Semiconductors and Silicon. Chemistry of Materials, 2016, 28, 3265-3275.	3.2	37
21418	Bacteria Absorption-Based Mn₂P₂O₇â€“Carbon@Reduced Graphene Oxides for High-Performance Lithium-Ion Battery Anodes. ACS Nano, 2016, 10, 5516-5524.	7.3	81
21419	Evaluating silicene as a potential cathode host to immobilize polysulfides in lithiumâ€“sulfur batteries. Journal of Coordination Chemistry, 2016, 69, 2090-2105.	0.8	37
21420	Theoretical investigations on vibrational properties and thermal conductivities of ternary antimonides TiXSb, ZrXSb and HfXSb (X = Si, Ge). Philosophical Magazine, 2016, 96, 1712-1723.	0.7	10
21421	Interaction of boron with graphite: A van der Waals density functional study. Applied Surface Science, 2016, 379, 402-410.	3.1	15
21422	The adsorption of CO and NO on the MoS2 monolayer doped with Au, Pt, Pd, or Ni: A first-principles study. Applied Surface Science, 2016, 383, 98-105.	3.1	321
21423	Structural and mechanical properties of NbN and Nb-Si-N films: Experiment and molecular dynamics simulations. Ceramics International, 2016, 42, 11743-11756.	2.3	63
21424	Opportunities and challenges in the electrocatalysis of CO2 and CO reduction using bifunctional surfaces: A theoretical and experimental study of Auâ€“Cd alloys. Journal of Catalysis, 2016, 343, 215-231.	3.1	115
21425	Nonradiative Relaxation of Photoexcited Black Phosphorus Is Reduced by Stacking with MoS₂: A Time Domain ab Initio Study. Journal of Physical Chemistry Letters, 2016, 7, 1830-1835.	2.1	36
21426	Sublattice effect on the formation of the band structure of crystals with the chalcopyrite lattice: B2CN, BC2N, BCN2. Journal of Structural Chemistry, 2016, 57, 8-13.	0.3	6
21427	Direct Exfoliation of Graphite into Graphene by Pyrene-Based Molecules as Molecular-Level Wedges: A Tribological View. Tribology Letters, 2016, 62, 1.	1.2	7

#	Article	IF	Citations
21428	Molecular dynamics simulation of nano-indentation of (111) cubic boron nitride with optimized Tersoff potential. Applied Surface Science, 2016, 382, 309-315.	3.1	35
21429	Hydrostatic Pressure Effects on Structural and Electronic Properties of ETN and PETN from First-Principles Calculations. Journal of Physical Chemistry A, 2016, 120, 3710-3717.	1.1	8
21430	A comparative study on the functionality of S- and P-based lubricant additives by combined first principles and experimental analysis. RSC Advances, 2016, 6, 47753-47760.	1.7	25
21431	Effect of lithium intercalation on the structural and electronic properties of layered LiFeSO4OH and layered FeSO4OH using first-principle calculations. Computational Materials Science, 2016, 119, 144-151.	1.4	9
21432	van der Waals forces and confinement in carbon nanopores: Interaction between CH4, COOH, NH3, OH, SH and single-walled carbon nanotubes. Chemical Physics Letters, 2016, 652, 22-26.	1.2	4
21433	The detailed crystal and electronic structures of the cotunnite-type ZrO2. Solid State Communications, 2016, 239, 27-31.	0.9	3
21434	Achirality in the low temperature structure and lattice modes of tris(acetylacetonate)iron(iii). Dalton Transactions, 2016, 45, 8278-8283.	1.6	0
21435	Why host to dopant energy transfer is absent in the MgAl₂O₄:Eu³⁺ spinel? And exploring Eu³⁺ site distribution and local symmetry through its photoluminescence: interplay of experiment and theory. RSC Advances, 2016, 6, 42923-42932.	1.7	46
21436	Understanding and Tuning the Hydrogen Evolution Reaction on Pt-Covered Tungsten Carbide Cathodes. Journal of the Electrochemical Society, 2016, 163, F629-F636.	1.3	15
21437	Combining solid-state NMR spectroscopy with first-principles calculations â€“ a guide to NMR crystallography. Chemical Communications, 2016, 52, 7186-7204.	2.2	202
21438	A graphene-coupled Bi₂WO₆ nanocomposite with enhanced photocatalytic performance: a first-principles study. Physical Chemistry Chemical Physics, 2016, 18, 14113-14121.	1.3	27
21439	Binding TiO₂-B nanosheets with N-doped carbon enables highly durable anodes for lithium-ion batteries. Journal of Materials Chemistry A, 2016, 4, 8172-8179.	5.2	47
21440	Analysis of adsorption properties of typical partial discharge gases on Ni-SWCNTs using density functional theory. Applied Surface Science, 2016, 379, 47-54.	3.1	104
21441	Effects of alloying on the behavior of B and S at Î£5 (2 1 0) grain boundary in Î³-Fe. Computational Materials Science, 2016, 115, 170-176.	1.4	24
21442	Mechanism studies concerning carbon deposition effect of CO methanation on Ni-based catalyst through DFT and TPSR methods. International Journal of Hydrogen Energy, 2016, 41, 8401-8411.	3.8	19
21443	Doping-induced stability in vanadium-doped ZnO quantum well wires (QWW): Combination of DFT calculations within experimental measurements. Solid State Sciences, 2016, 57, 33-37.	1.5	2
21444	First-principles study on the structural, elastic and electronic properties of Ti2SiN under high pressure. Solid State Communications, 2016, 237-238, 24-27.	0.9	12
21445	Atomistic-Scale Analysis of Carbon Coating and Its Effect on the Oxidation of Aluminum Nanoparticles by ReaxFF-Molecular Dynamics Simulations. Journal of Physical Chemistry C, 2016, 120, 9464-9474.	1.5	116

#	Article	IF	Citations
21446	Ab Initio Study of Layered Double Hydroxides Containing Iron and Its Potential Use as Fertilizer. Journal of Physical Chemistry C, 2016, 120, 9965-9974.	1.5	26
21447	Manipulation of birefringence via substitution of Sr²⁺by Pb²⁺based on the structure model of LiSr_{1â^'x}Pb_xBO₃(0 â‰¤ x â‰¤ 0.5). New Journal of Chemistry, 2016, 40, 6120-6126.	1.4	5
21448	Experimental and theoretical approach to account for green luminescence from Gd₂Zr₂O₇ pyrochlore: exploring the site occupancy and origin of host-dopant energy transfer in Gd₂Zr₂O₇:Eu³⁺. RSC Advances, 2016, 6, 44908-44920.	1.7	64
21449	Surface defect chemistry of Y-substituted and hydrated BaZrO₃ with subsurface space-charge regions. Journal of Materials Chemistry A, 2016, 4, 7437-7444.	5.2	38
21450	The high-pressure semiconducting phase of LiBC. Europhysics Letters, 2016, 114, 16001.	0.7	8
21451	Strain and carrier-induced coexistence of topologically insulating and superconducting phase in iodized Si(111) films. Nano Research, 2016, 9, 1578-1589.	5.8	6
21452	Effect of electron-electron correlation and site disorder on the magnetic moment and half-metallicity of Co 2 FeGa 1â^'x Si x alloys. Materials Chemistry and Physics, 2016, 177, 564-569.	2.0	5
21453	Diverse anisotropy of phonon transport in two-dimensional group IVâ€“VI compounds: A comparative study. Nanoscale, 2016, 8, 11306-11319.	2.8	234
21454	Investigations of the band structures of edge-defect zigzag graphene nanoribbons using density functional theory. RSC Advances, 2016, 6, 39587-39594.	1.7	18
21455	Electronic structure and optical properties of Î±-RDX crystal under pressure from first-principles calculations. Molecular Physics, 2016, 114, 1931-1938.	0.8	2
21456	A van der Waals DFT study of PtH 2 systems absorbed on pristine and defective graphene. Applied Surface Science, 2016, 382, 80-87.	3.1	27
21457	Optical vibrational modes of Ge nanowires: A computational approach. Microelectronic Engineering, 2016, 159, 215-220.	1.1	7
21458	High-Pressure Crystal Structure, Lattice Vibrations, and Band Structure of BiSbO₄. Inorganic Chemistry, 2016, 55, 4958-4969.	1.9	60
21459	Effect of the Exchange-Correlation Potential on the Transferability of BrÃ¸nstedâ€“Evansâ€“Polanyi Relationships in Heterogeneous Catalysis. Journal of Chemical Theory and Computation, 2016, 12, 2121-2126.	2.3	20
21460	Electrochemical Surface Stress Development during CO and NO Oxidation on Pt. Journal of Physical Chemistry C, 2016, 120, 8674-8683.	1.5	22
21461	Coincidence Lattices of 2D Crystals: Heterostructure Predictions and Applications. Journal of Physical Chemistry C, 2016, 120, 10895-10908.	1.5	68
21462	Theoretical characterization of the surface composition of ruthenium nanoparticles in equilibrium with syngas. Nanoscale, 2016, 8, 10974-10992.	2.8	43
21463	Point defect interactions in iron lattice: a first-principles study. RSC Advances, 2016, 6, 45250-45258.	1.7	21

#	Article	IF	Citations
21464	Thermal conductivity and mechanical properties of nitrogenated holey graphene. Carbon, 2016, 106, 1-8.	5.4	118
21465	Structural, electronic, bonding and thermo-elastic properties of orthorhombic and cubic CeO 2 compound. Chinese Journal of Physics, 2016, 54, 1-11.	2.0	8
21466	Mechanical and electronic properties of Si Ge alloy in Cmmm structure. Chinese Journal of Physics, 2016, 54, 298-307.	2.0	12
21467	Photochemical route for synthesizing atomically dispersed palladium catalysts. Science, 2016, 352, 797-800.	6.0	1,540
21468	Electronic band alignment at CuGaS2 chalcopyrite interfaces. Computational Materials Science, 2016, 121, 79-85.	1.4	16
21469	High-pressure behavior of solid nitrobenzene: Combined Raman spectroscopy and DFT-D calculations study. Solid State Communications, 2016, 242, 63-67.	0.9	2
21470	Cleavage of the Câ€“C Bond in the Ethanol Oxidation Reaction on Platinum. Insight from Experiments and Calculations. Journal of Physical Chemistry C, 2016, 120, 11590-11597.	1.5	47
21471	Band Gap Opening of Graphene by Forming Heterojunctions with the 2D Carbonitrides Nitrogenated Holey Graphene, g-C₃N₄, and g-CN: Electric Field Effect. Journal of Physical Chemistry C, 2016, 120, 11299-11305.	1.5	40
21472	Diffusive nature of thermal transport in stanene. Physical Chemistry Chemical Physics, 2016, 18, 14257-14263.	1.3	34
21473	First principles investigation of helium physisorption on an Î±-Al₂O₃(0001) surface. Physical Chemistry Chemical Physics, 2016, 18, 15711-15718.	1.3	8
21474	First principles study of nanoscale mechanism of oxygen adsorption on lanthanum zirconate surfaces. Physica E: Low-Dimensional Systems and Nanostructures, 2016, 83, 36-40.	1.3	4
21475	(Nb_x, Zr_{1â€“x})₄AlC₃ MAX Phase Solid Solutions: Processing, Mechanical Properties, and Density Functional Theory Calculations. Inorganic Chemistry, 2016, 55, 5445-5452.	1.9	54
21476	Strain and Spinâ€“Orbital Coupling Effects on Electronic Structures and Magnetism of Semi-Hydrogenated Stanene. Journal of Physical Chemistry C, 2016, 120, 10622-10628.	1.5	34
21477	Hydrogenation of Penta-Graphene Leads to Unexpected Large Improvement in Thermal Conductivity. Nano Letters, 2016, 16, 3925-3935.	4.5	142
21478	â€œXA6â€•octahedra influencing the arrangement of anionic groups and optical properties in inverse-perovskite [B6O10]XA3(X = Cl, Br; A = alkali metal). Physical Chemistry Chemical Physics, 2016, 18, 15394-15398.	1.3	16
21479	Room temperature ferromagnetic properties of dysprosium-doped tris(8-hydroxyquinoline) aluminum: experimental and theoretical investigation. RSC Advances, 2016, 6, 43780-43785.	1.7	4
21480	Ferromagnetic interlayer interaction in KCo2Se2â^'xSx (0 â‰¤ x â‰¤ 2) and its chemical origin. Dalton Transactions, 2016, 45, 8248-8252.	1.6	15
21481	Concentration Effect of Reducing Agents on Green Synthesis of Gold Nanoparticles: Size, Morphology, and Growth Mechanism. Nanoscale Research Letters, 2016, 11, 230.	3.1	76

#	Article	IF	Citations
21482	Na+ as a probe to structural investigation of dehydrated smectites using NMR spectra calculated by DFT. Applied Clay Science, 2016, 126, 132-140.	2.6	16
21483	Band Alignments, Valence Bands, and Core Levels in the Tin Sulfides SnS, SnS₂, and Sn₂S₃: Experiment and Theory. Chemistry of Materials, 2016, 28, 3718-3726.	3.2	172
21484	Localization versus Delocalization in Chiral Single Component Conductors of Gold Bis(dithiolene) Complexes. Journal of the American Chemical Society, 2016, 138, 6838-6851.	6.6	43
21485	Solubility of transition metal interstitials in proton conducting BaZrO₃ and similar perovskite oxides. Journal of Materials Chemistry A, 2016, 4, 8105-8112.	5.2	44
21486	Wavelength-dependent optical transition mechanisms for light-harvesting of perovskite MAPbI3 solar cells using first-principles calculations. Journal of Materials Chemistry C, 2016, 4, 5248-5254.	2.7	11
21487	Origin of the hardest c-axis and softest a-axis and lowest transition pressure of Mo₂Ga₂C from first principles. Modern Physics Letters B, 2016, 30, 1650105.	1.0	14
21488	First-principles characterisation of the pressure-dependent elastic anisotropy of SnO₂ polymorphs. Philosophical Magazine, 2016, 96, 1861-1882.	0.7	17
21489	Pressure-driven suppression of the Jahnâ€“Teller effects and structural changes in cupric oxide. Journal of Physics Condensed Matter, 2016, 28, 025401.	0.7	7
21490	Ab-initio study of the Y adsorption and YN formation on the GaN(000<mml:math) Tj ETQq0 0 0 rgBT /Overlock 10 Tf 50 437 Td (xmlns:m Diffusion pathways and stability. Superlattices and Microstructures, 2016, 96, 67-74.	1.4	4
21491	In-plane interfacing effects of two-dimensional transition-metal dichalcogenide heterostructures. Physical Chemistry Chemical Physics, 2016, 18, 15632-15638.	1.3	46
21492	Intrinsic quantum spin Hall and anomalous Hall effects in h-Sb/Bi epitaxial growth on a ferromagnetic MnO₂thin film. Nanoscale, 2016, 8, 11202-11209.	2.8	16
21493	Theoretical studies of the adsorption of hydroxymethylidyne (COH) on Pt-alloy surfaces using density functional theory. Physica Scripta, 2016, 91, 025803.	1.2	5
21494	First-principles study of the elastic and thermodynamic properties of thorium hydrides at high pressure. Chinese Physics B, 2016, 25, 057102.	0.7	1
21495	Ab Initio Study of Structure, Electronic and Magnetic Properties of YFe5 Phase Compound in the DFT Formalism. Archives of Metallurgy and Materials, 2016, 61, 369-374.	0.6	4
21496	On the morphology of BaMoO₄ crystals: A theoretical and experimental approach. Crystal Research and Technology, 2016, 51, 634-644.	0.6	24
21497	A theoretical understanding on the CO-tolerance mechanism of the WC(0001) supported Pt monolayer: Some improvement strategies. Applied Surface Science, 2016, 389, 455-461.	3.1	22
21498	Understanding the photoelectrochemical properties of nanostructured CeO2/Cu2O heterojunction photoanode for efficient photoelectrochemical water splitting. International Journal of Hydrogen Energy, 2016, 41, 18339-18350.	3.8	48
21499	Theoretical study of B3-to-B1 phase transition in ZnS. Physics Letters, Section A: General, Atomic and Solid State Physics, 2016, 380, 3696-3702.	0.9	3

#	Article	IF	Citations
21500	Few-Layer Tin Sulfide: A New Black-Phosphorus-Analogue 2D Material with a Sizeable Band Gap, Oddâ€“Even Quantum Confinement Effect, and High Carrier Mobility. Journal of Physical Chemistry C, 2016, 120, 22663-22669.	1.5	130
21501	Anhydrous Calcium Oxalate Polymorphism: A Combined Computational and Synchrotron X-ray Diffraction Study. Crystal Growth and Design, 2016, 16, 5954-5965.	1.4	18
21502	Hybridization Effects between Silicene/Silicene Oxides and Ag(111). Journal of Physical Chemistry C, 2016, 120, 20192-20198.	1.5	10
21503	The role of the crystalline face in the ordering of 6-mercaptopurine self-assembled monolayers on gold. Nanoscale, 2016, 8, 17231-17240.	2.8	16
21504	Novel Laves phase superconductor NbBe 2 : A theoretical investigation. Computational Condensed Matter, 2016, 8, 7-13.	0.9	32
21505	Mononuclear, tetranuclear and polymeric cadmium(II) complexes with the 3,6-bis(2-pyridyl)-1,2,4,5-tetrazine ligand: Synthesis, crystal structure, spectroscopic and DFT studies. Polyhedron, 2016, 119, 160-174.	1.0	17
21506	Density functional theory simulation of the adsorption of sulphur multilayers on Au(100). Physical Chemistry Chemical Physics, 2016, 18, 29987-29998.	1.3	4
21507	First-principles and experimental study of nitrogen/sulfur co-doped carbon nanosheets as anodes for rechargeable sodium ion batteries. Journal of Materials Chemistry A, 2016, 4, 15565-15574.	5.2	128
21508	Influence of strain relaxation on the relative orientation of ZnO and ZnMnO wurtzite lattice with respect to sapphire substrates. Materials Research Express, 2016, 3, 095902.	0.8	3
21509	Mechanical and electronic properties of Câ€“Si alloys in the P222 1 structure. Chinese Journal of Physics, 2016, 54, 700-710.	2.0	8
21510	6-Aminopenicillanic acid revisited: A combined solid state NMR and in silico refinement. Chemical Physics Letters, 2016, 660, 214-220.	1.2	2
21511	Role of surface fluorine in improving the electrochemical properties of Fe/MWCNT electrodes. Journal of Industrial and Engineering Chemistry, 2016, 43, 78-85.	2.9	14
21512	Electrochemical and DFT study of an anticancer and active anthelmintic drug at carbon nanostructured modified electrode. Materials Science and Engineering C, 2016, 69, 1345-1353.	3.8	26
21513	Dynamic Behavior of Single Fe Atoms Embedded in Graphene. Journal of Physical Chemistry C, 2016, 120, 21998-22003.	1.5	25
21514	Elastic Properties, Defect Thermodynamics, Electrochemical Window, Phase Stability, and Li⁺ Mobility of Li₃PS₄: Insights from First-Principles Calculations. ACS Applied Materials & Interfaces, 2016, 8, 25229-25242.	4.0	114
21515	Ultra-weak interlayer coupling in two-dimensional gallium selenide. Physical Chemistry Chemical Physics, 2016, 18, 25401-25408.	1.3	22
21516	Hydrogenated borophene as a stable two-dimensional Dirac material with an ultrahigh Fermi velocity. Physical Chemistry Chemical Physics, 2016, 18, 27284-27289.	1.3	167
21517	The temperature-dependent dislocation properties of aluminum from the improved Peierlsâ€“Nabarro model and first-principles. Philosophical Magazine, 2016, 96, 2829-2852.	0.7	11

#	Article	IF	Citations
21518	Role of Ti doping and Al and B vacancies in the dehydrogenation of Al(BH4)3. Journal of Chemical Sciences, 2016, 128, 1651-1662.	0.7	3
21519	Thermal and Chemical Stability of n -Hexadecanethiol Monolayers on Au(111) in O 2 Environments. Electrochimica Acta, 2016, 215, 313-325.	2.6	6
21520	Peierlsâ€Distorted Ruâ€Chains and Boron Dumbbells in Nb₂RuB₂ and Ta₂RuB₂ from Firstâ€Principles Calculations and Experiments. European Journal of Inorganic Chemistry, 2016, 2016, 4104-4110.	1.0	6
21521	A new look at NaBrF4: the most BrF3-rich tetrafluoridobromate(III) by mass. Monatshefte FÃ¼r Chemie, 2016, 147, 1661-1668.	0.9	11
21522	The mechanism of oxygen activation on single Pt-atom doped SnO2(110) surface. Journal of Materials Science, 2016, 51, 10400-10407.	1.7	32
21523	Electronic and magnetic structures and bonding properties of Ce 2 CrN 3 and U 2 CrN 3 from first principles. Computational Condensed Matter, 2016, 9, 13-18.	0.9	3
21524	The strain effect on lithium ion migration in Li-Si alloys: A first-principles study. Solid State Communications, 2016, 247, 47-52.	0.9	4
21525	Determining a Structural Distortion and Anion Ordering in La2Si4N6C via Computation and Experiment. Inorganic Chemistry, 2016, 55, 9454-9460.	1.9	6
21526	Improving the photocatalytic activity of s-triazine based graphitic carbon nitride through metal decoration: an ab initio investigation. Physical Chemistry Chemical Physics, 2016, 18, 26466-26474.	1.3	16
21527	AMgPO₄Â·6H₂O (A = Rb, Cs): strong SHG responses originated from orderly PO₄groups. Journal of Materials Chemistry C, 2016, 4, 9219-9226.	2.7	44
21528	The role of interstitial native defects in the topological insulator Bi₂Se₃. Journal of Physics Condensed Matter, 2016, 28, 425801.	0.7	13
21529	Photoemission simulation for photocathode design: theory and application to copper and silver surfaces. Computational Materials Science, 2016, 122, 331-340.	1.4	19
21530	The possible formation of a magnetic FeS2 phase in the two-dimensional MoS2 matrix. Physical Chemistry Chemical Physics, 2016, 18, 26956-26959.	1.3	1
21531	Bilayered graphene as a platform of nanostructures with folded edge holes. Physical Chemistry Chemical Physics, 2016, 18, 27432-27441.	1.3	21
21532	Plasmon Modes of Graphene Nanoribbons with Periodic Planar Arrangements. Physical Review Letters, 2016, 117, 116801.	2.9	52
21533	High-pressure elastic properties of cubic Ir 2 P from ab initio calculations. Physics Letters, Section A: General, Atomic and Solid State Physics, 2016, 380, 3672-3677.	0.9	13
21534	Iodine Anions beyond âˆ’1: Formation of LinI (n = 2â€“5) and Its Interaction with Quasiatoms. Inorganic Chemistry, 2016, 55, 9377-9382.	1.9	16
21535	Eight-Dimensional Quantum Dynamics Study of CH₄ and CD₄ Dissociation on Ni(100) Surface. Journal of Physical Chemistry C, 2016, 120, 20199-20205.	1.5	12

#	Article	IF	Citations
21536	New insight on cubicâ€“tetragonalâ€“monoclinic phase transitions in ZrO₂: ab initio study and symmetry analysis. Journal of Applied Crystallography, 2016, 49, 1572-1578.	1.9	10
21537	The application of plasma treatment for Ti3+ modified TiO2 nanowires film electrode with enhanced lithium-storage properties. Electrochimica Acta, 2016, 211, 395-403.	2.6	21
21538	Low charge overpotential of lithium-oxygen batteries with metallic Co encapsulated in single-layer graphene shell as the catalyst. Nano Energy, 2016, 30, 877-884.	8.2	67
21539	Reactivity of Two-Dimensional Au₉, Pt₉, and Au₁₈Pt₁₈ against Common Molecules. Inorganic Chemistry, 2016, 55, 9410-9416.	1.9	2
21540	Mechanical properties of monolayer penta-graphene and phagraphene: a first-principles study. Physical Chemistry Chemical Physics, 2016, 18, 26736-26742.	1.3	106
21541	Design of lateral heterostructure from arsenene and antimonene. 2D Materials, 2016, 3, 035017.	2.0	66
21542	Long-range antiferromagnetic order in epitaxial<mml:math xmlns:mml="http://www.w3.org/1998/Math/MathML"><mml:mrow><mml:msub><mml:mi>Mn</mml:mi><mml:mn>2</mml:mn></mml: films from neutron reflectometry. Physical Review B, 2016, 94, .	1.1	28
21543	Valley contrasting in epitaxial growth of In/Tl homoatomic monolayer with anomalous Nernst conductance. Physical Review B, 2016, 94, .	1.1	7
21544	Theoretical Investigation on the Reaction Pathways of the Oxygen Reduction Reaction on Graphene Codoped with Manganese and Phosphorus as a Potential Nonprecious Metal Catalyst. ChemCatChem, 2016, 8, 3353-3360.	1.8	10
21545	The effect of concentration of H 2 physisorption on the currentâ€“voltage characteristic of armchair BN nanotubes in CNTâ€“BNNTâ€“CNT set. Pramana - Journal of Physics, 2016, 87, 1.	0.9	8
21546	Application of the Peierlsâ€“Nabarro Model to Symmetric Tilt Low-Angle Grain Boundary with Full <a> Dislocation in Pure Magnesium. Acta Metallurgica Sinica (English Letters), 2016, 29, 1053-1063.	1.5	0
21547	Electronic and optical properties of MAPbX₃ perovskites (X = I, Br, Cl): a unified DFT and GW theoretical analysis. Physical Chemistry Chemical Physics, 2016, 18, 27158-27164.	1.3	140
21548	First-principles electronic structure calculations for the whole spinel oxide solid solution range Mn_xCo_{3â^'x}O₄ (0 â‰¤ x â‰¤ 3) and their comparison with experimental data. Physical Chemistry Chemical Physics, 2016, 18, 26166-26176.	1.3	11
21549	Adsorption and heterogeneous reactions of ClONO₂ and N₂O₅ on/with NaCl aerosol. RSC Advances, 2016, 6, 46336-46344.	1.7	3
21550	First-principles investigation of a novel organic-inorganic strontium halide perovskites and CH₃NH₃Pb_{1-x}Sr_xI₃solid solution. Integrated Ferroelectrics, 2016, 175, 193-201.	0.3	1
21551	Interfacial properties of staneneâ€“metal contacts. 2D Materials, 2016, 3, 035020.	2.0	26
21552	Electronic and magnetic properties of spiral spin-density-wave states in transition-metal chains. Physical Review B, 2016, 94, .	1.1	4
21553	Extreme Mechanics of Probing the Ultimate Strength of Nanotwinned Diamond. Physical Review Letters, 2016, 117, 116103.	2.9	75

#	Article	IF	Citations
21554	New insights into the structure-nonlinear mechanical property relations for graphene allotropes. Carbon, 2016, 110, 443-457.	5.4	32
21555	Nanolayered solid electrolyte (GeSe2)30(Sb2Se3)30(AgI)40/AgI: A new hypothesis for the conductivity mechanism in layered AgI. Solid State Ionics, 2016, 294, 82-89.	1.3	9
21556	An atomically thin ferromagnetic half-metallic pyrazine-fused Mn-porphyrin sheet: a slow spin relaxation system. Journal of Materials Chemistry C, 2016, 4, 9069-9077.	2.7	18
21557	The structural, elastic, electronic and optical properties of MgCu under pressure: A first-principles study. International Journal of Modern Physics B, 2016, 30, 1650199.	1.0	73
21558	Exfoliated Metal Oxide Nanosheets as Effective and Applicable Substrates for Atomically Dispersed Metal Nanoparticles with Tailorable Functionalities. Advanced Materials Interfaces, 2016, 3, 1600661.	1.9	5
21559	Hydrogenation of Hydrogen Cyanide to Methane and Ammonia by a Metal Catalyst: Insight from First-Principles Calculations. Journal of Physical Chemistry C, 2016, 120, 22946-22956.	1.5	8
21560	A Computational and Experimental Study on the Binding of Dithio Ligands to Sperrylite, Pentlandite, and Platinum. Journal of Physical Chemistry C, 2016, 120, 22476-22488.	1.5	16
21561	Insight into CH x formation in Fischerâ€“Tropsch synthesis on the hexahedron Co catalyst: Effect of surface structure on the preferential mechanism and existence form. Applied Catalysis A: General, 2016, 525, 76-84.	2.2	18
21562	Reaction mechanism of ethylene glycol decomposition on Pt model catalysts: A density functional theory study. Applied Surface Science, 2016, 390, 1015-1022.	3.1	2
21563	DFT + U investigation on the adsorption and initial decomposition of methylamine by a Pt single-atom catalyst supported on rutile (110) TiO2. Applied Surface Science, 2016, 389, 411-418.	3.1	14
21564	Ab initio computations of the linear and nonlinear optical properties of stable compounds in AlInN system. Current Applied Physics, 2016, 16, 1277-1283.	1.1	8
21565	Chirality effect on nearly half-metallic properties in systematic endo-doping of 3d transition metals of narrow carbon nanotubes. Chemical Physics, 2016, 478, 62-68.	0.9	1
21566	(10, 10) Single walled carbon nanotube consisted of chemisorbed oxygen atoms as a promising supercapacitor electrode material: A first principles study. Chemical Physics Letters, 2016, 664, 96-100.	1.2	5
21567	Robust diamond-like Fe-Si network in the zero-strain Na FeSiO4 cathode. Electrochimica Acta, 2016, 212, 934-940.	2.6	30
21568	Electron coincidence studies of sulfur-overlayers on Cu(001) and Ni(001) surfaces. Journal of Electron Spectroscopy and Related Phenomena, 2016, 211, 32-40.	0.8	6
21569	Water partitioning between bridgmanite and postperovskite in the lowermost mantle. Earth and Planetary Science Letters, 2016, 454, 20-27.	1.8	28
21570	The effect of titanium doping on carbon behavior in tungsten: A first-principles study. Fusion Engineering and Design, 2016, 112, 123-129.	1.0	5
21571	Relationship of the longer wavelength threshold and the narrower surface band gap: For GaN and GaAlN photocathodes. Optik, 2016, 127, 10710-10715.	1.4	11

#	Article	IF	Citations
21572	Solubility and partitioning of impurities in Be alloys. Journal of Alloys and Compounds, 2016, 688, 382-385.	2.8	4
21573	Overcoming the minimum image constraint using the closest point search. Journal of Molecular Graphics and Modelling, 2016, 68, 197-205.	1.3	2
21574	Characterizing magnesiumâ€“silicon binaries in Alâ€“Mgâ€“Si supersaturated solid solution by first-principles calculations. Journal of Science: Advanced Materials and Devices, 2016, 1, 527-530.	1.5	3
21575	Phase stability, elastic and electronic properties of Cr2TiAlC2: A new ordered layered ternary carbide. Materials Letters, 2016, 185, 389-391.	1.3	7
21576	The mechanism and process of spontaneous boron doping in graphene in the theoretical perspective. Physics Letters, Section A: General, Atomic and Solid State Physics, 2016, 380, 3384-3388.	0.9	2
21577	First-principles study of the crystal structures and physical properties of H18-BN and Rh6-BN. Physics Letters, Section A: General, Atomic and Solid State Physics, 2016, 380, 3891-3896.	0.9	16
21578	Theoretical Calculations on Electronic Structure and Optical Properties of Orthorhombic SrHfO3 in Cmcm Space Group. Rare Metal Materials and Engineering, 2016, 45, 881-884.	0.8	0
21579	The Key Indicator for the Control of Metal Particle Sizes on Supports from First-Principles and Experimental Observation. Journal of Physical Chemistry C, 2016, 120, 21879-21887.	1.5	5
21580	Modeling composite electrolytes for low-temperature solid oxide fuel cell application: structural, vibrational and electronic features of carbonateâ€“oxide interfaces. Journal of Materials Chemistry A, 2016, 4, 17473-17482.	5.2	6
21581	Topological semimetal to insulator quantum phase transition in the Zintl compounds<mml:math xmlns:mml="http://www.w3.org/1998/Math/MathML"><mml:mrow><mml:mi mathvariant="normal">B</mml:mi><mml:msub><mml:mi mathvariant="normal">a</mml:mi><mml:mn>2</mml:mn></mml:msub><mml:mi>X</mml:mi><mml:mrow><mml:mo>(</mml:mo><mml:mo><mml:mo>)</mml:mo></mml:mrow></mml:mrow></mml:math>. Physical Review B, 2016, 94, .	1.1	24
21582	Halogen diffusion on a Ga-stabilized Î¶-GaAs(001)â€“(4 Ã— 2) surface. Semiconductors, 2016, 50, 1131-1136.	0.2	0
21583	Dynamic Surface Stress Response during Reversible Mg Electrodeposition and Stripping. Journal of the Electrochemical Society, 2016, 163, A2679-A2684.	1.3	9
21584	Effect of Mn doping on the electronic structure and absorption spectrum of Ba 2 SiO 4 :Eu 2+ phosphor. Chinese Journal of Physics, 2016, 54, 931-939.	2.0	5
21585	The electronic and structural properties in Ca 2 TiMnO 6 double perovskite: The first principle study. Computational Condensed Matter, 2016, 9, 35-39.	0.9	9
21586	Theoretical study of disorder-order transition of sodium borohydride. Computational Materials Science, 2016, 124, 87-91.	1.4	3
21587	Strong correlation effect on the thermodynamic and mechanical properties of ytterbium dihydride. International Journal of Hydrogen Energy, 2016, 41, 21286-21292.	3.8	1
21588	Influence of basicity on 1,3-butadiene formation from catalytic 2,3-butanediol dehydration over Î³-alumina. Journal of Catalysis, 2016, 344, 77-89.	3.1	23
21589	Formation, Structures and Electronic Properties of Silicene Oxides on Ag(111). Journal of Materials Science and Technology, 2017, 33, 751-757.	5.6	12

#	Article	IF	Citations
21590	Phonons and stability of infinite-layer iron oxides SrFeO2 and CaFeO2. Solid State Communications, 2016, 241, 43-55.	0.9	1
21591	Hydrogen diffusion on Fe surface and into subsurface from first principles. Surface Science, 2016, 654, 48-55.	0.8	21
21592	Measurement of the dielectric function of Î±-Al2O3 by transmission electron microscopy â€“ Electron energy-loss spectroscopy without Cerenkov radiation effects. Ultramicroscopy, 2016, 169, 37-43.	0.8	3
21593	Structural, elastic, electronic and optical properties of black phosphorus, TiP and VP; ab initio study. Chinese Journal of Physics, 2016, 54, 734-743.	2.0	2
21594	Perovskite-based nanocubes with simultaneously improved visible-light absorption and charge separation enabling efficient photocatalytic CO2 reduction. Nano Energy, 2016, 30, 59-68.	8.2	92
21595	Water Oxidation Catalyzed by Cobalt Oxide Supported on the Mattagamite Phase of CoTe₂. ACS Catalysis, 2016, 6, 7393-7397.	5.5	39
21596	Size-dependent commensurability and its possible role in determining the frictional behavior of adsorbed systems. Physical Chemistry Chemical Physics, 2016, 18, 28997-29004.	1.3	8
21597	Spectroscopic and theoretical studies on the counterion effect of Cu(<scp>ii</scp>) ion and graphene oxide interaction with titanium dioxide. Environmental Science: Nano, 2016, 3, 1361-1368.	2.2	77
21598	First principles study of silicene symmetrically and asymmetrically functionalized with halogen atoms. RSC Advances, 2016, 6, 95846-95854.	1.7	63
21599	First-principles study on the electronic, elastic and thermodynamic properties of three novel germanium nitrides. Journal of Semiconductors, 2016, 37, 072002.	2.0	0
21600	Theoretical Analysis of Thermal Transport in Graphene Supported on Hexagonal Boron Nitride: The Importance of Strong Adhesion Due to<mml:math xmlns:mml="http://www.w3.org/1998/Math/MathML" display="inline"><mml:mi>Ï€</mml:mi></mml:math>-Bond Polarization. Physical Review Applied, 2016, 6, .	1.5	23
21601	Hydrogen-induced ferromagnetism in two-dimensional Pt dichalcogenides. Physical Review B, 2016, 94, .	1.1	46
21602	Manipulating charge density waves in<mml:math xmlns:mml="http://www.w3.org/1998/Math/MathML"><mml:mrow><mml:mn>1</mml:mn><mml:mi>T</mml:mi></mml:mrow></mml:mtext>â^'</mm charge-carrier doping: A first-principles investigation. Physical Review B, 2016, 94, .	1.1	43
21603	Structural, vibrational and bonding properties of hydro-nitrogen solids under high pressure: An ab-initio study. Journal of Chemical Sciences, 2016, 128, 1631-1639.	0.7	4
21604	Prediction of indirect to direct band gap transition under tensile biaxial strain in type-I guest-free silicon clathrate Si46: A first-principles approach. Superlattices and Microstructures, 2016, 100, 296-305.	1.4	4
21605	Discovery of a Red-Emitting Li₃RbGe₈O₁₈:Mn⁴⁺ Phosphor in the Alkali-Germanate System: Structural Determination and Electronic Calculations. Inorganic Chemistry, 2016, 55, 10310-10319.	1.9	77
21606	Calcium-decorated carbon nanostructures for the selective capture of carbon dioxide. Physical Chemistry Chemical Physics, 2016, 18, 29086-29091.	1.3	15
21607	Surface and shape modification of mackinawite (FeS) nanocrystals by cysteine adsorption: a first-principles DFT-D2 study. Physical Chemistry Chemical Physics, 2016, 18, 32007-32020.	1.3	35

#	Article	IF	Citations
21608	Ammonia and iron cointercalated iron sulfide (NH₃)Fe_{0.25}Fe₂S₂: hydrothermal synthesis, crystal structure, weak ferromagnetism and crossover from a negative to positive magnetoresistance. RSC Advances, 2016, 6, 81886-81893.	1.7	11
21609	First-principles study of fluorination of azobenzene. Molecular Crystals and Liquid Crystals, 2016, 634, 91-96.	0.4	0
21610	On the rich magnetic phase diagram of (Ni, Co)â€“Mnâ€“Sn Heusler alloys. Journal Physics D: Applied Physics, 2016, 49, 395001.	1.3	18
21611	Simulation of structure and stability of carbon nanoribbons. Russian Journal of General Chemistry, 2016, 86, 1777-1786.	0.3	2
21612	Impact of uniaxial compressive strain on physical and electronic parameters of a 10Ânm germanene nanoribbon field effect transistor. Superlattices and Microstructures, 2016, 100, 198-208.	1.4	17
21613	Systematic Approach To Calculate the Band Gap Energy of a Disordered Compound with a Low Symmetry and Large Cell Size via Density Functional Theory. ACS Omega, 2016, 1, 483-490.	1.6	14
21614	Nanostructural adsorption of vanadium oxide on functionalized graphene: a DFT study. Physical Chemistry Chemical Physics, 2016, 18, 29208-29217.	1.3	8
21615	Doping Mechanism in Transparent, Conducting Tantalum Doped ZnO Films Deposited Using Atomic Layer Deposition. Advanced Materials Interfaces, 2016, 3, 1600496.	1.9	15
21616	Selective Dehydrogenation of HCOOH on Zn-Decorated Pd(111) Surface Studied by First-Principles Calculations. Catalysis Letters, 2016, 146, 2348-2356.	1.4	6
21617	Theory for Modeling of High Resolution Resonant and Nonresonant Raman Images. Journal of Chemical Theory and Computation, 2016, 12, 4986-4995.	2.3	24
21618	Integrated High-Performance Infrared Phototransistor Arrays Composed of Nonlayered PbSâ€“MoS₂ Heterostructures with Edge Contacts. Nano Letters, 2016, 16, 6437-6444.	4.5	98
21619	Efficient Blue Electroluminescence Using Quantum-Confined Two-Dimensional Perovskites. ACS Nano, 2016, 10, 9720-9729.	7.3	299
21620	Nitrogen-induced magnetism in stannates from first-principles calculations. International Journal of Modern Physics B, 2016, 30, 1650236.	1.0	1
21621	First-Principles Study of the Structural, Optical, Dynamical and Thermodynamic Properties of BaZn $$hbox {O}_{2}$$ O 2 Under Pressure. International Journal of Thermophysics, 2016, 37, 1.	1.0	6
21622	Thermodynamic Properties of Rutile $$(hbox {TiO}_{2})$$ (TiO 2) Within the Phonon Calculations. International Journal of Thermophysics, 2016, 37, 1.	1.0	6
21623	Ab initio study on gas sensing properties of group III (B, Al and Ga) doped graphene. Computational Condensed Matter, 2016, 9, 40-55.	0.9	36
21624	Structural, electronic, elastic, vibrational and thermodynamic properties of ZrNi and ZrNiH 3 : A comprehensive study through first principles approach. International Journal of Hydrogen Energy, 2016, 41, 20250-20260.	3.8	13
21625	Block Copolymer-Assisted Solvothermal Synthesis of Hollow Bi₂MoO₆ Spheres Substituted with Samarium. Langmuir, 2016, 32, 10967-10976.	1.6	24

#	Article	IF	Citations
21626	Dry Reforming of Ethane and Butane with CO₂ over PtNi/CeO₂ Bimetallic Catalysts. ACS Catalysis, 2016, 6, 7283-7292.	5.5	103
21627	A first-principles based study of ns²containing ternary iodides and their possibility of scintillation. Journal Physics D: Applied Physics, 2016, 49, 395103.	1.3	9
21628	First-principles studies of effects of interstitial boron and carbon on the structural, elastic, and electronic properties of Ni solution and Ni ₃ Al intermetallics. Chinese Physics B, 2016, 25, 107104.	0.7	5
21629	Higher-order elastic constants and megabar pressure effects of bcc tungsten:Ab initiocalculations. Physical Review B, 2016, 94, .	1.1	21
21630	Impact of anharmonic effects on the phase stability, thermal transport, and electronic properties of AlN. Physical Review B, 2016, 94, .	1.1	20
21631	Anisotropic elastic properties of FexB (x = 1, 2, 3) under pressure. First-principles study. Materials Science-Poland, 2016, 34, 503-516.	0.4	9
21632	Optoelectronic properties of naphtho[2, 1-b:6, 5-bâ€²]difuran derivatives for photovoltaic application: a computational study. Journal of Molecular Modeling, 2016, 22, 248.	0.8	24
21633	Indium-defect interactions in FCC and BCC metals studied using the modified embedded atom method. Hyperfine Interactions, 2016, 237, 1.	0.2	1
21634	Ab initio investigations of the structural, electronic, and thermoelectric properties of Fe2NbAl-based alloys. Journal of Materials Science, 2016, 51, 10887-10896.	1.7	16
21635	Part I: C2C4 hydrocarbons separation addressed via molecular cluster models carved out from periodic MOF-74-Mg/Zn structures. Chemical Physics Letters, 2016, 660, 313-319.	1.2	5
21636	Supercell design for first-principles simulations of solids and application to diamond, silica, and superionic water. High Energy Density Physics, 2016, 21, 8-15.	0.4	6
21637	First-principles Debyeâ€“Callaway approach to lattice thermal conductivity. Journal of Materiomics, 2016, 2, 237-247.	2.8	53
21638	Structure determination and stability for Pa-Si, Np-Si and U-X-Si (XÂ=ÂMo, Th, Np) phases from first-principles. Journal of Nuclear Materials, 2016, 479, 593-607.	1.3	4
21639	A computational study on the SO2 adsorption by the pristine, Al, and Si doped BN nanosheets. Superlattices and Microstructures, 2016, 100, 350-357.	1.4	132
21640	Investigation of the energy and structural parameters of strained (Î²-InSe) /(In4Se3) superlattices. Superlattices and Microstructures, 2016, 100, 448-457.	1.4	1
21641	Lattice Dynamics of the Rhombohedral Polymorphs of CaSi₂. Inorganic Chemistry, 2016, 55, 10203-10207.	1.9	35
21642	Polymorphism in Strontium Tungstate SrWO₄ under Quasi-Hydrostatic Compression. Inorganic Chemistry, 2016, 55, 10406-10414.	1.9	25
21643	Molecular simulations of nitrogen-doped hierarchical carbon adsorbents for post-combustion CO₂ capture. Physical Chemistry Chemical Physics, 2016, 18, 28747-28758.	1.3	21

#	Article	IF	Citations
21644	Defects induced changes in the electronic structures of MgO and their correlation with the optical properties: a special case of electronâ€“hole recombination from the conduction band. RSC Advances, 2016, 6, 96398-96415.	1.7	78
21645	Topological insulators in the ordered double transition metals<mml:math xmlns:mml="http://www.w3.org/1998/Math/MathML"><mml:mrow><mml:msubsup><mml:mi>M</mml:mi><mml:mn>2</mml:mn><mml:mn mathvariant="normal">C</mml:mi><mml:mn>2</mml:mn></mml:msub></mml:mrow></mml:math>MXenes		

#	Article	IF	Citations
21662	Vibrational contributions to phase stability in the Mo-Ru system. Journal of Alloys and Compounds, 2016, 689, 969-976.	2.8	5
21663	Structural stability, electronic, magnetic and optical properties of zincblende Zn 0.5 V 0.5 Te under pressure. Physics Letters, Section A: General, Atomic and Solid State Physics, 2016, 380, 3683-3689.	0.9	4
21664	Drastic changes of electronic structure and crystal chemistry upon oxidation of SnII2TiO4E2 into SnIV2TiO6: An ab initio study. Solid State Sciences, 2016, 59, 25-31.	1.5	2
21665	Nonlinear Stark effect observed for carbon monoxide chemisorbed on gold core/palladium shell nanoparticle film electrodes, using in situ surface-enhanced Raman spectroscopy. Chinese Journal of Catalysis, 2016, 37, 1156-1165.	6.9	7
21666	Structural, Electronic, and Optical Properties of Bulk Boric Acid 2A and 3T Polymorphs: Experiment and Density Functional Theory Calculations. Crystal Growth and Design, 2016, 16, 6631-6640.	1.4	13
21667	DFT Perspective on the Thermochemistry of Carbon Nitride Synthesis. Journal of Physical Chemistry C, 2016, 120, 24542-24550.	1.5	21
21668	Theoretical Survey of the Thiophene Hydrodesulfurization Mechanism on Clean and Single-Sulfur-Atom-Modified MoP(001). Journal of Physical Chemistry C, 2016, 120, 23009-23023.	1.5	22
21669	Photocatalytic Properties of g-C₆N₆/g-C₃N₄ Heterostructure: A Theoretical Study. Journal of Physical Chemistry C, 2016, 120, 24023-24029.	1.5	78
21670	Mechanism of Isobutanalâ€“Isobutene Prins Condensation Reactions on Solid BrÃ¸nsted Acids. ACS Catalysis, 2016, 6, 7664-7684.	5.5	25
21671	Evolutionary design of interfacial phase change van der Waals heterostructures. Nanoscale, 2016, 8, 18212-18220.	2.8	28
21672	Room temperature observation of the correlation between atomic and electronic structure of graphene on Cu(110). RSC Advances, 2016, 6, 98001-98009.	1.7	2
21673	Intense conductivity suppression by edge defects in zigzag MoS₂and WSe₂nanoribbons: a density functional based tight-binding study. Nanotechnology, 2016, 27, 445202.	1.3	8
21674	On the implication of solute contents and grain boundaries on the Hall-Petch relationship of nanocrystalline Ni-W alloys. Materials Science & Engineering A: Structural Materials: Properties, Microstructure and Processing, 2016, 678, 204-214.	2.6	13
21675	Highly Efficient Free Energy Calculations of the Fe Equation of State Using Temperature-Dependent Effective Potential Method. Journal of Physical Chemistry A, 2016, 120, 8761-8768.	1.1	6
21676	How Should Iron and Titanium be Combined in Oxides to Improve Photoelectrochemical Properties?. Journal of Physical Chemistry C, 2016, 120, 24521-24532.	1.5	35
21677	Cobalt carbide nanoprisms for direct production of lower olefins from syngas. Nature, 2016, 538, 84-87.	13.7	647
21678	Global minimum of two-dimensional FeB₆and an oxidization induced negative Poisson's ratio: a new stable allotrope. Journal of Materials Chemistry C, 2016, 4, 9613-9621.	2.7	29
21679	The structural stabilities, mechanical properties and hardness of chromium tetraboride: Compared with low-B borides. International Journal of Modern Physics B, 2016, 30, 1650201.	1.0	16

#	Article	IF	Citations
21681	Mechanical and electronic properties of graphitic carbon nitride sheet: First-principles calculations. Solid State Communications, 2016, 248, 144-150.	0.9	35
21682	Dimensionality and Valency Dependent Quantum Growth of Metallic Nanostructures: A Unified Perspective. Nano Letters, 2016, 16, 6628-6635.	4.5	4
21683	Effect of lead and caesium on the mechanical, vibrational and thermodynamic properties of hexagonal fluorocarbonates: a comparative first principles study. RSC Advances, 2016, 6, 99885-99897.	1.7	14
21684	Electronic and optical properties of pristine and oxidized borophene. 2D Materials, 2016, 3, 045006.	2.0	123
21685	Tight-binding theory of NMR shifts in topological insulators<mml:math xmlns:mml="http://www.w3.org/1998/Math/MathML"><mml:mrow><mml:msub><mml:mi mathvariant="bold">Bi</mml:mi><mml:mn>2</mml:mn></mml:msub><mml:msub><mml:mi mathvariant="bold">Se</mml:mi><mml:mn>3</mml:mn></mml:msub></mml:mrow></mml:math>and<mml:math xmlns:mml="http://www.w3.org/1998/Math/MathML"><mml:mrow><mml:msub><mml:mi mathvariant="bold">Bi</mml:mi><mml:mn>2</mml:mn></mml:msub><mml:msub><mml:mi mathvariant="bold">	1.1	15
21686	Effect of strain, thickness, and local surface environment on electron transport properties of oxygen-terminated copper thin films. Physical Review B, 2016, 94, .	1.1	8
21687	First principles investigation of structural, elastic, electronic and optical properties of HgGeB 2 (B P,) Tj ETQq0 0 0 rgBT /Overlock 10 Tf 5	0.9	24
21688	Mapping nanometric electronic property changes induced by an aryl diazonium sub-monolayer on HOPG. Physical Chemistry Chemical Physics, 2016, 18, 29218-29225.	1.3	11
21689	Layer-dependent properties of<mml:math xmlns:mml="http://www.w3.org/1998/Math/MathML"><mml:msub><mml:mi mathvariant="bold">SnS</mml:mi><mml:mn>2</mml:mn></mml:msub></mml:math>and<mml:math xmlns:mml="http://www.w3.org/1998/Math/MathML"><mml:msub><mml:mi mathvariant="bold">SnSe</mml:mi><mml:mn>2</mml:mn></mml:msub></mml:math>two-dimensional materials. Physical Review B, 2016, 94, .	1.1	267
21690	Structural and electronic phase transitions of<mml:math xmlns:mml="http://www.w3.org/1998/Math/MathML"><mml:msub><mml:mi>ThS</mml:mi><mml:mn>2</mml:mn></mml:msub></mml:math>from first-principles calculations. Physical Review B, 2016, 94, .	1.1	11
21691	Chemical Trend of Superconducting Critical Temperatures in Hole-Doped CuBO₂, CuAlO₂, CuGaO₂, and CuInO₂. Journal of the Physical Society of Japan, 2016, 85, 094711.	0.7	7
21692	Toughening of Î±-Nb5Si3 by Ti. Journal of Alloys and Compounds, 2016, 689, 296-301.	2.8	36
21693	Polar phase transitions and physical properties in fresnoite A2TiSi2O8 (A= Ba, Sr) by first principles calculations. Journal of Solid State Chemistry, 2016, 242, 136-142.	1.4	4
21694	DFT Study on the Methane Synthesis from Syngas on a Cerium-Doped Ni(111) Surface. Journal of Physical Chemistry C, 2016, 120, 23030-23043.	1.5	19
21695	Ethylene decomposition over Pt(100): A mechanism study from first principle calculation. Applied Surface Science, 2016, 390, 984-992.	3.1	3
21696	Insight into the Origin of Boosted Photosensitive Efficiency of Graphene from the Cooperative Experiment and Theory Study. Journal of Physical Chemistry C, 2016, 120, 27091-27103.	1.5	37
21697	Structure and Reducibility of CeO₂ Doped with Trivalent Cations. Journal of Physical Chemistry C, 2016, 120, 23430-23440.	1.5	66
21698	First-principle study for influence of an external electric field on the electronic structure and optical properties of TiO₂. RSC Advances, 2016, 6, 98908-98915.	1.7	13

#	Article	IF	Citations
21699	Firstâ€principles prediction of mechanical and bonding characteristics of new T₂ superconductor Ta₅GeB₂. Physica Status Solidi (B): Basic Research, 2016, 253, 2020-2026.	0.7	61
21700	Density functional theory study on Hg removal mechanisms of Cu-impregnated activated carbon prepared by simplified method. Korean Journal of Chemical Engineering, 2016, 33, 2869-2877.	1.2	4
21701	Engendering anion immunity in oxygen consuming cathodes based on Fe-Nx electrocatalysts: Spectroscopic and electrochemical advanced characterizations. Applied Catalysis B: Environmental, 2016, 198, 318-324.	10.8	53
21702	Revisiting thermodynamics and kinetic diffusivities of uraniumâ€“niobium with Bayesian uncertainty analysis. Calphad: Computer Coupling of Phase Diagrams and Thermochemistry, 2016, 55, 219-230.	0.7	46
21703	First principles study of AlH3 vacancy mediated mechanism in dehydriding of NaAlH4. International Journal of Hydrogen Energy, 2016, 41, 16966-16973.	3.8	1
21704	Near-Edge X-ray Absorption Fine Structure Investigation of the Quasi-One-Dimensional Organic Conductor (TMTSF)₂PF₆. Journal of Physical Chemistry A, 2016, 120, 8574-8583.	1.1	6
21705	Supported Sub-Nanometer Gold Cluster Catalyzed Transfer Hydrogenation of Aldehydes to Alcohols. Journal of Physical Chemistry C, 2016, 120, 24449-24456.	1.5	14
21706	Coexistence of Two Electronic Nano-Phases on a CH₃NH₃PbI_{3â€“x}Cl_x Surface Observed in STM Measurements. ACS Applied Materials & Interfaces, 2016, 8, 29110-29116.	4.0	21
21707	Native defects as sources of optical transitions in MgAl₂O₄spinel. Materials Research Express, 2016, 3, 076202.	0.8	27
21708	Electronic Structures of Silicene Nanoribbons: Two-Edge-Chemistry Modification and First-Principles Study. Nanoscale Research Letters, 2016, 11, 371.	3.1	22
21709	LiSr_{2â€“x}Eu_xGe₃: Light on the Europium Site Preferences. Journal of Physical Chemistry C, 2016, 120, 23121-23128.	1.5	2
21710	Hybridization of inorganic CoB noncrystal with graphene and its Kubas-enhanced hydrogen adsorption at room temperature. RSC Advances, 2016, 6, 93238-93244.	1.7	7
21711	The interface of SrTiO ₃ and H ₂ O from density functional theory molecular dynamics. Proceedings of the Royal Society A: Mathematical, Physical and Engineering Sciences, 2016, 472, 20160293.	1.0	21
21712	Nature of charge density waves and superconductivity in<mml:math xmlns:mml="http://www.w3.org/1998/Math/MathML"><mml:mn>1</mml:mn><mml:mrow><mml:mi>T</mml:mi><mml:mo>’</mml:mo></mml:mrow></mml:math>-TaS2. Physical Review B, 2016, 94, .	1.1	27
21713	Two-dimensional SiS as a potential anode material for lithium-based batteries: A first-principles study. Journal of Power Sources, 2016, 331, 391-399.	4.0	46
21714	Uncloaking the Thermodynamics of the Studtite to Metastudtite Shear-Induced Transformation. Journal of Physical Chemistry C, 2016, 120, 16553-16560.	1.5	34
21715	Geometric, Electronic, and Magnetic Properties of MgH₂: Influence of Charged Defects. Journal of Physical Chemistry C, 2016, 120, 22844-22851.	1.5	3
21716	DFT investigation of Ni-doped graphene: catalytic ability to CO oxidation. New Journal of Chemistry, 2016, 40, 9361-9369.	1.4	85

#	Article	IF	Citations
21717	Strain controlled ferromagneticâ€“ferrimagnetic transition and vacancy formation energy of defective graphene. Nanotechnology, 2016, 27, 435206.	1.3	9
21718	A benchmark for the non-covalent interaction (NCI) index orâ€¦ is it really all in the geometry?. Theoretical Chemistry Accounts, 2016, 135, 1.	0.5	124
21719	Electronic, elastic, and optical properties of monolayer BC2N. Journal of Solid State Chemistry, 2016, 244, 120-128.	1.4	26
21720	Enhancing the Spinâ€“Orbit Coupling in Fe₃O₄ Epitaxial Thin Films by Interface Engineering. ACS Applied Materials & Interfaces, 2016, 8, 27353-27359.	4.0	20
21721	Molecular mechanisms for initial step of methanol dehydrogenation on metal surface. Journal of Power Sources, 2016, 332, 30-36.	4.0	5
21722	Promoting oxygen vacancy formation and p-type conductivity in SrTiO₃via alkali metal doping: a first principles study. Physical Chemistry Chemical Physics, 2016, 18, 28951-28959.	1.3	17
21723	First-principles study of the structural, elastic, vibrational, thermodynamic and electronic properties of the Mo2B intermetallic under pressure. Journal of Molecular Structure, 2016, 1125, 350-357.	1.8	7
21724	Driving electrocatalytic activity by interface electronic structure control in a metalloprotein hybrid catalyst for efficient hydrogen evolution. Physical Chemistry Chemical Physics, 2016, 18, 23220-23230.	1.3	6
21725	A new 2D monolayer BiXene, M₂C (M = Mo, Tc, Os). Nanoscale, 2016, 8, 15753-15762.	2.8	46
21726	Ab initio modelling of oxygen vacancies and protonic defects in La_{1â^'x}Sr_xFeO_{3â^'Î´} perovskite solid solutions. Journal of Materials Chemistry A, 2016, 4, 13093-13104.	5.2	33
21727	Tuning the work function of graphene with the adsorbed organic molecules: first-principles calculations. Molecular Physics, 2016, 114, 2993-2998.	0.8	5
21728	The structures of interstitial hydrogen centers in VO₂in the dilute limit from their vibrational properties and theory. Journal of Physics Condensed Matter, 2016, 28, 395401.	0.7	2
21729	Heterostructures based on graphene and MoS2layers decorated by C60fullerenes. Nanotechnology, 2016, 27, 365201.	1.3	11
21730	Mechanistic Insights on Ternary Ni_{2â^'}_xCo_xP for Hydrogen Evolution and Their Hybrids with Graphene as Highly Efficient and Robust Catalysts for Overall Water Splitting. Advanced Functional Materials, 2016, 26, 6785-6796.	7.8	500
21731	General approach for band gap calculation of semiconductors and insulators. Physica Status Solidi (A) Applications and Materials Science, 2016, 213, 2834-2837.	0.8	8
21732	The interaction of cyanide with pyrite, marcasite and pyrrhotite. Minerals Engineering, 2016, 95, 131-137.	1.8	32
21733	Adsorption of H2, Cl2, and HCl molecules on Î±-Cr2O3(0001) surfaces: AÂdensity functional theory investigation. Surface Science, 2016, 653, 211-221.	0.8	11
21734	Fluorine and Oxygen Adsorption and Their Coadsorption on the (111) Surface of InAs and GaAs. Journal of Physical Chemistry C, 2016, 120, 17491-17500.	1.5	11

#	Article	IF	Citations
21735	van der Waals density functionals applied to corundum-type sesquioxides: bulk properties and adsorption of CH₃ and C₆H₆ on (0001) surfaces. Physical Chemistry Chemical Physics, 2016, 18, 23139-23146.	1.3	7
21736	Hybrid improper ferroelectricity in SrZrO₃/BaZrO₃ superlattice. Physical Chemistry Chemical Physics, 2016, 18, 24024-24032.	1.3	7
21737	Molybdenum Disulfideâ€Coated Lithium Vanadium Fluorophosphate Anode: Experiments and Firstâ€Principles Calculations. ChemSusChem, 2016, 9, 2122-2128.	3.6	25
21738	A theoretical study of dye molecules adsorbed onto diamond (111) surfaces. Physica Status Solidi (A) Applications and Materials Science, 2016, 213, 2105-2111.	0.8	2
21739	Theoretical mechanistic insights into propylene epoxidation on Au-based catalysts: Surface O versus OOH as oxidizing agents. Catalysis Today, 2016, 278, 45-55.	2.2	21
21740	H 2 flux inhibition and stability of Pd-Ag membranes under exposure to trace amounts of NH 3. Fuel Processing Technology, 2016, 152, 259-265.	3.7	12
21741	Adsorption of Alizarin Red S Dye by Carbon Nanotubes: An Experimental and Theoretical Investigation. Journal of Physical Chemistry C, 2016, 120, 18296-18306.	1.5	103
21742	Enhanced electrocatalytic CO2 reduction via field-induced reagent concentration. Nature, 2016, 537, 382-386.	13.7	1,429
21743	Stacking fault energy of face-centered cubic metals: thermodynamic andab initioapproaches. Journal of Physics Condensed Matter, 2016, 28, 395001.	0.7	43
21744	Quantifying uncertainties in first-principles alloy thermodynamics using cluster expansions. Journal of Computational Physics, 2016, 323, 17-44.	1.9	17
21745	Phase equilibria in the U-Si system from first-principles calculations. Journal of Nuclear Materials, 2016, 479, 216-223.	1.3	68
21746	Eu³⁺-Doped Wide Band Gap Zn₂SnO₄ Semiconductor Nanoparticles: Structure and Luminescence. Journal of Physical Chemistry C, 2016, 120, 18887-18894.	1.5	43
21747	Novel room-temperature spin-valve-like magnetoresistance in magnetically coupled nano-column Fe₃O₄/Ni heterostructure. Nanoscale, 2016, 8, 15737-15743.	2.8	9
21748	Electronic and magnetic properties of the Co₂-based Heusler compounds under pressure: first-principles and Monte Carlo studies. Journal Physics D: Applied Physics, 2016, 49, 355004.	1.3	41
21749	Performance Upper Limit of subâ€10 nm Monolayer MoS₂ Transistors. Advanced Electronic Materials, 2016, 2, 1600191.	2.6	97
21750	Structural, Electronic, and Li Migration Properties of RE-Doped (RE = Ce, La) LiCoO₂for Li-ion Batteries: A First-Principles Investigation. Journal of Physical Chemistry C, 2016, 120, 18428-18434.	1.5	48
21751	Moderate Humidity Delays Electronâ€“Hole Recombination in Hybrid Organicâ€–Inorganic Perovskites: Time-Domain Ab Initio Simulations Rationalize Experiments. Journal of Physical Chemistry Letters, 2016, 7, 3215-3222.	2.1	139
21752	Structural dependence of the photocatalytic properties of double perovskite compounds A₂InTaO₆ (A = Sr or Ba) doped with nickel. Physical Chemistry Chemical Physics, 2016, 18, 21491-21499.	1.3	35

#	Article	IF	Citations
21753	New family of Dirac and Weyl semimetals in XAuTe (X = Na, K, Rb) ternary honeycomb compounds. Science China: Physics, Mechanics and Astronomy, 2016, 59, 1.	2.0	5
21754	Calcium decorated two dimensional carbon allotropes for hydrogen storage: A first-principles study. Computational Materials Science, 2016, 124, 106-113.	1.4	25
21755	Structural, electronic properties, and quantum capacitance of B, N and P-doped armchair carbon nanotubes. Physics Letters, Section A: General, Atomic and Solid State Physics, 2016, 380, 3378-3383.	0.9	57
21756	Enhanced Sensitivity of Epitaxial Graphene to NO₂ by Water Coadsorption. Journal of Physical Chemistry C, 2016, 120, 19107-19112.	1.5	10
21757	Feâ€“Si networks in Na₂FeSiO₄ cathode materials. Physical Chemistry Chemical Physics, 2016, 18, 23916-23922.	1.3	27
21758	ltinerant<mml:math xmlns:mml="http://www.w3.org/1998/Math/MathML"><mml:mi>G</mml:mi></mml:math>-type antiferromagnetism in<mml:math xmlns:mml="http://www.w3.org/1998/Math/MathML"><mml:mrow><mml:mi>D</mml:mi><mml:msub><mml:mn>0</mml:mn><mml:mml xmlns:mml="http://www.w3.org/1998/Math/MathML"><mml:mrow><mml:msub><mml:mi		

#	Article	IF	Citations
21771	Selective Activation of Alcohols in the Presence of Reactive Amines over Intermetallic PdZn: Efficient Catalysis for Alcohol-Based N-Alkylation of Various Amines. ACS Catalysis, 2016, 6, 5946-5953.	5.5	62
21772	Ab initio investigation on the stability of H-6 Carbon. RSC Advances, 2016, 6, 78187-78193.	1.7	7
21773	Strain effects on the electronic and transport properties of TiO₂ nanotubes. RSC Advances, 2016, 6, 80431-80437.	1.7	5
21774	Ab initio molecular dynamics of solvation effects on reactivity at electrified interfaces. Proceedings of the National Academy of Sciences of the United States of America, 2016, 113, E4937-45.	3.3	57
21775	Effects of quantum confinement on excited state properties of<mml:math xmlns:mml="http://www.w3.org/1998/Math/MathML"><mml:msub><mml:mi>SrTiO</mml:mi><mml:mn>3</mml:mn></mml:msub></m<i>initio</i>many-body perturbation theory. Physical Review B, 2016, 94, .	1.1	14
21776	Thermally Driven Electronic Topological Transition in FeTi. Physical Review Letters, 2016, 117, 076402.	2.9	3
21777	Stability of B2â€type FeS at Earth's inner core pressures. Geophysical Research Letters, 2016, 43, 8435-8440.	1.5	10
21778	The Effects of Percent and Position of Nitrogen Atoms on Electronic and Thermoelectric Properties of Graphene Nanoribbons. Journal of Inorganic and Organometallic Polymers and Materials, 2016, 26, 1095-1100.	1.9	3
21779	Comparative Analysis of Reactant and Product Adsorption Energies in the Selective Oxidative Coupling of Alcohols to Esters on Au(111). Topics in Catalysis, 2016, 59, 1383-1393.	1.3	3
21780	Improvement of p -type conductivity in Al-rich AlGaN substituted by Mg Ga Î´-doping (AlN) m /(GaN) n (m) Tj ETQq1 1 0.784314 rgBT /C	2.8	5
21781	Theoretical investigation of the structural, electronic, magnetic and elastic properties of binary cubic C15-Laves phases TbX2 (XÂ=ÂCo and Fe). Journal of Alloys and Compounds, 2016, 689, 885-893.	2.8	38
21782	First-principles study of sulfur atom doping and adsorption on Î±â€“Fe2O3 (0001) film. Physics Letters, Section A: General, Atomic and Solid State Physics, 2016, 380, 3149-3154.	0.9	7
21783	Origins of the Relative Stabilities of Anhydrous and Hydrated <scp>d</scp>-Mannitol Crystals. Journal of Physical Chemistry A, 2016, 120, 6629-6636.	1.1	15
21784	Influences of the Pb 6s² lone pair effect and quantum size effect on the diffusion of oxygen atoms on Pb(111) films. RSC Advances, 2016, 6, 78755-78761.	1.7	1
21785	Immobilization of Au nanoparticles on graphite tunnels through nanocapillarity. RSC Advances, 2016, 6, 77195-77200.	1.7	12
21786	First principles characterisation of brittle transgranular fracture of titanium hydrides. Acta Materialia, 2016, 118, 362-373.	3.8	29
21787	Deformation mechanisms of D022 ordered intermetallic phase in superalloys. Acta Materialia, 2016, 118, 350-361.	3.8	41
21788	Interaction between bimetal cluster Ni2Co2 and MgO and its effect on H adsorption and H2 dissociation: A DFT study. Applied Surface Science, 2016, 390, 7-16.	3.1	12

#	Article	IF	Citations
21789	Preparations of an inorganic-framework proton exchange nanochannel membrane. Journal of Power Sources, 2016, 326, 466-475.	4.0	15
21790	Can the state of platinum species be unambiguously determined by the stretching frequency of an adsorbed CO probe molecule?. Physical Chemistry Chemical Physics, 2016, 18, 22108-22121.	1.3	113
21791	Ab initiostudy of magnetoelectric coupling in La_{0.66}Sr_{0.33}MnO₃â€‰/â€‰PbZr_{0.2}Ti_{0.8}O₃multiferroi heterostructures. Journal of Physics Condensed Matter, 2016, 28, 396004.	1.8	18
21792	Electrophobic interaction induced impurity clustering in metals. Acta Materialia, 2016, 119, 1-8.	3.8	36
21793	First-principles study of the negative thermal expansion of PbTiO3. Computational Materials Science, 2016, 124, 92-97.	1.4	11
21794	Comparing the catalytic activity of the water gas shift reaction on Cu(3 2 1) and Cu(1 1 1) surfaces: Step sites do not always enhance the overall reactivity. Journal of Catalysis, 2016, 342, 75-83.	3.1	30
21795	A comparative first-principles study on electronic structures and mechanical properties of ternary intermetallic compounds Al8Cr4Y and Al8Cu4Y: Pressure and tension effects. Journal of Physics and Chemistry of Solids, 2016, 98, 298-308.	1.9	15
21796	A multifunctional material of two-dimensional g-C₄N₃/graphene bilayer. Physical Chemistry Chemical Physics, 2016, 18, 25388-25393.	1.3	20
21797	Strain-controlled fundamental gap and structure of bulk black phosphorus. Physical Review B, 2016, 94, .	1.1	40
21798	Vacancies and oxidation of two-dimensional group-IV monochalcogenides. Physical Review B, 2016, 94, .	1.1	77
21799	Fabrication and Characterization of p-Type SnO Thin Film with High c-Axis Preferred Orientation. Journal of Electronic Materials, 2016, 45, 5967-5973.	1.0	14
21800	The realization of half-metal and spin-semiconductor for metal adatoms on arsenene. Applied Surface Science, 2016, 390, 60-67.	3.1	31
21801	Molecular simulation of CH4, CO2, H2O and N2 molecules adsorption on heterogeneous surface models of coal. Applied Surface Science, 2016, 389, 894-905.	3.1	121
21802	Na0.282V2O5: A high-performance cathode material for rechargeable lithium batteries and sodium batteries. Journal of Power Sources, 2016, 328, 241-249.	4.0	37
21803	A Multi-Technique Experimental and Computational Approach To Study the Dehydration Processes in the Crystals of Endomorphin Opioid Peptide Derivative. Crystal Growth and Design, 2016, 16, 5312-5322.	1.4	7
21804	Effect of alloying elements on the ideal strength and charge redistribution of Î³â€²-Ni₃Al: a first-principles study of tensile deformation. RSC Advances, 2016, 6, 77489-77498.	1.7	17
21805	A first-principles study of oxygen adsorption on Ir(111) surface. Applied Surface Science, 2016, 389, 211-215.	3.1	14
21806	Ab initio investigation into structural, mechanical and electronic properties of low pressure, high pressure and high pressure-high temperature phases of Indium Selenide. Computational Materials Science, 2016, 124, 62-77.	1.4	16

#	Article	IF	Citations
21807	Effects of pressure on anisotropic elastic properties and minimum thermal conductivity of D022-Ni3Nb phase: First-principles calculations. Journal of Alloys and Compounds, 2016, 688, 285-293.	2.8	38
21808	Crystal and electronic structure changes during the charge-discharge process of Na4Co3(PO4)2P2O7. Journal of Power Sources, 2016, 326, 220-225.	4.0	32
21809	Ab initio study on structural, electronic properties, and hardness of re-doped W2B5. Solid State Communications, 2016, 245, 60-64.	0.9	5
21810	Is Spillover Relevant for Hydrogen Adsorption and Storage in Porous Carbons Doped with Palladium Nanoparticles?. Journal of Physical Chemistry C, 2016, 120, 17357-17364.	1.5	51
21811	Structural Studies of Polyaramid Fibers: Solid-State NMR and First-Principles Modeling. Macromolecules, 2016, 49, 5548-5560.	2.2	12
21812	C₂H₄ adsorption on Cu(210), revisited: bonding nature and coverage effects. Physical Chemistry Chemical Physics, 2016, 18, 23621-23627.	1.3	6
21813	Polarization and valley switching in monolayer group-IV monochalcogenides. Physical Review B, 2016, 94, .	1.1	122
21814	Emerging Diluted Ferromagnetism in Highâ€T_c Superconductors Driven by Point Defect Clusters. Advanced Science, 2016, 3, 1500295.	5.6	41
21815	Formation and Stability of Lowâ€Dimensional Structures for Group VIIIB and IB Transition Metals: The Role of sd⁴ Hybridization. Advanced Science, 2016, 3, 1500314.	5.6	7
21816	Designing efficient doped NiOOH catalysts for water splitting with first principles calculations. ChemistrySelect, 2016, 1, 911-916.	0.7	26
21817	CdTe/Si Composite Substrate and HgCdTe Epitaxy. , 2016, , 121-263.		0
21818	Dead layer effect and its elimination in ferroelectric thin film with oxide electrodes. Acta Materialia, 2016, 112, 216-223.	3.8	30
21819	First-principles study of phase equilibrium in Tiâ€“V, Tiâ€“Nb, and Tiâ€“Ta alloys. Calphad: Computer Coupling of Phase Diagrams and Thermochemistry, 2016, 54, 125-133.	0.7	42
21820	Two-dimensional metallic MoS2: A DFT study. Computational Materials Science, 2016, 124, 49-53.	1.4	22
21821	Hydrogen adsorption on boron nitride nanotubes functionalized with transition metals. International Journal of Hydrogen Energy, 2016, 41, 13531-13539.	3.8	59
21822	Point defects in thorium nitride: A first-principles study. Journal of Nuclear Materials, 2016, 480, 1-6.	1.3	19
21823	Refined Synthesis and Crystal Growth of Pb₂P₂Se₆ for Hard Radiation Detectors. Crystal Growth and Design, 2016, 16, 5100-5109.	1.4	12
21824	Surface Structure and Acidity Properties of Mesoporous Silica SBA-15 Modified with Aluminum and Titanium: First-Principles Calculations. Journal of Physical Chemistry C, 2016, 120, 18105-18114.	1.5	21

#	Article	IF	Citations
21825	Chemically-doped graphene with improved surface plasmon characteristics: an optical near-field study. Nanoscale, 2016, 8, 16621-16630.	2.8	14
21826	Ductile-to-brittle transition and materialsâ€™ resistance to amorphization by irradiation damage. RSC Advances, 2016, 6, 44561-44568.	1.7	14
21827	Lattice dynamics of neodymium: Influence of<mml:math xmlns:mml="http://www.w3.org/1998/Math/MathML"><mml:mrow><mml:mn>4</mml:mn><mml:mi>f</mml:mi></mml:mrow></mml:m correlations. Physical Review B, 2016, 94, .	1.1	10
21828	Effects of oxygen contamination on monolayer GeSe: A computational study. Physical Review B, 2016, 94, .	1.1	28
21829	Microscopic dielectric permittivities of graphene nanoribbons and graphene. Physical Review B, 2016, 94, .	1.1	42
21830	Ferromagnetic Quantum Critical Point Avoided by the Appearance of Another Magnetic Phase in<mml:math xmlns:mml="http://www.w3.org/1998/Math/MathML" display="inline"><mml:mrow><mml:msub><mml:mrow><mml:mi>LaCrGe</mml:mi></mml:mrow><mml:mrow><mml:mn>3</mml:mn></mml:mr Pressure. Physical Review Letters, 2016, 117, 037207.	2.9	47
21831	Adsorption of Noble-Gas Atoms on the TiO₂(110) Surface: An Ab Initio-Assisted Study with van der Waals-Corrected DFT. Journal of Physical Chemistry C, 2016, 120, 18126-18139.	1.5	51
21832	The electronic structure, elastic and optical properties of Cu₂ZnGe(Se_xS_{1 â’} _x)₄ alloys: density functional calculations. Molecular Physics, 2016, 114, 2948-2957.	0.8	6
21833	First-principles simulations of PVDF copolymers with high dielectric energy density: PVDF-HFP and PVDF-BTFE. Physical Review B, 2016, 94, .	1.1	7
21834	Structural and thermoelectric properties of zintl-phase CaLiPn (Pn=As, Sb, Bi). Journal of Solid State Chemistry, 2016, 243, 198-206.	1.4	10
21835	Unexpected Epitaxial Growth of a Few WS₂ Layers on {11Ì…00} Facets of ZnO Nanowires. Journal of Physical Chemistry C, 2016, 120, 21451-21459.	1.5	22
21836	Structural evolution of concave trimetallic nanocubes with tunable ultra-thin shells for oxygen reduction reaction. Nanoscale, 2016, 8, 16640-16649.	2.8	32
21837	Antiferromagnetic MnN layer on the MnGa(001) surface. Applied Surface Science, 2016, 390, 328-332.	3.1	11
21838	Dissociation of N2O on anatase TiO2 (001) surface â€“ The effect of oxygen vacancy and presence of Ag cluster. Applied Surface Science, 2016, 389, 1220-1232.	3.1	13
21839	Stability of vacancy-oxygen complexes in bulk nickel: Atomistic and ab initio calculations. Computational Materials Science, 2016, 124, 428-437.	1.4	10
21840	A first combined electrochemical and modelling strategy on composite carbonate/oxide electrolytes for hybrid fuel cells. International Journal of Hydrogen Energy, 2016, 41, 18778-18787.	3.8	10
21841	Size dependent magnetic and optical properties in diamond shaped graphene quantum dots: A DFT study. Journal of Physics and Chemistry of Solids, 2016, 99, 34-42.	1.9	46
21842	Investigating and comparison of electronic and optical properties of MgO nanosheet in (100) and (111) structural directions based on the density functional theory. Physica B: Condensed Matter, 2016, 502, 61-67.	1.3	17

#	Article	IF	Citations
21843	Tunable donor and acceptor impurity states in a WSe₂ monolayer by adsorption of common gas molecules. RSC Advances, 2016, 6, 82793-82800.	1.7	43
21844	Electronic properties of the FeSe/STO interface from first-principle calculations. Superconductor Science and Technology, 2016, 29, 104005.	1.8	10
21845	Band structure and optical transitions in the Hg 3 Se 2 Cl 2 crystals. Journal of Physics and Chemistry of Solids, 2016, 99, 153-158.	1.9	5
21846	Influences of Stoneâ€“Wales defects on the structure, stability and electronic properties of antimonene: A first principle study. Physica B: Condensed Matter, 2016, 503, 126-129.	1.3	23
21847	DFT-D2 Study of the Adsorption and Dissociation of Water on Clean and Oxygen-Covered {001} and {011} Surfaces of Mackinawite (FeS). Journal of Physical Chemistry C, 2016, 120, 21441-21450.	1.5	34
21848	Optimizing Binding Energies of Key Intermediates for CO₂ Hydrogenation to Methanol over Oxide-Supported Copper. Journal of the American Chemical Society, 2016, 138, 12440-12450.	6.6	565
21849	Highly active and selective nickel molybdenum catalysts for direct hydrazine fuel cell. Electrochimica Acta, 2016, 215, 420-426.	2.6	59
21850	Synthesis and first-principle calculations of the structural and electronic properties of Ge-substituted type-VIII Ba8Ga16Sn30 clathrate. Physica B: Condensed Matter, 2016, 502, 25-31.	1.3	0
21851	Electronic and optical properties of beryllium sulfide monolayer: Under stress and strain conditions. Physics Letters, Section A: General, Atomic and Solid State Physics, 2016, 380, 3546-3552.	0.9	11
21852	Enhancement of the spin transfer torque efficiency in magnetic STM junctions. Physical Review B, 2016, 94, .	1.1	5
21853	Electronic Structure and Transport Properties of Doped Lead Chalcogenides from First Principles. MRS Advances, 2016, 1, 4003-4010.	0.5	1
21854	Piezoelectric properties of monolayer IIâ€“VI group oxides by firstâ€principles calculations. Physica Status Solidi (B): Basic Research, 2016, 253, 2534-2539.	0.7	43
21855	Two-dimensional boron nitride structures functionalization: first principles studies. Journal of Molecular Modeling, 2016, 22, 226.	0.8	11
21856	Structure and electronic properties of palladium chains supported by NiAl(1 1 0): A first-principles study. Computational Materials Science, 2016, 124, 398-402.	1.4	5
21857	Defective Hexagonal Boron Nitride Nanosheet on Ni(111) and Cu(111): Stability, Electronic Structures, and Potential Applications. ACS Applied Materials & Interfaces, 2016, 8, 24238-24247.	4.0	51
21858	Tuning the electronic and magnetic properties of graphene-like SiGe hybrid nanosheets by surface functionalization. Physical Chemistry Chemical Physics, 2016, 18, 26205-26212.	1.3	8
21859	Size-tunable synthesis of monolayer MoS₂nanoparticles and their applications in non-volatile memory devices. Nanoscale, 2016, 8, 16995-17003.	2.8	23
21860	Atomic scale mobility of the volatile fission products Xe, Kr and I in cubic SiC. Physical Chemistry Chemical Physics, 2016, 18, 16902-16911.	1.3	2

#	Article	IF	Citations
21861	The contact of graphene with Ni(111) surface: description by modern dispersive forces approaches. Theoretical Chemistry Accounts, 2016, 135, 1.	0.5	15
21862	DFT insights into the electronic and optical properties of fluorine-doped monoclinic niobium pentoxide (B-Nb2O5:F). Applied Physics A: Materials Science and Processing, 2016, 122, 1.	1.1	16
21863	Evaluation of the tantalum-titanium phase diagram from ab-initio calculations. Acta Materialia, 2016, 120, 255-263.	3.8	29
21864	Exotic quantum spin Hall effect and anisotropic spin splitting in carbon based TMC 6 (TMÂ=ÂMo, W) kagome monolayers. Carbon, 2016, 109, 788-794.	5.4	10
21865	Investigation on WC/TiC interface relationship in wear-resistant coating by first-principles. Surface and Coatings Technology, 2016, 305, 200-207.	2.2	44
21866	Stability and effects of carbon-induced surface reconstructions in cobalt Fischerâ€“Tropsch synthesis. Surface Science, 2016, 653, 82-87.	0.8	11
21867	Substituent Effects and Molecular Descriptors of Reactivity in Condensation and Esterification Reactions of Oxygenates on Acidâ€“Base Pairs at TiO₂ and ZrO₂ Surfaces. Journal of Physical Chemistry C, 2016, 120, 21589-21616.	1.5	44
21868	Photoelectrochemical and theoretical investigation of the photocatalytic activity of TiO₂â€‰:â€‰N. RSC Advances, 2016, 6, 89687-89698.	1.7	44
21869	Theoretical prediction of MoN₂ monolayer as a high capacity electrode material for metal ion batteries. Journal of Materials Chemistry A, 2016, 4, 15224-15231.	5.2	259
21870	Calculated high-pressure structural properties, lattice dynamics and quasi particle band structures of perovskite fluorides KZnF₃, CsCaF₃and BaLiF₃. Journal of Physics Condensed Matter, 2016, 28, 315403.	0.7	12
21871	Pseudogap formation and vacancy ordering in the new perovskite boride Zr2Ir6B. Acta Materialia, 2016, 120, 32-39.	3.8	4
21872	Effects of strain and electric field on electronic structures and Schottky barrier in graphene and SnS hybrid heterostructures. Carbon, 2016, 109, 737-746.	5.4	106
21873	Defect and functionalized graphene for supercapacitor electrodes. Superlattices and Microstructures, 2016, 98, 306-315.	1.4	32
21874	Tuning the Phase Stability of Sodium Metal Pyrophosphates for Synthesis of High Voltage Cathode Materials. Chemistry of Materials, 2016, 28, 6724-6730.	3.2	14
21875	High-Pressure Synthesis of Melilite-type Rare-Earth Nitridophosphates RE₂P₃N₇ and a Ba₂Cu[Si₂O₇]-type Polymorph. Inorganic Chemistry, 2016, 55, 9400-9409.	1.9	24
21876	Unraveling the Mechanism of the Zn-Improved Catalytic Activity of Pd-Based Catalysts for Waterâ€“Gas Shift Reaction. Journal of Physical Chemistry C, 2016, 120, 20181-20191.	1.5	9
21877	Dynamic Stereochemical Activity of the Sn²⁺ Lone Pair in Perovskite CsSnBr₃. Journal of the American Chemical Society, 2016, 138, 11820-11832.	6.6	217
21878	DFT study of Rh-decorated pristine, B-doped and vacancy defected graphene for hydrogen adsorption. RSC Advances, 2016, 6, 83926-83941.	1.7	39

#	Article	IF	Citations
21879	Solvation and surface effects on polymorph stabilities at the nanoscale. Chemical Science, 2016, 7, 6617-6627.	3.7	128
21880	Thin-Film Photoluminescent Properties and the Atomistic Model of Mg2TiO4 as a Non-rare Earth Matrix Material for Red-Emitting Phosphor. Journal of Electronic Materials, 2016, 45, 6214-6221.	1.0	2
21881	Structural, electronic and magnetic properties of transition metal atom-doped ZnS dilute magnetic semiconductors: A first-principles study. Materials Chemistry and Physics, 2016, 183, 201-209.	2.0	13
21882	EuAu₃Al₂: Crystal and Electronic Structures and Spectroscopic, Magnetic, and Magnetocaloric Properties. Inorganic Chemistry, 2016, 55, 9057-9064.	1.9	16
21883	Mechanistic Insight into the Chemical Exfoliation and Functionalization of Ti₃C₂ MXene. ACS Applied Materials & Interfaces, 2016, 8, 24256-24264.	4.0	221
21884	Mechanical properties of phosphorene nanotubes: a density functional tight-binding study. Nanotechnology, 2016, 27, 395701.	1.3	40
21885	Tunable electronic structures and magnetism in arsenene nanosheets via transition metal doping. Journal of Materials Science, 2016, 51, 9504-9513.	1.7	46
21886	Half-metallic and magnetic properties of AlN nanosheets doped with nonmagnetic metals: A first-principles study. Computational Materials Science, 2016, 124, 98-105.	1.4	14
21887	Comparison of mechanistic understanding and experiments for CO methanation over nickel. Journal of Catalysis, 2016, 342, 105-116.	3.1	41
21888	Pressure-Stabilized Ir3â€“in a Superconducting Potassium Iridide. Journal of Physical Chemistry C, 2016, 120, 20033-20039.	1.5	12
21889	Reconstructive Transitions from Rotations of Rigid Heteroanionic Polyhedra. Journal of the American Chemical Society, 2016, 138, 11882-11889.	6.6	13
21890	First-principles calculations of sulphur isotope fractionation in MX2 minerals, with M= Fe, Co, Ni and X2= AsS, SbS. Chemical Geology, 2016, 441, 204-211.	1.4	11
21891	Structural and electronic properties of B2N3 planar nanostructure: A computational investigation. Chemical Physics Letters, 2016, 660, 244-249.	1.2	3
21892	Structural, bonding, anisotropic mechanical and thermal properties of Al₄SiC₄ and Al₄Si₂C₅ by first-principles investigations. Journal of Asian Ceramic Societies, 2016, 4, 289-298.	1.0	11
21893	Lattice dynamics, thermodynamics and elastic properties of C22-Zr6FeSn2 from first-principles calculations. Journal of Nuclear Materials, 2016, 479, 461-469.	1.3	12
21894	Realizing half-metallicity in K₂CoF₄ exfoliated nanosheets via defect engineering. Physical Chemistry Chemical Physics, 2016, 18, 15765-15773.	1.3	3
21895	Directional dependence of the electronic and transport properties of 2D borophene and borophane. Physical Chemistry Chemical Physics, 2016, 18, 25491-25496.	1.3	92
21896	Modulation of doping and biaxial strain on the transition temperature of the charge density waveÂtransition in 1T-TiSe₂. RSC Advances, 2016, 6, 76972-76979.	1.7	20

#	Article	IF	Citations
21897	Ab initio investigation of the electronic, lattice dynamic and thermodynamic properties of ScCd intermetallic alloy. International Journal of Modern Physics B, 2016, 30, 1650175.	1.0	0
21898	Thermoelasticity of Fe³⁺â€•and Alâ€bearing bridgmanite: Effects of iron spin crossover. Geophysical Research Letters, 2016, 43, 5661-5670.	1.5	43
21899	Layered Antiferromagnetic Ordering in the Most Active Perovskite Catalysts for the Oxygen Evolution Reaction. ChemCatChem, 2016, 8, 2968-2974.	1.8	61
21900	Charge transfer and weak bonding between molecular oxygen and graphene zigzag edges at low temperatures. Carbon, 2016, 107, 800-810.	5.4	27
21901	Electronic and magnetic properties of MnF3(4) superhalogen cluster-sandwiched bilayer graphene: First-principles calculations. Computational Materials Science, 2016, 124, 316-322.	1.4	7
21902	Firstâ€"principle calculation of the elastic, band structure, electronic states, and optical properties of Cuâ€"doped ZnS nanolayers. Physica B: Condensed Matter, 2016, 501, 146-152.	1.3	26
21903	Multinuclear NMR as a tool for studying local order and dynamics in CH₃NH₃PbX₃ (X = Cl, Br, I) hybrid perovskites. Physical Chemistry Chemical Physics, 2016, 18, 27133-27142.	1.3	78
21904	Large enhancement in photocurrent by Mn doping in CdSe/ZTO quantum dot sensitized solar cells. Physical Chemistry Chemical Physics, 2016, 18, 26771-26776.	1.3	14
21905	Origins of phase separation in thermoelectric (Ti, Zr, Hf)NiSn half-Heusler alloys from first principles. Journal of Materials Chemistry A, 2016, 4, 13949-13956.	5.2	41
21906	Stannene: A Likely 2D Topological Insulator. Series in Materials Science and Engineering, 2016, , 379-408.	0.1	0
21907	Exchange coupling and spin structure in cobalt-on-chromia thin films. Europhysics Letters, 2016, 115, 17003.	0.7	6
21908	Quantum chemical simulations of doped ZnO nanowires for photocatalytic hydrogen generation. Physica Status Solidi (B): Basic Research, 2016, 253, 2120-2128.	0.7	16
21909	Hosting of La3+ guest ions in type-I Ge clathrates: A first-principles characterization for thermoelectric applications. Computational Materials Science, 2016, 122, 46-56.	1.4	4
21910	First-principles study of zinc-blende BxAlyIn1â^'xâ^'yN quaternary alloy: Alchemical mixing approximation approach. International Journal of Modern Physics B, 2016, 30, 1650191.	1.0	1
21911	Thermoelectric properties of bilayer phosphorene under tensile strain. Surface and Interface Analysis, 2016, 48, 1231-1234.	0.8	5
21912	Interaction of a Ti-doped semi-fullerene (TiC30) with molecules of CO and CO2. Journal of Molecular Modeling, 2016, 22, 223.	0.8	2
21913	Structural prediction for scandium carbide monolayer sheet. Chemical Physics Letters, 2016, 660, 238-243.	1.2	5
21914	Hydrogen intercalation in<mml:math xmlns:mml="http://www.w3.org/1998/Math/MathML"><mml:msub><mml:mi>MoS</mml:mi><mml:mn>2</mml:mn></mml:msub></mml:math>. Physical Review B, 2016, 94, .	1.1	15

#	Article	IF	Citations
21915	Electronic Structure and N-Type Doping in Diamond from First Principles. MRS Advances, 2016, 1, 1093-1098.	0.5	20
21916	Structural, electronic and magnetic properties of carbon doped boron nitride nanowire: Ab initio study. Journal of Solid State Chemistry, 2016, 243, 232-240.	1.4	7
21917	Electron States of 2D Metalâ€“Organic and Covalentâ€“Organic Honeycomb Frameworks: Ab Initio Results and a General Fitting Hamiltonian. Journal of Physical Chemistry C, 2016, 120, 19796-19803.	1.5	23
21918	The rapid growth of ADP single crystal. CrystEngComm, 2016, 18, 7530-7536.	1.3	24
21919	Valence and conduction band tuning in halide perovskites for solar cell applications. Journal of Materials Chemistry A, 2016, 4, 15997-16002.	5.2	132
21920	Ferromagnetic origin of Na and Mn codoped CaZn2As2 diluted magnetic semiconductor: A first-principles study. JETP Letters, 2016, 103, 631-635.	0.4	4
21921	Surface study of gallium- and aluminum- doped graphenes upon adsorption of cytosine: DFT calculations. Applied Surface Science, 2016, 390, 444-451.	3.1	48
21922	Effects of strain on the stability of tetragonal<mml:math xmlns:mml="http://www.w3.org/1998/Math/MathML"><mml:msub><mml:mtext>ZrO</mml:mtext><mml:mn>2</mml:mn></mml:msub> Physical Review B, 2016, 94, .	3.7	18
21923	Anharmonicity in the High-Temperature<mml:math xmlns:mml="http://www.w3.org/1998/Math/MathML" display="inline"><mml:mi>C</mml:mi><mml:mi>m</mml:mi><mml:mi>c</mml:mi><mml:mi>m</mml:mi></mml:math>Phase of SnSe: Soft Modes and Three-Phonon Interactions. Physical Review Letters, 2016, 117, 075502.	8.6	447
21924	First-principles investigation on the electronic property and bonding configuration of NbC (111)/NbN (111) interface. Journal of Alloys and Compounds, 2016, 689, 874-884.	2.8	50
21925	Thermodynamic properties of Î±-uranium. Journal of Nuclear Materials, 2016, 480, 80-87.	1.3	6
21926	Structural and electronic properties of V-doped cubic BN: A density functional theory study. Solid State Communications, 2016, 244, 23-27.	0.9	11
21927	Theoretical studies on the form and effect of N-doping in an ZnGa₂O₄ photocatalyst. RSC Advances, 2016, 6, 74483-74492.	1.7	9
21928	A new congruent-melting double phosphate PbCd(PO3)4 with photocatalytic activity. Journal of Alloys and Compounds, 2016, 689, 599-605.	2.8	8
21929	First-principles study of martensitic transformation and magnetic properties of carbon doped Niâ€“Mnâ€“Sn Heusler alloys. Physics Letters, Section A: General, Atomic and Solid State Physics, 2016, 380, 3414-3420.	0.9	19
21930	Curvature-Dependent Selectivity of CO₂ Electrocatalytic Reduction on Cobalt Porphyrin Nanotubes. ACS Catalysis, 2016, 6, 6294-6301.	5.5	113
21931	TM@gt-C₃N₃ monolayers: high-temperature ferromagnetism and high anisotropy. Journal of Materials Chemistry C, 2016, 4, 8253-8262.	2.7	26
21932	Pressure effect on the structural, electronic, and elastic properties and Debye temperature of Rh3Nb: first-principles calculations. RSC Advances, 2016, 6, 78028-78035.	1.7	6

#	Article	IF	Citations
21933	The influence of the electronic specific heat on swift heavy ion irradiation simulations of silicon. Journal of Physics Condensed Matter, 2016, 28, 395201.	0.7	23
21934	Firstâ€principles lattice dynamics and Raman scattering in ionic conductor Î²â€Ag₂S. Physica Status Solidi (B): Basic Research, 2016, 253, 2049-2055.	0.7	33
21935	Structural, electronic and adsorption properties of Rh(111)/Mo(110) bimetallic catalyst: A DFT study. Applied Surface Science, 2016, 389, 1094-1103.	3.1	10
21936	Evaluating the size of Fe nanoparticles for ammonia adsorption and dehydrogenation. Computational Materials Science, 2016, 124, 220-227.	1.4	13
21937	Chromate adsorption mechanism on nanodiamond-derived onion-like carbon. Journal of Hazardous Materials, 2016, 320, 368-375.	6.5	25
21938	Investigation on grain refinement mechanism of Ni-based coating with LaAlO3 by first-principles. Materials and Design, 2016, 110, 644-652.	3.3	23
21939	Crystal Growth, Structure, and Optical Properties of LiGaGe₂Se₆. Inorganic Chemistry, 2016, 55, 8672-8680.	1.9	37
21940	Unraveling the Catalytic Mechanism of Rutile RuO₂ for the Oxygen Reduction Reaction and Oxygen Evolution Reaction in Liâ€“O₂ Batteries. ACS Catalysis, 2016, 6, 6285-6293.	5.5	51
21941	Anisotropic thermal motion in transition-metal carbonyls from experiments and ab initio theory. Dalton Transactions, 2016, 45, 13680-13685.	1.6	15
21942	Pressure-induced formation of hydrogen bonds in KNH₂ studied by first principles. RSC Advances, 2016, 6, 78678-78683.	1.7	1
21943	Carbon-rich icosahedral boron carbides beyond<mml:math xmlns:mml="http://www.w3.org/1998/Math/MathML"><mml:mrow><mml:msub><mml:mi mathvariant="normal">B</mml:mi><mml:mn>4</mml:mn></mml:msub><mml:mi mathvariant="normal">C</mml:mi></mml:mrow></mml:math>and their thermodynamic stabilities at high temperature and pressure from first principles. Physical Review B, 2016, 94, .	1.1	21
21944	Quantification of uncertainty in first-principles predicted mechanical properties of solids: Application to solid ion conductors. Physical Review B, 2016, 94, .	1.1	25
21945	On the Structure Sensitivity of Formic Acid Decomposition on Cu Catalysts. Topics in Catalysis, 2016, 59, 1580-1588.	1.3	37
21946	A Density Functional Theory Study of the Ionic and Electronic Transport Mechanisms in LiFeBO₃ Battery Electrodes. Journal of Physical Chemistry C, 2016, 120, 18355-18364.	1.5	24
21947	Bifunctional Interface of Au and Cu for Improved CO₂ Electroreduction. ACS Applied Materials & Interfaces, 2016, 8, 23022-23027.	4.0	93
21948	Mechanistic Evaluation of Li_xO_y Formation on Î´-MnO₂ in Nonaqueous Liâ€“Air Batteries. ACS Applied Materials & Interfaces, 2016, 8, 23028-23036.	4.0	46
21949	Electronic structure and transport properties of antiferromagnetic double perovskite Y₂AlCrO₆. RSC Advances, 2016, 6, 80415-80423.	1.7	10
21950	The enhanced CO gas sensing performance of Pd/SnO₂ hollow sphere sensors under hydrothermal conditions. RSC Advances, 2016, 6, 80455-80461.	1.7	15

#	Article	IF	Citations
21951	Towards Direct Synthesis of Alane: A Predicted Defectâ€Mediated Pathway Confirmed Experimentally. ChemSusChem, 2016, 9, 2358-2364.	3.6	5
21952	Structure and stability of pyrophyllite edge surfaces: Effect of temperature and water chemical potential. Geochimica Et Cosmochimica Acta, 2016, 190, 100-114.	1.6	32
21953	The mechanical, thermodynamic, and electronic properties of cubic Au4Al crystal via first-principles calculations. Journal of Alloys and Compounds, 2016, 689, 857-864.	2.8	20
21954	Structural and mechanical properties of transition metal borides Nb2MB2 (M=Tc, Ru, and Os) under pressure. Solid State Communications, 2016, 244, 68-75.	0.9	1
21955	Study of the vibrational, dielectric and infrared properties of CdSiP 2 via first principles. Solid State Communications, 2016, 246, 88-93.	0.9	19
21956	First principle investigation of crystal lattice structure, thermodynamics and mechanical properties in ZnZrAl2 intermetallic compound. Solid State Communications, 2016, 247, 82-87.	0.9	6
21957	Low Valence Cation Doping of Bulk Cr₂O₃: Charge Compensation and Oxygen Vacancy Formation. Journal of Physical Chemistry C, 2016, 120, 19160-19174.	1.5	59
21958	Group Additivity for Thermochemical Property Estimation of Lignin Monomers on Pt(111). Journal of Physical Chemistry C, 2016, 120, 19234-19241.	1.5	18
21959	Co-adsorption of O₂ and H₂O on Al(111) surface: a vdW-DFT study. RSC Advances, 2016, 6, 79836-79843.	1.7	14
21960	Van der Waals molecular interactions in the organic functionalization of graphane, silicane, and germanane with alkene and alkyne molecules: a DFT-D2 study. Journal of Molecular Modeling, 2016, 22, 175.	0.8	9
21961	Investigation of adatom adsorption on single layer buckled germanium selenide. Applied Surface Science, 2016, 390, 185-189.	3.1	4
21962	Mechanical properties and electronic structures of diverse Pt Al intermetallics: First-principles calculations. Computational Materials Science, 2016, 124, 273-281.	1.4	21
21963	Effects of biaxial strains on the structural, electronic, elastic and lattice vibrational properties in t -BC 2 N and z -BC 2 N. Journal of Alloys and Compounds, 2016, 686, 914-922.	2.8	11
21964	Theoretical prediction of long-range ferromagnetism in transition-metal atom-doped d⁰ dichalcogenide single layers SnS₂ and ZrS₂. Physical Chemistry Chemical Physics, 2016, 18, 25151-25160.	1.3	18
21965	A Cr₂CO₂ monolayer as a promising cathode for lithium and non-lithium ion batteries: a computational exploration. RSC Advances, 2016, 6, 81591-81596.	1.7	29
21966	First-principle study on electronic structure and optical properties of GaN nanowires with different cross-sections. International Journal of Modern Physics B, 2016, 30, 1650136.	1.0	3
21967	Reaction mechanism of aqueous-phase conversion of Î³-valerolactone (GVL) over a Ru/C catalyst. Journal of Energy Chemistry, 2016, 25, 1008-1014.	7.1	15
21968	Pseudo-Hydrogen Passivation: A Novel Way to Calculate Absolute Surface Energy of Zinc Blende (111)/(Íž1) Tj ETQq1 1 0.784314 rgB	1.6	28

#	Article	IF	Citations
21969	Theoretical calculations of structural, electronic, and elastic properties of CdSe _{1â^' x} Te _x : A first principles study. Chinese Physics B, 2016, 25, 076104.	0.7	12
21970	Direct observation of incommensurate structure in Mo₃Si. Acta Crystallographica Section A: Foundations and Advances, 2016, 72, 660-666.	0.0	3
21971	Room temperatured⁰ferromagnetism in hole doped Y₂O₃: widening the choice of host to tailor DMS. Journal of Physics Condensed Matter, 2016, 28, 336001.	0.7	12
21972	Static and Dynamical Properties of heavy actinide Monopnictides of Lutetium. Scientific Reports, 2016, 6, 29309.	1.6	20
21973	Effects of La 5d and 4f states on the electronic and optical properties of LaAlO3. Physical Review B, 2016, 94, .	1.1	14
21974	First-Principles Study of Thermodynamical and Elastic Properties of Î·â€²-(Cu,Co)6Sn5 Ternary Alloys. Journal of Electronic Materials, 2016, 45, 4919-4927.	1.0	9
21975	Signature of coexistence of superconductivity and ferromagnetism in two-dimensional NbSe2 triggered by surface molecular adsorption. Nature Communications, 2016, 7, 11210.	5.8	85
21976	Ab initio molecular dynamic study of solid-state transitions of ammonium nitrate. Scientific Reports, 2016, 6, 18918.	1.6	5
21977	Electronic bonding analyses and mechanical strengths of incompressible tetragonal transition metal dinitrides TMN2 (TMâ€‰=â€‰Ti, Zr, and Hf). Scientific Reports, 2016, 6, 36911.	1.6	22
21978	Structural and Thermodynamic Stability of the â€œ1111â€•Structure Type: A Case Study of the EuFZnPn Series. Inorganic Chemistry, 2016, 55, 12409-12418.	1.9	13
21979	Structures and Catalytic Properties of Crâ€“Cu Embedded CeO₂ Surfaces with Different Cr/Cu Ratios. Journal of Physical Chemistry C, 2016, 120, 26852-26863.	1.5	20
21980	Two-dimensional Topological Crystalline Insulator Phase in Sb/Bi Planar Honeycomb with Tunable Dirac Gap. Scientific Reports, 2016, 6, 18993.	1.6	21
21981	Dirac fermions induced in strained zigzag phosphorus nanotubes and their applications in field effect transistors. Physical Chemistry Chemical Physics, 2016, 18, 32521-32527.	1.3	3
21982	First-principles study of electronic and optical properties of cubic AgTaO3 structure in paraelectric phase at different pressures. Ferroelectrics, 2016, 504, 130-138.	0.3	3
21983	Molecular Level Study of Graphene Networks Functionalized with Phenylenediamine Monomers for Supercapacitor Electrodes. Chemistry of Materials, 2016, 28, 9110-9121.	3.2	98
21984	Simple Synthesis of Nanocrystalline Tin Sulfide/N-Doped Reduced Graphene Oxide Composites as Lithium Ion Battery Anodes. ACS Nano, 2016, 10, 10778-10788.	7.3	178
21985	Optically switched magnetism in photovoltaic perovskite CH3NH3(Mn:Pb)I3. Nature Communications, 2016, 7, 13406.	5.8	106
21986	Improved p-type conductivity in Al-rich AlGaN using multidimensional Mg-doped superlattices. Scientific Reports, 2016, 6, 21897.	1.6	49

#	Article	IF	Citations
21987	Electron work functionâ€“a promising guiding parameter for material design. Scientific Reports, 2016, 6, 24366.	1.6	55
21988	Investigating the adsorption mechanism of glycine in comparison with catechol on cristobalite surface using density functional theory for bio-adhesive materials. RSC Advances, 2016, 6, 114313-114319.	1.7	5
21989	Mechanical properties and anisotropy of thermal conductivity of Fe_{3â€“x}Cr_xO₄(x= 0â€“3). Journal of Materials Research, 2016, 31, 3805-3813.	1.2	17
21990	Structural effects of substitutional impurities on MoO3 bilayers: A first principles study. Journal of the Korean Physical Society, 2016, 69, 1439-1444.	0.3	2
21991	Ab initio modelling of Yâ€“O cluster formation in Î³â€Fe lattice. Physica Status Solidi (B): Basic Research, 2016, 253, 2136-2143.	0.7	4
21992	Generalized Surface Coordination Number as an Activity Descriptor for CO₂ Reduction on Cu Surfaces. Journal of Physical Chemistry C, 2016, 120, 28125-28130.	1.5	77
21993	Effects of strong interactions between Ti and ceria on the structures of Ti/CeO₂. Physical Chemistry Chemical Physics, 2016, 18, 32494-32502.	1.3	6
21994	Modelling how incorporation of divalent cations affects calcite wettabilityâ€“implications for biomineralisation and oil recovery. Scientific Reports, 2016, 6, 28854.	1.6	53
21995	Pressure induced elastic softening in framework aluminosilicate- albite (NaAlSi3O8). Scientific Reports, 2016, 6, 34815.	1.6	19
21996	High-throughput combinatorial study of the effect of<mml:math xmlns:mml="http://www.w3.org/1998/Math/MathML"><mml:mi>M</mml:mi></mml:math>site alloying on the solid solution behavior of<mml:math xmlns:mml="http://www.w3.org/1998/Math/MathML"><mml:mrow><mml:msub><mml:mi>M</mml:mi><mml:mn>2</mml:mn></mml:msub></mml:mrow></mml:math> phases. Physical Review B, 2016, 94, .	1.1	38
21997	The Stability and Structural, Electronic and Topological Properties of Covellite (001) Surfaces.. ChemistrySelect, 2016, 1, 2730-2741.	0.7	15
21998	Nonlinear bandgap opening behavior of BN co-doped graphene. Carbon, 2016, 107, 857-864.	5.4	23
21999	Experiment and Mechanism Study on the Effect of Kaolin on Melting Characteristics of Zhundong Coal Ash. Energy & Fuels, 2016, 30, 7763-7769.	2.5	34
22000	Double-Hole-Mediated Codoping on KNbO₃ for Visible Light Photocatalysis. Inorganic Chemistry, 2016, 55, 9620-9631.	1.9	30
22001	Partial Oxidation of Methanol on MoO3 (010): A DFT and Microkinetic Study. ACS Catalysis, 2016, 6, 7260-7277.	5.5	57
22002	Effect of caffeic acid adsorption in controlling the morphology of gold nanoparticles: role of surface coverage and functional groups. Physical Chemistry Chemical Physics, 2016, 18, 27775-27783.	1.3	22
22003	Hydrogen production based on a photoactivated nanowire-forest. Journal of Materials Chemistry A, 2016, 4, 14988-14995.	5.2	5
22004	The Stoneâ€“Wales transformation: from fullerenes to graphite, from radiation damage to heat capacity. Philosophical Transactions Series A, Mathematical, Physical, and Engineering Sciences, 2016, 374, 20150317.	1.6	10

#	Article	IF	Citations
22005	Investigated electronic structure and magnetic ordering of rare earth impurities (Eu, Gd) in ZnO. International Journal of Modern Physics B, 2016, 30, 1650225.	1.0	15
22006	Low phonon conductivity of layered BiCuOS, BiCuOSe, and BiCuOTe from first principles. Physical Review B, 2016, 94, .	1.1	28
22007	Structural, electronic transport and optical properties of functionalized quasi-2D TiC2 from first-principles calculations. Applied Surface Science, 2016, 390, 1009-1014.	3.1	10
22008	Equilibrium zinc isotope fractionation in Zn-bearing minerals from first-principlesÂcalculations. Chemical Geology, 2016, 443, 87-96.	1.4	68
22009	Predictions of solar radiation shielding properties of KB 6 from first principles. Computational Condensed Matter, 2016, 9, 1-5.	0.9	4
22010	Tunable Gravimetric and Volumetric Hydrogen Storage Capacities in Polyhedral Oligomeric Silsesquioxane Frameworks. ACS Applied Materials & Interfaces, 2016, 8, 25219-25228.	4.0	14
22011	Understanding the surface segregation behavior of transition metals on Ni(111): a first-principles study. Physical Chemistry Chemical Physics, 2016, 18, 26616-26622.	1.3	35
22012	A ZrNiAl related high-pressure modification of CeRuSn. Dalton Transactions, 2016, 45, 14216-14229.	1.6	6
22013	Synergistic effect of Liâ€“Ti and Kâ€“Ti co-doping on the dehydrogenation properties of NaAlH₄: an ab initio study. RSC Advances, 2016, 6, 89895-89900.	1.7	0
22014	Distance- and spin-resolved spectroscopy of iridium atoms on an iron bilayer. Physical Review B, 2016, 94, .	1.1	2
22015	Effects of a magnetic Fe monolayer on the structural and surface electronic properties ofSb2Te3. Physical Review B, 2016, 94, .	1.1	4
22016	Deep-Ultraviolet Transparent Cs₂LiPO₄ Exhibits an Unprecedented Second Harmonic Generation. Chemistry of Materials, 2016, 28, 7110-7116.	3.2	130
22017	Ferromagnetic and Half-Metallic FeC₂ Monolayer Containing C₂ Dimers. ACS Applied Materials & Interfaces, 2016, 8, 26207-26212.	4.0	58
22018	p-Doped Graphene/Graphitic Carbon Nitride Hybrid Electrocatalysts: Unraveling Charge Transfer Mechanisms for Enhanced Hydrogen Evolution Reaction Performance. ACS Catalysis, 2016, 6, 7071-7077.	5.5	62
22019	Nonlinear Rashba spin splitting in transition metal dichalcogenide monolayers. Nanoscale, 2016, 8, 17854-17860.	2.8	60
22020	Density functional theory study of high-energy metal (Al, Mg, Ti, and Zr)/CuO composites. RSC Advances, 2016, 6, 90206-90211.	1.7	7
22021	Influence of FrÃ¶hlich polaron coupling on renormalized electron bands in polar semiconductors: Results for zinc-blende GaN. Physical Review B, 2016, 94, .	1.1	35
22022	Transitionâ€Metal Substitution Doping in Synthetic Atomically Thin Semiconductors. Advanced Materials, 2016, 28, 9735-9743.	11.1	208

#	Article	IF	Citations
22023	Density functional theory for molecular and periodic systems using density fitting and continuous fast multipole method: Analytical gradients. Journal of Computational Chemistry, 2016, 37, 2518-2526.	1.5	29
22024	Anisotropic electrical and lattice transport properties of ordered quaternary phases Cr2TiAlC2 and Mo2TiAlC2: A first principles study. Physics Letters, Section A: General, Atomic and Solid State Physics, 2016, 380, 3748-3755.	0.9	29
22025	Reducing CO₂ to CO and H₂O on Ni(110): The Influence of Subsurface Hydrogen. Journal of Physical Chemistry C, 2016, 120, 23061-23068.	1.5	26
22026	Superhalogens as building blocks of two-dimensional organicâ€“inorganic hybrid perovskites for optoelectronics applications. Nanoscale, 2016, 8, 17836-17842.	2.8	34
22027	Germanene: a new electronic gas sensing material. RSC Advances, 2016, 6, 102264-102271.	1.7	68
22028	Electronic structure of 2 H -NbSe ₂ single-layers in the CDW state. 2D Materials, 2016, 3, 035028.	2.0	50
22029	First-principles study of SnO under high pressure. International Journal of Modern Physics B, 2016, 30, 1650228.	1.0	14
22030	Study of hydrostatic pressure effect on structural, mechanical, electronic and optical properties of KMgF₃, K0.5Na0.5MgF₃ and NaMgF₃ cubic fluoro-perovskites via abÂinitio calculations. International Journal of Modern Physics B, 2016, 30, 1650230.	1.0	22
22031	Role of Metal-Lithium Oxide Interfaces in the Extra Lithium Capacity of Metal Oxide Lithium-Ion Battery Anode Materials. Journal of the Electrochemical Society, 2016, 163, A2172-A2178.	1.3	22
22032	EPW: Electronâ€“phonon coupling, transport and superconducting properties using maximally localized Wannier functions. Computer Physics Communications, 2016, 209, 116-133.	3.0	777
22033	Synthesis of carbon-doped BiVO₄@multi-walled carbon nanotubes with high visible-light absorption behavior, and evaluation of their photocatalytic properties. CrystEngComm, 2016, 18, 9007-9015.	1.3	33
22034	N₂ activation on Al metal clusters: catalyzing role of BN-doped graphene support. Physical Chemistry Chemical Physics, 2016, 18, 27721-27727.	1.3	36
22035	Experimental and theoretical evidence for competitive interactions of tetracycline and sulfamethazine with reduced graphene oxides. Environmental Science: Nano, 2016, 3, 1318-1326.	2.2	88
22036	Electron-doping induced half-metallicity in one-dimensional Co-dithiolene molecular wires. Journal of Materials Chemistry C, 2016, 4, 10209-10214.	2.7	9
22037	A model for the effects of germanium on silica biomineralization in choanoflagellates. Journal of the Royal Society Interface, 2016, 13, 20160485.	1.5	10
22038	Ab initiostudy of Cu impurity diffusion in bulk TiN. Physical Review B, 2016, 94, .	1.1	14
22039	Optical absorption and transmission in a molybdenum disulfide monolayer. Physical Review B, 2016, 94, .	1.1	26
22040	Machine Learning Energies of 2AMillion Elpasolite<mml:math xmlns:mml="http://www.w3.org/1998/Math/MathML" display="inline"><mml:mrow><mml:mo stretchy="false">(</mml:mo><mml:mi>A</mml:mi><mml:mi>B</mml:mi><mml:msub><mml:mrow><mml:mi>C</mml:mi></mml:mrow> 135502.	2.9	313

#	Article	IF	Citations
22041	First-principles calculation of the photothreshold of a Î²-GaS layered crystal. Physics of the Solid State, 2016, 58, 1764-1766.	0.2	4
22042	Metallic impurities induced electronic transport in WSe2: First-principle calculations. Chemical Physics Letters, 2016, 658, 83-87.	1.2	19
22043	Unraveling the different charge storage mechanism in T and H phases of MoS2. Electrochimica Acta, 2016, 217, 1-8.	2.6	37
22044	Investigation of electro-optical properties of InSb under the influence of spin-orbit interaction at room temperature. Materials Chemistry and Physics, 2016, 184, 41-48.	2.0	47
22045	Band gap engineering in penta-graphene by substitutional doping: first-principles calculations. Journal of Physics Condensed Matter, 2016, 28, 475001.	0.7	37
22046	Interplay between interstitial displacement and displacive lattice transformations. Physical Review B, 2016, 94, .	1.1	10
22047	A study of the structural and spectral characteristics of free and bound water in kaolinite. Optics and Spectroscopy (English Translation of Optika I Spektroskopiya), 2016, 121, 357-363.	0.2	15
22048	Copper(II) adsorption on the kaolinite(001) surface: Insights from first-principles calculations and molecular dynamics simulations. Applied Surface Science, 2016, 389, 316-323.	3.1	44
22049	Lattice vibrational behavior and thermodynamic properties of uranium disilicide USi 2. Solid State Communications, 2016, 248, 47-52.	0.9	6
22050	Corrosion of Concrete by Water-Induced Metalâ€“Proton Exchange. Journal of Physical Chemistry C, 2016, 120, 22455-22459.	1.5	18
22051	Investigation on the conversion of ethylene to ethylidyne on Pt(100) and Pd(100) using density functional theory. Physical Chemistry Chemical Physics, 2016, 18, 26949-26955.	1.3	5
22052	Tuning electronic structures of the stanene monolayer via defects and transition-metal-embedding: spinâ€“orbit coupling. Physical Chemistry Chemical Physics, 2016, 18, 28759-28766.	1.3	29
22053	Band structure engineering in a MoS₂/PbI₂ van der Waals heterostructure via an external electric field. Physical Chemistry Chemical Physics, 2016, 18, 28466-28473.	1.3	37
22054	Atomic configuration and properties of austenitic steels at finite temperature: Effect of longitudinal spin fluctuations. Physical Review B, 2016, 94, .	1.1	41
22055	Molecular dynamics simulation of O₂ adsorption on Ag(110) from first principles electronic structure calculations. Physical Chemistry Chemical Physics, 2016, 18, 27366-27376.	1.3	14
22056	Assessing Hubbard-corrected AM05+U and PBEsol+U density functionals for strongly correlated oxides CeO₂ and Ce₂O₃. Physical Chemistry Chemical Physics, 2016, 18, 26816-26826.	1.3	25
22057	Improving visible light photocatalytic activity of NaNbO₃: a DFT based investigation. RSC Advances, 2016, 6, 90188-90196.	1.7	21
22058	First-principles insight into the photoelectronic properties of Ge-based perovskites. RSC Advances, 2016, 6, 86976-86981.	1.7	51

#	Article	IF	Citations
22059	Modulation of the band structures and optical properties of holey C₂N nanosheets by alloying with group IV and V elements. Journal of Materials Chemistry C, 2016, 4, 9294-9302.	2.7	24
22060	Stability of two-dimensional BN-Si structures. Physical Review B, 2016, 94, .	1.1	30
22061	Ferromagnetism-dependent polytypism: CrAs versus MnAs. Solid State Communications, 2016, 247, 98-103.	0.9	5
22062	Investigation of novel crystal structures of Biâ€“Sb binaries predicted using the minima hopping method. Physical Chemistry Chemical Physics, 2016, 18, 29771-29785.	1.3	37
22063	Mechanical properties of zigzag-shaped carbon nanotubes: the roles of the geometric parameters. RSC Advances, 2016, 6, 27999-28004.	1.7	0
22064	Origin of low thermal conductivity in SnSe. Physical Review B, 2016, 94, .	1.1	287
22065	Effects of the volume changes and elastic-strain energies on the phase transition in the Li-Sn battery. Journal of Power Sources, 2016, 330, 111-119.	4.0	24
22066	Many-Body Dispersion Correction Effects on Bulk and Surface Properties of Rutile and Anatase TiO₂. Journal of Physical Chemistry C, 2016, 120, 21552-21560.	1.5	11
22067	Enhanced hydrogen desorption properties of LiAlH₄ by doping lithium metatitanate. Physical Chemistry Chemical Physics, 2016, 18, 27623-27629.	1.3	16
22068	BiOX/BiOY (X, Y = F, Cl, Br, I) superlattices for visible light photocatalysis applications. RSC Advances, 2016, 6, 91508-91516.	1.7	41
22069	The optical spectrum of ternary alloy BBi_{1â^'x}As_x. Materials Research Express, 2016, 3, 065901.	0.8	1
22070	Electronic and magnetic properties in Mnâ€doped IIIAâ€nitride monolayers. Physica Status Solidi (B): Basic Research, 2016, 253, 2001-2008.	0.7	8
22071	The effect of water molecules on the thiol collector interaction on the galena (PbS) and sphalerite (ZnS) surfaces: A DFT study. Applied Surface Science, 2016, 389, 103-111.	3.1	77
22072	Research on optoelectronic properties of GaN nanowires with N vacancy. Computational and Theoretical Chemistry, 2016, 1092, 19-24.	1.1	5
22073	Diversification of MgO//Mg interfacial crystal orientations during oxidation: A density functional theory study. Journal of Alloys and Compounds, 2016, 688, 1233-1240.	2.8	10
22074	Ab-initio investigation of spin-dependent transport properties in Fe-doped armchair graphyne nanoribbons. Journal of Magnetism and Magnetic Materials, 2016, 420, 56-61.	1.0	11
22075	Experimental and theoretical investigations of the polar intermetallics SrPt3Al2 and Sr2Pd2Al. Journal of Solid State Chemistry, 2016, 242, 143-150.	1.4	17
22076	Effect of single vacancy on the structural, electronic structure and magnetic properties of monolayer graphyne by first-principles. Materials Chemistry and Physics, 2016, 182, 439-444.	2.0	18

#	Article	IF	Citations
22077	Interaction of Pyridine and Water with the Reconstructed Surfaces of GaP(111) and CdTe(111) Photoelectrodes: Implications for CO2 Reduction. Chemistry of Materials, 2016, 28, 5799-5810.	3.2	42
22078	First-principles analysis of the spectroscopic limited maximum efficiency of photovoltaic absorber layers for CuAu-like chalcogenides and silicon. Physical Chemistry Chemical Physics, 2016, 18, 20542-20549.	1.3	54
22079	Theoretical study of electronic and mechanical properties of Fe₂B. RSC Advances, 2016, 6, 73576-73580.	1.7	13
22080	Borophene as an extremely high capacity electrode material for Li-ion and Na-ion batteries. Nanoscale, 2016, 8, 15340-15347.	2.8	396
22081	Synthesis and Characterization of Nanostructured Magnesium Oxide: Insight from Solid-State Density Functional Theory Calculations. Journal of Inorganic and Organometallic Polymers and Materials, 2016, 26, 1413-1420.	1.9	21
22082	A comprehensive comparative DFT study on adsorption and reactions involved in vinyl acetate synthesis from acetoxylation of ethylene on pure Pd(100) and Pd-Au(100): Elucidating the role of Au. Applied Surface Science, 2016, 387, 1021-1028.	3.1	22
22083	Electronic and optical properties of bilayer blue phosphorus. Computational Materials Science, 2016, 124, 23-29.	1.4	51
22084	La interactions with C and N in bcc Fe from first principles. Journal of Alloys and Compounds, 2016, 688, 261-269.	2.8	15
22085	Two Silver Coordination Network Compounds with Colorful Photoluminescence. Inorganic Chemistry, 2016, 55, 7954-7961.	1.9	20
22086	In situ TEM study of deformation-induced crystalline-to-amorphous transition in silicon. NPG Asia Materials, 2016, 8, e291-e291.	3.8	60
22087	The impact of carbon and oxygen in alpha-titanium:ab initiostudy of solution enthalpies and grain boundary segregation. Journal of Physics Condensed Matter, 2016, 28, 385001.	0.7	12
22088	Possibility of realizing quantum spin Hall effect at room temperature in<mml:math xmlns:mml="http://www.w3.org/1998/Math/MathML"><mml:mrow><mml:mtext>stanene</mml:mtext><mml:mo>/</mml:mo><mml:mathvariant="normal">A</mml:mi><mml:msub><mml:mi mathvariant="normal">I</mml:mi><mml:mn>2</mml:mn></mml:msub><mml:msub><mml:mi mathvariant="normal">O</mml:mi><mml:mn>3</mml:mn></mml:msub><mml:mrow><mml:mo>(</mml:mo><mml:mn>0001</mml:mn> Physical Review B, 2016, 94, .	1.1	32
22089	Density functional calculations of a staggered FeSe monolayer on aSrTiO3(110) surface. Physical Review B, 2016, 94, .	1.1	4
22090	Prediction of physical properties of XO (X = Am, Cd, Mg, Zr) compounds using density functional theory. European Physical Journal Plus, 2016, 131, 1.	1.2	12
22091	First-principles study of the cubic CaHfO3 (001) surface. International Journal of Modern Physics B, 2016, 30, 1650168.	1.0	5
22092	Barriers of Electrochemical CO₂ Reduction on Transition Metals. Organic Process Research and Development, 2016, 20, 1424-1430.	1.3	135
22093	Surface directed reversible imidazole ligation to nickel(<scp>ii</scp>) octaethylporphyrin at the solution/solid interface: a single molecule level study. Physical Chemistry Chemical Physics, 2016, 18, 20819-20829.	1.3	23
22094	Two energetic complexes incorporating 3,5-dinitrobenzoic acid and azole ligands: microwave-assisted synthesis, favorable detonation properties, insensitivity and effects on the thermal decomposition of RDX. New Journal of Chemistry, 2016, 40, 7779-7786.	1.4	20

#	Article	IF	Citations
22095	Suppressing cation segregation on lanthanum-based perovskite oxides to enhance the stability of solid oxide fuel cell cathodes. RSC Advances, 2016, 6, 69782-69789.	1.7	41
22096	First-principles study on the electronic and magnetic properties of the Zn0.75Mo0.25M(M = S,Se,Te). Modern Physics Letters B, 2016, 30, 1650249.	1.0	5
22097	Synthesis, Crystal Structure and Comparative DFT Studies of a 1D Ni(II) Polymeric Complex of 2-Hydroxypyridine-N-oxide. Journal of Chemical Crystallography, 2016, 46, 269-279.	0.5	1
22098	Thermal expansion and thermal diffusivity properties of Co-Si solid solutions and intermetallic compounds. Journal of Chemical Thermodynamics, 2016, 102, 1-8.	1.0	4
22099	Stabilizing Active Edge Sites in Semicrystalline Molybdenum Sulfide by Anchorage on Nitrogenâ€Doped Carbon Nanotubes for Hydrogen Evolution Reaction. Advanced Functional Materials, 2016, 26, 6766-6776.	7.8	110
22100	Structural, Elastic, and Electronic Properties of Newly Discovered Li2PtSi3 Superconductor: Effect of Transition Metals. Journal of Superconductivity and Novel Magnetism, 2016, 29, 2503-2508.	0.8	23
22101	Passivation of Nickel Vacancy Defects in Nickel Oxide Solar Cells by Targeted Atomic Deposition of Boron. Journal of Physical Chemistry C, 2016, 120, 16568-16576.	1.5	44
22102	Proximity-Induced Spin Polarization of Graphene in Contact with Half-Metallic Manganite. ACS Nano, 2016, 10, 7532-7541.	7.3	44
22103	Stability and geometry of silica nano-ribbons (SNRs): a first-principles study. Physical Chemistry Chemical Physics, 2016, 18, 21825-21832.	1.3	3
22104	A microscopic level insight into Pt doped TiZn (001) surface for hydrogen energy storage usage. RSC Advances, 2016, 6, 73566-73575.	1.7	1
22105	Modelling of an ultra-thin silicatene/silicon-carbide hybrid film. Journal of Physics Condensed Matter, 2016, 28, 364005.	0.7	3
22106	Competition between ferromagnetism and antiferromagnetism in the rutile<mml:math xmlns:mml="http://www.w3.org/1998/Math/MathML"><mml:mrow><mml:mi mathvariant="normal">C</mml:mi><mml:msub><mml:mi mathvariant="normal">r</mml:mi><mml:mrow><mml:mn>1</mml:mn><mml:mo>â^’</mml:mo><mml:mi>x</mml:mi></mml:mrow></mml:mrow></mml:msub><mml:mi mathvariant="normal">V</mml:mi><mml:mi>x</mml:mi></mml:msub><mml:mi	1.1	18
22107	Magnetically driven anisotropic structural changes in the atomic laminate<mml:math xmlns:mml="http://www.w3.org/1998/Math/MathML"><mml:mrow><mml:mi mathvariant="normal">M</mml:mi><mml:msub><mml:mi mathvariant="normal">n</mml:mi><mml:mn>2</mml:mn></mml:msub><mml:mi>GaC</mml:mi></mml:mrow></mml:math>. Physical Review B, 2016, 93, .	1.1	44
22108	Electronic, structural, and magnetic properties of<mml:math xmlns:mml="http://www.w3.org/1998/Math/MathML"><mml:msub><mml:mi>LaMnO</mml:mi><mml:mn>3</mml:mn></mml:msub> Giant biquadratic interaction-induced magnetic anisotropy in the iron-based superconductor<mml:math xmlns:mml="http://www.w3.org/1998/Math/MathML"><mml:mrow><mml:msub><mml:mi>A</mml:mi><mml:mi>x</mml:mi></mml:msub>	1.1	35
22109	<mml:msub><mml:mi mathvariant="normal">F</mml:mi><mml:mi mathvariant="normal">e</mml:mi><mml:mrow><mml:mn>2</mml:mn><mml:mo>â^’</mml:mo><mml:mi>y</mml:mi></mml:mrow></mml:msub><mml:msub><mml:mi mathvariant="normal">S</mml:mi><mml:mi mathvariant="normal">e</mml:mi><mml:mn>2	1.1	13
22110	42214 layered Fe-based superconductors: Ab initiostudy of their structural, magnetic, and electronic properties. Physical Review B, 2016, 93, .	1.1	3
22111	<mml:math xmlns:mml="http://www.w3.org/1998/Math/MathML"><mml:mrow><mml:mtext>Hubbard-</mml:mtext><mml:mi>U</mml:mi> Hamiltonians for non-self-consistent random-phase approximation total-energy calculations: A study of ZnS,<mml:math xmlns:mml="http://www.w3.org/1998/Math/MathML"><mml:msub><mml:mtext>TiO</mml:mtext><mml:mn>2</mml:mn>	1.1	19
22112	Charge transport properties of bulk<mml:math xmlns:mml="http://www.w3.org/1998/Math/MathML"><mml:mrow><mml:msub><mml:mi>Ta</mml:mi><mml:mn>3</mml:mn><mml:mi mathvariant="normal">N</mml:mi><mml:mn>5</mml:mn></mml:msub></mml:mrow></mml:math> from first principles. Physical Review B, 2016, 93, .	1.1	32

#	Article	IF	Citations
22113	Spilling of electronic states in Pb quantum wells. Physical Review B, 2016, 93, .	1.1	7
22114	Two-dimensional transition metal dichalcogenides with a hexagonal lattice: Room-temperature quantum spin Hall insulators. Physical Review B, 2016, 93, .	1.1	56
22115	Quantum spin Hall effect in<mml:math xmlns:mml="http://www.w3.org/1998/Math/MathML"><mml:mi>Î±</mml:mi><mml:mo>â^'</mml:mo><mml:mi mathvariant="normal">Sn</mml:mi><mml:mo>/</mml:mo><mml:mtext>CdTe</mml:mtext><mml:mo>(</mml:mo><mml:mn>001</mml:mn> structures. Physical Review B, 2016, 93, .	1.1	8
22116	Self-ordered nanoporous lattice formed by chlorine atoms on Au(111). Physical Review B, 2016, 93, .	1.1	12
22117	High-pressure structural study of<mml:math xmlns:mml="http://www.w3.org/1998/Math/MathML"><mml:msub><mml:mi>MnF</mml:mi><mml:mn>2</mml:mn></mml:msub></mm Physical Review B, 2016, 93, .	1.1	26
22118	Strain-induced nonsymmorphic symmetry breaking and removal of Dirac semimetallic nodal line in an orthoperovskite iridate. Physical Review B, 2016, 93, .	1.1	67
22119	Predicting density functional theory total energies and enthalpies of formation of metal-nonmetal compounds by linear regression. Physical Review B, 2016, 93, .	1.1	63
22120	Quasiparticle band gap of organic-inorganic hybrid perovskites: Crystal structure, spin-orbit coupling, and self-energy effects. Physical Review B, 2016, 93, .	1.1	67
22121	Surface phonon excitation on clean metal surfaces in scanning tunneling microscopy. Physical Review B, 2016, 93, .	1.1	13
22122	Effects of orbital composition in a pair of spin-orbit-split surface bands at Tl/Ge(111). Physical Review B, 2016, 93, .	1.1	10
22123	Highly anisotropic thermal conductivity of arsenene: Anab initiostudy. Physical Review B, 2016, 93, .	1.1	114
22124	GaN: From three- to two-dimensional single-layer crystal and its multilayer van der Waals solids. Physical Review B, 2016, 93, .	1.1	139
22125	Depth dependence of vacancy formation energy at (100), (110), and (111) Al surfaces: A first-principles study. Physical Review B, 2016, 93, .	1.1	24
22126	Calculations of planar defect energies in substitutional alloys using the special-quasirandom-structure approach. Physical Review B, 2016, 93, .	1.1	12
22127	High-pressure phases of<mml:math xmlns:mml="http://www.w3.org/1998/Math/MathML"><mml:mrow><mml:msub><mml:mi>Mg</mml:mi><mml:mn>2</mml:mn></mml:msub><mml:mn></mml: first principles. Physical Review B, 2016, 93, .	1.1	26
22128	Uniaxial pressure-induced half-metallic ferromagnetic phase transition in<mml:math xmlns:mml="http://www.w3.org/1998/Math/MathML"><mml:msub><mml:mi mathvariant="normal">LaMnO</mml:mi><mml:mn>3</mml:mn></mml:msub></mml:math>. Physical Review B, 2016, 93, .	1.1	19
22129	Prediction of a stable half-metal ferromagnetic BaCl solid. Physical Review B, 2016, 93, .	1.1	6
22130	Topological characters in<mml:math xmlns:mml="http://www.w3.org/1998/Math/MathML"><mml:mi mathvariant="normal">Fe</mml:mi><mml:mo>(</mml:mo><mml:mrow><mml:msub><mml:mi>Te</mml:mi><mml:mrow><mml:mn> films. Physical Review B, 2016, 93, .	1.1	125

#	Article	IF	Citations
22131	Quasiparticle bands and spectra of<mml:math xmlns:mml="http://www.w3.org/1998/Math/MathML"><mml:mrow><mml:msub><mml:mi>Ga</mml:mi><mml:mn>2</mml:mn></mml:msub><mml:msub><mml:mi mathvariant="normal">O</mml:mi><mml:mn>3</mml:mn></mml:msub></mml:mrow></mml:math>polymorphs. Physical Review B, 2016, 93, .	1.1	165
22132	Structural and excited-state properties of oligoacene crystals from first principles. Physical Review B, 2016, 93, .	1.1	89
22133	Cation diffusion and hybridization effects at the Mn-GaSe(0001) reacted interface:Ab initiocalculations and soft x-ray electron spectroscopy studies. Physical Review B, 2016, 93, .	1.1	3
22134	Stability investigations on the non-vdW-exfoliated surfaces of the topological insulatorBi2Te3: A first-principles study. Physical Review B, 2016, 93, .	1.1	6
22135	Thermodynamic stability of the<mml:math xmlns:mml="http://www.w3.org/1998/Math/MathML"><mml:msub><mml:mi>UO</mml:mi><mml:mn>2</mml:mn></mml:msub></mml:math>Interplay between over-stoichiometry and polarity compensation. Physical Review B, 2016, 93, .	1.1	54
22136	Atomic configurations of Au-induced nanowires on Ge(001) stabilized by higher Au coverages. Physical Review B, 2016, 93, .	1.1	8
22137	Atomic size effects studied by transport in single silicide nanowires. Physical Review B, 2016, 93, .	1.1	14
22138	Optical absorption and conductivity in quasi-two-dimensional crystals from first principles: Application to graphene. Physical Review B, 2016, 93, .	1.1	53
22139	Reliability of Raman measurements of thermal conductivity of single-layer graphene due to selective electron-phonon coupling: A first-principles study. Physical Review B, 2016, 93, .	1.1	101
22140	Hydrogen in vanadium: Site occupancy and isotope effects. Physical Review B, 2016, 93, .	1.1	12
22141	Ab initiostudy of the one-dimensional H-bonded ferroelectricCsH2PO4. Physical Review B, 2016, 93, .	1.1	17
22142	Theoretical study of negative optical mode splitting inLaAlO3. Physical Review B, 2016, 93, .	1.1	4
22143	Lattice dynamics and thermal expansion behavior in the metal cyanides<mml:math xmlns:mml="http://www.w3.org/1998/Math/MathML"><mml:mrow><mml:mi>M</mml:mi><mml:mi>CN</mml:mi></mml:mrow></mml:	1.1	26
22144	Possible half-metallic antiferromagnetism in an iridium double-perovskite material. Physical Review B, 2016, 93, .	1.1	27
22145	Magnetism and deformation of epitaxial Pd and Rh thin films. Physical Review B, 2016, 93, .	1.1	5
22146	Transient optical properties of semiconductors under femtosecond x-ray irradiation. Physical Review B, 2016, 93, .	1.1	14
22147	Ideal compressive strength of fcc Co, Ni, and Ni-rich alloys along the<mml:math xmlns:mml="http://www.w3.org/1998/Math/MathML"><mml:mrow><mml:mo>âŒ©</mml:mo><mml:mn>001</mml:mn><mml:mo>â	1.1	12
22148	Anharmonicity effects in the frictionlike mode of graphite. Physical Review B, 2016, 93, .	1.1	1

#	Article	IF	Citations
22149	Interatomic force constants including the DFT-D dispersion contribution. Physical Review B, 2016, 93, .	1.1	50
22150	Efficient generation of generalized Monkhorst-Pack grids through the use of informatics. Physical Review B, 2016, 93, .	1.1	149
22151	Efficient and accurate approach to modeling the microstructure and defect properties of<mml:math xmlns:mml="http://www.w3.org/1998/Math/MathML"><mml:msub><mml:mtext>LaCoO</mml:mtext><mml:mn>3</mml:mn></mml:msub></mml:math> Physical Review B, 2016, 93, .	1.1	16
22152	Electronic states in an atomistic carbon quantum dot patterned in graphene. Physical Review B, 2016, 93, .	1.1	8
22153	Self-assembly of nanoscale lateral segregation profiles. Physical Review B, 2016, 93, .	1.1	7
22154	Conduction mechanism of nitronyl-nitroxide molecular magnetic compounds. Physical Review B, 2016, 93, .	1.1	5
22155	Density functional theory study of the shallow boron impurity in<mml:math xmlns:mml="http://www.w3.org/1998/Math/MathML"><mml:mrow><mml:mn>3</mml:mn><mml:mi>C</mml:mi></mml:mrow></mml:math> and comparison with experimental data. Physical Review B, 2016, 93, .	1.1	10
22156	Multiferroic nature of intrinsic point defects in<mml:math xmlns:mml="http://www.w3.org/1998/Math/MathML"><mml:msub><mml:mi>BiFeO</mml:mi><mml:mn>3</mml:mn></mml:msub></mml:math> A hybrid Hartree-Fock density functional study. Physical Review B, 2016, 93, .	1.1	39
22157	First-principles study of atomic and electronic structures of<mml:math xmlns:mml="http://www.w3.org/1998/Math/MathML"><mml:msup><mml:mn>60</mml:mn><mml:mo>â˜</mml:mo></mml:msup></mml:math> and<mml:math xmlns:mml="http://www.w3.org/1998/Math/MathML"><mml:msup><mml:mn>30</mml:mn><mml:mo>â˜</mml:mo></mml:msup></mml:math> glide dislocations in CdTe. Physical Review B, 2016, 93, .	1.1	20
22158	Magnetic ground state and spin fluctuations in MnGe chiral magnet as studied by muon spin rotation. Physical Review B, 2016, 93, .	1.1	26
22159	Rare-earth silicide thin films on the Si(111) surface. Physical Review B, 2016, 93, .	1.1	28
22160	Structural and electronic properties of Li-intercalated graphene on SiC(0001). Physical Review B, 2016, 93, .	1.1	44
22161	Structure and stability of ultrathin Fe films on W(110). Physical Review B, 2016, 93, .	1.1	6
22162	Isolated energy level in the band gap of<mml:math xmlns:mml="http://www.w3.org/1998/Math/MathML"><mml:mrow><mml:msub><mml:mi>Yb</mml:mi><mml:mn>2</mml:mn></mml:msub></mml:math> mathvariant="normal">O</mml:mi><mml:mn>7</mml:mn></mml:msub></mml:mrow></mml:math>identified by electron energy-loss spectroscopy. Physical Review B, 2016, 93, .	1.1	7
22163	Nearly free electron states in MXenes. Physical Review B, 2016, 93, .	1.1	185
22164	Configuration dependence of band-gap narrowing and localization in dilute<mml:math xmlns:mml="http://www.w3.org/1998/Math/MathML"><mml:mrow><mml:msub><mml:mi>GaAs</mml:mi><mml:mrow> Physical Review B, 2016, 93, .	1.1	31
22165	More realistic band gaps from meta-generalized gradient approximations: Only in a generalized Kohn-Sham scheme. Physical Review B, 2016, 93, .	1.1	182
22166	Self-passivation rule and structure of CdTe Î£3 (112) grain boundaries. Physical Review B, 2016, 93, .	1.1	21

#	Article	IF	Citations
22167	Interpretation of unexpected behavior of infrared absorption spectra of<mml:math xmlns:mml="http://www.w3.org/1998/Math/MathML"><mml:msub><mml:mi>ScF</mml:mi><mml:mn>3</mml:mn></mml:msub></mml the quasiharmonic approximation. Physical Review B, 2016, 93, .	1.1	57
22168	Spin-phonon coupling and high-pressure phase transitions of<mml:math xmlns:mml="http://www.w3.org/1998/Math/MathML"><mml:mrow><mml:mi>R</mml:mi><mml:mi>Mn</mml:mi><mml:msub><mml mathvariant="normal">O</mml:mi><mml:mn>3</mml:mn></mml:msub></mml:mrow></mml:math>(<mml:math)	1.1	9
22169	First-principles calculation and experimental investigation of lattice dynamics in the rare-earth pyrochlores<mml:math xmlns:mml="http://www.w3.org/1998/Math/MathML"><mml:mrow><mml:msub><mml:mi>R</mml:mi><mml:mn>2</mml:mn></mml:m mathvariant="normal">O</mml:mi><mml:mn>7</mml:mn></mml:msub></mml:mrow></mml:math><mml:math		

#	Article	IF	Citations
22185	Multiferroic Two-Dimensional Materials. Physical Review Letters, 2016, 116, 206803.	2.9	187
22186	Unveiling the Room-Temperature Magnetoelectricity of Troilite FeS. Physical Review Letters, 2016, 116, 227601.	2.9	31
22187	Comment on â€œLine of Dirac Nodes in Hyperhoneycomb Latticesâ€• Physical Review Letters, 2016, 116, 249701.	2.9	3
22188	Anisotropy, phonon modes, and free charge carrier parameters in monoclinic<mml:math xmlns:mml="http://www.w3.org/1998/Math/MathML"><mml:mi>Î²</mml:mi></mml:math>-gallium oxide single crystals. Physical Review B, 2016, 93, .	1.1	147
22189	Ab initiocalculation of thermodynamic potentials and entropies for superionic water. Physical Review E, 2016, 93, 022140.	0.8	47
22190	Tuning the electronic structures and magnetism of two-dimensional porous C₂N via transition metal embedding. Physical Chemistry Chemical Physics, 2016, 18, 22678-22686.	1.3	54
22191	Phonon optics, thermal expansion tensor, thermodynamic and chemical bonding properties of Al₄SiC₄ and Al₄Si₂C₅: a first-principles study. RSC Advances, 2016, 6, 43191-43204.	1.7	11
22192	Lattice dynamical and thermodynamic properties of FeNi3, FeNi and Fe3Ni invar materials. Computational Materials Science, 2016, 123, 287-295.	1.4	35
22193	Combined EXAFS, XRD, DRIFTS, and DFT Study of Nano Copper-Based Catalysts for CO₂ Hydrogenation. ACS Catalysis, 2016, 6, 5823-5833.	5.5	51
22194	Charge Mediated Reversible Metalâ€“Insulator Transition in Monolayer MoTe₂ and W_xMo_{1â€“x}Te₂ Alloy. ACS Nano, 2016, 10, 7370-7375.	7.3	133
22195	First Principles Simulations of Cyclic Voltammograms on Stepped Pt(553) and Pt(533) Electrode Surfaces. ChemElectroChem, 2016, 3, 1609-1617.	1.7	47
22196	Transition metal doped arsenene: A first-principles study. Applied Surface Science, 2016, 389, 594-600.	3.1	102
22197	The half-metallic ferromagnetic characters of (001)-oriented thin films of the double perovskite Pb2FeMoO6. Thin Solid Films, 2016, 615, 318-323.	0.8	4
22198	Impact of surface arrangement and composition on ethylene adsorption over Pdâ€“Ag surface alloys: a computational study. RSC Advances, 2016, 6, 70932-70942.	1.7	4
22199	Oxidation of the titanium(0001) surface: diffusion processes of oxygen from DFT. RSC Advances, 2016, 6, 71311-71318.	1.7	21
22200	Single and bilayer bismuthene: Stability at high temperature and mechanical and electronic properties. Physical Review B, 2016, 94, .	1.1	295
22201	Dielectrics in a time-dependent electric field: A real-time approach based on density-polarization functional theory. Physical Review B, 2016, 94, .	1.1	20
22202	Excitons and optical spectra of phosphorene nanoribbons. Physical Review B, 2016, 94, .	1.1	37

#	Article	IF	Citations
22203	Theoretical Investigation of Mechanical, Electronic, and Thermal Properties of Fe2TiSi and Fe2TiSn Under Pressure. Journal of Electronic Materials, 2016, 45, 5104-5111.	1.0	8
22204	Graphdiyne-supported single-atom Sc and Ti catalysts for high-efficient CO oxidation. Carbon, 2016, 108, 343-350.	5.4	114
22205	A DFT study of thermal effects on the elastic properties of ZrO2 nanosheet. Journal of Alloys and Compounds, 2016, 687, 790-796.	2.8	7
22206	A study on the structural, electronic and optical properties of the Î±-AlF3 compound. Materials Research Bulletin, 2016, 83, 615-622.	2.7	5
22207	TiO2 anatase's bulk and (001) surface, structural and electronic properties: A DFT study on the importance of Hubbard and van der Waals contributions. Surface Science, 2016, 653, 187-196.	0.8	39
22208	Two-Dimensional Phosphorus Carbide: Competition between sp² and sp³ Bonding. Nano Letters, 2016, 16, 3247-3252.	4.5	137
22209	Pressure induced superconductivity and electronic structure properties of scandium hydrides using first principles calculations. RSC Advances, 2016, 6, 81534-81541.	1.7	17
22210	The Electronic, Magnetic, and Vibrational Properties of Ce3Co29Ge4B10. Lecture Notes in Electrical Engineering, 2016, , 1079-1087.	0.3	0
22211	On possibility of superconductivity in SnSb: A first principle study. Physica C: Superconductivity and Its Applications, 2016, 528, 56-59.	0.6	9
22212	How Does Nanoporous Gold Dissociate Molecular Oxygen?. Journal of Physical Chemistry C, 2016, 120, 16636-16640.	1.5	46
22213	Thermal Transition from a Disordered, 2D Network to a Regular, 1D, Fe(II)â€“DCNQI Coordination Network. Journal of Physical Chemistry C, 2016, 120, 16712-16721.	1.5	4
22214	Mechanism of Oxygen Reduction Reaction on Pt(111) in Alkaline Solution: Importance of Chemisorbed Water on Surface. Journal of Physical Chemistry C, 2016, 120, 15288-15298.	1.5	120
22215	The thermal properties and thermoelectric performance ofÎ³-graphyne nanoribbons. Journal Physics D: Applied Physics, 2016, 49, 145102.	1.3	19
22216	Thermal stability of mulliteRMn₂O₅(Râ€‰â€‰=â€‰â€‰Bi, Y, Pr, Sm or Gd): combined density functional theory and experimental study. Journal of Physics Condensed Matter, 2016, 28, 125602.	0.7	17
22217	Alternate to Molybdenum Disulfide: A 2D, Fewâ€Layer Transitionâ€Metal Thiophosphate and Its Hydrogen Evolution Reaction Activity over a Wide pH Range. ChemElectroChem, 2016, 3, 1392-1399.	1.7	44
22218	A Comparative Study of Structural Stability and Mechanical and Optical Properties of Fluorapatite (Ca5(PO4)3F) and Lithium Disilicate (Li2Si2O5) Components Forming Dental Glassâ€“Ceramics: First Principles Study. Journal of Electronic Materials, 2016, 45, 5082-5095.	1.0	32
22219	Effect of alloying on elastic properties of ternary Ni-Al-Ti system: Experimental validation. Journal of Alloys and Compounds, 2016, 688, 534-541.	2.8	7
22220	First-principles study of the stability and diffusion properties of hydrogen in zirconium carbide. Journal of Nuclear Materials, 2016, 479, 130-136.	1.3	14

#	Article	IF	Citations
22221	Nonmagnetic 2 p -block elements (B, C, N, and O)-doped AgCl for potential halide spintronic applications: A first-principles perspective. Physics Letters, Section A: General, Atomic and Solid State Physics, 2016, 380, 2968-2973.	0.9	5
22222	Crystal Structures, Stabilities, Electronic Properties, and Hardness of MoB₂: First-Principles Calculations. Inorganic Chemistry, 2016, 55, 7033-7040.	1.9	39
22223	Density Functional Theory Study for Ni Diffusion on Ni(111) Surface under Solid Oxide Fuel Cell Operating Condition. Journal of Physical Chemistry C, 2016, 120, 16641-16648.	1.5	5
22224	Towards an accurate specific reaction parameter density functional for water dissociation on Ni(111): RPBE versus PW91. Physical Chemistry Chemical Physics, 2016, 18, 21817-21824.	1.3	25
22225	Crystal structure and magnetic properties of new Fe₃Co₃X₂(Xâ€‰â€‰=â€‰â€‰Ti, Nb) intermetallic compounds. Journal Physics D: Applied Physics, 2016, 49, 175002.	1.3	11
22226	Analysis of the electronic structure of crystals through band structure unfolding. Physics of the Solid State, 2016, 58, 462-468.	0.2	2
22227	Thermo-elastic and optical properties of molybdenum nitride. Canadian Journal of Physics, 2016, 94, 902-912.	0.4	11
22228	Tuning chemical bonding of MnO2 through transition-metal doping for enhanced CO oxidation. Journal of Catalysis, 2016, 341, 82-90.	3.1	132
22229	Atomic diffusion mediated by vacancy defects in pure and transition element (TM)-doped (TM = Ti, Y, Zr) Tj ETQq0 0 0 rgBT /Overlock 10	3.3	16
22230	Structural, electronic and magnetic properties of the (Co, Ni) codoped ZnS: A first-principles study. Physics Letters, Section A: General, Atomic and Solid State Physics, 2016, 380, 2796-2802.	0.9	12
22231	Aliovalent Doping in Colloidal Quantum Dots and Its Manifestation on Their Optical Properties: Surface Attachment versus Structural Incorporation. Chemistry of Materials, 2016, 28, 5384-5393.	3.2	15
22232	Organic Dye Graphene Hybrid Structures with Spectral Color Selectivity. Advanced Functional Materials, 2016, 26, 6593-6600.	7.8	31
22233	Highâ€Performance Ru₁/CeO₂ Singleâ€Atom Catalyst for CO Oxidation: A Computational Exploration. ChemPhysChem, 2016, 17, 3170-3175.	1.0	47
22234	Water-driven stabilization of diphenylalanine nanotube structures. Theoretical Chemistry Accounts, 2016, 135, 1.	0.5	40
22235	Physical properties of the recently discovered Zr2(Al1â^'x Bi x)C MAX phases. Journal of Materials Science: Materials in Electronics, 2016, 27, 11925-11933.	1.1	71
22236	Point defects in hexagonal germanium carbide monolayer: A first-principles calculation. Applied Surface Science, 2016, 389, 1-6.	3.1	62
22237	A first-principles investigation on the luminescence emissions of BaZrO3 obtained by microwave-assisted hydrothermal method. Journal of Luminescence, 2016, 180, 73-80.	1.5	3
22238	Stable Calcium Nitrides at Ambient and High Pressures. Inorganic Chemistry, 2016, 55, 7550-7555.	1.9	88

#	Article	IF	Citations
22239	Benchmarking Density Functional Theory Based Methods To Model NiOOH Material Properties: Hubbard and van der Waals Corrections vs Hybrid Functionals. Journal of Chemical Theory and Computation, 2016, 12, 3807-3812.	2.3	47
22240	DFT Calculations with van der Waals Interactions of Hydrated Calcium Carbonate Crystals CaCO₃Â·(H₂O, 6H₂O): Structural, Electronic, Optical, and Vibrational Properties. Journal of Physical Chemistry A, 2016, 120, 5752-5765.	1.1	31
22241	Interface and Doping Effect on the Electrochemical Property of Graphene/LiFePO₄. Journal of Physical Chemistry C, 2016, 120, 17165-17174.	1.5	21
22242	Surface Proton Hopping and Fast-Kinetics Pathway of Water Oxidation on Co₃O₄ (001) Surface. ACS Catalysis, 2016, 6, 5610-5617.	5.5	83
22243	Structure and electronic properties of bilayer graphene functionalized with half-sandwiched transition metal-cyclopentadienyl complexes. Physical Chemistry Chemical Physics, 2016, 18, 22390-22398.	1.3	5
22244	AbÂInitioStudy of Water Adsorption and Reactivity on the (211) Surface of Anatase<mml:math xmlns:mml="http://www.w3.org/1998/Math/MathML" display="inline"><mml:mrow><mml:msub><mml:mrow><mml:mi>TiO</mml:mi></mml:mrow><mml:mrow><mml:mn>2</mml:mn></mml:mrow> Physical Review Applied, 2016, 5, .	1.5	12
22245	Elastic and Thermodynamic Properties of Complex Mg-Al Intermetallic Compounds via Orbital-Free Density Functional Theory. Physical Review Applied, 2016, 5, .	1.5	30
22246	Density-functional theory with screened van der Waals interactions applied to atomic and molecular adsorbates on close-packed and non-close-packed surfaces. Physical Review B, 2016, 93, .	1.1	90
22247	Prediction of two-dimensional topological insulator by forming a surface alloy on Au/Si(111) substrate. Physical Review B, 2016, 93, .	1.1	27
22248	Dielectric screening and plasmon resonances in bilayer graphene. Physical Review B, 2016, 93, .	1.1	27
22249	Classical and quantum aspects of spin interaction in<mml:math xmlns:mml="http://www.w3.org/1998/Math/MathML"><mml:mrow><mml:mn>3</mml:mn><mml:mi>d</mml:mi></mml:mrow></mml:m on a<mml:math xmlns:mml="http://www.w3.org/1998/Math/MathML"><mml:mrow><mml:mi mathvariant="normal">C</mml:mi><mml:msub><mml:mi mathvariant="normal">u</mml:mi><mml:mn>3</mml:mn></mml:msub><mml:mi mathvariant="normal">N</mml:mi></mml:mrow></mml:math>-Cu(110) molecular network. Physical Rev	1.1	11
22250	Valley physics in tin (II) sulfide. Physical Review B, 2016, 93, .	1.1	101
22251	Effect of thermal lattice expansion on the stacking fault energies of fcc Fe and<mml:math xmlns:mml="http://www.w3.org/1998/Math/MathML"><mml:mrow><mml:msub><mml:mi>Fe</mml:mi><mml:mn>1</mml:mn> Physical Review B, 2016, 93, .	1.1	20
22252	Statistical physics of multicomponent alloys using KKR-CPA. Physical Review B, 2016, 93, .	1.1	28
22253	Theoretical investigation of superconductivity in<mml:math xmlns:mml="http://www.w3.org/1998/Math/MathML"><mml:mrow><mml:msub><mml:mi>SrPd</mml:mi><mml:mn>2</mml:mn> <mml:math xmlns:mml="http://www.w3.org/1998/Math/MathML"><mml:mrow><mml:msub><mml:mi>SrPd</mml:mi><mml:mn>2</mml:mn> and<mml:math xmlns:mml="http://www.w3.org/1998. Physical Review B, 2016, 93, .	1.1	10
22254	Layered structures of organic/inorganic hybrid halide perovskites. Physical Review B, 2016, 93, .	1.1	31
22255	Adsorption of metal-phthalocyanine molecules onto the Si(111) surface passivated by<mml:math xmlns:mml="http://www.w3.org/1998/Math/MathML"><mml:mi>Î´</mml:mi></mml:math>doping:Ab initiocalculations. Physical Review B, 2016, 93, .	1.1	17
22256	Lattice dynamics and a high-field structural phase transition in the nickel orthoborate <mml:math xmlns:mml="http://www.w3.org/1998/Math/MathML"><mml:mrow><mml:mi mathvariant="normal">N</mml:mi><mml:msub><mml:mi mathvariant="normal">i</mml:mi><mml:mn>3</mml:mn></mml:msub><mml:msub><mml:mrow><mml:mo>(</mml:mo><mml:mrow>	1.1	14

#	Article	IF	Citations
22257	Anomalous magnetotransport behavior in Fe-doped MnNiGe alloys. Physical Review B, 2016, 93, .	1.1	24
22258	Structureâ€“Curie temperature relationships in<mml:math xmlns:mml="http://www.w3.org/1998/Math/MathML"><mml:msub><mml:mi>BaTiO</mml:mi><mml:mn>3</mml:mn></mml:msub><m ferroelectric perovskites: Anomalous behavior of<mml:math xmlns:mml="http://www.w3.org/1998/Math/MathML"><mml:mo>(</mml:mo><mml:mi>Ba</mml:mi><mml:mo>,</mml:mo><mml:mi>C DFT, statistical inference, and experiments. Physical Review B, 2016, 93, .	1.1	39
22259	General atomistic approach for modeling metal-semiconductor interfaces using density functional theory and nonequilibrium Green's function. Physical Review B, 2016, 93, .	1.1	137
22260	Electron and chemical reservoir corrections for point-defect formation energies. Physical Review B, 2016, 93, .	1.1	50
22261	Origin of ferroelectric polarization in tetragonal tungsten-bronze-type oxides. Physical Review B, 2016, 93, .	1.1	44
22262	Pressure-dependent optical investigations of<mml:math xmlns:mml="http://www.w3.org/1998/Math/MathML"><mml:mi>Î±</mml:mi><mml:mtext>â^'</mml:mtext><mml:mo>(</mml:mo><m /><mml:mn>2</mml:mn></mml:msub><mml:msub><mml:mi mathvariant="normal">I</mml:mi><mml:mn>3</mml:mn></mml:msub></mml:mrow></mml:math>: Tuning charge order and narrow gap towards a Dirac semimetal. Physical Review B, 2016, 93, .	1.1	42
22263	Different effects of electronic excitation on metals and semiconductors. Physical Review B, 2016, 93, .	1.1	16
22264	Phonons in nonlocal van der Waals density functional theory. Physical Review B, 2016, 93, .	1.1	17
22265	Two-dimensional topological insulators in group-11 chalcogenide compounds:<mml:math xmlns:mml="http://www.w3.org/1998/Math/MathML"><mml:mrow><mml:msub><mml:mi>M</mml:mi><mml:mn>2</mml:mn></mml:m width="0.28em" /><mml:mrow><mml:mo>(</mml:mo><mml:mrow><mml:mi>M</mml:mi><mml:mo>=</mml:mo><mml:mi>Cu</mml:mi><mml:mi><mml:mo>,</	1.1	34
22266	Electronic structure of interstitial hydrogen in lutetium oxide from<mml:math xmlns:mml="http://www.w3.org/1998/Math/MathML"><mml:mtext>DFT</mml:mtext><mml:mo>+</mml:mo><mml:mi>U</mml:mi></ and comparison study with<mml:math xmlns:mml="http://www.w3.org/1998/Math/MathML"><mml:mrow><mml:mi>Î¼</mml:mi><mml:mi>SR</mml:mi></mml:mrow></ Physical Review B, 2016, 94, .	1.1	21
22267	High-pressure polymorphism of<mml:math xmlns:mml="http://www.w3.org/1998/Math/MathML"><mml:mrow><mml:mi>Pb</mml:mi><mml:msub><mml:mi mathvariant="normal">F</mml:mi><mml:mn>2</mml:mn></mml:msub></mml:mrow></mml:math>to 75 GPa. Physical Review B, 2016, 94, .	1.1	9
22268	Direct evidence of metallic bands in a monolayer boron sheet. Physical Review B, 2016, 94, .	1.1	152
22269	Role of Tensorial Electronic Friction in Energy Transfer at Metal Surfaces. Physical Review Letters, 2016, 116, 217601.	2.9	85
22270	Correct Implementation of Polarization Constants in Wurtzite Materials and Impact on III-Nitrides. Physical Review X, 2016, 6, .	2.8	81
22271	Thermodynamic properties of ZnTe in zinc-blende and wurtzite phases. International Journal of Modern Physics B, 2016, 30, 1650147.	1.0	7
22272	Homologous Compounds ZnnIn2O3+n (n = 4, 5, and 7) Containing Laminated Functional Groups as Efficient Photocatalysts for Hydrogen Production. ACS Applied Materials & Interfaces, 2016, 8, 28700-28708.	4.0	24
22273	Structure and ferromagnetic instability of the oxygen-deficient<mml:math xmlns:mml="http://www.w3.org/1998/Math/MathML"><mml:msub><mml:mi>SrTiO</mml:mi><mml:mn>3</mml:mn></mml:msub></m Physical Review B, 2016, 94, .	1.1	5
22274	Effect of edge modification on the zigzag BC2N nanoribbons. Chemical Physics Letters, 2016, 658, 234-239.	1.2	6

#	Article	IF	Citations
22275	Edge preference and band gap characters of MoS2 and WS2 nanoribbons. Surface Science, 2016, 653, 107-112.	0.8	51
22276	Highly doped and exposed Cu(<scp>i</scp>)â€“N active sites within graphene towards efficient oxygen reduction for zincâ€“air batteries. Energy and Environmental Science, 2016, 9, 3736-3745.	15.6	374
22277	Natural Abundance ¹⁵N and ¹³C Solidâ€State NMR Chemical Shifts: High Sensitivity Probes of the Halogen Bond Geometry. Chemistry - A European Journal, 2016, 22, 16819-16828.	1.7	37
22278	Zintl Phases K_{4â€“x}Na_xSi₄ (1 â‰¤ x â‰¤ 2.2) and K₇NaSi₈: Synthesis, Crystal Structures, and Solidâ€State NMR Spectroscopic Investigations. European Journal of Inorganic Chemistry, 2016, 2016, 4674-4682.	1.0	8
22279	Optoelectronic properties of Mg doping GaN nanowires. Optical and Quantum Electronics, 2016, 48, 1.	1.5	5
22280	Optical Identification of Topological Defect Types in Monolayer Arsenene by First-Principles Calculation. Journal of Physical Chemistry C, 2016, 120, 24917-24924.	1.5	24
22281	Gold-supported cerium-doped NiOx catalysts for water oxidation. Nature Energy, 2016, 1, .	19.8	458
22282	Interfacial Properties of Monolayer and Bilayer MoS2 Contacts with Metals: Beyond the Energy Band Calculations. Scientific Reports, 2016, 6, 21786.	1.6	224
22283	Fe doped LaGaO₃: good white light emitters. RSC Advances, 2016, 6, 100230-100238.	1.7	35
22284	Lu₂CaMg₂(Si_{1â€“x}Ge_x)₃O₁₂:Ce³⁺solid-solu phosphors: bandgap engineering for blue-light activated afterglow applicable to AC-LED. Journal of Materials Chemistry C, 2016, 4, 10329-10338.	2.7	92
22285	Si-Doped single-walled carbon nanotubes interacting with isoniazid-a density functional and molecular docking study. RSC Advances, 2016, 6, 94651-94660.	1.7	10
22286	Early stages in the formation and burning of graphene on a Pt/Mg(Al)O dehydrogenation catalyst: A temperature- and time-resolved study. Journal of Catalysis, 2016, 344, 482-495.	3.1	27
22287	Conductive Boron-Doped Graphene as an Ideal Material for Electrocatalytically Switchable and High-Capacity Hydrogen Storage. ACS Applied Materials & Interfaces, 2016, 8, 32815-32822.	4.0	52
22288	Enhanced power factor via the control of structural phase transition in SnSe. Scientific Reports, 2016, 6, 26193.	1.6	32
22289	Metal-free half-metallicity in a high energy phase C-doped gh-C₃N₄ system: a high Curie temperature planar system. Journal of Materials Chemistry C, 2016, 4, 11530-11539.	2.7	32
22290	Experimental and theoretical studies on a novel helical architecture driven by hydrogen and halogen bonding interactions. Journal of Chemical Sciences, 2016, 128, 1895-1904.	0.7	1
22291	The plane-wave DFT investigations into the structure and the 11B solid-state NMR parameters of lithium fluorooxoborates. Chemical Physics Letters, 2016, 666, 22-27.	1.2	4
22292	Catalysis on solid acids: Mechanism and catalyst descriptors in oligomerization reactions of light alkenes. Journal of Catalysis, 2016, 344, 553-569.	3.1	80

#	Article	IF	Citations
22293	Synthesis, Structure, and Local Molecular Dynamics for Crystalline Rotors Based on Hecogenin/Botogenin Steroidal Frameworks. Crystal Growth and Design, 2016, 16, 5698-5709.	1.4	12
22294	Carbon incorporation effects and reaction mechanism of FeOCl cathode materials for chloride ion batteries. Scientific Reports, 2016, 6, 19448.	1.6	43
22295	Electronic structure of organometal halide perovskite CH3NH3BiI3 and optical absorption extending to infrared region. Scientific Reports, 2016, 6, 37425.	1.6	29
22296	Band gap engineering of ZnO substituted with nitrogen and fluorine, ZnO_{1â^'3x}N_{2x}F_x: a hybrid density functional study. RSC Advances, 2016, 6, 99088-99095.	1.7	5
22297	Theoretical study of phase stability and elastic properties ofT0.75Y0.75B14(Tâ€‰â€‰=â€‰â€‰Sc, Ti, V, Y, Zr, Nb, Si). Journal of Physics Condensed Matter, 2016, 28, 105501.	0.7	3
22298	Comparative study of the interfaces of graphene and hexagonal boron nitride with silver. Physical Review B, 2016, 94, .	1.1	18
22299	Assessing exchange-correlation functional performance for structure and property predictions of oxyfluoride compounds from first principles. Physical Review B, 2016, 94, .	1.1	27
22300	Superconductivity Emerging from an Electronic Phase Separation in the Charge Ordered Phase of <mml:math xmlns:mml="http://www.w3.org/1998/Math/MathML" display="inline"><mml:mrow><mml:msub><mml:mrow><mml:mi>RbFe</mml:mi></mml:mrow><mml:mrow><mml:mn>2</mml:mn></mml:mrow> Physical Review Letters, 2016, 117, 217001.	2.9	20
22301	Calculation of the electronic structure, lattice dynamics, and optical and magnetic properties of europium tetraborate EuB4O7. Physics of the Solid State, 2016, 58, 2300-2306.	0.2	1
22302	Relationship between acidity and catalytic reactivity of faujasite zeolite: A periodic DFT study. Journal of Catalysis, 2016, 344, 570-577.	3.1	72
22303	Design of Dipole-Allowed Direct Band Gaps in Ge/Sn Coreâ€“Shell Nanowires. Journal of Physical Chemistry C, 2016, 120, 28169-28175.	1.5	1
22304	High-Pressure Structural Response of an Insensitive Energetic Crystal: 1,1-Diamino-2,2-dinitroethene (FOX-7). Journal of Physical Chemistry C, 2016, 120, 27600-27607.	1.5	22
22305	Laser-Induced Explosion of Nitrated Carbon Nanotubes: Nonadiabatic and Reactive Molecular Dynamics Simulations. Journal of the American Chemical Society, 2016, 138, 15927-15934.	6.6	36
22306	Synthesis of sodium polyhydrides at high pressures. Nature Communications, 2016, 7, 12267.	5.8	79
22307	Prediction of Quantum Anomalous Hall Insulator in half-fluorinated GaBi Honeycomb. Scientific Reports, 2016, 6, 31317.	1.6	12
22308	Topological band-order transition and quantum spin Hall edge engineering in functionalized X-Bi(111) (Xâ€‰=â€‰Ga, In, and Tl) bilayer. Scientific Reports, 2016, 6, 33395.	1.6	7
22309	Phosphorus K4 Crystal: A New Stable Allotrope. Scientific Reports, 2016, 6, 37528.	1.6	13
22310	Spin-photon entanglement interfaces in silicon carbide defect centers. Nanotechnology, 2016, 27, 504001.	1.3	36

#	Article	IF	Citations
22311	Chirality effect on Lithiation of narrow carbon nanotubes; bond order MD and DFT studies. Materials Research Express, 2016, 3, 105015.	0.8	0
22312	Density functional theory study of bulk and single-layer magnetic semiconductor <mml:math xmlns:mml="http://www.w3.org/1998/Math/MathML"><mml:msub><mml:mi>CrPS</mml:mi><mml:mn>4</mml:mn></mml:msub></mml:math> Physical Review B, 2016, 94, .	1.1	53
22313	First-principles calculations of multivacancies in germanium. Japanese Journal of Applied Physics, 2016, 55, 011301.	0.8	9
22314	Exploring global phase stability of (VN)1/(InN)1 and (CrN)1/(GaN)1 superlattices from density-functional theory. Superlattices and Microstructures, 2016, 100, 667-672.	1.4	0
22315	Self-healing in B₁₂P₂ through Mediated Defect Recombination. Chemistry of Materials, 2016, 28, 8415-8428.	3.2	9
22316	Origin and Mechanism of Piezoelectricity in Î±-Quartz-type M^{III}X^VO₄ Compounds (M = B, Al, or Ga; X = P or As). Journal of Physical Chemistry C, 2016, 120, 26645-26651.	1.5	11
22317	Adsorption of Methyl Acetoacetate at Ni{111}: Experiment and Theory. Journal of Physical Chemistry C, 2016, 120, 27490-27499.	1.5	17
22318	Biomass-Derived Porous Fe₃C/Tungsten Carbide/Graphitic Carbon Nanocomposite for Efficient Electrocatalysis of Oxygen Reduction. ACS Applied Materials & Interfaces, 2016, 8, 32307-32316.	4.0	88
22319	Facet Energy versus Enzyme-like Activities: The Unexpected Protection of Palladium Nanocrystals against Oxidative Damage. ACS Nano, 2016, 10, 10436-10445.	7.3	247
22320	High-throughput screening of metal-porphyrin-like graphenes for selective capture of carbon dioxide. Scientific Reports, 2016, 6, 21788.	1.6	31
22321	Sn/Be Sequentially co-doped Hematite Photoanodes for Enhanced Photoelectrochemical Water Oxidation: Effect of Be2+ as co-dopant. Scientific Reports, 2016, 6, 23183.	1.6	75
22322	Bonding-restricted structure search for novel 2D materials with dispersed C2 dimers. Scientific Reports, 2016, 6, 29531.	1.6	14
22323	Sn doping induced intermediate band in CuGaS₂. RSC Advances, 2016, 6, 110511-110516.	1.7	16
22324	Proposed two-dimensional topological insulator in SiTe. Physical Review B, 2016, 94, .	1.1	45
22325	Lattice Vibrations Change the Solid Solubility of an Alloy at High Temperatures. Physical Review Letters, 2016, 117, 205502.	2.9	60
22326	Ab Initio Surface Phase Diagrams for Coadsorption of Aromatics and Hydrogen on the Pt(111) Surface. Journal of Physical Chemistry C, 2016, 120, 26249-26258.	1.5	22
22327	Unusually efficient photocurrent extraction in monolayer van der Waals heterostructure by tunnelling through discretized barriers. Nature Communications, 2016, 7, 13278.	5.8	120
22328	Quinary wurtzite Zn-Ga-Ge-N-O solid solutions and their photocatalytic properties under visible light irradiation. Scientific Reports, 2016, 6, 19060.	1.6	24

#	Article	IF	Citations
22329	Thermal Conductivity of Wurtzite Zinc-Oxide from First-Principles Lattice Dynamics â€“ a Comparative Study with Gallium Nitride. Scientific Reports, 2016, 6, 22504.	1.6	119
22330	The mechanism of large second harmonic generation enhancement activated by Zn²⁺substitution. Physical Chemistry Chemical Physics, 2016, 18, 32931-32936.	1.3	31
22331	Theoretical perspective of energy harvesting properties of atomically thin BiI₃. Journal of Materials Chemistry A, 2016, 4, 19086-19094.	5.2	47
22332	<mml:math xmlns:mml="http://www.w3.org/1998/Math/MathML"><mml:msub><mml:mi mathvariant="normal">Ru</mml:mi><mml:mn>2</mml:mn></mml:msub><mml:mtext>NbGa</mml:mtext></mml:math> : A Heusler-type compound with semimetallic characteristics. Physical Review B, 2016, 94, .	1.1	18
22333	Topological Surface States in Dense Solid Hydrogen. Physical Review Letters, 2016, 117, 206403.	2.9	10
22334	Physical properties of chalcopyrite-type Cu1â^'xAgxGaTe2 by first-principles study. Modern Physics Letters B, 2016, 30, 1650373.	1.0	5
22335	How far away are iron carbide clusters from the bulk?. Physical Chemistry Chemical Physics, 2016, 18, 32944-32951.	1.3	12
22336	Archimedean (4,8)-tessellation of haeckelite ultrathin nanosheets composed of boron and aluminum-group V binary materials. Nanoscale, 2016, 8, 19287-19301.	2.8	12
22337	Validity boundary of orbital-free molecular dynamics method corresponding to thermal ionization of shell structure. Physical Review B, 2016, 94, .	1.1	20
22338	Optical properties of single-layer and bilayer arsenene phases. Physical Review B, 2016, 94, .	1.1	67
22339	Changes in work function due to <mml:math xmlns:mml="http://www.w3.org/1998/Math/MathML"><mml:msub><mml:mi>NO</mml:mi><mml:mn>2</mml:mn></mml:msub></mml adsorption on monolayer and bilayer epitaxial graphene on SiC(0001). Physical Review B, 2016, 94, .	1.1	16
22340	Theoretical calculations of high-pressure phases of NiF2: An ab initio constant-pressure study. Russian Journal of Physical Chemistry A, 2016, 90, 2550-2555.	0.1	13
22341	NMR Spectral Parameters in Graphene, Graphite, and Related Materials: Ab Initio Calculations and Experimental Results. Journal of Physical Chemistry C, 2016, 120, 27707-27716.	1.5	44
22342	Evolution of crystal and electronic structures of magnesium dicarbide at high pressure. Scientific Reports, 2016, 5, 17815.	1.6	11
22343	Structural stability and electronic properties of multi-functionalized two-dimensional chromium carbides. Thin Solid Films, 2016, 619, 131-136.	0.8	33
22344	Suppression of radiation-induced point defects by rhenium and osmium interstitials in tungsten. Scientific Reports, 2016, 6, 36738.	1.6	28
22345	Contradictory nature of Co doping in ferroelectricBaTiO3. Physical Review B, 2016, 94, .	1.1	8
22346	Entropy-driven structural transition and kinetic trapping in formamidinium lead iodide perovskite. Science Advances, 2016, 2, e1601650.	4.7	203

#	Article	IF	Citations
22347	Structural, electronic and optical properties of the Zn0.5V0.5S in three phases. Modern Physics Letters B, 2016, 30, 1650356.	1.0	0
22348	Ideal shear strength and deformation behaviours of L10 TiAl from first-principles calculations. Bulletin of Materials Science, 2016, 39, 1411-1418.	0.8	2
22349	Defect and Substitution-Induced Silicene Sensor to Probe Toxic Gases. Journal of Physical Chemistry C, 2016, 120, 25256-25262.	1.5	81
22350	Oxygen- and Lithium-Doped Hybrid Boron-Nitride/Carbon Networks for Hydrogen Storage. Langmuir, 2016, 32, 13313-13321.	1.6	59
22351	Phononic Structure Engineering: the Realization of Einstein Rattling in Calcium Cobaltate for the Suppression of Thermal Conductivity. Scientific Reports, 2016, 6, 30530.	1.6	1
22352	Penta-BxNy sheet: a density functional theory study of two-dimensional material. Scientific Reports, 2016, 6, 31840.	1.6	65
22353	Unravelling the fundamentals of thermal and chemical expansion of BaCeO₃ from first principles phonon calculations. Physical Chemistry Chemical Physics, 2016, 18, 31296-31303.	1.3	14
22354	A computational study on the superionic behaviour of ThO₂. Physical Chemistry Chemical Physics, 2016, 18, 31494-31504.	1.3	17
22355	Predicted low thermal conductivities in antimony films and the role of chemical functionalization. Physical Chemistry Chemical Physics, 2016, 18, 30061-30067.	1.3	25
22356	Mechanisms of H- and OH-assisted CO activation as well as Câ€“C coupling on the flat Co(0001) surface â€“ revisited. Catalysis Science and Technology, 2016, 6, 8336-8343.	2.1	18
22357	Giant spinâ€“orbit coupling topological insulator h-Ga₂Bi₂with exotic O-bridge states. Nanoscale, 2016, 8, 19066-19074.	2.8	2
22358	Enhanced coking tolerance of a MgO-modified Ni cermet anode for hydrocarbon fueled solid oxide fuel cells. Journal of Materials Chemistry A, 2016, 4, 18031-18036.	5.2	45
22359	Large-scale room-temperature synthesis and optical properties of perovskite-related Cs₄PbBr₆fluorophores. Journal of Materials Chemistry C, 2016, 4, 10646-10653.	2.7	183
22360	Voltage-gated spin-filtering properties and global minimum of planar MnB₆, and half-metallicity and room-temperature ferromagnetism of its oxide sheet. Journal of Materials Chemistry C, 2016, 4, 10866-10875.	2.7	26
22361	First-principles calculations of the water molecules and hydroxylated iron surface. Integrated Ferroelectrics, 2016, 175, 247-254.	0.3	0
22362	Oxygen vacancy induced surface stabilization: (110) terminated magnetite. Physical Review B, 2016, 94, .	1.1	12
22363	Toward effective passivation of graphene to humidity sensing effects. , 2016, , .		3
22364	Atomistic simulation of transport properties of non-graphitic armchair nanotubes and effect of Stone-Wales defects. , 2016, , .		2

#	Article	IF	Citations
22365	The Influence of Surface Oxygen and Hydroxyl Groups on the Dehydrogenation of Ethylene, Acetic Acid and Hydrogenated Vinyl Acetate on Pd/Au(100): A DFT Study. Catalysis Letters, 2016, 146, 2516-2533.	1.4	6
22366	Origin of Surprising Attractive Interactions between Electronegative Oxygen Adatoms on Aluminum Surfaces. Journal of Physical Chemistry C, 2016, 120, 25915-25922.	1.5	9
22367	Structural and electronic properties of epitaxial multilayer h-BN on Ni(111) for spintronics applications. Scientific Reports, 2016, 6, 23547.	1.6	80
22368	The role of exchangeâ€“correlation functional on the description of multiferroic properties using density functional theory: the ATiO₃ (A = Mn, Fe, Ni) case study. RSC Advances, 2016, 6, 101216-101225.	1.7	26
22369	Tuning metal cluster catalytic activity with morphology and composition: a DFT study of O₂ dissociation at the global minimum of Pt_mPd_n (m + n = 5) clusters. RSC Advances, 2016, 6, 104388-104397.	1.7	19
22370	Comprehensive structureâ€“function correlation of photoactive ionic Ï€-conjugated supermolecular assemblies: an experimental and computational study. Journal of Materials Chemistry C, 2016, 4, 10223-10239.	2.7	32
22371	Metastable cobalt nitride structures with high magnetic anisotropy for rare-earth free magnets. Physical Chemistry Chemical Physics, 2016, 18, 31680-31690.	1.3	28
22372	Ab initio study on structural, elastic, electronic and optical properties of cuprate based superconductor. Cogent Physics, 2016, 3, .	0.7	1
22373	Antiferromagnetic andxyferro-orbital order in insulating SrRuO3thin films with SrO termination. Journal of Physics Condensed Matter, 2016, 28, 426004.	0.7	21
22374	Molecular Dynamics Simulation of Thermal Transport in <mml:math xmlns:mml="http://www.w3.org/1998/Math/MathML" display="inline"><mml:mrow><mml:msub><mml:mrow><mml:mi>UO</mml:mi></mml:mrow><mml:mrow><mml:mn>2</mml:mn></ Containing Uranium, Oxygen, and Fission-product Defects. Physical Review Applied, 2016, 6, .	1.5	39
22375	Quasi-two-dimensional Bose-Einstein condensation of spin triplets in the dimerized quantum magnet<mml:math xmlns:mml="http://www.w3.org/1998/Math/MathML"><mml:mrow><mml:msub><mml:mi>Ba</mml:mi><mml:mn>3</mml:mn></ mathvariant="normal">O</mml:mi><mml:mn>6</mml:mn></mml:msub><mml:msub><mml:mi>Cl</mml:mi><mml:mn>2</mml:mn></ Physical Review B, 2016, 94, .	1.1	11
22376	Pressure-induced phase transition in <mml:math xmlns:mml="http://www.w3.org/1998/Math/MathML"><mml:msub><mml:mi>LaCo</mml:mi><mml:mn>5</mml:mn></mml:msub></ studied by x-ray emission spectroscopy, x-ray diffraction, and density functional theory. Physical Review B, 2016, 94, .	1.1	7
22377	Resonant bonding driven giant phonon anharmonicity and low thermal conductivity of phosphorene. Physical Review B, 2016, 94, .	1.1	114
22378	Versatile van der Waals Density Functional Based on a Meta-Generalized Gradient Approximation. Physical Review X, 2016, 6, .	2.8	321
22379	Van der Waals metal-semiconductor junction: Weak Fermi level pinning enables effective tuning of Schottky barrier. Science Advances, 2016, 2, e1600069.	4.7	446
22380	Salt concentration effects on mechanical properties of LiPF6/poly(propylene glycol) diacrylate solid electrolyte: Insights from reactive molecular dynamics simulations. Electrochimica Acta, 2016, 221, 115-123.	2.6	10
22381	Electronic Properties of Carbon Nanotubes Intercalated with Li+ and Mg2+: Effects of Ion Charge and Ion Solvation. Journal of Physical Chemistry C, 2016, 120, 26514-26521.	1.5	15
22382	Bandgap- and Local Field-Dependent Photoactivity of Ag/Black Phosphorus Nanohybrids. ACS Catalysis, 2016, 6, 8009-8020.	5.5	132

#	Article	IF	Citations
22383	Atomistic clustering-ordering and high-strain deformation of an Al0.1CrCoFeNi high-entropy alloy. Scientific Reports, 2016, 6, 31028.	1.6	81
22384	Electronic structures and enhanced optical properties of blue phosphorene/transition metal dichalcogenides van der Waals heterostructures. Scientific Reports, 2016, 6, 31994.	1.6	192
22385	Plasticity mechanisms in HfN at elevated and room temperature. Scientific Reports, 2016, 6, 34571.	1.6	7
22386	Technetium incorporation in scheelite: insights from first-principles. Dalton Transactions, 2016, 45, 18171-18176.	1.6	8
22387	Electric and structural properties of polymeric graphite carbon nitride (g-C3N4): A Density Functional Theory study. Computational and Theoretical Chemistry, 2016, 1098, 41-49.	1.1	35
22388	Structural, Vibrational and Electronic properties of FeNi. Materials Today: Proceedings, 2016, 3, 3012-3017.	0.9	1
22389	Effect of Tin Coverage on Selectivity for Ethane Dehydrogenation over Platinumâ€“Tin Alloys. Journal of Physical Chemistry C, 2016, 120, 27307-27318.	1.5	50
22390	Oxygen Vacancy Structure Associated Photocatalytic Water Oxidation of BiOCl. ACS Catalysis, 2016, 6, 8276-8285.	5.5	333
22391	Superior thermoelasticity and shape-memory nanopores in a porous supramolecular organic framework. Nature Communications, 2016, 7, 11564.	5.8	58
22392	Discovery of Superconductivity in Hard Hexagonal Îµ-NbN. Scientific Reports, 2016, 6, 22330.	1.6	36
22393	First-principle study of CO adsorption influence on the properties of ferroelectric tunnel junctions. Physical Chemistry Chemical Physics, 2016, 18, 31115-31124.	1.3	0
22394	First principles studies on the thermoelectric properties of (SrO)_m(SrTiO₃)_n superlattice. RSC Advances, 2016, 6, 102172-102182.	1.7	11
22395	Biaxial strain effect on electronic structure tuning in antimonene-based van der Waals heterostructures. RSC Advances, 2016, 6, 102724-102732.	1.7	32
22396	Energetics of Sn²⁺ isomorphic substitution into hydroxylapatite: first-principles predictions. RSC Advances, 2016, 6, 107286-107292.	1.7	2
22397	Local heterojunctions of atomic Pt clusters boost the oxygen reduction activity of Rucore@Pdshell nanocrystallites. Journal of Materials Chemistry A, 2016, 4, 17848-17856.	5.2	3
22398	Electronics and optoelectronics of lateral heterostructures within monolayer indium monochalcogenides. Journal of Materials Chemistry C, 2016, 4, 11253-11260.	2.7	49
22399	Ab initiodetermination of the tractionâ€“separation curve for a metal grain boundary: a critical assessment of strategies. Modelling and Simulation in Materials Science and Engineering, 2016, 24, 085014.	0.8	8
22400	Energy Dissipation during Diffusion at Metal Surfaces: Disentangling the Role of Phonons versus Electron-Hole Pairs. Physical Review Letters, 2016, 117, 196001.	2.9	29

#	Article	IF	Citations
22401	Theoretical Investigation of the Structural, Elastic, and Thermodynamic Properties of MgAl₂O₄ Spinel under High Pressure. Journal of the Physical Society of Japan, 2016, 85, 114605.	0.7	32
22402	The diffusion behavior of Cr and Re in nickel-based superalloys at an atomic level. Computational and Theoretical Chemistry, 2016, 1097, 33-39.	1.1	4
22403	Local Electronic Structure in Î³-LiAlO₂ Studied by Single-Crystal ²⁷Al NMR and DFT Calculations. Journal of Physical Chemistry A, 2016, 120, 7839-7846.	1.1	8
22404	Diverse ruthenium nitrides stabilized under pressure: a theoretical prediction. Scientific Reports, 2016, 6, 33506.	1.6	23
22405	Hydrogenation-controlled phase transition on two-dimensional transition metal dichalcogenides and their unique physical and catalytic properties. Scientific Reports, 2016, 6, 34186.	1.6	61
22406	Investigation of hydrogen induced fluorescence in C₆₀and its potential use in luminescence down shifting applications. Nanoscale, 2016, 8, 18760-18770.	2.8	9
22407	Pressure induced structural and spin state transitions in Sr₃Fe₂O₅. RSC Advances, 2016, 6, 94105-94112.	1.7	3
22408	Band narrowing and Mott localization in isotropically superstrained graphene. Physical Review B, 2016, 94, .	1.1	7
22409	Ab initio study of electronic excitations and the dielectric function in molybdenum disulfide monolayer. Physical Review B, 2016, 94, .	1.1	14
22410	Effect of molecular bending and foreign molecules on electronic properties of molecular junctions. Organic Electronics, 2016, 39, 296-303.	1.4	1
22411	First-Principles Design of Iron-Based Active Catalysts for Adsorption and Dehydrogenation of H₂O Molecule on Fe(111), W@Fe(111), and W₂@Fe(111) Surfaces. Journal of Physical Chemistry C, 2016, 120, 25780-25788.	1.5	7
22412	Few-Layer Fe₃(PO₄)₂Â·8H₂O: Novel H-Bonded 2D Material and Its Abnormal Electronic Properties. Journal of Physical Chemistry C, 2016, 120, 26278-26283.	1.5	2
22413	Accelerated search for materials with targeted properties by adaptive design. Nature Communications, 2016, 7, 11241.	5.8	504
22414	Band engineering in a van der Waals heterostructure using a 2D polar material and a capping layer. Scientific Reports, 2016, 6, 27986.	1.6	5
22415	Magnetic moment collapse induced axial alternative compressibility of Cr2TiAlC2 at 420â€‰GPa from first principle. Scientific Reports, 2016, 6, 34092.	1.6	11
22416	The atomistic structure of yttria stabilised zirconia at 6.7 mol%: an ab initio study. Physical Chemistry Chemical Physics, 2016, 18, 31277-31285.	1.3	15
22417	First-principles study of the phase transition in Cd₂Ta₂O₇. Ferroelectrics, 2016, 502, 76-86.	0.3	0
22418	Coupling atomic scale modeling, fluid modeling and KPFM measurements to characterize an interface at nanoscale. , 2016, , .		4

#	Article	IF	Citations
22419	Theoretical Investigation on the Reaction Pathways for Oxygen Reduction Reaction on Silicon Doped Graphene as Potential Metal-Free Catalyst. Journal of the Electrochemical Society, 2016, 163, F1496-F1502.	1.3	23
22420	The Influence of Pt Layers in Ag@Pt_{nL}(111) (n = 1 and 2) on Oxygen Reduction Reaction: A Theoretical Study. Journal of the Electrochemical Society, 2016, 163, F945-F951.	1.3	7
22421	Substitution- and strain-induced magnetic phase transition in iron carbide. Journal of the Korean Physical Society, 2016, 69, 1335-1340.	0.3	0
22422	Theoretical and experimental determination of the crystal structures of cesiumâ€“molybdenum chloride. Japanese Journal of Applied Physics, 2016, 55, 075502.	0.8	12
22423	Investigation of a solid oxide fuel cells catalyst LaSrNiO4: Electronic structure, surface segregation, and oxygen adsorption. International Journal of Hydrogen Energy, 2016, 41, 21497-21502.	3.8	5
22424	Decomposition Mechanism of Anisole on Pt(111): Combining Single-Crystal Experiments and First-Principles Calculations. ACS Catalysis, 2016, 6, 8166-8178.	5.5	34
22425	Oxidation of InP nanowires: a first principles molecular dynamics study. Physical Chemistry Chemical Physics, 2016, 18, 31101-31106.	1.3	3
22426	Ethylene glycol reforming on Pt(111): first-principles microkinetic modeling in vapor and aqueous phases. Catalysis Science and Technology, 2016, 6, 8242-8256.	2.1	35
22427	Paving a way to suppress hydrogen blistering by investigating the hydrogenâ€“beryllium interaction in tungsten. RSC Advances, 2016, 6, 103622-103631.	1.7	6
22428	Nitrogen induced phosphorene formation on the boron phosphide (111) surface: a density functional theory study. RSC Advances, 2016, 6, 108621-108626.	1.7	2
22429	Spontaneous symmetry breaking on ordered, racemic monolayers of achiral theophylline: formation of unichiral stripes on Au(111). Nanoscale, 2016, 8, 19302-19313.	2.8	6
22430	Theoretics-directed effect of copper or aluminum content on the ductility characteristics of Al-based (Al ₃ Ti, AlTi, AlCu, AlTiCu ₂) intermetallic compounds. Chinese Physics B, 2016, 25, 113101.	0.7	4
22431	Enhanced superconductivity in atomically thin TaS2. Nature Communications, 2016, 7, 11043.	5.8	285
22432	Surface engineering of hierarchical platinum-cobalt nanowires for efficient electrocatalysis. Nature Communications, 2016, 7, 11850.	5.8	607
22433	Intermediate stages of electrochemical oxidation of single-crystalline platinum revealed by in situ Raman spectroscopy. Nature Communications, 2016, 7, 12440.	5.8	175
22434	Extending the applicability of the Goldschmidt tolerance factor to arbitrary ionic compounds. Scientific Reports, 2016, 6, 23592.	1.6	119
22435	Photochemical Copper Coating on 3D Printed Thermoplastics. Scientific Reports, 2016, 6, 31188.	1.6	17
22436	Reconciling Local Structure Disorder and the Relaxor State in (Bi1/2Na1/2)TiO3-BaTiO3. Scientific Reports, 2016, 6, 31739.	1.6	73

#	Article	IF	Citations
22437	Half-metallicity and ferromagnetism in penta-AlN2 nanostructure. Scientific Reports, 2016, 6, 33060.	1.6	33
22438	Assembling non-ferromagnetic materials to ferromagnetic architectures using metal-semiconductor interfaces. Scientific Reports, 2016, 6, 34404.	1.6	10
22439	Unravelling the Efficient Photocatalytic Activity of Boron-induced Ti3+ Species in the Surface Layer of TiO2. Scientific Reports, 2016, 6, 34765.	1.6	53
22440	Low viscosity and high attenuation in MgSiO3 post-perovskite inferred from atomic-scale calculations. Scientific Reports, 2016, 6, 34771.	1.6	22
22441	Investigating the coverage dependent behaviour of CO on Gd/Pt(111). Physical Chemistry Chemical Physics, 2016, 18, 29732-29739.	1.3	5
22442	The effect of the surface energy and structure of the SiC substrate on epitaxial graphene growth. RSC Advances, 2016, 6, 100908-100915.	1.7	13
22443	Nonlinear optical response mechanism of noncentrosymmetric lead borate Pb₆[B₄O₇(OH)₂]₃with three crystallographically independent [B₄O₇(OH)₂]^{4â¯}chains. RSC Advances, 2016, 6, 100849-100856.	1.7	6
22444	Strongly bound Mott-Wannier excitons in GeS and GeSe monolayers. Physical Review B, 2016, 94, .	1.1	76
22445	Electronic transitions induced by short-range structural order in amorphous<mml:math xmlns:mml="http://www.w3.org/1998/Math/MathML"><mml:msub><mml:mi>TiO</mml:mi><mml:mn>2</mml:mn></mml:msub></mml:math> Physical Review B, 2016, 94, .	1.1	37
22446	Investigation into the origin of high stability of Î´-MnO2 pseudo-capacitive electrode using operando Raman spectroscopy. Nano Energy, 2016, 30, 293-302.	8.2	109
22447	Effects of Stone-Wales defect on the electronic and transport properties of bilayer armchair graphene nanoribbons. Superlattices and Microstructures, 2016, 100, 739-748.	1.4	10
22448	A theoretical investigation of the Zn-doping influence on structural and electronic properties of BaTiO3. Solid State Ionics, 2016, 297, 36-42.	1.3	19
22449	Isotope analysis in the transmission electron microscope. Nature Communications, 2016, 7, 13040.	5.8	64
22450	Correlating the Energetics and Atomic Motions of the Metal-Insulator Transition of M1 Vanadium Dioxide. Scientific Reports, 2016, 6, 26391.	1.6	8
22451	Ordered Peierls distortion prevented at growth onset of GeTe ultra-thin films. Scientific Reports, 2016, 6, 32895.	1.6	20
22452	Large gap Quantum Spin Hall Insulators of Hexagonal III-Bi monolayer. Scientific Reports, 2016, 6, 34861.	1.6	6
22453	New ordered MAX phase Mo₂TiAlC₂: Elastic and electronic properties from first-principles. Chinese Physics B, 2016, 25, 107103.	0.7	36
22454	Atomistic description for temperature-driven phase transitions in <mml:math xmlns:mml="http://www.w3.org/1998/Math/MathML"><mml:msub><mml:mi>BaTiO</mml:mi><mml:mn>3</mml:mn></mml:msub></mml:math> Physical Review B, 2016, 94, .	1.1	52

#	Article	IF	Citations
22455	Ab initiodensity functional theory study on the atomic and electronic structure of GaP/Si(001) heterointerfaces. Physical Review B, 2016, 94, .	1.1	28
22456	Reflectance anisotropy spectroscopy of the <mml:math xmlns:mml="http://www.w3.org/1998/Math/MathML"><mml:mi mathvariant="normal">Si</mml:mi><mml:mo>(</mml:mo><mml:mn>111</mml:mn><mml:mo>)</mml:mo><mml:mtext>â˜’</mml:m mathvariant="normal">Au</mml:mi></mml:math> surface. Physical Review B, 2016, 94, .	1.1	13
22457	Study on the Reaction Species of 1, 3-Butadiene Formation from Bio-ethanol on ZrO2. Catalysis Letters, 2016, 146, 2450-2457.	1.4	8
22458	Theoretical Designs of Photoresponsive Energy-Storage Materials Based on Attachment of Ï€-Conjugated Molecules onto Sulfur-Doped Graphene. Journal of Physical Chemistry C, 2016, 120, 25131-25141.	1.5	12
22459	Polytypism and Unique Site Preference in LiZnSb: A Superior Thermoelectric Reveals Its True Colors. Journal of the American Chemical Society, 2016, 138, 14574-14577.	6.6	29
22460	Structures and Electronic Properties of Different CH3NH3PbI3/TiO2 Interface: A First-Principles Study. Scientific Reports, 2016, 6, 20131.	1.6	69
22461	Easily doped p-type, low hole effective mass, transparent oxides. Scientific Reports, 2016, 6, 20446.	1.6	60
22462	Pressure coefficients for direct optical transitions in MoS2, MoSe2, WS2, and WSe2 crystals and semiconductor to metal transitions. Scientific Reports, 2016, 6, 26663.	1.6	56
22463	Columnar shifts as symmetry-breaking degrees of freedom in molecular perovskites. Physical Chemistry Chemical Physics, 2016, 18, 31881-31894.	1.3	52
22464	Suppressing FePt order-disorder structural phase transition temperature by Ag doping: First principles investigation for enhancing magnetic recording density. Integrated Ferroelectrics, 2016, 175, 255-261.	0.3	1
22465	Monazite-type <mml:math xmlns:mml="http://www.w3.org/1998/Math/MathML"><mml:mrow><mml:mi>SrCr</mml:mi><mml:msub><mml:mi mathvariant="normal">O</mml:mi><mml:mn>4</mml:mn></mml:msub></mml:mrow></mml:math> under compression. Physical Review B, 2016, 94, .	1.1	30
22466	Giant tunneling electroresistance induced by ferroelectrically switchable two-dimensional electron gas at nonpolar<mml:math xmlns:mml="http://www.w3.org/1998/Math/MathML"><mml:mrow><mml:msub><mml:mi>BaTiO</mml:mi><mml:mn>3</mml:mn></mml:msub></mml:mrow></mml:math> Physical Review B, 2016, 94, .	1.1	15
22467	Pressure dependence of the band-gap energy in BiTeI. Physical Review B, 2016, 94, .	1.1	11
22468	Nanocluster-Assembled Materials. Series in Materials Science and Engineering, 2016, , 113-148.	0.1	3
22469	Computational Evaluation of Lithium-Functionalized Carbon Nitride (g-C₆N₈) Monolayer as an Efficient Hydrogen Storage Material. Journal of Physical Chemistry C, 2016, 120, 25180-25188.	1.5	76
22470	Heterometallic Metalâ€“Organic Frameworks of MOF-5 and UiO-66 Families: Insight from Computational Chemistry. Journal of Physical Chemistry C, 2016, 120, 24885-24894.	1.5	43
22471	CO Dissociation on Face-Centered Cubic and Hexagonal Close-Packed Nickel Catalysts: A First-Principles Study. Journal of Physical Chemistry C, 2016, 120, 24895-24903.	1.5	52
22472	Competition between Two High-Density Assemblies of Poly(phenyl)thiols on Au(111). Journal of Physical Chemistry C, 2016, 120, 25462-25472.	1.5	19

#	Article	IF	Citations
22473	Pressure dependency of localization degree in heavy fermion CeIn3: A density functional theory analysis. Scientific Reports, 2016, 6, 31734.	1.6	14
22474	First-Principles Study of Properties of Strained PbTiO ₃ /KTaO ₃ Superlattice. Chinese Physics Letters, 2016, 33, 026302.	1.3	3
22475	Determination of the vibrational contribution to the entropy change at the martensitic transformation in Niâ€“Mnâ€“Sn metamagnetic shape memory alloys: a combined approach of time-of-flight neutron spectroscopy andab initiocalculations. Journal of Physics Condensed Matter, 2016, 28, 205402.	0.7	8
22476	Improved pseudopotential transferability for magnetic and electronic properties of binary manganese oxides from <mml:math xmlns:mml="http://www.w3.org/1998/Math/MathML"><mml:mi mathvariant="normal">DFT</mml:mi><mml:mo>+</mml:mo><mml:mi>U</mml:mi><mml:mo>+</mml:mo><mml:mi>J</mml:mi></mml calculations. Physical Review B, 2016, 94, .	1.1	30
22477	Origin of unusual bandgap shift and dual emission in organic-inorganic lead halide perovskites. Science Advances, 2016, 2, e1601156.	4.7	307
22478	3D Metal Carbide@Mesoporous Carbon Hybrid Architecture as a New Polysulfide Reservoir for Lithiumâ€Sulfur Batteries. Advanced Functional Materials, 2016, 26, 8746-8756.	7.8	210
22479	Mechanism of Electroless Copper Deposition from [Cu^{II}EDTA]^{2â€“} Complexes Using Aldehyde-Based Reductants. Journal of Physical Chemistry C, 2016, 120, 24789-24793.	1.5	5
22480	Acidâ€“Base Interactions in Halobenzeneâ€“Ceria Systems: Insights into Oxidative Addition from Theory. Journal of Physical Chemistry C, 2016, 120, 25436-25444.	1.5	2
22481	Effects of ZnO Quantum Dots Decoration on the Field Emission Behavior of Graphene. ACS Applied Materials & Interfaces, 2016, 8, 31856-31862.	4.0	11
22482	Group precipitation and age hardening of nanostructured Fe-based alloys with ultra-high strengths. Scientific Reports, 2016, 6, 21364.	1.6	44
22483	Surface degeneration of W crystal irradiated with low-energy hydrogen ions. Scientific Reports, 2016, 6, 23738.	1.6	8
22484	Metal organic frameworks as sorption media for volatile and semi-volatile organic compounds at ambient conditions. Scientific Reports, 2016, 6, 27813.	1.6	132
22485	Spin-wave propagation steered by electric field modulated exchange interaction. Scientific Reports, 2016, 6, 31783.	1.6	6
22486	First-principles study of pressure-induced structural phase transitions in MnF₂. Physical Chemistry Chemical Physics, 2016, 18, 33250-33263.	1.3	24
22487	Dioxin sensing properties of graphene and hexagonal boron nitride based van der Waals solids: a first-principles study. RSC Advances, 2016, 6, 107114-107126.	1.7	5
22488	High-pressure phase of<mml:math xmlns:mml="http://www.w3.org/1998/Math/MathML"><mml:msub><mml:mi>LaPO</mml:mi><mml:mn>4</mml:mn></mml:msub></ by x-ray diffraction and second harmonic generation. Physical Review B, 2016, 94, .	1.1	21
22489	Elucidating Oligomer-Surface and Oligomer-Oligomer Interactions at a Lithiated Silicon Surface. Electrochimica Acta, 2016, 220, 312-321.	2.6	9
22490	Structural and elastic properties of BiOCu1-xS with Cu vacancies. Materials Today: Proceedings, 2016, 3, 2877-2882.	0.9	2

#	Article	IF	Citations
22491	Proton segregation and space-charge at the BaZrO3 (0 0 1)/MgO (0 0 1) heterointerface. Solid State Ionics, 2016, 297, 77-81.	1.3	11
22492	Defects and Oxide Ion Migration in the Solid Oxide Fuel Cell Cathode Material LaFeO₃. Chemistry of Materials, 2016, 28, 8210-8220.	3.2	95
22493	Comparative Theoretical Study of the Chemistry of Hydrogen Sulfide on Cu(100) and Au(100): Implications for Sulfur Tolerance of Water Gas Shift Nanocatalysts. Journal of Physical Chemistry C, 2016, 120, 25351-25360.	1.5	12
22494	H₂O Adsorption/Dissociation and H₂ Generation by the Reaction of H₂O with Al₂O₃ Materials: A First-Principles Investigation. Journal of Physical Chemistry C, 2016, 120, 21561-21570.	1.5	11
22495	CO Activation Determines Ultrafast Dynamics of CO Oxidation Reaction on Pd Nanoparticles. Journal of Physical Chemistry C, 2016, 120, 25806-25821.	1.5	3
22496	Surface Charge Transfer Doping via Transition Metal Oxides for Efficient p-Type Doping of IIâ€“VI Nanostructures. ACS Nano, 2016, 10, 10283-10293.	7.3	31
22497	An unforeseen polymorph of coronene by the application of magnetic fields during crystal growth. Nature Communications, 2016, 7, 11555.	5.8	68
22498	Atomic intercalation to measure adhesion of graphene on graphite. Nature Communications, 2016, 7, 13263.	5.8	35
22499	Dirac cone move and bandgap on/off switching of graphene superlattice. Scientific Reports, 2016, 6, 18869.	1.6	24
22500	Spin-orbital effects in metal-dichalcogenide semiconducting monolayers. Scientific Reports, 2016, 6, 24093.	1.6	60
22501	Ferromagnetism controlled by electric field in tilted phosphorene nanoribbon. Scientific Reports, 2016, 6, 26300.	1.6	16
22502	A Synthetic Pseudo-Rh: NOx Reduction Activity and Electronic Structure of Pdâ€“Ru Solid-solution Alloy Nanoparticles. Scientific Reports, 2016, 6, 28265.	1.6	44
22503	Tunable magnetism in metal adsorbed fluorinated nanoporous graphene. Scientific Reports, 2016, 6, 31841.	1.6	12
22504	Insights into the effect of Pt doping of Cu(110)/H2O for methanol decomposition: a density functional theory study. RSC Advances, 2016, 6, 109124-109131.	1.7	0
22505	Structural origin of the superionic Na conduction in Na₂B₁₀H₁₀closo-borates and enhanced conductivity by Na deficiency for high performance solid electrolytes. Journal of Materials Chemistry A, 2016, 4, 17740-17748.	5.2	59
22506	Interaction-induced metallic state in graphene on hexagonal boron nitride. Physical Review B, 2016, 94, .	1.1	7
22507	Theoretical Study of the Impact of Substitutional Dopants and Thermal Stress on the Behavior of Intrinsic Point Defects in Growing Single Crystal Silicon. Hyomen Kagaku, 2016, 37, 116-121.	0.0	0
22508	First-Principles Calculation Study of Epitaxial Graphene Layer on 4H-SiC (0001) Surface. E-Journal of Surface Science and Nanotechnology, 2016, 14, 107-112.	0.1	1

#	Article	IF	Citations
22509	Theoretical Investigation on Electronic and Magnetic Structures of FeRh. Journal of the Magnetics Society of Japan, 2016, 40, 77-80.	0.5	4
22510	A FP-LAPW Study of Structural and Electronic Properties of NdPd₃ Intermetallic Compound. Journal of Metastable and Nanocrystalline Materials, 0, 28, 5-7.	0.1	1
22511	Thermodynamical study of boron doped CeX3 (X=Pd, Rh). AIP Conference Proceedings, 2016, , .	0.3	0
22512	Electronic structure and magnetic properties of (Cu, N)-codoped 3C-SiC studied by first-principles calculations. Chinese Physics B, 2016, 25, 096108.	0.7	11
22513	Origin of the c-axis ultraincompressibility of Mo2GaC above about 15â€‰GPa from first principles. Journal of Applied Physics, 2016, 119, .	1.1	14
22514	Hydrogen diffusion in the magnesium titanium hydrides. , 2016, , .		0
22515	Density functional study for crystalline structures and electronic properties of Si1âˆ’xSnxbinary alloys. Japanese Journal of Applied Physics, 2016, 55, 08PE04.	0.8	16
22516	Tunable one-dimensional electron gas carrier densities at nanostructured oxide interfaces. Scientific Reports, 2016, 6, 25452.	1.6	6
22517	How does the spin-state of Co ions affect the insulator-metal transition in Bi2A2Co2O8 (Aâ€‰=â€‰Ca, Sr, Ba)?. Scientific Reports, 2016, 6, 38212.	1.6	6
22518	Interaction of NO2 and SO2 with ZnO [101Â¯0] surface using density functional theory. AIP Conference Proceedings, 2016, , .	0.3	1
22519	New transparent conducting oxide based on doped SnO<inf>2</inf> for solar cells. , 2016, , .		1
22520	Convergence rates of supercell calculations in the reduced Hartreeâˆ’Fock model. ESAIM: Mathematical Modelling and Numerical Analysis, 2016, 50, 1403-1424.	0.8	8
22521	Spin-glass behavior of Sn0.9Fe3.1N: An experimental and quantum-theoretical study. AIP Advances, 2016, 6, .	0.6	14
22522	Formation of star nanowires of sulfur-doped zinc oxide: Ab initio calculations. AIP Advances, 2016, 6, 095219.	0.6	2
22523	Effects of guest atomic species on the lattice thermal conductivity of type-I silicon clathrate studied via classical molecular dynamics. Journal of Chemical Physics, 2016, 145, 064702.	1.2	4
22524	Extent of hydrogen coverage of Si(001) under chemical vapor deposition conditions from ab initio approaches. Journal of Chemical Physics, 2016, 144, 204706.	1.2	10
22525	Anisotropic straining of graphene using micropatterned SiN membranes. APL Materials, 2016, 4, .	2.2	11
22526	Hydrogen-induced atomic structure evolution of the oxygen-chemisorbed Cu(110) surface. Journal of Chemical Physics, 2016, 145, 234704.	1.2	7

#	Article	IF	Citations
22527	Ab initiotensorial electronic friction for molecules on metal surfaces: Nonadiabatic vibrational relaxation. Physical Review B, 2016, 94, .	1.1	74
22528	Lattice thermal conduction in ultra-thin nanocomposites. Journal of Applied Physics, 2016, 119, 244309.	1.1	3
22529	Electronic properties of a new structured Sin/O superlattice. AIP Advances, 2016, 6, 115203.	0.6	0
22530	A comprehensive picture in the view of atomic scale on piezoelectricity of ZnO tunnel junctions: The first principles simulation. AIP Advances, 2016, 6, 065217.	0.6	1
22531	First-principles study of electronic structures of graphene on Y2O3. Japanese Journal of Applied Physics, 2016, 55, 06GF07.	0.8	2
22532	First-Principles Molecular Dynamics Study on Helium- filled Carbon Nanotube. Journal of Physics: Conference Series, 2016, 739, 012081.	0.3	3
22533	First-principles study on bottom-up fabrication process of atomically precise graphene nanoribbons. Japanese Journal of Applied Physics, 2016, 55, 06GF05.	0.8	2
22534	Ab Initio Elastic Properties calculation of Gold (Au). Journal of Physics: Conference Series, 2016, 739, 012068.	0.3	0
22535	Giant Phonon Anharmonicity and Anomalous Pressure Dependence of Lattice Thermal Conductivity in Y2Si2O7 silicate. Scientific Reports, 2016, 6, 29801.	1.6	24
22536	First-principles study of He trapping in Î· -Fe ₂ C. Chinese Physics B, 2016, 25, 116801.	0.7	1
22537	Trilayer Graphene as a Candidate Material for Phase-Change Memory Applications. MRS Advances, 2016, 1, 1487-1494.	0.5	0
22538	Theoretical approach to surface reconstruction of InN(0001) during raised-pressure metalorganic vapor-phase epitaxy. Japanese Journal of Applied Physics, 2016, 55, 05FM01.	0.8	4
22539	Supercell Calculations in the Reduced Hartreeâ€“Fock Model for Crystals with Local Defects. Applied Mathematics Research EXpress, 0, , .	1.0	3
22540	Lattice dynamics and baric behavior of phonons in Hg2Cl2 crystals at high hydrostatic pressures. Bulletin of the Russian Academy of Sciences: Physics, 2016, 80, 1033-1037.	0.1	6
22541	Magnetic properties of intrinsic vacancies on the GaN $$(10ar 10)$$ surface: a density-functional-theory study. Journal of the Korean Physical Society, 2016, 68, 420-424.	0.3	2
22542	Site preferences for La and Pr in Nd2Fe14B permanent magnet: A first principles study. Journal of the Korean Physical Society, 2016, 69, 1564-1570.	0.3	4
22543	First principles investigation of structural, elastic, electronic and optical properties of ABi2O6 (Aï¿½ï¿½=ï¿½ï¿½Mg, Zn) with trirutile-type structure. Cogent Physics, 2016, 3, .	0.7	8
22544	Ab-initio study on structural, elastic, electronic and optical properties of iron-based superconductor. Cogent Physics, 2016, 3, .	0.7	5

#	Article	IF	Citations
22545	Pressure induced magnetic phase transition in RhFe3N and IrFe3N: An ab-initio study. AIP Conference Proceedings, 2016, , .	0.3	0
22546	Thermal properties of layered oxychalcogenides BiCuOCh (Châ€‰=â€‰S, Se, and Te): A first-principles calculation. Journal of Applied Physics, 2016, 119, .	1.1	18
22547	Optical properties and lattice dynamics of CuZnGeSe quaternary semiconductor: A densityâ€functional study. Physica Status Solidi (B): Basic Research, 2016, 253, 323-328.	0.7	17
22548	Hâ€bond and electric field correlations for water in highly hydrated crystals. International Journal of Quantum Chemistry, 2016, 116, 67-80.	1.0	14
22549	Stability of atomic oxygen chemisorption on Pt-alloy surfaces. Surface and Interface Analysis, 2016, 48, 181-185.	0.8	3
22550	Interstitial Point Defect Scattering Contributing to High Thermoelectric Performance in SnTe. Advanced Electronic Materials, 2016, 2, 1600019.	2.6	235
22551	Efficient Photocatalytic Oxygen Production over Nitrogenâ€Doped Sr₄Nb₂O₉ under Visibleâ€Light Irradiation. ChemCatChem, 2016, 8, 615-623.	1.8	45
22552	On the Importance of Regulating Hydroxyl Coverage on the Basal Plane of Graphene Oxide for Supercapacitors. ChemElectroChem, 2016, 3, 741-748.	1.7	6
22553	Vibrational and reorientational dynamics, crystal structure and solidâ€“solid phase transition studies in [Ca(H₂O)₆]Cl₂ supported by theoretical (DFT) calculations. Journal of Raman Spectroscopy, 2016, 47, 591-601.	1.2	9
22554	Nanoscale Elastic Changes in 2D Ti₃C₂T_x (MXene) Pseudocapacitive Electrodes. Advanced Energy Materials, 2016, 6, 1502290.	10.2	117
22555	Exploring Scaling Relations for Chemisorption Energies on Transitionâ€Metalâ€Exchanged Zeolites ZSMâ€22 and ZSMâ€5. ChemCatChem, 2016, 8, 767-772.	1.8	18
22556	Role of Oxygen Defects on the Photocatalytic Properties of Mgâ€Doped Mesoporous Ta₃N₅. ChemSusChem, 2016, 9, 1403-1412.	3.6	78
22557	Structural stabilities, elastic and electronic properties of chromium tetraboride from first-principles calculations. International Journal of Modern Physics B, 2016, 30, 1650098.	1.0	3
22558	Lattice dynamics and anharmonicity of CaZrF6 from Raman spectroscopy and ab initio calculations. Materials Chemistry and Physics, 2016, 180, 213-218.	2.0	28
22559	Electronic and optical properties of CeO₂ from first principles calculations. Analytical Methods, 2016, 8, 5045-5052.	1.3	29
22560	Density functional theory study of Li, Na, and Mg intercalation and diffusion in MoS₂with controlled interlayer spacing. Materials Research Express, 2016, 3, 064001.	0.8	100
22561	Modeling of metastable phase formation diagrams for sputtered thin films. Science and Technology of Advanced Materials, 2016, 17, 210-219.	2.8	27
22562	Understanding the high p-type conductivity in Cu-excess CuAlS₂: A first-principles study. Applied Physics Express, 2016, 9, 031202.	1.1	5

#	Article	IF	Citations
22563	Origin of the strain glass transition in Ti50(Ni50â˜ÂD) alloys. Journal of Alloys and Compounds, 2016, 678, 325-328.	2.8	4
22564	First principles study of structural, electronic, mechanical and magnetic properties of actinide nitrides AnN (AnÂ=ÂU, Np and Pu). Journal of Nuclear Materials, 2016, 478, 197-206.	1.3	8
22565	A comparative study on ferromagnetic C/O-implanted GaN films by positron annihilation spectroscopy. Nuclear Instruments & Methods in Physics Research B, 2016, 375, 107-111.	0.6	1
22566	Study of the electronic structure and half-metallicity of CaMnO3/BaTiO3 superlattice. Superlattices and Microstructures, 2016, 97, 116-124.	1.4	23
22567	A force field for mackinawite surface simulations in an aqueous environment. Theoretical Chemistry Accounts, 2016, 135, 1.	0.5	4
22568	Propionic acid derivatives confined in mesoporous silica: monomers or dimers? The case of ibuprofen investigated by static and dynamic ab initio simulations. Theoretical Chemistry Accounts, 2016, 135, 1.	0.5	6
22569	Compressional behavior of MgCr2O4 spinel from first-principles simulation. Science China Earth Sciences, 2016, 59, 989-996.	2.3	14
22570	Adsorption and decomposition of H2O on cobalt surfaces: A DFT study. Applied Surface Science, 2016, 384, 10-17.	3.1	32
22571	Liquid-liquid extraction of lithium using lipophilic dibenzo-14-crown-4 ether carboxylic acid in hydrophobic room temperature ionic liquid. Hydrometallurgy, 2016, 164, 362-371.	1.8	48
22572	A novel candidate for hydrogen storage: Ca-decorated zigzag C3N nanotube. International Journal of Hydrogen Energy, 2016, 41, 7431-7437.	3.8	29
22573	Effect of Boron Doping on the CVD Growth Rate of Diamond. Journal of Physical Chemistry C, 2016, 120, 10658-10666.	1.5	19
22574	Electrodeposition and ab Initio Studies of Metastable Orthorhombic Bi₂Se₃: A Novel Semiconductor with Bandgap for Photovoltaic Applications. Journal of Physical Chemistry C, 2016, 120, 11797-11806.	1.5	32
22575	Assembling a bi-coordinated Cr complex for ferromagnetic nanorings: insight from first-principles calculations. Physical Chemistry Chemical Physics, 2016, 18, 17868-17874.	1.3	0
22576	First-principle study of electronic structures and optical properties of chromium and carbon co-doped anatase TiO2. Ceramics International, 2016, 42, 13900-13908.	2.3	14
22577	Anatase TiO2 codoping with sulfur and acceptor IIB metals for water splitting. International Journal of Hydrogen Energy, 2016, 41, 13050-13057.	3.8	22
22578	GGA+U study of uranium mononitride: A comparison of the U-ramping and occupation matrix schemes and incorporation energies of fission products. Journal of Nuclear Materials, 2016, 478, 119-124.	1.3	39
22579	Exploring the sodium storage mechanism in disodium terephthalate as anode for organic battery using density-functional theory calculations. Journal of Power Sources, 2016, 324, 572-581.	4.0	51
22580	Cluster-Inspired Design of High-Capacity Anode for Li-Ion Batteries. ACS Energy Letters, 2016, 1, 202-208.	8.8	23

#	Article	IF	Citations
22581	Hydroxyapatite substituted by transition metals: experiment and theory. Physical Chemistry Chemical Physics, 2016, 18, 16457-16465.	1.3	91
22582	Spectroscopic Raman characterization of rutherfordine: a combined DFT and experimental study. Physical Chemistry Chemical Physics, 2016, 18, 16575-16584.	1.3	43
22583	Quantum Monte Carlo analysis of a charge ordered insulating antiferromagnet: the Ti₄O₇ MagnÃ©li phase. Physical Chemistry Chemical Physics, 2016, 18, 18323-18335.	1.3	27
22584	First-principles investigation of LaGaO₃and LaInO₃lanthanum perovskite oxides. Philosophical Magazine, 2016, 96, 2040-2058.	0.7	18
22585	Influence of alloying elements upon the theoretical tensile strength of Ni-based model superalloy: Î³-Ni/Î³â€²-Ni3Al multilayer. Computational Materials Science, 2016, 119, 120-129.	1.4	11
22586	DFT based study of structural and magnetic properties of full-Heusler compounds. Materials Today: Proceedings, 2016, 3, 1840-1844.	0.9	7
22587	Structural phase transition, electronic and elastic properties of rocksalt structure SnAs and SnSb. Solid State Communications, 2016, 243, 16-22.	0.9	8
22588	A Deep-Ultraviolet Nonlinear Optical Crystal: Strontium Beryllium Borate Fluoride with Planar Be(O/F)₃ Groups. Chemistry of Materials, 2016, 28, 4563-4571.	3.2	47
22589	Elucidating the Role of the Electric Field at the Ni/YSZ Electrode: A DFT Study. Journal of Physical Chemistry C, 2016, 120, 14608-14620.	1.5	12
22590	Interfacial Properties of Monolayer MoSe₂â€“Metal Contacts. Journal of Physical Chemistry C, 2016, 120, 13063-13070.	1.5	70
22591	Double-hole codoped huge-gap semiconductor ZrO₂ for visible-light photocatalysis. Physical Chemistry Chemical Physics, 2016, 18, 17517-17524.	1.3	32
22592	First principles calculations of solid-state thermionic transport in layered van der Waals heterostructures. Nanoscale, 2016, 8, 14695-14704.	2.8	33
22593	DFT simulations of⁷Li solid state NMR spectral parameters and Li⁺ion migration barriers in Li₂ZrO₃. RSC Advances, 2016, 6, 41015-41024.	1.7	5
22594	A novel theoretical study of thermally-induced reaction and vibration dynamics of methanol dissociative adsorption onto a Si(001) surface. RSC Advances, 2016, 6, 1491-1502.	1.7	5
22595	Transition-metal embedded carbon nitride monolayers: high-temperature ferromagnetism and half-metallicity. Nanoscale, 2016, 8, 14117-14126.	2.8	49
22596	A comparative investigation of the behaviors of H in Au and Ag from first principles. Modelling and Simulation in Materials Science and Engineering, 2016, 24, 045009.	0.8	4
22597	Effect of pressure on electronic and thermoelectric properties of magnesium silicide: A density functional theory study. Chinese Physics B, 2016, 25, 056401.	0.7	19
22598	First principles study of the diffusional phenomena across the clean and Re-doped Î³ -Ni/ Î³ â€™-Ni ₃ Al interface of Ni-based single crystal superalloy. Chinese Physics B, 2016, 25, 067104.	0.7	6

#	Article	IF	Citations
22599	Electronic Properties of MoS₂/MX₂/MoS₂Trilayer Heterostructures: A First Principle Study. ECS Journal of Solid State Science and Technology, 2016, 5, Q3001-Q3007.	0.9	6
22600	The stability of TiC surfaces in the environment with various carbon chemical potential and surface defects. Applied Surface Science, 2016, 386, 202-209.	3.1	18
22601	A DFT+U study on the contribution of 4f electrons to oxygen vacancy formation and migration in Ln-doped CeO₂. Physical Chemistry Chemical Physics, 2016, 18, 12938-12946.	1.3	43
22602	Tunneling spectra of graphene on copper unraveled. Physical Chemistry Chemical Physics, 2016, 18, 17081-17090.	1.3	2
22603	Structural, electronic, optical, vibrational and transport properties of CuBX₂ (X = S, Se,) Tj ETQq0 0 0 rgBT /Overlock 10 Tf	1.7	17
22604	A DFT study of pressure-induced phase transitions, structural and electronic properties of Cu₂ZnSnS₄. Modern Physics Letters B, 2016, 30, 1650176.	1.0	4
22605	Interfacial properties and electron structure of Al/B4C interface: A first-principles study. Journal of Nuclear Materials, 2016, 478, 227-235.	1.3	63
22606	First-principles study of size-, surface- and mechanical strain-dependent electronic properties of wurtzite and zinc-blende InSb nanowires. Physics Letters, Section A: General, Atomic and Solid State Physics, 2016, 380, 2678-2684.	0.9	3
22607	Extended homologous series of Snâ€“O layered systems: A first-principles study. Solid State Communications, 2016, 243, 36-43.	0.9	14
22608	Phonon properties of Î²-Ag2MoO4: Raman spectroscopy and ab initio calculations. Vibrational Spectroscopy, 2016, 86, 97-102.	1.2	33
22609	Theoretical Optimization of Pore Size and Chemistry in SIFSIX-3-M Hybrid Ultramicroporous Materials. Crystal Growth and Design, 2016, 16, 3890-3897.	1.4	37
22610	Experimental and theoretical studies on the linear and nonlinear optical properties of lead phosphate crystals LiPbPO₄. Physical Chemistry Chemical Physics, 2016, 18, 19123-19129.	1.3	61
22611	Thermoelectric properties of stannite-phase CuZn₂AS₄ (CZAS; A=Al, Ga and In) nanocrystals for solar energy conversion applications. Philosophical Magazine, 2016, 96, 2280-2299.	0.7	16
22612	First-principles study of nitrogen and carbon monoxide adsorptions on silicene. International Journal of Modern Physics B, 2016, 30, 1650176.	1.0	7
22613	First-Principles Calculations of the Mechanical and Elastic Properties of 2H_c- and 2H_a-WS₂/CrS₂ Under Pressure. Zeitschrift Fur Naturforschung - Section A Journal of Physical Sciences, 2016, 71, 517-524.	0.7	2
22614	Electronic, Magnetic and Optical Properties of Rutile Ti1-x TM x O2 (TM = V, Fe, Co, Ni) Using Tran and Blahaâ€™s Modified Beckeâ€“Johnson Exchange Potential Model. Journal of Superconductivity and Novel Magnetism, 2016, 29, 2641-2650.	0.8	2
22615	Adsorption of alkali and alkaline-earth metal atoms on stanene: A first-principles study. Materials Chemistry and Physics, 2016, 180, 326-331.	2.0	33
22616	Resonance Raman Optical Activity of Single Walled Chiral Carbon Nanotubes. Journal of Physical Chemistry A, 2016, 120, 5527-5538.	1.1	9

#	Article	IF	Citations
22617	Adsorption of gold subnano-structures on a magnetite(111) surface and their interaction with CO. Physical Chemistry Chemical Physics, 2016, 18, 18169-18179.	1.3	14
22618	Wedge energy bands of monolayer black phosphorus: a first-principles study. Journal of Physics Condensed Matter, 2016, 28, 305301.	0.7	1
22619	Engineering magnetism and electronic properties of silicene by changing adsorption coverage. Applied Surface Science, 2016, 384, 65-72.	3.1	18
22620	The nucleation and growth of H blisters in dislocation loops in W{110}. Journal of Nuclear Materials, 2016, 478, 222-226.	1.3	3
22621	Structural and mechanical properties of nitrogen-deficient cubic Crâ€“Moâ€“N and Crâ€“Wâ€“N systems. Scripta Materialia, 2016, 123, 34-37.	2.6	23
22622	SiTe monolayers: Si-based analogues of phosphorene. Journal of Materials Chemistry C, 2016, 4, 6353-6361.	2.7	54
22623	Interpretation of Raman spectra of the zirconâ€“hafnon solid solution. European Journal of Mineralogy, 2016, 28, 721-733.	0.4	9
22624	Monolayer MoS2 Nanoribbons as a Promising Material for Both n-type and p-type Legs in Thermoelectric Generators. Journal of Electronic Materials, 2016, 45, 5253-5263.	1.0	12
22625	Assessment of Different Quantum Mechanical Methods for the Prediction of Structure and Cohesive Energy of Molecular Crystals. Journal of Chemical Theory and Computation, 2016, 12, 3340-3352.	2.3	85
22626	Direct growth of Ge quantum dots on a graphene/SiO₂/Si structure using ion beam sputtering deposition. Nanotechnology, 2016, 27, 305601.	1.3	11
22627	First principle investigation of the electronic and thermoelectric properties of Mg ₂ C. Chinese Physics B, 2016, 25, 026402.	0.7	18
22628	A Honeycomb BeN₂ Sheet with a Desirable Direct Band Gap and High Carrier Mobility. Journal of Physical Chemistry Letters, 2016, 7, 2664-2670.	2.1	100
22629	Methylation of olefins with ketene in zeotypes and its implications for the direct conversion of syngas to light olefins: a periodic DFT study. Catalysis Science and Technology, 2016, 6, 6644-6649.	2.1	36
22630	Ab-initio study of surface oxide formation in Pt(111) electrocatalyst under influences of O2-containing intermediates of oxygen reduction reaction. Journal of Applied Electrochemistry, 2016, 46, 1031-1038.	1.5	4
22631	Pressure and temperature induced phase transition in WB4: A first principles study. Journal of Alloys and Compounds, 2016, 687, 579-585.	2.8	23
22632	Suppression of Jahnâ€“Teller Distortions and Origin of Piezochromism and Thermochromism in Cuâ€“Cl Hybrid Perovskite. Inorganic Chemistry, 2016, 55, 6817-6824.	1.9	24
22633	MXene: a promising photocatalyst for water splitting. Journal of Materials Chemistry A, 2016, 4, 11446-11452.	5.2	569
22634	Hydrogen adsorption on pristine, defected, and 3d-block transition metal-doped penta-graphene. International Journal of Hydrogen Energy, 2016, 41, 12157-12166.	3.8	78

#	Article	IF	Citations
22635	Unraveling the Coupled Processes of (De)hydration and Structural Changes in Na⁺-Saturated Montmorillonite. Journal of Physical Chemistry C, 2016, 120, 15282-15287.	1.5	16
22636	Valence Band Control of Metal Silicide Films via Stoichiometry. Journal of Physical Chemistry Letters, 2016, 7, 2573-2578.	2.1	6
22637	Control of Triboelectrification by Engineering Surface Dipole and Surface Electronic State. ACS Applied Materials & Interfaces, 2016, 8, 18519-18525.	4.0	100
22638	Band Edge Engineering in BiVO₄/TiO₂ Heterostructure: Enhanced Photoelectrochemical Performance through Improved Charge Transfer. ACS Catalysis, 2016, 6, 5311-5318.	5.5	117
22639	Enormous lattice distortion through an isomorphous phase transition in an organicâ€“inorganic hybrid based on haloantimonate(<scp>iii</scp>). CrystEngComm, 2016, 18, 6184-6194.	1.3	22
22640	Repairing sulfur vacancies in the MoS₂ monolayer by using CO, NO and NO₂ molecules. Journal of Materials Chemistry C, 2016, 4, 7093-7101.	2.7	111
22641	A computational study on the adsorption configurations and reactions of SiHx(x = 1-4) on clean and H-covered Si(100) surfaces. Applied Surface Science, 2016, 387, 546-556.	3.1	4
22642	Grain boundary and curvature enhanced lithium adsorption on carbon. Carbon, 2016, 107, 557-563.	5.4	17
22643	Spin-polarized transport properties of Fe-oligoporphyrin dimer-based molecular device. Organic Electronics, 2016, 36, 160-165.	1.4	10
22644	Highly Active Au/Î´-MoC and Cu/Î´-MoC Catalysts for the Conversion of CO₂: The Metal/C Ratio as a Key Factor Defining Activity, Selectivity, and Stability. Journal of the American Chemical Society, 2016, 138, 8269-8278.	6.6	140
22645	H₂/D₂ exchange reaction on mono-disperse Pt clusters: enhanced activity from minute O₂ concentrations. Catalysis Science and Technology, 2016, 6, 6893-6900.	2.1	9
22646	Doping enhanced ferromagnetism and induced half-metallicity in CrI ₃ monolayer. Europhysics Letters, 2016, 114, 47001.	0.7	146
22647	Electronic and Thermoelectric Properties of Al doped Mg2Si Material: DFT Study. Materials Today: Proceedings, 2016, 3, 1785-1791.	0.9	6
22648	Chiral vectors-tunable electronic property of MoS2 nanotubes. Physica E: Low-Dimensional Systems and Nanostructures, 2016, 84, 196-201.	1.3	6
22649	The interaction between light impurities and vacancies in titanium and aluminum metals: A DFT study. St Petersburg Polytechnical University Journal Physics and Mathematics, 2016, 2, 96-102.	0.3	3
22650	Be₂BO₃F: A Phase of Beryllium Fluoride Borate Derived from KBe₂BO₃F₂ with Short UV Absorption Edge. Inorganic Chemistry, 2016, 55, 6586-6591.	1.9	36
22651	Deposition Order Controls the First Stages of a Metalâ€“Organic Coordination Network on an Insulator Surface. Journal of Physical Chemistry C, 2016, 120, 14730-14735.	1.5	12
22652	Ionic Graphitization of Ultrathin Films of Ionic Compounds. Journal of Physical Chemistry Letters, 2016, 7, 2659-2663.	2.1	9

#	Article	IF	Citations
22653	High-coverage stable structures of 3d transition metal intercalated bilayer graphene. Physical Chemistry Chemical Physics, 2016, 18, 14244-14251.	1.3	9
22654	Preparation, structure and properties of Na₂Mn₃(SO₄)₄: a new potential candidate with high voltage for Na-ion batteries. Journal of Materials Chemistry A, 2016, 4, 11870-11877.	5.2	24
22655	Investigations on structural, elastic, thermodynamic and electronic properties of TiN, Ti2N and Ti3N2 under high pressure by first-principles. Journal of Physics and Chemistry of Solids, 2016, 98, 10-19.	1.9	62
22656	Transition-metal-decorated germanene as promising catalyst for removing CO contamination in H2. Materials and Design, 2016, 107, 82-89.	3.3	17
22657	Stability and hydrogen adsorption properties of Mg/TiMn2 interface by first principles calculation. Surface Science, 2016, 653, 22-26.	0.8	12
22658	Combined Theoretical and Experimental Approach to the Discovery of Electrochemically Active Mixed Polyanionic Phosphatonitrates, AFePO₄NO₃ (A = NH₄/Li, K). Chemistry of Materials, 2016, 28, 5029-5036.	3.2	22
22659	Proposed Modification of the Graphene Analogue Ni₃(HITP)₂ To Yield a Semiconducting Material. Journal of Physical Chemistry C, 2016, 120, 15001-15008.	1.5	67
22660	Structure and bonding in crystalline cesium uranyl tetrachloride under pressure. Physical Chemistry Chemical Physics, 2016, 18, 18398-18405.	1.3	7
22661	Colloidal CuFeS₂ Nanocrystals: Intermediate Fe d-Band Leads to High Photothermal Conversion Efficiency. Chemistry of Materials, 2016, 28, 4848-4858.	3.2	126
22662	First-principles study of the structural, electronic, and magnetic properties of double perovskite Sr 2 FeReO 6 containing various imperfections. Chinese Physics B, 2016, 25, 058102.	0.7	2
22663	Room temperature quantum spin Hall states in two-dimensional crystals composed of pentagonal rings and their quantum wells. NPG Asia Materials, 2016, 8, e264-e264.	3.8	65
22664	Hybrid functional calculations on the band gap bowing parameters of InxGa1â^'xN. Journal of Semiconductors, 2016, 37, 042001.	2.0	1
22665	The coloring problem in the solid-state metal boride carbide ScB₂C₂: a theoretical analysis. Zeitschrift Fur Naturforschung - Section B Journal of Chemical Sciences, 2016, 71, 593-601.	0.3	5
22666	Alloying Mg with Gd and Y: Increasing both plasticity and strength. Computational Materials Science, 2016, 115, 85-91.	1.4	46
22667	Electronic and magnetic properties of a new diluted magnetic semiconductor Li(Zn,TM)As (TM:V, Cr,) Tj ETQq0 0 0 rgBT /Overlock 10 Tf	1.2	2
22668	Mechanical properties of Wâ€“Ti alloys from first-principles calculations. Fusion Engineering and Design, 2016, 106, 34-39.	1.0	46
22669	Elastic and mechanical properties of Mg3Rh intermetallic compound: An ab initio study. Journal of Magnesium and Alloys, 2016, 4, 123-127.	5.5	6
22670	First-principles prediction of MgB2-like NaBC: A more promising high-temperature superconducting material than LiBC. Solid State Communications, 2016, 233, 30-34.	0.9	7

#	Article	IF	Citations
22671	Association of oxygen vacancies with carbon impurity in strontium titanate: first principles calculations. Ferroelectrics, 2016, 497, 9-14.	0.3	1
22672	Laser lap welding quality of steel/aluminum dissimilar metal joint and its electronic simulations. International Journal of Advanced Manufacturing Technology, 2016, 86, 2231-2242.	1.5	11
22673	A comparative study based on the first principles calculations of ATiO3 (AÂ=ÂBa, Ca, Pb and Sr) perovskite structure. Indian Journal of Physics, 2016, 90, 1105-1113.	0.9	22
22674	First principles prediction of a new high-pressure phase and transport properties of Mg2Si. Indian Journal of Physics, 2016, 90, 1403-1415.	0.9	5
22675	Complex Precipitation Sequences of Al-Cu-Li-(Mg) Alloys Characterized in Relation to Thermal Ageing Processes. Acta Metallurgica Sinica (English Letters), 2016, 29, 94-103.	1.5	34
22676	First-principles study on the stability and electronic structure of Mg/ZrB2 interfaces. Science China Materials, 2016, 59, 28-37.	3.5	29
22677	Molecular dynamics and first-principles studies of structural change in 1,3,5-triamino-2,4,6-trinitrobenzene (TATB) in crystalline state under high pressure: Comparison of hydrogen bond systems of TATB versus 1,3-diamino-2,4,6-trinitrobenzene (DATB). Chemical Physics, 2016, 472, 163-172.	0.9	19
22678	First principle calculations on the adsorption of molecular H2 in the largest pore of Co[Fe(CN)5NO] and Ni[Fe(CN)5NO] metal nitroprussides. Effect of the charged cavities on the adsorption and H2-host interactions. Computational Materials Science, 2016, 114, 102-111.	1.4	3
22679	The carbon-substitutionalâ€“carbon-interstitial (CsCi) defect pair in silicon from hybrid functional calculations. Computational Materials Science, 2016, 118, 338-341.	1.4	6
22680	Adsorption and migration behaviours of Nbâ€“C atoms on clean diamond (0 0 1) surface: A first principles study. Computational Materials Science, 2016, 121, 159-166.	1.4	10
22681	Point defects and Zn-doping in defective Laves phase C15 MgCu2: A first-principles study. Computational Materials Science, 2016, 122, 159-166.	1.4	10
22682	A first principles study of O2 dissociation on Pt modified ZrC(100) surface. Chemical Physics Letters, 2016, 649, 141-147.	1.2	11
22683	Strain modulating half-metallicity of semifluorinated GaN nanosheets. Chemical Physics Letters, 2016, 653, 42-46.	1.2	4
22684	Collision-induced fusion of two single-walled carbon nanotubes: A quantitative study. Chemical Physics Letters, 2016, 657, 184-189.	1.2	2
22685	Activation Effect of Electrochemical Cycling on Gold Nanoparticles towards the Hydrogen Evolution Reaction in Sulfuric Acid. Electrochimica Acta, 2016, 209, 440-447.	2.6	32
22686	Experimental and ab-initio study of the Zr- and Cr-enriched aluminide layer produced on an IN 713C Inconel substrate by CVD; investigations of the layer morphology, structural stability, mechanical properties, and corrosion resistance. Intermetallics, 2016, 74, 15-24.	1.8	11
22687	The distribution trends and site preferences of alloying elements in precipitates within a Zr alloy: A combined first-principles and experimental study. Journal of Alloys and Compounds, 2016, 678, 456-462.	2.8	10
22688	Ab-initio study of C and O impurities in uranium nitride. Journal of Nuclear Materials, 2016, 478, 112-118.	1.3	20

#	Article	IF	Citations
22689	Temperature-Dependent Hole Mobility and Its Limit in Crystal-Phase P3HT Calculated from First Principles. Journal of Physical Chemistry B, 2016, 120, 5572-5580.	1.2	10
22690	Defect Formation and Diffusion on the (001) Surface of LiKCO3 for Fuel Cell Applications: Insight from Hybrid DFT. Journal of Physical Chemistry C, 2016, 120, 12941-12951.	1.5	7
22691	Size-selective electrocatalytic activity of (Pt)_n/MoS₂ for oxygen reduction reaction. Catalysis Science and Technology, 2016, 6, 6389-6395.	2.1	16
22692	Effect of compression on the electronic, optical and transport properties of MoS ₂ /graphene-based junctions. 2D Materials, 2016, 3, 025018.	2.0	40
22693	The structural stability, mechanical properties and stacking fault energy of Al3Zr precipitates in Al-Cu-Zr alloys: HRTEM observations and first-principles calculations. Journal of Alloys and Compounds, 2016, 681, 96-108.	2.8	49
22694	Intrinsic reactivity of Ni, Pd and Pt surfaces in dry reforming and competitive reactions: Insights from first principles calculations and microkinetic modeling simulations. Journal of Catalysis, 2016, 343, 196-207.	3.1	156
22695	Direct time-domain observation of attosecond final-state lifetimes in photoemission from solids. Science, 2016, 353, 62-67.	6.0	181
22696	Short-range effect at the semi-coherent metal/its native oxide interface. Applied Surface Science, 2016, 378, 451-459.	3.1	3
22697	Structural, functional and mechanical properties of spark plasma sintered gadolinia (Gd 2 O 3). Ceramics International, 2016, 42, 1384-1391.	2.3	17
22698	First-principles calculations of generalized-stacking-fault-energy of Co-based alloys. Computational Materials Science, 2016, 121, 86-96.	1.4	67
22699	First principles phonon calculations of dielectric properties in Ba2MWO6 (M = Mg, Zn). Computational Materials Science, 2016, 122, 146-149.	1.4	8
22700	Metal-modified niobium carbides as low-cost and impurity-resistant electrocatalysts for hydrogen evolution in acidic and alkaline electrolytes. International Journal of Hydrogen Energy, 2016, 41, 5948-5954.	3.8	21
22701	First principles design of Li functionalized hydrogenated h-BN nanosheet for hydrogen storage. International Journal of Hydrogen Energy, 2016, 41, 14437-14446.	3.8	65
22702	Effect of Si substitution on structural, electronic and optical properties of YNi4Si-type DyNi5â^'Si (x=0,) Tj ETQq1 1 0.784314 rgBT /Ov	1.0	4
22703	A comparison study of oxygen reduction on the supported Pt, Pd, Au monolayer on WC(0001). Journal of Power Sources, 2016, 321, 163-173.	4.0	34
22704	Strong influence of off-site symmetry positions of hydrogen atoms in ScH3 hcp phases. Solid State Communications, 2016, 225, 48-55.	0.9	3
22705	First-principles study on reconstruction of 4H-SiC(0001) and (000<mml:math) Tj ETQq0 0 0 rgBT /Overlock 10 Tf 50 112 Td (xmlns:mml Surface Science, 2016, 647, 45-50.	0.8	9
22706	The structure and electronic properties of Ge/SrZrO 3. Vacuum, 2016, 130, 165-173.	1.6	2

#	Article	IF	Citations
22707	First-principles studies on the charge density wave in uranium. Modelling and Simulation in Materials Science and Engineering, 2016, 24, 055011.	0.8	4
22708	Surface reactivity of Ge[111] for organic functionalization by means of a radical-initiated reaction: A DFT study. Applied Surface Science, 2016, 379, 14-22.	3.1	4
22709	Charge transfer of edge states in zigzag silicene nanoribbons with Stoneâ€“Wales defects from first-principles. Applied Surface Science, 2016, 383, 310-316.	3.1	9
22710	Formation of InN atomic-size wires by simple N adsorption on the In/Si(111)â€“(4 Ã— 1) surface. Applied Surface Science, 2016, 385, 318-323.	3.1	3
22711	CO2 stability on the Ni low-index surfaces: van der Waals corrected DFT analysis. Catalysis Communications, 2016, 80, 33-38.	1.6	40
22712	Ab initio proposition of novel BCN3 hard material based on the intergrowth of wurtzite and pyrite-like motifs. Computational Condensed Matter, 2016, 7, 14-19.	0.9	2
22713	First principles calculations of SrZrO3 bulk and ZrO2-terminated (001) surface F centers. Computational Condensed Matter, 2016, 7, 1-6.	0.9	26
22714	Density functional theory calculations of the nitrogen-rich energetic compound 3,4-diamino-1,2,4-triazolium 1-aminotetrazol-5-oneate. Computational Materials Science, 2016, 121, 225-231.	1.4	1
22715	Adsorption of H 2 S on Î± -Cr 2 O 3 (0001) surfaces: A density functional theory investigation. Corrosion Science, 2016, 111, 1-12.	3.0	10
22716	Intriguing luminescence properties of (Ba, Sr)3Si6O9N4: Eu2+ phosphors via modifying synthesis method and cation substitution. Journal of Alloys and Compounds, 2016, 682, 481-488.	2.8	31
22717	Exploring phase stability, electronic and mechanical properties of Ceâ€“Pb intermetallic compounds using first-principles calculations. Journal of Solid State Chemistry, 2016, 237, 385-393.	1.4	11
22718	Effect of substitutional impurities on the electronic transport properties of graphene. Physica E: Low-Dimensional Systems and Nanostructures, 2016, 84, 22-26.	1.3	20
22719	Mechanical properties of Bi2Te3 topological insulator investigated by density functional theory and nanoindentation. Scripta Materialia, 2016, 121, 50-55.	2.6	22
22720	Structural and mechanical properties of alkali hydrides investigated by the first-principles calculations and principal component analysis. Solid State Sciences, 2016, 58, 30-36.	1.5	6
22721	Enhanced interfacial proton migration on BaZr(Y)O3 by molten carbonate: A first principles study. Solid State Ionics, 2016, 289, 48-54.	1.3	7
22722	Adsorption and decomposition of monopropellant molecule HAN on Pd(100) and Ir(100) surfaces: A DFT study. Surface Science, 2016, 653, 1-10.	0.8	10
22723	Bending rigidity of transition metal dichalcogenide monolayers from first-principles. Journal Physics D: Applied Physics, 2016, 49, 185301.	1.3	33
22724	Chiral vectors-tunable electronic property of MoS2 nanotubes. Physica E: Low-Dimensional Systems and Nanostructures, 2016, 83, 232-237.	1.3	6

#	Article	IF	Citations
22725	First-principles study of thermal expansion and thermomechanics of single-layer black and blue phosphorus. Physics Letters, Section A: General, Atomic and Solid State Physics, 2016, 380, 2098-2104.	0.9	60
22726	Revisiting Ir(CO)3Cl. Polyhedron, 2016, 103, 141-149.	1.0	11
22727	Synthesis and structure of a new halophosphate Sr 3 P 3 O 10 Cl with the flexible [P 3 O 10] 5â˜ anions. Solid State Sciences, 2016, 55, 159-163.	1.5	7
22728	Electronic properties of surface/bulk iodine defects of CsSnBr3 perovskite. Surface and Coatings Technology, 2016, 306, 159-163.	2.2	17
22729	A first-principles study on interaction of Mg/Ni interface and its hydrogen absorption characteristics. Surface Science, 2016, 649, 133-137.	0.8	5
22730	Superlattice supertoughness of TiN/MN (M = V, Nb, Ta, Mo, and W): First-principles study. Thin Solid Films, 2016, 607, 59-66.	0.8	23
22731	First-principles investigation of mechanical and electronic properties of LaAg5 Laves phase under pressure. Journal of Rare Earths, 2016, 34, 105-112.	2.5	0
22732	Proteinâ€“Support Interactions for Rationally Designed Bilirubin Oxidase Based Cathode: A Computational Study. Journal of Physical Chemistry B, 2016, 120, 3634-3641.	1.2	24
22733	Effects of Chain Length on the Mechanism and Rates of Metal-Catalyzed Hydrogenolysis of n-Alkanes. Journal of Physical Chemistry C, 2016, 120, 8125-8138.	1.5	49
22734	Role of Cations on the Electronic Transport and Optical Properties of Lead-Iodide Perovskites. Journal of Physical Chemistry C, 2016, 120, 16259-16270.	1.5	56
22735	Metal Adatoms and Clusters on Ultrathin Zirconia Films. Journal of Physical Chemistry C, 2016, 120, 9920-9932.	1.5	18
22736	Synthesis, Characterization, and Theoretical Studies of (Pb₄O)Pb₂B₆O₁₄: A New Lead(II) Borate with Isolated Oxygen-Centered Pb₄O Tetrahedra and Large Second Harmonic Generation Response. Journal of Physical Chemistry C, 2016, 120, 12757-12764.	1.5	39
22737	How Does the Surface Structure of Ptâ€“Ni Alloys Control Water and Hydrogen Peroxide Formation?. ACS Catalysis, 2016, 6, 5641-5650.	5.5	9
22738	Dilute Magnetic Semiconductor and Half-Metal Behaviors in 3d Transition-Metal Doped Black and Blue Phosphorenes: A First-Principles Study. Nanoscale Research Letters, 2016, 11, 77.	3.1	99
22739	Tension-Enhanced Hydrogen Evolution Reaction on Vanadium Disulfide Monolayer. Nanoscale Research Letters, 2016, 11, 113.	3.1	37
22740	Ferromagnetism in Transitional Metal-Doped MoS2 Monolayer. Nanoscale Research Letters, 2016, 11, 154.	3.1	103
22741	Sound velocities of bridgmanite from density of states determined by nuclear inelastic scattering and first-principles calculations. Progress in Earth and Planetary Science, 2016, 3, .	1.1	6
22742	Defect energetics and magnetic properties of 3d-transition-metal-doped topological crystalline insulator SnTe. Science China: Physics, Mechanics and Astronomy, 2016, 59, 1.	2.0	3

#	Article	IF	Citations
22743	Interface properties of Ge on cubic SrHfO3 (001). Journal of Crystal Growth, 2016, 443, 66-74.	0.7	2
22744	Ab initio simulations of the structure, energetics and mobility of radiation-induced point defects in bcc Nb. Journal of Nuclear Materials, 2016, 478, 185-196.	1.3	21
22745	Interaction of Adatoms and Molecules with Single-Layer Arsenene Phases. Journal of Physical Chemistry C, 2016, 120, 14345-14355.	1.5	98
22746	Microwave-Assisted Synthesis of Pd_xAu_{100â€“x} Alloy Nanoparticles: A Combined Experimental and Theoretical Assessment of Synthetic and Compositional Effects upon Catalytic Reactivity. ACS Catalysis, 2016, 6, 4882-4893.	5.5	54
22747	Adding a new dimension to the chemistry of phosphorus and arsenic. Physical Chemistry Chemical Physics, 2016, 18, 17586-17591.	1.3	39
22748	Towards more accurate prediction of activation energies for polyalcohol dehydrogenation on transition metal catalysts in water. Catalysis Science and Technology, 2016, 6, 6615-6624.	2.1	31
22749	The structure-dependent enhancement of the oxygen reduction reaction performance of Co-based low Pt catalysts through Au addition. Journal of Materials Chemistry A, 2016, 4, 11023-11029.	5.2	15
22750	Possible new metastable Mo2Ga2C and its phase transition under pressure: a density functional prediction. Journal of Materials Science, 2016, 51, 8452-8460.	1.7	8
22751	Comparisons between adsorption and diffusion of alkali, alkaline earth metal atoms on silicene and those on silicane: Insight from first-principles calculations. Chinese Physics B, 2016, 25, 067103.	0.7	17
22752	High-Pressure Crystal Structures of an Insensitive Energetic Crystal: 1,1-Diamino-2,2-dinitroethene. Journal of Physical Chemistry C, 2016, 120, 1218-1224.	1.5	42
22753	Structural optimization and physical properties of TcB3 and MoB3 at high-pressure: First-principles. International Journal of Modern Physics B, 2016, 30, 1650131.	1.0	6
22754	The plasticity of highly oriented nano-layered Zr/Nb composites. Acta Materialia, 2016, 115, 189-203.	3.8	60
22755	Ab-initio study of half-metallic ferromagnetism in Co/Ni substituted Li2X (X=S, Se, Te) compounds. Journal of Magnetism and Magnetic Materials, 2016, 418, 148-157.	1.0	2
22756	Electronic structure and magnetic properties of Co2TaAl from ab initio calculations. Journal of Science: Advanced Materials and Devices, 2016, 1, 286-289.	1.5	11
22757	Peculiar Piezoelectric Properties of Soft Two-Dimensional Materials. Journal of Physical Chemistry C, 2016, 120, 13948-13953.	1.5	50
22758	Understanding divergent behaviors in the photocatalytic hydrogen evolution reaction on CdS and ZnS: a DFT based study. Physical Chemistry Chemical Physics, 2016, 18, 16862-16869.	1.3	36
22759	Stabilization of alkali metal ions interaction with OH-functionalized graphene via clustering of OH groups â€“ implications in charge storage applications. RSC Advances, 2016, 6, 57910-57919.	1.7	25
22760	Probing the local environment of substitutional Al $$^{3+}$$ 3 + in goethite using X-ray absorption spectroscopy and first-principles calculations. Physics and Chemistry of Minerals, 2016, 43, 217-227.	0.3	15

#	Article	IF	Citations
22762	First-Principles Calculations of the Dynamical and Thermodynamic Properties of Yttrium Compounds YX (XÂ=ÂN, P, As and Sb). Journal of Phase Equilibria and Diffusion, 2016, 37, 336-344.	0.5	9
22763	Enthalpies of formation of TMâ€“X compounds (X=Al, Ga, Si, Ge, Sn). Comparison of ab-initio values and experimental data. Calphad: Computer Coupling of Phase Diagrams and Thermochemistry, 2016, 54, 16-34.	0.7	12
22764	Mechanical properties study for new hypothetical crystalline phases of ReB2: A computational approach using density functional theory. Computational Materials Science, 2016, 122, 240-248.	1.4	8
22765	Tolerance of non-platinum group metals cathodes proton exchange membrane fuel cells to air contaminants. Journal of Power Sources, 2016, 324, 556-571.	4.0	34
22766	Interaction between fullerene-wheeled nanocar and gold substrate: A DFT study. Physica E: Low-Dimensional Systems and Nanostructures, 2016, 83, 174-179.	1.3	15
22767	A DFT study of the adsorption of O₂ and H₂O on Al(111) surfaces. RSC Advances, 2016, 6, 56303-56312.	1.7	37
22768	Systematic Theoretical Study of Ethylene Adsorption on Î´-MoC(001), TiC(001), and ZrC(001) Surfaces. Journal of Physical Chemistry C, 2016, 120, 13531-13540.	1.5	19
22769	Tuning the Electronic Structure of the Metalâ€“Oxygen Group by Silicon Substitution in Lithium-Rich Manganese-Based Oxides for Superior Performance. Journal of Physical Chemistry C, 2016, 120, 13421-13426.	1.5	23
22770	A first-principles study of the tuning effect of a Fe₂O₃ cluster on the dehydrogenation properties of a LiBH₄ (001) surface. Dalton Transactions, 2016, 45, 10954-10959.	1.6	10
22771	Density Functional Theory Study of Hydrogen Adsorption in a Tiâ€Decorated Mgâ€Based Metalâ€“Organic Frameworkâ€74. ChemPhysChem, 2016, 17, 879-884.	1.0	25
22772	Application of zoneâ€folding approach to the firstâ€principles estimation of thermodynamic properties of carbon and <scp>ZrS</scp>₂â€based nanotubes. Journal of Computational Chemistry, 2016, 37, 641-652.	1.5	13
22773	Firstâ€principles Study of Stability of Cu in the Ndâ€rich and Nd Oxide Phases of Ndâ€Feâ€B Permanent Magnet. Journal of the Chinese Chemical Society, 2016, 63, 506-512.	0.8	7
22774	CO gas optoâ€electronic sensor using semiconductor graphene nanoribbons: A firstâ€principles study. Physica Status Solidi (B): Basic Research, 2016, 253, 559-565.	0.7	3
22775	Magnetotransport properties of corrugated stanene in the presence of electric modulation and tilted magnetic field. Physica Status Solidi (B): Basic Research, 2016, 253, 300-307.	0.7	8
22776	Site preference of manganese in Mn-alloyed cementite. Physica Status Solidi (B): Basic Research, 2016, 253, 1623-1628.	0.7	7
22777	First-principles and molecular dynamics studies on structural, electronic, and magnetic characteristics of (CaC)1/(SiC)1and (KC)1/(SiC)1in wurtzite structure. Physica Status Solidi (B): Basic Research, 2016, 253, 1734-1742.	0.7	2
22778	New description of metastable hcp phase for unaries Fe and Mn: Coupling between first-principles calculations and CALPHAD modeling. Physica Status Solidi (B): Basic Research, 2016, 253, 1830-1836.	0.7	34
22779	The structural, electronic, and magnetic properties of the stoichiometric (001) surface of double perovskite <scp>Sr₂FeMoO₆</scp>. Surface and Interface Analysis, 2016, 48, 1040-1047.	0.8	3

#	Article	IF	Citations
22780	Phase dependent structural and electronic properties of lanthanum orthophosphate (LaPO₄). Journal of Physics Condensed Matter, 2016, 28, 205501.	0.7	15
22781	First-principles study of lattice thermal conductivity of Tdâ€“WTe₂. New Journal of Physics, 2016, 18, 033017.	1.2	31
22782	Structural and electronic properties of Er_{0.5}Lu_{0.5}B₂and LuB₂compounds by using the PBE0 hybrid functional. Journal of Physics: Conference Series, 2016, 687, 012053.	0.3	1
22783	A density functional theory study of propylene epoxidation on RuO2(110) surface. Applied Surface Science, 2016, 385, 99-105.	3.1	17
22784	Structural, electronic, optical and bonding properties of strontianite, SrCO3: First-principles calculations. Journal of Physics and Chemistry of Solids, 2016, 98, 65-70.	1.9	10
22785	Halide Free M(BH₄)₂ (M = Sr, Ba, and Eu) Synthesis, Structure, and Decomposition. Inorganic Chemistry, 2016, 55, 7090-7097.	1.9	26
22786	Reaction Mechanism of Ethanol on Model Cobalt Catalysts: DFT Calculations. Journal of Physical Chemistry C, 2016, 120, 14198-14208.	1.5	19
22787	Revealing the Multibonding State between Hydrogen and Graphene-Supported Ti Clusters. Journal of Physical Chemistry C, 2016, 120, 12974-12979.	1.5	21
22788	Catalyst Site Selection via Control over Noncovalent Interactions in Self-Assembled Monolayers. ACS Catalysis, 2016, 6, 5086-5094.	5.5	44
22789	A periodic DFT study of adsorption of water on sodium-montmorillonite (001) basal and (010) edge surface. Applied Surface Science, 2016, 387, 308-316.	3.1	94
22790	Machine Learning Assisted Predictions of Intrinsic Dielectric Breakdown Strength of ABX₃ Perovskites. Journal of Physical Chemistry C, 2016, 120, 14575-14580.	1.5	147
22791	Can singly charged oxygen vacancies induce ferromagnetism in biaxial strained ZnO?. Physica Scripta, 2016, 91, 045801.	1.2	0
22792	Dispersion-corrected DFT investigation on defect chemistry and potassium migration in potassium-graphite intercalation compounds for potassium ion batteries anode materials. Carbon, 2016, 107, 885-894.	5.4	83
22793	Strong adsorption of Al-doped carbon nanotubes toward cisplatin. Chemical Physics Letters, 2016, 658, 162-167.	1.2	12
22794	First-principles calculations of the structural, elastic and thermodynamic properties of tetragonal copper-titanium intermetallic compounds. Journal of Alloys and Compounds, 2016, 687, 984-989.	2.8	22
22795	Lattice thermal conductivity of NiTiSn half-Heusler thermoelectric materials from first-principles calculations. Journal of Alloys and Compounds, 2016, 688, 248-252.	2.8	21
22796	Characterization of LSMO/C60 spinterface by first-principle calculations. Organic Electronics, 2016, 37, 55-60.	1.4	6
22797	Surface Doping of Sn in Orthorhombic CH3NH3PbI3 for Potential Perovskite Solar Cells: First Principles Study. Surface and Coatings Technology, 2016, 306, 285-289.	2.2	14

#	Article	IF	Citations
22798	Momentum-dependent band spin splitting in semiconducting MnO₂: a density functional calculation. Physical Chemistry Chemical Physics, 2016, 18, 13294-13303.	1.3	39
22799	An Organic Spin Valve Embedding a Selfâ€Assembled Monolayer of Organic Radicals. Advanced Materials Interfaces, 2016, 3, 1500855.	1.9	32
22800	Effects of Ga doping on Pt/CeO₂â€Al₂O₃ catalysts for propane dehydrogenation. AIChE Journal, 2016, 62, 4365-4376.	1.8	79
22801	Spatially Resolved Quantification of the Surface Reactivity of Solid Catalysts. Angewandte Chemie, 2016, 128, 6347-6351.	1.6	21
22802	Nitrogenâ€Rich Manganese Oxynitrides with Enhanced Catalytic Activity in the Oxygen Reduction Reaction. Angewandte Chemie - International Edition, 2016, 55, 7963-7967.	7.2	52
22803	Existence patterns of Dy in Î²-NiAl from first-principles calculations. Rare Metals, 2016, 35, 356-360.	3.6	2
22804	Transition Metal Nitrides: A First Principles Study. High Temperature Materials and Processes, 2016, 35, 389-398.	0.6	8
22805	Understanding the unusual friction behavior of hydrogen-free diamond-like carbon films in oxygen atmosphere by first-principles calculations. Carbon, 2016, 100, 556-563.	5.4	50
22806	Enhancing the Photocatalytic Activity of BiVO₄ for Oxygen Evolution by Ce Doping: Ce³⁺ Ions as Hole Traps. Journal of Physical Chemistry C, 2016, 120, 2058-2063.	1.5	121
22807	Spinâ€“orbit coupling effects on electronic structures in stanene nanoribbons. Physical Chemistry Chemical Physics, 2016, 18, 6534-6540.	1.3	42
22808	The bifurcation point of the oxygen reduction reaction on Auâ€“Pd nanoalloys. Faraday Discussions, 2016, 188, 257-278.	1.6	26
22809	Optical phonons in the kesterite Cu₂ZnGeS₄semiconductor: polarized Raman spectroscopy and first-principle calculations. RSC Advances, 2016, 6, 13278-13285.	1.7	35
22810	2D transition-metal diselenides: phase segregation, electronic structure, and magnetism. Journal of Physics Condensed Matter, 2016, 28, 064002.	0.7	17
22811	Effect of pressure on structural, electronic, mechanical and optical properties of ruthenium diboride with oP12-type structure. Indian Journal of Physics, 2016, 90, 767-779.	0.9	3
22812	Suppression of surface recombination in CuInSe2 (CIS) thin films via Trioctylphosphine Sulfide (TOP:S) surface passivation. Acta Materialia, 2016, 106, 171-181.	3.8	13
22813	Impurity-induced ferromagnetism and metallicity of WS2 monolayer. Ceramics International, 2016, 42, 2364-2369.	2.3	25
22814	Effects of oxygen vacancy on 3d transition-metal doped anatase TiO2: First principles calculations. Chemical Physics Letters, 2016, 647, 36-41.	1.2	29
22815	A DFT study of atomic structure and adhesion at the Fe(BCC)/Fe3O4 interfaces. Surface Science, 2016, 647, 55-65.	0.8	12

#	Article	IF	Citations
22816	Synthesis and Reaction Mechanism of Novel Fluorinated Carbon Fiber as a High-Voltage Cathode Material for Rechargeable Na Batteries. Chemistry of Materials, 2016, 28, 1026-1033.	3.2	53
22817	Low-Frequency Interlayer Raman Modes to Probe Interface of Twisted Bilayer MoS₂. Nano Letters, 2016, 16, 1435-1444.	4.5	177
22818	Lithiumâ€“Boron (Liâ€“B) Monolayers: First-Principles Cluster Expansion and Possible Two-Dimensional Superconductivity. ACS Applied Materials & Interfaces, 2016, 8, 2526-2532.	4.0	49
22819	First-principles study of structural, elastic, electronic and thermodynamic properties of topological insulator Bi₂Se₃under pressure. Philosophical Magazine, 2016, 96, 208-222.	0.7	39
22820	Stacking dependence of carrier transport properties in multilayered black phosphorous. Journal of Physics Condensed Matter, 2016, 28, 075001.	0.7	13
22821	Enhanced near-infrared shielding ability of (Li,K)-codoped WO₃for smart windows: DFT prediction validated by experiment. Nanotechnology, 2016, 27, 075203.	1.3	28
22822	A new family of sp 3 -hybridized carbon phases. Chinese Physics B, 2016, 25, 016103.	0.7	8
22823	Electronic structure and elastic properties of AgZn under pressure from first-principles calculations. Canadian Journal of Physics, 2016, 94, 328-333.	0.4	2
22824	A comparison of mechanical properties between Al and Al3Mg. International Journal of Modern Physics B, 2016, 30, 1550243.	1.0	7
22825	Interfacial structure, ferroelectric stability, and magnetoelectric effect of magnetoelectric junction FeCo/BaTiO3/FeCo with alloy electrode. Journal of Materials Science, 2016, 51, 3297-3302.	1.7	3
22826	Insigths into the Tribochemistry of Silicon-doped Carbon-Based Films by Ab Initio Analysis of Waterâ€“Surface Interactions. Tribology Letters, 2016, 61, 1.	1.2	17
22827	Different spin textures in one-dimensional electronic bands on Si(553)-Au surface. Applied Surface Science, 2016, 373, 26-31.	3.1	17
22828	Physical properties of predicted Ti2CdN versus existing Ti2CdC MAX phase: An ab initio study. Computational Materials Science, 2016, 113, 148-153.	1.4	101
22829	Site preference and diffusion of hydrogen during hydrogenation of Mg: A first-principles study. International Journal of Hydrogen Energy, 2016, 41, 3508-3516.	3.8	12
22830	First-principles investigation on the interaction of Boron atom with Nickel part I: From surface adsorption to bulk diffusion. Journal of Alloys and Compounds, 2016, 663, 116-122.	2.8	8
22831	A new approach for fabricating germanene with Dirac electrons preserved: a first principles study. Journal of Materials Chemistry C, 2016, 4, 1736-1740.	2.7	18
22832	Interface morphology and composition of Ga(NAsP) quantum well structures for monolithically integrated LASERs on silicon substrates. Journal Physics D: Applied Physics, 2016, 49, 075108.	1.3	18
22833	DFT study of catalytic activity of an ultrathin TiO2(110) layer covering Au(112): O2 activation, CO oxidation, and replacing Au with Ag. Catalysis Communications, 2016, 77, 79-82.	1.6	14

#	Article	IF	Citations
22834	Lower temperature deformation mechanisms in a Î³â€³-strengthened Ni-base superalloy. Scripta Materialia, 2016, 115, 108-112.	2.6	28
22835	Catalytic Activity of MS₂ Monolayer for Electrochemical Hydrogen Evolution. Journal of Physical Chemistry C, 2016, 120, 1623-1632.	1.5	75
22836	Sc-Decorated WS ₂ Nanoribbons as Hydrogen Storage Media. Chinese Physics Letters, 2016, 33, 016802.	1.3	4
22837	Molecular Dynamics Simulations on O 2 Permeation through Nafion Ionomer on Platinum Surface. Electrochimica Acta, 2016, 188, 767-776.	2.6	198
22838	N-heterocycles as corrosion inhibitors for mild steel in acid medium. Journal of Molecular Liquids, 2016, 216, 42-52.	2.3	94
22839	Comparison of Storage Mechanisms in RuO₂, SnO₂, and SnS₂for Lithium-Ion Battery Anode Materials. Journal of Physical Chemistry C, 2016, 120, 2036-2046.	1.5	54
22840	Defects-assisted ferromagnetism due to bound magnetic polarons in Ce into Fe, Co:ZnO nanoparticles and first-principle calculations. Physical Chemistry Chemical Physics, 2016, 18, 5647-5657.	1.3	38
22841	Stabilities and defect-mediated lithium-ion conduction in a ground state cubic Li₃N structure. Physical Chemistry Chemical Physics, 2016, 18, 4185-4190.	1.3	5
22842	Tuning the Nanofriction Between Two Graphene Layers by External Electric Fields: A Density Functional Theory Study. Tribology Letters, 2016, 61, 1.	1.2	15
22843	The influence of alloying elements on the corrosion of Zr alloys. Corrosion Science, 2016, 105, 36-43.	3.0	40
22844	Pressure-induced reappearance of superconductivity in the oC24 phase of lithium. Solid State Communications, 2016, 225, 7-11.	0.9	3
22845	Neutron diffraction study of the itinerant-electron metamagnetic Hf0.825Ta0.175Fe2 compound. Solid State Communications, 2016, 229, 16-21.	0.9	11
22846	Multigrid-Based Methodology for Implicit Solvation Models in Periodic DFT. Journal of Chemical Theory and Computation, 2016, 12, 1331-1341.	2.3	61
22847	Organic Pollutant Photodecomposition by Ag/KNbO₃ Nanocomposites: A Combined Experimental and Theoretical Study. Journal of Physical Chemistry C, 2016, 120, 2777-2786.	1.5	50
22848	On the nature of the solvated electron in ice I_h. Physical Chemistry Chemical Physics, 2016, 18, 4652-4658.	1.3	6
22849	Amino acid modified copper electrodes for the enhanced selective electroreduction of carbon dioxide towards hydrocarbons. Energy and Environmental Science, 2016, 9, 1687-1695.	15.6	290
22850	Phonon transport at the interfaces of vertically stacked graphene and hexagonal boron nitride heterostructures. Nanoscale, 2016, 8, 4037-4046.	2.8	38
22851	Contact-dependent mechanical properties of graphene nanoribbons: anab initiostudy. Nanotechnology, 2016, 27, 025702.	1.3	1

#	Article	IF	Citations
22852	Structural, anisotropic and electronic properties of C96 under pressure. European Physical Journal B, 2016, 89, 1.	0.6	6
22853	Elasticity, ideal tensile strength and lattice dynamics of LuH 2 dihydride from first-principles investigations. International Journal of Hydrogen Energy, 2016, 41, 2720-2726.	3.8	3
22854	Adsorption of uranyl species on hydroxylated titanium carbide nanosheet: A first-principles study. Journal of Hazardous Materials, 2016, 308, 402-410.	6.5	115
22855	Luminescence Properties of SrZrO₃/Tb³⁺ Perovskite: Host-Dopant Energy-Transfer Dynamics and Local Structure of Tb³⁺. Inorganic Chemistry, 2016, 55, 1728-1740.	1.9	96
22856	Structural and electronic properties of zigzag InP nanoribbons with Stoneâ€“Wales type defects. Journal of Physics Condensed Matter, 2016, 28, 065503.	0.7	1
22857	Electronic and optical properties of NH4NO3 and NaNO3: an ab initio study. Indian Journal of Physics, 2016, 90, 861-867.	0.9	2
22858	Control of crystallite and particle size in the synthesis of layered double hydroxides: Macromolecular insights and a complementary modeling tool. Journal of Colloid and Interface Science, 2016, 468, 86-94.	5.0	66
22859	Interaction of Al, Ti, and Cu Atoms with Boron Nitride Nanotubes: A Computational Investigation. Journal of Physical Chemistry C, 2016, 120, 3509-3518.	1.5	12
22860	First-Principle Study of Adsorption and Desorption of Chlorine on Cu(111) Surface: Does Chlorine or Copper Chloride Desorb?. Journal of Physical Chemistry C, 2016, 120, 2829-2836.	1.5	13
22861	Structural, electronic and optical properties of hexagonal TaN compound. International Journal of Modern Physics B, 2016, 30, 1650010.	1.0	4
22862	Mechanical properties of the interface structure of nanodiamond composite films: First-principles studies. Applied Surface Science, 2016, 363, 522-531.	3.1	2
22863	Understanding the stability of Fe incorporation within Mn3N2(001) surfaces: An ab-initio study. Applied Surface Science, 2016, 363, 651-658.	3.1	3
22864	Force-based optimization of pseudopotentials for non-equilibrium configurations. Computer Physics Communications, 2016, 201, 106-118.	3.0	4
22865	Mechanical properties of the hypereutectoid Feâ€“Crâ€“C hardfacing coatings with different nano-Y2O3 additives and the mechanism analysis. Materials Science & Engineering A: Structural Materials: Properties, Microstructure and Processing, 2016, 655, 346-354.	2.6	12
22866	Prediction of topological phase transition in X2â€“SiGe monolayers. Physical Chemistry Chemical Physics, 2016, 18, 3669-3674.	1.3	14
22867	Tuning band inversion symmetry of buckled III-Bi sheets by halogenation. Nanotechnology, 2016, 27, 055704.	1.3	42
22868	First-principles investigation on mechanical behaviors of Wâ€“Cr/Ti binary alloys. Journal of Nuclear Materials, 2016, 468, 105-112.	1.3	22
22869	Kinetics of Topological Stoneâ€“Wales Defect Formation in Single-Walled Carbon Nanotubes. Journal of Physical Chemistry C, 2016, 120, 1989-1993.	1.5	17

#	Article	IF	Citations
22870	A computational study of quantum transport properties of hydrogen passivated graphene monoxide: NDR and rectification. Canadian Journal of Physics, 2016, 94, 343-347.	0.4	1
22871	Density functional theory calculations for estimation of gettering sites of C, H, intrinsic point defects and related complexes in Si wafers. Materials Science in Semiconductor Processing, 2016, 44, 13-17.	1.9	24
22872	Isotropic strains tuned hole-mediated ferromagnetism in nitrogen-doped ZnO. Physics Letters, Section A: General, Atomic and Solid State Physics, 2016, 380, 465-469.	0.9	0
22873	Structure and Properties of Egyptian Blue Monolayer Family: XCuSi₄O₁₀ (X =) Tj ETQq1 1 0.784314 rgBT /O	2.1	24
22874	Nickel supported on nitrogen-doped carbon nanotubes as hydrogen oxidation reaction catalyst in alkaline electrolyte. Nature Communications, 2016, 7, 10141.	5.8	368
22875	Probing the electrochemical capacitance of MXene nanosheets for high-performance pseudocapacitors. Physical Chemistry Chemical Physics, 2016, 18, 4460-4467.	1.3	65
22876	Metalâ€“semiconductorâ€“metal transition in zigzag carbon nanoscrolls. Nanoscale, 2016, 8, 2887-2891.	2.8	3
22877	Defect charge states in Si doped hexagonal boron-nitride monolayer. Journal of Physics Condensed Matter, 2016, 28, 055501.	0.7	13
22878	Crystal structures and mechanical properties of M (Mg, Sr, Ba, La) x Ca 1â^'x B 6 solid solution: A first principles study. Ceramics International, 2016, 42, 6632-6639.	2.3	10
22879	Insights into the synergistic role of metalâ€“lattice oxygen site pairs in four-centered Câ€“H bond activation of methane: the case of CuO. Catalysis Science and Technology, 2016, 6, 3984-3996.	2.1	59
22880	Tuning the electronic and optical properties of phosphorene by transition-metal and nonmetallic atom co-doping. RSC Advances, 2016, 6, 10919-10929.	1.7	53
22881	The first principle study of electronic and optical properties in rhombohedral BiAlO₃. Modern Physics Letters B, 2016, 30, 1650006.	1.0	8
22882	Combined atom probe tomography and density functional theory investigation of the Al off-stoichiometry of Îº-carbides in an austenitic Feâ€“Mnâ€“Alâ€“C low density steel. Acta Materialia, 2016, 106, 229-238.	3.8	97
22883	Solubility, permeation, and capturing of impurity oxygen in Au/Ag: A comparative investigation from first-principles. Computational Materials Science, 2016, 114, 79-85.	1.4	13
22884	Phase stability, elastic properties and martensitic transformation temperature of Zr50Pd50â€“xRux alloys from first-principles calculations. Journal of Alloys and Compounds, 2016, 662, 484-488.	2.8	11
22885	Ab Initio Structure Determination and Photoluminescent Properties of an Efficient, Thermally Stable Blue Phosphor, Ba₂Y₅B₅O₁₇:Ce³⁺. Chemistry of Materials, 2016, 28, 1121-1127.	3.2	78
22886	Nanoscale stabilization of zintl compounds: 1D ionic Liâ€“P double helix confined inside a carbon nanotube. Nanoscale, 2016, 8, 3454-3460.	2.8	14
22887	Microalloying for the controllable delay of precipitate formation in metal alloys. Acta Materialia, 2016, 106, 117-128.	3.8	32

#	Article	IF	Citations
22888	Intrinsic strength and failure behaviors of ultra-small single-walled carbon nanotubes. Computational Materials Science, 2016, 114, 167-171.	1.4	16
22889	Carbon adsorption on tungsten and electronic field emission. Surface Science, 2016, 645, 56-62.	0.8	11
22890	Hydrogen Bond Symmetrization in Glycinium Oxalate under Pressure. Journal of Physical Chemistry B, 2016, 120, 851-859.	1.2	37
22891	A pH-Sensitive Supramolecular Switch Based on Mixed Carboxylic Acid Terminated Self-Assembled Monolayers on Au(111). Langmuir, 2016, 32, 947-953.	1.6	19
22892	Experimental and Computational Investigation of Acetic Acid Deoxygenation over Oxophilic Molybdenum Carbide: Surface Chemistry and Active Site Identity. ACS Catalysis, 2016, 6, 1181-1197.	5.5	76
22893	Electrocatalytic Oxygen Evolution with an Atomically Precise Nickel Catalyst. ACS Catalysis, 2016, 6, 1225-1234.	5.5	104
22894	Bottom-up fabrication of graphene nanostructures on Ru$left(10ar{1}0ight)$. Nanotechnology, 2016, 27, 055602.	1.3	4
22895	DFT study on the galvanic interaction between pyrite (100) and galena (100) surfaces. Applied Surface Science, 2016, 367, 270-276.	3.1	51
22896	New ternary tantalum borides containing boron dumbbells: Experimental and theoretical studies of Ta2OsB2 and TaRuB. Journal of Solid State Chemistry, 2016, 242, 28-33.	1.4	10
22897	Surface properties of NpO 2 and water reacting with stoichiometric and reduced NpO 2 (111), (110), and (100) surfaces from ab initio atomistic thermodynamics. Surface Science, 2016, 644, 153-164.	0.8	16
22898	Ab initio study of structural, mechanical, thermal and electronic properties of perovskites Sr(Li,Pd)H₃. International Journal of Modern Physics B, 2016, 30, 1650003.	1.0	8
22899	Ab initio study of chemical bond interactions between covalently functionalized carbon nanotubes via amide, ester and anhydride linkages. Solid State Sciences, 2016, 53, 56-62.	1.5	3
22900	Stable Monolayer Transition Metal Dichalcogenide Ordered Alloys with Tunable Electronic Properties. Journal of Physical Chemistry C, 2016, 120, 2501-2508.	1.5	51
22901	Ab initiomodelling of the interaction of H interstitials with grain boundaries in bcc Fe. Molecular Physics, 2016, 114, 1502-1512.	0.8	15
22902	Fermi resonance in the phonon spectra of quaternary chalcogenides of the type Cu₂ZnGeS₄. Journal of Physics Condensed Matter, 2016, 28, 065401.	0.7	27
22903	The fingerprint of Te-rich and stoichiometric Bi₂Te₃nanowires by Raman spectroscopy. Nanotechnology, 2016, 27, 075706.	1.3	33
22904	Ab initio study of electronic, magnetic, elastic and optical properties of full Heusler Co2MnSb. Indian Journal of Physics, 2016, 90, 909-916.	0.9	31
22905	Spin-polarized gapped Dirac spectrum of unsupported silicene. Applied Surface Science, 2016, 373, 45-50.	3.1	7

#	Article	IF	Citations
22906	Formation, Migration, and Reactivity of Auâ€“CO Complexes on Gold Surfaces. Journal of the American Chemical Society, 2016, 138, 1518-1526.	6.6	74
22907	Quaternary Iodides A(BaSr)I₅:Eu²⁺ (A = K, Cs) as Scintillators for Radiation Detection. Journal of Physical Chemistry C, 2016, 120, 1225-1236.	1.5	13
22908	Elastic and thermodynamic properties of Fe3Ga from first-principles calculations. Solid State Communications, 2016, 230, 43-48.	0.9	9
22909	Fabrication of a Homogeneous, Integrated, and Compact Film of Organicâ€“Inorganic Hybrid Ni(en)₃Ag₂I₄ with Near-Infrared Absorbance and Semiconducting Features. Inorganic Chemistry, 2016, 55, 1230-1235.	1.9	12
22910	Adsorption of NO2, NH3 on monolayer MoS2 doped with Al, Si, and P: A first-principles study. Chemical Physics Letters, 2016, 643, 27-33.	1.2	129
22911	pH and Alkali Cation Effects on the Pt Cyclic Voltammogram Explained Using Density Functional Theory. Journal of Physical Chemistry C, 2016, 120, 457-471.	1.5	145
22912	Inter- versus Intramolecular Structural Manipulation of a Dichromium(II) Pacman Complex through Pressure Variation. Inorganic Chemistry, 2016, 55, 214-220.	1.9	6
22913	Hydrophobic and antioxidant effects in In, Sn, and Sb based two dimensional materials. Dalton Transactions, 2016, 45, 3244-3246.	1.6	5
22914	First principles study on the interfacial properties of NM/graphdiyne (NM = Pd, Pt, Rh and Ir): The implications for NM growing. Applied Surface Science, 2016, 360, 1-7.	3.1	90
22915	Activation and mechanochemical breaking of Câ€“C bonds initiate wear of diamond (110) surfaces in contact with silica. Carbon, 2016, 98, 474-483.	5.4	61
22916	Decomposition of activated CO2 species on Ni(110): Role of surface diffusion in the reaction mechanism. Catalysis Communications, 2016, 74, 65-70.	1.6	25
22917	Origin of distinct hydrogen absorption behavior of Zr2Pd and ZrPd2. International Journal of Hydrogen Energy, 2016, 41, 1736-1743.	3.8	4
22918	Improving the electrical conductivity and structural stability of the Li 2 MnO 3 cathode via P doping. Journal of Alloys and Compounds, 2016, 658, 818-823.	2.8	29
22919	High pressure behaviour and elastic properties of a dense inorganicâ€“organic framework. Dalton Transactions, 2016, 45, 4303-4308.	1.6	26
22920	Phonon Spectrum in Hydroxyapatite: Calculations and EPR Study at Low Temperatures. Journal of Low Temperature Physics, 2016, 185, 627-632.	0.6	7
22921	An investigation into the influence of grain boundary misorientation on the tensile strength of SiC bicrystals. Mechanics of Advanced Materials and Structures, 2016, 23, 494-502.	1.5	7
22922	Computational Studies of Bismuth-Doped Zinc Oxide Nanowires. Nanoscience and Technology, 2016, , 401-421.	1.5	1
22923	Examining the Performance of Refractory Conductive Ceramics as Plasmonic Materials: A Theoretical Approach. ACS Photonics, 2016, 3, 43-50.	3.2	126

#	Article	IF	Citations
22924	Prospects of Spin Catalysis on Spin-Polarized Graphene Heterostructures. Australian Journal of Chemistry, 2016, 69, 753.	0.5	2
22925	Carbon dioxide adsorption on lanthanum zirconate nanostructured coating surface: a DFT study. Adsorption, 2016, 22, 159-163.	1.4	6
22926	Atomistic mechanism of nano-scale phase separation in fcc-based high entropy alloys. Journal of Alloys and Compounds, 2016, 663, 340-344.	2.8	16
22927	An ab initio study of the structural, elastic, electronic, optical properties and phonons of the double perovskite oxides Sr 2 AlXO 6 (X =Ta, Nb, V). Materials Science in Semiconductor Processing, 2016, 42, 405-412.	1.9	10
22928	Surface Structure and Chemistry of Alkanethiols on Au(100)-(1 Ã— 1) Substrates. Journal of Physical Chemistry C, 2016, 120, 291-296.	1.5	28
22929	Exploring Interfacial Events in Gold-Nanocluster-Sensitized Solar Cells: Insights into the Effects of the Cluster Size and Electrolyte on Solar Cell Performance. Journal of the American Chemical Society, 2016, 138, 390-401.	6.6	137
22930	Interlayer interaction and related properties of bilayer hexagonal boron nitride: ab initio study. RSC Advances, 2016, 6, 6423-6435.	1.7	37
22931	First-principles investigations on the electronic structures of U3Si2. Journal of Nuclear Materials, 2016, 469, 194-199.	1.3	65
22932	Methanol formation from CO₂catalyzed by Fe₃S₄{111}: formate versus hydrocarboxyl pathways. Faraday Discussions, 2016, 188, 161-180.	1.6	29
22933	Crystal structure, equation of state, and elasticity of hydrous aluminosilicate phase, topaz-OH (Al2SiO4(OH)2) at high pressures. Physics of the Earth and Planetary Interiors, 2016, 251, 24-35.	0.7	18
22934	First-principles study of electronic structure, phonons and electron-phonon interaction in hexagonal PdTe. Physica C: Superconductivity and Its Applications, 2016, 520, 19-23.	0.6	5
22935	Facet-dependent solar ammonia synthesis of BiOCl nanosheets via a proton-assisted electron transfer pathway. Nanoscale, 2016, 8, 1986-1993.	2.8	242
22936	Synthesis of urchin-like rutile titania carbon nanocomposites by iron-facilitated phase transformation of MXene for environmental remediation. Journal of Materials Chemistry A, 2016, 4, 489-499.	5.2	170
22937	Structure-sensitive electroreduction of acetaldehyde to ethanol on copper and its mechanistic implications for CO and CO 2 reduction. Catalysis Today, 2016, 262, 90-94.	2.2	132
22938	Magnetic reconstruction induced magnetoelectric coupling and spin-dependent tunneling in Ni/KNbO3/Ni multiferroic tunnel junctions. Journal of Magnetism and Magnetic Materials, 2016, 404, 1-6.	1.0	2
22939	Nanostructured BNâ€“Mg composites: features of interface bonding and mechanical properties. Physical Chemistry Chemical Physics, 2016, 18, 965-969.	1.3	12
22940	Syntheses, crystal structures and physical properties of three new chalcogenides: NaGaGe₃Se₈, K₃Ga₃Ge₇S₂₀, and K₃Ga₃Ge₇Se₂₀. Dalton Transactions, 2016, 45, 532-538.	1.6	13
22941	The electron transport properties of zigzag graphene nanoribbons with upright standing linear carbon chains. Solid State Communications, 2016, 227, 28-32.	0.9	5

#	Article	IF	Citations
22942	High pressure structural, electronic and vibrational properties of InN and InP. Phase Transitions, 2016, 89, 283-309.	0.6	4
22943	Interfacial electronic structure and charge transfer of hybrid graphene quantum dot and graphitic carbon nitride nanocomposites: insights into high efficiency for photocatalytic solar water splitting. Physical Chemistry Chemical Physics, 2016, 18, 1050-1058.	1.3	57
22944	Theoretical insights into a potential lead-free hybrid perovskite: substituting Pb²⁺with Ge²⁺. Nanoscale, 2016, 8, 1503-1512.	2.8	247
22945	Impact of vacancy defects in single-walled carbon nanotube on the structural properties of covalently attached aromatic diisocyanates. Applied Surface Science, 2016, 362, 1-10.	3.1	4
22946	First-principles study of the influence of doping elements on phase stability, crystal and electronic structure of Al 2 Cu (Î¸) phase. Computational Materials Science, 2016, 111, 328-333.	1.4	21
22947	Atomic investigation of alloying Cr, Ti, Y additions in a grain boundary of vanadium. Journal of Nuclear Materials, 2016, 468, 147-152.	1.3	14
22948	Kinetic Monte Carlo simulations of the water gas shift reaction on Cu(1 1 1) from density functional theory based calculations. Journal of Catalysis, 2016, 333, 217-226.	3.1	53
22949	Structural, electronic, magnetic and chemical properties of B-, C- and N-doped MgO(001) surfaces. Physical Chemistry Chemical Physics, 2016, 18, 426-435.	1.3	7
22950	Quaternary Al-Cu-Mg-Si Q Phase: Sample Preparation, Heat Capacity Measurement and First-Principles Calculations. Journal of Phase Equilibria and Diffusion, 2016, 37, 119-126.	0.5	12
22951	First-principles study of the origin of magnetism induced by intrinsic defects in monolayer MoS2. Applied Surface Science, 2016, 361, 199-205.	3.1	61
22952	First principles study of the spinâ€“orbit interaction effect on the opto-electric properties of lead telluride. Materials Science in Semiconductor Processing, 2016, 41, 83-88.	1.9	4
22953	Electronic and magnetic properties of germanene: Surface functionalization and strain effects. Solid State Communications, 2016, 226, 19-24.	0.9	36
22954	A Theoretical and Experimental In-Situ Electrochemical Infrared Spectroscopy Study of Adsorbed CO on Pt Dendrimer-Encapsulated Nanoparticles. Journal of the Electrochemical Society, 2016, 163, H3061-H3065.	1.3	10
22955	A first principles study of cohesive, elastic and electronic properties of binary Feâ€“Zr intermetallics. Computational Materials Science, 2016, 112, 52-66.	1.4	42
22956	Pressure effect on the structural, electronic, optical and elastic properties of Zn0.75Be0.25O from first-principles calculations. Optik, 2016, 127, 1754-1761.	1.4	9
22957	First-principle calculations of the structural, elastic and bonding properties of Cs2NaLnCl6 (Ln=Laâ€“Lu) cubic elpasolites. Journal of Luminescence, 2016, 169, 415-418.	1.5	4
22958	Development of a ReaxFF potential for Ag/Zn/O and application to Ag deposition on ZnO. Surface Science, 2016, 645, 67-73.	0.8	35
22959	Effects of Charging and Perpendicular Electric Field on Graphene Oxide. Nanoscience and Technology, 2016, , 261-290.	1.5	4

#	Article	IF	Citations
22960	Material synthesis and design from first principle calculations and machine learning. Computational Materials Science, 2016, 112, 364-367.	1.4	45
22961	Structural stability, electronic, mechanical and superconducting properties of CrC and MoC. Materials Chemistry and Physics, 2016, 169, 71-81.	2.0	30
22962	Crystal structure, electronic and magnetic properties of double perovskite Ba2FeWO6: A combined experimentalâ€“theoretical study. Physica B: Condensed Matter, 2016, 481, 217-223.	1.3	11
22963	Zn effect on STM imaging of brass surfaces. Surface Science, 2016, 644, 148-152.	0.8	7
22964	Neutron powder diffraction and theory-aided structure refinement of rubidium and cesium ureate. Zeitschrift Fur Naturforschung - Section B Journal of Chemical Sciences, 2016, 71, 431-438.	0.3	5
22965	First-principles study of defect formation in the photovoltaic semiconductor Cu2SnS3for comparison with Cu2ZnSnS4and CuInSe2. Japanese Journal of Applied Physics, 2016, 55, 04ES08.	0.8	9
22966	Magnetic properties in BiFeO3 doped with Cu and Zn first-principles investigation. Journal of Alloys and Compounds, 2016, 674, 463-469.	2.8	17
22967	Theoretical investigation of superconductivity in ternary silicide NaAlSi with layered diamond-like structure. Philosophical Magazine, 2016, 96, 1006-1019.	0.7	7
22968	First-principles study of the high-temperature behaviors of the willemite-II and post-phenacite phases of silicon nitride. Journal Wuhan University of Technology, Materials Science Edition, 2016, 31, 74-79.	0.4	1
22969	Density functional theory study of the adsorption and incorporation of Sc and Y on the AlN(0001) surface. Journal of Crystal Growth, 2016, 443, 1-7.	0.7	7
22970	Structural analysis and atomic simulation of Ag/BN nanoparticle hybrids obtained by Ag ion implantation. Materials and Design, 2016, 98, 167-173.	3.3	16
22971	Density Functional Theory Study of Elemental Mercury Adsorption on Fe₂O₃[104] and Its Effect on Carbon Deposit during Chemical Looping Combustion. Energy & Fuels, 2016, 30, 3413-3418.	2.5	12
22972	Long Range Functionalization of h-BN Monolayer by Carbon Doping. Journal of Physical Chemistry C, 2016, 120, 15993-16001.	1.5	42
22973	First principles analysis of oxygen vacancy formation and migration in Sr₂BMoO₆ (BA= Mg, Co, Ni). RSC Advances, 2016, 6, 31968-31975.	1.7	15
22974	Oxidation behaviour of lattice oxygen in Li-rich manganese-based layered oxide studied by hard X-ray photoelectron spectroscopy. Journal of Materials Chemistry A, 2016, 4, 5909-5916.	5.2	48
22975	Insight into the Reaction Mechanisms of Methanol on PtRu/Pt(111): A Density Functional Study. Applied Surface Science, 2016, 369, 257-266.	3.1	16
22976	Borophene: A promising anode material offering high specific capacity and high rate capability for lithium-ion batteries. Nano Energy, 2016, 23, 97-104.	8.2	454
22977	Segregation and Migration of the Oxygen Vacancies in the Î£3 (111) Tilt Grain Boundaries of Ceria. Journal of Physical Chemistry C, 2016, 120, 6625-6632.	1.5	11

#	Article	IF	Citations
22978	Structural, electronic, and magnetic properties of Mn-Doped InP nanowire. Superlattices and Microstructures, 2016, 92, 134-142.	1.4	8
22979	Reversible Hydrogen Uptake by BN and BC₃ Monolayers Functionalized with Small Fe Clusters: A Route to Effective Energy Storage. Journal of Physical Chemistry A, 2016, 120, 2009-2013.	1.1	39
22980	Influence of Interface Structure on Magnetic Proximity Effect in Pt/Y₃Fe₅O₁₂ Heterostructures. ACS Applied Materials & Interfaces, 2016, 8, 8175-8183.	4.0	36
22981	Raman Shifts in Electron-Irradiated Monolayer MoS₂. ACS Nano, 2016, 10, 4134-4142.	7.3	311
22982	Thermodynamic reassessment of the Auâ€“Dy system supported by first-principles calculations. Calphad: Computer Coupling of Phase Diagrams and Thermochemistry, 2016, 53, 49-54.	0.7	4
22983	Local charge states in hexagonal boron nitride with Stoneâ€“Wales defects. Nanoscale, 2016, 8, 8210-8219.	2.8	43
22984	Site preference and alloying effect of tungsten in the Î¼ phase of Co₇Mo₆. Philosophical Magazine Letters, 2016, 96, 1-8.	0.5	12
22985	Structural, electronic and optical properties of YNi4Si-type RNi4Si compounds (RÂ=ÂLa and Gd): a new orthorhombic derivative of CaCu5 structure. Journal of Materials Science, 2016, 51, 868-875.	1.7	4
22986	A DFT+U study of the Mars Van Krevelen mechanism of CO oxidation on Au/TiO2 catalysts. Applied Catalysis A: General, 2016, 519, 27-33.	2.2	39
22987	Evidence of the stability of Mo2TiAlC2 from first principles calculations and its thermodynamical and optical properties. Computational Materials Science, 2016, 118, 77-86.	1.4	28
22988	Charge-Transfer-Induced Magic Cluster Formation of Azaborine Heterocycles on Noble Metal Surfaces. Journal of Physical Chemistry C, 2016, 120, 6020-6030.	1.5	23
22989	Pseudo-Jahnâ€“Teller Distortion in Two-Dimensional Phosphorus: Origin of Black and Blue Phases of Phosphorene and Band Gap Modulation by Molecular Charge Transfer. Journal of Physical Chemistry Letters, 2016, 7, 1288-1297.	2.1	73
22990	Monoclinic C2/m-20 carbon: a novel superhard sp³carbon allotrope. RSC Advances, 2016, 6, 32740-32745.	1.7	29
22991	Mo₂C as a high capacity anode material: a first-principles study. Journal of Materials Chemistry A, 2016, 4, 6029-6035.	5.2	249
22992	Bond formation, electronic structure, and energy storage properties on polyoxometalateâ€“carbon nanocomposites. Theoretical Chemistry Accounts, 2016, 135, 1.	0.5	22
22993	Halogenated arsenenes as Dirac materials. Applied Surface Science, 2016, 376, 286-289.	3.1	49
22994	First-principles studies on substitutional doping by group IV and VI atoms in the two-dimensional arsenene. Applied Surface Science, 2016, 378, 350-356.	3.1	36
22995	Magnetism in transition-metal-doped germanene: A first-principles study. Computational Materials Science, 2016, 118, 112-116.	1.4	69

#	Article	IF	Citations
22996	Trigonal BiPO4: A potential piezoelectric for low-temperatures. Computational Materials Science, 2016, 118, 1-3.	1.4	3
22997	Understanding mechanisms of carbon dioxide conversion into methane for designing enhanced catalysts from first-principles. Computational and Theoretical Chemistry, 2016, 1083, 31-37.	1.1	17
22998	Electronic properties of GaPxAs1-x ternary alloy: A first-principles study. Journal of Alloys and Compounds, 2016, 675, 86-93.	2.8	9
22999	Catalytic Upgrading of Methane to Higher Hydrocarbon in a Nonoxidative Chemical Conversion. Energy & Fuels, 2016, 30, 2584-2593.	2.5	26
23000	NO Reduction by H₂ on the Rh(111) and Rh(221) Surfaces: A Mechanistic and Kinetic Study. Journal of Physical Chemistry C, 2016, 120, 5410-5419.	1.5	28
23001	Local structures and TWC activity of Pd supported on Ni-substituted aluminium oxide borates. Catalysis Science and Technology, 2016, 6, 5464-5472.	2.1	5
23002	Mode specificity for the dissociative chemisorption of H₂O on Cu(111): a quantum dynamics study on an accurately fitted potential energy surface. Physical Chemistry Chemical Physics, 2016, 18, 8537-8544.	1.3	33
23003	Homogeneously dispersed multimetal oxygen-evolving catalysts. Science, 2016, 352, 333-337.	6.0	1,948
23004	Density functional theoretical studies on the methanol adsorption and decomposition on Ru(0001) surfaces. Chemical Research in Chinese Universities, 2016, 32, 234-241.	1.3	4
23005	Water splitting and the band edge positions of TiO2. Electrochimica Acta, 2016, 199, 27-34.	2.6	64
23006	Effect and controlling mechanism of vanadium on Feâ€“Al interface reaction in Alâ€“Zn bath. Surface and Coatings Technology, 2016, 306, 408-417.	2.2	8
23007	Electronic structure of transition metal ions in GaN and AlN: Comparing GGA+U with experiment. Journal of Alloys and Compounds, 2016, 664, 565-579.	2.8	25
23008	Doping-Induced Room Temperature Stabilization of Metastable Î²-Ag₂WO₄ and Origin of Visible Emission in Î±- and Î²-Ag₂WO₄: Low Temperature Photoluminescence Studies. Journal of Physical Chemistry C, 2016, 120, 7265-7276.	1.5	46
23009	Two novel silicon phases with direct band gaps. Physical Chemistry Chemical Physics, 2016, 18, 12905-12913.	1.3	50
23010	On the mechanism of high product selectivity for HCOOH using Pb in CO₂ electroreduction. Physical Chemistry Chemical Physics, 2016, 18, 9652-9657.	1.3	60
23011	Mixed Valence Tin Oxides as Novel van der Waals Materials: Theoretical Predictions and Potential Applications. Advanced Energy Materials, 2016, 6, 1501190.	10.2	79
23012	Rhenium monoselenide: An investigation by density functional theory. Physica Status Solidi (B): Basic Research, 2016, 253, 1461-1464.	0.7	1
23013	Comprehensive electronic structure characterization of pristine and nitrogen/phosphorus doped carbon nanocages. Carbon, 2016, 103, 480-487.	5.4	23

#	Article	IF	Citations
23014	Investigation of microstructure evolution during self-annealing in thin Cu films by combining mesoscale level set and ab initio modeling. Journal of the Mechanics and Physics of Solids, 2016, 90, 160-178.	2.3	24
23015	Crystal Structure, Electronic Structure, and Photocatalytic Activity of Oxysulfides: La₂Ta₂ZrS₂O₈, La₂Ta₂TiS₂O₈, and La₂Nb₂TiS₂O₈. Inorganic Chemistry, 2016, 55, 3674-3679.	1.9	25
23016	Dissociative Adsorption of H₂ on PtRu Bimetallic Surfaces. Journal of Physical Chemistry C, 2016, 120, 7201-7212.	1.5	6
23017	First-principles investigations of transition-metal doped bilayer WS₂. Physical Chemistry Chemical Physics, 2016, 18, 10152-10157.	1.3	21
23018	The effect of hydrogen on the evolution of intergranular cracking: a cross-scale study using first-principles and cohesive finite element methods. RSC Advances, 2016, 6, 27282-27292.	1.7	19
23019	Density functional theory study of structural, electronic, and thermal properties of Pt, Pd, Rh, Ir, Os and PtPd X (X = Ir, Os, and Rh) alloys. Chinese Physics B, 2016, 25, 036501.	0.7	5
23020	Ab Initio Calculations on the Structural, Mechanical, Electronic, Dynamic, and Optical Properties of Semiconductor Half-Heusler Compound ZrPdSn. Zeitschrift Fur Naturforschung - Section A Journal of Physical Sciences, 2016, 71, 135-143.	0.7	2
23021	Consideration about the synthesis pressure effect on lattice defects of Mg2Si using 1st principle calculations. Journal of Alloys and Compounds, 2016, 664, 369-377.	2.8	20
23022	Understanding the enhanced catalytic activity of Cu1@Pd3(111) in formic acid dissociation, a theoretical perspective. Journal of Power Sources, 2016, 316, 8-16.	4.0	37
23023	Density functional theory study of nitrogen atoms and molecules interacting with Fe(1 1 1) surfaces. Nuclear Instruments & Methods in Physics Research B, 2016, 382, 105-109.	0.6	6
23024	Band Structure Engineering: Insights from Defects, Band Gap, and Electron Mobility, from Study of Magnesium Tantalate. Journal of Physical Chemistry C, 2016, 120, 6930-6937.	1.5	26
23025	RuO₂ Monolayer: A Promising Bifunctional Catalytic Material for Nonaqueous Lithiumâ€“Oxygen Batteries. Journal of Physical Chemistry C, 2016, 120, 6356-6362.	1.5	39
23026	Molecular Engineering as an Approach To Design a New Beryllium-Free Fluoride Carbonate as a Deep-Ultraviolet Nonlinear Optical Material. Chemistry of Materials, 2016, 28, 2301-2307.	3.2	85
23027	Multistable Rippling of Graphene on SiC: A Density Functional Theory Study. Journal of Physical Chemistry C, 2016, 120, 7670-7677.	1.5	17
23028	Electronic, Crystal Chemistry, and Nonlinear Optical Property Relationships in the Dugganite A₃B₃CD₂O₁₄ Family. Journal of the American Chemical Society, 2016, 138, 4984-4989.	6.6	118
23029	First principles study of confinement effects for oxygen vacancies in BaZrO₃ (001) ultra-thin films. Physical Chemistry Chemical Physics, 2016, 18, 9902-9908.	1.3	20
23030	Investigation of fluorine adsorption on nitrogen doped MgAl 2 O 4 surface by first-principles. Applied Surface Science, 2016, 376, 97-104.	3.1	33
23031	Interfacial effect on the electrochemical properties of the layered graphene/metal sulfide composites as anode materials for Li-ion batteries. Surface Science, 2016, 651, 10-15.	0.8	27

#	Article	IF	Citations
23032	Isolation of pristine MXene from Nb₄AlC₃ MAX phase: a first-principles study. Physical Chemistry Chemical Physics, 2016, 18, 11073-11080.	1.3	47
23033	Active sites and mechanisms for H ₂ O ₂ decomposition over Pd catalysts. Proceedings of the National Academy of Sciences of the United States of America, 2016, 113, E1973-82.	3.3	171
23034	X-ray absorption spectroscopy and density functional analysis of the Fe3+ distribution profile on Al sites in a chrysoberyl crystal, BeAl2O4:Fe3+. Journal of Applied Crystallography, 2016, 49, 385-388.	1.9	2
23035	Dimethyl ether electro-oxidation on platinum surfaces. Nano Energy, 2016, 29, 428-438.	8.2	17
23036	Hindered Translator and Hindered Rotor Models for Adsorbates: Partition Functions and Entropies. Journal of Physical Chemistry C, 2016, 120, 9719-9731.	1.5	113
23037	Ab initio study of the linear and nonlinear optical responses in BiAlO3. Philosophical Magazine, 2016, 96, 190-207.	0.7	6
23038	Tunable electronic structures and magnetic properties in two-dimensional stanene with hydrogenation. Materials Chemistry and Physics, 2016, 173, 246-254.	2.0	30
23039	Prediction of metallic and non-metallic structure and elastic properties of <mml:math xmlns:mml="http://www.w3.org/1998/Math/MathML" altimg="si0032.gif" overflow="scroll"><mml:mrow><mml:msub subscriptshift="65%"><mml:mrow><mml:mi>Fe</mml:mi></mml:mrow><mml:mrow><mml:mn>2</mml:mn></mml:mrow></mml:msub><mml:msub subscriptshift="65%"><mml:mrow><mml:mi>Ti</mml:mi></mml:mrow><mml:mrow><mml:mn>1</mml:mn><mml:mo form="prefix">−</mml:mo><mml:mi>x</mml:mi></mml:mrow></mml:msub><mml:msub><mml:mrow><mml:mi mathvariant="normal">Al</mml:mi></mml:mrow><mml:mrow><mml:mi>x</mml:mi></mml:mrow></mml:msub></mml:mrow></mml:math> alloys: Physic	1.3	14
23040	Effects of Uniaxial and Biaxial Strain on Few-Layered Terrace Structures of MoS₂ Grown by Vapor Transport. ACS Nano, 2016, 10, 3186-3197.	7.3	83
23041	Crossover from metal to insulator in dense lithium-rich compound CLi ₄. Proceedings of the National Academy of Sciences of the United States of America, 2016, 113, 2366-2369.	3.3	21
23042	Direct Water Decomposition on Transition Metal Surfaces: Structural Dependence and Catalytic Screening. Catalysis Letters, 2016, 146, 718-724.	1.4	18
23043	Mechanisms of monovacancy diffusion in graphene. Chemical Physics Letters, 2016, 648, 161-165.	1.2	24
23045	Strong coupling between magnetization and electric polarization in BC3 sheet adsorbed with Li, Na, K, and Ca. Solid State Communications, 2016, 226, 13-18.	0.9	3
23046	Light adatoms influences on electronic structures of the two-dimensional arsenene nanosheets. Solid State Communications, 2016, 230, 6-10.	0.9	24
23047	Adsorption and coupling of 4-aminophenol on Pt(111) surfaces. Surface Science, 2016, 646, 5-12.	0.8	8
23048	Correlation of Methane Activation and Oxide Catalyst Reducibility and Its Implications for Oxidative Coupling. ACS Catalysis, 2016, 6, 1812-1821.	5.5	134
23049	Effect of particle size on the surface activity of TiCâ€“Ni composite coating via the interfacial valence electron localization. RSC Advances, 2016, 6, 18793-18799.	1.7	12
23050	Super-ion inspired colorful hybrid perovskite solar cells. Journal of Materials Chemistry A, 2016, 4, 4728-4737.	5.2	84

#	Article	IF	Citations
23051	Two-Dimensional Î³-Graphyne Suspended on Si(111): A Hybrid Device. Journal of Physical Chemistry C, 2016, 120, 4605-4611.	1.5	16
23052	Improvement of Hydrogen Vacancy Diffusion Kinetics in MgH₂ by Niobium- and Zirconium-Doping for Hydrogen Storage Applications. Journal of Physical Chemistry C, 2016, 120, 4806-4812.	1.5	48
23053	Long-Chain Polysulfide Retention at the Cathode of Liâ€“S Batteries. Journal of Physical Chemistry C, 2016, 120, 4296-4305.	1.5	85
23055	Quantum Coherence Facilitates Efficient Charge Separation at a MoS₂/MoSe₂ van der Waals Junction. Nano Letters, 2016, 16, 1996-2003.	4.5	225
23056	Sodium-Ion Intercalation Mechanism in MXene Nanosheets. ACS Nano, 2016, 10, 3334-3341.	7.3	448
23057	Engineering the electronic and magnetic properties of d⁰ 2D dichalcogenide materials through vacancy doping and lattice strains. Physical Chemistry Chemical Physics, 2016, 18, 7163-7168.	1.3	16
23058	First-principles analysis of seven novel phases of phosphorene with chirality. RSC Advances, 2016, 6, 22277-22284.	1.7	8
23059	Role of silicon dangling bonds in the electronic properties of epitaxial graphene on silicon carbide. Nanotechnology, 2016, 27, 125705.	1.3	12
23060	Simultaneous tunability of the electronic and phononic gaps in SnS ₂ under normal compressive strain. 2D Materials, 2016, 3, 015009.	2.0	16
23061	Mechanism of adhesion of the diglycidyl ether of bisphenol A (DGEBA) to the Fe(100) surface. Composites Science and Technology, 2016, 126, 9-16.	3.8	32
23062	Novel Î±- and Î²-type boron sheets: Theoretical insight into their structures, thermodynamic stability, and work functions. Chemical Physics Letters, 2016, 648, 81-86.	1.2	12
23063	Ground state properties from first principle calculations of CdSxTe1â^'x ternary semiconductors materials. Journal of Alloys and Compounds, 2016, 659, 295-301.	2.8	3
23064	Phase-driven magneto-electrical characteristics of single-layer MoS₂. Nanoscale, 2016, 8, 5627-5633.	2.8	26
23065	Co-doping of magnesium with indium in nitrides: first principle calculation and experiment. RSC Advances, 2016, 6, 5111-5115.	1.7	13
23066	Electronic and Magnetic Properties of Cr2GeC with GGA + U Approximation. Journal of Superconductivity and Novel Magnetism, 2016, 29, 1267-1272.	0.8	17
23067	Magnetic Properties, Possible Martensitic Transformation, and Elastic Properties of Heusler Alloy Fe2NiSb from First-Principles Calculations. Journal of Superconductivity and Novel Magnetism, 2016, 29, 1019-1024.	0.8	3
23068	A density functional study on properties of a Cu3Zn material and CO adsorption onto its surfaces. Applied Surface Science, 2016, 363, 128-139.	3.1	12
23069	Influence of interlayer cations on structural properties of montmorillonites: A dispersion-corrected density functional theory study. Computational Materials Science, 2016, 117, 33-39.	1.4	17

#	Article	IF	Citations
23070	Electronic Anisotropy at Vicinal Ag(1 1 n) Surfaces: Energetics of Hydrogen Adsorption. Journal of Physical Chemistry C, 2016, 120, 2109-2118.	1.5	4
23071	Electronic Reducibility Scales with Intergranular Interface Area in Consolidated In₂O₃ Nanoparticles Powders. Journal of Physical Chemistry C, 2016, 120, 4581-4588.	1.5	4
23072	Structural semiconductor-to-semimetal phase transition in two-dimensional materials induced by electrostatic gating. Nature Communications, 2016, 7, 10671.	5.8	318
23073	Interfacial interaction of Ag nanoparticles with graphene oxide supports for improving NH₃ and NO adsorption: a first-principles study. Physical Chemistry Chemical Physics, 2016, 18, 7797-7807.	1.3	20
23074	Ab Initio Study of Carbon Impurities in Cu$_2$ ZnSnS$_4$. IEEE Journal of Photovoltaics, 2016, 6, 562-570.	1.5	3
23075	CdSxTe1-x ternary semiconductors band gaps calculation using ground state and GW approximations. Journal of Alloys and Compounds, 2016, 671, 144-149.	2.8	1
23076	The group VA element non-compensated nâ€“p codoping in CuGaS2 for intermediate band materials. Solar Energy Materials and Solar Cells, 2016, 144, 664-670.	3.0	15
23077	Pressure-induced phase transitions and structural properties of CoF2: An ab-initio molecular dynamics study. Solid State Communications, 2016, 231-232, 17-25.	0.9	9
23078	Formation of two-dimensional SiNx layers on GaN nonpolar surfaces. Thin Solid Films, 2016, 603, 238-242.	0.8	0
23079	Predicting Single-Layer Technetium Dichalcogenides (TcX₂, X = S, Se) with Promising Applications in Photovoltaics and Photocatalysis. ACS Applied Materials & Interfaces, 2016, 8, 5385-5392.	4.0	100
23080	Investigation on the effect of Na doping on structure and Li-ion kinetics of layered LiNi0.6Co0.2Mn0.2O2 cathode material. Electrochimica Acta, 2016, 192, 120-126.	2.6	132
23081	From Organized High-Throughput Data to Phenomenological Theory using Machine Learning: The Example of Dielectric Breakdown. Chemistry of Materials, 2016, 28, 1304-1311.	3.2	184
23082	Adsorption of Acetonitrile on Platinum and its Effects on Oxygen Reduction Reaction in Acidic Aqueous Solutionsâ€”Combined Theoretical and Experimental Study. Electrocatalysis, 2016, 7, 235-248.	1.5	13
23083	Adsorption of ethyl xanthate on ZnS(110) surface in the presence of water molecules: A DFT study. Applied Surface Science, 2016, 370, 11-18.	3.1	76
23084	Pressure effects on hydrogen atoms near the metal plane in the HCP phase of rare-earth metal trihydrides. Solid State Communications, 2016, 231-232, 48-52.	0.9	1
23085	Theoretical Study of the Dissociative Adsorption of Methane on Ir(111): The Role of Steps and Surface Distortions at High Temperatures. Journal of Physical Chemistry C, 2016, 120, 3946-3954.	1.5	26
23086	Dual-doping to suppress cracking in spinel LiMn₂O₄: a joint theoretical and experimental study. Physical Chemistry Chemical Physics, 2016, 18, 6893-6900.	1.3	33
23087	Investigation of new phases in the Baâ€“Si phase diagram under high pressure using ab initio structural search. Physical Chemistry Chemical Physics, 2016, 18, 8108-8114.	1.3	15

#	Article	IF	Citations
23088	Performance of cubic ZrO2 doped CeO2: First-principles investigation on elastic, electronic and optical properties of Ce1â^' Zr O2. Journal of Alloys and Compounds, 2016, 671, 208-219.	2.8	39
23089	Cohesive properties of (Cu,Ni)â€“(In,Sn) intermetallics: Database, electron-density correlations and interpretation of bonding trends. Journal of Physics and Chemistry of Solids, 2016, 93, 40-51.	1.9	5
23090	Structural and electronic properties of AB- and AA-stacking bilayer-graphene intercalated by Li, Na, Ca, B, Al, Si, Ge, Ag, and Au atoms. Solid State Communications, 2016, 231-232, 57-63.	0.9	15
23091	RbIO₃ and RbIO₂F₂: Two Promising Nonlinear Optical Materials in Mid-IR Region and Influence of Partially Replacing Oxygen with Fluorine for Improving Laser Damage Threshold. Chemistry of Materials, 2016, 28, 1413-1418.	3.2	107
23092	Mechanochemical stability of sub-nm ZnO chains. Physical Chemistry Chemical Physics, 2016, 18, 7688-7694.	1.3	2
23093	Theoretical study on the surface stabilities, electronic structures and water adsorption behavior of the Ta₃N₅(110) surface. Physical Chemistry Chemical Physics, 2016, 18, 7938-7945.	1.3	8
23094	An insight to the role of Cr in the process of intrinsic point defects in Î±-Al₂O₃. Physical Chemistry Chemical Physics, 2016, 18, 6734-6741.	1.3	11
23095	Continuum-atomistic simulation of picosecond laser heating of copper with electron heat capacity from ab initio calculation. Chemical Physics Letters, 2016, 648, 109-113.	1.2	14
23096	Shuffling-controlled versus strain-controlled deformation twinning: The case for HCP Mg twin nucleation. International Journal of Plasticity, 2016, 82, 32-43.	4.1	71
23097	Preferential activation of CO near hydrocarbon chains during Fischerâ€“Tropsch synthesis on Ru. Journal of Catalysis, 2016, 337, 91-101.	3.1	54
23098	The Hakoniwa method, an approach to predict material properties based on statistical thermodynamics and ab initio calculations. Materials Science in Semiconductor Processing, 2016, 43, 209-213.	1.9	11
23099	Synthesis and phase transformation mechanism of Nb2C carbide phases. Journal of Alloys and Compounds, 2016, 671, 424-434.	2.8	30
23100	Piezoelectric Response in Î±-Quartz-Type GeO2. Journal of Physical Chemistry C, 2016, 120, 126-132.	1.5	13
23101	Designing Square Two-Dimensional Gold and Platinum. Crystal Growth and Design, 2016, 16, 1746-1750.	1.4	15
23102	Two-dimensional germanane and germanane ribbons: density functional calculation of structural, electronic, optical and transport properties and the role of defects. RSC Advances, 2016, 6, 28298-28307.	1.7	18
23103	Phase Transition of MoS₂ Bilayer Structures. Journal of Physical Chemistry C, 2016, 120, 3776-3780.	1.5	33
23104	M₂Ca₃B₁₆O₂₈(M = Rb, Cs): structures analogous to SBBO with three-dimensional open-framework layers. RSC Advances, 2016, 6, 14205-14210.	1.7	9
23105	Plasmaâ€“powder application of antifrictional babbitt coatings modified by carbon nanotubes. Russian Engineering Research, 2016, 36, 46-52.	0.2	11

#	Article	IF	Citations
23106	Insight into the Relationship Between Structural and Electronic Properties of Bimetallic RhnPt55â^'n (nÂ=Â0â€“55) Clusters with Cuboctahedral Structure: DFT Approaches. Journal of Cluster Science, 2016, 27, 895-911.	1.7	5
23107	First principle calculations of the adsorption of molecular H2 in Cu[Fe(CN)5NO] metal nitroprussides. An insight into H2â€“host interactions. Computational Materials Science, 2016, 117, 54-64.	1.4	1
23108	Supramolecular clusters and chains of 2,6-dimethylpyridine on Cu(110): Observation of dynamic configuration change with real-space surface science techniques and DFT calculations. Surface Science, 2016, 652, 82-90.	0.8	1
23109	Temperature Dependence of NMR Parameters Calculated from Path Integral Molecular Dynamics Simulations. Journal of Chemical Theory and Computation, 2016, 12, 968-973.	2.3	54
23110	Persistent Luminescence Hole-Type Materials by Design: Transition-Metal-Doped Carbon Allotrope and Carbides. ACS Applied Materials & Interfaces, 2016, 8, 5439-5444.	4.0	14
23111	Selective Growth of Noble Gases at Metal/Oxide Interface. ACS Applied Materials & Interfaces, 2016, 8, 3725-3729.	4.0	6
23112	Thermodynamic Constraints in Using AuM (M = Fe, Co, Ni, and Mo) Alloys as N₂ Dissociation Catalysts: Functionalizing a Plasmon-Active Metal. ACS Nano, 2016, 10, 2940-2949.	7.3	40
23113	Molecular docking sites designed for the generation of highly crystalline covalent organic frameworks. Nature Chemistry, 2016, 8, 310-316.	6.6	436
23114	Selective hydrogenation of acetylene over TiO₂-supported PdAg cluster: carbon species effect. RSC Advances, 2016, 6, 14593-14601.	1.7	12
23115	Interplay between surface chemistry and performance of rutile-type catalysts for halogen production. Chemical Science, 2016, 7, 2996-3005.	3.7	21
23116	U(<scp>v</scp>) in metal uranates: a combined experimental and theoretical study of MgUO₄, CrUO₄, and FeUO₄. Dalton Transactions, 2016, 45, 4622-4632.	1.6	45
23117	Examination of phonon deformation potentials for accurate strain measurements in siliconâ€“germanium alloys with the whole composition range by Raman spectroscopy. Japanese Journal of Applied Physics, 2016, 55, 026602.	0.8	8
23118	The influence of surface oxygen and hydroxyl groups on the dehydrogenation of ethylene, acetic acid and hydrogenated vinyl acetate on pure Pd(1 0 0): A DFT study. Applied Surface Science, 2016, 388, 455-460.	3.1	16
23119	Kinetic and Theoretical Insights into the Mechanism of Alkanol Dehydration on Solid BrÃ¸nsted Acid Catalysts. Journal of Physical Chemistry C, 2016, 120, 3371-3389.	1.5	42
23120	Origins of Large Voltage Hysteresis in High-Energy-Density Metal Fluoride Lithium-Ion Battery Conversion Electrodes. Journal of the American Chemical Society, 2016, 138, 2838-2848.	6.6	212
23121	Volume dependence of the dielectric properties of amorphous SiO₂. Physical Chemistry Chemical Physics, 2016, 18, 7483-7489.	1.3	20
23122	Incorrect DFT-GGA predictions of the stability of non-stoichiometric/polar dielectric surfaces: the case of Cu₂O(111). Physical Chemistry Chemical Physics, 2016, 18, 6729-6733.	1.3	46
23124	Electronic and optical properties of novel carbon allotropes. Carbon, 2016, 101, 77-85.	5.4	98

#	Article	IF	Citations
23125	Facet-dependent photocatalytic reduction of CO2 on BiOI nanosheets. Chemical Engineering Journal, 2016, 291, 39-46.	6.6	188
23126	Mechanical properties of layered oxysulfide CaZnOS from first principle calculations. Journal of Alloys and Compounds, 2016, 670, 41-47.	2.8	11
23127	Ab-initio calculations of semiconductor MgGeP2 and MgGeAs2. Materials Research Bulletin, 2016, 77, 300-306.	2.7	8
23128	Exploration of the Detailed Conditions for Reductive Stability of Mg(TFSI)₂ in Diglyme: Implications for Multivalent Electrolytes. Journal of Physical Chemistry C, 2016, 120, 3583-3594.	1.5	81
23129	Understanding Thermal Quenching of Photoluminescence in Oxynitride Phosphors from First Principles. Journal of Physical Chemistry C, 2016, 120, 4040-4047.	1.5	58
23130	Computational Analysis of Pressure-Dependent Optimal Pore Size for CO₂ Capture with Graphitic Surfaces. Journal of Physical Chemistry C, 2016, 120, 3978-3985.	1.5	15
23131	Molecular structure and vibrations of NTCDA monolayers on Ag(111) from density-functional theory and infrared absorption spectroscopy. Physical Chemistry Chemical Physics, 2016, 18, 6316-6328.	1.3	24
23132	Towards Next Generation Lithium-Sulfur Batteries: Non-Conventional Carbon Compartments/Sulfur Electrodes and Multi-Scale Analysis. Journal of the Electrochemical Society, 2016, 163, A730-A741.	1.3	43
23133	Prediction of the band structures of Bi2Te3-related binary and Sb/Se-doped ternary thermoelectric materials. Journal of the Korean Physical Society, 2016, 68, 115-120.	0.3	30
23134	First principles study of the behavior of hydrogen atoms in a W monovacancy. Journal of Materials Science, 2016, 51, 1445-1455.	1.7	14
23135	Elasticity, hardness, and thermal properties of ZrB n (n =1, 2, 12). Ceramics International, 2016, 42, 6624-6631.	2.3	21
23136	The effect of structural ordering on the magnetic, electronic, and optical properties of the LaPbMnSbO6 double perovskite. Journal of Alloys and Compounds, 2016, 671, 184-191.	2.8	15
23137	Electronic Structure and Phase Stability of PdPt Nanoparticles. Journal of Physical Chemistry Letters, 2016, 7, 736-740.	2.1	40
23138	Magnetostructural phase transition assisted by temperature in Agâ€“Î±MnO₂: a density functional theory study. Physical Chemistry Chemical Physics, 2016, 18, 7442-7448.	1.3	6
23139	Titanium induced polarity inversion in ordered (In,Ga)N/GaN nanocolumns. Nanotechnology, 2016, 27, 065705.	1.3	16
23140	Anisotropic and temperature-dependent growth mechanism of S-phase precipitates in Alâ€“Cuâ€“Mg alloy in relation with GPB zones. Transactions of Nonferrous Metals Society of China, 2016, 26, 1-11.	1.7	23
23141	Migration behaviour of carbon atoms on clean diamond (0 0 1) surface: A first principle study. Applied Surface Science, 2016, 362, 387-393.	3.1	3
23142	Interface effect on leakage current of ferroelectric film. Computational Materials Science, 2016, 115, 120-124.	1.4	7

#	Article	IF	Citations
23143	Simulation of the chemical interactions of luminescent lanthanide complexes series [Ln(cin)3(H2O)3]Â·Hcin and [Ln2(cin)6(bpy)2] using DFT calculations. Computational Materials Science, 2016, 115, 184-191.	1.4	2
23144	Influence of alloying elements on the stability and dehydrogenation properties on Y(BH4)3 by first principles calculations. International Journal of Hydrogen Energy, 2016, 41, 1662-1671.	3.8	2
23145	Cation ordering/disordering effects upon photocatalytic activity of CrNbO4, CrTaO4, Sr2CrNbO6 and Sr2CrTaO6. International Journal of Hydrogen Energy, 2016, 41, 1550-1558.	3.8	30
23146	Surfactant antimony enhanced indium incorporation on InGaN (<mml:math) Tj ETQq1 1 0.784314 rgBT /Overlock 10 Tf 50 637 Td (xmlns surface: A DFT study. Journal of Crystal Growth, 2016, 438, 43-48.	0.7	7
23147	On the electrochemical behavior of formamidine disulfide on gold electrodes in acid media. Journal of Electroanalytical Chemistry, 2016, 764, 79-87.	1.9	6
23148	Cathode reaction mechanism on the h-BN/Ni (111) heterostructure for the lithium-oxygen battery. Journal of Power Sources, 2016, 307, 379-384.	4.0	18
23149	An Insight into the Various Defects-Induced Emission in MgAl₂O₄ and Their Tunability with Phase Behavior: Combined Experimental and Theoretical Approach. Journal of Physical Chemistry C, 2016, 120, 4016-4031.	1.5	100
23150	Thermodynamic properties of pure and doped (B,ÂN) graphene. RSC Advances, 2016, 6, 12158-12168.	1.7	33
23151	Manipulation of carbon nanotube magnetism with metal-rich iron nanoparticles. Journal of Materials Chemistry C, 2016, 4, 1215-1227.	2.7	7
23152	Breakthrough of thep-type doping bottleneck in ZnO by inserting an ultrathin ZnX (Xâ€‰â€‰=â€‰â€‰S, Se and Te) layer doped with NXor AgZn. Journal Physics D: Applied Physics, 2016, 49, 095104.	1.3	5
23153	Manipulation of spin-flip in Co3O4: a first principles study. Journal of Materials Science, 2016, 51, 4691-4696.	1.7	12
23154	Theoretical Predictions for High-Pressure Elastic, Mechanical, and Phonon Properties of SiGe Alloy. Brazilian Journal of Physics, 2016, 46, 192-197.	0.7	13
23155	The transformation pathways for vitual long period stacking-ordered Mg: First-principles study. Computational Materials Science, 2016, 114, 1-12.	1.4	2
23156	First-principles calculations of phonons and Raman spectra in the Hg3Te2Cl2 crystals. Journal of Alloys and Compounds, 2016, 669, 161-166.	2.8	8
23157	Ab initio study of the trapping of polonium on noble metals. Journal of Nuclear Materials, 2016, 472, 35-42.	1.3	6
23158	Structural, elastic and thermodynamic properties of the tetragonal structure of germanium carbonitride. Journal of Physics and Chemistry of Solids, 2016, 91, 106-113.	1.9	12
23159	Energetic, electronic and optical properties of lanthanide doped TiO2: An ab initio LDA+U study. Journal of Solid State Chemistry, 2016, 237, 129-137.	1.4	32
23160	Augmenting the sensing aptitude of hydrogenated graphene by crafting with defects and dopants. Sensors and Actuators B: Chemical, 2016, 228, 317-321.	4.0	44

#	Article	IF	Citations
23161	A DFT study of the structural, electronic and optical properties of transition metal doped fluorite oxides: <mml:math xmlns:mml="http://www.w3.org/1998/Math/MathML" altimg="si0010.gif" overflow="scroll"><mml:msub><mml:mrow><mml:mi>Ce</mml:mi></mml:mrow><mml:mrow><mml:mn>0.75</mml:mn></mml:mrow> mathvariant="normal">M</mml:mi></mml:mrow><mml:mrow><mml:mn>0.25</mml:mn></mml:mrow></mml:msub><mml:msub><mml:mi mathvariant="normal">O</mml:mi></mml:mrow><mml:mrow><mm. Solid State Communications, 2016, 231-232, 68-79.	0.9	34
23162	Acid Dissociation of 3-Mercaptopropionic Acid Coated CdSeâ€“CdS/Cd_{0.5}Zn_{0.5}S/ZnS Coreâ€“Multishell Quantum Dot and Strong Ionic Interaction with Ca²⁺ Ion. Journal of Physical Chemistry C, 2016, 120, 3519-3529.	1.5	15
23163	Dielectric Enhancement in Graphene/Barium Titanate Nanocomposites. ACS Applied Materials & Interfaces, 2016, 8, 3340-3348.	4.0	47
23164	Nonequilibrium spin injection in monolayer black phosphorus. Physical Chemistry Chemical Physics, 2016, 18, 1601-1606.	1.3	45
23165	The conversion of CO₂ to methanol on orthorhombic Î²-Mo₂C and Cu/Î²-Mo₂C catalysts: mechanism for admetal induced change in the selectivity and activity. Catalysis Science and Technology, 2016, 6, 6766-6777.	2.1	101
23166	Methanol dissociation on bimetallic surfaces: validity of the general BrÃ¸nstedâ€“Evansâ€“Polanyi relationship for Oâ€“H bond cleavage. RSC Advances, 2016, 6, 18695-18702.	1.7	10
23167	Some thermodynamic properties of larnite (Î²-Ca₂SiO₄) constrained by highT/Pexperiment and/or theoretical simulation. American Mineralogist, 2016, 101, 277-288.	0.9	16
23168	Electronic, Structural, and Magnetic Properties of the Double Perovskite Ba2MnMoO6 in Different Phases Using Hubbard Model. Journal of Superconductivity and Novel Magnetism, 2016, 29, 1339-1346.	0.8	5
23169	First-principles study of structural and work function properties for nitrogen-doped single-walled carbon nanotubes. Applied Surface Science, 2016, 368, 477-482.	3.1	17
23170	First-principles study of Bi and Al in orthorhombic PbZrO3. Computational Materials Science, 2016, 115, 99-103.	1.4	8
23171	The effects of Br dopant on the photo-catalytic properties of Bi2WO6. Materials Science and Engineering B: Solid-State Materials for Advanced Technology, 2016, 206, 79-84.	1.7	24
23172	First-principles simulations on the new hybrid phases of germanene with alkali metal atoms coverage. Applied Surface Science, 2016, 360, 707-714.	3.1	21
23173	Flux Crystal Growth and the Electronic Structure of BaFe₁₂O₁₉ Hexaferrite. Journal of Physical Chemistry C, 2016, 120, 5114-5123.	1.5	96
23174	Li₂S Film Formation on Lithium Anode Surface of Liâ€“S batteries. ACS Applied Materials & Interfaces, 2016, 8, 4700-4708.	4.0	70
23175	NO₂ Gas Sensing Mechanism of ZnO Thin-Film Transducers: Physical Experiment and Theoretical Correlation Study. ACS Sensors, 2016, 1, 406-412.	4.0	65
23176	The stacking dependent electronic structure and optical properties of bilayer black phosphorus. Physical Chemistry Chemical Physics, 2016, 18, 6085-6091.	1.3	54
23177	Design of noncentrosymmetric perovskites from centric and acentric basic building units. Journal of Materials Chemistry C, 2016, 4, 4016-4027.	2.7	27
23178	First-principles study of electronic properties of B and C doped CuNNi3. Materials Research Express, 2016, 3, 026001.	0.8	0

#	Article	IF	Citations
23179	Deposition Morphology and Magnetism of Co, Pt Adatoms and Small CoPt Adclusters on Ni(100) Substrate. Journal of Cluster Science, 2016, 27, 947-964.	1.7	2
23180	First-principles modeling of energetic and mechanical properties of Niâ€“Cr, Niâ€“Re and Crâ€“Re random alloys. Computational Materials Science, 2016, 117, 45-53.	1.4	17
23181	Local and collective magnetism of gallium vacancies in GaN studied by GGA+U approach. Journal of Magnetism and Magnetic Materials, 2016, 401, 310-319.	1.0	2
23182	Atomistic modelling of zirconium and silicon segregation at twist and tilt grain boundaries in molybdenum. Journal of Materials Science, 2016, 51, 1873-1881.	1.7	15
23183	Thermodynamic stability of Mgâ€“Yâ€“Zn ternary alloys through first-principles. Intermetallics, 2016, 72, 25-29.	1.8	15
23184	Muon-spin relaxation study of the double perovskite insulators Sr₂BOsO₆(Bâ€‰â€‰=â€‰â€‰Fe, Y, In). Journal of Physics Condensed Matter, 2016, 28, 076001.	2.7	9
23185	The comparative theoretical study of the LaBO3 (001) (BÂ=ÂMn, Fe, Co, and Ni) surface properties and oxygen adsorption mechanisms. Ionics, 2016, 22, 1153-1158.	1.2	6
23186	Defect driven magnetism in doped SnO2 nanoparticles: Surface effects. Journal of Magnetism and Magnetic Materials, 2016, 407, 46-50.	1.0	7
23187	Benchmark Theoretical and Experimental Study on ¹⁵N NMR Shifts of Oxidatively Damaged Guanine. Journal of Physical Chemistry B, 2016, 120, 915-925.	1.2	10
23188	Origin of Chemical Order in a-Si_xC_yH_z: Density-Functional Tight-Binding Molecular Dynamics and Statistical Thermodynamics Calculations. Journal of Physical Chemistry C, 2016, 120, 2615-2627.	1.5	4
23189	Toward Atomic-Scale Patterned Atomic Layer Deposition: Reactions of Al₂O₃ Precursors on a Si(001) Surface with Mixed Functionalizations. Journal of Physical Chemistry C, 2016, 120, 2628-2641.	1.5	17
23190	Beyond Graphitic Carbon Nitride: Nitrogen-Rich Penta-CN₂ Sheet. Journal of Physical Chemistry C, 2016, 120, 3993-3998.	1.5	167
23191	Atomic-Scale Picture of the Composition, Decay, and Oxidation of Two-Dimensional Radioactive Films. ACS Nano, 2016, 10, 2152-2158.	7.3	5
23192	Intrinsic Selectivity and Structure Sensitivity of Rhodium Catalysts for C₂₊ Oxygenate Production. Journal of the American Chemical Society, 2016, 138, 3705-3714.	6.6	179
23193	Pyrrolic-nitrogen doped graphene: a metal-free electrocatalyst with high efficiency and selectivity for the reduction of carbon dioxide to formic acid: a computational study. Physical Chemistry Chemical Physics, 2016, 18, 5491-5498.	1.3	114
23194	A general view on the reactivity of the oxygen-functionalized graphene basal plane. Physical Chemistry Chemical Physics, 2016, 18, 6580-6586.	1.3	54
23195	Effects of Mo/W codoping on the visible-light photocatalytic activity of monoclinic BiVO₄ within the GGA + U framework. RSC Advances, 2016, 6, 12290-12297.	1.7	44
23196	First-principles assessment of potential ultrafast laser-induced structural transition in Ni. Applied Surface Science, 2016, 374, 365-369.	3.1	7

#	Article	IF	Citations
23197	Novel structures and superconductivities of calciumâ€“lithium alloys at high pressures: A first-principles study. Journal of Alloys and Compounds, 2016, 669, 101-107.	2.8	4
23198	Interaction of Oxygen with Î±-Rhombohedral Boron (001) Surface. Journal of Physical Chemistry C, 2016, 120, 5968-5979.	1.5	3
23199	Application of a Parallel Genetic Algorithm to the Global Optimization of Gas-Phase and Supported Goldâ€“Iridium Sub-Nanoalloys. Journal of Physical Chemistry C, 2016, 120, 3759-3765.	1.5	24
23200	High Catalytic Activity and Chemoselectivity of Sub-nanometric Pd Clusters on Porous Nanorods of CeO₂ for Hydrogenation of Nitroarenes. Journal of the American Chemical Society, 2016, 138, 2629-2637.	6.6	387
23201	Investigation of structural, mechanical, electronic, optical, and dynamical properties of cubic BaLiF₃, BaLiH₃, and SrLiH₃. Materials Research Express, 2016, 3, 036301.	0.8	25
23202	First-principles study of structural, electronic, elastic and phonon properties of AB2O4(A = Ge,Si;B =) Tj ETQq1 1 0.784314 rgBT /Over	1.0	9
23203	Buckminsterfullerene's movability on the Fe(001) surface. Journal of Magnetism and Magnetic Materials, 2016, 410, 41-46.	1.0	3
23204	Combining the Advantages of Powder X-ray Diffraction and NMR Crystallography in Structure Determination of the Pharmaceutical Material Cimetidine Hydrochloride. Crystal Growth and Design, 2016, 16, 1798-1804.	1.4	55
23205	Monolayer Phosphoreneâ€“Metal Contacts. Chemistry of Materials, 2016, 28, 2100-2109.	3.2	199
23206	Simultaneously Controllable Doping Sites and the Activity of a Wâ€“N Codoped TiO₂ Photocatalyst. ACS Catalysis, 2016, 6, 2745-2753.	5.5	84
23207	Theoretical and experimental investigations of the Li storage capacity in single-walled carbon nanotube bundles. RSC Advances, 2016, 6, 27260-27266.	1.7	9
23208	Formation mechanism of the Nb2C phase in the Nbâ€“1Zrâ€“0.1C (wt.%) alloy and interrelation between Î³, Î² and Î±-Nb2C carbide phases. Acta Materialia, 2016, 108, 186-196.	3.8	24
23209	Nanostructured BaTiO3/Cu2O heterojunction with improved photoelectrochemical activity for H2 evolution: Experimental and first-principles analysis. Applied Catalysis B: Environmental, 2016, 189, 75-85.	10.8	51
23210	Ab-initio study of structural phase transitions and optoelectronic properties in BeH2 at increasing pressure. Journal of Physics and Chemistry of Solids, 2016, 93, 14-21.	1.9	5
23211	Ab Initio Prediction and Characterization of Mo₂C Monolayer as Anodes for Lithium-Ion and Sodium-Ion Batteries. Journal of Physical Chemistry Letters, 2016, 7, 937-943.	2.1	334
23212	Periodic DFT study of the donor interactions with the MgCl₂surface in the Zieglerâ€“Natta catalytic system. RSC Advances, 2016, 6, 13137-13144.	1.7	9
23213	Intercalation of indigo carmine anions into zinc hydroxide salt: A novel alternative blue pigment. Dyes and Pigments, 2016, 128, 158-164.	2.0	28
23214	Structural, half-metallic magnetism and elastic properties of the KMnQ2 (Q=O, S, Se, Te) chalcogenides from first-principles calculations. Journal of Magnetism and Magnetic Materials, 2016, 408, 199-205.	1.0	11

#	Article	IF	Citations
23215	Design and Epitaxial Growth of MoSe₂â€“NiSe Vertical Heteronanostructures with Electronic Modulation for Enhanced Hydrogen Evolution Reaction. Chemistry of Materials, 2016, 28, 1838-1846.	3.2	310
23216	Structure simulation and study of electronic and dielectric properties of two derivatives of benzamide. Molecular Crystals and Liquid Crystals, 2016, 625, 195-201.	0.4	1
23217	Predicted superconductivity of Ni₂VAl and pressure dependence of superconductivity in Ni₂NbX (Xâ€‰â€‰=â€‰â€‰Al, Ga and Sn) and Ni₂VAl. Journal of Physics Condensed Matter, 2016, 28, 115703.	0.7	8
23218	Charge transfer and 2k_Fvs. 4k_Finstabilities in the NMP-TCNQ molecular metal and (NMP)_x(Phen)_{1â^'x}TCNQ solid solutions. Europhysics Letters, 2016, 113, 27006.	0.7	8
23219	Ni-containing Cu/SiO2 catalyst for the chemoselective synthesis of ethanol via hydrogenation of dimethyl oxalate. Catalysis Today, 2016, 276, 28-35.	2.2	46
23220	Effects of adatoms and physisorbed molecules on the physical properties of antimonene. Physical Review B, 2016, 93, .	1.1	84
23221	Mechanical and Electronic Properties of P4₂/mnm Silicon Carbides. Zeitschrift Fur Naturforschung - Section A Journal of Physical Sciences, 2016, 71, 387-396.	0.7	14
23222	Density functional theory study of water gas shift reaction on Cu/ZnO <mml:math xmlns:mml="http://www.w3.org/1998/Math/MathML" altimg="si1.gif" overflow="scroll"><mml:mrow><mml:mo		

#	Article	IF	Citations
23233	Reactivity of the Fe₂O₃(0001) Surface for Methane Oxidation: A GGA + U Study. Journal of Physical Chemistry C, 2016, 120, 6642-6650.	1.5	51
23234	Role of the capping agent in the interaction of hydrophilic Ag nanoparticles with DMPC as a model biomembrane. Environmental Science: Nano, 2016, 3, 462-472.	2.2	22
23235	Ca2O3Fe2.6S2: an antiferromagnetic Mott insulator at proximity to bad metal. Journal of Physics Condensed Matter, 2016, 28, 145701.	0.7	6
23236	Bulk electronic, elastic, structural, and dielectric properties of the Weyl semimetal TaAs. Physical Review B, 2016, 93, .	1.1	42
23237	Reviewâ€"Properties of Intrinsic Point Defects in Si and Ge Assessed by Density Functional Theory. ECS Journal of Solid State Science and Technology, 2016, 5, P3176-P3195.	0.9	16
23238	Computational Studies of Silicene on Silver Surfaces. Springer Series in Materials Science, 2016, , 203-213.	0.4	1
23239	Point defect-induced magnetic properties in CuAlO2 films without magnetic impurities. Applied Physics A: Materials Science and Processing, 2016, 122, 1.	1.1	10
23240	A novel fullerene-like B30N30 structure: Stability and electronic property. Carbon, 2016, 102, 273-278.	5.4	18
23241	First principle calculation of physical properties of barium based chalcogenides BaM 4 S 7 (M = Ga, Al); a DFT, DFT-D and hybrid functional HSE06 study. Optical Materials, 2016, 54, 269-275.	1.7	19
23242	Effect of the alloying element on the temperature-dependent ideal shear strength of Î³â€²-Ni3Al. RSC Advances, 2016, 6, 20551-20558.	1.7	13
23243	Oxygen adsorption and diffusion on an Al(111) surface and subsurface: a theoretical study. Canadian Journal of Chemistry, 2016, 94, 541-546.	0.6	6
23244	A Novel Theoretical Investigation of Electronic Structure and Half-Metallic Ferromagnetism in 3d (V)-Doped InP for Spintronic Applications. Journal of Superconductivity and Novel Magnetism, 2016, 29, 1813-1819.	0.8	8
23245	Thermodynamic properties of calcium ferrite-type MgAl2O4: A first principles study. Science China Earth Sciences, 2016, 59, 831-839.	2.3	4
23246	Towards three-dimensional Weyl-surface semimetals in graphene networks. Nanoscale, 2016, 8, 7232-7239.	2.8	188
23247	Ca-decorated novel boron sheet: A potential hydrogen storage medium. International Journal of Hydrogen Energy, 2016, 41, 5276-5283.	3.8	76
23248	Energy loss in gas-surface dynamics: Electronâ€"hole pair and phonon excitation upon adsorbate relaxation. Nuclear Instruments & Methods in Physics Research B, 2016, 382, 26-31.	0.6	19
23249	Theoretical Modeling of Tribochemical Reaction on Pt and Au Contacts: Mechanical Load and Catalysis. ACS Applied Materials & Interfaces, 2016, 8, 7529-7535.	4.0	23
23250	Phase stability and dynamics of hybrid organicâ€"inorganic crystals [(CH₃)₃PH][SbCl₄] and [(CH₃)₃PH][SbBr₄]: a computational and NMR approach. CrystEngComm, 2016, 18, 2413-2424.	1.3	8

#	Article	IF	Citations
23251	Role of 5f electrons in the structural stability of light actinide (Thâ€“U) mononitrides under pressure. Physical Chemistry Chemical Physics, 2016, 18, 8682-8691.	1.3	7
23252	Performance of field-effect transistors based on Nb_xW_{1â^'x}S₂monolayers. Nanoscale, 2016, 8, 6507-6513.	2.8	23
23253	Structural, electronic and optical properties of copper, silver and gold sulfide: a DFT study. Theoretical Chemistry Accounts, 2016, 135, 1.	0.5	35
23254	Structural and Electronic Properties of Graphene Oxide for Different Degree of Oxidation1. Materials Today: Proceedings, 2016, 3, 796-802.	0.9	38
23255	Pressure effect on the structural and electronic properties of CuInS 2. Solid State Sciences, 2016, 55, 42-47.	1.5	3
23256	Solution Combustion Synthesis, Characterization, and Photoelectrochemistry of CuNb₂O₆ and ZnNb₂O₆ Nanoparticles. Journal of Physical Chemistry C, 2016, 120, 16024-16034.	1.5	56
23257	Stabilities, Electronic and Optical Properties of SnSe_{2(1â€“x)}S_{2x} Alloys: A First-Principles Study. Journal of Physical Chemistry C, 2016, 120, 5839-5847.	1.5	45
23258	Calculation of dopant solubilities and phase diagrams of Xâ€“Pbâ€“Se (X = Br, Na) limited to defects with localized charge. Journal of Materials Chemistry C, 2016, 4, 1769-1775.	2.7	12
23259	Pressure-induced phase transition in Bi₂Se₃at 3 GPa: electronic topological transition or not?. Journal of Physics Condensed Matter, 2016, 28, 105401.	0.7	18
23260	Halogen adsorption at an As-stabilized Î²2â€“GaAs (001)â€“(2 Ã— 4) surface. Semiconductors, 2016, 50, 171-179.	0.2	4
23261	Enhancement of Thermoelectric Properties of Molybdenum Diselenide Through Combined Mg Intercalation and Nb Doping. Journal of Electronic Materials, 2016, 45, 2926-2934.	1.0	17
23262	Size effect on the magnetic and electronic properties of the monolayer lateral hetero-junction WS2-MoS2 nanoribbon. Applied Surface Science, 2016, 371, 376-382.	3.1	26
23263	Morphed graphene nanostructures: Experimental evidence for existence. Carbon, 2016, 102, 288-296.	5.4	37
23264	Effect of strain on the magnetic states of transition-metal atoms doped monolayer WS2. Computational Materials Science, 2016, 117, 354-360.	1.4	30
23265	First-principles study on the adsorption and dissociation of H2 molecules on Be(0 0 0 1) surfaces. Computational Materials Science, 2016, 117, 251-258.	1.4	6
23266	A computational study of adsorption and activation of CO 2 and H 2 over Fe(1 0 0) surface. Journal of CO2 Utilization, 2016, 15, 107-114.	3.3	38
23267	A density functional theory study of the structure of pure-silica and aluminium-substituted MFI nanosheets. Journal of Solid State Chemistry, 2016, 237, 192-203.	1.4	28
23268	Layer-by-layer design of nanostructured thermoelectrics: First-principles study of ZnO:organic superlattices fabricated by ALD/MLD. Nano Energy, 2016, 22, 338-348.	8.2	26

#	Article	IF	Citations
23269	Unusual electronic and mechanical properties of sodium chlorides at high pressures. Physics Letters, Section A: General, Atomic and Solid State Physics, 2016, 380, 1556-1561.	0.9	2
23270	Combined Molecular Dynamics and Density Functional Theory Study of Azobenzeneâ€“Graphene Interfaces. Journal of Physical Chemistry C, 2016, 120, 6651-6658.	1.5	16
23271	Structure and Proton-Transfer Mechanism in One-Dimensional Chains of Benzimidazoles. Journal of Physical Chemistry C, 2016, 120, 5804-5809.	1.5	8
23272	Response of Metal Sites toward Water Effects on Postcombustion CO₂ Capture in Metalâ€“Organic Frameworks. ACS Sustainable Chemistry and Engineering, 2016, 4, 2387-2394.	3.2	24
23273	Proton transfer aiding phase transitions in oxalic acid dihydrate under pressure. Physical Chemistry Chemical Physics, 2016, 18, 8065-8074.	1.3	35
23274	A promising anode material for sodium-ion battery with high capacity and high diffusion ability: graphyne and graphdiyne. RSC Advances, 2016, 6, 25594-25600.	1.7	115
23275	Nickel cluster functionalised carbon nanotube for CO molecule detection: a theoretical study. Molecular Physics, 2016, 114, 671-680.	0.8	8
23276	First-principles study on mono-vacancy self diffusion and recovery in tungsten crystal. Fusion Engineering and Design, 2016, 109-111, 569-573.	1.0	8
23277	Structure, electronic, mechanical and optical properties of ternary YAl3C3 carbide. Journal of Solid State Chemistry, 2016, 237, 336-342.	1.4	9
23278	An Ab-initio study of structural, elastic, electronic and thermodynamic properties of triclinic Cu 7 In 3. Materials Chemistry and Physics, 2016, 174, 70-80.	2.0	10
23279	Adsorption Behavior of Nonplanar Phthalocyanines: Competition of Different Adsorption Conformations. Journal of Physical Chemistry C, 2016, 120, 6869-6875.	1.5	10
23280	Visualizing Redox Dynamics of a Single Ag/AgCl Heterogeneous Nanocatalyst at Atomic Resolution. ACS Nano, 2016, 10, 3738-3746.	7.3	61
23281	Piezoelectric and non-linear optical properties of Î±-quartz type Si_{1â^'x}Ge_xO₂single crystals. CrystEngComm, 2016, 18, 2500-2508.	1.3	13
23282	The mechanism of controllable dehydrogenation: CPMD study of M(BH₄)_x(NH₃)_y (M = Li, Mg) decomposition. Physical Chemistry Chemical Physics, 2016, 18, 7015-7018.	1.3	10
23283	Bifunctional alloys for the electroreduction of CO₂and CO. Physical Chemistry Chemical Physics, 2016, 18, 9194-9201.	1.3	127
23284	Control of electronic properties of 2D carbides (MXenes) by manipulating their transition metal layers. Nanoscale Horizons, 2016, 1, 227-234.	4.1	394
23285	The nature of strong BrÃ¸nsted acidity of Ni-SMM clay. Applied Catalysis B: Environmental, 2016, 191, 62-75.	10.8	14
23286	woptic: Optical conductivity with Wannier functions and adaptive k-mesh refinement. Computer Physics Communications, 2016, 202, 1-11.	3.0	14

#	Article	IF	Citations
23287	Stabilization of BeZnO alloy by S incorporation: A density functional theory investigation. Journal of Alloys and Compounds, 2016, 658, 636-641.	2.8	9
23288	The effect of BiIn hetero-antisite defects in In1â€“PBi alloy. Journal of Alloys and Compounds, 2016, 674, 21-25.	2.8	10
23289	Electron Doping of Ultrathin Black Phosphorus with Cu Adatoms. Nano Letters, 2016, 16, 2145-2151.	4.5	196
23290	Geometry strategy for engineering the recombination possibility of excitons in nanowires. Nanoscale, 2016, 8, 7318-7325.	2.8	0
23291	Structural and electronic properties of InN_xP_{1-x}alloy in full range (0 â‰¤ x â‰¤1). Philosophical Magazine, 2016, 96, 991-1005.	0.7	3
23292	New ternary nanolaminated carbide Mo2Ga2C: A first-principles comparison with the MAX phase counterpart Mo2GaC. Computational Materials Science, 2016, 117, 422-427.	1.4	74
23293	Influence of pressure on the properties of GaN/AlN multi-quantum wells â€“ Ab initio study. Journal of Physics and Chemistry of Solids, 2016, 93, 100-117.	1.9	8
23294	Thermoelectric transport in graphene/h-BN/graphene heterostructures: A computational study. Physica E: Low-Dimensional Systems and Nanostructures, 2016, 81, 96-101.	1.3	24
23295	Hydrogenation-Induced Structure and Property Changes in the Rare-Earth Metal Gallide NdGa: Evolution of a [GaH]^{2â€“} Polyanion Containing Peierls-like Gaâ€“H Chains. Inorganic Chemistry, 2016, 55, 345-352.	1.9	15
23296	Highly Efficient and Stable Vanadiaâ€“Titaniaâ€“Sulfate Catalysts for Methanol Oxidation to Methyl Formate: Synthesis and Mechanistic Study. Journal of Physical Chemistry C, 2016, 120, 6591-6600.	1.5	22
23297	Insights into the Performance Limits of the Li₇P₃S₁₁ Superionic Conductor: A Combined First-Principles and Experimental Study. ACS Applied Materials & Interfaces, 2016, 8, 7843-7853.	4.0	169
23298	Combined experimental and density functional theory studies of an organicâ€“inorganic hybrid perovskite. Physical Chemistry Chemical Physics, 2016, 18, 9431-9436.	1.3	11
23299	Lattice dynamics, phonon vibrational spectra, and thermal properties of tetragonal SrPt3P: a first-principles study. RSC Advances, 2016, 6, 27060-27067.	1.7	6
23300	Investigations on Nb₂C monolayer as promising anode material for Li or non-Li ion batteries from first-principles calculations. RSC Advances, 2016, 6, 27467-27474.	1.7	147
23301	Prediction of large magnetoelectric coupling in Fe₄N/BaTiO₃ and MnFe₃N/BaTiO₃ junctions from a first-principles study. RSC Advances, 2016, 6, 29504-29511.	1.7	5
23302	Structural, elastic, electronic and optical properties of platinum-based superconductor SrPt3P under pressure: a first-principles study. Philosophical Magazine, 2016, 96, 399-412.	0.7	4
23303	A comparative computational study of lithium and sodium insertion into van der Waals and covalent tetracyanoethylene (TCNE)-based crystals as promising materials for organic lithium and sodium ion batteries. Physical Chemistry Chemical Physics, 2016, 18, 8874-8880.	1.3	37
23304	Enhancement of oxygen reduction reaction activities by Pt nanoclusters decorated on ordered mesoporous porphyrinic carbons. Journal of Materials Chemistry A, 2016, 4, 5869-5876.	5.2	17

#	Article	IF	Citations
23305	Many-body dispersion corrections for periodic systems: an efficient reciprocal space implementation. Journal of Physics Condensed Matter, 2016, 28, 045201.	0.7	86
23306	Two scale simulation of surface stress in solids and its effects. Applied Surface Science, 2016, 371, 343-348.	3.1	5
23307	Geometry and fast diffusion of AlCl4 cluster intercalated in graphite. Electrochimica Acta, 2016, 195, 158-165.	2.6	84
23308	Experimental and first-principles DFT study on oxygen vacancies on cerium dioxide and its effect on enhanced photocatalytic hydrogen production. International Journal of Hydrogen Energy, 2016, 41, 7919-7926.	3.8	23
23309	Computational design of smallest nanotube junctions in 0.3 nm diameter. Materials and Design, 2016, 95, 641-647.	3.3	9
23310	Single non-noble-metal cobalt atom stabilized by pyridinic vacancy graphene: An efficient catalyst for CO oxidation. Journal of Molecular Catalysis A, 2016, 417, 28-35.	4.8	68
23311	Sticking with the Pointy End? Molecular Configuration of Chloro Boron-Subphthalocyanine on Cu(111). Journal of Physical Chemistry C, 2016, 120, 7113-7121.	1.5	11
23312	Interface Magnetoelectric Coupling in Co/Pb(Zr,Ti)O₃. ACS Applied Materials & Interfaces, 2016, 8, 7553-7563.	4.0	19
23313	Charge- and thickness-dependent inplane deformation of multilayer graphene thin films. Physical Chemistry Chemical Physics, 2016, 18, 3694-3699.	1.3	4
23314	Effects of oxygen coverage, catalyst size, and core composition on Pt-alloy coreâ€“shell nanoparticles for oxygen reduction reaction. Catalysis Science and Technology, 2016, 6, 5168-5177.	2.1	22
23315	New insight into the intrinsic instability of fcc ZrH2 by energy-resolved local bonding analysis. RSC Advances, 2016, 6, 19150-19154.	1.7	4
23316	From benzodithiophene to diethoxy-benzodithiophene covalent organic frameworks â€“ structural investigations. CrystEngComm, 2016, 18, 4295-4302.	1.3	27
23317	Band gap bowing and crossing of B_xGa_{1â^'x}N alloy investigated by hybrid functional method. Journal of Semiconductors, 2016, 37, 023004.	2.0	3
23318	Ab initio calculations of half-metallic ferromagnetism in (VN)₁/(AlN)₁, (VN)₁/(GaN)₁and (VN)₁/(InN)₁superlattices. Journal of Physics: Conference Series, 2016, 687, 012069.	0.3	1
23319	A first-principles lattice dynamical study of type-I, type-II, and type-VIII silicon clathrates. Journal of Materials Science, 2016, 51, 4538-4548.	1.7	11
23320	Effect of MgO/Fe Interface Oxidation State on Electric-Field Modulation of Interfacial Magnetic Anisotropy. Journal of Electronic Materials, 2016, 45, 3162-3166.	1.0	5
23321	Lithium diffusion in graphene and graphite: Effect of edge morphology. Carbon, 2016, 103, 209-216.	5.4	53
23322	Ambient dissolutionâ€“recrystallization towards large-scale preparation of V2O5 nanobelts for high-energy battery applications. Nano Energy, 2016, 22, 583-593.	8.2	112

#	Article	IF	Citations
23323	Elucidating the fundamental forces in protein crystal formation: the case of crambin. Chemical Science, 2016, 7, 1496-1507.	3.7	21
23324	Influence of N-anion-doping on the production and the photoluminescence properties of Î³-Ca₂SiO₄:Ce³⁺ phosphors and the Î² â†' Î³ phase transformation. Journal of Materials Chemistry C, 2016, 4, 3313-3320.	2.7	18
23325	Germanene nanoribbon tunneling field effect transistor (GeNR-TFET) with a 10 nm channel length: analog performance, doping and temperature effects. Semiconductor Science and Technology, 2016, 31, 045009.	1.0	27
23326	Half-oxidized phosphorene: band gap and elastic properties modulation. Journal of Physics Condensed Matter, 2016, 28, 145501.	0.7	9
23327	Water at hydroxyapatite surfaces: the effect of coverage and surface termination as investigated by all-electron B3LYP-D* simulations. Theoretical Chemistry Accounts, 2016, 135, 1.	0.5	29
23328	Optical and electronic properties of B Al1â^'P alloys: A first principles study. Optik, 2016, 127, 3755-3761.	1.4	15
23329	Reforming and oxidative dehydrogenation of ethane with CO2 as a soft oxidant over bimetallic catalysts. Journal of Catalysis, 2016, 343, 168-177.	3.1	115
23330	First-principles study on magnetism and half-metallicity in bulk and various (001) surfaces of Heusler alloy Zr2VSn with Hg2CuTi-type structure. Journal of Magnetism and Magnetic Materials, 2016, 409, 28-33.	1.0	14
23331	Ruddlesdenâ€"Popper perovskite sulfides A3B2S7: A new family of ferroelectric photovoltaic materials for the visible spectrum. Nano Energy, 2016, 22, 507-513.	8.2	66
23332	Thermodynamic Properties of Molecular Crystals Calculated within the Quasi-Harmonic Approximation. Journal of Physical Chemistry A, 2016, 120, 2022-2034.	1.1	48
23333	Spectroscopic Investigation of Plasma-Fluorinated Monolayer Graphene and Application for Gas Sensing. ACS Applied Materials & Interfaces, 2016, 8, 8652-8661.	4.0	77
23334	Density functional theory approach to CO₂ adsorption on a spinel mineral: determination of binding coordination. RSC Advances, 2016, 6, 28607-28611.	1.7	8
23335	Structural morphology of carbon nanofibers grown on different substrates. Carbon, 2016, 98, 343-351.	5.4	25
23336	First principles calculations of magnetic, electronic and optical properties of (Mnâ€"Fe) co-doped SrTiO3. Optik, 2016, 127, 3055-3058.	1.4	9
23337	Theoretical investigation of the electronic and magnetic properties of TM (TM=Ti, V, and Cr)-doped w-BN compound. Journal of Magnetism and Magnetic Materials, 2016, 402, 156-160.	1.0	10
23338	Ab initio study of early stage Nb growth on MgO(001). Surface Science, 2016, 645, 80-87.	0.8	3
23339	Mechanisms of Si and Ge diffusion on surfactant terminated (111) silicon and germanium surfaces. Surface Science, 2016, 647, 12-16.	0.8	3
23340	Noble metal chain adsorption on graphene sheet. Surface Science, 2016, 647, 96-102.	0.8	11

#	Article	IF	Citations
23341	Thermal exfoliation of stoichiometric single-layer silica from the stishovite phase: insight from first-principles calculations. Nanoscale, 2016, 8, 10598-10606.	2.8	7
23342	Elastic, Electronic, Optical and Thermal Properties of Na2Po: An Ab Initio Study. Journal of Electronic Materials, 2016, 45, 435-443.	1.0	1
23343	Correlation between diffusion barriers and alloying energy in binary alloys. Physical Chemistry Chemical Physics, 2016, 18, 3302-3307.	1.3	33
23344	Adsorption of diazinon and hinosan molecules on the iron-doped boron nitride nanotubes surface in gas phase and aqueous solution: A computational study. Applied Surface Science, 2016, 364, 862-869.	3.1	22
23345	Insights into the behaviour of biomolecules on the early Earth: The concentration of aspartate by layered double hydroxide minerals. Geochimica Et Cosmochimica Acta, 2016, 176, 239-258.	1.6	18
23346	Structural and mechanical properties of Alâ€•Mgâ€•B films: Experimental study and first-principles calculations. Thin Solid Films, 2016, 599, 72-77.	0.8	10
23347	Defects in metalâ€“organic frameworks: a compromise between adsorption and stability?. Dalton Transactions, 2016, 45, 4352-4359.	1.6	140
23348	Elastic Properties of the Solid Electrolyte Li₇La₃Zr₂O₁₂(LLZO). Chemistry of Materials, 2016, 28, 197-206.	3.2	445
23349	Water Kinetics and Clustering on the (101) TiO₂ Anatase Surface. Journal of Physical Chemistry C, 2016, 120, 450-456.	1.5	14
23350	Defect-engineered graphene chemical sensors with ultrahigh sensitivity. Physical Chemistry Chemical Physics, 2016, 18, 14198-14204.	1.3	110
23351	Porous graphene for high capacity lithium ion battery anode material. Applied Surface Science, 2016, 363, 318-322.	3.1	19
23352	Phosphorous bonding in single wall carbon nanotubes studied by X-ray photoelectron spectroscopy and DFT calculations. Carbon, 2016, 99, 1-7.	5.4	17
23353	Theoretical study of the migration behaviour of Y-C atoms on diamond (001) surface. Diamond and Related Materials, 2016, 61, 102-108.	1.8	6
23354	An ab initio investgation of ideal tensile and shear strength of TiVNbMo high-entropy alloy. Materials Letters, 2016, 166, 271-275.	1.3	39
23355	Effect of halide-mixing on the electronic transport properties of organometallic perovskites. Solar Energy Materials and Solar Cells, 2016, 148, 2-10.	3.0	25
23356	Shear-Induced Structural Transformation for Tetragonal BC₄. Journal of Physical Chemistry C, 2016, 120, 581-586.	1.5	3
23357	Role of Branching on the Rate and Mechanism of Câ€“C Cleavage in Alkanes on Metal Surfaces. ACS Catalysis, 2016, 6, 469-482.	5.5	40
23358	Structure prediction of the solid forms of methanol: an ab initio random structure searching approach. Physical Chemistry Chemical Physics, 2016, 18, 2736-2746.	1.3	15

#	Article	IF	Citations
23359	Electronic structure and optical properties of Fe-doped SnS₂ from first-principle calculations. RSC Advances, 2016, 6, 3480-3486.	1.7	24
23360	High-performance x Li 2 MnO 3 Â·(1- x)LiMn 1/3 Co 1/3 Ni 1/3 O 2 (0.1 â¿ x â¿0.5) as Cathode Material for Lithium-ion Battery. Electrochimica Acta, 2016, 188, 686-695.	2.6	37
23361	Metalâ€“support interaction effects on chemoâ€“regioselectivity: Hydrogenation of crotonaldehyde on Pt 13 /CeO 2 (1 1 1). Journal of Catalysis, 2016, 334, 68-78.	3.1	31
23362	Prediction of novel phase of silicon and Siâ€“Ge alloys. Journal of Solid State Chemistry, 2016, 233, 471-483.	1.4	37
23363	Li₃AlSiO₅: the first aluminosilicate as a potential deep-ultraviolet nonlinear optical crystal with the quaternary diamond-like structure. Physical Chemistry Chemical Physics, 2016, 18, 4362-4369.	1.3	40
23364	Cation doping size effect for methane activation on alkaline earth metal doping of the CeO2 (111) surface. Catalysis Science and Technology, 2016, 6, 3544-3558.	2.1	20
23365	Gold assisted oxygen dissociation on a molybdenum-doped CaO(001) surface. Catalysis Science and Technology, 2016, 6, 6784-6793.	2.1	3
23366	Dehydration of AlPO₄-34 studied by variable-temperature NMR, XRD and first-principles calculations. New Journal of Chemistry, 2016, 40, 4178-4186.	1.4	24
23367	The electronic and transport properties of two-dimensional conjugated polymer networks including disorder. Nanoscale, 2016, 8, 1642-1651.	2.8	19
23368	Ab initio studies of isolated hydrogen vacancies in graphane. Physica E: Low-Dimensional Systems and Nanostructures, 2016, 79, 52-58.	1.3	15
23369	Luminescence of undoped and Eu³⁺ doped nanocrystalline SrWO₄ scheelite: time resolved fluorescence complimented by DFT and positron annihilation spectroscopic studies. RSC Advances, 2016, 6, 3792-3805.	1.7	57
23370	Distinct electron density topologies and elastic properties of two similar omega phases: Ï‰-Zr and Zr 2 Al. Journal of Alloys and Compounds, 2016, 660, 316-323.	2.8	5
23371	Thermoelectric Properties of Fe2VAl and Fe2V0.75M0.25Al (MÂ=ÂMo, Nb, Ta) Alloys: First-Principles Calculations. Journal of Electronic Materials, 2016, 45, 1101-1114.	1.0	16
23372	Computing the band structure and energy gap of penta-graphene by using DFT and G0W0 approximations. Solid State Communications, 2016, 229, 1-4.	0.9	53
23373	Density functional theory study of Oâ€“H and Câ€“H bond scission of methanol catalyzed by a chemisorbed oxygen layer on Cu(111). Surface Science, 2016, 646, 288-297.	0.8	16
23374	Evidence for Germanene growth on epitaxial hexagonal (h)-AlN on Ag(1 1 1). Journal of Physics Condensed Matter, 2016, 28, 045002.	0.7	57
23375	An ab initio study on electronic and magnetic properties of Cr, V doped Cd and Zn nitrides for spintronic applications. Journal of Magnetism and Magnetic Materials, 2016, 406, 48-59.	1.0	11
23376	A hybrid functional calculation of Tm3+ defects in germanium (Ge). Materials Science in Semiconductor Processing, 2016, 43, 129-133.	1.9	15

#	Article	IF	Citations
23377	Structural, electronic and optical properties of Li intercalated on MO3 (M: Mo, W): A first principle investigation. Solid State Communications, 2016, 229, 37-42.	0.9	6
23379	Determination of Precise Redox Properties of Oxygen-Doped Single-Walled Carbon Nanotubes Based on in Situ Photoluminescence Electrochemistry. Journal of Physical Chemistry C, 2016, 120, 15632-15639.	1.5	25
23380	Electron Transfer and Catalytic Mechanism of Organic Molecule-Adsorbed Graphene Nanoribbons as Efficient Catalysts for Oxygen Reduction and Evolution Reactions. Journal of Physical Chemistry C, 2016, 120, 2166-2175.	1.5	42
23381	Improving KNbO₃ photocatalytic activity under visible light. RSC Advances, 2016, 6, 9958-9966.	1.7	33
23382	Sulphur diffusion inÎ²-NiAl and effect of Pt additive: anab initiostudy. Journal Physics D: Applied Physics, 2016, 49, 055306.	1.3	4
23383	Novel hetero-bilayered materials for photovoltaics. Applied Materials Today, 2016, 2, 24-31.	2.3	23
23384	High-pressure phase diagram of gold from first-principles calculations: Converging to an isotropic atomic stacking order. Computational Materials Science, 2016, 114, 72-78.	1.4	13
23385	Ab initio calculations of surface phonons of the hydrogen-terminated Si(110)-(1 Ã— 1) surface. Surface Science, 2016, 647, 17-25.	0.8	3
23386	Unravelling the hydrogen absorption process in Pd overlayers on a Au(111) surface. Physical Chemistry Chemical Physics, 2016, 18, 3659-3668.	1.3	10
23387	Electron beam controlled covalent attachment of small organic molecules to graphene. Nanoscale, 2016, 8, 2711-2719.	2.8	28
23388	Density functional theory study of hydrogenation of S to H₂S on Ptâ€“Pd alloy surfaces. RSC Advances, 2016, 6, 6289-6299.	1.7	6
23389	Ab initio investigations of the phase stability in group IVB and VB transition metal carbides. Computational Materials Science, 2016, 112, 318-326.	1.4	77
23390	Photoelectrochemical (PEC) water splitting of BiOI{001} nanosheets synthesized by a simple chemical transformation. Journal of Alloys and Compounds, 2016, 665, 158-164.	2.8	47
23391	Structural and Energetic Trends of Ethylene Hydrogenation over Transition Metal Surfaces. Journal of Physical Chemistry C, 2016, 120, 995-1003.	1.5	39
23392	Interaction of a Self-Assembled Ionic Liquid Layer with Graphite(0001): A Combined Experimental and Theoretical Study. Journal of Physical Chemistry Letters, 2016, 7, 226-233.	2.1	68
23393	Dependence on size of supported Rh nanoclusters for CO adsorption. RSC Advances, 2016, 6, 3830-3839.	1.7	12
23394	Bifunctional application of sodium cobaltate as a catalyst and captor through CO oxidation and subsequent CO₂ chemisorption processes. RSC Advances, 2016, 6, 2162-2170.	1.7	27
23395	Electronic structure of iron-doped misfit-layered calcium cobaltite. Computational Materials Science, 2016, 114, 64-71.	1.4	7

#	Article	IF	Citations
23396	First principles study on optical response of graphene oxides: From reduced graphene oxide to the fully oxidized surface. Computational Materials Science, 2016, 114, 112-120.	1.4	26
23397	Study on the electronic structure of Î±-U2N3 by XPS and first principles. Journal of Alloys and Compounds, 2016, 664, 745-749.	2.8	20
23398	Conduction mechanism in mesoporous hematite thin films using low temperature electrical measurements and theoretical electronic band structure calculations. Journal of Alloys and Compounds, 2016, 664, 682-689.	2.8	10
23399	Density-functional theory study of high hydrogen content complex hydrides Mg(BH 4) 2 at low temperature. Renewable Energy, 2016, 90, 114-119.	4.3	16
23400	Mixed lithium-sodium (LiNaCO3) and lithium-potassium (LiKCO3) carbonates for low temperature electrochemical applications: Structure, electronic properties and surface reconstruction from ab-initio calculations. Surface Science, 2016, 647, 66-77.	0.8	18
23401	Glass-like Lattice Thermal Conductivity and Thermoelectric Properties of Incommensurate Chimney-Ladder Compound FeGe_{Î³}. Chemistry of Materials, 2016, 28, 529-533.	3.2	26
23402	Structural Analysis and Li Migration Pathways in Ramsdellite Li₂Ti₃O₇: A Theoretical Study. Journal of Physical Chemistry C, 2016, 120, 5-10.	1.5	17
23403	CuO Surfaces and CO₂ Activation: A Dispersion-Corrected DFT+U Study. Journal of Physical Chemistry C, 2016, 120, 2198-2214.	1.5	165
23404	Rationalizing the Hydrogen and Oxygen Evolution Reaction Activity of Two-Dimensional Hydrogenated Silicene and Germanene. ACS Applied Materials & Interfaces, 2016, 8, 1536-1544.	4.0	69
23405	First principles study of the adsorption and dissociation mechanisms of H₂S on a TiO₂anatase (001) surface. RSC Advances, 2016, 6, 7941-7949.	1.7	25
23406	Adsorption of proline, hydroxyproline and glycine on anatase (001) surface: a first-principle study. Theoretical Chemistry Accounts, 2016, 135, 1.	0.5	8
23407	Phase transition, thermodynamics properties and IR spectrum of Î±- and Î³-RDX: First principles and MD studies. Chemical Physics Letters, 2016, 644, 250-254.	1.2	10
23408	Fast and Huge Anisotropic Diffusion of Cu (Ag) and Its Resistance on the Sn Self-diffusivity in Solid Î²â€“Sn. Journal of Materials Science and Technology, 2016, 32, 121-128.	5.6	18
23409	First-Principles Design of New Electrodes for Proton-Conducting Solid-Oxide Electrochemical Cells: A-Site Doped Sr₂Fe_{1.5}Mo_{0.5}O_{6â^Î´} Perovskite. Chemistry of Materials, 2016, 28, 490-500.	3.2	86
23410	Connecting defects and amorphization in UiO-66 and MIL-140 metalâ€“organic frameworks: a combined experimental and computational study. Physical Chemistry Chemical Physics, 2016, 18, 2192-2201.	1.3	85
23411	Which wets TiB2 inoculant particles: Al or Al3Ti?. Journal of Alloys and Compounds, 2016, 664, 460-468.	2.8	44
23412	Stability and nucleation of Ir n (n = 1â€“5) clusters on different Î³ -Al 2 O 3 surfaces: A density functional theory study. Physics Letters, Section A: General, Atomic and Solid State Physics, 2016, 380, 718-725.	0.9	8
23413	Structural Transformation of MXene (V₂C, Cr₂C, and Ta₂C) with O Groups during Lithiation: A First-Principles Investigation. ACS Applied Materials & Interfaces, 2016, 8, 74-81.	4.0	159

#	Article	IF	Citations
23414	Oxygen Reduction Reaction on Pt Overlayers Deposited onto a Gold Film: Ligand, Strain, and Ensemble Effect. ACS Catalysis, 2016, 6, 671-676.	5.5	79
23415	Ligand Addition Energies and the Stoichiometry of Colloidal Nanocrystals. ACS Nano, 2016, 10, 1462-1474.	7.3	33
23416	Where does methanol lose hydrogen to trigger steam reforming? A revisit of methanol dehydrogenation on the PdZn alloy model obtained from kinetic Monte Carlo simulations. Physical Chemistry Chemical Physics, 2016, 18, 3936-3943.	1.3	3
23417	Understanding and solving disorder in the substitution pattern of amino functionalized MIL-47(V). Dalton Transactions, 2016, 45, 4309-4315.	1.6	5
23418	Discovery of a ternary pseudobrookite phase in the earth-abundant Tiâ€“Znâ€“O system. Dalton Transactions, 2016, 45, 1572-1581.	1.6	6
23419	Nanoscale cross-correlated AFM, Kelvin probe, elastic modulus and quantum mechanics investigation of clay mineral surfaces: The case of chlorite. Applied Clay Science, 2016, 131, 175-181.	2.6	30
23420	Electronic structure, magnetic and optical properties of Cr-doped GaAs using hybrid density functional. Computational Materials Science, 2016, 113, 75-79.	1.4	7
23421	Theoretical investigation of hydrogen absorption properties of rhodiumâ€“silver alloys. Journal of Alloys and Compounds, 2016, 662, 404-408.	2.8	5
23422	Initial stages of water solvation of stepped platinum surfaces. Physical Chemistry Chemical Physics, 2016, 18, 3416-3422.	1.3	32
23423	Multifunctional biosensors based on peptideâ€“polyelectrolyte conjugates. Physical Chemistry Chemical Physics, 2016, 18, 3223-3233.	1.3	30
23424	Electronic structure, photovoltage, and photocatalytic hydrogen evolution with p-CuBi₂O₄ nanocrystals. Journal of Materials Chemistry A, 2016, 4, 2936-2942.	5.2	158
23425	Tetrahedral tilting and ferroelectricity in Bi2AO5 (A=Si, Ge) from first principles calculations. Journal of Solid State Chemistry, 2016, 235, 68-75.	1.4	33
23426	High thermoelectric performance can be achieved in black phosphorus. Journal of Materials Chemistry C, 2016, 4, 991-998.	2.7	59
23427	Modulating electronic, magnetic and chemical properties of MoS2 monolayer sheets by substitutional doping with transition metals. Applied Surface Science, 2016, 364, 181-189.	3.1	161
23428	A DFT study of hydrogen storage in Zr(Cr 0.5 Ni 0.5) 2 Laves phase. International Journal of Hydrogen Energy, 2016, 41, 2700-2710.	3.8	19
23429	Ab initio study of electronic structure and lattice properties of ZnSe1â^'O. Optik, 2016, 127, 1889-1892.	1.4	3
23430	Adsorption of acridine orange and methylene blue synthetic dyes and anthracene on single wall carbon nanotubes: A first principle approach. Computational and Theoretical Chemistry, 2016, 1076, 42-50.	1.1	47
23431	Effect of temperature on the distribution and inhomogeneity degree of Se-S atoms in CuIn(Se1â^'xSx)2alloys. Journal Physics D: Applied Physics, 2016, 49, 025101.	1.3	3

#	Article	IF	Citations
23432	DFT theoretical and FT-IR spectroscopic investigations of the plasticity of clay minerals dispersions. Journal of Molecular Structure, 2016, 1109, 97-105.	1.8	21
23433	Adsorption of Water on the Fe₃O₄(111) Surface: Structures, Stabilities, and Vibrational Properties Studied by Density Functional Theory. Journal of Physical Chemistry C, 2016, 120, 1056-1065.	1.5	71
23434	Unexpectedly large impact of van der Waals interactions on the description of heterogeneously catalyzed reactions: the water gas shift reaction on Cu(321) as a case example. Physical Chemistry Chemical Physics, 2016, 18, 2792-2801.	1.3	22
23435	Predicted thermoelectric properties of olivine-type Fe₂GeCh₄(Châ€‰â€‰=â€‰â€‰S, Se and) Ti ETQq1	0.7	11
23436	Isovalent Ca and Ba substitutions in thermoelectric layer-structured oxyselenide Sr₂CoO₂Cu₂Se₂. Journal of Physics Condensed Matter, 2016, 28, 035802.	0.7	9
23437	Hierarchical sulfur-impregnated hydrogenated TiO₂mesoporous spheres comprising anatase nanosheets with highly exposed (001) facets for advanced Li-S batteries. Nanotechnology, 2016, 27, 045403.	1.3	40
23438	The bandgap distribution investigated across the strain-induced bending ZnO nanowire. Modern Physics Letters B, 2016, 30, 1650048.	1.0	4
23439	Association of defects in doped non-stoichiometric ceria from first principles. Physical Chemistry Chemical Physics, 2016, 18, 3804-3811.	1.3	35
23440	First-principle investigations of structure, elastic and bond hardness of FexB (x=1, 2, 3) under pressure. Journal of Magnetism and Magnetic Materials, 2016, 406, 192-199.	1.0	57
23441	Characterization of Phosphate Species on Hydrated Anatase TiO2 Surfaces. Langmuir, 2016, 32, 997-1008.	1.6	18
23442	Pyridine intercalated Bi2Se3heterostructures: controlling the topologically protected states. Nanotechnology, 2016, 27, 035704.	1.3	2
23443	Electrochemical and Computational Study of Oxygen Reduction Reaction on Nonprecious Transition Metal/Nitrogen Doped Carbon Nanofibers in Acid Medium. Journal of Physical Chemistry C, 2016, 120, 1586-1596.	1.5	148
23444	Geometry and Electronic Properties of Glycerol Adsorbed on Bare and Transition-Metal Surface-Alloyed Au(111): A Density Functional Theory Study. Journal of Physical Chemistry C, 2016, 120, 1749-1757.	1.5	18
23445	Ethene Oligomerization in Ni-Containing Zeolites: Theoretical Discrimination of Reaction Mechanisms. ACS Catalysis, 2016, 6, 1205-1214.	5.5	106
23446	Complex Stoichiometry-Dependent Reordering of 3,4,9,10-Perylenetetracarboxylic Dianhydride on Ag(111) upon K Intercalation. ACS Nano, 2016, 10, 2365-2374.	7.3	22
23447	Production of Highly Monolayer Enriched Dispersions of Liquid-Exfoliated Nanosheets by Liquid Cascade Centrifugation. ACS Nano, 2016, 10, 1589-1601.	7.3	365
23448	Adsorption mechanism of graphene-like ZnO monolayer towards CO₂molecules: enhanced CO₂capture. Nanotechnology, 2016, 27, 015502.	1.3	69
23449	Structural and electronic properties of metalloporphyrin (MP, M = Fe, Co and Zn) adsorbed on single walled BNNT and SiCNT. Applied Surface Science, 2016, 360, 69-76.	3.1	17

#	Article	IF	Citations
23450	Thermodynamic properties of nuclear material uranium carbide using density functional theory. Journal of Thermal Analysis and Calorimetry, 2016, 124, 11-20.	2.0	19
23451	Effect of crystal structure on the electronic transport properties of the organometallic perovskite CH3NH3PbI3. Solar Energy Materials and Solar Cells, 2016, 148, 60-66.	3.0	18
23452	Formation, structure and magnetism of the Î³-(Fe,M)23C6 (M = Cr, Ni) phases: A first-principles study. Acta Materialia, 2016, 103, 273-279.	3.8	38
23453	One-dimensional mercury(II) halide coordination polymers of 3,6-bis(2-pyridyl)-1,2,4,5-tetrazine ligand: Synthesis, crystal structure, spectroscopic and DFT studies. Journal of Solid State Chemistry, 2016, 233, 311-319.	1.4	16
23454	Bandgap engineering of different stacking WS2 bilayer under an external electric field. Solid State Communications, 2016, 225, 32-37.	0.9	27
23455	TiO2 nanosheets with exposed {001} facets for photocatalytic applications. Nano Research, 2016, 9, 3-27.	5.8	327
23456	Structural, electronic and optical properties of Zn0.5Cr0.5S from first-principles. Computational Materials Science, 2016, 112, 39-43.	1.4	11
23457	Electron tunneling in Fe/KNbO3/Fe multiferroic tunnel junctions. Computational Materials Science, 2016, 112, 257-262.	1.4	3
23458	Effects of defect on the storage and diffusion of Na and Mg interstitials in Si anode. Journal of Alloys and Compounds, 2016, 654, 157-162.	2.8	9
23459	Structure and magnetism of Mn, Fe, or Co adatoms on monolayer and bilayer black phosphorus. Journal of Magnetism and Magnetic Materials, 2016, 401, 706-710.	1.0	16
23460	Structural, electronic and magnetic properties of the Mn50Al46Ni4 alloy. Journal of Magnetism and Magnetic Materials, 2016, 401, 841-847.	1.0	25
23461	Hydrogen isotope dissolution, diffusion, and permeation in Er2O3. Journal of Power Sources, 2016, 303, 168-174.	4.0	13
23462	Theoretical investigations of the ternary compound LaUN3. Journal of Solid State Chemistry, 2016, 233, 484-491.	1.4	1
23463	Crystal structure and band gap studies of sodalite: experimental and calculated results. Journal of Molecular Structure, 2016, 1106, 59-63.	1.8	9
23464	Na Deposition on MnO(100). Surface Science, 2016, 645, 23-29.	0.8	11
23465	Effect of ternary additions to structural properties of NiTi alloys. Computational Materials Science, 2016, 112, 347-355.	1.4	40
23466	Optimization of halide perovskite solar cells based on nanocolumnar ZnO. Solar Energy Materials and Solar Cells, 2016, 158, 202-208.	3.0	10
23467	The temperature effect on mechanical properties of silicon carbide sheet based on density functional treatment. Solid State Communications, 2016, 227, 40-44.	0.9	8

#	Article	IF	Citations
23468	Characterization of Two Distinct Amorphous Forms of Valsartan by Solid-State NMR. Molecular Pharmaceutics, 2016, 13, 211-222.	2.3	30
23469	Reduction of interfacial friction in commensurate graphene/h-BN heterostructures by surface functionalization. Nanoscale, 2016, 8, 575-580.	2.8	43
23470	The acceleration of methanol synthesis and C2 oxygenates formation on copper grain boundary from syngas. Applied Catalysis A: General, 2016, 509, 97-104.	2.2	23
23471	Flatbands in 2D boroxine-linked covalent organic frameworks. Physical Chemistry Chemical Physics, 2016, 18, 1258-1264.	1.3	25
23472	Energetics and the magnetic state of Mn2 adsorbed on Au(111): Dimer bond distance dependence. Journal of Magnetism and Magnetic Materials, 2016, 403, 172-180.	1.0	4
23473	Defect-Mediated Gold Substitution Doping in ZnO Mesocrystals and Catalysis in CO Oxidation. ACS Catalysis, 2016, 6, 115-122.	5.5	54
23474	WO₃ with surface oxygen vacancies as an anode buffer layer for high performance polymer solar cells. Journal of Materials Chemistry A, 2016, 4, 894-900.	5.2	68
23475	The molecular understanding of interfacial interactions of functionalized graphene and chitosan. Applied Surface Science, 2016, 360, 715-721.	3.1	23
23476	Ab initio derived reaction mechanism for the dry reforming of methane on Rh doped pyrochlore catalysts. Journal of Catalysis, 2016, 333, 59-70.	3.1	31
23477	Structural, electronic, mechanical and magnetic properties of rare-earth nitrides REN (RE=Ce, Pr, Nd): A first principles study. Materials Science in Semiconductor Processing, 2016, 41, 17-25.	1.9	4
23478	Simulation, fabrication, and application of transparent conductive Mo-doped ZnO film in a solar cell. Solar Energy Materials and Solar Cells, 2016, 145, 171-179.	3.0	35
23479	The selectivity and activity of catalyst for CO hydrogenation to methanol and hydrocarbon: A comparative study on Cu, Co and Ni surfaces. Surface Science, 2016, 645, 30-40.	0.8	15
23480	Phase stability, mechanical and thermodynamic properties of orthorhombic and trigonal MgSiN₂: an ab initio study. Phase Transitions, 2016, 89, 480-513.	0.6	69
23481	Structural, energetic, and electronic properties of gyroidal graphene nanostructures. Carbon, 2016, 96, 998-1007.	5.4	9
23482	Understanding the thermodynamic pathways of SnO-to-SnO x phase transition. Computational Materials Science, 2016, 111, 359-365.	1.4	22
23483	The effects of uniaxial and biaxial strain on the electronic structure of germanium. Computational Materials Science, 2016, 112, 263-268.	1.4	16
23484	Study of interaction between transition metal atoms and bigraphene monovacancy by means of quantum chemistry. Computational Materials Science, 2016, 112, 269-275.	1.4	1
23485	A 45 Sc-NMR and DFT calculation study of crystalline scandium compounds. Solid State Sciences, 2016, 51, 1-7.	1.5	22

#	Article	IF	Citations
23486	Structure and stability of clean and adsorbate covered intermetallic PdGa surfaces: A first principles study. Surface Science, 2016, 644, 69-79.	0.8	7
23487	Phase transition and optoelectronic properties of MgH₂. Phase Transitions, 2016, 89, 437-447.	0.6	8
23488	Surface elasticity revisited in the context of second strain gradient theory. Mechanics of Materials, 2016, 93, 220-237.	1.7	21
23489	Interactions between C and Cu atoms in single-layer graphene: direct observation and modelling. Nanoscale, 2016, 8, 529-535.	2.8	21
23490	Does p-type ohmic contact exist in WSe₂â€“metal interfaces?. Nanoscale, 2016, 8, 1179-1191.	2.8	166
23491	Defect stabilized gold atoms on graphene as potential catalysts for ethylene epoxidation: a first-principles investigation. Catalysis Science and Technology, 2016, 6, 1632-1641.	2.1	43
23492	The effect of Mg, Cu and P impurities on dose response of LiF:Mg,Cu,P phosphors: simulation versus experiments. Radiation Protection Dosimetry, 2016, 168, 19-26.	0.4	2
23493	Structural stability of ultra-incompressible Mo2B: A combined experimental and theoretical study. Journal of Alloys and Compounds, 2016, 654, 554-560.	2.8	17
23494	Two-body potential model based on cosine series expansion for ionic materials. Computational Materials Science, 2016, 111, 54-63.	1.4	1
23495	Planar versus three-dimensional growth of metal nanostructures at graphene. Carbon, 2016, 96, 216-222.	5.4	7
23496	Stability and electronic structures of double-walled armchair germanium carbide nanotubes. Computational Materials Science, 2016, 111, 86-90.	1.4	11
23497	Charge-modulated permeability and selectivity in graphdiyne for hydrogen purification. Molecular Simulation, 2016, 42, 573-579.	0.9	24
23498	Prediction of half-metallic properties for the AMnSe2 (A=Rb, Cs) compounds from first-principle calculations. Journal of Magnetism and Magnetic Materials, 2016, 399, 179-184.	1.0	10
23499	Effect of charge redistribution factor on stacking-fault energies of Mg-based binary alloys. Scripta Materialia, 2016, 112, 101-105.	2.6	44
23500	DFT study of the water gas shift reaction on Ni(111), Ni(100) and Ni(110) surfaces. Surface Science, 2016, 644, 53-63.	0.8	84
23501	First-principles study of point defects in C14 MgZn2 Laves phase. Journal of Alloys and Compounds, 2016, 654, 475-481.	2.8	16
23502	Thermal neutron scattering cross sections of beryllium and magnesium oxides. Annals of Nuclear Energy, 2016, 87, 242-251.	0.9	9
23503	Interface Schottky barrier engineering via strain in metalâ€“semiconductor composites. Nanoscale, 2016, 8, 1352-1359.	2.8	45

#	Article	IF	Citations
23504	Ab initio study of lattice dynamics of CsH 2 PO 4 and CsD 2 PO 4 crystals. Computational Materials Science, 2016, 111, 301-309.	1.4	10
23505	Ca2SnS4: Crystal structure, optical property, and electronic structure. Journal of Crystal Growth, 2016, 434, 67-71.	0.7	2
23506	Chemical synthesis, characterization and theoretical investigations of stannite phase CuZn₂AlS₄ nanocrystals. New Journal of Chemistry, 2016, 40, 1149-1154.	1.4	13
23507	Phase equilibria and solidification characteristics of the Alâ€“Scâ€“Si alloys. Journal of Materials Science, 2016, 51, 1644-1658.	1.7	13
23508	Electronic and optical properties of Mg-, F-doped and Mgâ^–F-codoped M 1 -VO 2 via hybrid density functional calculations. Journal of Alloys and Compounds, 2016, 658, 569-575.	2.8	30
23509	Electronic structures, magnetic properties, half-metallicity and optical properties of the zincblende Zn 1â^'x Mo x S. Journal of Magnetism and Magnetic Materials, 2016, 401, 746-750.	1.0	4
23510	Enhancement of ferroelectric polarization in layered BaZrO3/BaTiO3 superlattices. Physics Letters, Section A: General, Atomic and Solid State Physics, 2016, 380, 299-303.	0.9	14
23511	Dirac-like fermions and node-loop features in bilayer BC 3 sheet sandwiching a triangular alkaline metal layer. Physics Letters, Section A: General, Atomic and Solid State Physics, 2016, 380, 475-479.	0.9	1
23512	Effects of A 3+ cations on hydration in A 2 M 3 O 12 family materials: A first-principles study. Computational Materials Science, 2016, 111, 28-33.	1.4	14
23513	First-principles study of structural, elastic and electronic properties of Î±-, Î²- and Î³-graphyne. Carbon, 2016, 96, 879-887.	5.4	235
23514	First principle calculations of solid nitrobenzene under high pressure. Computational and Theoretical Chemistry, 2016, 1075, 98-103.	1.1	4
23515	Structural phase stability, electronic structure and mechanical properties of alkali metal hydrides AMH4 (A=Li, Na; M=B, Al). Journal of Physics and Chemistry of Solids, 2016, 88, 68-77.	1.9	5
23516	First-principles study of O2 adsorption on Al-doped ZnO(<mml:math) Tj ETQq0 0 0 rgBT /Overlock 10 Tf 50 282 Td (xmlns:mml="http://w surface. Sensors and Actuators B: Chemical, 2016, 224, 372-380.	4.0	25
23517	On the hydrogen adsorption and dissociation on Cu surfaces and nanorows. Surface Science, 2016, 646, 221-229.	0.8	37
23518	A noble 2-dimensional BN nano structure with tunable band gap by organic molecules. Computational Materials Science, 2016, 111, 366-373.	1.4	11
23519	Effect of Disorder on Electronic, Magnetic, and Optical Properties of Co2CrZ Heusler Alloys (Z = Al,) Tj ETQq1 1 0.784314 rgBT /Overl	0.8	21
23520	Influence of trap connectivity on H diffusion: Vacancy trapping. Acta Materialia, 2016, 103, 334-340.	3.8	38
23521	Multilayer heterostructures of magnetic Heusler and binary compounds from first principles. Journal of Magnetism and Magnetic Materials, 2016, 401, 138-143.	1.0	2

#	Article	IF	Citations
23522	Electronic and optical properties of<mml:math xmlns:mml="http://www.w3.org/1998/Math/MathML" altimg="si22.gif" overflow="scroll"><mml:mrow><mml:mtext>O</mml:mtext></mml:mrow></mml:math>-doped monolayer<mml:math xmlns:mml="http://www.w3.org/1998/Math/MathML" altimg="si1.gif" overflow="scroll"><mml:mrow><mml:msub><mml:mrow><mml:mtext>MoS</mml:mtext></mml:mrow><mml:mrow><mml:mn>2</mm Computational Materials Science, 2016, 111, 416-423.	1.4	47
23523	Long-range intercluster interactions of solute nanoprecipitates in Mgâ€“Y alloys: A first-principles study. Journal of Alloys and Compounds, 2016, 657, 662-670.	2.8	14
23524	Uniform graphene on liquid metal by chemical vapour deposition at reduced temperature. Carbon, 2016, 96, 799-804.	5.4	35
23525	Theoretical study of electronic structure and superconductivity in FeSe 0.9â^'x (Si/Sb) x alloys. Journal of Alloys and Compounds, 2016, 658, 1041-1059.	2.8	3
23526	Effects of La doping on structural, optical, electronic properties ofÂSr 2 Bi 2 O 5 photocatalyst. Journal of Alloys and Compounds, 2016, 658, 139-146.	2.8	24
23527	Adsorption of SO2 molecule on doped (8, 0) boron nitride nanotube: A first-principles study. Physica E: Low-Dimensional Systems and Nanostructures, 2016, 76, 47-51.	1.3	31
23528	Novel crystal structures for lithiumâ€“silicon alloy predicted by minima hopping method. Journal of Alloys and Compounds, 2016, 655, 147-154.	2.8	21
23529	Stability and electronic structure of MgAl2O4(1 1 1) surfaces: A first-principles study. Computational Materials Science, 2016, 112, 8-17.	1.4	24
23530	DFT calculations on electro-oxidations and dissolutions of Pt and Ptâ€“Au nanoparticles. Catalysis Today, 2016, 262, 100-109.	2.2	25
23531	First-principles study on surface stability of tantalum carbides. Surface Science, 2016, 644, 24-28.	0.8	16
23532	Synthesis, crystal structures, magnetic properties, and lattice dynamics of Ba2XCu(OH)[V2O7] with X=Cl, Br. Journal of Solid State Chemistry, 2016, 236, 69-77.	1.4	8
23533	Atomistic understanding of the origin of high oxygen reduction electrocatalytic activity of cuboctahedral Pt₃Coâ€“Pt coreâ€“shell nanoparticles. Catalysis Science and Technology, 2016, 6, 1393-1401.	2.1	17
23534	High-energy metalâ€“organic frameworks (HE-MOFs): Synthesis, structure and energetic performance. Coordination Chemistry Reviews, 2016, 307, 292-312.	9.5	259
23535	Preparation of porous carbons based on polyvinylidene fluoride for CO 2 adsorption: A combined experimental and computational study. Microporous and Mesoporous Materials, 2016, 219, 59-65.	2.2	28
23536	Electronic structure, optical dielectric constant and born effective charge of EuAlO. Journal of Physics and Chemistry of Solids, 2016, 88, 1-7.	1.9	9
23537	Partitioning of Cr and Si between cementite and ferrite derived from first-principles thermodynamics. Acta Materialia, 2016, 102, 241-250.	3.8	17
23538	Electronic Structure of Crystalline Buckyballs: fcc-C60. Journal of Electronic Materials, 2016, 45, 339-348.	1.0	26
23539	First-Principle Study of Structural, Electronic and Magnetic Properties in Pd1â^'x Fe x Te (x = 0, 0.0625,) Tj ETQq1 1 0.784314 rgBT /O	0.8	1

#	Article	IF	Citations
23540	First-principles investigation of mechanical, thermodynamic and electronic properties of FeSn 5 and CoSn 5 phases. Computational Materials Science, 2016, 111, 175-180.	1.4	11
23541	Hydrogen solubility and vacancy concentration in nickel single crystals at thermal equilibrium: New insights from statistical mechanics and ab initio calculations. Journal of Alloys and Compounds, 2016, 656, 555-567.	2.8	41
23542	Computational screening of alloying elements for the development of sustainable V-based hydrogen separation membranes. Journal of Membrane Science, 2016, 497, 270-281.	4.1	7
23543	A First-Principles Theoretical Study on the Thermoelectric Properties of the Compound Cu5AlSn2S8. Journal of Electronic Materials, 2016, 45, 1453-1458.	1.0	6
23544	Solid solution strengthening of hexagonal titanium alloys: Restoring forces and stacking faults calculated from first principles. Acta Materialia, 2016, 102, 304-314.	3.8	113
23545	Ab initio simulations on migration paths of interstitial oxygen in corundum. Nuclear Instruments & Methods in Physics Research B, 2016, 374, 29-34.	0.6	21
23546	Electronic and Magnetic Properties of the Bulk and Surfaces of Rock salt KM (M = Se and Te): A Density Functional Theory Study. Journal of Superconductivity and Novel Magnetism, 2016, 29, 215-226.	0.8	4
23547	The size-dependent site composition of FCC cobalt nanocrystals. Catalysis Today, 2016, 261, 48-59.	2.2	123
23548	TiC₂: a new two-dimensional sheet beyond MXenes. Nanoscale, 2016, 8, 233-242.	2.8	161
23549	Density functional investigation on electronic structure and elastic properties of BeX at high pressure. Indian Journal of Physics, 2016, 90, 271-281.	0.9	4
23550	Comparison of the coupling of ethylene with acetate species and ethylene dehydrogenation on Pdâ€“Au(100): a density functional study. Catalysis Science and Technology, 2016, 6, 555-568.	2.1	9
23551	Half-metallic ferromagnetic properties of Cr- and V-doped AlP semiconductors. Journal of Magnetism and Magnetic Materials, 2016, 397, 132-138.	1.0	19
23552	Pressureâ€“temperature dependence of thermodynamic properties of rutile (TiO2): A first-principles study. Pramana - Journal of Physics, 2016, 86, 117-126.	0.9	1
23553	Crystal growth and electronic structure of low-temperature phase SrMgF4. Journal of Solid State Chemistry, 2016, 236, 89-93.	1.4	11
23554	CO adsorption over Pd nanoparticles: A general framework for IR simulations on nanoparticles. Surface Science, 2016, 646, 210-220.	0.8	65
23555	Exploring pure and RE co-doped (Eu3+, Tb3+ and Dy3+) gadolinium scandate: Luminescence behaviour and dynamics of energy transfer. Chemical Engineering Journal, 2016, 283, 114-126.	6.6	51
23556	Butanethiol adsorption and dissociation on Ag (111): A periodic DFT study. Surface Science, 2016, 646, 247-252.	0.8	7
23557	Reaction mechanism of methyl nitrite dissociation during co catalytic coupling to dimethyl oxalate: A density functional theory study. Chinese Journal of Chemical Engineering, 2016, 24, 132-139.	1.7	19

#	Article	IF	Citations
23558	Quantum dynamics of polyatomic dissociative chemisorption on transition metal surfaces: mode specificity and bond selectivity. Chemical Society Reviews, 2016, 45, 3621-3640.	18.7	140
23559	Comparative ab initio calculations of SrTiO3/BaTiO3 and SrZrO3/PbZrO3 (0 0 1) heterostructures. Nuclear Instruments & Methods in Physics Research B, 2016, 374, 20-23.	0.6	15
23560	Tailoring physical properties of graphene: Effects of hydrogenation, oxidation, and grain boundaries by atomistic simulations. Computational Materials Science, 2016, 112, 527-546.	1.4	14
23561	Organic linkers on oxide surfaces: Adsorption and chemical bonding of phthalic anhydride on MgO(100). Surface Science, 2016, 646, 90-100.	0.8	7
23562	Composition, structure and stability of surfaces formed by Ni deposition on Pd(111). Surface Science, 2016, 646, 56-64.	0.8	7
23563	The structure and electronic properties of dislocations studied by first-principles and molecular dynamics. Molecular Simulation, 2016, 42, 102-109.	0.9	3
23564	Selective reduction of SWCNTs â€“ concepts and insights. Journal of Materials Chemistry C, 2017, 5, 3937-3947.	2.7	10
23565	Passivated co-doping approach to bandgap narrowing of titanium dioxide with enhanced photocatalytic activity. Applied Catalysis B: Environmental, 2017, 200, 1-9.	10.8	90
23566	MAGNETIC PROPERTIES OF Fe DEPOSITED ON W(110) SURFACE: EFFECTS OF O CONTAMINATION AND O₂ ADSORPTION. Surface Review and Letters, 2017, 24, 1750009.	0.5	1
23567	Formation, Stability, Geometry and Band Structure of Organically Surface-Modified Germanane. Journal of Materials Science and Technology, 2017, 33, 59-64.	5.6	12
23568	First Principles Calculations of Palladium Nanoparticle XANES Spectra. Topics in Catalysis, 2017, 60, 283-288.	1.3	28
23569	Feature engineering of machine-learning chemisorption models for catalyst design. Catalysis Today, 2017, 280, 232-238.	2.2	165
23570	Photocatalytic hydrogen production over solid solutions between BiFeO 3 and SrTiO 3. Applied Surface Science, 2017, 391, 535-541.	3.1	58
23571	Synthesis of Mn-doped ZnS microspheres with enhanced visible light photocatalytic activity. Applied Surface Science, 2017, 391, 557-564.	3.1	76
23572	Hexagonal Boron Nitride (hâ€BN) Sheets Decorated with OLi, ONa, and Li₂F Molecules for Enhanced Energy Storage. ChemPhysChem, 2017, 18, 513-518.	1.0	41
23573	Effects of applied strain and electric field on small-molecule sensing by stanene monolayers. Journal of Materials Science, 2017, 52, 5083-5096.	1.7	36
23574	Ab initio study on pressure induced structural sequence in LaF3 up to 2ÂMbar. Indian Journal of Physics, 2017, 91, 535-546.	0.9	4
23575	Defect engineering toward strong photocatalysis of Nb-doped anatase TiO2: Computational predictions and experimental verifications. Applied Catalysis B: Environmental, 2017, 206, 520-530.	10.8	62

#	Article	IF	Citations
23576	Effects of iron and chromium on the dynamic properties of oxygen in liquid leadâ€“bismuth eutectic alloy. Corrosion Science, 2017, 118, 1-11.	3.0	20
23577	A new interatomic pair potential for the modeling of crystalline Li2SiO3. Materials and Design, 2017, 118, 218-225.	3.3	7
23578	Ab initio modeling of point defects, self-diffusion, and incorporation of impurities in thorium. Solid State Communications, 2017, 252, 11-15.	0.9	6
23579	Chemical Insights into the Design and Development of Face-Centered Cubic Ruthenium Catalysts for Fischerâ€“Tropsch Synthesis. Journal of the American Chemical Society, 2017, 139, 2267-2276.	6.6	147
23580	Insights into the composition exploration of novel hydrogen storage alloys: evaluation of the Mgâ€“Niâ€“Ndâ€“H phase diagram. Journal of Materials Chemistry A, 2017, 5, 3848-3864.	5.2	62
23581	Theoretical Investigation of the Interfaces and Mechanisms of Induced Spin Polarization of 1D Narrow Zigzag Graphene- and h-BN Nanoribbons on a SrO-Terminated LSMO(001) Surface. Journal of Physical Chemistry A, 2017, 121, 680-689.	1.1	1
23582	Oxygen Binding to Active Sites of Feâ€“Nâ€“C ORR Electrocatalysts Observed by Ambient-Pressure XPS. Journal of Physical Chemistry C, 2017, 121, 2836-2843.	1.5	135
23583	Exchange and Dzyaloshinskii-Moriya interactions in bulk FeGe: Effects of atomic vacancies. AIP Advances, 2017, 7, 056412.	0.6	6
23584	Charge Ordering in K₄Fe₃F₁₂ from a First Principles Study. ChemistrySelect, 2017, 2, 714-719.	0.7	2
23585	Electron doped C2N monolayer as efficient noble metal-free catalysts for CO oxidation. Applied Surface Science, 2017, 418, 92-98.	3.1	24
23586	Effect of N impurity on the electronic structure and absorption spectrum of Ba2SiO4:Eu2+ phosphor. Optik, 2017, 134, 78-87.	1.4	8
23587	Investigations on molybdenum dinitride as a promising anode material for Na-ion batteries from first-principle calculations. Journal of Alloys and Compounds, 2017, 701, 875-881.	2.8	17
23588	Enhanced UV and ethanol vapour sensing of a single 3-D ZnO tetrapod alloyed with Fe2O3 nanoparticles. Sensors and Actuators B: Chemical, 2017, 245, 448-461.	4.0	46
23589	Atomic Adsorption on Nitrogenated Holey Graphene. Journal of Physical Chemistry C, 2017, 121, 3055-3061.	1.5	37
23590	Theoretical Study of the Interfacial Force-Field, Thermodynamic Property, and Heat Stress for Plastic Bonded Explosives. Journal of Physical Chemistry C, 2017, 121, 2778-2788.	1.5	13
23591	Electrocatalyst Design for Direct Borohydride Oxidation Guided by First Principles. Journal of Physical Chemistry C, 2017, 121, 2872-2881.	1.5	13
23592	Can a Black Phosphorus Schottky Barrier Transistor Be Good Enough?. ACS Applied Materials & Interfaces, 2017, 9, 3959-3966.	4.0	70
23593	Directional Charge-Carrier Transport in Oriented Benzodithiophene Covalent Organic Framework Thin Films. ACS Nano, 2017, 11, 2706-2713.	7.3	117

#	Article	IF	Citations
23594	Adsorption of oxygen and CO oxidation on Au/anatase(001) catalysts. A DFT+U study. New Journal of Chemistry, 2017, 41, 2073-2080.	1.4	12
23595	Ionicity and birefringence of Î±-LiNH₄SO₄crystals: ab initio DFT study, X-ray spectroscopy measurements. RSC Advances, 2017, 7, 6889-6901.	1.7	20
23596	Potential of Titania-covered Ag Catalysts for NO_x Reduction: A DFT Study. Chemistry Letters, 2017, 46, 456-459.	0.7	15
23597	Excitons in scintillator materials: Optical properties and electron-energy loss spectra of NaI, LaBr₃, BaI₂, and SrI₂. Journal of Materials Research, 2017, 32, 56-63.	1.2	6
23598	Ultrasmall CuCo₂S₄ Nanocrystals: Allâ€inâ€One Theragnosis Nanoplatform with Magnetic Resonance/Nearâ€Infrared Imaging for Efficiently Photothermal Therapy of Tumors. Advanced Functional Materials, 2017, 27, 1606218.	7.8	106
23599	Ellipsometric characterization of MoSe2 thin layers obtained by thermal treatment of molybdenum in selenium vapor. Applied Surface Science, 2017, 421, 310-314.	3.1	2
23600	Multithreaded conductive carbon: 1D conduction in 3D carbon. Carbon, 2017, 115, 584-588.	5.4	17
23601	Phase transformations, detwinning and superelasticity of shape-memory NiTi from MEAM with practical capability. Computational Materials Science, 2017, 130, 138-143.	1.4	24
23602	Evolution of the active species and catalytic mechanism of Ti doped NaAlH 4 for hydrogen storage. International Journal of Hydrogen Energy, 2017, 42, 6088-6095.	3.8	32
23603	Structural, elastic and magnetic properties of Mn and Sb doped chromium nitride â€“ An ab initio study. Materials Chemistry and Physics, 2017, 192, 291-298.	2.0	10
23604	A comparative study of atomic oxygen adsorption at Pd surfaces from Density Functional Theory. Surface Science, 2017, 658, 38-45.	0.8	10
23605	Hydrogen Oxidation and Water Dissociation over an Oxygen-Enriched Ni/YSZ Electrode in the Presence of an Electric Field: A First-Principles-Based Microkinetic Model. Industrial & Engineering Chemistry Research, 2017, 56, 1201-1213.	1.8	13
23606	Hydrides of Alkaline Earthâ€“Tetrel (AeTt) Zintl Phases: Covalent Ttâ€“H Bonds from Silicon to Tin. Inorganic Chemistry, 2017, 56, 1061-1071.	1.9	24
23607	Computational Search for Novel Hard Chromium-Based Materials. Journal of Physical Chemistry Letters, 2017, 8, 755-764.	2.1	62
23608	High-Dimensional Atomistic Neural Network Potentials for Moleculeâ€“Surface Interactions: HCl Scattering from Au(111). Journal of Physical Chemistry Letters, 2017, 8, 666-672.	2.1	94
23609	Hybridization of Zinc Oxide Tetrapods for Selective Gas Sensing Applications. ACS Applied Materials & Interfaces, 2017, 9, 4084-4099.	4.0	135
23610	Facile Synthesis of Vanadium-Doped Ni₃S₂ Nanowire Arrays as Active Electrocatalyst for Hydrogen Evolution Reaction. ACS Applied Materials & Interfaces, 2017, 9, 5959-5967.	4.0	196
23611	Chemical Functionalization of Pentagermanene Leads to Stabilization and Tunable Electronic Properties by External Tensile Strain. ACS Omega, 2017, 2, 171-180.	1.6	15

#	Article	IF	Citations
23612	Reaction mechanism of dimethyl ether carbonylation to methyl acetate over mordenite â€“ a combined DFT/experimental study. Catalysis Science and Technology, 2017, 7, 1141-1152.	2.1	54
23613	Stability and electronic properties of phosphorene oxides: from 0-dimensional to amorphous 2-dimensional structures. Nanoscale, 2017, 9, 2428-2435.	2.8	30
23614	A CO monolayer: first-principles design of a new direct band-gap semiconductor with excellent mechanical properties. Nanoscale, 2017, 9, 5445-5450.	2.8	33
23615	Screening novel candidates for mid-IR nonlinear optical materials from I₃â€“Vâ€“VI₄compounds. Journal of Materials Chemistry C, 2017, 5, 1963-1972.	2.7	32
23616	Electronic structure modeling of InAs/GaSb superlattices with hybrid density functional theory. Infrared Physics and Technology, 2017, 81, 27-31.	1.3	12
23617	Alloy engineering of electronic and optical properties of tetragonal monolayer zinc chalcogenides. Journal of Alloys and Compounds, 2017, 695, 1392-1396.	2.8	16
23618	Interstitial Fe-pairs in silicon. Journal of Crystal Growth, 2017, 468, 54-56.	0.7	3
23619	Intrasurface electron transition contribution to energy of adsorption of silicon at the SiC(0001) surface â€“ A density functional theory (DFT) study. Journal of Crystal Growth, 2017, 468, 870-873.	0.7	2
23620	Chemical beam epitaxy of GaAs 1-x N x using MMHy and DMHy precursors, modeled by ab initio study of GaAs(100) surfaces stability over As 2 , H 2 and N 2. Journal of Crystal Growth, 2017, 468, 557-561.	0.7	0
23621	Electronic and magnetic properties of bare armchair BC2N nanoribbons. Journal of Magnetism and Magnetic Materials, 2017, 426, 641-645.	1.0	4
23622	The direct exchange mechanism of induced spin polarization of low-dimensional Ï€-conjugated carbon- and h-BN fragments at LSMO(001) MnO-terminated interfaces. Journal of Magnetism and Magnetic Materials, 2017, 440, 23-29.	1.0	2
23623	Fission gas in thoria. Journal of Nuclear Materials, 2017, 485, 47-55.	1.3	13
23624	Waved graphene: Unique structure for the adsorption of small molecules. Materials Chemistry and Physics, 2017, 189, 111-117.	2.0	22
23625	Non-equilibrium vacancy formation energies in metastable alloys â€” A case study ofÂTi0.5Al0.5N. Materials and Design, 2017, 114, 484-493.	3.3	13
23626	Ab initio study of He-He interactions in homogeneous electron gas. Nuclear Instruments & Methods in Physics Research B, 2017, 393, 140-143.	0.6	2
23627	Adsorption of C 20 on two-dimensional materials. Physica E: Low-Dimensional Systems and Nanostructures, 2017, 87, 166-170.	1.3	2
23628	High resistance to sulfur poisoning of Ni with copper skin under electric field. Physics Letters, Section A: General, Atomic and Solid State Physics, 2017, 381, 671-678.	0.9	1
23629	n s 2 n p 4 (n Â=Â4, 5) lone pair triplets whirling in M*F 2 E 3 (M*Â=ÂKr, Xe): Stereochemistry and ab initio analyses. Solid State Sciences, 2017, 64, 114-124.	1.5	5

#	Article	IF	Citations
23630	Improving visible light photocatalytic activity of KTaO3 using cation-anion dopant pair. Solar Energy Materials and Solar Cells, 2017, 159, 590-598.	3.0	31
23631	Lattice dynamics and thermal conductivity of cesium chloride via first-principles investigation. Solid State Communications, 2017, 254, 31-36.	0.9	13
23632	Theoretical investigation on thermoelectric properties of Cu-based chalcopyrite compounds. Physical Review B, 2017, 95, .	1.1	19
23633	Enhanced Liâ€ion Accessibility in MXene Titanium Carbide by Steric Chloride Termination. Advanced Energy Materials, 2017, 7, 1601873.	10.2	212
23634	Electronic characteristics of p-type transparent SnO monolayer with high carrier mobility. Applied Surface Science, 2017, 401, 114-119.	3.1	36
23635	Structural, lattice dynamics and thermodynamic properties of Sr 2 VO 4 from first principles. Journal of Alloys and Compounds, 2017, 699, 98-105.	2.8	3
23636	First-principles investigations of electronic and magnetic properties of the FeRh/MgO (001) interface. Journal of Alloys and Compounds, 2017, 700, 191-197.	2.8	6
23637	Enhanced efficiency of solid-state NMR investigations of energy materials using an external automatic tuning/matching (eATM) robot. Journal of Magnetic Resonance, 2017, 275, 127-136.	1.2	41
23638	Theoretically designed metal-welded carbon nanotubes: Extraordinary electronic properties and promoted catalytic performance. Nano Energy, 2017, 32, 209-215.	8.2	17
23639	Titanium Trisulfide Monolayer as a Potential Thermoelectric Material: A First-Principles-Based Boltzmann Transport Study. ACS Applied Materials & Interfaces, 2017, 9, 2509-2515.	4.0	99
23640	Hardness of cubic solid solutions. Scientific Reports, 2017, 7, 40276.	1.6	14
23641	Internal dynamics in helical molecules studied by X-ray diffraction, NMR spectroscopy and DFT calculations. Physical Chemistry Chemical Physics, 2017, 19, 2900-2907.	1.3	33
23642	Electronic, magnetic and spectroscopic properties of doped Mn_(1â^'x)A_xWO₄(Aâ€‰â€‰=â€‰â€‰Co, Cu, Ni and Fe) multiferroic: an experimental and DFT study. Journal of Physics Condensed Matter, 2017, 29, 075901.	0.7	12
23643	Ab initiostudy of the nature and stability of the defects and multi-vacancies in TaN. Comparison with TiN. Journal of Physics Condensed Matter, 2017, 29, 075501.	0.7	3
23644	New method for calculations of nanostructure kinetic stability at high temperature. Journal of Magnetism and Magnetic Materials, 2017, 440, 167-170.	1.0	1
23645	Statistical mechanics study on wetting behaviors of Ne on Mg surface. Journal of Physics and Chemistry of Solids, 2017, 103, 123-131.	1.9	19
23646	Weak d ⁰ ferromagnetism: Zn vacancy condensation in ZnS nanocrystals. Journal of Physics Condensed Matter, 2017, 29, 025803.	0.7	3
23647	Local Bi ordering in MOVPE grown Ga(As,Bi) investigated by high resolution scanning transmission electron microscopy. Applied Materials Today, 2017, 6, 22-28.	2.3	21

#	Article	IF	Citations
23648	Surface half-metallicity and stability of zinc-blende sodium monoselenide. Applied Surface Science, 2017, 394, 282-287.	3.1	4
23649	Effects of annealing and conformal alumina passivation on anisotropy and hysteresis of magneto-optical properties of cobalt slanted columnar thin films. Applied Surface Science, 2017, 421, 320-324.	3.1	4
23650	First-principles study the behavior of oxygen vacancy on the surface of ZrO 2 and Zr 0.97 M 0.03 O 2. Computational Condensed Matter, 2017, 11, 1-10.	0.9	13
23651	Ferromagnetic orderings in Co Cu Zn1â^'(+)O by GGA and GGA+U formalisms within density functional theory. Computational Materials Science, 2017, 126, 344-350.	1.4	5
23652	Computational investigation of interstitial neon diffusion in pure hematite. Computational Materials Science, 2017, 128, 67-74.	1.4	11
23653	Structural evolution of (Ti0.5V0.5)+1GeC (n= 1â€“4) under pressure from first principles. Computational Materials Science, 2017, 127, 251-260.	1.4	18
23654	Band offset engineering in C-functionalized boronitrene. Computational Materials Science, 2017, 128, 373-378.	1.4	9
23655	Designing Mg7 cluster-assembled two dimensional crystal. FlatChem, 2017, 1, 57-59.	2.8	4
23656	Unraveling the Effects of Al Doping on the Electrochemical Properties of LiNi_{0.5}Co_{0.2}Mn_{0.3}O₂Using First Principles. Journal of the Electrochemical Society, 2017, 164, A6359-A6365.	1.3	118
23657	Systematic Search for Lithium Ion Conducting Compounds by Screening of Compositions Combined with Atomistic Simulation. MRS Advances, 2017, 2, 483-489.	0.5	3
23658	First-principle analysis of photoelectric properties of silicon-carbon materials with graphene-like honeycomb structure. Computational Materials Science, 2017, 126, 336-343.	1.4	12
23659	First principles study of mixed-stack charge-transfer pyromellitic diimide - diamino pyrene (PMDI - DAP) derivative. Chemical Physics Letters, 2017, 670, 89-94.	1.2	2
23660	Exploring metal decorated Porphyrin-like Porous Fullerene as catalyst for oxygen reduction reaction: A DFT study. International Journal of Hydrogen Energy, 2017, 42, 2278-2287.	3.8	47
23661	Carbon-rich superhard ruthenium carbides from first-principles. Materials and Design, 2017, 117, 353-362.	3.3	7
23662	Cooperativity and Dynamics Increase the Performance of NiFe Dry Reforming Catalysts. Journal of the American Chemical Society, 2017, 139, 1937-1949.	6.6	322
23663	Asymmetric interaction of point defects and heterophase interfaces in ZrN/TaN multilayered nanofilms. Scientific Reports, 2017, 7, 40044.	1.6	9
23664	Layered structure of the near-surface region of oxidized chalcopyrite (CuFeS₂): hard X-ray photoelectron spectroscopy, X-ray absorption spectroscopy and DFT+U studies. Physical Chemistry Chemical Physics, 2017, 19, 2749-2759.	1.3	21
23665	Engineering the electronic and optoelectronic properties of InX (X = S, Se, Te) monolayers via strain. Physical Chemistry Chemical Physics, 2017, 19, 4855-4860.	1.3	71

#	Article	IF	Citations
23666	A comparative study of hydrogen evolution reaction on pseudo-monolayer WS₂ and PtS₂: insights based on the density functional theory. Catalysis Science and Technology, 2017, 7, 687-692.	2.1	51
23667	5-fluorouracil adsorption on hydrated silica: density functional theory based-study. Adsorption, 2017, 23, 321-325.	1.4	10
23668	An interatomic potential for simulation of Zr-Nb system. Computational Materials Science, 2017, 129, 259-272.	1.4	38
23669	S/Te co-doping in tetragonal FeSe with unchanged lattice parameters: Effects on superconductivity and electronic structure. Journal of Alloys and Compounds, 2017, 700, 43-48.	2.8	13
23670	Role of Charge Transfer in Catalytic Hydrogen Oxidation over Platinum. Journal of Physical Chemistry C, 2017, 121, 2696-2701.	1.5	3
23671	Tetragonal-structured anisotropic 2D metal nitride monolayers and their halides with versatile promises in energy storage and conversion. Journal of Materials Chemistry A, 2017, 5, 2870-2875.	5.2	42
23672	Atomistic Modelingâ€Based Design of Novel Materials. Advanced Engineering Materials, 2017, 19, 1600688.	1.6	14
23673	Investigations on Magnetic Properties of Cr-Doped LiZnAs by First-Principle Calculations. Journal of Superconductivity and Novel Magnetism, 2017, 30, 1545-1549.	0.8	3
23674	Ruddlesden-Popper compounds in the double-perovskite family Sr2FeTaO6(SrO)n (n = 0, 1 and 2) and their photocatalytic properties. Applied Catalysis B: Environmental, 2017, 206, 35-43.	10.8	33
23675	First-principles study of mechanical and thermodynamic properties of Ti-Ga intermetallic compounds. Journal of Alloys and Compounds, 2017, 700, 208-214.	2.8	17
23676	Structural and optical characteristics of pre- and post-annealed sol-gel derived CoCu-oxide coatings. Journal of Alloys and Compounds, 2017, 701, 222-235.	2.8	12
23677	Development of a Classical Interatomic Potential for MAPbBr₃. Journal of Physical Chemistry C, 2017, 121, 3724-3733.	1.5	31
23678	Modeling Segregation on AuPd(111) Surfaces with Density Functional Theory and Monte Carlo Simulations. Journal of Physical Chemistry C, 2017, 121, 3479-3487.	1.5	48
23679	Revisiting CO Activation on Co Catalysts: Impact of Step and Kink Sites from DFT. ACS Catalysis, 2017, 7, 1984-1992.	5.5	64
23680	Ideal strength and elastic instability in single-layer 8-Pmmn borophene. RSC Advances, 2017, 7, 8654-8660.	1.7	53
23681	Thermoelectric properties of Mg2X (Xâ€‰=â€‰Si, Ge) based bulk and quantum well systems. Journal of Applied Physics, 2017, 121, .	1.1	6
23682	A first-principles model of copperâ€“boron interactions in Si: implications for the light-induced degradation of solar Si. Journal of Physics Condensed Matter, 2017, 29, 065701.	0.7	0
23683	Oxygen induced strong mobility modulation in few-layer black phosphorus. 2D Materials, 2017, 4, 021007.	2.0	45

#	Article	IF	Citations
23684	A Theoretical Investigation on CO Oxidation by Singleâ€Atom Catalysts M₁/Î³â€Al₂O₃ (M=Pd, Fe, Co, and Ni). ChemCatChem, 2017, 9, 1222-1229.	1.8	76
23685	Interface Effects in Hydrogen Elimination Reaction from Isopropanol by Ni₁₃ Cluster on Î³-Al₂O₃(010) Surface. Journal of Physical Chemistry C, 2017, 121, 3488-3495.	1.5	13
23686	Synthesis of Hf8O7, a new binary hafnium oxide, at high pressures and high temperatures. High Pressure Research, 2017, 37, 147-158.	0.4	3
23687	Atomic-scale imaging of few-layer black phosphorus and its reconstructed edge. Journal Physics D: Applied Physics, 2017, 50, 084003.	1.3	42
23688	First-principles study of structural, elastic and thermodynamic properties of Niâ€“Snâ€“P intermetallics. Journal of Materials Research, 2017, 32, 512-521.	1.2	4
23689	Adsorption of triclosan on single wall carbon nanotubes: A first principle approach. Applied Surface Science, 2017, 403, 519-524.	3.1	21
23690	First principles study on structural, electronic and optical properties of 3d transition metals-substituted CuGaSe2. Optik, 2017, 135, 346-352.	1.4	12
23691	Electronic and optical properties of Î± -InX (X = S, Se and Te) monolayer: Under strain conditions. Physics Letters, Section A: General, Atomic and Solid State Physics, 2017, 381, 1313-1320.	0.9	39
23692	Structural phase transitions of (Bi_{1â^'x}Sb_x)₂(Te_{1â^'y}Se_y)₃ compounds under high pressure and the influence of the atomic radius on the compression processes of tetradymites. Physical Chemistry Chemical Physics, 2017, 19, 2207-2216.	1.3	18
23693	An ab initio investigation of photoswitches adsorbed onto metal oxide surfaces: the case of donorâ€“acceptor Stenhouse adduct photochromes on TiO₂ anatase. Journal of Materials Chemistry C, 2017, 5, 1624-1631.	2.7	15
23694	Pressure-induced silica quartz amorphization studied by iterative stochastic surface walking reaction sampling. Physical Chemistry Chemical Physics, 2017, 19, 4725-4733.	1.3	32
23695	Elastic properties of amorphousT0.75Y0.75B14(Tâ€‰â€‰=â€‰â€‰Sc, Ti, V, Y, Zr, Nb) and the effect of O incorporation on bonding, density and elasticity (Tâ€²â€‰â€‰=â€‰â€‰Ti, Zr). Journal of Physics Condensed Matter, 2017, 29, 085404.	2	
23696	Comparative description of magnetic interactions in Sr₂CuTeO₆and Sr₂CuWO₆. Journal of Physics Condensed Matter, 2017, 29, 105801.	0.7	13
23697	DFT study of electronic and optical properties of paraelectric AgNbO3 crystal under 0â€“50ÂGPa pressure. Indian Journal of Physics, 2017, 91, 653-657.	0.9	3
23698	First-principles approach to design and evaluation of graphene as methane sensors. Materials and Design, 2017, 119, 397-405.	3.3	30
23699	M₄Mg₄(P₂O₇)₃ (M = K, Rb): Structural Engineering of Pyrophosphates for Nonlinear Optical Applications. Chemistry of Materials, 2017, 29, 1845-1855.	3.2	187
23700	Pressure-driven phase transition mechanisms revealed by quantum chemistry: <scp>l</scp>-serine polymorphs. Physical Chemistry Chemical Physics, 2017, 19, 6671-6676.	1.3	26
23701	Influences of the adsorption of different elements on the electronic structures of a tin sulfide monolayer. Physical Chemistry Chemical Physics, 2017, 19, 5423-5429.	1.3	17

#	Article	IF	Citations
23702	Neural network predictions of oxygen interactions on a dynamic Pd surface. Molecular Simulation, 2017, 43, 346-354.	0.9	58
23703	Automated firstâ€principles mapping for phaseâ€change materials. Journal of Computational Chemistry, 2017, 38, 620-628.	1.5	9
23704	Photoactive Semiconducting Oxides for Energy and Environment: Experimental and Theoretical Insights. , 2017, , 983-1030.		0
23705	Molecular Dynamics Simulation: From â€œAb Initioâ€•to â€œCoarse Grainedâ€• , 2017, , 337-396.		2
23706	Mechanism, kinetics and thermodynamics of carbon dioxide hydrogenation to methanol on Cu/ZnAl2O4 spinel-type heterogeneous catalysts. Applied Catalysis B: Environmental, 2017, 207, 267-278.	10.8	91
23707	An alkaline tin(II) halide compound Na 3 Sn 2 F 6 Cl: Synthesis, structure, and characterization. Journal of Solid State Chemistry, 2017, 248, 104-108.	1.4	7
23708	Al embedded MgO barrier MTJ: A first principle study for application in fast and compact STT-MRAMs. Superlattices and Microstructures, 2017, 103, 314-324.	1.4	5
23709	Isophorone on Au/MgO/Ag(001): Physisorption with Electrostatic Site Selection. Journal of Physical Chemistry C, 2017, 121, 10824-10831.	1.5	3
23710	Synthesis of ketones from biomass-derived feedstock. Nature Communications, 2017, 8, 14190.	5.8	115
23711	Size modulation electronic and optical properties of phosphorene nanoribbons: DFTâ€“BOLS approximation. Physical Chemistry Chemical Physics, 2017, 19, 5304-5309.	1.3	72
23712	Hexagonal Zn_{1â^'x}Cd_xS (0.2 â‰¤ x â‰¤ 1) solid solution photocatalysts for H₂ generation from water. Catalysis Science and Technology, 2017, 7, 982-987.	2.1	47
23713	Strain enhanced lithium adsorption and diffusion on silicene. Physical Chemistry Chemical Physics, 2017, 19, 6563-6568.	1.3	30
23714	On the electrostatic control achieved in transistors based on multilayered MoS2: A first-principles study. Journal of Applied Physics, 2017, 121, .	1.1	18
23715	A New Type of Scaling Relations to Assess the Accuracy of Computational Predictions of Catalytic Activities Applied to the Oxygen Evolution Reaction. ChemCatChem, 2017, 9, 1261-1268.	1.8	75
23716	A first-principles study on electronic structures and elastic properties of metal doped Î±-Fe(N) high nitrogen steel. Journal of Iron and Steel Research International, 2017, 24, 103-110.	1.4	4
23717	Characters of group V and VII atoms doped WSe 2 monolayer. Journal of Alloys and Compounds, 2017, 699, 291-296.	2.8	14
23718	Impact of grain boundary structures on trapping iron. Journal of Crystal Growth, 2017, 468, 448-451.	0.7	4
23719	First-principles investigation of the effect of oxidation on the electronic structure and magnetic properties at the FeRh/MgO (0 0 1) interface. Journal of Magnetism and Magnetic Materials, 2017, 432, 106-111.	1.0	2

#	Article	IF	Citations
23720	Tuning the electronic and magnetic properties of germanene by surface adsorption of small nitrogen-based molecules. Physica E: Low-Dimensional Systems and Nanostructures, 2017, 88, 237-242.	1.3	18
23721	Arsenene as a promising candidate for NO and NO 2 sensor: A first-principles study. Physics Letters, Section A: General, Atomic and Solid State Physics, 2017, 381, 1092-1096.	0.9	76
23722	CO₂ Electroreduction Performance of Phthalocyanine Sheet with Mn Dimer: A Theoretical Study. Journal of Physical Chemistry C, 2017, 121, 3963-3969.	1.5	95
23723	The electronic properties of the stanene/MoS₂ heterostructure under strain. RSC Advances, 2017, 7, 9176-9181.	1.7	34
23724	Charge Transfer Variability in Misfit Layer Compounds: Comparison of SnSâ€SnS₂ and LaSâ€TaS₂. Israel Journal of Chemistry, 2017, 57, 553-559.	1.0	10
23725	XPS-and-DFT analyses of the Pb 4f â€" Zn 3s and Pb 5d â€" O 2s overlapped ambiguity contributions to the final electronic structure of bulk and thin-film Pb-modulated zincite. Applied Surface Science, 2017, 405, 129-136.	3.1	30
23726	Structural, elastic, mechanical and thermodynamic properties of Terbium oxide: First-principles investigations. Results in Physics, 2017, 7, 709-714.	2.0	47
23727	Effects of oxygen vacancies on the structural and optical properties of Î²-Ga2O3. Scientific Reports, 2017, 7, 40160.	1.6	215
23728	Regulating Li deposition at artificial solid electrolyte interphases. Journal of Materials Chemistry A, 2017, 5, 3483-3492.	5.2	258
23729	Computational investigation of half-Heusler compounds for spintronics applications. Physical Review B, 2017, 95, .	1.1	208
23730	Three-dimensional organic Dirac-line materials due to nonsymmorphic symmetry: A data mining approach. Physical Review B, 2017, 95, .	1.1	29
23731	First principles study on the electronic structure properties of Keggin polyoxometalates on Carbon substrates for solid-state devices. Theoretical Chemistry Accounts, 2017, 136, 1.	0.5	12
23732	Theoretical band alignment in an intermediate band chalcopyrite based material. Applied Surface Science, 2017, 424, 132-136.	3.1	15
23733	Thermodynamic modelling of Ti-Zr-N system. Calphad: Computer Coupling of Phase Diagrams and Thermochemistry, 2017, 56, 102-107.	0.7	22
23734	Novel BTlGaN semiconducting materials for infrared opto-electronic devices. Infrared Physics and Technology, 2017, 81, 175-181.	1.3	13
23735	Doping and vacancy effects of graphyne on SO2 adsorption. Journal of Colloid and Interface Science, 2017, 493, 123-129.	5.0	30
23736	A first-principles study of the properties of four predicted novel phases of AlN. Journal of Physics and Chemistry of Solids, 2017, 104, 68-78.	1.9	31
23737	Structural and Vibrational Properties of the TiOPc Monolayer on Ag(111). Journal of Physical Chemistry C, 2017, 121, 1608-1617.	1.5	20

#	Article	IF	Citations
23738	Estimating carrier relaxation times in the Ba₈Ga₁₆Ge₃₀ clathrate in the extrinsic regime. Physical Chemistry Chemical Physics, 2017, 19, 3010-3018.	1.3	11
23739	Theoretical investigation of interactions between palladium and fullerene in polymer. RSC Advances, 2017, 7, 2202-2210.	1.7	20
23740	Zintl layer formation during perovskite atomic layer deposition on Ge (001). Journal of Chemical Physics, 2017, 146, 052817.	1.2	11
23741	Unravelling the interplay of geometrical, magnetic and electronic properties of metal-doped graphene nanomeshes. Journal of Physics Condensed Matter, 2017, 29, 055301.	0.7	7
23742	Mechanical properties and failure behavior of phosphorene with grain boundaries. Nanotechnology, 2017, 28, 075704.	1.3	21
23743	Interaction potential and friction of hydrogenated diamond surfaces at the atomic scale: first-principle calculation. Journal of Materials Science, 2017, 52, 1381-1389.	1.7	1
23744	Spontaneous formation of graphene on diamond (111) driven by B-doping induced surface reconstruction. Carbon, 2017, 115, 388-393.	5.4	18
23745	Structural, electronic, optical and mechanical properties of InP alloyed with Zn, Si, Sn and S under pressure: First-principles calculation. Journal of Alloys and Compounds, 2017, 700, 98-105.	2.8	17
23746	Multiscale Computational Design of Core/Shell Nanoparticles for Oxygen Reduction Reaction. Journal of Physical Chemistry C, 2017, 121, 1964-1973.	1.5	27
23747	Understanding the Structural and Electronic Effect of Zr⁴⁺-Doped KNb(Zr)O₃ Perovskite for Enhanced Photoactivity: A Combined Experimental and Computational Study. Journal of Physical Chemistry C, 2017, 121, 2597-2604.	1.5	9
23748	Layer-separable and gap-tunable topological insulators. Physical Chemistry Chemical Physics, 2017, 19, 3932-3936.	1.3	4
23749	Characteristics of lateral and hybrid heterostructures based on monolayer MoS₂: a computational study. Physical Chemistry Chemical Physics, 2017, 19, 4741-4750.	1.3	7
23750	The impact of hydrogenation on the thermal transport of silicene. 2D Materials, 2017, 4, 025002.	2.0	28
23751	First-principle studies on the Liâ€“Te system. Materials Research Express, 2017, 4, 015701.	0.8	0
23752	Ab initiostudy of doping effects in the 42214 compounds: A new family of layered iron-based superconductors. Physical Review B, 2017, 95, .	1.1	2
23753	Electronic and optical properties of Cr-, B-doped, and (Cr, B)-codoped SrTiO₃. International Journal of Modern Physics B, 2017, 31, 1750064.	1.0	2
23754	The Role of a Double Molecular Anchor on the Mobility and Selfâ€Assembly of Thiols on Au(111): The Case of Mercaptobenzoic Acid. ChemPhysChem, 2017, 18, 804-811.	1.0	7
23755	Electronic structure of stoichiometric and reduced ZnO from periodic relativistic all electron hybrid density functional calculations using numeric atomâ€centered orbitals. Journal of Computational Chemistry, 2017, 38, 523-529.	1.5	18

#	Article	IF	Citations
23756	Ab initio investigation of the surface properties of austenitic Fe-Ni-Cr alloys in aqueous environments. Applied Surface Science, 2017, 402, 108-113.	3.1	8
23757	A computational framework for automation of point defect calculations. Computational Materials Science, 2017, 130, 1-9.	1.4	131
23758	Insights into the mechanism of electrochemical ozone production via water splitting on the Ni and Sb doped SnO₂ catalyst. Physical Chemistry Chemical Physics, 2017, 19, 3800-3806.	1.3	18
23759	Strengthening materials by changing the number of valence electrons. Computational Materials Science, 2017, 129, 252-258.	1.4	7
23760	Prediction on technetium triboride from first-principles calculations. Solid State Communications, 2017, 252, 40-45.	0.9	20
23761	Full Mechanism of Zeolite Dealumination in Aqueous Strong Acid Medium: Ab Initio Periodic Study on H-Clinoptilolite. Journal of Physical Chemistry C, 2017, 121, 2652-2660.	1.5	20
23762	Impact of aluminum doping on the thermo-physical properties of refractory medium-entropy alloys. Journal of Applied Physics, 2017, 121, .	1.1	19
23763	Topological, Valleytronic, and Optical Properties of Monolayer PbS. Advanced Materials, 2017, 29, 1604788.	11.1	26
23764	First principles calculations of La2O3/GaAs interface properties under biaxial strain and hydrostatic pressure. Physica B: Condensed Matter, 2017, 510, 13-21.	1.3	5
23765	Strain Concentration at the Boundaries in 5-Fold Twins of Diamond and Silicon. ACS Applied Materials & Interfaces, 2017, 9, 4253-4258.	4.0	19
23766	Rhâ€“Agâ€“Si ternary composites: highly active hydrogen evolution electrocatalysts over Ptâ€“Agâ€“Si. Journal of Materials Chemistry A, 2017, 5, 1623-1628.	5.2	28
23767	First-principles study of interfacial interaction between carbon nanotube and Al2O3(0001). Journal of Applied Physics, 2017, 121, 025304.	1.1	7
23768	Exploring the potential of semiconducting BaSi₂for thin-film solar cell applications. Journal Physics D: Applied Physics, 2017, 50, 023001.	1.3	99
23769	Spinâ€“exciton interaction and related micro-photoluminescence spectra of ZnSe:Mn DMS nanoribbon. Nanotechnology, 2017, 28, 105202.	1.3	29
23770	Two-dimensional multiferroics in monolayer group IV monochalcogenides. 2D Materials, 2017, 4, 015042.	2.0	275
23771	Piezoelectricity in two-dimensional group III-V buckled honeycomb monolayers. Physica Status Solidi - Rapid Research Letters, 2017, 11, 1600412.	1.2	45
23772	Establishment of half-metallicity, ferrimagnetic ordering and double exchange interactions in Ni-doped BiFeO3 â€“ A first-principles study. Computational Materials Science, 2017, 130, 84-90.	1.4	13
23773	First-principles understanding of durable titanium nitride (TiN) electrocatalyst supports. Journal of Industrial and Engineering Chemistry, 2017, 49, 69-75.	2.9	34

#	Article	IF	Citations
23774	Electronic and spinâ€“orbit properties of the kagome MOF family M₃(1,2,5,6,9,) Tj ETQq0 0 0 rgBT /Overlock 10 Tf 50 747 2017, 29, 09LT01.	0.7	11
23775	Novel hybrid C/BN two-dimensional heterostructures. Nanotechnology, 2017, 28, 085205.	1.3	8
23776	Structural, mechanical, thermal and electronic properties of novel ternary carbide Al4Si2C5 under high pressure by DFT calculation. International Journal of Modern Physics B, 2017, 31, 1750012.	1.0	2
23777	Modulations of thermal properties of graphene by strain-induced phonon engineering. Japanese Journal of Applied Physics, 2017, 56, 025102.	0.8	14
23778	Ab initioprediction of a new allotrope of two-dimensional silicon. Physica Status Solidi - Rapid Research Letters, 2017, 11, 1600422.	1.2	9
23779	Improved HER activity of Ni and stainless steel electrodes activated by NiCoMo ionic activator â€“ A combined DFT and experimental study. International Journal of Hydrogen Energy, 2017, 42, 5072-5082.	3.8	7
23780	Electronic structure and optical properties of dilute boron-bismide quaternary alloys B Ga1â€“As1â€“Bi /GaAs for infrared optoelectronic devices. Optik, 2017, 135, 57-69.	1.4	14
23781	Structural, electronic, magnetic and optical properties of Zn 1-x Ni x O from first-principles. Journal of Physics and Chemistry of Solids, 2017, 104, 267-275.	1.9	5
23782	Influence of La/W ratio on electrical conductivity of lanthanum tungstate with high La/W ratio. Journal of Solid State Chemistry, 2017, 248, 1-8.	1.4	11
23783	Propelling polysulfides transformation for high-rate and long-life lithiumâ€“sulfur batteries. Nano Energy, 2017, 33, 306-312.	8.2	352
23784	Electrocatalytic Activities of Oxygen Reduction Reaction on Pd/C and Pdâ€“B/C Catalysts. Journal of Physical Chemistry C, 2017, 121, 3416-3423.	1.5	91
23785	Adsorption and Intermolecular Interaction of Cobalt Phthalocyanine on CoO(111) Ultrathin Films: An STM and DFT Study. Journal of Physical Chemistry C, 2017, 121, 2889-2895.	1.5	10
23786	Characterizing Substrateâ€“Surface Interactions on Alumina-Supported Metal Catalysts by Dynamic Nuclear Polarization-Enhanced Double-Resonance NMR Spectroscopy. Journal of the American Chemical Society, 2017, 139, 2702-2709.	6.6	59
23787	Surface reconstructions and related local properties of a BiFeO3 thin film. Scientific Reports, 2017, 7, 39698.	1.6	13
23788	Theoretical Study of Impact of Internal and External Stresses on Thermal Equilibrium Concentrations of Intrinsic Point Defects in Doped Si Crystals. ECS Journal of Solid State Science and Technology, 2017, 6, P78-P99.	0.9	4
23789	Magnetism and magnetocrystalline anisotropy in vacancy doped and (non)metal adsorbed single-layer PtSe2. Computational Materials Science, 2017, 129, 171-177.	1.4	14
23790	First-principles investigations on structure stability, elastic properties, anisotropy and Debye temperature of tetragonal LiFeAs and NaFeAs under pressure. Journal of Physics and Chemistry of Solids, 2017, 104, 243-251.	1.9	30
23791	Vibrational spectroscopy of orthorhombic Cu 2 ZnSiS 4 single crystal: Low-temperature polarized Raman scattering and first principle calculations. Vibrational Spectroscopy, 2017, 89, 81-84.	1.2	5

#	Article	IF	Citations
23792	Calculations of Oxygen Adsorption-Induced Surface Reconstruction and Oxide Formation on Cu(100). Chemistry of Materials, 2017, 29, 1472-1484.	3.2	12
23793	Site occupancy behaviours of ternary elements (Zr, Mo, Cr) in the Laves phase of C15 NbCo₂: a first-principles study. Philosophical Magazine, 2017, 97, 1012-1023.	0.7	3
23794	First-principles study on structural, thermal, mechanical and dynamic stability of Tâ€™-MoS₂. Journal of Physics Condensed Matter, 2017, 29, 095702.	0.7	14
23795	First-principles study on the dielectric and transport properties of the LiNbO₃-type CdPbO₃. International Journal of Modern Physics B, 2017, 31, 1750032.	1.0	0
23796	Effects of Bi doping on the microstructure, electrical and electrochemical properties of La 2-x Bi x Cu 0.5 Mn 1.5 O 6 (x = 0, 0.1 and 0.2) perovskites as novel cathodes for solid oxide fuel cells. Electrochimica Acta, 2017, 229, 429-437.	2.6	46
23797	Surface Reaction of CO on Carbide-Modified Mo(110). Journal of Physical Chemistry C, 2017, 121, 3133-3142.	1.5	1
23798	Effect of Ag and Pd promotion on CH₄selectivity in Fe(100) Fischerâ€“TrÃ¶psch catalysis. Physical Chemistry Chemical Physics, 2017, 19, 5495-5503.	1.3	4
23799	Pressure effect on the mechanical, electronic and thermodynamic properties of Ba2Bi3: First-principle calculations. Journal of Physics and Chemistry of Solids, 2017, 104, 293-303.	1.9	5
23800	Strained graphitic carbon nitride for hydrogen purification. Journal of Membrane Science, 2017, 528, 201-205.	4.1	23
23801	Atomic structures and electronic properties of interfaces between aluminum and carbides/nitrides: A first-principles study. Physica E: Low-Dimensional Systems and Nanostructures, 2017, 89, 15-20.	1.3	17
23802	Insight into the origin of magnetism in Iron-doped cadmium sulfide thin films from first principles calculations. Solid State Communications, 2017, 253, 10-13.	0.9	6
23803	Tuning Electronic Properties and Band Alignments of Phosphorene Combined With MoSe₂ and WSe₂. Journal of Physical Chemistry C, 2017, 121, 3862-3869.	1.5	55
23804	Is the Metallic Phosphorus Carbide (Î²₀-PC) Monolayer Stable? An Answer from a Theoretical Perspective. Journal of Physical Chemistry Letters, 2017, 8, 747-754.	2.1	47
23805	High mechanical strength in Zn₄B₆O₁₃with an unique sodalite-cage structure. RSC Advances, 2017, 7, 2038-2043.	1.7	7
23806	First principles study of structural and magnetic properties of transition metal nitrides TMN (TM =) Tj ETQq0 0 0 rgBT /Overlock 10 Tf 50	0.6	9
23807	An experimental and theoretical study of the optical, electronic, and magnetic properties of novel inverted Î±-Cr₂O₃@Î±-Mn_{0.35}Cr_{1.65}O_{2.94}core shell nanoparticles. Journal of Materials Research, 2017, 32, 269-278.	1.2	6
23808	An Î±-CrPO₄-type NaV₃(PO₄)₃ anode for sodium-ion batteries with excellent cycling stability and the exploration of sodium storage behavior. Journal of Materials Chemistry A, 2017, 5, 3839-3847.	5.2	24
23809	Determination of geometric and electronic structures of organic crystals from first principles: Role of the molecular configuration on the electronic structure. Journal of Applied Physics, 2017, 121, 045501.	1.1	14

#	Article	IF	Citations
23810	Antiperovskite Nitridophosphate Oxide Ho3[PN4]O by High-Pressure Metathesis. European Journal of Inorganic Chemistry, 2017, 2017, 1930-1937.	1.0	15
23811	Electronic structure, optical properties and band edges of layered MoO3: A first-principles investigation. Computational Materials Science, 2017, 130, 242-248.	1.4	76
23812	Estimation of graphene surface stability against the adsorption of environmental and technological chemical agents. Physica Status Solidi (B): Basic Research, 2017, 254, 1600702.	0.7	5
23813	Study of Pressure Effects on the Elastic Stability and Optical Treatment of Co2VAl using GGA+U. Silicon, 2017, 9, 431-437.	1.8	0
23814	A simple method to approximate electrode potential-dependent activation energies using density functional theory. Catalysis Today, 2017, 288, 63-73.	2.2	77
23815	Towards understanding the dissolving behaviors of oxygen at finite temperature in Au and Ag: First-principles total energy and phonon spectrum calculations. Chinese Journal of Physics, 2017, 55, 218-229.	2.0	0
23816	The electronic structure, optical absorption and photocatalytic water splitting of (FeÂ+ÂNi)-codoped TiO2: A DFT +U study. International Journal of Hydrogen Energy, 2017, 42, 4966-4976.	3.8	22
23817	Direct Writing on Copper Ion Doped Silica Films by Electrogeneration of Metallic Microstructures. Journal of Physical Chemistry C, 2017, 121, 1129-1139.	1.5	2
23818	Theoretically Manipulating Quantum Dots on Two-Dimensional TiO₂ Monolayer for Effective Visible Light Absorption. ACS Applied Materials & Interfaces, 2017, 9, 8255-8262.	4.0	39
23819	Insight into the topological defects and dopants in metal-free holey graphene for triiodide reduction in dye-sensitized solar cells. Journal of Materials Chemistry A, 2017, 5, 5952-5960.	5.2	49
23820	The elastic constants of rubrene determined by Brillouin scattering and density functional theory. Applied Physics Letters, 2017, 110, .	1.5	15
23821	Surface-gate-defined single-electron transistor in a MoS₂ bilayer. Nanotechnology, 2017, 28, 125203.	1.3	6
23822	Effect of Phosphorus Substitution on Stability, Electronic, and Magnetic Properties of SiC Hybrid. Journal of Superconductivity and Novel Magnetism, 2017, 30, 2099-2106.	0.8	1
23823	Insights on the extraordinary tolerance to alcohols of Fe-N-C cathode catalysts in highly performing direct alcohol fuel cells. Nano Energy, 2017, 34, 195-204.	8.2	113
23824	Scaling Relations for Adsorption Energies on Doped Molybdenum Phosphide Surfaces. ACS Catalysis, 2017, 7, 2528-2534.	5.5	39
23825	Room temperature organic magnets derived from sp3 functionalized graphene. Nature Communications, 2017, 8, 14525.	5.8	112
23826	The structural, electronic, elastic and dynamic properties of Co3W in the L12 phase. AIP Conference Proceedings, 2017, , .	0.3	1
23827	Effects of fluorine content on the elastic behavior of topaz [Al₂SiO₄(F,OH)₂]. American Mineralogist, 2017, 102, 347-356.	0.9	27

#	Article	IF	Citations
23828	Spectroscopic Observation of a Hydrogenated CO Dimer Intermediate During CO Reduction on Cu(100) Electrodes. Angewandte Chemie - International Edition, 2017, 56, 3621-3624.	7.2	366
23829	The investigation of adsorption and dissociation of H 2 O on Li 2 O (111) by ab initio theory. Applied Surface Science, 2017, 407, 44-51.	3.1	11
23830	The electronic structure and optical absorption of rutile TiO 2 with La and N dopants from first-principles calculation. Computational Materials Science, 2017, 131, 178-186.	1.4	12
23831	Structure and Characterization of a Zero-Dimensional Alkali Tin Dihalides Compound Cs₃Sn₃F₂Cl₇ with the [Sn₂F₂Cl₄]^{2â€“} Clusters. Inorganic Chemistry, 2017, 56, 3081-3086.	1.9	9
23832	Combination of Inelastic Neutron Scattering Experiments and ab Initio Quantum Calculations for the Study of the Hydration Properties of Oriented Saponites. Journal of Physical Chemistry C, 2017, 121, 5029-5040.	1.5	21
23833	Competition between Palladium Clusters and Hydrogen to Saturate Graphene Vacancies. Journal of Physical Chemistry C, 2017, 121, 10843-10850.	1.5	21
23834	Simulation calculations of efficiencies and silicon consumption for CH3NH3PbI3â^'xâ^'y Br x Cl y /crystalline silicon tandem solar cells. Journal Physics D: Applied Physics, 2017, 50, 155102.	1.3	3
23835	First-principles studies on facet-dependent photocatalytic properties of BiOI {001} surface. Journal of Materials Science, 2017, 52, 5686-5695.	1.7	22
23836	Newly synthesized Zr 2 AlC, Zr 2 (Al 0.58 Bi 0.42)C, Zr 2 (Al 0.2 Sn 0.8)C, and Zr 2 (Al 0.3 Sb 0.7)C MAX phases: A DFT based first-principles study. Computational Materials Science, 2017, 131, 139-145.	1.4	56
23837	Assessment of dispersion correction methods within density functional theory for energetic materials. Molecular Simulation, 2017, 43, 568-574.	0.9	27
23838	Behaviors of transmutation elements Re and Os and their effects on energetics and clustering of vacancy and self-interstitial atoms in W. Nuclear Fusion, 2017, 57, 046006.	1.6	32
23839	Zinc oxide for gas sensing of formaldehyde: Density functional theory modelling of the effect of nanostructure morphology and gas concentration on the chemisorption reaction. Materials Chemistry and Physics, 2017, 193, 274-284.	2.0	23
23840	Semimetal behavior of bilayer stanene. Physica E: Low-Dimensional Systems and Nanostructures, 2017, 89, 155-159.	1.3	4
23841	Unique Optoelectronic Structure and Photoreduction Properties of Sulfur-Doped Lead Chromates Explaining Their Instability in Paintings. Analytical Chemistry, 2017, 89, 3326-3334.	3.2	11
23842	Investigation of Structural Evolution of Li_{1.1}V₃O₈ by In Situ X-ray Diffraction and Density Functional Theory Calculations. Chemistry of Materials, 2017, 29, 2364-2373.	3.2	40
23843	Ab Initio Atomistic Thermodynamics Study of the (001) Surface of LiCoO₂ in a Water Environment and Implications for Reactivity under Ambient Conditions. Journal of Physical Chemistry C, 2017, 121, 5069-5080.	1.5	37
23844	Interfacial and Alloying Effects on Activation of Ethanol from First-Principles. Journal of Physical Chemistry C, 2017, 121, 5603-5611.	1.5	24
23845	Dispersion interactions in silicon allotropes. Physical Chemistry Chemical Physics, 2017, 19, 7699-7707.	1.3	7

#	Article	IF	Citations
23846	Computational study of phononic resonators and waveguides in monolayer transition metal dichalcogenides. Physical Chemistry Chemical Physics, 2017, 19, 8082-8090.	1.3	5
23847	Irradiation-induced void evolution in iron: A phase-field approach with atomistic derived parameters. Chinese Physics B, 2017, 26, 026102.	0.7	6
23848	Equilibrium crystal shape of BaZrO3 and space charge formation in the (011) surface by using ab-initio thermodynamics. Journal of the Korean Physical Society, 2017, 70, 75-80.	0.3	6
23849	Density function theory study of electronic, optical and thermodynamic properties of CaN2, SrN2 and BaN2. Journal Wuhan University of Technology, Materials Science Edition, 2017, 32, 100-105.	0.4	2
23850	Tuning electronic, magnetic and optical properties of germanene nanosheet with site dependent adatoms arsenic and gallium: A first principles study. Current Applied Physics, 2017, 17, 573-583.	1.1	20
23851	Tilt grain boundaries energy and structure in NiTi alloys. Computational Materials Science, 2017, 131, 108-119.	1.4	22
23852	High-pressure phases of AlxIn1â^'xN compounds: First principles calculations. Journal of Alloys and Compounds, 2017, 704, 160-169.	2.8	9
23853	Strong trapping and slow diffusion of helium in a tungsten grain boundary. Journal of Nuclear Materials, 2017, 487, 158-166.	1.3	38
23854	Magnetic engineering in 3d transition metals on phosphorene by strain. Physics Letters, Section A: General, Atomic and Solid State Physics, 2017, 381, 1236-1240.	0.9	16
23855	First-Principles Study of InVO₄ under Pressure: Phase Transitions from CrVO₄- to AgMnO₄-Type Structure. Inorganic Chemistry, 2017, 56, 2697-2711.	1.9	25
23856	Franckeite as a naturally occurring van der Waals heterostructure. Nature Communications, 2017, 8, 14409.	5.8	103
23857	Crystal shape controlled H2 storage rate in nanoporous carbon composite with ultra-fine Pt nanoparticle. Scientific Reports, 2017, 7, 42438.	1.6	6
23858	Are the experimentally observed 3-dimensional carbon honeycombs all-sp2 structures? The dangling p-orbital instability. RSC Advances, 2017, 7, 9790-9794.	1.7	14
23859	Temperature effect on lattice and electronic structures of WTe2 from first-principles study. Journal of Applied Physics, 2017, 121, .	1.1	11
23860	Ab initio study of the structural, electronic, elastic and thermal conductivity properties of SrClF with pressure effects. Philosophical Magazine, 2017, 97, 743-758.	0.7	8
23861	The effect of oxygen vacancies on the hyperfine properties of metal-doped SnO₂. Journal Physics D: Applied Physics, 2017, 50, 115103.	1.3	8
23862	Benchmarking Performance of a Gate-All-Around Germanium Nanotube Field Effect Transistor (GAA-GeNTFET) against GAA-CNTFET. ECS Journal of Solid State Science and Technology, 2017, 6, M24-M28.	0.9	12
23863	A Catalytic Etching-Wetting-Dewetting Mechanism in the Formation of Hollow Graphitic Carbon Fiber. CheM, 2017, 2, 299-310.	5.8	44

#	Article	IF	Citations
23864	Ab initio investigation into the structure and properties of Irâ€“Zr intermetallics for high-temperature structural applications. Computational Materials Science, 2017, 131, 146-159.	1.4	23
23865	Elastic, electronic and optical properties of cubic Mg2C under hydrostatic pressure: Modified Beckeâ€“Johnson calculations. Optik, 2017, 136, 411-420.	1.4	9
23866	Ferromagnetic Coupling in the Heterospin Bis-Catecholatoâ€“Manganese(IV) Complex with Pyridine Substituted by Nitronyl-nitroxide. Inorganic Chemistry, 2017, 56, 2426-2431.	1.9	18
23867	Wafer-scale two-dimensional semiconductors from printed oxide skin of liquid metals. Nature Communications, 2017, 8, 14482.	5.8	219
23868	A DFT+U investigation of hydrogen adsorption on the LaFeO₃(010) surface. Physical Chemistry Chemical Physics, 2017, 19, 7399-7409.	1.3	28
23869	Band gap scaling laws in group IV nanotubes. Nanotechnology, 2017, 28, 115202.	1.3	8
23870	Anisotropic mechanical and optical response and negative Poissonâ€™s ratio in Mo₂C nanomembranes revealed by first-principles simulations. Nanotechnology, 2017, 28, 115705.	1.3	57
23871	Band Structure and Optical Properties of Kesterite Type Compounds: first principle calculations. IOP Conference Series: Materials Science and Engineering, 2017, 175, 012014.	0.3	1
23872	High-temperature intrinsic quantum anomalous Hall effect in rare Earth monohalide. 2D Materials, 2017, 4, 021014.	2.0	28
23873	Magnetic coupling between 3d transition metal adatoms on graphene supported by metallic substrates. Carbon, 2017, 116, 599-605.	5.4	14
23874	Crystal structure, mechanical and thermal properties of Yb4Al2O9: A combination of experimental and theoretical investigations. Journal of the European Ceramic Society, 2017, 37, 2491-2499.	2.8	18
23875	Effect of the d electrons on the electronic band structure of the valence bands of IIbâ€“VIa<mml:math xmlns:mml="http://www.w3.org/1998/Math/MathML" altimg="si0033.gif" overflow="scroll"><mml:mrow><mml:mi>C</mml:mi><mml:mo stretchy="false">(</mml:mo><mml:mn>2</mml:mn><mml:mo>Ã—</mml:mo><mml:mn>2</mml:mn><mml:mo) Tj ETQq1 1 0.784314 Surface Science, 2017, 660, 47-55.	0.8	0
23876	Strain-Modulated Electronic Structure and Infrared Light Adsorption in Palladium Diselenide Monolayer. Scientific Reports, 2017, 7, 39995.	1.6	39
23877	Interface effects between germanene and Au(1â€†1â€†1) from first principles. Journal Physics D: Applied Physics, 2017, 50, 115301.	1.3	8
23878	Geometrically induced Ï€ -band splitting in graphene superlattices. Chinese Physics B, 2017, 26, 028103.	0.7	1
23879	Sb Doping of Metallic CuCr₂S₄ as a Route to Highly Improved Thermoelectric Properties. Chemistry of Materials, 2017, 29, 2988-2996.	3.2	68
23880	Zero Thermal Expansion and Semiconducting Properties in PbTiO₃â€“Bi(Co,) Tj ETQq0 0 0 rgBT /Overlock 10 Tf 50 102 Td	1.9	13
23881	Schiff Base-Functionalized Multi Walled Carbon Nano Tubes to Immobilization of Palladium Nanoparticles as Heterogeneous and Recyclable Nanocatalyst for Suzuki Reaction in Aqueous Media Under Mild Conditions. Catalysis Letters, 2017, 147, 976-986.	1.4	34

#	Article	IF	Citations
23882	First-Principles Study of Lattice Dynamics and Thermal Properties of Alkaline-Earth Metal Nitrides CaN, SrN, and BaN. Journal of Superconductivity and Novel Magnetism, 2017, 30, 2091-2097.	0.8	1
23883	Theoretical Predictions of Structural, Electronic, and Optical Properties of Dilute Bismide AlN1â^'x Bi x in Zinc-Blend Structures. Journal of Electronic Materials, 2017, 46, 1977-1983.	1.0	5
23884	Fe catalysts for methane decomposition to produce hydrogen and carbon nano materials. Applied Catalysis B: Environmental, 2017, 208, 44-59.	10.8	179
23885	Fourier transform infrared and Raman spectroscopy in the study of phase transitions in dipyrazolium iodide triiodide: Experimental and theoretical analysis. Spectrochimica Acta - Part A: Molecular and Biomolecular Spectroscopy, 2017, 179, 83-94.	2.0	0
23886	Nitrogen non-stoichiometric stabilization of UN 2. Solid State Communications, 2017, 254, 21-25.	0.9	4
23887	Electrochemical reduction of CO₂to synthesis gas with controlled CO/H₂ratios. Energy and Environmental Science, 2017, 10, 1180-1185.	15.6	341
23888	Impact of surface strain on the spin dynamics of deposited Co nanowires. Journal of Applied Physics, 2017, 121, 014306.	1.1	3
23889	Experimental and Firstâ€Principles Evidence for Interfacial Activity of Ru/TiO₂ for the Direct Conversion of mâ€Cresol to Toluene. ChemCatChem, 2017, 9, 2642-2651.	1.8	42
23890	On the junction physics of Schottky contact of (10, 10) MX2 (MoS2, WS2) nanotube and (10, 10) carbon nanotube (CNT): an atomistic study. Applied Physics A: Materials Science and Processing, 2017, 123, 1.	1.1	13
23891	Field Effect in Graphene-Based van der Waals Heterostructures: Stacking Sequence Matters. Nano Letters, 2017, 17, 2660-2666.	4.5	21
23892	Covalently Connected Carbon Nanotubes as Electrocatalysts for Hydrogen Evolution Reaction through Band Engineering. ACS Catalysis, 2017, 7, 2676-2684.	5.5	41
23893	Molecular and dissociative adsorption of water and hydrogen sulfide at perfect and defective Cu(110) surfaces. Physical Chemistry Chemical Physics, 2017, 19, 8111-8120.	1.3	20
23894	New high-pressure phases of <mml:math xmlns:mml="http://www.w3.org/1998/Math/MathML"><mml:msub><mml:mi>MoSe</mml:mi><mml:mn>2</mml:mn></mml:msub></m and <mml:math xmlns:mml="http://www.w3.org/1998/Math/MathML"><mml:msub><mml:mi>MoTe</mml:mi><mml:mn>2</mml:mn></mml:msub></m Physical Review B, 2017, 95, .	1.1	24
23895	Gate control of spin-polarized conductance in alloyed transitional metal nanocontacts. Physical Review B, 2017, 95, .	1.1	1
23896	Electronic Stopping of Slow Protons in Transition and Rare Earth Metals: Breakdown of the Free Electron Gas Concept. Physical Review Letters, 2017, 118, 103401.	2.9	52
23897	Tailoring magnetic behavior of CoFeMnNiX (XÂ= Al, Cr, Ga, and Sn) high entropy alloys by metal doping. Acta Materialia, 2017, 130, 10-18.	3.8	220
23898	Density-functional study of plutonium monoxide monohydride. Journal of Nuclear Materials, 2017, 485, 181-188.	1.3	4
23899	First principles study of inert-gas (helium, neon, and argon) interactions with hydrogen in tungsten. Journal of Nuclear Materials, 2017, 487, 128-134.	1.3	17

#	Article	IF	Citations
23900	Understanding the enhanced photoelectrochemical activity of Ta doped hematite. Journal of Molecular Structure, 2017, 1139, 104-110.	1.8	9
23901	Ligand-Induced Variations in Symmetry and Structural Dimensionality of Lead Oxide Carboxylates. Crystal Growth and Design, 2017, 17, 1574-1582.	1.4	11
23902	Ab Initio Molecular Dynamics Study of Dissociative Chemisorption and Scattering of CO₂ on Ni(100): Reactivity, Energy Transfer, Steering Dynamics, and Lattice Effects. Journal of Physical Chemistry C, 2017, 121, 5594-5602.	1.5	41
23903	Thermodynamic and Mechanical Properties of the Rutherfordine Mineral Based on Density Functional Theory. Journal of Physical Chemistry C, 2017, 121, 5994-6001.	1.5	41
23904	Al-Doped CoP nanoarray: a durable water-splitting electrocatalyst with superhigh activity. Nanoscale, 2017, 9, 4793-4800.	2.8	268
23905	High-index facet engineering of PtCu cocatalysts for superior photocatalytic reduction of CO₂ to CH₄. Journal of Materials Chemistry A, 2017, 5, 6686-6694.	5.2	93
23906	Hybrid n-type Sn_{1â^'x}Ta_xO₂ nanowalls bonded with graphene-like layers as high performance electrocatalysts for flexible energy conversion devices. Journal of Materials Chemistry A, 2017, 5, 6884-6892.	5.2	8
23907	Unprecedented Al supersaturation in single-phase rock salt structure VAlN films by Al+ subplantation. Journal of Applied Physics, 2017, 121, .	1.1	40
23908	Experimental and first-principles studies of high-pressure effects on the structural, electronic, and optical properties of semiconductors and lanthanide doped solids. Japanese Journal of Applied Physics, 2017, 56, 05FA02.	0.8	7
23909	Effects of Fluorine Doping and Pressure on the Electronic Structure of LaO1â^'x F x FeAs Superconductor: a First Principle Study. Journal of Superconductivity and Novel Magnetism, 2017, 30, 2065-2071.	0.8	1
23910	NO and NO 2 adsorption on subsurface doped MgO (100) and BaO (100) surfaces. A density functional study. Applied Surface Science, 2017, 404, 216-229.	3.1	12
23911	Mn 2 YGa (Y=Ir and Pt), a promising shape memory alloy by DFT methods. Chinese Journal of Physics, 2017, 55, 806-812.	2.0	6
23912	Catalytic effects of calcium and potassium on a curved char surface in fuel reburning: A first-principles study on the adsorption of nitric oxide on single-wall carbon nanotubes with metal decoration. Energy, 2017, 125, 459-469.	4.5	13
23913	Influence of interface geometry on phase stability and bandgap engineering in boron nitride substituted graphene: A combined first-principles and Monte Carlo study. Journal of Alloys and Compounds, 2017, 708, 437-443.	2.8	12
23914	Spin filtering effect in colorimetric chemosensor L-based molecular devices modulated with different transition metal ions. Physica B: Condensed Matter, 2017, 513, 10-14.	1.3	3
23915	Total Oxidation of Lean Methane over Cobalt Spinel Nanocubes Controlled by the Self-Adjusted Redox State of the Catalyst: Experimental and Theoretical Account for Interplay between the Langmuirâ€“Hinshelwood and Marsâ€“Van Krevelen Mechanisms. ACS Catalysis, 2017, 7, 2853-2867.	5.5	110
23916	Interactions between Er dopant and intrinsic point defects of ZnO: a first-principles study. Materials Research Express, 2017, 4, 035903.	0.8	11
23917	Optical properties of organically functionalized silicon surfaces: Uracil-like nucleobases on Si(001). Physical Review B, 2017, 95, .	1.1	11

#	Article	IF	Citations
23918	First-principles prediction and Monte Carlo study of half-metallic ferromagnetism of the C-doped honeycomb CdS monolayer. Japanese Journal of Applied Physics, 2017, 56, 041201.	0.8	2
23919	Oxygen Reduction in Alkaline Mediaâ€"a Discussion. Electrocatalysis, 2017, 8, 554-564.	1.5	17
23920	Structural, electronic, mechanical and magnetic properties of Mn based ferromagnetic half Heusler alloys: A first principles study. Journal of Alloys and Compounds, 2017, 708, 1216-1233.	2.8	35
23921	Ti-5Al-5Mo-5V-3Cr and similar Mo equivalent alloys: First principles calculations and experimental investigations. Journal of Applied Research and Technology, 2017, 15, 21-26.	0.6	10
23922	First-principles and experimental characterization of the electronic properties of CaGaSiN₃ and CaAlSiN₃: the impact of chemical disorder. Physical Chemistry Chemical Physics, 2017, 19, 9292-9299.	1.3	10
23923	Iron vacancy in tetragonal Fe_{1â^'x}S crystals and its effect on the structure and superconductivity. Physical Chemistry Chemical Physics, 2017, 19, 9000-9006.	1.3	18
23924	Thymine adsorption on two-dimensional boron nitride structures: first-principles studies. Journal of Molecular Modeling, 2017, 23, 109.	0.8	3
23925	Pressure and temperature dependence of the structural, elastic and thermodynamic properties of potassium telluride: First-principles calculations. Chinese Journal of Physics, 2017, 55, 769-779.	2.0	40
23926	Density functional theory study of stable configurations of substitutional and interstitial C and Sn atoms in Si and Ge crystals. Journal of Crystal Growth, 2017, 463, 110-115.	0.7	3
23927	Synergistic Strategy to Enhance the Thermoelectric Properties of CoSbS_{1â€"x}Se_x Compounds via Solid Solution. ACS Applied Materials & Interfaces, 2017, 9, 10595-10601.	4.0	38
23928	Phononic dissipation during â€œhotâ€•adatom motion: A QM/Me study of O2 dissociation at Pd surfaces. Journal of Chemical Physics, 2017, 146, 014702.	1.2	10
23929	Oxygen DX center in In0.17Al0.83N: Nonradiative recombination and persistent photoconductivity. Applied Physics Letters, 2017, 110, 072101.	1.5	4
23930	Low conductance of nickel atomic junctions in hydrogen atmosphere. Frontiers of Physics, 2017, 12, 1.	2.4	5
23931	Structural Tuning and Piezoluminescence Phenomenon in Trithiocyanuric Acid. Journal of Physical Chemistry C, 2017, 121, 1870-1875.	1.5	6
23932	Reinvestigation of Mechanical Properties and Shear-Induced Atomic Deformation of Tetragonal Superhard Semiconducting OsB4. Journal of Physical Chemistry C, 2017, 121, 6290-6299.	1.5	7
23933	Reliable current changes with selectivity ratio above 109 observed in lightly doped zinc oxide films. NPG Asia Materials, 2017, 9, e351-e351.	3.8	36
23934	KFeCuTe₂: a new compound to study the removal of interstitial Fe in layered tellurides. Dalton Transactions, 2017, 46, 3649-3654.	1.6	11
23935	Strong enhancement of spinâ€"orbit splitting induced by Ïƒâ€"Ï€ coupling in Pb-decorated silicene. RSC Advances, 2017, 7, 11761-11767.	1.7	1

#	Article	IF	Citations
23936	Clustering/anticlustering effects on the GeSi Raman spectra at moderate (Ge,Si) contents: Percolation scheme vs. ab initio calculations. Journal of Applied Physics, 2017, 121, .	1.1	7
23937	The photocatalytic mechanism of BiOI with oxygen vacancy and iodine self-doping. Chinese Journal of Physics, 2017, 55, 331-341.	2.0	5
23938	Electronic, dielectric and optical properties of orthorhombic lanthanum gallate perovskite. Journal of Alloys and Compounds, 2017, 708, 187-193.	2.8	16
23939	Ab initio study of the electronic and transport properties of waved graphene nanoribbons. Physica E: Low-Dimensional Systems and Nanostructures, 2017, 89, 170-176.	1.3	12
23940	Structures and Properties of As(OH)₃ Adsorption Complexes on Hydrated Mackinawite (FeS) Surfaces: A DFT-D2 Study. Environmental Science & Technology, 2017, 51, 3461-3470.	4.6	49
23941	Cluster Size Effects in Ethylene Hydrogenation over Palladium. Journal of Physical Chemistry C, 2017, 121, 10870-10875.	1.5	15
23942	Precise tuning in platinum-nickel/nickel sulfide interface nanowires for synergistic hydrogen evolution catalysis. Nature Communications, 2017, 8, 14580.	5.8	648
23943	Atomic scale structure of amorphous aluminum oxyhydroxide, oxide and oxycarbide films probed by very high field²⁷Al nuclear magnetic resonance. Physical Chemistry Chemical Physics, 2017, 19, 8101-8110.	1.3	23
23944	DFT investigation of capacious, ultrafast and highly conductive hexagonal Cr₂C and V₂C monolayers as anode materials for high-performance lithium-ion batteries. Physical Chemistry Chemical Physics, 2017, 19, 7807-7819.	1.3	59
23945	A DFT study of the interplay between dopants and oxygen functional groups over the graphene basal plane â€“ implications in energy-related applications. Physical Chemistry Chemical Physics, 2017, 19, 8530-8540.	1.3	56
23946	Site preference of ternary alloying elements in Ni3Al-X (Xâ€‰â€‰=â€‰â€‰Co,Nb): a first-principles calculations in combination with XPS study. Materials Research Express, 2017, 4, 025016.	0.8	3
23947	First-principles and Monte Carlo studies of the Ni₂(Mn,Cr)Ga Heusler alloys electronic and magnetic properties. Materials Research Express, 2017, 4, 026105.	0.8	10
23948	Stratified construction of neural network based interatomic models for multicomponent materials. Physical Review B, 2017, 95, .	1.1	67
23949	Thermodynamic stability and properties of boron subnitrides from first principles. Physical Review B, 2017, 95, .	1.1	13
23950	Strain-induced indirect-to-direct band-gap transition in bulk <mml:math xmlns:mml="http://www.w3.org/1998/Math/MathML"><mml:msub><mml:mi>SnS</mml:mi><mml:mn>2</mml:mn></mml:msub></mml:math> Physical Review B, 2017, 95, .	1.1	49
23951	<mml:math xmlns:mml="http://www.w3.org/1998/Math/MathML"><mml:mrow><mml:mi>Î²</mml:mi><mml:mo>â^'</mml:mo><mml:mi mathvariant="normal">G</mml:mi><mml:msub><mml:mi mathvariant="normal">a</mml:mi><mml:mn>2</mml:mn></mml:msub><mml:msub><mml:mi mathvariant="normal">O</mml:mi><mml:mn>3</mml:mn></mml:msub></mml:mrow></mml:math>.	1.1	184
23952	Two-dimensional topological crystalline quantum spin Hall effect in transition metal intercalated compounds. Physical Review B, 2017, 95, .	1.1	10
23953	First-principles study of the electrical and lattice thermal transport in monolayer and bilayer graphene. Physical Review B, 2017, 95, .	1.1	35

#	Article	IF	Citations
23954	Efficient oxygen reduction catalysis by subnanometer Pt alloy nanowires. Science Advances, 2017, 3, e1601705.	4.7	330
23955	Edge-Reconstructed, Few-Layered Graphene Nanoribbons: Stability and Electronic Properties. Journal of Physical Chemistry C, 2017, 121, 5836-5840.	1.5	4
23956	Understanding Active Sites in the Waterâ€“Gas Shift Reaction for Ptâ€“Re Catalysts on Titania. ACS Catalysis, 2017, 7, 2597-2606.	5.5	34
23957	Formation mechanism of conduction path in titanium dioxide with Ti-interstitials-doped: Carâ€“Parrinello molecular dynamics. AIP Conference Proceedings, 2017, , .	0.3	1
23958	First principles calculation of the elasticity of ice VIII and X. Journal of Chemical Physics, 2017, 146, 014501.	1.2	11
23959	Structural and electronic properties of bulk and low-index surfaces of zincblende PtC. Journal of Physics Condensed Matter, 2017, 29, 125002.	0.7	2
23960	Planar heterostructures of single-layer transition metal dichalcogenides: Composite structures, Schottky junctions, tunneling barriers, and half metals. Physical Review B, 2017, 95, .	1.1	20
23961	Quantitative Agreement between Electron-Optical Phase Images of<mml:math xmlns:mml="http://www.w3.org/1998/Math/MathML" display="inline"><mml:mrow><mml:msub><mml:mrow><mml:mi>WSe</mml:mi></mml:mrow><mml:mrow><mml:mn>2</mml:mn></mml:mrow></mml:msub></mml:mrow></mml:math> Simulations Based on Electrostatic Potentials that Include Bonding Effects. Physical Review Letters, 2017, 118, 086101.	2.9	15
23962	DFT Study of Hydrostatic Pressure Effect on Cd 1 â^' x Z x X (Z = Cr, Mn; X = S, Se) DMSs. Journal of Superconductivity and Novel Magnetism, 2017, 30, 2175-2185.	0.8	7
23963	LaSrMnO₄: Reversible Electrochemical Intercalation of Fluoride Ions in the Context of Fluoride Ion Batteries. Chemistry of Materials, 2017, 29, 3441-3453.	3.2	101
23964	Functionalization of Single-Layer Nitrogene by Vacancy, Adatoms, and Molecules. Journal of Physical Chemistry C, 2017, 121, 6329-6338.	1.5	16
23965	Modulation of the electronic and mechanical properties of phagraphene via hydrogenation and fluorination. Physical Chemistry Chemical Physics, 2017, 19, 11771-11777.	1.3	35
23966	Absorption and reflectivity of the lithium niobate surface masked with a graphene layer. AIP Advances, 2017, 7, .	0.6	6
23967	Intermediate states and structure evolution in the free-falling process of the dislocation in graphene. Philosophical Magazine, 2017, 97, 759-774.	0.7	2
23968	Multiferroic properties of the PbTiO₃/La_{2/3}Sr_{1/3}MnO₃interface studied from first principles. Journal of Physics Condensed Matter, 2017, 29, 175801.	0.7	5
23969	Temperature and isotope effects on the thermoelectric properties in SnTe. Journal of Physics Condensed Matter, 2017, 29, 175701.	0.7	4
23970	Thermoelectric properties of layered calcium cobaltite<mml:math xmlns:mml="http://www.w3.org/1998/Math/MathML"><mml:mrow><mml:msub><mml:mi>Ca</mml:mi><mml:mn>3</mml:mn></mml:msub><mml:msub><mml:mi mathvariant="normal">O</mml:mi><mml:mn>9</mml:mn></mml:msub></mml:mrow></mml:math>from hybrid functional first-principles calculations. Physical Review B, 2017, 95, .	1.1	12
23971	Plasmon properties and hybridization effects in silicene. Physical Review B, 2017, 95, .	1.1	29

#	Article	IF	Citations
23972	Probing Intermolecular Coupled Vibrations between Two Molecules. Physical Review Letters, 2017, 118, 036801.	2.9	22
23973	Dirac Fermions in Borophene. Physical Review Letters, 2017, 118, 096401.	2.9	353
23974	Polar Oxides without Inversion Symmetry through Vacancy and Chemical Order. Journal of the American Chemical Society, 2017, 139, 2833-2841.	6.6	34
23975	Tuning the band gap and polarization of BaSnO₃/SrSnO₃ superlattices for photovoltaic applications. Physical Chemistry Chemical Physics, 2017, 19, 7032-7039.	1.3	29
23976	First principles investigation of copper and silver intercalated molybdenum disulfide. Journal of Applied Physics, 2017, 121, .	1.1	23
23977	Hydrogen passivation of vacancies in diamond: Electronic structure and stability from ab initio calculations. MRS Advances, 2017, 2, 309-314.	0.5	7
23978	Prediction and characterization of the marcasite phase of iron pernitride under high pressure. Journal of Alloys and Compounds, 2017, 702, 132-137.	2.8	20
23979	Fast Diffusion of O₂ on Nitrogen-Doped Graphene to Enhance Oxygen Reduction and Its Application for High-Rate Znâ€“Air Batteries. ACS Applied Materials & Interfaces, 2017, 9, 7125-7130.	4.0	52
23980	Large-area synthesis of high-quality monolayer 1Tâ€™-WTe ₂ flakes. 2D Materials, 2017, 4, 021008.	2.0	81
23981	Solar Cell Materials by Design: Hybrid Pyroxene Cornerâ€Sharing VO₄ Tetrahedral Chains. ChemSusChem, 2017, 10, 1931-1942.	3.6	10
23982	Stepwise dehydrogenation of ammonia on Fcc-Co surfaces: A DFT study. Applied Surface Science, 2017, 405, 71-78.	3.1	8
23983	First-principles investigation of adsorption and diffusion of Li on doped silicenes: Prospective materials for lithium-ion batteries. Materials Chemistry and Physics, 2017, 192, 125-130.	2.0	26
23984	Structural Evolution and Atom Clustering in Î²-SiAlON: Î²-Si_{6â€“z}Al_zO_zN_{8â€“z}. Inorganic Chemistry, 2017, 56, 2153-2158.	1.9	24
23985	Modeling Ironâ€“Gold Nanoparticles Using a Dedicated Semi-Empirical Potential: Application to the Stability of Coreâ€“Shell Structures. Journal of Physical Chemistry C, 2017, 121, 4680-4691.	1.5	16
23986	Aluminium and magnesium insertion in sulfur-based spinels: a first-principles study. Physical Chemistry Chemical Physics, 2017, 19, 6076-6081.	1.3	33
23987	Direct observation of site-selective hydrogenation and spin-polarization in hydrogenated hexagonal boron nitride on Ni(111). Nanoscale, 2017, 9, 2369-2375.	2.8	17
23988	Chemically induced topological zero mode at graphene armchair edges. Physical Chemistry Chemical Physics, 2017, 19, 5145-5154.	1.3	12
23989	A first-principles investigation of a new hard multi-layered MnB₂ structure. RSC Advances, 2017, 7, 10559-10563.	1.7	10

#	Article	IF	Citations
23990	Corrosion inhibition of copper in aqueous chloride solution by 1H-1,2,3-triazole and 1,2,4-triazole and their combinations: electrochemical, Raman and theoretical studies. Physical Chemistry Chemical Physics, 2017, 19, 6113-6129.	1.3	60
23991	The microscopic origin of low thermal conductivity for enhanced thermoelectric performance of Yb doped MgAgSb. Acta Materialia, 2017, 128, 227-234.	3.8	49
23992	New two-dimensional boron nitride allotropes with attractive electronic and optical properties. Solid State Communications, 2017, 253, 51-56.	0.9	53
23993	Challenges in calculating the bandgap of triazine-based carbon nitride structures. Journal of Materials Chemistry A, 2017, 5, 5115-5122.	5.2	34
23994	Hydrogen weakens interlayer bonding in layered transition metal sulfide Fe_{1+x}S. Journal of Materials Chemistry A, 2017, 5, 5030-5035.	5.2	11
23995	Enhanced Ferroelectric and Visibleâ€Light Photoelectric Properties in Multiferroic KBiFe₂O₅ via Pressureâ€Induced Phase Transition. Advanced Electronic Materials, 2017, 3, 1600498.	2.6	34
23996	Reactivity of phosphorene with a 3d element trioxide (CrO3) considering van der Waals molecular interactions: a DFT-D2 study. Journal of Molecular Modeling, 2017, 23, 49.	0.8	5
23997	A physical model of thermal vacancies within the CALPHAD approach. Scripta Materialia, 2017, 133, 5-8.	2.6	12
23998	Thermal expansion, heat capacity and GrÃ¼neisen parameter of iridium phosphide Ir 2 P from quasi-harmonic Debye model. Solid State Communications, 2017, 253, 19-23.	0.9	5
23999	Structure and Vibrational Dynamics of NASICON-Type LiTi₂(PO₄)₃. Journal of Physical Chemistry C, 2017, 121, 3697-3706.	1.5	42
24000	Factors Favoring Ferroelectricity in Hafnia: A First-Principles Computational Study. Journal of Physical Chemistry C, 2017, 121, 4139-4145.	1.5	158
24001	Improving the electrical properties of carbon nanotubes with interhalogen compounds. Nanoscale, 2017, 9, 3212-3221.	2.8	54
24002	2D lateral heterostructures of monolayer and bilayer phosphorene. Journal of Materials Chemistry C, 2017, 5, 2291-2300.	2.7	25
24003	The conventional cell and the primitive cell electronic structure of anatase titanium dioxide crystal. Materials Research Express, 2017, 4, 036301.	0.8	0
24004	Theoretical Clarification of the Coexistence of Cl Effects on Au/TiO2: The Interaction between Au Clusters and the TiO2 Surface, and the Aggregation of Au Clusters on the TiO2 Surface. Bulletin of the Chemical Society of Japan, 2017, 90, 506-519.	2.0	18
24005	Structural, Electronic, and Mechanical Properties of CoN and NiN: An Ab Initio Study. Zeitschrift Fur Naturforschung - Section A Journal of Physical Sciences, 2017, 72, 321-330.	0.7	5
24006	Thermodynamic stability of Al 11 RE 3 intermetallic compounds from first-principles calculations. Computational Materials Science, 2017, 131, 28-34.	1.4	19
24007	First-principles study of the structural, electronic, elastic, and thermodynamic properties of Rh3Sc compound under high pressure. Journal of Alloys and Compounds, 2017, 704, 484-490.	2.8	16

#	Article	IF	Citations
24008	First-principles calculations of Mg1â^'xCuxSiP2 alloys with xÂ=Â0.0, 0.25, 0.5, 0.75 and 1.0. Journal of Alloys and Compounds, 2017, 705, 211-217.	2.8	7
24009	Metal-like Boronic-Organic Frameworks: A Design and Computation. Inorganic Chemistry, 2017, 56, 2490-2495.	1.9	3
24010	Random Phase Approximation for Periodic Systems Employing Direct Coulomb Lattice Summation. Journal of Chemical Theory and Computation, 2017, 13, 1159-1175.	2.3	11
24011	A New Strategy to Design Highly Sustainable Sulfide PhotoCatalyst for Hydrogen Production. Chinese Journal of Chemistry, 2017, 35, 148-152.	2.6	8
24012	Investigation on the contact between graphdiyne and Cu (111) surface. Carbon, 2017, 117, 246-251.	5.4	26
24013	Insights on the Mechanism of Na-Ion Storage in Soft Carbon Anode. Chemistry of Materials, 2017, 29, 2314-2320.	3.2	177
24014	Atomic Structure and Dynamics of Single Platinum Atom Interactions with Monolayer MoS₂. ACS Nano, 2017, 11, 3392-3403.	7.3	126
24015	Influence of C substitution on the oxygen sites of TiO2 (001) surface. AIP Conference Proceedings, 2017, , .	0.3	0
24016	Machine learning based interatomic potential for amorphous carbon. Physical Review B, 2017, 95, .	1.1	431
24017	First-principles identification of charge-transition levels of native defects in BaF₂. Modern Physics Letters B, 2017, 31, 1750068.	1.0	0
24018	Enhanced electrochemical performance of LiMnBO3 with conductive glassy phase: a prospective cathode material for lithium-ion battery. Ionics, 2017, 23, 1645-1653.	1.2	16
24019	Ab-initio calculations on half-Heusler NiXSn (XÂ=ÂZr, Hf) compounds: electronic and optical properties under pressure. Indian Journal of Physics, 2017, 91, 773-778.	0.9	5
24020	Atomic structure and optoelectronic properties of In0.53Ga0.47As (100) reconstruction surfaces: A DFT study. Optik, 2017, 135, 290-297.	1.4	2
24021	Tuning magnetocrystalline anisotropy of Î±â€³-Fe 16 N 2 by interstitial impurity doping: A first principles study. Journal of Magnetism and Magnetic Materials, 2017, 433, 17-23.	1.0	12
24022	A first principles kinetic Monte Carlo investigation of the adsorption and mobility of gadolinium on the (100) surface of tungsten. Journal of Nuclear Materials, 2017, 488, 9-15.	1.3	0
24023	Influence of the Dimensionality and Organic Cation on Crystal and Electronic Structure of Organometallic Halide Perovskites. Journal of Physical Chemistry C, 2017, 121, 6569-6574.	1.5	47
24024	Chiral Self-Assembly of Nonplanar 10,10â€²-Dibromo-9,9â€²-bianthryl Molecules on Ag(111). Langmuir, 2017, 33, 2993-2999.	1.6	15
24025	Spin filter properties of armchair graphene nanoribbons with substitutional Fe atoms. Molecular Physics, 2017, 115, 2231-2241.	0.8	10

#	Article	IF	Citations
24026	First-principles study of paraelectric and ferroelectric<mml:math xmlns:mml="http://www.w3.org/1998/Math/MathML"><mml:mrow><mml:msub><mml:mi mathvariant="bold">CsH</mml:mi><mml:mn>2</mml:mn></mml:msub><mml:msub><mml:mi mathvariant="bold">PO</mml:mi><mml:mn>4</mml:mn></mml:msub></mml:mrow></mml:math>including dispersion forces: Stability and related vibrational, dielectric, and elastic properties. Physical Review B, 2017, 95, .	1.1	15
24027	Pentagons in the<mml:math xmlns:mml="http://www.w3.org/1998/Math/MathML"><mml:mrow><mml:mi>Si</mml:mi><mml:mo>(</mml:mo><mml:mn>331</mml:mn></mml:mrow></mml:math> reconstruction. Physical Review B, 2017, 95, .	1.1	33
24028	Firstâ€principles study of surface segregation in bimetallic Ni₃M (Mâ€‰=â€‰Mo, Co, Fe) alloys with chemisorbed atomic oxygen. Physica Status Solidi (B): Basic Research, 2017, 254, 1600810.	0.7	8
24029	Stability, electronic and thermodynamic properties of aluminene from first-principles calculations. Applied Surface Science, 2017, 409, 85-90.	3.1	72
24030	Experimental investigation and thermodynamic assessment of the Li-Sb system. Calphad: Computer Coupling of Phase Diagrams and Thermochemistry, 2017, 57, 28-36.	0.7	8
24031	Structural Polymorphism in â€œKesteriteâ€•Cu₂ZnSnS₄: Raman Spectroscopy and First-Principles Calculations Analysis. Inorganic Chemistry, 2017, 56, 3467-3474.	1.9	84
24032	CO Chemisorption on Ultrathin MgO-Supported Palladium Nanoparticles. Journal of Physical Chemistry C, 2017, 121, 5551-5564.	1.5	17
24033	Prediction of Single-Wall Boron Nanotube Structures and the Effects of Hydrogenation. Journal of Physical Chemistry C, 2017, 121, 5841-5847.	1.5	9
24034	Changes in the Electronic States of Low-Temperature Solid n-Tetradecane: Decrease in the HOMOâ€“LUMO Gap. ACS Omega, 2017, 2, 618-625.	1.6	25
24035	Structural stability and electronic properties of an octagonal allotrope of two dimensional boron nitride. Dalton Transactions, 2017, 46, 4259-4264.	1.6	15
24036	Preservation of electronic properties of double-decker complexes on metallic supports. Physical Chemistry Chemical Physics, 2017, 19, 8282-8287.	1.3	7
24037	Mechanisms of direct hydrogen peroxide synthesis on silicon and phosphorus dual-doped graphene: a DFT-D study. Physical Chemistry Chemical Physics, 2017, 19, 9007-9015.	1.3	18
24038	Detection of defect populations in superhard semiconductor boron subphosphide B₁₂P₂ through X-ray absorption spectroscopy. Journal of Materials Chemistry A, 2017, 5, 5737-5749.	5.2	7
24039	Magnetic stability of oxygen defects on the SiO2 surface. AIP Advances, 2017, 7, .	0.6	12
24040	Unveiling descriptors for predicting the bulk modulus of amorphous carbon. Physical Review B, 2017, 95, .	1.1	8
24041	Free energy calculation of mechanically unstable but dynamically stabilized bcc titanium. Physical Review B, 2017, 95, .	1.1	40
24042	Structural and electronic properties of monolayer group III monochalcogenides. Physical Review B, 2017, 95, .	1.1	294
24043	Exploring the effects of interlamellar binding modes on the hardness of ReB2 and MoB2 with laminar structure. Canadian Journal of Physics, 2017, 95, 621-624.	0.4	1

#	Article	IF	Citations
24044	Nitrogen-doped graphene-wrapped iron nanofragments for high-performance oxygen reduction electrocatalysts. Journal of Nanoparticle Research, 2017, 19, 1.	0.8	36
24045	First-principles prediction of magnetic salts: Case study of NaCl bulk and (0 0 1) surface doped with light non-metallic 2 p -block elements. Computational Materials Science, 2017, 132, 10-18.	1.4	2
24046	Structural and elastic properties of zinc-blende and wurtzite InN1-Bi alloys. Journal of Alloys and Compounds, 2017, 708, 323-327.	2.8	5
24047	Optical manifestation of buckled configurations in graphene-like materials. Superlattices and Microstructures, 2017, 104, 349-361.	1.4	4
24048	Phase Transformation, Vibrational and Electronic Properties of K₂Ce(PO₄)₂: A Combined Experimental and Theoretical Study. Inorganic Chemistry, 2017, 56, 3335-3348.	1.9	14
24049	Chemical and Lattice Stability of the Tin Sulfides. Journal of Physical Chemistry C, 2017, 121, 6446-6454.	1.5	73
24050	Excited-State N₂ Dissociation Pathway on Fe-Functionalized Au. Journal of the American Chemical Society, 2017, 139, 4390-4398.	6.6	76
24051	Quantitative and Atomic-Scale View of CO-Induced Pt Nanoparticle Surface Reconstruction at Saturation Coverage via DFT Calculations Coupled with in Situ TEM and IR. Journal of the American Chemical Society, 2017, 139, 4551-4558.	6.6	186
24052	To address surface reaction network complexity using scaling relations machine learning and DFT calculations. Nature Communications, 2017, 8, 14621.	5.8	399
24053	Thermal transport and anharmonic phonons in strained monolayer hexagonal boron nitride. Scientific Reports, 2017, 7, 43956.	1.6	17
24054	Alkaline-earth metal (Mg) polynitrides at high pressure as possible high-energy materials. Physical Chemistry Chemical Physics, 2017, 19, 9246-9252.	1.3	77
24055	One-atom-thick 2D copper oxide clusters on graphene. Nanoscale, 2017, 9, 3980-3985.	2.8	32
24056	Structural evolution of FeH₄ under high pressure. RSC Advances, 2017, 7, 12570-12575.	1.7	20
24057	Reversible structural transition in nanoconfined ice. Physical Review B, 2017, 95, .	1.1	28
24058	Exact Model of Vacancy-Mediated Solute Transport in Magnesium. Physical Review Letters, 2017, 118, 105901.	2.9	26
24059	Water graphene contact surface investigated by pairwise potentials from force-matching PAW-PBE with dispersion correction. Journal of Chemical Physics, 2017, 146, 054702.	1.2	28
24060	Electronâ€“Phonon Coupled Heat Transfer and Thermal Response Induced by Femtosecond Laser Heating of Gold. Journal of Heat Transfer, 2017, 139, .	1.2	6
24061	First-principles study of the Cu-Pd phase diagram. Calphad: Computer Coupling of Phase Diagrams and Thermochemistry, 2017, 56, 224-229.	0.7	13

#	Article	IF	Citations
24062	First-principles calculations of electronic structures and optical, phononic, and thermodynamic properties of monoclinic Î± -spodumene. Ceramics International, 2017, 43, 6312-6321.	2.3	57
24063	Investigation of structural, elastic, electronic, optical and vibrational properties of silver chromate spinels: Normal (CrAg2O4) and inverse (Ag2CrO4). Journal of Alloys and Compounds, 2017, 704, 101-108.	2.8	26
24064	Mechanistic analysis of the role of metal oxophilicity in the hydrodeoxygenation of anisole. Journal of Catalysis, 2017, 347, 102-115.	3.1	107
24065	First-principles calculation of atomic configurations of carbon and tin near the surface of a silicon thin film used for solar cells. Materials Science in Semiconductor Processing, 2017, 63, 45-51.	1.9	2
24066	Surface ferromagnetism in<mml:math xmlns:mml="http://www.w3.org/1998/Math/MathML" altimg="si0064.gif" overflow="scroll"><mml:msub subscriptshift="65%"><mml:mrow><mml:mi>HfO</mml:mi></mml:mrow><mml:mrow><mml:mn>2</mml:mn></mml:mrow></mml:ms by excess oxygen. Solid State Communications, 2017, 252, 33-39.	0.9	5
24067	Periodic domain boundary ordering in a dense molecular adlayer: Sub-saturation carbon monoxide on Pd(111). Surface Science, 2017, 658, 46-54.	0.8	1
24069	Searching for large-gap quantum spin hall insulators: boron-nitride/(Pb,) Tj ETQq0 0 0 rgBT /Overlock 10 Tf 50 502 Td (Sn)/Î±-Al<sub>2<	2.8	6
24070	Hypothetical planar and nanotubular crystalline structures with five interatomic bonds of Kepler nets type. AIP Advances, 2017, 7, 025202.	0.6	14
24071	Interlayer vacancy defects in AA-stacked bilayer graphene: density functional theory predictions. Journal of Physics Condensed Matter, 2017, 29, 155304.	0.7	8
24072	Structural inheritance and difference between Ti₂AlC, Ti₃AlC₂ÂandÂTi₅Al₂C₃ under pressure from first principles. Modern Physics Letters B, 2017, 31, 1750016.	1.0	10
24073	Width-dependent structural stability and magnetic properties ofÂmonolayer zigzag MoS₂ nanoribbons. Modern Physics Letters B, 2017, 31, 1750017.	1.0	12
24074	Atomic structure of self-organizing iridium induced nanowires on Ge(001). Applied Surface Science, 2017, 404, 12-17.	3.1	18
24075	Halogen-Bond-Based Molecular Self-Assembly on Graphene Surface: A First-Principles Study. Journal of Physical Chemistry C, 2017, 121, 4451-4461.	1.5	17
24076	Tunable thermal expansion in framework materials through redox intercalation. Nature Communications, 2017, 8, 14441.	5.8	95
24077	Use of site symmetry in supercell models of defective crystals: polarons in CeO₂. Physical Chemistry Chemical Physics, 2017, 19, 8340-8348.	1.3	20
24078	Selective hydrogenation of CO on Fe₃S₄{111}: a computational study. Faraday Discussions, 2017, 197, 325-336.	1.6	7
24079	Monoclinic Ga₂O₃ (100) surface as a robust photocatalyst for water-splitting. RSC Advances, 2017, 7, 4124-4134.	1.7	16
24080	Adsorption of Te atoms on Au(1â€‰1â€‰1) and the emergence of an adatom-induced bound state. Journal of Physics Condensed Matter, 2017, 29, 125001.	0.7	7

#	Article	IF	Citations
24081	Thermodynamic Properties of Compressed CuX (XÂ=ÂCl, Br) Compounds: Ab Initio Study. Journal of Electronic Materials, 2017, 46, 2521-2528.	1.0	31
24082	Ab initio modelling of the effects of varying Zr (Ti) concentrations on the atomic and electronic properties of stoichiometric PZT solid solutions. Computational and Theoretical Chemistry, 2017, 1104, 56-60.	1.1	6
24083	Density Functional Theory Study on the Role of Polyacetylene as a Promoter in Selective Hydrogenation of Styrene on a Pd Catalyst. Journal of Physical Chemistry C, 2017, 121, 4246-4252.	1.5	7
24084	Cross-Plane Seebeck Coefficient Measurement of Misfit Layered Compounds (SnSe)_n(TiSe₂)_n (n = 1,3,4,5). Nano Letters, 2017, 17, 1978-1986.	4.5	25
24085	A zero-thermal-quenching phosphor. Nature Materials, 2017, 16, 543-550.	13.3	748
24086	Rational design of super-alkalis and their role in CO₂activation. Nanoscale, 2017, 9, 4891-4897.	2.8	58
24087	High-pressure structural phase transition and electronic properties of the alkali hydrides compounds XH (X = Li, Na). Phase Transitions, 2017, 90, 914-927.	0.6	9
24088	A first-principles model for anomalous segregation in dilute ternary tungsten-rhenium-vacancy alloys. Journal of Physics Condensed Matter, 2017, 29, 145403.	0.7	49
24089	Differences in optoelectronic properties between H-saturated and unsaturated GaN nanowires with DFT method. International Journal of Modern Physics B, 2017, 31, 1750084.	1.0	3
24090	Self-healing Pd3Au@Pt/C core-shell electrocatalysts with substantially enhanced activity and durability towards oxygen reduction. Applied Catalysis B: Environmental, 2017, 206, 666-674.	10.8	14
24091	Luminescent metal-organic frameworks for the detection of nitrobenzene in aqueous media. Sensors and Actuators B: Chemical, 2017, 245, 305-313.	4.0	42
24092	Thermodynamic stability of cobalt oxide's low-index surfaces from density functional theory calculations. Surface and Coatings Technology, 2017, 320, 18-22.	2.2	5
24093	Water Adsorption on AnO₂ {111}, {110}, and {100} Surfaces (An = U and Pu): A Density Functional Theory + U Study. Journal of Physical Chemistry C, 2017, 121, 1675-1682.	1.5	48
24094	Toward an Understanding of the Electric Field-Induced Electrostatic Doping in van der Waals Heterostructures: A First-Principles Study. ACS Applied Materials & Interfaces, 2017, 9, 7725-7734.	4.0	20
24095	Adsorption dynamics of molecular nitrogen at an Fe(111) surface. Physical Chemistry Chemical Physics, 2017, 19, 7370-7379.	1.3	9
24096	Diffusion of tellurium at nickel grain boundaries: a first-principles study. RSC Advances, 2017, 7, 8421-8428.	1.7	17
24097	Topologically insulating states in ternary transition metal dichalcogenides. Journal of Applied Physics, 2017, 121, 024303.	1.1	5
24098	Single-crystal elasticity of SrCO₃ by Brillouin spectroscopy. High Pressure Research, 2017, 37, 181-192.	0.4	15

#	Article	IF	Citations
24099	Structural, electronic and optical properties of Bi₂O₃ polymorphs by first-principles calculations for photocatalytic water splitting. Materials Research Express, 2017, 4, 034002.	0.8	17
24100	High Current Density Electrical Breakdown of TiS₃ Nanoribbonâ€Based Fieldâ€Effect Transistors. Advanced Functional Materials, 2017, 27, 1605647.	7.8	52
24101	DFT Investigation on the Electronic and Water Adsorption Properties of Pristine and N-Doped TiO2 Nanotubes for Photocatalytic Water Splitting Applications. Journal of Electronic Materials, 2017, 46, 3592-3602.	1.0	24
24102	A first principles study of adhesion and electronic structure at Fe (110)/graphite (0001) interface. Applied Surface Science, 2017, 405, 497-502.	3.1	27
24103	First-Principles Study of the Charge Transport Mechanisms in Lithium Superoxide. Chemistry of Materials, 2017, 29, 2202-2210.	3.2	30
24104	Why Porous Materials Have Selective Adsorptions: A Rational Aspect from Electrodynamics. Inorganic Chemistry, 2017, 56, 2614-2620.	1.9	12
24105	Tuning Electronic Properties of Monolayer Hexagonal Boron Phosphide with Group IIIâ€“IVâ€“V Dopants. Journal of Physical Chemistry C, 2017, 121, 4583-4592.	1.5	49
24106	Charge transfer induced polymerization of EDOT confined between 2D titanium carbide layers. Journal of Materials Chemistry A, 2017, 5, 5260-5265.	5.2	142
24107	Ab-initio study of the structural, electronic, elastic and vibrational properties of HfX (X = Rh, Ru and) Tj ETQq0 0 0 rgBT /Overlock 10 Tf 5	0.5	11
24108	Segregation effects of Y, Ti, Cr and Si on the intergranular fracture of niobium. Journal of Alloys and Compounds, 2017, 711, 637-642.	2.8	17
24109	Electronic structure and phase transition in polar ScFeO3 from first principles calculations. Journal of Alloys and Compounds, 2017, 713, 187-193.	2.8	8
24110	Stability, bonding and electronic structures of halogenated MoS 2 monolayer: A first-principles study. Physica E: Low-Dimensional Systems and Nanostructures, 2017, 91, 8-14.	1.3	9
24111	Theoretical assessment of structural, mechanical, and thermodynamic properties of Pd 2 Al. Solid State Sciences, 2017, 68, 10-18.	1.5	1
24112	Atomistic Simulations of Methylammonium Lead Halide Layers on PbTiO₃ (001) Surfaces. Journal of Physical Chemistry C, 2017, 121, 9096-9109.	1.5	9
24113	Dynamic properties of IIIâ€“V polytypes from density-functional theory. Journal of Applied Physics, 2017, 121, .	1.1	18
24114	TiPdSn: A half Heusler compound with high thermoelectric performance. Europhysics Letters, 2017, 117, 47002.	0.7	50
24115	Energy Landscape of Displace Phase Transition of Î² to Ï‰ in Ti-V alloys. MRS Advances, 2017, 2, 1449-1454.	0.5	2
24116	First-principles study of defect formation in the photovoltaic semiconductors Cu₂GeS₃and Cu₂ZnGeS₄for comparison with Cu₂SnS₃, Cu₂ZnSnS₄, and CuInSe₂. Japanese Journal of Applied Physics, 2017, 56, 04CS08.	0.8	14

#	Article	IF	Citations
24117	Comparison of GaAs photocathode grown by MOCVD and MBE: a first-principle and experimental research. Journal of Materials Science: Materials in Electronics, 2017, 28, 7429-7436.	1.1	0
24118	Experimental and thermodynamic investigation of Al-Cu-Nd ternary system. Materials Chemistry and Physics, 2017, 195, 94-104.	2.0	3
24119	First-principle study of the lattice dynamic and thermodynamic properties of Zn-based semiconductors with wurtzite structure. Physica B: Condensed Matter, 2017, 515, 51-55.	1.3	2
24120	QM/MD Simulations on Graphene Hydrogenation/Deuteration: C_xH/D Formation Mechanism and Isotope Effect. Journal of Physical Chemistry C, 2017, 121, 8480-8489.	1.5	2
24121	From Twoâ€•to Threeâ€Ðimensional Structures of a Supertetrahedral Boran Using Density Functional Calculations. Angewandte Chemie - International Edition, 2017, 56, 10118-10122.	7.2	24
24122	Atomistic study of electrostatics and carrier transport properties of CNT@MS2 (MÂ=ÂMo, W) and CNT@BN coreá€“shell nanotubes. Journal of Materials Science, 2017, 52, 8119-8131.	1.7	6
24124	Error estimation in high-throughput density functional theory calculation for material property: elastic constants of cubic binary alloy case. Computational Materials Science, 2017, 134, 190-200.	1.4	6
24125	Exploring the effect of oxygen coverage on the electronic, magnetic and chemical properties of Ni(111) supported h -BN sheet: A density functional study. Chemical Physics Letters, 2017, 676, 124-128.	1.2	5
24126	Ideal strength, phonon stability and thermodynamics of the CrB-type CaX IV (X IV Â=ÂSi, Ge, and Sn) binary compounds. Journal of Alloys and Compounds, 2017, 712, 296-302.	2.8	4
24127	BaAu₂S₂: A Au-Based Intrinsic Photocatalyst for High-Performance Visible-Light Photocatalysis. Inorganic Chemistry, 2017, 56, 5173-5181.	1.9	16
24128	6-Mercaptopurine Self-Assembled Monolayers on Gold (001)-Hex: Revealing the Fate of Gold Adatoms. Journal of Physical Chemistry C, 2017, 121, 8938-8943.	1.5	8
24129	Promoted Electrochemical Performance of Î²-MnO₂ through Surface Engineering. ACS Applied Materials & Interfaces, 2017, 9, 15176-15181.	4.0	18
24130	Multiscale structural and electronic control of molybdenum disulfide foam for highly efficient hydrogen production. Nature Communications, 2017, 8, 14430.	5.8	488
24131	A density functional theory study of the influence of exchange-correlation functionals on the properties of FeAs. Journal of Physics Condensed Matter, 2017, 29, 215604.	0.7	5
24132	The influence of N content on structure, phase stability, elastic and electronic properties in Ti₃AlC_{2â^'x}N_x (xâ€‰=â€‰0â€“2). Physica Status Solidi (B): Basic Research, 2017, 254, 1700009.	1.7	10
24133	Novel electronic properties of a new MoS 2 /TiO 2 heterostructure and potential applications in solar cells and photocatalysis. Applied Surface Science, 2017, 414, 34-40.	3.1	36
24134	Probing the dynamics of complexed local anesthetics via neutron scattering spectroscopy and DFT calculations. International Journal of Pharmaceutics, 2017, 524, 397-406.	2.6	14
24135	Effect of Pt addition on resistance to carbon formation of Ni catalysts in methane dehydrogenation over Ni-Pt bimetallic surfaces: A density functional theory study. Molecular Catalysis, 2017, 434, 206-218.	1.0	48

#	Article	IF	Citations
24136	Modeling short-range substitution order and disorder in crystals: Application to the Ga/Si distribution in a natrolite zeolite. Solid State Nuclear Magnetic Resonance, 2017, 84, 182-195.	1.5	10
24137	Magnetic properties of atomic 3d transition-metal chains on S-vacancy-line templates of monolayer MoS2: effects of substrate and strain. Journal of Materials Chemistry C, 2017, 5, 4557-4564.	2.7	20
24138	On the lubricity of transition metal dichalcogenides: an ab initio study. Nanoscale, 2017, 9, 5597-5607.	2.8	32
24139	Magnetic properties and martensitic transformation of Niâ€“Mnâ€“Ge Heusler alloys from first-principles and Monte Carlo studies. Journal Physics D: Applied Physics, 2017, 50, 195001.	1.3	8
24140	Phase stability, Debye temperature and hardness of semiconducting manganese tetraboride MnB₄: First-principles investigations. International Journal of Modern Physics B, 2017, 31, 1750131.	1.0	3
24141	Density Functional study on the transesterification of triacetin assisted by cooperative weak interactions via a gold heterogeneous catalyst: Insights into biodiesel production mechanisms. Fuel, 2017, 202, 98-108.	3.4	11
24142	Pressure-Induced Stable Beryllium Peroxide. Inorganic Chemistry, 2017, 56, 5233-5238.	1.9	17
24143	Microscopic Properties of Mg in Li and Nb Sites of LiNbO₃ by First-Principle Hybrid Functional: Formation and Related Optical Properties. Journal of Physical Chemistry C, 2017, 121, 8968-8975.	1.5	21
24144	Negative differential resistance and bias-modulated metal-to-insulator transition in zigzag C2N-h2D nanoribbon. Scientific Reports, 2017, 7, 43922.	1.6	6
24145	Diffusion Pathways and Activation Energies in Crystalline Lithium-Ion Conductors. Zeitschrift Fur Physikalische Chemie, 2017, 231, 1279-1302.	1.4	9
24146	First-principles calculation of a negatively charged boron-vacancy center in diamond. Japanese Journal of Applied Physics, 2017, 56, 04CK02.	0.8	3
24147	Experimental and ab initio studies of nanostructured Cu2Sb produced by mechanical alloying. Materials Letters, 2017, 199, 110-112.	1.3	5
24148	Charge transport in C₆₀-based single-molecule junctions with graphene electrodes. Nanoscale, 2017, 9, 7217-7226.	2.8	11
24149	Multialloying effect on thermophysical properties of Cr₇C₃â€type carbides. Journal of the American Ceramic Society, 2017, 100, 1588-1597.	1.9	26
24150	Vibrational properties of Î²-KSiH₃and Î²-RbSiH₃: a combined Raman and inelastic neutron scattering study. Journal of Raman Spectroscopy, 2017, 48, 284-291.	1.2	4
24151	Unusual magnetic properties of Auâ€“Mn nanowires on copper and silicon substrates. Physica Status Solidi (B): Basic Research, 2017, 254, 1600850.	0.7	2
24152	Density functional study on the heterogeneous oxidation of NO over Î±-Fe 2 O 3 catalyst by H 2 O 2 : Effect of oxygen vacancy. Applied Surface Science, 2017, 413, 292-301.	3.1	56
24153	Electronic and magnetic properties of pristine and hydrogenated borophene nanoribbons. Physica E: Low-Dimensional Systems and Nanostructures, 2017, 91, 106-112.	1.3	60

#	Article	IF	Citations
24154	Raman and DRIFT spectra, vibrational assignments and quantum mechanical calculations of centrosymmetric meso -2,3-Dimercaptosuccinic acid. Spectrochimica Acta - Part A: Molecular and Biomolecular Spectroscopy, 2017, 183, 275-283.	2.0	7
24155	Bi₄TaO₈Cl Nano-Photocatalyst: Influence of Local, Average, and Band Structure. Inorganic Chemistry, 2017, 56, 5525-5536.	1.9	37
24156	Tunable Schottky Barrier at MoSe₂/Metal Interfaces with a Buffer Layer. Journal of Physical Chemistry C, 2017, 121, 9305-9311.	1.5	45
24157	A Simple Descriptor to Rapidly Screen CO Oxidation Activity on Rare-Earth Metal-Doped CeO2: From Experiment to First-Principles. ACS Applied Materials & Interfaces, 2017, 9, 15449-15458.	4.0	59
24158	Firstâ€principles investigations on elevated temperature elastic and thermodynamic properties of ZrB₂ and HfB₂. Journal of the American Ceramic Society, 2017, 100, 3662-3672.	1.9	22
24159	New Platinum Alloy Catalysts for Oxygen Electroreduction Based on Alkaline Earth Metals. Electrocatalysis, 2017, 8, 594-604.	1.5	23
24160	The first-principles study for the novel optical properties of LiTi 2 O 4 , Li 4 Ti 5 O 12 , Li 2 Ti 2 O 4 and Li 7 Ti 5 O 12. Chemical Physics Letters, 2017, 677, 114-119.	1.2	29
24161	Magnetic and thermoelectric properties of ordered double perovskite Ba 2 FeMoO 6. Journal of Alloys and Compounds, 2017, 714, 704-708.	2.8	53
24162	Mechanochemical synthesis of nanostructured metal nitrides, carbonitrides and carbon nitride: a combined theoretical and experimental study. Physical Chemistry Chemical Physics, 2017, 19, 12414-12424.	1.3	15
24163	The effect of atomic arrangement on photoabsorption of freestanding double-layer honeycomb sheets of zinc selenide. Journal of Materials Chemistry C, 2017, 5, 4505-4510.	2.7	8
24164	Electronic structures of rutile (011)(2 Ã— 1) surfaces: A many-body perturbation theory study. Journal of Chemical Physics, 2017, 146, 124702.	1.2	6
24165	Thermodynamic properties of gold-rare earthÂelements. European Physical Journal: Special Topics, 2017, 226, 1123-1135.	1.2	3
24166	Theoretical and experimental investigation of point defects in cubic boron nitride. MRS Advances, 2017, 2, 1545-1550.	0.5	3
24167	First-Principle Study of Electronic and Half-Metallic Ferromagnetic Properties of Vanadium (V)-Doped Cubic BP and InP. Journal of Superconductivity and Novel Magnetism, 2017, 30, 2855-2864.	0.8	6
24168	Surface Relaxations, Surface Energies and Electronic Structures of BaSnO3 (001) Surfaces: Ab Initio Calculations. Journal of Electronic Materials, 2017, 46, 4133-4139.	1.0	14
24169	Hydrogenated boron nitride monolayer functionalization: A density functional theory study. Computational and Theoretical Chemistry, 2017, 1111, 33-39.	1.1	5
24170	Doping-Concentration-Induced Ferromagnetism and Antiferromagnetism in In₂S₃:Dy³⁺ Quantum Dots. Journal of Physical Chemistry C, 2017, 121, 9648-9654.	1.5	7
24171	Topology and electronic structure of flexible (Nb,Ru)O₂thermoelectrics. Journal of Physics Condensed Matter, 2017, 29, 085701.	0.7	0

#	Article	IF	Citations
24172	The Investigation of Electronic Structure of Transition Metal Doped TiO 2 for Diluted Magnetic Semiconductor Applications: A First Principle Study. Procedia Engineering, 2017, 170, 141-147.	1.2	13
24173	Temperature independent Seebeck coefficient through quantum confinement modulation in amorphous Nb-O/Ni-Ta-O multilayers. Solid State Communications, 2017, 258, 33-37.	0.9	4
24174	State-of-the-Art Calculations of Sublimation Enthalpies for Selected Molecular Crystals and Their Computational Uncertainty. Journal of Chemical Theory and Computation, 2017, 13, 2840-2850.	2.3	48
24175	Yin and Yang Dual Characters of CuO_x Clusters for Câ€“C Bond Oxidation Driven by Visible Light. ACS Catalysis, 2017, 7, 3850-3859.	5.5	103
24176	Electronic and magnetic properties of graphene, silicene and germanene with varying vacancy concentration. AIP Advances, 2017, 7, .	0.6	58
24177	A first-principles study of NbSe₂monolayer as anode materials for rechargeable lithium-ion and sodium-ion batteries. Journal Physics D: Applied Physics, 2017, 50, 235501.	1.3	69
24178	Topological Insulators: Electronic Band Structure and Spectroscopy. IOP Conference Series: Materials Science and Engineering, 2017, 175, 012004.	0.3	5
24179	Effect of oxygen and magnesium vacancies on the d 0 magnetism of C-monodoped MgO using ab initio method. Journal of Alloys and Compounds, 2017, 712, 526-534.	2.8	11
24180	An atomic-scale modeling and experimental study of <mml:math xmlns:mml="http://www.w3.org/1998/Math/MathML" altimg="si0029.gif" overflow="scroll"><mml:mrow><mml:mo stretchy="false">ã€ˆ</mml:mo><mml:mi>c</mml:mi><mml:mo>+</mml:mo><mml:mi>a</mml:mi><mml:mo stretchy="false">ã€‰</mml:mo></mml:mrow></mml:math> dislocations in Mg. Materials Science & Engineering A: Structural Materials: Properties, Microstructure and Processing, 2017, 695, 270-278.	2.6	32
24181	Low thermal conductivity of monolayer ZnO and its anomalous temperature dependence. Physical Chemistry Chemical Physics, 2017, 19, 12882-12889.	1.3	55
24182	Exploring the orthorhombicâ€“tetragonal phase transition in CH3NH3PbI3: the role of atom kinetics. Nanoscale, 2017, 9, 5896-5903.	2.8	22
24183	Passivation effects of phosphorus on 4H-SiC (0001) Si dangling bonds: A first-principles study. Chinese Physics B, 2017, 26, 037104.	0.7	6
24184	From Twoâ€•to Threeâ€Dimensional Structures of a Supertetrahedral Boran Using Density Functional Calculations. Angewandte Chemie, 2017, 129, 10252-10256.	1.6	2
24185	Structural and thermodynamic investigation of the hydration-dehydration process of Na+-Montmorillonite using DFTÂcalculations. Applied Clay Science, 2017, 143, 212-219.	2.6	24
24186	Two-Dimensional Metal-Free Organic Multiferroic Material for Design of Multifunctional Integrated Circuits. Journal of Physical Chemistry Letters, 2017, 8, 1973-1978.	2.1	64
24187	Ab initio investigation of Jahnâ€“Teller-distortion-tuned Li-ion migration in Î»-MnO₂. Journal of Materials Chemistry A, 2017, 5, 9618-9626.	5.2	23
24188	Defect-mediated leakage in lithium intercalated bilayer graphene. AIP Advances, 2017, 7, .	0.6	5
24189	(110) Facet of rutile-structured GeO₂: anab initioinvestigation. Molecular Physics, 2017, 115, 1598-1605.	0.8	4

#	Article	IF	Citations
24190	The electronic band structure of Ge_{1â^'x}Sn_xin the full composition range: indirect, direct, and inverted gaps regimes, band offsets, and the Bursteinâ€“Moss effect. Journal Physics D: Applied Physics, 2017, 50, 195103.	1.3	76
24191	Sb Substitution Effect on Thermoelectric Properties of Mg2Si. Journal of Electronic Materials, 2017, 46, 4682-4689.	1.0	6
24192	Proton conduction across and along BaOâ€“ and ZrO2â€“terminated (001) BaZrO3 surfaces using density functional theory. Solid State Ionics, 2017, 306, 137-141.	1.3	7
24193	Consequences of Surface Oxophilicity of Ni, Ni-Co, and Co Clusters on Methane Activation. Journal of the American Chemical Society, 2017, 139, 6928-6945.	6.6	104
24194	An approximate full-dimensional quantum dynamics study of the mode specificity in the dissociative chemisorption of D₂O on rigid Cu(111). Physical Chemistry Chemical Physics, 2017, 19, 11960-11967.	1.3	9
24195	Theoretical study on the self-assembly of 1,3,5-triethynylbenzene on Si(100)2 Ã— 1 and in situ polymerization via reaction with CO to fabricate a single surface-grafted polymer. Journal of Materials Chemistry C, 2017, 5, 3585-3591.	2.7	6
24196	Nitrogen and fluorine dual-doped porous graphene-nanosheets as efficient metal-free electrocatalysts for hydrogen-evolution in acidic media. Catalysis Science and Technology, 2017, 7, 2228-2235.	2.1	37
24197	Effects of high-k dielectric environment on the full ballistic transport properties of monolayer MoS2 FETs. Journal of Applied Physics, 2017, 121, 144505.	1.1	6
24198	Synthesis, Crystal Structures, and Properties of Zeoliteâ€Like T₃(H₃O)₂[M(CN)₆]₂Â·uH₂O (T = Co, Zn; M = Ru, Os). European Journal of Inorganic Chemistry, 2017, 2017, 2980-2989.	1.0	13
24199	Effects of oxygen vacancy on the mechanical, electronic and optical properties of monoclinic BiVO4. Journal of Materials Science, 2017, 52, 8546-8555.	1.7	32
24200	Activity and electrochemical stability of a chromium modified nickel catalyst for oxygen reduction reaction. Electrochimica Acta, 2017, 236, 260-272.	2.6	10
24201	DFT study of the electronic structure and magnetism of defective graphene decorated with hydrogen-adatom. Physica E: Low-Dimensional Systems and Nanostructures, 2017, 91, 65-71.	1.3	6
24202	Size and strain tunable band alignment of blackâ€“blue phosphorene lateral heterostructures. Physical Chemistry Chemical Physics, 2017, 19, 12466-12472.	1.3	25
24203	Investigating anomalous thermal expansion of copper halides by inelastic neutron scattering and ab initio phonon calculations. Physical Chemistry Chemical Physics, 2017, 19, 12107-12116.	1.3	9
24204	SeO 2 adsorption on CaO surface: DFT study on the adsorption of a single SeO 2 molecule. Applied Surface Science, 2017, 413, 366-371.	3.1	45
24205	Density functional theory calculations on alkali and the alkaline Ca atoms adsorbed on graphene monolayers. Applied Surface Science, 2017, 413, 197-208.	3.1	15
24206	Mechanism of sodium adsorption on N-doped graphene nanoribbons for sodium ion battery applications: A density functional theory approach. Carbon, 2017, 119, 492-501.	5.4	68
24207	Pressure-Driven Isostructural Phase Transition in InNbO₄: In Situ Experimental and Theoretical Investigations. Inorganic Chemistry, 2017, 56, 5420-5430.	1.9	29

#	Article	IF	Citations
24208	First-Principles Study on CO Removing Mechanism on Pt-Decorated Oxygen-Rich Anode Surfaces (Pt2/o-MO2(110), M = Ru and Ir) in DMFC. Journal of Physical Chemistry C, 2017, 121, 9825-9832.	1.5	14
24209	Magnetism in the p-type Monolayer II-VI semiconductors SrS and SrSe. Scientific Reports, 2017, 7, 45869.	1.6	17
24210	A layered wide-gap oxyhalide semiconductor with an infinite ZnO2 square planar sheet: Sr2ZnO2Cl2. Chemical Communications, 2017, 53, 3826-3829.	2.2	13
24211	Insights into the thermoelectric properties of SnSe from ab initio calculations. Physical Chemistry Chemical Physics, 2017, 19, 12804-12815.	1.3	42
24212	Method for determining optimal supercell representation of interfaces. Journal of Physics Condensed Matter, 2017, 29, 185901.	0.7	59
24213	Nuclear quadrupolar spin-lattice relaxation with realistic phonon density of states in alkali halides. Canadian Journal of Physics, 2017, 95, 1042-1048.	0.4	2
24214	The effect of defects on Cu-doped CdS: A first-principles study. Europhysics Letters, 2017, 117, 57007.	0.7	14
24215	Enhanced carbon tolerance on Ni-based reforming catalyst with Ir alloying: A DFT study. Applied Surface Science, 2017, 419, 678-682.	3.1	11
24216	Interpreting radiation-induced segregation and enhanced radiation tolerance of single-phase concentrated solid-solution alloys from first principles. Materials Letters, 2017, 202, 120-122.	1.3	6
24217	Inferring Protonation States of Hydroxamate Adsorbates on TiO₂ Surfaces. Journal of Physical Chemistry C, 2017, 121, 11985-11990.	1.5	5
24218	The role of group III, IV elements in Nb₄AC₃MAX phases (A = Al, Si, Ga, Ge) and the unusual anisotropic behavior of the electronic and optical properties. Physical Chemistry Chemical Physics, 2017, 19, 15471-15483.	1.3	17
24219	A computational study of hydrogen detection by borophene. Journal of Materials Chemistry C, 2017, 5, 5426-5433.	2.7	18
24220	Role of Cr-d states in the electronic and optical properties of the CdCr2X4 (X = S, Se) normal ferromagnetic spinels using PBE+U and TB-mBJ potentials. Journal of Materials Research, 2017, 32, 2431-2437.	1.2	2
24221	Functionalization of Î³-graphyne by transition metal adatoms. Carbon, 2017, 120, 63-70.	5.4	81
24222	Tuning of Interlayer Coupling in Large-Area Graphene/WSe₂ van der Waals Heterostructure via Ion Irradiation: Optical Evidences and Photonic Applications. ACS Photonics, 2017, 4, 1531-1538.	3.2	75
24223	Group-IV (Si, Ge, and Sn)-doped AgAlTe₂for intermediate band solar cell from first-principles study. Semiconductor Science and Technology, 2017, 32, 065007.	1.0	12
24224	Silver cluster supported on nitrogen-doped graphene as an electrocatalyst with high activity and stability for oxygen reduction reaction. International Journal of Hydrogen Energy, 2017, 42, 14522-14533.	3.8	19
24225	Adsorption behavior of SO 2 on vacancy-defected graphene: A DFT study. Journal of Physics and Chemistry of Solids, 2017, 109, 40-45.	1.9	59

#	Article	IF	Citations
24226	Assessing the Performance of Eumelanin/Si Interface for Photovoltaic Applications. Journal of Physical Chemistry C, 2017, 121, 11576-11584.	1.5	15
24227	Bimetallic Nickelâ€Substituted Cobaltâ€Borate Nanowire Array: An Earthâ€Abundant Water Oxidation Electrocatalyst with Superior Activity and Durability at Near Neutral pH. Small, 2017, 13, 1700394.	5.2	95
24228	Crystal structure and mechanical properties of a new ternary phase in Mg-Zn-Y alloy solidified under high pressure. Journal of Alloys and Compounds, 2017, 717, 214-218.	2.8	19
24229	Ionization Energy as a Stability Criterion for Halide Perovskites. Journal of Physical Chemistry C, 2017, 121, 11977-11984.	1.5	42
24230	Anisotropic thermal expansion of SnSe from first-principles calculations based on GrÃ¼neisen's theory. Physical Chemistry Chemical Physics, 2017, 19, 15187-15193.	1.3	35
24231	Metal-free spin and spin-gapless semiconducting heterobilayers: monolayer boron carbonitrides on hexagonal boron nitride. Physical Chemistry Chemical Physics, 2017, 19, 14801-14810.	1.3	6
24233	Computational exploration of the structure, stability and adsorption properties of the ZIF-9 metal-organic framework. Microporous and Mesoporous Materials, 2017, 254, 170-177.	2.2	8
24234	Negative differential resistance in polymer tunnel diodes using atomic layer deposited, TiO2 tunneling barriers at various deposition temperatures. Organic Electronics, 2017, 47, 228-234.	1.4	7
24235	A first-principles high-pressure study of Hf 2 PX (X=B, C, N). Solid State Communications, 2017, 259, 45-49.	0.9	0
24236	Lattice and Valence Electronic Structures of Crystalline Octahedral Molybdenum Halide Clusters-Based Compounds, Cs₂[Mo₆X₁₄] (X = Cl, Br, I), Studied by Density Functional Theory Calculations. Inorganic Chemistry, 2017, 56, 6234-6243.	1.9	16
24237	Computational mining of photocatalysts for water splitting hydrogen production: two-dimensional InSe-family monolayers. Catalysis Science and Technology, 2017, 7, 2744-2752.	2.1	123
24238	One-step fabrication of CdS:Moâ€“CdMoO4coreâ€“shell nanoribbons for nonvolatile memory devices with high resistance switching. Journal of Materials Chemistry C, 2017, 5, 6156-6162.	2.7	8
24239	Experimental and computational study of the magnetic properties of ZrMn2â^'xCoxGe4O12. Dalton Transactions, 2017, 46, 6921-6933.	1.6	7
24240	Effect of an external electric field on the electronic properties of SnS₂/PbI₂ van der Waals heterostructures. RSC Advances, 2017, 7, 25582-25588.	1.7	20
24241	A Model for Estimating Chemical Potentials in Ternary Semiconductor Compounds: the Case of InGaAs. MRS Advances, 2017, 2, 2909-2914.	0.5	3
24242	Density Functional Theory Evaluated for Structural and Electronic Properties of 1T-Li_xTiS₂ and Lithium Ion Migration in 1T-Li_{0.94}TiS₂. Zeitschrift Fur Physikalische Chemie, 2017, 231, 1263-1278.	1.4	4
24243	Electronic, elastic, lattice dynamic and thermal conductivity properties of Na₃OBr via first principles. Physica Status Solidi (B): Basic Research, 2017, 254, 1700089.	0.7	15
24244	Structural, electronic and magnetic properties of the MnGa(111)-1 Ã— 2 and 2 Ã— 2 reconstructions: Spin polarized first principles total energy calculations. Applied Surface Science, 2017, 419, 286-293.	3.1	3

#	Article	IF	Citations
24245	Exploration of thermoelectricity in ScRhTe and ZrPtPb Half Heusler compounds: A first principle study. Journal of Alloys and Compounds, 2017, 715, 297-303.	2.8	14
24246	Mechanism of CO₂ Reforming of CH₄ on a Pt₄/ZrO₂(101) Surface: A Density Functional Theory Study. Journal of Physical Chemistry B, 2017, 121, 5238-5246.	1.2	9
24247	A comprehensive understanding of water photooxidation on Ag₃PO₄ surfaces. RSC Advances, 2017, 7, 23994-24003.	1.7	13
24248	Superhard three-dimensional B3N4 with two-dimensional metallicity. Journal of Materials Chemistry C, 2017, 5, 5897-5901.	2.7	16
24249	Adsorption of methylene blue and its N-demethylated derivatives on the (111) face of coinage metals: The importance of dispersion interactions. Journal of Chemical Physics, 2017, 146, 164701.	1.2	17
24250	Density Functional Theory Calculations of Atomic Configurations and Bandgaps of C-, Ge-, and Sn-Doped Si Crystals for Solar Cells. ECS Journal of Solid State Science and Technology, 2017, 6, P326-P331.	0.9	1
24251	Novel Hybrid Catalyst for the Oxidation of Organic Acids: Pd Nanoparticles Supported on Mnâ€Nâ€3Dâ€Graphene Nanosheets. ChemElectroChem, 2017, 4, 2336-2344.	1.7	5
24252	Effect of transition metal Fe adsorption on CeO 2 (110) surface in the methane activation and oxygen vacancy formation: A density functional theory study. Applied Surface Science, 2017, 416, 547-564.	3.1	41
24253	Neutron diffraction study of superconductingLa3Ni2B112N3â˜Î´. Journal of Alloys and Compounds, 2017, 716, 251-258.	2.8	0
24254	Fabrication and characterizations of nitrogen-doped BaSi2 epitaxial films grown by molecular beam epitaxy. Journal of Crystal Growth, 2017, 471, 37-41.	0.7	0
24255	Electronic properties and gas adsorption behaviour of pristine, silicon-, and boron-doped (8, 0) single-walled carbon nanotube: A first principles study. Journal of Molecular Graphics and Modelling, 2017, 75, 85-93.	1.3	45
24256	First-Principles Investigation of Adsorbateâ€“Adsorbate Interactions on Ni(111), Ni(211), and Ni(100) Surfaces. Industrial & Engineering Chemistry Research, 2017, 56, 5813-5820.	1.8	22
24257	Exploring Systematic Discrepancies in DFT Calculations of Chlorine Nuclear Quadrupole Couplings. Journal of Physical Chemistry A, 2017, 121, 4103-4113.	1.1	19
24258	Effect of Transition Metal Cations on Stability Enhancement for Molybdate-Based Hybrid Supercapacitor. ACS Applied Materials & Interfaces, 2017, 9, 17977-17991.	4.0	82
24259	Nanotubular Gamma Alumina with High-Energy External Surfaces: Synthesis and High Performance for Catalysis. ACS Catalysis, 2017, 7, 4083-4092.	5.5	41
24260	Self-assembly of glycine on Cu(001): the effect of temperature and polarity. RSC Advances, 2017, 7, 4116-4123.	1.7	3
24261	In Situ Phaseâ€Induced Spatial Charge Separation in Coreâ€“Shell Oxynitride Nanocube Heterojunctions Realizing Robust Solar Water Splitting. Advanced Energy Materials, 2017, 7, 1700171.	10.2	39
24263	A hybrid organic-inorganic perovskite dataset. Scientific Data, 2017, 4, 170057.	2.4	112

#	Article	IF	Citations
24264	The preparation, and structural and multiferroic properties of B-site ordered double-perovskite Bi₂FeMnO₆. Journal of Materials Chemistry C, 2017, 5, 5494-5500.	2.7	28
24265	Anisotropic features in the electronic structure of the two-dimensional transition metal trichalcogenide TiS ₃ : electron doping and plasmons. 2D Materials, 2017, 4, 025085.	2.0	24
24266	Strained rocksalt ScN:ab initiostudies of electronic structure and lattice-dynamical properties. Materials Research Express, 2017, 4, 055001.	0.8	2
24267	<scp>DFT</scp> Analysis of the Adsorption of Methyl Nitrate on <scp>Al₂O₃</scp> Surfaces. Bulletin of the Korean Chemical Society, 2017, 38, 625-631.	1.0	4
24268	Promotion of CO oxidation on the Fe/N X clusters embedded graphene. Applied Physics A: Materials Science and Processing, 2017, 123, 1.	1.1	5
24269	Electronic properties modifications of single-wall boron nitride with lithium atom intercalation. Journal of Molecular Modeling, 2017, 23, 175.	0.8	0
24270	Pressure effect on elastic and lattice dynamic properties of beryllium selenide from first principles. Journal Wuhan University of Technology, Materials Science Edition, 2017, 32, 378-381.	0.4	0
24271	First-principles study of transformation strains and phase stabilities in Î±â€³ and Î² Ti-Nb-X alloys. Journal of Alloys and Compounds, 2017, 716, 37-45.	2.8	12
24272	Enhanced atomic oxygen adsorption on defective nickel surfaces: An ab initio study. Surface Science, 2017, 663, 62-70.	0.8	5
24273	Surface-Engineering of Ultrathin Gold Nanowires: Tailored Self-Assembly and Enhanced Stability. Langmuir, 2017, 33, 5456-5463.	1.6	22
24274	Elucidating the Properties of Grapheneâ€“Deep Eutectic Solvents Interface. Langmuir, 2017, 33, 5154-5165.	1.6	42
24275	Understanding the Thermal Stability of Palladiumâ€“Platinum Coreâ€“Shell Nanocrystals by In Situ Transmission Electron Microscopy and Density Functional Theory. ACS Nano, 2017, 11, 4571-4581.	7.3	53
24276	Novel magnetic properties of CoTe nanorods and diversified CoTe₂ nanostructures obtained at different NaOH concentrations. Science and Technology of Advanced Materials, 2017, 18, 325-333.	2.8	29
24277	The electronic, optical, and thermodynamical properties of tetragonal, monoclinic, and orthorhombic M 3 N 4 (M = Si, Ge, Sn): A first-principles study. Chinese Physics B, 2017, 26, 046303.	0.7	1
24278	Noncovalent Interactions between Dopamine and Regular and Defective Graphene. ChemPhysChem, 2017, 18, 2065-2080.	1.0	27
24279	First principles modeling of 3d-metal doped three-layer fluorite-structured TiO2 (4,4) nanotube to be used for photocatalytic hydrogen production. Vacuum, 2017, 146, 562-569.	1.6	13
24280	Role of Local Carbon Structure Surrounding FeN₄ Sites in Boosting the Catalytic Activity for Oxygen Reduction. Journal of Physical Chemistry C, 2017, 121, 11319-11324.	1.5	150
24281	Engineering Pt/Pd Interfacial Electronic Structures for Highly Efficient Hydrogen Evolution and Alcohol Oxidation. ACS Applied Materials & Interfaces, 2017, 9, 18008-18014.	4.0	111

#	Article	IF	Citations
24282	Epitaxial growth and intrinsic nature of molybdenum disulfide on graphite. Applied Physics Express, 2017, 10, 055201.	1.1	3
24283	Experimental investigation and DFT calculation of different amine/ammonium salts adsorption on kaolinite. Applied Surface Science, 2017, 419, 241-251.	3.1	54
24284	Insights into the metal-support interaction between NiCu cluster and MgO as well as its effect on H adsorption and H2 dissociation. Molecular Catalysis, 2017, 436, 111-119.	1.0	5
24285	Adsorption and Decomposition of a Lignin Î²-O-4 Linkage Model, 2-Phenoxyethanol, on Pt(111): Combination of Experiments and First-Principles Calculations. Journal of Physical Chemistry C, 2017, 121, 9889-9900.	1.5	16
24286	Atomic motions in the layered copper pseudochalcogenide CuNCN indicative of a quantum spin-liquid scenario. Journal of Physics Condensed Matter, 2017, 29, 235701.	0.7	5
24287	A density functional theory based elementary reaction mechanism for early steps of Fischer-Tropsch synthesis over cobalt catalyst. 1. Reaction kinetics. Molecular Catalysis, 2017, 436, 218-227.	1.0	9
24288	A density functional theory based elementary reaction mechanism for early steps of Fischer-Tropsch synthesis over cobalt catalyst. 2. Microkinetic modeling of liquid-phase vs. gaseous-phase process. Molecular Catalysis, 2017, 436, 210-217.	1.0	6
24289	Adsorption Study of a Water Molecule on Vacancy-Defected Nonpolar CdS Surfaces. Journal of Physical Chemistry C, 2017, 121, 9815-9824.	1.5	8
24290	Lattice Defects and the Mechanical Anisotropy of Borophene. Journal of Physical Chemistry C, 2017, 121, 10224-10232.	1.5	112
24291	Purely one-dimensional bands with a giant spin-orbit splitting: Pb nanoribbons on Si(553) surface. Scientific Reports, 2017, 7, 46215.	1.6	26
24292	Structural stability and intriguing electronic properties of two-dimensional transition metal dichalcogenide alloys. Physical Chemistry Chemical Physics, 2017, 19, 13846-13854.	1.3	46
24293	Atomic structure and formation mechanism of sub-nanometer pores in 2D monolayer MoS₂. Nanoscale, 2017, 9, 6417-6426.	2.8	54
24294	Layer-dependent electronic properties of phosphorene-like materials and phosphorene-based van der Waals heterostructures. Nanoscale, 2017, 9, 8616-8622.	2.8	44
24295	The dynamics of benzene on Cu(111): a combined helium spin echo and dispersion-corrected DFT study into the diffusion of physisorbed aromatics on metal surfaces. Faraday Discussions, 2017, 204, 471-485.	1.6	11
24296	New hexagonal boron nitride polytypes with triple-layer periodicity. Journal of Applied Physics, 2017, 121, .	1.1	13
24297	Pressure-induced boron nitride nanotube derivatives: 3D metastable allotropes. Journal of Applied Physics, 2017, 121, .	1.1	25
24298	Tunable Schottky barrier in van der Waals heterostructures of graphene and g-GaN. Applied Physics Letters, 2017, 110, .	1.5	166
24299	Stability of bound species during alkene reactions on solid acids. Proceedings of the National Academy of Sciences of the United States of America, 2017, 114, E3900-E3908.	3.3	52

#	Article	IF	Citations
24300	Multiscale Simulation of Î±-Mg Dendrite Growth via 3D Phase Field Modeling and Ab Initio First Principle Calculations. Minerals, Metals and Materials Series, 2017, , 263-272.	0.3	2
24301	First-Principle Investigation of V and Cr Doping on the Dilute Magnetic Semiconducting Properties of Rutile SnO2: a Modified Becke-Johnson (TB-mBJ) Exchange Potential Study. Journal of Superconductivity and Novel Magnetism, 2017, 30, 3415-3422.	0.8	1
24302	Engineering a tubular mesoporous silica nanocontainer with well-preserved clay shell from natural halloysite. Nano Research, 2017, 10, 2782-2799.	5.8	71
24303	Effect of surface termination on ion intercalation selectivity of bilayer Ti 3 C 2 T 2 (T = F, O and OH) MXene. Applied Surface Science, 2017, 416, 725-730.	3.1	81
24304	High-quality PVD graphene growth by fullerene decomposition on Cu foils. Carbon, 2017, 119, 535-543.	5.4	29
24305	Trapping and diffusion of organic dyes inside of palygorskite clay: The ancient Maya Blue pigment. Microporous and Mesoporous Materials, 2017, 249, 111-117.	2.2	26
24306	Influence of trivalent doping on point and Frenkel defect formation in bulk chromium (III) oxide. Solid State Ionics, 2017, 307, 51-64.	1.3	7
24307	Effect of Water on the CO₂ Adsorption Capacity of Amine-Functionalized Carbon Sorbents. Industrial & Engineering Chemistry Research, 2017, 56, 6317-6325.	1.8	18
24308	Study of NaFâ€“AlF₃ Melts by Coupling Molecular Dynamics, Density Functional Theory, and NMR Measurements. Journal of Physical Chemistry C, 2017, 121, 10289-10297.	1.5	29
24309	Prediction on the light-assisted exfoliation of multilayered arsenene by the photo-isomerization of azobenzene. Nanoscale, 2017, 9, 7006-7011.	2.8	40
24310	Tunable electronic properties of monolayer silicane via fluorine doping: a first-principles study. Journal of Physics Condensed Matter, 2017, 29, 265501.	0.7	0
24311	Tunable structural and electrical properties of zigzag CdS nanotubes: A density functional study. Physica Status Solidi (B): Basic Research, 2017, 254, 1700038.	0.7	5
24312	A DFT study of ethane activation on IrO 2 (110) surface by precursor-mediated mechanism. Applied Catalysis A: General, 2017, 541, 8-14.	2.2	21
24313	Study of the elastic properties and wave velocities of rocksalt Mg1â^'xFexO: ab initio calculations. Chinese Journal of Physics, 2017, 55, 1423-1431.	2.0	14
24314	Morphology and location manipulation of Fe nanoparticles on carbon nanofibers as catalysts for ammonia decomposition to generate hydrogen. International Journal of Hydrogen Energy, 2017, 42, 17466-17475.	3.8	20
24315	Ni-doped SrBi2Nb2O9 â€“ Perovskite oxides with reduced band gap and stable ferroelectricity for photovoltaic applications. Journal of Alloys and Compounds, 2017, 724, 1093-1100.	2.8	25
24316	Polytypism-induced stabilization of hexagonal 2H, 4H and 6H phases of gold. Superlattices and Microstructures, 2017, 109, 170-175.	1.4	14
24317	Low-temperature Synthesis of Heterostructures of Transition Metal Dichalcogenide Alloys (W_xMo_{1â€“x}S₂) and Graphene with Superior Catalytic Performance for Hydrogen Evolution. ACS Nano, 2017, 11, 5103-5112.	7.3	157

#	Article	IF	Citations
24318	Investigating Sodium Storage Mechanisms in Tin Anodes: A Combined Pair Distribution Function Analysis, Density Functional Theory, and Solid-State NMR Approach. Journal of the American Chemical Society, 2017, 139, 7273-7286.	6.6	121
24319	Surfaces and morphologies of covellite (CuS) nanoparticles by means of ab initio atomistic thermodynamics. CrystEngComm, 2017, 19, 3078-3084.	1.3	38
24320	Lattice dynamics of the tin sulphides SnS₂, SnS and Sn₂S₃: vibrational spectra and thermal transport. Physical Chemistry Chemical Physics, 2017, 19, 12452-12465.	1.3	187
24321	A direct four-electron process on Feâ€“N₃ doped graphene for the oxygen reduction reaction: a theoretical perspective. RSC Advances, 2017, 7, 23812-23819.	1.7	33
24322	Thermal mismatch strain induced disorder of Y₂Mo₃O₁₂ and its effect on thermal expansion of Y₂Mo₃O₁₂/Al composites. Physical Chemistry Chemical Physics, 2017, 19, 11778-11785.	1.3	16
24323	Unexpected coordination number and phase diagram of niobium diselenide under compression. Physical Chemistry Chemical Physics, 2017, 19, 13219-13229.	1.3	9
24324	Theoretical study on in situ synthesis of Pt/Ni Al hydroxide composites by etching of Pt Ni nanoparticles. Chemical Physics Letters, 2017, 679, 200-206.	1.2	3
24325	Intrinsic Origin of Superior Catalytic Properties of Tungsten-based Catalysts in Dye-sensitized Solar Cells. Electrochimica Acta, 2017, 242, 390-399.	2.6	73
24326	Half metallicity in bare BC 2 N nanoribbons with zigzag edges. Physics Letters, Section A: General, Atomic and Solid State Physics, 2017, 381, 1820-1824.	0.9	3
24327	Computational Design of Ni-Zn Based Catalyst for Direct Hydrazine Fuel Cell Catalyst Using Density Functional Theory. Procedia Engineering, 2017, 170, 148-153.	1.2	10
24328	Vibrational spectroscopic and computational studies on diisopropylammonium bromide. Spectrochimica Acta - Part A: Molecular and Biomolecular Spectroscopy, 2017, 184, 211-219.	2.0	9
24329	Fast Prediction of CO Binding Energy via the Local Structure Effect on PtCu Alloy Surfaces. Langmuir, 2017, 33, 8700-8706.	1.6	24
24330	Effects of the capping ligands, linkers and oxide surface on the electron injection mechanism of copper sulfide quantum dot-sensitized solar cells. Physical Chemistry Chemical Physics, 2017, 19, 14580-14587.	1.3	12
24331	Single- and few-layer BiOI as promising photocatalysts for solar water splitting. RSC Advances, 2017, 7, 24446-24452.	1.7	59
24332	Dynamics of carbon monoxide dissociation on Co(112Ì„0). Physical Chemistry Chemical Physics, 2017, 19, 12826-12837.	1.3	9
24333	Phosphorus Nanostripe Arrays on Cu(110): A Case Study to Understand the Substrate Effect on the Phosphorus thin Film Growth. Advanced Materials Interfaces, 2017, 4, 1601167.	1.9	18
24334	Selfâ€Standing CoP Nanosheets Array: A Threeâ€Dimensional Bifunctional Catalyst Electrode for Overall Water Splitting in both Neutral and Alkaline Media. ChemElectroChem, 2017, 4, 1840-1845.	1.7	345
24335	Combined high-pressure and high-temperature vibrational studies of dolomite: phase diagram and evidence of a new distorted modification. Physics and Chemistry of Minerals, 2017, 44, 465-476.	0.3	26

#	Article	IF	Citations
24336	First-principles study of Pd-skin/Pd3Fe(111) electrocatalyst for oxygen reduction reaction. Journal of Applied Electrochemistry, 2017, 47, 747-754.	1.5	8
24337	Experimental and theoretical DFT+ D investigations regarding to various morphology of cuprous oxide nanoparticles: Growth mechanism of ionic liquid-assisted synthesis and photocatalytic activities. Chemical Engineering Journal, 2017, 324, 347-357.	6.6	31
24338	Strengthening mechanism of Ï‰-Zr. Computational Materials Science, 2017, 135, 134-140.	1.4	5
24339	Ab initio calculations of structural and magnetic properties of Ni-Co-Mn-Cr-Sn supercell. Intermetallics, 2017, 87, 55-60.	1.8	11
24340	DFT/PBE0 study on structural, electronic and dielectric properties of SnZr 0.50 Ti 0.50 O 3 lead-free ferroelectric material. Journal of Alloys and Compounds, 2017, 714, 553-559.	2.8	24
24341	Tailoring electronic structure of Î± -AlH 3 to enhance spin polarization: Insights from density functional calculations. Journal of Physics and Chemistry of Solids, 2017, 108, 9-14.	1.9	2
24342	Structural, phononic and electronic properties of Ge-doped Î³-graphynes: A first-principles study. Solid State Communications, 2017, 258, 38-44.	0.9	11
24343	H2O and CO coadsorption on Co (0001): The effect of intermolecular hydrogen bond. Surface Science, 2017, 663, 56-61.	0.8	9
24344	Li⁺ Defects in a Solid-State Li Ion Battery: Theoretical Insights with a Li₃OCl Electrolyte. Chemistry of Materials, 2017, 29, 4330-4340.	3.2	80
24345	Room-Temperature Ferromagnetism in Two-Dimensional Fe₂Si Nanosheet with Enhanced Spin-Polarization Ratio. Nano Letters, 2017, 17, 2771-2777.	4.5	200
24346	Borophane as a Benchmate of Graphene: A Potential 2D Material for Anode of Li and Na-Ion Batteries. ACS Applied Materials & Interfaces, 2017, 9, 16148-16158.	4.0	142
24347	Two-dimensional Mo1.33C MXene with divacancy ordering prepared from parent 3D laminate with in-plane chemical ordering. Nature Communications, 2017, 8, 14949.	5.8	525
24348	Tuning the electronic properties of monolayer and bilayer transition metal dichalcogenide compounds under direct out-of-plane compression. Physical Chemistry Chemical Physics, 2017, 19, 13333-13340.	1.3	20
24349	DFT-D3 study of H₂ and N₂ chemisorption over cobalt promoted Ta₃N₅-(100), (010) and (001) surfaces. Physical Chemistry Chemical Physics, 2017, 19, 11968-11974.	1.3	22
24350	Improved catalysts for hydrogen evolution reaction in alkaline solutions through the electrochemical formation of nickel-reduced graphene oxide interface. Physical Chemistry Chemical Physics, 2017, 19, 13281-13293.	1.3	45
24351	Magnetic structure and properties of centrosymmetric twisted-melilite K2CoP2O7. Dalton Transactions, 2017, 46, 6409-6416.	1.6	10
24352	Graphene-based CO₂ sensing and its cross-sensitivity with humidity. RSC Advances, 2017, 7, 22329-22339.	1.7	68
24353	Design of efficient mono-aminosilane precursors for atomic layer deposition of SiO₂ thin films. RSC Advances, 2017, 7, 22672-22678.	1.7	16

#	Article	IF	Citations
24354	Tunable bending stiffness of MoSe2/WSe2 heterobilayers from flexural wrinkling. Nanotechnology, 2017, 28, 195701.	1.3	8
24355	Mechanical and thermodynamic properties of intermetallic compounds in the Niâ€“Ti system. International Journal of Modern Physics B, 2017, 31, 1750161.	1.0	23
24356	Ab Initio Study of Structural and Electronic Properties of (ZnO) n â€œMagicalâ€•Nanoclusters nâ€‰=â€‰(34, 60). Nanoscale Research Letters, 2017, 12, 76.	3.1	19
24357	Enhanced Electrocatalysis for Energyâ€Efficient Hydrogen Production over CoP Catalyst with Nonelectroactive Zn as a Promoter. Advanced Energy Materials, 2017, 7, 1700020.	10.2	519
24358	An ab initio and experimental studies of the structure, mechanical parameters and state density on the refractory high-entropy alloy systems. Journal of Alloys and Compounds, 2017, 714, 668-680.	2.8	58
24359	A First Principle Study of the Electronic Structures of Transition Metal Doped GaN for Diluted Magnetic Semiconductor Applications. Procedia Engineering, 2017, 170, 124-130.	1.2	9
24360	First-principles calculations of electronic and optical properties of aluminum-doped Î²-Ga2O3 with intrinsic defects. Results in Physics, 2017, 7, 1582-1589.	2.0	76
24361	DFT-Based Comparative Study about the Influence of Fluorine and Hydroxyl Anions on Opto-Electric Properties of Borate Crystals: Choice for Better Anion. Inorganic Chemistry, 2017, 56, 5636-5645.	1.9	9
24362	A type-II GeSe/SnS heterobilayer with a suitable direct gap, superior optical absorption and broad spectrum for photovoltaic applications. Journal of Materials Chemistry A, 2017, 5, 13400-13410.	5.2	138
24363	Characteristics and transport mechanisms of triple switching regimes of TaOx memristor. Applied Physics Letters, 2017, 110, .	1.5	35
24364	Synthesis and physical properties of (Zr_{1â^'x},Ti_x)₃AlC₂<scp>MAX</scp> phases. Journal of the American Ceramic Society, 2017, 100, 3393-3401.	1.9	63
24365	A Novel Polymerization of Nitrogen in Beryllium Tetranitride at High Pressure. Journal of Physical Chemistry C, 2017, 121, 9766-9772.	1.5	67
24366	Exploration of crystal structures and phase transitions in Hf3N4. CrystEngComm, 2017, 19, 2608-2613.	1.3	5
24367	Interatomic potential to study plastic deformation in tungsten-rhenium alloys. Journal of Applied Physics, 2017, 121, .	1.1	38
24368	Hydrostatic Pressure Effect on Ga0.75Cr0.25As DMS: DFT Study. Journal of Superconductivity and Novel Magnetism, 2017, 30, 3079-3084.	0.8	2
24369	The effect of Nb on the corrosion and hydrogen pick-up of Zr alloys. Acta Materialia, 2017, 132, 425-431.	3.8	40
24370	Optical properties calculations of the phosphorene-CrO 3 system within the G 0 W 0 and BSE approximations. Applied Surface Science, 2017, 416, 266-272.	3.1	4
24372	Experimental and theoretical study of the structural, mechanical and electronic properties of the Fe y N (y=â€‰1, 2, 3, 4) phases. Chinese Journal of Physics, 2017, 55, 674-682.	2.0	2

#	Article	IF	Citations
24373	Towards a metal-semiconductor transition in two dimensions. Chemical Physics Letters, 2017, 679, 127-131.	1.2	4
24374	Structure, Stability, and (Non)Reactivity of the Low-Index Surfaces of Crystalline B₂O₃â€"I. Journal of Physical Chemistry C, 2017, 121, 11346-11354.	1.5	10
24375	Ground-State Structure of YN₂ Monolayer Identified by Global Search. Journal of Physical Chemistry C, 2017, 121, 10258-10264.	1.5	38
24376	Potassium adsorption behavior on hcp cobalt as model systems for the Fischerâ€"Tropsch synthesis: a density functional theory study. Physical Chemistry Chemical Physics, 2017, 19, 12246-12254.	1.3	13
24377	Reduction and oxidation of Au adatoms on the CeO₂(111) surface â€" DFT+U versus hybrid functionals. Physical Chemistry Chemical Physics, 2017, 19, 12546-12558.	1.3	12
24378	HCl dissociating on a rigid Au(111) surface: A six-dimensional quantum mechanical study on a new potential energy surface based on the RPBE functional. Journal of Chemical Physics, 2017, 146, 164706.	1.2	20
24379	Hardness and compression behavior of niobium carbide. High Pressure Research, 2017, 37, 244-255.	0.4	8
24380	Physical properties of the body-centred tetragonal. Philosophical Magazine, 2017, 97, 1866-1883.	0.7	9
24381	The application of tailor-made force fields and molecular dynamics for NMR crystallography: a case study of free base cocaine. IUCrJ, 2017, 4, 175-184.	1.0	10
24382	A first-principles study of structural and mechanical properties of Ti3AlCxN1-x alloys. European Physical Journal Plus, 2017, 132, 1.	1.2	5
24383	First Principles Modeling of Cathodic Reaction Thermodynamics in Dilute Magnesium Alloys. Corrosion, 2017, 73, 506-517.	0.5	27
24384	Steric and chemical effects on the hydrogen adsorption and dissociation on free and grapheneâ€"supported palladium clusters. Computational and Theoretical Chemistry, 2017, 1107, 23-29.	1.1	25
24385	The origin of negative stacking fault energies and nano-twin formation in face-centered cubic high entropy alloys. Scripta Materialia, 2017, 130, 96-99.	2.6	223
24386	Intrinsic half metallicity in lithium terminated zigzag graphene nanoribbons. Solid State Communications, 2017, 250, 112-118.	0.9	5
24387	Diamondâ€™s third-order elastic constants: ab initio calculations and experimental investigation. Journal of Materials Science, 2017, 52, 3447-3456.	1.7	16
24388	Theoretical studies of optical properties of Cu doped rocksalt CdS. Journal of Alloys and Compounds, 2017, 695, 3605-3611.	2.8	25
24389	ThCr2Si2-type Ru-based superconductors LaRu2M2 (MÂ=ÂP and As): An ab-initio investigation. Journal of Alloys and Compounds, 2017, 695, 2827-2834.	2.8	27
24390	Effect of twin boundary on crack propagation behavior in magnesium binary alloys; Experimental and calculation studies. Scripta Materialia, 2017, 130, 114-118.	2.6	28

#	Article	IF	Citations
24391	Modelling the electronic structure of orthorhombic LaMnO3. Solid State Ionics, 2017, 299, 13-17.	1.3	23
24392	Electronic and optical properties of pentagonal-B₂C monolayer: A first-principles calculation. International Journal of Modern Physics B, 2017, 31, 1750044.	1.0	32
24393	Structural, elastic and electronic properties of C14-type Al2M (M=Mg, Ca, Sr and Ba) Laves phases. Physica B: Condensed Matter, 2017, 507, 147-155.	1.3	41
24394	Facet Effect of Single-Crystalline Pd Nanocrystals for Aerobic Oxidation of 5-Hydroxymethyl-2-furfural. ACS Catalysis, 2017, 7, 421-432.	5.5	85
24395	Straintronics in two-dimensional in-plane heterostructures of transition-metal dichalcogenides. Physical Chemistry Chemical Physics, 2017, 19, 663-672.	1.3	56
24396	Ba_{n+2}Zn_n(BO₃)_n(B₂O₅)F_n(n) Tj ETQq1 1 0 Inorganic Chemistry Frontiers, 2017, 4, 281-288.	3.0	29
24397	An ab-initio calculation of half-metallic ferromagnetism in vanadium doped ZnS. Journal of Alloys and Compounds, 2017, 695, 3131-3138.	2.8	13
24398	Method Dependence of Proline Ring Flexibility in the Poly-<scp>l</scp>-Proline Type II Polymer. Journal of Chemical Theory and Computation, 2017, 13, 370-379.	2.3	16
24399	The mechanism of H₂ and H₂O desorption from bridging hydroxyls of a TiO₂(110) surface. Catalysis Science and Technology, 2017, 7, 251-264.	2.1	13
24400	First-principles study on codoping effect to enhance photocatalytic activity of anatase TiO₂. International Journal of Modern Physics B, 2017, 31, 1750036.	1.0	3
24401	Ammonothermal Synthesis of Novel Nitrides: Case Study on CaGaSiN₃. Chemistry - A European Journal, 2017, 23, 2583-2590.	1.7	42
24402	High-pressure phase behavior of SrCO3: an experimental and computational Raman scattering study. Physics and Chemistry of Minerals, 2017, 44, 335-343.	0.3	21
24403	Two-dimensional nitrogen-rich transition metal compounds: The case of TiN 2. Journal of Electron Spectroscopy and Related Phenomena, 2017, 219, 29-34.	0.8	3
24404	Oxygen vacancies enhance pseudocapacitive charge storage properties of MoO3â^'x. Nature Materials, 2017, 16, 454-460.	13.3	1,632
24405	Hydrogen divacancy diffusion: a new perspective on H migration in MgH₂ materials for energy storage. Physical Chemistry Chemical Physics, 2017, 19, 1174-1180.	1.3	6
24406	Trapping of gaseous pollutants on defective N-doped graphene. Physical Chemistry Chemical Physics, 2017, 19, 636-643.	1.3	10
24407	Water-Gas Shift Activity of Atomically Dispersed Cationic Platinum versus Metallic Platinum Clusters on Titania Supports. ACS Catalysis, 2017, 7, 301-309.	5.5	78
24408	Structural, mechanical, dynamical and electronic properties and high-pressure behavior of Mo2GeC: A first-principles study. Computational Materials Science, 2017, 137, 306-313.	1.4	7

#	Article	IF	Citations
24409	Quantification and modeling of nanomechanical properties of chlorpropamide Î±, Î², and Î³ conformational polymorphs. European Journal of Pharmaceutical Sciences, 2017, 110, 109-116.	1.9	9
24410	Synthesis, crystal structure, optical property and theoretical studies of a noncentrosymmetric telluromolybdate CoTeMoO6. Journal of Alloys and Compounds, 2017, 722, 381-386.	2.8	5
24411	Band gap engineering and visible light response for GaS monolayer by isovalent anion-cation codoping. Materials Chemistry and Physics, 2017, 198, 275-282.	2.0	19
24412	First-Principles Prediction of a Stable Hexagonal Phase of CH₃NH₃PbI₃. Chemistry of Materials, 2017, 29, 6003-6011.	3.2	62
24413	Anchoring Small Au Clusters on the Dehydroxylated and Hydroxylated SiO2 Î±-Quartz (001) Surface via Ti-Alloying. Journal of Physical Chemistry C, 2017, 121, 14717-14724.	1.5	9
24414	Intrinsically low thermal conductivity from a quasi-one-dimensional crystal structure and enhanced electrical conductivity network via Pb doping in SbCrSe3. NPG Asia Materials, 2017, 9, e387-e387.	3.8	37
24415	Surface lattice dynamics and electronâ€“phonon interaction in cesium ultra-thin films. Physical Chemistry Chemical Physics, 2017, 19, 16358-16364.	1.3	10
24416	CO adsorption, oxidation and carbonate formation mechanisms on Fe₃O₄ surfaces. Physical Chemistry Chemical Physics, 2017, 19, 17287-17299.	1.3	34
24417	Theoretical insights into the effect of terrace width and step edge coverage on CO adsorption and dissociation over stepped Ni surfaces. Physical Chemistry Chemical Physics, 2017, 19, 17918-17927.	1.3	6
24418	Impact of air exposure and surface chemistry on Liâ€“Li₇La₃Zr₂O₁₂ interfacial resistance. Journal of Materials Chemistry A, 2017, 5, 13475-13487.	5.2	300
24419	Effect of Cr addition on Î³â€“Î³â€² cobalt-based Coâ€“Moâ€“Alâ€“Ta class of superalloys: a combined experimental and computational study. Journal of Materials Science, 2017, 52, 11036-11047.	1.7	61
24420	Elastic and thermodynamic properties of new (Zr3âˆ’Ti)AlC2 MAX-phase solid solutions. Computational Materials Science, 2017, 137, 318-326.	1.4	119
24421	Electronic and optical properties of Zn-doped InGaAs emission layer with vacancy defects: A DFT study. Optik, 2017, 143, 135-141.	1.4	6
24422	Search for magnetism in transition metal atoms doped tetragonal graphene: A DFT approach. Journal of Magnetism and Magnetic Materials, 2017, 441, 523-530.	1.0	21
24423	Localized defects related to the 14N+ ion irradiation-induced magnetism in SiC. Physica E: Low-Dimensional Systems and Nanostructures, 2017, 93, 6-11.	1.3	2
24424	Adsorption and desorption of propane on Pd (111): A van der Waals density functional study. Energy binding sites and geometries. Surface Science, 2017, 664, 82-86.	0.8	2
24425	Bonding Properties of Aluminum Nitride at High Pressure. Inorganic Chemistry, 2017, 56, 7494-7500.	1.9	34
24426	Computational characterization of monolayer C3N: A two-dimensional nitrogen-graphene crystal. Journal of Materials Research, 2017, 32, 2993-3001.	1.2	110

#	Article	IF	Citations
24427	First principles study of organophosphorus additives in boundary lubrication conditions: Effects of hydrocarbon chain length. Lubrication Science, 2017, 29, 485-491.	0.9	17
24428	Theoretical evaluation on selective adsorption characteristics of alkali metal-based sorbents for gaseous oxidized mercury. Chemosphere, 2017, 184, 711-719.	4.2	38
24429	Anomalous lattice behavior of vanadium pentaoxide (V₂O₅): X-ray diffraction, inelastic neutron scattering and ab initio lattice dynamics. Physical Chemistry Chemical Physics, 2017, 19, 17967-17984.	1.3	20
24430	First-principles study of structure sensitivity of chain growth and selectivity in Fischerâ€“Tropsch synthesis using HCP cobalt catalysts. Catalysis Science and Technology, 2017, 7, 2967-2977.	2.1	30
24431	Preparation and temperature-dependent photoluminescence properties of ScF₃:Eu³⁺submicroparticles. New Journal of Chemistry, 2017, 41, 7915-7923.	1.4	15
24432	First-principles study of decomposition mechanisms of Mg(BH₄)₂Â·2NH₃ and LiMg(BH₄)₃Â·2NH₃. RSC Advances, 2017, 7, 31027-31032.	1.7	9
24433	Study of Niobium Diffusion and Clusterization in hcp Zr-Nb Dilute Alloys. Defect and Diffusion Forum, 2017, 375, 167-174.	0.4	1
24434	Adsorption behavior of formaldehyde on ZnO <mml:math xmlns:mml="http://www.w3.org/1998/Math/MathML" altimg="si8.gif" overflow="scroll"><mml:mrow><mml:mrow><mml:mo		

#	Article	IF	Citations
24445	Thermodynamic assessment of the Al-C-Fe system. Calphad: Computer Coupling of Phase Diagrams and Thermochemistry, 2017, 58, 34-49.	0.7	41
24446	The geometric and electronic transitions in body-centered-tetragonal C8: A first principle study. Carbon, 2017, 120, 89-94.	5.4	17
24447	How relevant is the adsorption bonding of imidazoles and triazoles for their corrosion inhibition of copper?. Corrosion Science, 2017, 124, 25-34.	3.0	64
24448	First principles study on Fe based ferromagnetic quaternary Heusler alloys. Journal of Magnetism and Magnetic Materials, 2017, 441, 21-38.	1.0	18
24449	Enhancing Dissociative Adsorption of Water on Cu(111) via Chemisorbed Oxygen. Journal of Physical Chemistry C, 2017, 121, 12117-12126.	1.5	17
24450	Hydrogen Chemical Configuration and Thermal Stability in Tungsten Disulfide Nanoparticles Exposed to Hydrogen Plasma. Journal of Physical Chemistry C, 2017, 121, 11747-11756.	1.5	6
24451	An Efficient Scheme for Crystal Structure Prediction Based on Structural Motifs. Journal of Physical Chemistry C, 2017, 121, 11891-11896.	1.5	7
24452	Optical determination of crystal phase in semiconductor nanocrystals. Nature Communications, 2017, 8, 14849.	5.8	29
24453	External electric field driving the ultra-low thermal conductivity of silicene. Nanoscale, 2017, 9, 7227-7234.	2.8	69
24454	Theoretical studies on mechanical and electronic properties of s-triazine sheet. Philosophical Magazine, 2017, 97, 2077-2088.	0.7	13
24455	Electronic Structure and Thermoelectric Power Factor of Na x CoO 2 from First-Principles Calculation. Chinese Physics Letters, 2017, 34, 037101.	1.3	0
24456	Exploring new phases of Fe_{3â^'x}Co_xC for rare-earth-free magnets. Journal Physics D: Applied Physics, 2017, 50, 215005.	1.3	11
24457	A time-dependent atomistic reconstruction of severe irradiation damage and associated property changes in nuclear graphite. Carbon, 2017, 120, 111-120.	5.4	23
24458	Adsorption studies of ethanol and butanol on Co 3 O 4 nanostructures â€“ A DFT study. Chemical Physics, 2017, 491, 61-68.	0.9	20
24459	First-principles thermoelasticity and stability of pyrite-type FeO 2 under high pressure and temperature. Journal of Alloys and Compounds, 2017, 719, 42-46.	2.8	10
24460	Enhanced optical absorption and photocatalytic activity of anatase TiO 2 through C Nd-codoped: A DFT+ U calculations. Journal of Physics and Chemistry of Solids, 2017, 109, 70-77.	1.9	6
24461	The role of surface O-vacancies in the photocatalytic oxidation of Methylene Blue by Zn-doped TiO 2 : A Mechanistic approach. Journal of Photochemistry and Photobiology A: Chemistry, 2017, 345, 36-53.	2.0	55
24462	Cleavage of rutile SiO 2 hemi-crystals: Insights from first-principles investigations. Solid State Sciences, 2017, 67, 119-124.	1.5	5

#	Article	IF	Citations
24463	Mechanism on M (M Ni, Mo, Ni Mo) as deep level impurity reducing the TCR of Si-rich Cr Si resistive films. Superlattices and Microstructures, 2017, 109, 217-228.	1.4	1
24464	Li₅(BH₄)₃NH: Lithium-Rich Mixed Anion Complex Hydride. Journal of Physical Chemistry C, 2017, 121, 11069-11075.	1.5	16
24465	Tuning magnetic properties in quasi-two-dimensional ferromagnetic Fe_{3â^'y}Ge_{1â^'x}As_xTe₂ (0â€‰â€‰â©½â€‰â€‰xâ€‰â€‰â©½â€‰â€‰ Research Express, 2017, 4, 036103.		
24466	The nitridoborate nitrides Mg₃[BN₂]N and Ca₃[BN₂]N â€“ electronic structure and chemical bonding. Zeitschrift Fur Naturforschung - Section B Journal of Chemical Sciences, 2017, 72, 433-439.	0.3	4
24467	Bonding analyses of unconventional carbon allotropes. Carbon, 2017, 121, 154-162.	5.4	19
24468	Reaction mechanisms of methanol synthesis from CO/CO 2 hydrogenation on Cu 2 O(111): Comparison with Cu(111). Journal of CO2 Utilization, 2017, 20, 59-65.	3.3	60
24469	Structural and low temperature transport properties of Fe 2 B and FeB systems at high pressure. Journal of Physics and Chemistry of Solids, 2017, 109, 18-25.	1.9	15
24470	Highly active Au/Î´-MoC and Au/Î²-Mo₂C catalysts for the low-temperature water gas shift reaction: effects of the carbide metal/carbon ratio on the catalyst performance. Catalysis Science and Technology, 2017, 7, 5332-5342.	2.1	39
24471	Surface structure and anion order of the oxynitride LaTiO₂N. Journal of Materials Chemistry A, 2017, 5, 11040-11046.	5.2	26
24472	Intrinsic valley polarization of magnetic VSe₂ monolayers. Journal of Physics Condensed Matter, 2017, 29, 255501.	0.7	73
24473	Adsorption characteristic of Pd-4 cluster carbon nanotube towards transformer oil dissolved components: A simulation. Applied Surface Science, 2017, 419, 802-810.	3.1	32
24474	Microstructure and thermal stability of nanocrystalline Mg-Gd-Y-Zr alloy processed by high pressure torsion. Journal of Alloys and Compounds, 2017, 721, 577-585.	2.8	54
24475	Solution and diffusion of hydrogen isotopes in tungsten-rhenium alloy. Journal of Nuclear Materials, 2017, 491, 206-212.	1.3	26
24476	First-principles study of noble gas atoms in bcc Fe. Journal of Nuclear Materials, 2017, 492, 134-141.	1.3	15
24477	Influence of Electrolyte Cations on Ni(Fe)OOH Catalyzed Oxygen Evolution Reaction. Chemistry of Materials, 2017, 29, 4761-4767.	3.2	105
24478	Competition and Cooperation of Hydrogenation and Deoxygenation Reactions during Hydrodeoxygenation of Phenol on Pt(111). Journal of Physical Chemistry C, 2017, 121, 12249-12260.	1.5	57
24479	Band gap modulation of SrTiO₃ upon CO₂ adsorption. Physical Chemistry Chemical Physics, 2017, 19, 16629-16637.	1.3	17
24480	Energetics of intrinsic point defects in aluminium via orbital-free density functional theory. Philosophical Magazine, 2017, 97, 2164-2181.	0.7	18

#	Article	IF	Citations
24481	The effect of point defect on mechanical properties of MoSi₂. International Journal of Modern Physics B, 2017, 31, 1744081.	1.0	3
24482	Increased Malleability in Tetragonal Zr x Ti1âˆ'x O2 Ternary Alloys: First-Principles Approach. Zeitschrift Fur Naturforschung - Section A Journal of Physical Sciences, 2017, 72, 567-572.	0.7	1
24483	Theoretical investigation of solid solution states of Ti1âˆ'V H2. Acta Materialia, 2017, 134, 274-282.	3.8	4
24484	Nonmagnetic Quantum Emitters in Boron Nitride with Ultranarrow and Sideband-Free Emission Spectra. ACS Nano, 2017, 11, 6652-6660.	7.3	105
24485	Room-temperature soft mode and ferroelectric like polarization in SrTiO3 ultrathin films: Infrared and ab initio study. Scientific Reports, 2017, 7, 2160.	1.6	19
24486	Phase stability, elastic and electronic properties of Hfâ€“Rh intermetallic compounds from first-principles calculations. RSC Advances, 2017, 7, 20241-20251.	1.7	4
24487	Effect of water on the effective Goldschmidt tolerance factor and photoelectric conversion efficiency of organicâ€“inorganic perovskite: insights from first-principles calculations. Physical Chemistry Chemical Physics, 2017, 19, 14955-14960.	1.3	10
24488	The effect of spin orbit interaction on the physical properties of LaTSi3 (T = Ir, Pd, and Rh): First-principles calculations. Journal of Applied Physics, 2017, 121, 193904.	1.1	7
24489	Oneâ€Step Synthesis of Highly Oxygenâ€Deficient Lithium Titanate Oxide with Conformal Amorphous Carbon Coating as Anode Material for Lithium Ion Batteries. Advanced Materials Interfaces, 2017, 4, 1700329.	1.9	38
24490	Hydrogenated Coreâ€“Shell MAX@K₂Ti₈O₁₇ Pseudocapacitance with Ultrafast Sodium Storage and Longâ€Term Cycling. Advanced Energy Materials, 2017, 7, 1700700.	10.2	54
24491	Li₁₂P₃N₉ with Nonâ€Condensed [P₃N₉]^{12â^'}â€Rings and its Highâ€Pressure Polymorph Li₄PN₃ with Infinite Chains of PN₄â€Tetrahedra. Chemistry - A European Journal, 2017, 23, 9592-9599.	1.7	24
24492	Prediction of Tâ€and Hâ€Phase Twoâ€Dimensional Transitionâ€Metal Carbides/Nitrides and Their Semiconductingâ€“Metallic Phase Transition. ChemPhysChem, 2017, 18, 1897-1902.	1.0	30
24493	Electronic optical, properties and widening band gap of graphene with Ge doping. Optical and Quantum Electronics, 2017, 49, 1.	1.5	39
24494	Functionalized carbon nitride (g-CN) monolayer as a promising energy storage material: A density functional theory study. Applied Surface Science, 2017, 419, 708-712.	3.1	22
24495	DFT study of methanol adsorption on PtCo(111). Applied Surface Science, 2017, 420, 383-389.	3.1	21
24496	Understanding of SF 6 decompositions adsorbed on cobalt-doped SWCNT: A DFT study. Applied Surface Science, 2017, 420, 371-382.	3.1	32
24497	Origin of enhanced piezoelectric constants of MgNbAlN studied by first-principles calculations. Japanese Journal of Applied Physics, 2017, 56, 058004.	0.8	13
24498	Structural, electronic, and magnetic properties of double perovskite Pb₂ FeReO₆ thin films with (001) orientation and three possible terminations. Surface and Interface Analysis, 2017, 49, 960-966.	0.8	1

#	Article	IF	Citations
24499	Ordered PbHPO4 nanowires: Crystal structure, energy bands and optical properties from first principles. Computational Materials Science, 2017, 138, 1-9.	1.4	11
24500	Describing the anisotropic 133Cs solid state NMR interactions in cesium chromate. Chemical Physics Letters, 2017, 684, 8-13.	1.2	4
24501	Distinct effects of Al3+ doping on the structure and properties of hexagonal turbostratic birnessite: A comparison with Fe3+ doping. Geochimica Et Cosmochimica Acta, 2017, 208, 268-284.	1.6	26
24502	Ab-initio calculations of elastic constants and thermodynamic properties of LuAuPb and YAuPb half-heusler compounds. Journal of Alloys and Compounds, 2017, 722, 544-548.	2.8	22
24503	Structural, mechanical and vibrational study of uranyl silicate mineral soddyite by DFT calculations. Journal of Solid State Chemistry, 2017, 253, 249-257.	1.4	39
24504	Van der Waals bilayer antimonene: A promising thermophotovoltaic cell material with 31% energy conversion efficiency. Nano Energy, 2017, 38, 561-568.	8.2	92
24505	Size effect on brittle and ductile fracture of two-dimensional interlinked carbon nanotube network. Physica B: Condensed Matter, 2017, 520, 82-88.	1.3	6
24506	Ab initio and classical atomistic modelling of structure and defects inÂcrystalline orthorhombic polyethylene: Twin boundaries, slip interfaces, and nature of barriers. Polymer, 2017, 121, 234-246.	1.8	19
24507	Impact of Mg-Doping Site Control in the Performance of Li₄Ti₅O₁₂ Li-Ion Battery Anode: First-Principles Predictions and Experimental Verifications. Journal of Physical Chemistry C, 2017, 121, 14994-15001.	1.5	15
24508	Methionine as a Friction Modifier for Tungsten Carbide-Functionalized Surfaces via in Situ Tribo-Chemical Reactions. ACS Sustainable Chemistry and Engineering, 2017, 5, 7030-7039.	3.2	6
24509	Nanometre-scale 3D defects in Cr2AlC thin films. Scientific Reports, 2017, 7, 984.	1.6	5
24510	Indium selenide: an insight into electronic band structure and surface excitations. Scientific Reports, 2017, 7, 3445.	1.6	60
24511	On the interaction of toxic Heavy Metals (Cd, Hg, Pb) with graphene quantum dots and infinite graphene. Scientific Reports, 2017, 7, 3934.	1.6	94
24512	Ultra-high electrocatalytic activity of VS₂ nanoflowers for efficient hydrogen evolution reaction. Journal of Materials Chemistry A, 2017, 5, 15080-15086.	5.2	189
24513	An investigation of Na-related defects in Cu₂ZnSnSe₄. Physical Chemistry Chemical Physics, 2017, 19, 17799-17804.	1.3	21
24514	Effects of organic cations on the defect physics of tin halide perovskites. Journal of Materials Chemistry A, 2017, 5, 15124-15129.	5.2	213
24515	The electronic and magnetic properties of Zn0.875Fe0.125Se alloy. AIP Conference Proceedings, 2017, , .	0.3	0
24516	Negligible spin-orbit coupling effect in the Mott-insulating antiferromagnet KRuO4. Journal of Applied Physics, 2017, 121, .	1.1	6

#	Article	IF	Citations
24517	Phase transition and electronic properties of SbI₃: First-principles calculations. Modern Physics Letters B, 2017, 31, 1750200.	1.0	4
24518	Electronic and structural investigation of buckled antimonene using density functional theory calculation. Pramana - Journal of Physics, 2017, 89, 1.	0.9	5
24519	Mechanistic insights into tunable luminescence and persistent luminescence of the full-color-emitting BCNO phosphors. Carbon, 2017, 122, 176-184.	5.4	18
24520	Effect of hydrostatic strain on the electronic transport properties of CsPbI3. Computational Materials Science, 2017, 137, 314-317.	1.4	12
24521	Synthesis, characterization and theoretical study in gaseous and solid phases of the imine 4-Acetyl-N-(4-methoxybenzylidene)aniline. Journal of Molecular Structure, 2017, 1147, 300-309.	1.8	2
24522	Understanding Selectivity for the Electrochemical Reduction of Carbon Dioxide to Formic Acid and Carbon Monoxide on Metal Electrodes. ACS Catalysis, 2017, 7, 4822-4827.	5.5	637
24523	Computational Study of MoS₂/HfO₂ Defective Interfaces for Nanometer-Scale Electronics. ACS Omega, 2017, 2, 2827-2834.	1.6	16
24524	Ordered hydroxyls on Ca3Ru2O7(001). Nature Communications, 2017, 8, 23.	5.8	12
24525	Active bialkali photocathodes on free-standing graphene substrates. Npj 2D Materials and Applications, 2017, 1, .	3.9	24
24526	Recent Progress in the Development of Semiconductorâ€Based Photocatalyst Materials for Applications in Photocatalytic Water Splitting and Degradation of Pollutants. Advanced Sustainable Systems, 2017, 1, 1700006.	2.7	144
24527	Investigation on native defects of Î± -MgAgSb and its effects on thermoelectric properties using first principles calculations. Current Applied Physics, 2017, 17, 1279-1287.	1.1	7
24528	Investigation of structural and multiferroic properties of three phases of BiFeO 3 using modified Becke Johnson potential technique. Journal of Physics and Chemistry of Solids, 2017, 110, 316-326.	1.9	16
24529	Optical properties of graphene, silicene, germanene, and stanene from IR to far UV â€“ A first principles study. Journal of Physics and Chemistry of Solids, 2017, 110, 307-315.	1.9	120
24530	Difficulty of long-standing n-type conductivity in equilibrium and non-equilibrium Î³ -CuCl: A first-principles study. Physics Letters, Section A: General, Atomic and Solid State Physics, 2017, 381, 2743-2747.	0.9	4
24531	Mechanical properties of atomically thin boron nitride and the role of interlayer interactions. Nature Communications, 2017, 8, 15815.	5.8	576
24532	Ab-initio study of ReCN in the bulk and as a new two dimensional material. Scientific Reports, 2017, 7, 2799.	1.6	2
24533	Electronic properties of blue phosphorene/graphene and blue phosphorene/graphene-like gallium nitride heterostructures. Physical Chemistry Chemical Physics, 2017, 19, 17324-17330.	1.3	180
24534	Defects in Na-, K-, and Cd-Doped CuInSe$_2$: Canonical Thermodynamics Based on Ab Initio Calculations. IEEE Journal of Photovoltaics, 2017, 7, 1143-1152.	1.5	5

#	Article	IF	Citations
24535	Dynamics of the Lithiation and Sodiation of Silicon Allotropes: From the Bulk to the Surface. Journal of the Electrochemical Society, 2017, 164, A1644-A1650.	1.3	6
24536	Metal Immiscibility Route to Synthesis of Ultrathin Carbides, Borides, and Nitrides. Advanced Materials, 2017, 29, 1700364.	11.1	61
24537	Effect of ordered B-site cations on the structure, elastic and thermodynamic properties of KTa0.5Nb0.5O3 crystal. Applied Physics A: Materials Science and Processing, 2017, 123, 1.	1.1	3
24538	A computational study of the optoelectronic and thermoelectric properties of HfIrX (X = As, Sb and) Tj ETQq1 1 0.784314 rgBT /Overlo	1.3	11
24539	The CiOi(SiI)2 defect in silicon: density functional theory calculations. Journal of Materials Science: Materials in Electronics, 2017, 28, 10295-10297.	1.1	8
24540	Vacancy mediated alloying strengthening effects on Î³/Î³â€² interface of Ni-based single crystal superalloys: A first-principles study. Acta Materialia, 2017, 135, 25-34.	3.8	61
24541	First-principles prediction of the stacking fault energy of gold at finite temperature. Acta Materialia, 2017, 135, 88-95.	3.8	16
24542	Two-dimensional germanium monochalcogenides for photocatalytic water splitting with high carrier mobility. Applied Catalysis B: Environmental, 2017, 217, 275-284.	10.8	197
24543	Photocatalytic hydrogen production over Aurivillius compound Bi3TiNbO9 and its modifications by Cr/Nb co-doping. Applied Catalysis B: Environmental, 2017, 217, 342-352.	10.8	62
24544	Giant dielectric permittivity and electronic structure in (A3+, Nb5+) co-doped TiO2 (A = Al, Ga and In). Ceramics International, 2017, 43, S265-S269.	2.3	52
24545	Identification of Mn site in Mn-doped SrTiO 3 : First principles study. Ceramics International, 2017, 43, S381-S385.	2.3	14
24546	Theoretical investigation of the crystal structure of AlOF. Chemical Physics, 2017, 491, 112-117.	0.9	5
24547	Structural properties and mechanical stability of lithium-ion based materials. A theoretical study. Computational Materials Science, 2017, 136, 271-279.	1.4	10
24548	First-principles study of fission product stability and clustering in ThO2. Computational Materials Science, 2017, 137, 186-194.	1.4	3
24549	Conversion of toluene into benzyl radical on anatase TiO 2 (0 0 1) surface. Computational and Theoretical Chemistry, 2017, 1115, 13-21.	1.1	1
24550	Experimental and first principles investigation of Bi1-xCexFeO3: Structure, electronic and optical properties. Journal of Alloys and Compounds, 2017, 721, 638-645.	2.8	22
24551	Semiconducting antiferromagnetism in MgH 2 doped with 3 d transition metals: A first-principles view. Journal of Magnetism and Magnetic Materials, 2017, 441, 799-805.	1.0	4
24552	Magnetic properties of isolated Re ion and Re-Re complex in ZnO studied by GGA+U approach. Journal of Magnetism and Magnetic Materials, 2017, 441, 436-442.	1.0	4

#	Article	IF	Citations
24553	Phonon states of B 12 P 2 crystals: Ab initio calculation and experiment. Journal of Physics and Chemistry of Solids, 2017, 110, 248-253.	1.9	5
24554	Effect of external strain on the charge transfer: Adsorption of gas molecules on monolayer GaSe. Materials Chemistry and Physics, 2017, 198, 49-56.	2.0	15
24555	Structural stability, mechanical properties, electronic structures and thermal properties of XS (X =) Tj ETQq0 0 0 rgBT /Overlock 10 Tf 50 Physics, 2017, 381, 2648-2657.	0.9	20
24556	Effect of interactions between elements on the diffusion of solutes in Ni X Y systems and Î³â€²-coarsening in model Ni-based superalloys. Scripta Materialia, 2017, 138, 100-104.	2.6	30
24557	The electronic structure of GeSe monolayer with light nonmetallic elements decoration. Superlattices and Microstructures, 2017, 109, 829-840.	1.4	13
24558	Molecular Construction Using (C₃N₃O₃)^{3â€“} Anions: Analysis and Prospect for Inorganic Metal Cyanurates Nonlinear Optical Materials. Crystal Growth and Design, 2017, 17, 4015-4020.	1.4	114
24559	Density Functional Theory Study of the Thermodynamic and Raman Vibrational Properties of Î³-UO₃ Polymorph. Journal of Physical Chemistry C, 2017, 121, 14507-14516.	1.5	43
24560	Theoretical Insights and the Corresponding Construction of Supported Metal Catalysts for Highly Selective CO₂ to CO Conversion. ACS Catalysis, 2017, 7, 4613-4620.	5.5	104
24561	Compressional pathways of Î±-cristobalite, structure of cristobalite X-I, and towards the understanding of seifertite formation. Nature Communications, 2017, 8, 15647.	5.8	33
24562	Multiferroic Phases and Transitions in Ferroelectric Lead Titanate Nanodots. Scientific Reports, 2017, 7, 45373.	1.6	7
24563	Density functional theory calculations for the band gap and formation energy of Pr_{4â^'x}Ca_xSi₁₂O_{3+x}N_{18â^'x}; a highly disordered compound with low symmetry and a large cell size. Physical Chemistry Chemical Physics, 2017, 19, 16702-16712.	1.3	17
24564	The magnetic proximity effect and electrical field tunable valley degeneracy in MoS₂/EuS van der Waals heterojunctions. Nanoscale, 2017, 9, 9502-9509.	2.8	64
24565	Atomic structure, electronic properties and generalized stacking fault energy of diamond/c-BN multilayer. RSC Advances, 2017, 7, 29599-29605.	1.7	6
24566	Energy landscapes and dynamics of glycine on Cu(110). Physical Chemistry Chemical Physics, 2017, 19, 16600-16605.	1.3	1
24567	Atomistic insight into the electrode reaction mechanism of the cathode in molten carbonate fuel cells. Journal of Materials Chemistry A, 2017, 5, 13763-13768.	5.2	18
24568	Enhancement of the thermoelectric performance of bulk SnTe alloys via the synergistic effect of band structure modification and chemical bond softening. Journal of Materials Chemistry A, 2017, 5, 14165-14173.	5.2	65
24569	Electronic structure, optical and magnetic studies of PLD-grown (Mn, P)-doped ZnO nanocolumns at room temperature. Journal Physics D: Applied Physics, 2017, 50, 295002.	1.3	2
24570	The effect of irradiation-induced point defects on energetics and kinetics of hydrogen in 3C-SiC in a fusion environment. Nuclear Fusion, 2017, 57, 066031.	1.6	11

#	Article	IF	Citations
24571	Ohmic contact in monolayer InSe-metal interface. 2D Materials, 2017, 4, 025116.	2.0	60
24572	New allotropic forms of carbon based on Đ¡60 and Đ¡20 fullerenes with specific mechanical characteristics. JETP Letters, 2017, 105, 419-425.	0.4	3
24573	Inâ€Plane Uniaxial Strain in Black Phosphorus Enables the Identification of Crystalline Orientation. Small, 2017, 13, 1700466.	5.2	29
24574	Crystal Structures of CaB₃N₃ at High Pressures. Inorganic Chemistry, 2017, 56, 7449-7453.	1.9	2
24575	Ground-State Crystal Structure of Strontium Peroxide Predicted from First Principles. Inorganic Chemistry, 2017, 56, 7545-7549.	1.9	7
24576	Taming interfacial electronic properties of platinum nanoparticles on vacancy-abundant boron nitride nanosheets for enhanced catalysis. Nature Communications, 2017, 8, 15291.	5.8	200
24577	Electronic and thermoelectric properties of Mg ₂ Ge _x Sn _{1â˜' x} (x = 0.25, 0.50, 0.75) solid solutions by first-principles calculations. Chinese Physics B, 2017, 26, 066103.	0.7	5
24578	Enhancement of hydrogen sorption on metal(Ni, Rh, Pd) functionalized carbon nanotubes: a DFT study. Chemical Research in Chinese Universities, 2017, 33, 422-429.	1.3	7
24579	Elastic constants and observed ferromagnetism in inverse Heusler alloy Ti2CoAs using kjpaw pseudopotentials: A first-principles approach. Journal of Alloys and Compounds, 2017, 722, 207-211.	2.8	10
24580	Solvation Effects on Methanol Decomposition on Pd(111), Pt(111), and Ru(0001). Journal of Physical Chemistry C, 2017, 121, 13803-13809.	1.5	49
24581	Monolayer Bismuthene-Metal Contacts: A Theoretical Study. ACS Applied Materials & Interfaces, 2017, 9, 23128-23140.	4.0	73
24582	Adsorption differences between low coverage enantiomers of alanine on the chiral Cu{421}^R surface. Physical Chemistry Chemical Physics, 2017, 19, 13562-13570.	1.3	6
24583	Uncovering the Thermo-Kinetic Origins of Phase Ordering in Mixed-Valence Antimony Tetroxide by First-Principles Modeling. Inorganic Chemistry, 2017, 56, 6545-6550.	1.9	3
24584	Raman Radial Mode Revealed from Curved Graphene. Journal of Physical Chemistry Letters, 2017, 8, 2597-2601.	2.1	8
24585	Which Oxide for Low-Emissivity Glasses? First-Principles Modeling of Silver Adhesion. ACS Applied Materials & Interfaces, 2017, 9, 18346-18354.	4.0	10
24586	Acidâ€"Base Reactivity of Perovskite Catalysts Probed via Conversion of 2-Propanol over Titanates and Zirconates. ACS Catalysis, 2017, 7, 4423-4434.	5.5	81
24587	Understanding trends in electrochemical carbon dioxide reduction rates. Nature Communications, 2017, 8, 15438.	5.8	527
24588	Superionic conduction in Î²-eucryptite: inelastic neutron scattering and computational studies. Physical Chemistry Chemical Physics, 2017, 19, 15512-15520.	1.3	14

#	Article	IF	Citations
24589	A computational study of the electronic properties, ionic conduction, and thermal expansion of Sm_{1â^'x}A_xCoO₃and Sm_{1â^'x}A_xCoO_{3â^'x/2}(A = Ba²⁺, Ca²⁺,) Tj ETQq0 0 0 rgBT /Overlock 1 Chemical Physics, 2017, 19, 13960-13969.	1.3	10
24590	GaS_{0.5}Te_{0.5} monolayer as an efficient water splitting photocatalyst. Physical Chemistry Chemical Physics, 2017, 19, 15394-15402.	1.3	17
24591	Phosphomolybdic acid supported atomically dispersed transition metal atoms (M = Fe, Co, Ni, Cu, Ru,) Tj ETQq0 0 0 rgBT /Overlock 10 T Advances, 2017, 7, 24925-24932.	1.7	23
24592	The investigation of electronic, mechanical and lattice dynamical properties of PdCoX (Xâ€‰=â€‰Si and Ge) half-Heusler metallics in Î±, Î² and Î³ structural phases: an ab initio study. Philosophical Magazine, 2017, 97, 2237-2254.	0.7	13
24593	Scrutinize the effect of Ge and Sn doping on electronic and thermoelectric properties of Mg2Si as thermoelectric material. Indian Journal of Physics, 2017, 91, 1305-1317.	0.9	2
24594	Interfacial void segregation of Cl in Cu-Sn micro-connects. Electronic Materials Letters, 2017, 13, 307-312.	1.0	6
24595	Microwave-induced activation of additional active edge sites on the MoS 2 surface for enhanced Hg 0 capture. Applied Surface Science, 2017, 420, 439-445.	3.1	25
24597	Ab initio DFT studies of adsorption characteristics of benzene on close-packed surfaces of transition metals. Computational Materials Science, 2017, 137, 10-19.	1.4	9
24598	Theoretical study of direct versus oxygen-assisted water dissociation on Co(0 0 0 1) surface. Chemical Physics Letters, 2017, 681, 29-35.	1.2	8
24599	Partitioning and diffusion of transition metal solutes in ternary model Ni-based single crystal superalloys. Materials and Design, 2017, 130, 157-165.	3.3	46
24600	Elasticity of phase-Pi (Al3Si2O7(OH)3) â€“ A hydrous aluminosilicate phase. Physics of the Earth and Planetary Interiors, 2017, 269, 91-97.	0.7	8
24601	Electronic and magnetic properties tuning of armchair BC 2 N nanoribbons by edge modification. Solid State Communications, 2017, 257, 27-31.	0.9	1
24602	Theoretical investigations on helium trapping in the Zr/Ti 2 AlC interface. Surface and Coatings Technology, 2017, 322, 19-24.	2.2	17
24603	Comparative Analysis of the Electronic Structure and Nonlinear Optical Susceptibility of Î±-TeO₂ and Î²-TeO₃ Crystals. Journal of Physical Chemistry C, 2017, 121, 12365-12374.	1.5	17
24604	First-principles study of the structural stability and electrochemical properties of Na₂MSiO₄ (M = Mn, Fe, Co and Ni) polymorphs. Physical Chemistry Chemical Physics, 2017, 19, 14462-14470.	1.3	31
24605	Cathode Properties of Perovskite-type NaMF3 (M= Fe, Mn, and Co) Prepared by Mechanical Ball Milling for Sodium-ion Battery. Electrochimica Acta, 2017, 245, 424-429.	2.6	24
24606	Improved electronic transport properties of tin-halide perovskites. Solar Energy Materials and Solar Cells, 2017, 170, 8-12.	3.0	14
24607	Thermal stability and oxidation resistance of sputtered Ti Al Cr N hard coatings. Surface and Coatings Technology, 2017, 324, 48-56.	2.2	68

#	Article	IF	Citations
24608	Periodic DFT Study of Rutile IrO₂: Surface Reactivity and Catechol Adsorption. Journal of Physical Chemistry C, 2017, 121, 13135-13143.	1.5	32
24609	Borophene as a Promising Material for Charge-Modulated Switchable CO₂ Capture. ACS Applied Materials & Interfaces, 2017, 9, 19825-19830.	4.0	83
24610	Achieving Remarkable Activity and Durability toward Oxygen Reduction Reaction Based on Ultrathin Rh-Doped Pt Nanowires. Journal of the American Chemical Society, 2017, 139, 8152-8159.	6.6	265
24611	General Oriented Formation of Carbon Nanotubes from Metalâ€“Organic Frameworks. Journal of the American Chemical Society, 2017, 139, 8212-8221.	6.6	777
24612	Novel magnesium borides and their superconductivity. Physical Chemistry Chemical Physics, 2017, 19, 14486-14494.	1.3	10
24613	Formation and structures of Auâ€“Rh bimetallic nanoclusters supported on a thin film of Al2O3/NiAl(100). Physical Chemistry Chemical Physics, 2017, 19, 14566-14579.	1.3	5
24614	Strain induced quantum spin Hall insulator in monolayer Î²-BiSb from first-principles study. RSC Advances, 2017, 7, 27816-27822.	1.7	26
24615	Nontrivial Berry phase in magnetic BaMnSb ₂ semimetal. Proceedings of the National Academy of Sciences of the United States of America, 2017, 114, 6256-6261.	3.3	71
24616	Comparison of nitrogen-vacancy complexes in diamond and cubic SiC: dose dependencies and spin-Hamiltonian parameters. Journal of Physics Condensed Matter, 2017, 29, 325506.	0.7	2
24617	Structural and electronic properties of low-index surfaces of NbAl3 intermetallic with first-principles calculations. Applied Surface Science, 2017, 419, 811-816.	3.1	29
24618	Effects of Rb Incorporation and Water Degradation on the Stability of the Cubic Formamidinium Lead Iodide Perovskite Surface: A First-Principles Study. Journal of Physical Chemistry C, 2017, 121, 12711-12717.	1.5	40
24619	Enhancing Enantiomeric Separation with Strain: The Case of Serine on Cu(531). Journal of the American Chemical Society, 2017, 139, 8167-8173.	6.6	12
24620	Exploring ion migration in Li₂MnSiO₄ for Li-ion batteries through strain effects. RSC Advances, 2017, 7, 26089-26096.	1.7	15
24621	Asymmetric passivation of edges: a route to make magnetic graphene nanoribbons. RSC Advances, 2017, 7, 27932-27937.	1.7	2
24622	A computational study of monolayer hexagonal WTe₂ to metal interfaces. Physica Status Solidi (B): Basic Research, 2017, 254, 1600837.	0.7	17
24623	Using density functional theory to increase the accuracy of experimental crystal structures: The case of potassium peroxocarbonate. Journal of Molecular Structure, 2017, 1146, 1-4.	1.8	1
24624	Tunable Type-I and Type-II Dirac Fermions in Graphene with Nitrogen Line Defects. Journal of Physical Chemistry C, 2017, 121, 12476-12482.	1.5	10
24625	Theoretical Determination of Band Edge Alignments at the Waterâ€“CuInS₂(112) Semiconductor Interface. Langmuir, 2017, 33, 9479-9489.	1.6	6

#	Article	IF	Citations
24626	Enhanced Energy-Storage Density and High Efficiency of Lead-Free CaTiO₃â€“BiScO₃ Linear Dielectric Ceramics. ACS Applied Materials & Interfaces, 2017, 9, 19963-19972.	4.0	145
24627	Extra electronic outer-shell peculiarities accessible under a joint XPS and DFT study. Physical Chemistry Chemical Physics, 2017, 19, 15842-15848.	1.3	5
24628	The structural, electronic, dynamical and thermal properties of LaSn3 and LaPb3. AIP Conference Proceedings, 2017, , .	0.3	1
24629	Theoretical investigation of the structural, electronic, dynamical and thermal properties of YSn3 and YPb3. AIP Conference Proceedings, 2017, , .	0.3	0
24630	Effective control of phosphorus clustersâ€™ electronic and spin properties in graphene/BN heterostructure via electric fields. Journal Physics D: Applied Physics, 2017, 50, 235003.	1.3	0
24631	Comparative studies about CO methanation over Ni(211) and Zr-modified Ni(211) surfaces: Qualitative insight into the effect of surface structure and composition. Molecular Catalysis, 2017, 438, 1-14.	1.0	19
24632	Adsorption of benzene on low index surfaces of platinum in the presence of van der Waals interactions. Surface Science, 2017, 664, 8-15.	0.8	7
24633	First principle study of electronic and optical properties of molecular ion (BF4â^') substituted hybrid perovskite (CH3NH3PbI3). AIP Conference Proceedings, 2017, , .	0.3	2
24634	Descriptors for predicting the lattice constant of body centered cubic crystal. Journal of Chemical Physics, 2017, 146, 204104.	1.2	22
24635	Evidence for the antiferromagnetic ground state of Zr2TiAl: a first-principles study. Journal of Physics Condensed Matter, 2017, 29, 265801.	0.7	5
24636	Pressure-induced phase transformations of LiGaO 2 : First principles study. Ceramics International, 2017, 43, S376-S380.	2.3	5
24637	Investigation of thermodynamic stability, mechanical and electronic properties of superhard tetragonal B 4 CO 4 compound: Ab initio calculations. Computational Condensed Matter, 2017, 12, 1-8.	0.9	7
24638	Possible origin and roles of nano-porosity in ZrO 2 scales for hydrogen pick-up in Zr alloys. Journal of Nuclear Materials, 2017, 492, 22-31.	1.3	13
24639	van Hove singularities and tight-binding model in high-temperature superconductor H 3 Se. Physics Letters, Section A: General, Atomic and Solid State Physics, 2017, 381, 2526-2530.	0.9	4
24640	Adsorption of heavy metals on a complex Al-Si-O bearing mineral system: Insights from theory and experiments. Separation and Purification Technology, 2017, 186, 28-38.	3.9	27
24641	Structural Instabilities Related to Highly Anharmonic Phonons in Halide Perovskites. Journal of Physical Chemistry Letters, 2017, 8, 2659-2665.	2.1	132
24642	Crystal Structure Induced Preferential Surface Alloying of Sb on Wurtzite/Zinc Blende GaAs Nanowires. Nano Letters, 2017, 17, 3634-3640.	4.5	14
24643	Electrochemical Activation of CO₂ through Atomic Ordering Transformations of AuCu Nanoparticles. Journal of the American Chemical Society, 2017, 139, 8329-8336.	6.6	529

#	Article	IF	Citations
24644	Exploring the potential of boron-doped nanographene as efficient charge transport and nonlinear optical material: A first-principles study. Journal of Molecular Graphics and Modelling, 2017, 75, 209-219.	1.3	29
24645	In-situ studies on the micro-structure evolution of A 2 W 2 O 7 (A = Li, Na, K) during melting by high temperature Raman spectroscopy and density functional theory. Spectrochimica Acta - Part A: Molecular and Biomolecular Spectroscopy, 2017, 185, 188-196.	2.0	18
24646	Density functional calculations of graphene-based humidity and carbon dioxide sensors: effect of silica and sapphire substrates. Surface Science, 2017, 663, 23-30.	0.8	9
24647	Tin-tellurium-phosphide: Investigation of composition dependent band structure and its experimental realization. Vacuum, 2017, 146, 444-454.	1.6	6
24648	Atomic layer etching of graphene through controlled ion beam for graphene-based electronics. Scientific Reports, 2017, 7, 2462.	1.6	31
24649	First-principles computational studies on layered Na₂Mn₃O₇ as a high-rate cathode material for sodium ion batteries. Journal of Materials Chemistry A, 2017, 5, 12752-12756.	5.2	39
24650	The A-center defect in diamond: quantum mechanical characterization through the infrared spectrum. Physical Chemistry Chemical Physics, 2017, 19, 14478-14485.	1.3	16
24651	Modeling ferroelectric film properties and size effects from tetragonal interlayer in Hf1â€“xZrxO2 grains. Journal of Applied Physics, 2017, 121, .	1.1	49
24652	Atomic structure of the Fe/Fe₃C interface with the Isaichev orientation in pearlite. Philosophical Magazine, 2017, 97, 2375-2386.	0.7	22
24653	Ab initiostudies of coherent spin transport in Fe-hBN/graphene van der Waals multilayers. Journal of Physics Condensed Matter, 2017, 29, 285302.	0.7	8
24654	Switch effect of the nonquantized intrinsic spin Hall conductivity in monolayered monoclinic transition metal dichalcogenides. Journal of Physics Condensed Matter, 2017, 29, 295302.	0.7	1
24655	Electrical and optical properties of Si-doped Ga₂O₃. Modern Physics Letters B, 2017, 31, 1750172.	1.0	9
24656	Variable electronic transport properties of double carbon-nanotube junctions via substitutional Fe, Co, and Mn atom doping. Physica Status Solidi (B): Basic Research, 2017, 254, 1700013.	0.7	0
24657	DFT study of coadsorption of water and oxygen on galena (PbS) surface: An insight into the oxidation mechanism of galena. Applied Surface Science, 2017, 420, 714-719.	3.1	41
24658	First principles study of electronic, phonon and elastic properties of rock-salt-phase MTe (MÂ=ÂMg, Ca,) Tj ETQq0 0 0 rgBT /Overlock 10	0.9	2
24659	Efficient Strategy for Enhancement of Visible Light Photocatalytic Activity of NaTaO₃ by a Significant Extent. Journal of Physical Chemistry C, 2017, 121, 12980-12990.	1.5	20
24660	Influence of Film and Substrate Structure on Photoelectron Momentum Maps of Coronene Thin Films on Ag(111). Journal of Physical Chemistry C, 2017, 121, 12285-12293.	1.5	14
24661	Formation of Germa-ketenimine on the Ge(100) Surface by Adsorption of tert-Butyl Isocyanide. Journal of the American Chemical Society, 2017, 139, 8758-8765.	6.6	6

#	Article	IF	Citations
24662	First-principles study on intrinsic defects of SnSe. RSC Advances, 2017, 7, 27612-27618.	1.7	69
24663	Ab initio mechanical and thermal properties of FeMnP1â^'xGaxcompounds as refrigerant for room-temperature magnetic refrigeration. RSC Advances, 2017, 7, 27454-27463.	1.7	5
24664	Pressure-induced phase transition and electronic properties of MgB2C2. Journal of Applied Physics, 2017, 121, 195102.	1.1	3
24665	Molybdenum Carbide: A Stable Topological Semimetal with Line Nodes and Triply Degenerate Points. Chinese Physics Letters, 2017, 34, 027102.	1.3	14
24666	Ab initio study of the structural stability, elastic, electronic and optical properties of NaMgHiFj [(i, j) = (3, 0), (2, 1), (1, 2), (0, 3)] compounds. Solid State Communications, 2017, 261, 10-16.	0.9	1
24667	Improve the performance of Cr-free passivation film through nanoelectrodeposition for replacement of toxic Cr 6+ passivation in electrogalvanizing process. Surface and Coatings Technology, 2017, 324, 146-152.	2.2	11
24668	A novel borophene featuring heptagonal holes: a common precursor of borospherenes. Physical Chemistry Chemical Physics, 2017, 19, 19890-19895.	1.3	12
24669	Structural, electronic and lattice dynamical properties of perovskite CaZrO3 under high pressure. AIP Conference Proceedings, 2017, , .	0.3	3
24670	The investigation of electronic, magnetic, mechanical, and lattice dynamical properties of PdMX(Mâ€‰â€‰=â€‰â€‰Cr, Fe andXâ€‰â€‰=â€‰â€‰Si and Ge) ferromagnetic half-Heusler metallics: an initiostudy. Materials Research Express, 2017, 4, 066504.	1.7	17
24671	Electronic and transport properties of heterophase compounds based on MoS2. JETP Letters, 2017, 105, 250-254.	0.4	9
24672	Effect of H-vacancy defect on the adsorption of CO and NO on graphane: A DFT study. Applied Surface Science, 2017, 420, 720-725.	3.1	18
24673	Mechanical stability and superconductivity of PbO-type phase of thorium monocarbide at high pressure. Computational Materials Science, 2017, 136, 238-242.	1.4	8
24674	A newly designed Sc-decorated covalent organic framework: A potential candidate for room-temperature hydrogen storage. Computational Materials Science, 2017, 137, 107-112.	1.4	10
24675	The diode characteristics and rectification effect of three nanodevice containing graphene and oxidized graphene nanoribbons: A density functional theory + non-equilibrium Greenâ€™s function study. Computational Materials Science, 2017, 137, 125-133.	1.4	2
24676	Computational study of structural, optoelectronic and nonlinear optical properties of dynamic solid-state chalcone derivatives. Journal of Molecular Graphics and Modelling, 2017, 75, 355-364.	1.3	16
24677	A promising single atom catalyst for CO oxidation: Ag on boron vacancies of h-BN sheets. Physical Chemistry Chemical Physics, 2017, 19, 16795-16805.	1.3	102
24678	Topologically nontrivial electronic states in CaSn3. Journal of Applied Physics, 2017, 121, .	1.1	14
24679	Temperature Sensitivity of Electrical Resistivity of Graphene/Copper Hybrid Nano Ribbon Interconnect: A First Principle Study. ECS Journal of Solid State Science and Technology, 2017, 6, P119-P124.	0.9	10

#	Article	IF	Citations
24681	Defect processes of M3AlC2 (M = V, Zr, Ta, Ti) MAX phases. Solid State Communications, 2017, 261, 54-56.	0.9	9
24682	Synthesis, structure and photocatalytic activity of layered LaOInS₂. Journal of Materials Chemistry A, 2017, 5, 14270-14277.	5.2	30
24683	Ab initiostudies of two Al grain boundaries subjected to mixed tension/shear mode loading: how shear may promote breakage. Modelling and Simulation in Materials Science and Engineering, 2017, 25, 064001.	0.8	3
24684	Unraveling the effect of uniaxial strain on thermoelectric properties of Mg ₂ Si: A density functional theory study. Chinese Physics B, 2017, 26, 066401.	0.7	1
24685	Ab initio calculations of phonon dispersion in CdGa2Se4. Semiconductors, 2017, 51, 556-558.	0.2	3
24686	Graphene-like MoS2 containing adsorbents for Hg0 capture at coal-fired power plants. Applied Energy, 2017, 207, 254-264.	5.1	64
24687	Adsorption, dissociation and diffusion of hydrogen on the ZrCo surface and subsurface: A comprehensive study using first principles approach. Applied Surface Science, 2017, 422, 394-405.	3.1	38
24688	Structural, elastic and magneto-electronic properties of half-metallic BaNpO 3 perovskite. Materials Chemistry and Physics, 2017, 198, 380-385.	2.0	60
24689	Optical, electronic and elastic properties of ScAlN alloys in WZ and ZB phases: Prospective material for optoelectronics and solar cell applications. Superlattices and Microstructures, 2017, 109, 915-926.	1.4	6
24690	Understanding effects of Cr content on the slurry erosion behavior of high-Cr cast irons through local property mapping and computational analysis. Wear, 2017, 376-377, 587-594.	1.5	17
24691	Polar Magnets in Double Corundum Oxides. Chemistry of Materials, 2017, 29, 5447-5457.	3.2	46
24692	Binary Compound Bilayer and Multilayer with Vertical Polarizations: Two-Dimensional Ferroelectrics, Multiferroics, and Nanogenerators. ACS Nano, 2017, 11, 6382-6388.	7.3	301
24693	First-principles study on structural, electronic, vibrational and thermodynamic properties of Sr₁₀(PO₄)₆X₂(X = F, Cl, Br). RSC Advances, 2017, 7, 30310-30319.	1.7	6
24694	Electronic structures of solids made of C20 clusters. AIP Advances, 2017, 7, 025103.	0.6	1
24695	High-pressure structures of yttrium hydrides. Journal of Physics Condensed Matter, 2017, 29, 325401.	0.7	17
24696	CO2 Activation and Hydrogenation: A Comparative DFT Study of Ru10/TiO2 and Cu10/TiO2 Model Catalysts. Catalysis Letters, 2017, 147, 1871-1881.	1.4	25
24697	Density-Functional-Theory Study of Cohesive, Structural and Electronic Properties of Ni-Sb Intermetallic Phases. Journal of Phase Equilibria and Diffusion, 2017, 38, 223-230.	0.5	0
24698	Interfacial electronic and structural properties of SiO2(010)/BaTiO3(001) from first-principles calculations. Ceramics International, 2017, 43, 12988-12991.	2.3	4

#	Article	IF	Citations
24699	Density functional theory study of adsorption geometries and electronic structures of azo-dye-based molecules on anatase TiO2 surface for dye-sensitized solar cell applications. Journal of Molecular Graphics and Modelling, 2017, 76, 551-561.	1.3	41
24700	Highly desirable semiconducting materials for mid-IR optoelectronics: Dilute bismide InAs1âˆ'Bi alloys. Materials Research Bulletin, 2017, 95, 588-596.	2.7	18
24701	Many-body mechanism of Guinier-Preston zones stabilization in Alâ€“Cu alloys. Scripta Materialia, 2017, 138, 130-133.	2.6	17
24702	Structure Prediction of Liâ€“Sn and Liâ€“Sb Intermetallics for Lithium-Ion Batteries Anodes. Chemistry of Materials, 2017, 29, 5787-5795.	3.2	37
24703	Structure, Bonding, and Catalytic Properties of Defect Graphene Coordinated Pdâ€“Ni Nanoparticles. Journal of Physical Chemistry C, 2017, 121, 14668-14677.	1.5	11
24704	High-pressure dynamic, thermodynamic properties, and hardness of CdP ₂. Chinese Physics B, 2017, 26, 046301.	0.7	4
24705	Use of Wyckoff position splittings in the supercell model of crystals with point defects. Journal of Applied Crystallography, 2017, 50, 893-900.	1.9	8
24706	Structural properties and mechanical stability of monoclinic lithium disilicate. Physica Status Solidi (B): Basic Research, 2017, 254, 1700108.	0.7	6
24707	Ab Initio Investigation of Vibrational, Optical and Thermodynamics Properties of Yttrium Arsenide. Journal of Electronic Materials, 2017, 46, 5670-5676.	1.0	4
24708	Electronic structure and optical properties of iron based chalcogenide FeX2 (XÂ=ÂS, Se, Te) for photovoltaic applications: a first principle study. Indian Journal of Physics, 2017, 91, 1339-1344.	0.9	22
24709	Catalytic growth of diamond-like carbon on Fe3C-containing carburized layer through a single-step plasma-assisted carburizing process. Carbon, 2017, 122, 1-8.	5.4	49
24710	Structural, elastic, electronic and optical properties of the novel quaternary diamond-like semiconductors Cu2MgSiS4 and Cu2MgGeS4. Solid State Sciences, 2017, 70, 21-35.	1.5	24
24711	Two-Dimensional MXenes as Catalysts for Electrochemical Hydrogen Evolution: A Computational Screening Study. Journal of Physical Chemistry C, 2017, 121, 13593-13598.	1.5	183
24712	The enhanced oxygen reduction reaction performance on PtSn nanowires: the importance of segregation energy and morphological effects. Journal of Materials Chemistry A, 2017, 5, 14355-14364.	5.2	23
24713	Revisit the electromigration effect: In situ synchrotron X-ray and scanning electron microscopy and ab initio calculations. , 2017, , .		0
24714	Firstâ€Principles Simulation of Raman Spectra of Adsorbates on Metal Surfaces. ChemPlusChem, 2017, 82, 924-932.	1.3	6
24715	Firstâ€principles modeling of hafniaâ€based nanotubes. Journal of Computational Chemistry, 2017, 38, 2088-2099.	1.5	7
24716	Density functional theory calculations of helium clustering in monoâ€, diâ€, and hexaâ€vacancy in silicon. Physica Status Solidi (A) Applications and Materials Science, 2017, 214, 1700263.	0.8	5

#	Article	IF	Citations
24717	CO Adsorption on (110)-(1 Ã— 2) Missing-Row Reconstructed Surfaces of Pd, Au, and Pd₃Au: Electronic Structures and Vibrational Frequencies. Journal of the Physical Society of Japan, 2017, 86, 044712.	0.7	3
24718	Effect of Sr-doping on the band structure of BaTiO 3 through density functional theoretical calculations. Computational Condensed Matter, 2017, 11, 27-32.	0.9	4
24719	Prediction of structure and elastic properties of AlCrFeNiTi system high entropy alloys. Intermetallics, 2017, 86, 134-146.	1.8	51
24720	The order-disorder transition in Cu 2 ZnSnS 4 : A theoretical and experimental study. Journal of Solid State Chemistry, 2017, 250, 140-144.	1.4	24
24721	First principles study of methane decomposition on B5 step-edge type site of Ru surface. Journal of Physics Condensed Matter, 2017, 29, 184001.	0.7	8
24722	Ï€ Magnetism of Carbon Monovacancy in Graphene by Hybrid Density Functional Calculations. Journal of Physical Chemistry C, 2017, 121, 8653-8661.	1.5	17
24723	Dirac Nodal Lines and Tilted Semi-Dirac Cones Coexisting in a Striped Boron Sheet. Journal of Physical Chemistry Letters, 2017, 8, 1707-1713.	2.1	81
24724	Testing the tools for revealing and characterizing the iodineâ€“iodine halogen bond in crystals. Acta Crystallographica Section B: Structural Science, Crystal Engineering and Materials, 2017, 73, 217-226.	0.5	45
24725	DENSITY FUNCTIONAL STUDY OF ELEMENTAL MERCURY ADSORPTION ON X (X=Mn, Si, Ti, Al, AND Zn)-DOPED CuO (110) SURFACE. Surface Review and Letters, 2017, 24, 1750119.	0.5	3
24726	Study of Structure and Deformation Pathways in Ti-7Al Using Atomistic Simulations, Experiments, and Characterization. Metallurgical and Materials Transactions A: Physical Metallurgy and Materials Science, 2017, 48, 2222-2236.	1.1	19
24727	Hybrid triazine-based graphitic carbon nitride and molybdenum disulfide bilayer with and without Li/Mg intercalation: Structural, electronic and optical properties. Computational Materials Science, 2017, 134, 84-92.	1.4	11
24728	The (2Ã—2) reconstructions on the surface of cobalt silicides: Atomic configuration at the annealed Co/Si(111) interface. Surface Science, 2017, 662, 6-11.	0.8	6
24729	Ab initioexplanation of disorder and off-stoichiometry in Fe-Mn-Al-C<mml:math xmlns:mml="http://www.w3.org/1998/Math/MathML"><mml:mi>Î</mml:mi></mml:math>carbides. Physical Review B, 2017, 95, .	1.1	29
24730	Firstâ€principles investigation of chemical stability and proton conductivity of Mâ€doped BaZrO₃ (M=K, Rb, and Cs). Journal of the American Ceramic Society, 2017, 100, 2997-3003.	1.9	19
24731	Ab initio determination of electron affinity of polar nitride surfaces, clean and under Cs coverage. Journal of Vacuum Science and Technology A: Vacuum, Surfaces and Films, 2017, 35, .	0.9	19
24732	Solidâ€State NMR Spectroscopy Proves the Presence of Pentaâ€coordinated Sc Sites in MILâ€100(Sc). Chemistry - A European Journal, 2017, 23, 9525-9534.	1.7	19
24733	Enhanced Photocatalytic Water Splitting in a C₂N Monolayer by Câ€Site Isoelectronic Substitution. ChemPhysChem, 2017, 18, 1526-1532.	1.0	46
24734	Sc₂C as a Promising Anode Material with High Mobility and Capacity: A Firstâ€Principles Study. ChemPhysChem, 2017, 18, 1627-1634.	1.0	88

#	Article	IF	Citations
24735	First-Principles Calculations of Defect Structures in B2 AlCo and GaCo. Journal of Phase Equilibria and Diffusion, 2017, 38, 143-150.	0.5	1
24736	First-principles study on segregation of ternary additions for MoSi2/Mo5Si3 interface. Calphad: Computer Coupling of Phase Diagrams and Thermochemistry, 2017, 56, 150-153.	0.7	2
24737	First-principles calculations on structural energetics of Cu-Ti binary system intermetallic compounds in Ag-Cu-Ti and Cu-Ni-Ti active filler metals. Ceramics International, 2017, 43, 7751-7761.	2.3	31
24738	The spectral adjustment in nanoscale transport combined with the density functional based tight binding method. Computational Materials Science, 2017, 133, 14-21.	1.4	3
24739	Phonon spectrum, IR and Raman modes, thermal expansion tensor and thermal physical properties of M 2 TiAlC 2 (M = Cr, Mo, W). Computational Materials Science, 2017, 134, 67-83.	1.4	11
24740	A low energy pathway to CuCl 2 : A theoretical investigation. Chemical Physics Letters, 2017, 672, 54-56.	1.2	0
24741	An extrapolation scheme for solid-state NMR chemical shift calculations. Chemical Physics Letters, 2017, 677, 99-106.	1.2	9
24742	The study of defect structure in tungsten: Rotation and migration property for the self-interstitial atoms. Fusion Engineering and Design, 2017, 124, 1122-1126.	1.0	6
24743	Structural dependence of photocatalytic hydrogen production over La/Cr co-doped perovskite compound ATiO 3 (A = Ca, Sr and Ba). International Journal of Hydrogen Energy, 2017, 42, 23539-23547.	3.8	39
24744	Impact of the clusterization on the solubility of oxygen and vacancy concentration in nickel: A multi-scale approach. Journal of Alloys and Compounds, 2017, 708, 1063-1072.	2.8	12
24745	Ab initio study of N-doped Î²-Ga 2 O 3 with intrinsic defects: the structural, electronic and optical properties. Journal of Alloys and Compounds, 2017, 712, 379-385.	2.8	88
24746	A first principles calculation of Ni-16Cr and Ni-16Mo alloys. Journal of Applied Research and Technology, 2017, 15, 78-82.	0.6	7
24747	SCDM-k: Localized orbitals for solids via selected columns of the density matrix. Journal of Computational Physics, 2017, 334, 1-15.	1.9	36
24748	Modelling of the electronic and ferroelectric properties of trichloroacetamide using Monte Carlo and first-principles calculations. Journal of Materiomics, 2017, 3, 130-134.	2.8	6
24749	Influence of the different strainsâ€™ components on the uniaxial magnetic anisotropy parameters for a (Ga,Mn)As bulk system: A first-principles study. Journal of Magnetism and Magnetic Materials, 2017, 432, 396-403.	1.0	3
24750	Edge eigen-stress and eigen-displacement of armchair molybdenum disulfide nanoribbons. Physics Letters, Section A: General, Atomic and Solid State Physics, 2017, 381, 1568-1572.	0.9	4
24751	Pressure effects on electronic, anisotropic elastic and thermal properties of Ti3AC2(A Si, Ge and Sn) by ab initio calculations. Results in Physics, 2017, 7, 1055-1065.	2.0	6
24752	Ab-initio study on the stability, electronic and mechanical properties of transition metal nitrides under external pressure. Solid State Sciences, 2017, 67, 13-18.	1.5	4

#	Article	IF	Citations
24753	A room-temperature-operated Si LED with Î²-FeSi2 nanocrystals in the active layer: Î¼W emission power at 1.5â€‰Î¼m. Journal of Applied Physics, 2017, 121, .	1.1	13
24754	Fast and accurate approximate quasiparticle band structure calculations of ZnO, CdO, and MgO polymorphs. Physical Review B, 2017, 95, .	1.1	23
24755	Structural, elastic and thermodynamic properties of iron carbide Fe 7 C 3 phases: An ab initio study. Chinese Journal of Physics, 2017, 55, 977-988.	2.0	4
24756	Exploring Doping Characteristics of Various Adatoms on Single-Layer Stanene. Journal of Physical Chemistry C, 2017, 121, 7667-7676.	1.5	31
24757	Schottky Barriers in Bilayer Phosphorene Transistors. ACS Applied Materials & Interfaces, 2017, 9, 12694-12705.	4.0	94
24758	Magnetic states of MnP: muon-spin rotation studies. Journal of Physics Condensed Matter, 2017, 29, 164003.	0.7	11
24759	Stability, electronic structures, and mechanical properties of Feâ€“Mnâ€“Al system from first-principles calculations. Chinese Physics B, 2017, 26, 037102.	0.7	4
24760	Active sites for CO ₂ hydrogenation to methanol on Cu/ZnO catalysts. Science, 2017, 355, 1296-1299.	6.0	1,180
24761	Systematic Density Functional Theory Investigation of Stability of Dopant Atoms in Ge Ultra-Thin Film Grown on Si Substrate. ECS Journal of Solid State Science and Technology, 2017, 6, P154-P160.	0.9	1
24762	Effect of the modulation ratio on the interface structure of TiAlN/TiN and TiAlN/ZrN multilayers: First-principles and experimental investigations. Acta Materialia, 2017, 130, 281-288.	3.8	88
24763	High-pressure induced phase transition of FeS2: Electronic, mechanical and thermoelectric properties. Journal of Alloys and Compounds, 2017, 710, 267-273.	2.8	13
24764	Effect of strain on electronic and magnetic properties of Fe-doped monolayer SnS 2. Physics Letters, Section A: General, Atomic and Solid State Physics, 2017, 381, 1732-1737.	0.9	19
24765	A theoretical simulation of small-molecules sensing on an S-vacancy SnS₂ monolayer. Physical Chemistry Chemical Physics, 2017, 19, 10470-10480.	1.3	52
24766	Fe atoms trapped on graphene as a potential efficient catalyst for room-temperature complete oxidation of formaldehyde: a first-principles investigation. Catalysis Science and Technology, 2017, 7, 2012-2021.	2.1	13
24767	The atomic simulation environmentâ€”a Python library for working with atoms. Journal of Physics Condensed Matter, 2017, 29, 273002.	0.7	1,933
24768	Effect of P impurity on NiAlÎ£5 grain boundary from first-principles study. Chinese Physics B, 2017, 26, 023101.	0.7	1
24769	Transport properties of C and O in UN fuels. Physical Review B, 2017, 95, .	1.1	7
24770	Systematics of Structural, Phase Stability, and Cohesive Properties of Î·â€²-Cu6(Sn,In)5 Compounds Occurring in In-Sn/Cu Solder Joints. Journal of Electronic Materials, 2017, 46, 4485-4496.	1.0	2

#	Article	IF	Citations
24771	Self-assembling of calcium salt of the new DNA base 5-carboxylcytosine. Applied Surface Science, 2017, 407, 297-306.	3.1	3
24772	Structural stability and the electronic and magnetic properties of ferrimagnetic Mn 4 N(0 0 1) surfaces. Applied Surface Science, 2017, 407, 209-212.	3.1	8
24773	Investigation of the structural anisotropy in a self-assembling glycinate layer on Cu(100) by scanning tunneling microscopy and density functional theory calculations. Applied Surface Science, 2017, 409, 111-116.	3.1	1
24774	Temperature-dependent dissolution and diffusion of H isotopes in iron for nuclear energy applications: First-principles and vibration spectrum predictions. International Journal of Hydrogen Energy, 2017, 42, 11560-11573.	3.8	11
24775	Mechanism of the Key Impact of Residual Carbon Content on the Reliability of Integrated Resistive Random Access Memory Arrays. Journal of Physical Chemistry C, 2017, 121, 7005-7014.	1.5	8
24776	PdAu Alloy Nanoparticle Catalysts: Effective Candidates for Nitrite Reduction in Water. ACS Catalysis, 2017, 7, 3268-3276.	5.5	89
24777	Practical principles of density functional theory for catalytic reaction simulations on metal surfaces â€“ from theory to applications. Molecular Simulation, 2017, 43, 861-885.	0.9	22
24778	DFT study of the intercalation of layered double hydroxides and layered hydroxide salts with dodecylsulfate and dodecylbenzene sulfonate: Exfoliation and hydrationÂproperties. Applied Clay Science, 2017, 143, 107-114.	2.6	19
24779	Spectroelectrochemical detection of specifically adsorbed cyanurate anions at gold electrodes with (111) orientation in contact with cyanate and cyanuric acid neutral solutions. Journal of Electroanalytical Chemistry, 2017, 800, 167-175.	1.9	8
24780	Enhanced spectral response of semiconducting BaSi 2 films by oxygen incorporation. Thin Solid Films, 2017, 629, 17-21.	0.8	14
24781	Synthesis and Mechanical Character of Hexagonal Phase Î´â€²WN. Inorganic Chemistry, 2017, 56, 3970-3975.	1.9	25
24782	Embedded silicene nanostructures in partly-dehydrogenated polysilane. Physical Chemistry Chemical Physics, 2017, 19, 10401-10405.	1.3	1
24783	Low-temperature features in the heat capacity of unary metals and intermetallics for the example of bulk aluminum and<mml:math xmlns:mml="http://www.w3.org/1998/Math/MathML"><mml:msub><mml:mi>Al</mml:mi><mml:mn>3</mml:mn></mml:msub><mml:m mathvariant="normal">Sc</mml:mi></mml:math>. Physical Review B, 2017, 95, .	1.1	12
24784	First principles study of the vibrational, dielectric and thermal properties of SrClF. European Physical Journal B, 2017, 90, 1.	0.6	5
24785	Embedded atom method interatomic potentials fitted upon density functional theory calculations for the simulation of binary Pt Ni nanoparticles. Computational Materials Science, 2017, 133, 185-193.	1.4	4
24786	Electronic structure of substitutionally doped diamond: Spin-polarized, hybrid density functional theory analysis. Diamond and Related Materials, 2017, 75, 146-151.	1.8	30
24787	Interrelations between EOS parameters and cohesive energy of transition metals: Thermostatistical approach, ab initio calculations and analysis of â€œuniversalityâ€•features. Journal of Physics and Chemistry of Solids, 2017, 107, 93-99.	1.9	10
24788	Local Structure Evolution and Modes of Charge Storage in Secondary Liâ€“FeS₂ Cells. Chemistry of Materials, 2017, 29, 3070-3082.	3.2	42

#	Article	IF	Citations
24789	First-Principles Calculations That Clarify Energetics and Reactions of Oxygen Adsorption and Carbon Desorption on 4H-SiC (112ì...0) Surface. Journal of Physical Chemistry C, 2017, 121, 3920-3928.	1.5	8
24790	Dissociative and non-dissociative adsorption of O₂ on Cu(111) and Cu_{ML}/Ru(0001) surfaces: adiabaticity takes over. Physical Chemistry Chemical Physics, 2017, 19, 10217-10221.	1.3	20
24791	New carbon allotropes with metallic conducting properties: a first-principles prediction. RSC Advances, 2017, 7, 17417-17426.	1.7	45
24792	Suppression of conductivity deterioration of copper thin films by coating with atomic-layer materials. Applied Physics Letters, 2017, 110, .	1.5	22
24793	The effects of magnetic moment collapse under high pressure, on physical properties in mono-borides TMB (TM = Mn, Fe): a first-principles. Phase Transitions, 2017, 90, 984-1000.	0.6	5
24794	Phonons and elasticity of cementite through the Curie temperature. Physical Review B, 2017, 95, .	1.1	8
24795	First-Principles Predictions of Phase Transition and Mechanical Properties of Tungsten Diboride under Pressure. Journal of Physical Chemistry C, 2017, 121, 7397-7403.	1.5	15
24796	Effect of pressure on two polymorphs of tolazamide: why no interconversion?. CrystEngComm, 2017, 19, 2243-2252.	1.3	27
24797	Theoretical investigation of CO catalytic oxidation by a Feâ€“PtSe₂ monolayer. RSC Advances, 2017, 7, 19630-19638.	1.7	10
24798	Comparison of Li, Na, Mg and Al-ion insertion in vanadium pentoxides and vanadium dioxides. RSC Advances, 2017, 7, 18643-18649.	1.7	66
24799	Landscape of DNA-like inorganic metal free double helical semiconductors and potential applications in photocatalytic water splitting. Journal of Materials Chemistry A, 2017, 5, 8484-8492.	5.2	22
24800	Role of phonons in negative thermal expansion and high pressure phase transitions in Î²-eucryptite: An ab-initio lattice dynamics and inelastic neutron scattering study. Journal of Applied Physics, 2017, 121, .	1.1	14
24801	Communication: Calculations of the (2 Ã— 1)-O reconstruction kinetics on Cu(110). Journal of Chemical Physics, 2017, 146, 111101.	1.2	8
24802	Excitonic effects in the optical properties of 2D materials:an equation of motion approach. 2D Materials, 2017, 4, 025086.	2.0	45
24803	Effect of the Ni size on CH 4 /CO 2 reforming over Ni/MgO catalyst: A DFT study. Chinese Journal of Chemical Engineering, 2017, 25, 1442-1448.	1.7	22
24804	Adhesion mechanism of bisphenol A diglycidyl ether (BADGE) on an Î±-Fe 2 O 3 (0001) surface. Journal of Industrial and Engineering Chemistry, 2017, 53, 62-67.	2.9	16
24805	Study of electronic and optical properties of two-layered hydrogenated aluminum nitrate nanosheet. Physica E: Low-Dimensional Systems and Nanostructures, 2017, 93, 234-237.	1.3	1
24806	Formation kinetics and mechanism of metastable vacancy-dioxygen complex in neutron irradiated Czochralski silicon. Superlattices and Microstructures, 2017, 107, 91-96.	1.4	4

#	Article	IF	Citations
24807	Tunability of the Adsorbate Binding on Bimetallic Alloy Nanoparticles for the Optimization of Catalytic Hydrogenation. Journal of the American Chemical Society, 2017, 139, 5538-5546.	6.6	96
24808	Electronic and optical properties of topological semimetal Cd3As2. Scientific Reports, 2017, 7, 45500.	1.6	39
24809	A kinetic model of water adsorption, clustering and dissociation on the Fe₃S₄{001} surface. Physical Chemistry Chemical Physics, 2017, 19, 12045-12055.	1.3	16
24810	Sulfur doped graphene as a promising metal-free electrocatalyst for oxygen reduction reaction: a DFT-D study. RSC Advances, 2017, 7, 20398-20405.	1.7	53
24811	First-principles identification of novel double perovskites for water-splitting applications. Journal of Materials Science, 2017, 52, 8518-8525.	1.7	10
24812	Synergetic control of band gap and structural transformation for optimizing TiO 2 photocatalysts. Applied Catalysis B: Environmental, 2017, 210, 513-521.	10.8	37
24813	Effect of the structure distortion on the high photocatalytic performance of C 60 /g-C 3 N 4 composite. Applied Surface Science, 2017, 414, 124-130.	3.1	74
24814	Adsorption of Zn(II) on the kaolinite(001) surfaces in aqueous environment: A combined DFT and molecular dynamics study. Applied Surface Science, 2017, 414, 405-412.	3.1	36
24815	Incipient FeO(1 1 1) monolayer formation during O-adsorption on Fe(1 1 0) surface. Computational Materials Science, 2017, 134, 109-115.	1.4	6
24816	Elastic, electronic and optical properties of stable pentagonal ZnO 2. Physica E: Low-Dimensional Systems and Nanostructures, 2017, 91, 82-87.	1.3	26
24817	Ru-Catalyzed Steam Methane Reforming: Mechanistic Study from First Principles Calculations. ACS Omega, 2017, 2, 1295-1301.	1.6	17
24818	Electric field effect of GaAs monolayer from first principles. AIP Advances, 2017, 7, .	0.6	25
24819	Spectroscopic Observation of a Hydrogenated CO Dimer Intermediate During CO Reduction on Cu(100) Electrodes. Angewandte Chemie, 2017, 129, 3675-3678.	1.6	112
24820	Modulation of electronic and optical properties of ZnO by inserting an ultrathin ZnX (XÂ= S, Se and Te) layer to form short-period (ZnO) 5 /(ZnX) 1 superlattice. Journal of Alloys and Compounds, 2017, 711, 581-591.	2.8	3
24821	Theoretical investigation of structural, elastic, and electronic properties of ternary boride MoAlB. Physica Status Solidi (B): Basic Research, 2017, 254, 1700010.	0.7	113
24822	A density functional theory study on the carbon chain growth of ethanol formation on Cu-Co (111) and (211) surfaces. Applied Surface Science, 2017, 412, 374-384.	3.1	27
24823	Electronic properties of MgZnPt 2 at extremely high temperatures and pressures. Chinese Journal of Physics, 2017, 55, 1011-1017.	2.0	0
24824	First-principles investigation on the geometries, stabilities and defective properties of fluoride surfaces. Computational Materials Science, 2017, 133, 159-166.	1.4	8

#	Article	IF	Citations
24825	Electronic and optical properties of paratellurite TeO2 under pressure: A first-principles calculation. Optik, 2017, 139, 9-15.	1.4	24
24826	Ab initio and experimental studies of polarization and polarization related fields in nitrides and nitride structures. AIP Advances, 2017, 7, .	0.6	23
24827	Platinum atomic contacts: From tunneling to contact. Physical Review B, 2017, 95, .	1.1	8
24828	Physical properties of ternary silicide superconductors Li₂XSi₃ (X = Rh, Os): An ab initio study. International Journal of Modern Physics B, 2017, 31, 1750135.	1.0	5
24829	Prediction on structural, mechanical and thermal properties of Al₄SiC₄, Al₄C₃ and 4H-SiC under high pressure by first-principles calculation. Modern Physics Letters B, 2017, 31, 1750080.	1.0	10
24830	Mechanism and Application of Carbon Nanotube Sensors in SF6 Decomposed Production Detection: a Review. Nanoscale Research Letters, 2017, 12, 177.	3.1	74
24831	Efficient photocatalytic hydrogen production over La/Rh co-doped Ruddlesden-Popper compound Sr 2 TiO 4. Applied Catalysis B: Environmental, 2017, 210, 149-159.	10.8	45
24832	Effects of halogens on interactions between a reduced TiO 2 (110) surface and noble metal atoms: A DFT study. Applied Surface Science, 2017, 411, 149-162.	3.1	21
24833	Structural, electronic and optical properties of monoclinic Na 2 Ti 3 O 7 from density functional theory calculations: A comparison with XRD and optical absorption measurements. Journal of Solid State Chemistry, 2017, 250, 68-74.	1.4	38
24834	Structural, electronic, mechanical and quantum transport of ultrathin gold nanowire: A density functional approach. Superlattices and Microstructures, 2017, 106, 206-215.	1.4	9
24835	Bonding interactions in Li/Na oxides, peroxides and superoxides and their implication to the performance of the Li/Na-air batteries. Solid State Ionics, 2017, 303, 24-28.	1.3	3
24836	Probing lattice vibration and surface electronic state in a layered (NH4)2V3O8 single crystal. Journal of Materials Chemistry C, 2017, 5, 4185-4189.	2.7	0
24837	Solid-State NMR Spectroscopy Study of Cation Dynamics in Layered Na₂Ti₃O₇ and Li₂Ti₃O₇. Zeitschrift Fur Physikalische Chemie, 2017, 231, 1243-1262.	1.4	4
24838	Density functional theory study of CO2 and H2O adsorption on a monoclinic WO3(001) surface. Chemical Research in Chinese Universities, 2017, 33, 255-260.	1.3	12
24839	The role of negatively charged oxygen vacancies upon Î²-MnO2 conductivity. Acta Materialia, 2017, 131, 88-97.	3.8	13
24840	Structural, elastic and electronic properties of B2-type modified by ternary additions FeAl-based intermetallics: First-principles study. Journal of Alloys and Compounds, 2017, 710, 581-588.	2.8	43
24841	Wide-range ideal 2D Rashba electron gas with large spin splitting in Bi2Se3/MoTe2 heterostructure. Npj Computational Materials, 2017, 3, .	3.5	25
24842	Electronic structure and multi-scale behaviour for the dislocationâ€“doping complex in the gamma phase of nickel-base superalloys. RSC Advances, 2017, 7, 19124-19135.	1.7	7

#	Article	IF	Citations
24843	Systematic density functional theory study of the structural and electronic properties of constrained and fully relaxed (0Â0Â1) surfaces of alumina and hematite. Molecular Simulation, 2017, 43, 406-419.	0.9	23
24844	Band engineering of the MoS₂/stanene heterostructure: strain and electrostatic gating. Nanotechnology, 2017, 28, 195702.	1.3	44
24845	First-principles calculation of lattice thermal conductivity in crystalline phase change materials: GeTe, <mml:math xmlns:mml="http://www.w3.org/1998/Math/MathML"><mml:mrow><mml:msub><mml:mi mathvariant="bold">Sb</mml:mi><mml:mn>2</mml:mn></mml:msub><mml:msub><mml:mi mathvariant="bold">Te</mml:mi><mml:mn>3</mml:mn></mml:msub></mml:mrow></mml:math> , and <mml:math xmlns:mml="http://www.w3.org/1998/Math/MathML"><mml:mrow><mml:msub><mml:mi mat	1.1	86
24846	Effects of Ga content on the stability of Fe-X (X = 6.25, 12.5, 18.75, 25 at.% Ga) alloys from first-principles calculations. Modern Physics Letters B, 2017, 31, 1750098.	1.0	2
24847	LaTiO_xN_y Thin Film Model Systems for Photocatalytic Water Splitting: Physicochemical Evolution of the Solidâ€“Liquid Interface and the Role of the Crystallographic Orientation. Advanced Functional Materials, 2017, 27, 1605690.	7.8	38
24848	Enhancing visible light photocatalytic activity of KNbO $$_{3}$$ 3 by Nâ€“F passivated co-doping for hydrogen generation by water splitting. Journal of Materials Science, 2017, 52, 5333-5344.	1.7	7
24849	Optical properties of (Pb 1- x Mn x S) 1- y Fe y materials from first-principles calculations. Chinese Journal of Physics, 2017, 55, 1032-1043.	2.0	36
24850	Enabling accurate first principle calculations of electronic properties with a corrected <mml:math xmlns:mml="http://www.w3.org/1998/Math/MathML" altimg="si3.gif" overflow="scroll"><mml:mrow><mml:mi mathvariant="bold">k</mml:mi><mml:mo>Â·</mml:mo><mml:mi mathvariant="bold">p</mml:mi></mml:mrow></mml:math> scheme. Computational Materials Science, 2017, 134, 17-24.	1.4	13
24851	The novel structure and superconductivity of zirconium hydride. Computational Materials Science, 2017, 134, 38-41.	1.4	5
24852	Efficiency evaluation on Cs x [NH 2 CH = NH 2] 1â^' x Pb(I 1â^' y Br y) 3 /crystalline silicon tandem solar cells. Solar Energy, 2017, 147, 432-438.	2.9	7
24853	Cr_{0.5}Nb_{24.5}O₆₂ Nanowires with High Electronic Conductivity for High-Rate and Long-Life Lithium-Ion Storage. ACS Nano, 2017, 11, 4217-4224.	7.3	121
24854	Na-rich layered Na2Ti1â^'xCrxO3â^'x/2 (xâ€‰=â€‰0, 0.06): Na-ion battery cathode materials with high capacity and long cycle life. Scientific Reports, 2017, 7, 373.	1.6	25
24855	Chemical states of 3d transition metal impurities in a liquid leadâ€“bismuth eutectic analyzed using first principles calculations. Physical Chemistry Chemical Physics, 2017, 19, 9945-9956.	1.3	16
24856	Femtosecond laser induced desorption of <mml:math xmlns:mml="http://www.w3.org/1998/Math/MathML"><mml:msub><mml:mi mathvariant="normal">H</mml:mi><mml:mn>2</mml:mn></mml:msub><mml:mo>,</mml:mo><mml:msub><mml:mi mathvariant="normal">D</mml:mi><mml:mn>2</mml:mn></mml:msub></mml:math> , and HD from Ru(0001): Dynamical promotion and suppression studied with ab initio molecular dynamics with electronic friction. Physical Review B, 2017, 95, .	1.1	26
24857	Electronic structure, lattice dynamics, and thermoelectric properties of bismuth nanowire from first-principles calculation. Journal of Materials Research, 2017, 32, 2405-2413.	1.2	3
24858	Fast hydrogen diffusion along Î£13 grain boundary of Î±-Al2O3 and its suppression by the dopant Cr: A first-principles study. International Journal of Hydrogen Energy, 2017, 42, 10124-10130.	3.8	10
24859	Electronic structure and magnetism of RbGd2Fe4As4O2. Journal of Alloys and Compounds, 2017, 708, 392-396.	2.8	7
24860	First-principles investigation of metal-doped cubic BaTiO 3. Materials Research Bulletin, 2017, 96, 372-378.	2.7	39

#	Article	IF	Citations
24861	First-principles study on doping of tetragonal ZnSe monolayers. Materials Today Chemistry, 2017, 4, 40-44.	1.7	13
24862	Goldâ€“Ligand-Catalyzed Selective Hydrogenation of Alkynes into cis-Alkenes via H₂ Heterolytic Activation by Frustrated Lewis Pairs. ACS Catalysis, 2017, 7, 2973-2980.	5.5	108
24863	Artificial neural network for the configuration problem in solids. Journal of Chemical Physics, 2017, 146, 064103.	1.2	10
24864	New ternary superconducting compound LaRu ₂ As ₂ : Physical properties from density functional theory calculations. Chinese Physics B, 2017, 26, 037103.	0.7	39
24865	Piezoelectricity in two-dimensional materials: Comparative study between lattice dynamics andab initiocalculations. Physical Review B, 2017, 95, .	1.1	36
24866	The Influence of Water on the Performance of Molybdenum Carbide Catalysts in Hydrodeoxygenation Reactions: A Combined Theoretical and Experimental Study. ChemCatChem, 2017, 9, 1985-1991.	1.8	29
24867	Ultra high stiffness and thermal conductivity of graphene like C3N. Carbon, 2017, 118, 25-34.	5.4	235
24868	An embedded atom method interatomic potential for the zirconium-iron system. Computational Materials Science, 2017, 133, 6-13.	1.4	5
24869	Investigation of Iron-based double perovskite oxides on the magnetic phase stability, mechanical, electronic and optical properties via first-principles calculation. Materials Chemistry and Physics, 2017, 193, 453-469.	2.0	68
24870	Thermodynamics of GaN(s)-NH 3 (v)+N 2 (v)+H 2 (v) system â€“ Electronic aspects of the processes at GaN(0001) surface. Surface Science, 2017, 662, 12-33.	0.8	12
24871	Dipole-Moment Reversal in a Polar Organic Monolayer Probed by Sum and Difference Frequency Spectroscopy. Journal of Physical Chemistry C, 2017, 121, 6692-6700.	1.5	4
24872	Towards high visible light photocatalytic activity in rare earth and N co-doped SrTiO₃: a first principles evaluation and prediction. RSC Advances, 2017, 7, 16282-16289.	1.7	28
24873	Unique topological surface states of full-Heusler topological crystalline insulators. Physical Review B, 2017, 95, .	1.1	10
24874	2D-ordered kinked carbyne chains: DFT modeling and Raman characterization. Carbon, 2017, 117, 271-278.	5.4	31
24875	Charge-induced electrochemical actuation of armchair carbon nanotube bundles. Carbon, 2017, 118, 278-284.	5.4	12
24876	In situ intercalation polymerization approach to polyamide-6/graphite nanoflakes for enhanced thermal conductivity. Composites Part B: Engineering, 2017, 117, 165-173.	5.9	92
24877	Luminescence of VO 4 3â^' centers in LiMgPO 4 and LiMgVO 4 : Effect of [PO 4] 3â^' /[VO 4] 3â^' substitution on the structure and optical properties. Journal of Alloys and Compounds, 2017, 709, 1-7.	2.8	15
24878	Structural, Electronic, and Optical Properties of Cu₂NiSnS₄: A Combined Experimental and Theoretical Study toward Photovoltaic Applications. Chemistry of Materials, 2017, 29, 3133-3142.	3.2	90

#	Article	IF	Citations
24879	Counterintuitive Adsorption of [PW₁₁O₃₉]^{7â€“} on Au(100). Inorganic Chemistry, 2017, 56, 3961-3969.	1.9	18
24880	High-Throughput Survey of Ordering Configurations in MXene Alloys Across Compositions and Temperatures. ACS Nano, 2017, 11, 4407-4418.	7.3	146
24881	Adsorption of small inorganic molecules on a defective MoS₂monolayer. Physical Chemistry Chemical Physics, 2017, 19, 9485-9499.	1.3	68
24882	The mechanism of hydrogen adsorption on transition metal dichalcogenides as hydrogen evolution reaction catalyst. Physical Chemistry Chemical Physics, 2017, 19, 10125-10132.	1.3	126
24883	Intrinsic defects and their effects on the optical properties in the nonlinear optical crystal CdSiP₂: a first-principles study. Physical Chemistry Chemical Physics, 2017, 19, 9558-9565.	1.3	14
24884	Orbitally driven low thermal conductivity of monolayer gallium nitride (GaN) with planar honeycomb structure: a comparative study. Nanoscale, 2017, 9, 4295-4309.	2.8	155
24885	Optimizing CdTeâ€“metal interfaces for high performance solar cells. Journal of Materials Chemistry A, 2017, 5, 7118-7124.	5.2	18
24886	Lattice dynamics and ferroelectric properties of the nitride perovskite <mml:math xmlns:mml="http://www.w3.org/1998/Math/MathML"><mml:msub><mml:mi>LaWN</mml:mi><mml:mn>3</mml:mn></mml:msub><m Physical Review B, 2017, 95, .	1.1	48
24887	Self-consistent mapping: Effect of local environment on formation of magnetic moment in <mml:math xmlns:mml="http://www.w3.org/1998/Math/MathML"><mml:mrow><mml:mi>Î±</mml:mi><mml:mo>â^’</mml:mo><mml:mn Physical Review B, 2017, 95, .	1.1	16
24888	Lattice-matched heterojunctions between topological and normal insulators: A first-principles study. Physical Review B, 2017, 95, .	1.1	6
24889	Stacking fault energies of nondilute binary alloys using special quasirandom structures. Physical Review B, 2017, 95, .	1.1	9
24890	Experimental synthesis and density functional theory investigation of radiation tolerance of Zr₃(Al_{1â€“}<scp>_xS</scp>i_x)C₂<scp>MAX</scp> phases. Journal of the American Ceramic Society, 2017, 100, 1377-1387.	1.9	45
24891	Influence of the external pressure on the quantum correlations of molecular magnets. Europhysics Letters, 2017, 117, 20004.	0.7	6
24892	First Principles Calculations of Transition Metal Binary Alloys: Phase Stability and Surface Effects. Journal of Electronic Materials, 2017, 46, 3776-3783.	1.0	13
24893	First-principles calculations and thermodynamic modeling of the Sn-Ta system. Calphad: Computer Coupling of Phase Diagrams and Thermochemistry, 2017, 57, 46-54.	0.7	4
24894	Reaction pathway of CH 4 /CO 2 reforming over Ni8/MgO(100). Surface Science, 2017, 660, 22-30.	0.8	13
24895	Size-Selective Reactivity of Subnanometer Ag₄ and Ag₁₆ Clusters on a TiO₂ Surface. Journal of Physical Chemistry C, 2017, 121, 6614-6625.	1.5	21
24896	First-Principles Study: Tuning the Redox Behavior of Lithium-Rich Layered Oxides by Chlorine Doping. Journal of Physical Chemistry C, 2017, 121, 7155-7163.	1.5	41

#	Article	IF	Citations
24897	Rare earth separations by selective borate crystallization. Nature Communications, 2017, 8, 14438.	5.8	125
24898	Solution of an elusive pigment crystal structure from a thin film: a combined X-ray diffraction and computational study. CrystEngComm, 2017, 19, 1902-1911.	1.3	15
24899	Determination of a complex crystal structure in the absence of single crystals: analysis of powder X-ray diffraction data, guided by solid-state NMR and periodic DFT calculations, reveals a new 2â€²-deoxyguanosine structural motif. Chemical Science, 2017, 8, 3971-3979.	3.7	62
24900	Cobalt-related defects in silicon. Journal of Applied Physics, 2017, 121, .	1.1	7
24901	Quantum anomalous Hall effect in ferromagnetic transition metal halides. Physical Review B, 2017, 95, .	1.1	110
24902	Density Functional Theory Study on Formation Energy and Diffusion Path of Metal Atom near Dopant in Si Crystals. ECS Journal of Solid State Science and Technology, 2017, 6, P125-P131.	0.9	6
24903	Cohesive Properties of Cu-X and Ni-X (In, Sn) Intermetallics: Ab Initio Systematics, Correlations and â€œUniversalityâ€•Features. Journal of Phase Equilibria and Diffusion, 2017, 38, 257-267.	0.5	2
24904	MoTe2 is a good match for GeI by preserving quantum spin Hall phase. Nano Research, 2017, 10, 2823-2832.	5.8	7
24905	Selectivity of CO and NO adsorption on ZnO (0002) surfaces: A DFT investigation. Applied Surface Science, 2017, 410, 373-382.	3.1	40
24906	Formation of indium arsenide atomic wires on the In/Si(111)-4ÂÃ—Â1 surface. Superlattices and Microstructures, 2017, 103, 19-27.	1.4	1
24907	Room-Temperature Magneto-dielectric Effect in LaGa_{0.7}Fe_{0.3}O_{3+Î³}; Origin and Impact of Excess Oxygen. Inorganic Chemistry, 2017, 56, 3809-3819.	1.9	14
24908	Structural, Electronic, and Thermodynamic Properties of the T and B Phases of Niobia: First-Principle Calculations. Journal of Physical Chemistry A, 2017, 121, 2399-2409.	1.1	26
24909	Monolayer Group IVâ€“VI Monochalcogenides: Low-Dimensional Materials for Photocatalytic Water Splitting. Journal of Physical Chemistry C, 2017, 121, 7615-7624.	1.5	154
24910	Atomic Layer Etching Mechanism of MoS₂ for Nanodevices. ACS Applied Materials & Interfaces, 2017, 9, 11967-11976.	4.0	81
24911	Nanostructured Bulk-Heterojunction Solar Cells Based on Amorphous Carbon. ACS Energy Letters, 2017, 2, 882-888.	8.8	3
24912	Modulation of electronic and optical properties in mixed halide perovskites CsPbCl3xBr3(1-x) and CsPbBr3xI3(1-x). Applied Physics Letters, 2017, 110, .	1.5	28
24913	Neutron filter efficiency of beryllium and magnesium fluorides. Journal of Applied Crystallography, 2017, 50, 441-450.	1.9	4
24914	Modulation of interfacial electronic properties in PbI 2 and BN van der Waals heterobilayer via external electric field. Applied Surface Science, 2017, 411, 46-52.	3.1	16

#	Article	IF	Citations
24915	Structural, electronic and magnetic properties of Ti-doped polar and nonpolar GaN surfaces. Journal of Crystal Growth, 2017, 467, 12-17.	0.7	6
24916	First-principles electrostatic potentials for reliable alignment at interfaces and defects. Journal of Chemical Physics, 2017, 146, 104109.	1.2	49
24917	Interplay of electronic, structural and magnetic properties as the driving feature of high-entropy CoCrFeNiPd alloys. Journal Physics D: Applied Physics, 2017, 50, 185002.	1.3	16
24918	Comparative study of Mo ₂ Ga ₂ C with superconducting MAX phase Mo ₂ GaC: First-principles calculations. Chinese Physics B, 2017, 26, 033102.	0.7	32
24919	Structural phase transition, electronic, elastic, and vibrational properties of LiAl intermetallic compound: insights from first-principles calculations. Canadian Journal of Physics, 2017, 95, 691-698.	0.4	4
24920	The Crystal Structure of Nitridomagnesogermanate Ba[Mg₃GeN₄]:Eu²⁺ and Theoretical Calculations of Its Electronic Properties. European Journal of Inorganic Chemistry, 2017, 2017, 2422-2427.	1.0	8
24921	Effect of Ti addition on the thermal expansion anisotropy of Mo5Si3. Acta Materialia, 2017, 132, 25-34.	3.8	12
24922	A DFT study and micro-kinetic analysis of acetylene selective hydrogenation on Pd-doped Cu(111) surfaces. Applied Surface Science, 2017, 410, 154-165.	3.1	42
24923	First-principles study of H, O, and N adsorption on metal embedded carbon nanotubes. Applied Surface Science, 2017, 403, 645-651.	3.1	6
24924	The effect of yttrium on the generalized stacking fault energies in Mg. Computational Materials Science, 2017, 133, 1-5.	1.4	15
24925	Chiral penta-graphene nanotubes: Structure, bonding and electronic properties. Computational and Theoretical Chemistry, 2017, 1108, 70-75.	1.1	21
24926	SPARC: Accurate and efficient finite-difference formulation and parallel implementation of Density Functional Theory: Extended systems. Computer Physics Communications, 2017, 216, 109-125.	3.0	109
24927	Very low dielectric loss and giant dielectric response with excellent temperature stability of Ga 3+ and Ta 5+ co-doped rutile-TiO 2 ceramics. Materials and Design, 2017, 123, 15-23.	3.3	114
24928	Atomistic modeling study of a strain-free stress driven grain boundary migration mechanism. Scripta Materialia, 2017, 134, 52-56.	2.6	10
24929	First principles study of effects of vacancies on electronic, magnetic and optical properties of InN nanosheet. Superlattices and Microstructures, 2017, 105, 99-109.	1.4	20
24930	First-Principles Calculations on the Crystal/Electronic Structure and Phase Stability of H-Doped SrFeO₂. Journal of Physical Chemistry C, 2017, 121, 7478-7484.	1.5	1
24931	Quartic Dispersion, Strong Singularity, Magnetic Instability, and Unique Thermoelectric Properties in Two-Dimensional Hexagonal Lattices of Group-VA Elements. Nano Letters, 2017, 17, 2589-2595.	4.5	33
24932	First-principles study of structural stability, dynamical and mechanical properties of Li₂FeSiO₄ polymorphs. RSC Advances, 2017, 7, 16843-16853.	1.7	32

#	Article	IF	Citations
24933	Dissipation of the excess energy of the adsorbate-thermalization via electron transfer. Physical Chemistry Chemical Physics, 2017, 19, 9149-9155.	1.3	4
24934	A first-principles comparative study of lithium, sodium, and magnesium storage in pure and gallium-doped germanium: Competition between interstitial and substitutional sites. Journal of Chemical Physics, 2017, 146, 034706.	1.2	17
24935	Efficient noble metal nanocatalysts supported on HfC(001) for O2 dissociation. AIP Advances, 2017, 7, .	0.6	6
24936	DFT and TPD study of the role of steps in the adsorption of CO on copper: Cu(4â€‰1â€‰0) versus Cu(1â€‰0â€‰0). Journal of Physics Condensed Matter, 2017, 29, 194001.	0.7	13
24937	First-principles study of the dynamic Jahn-Teller distortion of the neutral vacancy in diamond. Physical Review B, 2017, 95, .	1.1	23
24938	Optical absorbance and band-gap engineering of<mml:math xmlns:mml="http://www.w3.org/1998/Math/MathML"><mml:mrow><mml:msub><mml:mrow><mml:mo>(</mml:mo><mml:mi>BN</mml:mi></mml:mrow><mml:mrow><mml:mo>)</mml:mo><mml:mi>x</mml:mi></mml:mrow></mml:msub><mml:mo>(</mml:mo><mml:mi>C</mml:mi><mml:msub><mml:mrow><mml:mo>)</mml:mo><mml:mi>y</mml:mi></mml:mrow><mml:mrow><mml:mo>(</mml:mo><mml:mi>BN</mml:mi></mml:mrow></mml:msub></mml:mrow></mml:math> alloys: Phase s. Physical Review B, 2017, 95, .	1.1	24
24939	Tunable dynamics of a flake on graphene: Libration frequency. Physical Review B, 2017, 95, .	1.1	7
24940	Strain Effect on the Electronic and Optical Properties of CdSe Nanowires. Nanoscale Research Letters, 2017, 12, 178.	3.1	20
24941	n- and p-type dopants in the InSe monolayer via substitutional doping. Journal of Materials Science, 2017, 52, 7207-7214.	1.7	48
24942	Hydrogen Evolution Reaction on Nanostructures Electrodesâ€”a Scenario on Stepped Silver Surfaces. Electrocatalysis, 2017, 8, 587-593.	1.5	4
24943	Tailoring of the electronic properties of ZnO-polyacrylonitrile nanofibers: Experiment and theory. Applied Surface Science, 2017, 411, 494-501.	3.1	34
24944	Experimental study and thermodynamic modeling of the Al-Sc-Zr system. Computational Materials Science, 2017, 133, 82-92.	1.4	18
24945	The influence of spin orbit interaction on phonons and superconductivity in the noncentrosymmetric superconductors LaPt 3 Si and LaPtSi 3. Intermetallics, 2017, 86, 1-10.	1.8	10
24946	Nanolines of transition metals ruled by grain boundaries in graphene: An ab initio study. Materials Chemistry and Physics, 2017, 194, 118-127.	2.0	5
24947	Molecule-decorated rutile-type ZnF 2 (110): A periodic DFT study. Surface Science, 2017, 662, 34-41.	0.8	5
24948	Strain Controlled Ferromagnetic-Antiferromagnetic Transformation in Mn-Doped Silicene for Information Transformation Devices. Journal of Physical Chemistry Letters, 2017, 8, 1484-1488.	2.1	55
24949	Atomistic Insights into Nucleation and Formation of Hexagonal Boron Nitride on Nickel from First-Principles-Based Reactive Molecular Dynamics Simulations. ACS Nano, 2017, 11, 3585-3596.	7.3	55
24950	Optimizing Charge Injection across Transition Metal Dichalcogenide Heterojunctions: Theory and Experiment. ACS Nano, 2017, 11, 3904-3910.	7.3	29

#	Article	IF	Citations
24951	LiSr₃Be₃B₃O₉F₄: a new ultraviolet nonlinear optical crystal for fourth-harmonic generation of Nd:YAG lasers. New Journal of Chemistry, 2017, 41, 4269-4272.	1.4	18
24952	Combined experiment and first-principles study of the formation of the Al₂O₃ layer in alumina-forming austenitic stainless steel. RSC Advances, 2017, 7, 15727-15734.	1.7	9
24953	Beyond lithium-ion batteries: A computational study on Na-S and Na-O batteries. IOP Conference Series: Materials Science and Engineering, 2017, 169, 012001.	0.3	4
24954	Rapid Ultrasoundâ€Assisted Synthesis of Mesoporous Manganese Oxides for Lowâ€Concentration NO Elimination with Superior Waterâ€Resistance. European Journal of Inorganic Chemistry, 2017, 2017, 2573-2579.	1.0	1
24955	Layer effect on catalytic activity of Pd-Cu bimetal for CO oxidation. Applied Catalysis A: General, 2017, 538, 66-73.	2.2	8
24956	Effect of nanostructuring of ZnO for gas sensing of nitrogen dioxide. Computational Materials Science, 2017, 132, 104-115.	1.4	23
24957	Biaxial tensile strain modulates magnetic properties of the 3d transition metal doped stanene. Superlattices and Microstructures, 2017, 106, 33-49.	1.4	4
24958	Hierarchical on-surface synthesis and electronic structure of carbonyl-functionalized one- and two-dimensional covalent nanoarchitectures. Nature Communications, 2017, 8, 14765.	5.8	120
24959	First-principles investigation of point defect and atomic diffusion in Al 2 Ca. Journal of Physics and Chemistry of Solids, 2017, 103, 6-12.	1.9	8
24960	Study of the thermal stability of studtite by in situ Raman spectroscopy and DFT calculations. Spectrochimica Acta - Part A: Molecular and Biomolecular Spectroscopy, 2017, 174, 245-253.	2.0	46
24961	New insight into Li/Ni disorder in layered cathode materials for lithium ion batteries: a joint study of neutron diffraction, electrochemical kinetic analysis and first-principles calculations. Journal of Materials Chemistry A, 2017, 5, 1679-1686.	5.2	73
24962	Microstructure, mechanical properties, and electronic simulations of steel/aluminum alloy joint during deep penetration laser welding. International Journal of Advanced Manufacturing Technology, 2017, 89, 377-387.	1.5	9
24963	X-ray diffraction data-assisted structure searches. Computer Physics Communications, 2017, 213, 40-45.	3.0	30
24964	Elastic properties of cubic K2B12H12 from theoretical calculations. Journal of Alloys and Compounds, 2017, 695, 2916-2922.	2.8	16
24965	Solution-processable exfoliation and photoelectric properties of two-dimensional layered MoS2 photoelectrodes. Journal of Colloid and Interface Science, 2017, 490, 287-293.	5.0	25
24966	Li ion diffusion dynamics on Li oxides and peroxides surfaces. Materials Letters, 2017, 188, 208-211.	1.3	2
24967	Formation of New Phases to Improve the Visible-Light Photocatalytic Activity of Tio₂ (B) Via Introducing Alien Elements. Journal of Physical Chemistry C, 2017, 121, 52-59.	1.5	1
24968	Anisotropic Electronic Structure and Transport Properties of the H-0 Hyperhoneycomb Lattice. Journal of Physical Chemistry C, 2017, 121, 1928-1933.	1.5	1

#	Article	IF	Citations
24969	Edge-Controlled Growth and Etching of Two-Dimensional GaSe Monolayers. Journal of the American Chemical Society, 2017, 139, 482-491.	6.6	65
24970	Topological insulating states in 2D transition metal dichalcogenides induced by defects and strain. Nanoscale, 2017, 9, 562-569.	2.8	28
24971	Softening and hardening of yield stress by hydrogenâ€“solute interactions. Philosophical Magazine, 2017, 97, 400-418.	0.7	34
24972	Two-dimensional SiP: an unexplored direct band-gap semiconductor. 2D Materials, 2017, 4, 015030.	2.0	78
24973	First-Principles Investigations on Structural, Elastic, Dynamical, and Thermal Properties of Earth-Abundant Nitride Semiconductor CaZn₂N₂ under Pressure. Zeitschrift Fur Naturforschung - Section A Journal of Physical Sciences, 2017, 72, 39-49.	0.7	8
24974	Effect of transition metal-doped Ni(211) for CO dissociation: Insights from DFT calculations. Applied Surface Science, 2017, 399, 255-264.	3.1	12
24975	Determination of Bulk and Surface Atomic Arrangement in Niâ€“Zn Î³-Brass Phase at Different Ni to Zn Ratios. Chemistry of Materials, 2017, 29, 504-512.	3.2	17
24976	Photoelectrochemical Properties and Behavior of Î±-SnWO₄ Photoanodes Synthesized by Hydrothermal Conversion of WO₃ Films. ACS Applied Materials & Interfaces, 2017, 9, 1459-1470.	4.0	42
24977	Nanopatterning of Group V Elements for Tailoring the Electronic Properties of Semiconductors by Monolayer Doping. ACS Applied Materials & Interfaces, 2017, 9, 1922-1928.	4.0	9
24978	Chemical Vapor Deposition Growth of Few-Layer MoTe₂ in the 2H, 1Tâ€², and 1T Phases: Tunable Properties of MoTe₂ Films. ACS Nano, 2017, 11, 900-905.	7.3	173
24979	Auâ€“Ge MEAM potential fitted to the binary phase diagram. Modelling and Simulation in Materials Science and Engineering, 2017, 25, 025004.	0.8	5
24980	The structural, elastic, electronic and dynamical properties of chalcopyrite semiconductor BeGeAs2 from first-principles calculations. Applied Physics A: Materials Science and Processing, 2017, 123, 1.	1.1	3
24981	Exploring novel phases of Cdâ€“O system at ambient pressure. Physics Letters, Section A: General, Atomic and Solid State Physics, 2017, 381, 685-688.	0.9	6
24982	Can a Photosensitive Oxide Catalyze Decomposition of Energetic Materials?. Journal of Physical Chemistry C, 2017, 121, 1153-1161.	1.5	12
24983	High-Mobility Transport Anisotropy in Few-Layer MoO₃ and Its Origin. ACS Applied Materials & Interfaces, 2017, 9, 1702-1709.	4.0	51
24984	Hydrogenâ€“vacancyâ€“dislocation interactions inÎ±-Fe. Modelling and Simulation in Materials Science and Engineering, 2017, 25, 025001.	0.8	28
24985	Half-metallic ferromagnetic features in d0 quaternary-Heusler compounds KCaCF and KCaCCl: A first-principles description. Journal of Magnetism and Magnetic Materials, 2017, 428, 250-254.	1.0	27
24986	First-principles predictions of ruthenium-phosphorus and ruthenium-boron glassy structures and chemical vapor deposition of thin amorphous ruthenium-boron alloy films. Thin Solid Films, 2017, 622, 56-64.	0.8	4

#	Article	IF	Citations
24987	Theory and Applications of Generalized Pipekâ€“Mezey Wannier Functions. Journal of Chemical Theory and Computation, 2017, 13, 460-474.	2.3	32
24988	Time-Domain ab Initio Modeling of Electronâ€“Phonon Relaxation in High-Temperature Cuprate Superconductors. Journal of Physical Chemistry Letters, 2017, 8, 193-198.	2.1	20
24989	The effect of pressure on the structural, electronic, magnetic, and thermodynamic properties of the Mn2RuGe inverse Heusler alloy. Journal of Magnetism and Magnetic Materials, 2017, 428, 287-292.	1.0	8
24990	Size-Dependent Structure Relations between Nanotubes and Encapsulated Nanocrystals. Nano Letters, 2017, 17, 805-810.	4.5	24
24991	First-Principles Investigation of the Epitaxial Stabilization of Oxide Polymorphs: TiO₂ on (Sr,Ba)TiO₃. ACS Applied Materials & Interfaces, 2017, 9, 4106-4118.	4.0	17
24992	A new quaternary semiconductor compound (Ba2Sb4GeS10): Ab initio study. Philosophical Magazine, 2017, 97, 549-560.	0.7	5
24993	The tunneling magnetoresistance and spin-polarized optoelectronic properties of graphyne-based molecular magnetic tunnel junctions. Journal Physics D: Applied Physics, 2017, 50, 075103.	1.3	5
24994	Activating Basal Planes and Sâ€Terminated Edges of MoS₂ toward More Efficient Hydrogen Evolution. Advanced Functional Materials, 2017, 27, 1604943.	7.8	131
24995	Metamorphosis in carbon network: From penta-graphene to biphenylene under uniaxial tension. FlatChem, 2017, 1, 65-73.	2.8	46
24996	Pressure dependence of thermal physical properties of A-type R 2 O 3 (R=Y, La): A first-principles study. Journal of Physics and Chemistry of Solids, 2017, 103, 49-58.	1.9	7
24997	Ab initio study of He trapping, diffusion and clustering in Y2O3. Nuclear Instruments & Methods in Physics Research B, 2017, 393, 82-87.	0.6	6
24998	First-principles study of Al 2 Sm intermetallic compound on structural, mechanical properties and electronic structure. Solid State Communications, 2017, 251, 98-103.	0.9	8
24999	New Class of 3D Topological Insulator in Double Perovskite. Journal of Physical Chemistry Letters, 2017, 8, 332-339.	2.1	27
25000	Acetylene adsorption on Î´-MoC(001), TiC(001) and ZrC(001) surfaces: a comprehensive periodic DFT study. Physical Chemistry Chemical Physics, 2017, 19, 1571-1579.	1.3	13
25001	Theoretical stability and materials synthesis of a chemically ordered MAX phase, Mo2ScAlC2, and its two-dimensional derivate Mo2ScC2 MXene. Acta Materialia, 2017, 125, 476-480.	3.8	185
25002	Stability and properties of the friendly environmental Zintl phases: Ca3Si4 and Ca14Si19. Acta Materialia, 2017, 125, 490-497.	3.8	7
25003	First-principles calculations for the mechanical properties of Ti-Nb-B2 solid solutions. Computational Materials Science, 2017, 129, 82-88.	1.4	11
25004	Multi-fidelity machine learning models for accurate bandgap predictions of solids. Computational Materials Science, 2017, 129, 156-163.	1.4	235

#	Article	IF	Citations
25005	An experimental and theoretical investigation on the optical and photocatalytic properties of ZnS nanoparticles. Journal of Physics and Chemistry of Solids, 2017, 103, 179-189.	1.9	46
25006	Simultaneously efficient light absorption and charge transport of phosphate and oxygen-vacancy confined in bismuth tungstate atomic layers triggering robust solar CO2 reduction. Nano Energy, 2017, 32, 359-366.	8.2	208
25007	A structural insight into mechanical strength of graphene-like carbon and carbon nitride networks. Nanotechnology, 2017, 28, 055707.	1.3	32
25008	Methanol decomposition on low index and stepped CeO 2 surfaces from GGA+ U. Applied Surface Science, 2017, 394, 509-518.	3.1	8
25009	Influence of point defects on optical properties of GaN-based materials by first principle study. Computational Materials Science, 2017, 129, 49-54.	1.4	14
25010	Density functional theory study on the effect of OH and Cl adsorption on the surface structure of Î±-Fe2O3. Computational and Theoretical Chemistry, 2017, 1100, 91-101.	1.1	22
25011	First principles study of the crystal, electronic structure, and diffusion mechanism of polaron-Na vacancy of Na₃MnPO₄CO₃for Na-ion battery applications. Journal Physics D: Applied Physics, 2017, 50, 045502.	1.3	18
25012	Elastic and electronic properties of oxygen plasma-treated graphene sheets from first principles. International Journal of Modern Physics B, 2017, 31, 1750054.	1.0	0
25013	Multifunctional Materials: A Case Study of the Effects of Metal Doping on ZnO Tetrapods with Bismuth and Tin Oxides. Advanced Functional Materials, 2017, 27, 1604676.	7.8	140
25014	Theoretical study of the impact of stress and interstitial oxygen on the behavior of intrinsic point defects in growing Czochralski Si crystals. Journal of Crystal Growth, 2017, 474, 89-95.	0.7	8
25015	Experimental and Theoretical Investigation of the Restructuring Process Induced by CO at Near Ambient Pressure: Pt Nanoclusters on Graphene/Ir(111). ACS Nano, 2017, 11, 1041-1053.	7.3	29
25016	Investigation of intrinsic defect magnetic properties in wurtzite ZnO materials. Journal of Magnetism and Magnetic Materials, 2017, 440, 5-9.	1.0	19
25017	Magnesium carbide monolayer: A novel quasi-planar semiconductor. Superlattices and Microstructures, 2017, 102, 134-140.	1.4	18
25018	Toward Two-Dimensional Superatomic Honeycomb Structures. Evaluation of [Ge₉(Si(SiMe₃))₃]^{â^'} as Source of Ge₉â€“Cluster Building Blocks for Extended Materials. Journal of Physical Chemistry C, 2017, 121, 1934-1940.	1.5	12
25019	Edge-Modified Graphene Nanoribbons: Appearance of Robust Spiral Magnetism. Journal of Physical Chemistry C, 2017, 121, 1371-1376.	1.5	12
25020	Graphene-family nanomaterials assembled with cobalt oxides and cobalt nanoparticles as hybrid supercapacitive electrodes and enzymeless glucose detection platforms. Journal of Materials Research, 2017, 32, 301-322.	1.2	25
25021	A new carbon allotrope: Penta-graphene as a metal-free catalyst for CO oxidation. Carbon, 2017, 114, 465-472.	5.4	91
25022	Single Pd atoms supported by graphitic carbon nitride, a potential oxygen reduction reaction catalyst from theoretical perspective. Carbon, 2017, 114, 619-627.	5.4	78

#	Article	IF	Citations
25023	Crystal and electronic structures of substituted halide perovskites based on density functional calculation and molecular dynamics. Chemical Physics, 2017, 485-486, 22-28.	0.9	12
25024	Thermal quenching of Eu 2+ emission in Ca- and Sr-Ga 2 S 4 in relation with VRBE schemes. Journal of Luminescence, 2017, 184, 256-261.	1.5	11
25025	First-principles calculations of typical anisotropic cubic and hexagonal structures and homogenized moduli estimation based on the Y-parameter: Application to CaO, MgO, CH and Calcite CaCO3. Journal of Physics and Chemistry of Solids, 2017, 101, 74-89.	1.9	41
25026	Single-layer ZnS supported on Au(111): A combined XPS, LEED, STM and DFT study. Surface Science, 2017, 658, 9-14.	0.8	20
25027	Binding Sites, Geometry, and Energetics of Propene at Nanoparticulate Au/TiO₂. Journal of Physical Chemistry C, 2017, 121, 1683-1689.	1.5	15
25028	Catalytic selectivity of Rh/TiO₂catalyst in syngas conversion to ethanol: probing into the mechanism and functions of TiO₂support and promoter. Catalysis Science and Technology, 2017, 7, 1073-1085.	2.1	31
25029	Understanding the interfacial interactions between dopamine and different graphenes for biomedical materials. Materials Chemistry Frontiers, 2017, 1, 1156-1164.	3.2	18
25030	Quantum Transport in Gated Dangling-Bond Atomic Wires. Nano Letters, 2017, 17, 322-327.	4.5	28
25031	The work function of few-layer graphene. Journal of Physics Condensed Matter, 2017, 29, 035003.	0.7	56
25032	From Activeâ€Site Models to Real Catalysts: Importance of the Material Gap in the Design of Pd Catalysts for Methane Oxidation. ChemCatChem, 2017, 9, 1594-1600.	1.8	15
25033	In-situhigh temperature Raman spectroscopic study on the structural evolution of Na₂W₂O₇from the crystalline to molten states. Journal of Raman Spectroscopy, 2017, 48, 298-304.	1.2	23
25034	Boron carbide nanoparticles for high-hardness ceramics: Crystal lattice defects after treatment in a planetary ball mill. Journal of the European Ceramic Society, 2017, 37, 1349-1353.	2.8	23
25035	Structure and magnetism of the solid solution Ge_xFe_{4â^'x}N_y (0 â‰¤ x) Tj ETQq0 0 0 rgBT /Overlo	2.7	8
25036	The influence of carbon on the seismic properties of solid iron. Geophysical Research Letters, 2017, 44, 128-134.	1.5	15
25037	Optical, elastic and thermal properties of ZB-AlN semiconductor from first-principle calculations. Indian Journal of Physics, 2017, 91, 445-451.	0.9	11
25038	Hydrodeoxygenation of acrylic acid using Mo2C/Al2O3. Applied Catalysis A: General, 2017, 531, 69-78.	2.2	22
25039	Mechanistic study for enhanced CO oxidation activity on (Mn,Fe) co-doped CeO 2 (111). Catalysis Today, 2017, 293-294, 82-88.	2.2	32
25040	Atomic and Local Electronic Structures of Ca₂AlMnO_{5+Î´} as an Oxygen Storage Material. Chemistry of Materials, 2017, 29, 648-655.	3.2	12

#	Article	IF	Citations
25041	Strain-mediated type-I/type-II transition in MXene/Blue phosphorene van der Waals heterostructures for flexible optical/electronic devices. Journal of Materials Chemistry C, 2017, 5, 978-984.	2.7	155
25042	A first-principles study of Sc-decorated graphene with pyridinic-N defects for hydrogen storage. International Journal of Hydrogen Energy, 2017, 42, 3106-3113.	3.8	47
25043	Structural, electronic and magnetic properties of the Mn 54â˜x Al 46 Ti x (xÂ=Â2; 4) alloys. Intermetallics, 2017, 82, 101-106.	1.8	18
25044	Experimental and theoretical assessment of the mechanism and site requirements for ketonization of carboxylic acids on oxides. Journal of Catalysis, 2017, 345, 183-206.	3.1	95
25045	Importance of metal-oxide interfaces in heterogeneous catalysis: A combined DFT, microkinetic, and experimental study of water-gas shift on Au/MgO. Journal of Catalysis, 2017, 345, 157-169.	3.1	109
25046	First-principles investigation of the energetics of point defects at a grain boundary in tungsten. Nuclear Instruments & Methods in Physics Research B, 2017, 393, 144-149.	0.6	18
25047	Micro-kinetic simulations of the catalytic decomposition of hydrazine on the Cu(111) surface. Faraday Discussions, 2017, 197, 41-57.	1.6	14
25048	Mechanism of enhancing visible-light photocatalytic activity of BiVO₄via hybridization of graphene based on a first-principles study. RSC Advances, 2017, 7, 4395-4401.	1.7	26
25049	Dualâ€Functional N Dopants in Edges and Basal Plane of MoS₂ Nanosheets Toward Efficient and Durable Hydrogen Evolution. Advanced Energy Materials, 2017, 7, 1602086.	10.2	286
25050	Doped 1D Nanostructures of Transitionâ€metal Oxides: Firstâ€principles Evaluation of Photocatalytic Suitability. Israel Journal of Chemistry, 2017, 57, 461-476.	1.0	15
25051	Deformation Microstructure and Deformation-Induced Martensite in Austenitic Fe-Cr-Ni Alloys Depending on Stacking Fault Energy. Metallurgical and Materials Transactions A: Physical Metallurgy and Materials Science, 2017, 48, 1-7.	1.1	150
25052	DFT study of the role of N- and B-doping on structural, elastic and electronic properties of Î±-, Î²- and Î³-graphyne. Carbon, 2017, 114, 301-310.	5.4	71
25053	Effect of Cu 2+ doping on the structural, electronic and optical properties of ZnAl 2 O 4 : A combined experimental and DFT+ U study. Journal of Luminescence, 2017, 184, 7-16.	1.5	20
25054	Activation of Oxygen in Ce₂Zr₂O_{7+x} across Pyrochlore to Fluorite Structural Transformation: First-Principles Analysis. Journal of Physical Chemistry C, 2017, 121, 1803-1808.	1.5	12
25055	BN-schwarzite: novel boron nitride spongy crystals. Physical Chemistry Chemical Physics, 2017, 19, 1167-1173.	1.3	8
25056	Reaction of CO, H₂O, H₂ and CO₂ on the clean as well as O, OH and H precovered Fe(100) and Fe(111) surfaces. Catalysis Science and Technology, 2017, 7, 427-440.	2.1	22
25057	ScVO₄under non-hydrostatic compression: a new metastable polymorph. Journal of Physics Condensed Matter, 2017, 29, 055401.	0.7	29
25058	How strong are H-bonds at the fully hydroxylated silica surfaces? Insights from the B3LYP electron density topological analysis. Structural Chemistry, 2017, 28, 1009-1015.	1.0	15

#	Article	IF	Citations
25059	Redox behavior of a low-doped Pr-CeO2(111) surface. A DFT+U study. Applied Surface Science, 2017, 401, 206-217.	3.1	22
25060	Bi24Ga2O39 for visible light photocatalytic reduction of Cr(VI): Controlled synthesis, facet-dependent activity and DFT study. Chemical Engineering Journal, 2017, 314, 249-256.	6.6	91
25061	A coupled experimental and thermodynamic study of the Al-Cr and Al-Cr-Mg systems. Journal of Alloys and Compounds, 2017, 698, 1038-1057.	2.8	26
25062	Highly active and stable single iron site confined in graphene nanosheets for oxygen reduction reaction. Nano Energy, 2017, 32, 353-358.	8.2	234
25063	Synthesis and investigations of In₂S₃:Ho³⁺quantum dots on doping induced changes. CrystEngComm, 2017, 19, 853-859.	1.3	14
25064	Hydrogen diffusion into the subsurfaces of model metal catalysts from first principles. Physical Chemistry Chemical Physics, 2017, 19, 3557-3564.	1.3	21
25065	Promoting the oxygen reduction reaction with gold at step/edge sites of Ni@AuPt coreâ€“shell nanoparticles. Catalysis Science and Technology, 2017, 7, 596-606.	2.1	27
25066	Atomic interpretation of high activity on transition metal and nitrogen-doped carbon nanofibers for catalyzing oxygen reduction. Journal of Materials Chemistry A, 2017, 5, 3336-3345.	5.2	88
25067	Stability and electronic properties of two-dimensional indium iodide. Physical Review B, 2017, 95, .	1.1	10
25068	Oxygen Vacancy Formation, Mobility, and Hydrogen Pick-up during Oxidation of Zirconium by Water. Oxidation of Metals, 2017, 87, 355-365.	1.0	22
25069	Dataset on the structure and thermodynamic and dynamic stability of Mo 2 ScAlC 2 from experiments and first-principles calculations. Data in Brief, 2017, 10, 576-582.	0.5	3
25070	Structural Modulation of Nitrate Group with Cations to Affect SHG Responses in RE(OH)₂NO₃ (RE = La, Y, and Gd): New Polar Materials with Large NLO Effect after Adjusting pH Values of Reaction Systems. Chemistry of Materials, 2017, 29, 896-903.	3.2	107
25071	Two Phosphates: Noncentrosymmetric Cs₆Mg₆(PO₃)₁₈ and Centrosymmetric Cs₂MgZn₂(P₂O₇)₂. Inorganic Chemistry, 2017, 56, 845-851.	1.9	48
25072	How Density Functional Theory Surface Energies May Explain the Morphology of Particles, Nanosheets, and Conversion Films Based on Layered Double Hydroxides. Journal of Physical Chemistry C, 2017, 121, 2211-2220.	1.5	29
25073	Tunable Broadband Nanocarbon Transparent Conductor by Electrochemical Intercalation. ACS Nano, 2017, 11, 788-796.	7.3	31
25074	Water-gas-shift reaction on reduced gold-substituted Ce1â^'xO2(111) surfaces: the role of Au charge. Physical Chemistry Chemical Physics, 2017, 19, 2201-2206.	1.3	10
25075	Intrinsic localized mode and low thermal conductivity of PbSe. Physical Review B, 2017, 95, .	1.1	84
25076	Experimental and theoretical analysis of electronic and optical properties of MgWO4. Journal of Materials Science, 2017, 52, 4934-4943.	1.7	28

#	Article	IF	Citations
25077	Electronic, optical and thermoelectric properties of bulk and surface (001) CuInTe 2 : A first principles study. Journal of Alloys and Compounds, 2017, 699, 1003-1011.	2.8	15
25078	First-principles calculations on the structural and electronic properties of cubic KCaF 3 and NaCaF 3 (001) surfaces. Physics Letters, Section A: General, Atomic and Solid State Physics, 2017, 381, 890-895.	0.9	11
25079	Solution-Synthesized In4SnSe4 Semiconductor Microwires with a Direct Band Gap. Chemistry of Materials, 2017, 29, 1095-1098.	3.2	12
25080	Impact of Vacancies on the Mechanical Properties of Ultraincompressible, Hard Rhenium Subnitrides: Re₂N and Re₃N. Chemistry of Materials, 2017, 29, 2542-2549.	3.2	17
25081	Structural Stabilities and Electronic Properties of High-Angle Grain Boundaries in Perovskite Cesium Lead Halides. Journal of Physical Chemistry C, 2017, 121, 1715-1722.	1.5	99
25082	Native point defects in Ti3GeC2 and Ti2GeC. Computational Materials Science, 2017, 128, 103-108.	1.4	3
25083	Determination of Krypton Diffusion Coefficients in Uranium Dioxide Using Atomic Scale Calculations. Inorganic Chemistry, 2017, 56, 125-137.	1.9	30
25084	Effects of High and Low Salt Concentration in Electrolytes at Lithiumâ€“Metal Anode Surfaces. Journal of Physical Chemistry C, 2017, 121, 182-194.	1.5	128
25085	An Aza-Fused Ï€-Conjugated Microporous Framework Catalyzes the Production of Hydrogen Peroxide. ACS Catalysis, 2017, 7, 1015-1024.	5.5	83
25086	Twoâ€Dimensional Singleâ€Layer Organicâ€“Inorganic Hybrid Perovskite Semiconductors. Advanced Energy Materials, 2017, 7, 1601731.	10.2	93
25087	Experimental and DFT high pressure study of fluorinated graphite (C2F)n. Carbon, 2017, 114, 690-699.	5.4	20
25088	A first-principle study of the structural, elastic, lattice dynamical and thermodynamic properties of <mml:math xmlns:mml="http://www.w3.org/1998/Math/MathML" altimg="si4.gif" overflow="scroll"><mml:mrow><mml:msup><mml:mrow><mml:mi>Î±</mml:mi></mml:mrow><mml:mrow><mml:mo>â€³</mml:mo><mml:mi mathvariant="italic">Fe</mml:mi></mml:mrow><mml:mrow><mml:mn>16</mml:mn></mml:mrow></mml:msub><mml:msub><mml:m Computational Materials Science, 2017, 128, 278-286.	1.4	19
25089	Ab-initio design of 3D carbyne-based material. Computational Materials Science, 2017, 128, 223-228.	1.4	3
25090	CPA descriptions of random Cu-Au alloys in comparison with SQS approach. Computational Materials Science, 2017, 128, 302-309.	1.4	21
25091	Crystal structure and bonding characteristics of transformation products of bcc Î² in Ti-Mo alloys. Journal of Alloys and Compounds, 2017, 705, 769-781.	2.8	25
25092	Adsorption of Benzene on the RuO₂(110) Surface. Journal of Physical Chemistry C, 2017, 121, 1585-1590.	1.5	5
25093	Atomic H-Induced Mo₂C Hybrid as an Active and Stable Bifunctional Electrocatalyst. ACS Nano, 2017, 11, 384-394.	7.3	149
25094	Electrolyte-controlled discharge product distribution of Naâ€“O₂batteries: a combined computational and experimental study. Physical Chemistry Chemical Physics, 2017, 19, 2940-2949.	1.3	14

#	Article	IF	Citations
25095	Solution-based synthesis and processing of Sn- and Bi-doped Cu₃SbSe₄nanocrystals, nanomaterials and ring-shaped thermoelectric generators. Journal of Materials Chemistry A, 2017, 5, 2592-2602.	5.2	73
25096	Anisotropic intrinsic lattice thermal conductivity of borophane from first-principles calculations. Physical Chemistry Chemical Physics, 2017, 19, 2843-2849.	1.3	40
25097	Strain-induced phonon shifts in tungsten disulfide nanoplatelets and nanotubes. 2D Materials, 2017, 4, 015007.	2.0	85
25098	Two-dimensional crystal CuSâ€"electronic and structural properties. 2D Materials, 2017, 4, 015041.	2.0	20
25099	DFT investigation of electronic structures and magnetic properties of halides family MeHal3 (Me=Ti,) Tj ETQq0 0 0 rgBT /Overlock 10 Tf 2017, 440, 93-96.	1.0	4
25100	Partial-Redox-Promoted Mn Cycling of Mn(II)-Doped Heterogeneous Catalyst for Efficient H₂O₂-Mediated Oxidation. ACS Applied Materials & Interfaces, 2017, 9, 371-380.	4.0	31
25101	Interfacial Multiferroics of TiO₂/PbTiO₃ Heterostructure Driven by Ferroelectric Polarization Discontinuity. ACS Applied Materials & Interfaces, 2017, 9, 1899-1906.	4.0	23
25102	Sm³⁺ and Eu³⁺ codoped SrBi₂B₂O₇: a red-emitting phosphor with improved thermal stability. RSC Advances, 2017, 7, 1146-1153.	1.7	43
25103	Enhanced strength and temperature dependence of mechanical properties of Li at small scales and its implications for Li metal anodes. Proceedings of the National Academy of Sciences of the United States of America, 2017, 114, 57-61.	3.3	206
25104	The Effect of Hydrostatic Pressure on the Superconducting and Structural Properties of Nb $_3$Sn: Ab-initio Modeling and SR-XRD Investigation. IEEE Transactions on Applied Superconductivity, 2017, 27, 1-5.	1.1	7
25105	Sodium Passivation of the Grain Boundaries in CuInSe₂ and Cu₂ZnSnS₄ for Highâ€Efficiency Solar Cells. Advanced Energy Materials, 2017, 7, 1601457.	10.2	56
25106	Morphological effects of Au 13 clusters on the adsorption of CO 2 over anatase TiO 2 (101). Applied Surface Science, 2017, 399, 469-479.	3.1	21
25107	Metastable phases, phase transformation and properties of AlAs based on first-principle study. Computational Materials Science, 2017, 128, 337-342.	1.4	20
25108	Theoretical study of the elasticity, ideal strength and thermal conductivity of a pure sp2 carbon. Diamond and Related Materials, 2017, 71, 73-78.	1.8	17
25109	Molecular and dissociative adsorption of water at a defective Cu(110) surface. Surface Science, 2017, 658, 1-8.	0.8	15
25110	Structural and thermoelectric properties of n-type isocubanite CuFe₂S₃. Inorganic Chemistry Frontiers, 2017, 4, 424-432.	3.0	40
25111	Porphyrin molecules boost the sensitivity of epitaxial graphene for NH₃detection. Journal of Physics Condensed Matter, 2017, 29, 065001.	0.7	9
25112	Defect character at grain boundary facet junctions: Analysis of an asymmetric Î£Â=Â5 grain boundary in Fe. Acta Materialia, 2017, 124, 383-396.	3.8	49

#	Article	IF	Citations
25113	Electronic properties of layered phosphorus heterostructures. Physical Chemistry Chemical Physics, 2017, 19, 1229-1235.	1.3	10
25114	Passivation of Black Phosphorus via Selfâ€Assembled Organic Monolayers by van der Waals Epitaxy. Advanced Materials, 2017, 29, 1603990.	11.1	113
25115	Investigation of structural, electronic and anisotropic elastic properties of Ru -doped WB 2 compound by increased valence electron concentration. Materials Chemistry and Physics, 2017, 189, 90-95.	2.0	21
25116	Origin of Blue-Green Emission in Î±-Zn₂P₂O₇ and Local Structure of Ln³⁺ Ion in Î±-Zn₂P₂O₇:Ln³⁺ (Ln = Sm,) Tj ETQq1 1 0.784314 rgBT 167-178.	1.9	53
25117	Bond Order Conservation Strategies in Catalysis Applied to the NH₃ Decomposition Reaction. ACS Catalysis, 2017, 7, 864-871.	5.5	25
25118	Adsorption and dehydrogenation of ethane, propane and butane on Rh13 clusters supported on unzipped graphene oxide and TiO2(110) â€“ a DFT study. Physical Chemistry Chemical Physics, 2017, 19, 4989-4996.	1.3	11
25119	Competing antiferromagnetism in a quasi-2D itinerant ferromagnet: Fe ₃ GeTe ₂. 2D Materials, 2017, 4, 011005.	2.0	123
25120	Characteristics of Interlayer Tunneling Field-Effect Transistors Computed by a â€œDFT-Bardeenâ€•Method. Journal of Electronic Materials, 2017, 46, 1378-1389.	1.0	5
25121	Dioxygen molecule adsorption and oxygen atom diffusion on clean and defective aluminum(111) surface using first principles calculations. Surface Science, 2017, 657, 79-89.	0.8	16
25122	On the Preferred Active Sites of Promoted MoS₂ for Hydrodesulfurization with Minimal Organonitrogen Inhibition. ACS Catalysis, 2017, 7, 501-509.	5.5	78
25123	Zinc-Blende MnTe Under Pressure: Structural, Mechanical, and Optical Properties from Ab Initio Calculation. Journal of Superconductivity and Novel Magnetism, 2017, 30, 1533-1538.	0.8	3
25124	Diffusion and retention of hydrogen in vanadium in presence of Ti and Cr: First-principles investigations. Journal of Nuclear Materials, 2017, 484, 276-282.	1.3	11
25125	Study of dimethyl ester interaction on the surface of Ga-doped graphene: Application of density functional theory. Journal of Molecular Liquids, 2017, 229, 1-5.	2.3	16
25126	A theoretical study of perovskite CsXCl3 (X=Pb, Cd) within first principles calculations. Physica B: Condensed Matter, 2017, 510, 60-73.	1.3	38
25127	Engineering the electronic structure of zigzag graphene nanoribbons with periodic line defect. Physics Letters, Section A: General, Atomic and Solid State Physics, 2017, 381, 307-313.	0.9	16
25128	Effects of reduced dimensionality on the properties of magnesium hydroxide and calcium hydroxide nanostructures. Physical Chemistry Chemical Physics, 2017, 19, 1963-1974.	1.3	9
25129	Computational search for two-dimensional intrinsic half-metals in transition-metal dinitrides. Journal of Materials Chemistry C, 2017, 5, 727-732.	2.7	61
25130	Probing hydrogen adsorption behaviors of Ti- and Ni-decorated carbon nanotube by density functional theory. Journal of Theoretical and Computational Chemistry, 2017, 16, 1750065.	1.8	12

#	Article	IF	Citations
25131	Exceptional Optical Response of Archimedean Boron and Group-V Ultrathin Nanosheets. Journal of Physical Chemistry C, 2017, 121, 24489-24494.	1.5	1
25132	Towards lead-free perovskite photovoltaics and optoelectronics by ab-initio simulations. Scientific Reports, 2017, 7, 14025.	1.6	310
25133	Novel optical properties of CdS:Zn rocksalt system (a theoretical study). Materials Research Express, 2017, 4, 115901.	0.8	3
25134	Exceptional ring topology makes diamond allotropes as light-weight superhard materials. Diamond and Related Materials, 2017, 80, 140-146.	1.8	0
25135	Structural and Electronic Features of Nb-Doped SrCoO₃: Insight from First-Principles Calculations. Journal of Physical Chemistry C, 2017, 121, 24987-24993.	1.5	4
25136	Tuning methane decomposition on stepped Ni surface: The role of subsurface atoms in catalyst design. Scientific Reports, 2017, 7, 13963.	1.6	41
25137	Tuning the electronic and quantum transport properties of nitrogenated holey graphene nanoribbons. Journal of Materials Chemistry C, 2017, 5, 11856-11866.	2.7	13
25138	Stability and the Electronic Structure of XB2 (X = Pt, Ir, Pd, Rh, Os) Diborides. Latvian Journal of Physics and Technical Sciences, 2017, 54, 49-57.	0.4	2
25139	Origin of ferromagnetism in Cu doped rutile TiO 2 - An ab-initio approach. Computational Condensed Matter, 2017, 13, 127-130.	0.9	21
25140	C₂ Oxygenate Synthesis via Fischerâ€“Tropsch Synthesis on Co₂C and Co/Co₂C Interface Catalysts: How To Control the Catalyst Crystal Facet for Optimal Selectivity. ACS Catalysis, 2017, 7, 8285-8295.	5.5	81
25141	Entropies of defect association in ceria from first principles. Physical Chemistry Chemical Physics, 2017, 19, 29625-29628.	1.3	3
25142	Ab initiothermodynamic properties and their uncertainties for crystalline Î±-methanol. Physical Chemistry Chemical Physics, 2017, 19, 29940-29953.	1.3	29
25143	Rational design of exfoliated 1T MoS₂@CNT-based bifunctional separators for lithium sulfur batteries. Journal of Materials Chemistry A, 2017, 5, 23909-23918.	5.2	111
25144	First-principles analysis of the structural, electronic, and elastic properties of cubic organicâ€“inorganic perovskite HC(NH ₂) ₂ PbI ₃. Chinese Physics B, 2017, 26, 106301.	0.7	19
25145	Porous germanene as a highly efficient gas separation membrane. Nanoscale, 2017, 9, 17505-17512.	2.8	12
25146	Thermodynamic modeling of phase equilibria and defect chemistry in the Zn-S system. Calphad: Computer Coupling of Phase Diagrams and Thermochemistry, 2017, 59, 171-181.	0.7	8
25147	Ultrahigh power factors in P-type 1T-ZrX2 (Xâ€¯=â€¯S, Se) single layers. Science Bulletin, 2017, 62, 1530-1537.	4.3	25
25148	Role of Point Defects in Spinel Mg Chalcogenide Conductors. Chemistry of Materials, 2017, 29, 9657-9667.	3.2	56

#	Article	IF	Citations
25149	Novel Ba-hexaferrite structural variations stabilized on the nanoscale as building blocks for epitaxial bi-magnetic hard/soft sandwiched maghemite/hexaferrite/maghemite nanoplatelets with out-of-plane easy axis and enhanced magnetization. Nanoscale, 2017, 9, 17551-17560.	2.8	16
25150	Dependence of the constitution, microstructure and electrochemical behaviour of magnetron sputtered Liâ€“Niâ€“Mnâ€“Coâ€“O thin film cathodes for lithium-ion batteries on the working gas pressure and annealing conditions. International Journal of Materials Research, 2017, 108, 879-886.	0.1	3
25152	Modeling of oxygen incorporation in Th, ThC, and ThN by density functional theory calculations. Journal of Nuclear Materials, 2017, 496, 124-128.	1.3	2
25153	Computational Design of Perovskite Ba_xSr_{1â€“x}SnO₃ Alloys as Transparent Conductors and Photocatalysts. Journal of Physical Chemistry C, 2017, 121, 26446-26456.	1.5	14
25154	Vibrational states of nano-confined water molecules in beryl investigated by first-principles calculations and optical experiments. Physical Chemistry Chemical Physics, 2017, 19, 30740-30748.	1.3	16
25155	The effects of He clusters on the mechanical properties of Ti₃AC₂ (A = Ge, Si): first-principles studies. RSC Advances, 2017, 7, 48437-48443.	1.7	4
25156	First-principles calculation of the structure and electronic properties of Fe-substituted Bi₂Ti₂O₇. Semiconductor Science and Technology, 2017, 32, 125007.	1.0	7
25157	Pressure-induced improvement in symmetry and change in electronic properties of SnSe. Journal of Molecular Modeling, 2017, 23, 319.	0.8	7
25158	The structural, magnetic and electronic properties of p-type and n-type doped monolayer WS 2 systems. Superlattices and Microstructures, 2017, 112, 619-627.	1.4	14
25159	Stretching Epitaxial La_{0.6}Sr_{0.4}CoO_{3â^Î´} for Fast Oxygen Reduction. Journal of Physical Chemistry C, 2017, 121, 25651-25658.	1.5	38
25160	Giant Piezoelectric Effects in Monolayer Group-V Binary Compounds with Honeycomb Phases: A First-Principles Prediction. Journal of Physical Chemistry C, 2017, 121, 25576-25584.	1.5	78
25161	Phonon-mediated superconductivity in Mg intercalated bilayer borophenes. Physical Chemistry Chemical Physics, 2017, 19, 29237-29243.	1.3	39
25162	Atmospheric pressure chemical vapor deposition of methylammonium bismuth iodide thin films. Journal of Materials Chemistry A, 2017, 5, 24728-24739.	5.2	41
25163	Effects of impurity adsorption on topological surface states of Bi 2 Te 3. Europhysics Letters, 2017, 119, 47001.	0.7	3
25164	First-principles investigation of Pd3Bi as a catalyst for the oxygen reduction reaction. International Journal of Hydrogen Energy, 2017, 42, 30359-30363.	3.8	4
25165	Experimental and theoretical assessment of the mechanism of hydrogen transfer in alkane-alkene coupling on solid acids. Journal of Catalysis, 2017, 354, 287-298.	3.1	7
25166	Effect of alloying elements on grain boundary sliding in magnesium binary alloys: Experimental and numerical studies. Materials Science & Engineering A: Structural Materials: Properties, Microstructure and Processing, 2017, 708, 267-273.	2.6	32
25167	Mechanism of Y2O3 as heterogeneous nucleus of TiC in hypereutectic Fe-Cr-C-Ti-Y2O3 coating: First principle calculation and experiment research. Materials Today Communications, 2017, 13, 80-91.	0.9	26

#	Article	IF	Citations
25168	First-principles insight into the structural fundamental of super ionic conducting in NASICON MTi2(PO4)3 (M = Li, Na) materials for rechargeable batteries. Nano Energy, 2017, 41, 626-633.	8.2	67
25169	Study of pressure variation effect on structural, opto-electronic, elastic, mechanical, and thermodynamic properties of SrLiF 3. Physica B: Condensed Matter, 2017, 525, 60-69.	1.3	15
25170	Electronic and phononic modulation of MoS2 under biaxial strain. Physica B: Condensed Matter, 2017, 526, 96-101.	1.3	12
25171	Adsorption of atoms and molecules on s-triazine sheet with embedded manganese atom: First-principles calculations. Physics Letters, Section A: General, Atomic and Solid State Physics, 2017, 381, 3664-3674.	0.9	15
25172	Role of metal impurity in hydrogen diffusion from surface into bulk magnesium: A theoretical study. Physics Letters, Section A: General, Atomic and Solid State Physics, 2017, 381, 3696-3700.	0.9	5
25173	Elastic, thermodynamic and optical behavior of V2AC (A= Al, Ga) MAX phases. Results in Physics, 2017, 7, 3634-3639.	2.0	31
25174	Ab initio study of structural, electronic and elastic properties of CdSe 1â^'x S x semiconductor. Solar Energy, 2017, 158, 63-70.	2.9	9
25175	Unexpected Roles of Interstitially Doped Lithium in Blue and Green Light Emitting Y₂O₃:Bi³⁺: A Combined Experimental and Computational Study. Inorganic Chemistry, 2017, 56, 12139-12147.	1.9	14
25176	Degradation Mechanism of Dimethyl Carbonate (DMC) Dissociation on the LiCoO₂ Cathode Surface: A First-Principles Study. ACS Applied Materials & Interfaces, 2017, 9, 36377-36384.	4.0	10
25177	Spinel-Structured ZnCr₂O₄ with Excess Zn Is the Active ZnO/Cr₂O₃ Catalyst for High-Temperature Methanol Synthesis. ACS Catalysis, 2017, 7, 7610-7622.	5.5	109
25178	Atomic Reconfiguration of van der Waals Gaps as the Key to Switching in GeTe/Sb₂Te₃ Superlattices. ACS Omega, 2017, 2, 6223-6232.	1.6	58
25179	Correlation between the structural change and the electrical transport properties of indium nitride under high pressure. Physical Chemistry Chemical Physics, 2017, 19, 26758-26764.	1.3	1
25180	Enhancing the solar energy conversion efficiency of solution-deposited Bi₂S₃ thin films by annealing in sulfur vapor at elevated temperature. Sustainable Energy and Fuels, 2017, 1, 2134-2144.	2.5	25
25181	A correlative experimental and ab initio approach to improve the fracture behavior of Mo thin films by alloying with Cu. Applied Physics Letters, 2017, 111, 134101.	1.5	5
25182	Ab initiostudy of hydrogen storage in TiFe intermetallic. Materials Research Express, 2017, 4, 106513.	0.8	1
25183	First-principles investigations of the electronic and magnetic structures and the bonding properties of uranium nitride fluoride (UNF). Zeitschrift Fur Naturforschung - Section B Journal of Chemical Sciences, 2017, 72, 725-730.	0.3	1
25184	Growth pattern and orientation selection of magnesium alloy dendrite: From 3-D experimental characterization to theoretical atomistic simulation. Materials Today Communications, 2017, 13, 155-162.	0.9	17
25185	Compressed tetragonal phase in XFe2As2 (X=Na , K, Rb, Cs) and in the alloy Na0.5K0.5Fe2As2. Physical Review B, 2017, 95, .	1.1	6

#	Article	IF	Citations
25186	Insights into Electrochemistry and Mechanical Stability of Î±- and Î²-Li₂MnP₂O₇ for Lithium-Ion Cathode Materials: First-Principles Comparison. Journal of Physical Chemistry C, 2017, 121, 22656-22664.	1.5	12
25187	Catalytic CO₂ reduction to valuable chemicals using NiFe-based nanoclusters: a first-principles theoretical evaluation. Physical Chemistry Chemical Physics, 2017, 19, 28344-28353.	1.3	18
25188	Predicting displacements of octahedral cations in ferroelectric perovskites using machine learning. Acta Crystallographica Section B: Structural Science, Crystal Engineering and Materials, 2017, 73, 962-967.	0.5	21
25189	Ab initio study of the dolomite to dolomite-II high-pressure phase transition. European Journal of Mineralogy, 2017, 29, 227-238.	0.4	18
25190	Level Alignment as Descriptor for Semiconductor/Catalyst Systems in Water Splitting: The Case of Hematite/Cobalt Hexacyanoferrate Photoanodes. ChemSusChem, 2017, 10, 4552-4560.	3.6	33
25191	Screening Divalent Metals for A- and B-Site Dopants in LaFeO₃. Chemistry of Materials, 2017, 29, 8147-8157.	3.2	50
25192	Flexible and Anisotropic Properties of Monolayer MX₂ (M = Tc and Re; X = S, Se). Journal of Physical Chemistry C, 2017, 121, 23744-23751.	1.5	35
25193	A new layered titanate Na₂Li₂Ti₅O₁₂as a high-performance intercalation anode for sodium-ion batteries. Journal of Materials Chemistry A, 2017, 5, 22208-22215.	5.2	18
25194	Effects of structural imperfection on the electronic properties of graphene/WSe₂ heterostructures. Journal of Materials Chemistry C, 2017, 5, 10383-10390.	2.7	131
25195	Ab initio study of lattice instabilities of zinc chalcogenides ZnX (X=O, S, Se, Te) induced by ultrafast intense laser irradiation. AIP Advances, 2017, 7, 095021.	0.6	5
25196	Face-to-face crosslinking of graphdiyne and related carbon sheets toward integrated graphene nanoribbon arrays. Carbon, 2017, 125, 536-543.	5.4	19
25197	Hydrostatic pressure effects on the kinetic parameters of hydrogen evolution and permeation in Armco iron. Electrochimica Acta, 2017, 255, 230-238.	2.6	25
25198	First-principles investigation of H₂S adsorption and dissociation on titanium carbide surfaces. Physical Chemistry Chemical Physics, 2017, 19, 27116-27122.	1.3	8
25199	Coupling of quantum well states and phonons in thin multilayer Pb films on Si(111). Physical Review B, 2017, 96, .	1.1	6
25200	Magnetic and structural properties of <mml:math xmlns:mml="http://www.w3.org/1998/Math/MathML"><mml:mrow><mml:mi>FeC</mml:mi><mml:msub><mml:mi mathvariant="normal">O</mml:mi><mml:mn>3</mml:mn></mml:msub></mml:mrow></mml:math> at high pressures. Physical Review B, 2017, 96, .	1.1	13
25201	Two-dimensional square buckled Rashba lead chalcogenides. Physical Review B, 2017, 96, .	1.1	29
25202	The tuning effect of the electric field on the physical properties of some typical wurtzite semiconductors. Modern Physics Letters B, 2017, 31, 1750310.	1.0	1
25203	First-principles study of copper nanoclusters for enhanced electrochemical CO2 reduction to CH4. Computational and Theoretical Chemistry, 2017, 1120, 84-90.	1.1	25

#	Article	IF	Citations
25204	Metal Borohydrides as Electrolytes for Solid-State Li, Na, Mg, and Ca Batteries: A First-Principles Study. Chemistry of Materials, 2017, 29, 9308-9319.	3.2	115
25205	Chemical Insights from Theoretical Electronic States in Nickel Hydroxide and Monolayer Surface Model. Journal of Physical Chemistry C, 2017, 121, 24603-24611.	1.5	5
25206	Thermoelectric properties of Se and Zn/Cd/Sn double substituted Co₄Sb₁₂ skutterudite compounds. Physical Chemistry Chemical Physics, 2017, 19, 28116-28126.	1.3	10
25207	First-principles study of helium clustering at initial stage in ThO 2. Chinese Physics B, 2017, 26, 097101.	0.7	5
25208	Structural, electronic, elastic and thermodynamic properties of Li 2 ZrO 3 : A comprehensive study using DFT formalism. Journal of Nuclear Materials, 2017, 496, 286-292.	1.3	10
25209	VS₂/Graphene Heterostructures as Promising Anode Material for Li-Ion Batteries. Journal of Physical Chemistry C, 2017, 121, 24179-24184.	1.5	73
25210	Surface Density-of-States Engineering of Anatase TiO₂ by Small Polyols for Enhanced Visible-Light Photocurrent Generation. ACS Omega, 2017, 2, 6309-6313.	1.6	3
25211	Ambient Humidity Influence on CO Detection with SnO₂ Gas Sensing Materials. A Combined DRIFTS/DFT Investigation. Journal of Physical Chemistry C, 2017, 121, 25064-25073.	1.5	82
25212	Mechanistic Insights Evaluating Ag, Pb, and Ni as Electrocatalysts for Furfural Reduction from First-Principles Methods. Journal of Physical Chemistry C, 2017, 121, 25768-25777.	1.5	35
25213	Dissociative Adsorption of Molecular Hydrogen on BN-Doped Graphene-Supported Aluminum Clusters. Journal of Physical Chemistry C, 2017, 121, 26493-26498.	1.5	9
25214	Electric field effect on the magnetic properties of zigzag MoS2 nanoribbons with different edge passivation. Physical Chemistry Chemical Physics, 2017, 19, 30814-30821.	1.3	4
25215	First-Principles Analysis on Ï€-bonded Chain Structure on Several Polytypes of SiC Surfaces: Importance of Stacking Sequence on Energetics and Electronic Structures. Journal of the Physical Society of Japan, 2017, 86, 094708.	0.7	2
25216	The study of the interactions between graphene and Ge(001)/Si(001). Nano Research, 2017, 10, 3648-3661.	5.8	23
25217	Structure and stability of hcp iron carbide precipitates: A first-principles study. Heliyon, 2017, 3, e00408.	1.4	6
25218	Ultrathin Lanthanum Tantalate Perovskite Nanosheets Modified by Nitrogen Doping for Efficient Photocatalytic Water Splitting. ACS Nano, 2017, 11, 11441-11448.	7.3	96
25219	Universal Dynamics of Molecular Reorientation in Hybrid Lead Iodide Perovskites. Journal of the American Chemical Society, 2017, 139, 16875-16884.	6.6	129
25220	Chemically induced large-gap quantum anomalous Hall insulator states in III-Bi honeycombs. Npj Computational Materials, 2017, 3, .	3.5	15
25221	Exploring the geometric, magnetic and electronic properties of Hofmann MOFs for drug delivery. Physical Chemistry Chemical Physics, 2017, 19, 31316-31324.	1.3	14

#	Article	IF	Citations
25222	Mechanistic insights on ethanol dehydrogenation on Pdâ€“Au model catalysts: a combined experimental and DFT study. Physical Chemistry Chemical Physics, 2017, 19, 30578-30589.	1.3	57
25223	Compressive strain induced dynamical stability of monolayer 1T-MX2 (Mâ€‰â€‰=â€‰â€‰Mo, W; Xâ€‰â€‰=â€‰â€‰S, Se). Ma Research Express, 2017, 4, 115018.	0.8	13
25224	Extremely large magnetoresistance and Kohler's rule in <mml:math xmlns:mml="http://www.w3.org/1998/Math/MathML"><mml:msub><mml:mi>PdSn</mml:mi><mml:mn>4</mml:mn></mml:msub></mm : A complete study of thermodynamic, transport, and band-structure properties. Physical Review B, 2017, 96, .	1.1	69
25225	Defect physics in intermediate-band materials: Insights from an optimized hybrid functional. Physical Review B, 2017, 96, .	1.1	13
25226	High pressure in-situ synthesis and physical properties of Cr3C2-Ni cermets. Ceramics International, 2017, 43, 17202-17205.	2.3	15
25227	Mechanical properties of Ni-based solid solution alloys: A first principles study. Journal of Applied Research and Technology, 2017, 15, 449-453.	0.6	10
25228	Enhanced thermoelectric properties of penta-graphene by strain effects process. Materials Research Express, 2017, 4, 105031.	0.8	12
25230	Determination of the ³¹P and ²⁰⁷Pb Chemical Shift Tensors in Pyromorphite, Pb₅(PO₄)₃Cl, by Singleâ€Crystal NMR Measurements and DFT Calculations. Zeitschrift Fur Anorganische Und Allgemeine Chemie, 2017, 643, 1635-1641.	0.6	7
25231	Giant thermoelectric performance of novel TaIrSn Half Heusler compound. Physics Letters, Section A: General, Atomic and Solid State Physics, 2017, 381, 3760-3765.	0.9	45
25232	Atomic-Step-Induced Local Nonequilibrium Effects on Surface Oxidation. Journal of Physical Chemistry C, 2017, 121, 22846-22853.	1.5	10
25233	Dioxygen Activation Pathways over Cobalt Spinel Nanocubesâ€”From Molecular Mechanism into Ab Initio Thermodynamics and ¹⁶O₂/¹⁸O₂ Exchange Microkinetics. Journal of Physical Chemistry C, 2017, 121, 24128-24143.	1.5	22
25234	Impact of Intrinsic Structural Properties on the Hydration of 2:1 Layer Silicates. ACS Earth and Space Chemistry, 2017, 1, 608-620.	1.2	10
25235	Strain induced atomic structure at the Ir-doped LaAlO₃/SrTiO₃ interface. Physical Chemistry Chemical Physics, 2017, 19, 28676-28683.	1.3	7
25236	Identification of activity trends for CO oxidation on supported transition-metal single-atom catalysts. Catalysis Science and Technology, 2017, 7, 5860-5871.	2.1	69
25237	Layered tetragonal zinc chalcogenides for energy-related applications: from photocatalysts for water splitting to cathode materials for Li-ion batteries. Nanoscale, 2017, 9, 17303-17311.	2.8	29
25238	Indole-based conjugated macromolecules as a redox-mediated electrolyte for an ultrahigh power supercapacitor. Energy and Environmental Science, 2017, 10, 2441-2449.	15.6	68
25239	An ab-initio study of optical properties of Co2VSi and Co2VGe alloys. AIP Conference Proceedings, 2017, , .	0.3	1
25240	Iron disulfide compound: a promising thermoelectric material. Materials Research Express, 2017, 4, 105907.	0.8	7

#	Article	IF	Citations
25241	Atomistic simulations and experimental measurements of helium nano-bubbles in nickel. Journal of Nuclear Materials, 2017, 495, 475-483.	1.3	23
25242	Dual-Phase Mechanism for the Catalytic Conversion of n-Butane to Maleic Anhydride by the Vanadyl Pyrophosphate Heterogeneous Catalyst. Journal of Physical Chemistry C, 2017, 121, 24069-24076.	1.5	14
25243	Scaling Relations for Acidity and Reactivity of Zeolites. Journal of Physical Chemistry C, 2017, 121, 23520-23530.	1.5	74
25244	The interaction of halogen atoms and molecules with borophene. Physical Chemistry Chemical Physics, 2017, 19, 28963-28969.	1.3	28
25245	Anisotropy, phonon modes, and lattice anharmonicity from dielectric function tensor analysis of monoclinic cadmium tungstate. Physical Review B, 2017, 95, .	1.1	22
25246	Structure Evolution and Spin-Glass Transition of Layered Compounds ALiFeSe₂ (A = Na, K,) Tj ETQq1 1 0.784314 rgBT /O	1.9	14
25247	Configurational Energies of Nanoparticles Based on Metalâ€“Metal Coordination. Journal of Physical Chemistry C, 2017, 121, 23002-23010.	1.5	40
25248	Facile synthesis of a molybdenum phosphide (MoP) nanocomposite Pt support for high performance methanol oxidation. Catalysis Science and Technology, 2017, 7, 5974-5981.	2.1	28
25249	A novel explanation for the increased conductivity in annealed Al-doped ZnO: an insight into migration of aluminum and displacement of zinc. Physical Chemistry Chemical Physics, 2017, 19, 27866-27877.	1.3	37
25250	A thermodynamic structural model of graphene oxide. Journal of Applied Physics, 2017, 122, .	1.1	12
25251	The Nextâ€Generation of Nonlinear Optical Materials: Rb₃Ba₃Li₂Al₄B₆O₂₀Fâ€”Synthesis, Characterization, and Crystal Growth. Advanced Optical Materials, 2017, 5, 1700840.	3.6	68
25252	A superhard sp3 microporous carbon with direct bandgap. Chemical Physics Letters, 2017, 689, 68-73.	1.2	39
25253	Tuned thermoelectric transport properties of Co2.0Sb1.6Se2.4 and Co2.0Sb1.5M0.1Se2.4 (M=Zn, Sn): Compounds with high phonon scattering. Journal of Alloys and Compounds, 2017, 729, 303-312.	2.8	5
25254	First-Principles Chemical Bonding Study of Manganese Carbodiimide, MnNCN, As Compared to Manganese Oxide, MnO. Journal of Physical Chemistry A, 2017, 121, 7778-7786.	1.1	22
25255	Selective Hydrogenation of Acetylene over Pd-In/Al₂O₃ Catalyst: Promotional Effect of Indium and Composition-Dependent Performance. ACS Catalysis, 2017, 7, 7835-7846.	5.5	194
25256	First-principles calculation of intrinsic defect chemistry and self-doping in PbTe. Npj Computational Materials, 2017, 3, .	3.5	62
25257	Understanding the spin-dependent electronic properties of symmetrically far-edge doped zigzag graphene nanoribbon from a first principles study. RSC Advances, 2017, 7, 46604-46614.	1.7	10
25258	Role of descriptors in predicting the dissolution energy of embedded oxides and the bulk modulus of oxide-embedded iron. Physical Review B, 2017, 95, .	1.1	9

#	Article	IF	Citations
25259	Thermal rectification in restructured graphene with locally modulated temperature dependence of thermal conductivity. Physical Review B, 2017, 96, .	1.1	19
25260	Atomic oxygen adsorption on Pb(1 0 0). European Physical Journal B, 2017, 90, 1.	0.6	0
25261	Phase transition and high-pressure thermodynamic properties of CdN derived from first-principles and quasi-harmonic Debye model. Computational and Theoretical Chemistry, 2017, 1120, 91-95.	1.1	3
25262	Site-specific equilibrium isotopic fractionation of oxygen, carbon and calcium in apatite. Geochimica Et Cosmochimica Acta, 2017, 219, 57-73.	1.6	13
25263	First-principles study on the initial decomposition process of CH3NH3PbI3. Journal of Chemical Physics, 2017, 147, 124702.	1.2	10
25264	Influence of point defects on the near edge structure of hexagonal boron nitride. Physical Review B, 2017, 96, .	1.1	59
25265	Elastic properties of noncarbon nanotubes as compared to carbon nanotubes. Physical Review B, 2017, 96, .	1.1	26
25266	Multiband <mml:math xmlns:mml="http://www.w3.org/1998/Math/MathML"><mml:mrow><mml:mi mathvariant="bold">k</mml:mi><mml:mo>Â·</mml:mo><mml:mi mathvariant="bold">p</mml:mi></mml:mrow></mml:math> theory of monolayer <mml:math xmlns:mml="http://www.w3.org/1998/Math/MathML"><mml:mrow><mml:mi>X</mml:mi><mml:mi>Se</mml:mi></mml:mrow></mml:m		

#	Article	IF	Citations
25277	Diffusion of interstitials in metallic systems, illustration of a complex study case: aluminum. Journal of Physics Condensed Matter, 2017, 29, 455703.	0.7	14
25278	Stability and band offsets between Si and LaAlO3. European Physical Journal B, 2017, 90, 1.	0.6	2
25279	DFT study of anisotropy effects on the electronic properties of diamond nanowires with nitrogen-vacancy center. Journal of Molecular Modeling, 2017, 23, 292.	0.8	1
25280	New Solid Electrolyte Na₉Al(MoO₄)₆: Structure and Na⁺ Ion Conductivity. Chemistry of Materials, 2017, 29, 8901-8913.	3.2	29
25281	Nature of Interlayer Binding and Stacking of spâ€“sp² Hybridized Carbon Layers: A Quantum Monte Carlo Study. Journal of Chemical Theory and Computation, 2017, 13, 5639-5646.	2.3	27
25282	Zerovalent Selenium Adsorption Mechanisms on CaO Surface: DFT Calculation and Experimental Study. Journal of Physical Chemistry A, 2017, 121, 7385-7392.	1.1	15
25283	Naphthalene on Ni(111): Experimental and Theoretical Insights into Adsorption, Dehydrogenation, and Carbon Passivation. Journal of Physical Chemistry C, 2017, 121, 22199-22207.	1.5	13
25284	High selectivity for n-dodecane hydroisomerization over highly siliceous ZSM-22 with low Pt loading. Catalysis Science and Technology, 2017, 7, 5055-5068.	2.1	42
25285	A two-dimensional layered CdS/C₂N heterostructure for visible-light-driven photocatalysis. Physical Chemistry Chemical Physics, 2017, 19, 28216-28224.	1.3	75
25286	Probing surface oxide formations on SiO₂-supported platinum nanocatalysts under CO oxidation. RSC Advances, 2017, 7, 45003-45009.	1.7	26
25287	Disorder-order phase transition at high pressure in ammonium fluoride. Physical Review B, 2017, 96, .	1.1	7
25288	High-Coverage H₂ Adsorption on the Reconstructed Cu₂O(111) Surface. Journal of Physical Chemistry C, 2017, 121, 22081-22091.	1.5	50
25289	Chemisorption of Pentacene on Pt(111) with a Little Molecular Distortion. Journal of Physical Chemistry C, 2017, 121, 22797-22805.	1.5	17
25290	Robust quasi-ohmic contact against angle rotation in noble transition-metal-dichalcogenide/graphene heterobilayers. RSC Advances, 2017, 7, 45896-45901.	1.7	8
25291	Effect of lithium-trapping on nitrogen-doped graphene as an anchoring material for lithiumâ€“sulfur batteries: a density functional theory study. Physical Chemistry Chemical Physics, 2017, 19, 28189-28194.	1.3	56
25292	Ab initio coverage-dependent microkinetic modeling of benzene hydrogenation on Pd(111). Catalysis Science and Technology, 2017, 7, 5267-5283.	2.1	19
25293	Compositional tuning in sputter-grown highly-oriented Biâ€“Te films and their optical and electronic structures. Nanoscale, 2017, 9, 15115-15121.	2.8	19
25294	High-throughput screening of bimetallic catalysts enabled by machine learning. Journal of Materials Chemistry A, 2017, 5, 24131-24138.	5.2	246

#	Article	IF	Citations
25295	Non-enzymatic glucose sensing properties of MoO3 nanorods: experimental and density functional theory investigations. Journal Physics D: Applied Physics, 2017, 50, 475401.	1.3	15
25296	Bilayers of Ni₃C₁₂S₁₂and Pt₃C₁₂S₁₂: graphene-like 2D topological insulators tunable by electric fields. Journal of Physics Condensed Matter, 2017, 29, 465502.	0.7	8
25297	Stabilizing the Ag Electrode and Reducing Jâ€“V Hysteresis through Suppression of Iodide Migration in Perovskite Solar Cells. ACS Applied Materials & Interfaces, 2017, 9, 36338-36349.	4.0	129
25298	Impact of Layer Alignment on the Behavior of <mml:math xmlns:mml="http://www.w3.org/1998/Math/MathML" display="inline"><mml:mrow><mml:msub><mml:mrow><mml:mi>MoS</mml:mi></mml:mrow><mml:mrow><mml:mn>2</mml:mn></ Tunnel Field-Effect Transistors: An AbÂInitio Study. Physical Review Applied, 2017, 8, .	1.5	16
25299	Rashba-like dispersion in buckled square lattices. Physical Review B, 2017, 96, .	1.1	6
25300	Cost-effective liquid-phase exfoliation of molybdenum disulfide by prefreezing and thermal-shock. Advanced Powder Technology, 2017, 28, 2996-3003.	2.0	3
25301	Effect of beryllium doping and vacancy in band structure, magnetic and optical properties of free standing germanene. Current Applied Physics, 2017, 17, 1589-1600.	1.1	18
25302	First principles study of the structural, elastic, electronic, optical and thermodynamic properties of SrRh 2 laves phase intermetallic compound. Computational Condensed Matter, 2017, 13, 65-71.	0.9	16
25303	Structure and electronic properties of perylene and coronene under pressure: First-principles calculations. Computational Materials Science, 2017, 139, 252-259.	1.4	15
25304	Magnetic, electrochemical and thermoelectric properties of <mml:math xmlns:mml="http://www.w3.org/1998/Math/MathML" altimg="si1.gif" overflow="scroll"><mml:mrow><mml:mtext>P</mml:mtext><mml:mn>2</mml:mn><mml:mo>-</mml:mo><mml:msub><mml:mrow>		

#	Article	IF	Citations
25313	Dopants Promoting Ferroelectricity in Hafnia: Insights from a comprehensive Chemical Space Exploration. Chemistry of Materials, 2017, 29, 9102-9109.	3.2	139
25314	Intragranular Phase Proton Conduction in Crystalline Sn_{1â€“x}In_xP₂O₇ (x = 0 and 0.1). Journal of Physical Chemistry C, 2017, 121, 23896-23905.	1.5	15
25315	Computational modeling of high-entropy alloys: Structures, thermodynamics and elasticity. Journal of Materials Research, 2017, 32, 3627-3641.	1.2	56
25316	Jahnâ€“Teller distortion affected Li ion migration in spinel TiO2. Solid State Ionics, 2017, 312, 17-20.	1.3	2
25317	Charge-Transfer-Induced Lattice Collapse in Ni-Rich NCM Cathode Materials during Delithiation. Journal of Physical Chemistry C, 2017, 121, 24381-24388.	1.5	242
25318	First-principles investigation of competing magnetic interactions in <mml:math xmlns:mml="http://www.w3.org/1998/Math/MathML"><mml:mrow><mml:mo>(</mml:mo><mml:mi>Mn</mml:mi><mml:mo>, Heusler solid solutions. Physical Review B, 2017, 96, .	1.1	7
25319	Band-gap engineering of halogenated silicon nanowires through molecular doping. Journal of Molecular Modeling, 2017, 23, 314.	0.8	7
25320	Stability, local structure and electronic properties of borane radicals on the Si(1 0 0) 2 Ã— 1:H surface: A first-principles study. Computational Materials Science, 2017, 140, 253-260.	1.4	3
25321	Alkylation of toluene with cyclohexene over phosphotungstic acid: A combined experimental and computational study. Journal of Catalysis, 2017, 355, 145-155.	3.1	10
25322	Ab initio study of ionic nature of 0.75AgI:0.25AgCl. Solid State Ionics, 2017, 310, 56-61.	1.3	1
25323	Location, distribution and acidity of Al substitution in ZSM-5 with different Si/Al ratios â€“ a periodic DFT computation. Catalysis Science and Technology, 2017, 7, 5694-5708.	2.1	30
25324	Quantum anomalous Hall insulator phase in asymmetrically functionalized germanene. Physical Review B, 2017, 96, .	1.1	18
25325	The pressure dependence of physical properties of (W2/3Ti1/3)3AlC2 and its counterpart W3AlC2 by first-principles calculations. Modern Physics Letters B, 2017, 31, 1750326.	1.0	4
25326	Assessing the thermoelectric properties of ScRhTe half-heusler compound. Computational Condensed Matter, 2017, 13, 120-126.	0.9	10
25327	Boron-Doped Graphene as a Promising Anode Material for Potassium-Ion Batteries with a Large Capacity, High Rate Performance, and Good Cycling Stability. Journal of Physical Chemistry C, 2017, 121, 24418-24424.	1.5	118
25328	Three-Dimensionally Hierarchical Ni/Ni₃S₂/S Cathode for Lithiumâ€“Sulfur Battery. ACS Applied Materials & Interfaces, 2017, 9, 38477-38485.	4.0	60
25329	Structure and Electronic Properties of Interface-Confined Oxide Nanostructures. ACS Nano, 2017, 11, 11449-11458.	7.3	23
25330	DFT study of CO₂ conversion on InZr₃(110) surface. Physical Chemistry Chemical Physics, 2017, 19, 28917-28927.	1.3	23

#	Article	IF	Citations
25331	Vanadium supersaturated silicon system: a theoretical and experimental approach. Journal Physics D: Applied Physics, 2017, 50, 495101.	1.3	10
25332	Modulating the electronic and optical properties of monolayer arsenene phases by organic molecular doping. Nanotechnology, 2017, 28, 495202.	1.3	22
25333	Surface state mediated plasmon decay in Al(100). Physical Review B, 2017, 95, .	1.1	4
25334	Convergence behavior of the random phase approximation renormalized correlation energy. Physical Review B, 2017, 95, .	1.1	15
25335	Improving Sensing of Sulfur-Containing Gas Molecules with ZnO Monolayers by Implanting Dopants and Defects. Journal of Physical Chemistry C, 2017, 121, 24365-24375.	1.5	35
25336	Cp-Graphyne: A Low-Energy Graphyne Polymorph with Double Distorted Dirac Points. ACS Omega, 2017, 2, 6822-6830.	1.6	41
25337	DFT insights into the electronic properties and adsorption of NO₂ on metal-doped carbon nanotubes for gas sensing applications. New Journal of Chemistry, 2017, 41, 14936-14944.	1.4	27
25338	Helical graphite metamaterials for intense and locally controllable magnetic fields. RSC Advances, 2017, 7, 49041-49047.	1.7	3
25339	Thermodynamic assessment of the oxygen reduction activity in aqueous solutions. Physical Chemistry Chemical Physics, 2017, 19, 29381-29388.	1.3	43
25340	Unexpected Crystallization Patterns of Zinc Boron Imidazolate Framework ZBIFâ€1: NMR Crystallography of Integrated Metalâ€“Organic Frameworks. ChemPhysChem, 2017, 18, 3576-3582.	1.0	6
25341	Syntheses and Crystal Structures of Sodium Hydrogen Fluorides NaFÂ·nHF (n= 2, 3, 4). Zeitschrift Fur Anorganische Und Allgemeine Chemie, 2017, 643, 1436-1443.	0.6	9
25342	Density functional theory study of defective silicenes as anode materials for lithium ion batteries. Journal of Molecular Graphics and Modelling, 2017, 78, 206-212.	1.3	4
25343	Synthesis and crystal structure of Fe[(Te 1.5 Se 0.5)O 5]Cl, the first iron compound with selenate(IV) and tellurate(IV) groups. Solid State Sciences, 2017, 74, 37-43.	1.5	3
25344	Facile Synthesis of Ru-Based Octahedral Nanocages with Ultrathin Walls in a Face-Centered Cubic Structure. Chemistry of Materials, 2017, 29, 9227-9237.	3.2	55
25345	LiGaGe₂S₆: A Chalcogenide with Good Infrared Nonlinear Optical Performance and Low Melting Point. Inorganic Chemistry, 2017, 56, 13267-13273.	1.9	51
25346	Wafer-Scale Synthesis of Semiconducting SnO Monolayers from Interfacial Oxide Layers of Metallic Liquid Tin. ACS Nano, 2017, 11, 10974-10983.	7.3	122
25347	A doping-less junction-formation mechanism between n-silicon and an atomically thin boron layer. Scientific Reports, 2017, 7, 13247.	1.6	8
25348	Density-Functional-Theory Modeling of Cation Diffusion in Bulk <mml:math xmlns:mml="http://www.w3.org/1998/Math/MathML" display="inline"><mml:mrow><mml:msub><mml:mrow><mml:mi>La</mml:mi></mml:mrow><mml:mrow><mml:mn>1</mml:mn><mml:mn> Physical Review Applied, 2017, 8, .	1.5	11

#	Article	IF	Citations
25349	Long-wavelength deformations and vibrational modes in empty and liquid-filled microtubules and nanotubes: A theoretical study. Physical Review B, 2017, 95, .	1.1	8
25350	Ru doping in iron-based pnictides: The â€œunfoldedâ€•dominant role of structural effects for superconductivity. Physical Review B, 2017, 95, .	1.1	11
25351	Hybrid solvation models for bulk, interface, and membrane: Reference interaction site methods coupled with density functional theory. Physical Review B, 2017, 96, .	1.1	131
25352	Anisotropic thermal expansion in flexible materials. Physical Review B, 2017, 96, .	1.1	21
25353	Phonon spectra in the parent superconducting iron-tuned telluride Fe1+xTe from inelastic neutron scattering and ab initio calculations. Physical Review B, 2017, 96, .	1.1	2
25354	Proximity Effect Induced Spin Injection in Phosphorene on Magnetic Insulator. ACS Applied Materials & Interfaces, 2017, 9, 38999-39010.	4.0	22
25355	The origin of uniaxial negative thermal expansion in layered perovskites. Npj Computational Materials, 2017, 3, .	3.5	38
25356	Correlation between crystallographic anisotropy and dendritic orientation selection of binary magnesium alloys. Scientific Reports, 2017, 7, 13600.	1.6	29
25357	Thermodynamic foundations of applications of ab initio methods for determination of the adsorbate equilibria: hydrogen at the GaN(0001) surface. Physical Chemistry Chemical Physics, 2017, 19, 29676-29684.	1.3	14
25358	Crystal-Chemical Composition of Dicoctahedral Smectites: An Energy-Based Assessment of Empirical Relations. ACS Earth and Space Chemistry, 2017, 1, 629-636.	1.2	6
25359	Transmutation effects on long-term Cs retention in phyllosilicate minerals from first principles. Physical Chemistry Chemical Physics, 2017, 19, 27007-27014.	1.3	4
25360	Strain effects on oxygen vacancy formation energy in perovskites. Solid State Ionics, 2017, 311, 105-117.	1.3	36
25361	Theoretical Design of Robust Ferromagnetism and Bipolar Semiconductivity in Graphene-Based Nanoroads. Journal of Physical Chemistry C, 2017, 121, 24824-24830.	1.5	5
25362	Dissociation mechanism of H₂ molecule on the Li₂O/hydrogenated-Li₂O (111) surface from first principles calculations. RSC Advances, 2017, 7, 35239-35250.	1.7	10
25363	First principle study of edge topological defect-modulated electronic and magnetic properties in zigzag graphene nanoribbons. Chinese Physics B, 2017, 26, 103103.	0.7	5
25364	Impact of strain on electronic and transport properties of 6â€‰nm hydrogenated germanane nano-ribbon channel double gate field effect transistor. Materials Research Express, 2017, 4, 114005.	0.8	2
25365	Effects of Defects on the Temperatureâ€Đependent Thermal Conductivity of Suspended Monolayer Molybdenum Disulfide Grown by Chemical Vapor Deposition. Advanced Functional Materials, 2017, 27, 1704357.	7.8	44
25366	From 3D to 2D Co and Ni Oxyhydroxide Catalysts: Elucidation of the Active Site and Influence of Doping on the Oxygen Evolution Activity. ACS Catalysis, 2017, 7, 8558-8571.	5.5	50

#	Article	IF	Citations
25367	DFT investigation on electronic, magnetic, mechanical and thermodynamic properties under pressure of some EuMO₃(Mâ€‰â€‰=â€‰â€‰Ga, In) perovskites. Materials Research Express, 2017, 4, 106104.	0.8	46
25368	Structural Evolution in BaSn₂F₅X (X = Cl, Br, I): A Family of Alkaline Earth Metal Tin Mixed Halides. Inorganic Chemistry, 2017, 56, 13593-13599.	1.9	11
25369	Interplay between Halogen and Hydrogen Bonds in 2D Self-Assembly on the Gold Surface: A First-Principles Investigation. Journal of Physical Chemistry C, 2017, 121, 24707-24720.	1.5	11
25370	Unravelling the mechanisms of CO₂ hydrogenation to methanol on Cu-based catalysts using first-principles multiscale modelling and experiments. Catalysis Science and Technology, 2017, 7, 5900-5913.	2.1	85
25371	High density oxidative plasma unzipping of multiwall carbon nanotubes. RSC Advances, 2017, 7, 48268-48274.	1.7	10
25372	Growth and characterization of BaZnGa. Philosophical Magazine, 2017, 97, 3317-3324.	0.7	0
25373	On atomic mechanisms governing the oxidation of Bi₂Te₃. Journal of Physics Condensed Matter, 2017, 29, 485705.	0.7	30
25374	Adsorption of oxygen on low-index surfaces of Ti3Al alloy. Physics of the Solid State, 2017, 59, 1852-1866.	0.2	9
25375	Enhancing Charge Carrier Lifetime in Metal Oxide Photoelectrodes through Mild Hydrogen Treatment. Advanced Energy Materials, 2017, 7, 1701536.	10.2	104
25376	Firstâ€Principles Study of Superconducting ScRhP and ScIrP pnictides. Physica Status Solidi (B): Basic Research, 2017, 254, 1700336.	0.7	39
25377	The comparative study on bulk-PtSe2 and 2D 1-Layer-PtSe2 under high pressure via first-principle calculations. Theoretical Chemistry Accounts, 2017, 136, 1.	0.5	4
25378	Mechanical characteristics of FeAl2O4 and AlFe2O4 spinel phases in coatings â€“ A study combining experimental evaluation and first-principles calculations. Ceramics International, 2017, 43, 16094-16100.	2.3	19
25379	DynaPhoPy: A code for extracting phonon quasiparticles from molecular dynamics simulations. Computer Physics Communications, 2017, 221, 221-234.	3.0	105
25380	CO₂ Reduction Mechanism on the Pb(111) Surface: Effect of Solvent and Cations. Journal of Physical Chemistry C, 2017, 121, 19767-19773.	1.5	47
25381	Atomic Structure of Submonolayer NaCl Grown on Ag(110) Surface. Journal of Physical Chemistry C, 2017, 121, 20272-20278.	1.5	9
25382	Effect of Surface Structure of TiO₂ Nanoparticles on CO₂ Adsorption and SO₂ Resistance. ACS Sustainable Chemistry and Engineering, 2017, 5, 9295-9306.	3.2	49
25383	An all-carbon vdW heterojunction composed of penta-graphene and graphene: Tuning the Schottky barrier by electrostatic gating or nitrogen doping. Applied Physics Letters, 2017, 111, .	1.5	30
25384	Robust theoretical modelling of core ionisation edges for quantitative electron energy loss spectroscopy of B- and N-doped graphene. Journal of Physics Condensed Matter, 2017, 29, 225303.	0.7	8

#	Article	IF	Citations
25385	Electronic transport properties of graphene doped by gallium. Nanotechnology, 2017, 28, 415203.	1.3	14
25386	New phases of osmium carbide from evolutionary algorithm andab initiocomputations. Materials Research Express, 2017, 4, 096503.	0.8	0
25387	Raman Spectra of Polycrystalline CeO₂: A Density Functional Theory Study. Journal of Physical Chemistry C, 2017, 121, 20834-20849.	1.5	278
25388	Enhanced Stability and Electrochemical Performance of Carbonâ€Coated Ti³⁺ Selfâ€Doped TiO₂â€Reduced Graphene Oxide Hollow Nanostructureâ€Supported Ptâ€Catalyzed Fuel Cell Electrodes. Advanced Materials Interfaces, 2017, 4, 1700564.	1.9	15
25389	First-principles study on half-metallic ferromagnetic properties of Zn1â^'x V x Se ternary alloys. Applied Physics A: Materials Science and Processing, 2017, 123, 1.	1.1	10
25390	Ti based half Heusler compounds: A new on the screen with robustic thermoelectric performance. Journal of Alloys and Compounds, 2017, 727, 1171-1177.	2.8	28
25391	Effect of exposed facets and oxygen vacancies on the catalytic activity of Pd_xCe_{1â^'x}O_{2â^'Î´} catalysts: a combined experimental and theoretical study. Catalysis Science and Technology, 2017, 7, 4462-4469.	2.1	11
25392	Theoretical studies on the electronic structure and optical absorption property of (Ni, C) co-doped anatase TiO 2. Computational Condensed Matter, 2017, 13, 16-28.	0.9	7
25393	Barrier effect of oxide on Cu permeation on Be surface. Physics Letters, Section A: General, Atomic and Solid State Physics, 2017, 381, 3211-3216.	0.9	3
25394	First-principles study of SO2 sensors based on phosphorene and its isoelectronic counterparts: GeS, GeSe, SnS, SnSe. Chemical Physics Letters, 2017, 686, 83-87.	1.2	51
25395	A new Ca3MgSi2O8 compound and some of its thermodynamic properties. Journal of Solid State Chemistry, 2017, 255, 145-149.	1.4	7
25396	First principles studies on the selectivity of dimethoxymethane and methyl formate in methanol oxidation over V₂O₅/TiO₂-based catalysts. Physical Chemistry Chemical Physics, 2017, 19, 19393-19406.	1.3	9
25397	Thermoelectric and piezoelectric properties of the predicted Al_xIn_{1â^'x}N composites based on ab initio calculations. Physical Chemistry Chemical Physics, 2017, 19, 24613-24625.	1.3	4
25398	Biofunctionalized conductive polymers enable efficient CO ₂ electroreduction. Science Advances, 2017, 3, e1700686.	4.7	89
25399	The GGA+U method studied the effects of Cu doping on the formation energy, electronic and optical properties of V-doped ZnO. Optical and Quantum Electronics, 2017, 49, 1.	1.5	3
25400	DFTÂ+ U and ab initio atomistic thermodynamics approache for mixed transitional metallic oxides: A case study of CoCu 2 O 3 surface terminations. Materials Chemistry and Physics, 2017, 201, 241-250.	2.0	13
25401	Acetylene and Ethylene Adsorption on a Î²-Mo₂C(100) Surface: A Periodic DFT Study on the Role of C- and Mo-Terminations for Bonding and Hydrogenation Reactions. Journal of Physical Chemistry C, 2017, 121, 19786-19795.	1.5	22
25402	Structural, electronic, and magnetic properties of non-planar doping of BeO in graphene: a DFT study. New Journal of Chemistry, 2017, 41, 10780-10789.	1.4	7

#	Article	IF	Citations
25403	First-principles study on the electronic, optical and thermodynamic properties of ABO₃ (AÂ= La,Sr, B = Fe,Co) perovskites. RSC Advances, 2017, 7, 38798-38804.	1.7	51
25404	Elastic, vibrational, and thermodynamic properties of Sr 10 (PO 4) 6 F 2 and Ca 10 (PO 4) 6 F 2 from first principles. Chinese Physics B, 2017, 26, 086301.	0.7	1
25405	Orientation-dependent properties of epitaxially strained perovskite oxide thin films: Insights from first-principles calculations. Physical Review B, 2017, 95, .	1.1	22
25406	Time-dependent density functional theory calculations for the excitation spectra of III-V ternary alloys. Physical Review B, 2017, 96, .	1.1	7
25407	Experimental and theoretical investigation of Nd doped ZnO. Journal of Magnetism and Magnetic Materials, 2017, 444, 416-420.	1.0	14
25408	Effect of the interfacial O and Mg vacancies on electronic structure and transport properties of the FeRh/MgO/FeRh (0 0 1) magnetic tunnel junction: DFT calculations. Journal of Magnetism and Magnetic Materials, 2017, 444, 394-400.	1.0	1
25409	Effects of monolayer Bi on the self-assembly of DBBA on Au(111). Surface Science, 2017, 665, 89-95.	0.8	30
25410	Dense CO Adlayers as Enablers of CO Hydrogenation Turnovers on Ru Surfaces. Journal of the American Chemical Society, 2017, 139, 11789-11802.	6.6	54
25411	Pressure-induced abnormal insulating state in triangular layered cobaltite Li_xCoO₂ (x = 0.9). Journal of Materials Chemistry A, 2017, 5, 19390-19397.	5.2	9
25412	Surface structures and compositions of Auâ€“Rh bimetallic nanoclusters supported on thin-film Al2O3/NiAl(100) probed with CO. Journal of Chemical Physics, 2017, 147, 044704.	1.2	4
25413	Polar ordering and structural distortion in electronic domain-wall properties of BiFeO3. Journal of Applied Physics, 2017, 122, 075103.	1.1	9
25414	Redox properties of birnessite from a defect perspective. Proceedings of the National Academy of Sciences of the United States of America, 2017, 114, 9523-9528.	3.3	50
25415	Theoretical study of the thickness dependence of the metal-insulator transition in <mml:math xmlns:mml="http://www.w3.org/1998/Math/MathML"><mml:mrow><mml:msub><mml:mi>Bi</mml:mi><mml:mn>2</mml:mn></mml:n mathvariant="normal">O</mml:mi><mml:mn>8</mml:mn></mml:msub></mml:mrow></mml:math> nanosheets. Physical Review B, 2017, 96, .	1.1	1
25416	Phase transition of tetragonal copper sulfide <mml:math xmlns:mml="http://www.w3.org/1998/Math/MathML"><mml:mrow><mml:msub><mml:mi>Cu</mml:mi><mml:mn>2</mml:mn></mml:mr mathvariant="normal">S</mml:mi></mml:mrow></mml:math> at low temperatures. Physical Review B, 2017, 96, .	1.1	15
25417	GrÃ¼neisen parameters and thermal conductivity in the phase change compound GeTe. Journal of Computational Electronics, 2017, 16, 997-1002.	1.3	13
25418	A first-principles study of aryloxyanthraquinone-based optical molecular switch. Chemical Physics Letters, 2017, 686, 140-147.	1.2	14
25419	A comparative study on magnetic properties of Mo doped AlN, GaN and InN monolayers from first-principles. Physica B: Condensed Matter, 2017, 524, 47-52.	1.3	10
25420	Influence of Intramolecular Charge Transfer and Nuclear Quantum Effects on Intramolecular Hydrogen Bonds in Azopyrimidines. Journal of Organic Chemistry, 2017, 82, 10350-10359.	1.7	15

#	Article	IF	Citations
25421	Magnetism and spin entropy in Ru doped Na0.5CoO2. Physical Chemistry Chemical Physics, 2017, 19, 23425-23430.	1.3	7
25422	Black phosphorus transistors with van der Waals-type electrical contacts. Nanoscale, 2017, 9, 14047-14057.	2.8	76
25423	Auxiliary-field quantum Monte Carlo calculations with multiple-projector pseudopotentials. Physical Review B, 2017, 95, .	1.1	20
25424	Phonon spectra, electronic, and thermodynamic properties of WS₂ nanotubes. Journal of Computational Chemistry, 2017, 38, 2581-2593.	1.5	24
25425	Energetics of halogen impurities in thorium dioxide. Journal of Nuclear Materials, 2017, 495, 192-201.	1.3	5
25426	Electronic transport properties and first-principles study of Î³-graphyne, and Î³-BN graphyne monolayers. Superlattices and Microstructures, 2017, 111, 1162-1171.	1.4	4
25427	Facet-Dependent Diol-Induced Density of States of Anatase TiO₂ Crystal Surface. ACS Omega, 2017, 2, 4032-4038.	1.6	12
25428	A first-principles study of anionic (S) and cationic (V/Nb) doped Sr₂Ta₂O₇ for visible light photocatalysis. RSC Advances, 2017, 7, 40922-40928.	1.7	13
25429	Li states on a Câ€“H vacancy in graphane: a first-principles study. RSC Advances, 2017, 7, 39748-39757.	1.7	7
25430	Defects and oxidation resilience in InSe. Physical Review B, 2017, 96, .	1.1	44
25431	General procedure for the calculation of accurate defect excitation energies from DFT-1/2 band structures: The case of the <mml:math xmlns:mml="http://www.w3.org/1998/Math/MathML"><mml:msup><mml:mrow><mml:mi>NV</mml:mi></mml:mrow><mml:mo>â^’</m center in diamond. Physical Review B, 2017, 96, .	1.1	19
25432	Stacking in incommensurate graphene/hexagonal-boron-nitride heterostructures based on ab initio study of interlayer interaction. Physical Review B, 2017, 96, .	1.1	23
25433	Ab initio study of the electron energy loss function in a graphene-sapphire-graphene composite system. Physical Review B, 2017, 96, .	1.1	22
25434	Insight into electrochemical and elastic properties in AFe1-M SO4F (A = Li, Na; M = Co, Ni, Mg) cathode materials: A first principle study. Electrochimica Acta, 2017, 251, 316-323.	2.6	10
25435	Highly active, bi-functional and metal-free B 4 C-nanoparticle-modified graphite felt electrodes for vanadium redox flow batteries. Journal of Power Sources, 2017, 365, 34-42.	4.0	75
25436	Synthesis and characterization of two lead-containing metal chalcogenides: Ba5Pb2Sn3S13 and Ba6PbSn3Se13. Journal of Solid State Chemistry, 2017, 255, 133-138.	1.4	6
25437	Modelling oxygen defects in orthorhombic LaMnO₃ and its low index surfaces. Physical Chemistry Chemical Physics, 2017, 19, 24636-24646.	1.3	25
25438	New insights into the electronic structures and optical properties in the orthorhombic perovskite MAPbI₃: a mixture of Pb and Ge/Sn. New Journal of Chemistry, 2017, 41, 11413-11421.	1.4	27

#	Article	IF	Citations
25439	Exploring an effective oxygen reduction reaction catalyst via 4eâ˜ process based on waved-graphene. Science China Materials, 2017, 60, 739-746.	3.5	11
25440	First-principles study on the electronic and optical properties of WS2 and MoS2 monolayers. Chinese Journal of Physics, 2017, 55, 1930-1937.	2.0	36
25441	Band gap modulation and indirect to direct band gap transition in ZnS/Si and Si/ZnS core/shell nanowires. Physica B: Condensed Matter, 2017, 524, 163-172.	1.3	11
25442	Ab Initio Study of Stability of Na₂Fe₂(SO₄)₃, a High Potential Na-Ion Battery Cathode Material. Journal of Physical Chemistry C, 2017, 121, 20067-20074.	1.5	15
25443	Role of Carbon Support for Subnanometer Gold-Cluster-Catalyzed Disiloxane Synthesis from Hydrosilane and Water. Journal of Physical Chemistry C, 2017, 121, 20101-20112.	1.5	9
25444	Initial-Stage Oxidation of Ni₃Al(100) and -(110) from Ab Initio Thermodynamics. Journal of Physical Chemistry C, 2017, 121, 19191-19200.	1.5	12
25445	Ab Initio Simulations of Copper Oxide Nanowires and Clusters on TiO₂ (101) Anatase Surface. Journal of Physical Chemistry C, 2017, 121, 20359-20365.	1.5	10
25446	First principles study of the Mn-doping effect on the physical and chemical properties of mullite-family Al₂SiO₅. Physical Chemistry Chemical Physics, 2017, 19, 24991-25001.	1.3	5
25447	Density functional study on the resistance to sulfur poisoning of Ptx (x = 0, 1, 4 and 8) modified Î±-Mo2C(0001) surfaces. Physical Chemistry Chemical Physics, 2017, 19, 24879-24885.	1.3	1
25448	Functionalizing Fe adatoms on Cu(001) as a nanoelectromechanical system. New Journal of Physics, 2017, 19, 073016.	1.2	3
25449	Quantum Dot Self-Assembly Driven by a Surfactant-Induced Morphological Instability. Physical Review Letters, 2017, 119, 086101.	2.9	18
25450	Structural, mechanical and electronic properties of CaB ₂ C ₂ at high pressure. Europhysics Letters, 2017, 118, 66001.	0.7	2
25451	Piezoelectric coefficients of bulk 3R transition metal dichalcogenides. Japanese Journal of Applied Physics, 2017, 56, 098002.	0.8	9
25452	Pressure-induced stable BeN 4 as a high-energy density material. Journal of Power Sources, 2017, 365, 155-161.	4.0	43
25453	A first-principles study on zigzag phosphorene nanoribbons passivated by iron-group atoms. Physical Chemistry Chemical Physics, 2017, 19, 25441-25445.	1.3	11
25454	Efficient diagnostics of the electronic and optical properties of defective ZnO nanoparticles synthesized using the solâ€“gel method: experimental and theoretical studies. Materials Research Express, 2017, 4, 085908.	0.8	26
25455	Prediction and synthesis of a family of atomic laminate phases with KagomÃ©-like and in-plane chemical ordering. Science Advances, 2017, 3, e1700642.	4.7	156
25456	Elastic anisotropy and stability of Rh 2 B and RhB 2 at high pressures. Chinese Journal of Physics, 2017, 55, 1981-1987.	2.0	3

#	Article	IF	Citations
25457	Finding and characterization of an energetically favorable cubic Ce0.75Zr0.25O2 solid solution using genetic algorithm and density functional theory. Computational Materials Science, 2017, 138, 219-224.	1.4	5
25458	An experimental and first-principles investigation of noncentrosymmetric cubic Re3W. Journal of Alloys and Compounds, 2017, 728, 984-991.	2.8	3
25459	Hg-Based Infrared Nonlinear Optical Material KHg₄Ga₅Se₁₂ Exhibits Good Phase-Matchability and Exceptional Second Harmonic Generation Response. Chemistry of Materials, 2017, 29, 7993-8002.	3.2	85
25460	Computational Characterization of the Dependence of Halide Perovskite Effective Masses on Chemical Composition and Structure. Journal of Physical Chemistry C, 2017, 121, 23886-23895.	1.5	38
25461	Geometric and electronic properties of ultrathin anatase TiO₂(001) films. Physical Chemistry Chemical Physics, 2017, 19, 25456-25462.	1.3	15
25462	Experimental and ab initio studies of Cd₅(BO₃)₃Cl: the first cadmium borate chlorine NLO material with isolated BO₃groups. Dalton Transactions, 2017, 46, 15228-15234.	1.6	18
25463	Effects of the Hubbard U on density functional-based predictions of BiFeO₃properties. Journal of Physics Condensed Matter, 2017, 29, 445501.	0.7	25
25464	Ab initio study of ceria films for resistive switching memory applications. Materials Research Express, 2017, 4, 106301.	0.8	11
25465	Birefringent Stable Glass with Predominantly Isotropic Molecular Orientation. Physical Review Letters, 2017, 119, 095502.	2.9	28
25466	Investigation of cobalt doped tin dioxide structure and defects: Density functional theory and empirical force fields. Journal of Contemporary Physics, 2017, 52, 227-233.	0.1	8
25467	Lithium and sodium adsorption properties of monolayer antimonene. Materials Today Energy, 2017, 5, 347-354.	2.5	62
25468	Surface Chemistry Mechanism of Ultra-Low Interfacial Resistance in the Solid-State Electrolyte Li₇La₃Zr₂O₁₂. Chemistry of Materials, 2017, 29, 7961-7968.	3.2	612
25469	Probing Biomolecular Interactions with Gold Nanoparticle-Decorated Single-Walled Carbon Nanotubes. Journal of Physical Chemistry C, 2017, 121, 20813-20820.	1.5	9
25470	Theoretical prediction of the mechanical properties of zeolitic imidazolate frameworks (ZIFs). RSC Advances, 2017, 7, 41499-41503.	1.7	18
25471	Mechanical anisotropy and strain-tailored band structures of pentagonal boron nitride monolayers. Journal of Applied Physics, 2017, 122, 094302.	1.1	9
25472	Charge state of vacancy defects in Eu-doped GaN. Physical Review B, 2017, 96, .	1.1	20
25473	Exchange constants in molecule-based magnets derived from density functional methods. Physical Review B, 2017, 96, .	1.1	8
25474	Raman spectroscopy and x-ray diffraction of <mml:math xmlns:mml="http://www.w3.org/1998/Math/MathML"><mml:mrow><mml:msup><mml:mrow><mml:mi mathvariant="italic">sp</mml:mi></mml:mrow><mml:mn>3</mml:mn></mml:msup><mml:mspace width="4pt" /><mml:mi>CaC</mml:mi><mml:msub><mml:mi mathvariant="normal">O</mml:mi><mml:mn>3</mml:mn></mml:msub></mml:mrow></mml:math> at lower mantle pressures. Physical Review B, 2017, 96, .	1.1	54

#	Article	IF	Citations
25475	Friction Regimes of Water-Lubricated Diamond (111): Role of Interfacial Ether Groups and Tribo-Induced Aromatic Surface Reconstructions. Physical Review Letters, 2017, 119, 096101.	2.9	63
25476	Low-energy transmission electron diffraction and imaging of large-area graphene. Science Advances, 2017, 3, e1603231.	4.7	35
25477	Stability, magnetic and electronic properties of SiC sheet doped with B, N, Al and P. Bulletin of Materials Science, 2017, 40, 1081-1086.	0.8	11
25478	A curved pathway for oxygen interstitial diffusion in aluminum. Computational Materials Science, 2017, 140, 47-54.	1.4	10
25479	First-principles calculations on the stacking fault energy, surface energy and dislocation properties of NbCr2 and HfCr2. Computational Materials Science, 2017, 140, 334-343.	1.4	13
25480	Effects of boron and carbon on the ideal strength of Ni solution and Ni3Al intermetallics: A first-principles study of tensile deformation. Computational Materials Science, 2017, 140, 140-147.	1.4	15
25481	The investigation on a universal local structural feature in Mgâ€“Al alloys. Computational Materials Science, 2017, 140, 224-234.	1.4	5
25482	Insights into the physics of interaction between borophene and O2-first-principles investigation. Computational Materials Science, 2017, 140, 261-266.	1.4	19
25483	Porous graphene and graphenylene nanotubes: Electronic structure and strain effects. Computational Materials Science, 2017, 140, 344-355.	1.4	10
25484	Electronic structural, optical and phonon lattice dynamical properties of pure- and La-doped SrTiO 3 : An ab initio thermodynamics study. Journal of Solid State Chemistry, 2017, 256, 239-251.	1.4	32
25485	Synthesis and Microwave Absorption Properties of BiFeO₃ Nanowire-RGO Nanocomposite and First-Principles Calculations for Insight of Electromagnetic Properties and Electronic Structures. Journal of Physical Chemistry C, 2017, 121, 21290-21304.	1.5	102
25486	Phase Stability, Phase Mixing, and Phase Separation in Fluorinated Alkaline Earth Hydrides. Journal of Physical Chemistry C, 2017, 121, 21806-21820.	1.5	6
25487	Ionic Conductivity in Ti-Doped KFeO₂: Experiment and Mathematical Modeling. Journal of Physical Chemistry C, 2017, 121, 21128-21135.	1.5	16
25488	The Positive Role of Hydrogen on the Dehydrogenation of Propane on Pt(111). ACS Catalysis, 2017, 7, 7495-7508.	5.5	95
25489	Chemical and Electronic Repair Mechanism of Defects in MoS₂ Monolayers. ACS Nano, 2017, 11, 9989-9996.	7.3	80
25490	In situ atomic-scale imaging of the metal/oxide interfacial transformation. Nature Communications, 2017, 8, 307.	5.8	79
25491	First-principles study of crystallographic slip modes in Ï‰-Zr. Scientific Reports, 2017, 7, 8932.	1.6	10
25492	Extremely high electrical conductance of microporous 3D graphene-like zeolite-templated carbon framework. Scientific Reports, 2017, 7, 11460.	1.6	23

#	Article	IF	Citations
25493	The role of metal oxide interactions: revisiting Pt growth on the TiO₂ surface in the process of impregnation method. Nanoscale, 2017, 9, 14272-14279.	2.8	22
25494	Two-dimensional VS₂ monolayers as potential anode materials for lithium-ion batteries and beyond: first-principles calculations. Journal of Materials Chemistry A, 2017, 5, 21370-21377.	5.2	176
25495	First principles studies of CO₂ and O₂ chemisorption on La₂O₃ surfaces. Physical Chemistry Chemical Physics, 2017, 19, 26799-26811.	1.3	21
25496	Ultrathin Î²-tellurium layers grown on highly oriented pyrolytic graphite by molecular-beam epitaxy. Nanoscale, 2017, 9, 15945-15948.	2.8	136
25497	Hierarchical cobaltâ€“nitride and â€“oxide co-doped porous carbon nanostructures for highly efficient and durable bifunctional oxygen reaction electrocatalysts. Nanoscale, 2017, 9, 15846-15855.	2.8	29
25498	Energy level alignment at semiconductorâ€“water interfaces from atomistic and continuum solvation models. RSC Advances, 2017, 7, 43660-43670.	1.7	16
25499	Magnetic two-dimensional organic topological insulator: Auâ€“1,3,5-triethynylbenzene framework. Journal of Chemical Physics, 2017, 147, 104704.	1.2	9
25500	First principles study of structural, magnetic and electronic properties of CrAs. Philosophical Magazine, 2017, 97, 3276-3295.	0.7	23
25501	AbÂinitio Surface Phase Diagram of Sn/Cu(001) : Reconciling Experiments with Theory. Physical Review Applied, 2017, 8, .	1.5	2
25502	Defect Engineering by Codoping in <mml:math xmlns:mml="http://www.w3.org/1998/Math/MathML" display="inline"><mml:mrow><mml:mrow><mml:msub><mml:mrow><mml:mi>KCaI</mml:mi></mml:mrow><mml:mrow><mml:mn> Single-Crystalline Scintillators. Physical Review Applied, 2017, 8, .	1.5	10
25503	Three-dimensional topological critical Dirac semimetal in <mml:math xmlns:mml="http://www.w3.org/1998/Math/MathML"><mml:mrow><mml:mi>A</mml:mi><mml:mi>MgBi</mml:mi></mml:mrow><mml:mm width="0.16em" /><mml:mo>(</mml:mo><mml:mrow><mml:mi>A</mml:mi><mml:mo>=</mml:mo></mml:mrow></mml:math>) Tj ETQq0 0 0 rgBT /Ov	1.1	39
25504	Tuning the topological states in metal-organic bilayers. Physical Review B, 2017, 96, .	1.1	15
25505	First-principles study on electronic properties of stanene/WS₂ monolayer. Modern Physics Letters B, 2017, 31, 1750271.	1.0	7
25506	The Synthesis and Mechanism of (001)-Orientated Hematite Nano Rings: A Combined Theoretical and Experimental Investigation. Nano, 2017, 12, 1750111.	0.5	2
25507	Exact location of dopants below the Si(001):H surface from scanning tunneling microscopy and density functional theory. Physical Review B, 2017, 95, .	1.1	10
25508	Quantum chemical calculations of thermodynamic and mechanical properties of the intermetallic phases in copperâ€“scandium alloy. Journal of Theoretical and Computational Chemistry, 2017, 16, 1750056.	1.8	4
25509	Elastic knowledge base of bcc Ti alloys from first-principles calculations and CALPHAD-based modeling. Computational Materials Science, 2017, 140, 121-139.	1.4	30
25510	Point defects in buckled and asymmetric washboard phases of arsenic phosphorus: A first principles study. Computational Materials Science, 2017, 140, 290-298.	1.4	19

#	Article	IF	Citations
25511	New Oxide-Ion Conductor SrYbInO₄ with Partially Cation-Disordered CaFe₂O₄-Type Structure. Journal of Physical Chemistry C, 2017, 121, 21272-21280.	1.5	24
25512	Electronic structure of boron based single and multi-layer two dimensional materials. Journal of Applied Physics, 2017, 122, 104302.	1.1	1
25513	Nonequilibrium ab initio molecular dynamics determination of Ti monovacancy migration rates in <mml:math xmlns:mml="http://www.w3.org/1998/Math/MathML"><mml:mrow><mml:mi>B</mml:mi><mml:mn>1</mml:mn></mml:mrow></mml:m TiN. Physical Review B, 2017, 96, .	1.1	15
25514	Towards understanding MgO/Fe interface formation: Adsorption of O and Mg atoms on an Fe(001) surface. Physical Review B, 2017, 96, .	1.1	6
25515	Improvements in the <mml:math xmlns:mml="http://www.w3.org/1998/Math/MathML"><mml:mrow><mml:mi>G</mml:mi><mml:mi>W</mml:mi></mml:mrow></mml:m and Bethe-Salpeter-equation calculations on phosphorene. Physical Review B, 2017, 96, .	1.1	82
25516	Enthalpies of formation of layered LiNixMnxCo1â€“2xO2 (0 â‰¤ x â‰¤ 0.5) compounds as lithium ion battery cathode materials. International Journal of Materials Research, 2017, 108, 869-878.	0.1	16
25517	Creation of models and parametrization of a classical force field for amorphous Al2O3/water interfaces based on Density Functional Theory. Computational Materials Science, 2017, 140, 307-314.	1.4	10
25518	Identifying the Ground State Geometry of a MoN₂ Sheet through a Global Structure Search and Its Tunable p-Electron Half-Metallicity. Chemistry of Materials, 2017, 29, 8588-8593.	3.2	44
25519	Tailoring the Electronic Band Gap and Band Edge Positions in the C₂N Monolayer by P and As Substitution for Photocatalytic Water Splitting. Journal of Physical Chemistry C, 2017, 121, 22216-22224.	1.5	80
25520	Formation and Characterization of Hydrogen Boride Sheets Derived from MgB₂ by Cation Exchange. Journal of the American Chemical Society, 2017, 139, 13761-13769.	6.6	157
25521	Toward rational nanoparticle synthesis: predicting surface intermixing in bimetallic alloy nanocatalysts. Nanoscale, 2017, 9, 15005-15017.	2.8	24
25522	Effect of oxygen vacancy and surface plasmon resonance: a photocatalytic activity study on Ag/Bi4Ti3O12 nanocomposites. Journal of Materials Science: Materials in Electronics, 2017, 28, 17896-17907.	1.1	9
25523	Quantitative evaluation of hydrogen atoms trapped at single vacancies in tungsten using positron annihilation lifetime measurements: Experiments and theoretical calculations. Journal of Nuclear Materials, 2017, 496, 9-17.	1.3	12
25524	Dislocation core structures of tungsten with dilute solute hydrogen. Journal of Nuclear Materials, 2017, 496, 362-366.	1.3	3
25525	First-principle calculations of structural, electronic, optical and thermal properties of hydrogenated graphene. Materials Science and Engineering B: Solid-State Materials for Advanced Technology, 2017, 226, 64-71.	1.7	24
25526	Group 10 Metal Benzene-1,2-dithiolate Derivatives in the Synthesis of Coordination Polymers Containing Potassium Countercations. Inorganic Chemistry, 2017, 56, 11810-11818.	1.9	12
25527	Differentiating Intrinsic Reactivity of Copper, Copperâ€“Zinc Alloy, and Copper/Zinc Oxide Interface for Methanol Steam Reforming by First-Principles Theory. Journal of Physical Chemistry C, 2017, 121, 21553-21559.	1.5	37
25528	Electronic Interactions of Size-Selected Oxide Clusters on Metallic and Thin Film Oxide Supports. Journal of Physical Chemistry C, 2017, 121, 22234-22247.	1.5	12

#	Article	IF	Citations
25529	Formic acid oxidation on platinum electrodes: a detailed mechanism supported by experiments and calculations on well-defined surfaces. Journal of Materials Chemistry A, 2017, 5, 21773-21784.	5.2	77
25530	Arsenene/Ca(OH)₂ van der Waals heterostructure: strain tunable electronic and photocatalytic properties. RSC Advances, 2017, 7, 44394-44400.	1.7	36
25531	BNC nanoshells: a novel structure for atomic storage. Nanotechnology, 2017, 28, 465201.	1.3	3
25532	First-principles calculations of Co 7 W 6 doped with Re: Site occupancy and electronic properties. Computational Condensed Matter, 2017, 13, 36-40.	0.9	4
25533	Theoretical insights on the reaction pathways of the oxygen reduction reaction on yttrium doped graphene as a catalyst in fuel cells. Synthetic Metals, 2017, 232, 131-137.	2.1	1
25534	Strain-induced ferroelectricity and lattice coupling in BaSnO3 and SrSnO3. Physical Chemistry Chemical Physics, 2017, 19, 26047-26055.	1.3	18
25535	Electronic structure, magnetic properties, and mixed valence character of Ce₂Ni₃Si₅ from first principles calculations. Journal of Computational Chemistry, 2017, 38, 2475-2480.	1.5	3
25536	First-principles study of structural, elastic, electronic, thermodynamic and optical properties of Sc 3 Sn X (X Â=ÂB, C). Computational Condensed Matter, 2017, 13, 41-48.	0.9	5
25537	First principles study of dehydrogenation properties of alkali/alkali-earth metal doped Mg7TiH16. Journal of Alloys and Compounds, 2017, 728, 1016-1022.	2.8	4
25538	Water adsorption on Î±-V2O5 surface and absorption in V2O5â˜™nH2O xerogel: DFT study of electronic structure. Surface Science, 2017, 666, 76-83.	0.8	4
25539	Perovskite-Type InCoO3 with Low-Spin Co3+: Effect of Inâ€“O Covalency on Structural Stabilization in Comparison with Rare-Earth Series. Inorganic Chemistry, 2017, 56, 11113-11122.	1.9	7
25540	First-Principles Investigation of Lithium Polysulfide Structure and Behavior in Solution. Journal of Physical Chemistry C, 2017, 121, 21105-21117.	1.5	53
25541	Structure and crystallization of SiO₂and B₂O₃doped lithium disilicate glasses from theory and experiment. Physical Chemistry Chemical Physics, 2017, 19, 25298-25308.	1.3	0
25542	Recipe for generating Weyl semimetals with extended topologically protected features. Physical Review B, 2017, 96, .	1.1	6
25543	First principles study on HenV clusters in Î±-Fe bulk and grain boundaries. Computational Materials Science, 2017, 139, 419-429.	1.4	5
25544	A comparison study of decomposition mechanisms of single-cation and double-cations (Li, Al) ammine borohydrides. International Journal of Hydrogen Energy, 2017, 42, 24861-24867.	3.8	1
25545	Iron Intercalation in Covalentâ€“Organic Frameworks: A Promising Approach for Semiconductors. Journal of Physical Chemistry C, 2017, 121, 21160-21170.	1.5	46
25546	Computational Discovery of Nickel-Based Catalysts for CO₂ Reduction to Formic Acid. Journal of Physical Chemistry C, 2017, 121, 20865-20870.	1.5	39

#	Article	IF	Citations
25547	Interaction between H₂O, N₂, CO, NO, NO₂ and N₂O molecules and a defective WSe₂ monolayer. Physical Chemistry Chemical Physics, 2017, 19, 26022-26033.	1.3	60
25548	Atomic-scale friction behavior of layered graphene and graphene-like BN materials modulated by interaction potential. AIP Advances, 2017, 7, .	0.6	3
25549	BulkÎ²-Te to few layeredÎ²-tellurenes: indirect to direct band-Gap transitions showing semiconducting property. Materials Research Express, 2017, 4, 095902.	0.8	58
25550	Ab initio simulation of dissolution energy and carbon activity in fcc Fe. Physics of the Solid State, 2017, 59, 1279-1284.	0.2	6
25551	Migration properties of mono-vacancy in W-4d/5d transition metal alloys. Journal of Alloys and Compounds, 2017, 728, 363-367.	2.8	6
25552	Efficient Yellow-Orange Phosphor Lu₄Ba₂[Si₉ON₁₆]O:Eu²⁺ and Orange-Red Emitting Y₄Ba₂[Si₉ON₁₆]O:Eu²⁺: Two Oxonitridosilicate Oxides with Outstanding Structural Variety. Chemistry of Materials, 2017, 29, 8277-8284.	3.2	34
25553	Crystal Structure, Stability, and Physical Properties of Metastable Electron-Poor Narrow-Gap AlGe Semiconductor. Inorganic Chemistry, 2017, 56, 11591-11602.	1.9	4
25554	Phase-Field Based Multiscale Modeling of Heterogeneous Solid Electrolytes: Applications to Nanoporous Li₃PS₄. ACS Applied Materials & Interfaces, 2017, 9, 33341-33350.	4.0	21
25555	First-principles calculations of oxygen interstitials in corundum: a site symmetry approach. Physical Chemistry Chemical Physics, 2017, 19, 25245-25251.	1.3	19
25556	Hybrid density functional theory insight into the stability and microscopic properties of Bi-doped <mml:math xmlns:mml="http://www.w3.org/1998/Math/MathML"><mml:msub><mml:mi>LiNbO</mml:mi><mml:mn>3</mml:mn></mml:msub></mml: : Lone electron pair effect. Physical Review B, 2017, 96, .	1.1	20
25557	A-Site Ordered Double Perovskite CaMnTi₂O₆ as a Multifunctional Piezoelectric and Ferroelectricâ€“Photovoltaic Material. Inorganic Chemistry, 2017, 56, 11854-11861.	1.9	54
25558	Passivation Mechanism of the Native Oxide/InAs Interface by Fluorine. Journal of Physical Chemistry C, 2017, 121, 20744-20750.	1.5	8
25559	Ab Initio Thermodynamic Investigation of Monolayer Stability of Multicomponent Metal Oxides: M_xO_y/ZnO(0001) and M_xO_y/TiO₂(110) (M = Pd, Ru, Ni, Pt, Au, Zn). Journal of Physical Chemistry C, 2017, 121, 21439-21448.	1.5	5
25560	Catalysis at the Rim: A Mechanism for Low Temperature CO Oxidation over Pt₃Sn. ACS Catalysis, 2017, 7, 7431-7441.	5.5	32
25561	Structural, mechanical, electronic and thermal properties of the newly predicted NB2 from ab initio calculations. Chinese Journal of Physics, 2017, 55, 2540-2547.	2.0	5
25562	Magnetic polaritons enhanced absorption of phosphorene in the near-infrared and visible region. Materials Science and Engineering B: Solid-State Materials for Advanced Technology, 2017, 226, 24-28.	1.7	4
25563	Novel Au Catalysis Strategy for the Synthesis of Au@Pt Coreâ€“Shell Nanoelectrocatalyst with Self-Controlled Quasi-Monolayer Pt Skin. ACS Applied Materials & Interfaces, 2017, 9, 32688-32697.	4.0	23
25564	Diffusion in energy materials: Governing dynamics from atomistic modelling. Applied Physics Reviews, 2017, 4, .	5.5	22

#	Article	IF	Citations
25565	Uric Acid as an Electrochemically Active Compound for Sodium-Ion Batteries: Stepwise Na⁺-Storage Mechanisms of Ï€-Conjugation and Stabilized Carbon Anion. ACS Applied Materials & Interfaces, 2017, 9, 33934-33940.	4.0	13
25566	Multi-orbital charge transfer at highly oriented organic/metal interfaces. Nature Communications, 2017, 8, 335.	5.8	45
25567	A rechargeable iodine-carbon battery that exploits ion intercalation and iodine redox chemistry. Nature Communications, 2017, 8, 527.	5.8	176
25568	Prediction of a room-temperature eight-coordinate two-dimensional topological insulator: penta-RuS4 monolayer. Npj 2D Materials and Applications, 2017, 1, .	3.9	18
25569	Facile microwave synthesis of ScPO₄Â·2H₂O flowerlike superstructures: morphology control, electronic structure and multicolor tunable luminescent properties. CrystEngComm, 2017, 19, 5787-5796.	1.3	8
25570	Periodic DFT+U investigation of the bulk and surface properties of marcasite (FeS2). Physical Chemistry Chemical Physics, 2017, 19, 27478-27488.	1.3	32
25571	Tuning the p-type Schottky barrier in 2D metal/semiconductor interface:boron-sheet on MoSe2, and WSe2. Journal of Physics Condensed Matter, 2017, 29, 405002.	0.7	3
25572	Local inversion symmetry breaking and spin-phonon coupling in the perovskite <mml:math xmlns:mml="http://www.w3.org/1998/Math/MathML"><mml:msub><mml:mi>GdCrO</mml:mi><mml:mn>3</mml:mn></mml:msub> Physical Review B, 2017, 96, .	1.1	43
25573	First-principles calculations on the origin of ferromagnetism in transition-metal doped Ge. Physical Review B, 2017, 96, .	1.1	10
25574	Computational Identification of a New Form of Li₂MnSiO₄ for Battery Applications. Solid State Phenomena, 2017, 263, 160-164.	0.3	0
25575	Anomalous random correlations of force constants on the lattice dynamical properties of disordered Au-Fe alloys. Physical Review B, 2017, 96, .	1.1	7
25576	Structural and electronic properties of <mml:math xmlns:mml="http://www.w3.org/1998/Math/MathML"><mml:mi>Î±</mml:mi></mml:math> -(BEDT-TTF) <mml:math xmlns:mml="http://www.w3.org/1998/Math/MathML"><mml:mrow><mml:msub><mml:mrow /><mml:mn>2</mml:mn></mml:msub><mml:msub><mml:mi mathvariant="normal">I</mml:mi><mml:mn>3</mml:mn></mml:msub></mml:mrow></mml:math> , <mml:math xmlns:mml="http://www.w3.org/1998/Math/MathML"><mml:mi>Î²</mml:mi></mml:math>		

#	Article	IF	Citations
25583	Polarizing Oxygen Vacancies in Insulating Metal Oxides under a High Electric Field. Physical Review Letters, 2017, 119, 126002.	2.9	42
25584	A First-Principles Study of O₂ Dissociation on Platinum Modified Titanium Carbide: A Possible Efficient Catalyst for the Oxygen Reduction Reaction. Journal of Physical Chemistry C, 2017, 121, 21333-21342.	1.5	18
25585	Supertetrahedral Aluminum â€“ A New Allotropic Ultralight Crystalline Form of Aluminum. Journal of Physical Chemistry C, 2017, 121, 22187-22190.	1.5	11
25586	High thermoelectric performances of monolayer SnSe allotropes. Nanoscale, 2017, 9, 16093-16100.	2.8	111
25587	First principles study and comparison of vibrational and thermodynamic properties of X Bi () Tj ETQq0 0 0 rgBT /Overlock 10 Tf 50	0.7	17
25588	Exploiting Diffusion Barrier and Chemical Affinity of Metalâ€“Organic Frameworks for Efficient Hydrogen Isotope Separation. Journal of the American Chemical Society, 2017, 139, 15135-15141.	6.6	125
25589	A new phase-matchable nonlinear optical silicate: Rb₂ZnSi₃O₈. Journal of Materials Chemistry C, 2017, 5, 11025-11029.	2.7	21
25590	Dielectric breakdown field of strained silicon under hydrostatic pressure. Applied Physics Letters, 2017, 111, 112904.	1.5	3
25591	Mechanical Anisotropic and Electronic Properties ofAmm2-carbon under Pressure[*]. Communications in Theoretical Physics, 2017, 68, 395.	1.1	8
25592	Finite-temperature H behaviors in tungsten and molybdenum: first-principles total energy and vibration spectrum calculations. Nuclear Fusion, 2017, 57, 126024.	1.6	8
25593	Boron Triangular Kagome Lattice with Half-Metallic Ferromagnetism. Scientific Reports, 2017, 7, 7279.	1.6	14
25594	Gapless edge states in (C,O,H)-built molecular system with p-stacking and hydrogen bonds. Scientific Reports, 2017, 7, 9888.	1.6	2
25595	Stability and optical properties of plutonium monoxide from first-principle calculation. Scientific Reports, 2017, 7, 12167.	1.6	13
25596	Electronic Dynamics in Graphene and MoS₂ Systems. Physica Status Solidi (B): Basic Research, 2017, 254, 1700179.	0.7	3
25597	Intergranular fracture of tungsten containing phosphorus impurities: A first principles investigation. Computational Materials Science, 2017, 139, 368-378.	1.4	12
25598	Ruddlesden-Popper compounds (SrO)(LaFeO3)n (n = 1 and 2) as p-type semiconductors for photocatalytic hydrogen production. Electrochimica Acta, 2017, 252, 138-146.	2.6	29
25599	Tetragonal-prism-like Guinierâ€“Prestonâ€“Bagaryatsky zones in an AlCuMg alloy. Materials Characterization, 2017, 132, 139-144.	1.9	20
25600	Nitrogen-vacancy diamond sensor: novel diamond surfaces from ab initio simulations. MRS Communications, 2017, 7, 551-562.	0.8	25

#	Article	IF	Citations
25601	Performance evaluation of catalysts in the dry reforming reaction of methane via the ratings concept. Reaction Kinetics, Mechanisms and Catalysis, 2017, 122, 53-68.	0.8	8
25602	Theoretical study on hydrogen storage capacity of expanded h-BN systems. Computational Materials Science, 2017, 139, 335-340.	1.4	32
25603	Tuning electronic and magnetic properties in monolayer MoSe2 by metal adsorption. Chemical Physics Letters, 2017, 687, 54-59.	1.2	12
25604	Doping and defect-induced germanene: A superior media for sensing H 2 S, SO 2, and CO 2 gas molecules. Surface Science, 2017, 665, 96-102.	0.8	76
25605	Surface Structure of 4-Mercaptopyridine on Au(111): A New Dense Phase. Langmuir, 2017, 33, 9565-9572.	1.6	24
25606	Fast kinetics of magnesium monochloride cations in interlayer-expanded titanium disulfide for magnesium rechargeable batteries. Nature Communications, 2017, 8, 339.	5.8	304
25607	Properties of hydrogen doped Cu nanowires and nanocontacts: a density-functional theory study. Materials Research Express, 2017, 4, 095010.	0.8	3
25608	Gauge-including projector augmented-wave NMR chemical shift calculations with DFT+ <mml:math xmlns:mml="http://www.w3.org/1998/Math/MathML"><mml:mi>U</mml:mi></mml:math>. Physical Review B, 2017, 96, .	1.1	7
25609	Native defects in the <mml:math xmlns:mml="http://www.w3.org/1998/Math/MathML"><mml:mrow><mml:msub><mml:mi>Co</mml:mi><mml:mn>2</mml:mn></mml: <mml:math xmlns:mml="http://www.w3.org/1998/Math/MathML"><mml:mo>(</mml:mo><mml:mrow><mml:mi>Z</mml:mi><mml:mo>=</mml:mo> full Heusler alloys: Formation and. Physical Review B, 2017, 96, .	1.1	24
25610	CO oxidation on Mn-N4 porphyrin-like carbon nanotube: A DFT-D study. Applied Surface Science, 2017, 426, 1232-1240.	3.1	99
25611	Graphene-wrapped Porous Sb Anodes for Sodium-Ion Batteries by Mechanochemical Compositing and Metallomechanical Reduction of Sb2O3. Electrochimica Acta, 2017, 252, 25-32.	2.6	21
25612	First principle and tight-binding study of strained SnC. Journal of Physics and Chemistry of Solids, 2017, 111, 458-463.	1.9	23
25613	High pressure elasticity of FeCO 3 -MgCO 3 carbonates. Physics of the Earth and Planetary Interiors, 2017, 271, 57-63.	0.7	22
25614	First-principle study of pressure-induced phase transitions and electronic properties of electride Y2C. Solid State Communications, 2017, 266, 34-38.	0.9	5
25615	Enhanced optical absorption via cation doping hybrid lead iodine perovskites. Scientific Reports, 2017, 7, 7843.	1.6	61
25617	Manipulating the Magnetic Moment of Palladium Clusters by Adsorption and Dissociation of Molecular Hydrogen. Journal of Physical Chemistry C, 2017, 121, 20756-20762.	1.5	12
25618	Durable and self-hydrating tungsten carbide-based composite polymer electrolyte membrane fuel cells. Nature Communications, 2017, 8, 418.	5.8	42
25619	A new insight for ohmic contacts to MoS₂: by tuning MoS₂ affinity energies but not metal work-functions. Physical Chemistry Chemical Physics, 2017, 19, 26151-26157.	1.3	18

#	Article	IF	Citations
25620	How thin barrier metal can be used to prevent Co diffusion in the modern integrated circuits?. Journal Physics D: Applied Physics, 2017, 50, 455103.	1.3	7
25621	Theoretical realization of Mo2P; a novel stable 2D material with superionic conductivity and attractive optical properties. Applied Materials Today, 2017, 9, 292-299.	2.3	43
25622	Tuning magnetic properties of Cr2M2C3T2 (M = Ti and V) using extensile strain. Computational Materials Science, 2017, 139, 313-319.	1.4	40
25623	First-principles calculations of the structural, elastic and thermodynamic properties of mackinawite (FeS) and pyrite (FeS 2). Physica B: Condensed Matter, 2017, 525, 119-126.	1.3	28
25624	Semimetallic behavior in Heusler-type Ru2TaAl and thermoelectric performance improved by off-stoichiometry. Physical Review B, 2017, 96, .	1.1	19
25625	New scheme for calculating the kinetic coefficients in CdTe based on first-principle wave function. Computational Materials Science, 2017, 139, 387-394.	1.4	14
25626	Oxygen adsorption at heterophase boundaries of the oxygenated Cu(110). Surface Science, 2017, 666, 28-43.	0.8	11
25627	Defects Slow Down Nonradiative Electronâ€“Hole Recombination in TiS₃ Nanoribbons: A Time-Domain Ab Initio Study. Journal of Physical Chemistry Letters, 2017, 8, 4522-4529.	2.1	16
25628	Confined Catalysis in the g-C₃N₄/Pt(111) Interface: Feasible Molecule Intercalation, Tunable Moleculeâ€“Metal Interaction, and Enhanced Reaction Activity of CO Oxidation. ACS Applied Materials & Interfaces, 2017, 9, 33267-33273.	4.0	40
25629	Stable reconstruction of the (110) surface and its role in pseudocapacitance of rutile-like RuO2. Scientific Reports, 2017, 7, 10357.	1.6	30
25630	Tuning the surface structure and conductivity of niobium-doped rutile TiO₂ single crystals via thermal reduction. Physical Chemistry Chemical Physics, 2017, 19, 30339-30350.	1.3	9
25631	General promoting effect of polydopamine on supported noble metal catalysts. Journal of Materials Chemistry A, 2017, 5, 20789-20796.	5.2	26
25632	Synergy of van der Waals and self-interaction corrections in transition metal monoxides. Physical Review B, 2017, 96, .	1.1	50
25633	Understanding the photoemission distribution of strongly interacting two-dimensional overlayers. Physical Review B, 2017, 96, .	1.1	25
25634	Theoretical Study of Nitrogen Absorption in Metals. Journal of Physical Chemistry C, 2017, 121, 17016-17028.	1.5	5
25635	Mechanical properties and electronic structure of edge-doped graphene nanoribbons with F, O, and Cl atoms. Physical Chemistry Chemical Physics, 2017, 19, 21474-21480.	1.3	2
25636	Approaching complexity of alkyl hydrogenation on Pd via density-functional modelling. Physical Chemistry Chemical Physics, 2017, 19, 21514-21521.	1.3	3
25637	Elucidation of the higher coking resistance of small versus large nickel nanoparticles in methane dry reforming via computational modeling. Catalysis Science and Technology, 2017, 7, 3339-3347.	2.1	15

#	Article	IF	Citations
25638	The tunable effect of nitrogen and boron dopants on a single walled carbon nanotube support on the catalytic properties of a single gold atom catalyst: a first principles study of CO oxidation. Journal of Materials Chemistry A, 2017, 5, 16653-16662.	5.2	58
25639	A fast hybrid methodology based on machine learning, quantum methods, and experimental measurements for evaluating material properties. Modelling and Simulation in Materials Science and Engineering, 2017, 25, 065014.	0.8	3
25640	The effect of carbon defects on Cl anion diffusion in graphene based on first principles calculations. Materials Research Express, 2017, 4, 075604.	0.8	0
25641	Orientation-dependent behaviors of H dissolution and diffusion near W surfaces: A first-principles study. International Journal of Modern Physics C, 2017, 28, 1750090.	0.8	4
25642	Ab initio hybrid DFT calculations of BaTiO₃ bulk and BaO-terminated (001) surface F-centers. International Journal of Modern Physics B, 2017, 31, 1750251.	1.0	22
25643	Isomorphic substitution and intermediary energy levels: A new application of DFT modelling and semiconductor theory to describe p-n type junctions interface in heterostructures. Physica Status Solidi (B): Basic Research, 2017, 254, 1700119.	0.7	6
25644	Facile Hydrothermal Synthesis of MnWO₄ Nanorods for Nonâ€Enzymatic Glucose Sensing and Supercapacitor Properties with Insights from Density Functional Theory Simulations. ChemistrySelect, 2017, 2, 5707-5715.	0.7	26
25645	Covalency Competition in the Quadruple Perovskite CdCu₃Fe₄O₁₂. Inorganic Chemistry, 2017, 56, 9303-9310.	1.9	14
25646	Initial Reduction of CO₂ on Pd-, Ru-, and Cu-Doped CeO₂(111) Surfaces: Effects of Surface Modification on Catalytic Activity and Selectivity. ACS Applied Materials & Interfaces, 2017, 9, 26107-26117.	4.0	61
25647	Different catalytic behaviors of Pd and Pt metals in decalin dehydrogenation to naphthalene. Catalysis Science and Technology, 2017, 7, 3728-3735.	2.1	38
25648	Ab initio velocity-field curves in monoclinic Î²-Ga2O3. Journal of Applied Physics, 2017, 122, .	1.1	116
25649	Second-order structural phase transitions, free energy curvature, and temperature-dependent anharmonic phonons in the self-consistent harmonic approximation: Theory and stochastic implementation. Physical Review B, 2017, 96, .	1.1	100
25650	Colossal Stability of Gasâ€Phase Trianions: Superâ€Pnictogens. Angewandte Chemie, 2017, 129, 13606-13610.	1.6	6
25651	Colossal Stability of Gasâ€Phase Trianions: Superâ€Pnictogens. Angewandte Chemie - International Edition, 2017, 56, 13421-13425.	7.2	23
25652	A first-principles study of bulk and surface Sn-doped LiFePO₄ : The role of intermediate valence component in the multivalent doping. Physica Status Solidi (B): Basic Research, 2017, 254, 1700041.	0.7	10
25653	Effect of two identical 3d transition-metal atoms M doping (Mâ€‰=â€‰V, Cr, Mn, Fe, Co, and Ni) on the structural, electronic, and magnetic properties of ZnO. Physica Status Solidi (B): Basic Research, 2017, 254, 1700098.	0.7	11
25654	Exploring the stability and reactivity of Ni2P and Mo2C catalysts using ab initio atomistic thermodynamics and conceptual DFT approaches. Biomass Conversion and Biorefinery, 2017, 7, 377-383.	2.9	3
25655	Identification of a ternary Î¼-phase in the Co-Ti-W system â€“ An advanced correlative thin-film and bulk combinatorial materials investigation. Acta Materialia, 2017, 138, 100-110.	3.8	12

#	Article	IF	Citations
25656	The effect of the adsorbate layer on the work function reduction of gold substrates under external electric fields. Applied Surface Science, 2017, 425, 776-780.	3.1	1
25657	The effect of surface structure on Ag atom adsorption over CuO(111) surfaces: A first principles study. Applied Surface Science, 2017, 425, 1111-1117.	3.1	13
25658	A DFT study of hydrogen electroadsorption on the missing row Pt(1 1 0)-(1<mml:math) Tj ETQq0 0 0 rgBT /Overlock 10 Tf 50 672 Td (xr Computational Materials Science, 2017, 138, 295-301.	1.4	10
25659	Investigation of the adhesion mechanism of Marine Musselâ€™s foot protein: Adsorption of L-dopa on silica Î±- & Î²-cristobalite using density functional theory (DFT). Materials Today: Proceedings, 2017, 4, 4912-4918.	0.9	3
25660	The design of a macromolecular depressant for galena based on DFT studies and its application. Minerals Engineering, 2017, 112, 50-56.	1.8	35
25661	Development of a Transferable Reactive Force Field of P/H Systems: Application to the Chemical and Mechanical Properties of Phosphorene. Journal of Physical Chemistry A, 2017, 121, 6135-6149.	1.1	38
25662	Molybdenum Carbide Modified Nanocarbon Catalysts for Alkane Dehydrogenation Reactions. ACS Catalysis, 2017, 7, 5820-5827.	5.5	55
25663	Atomic-scale computational design of hydrophobic RE surface-doped Al2O3 and TiO2. Physical Chemistry Chemical Physics, 2017, 19, 21119-21126.	1.3	7
25664	In- and Ga-based inorganic double perovskites with direct bandgaps for photovoltaic applications. Physical Chemistry Chemical Physics, 2017, 19, 21691-21695.	1.3	37
25665	Defect induced charge trapping in C-doped Î±-Al2O3. Journal of Applied Physics, 2017, 122, 025702.	1.1	6
25666	Effects of Sm doping content on the ionic conduction of CeO2 in SOFCs from first principles. Applied Physics Letters, 2017, 111, .	1.5	20
25667	Adsorption of CO₂ on Fe-doped graphene nano-ribbons: Investigation of transport properties. Journal of Physics: Conference Series, 2017, 869, 012041.	0.3	1
25668	Optical and structural study of the pressure-induced phase transition of <mml:math xmlns:mml="http://www.w3.org/1998/Math/MathML"><mml:msub><mml:mi>CdWO</mml:mi><mml:mn>4</mml:mn></mml:msub></ Physical Review B, 2017, 95, .	1.1	23
25669	Ab initio study of the lattice thermal conductivity of <mml:math xmlns:mml="http://www.w3.org/1998/Math/MathML"><mml:mrow><mml:msub><mml:mi>Cu</mml:mi><mml:mn>2</mml:mn></mml:mr mathvariant="normal">O</mml:mi></mml:mrow></mml:math> using the generalized gradient approximation and hybrid density functional methods. Physical Review B, 2017, 96, .	1.1	46
25670	First-principles prediction of stabilities and instabilities of compounds and alloys in the ternary B-As-P system. Physical Review B, 2017, 96, .	1.1	18
25671	Impurity band effects on transport and thermoelectric properties of Fe2â^'xNixVAl. Physical Review B, 2017, 96, .	1.1	26
25672	Ab initio molecular dynamics simulation of pressure-induced phase transition in MgS. Russian Journal of Physical Chemistry A, 2017, 91, 1408-1413.	0.1	0
25673	Nitrogen Doped Carbon Nanosheets Coupled Nickelâ€“Carbon Pyramid Arrays Toward Efficient Evolution of Hydrogen. Advanced Sustainable Systems, 2017, 1, 1700032.	2.7	12

#	Article	IF	Citations
25674	High coverage water adsorption on the CuO(111) surface. Applied Surface Science, 2017, 425, 803-810.	3.1	50
25675	A first-principles investigation of structural properties, electronic structures and optical properties of Î²- and Î³-LiAl(SiO3)2. Ceramics International, 2017, 43, 13948-13955.	2.3	22
25676	Effect of Interfacial Lithium Insertion on the Stability and Electronic Structure of Graphene/LiFePO4. Electrochimica Acta, 2017, 247, 1030-1037.	2.6	15
25677	Reaction and free-energy pathways of hydrogen activation on partially promoted metal edge of CoMoS and NiMoS: A DFT and thermodynamics study. Fuel Processing Technology, 2017, 166, 217-227.	3.7	19
25678	Spin-dependent structural, electronic and transport properties of armchair graphyne nanoribbons doped with single transition-metal atom, using DFT calculations. Journal of Magnetism and Magnetic Materials, 2017, 443, 96-103.	1.0	6
25679	Zn vacancy ferromagnetism in ZnS nanocrystals. Journal of Magnetism and Magnetic Materials, 2017, 443, 9-12.	1.0	1
25680	Development of spontaneous magnetism and half-metallicity in monolayer MoS2. Journal of Magnetism and Magnetic Materials, 2017, 443, 343-351.	1.0	15
25681	Phase stability of the Cu-Sn-S system and optimal growth conditions for earth-abundant Cu2SnS3 solar materials. Solar Energy, 2017, 155, 745-757.	2.9	29
25682	Magnetic Moment Controlling Desorption Temperature in Hydrogen Storage: A Case of Zirconium-Doped Graphene as a High Capacity Hydrogen Storage Medium. Journal of Physical Chemistry C, 2017, 121, 16721-16730.	1.5	59
25683	Phosphorus-Doped SnTe-Type Needle-like Crystals: Band Structure Modifications and Electronic Properties. Journal of Physical Chemistry C, 2017, 121, 18263-18273.	1.5	17
25684	Reducing Reaction Temperature, Steam Requirements, and Coke Formation During Methane Steam Reforming Using Electric Fields: A Microkinetic Modeling and Experimental Study. ACS Catalysis, 2017, 7, 6957-6968.	5.5	30
25685	Electronâ€“phonon interaction and superconductivity in the borocarbide superconductor. Philosophical Magazine, 2017, 97, 2669-2688.	0.7	8
25686	Strain engineering on thermoelectric performance of Mg2Si. Materials Research Express, 2017, 4, 075509.	0.8	11
25687	Intermediate bands in type-II silicon clathrate with Cu and Ag guest atoms. Physical Review B, 2017, 95, .	1.1	0
25688	Reduction in Modulus of Suspended Subâ€2 nm Single Crystalline Silicon Nanomembranes. Advanced Materials Interfaces, 2017, 4, 1700529.	1.9	3
25689	First-principles study of the small molecule adsorption on the InSe monolayer. Applied Surface Science, 2017, 426, 244-252.	3.1	100
25690	Reduced band gap & charge recombination rate in Se doped Î±-Bi 2 O 3 leads to enhanced photoelectrochemical and photocatalytic performance: Theoretical & experimental insight. International Journal of Hydrogen Energy, 2017, 42, 20638-20648.	3.8	52
25691	Structure of graphite-like BC 2 layer in Sc 2 B 1.1 C 3.2 : An intermediate between BC and BC 3. Journal of Solid State Chemistry, 2017, 254, 144-149.	1.4	3

#	Article	IF	Citations
25692	Two novel Ge phases and their Si Ge alloys with excellent electronic and optical properties. Materials and Design, 2017, 132, 539-551.	3.3	27
25693	Effects of alloying elements X (X=Zr, V, Cr, Mn, Mo, W, Nb, Y) on ferrite/TiC heterogeneous nucleation interface: first-principles study. Journal of Iron and Steel Research International, 2017, 24, 328-334.	1.4	21
25694	A New KBBF-Family Nonlinear Optical Material with Strong Interlayer Bonding. Crystal Growth and Design, 2017, 17, 4422-4427.	1.4	42
25695	Structures of defects on anatase TiO₂(001) surfaces. Nanoscale, 2017, 9, 11553-11565.	2.8	28
25696	Structures, phase transitions, and magnetic properties of Co3Si from first-principles calculations. Physical Review B, 2017, 96, .	1.1	8
25697	Relativistic response and novel spin-charge plasmon at the Tl/Si(111) surface. Physical Review B, 2017, 96, .	1.1	5
25698	Structural, electronic and magnetic properties of Fe, Co, Ni monatomic nanochains encapsulated in armchair LiF nanotubes. Materials Science-Poland, 2017, 35, 283-290.	0.4	1
25699	3R and 2H polytypes of MoS2: DFT and DFPT calculations of structural, optoelectronic, vibrational and thermodynamic properties. Journal of Physics and Chemistry of Solids, 2017, 111, 25-33.	1.9	35
25700	Pressure-induced structural transformations and polymerization in ThC2. Scientific Reports, 2017, 7, 45872.	1.6	13
25701	Hydrogenated carbon nanotube-based spin caloritronics. Physical Chemistry Chemical Physics, 2017, 19, 21507-21513.	1.3	14
25702	Intrinsic magnetism of graphdiyne. Applied Physics Letters, 2017, 111, .	1.5	45
25703	Topological Nodal Line Semimetal in Non-Centrosymmetric PbTaS${}_{2}$. Chinese Physics Letters, 2017, 34, 077101.	1.3	7
25704	Density functional investigation on structural, elastic, thermal and mechanical properties of NiTi intermetallic compound. Journal of Physics: Conference Series, 2017, 836, 012037.	0.3	1
25705	Binding mechanisms of DNA/RNA nucleobases adsorbed on graphene under charging: first-principles van der Waals study. Materials Research Express, 2017, 4, 065401.	0.8	23
25706	Electric-field noise from carbon-adatom diffusion on a Au(110) surface: First-principles calculations and experiments. Physical Review A, 2017, 95, .	1.0	20
25707	Nitrogenâ€Doped Graphene with a Threeâ€Dimensional Architecture Assisted by Carbon Nitride Tetrapods as an Efficient Metalâ€Free Electrocatalyst for Hydrogen Evolution. ChemElectroChem, 2017, 4, 2643-2652.	1.7	29
25708	Insight into carbon formation from acetic acid decomposition over Pd(100) via density functional theory calculations. Surface Science, 2017, 664, 226-232.	0.8	3
25709	Low-Temperature Oxygen Storage of Cr^{IV}â€“Cr^V Mixed-Valence YCr_{1â€“x}P_xO_{4â^'Î´} Driven by Local Condensation around Oxygen-Deficient Orthochromite. Journal of the American Chemical Society, 2017, 139, 11197-11206.	6.6	8

#	Article	IF	Citations
25710	Metallic surface states in elemental electrides. Physical Review B, 2017, 96, .	1.1	6
25711	Elasticity of Îµâ€FeOOH: Seismic implications for Earth's lower mantle. Journal of Geophysical Research: Solid Earth, 2017, 122, 5038-5047.	1.4	24
25712	Lattice dynamics and thermodynamic properties of alkaline-earth metal carbides XC ($$hbox) Tj ETQq0 0 0 rgBT /Overlock 10 Tf 50 667 Computational Electronics, 2017, 16, 526-534.	1.3	2
25713	Electronic, optical and thermal properties of highly stretchable 2D carbon Ene-yne graphyne. Carbon, 2017, 123, 344-353.	5.4	46
25714	Effects of Adsorbates (CO, COH, and HCO) on the Arrangement of Pd Atoms in PdCu(111). Journal of Physical Chemistry C, 2017, 121, 17818-17826.	1.5	11
25715	Performance improvement of perovskite solar cells by employing a CdSe quantum dot/PCBM composite as an electron transport layer. Journal of Materials Chemistry A, 2017, 5, 17499-17505.	5.2	293
25716	Design of <mml:math xmlns:mml="http://www.w3.org/1998/Math/MathML"><mml:mi>n</mml:mi></mml:math> - and <mml:math xmlns:mml="http://www.w3.org/1998/Math/MathML"><mml:mi>p</mml:mi></mml:math> -type oxide thermoelectrics in <mml:math xmlns:mml="http://www.w3.org/1998/Math/MathML"><mml:msub><mml:mi>LaNiO</mml:mi><mml:mn>3</mml:mn></mml:msub><m Physical Review B, 2017, 95, .	1.1	38
25717	Stability of Weyl points in magnetic half-metallic Heusler compounds. Physical Review B, 2017, 96, .	1.1	32
25718	First-principles study of the stability, magnetic and electronic properties of Fe and Co monoatomic chains encapsulated into copper nanotube. European Physical Journal B, 2017, 90, 1.	0.6	0
25719	Investigation of electronic structure and half-metallic ferromagnetic behavior with large half-metallic gap in $$hbox {Sr}_{1-x}hbox {V}_{x}hbox {O}$$ Sr 1 - x. Journal of Computational Electronics, 2017, 16, 542-547.	1.3	21
25720	THD-graphene used for a selective gas detector. Materials Chemistry and Physics, 2017, 200, 50-56.	2.0	15
25721	Properties of Lead-Free Hybrid Organic-Inorganic Halide Perovskite CH3NH3BX3 Using Density Functional Theory. Materials Today: Proceedings, 2017, 4, 5154-5160.	0.9	4
25722	Quasiparticle approximation electronic structure of the Ge/Si heterojunction to correct the local-density approximation band alignments. Superlattices and Microstructures, 2017, 111, 889-898.	1.4	2
25723	Predicting Selectivity for Ethane Dehydrogenation and Coke Formation Pathways over Model Ptâ€“M Surface Alloys with ab Initio and Scaling Methods. Journal of Physical Chemistry C, 2017, 121, 17882-17892.	1.5	42
25724	Promoter Effects of Alkali Metal Cations on the Electrochemical Reduction of Carbon Dioxide. Journal of the American Chemical Society, 2017, 139, 11277-11287.	6.6	653
25725	Surface configuration and wettability of nickel(oxy)hydroxides: a first-principles investigation. Physical Chemistry Chemical Physics, 2017, 19, 22659-22669.	1.3	31
25726	Polarity control of GaN epitaxial films grown on LiGaO₂(001) substrates and its mechanism. Physical Chemistry Chemical Physics, 2017, 19, 21467-21473.	1.3	5
25727	First-principles study of nitrogen-doped nanographene as an efficient charge transport and nonlinear optical material. RSC Advances, 2017, 7, 36632-36643.	1.7	25

#	Article	IF	Citations
25728	Electrons on the surface of 2D materials: from layered electrides to 2D electrenes. Journal of Materials Chemistry C, 2017, 5, 11196-11213.	2.7	45
25729	Interpretation of x-ray absorption spectroscopy in the presence of surface hybridization. Journal of Chemical Physics, 2017, 146, 214701.	1.2	31
25730	Energy jump during bond breaking. Physical Review B, 2017, 96, .	1.1	2
25731	Properties at the interface of graphene and <mml:math xmlns:mml="http://www.w3.org/1998/Math/MathML"><mml:mrow><mml:msub><mml:mi>Ti</mml:mi><mml:mn>2</mml:mn></mml:msub><mml:mi mathvariant="normal">C</mml:mi></mml:mrow></mml:math> MXene. Physical Review B, 2017, 96, .	1.1	20
25732	Site preference, structural and magnetic properties of La3Co29â^'Ni Si4B10 predicted by first-principles calculations. Computational Materials Science, 2017, 138, 412-418.	1.4	1
25733	Prediction of Novel High-Pressure Structures of Magnesium Niobium Dihydride. ACS Applied Materials & Interfaces, 2017, 9, 26169-26176.	4.0	16
25734	Ab initio calculation of magnetic properties in B, Al, C, Si, N, P and As-doped rutile TiO₂. International Journal of Modern Physics B, 2017, 31, 1750227.	1.0	32
25735	Rhodium clustering process on defective (8,0) SWCNT: Analysis of chemical and physical properties using density functional theory. Applied Surface Science, 2017, 425, 823-832.	3.1	15
25736	Facile synthesis of FeSi4P4 and its Sodium Ion Storage Performance. Electrochimica Acta, 2017, 247, 820-825.	2.6	11
25737	The effect of inert gas pre-irradiation on the retention of deuterium in tungsten: A TMAP investigation combined with first-principles method. Fusion Engineering and Design, 2017, 121, 342-347.	1.0	4
25738	Tunable electronic properties of CdS nanoribbons by edge effects. Solid State Communications, 2017, 262, 40-43.	0.9	2
25739	Thermodynamic Routes to Novel Metastable Nitrogen-Rich Nitrides. Chemistry of Materials, 2017, 29, 6936-6946.	3.2	121
25740	Comparison of Intermolecular Forces in Anhydrous Sorbitol and Solvent Cocrystals. Journal of Physical Chemistry A, 2017, 121, 5720-5727.	1.1	10
25741	Lattice Thermal Conductivity of MgSiO3 Perovskite from First Principles. Scientific Reports, 2017, 7, 5417.	1.6	23
25742	The adsorption and diffusion behavior of noble metal adatoms (Pd, Pt, Cu, Ag and Au) on a MoS₂ monolayer: a first-principles study. Physical Chemistry Chemical Physics, 2017, 19, 20713-20722.	1.3	135
25743	New allotropes of Li₂MnO₃ as cathode materials with better cycling performance predicted in high pressure synthesis. Journal of Materials Chemistry A, 2017, 5, 16936-16943.	5.2	17
25744	Theab initiostudy of unconventional superconductivity in CeCoIn5and FeSe. New Journal of Physics, 2017, 19, 063039.	1.2	25
25745	Carrier-Induced Band-Gap Variation and Point Defects in <mml:math xmlns:mml="http://www.w3.org/1998/Math/MathML" display="inline"><mml:mrow><mml:msub><mml:mrow><mml:mi>Zn</mml:mi></mml:mrow><mml:mrow><mml:mn>3</mml:mn></mml:mrow></mml:msub><mml:msub><mml:mrow><mml:mi mathvariant="normal">N</mml:mi></mml:mrow><mml:mrow><mml:mn>2</mml:mn></mml:mrow></mml:msub></mml:mrow></mml:math> from First Principles. Physical Review Applied, 2017, 8, .	4.6	28

#	Article	IF	Citations
25746	Coexistence of topological nodal lines, Weyl points, and triply degenerate points in TaS. Physical Review B, 2017, 96, .	1.1	39
25747	Part II: Quantum mechanical prediction of heats of adsorption for C2-C4 hydrocarbons in MOF-74-Mg/Zn periodic structures. Chemical Physics Letters, 2017, 682, 168-174.	1.2	3
25748	Mechanical behavior, bonding nature and defect processes of Mo2ScAlC2: A new ordered MAX phase. Journal of Alloys and Compounds, 2017, 724, 1167-1175.	2.8	52
25749	Density functional theory and reactive dynamics study of catalytic performance of TiO2 on CO2 desorption process with KHCO3/TiO2/Al2O3 sorbent. Molecular Catalysis, 2017, 439, 143-154.	1.0	14
25750	The electronic structures and ferromagnetism of Fe-doped GaSb: The first-principle calculation study. Physica B: Condensed Matter, 2017, 521, 371-375.	1.3	9
25751	Adsorption and dissociation of H 2 S on Rh(100) surface by First-principle study. Applied Surface Science, 2017, 425, 367-376.	3.1	15
25752	Insight into carbon deposition associated with NiCo/MgO catalyzed CH4/CO2 reforming by using density functional theory. Applied Surface Science, 2017, 423, 1080-1089.	3.1	14
25753	Site symmetry approach in the supercell model of carbon-doped ZnO bulk. Chemical Physics Letters, 2017, 682, 91-95.	1.2	6
25754	Hydrogen diffusion mechanism on Î±-AlPO4 (0001)/Î±-Al2O3 (0001) interface: A first-principles study. Fusion Engineering and Design, 2017, 125, 582-587.	1.0	4
25755	Synthesis and characterization of a new beryllium-free deep-ultraviolet nonlinear optical material: Na2GdCO3F3. Journal of Alloys and Compounds, 2017, 724, 1057-1063.	2.8	29
25756	Theoretical investigation on the point defect formation energies in beryllium and comparison with experiments. Nuclear Materials and Energy, 2017, 12, 453-457.	0.6	14
25757	Enhanced clustering tendency of Cu-impurities with a number of oxygen vacancies in heavy carbon-loaded TiO2 - the bulk and surface morphologies. Solid State Sciences, 2017, 71, 130-138.	1.5	5
25758	Experimental and Theoretical Evidence for the Reactivity of Bound Intermediates in Ketonization of Carboxylic Acids and Consequences of Acidâ€“Base Properties of Oxide Catalysts. Journal of Physical Chemistry C, 2017, 121, 18030-18046.	1.5	33
25759	Tracer diffusion of⁹⁶Zr and¹³⁴Ba in polycrystalline BaZrO₃. Physical Chemistry Chemical Physics, 2017, 19, 21878-21886.	1.3	22
25760	Why is sodium-intercalated graphite unstable?. RSC Advances, 2017, 7, 36550-36554.	1.7	194
25761	Non-classical behaviour of higher valence dopants in chromium (III) oxide by a Cr vacancy compensation mechanism. Journal of Physics Condensed Matter, 2017, 29, 415501.	0.7	2
25762	Simulations of twisted bilayer orthorhombic black phosphorus. Physical Review B, 2017, 96, .	1.1	20
25763	Valley-Polarized Quantum Anomalous Hall Effect in Ferrimagnetic Honeycomb Lattices. Physical Review Letters, 2017, 119, 046403.	2.9	64

#	Article	IF	Citations
25764	Bandgap engineering of SrTiO₃ /NaTaO₃ heterojunction for visible light photocatalysis. International Journal of Quantum Chemistry, 2017, 117, e25424.	1.0	17
25765	DFT-D study of adsorption of diaminoethane and propylamine molecules on anatase (101) TiO 2 surface. Applied Surface Science, 2017, 426, 107-115.	3.1	25
25766	Theoretical insights into the uranyl adsorption behavior on vanadium carbide MXene. Applied Surface Science, 2017, 426, 572-578.	3.1	83
25767	Effect of Ti content and nitrogen on the high-temperature oxidation behavior of (Mo,Ti)5Si3. Intermetallics, 2017, 90, 103-112.	1.8	18
25768	Structural stability and the alloying effect of TiB polymorphs in TiAl alloys. Intermetallics, 2017, 90, 97-102.	1.8	35
25769	Thermoelectric properties of n and p-type cubic and tetragonal <mml:math xmlns:mml="http://www.w3.org/1998/Math/MathML" altimg="si0025.gif" overflow="scroll"><mml:mrow><mml:mi>X</mml:mi><mml:msub><mml:mrow><mml:mi>TiO</mml:mi></mml:mrow><mml:mrow><mml:mn> (X = Ba,Pb): A density functional theory study. Physica B: Condensed Matter, 2017, 526, 122-126.	1.3	12
25770	Role of Transient Co-Subcarbonyls in Ostwald Ripening Sintering of Cobalt Supported on Î³-Alumina Surfaces. Journal of Physical Chemistry C, 2017, 121, 16739-16753.	1.5	22
25771	Two-Dimensional Intrinsic Half-Metals With Large Spin Gaps. Nano Letters, 2017, 17, 5251-5257.	4.5	172
25772	Modifying Surface Chemistry of Metal Oxides for Boosting Dissolution Kinetics in Water by Liquid Cell Electron Microscopy. ACS Nano, 2017, 11, 8018-8025.	7.3	39
25773	Participation of interfacial hydroxyl groups in the water-gas shift reaction over Au/MgO catalysts. Catalysis Science and Technology, 2017, 7, 5257-5266.	2.1	19
25774	A CNH monolayer: a direct gap 2D semiconductor with anisotropic electronic and optical properties. Journal of Materials Chemistry C, 2017, 5, 8498-8503.	2.7	13
25775	Comparative research on the influence of varied Al component on the active layer of AlGaN photocathode. Journal of Semiconductors, 2017, 38, 063004.	2.0	0
25776	Gate induced monolayer behavior in twisted bilayer black phosphorus. 2D Materials, 2017, 4, 035025.	2.0	18
25777	Experimental investigation and thermodynamic assessment of Alâ€“Caâ€“Ni ternary system. Journal of Materials Science, 2017, 52, 12409-12426.	1.7	12
25778	New insights into canted spiro carbon interstitial in graphite. Applied Surface Science, 2017, 426, 238-243.	3.1	9
25779	Electric field tunable band-gap crossover in black(blue) phosphorus/g-ZnO van der Waals heterostructures. RSC Advances, 2017, 7, 34584-34590.	1.7	34
25780	Explorations of new UV nonlinear optical materials in the Na₂CO₃â€“CaCO₃system. Journal of Materials Chemistry C, 2017, 5, 8758-8764.	2.7	25
25781	Hydrogenation of silicene on Ag(111) and formation of half-silicane. Journal of Materials Chemistry A, 2017, 5, 18128-18137.	5.2	18

#	Article	IF	Citations
25782	The stabilization of the rocksalt structured tantalum nitride. Journal of Applied Physics, 2017, 122, .	1.1	9
25783	Thermal expansion coefficient of WRe alloys from first principles. Physical Review B, 2017, 96, .	1.1	17
25784	Enhancing photocatalytic activity for hydrogen production and pollutant degradation by modifying tetragonal ZrO2 with monolayers slab surface of BiVO4, Ag3PO4, SrTiO3 and WO3: A first-principles study. Computational Materials Science, 2017, 138, 462-473.	1.4	16
25785	A First-Principles Study of Hydrogen Diffusivity and Dissociation on Î´-Pu (100) and (111) Surfaces. Journal of Physical Chemistry C, 2017, 121, 17950-17957.	1.5	21
25786	Optical properties and magnetic flux-induced electronic band tuning of a T-graphene sheet and nanoribbon. Physical Chemistry Chemical Physics, 2017, 19, 21584-21594.	1.3	28
25787	The pressureâ€“temperature phase diagram of pure Co based on first-principles calculations. Physical Chemistry Chemical Physics, 2017, 19, 22061-22068.	1.3	2
25788	The effect of defects on the catalytic activity of single Au atom supported carbon nanotubes and reaction mechanism for CO oxidation. Physical Chemistry Chemical Physics, 2017, 19, 22344-22354.	1.3	38
25789	First-principles study of electronic, mechanical and optical properties of mixed valence SmB6. IOP Conference Series: Materials Science and Engineering, 2017, 207, 012084.	0.3	3
25790	Influence of adsorbate and defect on structural and electronic properties of ultrathin silver nanotube. Journal of Physics and Chemistry of Solids, 2017, 111, 135-141.	1.9	1
25791	First-principles study on interlayer state in alkali and alkaline earth metal atoms intercalated bilayer graphene. Surface Science, 2017, 665, 1-9.	0.8	19
25792	Adsorption of Metallic, Metalloidic, and Nonmetallic Adatoms on Two-Dimensional C₃N. Journal of Physical Chemistry C, 2017, 121, 18575-18583.	1.5	111
25793	Structural Dependence of the Sulfur Reduction Mechanism in Carbon-Based Cathodes for Lithiumâ€“Sulfur Batteries. Journal of Physical Chemistry C, 2017, 121, 18369-18377.	1.5	17
25794	Dynamic Disorder and Potential Fluctuation in Two-Dimensional Perovskite. Journal of Physical Chemistry Letters, 2017, 8, 3875-3880.	2.1	31
25795	Disentangling the intricate atomic short-range order and electronic properties in amorphous transition metal oxides. Scientific Reports, 2017, 7, 2044.	1.6	19
25796	Giant Rashba effect at the topological surface of PrGe revealing antiferromagnetic spintronics. Scientific Reports, 2017, 7, 4120.	1.6	11
25797	The electromigration effect revisited: non-uniform local tensile stress-driven diffusion. Scientific Reports, 2017, 7, 3082.	1.6	30
25798	One-dimensional electron gas in strained lateral heterostructures of single layer materials. Scientific Reports, 2017, 7, 4316.	1.6	4
25799	Thermal conductivities of phosphorene allotropes from first-principles calculations: a comparative study. Scientific Reports, 2017, 7, 4623.	1.6	36

#	Article	IF	Citations
25800	On the stochastic phase stability of Ti2AlC-Cr2AlC. Scientific Reports, 2017, 7, 5138.	1.6	16
25801	Electronic Structure of Polyethylene: Role of Chemical, Morphological and Interfacial Complexity. Scientific Reports, 2017, 7, 6128.	1.6	53
25802	Transition metal alloying effect on the phosphoric acid adsorption strength of Pt nanoparticles: an experimental and density functional theory study. Scientific Reports, 2017, 7, 7186.	1.6	17
25803	Room temperature ferroelectricity in fluoroperovskite thin films. Scientific Reports, 2017, 7, 7182.	1.6	19
25804	Structural, electronic, mechanical, and thermoelectric properties of a novel half Heusler compound HfPtPb. Journal of Applied Physics, 2017, 122, .	1.1	34
25805	Adsorption sites of individual metal atoms on ultrathin MgO(100) films. Physical Review B, 2017, 96, .	1.1	25
25806	Selfâ€Templating Construction of Hollow Amorphous CoMoS₄ Nanotube Array towards Efficient Hydrogen Evolution Electrocatalysis at Neutral pH. Chemistry - A European Journal, 2017, 23, 12718-12723.	1.7	48
25807	Electronic and optical properties of Î²-graphyne nanotubes and their BN analogues. Journal of Materials Science, 2017, 52, 13133-13148.	1.7	7
25808	Supercell size convergence testing in uniaxial tensile test studies of an Al grain boundary: A proposed path to a robust analysis. Computational Materials Science, 2017, 139, 39-47.	1.4	8
25809	First-principles prediction of a novel cadmium disulfide monolayer (penta-CdS2): Indirect to direct band gap transition by strain engineering. Chemical Physics Letters, 2017, 685, 310-315.	1.2	45
25810	Potassium isotope fractionation between K-salts and saturated aqueous solutions at room temperature: Laboratory experiments and theoretical calculations. Geochimica Et Cosmochimica Acta, 2017, 214, 1-13.	1.6	38
25811	Dissociative Adsorption of Water at (211) Stepped Metallic Surfaces by First-Principles Simulations. Journal of Physical Chemistry C, 2017, 121, 16783-16791.	1.5	11
25812	Size-Dependence of the Adsorption Energy of CO on Pt Nanoparticles: Tracing Two Intersecting Trends by DFT Calculations. Journal of Physical Chemistry C, 2017, 121, 17371-17377.	1.5	39
25813	Evolution of the linear band dispersion of monolayer and bilayer germanene on Cu(111). Physical Chemistry Chemical Physics, 2017, 19, 22844-22851.	1.3	13
25814	A critical role of catalyst morphology in low-temperature synthesis of carbon nanotubeâ€“transition metal oxide nanocomposite. Nanoscale, 2017, 9, 12416-12424.	2.8	14
25815	Diverse polarization bi-stability in ferroelectric tunnel junctions due to the effects of the electrode and strain: an ab initio study. Physical Chemistry Chemical Physics, 2017, 19, 20147-20159.	1.3	2
25816	Diffusion and reaction pathways of water near fully hydrated TiO2 surfaces from ab initio molecular dynamics. Journal of Chemical Physics, 2017, 147, 024704.	1.2	55
25817	Third nearest neighbor parameterized tight binding model for graphene nano-ribbons. AIP Advances, 2017, 7, .	0.6	27

#	Article	IF	Citations
25818	Modeling of the interface formation during CuO deposition on Al(111) substrate: linking material design and elaboration process parameters through multi-levels approach. Modelling and Simulation in Materials Science and Engineering, 2017, 25, 064005.	0.8	1
25819	In-plane commensurate GaN/AlN junctions: Single-layer composite structures, single and multiple quantum wells and quantum dots. Physical Review B, 2017, 95, .	1.1	20
25820	Si(111) strained layers on Ge(111): Evidence for <mml:math xmlns:mml="http://www.w3.org/1998/Math/MathML"><mml:mi>c</mml:mi></mml:math> (<mml:math) Tj ETQq0 0 0 rgBT /Overlock 10	1.1	11
25821	Heat confinement of phase-change memory using graphene. , 2017, , .		2
25822	Electron correlation and spin-orbit coupling effects in scandium intermetallic compounds ScTM (TM) Tj ETQq0 0 0 rgBT /Overlock 10 Tf 5	1.0	5
25823	An ab-initio study of the energetics and geometry of sulfide, sulfite, and sulfate incorporation into apatite: The thermodynamic basis for using this system as an oxybarometer. American Mineralogist, 2017, 102, 1646-1656.	0.9	29
25824	A strain-induced new phase diagram and unusually high Curie temperature in manganites. Journal of Materials Chemistry C, 2017, 5, 7813-7819.	2.7	6
25825	Self-interaction free local exchange potentials applied to metallic systems. Journal of Physics Condensed Matter, 2017, 29, 374002.	0.7	4
25826	Topological phases in double layers of bismuthene and antimonene. Nanotechnology, 2017, 28, 395706.	1.3	24
25827	Improved sensing characteristics of methane over ZnO nano sheets upon implanting defects and foreign atoms substitution. Nanotechnology, 2017, 28, 415502.	1.3	17
25828	Characterization of the liquid Li-solid Mo (1â€‰1â€‰0) interface from classical molecular dynamics for plasma-facing applications. Nuclear Fusion, 2017, 57, 116036.	1.6	7
25829	Anomalous vibrational modes in few layer WTe ₂ revealed by polarized Raman scattering and first-principles calculations. 2D Materials, 2017, 4, 035024.	2.0	27
25830	Simulation of Youngâ€™s moduli for hexagonal ZnO [0â€‰0â€‰0â€‰1]-oriented nanowires: first principles and molecular mechanical calculations. Materials Research Express, 2017, 4, 085014.	0.8	10
25831	Mechanism of the high transition temperature for the 1111-type iron-based superconductors <mml:math xmlns:mml="http://www.w3.org/1998/Math/MathML"><mml:mrow><mml:mi>R</mml:mi><mml:mi>FeAsO</mml:mi></mml:mrow><mml:m <mml:math xmlns:mml="http://www.w3.org/1998/Math/MathML"><mml:mo>(</mml:mo><mml:mrow><mml:mi>R</mml:mi><mml:mo>=</mml:mo> Overview	1.1	8
25832	Insight into the influence of addition of a second metal Fe and supports with different morphology on H 2 dissociation over Ni/MgO catalysts. Applied Surface Science, 2017, 426, 827-832.	3.1	1
25833	Atomic and electronic structure of a copper/graphene interface as prepared and 1.5 years after. Applied Surface Science, 2017, 426, 1167-1172.	3.1	18
25834	Theoretical study of new potential semiconductor surfaces performance for dye sensitized solar cell usage: TiO2-B (001), (100) and H2Ti3O7 (100). Applied Surface Science, 2017, 426, 1182-1189.	3.1	23
25835	The effect of titanium(Ti) doping on hydrogen incorporation in tungsten(W)ï¼šFirst-principles calculations. Fusion Engineering and Design, 2017, 121, 227-234.	1.0	16

#	Article	IF	Citations
25836	Giant ferroelectric polarization and electric reversal of strong spontaneous magnetization in multiferroic Bi 2 FeMoO 6. Journal of Magnetism and Magnetic Materials, 2017, 441, 497-502.	1.0	9
25837	Study on the interactions of Ag nanoparticles with low molecular weight organic matter using first principles calculations. Materials Chemistry and Physics, 2017, 200, 270-279.	2.0	8
25838	Effects of Vanadium Substitution in the Layered LiFeSO 4 OH: A First Principles Investigation. Materials Today: Proceedings, 2017, 4, 5108-5115.	0.9	5
25839	Band offsets in La2O3/InN heterostructures. Solid State Communications, 2017, 265, 19-22.	0.9	0
25840	The effect of silicon on spangle size in hot-dipped 55 wt%Al-Zn coatings. Surface and Coatings Technology, 2017, 327, 110-117.	2.2	5
25841	Effects of substitution of X (X=rhenium, chromium and zirconium) on the properties of Co₇Mo₆ Î¼ phase: A firstâ€principles study. Materialwissenschaft Und Werkstofftechnik, 2017, 48, 570-576.	0.5	0
25842	Reaction mechanisms of acetylene hydrochlorination catalyzed by AuCl3/C catalysts: A density functional study. Catalysis Communications, 2017, 101, 120-124.	1.6	11
25843	Mechanism study on flotation separation of molybdenite from chalcocite using thioglycollic acid as depressant. International Journal of Mining Science and Technology, 2017, 27, 1043-1049.	4.6	28
25844	Bandgap Engineering of the g-ZnO Nanosheet via Cationicâ€“Anionic Passivated Codoping for Visible-Light-Driven Photocatalysis. Journal of Physical Chemistry C, 2017, 121, 18534-18543.	1.5	33
25845	The interaction of CO molecules on Auâ€“Rh bimetallic nanoclusters supported on a thin film of Al₂O₃/NiAl(100). RSC Advances, 2017, 7, 13362-13371.	1.7	6
25846	Wide band gap design of new chalcogenide compounds: KSrPS₄ and CsBaAsS₄. RSC Advances, 2017, 7, 38044-38051.	1.7	20
25847	Optical, electronic, and elastic properties of some A⁵B⁶C⁷ferroelectrics (A=Sb, Bi; B=S, Se; C=I, Br, Cl): First principle calculation. Ferroelectrics, 2017, 511, 22-34.	0.3	13
25848	Theoretical investigation of phase separation in thermoelectric AgSbTe2. Japanese Journal of Applied Physics, 2017, 56, 081201.	0.8	1
25849	Powerful recombination centers resulting from reactions of hydrogen with carbonâ€“oxygen defects in nâ€type Czochralskiâ€grown silicon. Physica Status Solidi - Rapid Research Letters, 2017, 11, 1700133.	1.2	13
25850	Atomistic Origin of Phase Stability in Oxygen-Functionalized MXene: A Comparative Study. Journal of Physical Chemistry C, 2017, 121, 18947-18953.	1.5	44
25851	Multiple resistive switching in coreâ€“shell ZnO nanowires exhibiting tunable surface states. Journal of Materials Chemistry C, 2017, 5, 10517-10523.	2.7	40
25852	Optical properties of <mml:math xmlns:mml="http://www.w3.org/1998/Math/MathML"><mml:mrow><mml:msub><mml:mi>Ti</mml:mi><mml:mi>x</mml:mi></mml:ms mathvariant="normal">O</mml:mi><mml:mn>2</mml:mn></mml:msub></mml:mrow></mml:math> solid solutions. Physical Review B, 2017, 95, .	1.1	9
25853	Edge magnetism modulation of graphene nanoribbons via planar tetrahedral coordinated atoms embedding. Journal of Materials Science, 2017, 52, 12307-12313.	1.7	3

#	Article	IF	Citations
25854	Stability and Elastic, Electronic, and Thermodynamic Properties of Fe2TiSi1â^'x Sn x Compounds. Journal of Electronic Materials, 2017, 46, 6038-6044.	1.0	9
25855	Ab Initio Investigation on Structural, Elastic and Electronic Properties of Î·-Phase Cu4.5Ni1Au0.5Sn5 and Cu5Ni1Sn4.5In0.5 Intermetallic Compounds. Journal of Electronic Materials, 2017, 46, 5684-5692.	1.0	1
25856	Intrinsic point defects in ternary MgCaSi: Ab initio investigation. Journal of Materials Research, 2017, 32, 3723-3731.	1.2	3
25857	Optical properties of LiGaSe2 noncentrosymmetric crystal. Optical Materials, 2017, 72, 795-804.	1.7	23
25858	Dramatic Drop of d⁰ Ferromagnetism with ZnO Nanocrystal Size in Vacuum and Air. Journal of Physical Chemistry C, 2017, 121, 19401-19406.	1.5	7
25859	Electrical Contacts in Monolayer Arsenene Devices. ACS Applied Materials & Interfaces, 2017, 9, 29273-29284.	4.0	76
25860	In situ atomic-scale observation of oxygen-driven core-shell formation in Pt3Co nanoparticles. Nature Communications, 2017, 8, 204.	5.8	102
25861	Electronic structure of charged bilayer and trilayer phosphorene. Physical Review B, 2017, 96, .	1.1	15
25862	Ab initio study of new sp3 silicon and germanium allotropes predicted from the zeolite topologies. European Physical Journal B, 2017, 90, 1.	0.6	8
25863	Influence of Cu Doping on the Electronic Structure and Magnetic Properties of the Mn₂VAl Heusler Compound. Physica Status Solidi (B): Basic Research, 2017, 254, 1700160.	0.7	4
25864	High-pressure synthesis of tetragonal iron aluminide FeAl2. Scripta Materialia, 2017, 141, 107-110.	2.6	10
25865	Role of the Band Gap for the Interaction Energy of Coadsorbed Fragments. Journal of Physical Chemistry C, 2017, 121, 18608-18614.	1.5	15
25866	Hysteresis and bonding reconstruction in the pressure-induced B3â€"B1 phase transition of 3C-SiC. Physical Chemistry Chemical Physics, 2017, 19, 22887-22894.	1.3	8
25867	Structural and electrical analysis of epitaxial 2D/3D vertical heterojunctions of monolayer MoS2 on GaN. Applied Physics Letters, 2017, 111, .	1.5	27
25868	Electronic and optical properties of GaN under pressure: DFT calculations. International Journal of Modern Physics B, 2017, 31, 1750261.	1.0	2
25869	Ab initio triangle maps for new insights into the crystal wave functions of carbon allotropes. Carbon, 2017, 123, 708-716.	5.4	3
25870	Adsorption of chloroform on N-doped and Al-doped graphene: A first-principle study. Chemical Physics Letters, 2017, 685, 344-348.	1.2	19
25871	High performance material for hydrogen storage: Graphenelike Si2BN solid. International Journal of Hydrogen Energy, 2017, 42, 22942-22952.	3.8	50

#	Article	IF	Citations
25872	A first principles study of hydrogen storage inÂlithium decorated defective phosphorene. International Journal of Hydrogen Energy, 2017, 42, 23018-23027.	3.8	56
25873	First principles investigations of the magnetic properties and martensitic transformation in Mn2NiB Heusler alloy. Journal of Magnetism and Magnetic Materials, 2017, 444, 43-48.	1.0	2
25874	Enhanced Pseudocapacitance of MoO₃-Reduced Graphene Oxide Hybrids with Insight from Density Functional Theory Investigations. Journal of Physical Chemistry C, 2017, 121, 18992-19001.	1.5	51
25875	Charge Transfer at the PTCDA/Black Phosphorus Interface. Journal of Physical Chemistry C, 2017, 121, 18084-18094.	1.5	46
25876	Deformation behavior of Re alloyed Mo thin films on flexible substrates: In situ fragmentation analysis supported by first-principles calculations. Scientific Reports, 2017, 7, 7374.	1.6	17
25877	Tunable interaction between metal clusters and graphene. Physical Chemistry Chemical Physics, 2017, 19, 22153-22160.	1.3	8
25878	Electric field modulations of band alignments in arsenene/Ca(OH)₂heterobilayers for multi-functional device applications. Journal Physics D: Applied Physics, 2017, 50, 415304.	1.3	12
25879	Theoretical Investigation of Strain and Doping on the Raman Spectra of Monolayer MoS₂. Physica Status Solidi (B): Basic Research, 2017, 254, 1700184.	0.7	49
25880	Metal-organic frameworks derived (Cu 0.30 Co 0.7)Co 2 O 4 /CuO composite rectangular pyramid grass as high performance anode materials for lithium ion battery. Electrochimica Acta, 2017, 250, 35-41.	2.6	8
25881	Probing Ï€-Ï€ stacking modulation of g-C3N4/graphene heterojunctions and corresponding role of graphene on photocatalytic activity. Journal of Colloid and Interface Science, 2017, 508, 274-281.	5.0	67
25882	First principles study of oxygen molecule interaction with the graphitic active sites of a boron-doped pyrolyzed Feâ€“Nâ€“C catalyst. Physical Chemistry Chemical Physics, 2017, 19, 23497-23504.	1.3	36
25883	Chemically fluorinated graphene oxide for room temperature ammonia detection at ppb levels. Journal of Materials Chemistry A, 2017, 5, 19116-19125.	5.2	83
25884	IIâ€“IVâ€“V₂ and IIIâ€“IIIâ€“V₂ Polytypes as Light Absorbers for Single Junction and Tandem Photovoltaic Devices. Journal of Physical Chemistry C, 2017, 121, 17780-17786.	1.5	18
25885	A computational approach towards understanding hydrogen gas adsorption in Coâ€“MIL-88A. RSC Advances, 2017, 7, 39583-39593.	1.7	7
25886	Shallow trapping vs. deep polarons in a hybrid lead halide perovskite, CH₃NH₃PbI₃. Physical Chemistry Chemical Physics, 2017, 19, 27184-27190.	1.3	18
25887	High-temperature superconducting phase of HBr under pressure predicted by first-principles calculations. Physical Review B, 2017, 96, .	1.1	8
25888	Rheniumâ€Loaded TiO₂: A Highly Versatile and Chemoselective Catalyst for the Hydrogenation of Carboxylic Acid Derivatives and the Nâ€Methylation of Amines Using H₂ and CO₂. Chemistry - A European Journal, 2017, 23, 14848-14859.	1.7	76
25889	DFT-based calculations of the adsorptions of acetic acid, triacetin, methanol and the alkoxide formation on the surfaces of zinc acetate. Molecular Catalysis, 2017, 440, 43-49.	1.0	9

#	Article	IF	Citations
25890	Structural phase transition, electronic and superconducting properties of ScBi and YBi. Solid State Communications, 2017, 266, 39-45.	0.9	10
25891	Electronic Structure of Transition-Metal Based Cu₂GeTe₃ Phase Change Material: Revealing the Key Role of Cu d Electrons. Chemistry of Materials, 2017, 29, 7440-7449.	3.2	24
25892	ScRu2B3 and Sc2RuB6: Borides Featuring a 2D Infinite Boron Clustering. Inorganic Chemistry, 2017, 56, 10549-10558.	1.9	6
25893	Interaction and Quantum Capacitance of Nitrogen/Sulfur Co-Doped Graphene: A Theoretical Calculation. Journal of Physical Chemistry C, 2017, 121, 18344-18350.	1.5	40
25894	Insight into metallic behavior in epitaxial half-metallic NiCo₂O₄ films. RSC Advances, 2017, 7, 36026-36033.	1.7	38
25895	Electronic structures at the interface between CuPc and black phosphorus. Journal of Chemical Physics, 2017, 147, 064702.	1.2	12
25896	Structural transformations and adsorption properties of PtNi nanoalloy thin film electrocatalysts prepared by magnetron co-sputtering. Electrochimica Acta, 2017, 251, 427-441.	2.6	15
25897	First hafnium-based MAX phase in the 312 family, Hf3AlC2: A first-principles study. Journal of Alloys and Compounds, 2017, 727, 616-626.	2.8	95
25898	Enhanced photoelectrochemical performance of anatase TiO₂ for water splitting via surface codoping. RSC Advances, 2017, 7, 39877-39884.	1.7	25
25899	Structural, mechanical and electronic properties of Nb₂C: first-principles calculations. RSC Advances, 2017, 7, 33402-33407.	1.7	14
25900	Understanding the Oxygen Evolution Reaction on a Twoâ€Dimensional NiO₂ Catalyst. ChemElectroChem, 2017, 4, 2764-2770.	1.7	29
25901	A density functional study of chalcopyrite MgGeSb2. Indian Journal of Physics, 2017, 91, 1487-1492.	0.9	0
25902	AELAS: Automatic ELAStic property derivations via high-throughput first-principles computation. Computer Physics Communications, 2017, 220, 403-416.	3.0	84
25903	Positron annihilation analysis of the atomic scale changes in oxidized Zircaloy-4 samples. Journal of Nuclear Materials, 2017, 495, 172-180.	1.3	12
25904	Effect of pressure on structural, elastic and mechanical properties of transition metal hydrides Mg7TMH16 (TMÂ=ÂSc, Ti, V, Y, Zr and Nb): First-principles investigation. Journal of Physics and Chemistry of Solids, 2017, 111, 229-237.	1.9	7
25905	Strain modulations of magnetism in Fe-doped InSe monolayer. Physica E: Low-Dimensional Systems and Nanostructures, 2017, 94, 153-157.	1.3	4
25906	A first principles study of p-type defects in LaCrO₃. Physical Chemistry Chemical Physics, 2017, 19, 22870-22876.	1.3	18
25907	Spectroscopic characterization of the on-surface induced (cyclo)dehydrogenation of a N-heteroaromatic compound on noble metal surfaces. Physical Chemistry Chemical Physics, 2017, 19, 22454-22461.	1.3	3

#	Article	IF	Citations
25908	Crystallographic structure and energetics of the Rh(1â€‰0â€‰0)-(3 Ã— 1)-2O phase. Journal of Physics Condensed Matter, 2017, 29, 365001.	0.7	0
25909	A comprehensive study of piezomagnetic response in CrPS₄monolayer: mechanical, electronic properties and magnetic ordering under strains. Journal of Physics Condensed Matter, 2017, 29, 405801.	0.7	28
25910	Ab initio investigation on the slip preference of ã€ˆaã€‰-dislocations in hexagonal metals and alloys. Computational Materials Science, 2017, 139, 209-215.	1.4	4
25911	Functionalized graphene for sodium battery applications: the DFT insights. Electrochimica Acta, 2017, 250, 185-195.	2.6	43
25912	Ullmann Reaction Catalyzed by Heterogeneous Mesoporous Copper/Manganese Oxide: A Kinetic and Mechanistic Analysis. Inorganic Chemistry, 2017, 56, 10290-10297.	1.9	36
25913	Cytocompatibility of Ti₃AlC₂, Ti₃SiC₂, and Ti₂AlN: In Vitro Tests and First-Principles Calculations. ACS Biomaterials Science and Engineering, 2017, 3, 2293-2301.	2.6	75
25914	Activation of chrysocolla flotation by organic chelating agents. RSC Advances, 2017, 7, 35608-35612.	1.7	7
25915	A machine learning approach to graph-theoretical cluster expansions of the energy of adsorbate layers. Journal of Chemical Physics, 2017, 147, 054106.	1.2	31
25916	Structural and electronic properties of MoS2, WS2, and WS2/MoS2 heterostructures encapsulated with hexagonal boron nitride monolayers. Journal of Applied Physics, 2017, 122, .	1.1	49
25917	Molecular beam epitaxy growth and structure of self-assembled Bi₂Se₃/Bi₂MnSe₄ multilayer heterostructures. New Journal of Physics, 2017, 19, 085002.	1.2	58
25918	Structural phase transition of BeTe: an ab initio molecular dynamics study. Journal of Molecular Modeling, 2017, 23, 261.	0.8	1
25919	Diffusion of a Single Platinum Atom on Light-Element-Doped Graphene. Journal of Physical Chemistry C, 2017, 121, 17787-17795.	1.5	21
25920	First-Principles Study on O2 Adsorption and Dissociation Processes over Rh(100) and Rh(111) Surfaces. Langmuir, 2017, 33, 11156-11163.	1.6	8
25921	Exceptional thermoelectric performance of a â€œstar-likeâ€•SnSe nanotube with ultra-low thermal conductivity and a high power factor. Physical Chemistry Chemical Physics, 2017, 19, 23247-23253.	1.3	7
25922	Formaldehyde adsorption on graphane. Computational and Theoretical Chemistry, 2017, 1117, 119-123.	1.1	14
25923	Catalytic Semihydrogenation of Acetylene on the (100) Surface of the o-Al₁₃Co₄ Quasicrystalline Approximant: Density Functional Theory Study. Journal of Physical Chemistry C, 2017, 121, 18738-18745.	1.5	12
25924	Unveiling universal trends for the energy level alignment in organic/oxide interfaces. Physical Chemistry Chemical Physics, 2017, 19, 24412-24420.	1.3	9
25925	Uniaxial strain-modulated electronic structures of Cd X (X = S, Se, Te) from first-principles calculations: A comparison between bulk and nanowires. Chinese Physics B, 2017, 26, 087103.	0.7	1

#	Article	IF	Citations
25926	Ab initio modelling of the early stages of precipitation in Al-6000 alloys. Acta Materialia, 2017, 140, 240-249.	3.8	14
25927	Stability of edge magnetism in functionalized zigzag graphene nanoribbons. Carbon, 2017, 124, 123-132.	5.4	21
25928	High temperature thermoelectric performance of p-type TaRhSn half Heusler compound: A computational assessment. Ceramics International, 2017, 43, 15160-15166.	2.3	26
25929	First-principle investigation 3,4-ethylenedioxythiophene molecule adsorption on Cu(110)-(2 â€¯Ã—â€¯ 1)O surface. Surface Science, 2017, 665, 83-88.	0.8	2
25930	Tuning the Electronic and Optical Properties of Monolayers As, Sb, and Bi via Surface Charge Transfer Doping. Journal of Physical Chemistry C, 2017, 121, 19530-19537.	1.5	35
25931	Dissociative adsorption dynamics of nitrogen on a Fe(111) surface. Physical Chemistry Chemical Physics, 2017, 19, 24626-24635.	1.3	9
25932	The diffusion of a Ga atom on GaAs(001)Î²2(2 Ã— 4): Local superbasin kinetic Monte Carlo. Journal of Chemical Physics, 2017, 147, 152711.	1.2	3
25933	First-principles study of charged steps on 180Â° domain walls in ferroelectric PbTiO3. Journal of Applied Physics, 2017, 122, .	1.1	9
25934	The effect of C, Si, N, and P impurities on structural and electronic properties of armchair boron nanotube. Journal of Nanostructure in Chemistry, 2017, 7, 243-248.	5.3	7
25935	A key role of tensile strain and surface termination in formation and properties of La0.7Sr0.3MnO3 composites with carbon nanotubes. Computational Materials Science, 2017, 139, 125-131.	1.4	1
25936	Mechanism of ethylene oxychlorination over ruthenium oxide. Journal of Catalysis, 2017, 353, 171-180.	3.1	12
25937	Alloyed surfaces: New substrates for graphene growth. Surface Science, 2017, 665, 28-31.	0.8	2
25938	Metaheuristics-Assisted Combinatorial Screening of Eu²⁺-Doped Caâ€“Srâ€“Baâ€“Liâ€“Mgâ€“Alâ€“Siâ€“Geâ€“N Compositional Space in Search of a Narrow-Band Green Emitting Phosphor and Density Functional Theory Calculations. Inorganic Chemistry, 2017, 56, 9814-9824.	1.9	23
25939	Data Mining for Three-Dimensional Organic Dirac Materials: Focus on Space Group 19. Scientific Reports, 2017, 7, 7298.	1.6	25
25940	The effect of vacancies and the substitution of p-block atoms on single-layer buckled germanium selenide. RSC Advances, 2017, 7, 37815-37822.	1.7	20
25941	First-Principles Investigations of TiGe/Ge Interface and Recipes to Reduce the Contact Resistance. IEEE Transactions on Electron Devices, 2017, 64, 3775-3780.	1.6	11
25942	From isolated diamondoids to a van-der-Waals crystal: A theoretical and experimental analysis of a trishomocubane and a diamantane dimer in the gas and solid phase. Journal of Chemical Physics, 2017, 147, 044303.	1.2	4
25943	Antiferromagnetism in <mml:math xmlns:mml="http://www.w3.org/1998/Math/MathML"><mml:mrow><mml:msub><mml:mi mathvariant="bold">Sr</mml:mi><mml:mn>3</mml:mn></mml:msub><mml:msub><mml:mi mathvariant="bold">Ru</mml:mi><mml:mn>2</mml:mn></mml:msub><mml:msub><mml:mi mathvariant="bold">O</mml:mi><mml:mn>7</mml:mn></mml:msub></mml:mrow></mml:math>. Physical Review B, 2017, 95, .	1.1	10

#	Article	IF	Citations
25944	Growth mechanism, dielectric, elastic and thermal properties of zinc cadmium thiocyanate crystal as a potential piezoelectric crystal. Chemical Physics Letters, 2017, 685, 401-409.	1.2	0
25945	Phase stability and thermodynamic properties of FeS polymorphs. Journal of Physics and Chemistry of Solids, 2017, 111, 317-323.	1.9	10
25946	Van der Waals Interaction Really Matters: Energetics of Benzoic Acid on TiO₂ Rutile Surfaces. Journal of Physical Chemistry C, 2017, 121, 17207-17214.	1.5	14
25947	Synergetic Effects toward Catalysis and Confinement of Magnesium Hydride on Modified Graphene: A First-Principles Study. Journal of Physical Chemistry C, 2017, 121, 18401-18411.	1.5	13
25948	Importance of Angelica Lactone Formation in the Hydrodeoxygenation of Levulinic Acid to Î³-Valerolactone over a Ru(0001) Model Surface. Journal of Physical Chemistry C, 2017, 121, 18746-18761.	1.5	21
25949	Increased thermal stability of activated N2 adsorbed on K-promoted Ni{110}. Physical Chemistry Chemical Physics, 2017, 19, 21848-21855.	1.3	3
25950	Effect of Ti doping on mechanical and optical properties of super-hard I2d-CN2 materials. RSC Advances, 2017, 7, 37943-37951.	1.7	3
25951	A wide visible light driven complex perovskite Ba(Mg_{1/3}Ta_{2/3})O_{3âˆ'x}N_y photocatalyst for water oxidation and reduction. Journal of Materials Chemistry A, 2017, 5, 18870-18877.	5.2	20
25952	Anisotropic carrier mobility in two-dimensional materials with tilted Dirac cones: theory and application. Physical Chemistry Chemical Physics, 2017, 19, 23942-23950.	1.3	69
25953	Insight into the preferred formation mechanism of long-chain hydrocarbons in Fischerâ€“Tropsch synthesis on Hcp Co(10âˆ'11) surfaces from DFT and microkinetic modeling. Catalysis Science and Technology, 2017, 7, 3758-3776.	2.1	39
25954	Visible light absorption of (Fe, C/N) co-doped NaTaO${}_{3}$: DFT+ U *. Chinese Physics B, 2017, 26, 087102.	0.7	5
25955	Lattice stability and the effect of Co and Re on the ideal strength of Ni: First-principles study of uniaxial tensile deformation. Chinese Physics B, 2017, 26, 093106.	0.7	4
25956	Hybrid density functional study of bandgaps for 27 new proposed half-Heusler semiconductors. Journal of Applied Physics, 2017, 122, .	1.1	28
25957	Pressure-induced magnetic moment abnormal increase in Mn2FeAl and non-continuing decrease in Fe2MnAl via first principles. Scientific Reports, 2017, 7, 16522.	1.6	12
25958	Efficient approach to compute melting properties fully from ab initio with application to Cu. Physical Review B, 2017, 96, .	1.1	53
25959	Chiral magnetic interactions in graphene nanoribbons on topological insulator substrates. Physical Review B, 2017, 96, .	1.1	6
25960	Ab initio model for GaAs_{1âˆ'}_xN_xchemical beam epitaxy using GaAs(100) surface stability over As₂, H₂, and N₂. Japanese Journal of Applied Physics, 2017, 56, 060306.	0.8	1
25961	First principles study on superconductivity of distorted bcc phase in phosphorus. Journal of Physics: Conference Series, 2017, 950, 042011.	0.3	1

#	Article	IF	Citations
25962	Low-temperature structure and the ferroelectric phase transitions in the <mml:math xmlns:mml="http://www.w3.org/1998/Math/MathML"><mml:mrow><mml:mi>CdTi</mml:mi><mml:msub><mml:mi mathvariant="normal">O</mml:mi><mml:mn>3</mml:mn></mml:msub></mml:mrow></mml:math> perovskite. Physical Review B, 2017, 96, .	1.1	12
25963	Orbital-based charge self-consistent Blackman-Esterling-Berk coherent potential approximation approach to substitutional disorder within a pseudopotential framework. Physical Review B, 2017, 96, .	1.1	2
25964	Effect of solid electrolyte interphase on the reactivity of polysulfide over lithium-metal anode. Electrochimica Acta, 2017, 258, 1320-1328.	2.6	13
25965	Predicting the Double Layer Width on Pt(111) in Acid and Base with Theory and Extracting It from Experimental Voltammograms. Journal of Physical Chemistry C, 2017, 121, 28051-28064.	1.5	3
25966	Mechanical properties of Fe rich Feâ€“Si alloys:ab initiolocal bulk-modulus viewpoint. Materials Research Express, 2017, 4, 116518.	0.8	9
25967	Thermal conductivity of type-I, type-II, and type-VIII pristine silicon clathrates: A first-principles study. Physical Review B, 2017, 96, .	1.1	14
25968	Decomposition of Ionic Liquids at Lithium Interfaces. 1. Ab Initio Molecular Dynamics Simulations. Journal of Physical Chemistry C, 2017, 121, 28214-28234.	1.5	68
25969	Deciphering the Electrocatalytic Activity of Nitrogen-Doped Carbon Embedded with Cobalt Nanoparticles and the Reaction Mechanism of Triiodide Reduction in Dye-Sensitized Solar Cells. Journal of Physical Chemistry C, 2017, 121, 27332-27343.	1.5	18
25970	Oxygen Evolution via the Bridging Inequivalent Dual-Site Reaction: First-Principles Study of a Quadruple-Perovskite Oxide Catalyst. Journal of Physical Chemistry C, 2017, 121, 28403-28411.	1.5	29
25971	Vacuum level dependent photoluminescence in chemical vapor deposition-grown monolayer MoS 2. Scientific Reports, 2017, 7, 16714.	1.6	27
25972	Research on c-HfO2 (0 0 1)/Î±-Al2O3 (1 -1 0 2) interface in CTM devices based on first principle theory. AIP Advances, 2017, 7, 125001.	0.6	6
25973	Surface magnetism of gallium arsenide nanofilms. Physical Review B, 2017, 96, .	1.1	1
25974	Point defects in the <mml:math xmlns:mml="http://www.w3.org/1998/Math/MathML"><mml:mrow><mml:mn>1</mml:mn><mml:msup><mml:mi>T</mml:mi><mml:mo and <mml:math xmlns:mml="http://www.w3.org/1998/Math/MathML"><mml:mrow><mml:mn>2</mml:mn><mml:mi>H</mml:mi></mml:mrow></mml:m phases of single-layer <mml:math xmlns:mml="http://www.w3.org/1998/Math/MathML"><mml:msub><mml:mi>MoS</mml:mi><mml:mn>2</mml:mn></mml:msub></mm	1.1	48
25975	Probing the Electric Field Effect on the Catalytic Performance of Mn-Doped Graphene to CO Oxidation. Journal of Physical Chemistry C, 2017, 121, 27983-27991.	1.5	19
25976	From Multiple Nodal Chain to Dirac/Weyl Semimetal and Topological Insulator in Ternary Hexagonal Materials. Journal of Physical Chemistry C, 2017, 121, 28587-28593.	1.5	21
25977	Molecular and Ionic Dipole Effects on the Electronic Properties of Si-/SiO₂-Grafted Alkylamine Monolayers. ACS Applied Materials & Interfaces, 2017, 9, 44873-44879.	4.0	10
25978	The electron-phonon interaction at deep Bi 2 Te3-semiconductor interfaces from Brillouin light scattering. Scientific Reports, 2017, 7, 16449.	1.6	10
25979	First-principles investigation of the orientation influenced He dissolution and diffusion behaviors onÂW surfaces. RSC Advances, 2017, 7, 25789-25795.	1.7	12

#	Article	IF	Citations
25980	Wurtzite BAlN and BGaN alloys for heterointerface polarization engineering. Applied Physics Letters, 2017, 111, .	1.5	37
25981	Thermophysical properties of paramagnetic Fe from first principles. Physical Review B, 2017, 96, .	1.1	21
25982	Energy Band Structure of Beâ€“(C, Si, Ge, Sn)â€“N2 Crystals. Russian Physics Journal, 2017, 60, 900-907.	0.2	12
25983	Atomistic Determination of Anisotropic Surface Energy-Associated Growth Patterns of Magnesium Alloy Dendrites. ACS Omega, 2017, 2, 8803-8809.	1.6	27
25984	Large guanidinium cation mixed with methylammonium in lead iodide perovskites for 19% efficient solar cells. Nature Energy, 2017, 2, 972-979.	19.8	445
25985	Geometric and electronic structures of iridium(III) acetylacetonate in atomic layer deposition of iridium: a first-principles study. Materials Research Express, 2017, 4, 106403.	0.8	2
25986	Synthesis and Characterization of Folate Conjugated Boron Nitride Nanocarriers for Targeted Drug Delivery. Journal of Physical Chemistry C, 2017, 121, 28096-28105.	1.5	29
25987	Topologically frustrated ionisation in a water-ammonia ice mixture. Nature Communications, 2017, 8, 1065.	5.8	21
25988	Changing the gap type of solid state boric acid by heating: a dispersion-corrected density functional study of Î±-, Î²-, and Î³-metaboric acid polymorphs. New Journal of Chemistry, 2017, 41, 15533-15544.	1.4	4
25989	First-principles study of solute diffusion in Ni ₃ Al. Chinese Physics B, 2017, 26, 093102.	0.7	3
25990	Energetic consideration of compounds at Mg₂Siâ€“Ni electrode interlayer produced by spark-plasma sintering. Japanese Journal of Applied Physics, 2017, 56, 05DC03.	0.8	8
25991	Relative Thermal Stability of Thiolate- and Selenolate-Bonded Aromatic Monolayers on the Au(111) Substrate. Journal of Physical Chemistry C, 2017, 121, 28031-28042.	1.5	33
25992	Dehydrogenation Selectivity of Ethanol on Close-Packed Transition Metal Surfaces: A Computational Study of Monometallic, Pd/Au, and Rh/Au Catalysts. Journal of Physical Chemistry C, 2017, 121, 27504-27510.	1.5	96
25993	Crystallite size-dependent metastable phase formation of TiAlN coatings. Scientific Reports, 2017, 7, 16096.	1.6	34
25994	Properties of Single-Layer Boron Sheets: First-Principle Study through MatCloud Platform. Communications in Theoretical Physics, 2017, 68, 125.	1.1	2
25995	A New Dirac Semimetal in Hexagonal BaGaSnH. Journal of the Physical Society of Japan, 2017, 86, 124714.	0.7	3
25996	Carbon adsorption on doped cementite surfaces for effective catalytic growth of diamond-like carbon: a first-principles study. Physical Chemistry Chemical Physics, 2017, 19, 32341-32348.	1.3	13
25997	Regio- and Chemoselective Hydrogenation of Dienes to Monoenes Governed by a Well-Structured Bimetallic Surface. Journal of the American Chemical Society, 2017, 139, 18231-18239.	6.6	48

#	Article	IF	Citations
25998	Computational investigations of electronic structure modifications of ferrocene-terminated self-assembled monolayers: effects of electron donating/withdrawing functional groups attached on the ferrocene moiety. Physical Chemistry Chemical Physics, 2017, 19, 32715-32722.	1.3	7
25999	Prediction of optically-active transitions in type-VIII guest-free silicon clathrate Si46: A comparative study of its physical properties with type-I counterpart through first-principles. Journal of Applied Physics, 2017, 122, .	1.1	7
26000	First principles investigation of structural, mechanical, dynamical and thermodynamic properties of AgMg under pressure. Materials Research Express, 2017, 4, 126507.	0.8	0
26001	Acetylene chain reaction on hydrogenated boron nitride monolayers: a density functional theory study. Journal of Molecular Modeling, 2017, 23, 359.	0.8	5
26002	Uniform Surface Modification of Li₂ZnTi₃O₈ by Liquated Na₂MoO₄ To Boost Electrochemical Performance. ACS Applied Materials & Interfaces, 2017, 9, 43603-43613.	4.0	18
26003	Chemical Welding on Semimetallic TiS2 Nanosheets for High-Performance Flexible n-Type Thermoelectric Films. ACS Applied Materials & Interfaces, 2017, 9, 42430-42437.	4.0	31
26004	Insights into the increased degradation rate of CH₃NH₃PbI₃ solar cells in combined water and O₂ environments. Journal of Materials Chemistry A, 2017, 5, 25469-25475.	5.2	52
26005	Effect of Platinum, Gold, and Potassium Additives on the Surface Chemistry of CdI₂-Antitype Mo₂C. ACS Omega, 2017, 2, 7976-7984.	1.6	2
26006	Scaling relationships and theory for vibrational frequencies of adsorbates on transition metal surfaces. Nature Communications, 2017, 8, 1842.	5.8	23
26007	Identifying light impurities in transition metal dichalcogenides: the local vibrational modes of S and O in ReSe2 and MoSe2. Npj 2D Materials and Applications, 2017, 1, .	3.9	5
26008	Work function and surface stability of tungsten-based thermionic electron emission cathodes. APL Materials, 2017, 5, .	2.2	52
26009	First-principles Green's-function method for surface calculations: A pseudopotential localized basis set approach. Physical Review B, 2017, 96, .	1.1	211
26010	Dirac cones in two-dimensional borane. Physical Review B, 2017, 96, .	1.1	17
26011	First-principles study on the structural, elastic and electronic properties of Ti4N3 and Ti6N5 under high pressure. Modern Physics Letters B, 2017, 31, 1750349.	1.0	4
26012	Disparity in Photoexcitation Dynamics between Vertical and Lateral MoS₂/WSe₂ Heterojunctions: Time-Domain Simulation Emphasizes the Importance of Donorâ€“Acceptor Interaction and Band Alignment. Journal of Physical Chemistry Letters, 2017, 8, 5771-5778.	2.1	52
26013	Catalytically Active Boron Nitride in Acetylene Hydrochlorination. ACS Catalysis, 2017, 7, 8572-8577.	5.5	54
26014	Control of interfacial reactions for the growth of high-quality AlN epitaxial films on Cu(111) substrates. CrystEngComm, 2017, 19, 7307-7315.	1.3	7
26015	Novel penta-graphene nanotubes: strain-induced structural and semiconductorâ€“metal transitions. Nanoscale, 2017, 9, 19310-19317.	2.8	18

#	Article	IF	Citations
26016	Effects of hydrostatic pressure on the thermoelectric properties of the Ïµ-polytype of InSe, GaSe, and InGaSe2 semiconductor compounds: anab initiostudy. Materials Research Express, 2017, 4, 125901.	0.8	0
26017	Absorption and Mid-IR SHG in Two-Dimensional Halogen and Hydrogen Saturated Silicene Series. Journal of Physical Chemistry C, 2017, 121, 27139-27146.	1.5	10
26018	Thermal expansion of Pd-based metallic glasses by ab initio methods and high energy X-ray diffraction. Scientific Reports, 2017, 7, 15744.	1.6	14
26019	Towards identifying the active sites on RuO₂(110) in catalyzing oxygen evolution. Energy and Environmental Science, 2017, 10, 2626-2637.	15.6	278
26020	3d transition metal doping-induced electronic structures and magnetism in 1T-HfSe₂ monolayers. RSC Advances, 2017, 7, 52747-52754.	1.7	15
26021	First-principles-based Landau-Devonshire potential for <mml:math xmlns:mml="http://www.w3.org/1998/Math/MathML"><mml:msub><mml:mi>BiFeO</mml:mi><mml:mn>3</mml:mn></mml:msub><m Physical Review B, 2017, 96, .	1.1	18
26022	Calibration of the fine-structure constant of graphene by time-dependent density-functional theory. Physical Review B, 2017, 96, .	1.1	24
26023	Enhanced Magnetic Hybridization of a Spinterface through Insertion of a Two-Dimensional Magnetic Oxide Layer. Nano Letters, 2017, 17, 7440-7446.	4.5	17
26024	Tunable electronic and magnetic properties of arsenene nanoribbons. RSC Advances, 2017, 7, 51935-51943.	1.7	8
26025	Adsorption and diffusion of hydrogen and oxygen in FCC-Co: a first-principles study. Physical Chemistry Chemical Physics, 2017, 19, 32404-32411.	1.3	11
26026	Sulfide perovskites for solar energy conversion applications: computational screening and synthesis of the selected compound LaYS₃. Energy and Environmental Science, 2017, 10, 2579-2593.	15.6	91
26027	Low-frequency optical phonon modes and carrier mobility in the halide perovskite CH3NH3PbBr3 using terahertz time-domain spectroscopy. Applied Physics Letters, 2017, 111, .	1.5	54
26028	First-principles calculations of structural and thermodynamic properties of Î² -PbO. Chinese Physics B, 2017, 26, 116501.	0.7	5
26029	Single layers and multilayers of GaN and AlN in square-octagon structure: Stability, electronic properties, and functionalization. Physical Review B, 2017, 96, .	1.1	25
26030	Chemically Tunable Properties of Graphene Covered Simultaneously with Hydroxyl and Epoxy Groups. Journal of Physical Chemistry C, 2017, 121, 27603-27611.	1.5	6
26031	Features of Electronic, Mechanical, and Electromechanical Properties of Fluorinated Diamond Films of Nanometer Thickness. Journal of Physical Chemistry C, 2017, 121, 28484-28489.	1.5	29
26032	Oxidation behavior of graphene-coated copper at intrinsic graphene defects of different origins. Nature Communications, 2017, 8, 1549.	5.8	60
26033	Two-Dimensional Co2S2 monolayer with robust ferromagnetism. Scientific Reports, 2017, 7, 15993.	1.6	23

#	Article	IF	Citations
26034	Computational design of enhanced photocatalytic activity of two-dimensional cadmium iodide. RSC Advances, 2017, 7, 53653-53657.	1.7	12
26035	Toward the Realization of 2D Borophene Based Gas Sensor. Journal of Physical Chemistry C, 2017, 121, 26869-26876.	1.5	148
26036	DFT study of key elementary steps for C2+ alcohol synthesis on bimetallic sites of Cu-Co shell-core structure from syngas. Molecular Catalysis, 2017, 443, 165-174.	1.0	6
26037	Pressure Driven Enhancement of Ideal Shear Strength in bc8-Carbon and Diamond. Journal of Physical Chemistry C, 2017, 121, 26457-26464.	1.5	9
26038	Anisotropic attosecond charge carrier dynamics and layer decoupling in quasi-2D layered SnS2. Nature Communications, 2017, 8, 1369.	5.8	27
26039	Germanene nanomeshes: Cooperative effects of degenerate perturbation and uniaxial strain on tuning bandgap. Chinese Physics B, 2017, 26, 108101.	0.7	3
26040	Giant Valley Splitting and Valley Polarized Plasmonics in Group V Transition-Metal Dichalcogenide Monolayers. Journal of Physical Chemistry Letters, 2017, 8, 5764-5770.	2.1	19
26041	Impurity states in InSe monolayers doped with group II and IV elements. Journal of Applied Physics, 2017, 122, 185702.	1.1	5
26042	Discovery and Characterization of a Pourbaix-Stable, 1.8 eV Direct Gap Bismuth Manganate Photoanode. Chemistry of Materials, 2017, 29, 10027-10036.	3.2	17
26043	First-Principles Analysis of Li Intercalation in VO₂(B). Chemistry of Materials, 2017, 29, 10075-10087.	3.2	28
26044	Fe-Cluster Compounds of Chalcogenides: Candidates for Rare-Earth-Free Permanent Magnet and Magnetic Nodal-Line Topological Material. Inorganic Chemistry, 2017, 56, 14577-14583.	1.9	4
26045	Crystal structure and chemical bonding in the mixed anion compound BaSF. Dalton Transactions, 2017, 46, 16244-16250.	1.6	11
26046	Metalâ€“semiconductor transition of two-dimensional Mg₂C monolayer induced by biaxial tensile strain. Physical Chemistry Chemical Physics, 2017, 19, 32086-32090.	1.3	16
26047	Superhard B₂CO phases derived from carbon allotropes. RSC Advances, 2017, 7, 52192-52199.	1.7	12
26048	Tuning the piezoelectric and mechanical properties of the AlN system via alloying with YN and BN. Journal of Applied Physics, 2017, 122, .	1.1	49
26049	Anharmonic, dimensionality and size effects in phonon transport. Journal of Physics Condensed Matter, 2017, 29, 505703.	0.7	12
26050	Strain-induced polar discontinuities in two-dimensional materials from combined first-principles and SchrÃ¶dinger-Poisson simulations. Physical Review B, 2017, 96, .	1.1	13
26051	Theory of Hydrogen Deposition and Evolution on Cu(111) Electrodes. Journal of the Electrochemical Society, 2017, 164, H691-H695.	1.3	6

#	Article	IF	Citations
26052	Identifying â€œOptimalâ€•Electrocatalysts: Impact of Operating Potential and Charge Transfer Model. ACS Catalysis, 2017, 7, 8641-8652.	5.5	21
26053	A light-driven modulation of electric conductance through the adsorption of azobenzene onto silicon-doped- and pyridine-like N3-vacancy graphene. Nanoscale, 2017, 9, 19017-19025.	2.8	5
26054	Magnetic structure of the mixed antiferromagnet <mml:math xmlns:mml="http://www.w3.org/1998/Math/MathML"><mml:mrow><mml:msub><mml:mi>NdMn</mml:mi><mml:mrow><mml:mn>0.8 mathvariant="normal">O</mml:mi><mml:mn>3</mml:mn></mml:msub></mml:mrow></mml:math>. Physical Review B, 2017, 96, .	1.1	7
26055	Role of defects in enhanced Fermi level pinning at interfaces between metals and transition metal dichalcogenides. Physical Review B, 2017, 96, .	1.1	26
26056	Evaluation of energy band offset of Si1â^'xSnxsemiconductors by numerical calculation using density functional theory. Japanese Journal of Applied Physics, 2017, 56, 04CR10.	0.8	3
26057	Effects of the Be ₂₂ W phase formation on hydrogen retention and blistering in mixed Be/W systems. Chinese Physics B, 2017, 26, 076801.	0.7	0
26058	Ferromagnetic Weyl semimetal phase in a tetragonal structure. Physical Review B, 2017, 96, .	1.1	48
26059	Quantum Capacitance of Hybrid Graphene Copper Nanoribbon. ECS Journal of Solid State Science and Technology, 2017, 6, M133-M138.	0.9	5
26060	First principles prediction of CH₄ reactivities with Co₃O₄ nanocatalysts of different morphologies. Physical Chemistry Chemical Physics, 2017, 19, 30874-30882.	1.3	12
26061	Investigation of chloride ion adsorption onto Ti₂C MXene monolayers by first-principles calculations. Journal of Materials Chemistry A, 2017, 5, 24720-24727.	5.2	57
26062	Tunable band structures in digital oxides with layered crystal habits. Physical Review B, 2017, 96, .	1.1	0
26063	Thermal conductivity changes across a structural phase transition: The case of high-pressure silica. Physical Review B, 2017, 96, .	1.1	13
26064	Theoretical analysis of the structural, electronic and optical properties of tetragonal Sr2GaSbO6. Chinese Journal of Physics, 2017, 55, 2476-2483.	2.0	19
26065	Comparative Kinetic Monte Carlo Study of Acetic Acid Decomposition to Surface Carbon Species and Undesirable Byproducts on Pd(100) and Pd/Au(100) from Density Functional Theory-Based Calculations. Journal of Physical Chemistry C, 2017, 121, 26733-26741.	1.5	11
26066	Mechanistic Study of Pdâ€“Cu Bimetallic Catalysts for Methanol Synthesis from CO₂ Hydrogenation. Journal of Physical Chemistry C, 2017, 121, 26287-26299.	1.5	60
26067	Tension-Tailored Electronic and Magnetic Switching of 2D Ti₂NO₂. Journal of Physical Chemistry C, 2017, 121, 25729-25735.	1.5	33
26068	Synthesis of Multilayer Silicene on Si(111)â^š3 Ã— â^š3-Ag. Journal of Physical Chemistry C, 2017, 121, 27182-27190.	1.5	34
26069	Dominant Kinetic Pathways of Graphene Growth in Chemical Vapor Deposition: The Role of Hydrogen. Journal of Physical Chemistry C, 2017, 121, 25949-25955.	1.5	61

#	Article	IF	Citations
26070	Ferroelectricity in Ruddlesdenâ€“Popper Chalcogenide Perovskites for Photovoltaic Application: The Role of Tolerance Factor. Journal of Physical Chemistry Letters, 2017, 8, 5834-5839.	2.1	35
26071	On-Surface Cyclization of ortho-Dihalotetracenes to Four- and Six-Membered Rings. Journal of the American Chemical Society, 2017, 139, 17617-17623.	6.6	68
26072	Elucidating electrolyte decomposition under electron-rich environments at the lithium-metal anode. Physical Chemistry Chemical Physics, 2017, 19, 30861-30873.	1.3	65
26073	A quantum chemical analysis of Zn and Sb doping and co-doping in SnO2. AIP Advances, 2017, 7, .	0.6	11
26074	Moving towards the magnetoelectric graphene transistor. Applied Physics Letters, 2017, 111, 182402.	1.5	19
26075	Strain-induced improper ferroelectricity in Ruddlesden-Popper perovskite halides. Physical Review B, 2017, 96, .	1.1	14
26076	Nonadiabatic Vibrational Damping of Molecular Adsorbates: Insights into Electronic Friction and the Role of Electronic Coherence. Physical Review Letters, 2017, 119, 176808.	2.9	18
26077	The surface structures growthâ€™s features caused by Ge adsorption on the Au(111) surface. JETP Letters, 2017, 106, 217-222.	0.4	11
26078	Adsorption of Water onto SrTiO₃ from Periodic MÃ¸llerâ€“Plesset Second-Order Perturbation Theory. Journal of Chemical Theory and Computation, 2017, 13, 6301-6307.	2.3	1
26079	I, N-Codoping Modification of TiO₂ for Enhanced Photoelectrochemical H₂O Splitting in Visible-Light Region. Journal of Physical Chemistry C, 2017, 121, 26202-26208.	1.5	11
26080	Cluster-Expansion Model for Complex Quinary Alloys: Application to Alnico Permanent Magnets. Physical Review Applied, 2017, 8, .	1.5	7
26081	Vibrational Properties of a Monolayer Silicene Sheet Studied by Tip-Enhanced Raman Spectroscopy. Physical Review Letters, 2017, 119, 196803.	2.9	74
26082	Catalytic effect of nickel phthalocyanine on hydrogen storage properties of magnesium hydride: Experimental and first-principles studies. International Journal of Hydrogen Energy, 2017, 42, 28485-28497.	3.8	12
26083	DFT Study of Mechanical Properties and Stability of Cubic Methylammonium Lead Halide Perovskites (CH₃NH₃PbX₃, X = I, Br, Cl). Journal of Physical Chemistry C, 2017, 121, 27059-27070.	1.5	73
26084	Hydride Transfer versus Deprotonation Kinetics in the Isobutaneâ€“Propene Alkylation Reaction: A Computational Study. ACS Catalysis, 2017, 7, 8613-8627.	5.5	49
26085	Hydrogenation of CO to Methanol on Ni(110) through Subsurface Hydrogen. Journal of the American Chemical Society, 2017, 139, 17582-17589.	6.6	35
26086	Retention of contaminants Cd and Hg adsorbed and intercalated in aluminosilicate clays: A first principles study. Journal of Chemical Physics, 2017, 147, 174704.	1.2	5
26087	Half metallicity and pressure-induced electronic structure of monolayer FeX2 (X = S, Se). Materials Research Express, 2017, 4, 116305.	0.8	6

#	Article	IF	Citations
26088	Reducing the stochasticity of crystal nucleation to enable subnanosecond memory writing. Science, 2017, 358, 1423-1427.	6.0	458
26089	Chemisorption of a hydrogen adatom on metal doped Î± -Zr (0Â0Â0Â1) surfaces in a vacuum and an implicit solvation environment. Nuclear Materials and Energy, 2017, 13, 28-34.	0.6	6
26090	Potential- and Rate-Determining Step for Oxygen Reduction on Pt(111). Journal of Physical Chemistry C, 2017, 121, 26785-26793.	1.5	56
26091	Copper-Based Intermetallic Electride Catalyst for Chemoselective Hydrogenation Reactions. Journal of the American Chemical Society, 2017, 139, 17089-17097.	6.6	90
26092	SU-8 based pyrolytic carbon for the electrochemical detection of dopamine. Journal of Materials Chemistry B, 2017, 5, 9033-9044.	2.9	30
26093	Order parameters for symmetry-breaking structural transitions: The tetragonal-monoclinic transition in <mml:math xmlns:mml="http://www.w3.org/1998/Math/MathML"><mml:msub><mml:mi>ZrO</mml:mi><mml:mn>2</mml:mn></mml:msub></m Physical Review B, 2017, 96, .	1.1	12
26094	Ferromagnetism in ferroelectric <mml:math xmlns:mml="http://www.w3.org/1998/Math/MathML"><mml:msub><mml:mi>BaTiO</mml:mi><mml:mn>3</mml:mn></mml:msub></m induced by vacancies: Sensitive dependence on charge state, origin of magnetism, and temperature range of existence. Physical Review B, 2017, 96, .	1.1	20
26095	Confinement and fermion doubling problem in Dirac-like Hamiltonians. Physical Review B, 2017, 96, .	1.1	16
26096	Electronic Stopping of Slow Protons in Oxides: Scaling Properties. Physical Review Letters, 2017, 119, 163401.	2.9	34
26097	Adsorption of gas molecules on a graphitic GaN sheet and its implications for molecule sensors. RSC Advances, 2017, 7, 51027-51035.	1.7	97
26098	Valence band splitting in bulk dilute bismides. Applied Physics Letters, 2017, 111, 182103.	1.5	7
26099	First principles study of the structural and magnetic properties of Fe(Rh, Pd) and Fe(Rh, Ni) alloys. Materials Today: Proceedings, 2017, 4, 4642-4646.	0.9	11
26100	DFT - based study of electronic structures and mechanical properties of LiTaO₃: ferroelectric and paraelectric phases. Philosophical Magazine, 2017, 97, 2469-2483.	0.7	6
26101	DFT study of Î²-d-glucose adsorption on single-walled carbon nanotubes decorated with platinum. A bonding analysis. Applied Surface Science, 2017, 423, 542-548.	3.1	7
26102	Unraveling the Magnesium-Ion Intercalation Mechanism in Vanadium Pentoxide in a Wet Organic Electrolyte by Structural Determination. Inorganic Chemistry, 2017, 56, 7668-7678.	1.9	63
26103	Density Functional Analysis of Fluorite-Structured (Ce, Zr)O₂/CeO₂ Interfaces. Journal of Physical Chemistry C, 2017, 121, 14678-14687.	1.5	12
26104	Tunable photoluminescence and room temperature ferromagnetism of In₂S₃:Dy³⁺,Tb³⁺ nanoparticles. Physical Chemistry Chemical Physics, 2017, 19, 16758-16764.	1.3	18
26105	Insight into thiophene hydrodesulfurization on clean and S-modified MoP(010): a periodic density functional theory study. Physical Chemistry Chemical Physics, 2017, 19, 17449-17460.	1.3	14

#	Article	IF	Citations
26106	Doping as a means to probe the potential dependence of dopamine adsorption on carbon-based surfaces: A first-principles study. Journal of Chemical Physics, 2017, 146, 234704.	1.2	13
26107	Water dissociation on multimetallic catalysts. Applied Catalysis B: Environmental, 2017, 218, 199-207.	10.8	14
26108	The structural and electronic properties of metal atoms adsorbed on graphene. Physica E: Low-Dimensional Systems and Nanostructures, 2017, 93, 265-270.	1.3	9
26109	Band structure modification of the thermoelectric Heusler-phase TiFe₂Sn via Mn substitution. Physical Chemistry Chemical Physics, 2017, 19, 18273-18278.	1.3	9
26110	Understanding the mechanism of enhanced charge separation and visible light photocatalytic activity of modified wurtzite ZnO with nanoclusters of ZnS and graphene oxide: from a hybrid density functional study. New Journal of Chemistry, 2017, 41, 8140-8155.	1.4	69
26111	Thermal transport in monolayer InSe. Journal of Physics Condensed Matter, 2017, 29, 335702.	0.7	37
26112	Ab initio studies on phonon, dielectric, and piezoelectric responses in perovskiteâ€like bismuth aluminate. International Journal of Applied Ceramic Technology, 2017, 14, 976-981.	1.1	4
26113	Temperature effects on the friction-like mode of graphite. Theoretical Chemistry Accounts, 2017, 136, 1.	0.5	0
26114	Substrate-mediated single-atom isolation: dispersion of Ni and La on Î³-graphyne. Theoretical Chemistry Accounts, 2017, 136, 1.	0.5	14
26115	Ferroelectric $$pi $$ Ï€ -stacks of molecules with the energy gaps in the sunlight range. Journal of Materials Science, 2017, 52, 4378-4388.	1.7	2
26116	Defect processes in Li2ZrO3: insights from atomistic modelling. Journal of Materials Science: Materials in Electronics, 2017, 28, 11789-11793.	1.1	7
26117	Properties of Alumina/Chromia Scales in N2-Containing Low Oxygen Activity Environment Investigated by Experiment and Theory. Oxidation of Metals, 2017, 87, 321-332.	1.0	10
26118	Cr3+ and Nb5+ co-doped Ti2Nb10O29 materials for high-performance lithium-ion storage. Journal of Power Sources, 2017, 360, 470-479.	4.0	85
26119	Strontium manganese vanadates from hydrothermal brines: Synthesis and structure of Sr2Mn2(V3O10)(VO4), Sr3Mn(V2O7)2, and Sr2Mn(VO4)2(OH). Journal of Solid State Chemistry, 2017, 255, 225-233.	1.4	10
26120	First-principles study of band structures of anthracene and tetracene under pressure. Materials Chemistry and Physics, 2017, 199, 173-178.	2.0	5
26121	Promising optical characteristics of zinc peroxide from first-principles investigation. Solid State Communications, 2017, 263, 6-9.	0.9	1
26122	Atomic Structure and Dynamics of Defects in 2D MoS₂ Bilayers. ACS Omega, 2017, 2, 3315-3324.	1.6	32
26123	Two prospective Li-based half-Heusler alloys for spintronic applications based on structural stability and spinâ€“orbit effect. Journal of Applied Physics, 2017, 122, 013901.	1.1	11

#	Article	IF	Citations
26124	Superconductivity and unexpected chemistry of germanium hydrides under pressure. Physical Review B, 2017, 95, .	1.1	16
26125	A DFT+U study of the structures and reactivities of polar CeO 2 (100) surfaces. Chinese Journal of Catalysis, 2017, 38, 1138-1147.	6.9	12
26126	Adsorption and migration behavior of Si atoms on the hydrogen-terminated diamond (001) surface: A first principles study. Applied Surface Science, 2017, 420, 542-549.	3.1	20
26127	Identification of surface species by vibrational normal mode analysis. A DFT study. Surface Science, 2017, 664, 233-240.	0.8	1
26128	Role of Lone Pair Cations in Ferroelectric Tungsten Bronzes. Chemistry of Materials, 2017, 29, 6414-6424.	3.2	20
26129	Globally-Optimized Local Pseudopotentials for (Orbital-Free) Density Functional Theory Simulations of Liquids and Solids. Journal of Chemical Theory and Computation, 2017, 13, 3684-3695.	2.3	18
26130	Surface evolution of a Ptâ€“Pdâ€“Au electrocatalyst for stable oxygen reduction. Nature Energy, 2017, 2, .	19.8	302
26131	Nonequilibrium phonon dynamics beyond the quasiequilibrium approach. Physical Review B, 2017, 96, .	1.1	12
26132	Magnetism and energetics for vacancy and helium impurity in Fe-9Cr alloy: A first-principles study. Computational Materials Science, 2017, 138, 267-276.	1.4	10
26133	Os/Si nanocomposites as excellent hydrogen evolution electrocatalysts with thermodynamically more favorable hydrogen adsorption free energy than platinum. Nano Energy, 2017, 39, 284-290.	8.2	40
26134	Strain effect on SnS2 nanoribbons: Robust direct bandgap of zigzag-edge and sensitive indirect semiconductor with armchair-edge states. Superlattices and Microstructures, 2017, 111, 480-486.	1.4	5
26135	High coverage water adsorption on CuO(011) surface. Physical Chemistry Chemical Physics, 2017, 19, 18652-18659.	1.3	19
26136	Theoretical study of the phononâ€“phonon scattering mechanism and the thermal conductive coefficients for energetic material. Philosophical Magazine, 2017, 97, 2575-2595.	0.7	8
26137	Enhanced superconductivity in SnSb under pressure: a first principles study. Journal of Physics Condensed Matter, 2017, 29, 405502.	0.7	4
26138	Electronic structure & yield strength prediction for dislocationâ€“Mo complex in the Î³ phase of nickel-based superalloys. Chinese Physics B, 2017, 26, 076104.	0.7	1
26139	Density functional theory investigation of carbon monoxide adsorption on the kaolinite (001) surface. Chinese Physics B, 2017, 26, 079101.	0.7	4
26140	Prediction of measurable two-dimensional plasmons in Li-intercalated graphene<mml:math xmlns:mml="http://www.w3.org/1998/Math/MathML"><mml:msub><mml:mi>LiC</mml:mi><mml:mn>2</mml:mn></mml:msub></mml Physical Review B, 2017, 95, .	1.1	20
26141	Electronic properties of superconducting FeS. Physical Review B, 2017, 95, .	1.1	10

#	Article	IF	Citations
26142	Ideal strength and ductility in metals from second- and third-order elastic constants. Physical Review B, 2017, 96, .	1.1	31
26143	Indium coverage of the Si(111)- <mml:math xmlns:mml="http://www.w3.org/1998/Math/MathML"><mml:mrow><mml:msqrt><mml:mn>7</mml:mn></mml:msqrt><mml:mo>Ã—</mml:mo> -In surface. Physical Review B, 2017, 96, .	1.1	15
26144	Ab initio assisted design of quinary dual-phase high-entropy alloys with transformation-induced plasticity. Acta Materialia, 2017, 136, 262-270.	3.8	275
26145	High Reactivity of the ZnO(0001) Polar Surface: The Role of Oxygen Adatoms. Journal of Physical Chemistry C, 2017, 121, 15711-15718.	1.5	11
26146	Understanding the Influence of [EMIM]Cl on the Suppression of the Hydrogen Evolution Reaction on Transition Metal Electrodes. Langmuir, 2017, 33, 9464-9471.	1.6	50
26147	Direct Observation of â€œPac-Manâ€•Coarsening. Nano Letters, 2017, 17, 4661-4664.	4.5	3
26148	Systematic First-Principles Study of Binary Metal Hydrides. ACS Combinatorial Science, 2017, 19, 513-523.	3.8	26
26149	Au cluster adsorption on perfect and defective MoS₂ monolayers: structural and electronic properties. Physical Chemistry Chemical Physics, 2017, 19, 20735-20748.	1.3	103
26150	Tuning band gaps and optical absorption of BiOCl through doping and strain: insight form DFT calculations. Physical Chemistry Chemical Physics, 2017, 19, 20968-20973.	1.3	34
26151	The impact of Ti and temperature on the stability of Nb₅Si₃ phases: a first-principles study. Science and Technology of Advanced Materials, 2017, 18, 467-479.	2.8	38
26152	Possible superconductivity in the electron-doped chromium pnictide LaOCrAs. Physical Review B, 2017, 95, .	1.1	10
26153	First-principles modeling of the Invar effect in <mml:math xmlns:mml="http://www.w3.org/1998/Math/MathML"><mml:mrow><mml:msub><mml:mi>Fe</mml:mi><mml:mn>65</mml:mn></mml:msub><mml:mn></mml:mn></mml:mrow></mml:math> by the spin-wave method. Physical Review B, 2017, 95, .	1.1	22
26154	Anomalously temperature-dependent thermal conductivity of monolayer GaN with large deviations from the traditional <mml:math xmlns:mml="http://www.w3.org/1998/Math/MathML"><mml:mn>1</mml:mn><mml:mo>/</mml:mo><mml:mi>T</mml:mi></mml:math> law. Physical Review B, 2017, 95, .	1.1	101
26155	Rh-MnO Interface Sites Formed by Atomic Layer Deposition Promote Syngas Conversion to Higher Oxygenates. ACS Catalysis, 2017, 7, 5746-5757.	5.5	66
26156	Electronic bandstructure and van der Waals coupling of ReSe2 revealed by high-resolution angle-resolved photoemission spectroscopy. Scientific Reports, 2017, 7, 5145.	1.6	32
26157	Enhancing the oxygen vacancy formation and migration in bulk chromium(<scp>iii</scp>) oxide by alkali metal doping: a change from isotropic to anisotropic oxygen diffusion. Journal of Materials Chemistry A, 2017, 5, 15613-15630.	5.2	36
26158	The origin of high electrocatalytic activity of hydrogen peroxide reduction reaction by a g-C₃N₄/HOPG sensor. Nanoscale, 2017, 9, 11170-11179.	2.8	20
26159	Electronic and protonic conduction in LaFeO₃. Journal of Materials Chemistry A, 2017, 5, 15367-15379.	5.2	48

#	Article	IF	Citations
26160	First-Principles Vibrational Electron Energy Loss Spectroscopy of <mml:math xmlns:mml="http://www.w3.org/1998/Math/MathML" display="inline"><mml:mi>Î²</mml:mi></mml:math> -Guanine. Physical Review Letters, 2017, 119, 027402.	2.9	19
26161	Critical Temperature for the Conversion from Wurtzite to Zincblende of the Optical Emission of InAs Nanowires. Journal of Physical Chemistry C, 2017, 121, 16650-16656.	1.5	2
26162	Carboxylic acid formation by hydroxyl insertion into acyl moieties on late transition metals. Catalysis Science and Technology, 2017, 7, 5365-5375.	2.1	2
26163	Exploring the driving forces behind the structural assembly of biphenylthiolates on Au(111). Journal of Chemical Physics, 2017, 147, 024706.	1.2	8
26164	Extended metastable Al solubility in cubic VAlN by metal-ion bombardment during pulsed magnetron sputtering: film stress vs subplantation. Journal of Applied Physics, 2017, 122, .	1.1	19
26165	Antiferromagnetism in the van der Waals layered spin-lozenge semiconductor <mml:math xmlns:mml="http://www.w3.org/1998/Math/MathML"><mml:msub><mml:mi mathvariant="bold">CrTe</mml:mi><mml:mn>3</mml:mn></mml:msub></mml:math>. Physical Review B, 2017, 95, .	1.1	44
26166	Electronic structure, lattice dynamics, and optical properties of a novel van der Waals semiconductor heterostructure: <mml:math xmlns:mml="http://www.w3.org/1998/Math/MathML"><mml:msub><mml:mi>InGaSe</mml:mi><mml:mn>2</mml:mn></mml:msub></ Physical Review B, 2017, 96, .	1.1	13
26167	Evolution of microstructure and radiative property of metal silicideâ€“glass hybrid coating for fibrous ZrO 2 ceramic during high temperature oxidizing atmosphere. Corrosion Science, 2017, 126, 78-93.	3.0	19
26168	Flexible Force Field Parameterization through Fitting on the Ab Initio-Derived Elastic Tensor. Journal of Chemical Theory and Computation, 2017, 13, 3722-3730.	2.3	13
26169	First-Principles Calculation of Charge Transfer at the Siliconâ€“Organic Interface. Journal of Physical Chemistry C, 2017, 121, 15529-15537.	1.5	10
26170	Structural, Vibrational, and Elastic Properties of Yttrium Orthoaluminate Nanoperovskite at High Pressures. Journal of Physical Chemistry C, 2017, 121, 15353-15367.	1.5	13
26171	Electron-phonon superconductivity in the filled skutterudites <mml:math xmlns:mml="http://www.w3.org/1998/Math/MathML"><mml:mrow><mml:msub><mml:mi>LaRu</mml:mi><mml:mn>4</mml:mn></ mathvariant="normal">P</mml:mi><mml:mn>12</mml:mn></mml:msub></mml:mrow><mml:mo>,</mml:mo><mml:mo>Â</mml:mo> . and <mml:math xmlns:mml="http://www.w3.or. Physical Review B, 2017, 95, .	1.1	14
26172	Investigation on formation mechanism of T1 precipitate in an Al-Cu-Li alloy. Journal of Alloys and Compounds, 2017, 723, 661-666.	2.8	72
26173	Structure, electronic and mechanical properties of Ga 1â^'x B x P alloys. Physica B: Condensed Matter, 2017, 521, 295-304.	1.3	2
26174	Formation of resonant bonding during growth of ultrathin GeTe films. NPG Asia Materials, 2017, 9, e396-e396.	3.8	25
26175	Ab initiodensity functional theory calculation of La₅Ti₂Cu_{1â^'x}Ag_xS₅O₇solid solution semiconductor photocatalysts for water splitting. Journal Physics D: Applied Physics, 2017, Identification	1.3	3
26176	of hydrogen defects in<mml:math xmlns:mml="http://www.w3.org/1998/Math/MathML"><mml:mrow><mml:mi>Î±</mml:mi><mml:mtext>â^'</mml:mtext><mml:mi mathvariant="normal">A</mml:mi><mml:msub><mml:mi mathvariant="normal">I</mml:mi><mml:mn>2</mml:mn></mml:msub><mml:msub><mml:mi mathvariant="normal">O</mml:mi><mml:mn>3</mml:mn></mml:msub></mml:mrow></mml:math>by first-principles local vibration mode calculations. Physical Review B, 2017, 95, .	1.1	12
26177	Theoretical search for possible Au-Si crystal structures using a genetic algorithm. Physical Review B, 2017, 95, .	1.1	9

#	Article	IF	Citations
26178	First-principles study on the adsorption energy of Fe on the N-doped CNT bus-bar. Chinese Journal of Physics, 2017, 55, 1162-1169.	2.0	0
26179	Comparative study on structural, elastic, dynamical, and thermodynamic properties of Weyl semimetals MX (M = Ta or Nb; X = As or P). Solid State Communications, 2017, 263, 10-18.	0.9	14
26180	Density Functional Theory Study of Interface Interactions in Hydroxyapatite/Rutile Composites for Biomedical Applications. Journal of Physical Chemistry C, 2017, 121, 15687-15695.	1.5	16
26181	First-Principles Calculation of Pt Surface Energies in an Electrochemical Environment: Thermodynamic Driving Forces for Surface Faceting and Nanoparticle Reconstruction. Langmuir, 2017, 33, 7043-7052.	1.6	31
26182	Dramatic band gap reduction incurred by dopant coordination rearrangement in Co-doped nanocrystals of CeO2. Scientific Reports, 2017, 7, 4715.	1.6	25
26183	Origin of long lifetime of band-edge charge carriers in organicâ€“inorganic lead iodide perovskites. Proceedings of the National Academy of Sciences of the United States of America, 2017, 114, 7519-7524.	3.3	137
26184	Distinguishing attosecond electronâ€“electron scattering and screening in transition metals. Proceedings of the National Academy of Sciences of the United States of America, 2017, 114, E5300-E5307.	3.3	55
26185	Contribution to the study of structural and elastic properties of wÃ¼stite under pressure up to 140ÂGPa by pseudopotential calculations. Phase Transitions, 2017, , 1-12.	0.6	0
26186	Hydrogenation and hydrogen intercalation of hexagonal boron nitride on Ni(1â€‰1â€‰1): reactivity and electronic structure. 2D Materials, 2017, 4, 035026.	2.0	28
26187	Phase-field study of ripening and rearrangement of precipitates under chemomechanical coupling. Physical Review B, 2017, 95, .	1.1	14
26188	A potential descriptor for the CO2 hydrogenation to CH4 over Al2O3 supported Ni and Ni-based alloy catalysts. Applied Catalysis B: Environmental, 2017, 218, 525-537.	10.8	83
26189	Evaluation of hydrogen bond networks in cellulose Iˆ² and II crystals using density functional theory and Carâ€“Parrinello molecular dynamics. Carbohydrate Research, 2017, 449, 103-113.	1.1	24
26190	Hybrid organic-inorganic lead and tin halide perovskites with saturated heterocyclic cations (CH2)nNH2+ and (CH2)nOH+, (n = 2â€“6): Ab initio study. Computational Materials Science, 2017, 138, 99-104.	1.4	5
26191	Quasiparticle and optical properties of strained stanene and stanane. Scientific Reports, 2017, 7, 3912.	1.6	40
26192	Structures, stabilities and work functions of alkali-metal-adsorbed boron Î± 1-sheets. Chemical Research in Chinese Universities, 2017, 33, 631-637.	1.3	8
26193	Molecular adsorption properties of CO and H 2 O on Au-, Cu-, and Au x Cu y -doped MoS 2 monolayer. Applied Surface Science, 2017, 425, 246-253.	3.1	21
26194	Theoretical investigation of lithium adsorption, diffusion and coverage on MX 2 (M = Mo, W; X = O, S,) Tj ETQq0 0 0 rgBT /Overlock 10 T	3.1	55
26195	Density functional theory study of a new Bi-based (K1.00)(Ba1.00)3(Bi0.89Na0.11)4O12 double perovskite superconductor. Computational Materials Science, 2017, 138, 160-165.	1.4	45

#	Article	IF	Citations
26196	Effect of interstitial carbon distribution and nickel substitution on the tetragonality of martensite: A first-principles study. Intermetallics, 2017, 89, 92-99.	1.8	30
26197	Two-dimensional metallicity and ferromagnetic ordering in monoatomic-thick Ce layer on Si(111). Materials Chemistry and Physics, 2017, 199, 225-229.	2.0	1
26198	TiS₃ Magnesium Battery Material: Atomic-Scale Study of Maximum Capacity and Structural Behavior. Journal of Physical Chemistry C, 2017, 121, 15509-15515.	1.5	39
26199	Invariant wide bandgaps in honeycomb monolayer and single-walled nanotubes of IIBâ€“VI semiconductors. Nanotechnology, 2017, 28, 355201.	1.3	2
26200	Absence of magnetism in the superconductor <mml:math xmlns:mml="http://www.w3.org/1998/Math/MathML"><mml:mrow><mml:mi mathvariant="normal">B</mml:mi><mml:msub><mml:mi mathvariant="normal">a</mml:mi><mml:mn>2</mml:mn></mml:msub><mml:mi mathvariant="normal">T</mml:mi><mml:msub><mml:mi mathvariant="normal">i</mml:mi><mml:mn>2</mml:mn></mml:msub><mml:mi mathvariant="normal">P	1.1	6
26201	First-principles based analysis of the piezoelectric response in <mml:math xmlns:mml="http://www.w3.org/1998/Math/MathML" altimg="si1.gif" overflow="scroll"><mml:mrow><mml:mi>Î±</mml:mi></mml:mrow></mml:math>-LiIO3. Computational Materials Science, 2017, 138, 199-203.	1.4	5
26202	Effects of alloying elements on the structural, elastic and thermodynamic properties of Co3Ta compounds from first-principlesÂcalculations. Journal of Alloys and Compounds, 2017, 726, 490-497.	2.8	5
26203	Automatic numerical evaluation of vacancy-mediated transport for arbitrary crystals: Onsager coefficients in the dilute limit using a Green function approach. Philosophical Magazine, 2017, 97, 2514-2563.	0.7	38
26204	Lattice thermal conductivity evaluated using elastic properties. Physical Review B, 2017, 95, .	1.1	114
26205	Ab initio lattice thermal conductivity of MgO from a complete solution of the linearized Boltzmann transport equation. Physical Review B, 2017, 95, .	1.1	24
26206	Bonding and electronics of the MoTe2/Ge interface under strain. Physical Review B, 2017, 95, .	1.1	11
26207	First-principles study on <mml:math xmlns:mml="http://www.w3.org/1998/Math/MathML"><mml:mrow><mml:msub><mml:mi>Ni</mml:mi><mml:mn>3</mml:mn></mml:msub></mml:mrow></mml:math> antiphase boundary with Ti and Hf impurities. Physical Review B, 2017, 95, .	1.1	22
26208	Accuracy of <mml:math xmlns:mml="http://www.w3.org/1998/Math/MathML"><mml:mrow><mml:mi>G</mml:mi><mml:mi>W</mml:mi></mml:mrow></mml:math> for calculating defect energy levels in solids. Physical Review B, 2017, 96, .	1.1	27
26209	Ab initio prediction of the high-pressure phase diagram of BaBiO3. Physical Review B, 2017, 96, .	1.1	8
26210	Comparison of the conversion of ethylene to ethylidyne on Pd-Au(100): A density functional study. Applied Surface Science, 2017, 423, 762-770.	3.1	8
26211	Adsorption behavior of 2, 3, 7, 8-tetrachlorodibenzo-p-dioxin on pristine and doped black phosphorene: A DFT study. Chemosphere, 2017, 185, 509-517.	4.2	21
26212	Se-Ni(OH)2-shelled vertically oriented NiSe nanowires as a superior electrocatalyst toward urea oxidation reaction of fuel cells. Electrochimica Acta, 2017, 248, 243-249.	2.6	77
26213	Fe Oxides on Ag Surfaces: Structure and Reactivity. Topics in Catalysis, 2017, 60, 492-502.	1.3	10

#	Article	IF	Citations
26214	Two-dimensional square transition metal dichalcogenides with lateral heterostructures. Nano Research, 2017, 10, 3909-3919.	5.8	17
26215	Fates of Hydrogen During Alumina Growth Below Yttria Nodules in FeCrAl(RE) at Low Partial Pressures of Water. Electrocatalysis, 2017, 8, 565-576.	1.5	6
26216	Surface structures of L10-MnGa (001) by scanning tunneling microscopy and first-principles theory. Applied Surface Science, 2017, 422, 985-989.	3.1	9
26217	Crystal structure of and displacive phase transition in tungsten nitride WN. Journal of Alloys and Compounds, 2017, 722, 517-524.	2.8	17
26218	Synergistically optimizing thermoelectric transport properties of n-type PbTe via Se and Sn co-alloying. Journal of Alloys and Compounds, 2017, 724, 208-221.	2.8	59
26219	Rare earth interstitial-complexes in Ge: Hybrid density functional studies. Nuclear Instruments & Methods in Physics Research B, 2017, 409, 9-13.	0.6	4
26220	Rare earth substitutional impurities in germanium: A hybrid density functional theory study. Nuclear Instruments & Methods in Physics Research B, 2017, 409, 31-35.	0.6	3
26221	Layer-controlled band alignment, work function and optical properties of few-layer GeSe. Physica B: Condensed Matter, 2017, 519, 90-94.	1.3	27
26222	Hydrogen scattering from a cesiated surface model. Surface Science, 2017, 664, 194-200.	0.8	20
26223	Graphenylene Monolayers Doped with Alkali or Alkaline Earth Metals: Promising Materials for Clean Energy Storage. Journal of Physical Chemistry C, 2017, 121, 14393-14400.	1.5	65
26224	Effects of Embedded Dipole Layers on Electrostatic Properties of Alkanethiolate Self-Assembled Monolayers. Journal of Physical Chemistry C, 2017, 121, 15815-15830.	1.5	45
26225	Manipulating the Bulk Band Structure of Artificially Constructed van der Waals Chalcogenide Heterostructures. ACS Applied Materials & Interfaces, 2017, 9, 23918-23925.	4.0	17
26226	High Tolerance to Iron Contamination in Lead Halide Perovskite Solar Cells. ACS Nano, 2017, 11, 7101-7109.	7.3	90
26227	Exsolution trends and co-segregation aspects of self-grown catalyst nanoparticles in perovskites. Nature Communications, 2017, 8, 15967.	5.8	305
26228	Prediction of metallic nanotube reactivity for H2O activation. Physical Chemistry Chemical Physics, 2017, 19, 19188-19195.	1.3	1
26229	All-solid-state disordered LiTiS2pseudocapacitor. Journal of Materials Chemistry A, 2017, 5, 15661-15668.	5.2	13
26230	Thermoelectric properties of ZrNiSn Half-Heusler system: An ab-initio study. AIP Conference Proceedings, 2017, , .	0.3	0
26231	2D halide perovskite-based van der Waals heterostructures: contact evaluation and performance modulation. 2D Materials, 2017, 4, 035009.	2.0	23

#	Article	IF	Citations
26232	A DFT+U investigation on methylamine decomposition catalyzed by Pt4 cluster supported on oxygen defective rutile(110) TiO2. Chemical Research in Chinese Universities, 2017, 33, 406-414.	1.3	2
26233	A Density Functional +UAssessment of Oxygen Evolution Reaction Mechanisms on Î²-NiOOH. ACS Catalysis, 2017, 7, 5329-5339.	5.5	110
26234	Theoretical investigation on radiation tolerance of ${{oldsymbol{M}}}_{{oldsymbol{n}}+1}{{oldsymbol{AX}}}_{{oldsymbol{n}}}$ phases. Chinese Physics B, 2017, 26, 060703.	0.7	1
26235	Structural transformations on an oxidized Ag(111) surface. JETP Letters, 2017, 105, 292-296.	0.4	6
26236	Effects of Cr on H and He trapping and vacancy complexes in V in a fusion environment: a first-principles study. European Physical Journal B, 2017, 90, 1.	0.6	2
26237	DFT study of the effect of BN pair doping on the electronic and optical properties of graphyne nanosheets. Journal of Materials Science, 2017, 52, 10294-10307.	1.7	21
26238	The Third-Order Elastic Moduli and Debye Temperature of SrFe2As2 and BaFe2As2: a First-Principles Study. Journal of Superconductivity and Novel Magnetism, 2017, 30, 1749-1756.	0.8	10
26239	Effect of Titanium Addition on the Elemental Partitioning Behavior of Silicon in Ni-19 At. Pct Al-xSi-yTi Alloys. Metallurgical and Materials Transactions A: Physical Metallurgy and Materials Science, 2017, 48, 3920-3926.	1.1	1
26240	The Preferable F2dd Phase for Ca(BH4)2 Crystal Under Hydrostatic Pressures. Journal of Electronic Materials, 2017, 46, 3479-3483.	1.0	1
26241	Can uranyl complexes encapsulate to carbon nanotubes? A periodic DFT study. Journal of Chemical Sciences, 2017, 129, 783-790.	0.7	2
26242	First-principles calculations of stacking fault energies in Mg-Y, Mg-Al and Mg-Zn alloys and implications for <mml:math xmlns:mml="http://www.w3.org/1998/Math/MathML" altimg="si1.gif" overflow="scroll"><mml:mrow><mml:mo>â€ˆ</mml:mo><mml:mi mathvariant="bold">c</mml:mi><mml:mo>+</mml:mo><mml:mi mathvariant="bold">a</mml:mi><mml:mo>â€‰</mml:mo></mml:mrow></mml:math> activity. Acta Materialia, 2017, 136, 249-261.	3.8	84
26243	Design of lithium selective crown ethers: Synthesis, extraction and theoretical binding studies. Chemical Engineering Journal, 2017, 326, 921-933.	6.6	78
26244	Mechanism of photoluminescence in intrinsically disordered CaZrO3 crystals: First principles modeling of the excited electronic states. Journal of Alloys and Compounds, 2017, 722, 981-995.	2.8	16
26245	Enhanced Nonenzymatic Glucose-Sensing Properties of Electrodeposited NiCo₂O₄â€“Pd Nanosheets: Experimental and DFT Investigations. ACS Applied Materials & Interfaces, 2017, 9, 23894-23903.	4.0	97
26246	The pyrite-type high-pressure form of FeOOH. Nature, 2017, 547, 205-208.	13.7	123
26247	Phonon-induced topological transition to a type-II Weyl semimetal. Physical Review B, 2017, 95, .	1.1	18
26248	Origin of Structural Modulations in Ultrathin Fe Films on Cu(001). Physical Review Letters, 2017, 118, 236101.	2.9	5
26249	Dielectric Anisotropy of the <mml:math xmlns:mml="http://www.w3.org/1998/Math/MathML" display="inline"><mml:mrow><mml:mi>GaP</mml:mi><mml:mo>/</mml:mo><mml:mi>Si</mml:mi><mml:mo stretchy="false">(</mml:mo><mml:mn>001</mml:mn><mml:mo> Tj ETQq1 1 0.784314 rgBT /Overlock 10 Tf 50 52 Td (stretchy="false" Physical Review Letters, 2017, 118, 237403.	7.5	11

#	Article	IF	Citations
26250	First principle calculations of iron and iron-boron transition levels in Si1â^'x Ge x alloy. European Physical Journal B, 2017, 90, 1.	0.6	2
26251	Investigation on the formation of lonsdaleite from graphite. Journal of Experimental and Theoretical Physics, 2017, 124, 265-274.	0.2	23
26252	Density Functional Theory Study of the Stress Impact on Formation Enthalpy of Intrinsic Point Defect around Dopant Atom in Ge Crystal. ECS Journal of Solid State Science and Technology, 2017, 6, P383-P398.	0.9	0
26253	Thermomechanical Stability of Carbyne-Based Nanodevices. Nanoscale Research Letters, 2017, 12, 327.	3.1	20
26254	Structure and Electronic Properties of Transition Metal Doped Kaolinite Nanoclay. Nanoscale Research Letters, 2017, 12, 411.	3.1	18
26255	Ferromagnetism and Halfâ€Metallicity in Atomically Thin Holey Nitrogenated Graphene Based Systems. ChemPhysChem, 2017, 18, 2336-2346.	1.0	12
26256	First-principles examination of low tolerance factor perovskites. International Journal of Quantum Chemistry, 2017, 117, e25420.	1.0	6
26257	First-Principles Study of Structural, Electronic, Mechanical, Thermal, and Phonon Properties of III-Phosphides (BP, AlP, GaP, and InP). Journal of Electronic Materials, 2017, 46, 6214-6223.	1.0	13
26258	Active {010} facet-exposed Cu2MoS4 nanotube as high-efficiency photocatalyst. Nano Research, 2017, 10, 3817-3825.	5.8	22
26259	A first principles investigation of the oxygen adsorption on Zr(0001) surface using cluster expansions. Applied Surface Science, 2017, 423, 1035-1044.	3.1	17
26260	Stability of the Al/TiB 2 interface and doping effects of Mg/Si. Applied Surface Science, 2017, 425, 639-645.	3.1	42
26261	Density functional study on H2S adsorption on Pd(111) and Pd/Î³-Al2O3(110) surfaces. Applied Surface Science, 2017, 423, 592-601.	3.1	13
26262	First-principles investigation on crystal structure and physical properties of HfB4. Journal of Alloys and Compounds, 2017, 723, 802-810.	2.8	21
26263	Electrochemical properties and lithium ion diffusion in Li4FeSbO6 studied by first principle. Journal of Solid State Chemistry, 2017, 254, 132-137.	1.4	5
26264	Impact of isovalent doping on the formation of the C i O i (Si I) n defects in silicon. Solid State Communications, 2017, 263, 19-22.	0.9	9
26265	Methylbenzenes on graphene. Surface Science, 2017, 664, 162-167.	0.8	15
26266	Conformational effects on hydrazine and OH coadsorption on Ni(111): A first-principles investigation. Surface Science, 2017, 664, 185-193.	0.8	16
26267	Development of Theoretical Descriptors for Cytotoxicity Evaluation of Metallic Nanoparticles. Chemical Research in Toxicology, 2017, 30, 1549-1555.	1.7	14

#	Article	IF	Citations
26268	Defect Interactions in the CeO₂â€“ZrO₂â€“Y₂O₃ Solid Solution. Journal of Physical Chemistry C, 2017, 121, 15078-15084.	1.5	17
26269	A Discovery of Strong Metalâ€“Support Bonding in Nanoengineered Auâ€“Fe₃O₄ Dumbbell-like Nanoparticles by in Situ Transmission Electron Microscopy. Nano Letters, 2017, 17, 4576-4582.	4.5	27
26270	Understanding the Unusual Response to High Pressure in KBe2BO3F2. Scientific Reports, 2017, 7, 4027.	1.6	2
26271	The formation mechanism of the initial Câ€“C chain in ethanol synthesis on Î³-AlOOH(100). Physical Chemistry Chemical Physics, 2017, 19, 19300-19307.	1.3	14
26272	Influence of transition metal doping on the electronic and optical properties of ReS₂and ReSe₂monolayers. Physical Chemistry Chemical Physics, 2017, 19, 19050-19057.	1.3	46
26273	The transition metal surface dependent methane decomposition in graphene chemical vapor deposition growth. Nanoscale, 2017, 9, 11584-11589.	2.8	76
26274	MD simulation of steady shock-wave fronts with phase transition in single-crystal iron. AIP Conference Proceedings, 2017, , .	0.3	12
26275	Dibromobianthryl ordering and polymerization on Ag(100). Journal of Chemical Physics, 2017, 146, .	1.2	2
26276	Charge ordering and magnetic frustration in CsFe₂F₆. Journal of Physics Condensed Matter, 2017, 29, 315501.	0.7	3
26277	Influences of pressure on methyl group, elasticity, sound velocity and sensitivity of solid nitromethane. European Physical Journal B, 2017, 90, 1.	0.6	14
26278	Vibrational and dielectric properties and ideal strength of Si2N2O ceramic from first principles. Ceramics International, 2017, 43, 10006-10012.	2.3	9
26279	Electronic and gap properties of lead-free perfect and mixed hybrid halide perovskites: An ab-initio study. Computational Materials Science, 2017, 138, 92-98.	1.4	24
26280	Mechanism of dicarbonyl(2,4-pentanedionato)iridium(I) decomposition on iron surface and in gas phase: Complex experimental and theoretical study. Journal of Molecular Structure, 2017, 1146, 677-683.	1.8	4
26281	Experimental and Theoretical Insights into Influence of Hydrogen and Nitrogen Plasma on the Water Splitting Performance of ALD Grown TiO₂ Thin Films. Journal of Physical Chemistry C, 2017, 121, 15538-15548.	1.5	13
26282	Periodic Arrays of Phosphorene Nanopores as Antidot Lattices with Tunable Properties. ACS Nano, 2017, 11, 7494-7507.	7.3	42
26283	Manipulating the mechanical properties of <mml:math xmlns:mml="http://www.w3.org/1998/Math/MathML"><mml:mrow><mml:msub><mml:mi>Ti</mml:mi><mml:mn>2</mml:mn></mml:msub><mml:mi mathvariant="normal">C</mml:mi></mml:mrow></mml:math> MXene: Effect of substitutional doping. Physical Review B, 2017, 95, .	1.1	65
26284	Highly responsive ground state of <mml:math xmlns:mml="http://www.w3.org/1998/Math/MathML"><mml:msub><mml:mi>PbTaSe</mml:mi><mml:mn>2</mml:mn></mml:msub></mml:math> : Structural phase transition and evolution of superconductivity under pressure. Physical Review B, 2017, 95, .	1.1	13
26285	DFT and Monte Carlo study of the W(001) surface reconstruction. European Physical Journal B, 2017, 90, 1.	0.6	2

#	Article	IF	Citations
26286	Half Metallic Behavior in H-Terminated Zigzag BC₂N Nanoribbons. Applied Mechanics and Materials, 2017, 864, 30-35.	0.2	0
26287	Tunable electronic and magnetic properties from structure phase transition of layered vanadium diselenide. Journal Wuhan University of Technology, Materials Science Edition, 2017, 32, 574-578.	0.4	9
26288	An ab initio investigation of phosphorene/hexagonal boron nitride heterostructures with defects for high performance photovoltaic applications. Applied Surface Science, 2017, 423, 1003-1011.	3.1	9
26289	Phonon and phonon-related properties of MgSiN 2 and MgGeN 2 ceramics: First principles studies. Ceramics International, 2017, 43, S444-S448.	2.3	11
26290	Elastic, electronic and optical properties of anatase TiO2 under pressure: A DFT approach. Chinese Journal of Physics, 2017, 55, 1252-1263.	2.0	15
26291	Hydroxyurea electrooxidation at gold electrodes. In situ infrared spectroelectrochemical and DFT characterization of adsorbed intermediates. Electrochimica Acta, 2017, 246, 951-962.	2.6	8
26292	Enhanced catalytic behavior of Ni alloys in steam methane reforming. Journal of Power Sources, 2017, 359, 450-457.	4.0	35
26293	Ï^-Graphene: A New Metallic Allotrope of Planar Carbon with Potential Applications as Anode Materials for Lithium-Ion Batteries. Journal of Physical Chemistry Letters, 2017, 8, 3234-3241.	2.1	205
26294	Structure- and Coverage-Sensitive Mechanism of NO Reduction on Platinum Electrodes. ACS Catalysis, 2017, 7, 4660-4667.	5.5	118
26295	Layer-dependent semiconductor-metal transition of SnO/Si(001) heterostructure and device application. Scientific Reports, 2017, 7, 2570.	1.6	5
26296	Stochastic surface walking reaction sampling for resolving heterogeneous catalytic reaction network: A revisit to the mechanism of water-gas shift reaction on Cu. Journal of Chemical Physics, 2017, 147, 152706.	1.2	22
26297	Structural, elastic, and vibrational properties of phase H: A first-principles simulation. Chinese Physics B, 2017, 26, 067401.	0.7	5
26298	Localization of Electronic States in III-V Semiconductor Alloys: A Comparative Study. Physical Review Applied, 2017, 7, .	1.5	22
26299	Electronic and optical properties of the monolayer group-IV monochalcogenides <mml:math xmlns:mml="http://www.w3.org/1998/Math/MathML"><mml:mrow><mml:mi>M</mml:mi><mml:mi>X</mml:mi></mml:mrow></mml:m		

#	Article	IF	Citations
26304	Crystal structure and electronic spectrum of InGaSe2. Inorganic Materials, 2017, 53, 670-674.	0.2	1
26305	Structural, electrical and optical properties of $$hbox {InGaZnO}_{4}$$ InGaZnO 4 and $$hbox {In}_{29}hbox {Sn}_{3}hbox {O}_{48}$$. Journal of Computational Electronics, 2017, 16, 280-286.	1.3	1
26306	Suppression of Defects and Deep Levels Using Isoelectronic Tungsten Substitution in Monolayer MoSe₂. Advanced Functional Materials, 2017, 27, 1603850.	7.8	84
26307	Phosphorene as a Polysulfide Immobilizer and Catalyst in Highâ€Performance Lithiumâ€“Sulfur Batteries. Advanced Materials, 2017, 29, 1602734.	11.1	289
26308	The adsorption of CaOH⁺on (001) basal and (010) edge surface of Na-montmorillonite: a DFT study. Surface and Interface Analysis, 2017, 49, 267-277.	0.8	49
26309	First-principles investigation of half-metallicity of Mn2Co1â^'xCrxAl. Computational Materials Science, 2017, 127, 15-21.	1.4	2
26310	Structural, electronic properties of microscale (NH4)2V3O8 fabricated using a novel preparation method. Journal of Physics and Chemistry of Solids, 2017, 101, 58-64.	1.9	6
26311	First-principles study of Frenkel pair recombination in tungsten. Nuclear Instruments & Methods in Physics Research B, 2017, 393, 190-194.	0.6	8
26312	Point defect properties of ternary fcc Fe-Cr-Ni alloys. Nuclear Instruments & Methods in Physics Research B, 2017, 393, 126-129.	0.6	6
26313	Identification of the catalytically active component of Cuâ€“Zrâ€“O catalyst for the hydrogenation of levulinic acid to Î³-valerolactone. Green Chemistry, 2017, 19, 225-236.	4.6	68
26314	Adsorption of alkali and alkaline earth metal atoms and dimers on monolayer germanium carbide. Philosophical Magazine, 2017, 97, 155-167.	0.7	14
26315	Brittle Fracture of 2D MoSe₂. Advanced Materials, 2017, 29, 1604201.	11.1	138
26316	A computational high-throughput search for new ternary superalloys. Acta Materialia, 2017, 122, 438-447.	3.8	70
26317	First principles study of adsorption and oxidation mechanism of elemental mercury by HCl over MoS 2 (1 0 0) surface. Chemical Engineering Journal, 2017, 308, 1225-1232.	6.6	31
26318	Density functional calculations of carbon substituting for Zr in barium zirconate. Journal of Crystal Growth, 2017, 468, 728-731.	0.7	1
26319	Theoretical study of Sn adsorbed on the Au(1 1 1) surface. Computational Materials Science, 2017, 127, 48-59.	1.4	11
26320	Effect of edge passivation on the mechanical properties of phosphorene nanoribbons. Extreme Mechanics Letters, 2017, 14, 2-9.	2.0	10
26321	Selectivity of Pd-Functionalized PtNi(111) Surface: cis -3-Hexenoic Acid Adsorption. Catalysis Letters, 2017, 147, 58-61.	1.4	0

#	Article	IF	Citations
26322	Electronic and Ferromagnetic Properties of 3d(V)-Doped (BaS) Barium Sulfide. Journal of Superconductivity and Novel Magnetism, 2017, 30, 917-923.	0.8	25
26323	Flexible highly-effective energy harvester via crystallographic and computational control of nanointerfacial morphotropic piezoelectric thin film. Nano Research, 2017, 10, 437-455.	5.8	86
26324	Strength and ductility of niobium alloys with nonmetallic elements: A first-principles study. Materials Letters, 2017, 189, 310-312.	1.3	21
26325	Growth, structure, optical and thermal properties of three new organicâ€“inorganic hybrid crystals: (C2H7N4S)3BiCl6Â·H2O, (C2H7N4S)2BiBr5, and (C2H5N4S)2BiI5. Polyhedron, 2017, 127, 478-488.	1.0	13
26326	A systematic study of ²⁵Mg NMR in paramagnetic transition metal oxides: applications to Mg-ion battery materials. Physical Chemistry Chemical Physics, 2017, 19, 613-625.	1.3	50
26327	Coincidence Lattices and Interlayer Twist in van der Waals Heterostructures: Application of the Coincidence Lattice Method on $$hbox {hBN/MoSe}_2$$ hBN/MoSe 2 Heterobilayer Systems. Journal of Electronic Materials, 2017, 46, 3910-3916.	1.0	9
26328	Tunable Rashba spin splitting in quantum-spin Hall-insulator AsF bilayers. Nano Research, 2017, 10, 491-502.	5.8	16
26329	Exploring the catalytic activity of pristine T6[100] surface for oxygen reduction reaction: A first-principles study. Applied Surface Science, 2017, 418, 56-63.	3.1	5
26330	The sensitive detection of formaldehyde in aqueous media using zirconium-based metal organic frameworks. Sensors and Actuators B: Chemical, 2017, 241, 938-948.	4.0	96
26331	Theoretical insights into the energetics and electronic properties of MPt12 (M = Fe, Co, Ni, Cu, and Pd) nanoparticles supported by N-doped defective graphene. Applied Surface Science, 2017, 397, 199-205.	3.1	25
26332	Product tunable behavior of carbon nanotubes-supported Niâ€“Fe catalysts for guaiacol hydrodeoxygenation. Applied Catalysis A: General, 2017, 529, 20-31.	2.2	153
26333	Ab-initio investigation of adsorption of CO and CO 2 molecules on graphene: Role of intrinsic defects on gas sensing. Applied Surface Science, 2017, 394, 219-230.	3.1	87
26334	Many-body dispersion effects on the binding of TCNQ and F4-TCNQ with graphene. Carbon, 2017, 111, 513-518.	5.4	14
26335	Methane formation from successive hydrogenation of C over stepped Ni and Ni3Fe surfaces: Effect of surface composition. International Journal of Hydrogen Energy, 2017, 42, 914-927.	3.8	9
26336	Tuning the band gap and optical spectra of silicon-doped graphene: Many-body effects and excitonic states. Journal of Alloys and Compounds, 2017, 693, 1185-1196.	2.8	119
26337	Effects of alloying elements concentrations and temperatures on the stacking fault energies of Co-based alloys by computational thermodynamic approach and first-principles calculations. Journal of Alloys and Compounds, 2017, 694, 1265-1279.	2.8	56
26338	DFT and spectroelectrochemical study of cyanate adsorption on gold single crystal electrodes in neutral medium. Journal of Electroanalytical Chemistry, 2017, 793, 147-156.	1.9	9
26339	Effect of Ti/Cr additive on helium diffusion and segregation in dilute vanadium alloys. Nuclear Instruments & Methods in Physics Research B, 2017, 393, 130-134.	0.6	10

#	Article	IF	Citations
26340	First-principles study of nanotubes within the tetragonal, hexagonal and dodecagonal cycle structures. Physica E: Low-Dimensional Systems and Nanostructures, 2017, 86, 129-135.	1.3	3
26341	Bubble growth from clustered hydrogen and helium atoms in tungsten under a fusion environment. Nuclear Fusion, 2017, 57, 016006.	1.6	23
26342	Trilayer TMDC Heterostructures for MOSFETs and Nanobiosensors. Journal of Electronic Materials, 2017, 46, 1248-1260.	1.0	20
26343	Adjusting band gap and charge transfer of organometallic complex adsorbed on MoS₂monolayer using vertical electric-field: a first-principles investigation. Journal of Physics Condensed Matter, 2017, 29, 015003.	0.7	2
26344	CO-induced Pd segregation and the effect of subsurface Pd on CO adsorption on CuPd surfaces. Journal of Physics Condensed Matter, 2017, 29, 025005.	0.7	11
26345	Firstâ€principles Study of Perovskite Ultrathin Films: Stability and Confinement Effects. Israel Journal of Chemistry, 2017, 57, 509-521.	1.0	7
26346	Theoretical study of the atrazine pesticide interaction with pyrophyllite and Ca²⁺-montmorillonite clay surfaces. Journal of Computational Chemistry, 2017, 38, 133-143.	1.5	35
26347	Theoretical investigations on novel SiC5 siligraphene as gas sensor for air pollutants. Carbon, 2017, 113, 114-121.	5.4	64
26348	Quantum-chemical prediction of the effects of Ni-loading on the hydrogenation and water-splitting efficiency of TiO2 nanoparticles with an experimental test. Chemical Physics Letters, 2017, 667, 278-283.	1.2	4
26349	First-principles structure optimization of scandium and lutetium trihydrides. Journal of Alloys and Compounds, 2017, 696, 96-101.	2.8	0
26350	Mechanical properties of refractory high-entropy alloys: Experiments and modeling. Journal of Alloys and Compounds, 2017, 696, 1139-1150.	2.8	307
26351	One-step electrodeposited 3D-ternary composite of zirconia nanoparticles, rGO and polypyrrole with enhanced supercapacitor performance. Nano Energy, 2017, 31, 225-232.	8.2	86
26352	New ultra-incompressible phases of NbB4 predicted from first principles. Physics Letters, Section A: General, Atomic and Solid State Physics, 2017, 381, 362-367.	0.9	7
26353	Two single-layer porous gallium nitride nanosheets: A first-principles study. Solid State Communications, 2017, 250, 18-22.	0.9	28
26354	Metallic NiPS₃@NiOOH Coreâ€“Shell Heterostructures as Highly Efficient and Stable Electrocatalyst for the Oxygen Evolution Reaction. ACS Catalysis, 2017, 7, 229-237.	5.5	233
26355	Improving Ni Catalysts Using Electric Fields: A DFT and Experimental Study of the Methane Steam Reforming Reaction. ACS Catalysis, 2017, 7, 551-562.	5.5	73
26356	Structural and optical properties of the recently synthesized (Zr3âˆ'x Ti x)AlC2 MAX phases. Journal of Materials Science: Materials in Electronics, 2017, 28, 3386-3393.	1.1	27
26357	Rare Earth Interstitials in Ge: A Hybrid Density Functional Theory Study. Journal of Electronic Materials, 2017, 46, 1022-1029.	1.0	8

#	Article	IF	Citations
26358	First principles study of electronic structure dependent optical properties of oxychalcogenides BiOCuCh (ChÂ=ÂS, Se, Te). Indian Journal of Physics, 2017, 91, 403-412.	0.9	9
26359	Structural and electronic properties of zigzag and armchair WSe2 nanotubes. Journal of Alloys and Compounds, 2017, 695, 2751-2756.	2.8	9
26360	The helium effect at grain boundaries in Fe-Cr alloys: A first-principles study. Nuclear Instruments & Methods in Physics Research B, 2017, 393, 118-121.	0.6	2
26361	Electronic transport properties and first-principles study of graphene/h-BN and h-BN bilayers. Physica E: Low-Dimensional Systems and Nanostructures, 2017, 87, 312-316.	1.3	9
26362	Surface charge transfer doping induced inversion layer for high-performance graphene/silicon heterojunction solar cells. Journal of Materials Chemistry A, 2017, 5, 285-291.	5.2	52
26363	Comparative study on hydrogenation of propanal on Ni(111) and Cu(111) from density functional theory. Applied Surface Science, 2017, 394, 333-339.	3.1	22
26364	Structural stability and mechanical properties of Ti2AlX (XÂ=ÂHf, Re) intermetallics: A DFT study. Journal of Alloys and Compounds, 2017, 695, 35-44.	2.8	3
26365	Ab initio study of structural, electronic, and thermal properties of Pt1â^'xPdx alloys. International Journal of Modern Physics B, 2017, 31, 1650243.	1.0	1
26366	Precipitation in a copper matrix modeled byab initiocalculations and atomistic kinetic Monte Carlo simulations. Physica Status Solidi (B): Basic Research, 2017, 254, 1600407.	0.7	7
26367	A comparative study of NbAl3 and Nb3Al intermetallic compounds under pressure. Computational Materials Science, 2017, 126, 280-286.	1.4	18
26368	Improvements on non-equilibrium and transport Green function techniques: The next-generation transiesta. Computer Physics Communications, 2017, 212, 8-24.	3.0	256
26369	Welcoming natural isotopic abundance in solid-state NMR: probing Ï€-stacking and supramolecular structure of organic nanoassemblies using DNP. Chemical Science, 2017, 8, 974-987.	3.7	48
26370	Electronâ€“phonon interaction and superconductivity in the. Philosophical Magazine, 2017, 97, 128-143.	0.7	3
26371	Does aluminum play well with others? Intrinsic Al-A alloying behavior in 211/312 MAX phases. Materials Research Letters, 2017, 5, 170-178.	4.1	20
26372	Platinum adsorption on ceria: A comparative theoretical study of different surfaces. Applied Surface Science, 2017, 394, 47-57.	3.1	11
26373	Surface regulated arsenenes as Dirac materials: From density functional calculations. Applied Surface Science, 2017, 394, 625-629.	3.1	17
26374	Reduced work function of graphene by metal adatoms. Applied Surface Science, 2017, 394, 98-107.	3.1	36
26375	Electronic and optical properties of AlN under pressure: DFT calculations. International Journal of Modern Physics B, 2017, 31, 1650255.	1.0	0

#	Article	IF	Citations
26376	Metalâ€Free Dual Modal Contrast Agents Based on Fluorographene Quantum Dots. Particle and Particle Systems Characterization, 2017, 34, 1600221.	1.2	25
26377	Spinel and post-spinel phase assemblages in Zn2TiO4: an experimental and theoretical study. Physics and Chemistry of Minerals, 2017, 44, 109-123.	0.3	9
26378	Dissociation and diffusion of hydrogen on defect-free and vacancy defective Mg (0001) surfaces: A density functional theory study. Applied Surface Science, 2017, 394, 371-377.	3.1	33
26379	Pressure induced structural and optical properties of cubic phase SnSe: An investigation for the infrared/mid-infrared optoelectronic devices. Journal of Alloys and Compounds, 2017, 695, 194-201.	2.8	45
26380	Enhanced superconductivity in the high pressure phase of SnAs studied from first principles. Physica B: Condensed Matter, 2017, 505, 33-40.	1.3	9
26381	Molecular dynamics simulation of nano-indentation on Ti-V multilayered thin films. Physica E: Low-Dimensional Systems and Nanostructures, 2017, 87, 213-219.	1.3	17
26382	Robust Ferromagnetism of Chromium Nanoparticles Formed in Superfluid Helium. Advanced Materials, 2017, 29, 1604277.	11.1	19
26383	Substrate-Induced Synthesis of Nitrogen-Doped Holey Graphene Nanocapsules for Advanced Metal-Free Bifunctional Electrocatalysts. Particle and Particle Systems Characterization, 2017, 34, 1600207.	1.2	15
26384	Density functional theory calculations on transition metal atoms adsorbed on graphene monolayers. Applied Surface Science, 2017, 421, 252-259.	3.1	28
26385	DFT study of the adsorption of 2,3,7,8-tetrachlorodibenzo-p-dioxin on pristine and Ni-doped boron nitride nanotubes. Chemosphere, 2017, 168, 18-24.	4.2	32
26386	Hydrogen storage on bare Cu atom and Cu-functionalized boron-doped graphene: A first principles study. International Journal of Hydrogen Energy, 2017, 42, 4233-4243.	3.8	68
26387	Effect of local environment on moment formation in iron silicides. Journal of Alloys and Compounds, 2017, 695, 1213-1222.	2.8	18
26388	Mechanical properties and electronic structures of Fe-Al intermetallic. Physica B: Condensed Matter, 2017, 506, 1-11.	1.3	82
26389	First-Principles Study of Substitution of Cu and Au for Ni in Ni3Sn2. Journal of Electronic Materials, 2017, 46, 616-626.	1.0	2
26390	Tuning the magnetic properties of pure hafnium by high pressure torsion. Acta Materialia, 2017, 123, 206-213.	3.8	14
26391	Ab initio calculations of the lattice parameter and elastic stiffness coefficients of bcc Fe with solutes. Computational Materials Science, 2017, 126, 503-513.	1.4	36
26392	Low temperature metal free growth of graphene on insulating substrates by plasma assisted chemical vapor deposition. 2D Materials, 2017, 4, 015009.	2.0	38
26393	Phase stability, electronic structures, and superconductivity properties of the BaPb_{1â^'x}Bi_xO₃ and Ba_{1â^'x}K_xBiO₃ perovskites. Journal of the American Ceramic Society, 2017, 100, 1221-1230.	1.9	29

#	Article	IF	Citations
26394	Comprehensive first-principles study of stable stacking faults in hcp metals. Acta Materialia, 2017, 123, 223-234.	3.8	139
26395	The effect of porosity on the vibrational and low temperature equilibrium thermodynamic properties of amorphous silicon via computer simulation. Journal of Non-Crystalline Solids, 2017, 455, 42-51.	1.5	1
26396	Helium diffusion in pure hematite (Î±-Fe2O3) for thermochronometric applications: A theoretical multi-scale study. Computational and Theoretical Chemistry, 2017, 1099, 21-28.	1.1	23
26397	Doping induced dimensionality reduction of the magnetic order in DyFe1-In O3. Journal of Alloys and Compounds, 2017, 695, 1699-1705.	2.8	2
26398	Detection of CO2 using CNT-based sensors: Role of Fe catalyst on sensitivity and selectivity. Materials Chemistry and Physics, 2017, 186, 353-364.	2.0	33
26399	First-principles study of structural, mechanical, lattice dynamical and thermal properties of nodal-line semimetals ZrXY (X=Si,Ge; Y=S,Se). Philosophical Magazine, 2017, 97, 175-186.	0.7	31
26400	A theoretical study of the electrical contact between metallic and semiconducting phases in monolayer MoS ₂. 2D Materials, 2017, 4, 015014.	2.0	21
26401	Electronic Structure, Phase Stability, and Elastic Properties of Inverse Heusler Compound Mn2RuSi at High Pressure. Journal of Superconductivity and Novel Magnetism, 2017, 30, 951-958.	0.8	7
26402	Effects of gold based dimers on structural and electronic properties of MoS2. Applied Surface Science, 2017, 396, 455-460.	3.1	8
26403	Quest of thermoelectricity in topological insulators: A density functional theory study. Applied Surface Science, 2017, 418, 232-237.	3.1	9
26404	Anisotropic optical constants and inter-band optical transitions in layered semiconductor TlGaSe2. Applied Surface Science, 2017, 421, 788-793.	3.1	5
26405	Hydrothermal preparation of hierarchical MoS2-reduced graphene oxide nanocomposites towards remarkable enhanced visible-light photocatalytic activity. Ceramics International, 2017, 43, 2384-2388.	2.3	20
26406	Investigation on WC/LaAlO3 heterogeneous nucleation interface by first-principles. Journal of Alloys and Compounds, 2017, 695, 1753-1762.	2.8	28
26407	Robust ruthenium catalysts for the selective conversion of stearic acid to diesel-range alkanes. Applied Catalysis B: Environmental, 2017, 201, 137-149.	10.8	60
26408	Superhard orthorhombic phase of B 2 CO compound. Diamond and Related Materials, 2017, 73, 87-92.	1.8	18
26409	Synthetic mimetics of the endogenous gastrointestinal nanomineral: Silent constructs that trap macromolecules for intracellular delivery. Nanomedicine: Nanotechnology, Biology, and Medicine, 2017, 13, 619-630.	1.7	17
26410	Thermoelectric and mechanical properties of gapless Zr2MnAl compound. Indian Journal of Physics, 2017, 91, 33-41.	0.9	57
26411	Effects of structure and size of Ni nanocatalysts on hydrogen selectivity via water-gas-shift reactionâ€"A first-principles-based kinetic study. Catalysis Today, 2017, 280, 210-219.	2.2	24

#	Article	IF	Citations
26412	Modulating the phases of iron carbide nanoparticles: from a perspective of interfering with the carbon penetration of Fe@Fe₃O₄ by selectively adsorbed halide ions. Chemical Science, 2017, 8, 473-481.	3.7	105
26413	Ab initio study of the electronic, optical and thermodynamic properties of the ternary phosphides LiAeP (AeÂ=ÂSr, Ba). Indian Journal of Physics, 2017, 91, 157-167.	0.9	9
26414	First-Principles Study of Structural, Optical, and Thermodynamic Properties of ZnIn2X4 (XÂ=ÂSe, Te) Compounds with DC or DF Structure. Journal of Electronic Materials, 2017, 46, 401-412.	1.0	5
26415	Efficient photocatalytic hydrogen production over solid solutions Sr1-xBixTi1-xFexO3 (0 â‰¤ x â‰¤ 0.5). Applied Catalysis B: Environmental, 2017, 200, 412-419.	10.8	67
26416	Combined effect of Mg and vacancy on the generalized planar fault energy of Al. Journal of Alloys and Compounds, 2017, 690, 841-850.	2.8	21
26417	Hydrogenated and halogenated blue phosphorene as Dirac materials: A first principles study. Applied Surface Science, 2017, 392, 46-50.	3.1	64
26418	Electronic and Magnetic Properties of Co2CrGa1â^'x Si x Heusler Alloys. Journal of Superconductivity and Novel Magnetism, 2017, 30, 421-424.	0.8	46
26419	Origins of Bistability and Na Ion Mobility Difference in P2â€•and O3â€Na_{2/3}Fe_{2/3}Mn_{1/3}O₂ Cathode Polymorphs. Advanced Energy Materials, 2017, 7, 1601477.	10.2	101
26420	Strategy to improve catalytic trend predictions for methane oxidation and reforming. AICHE Journal, 2017, 63, 66-77.	1.8	15
26421	Phase formation of Nb2AlC investigated by combinatorial thin film synthesis and ab initio calculations. Journal of the European Ceramic Society, 2017, 37, 35-41.	2.8	7
26422	Structural, electronic and elastic properties of REIr2 (REÂ=ÂSc, Y and La) Laves phase compounds under pressure. Indian Journal of Physics, 2017, 91, 183-190.	0.9	7
26423	First Principles Study of Molecular O2 Adsorption on the PdO(101) Surface. Topics in Catalysis, 2017, 60, 401-412.	1.3	9
26424	Study of the electronic, bonding, elastic and acoustic properties of covellite via first principles. Journal of Alloys and Compounds, 2017, 692, 440-447.	2.8	20
26425	Lithium ion adsorption and diffusion on black phosphorene nanotube: A first-principles study. Applied Surface Science, 2017, 392, 88-94.	3.1	32
26426	Bandgap engineering in semiconducting one to few layers of SnS and SnSe. Physica Status Solidi (B): Basic Research, 2017, 254, 1600379.	0.7	43
26427	Influence of O2 exposure on the interaction between CH4 and amorphous AlYB14. Applied Surface Science, 2017, 392, 1165-1172.	3.1	5
26428	Sign-tunable Poisson's ratio in semi-fluorinated graphene. Nanoscale, 2017, 9, 128-133.	2.8	33
26429	Structural, mechanical, electronic, and thermodynamic properties of dense B₃N₄ under high pressure predicted from first principles. Physica Status Solidi (B): Basic Research, 2017, 254, 1600312.	0.7	1

#	Article	IF	Citations
26430	Experimental and DFT investigation of (Cr,Ti)₃AlC₂ MAX phases stability. Materials Research Letters, 2017, 5, 144-157.	4.1	27
26431	In situ synthesis, structure, and properties of bulk nanolaminate YAl3C3 ceramic. Journal of the European Ceramic Society, 2017, 37, 83-89.	2.8	17
26432	Role of grain boundary character on oxygen and hydrogen segregation-induced embrittlement in polycrystalline Ni. Journal of Materials Science, 2017, 52, 30-45.	1.7	30
26433	Simulated Temperature Programmed Desorption of Acetaldehyde on CeO2(111): Evidence for the Role of Oxygen Vacancy and Hydrogen Transfer. Topics in Catalysis, 2017, 60, 446-458.	1.3	15
26434	Theoretical investigation of stabilities and physical properties of low cost Fe-based full-Heusler materials. Journal of Alloys and Compounds, 2017, 693, 462-467.	2.8	27
26435	Characterizing chemical stability and proton conductivity of B-site doped barium hafnate (BaHfO3) and barium stannate (BaSnO3) with first principles modeling. Journal of Alloys and Compounds, 2017, 693, 738-743.	2.8	22
26436	Composition-induced influence on the electronic band structure, optical and thermoelectric coefficients of the highly mismatched GaNSb alloy over the entire range: A DFT analysis. Journal of Alloys and Compounds, 2017, 693, 1020-1027.	2.8	38
26437	Chlorine Incorporation in the CH₃NH₃PbI₃ Perovskite: Small Concentration, Big Effect. Inorganic Chemistry, 2017, 56, 74-83.	1.9	40
26438	Bulk modulus and thermodynamic properties of L21 Ni2 XY (XÂ=ÂMn, Fe, Co, YÂ=ÂGa, In) compounds studied by first-principles calculations. Journal of Materials Science, 2017, 52, 1149-1155.	1.7	2
26439	The adsorption and dissociation of water molecule on goethite (010) surface: A DFT approach. Applied Surface Science, 2017, 392, 760-767.	3.1	30
26440	Electronic charge transfer contribution in adsorption of silicon at the SiC(0001) surfaceâ€"A density functional theory (DFT) study. Applied Surface Science, 2017, 393, 168-179.	3.1	8
26441	Thermodynamic reassessment of the Niâ€"Siâ€"Ti system using a four-sublattice model for ordered/disordered fcc phases supported by first-principles calculations. Journal of Alloys and Compounds, 2017, 693, 344-356.	2.8	21
26442	Helimagnetic order in bulk MnSi and CoSi/MnSi superlattices. Journal of Magnetism and Magnetic Materials, 2017, 421, 31-38.	1.0	5
26443	High-pressure behavior of Î±-boron studied on single crystals by X-ray diffraction, Raman and IR spectroscopy. Journal of Solid State Chemistry, 2017, 245, 50-60.	1.4	9
26444	Precipitate formations with self-adaptive elemental diffusion and segregation in T92 steel. Journal of Alloys and Compounds, 2017, 693, 264-278.	2.8	10
26445	Theoretical study of high-pressure phase stability of NaZr2(PO4)3 via elastic constants and equation of state. Indian Journal of Physics, 2017, 91, 277-286.	0.9	1
26446	Density functional theory study on the heterogeneous reaction between Hg 0 and HCl over spinel-type MnFe 2 O 4. Chemical Engineering Journal, 2017, 308, 897-903.	6.6	81
26447	First-principles and classical molecular dynamics study of threshold displacement energy in beryllium. Nuclear Instruments & Methods in Physics Research B, 2017, 393, 195-199.	0.6	8

#	Article	IF	Citations
26448	Structural, energetic and dynamical properties of ordered and disordered bcc Fe25at.%Ni alloys: A first-principles study. Computational Materials Science, 2017, 126, 82-89.	1.4	4
26449	First-principles study on the adhesive properties of Al/TiC interfaces: Revisited. Computational Materials Science, 2017, 126, 108-120.	1.4	23
26450	Adsorption and dissociation of molecular hydrogen on orthorhombic Î²-Mo2C and cubic Î´-MoC (001) surfaces. Surface Science, 2017, 656, 24-32.	0.8	50
26451	Investigation of visibleâ€light absorption in Cu₂O/TiO₂ heterojunctions with an interstitial at the interface. Physica Status Solidi (B): Basic Research, 2017, 254, 1600420.	0.7	1
26452	First-principles investigation on slip systems and twinnability of TiC. Computational Materials Science, 2017, 126, 103-107.	1.4	14
26453	Electrochemical Effects at Surfactantâ€“Platinum Nanoparticle Interfaces Boost Catalytic Performance. ChemCatChem, 2017, 9, 604-609.	1.8	14
26454	Doping effect of copper zinc tin sulphide counter electrode for dye-sensitized solar cells. Computational Materials Science, 2017, 126, 160-169.	1.4	6
26455	Understanding the thermal stability and bonding characteristic of Li x Ni0.5Mn1.5O4 as cathode materials for lithium-ion battery from first principles. Ionics, 2017, 23, 559-565.	1.2	3
26456	Geometry dependent structural and electronic properties of CdS nanowires: An ab-inito study. Superlattices and Microstructures, 2017, 101, 306-314.	1.4	3
26457	A first-principles study on the origin of magnetism induced by intrinsic defects in monolayer SnS2. Computational Materials Science, 2017, 126, 52-58.	1.4	31
26458	Silicon nanowires as potential gas sensors: A density functional study. Sensors and Actuators B: Chemical, 2017, 242, 1246-1250.	4.0	39
26459	Single-atom catalysts for CO₂ electroreduction with significant activity and selectivity improvements. Chemical Science, 2017, 8, 1090-1096.	3.7	430
26460	Magnetic properties of the 2D Fen core Xm (X = C, N, O, Cl, S and F) shell clusters embedded in graphene. Applied Surface Science, 2017, 392, 277-285.	3.1	5
26461	Interplay of Cation Ordering and Ferroelectricity in Perovskite Tin Iodides: Designing a Polar Halide Perovskite for Photovoltaic Applications. Inorganic Chemistry, 2017, 56, 26-32.	1.9	37
26462	Computational investigation of the kinetics and mechanism of the initial steps of the Fischerâ€“Tropsch synthesis on cobalt. Faraday Discussions, 2017, 197, 117-151.	1.6	37
26463	Unprecedented thermal stability of inherently metastable titanium aluminum nitride by point defect engineering. Materials Research Letters, 2017, 5, 158-169.	4.1	73
26464	Structural Stabilities and Elastic Thermodynamic Properties of SrTe Compound and SrTe1â^'x Ca x Alloy Under High Pressure. Journal of Electronic Materials, 2017, 46, 766-774.	1.0	0
26465	An Ab Initio Study of Carbon-Induced Ordering in Austenitic Fe-Mn-Al-C Alloys. Steel Research International, 2017, 88, 1600292.	1.0	14

#	Article	IF	Citations
26466	Phase Transitions and Electronic Properties for Zincblende-Derived and Wurtzite-Derived Stannite Cu2ZnSnS4 Under Pressure. Journal of Electronic Materials, 2017, 46, 2812-2821.	1.0	4
26467	DFT investigation of structural, electronic and optical properties of pure and Er-doped ZnO: Modified Becke-Johnson exchange potential. Optik, 2017, 128, 274-280.	1.4	19
26468	Adsorption and Dimerization of Late Transition Metal Atoms on the Regular and Defective Quartz (001) Surface. Topics in Catalysis, 2017, 60, 459-470.	1.3	13
26469	A computational quest for Nd2Fe14B-type Ce and Nd phases. Journal of Alloys and Compounds, 2017, 693, 238-244.	2.8	15
26470	Dissociation and reconstruction of double-decker bis(phthalocyaninato) terbium(III) complex (TbPc2) on Pd(001): A theoretical investigation. Surface Science, 2017, 655, 12-16.	0.8	4
26471	Characterization of Al-Mg-B-C films based on experimental and first-principles investigations. Surface and Coatings Technology, 2017, 309, 164-171.	2.2	4
26472	An experimental and theoretical study of glycerol oxidation to 1,3â€dihydroxyacetone over bimetallic Ptâ€Bi catalysts. AICHE Journal, 2017, 63, 705-715.	1.8	60
26473	DFT CALCULATIONS OF THE ELECTRONIC STRUCTURE AND INTERLAYER INTERACTION IN THE Li-INTERCALATED GRAPHENE BILAYER. Surface Review and Letters, 2017, 24, 1750020.	0.5	7
26474	Long-ranged interactions in bcc NbMoTaW high-entropy alloys. Materials Research Letters, 2017, 5, 35-40.	4.1	86
26475	Penetration and diffusion of hydrogen in Mg2Ni: A first-principles investigation. International Journal of Hydrogen Energy, 2017, 42, 3097-3105.	3.8	8
26476	Density functional theory study of dopant effect on formation energy of intrinsic point defects in germanium crystals. Journal of Crystal Growth, 2017, 474, 104-109.	0.7	4
26477	The simulation of interface structure, energy and electronic properties of TaN/ReB 2 multilayers using first-principles. Surface and Coatings Technology, 2017, 326, 417-423.	2.2	13
26478	The properties of isolated dangling bonds on hydrogenated 2H-SiC surfaces. Surface Science, 2017, 656, 109-114.	0.8	5
26479	LEED â€“ IV and DFT study of the co-adsorption of chlorine and water on Cu(100). Surface Science, 2017, 657, 51-57.	0.8	4
26480	Theoretical Investigation of the Hydrodeoxygenation of Levulinic Acid to Î³-Valerolactone over Ru(0001). ACS Catalysis, 2017, 7, 215-228.	5.5	65
26481	First-principles studies of the structural, elastic, and lattice dynamical properties of ZrMo₂ and HfMo₂. Phase Transitions, 2017, 90, 598-609.	0.6	21
26482	Structural stability, electronic structure, and novel transport properties with high thermoelectric performances of ZrIrX (X $$=$$ = As, Bi, and Sb). Journal of Computational Electronics, 2017, 16, 1-11.	1.3	22
26483	Surface excess elasticity of gold: Ab initio coefficients and impact on the effective elastic response of nanowires. Acta Materialia, 2017, 124, 468-477.	3.8	32

#	Article	IF	Citations
26484	First-principles study of structural, mechanical, and thermodynamic properties of cubic Y2O3 under high pressure. Ceramics International, 2017, 43, 3346-3355.	2.3	32
26485	New quasi-2D nickel-gallium mixed chalcogenides based on the Cu3Au-type extended fragments. Journal of Alloys and Compounds, 2017, 696, 413-422.	2.8	13
26486	Thermal equilibrium concentration of intrinsic point defects in heavily doped silicon crystals - Theoretical study of formation energy and formation entropy in area of influence of dopant atoms-. Journal of Crystal Growth, 2017, 474, 110-120.	0.7	4
26487	Electronic theoretical study of the influences of O adsorption on the electronic structure and optical properties of graphene. Physica B: Condensed Matter, 2017, 506, 156-162.	1.3	11
26488	Ab initio study of interstitial cluster interaction with Re, Os, and TaÂinÂW. Journal of Nuclear Materials, 2017, 484, 30-41.	1.3	42
26489	Band gap engineering and optical response of the ACr 2 S 4 (A=Fe, Co) normal spinels using PBE+U and TB-mBJ potentials. Journal of Physics and Chemistry of Solids, 2017, 102, 130-135.	1.9	4
26490	Electronic Structures and Magnetism of Rutile TiO2 with Vacancy Defects from First Principles: GGA + U Calculations. Journal of Superconductivity and Novel Magnetism, 2017, 30, 243-249.	0.8	7
26491	Prospects of asymmetrically H-terminated zigzag germanene nanoribbons for spintronic application. Applied Surface Science, 2017, 396, 1352-1359.	3.1	15
26492	First-principles investigation of the thermodynamic properties of two-dimensional MoS 2. Chinese Journal of Physics, 2017, 55, 105-114.	2.0	5
26493	Comparison of performance of van der Waals-corrected exchange-correlation functionals for interlayer interaction in graphene and hexagonal boron nitride. Computational Materials Science, 2017, 128, 45-58.	1.4	72
26494	Comparison of hydrogen absorption in metallic and semiconductor single-walled Ge- and GeO2-doped carbon nanotubes. International Journal of Hydrogen Energy, 2017, 42, 969-977.	3.8	9
26495	On the photophysics and speciation of actinide ion in MgAl2O4 spinel using photoluminescence spectroscopy and first principle calculation: A case study with uranium. Journal of Alloys and Compounds, 2017, 695, 337-343.	2.8	16
26496	Modeling the elastic anisotropies and mechanical strengths of Ir3X intermetallics. Journal of Alloys and Compounds, 2017, 696, 611-618.	2.8	7
26497	Shape, electronic structure and steric effects of organometallic nanocatalysts: relevant tools to improve the synergy between theory and experiment. Dalton Transactions, 2017, 46, 378-395.	1.6	17
26498	Two-dimensional hexagonal CrN with promising magnetic and optical properties: A theoretical prediction. Nanoscale, 2017, 9, 621-630.	2.8	66
26499	Boron phosphide monolayer as a potential anode material for alkali metal-based batteries. Journal of Materials Chemistry A, 2017, 5, 672-679.	5.2	217
26500	An ab initio investigation of Bi₂Se₃ topological insulator deposited on amorphous SiO₂. Journal of Physics Condensed Matter, 2017, 29, 045302.	0.7	3
26501	Engineering of highly mismatched alloy with semiconductor and semi-metallic substituent's for photovoltaic applications. Current Applied Physics, 2017, 17, 162-168.	1.1	39

#	Article	IF	Citations
26502	About copper promotion in CH 4 formation from CO hydrogenation on Fe(100): A density functional theory study. Applied Catalysis A: General, 2017, 530, 83-92.	2.2	16
26503	Screening of active metals for reactive adsorption desulfurization adsorbent using density functional theory. Applied Surface Science, 2017, 399, 440-450.	3.1	31
26504	Analysis and prediction of mid-IR nonlinear optical metal sulfides with diamond-like structures. Coordination Chemistry Reviews, 2017, 333, 57-70.	9.5	278
26505	Electronic and optical properties of cubic SrHfO3 at different pressures: A first principles study. Materials Chemistry and Physics, 2017, 186, 620-626.	2.0	43
26506	Magnetism of 3d Transition Metals Doped 2H, 4H and 6H-GaN Polytypes. Journal of Superconductivity and Novel Magnetism, 2017, 30, 1195-1199.	0.8	2
26507	Crystal facet-dependent reactivity of Î±-Mn2O3 microcrystalline catalyst for soot combustion. Applied Catalysis B: Environmental, 2017, 204, 374-384.	10.8	141
26508	CO adsorption on W(100) during temperature-programmed desorption: A combined density functional theory and kinetic Monte Carlo study. Applied Surface Science, 2017, 396, 1282-1288.	3.1	13
26509	Influence of phonon and electron excitations on the free energy of defect clusters in solids: A first-principles study. Computational Materials Science, 2017, 127, 284-294.	1.4	8
26510	Formation of cyanuric acid from cyanate adsorbed at gold electrodes. Electrochemistry Communications, 2017, 74, 1-4.	2.3	5
26511	4-d magnetism: Electronic structure and magnetism of some Mo-based alloys. Journal of Magnetism and Magnetic Materials, 2017, 423, 12-19.	1.0	4
26512	Elasticity, Hardness and Thermal Conductivity of Si-Ge-Based Oxynitrides (SiGeN2O). Journal of Electronic Materials, 2017, 46, 510-519.	1.0	2
26513	Hydrogen adsorption and storage on Palladium â€“ functionalized graphene with NH-dopant: A first principles calculation. Applied Surface Science, 2017, 392, 362-374.	3.1	84
26514	DFT calculation, electric and luminescent property of titanate solid state electrolytes based red emitting phosphor A 2 La 2 Ti 3 O 10 :Eu 3+ (AÂ=ÂNa, K). Dyes and Pigments, 2017, 136, 601-611.	2.0	25
26515	A theoretical study of dielectric tensor, Born effective charges, LO-TO splitting and infrared response of Al4SiC4 and Al4Si2C5. Journal of Alloys and Compounds, 2017, 692, 713-719.	2.8	8
26516	Atomistic investigations of Î¹-carbide precipitation in austenitic Fe-Mn-Al-C lightweight steels and the effect of Mo addition. Scripta Materialia, 2017, 127, 97-101.	2.6	80
26517	First-principles study on LaYbO3 as the localized f electrons containing system with MBJâ€“LDA +U approach. Computational Materials Science, 2017, 126, 7-11.	1.4	7
26518	Upconversion luminescence properties of Er 3+ in SrLaMgTaO 6 double perovskite phosphor. Materials Research Bulletin, 2017, 85, 216-221.	2.7	11
26519	Mechanistic studies of mercury adsorption and oxidation by oxygen over spinel-type MnFe2O4. Journal of Hazardous Materials, 2017, 321, 154-161.	6.5	184

#	Article	IF	Citations
26520	An investigation of electronic and optical properties of InN nanosheet by first principle study. Optics Communications, 2017, 395, 293-300.	1.0	21
26521	Strainâ€engineered atomicâ€layer movements and valenceâ€band maximum shifts in a twoâ€dimensional single quintuple film of Bi₂Te₃. Physica Status Solidi (B): Basic Research, 2017, 254, 1600362.	0.7	2
26522	First-Principles Study on the Half-Metallic Ferromagnetism and Optical Properties of Fe-Doped CdSe and Co-Doped CdSe. Journal of Superconductivity and Novel Magnetism, 2017, 30, 521-528.	0.8	18
26523	Alloying element's substitution in titanium alloy with improved oxidation resistance and enhanced magnetic properties. Journal of Magnetism and Magnetic Materials, 2017, 422, 20-24.	1.0	4
26524	Study of the orpiment and anorpiment phases of As2S3 under pressure. Journal of Physics: Conference Series, 2017, 950, 042018.	0.3	4
26525	A DFT +Ustudy on structural, electronic, vibrational and thermodynamic properties of TiO₂polymorphs and hydrogen titanate: tuning the Hubbard â€˜U-termâ€™. Journal of Physics Communications, 2017, 1, 055006.	0.5	45
26526	Mechanical, elastic, anisotropy, and electronic properties of monoclinic phase of m -Si _x Ge _{3â^’ x} N ₄. Chinese Physics B, 2017, 26, 126105.	0.7	3
26527	Oxidation Mechanism of Arsenopyrite in the Presence of Water. Journal of Physical Chemistry C, 2017, 121, 26887-26894.	1.5	14
26528	Tunable electronic and optical properties of gas molecules adsorbed monolayer graphitic ZnO: Implications for gas sensor and environment monitoring. Journal of Applied Physics, 2017, 122, .	1.1	11
26529	Plasmon properties of doped or gated graphene nanoribbon arrays with armchair shaped edges. , 2017, , .		1
26530	Ab initio calculations of exciton effects in optical spectra of an Î±-B12 crystal. Journal of Experimental and Theoretical Physics, 2017, 125, 495-501.	0.2	1
26531	Thermal transport properties of bulk and monolayer MoS₂: an ab-initio approach. Journal of Physics: Conference Series, 2017, 836, 012052.	0.3	11
26532	Dynamic instabilities in strongly correlated <mml:math xmlns:mml="http://www.w3.org/1998/Math/MathML"><mml:msub><mml:mtext>VSe</mml:mtext><mml:mn>2</mml:mn></mml:msub monolayers and bilayers. Physical Review B, 2017, 96, .	1.1	41
26533	Modification of electronic structure, magnetic structure, and topological phase of bismuthene by point defects. Physical Review B, 2017, 96, .	1.1	54
26534	Ab initio calculation of thermal boundary resistance at the interface of metals with GeTe, In $$_3$$ 3 SbTe $$_2$$. Journal of Computational Electronics, 2017, 16, 1003-1010.	1.3	6
26535	Periodic modeling of zeolite Ti-LTA. Journal of Chemical Physics, 2017, 147, 074701.	1.2	11
26536	Revisiting the ground state phase stability of super-heavy element Flerovium. Cogent Physics, 2017, 4, 1380454.	0.7	1
26537	Electronic, Elastic and Piezoelectric Properties of Two-Dimensional Group-IV Buckled Monolayers*. Chinese Physics Letters, 2017, 34, 087701.	1.3	19

#	Article	IF	Citations
26538	Molecular Adsorption, Hindered Rotation, and Species Separation of H₂/SrTiO₃(001). Journal of the Physical Society of Japan, 2017, 86, 073601.	0.7	3
26539	Two-dimensional carbon structures study within density functional theory. AIP Conference Proceedings, 2017, , .	0.3	0
26540	Defect processes in Be₁₂X (XÂ=ÂTi, Mo, V, W). Nuclear Fusion, 2017, 57, 086049.	1.6	19
26541	Dual effects of lone-pair electrons and rattling atoms in <mml:math xmlns:mml="http://www.w3.org/1998/Math/MathML"><mml:msub><mml:mi>CuBiS</mml:mi><mml:mn>2</mml:mn></mml:msub> on its ultralow thermal conductivity. Physical Review B, 2017, 96, .	1.1	52
26542	Two-Dimensional Tetragonal GaN as Potential Molecule Sensors for NO and NO₂ Detection: A First-Principle Study. ACS Omega, 2017, 2, 8888-8895.	1.6	75
26543	Strain-induced negative differential resistance in ultrasmall carbon nanotube. Modern Physics Letters B, 2017, 31, 1750217.	1.0	1
26544	Theoretical Investigations of the Electrochemical Reduction of CO on Single Metal Atoms Embedded in Graphene. ACS Central Science, 2017, 3, 1286-1293.	5.3	54
26545	The chirality of metal-encapsulated silicene-like nanotubes. Fullerenes Nanotubes and Carbon Nanostructures, 2017, 25, 699-703.	1.0	1
26546	Prediction of Mechanical Twinning in Magnesium Silicate Post-Perovskite. Scientific Reports, 2017, 7, 17640.	1.6	5
26547	Accuracy and Transferability ofAb InitioElectronic Band Structure Calculations for Doped BiFeO3. Journal of Physics: Conference Series, 2017, 921, 012009.	0.3	4
26548	Hydrogen and nitrogen codoping of anatase TiO2 for efficiency enhancement in organic solar cells. Scientific Reports, 2017, 7, 17839.	1.6	24
26549	Influence of external electric field on the electronic structure and optical properties of pyrite. RSC Advances, 2017, 7, 56676-56681.	1.7	11
26550	Carbon effect on the survival of vacancies in Czochralski silicon during rapid thermal anneal. Journal of Applied Physics, 2017, 122, 045705.	1.1	1
26551	Visualising crystal packing interactions in solid-state NMR: Concepts and applications. Journal of Chemical Physics, 2017, 147, 144203.	1.2	19
26552	A first principles study on the electronic origins of silver segregation at the Ag-Au (111) surface. Journal of Applied Physics, 2017, 122, 235303.	1.1	10
26553	First principles study of tunable band gap in bi layer Graphene (BLG). Materials Today: Proceedings, 2017, 4, 7586-7591.	0.9	1
26554	DFT study of electronic properties of noble d-metallic surface structures. Materials Today: Proceedings, 2017, 4, 12343-12348.	0.9	1
26555	A first-principles study of displacive Î² to Ï‰ transition in Ti-V alloys. Progress in Natural Science: Materials International, 2017, 27, 703-708.	1.8	5

#	Article	IF	Citations
26557	Doping stability and charge-density-wave transition of strained 1T-TiSe ₂. Europhysics Letters, 2017, 120, 17006.	0.7	6
26558	First principles study of oxidation of Si-segregated Î±-Ti(0001) surfaces. Japanese Journal of Applied Physics, 2017, 56, 125701.	0.8	10
26559	The Zn12O12 cluster-assembled nanowires as a highly sensitive and selective gas sensor for NO and NO2. Scientific Reports, 2017, 7, 17505.	1.6	32
26560	Characterizing the geometric and electronic structure of defects in the â€œ29â€•copper surface oxide. Journal of Chemical Physics, 2017, 147, 224706.	1.2	9
26561	Atomistic study of inelastic deformation in aluminium grain boundary fractures. Philosophical Magazine Letters, 2017, 97, 476-485.	0.5	2
26562	Band-to-band transitions, selection rules, effective mass, and excitonic contributions in monoclinic <mml:math xmlns:mml="http://www.w3.org/1998/Math/MathML"><mml:mrow><mml:mi>Î²</mml:mi><mml:mtext>â^'</mml:mtext><mml:msub><mml:mi mathvariant="normal">O</mml:mi><mml:mn>3</mml:mn></mml:msub></mml:mrow></mml:math>. Physical Review B, 2017, 96, .	1.1	17
26563	Identification of conjugate electron transitions in X-ray photoelectron spectra. Journal of Structural Chemistry, 2017, 58, 1160-1165.	0.3	3
26564	Effects of Mn dopant locations on the electronic bandgap of PbS quantum dots. Applied Physics Letters, 2017, 111, .	1.5	8
26565	First Principles Study of Electronic Band Structure and Structural Stability of Al2C Monolayer and Nanotubes. Journal of Physics: Conference Series, 2017, 901, 012171.	0.3	0
26566	Prediction and characterization of an Mg-Al intermetallic compound with potentially improved ductility via orbital-free and Kohn-Sham density functional theory. Modelling and Simulation in Materials Science and Engineering, 2017, 25, 075002.	0.8	11
26567	Versatile electronic and magnetic properties of chemically doped 2D platinum diselenide monolayers: A first-principles study. AIP Advances, 2017, 7, 125126.	0.6	4
26568	Structural, electronic, and thermodynamic properties of curium dioxide: Density functional theory calculations. Physical Review B, 2017, 96, .	1.1	36
26569	Spin-Orbit Semimetal <mml:math xmlns:mml="http://www.w3.org/1998/Math/MathML" display="inline"><mml:msub><mml:mi>SrIrO</mml:mi><mml:mn>3</mml:mn></mml:msub></mml:math> in the Two-Dimensional Limit. Physical Review Letters, 2017, 119, 256403.	2.9	83
26570	Prediction of a low-temperature N ₂ dissociation catalyst exploiting near-IRâ€“toâ€“visible light nanoplasmonics. Science Advances, 2017, 3, eaao4710.	4.7	74
26571	Haeckelite and N-Doped Haeckelite as Catalysts for Oxygen Reduction Reaction: Theoretical Studies. Journal of Physical Chemistry C, 2017, 121, 28339-28347.	1.5	8
26572	Enhanced competitive adsorption of CO2 and H2 on graphyne: A density functional theory study. AIP Advances, 2017, 7, .	0.6	15
26573	Exploring the electronic structure and optical properties of double perovskite Ba₂RESbO₆ (RE = Ho, Er) from first-principles calculations. Ferroelectrics, 2017, 518, 163-170.	0.3	2
26574	Microstructural characterization of the Î·-Ni₃(Ti, Al) phase in a long-term-aged Ni-based superalloy. Philosophical Magazine Letters, 2017, 97, 442-449.	0.5	5

#	Article	IF	Citations
26575	Spatial charge inhomogeneity and defect states in topological Dirac semimetal thin films of Na ₃ Bi. Science Advances, 2017, 3, eaao6661.	4.7	15
26576	A two-dimensional ON/OFF switching device based on anisotropic interactions of atomic quantum dots on Si(100):H. Nature Communications, 2017, 8, 2211.	5.8	14
26577	Robust ferromagnetism and half-metallicity in fluorinated two-dimensional BeN2 sheets. Applied Physics Letters, 2017, 111, .	1.5	8
26578	Electronic and spin dynamics in the insulating iron pnictide<mml:math xmlns:mml="http://www.w3.org/1998/Math/MathML"><mml:mrow><mml:msub><mml:mi>NaFe</mml:mi><mml:mrow><mml:mn>0.5</mml:mn> Physical Review B, 2017, 96, .	1.1	4
26579	Implications of X-ray thermal diffuse scattering in integrated Bragg intensities of silicon and cubic boron nitride. Journal of Applied Crystallography, 2017, 50, 1791-1799.	1.9	6
26580	Thermodynamic analysis of (0001) and $(000ar{1})$ GaN metalorganic vapor phase epitaxy. Japanese Journal of Applied Physics, 2017, 56, 070304.	0.8	27
26581	Theoretical investigation on the adsorption of DNA bases on B/N-doped SWCNT surface by the first principle. AIP Advances, 2017, 7, 105004.	0.6	4
26582	Effect of ionic substitutions on the magnetic properties of strontium hexaferrite: A first principles study. AIP Advances, 2017, 7, 115209.	0.6	15
26583	Thermal resistances of crystalline and amorphous few-layer oxide thin films. AIP Advances, 2017, 7, .	0.6	8
26584	Inelastic electron tunneling mediated by a molecular quantum rotator. Physical Review B, 2017, 96, .	1.1	5
26585	Lithium Diffusion Mechanisms in Î²-LiMO₂ (M = Al, Ga): A Combined Experimental and Theoretical Study. Journal of Physical Chemistry C, 2017, 121, 27788-27796.	1.5	10
26586	Impact of Coulomb Correlations on Magnetic Anisotropy in Mn3Ga Ferrimagnet. Scientific Reports, 2017, 7, 13221.	1.6	4
26587	Ordered and Disordered Phases in Mo1â^'xWxS2 Monolayer. Scientific Reports, 2017, 7, 15124.	1.6	21
26588	Class of diatomic ferroelectrics with multifunctional properties: IV-VI compounds in the distorted NiAs-type structure. Physical Review B, 2017, 96, .	1.1	4
26589	Breakdown of the Chiral Anomaly in Weyl Semimetals in a Strong Magnetic Field. Physical Review Letters, 2017, 119, 266401.	2.9	38
26590	Adsorption effect on the formation of conductive path in defective TiO₂: ab initio calculations. EPJ Applied Physics, 2017, 80, 10104.	0.3	0
26591	Simulation of crystal and electronic structures of octahedral molybdenum cluster complex compound Cs₂[Mo₆Cl₁₄] using various DFT functionals. Journal of the Ceramic Society of Japan, 2017, 125, 753-759.	0.5	5
26592	Origin of the type-II band offset between rutile and anatase titanium dioxide: Classical and quantum-mechanical interactions between O ions. Physical Review B, 2017, 95, .	1.1	11

#	Article	IF	Citations
26593	AuNx stabilization with interstitial nitrogen atoms: A Density Functional Theory Study. Journal of Physics: Conference Series, 2017, 850, 012002.	0.3	0
26594	A first-principle study of the adsorption behavior of NO gas molecules on pristine and Al-doped penta-graphene. , 2017, , .		8
26595	First-principles calculation of M₃Ta₆Si₄O₂₆ (M = Ba,) Tj ETQq0 0 0 rgBT /Overlock	0.5	0
26596	A Density Functional Theory Study of Adsorption States of Hydrogen Molecules on Ice Surfaces. Journal of the Vacuum Society of Japan, 2017, 60, 249-255.	0.3	2
26597	Symmetry Breaking-induced Band-splitting in GaAs Thin Film by First-principles Calculations. Journal of the Vacuum Society of Japan, 2017, 60, 445-449.	0.3	3
26598	Titaniaâ€Supported Singleâ€Atom Platinum Catalyst for Waterâ€Gas Shift Reaction. Chemie-Ingenieur-Technik, 2017, 89, 1343-1349.	0.4	22
26599	Electronic structure and effective masses of TlInSe₂ under pressure. Materials Science-Poland, 2017, 35, 857-860.	0.4	4
26600	The electronic structure of ultrathin [111]-oriented tin nanowire with hydrogen passivation. AIP Conference Proceedings, 2017, , .	0.3	0
26601	Investigation of the charge distribution in small cluster ions Ar 13 + and Ar 19 +. Moscow University Physics Bulletin (English Translation of Vestnik Moskovskogo Universiteta, Fizika), 2017, 72, 470-473.	0.1	0
26602	The Pressure Dependence of Structural, Electronic, Mechanical, Vibrational, and Thermodynamic Properties of Palladium-Based Heusler Alloys. Zeitschrift Fur Naturforschung - Section A Journal of Physical Sciences, 2017, 72, 843-853.	0.7	4
26603	Ab initio crystal structure and elasticity of tuite, Î³-Ca3(PO4)2, with implications for trace element partitioning in the lower mantle. Contributions To Mineralogy and Petrology, 2017, 172, 1.	1.2	4
26604	First Principles Investigation of the Magnetic, Magnetoelectric, and Optical Properties of Double Perovskites Containing Ions of Transition Metals LaPbTSbO6 (T = Fe, Co, Ni). Journal of Experimental and Theoretical Physics, 2017, 125, 1116-1126.	0.2	0
26605	Effects of alloying element on stabilities, electronic structures, and mechanical properties of Pdâ€“based superalloys. Chinese Physics B, 2017, 26, 126202.	0.7	2
26606	Ab-initio study of substitutional doping of Mg in In<inf>0.5</inf>Ga<inf>0.5</inf>N. , 2017, , .		0
26607	Energy loss and surface temperature effects in ab initio molecular dynamics simulations: N adsorption on Ag(111) as a case study. Physical Review B, 2017, 96, .	1.1	19
26608	Graphdiyne nanoribbons with open hexagonal rings: Existence of topological unprotected edge states. Physics Letters, Section A: General, Atomic and Solid State Physics, 2017, 381, 3337-3341.	0.9	12
26609	Elastic, thermodynamic, electronic, and optical properties of recently discovered superconducting transition metal boride NbRuB: An ab-initio investigation. Chinese Physics B, 2017, 26, 106201.	0.7	31
26610	Tuning the growth and strain relaxation of ferroelectric BaTiO₃ thin films on SrRuO₃ electrode: influence on electrical properties. EPJ Applied Physics, 2017, 80, 30303.	0.3	6

#	Article	IF	Citations
26611	Ab initio study of phonon dispersion and thermodynamic properties of pure and doped pyrites. European Physical Journal B, 2017, 90, 1.	0.6	7
26612	Novel electronic properties of 2D MoS2/TiO2van der Waals heterostructure. Semiconductor Science and Technology, 2017, 32, 105011.	1.0	13
26613	Effect of B on Growth of Recrystallized Grain of Ti-added Ultra-low Carbon Cold-rolled Steel Sheets. Tetsu-To-Hagane/Journal of the Iron and Steel Institute of Japan, 2017, 103, 221-229.	0.1	2
26614	g-C3N4/SnS2 Heterostructure: a Promising Water Splitting Photocatalyst. Chinese Journal of Chemical Physics, 2017, 30, 36-42.	0.6	25
26615	DFT+U Analysis on Stability of Low-Index Facets in Hexagonal LaCoO3 Perovskite: Effect of Co3+ Spin States. Chinese Journal of Chemical Physics, 2017, 30, 295-302.	0.6	9
26616	The Reactivity of Anatase TiO2 (211) Surface and the Bond- Charge Counting Model. , 2017, , .		2
26617	Electronic Structure and Thermoelectric Properties of Pseudogap Intermetallic Compound Al₅Co₂. Nippon Kinzoku Gakkaishi/Journal of the Japan Institute of Metals, 2017, 81, 55-59.	0.2	1
26618	Impact of carbon-ion implantation on the nonlinear optical susceptibility of LiNbO_3. Optics Express, 2017, 25, 21444.	1.7	4
26619	Enhanced Framework Rigidity of a Zeolitic Metal-Azolate via Ligand Substitution. Crystals, 2017, 7, 99.	1.0	11
26620	Si- and Sn-containing SiOCN-based nanocomposites as anode materials for lithium ion batteries: synthesis, thermodynamic characterization and modeling. International Journal of Materials Research, 2017, 108, 920-932.	0.1	8
26621	Intercalation of Si between MoS₂ layers. Beilstein Journal of Nanotechnology, 2017, 8, 1952-1960.	1.5	27
26622	Structural model of silicene-like nanoribbons on a Pb-reconstructed Si(111) surface. Beilstein Journal of Nanotechnology, 2017, 8, 1836-1843.	1.5	7
26623	Exploring the Mechanical Anisotropy and Ideal Strengths of Tetragonal B4CO4. Materials, 2017, 10, 128.	1.3	20
26624	Al-Doped ZnO Monolayer as a Promising Transparent Electrode Material: A First-Principles Study. Materials, 2017, 10, 359.	1.3	42
26625	Deformation Modes and Anisotropy of Anti-Perovskite Ti3AN (A = Al, In and Tl) from First-Principle Calculations. Materials, 2017, 10, 362.	1.3	9
26626	Theoretical Investigations of Si-Ge Alloys in P42/ncm Phase: First-Principles Calculations. Materials, 2017, 10, 599.	1.3	14
26627	Comparative Study on ZnO Monolayer Doped with Al, Ga and In Atoms as Transparent Electrodes. Materials, 2017, 10, 703.	1.3	16
26628	Mechanical, Anisotropic, and Electronic Properties of XN (X = C, Si, Ge): Theoretical Investigations. Materials, 2017, 10, 912.	1.3	3

#	Article	IF	Citations
26629	Modeling the Non-Equilibrium Process of the Chemical Adsorption of Ammonia on GaN(0001) Reconstructed Surfaces Based on Steepest-Entropy-Ascent Quantum Thermodynamics. Materials, 2017, 10, 948.	1.3	12
26630	A First-Principle Theoretical Study of Mechanical and Electronic Properties in Graphene Single-Walled Carbon Nanotube Junctions. Materials, 2017, 10, 1300.	1.3	15
26631	Formation of Surface and Quantum-Well States in Ultra Thin Pt Films on the Au(111) Surface. Materials, 2017, 10, 1409.	1.3	5
26632	Two B-C-O Compounds: Structural, Mechanical Anisotropy and Electronic Properties under Pressure. Materials, 2017, 10, 1413.	1.3	23
26633	Mechanical, Thermodynamic and Electronic Properties of Wurtzite and Zinc-Blende GaN Crystals. Materials, 2017, 10, 1419.	1.3	52
26634	The Role of Î²-Carbides as Hydrogen Traps in High-Mn Steels. Metals, 2017, 7, 264.	1.0	27
26635	DFT Modelling of Cu Segregation in Al-Cu Alloys Covered by an Ultrathin Oxide Film and Possible Links with Passivity. Metals, 2017, 7, 366.	1.0	9
26636	Na-Montmorillonite Edge Structure and Surface Complexes: An Atomistic Perspective. Minerals (Basel,) Tj ETQq1 1 0.784314 rgBT /Ov	0.8	17
26637	First Principles Thermodynamics of Minerals at HPâ€“HT Conditions: MgO as a Prototypical Material. Minerals (Basel, Switzerland), 2017, 7, 183.	0.8	22
26638	Pnma-BN: Another Boron Nitride Polymorph with Interesting Physical Properties. Nanomaterials, 2017, 7, 3.	1.9	41
26639	Changes in the reflectivity of a lithium niobate crystal decorated with a graphene layer. Journal of Physics: Conference Series, 2017, 792, 012069.	0.3	2
26640	Graphene-based materials and their potential applications. , 2017, , 267-287.		2
26641	Theoretical Prediction of Electronic Structures and Phonon Dispersion of Ce2XN2 (X = S, Se, and Te) Ternary. Computation, 2017, 5, 29.	1.0	2
26642	Ab Initio Study of the Elastic and Mechanical Properties of B19 TiAl. Crystals, 2017, 7, 39.	1.0	35
26643	First-Principles Investigations on Structural and Elastic Properties of Orthorhombic TiAl under Pressure. Crystals, 2017, 7, 111.	1.0	27
26644	Elastic, Mechanical and Phonon Behavior of Wurtzite Cadmium Sulfide under Pressure. Crystals, 2017, 7, 164.	1.0	22
26645	First Principles Study on Structure Stability and Mechanical Properties of YNi2B2C and LuNi2B2C under Pressure. Crystals, 2017, 7, 173.	1.0	3
26646	First-Principles Study of the Nonlinear Elasticity of Rare-Earth Hexaborides REB6 (RE = La, Ce). Crystals, 2017, 7, 320.	1.0	5

#	Article	IF	Citations
26647	Insulation Strength and Decomposition Characteristics of a C6F12O and N2 Gas Mixture. Energies, 2017, 10, 1170.	1.6	48
26648	Deciphering Molecular Mechanisms of Interface Buildup and Stability in Porous Si/Eumelanin Hybrids. International Journal of Molecular Sciences, 2017, 18, 1567.	1.8	15
26649	Nonlinear Elasticity of Borocarbide Superconductor YNi₂B₂C: A First-Principles Study. Advances in Materials Science and Engineering, 2017, 2017, 1-8.	1.0	0
26650	An Ab-initio study on UAl for nuclear applications. EPJ Web of Conferences, 2017, 154, 01021.	0.1	0
26651	The Adhesion Mechanism of Marine Mussel Foot Protein: Adsorption of L-Dopa on<mml:math xmlns:mml="http://www.w3.org/1998/Math/MathML" id="M1"><mml:mrow><mml:mi mathvariant="bold-italic">Î±</mml:mi></mml:mrow></mml:math>- andâ€‰<mml:math xmlns:mml="http://www.w3.org/1998/Math/MathML" id="M2"><mml:mrow><mml:mi mathvariant="bold-italic">Î²</mml:mi></mml:mrow></mml:math>-Cristobalite Silica Using Density Functional Theory. Journal of Chemistry, 2017, 2017, 1-6.	0.9	15
26652	Effect of (0001) Strain on the Electronic and Magnetic Properties of the Half-Metallic Ferromagnet Fe₂Si. Advances in Materials Science and Engineering, 2017, 2017, 1-7.	1.0	1
26653	A Multiscale Simulation Method and Its Application to Determine the Mechanical Behavior of Heterogeneous Geomaterials. Advances in Materials Science and Engineering, 2017, 2017, 1-12.	1.0	2
26654	Spectroscopic Characterization of Omeprazole and Its Salts. Journal of Spectroscopy, 2017, 2017, 1-11.	0.6	5
26655	Ab Initio Study of Electronic Transport in Cubic-HfO2 Grain Boundaries. Journal of Nanomaterials, 2017, 2017, 1-9.	1.5	3
26656	Tunable SnO₂ Nanoribbon by Electric Fields and Hydrogen Passivation. Journal of Nanomaterials, 2017, 2017, 1-12.	1.5	0
26657	A DFT study on the electronic structure of tungsten trioxide polymorphs. Turkish Journal of Physics, 2017, 41, 238-243.	0.5	5
26658	Atomistic study of comblike structure on the MoO2/Mo(110) surface by scanning tunneling microscopy and density functional theory calculations. Japanese Journal of Applied Physics, 2017, 56, 095501.	0.8	2
26659	Alane adsorption and dissociation on the Si(0â€‰0â€‰1) surface. Journal of Physics Condensed Matter, 2017, 29, 395001.	0.7	3
26660	Application of TiO2 Nanotubes Gas Sensors in Online Monitoring of SF6 Insulated Equipment. , 2017, , .		5
26661	Organic materials database: An open-access online database for data mining. PLoS ONE, 2017, 12, e0171501.	1.1	65
26662	A theoretical calculation of the electronic and magnetic behaviour of C-doped zincblende AlN. Journal of Physics: Conference Series, 2017, 935, 012001.	0.3	2
26663	A full understanding of oxygen reduction reaction mechanism on Au(1â€‰1â€‰1) surface. Journal of Physics Condensed Matter, 2017, 29, 365201.	0.7	7
26664	Design and adjustment of the graphene work function via size, modification, defects, and doping: a first-principle theory study. Nanoscale Research Letters, 2017, 12, 642.	3.1	28

#	Article	IF	Citations
26665	Possible bcc â† sc phase transitions in Caâ€“Sr solid solutions under pressure. Physics of Metals and Metallography, 2017, 118, 723-730.	0.3	1
26666	First-principles study of the stability of NbC-SiC solid solutions. , 2017, , .		1
26667	Complex interplay of interatomic bonding in a multi-component pyrophosphate crystal: K 2 Mg (H 2 P 2) Tj ETQq0 0 0 rgBT /Overlock 10	1.1	13
26668	Structural and electronic properties of Ir-doped zigzag silicene nanoribbons. , 2017, , .		0
26669	Thermal transport in high electron mobility transistors: A Boltzmann transport equation study. , 2017, , .		0
26670	Vibrational and Thermodynamic Properties of Layered LiM0.5Ni0.5O2 (M=Mn, Co) Cathode Materials for Li Ion Batteries. International Journal of Electrochemical Science, 2017, , 2963-2972.	0.5	1
26671	Clustering and spin interactions in Fe-doped diamond. Journal of Physics: Conference Series, 2017, 905, 012033.	0.3	3
26672	Structure and Optical Properties of K0.67Rb1.33Al2B2O7 Crystal. Crystals, 2017, 7, 104.	1.0	3
26673	First-Principles Calculation of Adsorption of Shale Gas on CaCO3 (100) Surfaces. Journal of Applied Biomaterials and Functional Materials, 2017, 15, 45-51.	0.7	2
26674	Stability of Montmorillonite Edge Faces Studied Using First-Principles Calculations. Clays and Clay Minerals, 2017, 65, 252-272.	0.6	3
26675	Theoretical Analysis of Elastic, Mechanical and Phonon Properties of Wurtzite Zinc Sulfide under Pressure. Crystals, 2017, 7, 161.	1.0	14
26676	Theoretical Studies of the Adsorption and Migration Behavior of Boron Atoms on Hydrogen-Terminated Diamond (001) Surface. Coatings, 2017, 7, 57.	1.2	8
26677	Manipulating polarized light with a planar slab of black phosphorus. Journal of Physics Communications, 2017, 1, 045003.	0.5	31
26678	Tunable plasmons in regular planar arrays of graphene nanoribbons with armchair and zigzag-shaped edges. Beilstein Journal of Nanotechnology, 2017, 8, 172-182.	1.5	18
26679	First-Principles Calculations of Ti₂N and Ti₂NT₂ (T = O, F, OH) Monolayers as Potential Anode Materials for Lithium-Ion Batteries and Beyond. Journal of Physical Chemistry C, 2017, 121, 13025-13034.	1.5	151
26680	New tetrahedral polymorphs of the group-14 elements. Journal of Physics: Conference Series, 2017, 950, 042010.	0.3	0
26681	Ab initiostudies of isolated boron substitutional defects ingraphane. Journal of Physics: Conference Series, 2017, 905, 012032.	0.3	0
26682	Unexpected robustness of the band gaps of TiO2 under high pressures. Journal of Physics Communications, 2017, 1, 055014.	0.5	3

#	Article	IF	Citations
26683	Infrared Investigations of the Neutral-Ionic Phase Transition in TTF-CA and Its Dynamics. Crystals, 2017, 7, 17.	1.0	15
26684	Infrared Spectroscopic and Computational Studies on Li₄FeH₆ with High Gravimetric Hydrogen Density. Materials Transactions, 2017, 58, 157-159.	0.4	4
26685	Novel band structures in germanene on aluminium nitride substrate. Japanese Journal of Applied Physics, 2017, 56, 095201.	0.8	2
26686	High coverage H2 adsorption and dissociation on fcc Co surfaces from DFT and thermodynamics. International Journal of Hydrogen Energy, 2018, 43, 5576-5590.	3.8	23
26687	Atomic cluster structures, phase stability and physicochemical properties of binary Mg-X (X= Ag, Al,) Tj ETQq0 0 0 rgBT /Overlock 10 Tf 5	£.8	34
26688	Two-site jumps in dimethyl sulfone studied by one- and two-dimensional 17O NMR spectroscopy. Journal of Magnetic Resonance, 2018, 288, 84-94.	1.2	16
26689	Lewis Base Passivation of Hybrid Halide Perovskites Slows Electronâ€“Hole Recombination: Time-Domain Ab Initio Analysis. Journal of Physical Chemistry Letters, 2018, 9, 1164-1171.	2.1	90
26690	Suppression of Cation Segregation in (La,Sr)CoO_{3â^'Î´} by Elastic Energy Minimization. ACS Applied Materials & Interfaces, 2018, 10, 8057-8065.	4.0	44
26691	Depolymerization of sodium polyphosphates on an iron oxide surface at high temperature. Physical Chemistry Chemical Physics, 2018, 20, 7819-7835.	1.3	15
26692	Ab initio understanding of magnetic properties in Zn2+ substitution of Fe3O4 ultra-thin film with dilute Zn substitution. AIP Advances, 2018, 8, .	0.6	4
26693	A Novel Interconnected Structure of Graphene-Carbon Nanotubes for the Application of Methane Adsorption. IEEE Sensors Journal, 2018, 18, 1555-1561.	2.4	5
26694	Electronic structure, magnetic, mechanical and thermo-physical behavior of double perovskite Ba2MgOsO6. European Physical Journal Plus, 2018, 133, 1.	1.2	34
26695	Structural and optical properties of Ni atoms and $$hbox {Ni}_{55}$$ Ni 55 cluster adsorbed on a rutile $$hbox {TiO}_{2}$$. Theoretical Chemistry Accounts, 2018, 137, 1.	0.5	2
26696	Adsorption of Carbohydrazide on Au(111) and Au3Ni(111) Surfaces. Catalysis Letters, 2018, 148, 1073-1079.	1.4	4
26697	Calculations of the Structural, Elastic, Magnetic, and Electronic Properties of the New Compound BaZr0.5Mn0.5O3 with Tetragonal Structure. Journal of Superconductivity and Novel Magnetism, 2018, 31, 3339-3346.	0.8	3
26698	First-principles investigation of quantum transport in GeP3 nanoribbon-based tunneling junctions. Frontiers of Physics, 2018, 13, 1.	2.4	6
26699	Structural, dynamical and thermodynamic properties of CdXP2 (XÂ=ÂSi, Ge) from first principles. Indian Journal of Physics, 2018, 92, 315-323.	0.9	5
26700	Tuning the magnetic properties of DyNiO3 by high-pressures. Computational Materials Science, 2018, 146, 213-219.	1.4	2

#	Article	IF	Citations
26701	Evaluation of H2S sensing characteristics of metalsâ€“doped graphene and metals-decorated graphene: Insights from DFT study. Physica E: Low-Dimensional Systems and Nanostructures, 2018, 99, 261-268.	1.3	64
26702	Structural analysis and electrical characterization of cation-substituted lithium ion conductors Li1â^'Ti1â^'MOPO4 (Mâ€¯=â€¯Nb, Ta, Sb). Solid State Ionics, 2018, 319, 170-179.	1.3	4
26703	Hybrid Dionâ€“Jacobson 2D Lead Iodide Perovskites. Journal of the American Chemical Society, 2018, 140, 3775-3783.	6.6	686
26704	A controllable robust multiferroic GaTeCl monolayer with colossal 2D ferroelectricity and desirable multifunctionality. Nanoscale, 2018, 10, 5990-5996.	2.8	59
26705	Novel electronic properties of two-dimensional As_xSb_y alloys studied using DFT. Journal of Materials Chemistry C, 2018, 6, 2854-2861.	2.7	17
26706	Room-temperature relaxor ferroelectricity and photovoltaic effects in tin titanate directly deposited on a silicon substrate. Physical Review B, 2018, 97, .	1.1	28
26707	Unconventional field induced phases in a quantum magnet formed by free radical tetramers. Physical Review B, 2018, 97, .	1.1	5
26708	Graphite as Cointercalation Electrode for Sodiumâ€ion Batteries: Electrode Dynamics and the Missing Solid Electrolyte Interphase (SEI). Advanced Energy Materials, 2018, 8, 1702724.	10.2	191
26709	First-principles study of the structural, elastic and electronic properties of SbXI (X=S, Se, Te) crystals. Journal of Molecular Modeling, 2018, 24, 66.	0.8	23
26710	Enhanced carbon monoxide sensing properties of TiO2 with exposed (0 0 1) facet: A combined first-principle and experimental study. Applied Surface Science, 2018, 442, 507-516.	3.1	85
26711	An ab initio study of mechanical and dynamical stability of MoSi2. Journal of Alloys and Compounds, 2018, 746, 720-728.	2.8	17
26712	Investigation on structure, electronic and magnetic properties of Cr doped (ZnO)12 clusters: First-principles calculations. Physica E: Low-Dimensional Systems and Nanostructures, 2018, 99, 51-57.	1.3	2
26713	Analysis of Photocatalytic Nitrogen Fixation on Rutile TiO₂(110). ACS Sustainable Chemistry and Engineering, 2018, 6, 4648-4660.	3.2	79
26714	Probing the interatomic potential of solids with strong-field nonlinear phononics. Nature, 2018, 555, 79-82.	13.7	105
26715	Effect of glycine functionalization of 2D titanium carbide (MXene) on charge storage. Journal of Materials Chemistry A, 2018, 6, 4617-4622.	5.2	103
26716	Structural and electronic properties of hydrogenated GaBi and InBi honeycomb monolayers with point defects. RSC Advances, 2018, 8, 7022-7028.	1.7	9
26717	Phonon glass behavior beyond traditional cage structures: synthesis, crystal and electronic structure, and properties of KMg4Sb3. Journal of Materials Chemistry A, 2018, 6, 4759-4767.	5.2	17
26718	New two-dimensional V-V binary compounds with a honeycomb-like structure: a first-principles study. Materials Research Express, 2018, 5, 035903.	0.8	34

#	Article	IF	Citations
26719	Oxidative dehydrogenation and dry reforming of n-butane with CO2 over NiFe bimetallic catalysts. Applied Catalysis B: Environmental, 2018, 231, 213-223.	10.8	33
26720	Spin polarization properties of benzene/graphene with transition metals as dopants: First principles calculations. Applied Surface Science, 2018, 439, 1158-1162.	3.1	14
26721	Effect of lattice structure changes caused by Al component on optical properties of AlGaN materials. Optik, 2018, 164, 72-77.	1.4	5
26722	New Iron-Based Intercalation Host for Lithium-Ion Batteries. Chemistry of Materials, 2018, 30, 1956-1964.	3.2	20
26723	Suppression of material transfer at contacting surfaces: the effect of adsorbates on Al/TiN and Cu/diamond interfaces from first-principles calculations. Journal of Physics Condensed Matter, 2018, 30, 105001.	0.7	7
26724	Modulation of electronic and magnetic properties in InSe nanoribbons: edge effect. Nanotechnology, 2018, 29, 205708.	1.3	15
26725	The effect of adding side group and changing contact geometry in single pyrene molecular devices. International Journal of Modern Physics B, 2018, 32, 1850078.	1.0	0
26726	The oxidation of methanol on hydroxylated m-ZrO2(â^Â1 1 1): a first-principles study. Theoretical Chemistry Accounts, 2018, 137, 1.	0.5	2
26727	Characterization of point defects in monolayer arsenene. Applied Surface Science, 2018, 443, 74-82.	3.1	31
26728	Optoelectronic properties of candidate photovoltaic Cu2PbSiS4, Ag2PbGeS4 and KAg2SbS4 semiconductors. Journal of Alloys and Compounds, 2018, 746, 405-412.	2.8	10
26729	Water Dissociative Adsorption on Î±-Al₂O₃(112Ì…0) Is Controlled by Surface Site Undercoordination, Density, and Topology. Journal of Physical Chemistry C, 2018, 122, 6573-6584.	1.5	17
26730	Combined Experimental and Theoretical Study of Methyl Acetoacetate Adsorption on Ni{100}. Journal of Physical Chemistry C, 2018, 122, 6186-6194.	1.5	6
26731	Switch in Relative Stability between cis and trans 2-Butene on Pt(111) as a Function of Experimental Conditions: A Density Functional Theory Study. ACS Catalysis, 2018, 8, 3067-3075.	5.5	8
26732	An atomic-scale view of single-site Pt catalysis for low-temperature CO oxidation. Nature Catalysis, 2018, 1, 192-198.	16.1	292
26733	First-principles study of the electronic and optical properties of Li(Nb,Os)O3 alloys. Applied Physics Letters, 2018, 112, .	1.5	7
26734	Quantum chemistry as a tool to assess energetic and spectroscopic properties of C1 and C2 hydrocarbons in MOF-74-Mg. Theoretical Chemistry Accounts, 2018, 137, 1.	0.5	1
26735	Lubrication of dislocation glide in MgO by hydrous defects. Physics and Chemistry of Minerals, 2018, 45, 713-726.	0.3	3
26736	Electronic structure and optical properties of Al0.25Ga0.75N with point defects and Mg-defect complexes. Optical and Quantum Electronics, 2018, 50, 1.	1.5	2

#	Article	IF	Citations
26737	The Structural Stability and Mechanical Properties of $$hbox {Cu}_{2}hbox {MnAl}$$ Cu 2 MnAl and $$hbox {Cu}_{2}hbox {MnIn}. Journal of Electronic Materials, 2018, 47, 3005-3017.	1.0	2
26738	Experimental and theoretical studies of magnetic properties for MnTeMoO6 crystal. Journal of Alloys and Compounds, 2018, 747, 591-594.	2.8	3
26739	Mn promoted Co catalysts for Fischer-Tropsch production of light olefins â€“ An experimental and theoretical study. Journal of Catalysis, 2018, 361, 23-32.	3.1	62
26740	A new flatland buddy as toxic gas scavenger: A first principles study. Journal of Hazardous Materials, 2018, 351, 337-345.	6.5	113
26741	Thickness-dependent surface energies of few-layered arsenene and antimonene films in Î± and Î² phases. Physica E: Low-Dimensional Systems and Nanostructures, 2018, 101, 38-43.	1.3	8
26742	Electrical Conductivity of Copper Hexamers Tuned by their Ground-State Valences. Inorganic Chemistry, 2018, 57, 3443-3450.	1.9	10
26743	Oxygen Vacancy Formation and Water Adsorption on Reduced AnO₂{111}, {110}, and {100} Surfaces (An = U, Pu): A Computational Study. Journal of Physical Chemistry C, 2018, 122, 7149-7165.	1.5	45
26744	Unveiling the Structural and Electronic Properties of the B-Nb₂O₅ Surfaces and Their Interaction with H₂O and H₂O₂. Journal of Physical Chemistry C, 2018, 122, 6618-6628.	1.5	18
26745	Electronic Origin and Kinetic Feasibility of the Lattice Oxygen Participation During the Oxygen Evolution Reaction on Perovskites. Journal of Physical Chemistry Letters, 2018, 9, 1473-1479.	2.1	62
26746	Metallic Bond-Enabled Wetting Behavior at the Liquid Ga/CuGa₂ Interfaces. ACS Applied Materials & Interfaces, 2018, 10, 9203-9210.	4.0	101
26747	Edge defect switched dual spin filter in zigzag hexagonal boron nitride nanoribbons. Physical Chemistry Chemical Physics, 2018, 20, 9241-9247.	1.3	11
26748	Effect of cation substitution on the pseudocapacitive performance of spinel cobaltite MCo₂O₄ (M = Mn, Ni, Cu, and Co). Journal of Materials Chemistry A, 2018, 6, 10674-10685.	5.2	266
26749	Transition-metal-doped group-IV monochalcogenides: a combination of two-dimensional triferroics and diluted magnetic semiconductors. Nanotechnology, 2018, 29, 215703.	1.3	41
26750	Theoretical study on electronic structure and thermoelectric properties of PbS _x Te _{1â" x} (x = 0.25, 0.5, and 0.75) solid solution. Chinese Physics B, 2018, 27, 026103.	0.7	4
26751	Crystal structure stability and electronic properties of the layered nickelate <mml:math xmlns:mml="http://www.w3.org/1998/Math/MathML"><mml:mrow><mml:msub><mml:mi>La</mml:mi><mml:mn>4</mml:mn></mml:r mathvariant="normal">O</mml:mi><mml:mn>10</mml:mn></mml:msub></mml:mrow></mml:math>. Physical Review B, 2018, 97, .	1.1	8
26752	Quartic Anharmonicity of Rattlers and Its Effect on Lattice Thermal Conductivity of Clathrates from First Principles. Physical Review Letters, 2018, 120, 105901.	2.9	130
26753	Elemental Ferroelectricity and Antiferroelectricity in Groupâ€V Monolayer. Advanced Functional Materials, 2018, 28, 1707383.	7.8	145
26754	Crystalline phase engineering on cocatalysts: A promising approach to enhancement on photocatalytic conversion of carbon dioxide to fuels. Applied Catalysis B: Environmental, 2018, 230, 145-153.	10.8	29

#	Article	IF	Citations
26755	Absolute band structure determination on naturally occurring rutile with complex chemistry: Implications for mineral photocatalysis on both Earth and Mars. Applied Surface Science, 2018, 439, 660-671.	3.1	12
26756	Study of electron transport in the functionalized nanotubes and their impact on the electron transfer in the active site of horseradish peroxidase. Journal of Physics and Chemistry of Solids, 2018, 116, 313-323.	1.9	8
26757	Pushing Nonlinear Optical Oxides into the Mid-Infrared Spectral Region Beyond 10 Î¼m: Design, Synthesis, and Characterization of La₃SnGa₅O₁₄. Journal of the American Chemical Society, 2018, 140, 4684-4690.	6.6	117
26758	Theoretical study of tetrahedral site occupation by hydrogen in Pd nanoparticles. Journal of Chemical Physics, 2018, 148, 034705.	1.2	18
26759	Comparison of mechanical and thermodynamic properties of fcc and bcc titanium under high pressure. Materials Research Express, 2018, 5, 026527.	0.8	1
26760	First-principles momentum distributions and vibrationally corrected permittivities of hexagonal and cubic ice. Physical Review B, 2018, 97, .	1.1	3
26761	Exploring single-layered SnSe honeycomb polymorphs for optoelectronic and photovoltaic applications. Physical Review B, 2018, 97, .	1.1	45
26762	The characterization of the VN H defects in diamond through the infrared vibrational spectrum. A quantum mechanical investigation. Carbon, 2018, 132, 210-219.	5.4	20
26763	Atomic self-diffusion in TiNi. Computational Materials Science, 2018, 148, 1-9.	1.4	7
26764	P21/c-C2/c phase transition and mixing properties of the (Li,Na)FeGe2O6 solid solution: A calorimetric and thermodynamic study. Journal of Chemical Thermodynamics, 2018, 120, 123-140.	1.0	6
26765	Coralloid Carbon Fiber-Based Composite Lithium Anode for Robust Lithium Metal Batteries. Joule, 2018, 2, 764-777.	11.7	609
26766	Synthesis of armchair graphene nanoribbons from the 10,10â€²-dibromo-9,9â€²-bianthracene molecules on Ag(111): the role of organometallic intermediates. Scientific Reports, 2018, 8, 3506.	1.6	39
26767	Stability and electronic structure of hydrogen vacancies in ADP: hybrid DFT with vdW correction. RSC Advances, 2018, 8, 6931-6939.	1.7	11
26768	A theoretical insight into H accumulation and bubble formation by applying isotropic strain on the Wâ€“H system under a fusion environment. Nuclear Fusion, 2018, 58, 046014.	1.6	1
26769	Encapsulation of Cadmium Selenide Nanocrystals in Biocompatible Nanotubes: DFT Calculations, Xâ€ray Diffraction Investigations, and Confocal Fluorescence Imaging. ChemistryOpen, 2018, 7, 144-158.	0.9	15
26770	Structural, electronic and magnetic properties of Mn-doped and vacancy-doped 2D LiZnP. Journal of Magnetism and Magnetic Materials, 2018, 458, 129-133.	1.0	1
26771	Oxygen adsorption on the Al 0.25 Ga 0.75 N (0001) surface: A first-principles study. Solid State Communications, 2018, 272, 17-21.	0.9	3
26772	Molecules ionization at phase transition in warm dense hydrogen. Journal of Physics: Conference Series, 2018, 946, 012121.	0.3	0

#	Article	IF	Citations
26773	The structural, electronic and optical properties of Auâ€“ZnO interface structure from the first-principles calculation. Modern Physics Letters B, 2018, 32, 1850107.	1.0	3
26774	Design of Pd-Pb Catalysts for Glycerol and Ethylene Glycol Electrooxidation in Alkaline Medium. Electrocatalysis, 2018, 9, 480-485.	1.5	20
26775	First principles study of surface stability and segregation of PdRuRh ternary metal alloy system. Surface Science, 2018, 671, 51-59.	0.8	6
26776	Molecule-Adsorbed Topological Insulator and Metal Surfaces: A Comparative First-Principles Study. Chemistry of Materials, 2018, 30, 1849-1855.	3.2	10
26777	Thermodynamic Properties of Uranyl-Containing Materials Based on Density Functional Theory. Journal of Physical Chemistry C, 2018, 122, 5254-5267.	1.5	32
26778	Fe and Ni Dopants Facilitating Ammonia Synthesis on Mn₄N and Mechanistic Insights from First-Principles Methods. Journal of Physical Chemistry C, 2018, 122, 6109-6116.	1.5	32
26779	A beryllium-free deep-UV nonlinear optical material CsNaMgP₂O₇with honeycomb-like topological layers. Journal of Materials Chemistry C, 2018, 6, 3910-3916.	2.7	48
26780	Photo-Excited Surface Dynamics from Massively Parallel Constrained-DFT Calculations. , 2018, , 157-168.		0
26781	Single layer of carbon phosphide as an efficient material for optoelectronic devices. Journal of Materials Science, 2018, 53, 8314-8327.	1.7	41
26782	Experimental and Theoretical Investigation of Structures, Stoichiometric Diversity, and Bench Stability of Cocrystals with a Volatile Halogen Bond Donor. Crystal Growth and Design, 2018, 18, 2387-2396.	1.4	19
26783	Computational Screening of Hydration Reactions for Thermal Energy Storage: New Materials and Design Rules. Chemistry of Materials, 2018, 30, 2006-2017.	3.2	45
26784	Is ReO₃ a mixed ionicâ€“electronic conductor? A DFT study of defect formation and migration in a B^{VI}O₃ perovskite-type oxide. Physical Chemistry Chemical Physics, 2018, 20, 8008-8015.	1.3	16
26785	Rotational state modification and fast ortho-para conversion of <mml:math xmlns:mml="http://www.w3.org/1998/Math/MathML"><mml:msub><mml:mi mathvariant="normal">H</mml:mi><mml:mn>2</mml:mn></mml:msub></mml:math> trapped within the highly anisotropic potential of Pd(210). Physical Review B, 2018, 97, .	1.1	8
26786	Crown oxygen-doping graphene with embedded main-group metal atoms. European Physical Journal B, 2018, 91, 1.	0.6	3
26787	Atomic-scale distorted lattice in chemically disordered equimolar complex alloys. Acta Materialia, 2018, 150, 182-194.	3.8	89
26788	Contribution of lattice parameter and vacancies on anisotropic optical properties of tin sulphide. Journal of Alloys and Compounds, 2018, 746, 9-18.	2.8	9
26789	MoSe2 nanosheets for detection of methanol and ethanol vapors: A DFT study. Journal of Molecular Graphics and Modelling, 2018, 81, 97-105.	1.3	41
26790	Cathodic Corrosion at the Bismuthâ€“Ionic Liquid Electrolyte Interface under Conditions for CO₂ Reduction. Chemistry of Materials, 2018, 30, 2362-2373.	3.2	38

#	Article	IF	Citations
26791	Diboryne Nanostructures Stabilized by Multitopic N-Heterocyclic Carbenes: A Computational Study. Inorganic Chemistry, 2018, 57, 3931-3940.	1.9	9
26792	Enhanced Out-of-Plane Electrical Transport in n-Type SnSe Thermoelectrics Induced by Resonant States and Charge Delocalization. ACS Applied Materials & Interfaces, 2018, 10, 9889-9893.	4.0	16
26793	Trends in the Catalytic Activity of Hydrogen Evolution during CO₂ Electroreduction on Transition Metals. ACS Catalysis, 2018, 8, 3035-3040.	5.5	107
26794	Activating Layered Perovskite Compound Sr₂TiO₄ via La/N Codoping for Visible Light Photocatalytic Water Splitting. ACS Catalysis, 2018, 8, 3209-3221.	5.5	82
26795	Enhanced hydrogen permeability of hafnium nitride nanocrystalline membranes by interfacial hydride conduction. Journal of Materials Chemistry A, 2018, 6, 2730-2741.	5.2	16
26796	First principles analysis of the CDW instability of single-layer 1 T -TiSe ₂ and its evolution with charge carrier density. 2D Materials, 2018, 5, 025024.	2.0	20
26797	Revealing the correlation between real-space structure and chiral magnetic order at the atomic scale. Physical Review B, 2018, 97, .	1.1	7
26798	Atomically thin gallium layers from solid-melt exfoliation. Science Advances, 2018, 4, e1701373.	4.7	157
26799	In situ formation of molecular Ni-Fe active sites on heteroatom-doped graphene as a heterogeneous electrocatalyst toward oxygen evolution. Science Advances, 2018, 4, eaap7970.	4.7	176
26800	Mechanical and Thermophysical Properties of Cubic Rock-Salt AlN Under High Pressure. Journal of Electronic Materials, 2018, 47, 3430-3439.	1.0	13
26801	Effect of nitrogen doping on electronic and optical properties of ZnO sheet: DFT+U study. Computational Condensed Matter, 2018, 15, 1-6.	0.9	11
26802	Improving the mechanical processing of titanium by hydrogen doping: A first-principles study. International Journal of Hydrogen Energy, 2018, 43, 6756-6764.	3.8	15
26803	The thermodynamic, electronic and optical properties of GeP type ZnO under pressure calculated by Debye model and hybrid function. Materials Chemistry and Physics, 2018, 211, 206-213.	2.0	2
26804	Engineering phosphorus-doped LaFeO3-Î´ perovskite oxide as robust bifunctional oxygen electrocatalysts in alkaline solutions. Nano Energy, 2018, 47, 199-209.	8.2	202
26805	Ab initio modelling of the initial stages of the ODS particle formation process. Nuclear Instruments & Methods in Physics Research B, 2018, 435, 70-73.	0.6	5
26806	Spin-filtering, giant magnetoresistance, negative differential resistance effects and spin logic gate in P2TA-O2-based molecular junction with different transition metal atoms. Organic Electronics, 2018, 57, 104-109.	1.4	18
26807	Insights into exfoliation possibility of MAX phases to MXenes. Physical Chemistry Chemical Physics, 2018, 20, 8579-8592.	1.3	182
26808	Theoretical investigation of the structural, electronic, and thermodynamic properties of CdS1-xSex alloys. Journal of Applied Physics, 2018, 123, .	1.1	10

#	Article	IF	Citations
26809	Enhanced photocatalytic property of hybrid graphitic C3N4 and graphitic ZnO nanocomposite: the effects of interface and doping. Journal of Physics Condensed Matter, 2018, 30, 175001.	0.7	17
26810	Studying the properties of a predicted tetragonal silicon by first principles. Materials Research Express, 2018, 5, 035910.	0.8	1
26811	Half-metallic ferromagnetism prediction in MoS₂-based two-dimensional superlattice from first-principles. Modern Physics Letters B, 2018, 32, 1850098.	1.0	4
26812	A first-principle study on the electronic properties of substitutionally Cu (I, II)-doped LiNbO₃. Journal of Advanced Dielectrics, 2018, 08, 1820002.	1.5	18
26813	H₂S Sensing and Splitting on Atomâ€Functionalized Carbon Nanotubes: A Theoretical Study. Advanced Theory and Simulations, 2018, 1, 1700033.	1.3	15
26814	Effects of Oxygen on the Density of States and Elastic Properties of Hafniumâ€"First Principles Calculations. Minerals, Metals and Materials Series, 2018, , 389-397.	0.3	0
26815	Ultrasensitive H2S gas sensors based on p-type WS2 hybrid materials. Nano Research, 2018, 11, 4215-4224.	5.8	76
26816	Reversible K⁺-Insertion/Deinsertion and Concomitant Na⁺-Redistribution in Pâ€²3-Na_{0.52}CrO₂ for High-Performance Potassium-Ion Battery Cathodes. Chemistry of Materials, 2018, 30, 2049-2057.	3.2	76
26817	Anisotropic lattice softening near the structural phase transition in the thermosalient crystal 1,2,4,5-tetrabromobenzene. Physical Chemistry Chemical Physics, 2018, 20, 8523-8532.	1.3	31
26818	First-principles study of crystal structure, elastic stiffness constants, piezoelectric constants, and spontaneous polarization of orthorhombicPna2₁-M₂O₃(M) Tj ETQq1 1 0.784314 rgBT /Overlock 10 Tf 50	1.1	27
26819	Detection of sub-MeV dark matter with three-dimensional Dirac materials. Physical Review D, 2018, 97, .	1.6	142
26820	Reactive Dynamics Simulation Study on the Pyrolysis of Polymer Precursors To Generate Amorphous Silicon Oxycarbide Structures. Journal of Physical Chemistry C, 2018, 122, 5767-5773.	1.5	17
26821	Water Confined in Nanocapillaries: Two-Dimensional Bilayer Squarelike Ice and Associated Solidâ€"Liquidâ€"Solid Transition. Journal of Physical Chemistry C, 2018, 122, 6704-6712.	1.5	27
26822	Noble Metal Nanocluster Formation in Epitaxial Perovskite Thin Films. ACS Omega, 2018, 3, 2169-2173.	1.6	15
26823	Versatile two-dimensional silicon diphosphide (SiP₂) for photocatalytic water splitting. Nanoscale, 2018, 10, 6369-6374.	2.8	51
26824	A density functional study of the effect of hydrogen on electronic properties and band discontinuity at anatase TiO2/diamond interface. Journal of Applied Physics, 2018, 123, .	1.1	8
26825	Relativistic quasiparticle band structures of Mg2Si, Mg2Ge, and Mg2Sn: Consistent parameterization and prediction of Seebeck coefficients. Journal of Applied Physics, 2018, 123, .	1.1	18
26826	First-Principles Study of Helium Trapping in Carbide Precipitates (Cr23C6) in Ferritic-Martensitic Steels. Fusion Science and Technology, 2018, 74, 177-185.	0.6	5

#	Article	IF	Citations
26827	Direct Covalent Chemical Functionalization of Unmodified Two-Dimensional Molybdenum Disulfide. Chemistry of Materials, 2018, 30, 2112-2128.	3.2	93
26828	Engineering the Electronic Structure of Tin Sulfide Nanoribbons: A Computational Study. Journal of Physical Chemistry C, 2018, 122, 5731-5741.	1.5	18
26829	A Bit of Sugar on TiO₂: Quantum Chemical Insights on the Interfacial Interaction of Glycolaldehyde over Titanium Dioxide. Journal of Physical Chemistry C, 2018, 122, 6041-6051.	1.5	7
26830	Effect of Sn-Doping on Behavior of Li-Intercalation in V₂O₅ Cathode Materials of Li-Ion Batteries: A Computational Perspective. Journal of Physical Chemistry C, 2018, 122, 5896-5907.	1.5	24
26831	Enhanced CO₂ Conversion to CO by Silica-Supported Perovskite Oxides at Low Temperatures. ACS Catalysis, 2018, 8, 3021-3029.	5.5	87
26832	Computational evaluation of metal pentazolate frameworks: inorganic analogues of azolate metalâ€“organic frameworks. Chemical Science, 2018, 9, 3367-3375.	3.7	39
26833	First-principles studies of spontaneous polarization in mixed poly(vinylidene) Tj ETQq0 0 0 rgBT /Overlock 10 Tf 50 502 Td (fluoride)/2,3,	1.2	13
26834	Carbon monoxide sensing properties of B-, Al- and Ga-doped Si nanowires. Nanotechnology, 2018, 29, 204001.	1.3	13
26835	Study of quantum confinement effects in ZnO nanostructures. Materials Research Express, 2018, 5, 035032.	0.8	24
26836	Observation of soft phonon mode in <mml:math xmlns:mml="http://www.w3.org/1998/Math/MathML"><mml:mrow><mml:msub><mml:mi>TbFe</mml:mi><mml:mn>3</mml:mn></ by inelastic neutron scattering. Physical Review B, 2018, 97, .	1.1	1
26837	The Oxygen Reduction Reaction Mechanism on FeN₃Doped Divacancy Graphene: A Theoretical Perspective. Journal of the Electrochemical Society, 2018, 165, F145-F151.	1.3	18
26838	Structures of WxNy Crystals and Their Intrinsic Properties: First-Principles Calculations. Crystal Growth and Design, 2018, 18, 2270-2278.	1.4	20
26839	Ternary Bismuthide SrPtBi₂: Computation and Experiment in Synergism to Explore Solid-State Materials. Journal of Physical Chemistry C, 2018, 122, 5057-5063.	1.5	4
26840	Enhanced Hydrogen Production from Methanol Photolysis on a Formate-Modified Rutile-TiO₂(110) Surface. Journal of Physical Chemistry C, 2018, 122, 13774-13781.	1.5	7
26841	Optical properties of dense lithium in electride phases by first-principles calculations. Scientific Reports, 2018, 8, 3868.	1.6	14
26842	Sulfur film sandwiched between few-layered MoS₂ electrocatalysts and conductive reduced graphene oxide as a robust cathode for advanced lithiumâ€“sulfur batteries. Journal of Materials Chemistry A, 2018, 6, 5899-5909.	5.2	95
26843	Dopant-driven enhancements in the optoelectronic properties of laser ablated ZnO: Ga thin films. Journal of Applied Physics, 2018, 123, 161401.	1.1	10
26844	The role of dopant charge state on defect chemistry and grain growth of doped UO2. Acta Materialia, 2018, 150, 403-413.	3.8	51

#	Article	IF	Citations
26845	Site dependent enhancement of magnetic anisotropy in 4d and 5d impurity doped Î±â€³-Fe 16 N 2 : A first principles study. Current Applied Physics, 2018, 18, 526-533.	1.1	8
26846	Effects of pressure on the structural and electronic properties of linear carbon chains encapsulated in double wall carbon nanotubes. Carbon, 2018, 133, 446-456.	5.4	47
26847	Spontaneous antiferromagnetic order and strain effect on electronic properties of Î±-graphyne. Carbon, 2018, 131, 223-228.	5.4	19
26848	Electronic structure of Li+@C60: Photoelectron spectroscopy of the Li+@C60[PF6â^'] salt and STM of the single Li+@C60 molecules on Cu(111). Carbon, 2018, 133, 23-30.	5.4	17
26849	Mechanism of ferroelectric properties of (BaCa)(ZrTi)O3 from first-principles calculations. Ceramics International, 2018, 44, 9684-9688.	2.3	10
26850	Computational study of CNT based nanoscale reversible mass transport archival memory with Fe, Co and Ni nano-shuttles. Computational Materials Science, 2018, 146, 112-118.	1.4	3
26851	First-principles investigation of surface properties and adsorption of oxygen on Ni-22Cr and the role of molybdenum. Corrosion Science, 2018, 134, 103-111.	3.0	37
26852	Oxidation versus salt-film formation: Competitive adsorption on a series of metals from first-principles. Electrochimica Acta, 2018, 269, 93-101.	2.6	32
26853	Achieving highly efficient electrocatalytic oxygen evolution with ultrathin 2D Fe-doped nickel thiophosphate nanosheets. Nano Energy, 2018, 47, 257-265.	8.2	122
26854	Vanadium impurity effects on optical properties of Ti3N2 mono-layer: An ab-initio study. Results in Physics, 2018, 9, 270-274.	2.0	2
26855	Structural electronic and mechanical properties of YM2 (M=Mn, Fe, Co) laves phase compounds: First principle calculations analyzed with datamining approach. Solid State Communications, 2018, 274, 9-20.	0.9	8
26856	Theoretical study of methanol synthesis from CO2 and CO hydrogenation on the surface of ZrO2 supported In2O3 catalyst. Surface Science, 2018, 672-673, 7-12.	0.8	39
26857	On the Prediction of Water Contents in Na-Saturated Dioctahedral Smectites. Journal of Physical Chemistry C, 2018, 122, 7484-7493.	1.5	7
26858	Tunable Band Gaps of In_xGa_{1â€“x}N Alloys: From Bulk to Two-Dimensional Limit. Journal of Physical Chemistry C, 2018, 122, 6930-6942.	1.5	35
26859	Structural behaviour of copper chloride catalysts during the chlorination of CO to phosgene. Faraday Discussions, 2018, 208, 67-85.	1.6	3
26860	High-performance nonpolar a-plane GaN-based metalâ€“semiconductorâ€“metal UV photo-detectors fabricated on LaAlO₃ substrates. Journal of Materials Chemistry C, 2018, 6, 3417-3426.	2.7	40
26861	Magnetic and electronic properties of single-walled Mo₂C nanotube: a first-principles study. Journal of Physics Condensed Matter, 2018, 30, 155305.	0.7	6
26862	Structural, Electronic and Elastic Properties of Heavy Fermion YbTM2 (TM= Ir and Pt) Laves Phase Compounds. IOP Conference Series: Materials Science and Engineering, 2018, 310, 012054.	0.3	1

#	Article	IF	Citations
26863	Effects of Epitaxial Strain on Antiferrodistortion of AgNbO₃ from Firstâ€Principle Calculations. Physica Status Solidi - Rapid Research Letters, 2018, 12, 1800007.	1.2	7
26864	First-principles study on the structure and electronic property of gas molecules adsorption on Ge2Li2 monolayer. Applied Surface Science, 2018, 442, 390-397.	3.1	4
26865	The transport and optoelectronic properties of Î³-graphyne-based molecular magnetic tunnel junctions. Carbon, 2018, 132, 632-640.	5.4	20
26866	Observation of ferromagnetic ordering by fragmenting fluorine clusters in highly fluorinated graphene. Carbon, 2018, 132, 691-697.	5.4	13
26867	Stability, mechanical and electronic properties of ceramic interphases in biomedical composites via first-principles calculations. Ceramics International, 2018, 44, 9656-9663.	2.3	8
26868	Molecular-Level Insight into How Hydroxyl Groups Boost Catalytic Activity in CO2 Hydrogenation into Methanol. CheM, 2018, 4, 613-625.	5.8	110
26869	Half metallic ferromagnetism in Ni based half Heusler alloys. Computational Materials Science, 2018, 148, 87-103.	1.4	30
26870	Electrochemical and DFT studies of laser-alloyed TiB2/TiC/Al coatings on aluminium alloy. Corrosion Science, 2018, 136, 18-27.	3.0	21
26871	Theoretical study of the rutile based semiconductor with visible-light responsive photocatalytic activity for water splitting. International Journal of Hydrogen Energy, 2018, 43, 6131-6137.	3.8	1
26872	The defect chemistry of <mml:math xmlns:mml="http://www.w3.org/1998/Math/MathML" altimg="si1.gif" overflow="scroll"><mml:mrow><mml:mi mathvariant="normal">U</mml:mi><mml:msub><mml:mi mathvariant="normal">O</mml:mi><mml:mrow><mml:mn>2</mml:mn><mml:mo>Â±</mml:mo><mml:mi>x</mml:mi></mml:mrow></mml:msub></mml:mrow> from atomistic simulations. Journal of Nuclear Materials, 2018, 504, 251-260.	1.3	45
26873	Exploring the acid catalyzed isomerization of phenanthrene under confinement in mordenite. Microporous and Mesoporous Materials, 2018, 265, 241-249.	2.2	3
26874	First-principles predictions of structural, mechanical and electronic properties of Î²TiNb under high pressure. Superlattices and Microstructures, 2018, 116, 141-150.	1.4	7
26875	Lattice dynamics and thermal conductivity of lithium fluoride via first-principles calculations. Solid State Communications, 2018, 272, 28-32.	0.9	13
26876	Origin of enhanced catalytic activity of oxygen reduction reaction on zirconium oxynitrides: A first-principle study. Solid State Ionics, 2018, 317, 15-20.	1.3	6
26877	Imaging Catalytic Activation of CO₂ on Cu₂O (110): A First-Principles Study. Chemistry of Materials, 2018, 30, 1912-1923.	3.2	56
26878	Tunable Electronic and Optical Properties of Monolayer and Multilayer Janus MoSSe as a Photocatalyst for Solar Water Splitting: A First-Principles Study. Journal of Physical Chemistry C, 2018, 122, 6209-6216.	1.5	233
26879	Tuning Interfacial Magnetic Ordering via Polarization Control in Ferroelectric SrTiO₃/PbTiO₃ Heterostructure. ACS Applied Materials & Interfaces, 2018, 10, 10536-10542.	4.0	16
26880	Nucleobases-decorated boron nitride nanoribbons for electrochemical biosensing: a dispersion-corrected DFT study. Physical Chemistry Chemical Physics, 2018, 20, 8943-8950.	1.3	34

#	Article	IF	Citations
26881	Ab initio molecular dynamics study of 1-D superionic conduction and phase transition in Î²-eucryptite. Journal of Materials Chemistry A, 2018, 6, 5052-5064.	5.2	22
26882	The intrinsic interface properties of the top and edge 1T/2H MoS2 contact: A first-principles study. Journal of Applied Physics, 2018, 123, .	1.1	19
26883	Electron-phonon interaction and superconducting behaviour of ZrB and HfB: A first principle study. IOP Conference Series: Materials Science and Engineering, 2018, 310, 012023.	0.3	2
26884	Pourbaix Diagrams for H₂O Oxidation to Adsorbed OH on Pt(111) and Why They Differ from Those for Bulk Solids. Journal of Physical Chemistry C, 2018, 122, 9958-9964.	1.5	1
26885	Electrooxidation of Glycerol on Gold in Acidic Medium: A Combined Experimental and DFT Study. Journal of Physical Chemistry C, 2018, 122, 10489-10494.	1.5	32
26886	Improving Olefin Purification Using Metal Organic Frameworks with Open Metal Sites. ACS Applied Materials & Interfaces, 2018, 10, 16911-16917.	4.0	25
26887	Electronic and optical properties of boron phosphide/blue phosphorus heterostructures. Physical Chemistry Chemical Physics, 2018, 20, 12053-12060.	1.3	53
26888	Metalâ€“organic framework-derived integrated nanoarrays for overall water splitting. Journal of Materials Chemistry A, 2018, 6, 9009-9018.	5.2	74
26889	Titanium-related color centers in diamond: a density functional theory prediction. Journal of Materials Chemistry C, 2018, 6, 5261-5268.	2.7	26
26890	Insight into the structural, electronic, elastic and optical properties of the alkali hydride compounds, XH (X = Rb and Cs). AIP Advances, 2018, 8, 045017.	0.6	5
26891	Study of electronic and magnetic properties of h-BN on Ni surfaces: A DFT approach. AIP Conference Proceedings, 2018, , .	0.3	0
26892	Highly Sensitive Sensing of NO and NO₂ Gases by Monolayer C₃N. Advanced Theory and Simulations, 2018, 1, 1700008.	1.3	43
26893	Unveiling Hidden Catalysts for the Oxidative Coupling of Methane based on Combining Machine Learning with Literature Data. ChemCatChem, 2018, 10, 3223-3228.	1.8	62
26894	Combined DFT and Differential Electrochemical Mass Spectrometry Investigation of the Effect of Dopants in Secondary Zincâ€“Air Batteries. ChemSusChem, 2018, 11, 1933-1941.	3.6	23
26895	Planar metallic carbon allotrope from graphene-like nanoribbons. Carbon, 2018, 135, 21-28.	5.4	55
26896	Beryllium-Free Nonlinear Optical Crystals A₃Ba₃Li₂Ga₄B₆O₂₀F (A = K) Tj ETQq1 1 0.784314 rgBT Strong Covalent Connection between the _{âˆž}²[Li₂Ga₄B₆O₂₀F]^{9â€“} Double Layers. Inorganic Chemistry, 2018, 57, 5669-5676.	1.9	23
26897	New Insights into the Crystal Structures of Plutonium Hydrides from First-Principles Calculations. Journal of Physical Chemistry C, 2018, 122, 10103-10112.	1.5	15
26898	Unconventional strain-dependent conductance oscillations in pristine phosphorene. Physical Chemistry Chemical Physics, 2018, 20, 13508-13516.	1.3	26

#	Article	IF	Citations
26899	Repairing single and double atomic vacancies in a C₃N monolayer with CO or NO molecules: a first-principles study. Physical Chemistry Chemical Physics, 2018, 20, 13517-13527.	1.3	41
26900	Structural, electronic and thermal properties of super hard ternary boride, WAlB. AIP Conference Proceedings, 2018, , .	0.3	1
26901	Surface stress mediated image force and torque on an edge dislocation. Philosophical Magazine, 2018, 98, 1731-1743.	0.7	7
26902	Alkali-metal induced band structure deformation investigated by angle-resolved photoemission spectroscopy and first-principles calculations. Physical Review B, 2018, 97, .	1.1	5
26903	Location of the valence band maximum in the band structure of anisotropic <mml:math xmlns:mml="http://www.w3.org/1998/Math/MathML"><mml:mrow><mml:mn>1</mml:mn><mml:msup><mml:mi>T</mml:mi> Physical Review B, 2018, 97, .	1.1	11
26904	Configurational forces in electronic structure calculations using Kohn-Sham density functional theory. Physical Review B, 2018, 97, .	1.1	14
26905	Nonlocal and Nonadiabatic Effects in the Charge-Density Response of Solids: A Time-Dependent Density-Functional Approach. Physical Review Letters, 2018, 120, 166402.	2.9	16
26906	Bound nuclear spin states of H2 in an anisotropic potential induced by a stepped metal surface. Journal of Vacuum Science and Technology A: Vacuum, Surfaces and Films, 2018, 36, 030601.	0.9	5
26907	FP-LAPW investigation of Al₃(Sc1â^'xTix) alloys properties in L1₂ and D022 structures. International Journal of Modern Physics B, 2018, 32, 1850167.	1.0	12
26908	Toward the Effective Exploitation of Topological Phases of Matter in Catalysis: Chemical Reactions at the Surfaces of NbAs and TaAs Weyl Semimetals. Advanced Functional Materials, 2018, 28, 1800511.	7.8	40
26909	Multinuclear compounds of s-elements with sterically hindered Đ¾-semiquinonates and catecholates. Russian Chemical Bulletin, 2018, 67, 61-70.	0.4	3
26910	Surface states as electron transfer pathway enhanced charge separation in TiO2 nanotube water splitting photoanodes. Applied Catalysis B: Environmental, 2018, 234, 100-108.	10.8	77
26911	Evaluation of dry reforming reaction catalysts via computational screening. Catalysis Today, 2018, 312, 23-34.	2.2	8
26912	Epitaxial engineering of polar Îµ-Ga2O3 for tunable two-dimensional electron gas at the heterointerface. Applied Physics Letters, 2018, 112, .	1.5	77
26913	Effect on electronic and optical properties of Frenkel and Schottky defects in HfS2 monolayer. AIP Conference Proceedings, 2018, , .	0.3	5
26914	Theoretical study of methanol synthesis from CO2 hydrogenation on PdCu3(111) surface. Applied Surface Science, 2018, 451, 333-345.	3.1	43
26915	Oxygen reduction reaction on Pt(1â€¯1â€¯1), Pt(2â€¯2â€¯1), and Ni/Au1Pt3(2â€¯2â€¯1) surfaces: Probing scaling relationships of reaction energetics and interfacial composition. Chemical Engineering Science, 2018, 184, 239-250.	1.9	16
26916	Gate-tunable interfacial properties of in-plane ML MX₂ 1Tâ€²â€“2H heterojunctions. Journal of Materials Chemistry C, 2018, 6, 5651-5661.	2.7	54

#	Article	IF	Citations
26917	Dynamical simulation of electron transfer processes in self-assembled monolayers at metal surfaces using a density matrix approach. Journal of Chemical Physics, 2018, 148, 124705.	1.2	5
26918	Enhanced radial growth of Mg doped GaN nanorods: A combined experimental and first-principles study. Journal of Applied Physics, 2018, 123, .	1.1	6
26919	Currentâ€“Voltage Characteristics of the Aziridine-Based Nano-Molecular Wires: a Light-Driven Molecular Switch. Chinese Physics Letters, 2018, 35, 048501.	1.3	11
26920	The role of iron-oxide aerosols and sunlight in the atmospheric reduction of Hg(II) species: A DFT+U study. Applied Catalysis B: Environmental, 2018, 234, 347-356.	10.8	10
26921	Ohmic contacts between monolayer WSe2 and two-dimensional titanium carbides. Carbon, 2018, 135, 125-133.	5.4	55
26922	Study of the structural, vibrational and thermodynamic properties of natroxalate mineral using density functional theory. Journal of Solid State Chemistry, 2018, 263, 131-140.	1.4	23
26923	Surface structure analysis of Eu Zintl template on Ge(001). Surface Science, 2018, 674, 94-102.	0.8	9
26924	Quantum anomalous/valley Hall effect and tunable quantum state in hydrogenated arsenene decorated with a transition metal. Physical Chemistry Chemical Physics, 2018, 20, 12138-12148.	1.3	5
26925	Density-functional study on the dopant-segregation mechanism: Chemical potential dependence of dopant-defect complex at Si/SiO2 interface. Journal of Applied Physics, 2018, 123, 161425.	1.1	1
26926	Computational prediction of muon stopping sites using ab initio random structure searching (AIRSS). Journal of Chemical Physics, 2018, 148, 134114.	1.2	16
26927	Metal-nonmetal oscillations in doped blue phosphorene: a first-principles study. Materials Research Express, 2018, 5, 055007.	0.8	6
26928	Structures, Mechanical Properties and Band Structures of Pentagonal B<i>_x</i>N<i>_y</i> Monolayers. Materials Science Forum, 0, 913, 573-581.	0.3	3
26929	Buckminsterfullerene hybridized zinc oxide tetrapods: defects and charge transfer induced optical and electrical response. Nanoscale, 2018, 10, 10050-10062.	2.8	44
26930	Metallic Contact between MoS₂ and Ni via Au Nanoglue. Small, 2018, 14, e1704526.	5.2	32
26931	Facile preparation of novel hydrophobic sponges coated by Cu2O with different crystal facet structure for selective oil absorption and oil/water separation. Journal of Materials Science, 2018, 53, 10025-10038.	1.7	15
26932	Lattice Mismatch Drives Spatial Modulation of Corannulene Tilt on Ag(111). Journal of Physical Chemistry C, 2018, 122, 10365-10376.	1.5	8
26933	Break the Interacting Bridge between Eu3+ Ions in the 3D Network Structure of CdMoO4: Eu3+ Bright Red Emission Phosphor. Scientific Reports, 2018, 8, 5936.	1.6	31
26934	Nitrogen electroreduction and hydrogen evolution on cubic molybdenum carbide: a density functional study. Physical Chemistry Chemical Physics, 2018, 20, 14679-14687.	1.3	55

#	Article	IF	Citations
26935	Influence of defect distribution on the thermoelectric properties of FeNbSb based materials. Physical Chemistry Chemical Physics, 2018, 20, 14441-14449.	1.3	18
26936	The role of the solid electrolyte interphase layer in preventing Li dendrite growth in solid-state batteries. Energy and Environmental Science, 2018, 11, 1803-1810.	15.6	304
26937	Ultrathin tellurium dioxide: emerging direct bandgap semiconductor with high-mobility transport anisotropy. Nanoscale, 2018, 10, 8397-8403.	2.8	66
26938	Spatially resolved proton momentum distributions in KDP from first-principles. Journal of Chemical Physics, 2018, 148, 144708.	1.2	3
26939	Energetics of He and H Atoms in Wâ€“Ta Alloys: First-Principle Calculations. Chinese Physics Letters, 2018, 35, 047102.	1.3	4
26940	Low-dimensional quantum magnetism in <mml:math xmlns:mml="http://www.w3.org/1998/Math/MathML"><mml:mi>Cu</mml:mi><mml:msub><mml:mrow><mml:mo(</mml:mi><mml:mn><mm : A molecular framework material. Physical Review B, 2018, 97, .	1.1	19
26941	Experimental observation of node-line-like surface states in LaBi. Physical Review B, 2018, 97, .	1.1	17
26942	High-pressure polymorphs of LiPN2: A first-principles study. Frontiers of Physics, 2018, 13, 1.	2.4	5
26943	First-principles study on the electronic structure and elastic properties of Mo₂NiB₂doped with V. Modern Physics Letters B, 2018, 32, 1850065.	1.0	7
26944	Ab Initio Methods. , 2018, , 7-197.		2
26945	Adsorption of rare earth yttrium and ammonium ions on kaolinite surfaces: a DFT study. Theoretical Chemistry Accounts, 2018, 137, 1.	0.5	23
26946	Stability of X-C-vacancy complexes (X=H, He) in vanadium from first principles investigations. Journal of Nuclear Materials, 2018, 505, 119-126.	1.3	12
26947	Toupinâ€“Mindlin first strain gradient theory revisited for cubic crystals of hexoctahedral class: Analytical expression of the material parameters in terms of the atomic force constants and evaluation via ab initio DFT. Mechanics of Materials, 2018, 123, 19-29.	1.7	16
26948	Siligraphene as a promising anode material for lithium-ion batteries predicted from first-principles calculations. Nano Energy, 2018, 49, 67-76.	8.2	95
26949	First-principles study of Au-decorated carbon nanotubes. Physica E: Low-Dimensional Systems and Nanostructures, 2018, 101, 273-277.	1.3	3
26950	Dissolution of Complex Metal Oxides from First-Principles and Thermodynamics: Cation Removal from the (001) Surface of Li(Ni_{1/3}Mn_{1/3}Co_{1/3})O₂. Environmental Science & Technology, 2018, 52, 5792-5802.	4.6	57
26951	Asymmetric electric field screening in van der Waals heterostructures. Nature Communications, 2018, 9, 1271.	5.8	38
26952	A cation size effect on the framework structures in ABi₂SeO₃F₅(A = K and Rb): first examples of alkali metal bismuth selenite fluorides. Dalton Transactions, 2018, 47, 6598-6604.	1.6	12

#	Article	IF	Citations
26953	Direct transition of a HfGeTe₄ ternary transition-metal chalcogenide monolayer with a zigzag van der Waals gap. APL Materials, 2018, 6, 046104.	2.2	17
26954	Embedded atom method potential for studying mechanical properties of binary Cuâ€“Au alloys. Modelling and Simulation in Materials Science and Engineering, 2018, 26, 055006.	0.8	17
26955	Pressure-induced changes of the structure and properties of monoclinic Î± -chalcocite Cu2S. Physical Review B, 2018, 97, .	1.1	9
26956	Photocatalytic performance of TiO2 nanocrystals with/without oxygen defects. Chinese Journal of Catalysis, 2018, 39, 867-875.	6.9	106
26957	Magnetic moment collapse induced by high-pressure in semi-borides TM2B (TMâ€¯=â€¯Fe, Co). A first-principles study. Chinese Journal of Physics, 2018, 56, 944-957.	2.0	5
26958	Mechanism of Phosphorus Transport Through Silicon Oxide During Phosphonic Acid Monolayer Doping. Journal of Physical Chemistry C, 2018, 122, 10088-10095.	1.5	16
26959	HOMO Level Pinning in Molecular Junctions: Joint Theoretical and Experimental Evidence. Journal of Physical Chemistry Letters, 2018, 9, 2394-2403.	2.1	45
26960	Effects of Controlled Crystalline Surface of Hydroxyapatite on Methane Oxidation Reactions. ACS Catalysis, 2018, 8, 4493-4507.	5.5	30
26961	High pressure structural stability of the Na-Te system. AIP Advances, 2018, 8, 035123.	0.6	0
26962	First principles study of pressure induced polymorphic phase transition in trimethylamine. AIP Conference Proceedings, 2018, , .	0.3	3
26963	Electronic structure and hydrogen storage capability of zirconium decorated graphyne. AIP Conference Proceedings, 2018, , .	0.3	2
26964	Magnetic Compton profiles of disordered <mml:math xmlns:mml="http://www.w3.org/1998/Math/MathML"><mml:mrow><mml:msub><mml:mi>Fe</mml:mi><mml:mrow><mml:mn>0.5</mml:mn> and ordered FeNi alloys. Physical Review B, 2018, 97, .	1.1	5
26965	Modulating electronic and optical properties of black phosphorous carbide monolayers by molecular doping. Applied Surface Science, 2018, 448, 270-280.	3.1	11
26966	New clathrate-like compound Eu7Cu44Sb23-Î´: synthesis, crystal and electronic structure, and the effect of As-for-Sb substitution on the magnetic properties. Intermetallics, 2018, 98, 1-10.	1.8	2
26967	Structural and elastic properties of Mg3CuH0.6 ternary hydride by ab initio study. Journal of Magnesium and Alloys, 2018, 6, 90-94.	5.5	10
26968	Electronic properties of g-C3N4/CdS heterojunction from the first-principles. Physica E: Low-Dimensional Systems and Nanostructures, 2018, 103, 459-463.	1.3	26
26969	Role of Lattice Oxygen Participation in Understanding Trends in the Oxygen Evolution Reaction on Perovskites. ACS Catalysis, 2018, 8, 4628-4636.	5.5	339
26970	Active learning with non-ab initio input features toward efficient CO₂ reduction catalysts. Chemical Science, 2018, 9, 5152-5159.	3.7	82

#	Article	IF	Citations
26971	Modelling of adsorption and intercalation of hydrogen on/into tungsten disulphide multilayers and multiwall nanotubes. Physical Chemistry Chemical Physics, 2018, 20, 12061-12074.	1.3	6
26972	Ba₂ZnSc(BO₃)₃and Ba₄Zn₅Sc₂(BO₃)₈: first examples of borates in the Znâ€“Scâ€“Bâ€“O system featuring special structure configurations. Inorganic Chemistry Frontiers, 2018, 5, 1787-1794.	3.0	12
26973	First principle study of UHTC ternary diboride, Cr2AlB2. AIP Conference Proceedings, 2018, , .	0.3	2
26974	An ab-initio study of mechanical, dynamical and electronic properties of MgEu intermetallic. AIP Conference Proceedings, 2018, , .	0.3	0
26975	Band gap modulation of graphene by metal substrate: A first principles study. AIP Conference Proceedings, 2018, , .	0.3	1
26976	Magnetocrystalline anisotropy in cobalt based magnets: a choice of correlation parameters and the relativistic effects. Journal of Physics Condensed Matter, 2018, 30, 195801.	0.7	21
26977	First-principles calculations of dynamical and thermodynamic properties of cuprite doped with silver (Cu_{2(1â^'x)}Ag_{2x}O). Materials Research Express, 2018, 5, 045704.	0.8	5
26978	Anisotropy and phonon modes from analysis of the dielectric function tensor and the inverse dielectric function tensor of monoclinic yttrium orthosilicate. Physical Review B, 2018, 97, .	1.1	15
26979	Probing quasi-one-dimensional band structures by plasmon spectroscopy. Physical Review B, 2018, 97, .	1.1	19
26980	Hydrophobic Properties of Al₂O₃ Doped with Rareâ€Earth Metals: Ab Initio Modeling Studies. Physica Status Solidi (A) Applications and Materials Science, 2018, 215, 1700895.	0.8	4
26981	MoS 2 -CdS heterojunction with enhanced photocatalytic activity: A first principles study. Journal of Physics and Chemistry of Solids, 2018, 120, 52-56.	1.9	27
26982	The spin-dependent electronic transport properties of M(dcdmp) 2 (M = Cu, Au, Co, Ni) molecular devices based on zigzag graphene nanoribbon electrodes. Physics Letters, Section A: General, Atomic and Solid State Physics, 2018, 382, 1401-1408.	0.9	8
26983	How the H-Bond Layout Determines Mechanical Properties of Crystalline Amino Acid Hydrogen Maleates. Crystal Growth and Design, 2018, 18, 3366-3375.	1.4	19
26984	Atomistic Elucidation of Sorption Processes in Hydrogen Evolution Reaction on a van der Waals Heterostructure. Journal of Physical Chemistry C, 2018, 122, 10034-10041.	1.5	18
26985	Water dissociating on rigid Ni(100): A quantum dynamics study on a full-dimensional potential energy surface. Journal of Chemical Physics, 2018, 148, 144705.	1.2	20
26986	Lithium Hexastannate: A Potential Material for Energy Storage. Physica Status Solidi (B): Basic Research, 2018, 255, 1700669.	0.7	16
26987	Theoretical Design of the Absorber for Intermediate Band Solar Cells from Groupâ€IV (Si, Ge, and) Tj ETQq0 0 0 rgBT /Overlock 10 Tf 50	0.7	8
26988	Effect of strain on the intrinsic stacking fault energy of fcc Co: a first-principles study. Journal of Materials Science, 2018, 53, 10217-10230.	1.7	9

#	Article	IF	Citations
26989	First-principles study of phase transition, electronic, elastic and optical properties of defect chalcopyrite ZnGa 2 Te 4 semiconductor under different pressures. Journal of Physics and Chemistry of Solids, 2018, 119, 193-201.	1.9	21
26990	Tuning electronic, magnetic, and transport properties of blue phosphorene by substitutional doping: a first-principles study. Journal of Computational Electronics, 2018, 17, 499-513.	1.3	37
26991	Ferromagnetic Phase Stability, Magnetic, Electronic, Elasto-Mechanical and Thermodynamic Properties of BaCmO3 Perovskite Oxide. Journal of Electronic Materials, 2018, 47, 3809-3816.	1.0	20
26992	Crystal structures and thermodynamic stabilities of two new CaGe2 polymorphs. Acta Materialia, 2018, 151, 347-355.	3.8	13
26993	Applying isotropic strain on Mo to predict H solution behaviors for nuclear energy application: Temperature dependence. International Journal of Hydrogen Energy, 2018, 43, 3750-3760.	3.8	7
26994	Structure, morphology and photoluminescence emissions of ZnMoO4: RE 3+=Tb3+ - Tm3+ - X Eu3+ (xÂ= 1,) Tj ETQq1 1 0.784314 rgBT Compounds, 2018, 750, 55-70.	2.8	34
26995	Itinerant-electron metamagnetic phase transition in FeGe thin films. Journal of Magnetism and Magnetic Materials, 2018, 454, 207-214.	1.0	0
26996	Exchange and magnetic order in bulk and nanostructured Fe5Si3. Journal of Magnetism and Magnetic Materials, 2018, 460, 438-447.	1.0	12
26997	Electron-phonon interaction in the binary superconductor lutetium carbide LuC2 via first-principles calculations. Physica C: Superconductivity and Its Applications, 2018, 549, 131-138.	0.6	1
26998	Electronic and magnetic properties of transition metal decorated monolayer GaS. Physica E: Low-Dimensional Systems and Nanostructures, 2018, 101, 131-138.	1.3	5
26999	Experimental and Theoretical Study of Bi₂O₂Se Under Compression. Journal of Physical Chemistry C, 2018, 122, 8853-8867.	1.5	46
27000	Mapping Catalytically Relevant Edge Electronic States of MoS₂. ACS Central Science, 2018, 4, 493-503.	5.3	39
27001	Impact of Ba to Si deposition rate ratios during molecular beam epitaxy on carrier concentration and spectral response of BaSi2 epitaxial films. Journal of Applied Physics, 2018, 123, 045703.	1.1	55
27002	Atomistic models of Cu diffusion in CuInSe2 under variations in composition. Journal of Applied Physics, 2018, 123, 115116.	1.1	2
27003	Experimental and ab initio study of Mg doping in the intrinsic ferromagnetic semiconductor GdN. Journal of Applied Physics, 2018, 123, .	1.1	5
27004	Trends on band alignments: Validity of Anderson's rule in<mml:math xmlns:mml="http://www.w3.org/1998/Math/MathML"><mml:msub><mml:mi>SnS</mml:mi><mml:mn>2</mml:mn></mml:msub></mml:math> and<mml:math xmlns:mml="http://www.w3.org/1998/Math/MathML"><mml:msub><mml:mi>SnSe</mml:mi><mml:mn>2</mml:mn></mml:msub></mml:math> van der Waals heterostructures. Physical Review B, 2018, 97, .	1.1	57
27005	Dirac Cone Spin Polarization of Graphene by Magnetic Insulator Proximity Effect Probed with Outermost Surface Spin Spectroscopy. Advanced Functional Materials, 2018, 28, 1800462.	7.8	12
27006	Chirality, Rigidity, and Conjugation: A First-Principles Study of the Key Molecular Aspects of Lignin Depolymerization on Ni-Based Catalysts. ACS Catalysis, 2018, 8, 4230-4240.	5.5	24

#	Article	IF	Citations
27007	Molecular structure and interactions of water intercalated in nickel hydroxide. Physical Chemistry Chemical Physics, 2018, 20, 11444-11453.	1.3	14
27008	Revisiting the origin of satellites in core-level photoemission of transparent conducting oxides: The case of <mml:math xmlns:mml="http://www.w3.org/1998/Math/MathML"><mml:mi>n</mml:mi></mml:math> -doped <mml:math xmlns:mml="http://www.w3.org/1998/Math/MathML"><mml:msub><mml:mi>SnO</mml:mi><mml:mn>2</mml:mn></mml:msub></mml:math>. Physical Review B, 2018, 97, .	1.1	30
27009	Large Oblate Hemispheroidal Ruthenium Particles Supported on Calcium Amide as Efficient Catalysts for Ammonia Decomposition. Chemistry - A European Journal, 2018, 24, 7976-7984.	1.7	34
27010	Structural Stability, Electronic, and Optical Properties of BiVO₄ With Oxygen Vacancy Under Pressure. Physica Status Solidi (B): Basic Research, 2018, 255, 1700653.	0.7	8
27011	First principles calculations of the structural, electronic and optical properties of the mixed fluorides SrxCd1â^'xF2. Chinese Journal of Physics, 2018, 56, 1033-1044.	2.0	1
27012	Study of structural, elastic, electronic, mechanical, optical and thermodynamic properties of NdPb 3 intermetallic compound: DFT based calculations. Computational Condensed Matter, 2018, 15, 42-47.	0.9	24
27013	Pressure-induced phase transition of KTa1/2Nb1/2O3 solid solutions: A first-principles study. Chemical Physics Letters, 2018, 699, 80-84.	1.2	3
27014	Development of a Multicenter Density Functional Tight Binding Model for Plutonium Surface Hydriding. Journal of Chemical Theory and Computation, 2018, 14, 2652-2660.	2.3	27
27015	Tuning the Deoxygenation of Bulk-Dissolved Oxygen in Copper. Journal of Physical Chemistry C, 2018, 122, 8254-8261.	1.5	15
27016	Augmented Pairwise Additive Interaction Model for Lateral Adsorbate Interactions: The NOâ€“CO Reaction System on Rh(100) and Rh(111). Langmuir, 2018, 34, 5174-5183.	1.6	7
27017	Fast-Response Single-Nanowire Photodetector Based on ZnO/WS₂ Core/Shell Heterostructures. ACS Applied Materials & Interfaces, 2018, 10, 13869-13876.	4.0	60
27018	Epitaxial phase diagrams of SrTiO3,ÂCaTiO3 , and SrHfO3 : Computational investigation including the role of antiferrodistortive and A -site displacement modes. Physical Review B, 2018, 97, .	1.1	5
27019	Observation of direct evolution from antiferromagnetism to superconductivity in Cu1â^'xLixFeAs () Tj ETQq0 0 0 rgBT /Overlock 10 Tf 50	1.1	3
27020	Raman scattering and phase transitions in <scp>(NH₄)₃TiF₇</scp>. Journal of Raman Spectroscopy, 2018, 49, 1230-1235.	1.2	3
27021	1Tâ€²â€Mo_{1â^'x}W_xS₂/CdS Heterostructure Enabling Robust Photocatalytic Water Splitting: Unveiling the Interfacial Charge Polarization. Solar Rrl, 2018, 2, 1800032.	3.1	27
27022	Magnetic, Optoelectronic, and Thermodynamic Properties of Sr2CrXO6 (X = La and Y): Half-Metallic and Ferromagnetic Behavior. Journal of Superconductivity and Novel Magnetism, 2018, 31, 3965-3979.	0.8	12
27023	Substitutional nitrogen in diamond: A quantum mechanical investigation of the electronic and spectroscopic properties. Carbon, 2018, 134, 354-365.	5.4	42
27024	Structure and thermodynamic properties of zirconium hydrides by structure search method and first principles calculations. Computational Materials Science, 2018, 150, 77-85.	1.4	34

#	Article	IF	Citations
27025	Crystal structures of CsSi6 at high pressures. Computational Materials Science, 2018, 150, 144-148.	1.4	8
27026	Ethylene versus ethane: A DFT-based selectivity descriptor for efficient catalyst screening. Journal of Catalysis, 2018, 362, 18-24.	3.1	52
27027	Towards understanding the mechanism of rhenium and osmium precipitation in tungsten and its implication for tungsten-based alloys. Journal of Nuclear Materials, 2018, 505, 30-43.	1.3	29
27028	First-principles study of solvent-solute mixed dumbbells in body-centered-cubic tungsten crystals. Journal of Nuclear Materials, 2018, 505, 15-21.	1.3	18
27029	Insight into the structural and electronic properties of orthorhombic Cr 3 C 2 (001) surface. Journal of Physics and Chemistry of Solids, 2018, 118, 68-72.	1.9	7
27030	The structural, elastic and electronic properties of marcasite FeS 2 under pressure. Journal of Physics and Chemistry of Solids, 2018, 118, 88-94.	1.9	6
27031	A first principles theoretical study of the adsorption of SF6 decomposition gases on a cassiterite (110) surface. Materials Chemistry and Physics, 2018, 212, 453-460.	2.0	27
27032	Prediction study of structural, elastic and electronic properties of FeMP (Mâ€¯=â€¯Ti, Zr, Hf) compounds. Results in Physics, 2018, 9, 763-770.	2.0	1
27033	Interaction of the O atom with the InSe monolayer: A first-principles study. Vacuum, 2018, 153, 53-61.	1.6	6
27034	The influence of surface functionalization on thermal transport and thermoelectric properties of MXene monolayers. Nanoscale, 2018, 10, 8859-8868.	2.8	118
27035	Significant enhancement of the performance of hydrogen evolution reaction through shape-controlled synthesis of hierarchical dendrite-like platinum. Journal of Materials Chemistry A, 2018, 6, 8068-8077.	5.2	46
27036	Adsorption behaviour of SF₆ decomposed species onto Pd₄-decorated single-walled CNT: a DFT study. Molecular Physics, 2018, 116, 1749-1755.	0.8	31
27037	Exact exchange plane-wave-pseudopotential calculations for slabs: Extending the width of the vacuum. Physical Review B, 2018, 97, .	1.1	6
27038	Mechanistic understanding of methanol carbonylation: Interfacing homogeneous and heterogeneous catalysis via carbon supported Ir La. Journal of Catalysis, 2018, 361, 414-422.	3.1	28
27039	Origin of the monolayer Raman signature in hexagonal boron nitride: a first-principles analysis. Journal of Physics Condensed Matter, 2018, 30, 185701.	0.7	3
27040	Influence of impurity elements on the corrosion of Î±-uranium surface: a density functional theory study. Journal of Radioanalytical and Nuclear Chemistry, 2018, 317, 345-354.	0.7	1
27041	Low-energy 3D sp²carbons with versatile properties beyond graphite and graphene. Dalton Transactions, 2018, 47, 6233-6239.	1.6	7
27042	Mechanical and thermodynamic properties of plutonium dihydride. Journal of Alloys and Compounds, 2018, 750, 258-264.	2.8	9

#	Article	IF	Citations
27043	Anions induced evolution of Co3X4 (Xâ€¯=â€¯O, S, Se) as sodium-ion anodes: The influences of electronic structure, morphology, electrochemical property. Nano Energy, 2018, 48, 617-629.	8.2	227
27044	Electronic Topological Transitions in CuNiMnAl and CuNiMnSn under pressure from first principles study. Solid State Sciences, 2018, 80, 92-100.	1.5	2
27045	Observation of Quasi-Two-Dimensional Polar Domains and Ferroelastic Switching in a Metal, Ca₃Ru₂O₇. Nano Letters, 2018, 18, 3088-3095.	4.5	62
27046	Room-temperature ductile inorganic semiconductor. Nature Materials, 2018, 17, 421-426.	13.3	262
27047	Quantitative assessment of intermolecular interactions by atomic force microscopy imaging using copper oxide tips. Nature Nanotechnology, 2018, 13, 371-375.	15.6	67
27048	Effects of doping Na and Cl atom on electronic structure of silicene: Density functional theory calculation. AIP Conference Proceedings, 2018, , .	0.3	1
27049	Doping Induced Band-gap widening in Transition-metal doped ZnO Nanocrystals. MRS Advances, 2018, 3, 2643-2652.	0.5	2
27050	Wâ€Based Atomic Laminates and Their 2D Derivative W_{1.33}C MXene with Vacancy Ordering. Advanced Materials, 2018, 30, e1706409.	11.1	240
27051	Metalâ€Free Artificial Photosynthesis of Carbon Monoxide Using Nâ€Doped ZnTe Nanorod Photocathode Decorated with Nâ€Doped Carbon Electrocatalyst Layer. Advanced Energy Materials, 2018, 8, 1702636.	10.2	42
27052	Layer-Resolved Photoemission Study ofÂDoped Ag-Supported Ultrathin MgO Films. Springer Proceedings in Physics, 2018, , 265-274.	0.1	0
27053	First-principles calculations of crystal structure, electronic structure and optical properties of Ba2RETaO6 (REâ€‰=â€‰Y, La, Pr, Sm, Gd). Journal of Materials Science, 2018, 53, 9401-9410.	1.7	10
27054	The structural, elastic, electronic, magnetic and optical properties of the Zn0.75V0.25X (Xâ€‰=â€‰S, Se or Te). Journal of Materials Science: Materials in Electronics, 2018, 29, 10190-10203.	1.1	0
27055	First-principles study of hydrogen segregation at the MgZn2 precipitate in Al-Mg-Zn alloys. Computational Materials Science, 2018, 148, 301-306.	1.4	51
27056	Insight into the Bonding of Silanols to Oxidized Aluminum Surfaces. Journal of Physical Chemistry C, 2018, 122, 9417-9431.	1.5	25
27057	First-Principles Insights into Ammonia Decomposition Catalyzed by Ru Clusters Anchored on Carbon Nanotubes: Size Dependence and Interfacial Effects. Journal of Physical Chemistry C, 2018, 122, 9091-9100.	1.5	35
27058	Pressure-induced anomalies and structural instability in compressed Î²-Sb₂O₃. Physical Chemistry Chemical Physics, 2018, 20, 11430-11436.	1.3	6
27059	Activation of ultrathin SrTiO₃ with subsurface SrRuO₃ for the oxygen evolution reaction. Energy and Environmental Science, 2018, 11, 1762-1769.	15.6	83
27060	Control of thermal conductivity with species mass in transition-metal dichalcogenides. Journal of Applied Physics, 2018, 123, .	1.1	7

#	Article	IF	Citations
27061	Strength and texture of sodium chloride to 56â€‰GPa. Journal of Applied Physics, 2018, 123, 135901.	1.1	10
27062	Formation Dynamics of Potassium-Based Graphite Intercalation Compounds: An AbÂInitio Study. Physical Review Applied, 2018, 9, .	1.5	7
27063	Uncovering Periodicity and Hidden Trends Responsible for Predicting the Magnetic Moment of Body Centered Cubic Crystal. ChemPhysChem, 2018, 19, 1593-1598.	1.0	3
27064	From Metallic LnTt (Ln = La, Nd; Tt = Si, Ge, Sn) to Electronâ€precise Zintl Phase Hydrides LnTtH. Zeitschrift Fur Anorganische Und Allgemeine Chemie, 2018, 644, 1532-1539.	0.6	3
27065	Effect of atomic order/disorder on vacancy clustering in concentrated NiFe alloys. Computational Materials Science, 2018, 147, 194-203.	1.4	9
27066	Magneto-electronic and thermoelectric properties of some Fe-based Heusler alloys. Journal of Physics and Chemistry of Solids, 2018, 119, 251-257.	1.9	27
27067	Lithium doping and vacancy effects on the structural, electronic and magnetic properties of hexagonal boron nitride sheet: A first-principles calculation. Superlattices and Microstructures, 2018, 118, 185-195.	1.4	13
27068	Electrocapillary Coupling at Metal Surfaces from First Principles: On the Impact of Excess Charge on Surface Stress and Relaxation. Langmuir, 2018, 34, 4920-4928.	1.6	5
27069	Enhanced Electrochemical and Thermal Transport Properties of Graphene/MoS₂ Heterostructures for Energy Storage: Insights from Multiscale Modeling. ACS Applied Materials & Interfaces, 2018, 10, 14614-14621.	4.0	56
27070	Understanding the Mechanism of SiC Plasma-Enhanced Chemical Vapor Deposition (PECVD) and Developing Routes toward SiC Atomic Layer Deposition (ALD) with Density Functional Theory. ACS Applied Materials & Interfaces, 2018, 10, 15216-15225.	4.0	23
27071	Reducing Coercive-Field Scaling in Ferroelectric Thin Films via Orientation Control. ACS Nano, 2018, 12, 4736-4743.	7.3	47
27072	Combining CO2 reduction with propane oxidative dehydrogenation over bimetallic catalysts. Nature Communications, 2018, 9, 1398.	5.8	113
27073	Novel carbon polymorphs with cumulative double bonds in three-dimensional spâ€“sp² hybrid framework. Physical Chemistry Chemical Physics, 2018, 20, 15022-15029.	1.3	7
27074	Phonons, phase transitions and thermal expansion in LiAlO₂: an ab initio density functional study. Physical Chemistry Chemical Physics, 2018, 20, 12248-12259.	1.3	9
27075	Theoretical Insights into Oxidation States of Transition Metals at (001) and (111) LiNi0.5Mn1.5O4Spinel Surfaces. Journal of the Electrochemical Society, 2018, 165, A1099-A1103.	1.3	14
27076	Hydration of Concrete: The First Steps. Chemistry - A European Journal, 2018, 24, 8603-8608.	1.7	13
27077	Plasma phase transition in warm dense hydrogen. Contributions To Plasma Physics, 2018, 58, 122-127.	0.5	9
27078	A theoretical investigation of structural, electronic and optical properties of bulk copper nitrides. Journal of Alloys and Compounds, 2018, 753, 576-585.	2.8	8

#	Article	IF	Citations
27079	Electronic, bonding, linear, and nonlinear optical properties of Na2MGe2Q6 (M=Cd, Zn, Hg; Q=S, Se), Na2ZnSi2S6, and Na2ZnSn2S6 two metal-mixed chalcogenide compounds: Insights from an ab initio study. Journal of Physics and Chemistry of Solids, 2018, 119, 220-227.	1.9	14
27080	Magnetic anisotropy of ultrathin Pd 4 Co(111) film by first-principles calculations. Journal of Science: Advanced Materials and Devices, 2018, 3, 243-253.	1.5	1
27081	Pressure-Induced Topological Phase Transitions in CdGeSb₂ and CdSnSb₂. Journal of Physical Chemistry Letters, 2018, 9, 2202-2207.	2.1	14
27082	Inhibition of Surface Chemical Moieties by Tris(hydroxymethyl)aminomethane: A Key to Understanding Oxygen Reduction on Ironâ€“Nitrogenâ€“Carbon Catalysts. ACS Applied Energy Materials, 2018, 1, 1942-1949.	2.5	18
27083	Growth of vertically aligned nanowires in metalâ€“oxide nanocomposites: kinetic Monte-Carlo modeling versus experiments. Nanoscale, 2018, 10, 7666-7675.	2.8	22
27084	Enhanced interface interaction between modified carbon nanotubes and magnesium matrix. Composite Interfaces, 2018, 25, 1101-1114.	1.3	6
27085	Electron-Mediated Phonon-Phonon Coupling Drives the Vibrational Relaxation of CO on Cu(100). Physical Review Letters, 2018, 120, 156804.	2.9	26
27086	Hydride Shuttle Formation and Reaction with CO₂ on GaP(110). ChemSusChem, 2018, 11, 1558-1566.	3.6	19
27088	Half-metallic property of the bulk and (001) surfaces of MNaCs (Mâ€¯=â€¯P, As) half-Heusler alloys: A density functional theory approach. Surface Science, 2018, 674, 103-114.	0.8	22
27089	Structural, magnetic, and electronic properties of Fe82Si4B10P4 metallic glass. Scientific Reports, 2018, 8, 5680.	1.6	15
27090	Highly negative Poisson's ratio in a flexible two-dimensional tungsten carbide monolayer. Physical Chemistry Chemical Physics, 2018, 20, 18924-18930.	1.3	42
27091	Self-powered photogalvanic phosphorene photodetectors with high polarization sensitivity and suppressed dark current. Nanoscale, 2018, 10, 7694-7701.	2.8	49
27092	Construction of a stable lithium sulfide membrane to greatly confine polysulfides for high performance lithiumâ€“sulfur batteries. Journal of Materials Chemistry A, 2018, 6, 8655-8661.	5.2	13
27093	Electronic properties of two-dimensional in-plane heterostructures of WS₂/WSe₂/MoS₂. Materials Research Express, 2018, 5, 046307.	0.8	18
27094	A metallic peanut-shaped carbon nanotube and its potential for CO2 capture. Carbon, 2018, 132, 249-256.	5.4	13
27095	Nitrogen-doped penta-graphene as a superior catalytic activity for CO oxidation. Carbon, 2018, 132, 257-262.	5.4	51
27096	Lattice dynamics of Ru 2 FeX (X = Si, Ge) Full Heusler alloys. Physica B: Condensed Matter, 2018, 537, 225-227.	1.3	10
27097	The structural, electronic and magnetic properties of CoS 2 under pressure. Solid State Communications, 2018, 273, 60-65.	0.9	7

#	Article	IF	Citations
27098	Pb₂BO₃Br: a novel nonlinear optical lead borate bromine with a KBBF-type structure exhibiting strong nonlinear optical response. Inorganic Chemistry Frontiers, 2018, 5, 916-921.	3.0	90
27099	¹⁷O solid-state NMR spectroscopy of A₂B₂O₇oxides: quantitative isotopic enrichment and spectral acquisition?. RSC Advances, 2018, 8, 7089-7101.	1.7	13
27100	Evidence for a different electronic configuration as a primary effect during compression of orthorhombic perovskites: The case of NdM3+O3(M=Cr,Ga). Physical Review B, 2018, 97, .	1.1	1
27101	Strong anharmonic phonon scattering induced giant reduction of thermal conductivity in PbTe nanotwin boundary. Physical Review B, 2018, 97, .	1.1	34
27102	Probing nanoscale variations in strain and band structure of <mml:math xmlns:mml="http://www.w3.org/1998/Math/MathML"><mml:mrow><mml:mi>Mo</mml:mi><mml:msub><mml:mi mathvariant="normal">S</mml:mi><mml:mn>2</mml:mn></mml:msub></mml:mrow></mml:math> on Au nanopyramids using tip-enhanced Raman spectroscopy. Physical Review B, 2018, 97, .	1.1	9
27103	Imaging the dynamics of an individual hydrogen atom intercalated between two graphene sheets. Physical Review B, 2018, 97, .	1.1	7
27104	Theoretical investigation of anisotropic mechanical and thermal properties of ABO₃ (A=Sr, Ba; B=Ti, Zr, Hf) perovskites. Journal of the American Ceramic Society, 2018, 101, 3527-3540.	1.9	57
27105	Binding maps for the study and prediction of bimetallic catalyst surface reactions: The case of methanol oxidation. International Journal of Quantum Chemistry, 2018, 118, e25606.	1.0	3
27106	Mott Transition in GdMnO3: an Ab Initio Study. Brazilian Journal of Physics, 2018, 48, 126-129.	0.7	2
27107	DFT study of stabilization effects on N-doped graphene for ORR catalysis. Catalysis Today, 2018, 312, 118-125.	2.2	81
27108	Improving the functionality and performance of AA2024 corrosion sensing coatings with nanocontainers. Chemical Engineering Journal, 2018, 341, 526-538.	6.6	51
27109	Electronic and transport properties for Ti3C2O2 under the influence of a vertical electric field and stacking number. Computational Materials Science, 2018, 147, 186-193.	1.4	4
27110	Newly synthesized MgAl 2 Ge 2 : A first-principles comparison with its silicide and carbide counterparts. Journal of Physics and Chemistry of Solids, 2018, 117, 139-147.	1.9	24
27111	Ternary interfacial superstructure enabling extraordinary hydrogen evolution electrocatalysis. Materials Today, 2018, 21, 602-610.	8.3	48
27112	Effect of stacking order and in-plane strain on the electronic properties of bilayer GeSe. Physical Chemistry Chemical Physics, 2018, 20, 6929-6935.	1.3	31
27113	Quantum Conductance of Copperâ€“Carbon Nanotube Composites. Journal of Engineering Materials and Technology, Transactions of the ASME, 2018, 140, .	0.8	7
27114	Elasticity, Anisotropy and Magnetism of Anti-perovskite M3AlC (M=Ti, Fe, Sm) from First-Principle Calculations. Journal of Superconductivity and Novel Magnetism, 2018, 31, 2879-2887.	0.8	7
27115	Probing the entropy hypothesis in highly concentrated alloys. Acta Materialia, 2018, 148, 263-279.	3.8	39

#	Article	IF	Citations
27116	Structural phase transition, electronic and lattice dynamical properties of half-Heusler compound CaAuBi. Journal of Alloys and Compounds, 2018, 745, 240-246.	2.8	13
27117	Three-dimensional evaluation of compositional and structural changes in cycled LiNi1/3Co1/3Mn1/3O2 by atom probe tomography. Journal of Power Sources, 2018, 379, 160-166.	4.0	23
27118	A computational study of high pressure polymorphic transformations in monazite-type LaPO₄. Physical Chemistry Chemical Physics, 2018, 20, 7621-7634.	1.3	8
27119	Tuning the catalytic activity of colloidal noble metal nanocrystals by using differently charged surfactants. Nanoscale, 2018, 10, 5607-5616.	2.8	14
27120	A first-principles study of stability of surface confined mixed metal oxides with corundum structure (Fe2O3, Cr2O3, V2O3). Physical Chemistry Chemical Physics, 2018, 20, 7073-7081.	1.3	7
27121	Magnetism and piezoelectricity of hexagonal boron nitride with triangular vacancy. Chinese Physics B, 2018, 27, 016301.	0.7	13
27122	Structural, electronic, and mechanical properties of cubic TiO₂: A first-principles study. Chinese Physics B, 2018, 27, 017102.	0.7	11
27123	Quaternary Ammonium Cation Specific Adsorption on Platinum Electrodes: A Combined Experimental and Density Functional Theory Study. Journal of the Electrochemical Society, 2018, 165, F114-F121.	1.3	26
27124	Pd-Doped WO₃ Nanostructures as Potential Glucose Sensor with Insight from Electronic Structure Simulations. Journal of Physical Chemistry B, 2018, 122, 2737-2746.	1.2	47
27125	Epitaxial Growth of Flat Antimonene Monolayer: A New Honeycomb Analogue of Graphene. Nano Letters, 2018, 18, 2133-2139.	4.5	219
27126	Tracking the ultrafast XUV optical properties of x-ray free-electron-laser heated matter with high-order harmonics. Physical Review A, 2018, 97, .	1.0	16
27127	Gd impurities effect on $$hbox {Co}_{2}hbox {CrSi}$$ Co 2 CrSi alloy: first-principle calculations. Bulletin of Materials Science, 2018, 41, 1.	0.8	74
27128	Boosting photocatalytic water oxidation reactions over strontium tantalum oxynitride by structural laminations. Applied Catalysis B: Environmental, 2018, 228, 10-18.	10.8	62
27129	Towards a uniform distribution of zinc in the negative electrode for zinc bromine flow batteries. Applied Energy, 2018, 213, 366-374.	5.1	83
27130	The adsorption and dissociation of O2 on Pd and Pt modified TaC (1â€¯0â€¯0) surface: A first principles study. Applied Surface Science, 2018, 439, 845-851.	3.1	7
27131	Electrochemical properties of stanene as an efficient anode material for Na-ion batteries. Computational Condensed Matter, 2018, 14, 84-88.	0.9	9
27132	The effect of pressure on structural, electronic, elastic, vibration and optical properties of ScXSb (X=Ni, Pd, Pt) compounds. Computational Condensed Matter, 2018, 14, 176-185.	0.9	16
27133	Insight into electronic structure, magnetic, mechanical and thermodynamic properties of double perovskite Ba 2 MgReO 6 : A first-principles investigation. Computational Condensed Matter, 2018, 14, 137-143.	0.9	32

#	Article	IF	Citations
27134	Microstructural analysis and optical properties of the halide double perovskite Cs2BiAgBr6 single crystals. Chemical Physics Letters, 2018, 694, 18-22.	1.2	42
27135	A DFT study on modification mechanism of (N,S) interstitial co-doped rutile TiO2. Chemical Physics Letters, 2018, 695, 8-18.	1.2	17
27136	Mechanical responses of two-dimensional MoTe2; pristine 2H, 1T and 1Tâ€² and 1Tâ€²/2H heterostructure. Extreme Mechanics Letters, 2018, 20, 65-72.	2.0	34
27137	The effects of vacancies and surface hydroxyls on the interactions of hydrogen with rare earth oxides â€“ DFT calculations on gadolinium oxide. Journal of Alloys and Compounds, 2018, 740, 926-934.	2.8	6
27138	Three alkaline-rare earth cations carbonates with large birefringence in the deep UV range. Journal of Alloys and Compounds, 2018, 742, 587-593.	2.8	11
27139	Recently synthesized (Zr1-xTix)2AlC (0â€¯â‰¤â€¯xâ€¯â‰¤â€¯1) solid solutions: Theoretical study of the effects of M mixing on physical properties. Journal of Alloys and Compounds, 2018, 743, 146-154.	2.8	69
27140	On the mechanism of the electrochemical conversion of ammonia to dinitrogen on Pt(1â€¯0â€¯0) in alkaline environment. Journal of Catalysis, 2018, 359, 82-91.	3.1	62
27141	Hydrodeoxygenation of m-cresol over bimetallic NiFe alloys: Kinetics and thermodynamics insight into reaction mechanism. Journal of Catalysis, 2018, 359, 272-286.	3.1	95
27142	High-pressure and high-temperature physical properties of LiF studied by density functional theory calculations and molecular dynamics simulations. Journal of Physics and Chemistry of Solids, 2018, 116, 209-215.	1.9	7
27143	Boosted electrochemical performance of Li2ZnTi3O8 enabled by ion-conductive Li2ZrO3 concomitant with superficial Zr-doping. Journal of Power Sources, 2018, 379, 270-277.	4.0	32
27144	Effect of gradual ordering of Ge/Sb atoms on chemical bonding: A proposed mechanism for the formation of crystalline Ge2Sb2Te5. Journal of Solid State Chemistry, 2018, 260, 124-131.	1.4	7
27145	A simple descriptor for energetics at fcc-bcc metal interfaces. Materials and Design, 2018, 142, 158-165.	3.3	15
27146	Theoretical study of H2 adsorbed on monolayer MoS2 doped with N, Si, P. Microelectronic Engineering, 2018, 190, 63-67.	1.1	32
27147	First-principles study for the enhanced sulfur tolerance of Ni(1Â1Â1) surface alloyed with Pb. Surface Science, 2018, 670, 68-71.	0.8	6
27148	Stability and band offsets of nonpolar (11<mml:math) Tj ETQq0 0 0 rgBT /Overlock 10 Tf 50 197 Td (xmlns:mml="http://www.w3.org/19 ZnO on (001) LaAlO 3. Vacuum, 2018, 150, 29-34.	1.6	10
27149	Mechanistic Analysis of Oxygen Vacancy Formation and Ionic Transport in Sr₃Fe₂O_{7â^'Î´}. Journal of Physical Chemistry C, 2018, 122, 4172-4181.	1.5	20
27150	A photoemission moments model using density functional and transfer matrix methods applied to coating layers on surfaces: Theory. Journal of Applied Physics, 2018, 123, .	1.1	15
27151	Influence of strain on dislocation core in silicon. Philosophical Magazine, 2018, 98, 1151-1169.	0.7	2

#	Article	IF	Citations
27152	Synthesis, Structure and Electronic Properties of Li₄Ti₅O₁₂ Anode Material for Lithium Ion Batteries. Solid State Phenomena, 0, 271, 9-17.	0.3	8
27153	The role of Ag, Ca, Zr and Al in strengthening effects of ZK series alloys by altering G.P. zones stability. Acta Materialia, 2018, 147, 42-50.	3.8	15
27154	Sensing properties of pristine boron nitride nanostructures towards alkaloids: A first principles dispersion corrected study. Applied Surface Science, 2018, 441, 588-598.	3.1	20
27155	DFT study on bimetallic Pt/Cu(1â€¯1â€¯1) as efficient catalyst for H2 dissociation. Applied Surface Science, 2018, 441, 23-28.	3.1	9
27156	X-ray absorption spectroscopy investigation of relationship between Mg vacancy and magnetic properties of MgO powder. Journal of Magnetism and Magnetic Materials, 2018, 460, 327-333.	1.0	12
27157	Optical properties of B12P2 crystals: Ab initio calculation and EELS. Journal of Physics and Chemistry of Solids, 2018, 116, 331-337.	1.9	4
27158	Phonon-induced linewidth of quantum-well states in monolayer Pb on Si(111). Surface Science, 2018, 678, 86-90.	0.8	0
27159	The effect of d and f states of ytterbium on the electronic and magnetic properties of Al1â^'xYbxN: DFT+U study. International Journal of Modern Physics B, 2018, 32, 1850119.	1.0	9
27160	Ab initio periodic modelling of the vibrational spectra of molecular crystals: the case of uracil. Theoretical Chemistry Accounts, 2018, 137, 1.	0.5	7
27161	Martensitic transition in Fe via Bain path at finite temperatures: A comprehensive first-principles study. Acta Materialia, 2018, 147, 261-276.	3.8	44
27162	Label-free surface plasmon resonance biosensing with titanium nitride thin film. Biosensors and Bioelectronics, 2018, 106, 129-135.	5.3	20
27163	A CALPHAD assessment of the Alâ€“Mnâ€“C system supported by ab initio calculations. Calphad: Computer Coupling of Phase Diagrams and Thermochemistry, 2018, 60, 231-239.	0.7	10
27164	Diffusion and adsorption of dimers on reconstructed Pt(1 1 0) surfaces: First principle and EAM studies. Chemical Physics, 2018, 502, 96-101.	0.9	2
27165	First-principles study of the atomic and electronic properties of (1â€¯0â€¯0) stacking faults in BaSnO3 crystal. Chemical Physics Letters, 2018, 694, 65-69.	1.2	1
27166	Aggregation and ordering of helium in thoria. Journal of Alloys and Compounds, 2018, 743, 196-202.	2.8	4
27167	Ruddlesden-Popper compound Sr2TiO4 co-doped with La and Fe for efficient photocatalytic hydrogen production. Journal of Catalysis, 2018, 359, 112-121.	3.1	42
27168	Determination of the mechanical properties of SnSe, a novel layered semiconductor. Journal of Physics and Chemistry of Solids, 2018, 116, 306-312.	1.9	16
27169	High Hydrides of Scandium under Pressure: Potential Superconductors. Journal of Physical Chemistry C, 2018, 122, 6298-6309.	1.5	83

#	Article	IF	Citations
27170	Two-dimensional delocalized states in organometallic bis-acetylide networks on Ag(111). Nanoscale, 2018, 10, 3769-3776.	2.8	32
27171	A theoretical study on the electronic properties of in-plane CdS/ZnSe heterostructures: type-II band alignment for water splitting. Journal of Materials Chemistry A, 2018, 6, 4161-4166.	5.2	99
27172	Theoretical prediction of sandwiched two-dimensional phosphide binary compound sheets with tunable bandgaps and anisotropic physical properties. Nanotechnology, 2018, 29, 095703.	1.3	6
27173	Development of a machine learning potential for graphene. Physical Review B, 2018, 97, .	1.1	142
27174	Synergistically Enhanced Oxygen Reduction Electrocatalysis by Subsurface Atoms in Ternary PdCuNi Alloy Catalysts. Advanced Functional Materials, 2018, 28, 1707219.	7.8	58
27175	Electronic Properties of Csâ€Based Halide Perovskites: An Ab Initio Study. Physica Status Solidi (A) Applications and Materials Science, 2018, 215, 1700941.	0.8	6
27176	Edgeâ€Riched MoSe₂/MoO₂ Hybrid Electrocatalyst for Efficient Hydrogen Evolution Reaction. Small, 2018, 14, e1703798.	5.2	97
27177	Study of Electronic, Magnetic, and Thermoelectric Properties of 24 Valence-Electron Fe2TiSn Heusler Compound Using Modified Becke-Johnson Scheme. Journal of Superconductivity and Novel Magnetism, 2018, 31, 3263-3267.	0.8	2
27178	Solute segregation in Cu: DFT vs. Experiment. Acta Materialia, 2018, 147, 122-132.	3.8	45
27179	Investigations of the microstructure evolution and tensile deformation behavior of austenitic Fe-Mn-Al-C lightweight steels and the effect of Mo addition. Acta Materialia, 2018, 147, 226-235.	3.8	87
27180	Influence of hydrogen on the elastic properties of nickel single crystal: A numerical and experimental investigation. Acta Materialia, 2018, 148, 280-288.	3.8	47
27181	Effect of surface Fe-S hybrid structure on the activity of the perfect and reduced Î±-Fe2O3(001) for chemical looping combustion. Applied Surface Science, 2018, 440, 29-34.	3.1	15
27182	Ab initio study of electronic structure, elasticity, bonding features and mechanical behaviour of zinc intermetallics. Computational Condensed Matter, 2018, 14, 144-152.	0.9	6
27183	Conductive Nb25O62 and Nb12O29 anode materials for use in high-performance lithium-ion storage. Electrochimica Acta, 2018, 266, 202-211.	2.6	39
27184	First principles study on elastic and electronic properties of bialkali alanates M2Mâ€²AlH6. International Journal of Hydrogen Energy, 2018, 43, 3862-3870.	3.8	15
27185	High-pressure structural phase transitions and electronic properties of the alkali hydride compounds XH (X=K, Rb and Cs). Materials Chemistry and Physics, 2018, 208, 132-142.	2.0	3
27186	The adsorption and dissociation of oxygen on Ag (111) supported Ï‡ 3 borophene. Physica B: Condensed Matter, 2018, 537, 1-6.	1.3	18
27187	Tunable magnetism in the LaAlO 3 /SrTiO 3 heterostructure: Insights from first-principles calculations. Physica E: Low-Dimensional Systems and Nanostructures, 2018, 98, 120-124.	1.3	6

#	Article	IF	Citations
27188	Experimental realization of honeycomb borophene. Science Bulletin, 2018, 63, 282-286.	4.3	397
27189	Zintl Ions within Framework Channels: The Complex Structure and Low-Temperature Transport Properties of Na4Ge13. Inorganic Chemistry, 2018, 57, 2002-2012.	1.9	7
27190	Decomposition Mechanism of Zinc Ammine Borohydride: A First-Principles Calculation. Journal of Physical Chemistry C, 2018, 122, 4241-4249.	1.5	6
27191	Microkinetics of alcohol reforming for H2 production from a FAIR density functional theory database. Nature Communications, 2018, 9, 526.	5.8	38
27192	Comparison of the periodic slab approach with the finite cluster description of metalâ€“organic interfaces at the example of PTCDA on Ag(110). Journal of Computational Chemistry, 2018, 39, 844-852.	1.5	17
27193	First-principles calculations of electronic, elastic and thermal properties of magnesium doped with alloying elements. Journal Wuhan University of Technology, Materials Science Edition, 2018, 33, 198-203.	0.4	5
27194	Understanding bond formation and its impact on the capacitive properties of SiW12 polyoxometalates adsorbed on functionalized carbon nanotubes. Carbon, 2018, 130, 623-635.	5.4	24
27195	A theoretical study on reaction mechanisms and kinetics of thiophene hydrodesulfurization over MoS2 catalysts. Catalysis Today, 2018, 312, 158-167.	2.2	25
27196	Preparation of elongated mullite self-reinforced porous ceramics. Ceramics International, 2018, 44, 7500-7508.	2.3	32
27197	Electronic and gap properties of Sb and Bi based halide perovskites: An ab-initio study. Computational Condensed Matter, 2018, 14, 161-166.	0.9	14
27198	Predicting the structural and electronic properties of two-dimensional single layer boron nitride sheets. Chemical Physics Letters, 2018, 694, 102-106.	1.2	32
27199	Preparation and the superior oxygen permeability of a new CO2-resistant Ruddlesdenâ€“Popper composite oxide Pr2Ni0.9Mo0.1O4+. Journal of Alloys and Compounds, 2018, 742, 966-976.	2.8	13
27200	New insights into solidification and phase equilibria in the Al-Al3Zr system: Theoretical and experimental investigations. Journal of Alloys and Compounds, 2018, 743, 626-638.	2.8	18
27201	Top-seeded solution growth and morphology change of RbTiOPO4:Ta single crystal. Journal of Crystal Growth, 2018, 487, 87-91.	0.7	3
27202	All boron-based 2D material as anode material in Li-ion batteries. Journal of Energy Chemistry, 2018, 27, 1651-1654.	7.1	35
27203	Electronic, optical, infrared, and elastic properties of KCdCO3F from first principles. Journal of Physics and Chemistry of Solids, 2018, 116, 353-359.	1.9	2
27204	Structural investigation of chemically synthesized ferrite magnetic nanomaterials. Journal of Molecular Structure, 2018, 1160, 447-454.	1.8	9
27205	Strong spin-orbit effects in transition metal oxides with tetrahedral coordination. Physica B: Condensed Matter, 2018, 537, 184-187.	1.3	2

#	Article	IF	Citations
27206	Numerical study of the electronic structure, elastic and optical properties of defect quaternary semiconductor CuGaSnSe4. Results in Physics, 2018, 9, 49-54.	2.0	2
27207	Electrical and optical degradation study of methylammonium-based perovskite materials under ambient conditions. Solar Energy Materials and Solar Cells, 2018, 178, 179-185.	3.0	16
27208	Chemically stabilized epitaxial wurtzite-BN thin film. Superlattices and Microstructures, 2018, 115, 197-203.	1.4	5
27209	Changing the Usual Interpretation of the Structure and Ground State of Cu²⁺-Layered Perovskites. Journal of Physical Chemistry C, 2018, 122, 5071-5082.	1.5	51
27210	Effect of Bromine Substitution on the Ion Migration and Optical Absorption in MAPbI₃ Perovskite Solar Cells: The First-Principles Study. ACS Applied Energy Materials, 2018, 1, 1374-1380.	2.5	46
27211	Ultrahigh Storage and Fast Diffusion of Na and K in Blue Phosphorene Anodes. ACS Applied Materials & Interfaces, 2018, 10, 8630-8639.	4.0	143
27212	Modulating Reactivity and Selectivity of 2-Pyrone-Derived Bicyclic Lactones through Choice of Catalyst and Solvent. ACS Catalysis, 2018, 8, 2450-2463.	5.5	14
27213	Two-Dimensional Fluorinated Boron Sheets: Mechanical, Electronic, and Thermal Properties. ACS Omega, 2018, 3, 1815-1822.	1.6	53
27214	Anti-fouling graphene-based membranes for effective water desalination. Nature Communications, 2018, 9, 683.	5.8	197
27215	Metamagnetism stabilized giant magnetoelectric coupling in ferroelectric xBaTiO3â€“(1 â^' x)BiCoO3 solid solution. Physical Chemistry Chemical Physics, 2018, 20, 7021-7032.	1.3	8
27216	Tunable reactivity of supported single metal atoms by impurity engineering of the MgO(001) support. Physical Chemistry Chemical Physics, 2018, 20, 6337-6346.	1.3	4
27217	Design and synthesis of a nonlinear optical material BaAl₄S₇with a wide band gap inspired from SrB₄O₇. Journal of Materials Chemistry C, 2018, 6, 2684-2689.	2.7	51
27218	Tuning the electronic and magnetic properties of InSe nanosheets by transition metal doping. Physical Chemistry Chemical Physics, 2018, 20, 7532-7537.	1.3	15
27219	Structure formation and surface chemistry of ionic liquids on model electrode surfacesâ€”Model studies for the electrode | electrolyte interface in Li-ion batteries. Journal of Chemical Physics, 2018, 148, 193821.	1.2	17
27220	Two-dimensional MoS₂ electromechanical actuators. Journal Physics D: Applied Physics, 2018, 51, 075306.	1.3	71
27221	Magnetoelectric and Raman spectroscopic studies of monocrystalline <mml:math xmlns:mml="http://www.w3.org/1998/Math/MathML"><mml:mrow><mml:mi>MnC</mml:mi><mml:msub><mml:mi mathvariant="normal">r</mml:mi><mml:mn>2</mml:mn></mml:msub><mml:msub><mml:mi mathvariant="normal">O</mml:mi><mml:mn>4</mml:mn></mml:msub></mml:mrow></mml:math>.	1.1	18
27222	Ab initio investigation of the thermodynamics of cation distribution and of the electronic and magnetic structures in the <mml:math xmlns:mml="http://www.w3.org/1998/Math/MathML"><mml:mrow><mml:msub><mml:mi>LiMn</mml:mi><mml:mn>2</mml:mn></mml:msub><mml:msub><mml:mi mathvariant="normal">O</mml:mi><mml:mn>4</mml:mn></mml:msub></mml:mrow></mml:math> spinel. Physical Review B, 2018, 97, .	1.1	21
27223	Prediction of a <mml:math xmlns:mml="http://www.w3.org/1998/Math/MathML"><mml:msub><mml:mi>BeP</mml:mi><mml:mn>2</mml:mn></mml:msub></mml:math> monolayer with a compression-induced Dirac semimetal state. Physical Review B, 2018, 97, .	1.1	15

#	Article	IF	Citations
27224	Investigation of different physical aspects such as structural, mechanical, optical properties and Debye temperature of Fe₂ScM (M=P and As) semiconductors: A DFT-based first principles study. International Journal of Modern Physics B, 2018, 32, 1850121.	1.0	33
27225	A first-principles investigation on mechanical and metallic properties of titanium carbides under pressure. Journal of Materials Science and Technology, 2018, 34, 1953-1958.	5.6	13
27226	Density Functional Theory plus Hubbard U Study of the Segregation of Pt to the CeO_{2â€“x} Grain Boundary. Nano Letters, 2018, 18, 1668-1677.	4.5	12
27227	Geometric isotope effect of deuteration in a hydrogen-bonded hostâ€“guest crystal. Nature Communications, 2018, 9, 481.	5.8	76
27228	Magnetism and high magnetic-field-induced stability of alloy carbides in Fe-based materials. Scientific Reports, 2018, 8, 3049.	1.6	15
27229	Monolayer PdSe2: A promising two-dimensional thermoelectric material. Scientific Reports, 2018, 8, 2764.	1.6	133
27230	A DFT study of chlorine coverage over late transition metals and its implication on 1,2-dichloroethane hydrodechlorination. Catalysis Science and Technology, 2018, 8, 1555-1563.	2.1	16
27231	Structural, electronic, vibration and elastic properties of the layered AgInP₂S₆semiconducting crystal â€“ DFT approach. RSC Advances, 2018, 8, 6965-6977.	1.7	20
27232	Gold fillings unravel the vacancy role in the phase transition of GeTe. Applied Physics Letters, 2018, 112, 071902.	1.5	10
27233	Harmonizing Energy and Power Density toward 2.7 V Asymmetric Aqueous Supercapacitor. Advanced Energy Materials, 2018, 8, 1702630.	10.2	201
27234	Pressure-induced elastic, electronic and optical properties of Ba(Mg1/3Nb2/3)O3 using first principles calculations. Indian Journal of Physics, 2018, 92, 731-740.	0.9	7
27235	Solid-State Synapse Based on Magnetoelectrically Coupled Memristor. ACS Applied Materials & Interfaces, 2018, 10, 5649-5656.	4.0	55
27236	Intrinsic defect processes and elastic properties of Ti3AC2 (A = Al, Si, Ga, Ge, In, Sn) MAX phases. Journal of Applied Physics, 2018, 123, .	1.1	31
27237	Ab initio calculations of ideal strength and lattice instability in W-Ta and W-Re alloys. Physical Review B, 2018, 97, .	1.1	11
27238	Hydrogen Generation from Additive-Free Formic Acid Decomposition Under Mild Conditions by Pd/C: Experimental and DFT Studies. Topics in Catalysis, 2018, 61, 254-266.	1.3	68
27239	Reaction of Acetylenedicarboxylic Acid Made Easy: High-Pressure Route for Polymerization. Crystal Growth and Design, 2018, 18, 1425-1431.	1.4	12
27240	Emergent property of high hardness for C-rich ruthenium carbides: partial covalent Ruâ€“Ru bonds. Physical Chemistry Chemical Physics, 2018, 20, 6108-6115.	1.3	5
27241	Investigating the Reactivity of Single Atom Alloys Using Density Functional Theory. Topics in Catalysis, 2018, 61, 462-474.	1.3	117

#	Article	IF	Citations
27242	Accelerating evaluation of converged lattice thermal conductivity. Npj Computational Materials, 2018, 4, .	3.5	50
27243	Natural Intermediate Band in I 2 -II-IV-VI4 Quaternary Chalcogenide Semiconductors. Scientific Reports, 2018, 8, 1604.	1.6	15
27244	A Au monolayer on WC(0001) with unexpected high activity towards CO oxidation. Nanoscale, 2018, 10, 4753-4760.	2.8	15
27245	Polyselenide Anchoring Using Transition-Metal Disulfides for Enhanced Lithiumâ€“Selenium Batteries. Inorganic Chemistry, 2018, 57, 2149-2156.	1.9	19
27246	First-Principle Study of Li-Ion Storage of Functionalized Ti₂C Monolayer with Vacancies. ACS Applied Materials & Interfaces, 2018, 10, 6369-6377.	4.0	89
27247	Highly Dual-Heteroatom-Doped Ultrathin Carbon Nanosheets with Expanded Interlayer Distance for Efficient Energy Storage. ACS Sustainable Chemistry and Engineering, 2018, 6, 3143-3153.	3.2	38
27248	Multifunctionalities of an Azine-Linked Covalent Organic Framework: From Nanoelectronics to Nitroexplosive Detection and Conductance Switching. Journal of Physical Chemistry C, 2018, 122, 3245-3255.	1.5	27
27249	Monolayered Silicon and Germanium Monopnictide Semiconductors: Excellent Stability, High Absorbance, and Strain Engineering of Electronic Properties. ACS Applied Materials & Interfaces, 2018, 10, 5133-5139.	4.0	89
27250	Bimodal hole transport in bulk BiVO₄ from computation. Journal of Materials Chemistry A, 2018, 6, 3714-3723.	5.2	20
27251	DFT study of In₂O₃-catalyzed methanol synthesis from CO₂ and CO hydrogenation on the defective site. New Journal of Chemistry, 2018, 42, 3293-3300.	1.4	33
27252	Completely flat 2D Zn3O2 monolayer with triangle and pentangle coordinated networks. Journal of Physics Condensed Matter, 2018, 30, 095301.	0.7	1
27253	Ab-initiocalculation and experimental observation of room temperature ferromagnetism in 50 keV nitrogen implanted rutile TiO2. Materials Research Express, 2018, 5, 026104.	0.8	13
27254	Noble metal (Pt or Au)-doped monolayer MoS2 as a promising adsorbent and gas-sensing material to SO2, SOF2 and SO2F2: a DFT study. Applied Physics A: Materials Science and Processing, 2018, 124, 1.	1.1	105
27255	Insight into Structural, Electronic, Magnetic, Mechanical, and Thermodynamic Properties of Actinide Perovskite BaPuO3. Journal of Superconductivity and Novel Magnetism, 2018, 31, 3201-3208.	0.8	33
27256	Evaluation of the Giant Ferromagnetic Ï€â€“d Interaction in Iron-Phthalocyanine Molecule. Journal of Physical Chemistry A, 2018, 122, 1678-1690.	1.1	6
27257	Tuning the Electronic Structure of an Aluminum Phosphide Nanotube through Configuration of the Lattice Geometry. ACS Applied Nano Materials, 2018, 1, 501-504.	2.4	1
27258	Ab Initio Simulation Explains the Enhancement of Catalytic Oxygen Evolution on CaMnO₃. ACS Catalysis, 2018, 8, 2218-2224.	5.5	30
27259	An insight into the origin of room-temperature ferromagnetism in SnO₂ and Mn-doped SnO₂ quantum dots: an experimental and DFT approach. Physical Chemistry Chemical Physics, 2018, 20, 6500-6514.	1.3	24

#	Article	IF	Citations
27260	X-ray absorption near edge structure and first-principles spectral investigations of cationic disorder in MgAl₂O₄ induced by swift heavy ions. Physical Chemistry Chemical Physics, 2018, 20, 4962-4969.	1.3	7
27261	3D hybrid carbon composed of multigraphene bridged by carbon chains. AIP Advances, 2018, 8, 015019.	0.6	0
27262	Adsorption of HCN molecules on Ni, Pd and Pt-doped (7, 0) boron nitride nanotube: a DFT study. Molecular Physics, 2018, 116, 1320-1327.	0.8	11
27263	First-principles investigation on electronic structure, magnetic, mechanical and thermodynamic properties of SrPuO₃perovskite oxide. Materials Research Express, 2018, 5, 026106.	0.8	49
27264	Gold nanoparticles decorated on BaTiO₃as photocatalyst: effect of SPR and ferroelectricity. Materials Research Express, 2018, 5, 025505.	0.8	14
27265	First-principles Study of Mechanical and Electronic Properties of Co-Sn Intermetallics for Lithium Ion Battery Anode. Chemical Research in Chinese Universities, 2018, 34, 235-240.	1.3	14
27266	First-principles study of theÎ±-Ï‰phase transformation in Ti and Zr coupled to slip modes. Journal of Applied Physics, 2018, 123, 045903.	1.1	6
27267	Raman scattering study of the ferroelectric phase transition in <mml:math xmlns:mml="http://www.w3.org/1998/Math/MathML"><mml:mrow><mml:mi>BaT</mml:mi><mml:msub><mml:mi mathvariant="normal">i</mml:mi><mml:mn>2</mml:mn></mml:msub><mml:msub><mml:mi mathvariant="normal">O</mml:mi><mml:mn>5</mml:mn></mml:msub></mml:mrow></mml:math>. Physical Review B, 2018, 97, .	1.1	24
27268	Intermetallic Pd₃Pb Nanoplates Enhance Oxygen Reduction Catalysis with Excellent Methanol Tolerance. Small Methods, 2018, 2, 1700331.	4.6	66
27269	Unraveling the Role of Doping in Selective Stabilization of NaMnO₂ Polymorphs: Combined Theoretical and Experimental Study. Chemistry of Materials, 2018, 30, 1257-1264.	3.2	24
27270	Electronic Properties of Sulfur Covered Ru(0001) Surfaces. Journal of Physical Chemistry A, 2018, 122, 2232-2240.	1.1	2
27271	Structural Changes as a Function of Thickness in [(SnSe)1+Î´]mTiSe2 Heterostructures. ACS Nano, 2018, 12, 1285-1295.	7.3	11
27272	Net W monolayer: A high-performance electrode material for Li-ion batteries. Applied Physics Letters, 2018, 112, .	1.5	29
27273	Metastable state in a tensile-strained<mml:math xmlns:mml="http://www.w3.org/1998/Math/MathML"><mml:mrow><mml:mi>Cu</mml:mi><mml:mspace width="0.16em" /><mml:mi mathvariant="normal">Î£</mml:mi><mml:mn>5</mml:mn></mml:mrow></mml:math>grain boundary: A first-principles study. Physical Review B, 2018, 97, .	1.1	6
27274	Ab initio calculations of the concentration dependent band gap reduction in dilute nitrides. Physical Review B, 2018, 97, .	1.1	9
27275	Looking for $$sp^2$$ s p 2 carbon atoms in diamond: a quantum mechanical study of interacting vacancies. Theoretical Chemistry Accounts, 2018, 137, 1.	0.5	8
27276	Determination of latent hardening response for FeNiCoCrMn for twin-twin interactions. Acta Materialia, 2018, 147, 149-164.	3.8	43
27277	Adsorption of NO on Fe3O4(111). Chemical Physics Letters, 2018, 693, 84-87.	1.2	21

#	Article	IF	Citations
27278	Topological behaviour of ternary non-symmorphic crystals KZnX (X = P, As, Sb) under pressure and strain: a first principles study. Physical Chemistry Chemical Physics, 2018, 20, 5084-5102.	1.3	9
27279	Borophene hydride: a stiff 2D material with high thermal conductivity and attractive optical and electronic properties. Nanoscale, 2018, 10, 3759-3768.	2.8	109
27280	Efficient evaluation of atom tunneling combined with electronic structure calculations. Journal of Chemical Physics, 2018, 148, 102334.	1.2	23
27281	Designing a tunable magnet using cluster-assembled iron. Journal of Applied Physics, 2018, 123, .	1.1	0
27282	First principles predictions of magneto-optical data for semiconductor point defect identification: the case of divacancy defects in 4Hâ€“SiC. New Journal of Physics, 2018, 20, 023035.	1.2	39
27283	Systematic investigation of structural, electronic, optical and thermal properties of ternary MoAlB; an ab initio approach. Materials Research Express, 2018, 5, 025701.	0.8	6
27284	Depth of formation of super-deep diamonds: Raman barometry of CaSiO3-walstromite inclusions. American Mineralogist, 2018, 103, 69-74.	0.9	33
27285	How and Why Does Helium Permeate Nonporous Arsenolite Under High Pressure?. ChemPhysChem, 2018, 19, 857-864.	1.0	10
27286	Theoretical study of mechanical and thermodynamic properties of titanium oxides Ti x O y. Materials Chemistry and Physics, 2018, 213, 538-547.	2.0	9
27287	High-Throughput Computational Assessment of Previously Synthesized Semiconductors for Photovoltaic and Photoelectrochemical Devices. ACS Energy Letters, 2018, 3, 436-446.	8.8	51
27288	Tuning the Electronic and Magnetic Properties of CuAlO₂ Nanocrystals Using Magnetic Dopants. ACS Omega, 2018, 3, 509-513.	1.6	13
27289	Theoretical potential for low energy consumption phase change memory utilizing electrostatically-induced structural phase transitions in 2D materials. Npj Computational Materials, 2018, 4, .	3.5	40
27290	A theoretical study of the effect of a non-aqueous proton donor on electrochemical ammonia synthesis. Physical Chemistry Chemical Physics, 2018, 20, 4982-4989.	1.3	86
27291	A computational study of energy barriers of structural transformations and hydrogen transfer in boehmite. RSC Advances, 2018, 8, 2377-2384.	1.7	8
27292	Band gap engineering of SnS₂ nanosheets by anionâ€“anion codoping for visible-light photocatalysis. RSC Advances, 2018, 8, 3304-3311.	1.7	31
27293	Cobalt Spinel (111) Facets of Various Stoichiometryâ€”DFT+U and Ab Initio Thermodynamic Investigations. Journal of Physical Chemistry C, 2018, 122, 2866-2879.	1.5	19
27294	Introducing DDEC6 atomic population analysis: part 4. Efficient parallel computation of net atomic charges, atomic spin moments, bond orders, and more. RSC Advances, 2018, 8, 2678-2707.	1.7	129
27295	Tuning the pure monoclinic phase of WO3 and WO3-Ag nanostructures for non-enzymatic glucose sensing application with theoretical insight from electronic structure simulations. Journal of Applied Physics, 2018, 123, .	1.1	44

#	Article	IF	Citations
27296	KVP₂O₇ as a Robust Highâ€Energy Cathode for Potassiumâ€Ion Batteries: Pinpointed by a Full Screening of the Inorganic Registry under Specific Search Conditions. Advanced Energy Materials, 2018, 8, 1703099.	10.2	154
27297	Cl24â€Si: a Semiconducting Silicon Phase with an Allâ€sp³ Bonding Network. ChemistrySelect, 2018, 3, 451-455.	0.7	7
27298	Electron Pair Repulsion Responsible for the Peculiar Edge Effects and Surface Chemistry of Black Phosphorus. Journal of Physical Chemistry Letters, 2018, 9, 947-953.	2.1	15
27299	Unusual strain response of thermal transport in dimerized three-dimensional graphene. Nanoscale, 2018, 10, 5229-5238.	2.8	22
27300	First-principles study of Cs/Rb co-doped FAPbI₃ stability and degradation in the presence of water and oxygen. Materials Research Express, 2018, 5, 026203.	0.8	4
27301	First-principles studies on electronic structures and optical properties of two-dimensional Sn1â^'xTi(Zr)xS2 alloys. Modern Physics Letters B, 2018, 32, 1850092.	1.0	1
27302	Unique Zigzag-Shaped Buckling Zn₂C Monolayer with Strain-Tunable Band Gap and Negative Poisson Ratio. Inorganic Chemistry, 2018, 57, 1958-1963.	1.9	22
27303	Friction induced structural transformations of water monolayers at graphene/Cu interfaces. Physical Chemistry Chemical Physics, 2018, 20, 4137-4143.	1.3	8
27304	Interplay between strong correlation and adsorption distances: Co on Cu(001). Physical Review B, 2018, 97, .	1.1	8
27305	Phosphorus Dimerization in Gallium Phosphide at High Pressure. Inorganic Chemistry, 2018, 57, 2432-2437.	1.9	9
27306	Iodine chemistry determines the defect tolerance of lead-halide perovskites. Energy and Environmental Science, 2018, 11, 702-713.	15.6	480
27307	Atomicâ€Scale Insight into Structure and Interface of Al₂Y Phase in an Mgâ€“Alâ€“Y Alloy. Advanced Engineering Materials, 2018, 20, 1701015.	1.6	9
27308	Tailoring the Surface Chemical Reactivity of Transitionâ€Metal Dichalcogenide PtTe₂ Crystals. Advanced Functional Materials, 2018, 28, 1706504.	7.8	68
27309	Decomposition Mechanisms of Anti-wear Lubricant Additive Tricresyl Phosphate on Iron Surfaces Using DFT and Atomistic Thermodynamic Studies. Tribology Letters, 2018, 66, 1.	1.2	20
27310	Effect of sulphur vacancy and interlayer interaction on the electronic structure and spin splitting of bilayer MoS₂. Journal of Physics Condensed Matter, 2018, 30, 125302.	0.7	30
27311	Phosphorusâ€Related Complexes and Shallow Doping in Diamond. Physica Status Solidi - Rapid Research Letters, 2018, 12, 1700409.	1.2	8
27312	Band gap tuning of hydrogen- and oxygen-passivated zigzag graphene monoxide nanoribbon: ab initio computations. Applied Physics A: Materials Science and Processing, 2018, 124, 1.	1.1	2
27313	The oxygen reduction reaction on graphitic carbon nitride supported single Ce atom and CexPt6-x cluster catalysts from first-principles. Carbon, 2018, 130, 636-644.	5.4	30

#	Article	IF	Citations
27314	Adsorption of 3d transition metal atoms on graphene-like gallium nitride monolayer: A first-principles study. Superlattices and Microstructures, 2018, 115, 108-115.	1.4	32
27315	Theoretical simulations of the structural stabilities, elastic, thermodynamic and electronic properties of Pt 3 Sc and Pt 3 Y compounds. Solid State Communications, 2018, 273, 23-29.	0.9	11
27316	First stages of oxide growth on Al(1â€¯1â€¯0) and core-level shifts from density functional theory calculations. Applied Surface Science, 2018, 441, 174-186.	3.1	11
27317	Charged vacancy defects in an AlN nanosheet: A first-principles DFT study. Computational Condensed Matter, 2018, 14, 153-160.	0.9	10
27318	The reaction pathways of the oxygen reduction reaction on IrN 4 doped divacancy graphene: A theoretical study. Journal of Molecular Graphics and Modelling, 2018, 80, 293-298.	1.3	11
27319	Electronic, phonon and superconducting properties of LaPtBi half-Heusler compound. Solid State Communications, 2018, 273, 1-4.	0.9	22
27320	Adsorption Mechanisms of Lithium Polysulfides on Graphene-Based Interlayers in Lithium Sulfur Batteries. ACS Applied Energy Materials, 2018, 1, 455-463.	2.5	28
27321	High pressure and high temperature investigation of metallic perovskite SnTaO3. Journal of Molecular Modeling, 2018, 24, 52.	0.8	8
27322	A comprehensive study of the high-pressureâ€“temperature phase diagram of silicon. Journal of Materials Science, 2018, 53, 7475-7485.	1.7	14
27323	Segregation of alloying elements to planar faults in <mml:math xmlns:mml="http://www.w3.org/1998/Math/MathML" altimg="si1.gif" overflow="scroll"><mml:mrow><mml:mi>Î³</mml:mi><mml:mo>'</mml:mo></mml:mrow></mml:math>-Ni3Al. Acta Materialia, 2018, 148, 173-184.	3.8	70
27324	Transformation stress of shape memory alloy CuZnAl: Non-Schmid behavior. Acta Materialia, 2018, 149, 220-234.	3.8	19
27325	Role of potassium in the enhancement of the catalytic activity of calcium oxide towards tar reduction. Applied Catalysis B: Environmental, 2018, 229, 88-95.	10.8	51
27326	Fabrication of carbon bridged g-C3N4 through supramolecular self-assembly for enhanced photocatalytic hydrogen evolution. Applied Catalysis B: Environmental, 2018, 229, 114-120.	10.8	128
27327	Oxygen reduction reaction (orr) on bimetallic AuPt and AuPd(1 0 0)â€“electrodes: Effects of the heteroatomic junction on the reaction paths. Applied Surface Science, 2018, 441, 663-669.	3.1	11
27328	Enriching the hydrogen storage capacity of carbon nanotube doped with polylithiated molecules. Applied Surface Science, 2018, 444, 467-473.	3.1	24
27329	Hydrogen storage in N- and B-doped graphene decorated by small platinum clusters: A computational study. Applied Surface Science, 2018, 441, 607-612.	3.1	42
27330	Alcohol molecules adsorption on graphane nanosheets â€“ A first-principles investigation. Applied Surface Science, 2018, 441, 734-743.	3.1	36
27331	Penta-SiC 5 monolayer: A novel quasi-planar indirect semiconductor with a tunable wide band gap. Physics Letters, Section A: General, Atomic and Solid State Physics, 2018, 382, 710-715.	0.9	46

#	Article	IF	Citations
27332	Electronic and magnetic properties of MoSe 2 armchair nanoribbons controlled by the different edge structures. Superlattices and Microstructures, 2018, 115, 30-39.	1.4	11
27333	Electron transport in NH 3 /NO 2 sensed buckled antimonene. Solid State Communications, 2018, 272, 1-7.	0.9	10
27334	Clean Os(0001) electronic surface states: A first-principle fully relativistic investigation. Surface Science, 2018, 671, 17-26.	0.8	3
27335	Adsorption and Diffusion of Lithium and Sodium on Defective Rhenium Disulfide: A First Principles Study. ACS Applied Materials & Interfaces, 2018, 10, 5373-5384.	4.0	92
27336	Promising half-metallicity in ductile NbF₃: a first-principles prediction. Physical Chemistry Chemical Physics, 2018, 20, 4781-4786.	1.3	10
27337	Trends in adsorption of electrocatalytic water splitting intermediates on cubic ABO₃ oxides. Physical Chemistry Chemical Physics, 2018, 20, 3813-3818.	1.3	94
27338	Band alignment and charge transfer predictions of ZnO/ZnX (X = S, Se or Te) interfaces applied to solar cells: a PBE+U theoretical study. Physical Chemistry Chemical Physics, 2018, 20, 4953-4961.	1.3	21
27339	Polarization canting in ferroelectric diisopropylammonium-halide molecular crystals: a computational first principles study. Journal of Materials Chemistry C, 2018, 6, 1143-1152.	2.7	10
27340	Structural, elastic, electronic, optical and thermoelectric properties of the Zintl-phase Ae₃AlAs₃ (Ae = Sr, Ba). Philosophical Magazine, 2018, 98, 1217-1240.	0.7	17
27341	Electronic structure and optical properties of Ag-MoS₂ composite systems. Journal Physics D: Applied Physics, 2018, 51, 085303.	1.3	16
27342	First principles study on the structural stability and optoelectronic properties of InxGa1âˆ’xAs materials with different Indium component. Materials Research Express, 2018, 5, 015912.	0.8	6
27343	Powder chemistry effects on the sintering of MgOâ€doped specialty Al₂O₃. Journal of the American Ceramic Society, 2018, 101, 2739-2751.	1.9	4
27344	Comparative Study on the Charge-Ordered and Mixed-Valence Phases of LuFe2O4 via First-Principles Calculations. Journal of Superconductivity and Novel Magnetism, 2018, 31, 2915-2923.	0.8	0
27345	Insight into the C C chain growth in Fischer-Tropsch synthesis on HCP Co(10-10) surface: The effect of crystal facets on the preferred mechanism. Computational Materials Science, 2018, 145, 263-279.	1.4	16
27346	Hunting the Correlation between Fe₅C₂ Surfaces and Their Activities on CO: The Descriptor of Bond Valence. Journal of Physical Chemistry C, 2018, 122, 2806-2814.	1.5	26
27347	A Facile Space-Confined Solid-Phase Sulfurization Strategy for Growth of High-Quality Ultrathin Molybdenum Disulfide Single Crystals. Nano Letters, 2018, 18, 2021-2032.	4.5	42
27348	Ab Initio Thermodynamics of Hydrated Calcium Carbonates and Calcium Analogues of Magnesium Carbonates: Implications for Carbonate Crystallization Pathways. ACS Earth and Space Chemistry, 2018, 2, 210-224.	1.2	25
27349	Zr₂Si: an antiferromagnetic Dirac MXene. Physical Chemistry Chemical Physics, 2018, 20, 3946-3952.	1.3	19

#	Article	IF	Citations
27350	Verwey-type charge ordering transition in an open-shell p -electron compound. Science Advances, 2018, 4, eaap7581.	4.7	13
27351	First-principles study of defect formation in a photovoltaic semiconductor Cu₂ZnGeSe₄. Japanese Journal of Applied Physics, 2018, 57, 02CE06.	0.8	5
27352	Energetic consideration of defected rhenium disilicide, ReSi 2-x, and the electronic structure of Re 4 Si 7 (ReSi 1.75), revisited. Computational Condensed Matter, 2018, 14, 167-175.	0.9	1
27353	Path integral Monte Carlo simulations of dense carbon-hydrogen plasmas. Journal of Chemical Physics, 2018, 148, 102318.	1.2	33
27354	Effect of rattling motion without cage structure on lattice thermal conductivity in LaOBiS2â^'xSex. Applied Physics Letters, 2018, 112, .	1.5	29
27355	Influence of Cation Size on the Electronic and Magnetic Structure of M CoO3 (M = Bi, La) from Ab Initio Calculations. Journal of Superconductivity and Novel Magnetism, 2018, 31, 2925-2934.	0.8	2
27356	Detoxification of aflatoxins on prospective approach: effect on structural, mechanical, and optical properties under pressures. Interdisciplinary Sciences, Computational Life Sciences, 2018, 10, 311-319.	2.2	10
27357	Firstâ€Principles Characterization of Equilibrium Vacancy Concentration in Metamagnetic Shape Memory Alloys: An Example of Ni₂MnGa. Physica Status Solidi (B): Basic Research, 2018, 255, 1700523.	0.7	6
27358	Preferential horizontal growth of tungsten sulfide on carbon and insight into active sulfur sites for the hydrogen evolution reaction. Nanoscale, 2018, 10, 3838-3848.	2.8	31
27359	Tailored fabrication of a prospective acoustoâ€“optic crystal TiTe₃O₈endowed with high performance. Journal of Materials Chemistry C, 2018, 6, 2443-2451.	2.7	18
27360	Franck Condon shift assessment in 2D MoS₂. Journal of Physics Condensed Matter, 2018, 30, 095501.	0.7	8
27361	Nitrogen Doping of Hexagonal and Cubic Ge₂Sb₂Te₅ Nanocrystals: An Ab Initio Study. International Journal of Nanoscience, 2018, 17, 1850009.	0.4	3
27362	Magnetic Properties of La-Doped ZnO(0001)â€“Zn Polar Surface with and without Vacancies: a First-Principle Study. Journal of Superconductivity and Novel Magnetism, 2018, 31, 2897-2905.	0.8	7
27363	Visualization and manipulation of magnetic domains in the quasi-two-dimensional material <mml:math xmlns:mml="http://www.w3.org/1998/Math/MathML"><mml:mrow><mml:mi mathvariant="normal">F</mml:mi><mml:msub><mml:mi mathvariant="normal">e</mml:mi><mml:mn>3</mml:mn></mml:msub><mml:mi>GeT</mml:mi><mml:msub><mml:mi mathvariant="normal">e</mml:mi><mml:mn>2</mml:mn></mml:msub></mml:mrow></mml:math>. Physical Review B, 2018, 97, .	1.1	74
27364	Dopantâ€“dopant interactions in beryllium doped indium gallium arsenide: An ab initio study. Journal of Materials Research, 2018, 33, 401-413.	1.2	4
27365	Origin of the overpotentials for HCOO^{â^'} and CO formation in the electroreduction of CO₂ on Cu(211): the reductive desorption processes decide. Physical Chemistry Chemical Physics, 2018, 20, 5756-5765.	1.3	19
27366	Structural phase transition and bonding properties of high-pressure polymeric CaN3. RSC Advances, 2018, 8, 4314-4320.	1.7	14
27367	Symmetry-dependent topological phase transitions in PbTe layers. Materials Research Express, 2018, 5, 015051.	0.8	7

#	Article	IF	Citations
27368	Machine learning properties of binary wurtzite superlattices. Journal of Materials Science, 2018, 53, 6652-6664.	1.7	24
27369	Organic Cation Substitution in Hybrid Perovskite CH₃NH₃PbI₃ with Hydroxylammonium (NH₃OH⁺): A First-Principles Study. Journal of Physical Chemistry C, 2018, 122, 3548-3557.	1.5	13
27370	Identification of Killer Defects in Kesterite Thin-Film Solar Cells. ACS Energy Letters, 2018, 3, 496-500.	8.8	130
27371	Metallic Ti₃C₂T_x MXene Gas Sensors with Ultrahigh Signal-to-Noise Ratio. ACS Nano, 2018, 12, 986-993.	7.3	1,153
27372	Local Plasmon Engineering in Doped Graphene. ACS Nano, 2018, 12, 1837-1848.	7.3	25
27373	CO adsorption and oxygen activation on group 11 nanoparticles â€“ a combined DFT and high level CCSD(T) study about size effects and activation processes. Faraday Discussions, 2018, 208, 105-121.	1.6	16
27374	Band alignments and heterostructures of monolayer transition metal trichalcogenides MX₃ (M = Zr, Hf; X = S, Se) and dichalcogenides MX₂ (M = Tc, Re; X=S, Se) for solar applications. Nanoscale, 2018, 10, 3547-3555.	2.8	70
27375	Tunable magnetotransport in Fe/hBN/graphene/hBN/Pt(Fe) epitaxial multilayers. Journal Physics D: Applied Physics, 2018, 51, 095302.	1.3	8
27376	Approximate quasiparticle correction for calculations of the energy gap in two-dimensional materials. Physical Review B, 2018, 97, .	1.1	20
27377	Anion Order and Spontaneous Polarization in <mml:math xmlns:mml="http://www.w3.org/1998/Math/MathML" display="inline"><mml:mrow><mml:msub><mml:mrow><mml:mi>LaTiO</mml:mi></mml:mrow><mml:mrow><mml:mn>2</mml:mn></mml:mrow></mml:msub><mml:mi mathvariant="normal">N</mml:mi></mml:mrow></mml:math> Oxynitride Thin Films. Physical Review Letters, 2018, 120, 046001.	2.9	26
27378	Mechanistic origin and prediction of enhanced ductility in magnesium alloys. Science, 2018, 359, 447-452.	6.0	432
27379	Theoretical study of phase stability, crystal and electronic structure of MeMgN2 (MeÂ=ÂTi, Zr, Hf) compounds. Journal of Materials Science, 2018, 53, 4294-4305.	1.7	15
27380	A DFT approach for methanol synthesis via hydrogenation of CO on gallia, ceria and ZnO surfaces. Applied Surface Science, 2018, 436, 1003-1017.	3.1	10
27381	First-principles study of the structure properties of Al(111)/6H-SiC(0001) interfaces. Surface Science, 2018, 670, 1-7.	0.8	16
27382	Engineering an N-doped TiO₂@N-doped C butterfly-like nanostructure with long-lived photo-generated carriers for efficient photocatalytic selective amine oxidation. Journal of Materials Chemistry A, 2018, 6, 2091-2099.	5.2	67
27383	Controlling electronic properties of MoS₂/graphene oxide heterojunctions for enhancing photocatalytic performance: the role of oxygen. Physical Chemistry Chemical Physics, 2018, 20, 1974-1983.	1.3	24
27384	The Effect of Platinum on Î²-NiAl/Î±-Al2O3 Interfacial Tensile Stress: A Combined Ab Initio DFT and Mechanics-Based Model Study. Oxidation of Metals, 2018, 90, 65-82.	1.0	3
27385	Charge-modulated CO2 capture of C3N nanosheet: Insights from DFT calculations. Chemical Engineering Journal, 2018, 338, 92-98.	6.6	111

#	Article	IF	Citations
27386	A computational thermodynamic and kinetic study of chlorine binding to the Zr(0001) surface. Colloids and Surfaces A: Physicochemical and Engineering Aspects, 2018, 539, 92-100.	2.3	7
27387	Shaping the Magnetic Properties of BaFeO₃ Perovskite-Type by Alkaline-Earth Doping. Journal of Physical Chemistry C, 2018, 122, 2983-2989.	1.5	23
27388	Detection of gas molecules on single Mn adatom adsorbed graphyne: a DFT-D study. Journal Physics D: Applied Physics, 2018, 51, 065109.	1.3	56
27389	Segregation of Mg, Cu and their effects on the strength of Al Î£5 (210)[001] symmetrical tilt grain boundary. Acta Materialia, 2018, 145, 235-246.	3.8	101
27390	DFT calculation for stability and strength of iron borides. Computational Materials Science, 2018, 144, 147-153.	1.4	3
27391	Electronic, magnetic and mechanical properties of (Fe,Ni)2Nb from density functional theory. Journal of Magnetism and Magnetic Materials, 2018, 452, 219-229.	1.0	14
27392	Rediscovering the MP₁₅ Family (M = Li, Na, and K) as an Anisotropic Layered Semiconducting Material. Journal of Physical Chemistry Letters, 2018, 9, 732-738.	2.1	15
27393	The structural, electronic and magnetic properties of Co1â^'xFexS2. Materials Research Express, 2018, 5, 016507.	0.8	5
27394	CO oxidation on inverse Ce6O12/Cu(111) catalyst: role of copperâ€“ceria interactions. Journal of Molecular Modeling, 2018, 24, 20.	0.8	4
27395	Theoretical design of Li-doped ILCOF-1 for high H2 uptake at moderate temperature. Computational Materials Science, 2018, 143, 360-367.	1.4	5
27396	The cluster-plus-glue-atom models of solid solution CuNi alloys: A first-principles study. Computational Materials Science, 2018, 143, 439-445.	1.4	5
27397	C2x: A tool for visualisation and input preparation for Castep and other electronic structure codes. Computer Physics Communications, 2018, 225, 174-179.	3.0	45
27398	Theoretical investigation of the structural, elastic, electronic and optical properties of the ternary indium sulfide layered structures A InS 2 (A Â= K, Rb and Cs). Solid State Sciences, 2018, 76, 74-84.	1.5	12
27399	The Role of Adsorbed CN and Cl on an Au Electrode for Electrochemical CO₂ Reduction. ACS Catalysis, 2018, 8, 1178-1185.	5.5	98
27400	Manipulation of cation combinations and configurations of halide double perovskites for solar cell absorbers. Journal of Materials Chemistry A, 2018, 6, 1809-1815.	5.2	85
27401	Bipolar Magnetic Materials Based on 2D Ni[TCNE] Metalâ€“Organic Coordination Networks. Advanced Electronic Materials, 2018, 4, 1700323.	2.6	17
27402	Revealing Pseudocapacitive Mechanisms of Metal Dichalcogenide SnS₂/Grapheneâ€CNT Aerogels for Highâ€Energy Na Hybrid Capacitors. Advanced Energy Materials, 2018, 8, 1702488.	10.2	135
27403	Morphological and Compositional Design of Pdâ€“Cu Bimetallic Nanocatalysts with Controllable Product Selectivity toward CO₂ Electroreduction. Small, 2018, 14, 1703314.	5.2	84

#	Article	IF	Citations
27404	Size Effects on Cohesive Energy, Debye Temperature and Lattice Heat Capacity from First-Principles Calculations of Sn Nanoparticles. Proceedings of the National Academy of Sciences India Section A - Physical Sciences, 2018, 88, 629-632.	0.8	7
27405	Topological line defects in graphene for applications in gas sensing. Carbon, 2018, 129, 803-808.	5.4	42
27406	First principles study of structural and optoelectronic properties of Li based half Heusler alloys. Computational Condensed Matter, 2018, 14, 55-66.	0.9	54
27407	Cobalt-doped molybdenum disulfide in-situ grown on graphite paper with excellent electrocatalytic activity for triiodide evolution. Electrochimica Acta, 2018, 263, 328-337.	2.6	33
27408	Influence of point defects on optoelectronic properties of Al0.375Ga0.625N. Optik, 2018, 157, 16-24.	1.4	1
27409	Effective approach for reducing the migration of ions and improving the stability of organicâ€“inorganic perovskite solar cells. Journal of Alloys and Compounds, 2018, 741, 489-494.	2.8	20
27410	Chemical doping in pnictides superconductors: The case ofCa(Fe1-xXx)2As2, Xâ€¯=â€¯Co, Ni, Pt. Journal of Magnetism and Magnetic Materials, 2018, 452, 179-183.	1.0	2
27411	The effect of relativity on stability of Copernicium phases, their electronic structure and mechanical properties. Physica B: Condensed Matter, 2018, 536, 576-582.	1.3	0
27412	Migration of sodium and lithium interstitials in anatase TiO2. Solid State Ionics, 2018, 315, 40-43.	1.3	9
27413	NMR interaction tensors of 51V and 207Pb in vanadinite, Pb5(VO4)3Cl, determined from DFT calculations and single-crystal NMR measurements, using only one general rotation axis. Solid State Nuclear Magnetic Resonance, 2018, 89, 11-20.	1.5	9
27414	Electronâ€“Phonon Coupling and Polaron Mobility in Hybrid Perovskites from First Principles. Journal of Physical Chemistry C, 2018, 122, 1361-1366.	1.5	29
27415	Resonant Raman and Exciton Coupling in High-Quality Single Crystals of Atomically Thin Molybdenum Diselenide Grown by Vapor-Phase Chalcogenization. ACS Nano, 2018, 12, 740-750.	7.3	34
27416	First-principles energy and vibration spectrum simulations of Cr/V interacting with H in W-based alloy in a fusion reactor. Journal of Nuclear Science and Technology, 2018, 55, 123-137.	0.7	1
27417	Exploring the relevance of thiophene rings as bridge unit in acceptorâ€bridgeâ€donor dyes on selfâ€aggregation and performance in DSSCs. Journal of Computational Chemistry, 2018, 39, 685-698.	1.5	10
27418	Chemistry below graphene: Decoupling epitaxial graphene from metals by potential-controlled electrochemical oxidation. Carbon, 2018, 129, 837-846.	5.4	30
27419	Pt4, Pd4, Ni4, and Ti4 catalyzed hydrogen spillover on penta-graphene for hydrogen storage: The first-principles and kinetic Monte Carlo study. International Journal of Hydrogen Energy, 2018, 43, 2247-2255.	3.8	29
27420	Properties of Y2TiO5 and Y2Ti2O7 crystals: Development of novel interatomic potentials. Journal of Alloys and Compounds, 2018, 739, 1037-1047.	2.8	12
27421	Investigation of GaBi1-xSbx based highly mismatched alloys: Potential thermoelectric materials for renewable energy devices and applications. Journal of Alloys and Compounds, 2018, 739, 380-387.	2.8	14

#	Article	IF	Citations
27422	DFT studies on the Al, B, and P doping of silicene. Superlattices and Microstructures, 2018, 114, 242-250.	1.4	18
27423	Borophene and defective borophene as potential anchoring materials for lithiumâ€“sulfur batteries: a first-principles study. Journal of Materials Chemistry A, 2018, 6, 2107-2114.	5.2	127
27424	Exploring the transposition effects on the electronic and optical properties of Cs₂AgSbCl₆via a combined computational-experimental approach. Journal of Materials Chemistry A, 2018, 6, 2346-2352.	5.2	100
27425	Nitrogen doped BiFeO3 with enhanced magnetic properties and photo-Fenton catalytic activity for degradation of bisphenol A under visible light. Chemical Engineering Journal, 2018, 337, 709-721.	6.6	62
27426	Zn doping in the In0.53Ga0.47As(100)Î²2(2â€²Ã—â€²4) surface for negative electron affinity photocathode: A first-principles research. Optik, 2018, 158, 355-362.	1.4	6
27427	Mechanical, optoelectronic and transport properties of single-layer Ca2N and Sr2N electrides. Journal of Alloys and Compounds, 2018, 739, 643-652.	2.8	14
27428	Clarification of the interaction between Au atoms and the anatase TiO2 (112) surface using density functional theory. Surface Science, 2018, 670, 23-32.	0.8	16
27429	Ni-Doping Effects on Oxygen Removal from an Orthorhombic Mo₂C (001) Surface: A Density Functional Theory Study. Journal of Physical Chemistry C, 2018, 122, 1595-1603.	1.5	20
27430	Density-functional tight-binding investigation of the structure, stability and material properties of nickel hydroxide nanotubes. Nanotechnology, 2018, 29, 025708.	1.3	2
27431	Prediction of Half-Metallic Properties in Non-transition Metal-based Binary Compounds X Bi (X = Ba, Sr) Tj ETQq1 1 0.784314 rgBT /Ov Magnetism, 2018, 31, 2767-2776.	0.8	2
27432	Pressure-dependent mechanical and thermodynamic properties of newly discovered cubic Na 2 He. Chinese Journal of Physics, 2018, 56, 231-237.	2.0	16
27433	Ab-initio calculation of the magnetic properties of P and As doped SnO 2. Computational Condensed Matter, 2018, 14, 36-39.	0.9	17
27434	New predicted ground state and high pressure phases of TcB3 and TcB4: First-principles. Computational Materials Science, 2018, 144, 154-160.	1.4	4
27435	Role of Gold Adatoms in the Adsorption of Sulfide Species on the Gold(001)-hex Surface. Journal of Physical Chemistry C, 2018, 122, 2207-2214.	1.5	12
27436	Wannier Koopmans Method Calculations of 2D Material Band Gaps. Journal of Physical Chemistry Letters, 2018, 9, 281-285.	2.1	12
27437	Accelerating the discovery of hidden two-dimensional magnets using machine learning and first principle calculations. Journal of Physics Condensed Matter, 2018, 30, 06LT01.	0.7	23
27438	Structureâ€Sensitive Scaling Relations: Adsorption Energies from Surface Site Stability. ChemCatChem, 2018, 10, 1643-1650.	1.8	57
27439	Protons in cubic yttria-stabilized zirconia: Binding sites and migration pathways. Solid State Ionics, 2018, 315, 116-125.	1.3	9

#	Article	IF	Citations
27440	Two-Dimensional Metalâ€“Organic Half-metallic Antiferromagnet: CoFePz. Journal of Physical Chemistry C, 2018, 122, 1846-1851.	1.5	24
27441	Electric field effects on the electronic and optical properties in C2N/Sb van der Waals heterostructure. Carbon, 2018, 129, 738-744.	5.4	47
27442	Formation of ferromagnetic/ferrimagnetic epitaxial interfaces: Stability and magnetic properties. Computational Materials Science, 2018, 144, 294-303.	1.4	10
27443	Structural, mechanical and electronic properties of two-dimensional structure of III-arsenide (1 1 1) binary compounds: An ab-initio study. Computational Materials Science, 2018, 144, 285-293.	1.4	10
27444	Theoretical studies on electronic structure and optical properties of Bi2WO6. Optik, 2018, 158, 962-969.	1.4	22
27445	Ab initio simulations on charged interstitial oxygen migration in corundum. Nuclear Instruments & Methods in Physics Research B, 2018, 435, 74-78.	0.6	14
27446	The structural, magnetic, electronic and optical properties of the cluster Fe-X6 (X=S, N, O or F) doped monolayer WS2. Superlattices and Microstructures, 2018, 114, 274-283.	1.4	6
27447	Thermodynamic assessment of the Mo-S system and its application in thermal decomposition of MoS 2. Thermochimica Acta, 2018, 660, 44-55.	1.2	10
27448	Magnetic properties of coreâ€“shell nanoparticles possessing a novel Fe(<scp>ii</scp>)-chromia phase: an experimental and theoretical approach. Nanoscale, 2018, 10, 2138-2147.	2.8	23
27449	Atomically Thin Mesoporous In₂O_{3â€“}_x/In₂S₃ Lateral Heterostructures Enabling Robust Broadbandâ€Light Photoâ€Electrochemical Water Splitting. Advanced Energy Materials, 2018, 8, 1701114.	10.2	106
27450	Theoretical insights on the oxygen-reduction reaction mechanism of LaN4-embedded graphene. Journal of Molecular Modeling, 2018, 24, 14.	0.8	5
27451	Oxygen adsorption and diffusion on Î³-U(0â€¯0â€¯1) surface: Effect of titanium. Computational Materials Science, 2018, 144, 85-91.	1.4	13
27452	The effects of strain and vacancy defects on the electronic structure of Cr2O3. Computational Materials Science, 2018, 144, 64-69.	1.4	25
27453	Band alignments of graphene-like III-nitride semiconductors. Solid State Communications, 2018, 270, 147-150.	0.9	12
27454	Polymorph transitions in uranium at low temperatures: first-principles investigation. Modelling and Simulation in Materials Science and Engineering, 2018, 26, 025009.	0.8	5
27455	First-principles investigation on the structures, energies, electronic and defective properties of Ti 2 AlN surfaces. Applied Surface Science, 2018, 433, 1056-1066.	3.1	25
27456	First-principles study of structural phase transition, electronic, elastic and thermodynamic properties of C15-type Laves phase TiCr 2 under pressure. Physica B: Condensed Matter, 2018, 531, 79-84.	1.3	10
27457	Role of Lead Vacancies for Optoelectronic Properties of Lead-Halide Perovskites. Journal of Physical Chemistry C, 2018, 122, 5216-5226.	1.5	20

#	Article	IF	Citations
27458	Enhanced Switchable Ferroelectric Photovoltaic Effects in Hexagonal Ferrite Thin Films via Strain Engineering. ACS Applied Materials & Interfaces, 2018, 10, 1846-1853.	4.0	47
27459	Charge Order and Negative Thermal Expansion in V₂OPO₄. Journal of the American Chemical Society, 2018, 140, 636-641.	6.6	45
27460	Oxygen-induced degradation of the electronic properties of thin-layer InSe. Physical Chemistry Chemical Physics, 2018, 20, 2238-2250.	1.3	23
27461	Tunable Schottky contacts in MSe₂/NbSe₂ (M = Mo and W) heterostructures and promising application potential in field-effect transistors. Physical Chemistry Chemical Physics, 2018, 20, 1897-1903.	1.3	17
27462	Negative Poisson's ratio and high-mobility transport anisotropy in SiC₆siligraphene. Nanoscale, 2018, 10, 2108-2114.	2.8	51
27463	From quantum to continuum mechanics: studying the fracture toughness of transition metal nitrides and oxynitrides. Materials Research Letters, 2018, 6, 142-151.	4.1	30
27464	High-pressure structural and vibrational properties of monazite-type BiPO₄, LaPO₄, CePO₄, and PrPO₄. Journal of Physics Condensed Matter, 2018, 30, 065401.	0.7	28
27465	Molecular and dissociative adsorption of a single water molecule on a Î²â€dicalcium silicate (100) surface explored by a <scp>DFT</scp> approach. Journal of the American Ceramic Society, 2018, 101, 2428-2437.	1.9	17
27466	Elasticity, slowness, thermal conductivity and the anisotropies in the Mn₃Cu1â^'xGexN compounds. International Journal of Modern Physics B, 2018, 32, 1850071.	1.0	2
27467	First-principle analysis of the structural, mechanical, optical and electronic properties of wollastonite monoclinic polymorph. Computational Condensed Matter, 2018, 14, 20-26.	0.9	38
27468	Hidden spin polarization in the 1 T -phase layered transition-metal dichalcogenides MX 2 (M â€¯=â€¯Zr, Hf; X) Tj ETQq0 0 0 rgBT /Overlo	4.3	25
27469	Kinetics of Molecular Diffusion and Self-Assembly: Glycine on Cu{110}. Journal of Physical Chemistry C, 2018, 122, 782-797.	1.5	4
27470	First-Principles Study of the Interactions between Graphene Oxide and Amine-Functionalized Carbon Nanotube. Journal of Physical Chemistry C, 2018, 122, 1288-1298.	1.5	17
27471	Unsupported shaped cobalt nanoparticles as efficient and recyclable catalysts for the solvent-free acceptorless dehydrogenation of alcohols. Catalysis Science and Technology, 2018, 8, 562-572.	2.1	20
27472	NaCl-CsCl structural transition in Sr2PdO3 and Sr2TiO4. Journal of Alloys and Compounds, 2018, 737, 230-237.	2.8	1
27473	Theoretical investigations on mechanical and dynamical properties of MAlB (MÂ=ÂMo, W) nanolaminated borides at ground-states and elevated temperatures. Journal of Alloys and Compounds, 2018, 738, 461-472.	2.8	33
27474	Al-based composites reinforced with AlB2, AlN and BN phases: Experimental and theoretical studies. Materials and Design, 2018, 141, 88-98.	3.3	69
27475	Identifying the Thermal Decomposition Mechanism of Guaiacol on Pt(111): An Integrated X-ray Photoelectron Spectroscopy and Density Functional Theory Study. Journal of Physical Chemistry C, 2018, 122, 4261-4273.	1.5	5

#	Article	IF	Citations
27476	Different Topological Quantum States in Ternary Zintl compounds: BaCaX (X = Si, Ge, Sn and Pb). Journal of Physical Chemistry C, 2018, 122, 705-713.	1.5	14
27477	Local Electronic Structure of a Single-Layer Porphyrin-Containing Covalent Organic Framework. ACS Nano, 2018, 12, 385-391.	7.3	68
27478	Microscopic evidence for the dissociation of water molecules on cleaved GaN(11Ì„00). Physical Chemistry Chemical Physics, 2018, 20, 1261-1266.	1.3	6
27479	Theoretical study of nitride short period superlattices. Journal of Physics Condensed Matter, 2018, 30, 063001.	0.7	31
27480	Phonon-driven electron scattering and magnetothermoelectric effect in two-dimensional tin selenide. Journal of Physics Condensed Matter, 2018, 30, 055301.	0.7	7
27481	Tuning electronic and optical properties of arsenene/C₃N van der Waals heterostructure by vertical strain and external electric field. Nanotechnology, 2018, 29, 075201.	1.3	89
27482	Ab Initio Study of Iodine-Doped Carbon Nanotube Conductors. Journal of Engineering Materials and Technology, Transactions of the ASME, 2018, 140, .	0.8	5
27483	Isovalent doping and the CiOi defect in germanium. Journal of Materials Science: Materials in Electronics, 2018, 29, 4261-4265.	1.1	3
27484	Bond saturation significantly enhances thermal energy transport in two-dimensional pentagonal materials. Nano Energy, 2018, 45, 1-9.	8.2	15
27485	Selective adsorption of a supramolecular structure on flat and stepped gold surfaces. Surface Science, 2018, 670, 44-50.	0.8	3
27486	Reactivity of Substrate-Supported Graphene: A Case Study of Hydrogenation. Journal of Physical Chemistry C, 2018, 122, 2761-2772.	1.5	7
27487	Few-Layer Iron Selenophosphate, FePSe₃: Efficient Electrocatalyst toward Water Splitting and Oxygen Reduction Reactions. ACS Applied Energy Materials, 2018, 1, 220-231.	2.5	80
27488	Evaluating the Risk of Câ€“C Bond Formation during Selective Hydrogenation of Acetylene on Palladium. ACS Catalysis, 2018, 8, 1662-1671.	5.5	65
27489	Bulk and surface properties of the Ruddlesdenâ€“Popper oxynitride Sr₂TaO₃N. Physical Chemistry Chemical Physics, 2018, 20, 2771-2776.	1.3	17
27490	Interaction between functionalized graphene and sulfur compounds in a lithiumâ€“sulfur battery â€“ a density functional theory investigation. RSC Advances, 2018, 8, 2271-2279.	1.7	50
27491	Interface spacing, stability, band offsets, and electronic properties on a (001) SrHfO3/GaAs interface: First-principles calculations. Journal of Applied Physics, 2018, 123, 025306.	1.1	0
27492	Ferromagnetism in CVT grown tungsten diselenide single crystals with nickel doping. Nanotechnology, 2018, 29, 115701.	1.3	31
27493	Superconductivity proximate to antiferromagnetism in a copper-oxide monolayer grown on Bi2Sr2CaCu2O8+Î´. Physical Review B, 2018, 97, .	1.1	5

#	Article	IF	Citations
27494	Observation of a two-dimensional Fermi surface and Dirac dispersion in <mml:math xmlns:mml="http://www.w3.org/1998/Math/MathML"><mml:msub><mml:mi>YbMnSb</mml:mi><mml:mn>2</mml:mn></mml:msub>< Physical Review B, 2018, 97, .	1.1	54
27495	Unraveling Hidden Mgâ€“Mnâ€“H Phase Relations at High Pressures and Temperatures by in Situ Synchrotron Diffraction. Inorganic Chemistry, 2018, 57, 1614-1622.	1.9	9
27496	Designing half-metallic ferromagnetism by a new strategy: an example of superhalogen modified graphitic C₃N₄. Journal of Materials Chemistry C, 2018, 6, 1709-1714.	2.7	21
27497	Electronic, Magnetic, and Transport Properties of Polyacrylonitrile-Based Carbon Nanofibers of Various Widths: Density-Functional Theory Calculations. Physical Review Applied, 2018, 9, .	1.5	8
27498	Magnetic Behaviors of 3d Transition Metal-Doped Silicane: a First-Principle Study. Journal of Superconductivity and Novel Magnetism, 2018, 31, 2789-2795.	0.8	81
27499	Influence of doping concentration on mechanical properties of Mo2FeB2 alloyed with Cr and Ni from first-principle calculations. Computational Materials Science, 2018, 146, 18-25.	1.4	49
27500	Vibrational Properties of Bulk Boric Acid2Aand3TPolymorphs and Their Two-Dimensional Layers: Measurements and Density Functional Theory Calculations. Journal of Physical Chemistry A, 2018, 122, 1312-1325.	1.1	10
27501	First-principles study of alloying effects on fluorine incorporation in Al_xGa_{1â^'x}N alloys. Journal Physics D: Applied Physics, 2018, 51, 065108.	1.3	10
27502	Tunable magnetism and spin-polarized electronic transport in graphene mediated by molecular functionalization of extended defects. Physical Review B, 2018, 97, .	1.1	9
27503	Pressure dependent mechanical properties of calcium carbides. Ceramics International, 2018, 44, 7429-7434.	2.3	2
27504	Reduced sintering of mass-selected Au clusters on SiO₂by alloying with Ti: an aberration-corrected STEM and computational study. Nanoscale, 2018, 10, 2363-2370.	2.8	14
27505	Vibrational properties of the Au-(<mml:math) Tj ETQq1 1 0.784314 rgBT /Overlock 10 Tf 50 307 Td (xmlns:mml="http://www.w3.org/	1.1	10
27506	First-principles study on the stability and magnetoelectric properties of multiferroic materials XTiO3 (X = Mn, Fe, Co, Ni). International Journal of Modern Physics B, 2018, 32, 1850105.	1.0	3
27507	Oxygenâ€Vacancy Abundant Ultrafine Co₃O₄/Graphene Composites for Highâ€Rate Supercapacitor Electrodes. Advanced Science, 2018, 5, 1700659.	5.6	392
27508	Tuning the Carrier Confinement in GeS/Phosphorene van der Waals Heterostructures. Small, 2018, 14, 1703536.	5.2	48
27509	Strained zigzag graphene nanoribbon devices with vacancies as perfect spin filters. Journal of Molecular Modeling, 2018, 24, 35.	0.8	7
27510	Theoretical insights into the surface structure of In2O3(1â€¯1â€¯0) surface and its effect on methanol synthesis from CO2 hydrogenation. Computational and Theoretical Chemistry, 2018, 1126, 7-15.	1.1	30
27511	Strain control of oxygen kinetics in the Ruddlesden-Popper oxide La1.85Sr0.15CuO4. Nature Communications, 2018, 9, 92.	5.8	38

#	Article	IF	Citations
27512	Spin-coupling-induced Improper Polarizations and Latent Magnetization in Multiferroic BiFeO3. Scientific Reports, 2018, 8, 405.	1.6	5
27513	Improper magnetic ferroelectricity of nearly pure electronic nature in helicoidal spiral <mml:math xmlns:mml="http://www.w3.org/1998/Math/MathML"><mml:mrow><mml:msub><mml:mi mathvariant="bold">CaMn</mml:mi><mml:mn>7</mml:mn></mml:msub><mml:msub><mml:mi mathvariant="bold">O</mml:mi><mml:mn>12</mml:mn></mml:msub></mml:mrow></mml:math>. Physical Review B, 2018, 97, .	1.1	11
27514	Origamiâ€Inspired 3D Interconnected Molybdenum Carbide Nanoflakes. Advanced Materials Interfaces, 2018, 5, 1701113.	1.9	13
27515	A Dualâ€Insertion Type Sodiumâ€Ion Full Cell Based on Highâ€Quality Ternaryâ€Metal Prussian Blue Analogs. Advanced Energy Materials, 2018, 8, 1702856.	10.2	143
27516	Supercell-zone folding transformation for bulk crystals and nanotubes. Theoretical Chemistry Accounts, 2018, 137, 1.	0.5	6
27517	On the effect of the carbonaceous substrate in the nucleation of Sn nanoparticles for Li-ion anodes: experiments and first principles calculations. Journal of Solid State Electrochemistry, 2018, 22, 1721-1733.	1.2	2
27518	Transition metal decorated covalent triazine-based frameworks as a capacity hydrogen storage medium. International Journal of Hydrogen Energy, 2018, 43, 2823-2830.	3.8	27
27519	Experimental and first principle calculation study on titanium, zirconium and aluminum oxides in promoting ferrite nucleation. Journal of Alloys and Compounds, 2018, 742, 112-122.	2.8	18
27520	Janus Structures of Transition Metal Dichalcogenides as the Heterojunction Photocatalysts for Water Splitting. Journal of Physical Chemistry C, 2018, 122, 3123-3129.	1.5	246
27521	Reconfiguring crystal and electronic structures of MoS2 by substitutional doping. Nature Communications, 2018, 9, 199.	5.8	128
27522	Liquid-like thermal conduction in intercalated layered crystalline solids. Nature Materials, 2018, 17, 226-230.	13.3	136
27523	Interfacial Coupling Effect on Electron Transport in MoS2/SrTiO3 Heterostructure: An Ab-initio Study. Scientific Reports, 2018, 8, 714.	1.6	9
27524	Improvement of O₂ adsorption for Î±-MnO₂ as an oxygen reduction catalyst by Zr⁴⁺ doping. RSC Advances, 2018, 8, 2963-2970.	1.7	32
27525	Earth abundant perovskite oxides for low temperature CO₂conversion. Energy and Environmental Science, 2018, 11, 648-659.	15.6	93
27526	Enhanced photochemical performance of hexagonal WO3 by metal-assisted Sâ€“O coupling for solar-driven water splitting. Science China Materials, 2018, 61, 91-100.	3.5	4
27527	Probing interfacial electronic properties of graphene/CH3NH3PbI3 heterojunctions: A theoretical study. Applied Surface Science, 2018, 440, 35-41.	3.1	54
27528	Effects of methylating agent and BrÃ¸nsted acidity on methylation activity of olefins in CHA-structured zeolites: A periodic DFT study. Molecular Catalysis, 2018, 446, 106-114.	1.0	4
27529	Searching for Hidden Perovskite Materials for Photovoltaic Systems by Combining Data Science and First Principle Calculations. ACS Photonics, 2018, 5, 771-775.	3.2	70

#	Article	IF	Citations
27530	A new phase of the two-dimensional ReS₂ sheet with tunable magnetism. Journal of Materials Chemistry C, 2018, 6, 1248-1254.	2.7	35
27531	Transition-metal alloying of <mml:math xmlns:mml="http://www.w3.org/1998/Math/MathML"><mml:mrow><mml:msup><mml:mi>Î³</mml:mi><mml:mo>â€²</mml:mo></m : Effects on the ideal uniaxial compressive strength from first-principles calculations. Physical Review B, 2018, 97, .	1.1	21
27532	Carbon ene-yne graphyne monolayer as an outstanding anode material for Li/Na ion batteries. Applied Materials Today, 2018, 10, 115-121.	2.3	44
27533	Highly conductive and transparent films of HAuCl4-doped single-walled carbon nanotubes for flexible applications. Carbon, 2018, 130, 448-457.	5.4	68
27534	Heliumâ€“vacancy interactions in vanadium and tantalum. Computational Materials Science, 2018, 145, 197-207.	1.4	8
27535	Density functional studies on the binding of methanol and ethanol molecules to graphyne nanosheet. Computational and Theoretical Chemistry, 2018, 1125, 86-94.	1.1	57
27536	Magnetic and optical properties of carbon and silicon decorated free standing buckled germanene: A DFT approach. Journal of Physics and Chemistry of Solids, 2018, 115, 332-341.	1.9	15
27537	Feâ€“Porphyrin-like Nanostructures for Selective Ammonia Capture under Humid Conditions. Journal of Physical Chemistry C, 2018, 122, 2046-2052.	1.5	7
27538	Ab initio molecular dynamics study of the Eley-Rideal reaction of H + Clâ€“Au(111) â†' HCl + Au(111): Impact of energy dissipation to surface phonons and electron-hole pairs. Journal of Chemical Physics, 2018, 148, 014702.	1.2	25
27539	New structures of Fe₃S for rare-earth-free permanent magnets. Journal Physics D: Applied Physics, 2018, 51, 075001.	1.3	4
27540	Accelerated Discovery of Large Electrostrains in BaTiO₃â€Based Piezoelectrics Using Active Learning. Advanced Materials, 2018, 30, 1702884.	11.1	254
27541	Unraveling localized states in quasi free standing monolayer graphene by means of Density Functional Theory. Carbon, 2018, 130, 466-474.	5.4	7
27542	Study of the structural, elastic, electronic and optical properties of lead free halide double perovskites Cs 2 AgBiX 6 (X â€¯=â€¯ Br, Cl). Chinese Journal of Physics, 2018, 56, 323-330.	2.0	39
27543	The magnetic effects on the energetic landscape of Fe-Cu alloy: A model Hamiltonian approach. Computational Materials Science, 2018, 145, 163-173.	1.4	4
27544	Electronic transport calculations for CO2 adsorption on calcium-decorated graphene nanoribbons. Computational Materials Science, 2018, 145, 134-139.	1.4	6
27545	Design of highly efficient Ni-based water-electrolysis catalysts by a third transition metal addition into Ni 3 Mo. Intermetallics, 2018, 94, 99-105.	1.8	7
27546	Possibility of a ferromagnetic and conducting metal-organic network. Journal of Magnetism and Magnetic Materials, 2018, 453, 48-52.	1.0	12
27547	Structural and electronic properties of CdSe/ZnS and ZnS/CdSe core/shell nanowires via first principles study. Journal of Physics and Chemistry of Solids, 2018, 116, 37-42.	1.9	5

#	Article	IF	Citations
27548	Elucidating the Vibrational Fingerprint of the Flexible Metalâ€“Organic Framework MIL-53(Al) Using a Combined Experimental/Computational Approach. Journal of Physical Chemistry C, 2018, 122, 2734-2746.	1.5	70
27549	Massless Dirac Fermions in ZrTe₂ Semimetal Grown on InAs(111) by van der Waals Epitaxy. ACS Nano, 2018, 12, 1696-1703.	7.3	82
27550	BN nanoparticle/Ag hybrids with enhanced catalytic activity: theory and experiments. Catalysis Science and Technology, 2018, 8, 1652-1662.	2.1	23
27551	Investigation of novel inverted NiO@NixCo1-xO core-shell nanoparticles. AIP Advances, 2018, 8, 056305.	0.6	7
27552	FeRh ground state and martensitic transformation. Physical Review B, 2018, 97, .	1.1	28
27553	Theoretical Prediction of an Antimony-Silicon Monolayer $$(hbox {penta-Sb}_{2}hbox) Tj ETQq1 1 0.784314 rgBT /Overlock 10 Tf 50 5 2290-2297.	1.0	31
27554	First-principles atomistic Wulff constructions for an equilibrium rutile TiO2 shape modeling. Applied Surface Science, 2018, 436, 989-994.	3.1	43
27555	The Au modified Ge(1â€¯1â€¯0) surface. Applied Surface Science, 2018, 439, 101-105.	3.1	7
27556	Mechanistic Effects of Water on the Fe-Catalyzed Hydrodeoxygenation of Phenol. The Role of BrÃ¸nsted Acid Sites. ACS Catalysis, 2018, 8, 2200-2208.	5.5	50
27557	The improvement of photocatalytic activity of monolayer g-C3N4via surface charge transfer doping. RSC Advances, 2018, 8, 1899-1904.	1.7	19
27558	Strain tunable magnetic properties of 3d transition-metal ion doped monolayer MoS2: A first-principles study. AIP Advances, 2018, 8, 055917.	0.6	12
27559	Theoretical study of the phonon spectrum, phonon refraction and thermodynamic properties for explosive/additive interfaces. Modelling and Simulation in Materials Science and Engineering, 2018, 26, 015002.	0.8	9
27560	Mechanism of fast lattice diffusion of hydrogen in palladium: Interplay of quantum fluctuations and lattice strain. Physical Review B, 2018, 97, .	1.1	30
27561	Tuning spin transport across two-dimensional organometallic junctions. Physical Review B, 2018, 97, .	1.1	2
27562	Atlas for the properties of elemental two-dimensional metals. Physical Review B, 2018, 97, .	1.1	75
27563	Highly Efficient Ambient Temperature CO₂ Photomethanation Catalyzed by Nanostructured RuO₂ on Silicon Photonic Crystal Support. Advanced Energy Materials, 2018, 8, 1702277.	10.2	58
27564	Material Discovery and Design Principles for Stable, High Activity Perovskite Cathodes for Solid Oxide Fuel Cells. Advanced Energy Materials, 2018, 8, 1702708.	10.2	125
27565	Highly Stable, New, Organicâ€inorganic Perovskite (CH₃NH₃)₂PdBr₄: Synthesis, Structure, and Physical Properties. Chemistry - A European Journal, 2018, 24, 4991-4998.	1.7	25

#	Article	IF	Citations
27566	Polarized Raman, <scp>FTIR,</scp> and <scp>DFT</scp> study of <scp>Na₂Ti₃O₇</scp> microcrystals. Journal of Raman Spectroscopy, 2018, 49, 538-548.	1.2	54
27567	Phase stability and transformation in a light-weight high-entropy alloy. Acta Materialia, 2018, 146, 280-293.	3.8	131
27568	Spin state transition in Bi1â^'xLaxCoO3 perovskite alloys: DFT+U study. Materials Chemistry and Physics, 2018, 207, 507-512.	2.0	7
27569	AuPb₂I₇: A Narrow Bandgap Au³⁺ Iodide Semiconductor. Inorganic Chemistry, 2018, 57, 804-810.	1.9	3
27570	Pb₃(SeO₃)Br₄: a new nonlinear optical material with enhanced SHG response designedviaan ion-substitution strategy. Dalton Transactions, 2018, 47, 1911-1917.	1.6	29
27571	On the H₂ interactions with transition metal adatoms supported on graphene: a systematic density functional study. Physical Chemistry Chemical Physics, 2018, 20, 3819-3830.	1.3	22
27572	Effects of atoms and molecules adsorption on electronic and magnetic properties of s-triazine with embedded Fe atom: DFT investigations. Philosophical Magazine, 2018, 98, 1114-1129.	0.7	10
27573	Metalâ€“Organic Frameworkâ€Derived ZnO/ZnS Heteronanostructures for Efficient Visibleâ€Lightâ€Driven Photocatalytic Hydrogen Production. Advanced Science, 2018, 5, 1700590.	5.6	169
27574	Comparative study of the phase stability in SrTaO 2 N. Boletin De La Sociedad Espanola De Ceramica Y Vidrio, 2018, 57, 40-44.	0.9	2
27575	Combining nitrogen substitutional defects and oxygen intercalation to control the graphene corrugation and doping level. Carbon, 2018, 130, 362-368.	5.4	8
27576	Properties of a predicted tetragonal carbon allotrope: First principles study. Diamond and Related Materials, 2018, 82, 50-55.	1.8	17
27577	Molybdenum incorporation on AB2 alloys-Part II. On the synergetic effects of Laves and non-Laves phases. Journal of Alloys and Compounds, 2018, 737, 530-535.	2.8	5
27578	The sesame ball-like CoS/MoS2 nanospheres as efficient counter electrode catalysts for dye-sensitized solar cells. Journal of Alloys and Compounds, 2018, 739, 568-576.	2.8	23
27579	Modeling Polaron-Coupled Li Cation Diffusion in V₂O₅ Cathode Material. Journal of Physical Chemistry C, 2018, 122, 150-157.	1.5	26
27580	Self-Supported Ternary Niâ€“Sâ€“Se Nanorod Arrays as Highly Active Electrocatalyst for Hydrogen Generation in Both Acidic and Basic Media: Experimental Investigation and DFT Calculation. ACS Applied Materials & Interfaces, 2018, 10, 2430-2441.	4.0	83
27581	Silver Clusters as Robust Nodes and Ïâ€“Activation Sites for the Construction of Heterogeneous Catalysts for the Cycloaddition of Propargylamines. ACS Catalysis, 2018, 8, 1384-1391.	5.5	85
27582	Epitaxial Synthesis of Molybdenum Carbide and Formation of a Mo₂C/MoS₂ Hybrid Structure via Chemical Conversion of Molybdenum Disulfide. ACS Nano, 2018, 12, 338-346.	7.3	148
27583	Defects controlled hole doping and multivalley transport in SnSe single crystals. Nature Communications, 2018, 9, 47.	5.8	95

#	Article	IF	Citations
27584	First-principles simulation of local response in transition metal dichalcogenides under electron irradiation. Nanoscale, 2018, 10, 2388-2397.	2.8	34
27585	Tuning transport performance in two-dimensional metal-organic framework semiconductors: Role of the metal d band. Applied Physics Letters, 2018, 112, .	1.5	53
27586	A density functional theory parameterised neural network model of zirconia. Molecular Simulation, 2018, 44, 623-630.	0.9	20
27587	Interband <mml:math xmlns:mml="http://www.w3.org/1998/Math/MathML"><mml:mi>Ï€</mml:mi></mml:math> -like plasmon in silicene grown on silver. Physical Review B, 2018, 97, .	1.1	10
27588	Improved Photoactivity of Pyroxene Silicates by Cation Substitutions. ChemPhysChem, 2018, 19, 943-953.	1.0	2
27589	Metallized siligraphene nanosheets (SiC7) as high capacity hydrogen storage materials. Nano Research, 2018, 11, 3802-3813.	5.8	48
27590	Formic acid decomposition on Pt1/Cu (111) single platinum atom catalyst: Insights from DFT calculations and energetic span model analysis. Applied Surface Science, 2018, 436, 631-638.	3.1	30
27591	First principles studies on the elastic, thermodynamic properties and electronic structure of Ti 15â^'x Mo x Sn compounds. Current Applied Physics, 2018, 18, 280-288.	1.1	7
27592	Bifunctional CoNx embedded graphene electrocatalysts for OER and ORR: A theoretical evaluation. Carbon, 2018, 130, 112-119.	5.4	209
27593	Systematic Doping of Cobalt into Layered Manganese Oxide Sheets Substantially Enhances Water Oxidation Catalysis. Inorganic Chemistry, 2018, 57, 557-564.	1.9	43
27594	Charge Balance Controls the (100) Surface Structure of the Ba8Au5.25Ge40.75 Clathrate. Journal of Physical Chemistry C, 2018, 122, 2215-2220.	1.5	6
27595	Anchoring of Iron Oxyhydroxide Clusters at H and L Ferritin Subunits. ACS Biomaterials Science and Engineering, 2018, 4, 483-490.	2.6	5
27596	Tailoring electronic properties of multilayer phosphorene by siliconization. Physical Chemistry Chemical Physics, 2018, 20, 2075-2083.	1.3	25
27597	A Janus MoSSe monolayer: a potential wide solar-spectrum water-splitting photocatalyst with a low carrier recombination rate. Journal of Materials Chemistry A, 2018, 6, 2295-2301.	5.2	387
27598	Temperature dependence of magnetic excitations in the frustrated antiferromagnetic spinel <mml:math xmlns:mml="http://www.w3.org/1998/Math/MathML"><mml:mrow><mml:msub><mml:mi>ZnMn</mml:mi><mml:mn>2</mml:mn><mml:mi mathvariant="normal">O</mml:mi><mml:mn>4</mml:mn></mml:msub></mml:mrow></mml:math>. Physical Review B, 2018, 97, .	1.1	6
27599	Graphene on nickel (100) micrograins: Modulating the interface interaction by extended moirÃ© superstructures. Carbon, 2018, 130, 441-447.	5.4	27
27600	Ultrawide range tuning of direct band gap in MgZnO monolayer via electric field effect. RSC Advances, 2018, 8, 1392-1397.	1.7	15
27601	Thermoelasticity and anomalies in the pressure dependence of phonon velocities in niobium. Applied Physics Letters, 2018, 112, .	1.5	15

#	Article	IF	Citations
27602	Effects of chromium on the morphology and mechanical properties of Fe2B intermetallic in Fe-3.0B alloy. Journal of Materials Science, 2018, 53, 5329-5338.	1.7	28
27603	Oxygen vacancies driven size-dependent d0 room temperature ferromagnetism in well-dispersed dopant-free ZnO nanoparticles and density functional theory calculation. Journal of Alloys and Compounds, 2018, 739, 1080-1088.	2.8	54
27604	Polarization-dependent epitaxial growth and photocatalytic performance of ferroelectric oxide heterostructures. Nano Energy, 2018, 45, 304-310.	8.2	50
27605	Structural stability, elastic and thermodynamic properties of Auâ€“Cu alloys from first-principles calculations. Physica B: Condensed Matter, 2018, 533, 58-62.	1.3	27
27606	Electronic structure and superconducting behaviour of LuPtBi half-Heusler compound: A first principle study. Physica C: Superconductivity and Its Applications, 2018, 544, 22-26.	0.6	16
27607	First-principles study on the phase transitions, crystal stabilities and thermodynamic properties of TiN under high pressure. Physics Letters, Section A: General, Atomic and Solid State Physics, 2018, 382, 656-661.	0.9	7
27608	Lateral and Vertical Heterostructures of Transition Metal Dichalcogenides. Journal of Physical Chemistry C, 2018, 122, 1547-1555.	1.5	26
27609	Topological Insulator in Two-Dimensional SiGe Induced by Biaxial Tensile Strain. ACS Omega, 2018, 3, 1-7.	1.6	23
27610	Oxygen vacancy and doping atom effect on electronic structure and optical properties of Cd₂SnO₄. RSC Advances, 2018, 8, 640-646.	1.7	20
27611	A Combined Density Functional Theory and Monte Carlo Investigation of the Competitive Adsorption of Atomic Oxygen and Chlorine to the Ni (111) Surface. Journal of the Electrochemical Society, 2018, 165, C302-C309.	1.3	10
27612	Insight into the structure and morphology of Run clusters on Co(111) and Co(311) surfaces. Catalysis Science and Technology, 2018, 8, 2728-2739.	2.1	7
27613	Perforated N-doped monoclinic ZnWO₄ nanorods for efficient photocatalytic hydrogen generation and RhB degradation under natural sunlight. Catalysis Science and Technology, 2018, 8, 2909-2919.	2.1	33
27614	Second- and third-order elastic constants of kesterite CZTS and its electronic and optical properties under various strain rates. Energy Sources, Part A: Recovery, Utilization and Environmental Effects, 2018, 40, 977-986.	1.2	2
27615	Electronic and magnetic properties of BaUO3 by modified Beckeâ€“Johnson (mBJ) functional. Modern Physics Letters B, 2018, 32, 1850164.	1.0	1
27616	Î³-Al2O3:Ce3+Cu2+ as a phosphor material; DFT+U and experimental approach. ChemistrySelect, 2018, 3, .	0.7	1
27617	Adsorption and dissociation mechanism of SO2 and H2S on Pt decorated graphene: a DFT-D3 study. Applied Physics A: Materials Science and Processing, 2018, 124, 1.	1.1	32
27618	The Ideal Strengths of Superconducting MgCNi3 and CdCNi3. Journal of Superconductivity and Novel Magnetism, 2018, 31, 2355-2361.	0.8	2
27619	Electronic Band Structure of Rhenium Dichalcogenides. Journal of Electronic Materials, 2018, 47, 4314-4320.	1.0	14

#	Article	IF	Citations
27620	Tuning the electronic properties of germanene by molecular adsorption and under an external electric field. Journal of Materials Chemistry C, 2018, 6, 5937-5948.	2.7	35
27621	Thermodynamics of inversion-domain boundaries in aluminum nitride: Interplay between interface energy and electric dipole potential energy. Journal of Applied Physics, 2018, 123, .	1.1	3
27622	Electrical and material properties of hydrothermally grown single crystal (111) UO2. European Physical Journal B, 2018, 91, 1.	0.6	6
27623	Lithium and sodium adsorption properties of two-dimensional aluminum nitride. Applied Surface Science, 2018, 451, 141-147.	3.1	38
27624	Site symmetry approach applied to the supercell model of MgAl2O4 spinel with oxygen interstitials: Ab initio calculations. Computational Materials Science, 2018, 150, 517-523.	1.4	11
27625	First-principles study of mechanical and magnetic properties of transition metal (M) nitrides in the cubic M4N structure. Journal of Physics and Chemistry of Solids, 2018, 120, 197-206.	1.9	41
27626	High selectivity of N-doped ZnO nano-ribbons in detecting H2, O2 and CO2 molecules: Effect of negative-differential resistance on gas-sensing. Sensors and Actuators B: Chemical, 2018, 270, 167-178.	4.0	46
27627	Origin of Pronounced Nonlinear Band Gap Behavior in Leadâ€“Tin Hybrid Perovskite Alloys. Chemistry of Materials, 2018, 30, 3920-3928.	3.2	166
27628	Multilevel Molecular Modeling Approach for a Rational Design of Ionic Current Sensors for Nanofluidics. Journal of Chemical Theory and Computation, 2018, 14, 3113-3120.	2.3	6
27629	Buildup of the Solid Electrolyte Interphase on Lithium-Metal Anodes: Reactive Molecular Dynamics Study. Journal of Physical Chemistry C, 2018, 122, 10783-10791.	1.5	44
27630	Implanting Germanium into Graphene. ACS Nano, 2018, 12, 4641-4647.	7.3	86
27631	Ferromagnetism in half-metallic EuGaO3 perovskite: A combined DFT and DFT+U investigation. AIP Conference Proceedings, 2018, , .	0.3	1
27632	Interaction of volatile organic compounds (VOCs) emitted from banana on stanene nanosheetâ€”a first-principles studies. Structural Chemistry, 2018, 29, 1321-1332.	1.0	20
27633	La doping inhibits stress production at the grain boundaries in Niâ€“WC coating. Journal of Alloys and Compounds, 2018, 753, 688-694.	2.8	11
27634	Adsorption studies of volatile organic compounds on germanene nanotube emitted from banana fruit for quality assessment â€“ A density functional application. Journal of Molecular Graphics and Modelling, 2018, 82, 129-136.	1.3	19
27635	Influence of Fe substitution on structure and Raman spectra of La 0.67 Sr 0.33 MnO 3 : Experimental and density functional studies. Physica B: Condensed Matter, 2018, 541, 103-110.	1.3	3
27636	Ultralow Thermal Conductivity in Diamond-Like Semiconductors: Selective Scattering of Phonons from Antisite Defects. Chemistry of Materials, 2018, 30, 3395-3409.	3.2	28
27637	Crystal Orientation-Dependent Reactivity of Oxide Surfaces in Contact with Lithium Metal. ACS Applied Materials & Interfaces, 2018, 10, 17471-17479.	4.0	9

#	Article	IF	Citations
27638	Specific Metalâ€“Support Interactions between Nanoparticle Layers for Catalysts with Enhanced Methanol Oxidation Activity. ACS Catalysis, 2018, 8, 5391-5398.	5.5	63
27639	MoS₂/ZnO van der Waals heterostructure as a high-efficiency water splitting photocatalyst: a first-principles study. Physical Chemistry Chemical Physics, 2018, 20, 13394-13399.	1.3	292
27640	Feâ€“Si networks and charge/discharge-induced phase transitions in Li₂FeSiO₄ cathode materials. Physical Chemistry Chemical Physics, 2018, 20, 14557-14563.	1.3	12
27641	Decomposition of methanol-d₄ on Auâ€“Rh bimetallic nanoclusters on a thin film of Al₂O₃/NiAl(100). Physical Chemistry Chemical Physics, 2018, 20, 11260-11272.	1.3	6
27642	Influence of applied pressure on bond distortions and electronic band structure of GeTe: First principle calculations. AIP Conference Proceedings, 2018, , .	0.3	0
27643	Using first-principles calculations to screen for fragile magnetism: Case study of <mml:math xmlns:mml="http://www.w3.org/1998/Math/MathML"><mml:mrow><mml:msub><mml:mi mathvariant="normal">LaCrGe</mml:mi><mml:mn>3</mml:mn></mml:msub></mml:mrow></mml:math> and <mml:math xmlns:mml="http://www.w3.org/1998/Math/MathML"><mml:mrow><mml:msub><mml:mi mathvariant="normal">LaCrSb</mml:mi><mml:mn>3</mml:mn></mml:msub></mml:mrow></mml:math>. Physical Review B, 2018, 97, .	1.1	6
27644	First-principle calculations of electronic structures and polar properties of (Î²,Îµ)-Ga₂O₃. Applied Physics Express, 2018, 11, 061101.	1.1	53
27645	Electron-phonon interaction and superconductivity in representative AuCu3-type intermetallic compounds. Computational Materials Science, 2018, 150, 491-499.	1.4	8
27646	Development of Fe-C interatomic potential for carbon impurities in Î±-iron. Computational Materials Science, 2018, 150, 510-516.	1.4	13
27647	The adsorption geometry and molecular self-assembly of graphene for 1,3,5-triphenylbenzene on Cu(111). Surface Science, 2018, 675, 42-46.	0.8	3
27648	Lithiation Products of a Silicon Anode Based on Soft X-ray Emission Spectroscopy: A Theoretical Study. Journal of Physical Chemistry C, 2018, 122, 11096-11108.	1.5	8
27649	Electronic Structure of a Self-Assembled Monolayer with Two Surface Anchors: 6-Mercaptopurine on Au(111). Langmuir, 2018, 34, 5696-5702.	1.6	5
27650	Enhanced field-emission properties of buckled Î±-borophene by means of Li decoration: a first-principles investigation. Physical Chemistry Chemical Physics, 2018, 20, 15139-15148.	1.3	8
27651	Efficient nitrogen fixation to ammonia on MXenes. Physical Chemistry Chemical Physics, 2018, 20, 14504-14512.	1.3	82
27652	First principles understanding of structural electronic and magnetic properties of new quaternary Heusler alloy: FeVRuSi. Materials Research Express, 2018, 5, 056516.	0.8	32
27653	First-principles studies of the local structure and relaxor behavior of <mml:math xmlns:mml="http://www.w3.org/1998/Math/MathML"><mml:mrow><mml:msub><mml:mrow><mml:mi>Pb</mml:mi><mml:mi	1.1	17
27654	Understanding the fast phase-change mechanism of tetrahedrally bonded <mml:math xmlns:mml="http://www.w3.org/1998/Math/MathML"><mml:mrow><mml:msub><mml:mi>Cu</mml:mi><mml:mn>2</mml:mn></mml:msub	1.1	11
27655	Co on the H-passivated Si(001) surface: Density-functional calculations. Physica B: Condensed Matter, 2018, 542, 44-50.	1.3	1

#	Article	IF	Citations
27656	First-Principles and Microkinetic Simulation Studies of the Structure Sensitivity of Cu Catalyst for Methanol Steam Reforming. Journal of Physical Chemistry C, 2018, 122, 10811-10819.	1.5	20
27657	Physics-informed machine learning for inorganic scintillator discovery. Journal of Chemical Physics, 2018, 148, 241729.	1.2	28
27658	Passivation of carbon dimer defects in amorphous SiO ₂ /4Hâ€“SiC (0001) interface: A first-principles study. Chinese Physics B, 2018, 27, 047103.	0.7	11
27659	Nitrogen doping and CO2 adsorption on graphene: A thermodynamical study. Physical Review B, 2018, 97, .	1.1	19
27660	UV/IR Dual-Wavelength Photodetector Design Based on ZnO/PMMA/PbSe Nanocomposites. IEEE Nanotechnology Magazine, 2018, 17, 574-581.	1.1	6
27661	The mechanism of the high resistance to sulfur poisoning of the rhenium doped nickel/yttria-stabilized zirconia. Applied Surface Science, 2018, 447, 561-568.	3.1	8
27662	Tuning the electronic structures, work functions, optical properties and stability of bifunctional hybrid graphene oxide/Vâ€“doped NaNbO3 typeâ€“II heterostructures: A promising photocatalyst for H2 production. Carbon, 2018, 136, 187-195.	5.4	36
27663	Theoretical investigation of dephosphorylation of phosphate monoesters on CeO2(111). Catalysis Today, 2018, 312, 141-148.	2.2	16
27664	Effects of ternary element additions on the generalized-stacking fault energy of Ti5Si3 in prismatic {11Â¯00}[0001] slip system: A first-principles study. Computational Materials Science, 2018, 146, 255-260.	1.4	6
27665	First principles studies of superhard BC6N phases with unexpected 1D metallicity. Computational Materials Science, 2018, 148, 157-164.	1.4	13
27666	Modeling pseudo-elastic behavior in small-scale ThCr2Si2-type crystals. Computational Materials Science, 2018, 150, 86-95.	1.4	4
27667	Energy storage properties of selectively functionalized Cr-group MXenes. Computational Materials Science, 2018, 150, 236-243.	1.4	18
27668	Î³-Graphyne analogues based on As and Sb elements. Computational Materials Science, 2018, 150, 325-328.	1.4	0
27669	Computational study of the electronic, optical and photocatalytic properties of single-layer hexagonal zinc chalcogenides. Computational Materials Science, 2018, 150, 432-438.	1.4	24
27670	On real-space Density Functional Theory for non-orthogonal crystal systems: Kronecker product formulation of the kinetic energy operator. Chemical Physics Letters, 2018, 700, 156-162.	1.2	9
27671	A new orthorhombic ground-state phase and mechanical strengths of ternary B2CO compound. Chemical Physics Letters, 2018, 701, 86-92.	1.2	10
27672	The influence of nitrogen pressure on formation of niobium nitride by thermal processing. Journal of Alloys and Compounds, 2018, 746, 370-376.	2.8	6
27673	Material-genome perspective towards tunable thermal expansion of rare-earth di-silicates. Journal of the European Ceramic Society, 2018, 38, 3547-3554.	2.8	27

#	Article	IF	Citations
27674	Structural and electronic properties of SnS 2 stacked nanosheets: An ab-initio study. Journal of Physics and Chemistry of Solids, 2018, 120, 211-217.	1.9	11
27675	Effect of anti-site point defects on the mechanical and thermodynamic properties of MgZn2, MgCu2 Laves phases: A first-principle study. Journal of Solid State Chemistry, 2018, 263, 18-23.	1.4	13
27676	Eu2P7X and Ba2As7X (Xâ€¯=â€¯Br, I): Chiral double-Zintl salts containing heptapnictotricyclane clusters. Journal of Solid State Chemistry, 2018, 263, 195-202.	1.4	3
27677	Applying a new interatomic potential for the simulation of monoclinic and triclinic Li4SiO4. Materials Chemistry and Physics, 2018, 214, 548-556.	2.0	6
27678	Nanoindentation-induced phase transformation between SiC polymorphs. Materials Letters, 2018, 220, 152-155.	1.3	5
27679	Enhancing CO2 electrolysis performance with vanadium-doped perovskite cathode in solid oxide electrolysis cell. Nano Energy, 2018, 50, 43-51.	8.2	158
27680	S-graphite slit pore: A superior selective adsorbent for light hydrocarbons. Applied Surface Science, 2018, 444, 772-779.	3.1	18
27681	Thermodynamic stabilities in the Fe-Fe16C2 system: Influence of carbon-carbon interactions studied by DFT. Computational Materials Science, 2018, 150, 524-534.	1.4	6
27682	Site preference and diffusion behaviors of H influenced by the implanted-He in 3C-Î² SiC. Journal of Alloys and Compounds, 2018, 742, 226-231.	2.8	4
27683	Insight into the structural evolution during TiN film growth via atomic resolution TEM. Journal of Alloys and Compounds, 2018, 754, 257-267.	2.8	36
27684	A first principle study of the phase stability, ion transport and substitution strategy for highly ionic conductive sodium antipervoskite as solid electrolyte for sodium ion batteries. Journal of Power Sources, 2018, 390, 61-70.	4.0	31
27685	Functionalization of silicon surface by thiadiazole molecule: A DFT study. Surface Science, 2018, 674, 87-93.	0.8	7
27686	Highly nitrogen doped carbon nanofibers with superior rate capability and cyclability for potassium ion batteries. Nature Communications, 2018, 9, 1720.	5.8	871
27687	Half-metallicity and enhanced ferromagnetism in Li-adsorbed ultrathin chromium triiodide. Journal of Materials Chemistry C, 2018, 6, 5716-5720.	2.7	71
27688	Structural and dynamical properties of water adsorption on PtO₂(001). RSC Advances, 2018, 8, 15078-15086.	1.7	7
27689	Theoretical investigation on MgV₂O₆: ab-initio study. Philosophical Magazine, 2018, 98, 2077-2093.	0.7	6
27690	Large enhancement of superconductivity in Zr point contacts. Journal of Physics Condensed Matter, 2018, 30, 255002.	0.7	3
27691	Investigation of the GaN/Al₂O₃ Interface by First Principles Calculations. Physica Status Solidi (B): Basic Research, 2018, 255, 1700323.	0.7	14

#	Article	IF	Citations
27692	The pressure-induced mechanical and optoelectronic behavior of cubic perovskite PbSnO3 via ab-initio investigations. Ceramics International, 2018, 44, 13750-13756.	2.3	95
27693	A multidisciplinary approach to study precipitation kinetics and hardening in an Al-4Cu (wt. %) alloy. Journal of Alloys and Compounds, 2018, 757, 504-519.	2.8	49
27694	Insight into lead-free organic-inorganic hybrid perovskites for photovoltaics and optoelectronics: A first-principles study. Organic Electronics, 2018, 59, 99-106.	1.4	123
27695	The structural, elastic, electronic and optical properties of orthorhombic FeX 2 (X=S, Se, Te). Superlattices and Microstructures, 2018, 119, 201-211.	1.4	12
27696	Microstructure and properties investigation of garnet structured Li7La3Zr2O12 as electrolyte for all-solid-state batteries. Solid State Ionics, 2018, 321, 126-134.	1.3	32
27697	Growth study of para-sexiphenyl on Ag(001): From single molecule to crystalline film. Surface Science, 2018, 678, 149-156.	0.8	5
27698	Theoretical Insight into M₁TPyPâ€“M₂ (M₁, M₂ = Fe, Co) MOFs: Correlation between Electronic Structure and Catalytic Activity Extending to Potentiality in Capturing Flue Gases. Journal of Physical Chemistry C, 2018, 122, 9899-9908.	1.5	11
27699	Theoretical insight into the catalytic activities of oxygen reduction reaction on transition metalâ€“N₄ doped graphene. New Journal of Chemistry, 2018, 42, 9620-9625.	1.4	21
27700	Confinement boosts CO oxidation on an Ni atom embedded inside boron nitride nanotubes. Physical Chemistry Chemical Physics, 2018, 20, 17599-17605.	1.3	15
27701	Negative electron affinity from aluminium on the diamond (1â€‰0â€‰0) surface: a theoretical study. Journal of Physics Condensed Matter, 2018, 30, 235002.	0.7	15
27702	Revealing out-of-equilibrium hidden phases in Sr3Ru2O7 by applying stress. Physical Review B, 2018, 97, .	1.1	2
27703	Equation of state of hexagonal hydroxylapatite (P6₃) as obtained from density functional theory simulations. International Journal of Quantum Chemistry, 2018, 118, e25553.	1.0	15
27704	Effect of (Cd, Al) Co-doping and hydrogenation on the long-range ferromagnetic ordering of ZnO: Experimental and DFT studies. Journal of Alloys and Compounds, 2018, 753, 813-820.	2.8	7
27705	Three-dimensional N- and S-codoped graphene hydrogel with in-plane pores for high performance supercapacitor. Microporous and Mesoporous Materials, 2018, 268, 260-267.	2.2	39
27706	Microporosity as a new property control factor in graphene-like 2D allotropes. Journal of Materials Chemistry A, 2018, 6, 10348-10353.	5.2	18
27707	A first principle calculation of anisotropic elastic, mechanical and electronic properties of TiB. AIP Conference Proceedings, 2018, , .	0.3	0
27708	Electronic Structure and Elastic Properties of ZnCdSe2 Crystal with the Chalcopyrite Structure. Journal of Structural Chemistry, 2018, 59, 15-19.	0.3	2
27709	A cascading nonlinear magneto-optical effect in topological insulators. Scientific Reports, 2018, 8, 3908.	1.6	10

#	Article	IF	Citations
27710	Stanene nanomeshes as anode materials for Na-ion batteries. Journal of Materials Chemistry A, 2018, 6, 7933-7941.	5.2	72
27711	Lattice dynamical probe of phase transformations in niobium oxyfluoride Nb2O2F3. Physical Review B, 2018, 97, .	1.1	0
27712	An insight into the dopant selection for CeO2-based resistive-switching memory system: a DFT and experimental study. Applied Nanoscience (Switzerland), 2018, 8, 839-851.	1.6	16
27713	Embedded atom method potentials for Ce-Ni binary alloy. Computational Materials Science, 2018, 150, 1-8.	1.4	5
27714	Highly dispersed and COad-tolerant Ptshell-Pdcore catalyst for ethanol oxidation reaction: Catalytic activity and long-term durability. International Journal of Hydrogen Energy, 2018, 43, 11335-11344.	3.8	6
27715	Periodic Density Functional Theory Study of the Structure, Raman Spectrum, and Mechanical Properties of Schoepite Mineral. Inorganic Chemistry, 2018, 57, 4470-4481.	1.9	51
27716	Computational Design of Active Site Structures with Improved Transition-State Scaling for Ammonia Synthesis. ACS Catalysis, 2018, 8, 4017-4024.	5.5	80
27717	Validity of Weyl fermion picture for transition metals monopnictides TaAs, TaP, NbAs, and NbP from ab initio studies. Scientific Reports, 2018, 8, 3534.	1.6	41
27718	Ethane dehydrogenation on pristine and AlO_x decorated Pt stepped surfaces. Catalysis Science and Technology, 2018, 8, 2159-2174.	2.1	18
27719	First principles investigation of structural, vibrational and thermal properties of black and blue phosphorene. International Journal of Modern Physics B, 2018, 32, 1850151.	1.0	12
27720	Interfacial segregation and fracture in Mg-based binary alloys: Experimental and first-principles perspective. Acta Materialia, 2018, 151, 78-86.	3.8	74
27721	Highly uranium elimination by crab shells-derived porous graphitic carbon nitride: Batch, EXAFS and theoretical calculations. Chemical Engineering Journal, 2018, 346, 406-415.	6.6	64
27722	A comparison study of the structural and mechanical properties of cubic, tetragonal, monoclinic, and three orthorhombic phases of ZrO2. Journal of Alloys and Compounds, 2018, 749, 283-292.	2.8	46
27723	Intrinsic Role of Excess Electrons in Surface Reactions on Rutile TiO₂ (110): Using Water and Oxygen as Probes. Journal of Physical Chemistry C, 2018, 122, 8270-8276.	1.5	12
27724	Structural stability, electronic structures and enhanced photocatalytic properties of BiF3 nanowires: A first-principles study. Ceramics International, 2018, 44, 9623-9632.	2.3	5
27725	Mechanical strength and origin of the strengthening effect of tantalum in superhard W 0.5 Ta 0.5 B monoboride. Ceramics International, 2018, 44, 10463-10469.	2.3	20
27726	Thermo-mechanical properties of cubic lanthanide oxides. Thin Solid Films, 2018, 653, 37-48.	0.8	10
27727	Theoretical research on novel orthorhombic tungsten dinitride from first principles calculations. RSC Advances, 2018, 8, 9272-9276.	1.7	4

#	Article	IF	Citations
27728	Ab-initio study of (Ga,Cr)N and (Ga,Mn)N DMSs: under hydrostatic pressure. Materials Research Express, 2018, 5, 036104.	0.8	6
27729	Origin of photoluminescence in <mml:math xmlns:mml="http://www.w3.org/1998/Math/MathML"><mml:mrow><mml:mi>Î²</mml:mi><mml:mo>â^'</mml:mo><mml:mi mathvariant="normal">G</mml:mi><mml:msub><mml:mi mathvariant="normal">a</mml:mi><mml:mn>2</mml:mn></mml:msub><mml:msub><mml:mi mathvariant="normal">O</mml:mi><mml:mn>3</mml:mn></mml:msub></mml:mrow></mml:math>. Physical Review B, 2018, 97, .	1.1	104
27730	Stability of boron-doped graphene/copper interface: DFT, XPS and OSEE studies. Applied Surface Science, 2018, 441, 978-983.	3.1	19
27731	Modeling palladium surfaces with density functional theory, neural networks and molecular dynamics. Catalysis Today, 2018, 312, 132-140.	2.2	15
27732	Adsorption of 3d transition-metal atom on InSe monolayer: A first-principles study. Computational Materials Science, 2018, 150, 33-41.	1.4	38
27733	Strain-induced semiconductor-to-metal transitions in C36-based carbon peapods: Ab initio study. Diamond and Related Materials, 2018, 84, 112-118.	1.8	12
27734	Direct band gap narrowing and light-harvesting-potential in orthorhombic In-doped-AlFeO3 perovskite: A first principles study. Journal of Alloys and Compounds, 2018, 750, 312-319.	2.8	17
27735	Crystal structures and theoretical studies of polyphosphate LiZnP3O9 for nonlinear optical applications. Journal of Solid State Chemistry, 2018, 262, 313-319.	1.4	14
27736	High pressure in solid state chemistry: Combined experimental and modeling approaches for assessing and predicting properties. Solid State Sciences, 2018, 80, 178-195.	1.5	1
27737	Ultrathin palladium nanosheets with selectively controlled surface facets. Chemical Science, 2018, 9, 4451-4455.	3.7	89
27738	Rare earth indates (RE: Laâ€“Yb): influence of the synthesis route and heat treatment on the crystal structure. Dalton Transactions, 2018, 47, 6787-6799.	1.6	12
27739	Anharmonicity in a double hydrogen transfer reaction studied in a single porphycene molecule on a Cu(110) surface. Physical Chemistry Chemical Physics, 2018, 20, 12112-12119.	1.3	3
27740	Enhanced Piezoelectric Response of AlN via CrN Alloying. Physical Review Applied, 2018, 9, .	1.5	57
27741	Prediction of Intrinsic Ferromagnetic Ferroelectricity in a Transition-Metal Halide Monolayer. Physical Review Letters, 2018, 120, 147601.	2.9	217
27742	Stability of Excess Oxygen Atoms near Oxide Precipitate and Oxygen Solubility in Silicon Crystal. ECS Journal of Solid State Science and Technology, 2018, 7, P102-P108.	0.9	5
27743	Prediction of Quantum Anomalous Hall Effect in MBi and MSb (M:Ti, Zr, and Hf) Honeycombs. Nanoscale Research Letters, 2018, 13, 43.	3.1	12
27744	First principles study of the effect of hydrogen annealing on SiC MOSFETs. Japanese Journal of Applied Physics, 2018, 57, 04FR05.	0.8	0
27745	First-principles study on C=C defects near SiC/SiO₂interface: Defect passivation by double-bond saturation. Japanese Journal of Applied Physics, 2018, 57, 04FR09.	0.8	7

#	Article	IF	Citations
27746	DFT Application on the Interaction Properties of Ethanol Vapors with MnFe2O4 Nanostructures. Journal of Inorganic and Organometallic Polymers and Materials, 2018, 28, 1753-1763.	1.9	8
27747	Theoretical study of ozone adsorption on the surface of Fe, Co and Ni doped boron nitride nanosheets. Applied Surface Science, 2018, 444, 642-649.	3.1	25
27748	Rationally-designed configuration of directly-coated Ni3S2/Ni electrode by RGO providing superior sodium storage. Carbon, 2018, 133, 14-22.	5.4	67
27749	Nanoporous ZnO: Structural and electronic study under biaxial strain. Computational Materials Science, 2018, 149, 91-97.	1.4	0
27750	First principle investigation of the mechanical properties of natural layered nanocomposite: Clinochlore as a model system for heterodesmic structures. Composite Structures, 2018, 202, 551-558.	3.1	22
27751	Enhanced photoelectrochemical performance of TiO2 through controlled Ar+ ion irradiation: A combined experimental and theoretical study. International Journal of Hydrogen Energy, 2018, 43, 6936-6944.	3.8	11
27752	Methane storage capacity of carbon fullerenes and their mechanical and electronic properties: Experimental and theoretical study. Materials Chemistry and Physics, 2018, 211, 192-199.	2.0	8
27753	Hollow Mo-doped CoP nanoarrays for efficient overall water splitting. Nano Energy, 2018, 48, 73-80.	8.2	608
27754	Electronic and optical properties of hydrogenated silicon carbide nanosheets: A DFT study. Solid State Communications, 2018, 275, 1-7.	0.9	14
27755	The surface energy and stress of metals. Surface Science, 2018, 674, 51-68.	0.8	68
27756	Adamantane-Derived Carbon Nanothreads: High Structural Stability and Mechanical Strength. Journal of Physical Chemistry C, 2018, 122, 7945-7950.	1.5	7
27757	Interaction of Boron Nitride Nanotubes with Aluminum: A Computational Study. Journal of Physical Chemistry C, 2018, 122, 15226-15240.	1.5	6
27758	Investigation of the Water Adsorption Properties and Structural Stability of MIL-100(Fe) with Different Anions. Langmuir, 2018, 34, 4180-4187.	1.6	33
27759	Accessing Frustrated Lewis Pair Chemistry through Robust Gold@N-Doped Carbon for Selective Hydrogenation of Alkynes. ACS Catalysis, 2018, 8, 3516-3524.	5.5	88
27760	First-principles study of magnetic properties of ultra-thin MoSi2 films. Journal of Applied Physics, 2018, 123, 104304.	1.1	5
27761	Magnetism on a Boron-doped Si(111)- $$sqrt 3 imes sqrt 3 $$ 3 Ã— 3 Surface. Journal of the Korean Physical Society, 2018, 72, 577-581.	0.3	0
27762	Thermodynamic description of the Ti-Mo-Nb-Ta-Zr system and its implications for phase stability of Ti bio-implant materials. Calphad: Computer Coupling of Phase Diagrams and Thermochemistry, 2018, 61, 72-84.	0.7	28
27763	Single Pd atom and Pd dimer embedded graphene catalyzed formic acid dehydrogenation: AÂfirst-principles study. International Journal of Hydrogen Energy, 2018, 43, 6997-7006.	3.8	36

#	Article	IF	Citations
27764	The effect of martensitic phase transition from cubic to tetragonal on the physical properties of V 3 Si superconductor. Intermetallics, 2018, 96, 25-32.	1.8	5
27765	Electronic and magnetic properties of Fe-, Co-, and Ni-decorated BC 3 : A first-principles study. Physics Letters, Section A: General, Atomic and Solid State Physics, 2018, 382, 1395-1400.	0.9	3
27766	Ultrathin silica films on Pd(111): Structure and adsorption properties. Surface Science, 2018, 678, 118-123.	0.8	25
27767	Two Zinc(II)-Based Metal Complexes of New Pyrimidine Derived Ligand: Anion-Dependent Structural Variations and Charge Transport Property Analysis. Journal of Physical Chemistry C, 2018, 122, 8724-8734.	1.5	30
27768	Room-temperature ferromagnetism in Ni(<scp>ii</scp>)-chromia based coreâ€“shell nanoparticles: experiment and first principles calculations. Physical Chemistry Chemical Physics, 2018, 20, 10396-10406.	1.3	8
27769	A density functional study on the oxygen reduction reaction mechanism on FeN₂-doped graphene. New Journal of Chemistry, 2018, 42, 6873-6879.	1.4	41
27770	Identification of Pt-based catalysts for propane dehydrogenation via a probability analysis. Chemical Science, 2018, 9, 3925-3931.	3.7	106
27771	Theoretical insights into the minority carrier lifetime of doped Siâ€”A computational study. Journal of Applied Physics, 2018, 123, 161420.	1.1	2
27772	Enhanced electronic and magnetic properties by functionalization of monolayer GaS via substitutional doping and adsorption. Journal of Physics Condensed Matter, 2018, 30, 195805.	0.7	11
27773	Electronic-structure and thermodynamic properties of ZnS1â^'Se ternary alloys from the first-principles calculations. Computational Materials Science, 2018, 149, 386-396.	1.4	12
27774	First-principles study of the effect of Cr and Al on the oxidation resistance of WSi2. Chemical Physics Letters, 2018, 698, 211-217.	1.2	49
27775	A novel approach for detection of NO 2 and SO 2 gas molecules using graphane nanosheet and nanotubes - A density functional application. Diamond and Related Materials, 2018, 85, 53-62.	1.8	34
27776	Superior Na-ion storage achieved by Ti substitution in Na3V2(PO4)3. Energy Storage Materials, 2018, 15, 108-115.	9.5	100
27777	First-principles study the phase stability and mechanical properties of binary W-Mo alloys. Fusion Engineering and Design, 2018, 130, 56-61.	1.0	35
27778	First-principles analysis of ferroelectric transition in MnSnO3 and MnTiO3 perovskites. Journal of Solid State Chemistry, 2018, 262, 251-255.	1.4	7
27779	First-principles investigation of mechanical and electronic properties of tetragonal NbAl 3 under tension. Physica B: Condensed Matter, 2018, 538, 47-53.	1.3	7
27780	Promising Photocatalysts for Water Splitting in BeN₂ and MgN₂ Monolayers. Journal of Physical Chemistry C, 2018, 122, 8102-8108.	1.5	32
27781	Al₃ (A = As, Sb) Single Layers and Their vdW Heterostructure for Photocatalysis and Solar Cell Applications. Journal of Physical Chemistry C, 2018, 122, 7656-7663.	1.5	34

#	Article	IF	Citations
27782	Defected and Functionalized Germanene-based Nanosensors under Sulfur Comprising Gas Exposure. ACS Sensors, 2018, 3, 867-874.	4.0	53
27783	Bias-dependent transport properties of passivated tilted black phosphorene nanoribbons. Physical Chemistry Chemical Physics, 2018, 20, 11021-11027.	1.3	5
27784	Application of 3D hierarchical monoclinic-type structural Sb-doped WO₃ towards NO₂ gas detection at low temperature. Nanoscale, 2018, 10, 7440-7450.	2.8	54
27785	Study of water adsorption on graphene edges. RSC Advances, 2018, 8, 11216-11221.	1.7	12
27786	Sequential BN-doping induced tuning of electronic properties in zigzag-edged graphene nanoribbons: a computational approach. RSC Advances, 2018, 8, 10964-10974.	1.7	3
27787	Structure prediction of boron-doped graphene by machine learning. Journal of Chemical Physics, 2018, 148, 241716.	1.2	46
27788	Non-parametric correlative uncertainty quantification and sensitivity analysis: Application to a Langmuir bimolecular adsorption model. AIP Advances, 2018, 8, .	0.6	8
27789	Catalytic methane combustion over Pd/ZrO2 catalysts: Effects of crystalline structure and textural properties. Applied Catalysis B: Environmental, 2018, 232, 544-552.	10.8	86
27790	Using BrÃ¸nsted-Evans-Polanyi relations to predict electrode potential-dependent activation energies. Catalysis Today, 2018, 312, 82-91.	2.2	36
27791	Ab initio study of iron adatom-vacancies in armchair graphene nanoribbons. Solid State Communications, 2018, 276, 9-13.	0.9	4
27792	Ab-initio calculation of surface phonons at the Sb2Te3(111) surface. Surface Science, 2018, 678, 46-51.	0.8	7
27793	Tight-Binding Approximation-Enhanced Global Optimization. Journal of Chemical Theory and Computation, 2018, 14, 2797-2807.	2.3	31
27794	Computational Screening of Near-Surface Alloys for CO₂ Electroreduction. ACS Catalysis, 2018, 8, 3885-3894.	5.5	79
27795	Design of high-strength refractory complex solid-solution alloys. Npj Computational Materials, 2018, 4, .	3.5	56
27796	Generic approach to access barriers in dehydrogenation reactions. Communications Chemistry, 2018, 1, .	2.0	9
27797	Hittorf's violet phosphorene as a promising candidate for optoelectronic and photocatalytic applications: first-principles characterization. Physical Chemistry Chemical Physics, 2018, 20, 11967-11975.	1.3	45
27798	Large spontaneous polarization in polar perovskites of PbTiO₃â€“Bi(Zn_{1/2}Ti_{1/2})O₃. Inorganic Chemistry Frontiers, 2018, 5, 1277-1281.	3.0	15
27799	Electronic, magnetic, catalytic, and electrochemical properties of two-dimensional Janus transition metal chalcogenides. Journal of Materials Chemistry A, 2018, 6, 8021-8029.	5.2	53

#	Article	IF	Citations
27800	Phosphorene oxides as a promising cathode material for sealed non-aqueous Liâ€“oxygen batteries. Journal of Materials Chemistry A, 2018, 6, 7815-7826.	5.2	20
27801	Insight into fast Li diffusion in Li-excess spinel lithium manganese oxide. Journal of Materials Chemistry A, 2018, 6, 9893-9898.	5.2	51
27802	First-principles investigations on structural, elastic, electronic properties and Debye temperature of orthorhombic Ni₃Ta under pressure. Philosophical Magazine, 2018, 98, 1641-1655.	0.7	3
27803	Effect of vacancies on the mechanical properties of phosphorene nanotubes. Nanotechnology, 2018, 29, 235707.	1.3	7
27804	Towards a Strong Spinâ€“Orbit Coupling Magnetoelectric Transistor. IEEE Journal on Exploratory Solid-State Computational Devices and Circuits, 2018, 4, 1-9.	1.1	40
27805	Investigation of the physical properties of two Laves phase compounds HRh₂ (H = Ca and) Tj ETQq1 1 0.784314 rgBT /O	1.0	15
27806	Degeneracy Lifting of Adsorbate Orbitals Imaged by High-Resolution Momentum Microscopy. Journal of the Physical Society of Japan, 2018, 87, 061009.	0.7	3
27807	Optical study of cubic, and orthorhombic structures of XCaCl 3 (Xâ€¯=â€¯K, Rb) compounds: Comparative Ab initio calculations. Optik, 2018, 166, 169-176.	1.4	12
27808	First-principle survey of structural, electronic, and optical properties of zinc-blende<mml:math xmlns:mml="http://www.w3.org/1998/Math/MathML" altimg="si14.gif" overflow="scroll"><mml:mrow><mml:msub><mml:mrow><mml:mi>B</mml:mi></mml:mrow><mml:mrow><mml:mi>x</mml:mi></mml:mrow></mml:msub><mml:msub><mml:mrow><mml:mi mathvariant="italic">Al</mml:mi></mml:mrow><mml:mrow><mml:mi>y</mml:mi></mml:mrow></mml:msub><mml:msub><mml:mrow><mml:mi mathvariant="italic">Ga</mml:mi></mml:mrow><mml:mrow><mml:mn>1</mml:mn><mm. Materials Letters, 2018, 221, 330-335.	1.3	2
27809	Quantum chemical modeling of solid-state B 4 X structures containing tetrahedral B 4 units with X = B, C, Al, Si. Mendeleev Communications, 2018, 28, 173-175.	0.6	4
27810	C3N monolayers as promising candidates for NO2 sensors. Sensors and Actuators B: Chemical, 2018, 266, 664-673.	4.0	172
27811	DFT study of structural, electronic and elastic properties of two polymorphs of monoclinic CsGaQ2 (Qâ€¯=â€¯S, Se). Chinese Journal of Physics, 2018, 56, 1345-1352.	2.0	4
27812	Detection of nucleobases using 2D germanane nanosheet: A first-principles study. Computational and Theoretical Chemistry, 2018, 1130, 68-76.	1.1	31
27813	Half-metallic ferromagnetism and metalâ€“insulator transition in Sn-doped SrRuO3 perovskite oxides. Journal of Magnetism and Magnetic Materials, 2018, 460, 54-60.	1.0	13
27814	First-principles predictions on structural, elastic and half-metallic properties of Fe 2 LiAs Heusler compound. Journal of Magnetism and Magnetic Materials, 2018, 458, 235-240.	1.0	6
27815	First-principles calculations of electronic, acoustic and anharmonic properties of Mn 2 RuZ (Zâ€¯=â€¯Si and) Tj ETQq1 1 0.784314 rgB	1.0	11
27816	A first-principle investigation of the Li diffusion mechanism in the super-ionic conductor lithium orthothioborate Li3BS3 structure. Materials Letters, 2018, 219, 186-189.	1.3	9
27817	Simultaneous multi-wavelength ultraviolet excited single-phase white light emitting phosphor Ba1-x(Zr,Ti)Si3O9:xEu. Optical Materials, 2018, 79, 53-62.	1.7	6

#	Article	IF	Citations
27818	First-principle study of single TM atoms X (X=Fe, Ru or Os) doped monolayer WS2 systems. Superlattices and Microstructures, 2018, 117, 155-162.	1.4	14
27819	â€œPop-On and Pop-Offâ€•Surface Chemistry of Alanine on Ni{111} under Elevated Hydrogen Pressures. Journal of Physical Chemistry C, 2018, 122, 7720-7730.	1.5	5
27820	First-Principles Modeling of Bismuth Doping in the MAPbI₃ Perovskite. Journal of Physical Chemistry C, 2018, 122, 14107-14112.	1.5	64
27821	Construction of Polarized Carbonâ€“Nickel Catalytic Surfaces for Potent, Durable, and Economic Hydrogen Evolution Reactions. ACS Nano, 2018, 12, 4148-4155.	7.3	121
27822	A density functional study on the reactivity enhancement induced by gold in IrAu nanoalloys. RSC Advances, 2018, 8, 10450-10456.	1.7	2
27823	Spin-polarized two-dimensional <mml:math xmlns:mml="http://www.w3.org/1998/Math/MathML"><mml:msub><mml:mi>t</mml:mi><mml:mrow><mml:mn>2</mml:mn><mml:mn><mml: electron gas: Ab initio study of EuO interface with oxygen-deficient <mml:math xmlns:mml="http://www.w3.org/1998/Math/MathML"><mml:mrow><mml:mi>SrTi</mml:mi><mml:msub><mml:mi mathvariant="normal">O</mml:mi><mml:mn>3</mml:mn></mml:msub></mml:mrow></mml:math>.	1.1	9
27824	Magnetic properties of iron doped zirconia as a function of Fe concentration: From ab initio simulations to the growth of thin films by atomic layer deposition and their characterization by synchrotron radiation. Journal of Vacuum Science and Technology A: Vacuum, Surfaces and Films, 2018, 36, .	0.9	4
27825	Preparation and surface characteristics of Re3W matrix scandate cathode: An experimental and theoretical study. Applied Surface Science, 2018, 440, 763-769.	3.1	18
27826	Structural and electronic properties of PdS 2 nanoribbons. Journal of Magnetism and Magnetic Materials, 2018, 458, 310-316.	1.0	10
27827	Spin resolved electronic transport through N@C20 fullerene molecule between Au electrodes: A first principles study. Physica E: Low-Dimensional Systems and Nanostructures, 2018, 99, 43-50.	1.3	8
27828	Polypyrrole on graphene: A density functional theory study. Surface Science, 2018, 674, 1-5.	0.8	13
27829	Calculation of Entropy of Adsorption for Small Molecules on Mineral Surfaces. Journal of Physical Chemistry C, 2018, 122, 8236-8243.	1.5	38
27830	Experimental and Theoretical Investigation of the Function of 4-tert-Butyl Pyridine for Interface Energy Level Adjustment in Efficient Solid-State Dye-Sensitized Solar Cells. ACS Applied Materials & Interfaces, 2018, 10, 11572-11579.	4.0	15
27831	A first principle comparative study of the ionic diffusivity in LiAlO2 and NaAlO2 polymorphs for solid-state battery applications. Physical Chemistry Chemical Physics, 2018, 20, 9824-9832.	1.3	16
27832	Bubble-wrap carbon: an integration of graphene and fullerenes. Nanoscale, 2018, 10, 11328-11334.	2.8	15
27833	Highly infrared sensitive VO₂ nanowires for a nano-optical device. Physical Chemistry Chemical Physics, 2018, 20, 11109-11115.	1.3	11
27834	DFT calculations of strain and interface effects on electronic structures and magnetic properties of L10-FePt/Ag heterojunction of GMR applications. AIP Advances, 2018, 8, 035310.	0.6	1
27835	Penta-P2X (X=C, Si) monolayers as wide-bandgap semiconductors: A first principles prediction. Frontiers of Physics, 2018, 13, 1.	2.4	60

#	Article	IF	Citations
27836	Solute strengthening of basal slip in Mg alloys. Acta Materialia, 2018, 151, 56-66.	3.8	87
27837	Investigation of structural and electronic properties of Î²-â€‰HgS: Molecular dynamics simulations. Chinese Journal of Physics, 2018, 56, 783-792.	2.0	12
27838	Precipitation mechanism of Mg2Ni in Mg-Ni-Y studied by STEM, 3DAP and first-principles calculations. Journal of Alloys and Compounds, 2018, 750, 117-123.	2.8	28
27839	Cations controlled growth of Î²-MnO2 crystals with tunable facets for electrochemical energy storage. Nano Energy, 2018, 48, 301-311.	8.2	56
27840	Tuning electronic properties of silicane layers by tensile strain and external electric field: A first-principles study. Thin Solid Films, 2018, 654, 107-115.	0.8	36
27841	Bandgap Engineering of InSe Single Crystals through S Substitution. Crystal Growth and Design, 2018, 18, 2899-2904.	1.4	18
27842	From Isolated Anions to Polymer Structures through Linking with I₂: Synthesis, Structure, and Properties of Two Complex Bismuth(III) Iodine Iodides. Inorganic Chemistry, 2018, 57, 4077-4087.	1.9	68
27843	Designing Two-Dimensional KBBF Family Second-Harmonic Generation Monolayers. Journal of Physical Chemistry C, 2018, 122, 7992-7996.	1.5	14
27844	Potential Dependence of the Buckling Structure of the Interfacial Water Bilayer on a Graphene Electrode. Journal of Physical Chemistry C, 2018, 122, 7795-7800.	1.5	4
27845	Anharmonicity and Disorder in the Black Phases of Cesium Lead Iodide Used for Stable Inorganic Perovskite Solar Cells. ACS Nano, 2018, 12, 3477-3486.	7.3	546
27846	A distinct correlation between the vibrational and thermal transport properties of group VA monolayer crystals. Nanoscale, 2018, 10, 7803-7812.	2.8	35
27847	Ab initioquantum transport in polycrystalline graphene. Nanoscale, 2018, 10, 7759-7768.	2.8	8
27848	Tuning the optoelectronic characteristics of ionic organic crystalline assemblies. Journal of Materials Chemistry C, 2018, 6, 4041-4056.	2.7	15
27849	Freestanding Ï‡₃-borophene nanoribbons: a density functional theory investigation. Physical Chemistry Chemical Physics, 2018, 20, 10493-10501.	1.3	26
27850	Elastic and thermodynamic properties of alkali hydrides XH (Xâ€¯=â€¯K, Rb and Cs). Chinese Journal of Physics, 2018, 56, 830-843.	2.0	1
27851	Crystal Structures, Local Atomic Environments, and Ion Diffusion Mechanisms of Scandium-Substituted Sodium Superionic Conductor (NASICON) Solid Electrolytes. Chemistry of Materials, 2018, 30, 2618-2630.	3.2	109
27852	Microwave-assisted hydrothermal synthesis of cobalt phosphide nanostructures for advanced supercapacitor electrodes. CrystEngComm, 2018, 20, 2413-2420.	1.3	30
27853	Metallic VO₂ monolayer as an anode material for Li, Na, K, Mg or Ca ion storage: a first-principle study. RSC Advances, 2018, 8, 10848-10854.	1.7	51

#	Article	IF	Citations
27854	Molecular-dynamics simulations of binary Pd-Si metal alloys: Glass formation, crystallisation and cluster properties. Journal of Non-Crystalline Solids, 2018, 487, 72-86.	1.5	21
27855	Effect of solute segregation on the intrinsic stacking fault energy of Co-based binary alloys: A first-principles study. Journal of Alloys and Compounds, 2018, 748, 328-337.	2.8	19
27856	Hydrogen trapping in carbon supersaturated Î±â€˜iron and its decohesion effect in martensitic steel. Scripta Materialia, 2018, 149, 79-83.	2.6	40
27857	Diffusion of hydrogen into and through Î³-iron by density functional theory. Surface Science, 2018, 672-673, 56-61.	0.8	10
27858	A theoretical perspective of the enhanced photocatalytic properties achieved by forming tetragonal ZnS/ZnSe hetero-bilayer. Physical Chemistry Chemical Physics, 2018, 20, 9950-9956.	1.3	14
27859	Electronic structures and enhanced photocatalytic properties of blue phosphorene/BSe van der Waals heterostructures. Journal of Materials Chemistry A, 2018, 6, 8923-8929.	5.2	197
27860	Hindered rotation and nuclear spin isomers separation of molecularly chemisorbed H2 on Pd(210). Journal of Applied Physics, 2018, 123, .	1.1	5
27861	Electrically active induced energy levels and metastability of B and N vacancy-complexes in 4Hâ€“SiC. Journal of Physics Condensed Matter, 2018, 30, 185702.	0.7	4
27862	Investigation of strain effect on electronic, chemical bonding, magnetic and phonon properties of ScNiBi: a DFT study. Materials Research Express, 2018, 5, 046502.	0.8	2
27863	Rocksalt or cesium chloride: Investigating the relative stability of the cesium halide structures with random phase approximation based methods. Physical Review B, 2018, 97, .	1.1	13
27864	First-principles study of electronic structure modulations in graphene on Ru(0001) by Au intercalation. Physical Review B, 2018, 97, .	1.1	2
27865	Facile air oxidative induced dealloying of hierarchical branched PtCu nanodendrites with enhanced activity for hydrogen evolution. Applied Catalysis A: General, 2018, 557, 72-78.	2.2	22
27866	Trapping of volatile fission products by C60. Carbon, 2018, 132, 477-485.	5.4	16
27867	Adsorption behavior of CO2 on pristine and doped phosphorenes: A dispersion corrected DFT study. Journal of CO2 Utilization, 2018, 24, 463-470.	3.3	39
27868	Structural, electronic, optical, thermodynamic and elastic properties of the zinc-blende Al x In 1-x N ternary alloys: A first principles calculations. Journal of Physics and Chemistry of Solids, 2018, 119, 36-49.	1.9	10
27869	The Vanadium effect on the electronic and optical properties of Ti3C2 graphene like: Based DFT. Results in Physics, 2018, 8, 1209-1215.	2.0	7
27870	Towards the systematic crystallisation of molecular ionic cocrystals: insights from computed crystal form landscapes. Faraday Discussions, 2018, 211, 401-424.	1.6	20
27871	Methyl Butanoate Adsorption on MoS2 Surface: A Density Functional Theory Investigation. MATEC Web of Conferences, 2018, 156, 06009.	0.1	0

#	Article	IF	Citations
27872	Rich interfacial chemistry and properties of carbon-doped hexagonal boron nitride nanosheets revealed by electronic structure calculations. Japanese Journal of Applied Physics, 2018, 57, 04FL11.	0.8	3
27873	First-principles study of lithium-ion diffusion in Î² -Li 3 PS 4 for solid-state electrolytes. Current Applied Physics, 2018, 18, 541-545.	1.1	18
27874	Satellite valleys and strained band gap transition of bulk Ge: Impact of pseudopotential approximations on quasiparticle levels. Computational Materials Science, 2018, 149, 115-124.	1.4	1
27875	Cs_{0.9}Ni_{3.1}Se₃: A Ni-Based Quasi-One-Dimensional Conductor with Spin-Glass Behavior. Inorganic Chemistry, 2018, 57, 3798-3804.	1.9	7
27876	Exploring Defect-Induced Emission in ZnAl₂O₄: An Exceptional Color-Tunable Phosphor Material with Diverse Lifetimes. Inorganic Chemistry, 2018, 57, 3963-3982.	1.9	72
27877	Crystal structural analysis of methyl-substituted pyrazines with anilic acids: a combined diffraction, inelastic neutron scattering,¹H-NMR study and theoretical approach. CrystEngComm, 2018, 20, 2016-2028.	1.3	6
27878	Two-dimensional <mml:math xmlns:mml="http://www.w3.org/1998/Math/MathML"><mml:mi>n</mml:mi></mml:math> -InSe/ <mml:math xmlns:mml="http://www.w3.org/1998/Math/MathML"><mml:mi>p</mml:mi></mml:math> -GeSe(SnS) van der Waals heterojunctions: High carrier mobility and broadband performance. Physical Review B, 2018, 97, .	1.1	113
27879	Nonequilibrium BN-ZnO: Optical properties and excitonic effects from first principles. Physical Review B, 2018, 97, .	1.1	9
27880	Electronic, Magnetic and Optical Properties of 2D Metal Nanolayers: A DFT Study. Metals and Materials International, 2018, 24, 904-912.	1.8	6
27881	Preparation of lanthanum zirconate films with a widely controllable La/Zr ratio by LCVD. Ceramics International, 2018, 44, 10621-10627.	2.3	12
27882	Study of vacancy-(H,B,C,N,O) clusters in Al using DFT and statistical approaches: Consequences on solubility of solutes. Journal of Alloys and Compounds, 2018, 748, 12-25.	2.8	11
27883	High electrical transport properties performance enhanced by anti-site defects in single crystalline SnSe. Journal of Alloys and Compounds, 2018, 748, 80-86.	2.8	13
27884	Two-dimensional Co3W3C nanosheets on graphene nanocomposition: An Pt-like electrocatalyst toward hydrogen evolution reaction in wide pH range. Materials Today Energy, 2018, 8, 65-72.	2.5	21
27885	Superconducting critical temperature under pressure. Physica C: Superconductivity and Its Applications, 2018, 548, 132-137.	0.6	9
27886	Rydberg transitions as a probe for structural changes and phase transition at polymer surfaces: an ATR-FUV-DUV and quantum chemical study of poly(3-hydroxybutyrate) and its nanocomposite with graphene. Physical Chemistry Chemical Physics, 2018, 20, 8859-8873.	1.3	20
27887	In-plane electric field controlled ferromagnetism and anisotropic magnetoresistance in an LSMO/PMN-PT heterostructure. Nanotechnology, 2018, 29, 224003.	1.3	11
27888	Origin of band bending at domain boundaries of MoS2: First-principles study. Japanese Journal of Applied Physics, 2018, 57, 04FP09.	0.8	1
27889	Effect of multicomponent alloying with Ni, Mn and Mo on phase stability of bcc Fe-Cr alloys. Acta Materialia, 2018, 150, 117-129.	3.8	23

#	Article	IF	Citations
27890	DFT study of imidazoles adsorption on the grain boundary of Cu (100) surface. Corrosion Science, 2018, 137, 33-42.	3.0	50
27891	Physical properties and defect processes of M3SnC2 (MÂ= Ti, Zr, Hf) MAX phases: Effect of M-elements. Journal of Alloys and Compounds, 2018, 748, 804-813.	2.8	49
27892	Mn induced 1â€Ã—â€2 reconstruction in the Ï„ -MnAl(0â€0â€1) surface. Journal of Crystal Growth, 2018, 489, 26-30.	1.7	0
27893	The stability of vacancy clusters and their effect on helium behaviors in 3C-SiC. Journal of Nuclear Materials, 2018, 503, 271-278.	1.3	29
27894	Dopant-Dependent SFG Response of Rhenium CO₂ Reduction Catalysts Chemisorbed on SrTiO₃ (100) Single Crystals. Journal of Physical Chemistry C, 2018, 122, 13944-13952.	1.5	10
27895	Latent Order in High-Angle Grain Boundary of GaN. Scientific Reports, 2018, 8, 4647.	1.6	2
27896	Stability and band offsets between c-plane ZnO semiconductor and LaAlO3 gate dielectric. Journal of Applied Physics, 2018, 123, .	1.1	2
27897	Observations of non-linear plasmon damping in dense plasmas. Physics of Plasmas, 2018, 25, .	0.7	29
27898	Calculation of spin-spin zero-field splitting within periodic boundary conditions: Towards all-electron accuracy. Physical Review B, 2018, 97, .	1.1	17
27899	Methanol Oxidation to Formaldehyde Promoted at the Step Sites of Ultrathin ZnO. Topics in Catalysis, 2018, 61, 499-508.	1.3	11
27900	Ternary W-Ni-Fe tungsten heavy alloys: A first principles and experimental investigations. International Journal of Refractory Metals and Hard Materials, 2018, 75, 43-49.	1.7	21
27901	Tuning magnetic properties of two-dimensional MoTe2 monolayer by doping 3d transition metals: Insights from first principles calculations. Journal of Alloys and Compounds, 2018, 748, 938-942.	2.8	39
27902	Crystal structure, electronic structure and photoluminescence properties of KLaMgWO6:Eu3+ phosphors. Journal of Luminescence, 2018, 197, 270-276.	1.5	34
27903	DFT study of the polarization behaviors of various distorted barium titanate crystals: The role of atomic displacements. Physica B: Condensed Matter, 2018, 538, 120-130.	1.3	6
27904	Na2MnO3 as cathode materials for Na ion batteries: From first-principles investigations. Solid State Ionics, 2018, 320, 210-214.	1.3	31
27905	Electronic structure and photoluminescence properties of single component white emitting Sr₃LuNa(PO₄)₃F:Eu²⁺,Mn²⁺ phosphor for WLEDs. Journal of Materials Chemistry C, 2018, 6, 4435-4443.	2.7	39
27906	First-Principle Calculations on the Structural, Mechanical, and Electronic Properties of Mn2RuSi and Mn2RuGe Under Pressure. Journal of Superconductivity and Novel Magnetism, 2018, 31, 3667-3677.	0.8	4
27907	Spectral redshift mechanism of N doped Sr 2 SiO 4 :Eu 2+ phosphors. Optik, 2018, 164, 289-296.	1.4	1

#	Article	IF	Citations
27908	Ab initio study of two-dimensional PdPS as an ideal light harvester and promising catalyst for hydrogen evolution reaction. Materials Today Energy, 2018, 7, 136-140.	2.5	24
27909	Hydrodeoxygenation of guaiacol over bimetallic Fe-alloyed (Ni, Pt) surfaces: reaction mechanism, transition-state scaling relations and descriptor for predicting Câ€“O bond scission reactivity. Catalysis Science and Technology, 2018, 8, 2146-2158.	2.1	56
27910	Defective boron nitride nanotubes: mechanical properties, electronic structures and failure behaviors. Journal Physics D: Applied Physics, 2018, 51, 125303.	1.3	11
27911	Reaction paths of alane dissociation on the Si(0â€‰0â€‰1) surface. Journal of Physics Condensed Matter, 2018, 30, 105002.	0.7	1
27912	Experimental and theoretical study of Co sorption in clay montmorillonites. Materials Research Express, 2018, 5, 035519.	0.8	5
27913	First-principles study on the gas sensing property of the Ge, As, and Br doped PtSe₂. Materials Research Express, 2018, 5, 035037.	0.8	13
27914	Frustrated magnetism in the tetragonal CoSe analog of superconducting FeSe. Physical Review B, 2018, 97, .	1.1	35
27915	Spin Injection into Graphene from Heusler Alloy Co₂MnGe (111) Surface: A First Principles Study. Materials Science Forum, 0, 914, 111-116.	0.3	2
27916	Healable Structure Triggered by Thermal/Electrochemical Force in Layered GeSe₂ for High Performance Liâ€ion Batteries. Advanced Energy Materials, 2018, 8, 1703635.	10.2	59
27917	Sulfur/Oxygen Codoped Porous Hard Carbon Microspheres for Highâ€Performance Potassiumâ€ion Batteries. Advanced Energy Materials, 2018, 8, 1800171.	10.2	363
27918	Selective Semihydrogenation of Phenylacetylene to Styrene Catalyzed by Alloyed Palladium/Gold Catalysts Anchored on Cerium Oxide. ChemNanoMat, 2018, 4, 472-476.	1.5	11
27919	Detailed mechanism of the NOâ€¯+â€¯CO reaction on Rh(1 0 0) and Rh(1 1 1): A first-principles study. Applied Surface Science, 2018, 444, 276-286.	3.1	20
27920	Brillouin zone grid refinement for highly resolved ab initio THz optical properties of graphene. Computer Physics Communications, 2018, 228, 96-99.	3.0	2
27921	First-principles calculation of the structural, electronic, dynamical, and thermodynamic properties of Li 4 TiO 4. Fusion Engineering and Design, 2018, 129, 241-246.	1.0	6
27922	Adhesion, stability and electronic properties of Ti 2 AlN(0001)/TiAl(111) coherent interface from first-principles calculation. Intermetallics, 2018, 96, 49-57.	1.8	36
27923	The first principles study of the sulfur oxidation on Ni surface with H2O. Journal of Alloys and Compounds, 2018, 741, 1183-1187.	2.8	9
27924	Electronic structure, magnetism and thermoelectric properties of double perovskite Sr 2 HoNbO 6. Journal of Magnetism and Magnetic Materials, 2018, 458, 176-182.	1.0	63
27925	Unraveling the Hydrogen Bond Network in a Theophyllineâ€“Pyridoxine Salt Cocrystal by a Combined X-ray Diffraction, Solid-State NMR, and Computational Approach. Crystal Growth and Design, 2018, 18, 2225-2233.	1.4	25

#	Article	IF	Citations
27926	High-Throughput Description of Infinite Compositionâ€“Structureâ€“Propertyâ€“Performance Relationships of Lithiumâ€“Manganese Oxide Spinel Cathodes. Chemistry of Materials, 2018, 30, 2287-2298.	3.2	20
27927	Nonadiabatic Molecular Dynamics Simulation of Charge Separation and Recombination at a WS₂/QD Heterojunction. Journal of Physical Chemistry C, 2018, 122, 7041-7050.	1.5	16
27928	Photocatalytic Activity of Phosphorene Derivatives: Coverage, Electronic, Optical, and Excitonic Properties. Journal of Physical Chemistry C, 2018, 122, 7194-7202.	1.5	9
27929	Design of Metal-Halide Inverse-Hybrid Perovskites. Journal of Physical Chemistry C, 2018, 122, 13872-13883.	1.5	9
27930	Rapid Decoherence Suppresses Charge Recombination in Multi-Layer 2D Halide Perovskites: Time-Domain Ab Initio Analysis. Nano Letters, 2018, 18, 2459-2466.	4.5	114
27931	Linear magnetoresistivity in layered semimetallic CaAl2Si2. Scientific Reports, 2018, 8, 4102.	1.6	4
27932	Methanol decomposition reactions over a boron-doped graphene supported Ruâ€“Pt catalyst. Physical Chemistry Chemical Physics, 2018, 20, 9355-9363.	1.3	25
27933	On the hydrogen evolution reaction activity of grapheneâ€“hBN van der Waals heterostructures. Physical Chemistry Chemical Physics, 2018, 20, 15007-15014.	1.3	41
27934	Negative thermal expansion and electronic structure variation of chalcopyrite type LiGaTe₂. RSC Advances, 2018, 8, 9946-9955.	1.7	35
27935	2D carbon sheets with negative Gaussian curvature assembled from pentagonal carbon nanoflakes. Physical Chemistry Chemical Physics, 2018, 20, 9123-9129.	1.3	6
27936	First-principles investigations on elastic, thermodynamic and lattice thermal conductivity of topological insulator LaAs. Philosophical Magazine, 2018, 98, 1900-1918.	0.7	11
27937	First-principles study of polarization and piezoelectricity behavior in tetragonal PbTiO ₃ -based superlattices. Chinese Physics B, 2018, 27, 027701.	0.7	2
27938	The high-pressure stability of Ni2In-type structure of ZrO2 with respect to OII and Fe2P-type phases: A first-principles study. IOP Conference Series: Materials Science and Engineering, 2018, 305, 012016.	0.3	4
27939	Interplay of valley selection and helicity exchange of light in Raman scattering for graphene and <mml:math xmlns:mml="http://www.w3.org/1998/Math/MathML"><mml:msub><mml:mi>MoS</mml:mi><mml:mn>2</mml:mn></mml:msub></mml Physical Review B, 2018, 97, .	1.1	27
27940	N-Doped Hybrid Graphene and Boron Nitride Armchair Nanoribbons As Nonmagnetic Semiconductors with Widely Tunable Electronic Properties. Russian Journal of Physical Chemistry A, 2018, 92, 532-539.	0.1	4
27941	Point defect concentrations of L12-Al3X(Sc, Zr, Er). Rare Metals, 2018, 37, 699-706.	3.6	11
27942	Mechanistic Study of Nitric Oxide Reduction by Hydrogen on Pt(100) (I): A DFT Analysis of the Reaction Network. Journal of Physical Chemistry B, 2018, 122, 432-443.	1.2	29
27943	Density functional calculations of the MÃ¶ssbauer parameters in hexagonal ferrite SrFe 12 O 19. Physica B: Condensed Matter, 2018, 532, 20-23.	1.3	5

#	Article	IF	Citations
27944	Metal-organic framework-derived porous shuttle-like vanadium oxides for sodium-ion battery application. Nano Research, 2018, 11, 449-463.	5.8	108
27945	Oxygen Reduction Reaction Catalyzed by Small Gold Cluster on h-BN/Au(111) Support. Electrocatalysis, 2018, 9, 182-188.	1.5	14
27946	Systematic trends in (0 0 1) surface ab initio calculations of ABO 3 perovskites. Journal of Saudi Chemical Society, 2018, 22, 459-468.	2.4	135
27947	A DFT Study on Structural, Electronic Mechanical and Thermodynamic Properties of 5f-Electron System BaAmO3. Journal of Superconductivity and Novel Magnetism, 2018, 31, 141-149.	0.8	28
27948	Adsorption Geometry and Energy Level Alignment at the PTCDA/TiO2(110) Interface. Journal of Physical Chemistry B, 2018, 122, 534-542.	1.2	11
27949	First-Principle Calculations of Structural, Elastic, and Electronic Properties of Intermetallic Rare Earth R2Ni2Pb (R = Ho, Lu, and Sm) Compounds. Journal of Superconductivity and Novel Magnetism, 2018, 31, 395-403.	0.8	90
27950	Effect of pressure on the Raman-active modes of zircon (ZrSiO4): a first-principles study. Physics and Chemistry of Minerals, 2018, 45, 173-184.	0.3	12
27951	Strain and different edge terminations modulated electronic and magnetic properties of armchair AlN/SiC nanoribbons: first-principles study. Canadian Journal of Physics, 2018, 96, 30-35.	0.4	0
27952	A first principles study of energetics and electronic structural responses of uranium-based coordination polymers to Np incorporation. Radiochimica Acta, 2018, 106, 1-13.	0.5	5
27953	Surface Termination of Fe₃O₄(111) Films Studied by CO Adsorption Revisited. Journal of Physical Chemistry B, 2018, 122, 527-533.	1.2	46
27954	Stability, Magnetism and Hardness of Iron Carbides from First-Principles Calculations. Journal of Superconductivity and Novel Magnetism, 2018, 31, 353-364.	0.8	12
27955	Trends of Alkane Activation on Doped Cobalt (II,â€...III) Oxide from First Principles. ChemCatChem, 2018, 10, 244-249.	1.8	25
27956	High Naâ€ion conducting Na_{1+x}[Sn_xGe_{2â^'x}(<scp>PO</scp>₄)₃] glassâ€ceramic electrolytes: Structural and electrochemical impedance studies. Journal of the American Ceramic Society, 2018, 101, 167-177.	1.9	23
27957	Matildite Contact with Media: First-Principles Study of AgBiS₂ Surfaces and Nanoparticle Morphology. Journal of Physical Chemistry B, 2018, 122, 521-526.	1.2	15
27958	Native point defects in MoS 2 and their influences on optical properties by first principles calculations. Physica B: Condensed Matter, 2018, 532, 184-194.	1.3	11
27959	Three-layer phosphorene-metal interfaces. Nano Research, 2018, 11, 707-721.	5.8	72
27960	Density functional theory calculation of monolayer WTe 2 transition metal dichalcogenides doped with H, Li and Be. Physica B: Condensed Matter, 2018, 535, 167-170.	1.3	1
27961	Density functional theory study for the enhanced sulfur tolerance of Ni catalysts by surface alloying. Applied Surface Science, 2018, 429, 87-94.	3.1	26

#	Article	IF	Citations
27962	Al-doped B 80 fullerene as a suitable candidate for H 2 , CH 4 , and CO 2 adsorption for clean energy applications. Journal of Saudi Chemical Society, 2018, 22, 49-57.	2.4	14
27963	Effects of K adsorption on the CO-induced restructuring of Co(11-20). Catalysis Today, 2018, 299, 37-46.	2.2	9
27964	Interaction of Pd single atoms with different CeO 2 crystal planes: A first-principles study. Applied Surface Science, 2018, 433, 1036-1048.	3.1	17
27965	Hydrogen adsorption on decorated graphyne and its analogous with Na. Materials Research Bulletin, 2018, 98, 200-205.	2.7	14
27966	Giant permittivity and low dielectric loss of Fe doped BaTiO3 ceramics: Experimental and first-principles calculations. Journal of the European Ceramic Society, 2018, 38, 1562-1568.	2.8	54
27967	Structures and anti-inflammatory properties of 4-halogenated -mofebutazones. Journal of Molecular Structure, 2018, 1154, 204-218.	1.8	0
27968	Segregation and mechanical properties of Si, Fe and Ti on the Al/Al2.5X0.5Zr (X = Cu, Zn, Ag) coherent interfaces: First-principles calculations. Computational Materials Science, 2018, 141, 325-340.	1.4	6
27969	Electronic, magnetic and transport properties of transition metal-doped holely C 2 N- h 2D nanoribbons. Physica B: Condensed Matter, 2018, 528, 1-8.	1.3	7
27970	Mechanical failure of graphene and the anharmonic phonon coupling mechanisms. Carbon, 2018, 126, 404-409.	5.4	4
27971	Direct comparison among the formation of terephthalate- and carbonate-intercalated Mg-Al-LDH: The influence of the high aluminum content. Applied Clay Science, 2018, 151, 194-200.	2.6	13
27972	First principles investigation of structural, electronic and optical properties of NiV 2 O 6. Computational Condensed Matter, 2018, 15, 95-99.	0.9	6
27973	Mechanical switching of ferroelectric domains beyond flexoelectricity. Journal of the Mechanics and Physics of Solids, 2018, 111, 43-66.	2.3	37
27974	A first-principles study of gas adsorption on monolayer AlN sheet. Vacuum, 2018, 147, 18-23.	1.6	43
27975	Effects of alloying elements on the elastic properties of bcc Ti-X alloys from first-principles calculations. Computational Materials Science, 2018, 142, 215-226.	1.4	38
27976	Hard three-dimensional BN framework with one-dimensional metallicity. Journal of Alloys and Compounds, 2018, 731, 364-368.	2.8	27
27977	The phase diagrams of KCaF3 and NaMgF3 by ab initio simulations. Physics and Chemistry of Minerals, 2018, 45, 311-322.	0.3	15
27978	New metallic carbon: Three dimensionally carbon allotropes comprising ultrathin diamond nanostripes. Carbon, 2018, 126, 601-610.	5.4	36
27979	Structural, magnetic and thermodynamic properties of Mn3-X-C (X = Ga, Sn) compounds: ab initio study. Physica B: Condensed Matter, 2018, 549, 94-97.	1.3	1

#	Article	IF	Citations
27980	Magnetism induced by 3d transition metal atom doping in InSe monolayer. Journal of Materials Science, 2018, 53, 3500-3508.	1.7	14
27981	Surface termination analysis of stoichiometric metal hexaborides: Insights from first-principles and XPS measurements. Acta Materialia, 2018, 144, 187-201.	3.8	21
27982	CO adsorption, dissociation and coupling formation mechanisms on Fe2C(001) surface. Applied Surface Science, 2018, 434, 464-472.	3.1	29
27983	The Role of Sodium in Tuning Product Distribution in Syngas Conversion by Rh Catalysts. Catalysis Letters, 2018, 148, 289-297.	1.4	12
27984	Theoretical Study of Structural, Magnetic, Elastic, Phonon, and Thermodynamic Properties of Heusler Alloys Fe2CrX (X = Al, Ga). Journal of Superconductivity and Novel Magnetism, 2018, 31, 1791-1798.	0.8	12
27985	Theoretical study of the promotional effect of ZrO2 on In2O3 catalyzed methanol synthesis from CO2 hydrogenation. Applied Surface Science, 2018, 433, 780-789.	3.1	63
27986	The role of the intrinsic Se and In vacancies in the interaction of O2 and H2O molecules with the InSe monolayer. Applied Surface Science, 2018, 434, 215-227.	3.1	27
27987	Competitive adsorption of gases dissolved in transformer oil on Co-doped ZnO (0 0 0 1) surface. Computational Materials Science, 2018, 142, 72-81.	1.4	14
27988	High-temperature and high-pressure physical properties of CuI with zinc-blende phase by a systematic ab initio investigation. Optik, 2018, 155, 17-25.	1.4	12
27989	Phase equilibria of Mg-La-Zr system and thermal conductivity of selected alloys. Journal of Alloys and Compounds, 2018, 731, 784-795.	2.8	17
27990	Squaric acid adsorption and oxidation at gold and platinum electrodes. Journal of Electroanalytical Chemistry, 2018, 819, 178-186.	1.9	5
27991	Coverage evolution of the unoccupied Density of States in sulfur superstructures on Ru(0001). Applied Surface Science, 2018, 433, 300-305.	3.1	3
27992	Two-dimensional siligraphenes as cathode catalysts for nonaqueous lithium-oxygen batteries. Carbon, 2018, 126, 580-587.	5.4	40
27993	Structural, vibrational, and thermodynamic properties of Î³-Na2TiO3: First-principles and experimental studies. Ceramics International, 2018, 44, 2065-2073.	2.3	4
27994	The electrochemical stability of thiols on gold surfaces. Journal of Electroanalytical Chemistry, 2018, 819, 234-239.	1.9	24
27995	Effect of Al2O3 on phase formation and thermal expansion of a BaO-SrO-ZnO-SiO2 glass ceramic. Ceramics International, 2018, 44, 2098-2108.	2.3	7
27996	Electronic properties and the phonon band structure of PbTe. Computational Condensed Matter, 2018, 15, 90-94.	0.9	5
27997	Atomic structure, stability and electronic properties of S(Al2CuMg)/Al interface: A first-principles study. Intermetallics, 2018, 93, 329-337.	1.8	31

#	Article	IF	Citations
27998	First-principles calculation on the electronic structure and optical properties of Eu2+ doped Î³-AlON phosphor. Ceramics International, 2018, 44, 1461-1466.	2.3	9
27999	Elastic properties and plastic deformation of TiC- and VC-based pseudobinary alloys. Acta Materialia, 2018, 144, 376-385.	3.8	45
28000	Protomene: A new carbon allotrope. Carbon, 2018, 126, 574-579.	5.4	28
28001	First-Principles Study of MoO 3 /Graphene Composite as Cathode Material for High-Performance Lithium-Ion Batteries. Applied Surface Science, 2018, 433, 1083-1093.	3.1	27
28002	Thermoelectric power factor of La 0.9 M 0.1 FeO 3 (MÂ=ÂCa and Ba) system: Structural, band gap and electrical transport evaluations. Physica B: Condensed Matter, 2018, 529, 1-8.	1.3	13
28003	Electronic and Magnetic Investigations of Rare-Earth Tm-doped AlGaN Ternary Alloy. Journal of Superconductivity and Novel Magnetism, 2018, 31, 1767-1771.	0.8	28
28004	Reaction mechanism for oxygen evolution on RuO2, IrO2, and RuO2@IrO2 core-shell nanocatalysts. Journal of Electroanalytical Chemistry, 2018, 819, 296-305.	1.9	141
28005	Structural, electronic, elastic, vibrational and thermodynamic properties of U3Si2: A comprehensive study using DFT. Journal of Alloys and Compounds, 2018, 732, 160-166.	2.8	35
28006	Strengthening mechanism of aluminum on elastic properties of NbVTiZr high-entropy alloys. Intermetallics, 2018, 92, 7-14.	1.8	44
28007	Structural, elastic, electronic and vibrational properties of BaRh2P2 and SrIr2As2 superconductors: A DFT study. Journal of Alloys and Compounds, 2018, 740, 754-765.	2.8	27
28008	First-principles study of mechanical, thermodynamic, transport and superconducting properties of Sr3SnO. Journal of Alloys and Compounds, 2018, 730, 279-283.	2.8	18
28009	Elucidating the unintentional p-type nature of spinel Co3O4: A defect study using ab-initio calculation. Journal of the European Ceramic Society, 2018, 38, 629-635.	2.8	10
28010	Strained noble metal di chalcogenides PtX 2 (X = S, Se) mono-layer: Ab initio study of electronic and lattice dynamic properties. Physica E: Low-Dimensional Systems and Nanostructures, 2018, 95, 139-143.	1.3	16
28011	Electronic and optical properties of ultra-thin 2D tungsten disulfide for photovoltaic applications. Solar Energy Materials and Solar Cells, 2018, 174, 370-379.	3.0	80
28012	High Temperature Stability of BaZrO₃: An Ab Initio Thermodynamic Study. Physica Status Solidi (B): Basic Research, 2018, 255, 1700398.	0.7	4
28013	Analytical modeling of electron energy loss spectroscopy of graphene: Ab initio study versus extended hydrodynamic model. Ultramicroscopy, 2018, 184, 134-142.	0.8	13
28014	Honeycomb BeO monolayer on the Mo(112) surface: LEED and DFT study. Applied Surface Science, 2018, 428, 815-818.	3.1	17
28015	A new insight into the theoretical design of highly dispersed and stable ceria supported metal nanoparticles. Journal of Colloid and Interface Science, 2018, 512, 775-783.	5.0	8

#	Article	IF	Citations
28016	Structural, elastic and anisotropic properties of CuZr from first-principles calculations. Materials Chemistry and Physics, 2018, 203, 166-172.	2.0	5
28017	Electronic structure and H2S adsorption property of Pt3 cluster decorated (8, 0) SWCNT. Applied Surface Science, 2018, 428, 82-88.	3.1	30
28018	Adsorption and reaction of CO and H2O on WC(0001) surface: A first-principles investigation. Applied Surface Science, 2018, 428, 579-585.	3.1	8
28019	Computational study of Mn-doped GaN polar and non-polar surfaces. Computational Materials Science, 2018, 141, 68-74.	1.4	8
28020	The grain refinement performance of B-doped TiC on Zr-containing Al alloys. Journal of Alloys and Compounds, 2018, 731, 774-783.	2.8	22
28021	First-Principles Study of Pressure Dependence of Optical Spectra of MnS. Journal of Superconductivity and Novel Magnetism, 2018, 31, 1643-1647.	0.8	11
28022	Ferromagnetism and Halfâ€Metallicity in a Highâ€Bandâ€Gap Hexagonal Boron Nitride System. ChemPhysChem, 2018, 19, 153-161.	1.0	10
28023	Defect structure of oxygen-vacancy clusters in O18 and self ion implanted Fe(100) crystal by ion channeling and ab-initio study. Acta Materialia, 2018, 143, 198-204.	3.8	2
28024	Adsorption of bentazon on CAT and CARBOPAL activated carbon: Experimental and computational study. Applied Surface Science, 2018, 433, 487-501.	3.1	9
28025	Low temperature preparation of oxygen-deficient tin dioxide nanocrystals and a role of oxygen vacancy in photocatalytic activity improvement. Journal of Colloid and Interface Science, 2018, 512, 105-114.	5.0	59
28026	High-pressure phase transition and thermodynamic properties from first-principles calculations: Application to cubic copper iodide. Materials Chemistry and Physics, 2018, 203, 362-373.	2.0	15
28027	First-principles investigation of graphitic carbon nitride monolayer with embedded Fe atom. Surface Science, 2018, 667, 112-120.	0.8	20
28028	Effects of an electric field on the adsorption of water molecules on the Cd(0001) surface. Surface Science, 2018, 668, 1-6.	0.8	3
28029	Theoretical investigations of group IV alloys in the Lonsdaleite phase. Journal of Materials Science, 2018, 53, 2785-2801.	1.7	31
28030	Structure and transport properties of AgIâ€“AgClâ€“CsCl glasses: molecular dynamics study. Ionics, 2018, 24, 1371-1376.	1.2	6
28031	Formation of carbon composite structures on the Ge(110) surfaces. Current Applied Physics, 2018, 18, 96-101.	1.1	2
28032	Chromium-vacancy clusters in dilute bcc Fe-Cr alloys: An ab initio study. Journal of Nuclear Materials, 2018, 499, 613-621.	1.3	12
28033	A DFT study for adsorption of CO on Ni, Pd and Pt atoms doped (7, 0) boron nitride nanotube. Molecular Physics, 2018, 116, 204-211.	0.8	10

#	Article	IF	Citations
28034	Magnetic states and intervalence charge transfer of Ti and Fe defects in Î±-Al2O3: The origin of the blue in sapphire. Acta Materialia, 2018, 143, 248-256.	3.8	10
28035	A novel aluminum dual-ion battery. Energy Storage Materials, 2018, 11, 91-99.	9.5	123
28036	First-principles study of the electronic transport properties of a 1,3-diazabicyclo[3.1.0]hex-3-ene molecular optical switch. Optik, 2018, 153, 135-143.	1.4	14
28037	Molecular-level insights into mercury removal mechanism by pyrite. Journal of Hazardous Materials, 2018, 344, 104-112.	6.5	138
28038	The role of the anionic and cationic pt sites in the adsorption site preference of water and ethanol on defected Pt4/Pt(111) substrates: A density functional theory investigation within the D3 van der waals corrections. Surface Science, 2018, 667, 84-91.	0.8	6
28039	Band structure and optical properties of polyaniline polymer material. Polymer Bulletin, 2018, 75, 3023-3033.	1.7	36
28040	Doped phosphorene for hydrogen capture: A DFT study. Applied Surface Science, 2018, 433, 249-255.	3.1	48
28041	Oxygen vacancy chain and conductive filament formation in hafnia. Journal of Applied Physics, 2018, 123, .	1.1	34
28042	Physical Properties of Superhard Diamond-Like BC5 from a First-Principles Study. Journal of Electronic Materials, 2018, 47, 272-284.	1.0	5
28043	Simultaneous Detection and Removal of Formaldehyde at Room Temperature: Janus Au@ZnO@ZIF-8 Nanoparticles. Nano-Micro Letters, 2018, 10, 4.	14.4	84
28044	Layered heterostructures based on graphene, hexagonal zinc oxide and molybdenum disulfide: Modeling of geometry and electronic properties. Computational Materials Science, 2018, 142, 32-37.	1.4	7
28045	Magnetic behavior study of samarium nitride using density functional theory. Journal of Magnetism and Magnetic Materials, 2018, 448, 186-191.	1.0	11
28046	Defect pair formation in fluorine and nitrogen codoped TiO2. Journal of Applied Physics, 2018, 123, 161510.	1.1	9
28047	Accurate Bandgap of Zr x Al1â^'x N Using Modified Beckeâ€"Johnson (mBJ) Exchange Potential. Journal of Superconductivity and Novel Magnetism, 2018, 31, 1545-1548.	0.8	1
28048	Anionâ€"Anion Coâ€Đoped Monolayer MoS₂ for Visible Light Photocatalysis. Physica Status Solidi (B): Basic Research, 2018, 255, 1700413.	0.7	9
28049	Ab Initio Investigation on Electronic, Magnetic, Mechanical, and Thermodynamic Properties of AMO3 (A) Tj ETQq1 1 0.784314 rgBT /Ov	0.8	8
28050	Effects of dopant separation on electronic states and magnetism in monolayer MoS2. Applied Surface Science, 2018, 428, 226-232.	3.1	16
28051	DFT study on the interaction of TiO2 (001) surface with HCHO molecules. Applied Surface Science, 2018, 428, 954-963.	3.1	25

#	Article	IF	Citations
28052	Structural, electronic, elastic, optical and vibrational properties of MAl2O4 (M = Co and Mn) aluminate spinels. Ceramics International, 2018, 44, 310-316.	2.3	17
28053	DFT study on structural, electronic, and optical properties of cubic and monoclinic CuO. Journal of Computational Electronics, 2018, 17, 21-28.	1.3	29
28054	Asymmetric hydrogenation-induced ferromagnetism in stanene nanoribbons considering electric field and strain effects. Journal of Materials Science, 2018, 53, 657-666.	1.7	3
28055	Electronic structure and relative stability of the coherent and semi-coherent HfO2/III-V interfaces. Applied Surface Science, 2018, 427, 243-252.	3.1	6
28056	Density functional theory calculations of biomolecules adsorption on phosphorene for biomedical applications. Applied Surface Science, 2018, 427, 1227-1234.	3.1	32
28057	Stability enhancement and electronic tunability of two-dimensional SbIV compounds via surface functionalization. Applied Surface Science, 2018, 427, 363-368.	3.1	8
28058	Magnetism in non-metal atoms adsorbed graphene-like gallium nitride monolayers. Applied Surface Science, 2018, 427, 609-612.	3.1	79
28059	Electronic structure and optical properties of BiOI {001} monolayer under biaxial strain. Journal of Materials Science, 2018, 53, 708-715.	1.7	9
28060	First-principles calculations of high-pressure iron-bearing monoclinic dolomite and single-cation carbonates with internally consistent Hubbard U. Physics and Chemistry of Minerals, 2018, 45, 293-302.	0.3	11
28061	The location of excess electrons on H₂O/TiO₂(110) surface and its role in the surface reactions. Molecular Physics, 2018, 116, 171-178.	0.8	7
28062	Underpotential deposition and involved alloy formation of cadmium on silver particles modified HOPG substrates. Journal of Solid State Electrochemistry, 2018, 22, 193-202.	1.2	2
28063	Theoretical investigation of thermoelectric and elastic properties of intermetallic compounds ScTM (TM = Cu, Ag, Au and Pd). International Journal of Modern Physics B, 2018, 32, 1850004.	1.0	7
28064	Theoretical and experimental investigations of mercury adsorption on hematite surfaces. Journal of the Air and Waste Management Association, 2018, 68, 39-53.	0.9	13
28065	Electronic structure and thermoelectric properties of narrow-band-gap intermetallic compound Al2Fe3Si3. Journal of Thermal Analysis and Calorimetry, 2018, 131, 281-287.	2.0	20
28066	Ab Initio Prediction of the Structural, Electronic, Elastic, and Thermoelectric Properties of Half-Heusler Ternary Compounds TiIrX (XÂ=ÂAs and Sb). Journal of Electronic Materials, 2018, 47, 196-204.	1.0	25
28067	High-metallic-phase-concentration Mo1â€“xWxS2 nanosheets with expanded interlayers as efficient electrocatalysts. Nano Research, 2018, 11, 1687-1698.	5.8	37
28068	Influences of Electrode Potential on Mechanism of Oxygen Reduction Reaction on Pd-Skin/Pd3Fe(111) Electrocatalyst: Insights from DFT-Based Calculations. Electrocatalysis, 2018, 9, 10-21.	1.5	4
28069	Efficient defect-controlled photocatalytic hydrogen generation based on near-infrared Cu-In-Zn-S quantum dots. Nano Research, 2018, 11, 1379-1388.	5.8	41

#	Article	IF	Citations
28070	Oxidation mechanism of chalcopyrite revealed by X-ray photoelectron spectroscopy and first principles studies. Applied Surface Science, 2018, 427, 233-241.	3.1	46
28071	Theoretical Evidence behind Bifunctional Catalytic Activity in Pristine and Functionalized Al₂C Monolayers. ChemPhysChem, 2018, 19, 148-152.	1.0	11
28072	Electrical contacts in monolayer blue phosphorene devices. Nano Research, 2018, 11, 1834-1849.	5.8	55
28073	Elastic properties and thermal expansion of lead-free halide double perovskite Cs2AgBiBr6. Computational Materials Science, 2018, 141, 49-58.	1.4	87
28074	Understanding the synergistic effects, optical and electronic properties of ternary Fe/C/Sâ€doped TiO₂ anatase within the DFT + U approach. International Journal of Quantum Chemistry, 2018, 118, e25505.	1.0	12
28075	Self-supported CoMoS4 nanosheet array as an efficient catalyst for hydrogen evolution reaction at neutral pH. Nano Research, 2018, 11, 2024-2033.	5.8	147
28076	DFT study on the adsorption sensitivity of graphane doped with Cr and Mn toward H 2 CO molecule. Physica E: Low-Dimensional Systems and Nanostructures, 2018, 95, 16-21.	1.3	35
28077	Atomic and molecular adsorption on Fe(110). Surface Science, 2018, 667, 54-65.	0.8	49
28078	Phase transformations in the relaxor Na_{1/2}Bi_{1/2}TiO₃ studied by means of density functional theory calculations. Journal of the American Ceramic Society, 2018, 101, 472-482.	1.9	10
28079	Investigation of the structural and electronic properties of CdS under high pressure: an ab initio study. Canadian Journal of Physics, 2018, 96, 216-224.	0.4	20
28080	Comparison of standard DFT and Hubbard-DFT methods in structural and electronic properties of TiO2 polymorphs and H-titanate ultrathin sheets for DSSC application. Applied Surface Science, 2018, 428, 118-123.	3.1	50
28081	Effects of alloying elements on relative phase stability and elastic properties of L12 Co3V from first-principles calculations. Journal of Materials Science, 2018, 53, 1204-1216.	1.7	8
28082	First-Principle Predictions of Electronic Properties and Half-Metallic Ferromagnetism in Vanadium-Doped Rock-Salt SrO. Journal of Electronic Materials, 2018, 47, 449-456.	1.0	27
28083	Phase stability, elastic, anisotropic properties, lattice dynamical and thermodynamic properties of B12M (M=Th, U, Np, Pu) dodecaborides. Ceramics International, 2018, 44, 128-135.	2.3	33
28084	Adsorption characteristics of DNA nucleobases, aromatic amino acids and heterocyclic molecules on silicene and germanene monolayers. Sensors and Actuators B: Chemical, 2018, 255, 2713-2720.	4.0	56
28085	Effect of tetravalent dopants on hematite nanostructure for enhanced photoelectrochemical water splitting. Applied Surface Science, 2018, 427, 1203-1212.	3.1	51
28086	Enhanced catalytic performance by oxygen vacancy and active interface originated from facile reduction of OMS-2. Chemical Engineering Journal, 2018, 331, 626-635.	6.6	100
28087	Insights into the photocatalytic mechanism of mediator-free direct Z-scheme g-C3N4/Bi2MoO6(010) and g-C3N4/Bi2WO6(010) heterostructures: A hybrid density functional theory study. Applied Surface Science, 2018, 427, 487-498.	3.1	125

#	Article	IF	Citations
28088	Ab initio characterization and experimental validation on the roles of oxygen-containing groups in graphene based formaldehyde sensors. Analyst, The, 2018, 143, 106-115.	1.7	13
28089	Controlling phenolic hydrodeoxygenation by tailoring metalâ€“O bond strength via specific catalyst metal type andÂparticle size selection. Comptes Rendus Chimie, 2018, 21, 155-163.	0.2	30
28090	Predicted MAX Phase Sc₂InC: Dynamical Stability, Vibrational and Optical Properties. Physica Status Solidi (B): Basic Research, 2018, 255, 1700235.	0.7	39
28091	Combined theoretical and experimental study on alcoholysis of amides on CeO2 surface: A catalytic interplay between Lewis acid and base sites. Catalysis Today, 2018, 303, 256-262.	2.2	13
28092	CH4 dissociation in the early stage of graphene growth on Feâ€“Cu(100) surface: Theoretical insights. Applied Surface Science, 2018, 427, 953-960.	3.1	11
28093	Sodium storage mechanism of N, S co-doped nanoporous carbon: Experimental design and theoretical evaluation. Energy Storage Materials, 2018, 11, 274-281.	9.5	112
28094	Initial Stages in the Formation of Nickel Phosphides. Journal of Physical Chemistry B, 2018, 122, 672-678.	1.2	12
28095	Synthesis and characterization of rhodium nanoclusters on TiO2(110) surface using organometallic compounds. Surface Science, 2018, 667, 38-44.	0.8	2
28096	New Polymorph Form of Dexamethasone Acetate. Journal of Pharmaceutical Sciences, 2018, 107, 672-681.	1.6	8
28097	First principles and Debye model study of the thermodynamic, electronic and optical properties of MgO under high-temperature and pressure. International Journal of Modern Physics B, 2018, 32, 1850047.	1.0	0
28098	High Lithium Insertion Voltage Singleâ€Crystal H₂Ti₁₂O₂₅ Nanorods as a Highâ€Capacity and Highâ€Rate Lithiumâ€Ion Battery Anode Material. ChemSusChem, 2018, 11, 299-310.	3.6	18
28099	Substitution behavior of Si atoms in the Ti2AlC ceramics. Acta Materialia, 2018, 144, 543-551.	3.8	26
28100	Role of the X and n factors in ion-irradiation induced phase transformations of Mn+1AXn phases. Acta Materialia, 2018, 144, 432-446.	3.8	21
28101	Fluorine-graphite intercalation compound (C4F)n at high pressure: Experimental and theoretical study. Carbon, 2018, 127, 384-391.	5.4	12
28102	Efficient hydrogen evolution electrocatalysis in alkaline medium using Pd-modified zeolite X. Electrochimica Acta, 2018, 259, 882-892.	2.6	27
28103	Equilibrium nickel isotope fractionation in nickel sulfide minerals. Geochimica Et Cosmochimica Acta, 2018, 222, 1-16.	1.6	24
28104	Variation of the<mml:math xmlns:mml="http://www.w3.org/1998/Math/MathML" altimg="si1.gif" overflow="scroll"><mml:mrow><mml:mi>z</mml:mi><mml:mi>T</mml:mi></mml:mrow></mml:math>factor of SnSe with doping: A first-principles study. Journal of Alloys and Compounds, 2018, 732, 536-546.	2.8	9
28105	Prediction of novel stable Fe-V-Si ternary phase. Journal of Alloys and Compounds, 2018, 732, 567-572.	2.8	4

#	Article	IF	Citations
28106	Search for New Half-Metallic Ferromagnets in Quaternary Diamond-Like Compounds Iâ€“II2â€“IIIâ€“VI4 and I2â€“IIâ€“IVâ€“VI4 (I = Cu; II = Mn, Fe, Co; III = In; IV = Ge, Sn; VI = S, Se, Te). Journal of Superconductivity and Novel Magnetism, 2018, 31, 1941-1947.	0.8	18
28107	Adsorption of alkylamine cations on montmorillonite (001) surface: A density functional theory study. Applied Clay Science, 2018, 152, 249-258.	2.6	47
28108	Mechanistic insight into the synergetic catalytic effect of Pd and MnO2 for high-performance Liâ€“O2 cells. Energy Storage Materials, 2018, 12, 8-16.	9.5	23
28109	Electronic and magnetic behavior of transition metal-doped cubic gallium nitride: first-principles calculations. Journal of Magnetism and Magnetic Materials, 2018, 451, 295-299.	1.0	10
28110	Tuning the electronic properties of bilayer group-IV monochalcogenides by stacking order, strain and an electric field: a computational study. Physical Chemistry Chemical Physics, 2018, 20, 214-220.	1.3	32
28111	Morphological Changes in Electrografted Arylâ€Based Thin Films Induced by using Diazonium Salts or Aryl Iodides. ChemElectroChem, 2018, 5, 464-470.	1.7	7
28112	Ab-initio study of electronic and elastic properties of Mg(BH4)(NH2) complex hydride. International Journal of Hydrogen Energy, 2018, 43, 1587-1595.	3.8	3
28113	Theoretical study on the photocatalytic properties of graphene oxide with single Au atom adsorption. Surface Science, 2018, 669, 71-78.	0.8	18
28114	Discovery of 2D Anisotropic Dirac Cones. Advanced Materials, 2018, 30, 1704025.	11.1	91
28115	Hydrostatic pressure and temperature effect on the Raman spectra of the molecular crystal 2-amine-1,3,4-thiadiazole. Journal of Molecular Structure, 2018, 1156, 127-135.	1.8	4
28116	Ab initio study of structural and electronic properties of copper and nickel tungstate. Computational Materials Science, 2018, 143, 301-307.	1.4	9
28117	Effect of the Mechanism of H₂S on Elemental Mercury Removal Using the MnO₂ Sorbent during Coal Gasification. Energy & Fuels, 2018, 32, 4453-4460.	2.5	44
28118	Graphene Oxide Epoxy (GOâ€xy): GO as Epoxy Adhesive by Interfacial Reaction of Functionalities. Advanced Materials Interfaces, 2018, 5, 1700657.	1.9	19
28119	Theoretical study of the structural and electronic properties of novel stanene-based buckled nanotubes and their adsorption behaviors. Applied Surface Science, 2018, 435, 733-742.	3.1	22
28120	Dislocation nucleation facilitated by atomicÂsegregation. Nature Materials, 2018, 17, 56-63.	13.3	99
28121	A first-principles study on the interaction of biogas with noble metal (Rh, Pt, Pd) decorated nitrogen doped graphene as a gas sensor: A DFT study. Applied Surface Science, 2018, 435, 1199-1212.	3.1	66
28122	Water dissociation and CO oxidation over Au/anatase catalyst. A DFT-D2 study. Applied Surface Science, 2018, 435, 1168-1173.	3.1	10
28123	Revisiting intrinsic brittleness and deformation behavior of B2 NiAl intermetallic compound: A first-principles study. Journal of Materials Science and Technology, 2018, 34, 620-626.	5.6	16

#	Article	IF	Citations
28124	Pressure effect of magnetic and electronic properties of Mn 2 PtGa Heusler alloy. Physics Letters, Section A: General, Atomic and Solid State Physics, 2018, 382, 224-230.	0.9	9
28125	Stress and strain effects on the electronic structure and optical properties of ScN monolayer. Physics Letters, Section A: General, Atomic and Solid State Physics, 2018, 382, 339-345.	0.9	22
28126	Origin of enhanced BrÃ¸nsted acidity of NiF-modified synthetic micaâ€“montmorillonite clay. Catalysis Science and Technology, 2018, 8, 244-251.	2.1	8
28127	Confined Li ion migration in the silicon-graphene complex system: An ab initio investigation. Applied Surface Science, 2018, 436, 505-510.	3.1	14
28128	Jacobâ€™s Ladder as Sketched by Escher: Assessing the Performance of Broadly Used Density Functionals on Transition Metal Surface Properties. Journal of Chemical Theory and Computation, 2018, 14, 395-403.	2.3	60
28129	Adsorption and Desulfurization Mechanism of Thiophene on Layered FeS(001), (011), and (111) Surfaces: A Dispersion-Corrected Density Functional Theory Study. Journal of Physical Chemistry C, 2018, 122, 359-370.	1.5	24
28130	Co-doped phosphorene: Enhanced sensitivity of CO gas sensing. International Journal of Modern Physics B, 2018, 32, 1850068.	1.0	10
28131	Mapping the relationship among composition, stacking fault energy and ductility in Nb alloys: A first-principles study. Acta Materialia, 2018, 144, 853-861.	3.8	32
28132	The role of Ga in the acetylene adsorption on PdGa intermetallic. Applied Surface Science, 2018, 435, 568-573.	3.1	13
28133	Influence of nearest neighbor atoms and coordination polyhedron on atomic volume of sigma phases. Computational Materials Science, 2018, 143, 308-315.	1.4	3
28134	Experimental and theoretical study to explain the morphology of CaMoO 4 crystals. Journal of Physics and Chemistry of Solids, 2018, 114, 141-152.	1.9	42
28135	Investigation on AlP as the heterogeneous nucleus of Mg2Si in Alâ€“Mg2Si alloys by experimental observation and first-principles calculation. Results in Physics, 2018, 8, 146-152.	2.0	16
28136	Tin chemical shift anisotropy in tin dioxide: On ambiguity of CSA asymmetry derived from MAS spectra. Solid State Nuclear Magnetic Resonance, 2018, 89, 1-10.	1.5	3
28137	Elucidating the Crystal Structure of dl-Arginine by Combined Powder X-ray Diffraction Data Analysis and Periodic DFT-D Calculations. Crystal Growth and Design, 2018, 18, 42-46.	1.4	11
28138	The Doping Effect on Ferromagnetic Arrangement and Electronic Structure of Cubic AlAs with Low Concentration of 3d (V, Cr, and Mn) Impurities. Journal of Superconductivity and Novel Magnetism, 2018, 31, 2157-2163.	0.8	4
28139	Elastic, Optoelectronic and Thermoelectric Properties of the Lead-Free Halide Semiconductors Cs2AgBiX 6 (XÂ=ÂCl, Br): Ab Initio Investigation. Journal of Electronic Materials, 2018, 47, 1533-1545.	1.0	70
28140	Vibrational and reorientational dynamics and thermal properties in [Mg(H2O)4](ReO4)2 supported by periodic DFT study. Vibrational Spectroscopy, 2018, 94, 49-60.	1.2	5
28141	Oxygen Reduction Reaction on Ag(111) in Alkaline Solution: A Combined Density Functional Theory and Kinetic Monte Carlo Study. ChemCatChem, 2018, 10, 540-549.	1.8	18

#	Article	IF	Citations
28142	Influence of H 2 O and H 2 S on the composition, activity, and stability of sulfided Mo, CoMo, and NiMo supported on MgAl 2 O 4 for hydrodeoxygenation of ethylene glycol. Applied Catalysis A: General, 2018, 551, 106-121.	2.2	31
28143	Chlorinated paraffins wrapping of carbon nanotubes: A theoretical investigation. Applied Surface Science, 2018, 436, 277-282.	3.1	3
28144	Classical and quantum calculations of the temperature dependence of the free energy of argon. Computational Materials Science, 2018, 144, 36-41.	1.4	5
28145	Stability and electronic structure of two-dimensional arsenic phosphide monolayer. Materials Science and Engineering B: Solid-State Materials for Advanced Technology, 2018, 228, 206-212.	1.7	21
28146	Adsorption of H₂, O₂, H₂O, OH and H on monolayer MoS₂. Journal of Physics Condensed Matter, 2018, 30, 035003.	0.7	27
28147	Novel Theoretical Prediction of Structural Properties, Ferromagnetic Ordering, and Electronic Structure of Fe2PbC MAX Phase. Journal of Superconductivity and Novel Magnetism, 2018, 31, 2485-2490.	0.8	6
28148	Bandgap engineering and charge separation in two-dimensional GaS-based van der Waals heterostructures for photocatalytic water splitting. Applied Surface Science, 2018, 439, 374-379.	3.1	36
28149	Effects of Co for Mn substitution on the electronic properties of Mn2-xCoxVAl as probed by XPS. Intermetallics, 2018, 93, 155-161.	1.8	15
28150	Multiscale simulations of ligand adsorption and exchange on gold nanoparticles. Physical Chemistry Chemical Physics, 2018, 20, 1381-1394.	1.3	25
28151	A comparative DFT study on the dehydrogenation of methanol on Rh(100) and Rh(110). Applied Surface Science, 2018, 436, 268-276.	3.1	16
28152	Electronic structure, charge transfer, and intrinsic luminescence of gadolinium oxide nanoparticles: Experiment and theory. Applied Surface Science, 2018, 436, 697-707.	3.1	63
28153	A DFT study of the electronic structures and optical properties of (Cr, C) co-doped rutile TiO2. Chemical Physics, 2018, 501, 60-67.	0.9	17
28154	Discovering chemical site occupancy- modulus correlations in Ni based intermetallics via statistical learning methods. Computational Condensed Matter, 2018, 14, 8-14.	0.9	3
28155	A DFT study of the stability of SIAs and small SIA clusters in the vicinity of solute atoms in Fe. Journal of Nuclear Materials, 2018, 500, 92-109.	1.3	24
28156	Chemical Pressure Maps of Molecules and Materials: Merging the Visual and Physical in Bonding Analysis. Journal of Chemical Theory and Computation, 2018, 14, 104-114.	2.3	20
28157	Superior non-enzymatic glucose sensing properties of Ag-/Au-NiCo₂O₄ nanosheets with insight from electronic structure simulations. Analyst, The, 2018, 143, 571-579.	1.7	35
28158	Analytical modelling and simulation of gas adsorption effects on graphene nanoribbon electrical properties. Molecular Simulation, 2018, 44, 551-557.	0.9	8
28159	Density Functional Theory Study of the Formaldehyde Catalytic Oxidation Mechanism on a Au-Doped CeO2(111) Surface. Journal of Physical Chemistry C, 2018, 122, 438-448.	1.5	22

#	Article	IF	Citations
28160	Formation of Ag nanoparticles under electron beam irradiation: Atomistic origins from firstâ€principles calculations. International Journal of Quantum Chemistry, 2018, 118, e25551.	1.0	21
28161	Atomic and electronic structures of stable linear carbon chains on Ag-nanoparticles. Carbon, 2018, 128, 296-301.	5.4	32
28162	Nonmetal doping induced electronic and magnetic properties in MoSe2 monolayer. Chemical Physics Letters, 2018, 692, 69-74.	1.2	12
28163	In situ surface stress measurement and computational analysis examining the oxygen reduction reaction on Pt and Pd. Electrochimica Acta, 2018, 260, 400-406.	2.6	14
28164	First-principles investigation on stability and diffusion mechanism of helium impurities in 4H-SiC. Journal of Nuclear Materials, 2018, 499, 168-174.	1.3	6
28165	Impact of Coinage Metal Insertion on the Thermoelectric Properties of GeTe Solid-State Solutions. Journal of Physical Chemistry C, 2018, 122, 227-235.	1.5	49
28166	Phase-Dependent Formation of Coherent Interface Structure between PtO₂ and TiO₂ and Its Impact on Thermal Decomposition Behavior. Journal of Physical Chemistry C, 2018, 122, 662-669.	1.5	21
28167	Solid Synthesis of Ultrathin Palladium and Its Alloysâ€™ Nanosheets on RGO with High Catalytic Activity for Oxygen Reduction Reaction. ACS Catalysis, 2018, 8, 910-919.	5.5	56
28168	Achieving High Thermoelectric Figure of Merit in Polycrystalline SnSe via Introducing Sn Vacancies. Journal of the American Chemical Society, 2018, 140, 499-505.	6.6	180
28169	Ultralow and anisotropic thermal conductivity in semiconductor As₂Se₃. Physical Chemistry Chemical Physics, 2018, 20, 1809-1816.	1.3	16
28170	Graphene-induced band gap renormalization in polythiophene: a many-body perturbation study. Journal of Physics Condensed Matter, 2018, 30, 035002.	0.7	2
28171	Structural Phase Transition, Electronic, and Mechanical Properties of Beryllium Oxide: Temperature and Pressureâ€Induced Effects. Physica Status Solidi (B): Basic Research, 2018, 255, 1700524.	0.7	2
28172	First-Principles Calculations of van der Waals and Spin Orbit Effects on the Two-Dimensional Topological Insulator Stanene and Stanene on Ge(111) Substrate. Journal of Superconductivity and Novel Magnetism, 2018, 31, 2579-2588.	0.8	10
28173	Electronic, Mechanical and Thermodynamic Properties of Ceramic Compounds. Iranian Journal of Science and Technology, Transaction A: Science, 2018, 42, 2355-2363.	0.7	6
28174	CALPHAD modeling and ab initio calculations of the Np-U-Zr system. Computational Materials Science, 2018, 143, 505-514.	1.4	6
28175	Oxygen diffusion and migration in clean and defective uranium nitride UN (0â€¯0â€¯1) surfaces. Computational Materials Science, 2018, 144, 56-63.	1.4	2
28176	Surface modification of reconstruction by evolution process of the B/P_C dimer on diamond (001) surface. Journal of Alloys and Compounds, 2018, 737, 456-463.	2.8	3
28177	Cocrystals Help Break the â€œRulesâ€•of Isostructurality: Solid Solutions and Polymorphism in the Malic/Tartaric Acid System. Crystal Growth and Design, 2018, 18, 855-863.	1.4	27

#	Article	IF	Citations
28178	Labile Low-Valent Tin Azides: Syntheses, Structural Characterization, and Thermal Properties. Inorganic Chemistry, 2018, 57, 400-411.	1.9	6
28179	Diffusion Kinetics of Gold and Copper Atoms on Pristine and Reduced Rutile TiO₂ (110) Surfaces. Journal of Physical Chemistry C, 2018, 122, 3824-3837.	1.5	12
28180	Controllable dissociation of H₂O on a CeO₂(111) surface. Physical Chemistry Chemical Physics, 2018, 20, 1575-1582.	1.3	10
28181	Pressure-induced structural phase transition in transition metal carbides TMC (TM = Ru, Rh, Pd, Os, Ir,) Tj ETQq1 1 0.784314 rgBT /Ov	0.7	4
28182	Theoretical Analysis of the Electrical and Optical Properties of ZnS. Lecture Notes in Electrical Engineering, 2018, , 9-19.	0.3	5
28183	Highly efficient catalytic scavenging of oxygen free radicals with graphene-encapsulated metal nanoshields. Nano Research, 2018, 11, 2821-2835.	5.8	31
28184	Design lateral heterostructure of monolayer ZrS2 and HfS2 from first principles calculations. Applied Surface Science, 2018, 436, 919-926.	3.1	33
28185	Studies of O18 impurity trapping at interstitial dislocation loops in ion implanted Fe (1â€¯1â€¯0) by ion channeling and ab initio calculations. Nuclear Instruments & Methods in Physics Research B, 2018, 414, 141-145.	0.6	1
28186	Origin of n-type conductivity in two-dimensional InSe: In atoms from surface adsorption and van der Waals gap. Physica E: Low-Dimensional Systems and Nanostructures, 2018, 98, 66-73.	1.3	8
28187	Characterization of the B-Center Defect in Diamond through the Vibrational Spectrum: A Quantum-Mechanical Approach. Journal of Physical Chemistry A, 2018, 122, 594-600.	1.1	23
28188	Electronâ€“Hole-Pair-Induced Vibrational Energy Relaxation of Rhenium Catalysts on Gold Surfaces. Journal of Physical Chemistry Letters, 2018, 9, 406-412.	2.1	22
28189	Understanding All-Solid Frustrated-Lewis-Pair Sites on CeO₂ from Theoretical Perspectives. ACS Catalysis, 2018, 8, 546-554.	5.5	135
28190	First-principles studies on the electronic and optical properties of Fe-doped potassium dihydrogen phosphate crystal. Computational Materials Science, 2018, 143, 398-402.	1.4	16
28191	Atomistic simulation of cubic and tetragonal phases of U-Mo alloy: Structure and thermodynamic properties. Journal of Nuclear Materials, 2018, 499, 451-463.	1.3	47
28192	Surface alloy formation by adsorption of holmium on Ag/Mo(112) bimetallic surfaces. Surface Science, 2018, 669, 57-63.	0.8	2
28193	Comparative study on dynamical stability against strain of pristine and chemically functionalized monolayer honeycomb materials. Journal of Materials Science, 2018, 53, 4306-4315.	1.7	6
28194	The Electronic Structures and Ferromagnetism of Cu-Doped ZnO: the First-Principle Calculation Study. Journal of Superconductivity and Novel Magnetism, 2018, 31, 2103-2110.	0.8	7
28195	First-principles study of adsorption-induced magnetic properties of InSe monolayers. Applied Surface Science, 2018, 436, 419-423.	3.1	13

#	Article	IF	Citations
28196	First principles investigation on pressure induced phase transition and photocatalytic properties in RbPbCl3. Computational Materials Science, 2018, 143, 403-410.	1.4	11
28197	Tight binding parametrization of few-layer black phosphorus from first-principles calculations. Computational Materials Science, 2018, 143, 411-417.	1.4	12
28198	First-principles studies of K1â^'xMxMgH3 (MÂ=ÂLi, Na, Rb, or Cs) perovskite hydrides for hydrogen storage. International Journal of Hydrogen Energy, 2018, 43, 2232-2236.	3.8	24
28199	Solute â€“ ã€^111ã€‰ interstitial loop interaction in Î±-Fe: A DFT study. Journal of Nuclear Materials, 2018, 499, 582-594.	1.3	34
28200	Screening of rare-earth-lean intermetallic 1-11 and 1-11-X compounds of YNi9In2-type for hard-magnetic applications. Scripta Materialia, 2018, 154, 295-299.	2.6	14
28201	First principle study of structural, elastic and electronic properties of APt3 (A=Mg, Sc, Y and Zr). Philosophical Magazine, 2018, 98, 408-421.	0.7	5
28202	Physical properties of molybdenum monoboride: Ab-initio study. Philosophical Magazine, 2018, 98, 422-436.	0.7	7
28203	Weakly spin-dependent band structures of antiferromagnetic perovskite LaMO₃(Mâ€‰â€‰=â€‰â€‰Cr, Mn) Tj ETQq1	0.7	10
28204	The structural, electronic, magnetic, and mechanical properties of perovskite oxides PbM1/2Nb1/2O₃(M = Fe, Co and Ni). International Journal of Modern Physics B, 2018, 32, 1850057.	1.0	6
28205	Mapping deformation mechanisms in lamellar titanium aluminide. Acta Materialia, 2018, 144, 835-843.	3.8	27
28206	The mixing effect of organic cations on the structural, electronic and optical properties of FA_xMA_{1â^'x}PbI₃perovskites. Physical Chemistry Chemical Physics, 2018, 20, 941-950.	1.3	24
28207	First-Principles Study of Structural, Electronic, Optical, and Thermal Properties of BeSiSb2 and MgSiSb2. Journal of Electronic Materials, 2018, 47, 1904-1915.	1.0	2
28208	Theoretical prediction of novel two-dimensional planar aluminum nitride allotropes: first principles calculations. Indian Journal of Physics, 2018, 92, 343-348.	0.9	2
28209	Alloyed palladium-nickel hollow nanospheres with interatomic charge polarization for improved hydrolytic dehydrogenation of ammonia borane. International Journal of Hydrogen Energy, 2018, 43, 283-292.	3.8	30
28210	Analysis of the conformational properties of amine ligands at the gold/water interface with QM, MM and QM/MM simulations. Physical Chemistry Chemical Physics, 2018, 20, 3349-3362.	1.3	15
28211	Recovery Mechanism of Degraded Black Phosphorus Fieldâ€Effect Transistors by 1,2â€Ethanedithiol Chemistry and Extended Device Stability. Small, 2018, 14, 1703194.	5.2	23
28212	Oxidization of Al0.5Ga0.5As(001) surface: The electronic properties. Applied Surface Science, 2018, 436, 460-466.	3.1	7
28213	Strengthening effects of alloying elements W and Re on Ni3Al: A first-principles study. Computational Materials Science, 2018, 144, 23-31.	1.4	27

#	Article	IF	Citations
28214	First-principles mechanistic study of ring hydrogenation and deoxygenation reactions of eugenol over Ru(0001) catalysts. Journal of Catalysis, 2018, 358, 8-18.	3.1	37
28215	Magnetic states of Ni2MnZ and Ni2CrZ (Zâ€¯=â€¯Al, As, Bi, Ga, Ge, In, P, Pb, Sb, Si, Sn, Tl) Heusler alloys. Journal of Magnetism and Magnetic Materials, 2018, 459, 78-83.	1.0	11
28216	Alignment of Redox Levels at Semiconductorâ€“Water Interfaces. Chemistry of Materials, 2018, 30, 94-111.	3.2	74
28217	Novel Flexible Transparent Conductive Films with Enhanced Chemical and Electromechanical Sustainability: TiO₂ Nanosheetâ€“Ag Nanowire Hybrid. ACS Applied Materials & Interfaces, 2018, 10, 2688-2700.	4.0	44
28218	Passivation of Hydrated Cement. ACS Sustainable Chemistry and Engineering, 2018, 6, 727-737.	3.2	12
28219	Electronic and magnetic properties of monolayer Î±-RuCl₃: a first-principles and Monte Carlo study. Physical Chemistry Chemical Physics, 2018, 20, 997-1004.	1.3	57
28220	Stabilizing benzene-like planar N₆rings to form a single atomic honeycomb BeN₃sheet with high carrier mobility. Nanoscale, 2018, 10, 949-957.	2.8	18
28221	Nonplanar core structure of the screw dislocations in tantalum from the improved Peierlsâ€“Nabarro theory. Philosophical Magazine, 2018, 98, 484-516.	0.7	17
28222	Effect of alloying elements on stacking fault energy and ductility of tungsten. Journal of Alloys and Compounds, 2018, 737, 372-376.	2.8	42
28223	Fe X (Xâ€¯=â€¯B, N) binary compounds: First-principles calculations of electronic structures, theoretic hardness and magnetic properties. Journal of Magnetism and Magnetic Materials, 2018, 451, 761-769.	1.0	12
28224	Grain boundaries in bcc-Fe: a density-functional theory and tight-binding study. Modelling and Simulation in Materials Science and Engineering, 2018, 26, 025008.	0.8	37
28225	Direct observation of thermal disorder and decomposition of black phosphorus. Nanotechnology, 2018, 29, 065702.	1.3	4
28226	Onion-like carbon as dopant/modification-free electrocatalyst for [VO]2+/[VO2]+ redox reaction: Performance-control mechanism. Carbon, 2018, 127, 31-40.	5.4	11
28227	Helium behavior in oxide dispersion strengthened (ODS) steel: Insights from ab initio modeling. Journal of Nuclear Materials, 2018, 499, 71-78.	1.3	10
28228	Structural and electronic properties of MnSi under high pressure: A first-principles calculation. Computational Materials Science, 2018, 142, 285-289.	1.4	7
28229	First principles band gap engineering of [1â€¯1â€¯0] oriented 3C-SiC nanowires. Computational Materials Science, 2018, 142, 268-276.	1.4	12
28230	Water adsorption on the stoichiometric and defected Fe(110) surfaces. Surface Science, 2018, 668, 144-149.	0.8	15
28231	Electronic and Topological Analysis for New Phases of Chromium Nitride. Physica Status Solidi (A) Applications and Materials Science, 2018, 215, 1700576.	0.8	2

#	Article	IF	Citations
28232	Breathing bands due to molecular order in CH3NH3PbI3. Computational Materials Science, 2018, 142, 361-371.	1.4	14
28233	Room-temperature ferromagnetism in alkaline-earth-metal doped AlP: First-principle calculations. Computational Materials Science, 2018, 142, 338-345.	1.4	9
28234	Enhanced activity of ethanol oxidation reaction on PtM (M=Au, Ag and Sn): The importance of oxophilicity and surface oxygen containing species. Electrochimica Acta, 2018, 259, 733-741.	2.6	21
28235	Charge and Discharge Processes and Sodium Storage in Disodium Pyridineâ€2,5â€Dicarboxylate Anodeâ€"Insights from Experiments and Theory. Advanced Energy Materials, 2018, 8, 1701572.	10.2	40
28236	Adsorption of DNA/RNA nucleobases onto single-layer MoS2 and Li-Doped MoS2: A dispersion-corrected DFT study. Applied Surface Science, 2018, 434, 176-187.	3.1	34
28237	Energetics of silica lithiation and its applications to lithium ion batteries. Electrochimica Acta, 2018, 259, 1053-1058.	2.6	40
28238	Experimental and theoretical study of hydrogen desorption process from Mn(BH4)2. Journal of Alloys and Compounds, 2018, 735, 277-284.	2.8	6
28239	The spin-dependent transport and optoelectronic properties of the 6,6,12-graphyne-based magnetic tunnel junction devices. Organic Electronics, 2018, 53, 1-13.	1.4	5
28240	Electronic and magnetic properties of zigzag GaN nanoribbons with hydrogenation and fluorination. Physica E: Low-Dimensional Systems and Nanostructures, 2018, 97, 144-150.	1.3	11
28241	Nuclear quantum effects induce metallization of dense solid molecular hydrogen. Journal of Computational Chemistry, 2018, 39, 262-268.	1.5	16
28242	Adsorption of water, sulfates and chloride on arsenopyrite surface. Applied Surface Science, 2018, 434, 389-399.	3.1	20
28243	Energetics of defects formation and oxygen migration in pyrochlore compounds from first principles calculations. Journal of Nuclear Materials, 2018, 505, 255-261.	1.3	23
28244	Optimum Cu nanoparticle catalysts for CO2 hydrogenation towards methanol. Nano Energy, 2018, 43, 200-209.	8.2	133
28245	STRUCTURAL AND ELECTRONIC PROPERTIES OF Pd AND Au MONOLAYERS ADSORBED ON MoS₂: A COMPARATIVE STUDY FROM DFT CALCULATIONS. Surface Review and Letters, 2018, 25, 1850117.	0.5	0
28246	A stepwise thermodynamic modeling of the phase diagram for the Cuâ€"Be system. Journal of Materials Science, 2018, 53, 3756-3766.	1.7	7
28247	Theoretical prediction of borophene monolayer as anode materials for high-performance lithium-ion batteries. Ionics, 2018, 24, 1603-1615.	1.2	28
28248	High-performance MoS2-based nanocomposite anode prepared by high-energy mechanical milling: The effect of carbonaceous matrix on MoS2. Electrochimica Acta, 2018, 260, 129-138.	2.6	31
28249	Influencing factors of atomic order in the binary sigma phase. Intermetallics, 2018, 93, 6-19.	1.8	8

#	Article	IF	Citations
28250	Reduction, sintering and mechanical properties of rhenium-tungsten compounds. Journal of Alloys and Compounds, 2018, 735, 2685-2693.	2.8	24
28251	Oxygen-Driven Surface Evolution of Nanoporous Gold: Insights from Ab Initio Molecular Dynamics and Auger Electron Spectroscopy. Journal of Physical Chemistry C, 2018, 122, 5349-5357.	1.5	25
28252	Unconventional thermal transport enhancement with large atom mass: a comparative study of 2D transition dichalcogenides. 2D Materials, 2018, 5, 015022.	2.0	12
28253	Metal adsorption on monolayer blue phosphorene: A first principles study. Physics Letters, Section A: General, Atomic and Solid State Physics, 2018, 382, 205-209.	0.9	20
28254	The electronic structure of two-dimensional transition metal hydroxide monolayers and heterostructures. Solid State Ionics, 2018, 314, 149-155.	1.3	6
28255	On the stability and mobility of di-vacancies in tungsten. Nuclear Fusion, 2018, 58, 026004.	1.6	27
28256	Optical Properties of Free and Si(001)â€Adsorbed Pyrimidinic Nucleobases. Physica Status Solidi (B): Basic Research, 2018, 255, 1700497.	0.7	4
28257	Enhanced O2 reduction on atomically thin Pt-based nanoshells by integrating surface facet, interfacial electronic, and substrate stabilization effects. Nano Research, 2018, 11, 3313-3326.	5.8	21
28258	High-performance sub-10-nm monolayer black phosphorene tunneling transistors. Nano Research, 2018, 11, 2658-2668.	5.8	47
28259	Non-uniformly functionalized titanium carbide-based MXenes as an anchoring material for Li-S batteries: A first-principles calculation. Applied Surface Science, 2018, 435, 210-215.	3.1	51
28260	Optimal sample formulations for DNP SENS: The importance of radical-surface interactions. Current Opinion in Colloid and Interface Science, 2018, 33, 9-18.	3.4	42
28261	Structural, electronic, magnetic and optical properties of semiconductor Zn 1â^'x Mo x Te compound. Journal of Physics and Chemistry of Solids, 2018, 114, 240-245.	1.9	17
28262	A method to explore the quantitative interactions between metal and ceria for M/CeO2 catalysts. Surface Science, 2018, 669, 79-86.	0.8	7
28263	Mechanistic Insights into Solution-Phase Oxidative Esterification of Primary Alcohols on Pd(111) from First-Principles Microkinetic Modeling. ACS Catalysis, 2018, 8, 272-282.	5.5	8
28264	La₂CoO₄: a new intercalation based cathode material for fluoride ion batteries with improved cycling stability. Journal of Materials Chemistry A, 2018, 6, 4658-4669.	5.2	73
28265	Pressure-Dependent Electronic and Transport Properties of Bulk Platinum Oxide by Density Functional Theory. Journal of Electronic Materials, 2018, 47, 1293-1301.	1.0	2
28266	Nonlinear Optical Crystal Rb₄Sn₃Cl₂Br₈: Synthesis, Structure, and Characterization. Crystal Growth and Design, 2018, 18, 380-385.	1.4	22
28267	Elastic, electronic structure, and optical properties of orthorhombic Na3AlF6: a first-principles study. Ionics, 2018, 24, 1377-1383.	1.2	9

#	Article	IF	Citations
28268	Selectivity tuning over monometallic and bimetallic dehydrogenation catalysts: effects of support and particle size. Catalysis Science and Technology, 2018, 8, 314-327.	2.1	23
28269	First-Principles Calculations of Acoustic and Anharmonic Properties of Ferromagnetic Cu2MnZ (Z =) Tj ETQq1 1 0.784314 rgBT /Overlo	0.8	5
28270	Lattice dynamics and thermomechanical properties of zirconium(IV) chloride: Evidence for low-temperature negative thermal expansion. Chemical Physics Letters, 2018, 691, 98-102.	1.2	5
28271	Adsorption and charge transfer of lithium at electrified graphene/electrolyte interface. Electrochimica Acta, 2018, 259, 1089-1094.	2.6	2
28272	Exploring thermoelectric materials for renewable energy applications: The case of highly mismatched alloys based on AlBi1-xSbx and InBi1-xSbx. Intermetallics, 2018, 93, 235-243.	1.8	41
28273	First principles investigation of the electronic properties of graphitic carbon nitride with different building block and sheet staggered arrangement. Journal of Alloys and Compounds, 2018, 735, 131-139.	2.8	40
28274	Structural Insights from ⁵⁹Co Solidâ€State NMR Experiments on Organocobalt(I) Catalysts. ChemPhysChem, 2018, 19, 227-236.	1.0	8
28275	Insight into the effect of promoter Co on C2 oxygenate formation from syngas on CoCu(100) and Cu(100): A comparative DFT study. Applied Surface Science, 2018, 434, 28-39.	3.1	11
28276	Density functional study of the thermodynamic properties and phase diagram of the magnesium hydride. Calphad: Computer Coupling of Phase Diagrams and Thermochemistry, 2018, 60, 7-15.	0.7	4
28277	Adsorption mechanism of H2O molecule on the Li4SiO4 (0â€¯1â€¯0) surface from first principles. Chemical Physics Letters, 2018, 691, 1-7.	1.2	17
28278	Easily removable visible-light-driven photocatalyst of nickel modified SnS2 nanosheets for reduction of Cr(VI). Journal of Alloys and Compounds, 2018, 735, 1314-1318.	2.8	19
28279	Tunable thermal properties in yttrium silicates switched by anharmonicity of low-frequency phonons. Journal of the European Ceramic Society, 2018, 38, 2043-2052.	2.8	16
28280	Enhanced scintillation of Ba3In(B3O6)3 based on nitrogen doping. Journal of Solid State Chemistry, 2018, 258, 351-357.	1.4	9
28281	Tuning electronic and magnetic properties of V-, Cr-, and Mn-doped PbS via strain engineering: A first-principles proposal. Materials Science and Engineering B: Solid-State Materials for Advanced Technology, 2018, 228, 1-6.	1.7	12
28282	A reinvestigation of a superhard phase Cm-carbon. Computational Materials Science, 2018, 143, 32-42.	1.4	18
28283	Lithium halide monolayer sheets: First-principles many-body calculations. Computational Materials Science, 2018, 143, 103-111.	1.4	26
28284	Dehydrogenation properties of LiBH4 modified by Mg from first-principles calculations. Journal of Alloys and Compounds, 2018, 735, 668-676.	2.8	17
28285	PtPd(111) Surface versus PtAu(111) Surface: Which One Is More Active for Methanol Oxidation?. ACS Catalysis, 2018, 8, 132-143.	5.5	56

#	Article	IF	Citations
28286	High valence Mo-doped Na₃V₂(PO₄)₃/C as a high rate and stable cycle-life cathode for sodium battery. Journal of Materials Chemistry A, 2018, 6, 1390-1396.	5.2	129
28287	Robust electronic and mechanical properties to layer number in 2D wide-gap X(OH)₂ (Xâ€‰â€‰=â€‰â€‰Mg, Ca). Journal Physics D: Applied Physics, 2018, 51, 015107.	1.3	7
28288	Reversible Polymerization of Adamantaneâ€type [P₄N₁₀]^{10â^'} Anions to Honeycombâ€type [P₂N₅]^{5â^'} Layers under Highâ€Pressure. Chemistry - A European Journal, 2018, 24, 736-742.	1.7	13
28289	Impact of Co and Fe Doping on the Martensitic Transformation and the Magnetic Properties in Niâ€Mnâ€Based Heusler Alloys. Physica Status Solidi (B): Basic Research, 2018, 255, 1700455.	0.7	14
28290	Electronic structure of octagonal boron nitride nanotubes. International Journal of Quantum Chemistry, 2018, 118, e25542.	1.0	1
28291	Point defects at the <mml:math xmlns:mml="http://www.w3.org/1998/Math/MathML" altimg="si1.gif" overflow="scroll"><mml:mrow><mml:mtext>Î£</mml:mtext><mml:mn>5</mml:mn></mml:mrow></mml:math>(012)[100] grain boundary in TiN and the early stages of Cu diffusion: An ab initio study. Acta Materialia, 2018, 144, 496-504.	3.8	20
28292	Enhanced visible-light photocatalytic activity of Bi2MoO6 nanoplates with heterogeneous Bi2MoO6-x@Bi2MoO6 core-shell structure. Applied Catalysis B: Environmental, 2018, 224, 692-704.	10.8	116
28293	Computational thermodynamic and first-principles calculation of stacking fault energy on ternary Co-based alloys. Computational Materials Science, 2018, 143, 112-117.	1.4	31
28294	Revealing the multi hydrogen bonding state within iron doped amorphous carbon. Chemical Physics Letters, 2018, 691, 122-125.	1.2	1
28295	A hybrid functional study of native point defects in Cu₂SnS₃: implications for reducing carrier recombination. Physical Chemistry Chemical Physics, 2018, 20, 256-261.	1.3	12
28296	Mechanical Properties of Ti2AlNb and Ti2AlZr Intermetallics: A First Principles Study. , 2018, , 269-275.		0
28297	Elastic, electronic and optical properties of the two-dimensional PtX2 (Xâ€‰=â€‰S, Se, and Te) monolayer. Applied Surface Science, 2018, 435, 476-482.	3.1	89
28298	Carbon segregation at Î£3 {1â€¯1â€¯2} grain boundaries in silicon. Computational Materials Science, 2018, 143, 80-86.	1.4	13
28299	Tuning the electronic and optical properties of XP(Xâ€¯=â€¯Al,Ga) monolayer semiconductors using biaxial strain effect: Modified Becke-Johnson calculations. Chemical Physics Letters, 2018, 691, 181-189.	1.2	18
28300	Ethanol synthesis from syngas over Cu(Pd)-doped Fe(100): a systematic theoretical investigation. Physical Chemistry Chemical Physics, 2018, 20, 2492-2507.	1.3	21
28301	Magnetic, Mechanical, and Electronic Properties of RhH x (x = 0, 0.25, 0.75, 1) from First-Principles Calculations. Journal of Superconductivity and Novel Magnetism, 2018, 31, 799-803.	0.8	1
28302	Scaling behavior of the Compton profile of alkali metals. Physica A: Statistical Mechanics and Its Applications, 2018, 489, 18-27.	1.2	6
28303	Adsorption of Prototypical Asphaltenes on Silica: First-Principles DFT Simulations Including Dispersion Corrections. Journal of Physical Chemistry B, 2018, 122, 618-624.	1.2	21

#	Article	IF	Citations
28304	Structural and elastic properties of AIBIIIC 2 VI semiconductors. Indian Journal of Physics, 2018, 92, 29-35.	0.9	15
28305	Integrated investigation of the Li4Ti5O12 phase stability. Ionics, 2018, 24, 707-713.	1.2	9
28306	Emission and evaporation properties of 75 at.% Re-25 at.% W mixed matrix impregnated cathode. Applied Surface Science, 2018, 427, 874-882.	3.1	20
28307	Effect of carbon on behavior of helium in vanadium: A first-principles investigation. International Journal of Modern Physics B, 2018, 32, 1750269.	1.0	0
28308	Early days of quantum crystallography: A personal account. Journal of Computational Chemistry, 2018, 39, 1029-1037.	1.5	28
28309	Electronic properties of B and Al doped graphane : A hybrid density functional study. Physica B: Condensed Matter, 2018, 535, 287-292.	1.3	4
28310	Combined plane wave and localized orbital electronic structure calculation: Adsorption energy of hydrogen on Pd(111). International Journal of Quantum Chemistry, 2018, 118, e25452.	1.0	5
28311	Optimisation of stability and charge transferability of ferrocene-encapsulated carbon nanotubes. Molecular Physics, 2018, 116, 9-18.	0.8	4
28312	Microkinetic modeling of H2SO4 formation on Pt based diesel oxidation catalysts. Applied Catalysis B: Environmental, 2018, 220, 348-355.	10.8	4
28313	Computational study of binary titanium-based potential shape memory alloys. IOP Conference Series: Materials Science and Engineering, 2018, 430, 012020.	0.3	0
28314	First-Principles Study of BCC/FCC Phase Transition Promoted by Interstitial Carbon in Iron. Materials Transactions, 2018, 59, 870-875.	0.4	16
28315	Optical properties of Ga-doped silicene and as-doped silicene: First principle calculations. AIP Conference Proceedings, 2018, , .	0.3	6
28316	Multiscale energy density algorithm and application to surface structure of Ni matrix of superalloy. Chinese Physics B, 2018, 27, 097105.	0.7	0
28317	Study of ultra-hard materials of the B-C-N-O quaternary system. Results in Physics, 2018, 11, 984-993.	2.0	3
28318	Ab initio simulations of superionic H2O, H2O2, and H9O4 compounds. AIP Conference Proceedings, 2018, , .	0.3	1
28319	First principles study of the influence of metallic-doping on crystalline ZnS: From efficiency aspects for use in a ZnS based dye sensitized solar cell (DSSC). Integrated Ferroelectrics, 2018, 194, 96-103.	0.3	1
28320	Computer Simulation of Plastic Deformation in Tial Alloys in the Presence of Chromium. Defect and Diffusion Forum, 2018, 386, 383-387.	0.4	1
28321	New high-pressure phases in MOOH (M = Al, Ga, In). American Mineralogist, 2018, 103, 1906-1917.	0.9	14

#	Article	IF	Citations
28322	Mechanical properties and stability of TiPt-M (M = Ru, Co, Cu, Zr and Hf) for high temperature applications. IOP Conference Series: Materials Science and Engineering, 2018, 430, 012019.	0.3	4
28323	Directional detection of light dark matter with polar materials. Physical Review D, 2018, 98, .	1.6	90
28324	Effect of P impurity on mechanical properties of NiAl Î£5 grain boundary: From perspectives of stress and energy. Chinese Physics B, 2018, 27, 037105.	0.7	1
28325	First-principles predictions of electronic structure change in plasma-damaged materials. Japanese Journal of Applied Physics, 2018, 57, 06JD04.	0.8	9
28326	Pt-doped single-walled CNT as a superior media for evaluating the operation status of insulation devices: A first-principle study. AIP Advances, 2018, 8, .	0.6	13
28327	Unintentionally doped hydrogen removal mechanism in Li doped ZnO. AIP Advances, 2018, 8, .	0.6	6
28328	Epitaxially strained SnTiO ₃ at finite temperatures. Chinese Physics B, 2018, 27, 127702.	0.7	5
28329	Stability of charges in titanium compounds and charge transfer to oxygen in titanium dioxide. Journal of Physics: Conference Series, 2018, 1136, 012017.	0.3	12
28330	Isoelectronic Sn-Ge substitution effect on electronic and thermoelectric properties of ZrNiSn compounds: a DFT Study. IOP Conference Series: Materials Science and Engineering, 2018, 360, 012061.	0.3	0
28331	Structure and Stability of Intermediate (Fe, Cr)₇C₃ Carbides. Solid State Phenomena, 0, 284, 634-639.	0.3	1
28332	Calculation of Youngâ€™s Modulus of MoS2-Based Single-Wall Nanotubes Using Force-Field and Hybrid Density Functional Theory. Physics of the Solid State, 2018, 60, 2551-2558.	0.2	4
28333	Effect of Impurities on the Formation Energy of Point Defects in the Î³-TiAl Alloy. Journal of Experimental and Theoretical Physics, 2018, 127, 1046-1058.	0.2	13
28334	Strain Tunable Bandgap and High Carrier Mobility in SiAs and SiAs2 Monolayers from First-Principles Studies. Nanoscale Research Letters, 2018, 13, 404.	3.1	17
28335	A Universal Strategy for Constructing Seamless Graphdiyne on Metal Oxides to Stabilize the Electrochemical Structure and Interface. Advanced Materials, 2019, 31, e1806272.	11.1	59
28336	Electronic properties of boron doped single-layer graphene. AIP Conference Proceedings, 2018, , .	0.3	1
28337	BaTiO3 polar surface in ultrahigh vacuum calculated by local density functional theory with a large supercell. Ferroelectrics, 2018, 534, 183-189.	0.3	1
28338	Mechanical Properties of Y2Al Crystal. Moscow University Physics Bulletin (English Translation of) Tj ETQq0 0 0 rgBT /Overlock 10 Tf 50	0.1	2
28339	Electronic, mechanical, and optical properties of Ruddlesden-Popper perovskite sulfides: First principle calculation. Ferroelectrics, 2018, 535, 142-151.	0.3	2

#	Article	IF	Citations
28340	Modification of a Shockley-Type Surface State on Pt(111) upon Deposition of Gold Thin Layers. Materials, 2018, 11, 2569.	1.3	1
28341	Surface Strain Effects on the Adsorption of Au Adatoms on MgO(001) Surfaces with Surface O Vacancies. Journal of the Korean Physical Society, 2018, 73, 1324-1328.	0.3	0
28342	Ab-initio study on the electronic properties of perovskite structure-based ferroelectrics. Ferroelectrics, 2018, 535, 65-71.	0.3	3
28343	Simulation of electron energy loss spectra with the turboEELS and thermo_pw codes. Journal of Physics: Conference Series, 2018, 1136, 012008.	0.3	1
28344	A Computational Study of AlF3 and ACF Surfaces. Inorganics, 2018, 6, 124.	1.2	4
28345	Electronic, Thermal Expanding, and Optical Absorption Properties of Transition Metal Dichalcogenides: A First-principles Study. Journal Wuhan University of Technology, Materials Science Edition, 2018, 33, 1355-1359.	0.4	0
28346	NMR Crystallography of the Polymorphs of Metergoline. Crystals, 2018, 8, 378.	1.0	15
28347	Vibronic (pseudo Jahn-Teller) theory of ferroelectricity: Novel aspects and applications. Ferroelectrics, 2018, 536, 1-59.	0.3	18
28348	Adsorption Characteristics of Ge on 4H-SiC(0001) Surface: First-Principles Study. , 2018, , .		0
28349	A Deeper Insight on the Stability of Water-Induced Reconstruction of Anatase (001) Surface. Applied Sciences (Switzerland), 2018, 8, 2522.	1.3	2
28350	Multiscale Simulation of Precipitation in Copper-Alloyed Pipeline Steels and in Cu-Ni-Si Alloys. , 2018, , 1-41.		0
28351	First-principles evaluation of resistance contributions in Ruthenium interconnects for advanced technology nodes. , 2018, , .		1
28352	Ab Initio Study of the ZnSnSb2 Semiconductor. Semiconductors, 2018, 52, 1715-1720.	0.2	2
28353	Physical properties of ThCr₂Si₂-type Rh-based compounds ARh₂Ge₂(A = Ca, Sr, Y and Ba): DFT based first-principles investigation. International Journal of Modern Physics B, 2018, 32, 1850357.	1.0	15
28354	Precision and efficiency in solid-state pseudopotential calculations. Npj Computational Materials, 2018, 4, .	3.5	390
28355	Detecting decompositions of sulfur hexafluoride using Ge modified SWCNT: a theoretical evaluation. , 2018, , .		0
28356	Vacancy Induced Electron-Phonon Interaction of Single Layer Graphene. , 2018, , .		1
28357	Investigation of Carbon Interstitials in the Vicinity of the Si0₂/4H-SiC(0001) Interface. , 2018, , .		0

#	Article	IF	Citations
28358	Polymeric Nitrogen A7 Layers Stabilized in the Confinement of a Multilayer BN Matrix at Ambient Conditions. Scientific Reports, 2018, 8, 13758.	1.6	8
28359	Self-passivating (Re,Al)B2 coatings synthesized by magnetron sputtering. Scientific Reports, 2018, 8, 15570.	1.6	5
28360	Electronic structure and optical properties of novel monolayer gallium nitride and boron phosphide heterobilayers. Physical Chemistry Chemical Physics, 2018, 20, 28124-28134.	1.3	58
28361	Efficient green phosphor realized by Ce³⁺â†'Tb³⁺ energy transfer in Li₃Sc₂(PO₄)₃ for ultraviolet white light-emitting diodes. Physical Chemistry Chemical Physics, 2018, 20, 26995-27002.	1.3	36
28362	A molecular roundabout: triple cyclically arranged hydrogen bonds in light of experiment and theory. New Journal of Chemistry, 2018, 42, 19467-19477.	1.4	10
28363	Prediction of piezoelectric properties by first principles calculations and hydrothermal crystal growth of Si1â"xSnxO2 Î±-quartz phase. CrystEngComm, 2018, 20, 7479-7485.	1.3	1
28364	Spin density distributions on graphene clusters and ribbons with carbene-like active sites. Physical Chemistry Chemical Physics, 2018, 20, 26968-26978.	1.3	7
28365	Structural, vibrational and electronic properties of the superconductor Cu_xTiSe₂: theoretical and experimental insights. Physical Chemistry Chemical Physics, 2018, 20, 27011-27018.	1.3	10
28366	A density functional theory study of propylene epoxidation mechanism on Ag₂O(001) surface. Physical Chemistry Chemical Physics, 2018, 20, 26681-26687.	1.3	13
28367	A unique metallic phase of H₃S at high-pressure: sulfur in three different local environments. Physical Chemistry Chemical Physics, 2018, 20, 26344-26350.	1.3	8
28368	Edge morphology induced rectifier diode effect in C₃N nanoribbon. Physical Chemistry Chemical Physics, 2018, 20, 28759-28766.	1.3	7
28369	Atomistic Study of Acoustic Phonon Limited Mobility in Extremely Scaled Si and Ge Films. , 2018, , .		2
28370	Entropy Signatures of Topological Phase Transitions. Journal of Experimental and Theoretical Physics, 2018, 127, 958-983.	0.2	9
28371	Enhanced photothermal reduction of gaseous CO₂ over silicon photonic crystal supported ruthenium at ambient temperature. Energy and Environmental Science, 2018, 11, 3443-3451.	15.6	83
28372	Theoretical investigation of conversion between different C₂H_xspecies over Pdâ€"Ag/Pd(100) surface alloys: influence on the selectivity and transformation of carbonaceous species. New Journal of Chemistry, 2018, 42, 19827-19836.	1.4	4
28373	Significantly enhanced magnetoresistance in monolayer WTe2via heterojunction engineering: a first-principles study. Nanoscale, 2018, 10, 22231-22236.	2.8	11
28374	Discovery of a novel spin-polarized nodal ring in a two-dimensional HK lattice. Nanoscale, 2018, 10, 20748-20753.	2.8	54
28375	Effect of pressure on the structural, electronic and mechanical properties of ultraincompressible W₂B. RSC Advances, 2018, 8, 35664-35671.	1.7	9

#	Article	IF	Citations
28376	Structural and electronic properties of KY(BH₄)₄: DFT+U study. RSC Advances, 2018, 8, 34374-34379.	1.7	0
28377	Retention and diffusion of transmutation H and He atoms in Be₁₂Ti: first-principles calculations. RSC Advances, 2018, 8, 35735-35743.	1.7	12
28378	Simultaneous adsorption of SO₂ and CO₂ in an Ni(bdc)(ted)_{0.5} metalâ€“organic framework. RSC Advances, 2018, 8, 38648-38655.	1.7	10
28379	A facile synthesis methodology for preparation of Agâ€“Ni-reduced graphene oxide: a magnetically separable versatile nanocatalyst for multiple organic reactions and density functional study of its electronic structures. RSC Advances, 2018, 8, 37774-37788.	1.7	24
28380	Charge-induced electromechanical actuation of Mo- and W-dichalcogenide monolayers. RSC Advances, 2018, 8, 38667-38672.	1.7	16
28381	Enhanced visible light absorption performance of SnS₂and SnSe₂viasurface charge transfer doping. RSC Advances, 2018, 8, 40464-40470.	1.7	10
28382	Thickness-tunable coreâ€“shell Co@Pt nanoparticles encapsulated in sandwich-like carbon sheets as an enhanced electrocatalyst for the oxygen reduction reaction. Journal of Materials Chemistry A, 2018, 6, 21396-21403.	5.2	23
28383	Atomically manipulated proton transfer energizes water oxidation on silicon carbide photoanodes. Journal of Materials Chemistry A, 2018, 6, 24358-24366.	5.2	17
28384	First-principles characterization of two-dimensional (CH₃(CH₂)₃NH₃)₂(CH₃NH₃)_nâ^'1</s perovskite. Journal of Materials Chemistry A, 2018, 6, 24389-24396.	5.2	68
28385	Fabrication of a high performance ZnIn₂S₄/Si heterostructure photodetector array for weak signal detection. Journal of Materials Chemistry C, 2018, 6, 12928-12939.	2.7	25
28386	Ba₂M(C₃N₃O₃)₂ (M = Mg, Ca): potential UV birefringent materials with strengthened optical anisotropy originating from the (C₃N₃O₃)^{3â^'} group. Journal of Materials Chemistry C, 2018, 6, 12879-12887.	2.7	65
28387	Structure stabilization effect of configuration entropy in cubic WN. Physical Chemistry Chemical Physics, 2018, 20, 29243-29248.	1.3	3
28388	Atomistic determination of the surface structure of Cu₂O(111): experiment and theory. Physical Chemistry Chemical Physics, 2018, 20, 27456-27463.	1.3	33
28389	Transition from antiferromagnetic ground state to robust ferrimagnetic order with Curie temperatures above 420 K in manganese-based antiperovskite-type structures. Journal of Materials Chemistry C, 2018, 6, 13336-13344.	2.7	5
28390	Palladium catalyzed selective arylation of o-carboranes via B(4)â€“H activation: amide induced regioselectivity reversal. Chemical Communications, 2018, 54, 13603-13606.	2.2	53
28391	Ab initio investigation of O₂ adsorption on Ca-doped LaMnO₃ cathodes in solid oxide fuel cells. Physical Chemistry Chemical Physics, 2018, 20, 28685-28698.	1.3	9
28392	Tracking down the origin of peculiar vibrational spectra of aromatic self-assembled thiolate monolayers. Physical Chemistry Chemical Physics, 2018, 20, 29918-29930.	1.3	6
28393	The first stages of oxide growth at the low index Al surfaces (100), (110), (111): clusters and stripes vs. homogeneous growth. Physical Chemistry Chemical Physics, 2018, 20, 29549-29557.	1.3	7

#	Article	IF	Citations
28394	The crucial role of electron transfer from interfacial molecules in the negative potential shift of Au electrode immersed in ionic liquids. Physical Chemistry Chemical Physics, 2018, 20, 29362-29373.	1.3	4
28395	Determination of possible configurations for Li_{0.5}CoO₂delithiated Li-ion battery cathodesviaDFT calculations coupled with a multi-objective non-dominated sorting genetic algorithm (NSGA-III). Physical Chemistry Chemical Physics, 2018, 20, 26405-26413.	1.3	20
28396	Structural search for stable Mgâ€“Ca alloys accelerated with a neural network interatomic model. Physical Chemistry Chemical Physics, 2018, 20, 27545-27557.	1.3	19
28397	Phase transition and superconductivity in ReS2, ReSe2 and ReTe2. Physical Chemistry Chemical Physics, 2018, 20, 29472-29479.	1.3	15
28398	First-principle study of seven allotropes of arsenene and antimonene: thermodynamic, electronic and optical properties. Physical Chemistry Chemical Physics, 2018, 20, 30257-30266.	1.3	46
28399	First principles study on 2Hâ€“1Tâ€² transition in MoS₂ with copper. Physical Chemistry Chemical Physics, 2018, 20, 26986-26994.	1.3	39
28400	Dissociative chemisorption of hydrogen molecules on defective graphene-supported aluminium clusters: a computational study. Physical Chemistry Chemical Physics, 2018, 20, 26506-26512.	1.3	10
28401	Vibrationally induced metallisation of the energetic azide Î±-NaN₃. Physical Chemistry Chemical Physics, 2018, 20, 29061-29069.	1.3	21
28402	A comparative study of the structure, stability and energetic performance of 5,5â€²-bitetrazole-1,1â€²-diolate based energetic ionic salts: future high energy density materials. Physical Chemistry Chemical Physics, 2018, 20, 29693-29707.	1.3	34
28403	Enhanced CO catalytic oxidation over an Auâ€“Pt alloy supported on TiO₂ nanotubes: investigation of the hydroxyl and Au/Pt ratio influences. Catalysis Science and Technology, 2018, 8, 6109-6122.	2.1	25
28404	Mechanistic study of the ceria supported, re-catalyzed deoxydehydration of vicinal OH groups. Catalysis Science and Technology, 2018, 8, 5750-5762.	2.1	24
28405	Pyridinium lead tribromide and pyridinium lead triiodide: quasi-one-dimensional perovskites with an optically active aromatic Ï€-system. Dalton Transactions, 2018, 47, 16313-16319.	1.6	24
28406	Local environment of arsenic in sulfide minerals: insights from high-resolution X-ray spectroscopies, and first-principles calculations at the As K-edge. Journal of Analytical Atomic Spectrometry, 2018, 33, 2070-2082.	1.6	24
28407	Onset of vertical bonds in new GaN multilayers: beyond van der Waals solids. Nanoscale, 2018, 10, 21842-21850.	2.8	13
28408	3D to 2D reorganization of silverâ€“thiol nanostructures, triggered by solvent vapor annealing. Nanoscale, 2018, 10, 23018-23026.	2.8	3
28409	Transition metal attenuated mechanism for protective alumina formation from first principles. RSC Advances, 2018, 8, 41255-41269.	1.7	4
28410	Theoretical study on cation codoped SrTiO₃ photocatalysts for water splitting. Journal of Materials Chemistry A, 2018, 6, 24342-24349.	5.2	20
28411	Two-dimensional Î²-phase group-VA binary compounds for versatile electronic and optical properties. Journal of Materials Chemistry C, 2018, 6, 11694-11700.	2.7	28

#	Article	IF	Citations
28412	Bipolar magnetism in a two-dimensional NbS₂ semiconductor with high Curie temperature. Journal of Materials Chemistry C, 2018, 6, 11401-11406.	2.7	35
28413	Synthesis of a novel strontium-based wide-bandgap semiconductor via X-ray photochemistry under extreme conditions. Journal of Materials Chemistry C, 2018, 6, 12473-12478.	2.7	11
28414	Thermodynamic stability of doped FeAl-X (X = Pd, Ag, Pt and Ru) systems. IOP Conference Series: Materials Science and Engineering, 2018, 430, 012018.	0.3	0
28415	Ab-Initio Modeling of Lubricant Reactions with a Metal Al (111) Surface. , 2018, , .		0
28416	Structures and energetics of CO2 adsorption on the Fe3O4 (111) surface. Journal of Fuel Chemistry and Technology, 2018, 46, 1113-1120.	0.9	7
28417	Influence of Mn Doping on the Electronic Structure and Absorption Spectrum of Ca2SiO4:Eu2+ Phosphor. Rare Metal Materials and Engineering, 2018, 47, 729-735.	0.8	1
28418	Structural insights into T₂-cluster-containing chalcogenides with vertex-, edge- and face-sharing connection modes of NaQ₆ligands: Na₃ZnM^{III}Q₄(M^{III}= In, Ga; Q = S, Se). Dalton Transactions, 2018, 47, 15538-15544.	1.6	12
28419	An ultra-sensitive and selective nitrogen dioxide sensor based on a novel P₂C₂monolayer from a theoretical perspective. Nanoscale, 2018, 10, 21936-21943.	2.8	28
28420	Li₈NaRb₃(SO₄)₆Â·2H₂O as a new sulfate deep-ultraviolet nonlinear optical material. Journal of Materials Chemistry C, 2018, 6, 12240-12244.	2.7	66
28421	Ultralow Interlayer Friction of Layered Electride Ca2N: A Potential Two-Dimensional Solid Lubricant Material. Materials, 2018, 11, 2462.	1.3	15
28422	First-principles investigation of adsorption behaviors of small molecules on penta-graphene. Nanoscale Research Letters, 2018, 13, 264.	3.1	51
28423	Enhanced oxygen reduction on graphene via Y5Si3 electride substrate: A first-principles study. Chinese Journal of Chemical Physics, 2018, 31, 649-654.	0.6	6
28424	Modeling of Carbon Chain Device Employing Quantum Mechanical Method: A Hybrid Diode. , 2018, , .		0
28425	Electronic structure and optical properties of K2Ti6O13 doped with transition metal Fe or Ag. Chinese Journal of Chemical Physics, 2018, 31, 318-324.	0.6	4
28426	Au Atom Diffusions on Reduced and Cl-Adsorbed Rutile TiO₂(110) Surfaces: A DFT + <i>U</i> Study. E-Journal of Surface Science and Nanotechnology, 2018, 16, 267-273.	0.1	3
28427	Electronic structures and optical properties of Ga doped single-layer indium nitride. Chinese Journal of Chemical Physics, 2018, 31, 313-317.	0.6	4
28428	DFT calculations based insight into bonding character and strength of Fe2Al5 and Fe4Al13 intermetallics at Al-Fe joints. Procedia Manufacturing, 2018, 15, 1407-1415.	1.9	16
28429	First principles study on structural and electronic properties of Li, Na and K â€“ intercalated zinc phthalocyanine. Materials Today: Proceedings, 2018, 5, 14852-14856.	0.9	0

#	Article	IF	Citations
28430	Investigation of the Energy Band at the Molybdenum Disulfide and ZrO2 Heterojunctions. Nanoscale Research Letters, 2018, 13, 405.	3.1	4
28431	Crystalline, Electronic, and Vibrational Structures of Zinc Cyanides. Journal of Structural Chemistry, 2018, 59, 1761-1767.	0.3	2
28432	Effect of transition metal (TM) doping on structural and magnetic properties in hexagonal YMn0.917TM0.083O3 systems. Heliyon, 2018, 4, e00993.	1.4	3
28433	First-principles Study on Effect of Pressure and Temperature on Mechanical, Thermodynamic Properties, and Electronic Structure of Ni3Al Alloy. Rare Metal Materials and Engineering, 2018, 47, 3651-3658.	0.8	1
28434	A Hybrid Atomistic - Semi-Analytical Modeling on Schottky Barrier Au-MoS2-Au MOSFETs. , 2018, , .		2
28435	Performance Analysis of Schottky Barrier Height Modulation in Strained (10, 0) MoS2 Armchair Nano Ribbon-Metal Junction. , 2018, , .		1
28436	Hidden Resources of Coordinated XPS and DFT Studies. , 0, , .		0
28437	Elastic Constants and Homogenized Moduli of Monoclinic Structures Based on Density Functional Theory. , 2018, , .		1
28438	First-Principles microkinetic study of methanol synthesis on Cu(221) and ZnCu(221) surfaces. Chinese Journal of Chemical Physics, 2018, 31, 284-290.	0.6	13
28439	Theoretical Structural Stability of Small Molecules Water. IOP Conference Series: Earth and Environmental Science, 2018, 178, 012020.	0.2	1
28440	Effect of dispersion corrections on ab initio predictions of graphite and diamond properties under pressure. Physical Review B, 2018, 98, .	1.1	24
28441	Polytypism driven zero-field splitting of silicon vacancies in <mml:math xmlns:mml="http://www.w3.org/1998/Math/MathML"><mml:mrow><mml:mn>6</mml:mn><mml:mi>H</mml:mi></mml:mrow></mml -SiC. Physical Review B, 2018, 98, .	1.1	17
28442	Modulating temperature dependence of thermal conductivity by nanostructuring. Japanese Journal of Applied Physics, 2018, 57, 120312.	0.8	2
28443	Density-Functional Tight-Binding Study on the Effects of Interfacial Water in the Adhesion Force between Epoxy Resin and Alumina Surface. Langmuir, 2018, 34, 14428-14438.	1.6	27
28444	Ground-state crystal structures of superconducting Nb3Al and the phase transformation under high pressures. Journal of Applied Physics, 2018, 124, 173902.	1.1	7
28445	Influence of the Thickness of Nonmagnetic Spacer on the Magnetic Properties of Fe/Cu Multilayered Nanowires. Key Engineering Materials, 2018, 787, 93-98.	0.4	0
28446	Orange-Emitting Li₄Sr₄[Si₄O₄N₆]O:Eu²⁺â€"a Layered Lithium Oxonitridosilicate Oxide. Inorganic Chemistry, 2018, 57, 14304-14313.	1.9	4
28447	Design of 2D massless Dirac fermion systems and quantum spin Hall insulators based on spâ€"sp2 carbon sheets. Npj Computational Materials, 2018, 4, .	3.5	20

#	Article	IF	Citations
28448	First-principle atomistic thermodynamic study on the early-stage corrosion of NiCr alloy under fluoride salt environment. Physical Chemistry Chemical Physics, 2018, 20, 28832-28839.	1.3	11
28449	Optimizing special quasirandom structure (SQS) models for accurate functional property prediction in disordered 2D alloys. Journal of Physics Condensed Matter, 2018, 30, 485402.	0.7	4
28450	Two-Dimensional Titanium Carbonitride Mxene for High-Performance Sodium Ion Batteries. ACS Applied Nano Materials, 2018, 1, 6854-6863.	2.4	71
28451	Effects of Native Vacancies on Nb-Doped MgH2 Using Density Functional Theory Calculations. Journal of Physical Chemistry C, 2018, 122, 27955-27962.	1.5	6
28452	Ferromagnetism of 1Tâ€²-MoS₂ Nanoribbons Stabilized by Edge Reconstruction and Its Periodic Variation on Nanoribbons Width. Journal of the American Chemical Society, 2018, 140, 16206-16212.	6.6	39
28453	Enhancement of thermoelectric properties of SrTiO3 by single doping at Sr and Ti site with Ho. AIP Conference Proceedings, 2018, , .	0.3	1
28454	Characterization of Elastic Modulus Across the (Al_{1â€“<italic>x</italic>}Sc_{<italic>x</italic>})N System Using DFT and Substrate-Effect-Corrected Nanoindentation. IEEE Transactions on Ultrasonics, Ferroelectrics, and Frequency Control, 2018, 65, 2167-2175.	1.7	22
28455	The accuracy of standard enthalpies and entropies for phases of petrological interest derived from density-functional calculations. Contributions To Mineralogy and Petrology, 2018, 173, 90.	1.2	22
28456	The effect of hydrogen on the electronic, mechanical and phonon properties of LaMgNi4 and its hydrides for hydrogen storage applications. International Journal of Hydrogen Energy, 2018, 43, 23397-23408.	3.8	40
28457	Silicon-Doped Nitrogen-Coordinated Graphene as Electrocatalyst for Oxygen Reduction Reaction. Journal of Physical Chemistry C, 2018, 122, 27233-27240.	1.5	59
28458	First principles study of ground-state properties of Laves phase ZrMn2 and its hydride. EPJ Applied Physics, 2018, 84, 10901.	0.3	2
28459	Ab initio Calculations of Phonon Dispersion in CdGa2S4. Physics of the Solid State, 2018, 60, 2305-2309.	0.2	2
28460	Effect of U Content on the Activation of H₂O on Ce_{1â€“x}U_xO_{2+Î´} Surfaces. Chemistry of Materials, 2018, 30, 8650-8660.	3.2	8
28461	Effect of Dipole Corrections and Spin Orbit Coupling on Tungsten Dichalcogenides Monolayer: A in Silico First Principles Study. , 2018, , .		4
28462	Physical properties of niobium-based intermetallics (Nb3B; B = Os, Pt, Au): a DFT-based ab-initio study. European Physical Journal B, 2018, 91, 1.	0.6	27
28463	Elastic anisotropy and thermal properties of extended linear chain compounds MV2Ga4 (M = Sc, Zr, Hf) from ab-initio calculations. Materialia, 2018, 4, 529-539.	1.3	7
28464	Transformation of the Anion Sublattice in the Cation-Exchange Synthesis of Au2S from Cu2â€“xS Nanocrystals. Chemistry of Materials, 2018, 30, 8843-8851.	3.2	17
28465	V₂Te₂O: A Two-Dimensional van der Waals Correlated Metal. Inorganic Chemistry, 2018, 57, 14617-14623.	1.9	8

#	Article	IF	Citations
28466	Diversity of Adsorbed Hydrogen on the TiC(001) Surface at High Coverages. Journal of Physical Chemistry C, 2018, 122, 28013-28020.	1.5	17
28467	Mono- and Diatomic Reactive Oxygen Species Produced upon O₂ Interaction with the (111) Facet of Cobalt Spinel at Various Conditionsâ€"Molecular DFT and Atomistic Thermodynamic Investigations. Journal of Physical Chemistry C, 2018, 122, 27528-27539.	1.5	14
28468	Pressure-induced superconductivity in topological semimetal NbAs2. Npj Quantum Materials, 2018, 3, .	1.8	25
28469	Reversible superdense ordering of lithium between two graphene sheets. Nature, 2018, 564, 234-239.	13.7	178
28470	Antiferromagneticâ€"ferromagnetic transition in zigzag graphene nanoribbons induced by substitutional doping. Chinese Physics B, 2018, 27, 117102.	0.7	6
28471	The physical properties of ThCr₂Si₂-type superconductors MPd₂P₂ (M = Y, La): A theoretical investigation. International Journal of Modern Physics B, 2018, 32, 1850312.	1.0	3
28472	Spin Excitations in Solid from Many-Body Perturbation Theory. , 2018, , 1-39.		1
28473	Electronic structure, defect properties, and hydrogen storage capacity of 2H-WS2: A first-principles study. International Journal of Hydrogen Energy, 2018, 43, 23126-23134.	3.8	12
28474	High-Pressure Evolution of Unexpected Chemical Bonding and Promising Superconducting Properties of YB₆. Journal of Physical Chemistry C, 2018, 122, 27820-27828.	1.5	23
28475	Breaking H₂ with CeO₂: Effect of Surface Termination. ACS Omega, 2018, 3, 16063-16073.	1.6	47
28476	Synthesis, Structure, and Properties of the Layered Oxide Chalcogenides Sr₂CuO₂Cu₂S₂ and Sr₂CuO₂Cu₂Se₂. Inorganic Chemistry, 2018, 57, 15379-15388.	1.9	15
28477	Does the Mgâ€"I₂ Battery Suffer Severe Shuttle Effect?. Journal of Physical Chemistry C, 2018, 122, 28518-28527.	1.5	9
28478	Effects of Electric Field on the Electronic Structures of Broken-gap Phosphorene/ <mml:math xmlns:mml="http://www.w3.org/1998/Math/MathML" display="inline" overflow="scroll"><mml:mi>Sn</mml:mi><mml:msub><mml:mi>X</mml:mi><mml:mn>2</mml:mn></mml:msub></mml:math>		

#	Article	IF	Citations
28484	Abnormal subsurface hydrogen diffusion behaviors in heterogeneous hydrogenation reactions. Journal of Chemical Physics, 2018, 149, 174704.	1.2	10
28485	High-accuracy large-scale DFT calculations using localized orbitals in complex electronic systems: the case of grapheneâ€“metal interfaces. Journal of Physics Condensed Matter, 2018, 30, 505901.	0.7	9
28486	Dopant Control of Electronâ€“Hole Recombination in Cesiumâ€“Titanium Halide Double Perovskite by Time Domain Ab Initio Simulation: Codoping Supersedes Monodoping. Journal of Physical Chemistry Letters, 2018, 9, 6907-6914.	2.1	24
28487	Pulsed axial epitaxy of colloidal quantum dots in nanowires enables facet-selective passivation. Nature Communications, 2018, 9, 4947.	5.8	22
28488	Modified spinâ€“orbit couplings in uniaxially strained graphene. European Physical Journal B, 2018, 91, 1.	0.6	8
28489	DFT Calculations of Hydrogenation of 2(5H)-Furanone over Ni-, Rh-, Pd-, and Pt-Metal Surfaces Considering the Effects of Subsurface H Atoms. Journal of Physical Chemistry C, 2018, 122, 28182-28191.	1.5	5
28490	Theoretical Study on PdCu/CeO2-Catalyzed Waterâ€“Gas Shift Reaction: Crucial Role of the Metal/Ceria Interface and O2 Enhancement Effects. Journal of Physical Chemistry C, 2018, 122, 28868-28883.	1.5	12
28491	Engineering SrSnO₃ Phases and Electron Mobility at Room Temperature Using Epitaxial Strain. ACS Applied Materials & Interfaces, 2018, 10, 43802-43808.	4.0	37
28493	Ba8Au5.25Ge40.75(110): A Nano-Caged Surface Electronically Controlled by Barium and Gold Adatoms. Journal of Physical Chemistry C, 2018, 122, 29298-29306.	1.5	5
28494	Calculations of the pH-Dependent Onset Potential for CO Electrooxidation on Au(111). Langmuir, 2018, 34, 15268-15275.	1.6	18
28495	Recipe for Dirac Phonon States with a Quantized Valley Berry Phase in Two-Dimensional Hexagonal Lattices. Nano Letters, 2018, 18, 7755-7760.	4.5	54
28496	On the calculation of the stress tensor in real-space Kohn-Sham density functional theory. Journal of Chemical Physics, 2018, 149, 194104.	1.2	9
28497	Accurate ab initio determination of ballistic electron emission spectroscopy: Application to Au/Ge. Physical Review B, 2018, 98, .	1.1	4
28498	Ab Initio Studies of Hydrogen Ion Insertion into Î²-, R-, and Î³-MnO₂Polymorphs and the Implications for Shallow-Cycled Rechargeable Zn/MnO₂Batteries. Journal of the Electrochemical Society, 2018, 165, A3517-A3524.	1.3	16
28499	The Infrared spectrum of very large (periodic) systems: global versus fragment strategiesâ€”the case of three defects in diamond. Theoretical Chemistry Accounts, 2018, 137, 1.	0.5	10
28500	Enhanced Carrier Transport and Bandgap Reduction in Sulfur-Modified BiVO₄ Photoanodes. Chemistry of Materials, 2018, 30, 8630-8638.	3.2	39
28501	Enabling Electrocatalytic N₂ Reduction to NH₃ by Y₂O₃ Nanosheet under Ambient Conditions. Industrial & Engineering Chemistry Research, 2018, 57, 16622-16627.	1.8	39
28502	Oxygen vacancy induced photoconductivity enhancement in Bi1-xCaxFeO3-Î´ nanoparticle ceramics: A combined experimental and theoretical study. Journal of Applied Physics, 2018, 124, 195108.	1.1	12

#	Article	IF	Citations
28503	Electronic exchange-correlation, many-body effect issues on first-principles calculations of bulk SiC polytypes. International Journal of Modern Physics B, 2018, 32, 1850328.	1.0	2
28504	Cyano-Based Materials with Giant Optical Anisotropy and Second Harmonic-Generation Effect. Inorganic Chemistry, 2018, 57, 15001-15008.	1.9	16
28505	Cobalt Phosphate Nanostructures for Non-Enzymatic Glucose Sensing at Physiological pH. ACS Applied Materials & Interfaces, 2018, 10, 42786-42795.	4.0	64
28506	Inducing wetting morphologies and increased reactivities of small Au clusters on doped oxide supports. Journal of Chemical Physics, 2018, 149, 174701.	1.2	6
28507	Thermal transport crossover from crystalline to partial-crystalline partial-liquid state. Nature Communications, 2018, 9, 4712.	5.8	39
28508	An ab-initio investigation on SrLa intermetallic compound. AIP Conference Proceedings, 2018, , .	0.3	1
28509	First-principles calculation of electronic properties of fluorinated graphene. AIP Conference Proceedings, 2018, , .	0.3	0
28510	GGA-1/2 self-energy correction for accurate band structure calculations: the case of resistive switching oxides. Journal of Physics Communications, 2018, 2, 105005.	0.5	70
28511	Ab initio molecular dynamics simulation of irradiation particles behavior in tungsten. European Physical Journal B, 2018, 91, 1.	0.6	0
28512	Electronic and optical properties of V doped AlN nanosheet: DFT calculations. Chinese Journal of Physics, 2018, 56, 2698-2709.	2.0	22
28513	Defect-Mediated Alloying of Monolayer Transition-Metal Dichalcogenides. ACS Nano, 2018, 12, 12795-12804.	7.3	42
28514	Metastable silica high pressure polymorphs as structural proxies of deep Earth silicate melts. Nature Communications, 2018, 9, 4789.	5.8	39
28515	Discrete Superconducting Phases in FeSe-Derived Superconductors. Physical Review Letters, 2018, 121, 207003.	2.9	49
28516	Mono- and Bi-Molecular Adsorption of SF6 Decomposition Products on Pt Doped Graphene: A First-Principles Investigation. Applied Sciences (Switzerland), 2018, 8, 2010.	1.3	4
28517	Effects of ensembles, ligand, and strain on adsorbate binding to alloy surfaces. Journal of Chemical Physics, 2018, 149, 174705.	1.2	193
28518	Hybrid DFT study of MWCNT/Zr-doped SrTiO3 heterostructure: Hydrogen production, electronic properties and charge Carrier mediator role of Zr4+Âion. International Journal of Hydrogen Energy, 2018, 43, 22253-22264.	3.8	11
28519	First-principles investigation of Ag-, Co-, Cr-, Cu-, Fe-, Mn-, Ni-, Pd- and Rh-hexaaminobenzene 2D metal-organic frameworks. Materials Today Energy, 2018, 10, 336-342.	2.5	18
28520	Opto-Mechanics Driven Fast Martensitic Transition in Two-Dimensional Materials. Nano Letters, 2018, 18, 7794-7800.	4.5	38

#	Article	IF	Citations
28521	Chirality dependence of the tunneling current in graphene nano-gaps for peptide sequencing. AIP Conference Proceedings, 2018, , .	0.3	0
28522	Excitation properties of the divacancy in <mml:math xmlns:mml="http://www.w3.org/1998/Math/MathML"><mml:mrow><mml:mn>4</mml:mn><mml:mi>H</mml:mi></mml:mrow></mml:math> -SiC. Physical Review B, 2018, 98, .	1.1	34
28523	Melting Si: Beyond Density Functional Theory. Physical Review Letters, 2018, 121, 195701.	2.9	46
28524	H2 Thermal Desorption Spectra on Pt(111): A Density Functional Theory and Kinetic Monte Carlo Simulation Study. Catalysts, 2018, 8, 450.	1.6	14
28525	Strength and Brittleness of Interfaces in Fe-Al Superalloy Nanocomposites under Multiaxial Loading: An ab initio and Atomistic Study. Nanomaterials, 2018, 8, 873.	1.9	22
28526	Electronic and Vibrational Properties of TiS₂, ZrS₂, and HfS₂: Periodic Trends Studied by Dispersion-Corrected Hybrid Density Functional Methods. Journal of Physical Chemistry C, 2018, 122, 26835-26844.	1.5	34
28527	Theoretical Insights into Perovskite Compounds MAPb_{1â^'Î±}X_{Î±}I_{3â^'Î²}Y_{Î²} (X = Ge, Sn; Y = Cl, Br): An Exploration for Superior Optical Performance. Journal of Physical Chemistry C, 2018, 122, 27205-27213.	1.5	7
28528	Heterostructure-Promoted Oxygen Electrocatalysis Enables Rechargeable Zincâ€“Air Battery with Neutral Aqueous Electrolyte. Journal of the American Chemical Society, 2018, 140, 17624-17631.	6.6	258
28529	Polar metals as electrodes to suppress the critical-thickness limit in ferroelectric nanocapacitors. Journal of Applied Physics, 2018, 124, .	1.1	23
28530	Six-dimensional quantum dynamics for the dissociative chemisorption of HCl on rigid Ag(111) on three potential energy surfaces with different density functionals. Journal of Chemical Physics, 2018, 149, 174702.	1.2	7
28531	A Promising Gas Sensor Based on Monolayer $alpha $-SbN to Detect SO₂ Among SF₆ Decompositions. , 2018, 2, 1-4.		10
28532	Optical Properties of Silicene and Related Materials from First Principles. Nanoscience and Technology, 2018, , 73-98.	1.5	6
28533	Vibrational fingerprint of localized excitons in a two-dimensional metal-organic crystal. Nature Communications, 2018, 9, 4703.	5.8	18
28534	Adsorption of SF₆ Decomposed Products over ZnO(101Ì…0): Effects of O and Zn Vacancies. ACS Omega, 2018, 3, 18739-18752.	1.6	9
28535	General rules of the sub-band gaps in group-IV (Si, Ge, and Sn)-doped I-III-VI2-type chalcopyrite compounds for intermediate band solar cell: A first-principles study. Materials Science and Engineering B: Solid-State Materials for Advanced Technology, 2018, 236-237, 147-152.	1.7	17
28536	Water Adsorption on the Î²-Dicalcium Silicate Surface from DFT Simulations. Minerals (Basel,) Tj ETQq1 1 0.784314 rgBT /Overlock 10	0.8	21
28537	Characterization of scrutinyite SnO₂ and investigation of the transformation with ¹¹⁹Sn NMR and complex impedance method. AIP Advances, 2018, 8, 125226.	0.6	2
28538	A First-Principles Study of the Al (001)/Fe(0-11) Interface. Materials Science Forum, 0, 941, 2349-2355.	0.3	8

#	Article	IF	Citations
28539	First-Principles Study on Superconductivity of P- and Cl-Doped H₃S. Journal of the Physical Society of Japan, 2018, 87, 124711.	0.7	25
28540	Cage-like $ext{N}_{10}^{6-}$ salt with N-N single bonds. Europhysics Letters, 2018, 124, 67004.	0.7	3
28541	Thermal Transport by First-Principles Anharmonic Lattice Dynamics. , 2018, , 1-31.		1
28542	Ultralow thermal conductivity in a two-dimensional material due to surface-enhanced resonant bonding. Materials Today Physics, 2018, 7, 89-95.	2.9	12
28543	Ab initio (DFT) calculations of corundum (Î±-Al2O3) oxygen isotope fractionation. European Journal of Mineralogy, 2018, 30, 1063-1070.	0.4	3
28544	Absorption in Finite-Length Chevron-Type Graphene Nanoribbons. Semiconductors, 2018, 52, 1890-1893.	0.2	14
28545	Rheological properties of super critical CO2 with CuO: Multi-scale computational modeling. Journal of Chemical Physics, 2018, 149, 224702.	1.2	12
28546	Theoretical and Experimental Evidence for a Post-Cotunnite Phase Transition in Hafnia at High Pressures. Journal of Superhard Materials, 2018, 40, 374-383.	0.5	5
28547	Impact of Nano-Scale Distribution of Atoms on Electronic and Magnetic Properties of Phases in Fe-Al Nanocomposites: An Ab Initio Study. Nanomaterials, 2018, 8, 1059.	1.9	15
28548	First-principles study of thermal conductivities of uranium aluminides. Materialia, 2018, 4, 449-456.	1.3	8
28549	Geometrical and electronic properties of C-doped graphyne-like BN sheets. Integrated Ferroelectrics, 2018, 191, 180-188.	0.3	2
28550	Spin-dependent properties in zigzag graphene nanoribbons with phenyl-edge defects. Physical Review B, 2018, 98, .	1.1	34
28551	Ab initio calculation of the spin lattice relaxation time <mml:math xmlns:mml="http://www.w3.org/1998/Math/MathML"><mml:msub><mml:mi>T</mml:mi><mml:mn>1</mml:mn></mml:msub></mml:m for nitrogen-vacancy centers in diamond. Physical Review B, 2018, 98, .	1.1	16
28552	Unified theory of direct or indirect band-gap nature of conventional semiconductors. Physical Review B, 2018, 98, .	1.1	60
28553	Investigations of the hydrogen bond in the crystals of tropolone and thiotropolone via carâ€parrinello and path integral molecular dynamics. Journal of Computational Chemistry, 2019, 40, 671-687.	1.5	6
28554	Ab initio inspection of thermophysical experiments for molybdenum near melting. AIP Advances, 2018, 8, 125012.	0.6	18
28555	Spin Excitations in a <mml:math xmlns:mml="http://www.w3.org/1998/Math/MathML" display="inline"><mml:mn>4</mml:mn><mml:mi>f</mml:mi><mml:mo>â^'</mml:mo><mml:mn>3</mml:mn><mml:mi>d</mml:mi></m Heterodimer on MgO. Physical Review Letters, 2018, 121, 257202.	2.9	4
28556	Mechanical, Electronic and Optical Properties of Two Phases of NbB4: First-Principles Calculations. Zeitschrift Fur Naturforschung - Section A Journal of Physical Sciences, 2018, 73, 453-460.	0.7	3

#	Article	IF	Citations
28557	The New Candidate Materials for Infrared Optical Devices. , 2018, , .		0
28558	An Ab Initio Study of Electronic Structure of Lithium Metaborate. Journal of Structural Chemistry, 2018, 59, 1501-1506.	0.3	5
28559	Ideal intersecting nodal-ring phonons in bcc <mml:math xmlns:mml="http://www.w3.org/1998/Math/MathML"><mml:msub><mml:mi mathvariant="normal">C</mml:mi><mml:mn>8</mml:mn></mml:msub></mml:math>. Physical Review B, 2018, 98, .	1.1	51
28560	Generation of multiple plasmons in strontium niobates mediated by local field effects. Physical Review B, 2018, 98, .	1.1	20
28561	Magnetism in semiconducting molybdenum dichalcogenides. Science Advances, 2018, 4, eaat3672.	4.7	92
28562	Quantum-Mechanical Study of Nanocomposites with Low and Ultra-Low Interface Energies. Nanomaterials, 2018, 8, 1057.	1.9	13
28563	Acceptor levels of the carbon vacancy in 4H-SiC: Combining Laplace deep level transient spectroscopy with density functional modeling. Journal of Applied Physics, 2018, 124, 245701.	1.1	19
28564	Interfacial Interaction between Carbon Nanotube and Stoichio- and Nonstoichiometric Ceramic Surfaces by <i>Ab-Initio</i> Calculations. Materials Transactions, 2018, 59, 1684-1690.	0.4	3
28565	First-Principles Study on the Electronic Structure of Bulk and Single-Layer Boehmite. Nano, 2018, 13, 1850138.	0.5	1
28566	Anisotropic Thermal Conduction in Transition Metal Dichalcogenide Nanocomposites with Rough Interfaces. Nanomaterials, 2018, 8, 1054.	1.9	2
28567	Phonon and Thermodynamic Properties in YNi2B2C and LuNi2B2C from First-Principles Study. Journal of Superconductivity and Novel Magnetism, 2018, 31, 1925-1931.	0.8	1
28568	Anomalous diffusion along metal/ceramic interfaces. Nature Communications, 2018, 9, 5251.	5.8	51
28569	Spin-filter state of Au-Co nanowires. EPJ Web of Conferences, 2018, 185, 01019.	0.1	1
28570	Rare Helium-Bearing Compound <mml:math xmlns:mml="http://www.w3.org/1998/Math/MathML" display="inline"><mml:mrow><mml:mrow><mml:msub><mml:mrow><mml:mi>FeO</mml:mi></mml:mrow><mml:mrow><mml:mn> Stabilized at Deep-Earth Conditions. Physical Review Letters, 2018, 121, 255703.	2.9	68
28571	A complete DFT description on structural, electronic, elastic, mechanical and thermodynamic properties of some intermetallic AuX2 (X = Al, Ga, In) compounds. European Physical Journal Plus, 2018, 133, 1.	1.2	7
28572	Unexpectedly large energy variations from dopant interactions in ferroelectric HfO2 from high-throughput ab initio calculations. Npj Computational Materials, 2018, 4, .	3.5	18
28573	Machine Learning a General-Purpose Interatomic Potential for Silicon. Physical Review X, 2018, 8, .	2.8	222
28574	New Cr-Ni-Base Alloy for High-Temperature Applications Designed on the Basis of First Principles Calculations. Advances in Condensed Matter Physics, 2018, 2018, 1-8.	0.4	13

#	Article	IF	Citations
28575	Extraction Difficulty of Lithium Ions from Various Crystal Planes of Lithium Titanate. Journal Wuhan University of Technology, Materials Science Edition, 2018, 33, 1086-1091.	0.4	8
28576	Probing the upper band gap of atomic rhenium disulfide layers. Light: Science and Applications, 2018, 7, 98.	7.7	24
28577	Two-Dimensional Mechanical Metamaterials with Unusual Poisson Ratio Behavior. Physical Review Applied, 2018, 10, .	1.5	17
28578	Phase transition systematics in <mml:math xmlns:mml="http://www.w3.org/1998/Math/MathML"><mml:msub><mml:mi>BiVO</mml:mi><mml:mn>4</mml:mn></mml:msub></mml:math> by means of high-pressureâ€“high-temperature Raman experiments. Physical Review B, 2018, 98, .	1.1	24
28579	Breakdown of Herring's processes in cubic semiconductors for subterahertz longitudinal acoustic phonons. Physical Review B, 2018, 98, .	1.1	5
28580	Toward the Design of New Suitable Materials for Solar Water Splitting Using Density Functional Theory. ACS Omega, 2018, 3, 18117-18123.	1.6	15
28581	The ideal commensurate value of Sc and the superconducting phase under high pressure. Journal of Applied Physics, 2018, 124, 225901.	1.1	23
28582	First principles investigation of electronic properties and high refractive index of rutile TiO2 for photovoltaic applications. AIP Conference Proceedings, 2018, , .	0.3	4
28583	Revealing the role of nitrogen on hydride nucleation and stability in pure niobium using first-principles calculations. Superconductor Science and Technology, 2018, 31, 115007.	1.8	19
28584	What is the origin of macroscopic friction?. Science Advances, 2018, 4, eaav2268.	4.7	35
28585	Perspectives on the Theory of Defects. Frontiers in Materials, 2018, 5, .	1.2	21
28586	Peculiar magnetic properties of NC6 and NC12 layered compounds from first principles. Journal of Theoretical and Applied Physics, 2018, 12, 209-217.	1.4	0
28587	Pressure-induced multiple phase transformations of the BaBi3 superconductor. Physical Review B, 2018, 98, .	1.1	8
28589	Firstâ€Principles Study of Aziridinium Lead Iodide Perovskite for Photovoltaics. ChemPhysChem, 2019, 20, 602-607.	1.0	8
28590	Anisotropic lattice strain induced by the enhanced electronic hybridization in SrTiO3. Applied Physics Letters, 2018, 113, .	1.5	5
28591	Resistive switching in Si₂Te₃ nanowires. AIP Advances, 2018, 8, 125008.	0.6	13
28592	Zigzag sp² Carbon Chains Passing through an sp³ Framework: A Driving Force toward Room-Temperature Ferromagnetic Graphene. ACS Nano, 2018, 12, 12847-12859.	7.3	19
28593	An Efficient Way To Suppress the Competition between Adsorption of H₂ and Desorption of nH₂â€“Nb Complex from Graphene Sheet: A Promising Approach to H₂ Storage. Journal of Physical Chemistry C, 2018, 122, 28506-28517.	1.5	45

#	Article	IF	Citations
28594	Prediction of two-dimensional organic topological insulator in metal-DCB lattices. Applied Physics Letters, 2018, 113, .	1.5	12
28595	Quantum behavior of hydrogen-vacancy complexes in diamond. Physical Review B, 2018, 98, .	1.1	15
28596	Decoupling Carrier Concentration and Electron-Phonon Coupling in Oxide Heterostructures Observed with Resonant Inelastic X-Ray Scattering. Physical Review Letters, 2018, 121, 236802.	2.9	22
28597	Auxiliary-field quantum Monte Carlo calculations of the structural properties of nickel oxide. Journal of Chemical Physics, 2018, 149, 164102.	1.2	24
28598	Ab initio investigation of electron-phonon interaction in LaSn3 and CaSn3. Philosophical Magazine Letters, 2018, 98, 375-391.	0.5	3
28599	Phonon thermodynamics and elastic behavior of GaN at high temperatures and pressures. Physical Review B, 2018, 98, .	1.1	10
28600	Transport properties of Cu-AlF3-W and Cu-AlF3-Cu heterojunctions using STS measurements and a DFT-NEGF approach. Results in Physics, 2018, 10, 813-817.	2.0	2
28601	Computational modelling of Ti50Pt 50-XVx potential shape memory alloys. IOP Conference Series: Materials Science and Engineering, 2018, 430, 012021.	0.3	0
28602	Magnetic field effect on the chiral magnetism of noncentrosymmetric UPtGe: Experiment and theory. Physical Review B, 2018, 98, .	1.1	3
28603	First principles study on ferromagnetism of diluted magnetic semiconductor Li(Zn, Mn)N. Journal of Applied Physics, 2018, 124, 203901.	1.1	2
28604	Thermoelectric properties of four typical silicon allotropes. Modelling and Simulation in Materials Science and Engineering, 2018, 26, 085006.	0.8	7
28605	Nodeless High- <mml:math xmlns:mml="http://www.w3.org/1998/Math/MathML" display="inline"><mml:msub><mml:mi>T</mml:mi><mml:mi>c</mml:mi></mml:msub></mml:math> Superconductivity in the Highly Overdoped <mml:math xmlns:mml="http://www.w3.org/1998/Math/MathML" display="inline"><mml:mrow><mml:msub><mml:mrow><mml:mi>CuO</mml:mi></mml:mrow><mml:mrow><mml:mn>2</mml:mn></mml:mrow></mml:msub></mml:mrow></mml:math> Monolayer. Physical Review Letters, 2018, 121, 227002.	2.9	31
28606	Difluorophosphorane-Flattened Phosphorene through Difluorination. Journal of Physical Chemistry Letters, 2018, 9, 6963-6966.	2.1	7
28607	Reactive Molecular Dynamics Simulations of Thermal Film Growth from Di-tert-butyl Disulfide on an Fe(100) surface. Langmuir, 2018, 34, 15681-15688.	1.6	12
28608	Computational Chemistry Meets Experiments for Explaining the Geometry, Electronic Structure, and Optical Properties of Ca₁₀V₆O₂₅. Inorganic Chemistry, 2018, 57, 15489-15499.	1.9	18
28609	Structural, electronic and magnetic properties of MnxGa/Co2MnSi (xâ€‰=â€‰1, 3) bilayers. Scientific Reports, 2018, 8, 16530.	1.6	10
28610	Atomic and electronic structure of the Si(331)-(12 Ã— 1) surface. Journal of Chemical Physics, 2018, 149, 204702.	1.2	8
28611	Effect of stacking faults and surface roughness on the thermal conductivity of InAs nanowires. Journal of Applied Physics, 2018, 124, 205101.	1.1	3

#	Article	IF	Citations
28612	Influence of Pressure on the Mechanical and Electronic Properties of Wurtzite and Zinc-Blende GaN Crystals. Crystals, 2018, 8, 428.	1.0	2
28613	Binderâ€Free ZnO Cathode synthesized via ALD by Direct Growth of Hierarchical ZnO Nanostructure on Current Collector for Highâ€Performance Rechargeable Aluminiumâ€Ion Batteries. ChemistrySelect, 2018, 3, 12512-12523.	0.7	14
28614	Stone-Wales like defects formation, stability and reactivity in black phosphorene. Materials Science and Engineering B: Solid-State Materials for Advanced Technology, 2018, 236-237, 208-216.	1.7	14
28615	Phosphorus Adsorption on Fe(110): An ab Initio Comparative Study of Iron Passivation by Different Adsorbates. Journal of Physical Chemistry C, 2018, 122, 28105-28112.	1.5	16
28616	First-Principles Structural, Mechanical, and Thermodynamic Calculations of the Negative Thermal Expansion Compound Zr2(WO4)(PO4)2. ACS Omega, 2018, 3, 15780-15788.	1.6	8
28617	Molecular tunneling in large tubes of 3D nitrogenated micropore materials. Journal of Applied Physics, 2018, 124, 194303.	1.1	22
28618	Ab initio optical and energy loss spectra of transition metal monopnictides TaAs, TaP, NbAs, and NbP. Journal of Applied Physics, 2018, 124, .	1.1	6
28619	Energy adsorption of carbon-based material doping boron with Ti and Ni metal ion decoration for hydrogen storage application using density functional theory. IOP Conference Series: Materials Science and Engineering, 2018, 432, 012051.	0.3	3
28620	Evaluation of exchange-correlation functionals with multiple-shock conductivity measurements in hydrogen and deuterium at the molecular-to-atomic transition. Physical Review B, 2018, 98, .	1.1	17
28621	First-principles modeling of x-ray Raman scattering spectra. Physical Review B, 2018, 98, .	1.1	9
28622	Melting properties from ab initio free energy calculations: Iron at the Earth's inner-core boundary. Physical Review B, 2018, 98, .	1.1	43
28623	Difference analysis model for the mismatch effect and substrate-induced lattice deformation in atomically thin materials. Physical Review B, 2018, 98, .	1.1	7
28624	Investigating the Electronic Properties of Oxygen Vacancies in Anatase TiO2: An Ab Initio Study. , 2018, , .		1
28625	Exploratory Study of Substitutional Elements in Mg₂Si for Inducing State of Negative Chemical Pressure. Materials Transactions, 2018, 59, 1417-1422.	0.4	4
28626	Revealing Activity Trends of Metal Diborides Toward pHâ€Universal Hydrogen Evolution Electrocatalysts with Ptâ€Like Activity. Advanced Energy Materials, 2019, 9, 1803369.	10.2	111
28627	Cationic Pb2 Dumbbells Stabilized in the Highly Covalent Lead Nitridosilicate Pb2Si5N8. Angewandte Chemie, 2018, 131, 1446.	1.6	2
28628	Vibrational properties and magnetic specific heat of the covalent chain antiferromagnet RbFeSe2. Physical Review B, 2018, 98, .	1.1	5
28629	Effects of spin-orbit coupling on the optical response of a material. Physical Review B, 2018, 98, .	1.1	5

#	Article	IF	Citations
28630	A combined DFT, DFTâ€¯+â€¯U and mBJ investigation on electronic structure, magnetic, mechanical and thermodynamics of double perovskite Ba2ZnOsO6. Materials Science and Engineering B: Solid-State Materials for Advanced Technology, 2018, 236-237, 217-224.	1.7	11
28631	Air-stable phosphorus-doped molybdenum nitride for enhanced electrocatalytic hydrogen evolution. Communications Chemistry, 2018, 1, .	2.0	36
28632	Pressure tuning of the thermal conductivity of gallium arsenide from first-principles calculations. Physical Chemistry Chemical Physics, 2018, 20, 30331-30339.	1.3	16
28633	Electronic stopping power of protons and alpha particles in nickel. Physical Review B, 2018, 98, .	1.1	26
28634	Na4Yb(CO3)3F: A New UV Nonlinear Optical Material with a Large Second Harmonic Generation Response. Crystals, 2018, 8, 381.	1.0	5
28635	Lattice dynamics study of cubic Tb₂O₃. Journal of Raman Spectroscopy, 2018, 49, 2021-2027.	1.2	15
28636	Effect of Substrate Chemistry on Prenucleation. Metallurgical and Materials Transactions A: Physical Metallurgy and Materials Science, 2018, 49, 6231-6242.	1.1	42
28637	Combined theoretical and experimental studies of CO oxidation on PdRu nanoalloys. Applied Catalysis A: General, 2018, 568, 176-182.	2.2	4
28638	How hydrogen-storage material affects the decomposition of nitramine explosive: CPMD investigations of LAB-doped CL20. International Journal of Hydrogen Energy, 2018, 43, 19825-19840.	3.8	4
28639	Effect of disorder on magnetic properties and martensitic transformation of Co-doped Ni-Mn-Al Heusler alloy. Intermetallics, 2018, 102, 132-139.	1.8	12
28640	Hierarchical MoS2/Ni3S2 core-shell nanofibers for highly efficient and stable overall-water-splitting in alkaline media. Materials Today Energy, 2018, 10, 214-221.	2.5	16
28641	Theoretical Prediction of Janus MoSSe as a Potential Anode Material for Lithium-Ion Batteries. Journal of Physical Chemistry C, 2018, 122, 23899-23909.	1.5	56
28642	Optimized Pt-Based Catalysts for Oxygen Reduction Reaction in Alkaline Solution: A First Principle Study. Journal of the Electrochemical Society, 2018, 165, J3090-J3094.	1.3	13
28643	Si/C/H ReaxFF Reactive Potential for Silicon Surfaces Grafted with Organic Molecules. Journal of Physical Chemistry C, 2018, 122, 23515-23527.	1.5	33
28644	The Electronic Structures and Magnetic Properties in Ti-doped MgO. IOP Conference Series: Materials Science and Engineering, 0, 381, 012016.	0.3	1
28645	Extension of the modified effective medium approach to nanocomposites with anisotropic thermal conductivities. Physical Review B, 2018, 98, .	1.1	5
28646	Strain-tunable magnetic anisotropy in monolayer <mml:math xmlns:mml="http://www.w3.org/1998/Math/MathML"><mml:msub><mml:mi>CrCl</mml:mi><mml:mn>3</mml:mn></mml:msub></mm , <mml:math xmlns:mml="http://www.w3.org/1998/Math/MathML"><mml:msub><mml:mi>CrBr</mml:mi><mml:mn>3</mml:mn></mml:msub></mm , and <mml:math xmlns:mml="http://www.w3.org/1998/Math/MathML"><mml:msub><mml:mi>CrI</mml:mi><mml:mn>3</mml:mn></mml:msub></mml:	1.1	405
28647	Strain-Induced Quantum Spin Hall Effect in Two-Dimensional Methyl-Functionalized Silicene SiCH3. Nanomaterials, 2018, 8, 698.	1.9	4

#	Article	IF	Citations
28648	Quantum-Mechanical Modeling of the Elastic Properties of Aluminum-Based Metal-Organic Frameworks. Russian Journal of Physical Chemistry A, 2018, 92, 1940-1946.	0.1	3
28649	Temperature Effects on the Elastic Constants, Stacking Fault Energy and Twinnability of Ni3Si and Ni3Ge: A First-Principles Study. Crystals, 2018, 8, 364.	1.0	3
28650	Theoretical Investigations of the Hexagonal Germanium Carbonitride. Materials, 2018, 11, 655.	1.3	3
28651	Layer-Coupled States Facilitate Ultrafast Charge Transfer in a Transition Metal Dichalcogenide Trilayer Heterostructure. Journal of Physical Chemistry Letters, 2018, 9, 5970-5978.	2.1	16
28652	MoB2 Driven Metallic Behavior and Interfacial Charge Transport Mechanism in MoS2/MoB2 Heterostructure: A First-Principles Study. Scientific Reports, 2018, 8, 14444.	1.6	5
28653	High magnetoresistance in ultra-thin two-dimensional Cr-based MXenes. Nanoscale, 2018, 10, 19492-19497.	2.8	26
28654	Efficient lattice constants and energy bandgaps for condensed systems from a meta-GGA level screened range-separated hybrid functional. Journal of Chemical Physics, 2018, 149, 094105.	1.2	14
28655	Compression behavior and spectroscopic properties of insensitive explosive 1,3,5-triamino-2,4,6-trinitrobenzene from dispersion-corrected density functional theory. Chinese Physics B, 2018, 27, 056401.	0.7	4
28656	Electronic Structure, Optical Properties, and Pressure Behavior of the CdB4O7 and HgB4O7 Compounds. Physics of the Solid State, 2018, 60, 1704-1711.	0.2	0
28657	EvaluaciÃ³n de caminos de difusiÃ³n de Al en UAl4. Revista Materia, 2018, 23, .	0.1	0
28658	Multiscale Computational Simulation of Amorphous Silicatesâ€™ Structural, Dielectric, and Vibrational Spectroscopic Properties. Minerals (Basel, Switzerland), 2018, 8, 353.	0.8	6
28659	Role of Oxygen Vacancies on Oxygen Evolution Reaction Activity: Î²-Ga₂O₃ as a Case Study. Chemistry of Materials, 2018, 30, 7714-7726.	3.2	43
28660	Dominant Role of Entropy in Stabilizing Sugar Isomerization Transition States within Hydrophobic Zeolite Pores. Journal of the American Chemical Society, 2018, 140, 14244-14266.	6.6	83
28661	Theoretical predicted high-thermal-conductivity cubic Si3N4 and Ge3N4: promising substrate materials for high-power electronic devices. Scientific Reports, 2018, 8, 14374.	1.6	13
28662	Electronic fingerprints of Cr and V dopants in the topological insulator <mml:math xmlns:mml="http://www.w3.org/1998/Math/MathML"><mml:mrow><mml:msub><mml:mi>Sb</mml:mi><mml:mn>2</mml:mn></mml:msub></mml:mrow></mml:math> Physical Review B, 2018, 98, .	1.1	19
28663	Phosphorene as a nanoelectromechanical material. Physical Review B, 2018, 98, .	1.1	15
28664	Effects of different dopant elements on structures, electronic properties, and sensitivity characteristics of nitromethane. Journal of Molecular Modeling, 2018, 24, 295.	0.8	4
28665	Iodine defect energies and equilibria in ZrO2. Journal of Nuclear Materials, 2018, 511, 390-395.	1.3	4

#	Article	IF	Citations
28666	Density functional theory study of the point defect energetics in Î³-LiAlO2, Li2ZrO3 and Li2TiO3 materials. Journal of Nuclear Materials, 2018, 511, 375-389.	1.3	18
28667	Influence of deposition temperature on the properties of sputtered films grown from a Cu2O CdO TeO2 composite target: Electronic properties of CdTe2O5. Superlattices and Microstructures, 2018, 123, 403-413.	1.4	1
28668	Phonons and Thermal Expansion Behavior of NiSi and NiGe. Frontiers in Chemistry, 2018, 6, 331.	1.8	6
28669	Two-Dimensional Janus Transition Metal Oxides and Chalcogenides: Multifunctional Properties for Photocatalysts, Electronics, and Energy Conversion. ACS Applied Materials & Interfaces, 2018, 10, 35289-35295.	4.0	135
28670	Electric Control of the Edge Magnetization in Zigzag Stanene Nanoribbons from First Principles. Physical Review Applied, 2018, 10, .	1.5	14
28671	Application of density functional theory in studying CO2 capture with TiO2-supported K2CO3 being an example. Applied Energy, 2018, 231, 167-178.	5.1	18
28672	Electronic and optical properties of strained noble metals: Implications for applications based on LSPR. Nano Energy, 2018, 53, 932-939.	8.2	45
28673	Liquid-phase exfoliated ultrathin Bi nanosheets: Uncovering the origins of enhanced electrocatalytic CO2 reduction on two-dimensional metal nanostructure. Nano Energy, 2018, 53, 808-816.	8.2	247
28674	Novel Phase of AlN₄ as a Possible Superhard Material. Journal of Physical Chemistry C, 2018, 122, 22660-22666.	1.5	17
28675	Mechanical and electromechanical properties of functionalized hexagonal boron nitride nanosheet: A density functional theory study. Journal of Chemical Physics, 2018, 149, 114701.	1.2	23
28676	Adsorption of H on Cs/W(110): Impact of H on the Stability of Cs on the Surface. E-Journal of Surface Science and Nanotechnology, 2018, 16, 391-395.	0.1	6
28677	Catalytic CO oxidation on B-doped and BN co-doped penta-graphene: a computational study. Physical Chemistry Chemical Physics, 2018, 20, 26414-26421.	1.3	31
28678	The impact of substrate surface defects on the properties of two-dimensional van der Waals heterostructures. Nanoscale, 2018, 10, 19212-19219.	2.8	10
28679	A Computational Study of the Electronic and Magnetic Properties of Rare Earth (Er)-Doped InGaN. Spin, 2018, 08, 1850011.	0.6	3
28680	Abâ€Initio Investigation of the Electronic Structure, Optical Properties, and Lattice Dynamics of Î²â€Ag₂Te. Physica Status Solidi (B): Basic Research, 2018, 255, 1800344.	0.7	6
28681	Mechanistic Insight into Formate Production via CO₂ Reduction in Câ€“C Coupled Carbon Nanotube Molecular Junctions. Journal of Physical Chemistry C, 2018, 122, 23385-23392.	1.5	6
28682	Grain Boundary Facilitates Photocatalytic Reaction in Rutile TiO₂ Despite Fast Charge Recombination: A Time-Domain ab Initio Analysis. Journal of Physical Chemistry Letters, 2018, 9, 5884-5889.	2.1	27
28683	Understanding the Impact of Surface Reconstruction of Perovskite Catalysts on CH₄ Activation and Combustion. ACS Catalysis, 2018, 8, 10306-10315.	5.5	50

#	Article	IF	Citations
28684	Spin-momentum locking and spin-orbit torques in magnetic nano-heterojunctions composed of Weyl semimetal WTe2. Nature Communications, 2018, 9, 3990.	5.8	105
28685	A two-step mechanism in nucleation of solid silica from Fe-O-Si melt. Journal of Theoretical and Computational Chemistry, 2018, 17, 1850026.	1.8	1
28686	An Unlikely Route to Low Lattice Thermal Conductivity: Small Atoms in a Simple Layered Structure. Joule, 2018, 2, 1879-1893.	11.7	117
28687	Hydrogen production from formic acid decomposition in the liquid phase using Pd nanoparticles supported on CNFs with different surface properties. Sustainable Energy and Fuels, 2018, 2, 2705-2716.	2.5	37
28688	Ab initio study of <mml:math xmlns:mml="http://www.w3.org/1998/Math/MathML"><mml:mrow><mml:mi>A</mml:mi><mml:msub><mml:mi>BiO</mml:mi><mml:m (<mml:math) Tj ETQq0 0 0 rgBT /Overlock 10 Tf 50 577 Td (xmlns:mml="http://www.w3.org/1998/Math/MathML"><mml:mrow><mml:r	1.1	3
28689	Deorbitalized meta-GGA exchange-correlation functionals in solids. Physical Review B, 2018, 98, .	1.1	59
28690	Interface dominated cooperative nanoprecipitation in interstitial alloys. Nature Communications, 2018, 9, 4017.	5.8	12
28691	Local environment dependence of Mn magnetism in bcc iron-manganese alloys: A first-principles study. Physical Review B, 2018, 98, .	1.1	23
28692	Thermoelectric Transport Properties of SrTiO₃ Doped with Pm. Solid State Phenomena, 0, 280, 3-8.	0.3	6
28693	Insight into the Mechanism of the Ionic Conductivity for Ln-Doped Ceria (Ln = La, Pr, Nd, Pm, Sm, Gd, Tb,) Tj ETQq1 1 0.784314 rgBT /O	1.9	33
28694	Graphdiyne-Supported Single-Atom-Sized Fe Catalysts for the Oxygen Reduction Reaction: DFT Predictions and Experimental Validations. ACS Catalysis, 2018, 8, 10364-10374.	5.5	202
28695	Effect of Oxygen on the Quantum, Magnetic, and Thermodynamic Properties of Co Nanowires on the Reconstructed Anisotropic (1 Ã— 2)/Au(110) and (1 Ã— 2)/Pt(110) Surfaces: Ab Initio Approach. Journal of Experimental and Theoretical Physics, 2018, 127, 179-188.	0.2	4
28696	Tuning Structural and Compositional Effects in Pdâ€“Au Nanowires for Highly Selective and Active CO₂ Electrochemical Reduction Reaction. Advanced Energy Materials, 2018, 8, 1802238.	10.2	132
28697	High-Throughput Pressure-Dependent Density Functional Theory Investigation of Herringbone Polycyclic Aromatic Hydrocarbons: Part 2. Pressure-Dependent Electronic Properties. Journal of Physical Chemistry C, 2018, 122, 23828-23844.	1.5	11
28698	Enhancement of thermoelectric figure-of-merit of graphene upon BN-doping and sample length reduction. Journal of Applied Physics, 2018, 124, .	1.1	8
28699	Electronic structure based descriptor for characterizing local atomic environments. Physical Review B, 2018, 98, .	1.1	15
28700	The Fluoroperovskite TlMnF₃. Zeitschrift Fur Anorganische Und Allgemeine Chemie, 2018, 644, 1557-1561.	0.6	1
28701	Mechanistic Insight into the Modification of the Surface Stability of In2O3 Catalyst Through Metal Oxide Doping. Catalysis Letters, 2018, 148, 3723-3731.	1.4	14

#	Article	IF	Citations
28702	DFT Study of the Oxygen Reduction Reaction on Carbon-Coated Iron and Iron Carbide. ACS Catalysis, 2018, 8, 10521-10529.	5.5	46
28703	Engineering the activity of CoNx-graphene for hydrogen evolution. International Journal of Hydrogen Energy, 2018, 43, 20573-20579.	3.8	29
28704	Effect of the Processing Route on the Thermoelectric Performance of Nanostructured CuPb₁₈SbTe₂₀. Inorganic Chemistry, 2018, 57, 12976-12986.	1.9	29
28705	Quantum transport in a compensated semimetal <mml:math xmlns:mml="http://www.w3.org/1998/Math/MathML"><mml:mrow><mml:msub><mml:mi mathvariant="normal">W</mml:mi><mml:mn>2</mml:mn></mml:msub><mml:msub><mml:mi>As</mml:mi><mml:mn>3</mml:mn></ with nontrivial <mml:math xmlns:mml="http://www.w3.org/1998/Math/MathML"><mml:msub><mml:mi>Z</mml:mi><mml:mn>2</mml:mn></mml:msub></mm indices. Physical Review B, 2018, 98, .	1.1	8
28706	Beyond ideal two-dimensional metals: Edges, vacancies, and polarizabilities. Physical Review B, 2018, 98, .	1.1	13
28707	Density Functional Theory Investigation of Carbon Dots as Holeâ€transport Material in Perovskite Solar Cells. ChemPhysChem, 2018, 19, 3018-3023.	1.0	18
28708	Importance of Feature Selection in Machine Learning and Adaptive Design for Materials. Springer Series in Materials Science, 2018, , 59-79.	0.4	21
28709	First-principles study of the electronic structure, magnetism, and phonon dispersions for CaX (XÂ= C,) Tj ETQq1 1 0.784314 rgBT /Ov	0.9	12
28710	SnO2 quantum dots @ 3D sulfur-doped reduced graphene oxides as active and durable anode for lithium ion batteries. Electrochimica Acta, 2018, 291, 24-30.	2.6	37
28711	Cobalt polyoxometalate-derived CoWO4 oxygen-evolving catalysts for efficient electrochemical and photoelectrochemical water oxidation. Journal of Catalysis, 2018, 367, 212-220.	3.1	44
28712	Understanding of the Elastic Constants, Energetics, and Bonding in Dicalcium Silicate Using First-Principles Calculations. Journal of Physical Chemistry C, 2018, 122, 24235-24245.	1.5	14
28713	Unusual Ferroelectricity of Trans-Unitcell Ion-Displacement and Multiferroic Soliton in Sodium and Potassium Hydroxides. ACS Applied Materials & Interfaces, 2018, 10, 35361-35366.	4.0	10
28714	Electrical conductivity and magnetic dynamos in magma oceans of Super-Earths. Nature Communications, 2018, 9, 3883.	5.8	48
28715	Strong two-dimensional plasmon in Li-intercalated hexagonal boron-nitride film with low damping. Npj 2D Materials and Applications, 2018, 2, .	3.9	15
28716	The tunable bandgap effect of SnS films. Journal of Physics Condensed Matter, 2018, 30, 465302.	0.7	7
28717	Esfuerzo de corte en Interfaces Fe/Fe3O4. Revista Materia, 2018, 23, .	0.1	0
28718	Factors Controlling Oxygen Interstitial Diffusion in the Ruddlesdenâ€“Popper Oxide La_{2â€“x}Sr_xNiO_{4+Î´}. Chemistry of Materials, 2018, 30, 7166-7177.	3.2	28
28719	Chiral self-sorted multifunctional supramolecular biocoordination polymers and their applications in sensors. Nature Communications, 2018, 9, 3933.	5.8	85

#	Article	IF	Citations
28720	â€œHaeckeliteâ€, a new low dimensional cousin of boron nitride for biosensing with ultra-fast recovery time: a first principles investigation. Journal of Materials Chemistry B, 2018, 6, 6796-6807.	2.9	30
28721	Elastic properties of single crystal hydrogen sulfide: A Brillouin scattering study under high pressure-temperature. Journal of Applied Physics, 2018, 124, 125901.	1.1	2
28722	Subsurface reconstruction and saturation of surface bonds. Science Bulletin, 2018, 63, 1570-1575.	4.3	16
28723	Efficient Charge Separation in 2D Janus van der Waals Structures with Built-in Electric Fields and Intrinsic pâ€“n Doping. Journal of Physical Chemistry C, 2018, 122, 24520-24526.	1.5	79
28724	Engineering Defect Transition-Levels through the van der Waals Heterostructure. Journal of Physical Chemistry C, 2018, 122, 24475-24480.	1.5	27
28725	Structural and Computational Assessment of the Influence of Wet-Chemical Post-Processing of the Al-Substituted Cubic Li₇La₃Zr₂O₁₂. ACS Applied Materials & Interfaces, 2018, 10, 37188-37197.	4.0	30
28726	Theoretical investigation of the Ag filament morphology in conductive bridge random access memories. Journal of Applied Physics, 2018, 124, .	1.1	17
28727	Competing structural instabilities in<mml:math xmlns:mml="http://www.w3.org/1998/Math/MathML"><mml:mrow><mml:msub><mml:mi>Bi</mml:mi><mml:mn>2</mml:mn></mml:msub></mml:mrow></mml:math>Se₃: Physical Review B, 2018, 98, .	2.1	19
28728	Electronic structure of the topological superconductor candidate <mml:math xmlns:mml="http://www.w3.org/1998/Math/MathML"><mml:mrow><mml:msub><mml:mi>Au</mml:mi><mml:mn>2</mml:mn></mml:msub></mml:mrow></mml:math>Pb: Physical Review B, 2018, 98, .	2.1	16
28729	Adsorption Energetics of Atoms and Diatomic Gases with Electrocatalysis Approach towards Hydrogen and Oxygen Evolution Reaction on Pt Surfaces. ChemistrySelect, 2018, 3, 10515-10525.	0.7	8
28730	A detailed study of the microstructure and thermal stability of typical SiC fibers. Materials Characterization, 2018, 146, 91-100.	1.9	16
28731	Sr₂FeIrO₄: Square-Planar Ir(II) in an Extended Oxide. Inorganic Chemistry, 2018, 57, 13577-13585.	1.9	15
28732	Organicâ€“Organic Hybrid g-C₃N₄/Ethanediamine Nanosheets for Photocatalytic H₂ Evolution. Journal of Physical Chemistry C, 2018, 122, 24725-24731.	1.5	15
28733	High-Throughput Pressure-Dependent Density Functional Theory Investigation of Herringbone Polycyclic Aromatic Hydrocarbons: Part 1. Pressure-Dependent Structure Trends. Journal of Physical Chemistry C, 2018, 122, 23815-23827.	1.5	9
28734	Polypyrrole Nanoparticles Doped with Fullerene Uniformly Distributed in the Polymeric Phase: Synthesis, Morphology, and Electrochemical Properties. Journal of Physical Chemistry C, 2018, 122, 25539-25554.	1.5	17
28735	LiCrS₂ and LiMnS₂ Cathodes with Extraordinary Mixed Electronâ€“Ion Conductivities and Favorable Interfacial Compatibilities with Sulfide Electrolyte. ACS Applied Materials & Interfaces, 2018, 10, 36941-36953.	4.0	28
28736	Bonding mechanisms and electronic properties of HgIn2Te4 with Au doping: First-principles study. Journal of Applied Physics, 2018, 124, .	1.1	1
28737	UV-induced formation of oxygen-derived dangling bonds on hydroxyl-terminated SiC. Journal of Physics Condensed Matter, 2018, 30, 435002.	0.7	0

#	Article	IF	Citations
28738	Unusual optical isotropy in anisotropic alkali metal perchlorates MClO₄(Mâ€‰â€‰=â€‰â€‰Li, Na,) Tj ETQq0 0 0	0.7	3
28739	Electronic States of Nanostructured Systems: Titanium and Zirconia. Physics of the Solid State, 2018, 60, 1903-1907.	0.2	2
28740	Cobalt-doped MnO2 ultrathin nanosheets with abundant oxygen vacancies supported on functionalized carbon nanofibers for efficient oxygen evolution. Nano Energy, 2018, 54, 129-137.	8.2	182
28741	Understanding the Intrinsic P-Type Behavior and Phase Stability of Thermoelectric Î±-Mg₃Sb₂. ACS Applied Energy Materials, 2018, 1, 6600-6608.	2.5	28
28742	Hidden order in URu2Si2 : Symmetry-induced antitoroidal vortices. Physical Review B, 2018, 98, .	1.1	1
28743	Roomâ€Temperature Ultrabroadband Photodetection with MoS₂ by Electronicâ€Structure Engineering Strategy. Advanced Materials, 2018, 30, e1804858.	11.1	66
28744	A material genome approach towards exploration of Zn and Cd coordination complex polyester as dielectrics: Design, synthesis and characterization. Polymer, 2018, 159, 95-105.	1.8	7
28745	Electrocatalytic Study of the Oxygen Reduction Reaction at Gold Nanoparticles in the Absence and Presence of Interactions with SnO_x Supports. Journal of the American Chemical Society, 2018, 140, 13775-13785.	6.6	42
28746	Synthesis of Pure NiTiSn by Mechanical Alloying: An Investigation of the Optimal Experimental Conditions Supported by First Principles Calculations. Metals, 2018, 8, 835.	1.0	8
28747	A density functional theory study of reactions of relevance to catalytic hydrocarbon synthesis and combustion. Theoretical Chemistry Accounts, 2018, 137, 1.	0.5	3
28748	Femtosecond Laser-Induced Recombinative O + O = O₂ Reaction on Single Crystal Pd(100) Surface Requires Thermal Assistance. Journal of Physical Chemistry C, 2018, 122, 26039-26046.	1.5	2
28749	Low energy excitations in NiO based on a direct Î”-SCF approach. Journal of Physics Condensed Matter, 2018, 30, 495901.	0.7	16
28750	Phonon Angular Momentum Induced by the Temperature Gradient. Physical Review Letters, 2018, 121, 175301.	2.9	53
28751	Ab Initio Modeling of the Local Violation of a Peierls Transition at the Sb(111) Surface. JETP Letters, 2018, 107, 780-784.	0.4	2
28752	Computational mining of the pressure effect on thermodynamic and thermoelectric properties of cubic Ca ₂ Si. Europhysics Letters, 2018, 123, 67003.	0.7	3
28753	Structural, Elastic, Electronic and Optical Properties of SrTMO3 (TM = Rh, Zr) Compounds: Insights from FP-LAPW Study. Materials, 2018, 11, 2057.	1.3	38
28754	Discovery of Descriptors for Stable Monolayer Oxide Coatings through Machine Learning. ACS Applied Energy Materials, 2018, 1, 6217-6226.	2.5	13
28755	Breaking the scaling relationship via thermally stable Pt/Cu single atom alloys for catalytic dehydrogenation. Nature Communications, 2018, 9, 4454.	5.8	451

#	Article	IF	Citations
28756	First-principles investigation of activity and solubility of Si in Mo solid solution. International Journal of Modern Physics B, 2018, 32, 1850305.	1.0	4
28757	Dilute magnetic semiconductor and half-metal behaviors in C-codoped BeO nanotubes: A first principles simulations. Chinese Journal of Physics, 2018, 56, 3039-3045.	2.0	12
28758	First principles study of M2InC (Mâ€¯=â€¯Zr, Hf and Ta) MAX phases: The effect of M atomic species. Results in Physics, 2018, 11, 869-876.	2.0	45
28759	Mutual interactions in a ternary protein/bioprotectant/water system. Vibrational Spectroscopy, 2018, 99, 190-195.	1.2	1
28760	spâ€“sp² Carbon Sheets as Promising Anode Materials for Na-Ion Batteries. ACS Omega, 2018, 3, 14477-14481.	1.6	6
28761	Anomalous Lattice Dynamics in AgC4N3: Insights From Inelastic Neutron Scattering and Density Functional Calculations. Frontiers in Chemistry, 2018, 6, 544.	1.8	1
28762	Benchmarking the performance of plane-wave vs. localized orbital basis set methods in DFT modeling of metal surface: a case study for Fe-(110). Journal of Computational Science, 2018, 29, 163-167.	1.5	9
28763	Comparison of the outermost layer of MB2 (1 0 1Â¯ 0) and (0001) surfaces (M=Hf, Ta): A first-principles investigation. Materials Today Communications, 2018, 17, 474-479.	0.9	1
28764	Momentum-resolved TDDFT algorithm in atomic basis for real time tracking of electronic excitation. Journal of Chemical Physics, 2018, 149, 154104.	1.2	21
28765	First-Principles Study on the Stabilities, Electronic and Optical Properties of GexSn1-xSe Alloys. Nanomaterials, 2018, 8, 876.	1.9	1
28766	Optical properties of shortest-width zig-zag silicene nano-ribbons: Effects of local fields. Micro and Nano Engineering, 2018, 1, 37-41.	1.4	3
28767	Copper adparticle enabled selective electrosynthesis of n-propanol. Nature Communications, 2018, 9, 4614.	5.8	153
28768	Controlling reaction pathways of selective Câ€“O bond cleavage of glycerol. Nature Communications, 2018, 9, 4612.	5.8	54
28769	Properties of Novel Non-Silicon Materials for Photovoltaic Applications: A First-Principle Insight. Materials, 2018, 11, 2006.	1.3	11
28770	Pressure Effect on Elastic Constants and Related Properties of Ti3Al Intermetallic Compound: A First-Principles Study. Materials, 2018, 11, 2015.	1.3	46
28771	First-Principles Calculations on Structural Property and Anisotropic Elasticity of Î³1-Ti4Nb3Al9 under Pressure. Materials, 2018, 11, 2025.	1.3	2
28772	Electronic Structure of Polymer Dielectrics: The Role of Chemical and Morphological Complexity. Chemistry of Materials, 2018, 30, 7699-7706.	3.2	26
28773	Graphene Oxide-Supported Transition Metal Catalysts for Di-Nitrogen Reduction. Journal of Physical Chemistry C, 2018, 122, 25441-25446.	1.5	24

#	Article	IF	Citations
28774	Insights on the Aluminaâ€“Water Interface Structure by Direct Comparison of Density Functional Simulations with X-ray Reflectivity. Journal of Physical Chemistry C, 2018, 122, 26934-26944.	1.5	19
28775	Mechanistic Study of Lead Adsorption on Activated Carbon. Langmuir, 2018, 34, 13565-13573.	1.6	43
28776	Alkali Metal Cation Effects in Structuring Pt, Rh, and Au Surfaces through Cathodic Corrosion. ACS Applied Materials & Interfaces, 2018, 10, 39363-39379.	4.0	50
28777	Magnetic Anisotropy Controlled by Distinct Interfacial Lattice Distortions at the La_{1â€“x}Sr_xCoO₃/La_{2/3}Sr_{1/3}MnO₃ Interfaces. ACS Applied Materials & Interfaces, 2018, 10, 40951-40957.	4.0	20
28778	Metal and ligand effects on the stability and electronic properties of crystalline two-dimensional metal-benzenehexathiolate coordination compounds. Journal of Physics Condensed Matter, 2018, 30, 465301.	0.7	20
28779	Adsorption and diffusion of F 2 molecules on pristine graphene. Chinese Physics B, 2018, 27, 106801.	0.7	6
28780	Effect of Mn doping on mechanical properties and electronic structure of WCoB ternary boride by first-principles calculations. Chinese Physics B, 2018, 27, 107101.	0.7	6
28781	First-Principles Calculations of Band Offsets at Heterovalent <mml:math xmlns:mml="http://www.w3.org/1998/Math/MathML" display="inline" overflow="scroll"><mml:mi>Îµ</mml:mi></mml:math> - <mml:math xmlns:mml="http://www.w3.org/1998/Math/MathML" display="inline" overflow="scroll"><mml:msub><mml:mrow><mml:mi>Ge</mml:mi><mml:mi>In</mml:mi></mml:mrow><mml:mi>x</mml:mi></mml:mrow> Physical Review Applied, 2018, 10, .	1.5	3
28782	Metallicâ€like thermoelectric Ti-V oxide nanocomposites. Journal of Vacuum Science and Technology A: Vacuum, Surfaces and Films, 2018, 36, .	0.9	1
28783	Scalable Synthesis of Fe/Nâ€Doped Porous Carbon Nanotube Frameworks for Aqueous Znâ€“Air Batteries. Chemistry - A European Journal, 2019, 25, 635-641.	1.7	11
28784	Synergistic Effect of Doping and Compositing on Photocatalytic Efficiency: A Case Study of La₂Ti₂O₇. ACS Applied Materials & Interfaces, 2018, 10, 39327-39335.	4.0	17
28785	Rhombohedralâ€“Orthorhombic Ferroelectric Morphotropic Phase Boundary Associated with a Polar Vortex in BiFeO₃ Films. ACS Nano, 2018, 12, 11098-11105.	7.3	57
28786	Mechanical and Thermal Conductivity Properties of Enhanced Phases in Mg-Zn-Zr System from First Principles. Materials, 2018, 11, 2010.	1.3	8
28787	KCrS₂ Cathode with Considerable Cyclability and High Rate Performance: The First K⁺ Stoichiometric Layered Compound for Potassiumâ€ion Batteries. Small, 2018, 14, e1803495.	5.2	33
28788	Enhancing the Photocatalytic Performance of MXenes via Stoichiometry Engineering of Their Electronic and Optical Properties. ACS Applied Materials & Interfaces, 2018, 10, 39879-39889.	4.0	37
28789	Testing topological protection of edge states in hexagonal quantum spin Hall candidate materials. Physical Review B, 2018, 98, .	1.1	32
28790	Superconductivity of Bi-III phase of elemental bismuth: Insights from muon-spin rotation and density functional theory. Physical Review B, 2018, 98, .	1.1	12
28791	Insight into the catalytic activity of MXenes for hydrogen evolution reaction. Science Bulletin, 2018, 63, 1397-1403.	4.3	61

#	Article	IF	Citations
28792	Vibrational Spectroscopy of Sodalite: Theory and Experiments. Journal of Physical Chemistry C, 2018, 122, 24765-24779.	1.5	26
28793	An Unusual Red Carbon Nitride to Boost the Photoelectrochemical Performance of Wide Bandgap Photoanodes. Advanced Functional Materials, 2018, 28, 1805698.	7.8	94
28794	Surface Tuning of Solid Oxide Fuel Cell Cathode by Atomic Layer Deposition. Advanced Energy Materials, 2018, 8, 1802506.	10.2	48
28795	Tuning On-Surface Synthesis of Graphene Nanoribbons by Noncovalent Intermolecular Interactions. Journal of Physical Chemistry C, 2018, 122, 24415-24420.	1.5	6
28796	Solvent Tunes the Selectivity of Hydrogenation Reaction over Î±-MoC Catalyst. Journal of the American Chemical Society, 2018, 140, 14481-14489.	6.6	167
28797	Phase-selective synthesis of 1Tâ€² MoS2 monolayers and heterophase bilayers. Nature Materials, 2018, 17, 1108-1114.	13.3	348
28798	Water oxidation on a mononuclear manganese heterogeneous catalyst. Nature Catalysis, 2018, 1, 870-877.	16.1	244
28799	Investigation of CHF3 treatment on the energy band at the MoS2/HfZrO4 heterostructure. Applied Physics Letters, 2018, 113, 143506.	1.5	6
28800	Cubic Perovskite Pb(Mg_{1/3}Nb_{2/3})O₃: A Damage Tolerant, Machinable, and Thermal barrier coating material. Zeitschrift Fur Naturforschung - Section A Journal of Physical Sciences, 2018, 74, 71-81.	0.7	33
28801	Electronic Structure and Transport Properties of La₂Zr₂O₇ Pyrochlore from First Principles. Solid State Phenomena, 0, 281, 767-773.	0.3	3
28802	Mesoscale modeling of irradiation damage evolution in bcc iron and vanadium: A comparative study. Fusion Engineering and Design, 2018, 137, 303-311.	1.0	8
28803	Effect of Curvature on the Hydrogen Evolution Reaction of Graphene. Journal of Physical Chemistry C, 2018, 122, 25331-25338.	1.5	33
28804	Parity-breaking in single-element phases: ferroelectric-like elemental polar metals. Journal of Physics Condensed Matter, 2018, 30, 415504.	0.7	5
28805	Anomalous pressure effect on the thermal conductivity of ZnO, GaN, and AlN from first-principles calculations. Physical Review B, 2018, 98, .	1.1	42
28806	Effect of a Rare-Earth Ion on the Structural Instability in RFe3(BO3)4 Crystals. JETP Letters, 2018, 108, 116-120.	0.4	3
28807	Electronic and Magnetic Properties of Bulk and Monolayer CrSi2: A First-Principle Study. Applied Sciences (Switzerland), 2018, 8, 1885.	1.3	8
28808	Physical Properties and Photovoltaic Application of Semiconducting Pd2Se3 Monolayer. Nanomaterials, 2018, 8, 832.	1.9	16
28809	Structural, electronic and optical properties of Ca3Bi2: First-principles investigation. Chinese Journal of Physics, 2018, 56, 2796-2804.	2.0	2

#	Article	IF	Citations
28810	In-situ growth of metallic nanoparticles on perovskite parent as a hydrogen electrode for solid oxide cells. Journal of Power Sources, 2018, 405, 114-123.	4.0	45
28811	Enhancing Visible Light Absorption for Ferroelectric Sn₂P₂S₆ by Se Anion Substitution. Journal of Physical Chemistry C, 2018, 122, 25565-25572.	1.5	7
28812	Ligand-Capped Ru Nanoparticles as Efficient Electrocatalyst for the Hydrogen Evolution Reaction. ACS Catalysis, 2018, 8, 11094-11102.	5.5	70
28813	Tunable Ultrafast Nonlinear Optical Properties of Graphene/MoS₂ van der Waals Heterostructures and Their Application in Solid-State Bulk Lasers. ACS Nano, 2018, 12, 11376-11385.	7.3	113
28814	Effects of annealing with CO and CO2 molecules on oxygen vacancy defect density in amorphous SiO2 formed by thermal oxidation of SiC. Journal of Applied Physics, 2018, 124, 135701.	1.1	8
28815	Pressure induced structural phase transition in rare earth sesquioxide Tm2O3: Experiment and ab initio calculations. Journal of Applied Physics, 2018, 124, 155901.	1.1	15
28816	Lattice Instability during Solid-Solid Structural Transformations under a General Applied Stress Tensor: Example of <mml:math xmlns:mml="http://www.w3.org/1998/Math/MathML" display="inline"><mml:mrow><mml:mi>Si</mml:mi><mml:mtext>â€‰</mml:mtext><mml:mtext>â€‰</mml:mtext><mml:mi mathvariant="normal">I</mml:mi><mml:mo>â†’</mml:mo><mml:mi>Si</mml:mi><mml:mtext>â€‰</mml:mtext><mml:mtext>â€‰ with Metallization. Physical Review Letters, 2018, 121, 165701.	8.1	31
28817	Ultrathin Ti₂Nb₂O₉ Nanosheets with Pseudocapacitive Properties as Superior Anode for Sodiumâ€Ion Batteries. Advanced Materials, 2018, 30, e1804378.	11.1	117
28818	Insights on porphyrin-functionalized graphene: Theoretical study of substituent and metal-center effects on adsorption. Chemical Physics Letters, 2018, 713, 172-179.	1.2	14
28819	Prevalence of trans-Alkenes in Hydrogenation Processes on Metal Surfaces: A Density Functional Theory Study. Journal of Physical Chemistry C, 2018, 122, 25339-25348.	1.5	4
28820	Raman spectra and structural peculiarities of TeO₂â€“TeO₃mixed oxides. Journal of Physics Condensed Matter, 2018, 30, 475403.	0.7	12
28821	Catalytic Hydrogenation of Octanoic Acid in the Gaseous Phase on Ni Catalysts: The Effect of Support Species and Structure. Industrial & Engineering Chemistry Research, 2018, 57, 16272-16283.	1.8	7
28822	Density Functional Theory and Experimental Studies of the Molecular, Vibrational, and Crystal Structure of Bis-Oxadiazole-Bis-Methylene Dinitrate (BODN). Journal of Physical Chemistry A, 2018, 122, 9043-9053.	1.1	9
28823	Reactivity of Silver Iodide (Î²-AgI) Surfaces: A Density Functional Theory Study. Journal of Physical Chemistry C, 2018, 122, 26401-26408.	1.5	1
28824	Experimental and Theoretical Study of Doxorubicin Physicochemical Interaction with BN(O) Drug Delivery Nanocarriers. Journal of Physical Chemistry C, 2018, 122, 26409-26418.	1.5	14
28825	Monolayer Transition-Metal Dichalcogenide Mo_{1â€“x}W_xS₂Alloys as Efficient Anode Materials for Lithium-Ion Batteries. Journal of Physical Chemistry C, 2018, 122, 25837-25848.	1.5	28
28826	Magnetoelectric multipoles in metals. Philosophical Transactions Series A, Mathematical, Physical, and Engineering Sciences, 2018, 376, 20170450.	1.6	33
28827	Strong coupling and periodic potential at the Pb/Sb(111) interface. Physical Review B, 2018, 98, .	1.1	2

#	Article	IF	Citations
28828	Theoretical paradigm for the quantum spin Hall effect at high temperatures. Physical Review B, 2018, 98, .	1.1	55
28829	Structuralâ€Distortionâ€Driven Magnetic Transformation from Ferroâ€to Ferrimagnetic Iron Chains in B 6 â€based Nb 6 FeIr 6 B 8. Angewandte Chemie, 2018, 130, 10480-10484.	1.6	1
28830	Elasticity, lattice dynamics and ideal strengths of USi3 and U3Si via first principles calculations. Journal of Nuclear Materials, 2018, 512, 407-416.	1.3	7
28831	Efficient Nanoclay-Based Composite Photocatalyst: The Role of Nanoclay in Photogenerated Charge Separation. Journal of Physical Chemistry C, 2018, 122, 25900-25908.	1.5	24
28832	Improving the Electrocatalytic Activity and Durability of the La_{0.6}Sr_{0.4}Co_{0.2}Fe_{0.8}O_{3â^'Î´} Cathode by Surface Modification. ACS Applied Materials & Interfaces, 2018, 10, 39785-39793.	4.0	71
28833	Online Kinetics Study of Oxidative Coupling of Methane over La₂O₃ for Methane Activation: What Is Behind the Distinguished Light-off Temperatures?. ACS Catalysis, 2018, 8, 11761-11772.	5.5	60
28834	Synthesis of metastable B2-type Feâ€“Sn alloy epitaxial films and study of their magnetic properties. Japanese Journal of Applied Physics, 2018, 57, 120302.	0.8	9
28835	First principles calculations of interfacial properties and electronic structure of the AlN(0â€¯0â€¯0â€¯1)/Ti(0â€¯0â€¯0â€¯1) interface. Chemical Physics Letters, 2018, 713, 153-159.	1.2	15
28836	Surface Termination and Composition Control of Activity of the Co_xNi_{1â€“x}Fe₂O₄(001) Surface for Water Oxidation: Insights from DFT+U Calculations. ACS Catalysis, 2018, 8, 11773-11782.	5.5	59
28837	An electrochemical thermal transistor. Nature Communications, 2018, 9, 4510.	5.8	105
28838	Disentanglement via Entanglement: A Unified Method for Wannier Localization. Multiscale Modeling and Simulation, 2018, 16, 1392-1410.	0.6	25
28839	Search for new d0 half-metallic materials: theoretical investigation on KCaC1â^'xSi (x = 0; 0.25; 0.5; 0.75) Tj ETQq1 1 0.784314 rgBT /	2.0	7
28840	Lead Vacancy Can Explain the Suppressed Nonradiative Electronâ€“Hole Recombination in FAPbI₃ Perovskite under Iodine-Rich Conditions: A Time-Domain Ab Initio Study. Journal of Physical Chemistry Letters, 2018, 9, 6489-6495.	2.1	29
28841	Strain-Modulated Band Engineering in Two-Dimensional Black Phosphorus/MoS₂ van der Waals Heterojunction. ACS Omega, 2018, 3, 14641-14649.	1.6	22
28842	First-principles prediction of two hexagonal silicon crystals as potential absorbing layer materials for solar-cell application. Journal of Applied Physics, 2018, 124, .	1.1	10
28843	Effect of covalent bonding on the superconducting critical temperature of the H-S-Se system. Physical Review B, 2018, 98, .	1.1	54
28844	First-Principles and Thermodynamics Study of Compositionally Tuned Complex Metal Oxides: Cation Release from the (001) Surface of Mn-Rich Lithium Nickel Manganese Cobalt Oxide. Inorganic Chemistry, 2018, 57, 13300-13311.	1.9	33
28845	Solving the Puzzle of the Coexistence of Different Adsorption Geometries of Graphene on Ni(111). Journal of Physical Chemistry C, 2018, 122, 26105-26110.	1.5	9

#	Article	IF	Citations
28846	First-principles insights on the electronic and optical properties of ZnO@CNT core@shell nanostructure. Scientific Reports, 2018, 8, 15464.	1.6	14
28847	Equation of state of the<mml:math xmlns:mml="http://www.w3.org/1998/Math/MathML"><mml:mrow><mml:mi>Î±</mml:mi><mml:mtext>â^'</mml:mtext><mml:mi>Pt</mml:mi> mathvariant="normal">O</mml:mi><mml:mn>2</mml:mn></mml:msub></mml:mrow></mml:math>and<mml:math xmlns:mml="http://www.w3.org/1998/Math/MathML"><mml:mrow><mml:mi>P</mml:mi><mml:mi>a</mml:mi><mml:mover accent="true"><mml:mn>3</mml:mn><mml:mo>Â¯</mml:mo></mml:mover></mml:mrow></mml:math>-type phases of<mml:math xmlns:mml="http://www.w3.org/1998/. Physical Review B, 2018, 98, .	1.1	7
28848	Surface Modifications of Ti₂CO₂ for Obtaining High Hydrogen Evolution Reaction Activity and Conductivity: A Computational Approach. ChemPhysChem, 2018, 19, 3380-3387.	1.0	20
28849	CO Oxidation at SnO2/Pt3Sn(111) Interfaces. Topics in Catalysis, 2018, 61, 1458-1464.	1.3	4
28850	Role of Hydroxyl Groups in Low-Temperature CO Catalytic Oxidation over Zn₄Si₂O₇(OH)₂ Nanowire-Supported Gold Nanoparticles. Journal of Physical Chemistry C, 2018, 122, 25456-25466.	1.5	2
28851	Tuning hydrogen adsorption on pure and doped ZnO (000 1 Â¯) surfaces by a simple electron counting model. Journal of Applied Physics, 2018, 124, 155302.	1.1	2
28852	Effect of Hf additions on phase stability and mechanical properties of binary W-Hf alloys: A first-principles study. Fusion Engineering and Design, 2018, 137, 295-302.	1.0	12
28853	Synthesis of PdV/C nanoparticles using phase transfer method for oxygen reduction in alkaline electrolytes. International Journal of Hydrogen Energy, 2018, 43, 20712-20720.	3.8	4
28854	Temperature-dependent structural transformation and friction behavior of nanocomposite VCN-(Ag) coatings. Materials and Design, 2018, 160, 964-973.	3.3	29
28855	Initial Reduction of the PdO(101) Surface: Role of Oxygen Vacancy Formation Kinetics. Journal of Physical Chemistry C, 2018, 122, 26007-26017.	1.5	13
28856	How One-Dimensional Are Atomic Gold Chains on a Substrate?. Journal of Physical Chemistry C, 2018, 122, 25580-25588.	1.5	22
28857	Contact properties of a vdW heterostructure composed of penta-graphene and penta-BN2 sheets. Journal of Applied Physics, 2018, 124, .	1.1	16
28858	Infrared and Raman active vibrational modes in MoS 2 â€based nanotubes: Symmetry analysis and firstâ€principles calculations. Journal of Computational Chemistry, 2018, 39, 2163-2172.	1.5	8
28859	Mechanic, electronic and optical properties of silicides MSi (Mâ€¯=â€¯Re,Tc): First-principle calculations. Chinese Journal of Physics, 2018, 56, 2760-2772.	2.0	2
28860	Cr_{2.37}Ga₃Se₈: A Quasi-Two-Dimensional Magnetic Semiconductor. Inorganic Chemistry, 2018, 57, 14298-14303.	1.9	3
28861	Local structure of stoichiometric and oxygen-deficient A2Ti6O13 (Aâ€‰=â€‰Li, Na, and K) studied by X-ray absorption spectroscopy and first-principles calculations. Journal of Applied Physics, 2018, 124, 155101.	1.1	11
28862	Structure sensitivity of electronic transport across graphene grain boundaries. Physical Review B, 2018, 98, .	1.1	6
28863	Universality of electronic characteristics and photocatalyst applications in the two-dimensional Janus transition metal dichalcogenides. Physical Review B, 2018, 98, .	1.1	229

#	Article	IF	Citations
28864	Investigation, using density function theory, of coverage of the kaolinite (001) surface during hydrogen adsorption. Clay Minerals, 2018, 53, 393-402.	0.2	2
28865	Toward the design of interstitial nonmetals co-doping for Mg-based hydrides as hydrogen storage material. Journal of Materials Research, 2018, 33, 4080-4091.	1.2	7
28866	Adsorption of Transition Metals on Black Phosphorene: a First-Principles Study. Nanoscale Research Letters, 2018, 13, 282.	3.1	79
28867	Lattice relaxations in disordered Fe-based materials in the paramagnetic state from first principles. Physical Review B, 2018, 98, .	1.1	18
28868	Spin-polarized electron transport in highly reduced MgFe₂O_{4-Î´}. Materials Research Express, 2018, 5, 126301.	0.8	9
28869	First-principles calculations of electronic structures and ferromagnetism of Fe3Si(001)//MgO(001) films. International Journal of Modern Physics B, 2018, 32, 1850272.	1.0	0
28870	Design of Effective Catalysts for Selective Alkyne Hydrogenation by Doping of Ceria with a Single-Atom Promotor. Journal of the American Chemical Society, 2018, 140, 12964-12973.	6.6	204
28871	Magnetic field-induced ferroelectricity in Sâ€‰=â€‰1/2 kagome staircase compound PbCu3TeO7. Npj Quantum Materials, 2018, 3, .	1.8	25
28872	Intrinsic structural and electronic properties of the Buffer Layer on Silicon Carbide unraveled by Density Functional Theory. Scientific Reports, 2018, 8, 13097.	1.6	20
28873	Vapor-phase hydrothermal transformation of a nanosheet array structure Ni(OH)₂ into ultrathin Ni₃S₂ nanosheets on nickel foam for high-efficiency overall water splitting. Journal of Materials Chemistry A, 2018, 6, 19201-19209.	5.2	47
28874	Melts of CrCoNi-based high-entropy alloys: Atomic diffusion and electronic/atomic structure from ab initio simulation. Applied Physics Letters, 2018, 113, .	1.5	27
28875	Thermoelectric properties of topological insulators based on Ï€-stacked molecular and graphene-belt systems with hydrogen bonds. IOP Conference Series: Materials Science and Engineering, 2018, 369, 012028.	0.3	1
28876	Selective hydrogen adsorption on a buckled carbon nitride sheet: first-principles calculation. Materials Research Express, 2018, 5, 125605.	0.8	6
28877	A first-principles study of pristine and Al-doped activated carbon interacting with 5-Fluorouracil anticancer drug. European Physical Journal E, 2018, 41, 107.	0.7	10
28878	Computational characterization of a-Si:H/c-Si interfaces. Journal of Computational Electronics, 2018, 17, 1457-1469.	1.3	3
28879	Effects of point defects on the mechanical response of LaRu2P2. Acta Materialia, 2018, 160, 224-234.	3.8	7
28880	CS-AFM study on Pb-induced degradation of passive film on nickel-based alloy in high temperature and high pressure water. Corrosion Science, 2018, 144, 249-257.	3.0	8
28881	Temperature dependence of thermodynamic properties of MoS2 monolayer and single-wall nanotubes: Application of the developed three-body force field. Journal of Molecular Graphics and Modelling, 2018, 85, 212-222.	1.3	4

#	Article	IF	Citations
28882	Enhanced electrical transport properties via Pb vacancies in single crystalline PbTe prepared by Te-flux method. Physica B: Condensed Matter, 2018, 550, 9-14.	1.3	1
28883	Role of Ni in Bimetallic PdNi Catalysts for Ethanol Oxidation Reaction. Journal of Physical Chemistry C, 2018, 122, 22448-22459.	1.5	43
28884	Anhydrous Methanol and Ethanol Dehydrogenation at Cu(111) Step Edges. Journal of Physical Chemistry C, 2018, 122, 21952-21962.	1.5	21
28885	Density Functional Theory Prediction of the Second Harmonic Generation and Linear Pockels Effect in Trigonal BaZnO₂. Journal of Physical Chemistry C, 2018, 122, 21277-21283.	1.5	5
28886	Strong Topological States and High Charge Carrier Mobility in Tetraoxa[8]circulene Nanosheets. Journal of Physical Chemistry C, 2018, 122, 22216-22222.	1.5	25
28887	Oxygen Evolution Reaction on Perovskites: A Multieffect Descriptor Study Combining Experimental and Theoretical Methods. ACS Catalysis, 2018, 8, 9567-9578.	5.5	98
28888	First-Principles Analysis of Radiative Recombination in Lead-Halide Perovskites. ACS Energy Letters, 2018, 3, 2329-2334.	8.8	81
28889	Electronic structure of electron-irradiated graphene and effects of hydrogen passivation. Materials Research Express, 2018, 5, 115603.	0.8	9
28890	Magnetic Proximity Effect and Anomalous Hall Effect in <mml:math xmlns:mml="http://www.w3.org/1998/Math/MathML" display="inline" overflow="scroll"><mml:mi>Pt</mml:mi><mml:mo>/</mml:mo><mml:msub><mml:mrow><mml:mrow><mml:mi mathvariant="normal">Y</mml:mi></mml:mrow></mml:mrow><mml:mn>3</mml:mn></mml:msub><mml:msub><mml:mi>Fe</mml:mi> Physical Review Applied, 2018, 10, .	1.5	12
28891	Doping of <mml:math xmlns:mml="http://www.w3.org/1998/Math/MathML"><mml:msub><mml:mi>BiFeO</mml:mi><mml:mn>3</mml:mn></mml:msub> : A comprehensive study on substitutional doping. Physical Review B, 2018, 98, .	1.1	51
28892	Quantum friction between oscillating crystal slabs: Graphene monolayers on dielectric substrates. Physical Review B, 2018, 98, .	1.1	6
28893	Stability of Cu-Precipitates in Al-Cu Alloys. Applied Sciences (Switzerland), 2018, 8, 1003.	1.3	8
28894	A new porous metallic silicon dicarbide for highly efficient Li-ion battery anode identified by targeted structure search. Carbon, 2018, 140, 680-687.	5.4	25
28895	Design of active nickel single-atom decorated MoS2 as a pH-universal catalyst for hydrogen evolution reaction. Nano Energy, 2018, 53, 458-467.	8.2	222
28896	Stress Relief and Reactivity Loss of Hydrated Anatase (001) Surface. Journal of Physical Chemistry C, 2018, 122, 22407-22417.	1.5	6
28897	Structure and Raman scattering of chained carbon films on copper substrate: ab initio approach. IOP Conference Series: Materials Science and Engineering, 2018, 292, 012102.	0.3	2
28898	Phase diagram of oxygen at extreme pressure and temperature conditions: An ab initio study. Physical Review B, 2018, 98, .	1.1	2
28899	Band Topology and Linking Structure of Nodal Line Semimetals with <mml:math xmlns:mml="http://www.w3.org/1998/Math/MathML" display="inline"><mml:msub><mml:mi>Z</mml:mi><mml:mn>2</mml:mn></mml:msub></mml:math> Monopole Charges. Physical Review Letters, 2018, 121, 106403.	2.9	164

#	Article	IF	Citations
28900	Lightâ€Induced Spin Transitions in Copperâ€Nitroxideâ€Based Switchable Molecular Magnets: Insights from Periodic DFT+U Calculations. Chemistry - A European Journal, 2018, 24, 18988-18997.	1.7	3
28901	First-principles study of the nanotubes from the TiO2 hexagonal sheet. Journal of Materials Science, 2018, 53, 15530-15540.	1.7	4
28902	Superdense tI12 carbon: Unexpectedly high elastic moduli but low ideal strength. Physics Letters, Section A: General, Atomic and Solid State Physics, 2018, 382, 3125-3130.	0.9	8
28903	Theoretical study of CaO, CaS and CaSe via first-principles calculations. Results in Physics, 2018, 10, 934-945.	2.0	29
28904	Atomic and electronic structure of graphene oxide/Cu interface. Thin Solid Films, 2018, 665, 99-108.	0.8	10
28905	Thermodynamical Stability of Plutonium Monoxide with Carbon Substitution. Journal of Physical Chemistry C, 2018, 122, 22821-22828.	1.5	9
28906	Multifunctionality of Partially Reduced Graphene Oxideâ€“CrVO₄Nanocomposite: Electrochemical and Photocatalytic Studies with Theoretical Insight from Density Functional Theory. Journal of Physical Chemistry C, 2018, 122, 21140-21150.	1.5	25
28907	Two-Dimensional Titania: Structures and Properties Predicted by First Principle Calculation. Journal of Physical Chemistry C, 2018, 122, 22911-22919.	1.5	12
28908	Effect of pressure on physical properties of LuAsO₄ crystal. Materials Research Express, 2018, 5, 116204.	0.8	1
28909	Growth of a predicted two-dimensional topological insulator based on InBi-Si(111)- <mml:math xmlns:mml="http://www.w3.org/1998/Math/MathML"><mml:mrow><mml:msqrt><mml:mn>7</mml:mn></mml:msqrt><mml:mo>Ã— Physical Review B, 2018, 98, .	1.1	22
28910	Thermodynamic Evaluation of Trace-Amount Transition-Metal-Ion Doping in NiOOH Films. Journal of the Electrochemical Society, 2018, 165, F907-F913.	1.3	7
28911	Activating Aromatic Rings as Na-Ion Storage Sites to Achieve High Capacity. CheM, 2018, 4, 2463-2478.	5.8	82
28912	Predicting a two-dimensional P2S3 monolayer: A global minimum structure. Computational Materials Science, 2018, 155, 288-292.	1.4	8
28913	Suppressing heating rate-dependent martensitic stabilization in ductile Cu-Al-Mn shape memory alloys by Ni addition: An experimental and first-principles study. Materials Characterization, 2018, 145, 381-388.	1.9	9
28914	Changes to the dissociation barrier of H2 due to buckling induced by a chemisorbed hydrogen on a doped graphene surface. Journal of Molecular Modeling, 2018, 24, 244.	0.8	4
28915	Vibrational Modes and Phonon and Thermodynamic Properties of the Metaboric Acid Polymorphs Î±-, Î²-, and Î³-(BOH)₃O₃ within a Density Functional Theory Framework. Journal of Physical Chemistry A, 2018, 122, 7628-7645.	1.1	4
28916	CeO_x-Decorated NiFe-Layered Double Hydroxide for Efficient Alkaline Hydrogen Evolution by Oxygen Vacancy Engineering. ACS Applied Materials & Interfaces, 2018, 10, 35145-35153.	4.0	156
28917	Control of coordinatively unsaturated Zr sites in ZrO2 for efficient Câ€“H bond activation. Nature Communications, 2018, 9, 3794.	5.8	133

#	Article	IF	Citations
28918	Crosslinking chemistry of poly(vinylmethyl-co-methyl)silazanes toward low-temperature formable preceramic polymers as precursors of functional aluminium-modified Siâ€“Câ€“N ceramics. Dalton Transactions, 2018, 47, 14580-14593.	1.6	25
28919	Modulating the electronic properties of perovskite via Ïƒâ€“Ï€ interfacial interactions: A computational study. APL Materials, 2018, 6, .	2.2	6
28920	Strain-tunable molecular doping in germanane: a first-principles study. Nanotechnology, 2018, 29, 465202.	1.3	4
28921	Effect of pressure on the elastic properties and optoelectronic behavior of Zn ₄ B ₆ O ₁₃ : First-principles investigation. Chinese Physics B, 2018, 27, 057101.	0.7	2
28922	Why Tiâ€Doping Enhances the Efficiency of Hematite Photoanodes for Water Splittingâ€”The Full Picture. Advanced Functional Materials, 2018, 28, 1804472.	7.8	53
28923	Understanding the Role of Functional Groups in Polymeric Binder for Electrochemical Carbon Dioxide Reduction on Gold Nanoparticles. Advanced Functional Materials, 2018, 28, 1804762.	7.8	76
28924	Reversible Olefin Addition to Extended Lattices of a Nickelâ€“Selenium Framework. Journal of Physical Chemistry C, 2018, 122, 22424-22434.	1.5	2
28925	Unconventional lattice dynamics in few-layer h-BN and indium iodide crystals*. Chinese Physics B, 2018, 27, 086301.	0.7	2
28926	Reversible and Reproducible Hydrogen Storage in Single- Walled Carbon Nanotubes Functionalized with Borane. , 2018, , .		1
28927	Effects of Charge, Size, and Shape of Transition States, Bound Intermediates, and Confining Voids in Reactions of Alkenes on Solid Acids. ChemCatChem, 2018, 10, 4028-4037.	1.8	27
28928	Atomistic simulation study on the shear behavior of Ag/MgO interface. Computational Materials Science, 2018, 155, 116-128.	1.4	10
28929	Deformation criterion for face-centered-cubic metal nanowires. Materials Science & Engineering A: Structural Materials: Properties, Microstructure and Processing, 2018, 736, 431-437.	2.6	3
28930	Anionic Structure in Molten Cryoliteâ€“Alumina Systems. Journal of Physical Chemistry C, 2018, 122, 21807-21816.	1.5	11
28931	Holey single-walled carbon nanotubes for ultra-fast broadband bolometers. Nanoscale, 2018, 10, 18665-18671.	2.8	29
28932	Critical-point model dielectric function analysis of WO3 thin films deposited by atomic layer deposition techniques. Journal of Applied Physics, 2018, 124, .	1.1	5
28933	Site preferences of alloying transition metal elements in Ni-based superalloy: A first-principles study. Chinese Physics B, 2018, 27, 097102.	0.7	3
28934	Adsorptions of metal adatoms on graphene-like BC ₃ and their rich electronic properties: A first-principles study. Chinese Physics B, 2018, 27, 097311.	0.7	3
28935	Size and temperature transferability of direct and local deep neural networks for atomic forces. Physical Review B, 2018, 98, .	1.1	16

#	Article	IF	Citations
28936	Pressure-induced structural modulations in coesite. Physical Review B, 2018, 98, .	1.1	4
28937	Thermooptical and Dielectric Studies of a Calcium-Induced Ferroelectric Phase in a SrTiO3 Incipient Ferroelectric. Physics of the Solid State, 2018, 60, 1793-1806.	0.2	1
28938	Investigation of Charge-Transfer Interaction in Mixed Stack Donorâ€“Acceptor Cocrystals Toward Tunable Solid-State Emission Characteristics. Crystal Growth and Design, 2018, 18, 6001-6008.	1.4	51
28939	Computational Prediction and Experimental Realization of p-Type Carriers in the Wide-Band-Gap Oxide SrZn_{1â€“x}Li_xO₂. Inorganic Chemistry, 2018, 57, 11874-11883.	1.9	6
28940	First-Principles Investigations of the Temperature Dependence of Electronic Structure and Optical Properties of Rutile TiO₂. Journal of Physical Chemistry C, 2018, 122, 22642-22649.	1.5	18
28941	Kinetically Determined Phase Transition from Stage II (LiC₁₂) to Stage I (LiC₆) in a Graphite Anode for Li-Ion Batteries. Journal of Physical Chemistry Letters, 2018, 9, 5567-5573.	2.1	74
28942	Activity and Selectivity Control in CO₂ Electroreduction to Multicarbon Products over CuO_x Catalysts via Electrolyte Design. ACS Catalysis, 2018, 8, 10012-10020.	5.5	173
28943	Unraveling a novel ferroelectric GeSe phase and its transformation into a topological crystalline insulator under high pressure. NPG Asia Materials, 2018, 10, 882-887.	3.8	27
28944	Pressure dependence on electronic structures, charge distribution and bond orders of solid nitromethane using nonlocal DFT functional. Molecular Simulation, 2018, 44, 1454-1460.	0.9	2
28945	Computational investigation of inverse Heusler compounds for spintronics applications. Physical Review B, 2018, 98, .	1.1	69
28946	Study of the New Two-Dimensional Compound CoC. JETP Letters, 2018, 108, 13-17.	0.4	9
28947	Effect of manganese on the crystal structures and luminescence properties of mn doped Sr2SiO4:Eu2+ phosphors. Chinese Journal of Physics, 2018, 56, 1977-1984.	2.0	0
28948	Reactivity of Amorphous Carbon Surfaces: Rationalizing the Role of Structural Motifs in Functionalization Using Machine Learning. Chemistry of Materials, 2018, 30, 7446-7455.	3.2	77
28949	Sub-5 nm monolayer black phosphorene tunneling transistors. Nanotechnology, 2018, 29, 485202.	1.3	21
28950	Assessing the SCAN functional for itinerant electron ferromagnets. Physical Review B, 2018, 98, .	1.1	64
28951	Direct Magnetization-Polarization Coupling in <mml:math xmlns:mml="http://www.w3.org/1998/Math/MathML" display="inline"><mml:mrow><mml:msub><mml:mrow><mml:mi>BaCuF</mml:mi></mml:mrow><mml:mrow><mml:mn>4</mml:mn></mml:mrow> Physical Review Letters, 2018, 121, 117601.	2.0	18
28952	A first-principles study of the properties of two novel Si3P4 phases. International Journal of Modern Physics B, 2018, 32, 1850244.	1.0	3
28953	Influence of CO molecule on structure stability and electronic properties of silver nanotube. Chinese Journal of Physics, 2018, 56, 1999-2005.	2.0	0

#	Article	IF	Citations
28954	Three-dimensional pentagonal silicon: Stability and properties. Computational Materials Science, 2018, 155, 373-377.	1.4	8
28955	Analysis of the structural, electronic, elastic and thermodynamic properties of CuAl2X4 (Xâ€‰=â€‰O, S) spinel structure. Materials Research Bulletin, 2018, 108, 255-265.	2.7	22
28956	Database Screening of Ternary Chalcogenides for P-type Transparent Conductors. Chemistry of Materials, 2018, 30, 6794-6800.	3.2	32
28957	Rb₃SiF₇:Mn⁴⁺ and Rb₂CsSiF₇:Mn⁴⁺ Red-Emitting Phosphors with a Faster Decay Rate. Chemistry of Materials, 2018, 30, 6936-6944.	3.2	81
28958	Predicting Monolayer Oxide Stability over Low-Index Surfaces of TiO₂ Polymorphs Using ab Initio Thermodynamics. Langmuir, 2018, 34, 11685-11694.	1.6	8
28959	Hydrogenated Na₂Ti₃O₇ Epitaxially Grown on Flexible N-Doped Carbon Sponge for Potassium-Ion Batteries. ACS Applied Materials & Interfaces, 2018, 10, 37974-37980.	4.0	45
28960	Entropy contributions to phase stability in binary random solid solutions. Npj Computational Materials, 2018, 4, .	3.5	64
28961	Na1â^'xSn2P2 as a new member of van der Waals-type layered tin pnictide superconductors. Scientific Reports, 2018, 8, 12852.	1.6	22
28962	First-principles study of anion diffusion in lead-free halide double perovskites. Physical Chemistry Chemical Physics, 2018, 20, 24339-24344.	1.3	59
28963	Suppression by Pt of CO adsorption and dissociation and methane formation on Fe5C2(100) surfaces. Physical Chemistry Chemical Physics, 2018, 20, 25246-25255.	1.3	9
28964	Optical properties of In₂O₃ from experiment and first-principles theory: influence of lattice screening. New Journal of Physics, 2018, 20, 053016.	1.2	20
28965	Comparison of vibrational and thermodynamic properties of MoS₂ and WS₂ nanotubes: first principles study. Materials Research Express, 2018, 5, 115028.	0.8	10
28966	Atomistic underpinnings for growth direction and pattern formation of hcp magnesium alloy dendrite. Acta Materialia, 2018, 161, 35-46.	3.8	52
28967	Molecular dynamics study of hydrogen-vacancy interactions in Î±-zirconium. Journal of Nuclear Materials, 2018, 511, 341-352.	1.3	16
28968	Auâ€“Rh Surface Structures on Rh(111): DFT Insights into the Formation of an Ordered Surface Alloy. Journal of Physical Chemistry C, 2018, 122, 22435-22447.	1.5	5
28969	Structure and Activity Transition from Oxidized to Metallic Tungsten for Catalytic Hydrogenation: A Density Functional Theory Study. Journal of Physical Chemistry C, 2018, 122, 23053-23061.	1.5	4
28970	Simple Route to Metal cyclo-N₅^{â€“} Salt: High-Pressure Synthesis of CuN₅. Journal of Physical Chemistry C, 2018, 122, 22339-22344.	1.5	46
28971	Sheet-membrane Mn-doped nickel hydroxide encapsulated via heterogeneous Ni₃S₂ nanoparticles for efficient alkaline batteryâ€“supercapacitor hybrid devices. Journal of Materials Chemistry A, 2018, 6, 19020-19029.	5.2	55

#	Article	IF	Citations
28972	Atomically dispersed tungsten on metal halide monolayer as a ferromagnetic Chern insulator. Physical Review B, 2018, 98, .	1.1	5
28973	Electrical resistivity modulation of thermoelectric iron based nanocomposites. Vacuum, 2018, 157, 384-390.	1.6	3
28974	Step-like band alignment and stacking-dependent band splitting in trilayer TMD heterostructures. Physical Chemistry Chemical Physics, 2018, 20, 25000-25008.	1.3	13
28975	Adsorption of common solvent molecules on graphene and MoS2 from first-principles. Journal of Chemical Physics, 2018, 149, 094702.	1.2	17
28976	From one to three, exploring the rungs of Jacobâ€™s ladder in magnetic alloys. European Physical Journal B, 2018, 91, 1.	0.6	15
28977	In Situ Observations of Early Stage Oxidation of Ni-Cr and Ni-Cr-Mo Alloys. Corrosion, 2018, 74, 939-946.	0.5	39
28978	Materials Informatics for Dark Matter Detection. Physica Status Solidi - Rapid Research Letters, 2018, 12, 1800293.	1.2	30
28979	One-pot synthesized porous Ti-doped MoO2 anode material for high energy density lithium ion batteries. Journal of Materials Science: Materials in Electronics, 2018, 29, 17571-17579.	1.1	5
28980	Predictions for structural stability and electronic evolution in pressure-induced overdoped YBa2Cu3O7. Computational Materials Science, 2018, 155, 416-423.	1.4	2
28981	Magnetothermoelectric Properties of Ferrocene-Based Compounds Sandwiched by Transition Metals in the Presence of Gold Electrodes. Journal of Physical Chemistry C, 2018, 122, 22063-22072.	1.5	5
28982	Chemically Functionalized Penta-stanene Monolayers for Light Harvesting with High Carrier Mobility. Journal of Physical Chemistry C, 2018, 122, 21763-21769.	1.5	18
28983	Influence of crystallographic environment on scandium K-edge X-ray absorption near-edge structure spectra. Physical Chemistry Chemical Physics, 2018, 20, 23903-23912.	1.3	14
28984	Structural phase transition and electronic properties of CaO under high pressure. Materials Research Express, 2018, 5, 125903.	0.8	10
28985	Time-resolved X-ray absorption spectroscopy on Alâ€“Cu alloys â€“ from solute copper to stable precipitates. Journal of Applied Crystallography, 2018, 51, 1339-1351.	1.9	7
28986	Controlled Airâ€Etching Synthesis of Porousâ€Carbon Nanotube Aerogels with Ultrafast Charging at 1000 A g^{â^'1}. Small, 2018, 14, e1802394.	5.2	37
28987	Rapid communication: Permeability of hydrogen in two-dimensional graphene and hexagonal boron nitride sheets. Pramana - Journal of Physics, 2018, 91, 1.	0.9	4
28988	Intermetallic Growth and Interfacial Properties of the Grain Refiners in Al Alloys. Materials, 2018, 11, 636.	1.3	14
28989	The Effects of Radial Compression on the Electronic Properties and Hydrogen Adsorption of SiC Nanotubes. Physica Status Solidi (B): Basic Research, 2018, 255, 1800180.	0.7	1

#	Article	IF	Citations
28990	Synthesis and characterization of the pyridineâ€"bromine trifluoride (1/1) complex, [pyâ^™BrF3]. Journal of Fluorine Chemistry, 2018, 215, 17-24.	0.9	5
28991	In-situ investigation of pressure effect on structural evolution and conductivity of Na3SbS4 superionic conductor. Journal of Power Sources, 2018, 401, 111-116.	4.0	26
28992	Elastic properties of Mn-rich Î± intermetallic phase in engineering aluminum alloys: An ab initio study. Journal of Applied Physics, 2018, 124, .	1.1	5
28993	Far-infrared reflectivity spectra of nanotwinned GaV₄Se₈. Phase Transitions, 2018, 91, 942-952.	0.6	1
28994	A theoretical study of substitutional boronâ€"nitrogen clusters in diamond. Journal of Physics Condensed Matter, 2018, 30, 425501.	0.7	10
28995	Influence of Tm, Ho and Er dopants on the properties of Yb activated ZnTiO₃perovskite: a density functional theory insight. Materials Research Express, 2018, 5, 106202.	0.8	17
28996	First-principles calculations on phase transformation and elastic properties of CuO under pressure. Journal of Computational Electronics, 2018, 17, 1450-1456.	1.3	9
28997	Impact of point defects on the elastic properties of BaZrO3: Comprehensive insight from experiments and ab initio calculations. Acta Materialia, 2018, 160, 247-256.	3.8	21
28998	The crucial role of density functional nonlocality and on-axis CH3NH3 rotation induced I2 formation in hybrid organic-inorganic CH3NH3PbI3 cubic perovskite. Scientific Reports, 2018, 8, 13161.	1.6	12
28999	Temperature-programmed desorption studies of NH3 and H2O on the RuO2(110) surface: effects of adsorbate diffusion. Physical Chemistry Chemical Physics, 2018, 20, 24201-24209.	1.3	14
29000	First-principles calculations of the electronic properties of SiC-based bilayer and trilayer heterostructures. Physical Chemistry Chemical Physics, 2018, 20, 24726-24734.	1.3	77
29001	High energetic polymeric nitrogen sheet confined in a graphene matrix. RSC Advances, 2018, 8, 30912-30918.	1.7	14
29002	Pressure-induced structural and electronic transitions in kesterite-type Cu2ZnSnS4. Journal of Applied Physics, 2018, 124, 085905.	1.1	7
29003	DFT reveals concentration-dependent cathodic/anodic behaviour of lithiated titania. Materials Research Express, 2018, 5, 096301.	0.8	2
29004	Clustering of hydrogen, phosphorus, and vacancies in diamond: A density functional theory analysis. Physical Review B, 2018, 98, .	1.1	22
29005	End-member compounds of a 4-sublattice model of multicomponent BCC solid solutions. Data in Brief, 2018, 20, 1018-1022.	0.5	2
29006	Accounting for the thermo-stability of PdHx (xÂ=Â1â€"3) by density functional theory. International Journal of Hydrogen Energy, 2018, 43, 18372-18381.	3.8	12
29007	Morphology control of Co2C nanostructures via the reduction process for direct production of lower olefins from syngas. Journal of Catalysis, 2018, 366, 289-299.	3.1	52

#	Article	IF	Citations
29008	The dimensional and hydrogenating effect on the electronic properties of ZnSe nanomaterials: a computational investigation. Physical Chemistry Chemical Physics, 2018, 20, 24453-24464.	1.3	4
29009	Double-atom catalysts: transition metal dimer-anchored C₂N monolayers as N₂ fixation electrocatalysts. Journal of Materials Chemistry A, 2018, 6, 18599-18604.	5.2	224
29010	Impact ionization in Î²-Ga2O3. Journal of Applied Physics, 2018, 124, .	1.1	89
29011	Polyaniline (C3N) nanoribbons: Magnetic metal, semiconductor, and half-metal. Journal of Applied Physics, 2018, 124, .	1.1	26
29012	(BEDT-TTF)2Cu2(CN)3 Spin Liquid: Beyond the Average Structure. Crystals, 2018, 8, 158.	1.0	14
29013	Computational exploration of two-dimensional silicon diarsenide and germanium arsenide for photovoltaic applications. Beilstein Journal of Nanotechnology, 2018, 9, 1247-1253.	1.5	14
29014	Micropillar compression deformation of single crystals of Mo5SiB2 with the tetragonal D8 structure. Acta Materialia, 2018, 159, 416-428.	3.8	29
29015	Atomically sharp interlayer stacking shifts at anti-phase grain boundaries in overlapping MoS₂ secondary layers. Nanoscale, 2018, 10, 16692-16702.	2.8	22
29016	Electronic, elastic and X-ray spectroscopic properties of direct and inverse full Heusler compounds Co₂FeAl and Fe₂CoAl, promising materials for spintronic applications: a DFT+U approach. Journal of Materials Chemistry C, 2018, 6, 10341-10349.	2.7	41
29017	Functional thiols as repair and doping agents of defective MoS₂ monolayers. Journal of Physics Condensed Matter, 2018, 30, 235302.	0.7	8
29018	Mixedâ€valence Compounds: AuO₂ and AuS. ChemPhysChem, 2018, 19, 2989-2994.	1.0	7
29019	Theoretical calculations of elastic, mechanical and thermal properties of REPt3 (REâ€‰=â€‰Sc, Y and Lu) intermetallic compounds based on DFT. Indian Journal of Physics, 2018, 92, 1503-1513.	0.9	5
29020	Lattice distortion in a strong and ductile refractory high-entropy alloy. Acta Materialia, 2018, 160, 158-172.	3.8	325
29021	The role of Ni in modifying the order of the phase transition of La(Fe,Ni,Si)13. Acta Materialia, 2018, 160, 137-146.	3.8	45
29022	The deposition characteristics of PAN/PPY on SiO2 substrate by density functional theory (DFT) calculations. Applied Surface Science, 2018, 462, 890-895.	3.1	7
29023	Nature of localized phonon modes of tilt grain boundaries in graphene. Carbon, 2018, 140, 250-258.	5.4	18
29024	Effects of heteroatom doping on the performance of graphene in sodium-ion batteries: A density functional theory investigation. Carbon, 2018, 140, 276-285.	5.4	106
29025	Investigation of the initial stages of the montmorillonite acid-activation process using DFT calculations. Applied Clay Science, 2018, 165, 170-178.	2.6	16

#	Article	IF	Citations
29026	Fundamental properties and phase stability of B1 and B2 phases of MgO over a wide range of pressures and temperatures: A first-principles study. Computational Materials Science, 2018, 154, 159-168.	1.4	3
29027	DFT study on the adsorption of p-nitrophenol over vacancy and Pt-doped graphene sheets. Computational and Theoretical Chemistry, 2018, 1142, 88-96.	1.1	26
29028	Effects of interstitial atoms (N/O) in bcc Fe from first-principle calculations. Fusion Engineering and Design, 2018, 137, 22-29.	1.0	7
29029	Silicon atom and silicon oxide molecule, within the metallic and semiconducting carbon nanotubes as promising centers candidates for hydrogen adsorption: A DFT theoretical study. International Journal of Hydrogen Energy, 2018, 43, 18306-18315.	3.8	9
29030	Monatomic oxygen adsorption on halogen-substituted monovacant graphene. International Journal of Hydrogen Energy, 2018, 43, 17673-17681.	3.8	1
29031	Origin of low Young modulus of multicomponent, biomedical Ti alloys - Seeking optimal elastic properties through a first principles investigation. Journal of the Mechanical Behavior of Biomedical Materials, 2018, 88, 352-361.	1.5	15
29032	13C NMR spectrum of crystalline [Rh(Acac) (CO)2]: A contribution to the discussion on [Rh(Acac) (CO)2] molecular structure in the solid state. Journal of Organometallic Chemistry, 2018, 874, 70-73.	0.8	0
29033	Adsorption of Acetone on Rutile TiO₂: A DFT and FTIRS Study. Journal of Physical Chemistry C, 2018, 122, 19481-19490.	1.5	23
29034	Adsorption of Monocyclic Aromatics on Transition Metal Surfaces: Insight into Variation of Binding Strength from First-Principles. Journal of Physical Chemistry C, 2018, 122, 21897-21909.	1.5	39
29035	Evaluating the Stability of Single-Atom Catalysts with High Chemical Activity. Journal of Physical Chemistry C, 2018, 122, 21919-21926.	1.5	20
29036	Surface Adsorption Affects the Performance of Alkaline Anion-Exchange Membrane Fuel Cells. ACS Catalysis, 2018, 8, 9429-9439.	5.5	55
29037	Iridiumâ€“Tungsten Alloy Nanodendrites as pH-Universal Water-Splitting Electrocatalysts. ACS Central Science, 2018, 4, 1244-1252.	5.3	196
29038	Modulation of Hydrogen Evolution Catalytic Activity of Basal Plane in Monolayer Platinum and Palladium Dichalcogenides. ACS Omega, 2018, 3, 10058-10065.	1.6	46
29039	Color-stable highly luminescent sky-blue perovskite light-emitting diodes. Nature Communications, 2018, 9, 3541.	5.8	536
29040	Tunable interlayer coupling and Schottky barrier in graphene and Janus MoSSe heterostructures by applying an external field. Physical Chemistry Chemical Physics, 2018, 20, 24109-24116.	1.3	86
29041	A DFT investigation of the role of oxygen vacancies on the structural, electronic and magnetic properties of ATiO₃ (A = Mn, Fe, Ni) multiferroic materials. Physical Chemistry Chemical Physics, 2018, 20, 28382-28392.	1.3	26
29042	Rapid fabrication of SnO₂ nanoparticle photocatalyst: computational understanding and photocatalytic degradation of organic dye. Inorganic Chemistry Frontiers, 2018, 5, 3005-3014.	3.0	85
29043	Phase stability, electronic structure and mechanical properties of Cr and Ti doped Pt₃Al: first-principles calculations. Materials Research Express, 2018, 5, 106517.	0.8	3

#	Article	IF	Citations
29044	Current-density implementation for calculating flexoelectric coefficients. Physical Review B, 2018, 98, .	1.1	44
29045	Characterization of epitaxial silicene with Raman spectroscopy. Physical Review B, 2018, 98, .	1.1	7
29046	Gate-dependent vacancy diffusion in graphene. Physical Review B, 2018, 98, .	1.1	10
29047	Electronic properties of a Ï€-conjugated Cairo pentagonal lattice: Direct band gap, ultrahigh carrier mobility, and slanted Dirac cones. Physical Review B, 2018, 98, .	1.1	22
29048	Theory of Mn-Based High-Magnetization Alloys. IEEE Transactions on Magnetics, 2018, 54, 1-6.	1.2	8
29049	Ab Initio Monte Carlo Simulations of the Acidic Dissolution of Stainless Steels: Further Insights into the Mechanisms. Journal of the Electrochemical Society, 2018, 165, C703-C709.	1.3	3
29050	Physical Properties of Yttrium-Rhodium and Yttrium-Copper B2-Type Rare Earth Intermetallic Compounds: First Principles Study. , 0, , .		0
29051	Tuning carbon dioxide capture capability with structural and compositional design in mmenâ€(Mg,Zn)(dobpdc) metalâ€organic framework: density functional theory investigation. , 2018, 8, 580-586.		5
29052	Enthalpies of formation of rare-earth borides from first principles. Comparison with experimental values. Calphad: Computer Coupling of Phase Diagrams and Thermochemistry, 2018, 62, 49-60.	0.7	11
29053	Detail investigations of SmFeO 3 under extreme condition. Materials Chemistry and Physics, 2018, 215, 393-403.	2.0	10
29054	Efficient charge separation and visible-light response in bilayer HfS₂-based van der Waals heterostructures. RSC Advances, 2018, 8, 18889-18895.	1.7	20
29055	A tungsten-rhenium interatomic potential for point defect studies. Journal of Applied Physics, 2018, 123, .	1.1	22
29056	Construction of bilayer PdSe2 on epitaxial graphene. Nano Research, 2018, 11, 5858-5865.	5.8	84
29057	Segregation induced order-disorder transition in Cu(Au) surface alloys. Acta Materialia, 2018, 154, 220-227.	3.8	11
29058	Manipulating the stability of crystallographic and magnetic sub-lattices: A first-order magnetoelastic transformation in transition metal based Laves phase. Acta Materialia, 2018, 154, 365-374.	3.8	29
29059	Catalytic activity of Î³-AlOOH (0â€¯0â€¯1) surface in syngas conversion: Probing into the mechanism of carbon chain growth. Applied Surface Science, 2018, 455, 123-131.	3.1	14
29060	Structure, electricity, and bandgap modulation in Fe2O3â€“doped potassium sodium niobate ceramics. Ceramics International, 2018, 44, 16069-16075.	2.3	14
29061	High chemisorption abilities of hydrogen and oxygen on ultrasmall iron clusters: A first-principles study. Chemical Physics Letters, 2018, 705, 59-64.	1.2	3

#	Article	IF	Citations
29062	Synthesis and characterization of monodisperse yttrium aluminum garnet (YAG) micro-crystals with rhombic dodecahedron. Journal of Alloys and Compounds, 2018, 762, 537-547.	2.8	6
29063	Interaction of Imuran, Pentasa and Hyoscyamine drugs and solvent effects on graphdiyne nanotube as a drug delivery system - A DFT study. Journal of Molecular Liquids, 2018, 265, 199-207.	2.3	49
29064	Phase transition in metalâ€“organic complex trans-PtCl₂(PEt₃)₂ under pressure: insights into the molecular and crystal structure. CrystEngComm, 2018, 20, 3728-3740.	1.3	5
29065	Influence of the aggregate state on band structure and optical properties of C60 computed with different methods. Journal of Chemical Physics, 2018, 148, 204301.	1.2	10
29066	Structural differences between single crystal and polycrystalline UBe13. Philosophical Magazine, 2018, 98, 2003-2017.	0.7	4
29067	The unique photocatalysis properties of a 2D vertical MoO₂/WO₂ heterostructure: a first-principles study. Journal Physics D: Applied Physics, 2018, 51, 265106.	1.3	14
29068	Interaction of coadsorbed C and O atoms on W(100) surface: Implications of CO2 on the temperature-programmed desorption profile. Journal of Vacuum Science and Technology A: Vacuum, Surfaces and Films, 2018, 36, .	0.9	2
29069	First-principles study on the mechanism of lithium intercalation in cubic CoN. Modern Physics Letters B, 2018, 32, 1850184.	1.0	2
29070	Anchoring effects of S-terminated Ti2C MXene for lithium-sulfur batteries: A first-principles study. Applied Surface Science, 2018, 455, 522-526.	3.1	134
29071	Ab initio study of novel IIIâ€“V nitride alloys B1-Tl N for optoelectronic applications. Computational Condensed Matter, 2018, 16, e00309.	0.9	4
29072	Influence of cobalt doping on residual stress in ZnO nanorods. Materials Science in Semiconductor Processing, 2018, 84, 131-137.	1.9	28
29073	Identification of the Nearby Hydroxylsâ€™ Role in Promoting HCHO Oxidation over a Pt Catalyst. Industrial & Engineering Chemistry Research, 2018, 57, 8183-8189.	1.8	20
29074	Interstitial nitrogen atoms in diamond. A quantum mechanical investigation of its electronic and vibrational properties. Physical Chemistry Chemical Physics, 2018, 20, 16615-16624.	1.3	10
29075	Performance of various density-functional approximations for cohesive properties of 64 bulk solids. New Journal of Physics, 2018, 20, 063020.	1.2	185
29076	Electronic Structure of OR-AgInS2 and TiO2 Crystals and Its Differential Characteristics. Physics of the Solid State, 2018, 60, 858-864.	0.2	2
29077	Metal-substitution strategy to control the conductive path in titanium dioxide: ab initio calculations. European Physical Journal B, 2018, 91, 1.	0.6	4
29078	Sum-frequency ionic Raman scattering. Physical Review B, 2018, 97, .	1.1	55
29079	Muon contact hyperfine field in metals: A DFT calculation. Physical Review B, 2018, 97, .	1.1	19

#	Article	IF	Citations
29080	Single-crystal study of the charge density wave metal <mml:math xmlns:mml="http://www.w3.org/1998/Math/MathML"><mml:mtext>LuNiC</mml:mtext><mml:msub><mml:mrow /><mml:mn>2</mml:mn></mml:msub></mml:math>. Physical Review B, 2018, 97, .	1.1	17
29081	UV-active plasmons in alkali and alkaline-earth intercalated graphene. Physical Review B, 2018, 97, .	1.1	8
29082	Electronic, optical and mechanical properties of lead-free halide double perovskites using first-principles density functional theory. Materials Letters, 2018, 227, 289-291.	1.3	51
29083	Strain induced electronic structure variation in methyl-ammonium lead iodide perovskite. Scientific Reports, 2018, 8, 7760.	1.6	53
29084	Constructing oxygen-doped g-C₃N₄ nanosheets with an enlarged conductive band edge for enhanced visible-light-driven hydrogen evolution. Inorganic Chemistry Frontiers, 2018, 5, 1721-1727.	3.0	54
29085	Ab â€“ initio study of rare earth magnesium alloy: TbMg. AIP Conference Proceedings, 2018, , .	0.3	0
29086	Highâ€Pressure Synthesis of a Nitrogenâ€Rich Inclusion Compound ReN₈â‹…xâ€‰N₂ with Conjugated Polymeric Nitrogen Chains. Angewandte Chemie - International Edition, 2018, 57, 9048-9053.	7.2	70
29087	Chemical and substitutional doping, and anti-site and vacancy formation in monolayer AlN and GaN. Physical Chemistry Chemical Physics, 2018, 20, 16077-16091.	1.3	45
29088	Exploration of new UV nonlinear optical materials in the sodiumâ€“zinc fluoride carbonate system with the discovery of a new regulation mechanism for the arrangement of [CO₃]^{2â¯} groups. Journal of Materials Chemistry C, 2018, 6, 6526-6533.	2.7	19
29089	First-Principles Estimation of Electronic Temperature from X-Ray Thomson Scattering Spectrum of Isochorically Heated Warm Dense Matter. Physical Review Letters, 2018, 120, 205002.	2.9	20
29090	The matrixâ€“twin transition in a perfect Mg crystal: Ab initio study. International Journal of Plasticity, 2018, 108, 186-200.	4.1	4
29091	BaM2As2S6 (MÂ= Cd, Hg): Synthesis, crystal structure, optical and electronic properties. Journal of Alloys and Compounds, 2018, 762, 143-148.	2.8	14
29092	A new stable polycrystalline Be2C monolayer: A direct semiconductor with hexa-coordinate carbons. Physics Letters, Section A: General, Atomic and Solid State Physics, 2018, 382, 2144-2148.	0.9	26
29093	Highly Regular, Uniform K₃ScF₆:Mn⁴⁺ Phosphors: Facile Synthesis, Microstructures, Photoluminescence Properties, and Application in Light-Emitting Diode Devices. ACS Applied Materials & Interfaces, 2018, 10, 19783-19795.	4.0	171
29094	Narrow Gap Semiconducting Germanium Allotrope from the Oxidation of a Layered Zintl Phase in Ionic Liquids. Journal of the American Chemical Society, 2018, 140, 6785-6788.	6.6	16
29095	Lithiation-induced amorphization of Pd3P2S8 for highly efficient hydrogen evolution. Nature Catalysis, 2018, 1, 460-468.	16.1	247
29096	Doped boron nitride surfaces: potential metal free bifunctional catalysts for non-aqueous Liâ€“O₂ batteries. Physical Chemistry Chemical Physics, 2018, 20, 16485-16492.	1.3	10
29097	Theoretical modeling of tip-enhanced resonance Raman images of switchable azobenzene molecules on Au(111). Nanoscale, 2018, 10, 11850-11860.	2.8	12

#	Article	IF	Citations
29098	Phase transition studies of Na₃Bi system under uniaxial strain. Journal of Physics Condensed Matter, 2018, 30, 125502.	0.7	7
29099	Structural, electronic, and magnetic properties of the CrN (0â€¯0â€¯1) surface: First-principles studies. Applied Surface Science, 2018, 454, 350-357.	3.1	21
29100	A comparison study of the Born effective charges and dielectric properties of the cubic, tetragonal, monoclinic, ortho-I, ortho-II and ortho-III phases of zirconia. Solid State Sciences, 2018, 81, 58-65.	1.5	8
29101	A-Site Cation in Inorganic A₃Sb₂I₉ Perovskite Influences Structural Dimensionality, Exciton Binding Energy, and Solar Cell Performance. Chemistry of Materials, 2018, 30, 3734-3742.	3.2	134
29102	High-pressure-assisted X-ray-induced damage as a new route for chemical and structural synthesis. Physical Chemistry Chemical Physics, 2018, 20, 18949-18956.	1.3	14
29103	Developing descriptors for CO₂methanation and CO₂reforming of CH₄over Al₂O₃supported Ni and low-cost Ni based alloy catalysts. Physical Chemistry Chemical Physics, 2018, 20, 15939-15950.	1.3	26
29104	Adventures in boron chemistry â€“ the prediction of novel ultra-flexible boron oxide frameworks. Faraday Discussions, 2018, 211, 569-591.	1.6	5
29105	Thermodynamic Evaluation of the Co-Al-C System by Coupling Ab Initio Calculations and CALPHAD Approach. Journal of Phase Equilibria and Diffusion, 2018, 39, 538-548.	0.5	4
29106	Structural, elastic, electronic, phonon, dielectric and optical properties of Bi3TeBO9 from first-principles calculations. Journal of Physics and Chemistry of Solids, 2018, 121, 139-144.	1.9	17
29107	Computational study of some thiophene derivatives as aluminium corrosion inhibitors. Journal of Molecular Liquids, 2018, 265, 668-678.	2.3	66
29108	Atomic structure, electronic states, and optical properties of epitaxially grown Î²-Ga2O3 layers. Superlattices and Microstructures, 2018, 120, 90-100.	1.4	60
29109	Initial oxidation of Cu(100) studied by X-ray photo-electron spectroscopy and density functional theory calculations. Surface Science, 2018, 675, 64-69.	0.8	17
29110	Interfacial Properties of Monolayer SnSâ€“Metal Contacts. Journal of Physical Chemistry C, 2018, 122, 12322-12331.	1.5	15
29111	Molecular and dissociative O₂ adsorption on the Cu₂O(111) surface. Physical Chemistry Chemical Physics, 2018, 20, 20352-20362.	1.3	26
29112	The catalytic activity and mechanism of oxygen reduction reaction on P-doped MoS₂. Physical Chemistry Chemical Physics, 2018, 20, 18184-18191.	1.3	22
29113	Adsorption of Hydrogen Sulfide, Hydrosulfide and Sulfide at Cu(110) â€•Polarizability and Cooperativity Effects. First Stages of Formation of a Sulfide Layer.. ChemPhysChem, 2018, 19, 2159-2168.	1.0	13
29114	Evolution of crystal structures and electronic properties for TiS2 at high pressure. Journal of Alloys and Compounds, 2018, 757, 448-454.	2.8	18
29115	Efficient charge carrier separation and excellent visible light photoresponse in Cu2O nanowires. Nano Energy, 2018, 50, 118-125.	8.2	166

#	Article	IF	Citations
29116	Oxygen Vacancy Defect Migration in Titanate Perovskite Surfaces: Effect of the A-Site Cations. Journal of Physical Chemistry C, 2018, 122, 14590-14597.	1.5	28
29117	Barium in High Oxidation States in Pressure-Stabilized Barium Fluorides. Journal of Physical Chemistry C, 2018, 122, 12448-12453.	1.5	22
29118	Controlling the Reaction Steps of Bifunctional Molecules 1,5-Dibromo-2,6-dimethylnaphthalene on Different Substrates. Journal of Physical Chemistry C, 2018, 122, 13001-13008.	1.5	21
29119	Density functional theory characterization of the structures of H₃AsO₃ and H₃AsO₄ adsorption complexes on ferrihydrite. Environmental Sciences: Processes and Impacts, 2018, 20, 977-987.	1.7	20
29120	Mechanistic investigations of the Au catalysed Câ€“H bond activations in on-surface synthesis. Physical Chemistry Chemical Physics, 2018, 20, 15901-15906.	1.3	9
29121	Highly efficient hydrogen evolution triggered by a multi-interfacial Ni/WC hybrid electrocatalyst. Energy and Environmental Science, 2018, 11, 2114-2123.	15.6	224
29122	Transition metal anchored C₂N monolayers as efficient bifunctional electrocatalysts for hydrogen and oxygen evolution reactions. Journal of Materials Chemistry A, 2018, 6, 11446-11452.	5.2	223
29123	Temperature-induced band shift in bulk Î³-InSe by angle-resolved photoemission spectroscopy. AIP Advances, 2018, 8, 055123.	0.6	5
29124	Doping Cu Atoms Excel as the Functional Material to Tune the Wettability for TMeNs Hard Coating. Advanced Materials Interfaces, 2018, 5, 1800391.	1.9	4
29125	Infrared and Raman spectroscopy of Î±â€ZrW₂O₈: A comprehensive density functional perturbation theory and experimental study. Journal of Raman Spectroscopy, 2018, 49, 1373-1384.	1.2	18
29126	Discrete dislocation dynamics simulations of dislocation-Î¸â€² precipitate interaction in Al-Cu alloys. Journal of the Mechanics and Physics of Solids, 2018, 118, 228-244.	2.3	53
29127	Density Functional Theory Investigation of the Role of Cocatalytic Water in Methane Steam Reforming over Anatase TiO₂ (101). Industrial & Engineering Chemistry Research, 2018, 57, 8131-8143.	1.8	8
29128	Appearance of Lithium-Ion Conduction in a Laâ€“Liâ€“Coâ€“O Band Insulator: Possible Route to Oxide Electrolyte. ACS Applied Energy Materials, 2018, 1, 2546-2554.	2.5	8
29129	Synthesis of Ru Icosahedral Nanocages with a Face-Centered-Cubic Structure and Evaluation of Their Catalytic Properties. ACS Catalysis, 2018, 8, 6948-6960.	5.5	66
29130	Creating Cavities at Palladiumâ€“Phosphine Interfaces for Enhanced Selectivity in Heterogeneous Biomass Conversion. ACS Catalysis, 2018, 8, 6138-6145.	5.5	19
29131	Two-dimensional nitrides as highly efficient potential candidates for CO₂ capture and activation. Physical Chemistry Chemical Physics, 2018, 20, 17117-17124.	1.3	55
29132	Superior ionic and electronic properties of ReN₂ monolayers for Na-ion battery electrodes. Nanotechnology, 2018, 29, 325401.	1.3	17
29133	Induced electronic changes at the fluorinated polyphenylthiols on nanostructured Au(1â€¯1â€¯1) interfaces. Applied Surface Science, 2018, 452, 141-147.	3.1	1

#	Article	IF	Citations
29134	Structures and energetics of point defects with charge states in zircon: A first-principles study. Journal of Alloys and Compounds, 2018, 759, 60-69.	2.8	4
29135	Effects of surface and confinement on the optical vibrational modes and dielectric function of 3C porous silicon carbide: An ab-initio study. Physica B: Condensed Matter, 2018, 550, 420-427.	1.3	7
29136	Photoinduced Localized Hole Delays Nonradiative Electronâ€“Hole Recombination in Cesiumâ€“Lead Halide Perovskites: A Time-Domain Ab Initio Analysis. Journal of Physical Chemistry Letters, 2018, 9, 3021-3028.	2.1	22
29137	Enhancement of the spin polarization of an Fe₃O₄(100) surface by nitric oxide adsorption. Physical Chemistry Chemical Physics, 2018, 20, 15871-15875.	1.3	5
29138	Electronic properties of in-plane phase engineered 1Tâ€²/2H/1Tâ€² MoS2. AIP Conference Proceedings, 2018, , .	0.3	1
29139	First principle investigation of structural and optical properties of cubic titanium dioxide. AIP Conference Proceedings, 2018, , .	0.3	2
29140	First-principles calculations of CdS-based nanolayers and nanotubes. Materials Research Express, 2018, 5, 055036.	0.8	5
29141	Highâ€Pressure Synthesis of a Nitrogenâ€Rich Inclusion Compound ReN₈â‹…xâ€‰N₂ with Conjugated Polymeric Nitrogen Chains. Angewandte Chemie, 2018, 130, 9186-9191.	1.6	16
29142	Synthesis of Smâ€“Al metallic glasses designed by molecular dynamics simulations. Journal of Materials Science, 2018, 53, 11488-11499.	1.7	3
29143	Mechanistic roles of catalyst surface coating in nitrobenzene selective reduction: A first-principles study. Applied Catalysis B: Environmental, 2018, 236, 509-517.	10.8	19
29144	Tuning the electronic property of two dimensional SiSe monolayer by in-plane strain. Chemical Physics Letters, 2018, 705, 12-18.	1.2	13
29145	Gd(Co 1-x Ga x) 2 : Synthesis, crystal structures, and investigation of structural transformations and magnetic properties. Journal of Solid State Chemistry, 2018, 264, 68-76.	1.4	3
29146	Large positive linear magnetoresistance in the two-dimensional t 2g electron gas at the EuO/SrTiO3 interface. Scientific Reports, 2018, 8, 7721.	1.6	40
29147	Surface termination effects on the oxygen reduction reaction rate at fuel cell cathodes. Journal of Materials Chemistry A, 2018, 6, 11929-11940.	5.2	38
29148	Effects of surface motion and electron-hole pair excitations in CO2 dissociation and scattering on Ni(100). Journal of Chemical Physics, 2018, 148, 174702.	1.2	11
29149	Structural models of increasing complexity for icosahedral boron carbide with compositions throughout the single-phase region from first principles. Physical Review B, 2018, 97, .	1.1	9
29150	Tetrahexcarbon: A two-dimensional allotrope of carbon. Carbon, 2018, 137, 266-273.	5.4	91
29151	First-principles studies of SnS2, MoS2 and WS2 stacked van der Waals hetero-multilayers. Computational Condensed Matter, 2018, 16, e00303.	0.9	5

#	Article	IF	Citations
29152	Bandgap engineering of Janus MoSSe monolayer implemented by Se vacancy. Computational Materials Science, 2018, 152, 20-27.	1.4	46
29153	The methanol and CO electro-oxidation onto Ptpc/Co/Pt metallic multilayer nanostructured electrodes: An experimental and theoretical approach. Electrochimica Acta, 2018, 280, 197-205.	2.6	13
29154	Graphene Oxideâ€Template Controlled Cuboidâ€Shaped Highâ€Capacity VS₄ Nanoparticles as Anode for Sodiumâ€Ion Batteries. Advanced Functional Materials, 2018, 28, 1801806.	7.8	125
29155	Liquidâ€Phase Exfoliated Indiumâ€“Selenide Flakes and Their Application in Hydrogen Evolution Reaction. Small, 2018, 14, e1800749.	5.2	90
29156	New insights on the role of H2S and sulfur vacancies on dibenzothiophene hydrodesulfurization over MoS2 edges. Applied Catalysis A: General, 2018, 566, 164-173.	2.2	25
29157	Adsorption of NOx (xâ€¯=â€¯1, 2) gas molecule on pristine and B atom embedded Î³-graphyne based on first-principles study. Applied Surface Science, 2018, 455, 484-491.	3.1	35
29158	Insight into the physical properties of two niobium based compounds, Nb3Be and Nb3Be2, via a first principles calculation. Chinese Journal of Physics, 2018, 56, 1386-1393.	2.0	6
29159	Activation of hydrogen iodide on silver tetramers: Role of confinement. Chemical Physics Letters, 2018, 705, 71-77.	1.2	2
29160	Effect of interstitial nitrogen in Fe18Cr6Mn8 austenitic alloys from density functional theory. Journal of Magnetism and Magnetic Materials, 2018, 463, 57-63.	1.0	7
29161	Theoretical Investigations of Transition Metal Surface Energies under Lattice Strain and CO Environment. Journal of Physical Chemistry C, 2018, 122, 14481-14487.	1.5	14
29162	Enhanced electronic and optical properties of three TMD heterobilayers. Physical Chemistry Chemical Physics, 2018, 20, 16604-16614.	1.3	23
29163	Tailoring the hexagonal boron nitride nanomesh on Rh(111) with gold. Physical Chemistry Chemical Physics, 2018, 20, 15473-15485.	1.3	17
29164	Density functional study of the phase stability and Raman spectra of Yb₂O₃, Yb₂SiO₅ and Yb₂Si₂O₇ under pressure. Physical Chemistry Chemical Physics, 2018, 20, 16518-16527.	1.3	30
29165	Stability and local magnetic moment of bilayer graphene by intercalation: first principles study. RSC Advances, 2018, 8, 19732-19738.	1.7	7
29166	The electronic properties of CH₃NH₃PbI₃ perovskite surfaces tuned by inverted polarities of pyridine and ethylamine. Journal of Materials Chemistry C, 2018, 6, 6733-6738.	2.7	3
29167	Static and Fluctuating Magnetic Moments in the Ferroelectric Metal LiOsO3. , 2018, , .		3
29168	Atomic N-coordinated cobalt sites within nanomesh graphene as highly efficient electrocatalysts for triiodide reduction in dye-sensitized solar cells. Chemical Engineering Journal, 2018, 349, 782-790.	6.6	24
29169	Van der Waals interactions and the properties of graphite and 2H-, 3R- and 1T-MoS2: A comparative study. Computational Materials Science, 2018, 152, 146-150.	1.4	30

#	Article	IF	Citations
29170	Investigation of electrocatalytic activity on a N-doped reduced graphene oxide surface for the oxygen reduction reaction in an alkaline medium. International Journal of Hydrogen Energy, 2018, 43, 12129-12139.	3.8	33
29171	Silicene adsorption on the bismuth-passivated<mml:math xmlns:mml="http://www.w3.org/1998/Math/MathML" altimg="si1.gif" overflow="scroll"><mml:mrow><mml:mi>S</mml:mi><mml:mi>i</mml:mi><mml:mrow><mml:mo>(</mml:mo><mml:mrow><mml:m... A first-principles study. Materials Chemistry and Physics, 2018, 216, 8-13.	2.0	2
29172	Thermoelectric Properties of Doped-Cu₃SbSe₄ Compounds: A First-Principles Insight. Inorganic Chemistry, 2018, 57, 7321-7333.	1.9	36
29173	Indirect-to-Direct Band Gap Transition of Si Nanosheets: Effect of Biaxial Strain. Journal of Physical Chemistry C, 2018, 122, 15297-15303.	1.5	8
29174	Microscopic Insights into Hydrogen Permeation Through a Model PdCu Membrane from First-Principles Investigations. Journal of Physical Chemistry C, 2018, 122, 12920-12933.	1.5	11
29175	High photoluminescence quantum yield of 18.7% by using nitrogen-doped Ti₃C₂ MXene quantum dots. Journal of Materials Chemistry C, 2018, 6, 6360-6369.	2.7	159
29176	Influence of graphene thickness and grain boundaries on MoS₂ wrinkle nanostructures. Physical Chemistry Chemical Physics, 2018, 20, 17000-17008.	1.3	9
29177	Molybdenum substitution simultaneously induced band structure modulation and luminescence enhancement in LiLaMg(W, Mo)O6: Eu3+ red-emitting phosphor for near ultraviolet excited white light diodes. Journal of Alloys and Compounds, 2018, 763, 278-288.	2.8	25
29178	Effects of Dispersion Corrections and Nonlocality on Density Functional Predictions of Pressure-Induced Polymorphic Transitions of Crystalline Diborane. Journal of Physical Chemistry C, 2018, 122, 14781-14787.	1.5	5
29179	CO Oxidation on a Au/TiO₂ Nanoparticle Catalyst via the Au-Assisted Marsâ€“van Krevelen Mechanism. ACS Catalysis, 2018, 8, 6513-6525.	5.5	103
29180	Theoretical investigation of electronic performance, half-metallicity, and magnetic properties of Cr-substituted BaTe. Journal of Computational Electronics, 2018, 17, 909-919.	1.3	19
29181	Investigation on the stability and electronic properties of Penta-XP5 (Xâ€¯=â€¯Al, Ga, In) monolayer semiconductors by using first principles calculations. Chemical Physics Letters, 2018, 706, 99-106.	1.2	20
29182	A mechanistic study of CO oxidation over spinel MnFe2O4 surface during chemical-looping combustion. Fuel, 2018, 230, 410-417.	3.4	35
29183	Influence of Ti/Hf doping on hydrogen storage performance and mechanical properties of ZrCo compounds: A first principle study. International Journal of Hydrogen Energy, 2018, 43, 13328-13338.	3.8	34
29184	The electronic, magnetic and optical properties of Co doped marcasite FeS2. Journal of Physics and Chemistry of Solids, 2018, 121, 285-291.	1.9	4
29185	Quaternary rare-earth selenides Ba2REGaSe5 and Ba2REInSe5. Journal of Solid State Chemistry, 2018, 265, 167-175.	1.4	5
29186	Preparation of nano-Fe0 modified coal fly-ash composite and its application for U(VI) sequestration. Journal of Molecular Liquids, 2018, 266, 824-833.	2.3	21
29187	New Tungsten Borides, Their Stability and Outstanding Mechanical Properties. Journal of Physical Chemistry Letters, 2018, 9, 3470-3477.	2.1	61

#	Article	IF	Citations
29188	Light metal decorated graphdiyne nanosheets for reversible hydrogen storage. Nanotechnology, 2018, 29, 355401.	1.3	83
29189	Promotion of catalytic selectivity on transition metal oxide through restructuring surface lattice. Applied Catalysis B: Environmental, 2018, 237, 957-969.	10.8	20
29190	On the diversity in the thermal transport properties of graphene: A first-principles-benchmark study testing different exchange-correlation functionals. Computational Materials Science, 2018, 151, 153-159.	1.4	34
29191	Anhydrous proline crystals: Structural optimization, optoelectronic properties, effective masses and Frenkel exciton energy. Journal of Physics and Chemistry of Solids, 2018, 121, 36-48.	1.9	17
29192	CaCO3 phase diagram studied with Raman spectroscopy at pressures up to 50â€¯GPa and high temperatures and DFT modeling. Physics of the Earth and Planetary Interiors, 2018, 281, 31-45.	0.7	83
29193	Prediction of Enhanced Catalytic Activity for Hydrogen Evolution Reaction in Janus Transition Metal Dichalcogenides. Nano Letters, 2018, 18, 3943-3949.	4.5	267
29194	NiO nanoparticle surface energy studies using first principles calculations. New Journal of Chemistry, 2018, 42, 10791-10797.	1.4	16
29195	Cu atomic chains supported on Î²-borophene sheets for effective CO₂electroreduction. Nanoscale, 2018, 10, 11064-11071.	2.8	50
29196	Effect of tensile strain on the band structure and carrier transport of germanium monosulphide monolayer: a firstâ€principles study. Micro and Nano Letters, 2018, 13, 600-605.	0.6	14
29197	Investigation of electronic structure and chemical bonding of intermetallic Pd2HfIn: An ab-initio study. AIP Conference Proceedings, 2018, , .	0.3	1
29198	Ni doping effect on the electronic and sensing properties of 2D SnO2. AIP Conference Proceedings, 2018, , .	0.3	4
29199	Tunable optical and excitonic properties of phosphorene via oxidation. Journal of Physics Condensed Matter, 2018, 30, 255703.	0.7	14
29200	Role of spin-orbit coupling in the physical properties of <mml:math xmlns:mml="http://www.w3.org/1998/Math/MathML"><mml:mrow><mml:mi>La</mml:mi><mml:msub><mml:mi>X</mml:mi><mml:mn (<mml:math) Tj ETQq0 0 0 rgBT /Overlock 10 Tf 50 257 Td (xmlns:mml="http://www.w3.org/1998/Math/MathML"><mml:mi>X</mml:m	1.1	12
29201	Bifunctional Nitrogen and Cobalt Codoped Hollow Carbon for Electrochemical Syngas Production. Advanced Science, 2018, 5, 1800177.	5.6	96
29202	The first-principles calculations of Mg2-xTi1+xO4's novel optical properties. Journal of Alloys and Compounds, 2018, 756, 57-61.	2.8	8
29203	Stability, Elastic Properties, and Deformation of LiBN2: A Potential High-Energy Material. Inorganic Chemistry, 2018, 57, 6333-6339.	1.9	0
29204	Hydrogen Bond-Induced Nitric Oxide Dissociation on Cu(110). Journal of Physical Chemistry C, 2018, 122, 11814-11824.	1.5	11
29205	Mechanisms of Formation of H, HO, and Water and of Water Desorption in the Early Stages of Cellulose Pyrolysis. Journal of Physical Chemistry C, 2018, 122, 12168-12176.	1.5	16

#	Article	IF	Citations
29206	Multicenter Bonding Effects in Oxygen Vacancy in the Bulk and on the Surface of MgO. Journal of Physical Chemistry C, 2018, 122, 11933-11937.	1.5	12
29207	Three-Dimensional Spin Texture in Hybrid Perovskites and Its Impact on Optical Transitions. Journal of Physical Chemistry Letters, 2018, 9, 2903-2908.	2.1	50
29208	Thermodynamics of Alkanethiol Self-Assembled Monolayer Assembly on Pd Surfaces. Langmuir, 2018, 34, 6346-6357.	1.6	13
29209	Synthesis, structure, and polymorphic transitions of praseodymium(<scp>iii</scp>) and neodymium(<scp>iii</scp>) borohydride, Pr(BH₄)₃ and Nd(BH₄)₃. Dalton Transactions, 2018, 47, 8307-8319.	1.6	19
29210	Sustainable p-type copper selenide solar material with ultra-large absorption coefficient. Chemical Science, 2018, 9, 5405-5414.	3.7	20
29211	Truncated hexagonal bi-pyramidal gallium ferrite nanocrystals: integration of structural details with visible-light photo-activity and self-cleaning properties. Journal of Materials Chemistry A, 2018, 6, 13031-13040.	5.2	9
29212	Cu doped diamond: Effect of charge state and defect aggregation on spin interactions in a 3d transition metal doped wide band-gap semiconductor. Journal of Applied Physics, 2018, 123, .	1.1	3
29213	Performance of exchange-correlation functionals in density functional theory calculations for liquid metal: A benchmark test for sodium. Journal of Chemical Physics, 2018, 148, 144501.	1.2	5
29214	Cubic phase stability, optical and magnetic properties of Cu-stabilized zirconia nanocrystals. Journal Physics D: Applied Physics, 2018, 51, 225304.	1.3	8
29215	Theoretical investigation on elastic and thermal properties of layered ternary ceramic-Ti4AlN2.89 under high pressure. Materials Research Express, 2018, 5, 065202.	0.8	2
29216	Lattice anharmonicity, phonon dispersion, and thermal conductivity of PbTe studied by the phonon quasiparticle approach. Physical Review B, 2018, 97, .	1.1	42
29217	Detection of topological phase transitions through entropy measurements: The case of germanene. Physical Review B, 2018, 97, .	1.1	17
29218	Transition metal (Pd, Pt, Ag, Au) decorated InN monolayer and their adsorption properties towards NO2: Density functional theory study. Applied Surface Science, 2018, 455, 106-114.	3.1	48
29219	A new molecular pathway allows the chemoselective reduction of nitroaromatics on non-noble metal catalysts. Journal of Catalysis, 2018, 364, 19-30.	3.1	57
29220	2D metalâ€“organic-framework array-derived hierarchical network architecture of cobalt oxide flakes with tunable oxygen vacancies towards efficient oxygen evolution reaction. Journal of Catalysis, 2018, 364, 48-56.	3.1	56
29221	First-principles study on structural, mechanical and electronic properties of thorium dichalcogenides under high pressure. Journal of Nuclear Materials, 2018, 508, 147-153.	1.3	0
29222	First principles study of the physical properties of Ti3AC2/Zr (A = Si, Al) van der Waals heterojunctions. Journal of Physics and Chemistry of Solids, 2018, 121, 298-303.	1.9	6
29223	Computational study of lithium nucleation tendency in Li7La3Zr2O12 (LLZO) and rational design of interlayer materials to prevent lithium dendrites. Journal of Power Sources, 2018, 392, 79-86.	4.0	144

#	Article	IF	Citations
29224	Hot-Hole Cooling Controls the Initial Ultrafast Relaxation in Methylammonium Lead Iodide Perovskite. Scientific Reports, 2018, 8, 8115.	1.6	32
29225	Meâ€“Nâ€“C (Me = Fe, Cu, and Co) nanosheet as a promising charge-controlled CO2 capture material. Journal of Materials Chemistry A, 2018, 6, 12404-12410.	5.2	27
29226	First-principles study on the structure and electronic properties of stanane under electric fields. Materials Research Express, 2018, 5, 065023.	0.8	7
29227	Impact of thermal atomic displacements on the Curie temperature of <mml:math xmlns:mml="http://www.w3.org/1998/Math/MathML"><mml:mrow><mml:mn>3</mml:mn><mml:mi>d</mml:mi></mml:mrow></mml: transition metals. Physical Review B, 2018, 97, .	1.1	21
29228	A first-principle study of H adsorption and absorption under the influence of coverage. Applied Surface Science, 2018, 457, 280-286.	3.1	16
29229	A DFT study of Li adsorption on surface of Si clusters anchored N-doped defective graphene composite. Applied Surface Science, 2018, 457, 789-796.	3.1	19
29230	Spin-orbit coupling induced band splitting in bulk ferroelectric BiAlO3 with tetragonal phase. Journal of Alloys and Compounds, 2018, 765, 1003-1007.	2.8	0
29231	Lattice dynamics and thermodynamic properties of alkaline earth metal nitrates M(NO3)2 (M = Sr, Ba): A first principles study. Journal of Physics and Chemistry of Solids, 2018, 122, 268-277.	1.9	4
29232	Topological phases in Bi/Sb planar and buckled honeycomb monolayers. Physics Letters, Section A: General, Atomic and Solid State Physics, 2018, 382, 2952-2958.	0.9	9
29233	Enhanced sulfur resistance of Ni(1 1 1) surface alloyed with Ge: A first principles study. Surface Science, 2018, 677, 115-120.	0.8	6
29234	Influence of Tight Confinement on Selective Oxidative Dehydrogenation of Ethane on MoVTeNb Mixed Oxides. ACS Catalysis, 2018, 8, 7051-7067.	5.5	59
29235	Refining Defect States in W₁₈O₄₉ by Mo Doping: A Strategy for Tuning N₂ Activation towards Solar-Driven Nitrogen Fixation. Journal of the American Chemical Society, 2018, 140, 9434-9443.	6.6	722
29236	Metastable phase formation of Pt-X (Xâ€‰=â€‰Ir, Au) thin films. Scientific Reports, 2018, 8, 10198.	1.6	11
29237	Half-metallicity and spin-valley coupling in 5d transition metal substituted monolayer MnPSe₃. Journal of Materials Chemistry C, 2018, 6, 8092-8098.	2.7	23
29238	Transition metal inverse-hybrid perovskites. Journal of Materials Chemistry A, 2018, 6, 14560-14565.	5.2	11
29239	A first principle study of the perovskite lanthanum aluminate. Materials Research Express, 2018, 5, 086302.	0.8	10
29240	Temperature dependence of phonons in Pd3Fe through the Curie temperature. Physical Review B, 2018, 98, .	1.1	12
29241	The Effect of Anti-Site Disorder on Structural and Magnetic Properties of Niâ€“Coâ€“Mnâ€“In Alloys: <italic>Ab Initio</italic> and Monte Carlo Studies. IEEE Transactions on Magnetics, 2018, 54, 1-5.	1.2	5

#	Article	IF	Citations
29242	Mechanical properties and chemical bonding of M2B and M2B0.75C0.25(M = Fe, Cr, W, Mo, Mn) compounds. Journal of Materials Research, 2018, 33, 3665-3676.	1.2	4
29243	Elastic Constants and Related Properties of Compressed Rocksalt CuX (X =Cl, Br): Ab Initio Study. Zeitschrift Fur Naturforschung - Section A Journal of Physical Sciences, 2018, 73, 767-773.	0.7	8
29244	Direct Correlation between Adsorption Energetics and Nuclear Spin Relaxation in a Liquidâ€saturated Catalyst Material. ChemPhysChem, 2018, 19, 2472-2479.	1.0	40
29245	Interaction of metal phthalocyanines with carbon zigzag and armchair nanotubes with different diameters. Applied Surface Science, 2018, 457, 235-240.	3.1	16
29246	Theoretical and experimental evidences of defects in LiMgPO4. Journal of Alloys and Compounds, 2018, 766, 626-636.	2.8	27
29247	Oxygen Vacancies Mediated Complete Visible Light NO Oxidation via Side-On Bridging Superoxide Radicals. Environmental Science & Technology, 2018, 52, 8659-8665.	4.6	149
29248	Adsorption of Maleic Acid Monomer on the Surface of Hydroxyapatite and TiO2: A Pathway toward Biomaterial Composites. ACS Applied Materials & Interfaces, 2018, 10, 24382-24391.	4.0	11
29249	Interaction trends between single metal atoms and oxide supports identified with density functional theory and statistical learning. Nature Catalysis, 2018, 1, 531-539.	16.1	269
29250	Ab-initio study on electronic properties of rocksalt SnAs. AIP Conference Proceedings, 2018, , .	0.3	0
29251	The optical conductivity and electron energy loss of graphene under different hydrostatic pressures using first-principles. , 2018, , .		0
29252	Ab initio calculations of the mechanical and acoustic properties of Ti2-based Heusler alloys under pressures. European Physical Journal B, 2018, 91, 1.	0.6	10
29253	Effect of Cr doping on the mechanical properties and electronic structure of WCoB ternary boride by first-principles calculations. Modern Physics Letters B, 2018, 32, 1850240.	1.0	7
29254	Ab initio study of thermodynamic properties of bulk zinc-blende CdS: Comparing the LDA and GGA. International Journal of Modern Physics B, 2018, 32, 1850207.	1.0	11
29255	First principles calculation of the structure and quantum capacity of acidic functional groups on graphene-based capacitor. , 2018, , .		0
29256	Superior sensing affinities of acetone towards vacancy induced and metallized ZnO monolayers. Applied Surface Science, 2018, 456, 711-716.	3.1	15
29257	Lattice-matched heterojunctions between blue phosphorene and MXene Y2CX2 (Xâ€=â€F, O, and Yâ€=â€Zr, Hf). Computational Materials Science, 2018, 152, 256-261.	1.4	6
29258	Experimental and theoretical investigations of unusual enhancement of room temperature ferromagnetism in nickel-cobalt codoped CeO2 nanostructures. Journal of Magnetism and Magnetic Materials, 2018, 465, 756-761.	1.0	6
29259	Modelling and experimental analysis of the effect of solute iron in thermally grown Zircaloy-4 oxides. Journal of Nuclear Materials, 2018, 509, 114-123.	1.3	6

#	Article	IF	Citations
29260	Spin-Negative Differential Resistance in Zigzag Graphene Nanoribbons with Side-Attached Porphine Molecule. Journal of Physical Chemistry C, 2018, 122, 15911-15921.	1.5	14
29261	Calculation of strained BaTiO3 with different exchange correlation functionals examined with criterion by Ginzburg-Landau theory, uncovering expressions by crystallographic parameters. Journal of Chemical Physics, 2018, 148, 194702.	1.2	9
29262	A DFT perspective analysis of optical properties of defected germanene mono-layer. Physical Sciences Reviews, 2018, 3, .	0.8	1
29263	Probing Quantum Confinement and Electronic Structure at Polar Oxide Interfaces. Advanced Science, 2018, 5, 1800242.	5.6	9
29264	Revealing the novel fracture mechanism of the interfaces of TiB2/Fe composite from a first principles investigation. Acta Materialia, 2018, 156, 228-244.	3.8	75
29265	Electronic structures and transition temperatures of high-T cuprate superconductors from first-principles calculations and Landau theory. Journal of Alloys and Compounds, 2018, 764, 869-880.	2.8	11
29266	Electronic and mechanical properties of MgN compound: Prediction of stable half-metallic ferromagnet in NaCl and ZB phases. Journal of Magnetism and Magnetic Materials, 2018, 466, 28-37.	1.0	5
29267	Efficient Carrier Separation and Band Structure Tuning of Two-Dimensional C₂N/GaTe van der Waals Heterostructure. Journal of Physical Chemistry C, 2018, 122, 15892-15902.	1.5	55
29268	Pure CO₂ electrolysis over an Ni/YSZ cathode in a solid oxide electrolysis cell. Journal of Materials Chemistry A, 2018, 6, 13661-13667.	5.2	77
29269	Electronic and magnetic properties of semihydrogenated, fully hydrogenated monolayer and bilayer MoN ₂ sheets. Chinese Physics B, 2018, 27, 060306.	0.7	4
29270	Effect of substitution (Al and P) atoms in ZnO nanosheet on structural and electronic properties. Journal of Physics: Conference Series, 2018, 1032, 012045.	0.3	6
29271	Pressure-Induced Sublattice Disordering in SnO2 : Invasive Selective Percolation. Physical Review Letters, 2018, 120, 265702.	2.9	11
29272	Gradient-level and nonlocal density functional descriptions of Cu-Au intermetallic compounds. European Physical Journal B, 2018, 91, 1.	0.6	5
29273	Comparative study of 9R and 12R hexagonal diamond by first-principles calculations. International Journal of Modern Physics B, 2018, 32, 1850211.	1.0	2
29274	Two Novel Deepâ€Ultraviolet Nonlinear Optical Crystals with Shorter Phaseâ€Matching Second Harmonic Generation than KBe₂BO₃F₂: A Firstâ€Principles Prediction. Physica Status Solidi - Rapid Research Letters, 2018, 12, 1800276.	1.2	15
29275	Ab-initio based search for late blooming phase compositions in iron alloys. Journal of Nuclear Materials, 2018, 509, 225-236.	1.3	14
29276	Mechanical anisotropy and ideal strength of ThBC. Journal of Physics and Chemistry of Solids, 2018, 122, 203-209.	1.9	5
29277	A Cu based layered multifunctional material: (C₈H₁₂N)₂CuCl₄ Optical and electronic properties. Materials Research Express, 2018, 5, 076305.	0.8	3

#	Article	IF	Citations
29278	Strain-induced gauge and Rashba fields in ferroelectric Rashba lead chalcogenide <mml:math xmlns:mml="http://www.w3.org/1998/Math/MathML"><mml:mrow><mml:mi>Pb</mml:mi><mml:mi>X</mml:mi></mml:mrow></mml:m monolayers (<mml:math) Tj ETQq0 0 0 rgBT /Overlock 10 Tf 50 737 Td (xmlns:mml="http://www.w3.org/1998/Math/MathML"> <mml:m	1.2	
29279	Vanadium clusters formation in geometrically frustrated spinel oxide AlV2O4. Acta Crystallographica Section B: Structural Science, Crystal Engineering and Materials, 2018, 74, 337-353.	0.5	10
29280	Tunable Quasiâ€Oneâ€Dimensional Ribbon Enhanced Light Absorption in Sb₂Se₃ Thinâ€film Solar Cells Grown by Closeâ€Space Sublimation. Solar Rrl, 2018, 2, 1800128.	3.1	64
29281	First principles investigation of the structural and bonding properties of hydrated actinide (IV) oxalates, An(C2O4)2·6H2O (Anâ€=â€U, Pu). Computational Materials Science, 2018, 153, 146-152.	1.4	7
29282	New High Pressure Phases of Energetic Material TEX: Evidence from Raman Spectroscopy, X-ray Diffraction, and First-Principles Calculations. Journal of Physical Chemistry A, 2018, 122, 6236-6242.	1.1	13
29283	Electronic Structure of a Polybenzimidazole-Wrapped Single-Wall Carbon Nanotube. Journal of Physical Chemistry C, 2018, 122, 15979-15985.	1.5	7
29284	Ultrahigh Conductivity in Two-Dimensional InSe via Remote Doping at Room Temperature. Journal of Physical Chemistry Letters, 2018, 9, 3897-3903.	2.1	23
29285	Grain Boundaries Are Benign and Suppress Nonradiative Electronâ€“Hole Recombination in Monolayer Black Phosphorus: A Time-Domain Ab Initio Study. Journal of Physical Chemistry Letters, 2018, 9, 3856-3862.	2.1	54
29286	Simplest MOF Units for Effective Photodriven Hydrogen Evolution Reaction. Journal of the American Chemical Society, 2018, 140, 9159-9166.	6.6	59
29287	Ab initio design of light absorption through silver atomic cluster decoration of TiO₂. Physical Chemistry Chemical Physics, 2018, 20, 19110-19119.	1.3	31
29288	Engineering an effective noble-metal-free photocatalyst for hydrogen evolution: hollow hexagonal porous micro-rods assembled from In₂O₃@carbon coreâ€“shell nanoparticles. Journal of Materials Chemistry A, 2018, 6, 15747-15754.	5.2	75
29289	Negative Hydration Expansion in <mml:math xmlns:mml="http://www.w3.org/1998/Math/MathML" display="inline"><mml:mrow><mml:msub><mml:mrow><mml:mi>ZrW</mml:mi></mml:mrow><mml:mrow><mml:mn>2</mml:mn></ mathvariant="normal">O</mml:mi></mml:mrow><mml:mrow><mml:mn>8</mml:mn></mml:mrow></mml:msub></mml:mrow></mml: : Microscopic Mechanism, Spaghetti Dynamics, and Negative Thermal Expansion. Physical Review Letters, 2018, 120, 265501.	2.9	21
29290	The effect of Snâ€“VO defect clustering on Zr alloy corrosion. Corrosion Science, 2018, 141, 14-17.	3.0	5
29291	An examination of the structural, electronic, elastic, vibrational and thermodynamic properties of Ru2YGa (Yâ€=â€Sc, Ti and V) Heusler alloys. Chinese Journal of Physics, 2018, 56, 1772-1780.	2.0	11
29292	Insights into the plasticity of Ag3Sn from density functional theory. International Journal of Plasticity, 2018, 110, 57-73.	4.1	6
29293	Diffusion and adsorption of Au and Pt adatoms on ideal and missing row reconstructed surfaces of Au(110): DFT and EAM calculations. Surface Science, 2018, 677, 83-89.	0.8	3
29294	Atomistic simulation of phosphorus segregation to Î£3 (111) symmetrical tilt grain boundary in Î±-iron. Modelling and Simulation in Materials Science and Engineering, 2018, 26, 065005.	0.8	5
29295	Interfacial coupling induced direct Z-scheme water splitting in metal-free photocatalyst: C₃N/g-C₃N₄ heterojunctions. Nanotechnology, 2018, 29, 365401.	1.3	39

#	Article	IF	Citations
29296	First-principles study on Ge<inf>1â^'x</inf>Sn<inf>x</inf>-Si core-shell nanowire transistors. , 2018, , .		0
29297	First-Principles Calculations of the Structure Stability and Mechanical Properties of LiFeAs and NaFeAs under Pressure. Advances in Materials Science and Engineering, 2018, 2018, 1-9.	1.0	5
29298	Novel 2D Sb₂S₃ Nanosheet/CNT Coupling Layer for Exceptional Polysulfide Recycling Performance. Advanced Energy Materials, 2018, 8, 1800710.	10.2	93
29299	Exotic high-pressure behavior of double nitride CuPN2. Computational Materials Science, 2018, 152, 217-222.	1.4	0
29300	Atomistic simulation study of the hydrogen diffusion in nickel. Computational Materials Science, 2018, 152, 374-380.	1.4	22
29301	First-principles study of electronic and optical properties of <mml:math xmlns:mml="http://www.w3.org/1998/Math/MathML" altimg="si1.gif" overflow="scroll"><mml:mrow><mml:msub><mml:mrow><mml:mi mathvariant="italic">Ag</mml:mi></mml:mrow><mml:mrow><mml:mn>2</mml:mn></mml:mrow></mml:msub><mml:msub><mml:mi mathvariant="italic">CdSnS</mml:mi></mml:mrow><mml:mrow><mml:mn>4</mml:mn></mml:mrow></mml:msub></mml:mrow></mml:math> for photovoltaic applications. Computational Materials Science, 2018, 152, 291-299.	1.4	14
29302	First-principles predictions of the geometries and electronic structures of tungsten ditelluride nanoribbons. Physics Letters, Section A: General, Atomic and Solid State Physics, 2018, 382, 2754-2758.	0.9	6
29303	A study of ordered mesoporous carbon doped with Co and Ni as a catalyst of oxygen reduction reaction in both alkaline and acidic media. Surface and Coatings Technology, 2018, 349, 511-521.	2.2	24
29304	Mechanisms and Active Sites for Câ€“O Bond Rupture within 2-Methyltetrahydrofuran over Ni, Ni₁₂P₅, and Ni₂P Catalysts. ACS Catalysis, 2018, 8, 7141-7157.	5.5	29
29305	Revealing strong polytypism tendency in MgTe from first-principles. Journal of Applied Physics, 2018, 123, 235903.	1.1	3
29306	Modelling relativistic effects in momentum-resolved electron energy loss spectroscopy of graphene. Radiation Effects and Defects in Solids, 2018, 173, 8-21.	0.4	5
29307	Enhanced magnetic properties and tunable Dirac point of graphene/Mn-doped monolayer MoS₂ heterostructures. Journal of Physics Condensed Matter, 2018, 30, 305304.	0.7	6
29308	First-principles study of electronic structure and magnetic properties of SrTi1-xMxO3 (M = Cr, Mn, Fe,) Tj ETQq0 0 0 rgBT /Overlock 10 T	2.4	17
29309	Investigation on sustainable phosphate release in agriculture: Structural and thermodynamic study of stability, dehydration and anionic exchange of Mg-Al-HPO4 layered double hydroxide by DFT calculations. Applied Clay Science, 2018, 162, 428-434.	2.6	19
29310	Improvement of multiferroic property and change of magnetic ordering in new ANiO3 (Aâ€¯=â€¯Ti, Ge, Zr, Sn,) Tj ETQq0 0 0 rgBT /Overlo	1.4	13
29311	Toxic gases molecules (NH3, SO2 and NO2) adsorption on GeSe monolayer with point defects engineering. Chemical Physics Letters, 2018, 706, 501-508.	1.2	53
29312	Covalency is Frustrating: La₂Sn₂O₇ and the Nature of Bonding in Pyrochlores under High Pressureâ€“Temperature Conditions. Inorganic Chemistry, 2018, 57, 15051-15061.	1.9	10
29313	Adsorption of Li₂O₂, Na₂O₂, and NaO₂ on TiC(111) Surface for Metalâ€“Air Rechargeable Batteries: A Theoretical Study. Journal of Physical Chemistry C, 2018, 122, 16473-16480.	1.5	12

#	Article	IF	Citations
29314	Effect of Step Density and Orientation on the Apparent pH Dependence of Hydrogen and Hydroxide Adsorption on Stepped Platinum Surfaces. Journal of Physical Chemistry C, 2018, 122, 16756-16764.	1.5	50
29315	2D FeO: A New Member in 2D Metal Oxide Family. Journal of Physical Chemistry C, 2018, 122, 17389-17394.	1.5	16
29316	DFT investigation on the adsorption of munition compounds on Î±-Fe₂O₃: similarity and differences with Î±-Al₂O₃. Physical Chemistry Chemical Physics, 2018, 20, 18850-18861.	1.3	12
29317	Electronic properties of FeCl3 and CrO3 interacting with GaN nanotubes from density functional calculations. Journal of Molecular Modeling, 2018, 24, 192.	0.8	8
29318	Preparation and adsorption performance of a NiO/MgF2 composite adsorbent. Journal of Radioanalytical and Nuclear Chemistry, 2018, 317, 287-295.	0.7	1
29319	Properties of Feâ€“Mnâ€“Al alloys with different Mn contents using density functional theory. Rare Metals, 2018, , 1.	3.6	1
29320	Amorphous FeCoPOx nanowires coupled to g-C3N4 nanosheets with enhanced interfacial electronic transfer for boosting photocatalytic hydrogen production. Applied Catalysis B: Environmental, 2018, 238, 161-167.	10.8	49
29321	Electronic properties of porous graphene and its hydrogen storage potentials. Journal of Alloys and Compounds, 2018, 766, 104-111.	2.8	9
29322	Understanding the role of Ni-Sn interaction to design highly effective CO2 conversion catalysts for dry reforming of methane. Journal of CO2 Utilization, 2018, 27, 1-10.	3.3	68
29323	Bi2O3/Ni-Bi2O3 system obtained via Ni-doping for enhanced PEC and photocatalytic activity supported by DFT and experimental study. Solar Energy Materials and Solar Cells, 2018, 186, 208-216.	3.0	49
29324	Native Defects in Li₁₀GeP₂S₁₂ and Their Effect on Lithium Diffusion. Chemistry of Materials, 2018, 30, 4995-5004.	3.2	33
29325	Suppression of Hydrogen Evolution Reaction in Electrochemical N₂ Reduction Using Single-Atom Catalysts: A Computational Guideline. ACS Catalysis, 2018, 8, 7517-7525.	5.5	545
29326	Effect of transition-metal-ion dopants on the oxygen evolution reaction on NiOOH(0001). Physical Chemistry Chemical Physics, 2018, 20, 19525-19531.	1.3	33
29327	Effect of mixed surface terminations on the structural and electrochemical properties of two-dimensional Ti₃C₂T₂ and V₂CT₂ MXenes multilayers. Nanoscale, 2018, 10, 13520-13530.	2.8	143
29328	Effects of strain on electronic properties of Delta nitrogen-doped graphene nanoribbons. Ferroelectrics, 2018, 530, 1-10.	0.3	1
29329	MoS2/Phosphorene Heterostructure for Optical Absorption in Visible Region. IEEE Journal of Quantum Electronics, 2018, 54, 1-6.	1.0	25
29330	Oxoberyllates SrBeO₂ and Sr₁₂Be₁₇O₂₉ as Novel Host Materials for Eu²⁺ Luminescence. Chemistry - A European Journal, 2018, 24, 12678-12685.	1.7	11
29331	Impact of correlative defects induced by double Re-addition on the ideal shear strength of Î³â€²-Ni3Al phases. Computational Materials Science, 2018, 152, 408-416.	1.4	19

#	Article	IF	Citations
29332	Structure-property orientation relationship of a Î³/Î±2/Ti5Si3 in as-cast Ti-45Al-2Nb-0.7Cr-0.3Si intermetallic alloy. Journal of Alloys and Compounds, 2018, 765, 690-699.	2.8	22
29333	Investigation of spin polarized band structure, magnetism, and mechanical properties of new gapless Zr2NbX (X= Al, Ga, In) Heusler alloys. Journal of Alloys and Compounds, 2018, 766, 241-247.	2.8	9
29334	High pressure phonon and thermodynamic properties of Ru based intermetallics: A DFT investigation. Journal of Physics and Chemistry of Solids, 2018, 122, 246-254.	1.9	4
29335	A discussion of La doping on the nucleation of Î±-Al in Alâ€“Znâ€“Si coating. Materials Letters, 2018, 228, 411-413.	1.3	6
29336	A first-principles study of hypothetical Ti 4 AlB 3 and V 4 AlB 3 phases. Solid State Communications, 2018, 281, 17-21.	0.9	4
29337	Atomic Structures of Pt Nanoclusters Supported on Graphene Grown on Pt(111). Journal of Physical Chemistry C, 2018, 122, 16132-16141.	1.5	5
29338	Defect Evolution Enhanced Visible-Light Photocatalytic Activity in Nitrogen-Doped Anatase TiO₂ Thin Films. Journal of Physical Chemistry C, 2018, 122, 16600-16606.	1.5	19
29339	Excited-state vibrational dynamics toward the polaron in methylammonium lead iodide perovskite. Nature Communications, 2018, 9, 2525.	5.8	129
29340	On the possibility of an Eleyâ€“Rideal mechanism for ammonia synthesis on Mn₆N_{5+x} (x = 1)-(111) surfaces. Physical Chemistry Chemical Physics, 2018, 20, 18729-18736.	1.3	6
29341	Pressure induced evolution of structures and properties of iron tetraboride. CrystEngComm, 2018, 20, 3928-3935.	1.3	14
29342	Phase stability, electronic structures and elastic properties of (U,Np)O2 and (Th,Np)O2 mixed oxides. Physical Chemistry Chemical Physics, 2018, 20, 18707-18717.	1.3	9
29343	Spin splitting in band structures of BiTeX (X=Cl, Br, I) monolayers. IOP Conference Series: Materials Science and Engineering, 2018, 347, 012017.	0.3	5
29344	Ab Initio Study of the Structural, Magnetic, Electronic, and Thermodynamic Properties of Pd2MnZ (Z =) Tj ETQq0 0 0 rgBT /Overlock 10	0.2	8
29345	Enhanced Photocatalytic Properties by Forming Tetragonal ZnX/PbO (X = S, Se) Heteroâ€Bilayers: A Computational Prediction. Advanced Theory and Simulations, 2018, 1, 1800046.	1.3	9
29346	Hydrogen adsorption in the presence of coadsorbed CO on Pd(111). Electrochemistry Communications, 2018, 93, 100-103.	2.3	13
29347	Asymmetric covalence bonding between In 5s and O 2p states in ferroelectric InFeO3. Journal of Physics and Chemistry of Solids, 2018, 122, 1-7.	1.9	8
29348	Tuning the magnetic properties of the monolayer MoSe 2 by nonmetal doping: First-principles study. Solid State Communications, 2018, 281, 6-11.	0.9	19
29349	Graphene Oxide/Perovskite Interfaces For Photovoltaics. Journal of Physical Chemistry C, 2018, 122, 16715-16726.	1.5	22

#	Article	IF	Citations
29350	Insights into the Impact of Native Defects on the Conductivity of CuVO₃ Material for Photovoltaic Application: A First-Principles Computational Study. ACS Omega, 2018, 3, 6605-6610.	1.6	3
29351	Tuning the Pd-catalyzed electroreduction of CO₂to CO with reduced overpotential. Catalysis Science and Technology, 2018, 8, 3894-3900.	2.1	24
29352	First-principles calculations of iron-hydrogen reactions in silicon. Journal of Applied Physics, 2018, 123, .	1.1	3
29353	High-throughput functionalization of single-layer electride Ca2N. Materials Research Express, 2018, 5, 076306.	0.8	2
29354	Band-edge levels of the NaCl(100) surface: Self-consistent hybrid density functional theory compared to many-body perturbation theory. Physical Review B, 2018, 97, .	1.1	11
29355	Nodal line fermions in magnetic oxides. Physical Review B, 2018, 97, .	1.1	24
29356	Single atom accelerates ammonia photosynthesis. Science China Chemistry, 2018, 61, 1187-1196.	4.2	107
29357	Metal-doped graphitic carbon nitride (g-C3N4) as selective NO2 sensors: A first-principles study. Applied Surface Science, 2018, 455, 1116-1122.	3.1	71
29358	Electronic structure tuning of stanene monolayers from DFT calculations: Effects of substitutional elemental doping. Applied Surface Science, 2018, 456, 290-301.	3.1	38
29359	DFT modelling of ethanol on BaTiO3 (0â€¯0â€¯1) surface. Applied Surface Science, 2018, 456, 276-289.	3.1	18
29360	Theoretical and experimental investigations on high temperature mechanical and thermal properties of BaZrO3. Ceramics International, 2018, 44, 16475-16482.	2.3	56
29361	A modified CALPHAD model for thermal expansion coefficient in Invar Ni-Fe(FCC) alloys. Computational Materials Science, 2018, 152, 178-182.	1.4	3
29362	Magnetocrystalline effects on the subsurface hydrogen diffusion in Î³-Fe(0â€¯0â€¯1). Computational Materials Science, 2018, 153, 57-63.	1.4	4
29363	Novel method to detect the lung cancer biomarker volatiles using hydrogen vacant silicane nanosheets: A DFT investigation. Computational and Theoretical Chemistry, 2018, 1138, 107-116.	1.1	22
29364	Nano-laminated thin film metallic glass design for outstanding mechanical properties. Scripta Materialia, 2018, 155, 73-77.	2.6	23
29365	Nafion-Mediated Liquid-Phase Exfoliation of Transition Metal Dichalcogenides and Direct Application in Hydrogen Evolution Reaction. Chemistry of Materials, 2018, 30, 4658-4666.	3.2	30
29366	High-Efficiency Production of Graphene by Supercritical CO₂ Exfoliation with Rapid Expansion. Langmuir, 2018, 34, 7797-7804.	1.6	20
29367	2D SnSe-based vdW heterojunctions: tuning the Schottky barrier by reducing Fermi level pinning. Nanoscale, 2018, 10, 13767-13772.	2.8	32

#	Article	IF	Citations
29368	Computational realization of Dirac nodal point and Dirac nodal loop fermions in novel Î²-graphyne analogues. Journal of Materials Chemistry C, 2018, 6, 7626-7634.	2.7	20
29369	Intermediate-phase method for computing the natural band offset between two materials with dissimilar structures. Physical Review B, 2018, 97, .	1.1	5
29370	Importance of van der Waals interactions and cation-anion coupling in an organic quantum spin liquid. Physical Review B, 2018, 97, .	1.1	11
29371	Metal-Insulator Transition of Solid Hydrogen by the Antisymmetric Shadow Wave Function. Zeitschrift Fur Naturforschung - Section A Journal of Physical Sciences, 2018, 73, 845-858.	0.7	3
29372	Role of zirconium in direct CO2 hydrogenation to lower olefins on oxide/zeolite bifunctional catalysts. Journal of Catalysis, 2018, 364, 382-393.	3.1	174
29373	Structures and thermodynamic stability of cobalt molybdenum oxide (CoMoO4-II). Surface Science, 2018, 677, 52-59.	0.8	9
29374	Ferroelectricity and Ferroelasticity in Organic Inorganic Hybrid (Pyrrolidinium)₃[Sb₂Cl₉]. Chemistry of Materials, 2018, 30, 4597-4608.	3.2	65
29375	Asymmetry induced intrinsic magnetodielectric effects in manganite â€“ Barium titanate solid solutions. Journal of Magnetism and Magnetic Materials, 2018, 468, 168-174.	1.0	2
29376	Ultra-stable sodium ion battery cathode realized by Cu7S4 nanoparticles. Journal of Power Sources, 2018, 399, 105-114.	4.0	24
29377	Modeling Oxygen Ion Migration in the CeO₂â€“ZrO₂â€“Y₂O₃ Solid Solution. Journal of Physical Chemistry C, 2018, 122, 18809-18817.	1.5	19
29378	Theoretical Insights into the Interaction of Oxygenated Organic Molecules and Cobalt(II) Precursor with Î³-Al₂O₃Surfaces. Journal of Physical Chemistry C, 2018, 122, 19560-19574.	1.5	8
29379	Understanding W Doping in Wurtzite ZnO. Journal of Physical Chemistry C, 2018, 122, 19082-19089.	1.5	4
29380	Calcium Phosphate Deposition on Planar and Stepped (101) Surfaces of Anatase TiO₂: Introducing an Interatomic Potential for the TiO₂/Ca-PO₄/Water Interface. Langmuir, 2018, 34, 10144-10152.	1.6	5
29381	Deep-ultraviolet Raman scattering spectroscopy of monolayer WS2. Scientific Reports, 2018, 8, 11398.	1.6	15
29382	Phosphomolybdic acid supported single-metal-atom catalysis in CO oxidation: first-principles calculations. Physical Chemistry Chemical Physics, 2018, 20, 20661-20668.	1.3	34
29383	Cu dimer anchored on C₂N monolayer: low-cost and efficient Bi-atom catalyst for CO oxidation. Nanoscale, 2018, 10, 15696-15705.	2.8	68
29384	Computational exploration of borophane-supported single transition metal atoms as potential oxygen reduction and evolution electrocatalysts. Physical Chemistry Chemical Physics, 2018, 20, 21095-21104.	1.3	54
29385	Exploring the impact of hydrostatic pressure on the structural, electronic and mechanical properties of ZrNiPb half-Heusler alloy: A DFT approach. International Journal of Modern Physics B, 2018, 32, 1850248.	1.0	3

#	Article	IF	Citations
29386	The adsorption of CO, O2 and H2 on Liâ€“doped defective (8,0) SWCNT: A DFT study. Applied Surface Science, 2018, 459, 201-207.	3.1	15
29387	The electrochemical performance and CO2 reduction mechanism on strontium doped lanthanum ferrite fuel electrode in solid oxide electrolysis cell. Electrochimica Acta, 2018, 284, 159-167.	2.6	65
29388	Thermoelectric properties of rare-earth based RENi2 (REâ€¯=â€¯Dy, Ho and Er) Laves phase compounds. Journal of Magnetism and Magnetic Materials, 2018, 468, 123-131.	1.0	15
29389	Theory-guided metal-decoration of nanoporous carbon for hydrogen storage applications. Surface and Coatings Technology, 2018, 351, 42-49.	2.2	16
29390	Dirac semimetal in Î² -CuI without surface Fermi arcs. Proceedings of the National Academy of Sciences of the United States of America, 2018, 115, 8311-8315.	3.3	30
29391	Local atomic geometry and Ti <mml:math xmlns:mml="http://www.w3.org/1998/Math/MathML"><mml:mrow><mml:mn>1</mml:mn><mml:mi>s</mml:mi></mml:mrow></mml:m near-edge spectra in <mml:math xmlns:mml="http://www.w3.org/1998/Math/MathML"><mml:msub><mml:mi>PbTiO</mml:mi><mml:mn>3</mml:mn></mml:msub> and <mml:math xmlns:mml="http://www.w3.org/1998/Math/MathML"><mml:msub><mml:mi>SrTiO</mml:mi><mml:mn>3</mml:mn></mml:msub>	1.1	12
29392	Antiferroelectric distortion with anomalous phonon softening in the excitonic insulator <mml:math xmlns:mml="http://www.w3.org/1998/Math/MathML"><mml:mrow><mml:msub><mml:mi>Ta</mml:mi><mml:mn>2</mml:mn></mml:msub></mml:m Physical Review B, 2018, 98, .	1.1	52
29393	Electronic and Magnetic Properties of Stoneâ€“Wales Defected Graphene Decorated with the Half-Metallocene of M (M = Fe, Co, Ni): A First Principle Study. Nanomaterials, 2018, 8, 552.	1.9	19
29394	Enhanced efficiency in lead-free bismuth iodide with post treatment based on a hole-conductor-free perovskite solar cell. Nano Research, 2018, 11, 6283-6293.	5.8	72
29395	Analysis of mechanical, thermodynamic, and thermoelectric properties of ferromagnetic SrFe4As12 skutterudite. Journal of Solid State Chemistry, 2018, 266, 274-278.	1.4	10
29396	Water oxidation chemistry of oxynitrides and oxides: Comparing NaTaO3 and SrTaO2N. Surface Science, 2018, 677, 258-263.	0.8	16
29397	Distorted Janus Transition Metal Dichalcogenides: Stable Two-Dimensional Materials with Sizable Band Gap and Ultrahigh Carrier Mobility. Journal of Physical Chemistry C, 2018, 122, 19153-19160.	1.5	55
29398	Rapid Evaluation of Dynamic Electronic Disorder in Molecular Semiconductors. Journal of Physical Chemistry C, 2018, 122, 18336-18345.	1.5	37
29399	Synergistically Enhanced Oxygen Evolution Reaction Catalysis for Multielement Transition-Metal Oxides. ACS Applied Energy Materials, 2018, 1, 3711-3721.	2.5	53
29400	Bandgap tuning in MoSSe bilayers: synergistic effects of dipole moment and interlayer distance. Physical Chemistry Chemical Physics, 2018, 20, 20919-20926.	1.3	46
29401	Comparison of optical absorption spectra of organic molecules and aggregates computed from real frequency dependent polarizability to TD-DFT and the dipole approximation. Journal of Chemical Physics, 2018, 149, 044114.	1.2	10
29402	Thermoelectric properties of the novel cubic structured silicon monochalcogenides: A first-principles study. Journal of Alloys and Compounds, 2018, 769, 413-419.	2.8	8
29403	Generating Sub-nanometer Pores in Single-Layer MoS₂ by Heavy-Ion Bombardment for Gas Separation: A Theoretical Perspective. ACS Applied Materials & Interfaces, 2018, 10, 28909-28917.	4.0	37

#	Article	IF	Citations
29404	Energy-efficient CO2 hydrogenation with fast response using photoexcitation of CO2 adsorbed on metal catalysts. Nature Communications, 2018, 9, 3027.	5.8	86
29405	Hidden magnetic order in plutonium dioxide nuclear fuel. Physical Chemistry Chemical Physics, 2018, 20, 20943-20951.	1.3	35
29406	Two-dimensional zigzag-shaped Cd₂C monolayer with a desirable bandgap and high carrier mobility. Journal of Materials Chemistry C, 2018, 6, 9175-9180.	2.7	19
29407	Ionic vs. van der Waals layered materials: identification and comparison of elastic anisotropy. Journal of Materials Chemistry A, 2018, 6, 15828-15838.	5.2	22
29408	Hugoniot equation of state of Si-doped glow discharge polymer and scaling to other plastic ablators. Physics of Plasmas, 2018, 25, .	0.7	4
29409	Oxygen isotope fractionation during smithsonite formation from aqueous solutions. Chemical Geology, 2018, 495, 76-89.	1.4	5
29410	Self-assembly directed one-step synthesis of [4]radialene on Cu(100) surfaces. Nature Communications, 2018, 9, 3113.	5.8	41
29411	An atom-to-circuit modeling approach to all-2D metalâ€“insulatorâ€“semiconductor field-effect transistors. Npj 2D Materials and Applications, 2018, 2, .	3.9	20
29412	The effects of combining alloying elements on the elastic properties of Î³ -Ni in Ni-based superalloy: High-throughput first-principles calculations. Chinese Physics B, 2018, 27, 077104.	0.7	6
29413	Tailoring nonlinear optical crystal borophosphate through the introduction of transition metal d orbitals for improving optical anisotropy and SHG response: a first-principles investigation. Materials Research Express, 2018, 5, 096204.	0.8	0
29414	Unraveling the structure and bonding evolution of the newly discovered iron oxide <mml:math xmlns:mml="http://www.w3.org/1998/Math/MathML"><mml:msub><mml:mi>FeO</mml:mi><mml:mn>2</mml:mn></mml:msub></mm Physical Review B, 2018, 98, .	1.1	62
29415	Effects of Y doping with point defects on the ferromagnetic properties of ZnO(0001)-Zn polar surface. Applied Surface Science, 2018, 459, 393-396.	3.1	19
29416	Theoretical study of acetate decomposition on Au(111) surface: Oxygen-assisted Î³-CH activation mechanism. International Journal of Hydrogen Energy, 2018, 43, 17048-17056.	3.8	2
29417	Effect of strain and diameter on electronic and charge transport properties of indium arsenide nanowires. Solid-State Electronics, 2018, 149, 6-14.	0.8	6
29418	The role of metal-oxo intermediate to oxygen reduction reaction catalysis: A theoretical investigation using nitrogen-substituted carbon nanotube models. Surface Science, 2018, 677, 301-305.	0.8	2
29419	Increased Lattice Stiffness Suppresses Nonradiative Charge Recombination in MAPbI₃ Doped with Larger Cations: Time-Domain Ab Initio Analysis. ACS Energy Letters, 2018, 3, 2070-2076.	8.8	68
29420	Discovery of High-Performance Thermoelectric Chalcogenides through Reliable High-Throughput Material Screening. Journal of the American Chemical Society, 2018, 140, 10785-10793.	6.6	134
29421	Structure and properties of a novel boride: ThNi₁₂B₆. Dalton Transactions, 2018, 47, 12933-12943.	1.6	1

#	Article	IF	Citations
29422	Zero-strain K_{0.6}Mn₁F_{2.7} hollow nanocubes for ultrastable potassium ion storage. Energy and Environmental Science, 2018, 11, 3033-3042.	15.6	87
29423	Band gap reduction in van der Waals layered 2D materials via a de-charge transfer mechanism. Nanoscale, 2018, 10, 16759-16764.	2.8	25
29424	Electronic and mechanical properties of few-layer borophene. Physical Review B, 2018, 98, .	1.1	83
29425	Breaking the Limits of Ionic Liquidâ€Based Supercapacitors: Mesoporous Carbon Electrodes Functionalized with Manganese Oxide Nanosplotches for Dense, Stable, and Wideâ€Temperature Energy Storage. Advanced Functional Materials, 2018, 28, 1801298.	7.8	75
29426	A DFT Study of Methanol Synthesis from CO2 Hydrogenation on the Pd(111) Surface. Catalysis Letters, 2018, 148, 2935-2944.	1.4	26
29427	PdCu nanoalloy immobilized in ZIF-derived N-doped carbon/graphene nanosheets: Alloying effect on catalysis. Chemical Engineering Journal, 2018, 353, 311-318.	6.6	52
29428	The first principle calculations of structural, vibrational, elastic, thermodynamic and electronic properties of MgX (XÂ= La, Nd, Sm) intermetallics. Computational Condensed Matter, 2018, 16, e00324.	0.9	6
29429	Density functional theory based prediction of a new two-dimensional TeSe2 semiconductor: A case study on the electronic properties. Chemical Physics Letters, 2018, 707, 160-164.	1.2	12
29430	Electronic and vibrational properties of TMDs heterogeneous bilayers, nontwisted bilayers silicene/TMDs heterostructures and photovoltaic heterojunctions of fullerenes with TMDs monolayers. Physica E: Low-Dimensional Systems and Nanostructures, 2018, 104, 155-164.	1.3	30
29431	Toward a Robust Elastic Geobarometry of Kyanite Inclusions in Eclogitic Diamonds. Journal of Geophysical Research: Solid Earth, 2018, 123, 6411-6423.	1.4	19
29432	Chirality at two-dimensional surfaces: A perspective from small molecule alcohol assembly on Au(111). Journal of Chemical Physics, 2018, 149, 034703.	1.2	9
29433	First-principles calculations of structural, electronic, magnetic and elastic properties of Mo₂FeB₂under high pressure. Royal Society Open Science, 2018, 5, 172247.	1.1	7
29434	Electronic structure and nearly room-temperature ferromagnetism in V-doped monolayer and bilayer MoS2. International Journal of Modern Physics B, 2018, 32, 1850231.	1.0	13
29435	Hierarchical tandem assembly of planar [3Ã—3] building units into {3Ã—[3Ã—3]} oligomers: mixed-valency, electrical conductivity and magnetism. Chemical Science, 2018, 9, 7498-7504.	3.7	23
29436	Interplay of non-uniform charge distribution on the electrochemical modification of graphene. Nanoscale, 2018, 10, 15048-15057.	2.8	27
29437	Anisotropic elastic properties and ideal uniaxial compressive strength of TiB 2 from first principles calculations. Chinese Physics B, 2018, 27, 077103.	0.7	3
29438	Ab Initio Guided Low Temperature Synthesis Strategy for Smooth Faceâ€“Centred Cubic FeMn Thin Films. Metals, 2018, 8, 384.	1.0	8
29439	Fabrication of a Biocompatible Nanocomposite-Based Voltammetric Sensor for Sensitive Determination of Mercazole. Journal of Electronic Materials, 2018, 47, 6251-6259.	1.0	6

#	Article	IF	Citations
29440	Can an element form a two-dimensional nanosheet of type 15 pentagons?. Computational Materials Science, 2018, 154, 37-40.	1.4	34
29441	A comparative first-principles study of tetragonal TiAl and Ti4Nb3Al9 intermetallic compounds. Intermetallics, 2018, 101, 72-80.	1.8	13
29442	A promising high-efficiency photovoltaic alternative non-silicon material: A first-principle investigation. Scripta Materialia, 2018, 156, 134-137.	2.6	2
29443	Subtle Fluorination of Conjugated Molecules Enables Stable Nanoscale Assemblies on Metal Surfaces. Journal of Physical Chemistry C, 2018, 122, 18902-18911.	1.5	10
29444	Quantum Confinement in Oxide Heterostructures: Room-Temperature Intersubband Absorption in SrTiO₃/LaAlO₃ Multiple Quantum Wells. ACS Nano, 2018, 12, 7682-7689.	7.3	15
29445	Electronic and mechanical properties of C/Si phases with sp2 and sp3 hybridization: A first-principles study. AIP Advances, 2018, 8, 075326.	0.6	0
29446	Shallow electron traps formed by Gd2+ ions adjacent to oxygen vacancies in cerium-doped Gd3Al2Ga3O12 crystals. Applied Physics Letters, 2018, 113, 041906.	1.5	11
29447	Structural, vibrational, and electronic properties of single-layer hexagonal crystals of group IV and V elements. Physical Review B, 2018, 98, .	1.1	102
29448	Theoretical Study of Monolayer PtSe₂ as Outstanding Gas Sensor to Detect SF₆ Decompositions. IEEE Electron Device Letters, 2018, 39, 1405-1408.	2.2	67
29449	Peculiarities of Interactions of Alloying Elements with Grain Boundaries and the Formation of Segregations in Alâ€“Mg and Alâ€“Zn Alloys. Physics of Metals and Metallography, 2018, 119, 607-612.	0.3	10
29450	Realization of a New Topological Crystalline Insulator and Lifshitz Transition in PbTe. Advanced Functional Materials, 2018, 28, 1803188.	7.8	16
29451	Twoâ€Đimensional Phosphorus Carbide Polymorphs: Influence of Structural Motifs on the Band Gap. Physica Status Solidi (B): Basic Research, 2018, 255, 1800192.	0.7	4
29452	H2S adsorption and dissociation on Rh(110) surface: a first-principles study. Adsorption, 2018, 24, 563-574.	1.4	8
29453	Elucidating mechanisms of Li plating on Li anodes of lithium-based batteries. Electrochimica Acta, 2018, 284, 485-494.	2.6	19
29454	Upconversion luminescence properties of different Fluoride matrix materials NaREF4 (RE: Gd, Lu, Y) doped with Er3+/Yb3+. Journal of Luminescence, 2018, 204, 333-340.	1.5	23
29455	Germanene Growth on Al(111): A Case Study of Interface Effect. Journal of Physical Chemistry C, 2018, 122, 18669-18681.	1.5	17
29456	Classic papers published by Taiwanese scientists in the science citation index expanded: A bibliometric study. Collnet Journal of Scientometrics and Information Management, 2018, 12, 83-95.	0.4	6
29457	B-Splines and NURBS Based Finite Element Methods for Strained Electronic Structure Calculations. Journal of Applied Mechanics, Transactions ASME, 2018, 85, .	1.1	6

#	Article	IF	Citations
29458	(10.4) Face of Ordered and Disordered Dolomite, MgCa(CO3)2: A Computational Study to Reveal the Growth Mechanism. Minerals (Basel, Switzerland), 2018, 8, 323.	0.8	7
29459	Optical absorption coefficient red shift effect of iodine vacancy in MAPbI3. Computational Materials Science, 2018, 154, 138-142.	1.4	0
29460	High-temperature mechanical and thermodynamic properties of silicon carbide polytypes. Journal of Alloys and Compounds, 2018, 768, 722-732.	2.8	34
29461	A molecular dynamics framework to explore the structure and dynamics of layered double hydroxides. Applied Clay Science, 2018, 163, 164-177.	2.6	27
29462	Photocatalytic mechanism of Au or Cl adsorption on the 1I-terminated BiOI (0â€¯0â€¯1) surface. Chemical Physics Letters, 2018, 711, 48-54.	1.2	4
29463	Revealing the role of calcium codoping on optical and scintillation homogeneity in Lu2SiO5:Ce single crystals. Journal of Crystal Growth, 2018, 498, 362-371.	0.7	20
29464	A progressive metalâ€“semiconductor transition in two-faced Janus monolayer transition-metal chalcogenides. Physical Chemistry Chemical Physics, 2018, 20, 21113-21118.	1.3	16
29465	Scanning tunneling microscopy investigations of unoccupied surface states in two-dimensional semiconducting Î²-â^š3 Ã— â^š3-Bi/Si(111) surface. Physical Chemistry Chemical Physics, 2018, 20, 20188-20193.	1.3	8
29466	Water dissociation on K₂O-pre-adsorbed transition metals: a systematic theoretical study. Physical Chemistry Chemical Physics, 2018, 20, 19850-19859.	1.3	7
29467	Widely used hardly known. An insight into electric and dynamic properties of formamidinium iodide. RSC Advances, 2018, 8, 26506-26516.	1.7	9
29468	The nature of the intermediate phase in K₃Na(SeO₄)₂ crystals: three possible transition paths of the trigonal-monoclinic phaseÂtransition. Phase Transitions, 2018, 91, 1135-1146.	0.6	0
29469	IR spectral fingerprint of carbon monoxide in interstellar waterâ€“ice models. Monthly Notices of the Royal Astronomical Society, 2018, 480, 1427-1444.	1.6	26
29470	First-principles studies on the interface between light-absorbing layer and Mo back electrode in Cu(In,Ga)Se₂, Cu₂ZnSn(S,Se)₄, and Cu₂SnS₃ solar cells. Japanese Journal of Applied Physics, 2018, 57, 08RC17.	0.8	7
29471	Enhanced oxidation resistance of NaBH4-treated mackinawite (FeS): Application to Cr(VI) and As(III) removal. Chemical Engineering Journal, 2018, 353, 890-899.	6.6	36
29472	Electronic properties of graphene nanoribbons doped with zinc, cadmium, mercury atoms. Physica E: Low-Dimensional Systems and Nanostructures, 2018, 104, 124-129.	1.3	5
29473	Multiple spin-resolved negative differential resistance and electrically controlled spin-polarization in transition metal-doped [6]cycloparaphenylenes. Physics Letters, Section A: General, Atomic and Solid State Physics, 2018, 382, 2763-2768.	0.9	7
29474	Unraveling the Structureâ€“Raman Spectra Relationships in V₂O₅ Polymorphs via a Comprehensive Experimental and DFT Study. Inorganic Chemistry, 2018, 57, 9190-9204.	1.9	36
29475	Sea coral-like NiCo₂O₄@(Ni, Co)OOH heterojunctions for enhancing overall water-splitting. Catalysis Science and Technology, 2018, 8, 4151-4158.	2.1	16

#	Article	IF	Citations
29476	A comparative study on the photocatalytic degradation of organic dyes using hybridized 1T/2H, 1T/3R and 2H MoS₂ nano-sheets. RSC Advances, 2018, 8, 26364-26370.	1.7	63
29477	Two-dimensional multiferroic semiconductors with coexisting ferroelectricity and ferromagnetism. Applied Physics Letters, 2018, 113, .	1.5	114
29478	Exploring triazine and heptazine based self assembled molecular materials through first principles investigations. Journal of Molecular Modeling, 2018, 24, 217.	0.8	5
29479	Promoted methane activation on doped ceria via occupation of Pr(4f) states. Applied Surface Science, 2018, 458, 397-404.	3.1	9
29480	IodideÂ·Â·Â·Ï€ Interactions of Perhalogenated Quinoid Rings in Co-crystals with Organic Bases. Crystal Growth and Design, 2018, 18, 5182-5193.	1.4	19
29481	Determination of the Intrinsic Defect at the Origin of Poor H₂ Evolution Performance of the Monoclinic BiVO₄ Photocatalyst Using Density Functional Theory. Journal of Physical Chemistry C, 2018, 122, 18204-18211.	1.5	28
29482	Computational screening of organic polymer dielectrics for novel accelerator technologies. Scientific Reports, 2018, 8, 9258.	1.6	4
29483	Achieving ultrahigh carrier mobilities and opening the band gap in two-dimensional Si₂BN. Physical Chemistry Chemical Physics, 2018, 20, 21716-21723.	1.3	30
29484	Structural stability and thermodynamic properties of BSb under high pressure and temperature. Materials Research Express, 2018, 5, 085904.	0.8	17
29485	Temperature-dependent Raman linewidths in transition-metal dichalcogenides. Physical Review B, 2018, 98, .	1.1	7
29486	Behaviors of helium in Cr₂AlC from first principles. Journal of the American Ceramic Society, 2018, 101, 5771-5780.	1.9	10
29487	The mechanism of ethanol steam reforming on the Co0 and Co2+ sites: A DFT study. Journal of Catalysis, 2018, 365, 391-404.	3.1	33
29488	Strain-mediated stability and electronic properties of WS2, Janus WSSe and WSe2 monolayers. Superlattices and Microstructures, 2018, 122, 268-279.	1.4	51
29489	Calculated tunneling magnetoresistance ratio of FeRh/MgO/FeRh (001) magnetic tunnel junction. Superlattices and Microstructures, 2018, 122, 235-242.	1.4	2
29490	Carâ€“Parrinello and Path Integral Molecular Dynamics Study of the Proton Transfer in the Intramolecular Hydrogen Bonds in the Ketohydrazoneâ€“Azoenol System. Journal of Physical Chemistry B, 2018, 122, 7862-7873.	1.2	9
29491	Interaction of HCl with a CeO₂(111) Layer Supported on Ru(0001): A Theory and Experiment Combined Study. Journal of Physical Chemistry C, 2018, 122, 19584-19592.	1.5	6
29492	Identifying Influential Parameters of Octahedrally Coordinated Cations in Spinel ZnMn_xCo_{2â€“x}O₄ Oxides for the Oxidation Reaction. ACS Catalysis, 2018, 8, 8568-8577.	5.5	68
29493	The effect of strain and functionalization on the optical properties of borophene. Physical Chemistry Chemical Physics, 2018, 20, 21043-21050.	1.3	45

#	Article	IF	Citations
29494	Insight into lithium-ion mobility in Li₂La(TaTi)O₇. Journal of Materials Chemistry A, 2018, 6, 22152-22160.	5.2	16
29495	Becquerelite mineral phase: crystal structure and thermodynamic and mechanical stability by using periodic DFT. RSC Advances, 2018, 8, 24599-24616.	1.7	36
29496	Three-dimensional quantum anomalous Hall effect in ferromagnetic insulators. Physical Review B, 2018, 98, .	1.1	25
29497	Hydrogen Bonding Controls the Structural Evolution in Perovskite-Related Hybrid Platinum(IV) Iodides. Inorganic Chemistry, 2018, 57, 10375-10382.	1.9	40
29498	Exceptional Optical Absorption of Buckled Arsenene Covering a Broad Spectral Range by Molecular Doping. ACS Omega, 2018, 3, 8514-8520.	1.6	107
29499	Seawater desalination using pillared graphene as a novel nano-membrane in reverse osmosis process: nonequilibrium MD simulation study. Physical Chemistry Chemical Physics, 2018, 20, 22241-22248.	1.3	20
29500	Assessing the performance of the Tao-Mo semilocal density functional in the projector-augmented-wave method. Journal of Chemical Physics, 2018, 149, 044120.	1.2	50
29501	Functionalization of the electronic and magnetic properties of silicene by halogen atoms unilateral adsorption: a first-principles study. Journal of Physics Condensed Matter, 2018, 30, 365001.	0.7	5
29502	Effect of B on Growth of Recrystallized Grain of Ti-added Ultra-low Carbon Cold-rolled Steel Sheets. ISIJ International, 2018, 58, 1901-1909.	0.6	4
29503	Ammonothermal Synthesis, Optical Properties, and DFT Calculations of Mg₂PN₃ and Zn₂PN₃. Chemistry - A European Journal, 2018, 24, 13963-13970.	1.7	27
29504	Effect of an Al-adlayer in the c-plane ZnO/AlN heterostructure. Europhysics Letters, 2018, 122, 26003.	0.7	2
29505	Using Applications and Tools to Visualize ab initio Calculations Performed in VASP. Lecture Notes in Computer Science, 2018, , 489-496.	1.0	1
29506	Comparative study of Ti and Cr adhesion to the AlN ceramic: Experiments and calculations. Applied Surface Science, 2018, 457, 856-862.	3.1	19
29507	A high-performance dual-ion cell utilizing Si nanosphere@graphene anode. Electrochimica Acta, 2018, 282, 946-954.	2.6	13
29508	Surface Orientation Dependent Water Dissociation on Rutile Ruthenium Dioxide. Journal of Physical Chemistry C, 2018, 122, 17802-17811.	1.5	44
29509	Accuracy of Density Functional Theory for Predicting Kinetics of Methanol Synthesis from CO and CO₂ Hydrogenation on Copper. Journal of Physical Chemistry C, 2018, 122, 17942-17953.	1.5	31
29510	Principles of Design for Substrate-Supported Molecular Switches Based on Physisorbed and Chemisorbed States. ACS Applied Materials & Interfaces, 2018, 10, 26772-26780.	4.0	15
29511	Mechanistic Study of the Direct Hydrodeoxygenation of m-Cresol over WO_x-Decorated Pt/C Catalysts. ACS Catalysis, 2018, 8, 7749-7759.	5.5	87

#	Article	IF	Citations
29512	Classical interatomic potential for quaternary Niâ€“Feâ€“Crâ€“Pd solid solution alloys. Modelling and Simulation in Materials Science and Engineering, 2018, 26, 065014.	0.8	10
29513	Metastability of the boron-vacancy complex in silicon: Insights from hybrid functional calculations. Physical Sciences Reviews, 2018, 3, .	0.8	0
29514	First Principles Study of Topochemical Effects and Electronic Structure Relationships between ANCl and A2N2Se (A = Zr, Ce) Assimilated to Pseudo-Binaries: {AN}Cl and {A2N2}Se. Computation, 2018, 6, 30.	1.0	1
29515	Synthesis and Characterization of Barium Hexafluoridoosmates. Crystals, 2018, 8, 11.	1.0	8
29516	Theoretical and Experimental Investigations into Novel Oxynitride Discovery in the GaN-TiO2 System at High Pressure. Crystals, 2018, 8, 15.	1.0	5
29517	First-Principles Investigations of the Structural, Anisotropic Mechanical, Thermodynamic and Electronic Properties of the AlNi2Ti Compound. Crystals, 2018, 8, 93.	1.0	10
29518	Rhombohedral Distortion of the Cubic MgCu2-Type Structure in Ca2Pt3Ga and Ca2Pd3Ga. Crystals, 2018, 8, 186.	1.0	4
29519	Electrodynamics in Organic Dimer Insulators Close to Mott Critical Point. Crystals, 2018, 8, 190.	1.0	17
29520	Optical Absorption and Reflectivity of a Molecular Cluster of Lithium Niobate Adsorbed on a Graphene Layer. Crystals, 2018, 8, 208.	1.0	3
29521	High-Pressure Elastic, Vibrational and Structural Study of Monazite-Type GdPO4 from Ab Initio Simulations. Crystals, 2018, 8, 209.	1.0	10
29522	Boron Monochalcogenides; Stable and Strong Two-Dimensional Wide Band-Gap Semiconductors. Energies, 2018, 11, 1573.	1.6	32
29523	A density functional based tight binding (DFTB+) study on the sulfidization-amine flotation mechanism of smithsonite. Applied Surface Science, 2018, 458, 454-463.	3.1	52
29524	Thermodynamic optimization of Si-Zr-N system using Calphad approach coupled with ab initio methods. Calphad: Computer Coupling of Phase Diagrams and Thermochemistry, 2018, 62, 148-153.	0.7	4
29525	Clarifying the capacity deterioration mechanism sheds light on the design of ultra-long-life hydrogen storage alloys. Chemical Engineering Journal, 2018, 352, 325-332.	6.6	22
29526	Composition effect of oxygen reduction reaction on PtSn nanorods: An experimental and computational study. International Journal of Hydrogen Energy, 2018, 43, 14427-14438.	3.8	22
29527	The catalytic effect of the Au(111) and Pt(111) surfaces to the sodium borohydride hydrolysis reaction mechanism: A DFT study. International Journal of Hydrogen Energy, 2018, 43, 14347-14359.	3.8	17
29528	Enhanced gas-sensing performance of graphene by doping transition metal atoms: A first-principles study. Physics Letters, Section A: General, Atomic and Solid State Physics, 2018, 382, 2965-2973.	0.9	34
29529	Modeling laser-driven high-rate plasticity in BCC lead. AIP Conference Proceedings, 2018, , .	0.3	3

#	Article	IF	Citations
29530	Doping SnO2 crystal with increasing concentrations of Zn and Sb atoms: a quantum chemical analysis. Physica Scripta, 2018, 93, 095801.	1.2	5
29531	Hybrid <mml:math xmlns:mml="http://www.w3.org/1998/Math/MathML"><mml:mrow><mml:mi mathvariant="normal">k</mml:mi><mml:mo>Â·</mml:mo><mml:mi mathvariant="normal">p</mml:mi></mml:mrow></mml:math> tight-binding model for subbands and infrared intersubband optics in few-layer films of transition-metal dichalcogenides: <mml:math xmlns:mml="http://www.w3.org/1998/Math/MathML"><mml:msub><mml:mi>MoS</mml:mi><mml:mn>2</mml:mn></mml:msub></mml:m	1.1	34
29532	The elastic behaviors and theoretical tensile strength of <mml:math xmlns:mml="http://www.w3.org/1998/Math/MathML" altimg="si1.gif" overflow="scroll"><mml:mi>Î³</mml:mi></mml:math>-TiAl alloy from the first principles calculations. Intermetallics, 2018, 101, 1-7.	1.8	30
29533	Effect of Zr and Al addition on nanocluster formation in oxide dispersion strengthened steel - An ab initio study. Journal of Alloys and Compounds, 2018, 767, 122-130.	2.8	29
29534	Investigation of the Preferential Doping Site and Regulating on the Visible Light Response and Redox Performance for Fe- and/or La-Doped InNbO₄. Inorganic Chemistry, 2018, 57, 8558-8567.	1.9	10
29535	Polymorphism, Weak Interactions and Phase Transitions in Chalcogenâ€“Phosphorus Heterocycles. Chemistry - A European Journal, 2018, 24, 11067-11081.	1.7	4
29536	Highly conductive CrNb11O29 nanorods for use in high-energy, safe, fast-charging and stable lithium-ion batteries. Journal of Power Sources, 2018, 397, 231-239.	4.0	48
29537	Electronic structure, elastic and phonon properties of perovskite-type hydrides MgXH 3 (Xâ€¯=â€¯Fe, Co) for hydrogen storage. Solid State Communications, 2018, 281, 38-43.	0.9	36
29538	Preparation and electron correlation effects of the perovskite La0.8Ca0.1Pb0.1Fe1â^'Co O3 (0â€¯â‰¤â€¯xâ€¯â‰¤â€¯0.20). Solid State Ionics, 2018, 324, 157-162.	1.3	7
29539	Existence of an Electrochemically Inert CO Population on Cu Electrodes in Alkaline pH. ACS Catalysis, 2018, 8, 7507-7516.	5.5	176
29540	The prediction of a new high-pressure phase of hafnia using first-principles computations. IOP Conference Series: Materials Science and Engineering, 2018, 305, 012006.	0.3	5
29541	Crystal-plane-dependent metal oxide-support interaction in CeO2/g-C3N4 for photocatalytic hydrogen evolution. Applied Catalysis B: Environmental, 2018, 238, 111-118.	10.8	178
29542	Stability and electronic properties of sulfur terminated two-dimensional early transition metal carbides and nitrides (MXene). Computational Materials Science, 2018, 153, 303-308.	1.4	46
29543	An ab initio study on stacking and stability of TiAl3 phases. Computational Materials Science, 2018, 153, 309-314.	1.4	10
29544	Nucleobases adsorption studies on silicane layer: A first-principles investigation. Journal of Molecular Graphics and Modelling, 2018, 85, 48-55.	1.3	16
29545	Effects of the Aqueous Environment on the Stability and Chemistry of Î²-NiOOH Surfaces. Chemistry of Materials, 2018, 30, 5205-5219.	3.2	41
29546	Theoretical Investigation of Methane Oxidation on Pd(111) and Other Metallic Surfaces. Journal of Physical Chemistry C, 2018, 122, 16023-16032.	1.5	34
29547	Combining High Photocatalytic Activity and Stability via Subsurface Defects in TiO₂. Journal of Physical Chemistry C, 2018, 122, 17221-17227.	1.5	27

#	Article	IF	Citations
29548	Coincident modulation of lattice and electron thermal transport performance in MXenes via surface functionalization. Physical Chemistry Chemical Physics, 2018, 20, 19689-19697.	1.3	18
29549	Substrate-induced enhancement of the chemical reactivity in metal-supported graphene. Physical Chemistry Chemical Physics, 2018, 20, 19492-19499.	1.3	10
29550	Orbitronic effect on the magnetic reconstruction of monocell SrMnO3 on ferroelectric BaTiO3 substrate. Journal of Applied Physics, 2018, 124, 014101.	1.1	0
29551	Theoretical prediction electronic properties of Group-IV diamond nanothreads. AIP Advances, 2018, 8, 075107.	0.6	8
29552	Negative thermal expansion behavior in <mml:math xmlns:mml="http://www.w3.org/1998/Math/MathML"><mml:mrow><mml:mi>M</mml:mi><mml:mi>Zr</mml:mi><mml:msub><mml:mi mathvariant="normal">F</mml:mi><mml:mn>6</mml:mn></mml:msub></mml:mrow><mml:mspace width="4pt" /><mml:mo>(</mml:mo><mml:mrow><mml:mi>M</mml:mi><mml:mo>=</mml:mo><mml:mi>Ca</mml:mi><mml:mo>,</mml:mo><mml:mn : Ab initio lattice dynamical stud. Physical Review B, 2018, 98, .	1.1	13
29553	Strong Adsorption of Al-Doped Bilayer Graphene Toward Anticancer Cisplatin. Nano, 2018, 13, 1850068.	0.5	0
29554	First-Principles Calculations of Structural, Electronic, Magnetic and Elastic Properties of Heusler Alloys Ru₂CoZ (Z = Si, Ge and Sn). Spin, 2018, 08, 1850009.	0.6	11
29555	Electronic structure and magnetic ordering in gadolinium-doped AlGaN from LSDA + U calculations. International Journal of Computational Materials Science and Engineering, 2018, 07, 1850019.	0.5	7
29556	Ab Initio Molecular Dynamics Simulation of Tribochemical Reactions Involving Phosphorus Additives at Sliding Iron Interfaces. Lubricants, 2018, 6, 31.	1.2	29
29557	DFT Study on Intermetallic Pdâ€“Cu Alloy with Cover Layer Pd as Efficient Catalyst for Oxygen Reduction Reaction. Materials, 2018, 11, 33.	1.3	24
29558	The Electronic Structure and Optical Properties of Anatase TiO2 with Rare Earth Metal Dopants from First-Principles Calculations. Materials, 2018, 11, 179.	1.3	26
29559	Study of Electronic Structure, Thermal Conductivity, Elastic and Optical Properties of Î±, Î², Î³-Graphyne. Materials, 2018, 11, 188.	1.3	65
29560	The Electronic Properties of O-Doped Pure and Sulfur Vacancy-Defect Monolayer WS2: A First-Principles Study. Materials, 2018, 11, 218.	1.3	32
29561	Structural, Electronic, and Thermodynamic Properties of Tetragonal t-SixGe3â^'xN4. Materials, 2018, 11, 397.	1.3	7
29562	The CiCs(Sil)n Defect in Silicon from a Density Functional Theory Perspective. Materials, 2018, 11, 612.	1.3	6
29563	Polycyclic Aromatic Hydrocarbons Adsorption onto Graphene: A DFT and AIMD Study. Materials, 2018, 11, 726.	1.3	41
29564	On the Mnâ€“C Short-Range Ordering in a High-Strength High-Ductility Steel: Small Angle Neutron Scattering and Ab Initio Investigation. Metals, 2018, 8, 44.	1.0	20
29565	DFT Study of Azole Corrosion Inhibitors on Cu2O Model of Oxidized Copper Surfaces: I. Moleculeâ€“Surface and Clâ€“Surface Bonding. Metals, 2018, 8, 310.	1.0	30

#	Article	IF	Citations
29566	DFT Study of Azole Corrosion Inhibitors on Cu2O Model of Oxidized Copper Surfaces: II. Lateral Interactions and Thermodynamic Stability. Metals, 2018, 8, 311.	1.0	14
29567	Magnetic Isotropy/Anisotropy in Layered Metal Phosphorous Trichalcogenide MPS3 (M = Mn, Fe)Single Crystals. Micromachines, 2018, 9, 292.	1.4	26
29568	Magnetic Properties of Metalâ€“Organic Coordination Networks Based on 3d Transition Metal Atoms. Molecules, 2018, 23, 964.	1.7	9
29569	Tunable Electronic and Topological Properties of Germanene by Functional Group Modification. Nanomaterials, 2018, 8, 145.	1.9	19
29570	The Effects of Graphene Stacking on the Performance of Methane Sensor: A First-Principles Study on the Adsorption, Band Gap and Doping of Graphene. Sensors, 2018, 18, 422.	2.1	9
29571	Fe-N system at high pressure reveals a compound featuring polymeric nitrogen chains. Nature Communications, 2018, 9, 2756.	5.8	153
29572	Novel triadius-like N4 specie of iron nitride compounds under high pressure. Scientific Reports, 2018, 8, 10670.	1.6	36
29573	Role of transition metals in a charge transfer mechanism and oxygen removal in Li_{1.17}Ni_{0.17}Mn_{0.5}Co_{0.17}O₂: experimental and first-principles analysis. Physical Chemistry Chemical Physics, 2018, 20, 19606-19613.	1.3	6
29574	CO₂ interaction with violarite (FeNi₂S₄) surfaces: a dispersion-corrected DFT study. Physical Chemistry Chemical Physics, 2018, 20, 20439-20446.	1.3	15
29575	Precipitation strengthening in Cuâ€“Niâ€“Si alloys modeled with ab initio based interatomic potentials. Journal of Chemical Physics, 2018, 149, 024701.	1.2	5
29576	Electronic structure of single layer 1T-NbSe₂: interplay of lattice distortions, non-local exchange, and Mottâ€“Hubbard correlations. Journal of Physics Condensed Matter, 2018, 30, 325601.	0.7	25
29577	Structural and electronic properties of 5,5â€²-Hydrazinebistetrazole under high pressure: A DFT study. IOP Conference Series: Materials Science and Engineering, 2018, 377, 012107.	0.3	0
29578	Multiple topologically nontrivial bands in noncentrosymmetric YSn2. Physical Review B, 2018, 98, .	1.1	4
29579	First-principles calculations of structural, electronic, magnetic, elastic and optical properties of tetragonal zircon-type CeVO4. International Journal of Modern Physics B, 2018, 32, 1850239.	1.0	1
29580	Pressure-induced structural phase transformation of yttrium diborocarbide at high pressure. Europhysics Letters, 2018, 122, 36004.	0.7	2
29581	Role of Disorder in NaO₂ and Its Implications for Naâ€“O₂ Batteries. Journal of Physical Chemistry C, 2018, 122, 18829-18835.	1.5	0
29582	Assignment of the Raman Spectrum of Benzylic Amide [2]Catenane: Raman Microscopy Experiments and First-Principles Calculations. Journal of Physical Chemistry C, 2018, 122, 18102-18109.	1.5	4
29583	Microscopic Electrode Processes in the Four-Electron Oxygen Reduction on Highly Active Carbon-Based Electrocatalysts. ACS Catalysis, 2018, 8, 8162-8176.	5.5	54

#	Article	IF	Citations
29584	Origin of Chemically Ordered Atomic Laminates (i-MAX): Expanding the Elemental Space by a Theoretical/Experimental Approach. ACS Nano, 2018, 12, 7761-7770.	7.3	99
29585	Nanoscale surface dynamics of Bi₂Te₃(111): observation of a prominent surface acoustic wave and the role of van der Waals interactions. Nanoscale, 2018, 10, 14627-14636.	2.8	27
29586	Robust large gap quantum spin Hall insulators in methyl and ethynyl functionalized TlSb buckled honeycombs. Journal of Applied Physics, 2018, 124, .	1.1	5
29587	Structural, electronic and thermodynamic properties of bulk and surfaces of terbium dioxide (TbO₂). Materials Research Express, 2018, 5, 085901.	0.8	9
29588	Stability and mechanical properties of high-La content Laâ€“Ni phases by first-principles study. International Journal of Modern Physics B, 2018, 32, 1850242.	1.0	2
29589	Effects of Scandium Addition on the Structural Stability and Ideal Strengths of Magnesium-Lithium Alloys. Zeitschrift Fur Naturforschung - Section A Journal of Physical Sciences, 2018, 73, 947-956.	0.7	1
29590	Magnetic Properties and Spontaneous Polarization of La-, Mn- and N-Doped Tetragonal BiFeO3: A First-Principles Study. Materials, 2018, 11, 985.	1.3	9
29591	Uniaxial compression behavior and spectroscopic properties of the explosive pentaerythritol tetranitrate from first-principles calculations. Computational Materials Science, 2018, 153, 392-398.	1.4	4
29592	First-principles calculations on physical properties of Ni3Sn binary system intermetallic compounds and Ni/Ni3Sn interfaces in Nickel-Tin TLPS bonding layer. Intermetallics, 2018, 101, 27-38.	1.8	19
29593	A strategy for designing new AB 4.5 -type hydrogen storage alloys with high capacity and long cycling life. Journal of Power Sources, 2018, 398, 42-48.	4.0	26
29594	Effects of pressure on the structure and lattice dynamics of ammonium perchlorate: A combined experimental and theoretical study. Journal of Chemical Physics, 2018, 149, 034501.	1.2	6
29595	First-principles study of elastic and slip properties of non-canonical Î²-based Alâ€“Cuâ€“Fe approximants. Philosophical Magazine, 2018, 98, 2135-2150.	0.7	0
29596	Towards understanding the influence of Re on H dissolution and retention in W by investigating the interaction between dispersed/aggregated-Re and H. Nuclear Fusion, 2018, 58, 096026.	1.6	16
29597	Insights into the unconventional superconductivity in <mml:math xmlns:mml="http://www.w3.org/1998/Math/MathML"><mml:mrow><mml:msub><mml:mi>HfV</mml:mi><mml:mn>2</mml:mn></mml:m and <mml:math xmlns:mml="http://www.w3.org/1998/Math/MathML"><mml:mrow><mml:msub><mml:mi>ScV</mml:mi><mml:mn>2</mml:mn></mml:m from first-principles electronic-str. Physical Review B, 2018, 98, .	1.1	8
29598	Inâ€‰situ highâ€‰temperature Raman spectroscopic studies of the vibrational characteristics and microstructure evolution of sodium tungstate dihydrate crystal during heating and melting. Journal of Raman Spectroscopy, 2018, 49, 1693-1705.	1.2	15
29599	The adsorption and diffusion properties of scandium atom on the surfaces of tungsten and noble metals. Applied Surface Science, 2018, 457, 1057-1063.	3.1	5
29600	Computational calculation identified optimal binding sites in nano-sized magnetic-cored dendrimer. Chemosphere, 2018, 210, 287-295.	4.2	7
29601	First principles study of structural, mechanical and electronic properties of the ternary alkali metal oxides KNaO and RbNaO. Chemical Physics Letters, 2018, 706, 684-693.	1.2	5

#	Article	IF	Citations
29602	First-principles study of hydrogen retention and diffusion behaviors in 4H-SiC. Superlattices and Microstructures, 2018, 122, 362-370.	1.4	1
29603	Insights into the Charge-Transfer Stabilization of Heterostructure Components with Unstable Bulk Analogs. Chemistry of Materials, 2018, 30, 4738-4747.	3.2	12
29604	Improved Nonenzymatic Glucose Sensing Properties of Pd/MnO₂ Nanosheets: Synthesis by Facile Microwave-Assisted Route and Theoretical Insight from Quantum Simulations. Journal of Physical Chemistry B, 2018, 122, 7636-7646.	1.2	28
29605	Interface Engineering of Graphene/CH₃NH₃PbI₃ Heterostructure for Novel pâ€“iâ€“n Structural Perovskites Solar Cells. Journal of Physical Chemistry C, 2018, 122, 17228-17237.	1.5	22
29606	Concerted Ion-Exchange Mechanism for Sodium Diffusion and Its Promotion in Na₃V₂(PO₄)₃ Framework. Journal of Physical Chemistry C, 2018, 122, 16649-16654.	1.5	56
29607	Suppression of surfaces states at cubic perovskite (001) surfaces by CO2 adsorption. Physical Chemistry Chemical Physics, 2018, 20, 18828-18836.	1.3	13
29608	Defects in orthorhombic LaMnO₃ â€“ ionic versus electronic compensation. Physical Chemistry Chemical Physics, 2018, 20, 19257-19267.	1.3	3
29609	Indexing of grazing-incidence X-ray diffraction patterns: the case of fibre-textured thin films. Acta Crystallographica Section A: Foundations and Advances, 2018, 74, 373-387.	0.0	19
29610	Electronic structure of heterojunction MoO2/g-C3N4 catalyst for oxidative desulfurization. Applied Catalysis B: Environmental, 2018, 238, 263-273.	10.8	178
29611	Exploring interfacial stability of solid-state electrolytes at the lithium-metal anode surface. Journal of Power Sources, 2018, 396, 782-790.	4.0	73
29612	Density Functional Theory Study of Water Photo-Oxidation at Copper Oxide Nanostructures on the Anatase (101) Surface. Journal of Physical Chemistry C, 2018, 122, 16765-16771.	1.5	5
29613	Electrically Conductive Copper Coreâ€“Shell Nanowires through Benzenethiol-Directed Assembly. Nano Letters, 2018, 18, 4900-4907.	4.5	8
29614	Multilayered Platinum Nanotube for Oxygen Reduction in a Fuel Cell Cathode: Origin of Activity and Product Selectivity. ACS Applied Energy Materials, 2018, 1, 3890-3899.	2.5	10
29615	Unraveling the Mechanism of Photoinduced Charge-Transfer Process in Bilayer Heterojunction. ACS Applied Materials & Interfaces, 2018, 10, 25401-25408.	4.0	29
29616	Performance-improved Li-O₂ batteries by tailoring the phases of Mo_xC porous nanorods as an efficient cathode. Nanoscale, 2018, 10, 14877-14884.	2.8	28
29617	Understanding the loss of electrochemical activity of nanosized LiMn₂O₄particles: a combined experimental andab initioDFT study. Journal of Materials Chemistry A, 2018, 6, 14967-14974.	5.2	13
29618	Short-range ion dynamics in methylammonium lead iodide by multinuclear solid state NMR and¹²⁷I NQR. Physical Chemistry Chemical Physics, 2018, 20, 20043-20055.	1.3	42
29619	Hydrogen as a source of flux noise in SQUIDs. Physical Review B, 2018, 98, .	1.1	11

#	Article	IF	Citations
29620	Electronic Properties of Vanadium Atoms Adsorption on Clean and Graphene-Covered Cu(111) Surface. Nanoscale Research Letters, 2018, 13, 199.	3.1	4
29621	First-Principles Study of the Calcium Insertion in Layered and Non-Layered Phases of Vanadia. MRS Advances, 2018, 3, 3507-3512.	0.5	4
29622	Identification of anhydrous CaCl2 and KCaCl3 in natural inclusions by Raman spectroscopy. Chemical Geology, 2018, 493, 532-543.	1.4	9
29623	Structure and Optical Properties of the Li₂In₂GeSe₆ Crystal. Journal of Physical Chemistry C, 2018, 122, 17413-17422.	1.5	11
29624	Hydrogenation of Cyclohexene on the M/Pt(111) and Pt/M/Pt(111) (M = Fe, Co, Ni, and Cu) Surfaces from a Systematic DFT Study. Journal of Physical Chemistry C, 2018, 122, 16692-16703.	1.5	9
29625	Unusual Pressure-Induced Periodic Lattice Distortion in <mml:math xmlns:mml="http://www.w3.org/1998/Math/MathML" display="inline"><mml:mrow><mml:msub><mml:mrow><mml:mi>SnSe</mml:mi></mml:mrow><mml:mrow><mml:mn>2</mml:mn> Physical Review Letters, 2018, 121, 027003.	2.9	24
29626	Sulfurâ€Deficient Bismuth Sulfide/Nitrogenâ€Doped Carbon Nanofibers as Advanced Freeâ€Standing Electrode for Asymmetric Supercapacitors. Small, 2018, 14, e1801562.	5.2	117
29627	Monolayered semiconducting GeAsSe and SnSbTe with ultrahigh hole mobility. Frontiers of Physics, 2018, 13, 1.	2.4	11
29628	A unified model for the uniaxial and hydrostatic pressure dependence of T in YBa2Cu3O (xâ€‾â‰ˆâ€‾6.95â€“7.0). Computational Materials Science, 2018, 153, 268-274.	1.4	1
29629	K₂ZnGe₃S₈: A Congruent-Melting Infrared Nonlinear-Optical Material with a Large Band Gap. Inorganic Chemistry, 2018, 57, 9446-9452.	1.9	31
29630	WO₃ as a nucleating agent for BaO/SrO/ZnO/SiO₂ glasses â€“ experiments and simulations. CrystEngComm, 2018, 20, 4565-4574.	1.3	10
29631	Influence of the lattice constant on defects in cerium oxide. Physical Chemistry Chemical Physics, 2018, 20, 19792-19799.	1.3	7
29632	Relation between image charge and potential alignment corrections for charged defects in periodic boundary conditions. Journal of Chemical Physics, 2018, 149, 024103.	1.2	57
29633	First-Principles Study on Hydrogen Diffusivity in BCC, FCC, and HCP Iron. Metallurgical and Materials Transactions A: Physical Metallurgy and Materials Science, 2018, 49, 5015-5022.	1.1	63
29634	Ab initio study of the lattice dynamical and thermodynamic properties of SbXI (X= S, Se, Te) compounds. Computational Condensed Matter, 2018, 16, e00320.	0.9	7
29635	An insight to origin of ferromagnetism in ZnO and N implanted ZnO thin films: Experimental and DFT approach. Journal of Alloys and Compounds, 2018, 768, 323-328.	2.8	21
29636	Periodic and non-periodic DFT modeling of CO reduction on the surface of Ni-doped graphene nanosheet. Molecular Catalysis, 2018, 455, 239-249.	1.0	8
29637	Surface functionalization of coal and quartz with aniline: A study on work function and frictional charge. Powder Technology, 2018, 338, 233-242.	2.1	11

#	Article	IF	Citations
29638	Promotion Effect of Methane Activation on Cu(111) by the Surface-Active Oxygen Species: A Combination of DFT and ReaxFF Study. Journal of Physical Chemistry C, 2018, 122, 17338-17346.	1.5	23
29639	Insight into the enhanced photocatalytic activity of SrTiO3 in the presence of a (Ni, V/Nb/Ta/Sb) pair. Physical Chemistry Chemical Physics, 2018, 20, 20078-20087.	1.3	23
29640	Two-dimensional Au-1,3,5 triethynylbenzene organometallic lattice: Structure, half-metallicity, and gas sensing. Journal of Chemical Physics, 2018, 149, 024702.	1.2	5
29641	Band structure, electron-phonon interaction and superconductivity of yttrium hypocarbide. Current Applied Physics, 2018, 18, 1338-1344.	1.1	5
29642	Testing new chromophores for singlet fission: A computational protocol applied to 2,3-diamino-1,4-benzoquinone. Chemical Physics, 2018, 515, 635-642.	0.9	5
29643	The mechanism and kinetics of methyl isobutyl ketone synthesis from acetone over ion-exchanged hydroxyapatite. Journal of Catalysis, 2018, 365, 174-183.	3.1	25
29644	Disorder-Induced Breaking of the Local Inversion Symmetry in Rhombohedral Pyrochlores M₂La₃Sb₃O₁₄ (M = Mg or Ca): A Structural and Spectroscopic Investigation. Inorganic Chemistry, 2018, 57, 9241-9250.	1.9	13
29645	Predicted Binary Compounds of Tin and Sulfur. Journal of Physical Chemistry C, 2018, 122, 17067-17072.	1.5	6
29646	Pressure-Induced Topological Nontrivial Phase and Tunable Optical Properties in All-Inorganic Halide Perovskites. Journal of Physical Chemistry C, 2018, 122, 17718-17725.	1.5	40
29647	Mechanistic Complexity of Methane Oxidation with H₂O₂ by Single-Site Fe/ZSM-5 Catalyst. ACS Catalysis, 2018, 8, 7961-7972.	5.5	98
29648	C₂N-graphene supported single-atom catalysts for CO₂ electrochemical reduction reaction: mechanistic insight and catalyst screening. Nanoscale, 2018, 10, 15262-15272.	2.8	156
29649	Insights into structural, electronic, optical and thermoelectric properties of WB and WAlB: a first principle study. Philosophical Magazine, 2018, 98, 2657-2679.	0.7	9
29650	Induced ferromagnetism and metal-insulator transition due to a charge transfer effect in silver nanoparticle decorated <mml:math xmlns:mml="http://www.w3.org/1998/Math/MathML"><mml:mrow><mml:mi>Mo</mml:mi><mml:msub><mml:mi mathvariant="normal">S</mml:mi><mml:mn>2</mml:mn></mml:msub></mml:mrow></mml:math>. Physical Review B, 2018, 98, .	1.1	10
29651	Hydrogenated and halogenated MB (M=As, Sb and Bi) monolayers: Structural, electronic, optical and topological properties by first principles calculations. Journal of Alloys and Compounds, 2018, 767, 552-558.	2.8	8
29652	Robustness of surface activity electronic structure-based descriptors of transition metals. Physical Chemistry Chemical Physics, 2018, 20, 20548-20554.	1.3	12
29653	Unraveling reaction networks behind the catalytic oxidation of methane with H₂O₂ over a mixed-metal MIL-53(Al,Fe) MOF catalyst. Chemical Science, 2018, 9, 6765-6773.	3.7	67
29654	Theoretical study of the adsorption of hydrogen on cobalt clusters. Physical Chemistry Chemical Physics, 2018, 20, 21163-21176.	1.3	19
29655	Electron-donor doping enhanced Li storage in electride Ca₂N monolayer: a first-principles study. Journal of Physics Condensed Matter, 2018, 30, 345501.	0.7	6

#	Article	IF	Citations
29656	Ab initio study of the (2 Ã— 2) phase of barium on graphene. European Physical Journal B, 2018, 91, 1.	0.6	5
29657	Molecular Deformation, Charge Flow, and Spongelike Behavior in Anionâ€“Ï€ {[M(CN)₄]^{2â^'};[HAT(CN)₆]}_{âˆž} (M=Ni, Pd, Pt) Supramolecular Stacks. Chemistry - A European Journal, 2018, 24, 16302-16314.	1.7	10
29658	Theoretical and experimental investigations on H2 sensing properties of flower-like titanium dioxide. Materials Research Bulletin, 2018, 107, 139-146.	2.7	18
29659	Electrical contact resistance in graphiteâ€“graphene contacts from ab initio methods. Journal of Physics Condensed Matter, 2018, 30, 325302.	0.7	2
29660	Co-adsorption of O 2 and H 2 O on Î± -uranium (110) surface: A density functional theory study. Chinese Physics B, 2018, 27, 076501.	0.7	4
29661	First-Principles Calculations on the Wettability of Li Atoms on the (111) Surfaces of W and Mo Substrates. Plasma Physics Reports, 2018, 44, 692-701.	0.3	4
29662	Stability, Electronic Structure, and Dehydrogenation Properties of Pristine and Doped 2D MgH2 by the First Principles Study. Metals, 2018, 8, 482.	1.0	6
29663	Ultralow Overpotential of Hydrogen Evolution Reaction using Feâ€Doped Defective Graphene: A Density Functional Study. ChemCatChem, 2018, 10, 4450-4455.	1.8	22
29664	Sulfur dioxide adsorbed on pristine and Au dimer decorated Î³-graphyne: A density functional theory study. Applied Surface Science, 2018, 458, 781-789.	3.1	25
29665	DFT study of optoelectronic and magnetic properties of a novel type perovskites. Chemical Physics, 2018, 513, 120-128.	0.9	2
29666	Cobalt-iron (oxides) water oxidation catalysts: Tracking catalyst redox states and reaction dynamic mechanism. Journal of Catalysis, 2018, 365, 227-237.	3.1	28
29667	The pressure-induced indirect to direct bandgap transition and thermoelectric response in SrTiO3: An ab-initio study. Journal of Physics and Chemistry of Solids, 2018, 123, 70-75.	1.9	19
29668	Microscopic Mechanism of the Helix-to-Layer Transformation in Elemental Group VI Solids. Nano Letters, 2018, 18, 4908-4913.	4.5	19
29669	Modeling of Phase Transitions of Graphites to Diamond-Like Phases. Physics of the Solid State, 2018, 60, 1294-1302.	0.2	13
29670	The Anisotropic Thermal Expansion of Non-linear Optical Crystal BaAlBO3F2 Below Room Temperature. Frontiers in Chemistry, 2018, 6, 252.	1.8	1
29671	Three-dimensional phase field simulation of intragranular void formation and thermal conductivity in irradiated Î±-Fe. Journal of Materials Science, 2018, 53, 11002-11014.	1.7	15
29672	Single-layer graphdiyne-covered Pt(111) surface: improved catalysis confined under two-dimensional overlayer. Journal of Nanoparticle Research, 2018, 20, 1.	0.8	9
29673	First-principles calculations on interface structure and fracture characteristic of TiC/TiZrC nano-multilayer film based on virtual crystal approximation. Journal of Alloys and Compounds, 2018, 755, 211-223.	2.8	32

#	Article	IF	Citations
29674	CH₃Cl/Cu(410): Interaction and Adsorption Geometry. Journal of Physical Chemistry C, 2018, 122, 11825-11831.	1.5	8
29675	Polymorphism and metal-induced structural transformation in 5,5â€²-bis(4-pyridyl)(2,2â€²-bispyrimidine) adlayers on Au(111). Physical Chemistry Chemical Physics, 2018, 20, 15960-15969.	1.3	8
29676	Role of tailor-made additives in controlling vapour growth asymmetry along the polar axis of Î±-resorcinol crystals: a molecular-scale study. CrystEngComm, 2018, 20, 3673-3687.	1.3	6
29677	Fe effect on the process of intrinsic point defects in Î±-Al2O3. Journal of Materials Science, 2018, 53, 11194-11203.	1.7	12
29678	Insight into the role of the promoters Pt, Ru and B in inhibiting the deactivation of Co catalysts in Fischer-Tropsch synthesis. Applied Surface Science, 2018, 453, 309-319.	3.1	16
29679	N-graphdiyne two-dimensional nanomaterials: Semiconductors with low thermal conductivity and high stretchability. Carbon, 2018, 137, 57-67.	5.4	82
29680	Influence of dilute solute substitutions in Ni on its generalized stacking fault energies and ductility. Computational Materials Science, 2018, 150, 424-431.	1.4	16
29681	Full potential study of HoMg. Journal of Magnesium and Alloys, 2018, 6, 189-196.	5.5	7
29682	Density Functional Theory Investigation of the Role of Cocatalytic Water in the Water Gas Shift Reaction over Anatase TiO₂ (101). Industrial & Engineering Chemistry Research, 2018, 57, 6830-6841.	1.8	8
29683	Theoretical Prediction and Synthesis of (Cr_{2/3}Zr_{1/3})₂AlC i-MAX Phase. Inorganic Chemistry, 2018, 57, 6237-6244.	1.9	59
29684	Selective and Stable Electroreduction of CO₂ to CO at the Copper/Indium Interface. ACS Catalysis, 2018, 8, 6571-6581.	5.5	175
29685	Origin of anisotropic negative Poisson's ratio in graphene. Nanoscale, 2018, 10, 10365-10370.	2.8	43
29686	Proton transfer in guanineâ€“cytosine base pair analogues studied by NMR spectroscopy and PIMD simulations. Faraday Discussions, 2018, 212, 331-344.	1.6	28
29687	Stability and magnetic properties of SnSe monolayer doped by transition metal atom (Mn, Fe, and Co): a first-principles study. Journal Physics D: Applied Physics, 2018, 51, 245004.	1.3	18
29688	Thermodynamic consideration and ground-state search of icosahedral boron subselenide B12(B1â^'xSex)2 from a first-principles cluster expansion. Physical Review B, 2018, 97, .	1.1	2
29689	Chiral Spin Texture in the Charge-Density-Wave Phase of the Correlated Metallic <mml:math xmlns:mml="http://www.w3.org/1998/Math/MathML" display="inline"><mml:mrow><mml:mi>Pb</mml:mi><mml:mrow><mml:mo>/</mml:mo><mml:mi>Si</mml:mi><mml:mo stretchy="false">(</mml:mo><mml:mn>111</mml:mn><mml:mo) Tj ETQq1 1 0.784314 rgBT /Overlock 10 Tf 50 132 Td (stretchy="false Letters, 2018, 120, 196402.	8.6	15
29690	Selective adsorption of H2 on N-doped ZnO nano-ribbons: First-principle analysis. , 2018, , .		2
29692	First-principles simulation on thermoelectric propertiesof transition metal dichalcogenide monolayers. Japanese Journal of Applied Physics, 2018, 57, 06HE04.	0.8	4

#	Article	IF	Citations
29693	Electronic conductivity of solid and liquid (Mg, Fe)O computed from first principles. Earth and Planetary Science Letters, 2018, 490, 11-19.	1.8	18
29694	Coreâ€“Shell Nanocomposites for Improving the Structural Stability of Li-Rich Layered Oxide Cathode Materials for Li-Ion Batteries. ACS Applied Materials & Interfaces, 2018, 10, 19226-19234.	4.0	30
29695	Defects and lithium migration in Li2CuO2. Scientific Reports, 2018, 8, 6754.	1.6	30
29696	Enhanced Photocatalytic Hydrogen Evolution by Loading Cd0.5Zn0.5S QDs onto Ni2P Porous Nanosheets. Nanoscale Research Letters, 2018, 13, 31.	3.1	30
29697	Origin of the Magnetism in Undoped and Mn-Doped In 2 O 3 : A First-Principles Study. Journal of Superconductivity and Novel Magnetism, 2018, 31, 2437-2441.	0.8	2
29698	First principle calculations and opto-electric enhancement in laser ablated GZO thin films. Optical and Quantum Electronics, 2018, 50, 1.	1.5	5
29699	Theoretical Investigation of the Thermodynamic Properties of Î·â€²-(Cu, Co)6Sn5 Alloys. Journal of Electronic Materials, 2018, 47, 1383-1389.	1.0	2
29700	Photoelectron Energy Loss in Al(002) Revisited: Retrieval of the Single Plasmon Loss Energy Distribution by a Fourier Transform Method. Brazilian Journal of Physics, 2018, 48, 215-226.	0.7	7
29701	MoF5 revisited. A comprehensive study of MoF5. Journal of Fluorine Chemistry, 2018, 211, 171-179.	0.9	19
29702	Double Kagome Bands in a Two-Dimensional Phosphorus Carbide P₂C₃. Journal of Physical Chemistry Letters, 2018, 9, 2751-2756.	2.1	29
29703	Developing intercalation based anode materials for fluoride-ion batteries: topochemical reduction of Sr₂TiO₃F₂via a hydride based defluorination process. Journal of Materials Chemistry A, 2018, 6, 22013-22026.	5.2	27
29704	Engineering the electronic band structures of novel cubic structured germanium monochalcogenides for thermoelectric applications. Journal of Applied Physics, 2018, 123, .	1.1	11
29705	Impact of Hydroxylation and Hydration on the Reactivity of Î±â€Fe 2 O 3 (0001) and (102) Surfaces under Environmental and Electrochemical Conditions. Advanced Energy Materials, 2018, 8, 1800545.	10.2	9
29706	Trapping/detrapping kinetic rates of hydrogen around a vacancy in nickel and some consequences on the hydrogen-vacancy clusters thermodynamic equilibrium. Computational Materials Science, 2018, 151, 144-152.	1.4	20
29707	Chemical composition and stress dependence of the elastic properties of Îº-(Fe,Mn)3AlC thin films. Scripta Materialia, 2018, 153, 49-53.	2.6	7
29708	Nonmetallic FeH₆ under High Pressure. Journal of Physical Chemistry C, 2018, 122, 12022-12028.	1.5	29
29709	Modulating the electronic and magnetic properties of bilayer borophene via transition metal atoms intercalation: from metal to half metal and semiconductor. Nanotechnology, 2018, 29, 305706.	1.3	16
29710	Magnetism and multiferroic properties at MnTiO3 surfaces: A DFT study. Applied Surface Science, 2018, 452, 463-472.	3.1	45

#	Article	IF	Citations
29711	<mml:math xmlns:mml="http://www.w3.org/1998/Math/MathML" altimg="si1.gif" overflow="scroll"><mml:mrow><mml:mi>z</mml:mi><mml:mi>T</mml:mi></mml:mrow></mml:math> factors in Ag- and Na-doped SnSe: Chemical potentials, relaxation times and predictions for other dopant species. Journal of Alloys and Compounds, 2018, 757, 70-78.	2.8	6
29712	Potentially high-temperature superconductivity in K1â^'B6: A first-principles prediction. Physica C: Superconductivity and Its Applications, 2018, 551, 16-18.	0.6	2
29713	First-principles study of thermoelectric properties of Mg2Siâ€“Mg2Pb semiconductor materials. RSC Advances, 2018, 8, 17168-17175.	1.7	15
29714	Boronâ€“graphdiyne: a superstretchable semiconductor with low thermal conductivity and ultrahigh capacity for Li, Na and Ca ion storage. Journal of Materials Chemistry A, 2018, 6, 11022-11036.	5.2	104
29715	Lithium effect on the electronic properties of porous silicon for energy storage applications: a DFT study. Dalton Transactions, 2018, 47, 7505-7514.	1.6	12
29716	Combining batch technique with theoretical calculation studies to analyze the highly efficient enrichment of U(VI) and Eu(III) on magnetic MnFe2O4 nanocubes. Chemical Engineering Journal, 2018, 349, 347-357.	6.6	82
29717	Experimental and theoretical studies of the physicochemical and mechanical properties of multi-layered TiN/SiC films: Temperature effects on the nanocomposite structure. Composites Part B: Engineering, 2018, 142, 85-94.	5.9	98
29718	Tunable twin stability and an accurate magnesium interatomic potential for dislocation-twin interactions. Materials and Design, 2018, 153, 232-241.	3.3	16
29719	First-Principles Insight into Electrocatalytic Reduction of CO₂ to CH₄ on a Copper Nanoparticle. Journal of Physical Chemistry C, 2018, 122, 11392-11398.	1.5	56
29720	Stable holey two-dimensional <mml:math xmlns:mml="http://www.w3.org/1998/Math/MathML"><mml:mrow><mml:msub><mml:mi mathvariant="normal">C</mml:mi><mml:mn>2</mml:mn></mml:msub><mml:mi mathvariant="normal">N</mml:mi></mml:mrow></mml:math> structures with tunable electronic structure. Physical Review B, 2018, 97, .	1.1	13
29721	Microscopic description of orbital-selective spin ordering in BaMn2As2. Physical Review B, 2018, 97, .	1.1	4
29722	Local Electron Interaction with Point Defects in Sphalerite Zinc Selenide: Calculation from First Principles. Journal of Electronic Materials, 2018, 47, 4212-4218.	1.0	11
29723	Dry reforming of methane over CeO2-supported Pt-Co catalysts with enhanced activity. Applied Catalysis B: Environmental, 2018, 236, 280-293.	10.8	131
29724	Electron injection study of photoexcitation effects on supported subnanometer Pt clusters for CO2 photoreduction. Physical Chemistry Chemical Physics, 2018, 20, 15926-15938.	1.3	7
29725	Single-layer ZnMN₂ (M = Si, Ge, Sn) zinc nitrides as promising photocatalysts. Physical Chemistry Chemical Physics, 2018, 20, 14619-14626.	1.3	17
29726	Tl₂S: a metal-shrouded two-dimensional semiconductor. Physical Chemistry Chemical Physics, 2018, 20, 14778-14784.	1.3	11
29727	Monolayer tellureneâ€“metal contacts. Journal of Materials Chemistry C, 2018, 6, 6153-6163.	2.7	81
29728	Theoretical prediction of honeycomb carbon as Li-ion batteries anode material. European Physical Journal B, 2018, 91, 1.	0.6	11

#	Article	IF	Citations
29729	Density Functional Theory study of Cu doped {0001} and {01$overline 1 $2} surfaces of hematite for water splitting. MRS Advances, 2018, 3, 669-678.	0.5	12
29730	Numerical study of the defect adamantine compound CuGaGeSe4. Molecular Physics, 2018, 116, 1551-1557.	0.8	2
29731	Room-temperature <mml:math xmlns:mml="http://www.w3.org/1998/Math/MathML"><mml:msup><mml:mi>d</mml:mi><mml:mn>0</mml:mn></mml:msup></mml:m ferromagnetism in carbon-doped <mml:math xmlns:mml="http://www.w3.org/1998/Math/MathML"><mml:mrow><mml:msub><mml:mi mathvariant="normal">Y</mml:mi><mml:mn>2</mml:mn></mml:msub><mml:msub><mml:mi mathvariant="normal">O</mml:mi><mml:mn>3</mml:mn></mml:msub></mml:mrow></mml:math> for s	1.1	22
29732	Thermo-Optical Study of Short-Range Polar Order in a Ferroelectric Phase: The Ca2+ Impurity-Induced Ferroelectric Phase in SrTiO3. Bulletin of the Russian Academy of Sciences: Physics, 2018, 82, 273-279.	0.1	1
29733	A novel strategy to develop non-noble metal catalyst for CO2 electroreduction: Hybridization of metal-organic polymer. Applied Catalysis B: Environmental, 2018, 236, 154-161.	10.8	43
29734	High-throughput screening for superhard carbon and boron nitride allotropes with superior stiffness and strength. Carbon, 2018, 137, 156-164.	5.4	22
29735	Diffusion of helium, hydrogen and deuterium in diamond: Experiment, theory and geochemical applications. Geochimica Et Cosmochimica Acta, 2018, 232, 206-224.	1.6	11
29736	Adiabatic Connection without Coupling Constant Integration. Journal of Chemical Theory and Computation, 2018, 14, 2979-2990.	2.3	14
29737	F-Doping effects on carbon-coated Li3V2(PO4)3 as a cathode for high performance lithium rechargeable batteries: combined experimental and DFT studies. Physical Chemistry Chemical Physics, 2018, 20, 15192-15202.	1.3	16
29738	Computation of physical properties of ferroelectric RbNbO₃ under pressure. Ferroelectrics, 2018, 526, 120-139.	0.3	5
29739	Mechanisms for carbon adsorption on Au(110)-(2â€²Ã—â€²1): A work function analysis. Surface Science, 2018, 677, 232-238.	0.8	9
29740	Tuning Band Gap and Work Function Modulations in Monolayer hBN/Cu(111) Heterostructures with MoirÃ© Patterns. ACS Nano, 2018, 12, 9355-9362.	7.3	33
29741	Vibration analysis of hydrogen, deuterium and tritium in metals: consequences on the isotope effect. Journal of Physics Condensed Matter, 2018, 30, 335402.	0.7	12
29742	Magnetic and energetic properties of transition metal doped alumina. Journal of Physics Condensed Matter, 2018, 30, 395801.	0.7	5
29743	Impact of complex adatom-induced interactions on quantum spin Hall phases. Physical Review B, 2018, 98, .	1.1	17
29744	Tailoring the photocatalytic activity of WO3 by Nb-F codoping from first-principles calculations. Chinese Journal of Physics, 2018, 56, 2285-2290.	2.0	2
29745	Boron-Doped C₃N Monolayer as a Promising Metal-Free Oxygen Reduction Reaction Catalyst: A Theoretical Insight. Journal of Physical Chemistry C, 2018, 122, 20312-20322.	1.5	78
29746	Lithium Adsorption on Graphene at Finite Temperature. Journal of Physical Chemistry C, 2018, 122, 20800-20808.	1.5	11

#	Article	IF	Citations
29747	High-Pressure Studies of Hydrogen-Bonded Energetic Material 3,6-Dihydrazino-s-tetrazine Using DFT. ACS Omega, 2018, 3, 9388-9399.	1.6	19
29748	Type-II InSe/MoSe₂(WSe₂) van der Waals heterostructures: vertical strain and electric field effects. Journal of Materials Chemistry C, 2018, 6, 10010-10019.	2.7	59
29749	Ab-initio Study of Physical Properties of MgO/FeOx/Fe(001) Interfaces. Journal of the Korean Physical Society, 2018, 73, 320-324.	0.3	5
29750	Adsorption and Decomposition of Formic Acid on Cobalt(0001). Journal of Physical Chemistry C, 2018, 122, 20279-20288.	1.5	16
29751	First principles mechanistic study of self-limiting oxidative adsorption of remote oxygen plasma during the atomic layer deposition of alumina. Physical Chemistry Chemical Physics, 2018, 20, 22783-22795.	1.3	14
29752	Strain controlled electronic and transport anisotropies in two-dimensional borophene sheets. Physical Chemistry Chemical Physics, 2018, 20, 22952-22960.	1.3	53
29753	Analysis of the structure and abnormal photoluminescence of a red-emitting LiMgBO₃:Mn²⁺ phosphor. Dalton Transactions, 2018, 47, 13094-13105.	1.6	20
29754	Accumulation of beryllium and its effects on hydrogen retention in tungsten divertor. Nuclear Fusion, 2018, 58, 106015.	1.6	2
29755	Biaxial strain effects on the electronic properties of silicene: the density-functional-theory-based calculations. Journal of Physics: Conference Series, 2018, 1011, 012074.	0.3	9
29756	Elastic, magnetic and electronic properties of ferrimagnetic double perovskite Sr2MnWO6 using GGAâ€‰+â€‰U and mBJ-GGA. Applied Physics A: Materials Science and Processing, 2018, 124, 1.	1.1	4
29757	Study on synergistic effects of H and He in Î±-Fe. Nuclear Materials and Energy, 2018, 16, 212-216.	0.6	7
29758	Enhanced Photosensitive Schottky Diode Behavior of Pyrazine over 2-Aminopyrimidine Ligand in Copper(II)-Phthalate MOFs: Experimental and Theoretical Rationalization. ACS Omega, 2018, 3, 9160-9171.	1.6	26
29759	Effect of impurity carbon and oxygen atoms on the behavior of hydrogen in vanadium in a fusion environment: A first-principles study. International Journal of Modern Physics B, 2018, 32, 1850232.	1.0	1
29760	A DFT study of the electronic and magnetic properties of Cu2Cr1â^'xVxGa alloys. International Journal of Computational Materials Science and Engineering, 2018, 07, 1850022.	0.5	3
29761	Enhancement of the Magnetic Anisotropy in Rare-Earth-Free Multilayer Fe16N2/Ag/Fe16N2 and Fe16N2/Au/Fe16N2. Journal of the Korean Physical Society, 2018, 72, 1343-1349.	0.3	1
29762	Yellow Emission from Low Coordination Site of Sr₂SiO₄:Eu²⁺, Ce³⁺: Influence of Lanthanide Dopants on the Electron Density and Crystallinity in Crystal Site Engineering Approach. Chemistry - A European Journal, 2018, 24, 16149-16159.	1.7	20
29763	Interface reaction processes and reactive properties of Al/CuO nanothermite: An ab initio molecular dynamics simulation. Applied Surface Science, 2018, 459, 835-844.	3.1	16
29764	Two-dimensional sheet of germanium selenide as an anode material for sodium and potassium ion batteries: First-principles simulation study. Computational Materials Science, 2018, 154, 204-211.	1.4	74

#	Article	IF	Citations
29765	Antimonene nanosheet device for detection of explosive vapors â€“ A first-principles inspection. Chemical Physics Letters, 2018, 708, 130-137.	1.2	39
29766	First-principles calculations of interaction between solutes and dislocations in tungsten. Nuclear Materials and Energy, 2018, 16, 221-225.	0.6	13
29767	Corrosion protection of Al(111) by 8-hydroxyquinoline: a comprehensive DFT study. Physical Chemistry Chemical Physics, 2018, 20, 21474-21486.	1.3	10
29768	Theoretical discovery of novel two-dimensional V^A-N binary compounds with auxiticity. Physical Chemistry Chemical Physics, 2018, 20, 22027-22037.	1.3	52
29769	Synergistic Reducing Effect for Synthesis of Well-Defined Au Nanooctopods With Ultra-Narrow Plasmon Band Width and High Photothermal Conversion Efficiency. Frontiers in Chemistry, 2018, 6, 335.	1.8	9
29770	Quantum confinement effects on the harmfulâ€gasâ€sensing properties of silicon nanowires. International Journal of Quantum Chemistry, 2018, 118, e25713.	1.0	9
29771	A first-principle study of NaMPO4 (M = Mn, Fe, Co, Ni) possible novel structures as cathode materials for sodium-ion batteries: Structural and electrochemical characterisation. Materials Chemistry and Physics, 2018, 219, 212-221.	2.0	14
29772	First Principles Investigation of HCl, H₂, and Chlorosilane Adsorption on Cu₃Si Surfaces with Applications for Polysilicon Production. Journal of Physical Chemistry C, 2018, 122, 20252-20260.	1.5	9
29773	Unravelling the Effects of A-Site Cations on Nonradiative Electronâ€“Hole Recombination in Lead Bromide Perovskites: Time-Domain ab Initio Analysis. Journal of Physical Chemistry Letters, 2018, 9, 4834-4840.	2.1	24
29774	Understanding the apparent fractional charge of protons in the aqueous electrochemical double layer. Nature Communications, 2018, 9, 3202.	5.8	47
29775	Synthesis of multifunctional CuFe₂O₄â€“reduced graphene oxide nanocomposite: an efficient magnetically separable catalyst as well as high performance supercapacitor and first-principles calculations of its electronic structures. RSC Advances, 2018, 8, 27725-27739.	1.7	61
29776	Greater diffusion rate of carbon atoms from nonlinear migration in micro-cell and spatially heterogeneous stable states in FCC iron. Journal of Materials Science, 2018, 53, 15952-15968.	1.7	2
29777	Phase stability and mechanical properties of ternary transition elements X(Xâ€¯=â€¯Cu,Zn,Ag) in Al3Hf intermetallic from first-principles calculations. Computational Materials Science, 2018, 154, 266-275.	1.4	3
29778	Understanding the underlying mechanism of improved selectivity in pd1 single-atom catalyzed hydrogenation reaction. Journal of Catalysis, 2018, 366, 70-79.	3.1	70
29779	Ab initio calculations for the polar (0â€¯0â€¯1) surfaces of YAlO3. Nuclear Instruments & Methods in Physics Research B, 2018, 434, 1-5.	0.6	14
29780	First-principles calculations of structure and electronic properties of aluminum doped by Ge, Sn and Pb. Physica B: Condensed Matter, 2018, 547, 6-11.	1.3	3
29781	Electronic and optical properties of heterostructures based on transition metal dichalcogenides and graphene-like zinc oxide. Scientific Reports, 2018, 8, 12009.	1.6	173
29782	Synthesis of self-assembled PtPdAg nanostructures with a high catalytic activity for oxygen reduction reactions. Nanoscale, 2018, 10, 17140-17147.	2.8	11

#	Article	IF	Citations
29783	Low-temperature activation of methane on doped single atoms: descriptor and prediction. Physical Chemistry Chemical Physics, 2018, 20, 22909-22914.	1.3	62
29784	Density functional theory study of structural stability for gas hydrate. Chinese Physics B, 2018, 27, 043103.	0.7	7
29785	Spectroelectrochemical and Density Functional Theory Study of Squaric Acid Adsorption and Oxidation at Gold Thin Film and Single Crystal Electrodes. Journal of Physical Chemistry C, 2018, 122, 22352-22365.	1.5	5
29786	Chemical Bond Formation and Rupture Processes: An Application of DFTâ€“Chemical Pressure Approach. Journal of Physical Chemistry C, 2018, 122, 21216-21225.	1.5	9
29787	Pressure-induced phase transition, metallization and superconductivity in ZrS₂. Physical Chemistry Chemical Physics, 2018, 20, 23656-23663.	1.3	23
29788	Phase stability and interlayer interaction of blue phosphorene. Physical Review B, 2018, 98, .	1.1	19
29789	Propertyâ€“Activity Relations for Methane Activation by Dualâ€Metal Cuâ€“Oxo Trimers in ZSMâ€5 Zeolite. Small Methods, 2018, 2, 1800266.	4.6	21
29790	Robust Periodic Fock Exchange with Atom-Centered Gaussian Basis Sets. Journal of Chemical Theory and Computation, 2018, 14, 4567-4580.	2.3	17
29791	Stability, Structural, and Electronic Properties of Hausmannite (Mn₃O₄) Surfaces and Their Interaction with Water. Journal of Physical Chemistry C, 2018, 122, 20841-20849.	1.5	55
29792	New Understanding on Enhanced Photocatalytic Activity of g-C₃N₄/BiPO₄ Heterojunctions by Effective Interfacial Coupling. ACS Applied Nano Materials, 2018, 1, 5507-5515.	2.4	52
29793	Giant magnetoelectric effect at the graphone/ferroelectric interface. Scientific Reports, 2018, 8, 12448.	1.6	5
29794	Thermoelectric properties of two-dimensional selenene and tellurene from group-VI elements. Physical Chemistry Chemical Physics, 2018, 20, 24250-24256.	1.3	73
29795	Electronic structure of a buried two-dimensional antiferromagnetic layer: Experimental and theoretical investigation of Ag/Cr/Ag(001). Physical Review B, 2018, 98, .	1.1	4
29796	Activating Transition Metal Dichalcogenides by Substitutional Nitrogenâ€Doping for Potential ORR Electrocatalysts. ChemElectroChem, 2018, 5, 4029-4035.	1.7	27
29797	Arsenene Nanotube as a Chemical Sensor to Detect the Presence of Explosive Vapors: A First-Principles Insight. Journal of Inorganic and Organometallic Polymers and Materials, 2018, 28, 2844-2853.	1.9	30
29798	Stable Red Emission from Nanosheets of Molecularly Doped Hexagonal Boron Nitride. Journal of Physical Chemistry C, 2018, 122, 21076-21082.	1.5	6
29799	Wurtzite AlN(0001) Surface Oxidation: Hints from Ab Initio Calculations. ACS Applied Materials & Interfaces, 2018, 10, 30811-30818.	4.0	30
29800	Direct imaging of a single Ni atom cutting graphene to form a graphene nanomesh. Physical Chemistry Chemical Physics, 2018, 20, 26814-26818.	1.3	11

#	Article	IF	Citations
29801	Thermal neutron scattering cross sections of ²³⁸U and ²³⁵U in the Î³ phase. Journal of Physics Condensed Matter, 2018, 30, 415401.	0.7	4
29802	Candidate replacements for lead in CH3NH3PbI3 from first principles calculations. Computational Materials Science, 2018, 155, 69-73.	1.4	7
29803	Interface relationship between TiN and Ti substrate by first-principles calculation. Computational Materials Science, 2018, 155, 36-47.	1.4	25
29804	CO Direct versus H-Assisted Dissociation on Hydrogen Coadsorbed Ï‡-Fe₅C₂ Fischerâ€“Tropsch Catalysts. Journal of Physical Chemistry C, 2018, 122, 20907-20917.	1.5	23
29805	A roadmap of strain in doped anatase TiO2. Scientific Reports, 2018, 8, 12790.	1.6	27
29806	Six-dimensional potential energy surfaces of the dissociative chemisorption of HCl on Ag(111) with three density functionals. Journal of Chemical Physics, 2018, 149, 054702.	1.2	15
29807	Multiple triple-point fermions in Heusler compounds. Journal of Physics Condensed Matter, 2018, 30, 375702.	0.7	8
29808	Deformation twinning of ultrahigh strength aluminum nanowire. Acta Materialia, 2018, 160, 14-21.	3.8	30
29809	Exploring Multifunctional Applications of Hexagonal Boron Arsenide Sheet: A DFT Study. ACS Omega, 2018, 3, 9533-9543.	1.6	35
29810	Hybridization of Co₃O₄ and Î±-MnO₂ Nanostructures for High-Performance Nonenzymatic Glucose Sensing. ACS Sustainable Chemistry and Engineering, 2018, 6, 13248-13261.	3.2	54
29811	Interlayer coupling and external electric field tunable electronic properties of a 2D type-I Î±-tellurene/MoS₂ heterostructure. Journal of Materials Chemistry C, 2018, 6, 10256-10262.	2.7	56
29812	Tuning electronic transport properties of zigzag graphene nanoribbons with silicon doping and phosphorus passivation. AIP Advances, 2018, 8, 085123.	0.6	9
29813	Air molecules in XPbI3 (X=MA, FA, Cs) perovskite: A degradation mechanism based on first-principles calculations. Journal of Applied Physics, 2018, 124, .	1.1	15
29814	Magnetic phases of skyrmion-hosting<mml:math xmlns:mml="http://www.w3.org/1998/Math/MathML"><mml:mrow><mml:msub><mml:mi>GaV</mml:mi><mml:mn>4</mml:mn></mml:msub><mml:msub><mml:mi mathvariant="normal">S</mml:mi><mml:mrow><mml:mn>8</mml:mn><mml:mo>â¾</mml:mo><mml:mi>y</mml:mi></mml:mrow></mml:msub></mml:mrow></mml:math width="4pt"		

#	Article	IF	Citations
29819	The structural, electronic, magnetic and optical properties of the Zn0.75V0.25Te alloy under pressure. Materials Chemistry and Physics, 2018, 220, 66-74.	2.0	0
29820	Electronic structure of <mml:math xmlns:mml="http://www.w3.org/1998/Math/MathML" altimg="si1.gif" overflow="scroll"><mml:mrow><mml:msubsup><mml:mrow><mml:mtext>Mn</mml:mtext></mml:mrow><mml:mrow><mml:mtext>Al</mml:mtext></mml:mrow> and <mml:math xmlns:mml="http://www.w3.org/1998/Math/MathML" altimg="si2.gif" overflow="scroll"><mml:mrow><mml:msubsup><mml:mrow><mml:mtext>Mn</mml:mtext></mml:mrow><mml:mrow><mml:mtext>Ga</mml:mtext></mml:mrow> Optical Materials, 2018, 85, 162-166.	1.7	12
29821	Completing the Picture of 2-(Aminomethylpyridinium) Lead Hybrid Perovskites: Insights into Structure, Conductivity Behavior, and Optical Properties. Chemistry of Materials, 2018, 30, 6289-6297.	3.2	32
29822	Activity Trends for Catalytic CO and NO Co-Oxidation at Low Temperature Diesel Emission Conditions. Industrial & Engineering Chemistry Research, 2018, 57, 12715-12725.	1.8	13
29823	Thermodynamically Stable Orthorhombic Î³-CsPbI₃ Thin Films for High-Performance Photovoltaics. Journal of the American Chemical Society, 2018, 140, 11716-11725.	6.6	308
29824	Modulate the direct-current and alternating-current transport properties of magnetic Î³-graphyne heterojunctions by chemical modification. Journal of Applied Physics, 2018, 124, 084501.	1.1	2
29825	Electronic and structural peculiarities of Br2-embedded C2F: XPS and DFT study. AIP Advances, 2018, 8, 085319.	0.6	5
29826	Density functional theory based first principles electronic structure study on 112 Fe based superconductors: Fermiology and Lifshitz transition. AIP Conference Proceedings, 2018, , .	0.3	1
29827	Band offset and electronic properties at semipolar plane AlN($1ar{1}01$)/diamond heterointerface. Chinese Physics B, 2018, 27, 058101.	0.7	3
29828	Effects of the Fermi level energy on the adsorption of O ₂ to monolayer MoS ₂. 2D Materials, 2018, 5, 045025.	2.0	8
29829	Influence of substitutional atoms on the diffusion of oxygen in dilute iron alloys. Physical Review B, 2018, 98, .	1.1	13
29830	Structure and Properties of New High-Pressure Phases of Fe7N3. JETP Letters, 2018, 107, 379-383.	0.4	5
29831	Long triple carbon chains formation by heat treatment of graphene nanoribbon: Molecular dynamics study with revised Brenner potential. Carbon, 2018, 140, 543-556.	5.4	13
29832	A new antimony carbide monolayer: An indirect semiconductor with a tunable band gap. Chemical Physics Letters, 2018, 708, 188-193.	1.2	14
29833	Stress-controlled carbon diffusion channeling in bct-iron: A mean-field theory. Journal of Alloys and Compounds, 2018, 769, 1121-1131.	2.8	23
29834	Synthesis and characterization of pure and cobalt doped magnesium oxide nanoparticles: Insight from experimental and theoretical investigation. Superlattices and Microstructures, 2018, 122, 124-139.	1.4	36
29835	The effect of single pd atoms on the energetics of recombinative O2 desorption from Au(111). Surface Science, 2018, 677, 296-300.	0.8	20
29836	Expanding the Iâ€“IIâ€“V Phase Space: Soft Synthesis of Polytypic Ternary and Binary Zinc Antimonides. Chemistry of Materials, 2018, 30, 6173-6182.	3.2	15

#	Article	IF	Citations
29837	X-ray Absorption Near-Edge Spectroscopy Calculations on Pristine and Modified Chalcopyrite Surfaces. Journal of Physical Chemistry C, 2018, 122, 20200-20209.	1.5	8
29838	First-Principles Study of the Water Adsorption on Anatase(101) as a Function of the Coverage. Journal of Physical Chemistry C, 2018, 122, 20736-20744.	1.5	25
29839	Tuning transition metal carbide activity by surface metal alloying: a case study on CO₂capture and activation. Physical Chemistry Chemical Physics, 2018, 20, 22179-22186.	1.3	12
29840	Interlayer excitons in transition-metal dichalcogenide heterostructures with type-II band alignment. Journal of Physics Condensed Matter, 2018, 30, 374002.	0.7	9
29841	From charge- to orbital-ordered metal-insulator transition in alkaline-earth ferrites. Physical Review B, 2018, 98, .	1.1	20
29842	Ionic Modulation of the Interfacial Magnetism in a Bilayer System Comprising a Heavy Metal and a Magnetic Insulator for Voltageâ€Tunable Spintronic Devices. Advanced Materials, 2018, 30, e1802902.	11.1	22
29843	Structural and electronic properties of the <scp>Al₄Sr</scp>(001) surface: <scp>A</scp> firstâ€principles study. Surface and Interface Analysis, 2018, 50, 1296-1301.	0.8	1
29844	First-principles calculations on wetting interface between Ag-Cu-Ti filler metal and SiC ceramic: Ag (1â€¯1â€¯1)/SiC (1â€¯1â€¯1) interface and Ag (1â€¯1â€¯1)/TiC (1â€¯1â€¯1) interface. Applied Surface Science, 2018, 462, 55-64.	3.1	53
29845	Electronic structure and thermophysical properties of U3Si2: A systematic first principle study. Journal of Nuclear Materials, 2018, 510, 360-365.	1.3	15
29846	First-principles study of the structural and electronic properties of CoX0.25S1.75 (X = F, Cl, or Br). Journal of Physics and Chemistry of Solids, 2018, 123, 284-293.	1.9	0
29847	Atomic structure of manganese-doped yttrium orthoaluminate. Nuclear Instruments & Methods in Physics Research B, 2018, 434, 6-8.	0.6	5
29848	Electronic and Polar Properties of Vanadate Compounds Stabilized by Epitaxial Strain. Chemistry of Materials, 2018, 30, 5870-5877.	3.2	8
29849	Removal of A-Site Alkali and Alkaline Earth Metal Cations in KBe₂BO₃F₂-Type Layered Structures To Enhance the Deep-Ultraviolet Nonlinear Optical Capability. Inorganic Chemistry, 2018, 57, 11146-11156.	1.9	37
29850	Probing the chirality-dependent elastic properties and crack propagation behavior of single and bilayer stanene. Physical Chemistry Chemical Physics, 2018, 20, 22768-22782.	1.3	27
29851	Amino group promoted photocatalytic hydrogen evolution activity observed in two copper(ii)-based layered complexes. Dalton Transactions, 2018, 47, 12726-12733.	1.6	25
29852	Unravelling the electrochemical mechanisms for nitrogen fixation on single transition metal atoms embedded in defective graphitic carbon nitride. Journal of Materials Chemistry A, 2018, 6, 21941-21948.	5.2	161
29853	Rapid and durable electrochemical storage behavior enabled by V₄Nb₁₈O₅₅ beaded nanofibers: a joint theoretical and experimental study. Journal of Materials Chemistry A, 2018, 6, 17389-17400.	5.2	24
29854	Structures and magnetic properties of iron silicide from adaptive genetic algorithm and first-principles calculations. Journal of Applied Physics, 2018, 124, .	1.1	6

#	Article	IF	Citations
29855	Discovery of Two-Dimensional Quantum Spin Hall Effect in Triangular Transition-Metal Carbides. Chinese Physics Letters, 2018, 35, 087303.	1.3	6
29856	Mechanical properties of pristine and defective carbonâ€“phosphide monolayers: a density functional tight-binding study. Nanotechnology, 2018, 29, 435707.	1.3	7
29857	The Initial Steps of Hydrogenâ€“Metal Reactions: The Gd H2 as a Model System. , 2018, , 1-8.		0
29858	Self-assembly synthesis of boron-doped graphitic carbon nitride hollow tubes for enhanced photocatalytic NOx removal under visible light. Applied Catalysis B: Environmental, 2018, 239, 352-361.	10.8	154
29859	DFT study of [BH4]â^' rotation in pressure-driven phase transition of MBH4. Computational Materials Science, 2018, 154, 143-146.	1.4	1
29860	The effects of Fe@C nanoparticles on the lithium storage performance of VS4 anode. Journal of Alloys and Compounds, 2018, 768, 938-943.	2.8	11
29861	Prediction of Molybdenum Nitride from First-Principle Calculations: Crystal Structures, Electronic Properties, and Hardness. Journal of Physical Chemistry C, 2018, 122, 21039-21046.	1.5	13
29862	Simulations of Quantum Transport in Sub-5-nm Monolayer Phosphorene Transistors. Physical Review Applied, 2018, 10, .	1.5	144
29863	Many-body renormalization of forces in <mml:math xmlns:mml="http://www.w3.org/1998/Math/MathML"><mml:mi>f</mml:mi></mml:math> -electron materials. Physical Review B, 2018, 98, .	1.1	20
29864	IIIâ€Nitride Polymorphs: XN (X=Al, Ga, In) in the Pnma Phase. Chemistry - A European Journal, 2018, 24, 17280-17287.	1.7	46
29865	Ultrathin Molybdenum Dioxide Nanosheets as Uniform and Reusable Surfaceâ€Enhanced Raman Spectroscopy Substrates with High Sensitivity. Small, 2018, 14, e1802276.	5.2	80
29866	Two-dimensional group-VA porous crystals: Diverse electronic structures and photocatalytic properties. Computational Materials Science, 2018, 154, 459-463.	1.4	4
29867	Ab initio modelling of the Y, O, and Ti solute interaction in fcc-Fe matrix. Nuclear Instruments & Methods in Physics Research B, 2018, 433, 106-110.	0.6	3
29868	Terahertz spectroscopy of 2,4,6-trinitrotoluene molecular solids from first principles. Beilstein Journal of Organic Chemistry, 2018, 14, 381-388.	1.3	10
29869	First Principle Study of Ti₅₀Al₅₀ Alloys. Key Engineering Materials, 2018, 770, 224-229.	0.4	0
29870	Databaseâ€Driven Materials Selection for Semiconductor Heterojunction Design. Advanced Theory and Simulations, 2018, 1, 1800075.	1.3	23
29871	Local Charge Distribution Engineered by Schottky Heterojunctions toward Urea Electrolysis. Advanced Energy Materials, 2018, 8, 1801775.	10.2	266
29872	Effect of N-doping on hard carbon nano-balls as anode for Li-ion battery: improved hydrothermal synthesis and volume expansion study. Journal of Solid State Electrochemistry, 2018, 22, 3443-3455.	1.2	23

#	Article	IF	Citations
29873	The evolution in graphitic surface wettability with first-principles quantum simulations: the counterintuitive role of water. Physical Chemistry Chemical Physics, 2018, 20, 22636-22644.	1.3	23
29874	Discovery of a high-pressure phase of rutile-like CoO₂ and its potential as a cathode material. Journal of Materials Chemistry A, 2018, 6, 18449-18457.	5.2	9
29875	First-principles study of thermoelectric properties of blue phosphorene. Applied Physics Letters, 2018, 113, 063903.	1.5	12
29876	Communication: Dielectric properties of condensed systems composed of fragments. Journal of Chemical Physics, 2018, 149, 051101.	1.2	9
29877	Nonequilibrium optical properties of transition metals upon ultrafast electron heating. Journal of Physics Condensed Matter, 2018, 30, 385401.	0.7	29
29878	Correlation-Driven Dimerization and Topological Gap Opening in Isotropically Strained Graphene. Physical Review Letters, 2018, 121, 066402.	2.9	34
29879	The Mechanical Properties and Elastic Anisotropies of Cubic Ni3Al from First Principles Calculations. Crystals, 2018, 8, 307.	1.0	88
29880	Carbon doped hexagonal BN as a highly efficient metal-free base catalyst for Knoevenagel condensation reaction. Applied Catalysis B: Environmental, 2018, 239, 254-259.	10.8	102
29881	Efficient extraction of multivalent cations from aqueous solutions into sitinakite-based sorbents. Chemical Engineering Journal, 2018, 354, 727-739.	6.6	17
29882	First-principles prediction of ferromagnetism in transition-metal doped monolayer AlN. Superlattices and Microstructures, 2018, 122, 171-180.	1.4	18
29883	Theoretical Insights into 1D Transition-Metal Nanoalloys Grown on the NiAl(110) Surface. ACS Omega, 2018, 3, 8819-8828.	1.6	3
29884	Experimental and theoretical study of the energetic, morphological, and photoluminescence properties of CaZrO₃:Eu³⁺. CrystEngComm, 2018, 20, 5519-5530.	1.3	22
29885	Solution-derived glass-ceramic NaIÂ·Na₃SbS₄ superionic conductors for all-solid-state Na-ion batteries. Journal of Materials Chemistry A, 2018, 6, 17192-17200.	5.2	41
29886	Effect of defects on adsorption characteristics of AlN monolayer towards SO2 and NO2: Ab initio exposure. Applied Surface Science, 2018, 462, 615-622.	3.1	42
29887	Density functional theory-based ab initio molecular dynamics simulation of ionic conduction in N-/F-doped ZrO2 under epitaxial strain. Computational Materials Science, 2018, 154, 91-96.	1.4	3
29888	Structural, electronic and magnetic properties of the H- passivated armchair MoSe2 nanoribbons with the periodic vacancy. Superlattices and Microstructures, 2018, 122, 203-215.	1.4	1
29889	Crystal Engineering of Covalent Organic Frameworks Based on Hydrazine and Hydroxy-1,3,5-Triformylbenzenes. Crystal Growth and Design, 2018, 18, 5682-5689.	1.4	37
29890	Quantum anomalous Hall effect in metal-bis(dithiolene), magnetic properties, doping and interfacing graphene. Physical Chemistry Chemical Physics, 2018, 20, 22652-22659.	1.3	14

#	Article	IF	Citations
29891	Development of a ReaxFF reactive force field for lithium ion conducting solid electrolyte Li_{1+x}Al_xTi_{2â^'x}(PO₄)₃ (LATP). Physical Chemistry Chemical Physics, 2018, 20, 22134-22147.	1.3	30
29892	Combining nanostructuration with boron doping to alter sub band gap acceptor states in diamond materials. Journal of Materials Chemistry A, 2018, 6, 16645-16654.	5.2	14
29893	Î¼SR study of spin freezing and persistent spin dynamics in NaCaNi₂F₇. Journal of Physics Condensed Matter, 2018, 30, 385802.	0.7	3
29894	Spin-orbit coupling driven crossover from a starfruitlike nodal semimetal to Dirac and Weyl semimetal state in CaAuAs. Physical Review B, 2018, 98, .	1.1	29
29895	Edge-Oxidized Germanene Nanoribbons for Nanoscale Metal Interconnect Applications. IEEE Transactions on Electron Devices, 2018, 65, 3893-3900.	1.6	23
29896	Subsurface catalysis-mediated selectivity of dehydrogenation reaction. Science Advances, 2018, 4, eaar5418.	4.7	89
29897	Tunable band inversion in half-Heusler topological LuAuSn/LuPtBi superlattices. Applied Physics Express, 2018, 11, 095701.	1.1	3
29898	Curvature induced improvement of Li storage in Ca2N nanotubes. Applied Surface Science, 2018, 459, 406-410.	3.1	5
29899	Computational insight into the mechanism of O2 to H2O2 reduction on amino-groups-containing g-C3N4. Applied Surface Science, 2018, 462, 134-141.	3.1	29
29900	Adsorption of O3, SO2 and NO2 molecules on the surface of pure and Fe-doped silicon carbide nanosheets: A computational study. Applied Surface Science, 2018, 462, 685-692.	3.1	26
29901	Ideal adhesive and shear strengths of solid interfaces: A high throughput ab initio approach. Computational Materials Science, 2018, 154, 517-529.	1.4	22
29902	Nitrogen-Doped Carbon Nanomaterials as Highly Active and Specific Peroxidase Mimics. Chemistry of Materials, 2018, 30, 6431-6439.	3.2	236
29903	Microscopic Sources of Solid-State NMR Shielding in Titanate of Alkaline Earth Perovskite Metals. Journal of Physical Chemistry C, 2018, 122, 20589-20601.	1.5	8
29904	Ultrasharp h-BN Nanocones and the Origin of Their High Mechanical Stiffness and Large Dipole Moment. Journal of Physical Chemistry Letters, 2018, 9, 5086-5091.	2.1	11
29905	Ideal inert substrates for planar antimonene: h-BN and hydrogenated SiC(0001). Physical Chemistry Chemical Physics, 2018, 20, 23397-23402.	1.3	2
29906	Tunable stacking fault energies by tailoring local chemical order in CrCoNi medium-entropy alloys. Proceedings of the National Academy of Sciences of the United States of America, 2018, 115, 8919-8924.	3.3	495
29907	Role of Multiple Charge States of <mml:math xmlns:mml="http://www.w3.org/1998/Math/MathML" display="inline" overflow="scroll"><mml:mi>Ce</mml:mi></mml:math> in the Scintillation of <mml:math xmlns:mml="http://www.w3.org/1998/Math/MathML" display="inline" overflow="scroll"><mml:mi mathvariant="italic">AB</mml:mi><mml:msub><mml:mrow><mml:mrow><mml:mi	1.5	15
29908	Electronic and structural response to pressure in the hyperkagome lattice <mml:math xmlns:mml="http://www.w3.org/1998/Math/MathML"><mml:mrow><mml:msub><mml:mi>Na</mml:mi><mml:mn>3</mml:mn></mml:msub><mml:msub><mml:mi mathvariant="normal">O</mml:mi><mml:mn>8</mml:mn></mml:msub></mml:mrow></mml:math>. Physical Review B, 2018, 98, .	1.1	10

#	Article	IF	Citations
29909	Unexpected Ground-State Structure and Mechanical Properties of Ir2Zr Intermetallic Compound. Materials, 2018, 11, 103.	1.3	2
29910	Strain dependent electronic and optical properties of PtS2 monolayer. Chemical Physics Letters, 2018, 709, 65-70.	1.2	53
29911	Stability of U5Si4 phase in U-Si system: Crystal structure prediction and phonon properties using first-principles calculations. Journal of Nuclear Materials, 2018, 510, 331-336.	1.3	25
29912	Novel application of MgH2/MoS2 hydrogen storage materials to thiophene hydrodesulfurization: A combined experimental and theoretical case study. Materials and Design, 2018, 158, 213-223.	3.3	21
29913	Strain effect on the electronic properties of Ce-doped SnS2 monolayer. Physica B: Condensed Matter, 2018, 547, 1-5.	1.3	11
29914	Atomistic Sodiation Mechanism of a Phosphorene/Graphene Heterostructure for Sodium-Ion Batteries Determined by First-Principles Calculations. Journal of Physical Chemistry C, 2018, 122, 20653-20660.	1.5	35
29915	Theoretical Study of Propylene Epoxidation over Cu₂O(111) Surface: Activity of O^{2â€“}, O^{â€“}, and O₂^{â€“} Species. Journal of Physical Chemistry C, 2018, 122, 21500-21513.	1.5	34
29916	Toward Intrinsic Room-Temperature Ferromagnetism in Two-Dimensional Semiconductors. Journal of the American Chemical Society, 2018, 140, 11519-11525.	6.6	280
29917	Thermodynamic and Elastic Properties of Magnesite at Mantle Conditions: Firstâ€Principles Calculations. Geochemistry, Geophysics, Geosystems, 2018, 19, 2719-2731.	1.0	16
29918	First-principles and experimental studies of [ZrO(OH)]⁺ or ZrO(OH)₂ for enhancing CO₂ desorption kinetics â€“ imperative for significant reduction of CO₂ capture energy consumption. Journal of Materials Chemistry A, 2018, 6, 17671-17681.	5.2	13
29919	Comparative study of structural and electronic properties of GaSe and InSe polytypes. Journal of Chemical Physics, 2018, 149, 054106.	1.2	35
29920	Electronic structure and thermoelectric properties of monolayers of group V atoms. AIP Conference Proceedings, 2018, , .	0.3	5
29921	First principles study of the structural, electronic and optical properties of epitaxial GaSb_{1â^'x â^'y}N_yBi_x, lattice matched to GaSb. Materials Research Express, 2018, 5, 115901.	0.8	3
29922	Magnetic and electronic structure of the layered rare-earth pnictide <mml:math xmlns:mml="http://www.w3.org/1998/Math/MathML"><mml:mrow><mml:msub><mml:mi mathvariant="normal">EuCd</mml:mi><mml:mn>2</mml:mn></mml:msub><mml:msub><mml:mi mathvariant="normal">Sb</mml:mi><mml:mn>2</mml:mn></mml:msub></mml:mrow></mml:math>. Physical Review B, 2018, 98, .	1.1	20
29923	Interaction of water with stepped Co(0001): how is it different from flat Co(0001)?. European Physical Journal B, 2018, 91, 1.	0.6	2
29924	Experimental and theoretical study of Raman scattering spectra of ternary chalcogenides Tl₄HgI₆, Tl₄HgBr₆, and TlHgCl₃. Journal of Raman Spectroscopy, 2018, 49, 1840-1848.	1.2	7
29925	Theoretical investigations of HCOOH decomposition on ordered Cu-Pd alloy surfaces. Applied Surface Science, 2018, 462, 649-658.	3.1	13
29926	H2O adsorption on the Au and Pd single atom catalysts supported on ceria: A first-principles study. Applied Surface Science, 2018, 462, 399-408.	3.1	7

#	Article	IF	Citations
29927	Structural phase stability, elastic parameters and thermal properties of YN from first-principles calculation. Chinese Journal of Physics, 2018, 56, 1816-1825.	2.0	10
29928	Efficiency of Generalized Regular <mml:math xmlns:mml="http://www.w3.org/1998/Math/MathML" altimg="si1.gif" overflow="scroll"><mml:mrow><mml:mi mathvariant="bold">k</mml:mi></mml:mrow></mml:math>-point grids. Computational Materials Science, 2018, 153, 424-430.	1.4	26
29929	Thermodynamic properties of Pb3U11O36. Journal of Nuclear Materials, 2018, 510, 38-42.	1.3	0
29930	Li2SnO3 as a Cathode Material for Lithium-ion Batteries: Defects, Lithium Ion Diffusion and Dopants. Scientific Reports, 2018, 8, 12621.	1.6	34
29931	Enhanced Carrier Concentration and Electronic Transport by Inserting Graphene into van der Waals Heterostructures of Transition-Metal Dichalcogenides. Physical Review Applied, 2018, 10, .	1.5	19
29932	Strain enhancement of the electro-optical response in <mml:math xmlns:mml="http://www.w3.org/1998/Math/MathML"><mml:mrow><mml:mi>BaTi</mml:mi><mml:msub><mml:mi mathvariant="normal">O</mml:mi><mml:mn>3</mml:mn></mml:msub></mml:mrow></mml:math> films integrated on <mml:math xmlns:mml="http://www.w3.org/1998/Math/MathML"><mml:mrow><mml:mi>Si</mml:mi><mml:mo>(</mml:mo><mml:mn>001</mml:mn> Physical Review B, 2018, 98, .	1.1	21
29933	Computational Predictions and Microwave Plasma Synthesis of Superhard Boron-Carbon Materials. Materials, 2018, 11, 1279.	1.3	9
29934	Operando monitoring the lithium spatial distribution of lithium metal anodes. Nature Communications, 2018, 9, 2152.	5.8	96
29935	Electronic structure and magnetism of titanium substituted Cd3P2: An ab-initio study. AIP Conference Proceedings, 2018, , .	0.3	2
29936	Structural, electronic and optical properties of bandgap-tunable Cu 2 ZnSi x Sn 1â^' x Se 4 alloys. Chemical Physics Letters, 2018, 705, 92-96.	1.2	4
29937	Origin of H₂ Formation on Perfect SrTiO₃ (001) Surface: A First-principles Study. Journal of Physical Chemistry C, 2018, 122, 12951-12955.	1.5	1
29938	Suppressing Voltage Decay of a Lithium-Rich Cathode Material by Surface Enrichment with Atomic Ruthenium. ACS Applied Materials & Interfaces, 2018, 10, 21349-21355.	4.0	36
29939	Few-Layer PdSe₂ Sheets: Promising Thermoelectric Materials Driven by High Valley Convergence. ACS Omega, 2018, 3, 5971-5979.	1.6	87
29940	First principle study of structural, electronic and fermi surface properties of aluminum praseodymium. AIP Conference Proceedings, 2018, , .	0.3	0
29941	Structural, electronic and elastic properties of heavy fermion YbRh2 Laves phase compound. AIP Conference Proceedings, 2018, , .	0.3	1
29942	First-principles study of bandgap tuning in Ge1â^'xPbxSe. International Journal of Modern Physics B, 2018, 32, 1850076.	1.0	0
29943	Investigation of the mechanical and thermodynamic properties of the U3Pt4 and Th3Pt4. Journal of Alloys and Compounds, 2018, 763, 496-503.	2.8	3
29944	First principles study of vacancy-solute complexes in vanadium. Journal of Alloys and Compounds, 2018, 763, 861-866.	2.8	19

#	Article	IF	Citations
29945	Metalâ€“Insulator Transition and Heterostructure Formation by Glycines Self-Assembled on Defect-Patterned Graphene. Journal of Physical Chemistry C, 2018, 122, 14598-14605.	1.5	28
29946	Tuning the Optoelectronic Properties of Two-Dimensional Hybrid Perovskite Semiconductors with Alkyl Chain Spacers. Journal of Physical Chemistry Letters, 2018, 9, 3416-3424.	2.1	77
29947	A remarkable two-dimensional membrane for multifunctional gas separation: halogenated metal-free fused-ring polyphthalocyanine. Physical Chemistry Chemical Physics, 2018, 20, 18931-18937.	1.3	7
29948	Water adsorption on the Fe₃O₄(111) surface: dissociation and network formation. Physical Chemistry Chemical Physics, 2018, 20, 15764-15774.	1.3	26
29949	Strain and defect engineering on phase transition of monolayer black phosphorene. Physical Chemistry Chemical Physics, 2018, 20, 21832-21843.	1.3	8
29950	Anharmonic contribution to the stabilization of Mg(OH)2 from first principles. Physical Chemistry Chemical Physics, 2018, 20, 17799-17808.	1.3	10
29951	Rapid flame doping of Co to WS₂ for efficient hydrogen evolution. Energy and Environmental Science, 2018, 11, 2270-2277.	15.6	74
29952	Origin of spin polarization in an edge boron doped zigzag graphene nanoribbon: a potential spin filter. Nanotechnology, 2018, 29, 345203.	1.3	7
29953	Spectroscopic and theoretical investigation of the electronic states of layered perovskite oxyfluoride <mml:math xmlns:mml="http://www.w3.org/1998/Math/MathML"><mml:mrow><mml:mi mathvariant="normal">S</mml:mi><mml:msub><mml:mi mathvariant="normal">r</mml:mi><mml:mn>2</mml:mn></mml:msub><mml:mi>Ru</mml:mi><mml:msub><mml:mi mathvariant="normal">O</mml:mi><mml:mn>3</mml:mn></mml:msub><mml:msub><mml:mi mathvariant="normal">F</mml:mi><mml:mn>2</mml:mn></mml:msub></mml:mrow></mml:math> thin fi	1.1	6
29954	Charge transport in doped zigzag phosphorene nanoribbons. Physical Review B, 2018, 97, .	1.1	25
29955	High Thermoelectric Performance in Supersaturated Solid Solutions and Nanostructured nâ€Type PbTeâ€“GeTe. Advanced Functional Materials, 2018, 28, 1801617.	7.8	92
29956	Improvement of the Photophysical Performance of Platinumâ€Cyclometalated Complexes in Halogenâ€Bonded Adducts. Chemistry - A European Journal, 2018, 24, 11475-11484.	1.7	39
29957	Two-Dimensional Manganese Nitride Monolayer with Room Temperature Rigid Ferromagnetism under Strain. Journal of Physical Chemistry C, 2018, 122, 14918-14927.	1.5	50
29958	Graphdiyne as an ideal monolayer coating material for lithium-ion battery cathodes with ultralow areal density and ultrafast Li penetration. Journal of Materials Chemistry A, 2018, 6, 12630-12636.	5.2	24
29959	Hydrogen storage in Li, Na and Ca decorated and defective borophene: a first principles study. RSC Advances, 2018, 8, 20748-20757.	1.7	64
29960	Effects of external magnetic field and out-of-plane strain on magneto-optical Kerr spectra in CrI3 monolayer. Journal of Physics Condensed Matter, 2018, 30, 285303.	0.7	16
29961	Metal dopants adjusted perovskite stannates: Conductivity and optical properties. Ceramics International, 2018, 44, 16051-16057.	2.3	14
29962	First-principles investigation of structural, mechanical, electronic, and thermoelectric properties of Half-Heusler compounds RuVX (X=As, P, and Sb). Computational Condensed Matter, 2018, 16, e00312.	0.9	26

#	Article	IF	Citations
29963	Enhanced stability and induced magnetic moments of silicene by substitutional doping of nickel. Chemical Physics Letters, 2018, 706, 202-207.	1.2	13
29964	The synergistic effect of Ni promoter on Mo-S/CNT catalyst towards hydrodesulfurization and hydrogen evolution reactions. Fuel, 2018, 232, 36-44.	3.4	30
29965	A promising thermoelectric response of HfRhSb half Heusler compound at high temperature: A first principle study. Journal of Alloys and Compounds, 2018, 763, 1018-1023.	2.8	54
29966	Water activation by single Pt atoms supported on a Cu2O thin film. Journal of Catalysis, 2018, 364, 166-173.	3.1	18
29967	3D long-range magnetic ordering in (C2H5NH3)2CuCl4 compound revealed by internal magnetic field from muon spin rotation and first principal calculation. Physica B: Condensed Matter, 2018, 545, 76-79.	1.3	4
29968	External pressure effect on the electronic, optical and thermoelectric properties of the CdY2Ch4 (Ch) Tj ETQq1 1 0.784314 rgBT /Ove Matter, 2018, 545, 40-47.	1.3	9
29969	Structure and Reactivity of Anatase TiO₂(001)-(1 Ã— 4) Surface. Journal of Physical Chemistry C, 2018, 122, 14528-14536.	1.5	16
29970	Acetylene Adsorption on Pdâ€“Ag Alloys: Evidence for Limited Island Formation and Strong Reverse Segregation from Monte Carlo Simulations. Journal of Physical Chemistry C, 2018, 122, 15456-15463.	1.5	35
29971	Water Dissociation on Clean and Potassium Preadsorbed Transition Metals: A Systematic Theoretical Study. Journal of Physical Chemistry C, 2018, 122, 15474-15484.	1.5	16
29972	Sub-5 nm Monolayer Arsenene and Antimonene Transistors. ACS Applied Materials & Interfaces, 2018, 10, 22363-22371.	4.0	77
29973	Strain Tuning of the Anisotropy in the Optoelectronic Properties of TiS₃. ACS Photonics, 2018, 5, 3231-3237.	3.2	14
29974	Selecting electrode materials for monolayer ReS₂ with an Ohmic contact. Journal of Materials Chemistry C, 2018, 6, 6764-6770.	2.7	34
29975	Magnetic properties of X-C2N (X=Cl, Br and I) monolayers: A first-principles study. AIP Advances, 2018, 8, 055333.	0.6	4
29976	Diffusion quantum Monte Carlo and density functional calculations of the structural stability of bilayer arsenene. Journal of Chemical Physics, 2018, 148, 214706.	1.2	23
29977	Permeability of two-dimensional graphene and hexagonal-boron nitride to hydrogen atom. AIP Conference Proceedings, 2018, , .	0.3	2
29978	Structural, electronic and vibrational properties of LaF₃ according to density functional theory and Raman spectroscopy. Journal of Physics Condensed Matter, 2018, 30, 255901.	0.7	5
29979	Observation of a well-defined hybridization gap and in-gap states on the <mml:math xmlns:mml="http://www.w3.org/1998/Math/MathML"><mml:msub><mml:mi>SmB</mml:mi><mml:mn>6</mml:mn></mml:msub></mml (001) surface. Physical Review B, 2018, 97, .	1.1	20
29980	Computer Simulation of Energy Parameters and Magnetic Effects in Fe-Si-C Ternary Alloys. Russian Physics Journal, 2018, 61, 242-247.	0.2	0

#	Article	IF	Citations
29981	Localization effect of f-electron of heavier rare-earth atoms in RENi2 (RE= Dy, Ho and Er) Laves phase compounds. Computational Condensed Matter, 2018, 16, e00316.	0.9	3
29982	Equilibrium lithium isotope fractionation in Li-bearing minerals. Geochimica Et Cosmochimica Acta, 2018, 235, 360-375.	1.6	20
29983	Theoretical study on the reaction mechanism of carbon dioxide reforming of methane on La and La2O3 modified Ni(1â€¯1â€¯1) surface. Journal of Catalysis, 2018, 364, 248-261.	3.1	30
29984	Structural Characterization of Pristine and Defective [Zr₁₂(Î¼₃-O)₈(Î¼₃-OH)₈(Î¼₂-OH)₆ Double-Node Metalâ€“Organic Framework and Predicted Applications for Single-Site Catalytic Hydrolysis of Sarin. Chemistry of Materials, 2018, 30, 4432-4439.	3.2	42
29985	Nano-mechanical properties of Fe-Mn-Al-C lightweight steels. Scientific Reports, 2018, 8, 9065.	1.6	22
29986	Selective hydrogenation of 1,3-butadiene catalyzed by a single Pd atom anchored on graphene: the importance of dynamics. Chemical Science, 2018, 9, 5890-5896.	3.7	55
29987	Two-dimensional silicon carbide structure under uniaxial strains, electronic and bonding analysis. Computational Materials Science, 2018, 151, 288-295.	1.4	26
29988	On-Surface Synthesis of Spin Crossover Polymeric Chains. Journal of Physical Chemistry C, 2018, 122, 15033-15040.	1.5	17
29989	Role of Subsurface Oxygen on Cu Surfaces for CO₂ Electrochemical Reduction. Journal of Physical Chemistry C, 2018, 122, 16209-16215.	1.5	68
29990	High-Efficiency â€œWorking-in-Tandemâ€•Nitrogen Photofixation Achieved by Assembling Plasmonic Gold Nanocrystals on Ultrathin Titania Nanosheets. Journal of the American Chemical Society, 2018, 140, 8497-8508.	6.6	382
29991	Carbon nitride supported Fe2 cluster catalysts with superior performance for alkene epoxidation. Nature Communications, 2018, 9, 2353.	5.8	278
29992	Factors driving stable growth of He clusters in W: first-principles study. Nuclear Fusion, 2018, 58, 076024.	1.6	2
29993	Competition of lattice and spin excitations in the temperature dependence of spin-wave properties. Physical Review B, 2018, 97, .	1.1	5
29994	Structuralâ€Distortionâ€Driven Magnetic Transformation from Ferroâ€•to Ferrimagnetic Iron Chains in B 6 â€based Nb 6 FeIr 6 B 8. Angewandte Chemie - International Edition, 2018, 57, 10323-10327.	7.2	6
29995	Bandgap modulation of partially chlorinated graphene (C4Cl) nanosheets via biaxial strain and external electric field: a computational study. Applied Physics A: Materials Science and Processing, 2018, 124, 1.	1.1	20
29996	Structural, elastic and optoelectronic properties of Sr-based perovskite-type oxides SrXO3 (Mâ€¯=â€¯Th, Zr) via first-principles calculations. Chinese Journal of Physics, 2018, 56, 1515-1524.	2.0	10
29997	Mono and bi-layer germanene as prospective anode material for Li-ion batteries: A first-principles study. Computational Condensed Matter, 2018, 16, e00314.	0.9	25
29998	Methanol oxidation on the Au(3â€¯1â€¯0) surface: A theoretical study. Journal of Catalysis, 2018, 364, 216-227.	3.1	17

#	Article	IF	Citations
29999	Multiferroism and magnetic ordering in new NiBO3 (Bâ€¯=â€¯Ti, Ge, Zr, Sn, Hf and Pb) materials: A DFT study. Journal of Magnetism and Magnetic Materials, 2018, 465, 412-420.	1.0	13
30000	Boosting hot electron flux and catalytic activity at metalâ€“oxide interfaces of PtCo bimetallic nanoparticles. Nature Communications, 2018, 9, 2235.	5.8	80
30001	Optical properties of monolayer BeC under an external electric field: A DFT approach. Physical Sciences Reviews, 2018, 3, .	0.8	1
30002	Chemicalâ€Strain Induced Tilted Dirac Nodes in (BEDTâ€TTF)₂X₃ (Xâ€‰=â€‰I, Cl, Br, F) Based Chargeâ€Transfer Salts. Physica Status Solidi - Rapid Research Letters, 2018, 12, 1800081.	1.2	9
30003	A Neutron Diffraction and Quantumâ€Chemical Study of [Mn(ND₃)₆](N₃)₂. Zeitschrift Fur Anorganische Und Allgemeine Chemie, 2018, 644, 1349-1353.	0.6	0
30004	Electronic and magnetic properties of the [4Fe-4S] iron-sulfur clusters encapsulated in a single-walled semiconducting carbon nanotube. Current Applied Physics, 2018, 18, 1034-1040.	1.1	0
30005	Rational design of carbonaceous nanofiber/Ni-Al layered double hydroxide nanocomposites for high-efficiency removal of heavy metals from aqueous solutions. Environmental Pollution, 2018, 242, 1-11.	3.7	122
30006	Anisotropic mechanical properties and strain tuneable band-gap in single-layer SiP, SiAs, GeP and GeAs. Physica E: Low-Dimensional Systems and Nanostructures, 2018, 103, 273-278.	1.3	45
30007	Investigation of the initial reactions of lithium oxides on the graphitic carbon nitrides (g-C3N4) for catalyst in non-aqueous lithium - air batteries: A first-principles calculations. Thin Solid Films, 2018, 660, 186-190.	0.8	6
30008	Î±-Fe₂O₃ Nanoparticles as Oxygen Carriers for Chemical Looping Combustion: An Integrated Materials Characterization Approach to Understanding Oxygen Carrier Performance, Reduction Mechanism, and Particle Size Effects. Energy & Fuels, 2018, 32, 7959-7970.	2.5	33
30009	Computational predictions turning the isomers of alanine to generate distinct morphs of free-flowing salt crystals. Physical Chemistry Chemical Physics, 2018, 20, 17125-17131.	1.3	0
30010	Electronic and atomic structures of edge and screw dislocations in rock salt structured ionic crystals. Philosophical Magazine, 2018, 98, 2189-2204.	0.7	6
30011	Pressure induced phase transitions and elastic properties of CaCO₃polymorphs: a density functional theory study. Modelling and Simulation in Materials Science and Engineering, 2018, 26, 065004.	0.8	14
30012	Two-Dimensional Deep-Ultraviolet Beryllium-Free KBe₂BO₃F₂ Family Nonlinear-Optical Monolayer. Inorganic Chemistry, 2018, 57, 7503-7506.	1.9	30
30013	High-pressure phase diagram of hydrogen and deuterium sulfides from first principles: Structural and vibrational properties including quantum and anharmonic effects. Physical Review B, 2018, 97, .	1.1	38
30014	The promotion effect of oxygen on the dissociative adsorption of water to uranium dioxide surface: a GGAâ€‰+â€‰U study. Journal of Radioanalytical and Nuclear Chemistry, 2018, 317, 1013-1020.	0.7	2
30015	Combinatorial alloying improves bismuth vanadate photoanodes via reduced monoclinic distortion. Energy and Environmental Science, 2018, 11, 2444-2457.	15.6	21
30016	Piezoelectricity in WSe₂/MoS₂ heterostructure atomic layers. Nanoscale, 2018, 10, 12472-12479.	2.8	24

#	Article	IF	Citations
30017	Structure and vibrational properties of the dominant O-H center in Î²-Ga2O3. Applied Physics Letters, 2018, 112, .	1.5	83
30018	Chromium nanostructure formation on the GaAs(1â€¯1â€¯1)â€“(2â€¯Ã—â€¯2) surface: First principles studies. Applied Surface Science, 2018, 455, 1078-1085.	3.1	3
30019	Energetics of hydrogen and helium-vacancy complexes in bulk and near surfaces of tungsten: First-principles study. Journal of Applied Physics, 2018, 123, 215104.	1.1	13
30020	Effects of vacancy defects on Fe properties incorporated in MgO. Journal of Physics Condensed Matter, 2018, 30, 295701.	0.7	1
30021	Ab Initio Study of the Polarization, Electronic, Magnetic, and Optical Properties of Perovskite SrMO3 (M = Fe, Mn) Crystals and Thin Films Containing Magnetic Ions. Journal of Experimental and Theoretical Physics, 2018, 126, 497-505.	0.2	8
30022	Structural, Electronic and Elastic Properties of Half-Heusler Alloys CrNiZ (Z = Al, Si, Ge and As). Journal of the Korean Physical Society, 2018, 72, 1337-1342.	0.3	6
30023	Structural and magnetic properties of MoS 2 monolayer zigzag nanoribbon doped by Ti, V, Cr, and Mn. Physics Letters, Section A: General, Atomic and Solid State Physics, 2018, 382, 2354-2360.	0.9	14
30024	Interplay of water and reactive elements in oxidation of alumina-forming alloys. Nature Materials, 2018, 17, 610-617.	13.3	72
30025	Mechanistic study of dry reforming of ethane by CO₂ on a bimetallic PtNi(111) model surface. Catalysis Science and Technology, 2018, 8, 3748-3758.	2.1	24
30026	Removal of Cr(<scp>iii</scp>)/Cr(<scp>vi</scp>) from wastewater using defective porous boron nitride: a DFT study. Inorganic Chemistry Frontiers, 2018, 5, 1933-1940.	3.0	18
30027	Novel two-dimensional diamond like carbon nitrides with extraordinary elasticity and thermal conductivity. Carbon, 2018, 138, 319-324.	5.4	23
30028	Comprehensive Phase Diagrams of MoS₂ Edge Sites Using Dispersion-Corrected DFT Free Energy Calculations. Journal of Physical Chemistry C, 2018, 122, 15318-15329.	1.5	18
30029	Initial Oxygen Incorporation in the Prismatic Surfaces of Troilite FeS. Journal of Physical Chemistry C, 2018, 122, 12810-12818.	1.5	16
30030	In-Situ Formed Hydroxide Accelerating Water Dissociation Kinetics on Co₃N for Hydrogen Production in Alkaline Solution. ACS Applied Materials & Interfaces, 2018, 10, 22102-22109.	4.0	54
30031	Two-dimensional pentagonal CrX (X = S, Se or Te) monolayers: antiferromagnetic semiconductors for spintronics and photocatalysts. Physical Chemistry Chemical Physics, 2018, 20, 18348-18354.	1.3	26
30032	Highly efficient and ultra-stable boron-doped graphite felt electrodes for vanadium redox flow batteries. Journal of Materials Chemistry A, 2018, 6, 13244-13253.	5.2	97
30033	Hole-doping-induced half-metallic ferromagnetism in a highly-air-stable PdSe₂ monolayer under uniaxial stress. Journal of Materials Chemistry C, 2018, 6, 6792-6798.	2.7	38
30034	Stability of SnSe_{1â”’x}S_x solid solutions revealed by first-principles cluster expansion. Journal of Physics Condensed Matter, 2018, 30, 29LT01.	0.7	14

#	Article	IF	Citations
30035	Adaptive modulation in the <mml:math xmlns:mml="http://www.w3.org/1998/Math/MathML"><mml:mrow><mml:mi mathvariant="normal">N</mml:mi><mml:msub><mml:mi mathvariant="normal">i</mml:mi><mml:mn>2</mml:mn></mml:msub><mml:mi mathvariant="normal">M</mml:mi><mml:msub><mml:mi mathvariant="normal">n</mml:mi><mml:mrow><mml:mn>1.4</mml:mn></mml:mrow></mml:msub><mml:mi	1.1	18
30036	Origin of efficient oxygen reduction reaction on Pd monolayer supported on Pd-M (M=Ni, Fe) intermetallic alloy. Electrochimica Acta, 2018, 282, 680-686.	2.6	26
30037	A first principle study of the pristine InBi honeycomb film functionalized with fluorine atoms. Journal of Fluorine Chemistry, 2018, 212, 171-179.	0.9	12
30038	Stability of FeVO₄ under Pressure: An X-ray Diffraction and First-Principles Study. Inorganic Chemistry, 2018, 57, 7860-7876.	1.9	27
30039	Giant photovoltaic response in band engineered ferroelectric perovskite. Scientific Reports, 2018, 8, 8005.	1.6	36
30040	Density functional theory study of thermodynamic and kinetic isotope effects of H2/D2 dissociative adsorption on transition metals. Catalysis Science and Technology, 2018, 8, 3321-3335.	2.1	26
30041	Valley-selective circular dichroism and high carrier mobility of graphene-like BC₆N. Nanoscale, 2018, 10, 13179-13186.	2.8	37
30042	Pressure induced phase transition in CdTe nanowire: A DFT study. AIP Conference Proceedings, 2018, , .	0.3	0
30043	First-principles study of structural and electronic properties of Be0.25Zn0.75S mixed compound. AIP Conference Proceedings, 2018, , .	0.3	0
30044	From semilocal density functionals to random phase approximation renormalized perturbation theory: A methodological assessment of structural phase transitions. Physical Review B, 2018, 97, .	1.1	68
30045	Theoretical study of strain-induced modulation of the bandgap in SiC. Japanese Journal of Applied Physics, 2018, 57, 071301.	0.8	11
30046	Room-Temperature Methane Conversion by Graphene-Confined Single Iron Atoms. CheM, 2018, 4, 1902-1910.	5.8	350
30047	Stability of L21 (NiM)2TiAl (M=Co, Fe) in high-entropy alloys. Journal of Alloys and Compounds, 2018, 764, 650-655.	2.8	7
30048	Dioxygen activation routes in Mars-van Krevelen redox cycles catalyzed by metal oxides. Journal of Catalysis, 2018, 364, 228-247.	3.1	36
30049	Single-atom vacancy in monolayer phosphorene: A comprehensive study of stability and magnetism under applied strain. Journal of Magnetism and Magnetic Materials, 2018, 465, 546-553.	1.0	2
30050	Theoretical understanding of SnS monolayer as Li ion battery anode material. Journal of Physics and Chemistry of Solids, 2018, 121, 261-265.	1.9	22
30051	Remedies of capacity fading in room-temperature sodium-sulfur batteries. Journal of Power Sources, 2018, 396, 304-313.	4.0	45
30052	Adsorption of the Gas Molecules NH₃, NO, NO₂, and CO on Borophene. Journal of Physical Chemistry C, 2018, 122, 14665-14670.	1.5	91

#	Article	IF	Citations
30053	Theoretical Insight into Catalytic Propane Dehydrogenation on Ni(111). Journal of Physical Chemistry C, 2018, 122, 14678-14690.	1.5	43
30054	Thickness-Dependent Reactivity of O₂ on Cu Layers Grown on Ru(0001) Surfaces. Journal of Physical Chemistry C, 2018, 122, 15529-15538.	1.5	8
30055	New Deformation-Induced Nanostructure in Silicon. Nano Letters, 2018, 18, 4611-4617.	4.5	182
30056	Supported goldâ€“nickel nano-alloy as a highly efficient catalyst in levulinic acid hydrogenation with formic acid as an internal hydrogen source. Catalysis Science and Technology, 2018, 8, 4318-4331.	2.1	51
30057	NH4B11O16(OH)2: a new ammonium borate with wavy-shaped polycyclic 2âˆž[B11O16(OH)2] layers. New Journal of Chemistry, 2018, 42, 12091-12097.	1.4	20
30058	Experimental and computational conductivity study of multilayer graphene in polypropylene nanocomposites. Journal of Materials Chemistry C, 2018, 6, 7232-7241.	2.7	5
30059	A first-principles study of the electrically tunable band gap in few-layer penta-graphene. Physical Chemistry Chemical Physics, 2018, 20, 18110-18116.	1.3	14
30060	Electronic structure, bonding characteristics, and mechanical properties in (W_{2/3}Sc_{1/3})₂AlC and (W_{2/3}Y_{1/3})₂AlC i-MAX phases from first-principles calculations. Journal of Physics Condensed Matter, 2018, 30, 305502.	0.7	9
30061	Multiple water layers on AnO2 {111}, {110}, and {100} surfaces (An = U, Pu): A computational study. Journal of Vacuum Science and Technology A: Vacuum, Surfaces and Films, 2018, 36, .	0.9	9
30062	Photothreshold of an Î±-GeS Layered Crystal: First-Principles Calculation. Semiconductors, 2018, 52, 840-842.	0.2	1
30063	Facetâ€Đependent Phase Control by Band Filling and Anisotropic Electronâ€“Lattice Coupling in HVO₂ Epitaxial Films. Advanced Electronic Materials, 2018, 4, 1800128.	2.6	15
30064	Anisotropic charge transport properties of chrysene derivatives as organic semiconductor: A computational study. Journal of Physical Organic Chemistry, 2018, 31, e3859.	0.9	3
30065	Structural and electronic properties of point defects in Haeckelite GaN monolayer. Physica E: Low-Dimensional Systems and Nanostructures, 2018, 103, 289-293.	1.3	9
30066	Unexpected High-Pressure Phase of GeTe with an Origin of Low Ionicity and Electron Delocalization. Journal of Physical Chemistry C, 2018, 122, 15673-15677.	1.5	13
30067	Hot-Atom-Mediated Dynamical Displacement of CO Adsorbed on Cu(111) by Incident H Atoms: An Ab Initio Molecular Dynamics Study. Journal of Physical Chemistry C, 2018, 122, 15485-15493.	1.5	6
30068	Phase Coexistence and Strain-Induced Topological Insulator in Two-Dimensional BiAs. Journal of Physical Chemistry C, 2018, 122, 15047-15054.	1.5	33
30069	Sodiation and Desodiation via Helical Phosphorus Intermediates in High-Capacity Anodes for Sodium-Ion Batteries. Journal of the American Chemical Society, 2018, 140, 7994-8004.	6.6	85
30070	Spectral concentration of thermal conductivity in GaNâ€”A first-principles study. Applied Physics Letters, 2018, 112, .	1.5	18

#	Article	IF	Citations
30071	Flexible modulation of electronic and magnetic properties of zigzag H-MoS₂ nanoribbons by crack defects. Journal of Physics Condensed Matter, 2018, 30, 285302.	0.7	3
30072	Pressure and Strain Effects on the Structural, Electronic, and Optical Properties of K4 Phosphorus. Zeitschrift Fur Naturforschung - Section A Journal of Physical Sciences, 2018, 73, 661-668.	0.7	3
30073	Direct Observation at Room Temperature of the Orthorhombic Weyl Semimetal Phase in Thin Epitaxial MoTe₂. Advanced Functional Materials, 2018, 28, 1802084.	7.8	31
30074	Efficient Adsorption Characteristics of Pristine and Silverâ€Doped Graphene Oxide Towards Contaminants: A Potential Membrane Material for Water Purification?. ChemPhysChem, 2018, 19, 2250-2257.	1.0	14
30075	Computational investigations of mechanical and dynamical properties of gold-based compounds (X3Au, Xâ€¯=â€¯Ti, Zr and V). Chinese Journal of Physics, 2018, 56, 1508-1514.	2.0	3
30076	p- and n-type Doping Effects on the Electrical and Ionic Conductivities of Li4Ti5O12 Anode Materials. Journal of Physical Chemistry C, 2018, 122, 15155-15162.	1.5	10
30077	Enhanced Oxygen Reduction Activity by Selective Anion Adsorption on Non-Precious-Metal Catalysts. ACS Catalysis, 2018, 8, 7104-7112.	5.5	53
30078	Hydrogen-free defects in hydrogenated black TiO2. Physical Chemistry Chemical Physics, 2018, 20, 19871-19876.	1.3	6
30079	A new 3D Dirac nodal-line semi-metallic graphene monolith for lithium ion battery anode materials. Journal of Materials Chemistry A, 2018, 6, 13816-13824.	5.2	44
30080	Tuning the electronic and magnetic properties of graphene/h-BN hetero nanoribbon: A first-principles investigation. AIP Advances, 2018, 8, .	0.6	7
30081	Weak metal-metal transition in the vanadium oxytelluride <mml:math xmlns:mml="http://www.w3.org/1998/Math/MathML"><mml:mrow><mml:msub><mml:mi>Rb</mml:mi><mml:mrow><mml:mn>1</mml:mn></mml:mrow></mml:msub><mml:msub><mml:mi mathvariant="normal">V</mml:mi><mml:mn>2</mml:mn></mml:msub><mml:msub><mml:mi>Te</mml:mi><mml:mn>2</mml:mn></mml:msub><mml:msub><mml:mi mathvariant="normal">O</mml:mi></mml:mrow></mml:math>. Physical Review B, 2018, 97, .	1.1	9
30082	Polarization fluctuations in the perovskite-structured ferroelectric <mml:math xmlns:mml="http://www.w3.org/1998/Math/MathML"><mml:mrow><mml:mi>AgNb</mml:mi><mml:msub><mml:mi mathvariant="normal">O</mml:mi><mml:mn>3</mml:mn></mml:msub></mml:mrow></mml:math>. Physical Review B, 2018, 97, .	1.1	20
30083	Structural and mechanistic revelations on high capacity cation-disordered Li-rich oxides for rechargeable Li-ion batteries. Energy Storage Materials, 2019, 16, 354-363.	9.5	94
30084	Thermochemical conversion of carbon dioxide by reverse water-gas shift chemical looping using supported perovskite oxides. Catalysis Today, 2019, 323, 225-232.	2.2	51
30085	Photocatalytic water splitting of (F, Ti) codoped heptazine/triazine based g-C3N4 heterostructure: A hybrid DFT study. Applied Surface Science, 2019, 463, 809-819.	3.1	39
30086	Elucidating linear and nonlinear optical properties of defect chalcopyrite compounds ZnX2Te4 (X=Al,) Tj ETQq1 1 0.784314 rgBT /Ove	1.5	8
30087	Materials with honeycomb structures for gate dielectrics in two-dimensional Field Effect Transistors â€“ An ab initio study. Ceramics International, 2019, 45, 9339-9347.	2.3	6
30088	Ab Initio Calculations on the Electronic Structure and Photocatalytic Properties of Twoâ€Dimensional WS₂ (0001) Nanolayers of Varying Thickness. Physica Status Solidi - Rapid Research Letters, 2019, 13, 1800253.	1.2	16

#	Article	IF	Citations
30089	Improved oxidation of hydrogen off-gas by hydrophobic surface modification: A multiscale density functional theory study. Particuology, 2019, 44, 28-35.	2.0	4
30090	Graphene intercalated Ni-SiO2/GO-Ni-foam catalyst with enhanced reactivity and heat-transfer for CO2 methanation. Chemical Engineering Science, 2019, 194, 10-21.	1.9	43
30091	Adhesion and mechanical properties of layered nano films TiN/ZrN and TiN/Ti/ZrN: pseudopotential simulation. Composite Interfaces, 2019, 26, 97-106.	1.3	2
30092	Half-Metallic and Half-Semiconductor Gaps in Cr-Based Chalcogenides: DFT + U Calculations. Journal of Superconductivity and Novel Magnetism, 2019, 32, 635-649.	0.8	14
30093	BaNb3.6O10 nanowires with superior electrochemical performance towards ultrafast and highly stable lithium storage. Energy Storage Materials, 2019, 16, 400-410.	9.5	43
30094	Investigations on ferromagnetism of Li and Mn codoped LiZnN by firstâ€principles calculations. Journal of the American Ceramic Society, 2019, 102, 303-309.	1.9	2
30095	A new six-dimensional potential energy surface for NO/Au(111). Molecular Physics, 2019, 117, 42-57.	0.8	6
30096	Direct observation of Eu atoms in AlN lattice and the firstâ€principles simulations. Journal of the American Ceramic Society, 2019, 102, 310-319.	1.9	20
30097	Visible light absorption of surface-modified Al2O3 powders: A comparative DFT and experimental study. Microporous and Mesoporous Materials, 2019, 273, 41-49.	2.2	15
30098	Heterogeneous reaction mechanism of elemental mercury oxidation by oxygen species over MnO2 catalyst. Proceedings of the Combustion Institute, 2019, 37, 2967-2975.	2.4	80
30099	Ab initio study of the theoretical strength and magnetism of the Feâ^'Pd, Feâ^'Pt and Feâ^'Cu nanocomposites. Journal of Magnetism and Magnetic Materials, 2019, 469, 100-107.	1.0	3
30100	Structural and optical evolution in Pb100-Ag Se (xâ€¯=â€¯3, 6, 9 and 12) thin films by chemical bath deposition. Journal of Alloys and Compounds, 2019, 770, 649-654.	2.8	9
30101	Geometry, electronic structure, morphology, and photoluminescence emissions of BaW1-xMoxO4 (xâ€¯=â€¯0, 0.25, 0.50, 0.75, and 1) solid solutions: Theory and experiment in concert. Applied Surface Science, 2019, 463, 907-917.	3.1	24
30102	Theoretical Approach for Nanocarbon-Based Energy Catalyst Design. Nanostructure Science and Technology, 2019, , 159-174.	0.1	0
30103	First-principles assessment of the analogy between gas-phase and gas-solid H-abstraction reactions at graphene edges. Chemical Engineering Journal, 2019, 377, 119691.	6.6	6
30104	Effect of Fe and Ti Substitution Doping on Magnetic Property of Monolayer CrSi2: a First-Principle Investigation. Journal of Superconductivity and Novel Magnetism, 2019, 32, 1341-1346.	0.8	4
30105	Esterification of Tertiary Amides by Alcohols Through Câ^'N Bond Cleavage over CeO₂. ChemCatChem, 2019, 11, 449-456.	1.8	21
30106	The Preference of the Ferromagnetic Ordering for the Novel Heusler Rh 2 MnTi ${ext {Rh}}_{ext {2}}ext {MnTi}$ Compound. Journal of Superconductivity and Novel Magnetism, 2019, 32, 1415-1421.	0.8	6

#	Article	IF	Citations
30107	Effect of oxide additives on the hydrotalcite derived Ni catalysts for CO2 reforming of methane. Chemical Engineering Journal, 2019, 377, 119763.	6.6	97
30108	Understanding the formation thermodynamics of fresnoitic trivanadates: DFT calculations and soft base hydrolysis synthesis. Journal of Physics and Chemistry of Solids, 2019, 124, 7-12.	1.9	0
30109	Experimental and theoretical approaches for the investigation of proton conductive characteristics of La1-Ba YbO3-Î´. Journal of Alloys and Compounds, 2019, 770, 294-300.	2.8	11
30110	Magnetization on nitrogen in extended honeycomb carbon layers from first principles: Case studies of CxN (xâ€¯=â€¯2, 6, 12). Journal of Magnetism and Magnetic Materials, 2019, 469, 46-51.	1.0	3
30111	2-Amino-pentanoic acid and 1-Pyridiniumylacetate are new additives to generate distinct morphs of salt crystals: A combined computational and experimental study. Journal of Molecular Structure, 2019, 1175, 728-733.	1.8	0
30112	Activation energy calculation of NOâ€“CO reaction on rhodium surface by density functional theory. Catalysis Today, 2019, 332, 272-279.	2.2	5
30113	Insight into interfacial structure and bonding nature of diamond(001)/Cr3C2(001) interface. Journal of Alloys and Compounds, 2019, 770, 82-89.	2.8	12
30114	Facile synthesis of self-activated oxyfluorotungstate phosphor with high QE and its thermal quenching. Journal of Alloys and Compounds, 2019, 770, 559-563.	2.8	6
30115	Effects of transition metals on physical properties of M2BC (Mâ€¯=â€¯V, Nb, Mo and Ta): A DFT calculation. Journal of Alloys and Compounds, 2019, 770, 523-534.	2.8	46
30116	Vibrational response of strontianite at high pressures and high temperatures and construction of Pâ€“T phase diagram. Physics and Chemistry of Minerals, 2019, 46, 27-35.	0.3	9
30117	Equation of state and second-order elastic constants of portlandite Ca(OH)2 and brucite Mg(OH)2. Physics and Chemistry of Minerals, 2019, 46, 101-117.	0.3	16
30118	Reaction mechanism of spinel CuFe2O4 with CO during chemical-looping combustion: An experimental and theoretical study. Proceedings of the Combustion Institute, 2019, 37, 4399-4408.	2.4	59
30119	Density-functional study of the La2Zr2O7 low-index surfaces. Surface Science, 2019, 689, 121235.	0.8	2
30120	Electronic and mechanical responses of two-dimensional HfS2, HfSe2, ZrS2, and ZrSe2 from first-principles. Frontiers of Structural and Civil Engineering, 2019, 13, 486-494.	1.2	41
30121	Comparative study of polytype 2H-MoS2 and 3R-MoS2 systems by employing DFT. Physica E: Low-Dimensional Systems and Nanostructures, 2019, 106, 338-345.	1.3	30
30122	Ferromagnetism in (X, Y)-Codoped 4H-GaN Polytype X = Na and Mg, Y = Na and Mg: Ab Initio Study. Journal of Superconductivity and Novel Magnetism, 2019, 32, 335-340.	0.8	1
30123	Silicene band structure calculations using a semi-empirical pseudopotential method with spin and spin-orbital coupling included. Journal of Physics: Conference Series, 2019, 1199, 012019.	0.3	1
30124	First-Principles Determination of Oxygen and Silicon Î²-Factors for Zircon. Petrology, 2019, 27, 386-394.	0.2	2

#	Article	IF	Citations
30125	Insight into the Anchoring and Catalytic Effects of VO₂ and VS₂ Nanosheets as Sulfur Cathode Hosts for Liâ€“S Batteries. ChemSusChem, 2019, 12, 4671-4678.	3.6	50
30126	Currentâ€“voltage characteristics of Î²-ketoenamines molecular switches induced by intramolecular hydrogen transfer. Indian Journal of Physics, 2019, 93, 1527-1535.	0.9	7
30127	A first-principles molecular dynamics study on the surface lattice oxygen of ceria. Applied Surface Science, 2019, 496, 143712.	3.1	1
30128	Enantiospecific Adsorption and Decomposition of Cysteine Enantiomers on the Chiral Cu{421}^R Surface. Journal of Physical Chemistry C, 2019, 123, 20829-20837.	1.5	8
30129	Photochemistry of Plasmonic Titanium Nitride Nanocrystals. Journal of Physical Chemistry C, 2019, 123, 21796-21804.	1.5	33
30130	Orbital Pseudospin-Momentum Locking in Two-Dimensional Chiral Borophene. Nano Letters, 2019, 19, 6564-6568.	4.5	17
30131	Tuning the activity and selectivity of electroreduction of CO2 to synthesis gas using bimetallic catalysts. Nature Communications, 2019, 10, 3724.	5.8	156
30132	Directly transforming copper (I) oxide bulk into isolated single-atom copper sites catalyst through gas-transport approach. Nature Communications, 2019, 10, 3734.	5.8	276
30133	Ballistic transport simulation of acceptorâ€“donor C₃N/C₃B double-wall hetero-nanotube field effect transistors. Physical Chemistry Chemical Physics, 2019, 21, 19567-19574.	1.3	4
30134	Monitoring the electronic, thermal and optical properties of two-dimensional MoO₂ under strain via vibrational spectroscopies: a first-principles investigation. Physical Chemistry Chemical Physics, 2019, 21, 19904-19914.	1.3	24
30135	A charge optimized many-body potential for iron/iron-fluoride systems. Physical Chemistry Chemical Physics, 2019, 21, 20118-20131.	1.3	4
30136	Electronic, optical and thermoelectric properties of Fe₂ZrP compound determined via first-principles calculations. RSC Advances, 2019, 9, 25900-25911.	1.7	22
30137	Ab initio study of optoelectronic and magnetic properties of Mn-doped ZnS with and without vacancy defects. Journal of Physics Condensed Matter, 2019, 31, 485706.	0.7	6
30138	Coherent diffraction of hydrogen through the 246 pm lattice of graphene. New Journal of Physics, 2019, 21, 033004.	1.2	15
30139	Can photoemission tomography be useful for small, strongly-interacting adsorbate systems?. New Journal of Physics, 2019, 21, 043003.	1.2	9
30140	Putting the Squeeze on Lead Chromate Nanorods. Journal of Physical Chemistry Letters, 2019, 10, 4744-4751.	2.1	6
30141	Switching the Spin on a Ni Trimer within a Metalâ€“Organic Motif by Controlling the On-Top Bromine Atom. ACS Nano, 2019, 13, 9936-9943.	7.3	14
30142	Morphology evolution of Eu³⁺-activated NaTbF₄ nanorods: a highly-efficient near-ultraviolet light-triggered red-emitting platform towards application in white light-emitting diodes. Journal of Materials Chemistry C, 2019, 7, 10802-10809.	2.7	85

#	Article	IF	Citations
30143	Investigation of structural and mechanical properties of ferromagnetic Co2MnAs compound. AIP Conference Proceedings, 2019, , .	0.3	11
30144	Distorted structures in half-filled p-band materials. Journal of Physics Condensed Matter, 2019, 31, 465501.	0.7	7
30145	Structure-property correlation studies of alkaline-earth metalâ€"azides M(N₃)₂(Mâ€‰â€‰=â€‰â€‰Sr, Ba). Journal of Physics Condensed Matter, 2019, 31, 475402.	0.7	1
30146	Structural and topological phase transitions induced by strain in two-dimensional bismuth. Journal of Physics Condensed Matter, 2019, 31, 475001.	0.7	2
30147	DFT + U studies of the electronic and optical properties of ReS₂ mono-layer doped with lanthanide atoms. Materials Research Express, 2019, 6, 106307.	0.8	10
30148	Density functional perturbation theory for lattice dynamics with fully relativistic ultrasoft pseudopotentials: The magnetic case. Physical Review B, 2019, 100, .	1.1	9
30149	Symmetry-Protected Ideal Type-II Weyl Phonons in CdTe. Physical Review Letters, 2019, 123, 065501.	2.9	86
30150	Microscopic Nature of Magnetic Ground State in CeAuSb 2. Physica Status Solidi - Rapid Research Letters, 2019, 13, 1900304.	1.2	3
30151	First-Principles Study of Strain Engineered Electronic Properties of GeSe-SnS Hetero-bilayer. Journal of Electronic Materials, 2019, 48, 6735-6741.	1.0	9
30152	Magnetic moment of Mn in disordered Pd2MnGe Heusler alloy as studied by CPA and supercell modelling. Journal of Magnetism and Magnetic Materials, 2019, 491, 165638.	1.0	1
30153	A series of silver doped butterfly-like Ti₈Ag₂ clusters with two Ag ions panelled on a Ti₈ surface. Dalton Transactions, 2019, 48, 13423-13429.	1.6	26
30154	Flexible NO₂â€Functionalized Nâ€Heterocyclic Carbene Monolayers on Au (111) Surface. Chemistry - A European Journal, 2019, 25, 15067-15072.	1.7	39
30155	Unveiling the structures and electronic properties of CH3NH3PbI3 interfaces with TiO2, ZnO, and SnO2: a first-principles study. Journal of Materials Science, 2019, 54, 13594-13608.	1.7	5
30156	Efficient band structure engineering and visible-light response in SnS2/GaS heterostructure by electric field and biaxial strain. Superlattices and Microstructures, 2019, 134, 106210.	1.4	2
30157	The Electrochemical Mechanisms of Solidâ€"Electrolyte Interphase Formation in Lithium-Based Batteries. Journal of Physical Chemistry C, 2019, 123, 20084-20092.	1.5	19
30158	Linear Correlations between Adsorption Energies and HOMO Levels for the Adsorption of Small Molecules on TiO₂ Surfaces. Journal of Physical Chemistry C, 2019, 123, 20988-20997.	1.5	23
30159	Unidirectional Spinâ€"Orbit Interaction Induced by the Line Defect in Monolayer Transition Metal Dichalcogenides for High-Performance Devices. Nano Letters, 2019, 19, 6005-6012.	4.5	21
30160	Strengthening in multi-principal element alloys with local-chemical-order roughened dislocation pathways. Nature Communications, 2019, 10, 3563.	5.8	330

#	Article	IF	Citations
30161	Probing the active sites of newly predicted stable Janus scandium dichalcogenides for photocatalytic water-splitting. Catalysis Science and Technology, 2019, 9, 4981-4989.	2.1	28
30162	A Cuâ€“Pd single-atom alloy catalyst for highly efficient NO reduction. Chemical Science, 2019, 10, 8292-8298.	3.7	105
30163	Real-space exciton distribution in strained-siligraphene g-SiC7. Journal of Applied Physics, 2019, 126, .	1.1	8
30164	Hydroxylation of ZnO/Cu(1â€‰1â€‰1) inverse catalysts under ambient water vapor and the waterâ€“gas shift reaction. Journal Physics D: Applied Physics, 2019, 52, 454001.	1.3	8
30165	Detwinning Mechanism for Nanotwinned Cubic Boron Nitride with Unprecedented Strength: A First-Principles Study. Nanomaterials, 2019, 9, 1117.	1.9	5
30166	Temperature dependent GrÃ¼neisen parameter. Science China Technological Sciences, 2019, 62, 1565-1576.	2.0	15
30167	Vacuum-Level Shift at Al/LiF/Alq₃ Interfaces: A First-Principles Study. ACS Omega, 2019, 4, 13426-13434.	1.6	3
30168	Interaction of Oâ€“Y and Oâ€“Yâ€“Ti clusters embedded in bcc Fe with He, vacancies and self-interstitial atoms. Journal of Physics Condensed Matter, 2019, 31, 485702.	0.7	1
30169	Determining the Optimal Phase-Change Material via High-Throughput Calculations. MRS Advances, 2019, 4, 2679-2687.	0.5	4
30170	Atomic Substitution to Balance Hardness, Ductility, and Sustainability in Molybdenum Tungsten Borocarbide. Chemistry of Materials, 2019, 31, 7696-7703.	3.2	11
30171	Elucidating Structureâ€“Spectral Property Relationships of Negative Thermal Expansion Zr₂(WO₄)(PO₄)₂: A First-Principles Study with Experimental Validation. Journal of Physical Chemistry C, 2019, 123, 21607-21616.	1.5	2
30172	Fast Energy Storage in Two-Dimensional MoO₂ Enabled by Uniform Oriented Tunnels. ACS Nano, 2019, 13, 9091-9099.	7.3	59
30173	Computer-aided discovery of connected metal-organic frameworks. Nature Communications, 2019, 10, 3620.	5.8	71
30174	Liquid phase hydrogenation of CO₂ to formate using palladium and ruthenium nanoparticles supported on molybdenum carbide. New Journal of Chemistry, 2019, 43, 13985-13997.	1.4	18
30175	Effective cluster interactions and preâ€“precipitate morphology in binary Al-based alloys. Acta Materialia, 2019, 179, 70-84.	3.8	20
30176	Hydrogen storage in Na-decorated H4,4,4-graphyne: A density functional theory and Monte Carlo study. Applied Surface Science, 2019, 495, 143621.	3.1	20
30177	High temperatureâ€“high pressure phase transformation of Cu. Computational Materials Science, 2019, 170, 109154.	1.4	4
30178	Tuning the electronic and magnetic properties of zigzag silicene nanoribbons by 585 defects. Physics Letters, Section A: General, Atomic and Solid State Physics, 2019, 383, 125869.	0.9	6

#	Article	IF	Citations
30179	Prediction of C₇N₆ and C₉N₄: stable and strong porous carbon-nitride nanosheets with attractive electronic and optical properties. Journal of Materials Chemistry C, 2019, 7, 10908-10917.	2.7	57
30180	High-efficiency spin polarization in electron transport through the graphene nanoribbon coupled to chromium triiodide. Journal Physics D: Applied Physics, 2019, 52, 435304.	1.3	2
30181	Extraordinarily large kinetic isotope effect on alkene hydrogenation over Rh-based intermetallic compounds. Science and Technology of Advanced Materials, 2019, 20, 805-812.	2.8	6
30182	Theoretical studies on the hydrous lower mantle and Dâ€³ layer minerals. Earth and Planetary Science Letters, 2019, 525, 115753.	1.8	4
30183	Structural, elastic, electronic and vibrational properties of XAl2O4 (XÂ=ÂCa, Sr and Cd) semiconductors with orthorhombic structure. Journal of Alloys and Compounds, 2019, 809, 151773.	2.8	9
30184	Mechanism of Photocatalytic Reduction of CO₂ by Ag₃PO₄(111)/g-C₃N₄ Nanocomposite: A First-Principles Study. Journal of Physical Chemistry C, 2019, 123, 22191-22201.	1.5	38
30185	Dissociative Chemisorption of Methane on Stepped Ir(332) Surface: Density Functional Theory and Ab Initio Molecular Dynamics Studies. Journal of Physical Chemistry C, 2019, 123, 20893-20902.	1.5	12
30186	Oxidation Mechanism on One-Dimensional Pt-Induced Nanowires on Ge(001). Journal of Physical Chemistry C, 2019, 123, 21645-21650.	1.5	2
30187	Lattice Expansion in Hybrid Perovskites: Effect on Optoelectronic Properties and Charge Carrier Dynamics. Journal of Physical Chemistry Letters, 2019, 10, 5000-5007.	2.1	60
30188	Pb₇F₁₂Cl₂: a promising infrared nonlinear optical material with high laser damage threshold. Dalton Transactions, 2019, 48, 13529-13535.	1.6	13
30189	Investigation of structural, electronic, elastic, optical and dynamical properties of Ga_{1â^'x}Al_xN alloys. Materials Research Express, 2019, 6, 096318.	0.8	7
30190	Adsorption insights of amine vapors on black phosphorene nanotubesâ€”a first-principles study. Materials Research Express, 2019, 6, 105518.	0.8	10
30191	Electronic and Magnetic Properties of Fe2â^'xCoxTiSi (xâ€‰=â€‰0, 0.5, 1, 1.5, 2) Heusler Alloys. Journal of Electronic Materials, 2019, 48, 6753-6761.	1.0	4
30192	Ab-initio investigation of lithium adsorption on short carbon nanotubes considering effects of the tube length. Carbon, 2019, 155, 727-733.	5.4	12
30193	Influence of Anion Charge on Li Ion Diffusion in a New Solid-State Electrolyte, Li₃LaI₆. Chemistry of Materials, 2019, 31, 7425-7433.	3.2	71
30194	Spinodal Decomposition During Anion Exchange in Colloidal Mn²⁺-Doped CsPbX₃ (X = Cl, Br) Perovskite Nanocrystals. Chemistry of Materials, 2019, 31, 7711-7722.	3.2	36
30195	Material Consequences of Hydrogen Dissolution in Palladium Alloys Observed from First Principles. Journal of Physical Chemistry C, 2019, 123, 22158-22171.	1.5	8
30196	Encapsulating MnSe Nanoparticles Inside 3D Hierarchical Carbon Frameworks with Lithium Storage Boosted by in Situ Electrochemical Phase Transformation. ACS Applied Materials & Interfaces, 2019, 11, 33022-33032.	4.0	40

#	Article	IF	Citations
30197	Oxygen Evolution Reaction (OER) on Clean and Oxygen Deficient Low-Index SrTiO₃ Surfaces: A Theoretical Systematic Study. ACS Sustainable Chemistry and Engineering, 2019, 7, 15346-15353.	3.2	16
30198	Strain-tunable CO₂ storage by black phosphorene and Î±-PC from combined first principles and molecular dynamics studies. Physical Chemistry Chemical Physics, 2019, 21, 20107-20117.	1.3	11
30199	Investigation of half-metallic and magnetic phase transition in Co₂TiZ (Zâ€‰=â€‰Al, Ga, In) Heusler alloys. Phase Transitions, 2019, 92, 875-887.	0.6	9
30200	First principles study of interactions of oxygenâ€“carbonâ€“vacancy in bcc Fe*. Chinese Physics B, 2019, 28, 106102.	0.7	0
30201	Origin of lowered bandgap in Bi₂FeCrO₆ with alternate stacking of B-site cations by first-principles investigations. Materials Research Express, 2019, 6, 096112.	0.8	3
30202	Two-dimensional Weyl half-semimetal and tunable quantum anomalous Hall effect. Physical Review B, 2019, 100, .	1.1	101
30203	Interplay between in-plane and flexural phonons in electronic transport of two-dimensional semiconductors. Physical Review B, 2019, 100, .	1.1	11
30204	Ballistic thermoelectric properties of monolayer semiconducting transition metal dichalcogenides and oxides. Physical Review B, 2019, 100, .	1.1	60
30205	Exotic impurity-induced states in single-layer h -BN: The role of sublattice structure and intervalley interactions. Physical Review B, 2019, 100, .	1.1	6
30206	Cryogenic-temperature fracture toughness analysis of non-equi-atomic V10Cr10Fe45Co20Ni15 high-entropy alloy. Journal of Alloys and Compounds, 2019, 809, 151864.	2.8	57
30207	Organic-inorganic all-pseudocapacitive asymmetric energy storage devices. Nano Energy, 2019, 65, 104022.	8.2	52
30208	CO2 adsorption on hydroxylated In2O3(110). Physical Chemistry Chemical Physics, 2019, 21, 21698-21708.	1.3	23
30209	Catalytic manganese oxide nanostructures for the reverse water gas shift reaction. Nanoscale, 2019, 11, 16677-16688.	2.8	31
30210	Efficient ab initio plus analytic calculation of the effect of GaN layer tensile strain in AlGaN/GaN heterostructures. Japanese Journal of Applied Physics, 2019, 58, 094001.	0.8	6
30211	Site-Dependent Activity and Selectivity of H₂O₂ Formation from H₂ and O₂ over Au-Based Catalysts. Industrial & Engineering Chemistry Research, 2019, 58, 15119-15126.	1.8	15
30212	Uncovering the Surface and Phase Effect of Molybdenum Carbides on Hydrogen Evolution: A First-Principles Study. Journal of Physical Chemistry C, 2019, 123, 21878-21887.	1.5	23
30213	Surface-Plasmon-Induced Ammonia Decomposition on Copper: Excited-State Reaction Pathways Revealed by Embedded Correlated Wavefunction Theory. ACS Nano, 2019, 13, 9944-9957.	7.3	38
30214	DFT study of Au self-diffusion on Au(001) in the presence of a Cl adlayer. Journal of Chemical Physics, 2019, 151, 064709.	1.2	3

#	Article	IF	Citations
30215	Strong Electronic Interaction of Amorphous Fe₂O₃ Nanosheets with Singleâ€Atom Pt toward Enhanced Carbon Monoxide Oxidation. Advanced Functional Materials, 2019, 29, 1904278.	7.8	51
30216	Defect Induced Performance Enhancement of Monolayer MoS₂ for Li- and Na-Ion Batteries. Journal of Physical Chemistry C, 2019, 123, 21852-21865.	1.5	78
30217	Band Gap Engineering in Cs₂(Na_xAg_{1â€“x})BiCl₆ Double Perovskite Nanocrystals. Journal of Physical Chemistry Letters, 2019, 10, 5173-5181.	2.1	109
30218	Effects of Ni and Cu Antisite Substitution on the Phase Stability of CuGa2 from Liquid Ga/Cuâ€“Ni Interfacial Reaction. ACS Applied Materials & Interfaces, 2019, 11, 32523-32532.	4.0	10
30219	Anhydrous Phase B: Transmission Electron Microscope Characterization and Elastic Properties. Geochemistry, Geophysics, Geosystems, 2019, 20, 4059-4072.	1.0	1
30220	Functionalization of 2D materials for enhancing OER/ORR catalytic activity in Liâ€“oxygen batteries. Communications Chemistry, 2019, 2, .	2.0	61
30221	Lattice Dynamics and Electronic Properties of a BaGa2GeS6 Nonlinear Crystal: Raman Scattering, IR Reflection, and ab initio Calculations. Optics and Spectroscopy (English Translation of Optika I) Tj ETQq0 0 0 rgBT /Overlock 10 Tf 50 49	0.2	2
30222	Dental Resin Monomer Enables Unique NbO₂/Carbon Lithiumâ€Ion Battery Negative Electrode with Exceptional Performance. Advanced Functional Materials, 2019, 29, 1904961.	7.8	26
30223	Highly Enhanced Pseudocapacitive Performance of Vanadiumâ€Doped MXenes in Neutral Electrolytes. Small, 2019, 15, e1902649.	5.2	46
30224	p-Type Conductivity of Hydrated Amorphous V₂O₅ and Its Enhanced Photocatalytic Performance in ZnO/V₂O₅/rGO. ACS Applied Electronic Materials, 2019, 1, 1881-1889.	2.0	13
30225	Phenethylammonium bismuth halides: from single crystals to bulky-organic cation promoted thin-film deposition for potential optoelectronic applications. Journal of Materials Chemistry A, 2019, 7, 20733-20741.	5.2	38
30226	A three dimensional numerical quantum mechanical model of field electron emission from metallic surfaces covered with carbon adsorbates. Journal of Applied Physics, 2019, 126, .	1.1	7
30227	Electronic Structure of CO2 and CS2 Crystals. Journal of Structural Chemistry, 2019, 60, 1019-1026.	0.3	2
30228	Superoctahedral two-dimensional metallic boron with peculiar magnetic properties. Physical Chemistry Chemical Physics, 2019, 21, 19764-19771.	1.3	36
30229	Thermoradiative Cells Based on a p-type Cu3SbSe4 Semiconductor: Application of a Detailed Balance Model. Journal of Electronic Materials, 2019, 48, 6777-6785.	1.0	4
30230	First Principles Calculations of the Energetic, Structural, Electronic, and Magnetic Properties of Fe/Ir(100) System. Journal of Electronic Materials, 2019, 48, 6932-6939.	1.0	2
30231	Structural, elastic, thermal and lattice dynamic properties of new 321 MAX phases. Computational Materials Science, 2019, 170, 109144.	1.4	34
30232	Molecular Boolean logic gates based on spin caloritronic transport properties of planar four-coordinate Fe complex-based molecular devices. Chemical Physics Letters, 2019, 733, 136671.	1.2	4

#	Article	IF	Citations
30233	The tunable ferroelectricity and piezoelectricity of the KNN piezoceramics by Na concentrations: First-principles calculations. Journal of the European Ceramic Society, 2019, 39, 5252-5259.	2.8	12
30234	First-principles calculation on the adhesion strength, fracture mechanism, interfacial bonding of the NiTi (111)//Î±-Al2O3 (0001) interfaces. Materials and Design, 2019, 183, 108119.	3.3	48
30235	DFT + U and Low-Temperature XPS Studies of Fe-Depleted Chalcopyrite (CuFeS₂) Surfaces: A Focus on Polysulfide Species. Journal of Physical Chemistry C, 2019, 123, 21031-21041.	1.5	29
30236	Engineering Surface Structure of Spinel Oxides via High-Valent Vanadium Doping for Remarkably Enhanced Electrocatalytic Oxygen Evolution Reaction. ACS Applied Materials & Interfaces, 2019, 11, 33012-33021.	4.0	70
30237	High temperature shockwave stabilized single atoms. Nature Nanotechnology, 2019, 14, 851-857.	15.6	278
30238	DFT and microkinetic investigation of methanol synthesis via CO₂ hydrogenation on Ni(111)-based surfaces. Physical Chemistry Chemical Physics, 2019, 21, 20276-20286.	1.3	26
30239	Ab initio-informed phase-field modeling of dislocation core structures in equal-molar CoNiRu multi-principal element alloys. Modelling and Simulation in Materials Science and Engineering, 2019, 27, 084001.	0.8	23
30240	Platinum vs transition metal carbide surfaces as catalysts for olefin and alkyne conversion: binding and hydrogenation of ethylidyne. Journal of Physics: Conference Series, 2019, 1247, 012003.	0.3	5
30241	Wake potential in graphene-insulator-graphene composite systems. Physical Review B, 2019, 100, .	1.1	3
30242	Single pair of Weyl fermions in the half-metallic semimetal <mml:math xmlns:mml="http://www.w3.org/1998/Math/MathML"><mml:mrow><mml:mi>EuC</mml:mi><mml:msub><mml:mi mathvariant="normal">d</mml:mi><mml:mn>2</mml:mn></mml:msub><mml:mi mathvariant="normal">A</mml:mi><mml:msub><mml:mi mathvariant="normal">s</mml:mi><mml:mn>2</mml:mn></mml:msub></mml:mrow></mml:math>. Physical Review B, 2019, 99.	1.1	83
30243	Tuning the electronic and magnetic properties of Mn-doped graphene by gas adsorption and effect of external electric field: First-principles study. International Journal of Modern Physics B, 2019, 33, 1950166.	1.0	5
30244	Physical Properties of Group 14 in P6₂22 Phase: First-Principles Calculations*. Communications in Theoretical Physics, 2019, 71, 1036.	1.1	11
30245	Electronic properties of size-dependent MoTe 2 /WTe 2 heterostructure. Chinese Physics B, 2019, 28, 107101.	0.7	10
30246	From Electronic Structure to Design Principles for Photocathodes: <mml:math xmlns:mml="http://www.w3.org/1998/Math/MathML" display="inline" overflow="scroll"><mml:mi>Cu</mml:mi></mml:math> - <mml:math xmlns:mml="http://www.w3.org/1998/Math/MathML" display="inline" overflow="scroll"><mml:mi>Ba</mml:mi></mml:math> Alloys. Physical Review Applied, 2019, 11, .	1.5	2
30247	First-principles calculations of the atomic structure and electronic states of <mml:math xmlns:mml="http://www.w3.org/1998/Math/MathML"><mml:mrow><mml:msub><mml:mi>Li</mml:mi><mml:mi>x</mml:mi></mml:msub><mml:msub><mml:mi>Ni</mml:mi><mml:mn>3</mml:mn></mml:ms Physical Review B, 2019, 100, .		
30248	Sound velocity, shear modulus, and shock melting of beryllium along the Hugoniot. Physical Review B, 2019, 100, .	1.1	17
30249	Effect of Uniaxial Strain on Properties of Blue Phosphorene-CNT Heterojunction. , 2019, , .		0
30250	Thermodynamic Analysis for the Magnetic-Field-Induced Precipitation Behaviours in Steels. Metals, 2019, 9, 909.	1.0	8

#	Article	IF	Citations
30251	Structural and Optoelectronic Properties of the Î±-, Î²-, and Î³-Glycine Polymorphs and the Glycine Dihydrate Crystal: A DFT Study. Crystal Growth and Design, 2019, 19, 5204-5217.	1.4	13
30252	Interfacial Electronic Properties Dictate Li Dendrite Growth in Solid Electrolytes. Chemistry of Materials, 2019, 31, 7351-7359.	3.2	165
30253	Toward obtaining 2D and 3D and 1D PtPN with pentagonal pattern. Journal of Materials Science, 2019, 54, 14029-14037.	1.7	4
30254	Decoding Collagen Triple Helix Stability by Means of Hybrid DFT Simulations. Journal of Physical Chemistry B, 2019, 123, 7354-7364.	1.2	14
30255	Syngas Conversion to C₂ Oxygenates over the Cu/Î²-Mo₂C Catalyst: Probing into the Effect of the Interface between Cu and Î²-Mo₂C on Catalytic Performance. Journal of Physical Chemistry C, 2019, 123, 21022-21030.	1.5	8
30256	Electrocatalytic Production of H₂O₂ by Selective Oxygen Reduction Using Earth-Abundant Cobalt Pyrite (CoS₂). ACS Catalysis, 2019, 9, 8433-8442.	5.5	167
30257	Coverage dependent structure and energy of water dissociative adsorption on clean and O-pre-covered Ni (100) and Ni(110). Catalysis Science and Technology, 2019, 9, 4725-4743.	2.1	8
30258	Gold adatoms modulate sulfur adsorption on gold. Nanoscale, 2019, 11, 19341-19351.	2.8	7
30259	Density functional theory study of NOx adsorption on alkaline earth metal oxide and transition metal surfaces. Korean Journal of Chemical Engineering, 2019, 36, 1258-1266.	1.2	7
30260	Theoretical insights into nitrogen fixation on Ti₂C and Ti₂CO₂ in a lithiumâ€“nitrogen battery. Journal of Materials Chemistry A, 2019, 7, 19950-19960.	5.2	21
30261	Ab initio insights into Na-ion diffusion and intercalation mechanism in alluaudite Na Mn2(MoO4)3 as cathode material for sodium-ion batteries. Journal of Alloys and Compounds, 2019, 808, 151667.	2.8	12
30262	Theoretical prediction of thermal and electronic properties of metal-organic frameworks. Journal of Industrial and Engineering Chemistry, 2019, 80, 136-151.	2.9	10
30263	Ultrafine Defective RuO₂ Electrocatayst Integrated on Carbon Cloth for Robust Water Oxidation in Acidic Media. Advanced Energy Materials, 2019, 9, 1901313.	10.2	182
30264	Defect driven d0 ferromagnetism and colossal dielectric behavior in Bi(Zn0.5Ti0.5)O3â€“PbTiO3 ceramics. Ceramics International, 2019, 45, 22948-22955.	2.3	4
30265	A switchable-selectivity multiple-interface Ni-WC hybrid catalyst for efficient nitroarene reduction. Journal of Catalysis, 2019, 377, 174-182.	3.1	24
30266	Origin and evolution of ferroelectricity in the layered rare-earth-titanate,<mml:math xmlns:mml="http://www.w3.org/1998/Math/MathML" altimg="si210.svg"><mml:mrow><mml:msub><mml:mrow><mml:mi>R</mml:mi></mml:mrow><mml:mrow><mml:mn>2</mml:mn> Carpy-Galy phases. Polyhedron, 2019, 171, 181-192.	1.0	11
30267	Buckling strain effects on electronic and optical aspects of penta-graphene nanostructure. Superlattices and Microstructures, 2019, 133, 106217.	1.4	14
30268	Role of Inorganic Surface Layer on Solid Electrolyte Interphase Evolution at Li-Metal Anodes. ACS Applied Materials & Interfaces, 2019, 11, 31467-31476.	4.0	75

#	Article	IF	Citations
30269	Density Functional Study on the Formation of Sulfur-doped Configuration on the Active Site of Pyrolyzed Fe/N/C Catalyst. Journal of Physics: Conference Series, 2019, 1204, 012119.	0.3	5
30270	Antimonene on Pb quantum wells. 2D Materials, 2019, 6, 045028.	2.0	18
30271	Vibration signatures of the structural phase transition of Sn/Ge(111) compared to Sn/Si(111). Physical Review B, 2019, 100, .	1.1	3
30272	First-principles study of the structural and electronic properties of bulk ZnS and small <mml:math xmlns:mml="http://www.w3.org/1998/Math/MathML"><mml:mrow><mml:msub><mml:mi>Zn</mml:mi><mml:mi>n</mml:mi></mml:m mathvariant="normal">S</mml:mi><mml:mi>n</mml:mi></mml:msub></mml:mrow></mml:math> nanoclusters in the framework of the <mml:math xmlns:mml="http://www.w3.org/1998/Math/MathML"><mml:mrow><mml:mi>DFT</mml:mi><mml:mo>+</mml:mo><mml:mi>U</mml:mi></mml:m method. Physical Review B, 2019, 100, .	1.1	16
30273	First-principles study of the structural, electronic, magnetic, elastic and optical properties of CoFeZrSi1â^'xGex(x = 0.00, 0.25, 0.50, 0.75, 1.00). International Journal of Modern Physics B, 2019, 33, 1950158.	1.0	4
30274	Influence of spinâ€“orbit interaction on band structure of TlInSe₂. International Journal of Modern Physics B, 2019, 33, 1950161.	1.0	6
30275	Intermetallic M Pt₃ (M = Ti, Zr, Hf): Elastic, electronic, optical and thermal properties. International Journal of Modern Physics B, 2019, 33, 1950189.	1.0	10
30276	Electron structure and density of statesâ€™ calculations of Ag₂S and Ag₂Se crystals from first-principle. Modern Physics Letters B, 2019, 33, 1950242.	1.0	30
30277	Elastic properties of graphyne-based nanotubes. Computational Materials Science, 2019, 170, 109153.	1.4	25
30278	Thermoelectric transport behaviours of n-type Mg2 (Si,Sn,Ge) quaternary solid solutions. Journal of Magnesium and Alloys, 2019, 7, 514-521.	5.5	9
30279	LiB6Si: An indirect band gap semiconductor. Physics Letters, Section A: General, Atomic and Solid State Physics, 2019, 383, 125862.	0.9	3
30280	First-Principles Investigations on Sodium Superionic Conductor Na₁₁Sn₂PS₁₂. Chemistry of Materials, 2019, 31, 6066-6075.	3.2	23
30281	Impact of local composition on the energetics of E-centres in Si1â^'xGex alloys. Scientific Reports, 2019, 9, 10849.	1.6	4
30282	Suppression of platinum sintering on Ptâ€“M/ZSM-22 (M = Ce, La, and Re) catalyst for n-dodecane isomerization. New Journal of Chemistry, 2019, 43, 13967-13978.	1.4	16
30283	Janus single-layer group-III monochalcogenides: a promising visible-light photocatalyst. Journal Physics D: Applied Physics, 2019, 52, 455303.	1.3	26
30284	Exfoliation and characterization of a two-dimensional serpentine-based material. Nanotechnology, 2019, 30, 445705.	1.3	14
30285	Computer Modeling of Extended PnX3n + 2 Chains (X = F, Cl). Russian Journal of Inorganic Chemistry, 2019, 64, 780-785.	0.3	0
30286	Approaches on the understanding of nanoporous carbon reactivity with polyatomic ions. Applied Surface Science, 2019, 495, 143392.	3.1	3

#	Article	IF	Citations
30287	Giant spin splitting induced by a symmetry-braking van der Waals interaction. Applied Surface Science, 2019, 494, 619-626.	3.1	13
30288	Electronic and optical properties of graphane, silicane, MoS2 homo-bilayers and hetero-bilayers. Current Applied Physics, 2019, 19, 1222-1232.	1.1	10
30289	Electronic structures and magnetic properties of La(Zn,TM)AsO from first principles calculations (TMâ€¯=â€¯V, Cr, Mn, Fe, Co and Ni). Chemical Physics Letters, 2019, 732, 136654.	1.2	0
30290	Exploring the electronic, charge transport and lattice dynamic properties of two-dimensional phosphorene. Physica B: Condensed Matter, 2019, 572, 88-93.	1.3	9
30291	The electronic and microwave dielectric properties of Sr1-xCaxWO4 alloys by first principles calculations. Physica B: Condensed Matter, 2019, 572, 266-272.	1.3	5
30292	Mechanical and electronic properties of armchair graphene nanoribbons with symmetrically double-lines-doped BN under uniaxial tensile strain: Ab initio study. Solid State Communications, 2019, 300, 113644.	0.9	1
30293	Electronic structure and magnetic properties of few-layer Cr ₂ Ge ₂ Te ₆ : the key role of nonlocal electronâ€“electron interaction effects. 2D Materials, 2019, 6, 045042.	2.0	36
30294	Mechanism for unconventional nonlinear elasticity. Physical Review B, 2019, 100, .	1.1	4
30295	Ground states of Au2Pb and pressure-enhanced superconductivity. Physical Review B, 2019, 100, .	1.1	9
30296	Influence of crystal structure on charge carrier effective masses in <mml:math xmlns:mml="http://www.w3.org/1998/Math/MathML"><mml:msub><mml:mi>BiFeO</mml:mi><mml:mn>3</mml:mn></mml:msub><m Physical Review B, 2019, 100, .	1.1	11
30297	Layer-dependent intrinsic anomalous Hall effect in <mml:math xmlns:mml="http://www.w3.org/1998/Math/MathML"><mml:mrow><mml:msub><mml:mi>Fe</mml:mi><mml:mn>3</mml:mn></mml:msub><mml:m Physical Review B, 2019, 100, .	1.1	19
30298	Adsorption mechanism of NH3, NO, and O2 molecules over MnxOy/Ni (111) surface: a density functional theory study. Journal of Materials Science, 2019, 54, 14414-14430.	1.7	23
30299	The role of isotropic and anisotropic Hubbard corrections for the magnetic ordering and absolute band alignment of hematite Î±-Fe2O3(0001) surfaces. Progress in Natural Science: Materials International, 2019, 29, 349-355.	1.8	5
30300	Evidence of Topological Edge States in Buckled Antimonene Monolayers. Nano Letters, 2019, 19, 6323-6329.	4.5	61
30301	Design of metal contacts for monolayer Fe3GeTe2 based devices. Applied Physics Letters, 2019, 115, .	1.5	19
30302	Electronic and elastic properties of the multiferroic crystals with the Kagome type lattices -Mn₃V₂O₈ and Ni₃V₂O₈: First principle calculations. Ferroelectrics, 2019, 544, 11-19.	0.3	2
30303	From qualitative to quantitative description of the anomalous thermoelastic behavior of V, Nb, Ta, Pd and Pt. Journal of Physics Condensed Matter, 2019, 31, 225402.	0.7	8
30304	Structural phase transitions in malononitrile, CH2(CN)2: crystal structure of the Î´ phase by neutron powder diffraction, and ab initio calculations of the structures and phonons of the Î± and Î´ phases. Journal of Physics Condensed Matter, 2019, 31, 255401.	0.7	0

#	Article	IF	Citations
30305	Stability of pyridine-like and pyridinium-like nitrogen in graphene. Journal of Physics Condensed Matter, 2019, 31, 265403.	0.7	0
30306	Electronic and optical properties of SnX₂(X = S, Se)â€”InSe van der Waalâ€™s heterostructures from first-principle calculations. Physica Scripta, 2019, 94, 125806.	1.2	10
30307	First-Principles Calculations of the Structural, Magnetic, and Electronic Properties of $$hbox {Fe}_{2}hbox {MgB}$$ Full-Heusler Alloy. Journal of Electronic Materials, 2019, 48, 7258-7262.	1.0	4
30308	Formation and migration of helium pair in bcc Fe from first principle calculations. Computational Materials Science, 2019, 170, 109192.	1.4	3
30309	N, P dual-doped carbon nanotube with superior high-rate sodium storage performance for sodium ion batteries. Journal of Electroanalytical Chemistry, 2019, 850, 113392.	1.9	26
30310	Thermoelectric properties, optimal doping levels and high figure of merit in Cobalt-based Half/Full Heusler alloys by First-Principles calculations. Materials Science and Engineering B: Solid-State Materials for Advanced Technology, 2019, 248, 114409.	1.7	3
30311	First-principles studies on electronic structures of superatomic compounds [Co6Se8(PMe3)6][C60] in several cubic structures. Results in Physics, 2019, 15, 102595.	2.0	0
30312	Spin-Layer and Spin-Valley Locking in CVD-Grown AAâ€²- and AB-Stacked Tungsten-Disulfide Bilayers. Journal of Physical Chemistry C, 2019, 123, 21813-21821.	1.5	27
30313	Data-Driven Systematic Search of Promising Photocatalysts for Water Splitting under Visible Light. Journal of Physical Chemistry Letters, 2019, 10, 5211-5218.	2.1	31
30314	Anomalous Temperature-Dependent Charge Recombination in CH₃NH₃PbI₃ Perovskite: Key Roles of Charge Localization and Thermal Effect. ACS Applied Materials & Interfaces, 2019, 11, 32069-32075.	4.0	22
30315	Spinâ€“lattice and electronâ€“phonon coupling in 3d/5d hybrid Sr3NiIrO6. Npj Quantum Materials, 2019, 4, .	1.8	6
30316	Cohesive properties of the crystalline phases of twenty proteinogenic Î±-aminoacids from first-principles calculations. Physical Chemistry Chemical Physics, 2019, 21, 18501-18515.	1.3	18
30317	Transport properties of electron small polarons in a V₂O₅ cathode of Li-ion batteries: a computational study. RSC Advances, 2019, 9, 19483-19494.	1.7	31
30318	Descriptor for the Efficacy of Aliovalent Doping of Oxides and Its Application for the Charging of Supported Au Clusters. Journal of Physical Chemistry C, 2019, 123, 19794-19805.	1.5	4
30319	Efficient Base-Metal NiMn/TiO₂ Catalyst for CO₂ Methanation. ACS Catalysis, 2019, 9, 7823-7839.	5.5	124
30320	Structures and energetics of low-index stoichiometric BiPO₄surfaces. CrystEngComm, 2019, 21, 4730-4739.	1.3	9
30321	Implicit solvent effects in the determination of BrÃ¸nstedâ€“Evansâ€“Polanyi relationships for heterogeneously catalyzed reactions. Physical Chemistry Chemical Physics, 2019, 21, 17687-17695.	1.3	4
30322	The effect of compositional engineering of imidazolium lead iodide on the resistive switching properties. Nanoscale, 2019, 11, 14455-14464.	2.8	16

#	Article	IF	Citations
30323	Phonons and anisotropic thermal expansion behavior of NiX (Xâ€‰=â€‰S, Se, Te). Journal of Applied Physics, 2019, 125, .	1.1	2
30324	Predictions of the structures and properties of the substituted layered ternary compound series (Zr1â”x T x)3Al3C5 (Tâ€‰â€‰=â€‰â€‰Hf, Nb, and V) through first-principles studies. Journal of Physics Condensed Matter, 2019, 31, 385702.	0.7	2
30325	Temperature-induced phase transitions in the rock-salt type SiC: a first-principles study. Journal of Physics Condensed Matter, 2019, 31, 405401.	0.7	4
30326	Practical Considerations for Continuum Models Applied to Surface Electrochemistry. ChemPhysChem, 2019, 20, 3074-3080.	1.0	40
30327	DFT study of SF6 decomposed products on Pdâ€“TiO2: gas sensing mechanism study. Adsorption, 2019, 25, 1643-1653.	1.4	19
30328	First-principles study on stability, electronic, and mechanical properties of Laâ€“C and Ceâ€“C binary compounds. Journal of Iron and Steel Research International, 2019, 26, 771-778.	1.4	5
30329	Phase diagrams and mechanical properties of TiC-SiC solid solutions from first-principles. Calphad: Computer Coupling of Phase Diagrams and Thermochemistry, 2019, 66, 101643.	0.7	4
30330	The adsorption and dissolution properties of iron surfaces in liquid lithium and lead under a fusion environment. Journal of Nuclear Materials, 2019, 524, 200-208.	1.3	8
30331	Strain tuned electronic and magnetic anisotropy in SrTiO3 (110) surface. Physics Letters, Section A: General, Atomic and Solid State Physics, 2019, 383, 2685-2691.	0.9	1
30332	Unravelling the Effects of Pressure-Induced Suppressed Electronâ€“Hole Recombination in CsPbBr₃ Perovskite: Time-Domain ab Initio Analysis. Journal of Physical Chemistry Letters, 2019, 10, 4354-4361.	2.1	19
30333	Synthesis and structure of a new mixed metal iodate Ba₃Ga₂(IO₃)₁₂. CrystEngComm, 2019, 21, 4981-4986.	1.3	14
30334	Electron affinity of boron-terminated diamond (001) surfaces: a density functional theory study. Journal of Materials Chemistry C, 2019, 7, 9756-9765.	2.7	24
30335	Density functional study of Na doped Tin selenide. AIP Conference Proceedings, 2019, , .	0.3	1
30336	Cu Doped Crystalline Carbon-Conjugated g-C₃N₄, a Promising Oxygen Reduction Catalyst by Theoretical Study. Journal of the Electrochemical Society, 2019, 166, F755-F759.	1.3	14
30337	First Principles Study of the Vibrational and Thermal Properties of Sn-Based Type II Clathrates, CsxSn136 (0 â‰‰ x â‰‰ 24) and Rb24Ga24Sn112. Inorganics, 2019, 7, 74.	1.2	1
30338	Ultrahigh Thermoelectric Performance Realized in Black Phosphorus System by Favorable Band Engineering through Group VA Doping. Advanced Functional Materials, 2019, 29, 1904346.	7.8	41
30339	Improving the Calculations of Electronic and Magnetic Properties of Sr2CrMoO6 Double-Perovskite with LDA+U and mBJ Potential. Journal of Electronic Materials, 2019, 48, 6406-6413.	1.0	8
30340	Effect of organic spacers on electronic, optical and transport properties of two-dimensional layered lead-halide perovskites. Computational Materials Science, 2019, 169, 109130.	1.4	3

#	Article	IF	Citations
30341	A comparative study of Na3LiTi5O12 and Li4Ti5O12: Geometric and electronic structures obtained by density functional theory calculations. Chemical Physics Letters, 2019, 731, 136598.	1.2	9
30342	Finite temperature thermophysical properties of MgCu intermetallic compound from quasi-harmonic Debye model. Journal of Magnesium and Alloys, 2019, 7, 335-344.	5.5	14
30343	Nitrogen mustard gas molecules and Î±-arsenene nanosheet interaction studies â€“ A DFT insight. Journal of Molecular Graphics and Modelling, 2019, 92, 65-73.	1.3	23
30344	Band gap and magnetism engineering in Dirac half-metallic Na2C nanosheet via layer thickness, strain and point defects. Journal of Magnetism and Magnetic Materials, 2019, 491, 165565.	1.0	27
30345	The effect of Cr on He segregation and diffusion at Î£3(1â€¯1â€¯2) grain boundary in Î±-Fe. Nuclear Instruments & Methods in Physics Research B, 2019, 456, 7-11.	0.6	5
30346	Band gap tunability and structural stability of metal/nonmetal codoped group-IV tin nanotubes: Effect of spin-orbit coupling. Physica E: Low-Dimensional Systems and Nanostructures, 2019, 114, 113644.	1.3	13
30347	Biomimetic Superoxide Disproportionation Catalyst for Anti-Aging Lithiumâ€“Oxygen Batteries. ACS Nano, 2019, 13, 9190-9197.	7.3	29
30348	Superior Photo-thermionic electron Emission from Illuminated Phosphorene Surface. Scientific Reports, 2019, 9, 10307.	1.6	9
30349	The hot carrier dynamics of graphitic carbon nitride/molybdenum disulfide heterojunctions. Journal Physics D: Applied Physics, 2019, 52, 385107.	1.3	2
30350	Electronic and optical properties of TiO₂ by first-principle calculation (DFT-GW and BSE). Materials Research Express, 2019, 6, 095021.	0.8	10
30351	NiSe₂ as Coâ€Catalyst with CdS: Nanocomposites for Highâ€Performance Photodriven Hydrogen Evolution under Visibleâ€Light Irradiation. ChemPlusChem, 2019, 84, 999-1010.	1.3	12
30352	Correlation of electron density and bond length to band gap for binary oxides and halides. International Journal of Quantum Chemistry, 2019, 119, e26022.	1.0	1
30353	Universal building block for (1 1 0)-family silicon and germanium surfaces. Applied Surface Science, 2019, 494, 46-50.	3.1	11
30354	Experimental and theoretical insights into the cyclotrimerization of acetylene during vinyl acetate synthesis. Chemical Engineering Journal, 2019, 378, 122183.	6.6	9
30355	Synergistic effects of reduced graphene oxide with freeze drying tuned interfacial structure on performance of transparent and flexible supercapacitors. Journal of Colloid and Interface Science, 2019, 554, 650-657.	5.0	5
30356	A computational study of structural, electronic and carrier mobility of boron and phosphorus/nitrogen co-doped graphene. Physica B: Condensed Matter, 2019, 571, 291-295.	1.3	19
30357	Density functional theory model for carbon dot surfaces and their interaction with silver nanoparticles. Physica E: Low-Dimensional Systems and Nanostructures, 2019, 114, 113640.	1.3	18
30358	Outstanding Energy Exchange between Organic Molecules and Metal Surfaces: Decomposition Kinetics of Excited Vinyl Derivatives Driven by the Interaction with a Cu(111) Surface. Journal of Physical Chemistry C, 2019, 123, 19625-19636.	1.5	6

#	Article	IF	Citations
30359	Design of a Pdâ€“Au Nitrite Reduction Catalyst by Identifying and Optimizing Active Ensembles. ACS Catalysis, 2019, 9, 7957-7966.	5.5	160
30360	Methane Chemisorption on Oxideâ€Supported Pt Single Atom. ChemPhysChem, 2019, 20, 2217-2220.	1.0	19
30361	Direct synthesis of Hâ¯-encaged 12CaOÂ·7Al2O3 crystals by high-pressure processes. Ceramics International, 2019, 45, 16028-16031.	2.3	3
30362	Influence of Li ion implantation on LO phonon broadening and bandgap opening in ZnO thin films. Journal of Alloys and Compounds, 2019, 806, 1138-1145.	2.8	7
30363	Elastic, electronic, chemical bonding and thermodynamic properties of the ternary nitride Ca4TiN4: Ab initio predictions. Journal of Molecular Graphics and Modelling, 2019, 92, 74-85.	1.3	5
30364	Polymorphic Transformation of Drugs Induced by Glycopolymeric Vesicles Designed for Anticancer Therapy Probed by Solid-State NMR Spectroscopy. ACS Applied Materials & Interfaces, 2019, 11, 28278-28288.	4.0	17
30365	A₂Bi₂(SO₄)₂Cl₄(A = NH₄, K,) Tj ETQq0 0 0 rgBT /Overloc birefringence in sulfate nonlinear optical materials. Journal of Materials Chemistry C, 2019, 7, 9900-9907.	2.7	63
30366	Dry reforming activity due to ionic Ru in La_{1.99}Ru_{0.01}O₃: the role of specific carbonates. Physical Chemistry Chemical Physics, 2019, 21, 16726-16736.	1.3	8
30367	A study on magnetic, electronic, elastic and vibrational properties of Ir₂MnAl Heusler alloy for spintronic applications. Materials Research Express, 2019, 6, 096571.	0.8	6
30368	Temperature and Impurity Induced Stabilization of Cubic HfV2 Laves Phase. Condensed Matter, 2019, 4, 63.	0.8	3
30369	Quantitative and qualitative correlations by atomistic determination for the precipitated phases in Alâ€“Liâ€“Cu system. Intermetallics, 2019, 112, 106551.	1.8	7
30370	Mitigating Voltage Decay of Li-Rich Layered Oxide by Incorporation of 5d Metal Rhenium. Journal of Physical Chemistry C, 2019, 123, 18870-18876.	1.5	23
30371	A p-type thermoelectric material BaCu4S3 with high electronic band degeneracy. Journal of Applied Physics, 2019, 126, .	1.1	7
30372	First principles study of single and multi-site transition metal dopant ions in MoS2 monolayer. Computational Condensed Matter, 2019, 21, e00419.	0.9	30
30373	Structure and Composition Modification of Ultrasmall Palladium Nanoparticles upon Hydrogenation from First Principles. Journal of Physical Chemistry C, 2019, 123, 18609-18619.	1.5	2
30374	Strong Interplay between Sodium and Oxygen in Kesterite Absorbers: Complex Formation, Incorporation, and Tailoring Depth Distributions. Advanced Energy Materials, 2019, 9, 1900740.	10.2	20
30375	Theoretical investigation of elastic constants and related properties of compressed PbO2. Journal of Computational Electronics, 2019, 18, 1111-1118.	1.3	4
30376	Electronic structure and magnetic properties of 3d transition-metal atom adsorbed SnO monolayers. Applied Surface Science, 2019, 493, 404-410.	3.1	17

#	Article	IF	Citations
30377	Designing for high corrosion-resistant high nitrogen martensitic stainless steel based on DFT calculation and pressurized metallurgy method. Corrosion Science, 2019, 158, 108081.	3.0	61
30378	Toughening and maintaining strength of diamond with substitutional doping boron and nitrogen. Journal of Alloys and Compounds, 2019, 805, 1090-1095.	2.8	5
30379	CO₂ Conversion Performance of Perovskite Oxides Designed with Abundant Metals. Industrial & Engineering Chemistry Research, 2019, 58, 12551-12560.	1.8	16
30380	High temperature-mediated rocksalt to wurtzite phase transformation in cadmium oxide nanosheets and its theoretical evidence. Nanoscale, 2019, 11, 14802-14819.	2.8	15
30381	Two-dimensional ferroelastic topological insulator with tunable topological edge states in single-layer ZrAsX (X = Br and Cl). Journal of Materials Chemistry C, 2019, 7, 9743-9747.	2.7	15
30382	Single Pt atoms stabilized on Mo2TiC2O2 for hydrogen evolution: A first-principles investigation. Journal of Chemical Physics, 2019, 151, 024702.	1.2	22
30383	Electronic structural, lattice dynamics and superconducting properties of tife intermetallic compound: A first-principles study. AIP Conference Proceedings, 2019, , .	0.3	1
30384	The structural parameters of Lnn+1NinO2n+2 (Ln=La, Ce, Pr, Pm; n=3): An ab-initio approach. AIP Conference Proceedings, 2019, , .	0.3	0
30385	Oxygen and potassium vacancies in KTP calculated from first principles. Journal of Physics Condensed Matter, 2019, 31, 385401.	0.7	8
30386	First-principles calculations of the structural, elastic, vibrational and electronic properties of YB6 compound under pressure. European Physical Journal B, 2019, 92, 1.	0.6	10
30387	Spontaneous Non-stoichiometry and Ordering in Degenerate but Gapped Transparent Conductors. Matter, 2019, 1, 280-294.	5.0	27
30388	Adsorption and diffusion of Pt, Cu, Ag and Au on missing row reconstructed Pt(110) surfaces: An ab initio investigation. Surface Science, 2019, 690, 121463.	0.8	3
30389	P-Doped Ironâ€“Nickel Sulfide Nanosheet Arrays for Highly Efficient Overall Water Splitting. ACS Applied Materials & Interfaces, 2019, 11, 27667-27676.	4.0	155
30390	Building egg-tray-shaped graphenes that have superior mechanical strength and band gap. Npj Computational Materials, 2019, 5, .	3.5	19
30391	Ba₃Ca₄(BO₃)₃(SiO₄)Cl: a new non-centrosymmetric complex alkaline-earth metal borosilicate chloride with a deep-ultraviolet cut-off edge. Inorganic Chemistry Frontiers, 2019, 6, 2200-2208.	3.0	16
30392	Electronic Structure of a Semiconducting Imineâ€Covalent Organic Framework. Chemistry - an Asian Journal, 2019, 14, 4645-4650.	1.7	8
30393	Strain Engineering and Electric Field Tunable Electronic Properties of Janus MoSSe/WX₂ (Xâ€‰=â€‰S, Se) van der Waals Heterostructures. Physica Status Solidi (B): Basic Research, 2019, 256, 1900261.	0.7	16
30394	First-principles investigation of N-triphenylene-graphdiyne nanosheets as an anode material for Na, K, Mg and Ca storage. Computational Materials Science, 2019, 169, 109093.	1.4	19

#	Article	IF	Citations
30395	Giant anisotropy of thermal expansion and thermomechanical properties of monolayer Î±-antimonene: A first-principles study. Computational Materials Science, 2019, 169, 109132.	1.4	1
30396	MÃ¶ssbauerite as Iron-Only Layered Oxyhydroxide Catalyst for WO₃ Photoanodes. Inorganic Chemistry, 2019, 58, 9655-9662.	1.9	9
30397	Computational Investigation of Aqueous Phase Effects on the Dehydrogenation and Dehydroxylation of Polyols over Pt(111). Journal of Physical Chemistry C, 2019, 123, 19052-19065.	1.5	21
30398	Statics and dynamics of multivalley charge density waves in Sb(111). Npj Quantum Materials, 2019, 4, .	1.8	14
30399	Structure, stability and electronic properties of bimetallic atomic chains of Auâ€“Ag and Auâ€“Pt. Pramana - Journal of Physics, 2019, 93, 1.	0.9	2
30400	Assessments of molar volumes of Co-, Ni- and Ti- related bcc and fcc phases. Calphad: Computer Coupling of Phase Diagrams and Thermochemistry, 2019, 66, 101629.	0.7	7
30401	Potential and distance dependent charge transfer: Hybrid first-principles/continuum calculations. Computational Materials Science, 2019, 169, 109121.	1.4	1
30402	Oxidation simulation study of silicon carbide nanowires: A carbon-rich interface state. Applied Surface Science, 2019, 493, 882-888.	3.1	24
30403	Structural stability of scandium monochalcogeides ScS and ScSe under pressure and superconductivity: A first principles study. Computational Condensed Matter, 2019, 21, e00418.	0.9	6
30404	Understanding the magneto-structural coupling of Ni50Mn35.4In14.6 alloy from first-principles calculations. Journal of Magnetism and Magnetic Materials, 2019, 488, 165339.	1.0	9
30405	Interfacial engineering of oxygenated chemical bathâ€“deposited CdS window layer for highly efficient Sb2Se3 thin-film solar cells. Materials Today Physics, 2019, 10, 100125.	2.9	22
30406	Hydrodeoxygenation of phenol over Ni-based bimetallic single-atom surface alloys: mechanism, kinetics and descriptor. Catalysis Science and Technology, 2019, 9, 4314-4326.	2.1	65
30407	A first-principles study of interfacial fluorination at the HfO2/Al2O3 interface in charge trapping memory devices. Journal of Applied Physics, 2019, 125, 215303.	1.1	0
30408	Negative capacitance tunneling field effect transistors based on monolayer arsenene, antimonene, and bismuthene. Semiconductor Science and Technology, 2019, 34, 085006.	1.0	20
30409	Mechanical, thermal, electronic and optical properties of Cu₃NbS₄: an ab-initio study. Materials Research Express, 2019, 6, 096528.	0.8	2
30410	Lattice Dynamic and Instability in Pentasilicene: A Light Single-Element Ferroelectric Material With High Curie Temperature. Physical Review Applied, 2019, 11, .	1.5	24
30411	Theoretical and experimental refraction index of shock compressed and pre-compressed water in the megabar pressure range. Europhysics Letters, 2019, 126, 56001.	0.7	5
30412	Electronic structure, elastic and thermal transport properties of thorium monocarbide based on first-principles study. Journal of Nuclear Materials, 2019, 524, 141-148.	1.3	8

#	Article	IF	Citations
30413	Transition Metal-Functionalized Janus MoSSe Monolayer: A Magnetic and Efficient Single-Atom Photocatalyst for Water-Splitting Applications. Journal of Physical Chemistry C, 2019, 123, 18347-18354.	1.5	46
30414	Graphitic carbon nitride decorated with FeNi₃ nanoparticles for flexible planar micro-supercapacitor with ultrahigh energy density and quantum storage capacity. Dalton Transactions, 2019, 48, 12137-12146.	1.6	29
30415	Piezoelectric enhancement of a defect-mediated boron nitride nanotube. Journal Physics D: Applied Physics, 2019, 52, 335304.	1.3	3
30416	Effect of extended alkyl auxiliary groups on optical and electronic properties of Benzo[2,1-b:3,4-bâ€²:5,6-câ€³]trithiophene derivatives at bulk level: a first-principles study. Materials Research Express, 2019, 6, 095102.	0.8	2
30417	Unraveling anomalous isotope effect on hydrogen diffusivities in fcc metals from first principles including nuclear quantum effects. Physical Review B, 2019, 100, .	1.1	17
30418	Ferromagnetic nodal-line metal in monolayer <mml:math xmlns:mml="http://www.w3.org/1998/Math/MathML"><mml:mi>h</mml:mi></mml:math> -InC. Physical Review B, 2019, 100, .	1.1	14
30419	Firstâ€Principles Study on the Electronic, Magnetic, and Optical Properties in TM Atom Doped Cadmium Sulfide Nanosheets. Physica Status Solidi (B): Basic Research, 2019, 256, 1900182.	0.7	4
30420	A simple descriptor for binding and charge transfer at blue phosphorene-metal interfaces. Applied Surface Science, 2019, 492, 16-22.	3.1	5
30421	Aluminum intercalation and transport in TiO2(B) from first principles. Journal of Energy Storage, 2019, 24, 100800.	3.9	4
30422	Ab initio based modeling of interfacial segregation at Cu-rich precipitates in Feâ€“Cuâ€“Ni alloys. Nuclear Instruments & Methods in Physics Research B, 2019, 456, 32-36.	0.6	1
30423	Optoelectronic pressure dependent study of MgZrO3 oxide and ground state thermoelectric response using Ab-initio calculations. Opto-electronics Review, 2019, 27, 194-201.	2.4	16
30424	Theoretical Investigation of Propylene Epoxidation on Ag(111) by Molecular Oxygen: Na(K,Cl) Effects. Journal of Physical Chemistry C, 2019, 123, 17273-17282.	1.5	22
30425	Understanding the White-Emitting CaMoO₄ Co-Doped Eu³⁺, Tb³⁺, and Tm³⁺ Phosphor through Experiment and Computation. Journal of Physical Chemistry C, 2019, 123, 18536-18550.	1.5	45
30426	Structural and electronic properties of the incommensurate host-guest Bi-III phase. Physical Review B, 2019, 100, .	1.1	5
30427	Doping and Anisotropyâ€“Dependent Electronic Transport in Chalcogenide Perovskite CaZrSe₃ for High Thermoelectric Efficiency. Advanced Theory and Simulations, 2019, 2, 1900060.	1.3	14
30428	Adsorption of molecules on C3N nanosheet: A first-principles calculations. Chemical Physics, 2019, 526, 110442.	0.9	49
30429	New insights into the determination of maximum chemical potentials to account for alkali doping in <mml:math xmlns:mml="http://www.w3.org/1998/Math/MathML" altimg="si12.svg"><mml:mrow><mml:mi>I²</mml:mi><mml:mtext>-</mml:mtext><mml:msub><mml:mrow><mml:mi mathvariant="normal">In</mml:mi></mml:mrow><mml:mrow><mml:mn>2</mml:mn></mml:mrow></mml:msub><mml:msub><mml:m mathvariant="normal">S</mml:mi></mml:mrow><mml:mrow><mml:mn>3</mml:mn></mml:mrow></mml:msub></mml:mrow></mml:m by ab initio calculati. Computational Materials Science, 2019, 168, 221-228.	1.4	7
30430	Nitrided FeNi: Chemical versus magnetovolume effects from ab initio. Journal of Magnetism and Magnetic Materials, 2019, 491, 165555.	1.0	1

#	Article	IF	Citations
30431	Strain tunable structural, mechanical and electronic properties of monolayer tin dioxides and dichalcogenides SnX2 (X O, S, Se, Te). Materials Research Bulletin, 2019, 119, 110533.	2.7	20
30432	One-Pot Formation of Sbâ€“Carbon Microspheres with Graphene Sheets: Potassium-Ion Storage Properties and Discharge Mechanisms. ACS Applied Materials & Interfaces, 2019, 11, 27973-27981.	4.0	46
30433	First-principles study of Ni adatom migration on graphene with vacancies. RSC Advances, 2019, 9, 18823-18834.	1.7	7
30434	Nonlocal effects on the structural transition of gold clusters from planar to three-dimensional geometries. RSC Advances, 2019, 9, 20989-20999.	1.7	6
30435	Tailoring Storage Capacity and Ion Kinetics in Ti2CO2/ Graphene Heterostructures by Functionalization of Graphene. Physical Review Applied, 2019, 12, .	1.5	17
30436	Thermodynamic stability of hexagonal and rhombohedral boron nitride under chemical vapor deposition conditions from van der Waals corrected first principles calculations. Journal of Vacuum Science and Technology A: Vacuum, Surfaces and Films, 2019, 37, .	0.9	7
30437	Control of electric, optical, thermal properties of C60 films by electron-beam irradiation. Carbon, 2019, 152, 882-887.	5.4	15
30438	Puckered arsenene single-walled nanotubes: Stability, geometry, and electronic properties. Computational Materials Science, 2019, 169, 109108.	1.4	5
30439	Ab initio atomistic insights into lead-free formamidinium based hybrid perovskites for photovoltaics and optoelectronics. Computational Materials Science, 2019, 169, 109118.	1.4	50
30440	High rate and long cycle life in Li-O2 batteries with highly efficient catalytic cathode configured with Co3O4 nanoflower. Nano Energy, 2019, 64, 103896.	8.2	71
30441	Vibrational properties of uranium fluorides. Physica B: Condensed Matter, 2019, 570, 194-205.	1.3	5
30442	Manipulating electronic and magnetic properties of black phosphorene with 4d series transition metal adsorption. Physics Letters, Section A: General, Atomic and Solid State Physics, 2019, 383, 2765-2771.	0.9	13
30443	First-principles study of hydrogen-vacancy complexes in Be12Ti. Journal of Nuclear Materials, 2019, 525, 7-13.	1.3	8
30444	Density functional theory studies of the SrC and SrN compounds. Materials Chemistry and Physics, 2019, 237, 121875.	2.0	7
30445	Inactivation of HeLa cells on nanoporous gold. Materialia, 2019, 7, 100370.	1.3	3
30446	Scaling Relation of Oxygen Reduction Reaction Intermediates at Defective TiO₂ Surfaces. Journal of Physical Chemistry C, 2019, 123, 19486-19492.	1.5	20
30447	Understanding the Decomposition Mechanisms of LiNH₂, Mg(NH₂)₂, and NaNH₂: A Joint Experimental and Theoretical Study. Journal of Physical Chemistry C, 2019, 123, 18180-18186.	1.5	9
30448	Gallium Thiophosphate: An Emerging Bidirectional Auxetic Two-Dimensional Crystal with Wide Direct Band Gap. Journal of Physical Chemistry Letters, 2019, 10, 4455-4462.	2.1	35

#	Article	IF	Citations
30449	Structural stability and band alignment in the c-plane ZnO/GaN heterostructure. Semiconductor Science and Technology, 2019, 34, 095008.	1.0	1
30450	Electronic structure study of <mml:math xmlns:mml="http://www.w3.org/1998/Math/MathML"><mml:msub><mml:mi>LaCoIn</mml:mi><mml:mn>5</mml:mn></mml:msub> and its comparison with <mml:math xmlns:mml="http://www.w3.org/1998/Math/MathML"><mml:msub><mml:mi>CeCoIn</mml:mi><mml:mn>5</mml:mn></mml:msub> Physical Review B, 2019, 100, .	1.1	7
30451	Promoting Highly Reversible Sodium Storage of Iron Sulfide Hollow Polyhedrons via Cobalt Incorporation and Graphene Wrapping. Advanced Energy Materials, 2019, 9, 1901584.	10.2	71
30452	Hydrogen Oxidation in Alkaline Media: the Bifunctional Mechanism for Water Formation. Electrocatalysis, 2019, 10, 584-590.	1.5	7
30453	Efficient and Selective CO2 Reduction Integrated with Organic Synthesis by Solar Energy. CheM, 2019, 5, 2605-2616.	5.8	179
30454	Mechanical, electronic, optical, and thermodynamic properties of orthorhonmbic LiCuBiO4 crystal: a firstâ€“priciples study. Journal of Materials Research and Technology, 2019, 8, 3783-3794.	2.6	41
30455	Syntheses, crystal structures, and characterizations of three new pyrophosphates CsNaZnP2O7, RbNaZnP2O7, and RbLiMgP2O7. Solid State Sciences, 2019, 95, 105940.	1.5	4
30456	C₂ Oxygenates Formation from Syngas over the Cu-Rich and Rh-Rich Surfaces of Rh-Cu Bimetallic Catalysts: Probing into the Effects of the Surface Structure and Composition on the Catalytic Performance. Journal of Physical Chemistry C, 2019, 123, 19528-19539.	1.5	3
30457	Unraveling the Water Degradation Mechanism of CH₃NH₃PbI₃. Journal of Physical Chemistry C, 2019, 123, 19385-19394.	1.5	63
30458	Continuously Tuning Electronic Properties of Few-Layer Molybdenum Ditelluride with in Situ Aluminum Modification toward Ultrahigh Gain Complementary Inverters. ACS Nano, 2019, 13, 9464-9472.	7.3	36
30459	A semiconducting layered metal-organic framework magnet. Nature Communications, 2019, 10, 3260.	5.8	119
30460	Binding and activation of ethylene on tungsten carbide and platinum surfaces. Physical Chemistry Chemical Physics, 2019, 21, 17332-17342.	1.3	9
30461	Anion-mediated electronic effects in reducible oxides: Tuning the valence band of ceria via fluorine doping. Journal of Chemical Physics, 2019, 151, 044701.	1.2	4
30462	Anharmonic lattice relaxation during nonradiative carrier capture. Physical Review B, 2019, 100, .	1.1	34
30463	Strain Effect Of Band Gap In Snte Monolayer. , 2019, , .		0
30464	Edge effects on Li atom adsorption and migration of MoS2 zigzag nanoribbons. Applied Surface Science, 2019, 494, 223-229.	3.1	7
30465	Lithium and calcium decorated triphenylene-graphdiyne as potential high-capacity hydrogen storage medium: A first-principles prediction. Applied Surface Science, 2019, 494, 763-770.	3.1	35
30466	Al2O3/FeAl interfacial behaviors by yttrium doping in high temperature oxidation. Ceramics International, 2019, 45, 22273-22280.	2.3	12

#	Article	IF	Citations
30467	First-principles theoretical and experimental studies of effects of ruthenium on precipitation behavior of Î¼ phase and Î¼/matrix interface stability in Ni-based single crystal superalloys. Intermetallics, 2019, 113, 106556.	1.8	19
30468	Temperature dependence of thermodynamic stability and mechanical property of alloying Co3Ta compounds. Journal of Alloys and Compounds, 2019, 808, 151068.	2.8	3
30469	Thermodynamic description of the sintering aid system in silicon carbide ceramics with the addition of yttrium. Journal of the European Ceramic Society, 2019, 39, 4510-4519.	2.8	15
30470	Tuning the properties of hydrogenated graphene via interfacial contact of cubic BN (111). Physica B: Condensed Matter, 2019, 571, 257-262.	1.3	2
30471	Improving Electrochemical Pb²⁺ Detection Using a Vertically Aligned 2D MoS₂ Nanofilm. Analytical Chemistry, 2019, 91, 11770-11777.	3.2	73
30472	Inquisitive Geometric Sites in h-BN Monolayer for Alkali Earth Metal Ion Batteries. Journal of Physical Chemistry C, 2019, 123, 19340-19346.	1.5	18
30473	Computational Evaluation of Electrocatalytic Nitrogen Reduction on TM Single-, Double-, and Triple-Atom Catalysts (TM = Mn, Fe, Co, Ni) Based on Graphdiyne Monolayers. Journal of Physical Chemistry C, 2019, 123, 19066-19076.	1.5	224
30474	Enhancement of CO₂ Methanation over La-Modified Ni/SBA-15 Catalysts Prepared by Different Doping Methods. ACS Sustainable Chemistry and Engineering, 2019, 7, 14647-14660.	3.2	69
30475	Ab initio study of a 2D h-BAs monolayer: a promising anode material for alkali-metal ion batteries. Physical Chemistry Chemical Physics, 2019, 21, 18328-18337.	1.3	70
30476	Theoretical study on the intrinsic properties of In2Se3/MoS2 as a photocatalyst driven by near-infrared, visible and ultraviolet light. Catalysis Science and Technology, 2019, 9, 4659-4667.	2.1	31
30477	Validity of perturbative methods to treat the spinâ€“orbit interaction: application to magnetocrystalline anisotropy. New Journal of Physics, 2019, 21, 073054.	1.2	29
30478	Electronic and magnetic properties of CrI₃ nanoribbons and nanotubes*. Chinese Physics B, 2019, 28, 077301.	0.7	8
30479	Axial field induced spin response in Fe/hBN-based tunnel junctions. Physical Review B, 2019, 100, .	1.1	5
30480	Electronic Bands and Dielectric Functions of In0.5Tl0.5I Solid State Solution with Structural Defects. Journal of Electronic Materials, 2019, 48, 5586-5594.	1.0	12
30481	Acid-Free and Selective Extraction of Lithium from Spent Lithium Iron Phosphate Batteries via a Mechanochemically Induced Isomorphic Substitution. Environmental Science & Technology, 2019, 53, 9781-9788.	4.6	112
30482	Theoretical Insights into Li-Ion Transport in LiTa₂PO₈. Journal of Physical Chemistry C, 2019, 123, 19282-19287.	1.5	24
30483	Electrical Property Dominated Promising Half-Heusler Thermoelectrics through High-Throughput Material Computations. Journal of Physical Chemistry C, 2019, 123, 18824-18833.	1.5	32
30484	Methanol oxidation on the Pt(321) surface: a theoretical approach on the role of surface morphology and surface coverage effects. Physical Chemistry Chemical Physics, 2019, 21, 18227-18239.	1.3	14

#	Article	IF	Citations
30485	An electronic structure governed by the displacement of the indium site in Inâ€“S₆ octahedra: LnOInS₂ (Ln = La, Ce, and Pr). Dalton Transactions, 2019, 48, 12272-12278.	1.6	8
30486	First-principle study of zigzag GaN nanoribbons with Cl functionalization. AIP Conference Proceedings, 2019, , .	0.3	0
30487	First-principle Study on Sr-doped LiNi0.5Mn1.5O4. International Journal of Electrochemical Science, 2019, 14, 6315-6324.	0.5	7
30488	Anomalous elastic behavior of phase egg, AlSiO3(OH), at high pressures. American Mineralogist, 2019, 104, 130-139.	0.9	7
30489	Thermodynamic Properties of a GaAs Quantum Dot with an Effective-Parabolic Potential: Theory and Simulation. Journal of Low Temperature Physics, 2019, 197, 95-110.	0.6	30
30490	Adsorption of O3, SO3 and CH2O on two dimensional SnS monolayer: A first principles study. Physica B: Condensed Matter, 2019, 572, 12-17.	1.3	23
30491	AHgSnQ₄ (A = Sr, Ba; Q = S, Se): A Series of Hg-Based Infrared Nonlinear-Optical Materials with Strong Second-Harmonic-Generation Response and Good Phase Matchability. Inorganic Chemistry, 2019, 58, 10390-10398.	1.9	49
30492	Interface Engineering of Band Evolution and Transport Properties of Bilayer WSe2 under Different Electric Fields. Journal of Physical Chemistry C, 2019, 123, 19812-19819.	1.5	4
30493	TiCaPCON-Supported Pt- and Fe-Based Nanoparticles and Related Antibacterial Activity. ACS Applied Materials & Interfaces, 2019, 11, 28699-28719.	4.0	16
30494	RE(H2C3N3O3)2Â·(OH)Â·xH2O (RE = La, Y and Gd): potential UV birefringent materials with strong optical anisotropy originating from the (H2C3N3O3)â^' group. Dalton Transactions, 2019, 48, 12296-12302.	1.6	24
30495	The first principle study of the effect of Co dopant and C/Cu vacancy defect on the interfacial bonding of graphene-copper composites. Materials Research Express, 2019, 6, 095621.	0.8	2
30496	First principle study of the structural, electronic, optical and thermodynamic properties of the cubic Al1â^'xBxAs ternary alloys. Materials Research Express, 2019, 6, 105902.	0.8	4
30497	Pressure-Induced Hydrogen-Hydrogen Interaction in Metallic FeH Revealed by NMR. Physical Review X, 2019, 9, .	2.8	16
30498	Optimal transport and colossal ionic mechano-conductance in graphene crown ethers. Science Advances, 2019, 5, eaaw5478.	4.7	37
30499	Hybrid-Functional and Quasi-Particle Calculations of Band Structures of Mg2Si, Mg2Ge, and Mg2Sn. Journal of the Korean Physical Society, 2019, 75, 144-152.	0.3	20
30500	Firstâ€principles study of the atomic structures, electronic properties, and surface stability of BaTiO3(001) and (011) surfaces. Surface and Interface Analysis, 2019, 51, 1021-1032.	0.8	16
30501	Reaction paths for hydrodeoxygenation of furfuryl alcohol at TiO2/Pd interfaces. Journal of Catalysis, 2019, 377, 28-40.	3.1	17
30502	A first-principles study of Cu and Al doping in ZrO2 for RRAM device applications. Vacuum, 2019, 168, 108842.	1.6	24

#	Article	IF	Citations
30503	First-principles study of the mechanical and thermodynamic properties of Al4W, Al5W and Al12W under pressure. Vacuum, 2019, 169, 108844.	1.6	20
30504	Defect-enriched tunability of electronic and charge-carrier transport characteristics of 2D borocarbonitride (BCN) monolayers from ab initio calculations. Nanoscale, 2019, 11, 19398-19407.	2.8	18
30505	Off-the-shelf DFT-DISPersion methods: Are they now â€œon-trendâ€•for organic molecular crystals?. Journal of Chemical Physics, 2019, 151, 044106.	1.2	11
30506	Intrinsic point defects and the n - and p -type dopability of the narrow gap semiconductors GaSb and InSb. Physical Review B, 2019, 100, .	1.1	16
30507	First Principles Study of the Stability and Diffusion Mechanism of a Carbon Vacancy in the Vicinity of a SiO₂/4Hâ€“SiC Interface. Physica Status Solidi (A) Applications and Materials Science, 2019, 216, 1900328.	0.8	2
30508	First-principles study on the mechanical properties of interstitial solid solution Aluminumâ€“Boron alloy. Computational Materials Science, 2019, 170, 109159.	1.4	3
30509	Exploring mechanical, electronic, vibrational, and thermoelectric properties of CaGa2P2, CaGa2As2, and SrGa2As2. Solid State Sciences, 2019, 96, 105942.	1.5	5
30510	Assessment of thermodynamic data for CuCrO2 delafossite from calorimetric measurements. Thermochimica Acta, 2019, 680, 178345.	1.2	4
30511	Origins of Negative Differential Resistance in N-doped ZnO Nano-ribbons: Ab-initio Investigation. Scientific Reports, 2019, 9, 9914.	1.6	15
30512	Pinpointing the active sites and reaction mechanism of CO oxidation on NiO. Physical Chemistry Chemical Physics, 2019, 21, 17852-17858.	1.3	4
30513	Effect of substitutional impurities on vibrational properties of zircon: a first-principles study. Journal of Physics Condensed Matter, 2019, 31, 455402.	0.7	5
30514	New Findings on Multilayer Silicene on Si(111)âˆš3Ã—âˆš3R30Â°â€“Ag Template. Materials, 2019, 12, 2258.	1.3	14
30515	Electronic Structure and Lithium Diffusion in LiAl2(OH)6Cl Studied by First Principle Calculations. Molecules, 2019, 24, 2667.	1.7	10
30516	Water dissociative adsorption on the precovered Fe (100) surface from DFT computation. Indian Journal of Physics, 2019, 93, 1019-1029.	0.9	3
30517	Insight into the mechanism of CO2 and CO methanation over Cu(100) and Co-modified Cu(100) surfaces: A DFT study. Applied Surface Science, 2019, 495, 143457.	3.1	30
30518	Acrylonitrile vapor adsorption studies on armchair arsenene nanoribbon based on DFT study. Applied Surface Science, 2019, 494, 1148-1155.	3.1	23
30519	Structural and electronic properties of BN co-doped and BN analogue of twin graphene sheets: A density functional theory study. Journal of Physics and Chemistry of Solids, 2019, 135, 109115.	1.9	28
30520	Pronounced Negative Thermal Expansion in Lead-Free BiCoO₃-Based Ferroelectrics Triggered by the Stabilized Perovskite Structure. Chemistry of Materials, 2019, 31, 6187-6192.	3.2	14

#	Article	IF	Citations
30521	Phase Transition Pathway Sampling via Swarm Intelligence and Graph Theory. Journal of Physical Chemistry Letters, 2019, 10, 5019-5026.	2.1	10
30522	Oxidation and Corrosion of Platinumâ€“Nickel and Platinumâ€“Cobalt Nanoparticles in an Aqueous Acidic Medium. ACS Applied Energy Materials, 2019, 2, 7019-7035.	2.5	8
30523	Reexamination of the Schottky Barrier Heights in Monolayer MoS₂ Field-Effect Transistors. ACS Applied Nano Materials, 2019, 2, 4717-4726.	2.4	27
30524	Hollow Porous Ag Spherical Catalysts for Highly Efficient and Selective Electrocatalytic Reduction of CO₂ to CO. ACS Sustainable Chemistry and Engineering, 2019, 7, 14443-14450.	3.2	40
30525	Photocatalytic Facet Selectivity in BiVO4 Nanoparticles: Polaron Electronic Structure and Thermodynamic Stability Considerations for Photocatalysis. Journal of Physical Chemistry C, 2019, 123, 20142-20151.	1.5	18
30526	Nickel Metal Nanoparticles as Anode Electrocatalysts for Highly Efficient Direct Borohydride Fuel Cells. ACS Catalysis, 2019, 9, 8520-8528.	5.5	46
30527	Effect of External Electric Field on Methane Conversion on IrO₂(110) Surface: A Density Functional Theory Study. ACS Catalysis, 2019, 9, 8230-8242.	5.5	34
30528	Active Oxygen Species Promoted Catalytic Oxidation of 5-Hydroxymethyl-2-furfural on Facet-Specific Pt Nanocrystals. ACS Catalysis, 2019, 9, 8306-8315.	5.5	53
30529	Hydrogen physisorption on palygorskite dehydrated channels: A van der Waals density functional study. International Journal of Hydrogen Energy, 2019, 44, 21936-21947.	3.8	6
30530	Density functional study of structural, electronic and magnetic properties of new half-metallic ferromagnetic double perovskite Sr2MnVO6. Journal of Physics Condensed Matter, 2019, 31, 475501.	0.7	4
30531	Electronic and Optical Properties of Two-Dimensional Tellurene: From First-Principles Calculations. Nanomaterials, 2019, 9, 1075.	1.9	40
30532	Firstâ€Principles Prediction of the Structural, Electronic, and Magnetic Properties of Nonmetal Atoms Doped Singleâ€Layer CrS 2. Physica Status Solidi (B): Basic Research, 2019, 256, 1900149.	0.7	5
30533	DFT calculations in periodic boundary conditions of gas-phase acidities and of transition-metal anionic clusters: case study with carboxylate-stabilized ruthenium clusters. Theoretical Chemistry Accounts, 2019, 138, 1.	0.5	4
30534	Structural, elastic and dynamical properties of $$hbox { YP}_{1-x}hbox {As}_{x}$$ alloys from first principles calculations. Pramana - Journal of Physics, 2019, 93, 1.	0.9	3
30535	Azobenzene-based lustrous golden thin films fabricated by electrophoretic deposition. Colloids and Surfaces A: Physicochemical and Engineering Aspects, 2019, 579, 123705.	2.3	5
30536	Size-dependent bond dissociation enthalpies in single-walled carbon nanotubes. Chemical Physics Letters, 2019, 731, 136628.	1.2	2
30537	Transition-metal-element dependence of ideal shear strength and elastic behaviors of Î³â€²-Ni3Al: ab initio study to guide rational alloy design. Journal of Alloys and Compounds, 2019, 806, 1260-1266.	2.8	17
30538	The crystal shape algorithm as a tool for the characterization of agglomerated morphologies: Cubic and hexagonal crystal habits of LiMn2O4. Materials Research Bulletin, 2019, 119, 110535.	2.7	0

#	Article	IF	Citations
30539	Exploring the Mgâ€“Crâ€“H System at High Pressure and Temperature via in Situ Synchrotron Diffraction. Inorganic Chemistry, 2019, 58, 11043-11050.	1.9	6
30540	Synthesis, structure and characterization of M(IO₃)₂(HIO₃) (M =) Tj ETQq1 1 0.784314 rgBT /O Transactions, 2019, 48, 13074-13080.	1.6	7
30541	Unoccupied electronic band structure of pentagonal Si nanoribbons on Ag(110). Physical Chemistry Chemical Physics, 2019, 21, 17811-17820.	1.3	9
30542	Intrinsically low thermal conductivity of bismuth oxychalcogenides originating from interlayer coupling. Physical Chemistry Chemical Physics, 2019, 21, 18259-18264.	1.3	12
30543	Atomistic design favored compositions and atomic-level structure of Mgâ€“Caâ€“Ag ternary metallic glasses. AIP Advances, 2019, 9, .	0.6	3
30544	A comprehensive assessment of the low-temperature thermal properties and thermodynamic functions of CeO2. Journal of Chemical Physics, 2019, 151, 044202.	1.2	5
30545	Characterization of the energetics and configurations of hydrogen in vacancy clusters in tungsten. Nuclear Fusion, 2019, 59, 106032.	1.6	16
30546	The structural, electronic and optical properties of novel GaP/ZnS/AlP multilayer heterostructure: first-principles study. Materials Research Express, 2019, 6, 095912.	0.8	5
30547	Atomistic simulation of fracture in UO2 under tensile loading. Journal of Alloys and Compounds, 2019, 803, 42-50.	2.8	3
30548	Study of ferromagnetism, spin-polarization, thermoelectrics and thermodynamics of layered perovskite Ba2FeMnO6 under pressure and temperature. Journal of Physics and Chemistry of Solids, 2019, 135, 109079.	1.9	37
30549	Growth of Layered Copperâ€“Alkanethiolate Frameworks from Thin Anodic Copper Oxide Films. Journal of Physical Chemistry C, 2019, 123, 17283-17295.	1.5	6
30550	Electrochemical Synthesis of Cation Vacancy-Enriched Ultrathin Bimetallic Oxyhydroxide Nanoplatelets for Enhanced Water Oxidation. ACS Applied Materials & Interfaces, 2019, 11, 25958-25966.	4.0	25
30551	Impact of Transition Metal Carbide and Nitride Supports on the Electronic Structure of Thin Platinum Overlayers. ACS Catalysis, 2019, 9, 7090-7098.	5.5	30
30552	Tellurium Doping and the Structural, Electronic, and Optical Properties of NaYS_{2(1â€“x)}Te_{2x}Alloys. ACS Omega, 2019, 4, 11320-11331.	1.6	15
30553	Hydrogen bond dynamics and conformational flexibility in antipsychotics. Physical Chemistry Chemical Physics, 2019, 21, 15463-15470.	1.3	4
30554	Monte-Carlo simulation combined with density functional theory to investigate the equilibrium thermodynamics of electrode materials: lithium titanates as model compounds. Physical Chemistry Chemical Physics, 2019, 21, 15551-15559.	1.3	10
30555	Giant effective charges and piezoelectricity in gapped graphene. 2D Materials, 2019, 6, 045015.	2.0	23
30556	Magnon-polaron excitations in the noncollinear antiferromagnet Mn3Ge. Physical Review B, 2019, 99, .	1.1	18

#	Article	IF	Citations
30557	Structure and stability of (Cr, Fe)7C3 ternary carbides in solid and liquid state. Journal of Alloys and Compounds, 2019, 804, 566-572.	2.8	8
30558	Pressure-Controlled Migration of Paramagnetic Centers in a Heterospin Crystal. Inorganic Chemistry, 2019, 58, 9187-9194.	1.9	19
30559	Growth and theoretical study on the deep-ultraviolet transparent Î²-CsBa₂(PO₃)₅ nonlinear optical crystal. CrystEngComm, 2019, 21, 4690-4695.	1.3	8
30560	Single molybdenum center supported on N-doped black phosphorus as an efficient electrocatalyst for nitrogen fixation. Nanoscale, 2019, 11, 13600-13611.	2.8	102
30561	A two-dimensional MoS₂/C₃N broken-gap heterostructure, a first principles study. RSC Advances, 2019, 9, 19837-19843.	1.7	32
30562	Superflexible C₆₈-graphyne as a promising anode material for lithium-ion batteries. Journal of Materials Chemistry A, 2019, 7, 17357-17365.	5.2	19
30563	First-principles study of electronic, optical and thermal transport properties of group IIIâ€“VI monolayer MX (Mâ€‰=â€‰Ga, In; Xâ€‰=â€‰S, Se). Journal of Applied Physics, 2019, 125, .	1.1	61
30564	Structure and electron affinity of silicon and germanium terminated (0â€‰0â€‰1)-(2 Ã— 1) diamond surface. Journal of Physics Condensed Matter, 2019, 31, 395001.	0.7	3
30565	Basal dislocation/precipitate interactions in Mgâ€“Al alloys: an atomistic investigation. Modelling and Simulation in Materials Science and Engineering, 2019, 27, 075003.	0.8	22
30566	Antiferromagnetic Kitaev interaction in <mml:math xmlns:mml="http://www.w3.org/1998/Math/MathML"><mml:mi>f</mml:mi></mml:math> -electron based honeycomb magnets. Physical Review B, 2019, 99, .	1.1	50
30567	Creation of two-dimensional layered Zintl phase by dimensional manipulation of crystal structure. Science Advances, 2019, 5, eaax0390.	4.7	19
30568	Electronic Structure and Theoretical Aspects on Sensing Application of 2D Materials. , 2019, , 145-203.		7
30569	Dynamically Stable Topological Phase of Arsenene. Scientific Reports, 2019, 9, 7966.	1.6	21
30570	Effect of structure and composition on the electronic excitation induced amorphization of La2Ti2â^'xZrxO7 ceramics. Scientific Reports, 2019, 9, 8190.	1.6	11
30571	Transport and topological properties of ThOCh(Ch: S, Se and Te) in bulk and monolayer: a first principles study. Journal of Physics Condensed Matter, 2019, 31, 435504.	0.7	0
30572	Exchange-correlation thermal effects in shocked deuterium: Softening the principal Hugoniot and thermophysical properties. Physical Review B, 2019, 99, .	1.1	22
30573	High-Efficiency Visible Light Responsive Sulfide KSb5S8 Photocatalyst with a Layered Crystal Structure. Catalysts, 2019, 9, 529.	1.6	4
30574	Research on the Effect of Carbon Defects on the Hydrophilicity of Coal Pyrite Surface from the Insight of Quantum Chemistry. Molecules, 2019, 24, 2285.	1.7	7

#	Article	IF	Citations
30575	Chemisorption enhancement of single carbon and oxygen atoms near the grain boundary on Fe surface: ab initio study. Applied Surface Science, 2019, 493, 1042-1047.	3.1	18
30576	Three dimensional metallic porous SiC4 allotropes: Stability and battery applications. Nano Energy, 2019, 63, 103862.	8.2	15
30577	Enhanced Photo-Electrocatalytic Hydrogen Generation in Graphene/hBN van der Waals Structures. Journal of Physical Chemistry C, 2019, 123, 17249-17254.	1.5	6
30578	Core properties and the role of screw dislocations in the bulk n-type conductivity in InN. Physical Chemistry Chemical Physics, 2019, 21, 15767-15778.	1.3	2
30579	Oxygen migration and proton diffusivity in transition-metal (Mn, Fe, Co, and Cu) doped Ruddlesdenâ€“Popper oxides. Journal of Materials Chemistry A, 2019, 7, 18558-18567.	5.2	56
30580	High pressure theoretical and experimental analysis of the bandgap of BaMoO4, PbMoO4, and CdMoO4. Applied Physics Letters, 2019, 115, .	1.5	24
30581	Structure and Dynamic and Nonlinear Optical Properties of Hg2F2 Crystals. Journal of Experimental and Theoretical Physics, 2019, 128, 727-738.	0.2	1
30582	High Thermoelectric Performance in PbSeâ€“NaSbSe₂ Alloys from Valence Band Convergence and Low Thermal Conductivity. Advanced Energy Materials, 2019, 9, 1901377.	10.2	54
30583	Electronic and optical properties of C-doped BN nanotubes by adsorption of typical decomposition products of C3F7CN gas. Applied Surface Science, 2019, 491, 698-706.	3.1	11
30584	Effect of Co doping on martensitic transformation and magnetic properties of Ni50Mn35.4In14.6 alloy by first-principles calculations. Journal of Alloys and Compounds, 2019, 804, 111-118.	2.8	9
30585	Graphene/h-BN In-Plane Heterostructures: Stability and Electronic and Transport Properties. Journal of Physical Chemistry C, 2019, 123, 18600-18608.	1.5	5
30586	Revealing the Mechanism of Multiwalled Carbon Nanotube Growth on Supported Nickel Nanoparticles by in Situ Synchrotron X-ray Diffraction, Density Functional Theory, and Molecular Dynamics Simulations. ACS Catalysis, 2019, 9, 6999-7011.	5.5	36
30587	Exploring Metalâ€“Support Interactions To Immobilize Subnanometer Co Clusters on Î³â€“Mo₂N: A Highly Selective and Stable Catalyst for CO₂ Activation. ACS Catalysis, 2019, 9, 9087-9097.	5.5	50
30588	Interface-mediated Kirkendall effect and nanoscale void migration in bimetallic nanoparticles during interdiffusion. Nature Communications, 2019, 10, 2831.	5.8	42
30589	Tailoring phononic, electronic, and thermoelectric properties of orthorhombic GeSe through hydrostatic pressure. Scientific Reports, 2019, 9, 9490.	1.6	21
30590	Pdâ€“H and Niâ€“H phase diagrams using cluster variation method and Monte Carlo simulation. Philosophical Magazine, 2019, 99, 2376-2392.	0.7	4
30591	First principles investigations of the structural, elastic, vibrational, and thermodynamic properties of TiMg2O4 oxide spinels: cubic and tetragonal phases. Journal of Molecular Modeling, 2019, 25, 210.	0.8	1
30592	A first-principles simulation of the metal borohydride ammonia borane complex (LiBH4)2(NH3BH3) and the decomposition reaction pathway for hydrogen storage. International Journal of Hydrogen Energy, 2019, 44, 20121-20132.	3.8	3

#	Article	IF	Citations
30593	On the mechanism of alkyne hydrogenation catalyzed by Ga-doped ceria. Journal of Catalysis, 2019, 375, 410-418.	3.1	43
30594	Structural and electronic properties of monolayer group III-VII compounds: A first-principle study. Physica E: Low-Dimensional Systems and Nanostructures, 2019, 114, 113605.	1.3	2
30595	Edge-modulated dual spin-filter effect in zigzag-shaped buckling Ag₂S nanoribbons. Physical Chemistry Chemical Physics, 2019, 21, 15623-15629.	1.3	6
30596	Water oxidation catalysis on reconstructed NaTaO₃ (001) surfaces. Journal of Materials Chemistry A, 2019, 7, 16770-16776.	5.2	19
30597	H permeation in molybdenum: temperature dependence and compensation effect from first-principles simulation. Journal of Nuclear Science and Technology, 2019, 56, 1014-1028.	0.7	2
30598	Internal exchange interaction of Tb⁺³ ions and influence of Si substitution on structural, electronic, magnetic and optical properties of YNi₄Si -type TbNi_{5â^'x}Si_x (x = 0, 1, 2) compounds. Materials Research Express, 2019, 6, 086111.	0.8	2
30599	Investigation on mechanical and electronic properties of graphene-doped boron nitride nanotubes. Materials Research Express, 2019, 6, 1150c5.	0.8	3
30600	Comparative study of density functionals for the description of lithiumâ€graphite intercalation compounds. Journal of Computational Chemistry, 2019, 40, 2400-2412.	1.5	21
30601	Methylammonium Chloride Induces Intermediate Phase Stabilization for Efficient Perovskite Solar Cells. Joule, 2019, 3, 2179-2192.	11.7	1,228
30602	Electrochemical performance and computational analysis of an Al-based battery system using a cathode of graphene obtained from processed expandable graphite. Journal of Power Sources, 2019, 435, 226780.	4.0	7
30603	Enhancing electronic and optical properties of monolayer MoSe₂via a MoSe₂/blue phosphorene heterobilayer. Physical Chemistry Chemical Physics, 2019, 21, 15760-15766.	1.3	68
30604	Cable-like Ru/WNO@C nanowires for simultaneous high-efficiency hydrogen evolution and low-energy consumption chlor-alkali electrolysis. Energy and Environmental Science, 2019, 12, 2569-2580.	15.6	137
30605	High-throughput screening and classification of layered di-metal chalcogenides. Nanoscale, 2019, 11, 13924-13933.	2.8	11
30606	Designing ultrastrong 5d transition metal diborides with excellent stability for harsh service environments. Physical Chemistry Chemical Physics, 2019, 21, 16095-16107.	1.3	7
30607	Pressure-induced modification of the anomalous Hall effect in layered <mml:math xmlns:mml="http://www.w3.org/1998/Math/MathML"><mml:mrow><mml:msub><mml:mi>Fe</mml:mi><mml:mn>3</mml:mn></mml:msub></mml:r Physical Review B, 2019, 100, .	3.7	32
30608	Effects of Transition Metal Substituents on Interfacial and Electronic Structure of CH3NH3PbI3/TiO2 Interface: A First-Principles Comparative Study. Nanomaterials, 2019, 9, 966.	1.9	13
30609	Electronic structure and structural defects in 3d-metal doped In2O3. Journal of Materials Science: Materials in Electronics, 2019, 30, 14091-14098.	1.1	1
30610	Understanding how yttrium doping influences the properties of nickel ferrite â€“ Combined experimental and computational study. Ceramics International, 2019, 45, 20290-20296.	2.3	12

#	Article	IF	Citations
30611	Electronic band structure, thermodynamics and optical characteristics of BeO1â˜'A (Aâ€¯=â€¯S, Se, Te) alloys: Insights from ab initio study. Chemical Physics, 2019, 526, 110414.	0.9	39
30612	Mechanical elasticity and piezoelectricity in monolayer transition-metal dichalcogenide alloys. Journal of Physics and Chemistry of Solids, 2019, 135, 109081.	1.9	4
30613	Structure of Na₃[Al(L-Lactate)₃]₂Â·6H₂O Crystallized from Lohtragon AL 250â€"A Commercial Cement Adjuvant. Crystal Growth and Design, 2019, 19, 4557-4563.	1.4	1
30614	Density Functional Theory Study on the Reaction Mechanism of Spinel CoFe₂O₄ with CO during Chemical-Looping Combustion. Journal of Physical Chemistry C, 2019, 123, 17335-17342.	1.5	27
30615	Boosting the Curie Temperature of Two-Dimensional Semiconducting CrI₃ Monolayer through van der Waals Heterostructures. Journal of Physical Chemistry C, 2019, 123, 17987-17993.	1.5	74
30616	High-pressure synthesis of ultraincompressible hard rhenium nitride pernitride Re2(N2)(N)2 stable at ambient conditions. Nature Communications, 2019, 10, 2994.	5.8	65
30617	Dielectric properties and the role of grain boundaries in polycrystalline tetracene at high pressures. CrystEngComm, 2019, 21, 4507-4512.	1.3	6
30618	Pressure-induced Ge₂Se₃and Ge₃Se₄crystals with low superconducting transition temperatures. Physical Chemistry Chemical Physics, 2019, 21, 15417-15421.	1.3	1
30619	Lattice thermal conductivity of <mml:math xmlns:mml="http://www.w3.org/1998/Math/MathML"><mml:msub><mml:mi>TiS</mml:mi><mml:mn>2</mml:mn></mml:msub></mml , <mml:math xmlns:mml="http://www.w3.org/1998/Math/MathML"><mml:msub><mml:mi>ZrS</mml:mi><mml:mn>2</mml:mn></mml:msub></mml , and <mml:math xmlns:mml="http://www.w3.org/1998/Math/MathML"><mml:msub><mml:mi>HfS</mml:mi><mml:mn>2</mml:mn></mml:msub></mm	1.1	13
30620	Electronic Structure, Elastic and Optical Properties of AEuS 2 (Aâ€‰=â€‰Na,â€‰K, Rb, and Cs) Ternary Sulfides: Firstâ€Principles Study. Physica Status Solidi (B): Basic Research, 2019, 256, 1900136.	0.7	14
30621	Which phase of iron oxyhydroxides (FeOOH) is more competent in overall water splitting as a photocatalyst, goethite, akaganeite or lepidocrocite? A DFT-based investigation. Computational Materials Science, 2019, 169, 109110.	1.4	28
30622	Structural, electronic, and optical properties and bond stiffness of ScAl3C3-type LaCd3P3 phases: ab initio calculations. Journal of Physics and Chemistry of Solids, 2019, 134, 115-120.	1.9	3
30623	Revealing Atomic Structure and Oxidation States of Dopants in Charge-Ordered Nanoparticles for Migration-Promoted Oxygen-Exchange Capacity. Chemistry of Materials, 2019, 31, 5769-5777.	3.2	10
30624	Electrochemical Oxygen-Reduction Activity and Carbon Monoxide Tolerance of Iron Phthalocyanine Functionalized with Graphene Quantum Dots: A Density Functional Theory Approach. Journal of Physical Chemistry C, 2019, 123, 27483-27491.	1.5	10
30625	Iodine Adsorption on Ni(110): 2D-Phase Transitions and NiI₂ Growth. Journal of Physical Chemistry C, 2019, 123, 27659-27665.	1.5	3
30626	Gas-Induced Confinementâ€"Deconfinement Interplay in Organicâ€"Inorganic Hybrid Perovskite Thin Film Results in Systematic Band Modulation. ACS Applied Materials & Interfaces, 2019, 11, 43708-43718.	4.0	4
30627	Three-dimensional open nano-netcage electrocatalysts for efficient pH-universal overall water splitting. Nature Communications, 2019, 10, 4875.	5.8	253
30628	Dynamic oxygen adsorption on single-atomic Ruthenium catalyst with high performance for acidic oxygen evolution reaction. Nature Communications, 2019, 10, 4849.	5.8	416

#	Article	IF	Citations
30629	Gate voltage controllable device based on black phosphorus/blue phosphorus heterostructure. Journal Physics D: Applied Physics, 2019, 52, 505111.	1.3	2
30630	First principles calculations of the optoelectronic properties of magnesium substitutes in Lead based ABX₃ compounds. Journal of Physics: Conference Series, 2019, 1299, 012129.	0.3	9
30631	First-principles calculation on the structural, elastic and thermodynamic properties of Ti-Al intermetallics. Materials Research Express, 2019, 6, 1065a4.	0.8	18
30632	Spintronic transport in zigzag silicon carbide nanoribbons with edge hydrogenation. Materials Research Express, 2019, 6, 115040.	0.8	4
30633	Exploring optical properties of Gd doped zincblende GaN for novel optoelectronic applications (A) Tj ETQq0 0 0 rgBT /Overlock 10 Tf 50	0.8	8
30634	Rashba-like spin splitting along three momentum directions in trigonal layered PtBi2. Nature Communications, 2019, 10, 4765.	5.8	42
30635	Gas sensing of graphene and graphene oxide nanoplatelets to ClO2 and its decomposed species. Superlattices and Microstructures, 2019, 135, 106248.	1.4	19
30636	Molecular-Level Understanding of Hydroxyl Groups Boosted the Catalytic Activity of the CuZnAl Catalyst in the Conversion of Syngas to Ethanol. Industrial & Engineering Chemistry Research, 2019, 58, 19421-19433.	1.8	1
30637	Grazynes: Carbon-Based Two-Dimensional Composites with Anisotropic Properties. Journal of Physical Chemistry C, 2019, 123, 27140-27149.	1.5	14
30638	Identifying Adhesion Properties at Si/Polymer Interfaces with ReaxFF. Journal of Physical Chemistry C, 2019, 123, 27036-27047.	1.5	10
30639	n-Type TaCoSn-Based Half-Heuslers as Promising Thermoelectric Materials. ACS Applied Materials & Interfaces, 2019, 11, 41321-41329.	4.0	44
30640	Level the Conversion/Alloying Voltage Gap by Grafting the Endogenetic Sb₂Te₃ Building Block into Layered GeTe to Build Ge₂Sb₂Te₅ for Li-Ion Batteries. ACS Applied Materials & Interfaces, 2019, 11, 41374-41382.	4.0	15
30641	Thermoelectric Performance of Two-Dimensional AlX (X = S, Se, Te): A First-Principles-Based Transport Study. ACS Omega, 2019, 4, 17773-17781.	1.6	38
30642	Improved Oxygen Reduction Activity in Heteronuclear FeCo-Codoped Graphene: A Theoretical Study. ACS Sustainable Chemistry and Engineering, 2019, 7, 17273-17281.	3.2	56
30643	Atomic-scale measurement of polar entropy. Physical Review B, 2019, 100, .	1.1	7
30644	Electro-optical properties of a pressure-induced <mml:math xmlns:mml="http://www.w3.org/1998/Math/MathML"><mml:mrow><mml:mi>g</mml:mi><mml:mtext>â^'</mml:mtext><mml:msub> sheet from many-body perturbation theory. Physical Review B, 2019, 100, .	1.1	18
30645	Encapsulating Trogtalite CoSe₂ Nanobuds into BCN Nanotubes as High Storage Capacity Sodium Ion Battery Anodes. Advanced Energy Materials, 2019, 9, 1901778.	10.2	131
30646	Highly Stabilized Quantum Dot Ink for Efficient Infrared Light Absorbing Solar Cells. Advanced Energy Materials, 2019, 9, 1902809.	10.2	50

#	Article	IF	Citations
30647	ZnS coating of cathode facilitates leanâ€electrolyte Liâ€S batteries. , 2019, 1, 165-172.		87
30648	Unveiling the Origin of the High Catalytic Activity of Ultrathin 1T/2H MoSe₂ Nanosheets for the Hydrogen Evolution Reaction: A Combined Experimental and Theoretical Study. ChemSusChem, 2019, 12, 5015-5022.	3.6	48
30649	Elastic constants determination of anisotropic materials by depth-sensing indentation. SN Applied Sciences, 2019, 1, 1.	1.5	6
30650	Structural stability, electronic, optical and lattice thermal conductivity properties of bulk and monolayer PtS_2. Materials Today Communications, 2019, 21, 100661.	0.9	6
30651	Theoretical Investigation of the Role of the Nitride Ion in the Magnetism of Oxynitride MnTaO₂N. Journal of Physical Chemistry C, 2019, 123, 25379-25384.	1.5	3
30652	Hierarchical Flower-Like MoS₂ Microspheres and Their Efficient Al Storage Properties. Journal of Physical Chemistry C, 2019, 123, 26794-26802.	1.5	20
30653	Ferromagnetic, antiferromagnetic, and Peierls distortion states in IVA-VA nanoribbons. Applied Physics Letters, 2019, 115, .	1.5	1
30654	Machine-learning interatomic potential for radiation damage and defects in tungsten. Physical Review B, 2019, 100, .	1.1	79
30655	Exploiting the Novel Electronic and Magnetic Structure of C₃N via Functionalization and Conformation. Advanced Electronic Materials, 2019, 5, 1900459.	2.6	40
30656	Temperature-dependent nucleation kinetics of Guinier-Preston zones in Alâ€“Cu alloys: An atomistic kinetic Monte Carlo and classical nucleation theory approach. Acta Materialia, 2019, 179, 262-272.	3.8	31
30657	Designed materials with the giant magnetocaloric effect near room temperature. Acta Materialia, 2019, 180, 341-348.	3.8	73
30658	Thermodynamic and mechanical stability of Ni3X-type intermetallic compounds. Intermetallics, 2019, 114, 106604.	1.8	33
30659	Tuning the bandgap and introducing magnetism into monolayer BC3 by strain/defect engineering and adatom/molecule adsorption. Journal of Applied Physics, 2019, 126, .	1.1	56
30660	Theoretical Modeling of Defects, Dopants, and Diffusion in the Mineral Ilmenite. Minerals (Basel,) Tj ETQq1 1 0.784314 rgBT /Overloc	0.8	5
30661	Modified embedded-atom method potential for cadmium. Hyperfine Interactions, 2019, 240, 1.	0.2	0
30662	A comparative investigation of metal (Li, Ca and Sc)-decorated 6,6,12-graphyne monolayers and 6,6,12-graphyne nanotubes for hydrogen storage. Applied Surface Science, 2019, 498, 143763.	3.1	20
30663	Profound softening and shear-induced melting of diamond under extreme conditions: An ab-initio molecular dynamics study. Carbon, 2019, 155, 361-368.	5.4	9
30664	High-pressure, high temperature insertion of bismuth in the siliceous zeolite silicalite-1. Solid State Sciences, 2019, 97, 106001.	1.5	1

#	Article	IF	Citations
30665	Electronic structure and dielectric function of Mn-Bi-Te layered compounds. Journal of Vacuum Science and Technology B:Nanotechnology and Microelectronics, 2019, 37, .	0.6	21
30666	Experimental and Theoretical In Situ Spectral Magneto-Ellipsometry Study of Layered Ferromagnetic Structures. JETP Letters, 2019, 110, 166-172.	0.4	5
30667	Tomographic layer-by-layer analysis of epitaxial iron-silicide nanostructures by DFT-assisted STS. Applied Surface Science, 2019, 496, 143583.	3.1	4
30668	Single-Walled boron nitride nanotubes interaction with nickel, titanium, palladium, and gold metal atoms- A first-principles study. Results in Materials, 2019, 2, 100029.	0.9	7
30669	Structural, electronic and magnetic properties of the Fe8â˜Mn Rh8 compound: A density functional study. Results in Physics, 2019, 15, 102743.	2.0	1
30670	Rationalizing and engineering Rashba spin-splitting in ferroelectric oxides. Npj Quantum Materials, 2019, 4, .	1.8	59
30671	Novel high pressure structures and mechanical properties of rhenium diboride. Journal of Applied Physics, 2019, 126, .	1.1	3
30672	Synthesis and Properties of Orthorhombic MoAlB Coatings. Coatings, 2019, 9, 510.	1.2	17
30673	Ab initio calculation insights into the structural, elastic and mechanical properties of high-k dielectric gadolinium oxide (Gd2O3). Applied Physics A: Materials Science and Processing, 2019, 125, 1.	1.1	4
30674	LiZnN filled-tetrahedral compound: A first-principles study of the electronic, optical and effective mass properties. Journal of Solid State Chemistry, 2019, 280, 120974.	1.4	4
30675	A metal-semiconductor transition in helical graphene nanoribbon. Journal of Applied Physics, 2019, 126, 144303.	1.1	9
30676	First-Principles Calculations of Structural, Mechanical, and Electronic Properties of the B2-Phase NiTi Shape-Memory Alloy Under High Pressure. Computation, 2019, 7, 57.	1.0	11
30677	DFT Study into the Influence of Carbon Material on the Hydrophobicity of a Coal Pyrite Surface. Molecules, 2019, 24, 3534.	1.7	4
30678	First principles modeling of pure black phosphorus devices under pressure. Beilstein Journal of Nanotechnology, 2019, 10, 1943-1951.	1.5	5
30679	Optimized hybrid functionals for defect calculations in semiconductors. Journal of Applied Physics, 2019, 126, 130901.	1.1	27
30680	First-Principles Modeling of Atomic Structure and Chemical and Optical Properties of Î²-C3N4. Journal of Carbon Research, 2019, 5, 58.	1.4	1
30681	Noncollinear Magnetic Structure with Spin-dependent van der Waals Density Functional Approach: Î²-phase Solid Oxygen. Journal of the Physical Society of Japan, 2019, 88, 104601.	0.7	1
30682	Transition from ductilizing to hardening in tungsten: The dependence on rhenium distribution. Acta Materialia, 2019, 181, 110-123.	3.8	26

#	Article	IF	Citations
30683	First-principles study of ferromagnetic metal Fe5GeTe2. Nano Materials Science, 2019, 1, 299-303.	3.9	26
30684	Influence of Al on the Structure and in Vitro Behavior of Hydroxyapatite Nanopowders. Journal of Physical Chemistry B, 2019, 123, 9143-9154.	1.2	26
30685	On the Reactivity of the Cu/ZrO₂ System for the Hydrogenation of CO₂ to Methanol: A Density Functional Theory Study. Journal of Physical Chemistry C, 2019, 123, 26904-26911.	1.5	24
30686	Two-Dimensional Fe-Hexaaminobenzene Metalâ€“Organic Frameworks as Promising CO₂ Catalysts with High Activity and Selectivity. Journal of Physical Chemistry C, 2019, 123, 26460-26466.	1.5	16
30687	Hole Localization Inhibits Charge Recombination in Tinâ€“Lead Mixed Perovskites: Timeâ€“Domain ab Initio Analysis. Journal of Physical Chemistry Letters, 2019, 10, 6604-6612.	2.1	21
30688	Ensemble-Based Modeling of the NMR Spectra of Solid Solutions: Cation Disorder in Y₂(Sn,Ti)₂O₇. Journal of the American Chemical Society, 2019, 141, 17838-17846.	6.6	29
30689	In situ-grown compressed NiCo2S4 barrier layer for efficient and durable polysulfide entrapment. NPG Asia Materials, 2019, 11, .	3.8	27
30690	Influence of simple metals on the stability of <mml:math xmlns:mml="http://www.w3.org/1998/Math/MathML" altimg="si1.svg"><mml:mrow><mml:mrow><mml:mo>â€ˆ</mml:mo><mml:mrow><mml:mi>a</mml:mi></mml:mrow><mml:mo>â€ basal screw dislocations in hexagonal titanium alloys. Acta Materialia, 2019, 180, 42-50.	3.8	22
30691	Energetically-favorable distribution of oxygen vacancies and metal atoms in perovskite BaCe Zr0.85â^'Y0.15O2.925 solid solutions using a genetic algorithm and lattice statics. Computational Materials Science, 2019, 170, 109184.	1.4	6
30692	Ruthenium decorated boron-doped carbon nanotube for hydrogen storage: A first-principle study. International Journal of Hydrogen Energy, 2019, 44, 27853-27861.	3.8	41
30693	Atomic bonding and electronic stability of the binary sigma phase. Journal of Alloys and Compounds, 2019, 811, 152053.	2.8	7
30694	Effect of rock mineralogy on Hot-CO2 injection for enhanced gas recovery. Journal of Natural Gas Science and Engineering, 2019, 72, 103030.	2.1	19
30695	An unreported precipitate orientation relationship in Al-Zn-Mg based alloys. Materials Characterization, 2019, 158, 109958.	1.9	20
30696	Structural, electronic, elastic and vibrational properties of two dimensional graphene-like BN under high pressure. Solid State Communications, 2019, 303-304, 113740.	0.9	12
30697	Enhancing the Pharmaceutical Properties of Pirfenidone by Mechanochemical Cocrystallization. Crystal Growth and Design, 2019, 19, 6482-6492.	1.4	42
30698	(Cu)tet(Cr2â€“xSnx)octS4â€“ySey Spinels: Crystal Structure, Density Functional Theory Calculations, and Magnetic Behavior. Inorganic Chemistry, 2019, 58, 13945-13952.	1.9	6
30699	Coverage and Stability of NH_x-Terminated Cobalt and Ruthenium Surfaces: A First-Principles Investigation. Journal of Physical Chemistry C, 2019, 123, 25166-25175.	1.5	10
30700	Influence of Oxygenâ€“Sulfur Exchange on the Structural, Electronic, and Stability Properties of Alkali Hexastannates. Journal of Physical Chemistry C, 2019, 123, 24375-24382.	1.5	6

#	Article	IF	Citations
30701	Oxidation Driven Permeation of Iron Oxide Scales by Chloride from Experiment Guided First-Principles Modeling. Journal of Physical Chemistry C, 2019, 123, 25957-25966.	1.5	14
30702	FeP/MoS₂ Enriched with Dense Catalytic Sites and High Electrical Conductivity for the Hydrogen Evolution Reaction. ACS Sustainable Chemistry and Engineering, 2019, 7, 17671-17681.	3.2	24
30703	Statistical learning goes beyond the d-band model providing the thermochemistry of adsorbates on transition metals. Nature Communications, 2019, 10, 4687.	5.8	76
30704	The encapsulation selectivity for anionic fission products imparted by an electride. Scientific Reports, 2019, 9, 13612.	1.6	14
30705	Two novel superhard carbon allotropes with honeycomb structures. Journal of Applied Physics, 2019, 126, .	1.1	41
30706	Enhanced Absorption in MoS₂/Hg_{0.33}Cd_{0.66}Te Heterostructure for Application in Solar Cell Absorbers. IEEE Nanotechnology Magazine, 2019, 18, 989-994.	1.1	17
30707	First principle study on electronic, thermophysical and optical properties of ScAl3C3 and UAl3C3 under high pressure. Journal of Materials Research and Technology, 2019, 8, 5774-5780.	2.6	13
30708	LiCsPbP2O7: A new alkali metal lead pyrophosphate featuring two dimensional [LiP2O7]â^ž layer. Journal of Solid State Chemistry, 2019, 280, 120823.	1.4	0
30709	Effects of impurities on graphite shape during solidification of spheroidal graphite cast ions. Materialia, 2019, 8, 100471.	1.3	15
30710	Partial Oxidation of Methanol on the Fe3O4(111) Surface Studied by Density Functional Theory. Journal of Physical Chemistry C, 2019, 123, 8429-8438.	1.5	17
30711	First-Principles Computational Screening of Perovskite Hydrides for Hydrogen Release. ACS Combinatorial Science, 2019, 21, 736-742.	3.8	10
30712	Structural and electronic properties of liquid, amorphous, and supercooled liquid phases of In2Te5 from first-principles. Journal of Chemical Physics, 2019, 151, 134503.	1.2	8
30713	Effect of oxygen plasma modification on Pd/Al/Au Ohmic contacts on undoped AlN. Journal Physics D: Applied Physics, 2019, 52, 505106.	1.3	1
30714	Designing functional ferroelectric interfaces from first-principles: dipoles and band bending at oxide heterojunctions. New Journal of Physics, 2019, 21, 113005.	1.2	8
30715	Quasiparticle electronic structure of 1Tâ€™-MoS2 within GW approximation. Journal of Physics: Conference Series, 2019, 1245, 012085.	0.3	2
30716	Microstructural, electronic, and mechanical properties of L1₂ ordered Al₃Er and Al₃Yb intermetallics: an experimental and first-principles calculations. Materials Research Express, 2019, 6, 116516.	0.8	4
30717	Revealing atypical ground state structures of III-Ununpentium compounds. Materials Research Express, 2019, 6, 115922.	0.8	1
30718	Pd3Te2: an s-wave superconductor with Pd atom coordinated by five Te atoms. Journal of Physics Communications, 2019, 3, 095008.	0.5	1

#	Article	IF	Citations
30719	Atomic Nb Anchoring on Graphdiyne as a New Potential Electrocatalyst for Nitrogen Fixation: A Computational View. Advanced Theory and Simulations, 2019, 2, 1900132.	1.3	38
30720	On the Origin of the Large Remanent Polarization in La:HfO₂. Advanced Electronic Materials, 2019, 5, 1900303.	2.6	85
30721	Germanium Incorporation in Cu₂ZnSnS₄ and Formation of a Snâ€“Ge Gradient. Physica Status Solidi (A) Applications and Materials Science, 2019, 216, 1900492.	0.8	17
30722	DFT calculations of the structural, electronic, optical and vibrational properties of anhydrous orthorhombic L-threonine crystals. Computational and Theoretical Chemistry, 2019, 1170, 112621.	1.1	13
30723	One-step synthesized 2D heteroatom doped graphene for high throughput electrochemical biosensing: A combined experimental and computational studies. Diamond and Related Materials, 2019, 100, 107592.	1.8	10
30724	Enhanced Synergetic Catalytic Effect of Mo₂C/NCNTs@Co Heterostructures in Dye-Sensitized Solar Cells: Fine-Tuned Energy Level Alignment and Efficient Charge Transfer Behavior. ACS Applied Materials & Interfaces, 2019, 11, 42156-42171.	4.0	63
30725	Functionalized MXenes as ideal electrodes for Janus MoSSe. Physical Chemistry Chemical Physics, 2019, 21, 70-76.	1.3	35
30726	Single-molecule and -particle probing crystal edge/corner as highly efficient photocatalytic sites on a single TiO ₂ particle. Proceedings of the National Academy of Sciences of the United States of America, 2019, 116, 18827-18833.	3.3	54
30727	Effect of sub-surface hydrogen on intrinsic crack tip plasticity in aluminium. Philosophical Magazine, 2019, 99, 2355-2375.	0.7	1
30728	Rare-Earth Elements Modified 1T Phase Mos2 Synergy with Defects for Enhanced Hydrogen Evolution. IOP Conference Series: Earth and Environmental Science, 2019, 252, 022136.	0.2	1
30729	First-principle calculations of mechanical properties and electronic structure of WCoB and Cr doped WCoB under high pressure. Materials Research Express, 2019, 6, 116320.	0.8	5
30730	Theoretical investigation on the interaction between groups in LAP crystal and its linear optical properties. International Journal of Modern Physics B, 2019, 33, 1950156.	1.0	1
30731	First Principles Study of Penta-siligraphene as High-Performance Anode Material for Li-Ion Batteries. Nanoscale Research Letters, 2019, 14, 260.	3.1	25
30732	Crystal Structures of Al2Cu Revisited: Understanding Existing Phases and Exploring Other Potential Phases. Metals, 2019, 9, 1037.	1.0	26
30733	Reversing the charge transfer between platinum and sulfur-doped carbon support for electrocatalytic hydrogen evolution. Nature Communications, 2019, 10, 4977.	5.8	243
30734	An empirical law on the finite-size effects in electronic transport calculations of tungsten. AIP Advances, 2019, 9, .	0.6	5
30735	The Application of Periodic Density Functional Theory to the Study of Uranyl-Containing Materials: Thermodynamic Properties and Stability. , 2019, , .		0
30736	Electronic band structure of nitrogen diluted Ga(PAsN): Formation of the intermediate band, direct and indirect optical transitions, and localization of states. Journal of Applied Physics, 2019, 126, 175701.	1.1	8

#	Article	IF	Citations
30737	Interstitial sodium and lithium doping effects on the electronic and mechanical properties of silicon nanowires: a DFT study. Journal of Molecular Modeling, 2019, 25, 338.	0.8	5
30738	Synthesis and Fundamental Studies of Si-Compatible (Si)GeSn and GeSn Mid-IR Systems with Ultrahigh Sn Contents. Chemistry of Materials, 2019, 31, 9831-9842.	3.2	26
30739	First-principles calculation of the electronic and optical properties of a new two-dimensional carbon allotrope: tetra-penta-octagonal graphene. Physical Chemistry Chemical Physics, 2019, 21, 24758-24767.	1.3	20
30740	Interfacial aspect of ZnTe/In₂Te₃ heterostructures as an efficient catalyst for the hydrogen evolution reaction. Journal of Materials Chemistry A, 2019, 7, 27441-27449.	5.2	41
30741	Stabilities, and electronic and piezoelectric properties of two-dimensional tin dichalcogenide derived Janus monolayers. Journal of Materials Chemistry C, 2019, 7, 13203-13210.	2.7	72
30742	X-ray absorption near edge spectroscopy study of warm dense MgO. Physics of Plasmas, 2019, 26, 112703.	0.7	3
30743	Charge smoothening and band flattening due to Hartree corrections in twisted bilayer graphene. Physical Review B, 2019, 100, .	1.1	55
30744	Electronic structures and magnetic performance related to spintronics of Sr0.875Ti0.125S. Optical and Quantum Electronics, 2019, 51, 1.	1.5	7
30745	First-principles DFT insights into the structural, elastic, and optoelectronic properties ofÎ±andÎ²-ZnP₂: implications for photovoltaic applications. Journal of Physics Condensed Matter, 2019, 31, 265501.	0.7	4
30746	Calculating the Lattice Dynamics in the RFe3(BO3)4 Crystals in the Quasi-Harmonic Approximation. Physics of the Solid State, 2019, 61, 2019-2025.	0.2	3
30747	The system thorium-palladium-boron: A DFT study on the stability and properties of Th2Pd15B5. Journal of Alloys and Compounds, 2019, 811, 151578.	2.8	1
30748	Probing the low-symmetry structure determined anisotropic elastic properties of rhenium disulphide by first-principle calculations. Materials Today Communications, 2019, 21, 100684.	0.9	2
30749	Unified Approach to Implicit and Explicit Solvent Simulations of Electrochemical Reaction Energetics. Journal of Chemical Theory and Computation, 2019, 15, 6895-6906.	2.3	86
30750	Tailoring Alkane Uniaxial Self-Assembly via Polymer Modified Step Edges. Journal of Physical Chemistry C, 2019, 123, 28811-28815.	1.5	2
30751	CLEASE: a versatile and user-friendly implementation of cluster expansion method. Journal of Physics Condensed Matter, 2019, 31, 325901.	0.7	41
30752	High-T _c superconductivity in H₃S: pressure effects on the superconducting critical temperature and Cooper pair distribution function. Superconductor Science and Technology, 2019, 32, 125013.	1.8	10
30753	Electronic distribution and elastic properties of zinc-blende AlN and GaN. IOP Conference Series: Materials Science and Engineering, 2019, 563, 022009.	0.3	2
30754	Lead sulfide; a new candidate for optoelectronics applications in the ultra violet spectral range. Materials Research Express, 2019, 6, 116220.	0.8	10

#	Article	IF	Citations
30755	Compression of liquid Ni and Co under extreme conditions explored by x-ray absorption spectroscopy. Physical Review B, 2019, 100, .	1.1	8
30756	Smooth Flow in Diamond: Atomistic Ductility and Electronic Conductivity. Physical Review Letters, 2019, 123, 195504.	2.9	50
30757	CO Adsorption and Activation of Î·-Fe₂C Fischerâ€“Tropsch Catalyst. Industrial & Engineering Chemistry Research, 2019, 58, 21296-21303.	1.8	9
30758	Selective Hydrogenolysis of Î±-Câ€“O Bond in Biomass-Derived 2-Furancarboxylic Acid to 5-Hydroxyvaleric Acid on Supported Pt Catalysts at Near-Ambient Temperature. ACS Catalysis, 2019, 9, 11413-11425.	5.5	21
30759	Rational Design of Rhodiumâ€“Iridium Alloy Nanoparticles as Highly Active Catalysts for Acidic Oxygen Evolution. ACS Nano, 2019, 13, 13225-13234.	7.3	151
30760	Theoretical study on wetting behavior of B-SWNT: Effects of doping concentration. Applied Surface Science, 2019, 497, 143798.	3.1	6
30761	Energy propagation along polypeptide Î±-helix: Experimental data and ab initio zone structure. BioSystems, 2019, 185, 104016.	0.9	15
30762	Tuning the supercritical effective charge in gapless graphene via Fermi velocity modifying through the mechanical stretching. Diamond and Related Materials, 2019, 100, 107566.	1.8	4
30763	Tuning the Apparent Stability of Polymorphic Cocrystals through Mechanochemistry. Crystal Growth and Design, 2019, 19, 7271-7279.	1.4	23
30764	Dinitrogen Activation on Graphene Anchored Single Atom Catalysts: Local Site Activity or Surface Phenomena. Journal of Physical Chemistry C, 2019, 123, 27492-27500.	1.5	13
30765	Nanotribological Properties of the h-BN/Au(111) Interface: A DFT Study. Journal of Physical Chemistry C, 2019, 123, 28411-28418.	1.5	10
30766	Interfacial Charge Transfer Transitions in Colloidal TiO₂ Nanoparticles Functionalized with Salicylic acid and 5-Aminosalicylic acid: A Comparative Photoelectron Spectroscopy and DFT Study. Journal of Physical Chemistry C, 2019, 123, 29057-29066.	1.5	17
30767	Anisotropic Rashba effect and charge and spin currents in monolayer BiTeI by controlling symmetry. Physical Review B, 2019, 100, .	1.1	19
30768	Trigonal Tellurium Nanostructure Formation Energy and Band gap. , 2019, , .		1
30769	Atomistic Modeling Of Nanoscale Ferroelectric Capacitors Using a Density Functional Theory And Non-Equilibrium Greenâ€™s-Function Method. , 2019, , .		1
30770	Computational Modeling of Tensile Stress Effects on the Structure and Stability of Prototypical Covalent and Layered Materials. Nanomaterials, 2019, 9, 1483.	1.9	3
30771	Using Pd-Doped Î³-Graphyne to Detect Dissolved Gases in Transformer Oil: A Density Functional Theory Investigation. Nanomaterials, 2019, 9, 1490.	1.9	37
30772	Pressure-Induced Structural Transition to the Polar Phase in GdFe₃(BO₃)₄. Crystal Growth and Design, 2019, 19, 6935-6944.	1.4	2

#	Article	IF	Citations
30773	Phase Stability and Ordering in Rock Salt-Based Thermoelectrics: NaSbX₂, AgSbX₂, and Their Alloys with PbX and SnX (X = S, Se, Te). Chemistry of Materials, 2019, 31, 9445-9452.	3.2	15
30774	Elucidating the Electronic Structure and Magnetic and Conducting Properties of Î¼-Oxo Mn-phthalocyanine [MnPc(CN)]₂O Complex. Journal of Physical Chemistry C, 2019, 123, 28359-28369.	1.5	1
30775	Improved Prediction for the Methane Activation Mechanism on Rutile Metal Oxides by a Machine Learning Model with Geometrical Descriptors. Journal of Physical Chemistry C, 2019, 123, 28802-28810.	1.5	29
30776	Mysterious SiB₃: Identifying the Relation between Î±- and Î²-SiB₃. ACS Omega, 2019, 4, 18741-18759.	1.6	9
30777	Electric-Field-Controllable Conductance Switching of an Overcrowded Ethylene Self-Assembled Monolayer. Journal of the American Chemical Society, 2019, 141, 18544-18550.	6.6	17
30778	Theoretical prediction of a highly responsive material: Spin fluctuations and superconductivity in FeNiB2 system. Applied Physics Letters, 2019, 115, 182601.	1.5	4
30779	Structural and lattice dynamical study of half Heusler alloys RuMnX (X = P, As). AIP Conference Proceedings, 2019, , .	0.3	7
30780	Tuning topological surface states by cleavage angle in topological crystalline insulators. Physical Review B, 2019, 100, .	1.1	4
30783	Single and multi domain buckled germanene phases on Al(111) surface. Nano Research, 2019, 12, 2988-2996.	5.8	17
30784	Insights into the Most Suitable TiO₂ Surfaces for Photocatalytic O₂ and H₂ Evolution Reactions from DFT Calculations. Journal of Physical Chemistry C, 2019, 123, 28210-28218.	1.5	48
30785	Understanding the Water Splitting Mechanism on WO₃(001)â€"A Theoretical Approach. Journal of Physical Chemistry C, 2019, 123, 28233-28240.	1.5	20
30786	Moderate strain induced indirect bandgap and conduction electrons in MoS2 single layers. Npj 2D Materials and Applications, 2019, 3, .	3.9	45
30787	First-principles study of crystal structures and superconductivity of ternary <mml:math xmlns:mml="http://www.w3.org/1998/Math/MathML"><mml:msub><mml:mi>YSH</mml:mi><mml:mn>6</mml:mn></mml:msub></mm and <mml:math xmlns:mml="http://www.w3.org/1998/Math/MathML"><mml:msub><mml:mi>LaSH</mml:mi><mml:mn>6</mml:mn></mml:msub></mr at high pressures. Physical Review B, 2019, 100, .	1.1	33
30788	Influence of Inorganic Solution Components on Lithium Carbonate Crystal Growth. Crystal Growth and Design, 2019, 19, 6994-7006.	1.4	9
30789	Facile Electron Transfer to CO₂ during Adsorption at the Metal|Solution Interface. Journal of Physical Chemistry C, 2019, 123, 29278-29283.	1.5	36
30790	Ferroelectric Polarization Suppresses Nonradiative Electronâ€"Hole Recombination in CH₃NH₃PbI₃ Perovskites: A Time-Domain ab Initio Study. Journal of Physical Chemistry Letters, 2019, 10, 7237-7244.	2.1	17
30791	First-Principles Study of Structural, Elastic, Electronic and Optical Properties of Zinc Ferrite Spinel. IOP Conference Series: Materials Science and Engineering, 2019, 569, 022016.	0.3	4
30792	A computational study of the electronic structure and optical properties of the complex TeO2/TeO3 oxides as advanced materials for nonlinear optics. Materials Research Express, 2019, 6, 125903.	0.8	2

#	Article	IF	Citations
30793	Rashba-like spin-orbit and strain effects in tetragonal <mml:math xmlns:mml="http://www.w3.org/1998/Math/MathML"><mml:msub><mml:mi>PbTiO</mml:mi><mml:mn>3</mml:mn></mml:msub></m Physical Review B, 2019, 100, .	1.1	29
30794	Large Fermi arc and robust Weyl semimetal phase in Ag2S. Physical Review B, 2019, 100, .	1.1	6
30795	A Bespoke Force Field To Describe Biomolecule Adsorption at the Aqueous Boron Nitride Interface. Langmuir, 2019, 35, 16234-16243.	1.6	13
30796	A comprehensive study on the mechanism of ferroelectric phase formation in hafnia-zirconia nanolaminates and superlattices. Applied Physics Reviews, 2019, 6, .	5.5	73
30797	Ultrasmall Au clusters supported on pristine and defected CeO2: Structure and stability. Journal of Chemical Physics, 2019, 151, 174702.	1.2	8
30798	Understanding Structureâ€“Property Relationships of MoO₃-Promoted Rh Catalysts for Syngas Conversion to Alcohols. Journal of the American Chemical Society, 2019, 141, 19655-19668.	6.6	41
30799	Boron Phosphide van der Waals p-n Junction via Molecular Adsorption. Physical Review Applied, 2019, 12, .	1.5	10
30800	Degradation of Ka-Band GaN LNA Under High-Input Power Stress: Experimental and Theoretical Insights. IEEE Transactions on Electron Devices, 2019, 66, 5091-5096.	1.6	15
30801	Thermodynamic and kinetic behavior of low-alloy steels: An atomic level study using an Fe-Mn-Si-C modified embedded atom method (MEAM) potential. Materialia, 2019, 8, 100473.	1.3	15
30802	Single Au Anion Can Catalyze Acetylene Hydrochlorination: Tunable Catalytic Performance from Rational Doping. Journal of Physical Chemistry C, 2019, 123, 29203-29208.	1.5	26
30803	A new single-layer structure of MBene family: Ti₂B. Journal of Physics Condensed Matter, 2019, 31, 505401.	0.7	27
30804	An Ab-initio Study of Structural and Electronic Properties of CaTe under High Pressure. Russian Journal of Physical Chemistry A, 2019, 93, 2226-2232.	0.1	2
30805	Effect of Impurities on the Oxygen Adsorption Properties on the NiTi(110) Surface. Journal of Experimental and Theoretical Physics, 2019, 129, 413-420.	0.2	0
30806	Selenium Chemisorption Makes Iron Surfaces Slippery. Tribology Letters, 2019, 67, 1.	1.2	1
30807	Equilibrium hydrogen pressures in the Vâ€“H system from first principles. International Journal of Hydrogen Energy, 2019, 44, 28909-28918.	3.8	6
30808	First principles study of alkali and alkaline earth metal ions adsorption and diffusion on penta-graphene. Solid State Ionics, 2019, 342, 115062.	1.3	18
30809	Understanding X-ray Spectroscopy of Carbonaceous Materials by Combining Experiments, Density Functional Theory, and Machine Learning. Part I: Fingerprint Spectra. Chemistry of Materials, 2019, 31, 9243-9255.	3.2	62
30810	Activity Descriptors Derived from Comparison of Mo and Fe as Active Metal for Methane Conversion to Aromatics. Journal of the American Chemical Society, 2019, 141, 18814-18824.	6.6	52

#	Article	IF	Citations
30811	Probing changes in secondary electron yield from copper electrodes due to surface defects and changes in crystal orientation. Journal of Applied Physics, 2019, 126, .	1.1	11
30812	A review on computational modelling of individual device components and interfaces of perovskite solar cells using DFT. AIP Conference Proceedings, 2019, , .	0.3	5
30813	Strong acoustic plasmons in chemically doped graphene induced by a nearby metal surface. Physical Review B, 2019, 100, .	1.1	12
30814	Synergy of a Metallic NiCo Dimer Anchored on a C₂Nâ€“Graphene Matrix Promotes the Electrochemical CO₂ Reduction Reaction. ACS Sustainable Chemistry and Engineering, 2019, 7, 19113-19121.	3.2	91
30815	First-Principles Investigation on the Fully Compensated Ferrimagnetic Behavior in Ti2NbSb and TiZrNbSb. Chinese Physics Letters, 2019, 36, 067101.	1.3	0
30816	Physical properties of hexagonal BaPtAs with noncentrosymmetric SrPtSb-type and centrosymmetric YPtAs-type crystal structures: Effects of spin-orbit coupling. Physical Review B, 2019, 100, .	1.1	5
30817	Investigating the normal state and superconducting state properties of orthorhombic and hexagonal ZrRuP: A first-principles study. Physical Review B, 2019, 100, .	1.1	14
30818	Asymmetric Strainâ€Introduced Interface Effect on the Electronic and Optical Properties of the CsPbI 3 /SnS van der Waals Heterostructure. Advanced Materials Interfaces, 2019, 6, 1901330.	1.9	20
30819	Transition levels of intrinsic defects in type-II InAs/InAs0.5Sb0.5 strained-layer superlattices. Applied Physics Letters, 2019, 115, .	1.5	3
30820	Theoretical investigation on SiC(1 1 1)/Al4C3(0 0 0 1) interface using density functional theory calculations. Materials Today Communications, 2019, 21, 100743.	0.9	7
30821	Performance of Taoâ€“Mo Semilocal Functional with rVV10 Dispersion-Correction: Influence of Different Correlation. Journal of Physical Chemistry A, 2019, 123, 10582-10593.	1.1	14
30822	Quantitative Multilayer Cu(410) Structure and Relaxation Determined by QLEED. Scientific Reports, 2019, 9, 16882.	1.6	1
30823	Temperature-Dependent Magnetic Properties of Bi-Doped Fe₁₆N₂: First Principles and Atomistic Study. IEEE Transactions on Magnetics, 2019, 55, 1-5.	1.2	2
30824	Phase stability of an high-entropy Al-Cr-Fe-Ni-V alloy with exceptional mechanical properties: First-principles and APT investigations. Computational Materials Science, 2019, 170, 109161.	1.4	15
30825	Synthesis and Electronic Structure of a 3D Crystalline Stack of MXene-Like Sheets. Chemistry of Materials, 2019, 31, 9788-9796.	3.2	34
30826	IR Spectra of Crystalline Nucleobases: Combination of Periodic Harmonic Calculations with Anharmonic Corrections Based on Finite Models. Journal of Physical Chemistry B, 2019, 123, 10001-10013.	1.2	18
30827	Polarized Raman Reveals Alignment of Few-Layer MoS₂ Films. Journal of Physical Chemistry C, 2019, 123, 29468-29475.	1.5	14
30828	Tuning CO₂ Electroreduction of Cu Atoms on Triphenylene-Cored Graphdiyne. Journal of Physical Chemistry C, 2019, 123, 29776-29782.	1.5	12

#	Article	IF	Citations
30829	Electronic Property and Negative Thermal Expansion Behavior of Si136-xGex (x = 8, 32, 40, 104) Clathrate Solid Solution from First Principles. Nanomaterials, 2019, 9, 851.	1.9	1
30830	Stability of Coinage Metals Interacting with C60. Nanomaterials, 2019, 9, 1484.	1.9	4
30831	Metal-atom penetration and diffusion in organic solids: difference between Ïƒ- and Ï€- orbital molecular systems. Japanese Journal of Applied Physics, 2019, 58, SIIB28.	0.8	4
30832	Visualization of Dopant Oxygen Atoms in a Bi₂Sr₂CaCu₂O₈₊_{Î´} Superconductor. Advanced Functional Materials, 2019, 29, 1903843.	7.8	34
30833	XBi₄S₇ (X = Mn, Fe): New Costâ€Efficient Layered nâ€Type Thermoelectric Sulfides with Ultralow Thermal Conductivity. Advanced Functional Materials, 2019, 29, 1904112.	7.8	24
30834	Heavy Mn²⁺ Doped MgAl₂O₄ Phosphor for Highâ€Efficient Nearâ€Infrared Lightâ€Emitting Diode and the Nightâ€Vision Application. Advanced Optical Materials, 2019, 7, 1901105.	3.6	167
30835	Interface Effects on Epilayer Surface Density of States by Scanning Tunneling Spectroscopy and Density Functional Theory. Advanced Theory and Simulations, 2019, 2, 1900140.	1.3	2
30836	Nontoxic KBBF Family Member Zn₂BO₃(OH): Balance between Beneficial Layered Structure and Layer Tendency. Advanced Science, 2019, 6, 1901679.	5.6	56
30837	Influence of Orientational Disorder on the Optical Absorption Properties of the Hybrid Metalâ€Halide Perovskite CH₃NH₃PbI₃. ChemPhysChem, 2019, 20, 3228-3237.	1.0	2
30838	Uniform Ag Nanocubes Prepared by AgCl Particleâ€“Mediated Heterogeneous Nucleation and Disassembly and Their Mechanism Study by DFT Calculation. Small, 2019, 15, 1904031.	5.2	2
30839	Structural stability of uranium carbide (UC) under high pressure: ab-initio study. Computational Condensed Matter, 2019, 21, e00431.	0.9	8
30840	Using first principles density functional theory approach to model the thermal conductivity of diamond-like materials. Materials Today: Proceedings, 2019, 19, 2109-2111.	0.9	1
30841	Understanding why Alite is responsible of the main mechanical characteristics in Portland cement. Cement and Concrete Research, 2019, 126, 105916.	4.6	21
30842	Interaction properties of benzyl chloride and chlorobenzene on violet phosphorene sheets â€“ A first-principles perception. Computational and Theoretical Chemistry, 2019, 1165, 112563.	1.1	20
30843	Continuous/reversible phase transition behaviors and their effect on the hysteresis energy loss of the anodes in Na-ion batteries. Electrochimica Acta, 2019, 328, 135106.	2.6	5
30844	The active site of syngas conversion into ethanol over Cu/ZnO/Al2O3 ternary catalysts in slurry bed. Journal of Catalysis, 2019, 380, 68-82.	3.1	22
30845	A Density Functional Theory based Analysis on the Electronic, Mechanical, and Optical Properties of Cubic TiO2. Materials Today: Proceedings, 2019, 18, 596-605.	0.9	4
30846	DFT study of Ptn, Pdn, and Irn (n = 5, 6) clusters adsorbed on graphene: Structural and electronic properties. Physica B: Condensed Matter, 2019, 575, 411678.	1.3	6

#	Article	IF	Citations
30847	Prediction of a new direct-gap silicon phase: T36 silicon. Physics Letters, Section A: General, Atomic and Solid State Physics, 2019, 383, 125903.	0.9	2
30848	Scanning tunneling spectroscopy study of 20â€¯nm-thick nitrogen-doped lanthanum hexaboride thin film. Vacuum, 2019, 170, 108973.	1.6	4
30849	Postannealed Structural Relaxation and Phase Evolution of Quaternary Alloy BeMgZnO. ACS Applied Electronic Materials, 2019, 1, 2061-2068.	2.0	3
30850	Enhanced Iridium Mass Activity of 6H-Phase, Ir-Based Perovskite with Nonprecious Incorporation for Acidic Oxygen Evolution Electrocatalysis. ACS Applied Materials & Interfaces, 2019, 11, 42006-42013.	4.0	48
30851	Multifarious Interfaces, Band Alignments, and Formation Asymmetry of WSe₂â€“MoSe₂ Heterojunction Grown by Molecular-Beam Epitaxy. ACS Applied Materials & Interfaces, 2019, 11, 43766-43773.	4.0	8
30852	Ab Initio Calculation of Equilibrium Isotopic Fractionations of Potassium and Rubidium in Minerals and Water. ACS Earth and Space Chemistry, 2019, 3, 2601-2612.	1.2	49
30853	High thermoelectric properties in full-Heusler X₂YZ alloys (Xâ€‰â€‰=â€‰â€‰Ca, Sr, and Ba; Yâ€‰â€‰=â€‰â€‰Au	1.3	6
30854	First-principles studies on carbon diffusion in tungsten*. Chinese Physics B, 2019, 28, 116106.	0.7	4
30855	Effects of biaxial strain and functional groups on SiC/ti₃C₂ heterostructure: a first principle calculation. Materials Research Express, 2019, 6, 125070.	0.8	1
30856	Phase diagrams and electronic properties of B-S and H-B-S systems under high pressure. Physical Review B, 2019, 100, .	1.1	14
30857	Elastic Properties of Orthorhombic YBa2Cu3O7 under Pressure. Crystals, 2019, 9, 497.	1.0	22
30858	First-principle calculation of the pressure-induced variation in the formation energy of iron defect in Si1â^xGex alloy. Applied Physics A: Materials Science and Processing, 2019, 125, 1.	1.1	0
30859	KFeO2 with corner-shared FeO4 frameworks as a new type of cathode material in potassium-ion batteries. Journal of Solid State Electrochemistry, 2019, 23, 3135-3143.	1.2	19
30860	Stable structure of hydrogen atoms trapped in tungsten divacancy. Journal of Nuclear Materials, 2019, 527, 151825.	1.3	8
30861	Effects of transmutation elements on hydrogen trapping ability of vacancy in tungsten. Nuclear Instruments & Methods in Physics Research B, 2019, 461, 267-271.	0.6	1
30862	Electronic properties of novel bismuthene nanosheets with adsorption studies of G-series nerve agent molecules â€“ a DFT outlook. Physics Letters, Section A: General, Atomic and Solid State Physics, 2019, 383, 125975.	0.9	21
30863	Intrinsic Controllable Magnetism of Graphene Grown on Fe. Journal of Physical Chemistry C, 2019, 123, 26870-26876.	1.5	10
30864	Origin of Chemisorption Energy Scaling Relations over Perovskite Surfaces. Journal of Physical Chemistry C, 2019, 123, 28275-28283.	1.5	11

#	Article	IF	Citations
30865	Intrinsic Electric Field-Induced Properties in Janus MoSSe van der Waals Structures. Journal of Physical Chemistry Letters, 2019, 10, 559-565.	2.1	98
30866	Computational Design of Novel Hydrogen-Rich YSâ€“H Compounds. ACS Omega, 2019, 4, 14317-14323.	1.6	17
30867	Photoinduced hydrogen release from hydrogen boride sheets. Nature Communications, 2019, 10, 4880.	5.8	63
30868	DFT+U study of small ZnO nanoclusters. AIP Conference Proceedings, 2019, , .	0.3	0
30869	Electronic structure of YbB6 dependent on onsite Coulomb interaction U and internal parameter of B atom. Chinese Physics B, 2019, 28, 116201.	0.7	2
30870	Phonon dynamics in the layered negative thermal expansion compounds CuxNi2â^'x(CN)4. Physical Review B, 2019, 100, .	1.1	9
30871	Symmetry-adapted real-space density functional theory for cylindrical geometries: Application to large group-IV nanotubes. Physical Review B, 2019, 100, .	1.1	27
30872	Lattice dynamical properties of antiferromagnetic MnO, CoO, and NiO, and the lattice thermal conductivity of NiO. Physical Review B, 2019, 100, .	1.1	10
30873	Effect of confinement and octahedral rotations on the electronic, magnetic, and thermoelectric properties of correlated <mml:math xmlns:mml="http://www.w3.org/1998/Math/MathML"><mml:mrow><mml:mi>Sr</mml:mi><mml:mi>X</mml:mi><mml:msub><mml:mi mathvariant="normal">O</mml:mi><mml:mn>3</mml:mn></mml:msub><mml:mo>/</mml:mo><mml:msub><mml:mi>SrTiO</mml:mi>		

#	Article	IF	Citations
30884	Phonon-induced electronic relaxation in a strongly correlated system: The Sn/Si(111) <mml:math xmlns:mml="http://www.w3.org/1998/Math/MathML"><mml:mrow><mml:mo>(</mml:mo><mml:msqrt><mml:mn>3</mml:mn></mml: adlayer revisited. Physical Review B, 2019, 100, .	1.1	2
30885	High density of genuine growth twins in electrodeposited aluminum. Science Advances, 2019, 5, eaax3894.	4.7	17
30886	Ligand-Modified Boron-Doped Diamond Surface: DFT Insights into the Electronic Properties of Biofunctionalization. Materials, 2019, 12, 2910.	1.3	4
30887	Partitioning of Interstitial Segregants during Decohesion: A DFT Case Study of the Î£3 Symmetric Tilt Grain Boundary in Ferritic Steel. Materials, 2019, 12, 2971.	1.3	4
30888	Structural Stability, Electronic Structures, Mechanical Properties and Debye Temperature of Transition Metal Impurities in Tungsten: A First-Principles Study. Metals, 2019, 9, 967.	1.0	23
30889	Potential Application of Graphene/Antimonene Herterostructure as an Anode for Li-Ion Batteries: A First-Principles Study. Nanomaterials, 2019, 9, 1430.	1.9	20
30890	Intrinsic Thermal Shock Behavior of Common Rutile Oxides. Physics, 2019, 1, 290-300.	0.5	6
30891	Tunable Graphene Electronics with Local Ultrahigh Pressure. Advanced Functional Materials, 2019, 29, 1806715.	7.8	15
30892	Photo-absorption properties of van der Waals heterostructure of monolayer InSe with silicene, germanene and antimonene. Applied Surface Science, 2019, 475, 774-780.	3.1	12
30893	First-principles study of electronic and optical properties of sulfur doped tin monoxide: A potential applicant for optoelectronic devices. Ceramics International, 2019, 45, 7495-7503.	2.3	7
30894	Effect of stress layer on thermal properties of SnSe2 few layers. Journal of Alloys and Compounds, 2019, 783, 226-231.	2.8	11
30895	Effect of Ca doping on structural, magnetic and electronic properties of TbMnO3. Journal of Magnetism and Magnetic Materials, 2019, 477, 77-82.	1.0	4
30896	Mechanical behaviors, lattice thermal conductivity and vibrational properties of a new MAX phase Lu2SnC. Journal of Physics and Chemistry of Solids, 2019, 129, 162-171.	1.9	83
30897	Density functional theory study on the electronic structures and related properties of Ag-doped CH3NH3PbI3 perovskite. Results in Physics, 2019, 15, 102709.	2.0	10
30898	Atomic and electronic structure of domains walls in a polar metal. Physical Review B, 2019, 99, .	1.1	19
30899	Nonlinear Electronic Transport Behavior of <inline-formula> <tex-math notation="LaTeX">$Upsilon$ </tex-math> </inline-formula>-Graphyne Nanotubes. IEEE Transactions on Electron Devices, 2019, 66, 1584-1590.	1.6	10
30900	The alkali resistance of CuNbTi catalyst for selective reduction of NO by NH3: A comparative investigation with VWTi catalyst. Applied Catalysis B: Environmental, 2019, 246, 166-179.	10.8	96
30901	First-principles study of structure, mechanical and optical properties of La- and Sc-doped Y2O3. Journal of Rare Earths, 2019, 37, 879-885.	2.5	12

#	Article	IF	Citations
30902	h-C63: A new hexagonal superhard metallic carbon allotrope. Results in Physics, 2019, 15, 102738.	2.0	3
30903	Variability of Câ€“F Bonds Governs the Formation of Specific Structural Motifs in Fluorinated Graphenes. Journal of Physical Chemistry C, 2019, 123, 27896-27903.	1.5	22
30904	Translational Manipulation of Magnetic Cobalt Adatoms on the Si(100)-2 Ã— 1 Surface at 9 K. Journal of Physical Chemistry C, 2019, 123, 26415-26423.	1.5	3
30905	Quantitative Studies of the Coverage Effects on Microkinetic Simulations for NO Oxidation on Pt(111). Journal of Physical Chemistry C, 2019, 123, 27594-27602.	1.5	30
30906	Rational Design of Porous Nodal-Line Semimetallic Carbon for K-Ion Battery Anode Materials. Journal of Physical Chemistry Letters, 2019, 10, 6360-6367.	2.1	31
30907	Reshaping Dynamics of Gold Nanoparticles under H₂ and O₂ at Atmospheric Pressure. ACS Nano, 2019, 13, 2024-2033.	7.3	32
30908	Firstâ€principles Investigation of Frictional Characteristics of Brucite: An Application to Its Macroscopic Frictional Characteristics. Journal of Geophysical Research: Solid Earth, 2019, 124, 10423-10443.	1.4	7
30909	Physical properties of ternary thallium chalcogenes Tl 2 MQ 3 (M = Zr, Hf; Q = S, Se, Te) via ab - initio calculations. Chinese Physics B, 2019, 28, 106301.	0.7	1
30910	A study of properties of palladium metal as a component of fuel cells. Materials Research Express, 2019, 6, 105540.	0.8	7
30911	Anisotropy in elasticity and physical properties of Ti₂B under high pressure. Materials Research Express, 2019, 6, 1065c4.	0.8	5
30912	Structural, elastic, electronic and optical properties of lead-free halide double perovskite Cs₂AgBiX₆ (X = Cl, Br, and I). Materials Research Express, 2019, 6, 115517.	0.8	31
30913	The mechanical properties and strain effect on the electronic properties of III-nitride monolayers: ab-initio study. Materials Research Express, 2019, 6, 115915.	0.8	7
30914	The first principle study: electronic, optical and elastic properties of HfTe₅metal pentatelluride. Materials Research Express, 2019, 6, 116315.	0.8	3
30915	Theoretical and experimental investigation of structural and optical properties of lithium doped cadmium oxide thin films. Materials Research Express, 2019, 6, 116434.	0.8	24
30916	An ideal metal contact with monolayer Ti₂CO₂. Materials Research Express, 2019, 6, 1165a9.	0.8	1
30917	Electronic structures and magnetic behavior of Al-, Si-, P- and Cl-doped ZnS. Materials Research Express, 2019, 6, 116121.	0.8	1
30918	Tunneling anisotropic magnetoresistance of Pb and Bi adatoms and dimers on Mn/W(110): A first-principles study. Physical Review B, 2019, 100, .	1.1	3
30919	Crystalline phase transitions and vibrational spectra of silicon up to multiterapascal pressures. Physical Review B, 2019, 100, .	1.1	9

#	Article	IF	Citations
30920	Observation of topological transition in high- <mml:math xmlns:mml="http://www.w3.org/1998/Math/MathML"><mml:msub><mml:mi>T</mml:mi><mml:mi>c</mml:mi></mml:msub></mml:ma superconducting monolayer <mml:math xmlns:mml="http://www.w3.org/1998/Math/MathML"><mml:msub><mml:mi mathvariant="normal">FeTe</mml:mi><mml:mrow><mml:mn>1</mml:mn><mml:mo>â^'</mml:mo><mml:mi>x</mml:mi></mml:mrow> mathvariant="normal">Se</mml:mi><mml:mi>x</mml:mi></mml:msub></mml:math> films on <mml:math	1.1	37
30921	Magnetic instabilities in doped <mml:math xmlns:mml="http://www.w3.org/1998/Math/MathML"><mml:mrow><mml:msub><mml:mi>Fe</mml:mi><mml:mn>2</mml:mn></mml:msub> full-Heusler thermoelectric compounds. Physical Review B, 2019, 100, .	1.1	5
30922	Electronic and hyperbolic dielectric properties of <mml:math xmlns:mml="http://www.w3.org/1998/Math/MathML"><mml:mrow><mml:mi>Zr</mml:mi><mml:msub><mml:mi mathvariant="normal">S</mml:mi><mml:mn>2</mml:mn></mml:msub><mml:mo>/</mml:mo><mml:mi>Hf</mml:mi><mml:msub><mml:mi mathvariant="normal">S</mml:mi><mml:mn>2</mml:mn></mml:msub></mml:mrow></mml:math> heterostructures. Physical Review B, 2019, 100, .	1.1	12
30923	Mechanical properties of VMoNO as a function of oxygen concentration: Toward development of hard and tough refractory oxynitrides. Journal of Vacuum Science and Technology A: Vacuum, Surfaces and Films, 2019, 37, .	0.9	1
30924	Two-Dimensional SiP, SiAs, GeP and GeAs as Promising Candidates for Photocatalytic Applications. Coatings, 2019, 9, 522.	1.2	32
30925	Catalysis of material surface defects: Multiscale modeling of methanol synthesis by CO2 reduction on copper. Applied Surface Science, 2019, 497, 143783.	3.1	40
30926	Influence of graphene surface chemistry on Ir-catalyzed hydrogenation of p-chloronitrobenzene and cinnamaldehyde: Weak molecule-support interactions. Journal of Catalysis, 2019, 377, 524-533.	3.1	13
30927	Alkali metal-substituted bismuth-based perovskite compounds: A DFT study. Journal of Science: Advanced Materials and Devices, 2019, 4, 492-498.	1.5	6
30928	Phase transition and electronic properties of skutterudite-type IrP₃ under high pressure. Physical Chemistry Chemical Physics, 2019, 21, 21262-21266.	1.3	6
30929	Enhancing hydrogen evolution activity by doping and tuning the curvature of manganese-embedded carbon nanotubes. Catalysis Science and Technology, 2019, 9, 5301-5314.	2.1	23
30930	Novel High Efficiency Layered Oxide Photocatalyst Li2SnO3 for Rhodamine B and Tetracycline Degradation. Catalysts, 2019, 9, 712.	1.6	11
30931	Improved Moisture Stability of Perovskite Solar Cells Using N719 Dye Molecules. Solar Rrl, 2019, 3, 1900345.	3.1	30
30932	Experimental and ab-initio investigation of the microstructure and optoelectronic properties of FCMâ€“CVD-prepared Al-doped ZnO thin films. Applied Physics A: Materials Science and Processing, 2019, 125, 1.	1.1	27
30933	Experimental and Theoretical Investigations on the Influence of A on the Hydrogen Sorption Properties of ANiy Compounds, A = {Y, Sm, Gd}. Journal of Physical Chemistry C, 2019, 123, 23334-23341.	1.5	6
30934	Polarization Control of the Interface Ferromagnetic to Antiferromagnetic Phase Transition in Co/Pb(Zr,Ti)O₃. ACS Applied Materials & Interfaces, 2019, 11, 34399-34407.	4.0	6
30935	Structural and Electronic Properties of Iron-Doped Sodium Montmorillonite Clays: A First-Principles DFT Study. ACS Omega, 2019, 4, 14369-14377.	1.6	10
30936	New insights into the origin of unstable sodium graphite intercalation compounds. Physical Chemistry Chemical Physics, 2019, 21, 19378-19390.	1.3	68
30937	Transition metal embedded C₃N monolayers as promising catalysts for the hydrogen evolution reaction. Physical Chemistry Chemical Physics, 2019, 21, 20432-20441.	1.3	32

#	Article	IF	Citations
30938	Theoretical search for novel Au or Ag bimetallic alloys capable of transforming CO2 into hydrocarbons. Journal of Materials Chemistry A, 2019, 7, 20567-20573.	5.2	15
30939	Unusually strong heteroatomic bonding in the complex polyanion of intermetallic Ba₆Pt₂₂Al₅₃. Dalton Transactions, 2019, 48, 14103-14114.	1.6	3
30940	Designing an All-Carbon Membrane for Water Desalination. Physical Review Applied, 2019, 12, .	1.5	16
30941	Tetrahedron integration method for strongly varying functions: Application to the GT self-energy. Physical Review B, 2019, 100, .	1.1	15
30942	Rational Design Principles of the Quantum Anomalous Hall Effect in Superlatticelike Magnetic Topological Insulators. Physical Review Letters, 2019, 123, 096401.	2.9	104
30943	Materials Compatibility in Rechargeable Aluminum Batteries: Chemical and Electrochemical Properties between Vanadium Pentoxide and Chloroaluminate Ionic Liquids. Chemistry of Materials, 2019, 31, 7238-7247.	3.2	35
30944	Cohesive Properties of Ionic Liquids Calculated from First Principles. Journal of Chemical Theory and Computation, 2019, 15, 5563-5578.	2.3	23
30945	Computation-Guided Design of Niâ€“Mnâ€“Sn Ferromagnetic Shape Memory Alloy with Giant Magnetocaloric Effect and Excellent Mechanical Properties and High Working Temperature via Multielement Doping. ACS Applied Materials & Interfaces, 2019, 11, 34827-34840.	4.0	26
30946	Atomic and electronic modulation of self-supported nickel-vanadium layered double hydroxide to accelerate water splitting kinetics. Nature Communications, 2019, 10, 3899.	5.8	355
30947	First principle study of In/Ga-doped phosphorene. AIP Conference Proceedings, 2019, , .	0.3	0
30948	A new activity model for Mgâ€“Al biotites determined through an integrated approach. Contributions To Mineralogy and Petrology, 2019, 174, 76.	1.2	5
30949	Investigation of growth mechanism for highly oriented TiO2 nanorods: the role of reaction time and annealing temperature. SN Applied Sciences, 2019, 1, 1.	1.5	19
30950	Photooxidation of Water on Pristine, S- and N-Doped TiO₂(001) Nanotube Surfaces: A DFT + U Study. Journal of Physical Chemistry C, 2019, 123, 22691-22698.	1.5	15
30951	Enhanced Interactions of Amino Acids and Nucleic Acid Bases with Bare Black Phosphorene Monolayer Mediated by Coadsorbed Species. Journal of Physical Chemistry C, 2019, 123, 23691-23704.	1.5	10
30952	Carbon-Related Bilayers: Nanoscale Building Blocks for Self-Assembly Nanomanufacturing. Journal of Physical Chemistry C, 2019, 123, 23195-23204.	1.5	5
30953	Exploring the Catalytic Properties of Unsupported and TiO₂-Supported Cu₅ Clusters: CO₂ Decomposition to CO and CO₂ Photoactivation. Journal of Physical Chemistry C, 2019, 123, 23064-23074.	1.5	39
30954	Dendrite-Free Fluorinated Graphene/Lithium Anodes Enabling in Situ LiF Formation for High-Performance Lithiumâ€“Oxygen Cells. ACS Applied Materials & Interfaces, 2019, 11, 39737-39745.	4.0	23
30955	Surface Functionalization of Layered Molybdenum Disulfide for the Selective Detection of Volatile Organic Compounds at Room Temperature. ACS Applied Materials & Interfaces, 2019, 11, 34135-34143.	4.0	79

#	Article	IF	Citations
30956	A General Atomic Surface Modification Strategy for Improving Anchoring and Electrocatalysis Behavior of Ti₃C₂T₂ MXene in Lithiumâ€“Sulfur Batteries. ACS Nano, 2019, 13, 11078-11086.	7.3	232
30957	The influence of support materials on the structural and electronic properties of gold nanoparticles â€“ a DFT study. Physical Chemistry Chemical Physics, 2019, 21, 19011-19025.	1.3	39
30958	Theoretical Prediction of Martensitic Transformation in Mn3Si Heusler Alloy. Shape Memory and Superelasticity, 2019, 5, 258-262.	1.1	0
30959	In Situ EC-STM Study and DFT Modeling of the Adsorption of Glycerol on Cu(111) in NaOH Solution. Journal of Physical Chemistry C, 2019, 123, 22228-22238.	1.5	7
30960	Structural, mechanical, and electronic properties of 25 kinds of IIIâ€“V binary monolayers: A computational study with first-principles calculation*. Chinese Physics B, 2019, 28, 086105.	0.7	29
30961	Computational investigations of MnNiCuSb alloy for structural, elasto-mechanical and vibrational properties. Modern Physics Letters B, 2019, 33, 1950276.	1.0	3
30962	Electronic properties of vacancies in bilayer graphane. Physica B: Condensed Matter, 2019, 573, 67-71.	1.3	1
30963	Improving Predicted Nuclear Magnetic Resonance Chemical Shifts Using the Quasi-Harmonic Approximation. Journal of Chemical Theory and Computation, 2019, 15, 5259-5274.	2.3	11
30964	First-Principles Mapping of the Electronic Properties of Two-Dimensional Materials for Strain-Tunable Nanoelectronics. ACS Applied Nano Materials, 2019, 2, 5614-5624.	2.4	17
30965	Stabilizing honeycomb borophene by metal decoration: a computational study. Journal of Materials Chemistry C, 2019, 7, 11493-11499.	2.7	17
30966	Aluminum adsorption on graphene: Theoretical study of dispersion effects. Journal of Theoretical and Computational Chemistry, 2019, 18, 1950019.	1.8	3
30967	Facile and Versatile Functionalization of Twoâ€Đimensional Carbon Nitrides by Design: Magnetism/Multiferroicity, Valleytronics, and Photovoltaics. Advanced Functional Materials, 2019, 29, 1905752.	7.8	19
30968	Molecular Dynamics Study of Molecular and Dissociative Adsorption Using System-Specific Force Fields Based on Ab Initio Calculations: CO/Cu(110) and $$ext {CH}_4/ext {Pt(110)}$$. Topics in Catalysis, 2019, 62, 1044-1052.	1.3	8
30969	Rh nanoroses for isopropanol oxidation reaction. Applied Catalysis B: Environmental, 2019, 259, 118082.	10.8	44
30970	High-pressure stable phases in mercury azide. Computational Materials Science, 2019, 169, 109147.	1.4	6
30971	NaB6Si: A novel wide band gap semiconductor with great hardness. Physics Letters, Section A: General, Atomic and Solid State Physics, 2019, 383, 125901.	0.9	1
30972	Mechanistic Insights into Selective CO₂ Conversion via RWGS on Transition Metal Phosphides: A DFT Study. Journal of Physical Chemistry C, 2019, 123, 22918-22931.	1.5	25
30973	Cation Disorder and Lithium Insertion Mechanism of Wadsleyâ€“Roth Crystallographic Shear Phases from First Principles. Journal of the American Chemical Society, 2019, 141, 15121-15134.	6.6	69

#	Article	IF	Citations
30974	Ultrahigh-current-density niobium disulfide catalysts for hydrogen evolution. Nature Materials, 2019, 18, 1309-1314.	13.3	280
30975	Hydrogen in Î±-iron: role of phonons in the diffusion of interstitials at high temperature. Scientific Reports, 2019, 9, 12127.	1.6	5
30976	Pressure induced semiconductorâ€“semimetalâ€“superconductor transition of magnesium hexaborides. Dalton Transactions, 2019, 48, 14299-14305.	1.6	6
30977	Mechanisms of ammonia and hydrazine synthesis on Î·-Mn₃N₂-(100) surfaces. Physical Chemistry Chemical Physics, 2019, 21, 19365-19377.	1.3	4
30978	Monolayer Î²-tellurene: a promising p-type thermoelectric material via first-principles calculations. Nanoscale, 2019, 11, 18116-18123.	2.8	36
30979	Improved cycling stability in high-capacity Li-rich vanadium containing disordered rock salt oxyfluoride cathodes. Journal of Materials Chemistry A, 2019, 7, 21244-21253.	5.2	37
30980	Towards magnetic alumina: uncovering the roles of transition metal doping and electron hybridization in spin delocalization. Journal of Physics Condensed Matter, 2019, 31, 245801.	0.7	2
30981	Band structure of Ge_{1â^'x}Sn_x alloy: a full-zone 30-band k Â· p model. New Journal of Physics, 2019, 21, 073037.	1.2	24
30982	Hydrogen molecule adsorption on a Ti-doped graphene+ semi-fullerene surface.. Journal of Physics: Conference Series, 2019, 1221, 012081.	0.3	3
30983	Ab initio simulation of oxygen vacancies in LiMgPO₄. Materials Research Express, 2019, 6, 106304.	0.8	15
30984	Comparison of structural, mechanical and optical properties of tantalum hemicarbide with tantalum monocarbide: ab initio calculations. Journal of Physics Communications, 2019, 3, 055017.	0.5	16
30985	A robust algorithm for k-point grid generation and symmetry reduction. Journal of Physics Communications, 2019, 3, 065009.	0.5	8
30986	How to resolve a phonon-associated property into contributions of basic phonon modes. JPhys Materials, 2019, 2, 045005.	1.8	6
30987	Spectroscopic properties of few-layer tin chalcogenides. JPhys Materials, 2019, 2, 044005.	1.8	12
30988	Erasable and recreatable two-dimensional electron gas at the heterointerface of SrTiO ₃ and a water-dissolvable overlayer. Science Advances, 2019, 5, eaaw7286.	4.7	24
30989	Electronic and Magnetic Properties of Defected Monolayer WSe2 with Vacancies. Nanoscale Research Letters, 2019, 14, 192.	3.1	37
30990	Dependence of Electronic and Optical Properties of MoS2 Multilayers on the Interlayer Coupling and Van Hove Singularity. Nanoscale Research Letters, 2019, 14, 288.	3.1	27
30991	Lattice dynamics for isochorically heated metals: A model study. Journal of Applied Physics, 2019, 126, 075113.	1.1	9

#	Article	IF	Citations
30992	Phase stabilities of <mml:math xmlns:mml="http://www.w3.org/1998/Math/MathML"><mml:mrow><mml:mi>C</mml:mi><mml:mi>m</mml:mi><mml:mi>c</mml:mi><mml:mi> and <mml:math xmlns:mml="http://www.w3.org/1998/Math/MathML"><mml:mrow><mml:mi>P</mml:mi><mml:mi>n</mml:mi><mml:mi>m</mml:mi><mml:mi>	1.1	14
30993	Anomalous thermal expansion and dynamical instabilities in Mg(BH4)2. Physical Review B, 2019, 100, .	1.1	10
30994	First-Principles Study of Piezoelectric Properties and Bonding Analysis in (Mg, X, Al)N Solid Solutions (X = Nb, Ti, Zr, Hf). ACS Omega, 2019, 4, 15081-15086.	1.6	31
30995	Magnetic field-temperature phase diagram of multiferroic (NH4)2FeCl5Â·H2O. Npj Quantum Materials, 2019, 4, .	1.8	10
30996	Theoretical study of the photoconduction and photomagnetism of the BPY[Ni(dmit)2]2 molecular crystal. Dalton Transactions, 2019, 48, 13789-13798.	1.6	1
30997	NaSbSe2 as a promising light-absorber semiconductor in solar cells: First-principles insights. APL Materials, 2019, 7, 081122.	2.2	11
30998	Strain effects and electronic structures of narrow band P-R ferroelectrics: First principles calculation. Ferroelectrics, 2019, 544, 1-10.	0.3	0
30999	Imaging and Dynamics of Water Hexamer Confined in Nanopores. ACS Nano, 2019, 13, 10622-10630.	7.3	10
31000	Highly efficient decomposition of ammonia using high-entropy alloy catalysts. Nature Communications, 2019, 10, 4011.	5.8	376
31001	The influence of oxygen vacancy on the electronic and optical properties of ABO_{3â^'Î´} (A =) Tj ETQq1 1 0.784314 rgBT /Ov	1.3	41
31002	Rectification and negative differential effects of Si₂C₂ clusters: An abÂinitio study. International Journal of Modern Physics B, 2019, 33, 1950205.	1.0	0
31003	Quantum capacitance of transition metal and nitrogen co-doped graphenes as supercapacitors electrodes: A DFT study. Applied Surface Science, 2019, 496, 143659.	3.1	58
31004	Two-dimensional metal carbide comrade for tracing CO and CO2. Applied Surface Science, 2019, 496, 143685.	3.1	36
31005	Combined Experimental and Theoretical Insights into Energy Storage Applications of a VO₂(D)â€“Graphene Hybrid. Journal of Physical Chemistry C, 2019, 123, 24280-24288.	1.5	37
31006	Nickel Hydrides under High Pressure. Journal of Physical Chemistry C, 2019, 123, 24243-24247.	1.5	3
31007	Suppressed Carrier Recombination in Janus MoSSe Bilayer Stacks: A Time-Domain Ab Initio Study. Journal of Physical Chemistry Letters, 2019, 10, 5564-5570.	2.1	23
31008	A comprehensive study of the molecular vibrations in solid-state benzylic amide [2]catenane. Physical Chemistry Chemical Physics, 2019, 21, 19538-19547.	1.3	4
31009	Synthesis, structure and properties of a calcium oxonitridosilicate phosphor showing green or red luminescence upon doping with Eu²⁺ or Ce³⁺. Dalton Transactions, 2019, 48, 14069-14076.	1.6	5

#	Article	IF	Citations
31010	High performance P2 sodium layered oxides: an in-depth study into the effect of rationally selected stoichiometry. Journal of Materials Chemistry A, 2019, 7, 21812-21826.	5.2	11
31011	Electronic structure and atomic level complexity in Al0.5TiZrPdCuNi high-entropy alloy in glass phase. Journal of Applied Physics, 2019, 126, .	1.1	12
31012	Adsorption of Na atom on mono-layer gallenene. AIP Conference Proceedings, 2019, , .	0.3	2
31013	Edge phonons in layered orthorhombic GeS and GeSe monochalcogenides. Physical Review B, 2019, 100, .	1.1	22
31014	<mml:math xmlns:mml="http://www.w3.org/1998/Math/MathML"><mml:mrow><mml:msub><mml:mi>FeTi</mml:mi><mml:mn>2</mml:mn></mml:msub><mml:mathvariant="normal">O</mml:mi><mml:mn>5</mml:mn></mml:msub></mml:mrow></mml:math> : A spin Jahn-Teller transition enhanced by cation substitution. Physical Review B, 2019, 100, .	1.1	7
31015	Atomically precise, custom-design origami graphene nanostructures. Science, 2019, 365, 1036-1040.	6.0	156
31016	First-principles study of BiFeO₃and BaTiO₃in tetragonal structure. International Journal of Modern Physics B, 2019, 33, 1950231.	1.0	40
31017	Multiple fermions in MoP. Modern Physics Letters B, 2019, 33, 1950293.	1.0	0
31018	Defects, Diffusion, and Dopants in Li2Ti6O13: Atomistic Simulation Study. Materials, 2019, 12, 2851.	1.3	12
31019	Synthesis and structural characterization of 3-[1-[4-(2-methylpropyl)phenyl]ethyl]-6-(4-fluorophenyl)-1,2,4-triazolo[3,4-b]-1,3,4-thiadiazole. Powder Diffraction, 2019, 34, 325-330.	0.4	1
31020	Sub-nanocatalysis for Efficient Aqueous Nitrate Reduction: Effect of Strong Metalâ€“Support Interaction. ACS Applied Materials & Interfaces, 2019, 11, 33859-33867.	4.0	15
31021	Effect of vacancies on the structural and electronic properties of Ti₂CO₂. RSC Advances, 2019, 9, 27646-27651.	1.7	17
31022	Interfacial engineering to improve Cu2ZnSnX4 (X = S, Se) solar cell efficiency. APL Materials, 2019, 7, .	2.2	19
31023	Density functional theory study of the effect of Vanadium doping on electronic and optical properties of NiO. International Journal of Computational Materials Science and Engineering, 2019, 08, 1950007.	0.5	1
31024	Thermodynamics of graphite intercalation binary alloys of Li-Na, Na-K, and Li-K from van der Waals density functionals. Journal of Solid State Electrochemistry, 2019, 23, 2825-2834.	1.2	2
31025	Thermodynamics and kinetics of ordered and disordered Cu/Au alloys from first principles calculations. Journal of Alloys and Compounds, 2019, 809, 151615.	2.8	10
31026	Adsorption geometries and interface electronic structure of C60 on Si(100)2â€Ã—â€1 reconstruction surface. Surface Science, 2019, 690, 121484.	0.8	2
31027	Computational screening of transition-metal single atom doped C₉N₄ monolayers as efficient electrocatalysts for water splitting. Nanoscale, 2019, 11, 18169-18175.	2.8	56

#	Article	IF	Citations
31028	Toward rational catalyst design for partial hydrogenation of dimethyl oxalate to methyl glycolate: a descriptor-based microkinetic analysis. Catalysis Science and Technology, 2019, 9, 5763-5773.	2.1	19
31029	Study of interaction of nucleobases with ultrathin VO2 monoclinic nanowire. AIP Conference Proceedings, 2019, , .	0.3	0
31030	Orbital-Selective Kondo Entanglement and Antiferromagnetic Order in <mml:math xmlns:mml="http://www.w3.org/1998/Math/MathML" display="inline"><mml:mrow><mml:msub><mml:mrow><mml:mi>USb</mml:mi></mml:mrow><mml:mrow><mml:mn>2</mml:mn></m Physical Review Letters, 2019, 123, 106402.	2.9	21
31031	Computer Design of Two-Dimensional Monolayers with Octahedral 1,6-Carborane Units. Russian Journal of Inorganic Chemistry, 2019, 64, 1031-1034.	0.3	3
31032	Unusual lattice thermal conductivity in the simple crystalline compounds <mml:math xmlns:mml="http://www.w3.org/1998/Math/MathML"><mml:mrow><mml:mrow><mml:mi>Tl</mml:mi><mml:mi>X</mml:mi></mml:m mathvariant="normal">Te</mml:mi><mml:mn>2</mml:mn></mml:msub></mml:mrow><mml:mrow><mml:mo>(</mml:mo><mml:mrov Physical Review B, 2019, 100, .	1.1	16
31033	Band folding, strain, confinement, and surface relaxation effects on the electronic structure of GaAs and GaP: from bulk to nanowires. European Physical Journal B, 2019, 92, 1.	0.6	3
31034	Revelation of the Nature of the Ligandâ€“PbS Bond and Its Implication on Chemical Functionalization of PbS. Journal of Physical Chemistry C, 2019, 123, 22981-22988.	1.5	2
31035	Surface Pb-Dimer Passivated by Molecule Oxygen Notably Suppresses Charge Recombination in CsPbBr₃ Perovskites: Time-Domain Ab Initio Analysis. Journal of Physical Chemistry Letters, 2019, 10, 5499-5506.	2.1	22
31036	Computational Study of Ohmic Contact at Bilayer InSe-Metal Interfaces: Implications for Field-Effect Transistors. ACS Applied Nano Materials, 2019, 2, 6898-6908.	2.4	13
31037	First principles study of g-Mg₃N₂ as an anode material for Na-, K-, Mg-, Ca- and Al-ion storage. RSC Advances, 2019, 9, 27378-27385.	1.7	24
31038	Magnetoelectric Effect at the <mml:math xmlns:mml="http://www.w3.org/1998/Math/MathML" display="inline" overflow="scroll"><mml:mi>Ni</mml:mi><mml:mo>/</mml:mo><mml:msub><mml:mrow><mml:mi>Hf</mml:mi><mml:mi mathvariant="normal">O</mml:mi></mml:mrow><mml:mn>2</mml:mn></mml:msub></mml:math> Interface Induced by Ferroelectric Polarization. Physical Review Applied, 2019, 12, .	1.5	15
31039	Role of Co dopants on the structural, optical and magnetic properties of lead-free ferroelectric Na0.5Bi0.5TiO3 materials. Journal of Science: Advanced Materials and Devices, 2019, 4, 584-590.	1.5	9
31040	Polymer network of graphene oxide with covalently attached 2-(4â€²-Hydroxyphenyl)fulleropyrrolidine and Palladium: Synthesis, properties and theoretical studies. Materials Science and Engineering B: Solid-State Materials for Advanced Technology, 2019, 249, 114406.	1.7	5
31041	Computational studies of mono-chalcogenides ZnS and ZnSe at high-pressures. Results in Physics, 2019, 15, 102626.	2.0	13
31042	Atomic and Effective Pair Interactions in FeC Alloy with Point Defects: A Cluster Expansion Study. ISIJ International, 2019, 59, 2343-2351.	0.6	0
31043	DFT Calculations of the Structural, Mechanical, and Electronic Properties of TiV Alloy Under High Pressure. Symmetry, 2019, 11, 972.	1.1	8
31044	Atomistic Simulation of Anistropic Crystal Structures at Nanoscale. , 2019, , .		3
31045	First-principles calculations for Li, P dopants and vacancy defect in ultra-thin hydrogenated diamond nanofilms: Structural, electronic and optical properties. Diamond and Related Materials, 2019, 99, 107526.	1.8	14

#	Article	IF	Citations
31046	Reactivity and selectivity descriptors of dioxygen activation routes on metal oxides. Journal of Catalysis, 2019, 377, 692-710.	3.1	9
31047	Structure-property relationship of graphene coupled metal (Ni, Co, Fe) (oxy)hydroxides for efficient electrochemical evolution of oxygen. Journal of Catalysis, 2019, 377, 619-628.	3.1	15
31048	Electronic, elastic and piezoelectric properties of boron-V group binary and ternary monolayers. Physica B: Condensed Matter, 2019, 574, 311634.	1.3	23
31049	Zn-Doped Cu(100) facet with efficient catalytic ability for the CO₂ electroreduction to ethylene. Physical Chemistry Chemical Physics, 2019, 21, 21341-21348.	1.3	25
31050	Electric-field-tunable molecular adsorption on germanane. Physical Chemistry Chemical Physics, 2019, 21, 20287-20295.	1.3	7
31051	Nanoscale Active Sites for the Hydrogen Evolution Reaction on Low Carbon Steel. Journal of Physical Chemistry C, 2019, 123, 24146-24155.	1.5	54
31052	Surface Defect-Controlled Growth and High Photocatalytic H₂ Production Efficiency of Anatase TiO₂ Nanosheets. ACS Applied Materials & Interfaces, 2019, 11, 37256-37262.	4.0	32
31053	Highly Exposed Active Sites of Defect-Enriched Derived MOFs for Enhanced Oxygen Reduction Reaction. ACS Sustainable Chemistry and Engineering, 2019, 7, 17855-17862.	3.2	66
31054	Microstructure and surface control of MXene films for water purification. Nature Sustainability, 2019, 2, 856-862.	11.5	273
31055	Introducing novel electronic and magnetic properties in C₃N nanosheets by defect engineering and atom substitution. Physical Chemistry Chemical Physics, 2019, 21, 21070-21083.	1.3	57
31056	Intermediate band solar cell materials through the doping of group-VA elements (N, P, As and Sb) in Cu₂ZnSiSe₄. RSC Advances, 2019, 9, 28234-28240.	1.7	3
31057	Effect of doping Ti on the vacancy trapping mechanism for helium in ZrCo from first principles. Physical Chemistry Chemical Physics, 2019, 21, 20909-20918.	1.3	10
31058	Unravelling the effects of oxidation state of interstitial iodine and oxygen passivation on charge trapping and recombination in CH₃NH₃PbI₃ perovskite: a time-domain ab initio study. Chemical Science, 2019, 10, 10079-10088.	3.7	44
31059	Density functional theory study on the effect of Cu- and Na-substituted layers on spin-dependent transport and TMR in the Fe/ZnO/Fe MTJ. Journal of Theoretical and Applied Physics, 2019, 13, 375-382.	1.4	1
31060	Stability of non-metal dopants to tune the photo-absorption of TiO2 at realistic temperatures and oxygen partial pressures: A hybrid DFT study. Scientific Reports, 2019, 9, 11427.	1.6	17
31061	Callistemon-like Zn and S codoped CoP nanorod clusters as highly efficient electrocatalysts for neutral-pH overall water splitting. Journal of Materials Chemistry A, 2019, 7, 22453-22462.	5.2	76
31062	Limitations of In2O3 as a transparent conducting oxide. Applied Physics Letters, 2019, 115, .	1.5	14
31063	Structural Complexity and High Thermoelectric Performance of the Zintl Phase: Yb₂₁Mn₄Sb₁₈. Chemistry of Materials, 2019, 31, 8076-8086.	3.2	28

#	Article	IF	Citations
31064	Comprehensive understanding of intrinsic mobility in the monolayers of IIIâ€“VI group 2D materials. Physical Chemistry Chemical Physics, 2019, 21, 21898-21907.	1.3	32
31065	Electronic stripes and transport properties in borophene heterostructures. Nanoscale, 2019, 11, 17894-17903.	2.8	21
31066	An emerging Janus MoSeTe material for potential applications in optoelectronic devices. Journal of Materials Chemistry C, 2019, 7, 12312-12320.	2.7	85
31067	Magnetostriction, Soft Magnetism, and Microwave Properties in <mml:math xmlns:mml="http://www.w3.org/1998/Math/MathML" display="inline" overflow="scroll"><mml:mi>Co</mml:mi><mml:mtext>â^’</mml:mtext><mml:mi>Fe</mml:mi><mml:mtext>â^’</mml:mtext><mml:mi mathvariant="normal">C</mml:mi></mml:mrow></mml:mrow></mml:math> Alloy Films. Physical Review Applied, 2019, 12, .	4.6	16
31068	Adsorption Behavior of CH4 Gas Molecule on the MoX2(S, Se, Te) Monolayer: The DFT Study. Nanoscale Research Letters, 2019, 14, 293.	3.1	15
31069	Acrylic acid hydrodeoxygenation reaction mechanism over molybdenum carbide studied by DFT calculations. Journal of Molecular Modeling, 2019, 25, 309.	0.8	2
31070	Structural, electronic and optical properties of ABTe2 (A = Li, Na, K, Rb, Cs and B = Sc, Y, La): Insights from first-principles computations. Journal of Solid State Chemistry, 2019, 279, 120954.	1.4	13
31071	Synthesis of Tunable-Aspect-Ratio Calcite Nanoparticles via Mg2+ Doping. Crystal Growth and Design, 2019, 19, 6784-6791.	1.4	4
31072	Photoactive Ag(I)-Based Coordination Polymer as a Potential Semiconductor for Photocatalytic Water Splitting and Environmental Remediation: Experimental and Theoretical Approach. Journal of Physical Chemistry C, 2019, 123, 23940-23950.	1.5	12
31073	Transition Metal Substitution of Hollandite Î±-MnO₂: Enhanced Potential and Structural Stability on Lithiation from First-Principles Calculation. Journal of Physical Chemistry C, 2019, 123, 25042-25051.	1.5	14
31074	Frequencies and Thermal Stability of Isolated Surface Hydroxyls on Pyrogenic TiO₂ Nanoparticles. Journal of Physical Chemistry C, 2019, 123, 24533-24548.	1.5	30
31075	Influence of Native Defects on the Electronic and Magnetic Properties of CVD Grown MoSe₂ Single Layers. Journal of Physical Chemistry C, 2019, 123, 24855-24864.	1.5	22
31076	Passivating Grain Boundaries in Polycrystalline CdTe. Journal of Physical Chemistry C, 2019, 123, 23882-23889.	1.5	22
31077	Theoretical Investigation on the Single Transition-Metal Atom-Decorated Defective MoS₂ for Electrocatalytic Ammonia Synthesis. ACS Applied Materials & Interfaces, 2019, 11, 36506-36514.	4.0	88
31078	The Role of Ru in Improving the Activity of Pd toward Hydrogen Evolution and Oxidation Reactions in Alkaline Solutions. ACS Catalysis, 2019, 9, 9614-9621.	5.5	112
31079	Assessment of van der Waals inclusive density functional theory methods for adsorption and selective dehydrogenation of formic acid on Pt(111) surface. Physical Chemistry Chemical Physics, 2019, 21, 21049-21056.	1.3	23
31080	A type-II C₂N/Î±-Te van der Waals heterojunction with improved optical properties by external perturbation. Physical Chemistry Chemical Physics, 2019, 21, 21753-21760.	1.3	20
31081	Inhibitor, Co-Catalyst, or Co-Reactant? Probing the Different Roles of H₂S during CO₂ Hydrogenation on the MoS₂ Catalyst. ACS Catalysis, 2019, 9, 10044-10059.	5.5	24

#	Article	IF	Citations
31082	Practical band interpolation with a modified tight-binding method. Journal of Physics Condensed Matter, 2019, 31, 215501.	0.7	1
31083	Effect of Î± phase on evolution of oxygen-rich layer on titanium alloys. Transactions of Nonferrous Metals Society of China, 2019, 29, 534-545.	1.7	12
31084	First-principles calculations of the oxygen-diffusion mechanism in mixed Fe/Ti perovskites for solid-oxide fuel cells. Ceramics International, 2019, 45, 17646-17652.	2.3	14
31085	Paving the way for cristobalite TiO2 and GeO2 attainable under moderate tensile stress: A DFT study of transformation paths and activation barriers in cristobalite-rutile transformations of MO2 (Mâ€¯=â€¯Si, Ge,) Tj ETQq1 1 0.784314 rgB	1.1	13
31086	Electronic and magnetic properties of single-layer boron phosphide associated with materials processing defects. Computational Materials Science, 2019, 170, 109201.	1.4	63
31087	Temperature dependence of vacancy concentration and void growth mechanism in Al with constant hydrogen concentration: A first-principles study. Engineering Fracture Mechanics, 2019, 216, 106508.	2.0	4
31088	Realizing high thermoelectric properties of SnTe via synergistic band engineering and structure engineering. Nano Energy, 2019, 65, 104056.	8.2	116
31089	Insight into the Rapid Degradation Behavior of Nonprecious Metal Feâ€“Nâ€“C Electrocatalyst-Based Proton Exchange Membrane Fuel Cells. ACS Applied Materials & Interfaces, 2019, 11, 37779-37786.	4.0	41
31090	Nanoscale topological defects and improper ferroelectric domains in multiferroic barium hexaferrite nanocrystals. Physical Review B, 2019, 100, .	1.1	14
31091	Superconductivity with strong electron-phonon coupling in noncentrosymmetric <mml:math xmlns:mml="http://www.w3.org/1998/Math/MathML"><mml:mrow><mml:msub><mml:mi mathvariant="normal">W</mml:mi><mml:mn>3</mml:mn></mml:msub><mml:msub><mml:mi>Al</mml:mi><mml:mn>2</mml:mn><mml:mi mathvariant="normal">C</mml:mi></mml:mrow></mml:math>. Physical Review B, 2019, 100, .	1.1	13
31092	BaCoxFe0.7-xZr0.3O3-Î´(0.2â‰¤xâ‰¤0.5) as cathode materials for proton-based SOFCs. Ceramics International, 2019, 45, 23948-23953.	2.3	17
31093	Effect of hydrostatic pressure and the emergence of half metallic ferromagnetism in rhodium oxide - A DFT+U perspective. Computational Condensed Matter, 2019, 21, e00425.	0.9	0
31094	Noncovalent bonding of copper atoms to the nitrogen-containing sites of hydrogenated diamond surfaces. Mendeleev Communications, 2019, 29, 452-454.	0.6	7
31095	Influence of Excess Volumes Induced by Re and W on Dislocation Motion and Creep in Ni-Base Single Crystal Superalloys: A 3D Discrete Dislocation Dynamics Study. Metals, 2019, 9, 637.	1.0	9
31096	Adsorption and dissociation of NO2 on silicene. Applied Surface Science, 2019, 498, 143854.	3.1	9
31097	Synergistically Optimizing Carrier Concentration and Decreasing Sound Velocity in n-type AgInSe₂ Thermoelectrics. Chemistry of Materials, 2019, 31, 8182-8190.	3.2	23
31098	Oxygen Vacancy Promoted O₂ Activation over Perovskite Oxide for Low-Temperature CO Oxidation. ACS Catalysis, 2019, 9, 9751-9763.	5.5	296
31099	Composition dependence of phonon and thermodynamic properties of the ternary AlGaN mixed crystal. Results in Physics, 2019, 14, 102505.	2.0	12

#	Article	IF	Citations
31100	Ultranarrow heterojunctions of armchair-graphene nanoribbons as resonant-tunnelling devices. Physical Chemistry Chemical Physics, 2019, 21, 24867-24875.	1.3	2
31101	Fully spin-polarized open and closed nodal lines in <mml:math xmlns:mml="http://www.w3.org/1998/Math/MathML"><mml:mi>Î²</mml:mi></mml:math> -borophene by magnetic proximity effect. Physical Review B, 2019, 100, .	1.1	16
31102	Crystal Structure Exploration of Boron Nitride Polymorphs Using Anharmonic Downward Distortion Following Method with Potential Energy Surface Modified by the Inverse of Lattice Volume. Chemistry Letters, 2019, 48, 1288-1291.	0.7	4
31103	Theoretical and FTIR Investigations of the Acetonitrile Hydrogenation Pathways on Platinum. Topics in Catalysis, 2019, 62, 1076-1085.	1.3	11
31104	Deep Dehalogenation of Florfenicol Using Crystalline CoP Nanosheet Arrays on a Ti Plate via Direct Cathodic Reduction and Atomic H. Environmental Science & Technology, 2019, 53, 11932-11940.	4.6	67
31105	Oddâ€“Even Layer Effect of Bismuth Oxychalcogenide Nanosurfaces: A First-Principles Study. Journal of Physical Chemistry C, 2019, 123, 24024-24030.	1.5	5
31106	Structure-property correlations of bis(nitrofurazano) furazan(BNFF-1): A density functional theory study. AIP Conference Proceedings, 2019, , .	0.3	0
31107	Density functional theory calculations of generalized stacking fault energy surfaces for eight face-centered cubic transition metals. Journal of Applied Physics, 2019, 126, .	1.1	39
31108	Gaussian approximation potential for studying the thermal conductivity of silicene. Journal of Applied Physics, 2019, 126, .	1.1	21
31109	Adsorption, Absorption, Diffusion, and Permeation of Hydrogen and Its Isotopes in bcc Bulk Fe and Fe(100) Surface: Plane Wave-Based Density Functional Theoretical Investigations. Journal of Physical Chemistry C, 2019, 123, 23951-23966.	1.5	11
31110	Revealing the role of the 1T phase on the adsorption of organic dyes on MoS₂ nanosheets. RSC Advances, 2019, 9, 28345-28356.	1.7	19
31111	Mn promotes the rate of nucleation and growth of precipitates by increasing Frenkel pairs in Feâ€“Cu based alloys. RSC Advances, 2019, 9, 19620-19629.	1.7	1
31112	On a new nitrogen sX hydrate from ice XVII. Journal of Chemical Physics, 2019, 151, 104305.	1.2	8
31113	Ferromagnetic Half-Semiconductor (HSC) gaps in co-doped CdS: Ab-initio study. Chinese Journal of Physics, 2019, 61, 155-165.	2.0	9
31114	Antiferromagnetic semiconductor Eu3Sn2P4 with Snâ€“Sn dimer and crown-wrapped Eu. Journal of Materials Chemistry C, 2019, 7, 12650-12656.	2.7	5
31115	Valleyite: A new magnetic mineral with the sodalite-type structure. American Mineralogist, 2019, 104, 1238-1245.	0.9	11
31116	Thermodynamic Properties of Hexagonal Molybdenum Disulfide Calculated from First Principles. Powder Metallurgy and Metal Ceramics, 2019, 58, 230-236.	0.4	1
31117	Mechanistic Insights into the Pathways of Phenol Hydrogenation on Pd Nanostructures. ACS Sustainable Chemistry and Engineering, 2019, 7, 17126-17136.	3.2	57

#	Article	IF	Citations
31118	Evolution map of the memristor: from pure capacitive state to resistive switching state. Nanoscale, 2019, 11, 17222-17229.	2.8	45
31119	Spin polarization and tunable valley degeneracy in a MoS₂ monolayer via proximity coupling to a Cr₂O₃ substrate. Nanoscale, 2019, 11, 19536-19542.	2.8	14
31120	Multi-phonon (percolation) behavior and local clustering of CdxZn1â^'xSe-cubic mixed crystals (xâ€‰â‰€0.3): A Ramanâ€“ab initio study. Journal of Applied Physics, 2019, 126, .	1.1	5
31121	Diffusion Monte Carlo study of <mml:math xmlns:mml="http://www.w3.org/1998/Math/MathML"><mml:msub><mml:mi mathvariant="normal">O</mml:mi><mml:mn>2</mml:mn></mml:msub></mml:math> adsorption on single layer graphene. Physical Review B, 2019, 100, .	1.1	6
31122	Optical spectroscopy study of the topological property in PrSb. Physical Review B, 2019, 100, .	1.1	3
31123	Observation of a topological nodal-line semimetal in <mml:math xmlns:mml="http://www.w3.org/1998/Math/MathML"><mml:msub><mml:mi>YbMnSb</mml:mi><mml:mn>2</mml:mn></mml:msub> through optical spectroscopy. Physical Review B, 2019, 100, .	1.1	26
31124	First-Principles Study of Ferromagnetism in Iron Chromite Spinels: FeCr₂O₄ and CrFe₂O₄. Spin, 2019, 09, .	0.6	12
31125	Electronic Transport Properties of Silicane Determined from First Principles. Materials, 2019, 12, 2935.	1.3	14
31126	Magnetic, Electronic, Mechanic, Anisotropic Elastic and Vibrational Properties of Antiferromagnetic Ru2TGa (Tâ€‰=â€‰Cr, Mn, and Co) Heusler Alloys. Journal of Electronic Materials, 2019, 48, 7608-7622.	1.0	10
31127	Predicting the Structure Stability of Layered Heteroanionic Materials Exhibiting Anion Order. Inorganic Chemistry, 2019, 58, 13229-13240.	1.9	9
31128	Influence of the Cation on the Surface Electronic Band Structure and Magnetic Properties of Mn:ZnS and Mn:CdS Quantum Dot Thin Films. Journal of Physical Chemistry C, 2019, 123, 24890-24898.	1.5	10
31129	Transparent Conductive Films Derived from Single-Walled Aluminosilicate Nanotubes. ACS Applied Nano Materials, 2019, 2, 6677-6689.	2.4	5
31130	Density functional theory (DFT) study of BaScO₃H_{0.5} compound and its hydrogen storage properties. Canadian Journal of Physics, 2019, 97, 1191-1199.	0.4	6
31131	Sub-5 nm Monolayer BiH Transistors. ACS Applied Electronic Materials, 2019, 1, 2103-2108.	2.0	7
31132	Enhancing and controlling valley magnetic response in MoS2/WS2 heterostructures by all-optical route. Nature Communications, 2019, 10, 4226.	5.8	38
31133	Materials property prediction using symmetry-labeled graphs as atomic position independent descriptors. Physical Review B, 2019, 100, .	1.1	9
31134	Charge qubit in van der Waals heterostructures. Physical Review B, 2019, 100, .	1.1	15
31135	Selective oxidation of glycerol to carboxylic acids on Pt(111) in base-free medium: A periodic density functional theory investigation. Applied Surface Science, 2019, 497, 143661.	3.1	31

#	Article	IF	Citations
31136	Thermodynamic description of the Coâ€“Niâ€“Ta system. Calphad: Computer Coupling of Phase Diagrams and Thermochemistry, 2019, 66, 101649.	0.7	13
31137	Electronic and optical properties of HoNi₅ and HoNi₄Si: An LSDA + U study. Modern Physics Letters B, 2019, 33, 1950358.	1.0	2
31138	Mechanical and Electronic Stabilization of Solid Electrolyte Interphase with Sulfite Additive for Lithium Metal Batteries. Journal of the Electrochemical Society, 2019, 166, A3201-A3206.	1.3	8
31139	Structural, Electronic, Lattice Dynamic, and Elastic Properties of SnTiO₃ and PbTiO₃ Using Density Functional Theory. Advances in Condensed Matter Physics, 2019, 2019, 1-12.	0.4	24
31140	Electronic and Optical Properties of Cubic Perovskites CsPbCl_{3â^'} _yI_y (y = 0, 1, 2, 3). Zeitschrift Fur Naturforschung - Section A Journal of Physical Sciences, 2019, 74, 905-913.	0.7	19
31141	Bifunctional Electrocatalytic Activity of Bis(iminothiolato)nickel Monolayer for Overall Water Splitting. Journal of Physical Chemistry C, 2019, 123, 25651-25656.	1.5	17
31142	Improved CO Oxidation via Surface Stabilization of Ceria Nanoparticles Induced by Rare-Earth Metal Dopants. ACS Applied Nano Materials, 2019, 2, 6473-6481.	2.4	13
31143	Understanding CO₂ Adsorption on a M₁ (M₂)-Promoted (Doped) MgOâ€“CaO(100) Surface (M₁ = Li, Na, K, and Rb, M₂ = Sr): A DFT Theoretical Study. ACS Sustainable Chemistry and Engineering, 2019, 7, 16979-16984.	3.2	18
31144	Synthesis of clathrate cerium superhydride CeH9 at 80-100 GPa with atomic hydrogen sublattice. Nature Communications, 2019, 10, 4453.	5.8	117
31145	First-principles investigation on electronic properties and band alignment of group III monochalcogenides. Scientific Reports, 2019, 9, 13289.	1.6	23
31146	Sensing properties of Ni-doped boron nitride nanotube to SF6 decomposed components: A DFT study. AIP Advances, 2019, 9, .	0.6	30
31147	Ge3P2: New viable two-dimensional semiconductors with ultrahigh carrier mobility. Applied Surface Science, 2019, 497, 143803.	3.1	17
31148	Effects of co-doping on electronic structure and optical properties of 3C-SiC from first-principles method. Computational Materials Science, 2019, 170, 109172.	1.4	5
31149	Aluminium substituted Î²â€“type NaMn1-Al O2: A stable and enhanced electrochemical kinetic sodium-ion battery cathode. Journal of Power Sources, 2019, 438, 227025.	4.0	20
31150	Giant Magnetoelectric Coupling in Multiferroic PbTi_{1â€“x}V_xO₃ from Density Functional Calculations. ACS Omega, 2019, 4, 16743-16755.	1.6	1
31151	Ultrastable phonon frequencies in Î± -quartz-type BPO4 at high temperature. Applied Physics Letters, 2019, 115, .	1.5	3
31152	Prediction of 2D Li2X (X=Se, Te) monolayer semiconductors by first principles calculations. Physics Letters, Section A: General, Atomic and Solid State Physics, 2019, 383, 125992.	0.9	16
31153	Interaction of H₂O with the Platinum Pt (001), (011), and (111) Surfaces: A Density Functional Theory Study with Long-Range Dispersion Corrections. Journal of Physical Chemistry C, 2019, 123, 27465-27476.	1.5	33

#	Article	IF	Citations
31154	Compression Behavior of Copper Hydroxyfluoride CuOHF as a Case Study of the High-Pressure Responses of the Hydrogen-Bonded Two-Dimensional Layered Materials. Journal of Physical Chemistry C, 2019, 123, 25492-25500.	1.5	6
31155	Highly Water-Resistant La-Doped Co₃O₄ Catalyst for CO Oxidation. ACS Catalysis, 2019, 9, 10093-10100.	5.5	126
31156	PdMo bimetallene for oxygen reduction catalysis. Nature, 2019, 574, 81-85.	13.7	935
31157	Composition Optimum Design and Strengthening and Toughening Mechanisms of New Alumina-Forming Austenitic Heat-Resistant Steels. Metals, 2019, 9, 921.	1.0	5
31158	Rationally Designed High-Performance Spin Filter Based on Two-Dimensional Half-Metal Cr2NO2. Matter, 2019, 1, 1304-1315.	5.0	30
31159	Stabilizing Low-Coordinated O Ions To Operate Cationic and Anionic Redox Chemistry of Li-Ion Battery Materials. ACS Applied Materials & Interfaces, 2019, 11, 37768-37778.	4.0	13
31160	Organically interconnected graphene flakes: A flexible 3-D material with tunable electronic bandgap. Scientific Reports, 2019, 9, 13676.	1.6	5
31161	Magnon drag effect in Fe-Co alloys. Journal of Applied Physics, 2019, 126, 125107.	1.1	4
31162	Structural, Electronic, Mechanical, Thermodynamic, and Linear and Nonlinear Optical Properties of MoS2, MoSe2, and their MoS2xSe2(1â^'x) Alloys: Ab Initio Calculations. Journal of Electronic Materials, 2019, 48, 7977-7990.	1.0	12
31163	Boosting Sodium Storage of Fe1â^'xS/MoS2 Composite via Heterointerface Engineering. Nano-Micro Letters, 2019, 11, 80.	14.4	77
31164	Path integral study on C15-type Laves TiCr2 hydride. International Journal of Hydrogen Energy, 2019, 44, 23708-23715.	3.8	7
31165	Tuning of adsorption energies of CO2 and CH4 in borocarbonitrides BxCyNz: A first-principles study. Journal of Molecular Graphics and Modelling, 2019, 93, 107446.	1.3	10
31166	NiCoP nanopeapods embedded in carbon nanotube arrays as bifunctional catalysts for efficient overall water splitting. Materials Today Nano, 2019, 8, 100053.	2.3	17
31167	Structural, electronic, thermophysical properties and bond stiffness of ternary ceramic ScAl3C3 and UAl3C3: Ab initio calculations. Materials Letters, 2019, 255, 126610.	1.3	4
31168	Influence of the Iron Proportion on the Efficiency of an Oil-Soluble Niâ€“Fe Catalyst Applied in the Co-liquefaction of Lignite and Heavy Residue. Industrial & Engineering Chemistry Research, 2019, 58, 19072-19081.	1.8	9
31169	Active Sites in Single-Layer BiOX (X = Cl, Br, and I) Catalysts for the Hydrogen Evolution Reaction. Inorganic Chemistry, 2019, 58, 13195-13202.	1.9	29
31170	S-Functionalized Mo₂C Monolayer as a Novel Electrode Material in Li-Ion Batteries. Journal of Physical Chemistry C, 2019, 123, 25052-25060.	1.5	33
31171	Topological Phases in Hydrogenated Group 13 Monolayers. Journal of Physical Chemistry C, 2019, 123, 25985-25990.	1.5	4

#	Article	IF	Citations
31172	First-principles study of the structural, electronic, magnetic, and ferroelectric properties of a charge-ordered iron(ii)-iron(iii) formate framework. Journal of Chemical Physics, 2019, 151, 124704.	1.2	4
31173	Stabilization of E-type antiferromagnetic ordering in La and Y substituted orthorhombic LuMnO3: A first-principles study. Physics Letters, Section A: General, Atomic and Solid State Physics, 2019, 383, 125950.	0.9	4
31174	Net-Y as a high performance electrode material for Na-ion battery. Chemical Physics Letters, 2019, 734, 136733.	1.2	11
31175	Hybrid functional study of hydrogen passivation in carbon-oxygen related defect complexes in silicon. Physica B: Condensed Matter, 2019, 572, 238-241.	1.3	5
31176	Study on the control of porosity in films of polythiophene derivatives. Polymer, 2019, 182, 121858.	1.8	0
31177	Monolayer Nitrides Doped with Transition Metals as Efficient Catalysts for Water Oxidation: The Singular Role of Nickel. Journal of Physical Chemistry C, 2019, 123, 26289-26298.	1.5	12
31178	High-Pressure Study of Two Polymorphs of 2,4,6-Trinitrotoluene Using Neutron Powder Diffraction and Density Functional Theory Methods. Journal of Physical Chemistry C, 2019, 123, 26095-26105.	1.5	16
31179	Coexisting Charge States in a Unary Organic Monolayer Film on a Metal. Journal of Physical Chemistry Letters, 2019, 10, 6438-6445.	2.1	18
31180	Cs₂NaVCl₆: A Pb-Free Halide Double Perovskite with Strong Visible and Near-Infrared Light Absorption. ACS Applied Materials & Interfaces, 2019, 11, 38648-38653.	4.0	39
31181	Volcano Trend in Electrocatalytic CO₂ Reduction Activity over Atomically Dispersed Metal Sites on Nitrogen-Doped Carbon. ACS Catalysis, 2019, 9, 10426-10439.	5.5	142
31182	Surface Defect Dynamics in Organicâ€“Inorganic Hybrid Perovskites: From Mechanism to Interfacial Properties. ACS Nano, 2019, 13, 12127-12136.	7.3	56
31183	Elemental Substitution of Two-Dimensional Transition Metal Dichalcogenides (MoSe₂ and) Tj ETQq1 1 0.784314 rgBT /Ov	4.0	102
31184	Atomically ordered non-precious Co3Ta intermetallic nanoparticles as high-performance catalysts for hydrazine electrooxidation. Nature Communications, 2019, 10, 4514.	5.8	80
31185	Rhenium dinitride: Carrier transport in a novel transition metal dinitride layered crystal. APL Materials, 2019, 7, 101103.	2.2	7
31186	Ab Initio Study of Ternary W5Si3 Type TM5Sn2X Compounds (TM = Nb, Ti and X = Al, Si). Materials, 2019, 12, 3217.	1.3	5
31187	Ultrahigh-sensitive gas sensors based on doped phosphorene: A first-principles investigation. Applied Surface Science, 2019, 497, 143660.	3.1	35
31188	Tunable electronic structures in BP/MoSSe van der Waals heterostructures by external electric field and strain. Applied Surface Science, 2019, 497, 143809.	3.1	71
31189	Study of first principles on anisotropy and elastic constants of Y3Al2 compound. Chinese Journal of Physics, 2019, 61, 180-189.	2.0	2

#	Article	IF	Citations
31190	Crystal habit-directed gold deposition on pyrite: Surface chemical interpretation of the pyrite morphology indicative of gold enrichment. Geochimica Et Cosmochimica Acta, 2019, 264, 191-204.	1.6	24
31191	Thermodynamic modeling of YO1.5-TaO2.5 system and the effects of elastic strain energy and diffusion on phase transformation of YTaO4. Journal of the European Ceramic Society, 2019, 39, 5036-5047.	2.8	27
31192	A detailed physical analysis on the interaction between transition elements (3d, 4d and 5d) and point defects in molybdenum for nuclear material application. Journal of Nuclear Materials, 2019, 527, 151805.	1.3	6
31193	Carbon nanotube-supported bimetallic Cu-Fe catalysts for syngas conversion to higher alcohols. Molecular Catalysis, 2019, 479, 110610.	1.0	15
31194	Few-layer transition metal dichalcogenides (MoS2, WS2, and WSe2) for water splitting and degradation of organic pollutants: Understanding the piezocatalytic effect. Nano Energy, 2019, 66, 104083.	8.2	181
31195	SrI3O9H: A new alkaline earth metal iodate with two different anionic units using mild aqua-solution method. Solid State Sciences, 2019, 97, 105982.	1.5	5
31196	Insight into the pressure effect on the structural stability and physical properties of cubic sesquioxides X2O3 (X= Sc, Y and In). Vacuum, 2019, 168, 108855.	1.6	15
31197	Two-Dimensional CuTe₂X (X = Cl, Br, and I): Potential Photocatalysts for Water Splitting under the Visible/Infrared Light. Journal of Physical Chemistry C, 2019, 123, 25543-25548.	1.5	6
31198	Synthesis of magnesium-nitrogen salts of polynitrogen anions. Nature Communications, 2019, 10, 4515.	5.8	76
31199	Negative thermal expansion behavior in orthorhombic Sc2(MoO4)3 and Sc2(WO4)3. Journal of Applied Physics, 2019, 126, 125114.	1.1	11
31200	Structural and electronic properties of boron-induced defects on the Si(001) surface. Physical Review B, 2019, 100, .	1.1	0
31201	First-principles study of structural, electronic, elastic, thermodynamic and optical properties of LuPdBi half-Heusler compound. Modern Physics Letters B, 2019, 33, 1950378.	1.0	23
31202	Single Mn atom as a promising electrocatalyst for CO reduction to C2H5OH and C3H6: A computational study. Applied Surface Science, 2019, 498, 143868.	3.1	15
31203	An ab initio study on the transition path of carbon dioxide at high pressure: Evidence for a new intermediate P4â€¾m2 phase. Computational Condensed Matter, 2019, 21, e00429.	0.9	1
31204	Molecular speciation of phosphorus in phosphogypsum waste by solid-state nuclear magnetic resonance spectroscopy. Science of the Total Environment, 2019, 696, 133958.	3.9	17
31205	Controlled Single-Crystalline Polymerization of C₁₀H₈Â·C₁₀F₈ under Pressure. Macromolecules, 2019, 52, 7557-7563.	2.2	33
31206	Theoretical Study of GaN/BP van der Waals Nanocomposites with Strain-Enhanced Electronic and Optical Properties for Optoelectronic Applications. ACS Applied Nano Materials, 2019, 2, 6482-6491.	2.4	75
31207	Amorphous Surface PdO_X and Its Activity toward Methane Combustion. ACS Catalysis, 2019, 9, 10317-10323.	5.5	34

#	Article	IF	Citations
31208	Predicting the elastic, phonon and thermodynamic properties of cubic HfNiX (X = Ge and Sn) Half Heulser alloys: a DFT study. European Physical Journal B, 2019, 92, 1.	0.6	11
31209	Adsorption and Sensing Behaviors of Pd-Doped InN Monolayer upon CO and NO Molecules: A First-Principles Study. Applied Sciences (Switzerland), 2019, 9, 3390.	1.3	10
31210	Siâ€“Ge alloys in C2/c phase with tunable direct band gaps: A comprehensive study. Current Applied Physics, 2019, 19, 1325-1333.	1.1	17
31211	SnSe₂ Nanorods on Carbon Cloth as a Highly Selective, Active, and Flexible Electrocatalyst for Electrochemical Reduction of CO₂ into Formate. ACS Applied Energy Materials, 2019, 2, 7655-7662.	2.5	39
31212	Cooperation of Ni and CaO at Interface for CO₂ Reforming of CH₄: A Combined Theoretical and Experimental Study. ACS Catalysis, 2019, 9, 10060-10069.	5.5	68
31213	Epitaxial Synthesis of Monolayer PtSe₂ Single Crystal on MoSe₂ with Strong Interlayer Coupling. ACS Nano, 2019, 13, 10929-10938.	7.3	72
31214	Exploring the electronic, mechanical, and anisotropy properties of novel tetragonal B₂CO phase. Journal of Materials Research, 2019, 34, 3617-3626.	1.2	5
31215	Elementary kinetics of nitrogen electroreduction to ammonia on late transition metals. Catalysis Science and Technology, 2019, 9, 174-181.	2.1	47
31216	A dimer path for CO dissociation on PtSn. Catalysis Science and Technology, 2019, 9, 695-701.	2.1	9
31217	Molecular or dissociative adsorption of water on clean and oxygen pre-covered Ni(111) surfaces. Catalysis Science and Technology, 2019, 9, 199-212.	2.1	9
31218	Effective chemical potential for non-equilibrium systems and its application to molecular beam epitaxy of Bi₂Se₃. Nanoscale Advances, 2019, 1, 470-475.	2.2	6
31219	High-performance sub-10 nm monolayer Bi₂O₂Se transistors. Nanoscale, 2019, 11, 532-540.	2.8	196
31220	Enhanced photocatalytic activity for water splitting of blue-phase GeS and GeSe monolayers via biaxial straining. Nanoscale, 2019, 11, 2335-2342.	2.8	80
31221	Au decoration of a graphene microchannel for self-activated chemoresistive flexible gas sensors with substantially enhanced response to hydrogen. Nanoscale, 2019, 11, 2966-2973.	2.8	46
31222	A topological model for predicting adsorption energies of polycyclic aromatic hydrocarbons on late-transition metal surfaces. Reaction Chemistry and Engineering, 2019, 4, 410-417.	1.9	2
31223	Insights into the intrinsic capacity of interlayer-expanded MoS₂ as a Li-ion intercalation host. Journal of Materials Chemistry A, 2019, 7, 1187-1195.	5.2	32
31224	Charge carrier transport dynamics in W/Mo-doped BiVO₄: first principles-based mesoscale characterization. Journal of Materials Chemistry A, 2019, 7, 3054-3065.	5.2	51
31225	Carrier density control in Cu2HgGeTe4and discovery of Hg2GeTe4viaphase boundary mapping. Journal of Materials Chemistry A, 2019, 7, 621-631.	5.2	27

#	Article	IF	Citations
31226	Unique SchrÃ¶dinger semimetal state in ternary Be₂P₃N honeycomb lattice. Journal of Materials Chemistry C, 2019, 7, 4118-4123.	2.7	8
31227	Robust negative differential resistance and abnormal magnetoresistance effects in heteroatom-substituted zigzag Î³-graphyne nanoribbon homojunctions. Journal of Materials Chemistry C, 2019, 7, 1359-1369.	2.7	11
31228	A sub-10 nm monolayer ReS₂ transistor for low-power applications. Journal of Materials Chemistry C, 2019, 7, 1604-1611.	2.7	32
31229	Stress-Dependent Elasticity of TiAlN Coatings. Coatings, 2019, 9, 24.	1.2	20
31230	Vanadium Oxides: Synthesis, Properties, and Applications. , 2019, , 127-218.		8
31231	First-principles study of solid solution strengthening in Mgâ€“X (X=Al, Er) alloys. Bulletin of Materials Science, 2019, 42, 1.	0.8	8
31232	Precipitation during high temperature aging of Alâ€“Cu alloys: AÂmultiscale analysis based on first principles calculations. Acta Materialia, 2019, 167, 121-135.	3.8	70
31233	First-principles calculations on Ni/W interfaces in Steel/Ni/W hot isostatic pressure diffusion bonding layer. Applied Surface Science, 2019, 475, 906-916.	3.1	29
31234	Oxygenated (113) diamond surface for nitrogen-vacancy quantum sensors with preferential alignment and long coherence time from first principles. Carbon, 2019, 145, 273-280.	5.4	24
31235	Orbital selective bandwidth renormalization, Lifshitz transition in Rare Earth doped 112 iron based superconductors. Computational Materials Science, 2019, 160, 62-71.	1.4	13
31236	Magnetic properties of Ni-Ti clusters of the lower hierarchical level. Chemical Physics Letters, 2019, 716, 199-206.	1.2	1
31237	A site-sensitive quasi-in situ strategy to characterize Mo/HZSM-5 during activation. Journal of Catalysis, 2019, 370, 321-331.	3.1	40
31238	Mechanistic study of methanol synthesis from CO2 hydrogenation on Rh-doped Cu(111) surfaces. Molecular Catalysis, 2019, 466, 26-36.	1.0	60
31239	Electronic structure and magnetic order in Cu Zn(1â€²)O: A study GGA and GGAÂ+ÂU. Physica B: Condensed Matter, 2019, 557, 74-81.	1.3	7
31240	Sandwich-structured, damage-resistant TiN/graded TiSiN/TiSiN film. Results in Physics, 2019, 12, 543-554.	2.0	15
31241	First principles study of structural, electronic and mechanical properties of metal carbides M2C and MC2 (M= Os, Ir, Pt). Solid State Communications, 2019, 291, 43-50.	0.9	8
31242	Ultrasound exfoliation of graphite in biphasic liquid systems containing ionic liquids: A study on the conditions for obtaining large few-layers graphene. Ultrasonics Sonochemistry, 2019, 55, 279-288.	3.8	21
31243	BeO₆ Trigonal Prism with Ultralong Beâ€“O Bonds Observed in a Deep Ultraviolet Optical Crystal Li₁₃BeBe₆B₉O₂₇. Inorganic Chemistry, 2019, 58, 2201-2207.	1.9	9

#	Article	IF	Citations
31244	Terahertz Spectroscopy and Quantum Mechanical Simulations of Crystalline Copper-Containing Historical Pigments. Journal of Physical Chemistry A, 2019, 123, 1225-1232.	1.1	21
31245	Predictions of Hg⁰ and HgCl₂ Adsorption Properties in UiO-66 from Flue Gas Using Molecular Simulations. Journal of Physical Chemistry C, 2019, 123, 5972-5979.	1.5	18
31246	First-Principles Evaluation of the Morphology of WS₂ Nanotubes for Application as Visible-Light-Driven Water-Splitting Photocatalysts. ACS Omega, 2019, 4, 1434-1442.	1.6	27
31247	Observation of ballistic avalanche phenomena in nanoscale vertical InSe/BP heterostructures. Nature Nanotechnology, 2019, 14, 217-222.	15.6	153
31248	Terahertz-driven phonon upconversion in SrTiO3. Nature Physics, 2019, 15, 387-392.	6.5	128
31249	Magnetic structure of UO₂and NpO₂by first-principle methods. Physical Chemistry Chemical Physics, 2019, 21, 760-771.	1.3	31
31250	2D planar penta-MN₂ (M = Pd, Pt) sheets identified through structure search. Physical Chemistry Chemical Physics, 2019, 21, 246-251.	1.3	32
31251	Theoretical design of a series of 2D TMâ€“C₃N₄ and TMâ€“C₃N₄@graphene (TM = V, Nb and Ta) nanostructures with highly efficient catalytic activity for the hydrogen evolution reaction. Physical Chemistry Chemical Physics, 2019, 21, 1773-1783.	1.3	27
31252	VC₂ and V_{1/2}Mn_{1/2}C₂ nanosheets with robust mechanical and thermal properties as promising materials for Li-ion batteries. Physical Chemistry Chemical Physics, 2019, 21, 1606-1613.	1.3	8
31253	Screened hybrid meta-GGA exchangeâ€“correlation functionals for extended systems. Physical Chemistry Chemical Physics, 2019, 21, 3002-3015.	1.3	16
31254	Mechanical properties of anhydrous oxalic acid and oxalic acid dihydrate. Physical Chemistry Chemical Physics, 2019, 21, 2673-2690.	1.3	43
31255	Effects of the number of layers on the vibrational, electronic and optical properties of alpha lead oxide. Physical Chemistry Chemical Physics, 2019, 21, 3868-3876.	1.3	25
31256	Ferromagnetic ligand holes in cobalt perovskite electrocatalysts as an essential factor for high activity towards oxygen evolution. Physical Chemistry Chemical Physics, 2019, 21, 2977-2983.	1.3	32
31257	Effect of ammonia on cobalt Fischerâ€“Tropsch synthesis catalysts: a surface science approach. Catalysis Science and Technology, 2019, 9, 702-710.	2.1	5
31258	Phase evolution in calcium molybdate nanoparticles as a function of synthesis temperature and its electrochemical effect on energy storage. Nanoscale Advances, 2019, 1, 565-580.	2.2	49
31259	KTlO: a metal shrouded 2D semiconductor with high carrier mobility and tunable magnetism. Nanoscale, 2019, 11, 1131-1139.	2.8	50
31260	Insights into the roles of water on the aqueous phase reforming of glycerol. Reaction Chemistry and Engineering, 2019, 4, 383-392.	1.9	25
31261	Anion-order driven polar interfaces at LaTiO₂N surfaces. Journal of Materials Chemistry A, 2019, 7, 2129-2134.	5.2	9

#	Article	IF	Citations
31262	First-principles investigation on tunable electronic properties and magnetism by polarization in PbTiO₃/BiFeO₃ 2D ferroelectric heterostructures. Journal of Materials Chemistry C, 2019, 7, 463-473.	2.7	21
31263	Observation of a Dirac state in borophene hetero-bilayers by Cr intercalation. Journal of Materials Chemistry C, 2019, 7, 2068-2075.	2.7	7
31264	Microscopic origin of pressure-induced phase-transitions in urea: a detailed investigation through first principles calculations. Physical Chemistry Chemical Physics, 2019, 21, 884-900.	1.3	16
31265	Carbon chain growth by formyl coupling over the Cu/Î³-AlOOH(001) surface in syngas conversion. Physical Chemistry Chemical Physics, 2019, 21, 148-159.	1.3	12
31266	Achieving a direct band gap and high power conversion efficiency in an SbI₃/BiI₃ type-II vdW heterostructure via interlayer compression and electric field application. Physical Chemistry Chemical Physics, 2019, 21, 2619-2627.	1.3	13
31267	High-pressure behaviour of Prussian blue analogues: interplay of hydration, Jahn-Teller distortions and vacancies. Dalton Transactions, 2019, 48, 1647-1655.	1.6	31
31268	Pulsed-grown graphene for flexible transparent conductors. Nanoscale Advances, 2019, 1, 1215-1223.	2.2	12
31269	Effects of precursor pre-treatment on the vapor deposition of WS₂ monolayers. Nanoscale Advances, 2019, 1, 953-960.	2.2	17
31270	N-Doped carbon nanotubes enriched with graphitic nitrogen in a buckypaper configuration as efficient 3D electrodes for oxygen reduction to H₂O₂. Nanoscale, 2019, 11, 2829-2839.	2.8	54
31271	Strong interfacial interactions induced a large reduction in lateral thermal conductivity of transition-metal dichalcogenide superlattices. RSC Advances, 2019, 9, 1387-1393.	1.7	7
31272	A hypervalent and cubically coordinated molecular phase of IF₈predicted at high pressure. Chemical Science, 2019, 10, 2543-2550.	3.7	36
31273	Lone-pair effect on carrier capture in Cu₂ZnSnS₄solar cells. Journal of Materials Chemistry A, 2019, 7, 2686-2693.	5.2	55
31274	DFT study of electronic structure and optical properties of layered two-dimensional CH₃NH₃PbX₃ (X=Cl, Br, I). Energy Sources, Part A: Recovery, Utilization and Environmental Effects, 2019, 41, 2734-2745.	1.2	10
31275	Optical properties and lattice dynamics of a novel allotrope of orthorhombic elemental germanium. Journal of Physics Condensed Matter, 2019, 31, 135401.	0.7	3
31276	Intrinsic defects in and electronic properties of Î¸-Al13Fe4: an ab initio DFT study. JPhys Materials, 2019, 2, 015004.	1.8	9
31277	Heat and charge transport in bulk semiconductors with interstitial defects. Physical Review B, 2019, 99, .	1.1	10
31278	Lattice dynamics and negative thermal expansion in the framework compound <mml:math xmlns:mml="http://www.w3.org/1998/Math/MathML"><mml:mrow><mml:mi>ZnNi</mml:mi><mml:msub><mml:mrow><mml:mo>(</m with two-dimensional and three-dimensional local environments. Physical Review B, 2019, 99, .	1.1	26
31279	CO₂ Electrochemical Reduction Catalyzed by Graphene Supported Palladium Cluster: A Computational Guideline. ACS Applied Energy Materials, 2019, 2, 1544-1552.	2.5	17

#	Article	IF	Citations
31280	Electronic and optical properties of lead-free hybrid double perovskites for photovoltaic and optoelectronic applications. Scientific Reports, 2019, 9, 718.	1.6	130
31281	Selective control of molecule charge state on graphene using tip-induced electric field and nitrogen doping. Npj 2D Materials and Applications, 2019, 3, .	3.9	19
31282	New high-pressure phases of Fe7N3 and Fe7C3 stable at Earth's core conditions: evidences for carbonâ€“nitrogen isomorphism in Fe-compounds. RSC Advances, 2019, 9, 3577-3581.	1.7	15
31283	Soft X-ray Li-K and Si-L2, 3 Emission from Crystalline and Amorphous Lithium Silicides in Lithium-Ion Batteries Anode. Journal of the Electrochemical Society, 2019, 166, A5362-A5368.	1.3	3
31284	Probing cyanogen chloride gas molecules using blue phosphorene nanosheets based on adsorption properties: A first-principles study. Computational and Theoretical Chemistry, 2019, 1150, 63-70.	1.1	33
31285	Thermodynamic mixing properties of alunite supergroup minerals: Quantum-mechanical modeling and thermodynamic analysis of sulfate, chromate, selenate, phosphate, and arsenate solid solutions, as well as uranyl incorporation. Geochimica Et Cosmochimica Acta, 2019, 248, 138-160.	1.6	5
31286	Ab initio investigation of spin orbit coupling effect on the physical properties of IrGe superconductor. Intermetallics, 2019, 106, 107-114.	1.8	9
31287	Adsorption of NO and NO2 molecules on defected-graphene and ozone-treated graphene: First-principles analysis. Surface Science, 2019, 684, 28-36.	0.8	39
31288	van der Waals Stacking Induced Transition from Schottky to Ohmic Contacts: 2D Metals on Multilayer InSe. Journal of the American Chemical Society, 2019, 141, 3110-3115.	6.6	162
31289	Diffusion-free Grotthuss topochemistry for high-rate and long-life proton batteries. Nature Energy, 2019, 4, 123-130.	19.8	446
31290	Effects of pressure on the structure and lattice dynamics of Î±-glycine: a combined experimental and theoretical study. CrystEngComm, 2019, 21, 4457-4464.	1.3	16
31291	Strong decoupling between magnetic subsystems in the low-dimensional spin- <mml:math xmlns:mml="http://www.w3.org/1998/Math/MathML"><mml:mfrac><mml:mn>1</mml:mn><mml:mn>2</mml:mn></mml:mfrac></m antiferromagnet <mml:math xmlns:mml="http://www.w3.org/1998/Math/MathML"><mml:msub><mml:mi>SeCuO</mml:mi><mml:mn>3</mml:mn></mml:msub> Physical Review B, 2019, 99, .	1.1	8
31292	Density functional theory study explaining the underperformance of copper oxides as photovoltaic absorbers. Physical Review B, 2019, 99, .	1.1	40
31293	Synthesis, First-Principle Simulation, and Application of Three-Dimensional Ceria Nanoparticles/Graphene Nanocomposite for Non-Enzymatic Hydrogen Peroxide Detection. Journal of the Electrochemical Society, 2019, 166, H3167-H3174.	1.3	30
31294	Planar penta-transition metal phosphide and arsenide as narrow-gap semiconductors with ultrahigh carrier mobility. Journal of Materials Science, 2019, 54, 7035-7047.	1.7	20
31295	Chemisorption of carbon monoxide, carbon dioxide and â€œmethanephobiaâ€•on the [0001] titanium surface. Applied Surface Science, 2019, 478, 128-133.	3.1	3
31296	Application of highly stretchable and conductive two-dimensional 1T VS2 and VSe2 as anode materials for Li-, Na- and Ca-ion storage. Computational Materials Science, 2019, 160, 360-367.	1.4	60
31297	Negative Poisson's ratio in monolayer PdSe2. Computational Materials Science, 2019, 160, 309-314.	1.4	29

#	Article	IF	Citations
31298	Adjusting dispersion parameters for the density-functional tight-binding description of molecular crystals. Chemical Physics Letters, 2019, 718, 7-11.	1.2	5
31299	Geometry optimizations and evaluation of electronic properties of prism carbon tubes by density functional theory using plane waves. Chemical Physics Letters, 2019, 718, 32-37.	1.2	1
31300	Hydrogen adsorption, dissociation, and diffusion on high-index Mg(10<mml:math) Tj ETQq0 0 0 rgBT /Overlock 10 Tf 50 682 Td (xmlns:m and their comparisons with Mg(0001): A systematic first-principles study. International Journal of Hydrogen Energy, 2019, 44, 4897-4906.	3.8	11
31301	Interfacial electronic properties of ferroelectric nanocomposites for energy storage application. Materials Today Energy, 2019, 12, 136-145.	2.5	23
31302	Two-Dimensional Anti-Vanâ€™t Hoff/Le Bel Array AlB₆ with High Stability, Unique Motif, Triple Dirac Cones, and Superconductivity. Journal of the American Chemical Society, 2019, 141, 3630-3640.	6.6	154
31303	An ab initio study of sensing applications of MoB₂ monolayer: a potential gas sensor. Physical Chemistry Chemical Physics, 2019, 21, 4633-4640.	1.3	68
31304	The role of sp²and sp³hybridized bonds on the structural, mechanical, and electronic properties in a hard BN framework. RSC Advances, 2019, 9, 2657-2665.	1.7	17
31305	Giant enhancements in electronic transport and photoelectric properties of bismuth oxysulfide by pressure-driven 2Dâ€“3D structural reconstruction. Journal of Materials Chemistry A, 2019, 7, 4019-4025.	5.2	35
31306	Energy-level alignment at strongly coupled organicâ€“metal interfaces. Journal of Physics Condensed Matter, 2019, 31, 194002.	0.7	12
31307	Effect of transition metal (TM: Cr and Mn) doping on charge transport properties of ScNiBi: a density functional theory approach. Materials Research Express, 2019, 6, 056511.	0.8	1
31308	Magnesium based materials for hydrogen based energy storage: Past, present and future. International Journal of Hydrogen Energy, 2019, 44, 7809-7859.	3.8	460
31309	Eu3+ doped (Li, Na, K) LaMgWO6 red emission phosphors: An example to rational design with theoretical and experimental investigation. Journal of Alloys and Compounds, 2019, 785, 651-659.	2.8	36
31310	Microscopic calculation of the optical properties and intrinsic losses in the methylammonium lead iodide perovskite system. APL Materials, 2019, 7, 011107.	2.2	2
31311	Synergistic effect of surface oxygen vacancies and interfacial charge transfer on Fe(III)/Bi2MoO6 for efficient photocatalysis. Applied Catalysis B: Environmental, 2019, 247, 150-162.	10.8	185
31312	Effect of position and concentration of Li on ZnO physical properties: Density functional investigation. Chemical Physics Letters, 2019, 719, 45-53.	1.2	19
31313	Theoretical study of the structural and electronic properties of impurities in non-passivated silicon thin nanowires. Solid State Communications, 2019, 290, 1-6.	0.9	2
31314	Featuring IÂ·Â·Â·N Halogen Bond and Weaker Interactions in Iodoperfluoroalkylimidazoles: An Experimental and Theoretical Charge Density Study. Crystal Growth and Design, 2019, 19, 1621-1631.	1.4	12
31315	Strong Variation of Electronic Properties of MoS₂ and WS₂ Nanotubes in the Presence of External Electric Fields. Journal of Physical Chemistry C, 2019, 123, 3892-3899.	1.5	13

#	Article	IF	Citations
31316	Lithium Doping of ZnO for High Efficiency and Stability Fullerene and Non-fullerene Organic Solar Cells. ACS Applied Energy Materials, 2019, 2, 1663-1675.	2.5	52
31317	Approaching the Volcano Top: Iridium/Silicon Nanocomposites as Efficient Electrocatalysts for the Hydrogen Evolution Reaction. ACS Nano, 2019, 13, 2786-2794.	7.3	106
31318	Learning-in-Templates Enables Accelerated Discovery and Synthesis of New Stable Double Perovskites. Journal of the American Chemical Society, 2019, 141, 3682-3690.	6.6	27
31319	Perovskite-polymer composite cross-linker approach for highly-stable and efficient perovskite solar cells. Nature Communications, 2019, 10, 520.	5.8	405
31320	Synergy of the catalytic activation on Ni and the CeO₂â€“TiO₂/Ce₂Ti₂O₇ stoichiometric redox cycle for dramatically enhanced solar fuel production. Energy and Environmental Science, 2019, 12, 767-779.	15.6	90
31321	Exfoliation of borophenes from silver substrates assisted by Li/Mg atomsâ€”a density functional theory study. Journal of Materials Chemistry C, 2019, 7, 4043-4048.	2.7	15
31322	Design and characterization of novel polymorphs of single-layered tin-sulfide for direction-dependent thermoelectric applications using first-principles approaches. Physical Chemistry Chemical Physics, 2019, 21, 4624-4632.	1.3	37
31323	3D hierarchical porous indium catalyst for highly efficient electroreduction of CO₂. Journal of Materials Chemistry A, 2019, 7, 4505-4515.	5.2	134
31324	Thermoelectric properties of topological insulator lanthanum phosphide via first-principles study. Journal of Applied Physics, 2019, 125, .	1.1	16
31325	Equations of state of Co2TiO4-Sp, Co2TiO4-CM, and Co2TiO4-CT, and their phase transitions: an experimental and theoretical study. Physics and Chemistry of Minerals, 2019, 46, 571-582.	0.3	4
31326	Assessment of Constant-Potential Implicit Solvation Calculations of Electrochemical Energy Barriers for H₂ Evolution on Pt. Journal of Physical Chemistry C, 2019, 123, 4116-4124.	1.5	71
31327	Probing the Active Sites of MoS₂ Based Hydrotreating Catalysts Using Modulation Excitation Spectroscopy. ACS Catalysis, 2019, 9, 2568-2579.	5.5	43
31328	Simulating the Nanomechanical Response of Cyclooctatetraene Molecules on a Graphene Device. ACS Nano, 2019, 13, 1713-1718.	7.3	6
31329	Stability and magnetism of FeN high-pressure phases. Physical Chemistry Chemical Physics, 2019, 21, 5262-5273.	1.3	12
31330	Hybrid Organic-Inorganic Perovskites as Promising Substrates for Pt Single-Atom Catalysts. Physical Review Letters, 2019, 122, 046101.	2.9	25
31331	Optical Properties of Au-Based and Pt-Based Alloys for Infrared Device Applications: A Combined First Principle and Electromagnetic Simulation Study. Micromachines, 2019, 10, 73.	1.4	7
31332	Non-Monotonic Trends of Hydrogen Adsorption on Single Atom Doped g-C3N4. Catalysts, 2019, 9, 84.	1.6	19
31333	New Insights on the Role of Chloride During the Onset of Local Corrosion: TEM, APT, Surface Energy, and Morphological Instability. Corrosion, 2019, 75, 616-627.	0.5	15

#	Article	IF	Citations
31334	Ion Conductivity Enhancement in Antiâ€Spinel Li₃OBr with Intrinsic Vacancies. Advanced Theory and Simulations, 2019, 2, 1800138.	1.3	14
31335	Elastic properties of the TiZrNbTaMo multi-principal element alloy studied from first principles. Intermetallics, 2019, 106, 130-140.	1.8	29
31336	Ultrathin nanowire based on icosahedral W@Au12 and application as NO gas sensor. Journal of Physics and Chemistry of Solids, 2019, 127, 68-75.	1.9	16
31337	Functionalized Rutile TiO₂(110) as a Sorbent To Capture CO₂ through Noncovalent Interactions: A Computational Investigation. Journal of Physical Chemistry C, 2019, 123, 3491-3504.	1.5	16
31338	Effect of Net Charge on the Relative Stability of 2D Boron Allotropes. Nano Letters, 2019, 19, 1359-1365.	4.5	23
31339	New 2D Structural Materials: Carbonâ€“Gallium Nitride (CCâ€“GaN) and Boronâ€“Gallium Nitride (BNâ€“GaN) Heterostructuresâ€”Materials Design Through Density Functional Theory. ACS Omega, 2019, 4, 1722-1728.	1.6	11
31340	Breaking Long-Range Order in Iridium Oxide by Alkali Ion for Efficient Water Oxidation. Journal of the American Chemical Society, 2019, 141, 3014-3023.	6.6	337
31341	Hybrid hollow spheres of carbon@Co_xNi_{1â^'x}MoO₄ as advanced electrodes for high-performance asymmetric supercapacitors. Nanoscale, 2019, 11, 3281-3291.	2.8	79
31342	First-principles investigation of the electronic structures and Seebeck coefficients of PbTe/SrTe interfaces. Journal of Applied Physics, 2019, 125, 035107.	1.1	5
31343	Strain induced NDR and rectification behavior of the Î³-graphyne nanotubes. Materials Research Express, 2019, 6, 045050.	0.8	8
31344	First-principles localized cluster expansion study of the kinetics of hydrogen diffusion in homogeneous and heterogeneous Fe-Cr alloys. Physical Review B, 2019, 99, .	1.1	16
31345	Hybrid density functional theory study of vanadium doping in stoichiometric and congruent <mml:math xmlns:mml="http://www.w3.org/1998/Math/MathML"><mml:mrow><mml:mi>LiNb</mml:mi><mml:msub><mml:mi mathvariant="normal">O</mml:mi><mml:mn>3</mml:mn></mml:msub></mml:mrow></mml:math>. Physical Review B, 2019, 99, .	1.1	11
31347	Opto-electronic and thermoelectric properties of MgIn2X4 (XÂ= S, Se) spinels via ab-initio calculations. Journal of Molecular Graphics and Modelling, 2019, 88, 168-173.	1.3	42
31348	ASbF3Cl (A = Rb, Cs): Structural Evolution from Centrosymmetry to Noncentrosymmetry. Crystal Growth and Design, 2019, 19, 1874-1879.	1.4	8
31349	Surface Activity of Early Transition-Metal Oxycarbides: CO₂ Adsorption Case Study. Journal of Physical Chemistry C, 2019, 123, 3664-3671.	1.5	10
31350	Metal Chalcogenides Janus Monolayers for Efficient Hydrogen Generation by Photocatalytic Water Splitting. ACS Applied Nano Materials, 2019, 2, 890-897.	2.4	93
31351	A Picture of Disorder in Hydrous Wadsleyiteâ€”Under the Combined Microscope of Solid-State NMR Spectroscopy and Ab Initio Random Structure Searching. Journal of the American Chemical Society, 2019, 141, 3024-3036.	6.6	13
31352	Polymorphism in p-aminobenzoic acid. CrystEngComm, 2019, 21, 2034-2042.	1.3	30

#	Article	IF	Citations
31353	Single-layer ferromagnetic and piezoelectric CoAsS with pentagonal structure. APL Materials, 2019, 7, .	2.2	14
31354	Tuning the magnetocrystalline anisotropy ofFe3Snby alloying. Physical Review B, 2019, 99, .	1.1	17
31355	Exciton in phosphorene: Strain, impurity, thickness, and heterostructure. Physical Review B, 2019, 99, .	1.1	17
31356	Carbon Permeation: The Prerequisite Elementary Step in Iron-Catalyzed Fischerâ€“Tropsch Synthesis. Catalysis Letters, 2019, 149, 645-664.	1.4	19
31357	Graphene on the oxidized SiC surface and the impact of the metal intercalation. Carbon, 2019, 145, 603-613.	5.4	9
31358	A density functional theory analysis of the mechanical and dynamic stability and thermodynamic properties of pyrite-type ZnSe2 and ZnTe2. Computational Condensed Matter, 2019, 19, e00366.	0.9	0
31359	High-throughput fabrication of 3D N-doped graphenic framework coupled with Fe3C@porous graphite carbon for ultrastable potassium ion storage. Energy Storage Materials, 2019, 22, 185-193.	9.5	91
31360	Tunable band gap of N V co-doped Ca:TiO2B (CaTi5O11) for visible-light photocatalysis. International Journal of Hydrogen Energy, 2019, 44, 4716-4723.	3.8	12
31361	Theoretical study on stability, mechanical and thermodynamic properties of (Pu, Zr)N. Journal of Nuclear Materials, 2019, 516, 264-270.	1.3	11
31362	Mixed Cs and FA Cations Slow Electronâ€“Hole Recombination in FAPbI₃ Perovskites by Time-Domain Ab Initio Study: Lattice Contraction versus Octahedral Tilting. Journal of Physical Chemistry Letters, 2019, 10, 672-678.	2.1	29
31363	Prospects for experimental realization of two-dimensional aluminium allotropes. Journal of Materials Chemistry C, 2019, 7, 2666-2675.	2.7	24
31364	Electron density topological and adsorbate orbital analyses of water and carbon monoxide co-adsorption on platinum. Journal of Chemical Physics, 2019, 150, 024703.	1.2	6
31365	Perseverance of direct bandgap in multilayer 2D PbI ₂ under an experimental strain up to 7.69%. 2D Materials, 2019, 6, 025014.	2.0	20
31366	Single-Crystal Permanent Magnets: Extraordinary Magnetic Behavior in theTa-,Cu-, andFe-SubstitutedCeCo5Systems. Physical Review Applied, 2019, 11, .	1.5	15
31367	Effect of Mn and C on Age Hardening of Feâ€“Mnâ€“Alâ€“C Lightweight Steels. Metals and Materials International, 2019, 25, 683-696.	1.8	24
31368	Interfacial properties of two-dimensional graphene/ZrS2 and ScS2/ZrS2 contacts. Applied Surface Science, 2019, 476, 778-788.	3.1	11
31369	Encapsulation of cadmium telluride nanocrystals within single walled carbon nanotubes. Inorganica Chimica Acta, 2019, 488, 246-254.	1.2	8
31370	Theoretical study of electronic structure, thermoelectric and thermodynamic properties of 2H-AgAlO2. Physica B: Condensed Matter, 2019, 558, 109-115.	1.3	6

#	Article	IF	Citations
31371	Learning from Nature: Charge Transfer and Carbon Dioxide Activation at Single, Biomimetic Fe Sites in Tetrapyrroles on Graphene. Journal of Physical Chemistry C, 2019, 123, 3916-3922.	1.5	11
31372	Adsorption studies of dimethyl and methyl-ethyl ester molecules on silicene nanoring: Application of DFT study. Phosphorus, Sulfur and Silicon and the Related Elements, 2019, 194, 25-32.	0.8	12
31373	Strain Enhanced Visibleâ€“Ultraviolet Absorption of Blue Phosphorene/MoX 2 (Xâ€‰=â€‰S,Se) Heterolayers. Physica Status Solidi - Rapid Research Letters, 2019, 13, 1800659.	1.2	5
31374	The role of chemical disorder and structural freedom in radiation-induced amorphization of silicon carbide deduced from electron spectroscopy and ab initio simulations. Journal of Nuclear Materials, 2019, 514, 299-310.	1.3	9
31375	Microstructure, indentation and first principles study of AlCuFeMn alloy. Materialia, 2019, 5, 100206.	1.3	4
31376	The Janus structures of group-III chalcogenide monolayers as promising photocatalysts for water splitting. Applied Surface Science, 2019, 478, 522-531.	3.1	78
31377	Defect-rich activated carbons as active and stable metal-free catalyst for acetylene hydrochlorination. Carbon, 2019, 146, 406-412.	5.4	78
31378	Hydrogen adsorption on WS2 decorated by Na and Li. Superlattices and Microstructures, 2019, 128, 392-401.	1.4	31
31379	Microscopic Simulation of Methane Adsorption in Organic Matter. Industrial & Engineering Chemistry Research, 2019, 58, 3523-3530.	1.8	13
31380	Role of Long-Range Dispersion Forces in Modeling of MXenes as Battery Electrode Materials. Journal of Physical Chemistry C, 2019, 123, 4064-4071.	1.5	5
31381	Support Effects Examined by a Comparative Theoretical Study of Au, Cu, and CuAu Nanoclusters on Rutile and Anatase Surfaces. Journal of Physical Chemistry C, 2019, 123, 4892-4902.	1.5	11
31382	Cu-Based Single-Atom Catalysts Boost Electroreduction of CO₂ to CH₃OH: First-Principles Predictions. Journal of Physical Chemistry C, 2019, 123, 4380-4387.	1.5	68
31383	Structure- and Temperature-Dependence of Pt-Catalyzed Ammonia Oxidation Rates and Selectivities. ACS Catalysis, 2019, 9, 2407-2414.	5.5	58
31384	Defect Chemistry and Li-ion Diffusion in Li2RuO3. Scientific Reports, 2019, 9, 550.	1.6	28
31385	Metal/graphene heterobilayers as hydrogen evolution reaction cathodes: a first-principles study. Physical Chemistry Chemical Physics, 2019, 21, 4594-4599.	1.3	6
31386	Mg²⁺storage and mobility in anatase TiO₂: the role of frustrated coordination. Journal of Materials Chemistry A, 2019, 7, 3704-3713.	5.2	10
31387	Surface reactivity and cation non-stoichiometry in BaZr_{1â^'x}Y_xO_{3â^'Î´} (x = 0â€“0.2) exposed to CO₂ at elevated temperature. Journal of Materials Chemistry A, 2019, 7, 3848-3856.	5.2	21
31388	Effect of spin contamination error on surface catalytic reaction: NO reduction by core-shell catalysts. Molecular Physics, 2019, 117, 2251-2259.	0.8	22

#	Article	IF	Citations
31389	Negative linear compressibility in uranyl squarate monohydrate. Journal of Physics Condensed Matter, 2019, 31, 175701.	0.7	11
31390	Heterostructured Nanocubeâ€Shaped Binary Sulfide (SnCo)S₂ Interlaced with Sâ€Doped Graphene as a Highâ€Performance Anode for Advanced Na⁺ Batteries. Advanced Functional Materials, 2019, 29, 1807971.	7.8	154
31391	Effects of Electronic Delocalization and Hydrostatic Compression on Structure and Properties of Cage Compound 4â€Trinitroethylâ€2,6,8,10,12â€pentanitrohexaazaisowurtzitane. ChemistrySelect, 2019, 4, 1567-1575.	0.7	2
31392	A stable mesoporous super-acid nanocatalyst for eco-friendly synthesis of biodiesel. Chemical Engineering Journal, 2019, 364, 111-122.	6.6	38
31393	3D meso-nanostructures in cleaved and nanolithographed Mg-Al-hydroxysilicate (clinochlore): Topology, crystal-chemistry, and surface properties. Applied Clay Science, 2019, 169, 74-80.	2.6	11
31394	Roles of oxygen vacancies and pH induced size changes on photo- and radioluminescence of undoped and Eu3+-doped La2Zr2O7 nanoparticles. Journal of Luminescence, 2019, 209, 302-315.	1.5	36
31395	First-principles studies on mechanical properties and band structures of TMO2 (TM = Zr or Hf) nanostructures under high pressure. Physica B: Condensed Matter, 2019, 559, 1-7.	1.3	13
31396	Strain Engineering of Adsorbate Self-Assembly on Graphene for Band Gap Tuning. Journal of Physical Chemistry C, 2019, 123, 4475-4482.	1.5	18
31397	Comparing Rate and Mechanism of Ethane Hydrogenolysis on Transition-Metal Catalysts. Journal of Physical Chemistry C, 2019, 123, 5421-5432.	1.5	31
31398	ITO Work Function Tunability by Polarizable Chromophore Monolayers. Langmuir, 2019, 35, 2997-3004.	1.6	12
31399	Enhanced flexoelectricity at reduced dimensions revealed by mechanically tunable quantum tunnelling. Nature Communications, 2019, 10, 537.	5.8	64
31400	High selectivity n-type InSe monolayer toward decomposition products of sulfur hexafluoride: A density functional theory study. Applied Surface Science, 2019, 479, 852-862.	3.1	20
31401	First-principles calculations of aluminium nitride monolayer with chemical functionalization. Applied Surface Science, 2019, 481, 1549-1553.	3.1	36
31402	Role of external magnetic fields in determining the thermodynamic properties of iron carbides in steel. Acta Materialia, 2019, 167, 71-79.	3.8	14
31403	Screening of active center and reactivity descriptor in acetylene hydrochlorination on metal-free doped carbon catalysts from first principle calculations. Applied Surface Science, 2019, 478, 574-580.	3.1	21
31404	Optical properties and quasiparticle energies in the two-layered hydrogenated gallium nitrate nanosheet: A DFT study. Computational and Theoretical Chemistry, 2019, 1151, 31-35.	1.1	2
31405	Enhanced thermoelectric performance in the n-type NbFeSb half-Heusler compound with heavy element Ir doping. Materials Today Physics, 2019, 8, 62-70.	2.9	44
31406	The electronic properties in the hole-doped 1111 compounds: An ab-initio description. Physica C: Superconductivity and Its Applications, 2019, 559, 8-13.	0.6	1

#	Article	IF	Citations
31407	Mechanism of Sodium-Ion Diffusion in Alluaudite-Type Na₅Sc(MoO₄)₄ from NMR Experiment and Ab Initio Calculations. Journal of Physical Chemistry C, 2019, 123, 4729-4738.	1.5	16
31408	Theoretical Investigation of On-Purpose Propane Dehydrogenation over the Two-Dimensional Ruâ€“Pc Framework. Journal of Physical Chemistry C, 2019, 123, 4969-4976.	1.5	28
31409	Nanoclay-modulated oxygen vacancies of metal oxide. Communications Chemistry, 2019, 2, .	2.0	84
31410	Insight into the reaction mechanism of water, oxygen and nitrogen molecules on a tin iodine perovskite surface. Journal of Materials Chemistry A, 2019, 7, 5779-5793.	5.2	40
31411	Discovery of a ferroelastic topological insulator in a two-dimensional tetragonal lattice. Physical Chemistry Chemical Physics, 2019, 21, 5165-5169.	1.3	5
31412	Topologically nontrivial phases in superconducting transition metal carbides. Journal of Applied Physics, 2019, 125, 053903.	1.1	10
31413	Monitoring the Applied Strain in Monolayer Gallium Selenide through Vibrational Spectroscopies: A First-Principles Investigation. Physical Review Applied, 2019, 11, .	1.5	17
31414	Metric wave approach to flexoelectricity within density functional perturbation theory. Physical Review B, 2019, 99, .	1.1	15
31415	Effect of randomly distributed asymmetric stone-wales defect on electronic and transport properties of armchair graphene nanoribbon. Superlattices and Microstructures, 2019, 128, 116-126.	1.4	13
31416	Facile One-Pot Synthesis of Pd@Pt_{1L} Octahedra with Enhanced Activity and Durability toward Oxygen Reduction. Chemistry of Materials, 2019, 31, 1370-1380.	3.2	41
31417	XANES, EXAFS, EPR, and First-Principles Modeling on Electronic Structure and Ferromagnetism in Mn Doped SnO₂ Quantum Dots. Journal of Physical Chemistry C, 2019, 123, 3067-3075.	1.5	15
31418	Electronic and Magnetic Properties of Lanthanum and Strontium Doped Bismuth Ferrite: A First-Principles Study. Scientific Reports, 2019, 9, 194.	1.6	42
31419	Symmetry-breaking induced large piezoelectricity in Janus tellurene materials. Physical Chemistry Chemical Physics, 2019, 21, 1207-1216.	1.3	134
31420	Discovery of ABO₃ perovskites as thermal barrier coatings through high-throughput first principles calculations. Materials Research Letters, 2019, 7, 145-151.	4.1	60
31421	Local order in Cr-Fe-Co-Ni: Experiment and electronic structure calculations. Physical Review B, 2019, 99, .	1.1	40
31422	Ab initio study of the LiH phase diagram at extreme pressures and temperatures. Physical Review B, 2019, 99, .	1.1	5
31423	Magnetic order of Dy2Fe14B/Fe interface. International Journal of Applied Electromagnetics and Mechanics, 2019, 59, 145-150.	0.3	0
31424	Effects of Impurity Doping on the Luminescence Performance of Mn4+-Doped Aluminates with the Magnetoplumbite-Type Structure for Plant Cultivation. Materials, 2019, 12, 86.	1.3	17

#	Article	IF	Citations
31425	Al80Cr20N-layer thickness-dependent microstructure and mechanical properties of Al50Cr50N/Al80Cr20N nanomultilayered films. Vacuum, 2019, 162, 1-7.	1.6	5
31426	Tuning oxygen electrocatalysis via strain on LaNiO3(001). Physical Chemistry Chemical Physics, 2019, 21, 4738-4745.	1.3	14
31427	Rational design and observation of the tight interface between graphene and ligand protected nanocrystals. Physical Chemistry Chemical Physics, 2019, 21, 329-335.	1.3	2
31428	Coexistence of piezoelectricity and magnetism in two-dimensional vanadium dichalcogenides. Physical Chemistry Chemical Physics, 2019, 21, 132-136.	1.3	80
31429	Infrared and Raman spectroscopy of non-conventional hydrogen bonding between N,Nâ€²-disubstituted urea and thiourea groups: a combined experimental and theoretical investigation. Physical Chemistry Chemical Physics, 2019, 21, 3310-3317.	1.3	15
31430	Thermodynamic stability of non-stoichiometric SrFeO_{3â^'Î´}: a hybrid DFT study. Physical Chemistry Chemical Physics, 2019, 21, 3918-3931.	1.3	30
31431	Computational discovery and characterization of new B₂O phases. Physical Chemistry Chemical Physics, 2019, 21, 2499-2506.	1.3	7
31432	Sulfation of a PdO(101) methane oxidation catalyst: mechanism revealed by first principles calculations. Catalysis Science and Technology, 2019, 9, 232-240.	2.1	10
31433	Enhanced deep-red emission from Mn⁴⁺/Mg²⁺co-doped CaGdAlO₄phosphors for plant cultivation. Dalton Transactions, 2019, 48, 2455-2466.	1.6	50
31434	Molecular-scale structures of uranyl surface complexes on hematite facets. Environmental Science: Nano, 2019, 6, 892-903.	2.2	19
31436	Atomically dispersed Ni as the active site towards selective hydrogenation of nitroarenes. Green Chemistry, 2019, 21, 704-711.	4.6	98
31437	Germagraphene as a promising anode material for lithium-ion batteries predicted from first-principles calculations. Nanoscale Horizons, 2019, 4, 457-463.	4.1	48
31438	Catalytic performance of graphene quantum dot supported manganese phthalocyanine for efficient oxygen reduction: density functional theory approach. New Journal of Chemistry, 2019, 43, 348-355.	1.4	19
31439	Effects of pore surfaces on the electronic states of metal complexes formed on bipyridine periodic mesoporous organosilica. New Journal of Chemistry, 2019, 43, 2471-2478.	1.4	6
31440	Morphology controlled synthesis of low bandgap SnSe₂ with high photodetectivity. Nanoscale, 2019, 11, 870-877.	2.8	31
31441	Intrinsic multiferroicity in two-dimensional VOCl₂ monolayers. Nanoscale, 2019, 11, 1103-1110.	2.8	62
31442	Synthesis and characterization of methylammonium phosphates as crystalline approximants for anhydrous, low melting phosphate glasses. RSC Advances, 2019, 9, 1822-1830.	1.7	1
31443	Negative area compressibility of a hydrogen-bonded two-dimensional material. Chemical Science, 2019, 10, 1309-1315.	3.7	24

#	Article	IF	Citations
31444	Reductive diazotation of carbon nanotubes: an experimental and theoretical selectivity study. Chemical Science, 2019, 10, 706-717.	3.7	6
31445	How does graphene enhance the photoelectric conversion efficiency of dye sensitized solar cells? An insight from a theoretical perspective. Journal of Materials Chemistry A, 2019, 7, 2730-2740.	5.2	26
31446	Enhancement of photocatalytic H2 production by metal complex electrostatic adsorption on TiO2 (B) nanosheets. Journal of Materials Chemistry A, 2019, 7, 3797-3804.	5.2	11
31447	Uniform Pd_{0.33}Ir_{0.67} nanoparticles supported on nitrogen-doped carbon with remarkable activity toward the alkaline hydrogen oxidation reaction. Journal of Materials Chemistry A, 2019, 7, 3161-3169.	5.2	50
31448	Three-dimensional auxetic properties in group Vâ€“VI binary monolayer crystals X₃M₂ (X = S, Se; M = N, P, As). Physical Chemistry Chemical Physics, 2019, 21, 5916-5924.	1.3	10
31449	A density functional theory study of the hydrogenation and reduction of the thio-spinel Fe₃S₄{111} surface. Physical Chemistry Chemical Physics, 2019, 21, 2426-2433.	1.3	4
31450	Spin-filtering and tunneling magnetoresistance effects in 6,6,12-graphyne-based molecular magnetic tunnel junctions. Physical Chemistry Chemical Physics, 2019, 21, 2734-2742.	1.3	6
31451	Adsorption of CO and NO molecules on Al, P and Si embedded MoS2 nanosheets investigated by DFT calculations. Adsorption, 2019, 25, 1001-1017.	1.4	33
31452	A first principles calculation of site occupancy of the B2 phase in Ti2AlX (X=V, Cr, Fe, Mo, Ta, Nb, Zr, Hf) Tj ETQq0 0 0 rgBT /Overlock 10	2.0	17
31453	Electrochemically active novel amorphous carbon (a-C)/Cu3P peapod nanowires by low-temperature chemical vapor phosphorization reaction as high efficient electrocatalysts for hydrogen evolution reaction. Electrochimica Acta, 2019, 318, 374-383.	2.6	13
31454	Hydrogen induced structure and property changes in Eu3Si4. Journal of Solid State Chemistry, 2019, 277, 37-45.	1.4	0
31455	First principles investigation into the phase stability and enhanced hardness of TiN-ScN and TiN-YN alloys. Thin Solid Films, 2019, 688, 137284.	0.8	16
31456	Supramolecular Interactions of Group VI Metal Carbonyl Complexes: The Facilitating Role of 1,3-Bis(p-isocyanophenyl)urea. Inorganic Chemistry, 2019, 58, 8130-8139.	1.9	5
31457	Donorâ€“Acceptor Sequence Engineering in Ï€-Conjugated Polymers for Enhanced Hole Transport and Photocurrent. Journal of Physical Chemistry C, 2019, 123, 14253-14260.	1.5	4
31458	Gate tunable giant anisotropic resistance in ultra-thin GaTe. Nature Communications, 2019, 10, 2302.	5.8	72
31459	High-pressure polymorphism in l-threonine between ambient pressure and 22 GPa. CrystEngComm, 2019, 21, 4444-4456.	1.3	27
31460	Determination of elementâ€“deuterium bond lengths in Zintl phase deuterides by 2H-NMR. Physical Chemistry Chemical Physics, 2019, 21, 10594-10602.	1.3	2
31461	Crystal structure, hydrogen bonding, mechanical properties and Raman spectrum of the lead uranyl silicate monohydrate mineral kasolite. RSC Advances, 2019, 9, 15323-15334.	1.7	24

#	Article	IF	Citations
31462	Strain-induced electronic properties of van der Waals heterostructures based on tin dichalcogenides. AIP Advances, 2019, 9, .	0.6	11
31463	Two-dimensional antiferromagnetic boron form first principles. AIP Advances, 2019, 9, 055211.	0.6	2
31464	Effect of layer and stacking sequence in simultaneously grown 2H and 3R WS₂ atomic layers. Nanotechnology, 2019, 30, 345203.	1.3	16
31465	Molecular dynamic simulations of ether or ethanol coated aluminum nanoparticles for the application of hydrogenation: a comparison study. Materials Research Express, 2019, 6, 085083.	0.8	2
31466	Probing the Structural, Electronic, Mechanical Strength and Thermodynamic Properties of Tungsten-Based Oxide Perovskites RbWO3 and CsWO3: First-Principles Investigation. Journal of Electronic Materials, 2019, 48, 4886-4894.	1.0	8
31467	Fine-tuning the ductile-brittle transition temperature of Mg2Si intermetallic compound via Al doping. International Journal of Minerals, Metallurgy and Materials, 2019, 26, 507-515.	2.4	10
31468	The modulation of the magnetocrystalline anisotropy of the halogen functionalize metal-phthalocyanine networks. Chemical Physics Letters, 2019, 728, 181-185.	1.2	2
31469	Exploration of crystal structure and the origin of unexpected intrinsic ductility of Ï‡Co7Ta2. Journal of Alloys and Compounds, 2019, 797, 1198-1204.	2.8	5
31470	Theoretical study on Frenkel pair formation and recombination in single crystal silicon. Journal of Crystal Growth, 2019, 520, 1-10.	0.7	3
31471	Effects of Zr and V additions on the stability and migration of He in bcc W: A first-principles study. Physics Letters, Section A: General, Atomic and Solid State Physics, 2019, 383, 2777-2783.	0.9	5
31472	Structural and electronic properties of 2H phase Janus transition metal dichalcogenide bilayers. Superlattices and Microstructures, 2019, 131, 8-14.	1.4	23
31473	Impact of lattice relaxations on phase transitions in a high-entropy alloy studied by machine-learning potentials. Npj Computational Materials, 2019, 5, .	3.5	110
31474	Single Pt atom supported on penta-graphene as an efficient catalyst for CO oxidation. Physical Chemistry Chemical Physics, 2019, 21, 12201-12208.	1.3	27
31475	Electronic structure and high-temperature thermochemistry of BaZrO_{3â^'Î´}perovskite from first-principles calculations. Physical Chemistry Chemical Physics, 2019, 21, 12468-12476.	1.3	7
31476	Density functional study of methyl butanoate adsorption and its Câ€“O bonds cleavage on MoS₂-based catalyst with various loads of Ni promoters. Journal of Physics Condensed Matter, 2019, 31, 365001.	0.7	8
31477	Physical properties of epitaxial SrMnO_{2.5â^'Î´}F_{Î³} oxyfluoride films. Journal of Physics Condensed Matter, 2019, 31, 365602.	0.7	5
31478	First-principles study of structural, mechanical, and electronic properties of W alloying with Zr. Chinese Physics B, 2019, 28, 046301.	0.7	6
31479	Electronic and magnetic properties of graphene densely decorated with 3 d metallic adatomsâ€”the effect of structure privilege and spinâ€“orbit interaction. Electronic Structure, 2019, 1, 015006.	1.0	0

#	Article	IF	Citations
31480	Transformation of the Topological Phase and the Edge Modes of Double-Bilayer Bismuthene with Inter-Bilayer Spacing. Crystals, 2019, 9, 266.	1.0	1
31481	Molecular Modeling of Interactions between N-(Carboxymethyl)-N-tetradecylglycine and Fluorapatite. Minerals (Basel, Switzerland), 2019, 9, 278.	0.8	7
31482	Understanding of relationship between dopant and substitutional site to develop novel phase-change materials based on In₃SbTe₂. Japanese Journal of Applied Physics, 2019, 58, SBBB02.	0.8	15
31483	Interface reaction of high-strength low-alloy steel with Alâ€“43.4Znâ€“1.6Si (wt.%) metallic coating. Journal of Iron and Steel Research International, 2019, 26, 1304-1314.	1.4	2
31484	Mechanism insights into Hg(II) adsorption on kaolinite(001) surface: A density functional study. Applied Surface Science, 2019, 488, 494-502.	3.1	37
31485	Critical review of phase equilibria in the Ni-Si-Zn ternary system and its thermodynamic description supported by first-principles calculations. Calphad: Computer Coupling of Phase Diagrams and Thermochemistry, 2019, 66, 101622.	0.7	5
31486	Low Temperature Pyrolyzed Soft Carbon as High Capacity K-Ion Anode. ACS Applied Energy Materials, 2019, 2, 4053-4058.	2.5	44
31487	Theoretical phase diagram of boron carbide from ambient to high pressure and temperature. Journal of Applied Physics, 2019, 125, 185902.	1.1	24
31488	Antiferromagnetism and the emergence of frustration in the sawtooth lattice chalcogenide olivines <mml:math xmlns:mml="http://www.w3.org/1998/Math/MathML"><mml:mrow><mml:msub><mml:mi>Mn</mml:mi><mml:mn>2</mml:mn></mml:		

#	Article	IF	Citations
31498	Tuning the magnetism of two-dimensional hematene by ferroelectric polarization. Physical Chemistry Chemical Physics, 2019, 21, 12301-12309.	1.3	16
31499	Controlling the magnetocrystalline anisotropy of Îµ-Fe2O3. AIP Advances, 2019, 9, 035231.	0.6	3
31500	External strain-enhanced cysteine enantiomeric separation ability on alloyed stepped surfaces. Journal of Chemical Physics, 2019, 150, 154701.	1.2	4
31501	Sorption mechanism and dynamic behavior of graphene oxide as an effective adsorbent for the removal of chlorophenol based environmental-hormones: A DFT and MD simulation study. Chemical Engineering Journal, 2019, 375, 121964.	6.6	74
31502	Thermal expansion of energetic material TEX obtained from x-ray diffraction and first principles calculations. Journal of Molecular Structure, 2019, 1195, 859-862.	1.8	6
31503	Efficient band structure engineering and visible-light response in ZrS2/GaS heterobilayer by electrical field or external strains. Physics Letters, Section A: General, Atomic and Solid State Physics, 2019, 383, 2969-2973.	0.9	8
31504	Ab initio calculations of CaZrO₃, BaZrO₃, PbTiO₃ and SrTiO₃ (001), (011) and (111) surfaces as well as their (001) interfaces. Integrated Ferroelectrics, 2019, 196, 7-15.	0.3	10
31505	Structural stability of MoB up to 25 GPa: experiment and computation. Materials Research Express, 2019, 6, 096502.	0.8	4
31506	Tunable first order transition in La(Fe,Cr,Si)13 compounds: Retaining magnetocaloric response despite a magnetic moment reduction. Acta Materialia, 2019, 175, 406-414.	3.8	45
31507	Expanded hexagonal nanohelicenes of zigzag morphology under elastic strain: A quantum chemical study. Carbon, 2019, 152, 755-765.	5.4	11
31508	Reliable thermodynamic estimators for screening caloric materials. Journal of Alloys and Compounds, 2019, 802, 712-722.	2.8	22
31509	First-principles study of dopant stability and related optical properties in CdSiP2 crystal. Journal of Alloys and Compounds, 2019, 802, 310-317.	2.8	2
31510	Giant Magnetoelectric Coupling and Two-Dimensional Electron Gas Regulated by Polarization in BiFeO₃/LaFeO₃ Heterostructures. Journal of Physical Chemistry C, 2019, 123, 16393-16399.	1.5	18
31511	Trace doping of multiple elements enables stable battery cycling of LiCoO2 at 4.6â€‰V. Nature Energy, 2019, 4, 594-603.	19.8	572
31512	Anisotropic thermoelectric properties of Weyl semimetal NbX (X = P and As): a potential thermoelectric material. Physical Chemistry Chemical Physics, 2019, 21, 15167-15176.	1.3	31
31513	Nature of Bimetallic Oxide Sb₂MoO₆/rGO Anode for Highâ€Performance Potassiumâ€Ion Batteries. Advanced Science, 2019, 6, 1900904.	5.6	60
31514	Micromachining of ferrous metal with an ion implanted diamond cutting tool. Carbon, 2019, 152, 598-608.	5.4	27
31515	First-principle study on structural, linear and nonlinear optical properties of selenocyanate complex ZnCd(SeCN)4 crystal. Computational Materials Science, 2019, 168, 154-163.	1.4	4

#	Article	IF	Citations
31516	Organic Molecule Orientations and Rashbaâ€“Dresselhaus Effect in Î±-Formamidinium Lead Iodide. Journal of Physical Chemistry C, 2019, 123, 16508-16515.	1.5	16
31517	Singular Nonmagnetic Semiconductor ScH₃ Molecular Nanowire: A New Type of Room-Temperature Spintronic Material. Journal of Physical Chemistry C, 2019, 123, 16994-17001.	1.5	7
31518	Formation of Silicene on Ultrathin Pb(111) Films. Journal of Physical Chemistry C, 2019, 123, 17019-17025.	1.5	40
31519	Effect of Doped Metals on Hydrodeoxygenation of Phenol over Pt-Based Bimetallic Alloys: C_{aryl}â€“OH Versus C_{aliphatic}Hâ€“OH Bond Scission. Journal of Physical Chemistry C, 2019, 123, 16873-16882.	1.5	35
31520	Lattice Dynamics Study of Thermoelectric Oxychalcogenide BiCuChO (Ch = Se, S). Journal of Physical Chemistry C, 2019, 123, 16046-16057.	1.5	16
31521	Low Resistivity and High Breakdown Current Density of 10 nm Diameter van der Waals TaSe₃ Nanowires by Chemical Vapor Deposition. Nano Letters, 2019, 19, 4355-4361.	4.5	55
31522	PdAg nanoparticles supported on resorcinol-formaldehyde polymers containing amine groups: the promotional effect of phenylamine moieties on CO₂ transformation to formic acid. Journal of Materials Chemistry A, 2019, 7, 16356-16363.	5.2	39
31523	Fine tuning of Fermi level by charged impurity-defect cluster formation and thermoelectric properties in n-type PbTe-based compounds. Journal of Materials Chemistry A, 2019, 7, 16488-16500.	5.2	24
31524	Stable, one-dimensional suspended and supported monatomic chains of pnictogens: a metalâ€“insulator framework. Physical Chemistry Chemical Physics, 2019, 21, 14832-14845.	1.3	9
31525	Uniaxial strain induced topological phase transition in bismuthâ€“tellurohalideâ€“graphene heterostructures. Nanoscale, 2019, 11, 12704-12711.	2.8	10
31526	Inverse pressure-induced Mott transition in TiPO4. Physical Review B, 2019, 99, .	1.1	2
31527	Tunable Electronic Properties and Giant Spontaneous Polarization in Graphene/Monolayer GeS van der Waals Heterostructure. Physica Status Solidi (B): Basic Research, 2019, 256, 1900194.	0.7	6
31528	Anti-corrosive properties of quercetin and its derivatives on Fe(111) surface: a quantum chemical approach. SN Applied Sciences, 2019, 1, 1.	1.5	5
31529	CO₂ Activation and Reduction on Pt-CeO₂-Based Catalysts. Journal of Physical Chemistry C, 2019, 123, 17092-17101.	1.5	31
31530	Quantitative Understanding of the Sluggish Kinetics of Hydrogen Reactions in Alkaline Media Based on a Microscopic Hamiltonian Model for the Volmer Step. Journal of Physical Chemistry C, 2019, 123, 17325-17334.	1.5	38
31531	HLE17: An Efficient Way To Predict Band Gaps of Complex Materials. Journal of Physical Chemistry C, 2019, 123, 17416-17424.	1.5	26
31532	Role of Cation Vacancies in Cu₂SnSe₃ Thermoelectrics. ACS Applied Materials & Interfaces, 2019, 11, 24212-24220.	4.0	30
31533	Three-Dimensional Optical Anisotropy of Low-Symmetry Layered GeS. ACS Applied Materials & Interfaces, 2019, 11, 24247-24253.	4.0	27

#	Article	IF	Citations
31534	Plasmonic Photocatalysis of Nitrous Oxide into N₂ and O₂ Using Aluminumâ€“Iridium Antennaâ€“Reactor Nanoparticles. ACS Nano, 2019, 13, 8076-8086.	7.3	83
31535	K2[B4O5(OH)4]Â·H2O and K2[B4O5(OH)4]: two new hydrated potassium borates with isolated [B4O5(OH)4]2â^' units and different structural frameworks. New Journal of Chemistry, 2019, 43, 11660-11665.	1.4	3
31536	Real-time dynamic holographic display realized by bismuth and magnesium co-doped lithium niobate. Applied Physics Letters, 2019, 114, .	1.5	13
31537	Development of the Local (Site) Symmetry Method in the Supercell Model for a Crystal with an Impurity. Physics of the Solid State, 2019, 61, 994-1006.	0.2	0
31538	The Response to a Uniform Electric Field in Calculating the Electronic Structure of Crystals with a Basis of Localized Orbitals. Physics of the Solid State, 2019, 61, 987-993.	0.2	2
31539	A 3D and Stable Lithium Anode for Highâ€Performance Lithiumâ€“Iodine Batteries. Advanced Materials, 2019, 31, e1902399.	11.1	137
31540	Selective detection of SO2 in SF6 insulation devices by Rh-doped HfSe2 monolayer: a first-principles study. Applied Physics A: Materials Science and Processing, 2019, 125, 1.	1.1	12
31541	Strain-induced band modulation of surface F-functionalized two-dimensional Sc2C. Applied Surface Science, 2019, 491, 276-285.	3.1	23
31542	DFT study on electronic and optical properties of halogen-adsorbed hexagonal boron nitride. Computational Condensed Matter, 2019, 21, e00416.	0.9	15
31543	Effect of sulfur dopant atoms on the electronic band gap and optical properties of tin iodide. Chemical Physics Letters, 2019, 730, 557-561.	1.2	8
31544	Improving the accuracy of solid-state nuclear magnetic resonance chemical shift prediction with a simple molecular correction. Physical Chemistry Chemical Physics, 2019, 21, 14992-15000.	1.3	38
31545	Electronic and optical properties of van der Waals heterostructures of g-GaN and transition metal dichalcogenides. Applied Surface Science, 2019, 492, 513-519.	3.1	178
31546	Sublattice formation in CoCrFeNi high-entropy alloy. Intermetallics, 2019, 112, 106542.	1.8	20
31547	Insight into void formation near grain boundary from phase-field simulations. Nuclear Instruments & Methods in Physics Research B, 2019, 453, 50-55.	0.6	1
31548	Structural, electronic, and elastic properties of orthorhombic NaB3H8: A first-principles investigation. Solid State Communications, 2019, 299, 113653.	0.9	3
31549	Tuning the Electronic and Magnetic Properties of Graphene Flake Embedded in Boron Nitride Nanoribbons with Transverse Electric Fields: First-Principles Calculations. ACS Omega, 2019, 4, 10293-10301.	1.6	16
31550	First-Principles Study of Ferromagnetic KxCa1â^'xN Novel Alloy. Journal of Superconductivity and Novel Magnetism, 2019, 32, 3965-3969.	0.8	0
31551	Database of novel magnetic materials for high-performance permanent magnet development. Computational Materials Science, 2019, 168, 188-202.	1.4	41

#	Article	IF	Citations
31552	Elastic anisotropy and single-crystal moduli of solid argon up to 64ÂGPa from time-domain Brillouin scattering. Physical Review B, 2019, 99, .	1.1	10
31553	Uranium(IV) incorporation into inverse spinel magnetite ($$hbox {FeFe}_{2}hbox {O}_{4}$$): A charge-balanced substitution case analysis. Pramana - Journal of Physics, 2019, 93, 1.	0.9	1
31554	Site Occupation of Nb in Î³-TiAl: Beyond the Point Defect Gas Approximation. Acta Metallurgica Sinica (English Letters), 2019, 32, 1511-1520.	1.5	5
31555	Ferromagnetic topological crystalline insulating phase in the $$pi$$-stacked graphene nanobelts under a small pressure. SN Applied Sciences, 2019, 1, 1.	1.5	0
31556	Electronic structures, bonding natures and defect processes in Sn-based 211 MAX phases. Computational Materials Science, 2019, 168, 203-212.	1.4	17
31557	First-principle calculations of structural, electronic, optical and thermodynamical properties of fluorinated graphene. Materials Science and Engineering B: Solid-State Materials for Advanced Technology, 2019, 246, 127-135.	1.7	19
31558	A comparative first-principles study of orthorhombic and full-Heusler phases in Ti₂AlNb intermetallic. Materials Research Express, 2019, 6, 096510.	0.8	6
31559	Bonding and electronics of the silicene/MoTe2 interface under strain. Applied Surface Science, 2019, 491, 469-477.	3.1	16
31560	Density functional theory calculation on two-dimensional MoS2/BiOX (Xâ€¯=â€¯Cl, Br, I) van der Waals heterostructures for photocatalytic action. Applied Surface Science, 2019, 492, 157-165.	3.1	65
31561	Corrosion mechanism of annealed equiatomic AlCoCrFeNi tri-phase high-entropy alloy in 0.5 M H2SO4 aerated aqueous solution. Corrosion Science, 2019, 157, 462-471.	3.0	89
31562	Charge-controlled switchable H2 storage on conductive borophene nanosheet. International Journal of Hydrogen Energy, 2019, 44, 20150-20157.	3.8	26
31563	Tunable K vacancies in K1â^'Co2Se2 and their effects on structure and ferromagnetism. Journal of Magnetism and Magnetic Materials, 2019, 490, 165473.	1.0	2
31564	Strain effects on magnetic states of monolayer MoS2 doped with group IIIA to VA atoms. Physica E: Low-Dimensional Systems and Nanostructures, 2019, 114, 113609.	1.3	8
31565	True Polymorphic Phase Transition or Dynamic Crystal Disorder? An Investigation into the Unusual Phase Behavior of Barbituric Acid Dihydrate. Crystal Growth and Design, 2019, 19, 4745-4753.	1.4	6
31566	Turning a Methanation Co Catalyst into an Inâ€“Co Methanol Producer. ACS Catalysis, 2019, 9, 6910-6918.	5.5	88
31567	Effective Promotion of Oxygen Reduction Reaction by in Situ Formation of Nanostructured Catalyst. ACS Catalysis, 2019, 9, 7137-7142.	5.5	42
31568	Activity and Selectivity Trends in Electrocatalytic Nitrate Reduction on Transition Metals. ACS Catalysis, 2019, 9, 7052-7064.	5.5	369
31569	New two-dimensional carbon nitride allotrope with 1â€‰:â€‰1 stoichiometry featuring spine-like structures: a structural and electronic DFT-D study. Physical Chemistry Chemical Physics, 2019, 21, 15282-15285.	1.3	7

#	Article	IF	Citations
31570	Lithium oxide: a quantum-corrected and classical Monte Carlo study. Physical Chemistry Chemical Physics, 2019, 21, 14964-14972.	1.3	3
31571	Effect of toxic ligands on O2 binding to heme and their toxicity mechanism. Physical Chemistry Chemical Physics, 2019, 21, 14957-14963.	1.3	2
31572	Importance of zero-point energy for crystalline ice phases: A comparison of force fields and density functional theory. Journal of Chemical Physics, 2019, 150, 234504.	1.2	7
31573	Interaction of CO, O, and CO₂ with Cu cluster supported on Cu(1â€‰1â€‰1): a density functional theory study. Journal of Physics Condensed Matter, 2019, 31, 415201.	0.7	8
31574	Stable Dynamics Performance and High Efficiency of ABX₃â€Type Superâ€Alkali Perovskites First Obtained by Introducing H₅O₂ Cation. Advanced Energy Materials, 2019, 9, 1900664.	10.2	113
31575	Interface Engineering via Sputtered Oxygenated CdS:O Window Layer for Highly Efficient Sb₂Se₃ Thinâ€Film Solar Cells with Efficiency Above 7%. Solar Rrl, 2019, 3, 1900225.	3.1	42
31576	DFT Study of Pyrolysis Gasoline Hydrogenation on Pd(100), Pd(110) and Pd(111) Surfaces. Catalysis Letters, 2019, 149, 2226-2233.	1.4	3
31577	The Bonding Characteristics and Local Structure of Carbon in Solution and Iron Carbides in Iron Using C K-Edge X-Ray Absorption Spectroscopy Measurement and First-Principle Calculation. Metallurgical and Materials Transactions A: Physical Metallurgy and Materials Science, 2019, 50, 4435-4444.	1.1	7
31578	Structural, elastic, and quasiparticle bandstructure of 4,4â€²-Bis(nitramino)azofurazan from first principles theory. Computational Materials Science, 2019, 169, 109081.	1.4	5
31579	Modulating optoelectronic properties of organo-metal halide perovskites with unsaturated heterocyclic cations via ring substitution. Journal of Physics and Chemistry of Solids, 2019, 135, 109078.	1.9	3
31580	Simultaneous enzyme mimicking and chemical reduction mechanisms for nanoceria as a bio-antioxidant: a catalytic model bridging computations and experiments for nanozymes. Nanoscale, 2019, 11, 13289-13299.	2.8	100
31581	Shock compression of niobium from first-principles. Journal of Applied Physics, 2019, 125, .	1.1	11
31582	Spectral characterization of a Rh(110) photocathode: Band structure interpretation. AIP Advances, 2019, 9, 065305.	0.6	5
31583	Modulation of magnetocrystalline anisotropy in FePt/PbTiO₃ heterostructures by ferroelectric polarization. Journal of Physics Condensed Matter, 2019, 31, 395801.	0.7	2
31584	Temperature dependent transport spin-polarization in the low Curie temperature complex itinerant ferromagnet EuTi_{1â^’x}Nb_xO₃. Journal of Physics Condensed Matter, 2019, 31, 415601.	0.7	5
31585	Modulating the Electrical Transport in the Two-Dimensional Electron Gas at <mml:math xmlns:mml="http://www.w3.org/1998/Math/MathML" display="inline"><mml:mrow><mml:msub><mml:mrow><mml:mi>LaAlO</mml:mi></mml:mrow><mml:mrow><mml:mn>3</mml:mn></mml:mrow> Heterostructures by Interfacial Flexoelectricity. Physical Review Letters, 2019, 122, 257601.	2.9	72
31586	Exploratory Study of Substitutional Elements in Mg₂Si for Inducing State of Negative Chemical Pressure. Nippon Kinzoku Gakkaishi/Journal of the Japan Institute of Metals, 2019, 83, 243-249.	0.2	0
31587	Applying a machine learning interatomic potential to unravel theÂeffects of local lattice distortion on the elastic properties of multi-principal element alloys. Journal of Alloys and Compounds, 2019, 803, 1054-1062.	2.8	41

#	Article	IF	Citations
31588	Spin polarization effect on the ground state and electronic properties of ErCu using DFT and DFT+U approaches. Physica B: Condensed Matter, 2019, 570, 122-127.	1.3	5
31589	A theoretical approach of the ethanol adsorption on Au(100), Au(110) and Au(111) surfaces. Surface Science, 2019, 689, 121458.	0.8	5
31590	Novel Ordered Rocksalt-Type Lithium-Rich Li₂Ru_{1â€“x}Ni_xO_{3â^'Î´} (0.3 â‰¤ x â‰¤ 0.5) Cathode Material with Tunable Anionic Redox Potential. ACS Applied Energy Materials, 2019, 2, 5933-5944.	2.5	22
31591	Highly Active Pt₃Sn{110}-Excavated Nanocube Cocatalysts for Photocatalytic Hydrogen Production. ACS Applied Materials & Interfaces, 2019, 11, 25844-25853.	4.0	28
31592	Composition-dependent CO₂ electrochemical reduction activity and selectivity on Auâ€“Pd coreâ€“shell nanoparticles. Journal of Materials Chemistry A, 2019, 7, 16954-16961.	5.2	56
31593	Sulfurâ€“nitrogen co-doped porous carbon nanosheets to control lithium growth for a stable lithium metal anode. Journal of Materials Chemistry A, 2019, 7, 18267-18274.	5.2	71
31594	Characterization of Ni3Sn intermetallic nanoparticles fabricated by thermal plasma process and catalytic properties for methanol decomposition. Science and Technology of Advanced Materials, 2019, 20, 622-631.	2.8	13
31595	Enhanced lateral growth of AlN epitaxial layer on sapphire by introducing periodically pulsed-TMGa flows. Superlattices and Microstructures, 2019, 131, 59-65.	1.4	3
31596	Water-Mediated Reduction of Aqueous N-Nitrosodimethylamine with Pd. Environmental Science & Technology, 2019, 53, 7551-7563.	4.6	11
31597	General Atomic Neighborhood Fingerprint for Machine Learning-Based Methods. Journal of Physical Chemistry C, 2019, 123, 15859-15866.	1.5	33
31598	Chemical doping of the SnSe monolayer: a first-principle calculation. Physical Chemistry Chemical Physics, 2019, 21, 14629-14637.	1.3	9
31599	Electronic structure tuning of the anomalous thermoelastic behavior in Nb-X (Xâ€‰=â€‰Zr, V, Mo) solid solutions. Journal of Applied Physics, 2019, 125, 215103.	1.1	2
31600	Coupled Biphase (1Tâ€²2H)â€MoSe₂ on Mold Spore Carbon for Advanced Hydrogen Evolution Reaction. Small, 2019, 15, e1901796.	5.2	87
31601	First-principles study on the electronic and optical properties of the ZnTe/InP heterojunction. Journal of Computational Electronics, 2019, 18, 749-757.	1.3	16
31602	The deep oxidation of NO was realized by Sr multi-site doped g-C3N4 via photocatalytic method. Applied Catalysis B: Environmental, 2019, 256, 117825.	10.8	74
31603	The structural and optical properties of ternary mixed crystals In Ga1â^'As with zinc-blende structure by first-principle calculations. Physica B: Condensed Matter, 2019, 569, 87-95.	1.3	8
31604	Character of defect states in vacancy-doped MoTe2 monolayer: Spatial localization, flat bands and hybridization gap. Superlattices and Microstructures, 2019, 130, 528-538.	1.4	7
31605	Structural and Electronic Properties of Frenkel and Schottky Defects at the MgO{100} Surface: Spin Polarization, Mid-Band Gap States, and Charge Trapping at Vacancy Sites. Journal of Physical Chemistry C, 2019, 123, 14408-14420.	1.5	10

#	Article	IF	Citations
31606	Controlling the Infrared Dielectric Function through Atomic-Scale Heterostructures. ACS Nano, 2019, 13, 6730-6741.	7.3	33
31607	Deeply Nesting Zinc Sulfide Dendrites in Tertiary Hierarchical Structure for Potassium Ion Batteries: Enhanced Conductivity from Interior to Exterior. ACS Nano, 2019, 13, 6906-6916.	7.3	139
31608	Type I GaSb1-xBix/GaSb quantum wells dedicated for mid infrared laser applications: Photoreflectance studies of bandgap alignment. Journal of Applied Physics, 2019, 125, .	1.1	16
31609	A comparative study of the vibrational and thermodynamic properties of Î±-RDX and Î³-RDX under ambient conditions. Journal of Molecular Modeling, 2019, 25, 182.	0.8	7
31610	Manganeseâ€germanium nanostructure formation on the GaAs(111)â€"(1â€Ã—â€1)A surface: Stability and magnetic properties. Applied Surface Science, 2019, 491, 147-153.	3.1	10
31611	High-temperature and high-pressure thermophysical properties of AlP semiconducting material: A systematic ab initio study. Chemical Physics, 2019, 525, 110399.	0.9	14
31612	Electronic, mechanical and hydrogen storage properties of novel Mg3N2. Journal of Alloys and Compounds, 2019, 800, 8-15.	2.8	7
31613	Cobalt-catalyzed nitrile hydrogenation: Insights into the reaction mechanism and product selectivity from DFT analysis. Surface Science, 2019, 688, 31-44.	0.8	15
31614	Electrochemical Properties of Na_{0.66}V₄O₁₀ Nanostructures as Cathode Material in Rechargeable Batteries for Energy Storage Applications. ACS Omega, 2019, 4, 9878-9888.	1.6	15
31615	Tuning the electronic properties of the Î³-Al₂O₃surface by phosphorus doping. Physical Chemistry Chemical Physics, 2019, 21, 15080-15088.	1.3	11
31616	Crystal structure and photoluminescence tuning of novel single-phase Ca₈ZnLu(PO₄)₇:Eu²⁺,Mn²⁺ phosphors for near-UV converted white light-emitting diodes. Journal of Materials Chemistry C, 2019, 7, 8374-8382.	2.7	52
31617	First-principles calculations of the structural, electronic, and optical properties of a ZnS/GaP van der Waals heterostructure. Journal of Computational Electronics, 2019, 18, 758-769.	1.3	4
31618	Defect engineered MoSSe Janus monolayer as a promising two dimensional material for NO2 and NO gas sensing. Applied Surface Science, 2019, 490, 204-219.	3.1	65
31619	Thermodynamic stability of nitrogen functionalities and defects in graphene and graphene nanoribbons from first principles. Carbon, 2019, 152, 715-726.	5.4	22
31620	Synthesis and microstructure evolution of WCoB based cermets during spark plasma sintering. Ceramics International, 2019, 45, 17536-17544.	2.3	16
31621	Electronic transport properties of partially hydrogenated and fluorinated borophene, a DFT study. Computational Materials Science, 2019, 168, 74-80.	1.4	4
31622	DFT study of electronic and optical properties of silicene functionalized with chemical groups. Journal of Molecular Graphics and Modelling, 2019, 91, 72-79.	1.3	23
31623	Bilayer tellureneâ€"metal interfaces. Journal of Semiconductors, 2019, 40, 062003.	2.0	9

#	Article	IF	Citations
31625	Atomic and electronic structures of graphene-decorated graphitic carbon nitride (g-C3N4) as a metal-free photocatalyst under visible-light. Applied Catalysis B: Environmental, 2019, 256, 117850.	10.8	19
31626	Magnetoelectric composite films of La0.67Sr0.33MnO3 and Fe-substituted Bi4Ti3O12 fabricated by chemical solution deposition. Applied Surface Science, 2019, 491, 225-235.	3.1	6
31627	Effects of Defect, Doping, Geometrical Configuration, and Size on Plasmon Excitations for Three Silicon Nanostructures. Journal of Physical Chemistry C, 2019, 123, 15707-15716.	1.5	3
31628	Experimental and Theoretical Structural Characterization of Cuâ€“Au Tripods for Photothermal Anticancer Therapy. ACS Applied Nano Materials, 2019, 2, 3735-3742.	2.4	17
31629	Vibrational spectra of Pb2Bi2Te3, PbBi2Te4, and PbBi4Te7 topological insulators: temperature-dependent Raman and theoretical insights from DFT simulations. Physical Chemistry Chemical Physics, 2019, 21, 15030-15039.	1.3	21
31630	Prediction of low energy phase transition in metal doped MoTe2 from first principle calculations. Journal of Applied Physics, 2019, 125, .	1.1	5
31631	Interfacial Properties of Monolayer Antimonene Devices. Physical Review Applied, 2019, 11, .	1.5	22
31632	Lateral Spin Valve Based on the Two-Dimensional <mml:math xmlns:mml="http://www.w3.org/1998/Math/MathML" display="inline" overflow="scroll"><mml:mrow><mml:mi>Cr</mml:mi><mml:mi mathvariant="normal">N</mml:mi></mml:mrow></mml:math> / <mml:math xmlns:mml="http://www.w3.org/1998/Math/MathML" display="inline" overflow="scroll"><mml:mrow><mml:mi>Cr</mml:mi><mml:mi mathvariant="normal">P</mml:mi></mml:mrow>	1.5	37
31633	Structure and one-dimensional metallicity of rare-earth silicide nanowires on Si(001). Physical Review B, 2019, 99, .	1.1	9
31634	Quasiparticle electronic structure and optical spectra of single-layer and bilayer <mml:math xmlns:mml="http://www.w3.org/1998/Math/MathML"><mml:msub><mml:mi>PdSe</mml:mi><mml:mn>2</mml:mn></mml:msub></mml:math> : Proximity and defect-induced band gap renormalization. Physical Review B, 2019, 99, .	1.1	49
31635	Mixed Two-Dimensional Organic-Inorganic Halide Perovskites for Highly Efficient and Stable Photovoltaic Application. Molecules, 2019, 24, 2144.	1.7	2
31636	Energetic Stability of Vacancyâ€Carbon Clusters in Solid Solution Alloys: The Feâ€Crâ€C Case. Physica Status Solidi (B): Basic Research, 2019, 256, 1900130.	0.7	4
31637	Reststrahlen Band Studies of RuCrX (Xâ€‰=â€‰Si, Ge, Sn) Half Heusler Alloys. Journal of Electronic Materials, 2019, 48, 5323-5327.	1.0	7
31638	Chromium phosphide CrP as highly active and stable electrocatalysts for oxygen electroreduction in alkaline media. Applied Catalysis B: Environmental, 2019, 256, 117846.	10.8	20
31639	Initial stages of the epitaxial growth of MnN on the GaAs (001)-(2â€Ã—â€2) surface: First-principle study. Applied Surface Science, 2019, 489, 639-647.	3.1	9
31640	Computational study of metal/ceramic interfacial adhesion and barriers to shear displacement. Computational Materials Science, 2019, 168, 104-115.	1.4	12
31641	New stable structures of HeN3 predicted using first-principles calculations. Journal of Alloys and Compounds, 2019, 800, 505-511.	2.8	6
31642	Segregation of point defects at the CuInSe2(001)/GaAs(001) interface. Solid State Communications, 2019, 299, 113652.	0.9	1

#	Article	IF	Citations
31643	KBaTeBiO₆: A Lead-Free, Inorganic Double-Perovskite Semiconductor for Photovoltaic Applications. Chemistry of Materials, 2019, 31, 4769-4778.	3.2	46
31644	Theoretical Study on Sandwich-Like Transition-Metalâ€“Cyclooctatetraene Clusters and One-Dimensional Infinite Molecular Wires. ACS Omega, 2019, 4, 9739-9744.	1.6	8
31645	Stepwise on-surface dissymmetric reaction to construct binodal organometallic network. Nature Communications, 2019, 10, 2545.	5.8	26
31646	Synergistic effect of band convergence and carrier transport on enhancing the thermoelectric performance of Ga doped Cu2Te at medium temperatures. Scientific Reports, 2019, 9, 8180.	1.6	18
31647	Excellent Device Performance of Subâ€5â€nm Monolayer Tellurene Transistors. Advanced Electronic Materials, 2019, 5, 1900226.	2.6	65
31648	Exploring the catalytic activity of MXenes Mn+1CnO2 for hydrogen evolution. Journal of Materials Science, 2019, 54, 11378-11389.	1.7	14
31649	Pressure effect on the structural, elastic and thermodynamic properties of the BeP2N4 compound: First-principles investigation. Computational Condensed Matter, 2019, 21, e00408.	0.9	1
31650	Hydrogen distribution induced screw dislocation core spreading in tungsten. Journal of Nuclear Materials, 2019, 523, 71-79.	1.3	8
31651	The role of strong electron correlations in determination of band structure and charge distribution of transition metal dihalide monolayers. Journal of Physics and Chemistry of Solids, 2019, 134, 324-332.	1.9	23
31652	Anisotropic elasticity, electronic structure and thermodynamic properties of Al-Fe-Si intermetallic compounds from first principles calculations. Solid State Communications, 2019, 298, 113643.	0.9	4
31653	Prediction of Selective Formation of Chair- and Boat-Type Hydrogenated Graphene via Birch Reduction. Chemistry of Materials, 2019, 31, 4584-4590.	3.2	1
31654	Modifying the Magnetic Anisotropy of an Iron Porphyrin Molecule by an on-Surface Ring-Closure Reaction. Journal of Physical Chemistry C, 2019, 123, 14547-14555.	1.5	15
31655	Infinitesimal sulfur fusion yields quasi-metallic bulk silicon for stable and fast energy storage. Nature Communications, 2019, 10, 2351.	5.8	57
31656	Post-tilleyite, a dense calcium silicate-carbonate phase. Scientific Reports, 2019, 9, 7898.	1.6	18
31657	Theoretical study of the microscopic Doppler effect forÂenergetic material. Philosophical Magazine, 2019, 99, 1763-1786.	0.7	0
31658	Ab initio playing of pentagonal puzzles. Electronic Structure, 2019, 1, 015004.	1.0	7
31659	Sampling-dependent systematic errors in effective harmonic models. Physical Review B, 2019, 99, .	1.1	6
31660	Quantum phase transition and ferromagnetism in <mml:math xmlns:mml="http://www.w3.org/1998/Math/MathML"><mml:mrow><mml:mi mathvariant="normal">C</mml:mi><mml:msub><mml:mi mathvariant="normal">o</mml:mi><mml:mrow><mml:mn>1</mml:mn><mml:mo>+</mml:mo><mml:mi>x</mml:mi></mml:mrow><mml:m Physical Review B, 2019, 99, .	1.1	4

#	Article	IF	Citations
31661	Fermi-level Dirac crossings in <mml:math xmlns:mml="http://www.w3.org/1998/Math/MathML"><mml:mrow><mml:mn>4</mml:mn><mml:mi>d</mml:mi></mml:mrow></mml:r and <mml:math xmlns:mml="http://www.w3.org/1998/Math/MathML"><mml:mrow><mml:mn>5</mml:mn><mml:mi>d</mml:mi></mml:mrow></mml:r cubic metal oxides: <mml:math xmlns:mml="http://www.w3.org/1998/Math/MathML"><mml:mrow><mml:msub><mml:mi>NaPd</mml:mi><mml:mn>3</mml:mn></	1.1	7
31662	N-doped peanut-shaped carbon nanotubes for efficient CO2 electrocatalytic reduction. Carbon, 2019, 152, 241-246.	5.4	29
31663	First principles study on hydrogen storage in yttrium doped graphyne: Role of acetylene linkage in enhancing hydrogen storage. International Journal of Hydrogen Energy, 2019, 44, 16735-16744.	3.8	72
31664	Electrochemical Stability Window of Polymeric Electrolytes. Chemistry of Materials, 2019, 31, 4598-4604.	3.2	83
31665	Bulk Inclusions of Double Pyridazine Molecular Rotors in Hexagonal Tris(o-phenylene)cyclotriphosphazene. Journal of Organic Chemistry, 2019, 84, 8449-8467.	1.7	18
31666	Single Ru Sites-Embedded Rutile TiO2 Catalyst for Non-Oxidative Direct Conversion of Methane: A First-Principles Study. Journal of Physical Chemistry C, 2019, 123, 14391-14397.	1.5	13
31667	Optoelectronic Tunability of Hf-Doped ZnO for Photovoltaic Applications. Journal of Physical Chemistry C, 2019, 123, 15258-15266.	1.5	10
31668	Insights into Hydrogen Transport Behavior on Perovskite Surfaces: Transition from the Grotthuss Mechanism to the Vehicle Mechanism. Langmuir, 2019, 35, 9962-9969.	1.6	29
31669	Charge density wave and spin 1/2 insulating state in single layer 1T-NbS ₂. 2D Materials, 2019, 6, 035041.	2.0	27
31670	DFT study of Ni segregation at the B2-NiTi(110)/rutile-TiO2(110) interface. Applied Surface Science, 2019, 489, 287-296.	3.1	6
31671	Interstitialcy diffusion of fluoride ions in LaOF by DFT-based first-principles calculations. Computational Materials Science, 2019, 167, 92-99.	1.4	9
31672	Effect of doping and annealing on the electronic structure and magnetic properties of nanoscale Co and Zn co-doped SnO2: An experimental study and first-principles modeling. Journal of Alloys and Compounds, 2019, 799, 433-441.	2.8	8
31673	Oriented Attachment Revisited: Does a Chemical Reaction Occur?. Matter, 2019, 1, 690-704.	5.0	27
31674	Prediction of novel SiX2(Xâ€¯=â€¯S, Se) monolayer semiconductors by density functional theory. Physica E: Low-Dimensional Systems and Nanostructures, 2019, 114, 113581.	1.3	25
31675	Electrical transport and thermoelectric properties of Teâ€“Se solid solutions. Physics Letters, Section A: General, Atomic and Solid State Physics, 2019, 383, 2615-2620.	0.9	12
31676	Electrosynthesis of Y2O3 nanoparticles and its nanocomposite with POAP as high efficient electrode materials in energy storage device: Surface, density of state and electrochemical investigation. Solid State Ionics, 2019, 338, 87-95.	1.3	35
31677	Spinel-Type Sodium Titanium Oxide: A Promising Sodium-Insertion Material of Sodium-Ion Batteries. ACS Applied Energy Materials, 2019, 2, 4345-4353.	2.5	22
31678	Enhanced tetragonality and large negative thermal expansion in a new Pb/Bi-based perovskite ferroelectric of (1 â^) Tj ETQq1 1 0.784314 rgBT /Overlock 10 Tf 50 62 Td (x)PbTiO₃â€“xBi(Zn<sub>1/2</ Chemistry Frontiers, 2019, 6, 1990-1995.	3.0	8

#	Article	IF	Citations
31679	Dimension engineering of single-layer PtN 2 with the Cairo tessellation. Journal of Applied Physics, 2019, 125, 204302.	1.1	4
31680	The Effect of Pressure on Halogen Bonding in 4-Iodobenzonitrile. Molecules, 2019, 24, 2018.	1.7	11
31681	Structural, Elastic, Mechanical and Electronic Properties of NbWâ€Based Intermetallic Compounds: Firstâ€Principles Calculations. Physica Status Solidi (B): Basic Research, 2019, 256, 1800570.	0.7	1
31682	Electronic and Magnetic Properties of Mn-doped and (Mn,C)-codoped w-AlN with the Presence of N Vacancy. Journal of Superconductivity and Novel Magnetism, 2019, 32, 3691-3697.	0.8	9
31683	H2 Dissociation and Oxygen Vacancy Formation on Ce2O3 Surfaces. Topics in Catalysis, 2019, 62, 956-967.	1.3	9
31684	Adsorption of Polyaromatic Backbone Impacts the Performance of Anion Exchange Membrane Fuel Cells. Chemistry of Materials, 2019, 31, 4195-4204.	3.2	91
31685	Dynamics of Cluster Isomerization Induced by Hydrogen Adsorption. Journal of Physical Chemistry C, 2019, 123, 15236-15243.	1.5	12
31686	Physical Fingerprints of the 2O-tÎ±P Phase in Phosphorene Stacking. Journal of Physical Chemistry Letters, 2019, 10, 3190-3196.	2.1	4
31687	Mixing thermodynamics and electronic structure of the Pt_{1â^'x}Ni_x (0 â‰) Tj ETQq0 0 0 rgBT /Overlock 10 Tf 5	1.7	10
31688	Crystal structure, chemical bonding, and physical properties of layered AlrSn2 (Aâ€‰=â€‰Sr and Ba). Journal of Materials Science, 2019, 54, 11127-11133.	1.7	3
31689	Understanding the improved electrochemical performance of nitrogen-doped hard carbons as an anode for sodium ion battery. Electrochimica Acta, 2019, 317, 164-172.	2.6	70
31690	Prediction of stable high-pressure structures of tantalum nitride TaN2. Journal of Materials Science and Technology, 2019, 35, 2297-2304.	5.6	8
31691	Atomic scandium and nitrogen-codoped graphene for oxygen reduction reaction. Journal of Power Sources, 2019, 431, 265-273.	4.0	39
31692	Material design for Ge2Sb2Te5 phase-change material with thermal stability and lattice distortion. Scripta Materialia, 2019, 170, 16-19.	2.6	7
31693	Tuning Electrical and Raman Scattering Properties of Cadmium Sulfide Nanoribbons via Surface Charge Transfer Doping. Journal of Physical Chemistry C, 2019, 123, 15794-15801.	1.5	7
31694	Scalable Salt-Templated Synthesis of Nitrogen-Doped Graphene Nanosheets toward Printable Energy Storage. ACS Nano, 2019, 13, 7517-7526.	7.3	83
31695	Identification of the mechanism responsible for the boron oxygen light induced degradation in silicon photovoltaic cells. Journal of Applied Physics, 2019, 125, .	1.1	36
31696	A First Principle Study of Structural, Electronic, and Vibrational Properties of LuPdBi Halfâ€Heusler Alloy. Physica Status Solidi (B): Basic Research, 2019, 256, 1900117.	0.7	18

#	Article	IF	Citations
31697	Computationally predicting spin semiconductors and half metals from doped phosphorene monolayers. Frontiers of Physics, 2019, 14, 1.	2.4	14
31698	First-principle study of NO2 adsorption and detection on the edges of zigzag nitride nanoribbons. Physica E: Low-Dimensional Systems and Nanostructures, 2019, 114, 113575.	1.3	17
31699	Dynamics of dissociative chemisorption of O2 on Cu(100) surface: A theoretical study. Surface Science, 2019, 688, 45-50.	0.8	7
31700	Computational design of alkali metals decorated 2D GeSe for hydrogen storage: a first principle study. Materials Research Express, 2019, 6, 085538.	0.8	5
31701	Thermodynamic Properties of W x (TaTiVCr) 1â^' x Highâ€Entropy(â€Like) Alloy and Influence of Tungsten Content. Physica Status Solidi (B): Basic Research, 2019, 256, 1800741.	0.7	2
31702	Structural, Electronic, and Optical Properties of ZnO_{1â€‰â€“â€‰x}Te_x Alloys. Physica Status Solidi - Rapid Research Letters, 2019, 13, 1900155.	1.2	3
31703	Flexible Composite Energy Harvesters from Ferroelectric A₂MX₄-Type Hybrid Halogenometallates. Chemistry of Materials, 2019, 31, 4545-4552.	3.2	35
31704	Observation of Square-Planar Distortion in Lanthanide-Doped Skutterudite Crystals. Journal of Physical Chemistry C, 2019, 123, 14632-14638.	1.5	1
31705	Computational Study of the Bulk and Surface Properties of Minor Actinide Dioxides MAnO₂ (MAn = Np, Am, and Cm); Water Adsorption on Stoichiometric and Reduced {111}, {110}, and {100} Surfaces. Journal of Physical Chemistry C, 2019, 123, 15540-15550.	1.5	14
31706	Tuning Adsorption of Methylamine and Methanethiol on Twisted-Bilayer Graphene. Journal of Physical Chemistry C, 2019, 123, 15273-15283.	1.5	12
31707	Novel Metallic Clathrates of Group-IV Elements and Their Compounds in a Dense Hexagonal Lattice. Journal of Physical Chemistry C, 2019, 123, 15330-15338.	1.5	5
31708	Doping-Induced Rapid Decoherence Suppresses Charge Recombination in Mono/Divalent Cation Mixed Perovskites from Nonadiabatic Molecular Dynamics Simulation. Journal of Physical Chemistry Letters, 2019, 10, 3433-3439.	2.1	24
31709	Direct Oxidation of Methane to Methanol Enabled by Electronic Atomic Monolayerâ€“Metal Support Interaction. ACS Catalysis, 2019, 9, 6073-6079.	5.5	36
31710	SO₂-Induced Selectivity Change in CO₂ Electroreduction. Journal of the American Chemical Society, 2019, 141, 9902-9909.	6.6	102
31711	Surface oxidation mechanism of a refractory high-entropy alloy. Npj Materials Degradation, 2019, 3, .	2.6	42
31712	Surface phase diagrams of La-based perovskites towards the O-rich limit from first principles. Physical Chemistry Chemical Physics, 2019, 21, 12859-12871.	1.3	7
31713	Ab-initio calculation of band alignments for opto-electronic simulations. AIP Advances, 2019, 9, 055328.	0.6	1
31714	Single-layer BiOBr: An effective p-type 2D thermoelectric material. Journal of Applied Physics, 2019, 125, .	1.1	22

#	Article	IF	Citations
31715	Computing of 93Nb NMR Parameters of Solid-State Niobates. The Geometry Matters. Journal of Structural Chemistry, 2019, 60, 412-419.	0.3	3
31716	Computational Study of Ru₂TiZ (Z = Si, Ge, Sn) for Structural, Mechanical and Vibrational Properties. Zeitschrift Fur Naturforschung - Section A Journal of Physical Sciences, 2019, 74, 545-550.	0.7	4
31717	The influence of intermetallic ordering on wear and indentation properties of TiC-Ni3Al cermets. Wear, 2019, 426-427, 390-400.	1.5	18
31718	Magnetotransport properties of the correlated topological nodal-line semimetal YbCdGe. Physical Review B, 2019, 99, .	1.1	32
31719	First Principle Study of the Attachment of Graphene onto Different Terminated Diamond (111) Surfaces. Advances in Condensed Matter Physics, 2019, 2019, 1-9.	0.4	7
31720	Firstâ€Principles Calculations to Investigate the Refractive Index and Optical Dielectric Constant of Na₃SbX₄ (Xâ€‰=â€‰S, Se) Ternary Chalcogenides. Physica Status Solidi (B): Basic Research, 2019, 256, 1900131.	0.7	106
31721	Î²-PtO2: Phononic, thermodynamic, and elastic properties derived from first-principles calculations. Frontiers of Physics, 2019, 14, 1.	2.4	3
31722	Nuclear magnetic resonance and theoretical simulation study on Cs ion co-adsorbed with other alkali cations on illite. Applied Surface Science, 2019, 489, 766-775.	3.1	9
31723	Reversible hydrogen storage properties of defect-engineered <mml:math xmlns:mml="http://www.w3.org/1998/Math/MathML" altimg="si1.svg"><mml:mrow><mml:msub><mml:mrow><mml:mi mathvariant="bold">C</mml:mi></mml:mrow><mml:mrow><mml:mn mathvariant="bold">4</mml:mn></mml:mrow></mml:msub><mml:mi mathvariant="bold">N</mml:mi></mml:mrow></mml:math> nanosheets under ambient conditions. Car	5.4	69
31724	Study of the linear and nonlinear response properties of the zinc-blende AlP, GaP and their AlxGa1-xP ternary alloys using first principle calculations. Computational Condensed Matter, 2019, 21, e00410.	0.9	4
31725	First-principle studies of the magnetism and optical properties of (Sc, Y)-codoped anatase TiO2 (101) surface. Physics Letters, Section A: General, Atomic and Solid State Physics, 2019, 383, 2679-2684.	0.9	11
31726	Approaching the Intrinsic Limit in Transition Metal Diselenides via Point Defect Control. Nano Letters, 2019, 19, 4371-4379.	4.5	161
31727	pH Effects on Hydrogen Evolution and Oxidation over Pt(111): Insights from First-Principles. ACS Catalysis, 2019, 9, 6194-6201.	5.5	136
31728	Cuâ€“Al Spinel as a Highly Active and Stable Catalyst for the Reverse Water Gas Shift Reaction. ACS Catalysis, 2019, 9, 6243-6251.	5.5	76
31729	Defect-Mediated Charge-Carrier Trapping and Nonradiative Recombination in WSe₂ Monolayers. Journal of the American Chemical Society, 2019, 141, 10451-10461.	6.6	81
31730	Freestanding crystalline oxide perovskites down to the monolayer limit. Nature, 2019, 570, 87-90.	13.7	398
31731	Acetylenic linkage dependent electronic and optical behaviour of morphologically distinct â€˜ynesâ€™. Physical Chemistry Chemical Physics, 2019, 21, 13795-13808.	1.3	37
31732	Inducing magnetism in non-magnetic Î±-FeSi2 by distortions and/or intercalations. Physical Chemistry Chemical Physics, 2019, 21, 13835-13846.	1.3	4

#	Article	IF	Citations
31733	First-principles computational investigation of nitrogen-doped carbon nanotubes as anode materials for lithium-ion and potassium-ion batteries. RSC Advances, 2019, 9, 17299-17307.	1.7	11
31734	Electronic properties of spin excitation in multiferroics with a spinel structure: first principles calculation. Ferroelectrics, 2019, 539, 41-49.	0.3	0
31735	A DFT study about the effects of exchange-correlation functional on the structural and electronic properties of Anatase. Journal of Physics: Conference Series, 2019, 1219, 012019.	0.3	6
31736	Spin Transition in the Cu(hfac)2 Complex with (4-Ethylpyridin-3-yl)-Substituted Nitronyl Nitroxide Caused by the â€œAsymmetricâ€•Structural Rearrangement of Exchange Clusters in the Heterospin Molecule. Crystals, 2019, 9, 285.	1.0	9
31737	Electronic, Elastic, and Vibrational Properties of ZrBeSi via First Principles. Physica Status Solidi (B): Basic Research, 2019, 256, 1900118.	0.7	3
31738	Tunable Magnetism of Na0.5Bi0.5TiO3 Materials via Fe Defects. Journal of Superconductivity and Novel Magnetism, 2019, 32, 3011-3018.	0.8	23
31739	Calculation of the anisotropic coefficients of thermal expansion: A first-principles approach. Computational Materials Science, 2019, 167, 257-263.	1.4	16
31740	A first-principles study of the effect of surface oxygen during the early stage of graphene growth on a Cu(1â€¯1â€¯1) surface. Computational Materials Science, 2019, 168, 17-24.	1.4	8
31741	Electronic band gaps corrections using total energy with DFT/LDA-Â½ quasi-particle approximation. Computational Materials Science, 2019, 167, 228-236.	1.4	6
31742	Synthesis, crystal structure, spectroscopic properties, and thermal behavior of rare-earth oxide selenates, Ln2O2SeO4 (Ln = La, Pr, Nd): The new perspectives of solid-state double-exchange synthesis. Journal of Solid State Chemistry, 2019, 277, 163-168.	1.4	4
31743	Towards reliable ab initio sublimation pressures for organic molecular crystals â€“ are we there yet?. Physical Chemistry Chemical Physics, 2019, 21, 14799-14810.	1.3	17
31744	Propose two-dimensional Sb₂Te₂X (X = S, Se) with isotropic electron mobility and remarkable visible-light response. Physical Chemistry Chemical Physics, 2019, 21, 14904-14910.	1.3	2
31745	Influence of Ti on the dissolution and migration of He in ZrCo based on first principles investigation. Physical Chemistry Chemical Physics, 2019, 21, 14692-14700.	1.3	8
31746	Computational analysis of composition-structure-property-relationships in NZP-type materials for Li-ion batteries. Journal of Applied Physics, 2019, 125, .	1.1	6
31747	Lithium diffusion in <mml:math xmlns:mml="http://www.w3.org/1998/Math/MathML"><mml:mrow><mml:mi mathvariant="normal">L</mml:mi><mml:msub><mml:mi mathvariant="normal">i</mml:mi><mml:mn>2</mml:mn></mml:msub><mml:mi>X</mml:mi></mml:mrow></mml:math>		

#	Article	IF	Citations
31751	Atomic modeling for the initial stage of chromium passivation. International Journal of Minerals, Metallurgy and Materials, 2019, 26, 732-739.	2.4	8
31752	Effects of Y atom substitution on the structural, magnetic, electronic, elastic, mechanical, thermodynamic and thermoelectric properties of Co2YAl (YÂ= Cr, Mn) Full Heusler alloys from first principles investigations. Computational Condensed Matter, 2019, 21, e00412.	0.9	14
31753	Mixtures of lithium salts and ionic liquids at defected graphene walls. Journal of Molecular Liquids, 2019, 289, 111083.	2.3	6
31754	Oxygen vacancy enables electrochemical N2 fixation over WO3 with tailored structure. Nano Energy, 2019, 62, 869-875.	8.2	150
31755	Development and Assessment of a Criterion for the Application of BrÃ¸nstedâ€“Evansâ€“Polanyi Relations for Dissociation Catalytic Reactions at Surfaces. Industrial & Engineering Chemistry Research, 2019, 58, 9864-9874.	1.8	15
31756	Reduction and Oxidation of Maghemite (001) Surfaces: The Role of Iron Vacancies. Journal of Physical Chemistry C, 2019, 123, 15648-15658.	1.5	7
31757	Functionalization and Defect-Driven Water Splitting Mechanism on a Quasi-Two-Dimensional TiO2 Hexagonal Nanosheet. ACS Applied Energy Materials, 2019, 2, 5074-5082.	2.5	8
31758	Preparation of Pt-skin PtRhNi Nanoframes Decorated with Small SnO₂ Nanoparticles as an Efficient Catalyst for Ethanol Oxidation Reaction. ACS Applied Materials & Interfaces, 2019, 11, 22352-22363.	4.0	18
31759	Eu³⁺-Activated NaGdF₄ Nanorods for Near-Ultraviolet Light-Triggered Indoor Illumination. ACS Applied Nano Materials, 2019, 2, 4275-4285.	2.4	74
31760	Bonding in 2D Donorâ€“Acceptor Heterostructures. Journal of the American Chemical Society, 2019, 141, 10300-10308.	6.6	42
31761	Electronic structures and elastic properties of a family of metal-free perovskites. Materials Chemistry Frontiers, 2019, 3, 1678-1685.	3.2	46
31762	The influence of interaction between oxygen vacancies on set process in resistive switching: A case of MgO. AIP Advances, 2019, 9, 055230.	0.6	2
31763	Electronic structure and superconductivity in hexagonal Li3B2 and Li2B2H phases under pressure. Journal of Applied Physics, 2019, 125, 223902.	1.1	0
31764	Magnetic skyrmions in atomic thin CrI3 monolayer. Applied Physics Letters, 2019, 114, .	1.5	59
31765	Topological phase transition induced by magnetic proximity effect in two dimensions. Journal of Physics Condensed Matter, 2019, 31, 395502.	0.7	4
31766	Pressure-induced reentrant transition in <mml:math xmlns:mml="http://www.w3.org/1998/Math/MathML"><mml:mrow><mml:mi>Nb</mml:mi><mml:msub><mml:mi mathvariant="normal">S</mml:mi><mml:mn>3</mml:mn></mml:msub></mml:mrow></mml:math> phases: Combined Raman scattering and x-ray diffraction study. Physical Review B, 2019, 99, .	1.1	5
31767	Tuning the electronic properties of monolayer MoS2, MoSe2 and MoSSe by applying z-axial strain. Chemical Physics Letters, 2019, 730, 191-197.	1.2	29
31768	Mechanical Behavior of InP Twinning Superlattice Nanowires. Nano Letters, 2019, 19, 4490-4497.	4.5	18

#	Article	IF	Citations
31769	Quantum chemical models for the absorption of endohedral clusters on Si(111)-(7 Ã— 7): a subtle balance between Wâ€“Si and Siâ€“Si bonding. Physical Chemistry Chemical Physics, 2019, 21, 13686-13695.	1.3	0
31770	First-principles study of elastic and electronic properties of layered ternary nitride SrZrN₂ under pressure. Philosophical Magazine, 2019, 99, 2321-2339.	0.7	4
31771	Charge-induced ferromagnetic phase transition and anomalous Hall effect in full <mml:math xmlns:mml="http://www.w3.org/1998/Math/MathML"><mml:mi>d</mml:mi></mml:math> -band nonmagnetic metals. Physical Review B, 2019, 99, .	1.1	9
31772	Ultrasoft pseudopotentials with kinetic energy density support: Implementing the Tran-Blaha potential. Physical Review B, 2019, 99, .	1.1	10
31773	Effect of thickness and substrate type on the structure and low vacuum photoemission of carbyne-containing films. Carbon, 2019, 152, 388-395.	5.4	10
31774	Robust ferromagnetism and half-metallicity in hydrogenated monolayer-CdS. Physica B: Condensed Matter, 2019, 570, 209-216.	1.3	12
31775	Controlling the stability and the electronic structure of transition metal dichalcogenide single layer under chemical doping. Physics Letters, Section A: General, Atomic and Solid State Physics, 2019, 383, 2922-2927.	0.9	9
31776	Synthesis, structure and characterization of a new triphosphate: CsMg2P3O10. Solid State Sciences, 2019, 94, 133-137.	1.5	0
31777	The Oâ€“O Bonding and Hydrogen Storage in the Pyrite-type PtO₂. Inorganic Chemistry, 2019, 58, 8300-8307.	1.9	6
31778	Underlying Molecular Interactions between Sodium Montmorillonite Clay and Acidic Bitumen. Journal of Physical Chemistry C, 2019, 123, 15513-15522.	1.5	21
31779	Multi-Step Topochemical Pathway to Metastable Mo₂AlB₂ and Related Two-Dimensional Nanosheet Heterostructures. Journal of the American Chemical Society, 2019, 141, 10852-10861.	6.6	84
31780	Proton-assisted creation of controllable volumetric oxygen vacancies in ultrathin CeO2â^'x for pseudocapacitive energy storage applications. Nature Communications, 2019, 10, 2594.	5.8	75
31781	Band-gap engineering in AB(O_xS_{1â^'x})₃ perovskite oxysulfides: a route to strongly polar materials for photocatalytic water splitting. Journal of Materials Chemistry A, 2019, 7, 15741-15748.	5.2	45
31782	An optimized twist angle to find the twist-averaged correlation energy applied to the uniform electron gas. Journal of Chemical Physics, 2019, 150, 191101.	1.2	17
31783	The effect of grain boundary on the visible light absorption of BaTi_{1â€x}[Ni_{1/2}Nb_{1/2}]_xO_{3â€Î´} ferroelectric ceramics. Journal of the American Ceramic Society, 2019, 102, 7405-7413.	1.9	16
31784	Elastic Properties of Bilayer Graphene Nanostructures with Closed Holes. JETP Letters, 2019, 109, 472-477.	0.4	9
31785	Micro-Kinetic Modelling of CO-TPD from Fe(100)â€"Incorporating Lateral Interactions. Catalysts, 2019, 9, 310.	1.6	10
31786	Structural, Electronic, and Magnetic Properties of Hard Magnetic SmNi2Fe Compound: a DFT Study. Journal of Superconductivity and Novel Magnetism, 2019, 32, 3901-3905.	0.8	3

#	Article	IF	Citations
31787	Vacancy formation energy in CuNiCo equimolar alloy and CuNiCoFe high entropy alloy: ab initio based study. Calphad: Computer Coupling of Phase Diagrams and Thermochemistry, 2019, 66, 101634.	0.7	13
31788	Prediction of electronic structure in atomistic model using artificial neural network. Computational Materials Science, 2019, 168, 164-171.	1.4	10
31789	Structural, electronic, elastic and mechanical properties of novel ZrMnAs half Heusler alloy from first principles. Physica B: Condensed Matter, 2019, 571, 41-49.	1.3	8
31790	Stable group-IIB elements â€"Zn, Cd and Hg at terapascal pressures. Europhysics Letters, 2019, 126, 36001.	0.7	2
31791	Theoretical studies and tuning the electronic and optical properties of Zr2CO2 monolayer using biaxial strain effect: Modified Beckeâ€"Johnson calculation. Physica E: Low-Dimensional Systems and Nanostructures, 2019, 114, 113559.	1.3	30
31792	Enhanced photocatalytic N2 fixation by promoting N2 adsorption with a co-catalyst. Science Bulletin, 2019, 64, 918-925.	4.3	109
31793	Robust two-dimensional ferroelectricity in single-layer Î³-SbP and Î³-SbAs. Nanoscale, 2019, 11, 11864-11871.	2.8	27
31794	In situ formed ultrafine NbTi nanocrystals from a NbTiC solid-solution MXene for hydrogen storage in MgH₂. Journal of Materials Chemistry A, 2019, 7, 14244-14252.	5.2	114
31795	Improvement of high-temperature initial oxidation behavior of HR3C austenitic heat-resistant steel using silicon modification: experimental and first-principle study. Metallurgical Research and Technology, 2019, 116, 401.	0.4	1
31796	Anisotropic thermal expansion and thermodynamic properties of monolayer <mml:math xmlns:mml="http://www.w3.org/1998/Math/MathML"><mml:mi>Î²</mml:mi></mml:math> -Te. Physical Review B, 2019, 99, .	1.1	25
31797	A new BaCa(CO₃)₂polymorph. Acta Crystallographica Section B: Structural Science, Crystal Engineering and Materials, 2019, 75, 291-300.	0.5	5
31798	Simulation of the Crystal Structure of GelSimCn Compounds and the Study of Their Electronic Structure. Journal of Structural Chemistry, 2019, 60, 518-523.	0.3	1
31799	Oxygen reduction on bimodal nanoporous palladiumâ€"copper catalyst synthesized using sacrificial nanoporous copper. Journal of Materials Research, 2019, 34, 2086-2094.	1.2	3
31800	Constructing CoO/Co₃S₄ Heterostructures Embedded in Nâ€doped Carbon Frameworks for Highâ€Performance Sodiumâ€Ion Batteries. Advanced Functional Materials, 2019, 29, 1901925.	7.8	169
31801	Double-shelled hollow rods assembled from nitrogen/sulfur-codoped carbon coated indium oxide nanoparticles as excellent photocatalysts. Nature Communications, 2019, 10, 2270.	5.8	105
31802	Tuning the structural and electronic properties and chemical activities of stanene monolayers by embedding 4d Pd: a DFT study. RSC Advances, 2019, 9, 16069-16082.	1.7	40
31803	1D/2D nitrogen-doped carbon nanorod arrays/ultrathin carbon nanosheets: outstanding catalysts for the highly efficient electroreduction of CO₂ to CO. Journal of Materials Chemistry A, 2019, 7, 14895-14903.	5.2	46
31804	A hybrid niobium-based oxide with bio-based porous carbon as an efficient electrocatalyst in photovoltaics: a general strategy for understanding the catalytic mechanism. Journal of Materials Chemistry A, 2019, 7, 14864-14875.	5.2	74

#	Article	IF	Citations
31805	Selfâ€healing of TiSiN/Ag coatings induced by Ag. Journal of the American Ceramic Society, 2019, 102, 7521-7532.	1.9	6
31806	First-principles investigation of electronic, magnetic and half-metallic properties in Cr1-xPdxP (x =) Tj ETQq1 1 0.784314 rgBT /Overlock	1.2	3
31807	The Influence of Interface Structure on the Electrical Conductivity of Graphene Embedded in Aluminum Matrix. Advanced Materials Interfaces, 2019, 6, 1900468.	1.9	38
31808	Assessment of M2O(111) (Mâ€¯=â€¯Li and Na) surfaces for CO2 adsorption based on first-principles calculations. Applied Surface Science, 2019, 486, 571-577.	3.1	9
31809	Comparative electrochemical analysis of rGO-FeVO4 nanocomposite and FeVO4 for supercapacitor application. Applied Surface Science, 2019, 488, 221-227.	3.1	45
31810	Realization of spin-canted magnetism from lattice site specific spin structure in the double perovskite Nd2CoTiO6. Journal of Magnetism and Magnetic Materials, 2019, 488, 165338.	1.0	4
31811	Ammonothermal Crystal Growth of ATaN₂ with A = Na, K, Rb, and Cs and Their Optical and Electronic Properties. Crystal Growth and Design, 2019, 19, 3484-3490.	1.4	4
31812	Tunable Electronic and Optical Properties of a Planar Hydrogenated AsSi Hybrid Nanosheet: A Potential Wide Water-Splitting Photocatalyst. Journal of Physical Chemistry C, 2019, 123, 14999-15008.	1.5	8
31813	Mechanism and Kinetics of Methylating C₆â€“C₁₂ Methylbenzenes with Methanol and Dimethyl Ether in H-MFI Zeolites. ACS Catalysis, 2019, 9, 6444-6460.	5.5	45
31814	Discovery of hexagonal ternary phase Ti2InB2 and its evolution to layered boride TiB. Nature Communications, 2019, 10, 2284.	5.8	159
31815	Interface depended electronic and magnetic properties of vertical CrI₃/WSe₂ heterostructures. RSC Advances, 2019, 9, 14766-14771.	1.7	27
31816	Grapheneâ€“boron nitride hybrid-supported single Mo atom electrocatalysts for efficient nitrogen reduction reaction. Journal of Materials Chemistry A, 2019, 7, 15173-15180.	5.2	107
31817	Effect of point defects on electronic and magnetic properties of single-layer SiO. Philosophical Magazine, 2019, 99, 2340-2353.	0.7	3
31818	Defect Engineering in Two Common Types of Dielectric Materials for Electromagnetic Absorption Applications. Advanced Functional Materials, 2019, 29, 1901236.	7.8	469
31819	Modulation of New Excitons in Transition Metal Dichalcogenideâ€Perovskite Oxide System. Advanced Science, 2019, 6, 1900446.	5.6	6
31820	Sound Velocities and Elastic Moduli of Phases I and V of Silicon at High Pressures. Physica Status Solidi - Rapid Research Letters, 2019, 13, 1900173.	1.2	2
31821	Density functional theory of influence of methane adsorption on the electronic properties of a PbS cluster. Pramana - Journal of Physics, 2019, 93, 1.	0.9	8
31822	C2N monolayer as NH3 and NO sensors: A DFT study. Applied Surface Science, 2019, 487, 488-495.	3.1	146

#	Article	IF	Citations
31823	Theoretical study on hydrogen solubility and diffusivity in the Î³-TiAl L10 structure. International Journal of Hydrogen Energy, 2019, 44, 12215-12227.	3.8	15
31824	Ordered double-M elements MXenes TiMC: Large in-plane stiffness and ferromagnetism. Journal of Magnetism and Magnetic Materials, 2019, 486, 165280.	1.0	14
31825	Anisotropic thermophysical properties of U3Si2 fuel: An atomic scale study. Journal of Nuclear Materials, 2019, 521, 1-12.	1.3	21
31826	Tunable magnetism in defective MoS2 monolayer with nonmetal atoms adsorption. Superlattices and Microstructures, 2019, 130, 346-353.	1.4	4
31827	Sulfidation mitigates the passivation of zero valent iron at alkaline pHs: Experimental evidences and mechanism. Water Research, 2019, 159, 233-241.	5.3	97
31828	Understanding Hysteresis in Carbon Dioxide Sorption in Porous Metalâ€“Organic Frameworks. Inorganic Chemistry, 2019, 58, 6811-6820.	1.9	19
31829	Unveiling Oxygen Adsorption States on One-Dimensional Pt-Induced Nanowires on Ge(001). Journal of Physical Chemistry C, 2019, 123, 13263-13268.	1.5	1
31830	Selenium-Coupled Reduced Graphene Oxide as Single-Atom Site Catalyst for Direct Four-Electron Oxygen Reduction Reaction. ACS Applied Energy Materials, 2019, 2, 3624-3632.	2.5	19
31831	Dynamic Frustrated Lewis Pairs on Ceria for Direct Nonoxidative Coupling of Methane. ACS Catalysis, 2019, 9, 5523-5536.	5.5	54
31832	Tuning the electronic structure properties of MoS₂ monolayers with carbon doping. Physical Chemistry Chemical Physics, 2019, 21, 11168-11174.	1.3	10
31833	A theoretical study of adsorbed non-metallic atoms on magnesium chloride monolayers. New Journal of Chemistry, 2019, 43, 7778-7783.	1.4	10
31834	Effect of pressure on the mechanical and dynamical stability of NaAlSi. Philosophical Magazine Letters, 2019, 99, 29-38.	0.5	3
31835	Assessing the Role of Fluorine in the Performance of <mml:math xmlns:mml="http://www.w3.org/1998/Math/MathML" display="inline" overflow="scroll"><mml:msub><mml:mi>Al</mml:mi><mml:mi>x</mml:mi></mml:msub><mml:msub><mml:mi>Ga</mml:mi><mml:mrow><mml:mi mathvariant="normal">N</mml:mi></mml:mrow></mml:msub><mml:mo>/</mml:mo><mml:msub><mml:mi>Ga</mml:mi><mml:mi mathvariant="normal">N</mml:mi></mml:mat. Physical Review Applied, 2019, 11, .	1.5	11
31836	Explicating the Sodium Storage Kinetics and Redox Mechanism of Highly Pseudocapacitive Binary Transition Metal Sulfide via Operando Techniques and Ab Initio Evaluation. Small Methods, 2019, 3, 1900112.	4.6	21
31837	The effect of oxygen coverages on hydrogenation of Mg (0001) surface. Applied Surface Science, 2019, 487, 510-518.	3.1	8
31838	Topological analysis of CeMIn5 (Mâ€¯=â€¯Co, Rh) electron charge densities. Computational Materials Science, 2019, 164, 205-217.	1.4	3
31839	Computational prediction and characterization of two-dimensional pentagonal arsenopyrite FeAsS. Computational Materials Science, 2019, 166, 105-110.	1.4	9
31840	Ab initio study of diffusion of hydrogen, silver and lithium in PbS and Ag2S. Computational Materials Science, 2019, 166, 75-81.	1.4	9

#	Article	IF	Citations
31841	Cation substitution induced reactivity variation on the tricalcium silicate polymorphs determined from first-principles calculations. Construction and Building Materials, 2019, 216, 239-248.	3.2	17
31842	Penta-BeP2 monolayer: A new 2D beryllium phosphate with a narrow band gap. Chemical Physics Letters, 2019, 728, 136-141.	1.2	15
31843	Catalytic mechanism of silver in the oxidative dissolution process of chalcopyrite: Experiment and DFT calculation. Hydrometallurgy, 2019, 187, 18-29.	1.8	29
31844	Tuning CO2 hydrogenation selectivity via metal-oxide interfacial sites. Journal of Catalysis, 2019, 374, 60-71.	3.1	115
31845	Thermal conductivity and diffusion mechanisms of noble gases in uranium dioxide: A DFT+U study. Journal of Nuclear Materials, 2019, 521, 137-145.	1.3	21
31846	A study of ferroelectric and magnetic properties of rare earth (RE=La, Nd, Sm, Gd) doped BiFeO3 using modified Becke Johnson potential with SOC techniques. Materials Chemistry and Physics, 2019, 232, 460-470.	2.0	19
31847	Iron-Doping-Induced Phase Transformation in Dual-Carbon-Confined Cobalt Diselenide Enabling Superior Lithium Storage. ACS Nano, 2019, 13, 6113-6124.	7.3	108
31848	Cooperativity and coverage dependent molecular desorption in self-assembled monolayers: computational case study with coronene on Au(111) and HOPG. Physical Chemistry Chemical Physics, 2019, 21, 10505-10513.	1.3	11
31849	Understanding the high activity of mildly reduced graphene oxide electrocatalysts in oxygen reduction to hydrogen peroxide. Materials Horizons, 2019, 6, 1409-1415.	6.4	51
31850	Reduction of Fermi level pinning at Cuâ€“BP interfaces by atomic passivation. Nanoscale, 2019, 11, 11569-11576.	2.8	5
31851	First-principles study of the effect of compressive strain on oxygen adsorption in Pd/Ni/Cu-alloy-core@Pd/Ir-alloy-shell catalysts. New Journal of Chemistry, 2019, 43, 8195-8203.	1.4	7
31852	Enthalpy of Formation of NaxCoO2 and (Na, Mg)xCoO2 Systems: A First Principle Calculation Study. Journal of Physics: Conference Series, 2019, 1204, 012028.	0.3	1
31853	An ab-initio Investigation: The Physical Properties of ScIr2 Superconductor. Physics of the Solid State, 2019, 61, 530-536.	0.2	3
31854	First-principles calculations of the site preference, phase stability and brittle versus ductile behaviors of TiAl intermetallic alloyed with ternary elements. International Journal of Modern Physics B, 2019, 33, 1950097.	1.0	4
31855	ZnO nanorods decorated with nanocrystalline (nc) Au Particles:Electronic structure and magnetic behaviours. Journal of Alloys and Compounds, 2019, 797, 74-82.	2.8	7
31856	Unexpected capture of Guinier-Preston zone and Î³â€³ phase in as-cast Mg-Gd-Y-Zn-Ni-Mn alloy: Atomic-scale insights. Materials Characterization, 2019, 153, 103-107.	1.9	8
31857	Precisely-controlled, a few layers of iron titanate inverse opal structure for enhanced photoelectrochemical water splitting. Nano Energy, 2019, 62, 20-29.	8.2	24
31858	First-principles study on the electronic and optical properties of two-dimensional graphene-like Zn1â^'xVxO (xâ€¯=â€¯0.0625, 0.125) monolayer. Physica E: Low-Dimensional Systems and Nanostructures, 2019, 113, 143-151.	1.3	4

#	Article	IF	Citations
31859	New Paradigm for Gas Sensing by Two-Dimensional Materials. Journal of Physical Chemistry C, 2019, 123, 13104-13109.	1.5	24
31860	Engineering atomic-level complexity in high-entropy and complex concentrated alloys. Nature Communications, 2019, 10, 2090.	5.8	182
31861	Hydrogenation of CO2 to formic acid on the single atom catalysis Cu/C2N: A first principles study. Applied Surface Science, 2019, 488, 1-9.	3.1	45
31862	C2 oxygenates formation from syngas over the promoter M(Mâ€¯=â€¯Rh, Co) monolayer-modified Cu(111) surface: Probing into the role of monolayer promoter on the selectivity. Applied Surface Science, 2019, 488, 434-444.	3.1	6
31863	MnO2 polymorph selection for non-enzymatic glucose detection: An integrated experimental and density functional theory investigation. Applied Surface Science, 2019, 487, 1033-1042.	3.1	31
31864	Vacancy effect on the generalized stacking fault energy of alloyed Î³-Ni system: A first-principles study. Computational Materials Science, 2019, 166, 187-192.	1.4	11
31865	Hydrogen storage properties of Li-decorated B2S monolayers: A DFT study. International Journal of Hydrogen Energy, 2019, 44, 16803-16810.	3.8	53
31866	Ab initio study of the electronic, elastic, vibrational and dielectric properties of KBaBi. Journal of Solid State Chemistry, 2019, 276, 272-277.	1.4	3
31867	Effects of Solvent Stabilization on Pharmaceutical Crystallization: Investigating Conformational Polymorphism of Probucol Using Combined Solid-State Density Functional Theory, Molecular Dynamics, and Terahertz Spectroscopy. Journal of Physical Chemistry A, 2019, 123, 6937-6947.	1.1	21
31868	Strain vs. charge mediated magnetoelectric coupling across the magnetic oxide/ferroelectric interfaces. RSC Advances, 2019, 9, 13033-13041.	1.7	14
31869	Structural and electrical properties of Gaâ€“Te systems under high pressure. Chinese Physics B, 2019, 28, 056104.	0.7	6
31870	First-principles study of structural, electronic, elastic, thermodynamic and optical properties of topological superconductor LuPtBi. Computational Condensed Matter, 2019, 21, e00402.	0.9	40
31871	Characterization of two-dimensional Ga1â^'Al N ordered alloys with varying chemical composition. Computational Materials Science, 2019, 167, 13-18.	1.4	3
31872	Enhancing thermal properties of few-layer boron nitride by high-k Al2O3 capping layer. Journal of Alloys and Compounds, 2019, 797, 262-268.	2.8	5
31873	Electronic structure and optical properties of Cd co-doped wurtizte GaN exposed from first principles study. Results in Physics, 2019, 13, 102330.	2.0	9
31874	Structural, Electronic, and Mechanical Properties of A₃Mn₂O₇ (Aâ€‰=â€‰Sr, Ca): Ab Initio Calculation. Ferroelectrics, 2019, 538, 135-145.	0.3	8
31875	Interfacial structure and mechanical properties of a new Nb/Re laminated composite. Materials Research Express, 2019, 6, 1065b1.	0.8	1
31876	Structural, Magnetic and Electronic Properties of 3d Transition-Metal Atoms Adsorbed Monolayer BC2N: A First-principles Study. Materials, 2019, 12, 1601.	1.3	8

#	Article	IF	Citations
31877	Electronic Structure, Lattice Dynamics, and Superconducting Properties of Mercury-Alkaline Earth Metal Compounds: a First-Principles Study. Journal of Superconductivity and Novel Magnetism, 2019, 32, 3425-3430.	0.8	2
31878	DFT study for OH radical formation on SrTiO3(001) surface and the effect of Bi. Applied Surface Science, 2019, 487, 1394-1402.	3.1	7
31879	Graphene-like carbon-nitrogen materials as anode materials for Li-ion and mg-ion batteries. Applied Surface Science, 2019, 487, 1026-1032.	3.1	85
31880	An investigation of thin Zn films on 4H-SiC(0001) graphene. Applied Surface Science, 2019, 487, 1348-1355.	3.1	8
31881	Physical investigations and DFT model calculation on Zn2SnO4-ZnO (ZTO-ZO) alloy thin films for wettability and photocatalysis purposes. Optik, 2019, 187, 49-64.	1.4	10
31882	Sensing and elimination of the hazardous materials such as Sarin by metal functionalized Î³-graphyne surface: A DFT study. Journal of Molecular Liquids, 2019, 286, 110929.	2.3	20
31883	First-principles investigation of ternary two-dimensional (2D) AlxB1-x N monolayer alloys. Superlattices and Microstructures, 2019, 130, 249-257.	1.4	5
31884	Adsorption and Diffusion of H Atoms on Î²-PtO₂ Surface: The Role of Nuclear Quantum Effects. Journal of Physical Chemistry C, 2019, 123, 13804-13811.	1.5	9
31885	Sulfur-Doped Anatase TiO₂ as an Anode for High-Performance Sodium-Ion Batteries. ACS Applied Energy Materials, 2019, 2, 3791-3797.	2.5	46
31886	Theoretical Resolution of the Exceptional Oxygen Reduction Activity of Au(100) in Alkaline Media. ACS Catalysis, 2019, 9, 5567-5573.	5.5	93
31887	Two alkali calcium borates exhibiting second harmonic generation and deep-UV cutoff edges. New Journal of Chemistry, 2019, 43, 9354-9363.	1.4	2
31888	Strain induced electronic and magnetic properties of 2D magnet CrI₃: a DFT approach. Journal of Physics Condensed Matter, 2019, 31, 335802.	0.7	21
31889	Nonlinear elasticity of É› -Fe: The pressure effect. Physical Review B, 2019, 99, .	1.1	2
31890	Structural deformations and mechanical properties of <mml:math xmlns:mml="http://www.w3.org/1998/Math/MathML"><mml:mrow><mml:msub><mml:mi>Si</mml:mi><mml:mn>2</mml:mn></mml:msub></mml:mrow></mml:math> under uniaxial and uniform biaxial strain in comparison with graphene: An ab initio study. Physical Review B, 2019, 99, .	1.1	17
31891	Effect of SrO termination on electron transport of MoS2/SrTiO3 heterostructure: A DFT approach. Applied Surface Science, 2019, 487, 1403-1408.	3.1	4
31892	Ultrahigh stretching bond force constants of linear chains of carbon and boron nitride. Carbon, 2019, 150, 349-355.	5.4	5
31893	Study on the mechanism of phase transition and embrittlement for Î³-Fe by hydrogen with stress through the first principles method. Chinese Journal of Physics, 2019, 59, 242-249.	2.0	2
31894	Magnetism and ferroelectricity in BiFeO3 doped with Ga at Fe sites. Journal of Alloys and Compounds, 2019, 797, 117-121.	2.8	13

#	Article	IF	Citations
31895	Putting the Squeeze on Lead Iodide Perovskites: Pressure-Induced Effects To Tune Their Structural and Optoelectronic Behavior. Chemistry of Materials, 2019, 31, 4063-4071.	3.2	87
31896	Doping of epitaxial graphene by direct incorporation of nickel adatoms. Nanoscale, 2019, 11, 10358-10364.	2.8	21
31897	A novel two-dimensional Î´-InP₃ monolayer with high stability, tunable bandgap, high carrier mobility, and gas sensing of NO₂. Journal of Materials Chemistry C, 2019, 7, 7352-7359.	2.7	44
31898	Regularized SCAN functional. Journal of Chemical Physics, 2019, 150, 161101.	1.2	124
31899	An Ab Initio Study of Vacancies in Disordered Magnetic Systems: A Case Study of Fe-Rich Fe-Al Phases. Materials, 2019, 12, 1430.	1.3	11
31900	Generalized Stacking Fault Energy of {10-11}<11-23> Slip System in Mg-Based Binary Alloys: A First Principles Study. Materials, 2019, 12, 1548.	1.3	7
31901	High-performance Li-ion capacitor based on black-TiO2-x/graphene aerogel anode and biomass-derived microporous carbon cathode. Nano Research, 2019, 12, 1713-1719.	5.8	64
31902	Sulfur-deficient MoS2-x promoted lithium polysulfides conversion in lithium-sulfur battery: A first-principles study. Applied Surface Science, 2019, 487, 452-463.	3.1	58
31903	Why are trace amounts of chloride so highly surface-active?. Journal of Electroanalytical Chemistry, 2019, 847, 113128.	1.9	2
31904	The electronic, magnetic and optical properties of single-layer CrS2 with vacancy defects. Journal of Magnetism and Magnetic Materials, 2019, 487, 165300.	1.0	16
31905	Green synthesis of zinc doped cobalt ferrite nanoparticles: Structural, optical, photocatalytic and antibacterial studies. Nano Structures Nano Objects, 2019, 19, 100322.	1.9	98
31906	Activation mechanisms of silver toward CO oxidation by tungsten carbide substrate: A density functional theory study. Physics Letters, Section A: General, Atomic and Solid State Physics, 2019, 383, 2436-2442.	0.9	12
31907	Graphene-Nickel interaction in layered metal-matrix composites. Surface Science, 2019, 688, 1-6.	0.8	17
31908	Impact of Structural Transformation on Electrochemical Performances of Li-Rich Cathode Materials: The Case of Li₂RuO₃. Journal of Physical Chemistry C, 2019, 123, 13491-13499.	1.5	29
31909	Layered Phosphorus-Rich Phosphide Composite as a Stable, High-Capacity Anode for Sodium Ion Batteries. ACS Applied Energy Materials, 2019, 2, 4309-4315.	2.5	11
31910	Electronic Metalâ€“Support Interaction To Modulate MoS₂-Supported Pd Nanoparticles for the Degradation of Organic Dyes. ACS Applied Nano Materials, 2019, 2, 3385-3393.	2.4	43
31911	Nitrogen Loss and Oxygen Evolution Reaction Activity of Perovskite Oxynitrides. , 2019, 1, 52-57.		26
31912	First principles calculations of surface dependent electronic structures: a study on Î²-FeOOH and Î³-FeOOH. Physical Chemistry Chemical Physics, 2019, 21, 18486-18494.	1.3	17

#	Article	IF	Citations
31913	Novel MAB phases and insights into their exfoliation into 2D MBenes. Nanoscale, 2019, 11, 11305-11314.	2.8	120
31914	Ultrahigh-pressure induced decomposition of silicon disulfide into silicon-sulfur compounds with high coordination numbers. Physical Review B, 2019, 99, .	1.1	10
31915	The Fluorescent Quenching Mechanism of N and S Co-Doped Graphene Quantum Dots with Fe3+ and Hg2+ Ions and Their Application as a Novel Fluorescent Sensor. Nanomaterials, 2019, 9, 738.	1.9	32
31916	Electrolyte Effects on the Stability of Niâ^'Mo Cathodes for the Hydrogen Evolution Reaction. ChemSusChem, 2019, 12, 3491-3500.	3.6	37
31917	Boosting ORR/OER Activity of Graphdiyne by Simple Heteroatom Doping. Small Methods, 2019, 3, 1800550.	4.6	149
31918	Two dimensional InSe/C2N van der Waals heterojunction as enhanced visible-light-responsible photocatalyst for water splitting. Applied Surface Science, 2019, 485, 375-380.	3.1	61
31919	New aspects of the surface chemistry of sulfur on Au(111): Surface structures formed by gold-sulfur complexes. Applied Surface Science, 2019, 487, 848-856.	3.1	6
31920	First principles prediction of the solar cell efficiency of chalcopyrite materials AgMX2 (M=In, Al; X=S,) Tj ETQq1 1 0.784314 rgBT /Over	0.9	2
31921	Cubic Germanium monochalcogenides (Ï€-GeS and Ï€-GeSe): Emerging materials for optoelectronic and energy harvesting devices. Solar Energy, 2019, 185, 211-221.	2.9	19
31922	The enhanced ferromagnetism of single-layer CrX₃ (X = Br and I) via van der Waals engineering. Physical Chemistry Chemical Physics, 2019, 21, 11949-11955.	1.3	26
31923	Ethylene-glycol ligand environment facilitates highly efficient hydrogen evolution of Pt/CoP through proton concentration and hydrogen spillover. Energy and Environmental Science, 2019, 12, 2298-2304.	15.6	227
31924	Selectivity for ethanol partial oxidation: the unique chemistry of single-atom alloy catalysts on Au, Ag, and Cu(111). Journal of Materials Chemistry A, 2019, 7, 23868-23877.	5.2	80
31925	Direct evaluation of the isotope effect within the framework of density functional theory for superconductors. Journal of Physics Condensed Matter, 2019, 31, 334001.	0.7	2
31926	Electronic Structure and Dielectric Properties of Azides Ca(N3)2 and Sr(N3)2. Journal of Structural Chemistry, 2019, 60, 509-517.	0.3	1
31927	Promising thermoelectric materials of Cu3VX4 (X=S, Se, Te): A Cu-V-X framework plus void tunnels. International Journal of Modern Physics C, 2019, 30, 1950045.	0.8	10
31928	Hydrogenation Properties of LnAl2 (Ln = La, Eu, Yb), LaGa2, LaSi2 and the Crystal Structure of LaGa2H0.71(2). Crystals, 2019, 9, 193.	1.0	9
31929	Chiral Recognition of Hexahelicene on a Surface via the Forming of Asymmetric Heterochiral Trimers. International Journal of Molecular Sciences, 2019, 20, 2018.	1.8	13
31930	Hierarchical and ultrathin copper nanosheets synthesized via galvanic replacement for selective electrocatalytic carbon dioxide conversion to carbon monoxide. Applied Catalysis B: Environmental, 2019, 255, 117736.	10.8	56

#	Article	IF	Citations
31931	Adsorption and dissociation of water molecules at the Î±-Al2O3(0001) surface: A 2-dimensional hybrid self-consistent charge density functional based tight-binding/molecular mechanics molecular dynamics (2D SCC-DFTB/MM MD) simulation study. Computational Materials Science, 2019, 164, 195-204.	1.4	12
31932	Systematic first-principles study on the Ni and X (Xâ€¯=â€¯C, N, O, F, P, S, Cl, Se, and Te) codoped monolayer WS2 (W15Ni1S26X6). Journal of Magnetism and Magnetic Materials, 2019, 486, 165255.	1.0	5
31933	Tunable electronic structures and high efficiency obtained by introducing superalkali and superhalogen into AMX3-type perovskites. Journal of Power Sources, 2019, 429, 120-126.	4.0	43
31934	Ternary palladium â€“ Group 12 metal compounds of the Pd5TlAs-type: A case study. Journal of Solid State Chemistry, 2019, 276, 217-225.	1.4	5
31935	Computational Discovery of Transparent Conducting In-Plane Ordered MXene (i-MXene) Alloys. Chemistry of Materials, 2019, 31, 4124-4132.	3.2	19
31936	Arousing the Reactive Fe Sites in Pyrite (FeS₂) via Integration of Electronic Structure Reconfiguration and in Situ Electrochemical Topotactic Transformation for Highly Efficient Oxygen Evolution Reaction. Inorganic Chemistry, 2019, 58, 7615-7627.	1.9	53
31937	A critical assessment on the electron transport through dehydrogenated intrinsically conducting channels in graphane-graphene hybrids. Materials Research Express, 2019, 6, 085618.	0.8	1
31938	Interstitial Zn-modulated ferromagnetism in Co-doped ZnSe. Materials Research Express, 2019, 6, 106121.	0.8	2
31939	Large spin gaps in the half-metals <mml:math xmlns:mml="http://www.w3.org/1998/Math/MathML"><mml:mi>M</mml:mi><mml:msub><mml:mrow><mml:mi mathvariant="normal">N</mml:mi></mml:mrow><mml:mn>4</mml:mn></mml:msub></mml:math> () Tj ETQq0 0 0 rgBT /Overlock 10	1.1	10
31940	<mml:msub><mml:mrow><mml:mi mathvariant="n Proximity of Ferromagnetic Nickel to Paramagnetic Instability. JETP Letters, 2019, 109, 276-279.	0.4	1
31941	Gas Sensors Based on Mechanically Exfoliated MoS2 Nanosheets for Room-Temperature NO2 Detection. Sensors, 2019, 19, 2123.	2.1	70
31942	High pressure structural investigations on K2Zr(PO4)2. Journal of Solid State Chemistry, 2019, 276, 251-260.	1.4	4
31943	Self-Combustion Synthesis of Novel Metastable Ternary Molybdenum Nitrides. , 2019, 1, 64-70.		20
31944	Physical properties of B ₄ N ₄ -I and B ₄ N ₄ -II: First-principles study. Chinese Physics B, 2019, 28, 036101.	0.7	21
31945	Theoretical prediction of the structural, elastic, electronic, and thermodynamic properties of the Nowotny-Juza LiMgAsxSb1-x alloy. Computational Condensed Matter, 2019, 21, e00401.	0.9	5
31946	Formaldehyde adsorption on a hydrogenated aluminum nitride monolayer: A self-propagated reaction. Computational and Theoretical Chemistry, 2019, 1159, 18-22.	1.1	8
31947	First-principles study of the surface properties of Î³-LiAlO2: Stability and tritium adsorption. Journal of Nuclear Materials, 2019, 522, 1-10.	1.3	17
31948	Studying the insulating characters of cubic ZrO2 slabs with nine terminations within three lower index Miller planes (001), (110) and (111). Microelectronic Engineering, 2019, 213, 77-85.	1.1	9

#	Article	IF	Citations
31949	On the Models for the Investigation of Charged Defects in Solids: The Case of the VN^{â€“} Defect in Diamond. Journal of Physical Chemistry A, 2019, 123, 4806-4815.	1.1	4
31950	Chirality Transfer in Gold Nanoparticles by <scp>l</scp>-Cysteine Amino Acid: A First-Principles Study. Journal of Physical Chemistry C, 2019, 123, 13758-13764.	1.5	23
31951	Pressure dependence of direct optical transitions in ReS2 and ReSe2. Npj 2D Materials and Applications, 2019, 3, .	3.9	35
31952	Ab initio exploration and prediction of AE-containing nitrido(litho/magneso)tetrelates (AE = Ca,) Tj ETQq1 1 0.784314 rgBT /Over [Ge₂N₆]^{10â^’} units. Dalton Transactions, 2019, 48, 8671-8677.	1.6	2
31953	Insight into the role of Niâ€“Fe dual sites in the oxygen evolution reaction based on atomically metal-doped polymeric carbon nitride. Journal of Materials Chemistry A, 2019, 7, 14001-14010.	5.2	97
31954	First-Principles Investigation of the Stability of the Oxygen Framework of Li-Rich Battery Cathodes. MRS Advances, 2019, 4, 813-820.	0.5	4
31955	Ab initio based examination of the kinetics and thermodynamics of oxygen in Fe-Cr alloys. Physical Review B, 2019, 99, .	1.1	7
31956	Electronâ€”Phonon Interaction, Phonon and Electronic Structures of Layered Electride Ca2N. JETP Letters, 2019, 109, 606-609.	0.4	0
31957	DFT modelling of the edge dislocation in 4H-SiC. Journal of Materials Science, 2019, 54, 10737-10745.	1.7	13
31958	Super-stretchability in two-dimensional RuCl3 and RuBr3 confirmed by first-principles simulations. Physica E: Low-Dimensional Systems and Nanostructures, 2019, 113, 79-85.	1.3	9
31959	Spin-dependent transport properties of debrominated tetrabromopolyaromatic with Cu or Co doping embedded between zigzag graphene nanoribbon electrodes. Physics Letters, Section A: General, Atomic and Solid State Physics, 2019, 383, 2185-2192.	0.9	5
31960	The performance of adsorption, dissociation and diffusion mechanism of hydrogen on the Ti-doped ZrCo(110) surface. Physical Chemistry Chemical Physics, 2019, 21, 12597-12605.	1.3	14
31961	An ultra-high yield of spherical K₂NaScF₆:Mn⁴⁺ red phosphor and its application in ultra-wide color gamut liquid crystal displays. Journal of Materials Chemistry C, 2019, 7, 7237-7248.	2.7	76
31962	Stabilizing the metastable superhard material wurtzite boron nitride by three-dimensional networks of planar defects. Proceedings of the National Academy of Sciences of the United States of America, 2019, 116, 11181-11186.	3.3	19
31963	Alloy structure of rare earth Ce with Pt base metal, and the adsorption of CO. Materials Research Express, 2019, 6, 046538.	0.8	0
31964	Incipient adsorption of water and hydroxyl on hematite (0001) surface. Journal of Physics Communications, 2019, 3, 035023.	0.5	7
31965	A first-principles study on the structural, thermal and electronic properties of cerium oxides by using different functionals. Electronic Structure, 2019, 1, 015003.	1.0	6
31966	Lattice dynamics of orthorhombic <mml:math xmlns:mml="http://www.w3.org/1998/Math/MathML"><mml:msub><mml:mi>NdGaO</mml:mi><mml:mn>3</mml:mn></mml:msub> Physical Review B, 2019, 99, .	1.1	9

#	Article	IF	Citations
31967	First-principles investigation of the effect of substitution and surface adsorption on the magnetostrictive performance of Fe-Ga alloys. Physical Review B, 2019, 99, .	1.1	7
31968	Optical-Energy Properties of CdS Thin Films Obtained by the Method of High-Frequency Magnetron Sputtering. Optics and Spectroscopy (English Translation of Optika I Spektroskopiya), 2019, 126, 220-225.	0.2	28
31969	High Pressure Hydrocarbons Revisited: From van der Waals Compounds to Diamond. Geosciences (Switzerland), 2019, 9, 227.	1.0	18
31970	Structural Properties and Phase Stability of Primary Y Phase (Ti2SC) in Ti-Stabilized Stainless Steel from Experiments and First Principles. Materials, 2019, 12, 1118.	1.3	3
31971	Efficient Calculation Methods for the Diffusion Coefficient of Interstitial Solutes in Dilute Alloys. Materials, 2019, 12, 1491.	1.3	3
31972	The Effect of Alloying Elements on the Structural Stability, and Mechanical and Electronic Properties of Al3Sc: A First-Principles Study. Materials, 2019, 12, 1539.	1.3	7
31973	Exploring Accuracy Limits of Predictions of the 1H NMR Chemical Shielding Anisotropy in the Solid State. Molecules, 2019, 24, 1731.	1.7	11
31974	First-Principles Analysis of Vibrational Properties of Type II SiGe Alloy Clathrates. Nanomaterials, 2019, 9, 723.	1.9	3
31975	Structural Stability and Electronic and Optical Properties of Coinage-Metal (4, 2) Alloy Nanotubes: A First-Principles Study. Journal of the Korean Physical Society, 2019, 74, 555-562.	0.3	0
31976	A systematic study of the surface structures and energetics of CH3NO2 surfaces by first-principles calculations. Journal of Molecular Modeling, 2019, 25, 164.	0.8	4
31977	Perceptions on the adsorption of COPD biomarker vapors on violet phosphorene nanosheet - A first-principles study. Journal of Molecular Graphics and Modelling, 2019, 91, 22-29.	1.3	27
31978	High pressure structural stability of ThN: ab-initio study. Journal of Nuclear Materials, 2019, 521, 161-166.	1.3	7
31979	Structural and electronic properties of Nb-Cr-Si based alloys: First-principles calculations. Physica B: Condensed Matter, 2019, 568, 1-5.	1.3	2
31980	Interlayer vibration of twisted bilayer graphene: A first-principles study. Physics Letters, Section A: General, Atomic and Solid State Physics, 2019, 383, 2628-2632.	0.9	16
31981	Negative linear compressibility and structural phase transition in energetic silver azide under pressure: A first principles study. Solid State Communications, 2019, 297, 39-44.	0.9	5
31982	Surface chemistry of 2,3-dibromosubstituted norbornadiene/quadricyclane as molecular solar thermal energy storage system on Ni(111). Journal of Chemical Physics, 2019, 150, 184706.	1.2	17
31983	Densely Populated Isolated Single Coï£¿N Site for Efficient Oxygen Electrocatalysis. Advanced Energy Materials, 2019, 9, 1900149.	10.2	262
31984	Implications of Oxygenâ€“Sulfur Exchange on Structural, Electronic Properties, and Stability of Alkaliâ€Metal Hexatitanates. Physica Status Solidi (B): Basic Research, 2019, 256, 1800568.	0.7	7

#	Article	IF	Citations
31985	Oxygenationâ€Induced Twoâ€Dimensional Topological Insulators in Antimony Arsenide. Physica Status Solidi - Rapid Research Letters, 2019, 13, 1900146.	1.2	1
31986	Investigation on heterogeneous nucleation substrate of Y2O3 as NbC in hypereutectic Feâ€“Crâ€“C hardfacing coating by experiment and first-principles calculation. Journal of Materials Science, 2019, 54, 10102-10118.	1.7	9
31987	Ab initio studies of copper hydrides under high pressure. Frontiers of Physics, 2019, 14, 1.	2.4	9
31988	Covalent bonding versus total energy: On the attainability of certain predicted low-energy carbon allotropes. Carbon, 2019, 148, 151-158.	5.4	14
31989	Effect of mass transfer process on hydrogen adsorption on polycrystalline platinum electrode in sulfuric acid solution. Chinese Chemical Letters, 2019, 30, 1168-1172.	4.8	6
31990	Insight into the structural, elastic, electronic, thermoelectric, thermodynamic and optical properties of MRhSb (Mâ€¯=â€¯Ti, Zr, Hf) half-Heuslers from ab initio calculations. Chinese Journal of Physics, 2019, 59, 434-448.	2.0	17
31991	First principles comparative studies of thermoelectric and other properties in the cubic and hexagonal structure of CsCdCl3 halide perovskites. Computational Condensed Matter, 2019, 21, e00388.	0.9	8
31992	Selecting substituent elements for LiMnPO4 cathode materials combined with density functional theory (DFT) calculations and experiments. Journal of Alloys and Compounds, 2019, 793, 360-368.	2.8	31
31993	Theoretical studies on the electronic structures and optical properties of (Cu, C)-codoped rutile TiO2 from GGA+U calculations. Journal of Molecular Graphics and Modelling, 2019, 90, 104-108.	1.3	2
31994	Phase transition, structure and reorientational dynamics of H2O ligands and ReO4â¯ anions in [Ba(H2O)3](ReO4)2â‹…H2O. Journal of Molecular Structure, 2019, 1188, 173-184.	1.8	2
31995	C₃N Monolayer: Exploring the Emerging of Novel Electronic and Magnetic Properties with Adatom Adsorption, Functionalizations, Electric Field, Charging, and Strain. Journal of Physical Chemistry C, 2019, 123, 12485-12499.	1.5	78
31996	Understanding Oxygen Activation on Nanoporous Gold. ACS Catalysis, 2019, 9, 5204-5216.	5.5	26
31997	Discoloration Effect and One-Step Synthesis of Hydrogen Tungsten and Molybdenum Bronze (H_xMO₃) using Liquid Metal at Room Temperature. ACS Omega, 2019, 4, 7428-7435.	1.6	28
31998	Thermodynamics, kinetics and electronic properties of point defects in Î²-FeSi₂. Physical Chemistry Chemical Physics, 2019, 21, 10497-10504.	1.3	15
31999	Role of Sn promoter in Ni/Al₂O₃ catalyst for the deoxygenation of stearic acid and coke formation: experimental and theoretical studies. Catalysis Science and Technology, 2019, 9, 3361-3372.	2.1	33
32000	Band engineering realized by chemical combination in 2D group VAâ€“VA materials. Nanoscale Horizons, 2019, 4, 1145-1152.	4.1	15
32001	First principles study of graphene on metals with the SCAN and SCAN+rVV10 functionals. Journal of Chemical Physics, 2019, 150, 154702.	1.2	17
32002	Electronic structures and magnetic properties of (Al, Cr) co-doped 4H-SiC: a first-principles study. Materials Research Express, 2019, 6, 096316.	0.8	2

#	Article	IF	Citations
32003	Enhanced photovoltaic property based on reduced leakage current and band gap in Nd-doped BiFeO₃ films. Materials Research Express, 2019, 6, 086426.	0.8	9
32004	From an atomic layer to the bulk: Low-temperature atomistic structure and ferroelectric and electronic properties of SnTe films. Physical Review B, 2019, 99, .	1.1	39
32005	Structural, electronic, optical and elastic properties of layered rhombohedral compounds ALaSe₂(A=K, Rb): Insights from an ab initio study. International Journal of Modern Physics B, 2019, 33, 1950084.	1.0	9
32006	Structural and Electronic Properties of Qatranaite. Advances in Materials Science and Engineering, 2019, 2019, 1-6.	1.0	0
32007	Colossal magnetoresistance in the insulating ferromagnetic double perovskites Tl2NiMnO6: A neutron diffraction study. Acta Materialia, 2019, 173, 20-26.	3.8	11
32008	Optical properties of oxygen vacancy in gamma-LiAlO2: A computational study. Chemical Physics Letters, 2019, 727, 85-89.	1.2	5
32009	Seedâ€Layerâ€Free Atomic Layer Deposition of Highly Uniform Al₂O₃ Thin Films onto Monolayer Epitaxial Graphene on Silicon Carbide. Advanced Materials Interfaces, 2019, 6, 1900097.	1.9	24
32010	Suppressing the Pd-C interaction through B-doping for highly efficient oxygen reduction. Carbon, 2019, 149, 370-379.	5.4	32
32011	Investigation on new equiatomic quaternary Heusler compound CoCrIrSi via FP-LAPW calculations. Chemical Physics, 2019, 523, 130-137.	0.9	25
32012	Effect of Stone-Wales defect on an armchair graphene nanoribbon-based photodetector. Superlattices and Microstructures, 2019, 130, 127-138.	1.4	10
32013	Adhesion strength and stability of Cu(111)/TiC(111) interface in composite coatings by first principles study. Vacuum, 2019, 165, 215-222.	1.6	39
32014	Coexistence of Elastic Modulations in the Charge Density Wave State of 2H-NbSe₂. Nano Letters, 2019, 19, 3027-3032.	4.5	26
32015	Superstrong Noncovalent Interface between Melamine and Graphene Oxide. ACS Applied Materials & Interfaces, 2019, 11, 17068-17078.	4.0	18
32016	Computational study of the mixed B-site perovskite SmB_xCo_{1â”'x}O_{3â”'d} (B = Mn, Fe, Ni, Cu) for next generation solid oxide fuel cell cathodes. Physical Chemistry Chemical Physics, 2019, 21, 9407-9418.	1.3	20
32017	Magnetic orders and electronic behaviours of new chalcogenides Cu₃MnCh₄(Châ€‰=â€‰S, Se and Te): Anab initiostudy. Philosophical Magazine, 2019, 99, 1941-1955.	0.7	3
32018	Prediction of high-mobility two-dimensional electron gas at KTaO 3 -based heterointerfaces. Chinese Physics B, 2019, 28, 047101.	0.7	7
32019	Huge power factor in p-type half-Heusler alloys NbFeSb and TaFeSb. JPhys Materials, 2019, 2, 035002.	1.8	33
32020	Tunable Type-II <mml:math xmlns:mml="http://www.w3.org/1998/Math/MathML" display="inline" overflow="scroll"><mml:msub><mml:mrow><mml:mi>Bi</mml:mi><mml:mi>VO</mml:mi></mml:mrow><mml:mn>4</mml:mn></mml:msub></mml:math> /g-<mml:math xmlns:mml="http://www.w3.org/1998/Math/MathML" display="inline" overflow="scroll"><mml:msub><mml:mrow><mml:mrow><mml:mi mathvariant="normal">C</mml:mi></mml:mrow></mml:mrow><mml:mn>3</mml:mn></mml:msub></mml:math> Heterostructure for Photocatalytic Overall Water Splitting. Physical Review Applied, 201	1.5	23

#	Article	IF	Citations
32021	Shedding Light on the Intrinsic Characteristics of 3D Distorted Fluorite-Type Zirconium Tellurite Single Crystals. Inorganic Chemistry, 2019, 58, 7794-7802.	1.9	10
32022	Trap engineering in solution processed PbSe quantum dots for high-speed MID-infrared photodetectors. Journal of Materials Chemistry C, 2019, 7, 5658-5669.	2.7	36
32023	Ab initio calculation of multilayer magnetic structures by VASP on OpenPOWER high performance system. Journal of Physics: Conference Series, 2019, 1163, 012059.	0.3	0
32024	The Structural stabilities and Band Gap Engineering of Core-Shell Nanowires. IOP Conference Series: Materials Science and Engineering, 2019, 490, 022021.	0.3	1
32025	Fragility of Fermi arcs in Dirac semimetals. Physical Review B, 2019, 99, .	1.1	19
32026	Effects of the N/S codoping configuration and ternary doping on the quantum capacitance of graphene. Journal of Materials Science, 2019, 54, 8995-9003.	1.7	14
32027	Modeling of substitutionally modified graphene structures to prevent the shuttle mechanism in lithium-sulfur batteries. Electrochimica Acta, 2019, 309, 402-414.	2.6	21
32028	Tunable electronic structure and structural transition of GaAs clusters at high pressure and temperature. Journal of Alloys and Compounds, 2019, 791, 1159-1166.	2.8	8
32029	Unraveling the Hidden Martensitic Phase Transition in BaClF and PbClF under High Pressure Using an Ab Initio Evolutionary Approach. Inorganic Chemistry, 2019, 58, 5886-5899.	1.9	9
32030	Computational Screening of Defective Group IVA Monochalcogenides as Efficient Catalysts for Hydrogen Evolution Reaction. Journal of Physical Chemistry C, 2019, 123, 11791-11797.	1.5	24
32031	Adsorption of formaldehyde on transition metal doped monolayer MoS2: A DFT study. Applied Surface Science, 2019, 484, 1244-1252.	3.1	65
32032	Thermoelectric properties of KCaF3. Physica B: Condensed Matter, 2019, 565, 18-24.	1.3	22
32033	From the Terrace Contraction to the Hexameric Sulfur Phase in the Au(100) Surface: A Combined Density Functional Theory and Scanning Tunneling Microscopy Study. Journal of Physical Chemistry C, 2019, 123, 12183-12194.	1.5	0
32034	A New Magnetic Topological Quantum Material Candidate by Design. ACS Central Science, 2019, 5, 900-910.	5.3	63
32035	Valence Engineering via Selective Atomic Substitution on Tetrahedral Sites in Spinel Oxide for Highly Enhanced Oxygen Evolution Catalysis. Journal of the American Chemical Society, 2019, 141, 8136-8145.	6.6	220
32036	First-principles modeling of GaN(0001)/water interface: Effect of surface charging. Journal of Chemical Physics, 2019, 150, 154703.	1.2	6
32037	Theoretical Study of Sulphur Atomsâ€™ Adsorption and Migration Behaviors on Diamond (001) Surface. Coatings, 2019, 9, 184.	1.2	1
32038	First-Principles Study on the Mechanical Properties and Electronic Structure of V Doped WCoB and W2CoB2 Ternary Borides. Materials, 2019, 12, 967.	1.3	17

#	Article	IF	Citations
32039	CH4 Adsorption Probability on GaN(0001) and (000â¯1) during Metalorganic Vapor Phase Epitaxy and Its Relationship to Carbon Contamination in the Films. Materials, 2019, 12, 972.	1.3	10
32040	A Metastable Fo-III Wedge in Cold Slabs Subducted to the Lower Part of the Mantle Transition Zone: A Hypothesis Based on First-Principles Simulations. Minerals (Basel, Switzerland), 2019, 9, 186.	0.8	2
32041	A new stable BeP2C monolayer with visible light sensitivity: A first principles study. Chemical Physics Letters, 2019, 728, 14-18.	1.2	2
32042	First principles prediction of XI (X=Be, Mg) monolayer semiconductors: Modified Becke-Johnson approach. Optik, 2019, 186, 332-338.	1.4	0
32043	Thermodynamics, Electronic Structure, and Vibrational Properties of Snn(S1â€“xSex)m Solid Solutions for Energy Applications. Chemistry of Materials, 2019, 31, 3672-3685.	3.2	11
32044	Reshuffling of Electronic Environment by Introducing CH₃NH₂F⁺ as an Organic Cation for Enhanced Power Conversion Efficiency and Stability of the Designed Hybrid Organicâ€“Inorganic Perovskite. Journal of Physical Chemistry C, 2019, 123, 13385-13393.	1.5	5
32045	Resolving a Decade-Long Question of Oxygen Defects in Raman Spectra of Ceria-Based Catalysts at Atomic Level. Journal of Physical Chemistry C, 2019, 123, 18889-18894.	1.5	53
32046	Statistical Analysis of Tri-Cresyl Phosphate Conversion on an Iron Oxide Surface Using Reactive Molecular Dynamics Simulations. Journal of Physical Chemistry C, 2019, 123, 12886-12893.	1.5	18
32047	Growth of Germanene on Al(111) Hindered by Surface Alloy Formation. Journal of Physical Chemistry C, 2019, 123, 12910-12918.	1.5	20
32048	Electronically-Coupled Phase Boundaries in Î±-Fe₂O₃/Fe₃O₄ Nanocomposite Photoanodes for Enhanced Water Oxidation. ACS Applied Nano Materials, 2019, 2, 334-342.	2.4	32
32049	Gas reactions under intrapore condensation regime within tailored metalâ€“organic framework catalysts. Nature Communications, 2019, 10, 2076.	5.8	45
32050	First-principles studies of superhard BC8N structures. Journal of Applied Physics, 2019, 125, .	1.1	14
32051	A computational study of gadolinium-doped ceria: Relationship between atomic arrangement and electrostriction. APL Materials, 2019, 7, .	2.2	5
32052	The role of magnetic order in VOCl. Journal of Physics Condensed Matter, 2019, 31, 325502.	0.7	5
32053	Charge Delocalization, Oxidation States, and Silver Mobility in the Mixed Silverâ€“Copper Oxide AgCuO₂. Inorganic Chemistry, 2019, 58, 7026-7035.	1.9	5
32054	On the Stability Issues of TiO₂-Based Composites in View of Fuel Cell Application: A Combined Experimental and Theoretical Investigation. Journal of Physical Chemistry C, 2019, 123, 12573-12582.	1.5	3
32055	Stepwise Electrochemical Construction of FeOOH/Ni(OH)₂ on Ni Foam for Enhanced Electrocatalytic Oxygen Evolution. ACS Applied Energy Materials, 2019, 2, 3927-3935.	2.5	87
32056	Structureâ€“Property-Performance Relationship of Ultrathin Pdâ€“Au Alloy Catalyst Layers for Low-Temperature Ethanol Oxidation in Alkaline Media. ACS Applied Materials & Interfaces, 2019, 11, 24919-24932.	4.0	27

#	Article	IF	Citations
32057	Heterochiral Doped Supramolecular Coordination Networks for High-Performance Optoelectronics. ACS Applied Materials & Interfaces, 2019, 11, 20174-20182.	4.0	11
32058	Investigating Polaron Formation in Anatase and Brookite TiO₂ by Density Functional Theory with Hybrid-Functional and DFT + U Methods. ACS Omega, 2019, 4, 8056-8064.	1.6	34
32059	From Two- to Three-Dimensional van der Waals Layered Structures of Boron Crystals: An Ab Initio Study. ACS Omega, 2019, 4, 8015-8021.	1.6	19
32060	Lifetime of carbyne-based nanodevices: size and â€œeven-oddâ€•effects. European Physical Journal Plus, 2019, 134, 1.	1.2	7
32061	Rh Doping in Pd Nanocubes Optimizes the Adsorption of 3â€Nitrostyrene towards Selective Hydrogenation of Vinyl Group. ChemCatChem, 2019, 11, 2793-2798.	1.8	8
32062	Influence of Nb concentration on the structure, stability, and electronic and mechanical properties of D022 Al3Ti by first-principles calculations and experiments. Journal of Physics and Chemistry of Solids, 2019, 131, 243-253.	1.9	11
32063	Structural prediction for zirconium boride monolayer. Physica E: Low-Dimensional Systems and Nanostructures, 2019, 113, 43-46.	1.3	3
32064	Adsorption of toxic gas molecules on pristine and transition metal doped hexagonal GaN monolayer: A first-principles study. Vacuum, 2019, 165, 35-45.	1.6	74
32065	Oxygen Vacancies Promoted the Selective Photocatalytic Removal of NO with Blue TiO₂ via Simultaneous Molecular Oxygen Activation and Photogenerated Hole Annihilation. Environmental Science & Technology, 2019, 53, 6444-6453.	4.6	215
32066	Encapsulation of heavy metals by a nanoporous complex oxide 12CaOâ€‰Â·â€‰7Al2O3. Journal of Applied Physics, 2019, 125, .	1.1	7
32067	Negative Differential Resistance and Rectifying Effects of Diblock Co-Oligomer Molecule Devices Sandwiched between C 2 N- h 2D Electrodes. Chinese Physics Letters, 2019, 36, 047101.	1.3	2
32069	3D Stackable and Scalable Binary Ovonic Threshold Switch Devices with Excellent Thermal Stability and Low Leakage Current for Highâ€Density Crossâ€Point Memory Applications. Advanced Electronic Materials, 2019, 5, 1900196.	2.6	27
32070	WS₂ Nanosheets with Highlyâ€Enhanced Electrochemical Activity by Facile Control of Sulfur Vacancies. ChemCatChem, 2019, 11, 2667-2675.	1.8	57
32071	Transition metal substitution on Mg(101Â¯3) and Mg(0001) surfaces for improved hydrogenation and dehydrogenation: A systematic first-principles study. Applied Surface Science, 2019, 479, 626-633.	3.1	6
32072	Pressure effect on mechanical, magnetic and optoelectronic properties of SrCoO3-Perovskite: FP-(L)APW+lo investigation. Chinese Journal of Physics, 2019, 59, 625-640.	2.0	10
32073	Natural sulvanite Cu3MX4 (Mâ€¯=â€¯Nb, Ta; Xâ€¯=â€¯S, Se): Promising visible-light photocatalysts for water splitting. Computational Materials Science, 2019, 165, 137-143.	1.4	9
32074	Enhanced photovoltaic performance of dye-sensitized solar cells by the adsorption of Zn-porphyrin dye molecule on TiO2 surfaces. Journal of Alloys and Compounds, 2019, 794, 35-44.	2.8	4
32075	Energetics and kinetics of hydrogen at the grain boundary of the Ni alloys: A first-principles study. Journal of Alloys and Compounds, 2019, 795, 343-350.	2.8	8

#	Article	IF	Citations
32076	Ultralow lattice thermal conductivity induced high thermoelectric performance in the Î´-Cu₂S monolayer. Nanoscale, 2019, 11, 10306-10313.	2.8	43
32077	A novel cobalt-free cathode with triple-conduction for proton-conducting solid oxide fuel cells with unprecedented performance. Journal of Materials Chemistry A, 2019, 7, 16136-16148.	5.2	145
32078	Strengthening and toughening by partial slip in nanotwinned diamond. Carbon, 2019, 150, 1-7.	5.4	29
32079	Extensive stacking of DHI-like monomers as a model of out-of-plane complexity in eumelanin protomolecules: Chemical and structural sensitivity of optical absorption spectra. Chemical Physics, 2019, 524, 92-100.	0.9	8
32080	Ultra-fast NH4+ Storage: Strong H Bonding between NH4+ and Bi-layered V2O5. CheM, 2019, 5, 1537-1551.	5.8	207
32081	Ultrathin Amorphous Titania on Nanowires: Optimization of Conformal Growth and Elucidation of Atomic-Scale Motifs. Nano Letters, 2019, 19, 3457-3463.	4.5	14
32082	Enhancing electrostatic interactions to activate polar molecules: ammonia borane methanolysis on a Cu/Co(OH)₂ nanohybrid. Catalysis Science and Technology, 2019, 9, 2828-2835.	2.1	14
32083	Elastic and hydrostatic behaviour of a zinc dietary supplement, zinc glycinate hydrate. RSC Advances, 2019, 9, 13153-13158.	1.7	6
32084	Site preference and magnetic properties of Zn-Sn-substituted strontium hexaferrite. Journal of Applied Physics, 2019, 125, .	1.1	15
32085	Enhancing High Humidity Stability of Quasiâ€2D Perovskite Thin Films through Mixed Cation Doping and Solvent Engineering. ChemNanoMat, 2019, 5, 1280-1288.	1.5	13
32086	Ultrastable CsPbBr₃ Perovskite Quantum Dot and Their Enhanced Amplified Spontaneous Emission by Surface Ligand Modification. Small, 2019, 15, e1901173.	5.2	229
32087	First-principles study of CO and OH adsorption on in-doped ZnO surfaces. Journal of Physics and Chemistry of Solids, 2019, 132, 172-181.	1.9	8
32088	Electrodeposition of Tin-Based Electrocatalysts with Different Surface Tin Species Distributions for Electrochemical Reduction of CO₂ to HCOOH. ACS Sustainable Chemistry and Engineering, 2019, 7, 9360-9368.	3.2	85
32089	First-principles study of the layered thermoelectric material TiNBr. RSC Advances, 2019, 9, 12886-12894.	1.7	18
32090	Mo-based 2D MOF as a highly efficient electrocatalyst for reduction of N₂ to NH₃: a density functional theory study. Journal of Materials Chemistry A, 2019, 7, 14510-14518.	5.2	139
32091	Prediction of the terminations and Miller planes of the tetragonal zirconia thin films as a gate dielectric layer in integratedâ€circuit industry. Surface and Interface Analysis, 2019, 51, 774-782.	0.8	2
32092	First principle characterization of structural, electronic, mechanical, thermodynamic, linear and nonlinear optical properties of zinc blende InAs, InSb and their InAsxSb1-x ternary alloys. Journal of Physics and Chemistry of Solids, 2019, 132, 213-221.	1.9	16
32093	Two-Dimensional Silver(I)-Dithiocarboxylate Coordination Polymer Exhibiting Strong Near-Infrared Photothermal Effect. Inorganic Chemistry, 2019, 58, 6601-6608.	1.9	28

#	Article	IF	Citations
32094	Spin Polarization Enhancement of an Fe3O4(100) Surface by Coadsorption of Atomic Hydrogen and Molecular Nitric Oxide. Journal of Physical Chemistry C, 2019, , .	1.5	2
32095	Hydrogen Passivated Silicon Grain Boundaries Greatly Reduce Charge Recombination for Improved Silicon/Perovskite Tandem Solar Cell Performance: Time Domain Ab Initio Analysis. Journal of Physical Chemistry Letters, 2019, 10, 2445-2452.	2.1	14
32096	Tunable electronic properties of van der Waals heterostructures composed of stanene adsorbed on two-dimensional, graphene-like nitrides. Journal of Applied Physics, 2019, 125, 155301.	1.1	5
32097	Magnetoelectric Effects at the BiFeO3/Fe Interface: A First Principles Study. IOP Conference Series: Materials Science and Engineering, 2019, 493, 012142.	0.3	0
32098	Ab Initio Study of Elastic and Mechanical Properties in FeCrMn Alloys. Materials, 2019, 12, 1129.	1.3	8
32099	Crystal structure, optical and electronic properties studies on an hybrid multifunctional MnCl4-based material. Advanced Composites and Hybrid Materials, 2019, 2, 373-380.	9.9	8
32100	Ab initio study of interstitial helium clusters in 3C-SiC. Journal of Nuclear Materials, 2019, 521, 13-20.	1.3	12
32101	Regulating the Catalytic Performance of Single-Atomic-Site Ir Catalyst for Biomass Conversion by Metalâ€“Support Interactions. ACS Catalysis, 2019, 9, 5223-5230.	5.5	87
32102	Degenerately Doped Transition Metal Dichalcogenides as Ohmic Homojunction Contacts to Transition Metal Dichalcogenide Semiconductors. ACS Nano, 2019, 13, 5103-5111.	7.3	39
32103	Crystal water for high performance layered manganese oxide cathodes in aqueous rechargeable zinc batteries. Energy and Environmental Science, 2019, 12, 1999-2009.	15.6	269
32104	Birnessite Nanosheet Arrays with High K Content as a Highâ€Capacity and Ultrastable Cathode for Kâ€Ion Batteries. Advanced Materials, 2019, 31, e1900060.	11.1	183
32105	Gallium Polymorphs: Phaseâ€Dependent Plasmonics. Advanced Optical Materials, 2019, 7, 1900307.	3.6	25
32106	Identifying Catalytic Active Sites of Trimolybdenum Phosphide (Mo₃P) for Electrochemical Hydrogen Evolution. Advanced Energy Materials, 2019, 9, 1900516.	10.2	47
32107	Ab-initio calculation of the structural, electronic, optical and transport properties of SbNSr3 ternary nitride compound. Computational Condensed Matter, 2019, 21, e00395.	0.9	1
32108	Zinc substituted MgH2 - a potential material for hydrogen storage applications. International Journal of Hydrogen Energy, 2019, 44, 13632-13646.	3.8	5
32109	Phonon stability, electronic structure results, mechanical and thermodynamic properties of RbSbO3 and CsSbO3 perovskite oxides: Ab initio investigation. Journal of Molecular Graphics and Modelling, 2019, 90, 120-127.	1.3	11
32110	Atomic-scale friction adjustment enabled by doping-induced modification in graphene nanosheet. Applied Surface Science, 2019, 483, 742-749.	3.1	36
32111	Enhanced photocatalytic activity of single-layered Hittorfâ€™s violet phosphorene by isoelectronic doping and mechanical strain: A first-principles research. Computational Materials Science, 2019, 163, 209-217.	1.4	22

#	Article	IF	Citations
32112	Exploration of Properties from Both the Bulk and Surface of Iron Silicides: A Unified Theoretical Study. Journal of Physical Chemistry C, 2019, 123, 11939-11949.	1.5	4
32113	Energy, Phonon, and Dynamic Stability Criteria of Two-Dimensional Materials. ACS Applied Materials & Interfaces, 2019, 11, 24876-24884.	4.0	76
32114	A Li₂CuPS₄ superionic conductor: a new sulfide-based solid-state electrolyte. Journal of Materials Chemistry A, 2019, 7, 12645-12653.	5.2	31
32115	Separated and intermixed phases of borophene as anode material for lithium-Ion batteries. Journal Physics D: Applied Physics, 2019, 52, 245501.	1.3	19
32116	Stability and physical properties tuning via interstitials chemical engineering of Zr5Sn3: a first-principles study. Journal of Materials Science, 2019, 54, 10284-10296.	1.7	4
32117	The physical properties of bismuth replacement in lead halogen perovskite solar cells: CH3NH3Pb1â^'Bi I3 compounds by ab-initio calculations. Results in Physics, 2019, 13, 102278.	2.0	14
32118	Band Gap Tuning in Bismuth Oxide Carbodiimide Bi₂O₂NCN. Inorganic Chemistry, 2019, 58, 6467-6473.	1.9	28
32119	DFT Characterization of Metallole-Decorated Silicon (001) Surface. Journal of Physical Chemistry C, 2019, 123, 11639-11648.	1.5	0
32120	Effects of O₂ and H₂O in the Oxidative Steam-Reforming Reaction of Ethanol on Rh Catalysts. Journal of Physical Chemistry C, 2019, 123, 11649-11661.	1.5	10
32121	Multifidelity Information Fusion with Machine Learning: A Case Study of Dopant Formation Energies in Hafnia. ACS Applied Materials & Interfaces, 2019, 11, 24906-24918.	4.0	49
32122	Benzo-Fused Periacenes or Double Helicenes? Different Cyclodehydrogenation Pathways on Surface and in Solution. Journal of the American Chemical Society, 2019, 141, 7399-7406.	6.6	49
32123	Topological Dirac states in transition-metal monolayers on graphyne. Physical Chemistry Chemical Physics, 2019, 21, 9310-9316.	1.3	7
32124	Enhancing the photocatalytic activity of ZnSn(OH)₆ achieved by gradual sulfur doping tactics. Nanoscale, 2019, 11, 9444-9456.	2.8	19
32125	Anharmonic lattice dynamics of Te and its counter-intuitive strain dependent lattice thermal conductivity. Journal of Materials Chemistry C, 2019, 7, 5970-5974.	2.7	9
32126	Effects of the introduction of a chromium oxide monolayer at the C60/Fe(001) interface. Journal of Applied Physics, 2019, 125, 142907.	1.1	3
32127	Adsorption, diffusion, and limited dissociation of a single water molecule on the Î±-Pu₂O₃ (1â€‰1â€‰1) surface. Journal of Physics Condensed Matter, 2019, 31, 265001.	1.7	4
32128	Inducing <mml:math xmlns:mml="http://www.w3.org/1998/Math/MathML" display="inline" overflow="scroll"><mml:mi>n</mml:mi></mml:math> - and <mml:math xmlns:mml="http://www.w3.org/1998/Math/MathML" display="inline" overflow="scroll"><mml:mi>p</mml:mi></mml:math> -Type Thermoelectricity in Oxide Superlattices by Strain Tuning of Orbital-Selective Transport Resonances. Physical Review Applied, 2019, 11, .	1.5	21
32129	Transition Metal Dichalcogenide Anchored in 3D Nickel Framework with Graphene Support for Efficient Electrocatalytic Hydrogen Evolution. Advanced Sustainable Systems, 2019, 3, 1800168.	2.7	12

#	Article	IF	Citations
32130	Theoretical Investigation of The interaction Between Noble Metals (Ag, Au, Pd, Pt) and Stanene Nanosheets: A DFT Study. Journal of Inorganic and Organometallic Polymers and Materials, 2019, 29, 1895-1915.	1.9	20
32131	Atomistic simulation of the structural and conductance evolution of Au break junctions. Computational Materials Science, 2019, 164, 147-152.	1.4	1
32132	On the origin of the giant magnetocaloric effect in HoMn2O5 single crystals: First principles study and Monte Carlo simulations. Materials Chemistry and Physics, 2019, 231, 366-371.	2.0	9
32133	Electronic structures, mechanical properties and defect formation energies of U3Si5 from density functional theory calculations. Progress in Nuclear Energy, 2019, 116, 87-94.	1.3	6
32134	High-Pressure Single-Crystal X-ray Diffraction of Lead Chromate: Structural Determination and Reinterpretation of Electronic and Vibrational Properties. Inorganic Chemistry, 2019, 58, 5966-5979.	1.9	13
32135	Crystal Structures of Î±- and Î²-Nitrogen Trifluoride. Inorganic Chemistry, 2019, 58, 6422-6430.	1.9	4
32136	Approaching the Quantitative Description of Enantioselective Adsorption by the Density Functional Theory Means. Journal of Physical Chemistry C, 2019, 123, 11714-11722.	1.5	5
32137	A DFT study of the electronic, optical and topological properties of free and biaxially strained CuIn_{1â^'x}Al_xSe₂. Journal of Materials Chemistry C, 2019, 7, 5803-5815.	2.7	14
32138	Crystallographic orientation dependence of work function: carbon adsorption on Au surfaces. Molecular Physics, 2019, 117, 2157-2161.	0.8	7
32139	Versatile electrical behavior of <mml:math xmlns:mml="http://www.w3.org/1998/Math/MathML"><mml:mrow><mml:mn>1</mml:mn><mml:mi>T</mml:mi><mml:mtext>â^'</mml:mtext></mml:mrow></mml:math> elucidated from a theoretical study. Physical Review B, 2019, 99, .	3.7	11
32140	Surface stabilities of 3Câ€“SiC and H 2 O adsorption on the (110) surface. Journal of the American Ceramic Society, 2019, 102, 6256-6266.	1.9	7
32141	Deep-ultraviolet nonlinear optical crystal NaBe2BO3F2â€”Structure, growth and optical properties. Journal of Crystal Growth, 2019, 518, 45-50.	0.7	17
32142	Rhenium disulfide nanosheets/carbon composite as novel anodes for high-rate and long lifespan sodium-ion batteries. Nano Energy, 2019, 61, 626-636.	8.2	46
32143	Uniaxial compression behavior and spectroscopic properties of energetic 1,1-diamino-2,2-dinitroethylene (FOX-7) crystals from density functional theory calculations. Progress in Natural Science: Materials International, 2019, 29, 329-334.	1.8	7
32144	Electronic structure of REFe2 (REâ€¯=â€¯Dy, Ho and Er) intermetallic compounds: Ab initio spin-density functional theory. Solid State Communications, 2019, 296, 42-48.	0.9	11
32145	Theoretical Prediction and Experimental Evaluation of Topological Landscape and Thermodynamic Stability of a Fluorinated Zeolitic Imidazolate Framework. Chemistry of Materials, 2019, 31, 3777-3783.	3.2	31
32146	The Pressure Gap for Thiols: Methanethiol Self-Assembly on Au(111) from Vacuum to 1 bar. Journal of Physical Chemistry C, 2019, 123, 12382-12389.	1.5	7
32147	Elucidation of the Reaction Mechanism for High-Temperature Water Gas Shift over an Industrial-Type Copperâ€“Chromiumâ€“Iron Oxide Catalyst. Journal of the American Chemical Society, 2019, 141, 7990-7999.	6.6	60

#	Article	IF	Citations
32148	Insights into how the aqueous environment influences the kinetics and mechanisms of heterogeneously-catalyzed COH* and CH₃OH* dehydrogenation reactions on Pt(111). Physical Chemistry Chemical Physics, 2019, 21, 9895-9904.	1.3	13
32149	Design and synthesis of Ga-doped ZSM-22 zeolites as highly selective and stable catalysts forn-dodecane isomerization. Catalysis Science and Technology, 2019, 9, 2812-2827.	2.1	22
32150	Tuning the electronic and magnetic properties of antimonene nanosheets via point defects and external fields: first-principles calculations. Physical Chemistry Chemical Physics, 2019, 21, 10552-10566.	1.3	46
32151	Rigid-band electronic structure of scandium nitride across the <mml:math xmlns:mml="http://www.w3.org/1998/Math/MathML"><mml:mi>n</mml:mi></mml:math> -type to <mml:math xmlns:mml="http://www.w3.org/1998/Math/MathML"><mml:mi>p</mml:mi></mml:math> -type carrier transition regime. Physical Review B, 2019, 99, .	1.1	23
32152	Electronic and structural properties of H-intercalated graphene-SiC (0001) interface. Japanese Journal of Applied Physics, 2019, 58, 035001.	0.8	1
32153	Electronic and optical properties of the supercell of 8-Pmmn borophene modified on doping by H, Li, Be, and C: a DFT approach. Applied Physics A: Materials Science and Processing, 2019, 125, 1.	1.1	21
32154	Adsorption Ability of Germanane Nanosheets Towards Nitrogen and Sulfur Mustard Gas Molecules: A First-Principles Study. Journal of Inorganic and Organometallic Polymers and Materials, 2019, 29, 2035-2043.	1.9	12
32155	Outstanding strength, optical characteristics and thermal conductivity of graphene-like BC3 and BC6N semiconductors. Carbon, 2019, 149, 733-742.	5.4	126
32156	Coexistence of half-metallicity and martensitic transition in Co2VGa1Sb (xâ€¯=â€¯0, 0.25 and 0.5) Heusler alloys: First-principles calculations combined with structural experiments. Computational Materials Science, 2019, 165, 34-39.	1.4	9
32157	1T MoS2 nanosheets with extraordinary sodium storage properties via thermal-driven ion intercalation assisted exfoliation of bulky MoS2. Nano Energy, 2019, 61, 361-369.	8.2	157
32158	DFT Analysis of the Adsorption of Phenol on the Nonpolar (101Ì…0) ZnO Surface. Journal of Physical Chemistry C, 2019, 123, 12296-12304.	1.5	26
32159	Theoretical design of a technetium-like alloy and its catalytic properties. Chemical Science, 2019, 10, 5461-5469.	3.7	5
32160	Transition metal-embedded two-dimensional C₃N as a highly active electrocatalyst for oxygen evolution and reduction reactions. Journal of Materials Chemistry A, 2019, 7, 12050-12059.	5.2	123
32161	Tunable electronic and optical properties of novel ZnSe/AlP van der Waals heterostructure. Materials Research Express, 2019, 6, 075907.	0.8	10
32162	First principles investigations of the structural, elastic, electronic, vibrational and thermodynamic properties of hexagonal XAl₂O₄ (X = Cd, Ca and Sr). Materials Research Express, 2019, 6, 085518.	0.8	2
32163	Role of Loneâ€Pairs in Driving Ferroelectricity of Perovskite Oxides: An Orbital Selective External Potential Study. Advanced Theory and Simulations, 2019, 2, 1900029.	1.3	11
32164	Chemical response of thioaldehydes to compression between magnesium oxide surfaces: A first-principles molecular dynamics study. Surface Science, 2019, 687, 7-16.	0.8	2
32165	First-principles study of hydrogen diffusion and self-clustering below tungsten surfaces. Journal of Applied Physics, 2019, 125, .	1.1	18

#	Article	IF	Citations
32166	Ab-initio investigations of structural, optoelectronic and thermoelectric properties of AIn2Se4 (A =) Tj ETQq0 0 0 rgBT /Overlock 10 Tf 50	0.8	2
32167	Orientation dependent electronic and optical properties of ZnS nanowires and ZnSâ€"Si core shell nanowires. Applied Surface Science, 2019, 486, 539-545.	3.1	14
32168	Magnetic properties of transition metal doped SnO2: A detailed theoretical study. Computational Condensed Matter, 2019, 21, e00393.	0.9	19
32169	First-principles study on the two-dimensional siligene (2D SiGe) as an anode material of an alkali metal ion battery. Computational Materials Science, 2019, 165, 121-128.	1.4	60
32170	Modified band alignment at multilayer MoS2/Al2O3 heterojunctions by nitridation treatment. Journal of Alloys and Compounds, 2019, 793, 599-603.	2.8	10
32171	Effect of Al solute concentration on mechanical properties of AlxFeCuCrNi high-entropy alloys: A first-principles study. Physica B: Condensed Matter, 2019, 566, 30-37.	1.3	30
32172	Electron-Beam-Driven Structure Evolution of Single-Layer MoTe₂ for Quantum Devices. ACS Applied Nano Materials, 2019, 2, 3262-3270.	2.4	39
32173	B₃S monolayer: prediction of a high-performance anode material for lithium-ion batteries. Journal of Materials Chemistry A, 2019, 7, 12706-12712.	5.2	59
32174	Benzyl alcohol oxidation with Pd-Zn/TiO2: computational and experimental studies. Science and Technology of Advanced Materials, 2019, 20, 367-378.	2.8	26
32175	Syntheses of Colloidal F:In₂O₃ Cubes: Fluorine-Induced Faceting and Infrared Plasmonic Response. Chemistry of Materials, 2019, 31, 2661-2676.	3.2	41
32176	Unexpected Xe Cations and Superconductivity in Yâ€"Xe Intermediate Compounds under Pressure. Journal of Physical Chemistry C, 2019, 123, 9323-9330.	1.5	6
32177	CO, CO2, and H2 Interactions with (0001) and (001) Tungsten Carbide Surfaces: Importance of Carbon and Metal Sites. Journal of Physical Chemistry C, 2019, 123, 8871-8883.	1.5	30
32178	Exploring the Compositional Ternary Diagram of Ge/S/Cu Glasses for Resistance Switching Memories. Journal of Physical Chemistry C, 2019, 123, 9486-9495.	1.5	6
32179	DFT-GIPAW 27Al NMR Simulations for Intermetallics: Accuracy Issues and Magnetic Screening Mechanisms. Journal of Physical Chemistry C, 2019, 123, 9371-9381.	1.5	5
32180	Anisotropic atomistic evolution during the sublimation of polar InAs nanowires. Nanoscale, 2019, 11, 6685-6692.	2.8	6
32181	Synthesis, characterization, and post-synthetic modification of a micro/mesoporous zirconiumâ€"tricarboxylate metalâ€"organic framework: towards the addition of acid active sites. CrystEngComm, 2019, 21, 3014-3030.	1.3	38
32182	DHQ-graphene: a novel two-dimensional defective graphene for corrosion-resistant coating. Journal of Materials Chemistry A, 2019, 7, 8967-8974.	5.2	33
32183	Charge-mediated cation deposition on metallic surfaces. Journal of Materials Chemistry A, 2019, 7, 8527-8539.	5.2	13

#	Article	IF	Citations
32184	Modulation of the electronic properties of pristine and AlP-codoped stanene monolayers by the adsorption of CH₂O and CH₄ molecules: a DFT study. Materials Research Express, 2019, 6, 076410.	0.8	21
32185	Synthesis, Hirshfeld surface analysis, optical and electronic properties of the functional hybrid perovskite [NH₃â€“(CH₂)₂â€“NH₃] CdCl₄: a combined experimental and theoretical study. Materials Research Express, 2019, 6, 076301.	0.8	4
32186	Giant conductivity enhancement: Pressure-induced semiconductor-metal phase transition in Cd0.90Zn0.1Te. Physical Review B, 2019, 99, .	1.1	6
32187	Kagome bands disguised in a coloring-triangle lattice. Physical Review B, 2019, 99, .	1.1	42
32188	Monopole mining method for high-throughput screening for Weyl semimetals. Physical Review B, 2019, 99, .	1.1	10
32189	Static subspace approximation for the evaluation of <mml:math xmlns:mml="http://www.w3.org/1998/Math/MathML"><mml:mrow><mml:msub><mml:mi>G</mml:mi><mml:mn>0</mml:mn></mml:msub></mml:mrow></mml:math> quasiparticle energies within a sum-over-bands approach. Physical Review B, 2019, 99, .	1.1	13
32190	High-pressure structural phase transitions, electronic properties, and intermediate states of CaSe. Canadian Journal of Physics, 2019, 97, 797-802.	0.4	2
32191	Study of thermo-elastic and lattice dynamics properties of half-Heusler compounds XMgAl (X = Li, Na) by computational investigations. Modern Physics Letters B, 2019, 33, 1950093.	1.0	8
32192	Elastic constants of Dy2Fe14B crystal by ab-initio calculations. International Journal of Applied Electromagnetics and Mechanics, 2019, 59, 151-156.	0.3	0
32193	Plasma phase transition (by the fiftieth anniversary of the prediction). Contributions To Plasma Physics, 2019, 59, e201800182.	0.5	6
32194	Periodic density functional theory study of the Raman spectrum of the hydrated uranyl oxyhydroxide mineral becquerelite. Theoretical Chemistry Accounts, 2019, 138, 1.	0.5	12
32195	Revealing the Mechanism of Graphene Oxide Reduction by Supercritical Ethanol with First-Principles Calculations. Journal of Physical Chemistry C, 2019, 123, 8932-8942.	1.5	5
32196	How far does the defect tolerance of lead-halide perovskites range? The example of Bi impurities introducing efficient recombination centers. Journal of Materials Chemistry A, 2019, 7, 23838-23853.	5.2	57
32197	Morphology evolution of fcc Ru nanoparticles under hydrogen atmosphere. Nanoscale, 2019, 11, 8037-8046.	2.8	18
32198	Study of Structural, Electronic and Vibrational Properties of Porous Silicon with Different Porosity. Silicon, 2019, 11, 2505-2515.	1.8	4
32199	Insights into graphene wettability transparency by locally probing its surface free energy. Nanoscale, 2019, 11, 7944-7951.	2.8	25
32200	Phase stability of three-dimensional bulk and two-dimensional monolayer As_{1â^'x}Sb_x solid solutions from first principles. Journal of Physics Condensed Matter, 2019, 31, 245702.	0.7	6
32201	Plasmon damping depends on the chemical nature of the nanoparticle interface. Science Advances, 2019, 5, eaav0704.	4.7	128

#	Article	IF	Citations
32202	Comprehensive study of the promotional mechanism of F on Ceâ€“Mo/TiO₂ catalysts for wide temperature NH₃-SCR performance: the activation of surface î€,Tiâ€“F bonds. Catalysis Science and Technology, 2019, 9, 2231-2244.	2.1	18
32203	Microstructural Evolution and Mechanical Properties of Intermetallics at the CuW/Al Interface with a Ni Interlayer. Advanced Engineering Materials, 2019, 21, 1801273.	1.6	4
32204	Vibrational and Thermodynamical Properties of MgO Nanosheets of (111) and (100) Facets by Density Functional Theory. Journal of Electronic Materials, 2019, 48, 3816-3822.	1.0	14
32205	One-pot synthesis of porous 1T-phase MoS2 integrated with single-atom Cu doping for enhancing electrocatalytic hydrogen evolution reaction. Applied Catalysis B: Environmental, 2019, 251, 87-93.	10.8	160
32206	First-principles investigations of structural and elastic properties of LiGaO2 under pressure. Computational Condensed Matter, 2019, 20, e00385.	0.9	1
32207	First-principle study of the oxidation mechanism of formaldehyde and hypophosphite for copper and nickel electroless deposition process. Electrochimica Acta, 2019, 307, 536-542.	2.6	12
32208	A comparison study of the structural, electronic and magnetic properties in zinc-blende PtxCr1-xP and RhxCr1-xP (xâ€¯=â€¯0.125, 0.25), and half-Heusler XCrP (Xâ€¯=â€¯Pt, Rh): First principles calculations. Materials Chemistry and Physics, 2019, 230, 151-161.	2.0	3
32209	Unraveling the Charge State of Oxygen Vacancies in ZrO_{2â€“x} on the Basis of Synergistic Computational and Experimental Evidence. Journal of Physical Chemistry C, 2019, 123, 11581-11590.	1.5	31
32210	Modeling Key Pathways Proposed for the Formation and Evolution of â€œCocktailâ€•Type Systems in Pd-Catalyzed Reactions Involving ArX Reagents. ACS Catalysis, 2019, 9, 3991-4005.	5.5	63
32211	The first principle calculations of magnetic and thermoelectric properties of Ba2CeCoO6 with GGA and mBJ approximations. Computational Condensed Matter, 2019, 19, e00380.	0.9	5
32212	Novel hybrid semiconducting lead and tin halide perovskites with saturated heterocyclic cations (CH2)nPH2+ and (CH2)nSH+, (n=2â€“6): Ab initio study. Materials Chemistry and Physics, 2019, 229, 387-391.	2.0	2
32213	Ab initio modeling of oxygen ion migration in non-stoichiometric bismuth titanate pyrochlore Bi1.5Ti2O6.25. Solid State Ionics, 2019, 335, 135-141.	1.3	12
32214	Wettability of Fully Hydroxylated and Alkylated (001) Î±-Quartz Surface in Carbon Dioxide Atmosphere. Journal of Physical Chemistry C, 2019, 123, 9027-9040.	1.5	69
32215	Experimental and Computational Design of Highly Active Ceâ€“ZrO2â€“GO Photocatalyst for Eosin Yellow Dye Degradation: The Role of Interface and Ce3+ Ion. Catalysis Letters, 2019, 149, 1633-1650.	1.4	18
32216	Tetra-SiC â€“ New allotrope of 2D silicon carbide. Computational Materials Science, 2019, 162, 236-244.	1.4	8
32217	Synergistic effect of metal-nonmetal substitution on oxygen activation in Pd/C- and Pd/N-substituted TiO2. Computational Materials Science, 2019, 162, 349-358.	1.4	3
32218	Optimized band gap and fast interlayer charge transfer in two-dimensional perovskite oxynitride Ba2NbO3N and Sr2NbO3/Ba2NbO3N bonded heterostructure visible-light photocatalysts for overall water splitting. Journal of Colloid and Interface Science, 2019, 546, 20-31.	5.0	26
32219	DFT study of the electronic and vibrational properties of silicene/stanene heterobilayer. Physica E: Low-Dimensional Systems and Nanostructures, 2019, 111, 127-129.	1.3	10

#	Article	IF	Citations
32220	Scattering of conduction electrons on the W(001) surface covered with the ordered deuterium monolayer. Surface Science, 2019, 685, 13-18.	0.8	1
32221	Pervasive Ohmic Contacts in Bilayer Bi₂O₂Seâ€“Metal Interfaces. Journal of Physical Chemistry C, 2019, 123, 8923-8931.	1.5	17
32222	Tunable Dipole Moment in Janus Single-Layer MoSSe via Transition-Metal Atom Adsorption. Journal of Physical Chemistry C, 2019, 123, 9059-9065.	1.5	42
32223	Machine-Learning-Assisted Development and Theoretical Consideration for the Al₂Fe₃Si₃ Thermoelectric Material. ACS Applied Materials & Interfaces, 2019, 11, 11545-11554.	4.0	69
32224	Influence of Atomic Surface Structure on the Activity of Ag for the Electrochemical Reduction of CO₂ to CO. ACS Catalysis, 2019, 9, 4006-4014.	5.5	119
32225	Superoxide/Peroxide Chemistry Extends Charge Carriersâ€™ Lifetime but Undermines Chemical Stability of CH₃NH₃PbI₃ Exposed to Oxygen: Time-Domain ab Initio Analysis. Journal of the American Chemical Society, 2019, 141, 5798-5807.	6.6	102
32226	Unified picture of anionic redox in Li/Na-ion batteries. Nature Materials, 2019, 18, 496-502.	13.3	335
32227	Exploring T-carbon for energy applications. Nanoscale, 2019, 11, 5798-5806.	2.8	38
32228	First-principles characterization of reversible martensitic transformations. Physical Review B, 2019, 99, .	1.1	12
32229	Vacancy mediated magnetization and healing of a graphene monolayer. Physical Review B, 2019, 99, .	1.1	9
32230	Stable structure and electronic properties of Ru 1â^' x Ti x O 2 rutile type solid solutions from DFT calculations. Journal of the American Ceramic Society, 2019, 102, 4976-4989.	1.9	8
32231	A synergistic reinforcement of Re and W for ideal shear strengths of Î³â€²-Ni3Al phases. Journal of Physics and Chemistry of Solids, 2019, 131, 34-43.	1.9	18
32232	Properties of M₂O₃/Au(111) Honeycomb Monolayers (M = Sc, Ti, V, Cr, Mn, Fe,) Tj ETQq0 0 0 rgBT /Overlock	1.5	21
32233	Symmetry Breaking at MAPbI₃ Perovskite Grain Boundaries Suppresses Charge Recombination: Time-Domain ab Initio Analysis. Journal of Physical Chemistry Letters, 2019, 10, 1617-1623.	2.1	65
32234	1 + 1â€² > 2: Heteronuclear Biatom Catalyst Outperforms Its Homonuclear Counterparts for CO Oxidation. Small Methods, 2019, 3, 1800480.	4.6	92
32235	Sintering behavior of high-concentration Li2CO3-doped BaTiO3 ceramics. Applied Physics A: Materials Science and Processing, 2019, 125, 1.	1.1	5
32236	First-Principle Predictions of Electronic Properties and Half-Metallic Ferromagnetism in Vanadium-Doped Rock-Salt CaS. Journal of Electronic Materials, 2019, 48, 3276-3284.	1.0	12
32237	First-principles study of the ferroelectric phase of AgNbO3. , 2019, , 137-159.		0

#	Article	IF	Citations
32238	2D Li2S monolayer: A global minimum lithium sulfide sandwich. Chemical Physics Letters, 2019, 722, 58-63.	1.2	12
32239	First-principles study of structural, electronic and optical properties of doped Ti2CF2 MXenes. Physica B: Condensed Matter, 2019, 561, 90-96.	1.3	10
32240	Perfect mechanical and robust electronic properties of new carbon nanothreads: A first principles study. Physica E: Low-Dimensional Systems and Nanostructures, 2019, 111, 37-43.	1.3	8
32241	First-Principles Study of the Effect of Nonmetallic Si Doping on Tritium Release from Li₂TiO₃(001) Surface. Journal of Physical Chemistry C, 2019, 123, 6477-6486.	1.5	8
32242	The basis for reevaluating the reactivity of pyrite surfaces: spin states and crystal field d-orbital splitting energies of bulk, terrace, edge, and corner Fe(<scp>ii</scp>) ions. Physical Chemistry Chemical Physics, 2019, 21, 6415-6431.	1.3	8
32243	Design of Pd-based pseudo-binary alloy catalysts for highly active and selective NO reduction. Chemical Science, 2019, 10, 4148-4162.	3.7	41
32244	Single metal atoms regulated flexibly by a 2D InSe substrate for CO₂ reduction electrocatalysts. Journal of Materials Chemistry A, 2019, 7, 8210-8217.	5.2	26
32245	Hybrid 2D nanodevices (graphene/h-BN): selecting NO_x gas through the device interface. Journal of Materials Chemistry A, 2019, 7, 8905-8911.	5.2	29
32246	Strain-driven thermodynamic stability and electronic transitions in ZnX (Xâ€‰=â€‰O, S, Se, and Te) monolayers. Journal of Applied Physics, 2019, 125, .	1.1	29
32247	An insight into optical properties of Pb:CdS system (a theoretical study). Materials Research Express, 2019, 6, 065904.	0.8	8
32248	Electronic Properties of SbTa₁₋_xNb_xO₄: Phase-Related Distortions. Journal of the Electrochemical Society, 2019, 166, H3195-H3201.	1.3	6
32249	Phase Stability and Mechanical Properties of Al8Fe4RE via First-Principle Calculations. Materials, 2019, 12, 701.	1.3	4
32250	Scalable Synthesis of Ultrathin Mn₃N₂ Exhibiting Roomâ€Temperature Antiferromagnetism. Advanced Functional Materials, 2019, 29, 1809001.	7.8	67
32251	First-principles study of mechanical, electronic properties and anisotropic deformation mechanisms of TiB under uniaxial compressions. Applied Physics A: Materials Science and Processing, 2019, 125, 1.	1.1	5
32252	Design of high efficient oxygen reduction catalyst from the transition metal dimer phthalocyanine monolayer. Applied Surface Science, 2019, 480, 905-911.	3.1	12
32253	Nucleation of Y-X-O (X=Al, Ti, or Zr) NCs in nano-structured ferritic alloys: A first principles comparative study. Journal of Nuclear Materials, 2019, 518, 140-148.	1.3	18
32254	Crystal and Magnetic Structures of Melilite-Type Ba₂MnSi₂O₇. Inorganic Chemistry, 2019, 58, 4164-4172.	1.9	8
32255	Assessing structure and stability of polymer/lithium-metal interfaces from first-principles calculations. Journal of Materials Chemistry A, 2019, 7, 8394-8404.	5.2	77

#	Article	IF	Citations
32256	Data-enabled structureâ€“property mappings for lanthanide-activated inorganic scintillators. Journal of Materials Science, 2019, 54, 8361-8380.	1.7	9
32257	Effects of Solute Atoms on 9R Phase Stabilization in High-Performance Al Alloys: A First-Principles Study. Jom, 2019, 71, 2047-2053.	0.9	8
32258	Monolayer Zr2B2: A promising two-dimensional anode material for Li-ion batteries. Applied Surface Science, 2019, 480, 448-453.	3.1	63
32259	Adsorption and migration of selenium atoms on a hydrogen-terminated diamond (0â€¯0â€¯1) surface: A first-principles study. Computational Materials Science, 2019, 162, 186-198.	1.4	4
32260	Structural stability, electronic structure, and superconductivity of cubic sodium hexaboride NaB6 from first-principle calculations. Chemical Physics Letters, 2019, 722, 80-84.	1.2	8
32261	Origin of anisotropy and compositional dependence of phonon and electron transport in ZnO based natural superlattices and role of atomic layer interfaces. Nano Energy, 2019, 59, 651-666.	8.2	5
32262	Investigations of physical aspects of spinel ABi2O4 (A=Zn, Cd) oxides via ab-initio calculations. Physics Letters, Section A: General, Atomic and Solid State Physics, 2019, 383, 1810-1815.	0.9	6
32263	Structural, electronic, magnetic, and optical properties of monolayer WS2 doped with Co-X6 (Xâ€¯=â€¯S, N,) Tj ETQq1 1 0.784314 rgBT	0.8	10
32264	Atomically Layered and Ordered Rare-Earth i-MAX Phases: A New Class of Magnetic Quaternary Compounds. Chemistry of Materials, 2019, 31, 2476-2485.	3.2	89
32265	Double-Spiral Hexagonal Boron Nitride and Shear Strained Coalescence Boundary. Nano Letters, 2019, 19, 4229-4236.	4.5	15
32266	The Opposite Anisotropic Piezoresistive Effect of ReS₂. ACS Nano, 2019, 13, 3310-3319.	7.3	55
32267	Prediction of Weyl semimetal and antiferromagnetic topological insulator phases in Bi2MnSe4. Npj Computational Materials, 2019, 5, .	3.5	47
32268	Strain-induced indirect-to-direct bandgap transition in an np-type LaAlO3/SrTiO3(110) superlattice. Physical Chemistry Chemical Physics, 2019, 21, 7075-7082.	1.3	2
32269	Adsorption and migration of alkali metals (Li, Na, and K) on pristine and defective graphene surfaces. Nanoscale, 2019, 11, 5274-5284.	2.8	149
32270	Computational understanding of the structural and electronic properties of the GeSâ€“graphene contact. Physical Chemistry Chemical Physics, 2019, 21, 7447-7453.	1.3	62
32271	Deprotonation and vacancies at the CH3NH3PbI3/ZnO and CH3NH3PbI3/GaN interfaces, detected in their theoretical XANES. Journal of Materials Chemistry C, 2019, 7, 5307-5313.	2.7	2
32272	Exciton states and oscillator strength in few-layer Î±-tellurene. Applied Physics Letters, 2019, 114, .	1.5	14
32273	Tunable 2D-gallium arsenide and graphene bandgaps in a graphene/GaAs heterostructure: anab initiostudy. Journal of Physics Condensed Matter, 2019, 31, 265502.	0.7	6

#	Article	IF	Citations
32274	Liquid-glass transition in monoatomic vanadium: A first-principles study. Physical Review B, 2019, 99, .	1.1	6
32275	Li and Na Adsorption on Graphene and Graphene Oxide Examined by Density Functional Theory, Quantum Theory of Atoms in Molecules, and Electron Localization Function. Molecules, 2019, 24, 754.	1.7	39
32276	A First-Principles Study on the Multiferroic Property of Two-Dimensional BaTiO3 (001) Ultrathin Film with Surface Ba Vacancy. Nanomaterials, 2019, 9, 269.	1.9	9
32277	Ordered Mesoporous CeO₂â€supported Ag as an Effective Catalyst for Carboxylative Coupling Reaction Using CO₂. ChemCatChem, 2019, 11, 2089-2098.	1.8	24
32278	Interfacial Properties for a Monolayer CrS 2 Contact with Metal: A Theoretical Perspective. Physica Status Solidi (B): Basic Research, 2019, 256, 1800597.	0.7	8
32279	Understanding the role of Ru dopant on selective catalytic reduction of NO with NH3 over Ru-doped CeO2 catalyst. Chemical Engineering Journal, 2019, 369, 124-133.	6.6	33
32280	The physical properties of ThCr2Si2- type nickel-based superconductors BaNi2T2 (Tâ€¯=â€¯P, As): An ab-initio study. Chinese Journal of Physics, 2019, 59, 58-69.	2.0	11
32281	Hydrogen storage on graphitic carbon nitride and its palladium nanocomposites: A multiscale computational approach. International Journal of Hydrogen Energy, 2019, 44, 8325-8340.	3.8	32
32282	Theoretical investigation of superconductivity mechanism in the filled skutterudites YRu4P12, YOs4P12, LaOs1P12 and LaOs4As12. Journal of Physics and Chemistry of Solids, 2019, 130, 197-209.	1.9	3
32283	A metal-semiconductor transition triggered by atomically flat zigzag edge in monolayer transition-metal dichalcogenides. Physics Letters, Section A: General, Atomic and Solid State Physics, 2019, 383, 1636-1641.	0.9	2
32284	Effects of Dimethyl Disulfide Cosolvent on Liâ€“S Battery Chemistry and Performance. Chemistry of Materials, 2019, 31, 2377-2389.	3.2	11
32285	Characterization of Phonon Vibrations of Silica Bilayer Films. Journal of Physical Chemistry C, 2019, 123, 7110-7117.	1.5	8
32286	Revealing the Synergy between Oxide and Alloy Phases on the Performance of Bimetallic Inâ€“Pd Catalysts for CO₂ Hydrogenation to Methanol. ACS Catalysis, 2019, 9, 3399-3412.	5.5	173
32287	Structureâ€“Activity Relationships That Identify Metalâ€–Organic Framework Catalysts for Methane Activation. ACS Catalysis, 2019, 9, 3576-3587.	5.5	105
32288	Graphene-assisted quasi-van der Waals epitaxy of AlN film for ultraviolet light emitting diodes on nano-patterned sapphire substrate. Applied Physics Letters, 2019, 114, .	1.5	76
32289	Magnetic and electronic properties of Cr2Ge2Te6 monolayer by strain and electric-field engineering. Applied Physics Letters, 2019, 114, .	1.5	69
32290	Self-consistent site-dependent DFT+ <mml:math xmlns:mml="http://www.w3.org/1998/Math/MathML"><mml:mi>U</mml:mi></mml:math> study of stoichiometric and defective <mml:math xmlns:mml="http://www.w3.org/1998/Math/MathML"><mml:msub><mml:mi>SrMnO</mml:mi><mml:mn>3</mml:mn></mml:msub></m Physical Review B, 2019, 99, .	1.1	39
32291	Microscopic theory of electric polarization induced by skyrmionic order in <mml:math xmlns:mml="http://www.w3.org/1998/Math/MathML"><mml:mrow><mml:msub><mml:mi>GaV</mml:mi><mml:mn>4</mml:mn></mml:m mathvariant="normal">S</mml:mi><mml:mn>8</mml:mn></mml:msub></mml:mrow></mml:math>. Physical Review B, 2019, 99, .	1.1	18

#	Article	IF	Citations
32292	Ab Initio Study of the Combined Effects of Alloying Elements and H on Grain Boundary Cohesion in Ferritic Steels. Metals, 2019, 9, 291.	1.0	14
32293	Surface Instability and Chemical Reactivity of ZrSiS and ZrSiSe Nodalâ€Line Semimetals. Advanced Functional Materials, 2019, 29, 1900438.	7.8	6
32294	Nanoporous graphene: A 2D semiconductor with anisotropic mechanical, optical and thermal conduction properties. Carbon, 2019, 147, 377-384.	5.4	46
32295	Phase diagram and bonding states of Ir-P binary compounds at high pressures. Journal of Alloys and Compounds, 2019, 791, 1257-1262.	2.8	7
32296	Diversity of structural and electronic properties ofPâ€“AuBr of different dimensions. Materials Research Express, 2019, 6, 065010.	0.8	1
32297	Strain and screening: Optical properties of a small-diameter carbon nanotube from first principles. Physical Review B, 2019, 99, .	1.1	10
32298	Ultrafast electron calorimetry uncovers a new long-lived metastable state in 1 T -TaSe ₂ mediated by mode-selective electron-phonon coupling. Science Advances, 2019, 5, eaav4449.	4.7	43
32299	Ab Initio Study on the Oxidation Mechanism of Millerite. Minerals, Metals and Materials Series, 2019, , 1037-1044.	0.3	1
32300	Exploring reaction mechanisms for CO oxidation on boron-doped carbon nanotubes: A computational approach. Applied Surface Science, 2019, 480, 63-69.	3.1	8
32301	First principles calculations on CeO2 doped with Tb3+ ions. Optical Materials, 2019, 90, 76-83.	1.7	3
32302	Adsorption of Ethene-1,2-Dione on Materials Based on Graphene. Journal of Physical Chemistry C, 2019, 123, 6316-6325.	1.5	1
32303	High-Throughput 2D Heteroatom Graphene Bioelectronic Nanosculpture: A Combined Experimental and Theoretical Study. ACS Applied Materials & Interfaces, 2019, 11, 11238-11250.	4.0	5
32304	Martensitic transformation of Ti50(Ni50â^'xCux) and Ni50(Ti50â^'xZrx) shape-memory alloys. Scientific Reports, 2019, 9, 3221.	1.6	13
32305	Electronic and optical properties of perovskite compounds MA_{1â^'Î±}FA_{Î±}PbI_{3â^'Î²}X_{Î²} (X = Cl, Br) explored for photovoltaic applications. RSC Advances, 2019, 9, 7015-7024.	1.7	20
32306	Functionalization of monolayer AsP phases by adatoms: a first-principles study. Materials Research Express, 2019, 6, 065032.	0.8	5
32307	Enhancement in hydrogen storage capacities of light metal functionalized Boronâ€“Graphdiyne nanosheets. Carbon, 2019, 147, 199-205.	5.4	100
32308	Realizing discrete growth of thin Li2O2 sheets on black phosphorus quantum dots-decorated Î´-MnO2catalyst for long-life lithiumâ€“oxygen cells. Energy Storage Materials, 2019, 23, 684-692.	9.5	24
32309	Correlating structural and mechanical properties of AlN/TiN superlattice films. Scripta Materialia, 2019, 165, 159-163.	2.6	29

#	Article	IF	Citations
32310	Structural principles to steer the selectivity of the electrocatalytic reduction of aliphatic ketones on platinum. Nature Catalysis, 2019, 2, 243-250.	16.1	95
32311	Promoting nitrogen electroreduction to ammonia with bismuth nanocrystals and potassium cations in water. Nature Catalysis, 2019, 2, 448-456.	16.1	642
32312	The potential application of black and blue phosphorene as cathode materials in rechargeable aluminum batteries: a first-principles study. Physical Chemistry Chemical Physics, 2019, 21, 7021-7028.	1.3	24
32313	The mechanism and activity of oxygen reduction reaction on single atom doped graphene: a DFT method. RSC Advances, 2019, 9, 7086-7093.	1.7	31
32314	Strain effects on electronic and magnetic properties of the monolayer Î±-RuCl3: A first-principles and Monte Carlo study. Journal of Applied Physics, 2019, 125, .	1.1	32
32315	Role of intrinsic defects on the persistent luminescence of pristine and Mn doped ZnGa2O4. Journal of Applied Physics, 2019, 125, .	1.1	9
32316	First-principles study of localized and delocalized electronic states in crystallographic shear phases of niobium oxide. Physical Review B, 2019, 99, .	1.1	30
32317	Carbon in GaN: Calculations with an optimized hybrid functional. Physical Review B, 2019, 99, .	1.1	32
32318	Engineering Vacancies in Bi₂S₃ yielding Subâ€Bandgap Photoresponse and Highly Sensitive Shortâ€Wave Infrared Photodetectors. Advanced Optical Materials, 2019, 7, 1900258.	3.6	37
32319	Theoretical Investigation of the Electronic Structure and Magnetic Properties in Ferromagnetic Rock-Salt and Zinc Blende Structures of 3d (V)-Doped MgS. Journal of Electronic Materials, 2019, 48, 3794-3804.	1.0	10
32320	Microscopic mechanisms of Si(111) surface nitridation and energetics of Si3N4/Si(111) interface. Applied Surface Science, 2019, 483, 302-312.	3.1	3
32321	Amorphous phosphorus-carbon nanotube hybrid anode with ultralong cycle life and high-rate capability for lithium-ion batteries. Carbon, 2019, 148, 518-524.	5.4	65
32322	A novel anions and cations co-doped strategy for developing high-performance cobalt-free cathode for intermediate-temperature proton-conducting solid oxide fuel cells. International Journal of Hydrogen Energy, 2019, 44, 11079-11087.	3.8	24
32323	Interfacial structure and electronic properties of TiO2/ZnO/TiO2 for photocatalytic and photovoltaic applications: A theoretical study. Surface Science, 2019, 686, 10-16.	0.8	29
32324	Investigation of half-metallicity and magnetism of bulk and (111)-surfaces of Fe2MnP full Heusler alloy. Vacuum, 2019, 164, 336-342.	1.6	37
32325	High-Pressure Behavior of C2I2 and Polymerization to a Conductive Polymer. Journal of Physical Chemistry C, 2019, 123, 11369-11377.	1.5	14
32326	DFT Study of Layered Double Hydroxides with Cation Exchange Capacity: (A⁺(H₂O)₆)[M₆²⁺Al₃(OH)₁₈(SO₄<s (M²⁺ = Mg, Zn and A⁺ = Na, K). Journal of Physical Chemistry C, 2019, 123, 9838-9845.	1.5	15
32327	Mechanical, Electronic, and Magnetic Properties of NiX₂ (X = Cl, Br, I) Layers. ACS Omega, 2019, 4, 5714-5721.	1.6	40

#	Article	IF	Citations
32328	Colossal barocaloric effects in plastic crystals. Nature, 2019, 567, 506-510.	13.7	253
32329	Effects of iron spin transition on the electronic structure, thermal expansivity and lattice thermal conductivity of ferropericlase: a first principles study. Scientific Reports, 2019, 9, 4172.	1.6	10
32330	Excellent catalysis of TiO₂ nanosheets with high-surface-energy {001} facets on the hydrogen storage properties of MgH₂. Nanoscale, 2019, 11, 7465-7473.	2.8	89
32331	Nanotube-assembled pine-needle-like CuS as an effective energy booster for sodium-ion storage. Journal of Materials Chemistry A, 2019, 7, 10619-10628.	5.2	70
32332	Sodium bismuth dichalcogenides: candidates for ferroelectric high-mobility semiconductors for multifunctional applications. Physical Chemistry Chemical Physics, 2019, 21, 8553-8558.	1.3	21
32333	Hybrid-functional calculations of electronic structure and phase stability of MO (M = Zn, Cd, Be, Mg,) Tj ETQq1 1 0.784314 rgBT /Ove 8507-8514.	1.7	9
32334	First-principles study of the effect of dopants (Pd, Ni) on the formation and desorption of T₂O from a Li₂TiO₃ (001) surface. RSC Advances, 2019, 9, 8490-8497.	1.7	5
32335	Molecular dynamics simulations for hydrogen adsorption in low energy collisions with carbon and boron-nitride nanotubes. Journal of Applied Physics, 2019, 125, 094506.	1.1	3
32336	The diverse electronic properties of C/BN heteronanotubes with polar discontinuity. Journal Physics D: Applied Physics, 2019, 52, 215302.	1.3	2
32337	BEEF-vdW+U method applied to perovskites: thermodynamic, structural, electronic, and magnetic properties. Journal of Physics Condensed Matter, 2019, 31, 145901.	0.7	11
32338	Hydrogenated antimonene as quantum spin Hall insulator: A first-principles study. Chinese Physics B, 2019, 28, 037301.	0.7	10
32339	First-principles bulk-layer model for dielectric and piezoelectric responses in superlattices. Physical Review B, 2019, 99, .	1.1	3
32340	Synthesis and physical properties of the 10.6 K ferromagnet <mml:math xmlns:mml="http://www.w3.org/1998/Math/MathML"><mml:mrow><mml:mi>Nd</mml:mi><mml:msub><mml:mi>Ir</mml:mi><mml:mi><mml:m Physical Review B, 2019, 99, .	1.1	4
32341	Fermi surface properties of the bifunctional organic metal <mml:math xmlns:mml="http://www.w3.org/1998/Math/MathML"><mml:mrow><mml:mi>Î²</mml:mi><mml:mtext>â^'</mml:mtext><mml:msub> mathvariant="normal">N</mml:mi><mml:msub><mml:mrow><mml:mo>(</mml:mo><mml:mi>CN</mml:mi><mml:mo>)</mml:mo> Physical Review B, 2019, 99, .	1.1	3
32342	Anharmonic and Anomalous Trends in the High-Pressure Phase Diagram of Silicon. Physical Review Letters, 2019, 122, 125701.	2.9	15
32343	A Preview of a Construction of a Crystal Lattice Based on Intermolecular Interactions. Crystals, 2019, 9, 159.	1.0	0
32344	C H versus O H bond scission in methanol decomposition on Pt(111): Role of the dispersion interaction. Applied Surface Science, 2019, 481, 1327-1334.	3.1	17
32345	Computational study of electronic and optical properties of p-group atomic adsorption on Î±-Al2O3 (0001). Computational and Theoretical Chemistry, 2019, 1155, 101-108.	1.1	5

#	Article	IF	Citations
32346	Theoretical understanding of atomic and electronic structures of the ZrC(111)/Cu(111) interface. Journal of Alloys and Compounds, 2019, 791, 431-437.	2.8	23
32347	Fluorescent silicon nanomaterials: from synthesis to functionalization and application. Nano Today, 2019, 26, 149-163.	6.2	53
32348	H₂ Dissociation on Noble Metal Single Atom Catalysts Adsorbed on and Doped into CeO₂ (111). Journal of Physical Chemistry C, 2019, 123, 9875-9883.	1.5	33
32349	BX₁â€“BX₂ (X₁, X₂ = P, As, Sb) lateral heterostructure: novel and efficient two-dimensional photovoltaic materials with ultra-high carrier mobilities. Journal of Materials Chemistry A, 2019, 7, 10684-10695.	5.2	30
32350	Theoretical assessment of wettability on silane coatings: from hydrophilic to hydrophobic. Physical Chemistry Chemical Physics, 2019, 21, 8257-8263.	1.3	4
32351	Grain-boundary segregation of 3d-transition metal solutes in bcc Fe: ab initio local-energy and d-electron behavior analysis. Journal of Physics Condensed Matter, 2019, 31, 115001.	0.7	23
32352	New Strategy to Overcome the Instability That Could Speed up the Commercialization of Perovskite Solar Cells. Advanced Materials Interfaces, 2019, 6, 1900134.	1.9	11
32353	Two-dimensional haeckelite h567: A promising high capacity and fast Li diffusion anode material for lithium-ion batteries. Carbon, 2019, 148, 344-353.	5.4	59
32354	First-principles study on the structure and electronic properties of Ge2H2 and Ge2Li2 nanosheets under electric fields. Physica B: Condensed Matter, 2019, 567, 95-99.	1.3	4
32355	Mass Transfer of Divalent Ions in an Oxide Host: Comparison of Mg²⁺ and Zn²⁺ Diffusion in Hexagonal K_xW₃O₉ Bronze. Chemistry of Materials, 2019, 31, 2296-2307.	3.2	11
32356	Structural and Electronic Properties of Double-Walled Black Phosphorene Nanotubes: A Density Functional Theory Study. Journal of Physical Chemistry C, 2019, 123, 7217-7224.	1.5	12
32357	Reinterpretation of Single-Wall Carbon Nanotubes by Raman Spectroscopy. Journal of Physical Chemistry C, 2019, 123, 14003-14009.	1.5	25
32358	Heterogeneous Additive-Free Hydroboration of Alkenes Using Cuâ€“Ni/Al₂O₃: Concerted Catalysis Assisted by Acidâ€“Base Properties and Alloying Effects. ACS Catalysis, 2019, 9, 5096-5103.	5.5	22
32359	The effect of protons on the Mg²⁺ migration in an Î±-V₂O₅ cathode for magnesium batteries: a first-principles investigation. Physical Chemistry Chemical Physics, 2019, 21, 7406-7411.	1.3	18
32360	MoSSe nanotube: a promising photocatalyst with an extremely long carrier lifetime. Journal of Materials Chemistry A, 2019, 7, 7885-7890.	5.2	52
32361	SIMPLE code: Optical properties with optimal basis functions. Computer Physics Communications, 2019, 240, 106-119.	3.0	21
32362	Tuning the n-type contact of graphene on Janus MoSSe monolayer by strain and electric field. Physica E: Low-Dimensional Systems and Nanostructures, 2019, 110, 148-152.	1.3	20
32363	Quantifying the Impact of Magnesium on the Stability and Water Binding Energy of Hydrated Calcium Carbonates by Ab Initio Thermodynamics. Journal of Physical Chemistry A, 2019, 123, 2908-2923.	1.1	11

#	Article	IF	Citations
32364	Effect of encapsulation on electronic transport properties of nanoscale Cu(111) films. Scientific Reports, 2019, 9, 3488.	1.6	5
32365	First-principles calculations of photoluminescence and defect states of <mml:math xmlns:mml="http://www.w3.org/1998/Math/MathML"><mml:mrow><mml:mi mathvariant="normal">C</mml:mi><mml:msup><mml:mrow><mml:mi mathvariant="normal">e</mml:mi></mml:mrow><mml:mrow><mml:mn>3</mml:mn><mml:mo>+</mml:mo></mml:mrow></mml:msup> -doped <mml:math		

#	Article	IF	Citations
32382	Enhanced photocatalysis for water splitting in layered tin chalcogenides with high carrier mobility. Physical Chemistry Chemical Physics, 2019, 21, 7559-7566.	1.3	36
32383	The electric field modulation of electronic properties in a type-II phosphorene/PbI₂ van der Waals heterojunction. Physical Chemistry Chemical Physics, 2019, 21, 7765-7772.	1.3	25
32384	Unique Thickness-Dependent Properties of the van der Waals Interlayer Antiferromagnet <mml:math xmlns:mml="http://www.w3.org/1998/Math/MathML" display="inline"><mml:mrow><mml:msub><mml:mrow><mml:mi>MnBi</mml:mi></mml:mrow><mml:mrow><mml:mn>2</mml:mn></mml:mrow></mml:msub></mml:mrow></mml:math> Films. Physical Review Letters, 2019, 122, 107202.	2.9	415
32385	Itinerant ferromagnetism induced by electron doping in SrCo2As2. Inorganic Chemistry Communication, 2019, 103, 25-29.	1.8	6
32386	A theoretical investigation of ThCr2Si2-type Pd-based superconductors XPd2Ge2 (Xâ€¯=â€¯Ca, Sr, La, Nd). Physica C: Superconductivity and Its Applications, 2019, 561, 35-44.	0.6	9
32387	Structural, vibrational and optoelectronic properties of buckled metallic FeGe monolayer. Superlattices and Microstructures, 2019, 129, 62-68.	1.4	3
32388	Computational MitoTarget Scanning Based on Topological Vacancies of Single-Walled Carbon Nanotubes with the Human Mitochondrial Voltage-Dependent Anion Channel (hVDAC1). Chemical Research in Toxicology, 2019, 32, 566-577.	1.7	4
32389	Enhancing the Dynamics of Water Confined between Graphene Oxide Surfaces with Janus Interfaces: A Molecular Dynamics Study. Journal of Physical Chemistry B, 2019, 123, 2978-2993.	1.2	24
32390	Theoretical Insights of Ni₂P (0001) Surface toward Its Potential Applicability in CO₂ Conversion via Dry Reforming of Methane. ACS Catalysis, 2019, 9, 3487-3497.	5.5	36
32391	IrF₈ Molecular Crystal under High Pressure. Journal of the American Chemical Society, 2019, 141, 5409-5414.	6.6	40
32392	Double-well potential energy surface in the interaction between h-BN and Ni(111). Physical Chemistry Chemical Physics, 2019, 21, 10888-10894.	1.3	7
32393	Insulating titanium oxynitride for visible light photocatalysis. Physical Review B, 2019, 99, .	1.1	12
32394	Dependence of Carbon Concentration and Alloying Elements on the Stability of Iron Carbides. ISIJ International, 2019, 59, 1128-1135.	0.6	16
32395	Theoretical Study of As2O3 Adsorption Mechanisms on CaO surface. Materials, 2019, 12, 677.	1.3	29
32396	DFT Computed Dielectric Response and THz Spectra of Organic Co-Crystals and Their Constituent Components. Molecules, 2019, 24, 959.	1.7	2
32397	The Modulation Effect of MoS2 Monolayers on the Nucleation and Growth of Pd Clusters: First-Principles Study. Nanomaterials, 2019, 9, 395.	1.9	13
32398	Mechanistic Insights into the Formation of Lithium Fluoride Nanotubes. Chemistry - A European Journal, 2019, 25, 5269-5279.	1.7	4
32399	Understanding the Thermodynamics and Crystal Structure of Complex Fe Containing Intermetallic Phases Formed on Solidification of Aluminium Alloys. Jom, 2019, 71, 1731-1736.	0.9	14

#	Article	IF	Citations
32400	Dispersoid composition in zirconium containing Al-Zn-Mg-Cu (AA7010) aluminium alloy. Acta Materialia, 2019, 169, 135-146.	3.8	51
32401	Electronic correlation and spin-orbit coupling in J1-J2 square lattice antiferromagnetism MoOPO4. Journal of Applied Physics, 2019, 125, .	1.1	2
32402	Adsorption behaviors of ether and aluminum surface: A molecular dynamics study. International Journal of Modern Physics B, 2019, 33, 1950028.	1.0	6
32403	Flexible and Ultrasoft Inorganic 1D Semiconductor and Heterostructure Systems Based on SnIP. Advanced Functional Materials, 2019, 29, 1900233.	7.8	37
32404	Thermodynamic stability and pressure dependence of FePO4 polymorphs. Computational and Theoretical Chemistry, 2019, 1155, 67-74.	1.1	12
32405	Role of coupling between surface orbitals in SOC enhanced spin splitting. Surface Science, 2019, 684, 12-17.	0.8	4
32406	Free Energies of Catalytic Species Adsorbed to Pt(111) Surfaces under Liquid Solvent Calculated Using Classical and Quantum Approaches. Journal of Chemical Information and Modeling, 2019, 59, 2190-2198.	2.5	37
32407	Modeling of Nanosheets Based on Transition-Metal Dichalcogenides for Spintronic Applications: Insights From First-Principles. , 2019, , 207-218.		4
32408	Local Lattice Strains Around Alloying Elements in Metals. , 2019, , 221-260.		1
32409	Theoretical realization of two-dimensional M3(C6X6)2 (M = Co, Cr, Cu, Fe, Mn, Ni, Pd, Rh and X = O, S,) Tj ETQq1 1 0.784314 rgBT /O	2.3	37
32410	Simple and Cost-Effective Approach To Dramatically Enhance the Durability and Capability of a Layered Î´-MnO₂ Based Electrode for Pseudocapacitors: A Practical Electrochemical Test and Mechanistic Revealing. ACS Applied Energy Materials, 2019, 2, 2743-2750.	2.5	17
32411	Orbital magneto-optical response of periodic insulators from first principles. Npj Computational Materials, 2019, 5, .	3.5	5
32412	The effect of Fe vacancies and Cu adhesion on the magnetic properties of Fe₃GeTe₂. Physical Chemistry Chemical Physics, 2019, 21, 7588-7593.	1.3	11
32413	Bilayer phosphorene under high pressure: in situ Raman spectroscopy. Physical Chemistry Chemical Physics, 2019, 21, 7298-7304.	1.3	19
32414	Effect of addition of Co on the magnetic properties of MnSb. AIP Advances, 2019, 9, 035217.	0.6	4
32415	Unusual Fermiâ€Level Pinning and Ohmic Contact at Monolayer Bi 2 O 2 Seâ€“Metal Interface. Advanced Theory and Simulations, 2019, 2, 1800178.	1.3	20
32416	Identification of Phase Control of Carbonâ€Confined Nb₂O₅ Nanoparticles toward Highâ€Performance Lithium Storage. Advanced Energy Materials, 2019, 9, 1802695.	10.2	161
32417	The Solâ€“gel method synthesis of Bi4NbO8Cl with (001) facets exposed for high visible-light activity. Journal of Materials Science: Materials in Electronics, 2019, 30, 7907-7915.	1.1	4

#	Article	IF	Citations
32418	Materials Discovery of Stable and Nontoxic Halide Perovskite Materials for Highâ€Efficiency Solar Cells. Advanced Functional Materials, 2019, 29, 1804354.	7.8	61
32419	Pressureâ€Induced Formation of Quaternary Compound and Inâ^'N Distribution in InGaAsN Zincblende from Ab Initio Calculation. ChemistryOpen, 2019, 8, 393-398.	0.9	8
32420	DFT investigation of metal doped graphene capacity for adsorbing of ozone, nitrogen dioxide and sulfur dioxide molecules. Adsorption, 2019, 25, 661-667.	1.4	11
32421	Single-layer Ag6S2: First principles investigation of a new two-dimensional direct bandgap semiconductor. Computational Materials Science, 2019, 163, 278-281.	1.4	13
32422	Cooper pair distribution function of misaligned graphene sheets and determination of superconducting properties. Diamond and Related Materials, 2019, 95, 109-114.	1.8	5
32423	Improving hydrogen evolution activity of perovskite BaTiO3 with Mo doping: Experiments and first-principles analysis. International Journal of Hydrogen Energy, 2019, 44, 11695-11704.	3.8	34
32424	Two-dimensional copper nanosheets for electrochemical reduction of carbon monoxide to acetate. Nature Catalysis, 2019, 2, 423-430.	16.1	368
32425	Synthesis of large-scale few-layer PtS2 films by chemical vapor deposition. AIP Advances, 2019, 9, .	0.6	42
32426	Spin structure and optical properties of cobalt octaethylporphyrin. Modern Physics Letters B, 2019, 33, 1950134.	1.0	0
32427	DFT study of CuCoMnX (X = Si, Sn, Sb) quaternary Heusler alloys for phonon spectra. Modern Physics Letters B, 2019, 33, 1950155.	1.0	4
32428	Molecular dynamics study of a new metastable allotropic crystalline form of galliumâ€"supertetrahedral gallium. Journal of Computational Chemistry, 2019, 40, 1861-1865.	1.5	4
32429	QTAIM method for accelerated prediction of band gaps in perovskites. Theoretical Chemistry Accounts, 2019, 138, 1.	0.5	5
32430	Strain Modulated Optoelectronic Properties of CdO Monolayer. Journal of Electronic Materials, 2019, 48, 3963-3969.	1.0	15
32431	The Effect of Pressure on Elastic Anisotropy, Vibration and Optical Properties of a AgScSi Compound. Journal of Electronic Materials, 2019, 48, 4050-4056.	1.0	9
32432	Thermodynamic modelling of Al-B-N system. Calphad: Computer Coupling of Phase Diagrams and Thermochemistry, 2019, 65, 291-298.	0.7	9
32433	Co, Fe, and Mn in La-perovskite oxides for low temperature thermochemical CO2 conversion. Catalysis Today, 2019, 338, 52-59.	2.2	40
32434	Hydrogen chloride adsorption on large defective PAHs modeling soot surfaces and influence on water trapping: A DFT and AIMD study. Chemical Physics, 2019, 523, 18-27.	0.9	9
32435	First-principles study on the structural, elastic, electronic and optical properties of LiNbO3. Heliyon, 2019, 5, e01436.	1.4	43

#	Article	IF	Citations
32436	Physical properties of alkali metals-based iodides via Ab-initio calculations. Journal of Physics and Chemistry of Solids, 2019, 132, 68-75.	1.9	6
32437	The physical properties of ThCr2Si2-type Ru-based compounds SrRu2X2 (X = P, Ge, As): An ab-inito investigation. Physica C: Superconductivity and Its Applications, 2019, 562, 48-55.	0.6	4
32438	The effect of Al and Cr elements on the oxidation resistance of MoSi2 via first-principles calculation. Progress in Natural Science: Materials International, 2019, 29, 65-70.	1.8	8
32439	A Guideline for Tailoring Lattice Oxygen Activity in Lithium-Rich Layered Cathodes by Strain. Journal of Physical Chemistry Letters, 2019, 10, 2202-2207.	2.1	6
32440	Selective Oxidation of Acetaldehyde to Acetic Acid on Pdâ€“Au Bimetallic Model Catalysts. ACS Catalysis, 2019, 9, 4360-4368.	5.5	26
32441	The adsorption properties of Fe, Co, and Ni atoms onÎ±-WC(0001) surface: a first principles study. Materials Research Express, 2019, 6, 075609.	0.8	3
32442	Identification of a monoclinic metallic state in VO2 from a modified first-principles approach. Modern Physics Letters B, 2019, 33, 1950148.	1.0	0
32443	Moderate Adsorption of Oxygen Molecular Induced Better Performance of Oxygen Reduction Reaction. Journal of the Electrochemical Society, 2019, 166, F386-F392.	1.3	8
32444	A Comprehensive Study on the Reductive Amination of 5â€Hydroxymethylfurfural into 2,5â€Bisaminomethylfuran over Raney Ni Through DFT Calculations. ChemCatChem, 2019, 11, 2649-2656.	1.8	43
32445	Role of defects in tuning the adsorption of CO over graphene-supported Co13 cluster. Applied Surface Science, 2019, 481, 1080-1088.	3.1	16
32446	Superconductivity at 23â€¯K in MgLi compound at ultrahigh pressure. Computational Materials Science, 2019, 164, 158-165.	1.4	0
32447	A framework for optimizing oxygen vacancy formation in doped perovskites. Computers and Chemical Engineering, 2019, 126, 168-177.	2.0	20
32448	Theoretical investigation of antisymmetric spin-orbit coupling effect on the physical properties of noncentrosymmetric BaPtSb superconductor. Intermetallics, 2019, 108, 109-116.	1.8	7
32449	Electronic and magnetic properties of MoS2 monolayers with antisite defects. Journal of Physics and Chemistry of Solids, 2019, 131, 119-124.	1.9	15
32450	Phase stability and physical properties of (Zr1-Nb)2AlC MAX phases. Journal of Physics and Chemistry of Solids, 2019, 132, 38-47.	1.9	32
32451	Electronic structures of two-dimensional hydrogenated bilayer diamond films with Si dopant and Si-V center. Results in Physics, 2019, 13, 102240.	2.0	14
32452	Elastic properties of the Î±' martensitic phase in the Ti-6Al-4V alloy obtained by additive manufacturing. Scripta Materialia, 2019, 167, 115-119.	2.6	32
32453	MgCu2-type laves phases CaPt2, SrPd2 and SrPt2: A DFT based ab-initio investigation. Solid State Communications, 2019, 296, 1-7.	0.9	4

#	Article	IF	Citations
32454	First-principles study on magnetoelectric coupling effect of M/BiFeO3 (M = Co, Fe) multiferroic superlattice. Vacuum, 2019, 165, 105-112.	1.6	43
32455	Effect of trace Ni on the resistance of high-Cr cast iron to slurry erosion. Wear, 2019, 426-427, 605-611.	1.5	11
32456	RuN₄ Doped Graphene Oxide, a Highly Efficient Bifunctional Catalyst for Oxygen Reduction and CO₂ Reduction from Computational Study. ACS Sustainable Chemistry and Engineering, 2019, 7, 8136-8144.	3.2	29
32457	In-situ local phase-transitioned MoSe2 in La0.5Sr0.5CoO3-Î´ heterostructure and stable overall water electrolysis over 1000 hours. Nature Communications, 2019, 10, 1723.	5.8	143
32458	Dual effect of humidity on cesium lead bromide: enhancement and degradation of perovskite films. Journal of Materials Chemistry A, 2019, 7, 12292-12302.	5.2	74
32459	In situ exsolved FeNi₃ nanoparticles on nickel doped Sr₂Fe_{1.5}Mo_{0.5}O_{6â^'Î´} perovskite for efficient electrochemical CO₂ reduction reaction. Journal of Materials Chemistry A, 2019, 7, 11967-11975.	5.2	159
32460	First Principle Calculation of Electromagnetic Mechanism for Fe2Si Bulk Material. Journal Wuhan University of Technology, Materials Science Edition, 2019, 34, 64-68.	0.4	3
32461	Mechanisms of Transforming CHx to CO on Ni(111) Surface by Density Functional Theory. Transactions of Tianjin University, 2019, 25, 330-339.	3.3	2
32462	Effect of doping Hf on the hydrogen dissociation and diffusion mechanism on the ZrCo (110) surface. Applied Surface Science, 2019, 483, 383-390.	3.1	23
32463	Ab initio study on the role of the crystalline symmetry in the stabilization of the magnetic order in Al-doped SnS. Journal of Magnetism and Magnetic Materials, 2019, 484, 146-153.	1.0	3
32464	SnTe monolayer: Tuning its electronic properties with doping. Superlattices and Microstructures, 2019, 130, 12-19.	1.4	8
32465	MBe20N14:Eu2+ (M = Sr, Ba): Highly Condensed Nitridoberyllates with Exceptional Highly Energetic Eu2+ Luminescence. Chemistry of Materials, 2019, 31, 3174-3182.	3.2	24
32466	Correlation between Composition and Mechanical Properties of Calcium Silicate Hydrates Identified by Infrared Spectroscopy and Density Functional Theory. Journal of Physical Chemistry C, 2019, 123, 10868-10873.	1.5	25
32467	New Phosphorene by Phase Combination with Tunable Electronic and Mechanical Properties. Journal of Physical Chemistry C, 2019, 123, 10788-10794.	1.5	13
32468	Application of the CLAYFF and the DREIDING Force Fields for Modeling of Alkylated Quartz Surfaces. Langmuir, 2019, 35, 5746-5752.	1.6	15
32469	Exploration of Long-Life Pt/Heteroatom-Doped Graphene Catalysts in Hydrogen Atmosphere. ACS Omega, 2019, 4, 6573-6584.	1.6	2
32470	Structural, electronic, and optical properties of Î±-Te tubular nanostructures: A first-principles study. APL Materials, 2019, 7, .	2.2	8
32471	Scalable and efficient Sb2S3 thin-film solar cells fabricated by close space sublimation. APL Materials, 2019, 7, .	2.2	72

#	Article	IF	Citations
32472	Dislocation structures, interfacing, and magnetism in the L10â^' MnGa on Î·âŠ¥â^' Mn3N2 bilayer. Journal of Vacuum Science and Technology A: Vacuum, Surfaces and Films, 2019, 37, 031102.	0.9	8
32473	Magnification Effects in Scanning Tunneling Microscopy: the Role of Surface Radicals. Journal of Experimental and Theoretical Physics, 2019, 128, 94-97.	0.2	2
32474	van der Waals exchange-correlation functionals over bulk and surface properties of transition metals. Journal of Physics Condensed Matter, 2019, 31, 315501.	0.7	10
32475	Main-group test set for materials science and engineering with user-friendly graphical tools for error analysis: systematic benchmark of the numerical and intrinsic errors in state-of-the-art electronic-structure approximations. New Journal of Physics, 2019, 21, 013025.	1.2	15
32476	Electronic structure and magnetic ordering of NiN and Ni ₂ N from first principles. Electronic Structure, 2019, 1, 015002.	1.0	6
32477	Precipitation, planar defects and dislocations in alloys: Simulations on Ni3Si and Ni3Al precipitates. European Physical Journal: Special Topics, 2019, 227, 1559-1574.	1.2	6
32478	Strain-dependent electronic structure and optical properties of monolayer indium selenide: A density functionalâ€¯+â€¯tight-binding modelâ€¯+â€¯many-body perturbation theory study. FlatChem, 2019, 15, 100092.	2.8	3
32479	First-principle study of metal-organic frameworks of the 4d and 5d transition metal series with phthalocyanine and tetracyanobenzene. Superlattices and Microstructures, 2019, 130, 122-126.	1.4	3
32480	Modification of Electrical and Magnetic Properties of Fe₃O₄ Epitaxial Thin Films by Nitrogen Substitution for Oxygen. ACS Applied Electronic Materials, 2019, 1, 595-599.	2.0	3
32481	Stretchable and dynamically stable promising two-dimensional thermoelectric materials: ScPÂand ScAs. Journal of Materials Chemistry A, 2019, 7, 12604-12615.	5.2	40
32482	Novel two-dimensional molybdenum carbides as high capacity anodes for lithium/sodium-ion batteries. Journal of Materials Chemistry A, 2019, 7, 12145-12153.	5.2	106
32483	Structural and electronic properties of T graphene nanotubes: a first-principles study. New Journal of Physics, 2019, 21, 053015.	1.2	12
32484	Electronic, elastic and lattice dynamic properties of the topological Dirac semimetal Na₃Bi. Materials Research Express, 2019, 6, 076308.	0.8	4
32485	Double dependence of H diffusion in tungsten from first-principles determination: strain and temperature. Materials Research Express, 2019, 6, 075520.	0.8	1
32486	New insights on the GeSe _x Te_{1â^'x} phase diagram from theory and experiment. Acta Crystallographica Section B: Structural Science, Crystal Engineering and Materials, 2019, 75, 246-256.	0.5	6
32487	Diethanolamine and quaternium-15 interaction studies on antimonene nanosheet based on first-principles studies. Computational and Theoretical Chemistry, 2019, 1157, 19-27.	1.1	25
32488	Network topological model of reconstructive solid-state transformations. Scientific Reports, 2019, 9, 6007.	1.6	21
32489	Carboxylic acid-capped ruthenium nanoparticles: experimental and theoretical case study with ethanoic acid. Nanoscale, 2019, 11, 9392-9409.	2.8	19

#	Article	IF	Citations
32490	Structural, electronic, and dynamical properties of the tetragonal and collapsed tetragonal phases of KFe2As2. Physical Review B, 2019, 99, .	1.1	10
32491	Ab initio Study of Anchoring Groups for CuGaO2 Delafossite-Based p-Type Dye Sensitized Solar Cells. Frontiers in Chemistry, 2019, 7, 158.	1.8	15
32492	Oxygen Functionalization of Hexagonal Boron Nitride on Ni(111). Chemistry - A European Journal, 2019, 25, 8884-8893.	1.7	10
32493	Two-dimensional graphyne-like carbon nitrides: Moderate band gaps, high carrier mobility, high flexibility and type-II band alignment. Carbon, 2019, 149, 234-241.	5.4	38
32494	Dominant in-plane cleavage direction of CrPS4. Computational Materials Science, 2019, 162, 277-280.	1.4	6
32495	Theoretical predictions on intrinsic lattice thermal conductivity of ZrB2. Journal of the European Ceramic Society, 2019, 39, 2982-2988.	2.8	18
32496	Strain effects on the mechanical properties of Group-V monolayers with buckled honeycomb structures. Physica E: Low-Dimensional Systems and Nanostructures, 2019, 112, 59-65.	1.3	20
32497	Chemical Properties of Metal-Silicates Rendered by Metal Exchange Reaction. ACS Sustainable Chemistry and Engineering, 2019, 7, 8449-8457.	3.2	10
32498	Theoretical characterization of C doped SiGe monolayer. Journal of Applied Physics, 2019, 125, 145703.	1.1	4
32499	Polarization branches and optimization calculation strategy applied to ABO3 ferroelectrics. Modelling and Simulation in Materials Science and Engineering, 2019, 27, 045008.	0.8	5
32500	Bifunctional oxygen evolution and supercapacitor electrode with integrated architecture of NiFe-layered double hydroxides and hierarchical carbon framework. Nanotechnology, 2019, 30, 325402.	1.3	14
32501	Electrical resistivity of liquid expanded metals by Ziman approach. Journal of Physics: Conference Series, 2019, 1147, 012005.	0.3	1
32502	Diffusion of Alkali Metals in Polycrystalline CuInSe₂ and Their Role in the Passivation of Grain Boundaries. ACS Applied Materials & Interfaces, 2019, 11, 14821-14829.	4.0	23
32503	Novel graphene-like two-dimensional bilayer germanene dioxide: electronic structure and optical properties. RSC Advances, 2019, 9, 9633-9639.	1.7	4
32504	Penta-PdX₂ (X = S, Se, Te) monolayers: promising anisotropic thermoelectric materials. Journal of Materials Chemistry A, 2019, 7, 11134-11142.	5.2	117
32505	Bandgap tailoring of tetragonal BiFeO3 with different magnetic orders calculated by firstâ€“principles calculations. Materials Research Express, 2019, 6, 045907.	0.8	0
32506	DFT calculations on the structural and electronic properties of vacancy effects in the silicon nanowires. European Physical Journal B, 2019, 92, 1.	0.6	2
32507	Toward an Understanding of Capping Molecules on Pt Nanoparticles for Hydrogenation: the Key Role of Hydroxyl Groups. ChemistrySelect, 2019, 4, 3505-3514.	0.7	1

#	Article	IF	Citations
32508	Structural, Elastic, Electronic, and Magnetic Properties of a New Full-Heusler Alloy Mn2MgGe: First-Principles Calculations. Journal of Superconductivity and Novel Magnetism, 2019, 32, 3001-3008.	0.8	9
32509	Electronic and magnetic properties of Fe2â^'xCoxTiGe (xâ€¯=â€¯0, 0.5, 1, 1.5, 2) full Heusler alloys. Chinese Journal of Physics, 2019, 59, 166-174.	2.0	8
32510	Mechanism for the Structural Transformation to the Modulated Superconducting Phase of Compressed Hydrogen Sulfide. Scientific Reports, 2019, 9, 5023.	1.6	12
32511	Copperâ€"nitroxide based breathing crystals: a unified mechanism of gradual magnetostructural transition supported by quantum chemistry calculations. Inorganic Chemistry Frontiers, 2019, 6, 1228-1237.	3.0	5
32512	Hexagonal MASnI3 exhibiting strong absorption of ultraviolet photons. Applied Physics Letters, 2019, 114, .	1.5	5
32513	First principles study on new half-metallic ferromagnetic ternary zinc-based sulfide and telluride (Zn₃VS₄ and Zn₃VTe₄). Materials Research Express, 2019, 6, 076107.	0.8	5
32514	Evolution of elastic moduli through a two-dimensional structural transformation. Physical Review B, 2019, 99, .	1.1	12
32515	First-Principle Simulation of Ferromagnetism in Gd-Doped Mg₂X (X=Si, Ge and Sn). Spin, 2019, 09, .	0.6	2
32516	Understanding the thermal conductivity of Diamond/Copper composites by first-principles calculations. Carbon, 2019, 148, 249-257.	5.4	51
32517	First-principles study of a vertical spin switch in atomic scale two-dimensional platform. Journal of Magnetism and Magnetic Materials, 2019, 484, 462-471.	1.0	6
32518	First-principles study on the influence of compressive deformation on the oxygen adsorption energy and electrical properties of phosphorene. Physica B: Condensed Matter, 2019, 563, 72-78.	1.3	2
32519	First-principles calculations of iodine-related point defects in CsPbI₃. Physical Chemistry Chemical Physics, 2019, 21, 7841-7846.	1.3	29
32520	Defect structure in Î´-Bi₅PbY₂O_{11.5}. RSC Advances, 2019, 9, 9640-9653.	1.7	6
32521	First principles study of H₂ adsorption on Ni-decorated silicene. Materials Research Express, 2019, 6, 055509.	0.8	12
32522	Surface properties enhanced MnxAlO oxide catalysts derived from MnxAl layered double hydroxides for acetone catalytic oxidation at low temperature. Applied Catalysis B: Environmental, 2019, 251, 295-304.	10.8	62
32523	Understanding the role of Au in the selective hydrogenation of acetylene on trimetallic PdAgAu catalytic surface. Catalysis Communications, 2019, 124, 41-45.	1.6	16
32524	Kinetic study on the anisotropic grain growth of elongated iron-containing mullite. Ceramics International, 2019, 45, 12934-12941.	2.3	9
32525	Reaction mechanism and kinetics for Pt/CNTs catalyzed base-free oxidation of glycerol. Chemical Engineering Science, 2019, 203, 228-236.	1.9	32

#	Article	IF	Citations
32526	Lattice Green function methods for atomistic/continuum coupling: Theory and data-sparse implementation. Computer Methods in Applied Mechanics and Engineering, 2019, 348, 1039-1075.	3.4	6
32527	Electronic and structural properties of vacancy endowed BCN heterostructures. Chemical Physics Letters, 2019, 724, 103-109.	1.2	7
32528	Integrated modeling of molar volume of the sigma phase aided by first-principles calculations. Journal of Alloys and Compounds, 2019, 791, 994-1004.	2.8	6
32529	Structural and electronic properties of the Î±-GeSe surface. Surface Science, 2019, 686, 17-21.	0.8	4
32530	Spin-polarized electronic surface states of Re(0001): An ab-initio investigation. Surface Science, 2019, 686, 22-29.	0.8	7
32531	Structureâ€“Property Correlation Studies of Potassium 4,4â€²-Bis(dinitromethyl)-3,3â€²-azofurazanate: A Noncentrosymmetric Primary Explosive. Journal of Physical Chemistry C, 2019, 123, 10034-10050.	1.5	10
32532	Metalâ€“polymer hybrid nanomaterials for plasmonic ultrafast hydrogen detection. Nature Materials, 2019, 18, 489-495.	13.3	227
32533	A new device concept for bacterial sensing by Raman spectroscopy and voltage-gated monolayer graphene. Nanoscale, 2019, 11, 8528-8537.	2.8	15
32534	Stability and band offsets between GaAs semiconductor and CeO2 gate dielectric. AIP Advances, 2019, 9, 025117.	0.6	4
32535	Solid state properties of hydroxyurea: Optical absorption measurement and DFT calculations. Journal of Applied Physics, 2019, 125, 134901.	1.1	4
32536	High-pressure characterization of the optical and electronic properties of InVO4, InNbO4, and InTaO4. SN Applied Sciences, 2019, 1, 1.	1.5	42
32537	Improving the electrochemical oxidation of formic acid by tuning the electronic properties of Pd-based bimetallic nanoparticles. Applied Catalysis B: Environmental, 2019, 254, 685-692.	10.8	73
32538	Two-dimensional blue-phosphorene-phase germanium monochalcogenide photocatalysts for water splitting: From ultraviolet to visible absorption. Journal of Catalysis, 2019, 373, 67-74.	3.1	26
32539	Experimental and DFT study of CoCuMo ternary ionic activator for alkaline HER on Ni cathode. Journal of Electroanalytical Chemistry, 2019, 839, 224-230.	1.9	2
32540	High-throughput first-principles investigation of GaN-AlN ternary system. Superlattices and Microstructures, 2019, 129, 226-229.	1.4	3
32541	Electronic structure evolution at DBBA/Au(111) interface W/O Bismuth insertion layer. Synthetic Metals, 2019, 251, 24-29.	2.1	10
32542	BaHgGeSe₄ and SrHgGeSe₄: Two New Hg-Based Infrared Nonlinear Optical Materials. Chemistry of Materials, 2019, 31, 3034-3040.	3.2	104
32543	Growth Kinetics of Individual Co Particles Ex-solved on SrTi_{0.75}Co_{0.25}O_{3-Î´} Polycrystalline Perovskite Thin Films. Journal of the American Chemical Society, 2019, 141, 6690-6697.	6.6	75

#	Article	IF	Citations
32544	Layered Tl₂O: a model thermoelectric material. Journal of Materials Chemistry C, 2019, 7, 5094-5103.	2.7	46
32545	Electronic and magnetic properties of the one-dimensional interfaces of two-dimensional lateral GeC/BP heterostructures. Physical Chemistry Chemical Physics, 2019, 21, 8856-8864.	1.3	7
32546	Electronic Structure and Optical Property Calculation of an Oxygen Vacancy in NH 4 H 2 PO 4 Crystals *. Chinese Physics Letters, 2019, 36, 037801.	1.3	1
32547	Mapping multi-valley Lifshitz transitions induced by field-effect doping in strained MoS₂ nanolayers. Journal of Physics Condensed Matter, 2019, 31, 114002.	0.7	13
32548	Local magnetism, magnetic order and spin freezing in the â€˜nonmetallic metalâ€™ FeCrAs. Journal of Physics Condensed Matter, 2019, 31, 285803.	0.7	8
32549	Optical, charge transport and magnetic properties of palladium retrieved from photometric measurements: approaching the quantum mechanics background. Physica Scripta, 2019, 94, 055101.	1.2	3
32550	First-principles investigations on the visible light photocatalytic activity of NaNbO3 by N and F doping. European Physical Journal B, 2019, 92, 1.	0.6	4
32551	Effects of Hydrostatic Pressure and Biaxial Strains on the Elastic, Electronic and Lattice Vibrational Properties of Trigonal Boron Nitride. Physica Status Solidi (B): Basic Research, 2019, 256, 1800699.	0.7	2
32552	Functionalization of silicene and silicane with benzaldehyde. Journal of Molecular Modeling, 2019, 25, 109.	0.8	8
32553	Grain growth and solid-state dewetting of Bi-Crystal Ni-Fe thin films on sapphire. Acta Materialia, 2019, 168, 237-249.	3.8	17
32554	First-principles study, fabrication and characterization of (Zr0.25Nb0.25Ti0.25V0.25)C high-entropy ceramics. Acta Materialia, 2019, 170, 15-23.	3.8	294
32555	Thermodynamic and physical properties of Zr3Fe and ZrFe2 intermetallic compounds. Intermetallics, 2019, 109, 189-196.	1.8	14
32556	P doped MoS2 nanoplates embedded in nitrogen doped carbon nanofibers as an efficient catalyst for hydrogen evolution reaction. Journal of Colloid and Interface Science, 2019, 547, 291-298.	5.0	33
32557	Physical properties of ThCr2Si2-type Ni-based compounds SrNi2M2 (M= As and Ge): DFT based Ab-inito calculations. Physica C: Superconductivity and Its Applications, 2019, 560, 19-25.	0.6	2
32558	Intermediate band insertion by group-IIIA elements alloying in a low cost solar cell absorber CuYSe2: A first-principles study. Physics Letters, Section A: General, Atomic and Solid State Physics, 2019, 383, 1972-1976.	0.9	6
32559	Chlorine Passivation of Grain Boundary Suppresses Electronâ€“Hole Recombination in CsPbBr₃ Perovskite by Nonadiabatic Molecular Dynamics Simulation. ACS Applied Energy Materials, 2019, 2, 3419-3426.	2.5	32
32560	Intercalation of first row transition metals inside covalent-organic frameworks (COFs): a strategy to fine tune the electronic properties of porous crystalline materials. Physical Chemistry Chemical Physics, 2019, 21, 8785-8796.	1.3	28
32561	The importance of phase equilibrium for doping efficiency: iodine doped PbTe. Materials Horizons, 2019, 6, 1444-1453.	6.4	42

#	Article	IF	Citations
32562	MnB₂ nanosheet and nanotube: stability, electronic structures, novel functionalization and application for Li-ion batteries. Nanoscale, 2019, 11, 7857-7865.	2.8	18
32563	DFT calculations of energetic stability and geometry of O-terminated B- and N-doped diamond (1â€‰1â€‰1)-1â€‰â€‰Ã—â€‰â€‰ surfaces. Journal of Physics Condensed Matter, 2019, 31, 265002.	0.7	6
32564	Correlative Experimental and Theoretical Investigation of the Angle-Resolved Composition Evolution of Thin Films Sputtered from a Compound Mo2BC Target. Coatings, 2019, 9, 206.	1.2	10
32565	Predicting Adsorption Properties of Catalytic Descriptors on Bimetallic Nanoalloys with Site-Specific Precision. Journal of Physical Chemistry Letters, 2019, 10, 1852-1859.	2.1	41
32566	Quantum Enhancement of Charge Density Wave in NbS₂ in the Two-Dimensional Limit. Nano Letters, 2019, 19, 3098-3103.	4.5	62
32567	Synergic effect of adsorbed gas and charging on surface flashover. Scientific Reports, 2019, 9, 5464.	1.6	35
32568	The Effect of Dopants on Diamond Surface Properties and Growth. Topics in Applied Physics, 2019, , 31-52.	0.4	0
32569	Elastic, piezoelectric and thermal properties of zinc-blende AlN under pressure. Theoretical Chemistry Accounts, 2019, 138, 1.	0.5	11
32570	Origin of the R(15â€¯Ã—â€¯3) surface reconstruction of carburized W(110) - revisited. Surface Science, 2019, 682, 33-37.	0.8	3
32571	Different doping of penta-graphene as adsorbent and gas sensing material for scavenging and detecting SF6 decomposed species. Sustainable Materials and Technologies, 2019, 21, e00100.	1.7	11
32572	Structural, electronic, optical and lattice dynamic properties of the different WO3 phases: First-principle calculation. Vacuum, 2019, 164, 411-420.	1.6	37
32573	Two Deep Ultraviolet Hydrated Borate Crystals: Centrosymmetric LiRbB₅O₈(OH)Â·H₂O and Non-Centrosymmetric K₂B₅O₈(OH)Â·2H₂O. Crystal Growth and Design, 2019, 19, 3052-3059.	1.4	5
32574	Influence of Cobalt Crystal Structures on Activation of Nitrogen Molecule: A First-Principles Study. Journal of Physical Chemistry C, 2019, 123, 10956-10966.	1.5	19
32575	Anomalously Low Barrier for Water Dimer Diffusion on Cu(111). Nano Letters, 2019, 19, 3049-3056.	4.5	20
32576	Noble gas as a functional dopant in ZnO. Npj Computational Materials, 2019, 5, .	3.5	9
32577	Ligand induced structure and property changes of 1T-MoS2. Physical Chemistry Chemical Physics, 2019, 21, 9391-9398.	1.3	15
32578	General scaling relations and prediction of transition state energies in CHA/AlPO-34-structured zeolite catalysis related to the methanol-to-olefins conversion. Catalysis Science and Technology, 2019, 9, 2245-2252.	2.1	13
32579	Bandgap engineering of PbTe ultra-thin layers by surface passivations. Journal of Physics Condensed Matter, 2019, 31, 295503.	0.7	2

#	Article	IF	Citations
32580	Electronic properties of several two dimensional halides from ab initio calculations. Beilstein Journal of Nanotechnology, 2019, 10, 823-832.	1.5	24
32581	Modeling halogen bonding with planewave density functional theory: Accuracy and challenges. Journal of Computational Chemistry, 2019, 40, 1829-1835.	1.5	6
32582	The effect of surface vacancies on the interactions of Cl with a Î±-Fe2O3 (0001) surface and the role of Cl in depassivation. Corrosion Science, 2019, 154, 61-69.	3.0	30
32583	Oxygen-vacancies-engaged efficient carrier utilization for the photocatalytic coupling reaction. Journal of Catalysis, 2019, 373, 116-125.	3.1	33
32584	First-principles investigation of electronic structure and derived structural and magnetic properties of HgTe alloyed with Mn transition metal. Solid State Communications, 2019, 295, 26-31.	0.9	8
32585	Predicting two-dimensional pentagonal transition metal monophosphides for efficient electrocatalytic nitrogen reduction. Journal of Materials Chemistry A, 2019, 7, 11444-11451.	5.2	49
32586	Effect of M elements (Mâ€‰â€‰=â€‰â€‰Ti, Zr, and Hf) on thermoelectric performance of the half-Heusler compounds MCoBi. Journal Physics D: Applied Physics, 2019, 52, 255501.	1.3	26
32587	Equation of state of boron nitride combining computation, modeling, and experiment. Physical Review B, 2019, 99, .	1.1	28
32588	Stability of graphite-like ZnO film with Cu doping: First principle study. European Physical Journal Plus, 2019, 134, 1.	1.2	3
32589	Ab initio investigation of the optical properties of layered MoSxSe(2âˆ’x) (0 â‰‰ x â‰‰ 2): By GGA and mBJ approaches. International Journal of Modern Physics B, 2019, 33, 1950062.	1.0	1
32590	Electronic and Vibrational Properties of LiBO2 Crystals. Russian Physics Journal, 2019, 61, 1868-1875.	0.2	8
32591	Novel 2D materials from exfoliation of layered hydroxide salts: A theoretical study. Applied Surface Science, 2019, 483, 762-771.	3.1	14
32592	Physical properties of Ima2-BN under pressure: First principles calculations. Chinese Journal of Physics, 2019, 59, 317-324.	2.0	22
32593	Achieving high transparent Î²-Ga2O3 through AlGa-InGa-VO. Journal of Alloys and Compounds, 2019, 792, 405-410.	2.8	8
32594	Free-standing integrated cathode derived from 3D graphene/carbon nanotube aerogels serving as binder-free sulfur host and interlayer for ultrahigh volumetric-energy-density lithium sulfur batteries. Nano Energy, 2019, 60, 743-751.	8.2	151
32595	First-principles study of the reorientational motion of the [BH4]- groups in CsBH4's fractionally occupied ground-state phase and the thermal properties. Physica B: Condensed Matter, 2019, 564, 69-79.	1.3	1
32596	Study of mechanical and electronic properties of single-layer FeB2. Physica E: Low-Dimensional Systems and Nanostructures, 2019, 112, 71-77.	1.3	12
32597	Sublimation growth and property characterization of p-type 4H-SiC by Al B co-doping technique. Scripta Materialia, 2019, 167, 76-80.	2.6	7

#	Article	IF	Citations
32598	1Tâ€²-MoS₂, A Promising Candidate for Sensing NO_x. Journal of Physical Chemistry C, 2019, 123, 10339-10345.	1.5	31
32599	Modeling the effect of surface CO coverage on the electrocatalytic reduction of CO₂ to CO on Pd surfaces. Physical Chemistry Chemical Physics, 2019, 21, 9876-9882.	1.3	34
32600	Graphene and novel graphitic ZnO and ZnS nanofilms: the energy landscape, non-stoichiometry and water dissociation. Nanoscale Advances, 2019, 1, 1924-1935.	2.2	6
32601	A two-dimensional GeSe/SnSe heterostructure for high performance thin-film solar cells. Journal of Materials Chemistry A, 2019, 7, 11265-11271.	5.2	88
32602	Uncovering the Effect of Lattice Strain and Oxygen Deficiency on Electrocatalytic Activity of Perovskite Cobaltite Thin Films. Advanced Science, 2019, 6, 1801898.	5.6	136
32603	Sc2CO2 and Mn-doped Sc2CO2 as gas sensor materials to NO and CO: A first-principles study. Physica E: Low-Dimensional Systems and Nanostructures, 2019, 111, 84-90.	1.3	54
32604	Crystallography-Derived Youngâ€™s Modulus and Tensile Strength of AlN Nanowires as Revealed by in Situ Transmission Electron Microscopy. Nano Letters, 2019, 19, 2084-2091.	4.5	11
32605	Proximity-Induced Colossal Conductivity Modulation in Phosphorene. Physical Review Applied, 2019, 11, .	1.5	21
32606	Bond-Selected Photodissociation of Single Molecules Adsorbed on Metal Surfaces. Physical Review Letters, 2019, 122, 077401.	2.9	15
32607	Schottky Contact in Monolayer WS₂ Fieldâ€Effect Transistors. Advanced Theory and Simulations, 2019, 2, 1900001.	1.3	42
32608	Mechanism of hardening and damage initiation in oxygen embrittlement of body-centred-cubic niobium. Acta Materialia, 2019, 168, 331-342.	3.8	60
32609	Effects of strain and surface modification on stability, electronic and optical properties of GaN monolayer. Applied Surface Science, 2019, 479, 475-481.	3.1	129
32610	Amino acids-clay interaction at the nano-atomic scale: The l-alanine-chlorite system. Applied Clay Science, 2019, 172, 28-39.	2.6	13
32611	Magnetic, electronic, ferroelectric, structural and topological analysis of AlFeO3, FeAlO3, FeVO3, BiFeO3 and PbFeO3 materials: Theoretical evidences of magnetoelectric coupling. Journal of Magnetism and Magnetic Materials, 2019, 480, 199-208.	1.0	27
32612	Reaction Mechanisms for Long-Life Rechargeable Zn/MnO₂ Batteries. Chemistry of Materials, 2019, 31, 2036-2047.	3.2	195
32613	Ba₂ScHO₃: H^{â€“} Conductive Layered Oxyhydride with H^{â€“} Site Selectivity. Inorganic Chemistry, 2019, 58, 4431-4436.	1.9	41
32614	Chemical Functionalization of ZnS: A Perspective from the Ligandâ€“ZnS Bond Character. Journal of Physical Chemistry C, 2019, 123, 6054-6061.	1.5	4
32615	Phase stability of intercalated V₂O₅ battery cathodes elucidated through the Goldschmidt tolerance factor. Physical Chemistry Chemical Physics, 2019, 21, 7732-7744.	1.3	9

#	Article	IF	Citations
32616	Site stability and pipe diffusion of hydrogen under localised shear in aluminium. Philosophical Magazine, 2019, 99, 1184-1205.	0.7	4
32617	Ferroelectricity of stress-free and strained pure SrTiO3 revealed by ab initio calculations with hybrid and density functionals. Physical Review B, 2019, 99, .	1.1	8
32618	Theoretical Investigation of Phase Transitions of Graphite and Cubic 3C Diamond Into Hexagonal 2H Diamond Under High Pressures. Physica Status Solidi (B): Basic Research, 2019, 256, 1800575.	0.7	10
32619	Modulating the electronic and magnetic properties of the marcasite FeS2 via transition metal atoms doping. Journal of Materials Science: Materials in Electronics, 2019, 30, 5891-5901.	1.1	3
32620	Substitutional boron and nitrogen pairs in diamond. A quantum mechanical vibrational analysis. Carbon, 2019, 146, 709-716.	5.4	10
32621	Hydrostatic-pressure-dependent electronic and optical properties of tungstate MnWO4: A first-principles study. Chinese Journal of Physics, 2019, 57, 157-164.	2.0	3
32622	A density functional theory study on ethylene decomposition to carbon monomer on Cu(410) surface. Computational Materials Science, 2019, 161, 321-329.	1.4	1
32623	A first-principles study of the electronic and optical properties of monolayer Î±-PbO. Chemical Physics Letters, 2019, 721, 27-32.	1.2	10
32624	Surface Morphology and Sulfur Reduction Pathways of MoS₂ Mo Edges of the Monolayer and (100) and (103) Surfaces by Molecular Hydrogen: A DFT Study. ACS Omega, 2019, 4, 4023-4028.	1.6	7
32625	Uncovering and tailoring hidden Rashba spinâ€“orbit splitting in centrosymmetric crystals. Nature Communications, 2019, 10, 906.	5.8	53
32626	Observation of Restored Topological Surface States in Magnetically Doped Topological Insulator. Scientific Reports, 2019, 9, 1331.	1.6	17
32627	A first-principles study of doped black phosphorus carbide monolayers as NO2 and NH3 sensors. Journal of Applied Physics, 2019, 125, .	1.1	17
32628	Candidate Inorganic Photovoltaic Materials from Electronic Structure-Based Optical Absorption and Charge Transport Proxies. Chemistry of Materials, 2019, 31, 1561-1574.	3.2	40
32629	Electron engineering of metallic multiferroic polarons in epitaxial BaTiO3. Npj Computational Materials, 2019, 5, .	3.5	14
32630	Interplay Between Site Activity and Density of BCC Iron for Ammonia Synthesis Based on Firstâ€Principles Theory. ChemCatChem, 2019, 11, 1928-1934.	1.8	20
32631	Prediction of robustness of electronic, magnetic and thermoelectric properties under pressure and temperature variation in Co2MnAs alloy. Computational Condensed Matter, 2019, 19, e00375.	0.9	34
32632	Effect of carbon on elastic properties and microstructure of maraging steel: First-principles and phase-field study. Computational Materials Science, 2019, 162, 1-11.	1.4	5
32633	Effects of different phases, compositional change, and doping on ductility improvement of NbAl3 phases. Journal of Alloys and Compounds, 2019, 788, 172-182.	2.8	5

#	Article	IF	Citations
32634	Synthesis, crystallographic structure and thermodynamic properties of T2-Al2MgC2. Journal of Solid State Chemistry, 2019, 273, 150-157.	1.4	8
32635	Ab initio investigation of mechanical and thermodynamic properties of vanadium-nitride. Materials Chemistry and Physics, 2019, 228, 237-243.	2.0	9
32636	Comparative study of Cs,O coadsorption on Ga0.75Al0.25N (0001) and (001) surfaces. Optical and Quantum Electronics, 2019, 51, 1.	1.5	4
32637	Vanadium carbide coating as hydrogen permeation barrier: A DFT study. International Journal of Hydrogen Energy, 2019, 44, 6093-6102.	3.8	27
32638	Oxygen vacancy enhancing mechanism of nitrogen reduction reaction property in Ru/TiO2. Journal of Energy Chemistry, 2019, 39, 144-151.	7.1	79
32639	Silanization of superficially porous silica particles with p-aminophenyltrimethoxysilane. Microchemical Journal, 2019, 147, 263-268.	2.3	8
32640	Surface Diffusion of Fe and Cu on Fe (001) Under Electric Field Using First-Principles Calculations. Microscopy and Microanalysis, 2019, 25, 547-553.	0.2	7
32641	A DFT/ZORA Study of Cadmium Magnetic Shielding Tensors: Analysis of Relativistic Effects and Electronic-State Approximations. Journal of Chemical Theory and Computation, 2019, 15, 1785-1797.	2.3	5
32642	Mechanism of Nitric Oxide Reduction by Hydrogen on Ni(110) and Ir/Ni(110): First Principles and Microkinetic Modeling. Journal of Physical Chemistry C, 2019, 123, 4825-4836.	1.5	12
32643	Magnetic Polymer Chains of Transition Metal Atoms and Zwitterionic Quinone. Journal of Physical Chemistry C, 2019, 123, 4582-4589.	1.5	13
32644	Unusual oxidation-induced core-level shifts at the HfO2/InP interface. Scientific Reports, 2019, 9, 1462.	1.6	9
32645	N-, B-, P-, Al-, As-, and Ga-graphdiyne/graphyne lattices: first-principles investigation of mechanical, optical and electronic properties. Journal of Materials Chemistry C, 2019, 7, 3025-3036.	2.7	41
32646	Impact of iron composition on the calculated electronic and magnetic properties of Fe_{3â^'x}Ni_xSi. Molecular Physics, 2019, 117, 2570-2576.	0.8	1
32647	Phonon-driven phase transitions in calcite, dolomite, and magnesite. Physical Review B, 2019, 99, .	1.1	7
32648	First-principles anharmonic vibrational study of the structure of calcium silicate perovskite under lower mantle conditions. Physical Review B, 2019, 99, .	1.1	3
32649	First-Principles Investigation on Type-II Aluminum-Substituted Ternary and Quaternary Clathrate Semiconductors R8Al8Si128 (R = Cs, Rb), Cs8Na16Al24Si112. Applied Sciences (Switzerland), 2019, 9, 125.	1.3	1
32650	The band alignments modulation of gâ€“MoTe2/WTe2 van der Waals heterostructures. Applied Physics A: Materials Science and Processing, 2019, 125, 1.	1.1	5
32651	Intrinsic magnetic properties of SmFe12â^'V alloys with reduced V-concentration. Journal of Alloys and Compounds, 2019, 786, 969-974.	2.8	45

#	Article	IF	Citations
32652	Benchmarking Density Functional Theory Functionals for Polarons in Oxides: Properties of CeO₂. Journal of Physical Chemistry C, 2019, 123, 5164-5175.	1.5	28
32653	Nonhexagonal Na Sublattice Reconstruction in the Super-Ionic Conductor Na2Zn2TeO6: Insights from Ab Initio Molecular Dynamics. Journal of Physical Chemistry C, 2019, 123, 4654-4663.	1.5	9
32654	Asymmetric MXene/monolayer transition metal dichalcogenide heterostructures for functional applications. Npj Computational Materials, 2019, 5, .	3.5	23
32655	Computational design of CO-tolerant Pt₃M anode electrocatalysts for proton-exchange membrane fuel cells. Physical Chemistry Chemical Physics, 2019, 21, 4046-4052.	1.3	14
32656	Electronic structure and <mml:math xmlns:mml="http://www.w3.org/1998/Math/MathML"><mml:mrow><mml:mn>4</mml:mn><mml:mi>f</mml:mi></mml:mrow></mml:m -electron character in <mml:math xmlns:mml="http://www.w3.org/1998/Math/MathML"><mml:mrow><mml:msub><mml:mi>Ce</mml:mi><mml:mn>2</mml:mn></mml:m studied by angle-resolved photoemission spectroscopy. Physical Review B, 2019, 99, .	1.1	14
32657	Insight into the structures, melting points, and mechanical properties of NbSi₂ from firstâ€principles calculations. Journal of the American Ceramic Society, 2019, 102, 4822-4834.	1.9	69
32658	Selective electroreduction of carbon dioxide to methanol on copper selenide nanocatalysts. Nature Communications, 2019, 10, 677.	5.8	258
32659	Electronic origin of antimicrobial activity owing to surface effect. Scientific Reports, 2019, 9, 1091.	1.6	6
32660	Living in the salt-cocrystal continuum: indecisive organic complexes with thermochromic behaviour. CrystEngComm, 2019, 21, 1626-1634.	1.3	28
32661	Crystal and electronic structure studies on transparent conducting nitrides A ₃N₂ (A = Mg, Zn and Sn) and Sn₃N₄. Materials Research Express, 2019, 6, 055912.	0.8	5
32662	Robust Twin Pairs of Weyl Fermions in Ferromagnetic Oxides. Physical Review Letters, 2019, 122, 057205.	2.9	14
32663	Spin polarization in graphene nanoribbons functionalized with nitroxide. Journal of Molecular Modeling, 2019, 25, 58.	0.8	10
32664	Impact of position and concentration of sodium on the photovoltaic properties of zinc oxide solar cells. Physica B: Condensed Matter, 2019, 560, 28-36.	1.3	21
32665	Intricacies of DFT+U, Not Only in a Numeric Atom Centered Orbital Framework. Journal of Chemical Theory and Computation, 2019, 15, 1705-1718.	2.3	41
32666	Thermoelectric and electronic properties of B-doped graphene nanoribbon. Canadian Journal of Physics, 2019, 97, 1027-1030.	0.4	3
32667	Spin Polarization and Magnetic Properties of VGaON and VGaONInGa in GaN: GGA+U Approach. Journal of Superconductivity and Novel Magnetism, 2019, 32, 2661-2672.	0.8	0
32668	Semimetallic Si3C as a high capacity anode material for advanced lithium ion batteries. Applied Surface Science, 2019, 479, 519-524.	3.1	33
32669	Structural patterns in carbon chemisorption on ultrasmall iron clusters: A first-principles study. Computational and Theoretical Chemistry, 2019, 1150, 49-56.	1.1	0

#	Article	IF	Citations
32670	Germanium-substituted Zn2TiO4 solid solution photocatalyst for conversion of CO2 into fuels. Journal of Catalysis, 2019, 371, 144-152.	3.1	23
32671	Multi Band Gap Electronic Structure in CH3NH3PbI3. Scientific Reports, 2019, 9, 2144.	1.6	26
32672	The Influence of Boron Dopant on the Structural and Mechanical Properties of Silicon: First Principles Study. Minerals, Metals and Materials Series, 2019, , 191-199.	0.3	1
32673	Design of pentagonal NbX monolayers for electronics and electrocatalysis. Applied Surface Science, 2019, 479, 595-600.	3.1	14
32674	Cd complexation with mercapto-functionalized attapulgite (MATP): Adsorption and DFT study. Chemical Engineering Journal, 2019, 366, 569-576.	6.6	51
32675	An ab initio study of spectroscopic and thermodynamic characteristics of MgH2 and TiC systems. International Journal of Hydrogen Energy, 2019, 44, 6756-6762.	3.8	8
32676	Temperature dependent magnetic properties of Dy-doped Fe16N2: Potential rare-earth-lean permanent magnet. Intermetallics, 2019, 108, 25-31.	1.8	4
32677	Double-shell Li-rich layered oxide hollow microspheres with sandwich-like carbon@spinel@layered@spinel@carbon shells as high-rate lithium ion battery cathode. Nano Energy, 2019, 59, 184-196.	8.2	194
32678	Structural, optoelectronic and thermoelectric properties of antiperovskite compounds Ae3PbS (Ae =) Tj ETQq0 0 0 rgBT /Overlock 10 Tf Physics, 2019, 383, 1648-1654.	0.9	22
32679	Interface-Driven Phase Transition of Phase-Change Material. Crystal Growth and Design, 2019, 19, 2123-2130.	1.4	5
32680	Origin of Room-Temperature Ferromagnetism in Hydrogenated Epitaxial Graphene on Silicon Carbide. Nanomaterials, 2019, 9, 228.	1.9	2
32681	The Influence of Phosphorus Dopant on the Structural and Mechanical Properties of Silicon. Minerals, Metals and Materials Series, 2019, , 201-211.	0.3	0
32682	Transition Metal Doped ZnS Monolayer: The First Principles Insights. Springer Proceedings in Physics, 2019, , 49-56.	0.1	2
32683	Effects of finite temperature on the surface energy in Al alloys from first-principles calculations. Applied Surface Science, 2019, 479, 499-505.	3.1	22
32684	Convergence and machine learning predictions of Monkhorst-Pack k-points and plane-wave cut-off in high-throughput DFT calculations. Computational Materials Science, 2019, 161, 300-308.	1.4	68
32685	On the possibility of severe corrosion of a Ni-W-Cr alloy in fluoride molten salts at high temperature. Corrosion Science, 2019, 149, 218-225.	3.0	42
32686	Thermodynamic and Mechanical Stability of Crystalline Phases of Li2S2. Journal of Physical Chemistry C, 2019, 123, 4674-4681.	1.5	16
32687	Toward Understanding the Kinetics of CO₂ Capture on Sodium Carbonate. ACS Applied Materials & Interfaces, 2019, 11, 9033-9041.	4.0	21

#	Article	IF	Citations
32688	Role of defects in determining the magnetic ground state of ytterbium titanate. Nature Communications, 2019, 10, 637.	5.8	28
32689	Phonon thermal conductance across GaN-AlN interfaces from first principles. Physical Review B, 2019, 99, .	1.1	42
32690	Ab initio study of structural, elastic, and electronic properties of Mo3.46B12 under high pressure. European Physical Journal B, 2019, 92, 1.	0.6	6
32691	Configurational Entropy in Multicomponent Alloys: Matrix Formulation from Ab Initio Based Hamiltonian and Application to the FCC Cr-Fe-Mn-Ni System. Entropy, 2019, 21, 68.	1.1	24
32692	Manipulation of Bi³⁺/In³⁺ Transmutation and Mn²⁺â€Doping Effect on the Structure and Optical Properties of Double Perovskite Cs₂NaBi_{1â€«}_xIn_xCl₆. Advanced Optical Materials, 2019, 7, 1801435.	3.6	157
32693	Dopantâ€Dependent Stability of Garnet Solid Electrolyte Interfaces with Lithium Metal. Advanced Energy Materials, 2019, 9, 1803440.	10.2	217
32694	Tailoring Active Sites in Mesoporous Defectâ€Rich NC/V_oâ€WON Heterostructure Array for Superior Electrocatalytic Hydrogen Evolution. Advanced Energy Materials, 2019, 9, 1803693.	10.2	66
32695	Synthesis and Characterization of [Br 3][MF 6] (M=Sb, Ir), as well as Quantum Chemical Study of [Br 3] + Structure, Chemical Bonding, and Relativistic Effects Compared with [XBr 2] + (X=Br, I, At, Ts) and [TsZ 2] + (Z=F, Cl, Br, I, At, Ts). Chemistry - A European Journal, 2019, 25, 5793-5802.	1.7	10
32696	Big to Small: Ultrafine Mo₂C Particles Derived from Giant Polyoxomolybdate Clusters for Hydrogen Evolution Reaction. Small, 2019, 15, e1900358.	5.2	53
32697	Nitrogen Soaking Promotes Lattice Recovery inÂPolycrystalline Hybrid Perovskites. Advanced Energy Materials, 2019, 9, 1803450.	10.2	46
32698	Revealing the factors influencing grain boundary segregation of P, As in Si: Insights from first-principles. Acta Materialia, 2019, 168, 52-62.	3.8	26
32699	Phase stabilities and vibrational analysis of hydrogenated diamondized bilayer graphenes: A first principles investigation. Carbon, 2019, 146, 468-475.	5.4	43
32700	First principle study of the structural, electronic, vibrational, thermodynamic, linear and nonlinear optical properties of zinc-blende ZnSe and ZnTe semiconductors. Computational Condensed Matter, 2019, 19, e00372.	0.9	9
32701	High Rate Li-Ion Batteries with Cation-Disordered Cathodes. Joule, 2019, 3, 1064-1079.	11.7	12
32702	Exploring new insights in BAlN from evolutionary algorithms ab initio computations. Physics Letters, Section A: General, Atomic and Solid State Physics, 2019, 383, 1385-1388.	0.9	8
32703	Structural evolution and electronic properties of CaS: An ab initio study. Solid State Sciences, 2019, 90, 14-20.	1.5	9
32704	Vibrational and thermodynamic properties of pure and gold adsorbed graphene. Vacuum, 2019, 166, 405-412.	1.6	9
32705	Multifunctional Copper(I) Coordination Polymers with Aromatic Mono- and Ditopic Thioamides. Inorganic Chemistry, 2019, 58, 3290-3301.	1.9	42

#	Article	IF	Citations
32706	ReGa0.4Ge0.6: Intermetallic Compound with Pronounced Covalency in the Bonding Pattern. Inorganic Chemistry, 2019, 58, 2822-2832.	1.9	3
32707	Rhodium and Nitrogen Codoped Graphene as a Bifunctional Electrocatalyst for the Oxygen Reduction Reaction and CO₂ Reduction Reaction: Mechanism Insights. Journal of Physical Chemistry C, 2019, 123, 5176-5187.	1.5	44
32708	Enhanced Performances of PbS Quantum-Dots-Modified MoS₂ Composite for NO₂ Detection at Room Temperature. ACS Applied Materials & Interfaces, 2019, 11, 9438-9447.	4.0	102
32709	Neurotransmitter-Functionalized Boron Nitride Nanoribbons as Biological Cargo Carriers: Analysis by Density Functional Theory. ACS Applied Nano Materials, 2019, 2, 1552-1561.	2.4	11
32710	Water Adsorption on MO₂ (M = Ti, Ru, and Ir) Surfaces. Importance of Octahedral Distortion and Cooperative Effects. ACS Omega, 2019, 4, 2989-2999.	1.6	28
32711	eg occupancy as an effective descriptor for the catalytic activity of perovskite oxide-based peroxidase mimics. Nature Communications, 2019, 10, 704.	5.8	199
32712	First-principles-based prediction of yield strength in the RhIrPdPtNiCu high-entropy alloy. Npj Computational Materials, 2019, 5, .	3.5	86
32713	A weak topological insulator state in quasi-one-dimensional bismuth iodide. Nature, 2019, 566, 518-522.	13.7	119
32714	Relevance of silica surface morphology in Ampyra adsorption. Insights from quantum chemical calculations. RSC Advances, 2019, 9, 4415-4421.	1.7	3
32715	Tetragonal C₂₄: a topological nodal-surface semimetal with potential as an anode material for sodium ion batteries. Journal of Materials Chemistry A, 2019, 7, 5733-5739.	5.2	72
32716	Band gap and band alignment prediction of nitride-based semiconductors using machine learning. Journal of Materials Chemistry C, 2019, 7, 3238-3245.	2.7	48
32717	Tailoring widely used ammonia synthesis catalysts for H and N poisoning resistance. Physical Chemistry Chemical Physics, 2019, 21, 5117-5122.	1.3	13
32718	Electrochemical synthesis of nitric acid from air and ammonia through waste utilization. National Science Review, 2019, 6, 730-738.	4.6	296
32719	Polarization dependence of angle-resolved photoemission with submicron spatial resolution reveals emerging one-dimensionality of electrons in <mml:math xmlns:mml="http://www.w3.org/1998/Math/MathML"><mml:msub><mml:mi>NbSe</mml:mi><mml:mn>3</mml:mn></mml:msub></m Physical Review B, 2019, 99, .	1.1	11
32720	Quantitative modeling of secondary electron emission from slow-ion bombardment on semiconductors. Physical Review B, 2019, 99, .	1.1	9
32721	Ab initio study of the structural, electronic, magnetic, and optical properties of silicene nanoribbons. Physical Review B, 2019, 99, .	1.1	15
32722	First-Principles Investigation of the Mechanical and Thermodynamic Properties of the Metal-Borohydrides as Electrolytes for Solid-State Batteries. Journal of the Electrochemical Society, 2019, 166, A493-A500.	1.3	10
32723	First-Principles Study of the Electronic, Vibrational Properties and Anharmonic Effects of Some Si-Based Type-II Binary Clathrates. Materials, 2019, 12, 536.	1.3	2

#	Article	IF	Citations
32724	Layered Compounds BaFMgPn (Pn = P, As, Sb, and Bi), Transition-Metal-Free Representatives of the 1111 Structure Type. Inorganic Chemistry, 2019, 58, 3435-3443.	1.9	8
32725	Role of Methylammonium Rotation in Hybrid Halide MAPbX₃ (X = I, Br, and Cl) Perovskites by a Density Functional Theory Approach: Optical and Electronic Properties. Journal of Physical Chemistry C, 2019, 123, 6725-6734.	1.5	23
32726	Potential Applications of Halide Double Perovskite Cs₂AgInX₆ (X = Cl, Br) in Flexible Optoelectronics: Unusual Effects of Uniaxial Strains. Journal of Physical Chemistry Letters, 2019, 10, 1120-1125.	2.1	44
32727	Effects of Phosphorus Doping and Postgrowth Laser Annealing on the Structural, Electrical, and Chemical Properties of Phosphorus-Doped Silicon Films. ACS Applied Electronic Materials, 2019, 1, 288-301.	2.0	31
32728	Versatile Graphene-Based Platform for Robust Nanobiohybrid Interfaces. ACS Omega, 2019, 4, 3287-3297.	1.6	9
32729	Boronâ€“Carbonâ€“Nitride Sheet as a Novel Surface for Biological Applications: Insights from Density Functional Theory. ACS Omega, 2019, 4, 3732-3738.	1.6	29
32730	Bandgap prediction by deep learning in configurationally hybridized graphene and boron nitride. Npj Computational Materials, 2019, 5, .	3.5	86
32731	Fundamentals of Câ€“O bond activation on metal oxide catalysts. Nature Catalysis, 2019, 2, 269-276.	16.1	82
32732	Oxygen-functionalized TlTe buckled honeycomb from first-principles study. Physical Chemistry Chemical Physics, 2019, 21, 5689-5694.	1.3	2
32733	Surface P atom grafting of g-C₃N₄ for improved local spatial charge separation and enhanced photocatalytic H₂ production. Journal of Materials Chemistry A, 2019, 7, 7628-7635.	5.2	50
32734	Size dependence in two-dimensional lateral heterostructures of transition metal dichalcogenides. Journal of Materials Chemistry C, 2019, 7, 3837-3842.	2.7	7
32735	Band structures and optical properties related to substitutional impurities in TlGaSe₂ layered crystals: first-principles study. Phase Transitions, 2019, 92, 451-460.	0.6	6
32736	The Basics of Electronic Structure Theory for Periodic Systems. Frontiers in Chemistry, 2019, 7, 106.	1.8	57
32737	Density Functional Theory Study on Defect Behavior Related to the Bulk Lifetime of Silicon Crystals for Power Device Application. Physica Status Solidi (A) Applications and Materials Science, 2019, 216, 1800615.	0.8	6
32738	Tuning the electronic transport anisotropy in borophene via oxidation strategy. Science China Technological Sciences, 2019, 62, 799-810.	2.0	14
32739	Ferromagnetism in p-block-element doped ZnO: An ab-initio approach. Computational Condensed Matter, 2019, 19, e00376.	0.9	3
32740	Point defect interactions with Guinier-Preston zones in Al-Cu based alloys: Vacancy mediated GPZ to Î¸â€²-phase transformation. Scripta Materialia, 2019, 165, 123-127.	2.6	8
32741	Quasi-Ballistic Thermal Transport Across MoS₂ Thin Films. Nano Letters, 2019, 19, 2434-2442.	4.5	61

#	Article	IF	Citations
32742	Dual Lithiophilic Structure for Uniform Li Deposition. ACS Applied Materials & Interfaces, 2019, 11, 10616-10623.	4.0	43
32743	Subnanometer cobalt oxide clusters as selective low temperature oxidative dehydrogenation catalysts. Nature Communications, 2019, 10, 954.	5.8	38
32744	Density functional theory prediction of Mg₃N₂ as a high-performance anode material for Li-ion batteries. Physical Chemistry Chemical Physics, 2019, 21, 7053-7060.	1.3	16
32745	Electron-phonon properties, structural stability, and superconductivity of doped antimonene. Physical Review B, 2019, 99, .	1.1	27
32746	First-Principles Calculation for the Influence of C and O on the Mechanical Properties of Î³-TiAl Alloy at High Temperature. Metals, 2019, 9, 262.	1.0	5
32747	Defects, Lithium Mobility and Tetravalent Dopants in the Li3NbO4 Cathode Material. Scientific Reports, 2019, 9, 2192.	1.6	28
32748	Ultrahigh Electrical Conductivity of Graphene Embedded in Metals. Advanced Functional Materials, 2019, 29, 1806792.	7.8	126
32749	Carbonâ€Nanotubeâ€Cored Cobalt Porphyrin as a 1D Nanohybrid Strategy for Highâ€Performance Lithiumâ€Ion Battery Anodes. Advanced Functional Materials, 2019, 29, 1806937.	7.8	35
32750	LiFePO₄ Particles Embedded in Fast Bifunctional Conductor rGO&C@Li₃V₂(PO₄)₃ Nanosheets as Cathodes for Highâ€Performance Liâ€Ion Hybrid Capacitors. Advanced Functional Materials, 2019, 29, 1807895.	7.8	42
32751	Polarizationâ€Sensitive Ultraviolet Photodetection of Anisotropic 2D GeS₂. Advanced Functional Materials, 2019, 29, 1900411.	7.8	120
32752	Lattice Structure and Bandgap Control of 2D GaN Grown on Graphene/Si Heterostructures. Small, 2019, 15, e1802995.	5.2	58
32753	Landauâ€“Devonshire thermodynamic potentials for displacive perovskite ferroelectrics from first principles. Journal of Materials Science, 2019, 54, 8381-8400.	1.7	10
32754	Charge transference and conformational stress influence on the electronic properties of zigzag carbon nanowires. Journal of Nanoparticle Research, 2019, 21, 1.	0.8	1
32755	Investigation of structural, electronic, elastic and phonon properties of cubic spinel ZnM2O4(Mâ€¯=â€¯Co,) Tj ETQq1 1 0.784314 rgB	2.0	3
32756	Interfacial wetting behaviors of liquid Ga alloys/FeGa3 based on metallic bond interaction. Colloids and Surfaces A: Physicochemical and Engineering Aspects, 2019, 569, 102-109.	2.3	27
32757	Determination of second- and third-order elastic constants for energetic materials. Computational Materials Science, 2019, 161, 379-384.	1.4	12
32758	Electron-affinity and surface-stability of aluminium-oxide terminated diamond surfaces. Diamond and Related Materials, 2019, 94, 137-145.	1.8	11
32759	Ruthenium decorated single walled carbon nanotube for molecular hydrogen storage: A first-principle study. International Journal of Hydrogen Energy, 2019, 44, 8376-8383.	3.8	36

#	Article	IF	Citations
32760	Theoretical investigation of electron-phonon interaction in the orthorhombic phase of Mo2C. Journal of Alloys and Compounds, 2019, 788, 842-851.	2.8	13
32761	A theoretical explanation of the effect of oxygen poisoning on industrial Haber-Bosch catalysts. Journal of Catalysis, 2019, 372, 33-38.	3.1	40
32762	The effect of phase composition and crystallite size on activity and selectivity of ZrO2 in non-oxidative propane dehydrogenation. Journal of Catalysis, 2019, 371, 313-324.	3.1	74
32763	The electronic, half-metallic, and magnetic properties of Ca1-Cr S ternary alloys: Insights from the first-principle calculations. Journal of Molecular Graphics and Modelling, 2019, 89, 22-32.	1.3	43
32764	Large-Stokes-Shifted Infrared-Emitting InAsâ€“In(Zn)Pâ€“ZnSeâ€“ZnS Giant-Shell Quantum Dots by One-Pot Continuous-Injection Synthesis. Chemistry of Materials, 2019, 31, 2019-2026.	3.2	21
32765	First-Principles Insights into the Structural and Electronic Properties of Polytetrafluoroethylene in Its High-Pressure Phase (Form III). Journal of Physical Chemistry C, 2019, 123, 6250-6255.	1.5	10
32766	Unique crystal field splitting and multiband RKKY interactions in Ni-doped EuRbFe4As4. Communications Physics, 2019, 2, .	2.0	17
32767	Synthesis and characterisation of a quaternary nitride series with spin-glass behaviour: Sn_xGe_{1â^'x}Fe₃N. Journal of Materials Chemistry C, 2019, 7, 3822-3828.	2.7	4
32768	Sn₂B₇O₁₂F with a 2â^ž[B₁₄O₂₄]^{6â^'} layer constructed from the unprecedented [B₇O₁₆]^{11â^'} fundamental building block. Inorganic Chemistry Frontiers, 2019, 6, 996-1002.	3.0	17
32769	Tunable electronic properties in stanene and two dimensional silicon-carbide heterobilayer: A first principles investigation. AIP Advances, 2019, 9, .	0.6	37
32770	Two-phase equation of state for lithium fluoride. Journal of Chemical Physics, 2019, 150, 074506.	1.2	10
32771	Computational Investigation on the Electronic Structure and Functionalities of a Thiophene-Based Covalent Triazine Framework. ACS Omega, 2019, 4, 3556-3564.	1.6	12
32772	Thermoelasticity of Ironâ€•and Aluminumâ€Bearing MgSiO₃ Postperovskite. Journal of Geophysical Research: Solid Earth, 2019, 124, 2417-2427.	1.4	5
32773	Interface Schottky barrier in Hf₂NT₂/MSSe (T = F, O, OH; M = Mo, W) heterostructures. Physical Chemistry Chemical Physics, 2019, 21, 5394-5401.	1.3	19
32774	Electronic Transport in the V-Shaped Edge Distorted Zigzag Graphene Nanoribbons with Substitutional Doping. Advances in Condensed Matter Physics, 2019, 2019, 1-8.	0.4	2
32775	Temperature effects on the structural phase transitions of gallium phosphide. Computational Materials Science, 2019, 161, 265-275.	1.4	8
32776	Lifshitz transition in new doped 112 superconductors. Intermetallics, 2019, 107, 126-136.	1.8	12
32777	Electric field effects on the electronic structures of MoS2/antimonene van der Waals heterostructure. Solid State Communications, 2019, 293, 28-32.	0.9	8

#	Article	IF	Citations
32778	First-principles study of elastic, thermal and optical properties of a metal-shrouded two-dimensional semiconductor Tl2O. Solid State Communications, 2019, 293, 40-47.	0.9	6
32779	Structure dependent effect of silicon on the oxidation of Al(111) and Al(100). Surface Science, 2019, 684, 1-11.	0.8	2
32780	Adsorption and Reaction of Water on the AlN(0001) Surface from First Principles. Journal of Physical Chemistry C, 2019, 123, 5460-5468.	1.5	17
32781	Solventâ€“Adsorbate Interactions and Adsorbate-Specific Solvent Structure in Carbon Dioxide Reduction on a Stepped Cu Surface. Journal of Physical Chemistry C, 2019, 123, 5999-6009.	1.5	63
32782	CO Stretch Vibration Lives Long on Au(111). Journal of Physical Chemistry Letters, 2019, 10, 1043-1047.	2.1	21
32783	High performance of PtCu@TiO₂ nanocatalysts toward methanol oxidation reaction: from synthesis to molecular picture insight. RSC Advances, 2019, 9, 2073-2080.	1.7	18
32784	Modulating charge transfer dynamics for g-C₃N₄ through a dimension and interface engineered transition metal phosphide co-catalyst for efficient visible-light photocatalytic hydrogen generation. Journal of Materials Chemistry A, 2019, 7, 6939-6945.	5.2	64
32785	Density functional theory description of random Cu-Au alloys. Physical Review B, 2019, 99, .	1.1	5
32786	Revealing the Nature of Antiferroquadrupolar Ordering in Cerium Hexaboride: <mml:math xmlns:mml="http://www.w3.org/1998/Math/MathML" display="inline"><mml:mrow><mml:msub><mml:mrow><mml:mi>CeB</mml:mi></mml:mrow><mml:mrow><mml:mn>6</mml:mn></m Physical Review Letters, 2019, 122, 076401.	2.9	14
32787	Stability, Mechanical Properties and Anisotropic Elastic Properties of GaxMgy Compounds. Materials Research, 2019, 22, .	0.6	12
32788	Hydrated Intercalation for Highâ€Performance Aqueous Zinc Ion Batteries. Advanced Energy Materials, 2019, 9, 1900083.	10.2	243
32789	Spin Excitations in Solid from Many-Body Perturbation Theory. , 2019, , 1-39.		1
32790	The effects of non-hydrostatic stress on the structure and properties of alpha-quartz. Physics and Chemistry of Minerals, 2019, 46, 487-499.	0.3	27
32791	Theoretical studies of photocatalytic behaviors of isoelectronic C/Si/Ge/Sn-doped TiO2: DFTâ€¯+â€¯U. Applied Surface Science, 2019, 484, 1304-1309.	3.1	19
32792	Combined effect of point defects and layer number on the adsorption of benzene and toluene on graphene. Applied Surface Science, 2019, 480, 1063-1069.	3.1	12
32793	Fabrication of SnS₂/Mn₂SnS₄/Carbon Heterostructures for Sodium-Ion Batteries with High Initial Coulombic Efficiency and Cycling Stability. ACS Nano, 2019, 13, 3666-3676.	7.3	205
32794	Effect of nitrogen-doping configuration in graphene on the oxygen reduction reaction. RSC Advances, 2019, 9, 6035-6041.	1.7	21
32795	Increasing the optical response of TiO₂ and extending it into the visible region through surface activation with highly stable Cu₅ clusters. Journal of Materials Chemistry A, 2019, 7, 7489-7500.	5.2	35

#	Article	IF	Citations
32796	Theoretical study on halide and mixed halide Perovskite solar cells: Effects of halide atoms on the stability and electronic properties. Journal of the Chinese Chemical Society, 2019, 66, 575-582.	0.8	10
32797	Firstâ€principles studies of lithium adsorption and diffusion on silicene with grain boundaries. International Journal of Quantum Chemistry, 2019, 119, e25913.	1.0	11
32798	A First Principle Study of Graphene/Metal-Oxides as Nano-Composite Electrode Materials for Supercapacitors. Journal of Electronic Materials, 2019, 48, 2343-2349.	1.0	13
32799	The partial reduction of clean and doped Î±-Fe2O3(0001) from first principles. Applied Catalysis A: General, 2019, 582, 116989.	2.2	6
32800	Hydrazine adsorption on perfect and defective fcc nickel (100), (110) and (111) surfaces: A dispersion corrected DFT-D2 study. Applied Surface Science, 2019, 480, 1014-1024.	3.1	13
32801	Highly absorbent cubic structured Silicon-monochalcogenides: Promising materials for photovoltaic applications. Ceramics International, 2019, 45, 8971-8978.	2.3	7
32802	An experimental and theoretical study on the crystal structure and elastic properties of Ta1â^'xOx coatings. Surface and Coatings Technology, 2019, 364, 289-297.	2.2	1
32803	Methane Dissociation on Î±-Fe₂O₃(0001) and Fe₃O₄(111) Surfaces: First-Principles Insights into Chemical Looping Combustion. Journal of Physical Chemistry C, 2019, 123, 6450-6463.	1.5	23
32804	Charge Transfer Dynamics of Phase-Segregated Halide Perovskites: CH₃NH₃PbCl₃ and CH₃NH₃PbI₃ or (C₄H₉NH₃)₂(CH₃NH₃)_{nâ^'1}Pb<s Mixtures. ACS Applied Materials & Interfaces, 2019, 11, 9583-9593.	4.0	14
32805	Water Splitting Reaction at Polar Lithium Niobate Surfaces. ACS Omega, 2019, 4, 3850-3859.	1.6	16
32806	Phonon spectrum attributes for the negative thermal expansion of MZrF₆ (M = Ca, Mnâ€“Ni,) Tj ETQq0 0 0 rgBT /Overlock	3.0	2
32807	Theoretical study of single transition metal atom modified MoP as a nitrogen reduction electrocatalyst. Physical Chemistry Chemical Physics, 2019, 21, 5950-5955.	1.3	43
32808	A coordination-based model for transition metal alloy nanoparticles. Nanoscale, 2019, 11, 4438-4452.	2.8	34
32809	High spin polarization in all-3d-metallic Heusler compounds: the case of Fe₂CrZ and Co₂CrZ (Zâ€‰â€‰=â€‰â€‰Sc,Ti,V). Journal Physics D: Applied Physics, 2019, 52, 205003.	1.3	16
32810	Biogas detection on carbon nitride sheet with embedded Mn atom: dispersion-corrected density functional theory. Materials Research Express, 2019, 6, 065603.	0.8	4
32811	Tunable intrinsic strain in two-dimensional transition metal electrocatalysts. Science, 2019, 363, 870-874.	6.0	384
32812	Facet selectivity of Cu current collector for Li electrodeposition. Energy Storage Materials, 2019, 19, 154-162.	9.5	57
32813	Adsorption of hydrazine on XC3 (X = B, Al, N, Si, and Ge) nanosheets: A computational study. International Journal of Hydrogen Energy, 2019, 44, 6055-6064.	3.8	25

#	Article	IF	Citations
32814	First-principles rational design of M-doped LiBH4(010) surface for hydrogen release: Role of strain and dopants (M=Na, K, Al, F, or Cl). International Journal of Hydrogen Energy, 2019, 44, 6065-6073.	3.8	7
32815	Study of the NaF-ScF3 system as a molten bath for production of Sc alloys: A combination of NMR and molecular dynamics simulations. Journal of Alloys and Compounds, 2019, 786, 953-959.	2.8	8
32816	New approaches to consider electrical properties, band gaps and rate capability of same-structured cathode materials using density of states diagrams: Layered oxides as a case study. Journal of Alloys and Compounds, 2019, 787, 738-743.	2.8	30
32817	Structural, phonon, elastic, thermodynamic and electronic properties of Mgâ€“X (Xâ€¯=â€¯La, Nd, Sm) intermetallics: The first principles study. Journal of Magnesium and Alloys, 2019, 7, 166-185.	5.5	31
32818	Determination of an adequate bornite model for computational simulations â€“ Cu5FeS4 or Cu8Fe4S8. Journal of Molecular Structure, 2019, 1184, 72-78.	1.8	0
32819	Overall structural modification of a layered Ni-rich cathode for enhanced cycling stability and rate capability at high voltage. Journal of Materials Chemistry A, 2019, 7, 6080-6089.	5.2	112
32820	Space partitioning of exchange-correlation functionals with the projector augmented-wave method. Journal of Chemical Physics, 2019, 150, 054101.	1.2	8
32821	The impact of lattice vibrations on the macroscopic breathing behavior of MIL-53(Al). Zeitschrift Fur Kristallographie - Crystalline Materials, 2019, 234, 529-545.	0.4	22
32822	Strain-Tunable Visible-Light-Responsive Photocatalytic Properties of Two-Dimensional CdS/g-C3N4: A Hybrid Density Functional Study. Nanomaterials, 2019, 9, 244.	1.9	46
32823	Intrinsic Halfâ€Metallicity in 2D Ternary Chalcogenides with High Critical Temperature and Controllable Magnetization Direction. Advanced Functional Materials, 2019, 29, 1808380.	7.8	68
32824	Influences of pressure on structural and electronic properties of four types of HMX. Journal of Molecular Modeling, 2019, 25, 63.	0.8	3
32825	Phosphorene: A promising metal free cathode material for proton exchange membrane fuel cell. Applied Surface Science, 2019, 479, 590-594.	3.1	26
32826	Fabrication and reduction process of dispersive Er2O3 doped Mo super-fine powders comparing with La2O3 doped Mo powders. Powder Technology, 2019, 346, 78-84.	2.1	9
32827	Tuning the Hematite (110) Surface Properties To Enhance Its Efficiency in Photoelectrochemistry. Journal of Physical Chemistry C, 2019, 123, 5401-5410.	1.5	10
32828	Jahnâ€“Teller type small polaron assisted Na diffusion in NaMnO₂as a cathode material for Na-ion batteries. Journal of Materials Chemistry A, 2019, 7, 6053-6061.	5.2	27
32829	On the prevalence of smooth polymorphs at the nanoscale: implications for pharmaceuticals. CrystEngComm, 2019, 21, 2203-2211.	1.3	20
32830	Sr- and Co-doped LaGaO_{3â^Î´} with high O₂ and H₂ yields in solar thermochemical water splitting. Journal of Materials Chemistry A, 2019, 7, 6099-6112.	5.2	46
32831	Weyl-loop half-metal in <mml:math xmlns:mml="http://www.w3.org/1998/Math/MathML"><mml:mrow><mml:msub><mml:mrow><mml:mi>Li</mml:mi></mml:mrow> Physical Review B, 2019, 99, .	3.1	61

#	Article	IF	Citations
32832	3D Printing of a Thermoâ€•and Solvatochromic Composite Material Based on a Cu(II)â€“Thymine Coordination Polymer with Moisture Sensing Capabilities. Advanced Functional Materials, 2019, 29, 1808424.	7.8	35
32833	New insight into the effect of fluorine doping and oxygen vacancies on electrochemical performance of Co2MnO4 for flexible quasi-solid-state asymmetric supercapacitors. Energy Storage Materials, 2019, 22, 384-396.	9.5	189
32834	First principle studies of ZnO1-xSx alloys under high pressure. Journal of Alloys and Compounds, 2019, 788, 905-911.	2.8	6
32835	Oxygen species stabilized on the cobalt spinel nano-octahedra at various reaction conditions and their role in catalytic CO and CH4 oxidation, N2O decomposition and oxygen isotopic exchange. Journal of Catalysis, 2019, 371, 224-235.	3.1	26
32836	Electrical properties of yttrium calcium oxyborate crystal annealed at high temperature and low oxygen partial pressure. Journal of Materiomics, 2019, 5, 363-371.	2.8	9
32837	Suzukiâ€“Miyaura reaction by heterogeneously supported Pd nanoparticles on thio-modified multi walled carbon nanotubes as efficient nanocatalyst. Polyhedron, 2019, 162, 240-244.	1.0	25
32838	Pressure-induced formation of bulk Ge-Sn compounds with high concentration of Sn. Solid State Communications, 2019, 293, 48-52.	0.9	1
32839	Rapid Prediction of Anisotropic Lattice Thermal Conductivity: Application to Layered Materials. Chemistry of Materials, 2019, 31, 2048-2057.	3.2	20
32840	First-Principles Calculations on Polymorphs of Dicalcium Silicateâ€”Belite, a Main Component of Portland Cement. Journal of Physical Chemistry C, 2019, 123, 6768-6777.	1.5	17
32841	Water adsorption on olivine(010) surfaces: Effect of alkali and transition metal cation doping. Journal of Chemical Physics, 2019, 150, 044703.	1.2	4
32842	Study on the strain-induced mechanical property modulations in monolayer Tellurene. Journal of Applied Physics, 2019, 125, .	1.1	41
32843	Interfacial properties of penta-graphene-metal contacts. Journal of Applied Physics, 2019, 125, .	1.1	11
32844	Electronic structure and optical properties of CsSnI3â^'yBry (y = 0, 1, 2, 3) perovskites. International Journal of Modern Physics B, 2019, 33, 1950003.	1.0	5
32845	The Study for Two-dimensional PtX2 (X=S Se Te) Which Have Geometrical Structures Fully Composed of Pentagons.. IOP Conference Series: Materials Science and Engineering, 2019, 631, 042010.	0.3	4
32846	Electrostatics of Double Channel Bipolar FET. , 2019, , .		0
32847	Role of spin-orbit coupling in semimetallic bulk Bismuth. IOP Conference Series: Materials Science and Engineering, 2019, 577, 012072.	0.3	1
32848	Thickness-dependent Strengthening Effect of Grain Refiner Al3Zr and Al3(Zr,Sc) in Al Alloys. IOP Conference Series: Materials Science and Engineering, 2019, 585, 012027.	0.3	0
32849	Theoretical Studies of the Structural, Mechanical and Raman Spectroscopic Properties of Uranyl-Containing Minerals. , 0, , .		0

#	Article	IF	Citations
32850	Graphene crumpling as a method of hydrogen storage: Simulation results. Journal of Micromechanics and Molecular Physics, 2019, 04, 1950009.	0.7	4
32851	Structure and Stability of the Stoichiometric Al3Fe Phase. Metals, 2019, 9, 1322.	1.0	8
32852	Positron annihilation study on the phase transition of thermally aged Fe-Cr binary alloys at 748K. Philosophical Magazine Letters, 2019, 99, 360-371.	0.5	2
32853	Optical Properties and Band Structure of Cu7SiS5I Crystal. , 2019, , .		0
32854	Activating inert basal plane of MoS2 for H2O dissociation and HER via formation of vacancy defects: A DFT study*. , 2019, , .		0
32855	Tailoring Donor-Acceptor Pairs of Tungsten-based Transition Metal Di-Chalcogenides (TMDCs) for Improved Photovoltaic Current Generation. , 2019, , .		0
32856	Prediction of Strain Effect on Hydrogen Evolution Reaction on VMO-SLMOS2 *. , 2019, , .		0
32857	Structural, electronic and energetic properties of uraniumâ€“americium mixed oxides ${m U}_{1-y}{m Am}_y{m O}_2$ using DFT$+{U}$ calculations. Journal of Physics Condensed Matter, 2019, 31, 485501.	0.7	7
32858	A Combined Experimental and Theoretical Study on the Mechanisms Behind Tribocharging Phenomenon and the Influence of Triboemission. Tribology Online, 2019, 14, 367-374.	0.2	5
32859	Investigation of NbC/TiC Heterogeneous Nucleation Interface by First-Principles and Experimental Methods. Metals, 2019, 9, 1265.	1.0	6
32860	Role of generated free radicals in synthesis of amorphous hydrogenated boron carbide from orthocarborane using argon bombardment: a ReaxFF molecular dynamics study. Materials Research Express, 2019, 6, 126461.	0.8	0
32861	Broken translational and rotational symmetries in LiMn1.5Ni0.5O4 spinel. Journal of Physics Condensed Matter, 2019, 31, 395701.	0.7	4
32862	Prediction of colossal magnetocrystalline anisotropy for transition metal triiodides. Journal of Physics Condensed Matter, 2019, 31, 295801.	0.7	7
32863	Ab Initio Monte Carlo Simulations of the Acidic Dissolution of Stainless Steels Effect of Mechanical Deformation. Journal of the Electrochemical Society, 2019, 166, C564-C570.	1.3	2
32864	A study of structural phase transitions and optoelectronic properties of perovskite-type hydride MgFeH₃: ab initio calculations. Journal of Physics Condensed Matter, 2019, 31, 305401.	0.7	11
32865	Ab initio study of negative electron affinity from light metals on the oxygen-terminated diamond (1â€‰1â€‰1) surface. Journal of Physics Condensed Matter, 2019, 31, 295002.	0.7	10
32866	Tunability of Mg₂Si Bandgap by Formation of Mg₂(Si, C) with an Anti-Fluorite Structure Examined by First-Principles Calculations. Materials Transactions, 2019, 60, 1873-1880.	0.4	1
32868	A Theoretical Study of the Energetic Stability and Geometry of Silicon-Vacancy Color Centers in Diamond (001) Surfaces. Applied Sciences (Switzerland), 2019, 9, 5471.	1.3	4

#	Article	IF	Citations
32869	First-Principles Investigations on Structural, Elastic, and Thermodynamic Properties of CaX (X = S, Se,) Tj ETQq0 0 0 rgBT /Overlock 10 Tf	0.1	7
32870	First-Principles Investigation of Electronic Properties of GaAsxSb1 â€“x Ternary Alloys. Semiconductors, 2019, 53, 1731-1739.	0.2	2
32871	Development of a CALPHAD Thermodynamic Database for Pu-U-Fe-Ga Alloys. Applied Sciences (Switzerland), 2019, 9, 5040.	1.3	17
32872	Computational Study of Lithium Intercalation in Silicene Channels on a Carbon Substrate after Nuclear Transmutation Doping. Computation, 2019, 7, 60.	1.0	14
32873	Novel elastic evolution of carbide Mo2Ga2C under pressure: Ab initio theoretical investigation. International Journal of Modern Physics B, 2019, 33, 1950358.	1.0	1
32874	Effect of a small amount of Fe-addition on intergranular fracture of Alâ€“7.3â€‰mass%Mg alloys. Keikinzoku/Journal of Japan Institute of Light Metals, 2019, 69, 457-464.	0.1	5
32875	Influence of Octahedral Cation Distribution in Montmorillonite on Interlayer Hydrogen Counter-Ion Retention Strength via First-Principles Calculations. Clays and Clay Minerals, 2019, 67, 439-448.	0.6	4
32877	An ab initio Study of Cr and Mn Doped MAX Phase TiMSiB. , 2019, , .		0
32878	The mechanical and electronic properties of spinel oxides VX2O4 (X = Mn and Fe) by first principle calculations. AIP Conference Proceedings, 2019, , .	0.3	3
32879	Elastic, Electronic, and Optical properties of NaSnX (X=Sb, Bi, As): First principle calculations. IOP Conference Series: Materials Science and Engineering, 2019, 613, 012011.	0.3	1
32880	Solid Solutions PdTe1â€“ xBix (x < 0.8) with the NiAs Structure in the Pdâ€“Biâ€“Te System. Russian Journal of Inorganic Chemistry, 2019, 64, 1486-1493.	0.3	2
32881	Research on monolayer h-BN cell strain effect vacancy stability. Journal of Physics: Conference Series, 2019, 1353, 012020.	0.3	0
32882	Effects of increasing the concentration of Cr in the alloys Nb1-xCrxN. Journal of Physics: Conference Series, 2019, 1386, 012027.	0.3	0
32883	Comparative study of the effect of the exchange-correlation functional on the structural and electronic properties of rutile. Journal of Physics: Conference Series, 2019, 1386, 012074.	0.3	1
32884	Phonons in short-period (GaN)_m(AlN)_n superlattices: ab initio calculations and group-theoretical analysis of modes and their genesis. Journal of Physics: Conference Series, 2019, 1400, 066016.	0.3	3
32885	Forming the GaN Nanocrystals on the Graphene-Like g-AlN and g-Si3N3 Surface. Physics of the Solid State, 2019, 61, 2329-2334.	0.2	1
32886	Flat Band and Hole-induced Ferromagnetism in a Novel Carbon Monolayer. Scientific Reports, 2019, 9, 20116.	1.6	19
32889	Engineering the Interfacial Electronic Structure of Epitaxial Ge/AlAs(001) Heterointerfaces via Substitutional Boron Incorporation: The Roles of Doping and Interface Stoichiometry. ACS Applied Electronic Materials, 2019, 1, 2646-2654.	2.0	7

#	Article	IF	Citations
32890	Mechanism of the transition of solid hydrogen to the conducting state at high pressures. Journal of Physics: Conference Series, 2019, 1147, 012002.	0.3	0
32891	Systematic trends in YAlO₃, SrTiO₃, BaTiO₃, BaZrO₃ (001) and (111) surface ab initio calculations. International Journal of Modern Physics B, 2019, 33, 1950390.	1.0	11
32892	Directed Molecular Stacking for Engineered Fluorescent Threeâ€Dimensional Reduced Graphene Oxide and Coronene Frameworks. ChemistryOpen, 2019, 8, 1383-1398.	0.9	5
32893	Size Matters: New Zintl Phase Hydrides of REGa (RE = Y, La, Tm) and RESi (RE = Y, Er, Tm) with Large and Small Cations. Crystals, 2019, 9, 600.	1.0	0
32894	First-principles calculations of elastic properties and electronic structure of Î±-CoSn3 IMC. , 2019, , .		1
32895	First-Principles Study of the Stability of the TiC-ZrC Solid Solutions. , 2019, , .		0
32896	Hardening tungsten carbide by alloying elements with high work function. Acta Crystallographica Section B: Structural Science, Crystal Engineering and Materials, 2019, 75, 994-1002.	0.5	2
32897	Towards Control of Band Gap in Two-Dimensional Hexagonal Boron Nitride by Doping. , 2019, , .		1
32898	Ultimate Mechanical Properties of Forsterite. Minerals (Basel, Switzerland), 2019, 9, 787.	0.8	12
32899	Electrostatic Potential Anomaly in 2D Janus Transition Metal Dichalcogenides. Annalen Der Physik, 2019, 531, 1900369.	0.9	13
32900	First principles investigations of hydrogen interaction with vacancy-oxygen complexes in vanadium alloys. International Journal of Hydrogen Energy, 2019, 44, 26637-26645.	3.8	11
32901	Coordination Geometry Engineering in a Doped Disordered Matrix for Tunable Optical Response. Journal of Physical Chemistry C, 2019, 123, 29343-29352.	1.5	10
32902	Superconducting Single-Layer T-Graphene and Novel Synthesis Routes*. Chinese Physics Letters, 2019, 36, 097401.	1.3	61
32903	Experimental evidence of crystal symmetry protection for the topological nodal line semimetal state in ZrSiS. Physical Review B, 2019, 100, .	1.1	19
32904	Birefringence of Tl₄HgI₆ Crystal. , 2019, , .		2
32905	Passivating Surface States on Water Splitting Cuprous Oxide Photocatalyst with Bismuth Decoration. Molecules, 2019, 24, 4156.	1.7	2
32906	Prediction of Transition-State Energies of Hydrodeoxygenation Reactions on Transition-Metal Surfaces Based on Machine Learning. Journal of Physical Chemistry C, 2019, 123, 29804-29810.	1.5	21
32907	Fullerene-Based Switching Molecular Diodes Controlled by Oriented External Electric Fields. Journal of the American Chemical Society, 2019, 141, 19644-19654.	6.6	59

#	Article	IF	Citations
32908	Elucidating the origin of magnetic ordering in ferroelectric BaTiO₃₋ d thin film via electronic structure modification. Journal of Physics Condensed Matter, 2019, 31, 205001.	0.7	13
32909	P2 Type Layered Solid-State Electrolyte Na₂Zn₂TeO₆: Crystal Structure and Stacking Faults. Journal of the Electrochemical Society, 2019, 166, A3830-A3837.	1.3	10
32910	Effects of Lattice O Atom Coordination and Pore Confinement on Selectivity Limitations for Ethane Oxidative Dehydrogenation Catalyzed by Vanadium-Oxo Species. Journal of Physical Chemistry C, 2019, 123, 28168-28191.	1.5	20
32911	Analysis of Dihydrogen Bonding in Ammonium Borohydride. Journal of Physical Chemistry C, 2019, 123, 28631-28639.	1.5	22
32912	Low-Temperature Catalytic NO Reduction with CO by Subnanometric Pt Clusters. ACS Catalysis, 2019, 9, 11530-11541.	5.5	70
32913	A Comparative Computational Study of the Adsorption of TCNQ and F4-TCNQ on the Coinage Metal Surfaces. ACS Omega, 2019, 4, 16906-16915.	1.6	9
32914	Absorption enhancement by transition metal doping in ZnS. Materials Research Express, 2019, 6, 126550.	0.8	7
32915	Stability and interatomic potentials for M-doped TiV alloys (M=H, He, C, O) by first-principles simulations. European Physical Journal D, 2019, 73, 1.	0.6	5
32916	Multilayered stable 2D nano-sheets of Ti2NTx MXene: synthesis, characterization, and anticancer activity. Journal of Nanobiotechnology, 2019, 17, 114.	4.2	63
32917	The Nucleation and the Intrinsic Microstructure Evolution of Martensite from 332113Î² Twin Boundary in Î² Titanium: First-Principles Calculations. Metals, 2019, 9, 1202.	1.0	6
32918	Study of the Structural, Elastic, Electronic and Optical Properties of the Ternary Acetylides A2MC2 (A) Tj ETQq0 0 0 rgBT /Overlock 10 Tf	0.3	0
32919	The high-pressure study of energetic compound DMNA by dispersion-corrected density functional theory calculations. Computational and Theoretical Chemistry, 2019, 1167, 112603.	1.1	2
32920	Single-atom cobalt array bound to distorted 1T MoS2 with ensemble effect for hydrogen evolution catalysis. Nature Communications, 2019, 10, 5231.	5.8	371
32921	Super-resolution energy spectra from neutron direct-geometry spectrometers. Review of Scientific Instruments, 2019, 90, 105109.	0.6	9
32922	Blue phosphorene nanoribbon for detection of chloroform vapours â€“ a first-principles study. International Journal of Environmental Analytical Chemistry, 2019, , 1-13.	1.8	13
32923	Removing all periodic boundary conditions: Efficient nonequilibrium Green's function calculations. Physical Review B, 2019, 100, .	1.1	9
32924	Hybrid neural network potential for multilayer graphene. Physical Review B, 2019, 100, .	1.1	38
32925	Topological Phase Diagram of BiTeXâ€“Graphene Hybrid Structures. Applied Sciences (Switzerland), 2019, 9, 4330.	1.3	3

#	Article	IF	Citations
32926	Ab initio theory of the nitrogen-vacancy center in diamond. Nanophotonics, 2019, 8, 1907-1943.	2.9	140
32927	First-principles calculations of mechanical and thermodynamic properties of tungsten-based alloy. Nanotechnology Reviews, 2019, 8, 258-265.	2.6	10
32928	Effective lattice model of graphene moirÃ© superlattices on hexagonal boron nitride. Physical Review B, 2019, 100, .	1.1	17
32929	Dielectric function spectra and optical transitions in thallium bromide crystals for radiation detectors. Journal of Vacuum Science and Technology B:Nanotechnology and Microelectronics, 2019, 37, 061207.	0.6	0
32930	First Principles Investigation of Anomalous Pressure-Dependent Thermal Conductivity of Chalcopyrites. Materials, 2019, 12, 3491.	1.3	8
32931	High-Throughput Screening of Rare-Earth-Lean Intermetallic 1-13-X Compounds for Good Hard-Magnetic Properties. Metals, 2019, 9, 1096.	1.0	7
32932	Giant Rashba spin splitting induced by heavy element adsorption at germanene. FlatChem, 2019, 18, 100141.	2.8	7
32933	Characterization and Stability of Janus TiXY (X/Y = S, Se, and Te) Monolayers. Journal of Physical Chemistry C, 2019, 123, 29922-29931.	1.5	30
32934	Nonvolatile Balanced Ternary Memory Based on The Multiferroelectric Material GeSnTe2. Journal of Physical Chemistry Letters, 2019, 10, 7470-7474.	2.1	6
32935	Improved thermoelectric performance of p-doped half-Heusler Ti0.5Zr0.5CoSb0.5P0.5, Ti0.5Hf0.5CoSb0.5P0.5, and Zr0.5Hf0.5CoSb0.5P0.5 compounds. Materials Research Express, 2019, 6, 126305.	0.8	5
32936	Defect processes in F and Cl doped anatase TiO2. Scientific Reports, 2019, 9, 19970.	1.6	35
32937	Single-layer LaBr2: Two-dimensional valleytronic semiconductor with spontaneous spin and valley polarizations. Applied Physics Letters, 2019, 115, .	1.5	100
32938	First-Principles study of two dimensional transition metal phthalocyanine-based metal-organic frameworks in kagome lattice. Chinese Journal of Chemical Physics, 2019, 32, 563-571.	0.6	8
32939	Efficient method for grand-canonical twist averaging in quantum Monte Carlo calculations. Physical Review B, 2019, 100, .	1.1	16
32940	Effect of strain on the structural and electronic properties of graphene-like GaN: A DFT study. International Journal of Modern Physics B, 2019, 33, 1950281.	1.0	1
32941	Effect of rare earth (Sc, Y, La, Sm and Gd) doping on mechanical and thermodynamic properties of Al12Mg17 intermetallic compounds. Modern Physics Letters B, 2019, 33, 1950442.	1.0	1
32942	Theoretical Investigation on the Elastic Properties, Bond Stiffness and Hardness of WX2 (X = B and N). Journal of Superhard Materials, 2019, 41, 434-440.	0.5	1
32943	First-Principles Study of Alkyl Derivatives of Boehmite. Journal of the Korean Physical Society, 2019, 75, 490-493.	0.3	1

#	Article	IF	Citations
32944	Theory of Carbon-Vacancy Diffusion at the SiO₂/4H-SiC Interface. Materials Science Forum, 0, 963, 204-207.	0.3	0
32945	Water interaction and dissociation on stoichiometric and defective Mn- and Fe-doped CeO2 surfaces. Materials Today Communications, 2019, 21, 100703.	0.9	2
32946	Photorealistic modelling of metals from first principles. Npj Computational Materials, 2019, 5, .	3.5	21
32947	Charge-induced electromechanical actuation of two-dimensional hexagonal and pentagonal materials. Physical Chemistry Chemical Physics, 2019, 21, 22377-22384.	1.3	15
32948	Structural and electronic transport properties of a SiC chain encapsulated inside a SiC nanotube: first-principles study. Physical Chemistry Chemical Physics, 2019, 21, 25548-25557.	1.3	4
32949	Chemical origin of differences in steel corrosion behaviors of s-electron and p-electron liquid metals by first-principles calculation. Physical Chemistry Chemical Physics, 2019, 21, 25916-25924.	1.3	1
32950	Electronic engineering of a tetrathiafulvalene charge-transfer salt via reduced symmetry induced by combined substituents. Physical Chemistry Chemical Physics, 2019, 21, 22639-22646.	1.3	10
32951	The unexpected effect of vacancies and wrinkling on the electronic properties of MoS₂ layers. Physical Chemistry Chemical Physics, 2019, 21, 24731-24739.	1.3	5
32952	Bimetallic Alâ€“Sn clusters: mixing at the nanoscale. Physical Chemistry Chemical Physics, 2019, 21, 22919-22929.	1.3	8
32953	First-principles theory of atomic-scale friction explored by an intuitive charge density fluctuation surface. Physical Chemistry Chemical Physics, 2019, 21, 24565-24571.	1.3	13
32954	Dramatic magnetic phase designing in phosphorene. Physical Chemistry Chemical Physics, 2019, 21, 23713-23719.	1.3	26
32955	Size-controlled excitonic effects on electronic and optical properties of Sb₂S₃ nanowires. Physical Chemistry Chemical Physics, 2019, 21, 26515-26524.	1.3	14
32956	Mechanisms of alumina growth via atomic layer deposition on nickel oxide and metallic nickel surfaces. Physical Chemistry Chemical Physics, 2019, 21, 24543-24553.	1.3	5
32957	Synthesis, crystal and electronic structures of Pt-rich phosphides EuPt₃P and EuPt₆P₂. Dalton Transactions, 2019, 48, 15272-15282.	1.6	3
32958	Surface structural phase transition induced by the formation of metalâ€“organic networks on the Si(111)–In surface. Nanoscale, 2019, 11, 21790-21798.	2.8	4
32959	Promoting polysulfide conversion by catalytic ternary Fe₃O₄/carbon/graphene composites with ordered microchannels for ultrahigh-rate lithiumâ€“sulfur batteries. Journal of Materials Chemistry A, 2019, 7, 25078-25087.	5.2	68
32960	Topological dual double node-line semimetals NaAlSi(Ge) and their potential as cathode material for sodium ion batteries. Journal of Materials Chemistry C, 2019, 7, 15375-15381.	2.7	34
32961	The mechanical, electronic and optical properties of two-dimensional transition metal chalcogenides MX₂ and M₂X₃ (M = Ni, Pd; X = S, Se, Te) with hexagonal and orthorhombic structures. Journal of Materials Chemistry C, 2019, 7, 13518-13525.	2.7	58

#	Article	IF	Citations
32962	Investigations of fundamental physical and thermoelectric properties of methylammonium lead iodide (CH₃NH₃PbI₃) perovskites. Materials Research Express, 2019, 6, 126323.	0.8	17
32963	Effect of S-vacancy on the oxidation state of Ce in monolayer SnS₂. International Journal of Modern Physics B, 2019, 33, 1950308.	1.0	3
32964	Ab Initio Molecular Dynamics Study of Alignment-Resolved O₂ Scattering from Highly Oriented Pyrolytic Graphite. Journal of Physical Chemistry C, 2019, 123, 31094-31102.	1.5	15
32965	Computational Simulation of Trapped Charge Carriers in TiO₂ and Their Impacts on Photocatalytic Water Splitting. ACS Symposium Series, 2019, , 67-100.	0.5	1
32966	Time-Domain ab Initio Studies of Excited State Dynamics at Nanoscale Interfaces. ACS Symposium Series, 2019, , 101-136.	0.5	2
32967	Comprehensive Study of Multiple Exciton Generation in Chiral Carbon Nanotubes Using Many-Body Perturbation Theory Based on Density Functional Theory Simulations. ACS Symposium Series, 2019, , 157-179.	0.5	0
32968	A computational-experimental investigation on high ethylene selectivity in ethanol dehydration reaction found on WOx/ZrO2-activated carbon bi-support systems. Scientific Reports, 2019, 9, 19738.	1.6	8
32969	Theoretical investigation of the vertical dielectric screening dependence on defects for few-layered van der Waals materials. RSC Advances, 2019, 9, 40309-40315.	1.7	12
32970	Atomic interactions between Si and Mn during eutectoid transformation in high-carbon pearlitic steel. Journal of Applied Physics, 2019, 126, .	1.1	5
32971	The electronic behaviors and charge transfer mechanism at the interface of metals: A first-principles perspective. Journal of Applied Physics, 2019, 126, 205301.	1.1	2
32972	Enhanced ductility of III-V covalent semiconductors from electrons and holes. Journal of Applied Physics, 2019, 126, .	1.1	5
32973	Low compressible Î²-BP3N6. AIP Advances, 2019, 9, .	0.6	3
32974	Influence of Ni doping in a lead-halide and a lead-free halide perovskites for optoelectronic applications. AIP Advances, 2019, 9, .	0.6	56
32975	Attaching titania clusters of various size to reduced graphene oxide and its impact on the conceivable photocatalytic behavior of the junctionsâ€”a DFT/Dâ€‰â€‰+â€‰â€‰U and TD DFTB modeling. Journal of Physics: Condensed Matter, 2019, 31, 404001.	1.7	11
32976	<mml:math xmlns:mml="http://www.w3.org/1998/Math/MathML"><mml:mi mathvariant="script">PT</mml:mi></mml:math> -symmetry-protected Dirac states in strain-induced hidden <mml:math xmlns:mml="http://www.w3.org/1998/Math/MathML"><mml:mrow><mml:mi>Mo</mml:mi><mml:msub><mml:mi mathvariant="normal">S</mml:mi><mml:mn>2</mml:mn></mml:msub></mml:mrow></mml:math> monolayer. Physical Review B, 2019, 100, .	1.1	9
32977	First-principle study of the structural, mechanical, electronic and thermodynamic properties of intermetallic compounds: Pd₃M (M=Sc, Y). International Journal of Modern Physics B, 2019, 33, 1950321.	1.0	3
32978	Contact-Induced Phase Separation of Alloy Catalyst to Promote Carbon Nanotube Growth. Physical Review Letters, 2019, 123, 256101.	2.9	17
32979	Two-Dimensional Second-Order Topological Insulator in Graphdiyne. Physical Review Letters, 2019, 123, 256402.	2.9	193

#	Article	IF	Citations
32980	The Flexible Lubrication Performance of Graphene Used in Diamond Interface as a Solid Lubricant: First-Principles Calculations. Nanomaterials, 2019, 9, 1784.	1.9	4
32981	Theoretical Investigation of NiI₂ Based Bilayer Heterostructures. Key Engineering Materials, 0, 806, 10-16.	0.4	0
32982	Modeling of Photooxidative Degradation of Aromatics in Water Matrix: A Quantitative Structureâ^'Property Relationship Approach. ACS Symposium Series, 2019, , 257-292.	0.5	0
32983	Functionalized Carbon Nanotube Excited States and Optical Properties. ACS Symposium Series, 2019, , 181-207.	0.5	1
32984	Towards a transferable design of solid-state embedding models on the example of a rutile TiO2 (110) surface. Journal of Chemical Physics, 2019, 151, 184114.	1.2	12
32985	Bowing of the band gap and spin-orbit splitting energy in BGaAs. Materials Research Express, 2019, 6, 125913.	0.8	8
32986	A first-principles study of magnetic properties of Zn_{0.94}Mg_{0.01}Mn_{0.05}O. Materials Research Express, 2019, 6, 126118.	0.8	4
32987	A computational approach to study the optoelectronic properties of F-BODIPY derivatives at the bulk level for photovoltaic applications. Materials Research Express, 2019, 6, 125110.	0.8	2
32988	Electronic Structure and Excited State Dynamics of TiO₂Nanowires. ACS Symposium Series, 2019, , 23-46.	0.5	0
32989	Optical Properties of the TiO₂(110) Surface with Adsorbed Ag Atoms Relevant to Photocatalysis and Photovoltaics. ACS Symposium Series, 2019, , 47-66.	0.5	1
32990	Physical Properties of Conjugated Nanopore Materials. ACS Symposium Series, 2019, , 293-308.	0.5	0
32991	Photo-induced Charge Separation and Photoredox Catalysis in Cerium-Based Metalâ€“Organic Frameworks. ACS Symposium Series, 2019, , 309-326.	0.5	5
32992	Excited State Electronic Structure of Single-Site Vanadium Oxide Photocatalysts Supported on Mesoporous Silica. ACS Symposium Series, 2019, , 327-341.	0.5	2
32993	Effect of doping on nanoindentation induced incipient plasticity in InP crystal. AIP Advances, 2019, 9, .	0.6	4
32994	Polarization Selectivity in Vibrational Electron-Energy-Loss Spectroscopy. Physical Review Letters, 2019, 123, 256001.	2.9	16
32995	Strong Valence Electrons Dependent and Logical Relations of Elemental Impurities in 2D Binary Semiconductor: a Case of GeP3 Monolayer from Ab Initio Studies. Nanoscale Research Letters, 2019, 14, 307.	3.1	2
32996	Phonon-Mediated Ultrafast Hole Transfer from Photoexcited CdSe Quantum Dots to Black Dye. ACS Symposium Series, 2019, , 137-156.	0.5	4
32997	Carbon sp chains in diamond nanocavities. Physical Chemistry Chemical Physics, 2019, 21, 21814-21823.	1.3	3

#	Article	IF	Citations
32998	Interface-induced enhancement of piezoelectricity in the (SrTiO₃)_m/(BaTiO₃)_{Mâ^'m} superlattice for energy harvesting applications. Physical Chemistry Chemical Physics, 2019, 21, 23541-23551.	1.3	9
32999	Interpenetrating graphene network bct-C₄₀: a promising anode material for Li ion batteries. Physical Chemistry Chemical Physics, 2019, 21, 23485-23491.	1.3	9
33000	Accurate K-edge X-ray photoelectron and absorption spectra of g-C₃N₄ nanosheets by first-principles simulations and reinterpretations. Physical Chemistry Chemical Physics, 2019, 21, 22819-22830.	1.3	70
33001	Mechanical properties and superconductivity in two-dimensional B2O under extreme strain. Physical Chemistry Chemical Physics, 2019, 21, 25859-25864.	1.3	4
33002	Thickness biased capture of CO₂ on carbide MXenes. Physical Chemistry Chemical Physics, 2019, 21, 23136-23142.	1.3	55
33003	Two-dimensional ZrB₂C₂ with multiple tunable Dirac states. Physical Chemistry Chemical Physics, 2019, 21, 24212-24217.	1.3	10
33004	Theoretical study of the optical and thermodynamic properties of La_xSr_{1â^'x}Co_{1â^'y}Fe_yO_{3â^'Î´} (x/y =) ïBETQq0 0 0 rgBT /C		
33005	Structural transition induced by compression and stretching of puckered arsenene nanotubes. Physical Chemistry Chemical Physics, 2019, 21, 22467-22474.	1.3	6
33006	Potential hydrogen storage materials from metal decorated 2D-C₂N: an ab initio study. Physical Chemistry Chemical Physics, 2019, 21, 25311-25322.	1.3	53
33007	Experimental and theoretical investigation of lithium-ion conductivity in Li₂LaNbTiO₇. Dalton Transactions, 2019, 48, 17281-17290.	1.6	6
33008	An experimental and theoretical study of metallorganic coordination networks of tetrahydroxyquinone on Cu(111). New Journal of Chemistry, 2019, 43, 19186-19192.	1.4	3
33009	Raman and electrical transport properties of few-layered arsenic-doped black phosphorus. Nanoscale, 2019, 11, 18449-18463.	2.8	27
33010	Design of high-performance MoS₂ edge supported single-metal atom bifunctional catalysts for overall water splitting via a simple equation. Nanoscale, 2019, 11, 20228-20237.	2.8	57
33011	The preparation and mechanistic study of highly effective PtSnRu ternary nanorod catalysts toward the ethanol oxidation reaction. Sustainable Energy and Fuels, 2019, 3, 3352-3362.	2.5	9
33012	Laser-engineered oxygen vacancies for improving the NO₂ sensing performance of SnO₂ nanowires. Journal of Materials Chemistry A, 2019, 7, 27205-27211.	5.2	33
33013	Itinerant ferromagnetic half metallic cobaltâ€“iron couples: promising bifunctional electrocatalysts for ORR and OER. Journal of Materials Chemistry A, 2019, 7, 27175-27185.	5.2	122
33014	Isomorphism combined with intercalation methods to construct a hybrid electrode material for high-energy storage capacitors. Journal of Materials Chemistry A, 2019, 7, 25120-25131.	5.2	23
33015	Self energy and excitonic effect in (un)doped TiO₂ anatase: a comparative study of hybrid DFT, GW and BSE to explore optical properties. Journal of Materials Chemistry C, 2019, 7, 14284-14293.	2.7	24

#	Article	IF	Citations
33016	Orbitally dominated Rashba-Edelstein effect in noncentrosymmetric antiferromagnets. Nature Communications, 2019, 10, 5381.	5.8	47
33017	First principle study of HF molecule adsorption on TiO2 (110) surface. IOP Conference Series: Materials Science and Engineering, 2019, 655, 012043.	0.3	2
33018	Bilayer MoSe2/HfS2 Nanocomposite as a Potential Visible-Light-Driven Z-Scheme Photocatalyst. Nanomaterials, 2019, 9, 1706.	1.9	20
33019	Non-Fermi-liquid types of behavior associated with a magnetic quantum critical point in <mml:math xmlns:mml="http://www.w3.org/1998/Math/MathML"><mml:mrow><mml:mi>Sr</mml:mi><mml:msub><mml:mrow><mml:mi></mml:mi></mml:mrow><mml:mn>(</mml:mn> Physical Review B, 2019, 100, .	1.1	19
33020	Density Functional Theory Analysis of the Adsorption Interactions of Carbon Impurities in Coal-associated Kaolinite. Processes, 2019, 7, 782.	1.3	3
33021	Stabilizer-Free CuIr Alloy Nanoparticle Catalysts. Chemistry of Materials, 2019, 31, 10225-10235.	3.2	16
33022	A systematic study of the negative thermal expansion in zinc-blende and diamond-like semiconductors. New Journal of Physics, 2019, 21, 123015.	1.2	10
33023	Density Functional Study of the Electronic, Elastic and Optical Properties of Bi₂O₂Te. Zeitschrift Fur Naturforschung - Section A Journal of Physical Sciences, 2019, 75, 73-80.	0.7	6
33024	Real-space observation of far- and near-field-induced photolysis of molecular oxygen on an Ag(110) surface by visible light. Journal of Chemical Physics, 2019, 151, 144705.	1.2	14
33025	Possible enhancement of superconductivity by Sb doping in rare earth doped 112 compounds: an ab-initio study. International Journal of Environmental Analytical Chemistry, 2019, , 1-12.	1.8	1
33026	Theoretical study of the insertion and diffusivity of hydrogen in the Ti3Al-D019 system: Comparison with Ti-hcp and TiAl-L10 systems. International Journal of Hydrogen Energy, 2019, 44, 32307-32322.	3.8	11
33027	Facile high-yield synthesis of MoS₂ nanosheets with enhanced photocatalytic performance using ultrasound driven exfoliation technique. Materials Research Express, 2019, 6, 125079.	0.8	10
33028	Theoretical design of a novel 2D tetragonal ZnS/SnO hetero-bilayer as a promising photocatalyst for solar water splitting. International Journal of Hydrogen Energy, 2019, 44, 27816-27824.	3.8	11
33029	Effects of Gas-Phase Conditions and Particle Size on the Properties of Cu(111)-Supported Zn_yO_x Particles Revealed by Global Optimization and Ab Initio Thermodynamics. Journal of Physical Chemistry C, 2019, 123, 30903-30916.	1.5	17
33030	Imaging individual solute atoms at crystalline imperfections in metals. New Journal of Physics, 2019, 21, 123020.	1.2	26
33031	Effect of electric field on optoelectronic properties of indiene monolayer for photoelectric nanodevices. Scientific Reports, 2019, 9, 17300.	1.6	18
33032	Plasma Surface Polymerized and Biomarker Conjugated Boron Nitride Nanoparticles for Cancer-Specific Therapy: Experimental and Theoretical Study. Nanomaterials, 2019, 9, 1658.	1.9	6
33033	Ultralow lattice thermal conductivity of chalcogenide perovskite CaZrSe3 contributes to high thermoelectric figure of merit. Npj Computational Materials, 2019, 5, .	3.5	31

#	Article	IF	Citations
33034	Oxidized Silicon Sulfide: Stability and Electronic Properties of a Novel Two-Dimensional Material. Journal of Physical Chemistry C, 2019, 123, 29986-29993.	1.5	2
33035	Probing Structural Reconstruction of Metal Nanoparticles under Annealing and Water Vapor Conditions: A Theoretical Study. Journal of Physical Chemistry C, 2019, 123, 29783-29793.	1.5	7
33036	Optimization of Defects in Large-Area Synthetic MoS₂ Thin Films by CS₂ Treatment for Switching and Sensing Devices. ACS Applied Nano Materials, 2019, 2, 7810-7818.	2.4	15
33037	Conducting and Lithiophilic MXene/Graphene Framework for High-Capacity, Dendrite-Free Lithiumâ€“Metal Anodes. ACS Nano, 2019, 13, 14308-14318.	7.3	155
33038	A â€œOne-Potâ€•Route for the Synthesis of Snowflake-like Dendritic CoNi Alloy-Reduced Graphene Oxide-Based Multifunctional Nanocomposites: An Efficient Magnetically Separable Versatile Catalyst and Electrode Material for High-Performance Supercapacitors. ACS Omega, 2019, 4, 20672-20689.	1.6	22
33039	Lattice Thermal Conductivity of MgSiO₃ Postperovskite Under the Lowermost Mantle Conditions From Ab Initio Anharmonic Lattice Dynamics. Geophysical Research Letters, 2019, 46, 12919-12926.	1.5	17
33040	Dual phases of crystalline and electronic structures in the nanocrystalline perovskite CsPbBr3. NPG Asia Materials, 2019, 11, .	3.8	41
33041	Influence of confinement on free radical chemistry in layered nanostructures. Scientific Reports, 2019, 9, 17165.	1.6	3
33042	Negative thermal expansion of Cu2O studied by quasi-harmonic approximation and cubic force-constant method. Journal of Chemical Physics, 2019, 151, 184109.	1.2	8
33043	Interrelation between the grain boundary energy and the packing density in Î±-Fe. AIP Conference Proceedings, 2019, , .	0.3	1
33044	First-principles analysis of ferromagnetic properties of molybdenum-doped wide-band-gap oxides. Philosophical Magazine Letters, 2019, 99, 326-337.	0.5	19
33045	Strain Controls Charge Carrier Lifetimes in Monolayer WSe₂: Ab Initio Time Domain Analysis. Journal of Physical Chemistry Letters, 2019, 10, 7732-7739.	2.1	36
33046	In situ formation of mononuclear complexes by reaction-induced atomic dispersion of supported noble metal nanoparticles. Nature Communications, 2019, 10, 5281.	5.8	57
33047	Six-dimensional potential energy surfaces for the dissociative chemisorption of HCl on rigid Ag(100) and Ag(110) surfaces. Journal of Chemical Physics, 2019, 151, 144707.	1.2	10
33048	Spin-dependent Dirac electrons and valley polarization in the ferromagnetic stanene/ <mml:math xmlns:mml="http://www.w3.org/1998/Math/MathML"><mml:mrow><mml:mi>Cr</mml:mi><mml:msub><mml:mi mathvariant="normal">I</mml:mi><mml:mn>3</mml:mn></mml:msub></mml:mrow></mml:math> van der Waals heterostructure. Physical Review B, 2019, 100, .	1.1	35
33049	Charge density wave hampers exciton condensation in <mml:math xmlns:mml="http://www.w3.org/1998/Math/MathML"><mml:mrow><mml:mn>1</mml:mn><mml:mi>T</mml:mi><mml:mtext> â^’ </mml:mtext></mml:mrow></mml:math> Physical Review B, 2019, 100, .	1.1	18
33050	Higher-Order Topological Insulator in Twisted Bilayer Graphene. Physical Review Letters, 2019, 123, 216803.	2.9	173
33051	Quantum Phase Transition of Correlated Iron-Based Superconductivity in <mml:math xmlns:mml="http://www.w3.org/1998/Math/MathML" display="inline"><mml:mrow><mml:msub><mml:mrow><mml:mi>LiFe</mml:mi></mml:mrow><mml:mrow><mml:mn>1</mml:mn></mml:mrow> Physical Review Letters, 2019, 123, 217004.	2.9	19

#	Article	IF	Citations
33052	Ground-State Magnetic Phase in Transition-Metal-Doped Boron Nitride Nanosheet With (5,0) Chirality. IEEE Magnetics Letters, 2019, 10, 1-4.	0.6	16
33053	Adsorption of carbon dioxide and ammonia in transition metalâ€“doped boron nitride nanotubes. Journal of Molecular Modeling, 2019, 25, 359.	0.8	9
33054	Computation of formation enthalpies and molar volumes of halides. Solid State Ionics, 2019, 343, 115081.	1.3	0
33055	Two-Dimensional Covalent Triazine Framework as a Promising Anode Material for Li-Ion Batteries. Journal of Physical Chemistry C, 2019, 123, 30155-30164.	1.5	34
33056	The CeFe₁₁Ti permanent magnet: a closer look at the microstructure of the compound. Journal of Physics Condensed Matter, 2019, 31, 505505.	0.7	6
33057	Adsorption of thiophene and SO_x molecules on Cr-doped and Ti-doped graphene nanosheets: a DFT study. Materials Research Express, 2019, 6, 125067.	0.8	6
33058	Experimental and theoretical investigations on the composition-dependent structural phase transition in Cu₂Cd_xZn_{1â^'x}SnS₄. Materials Research Express, 2019, 6, 125525.	0.8	9
33059	Spin reorientation in one-dimensional transition metal cyanides: Behavior of the trimetallic cyanide <mml:math xmlns:mml="http://www.w3.org/1998/Math/MathML"><mml:mrow><mml:mi mathvariant="normal">C</mml:mi><mml:msub><mml:mi mathvariant="normal">u</mml:mi><mml:mrow><mml:mn>1</mml:mn><mml:mo>/</mml:mo><mml:mn>3</mml:mn></mml:mrow>	1.1	3
33060	Sandwiched NiO/Î²â€Mo₂C/RGO as Improved Electrocatalyst for Hydrogen Evolution Reaction: Solvothermalâ€Assisted Selfâ€Assembly and Catalytic Mechanism. ChemElectroChem, 2019, 6, 5958-5966.	1.7	12
33061	Electronic Structural Origin of the Catalytic Activity Trend of Transition Metals for Electrochemical Nitrogen Reduction. Journal of Physical Chemistry C, 2019, 123, 31026-31031.	1.5	16
33062	First-principles investigation of the ferroelectric, piezoelectric and nonlinear optical properties of LiNbO3-type ZnTiO3. Scientific Reports, 2019, 9, 17632.	1.6	12
33063	Electronic and mechanical properties of Al (100)/6Hâ€“SiC (0001) interfaces: a first-principles study. Materials Research Express, 2019, 6, 126316.	0.8	3
33064	Boson Peak Related to Ga Nanoclusters in AlGaN Layers Grown by Plasma-Assisted Molecular Beam Epitaxy at Ga-Rich Conditions. Semiconductors, 2019, 53, 1479-1488.	0.2	1
33065	First-principles electronic structure in second-moment calculation of mode frequencies: Failure of quasiharmonic approximation in silicon. Physical Review B, 2019, 100, .	1.1	2
33066	Pressure-induced superconductivity in GeAs. Physical Review B, 2019, 100, .	1.1	9
33067	Anisotropic magnetoresistance and nontrivial spin Hall magnetoresistance in <mml:math xmlns:mml="http://www.w3.org/1998/Math/MathML"><mml:mrow><mml:mi>Pt</mml:mi><mml:mo>/</mml:mo><mml:mi>Î±</mml:mi><mml:mi mathvariant="normal">F</mml:mi><mml:msub><mml:mi mathvariant="normal">e</mml:mi><mml:mn>2</mml:mn></mml:msub><mml:msub><mml:mi mathvariant="normal">O</mml:mi><mml:mn>3</mml:mn></mml:msub></mml:mrow></mml:math>	1.1	35
33068	First-principles study of high-pressure phase stability and superconductivity of <mml:math xmlns:mml="http://www.w3.org/1998/Math/MathML"><mml:mrow><mml:msub><mml:mi>Bi</mml:mi><mml:mn>4</mml:mn></mml:msub><mml:msub><mml:mi mathvariant="normal">I</mml:mi><mml:mn>4</mml:mn></mml:msub></mml:mrow></mml:math>. Physical Review B, 2019, 100, .	1.1	9
33069	Interfacial coupling induced critical thickness for the ferroelectric bistability of two-dimensional ferromagnet/ferroelectric van der Waals heterostructures. Physical Review B, 2019, 100, .	1.1	30

#	Article	IF	Citations
33070	Vibrational response and motion of carbon monoxide on Cu(100) driven by femtosecond laser pulses: Molecular dynamics with electronic friction. Physical Review B, 2019, 100, .	1.1	16
33072	Conjugates of Gold Nanoparticles and Antitumor Gold(III) Complexes as a Tool for Their AFM and SERS Detection in Biological Tissue. International Journal of Molecular Sciences, 2019, 20, 6306.	1.8	6
33073	Theoretical Study of Zirconium Isomorphous Substitution into Zeolite Frameworks. Molecules, 2019, 24, 4466.	1.7	3
33074	Electronic Structure and Polarization of Polar BiOIO3. Journal of the Korean Physical Society, 2019, 75, 990-996.	0.3	6
33075	Atomistic Simulations of Plasmon Mediated Photochemistry. ACS Symposium Series, 2019, , 239-256.	0.5	2
33077	First-principles soft-mode lattice dynamics of <mml:math xmlns:mml="http://www.w3.org/1998/Math/MathML"><mml:mrow><mml:msub><mml:mi>PbZr</mml:mi><mml:mrow><mml:mn>0.<mathvariant="normal">O</mml:mi><mml:mn>3</mml:mn></mml:msub></mml:mrow></mml:math> and shortcomings of the virtual crystal approximation. Physical Review B, 2019, 100, .	1.1	5
33078	Alloying Element Segregation and Grain Boundary Reconstruction, Atomistic Modeling. Metals, 2019, 9, 1319.	1.0	7
33079	The first principles calculations of CO2 adsorption on (101Â¯0) ZnO surface. AIP Conference Proceedings, 2019, , .	0.3	9
33080	Disorder-induced localisation and suppression of superconductivity in YSr₂Cu₃O_{6+x}. Journal of Physics Condensed Matter, 2019, 31, 284001.	0.7	1
33081	Phase transitions in titanium with an analytic bond-order potential. Modelling and Simulation in Materials Science and Engineering, 2019, 27, 085008.	0.8	3
33082	First principle investigation of the exposed surfaces and morphology of Î²-ZnMoO4. Journal of Applied Physics, 2019, 126, 235301.	1.1	14
33083	Catalytic Reaction Mechanism of NOâ€“CO on the ZrO2 (110) and (111) Surfaces. International Journal of Molecular Sciences, 2019, 20, 6129.	1.8	6
33084	First-Principles Calculations of Thermoelectric PbSe₂ Compound to Predict its Elastic Properties. Materials Science Forum, 2019, 956, 46-54.	0.3	3
33085	First-principle calculations of electronic, vibrational, and thermodynamic properties of 1,3-diamino-2,4,6-trinitrobenzene. Journal of Molecular Modeling, 2019, 25, 356.	0.8	4
33086	Understanding the Electrochemical Reduction of Carbon Dioxide at Copper Surfaces. ACS Symposium Series, 2019, , 209-223.	0.5	1
33087	Large magnetic gap at the Dirac point in Bi2Te3/MnBi2Te4 heterostructures. Nature, 2019, 576, 423-428.	13.7	189
33088	Distinct dependence on size of Pt and Rh nanoclusters on graphene/Pt(111) in the decomposition of methanol-d4. Journal of Chemical Physics, 2019, 151, 224707.	1.2	19
33089	First principles evaluation on photocatalytic suitability of 2H structured and [0001] oriented WS2 nanosheets and nanotubes. IOP Conference Series: Materials Science and Engineering, 2019, 503, 012002.	0.3	4

#	Article	IF	Citations
33090	Two-Dimensional Fluorine Distribution in a Heavily Distorted Perovskite Nickel Oxyfluoride Revealed by First-Principles Calculation. Journal of Physical Chemistry C, 2019, 123, 31190-31195.	1.5	4
33091	Structural evolution and the role of native defects in subnanometer MoS nanowires. Physical Review B, 2019, 100, .	1.1	7
33092	Electronic properties of Pb-I deficient lead halide perovskites. Journal of Chemical Physics, 2019, 151, 234704.	1.2	7
33093	Mechanical properties of 1T-, 1Tâ€²-, and 1H-MX2 monolayers and their 1H/1Tâ€²-MX2 (M = Mo, W and X = S, Se, Te) heterostructures. AIP Advances, 2019, 9, .	0.6	13
33094	Spin-Unrestricted and Spinor Nonradiative Relaxation Dynamics in Functionalized Semiconductors. ACS Symposium Series, 2019, , 1-22.	0.5	1
33095	K₅(W₃O₉F₄)(IO₃): An Efficient Mid-Infrared Nonlinear Optical Compound with High Laser Damage Threshold. Chemistry of Materials, 2019, 31, 10100-10108.	3.2	92
33096	3d Transition Metal-Metallofullerene-Ligand Molecular Wires: Robust One-Dimensional Antiferromagnetic Semiconductors. Journal of Physical Chemistry C, 2019, 123, 30571-30577.	1.5	6
33097	Ultrahigh-pressure isostructural electronic transitions in hydrogen. Nature, 2019, 573, 558-562.	13.7	78
33098	Real-space charge-density imaging with sub-Ã¥ngstrÃ¶m resolution by four-dimensional electron microscopy. Nature, 2019, 575, 480-484.	13.7	127
33099	Pressure-induced polymorphism in <mml:math xmlns:mml="http://www.w3.org/1998/Math/MathML"><mml:msub><mml:mi>SrB</mml:mi><mml:mn>6</mml:mn></mml:msub></m and deformation mechanisms of covalent networks. Physical Review B, 2019, 100, .	1.1	31
33100	Magnetic and atomic short range order in Fe1â^'xCrx alloys. Physical Review B, 2019, 100, .	1.1	6
33101	Defect calculations with hybrid functionals in layered compounds and in slab models. Physical Review B, 2019, 100, .	1.1	9
33102	Improved Moisture Stability of Perovskite Solar Cells Using N719 Dye Molecules. Solar Rrl, 2019, 3, 1970115.	3.1	1
33103	Polymorphism and Temperature-Induced Phase Transitions of Na₂CoP₂O₇. Inorganic Chemistry, 2019, 58, 16823-16830.	1.9	3
33104	Toward ab Initio Ground States of Gold Clusters via Neural Network Modeling. Journal of Physical Chemistry C, 2019, 123, 30088-30098.	1.5	21
33105	Elastic and bandgap modulation of hexagonal C6 from first-principles calculations. Journal of Applied Physics, 2019, 126, 205108.	1.1	2
33106	Incommensurate Phase Transition and Electronic Properties of BaMnF4. IOP Conference Series: Materials Science and Engineering, 2019, 613, 012014.	0.3	0
33107	Ab initio prediction of a two-dimensional variant of the iridate <mml:math xmlns:mml="http://www.w3.org/1998/Math/MathML"><mml:msub><mml:mi>IrO</mml:mi><mml:mn>2</mml:mn></mml:msub></m Physical Review B, 2019, 100, .	1.1	3

#	Article	IF	Citations
33108	Realistic indirect spin interactions between magnetic impurities on a metallic Pb(110) surface. Physical Review B, 2019, 100, .	1.1	1
33109	First-Principles Investigation of Electronic Properties of GaAsxSb1 â€“x Ternary Alloys. Semiconductors, 2019, 53, 1584-1592.	0.2	8
33110	312 MAX Phases: Elastic Properties and Lithiation. Materials, 2019, 12, 4098.	1.3	20
33111	Semiconducting SiGeSn high-entropy alloy: A density functional theory study. Journal of Applied Physics, 2019, 126, 225703.	1.1	12
33112	Plasmon oscillations in two-dimensional arrays of ultranarrow graphene nanoribbons. Physical Review B, 2019, 100, .	1.1	13
33113	Honeycomb silicon on alumina: Massless Dirac fermions in silicene on substrate. Physical Review B, 2019, 100, .	1.1	17
33114	Effect of Oxygen Interstitial Ordering on Multiple Order Parameters in Rare Earth Ferrite. Physical Review Letters, 2019, 123, 247601.	2.9	13
33115	A High-Pressure Investigation of the Synthetic Analogue of Chalcomenite, CuSeO3â^™2H2O. Crystals, 2019, 9, 643.	1.0	8
33116	Mechanistic Landscape of HCl-Mediated Hg⁰ Capture by Magnetite. Journal of Physical Chemistry C, 2019, 123, 30434-30442.	1.5	7
33117	Can Single-Walled Carbon Nanotube Diameter Be Defined by Catalyst Particle Diameter?. Journal of Physical Chemistry C, 2019, 123, 30305-30317.	1.5	17
33118	Transformation of Optical Anisotropy Origins in Perovskite-Related Materials: A First-Principles Study. Journal of Physical Chemistry C, 2019, 123, 31167-31174.	1.5	14
33119	Lateral InSe pâ€“n Junction Formed by Partial Doping for Use in Ultrathin Flexible Solar Cells. Journal of Physical Chemistry Letters, 2019, 10, 7712-7718.	2.1	20
33120	Temperature dependence of spherical electron transfer in a nanosized [Fe14] complex. Nature Communications, 2019, 10, 5510.	5.8	12
33121	Two-dimensional carbon nitride (2DCN) nanosheets: Tuning of novel electronic and magnetic properties by hydrogenation, atom substitution and defect engineering. Journal of Applied Physics, 2019, 126, .	1.1	70
33122	CALPHAD assessment of bio-oriented Tiâ€“Zrâ€“Sn system and experimental validation in Ti/Zr-rich alloys. Calphad: Computer Coupling of Phase Diagrams and Thermochemistry, 2019, 67, 101686.	0.7	12
33123	Effect of Competitive Adsorption at the Interface between Aqueous Electrolyte and Solid Electrode. ACS Symposium Series, 2019, , 225-238.	0.5	5
33124	Optimizing bidentate N-heterocyclic carbene ligands for the modification of late transition metal surfaces â€“ new insights through theory. Physical Chemistry Chemical Physics, 2019, 21, 24926-24934.	1.3	3
33125	TiO₂-supported Pt single atoms by surface organometallic chemistry for photocatalytic hydrogen evolution. Physical Chemistry Chemical Physics, 2019, 21, 24429-24440.	1.3	32

#	Article	IF	Citations
33126	Ferromagnetism in 2D organic iron hemoglobin crystals based on nitrogenated conjugated micropore materials. Physical Chemistry Chemical Physics, 2019, 21, 25820-25825.	1.3	4
33127	The role of metastability in enhancing water-oxidation activity. Physical Chemistry Chemical Physics, 2019, 21, 24354-24360.	1.3	10
33128	Molecular behaviour of phenol in zeolite Beta catalysts as a function of acid site presence: a quasielastic neutron scattering and molecular dynamics simulation study. Catalysis Science and Technology, 2019, 9, 6700-6713.	2.1	12
33129	Direct synthesis of acetic acid from carbon dioxide and methane over Cu-modulated BEA, MFI, MOR and TON zeolites: a density functional theory study. Catalysis Science and Technology, 2019, 9, 6613-6626.	2.1	26
33130	The layered uranyl silicate mineral uranophane-Î²: crystal structure, mechanical properties, Raman spectrum and comparison with the Î±-polymorph. Dalton Transactions, 2019, 48, 16722-16736.	1.6	20
33131	Insight into the structure and bonding of copper(i) iodide clusters and a cluster-based coordination polymer. New Journal of Chemistry, 2019, 43, 16176-16187.	1.4	4
33132	Ironâ€“magnesium compounds under high pressure. New Journal of Chemistry, 2019, 43, 17403-17407.	1.4	7
33133	Electronic properties of polymorphic two-dimensional layered chromium disulphide. Nanoscale, 2019, 11, 20123-20132.	2.8	72
33134	Modulated thermal conductivity of 2D hexagonal boron arsenide: a strain engineering study. Nanoscale, 2019, 11, 21799-21810.	2.8	43
33135	Thermally reduced fluorographenes as efficient electrode materials for supercapacitors. Nanoscale, 2019, 11, 21364-21375.	2.8	15
33136	Sub-10 nm tunneling field-effect transistors based on monolayer group IV mono-chalcogenides. Nanoscale, 2019, 11, 23392-23401.	2.8	30
33137	Electronic structure and transport properties of 2D RhTeCl: a NEGF-DFT study. Nanoscale, 2019, 11, 20461-20466.	2.8	8
33138	X-ray absorption near edge structure simulation of LiNi_{0.5}Co_{0.2}Mn_{0.3}O₂via first-principles calculation. RSC Advances, 2019, 9, 35655-35661.	1.7	6
33139	Electron delocalization in single-layer phthalocyanine-based covalent organic frameworks: a first principle study. RSC Advances, 2019, 9, 29440-29447.	1.7	11
33140	Development of a robust tool to extract Mulliken and LÃ¶wdin charges from plane waves and its application to solid-state materials. RSC Advances, 2019, 9, 29821-29830.	1.7	77
33141	Investigation of the structural, electronic, and optical properties of Mn-doped CsPbCl₃: theory and experiment. RSC Advances, 2019, 9, 29556-29565.	1.7	52
33142	Prediction of pressure-induced phase transformations in Mg₃As₂. RSC Advances, 2019, 9, 34401-34405.	1.7	2
33143	First-principles study of vanadium carbides as electrocatalysts for hydrogen and oxygen evolution reactions. RSC Advances, 2019, 9, 37467-37473.	1.7	16

#	Article	IF	Citations
33144	Study of half metallicity, structural and mechanical properties in inverse Heusler alloy Mn₂ZnSi_(1â^'x)Ge_x and a superlattice. RSC Advances, 2019, 9, 36680-36689.	1.7	8
33145	Halogenation of graphene triggered by heteroatom doping. RSC Advances, 2019, 9, 37507-37511.	1.7	10
33146	A collection of forcefield precursors for metalâ€"organic frameworks. RSC Advances, 2019, 9, 36492-36507.	1.7	21
33147	Large bandgap quantum spin Hall insulator in methyl decorated plumbene monolayer: a first-principles study. RSC Advances, 2019, 9, 42194-42203.	1.7	11
33148	Electronic properties of Î±-graphyne on hexagonal boron nitride and Î±-BNyne substrates. RSC Advances, 2019, 9, 35297-35303.	1.7	3
33149	Azugraphene: a new graphene-like hexagonal carbon allotrope with Dirac cones. RSC Advances, 2019, 9, 34481-34485.	1.7	17
33150	First principles calculations of the thermodynamic stability of Ba, Zr, and O vacancies in BaZrO3. RSC Advances, 2019, 9, 34158-34165.	1.7	6
33151	Comparative study on the electronic structures and redox reactions in LiCrX₂ and NaCrX₂ (X = O and S). RSC Advances, 2019, 9, 36867-36874.	1.7	2
33152	Tunable magnetic ground states of iron monolayer on nonmagnetic metallic substrates by small in-plane strains. RSC Advances, 2019, 9, 41099-41106.	1.7	4
33153	Atomic-level understanding of interface interactions in a halloysite nanotubesâ€"PLA nanocomposite. RSC Advances, 2019, 9, 39505-39514.	1.7	23
33154	Structural, mechanical, spectroscopic and thermodynamic characterization of the copper-uranyl tetrahydroxide mineral vandenbrandeite. RSC Advances, 2019, 9, 40708-40726.	1.7	10
33155	Two-dimensional magnetic metalâ€"organic frameworks with the Shastry-Sutherland lattice. Chemical Science, 2019, 10, 10381-10387.	3.7	21
33156	Halogen-bond driven self-assembly of perfluorocarbon monolayers on silicon nitride. Journal of Materials Chemistry A, 2019, 7, 24445-24453.	5.2	10
33157	Revealing Ni-based layered double hydroxides as high-efficiency electrocatalysts for the oxygen evolution reaction: a DFT study. Journal of Materials Chemistry A, 2019, 7, 23091-23097.	5.2	75
33158	Sr₂Fe_{1.4}Mn_{0.1}Mo_{0.5}O_{6â^'Î´} perovskite cathode for highly efficient CO₂ electrolysis. Journal of Materials Chemistry A, 2019, 7, 22939-22949.	5.2	68
33159	Two-dimensional transition metal diborides: promising Dirac electrocatalysts with large reaction regions toward efficient N₂ fixation. Journal of Materials Chemistry A, 2019, 7, 25887-25893.	5.2	45
33160	Zr vacancy interfaces: an effective strategy for collaborative optimization of ZrNiSn-based thermoelectric performance. Journal of Materials Chemistry A, 2019, 7, 26053-26061.	5.2	16
33161	Topological nodal lines and nodal points in the antiferromagnetic material Î²-Fe₂PO₅. Journal of Materials Chemistry C, 2019, 7, 12657-12663.	2.7	50

#	Article	IF	Citations
33162	Topological semi-metal Na3Bi as efficient spin injector in current driven magnetic tunnel junction. Journal of Applied Physics, 2019, 126, .	1.1	5
33163	Successive orbital ordering transitions in FeV2O4 from first-principles calculation. Journal of Applied Physics, 2019, 126, .	1.1	2
33164	Enhanced catalytic hydrogen evolution reaction in phosphorene nanosheet via cobalt intercalation. Chinese Journal of Chemical Physics, 2019, 32, 572-578.	0.6	4
33165	Density functional theory study of TiPd alloying with Os as potential high temperature shape memory alloys. IOP Conference Series: Materials Science and Engineering, 2019, 655, 012042.	0.3	1
33166	Electrons and Phonons Cooperate in the Laser-Induced Desorption of CO from Pd(111). Physical Review Letters, 2019, 123, 246802.	2.9	15
33167	Density Functional Theory Study on Stability of Fe, Cu, and Ni Atoms Near (001) Surface of Si Wafer. ECS Journal of Solid State Science and Technology, 2019, 8, P573-P579.	0.9	3
33168	The electronic and optical properties of 3d transition metals doped silicene sheet: A DFT study. Materials Research Express, 2019, 6, 126326.	0.8	5
33169	Spin transport properties in zigzag silicon carbide nanoribbon nanojunctions by asymmetric hydrogenation and BN doping. Materials Research Express, 2019, 6, 1250a4.	0.8	3
33170	Crystal and Electronic Structures of Alluaudite-Type Double Molybdates of Scandium and Indium. Journal of Structural Chemistry, 2019, 60, 1868-1876.	0.3	3
33171	First-principles calculations on structure and electronic properties of Î±-zirconium hydrogen phosphate. MRS Advances, 2019, 4, 2699-2707.	0.5	0
33172	Behavior of Eu ions in SrSnO3: Optical properties, XPS experiments and DFT calculations. Journal of Alloys and Compounds, 2019, 771, 162-168.	2.8	36
33173	Correlation effects on the electronic structure of Co2VGa1âˆ’xSix (xâ€¯=â€¯0, 0.25, 0.5, 0.75 and 1) quaternary Heusler alloys: First-principles calculations. Journal of Alloys and Compounds, 2019, 771, 1062-1071.	2.8	15
33174	Combustion synthesis of AlN doped with carbon and oxygen. Journal of the American Ceramic Society, 2019, 102, 524-532.	1.9	7
33175	Y₂₃Sr₁₇[Si₃₈O₁₈N₆₇]O₉ â€“ An Oxonitridosilicate Oxide with a Unique Layered Structure. Zeitschrift Fur Anorganische Und Allgemeine Chemie, 2019, 645, 182-187.	0.6	3
33176	First principles calculations of the adsorption and migration behaviors of N atoms on the H-terminated diamond (0â€¯0â€¯1) surface. Applied Surface Science, 2019, 463, 668-678.	3.1	9
33177	Theoretical research on structural, electronic, mechanical, lattice dynamical and thermodynamic properties of layered ternary nitrides Ti2AN (Aâ€¯=â€¯Si, Ge and Sn). Journal of Alloys and Compounds, 2019, 771, 664-673.	2.8	34
33178	Ab-initio studies of electronic, structural and thermophysical properties of the Sr2TiMoO6 double perovskite. Journal of Alloys and Compounds, 2019, 771, 1080-1089.	2.8	16
33179	Point defects induced magnetism in CdO monolayer: A theoretical study. Journal of Magnetism and Magnetic Materials, 2019, 469, 279-288.	1.0	34

#	Article	IF	Citations
33180	Adsorption of water on fluorinated graphene. Journal of Physics and Chemistry of Solids, 2019, 124, 54-59.	1.9	16
33181	Arsenene and antimonene doped by group-VA atoms: First-principles studies of the geometric structures, electronic properties and STM images. Physica B: Condensed Matter, 2019, 553, 195-201.	1.3	16
33182	Density functional theory study of small Ag cluster adsorbed on graphyne. Applied Surface Science, 2019, 465, 93-102.	3.1	46
33183	Copper(<scp>i</scp>) sulfide: a two-dimensional semiconductor with superior oxidation resistance and high carrier mobility. Nanoscale Horizons, 2019, 4, 223-230.	4.1	51
33184	Sr substitution effects on atomic and local electronic structure of Ca₂AlMnO_{5+Î´}. Surface and Interface Analysis, 2019, 51, 65-69.	0.8	4
33185	Arsenic-induced faceted lateral nanoprisms array on Si (1â€¯0â€¯3) surface. Applied Surface Science, 2019, 463, 713-720.	3.1	0
33186	A dual approach to study the key features of nickel (II) and copper (II) coordination complexes: Synthesis, crystal structure, optical and nonlinear properties. Inorganica Chimica Acta, 2019, 484, 148-159.	1.2	39
33187	Induced defect levels of P and Al vacancy-complexes in <mml:math xmlns:mml="http://www.w3.org/1998/Math/MathML" altimg="si0060.gif" overflow="scroll"><mml:mrow><mml:mn>4</mml:mn><mml:mspace width="0.25em" /><mml:mi>H</mml:mi></mml:mrow></mml:math>-SiC: A hybrid functional study. Materials Science in Semiconductor Processing, 2019, 89, 77-84.	1.9	4
33188	Characterization of the electronic and vibrational properties of ZnxCd1âˆ’xSySe1âˆ’y (yâ€‰=â€‰0.25, 0.75) mixed crystals by a first-principles method. Journal of Materials Science, 2019, 54, 1382-1394.	1.7	4
33189	DFT study of Rh and Ti dimers decorating N-doped pyridinic and pyrrolic graphene for molecular and dissociative hydrogen adsorption. Applied Surface Science, 2019, 464, 243-254.	3.1	23
33190	Investigation of the Substituting Effect of Chromium on the Electronic Structures and the Half-Metallic Ferromagnetic Properties of BaO. Journal of Superconductivity and Novel Magnetism, 2019, 32, 1781-1790.	0.8	11
33191	Thermodynamic properties and phase stability of the Ba-Bi system: A combined computational and experimental study. Journal of Alloys and Compounds, 2019, 771, 281-289.	2.8	4
33192	Magnetic semiconducting and strain-induced semiconductingâ€“metallic transition in Cu-doped single-layer WSe2. Journal of Materials Science, 2019, 54, 529-539.	1.7	7
33193	Enhancement of red emission and site analysis in Eu2+ doped new-type structure Ba3CaK(PO4)3 for plant growth white LEDs. Chemical Engineering Journal, 2019, 356, 236-244.	6.6	160
33194	High-voltage performance of LiCoO2 cathode studied by single particle microelectrodes â€“influence of surface modification with TiO2. Electrochimica Acta, 2019, 295, 1017-1026.	2.6	33
33195	STM and DFT studies of CO2 adsorption on O-Cu(100) surface. Surface Science, 2019, 679, 50-55.	0.8	15
33196	Piezoelectricity and dipolar polarization of group V-IV-III-VI sheets: A first-principles study. Applied Surface Science, 2019, 463, 918-922.	3.1	15
33197	(0001) Interfaces between M2O3 corundum oxides (MÂ=ÂAl, Ti, V, Cr, Fe).. Surface Science, 2019, 679, 17-23.	0.8	12

#	Article	IF	Citations
33198	Influence of hydrogen and halogen adsorption on the photocatalytic water splitting activity of C2N monolayer: A first-principles study. Carbon, 2019, 141, 50-58.	5.4	54
33199	Light absorption optimizing in (La0.25Bi0.75)2FeCrO6 active layers: GGAâ€‰+â€‰U study. Indian Journal of Physics, 2019, 93, 327-333.	0.9	0
33200	Two-dimensional Ï€-conjugated metalâ€“organic nanosheets as single-atom catalysts for the hydrogen evolution reaction. Nanoscale, 2019, 11, 454-458.	2.8	65
33201	Insight into the structural, elastic and electronic properties of tetragonal inter-alkali metal chalcogenides CsNaX (X=S, Se, and Te) from first-principles calculations. Materials Chemistry and Physics, 2019, 221, 125-137.	2.0	16
33202	Prediction of a flexible anode material for Li/Na ion batteries: Phosphorous carbide monolayer (Î±-PC). Carbon, 2019, 141, 444-450.	5.4	70
33203	Influence of electric charge on the stability of graphite-like BC2. Journal of Solid State Chemistry, 2019, 269, 113-117.	1.4	2
33204	Rational design of C₂N-based type-II heterojunctions for overall photocatalytic water splitting. Nanoscale Advances, 2019, 1, 154-161.	2.2	70
33205	Three-dimensional honeycomb carbon: Junction line distortion and novel emergent fermions. Carbon, 2019, 141, 417-426.	5.4	48
33206	Diffusion of interstitial species (H and O atoms) in fcc systems (Al, Cu, Co, Ni and Pd): Contribution of first and second order transition states. Journal of Alloys and Compounds, 2019, 772, 280-287.	2.8	15
33207	The electronic, elastic and thermodynamic properties of carbon-and nitrogen-doped Hf2PB: a theoretical approach. Materials Research Express, 2019, 6, 056507.	0.8	4
33208	Electrocatalytic Reduction of Carbon Dioxide to Methane on Single Transition Metal Atoms Supported on a Defective Boron Nitride Monolayer: First Principle Study. Advanced Theory and Simulations, 2019, 2, 1800094.	1.3	33
33209	Relative stabilities of various fully functionalized graphene polymorphs under mechanical strain and electric field. Applied Surface Science, 2019, 463, 1051-1057.	3.1	19
33210	Co9S8@carbon yolk-shell nanocages as a high performance direct conversion anode material for sodium ion batteries. Energy Storage Materials, 2019, 18, 51-58.	9.5	89
33211	First-principles analysis of acetonitrile reaction pathways to primary, secondary, and tertiary amines on Pd(111). Surface Science, 2019, 682, 84-98.	0.8	14
33212	Kinetic suppression of boronâ€“oxygen complexes in p-type Czochralski silicon by tin doping. Applied Physics Express, 2019, 12, 011005.	1.1	0
33213	First-principles study of structural, mechanical, and electronic properties of typical iron-containing phases in Al-Cu alloys under different pressures. Physica B: Condensed Matter, 2019, 555, 112-117.	1.3	4
33214	DFT study of the effects of Al P pair doping on the structural and electronic properties of stanene nanosheets. Physica E: Low-Dimensional Systems and Nanostructures, 2019, 108, 34-43.	1.3	46
33215	Probing the Accuracy of First-Principles Modeling of Molecular Crystals: Calculation of Sublimation Pressures. Crystal Growth and Design, 2019, 19, 808-820.	1.4	10

#	Article	IF	Citations
33216	Prediction of Stable and Active (Oxy-Hydro) Oxide Nanoislands on Noble-Metal Supports for Electrochemical Oxygen Reduction Reaction. ACS Applied Materials & Interfaces, 2019, 11, 2006-2013.	4.0	24
33217	The adsorption of a single water molecule on low-index C3S surfaces: A DFT approach. Applied Surface Science, 2019, 471, 658-663.	3.1	20
33218	The stability and reactivity of transition metal atoms supported mono and di vacancies defected carbon based materials revealed from first principles study. Applied Surface Science, 2019, 473, 777-784.	3.1	30
33219	Improved catalytic performance of monolayer nano-triangles WS2 and MoS2 on HER by 3d metals doping. Computational Materials Science, 2019, 159, 333-340.	1.4	31
33220	Exploring the electronic and magnetic properties of new metal halides from bulk to two-dimensional monolayer: RuX3 (Xâ€¯=â€¯Br, I). Journal of Magnetism and Magnetic Materials, 2019, 476, 111-119.	1.0	48
33221	Hydrogen reduction characteristics of WO3 based on density functional theory. Results in Physics, 2019, 12, 896-902.	2.0	11
33222	Enhanced hardness and age-hardening of TiAlN coatings through Ru-addition. Scripta Materialia, 2019, 162, 382-386.	2.6	21
33223	Fundamental Mechanisms of Reversible Dehydrogenation of Formate on N-Doped Graphene-Supported Pd Nanoparticles. Journal of Physical Chemistry C, 2019, 123, 1539-1549.	1.5	28
33224	Mechanically-Controllable Strong 2D Ferroelectricity and Optical Properties of Semiconducting BiN Monolayer. ACS Applied Nano Materials, 2019, 2, 58-63.	2.4	14
33225	Orbitonâ€“phonon coupling in Ir⁵⁺(5d ⁴) double perovskite Ba₂YIrO₆. Journal of Physics Condensed Matter, 2019, 31, 065603.	0.7	8
33226	Anomalous mechanical behavior of the deltic, squaric and croconic cyclic oxocarbon acids. Materials Research Express, 2019, 6, 045610.	0.8	23
33227	Key Factor for the Transformation from hcp to 18R-Type Long-Period Stacking Ordered Structure in Mg Alloys. Materials Transactions, 2019, 60, 237-245.	0.4	12
33228	Impact of surface adsorbed gases on hydrogen diffusion into Pd(1â€“0â€“0) subsurface from first principles. Applied Surface Science, 2019, 473, 476-485.	3.1	8
33229	A MnN4 moiety embedded graphene as a magnetic gas sensor for CO detection: A first principle study. Applied Surface Science, 2019, 473, 820-827.	3.1	67
33230	Structures of quaternary chromium silicides revealed by a combination of resonant X-ray diffraction and ab initio calculations. Intermetallics, 2019, 105, 130-138.	1.8	1
33231	First-principles study on electronic and magnetic properties of (Al,Mn) codoped BaZn2As2. Journal of Alloys and Compounds, 2019, 783, 387-392.	2.8	4
33232	Li3SbO4 lithium-ion battery material: Defects, lithium ion diffusion and tetravalent dopants. Materials Chemistry and Physics, 2019, 225, 34-41.	2.0	22
33233	Quantitative determination of the lattice constant in high entropy alloys. Scripta Materialia, 2019, 162, 468-471.	2.6	40

#	Article	IF	Citations
33234	Overcoming the Memory Bottleneck in Auxiliary Field Quantum Monte Carlo Simulations with Interpolative Separable Density Fitting. Journal of Chemical Theory and Computation, 2019, 15, 256-264.	2.3	38
33235	First principles studies of self-diffusion processes on metallic lithium surfaces. Journal of Chemical Physics, 2019, 150, 041723.	1.2	34
33236	Electronic structure, elastic, mechanical, thermodynamic and thermoelectric investigations of Mn2PtX (X=Rh, Pd) Heusler alloys. Solid State Communications, 2019, 290, 12-21.	0.9	20
33237	How Silver Grows on the Silicon (001) Surface: A Theoretical and Experimental Investigation. ACS Applied Electronic Materials, 2019, 1, 122-131.	2.0	4
33238	Elucidating the Role of Support Oxygen in the Waterâ€“Gas Shift Reaction over Ceria-Supported Gold Catalysts Using Operando Spectroscopy. ACS Catalysis, 2019, 9, 1159-1171.	5.5	49
33239	Electronic and Optical Properties of CsSnI3â^'yCly (yâ€‰=â€‰0, 1, 2, 3) Perovskites: a DFT Study. Journal of Electronic Materials, 2019, 48, 1243-1251.	1.0	24
33240	Edge modification induced giant rectification effect in armchair C2N-h2D nanoribbons. Solid State Communications, 2019, 289, 61-66.	0.9	2
33241	Electronic Origin of Oxygen Transport Behavior in La-Based Perovskites: A Density Functional Theory Study. Journal of Physical Chemistry C, 2019, 123, 275-290.	1.5	25
33242	Generalized stacking fault energy of carbon-alloyed paramagnetic $ gamma $ -Fe. Journal of Physics Condensed Matter, 2019, 31, 065703.	0.7	5
33243	Ab initiocalculations of hardness, elastic, thermodynamic and electronic properties of metal nitrides (XN₂; X = Pd, Pt) under high-pressure. Materials Research Express, 2019, 6, 045904.	0.8	2
33244	Tin Intercalated Ultrathin MoO₃ Nanoribbons for Advanced Lithiumâ€“Sulfur Batteries. Advanced Energy Materials, 2019, 9, 1803137.	10.2	126
33245	Lattice dynamics of Bi3TeBO9 microcrystals: Î¼-Raman/IR spectroscopic investigation and ab initio analysis. Journal of Alloys and Compounds, 2019, 782, 488-495.	2.8	9
33246	Insight into electronic, magnetic and optical properties of magnetically ordered Bi2Fe4O9. Journal of Magnetism and Magnetic Materials, 2019, 475, 695-702.	1.0	18
33247	Adsorption effect of a chromium atom on the structure and electronic properties of a single ZnO monolayer. Physica B: Condensed Matter, 2019, 565, 44-47.	1.3	5
33248	Ab initio investigation into the physisorption of noble gases on graphene. Surface Science, 2019, 682, 38-42.	0.8	12
33249	Pressure-Induced Band Structure Evolution of Halide Perovskites: A First-Principles Atomic and Electronic Structure Study. Journal of Physical Chemistry C, 2019, 123, 739-745.	1.5	53
33250	Resonance Raman Spectroscopy of Silicene and Germanene. Journal of Physical Chemistry C, 2019, 123, 1995-2008.	1.5	8
33251	One-Pot Synthesis of Co-Doped VSe₂ Nanosheets for Enhanced Hydrogen Evolution Reaction. ACS Applied Energy Materials, 2019, 2, 644-653.	2.5	59

#	Article	IF	Citations
33252	Using Single-Layer HfS₂ as Prospective Sensing Device Toward Typical Partial Discharge Gas in SF₆-Based Gas-Insulated Switchgear. IEEE Transactions on Electron Devices, 2019, 66, 689-695.	1.6	26
33253	Carrier Transport and Thermoelectric Properties of Differently Shaped Germanene (Ge) and Silicene (Si) Nanoribbon Interconnects. IEEE Transactions on Electron Devices, 2019, 66, 664-669.	1.6	3
33254	Strain-modulated mechanical, electronic, and thermal transport properties of two-dimensional PdS2 from first-principles investigations. Applied Physics A: Materials Science and Processing, 2019, 125, 1.	1.1	13
33255	Modeling of metastable phase formation for sputtered Ti1-xAlxN thin films. Acta Materialia, 2019, 165, 615-625.	3.8	34
33256	Thermal neutron scattering kernels for uranium mono-nitride: A potential advanced tolerant fuel candidate for light water reactors. Annals of Nuclear Energy, 2019, 127, 68-78.	0.9	8
33257	Binding of hydrogen to phosphorus dopant in phosphorus-doped diamond surfaces: A density functional theory study. Applied Surface Science, 2019, 471, 309-317.	3.1	12
33258	BH4 dissociation on various metal (1â€¯1â€¯1) surfaces: A DFT study. Applied Surface Science, 2019, 473, 681-692.	3.1	14
33259	Dopamine sensing by boron and nitrogen co-doped single-walled carbon nanotubes: A first-principles study. Applied Surface Science, 2019, 473, 59-64.	3.1	28
33260	Spin dependent resonant electron tunneling through planar graphene barriers. Carbon, 2019, 144, 362-369.	5.4	1
33261	Accurate semiempirical analytical formulas for spontaneous polarization by crystallographic parameters of SrTiO3-BaTiO3 system by ab initio calculations. Computational Materials Science, 2019, 158, 315-323.	1.4	4
33262	Role of heteroatoms in the adsorption of thiazole on Cu (1 1 1) surface: First principles study. Corrosion Science, 2019, 148, 171-177.	3.0	15
33263	Sodium storage via single epoxy group on graphene â€“ The role of surface doping. Electrochimica Acta, 2019, 297, 523-528.	2.6	14
33264	Influence of heavy metal sorption pathway on the structure of biogenic birnessite: Insight from the band structure and photostability. Geochimica Et Cosmochimica Acta, 2019, 256, 116-134.	1.6	23
33265	Short-range order formation in Fe-Co alloys: NMR study and first-principles calculations. Journal of Alloys and Compounds, 2019, 782, 1008-1014.	2.8	5
33266	Kinetics of interaction of impurity interstitials with dislocations revisited. Progress in Materials Science, 2019, 101, 172-206.	16.0	34
33267	Electrochemical Properties and Theoretical Capacity for Sodium Storage in Hard Carbon: Insights from First Principles Calculations. Chemistry of Materials, 2019, 31, 658-677.	3.2	60
33268	Computationally Designed Crystal Structures of the Supertetrahedral Al₄X (X = B, C, Al,) Tj ETQq0 0 0 rgBT /Overlock 10 Tf	1.1	5
33269	Theoretical Investigation: 2D N-Graphdiyne Nanosheets as Promising Anode Materials for Li/Na Rechargeable Storage Devices. ACS Applied Nano Materials, 2019, 2, 127-135.	2.4	56

#	Article	IF	Citations
33270	Spin dependent transport in hybrid one dimensional BNC systems. Semiconductor Science and Technology, 2019, 34, 015004.	1.0	2
33271	Electric field mediated large valley splitting in the van der Waals heterostructure WSe₂/CrI₃. Japanese Journal of Applied Physics, 2019, 58, 010906.	0.8	24
33272	Structural phase transitions and superconductivity of YC2 from first-principles calculations. Computational Materials Science, 2019, 159, 120-126.	1.4	4
33273	Barriers to achieving highly dispersed graphene oxide in cementitious composites: An experimental and computational study. Construction and Building Materials, 2019, 199, 269-278.	3.2	60
33274	Single-Atom Electroplating on Two Dimensional Materials. Chemistry of Materials, 2019, 31, 429-435.	3.2	55
33275	Tunable Direct Semiconductor Gap and High Carrier Mobility of Mo6Br6S3 Monolayer. Journal of Physical Chemistry C, 2019, 123, 791-797.	1.5	0
33276	Energy Band Gap Modulation in Nd-Doped BiFeO₃/SrRuO₃ Heteroepitaxy for Visible Light Photoelectrochemical Activity. ACS Applied Materials & Interfaces, 2019, 11, 1655-1664.	4.0	25
33277	Effects of hydrostaticity on the structural stability of carbonates at lower mantle pressures: the case study of dolomite. High Pressure Research, 2019, 39, 36-49.	0.4	9
33278	Co-doped 1T-MoS2 nanosheets embedded in N, S-doped carbon nanobowls for high-rate and ultra-stable sodium-ion batteries. Nano Research, 2019, 12, 2218-2223.	5.8	88
33279	The MN effect on Electronic, optical and thermoelectric properties of Ti2N graphene: by DFT. Chinese Journal of Physics, 2019, 57, 240-249.	2.0	1
33280	On the fast kinetics of B2â€“L21 ordering in Ni-Co-Mn-In metamagnetic shape memory alloys. Journal of Alloys and Compounds, 2019, 781, 479-489.	2.8	10
33281	Initial stages of the epitaxial growth of AlN on GaN (1â€¯1â€¯1)-(2â€¯Ã—â€¯2) surface: Ab-initio studies. Journal of Crystal Growth, 2019, 507, 370-378.	0.7	8
33282	Detection of trace level of hazardous phosgene gas on antimonene nanotube based on first-principles method. Journal of Molecular Graphics and Modelling, 2019, 88, 32-40.	1.3	43
33283	Structural and Physical Properties of ZrSi2 under High Pressure: Experimental Study and First-Principles Calculations. Inorganic Chemistry, 2019, 58, 405-410.	1.9	8
33284	Competitive Hydrogenation between Linear Alkenes and Aromatics on Close-Packed Late Transition Metal Surfaces. Journal of Physical Chemistry C, 2019, 123, 8370-8378.	1.5	5
33285	Piezoelectric Effects in Surface-Engineered Two-Dimensional Group III Nitrides. ACS Applied Materials & Interfaces, 2019, 11, 1033-1039.	4.0	47
33286	Bulk and few-layer MnPS₃: a new candidate for field effect transistors and UV photodetectors. Journal of Materials Chemistry C, 2019, 7, 324-329.	2.7	82
33287	Phase diagram of magnetostrictive Fe-Ga alloys: insights from theory and experiment. Phase Transitions, 2019, 92, 101-116.	0.6	33

#	Article	IF	Citations
33288	High pressure structural investigations on hexagonal YInO₃. High Pressure Research, 2019, 39, 17-35.	0.4	6
33289	Magnetostriction of Fe100-xGax alloys from first principles calculations. Journal of Magnetism and Magnetic Materials, 2019, 476, 120-123.	1.0	7
33290	First-principles calculations of methane adsorption at different coverage on the kaolinite (001) surface. Materials Today Communications, 2019, 18, 199-205.	0.9	10
33291	A first principles study on spin resolved electronic properties of X@C70 (Xâ€¯=â€¯N, B) endohedral fullerene based molecular devices. Physica E: Low-Dimensional Systems and Nanostructures, 2019, 108, 83-89.	1.3	6
33292	Adsorption of CO gas molecules on zigzag BN/AlN nanoribbons for nano sensor applications. Physics Letters, Section A: General, Atomic and Solid State Physics, 2019, 383, 532-538.	0.9	43
33293	Connecting Oxide Nucleation and Growth to Oxygen Diffusion Energetics on Stepped Cu(011) Surfaces: An Experimental and Theoretical Study. Journal of Physical Chemistry C, 2019, 123, 452-463.	1.5	19
33294	Formation of Feâ€“Fe Antiferromagnetic Dimers in Doped TiO2:Fe Nanoparticles. Journal of Physical Chemistry C, 2019, 123, 1494-1505.	1.5	9
33296	Twoâ€Đimensional GaX/SnS₂ (Xâ€‰=â€‰S, Se) van der Waals Heterostructures for Photovoltaic Application: Heteroatom Doping Strategy to Boost Power Conversion Efficiency. Physica Status Solidi - Rapid Research Letters, 2019, 13, 1800565.	1.2	35
33297	First-Principles Modeling of Interface Effects in Oxides. , 2019, , 1-30.		0
33298	Magnetic coupling in 3D-hierarchical MnO2 microsphere. Journal of Materials Science: Materials in Electronics, 2019, 30, 2802-2808.	1.1	7
33299	Detection of gas molecule using C3N island single electron transistor. Carbon, 2019, 144, 235-240.	5.4	33
33300	The physics of single-side fluorination of graphene: DFT and DFTÂ+ U studies. Carbon, 2019, 144, 615-627.	5.4	30
33301	Electronic structure and thermoelectric properties of Ta-based half-Heusler compounds with 18 valence electrons. Computational Materials Science, 2019, 159, 470-477.	1.4	41
33302	Ag monolayer doped by Pt atom on WC (0001) surface: A good catalyst for H2 dissociation with high sulfur tolerance. International Journal of Hydrogen Energy, 2019, 44, 3115-3120.	3.8	9
33303	Effect of oxygen concentration on the tension and shear strength of Zr-O system: A first-principles study. Journal of Alloys and Compounds, 2019, 781, 919-928.	2.8	8
33304	Understanding structure, optical, and electrical properties of In4Sn3O12 and In4.5Sn2M0.5O12 (Mâ€¯=â€¯Nb) Tj ETQq1 1 0.784314	2.8	5
33305	First-principles predictions for stabilizations of multilayer nanotwins in Al alloys at finite temperatures. Journal of Alloys and Compounds, 2019, 783, 765-771.	2.8	20
33306	Elastic, electronic and thermoelectric properties of Sr3MN (MÂ= Sb, Bi) under pressure. Journal of Alloys and Compounds, 2019, 783, 593-600.	2.8	13

#	Article	IF	Citations
33307	Low-temperature nanostructured bainite transformation: The effect of magnetic field. Materials Letters, 2019, 240, 66-68.	1.3	13
33308	Controllable tuning of Fe-N nanosheets by Co substitution for enhanced oxygen evolution reaction. Nano Energy, 2019, 57, 644-652.	8.2	90
33309	Crystal structures of silicon-rich lithium silicides at high pressure. Physics Letters, Section A: General, Atomic and Solid State Physics, 2019, 383, 1047-1051.	0.9	4
33310	Multiscale modeling of PEEK using reactive molecular dynamics modeling and micromechanics. Polymer, 2019, 163, 96-105.	1.8	40
33311	Coadsorbed oligolayers of beryllium and oxygen on molybdenum (1 1 2) surface: Formation and chemical composition, atomic structure and evaporation. Surface Science, 2019, 682, 14-24.	0.8	5
33312	Interface properties of nonpolar LiAlO2/SrTiO3 heterostructures. Vacuum, 2019, 161, 98-102.	1.6	2
33313	p-Type Conductivity and Room-Temperature Ferrimagnetism in Spinel MoFe₂O₄ Epitaxial Thin Film. Crystal Growth and Design, 2019, 19, 902-906.	1.4	11
33314	Uncovering New Buckled Structures of Bilayer GaN: A First-Principles Study. Journal of Physical Chemistry C, 2019, 123, 1939-1947.	1.5	6
33315	Acetonitrile Adsorption on Pt Single-Crystal Electrodes and Its Effect on Oxygen Reduction Reaction in Acidic and Alkaline Aqueous Solutions. Journal of Physical Chemistry C, 2019, 123, 2300-2313.	1.5	19
33316	Functionalized Single-Atom-Embedded Bilayer Graphene and Hexagonal Boron Nitride. ACS Applied Electronic Materials, 2019, 1, 2-6.	2.0	1
33317	Millimeter-Scale Growth of Single-Oriented Graphene on a Palladium Silicide Amorphous Film. ACS Nano, 2019, 13, 1127-1135.	7.3	1
33318	pH effects on the electrochemical reduction of CO(2) towards C2 products on stepped copper. Nature Communications, 2019, 10, 32.	5.8	371
33319	Identification of single-atom active sites in carbon-based cobalt catalysts during electrocatalytic hydrogen evolution. Nature Catalysis, 2019, 2, 134-141.	16.1	629
33320	Theoretical insights into photo-induced electron transfer at BiOX (X = F, Cl, Br, I) (001) surfaces and interfaces. Physical Chemistry Chemical Physics, 2019, 21, 868-875.	1.3	51
33321	Atomistic study of an ideal metal/thermoelectric contact: The full-Heusler/half-Heusler interface. APL Materials, 2019, 7, 013202.	2.2	7
33322	Phonon properties and thermal conductivity from first principles, lattice dynamics, and the Boltzmann transport equation. Journal of Applied Physics, 2019, 125, .	1.1	141
33323	Effect of external stresses on the optical and electronic properties of potassium dihydrogen phosphate crystals. Materials Research Express, 2019, 6, 045026.	0.8	0
33324	Insight into structural, electronic and thermoelectric properties of Zr2MnX (X = Ga, In) Heuslers. Materials Research Express, 2019, 6, 046530.	0.8	4

#	Article	IF	Citations
33325	Polarization rotation in Bi4Ti3O12 by isovalent doping at the fluorite sublattice. Physical Review B, 2019, 99, .	1.1	16
33326	Emergence of glassy features in halomethane crystals. Physical Review B, 2019, 99, .	1.1	29
33327	X3N (X=C and Si) monolayers and their van der Waals Heterostructures with graphene and h-BN: Emerging tunable electronic structures by strain engineering. Carbon, 2019, 145, 1-9.	5.4	36
33328	A comparative ab initio study of the structural, mechanical, electronic and optical behaviors of ZnO:Ni thin films with nanometer scale. Chinese Journal of Physics, 2019, 57, 61-71.	2.0	1
33329	Development of an interatomic potential for titanium with high predictive accuracy of thermal properties up to melting point. Computational Materials Science, 2019, 160, 30-41.	1.4	11
33330	Tuning nitrogen species in three-dimensional porous carbon via phosphorus doping for ultra-fast potassium storage. Nano Energy, 2019, 57, 728-736.	8.2	323
33331	Assessing Correlations of Perovskite Catalytic Performance with Electronic Structure Descriptors. Chemistry of Materials, 2019, 31, 785-797.	3.2	106
33332	Edge-State-Enhanced CO₂ Electroreduction on Topological Nodal-Line Semimetal Cu₂Si Nanoribbons. Journal of Physical Chemistry C, 2019, 123, 2837-2842.	1.5	26
33333	Switchable Schottky Contacts: Simultaneously Enhanced Output Current and Reduced Leakage Current. Journal of the American Chemical Society, 2019, 141, 1628-1635.	6.6	43
33334	Metal Hexaboride Work Functions: Surface Configurations and the Electrical Double Layer from Firstâ€Principles. Advanced Electronic Materials, 2019, 5, 1800074.	2.6	9
33335	Reaction mechanism for NH3-SCR of NOx over CuMn2O4 catalyst. Chemical Engineering Journal, 2019, 361, 578-587.	6.6	146
33336	Systematic analysis of the fine structure of energy levels and spin-Hamiltonian parameters of V3+ ion in corundum with dynamic Jahn-Teller effect. Journal of Luminescence, 2019, 208, 273-278.	1.5	1
33337	First-principles study on the stability and properties of Î²-SiC/M+1AlC (M=Sc, Ti, V, Cr, Zr, Nb, Mo, Hf, Ta;) Tj ETQq0 0 0 rgBT /Overlock 1	1.9	5
33338	Investigation of structural models for Oâ€“Y and Oâ€“Yâ€“Ti clusters in bcc Fe: a density functional theory study. Journal of Physics Condensed Matter, 2019, 31, 095701.	0.7	3
33339	Ideal half-filled intermediate band position in CuGaS₂ generated by Sb-related defect complex: a first-principles study. Applied Physics Express, 2019, 12, 021002.	1.1	3
33340	Structural and thermodynamic properties of cubic sphalerite aluminum nitride under hydrostatic compression. Computational Condensed Matter, 2019, 19, e00359.	0.9	13
33341	Phase Stability Analysis of Ternary Alkaline-Earth Hexaborides: Insights from DFT Calculations. ACS Applied Electronic Materials, 2019, 1, 105-112.	2.0	2
33342	High-Magnetization Tetragonal Ferrite-Based Films Induced by Carbon and Oxygen Vacancy Pairs. ACS Applied Materials & Interfaces, 2019, 11, 1049-1056.	4.0	5

#	Article	IF	Citations
33343	Graphene and graphene nanomesh supported nickel clusters: electronic, magnetic, and hydrogen storage properties. Nanotechnology, 2019, 30, 085709.	1.3	10
33344	Investigation on probing explosive nitroaromatic compound vapors using graphyne nanosheet: a first-principle study. Structural Chemistry, 2019, 30, 657-667.	1.0	22
33345	Synthesis, characterization and thermodynamic stability of nanostructured Îµ-iron carbonitride powder prepared by a solid-state mechanochemical route. Journal of Alloys and Compounds, 2019, 778, 327-336.	2.8	6
33346	Band manipulation for high thermoelectric performance in SnTe through heavy CdSe-alloying. Journal of Materiomics, 2019, 5, 111-117.	2.8	17
33347	First-principles study of surface properties of uranium silicides. Journal of Nuclear Materials, 2019, 513, 192-197.	1.3	9
33348	First-principles study of thermophysical properties of interaction layer products in U-Mo/Al dispersion fuel. Journal of Nuclear Materials, 2019, 513, 94-101.	1.3	1
33349	Unobvious elastic anisotropy of measured singleâ€“crystal cementite. Materials Research Express, 2019, 6, 016531.	0.8	0
33350	Adsorption and catalytic decomposition of hydrazine on metal-free SiC3 siligraphene. Applied Surface Science, 2019, 469, 316-324.	3.1	16
33351	Single-layer planar penta-X2N4 (Xâ€¯=â€¯Ni, Pd and Pt) as direct-bandgap semiconductors from first principle calculations. Applied Surface Science, 2019, 469, 456-462.	3.1	48
33352	Insights into unidirectional migration of photo-excited electrons at ZnFe2O4/graphene van der Waals interface. Computational Materials Science, 2019, 157, 60-66.	1.4	7
33353	Identification of Distinct Framework Aluminum Sites in Zeolite ZSM-23: A Combined Computational and Experimental ²⁷Al NMR Study. Journal of Physical Chemistry C, 2019, 123, 7831-7844.	1.5	19
33354	Design of Singleâ€Molecule Multiferroics for Efficient Ultrahighâ€Density Nonvolatile Memories. Advanced Science, 2019, 6, 1801572.	5.6	41
33355	Efficient and selective sensing of nitrogen-containing gases by Si2BN nanosheets under pristine and pre-oxidized conditions. Applied Surface Science, 2019, 469, 775-780.	3.1	78
33356	Potassium-Promoted Reduction of Cu₂O/Cu(111) by CO. Journal of Physical Chemistry C, 2019, 123, 8057-8066.	1.5	20
33357	Interplay of solute-mixed self-interstitial atoms and substitutional solutes with interstitial and substitutional helium atoms in tungsten-transition metal alloys. Nuclear Fusion, 2019, 59, 026002.	1.6	8
33358	Dehydrated Na₆[AlSiO₄]₆ sodalite as a promising SO₂ sorbent material: A first principles thermodynamics prediction. Journal of the American Ceramic Society, 2019, 102, 3663-3672.	1.9	9
33359	Defects guided wrinkling in graphene on copper substrate. Carbon, 2019, 143, 736-742.	5.4	27
33360	Ab-initio DFT based investigation of double perovskite oxide Ba2CdOsO6 with cubic structure. Computational Condensed Matter, 2019, 18, e00351.	0.9	25

#	Article	IF	Citations
33361	Atomistic understanding of helium behaviors at grain boundaries in vanadium. Computational Materials Science, 2019, 158, 296-306.	1.4	12
33362	Fluorination of graphene oxide at ambient conditions. Diamond and Related Materials, 2019, 91, 107-111.	1.8	3
33363	Pressure effects on the optical and electronic aspects of T-Carbon: A first principles calculation. Optik, 2019, 180, 125-133.	1.4	22
33364	A review on density functional theoryâ€“based study on two-dimensional materials used in batteries. Materials Today Chemistry, 2019, 11, 94-111.	1.7	42
33365	Band structure and giant Stark effect in two-dimensional transition-metal dichalcogenides. Electronic Structure, 2019, 1, 015005.	1.0	5
33366	Local Electronic Structure of Molecular Heterojunctions in a Singleâ€Layer 2D Covalent Organic Framework. Advanced Materials, 2019, 31, e1805941.	11.1	74
33367	Elastomer-like deformation in high-Poisson's-ratio graphene allotropes may allow tensile strengths beyond theoretical cohesive strength limits. Carbon, 2019, 143, 752-761.	5.4	8
33368	Enhanced thermal conductivity of MoS2/InSe-nanoparticles/MoS2 hybrid sandwich structure. Journal of Alloys and Compounds, 2019, 777, 1145-1151.	2.8	4
33369	Challenges in Modeling Electrochemical Reaction Energetics with Polarizable Continuum Models. ACS Catalysis, 2019, 9, 920-931.	5.5	153
33370	Enhanced lithium storage capability of FeF3Â·0.33H2O single crystal with active insertion site exposed. Nano Energy, 2019, 56, 884-892.	8.2	55
33371	Electrocatalytic Hydrogenation of N₂ to NH₃ by MnO: Experimental and Theoretical Investigations. Advanced Science, 2019, 6, 1801182.	5.6	117
33372	Atomic-level insights into the adsorption of rare earth Y(OH)3-nn+ (nâ€¯=â€¯1â€“3) ions on kaolinite surface. Applied Surface Science, 2019, 469, 357-367.	3.1	31
33373	tâ€Si₆₄: A Novel Silicon Allotrope. ChemPhysChem, 2019, 20, 128-133.	1.0	45
33374	First principles study of structural, elastic and electronic structural properties of strontium chalcogenides. Chinese Journal of Physics, 2019, 57, 418-434.	2.0	10
33375	Quasiparticle electronic structure of honeycomb C ₃ N: from monolayer to bulk. 2D Materials, 2019, 6, 015018.	2.0	20
33376	Massively parallelization strategy for material simulation using highâ€dimensional neural network potential. Journal of Computational Chemistry, 2019, 40, 1091-1096.	1.5	13
33377	SiP2S monolayer: A two dimensional semiconductor with a moderate band gap. Chemical Physics Letters, 2019, 715, 100-104.	1.2	5
33378	Spin resolved electronic structure and transport properties of zinc oxide nanoribbon based devices. Physica E: Low-Dimensional Systems and Nanostructures, 2019, 107, 67-72.	1.3	7

#	Article	IF	Citations
33379	Two-dimensional lead-free hybrid halide perovskite using superatom anions with tunable electronic properties. Solar Energy Materials and Solar Cells, 2019, 191, 33-38.	3.0	90
33380	Firstâ"principles study: Structural, mechanical, electronic and thermodynamic properties of simpleâ"cubicâ"perovskite (Ba0.62K0.38)(Bi0.92Mg0.08)O3. Solid State Communications, 2019, 288, 22-27.	0.9	22
33381	The Coulomb interaction in van der Waals heterostructures. Science China: Physics, Mechanics and Astronomy, 2019, 62, 1.	2.0	25
33382	Atomistic modelling of the diffusion of C in Fe Cr alloys. Acta Materialia, 2019, 165, 638-653.	3.8	13
33383	Br-doped Bi2O2CO3 nanosheets with improved electronic structure and accelerated charge migration for outstanding photocatalytic behavior. Applied Surface Science, 2019, 470, 63-73.	3.1	53
33384	Unlocking the nature of the co-doping effect on the ionic conductivity of CeO2-based electrolyte. Ceramics International, 2019, 45, 3977-3985.	2.3	27
33385	First-principles study of structural, elastic, electronic, vibrational and thermodynamic properties of uranium aluminides. Computational Materials Science, 2019, 158, 26-31.	1.4	15
33386	Defective GP-zones and their evolution in an Al-Cu-Mg alloy during high-temperature aging. Journal of Alloys and Compounds, 2019, 774, 988-996.	2.8	37
33387	One-for-multiple substitution of large atoms in beryllium. Scripta Materialia, 2019, 162, 172-175.	2.6	1
33388	Ferromagnetism induced by vacancies in (N, Al)-codoped 6H-SiC. Solid State Communications, 2019, 288, 28-32.	0.9	3
33389	Half-Metallic Ferromagnetism Character in Cr-Doped CaS Diluted Magnetic Insulator and Semiconductor: an Ab Initio Study. Journal of Superconductivity and Novel Magnetism, 2019, 32, 2155-2164.	0.8	10
33390	Conjugation of biomolecules onto antimonene surface for biomedical prospects: A DFT study. Chemical Physics Letters, 2019, 715, 115-122.	1.2	5
33391	First principles study of the structural, electronic and magnetic properties of w-CoS. Physica B: Condensed Matter, 2019, 554, 165-172.	1.3	6
33392	Synthesis and magnetic properties of Feâ€doped CdS nanorods. Micro and Nano Letters, 2019, 14, 275-279.	0.6	1
33393	Thermal Behavior and Detonation Characterization of 3,3â€Dinitroazetidinium Salicylate. Propellants, Explosives, Pyrotechnics, 2019, 44, 175-180.	1.0	3
33394	Pure and M-doped (M=Zn, Cu, Ni, Co) cadmium oxide nanosheets, novel adsorbents for the adsorption of ethyl benzene and ortho, meta, para xylene: a theoretical study. Adsorption, 2019, 25, 51-62.	1.4	0
33395	The initial stage of OH adsorption on Ni(111). Journal of Electroanalytical Chemistry, 2019, 832, 137-141.	1.9	7
33396	On the presence of antisite defect in monoclinic Li2FeSiO4 â€" A combined X-Ray diffraction and DFT study. Solid State Sciences, 2019, 87, 81-86.	1.5	2

#	Article	IF	Citations
33397	Fe-porphyrin carbon matrix as a bifunctional catalyst for oxygen reduction and CO₂ reduction from theoretical perspective. Molecular Physics, 2019, 117, 1805-1812.	0.8	12
33398	Boosting the Photocatalytic Ability of Cu₂O Nanowires for CO₂ Conversion by MXene Quantum Dots. Advanced Functional Materials, 2019, 29, 1806500.	7.8	354
33399	Nonâ€Đestructive Surface Energy Measurements on (1Â0Â0) Galfenol. Advanced Theory and Simulations, 2019, 2, 1800043.	1.3	4
33400	Electronic Structures and Ferromagnetic Properties of 3d (Cr)-Doped BaSe Barium Selenide. Journal of Superconductivity and Novel Magnetism, 2019, 32, 2185-2192.	0.8	14
33401	Ab-initio modeling and experimental investigation of properties of ultra-high temperature solid solutions TaxZr1-xC. Journal of Alloys and Compounds, 2019, 778, 480-486.	2.8	22
33402	Electronic, transport, and optical properties of atomically thin silicon phosphide: first-principles calculations. Materials Research Express, 2019, 6, 026428.	0.8	7
33403	Comprehensive theoretical analysis of the influence of surface alloying by zinc on the catalytic performance of Cu(1â€¯1â€¯0) for the production of methanol from CO2 selective hydrogenation: Part 1 â€“ Thermochemical aspects. Applied Surface Science, 2019, 469, 841-853.	3.1	13
33404	Pressure effect on the band structure and topological properties of the electron density of pyrene: First-principles calculations. Chemical Physics, 2019, 518, 8-14.	0.9	5
33405	A DFT based prediction of a new 2D zirconium disulfide Pmmm-ZrS2 monolayer: A quasi direct band gap semiconductor. Results in Physics, 2019, 12, 903-907.	2.0	10
33406	Press-engineered funnel effect in MoS2 monolayer homojunction. Journal Physics D: Applied Physics, 2019, 52, 055103.	1.3	1
33407	Bond length anomaly in TiB2 at high pressure: first principles calculations. Materials Research Express, 2019, 6, 026531.	0.8	4
33408	Glycine self-assembled on graphene enhances the solar absorbance performance. Carbon, 2019, 143, 329-334.	5.4	21
33409	Superprismane: A porous carbon allotrope. Chemical Physics Letters, 2019, 715, 29-33.	1.2	12
33410	Ultrathin Sb2S3 nanosheet anodes for exceptional pseudocapacitive contribution to multi-battery charge storage. Energy Storage Materials, 2019, 20, 36-45.	9.5	51
33411	Theoretical investigations of TiNbC MXenes as anode materials for Li-ion batteries. Journal of Alloys and Compounds, 2019, 778, 53-60.	2.8	49
33412	Pd-Ga model SCALMS: Characterization and stability of Pd single atom sites. Journal of Catalysis, 2019, 369, 33-46.	3.1	33
33413	Tribo-piezoelectricity in Janus transition metal dichalcogenide bilayers: A first-principles study. Nano Energy, 2019, 56, 33-39.	8.2	58
33414	In-situ fabrication and characteristics of an Al4W/Al12W composite using infiltration method. Vacuum, 2019, 160, 95-101.	1.6	12

#	Article	IF	Citations
33415	Epitaxial Heterogeneous Interfaces on Nâ€NiMoO₄/NiS₂ Nanowires/Nanosheets to Boost Hydrogen and Oxygen Production for Overall Water Splitting. Advanced Functional Materials, 2019, 29, 1805298.	7.8	378
33416	Effects of vacancies at Al(1â€¯1â€¯1)/6H-SiC(0001) interfaces on deformation behavior: A first-principle study. Computational Materials Science, 2019, 158, 110-116.	1.4	16
33417	Structural and electronic properties of BiOF with two-dimensional layered structure under high pressure: Ab initio study. Solid State Communications, 2019, 288, 33-37.	0.9	11
33418	Silver atom, trimer and tetramer species supported on a ceria nanoparticle: A density functional study. Surface Science, 2019, 681, 38-46.	0.8	8
33419	Two-dimensional phosphorene/C3N p-n heterostructure: Effect of contact type on electronic and optical properties. Science China Technological Sciences, 2019, 62, 478-489.	2.0	2
33420	DFT Calculation about Oxygen Vacancy to Promote Adsorption of a CO Molecule on Single Auâ€supported Titanium Dioxide. Physica Status Solidi (B): Basic Research, 2019, 256, 1800386.	0.7	7
33421	Formation and temporal evolution of modulated structure in high Nb-containing lamellar Î³-TiAl alloy. Acta Materialia, 2019, 165, 215-227.	3.8	35
33422	The investigations on optical properties of TiN1âˆ’xCx ternary alloys. Physica B: Condensed Matter, 2019, 556, 61-65.	1.3	3
33423	First principles study of the electronic structure and optical properties of chrysene under pressure. Molecular Simulation, 2019, 45, 147-153.	0.9	0
33424	CO2 reduction by H2 to CHO on Ru(0001): DFT evaluation of three pathways. Surface Science, 2019, 681, 54-58.	0.8	11
33425	Growth and Isolation of Large Area Boronâ€Doped Nanocrystalline Diamond Sheets: A Route toward Diamondâ€onâ€Graphene Heterojunction. Advanced Functional Materials, 2019, 29, 1805242.	7.8	22
33426	Magnetic properties of diluted magnetic semiconductors Li(Zn,TM)N with decoupled charge and spin doping (TM: V, Cr, Mn, Fe, Co and Ni). Computational Materials Science, 2019, 158, 260-264.	1.4	12
33427	Penta-AlN2 monolayer: A ferromagnetic insulator. Journal of Magnetism and Magnetic Materials, 2019, 475, 83-87.	1.0	7
33428	Energetics and kinetics of metal impurities in the low-temperature ordered phase of V2C from first-principles calculations. Journal of Nuclear Materials, 2019, 513, 185-191.	1.3	1
33429	Basal slip of âŸ¨aâŸ© screw dislocations in hexagonal titanium. Scripta Materialia, 2019, 162, 296-299.	2.6	22
33430	Atomistic origins of Guinier-Preston zone formation and morphology in Al-Cu and Al-Ag alloys from first principles. Scripta Materialia, 2019, 162, 235-240.	2.6	13
33431	Layered lithium niobium (III) oxideâ€”LiNbO₂ as a visible-light-driven photocatalyst for H₂ evolution. JPhys Energy, 2019, 1, 015001.	2.3	3
33432	First principle analysis for magnetic properties of noble metal doped rutile TiO2. Computational Condensed Matter, 2019, 18, e00349.	0.9	9

#	Article	IF	Citations
33433	Corrosion resistance enhancement of WC cermet coating by carbides alloying. Corrosion Science, 2019, 147, 372-383.	3.0	24
33434	A study on quercetin and 5-fluorouracil drug interaction on graphyne nanosheets and solvent effects â€" A first-principles study. Journal of Molecular Liquids, 2019, 275, 713-722.	2.3	45
33435	Immobilization of palladium nanoparticles on Metformin-functionalized graphene oxide as a heterogeneous and recyclable nanocatalyst for Suzuki coupling reactions and reduction of 4-nitrophenol. Polyhedron, 2019, 158, 414-422.	1.0	78
33436	Hydrogen storage in MIL-88 series. Journal of Materials Science, 2019, 54, 3994-4010.	1.7	27
33437	Photo-induced negative differential resistance in a resistive switching memory device based on BiFeO3/ZnO heterojunctions. Applied Materials Today, 2019, 14, 21-28.	2.3	76
33438	A kinetic Monte Carlo study of vacancy diffusion in non-dilute Ni-Re alloys. Materials Science & Engineering A: Structural Materials: Properties, Microstructure and Processing, 2019, 743, 265-273.	2.6	15
33439	Computational investigations of XMgGa (Xâ€¯=â€¯Li, Na) half Heusler compounds for thermo-elastic and vibrational properties. Physica B: Condensed Matter, 2019, 554, 102-106.	1.3	10
33440	Elastic constants of graphene: Comparison of empirical potentials and DFT calculations. Physica E: Low-Dimensional Systems and Nanostructures, 2019, 108, 326-338.	1.3	47
33441	2 Ã— 2 charge density wave in single-layer TiTe ₂. 2D Materials, 2019, 6, 015027.	2.0	20
33442	Prediction of a Dynamically Stable New Half-Metallic Phase for the BaN and BaC Compounds. Journal of Superconductivity and Novel Magnetism, 2019, 32, 2031-2044.	0.8	3
33443	DFT study on the influence of sulfur on the hydrophobicity of pyrite surfaces in the process of oxidation. Applied Surface Science, 2019, 466, 964-969.	3.1	19
33444	First principles investigation of the surface stability and equilibrium morphology of MoO3. Applied Surface Science, 2019, 467-468, 753-759.	3.1	20
33445	Novel carbon-rich nitride C3N: A superhard phase in monoclinic symmetry. Computational Materials Science, 2019, 158, 170-177.	1.4	19
33446	Vacancy-ordered yttria stabilized zirconia as a low-temperature electronic conductor achieved by laser melting. Journal of the European Ceramic Society, 2019, 39, 1374-1380.	2.8	10
33447	Rational Band Design in Metal Chalcogenide Ba₆Zn₆HfS₁₄: Splitting Orbitals, Narrowing the Forbidden Gap, and Boosting Photocatalyst Properties. Crystal Growth and Design, 2019, 19, 193-199.	1.4	5
33448	The electronic and elasticity properties of new half-metallic chalcogenides Cu₃TMCh₄(TMâ€‰=â€‰Cr, Fe and Châ€‰=â€‰S, Se, Te): anab initiostudy. Philosophical Magazine, 2019, 99, 513-529.	1.7	12
33449	Effect of pressure on the physical properties of the superconductor NiBi₃. Journal of Physics Condensed Matter, 2019, 31, 035701.	0.7	9
33450	Ensemble Design in Nickel Phosphide Catalysts for Alkyne Semiâ€Hydrogenation. ChemCatChem, 2019, 11, 457-464.	1.8	25

#	Article	IF	Citations
33451	Methyl-terminated germanane GeCH3 synthesized by solvothermal method with improved photocatalytic properties. Applied Surface Science, 2019, 467-468, 881-888.	3.1	30
33452	Prediction of Li2B novel phases and superconductivity under varying pressures. Computational Materials Science, 2019, 158, 255-259.	1.4	6
33453	Complete martensitic transformation sequence and magnetic properties of non-stoichiometric Ni2Mn1.2Ga0.8 alloy by first-principles calculations. Journal of Magnetism and Magnetic Materials, 2019, 473, 360-364.	1.0	22
33454	First-principle study of the polarization, atomic displacements and electronic structure of angular-deformed barium titanate. Physica B: Condensed Matter, 2019, 553, 96-104.	1.3	1
33455	Effect of trace potassium on hydrogen adsorption and dissociation on hcp cobalt: A density functional theory study. Surface Science, 2019, 681, 24-31.	0.8	9
33456	Heterogeneous Coâ€“N/C Electrocatalysts with Controlled Cobalt Site Densities for the Hydrogen Evolution Reaction: Structureâ€“Activity Correlations and Kinetic Insights. ACS Catalysis, 2019, 9, 83-97.	5.5	122
33457	Origin of Blue Luminescence in <mml:math xmlns:mml="http://www.w3.org/1998/Math/MathML" display="inline" overflow="scroll"><mml:mi>Mg</mml:mi></mml:math> -Doped <mml:math xmlns:mml="http://www.w3.org/1998/Math/MathML" display="inline" overflow="scroll"><mml:mi>Ga</mml:mi><mml:mi mathvariant="normal">N</mml:mi></mml:math>. Physical Review Applied, 2019, 11, .	1.5	19
33458	Ultrafast Transient Dynamics of Adsorbates on Surfaces Deciphered: The Case of CO on Cu(100). Physical Review Letters, 2019, 122, 016806.	2.9	29
33459	Effect of Defects on Spontaneous Polarization in Pure and Doped LiNbO3: First-Principles Calculations. Materials, 2019, 12, 100.	1.3	19
33460	Synthesis of Nickelâ€Doped Ceria Catalysts for Selective Acetylene Hydrogenation. ChemCatChem, 2019, 11, 1526-1533.	1.8	30
33461	Abâ€initio study of electronic, optical, thermal, and transport properties of Cr4AlB6. International Journal of Quantum Chemistry, 2019, 119, e25897.	1.0	1
33462	New insights into adsorption bonding of imidazole: A viable C2â€“H bond cleavage on copper surfaces. Applied Surface Science, 2019, 479, 463-468.	3.1	13
33463	Germanane nanosheet as a novel biosensor for liver cirrhosis based on adsorption of biomarker volatiles â€“ A DFT study. Applied Surface Science, 2019, 475, 990-998.	3.1	56
33464	Effective mass and optical properties of orthorhombic Al1â^'xInxFeO3 perovskite: An ab-initio study. Computational Materials Science, 2019, 159, 222-227.	1.4	8
33465	First-principles investigation of native point defects in two-dimensional Ti3C2. Computational and Theoretical Chemistry, 2019, 1150, 26-39.	1.1	9
33466	Energy Gap-Modulated Blue Phosphorene as Flexible Anodes for Lithium- and Sodium-Ion Batteries. Journal of Physical Chemistry C, 2019, 123, 2808-2819.	1.5	29
33467	Toward Fundamentals of Confined Electrocatalysis in Nanoscale Reactors. Journal of Physical Chemistry Letters, 2019, 10, 533-539.	2.1	18
33468	Doping of Monolayer Transition-Metal Dichalcogenides via Physisorption of Aromatic Solvent Molecules. Journal of Physical Chemistry Letters, 2019, 10, 540-547.	2.1	52

#	Article	IF	Citations
33469	Effect of surface-bound sulfide on oxygen reduction reaction on Pt: Breaking the scaling relationship and mechanistic insights. Journal of Chemical Physics, 2019, 150, 041728.	1.2	17
33470	High-pressure phases of MnCO3 by random structure search. Physical Review B, 2019, 99, .	1.1	3
33471	Transport properties of doped zigzag graphene nanoribbons. Chinese Journal of Physics, 2019, 57, 47-52.	2.0	7
33472	Dense Electronâ€“Hole Plasma Formation and Ultralong Charge Lifetime in Monolayer MoS₂ via Material Tuning. Nano Letters, 2019, 19, 1104-1111.	4.5	41
33473	F-Doped NaTi₂(PO₄)₃/C Nanocomposite as a High-Performance Anode for Sodium-Ion Batteries. ACS Applied Materials & Interfaces, 2019, 11, 3116-3124.	4.0	52
33474	Silicate-mediated interstellar water formation: a theoretical study. Monthly Notices of the Royal Astronomical Society, 2019, 482, 5389-5400.	1.6	22
33475	Thermodynamic assessment of the Co-Ta system. Calphad: Computer Coupling of Phase Diagrams and Thermochemistry, 2019, 64, 205-212.	0.7	17
33476	Tuning the electronic and magnetic properties of Fe atom embedded heptazine sheet by atomic and molecular adsorption: First-principles calculations. Chinese Journal of Physics, 2019, 57, 1-5.	2.0	4
33477	Surface thermodynamic stability of Li-rich Li2MnO3: Effect of defective graphene. Energy Storage Materials, 2019, 22, 113-119.	9.5	45
33478	Fast and Accurate Uncertainty Estimation in Chemical Machine Learning. Journal of Chemical Theory and Computation, 2019, 15, 906-915.	2.3	102
33479	The Crystal Structures of Î±â€•and Î²â€Ť₂ Revisited. Chemistry - A European Journal, 2019, 25, 3310-3317.	1.7	9
33480	Effects of substitutional Mo and Cr on site occupation and diffusion of hydrogen in the Î²-phase vanadium hydride by first principles calculations. Theoretical Chemistry Accounts, 2019, 138, 1.	0.5	3
33481	Electronic structure, magnetism properties and optical absorption of organometal halide perovskite CH3NH3XI3 (Xâ€‰=â€‰Fe, Mn). Applied Physics A: Materials Science and Processing, 2019, 125, 1.	1.1	11
33482	First-principles study of the surface reparation of ultrathin InSe with Se-atom vacancies by thiol chemistry. Applied Surface Science, 2019, 475, 487-493.	3.1	6
33483	Theoretical investigations on physical properties of SrFCuCh (Ch=S and Se). Journal of Solid State Chemistry, 2019, 271, 191-198.	1.4	2
33484	Few-Nanometer-Sized Î±-CsPbI₃ Quantum Dots Enabled by Strontium Substitution and Iodide Passivation for Efficient Red-Light Emitting Diodes. Journal of the American Chemical Society, 2019, 141, 2069-2079.	6.6	218
33485	Interfacial electric field and spin-orbitronic properties of heavy-metal/CoFe bilayers. Applied Physics Letters, 2019, 114, .	1.5	9
33486	Bulk properties of the van der Waals hard ferromagnet <mml:math xmlns:mml="http://www.w3.org/1998/Math/MathML"><mml:msub><mml:mi>VI</mml:mi><mml:mn>3</mml:mn></mml:msub></mml:math> Physical Review B, 2019, 99, .	1.1	98

#	Article	IF	Citations
33487	Stability, Electronic and Magnetic Properties of Rare Earth (Eu, Tm) Implanted InGaN. Journal of Superconductivity and Novel Magnetism, 2019, 32, 2515-2519.	0.8	4
33488	Molecular adsorption and surface formation reactions of HCl, H2 and chlorosilanes on Si(100)-c(4â€Ã—â€2) with applications for high purity silicon production. Applied Surface Science, 2019, 475, 124-134.	3.1	14
33489	Uniform MoS2 nanolayer with sulfur vacancy on carbon nanotube networks as binder-free electrodes for asymmetrical supercapacitor. Applied Surface Science, 2019, 475, 793-802.	3.1	69
33490	First-principles investigations on elasticity properties of FeSi under high pressure and temperature. Physica B: Condensed Matter, 2019, 557, 82-87.	1.3	4
33491	Structural, elastic, thermoelastic and electronic properties of M2O3 (Mâ€=â€Cr, Fe, Al) compounds: Experimental and theoretical study. Results in Physics, 2019, 12, 725-731.	2.0	1
33492	Surface-Templated Assembly of Molecular Methanol on the Thin Film â€œ29â€•Cu(111) Surface Oxide. Journal of Physical Chemistry C, 2019, 123, 2911-2921.	1.5	9
33493	Transferability of the Specific Reaction Parameter Density Functional for H2 + Pt(111) to H2 + Pt(211). Journal of Physical Chemistry C, 2019, 123, 2973-2986.	1.5	18
33494	Equation of state and structural characterization of Cu₄I₄{PPh₂(CH₂CHâ€‰=â€‰CH₂)}₄ under pressure. High Pressure Research, 2019, 39, 69-80.	0.9	5
33495	Tailoring Lithium Deposition via an SEIâ€Functionalized Membrane Derived from LiF Decorated Layered Carbon Structure. Advanced Energy Materials, 2019, 9, 1802912.	10.2	98
33496	First-Principles Study of the Structural Stability and Dynamic Properties of Li2MSiO4 (M = Mn, Co, Ni) Polymorphs. Energies, 2019, 12, 224.	1.6	7
33497	Phase transition in two-dimensional tellurene under mechanical strain modulation. Nano Energy, 2019, 58, 202-210.	8.2	43
33498	A theoretical study of electrocatalytic ammonia synthesis on single metal atom/MXene. Chinese Journal of Catalysis, 2019, 40, 152-159.	6.9	76
33499	Rational Design via Synergistic Combination Leads to an Outstanding Deep-Ultraviolet Birefringent Li₂Na₂B₂O₅ Material with an Unvalued B₂O₅ Functional Gene. Journal of the American Chemical Society, 2019, 141, 3258-3264.	6.6	177
33500	Distortion-stabilized ordered structures in A2BBâ€™O7 mixed pyrochlores. Npj Computational Materials, 2019, 5, .	3.5	23
33501	Quasi-one-dimensional silicon nanostructures for gas molecule adsorption: a DFT investigation. Applied Surface Science, 2019, 475, 278-284.	3.1	14
33502	Shapeâ€Controlled CO₂ Electrochemical Reduction on Nanosized Pd Hydride Cubes and Octahedra. Advanced Energy Materials, 2019, 9, 1802840.	10.2	132
33503	Transition metal-doped 3C-SiC as a promising material for intermediate band solar cells. Optical and Quantum Electronics, 2019, 51, 1.	1.5	15
33504	Enhanced Stability and Optical Absorption in the Perovskiteâ€Based Compounds MA 1â^' x Cs x PbI 3â^' y Br y. ChemPhysChem, 2019, 20, 489-498.	1.0	6

#	Article	IF	Citations
33505	Synthesis of SrCoO3 perovskite as W-based double perovskite and its structural properties. Journal of Materials Science: Materials in Electronics, 2019, 30, 4270-4278.	1.1	2
33506	Using First-Principles Calculations in CALPHAD Models to Determine Carrier Concentration of the Binary PbSe Semiconductor. Journal of Electronic Materials, 2019, 48, 1031-1043.	1.0	8
33507	Effect of atom adsorption on the electronic, magnetic, and optical properties of the GeP monolayer: A first-principle study. Applied Surface Science, 2019, 475, 863-872.	3.1	14
33508	First-principles study of the electronic structure and optical properties of Eu2+â€“M (M = Mn2+, Mg2+,) Tj ETQq1 1 0.784314 rgBT /O	2.3	6
33509	First-principles calculations of vacancy-O-He and vacancy-N-He complexes in vanadium. Computational Materials Science, 2019, 160, 180-185.	1.4	14
33510	A proof of concept: Thermodynamics of aluminum â€“ transition metal highly concentrated alloys. Journal of Alloys and Compounds, 2019, 781, 595-605.	2.8	10
33511	Green luminescence and calculated optical properties of Cu ions in ZnO. Journal of Alloys and Compounds, 2019, 782, 1024-1030.	2.8	6
33512	AlÂâ˜ BN interaction in a high-strength lightweight Al/BN metal-matrix composite: Theoretical modelling and experimental verification. Journal of Alloys and Compounds, 2019, 782, 875-880.	2.8	20
33513	Thermal stability of ternary compounds in the Cu-Li-Sn system and phase transition of the Cu6Sn5 electrode: First-principles calculations and experiment. Journal of Alloys and Compounds, 2019, 783, 44-54.	2.8	2
33514	Theoretical study of structural, electronic, phonon and thermoelectric properties of KScX (X=Sn and) Tj ETQq1 1 0.784314 rgBT /Ove and Compounds, 2019, 784, 319-329.	2.8	44
33515	Reactions of KBrF4 with platinum metals. Journal of Fluorine Chemistry, 2019, 218, 11-20.	0.9	8
33516	Theory-guided bottom-up design of the FeCrAl alloys as accident tolerant fuel cladding materials. Journal of Nuclear Materials, 2019, 516, 63-72.	1.3	27
33517	Influence of hydrostatic strain on the behaviors of rhenium and osmium in tungsten. Journal of Nuclear Materials, 2019, 516, 111-117.	1.3	1
33518	Electronic and optical properties of double perovskite oxide Pb2ScMO6 (M = Ta, Sb) using a first principles approach. Journal of Physics and Chemistry of Solids, 2019, 129, 188-195.	1.9	11
33519	Unusual pressure-induced electronic structure evolution in organometal halide perovskite predicted from first-principles. Organic Electronics, 2019, 67, 89-94.	1.4	23
33520	Supercritical water gasification of phenol over Ni-Ru bimetallic catalysts. Water Research, 2019, 152, 12-20.	5.3	34
33521	Size-Dependent Adsorption of Styrene on Pd Clusters: A Density Functional Theory Study. Journal of Physical Chemistry C, 2019, 123, 2182-2188.	1.5	12
33522	Effect of Interstitial Hydrogen on the Mechanical and Thermal Properties of Tungsten: A First-Principles Study. Journal of Physical Chemistry C, 2019, 123, 1913-1921.	1.5	13

#	Article	IF	Citations
33523	Polymorphism, Phase Transition, and Lattice Dynamics of Energetic Oxidizer Ammonium Perchlorate under High Pressure. Journal of Physical Chemistry C, 2019, 123, 2114-2126.	1.5	16
33524	Achieving Fast Kinetics and Enhanced Li Storage Capacity for Ti3C2O2 by Intercalation of Quinone Molecules. ACS Applied Energy Materials, 2019, 2, 1251-1258.	2.5	19
33525	Artificial Second-Order Nonlinear Optics in a Centrosymmetric Optical Material BiVO₄: Breaking the Prerequisite for Nonlinear Optical Materials. ACS Omega, 2019, 4, 1045-1052.	1.6	6
33526	Interaction of Hydrogen with MB6 (M = Ba, Ca, La, and Sr) Surfaces from First Principles. ACS Omega, 2019, 4, 65-72.	1.6	5
33527	Phonon coherences reveal the polaronic character of excitons in two-dimensional lead halide perovskites. Nature Materials, 2019, 18, 349-356.	13.3	257
33528	A comparative study of mechanisms of the adsorption of CO₂ confined within grapheneâ€“MoS₂ nanosheets: a DFT trend study. Nanoscale Advances, 2019, 1, 1442-1451.	2.2	22
33529	Self-assembling of formic acid on the partially oxidizedp(2 Ã— 1) Cu(110) surface reconstruction at low coverages. Journal of Chemical Physics, 2019, 150, 041720.	1.2	3
33530	First principles study of hBN-AlN short-period superlattice heterostructures. Applied Physics Letters, 2019, 114, 011903.	1.5	5
33531	Strain-engineering the anisotropic electrical properties of low-symmetry bilayer GeSe. Journal of Applied Physics, 2019, 125, .	1.1	5
33532	Phase transition of ZrN under pressure. Philosophical Magazine, 2019, 99, 942-955.	0.7	3
33533	Tuneable thermal expansion of poly (3,4-ethylenedioxythiophene) polystyrene sulfonate. Journal of Physics Condensed Matter, 2019, 31, 125101.	0.7	7
33534	Air-stable n-doped black phosphorus transistor by thermal deposition of metal adatoms. Nanotechnology, 2019, 30, 135201.	1.3	16
33535	Can we rely on hybrid-DFT energies of solid-state problems with local-DFT geometries?. Electronic Structure, 2019, 1, 015008.	1.0	18
33536	Adsorption and migration behavior of molybdenum atom on graphite (0001) surface. Applied Surface Science, 2019, 470, 1064-1070.	3.1	14
33537	Manganese speciation in Mn-rich CaCO3: A density functional theory study. Geochimica Et Cosmochimica Acta, 2019, 248, 231-241.	1.6	9
33538	Predicting the Electrochemical Synthesis of 2D Materials from First Principles. Journal of Physical Chemistry C, 2019, 123, 3180-3187.	1.5	34
33539	Influence of Cu(111) and Ni(111) Substrates on the Capacitances of Monolayer and Bilayer Graphene Supercapacitor Electrodes. Journal of Physical Chemistry C, 2019, 123, 2783-2791.	1.5	7
33540	Tailoring the Bactericidal Activity of Ag Nanoparticles/Î±-Ag₂WO₄ Composite Induced by Electron Beam and Femtosecond Laser Irradiation: Integration of Experiment and Computational Modeling. ACS Applied Bio Materials, 2019, 2, 824-837.	2.3	30

#	Article	IF	Citations
33541	Thickness dependent electronic properties of Pt dichalcogenides. Npj 2D Materials and Applications, 2019, 3, .	3.9	138
33542	Initial stages of graphene oxide cracking in basic media. Carbon, 2019, 142, 217-223.	5.4	3
33543	First-principles study of elastic, electronic, and optical properties of Î±-TeO2 under pressure. Journal of Alloys and Compounds, 2019, 776, 417-427.	2.8	5
33544	Electronic, magnetic and transport properties of zigzag silicene nanoribbon adsorbed with Cu atom: A first-principles calculation. Journal of Magnetism and Magnetic Materials, 2019, 473, 306-311.	1.0	12
33545	First-principle studies on the mechanical, thermodynamic and electronic properties of Î²â€³-Mg3Gd and Î²â€²-Mg7Gd alloys under pressure. Journal of Physics and Chemistry of Solids, 2019, 125, 115-122.	1.9	14
33546	First-principles study on stability, electronic, mechanical and thermodynamic properties of Al-Cu-RE ternary compounds. Solid State Communications, 2019, 287, 63-67.	0.9	7
33547	Elucidating Molecular Interactions in Glycerol Adsorption at the Metalâ€“Water Interface with Density Functional Theory. Langmuir, 2019, 35, 4791-4805.	1.6	10
33548	Theoretical investigation of superconductivity in the non-centrosymmetric SrPtGe₃ and CaPtSi₃ compounds. Philosophical Magazine, 2019, 99, 198-223.	0.7	5
33549	The interactions between fine particles of coal and kaolinite in aqueous, insights from experiments and molecular simulations. Applied Surface Science, 2019, 467-468, 12-21.	3.1	46
33550	Detecting Decompositions of Sulfur Hexafluoride Using MoS₂ Monolayer as Gas Sensor. IEEE Sensors Journal, 2019, 19, 39-46.	2.4	51
33551	The Structural, Electronic, and Magnetic Properties of Cobalt Disulfide Doped with Oxygen, Selenium, or Tellurium. Journal of Electronic Materials, 2019, 48, 483-493.	1.0	0
33552	Tuning the electronic and structural properties of Gd-TiO2-GO nanocomposites for enhancing photodegradation of IC dye: The role of Gd3+ ion. Applied Catalysis B: Environmental, 2019, 243, 106-120.	10.8	60
33553	Ab-initio study of electronic properties of Si(C) honeycomb structures. Chinese Journal of Physics, 2019, 57, 479-489.	2.0	4
33554	Theoretical analysis of the adsorption of ammoniaâ€“borane and their dehydrogenation products on the (001) surface of TiC and ZrC. Surface Science, 2019, 680, 95-106.	0.8	9
33555	Elastic and electronic properties of C₂N monolayer: first-principles calculation. Materials Research Express, 2019, 6, 025601.	0.8	6
33556	Combining the Physics of Metal/Oxide Heterostructure, Interface Dipole, Band Bending, Crystallography, and Surface State to Understand Heterogeneity Contrast in Oxidation and Corrosion. Corrosion, 2019, 75, 152-166.	0.5	12
33557	Electronic and Interface Properties in Graphene Oxide/Hydrogenâ€Passivated Ge Heterostructure. Physica Status Solidi - Rapid Research Letters, 2019, 13, 1800461.	1.2	31
33558	Density functional investigation on hexagonal nanosheets and bulk thallium nitrides for possible thermoelectric applications. Applied Nanoscience (Switzerland), 2019, 9, 33-42.	1.6	8

#	Article	IF	Citations
33559	Unsaturated edge-anchored Ni single atoms on porous microwave exfoliated graphene oxide for electrochemical CO2. Applied Catalysis B: Environmental, 2019, 243, 294-303.	10.8	243
33560	Theoretical investigation on vanadium dinitrides from first-principles calculations. Ceramics International, 2019, 45, 2457-2465.	2.3	6
33561	Energetics of helium-vacancy complexes in Fe-9Cr alloys from first-principles calculations. Journal of Nuclear Materials, 2019, 513, 143-151.	1.3	26
33562	Planar net-Ï„: A new high-performance metallic carbon anode material for lithium-ion batteries. Carbon, 2019, 142, 438-444.	5.4	63
33563	Effect of additional solute elements (X= Al, Ca, Y, Ba, Sn, Gd and Zn) on crystallographic anisotropy during the dendritic growth of magnesium alloys. Journal of Alloys and Compounds, 2019, 775, 322-329.	2.8	15
33564	On the stacking fault energy related deformation mechanism of nanocrystalline Cu and Cu alloys: A first-principles and TEM study. Journal of Alloys and Compounds, 2019, 776, 807-818.	2.8	36
33565	Modeling of the Coadsorption of Chloride and Hydrogen Ions on Copper Electrode Surface. Journal of the Electrochemical Society, 2019, 166, D3042-D3048.	1.3	1
33566	First Principles Simulations on Migration Paths of Oxygen Interstitials in MgAl₂O₄. Physica Status Solidi (B): Basic Research, 2019, 256, 1800282.	0.7	7
33567	Zig-zag boron nitride nanotubes functionalization with acetylene molecules: a density functional theory study. Adsorption, 2019, 25, 63-74.	1.4	4
33568	Error controlling of the combined Cluster-Expansion and Wangâ€“Landau Monte-Carlo method and its application to FeCo. Computer Physics Communications, 2019, 235, 95-101.	3.0	10
33569	A hybrid density functional study of optical and electronic properties of AlGa-codoped ZnO. Optik, 2019, 179, 566-573.	1.4	8
33570	Electronic origins of the giant volume collapse in the pyrite mineral <mml:math xmlns:mml="http://www.w3.org/1998/Math/MathML" altimg="si0047.gif" overflow="scroll"><mml:msub><mml:mrow><mml:mi>MnS</mml:mi></mml:mrow><mml:mrow><mml:mn>2</mml:mn></mml:mrow> Journal of Solid State Chemistry, 2019, 269, 540-546.	1.4	7
33571	First principles study of the electronic and magnetic properties of Zn1-xCoxSe alloys. Solid State Communications, 2019, 287, 48-53.	0.9	4
33572	Coupling of Acetaldehyde to Crotonaldehyde on CeO_{2â€“x}(111): Bifunctional Mechanism and Role of Oxygen Vacancies. Journal of Physical Chemistry C, 2019, 123, 8273-8286.	1.5	23
33573	Basics of semiconducting metal oxideâ€“based gas sensors. , 2019, , 61-165.		17
33574	Surface characterization of face-centered cubic crystals. Mechanics of Materials, 2019, 129, 15-22.	1.7	13
33575	Ab initio and Monte Carlo studies of phase transitions and magnetic properties of YCrO3: Heisenberg model. Physics Letters, Section A: General, Atomic and Solid State Physics, 2019, 383, 121-126.	0.9	3
33576	Analysis of dynamic decomposition for barium dimethyl-naphthalene-sulfonate on an Al3Mg (0â€¯0â€¯1) surface from ab-initio molecular dynamics. Applied Surface Science, 2019, 466, 772-779.	3.1	2

#	Article	IF	Citations
33577	Adsorption of dimethyl sulfoxide on blue phosphorene. Surface Science, 2019, 680, 88-94.	0.8	10
33578	Intrinsic Properties of Pure and Mixed Monolayer Oxides in the Honeycomb Structure: M₂O₃ and MMâ€²O₃ (M, Mâ€² = Ti, V, Cr, Fe). Journal of Physical Chemistry C, 2019, 123, 7898-7910.	1.5	13
33579	Mechanism for Zr poisoning of Al-Ti-B based grain refiners. Acta Materialia, 2019, 164, 428-439.	3.8	105
33580	Effects of temperature and O partial pressure on the atomic structure of Al2O3 (0â€¯0â€¯0â€¯1) surface. Computational Materials Science, 2019, 157, 37-42.	1.4	6
33581	First-principles study of fracture toughness enhancement in transition metal nitrides. Surface and Coatings Technology, 2019, 357, 903-909.	2.2	26
33582	Effect of vacancies on spin transport characteristics of zigzag WS₂ nanoribbon. Materials Research Express, 2019, 6, 025013.	0.8	7
33583	First-Principles Study on Optical and Thermodynamic Behaviour of Multiferroic BiFeO3 Using LSDA+ U and TB-mBJ Methods. Journal of Electronic Materials, 2019, 48, 621-633.	1.0	10
33584	Density functional theory calculation on facet-dependent photocatalytic activity of MoS2/CdS heterostructures. Applied Surface Science, 2019, 469, 27-33.	3.1	63
33585	Measured and calculated properties of B-doped Ï„-phase MnAl â€“ A rare earth free permanent magnet. Journal of Magnetism and Magnetic Materials, 2019, 474, 591-598.	1.0	7
33586	Highly stable tungsten disulfide supported on a self-standing nickel phosphide foam as a hybrid electrocatalyst for efficient electrolytic hydrogen evolution. Nano Energy, 2019, 55, 193-202.	8.2	59
33587	Tuning the electronic and optical properties of GaAs nanowire (10-10) surfaces by Zn doping: First-principles study. Solid State Communications, 2019, 288, 43-47.	0.9	7
33588	Adsorption and dissociation of H₂S on the anatase TiO₂ (100) surface: DFT + U study. Materials Research Express, 2019, 6, 025510.	0.8	7
33589	Ab initio molecular dynamics simulation of methanol and acetonitrile: The effect of van der Waals interactions. Chemical Physics Letters, 2019, 714, 172-177.	1.2	5
33590	Prediction of Ti3C2O2 MXene as an effective capturer of formaldehyde. Applied Surface Science, 2019, 469, 770-774.	3.1	40
33591	Understanding the synergetic interaction within Î±-MoC/Î²-Mo2C heterostructured electrocatalyst. Journal of Energy Chemistry, 2019, 35, 66-70.	7.1	30
33592	Stable monolayer of the RuO₂ structure by the Peierls distortion. Philosophical Magazine, 2019, 99, 376-385.	0.7	18
33593	Calculation of the stability and mechanical and phonon properties of NbRuB, TaRuB, and NbOsB compounds. Philosophical Magazine, 2019, 99, 328-346.	0.7	11
33594	Fundamental Insights into the Performance Deterioration of Phosphorene due to Oxidation: A GW Method Investigation. Advanced Materials Interfaces, 2019, 6, 1801175.	1.9	12

#	Article	IF	Citations
33595	The preferred slip plane of nuclear material of Hafnium: A first-principles study. Computational Materials Science, 2019, 157, 25-30.	1.4	7
33596	Phosphorous-containing oxygen-deficient cobalt molybdate as an advanced electrode material for supercapacitors. Energy Storage Materials, 2019, 19, 186-196.	9.5	145
33597	The effect of pressure on the structural, elastic, electronic, magnetic, and optical properties of Mo-doped ZnSe alloy. Journal of Magnetism and Magnetic Materials, 2019, 474, 14-24.	1.0	5
33598	Exploration the p-type doping mechanism of GaAs nanowires from first-principles study. Physics Letters, Section A: General, Atomic and Solid State Physics, 2019, 383, 202-209.	0.9	26
33599	Quantum-chemical-based microkinetics simulations of syngas conversion over MoS2(1â€¯0â€¯0) surface. Chemical Engineering Science, 2019, 198, 166-183.	1.9	5
33600	Strain-mediated point defects in thermoelectric p-type bismuth telluride polycrystalline. Nano Energy, 2019, 55, 486-493.	8.2	32
33601	Solvent polarity-induced photoluminescence enhancement (SPIPE): A method enables several-fold increase in quantum yield of silicon nanoparticles. Nano Research, 2019, 12, 315-322.	5.8	12
33602	Effect of graphene oxide loading on TiO2: Morphological, optical, interfacial charge dynamics-A combined experimental and theoretical study. Carbon, 2019, 143, 51-62.	5.4	37
33603	Influences of isotropic strain on the electronic and magnetic properties of Fe-, Co-, and Ni-doped PbS revealed by density functional calculations. Materials Chemistry and Physics, 2019, 223, 133-139.	2.0	1
33604	Synthesis, crystal structure, microstructure and mechanical properties of (Ti1-Zr)3SiC2 MAX phase solid solutions. Ceramics International, 2019, 45, 1400-1408.	2.3	21
33605	Strain effect of high Tc ferromagnetism in Mo-doped SnS2 monolayer. Computational Materials Science, 2019, 156, 321-324.	1.4	11
33606	High activity of Au monolayer doped by Pt atom on WC (0001) surface towards H2 dissociation and high tolerance of sulfur poisoning. Journal of Alloys and Compounds, 2019, 775, 330-334.	2.8	10
33607	Selective hydrogenation of 1,3-butadiene over single Pt1/Cu(1â€¯1â€¯1) model catalysts: A DFT study. Applied Surface Science, 2019, 466, 946-955.	3.1	23
33608	The mechanism of defect induced hydroxylation on pyrite surfaces and implications for hydroxyl radical generation in prebiotic chemistry. Geochimica Et Cosmochimica Acta, 2019, 244, 163-172.	1.6	26
33609	First-principle studies of optical properties of Be Zn1-O ternary mixed crystal. Optik, 2019, 178, 691-697.	1.4	10
33610	Phase transition, mechanical stability and optical response of MnSe: Pressure effect. Physica B: Condensed Matter, 2019, 553, 6-10.	1.3	4
33611	Electronic Structure and Optical Absorption in Gdâ€‰implanted Silica Glasses. Physica Status Solidi (A) Applications and Materials Science, 2019, 216, 1800522.	0.8	10
33612	Mn- and N- doped carbon as promising catalysts for oxygen reduction reaction: Theoretical prediction and experimental validation. Applied Catalysis B: Environmental, 2019, 243, 195-203.	10.8	170

#	Article	IF	Citations
33613	Toward barrier free contact to MoSe2/WSe2 heterojunctions using two-dimensional metal electrodes. Nanotechnology, 2019, 30, 015707.	1.3	5
33614	Thermoelectricity in B80-based single-molecule junctions: First-principles investigation. Frontiers of Physics, 2019, 14, 1.	2.4	4
33615	First-principles calculation of multiple hydrogen segregation along aluminum grain boundaries. Computational Materials Science, 2019, 156, 368-375.	1.4	45
33616	Understanding interfacial interactions of polydopamine and glass fiber and their enhancement mechanisms in epoxy-based laminates. Composites Part A: Applied Science and Manufacturing, 2019, 116, 62-71.	3.8	45
33617	Raman, infrared and NMR spectra, vibrational assignments and quantum mechanical calculations of centrosymmetric 3,6-Dicholoro-1,2,4,5-tetrazine. Journal of Molecular Structure, 2019, 1178, 298-304.	1.8	1
33618	DFT study of the dimethyl sulfoxide reduction on silicene. Applied Surface Science, 2019, 467-468, 261-267.	3.1	7
33619	Mechanical and strain-tunable electronic properties of the SnS monolayer. Journal of Physics and Chemistry of Solids, 2019, 126, 43-54.	1.9	15
33620	Lewis Acid Site and Hydrogen-Bond-Mediated Polarization Synergy in the Catalysis of Dielsâ€“Alder Cycloaddition by Band-Gap Transition-Metal Oxides. ACS Catalysis, 2019, 9, 701-715.	5.5	15
33621	Multi-site electrocatalysts for hydrogen evolution in neutral media by destabilization of water molecules. Nature Energy, 2019, 4, 107-114.	19.8	470
33622	Ceramic phases with one-dimensional long-range order. Nature Materials, 2019, 18, 19-23.	13.3	18
33623	Energy level engineering in transition-metal doped spinel-structured nanosheets for efficient overall water splitting. Journal of Materials Chemistry A, 2019, 7, 827-833.	5.2	52
33624	Band gap modulation of ZrX₂ (X = S, Se, Te) mono-layers under biaxial strain and transverse electric field and its lattice dynamic properties: a first principles study. Materials Research Express, 2019, 6, 036308.	0.8	10
33625	Calculation of the Infrared Intensity of Crystalline Systems. A Comparison of Three Strategies Based on Berry Phase, Wannier Function, and Coupled-Perturbed Kohnâ€“Sham Methods. Journal of Physical Chemistry C, 2019, 123, 8336-8346.	1.5	24
33626	New Assembly-Free Bulk Layered Inorganic Vertical Heterostructures with Infrared and Optical Bandgaps. Nano Letters, 2019, 19, 142-149.	4.5	3
33627	Atomistic Mechanisms of Mg Insertion Reactions in Group XIV Anodes for Mg-Ion Batteries. ACS Applied Materials & Interfaces, 2019, 11, 774-783.	4.0	18
33628	Endogenous Dynamic Nuclear Polarization for Natural Abundance ¹⁷O and Lithium NMR in the Bulk of Inorganic Solids. Journal of the American Chemical Society, 2019, 141, 451-462.	6.6	69
33629	Temperature induced twinning in aragonite: transmission electron microscopy experiments and ab initio calculations. Zeitschrift Fur Kristallographie - Crystalline Materials, 2019, 234, 79-84.	0.4	4
33630	A Comparative First-Principles Study of Lithium, Sodium and Magnesium Insertion Energetics in Brookite Titanium Dioxide. MRS Advances, 2019, 4, 837-842.	0.5	6

#	Article	IF	Citations
33631	Insights into the Li-Metal/Organic Carbonate Interfacial Chemistry by Combined First-Principles Theory and X-ray Photoelectron Spectroscopy. Journal of Physical Chemistry C, 2019, 123, 347-355.	1.5	10
33632	Properties of NTCDA Thin Films on Ag(110): Scanning Tunneling Microscopy, Photoemission, Near-Edge X-ray Fine Structure, and Density Functional Theory Investigations. Journal of Physical Chemistry C, 2019, 123, 379-386.	1.5	5
33633	Coherent Topotactic Interface between Corundum and Rutile Structures. Journal of Physical Chemistry C, 2019, 123, 534-540.	1.5	3
33634	Influence of Disorder and Anharmonic Fluctuations on the Dynamical Rashba Effect in Purely Inorganic Lead-Halide Perovskites. Journal of Physical Chemistry C, 2019, 123, 291-298.	1.5	32
33635	Termination Effects of Pt/v-Ti_{n+1}C_nT₂ MXene Surfaces for Oxygen Reduction Reaction Catalysis. ACS Applied Materials & Interfaces, 2019, 11, 1638-1644.	4.0	88
33636	High Hole Mobility and Nonsaturating Giant Magnetoresistance in the New 2D Metal NaCu4Se4 Synthesized by a Unique Pathway. Journal of the American Chemical Society, 2019, 141, 635-642.	6.6	14
33637	Defected Graphene as Ammonia Sensor: Theoretical Insight. IEEE Sensors Journal, 2019, 19, 2031-2038.	2.4	17
33638	Investigation of half-metallic ferromagnetism in hafnium and tantalum doped NiO for spintronic applications: A DFT study. Current Applied Physics, 2019, 19, 357-362.	1.1	4
33639	Extreme static compression of carbon to terapascal pressures. Carbon, 2019, 144, 161-170.	5.4	8
33640	Rattling Heusler semiconductors' thermoelectric properties: First-principles prediction. Chinese Journal of Physics, 2019, 57, 195-210.	2.0	19
33641	Theoretical study of elastic and thermodynamic properties of CuSc intermetallic compound under high pressure. Chinese Journal of Physics, 2019, 57, 179-188.	2.0	12
33642	Elastic and thermophysical properties of BAs under high pressure and temperature. Chinese Journal of Physics, 2019, 57, 165-178.	2.0	14
33643	Chemical inactivity of GaN(0001) surface â€“ The role of oxygen adsorption â€“ Ab initio picture. Materials Science in Semiconductor Processing, 2019, 91, 252-259.	1.9	8
33644	Electrocatalytic N₂ Fixation over Hollow VO₂ Microspheres at Ambient Conditions. ChemElectroChem, 2019, 6, 1014-1018.	1.7	59
33645	Band structure tuning and charge separation of MNX monolayers and MNX/GaS van der Waals heterostructures. Physica E: Low-Dimensional Systems and Nanostructures, 2019, 108, 44-52.	1.3	2
33646	Noncollinear Relativistic DFT + U Calculations of Actinide Dioxide Surfaces. Journal of Physical Chemistry C, 2019, 123, 356-366.	1.5	14
33647	Anion-dependent Hot Carrier Dynamics in Chalcogenide Perovskites SrSnX₃ (X = S, Se). Journal of Physical Chemistry C, 2019, 123, 29-35.	1.5	8
33648	A Study on the Weak Ferromagnetism of Nanocrystalline Stannous Oxide Induced by L-Shaped Oâ€“Snâ€“O Vacancies. Journal of Physical Chemistry C, 2019, 123, 719-724.	1.5	4

#	Article	IF	Citations
33649	Boron and Nitrogen Co-Doping of Graphynes without Inducing Empty or Doubly Filled States in Ï€-Conjugated Systems. Journal of Physical Chemistry C, 2019, 123, 625-630.	1.5	2
33650	Facile Production of Mesoporous WO₃-rGO Hybrids for High-Performance Supercapacitor Electrodes: An Experimental and Computational Study. ACS Sustainable Chemistry and Engineering, 2019, 7, 2350-2359.	3.2	75
33651	Unraveling Oxygen Evolution on Iron-Doped Î²-Nickel Oxyhydroxide: The Key Role of Highly Active Molecular-like Sites. Journal of the American Chemical Society, 2019, 141, 693-705.	6.6	176
33652	The Sommerfeld ground-wave limit for a molecule adsorbed at a surface. Science, 2019, 363, 158-161.	6.0	43
33653	On the heat of formation of ye'elimite Ca4Al6O12.SO4 using density functional theory. Advances in Cement Research, 2019, 31, 106-112.	0.7	4
33654	Reconciling Experimental and Theoretical Data in the Structural Analysis of Tiâ€“Ta Shape-Memory Alloys. Shape Memory and Superelasticity, 2019, 5, 6-15.	1.1	5
33655	Metal functionalized inorganic nano-sheets as promising materials for clean energy storage. Applied Surface Science, 2019, 471, 887-892.	3.1	39
33656	Density-functional-studying of oP8â€“, tI16â€“, and tP4â€“B2CO physical properties under pressure. Journal of Solid State Chemistry, 2019, 270, 642-650.	1.4	20
33657	CO Adsorption on Au(332): Combined Infrared Spectroscopy and Density Functional Theory Study. Journal of Physical Chemistry C, 2019, 123, 8187-8197.	1.5	7
33658	TiS₂ Monolayer as an Emerging Ultrathin Bifunctional Catalyst: Influence of Defects and Functionalization. ChemPhysChem, 2019, 20, 608-617.	1.0	24
33659	Atomic Layer Deposition of Al₂O₃ Using Aluminum Triisopropoxide (ATIP): A Combined Experimental and Theoretical Study. Journal of Physical Chemistry C, 2019, 123, 485-494.	1.5	9
33660	Machine-Learning Identification of the Sensing Descriptors Relevant in Molecular Interactions with Metal Nanoparticle-Decorated Nanotube Field-Effect Transistors. ACS Applied Materials & Interfaces, 2019, 11, 1219-1227.	4.0	25
33661	Computational assessment on the interaction of amantadine drug with B12N12 and Zn12O12 nanocages and improvement in adsorption behaviors by impurity Al doping. Theoretical Chemistry Accounts, 2019, 138, 1.	0.5	27
33662	First-principles study of elastic, electronic, optical and thermoelectric properties of newly synthesized K2Cu2GeS4 chalcogenide. Journal of Alloys and Compounds, 2019, 781, 37-46.	2.8	34
33663	Physical properties of spinel-type superconductors CuRh2S4 and CuRh2Se4: A DFT study. Results in Physics, 2019, 12, 73-82.	2.0	17
33664	A DFT study of CO adsorption on pt (111) using van der Waals functionals. Surface Science, 2019, 681, 143-148.	0.8	15
33665	Modulating Hardness in Molybdenum Monoborides by Adjusting an Array of Boron Zigzag Chains. Chemistry of Materials, 2019, 31, 200-206.	3.2	22
33666	Synergistic Contribution of the Acidic Metal Oxideâ€“Metal Couple and Solvent Environment in the Selective Hydrogenolysis of Glycerol: A Combined Experimental and Computational Study Using ReO_xâ€“Ir as the Catalyst. ACS Catalysis, 2019, 9, 485-503.	5.5	40

#	Article	IF	Citations
33667	Largely Increased Lithium Storage Ability of Mangnese Oxide through a Continuous Electronic Structure Modulation and Elevated Capacitive Contribution. ACS Sustainable Chemistry and Engineering, 2019, 7, 740-747.	3.2	18
33668	Computational design of GeSe/graphene heterojunction based on density functional theory. Materials Research Express, 2019, 6, 036305.	0.8	9
33669	Cationic Pb₂ Dumbbells Stabilized in the Highly Covalent Lead Nitridosilicate Pb₂Si₅N₈. Angewandte Chemie - International Edition, 2019, 58, 1432-1436.	7.2	12
33670	Hydrogen in Ga2O3. , 2019, , 191-210.		6
33671	Combined experimental and theoretical studies on adsorption mechanisms of gaseous mercury(II) by calcium-based sorbents: The effect of unsaturated oxygen sites. Science of the Total Environment, 2019, 656, 937-945.	3.9	27
33672	Adsorption properties of the tetragonal P4/nmm WO3 (100) surface toward molecules involved in the hydration of ethylene. Surface Science, 2019, 681, 149-157.	0.8	5
33673	First principles study of structural, electronic and optical properties of Cs-doped CH3NH3PbI3 for photovoltaic applications. Vacuum, 2019, 160, 440-444.	1.6	18
33674	Computational Screening of Electrocatalytic Materials for Hydrogen Evolution: Platinum Monolayer on Transitional Metals. Journal of Physical Chemistry C, 2019, 123, 495-503.	1.5	15
33675	Phosphorene as a Catalyst for Highly Efficient Nonaqueous Liâ€“Air Batteries. ACS Applied Materials & Interfaces, 2019, 11, 499-510.	4.0	27
33676	Hydrogen Production via Efficient Formic Acid Decomposition: Engineering the Surface Structure of Pd-Based Alloy Catalysts by Design. ACS Catalysis, 2019, 9, 781-790.	5.5	62
33677	Elementary kinetics of nitrogen electroreduction on Fe surfaces. Journal of Chemical Physics, 2019, 150, 041708.	1.2	32
33678	Mode confinement, interface mass-smudging, and sample length effects on phonon transport in thin nanocomposite superlattices. Journal of Physics Condensed Matter, 2019, 31, 055303.	0.7	4
33679	Pmma-XO (X = C, Si, Ge) monolayer as promising anchoring materials for lithiumâ€“sulfur battery: a first-principles study. Nanotechnology, 2019, 30, 085405.	1.3	8
33680	Experimental and Theoretical Investigation on the Origin of the High Intercalation Voltage of K₂Zn₃[Fe(CN)₆]₂ Cathode. Journal of the Electrochemical Society, 2019, 166, A5139-A5145.	1.3	18
33681	Thermal diffusivity and thermal conductivity in layered ferrielectric materials M¹⁺M³⁺P₂(S,Se)₆ (M¹⁺â€‰=â€‰Cu, Ag;) Tj ET Q q 0 0 0 rg BT /Overl		
33682	High Selective SO₂ Gas Sensor Based on Monolayer <inline-formula> <tex-math notation="LaTeX">eta </tex-math> </inline-formula>-AsSb to Detect SF₆ Decompositions. IEEE Sensors Journal, 2019, 19, 1215-1223.	2.4	21
33683	An NMR crystallography investigation of furosemide. Magnetic Resonance in Chemistry, 2019, 57, 191-199.	1.1	10
33684	Thermodynamic analysis of the topologically close packed Ïƒ phase in the Co Cr system. Intermetallics, 2019, 105, 13-20.	1.8	17

#	Article	IF	Citations
33685	First-principles studies of Mg17Al12,Mg2Al3,Mg2Sn,MgZn2,Mg2Ni and Al3Ni phases. Physica B: Condensed Matter, 2019, 560, 255-260.	1.3	21
33686	First principles investigations of Fe, Co, Ni in model honeycomb carbon networks. Solid State Sciences, 2019, 87, 155-162.	1.5	2
33687	Can microsolvation effects be estimated from vacuum computations? A case-study of alcohol decomposition at the H₂O/Pt(111) interface. Physical Chemistry Chemical Physics, 2019, 21, 5368-5377.	1.3	25
33688	Structural, electronic, and mechanical properties of anatase titanium dioxide. Multidiscipline Modeling in Materials and Structures, 2019, 15, 306-316.	0.6	8
33689	Germanene nanotube electroresistive molecular device for detection of NO2 and SO2 gas molecules: a first-principles investigation. Journal of Computational Electronics, 2019, 18, 308-318.	1.3	27
33690	The hardness mechanism and bonding properties of CrN2: A first principle study. Computational Materials Science, 2019, 158, 282-288.	1.4	2
33691	First-principles study of thermal expansion and thermomechanics of group-V monolayers: blue phosphorene, arsenene, and antimonene. Journal of Physics Condensed Matter, 2019, 31, 065302.	0.7	11
33692	Effect of Zr additions on crystal structures and mechanical properties of binary Wâ€“Zr alloys: A first-principles study. Journal of Materials Research, 2019, 34, 290-300.	1.2	19
33693	The adsorption of dodecylamine and oleic acid on kaolinite surfaces: Insights from DFT calculation and experimental investigation. Applied Surface Science, 2019, 470, 27-35.	3.1	38
33694	Structural tuning and catalysis of tungsten carbides for the regioselective cleavage of C O bonds. Journal of Catalysis, 2019, 369, 283-295.	3.1	38
33695	Half-metallic compensated ferrimagnetism in the Mn-Co-V-Al Heusler alloys. Journal of Magnetism and Magnetic Materials, 2019, 475, 229-233.	1.0	15
33696	Towards enhancing the magnetic properties by morphology control of ATiO3 (Aâ€¯=â€¯Mn, Fe, Ni) multiferroic materials. Journal of Magnetism and Magnetic Materials, 2019, 475, 544-549.	1.0	29
33697	Cluster formation and eventual mobility of helium in a tungsten grain boundary. Journal of Nuclear Materials, 2019, 514, 171-180.	1.3	17
33698	Brownian-snowball-mechanism-induced hierarchical cobalt sulfide for supercapacitors. Journal of Power Sources, 2019, 412, 321-330.	4.0	31
33699	Width dependent structural and electrical properties of zigzag ZnTe nanoribbons. Physics Letters, Section A: General, Atomic and Solid State Physics, 2019, 383, 748-753.	0.9	4
33700	Tailoring the capability of carbon nitride (C₃N) nanosheets toward hydrogen storage upon light transition metal decoration. Nanotechnology, 2019, 30, 075404.	1.3	40
33701	Structure Distortion Induced Monoclinic Nickel Hexacyanoferrate as Highâ€Performance Cathode for Naâ€Ion Batteries. Advanced Energy Materials, 2019, 9, 1803158.	10.2	93
33702	Role of Co₂C in ZnOâ€promoted Co Catalysts for Alcohol Synthesis from Syngas. ChemCatChem, 2019, 11, 799-809.	1.8	26

#	Article	IF	Citations
33703	Two-dimensional CdS/g-C6N6 heterostructure used for visible light photocatalysis. Applied Surface Science, 2019, 471, 162-167.	3.1	72
33704	Mechanistic studies of the influence of halogen substituents on the corrosion inhibitive efficiency of selected imidazole molecules: A synergistic computational and experimental approach. Applied Surface Science, 2019, 471, 494-505.	3.1	51
33705	Acoustical characteristics of single-walled noncarbon nanotubes: Longitudinal and torsional waves. Computational Condensed Matter, 2019, 18, e00350.	0.9	2
33706	A new diagrammatic method for the prediction of solid solubility in Mg alloys based on the short-range ordered structure. Computational Materials Science, 2019, 159, 32-42.	1.4	5
33707	Tailor-made metal-nitrogen-carbon bifunctional electrocatalysts for rechargeable Zn-air batteries via controllable MOF units. Energy Storage Materials, 2019, 17, 46-61.	9.5	70
33708	Cobalt nitride nanoparticles embedded in porous carbon nanosheet arrays propelling polysulfides conversion for highly stable lithiumâ€“sulfur batteries. Energy Storage Materials, 2019, 21, 210-218.	9.5	79
33709	Structural, elastic, electronic, thermodynamic, and optical properties of layered BaPd2As2 pnictide superconductor: A first principles investigation. Journal of Alloys and Compounds, 2019, 780, 452-460.	2.8	61
33710	The electronic structure and magnetic property of the Mn doped Î²-Ga2O3. Superlattices and Microstructures, 2019, 125, 330-337.	1.4	16
33711	Adsorption of phenol, hydrazine and thiophene on stanene monolayers: A computational investigation. Synthetic Metals, 2019, 247, 26-36.	2.1	52
33712	Interaction between Ruthenium Oxide Surfaces and Water Molecules. Effect of Surface Morphology and Water Coverage. Journal of Physical Chemistry C, 2019, 123, 7786-7798.	1.5	18
33713	Partitioning of C into Îº-carbides by Si addition and its effect on the initial deformation mechanism of Fe-Mn-Al-C lightweight steels. Journal of Alloys and Compounds, 2019, 775, 554-564.	2.8	43
33714	Structural, spectroscopic, and thermodynamic characterization of ammonium oxalate monohydrate mineral using theoretical solid-state methods. Journal of Physics and Chemistry of Solids, 2019, 125, 31-42.	1.9	14
33715	ab initio study of the exo-hydrogenated single wall carbon nanotubes. Physica B: Condensed Matter, 2019, 552, 124-129.	1.3	3
33716	Suppressed and enhanced spin polarization in the 1ML-Pb/Ge(1 1 1)-1â€Ã—â€1 system. Applied Surface Science, 2019, 466, 224-229.	3.1	7
33717	Formation and migration of point defects in tungsten carbide: Unveiling the sluggish bulk self-diffusivity of WC. Journal of the European Ceramic Society, 2019, 39, 165-172.	2.8	19
33718	Tuning electronic and magnetic properties of single-layer PN phases by point defects. Journal of Physics and Chemistry of Solids, 2019, 125, 80-89.	1.9	3
33719	Ab Initio Modeling of Y and O Solute Atom Interaction in Small Clusters within the bcc Iron Lattice. Physica Status Solidi (B): Basic Research, 2019, 256, 1800346.	0.7	2
33720	Interaction between polysaccharide monomer and SiO2/Al2O3/CaCO3 surfaces: A DFT theoretical study. Applied Surface Science, 2019, 466, 607-614.	3.1	19

#	Article	IF	Citations
33721	An automated algorithm for reliable equation of state fitting of magnetic systems. Computational Materials Science, 2019, 156, 121-128.	1.4	2
33722	Development of a pair potential for Ta-He system. Computational Materials Science, 2019, 156, 268-272.	1.4	4
33723	Elements (Si, Sn, and Mg) doped Î±-Ga2O3: First-principles investigations and predictions. Computational Materials Science, 2019, 156, 273-279.	1.4	38
33724	Electronic structure and photoluminescence properties of a novel single-phased color tunable phosphor KAlGeO4:Bi3+,Eu3+ for WLEDs. Journal of Alloys and Compounds, 2019, 774, 477-486.	2.8	69
33725	First-principles study the structures and mechanical properties of binary W-V alloys. Physica B: Condensed Matter, 2019, 552, 165-169.	1.3	17
33726	DFT investigation of elastic, mechanical, vibrational and thermodynamic properties of cadmium dichalcogenides. Physica B: Condensed Matter, 2019, 552, 159-164.	1.3	7
33727	Interactions between dislocations and twins in deformed titanium aluminide crystals. Journal of Materials Science and Technology, 2019, 35, 402-408.	5.6	10
33728	Atomic structure and electronic properties of Ag(111)/TiC(111) interface: Insights from first-principles simulations. Journal of Physics and Chemistry of Solids, 2019, 124, 212-220.	1.9	26
33729	Can fluorine and chlorine functionalization stabilize the graphene like borophene?. Computational Materials Science, 2019, 156, 56-66.	1.4	34
33730	Analysis of the structural, anisotropic elastic and electronic properties of Î²-Ga2O3 with various pressures. Journal of Crystal Growth, 2019, 505, 74-81.	0.7	26
33731	Reversible hydrogen storage behaviors of Ti2N MXenes predicted by first-principles calculations. Journal of Materials Science, 2019, 54, 493-505.	1.7	38
33732	Computational predictions of electronic properties of graphene with defects, adsorbed transition metal-oxides and water using density functional theory. Applied Surface Science, 2019, 467-468, 760-772.	3.1	12
33733	Quantum confinement luminescence of trigonal cesium lead bromide quantum dots. Applied Surface Science, 2019, 466, 119-125.	3.1	22
33734	Identification of a narrow band red light-emitting phosphor using computational screening of ICSD: Its synthesis and optical characterization. Journal of Alloys and Compounds, 2019, 774, 338-346.	2.8	13
33735	Pristine and Cu decorated hexagonal InN monolayer, a promising candidate to detect and scavenge SF6 decompositions based on first-principle study. Journal of Hazardous Materials, 2019, 363, 346-357.	6.5	146
33736	Experimental and first principle study of room temperature ferromagnetism in carbon-doped rutile TiO2. Materials Research Bulletin, 2019, 110, 13-17.	2.7	24
33737	Band alignment of nonpolar (10<mml:math xmlns:mml="http://www.w3.org/1998/Math/MathML") Tj ETQq0 0 0 rgBT /Overlock 10 Tf 50 ZnO on (112) LaAlO3. Solid State Communications, 2019, 287, 23-26.	0.9	3
33738	Anisotropy of the proton kinetic energy in ice Ih. Surface Science, 2019, 679, 174-179.	0.8	2

#	Article	IF	Citations
33739	Electronic structure of Lanthanum induced Ï€-bonded Seiwatz chains on the Si(111)-(2â€²â€²Ã—â€²â€²3) surface. Surface Science, 2019, 679, 214-217.	0.8	3
33740	Mn doped GaSb may be a good candidate for ferromagnetic semiconductor predicted by the DFT + U approach. Materials Research Express, 2019, 6, 015901.	0.8	5
33741	Understanding the role of Pd:Cu ratio, surface and electronic structures in Pd-Cu alloy material applied in direct formic acid fuel cells. Applied Surface Science, 2019, 465, 730-739.	3.1	44
33742	A comparative first-principles study of point defect properties in the layered MX2 (Mâ€²=â€²Mo, W; Xâ€²=â€²S, Te): Substitution by the groups III, V and VII elements. Computational Materials Science, 2019, 156, 280-285.	1.4	3
33743	Effect of vacancy on adsorption/dissociation and diffusion of H2S on Fe(1â€²0â€²0) surfaces: A density functional theory study. Applied Surface Science, 2019, 465, 833-845.	3.1	27
33744	Tuning the photoluminescence of graphene oxide quantum dots by photochemical fluorination. Carbon, 2019, 141, 331-338.	5.4	31
33745	N-, P-, As-triphenylene-graphdiyne: Strong and stable 2D semiconductors with outstanding capacities as anodes for Li-ion batteries. Carbon, 2019, 141, 291-303.	5.4	73
33746	Exploring the sensitivity of nanodiamond to sarafloxacin: A DFT approach. Journal of Physics and Chemistry of Solids, 2019, 124, 235-241.	1.9	2
33747	First-principles calculations of half-metallic ferromagnetism of AlC0.0625N0.9375 and AlC0.125N0.875-zincblende. Physica B: Condensed Matter, 2019, 552, 84-87.	1.3	2
33748	Sub-10â€²nm vertical tunneling transistors based on layered black phosphorene homojunction. Applied Surface Science, 2019, 465, 895-901.	3.1	17
33749	DFT studies on the key competing reaction steps towards complete ethanol oxidation on transition metal catalysts. Computational Materials Science, 2019, 156, 175-186.	1.4	29
33750	First-principles study of the vibrational characteristics of the heavy element substitution on Cu3SbSe3. Computational Materials Science, 2019, 156, 167-174.	1.4	4
33751	Multiple topological states in iron-based superconductors. Nature Physics, 2019, 15, 41-47.	6.5	170
33752	Elemental site occupancy in the L12 A3B ordered intermetallic phase in Co-based superalloys and its influence on the microstructure. Acta Materialia, 2019, 163, 140-153.	3.8	65
33753	Hydrogen adsorption on alkali metal decorated blue phosphorene nanosheets. Applied Surface Science, 2019, 465, 440-449.	3.1	28
33754	Phase stability, mechanical properties and electronic structures of Ti Al binary compounds by first principles calculations. Materials Chemistry and Physics, 2019, 221, 311-321.	2.0	57
33755	First-principle calculations of electronic and optical properties of CdCr2Te4 spinel: use of mBJâ€‰+â€‰U potential in narrow band gap semiconductors. Indian Journal of Physics, 2019, 93, 335-341.	0.9	2
33756	Theoretical investigation of the effect of phosphate doping on the aggregation of Au atoms on an Al2O3 (0001) surface. Applied Surface Science, 2019, 465, 1003-1013.	3.1	5

#	Article	IF	Citations
33757	Electronic and magnetic properties of the adsorption of As harmful species on zero-valent Fe surfaces, clusters and nanoparticules. Applied Surface Science, 2019, 465, 715-723.	3.1	11
33758	First-principles investigation of water adsorption on FeCrAl (1â€¯1â€¯0) surfaces. Applied Surface Science, 2019, 465, 259-266.	3.1	8
33759	Surface modification vs sorption strength: Study of nedaplatin drug supported on silica. Applied Surface Science, 2019, 465, 693-699.	3.1	7
33760	First-principles study of pressure-induced phase transformations in thermoelectric Mg2Si. Journal of Alloys and Compounds, 2019, 773, 988-996.	2.8	9
33761	CO Oxidation over Unsupported Group 11 Metal Catalysts: New Mechanistic Insight from First-Principles. Journal of Physical Chemistry C, 2019, 123, 7818-7830.	1.5	8
33762	Mutual modulation of F-distribution and N-configuration in F and N dual-functionalized graphene. Applied Surface Science, 2019, 465, 880-887.	3.1	2
33763	Functionalization Ti3C2 MXene by the adsorption or substitution of single metal atom. Applied Surface Science, 2019, 465, 911-918.	3.1	63
33764	Beryllium chloride monolayer as a direct semiconductor with a tunable band gap: First principles study. Optik, 2019, 176, 579-585.	1.4	2
33765	Enhancement of electrical performance via carrier modulation in single crystalline PbTe prepared by Pb-flux method. Journal of Alloys and Compounds, 2019, 774, 282-289.	2.8	9
33766	Experimental and theoretical interpretation of magnetic ground state of FeMnO3. Journal of Alloys and Compounds, 2019, 774, 290-298.	2.8	13
33767	Effect of Cl on Softening and Melting Behaviors of BF Burden. High Temperature Materials and Processes, 2019, 38, 273-279.	0.6	2
33768	Cyclic oxidation of Ti3Al-based materials. Ceramics International, 2019, 45, 9423-9438.	2.3	8
33769	First-principles study of structural, elastic, and electronic properties of triclinic TATB under different pressures. Physica B: Condensed Matter, 2019, 552, 151-158.	1.3	22
33770	First-principles calculation of quantum capacitance of metals doped graphenes and nitrogen/metals co-doped graphenes: designing strategies for supercapacitor electrodes. Journal of Materials Science, 2019, 54, 483-492.	1.7	23
33771	Surface-loaded metal nanoparticles for peroxymonosulfate activation: Efficiency and mechanism reconnaissance. Applied Catalysis B: Environmental, 2019, 241, 561-569.	10.8	260
33772	Improved selectivity and coke resistance of core-shell alloy catalysts for propane dehydrogenation from first principles and microkinetic analysis. Chemical Engineering Journal, 2019, 377, 120049.	6.6	42
33773	Mg-X (X = Ni, Pd, Ti, Nb) interface and atomic mixture effect: a first-principles study. Materials Research Express, 2019, 6, 016305.	0.8	1
33774	Unexpected ground-state crystal structures and mechanical properties of transition metal pernitrides MN2 (M= Ti, Zr, and Hf). Journal of Alloys and Compounds, 2019, 774, 918-925.	2.8	37

#	Article	IF	Citations
33775	Determination of Silica and Germania Film Network Structures on Ru(0001) at the Atomic Scale. Journal of Physical Chemistry C, 2019, 123, 7889-7897.	1.5	14
33776	Topological critical materials of ternary compounds. Journal of Physics and Chemistry of Solids, 2019, 128, 218-224.	1.9	4
33777	Magnetic properties of Fe100â^'Ga : Ab initio and Monte Carlo study. Journal of Magnetism and Magnetic Materials, 2019, 470, 118-122.	1.0	8
33778	Facet design promotes electroreduction of carbon dioxide to carbon monoxide on palladium nanocrystals. Chemical Engineering Science, 2019, 194, 29-35.	1.9	34
33779	First principle study of native point defects in (ZnO)n nanoclusters (nâ€‰=â€‰34, 60). Applied Nanoscience (Switzerland), 2019, 9, 1067-1074.	1.6	6
33780	VSe2-reduced graphene oxide as efficient cathode material for field emission. Journal of Physics and Chemistry of Solids, 2019, 128, 384-390.	1.9	31
33781	Spin-orbit enhanced carrier lifetimes in noncentrosymmetric semiconductors. Journal of Physics and Chemistry of Solids, 2019, 128, 225-230.	1.9	1
33782	Electronic and magnetic properties of <mml:math xmlns:mml="http://www.w3.org/1998/Math/MathML" altimg="si1.gif" overflow="scroll"><mml:mrow><mml:mi>A</mml:mi><mml:mi>I</mml:mi></mml:mrow></mml:math> doped (<mml:math xmlns:mml="http://www.w3.org/1998/Math/MathML" altimg="si2.gif") Tj ETQq1 1 0.784314 rgBT /Overlock 10 Tf 5 with intrinsic vacancy. Superlattices and Microstructures, 2019, 127, 186-190.	1.4	15
33783	Combining Theory and Experiment for Multitechnique Characterization of Activated CO₂ on Transition Metal Carbide (001) Surfaces. Journal of Physical Chemistry C, 2019, 123, 7567-7576.	1.5	22
33784	Ab initio STUDY OF POINT DEFECTS IN 2D GRAPHENE LAYER. Surface Review and Letters, 2019, 26, 1850142.	0.5	6
33785	Ab initio study of mono-layer 2-D insulators (X-(OH)2 and h-BN) and their use in MTJ memory device. Microsystem Technologies, 2019, 25, 1909-1917.	1.2	8
33786	Off-Plane Dielectric Screening of Few-Layer Graphdiyne and Its Family. ACS Applied Materials & Interfaces, 2019, 11, 2571-2578.	4.0	13
33787	High-pressure yield strength of rocksalt structures using quartz Raman piezometry. Comptes Rendus - Geoscience, 2019, 351, 71-79.	0.4	4
33788	Tailoring magnetic characteristics of phosphorene by the doping of Ce and Ti: A DFT study. Physica E: Low-Dimensional Systems and Nanostructures, 2019, 106, 352-356.	1.3	5
33789	Immobilized Ferrous Ion and Glucose Oxidase on Graphdiyne and Its Application on One-Step Glucose Detection. ACS Applied Materials & Interfaces, 2019, 11, 2647-2654.	4.0	86
33790	How Does Collagen Adsorb on Hydroxyapatite? Insights From Ab Initio Simulations on a Polyproline Type II Model. Journal of Physical Chemistry C, 2019, 123, 7540-7550.	1.5	31
33791	Computational analysis of the intermetallic formation during the dissimilar metal aluminum-to-steel friction stir welding process. Proceedings of the Institution of Mechanical Engineers, Part L: Journal of Materials: Design and Applications, 2019, 233, 1080-1100.	0.7	4
33792	Structural stability of Lanthanum-based oxygen-deficient perovskites in redox catalysis: A density functional theory study. Catalysis Today, 2020, 347, 142-149.	2.2	18

#	Article	IF	Citations
33793	High Coverage CO Adsorption on Fe6O6 Cluster Using GGAâ€‰+â€‰U. Journal of Cluster Science, 2020, 31, 591-600.	1.7	5
33794	Mo2TiC2 MXene: A Promising Catalyst for Electrocatalytic Ammonia Synthesis. Catalysis Today, 2020, 339, 120-126.	2.2	102
33795	Thermodynamic and kinetic roles of H2 in structure evolution of urchin-like Co: A density functional theory study. Particuology, 2020, 48, 2-12.	2.0	2
33796	Mechanistic pathways for oxygen removal on Pt-doped Co(111) in the Fischer-Tropsch reaction. Catalysis Today, 2020, 342, 142-151.	2.2	16
33797	Adsorption behaviour of SO₂ and SOF₂ gas on Rh-doped BNNT: a DFT study. Molecular Physics, 2020, 118, e1580394.	0.8	32
33798	Scaling law of hydrogen evolution reaction for InSe monolayer with 3d transition metals doping and strain engineering. Journal of Energy Chemistry, 2020, 41, 107-114.	7.1	34
33799	Platinum in-situ catalytic oleylamine combustion removal process for carbon supported platinum nanoparticles. Journal of Energy Chemistry, 2020, 41, 120-125.	7.1	13
33800	Reshaping of Rh nanoparticles in operando conditions. Catalysis Today, 2020, 350, 184-191.	2.2	3
33801	Hybrid Cu⁰ and Cu^x⁺ as Atomic Interfaces Promote Highâ€Selectivity Conversion of CO₂ to C₂H₅OH at Low Potential. Small, 2020, 16, e1901981.	5.2	92
33802	Interaction of hydrogen with flat (0001) and corrugated (11â€“20) and (10â€“12) cobalt surfaces: Insights from experiment and theory. Catalysis Today, 2020, 342, 124-130.	2.2	24
33803	First-principles prediction of crystal structure and physical properties of ScB₃. Molecular Physics, 2020, 118, .	0.8	9
33804	Total oxidation of lean methane over cobalt spinel nanocubesâ€”Mechanistic vistas gained from DFT modeling and catalytic isotopic investigations. Catalysis Today, 2020, 354, 183-195.	2.2	11
33805	Structural, elastic, electronic, andoptical properties of layered TiNX (Xâ€‰=â€‰F,â€‰Cl,â€‰Br,â€‰I) compounds: a density functional theory study. Molecular Physics, 2020, 118, e1609706.	0.8	21
33806	Theoretical Investigation of Dielectric Materials for Twoâ€Dimensional Fieldâ€Effect Transistors. Advanced Functional Materials, 2020, 30, 1808544.	7.8	15
33807	Investigation of the Structural, Electronic and Mechanical Properties of Type-VIII Ba8Si46 Clathrate under High-Pressure through First-Principles. Silicon, 2020, 12, 381-391.	1.8	6
33808	Precipitates and alloying elements distribution in near Î± titanium alloy Ti65. Journal of Materials Science and Technology, 2020, 36, 91-96.	5.6	39
33809	First-principles based microkinetic modeling of transient kinetics of CO hydrogenation on cobalt catalysts. Catalysis Today, 2020, 342, 131-141.	2.2	29
33810	Shape selectivity in acidic zeolite catalyzed 2-pentene skeletal isomerization from first principles. Catalysis Today, 2020, 347, 115-123.	2.2	7

#	Article	IF	Citations
33811	Modeling study of adhesion in the TiN/Ti, TiN/ZrN, TiN/Ti/ZrN, and TiN/Zr/ZrN layered systems. Journal of Adhesion, 2020, 96, 633-646.	1.8	3
33812	Ab initio calculations of CaZrO3 (011) surfaces: systematic trends in polar (011) surface calculations of ABO3 perovskites. Journal of Materials Science, 2020, 55, 203-217.	1.7	23
33813	In silicohigh throughput screening of bimetallic and single atom alloys using machine learning andab initiomicrokinetic modelling. Journal of Materials Chemistry A, 2020, 8, 107-123.	5.2	48
33814	Black reduced porous SnO2 nanosheets for CO2 electroreduction with high formate selectivity and low overpotential. Applied Catalysis B: Environmental, 2020, 260, 118134.	10.8	107
33815	High anisotropy in the electronic and thermoelectric properties of layered oxysulfides: A case study of LaOPbBiS3. Journal of Alloys and Compounds, 2020, 814, 152137.	2.8	5
33816	Study on the stability of organicâ€“inorganic perovskite solar cell materials based on first principle. Molecular Physics, 2020, 118, e1665200.	0.8	12
33817	A theoretical study on the chirality detection of serine amino acid based on carbon nanotubes with and without Stone-Wales defects. Structural Chemistry, 2020, 31, 455-464.	1.0	7
33818	Investigation of the thermodynamic properties of Al4C3: A combined DFT and DSC study. Computational Materials Science, 2020, 171, 109100.	1.4	9
33819	Field-assisted suppression of coke in the methane steam reforming reaction. Applied Catalysis B: Environmental, 2020, 260, 118132.	10.8	20
33820	Novel two-dimensional MOF as a promising single-atom electrocatalyst for CO2 reduction: A theoretical study. Applied Surface Science, 2020, 500, 143993.	3.1	74
33821	Insights on the stability of cuprous chloride under high pressure: An equilibrium ab initio atomistic thermodynamics study. Journal of Physics and Chemistry of Solids, 2020, 136, 109158.	1.9	1
33822	Isocyanic acid (HNCO) adsorption on the flat and defective Rh(001) surfaces: Pure DFT and DFT+vdW calculations. Journal of Physics and Chemistry of Solids, 2020, 138, 109162.	1.9	4
33823	Semiconducting SN₂ monolayer with three-dimensional auxetic properties: a global minimum with tetracoordinated sulfurs. Nanoscale, 2020, 12, 85-92.	2.8	21
33824	Water Adsorption on Ideal Anatase-TiO₂(101) â€“ An Embedded Cluster Model for Accurate Adsorption Energetics and Excited State Properties. Zeitschrift Fur Physikalische Chemie, 2020, 234, 813-834.	1.4	16
33825	The nano gold rush: Graphynes as atomic sieves for coinage and Pt-group transition metals. Applied Surface Science, 2020, 499, 143927.	3.1	5
33826	Exploring the stability and electronic properties of Zn-doped hematite surfaces for photoelectrochemical water splitting. Journal of Physics and Chemistry of Solids, 2020, 136, 109159.	1.9	9
33827	Structural, magnetic, electronic and elastic properties of half-metallic ferromagnetism full-Heusler alloys: Normal-Co2TiSn and inverse- Zr2RhGa using FP-LAPW method. Materials Chemistry and Physics, 2020, 240, 122122.	2.0	15
33828	Extreme negative mechanical phenomena in the zinc and cadmium anhydrous metal oxalates and lead oxalate dihydrate. Journal of Materials Science, 2020, 55, 218-236.	1.7	17

#	Article	IF	Citations
33829	Temperature dependence of the optical properties of MgO: Ab initio molecular dynamics calculations. Optik, 2020, 200, 163421.	1.4	4
33830	Temperature and doping effects on the transport properties of SrIn2P2 Zintl compound. Journal of Alloys and Compounds, 2020, 815, 152384.	2.8	9
33831	A DFT study on corrosion mechanism of steel bar under water-oxygen interaction. Computational Materials Science, 2020, 171, 109265.	1.4	22
33832	Co single-atom anchored on Co3O4 and nitrogen-doped active carbon toward bifunctional catalyst for zinc-air batteries. Applied Catalysis B: Environmental, 2020, 260, 118188.	10.8	163
33833	Structural, electronic and transport properties of a single 1,4-benzenediamine molecule attached to metal contacts of Au, Ag and Cu. Computational Materials Science, 2020, 171, 109212.	1.4	3
33834	Projector augmented-wave pseudopotentials for uranium-based compounds. Computational Materials Science, 2020, 171, 109237.	1.4	26
33835	Activation volume dominated diffusivity of Ni50Al50 melt under extreme conditions. Computational Materials Science, 2020, 171, 109263.	1.4	5
33836	Effect of Mo and aging temperature on corrosion behavior of (CoCrFeNi)100-Mo high-entropy alloys. Journal of Alloys and Compounds, 2020, 812, 152139.	2.8	77
33837	Electronic structures and magnetic properties in transition metal adsorbed gt-C3N4 monolayer. Journal of Magnetism and Magnetic Materials, 2020, 493, 165745.	1.0	5
33838	Half metallic ferromagnetic and optical properties of ruthenium-doped zincblende ZnS: A first principles study. Journal of Physics and Chemistry of Solids, 2020, 136, 109175.	1.9	21
33839	Half-metallicity and magnetism of CoFeHfGe novel quaternary Heusler alloy in bulk form as well as (100) and (001) surfaces: An ab initio study. Journal of Physics and Chemistry of Solids, 2020, 136, 109190.	1.9	21
33840	Functionalization of two-dimensional C4N by atoms adsorption: A first-principles investigation. Physica E: Low-Dimensional Systems and Nanostructures, 2020, 115, 113649.	1.3	6
33841	Facile constructing of isotype g-C3N4(bulk)/g-C3N4(nanosheet) heterojunctions through thermal polymerization of single-source glucose-modified melamine: An efficient charge separation system for photocatalytic hydrogen production. Applied Surface Science, 2020, 500, 143985.	3.1	58
33842	The structure and stability of the low-index surfaces of D8m-Mo5Si3 by first-principles calculations. Ceramics International, 2020, 46, 877-887.	2.3	7
33843	Promotion effect with dispersed Fe-Ni-S catalyst to facilitate hydrogenolysis of lignite and heavy residue. Fuel, 2020, 259, 116303.	3.4	11
33844	Steering elementary steps towards efficient alkaline hydrogen evolution via size-dependent Ni/NiO nanoscale heterosurfaces. National Science Review, 2020, 7, 27-36.	4.6	192
33845	Controlling electronic structure of single-layered $${hbox {HfX}}_{3}$$ ($$hbox {X=S}$$, Se) trichalcogenides through systematic Zr doping. Journal of Materials Science, 2020, 55, 660-669.	1.7	12
33846	Strain engineering of selective chemical adsorption on monolayer black phosphorous. Applied Surface Science, 2020, 503, 144033.	3.1	25

#	Article	IF	Citations
33847	Hydrogen evolution reaction electrocatalysis trends of confined gallium phosphide with substitutional defects. International Journal of Hydrogen Energy, 2020, 45, 23928-23936.	3.8	10
33848	Electronic and magnetic properties of 3d transition metal doped MoSe2 monolayer. Physica E: Low-Dimensional Systems and Nanostructures, 2020, 116, 113745.	1.3	29
33849	Generalized Stress-Redox Equivalence: A Chemical Link between Pressure and Electronegativity in Inorganic Crystals. Inorganic Chemistry, 2020, 59, 5281-5291.	1.9	21
33850	Mindlinâ€“Eringen anisotropic micromorphic elasticity and lattice dynamics representation. Philosophical Magazine, 2020, 100, 157-193.	0.7	7
33851	Intrinsic properties of nitrogen-rich carbon nitride for oxygen reduction reaction. Applied Surface Science, 2020, 500, 144020.	3.1	21
33852	First principle study of feasibility of dinitrogen reduction to ammonia on two-dimensional transition metal phthalocyanine monolayer. Applied Surface Science, 2020, 500, 144032.	3.1	34
33853	Understanding ferromagnetism in Ni-doped MoS2 monolayer from first principles. Chemical Physics, 2020, 528, 110501.	0.9	16
33854	Theory of atomic scale quantum dots in silicon: Dangling bond quantum dots on silicon surface. Solid State Communications, 2020, 305, 113752.	0.9	4
33855	A DFT study of dissolved gas (C2H2, H2, CH4) detection in oil on CuO-modified BNNT. Applied Surface Science, 2020, 500, 144030.	3.1	123
33856	Density functional theory study on the dehydrogenation of 1,2-dimethyl cyclohexane and 2-methyl piperidine on Pd and Pt catalysts. Catalysis Today, 2020, 352, 345-353.	2.2	30
33857	A DFT investigation on electronic structure, charge density, mechanical stability and thermodynamic properties of XAl3 (XÂ=Sc, Yb and Lu) intermetallic compounds. Journal of Molecular Graphics and Modelling, 2020, 94, 107463.	1.3	9
33858	Insight into the structural, vibrational and thermodynamic properties of SmX (X = S, Se, Te) chalcogenides: First-principles investigations. Physica B: Condensed Matter, 2020, 576, 411715.	1.3	3
33859	Synergetic donorâ€“donor codoping strategy for enhanced photoelectrochemical activity of hematite. Applied Catalysis B: Environmental, 2020, 260, 118186.	10.8	5
33860	Pseudopotential for plane-wave density functional theory studies of metallic uranium. Computational Materials Science, 2020, 171, 109221.	1.4	11
33861	Polytypism in calcium oxide compound: Mechanical and dynamical evidence of structural stability. Journal of Alloys and Compounds, 2020, 815, 152424.	2.8	8
33862	Exploring the effect of mono- and di-fluorinated triphenylamine-based molecules as electron donors for dye-sensitised solar cells. Molecular Simulation, 2020, 46, 41-53.	0.9	9
33863	Identification of the most active sites for tetrahydropyranylation in zeolites: MFI as a test case. Catalysis Today, 2020, 345, 165-174.	2.2	4
33864	Enhanced visible-light photocatalytic H2 production of hierarchical g-C3N4 hexagon by one-step self-assembly strategy. Applied Surface Science, 2020, 499, 143942.	3.1	16

#	Article	IF	Citations
33865	Study of transport properties in Se-deficient and Fe-intercalated NbSe2 single crystals: experiment and theory. Journal of Materials Science, 2020, 55, 250-262.	1.7	5
33866	Modeling of alloying effect on elastic properties in BCC Nb-Ti-V-Zr solid solution: From unary to quaternary. Computational Materials Science, 2020, 172, 109289.	1.4	48
33867	A new trick for an old support: Stabilizing gold single atoms on LaFeO3 perovskite. Applied Catalysis B: Environmental, 2020, 261, 118178.	10.8	31
33868	First-principles study: Effect of lithium and sodium intercalation in transition metal phosphates, MPO4 (M: Mn, Fe, Co). Computational Condensed Matter, 2020, 22, e00437.	0.9	10
33869	Boron trifluoride interaction studies on graphdiyne nanotubes â€“ A first-principles insight. Chemical Physics Letters, 2020, 738, 136841.	1.2	41
33870	Thermoelectric properties of strontium sulfide via first-principles calculations. Solid State Communications, 2020, 305, 113755.	0.9	10
33871	MXenes as promising catalysts for water dissociation. Applied Catalysis B: Environmental, 2020, 260, 118191.	10.8	94
33872	Probing the 91Zr NMR parameters in the solid state by a combination of DFT calculations and experiments. Chemical Physics Letters, 2020, 738, 136855.	1.2	0
33873	Impact of Re-clustering on resistances to dislocation slip mediated plastic deformations in Î³ matrix phases. Computational Materials Science, 2020, 172, 109314.	1.4	6
33874	Site preference and brittleâ€“ductile transition mechanism of B2-NiAl with ternary elements additions form first-principles calculations. Physica B: Condensed Matter, 2020, 576, 411703.	1.3	6
33875	Effect of zinc-doping on tensile strength of Î£5 bcc Fe symmetric tilt grain boundary. Computational Materials Science, 2020, 171, 109204.	1.4	25
33876	Effective Coulomb interaction in actinides from linear response approach. Computational Materials Science, 2020, 171, 109270.	1.4	14
33877	First-principles investigations of effects of solute elements on stability and electronic structure of laves phase/matrix interface in Ni-based superalloys. Journal of Physics and Chemistry of Solids, 2020, 136, 109166.	1.9	18
33878	Experimental and theoretical study on elastic properties of crystalline alkali silicate hydrate. Materials and Design, 2020, 185, 108240.	3.3	1
33879	LiGaOS is a fast Li-Ion conductor: A first-principles prediction. Materials and Design, 2020, 185, 108264.	3.3	6
33880	The Comparison between Single Atom Catalysis and Surface Organometallic Catalysis. Chemical Reviews, 2020, 120, 734-813.	23.0	201
33881	Graphitic carbon nitride catalyzes selective oxidative dehydrogenation of propane. Applied Catalysis B: Environmental, 2020, 262, 118277.	10.8	47
33882	NaTaO3 cubic and orthorhombic surfaces: An intrinsic improvement of photocatalytic properties. Applied Surface Science, 2020, 502, 144206.	3.1	32

#	Article	IF	Citations
33883	Morphology prediction of portlandite: Atomistic simulations and experimental research. Applied Surface Science, 2020, 502, 144296.	3.1	16
33884	Strain-tunable magnetic order and electronic structure in 2D CrAsS4. Journal of Magnetism and Magnetic Materials, 2020, 497, 165941.	1.0	8
33885	B, Nâ€coâ€doped grapheneâ€supported Ir and Pt clusters for methane activation and Câ”€C coupling: A density functional theory study. Journal of Computational Chemistry, 2020, 41, 194-202.	1.5	9
33886	Theoretical Investigation on Denitrification Mechanism of Piperidine: Effects of Methylation Versus Protonation on Câ€“N Bond Activation. Catalysis Letters, 2020, 150, 631-639.	1.4	1
33887	Modifying effects and mechanisms of graphene on dehydrogenation properties of sodium borohydride. Journal of Materials Science, 2020, 55, 1959-1972.	1.7	12
33888	Performance of ZIF-67 â€“ Derived fold polyhedrons for enhanced photocatalytic hydrogen evolution. Chemical Engineering Journal, 2020, 382, 123051.	6.6	165
33889	Predicting magnetization of ferromagnetic binary Fe alloys from chemical short range order. Computational Materials Science, 2020, 172, 109344.	1.4	10
33890	DFT-FE â€“ A massively parallel adaptive finite-element code for large-scale density functional theory calculations. Computer Physics Communications, 2020, 246, 106853.	3.0	119
33891	Theoretical investigation of phonon contributions to thermal expansion coefficients for rare earth monosilicates RE2SiO5 (RE = Dy, Ho, Er, Tm, Yb and Lu). Journal of the European Ceramic Society, 2020, 40, 2658-2666.	2.8	41
33892	Structural and magnetic investigations on Cu-doped MnV2O6 compound: Experiment and theory. Journal of Magnetism and Magnetic Materials, 2020, 497, 165995.	1.0	3
33893	Structure Evolution, Elastic and Electronic Properties of Ptâ€Ðoped Ti Alloy under Pressure. Physica Status Solidi (B): Basic Research, 2020, 257, 1900360.	0.7	2
33894	Benzyl Chloride and Chlorobenzene Adsorption Studies on Bismuthene Nanosheet: A DFT Study. Journal of Inorganic and Organometallic Polymers and Materials, 2020, 30, 1888-1897.	1.9	15
33895	First-principles calculations of the electronic, magnetic and optical properties of rhenium-doped alkaline earth oxides. Physica Scripta, 2020, 95, 025801.	1.2	6
33896	Chemical and structural stability of superconducting In5Bi3 driven by spinâ€“orbit coupling. JPhys Materials, 2020, 3, 015007.	1.8	1
33897	Relative Efficacy of Coâ^'X₄ Embedded Graphene (X=N, S, B, and P) Electrocatalysts towards Hydrogen Evolution Reaction: Is Nitrogen Really the Best Choice?. ChemCatChem, 2020, 12, 536-543.	1.8	32
33898	The structure and electronic structure of tin oxides. , 2020, , 11-39.		8
33899	Study of the stability of Î±-Fe/MnS interfaces from first principles and experiment. Applied Surface Science, 2020, 501, 144017.	3.1	26
33900	Investigation of the structural and electronic properties of pristine and Au-embedded MoS2/C60 and WSe2/C60 van der Waals heterostructures: A first-principles study. Applied Surface Science, 2020, 503, 144328.	3.1	17

#	Article	IF	Citations
33901	Surface-scale affinity and adsorption selectivity of alkaline earth metal oxides to H2O and CO2: Insight into SOFC anode modification. Applied Surface Science, 2020, 503, 144333.	3.1	10
33902	A first-principles study of the effects of atom impurities, defects, strain, electric field and layer thickness on the electronic and magnetic properties of the C2N nanosheet. Carbon, 2020, 157, 371-384.	5.4	114
33903	Ab-initio approach to the stability and the structural, electronic and magnetic properties of the (001) Znfe2O4 surface terminations. Applied Surface Science, 2020, 499, 143859.	3.1	10
33904	Ab initio study of the adsorption and dissociation of NO2 on pristine and Cu decorated ZnO(0001)-3â€Ã—â€3. Applied Surface Science, 2020, 500, 144031.	3.1	7
33905	The effect of thermal annealing on the magnetic properties of graphene oxide quantum dots. Applied Surface Science, 2020, 501, 144234.	3.1	5
33906	Adsorption properties of dopamine derivatives using carbon nanotubes: A first-principles study. Applied Surface Science, 2020, 501, 144249.	3.1	16
33907	A first-principles investigation of double transition metal atoms embedded C2N monolayer as a promising SF6 gas adsorbent and scavenger. Materials Chemistry and Physics, 2020, 240, 122184.	2.0	17
33908	A DFT+U study to report magnetic phase transition, electronic properties and half metallic ferromagnetism in palladium oxide using Hubbard method. Materials Chemistry and Physics, 2020, 241, 122263.	2.0	7
33909	Coadsorption of hydrazine (N2H4) and OH on NiZn surface: A DFT-based study. Surface Science, 2020, 691, 121505.	0.8	5
33910	Influence of the segregation of 3d transition metal solutes on the elastic modulus of a tilt grain boundary in bcc Fe: ab initio local analysis. Journal of Materials Science, 2020, 55, 3056-3063.	1.7	2
33911	First-principles study of structural and optoelectronic properties of CsSnI3â^'yFy (yâ€‰=â€‰0, 1, 2, 3) perovskites. Indian Journal of Physics, 2020, 94, 1351-1359.	0.9	6
33912	Uncovering the electrochemical mechanisms for hydrogen evolution reaction of heteroatom doped M2C MXene (Mâ€=â€Ti, Mo). Applied Surface Science, 2020, 500, 143987.	3.1	93
33913	DFT studies of adsorption properties and bond strengths of H2S, HCN and NH3 on Fe(1â€0â€0). Applied Surface Science, 2020, 500, 144232.	3.1	39
33914	DFT study of ethanol adsorption on CaO(0â€0â€1) surface. Applied Surface Science, 2020, 500, 144254.	3.1	25
33915	Energy-level engineered hollow N-doped NiS1.03 for Znâ€“Air batteries. Energy Storage Materials, 2020, 25, 202-209.	9.5	62
33916	Evidence of inter-species swing adsorption between aromatic hydrocarbons. Environmental Research, 2020, 181, 108814.	3.7	13
33917	Hydrogen evolution reaction of metal di-chalcogenides: ZrS2, ZrSe2 and Janus ZrSSe. International Journal of Hydrogen Energy, 2020, 45, 23920-23927.	3.8	43
33918	Bond relaxation and electronic and magnetic properties of Sc atoms adsorbed on the Li (1â€1â€0) surface. Journal of Magnetism and Magnetic Materials, 2020, 496, 165910.	1.0	4

#	Article	IF	Citations
33919	New candidate to reach Shockleyâ€“Queisser limit: The DFT study of orthorhombic silicon allotrope Si(oP32). Journal of Physics and Chemistry of Solids, 2020, 137, 109219.	1.9	15
33920	Preparation, Structure, and enhanced thermoelectric properties of Sm-doped BiCuSeO oxyselenide. Materials and Design, 2020, 185, 108263.	3.3	29
33921	Novel process for decontamination and additional valorization of steel making dust processing using two-step correlative leaching. Journal of Hazardous Materials, 2020, 384, 121442.	6.5	6
33922	Magnetic phase stability of transition metals doped (4,4) AlN nanosheet. Journal of Magnetism and Magnetic Materials, 2020, 497, 166028.	1.0	18
33923	Two-dimensional carbon nitride (C3N) nanosheets as promising materials for H2S and NH3 elimination: A computational approach. Physica E: Low-Dimensional Systems and Nanostructures, 2020, 117, 113794.	1.3	31
33924	Theoretical study of hydrocarbon functional groups on elemental mercury adsorption on carbonaceous surface. Chemical Engineering Journal, 2020, 380, 122505.	6.6	22
33926	Edge promotion and basal plane activation of MoS2 catalyst by isolated Co atoms for hydrodesulfurization and hydrodenitrogenation. Catalysis Today, 2020, 350, 56-63.	2.2	5
33927	Ï€-Complexation for olefin/paraffin separation using aluminosilicates. Chemical Engineering Journal, 2020, 380, 122482.	6.6	28
33928	Hydrogen evolution and oxygen evolution reactions of pristine and alkali metal doped SnSe2 monolayer. International Journal of Hydrogen Energy, 2020, 45, 18657-18665.	3.8	32
33929	Electron transport properties of silicene: Intrinsic and dirty cases with screening effects. Journal of Molecular Structure, 2020, 1199, 126878.	1.8	3
33930	First-principles study on stability, structural and electronic properties of monolayers and nanotubes based on pure Mo(W)S(Se)2 and mixed (Janus) Mo(W)SSe dichalcogenides. Physica E: Low-Dimensional Systems and Nanostructures, 2020, 115, 113681.	1.3	22
33931	An insight of Mg doped ZnO thin films: A comparative experimental and first-principle investigations. Physica E: Low-Dimensional Systems and Nanostructures, 2020, 115, 113658.	1.3	20
33932	Confined seeds derived sodium titanate/graphene composite with synergistic storage ability toward high performance sodium ion capacitors. Chemical Engineering Journal, 2020, 379, 122418.	6.6	23
33933	Theoretical investigations on the U2Mo3Si4 compound from first-principles calculations. Progress in Nuclear Energy, 2020, 118, 103121.	1.3	2
33934	Study of first principles on anisotropy and elastic constants of YAl₃ compound. Canadian Journal of Physics, 2020, 98, 357-363.	0.4	10
33935	Selective extraction of titanium from Ti-bearing slag via the enhanced depolarization effect of liquid copper cathode. Journal of Energy Chemistry, 2020, 42, 43-48.	7.1	23
33936	Interaction of VSe₂ with Ambient Gases: Stability and Chemical Reactivity. Physica Status Solidi - Rapid Research Letters, 2020, 14, 1900332.	1.2	10
33937	First-principles investigation of structural, electronic and mechanical properties of some Dysprosium chalcogenides, DyX (Xâ€‰=â€‰S, Se and Te). Indian Journal of Physics, 2020, 94, 1195-1201.	0.9	4

#	Article	IF	Citations
33938	O-assisted and pristine Au-Pt(100) surfaces: A platform for adsorption and decomposition of H2O. International Journal of Hydrogen Energy, 2020, 45, 18666-18675.	3.8	6
33939	Controlling the strength of Zr (10 <mml:math xmlns:mml="http://www.w3.org/1998/Math/MathML") Tj ETQq1 1 0.784314 rgBT /Ove lo boundary by nonmetallic impurities doping: A DFT study. Journal of Materials Science and Technology, 2020, 36, 140-148.	5.6	12
33940	Prenucleation at the liquid-Al/Î±-Al2O3 and the liquid-Al/MgO interfaces. Computational Materials Science, 2020, 171, 109258.	1.4	20
33941	Intriguing p-orbital magnetic semiconductors and carrier induced half-metallicity in surface oxygen-functionalized two-dimensional <mml:math xmlns:mml="http://www.w3.org/1998/Math/MathML" altimg="si27.svg"><mml:mrow><mml:msub><mml:mrow><mml:mi>X</mml:mi></mml:mrow><mml:mrow><mml:mn>2</mml:mn><m		

#	Article	IF	Citations
33956	First-Principles Investigation of Thermodynamic Decomposition of Interfacial Oxides in Hot Compression Bonding. Metallurgical and Materials Transactions A: Physical Metallurgy and Materials Science, 2020, 51, 874-886.	1.1	9
33957	First-principles density-functional-theory calculations of formation and dissociation energies in germanene multivacancies. Materials Today Communications, 2020, 22, 100754.	0.9	3
33958	Ab-Initio Simulations of Monolayer InSe and MoS2 Strain Effect: From Electron Mobility to Photoelectric Effect. Journal of Electronic Materials, 2020, 49, 559-565.	1.0	14
33959	Adsorption of NH3 onto vacancy-defected Ti2CO2 monolayer by first-principles calculations. Applied Surface Science, 2020, 504, 144325.	3.1	18
33960	Impact of the voids on the cracking behavior of the duplex oxide scale on the 18%Cr austenite alloy surface. Corrosion Science, 2020, 163, 108298.	3.0	5
33961	First-principles calculations on formation and electronic properties of edge-functionalized arsenene nanoribbons. Physica B: Condensed Matter, 2020, 577, 411749.	1.3	4
33962	Cohesion strength and fracture toughness of Mo-TiC interfaces. Surface and Coatings Technology, 2020, 382, 125158.	2.2	14
33963	QuantumATK: an integrated platform of electronic and atomic-scale modelling tools. Journal of Physics Condensed Matter, 2020, 32, 015901.	0.7	771
33964	Tailoring electronic properties and kinetics behaviors of Pd/Nâ€CNTs catalysts for selective hydrogenation of acetylene. AICHE Journal, 2020, 66, e16857.	1.8	28
33965	Highly Efficient Polarized GeS/MoSe₂ van der Waals Heterostructure for Water Splitting from Ultraviolet to Nearâ€Infrared Light. Physica Status Solidi - Rapid Research Letters, 2020, 14, 1900582.	1.2	14
33966	Electrical conduction mechanism of rare-earth calcium oxyborate high temperature piezoelectric crystals. Acta Materialia, 2020, 183, 165-171.	3.8	14
33967	First-principles investigation of CO and CO2 adsorption on <mml:math xmlns:mml="http://www.w3.org/1998/Math/MathML" altimg="si61.svg"><mml:mrow><mml:mi>Î³</mml:mi></mml:mrow></mml:math>-Al2O3 supported monoatomic and diatomic Pt clusters. Applied Surface Science, 2020, 499, 143968.	3.1	10
33968	Anti-perovskite carbides and nitrides A3BX: A new family of damage tolerant ceramics. Journal of Materials Science and Technology, 2020, 40, 64-71.	5.6	15
33969	Beyond the Vegard's law: solid mixing excess volume and thermodynamic potentials prediction, from end-members. Physics Letters, Section A: General, Atomic and Solid State Physics, 2020, 384, 126059.	0.9	2
33970	Discovery of space aromaticity in transitionâ€“metal monoxide crystal Nb3O3 enabled by octahedral Nb6 structural units. Science Bulletin, 2020, 65, 367-372.	4.3	3
33971	Ab initio dielectric response function of diamond and other relevant high pressure phases of carbon. Journal of Physics Condensed Matter, 2020, 32, 095401.	0.7	17
33972	First-principles insight into hydrogen adsorption over Co4 anchored on defective graphene. Applied Surface Science, 2020, 504, 144413.	3.1	12
33973	Realization of noble heterobilayers with enhanced optoelectronic properties. Applied Surface Science, 2020, 505, 144530.	3.1	4

#	Article	IF	Citations
33974	Dielectric, piezoelectric and nonlinear optical properties of polar iodate BiO(IO3) from first-principles studies. Journal of Solid State Chemistry, 2020, 281, 121057.	1.4	8
33975	Electronic and optical properties of SrS nanosheet in 001 and 101 directions. Computational Condensed Matter, 2020, 22, e00445.	0.9	5
33976	2D Hexagonal Boron Nitride/Cadmium Sulfide Heterostructure as a Promising Waterâ€Splitting Photocatalyst. Physica Status Solidi (B): Basic Research, 2020, 257, 1900431.	0.7	22
33977	Ferroelectric and dipole control of band alignment in the two dimensional InTe/In₂Se₃ heterostructure. Journal of Physics Condensed Matter, 2020, 32, 055703.	0.7	19
33978	Room-temperature multiferroicity and diversified magnetoelectric couplings in 2D materials. National Science Review, 2020, 7, 373-380.	4.6	50
33979	Electrochemically Derived Grapheneâ€Like Carbon Film as a Superb Substrate for Highâ€Performance Aqueous Znâ€Ion Batteries. Advanced Functional Materials, 2020, 30, 1907120.	7.8	78
33980	Study on mechanism of hydrogen adsorption on WO3, W20O58, and W18O49. International Journal of Quantum Chemistry, 2020, 120, e26072.	1.0	3
33981	External electric field effect on electronic properties and charge transfer in CoI₂/NiI₂ spinterface. International Journal of Quantum Chemistry, 2020, 120, e26092.	1.0	3
33982	Atomic scale configuration of planar defects in the Nb-rich C14 Laves phase NbFe2. Acta Materialia, 2020, 183, 362-376.	3.8	29
33983	A theoretical study of gas adsorption on calcite for CO2 enhanced natural gas recovery. Applied Surface Science, 2020, 504, 144575.	3.1	28
33984	Investigation of structural, electronic, magnetic and half-metallic properties in ternary zinc blende CrMoO and ScMoO by GGA and GGA+U method: First principles study. Journal of Molecular Graphics and Modelling, 2020, 95, 107490.	1.3	3
33985	Electronic structure based design of thin film metallic glasses with superior fracture toughness. Materials and Design, 2020, 186, 108327.	3.3	13
33986	Effect of halogens in MgO to predict half-metallic ferromagnetism: By first principles calculations. Solid State Sciences, 2020, 99, 106048.	1.5	7
33987	Elastic properties of the molecular crystals of hydrocarbons from first principles calculations. Journal of Physics Condensed Matter, 2020, 32, 085704.	0.7	3
33988	Tuning the Catalytic Preference of Ruthenium Catalysts for Nitrogen Reduction by Atomic Dispersion. Advanced Functional Materials, 2020, 30, 1905665.	7.8	159
33989	A Firstâ€Principles Study of C₃N Nanostructures: Control and Engineering of the Electronic and Magnetic Properties of Nanosheets, Tubes and Ribbons. ChemPhysChem, 2020, 21, 164-174.	1.0	34
33990	PbF[Br 2 F 7], a Fluoridobromate(III) of a pâ€Block Metal. European Journal of Inorganic Chemistry, 2020, 2020, 64-70.	1.0	6
33991	Surface speciation of Co based Fischer-Tropsch catalyst under reaction conditions: Deactivation by coke or by oxidation?. Applied Catalysis A: General, 2020, 590, 117332.	2.2	9

#	Article	IF	Citations
33992	Release and migration characteristics of sodium and potassium in high alkali coal under oxy-fuel fluidized bed combustion condition. Fuel, 2020, 262, 116413.	3.4	16
33993	First-principles investigation on the atomic structure, stability and electronic property of O(001)/B2(110) interface in Ti2AlNb alloys. Journal of Alloys and Compounds, 2020, 817, 152734.	2.8	12
33994	Metal oxide sub-nanoclusters decorated Ni catalyst for selective hydrogenation of adiponitrile to hexamethylenediamine. Journal of Catalysis, 2020, 381, 14-25.	3.1	22
33995	Broadband CrOCl Saturable Absorber with a Spectral Region Extension to 10.6 Âµm. Advanced Optical Materials, 2020, 8, 1901446.	3.6	15
33996	Probing the efficiency of platinum nanotubes for the H2 production by water gas shift reaction: A DFT study. Applied Catalysis B: Environmental, 2020, 263, 118301.	10.8	19
33997	Understanding oxygen vacancies in disorder-engineered surface and subsurface of CaTiO3 nanosheets on photocatalytic hydrogen evolution. Applied Catalysis B: Environmental, 2020, 267, 118378.	10.8	86
33998	First-principles study of surface properties of crystalline and amorphous uranium aluminides. Applied Surface Science, 2020, 502, 144132.	3.1	5
33999	Rational design of a PC3 monolayer: A high-capacity, rapidly charging anode material for sodium-ion batteries. Carbon, 2020, 157, 420-426.	5.4	49
34000	Electrochemical properties and sodium ion diffusion in Na3V(PO4)2. Journal of Solid State Chemistry, 2020, 281, 121047.	1.4	2
34001	Combined DFT and experimental investigation on ion isomorphic substitution of aluminophosphate microporous crystals. Microporous and Mesoporous Materials, 2020, 294, 109859.	2.2	6
34002	Physico-chemical properties of CrMoN coatings - combined experimental and computational studies. Thin Solid Films, 2020, 693, 137671.	0.8	13
34003	Solute segregation induced sandwich structure in Al-Cu(-Au) alloys. Acta Materialia, 2020, 184, 17-29.	3.8	28
34004	Two-dimensional H-TiO2/MoS2(WS2) van der Waals heterostructures for visible-light photocatalysis and energy conversion. Applied Surface Science, 2020, 504, 144425.	3.1	48
34005	Synergistic band convergence and endotaxial nanostructuring: Achieving ultralow lattice thermal conductivity and high figure of merit in eco-friendly SnTe. Nano Energy, 2020, 67, 104261.	8.2	72
34006	Pressure induced superconductive 10-fold coordinated TaS₂: a first-principles study. Journal of Physics Condensed Matter, 2020, 32, 085402.	0.7	7
34007	Prediction of staggered stacking 2D BeP semiconductor with unique anisotropic electronic properties. Journal of Physics Condensed Matter, 2020, 32, 085301.	0.7	2
34008	First-principles study on the electronic and magnetic properties of P edge-doped armchair germanium selenide nanoribbon. Computational Materials Science, 2020, 172, 109348.	1.4	16
34009	New aluminium hydroxide at multimegabar pressures: Implications for water reservoirs in deep planetary interiors. Icarus, 2020, 338, 113539.	1.1	5

#	Article	IF	Citations
34010	Crystal facets engineering and rGO hybridizing for synergistic enhancement of photocatalytic activity of nickel disulfide. Journal of Hazardous Materials, 2020, 384, 121402.	6.5	11
34011	Electronic Structures and Catalytic Activities of Niobium Oxides as Electrocatalysts in Liquidâ€Junction Photovoltaic Devices. Solar Rrl, 2020, 4, 1900430.	3.1	29
34012	Surface Ni-rich engineering towards highly stable Li1.2Mn0.54Ni0.13Co0.13O2 cathode materials. Energy Storage Materials, 2020, 25, 76-85.	9.5	47
34013	Effect of tungsten on the vacancy behaviors in Taâ€“W alloys from first-principles calculations. Solid State Communications, 2020, 306, 113767.	0.9	11
34014	First-principles Predictions on Half-Metallic, Mechanical, and Acoustic Properties of CuHg2Ti-Type Mn2LiZ (Z=As, Sb) Compounds. Journal of Superconductivity and Novel Magnetism, 2020, 33, 1065-1072.	0.8	3
34015	The gas sensing performance of borophene/MoS2 heterostructure. Applied Surface Science, 2020, 504, 144412.	3.1	59
34016	Towards stable Na-rich layered transition metal oxides for high energy density sodium-ion batteries. Energy Storage Materials, 2020, 25, 62-69.	9.5	27
34017	Exploring the hidden catalyst from boron pnictide family for HER and OER. International Journal of Hydrogen Energy, 2020, 45, 18612-18622.	3.8	12
34018	Modelling of antimonene as an anode material in sodium-ion battery: A first-principles study. Materials Chemistry and Physics, 2020, 241, 122381.	2.0	27
34019	Electronic structure, magnetism and elastic properties of Inverse Perovskite Carbide: A first principles study. Physica B: Condensed Matter, 2020, 578, 411839.	1.3	14
34020	Effects of vacancy defects on electronic properties of 2D group-IV Tellurides (XTe, X = Si, Ge, Sn and) Tj ETQq0 0 0 rgBT /Overlock 10 Tf	1.4	3
34021	Silicene, Siloxene, or Silicane? Revealing the Structure and Optical Properties of Silicon Nanosheets Derived from Calcium Disilicide. Chemistry of Materials, 2020, 32, 795-804.	3.2	59
34022	Cobalt atoms drive the anchoring of Co-TPP molecules to the oxygen-passivated Fe(0â€¯0â€¯1) surface. Applied Surface Science, 2020, 505, 144213.	3.1	21
34023	Superhard conductive orthorhombic carbon polymorphs. Carbon, 2020, 158, 546-552.	5.4	27
34024	First-principles study of the electronic, magnetic and optical properties of Fe3Se4 in its monoclinic phase. Journal of Magnetism and Magnetic Materials, 2020, 498, 166157.	1.0	6
34025	Electronic structure and optical properties of two-dimensional tetragonal and hexagonal ScN monolayers: Impact of strain. Journal of Physics and Chemistry of Solids, 2020, 138, 109270.	1.9	10
34026	Unveiling the Working Mechanism of Graphene Bubble Film/Silicon Composite Anodes in Li-Ion Batteries: From Experiment to Modeling. ACS Applied Energy Materials, 2020, 3, 521-531.	2.5	24
34027	The energy band engineering for the high-performance infrared photodetectors constructed by CdTe/MoS₂ heterojunction. Journal of Physics Condensed Matter, 2020, 32, 065004.	0.7	20

#	Article	IF	Citations
34028	A Mechanism Investigation of how the Alloying Effect Improves the Photocatalytic Nitrate Reduction Activity of Bismuth Oxyhalide Nanosheets. ChemPhotoChem, 2020, 4, 110-119.	1.5	16
34029	Quantitative analysis of plasmon excitations in hard x-ray photoelectron spectra of bulk black phosphorus. Applied Surface Science, 2020, 505, 144385.	3.1	7
34030	Tunable electronic properties in bismuthene/2D silicon carbide van der Waals heterobilayer. Japanese Journal of Applied Physics, 2020, 59, SCCC03.	0.8	18
34031	A theoretical study of the reverse waterâ€gas shift reaction on Ni(111) and Ni(311) surfaces. Canadian Journal of Chemical Engineering, 2020, 98, 740-748.	0.9	25
34032	Firstâ€Principles Calculation of Bandgaps of Al 1â^' x In x N Alloys and Shortâ€Period Al 1â^' x In x N/Al 1â^' y In y N Superlattices. Physica Status Solidi (B): Basic Research, 2020, 257, 1900530.	0.7	3
34033	CrAs Monolayer: Low Buckled 2D Halfâ€Metal Ferromagnet. Physica Status Solidi - Rapid Research Letters, 2020, 14, 1900509.	1.2	4
34034	Temperature dependence on phase evolution in the BaTiO₃ polytypes studied using ab initio calculations. International Journal of Quantum Chemistry, 2020, 120, e26054.	1.0	23
34035	Nature of Nitrogen Incorporation in BiVO4Photoanodes through Chemical and Physical Methods. Solar Rrl, 2020, 4, 1900290.	3.1	23
34036	First principles study on the functionalization of graphene with Fe catalyst for the detection of CO2: Effect of catalyst clustering. Applied Surface Science, 2020, 502, 144153.	3.1	18
34038	Systematic computational investigation of an Ni3Fe catalyst for the OER. Catalysis Today, 2020, 345, 220-226.	2.2	9
34039	Interface microstructure evolution of a novel CuW/Al composite fabricated by an infiltration method. Journal of Alloys and Compounds, 2020, 816, 152506.	2.8	8
34040	Magnetism, half-metallicity and bonding in AlFeO3 and the impact of In-doping. Journal of Magnetism and Magnetic Materials, 2020, 497, 165909.	1.0	8
34041	Point-defect engineering of MoN/TaN superlattice films: A first-principles and experimental study. Materials and Design, 2020, 186, 108211.	3.3	11
34042	Spectral characterization, thermochemical studies, periodic SAPT calculations and detailed quantum mechanical profiling various physico-chemical properties of 3,4-dichlorodiuron. Spectrochimica Acta - Part A: Molecular and Biomolecular Spectroscopy, 2020, 228, 117580.	2.0	26
34043	Electronic structure and magnetism of Al-doped tris(8-hydroxyquinoline)iron investigated by experiment and first-principle calculation. Journal of Magnetism and Magnetic Materials, 2020, 497, 165969.	1.0	3
34044	Effect of van der Waals interactions to structures and properties of 3,<mml:math xmlns:mml="http://www.w3.org/1998/Math/MathML" display="inline" id="d1e5014" altimg="si4.svg"><mml:msup><mml:mrow><mml:mn>3</mml:mn></mml:mrow><mml:mrow><mml:mo>â€²</mml:mo></mml:mrow> <mml:math xmlns:mml="http://www.w3.org/1998/Math/MathML" display="inline" id="d1e5024" altimg="si5.svg"><mml:msup><mml:mrow><mml:mn>5</mml:mn></mml:mrow><mml:mrow><mml:mo>â€²</mml:mo></mml:mrow> Materials Chemistry and Physics, 2020, 240, 122175.	2.0	13
34045	Adsorption behaviors of HCN, SO2, H2S and NO molecules on graphitic carbon nitride with Mo atom decoration. Applied Surface Science, 2020, 501, 144199.	3.1	38
34046	Equilibrium morphology evolution of FCC cobalt nanoparticle under CO and hydrogen environments. Applied Surface Science, 2020, 504, 144469.	3.1	9

#	Article	IF	Citations
34047	Ferromagnetic ordering in cobalt doped methylammonium lead bromide: An ab-initio study. Computational Condensed Matter, 2020, 22, e00444.	0.9	3
34048	Structural, mechanical and electronic properties study on group 5 transition metals ternary mononitrides from first-principles calculations. Journal of Alloys and Compounds, 2020, 813, 152246.	2.8	13
34049	Comparative study of sonochemically synthesized Co-Zr and Ni-Zr substituted Sr-hexaferrites: Magnetic and structural investigations. Journal of Magnetism and Magnetic Materials, 2020, 497, 165996.	1.0	24
34050	Nitrogen induced half metallic ferromagnetism in oxides of calcium and cadmium: A DFT perspective. Materials Chemistry and Physics, 2020, 243, 122336.	2.0	2
34051	A novel metallic silicon hexaboride, Cmca-B6Si. Physics Letters, Section A: General, Atomic and Solid State Physics, 2020, 384, 126075.	0.9	7
34052	Visible-blind UV-Detector properties of monolayer calcium chloride: DFT calculations of its structural, mechanical, electronic and optical properties. Solid State Communications, 2020, 306, 113771.	0.9	3
34053	Thermodynamics of low-index surfaces and particle shapes of Y(OH)3 under typical hydrothermal conditions. Surface Science, 2020, 691, 121490.	0.8	1
34054	Carbon vs silicon polyprismanes: a comparative study of metallic sp³-hybridized allotropes. Fullerenes Nanotubes and Carbon Nanostructures, 2020, 28, 97-103.	1.0	18
34055	Influence of defect pairs in Ga-based ordered defect compounds: a hybrid density functional study. Canadian Journal of Physics, 2020, 98, 770-777.	0.4	0
34056	Tunable electric properties of bilayer MX2 (Mâ€¯=â€¯Ge, Sn; Xâ€¯=â€¯S, Se) with different strain and external electric field. Physica B: Condensed Matter, 2020, 581, 411673.	1.3	5
34057	Probing the active sites of site-specific nitrogen doping in metal-free graphdiyne for electrochemical oxygen reduction reactions. Science Bulletin, 2020, 65, 45-54.	4.3	52
34058	Exploration of pressure induced phase transitions and thermo-mechanical properties in LuX (X=As, Sb,) Tj ETQq1 1 0.784314 rgBT /Ov	0.9	0
34059	Formaldehyde adsorption on a hydrogenated gallium nitride monolayer: A density functional theory study. Applied Surface Science, 2020, 506, 144944.	3.1	13
34060	Electronic structure and spin texture of Mo/N co-doped polar 2D-SiC. Applied Surface Science, 2020, 509, 145193.	3.1	3
34061	Shape change of submicron nickel particles under hydrogen and nickel chloride vapor. Applied Surface Science, 2020, 509, 145274.	3.1	4
34062	Segregation of S at Mo(001)/MoSi2(001) interface. Ceramics International, 2020, 46, 5050-5057.	2.3	8
34063	First-principles study of the insertion and diffusion of interstitial atoms (H, C, N and O) in nickel. Journal of Alloys and Compounds, 2020, 822, 153555.	2.8	14
34065	Remarkably High Thermoelectric Efficiencies of the Half-Heusler Compounds BXGa (X = Be, Mg, and Ca). ACS Applied Materials & Interfaces, 2020, 12, 5838-5846.	4.0	39

#	Article	IF	Citations
34066	Theoretical Insight into the Role of Defects and Facets in the Selectivity of Products in Water Oxidation over Bismuth Vanadate (BiVO₄). ACS Sustainable Chemistry and Engineering, 2020, 8, 1980-1988.	3.2	15
34067	Li2S growth on graphene: Impact on the electrochemical performance of Li-S batteries. Journal of Chemical Physics, 2020, 152, 014701.	1.2	10
34068	Efficient metal overlayer catalysts on the Nb2C monolayer for CO oxidation from first-principles screening. Journal of Physics Condensed Matter, 2020, 32, 175201.	0.7	5
34069	Enhanced electrochemical hydrogen evolution performance of WS2 nanosheets by Te doping. Journal of Catalysis, 2020, 382, 204-211.	3.1	51
34070	Promoted CO2 electroreduction over indium-doped SnP3: A computational study. Journal of Energy Chemistry, 2020, 48, 1-6.	7.1	19
34071	The trend of chemisorption of hydrogen and oxygen atoms on pure transition metals: Magnetism justifies unexpected behaviour of Mn and Cr. Materials Today Communications, 2020, 23, 100894.	0.9	9
34072	Quasi van der Waals epitaxy nitride materials and devices on two dimension materials. Nano Energy, 2020, 69, 104463.	8.2	48
34073	Introduction to Carbon-Based Nanostructures. , 2020, , 1-10.		0
34074	The New Family of Two-Dimensional Materials and van der Waals Heterostructures. , 2020, , 70-91.		0
34075	Quantum Transport: General Concepts. , 2020, , 92-119.		0
34076	Klein Tunneling and Ballistic Transport in Graphene and Related Materials. , 2020, , 120-144.		0
34077	Quantum Transport in Disordered Graphene-Based Materials. , 2020, , 145-209.		0
34078	Structure and Chemical State of Cesium on Well-Defined Cu(111) and Cu₂O/Cu(111) Surfaces. Journal of Physical Chemistry C, 2020, 124, 3107-3121.	1.5	16
34079	Ultrafast charge ordering by self-amplified excitonâ€“phonon dynamics in TiSe2. Nature Communications, 2020, 11, 43.	5.8	53
34080	Electronic structures of 24-valence-electron full Heusler compounds investigated by density functional and GW calculations. Journal of Physics Condensed Matter, 2020, 32, 175501.	0.7	4
34081	Identifying aspirin polymorphs from combined DFTâ€based crystal structure prediction and solidâ€state NMR. Magnetic Resonance in Chemistry, 2020, 58, 1018-1025.	1.1	6
34082	Exploring the Reliability of DFT Calculations of the Infrared and Terahertz Spectra of Sodium Peroxodisulfate. Journal of Infrared, Millimeter, and Terahertz Waves, 2020, 41, 382-413.	1.2	14
34083	Time-Domain Terahertz Spectroscopy and Solid-State Density Functional Theory Analysis of p-Nitrophenol Polymorphs. Journal of Infrared, Millimeter, and Terahertz Waves, 2020, 41, 1337-1354.	1.2	2

#	Article	IF	Citations
34084	Evolution and Growth Mechanism of Cu2(In,Sn) Formed Between In-48Sn Solder and Polycrystalline Cu During Long-Time Liquid-State Aging. Journal of Electronic Materials, 2020, 49, 2651-2659.	1.0	4
34085	An integrated experimental and computational study of diffusion and atomic mobility of the aluminumâ€“magnesium system. Acta Materialia, 2020, 189, 214-231.	3.8	29
34086	Accelerated design of novel W-free high-strength Co-base superalloys with extremely wide Î³/Î³Ê¹ region by machine learning and CALPHAD methods. Acta Materialia, 2020, 186, 425-433.	3.8	57
34087	Catalytic formation of narrow Nb nanowires inside carbon nanotubes. Carbon, 2020, 159, 195-200.	5.4	3
34088	Zirconia (1Â1Â0) surface adsorption behavior â€“ A density functional theory study. Computational and Theoretical Chemistry, 2020, 1173, 112702.	1.1	4
34089	Optoelectronic, thermoelectric and thermodynamic properties of AgBO2 delafossite structure: An ab initio comparative study with AgAlO2. Optik, 2020, 204, 164158.	1.4	1
34090	The structural, electronic and dynamical investigations of NdMn2O5 and La2CoMnO6 for optoelectronic applications: A first principles study. Optik, 2020, 204, 164165.	1.4	11
34091	Adsorption characteristics composition of Ge and Si on 4H-SiC(0Â0Â0Â1) surface. Journal of Crystal Growth, 2020, 531, 125370.	0.7	1
34092	Anatomy of large perpendicular magnetic anisotropy in free-standing Co/Ni (1 1 1) multilayer. Journal of Magnetism and Magnetic Materials, 2020, 500, 166357.	1.0	5
34093	Effects of gas adsorption on electronic and optical properties of palladium-doped graphene: First-principles study. Physica E: Low-Dimensional Systems and Nanostructures, 2020, 118, 113879.	1.3	21
34094	The spin-dependent transport properties of endohedral transition-metal-fullerene X@C66H4 (X=Fe, Co,) Tj ETQq0 0 0 rgBT /Overlock 10	0.9	1
34095	A special triple point in non-centrosymmetric materials Zn3In2Se6 and In2Se3. Physics Letters, Section A: General, Atomic and Solid State Physics, 2020, 384, 126216.	0.9	1
34096	Computational Screening of Single Non-Noble Transition-Metal Atoms Confined Inside Boron Nitride Nanotubes for CO Oxidation. Journal of Physical Chemistry C, 2020, 124, 2030-2038.	1.5	10
34097	Changing the Phosphorus Allotrope from a Square Columnar Structure to a Planar Zigzag Nanoribbon by Increasing the Diameter of Carbon Nanotube Nanoreactors. Nano Letters, 2020, 20, 1280-1285.	4.5	29
34098	New Dimorphs of Na₅V(PO₄)₂F₂ as an Ultrastable Cathode Material for Sodium-Ion Batteries. ACS Applied Energy Materials, 2020, 3, 1181-1189.	2.5	16
34099	Unravelling the early oxidation mechanism of zinc phosphide (Zn₃P₂) surfaces by adsorbed oxygen and water: a first-principles DFT-D3 investigation. Physical Chemistry Chemical Physics, 2020, 22, 1444-1456.	1.3	15
34100	Strain-engineered BluePâ€“MoS2 van der Waals heterostructure with improved lithiation/sodiation for LIBs and SIBs. Physical Chemistry Chemical Physics, 2020, 22, 1701-1714.	1.3	19
34101	Combined density functional theory and molecular dynamics study of Sm_{0.75}A_{0.25}Co_{1â^'x}Mn_xO_{2.88} (A = Ca, Sr;) Tj ETQq1 1 0.784314	1.3	10

Chemical Physics, 2020, 22, 692-699.

#	Article	IF	Citations
34102	A first-principles study of the thermoelectric properties of rhombohedral GeSe. Physical Chemistry Chemical Physics, 2020, 22, 1911-1922.	1.3	32
34103	Coexistence of three types of sodium motion in double molybdate Na₉Sc(MoO₄)₆: ²³Na and ⁴⁵Sc NMR data and ab initio calculations. Physical Chemistry Chemical Physics, 2020, 22, 144-154.	1.3	9
34104	Effects of a graphene substrate on the structure and properties of atomically thin metal sheets. Physical Chemistry Chemical Physics, 2020, 22, 667-673.	1.3	6
34105	On the stability of hydroxyl groups on substituted titania. Physical Chemistry Chemical Physics, 2020, 22, 1250-1257.	1.3	1
34106	Discovery of twin orbital-order phases in ferromagnetic semiconducting VI₃ monolayer. Physical Chemistry Chemical Physics, 2020, 22, 512-517.	1.3	29
34107	From the perspectives of DFT calculations, thermodynamic modeling, and kinetic Monte Carlo simulations: the interaction between hydrogen and Sc₂C monolayers. Physical Chemistry Chemical Physics, 2020, 22, 4387-4401.	1.3	4
34108	How coverage influences thermodynamic and kinetic isotope effects for H₂/D₂ dissociative adsorption on transition metals. Catalysis Science and Technology, 2020, 10, 671-689.	2.1	26
34109	FSI-inspired solvent and â€œfull fluorosulfonylâ€•electrolyte for 4 V class lithium-metal batteries. Energy and Environmental Science, 2020, 13, 212-220.	15.6	198
34110	Computational screening of transition metal-doped phthalocyanine monolayers for oxygen evolution and reduction. Nanoscale Advances, 2020, 2, 710-716.	2.2	30
34111	Highly stable two-dimensional gold selenide with large in-plane anisotropy and ultrahigh carrier mobility. Nanoscale Horizons, 2020, 5, 366-371.	4.1	28
34112	Predictive theoretical screening of phase stability for chemical order and disorder in quaternary 312 and 413 MAX phases. Nanoscale, 2020, 12, 785-794.	2.8	56
34113	Trace fluorinated-carbon-nanotube-induced lithium dendrite elimination for high-performance lithiumâ€“oxygen cells. Nanoscale, 2020, 12, 3424-3434.	2.8	14
34114	Hot carrier relaxation in Cs₂TiI_yBr_{6â^'y} (y = 0, 2 and 6) by a time-domain ab initio study. RSC Advances, 2020, 10, 958-964.	1.7	10
34115	Interlayer separation in hydrogen titanates enables electrochemical proton intercalation. Journal of Materials Chemistry A, 2020, 8, 412-421.	5.2	28
34116	Interfacial stability and ionic conductivity enhanced by dopant segregation in eutectic ceramics: the role of Gd segregation in doped CeO₂/CoO and CeO₂/NiO interfaces. Journal of Materials Chemistry A, 2020, 8, 2591-2601.	5.2	5
34117	Câ€“Hâ€¦N hydrogen bonding in an overlayer of s-triazine physisorbed on a graphite surface. Molecular Physics, 2020, 118, e1706777.	0.8	4
34118	Role of W-site substitution on mechanical and electronic properties of cubic tungsten carbide. Journal of Physics Condensed Matter, 2020, 32, 145701.	0.7	5
34119	Investigations on p- and n-type diluted magnetic semiconductors X/Mn-codoped LiZnN (X= Li, Na and K). Journal of Alloys and Compounds, 2020, 821, 153235.	2.8	0

#	Article	IF	Citations
34120	Gallium Composition-Dependent Structural Phase Transitions in HoFe_{3â€“x}Ga_x(BO₃)₄ Solid Solutions: Crystal Growth, Structure, and Raman Spectroscopy Study. Crystal Growth and Design, 2020, 20, 1058-1069.	1.4	6
34121	Facile One-Step Syntheses of Several Complex Ionic Lithium Gallates from LiGa as Intermetallic Precursors. Chemistry of Materials, 2020, 32, 866-873.	3.2	8
34122	Origin of Electronic Modification of Platinum in a Pt₃V Alloy and Its Consequences for Propane Dehydrogenation Catalysis. ACS Applied Energy Materials, 2020, 3, 1410-1422.	2.5	41
34123	Role of Transition Metals in Layered Double Hydroxides for Differentiating the Oxygen Evolution and Nonenzymatic Glucose Sensing. ACS Applied Materials & Interfaces, 2020, 12, 6193-6204.	4.0	48
34124	Orpiment under compression: metavalent bonding at high pressure. Physical Chemistry Chemical Physics, 2020, 22, 3352-3369.	1.3	20
34125	Tuning ferroelectricity by charge doping in two-dimensional SnSe. Journal of Applied Physics, 2020, 127, 014101.	1.1	12
34126	Understanding bisphenol-A adsorption in magnetic modified covalent organic frameworks: Experiments coupled with DFT calculations. Journal of Molecular Liquids, 2020, 301, 112431.	2.3	52
34127	First-principles study of the electronic and optical properties of nitrogen and gold co-doped graphene. Superlattices and Microstructures, 2020, 139, 106363.	1.4	4
34128	Experimental and Computational Studies of CO and NO Adsorption Properties on Rh-Based Single Nanosized Catalysts. Journal of Physical Chemistry C, 2020, 124, 2953-2960.	1.5	8
34129	Three-Dimensional Superlithiophilic Interphase for Dendrite-Free Lithium Metal Anodes. ACS Applied Materials & Interfaces, 2020, 12, 5767-5774.	4.0	36
34130	Hybrid activation mechanism of thermal annealing for hydrogen storage of magnesium based on experimental evidence and theoretical validation. Applied Surface Science, 2020, 504, 144491.	3.1	19
34131	Theoretical dopant screening and processing optimization for vanadium disulfide as cathode material for Li-air batteries: A density functional theory study. Applied Surface Science, 2020, 508, 145276.	3.1	8
34132	A-site deficient perovskite with nano-socketed Ni-Fe alloy particles as highly active and durable catalyst for high-temperature CO2 electrolysis. Electrochimica Acta, 2020, 335, 135683.	2.6	38
34133	Anomalous lattice compression in the hexagonal La2O3â€“ A high pressure X-ray diffraction, Raman spectroscopy and first principle study. Journal of Alloys and Compounds, 2020, 822, 153657.	2.8	17
34136	Electronic Properties of Carbon-Based Nanostructures. , 2020, , 11-69.		0
34137	Quantum Hall Effects in Graphene. , 2020, , 210-236.		0
34138	Spin-Related Phenomena. , 2020, , 237-277.		0
34139	Ab Initio and Multiscale Quantum Transport in Graphene-Based Materials. , 2020, , 293-353.		0

#	Article	IF	Citations
34143	Optical absorption in array of Ge/Al-shell nanoparticles in an Alumina matrix. Scientific Reports, 2020, 10, 65.	1.6	7
34144	Realizing high-efficiency power generation in low-cost PbS-based thermoelectric materials. Energy and Environmental Science, 2020, 13, 579-591.	15.6	101
34145	From Trigonal to Cubic LiVO₂: A High-Energy Phase Transition toward Disordered Rock Salt Materials. Journal of Physical Chemistry C, 2020, 124, 2229-2237.	1.5	14
34146	Control of C₃N₄and C₄N₃carbon nitride nanosheetsâ€™ electronic and magnetic properties through embedded atoms. Physical Chemistry Chemical Physics, 2020, 22, 2249-2261.	1.3	49
34147	Carbon at the nanoscale: Ultrastiffness and unambiguous definition of incompressibility. Carbon, 2020, 160, 228-235.	5.4	10
34148	Effects of Si concentration on electronic structure and optical gap of Si-doped Î²-Ga2O3. Computational Materials Science, 2020, 174, 109505.	1.4	17
34149	Electronic and transport properties of blue phosphorene in presence of point defects: A first-principles study. Physica E: Low-Dimensional Systems and Nanostructures, 2020, 118, 113938.	1.3	16
34150	Elastic properties of long-period stacking ordered phases in Mgâ€“Znâ€“Y and Mgâ€“Niâ€“Y alloys: A first-principles study. Scripta Materialia, 2020, 178, 422-427.	2.6	69
34151	Mixed 4f population of Tm adatoms on insulating Cu₂N islands. Physical Chemistry Chemical Physics, 2020, 22, 196-202.	1.3	3
34152	High-throughput HSE study on the doping effect in anatase TiO₂. Physical Chemistry Chemical Physics, 2020, 22, 39-53.	1.3	30
34153	Structure, elastic characteristic, ideal strengths, and phonon stability of binary uranium intermetallic UGe₃ of AuCu₃-type. Physical Chemistry Chemical Physics, 2020, 22, 1381-1391.	1.3	4
34154	p-Type conductivity mechanism and defect structure of nitrogen-doped LiNbO3 from first-principles calculations. Physical Chemistry Chemical Physics, 2020, 22, 20-27.	1.3	8
34155	Control of the deprotonation of terephthalic acid assemblies on Ag(111) studied by DFT calculations and low temperature scanning tunneling microscopy. Physical Chemistry Chemical Physics, 2020, 22, 3173-3183.	1.3	3
34156	The catalytic mechanism of the Au@TiO_{2â^'x}/ZnO catalyst towards a low-temperature water-gas shift reaction. Catalysis Science and Technology, 2020, 10, 768-775.	2.1	9
34157	A systematic theoretical study of the water gas shift reaction on the Pt/ZrO₂ interface and Pt(111) face: key role of a potassium additive. Catalysis Science and Technology, 2020, 10, 876-892.	2.1	22
34158	Substituent group-tunable hydrogen evolution activity observed in isostructural Cu(<scp>ii</scp>)-based coordination polymer photocatalysts. Dalton Transactions, 2020, 49, 1674-1680.	1.6	4
34159	Self-doped pâ€“n junctions in two-dimensional In₂X₃ van der Waals materials. Materials Horizons, 2020, 7, 504-510.	6.4	42
34160	Experimental evidence of a new class of massless fermions. Nanoscale Horizons, 2020, 5, 679-682.	4.1	5

#	Article	IF	Citations
34161	Ferroelastic domains drive charge separation and suppress electronâ€“hole recombination in all-inorganic halide perovskites: time-domain ab initio analysis. Nanoscale Horizons, 2020, 5, 683-690.	4.1	20
34162	Boron-decorated C₉N₄ monolayers as promising metal-free catalysts for electrocatalytic nitrogen reduction reaction: a first-principles study. New Journal of Chemistry, 2020, 44, 422-427.	1.4	34
34163	Temperature, strain and charge mediated multiple and dynamical phase changes of selenium and tellurium. Nanoscale, 2020, 12, 3249-3258.	2.8	8
34164	Metal-free highly efficient photocatalysts for overall water splitting: C₃N₅ multilayers. Nanoscale, 2020, 12, 306-315.	2.8	57
34165	Theoretical insights into nonprecious oxygen-evolution active sites in Tiâ€“Ir-Based perovskite solid solution electrocatalysts. Journal of Materials Chemistry A, 2020, 8, 218-223.	5.2	15
34166	Local mobility in electrochemically inactive sodium in hard carbon anodes after the first cycle. Journal of Materials Chemistry A, 2020, 8, 743-749.	5.2	28
34167	W supported on g-CN manifests high activity and selectivity for N₂electroreduction to NH₃. Journal of Materials Chemistry A, 2020, 8, 1378-1385.	5.2	93
34168	Bottom-top channeling Li nucleation and growth by a gradient lithiophilic 3D conductive host for highly stable Li-metal anodes. Journal of Materials Chemistry A, 2020, 8, 1678-1686.	5.2	31
34169	Partial sulfuration-induced defect and interface tailoring on bismuth oxide for promoting electrocatalytic CO₂reduction. Journal of Materials Chemistry A, 2020, 8, 2472-2480.	5.2	82
34170	A vanadiumâ€“nickel oxynitride layer for enhanced electrocatalytic nitrogen fixation in neutral media. Journal of Materials Chemistry A, 2020, 8, 91-96.	5.2	42
34171	In situ engineered ZnSâ€“FeS heterostructures in N-doped carbon nanocages accelerating polysulfide redox kinetics for lithium sulfur batteries. Journal of Materials Chemistry A, 2020, 8, 433-442.	5.2	118
34172	Insights into the vacancy behaviour at the interface of Asâ€“Sb lateral heterostructures. Journal of Materials Chemistry C, 2020, 8, 650-662.	2.7	4
34173	Broadband near-infrared (NIR) emission realized by the crystal-field engineering of Y_{3â^'x}Ca_xAl_{5â^'x}Si_xO₁₂:Cr³⁺(x=	2.7	36
34174	As₂S₃, As₂Se₃ and As₂Te₃ nanosheets: superstretchable semiconductors with anisotropic carrier mobilities and optical properties. Journal of Materials Chemistry C, 2020, 8, 2400-2410.	2.7	45
34175	First-principles investigation of bandgap tailoring in tetragonal Bi₂FeCrO₆ by magnetic ordering and B-site-cation ordering. Functional Materials Letters, 2020, 13, 1950092.	0.7	4
34176	Effects of Li Confined Motion on NMR Quadrupolar Interactions: A Combined 7 Li NMR and DFTâ€MD Study of LiR 2 (PO 4) 3 (R=Ti or Zr) Phases. ChemSusChem, 2020, 13, 1027-1036.	3.6	4
34177	Unusual Effect of Trace Water on the Structure and Activity of Ni x Co 1â^' x Electrocatalysts for the Methanol Oxidation Reaction. ChemSusChem, 2020, 13, 964-973.	3.6	14
34178	Cu 2 MgO 3 Electronic and Magnetic Properties â€“ a DFT Study. Israel Journal of Chemistry, 2020, 60, 863-869.	1.0	2

#	Article	IF	Citations
34179	Pressureâ€Dependent Mechanical Properties of Nb 5 Si 3 Phase from Firstâ€Principles Calculations. Physica Status Solidi (B): Basic Research, 2020, 257, 1900754.	0.7	2
34180	A Theoretical Study of Pressure-Induced Effects on Phase Transition and Elastic Properties of AsTh Compound. Journal of Electronic Materials, 2020, 49, 2086-2094.	1.0	3
34181	Mechanisms behind the spontaneous growth of Tin whiskers on the Ti2SnC ceramics. Acta Materialia, 2020, 185, 433-440.	3.8	34
34182	Environmentally benign synthesis of a PGM-free catalyst for low temperature CO oxidation. Applied Catalysis B: Environmental, 2020, 264, 118547.	10.8	20
34183	Phosphorus-doped graphite felt allowing stabilized electrochemical interface and hierarchical pore structure for redox flow battery. Applied Energy, 2020, 261, 114369.	5.1	69
34184	The adsorption properties of environmentally friendly insulation gas C4F7N on Zn (0A0A0A1) and ZnO (1Â0Â<mml:math xmlns:mml="http://www.w3.org/1998/Math/MathML" altimg="si1.svg"><mml:mover) Tj ETQq1 1 0.784314 rgBT /Ov study. Applied Surface Science, 2020, 509, 144854.	3.1	10
34185	Investigation of the electronic and structural properties of graphyne oxide toward CO, CO2 and NH3 adsorption: A DFT and MD study. Applied Surface Science, 2020, 507, 145134.	3.1	46
34186	A hybrid Co NPs@CNT nanocomposite as highly efficient electrocatalyst for oxygen evolution reaction. Applied Surface Science, 2020, 507, 145155.	3.1	34
34187	The VN2 negatively charged defect in diamond. A quantum mechanical investigation of the EPR response. Carbon, 2020, 159, 443-450.	5.4	17
34188	Connecting theory with experiment to understand the photocatalytic activity of CuOâ€“ZnO heterostructure. Ceramics International, 2020, 46, 9446-9454.	2.3	50
34189	First-principles calculation of elastic properties of Cu-Zn intermetallic compounds for improving the stiffness of aluminum alloys. Computational Materials Science, 2020, 174, 109479.	1.4	11
34190	Silicon rebirth: Ab initio prediction of metallic sp3-hybridized silicon allotropes. Computational Materials Science, 2020, 174, 109480.	1.4	12
34191	Machine learning models for the prediction of energy, forces, and stresses for Platinum. Computational Materials Science, 2020, 174, 109483.	1.4	17
34192	Elastic constants of pure body-centered cubic Mg in nanolaminates. Computational Materials Science, 2020, 174, 109501.	1.4	18
34193	Direct Z-scheme photocatalytic overall water splitting on two dimensional MoSe2/SnS2 heterojunction. International Journal of Hydrogen Energy, 2020, 45, 2785-2793.	3.8	54
34194	Remarkable improvement in hydrogen storage capacities of two-dimensional carbon nitride (g-C3N4) nanosheets under selected transition metal doping. International Journal of Hydrogen Energy, 2020, 45, 3035-3045.	3.8	110
34195	High pressure phase transitions and physical properties of Li2MgH4; implications for hydrogen storage. International Journal of Hydrogen Energy, 2020, 45, 4720-4730.	3.8	27
34196	Ab-initio revelation on the origins of Ti substitution for Ga, Mn and Ni on ferromagnetism, phase stability and elastic properties in Ni2MnGa. Journal of Alloys and Compounds, 2020, 821, 153481.	2.8	27

#	Article	IF	Citations
34197	Insights into the active sites and catalytic mechanism of oxidative esterification of 5-hydroxymethylfurfural by metal-organic frameworks-derived N-doped carbon. Journal of Catalysis, 2020, 381, 570-578.	3.1	56
34198	The position of lysine controls the catechol-mediated surface adhesion and cohesion in underwater mussel adhesion. Journal of Colloid and Interface Science, 2020, 563, 168-176.	5.0	51
34199	Ta-based 413 and 211 MAX phase solid solutions with Hf and Nb. Journal of the European Ceramic Society, 2020, 40, 1829-1838.	2.8	31
34200	A DFT investigation on magnetoelectric coupling in PbBO3 (BÂ=ÂV, Cr, Mn, Co, and Cu) materials: The influence on multiferroic properties. Journal of Magnetism and Magnetic Materials, 2020, 500, 166364.	1.0	9
34201	Hydrogen isotope role in the crystal orientation change of erbium oxide coatings. Journal of Nuclear Materials, 2020, 528, 151871.	1.3	4
34202	Prediction of a novel carbon allotrope from first-principle calculations: A potential superhard material in monoclinic symmetry. Materials Chemistry and Physics, 2020, 242, 122480.	2.0	47
34203	Calculated infrared and Raman signatures of Ag+, Cd2+, Pb2+, Hg2+, Ca2+, Mg2+, and K+ sodalites. Microporous and Mesoporous Materials, 2020, 296, 109983.	2.2	9
34204	Complex water dynamics in crystalline [Ca(H2O)2](ReO4)2, studied by the vibrational spectroscopy and proton magnetic resonance. Journal of Molecular Structure, 2020, 1205, 127610.	1.8	2
34205	Investigation of structural, mechanical, dynamic, electronic and optical properties of seleno-germanates A<mml:math xmlns:mml="http://www.w3.org/1998/Math/MathML" altimg="si1.svg"><mml:msub><mml:mrow /><mml:mn>2</mml:mn></mml:msub></mml:math>GeSe<mml:math xmlns:mml="http://www.w3.org/1998/Math/MathML" altimg="si2.svg"><mml:msub><mml:mrow		

#	Article	IF	Citations
34215	Artificial Intelligence to Accelerate the Discovery of N₂ Electroreduction Catalysts. Chemistry of Materials, 2020, 32, 709-720.	3.2	59
34216	Pressure-Induced Phase Changes in Cesium Lead Bromide Perovskite Nanocrystals with and without Ruddlesdenâ€“Popper Faults. Chemistry of Materials, 2020, 32, 785-794.	3.2	25
34217	Experimental and Theoretical Study of SbPO4 under Compression. Inorganic Chemistry, 2020, 59, 287-307.	1.9	14
34218	Synthesis and Catalytic Properties of Porous Metal Silica Materials Templated and Functionalized by Extended Coordination Cages. Inorganic Chemistry, 2020, 59, 767-776.	1.9	16
34219	Aurivillius Halide Perovskite: A New Family of Two-Dimensional Materials for Optoelectronic Applications. Journal of Physical Chemistry C, 2020, 124, 1788-1793.	1.5	13
34220	Nature of Interactions between Epoxides in Graphene Oxide. Journal of Physical Chemistry C, 2020, 124, 1695-1703.	1.5	5
34221	Two-Dimensional Transition Metal Porphyrin Sheets as a Promising Single-Atom-Catalyst for Dinitrogen Electrochemical Reduction to Ammonia: A Theoretical Study. Journal of Physical Chemistry C, 2020, 124, 1492-1499.	1.5	30
34222	Covalent Functionalized Black Phosphorus Greatly Inhibits Nonradiative Charge Recombination: A Time Domain Ab Initio Study. Journal of Physical Chemistry Letters, 2020, 11, 478-484.	2.1	22
34223	Two-Dimensional (001) LaAlO₃/SrTiO₃ Heterostructures with Adjustable Band Gap and Magnetic Properties. ACS Applied Materials & Interfaces, 2020, 12, 3134-3139.	4.0	11
34224	Unraveling the Surface Chemistry and Structure in Highly Active Sputtered Pt₃Y Catalyst Films for the Oxygen Reduction Reaction. ACS Applied Materials & Interfaces, 2020, 12, 4454-4462.	4.0	16
34225	Bioinspired Electrocatalyst for Electrochemical Reduction of N₂ to NH₃ in Ambient Conditions. ACS Applied Materials & Interfaces, 2020, 12, 2445-2451.	4.0	39
34226	Ultrafine Tungsten Oxide Nanowires: Synthesis and Highly Selective Acetone Sensing and Mechanism Analysis. ACS Applied Materials & Interfaces, 2020, 12, 3755-3763.	4.0	58
34227	Ultrastrong Ï€-Bonded Interface as Ductile Plastic Flow Channel in Nanostructured Diamond. ACS Applied Materials & Interfaces, 2020, 12, 4135-4142.	4.0	7
34228	N/P-Dual-Doped Carbon-Coated Na₃V₂(PO₄)₂O₂F Microspheres as a High-Performance Cathode Material for Sodium-Ion Batteries. ACS Applied Materials & Interfaces, 2020, 12, 3670-3680.	4.0	63
34229	Variation in the In₂O₃ Crystal Phase Alters Catalytic Performance toward the Reverse Water Gas Shift Reaction. ACS Catalysis, 2020, 10, 3264-3273.	5.5	112
34230	Thiocyanate-Modified Silver Nanofoam for Efficient CO₂ Reduction to CO. ACS Catalysis, 2020, 10, 1444-1453.	5.5	51
34231	Effect of Manganese on the Selective Catalytic Hydrogenation of COx in the Presence of Light Hydrocarbons Over Ni/Al2O3: An Experimental and Computational Study. ACS Catalysis, 2020, 10, 1535-1547.	5.5	24
34232	Harvesting Delayed Fluorescence in Perovskite Nanocrystals Using Spin-Forbidden Mn d States. ACS Energy Letters, 2020, 5, 353-359.	8.8	18

#	Article	IF	Citations
34233	Synergetic Effect of Nitrogen/Sulfur Dual-Doped Hierarchically Porous Carbon Networks for Liâ€“S Batteries. ACS Sustainable Chemistry and Engineering, 2020, 8, 749-758.	3.2	23
34234	Nanoscale percolation in doped BaZrO3 for high proton mobility. Nature Materials, 2020, 19, 338-346.	13.3	73
34235	Targeted chemical pressure yields tuneable millimetre-wave dielectric. Nature Materials, 2020, 19, 176-181.	13.3	27
34236	GeI₂ monolayer: a model thermoelectric material from 300 to 600â€…K. Philosophical Magazine, 2020, 100, 782-796.	0.7	18
34237	Mechanistic Study of Radium Adsorption onto Goethite. Journal of Physical Chemistry C, 2020, 124, 805-814.	1.5	4
34238	A-site deficient/excessive effects of LaMnO3 perovskite as bifunctional oxygen catalyst for zinc-air batteries. Electrochimica Acta, 2020, 333, 135566.	2.6	71
34239	Synthesis, structure and physical properties of layered quaternary sulfides NaLiMS2 (MÂ= Mn, Fe, Co). Journal of Alloys and Compounds, 2020, 822, 153613.	2.8	4
34240	Theoretical investigation of structural, electronic and thermoelectric properties of $$p{-}n$$ type $$hbox {Mg}_{2}hbox {Si}_{1-x}hbox {Sn}_{x}$$ system. Pramana - Journal of Physics, 2020, 94, 1.	0.9	2
34241	Competition between the hcp nonmagnetic and antiferromagnetic phases in the transition path of Fe under pressure. Journal of Magnetism and Magnetic Materials, 2020, 499, 166312.	1.0	3
34242	A comparable study of Fe//MCs (M = Ti, V) interfaces by first-principles method: The chemical bonding, work of adhesion and electronic structures. Journal of Physics and Chemistry of Solids, 2020, 138, 109292.	1.9	18
34243	Adsorption of small molecules on a Pmma CO monolayer. Journal of Physics and Chemistry of Solids, 2020, 139, 109300.	1.9	0
34244	Selective Synthesis of a Salt and a Cocrystal of the Ethionamideâ€“Salicylic Acid System. Crystal Growth and Design, 2020, 20, 906-915.	1.4	49
34245	Bis(iminothiolato)-Based One-Dimensional Metalâ€“Organic Framework: Robust Bipolar Magnetic Semiconductor with Reversal of Spin Polarization. Journal of Physical Chemistry C, 2020, 124, 37-43.	1.5	14
34246	Unraveling the Mechanism of Water-Mediated Sulfur Tolerance via Operando Surface-Enhanced Raman Spectroscopy. ACS Applied Materials & Interfaces, 2020, 12, 2370-2379.	4.0	17
34247	DFT-investigation on anisotropy degree of electronic, optical, and mechanical properties of olivine ZnRE2S4 (RE = Er, Tm) compounds. Materials Research Express, 2020, 7, 016305.	0.8	3
34248	Theoryâ€Guided Defect Tuning through Topochemical Reactions for Accelerated Discovery of UVC Persistent Phosphors. Advanced Optical Materials, 2020, 8, 1901727.	3.6	20
34249	Strain-tunable electronic and optical properties in two dimensional GaSe/g-C3N4 van der Waals heterojunction as photocatalyst for water splitting. Physica E: Low-Dimensional Systems and Nanostructures, 2020, 118, 113896.	1.3	22
34250	Crystalline and Electronic Structures of the Al1+xV2Sn2â€“x (x = 0.19) Intermetallic Compound. Inorganic Chemistry, 2020, 59, 360-366.	1.9	0

#	Article	IF	Citations
34251	Combined Experimental and Theoretical Assessment of WX_y (X = C, N, S, P) for Hydrogen Evolution Reaction. ACS Applied Energy Materials, 2020, 3, 1082-1088.	2.5	32
34252	Theoretical study of adatom stability on polar GaN surfaces during MBE and MOVPE. Applied Surface Science, 2020, 502, 144205.	3.1	13
34253	RE (La, Nd and Yb) doped CeO2 abrasive particles for chemical mechanical polishing of dielectric materials: Experimental and computational analysis. Applied Surface Science, 2020, 506, 144668.	3.1	50
34254	Nanoscale electrochemical visualization of grain-dependent anodic iron dissolution from low carbon steel. Electrochimica Acta, 2020, 332, 135267.	2.6	48
34255	Investigating hydrogen evolution reaction properties of a new honeycomb 2D AlC. International Journal of Hydrogen Energy, 2020, 45, 18602-18611.	3.8	11
34256	Thermodynamic modelling of the Niâ€“Zr system. Intermetallics, 2020, 116, 106640.	1.8	8
34257	Crystal plane dependent electrocatalytic performance of NiS2 nanocrystals for hydrogen evolution reaction. Journal of Catalysis, 2020, 381, 63-69.	3.1	25
34258	Ni clusters embedded in multivacancy graphene substrates. Journal of Physics and Chemistry of Solids, 2020, 138, 109258.	1.9	7
34259	Magnetic properties in Nb/Tc adsorbed gt-C3N4 monolayer. Physica E: Low-Dimensional Systems and Nanostructures, 2020, 116, 113753.	1.3	2
34260	M-porphyrin (Mâ€‰=â€‰Mn, Co) carbon materials as oxygen reduction catalysts from density functional studies. Molecular Physics, 2020, 118, e1687949.	0.8	4
34261	Zr vacancies and their complexes with hydrogen in monoclinic zirconia: formation energies and positron lifetimes. Physica Scripta, 2020, 95, 035801.	1.2	0
34262	PdTe₂ Transitionâ€Metal Dichalcogenide: Chemical Reactivity, Thermal Stability, and Device Implementation. Advanced Functional Materials, 2020, 30, 1906556.	7.8	27
34263	Strain Engineering for 2D Ferroelectricity in Lead Chalcogenides. Advanced Electronic Materials, 2020, 6, 1900932.	2.6	17
34264	The effects of Zn²⁺ and ClO₄^{â¯} in the excellent primary explosive Zn(CHZ)₃(ClO₄)₂. International Journal of Quantum Chemistry, 2020, 120, e26107.	1.0	3
34265	In situ formation of N-doped carbon-coated porous MoP nanowires: a highly efficient electrocatalyst for hydrogen evolution reaction in a wide pH range. Applied Catalysis B: Environmental, 2020, 263, 118358.	10.8	112
34266	In-situ synthesis of Bi2S3 quantum dots for enhancing photodegradation of organic pollutants. Applied Surface Science, 2020, 501, 144047.	3.1	19
34267	Catalyst-induced gas-sensing selectivity in ZnO nanoribbons: Ab-initio investigation at room temperature. Applied Surface Science, 2020, 505, 144602.	3.1	8
34268	Site preference of V and its influence on the elastic properties in the boride series VxMo5â€“xSiB2 as studied by first principles density functional theory. Journal of Alloys and Compounds, 2020, 819, 153041.	2.8	3

#	Article	IF	Citations
34269	Reversal Topotactic Removal of Acetone from (HMTH)2BiI5Â·(CH3)2Câ•O Accompanied by Rearrangement of Weak Bonds, from 1D to 3D Patterns. Crystal Growth and Design, 2020, 20, 87-94.	1.4	11
34270	Tunable quadruple-well ferroelectric van der Waals crystals. Nature Materials, 2020, 19, 43-48.	13.3	140
34271	Structural and electronic properties of tungsten oxides under high pressures. Journal of Physics Condensed Matter, 2020, 32, 085403.	0.7	2
34272	The Dopant Local Effect on the Stability of an Oxygen Vacancy and the Reliability of a Conductive Filament in Rutile Titanium Dioxide. Physica Status Solidi (B): Basic Research, 2020, 257, 1900455.	0.7	3
34273	Insights into the mechanism of formic acid dehydrogenation on Pd-Co@Pd core-shell catalysts: A theoretical study. Applied Surface Science, 2020, 505, 144532.	3.1	10
34274	Nitrogen-Doped graphene coated FeS2 microsphere composite as high-performance anode materials for sodium-ion batteries enhanced by the chemical and structural synergistic effect. Applied Surface Science, 2020, 505, 144633.	3.1	18
34275	Discovering the root of the stability of hexagonal WO3 surfaces from a periodic DFT perspective. Applied Surface Science, 2020, 506, 144719.	3.1	13
34276	H induced decohesion of an Al grain boundary investigated with first principles: General conditions for instant breakage and local delayed fracture. Computational Materials Science, 2020, 173, 109403.	1.4	2
34277	Experimental and theoretical modelling of kinetic and equilibrium Ba isotope fractionation during calcite and aragonite precipitation. Geochimica Et Cosmochimica Acta, 2020, 269, 566-580.	1.6	26
34278	Insight into the effect of high pressure on multiferroic properties of TmNiO3. Journal of Alloys and Compounds, 2020, 815, 152351.	2.8	2
34279	Dual acceptor (N, Cu) doping effects on the electronic and optical properties of ZnO. Materials Chemistry and Physics, 2020, 242, 122463.	2.0	22
34280	Optical characteristics of dilute gallium phosphide bismide: Promising material for near-infra photonic device applications. Physics Letters, Section A: General, Atomic and Solid State Physics, 2020, 384, 126147.	0.9	8
34281	Spiroâ€Carbon: A Metallic Carbon Allotrope Predicted from First Principles Calculations. ChemPhysChem, 2020, 21, 59-64.	1.0	6
34282	Tunable electronic and magnetic properties of graphene/carbon-nitride van der Waals heterostructures. Applied Surface Science, 2020, 505, 144450.	3.1	61
34283	High crystalline aluminum nitride via highly enhanced adatom diffusion driven by point defect complex. Applied Surface Science, 2020, 505, 144615.	3.1	6
34284	Density functional theory analysis of the effect of structural configurations on the stability of GaAsBi compounds. Computational Materials Science, 2020, 173, 109401.	1.4	0
34285	Electronic, structural, and optical properties of Y2WO6, a host material for inorganic phosphors. Journal of Alloys and Compounds, 2020, 819, 152958.	2.8	3
34286	Properties of monolayer black phosphorus affected by uniaxial strain. Physica E: Low-Dimensional Systems and Nanostructures, 2020, 117, 113834.	1.3	5

#	Article	IF	Citations
34287	Dipole moment effects in dopamine/N-doped-graphene systems. Surface Science, 2020, 693, 121546.	0.8	6
34288	On the piezotronic behaviours of wurtzite coreâ€“shell nanowires. Nanotechnology, 2020, 31, 095407.	1.3	6
34289	Conformational investigation of peptides using solidâ€state NMR spectroscopyâ€”A study of polymorphism of Î²â€turn peptides containing diprolines. Chemical Biology and Drug Design, 2020, 95, 394-407.	1.5	3
34290	Elastic anisotropy and physical properties of semi-transition-metal borides: first-principles calculation. Applied Physics Express, 2020, 13, 015501.	1.1	7
34291	Sn-Doped Hematite for Photoelectrochemical Water Splitting: The Effect of Sn Concentration. Zeitschrift Fur Physikalische Chemie, 2020, 234, 683-698.	1.4	10
34292	The effect of chemical disorder on defect formation and migration in disordered max phases. Acta Materialia, 2020, 184, 50-58.	3.8	15
34293	Designing strained C2N/GaTe(InTe) heterostructures for photovoltaic and photocatalytic application. Journal of Alloys and Compounds, 2020, 816, 152559.	2.8	20
34294	Nâ€Doped Graphene Supported on Metalâ€Iron Carbide as a Catalyst for the Oxygen Reduction Reaction: Density Functional Theory Study. ChemSusChem, 2020, 13, 996-1005.	3.6	21
34295	Defect-Mediated Room Temperature Ferromagnetism in Lead-Free Ferroelectric Na0.5Bi0.5TiO3 Materials. Journal of Superconductivity and Novel Magnetism, 2020, 33, 911-920.	0.8	20
34296	Binding and 2D organization of arginine on Cu(1Â1Â0). Applied Surface Science, 2020, 509, 144865.	3.1	2
34297	Two-dimensional porphyrin sheet as an electric and optical sensor material for pH detection: A DFT study. Computational Materials Science, 2020, 174, 109485.	1.4	17
34298	ÎÎ¦: Solid state package allowing Bardeenâ€“Cooperâ€“Schrieffer and magnetic superstructure electronic states. Computer Physics Communications, 2020, 251, 107079.	3.0	4
34299	Theoretical investigations on structural, electronic and optical properties of wurtzite AlxGa1-xN (x=0, 0.25, 0.5, 0.75 and 1). Optik, 2020, 203, 164035.	1.4	0
34300	Theoretical study of the electronic, thermodynamic, and thermo-conductive properties of Î³-LiAlO2 with 6Li isotope substitutions for tritium production. Journal of Nuclear Materials, 2020, 530, 151963.	1.3	11
34301	Intrinsic point defects in half-Heusler AuMnSn. Journal of Physics and Chemistry of Solids, 2020, 139, 109328.	1.9	10
34302	Computational insights into nitrogen reduction reaction catalyzed by transition metal doped graphene: Comparative investigations. Materials Chemistry and Physics, 2020, 243, 122622.	2.0	27
34303	Light-driven methane dry reforming with single atomic site antenna-reactor plasmonic photocatalysts. Nature Energy, 2020, 5, 61-70.	19.8	466
34304	Synergistic enhancement of electrocatalytic CO2 reduction to C2 oxygenates at nitrogen-doped nanodiamonds/Cu interface. Nature Nanotechnology, 2020, 15, 131-137.	15.6	169

#	Article	IF	Citations
34305	A narrow-band ultra-bright green phosphor for LED-based applications. Dalton Transactions, 2020, 49, 1935-1946.	1.6	15
34306	A first-principles study on the influences of metal species Al, Zr, Mo and Tc on the mechanical properties of U₃Si₂. Physical Chemistry Chemical Physics, 2020, 22, 1833-1840.	1.3	8
34307	Pressure-stabilized polymerization of nitrogen in alkaline-earth-metal strontium nitrides. Physical Chemistry Chemical Physics, 2020, 22, 5242-5248.	1.3	25
34308	Investigation of the mechanism of overall water splitting in UV-visible and infrared regions with SnC/arsenene vdW heterostructures in different configurations. Physical Chemistry Chemical Physics, 2020, 22, 1045-1052.	1.3	22
34309	Theoretically predicted surface morphology of FCC cobalt nanoparticles induced by Ru promoter. Catalysis Science and Technology, 2020, 10, 187-195.	2.1	9
34310	Strain-induced phase transition and giant piezoelectricity in monolayer tellurene. Nanoscale, 2020, 12, 167-172.	2.8	25
34311	Highly efficient N₂ fixation catalysts: transition-metal carbides M₂C (MXenes). Nanoscale, 2020, 12, 538-547.	2.8	71
34312	RbNa(HC₃N₃O₃)Â·2H₂O exhibiting a strong second harmonic generation response and large birefringence as a new potential UV nonlinear optical material. Inorganic Chemistry Frontiers, 2020, 7, 150-156.	3.0	49
34313	Strain-engineering enables reversible semiconductorâ€“metal transition of skutterudite IrAs3. Inorganic Chemistry Frontiers, 2020, 7, 1108-1114.	3.0	1
34314	Application of organicâ€“graphene hybrids in high performance photodetectors. Materials Chemistry Frontiers, 2020, 4, 354-368.	3.2	16
34315	Elucidating the unexpected electrocatalytic activity of nanoscale PdO layers on Pd electrocatalysts towards ethanol oxidation in a basic solution. Sustainable Energy and Fuels, 2020, 4, 1118-1125.	2.5	22
34316	Thermal, electronic and thermoelectric properties of TiNiSn and TiCoSb based quaternary half Heusler alloys obtained fromab initiocalculations. Sustainable Energy and Fuels, 2020, 4, 895-910.	2.5	15
34317	Strain-tunable electronic properties and lithium storage of 2D transition metal carbide (MXene) Ti₂CO₂ as a flexible electrode. Journal of Materials Chemistry A, 2020, 8, 760-769.	5.2	35
34318	Ab initio prediction of two-dimensional Si₃C enabling high specific capacity as an anode material for Li/Na/K-ion batteries. Journal of Materials Chemistry A, 2020, 8, 4274-4282.	5.2	68
34319	Enhanced Na⁺ pseudocapacitance in a P, S co-doped carbon anode arising from the surface modification by sulfur and phosphorus with Câ€“Sâ€“P coupling. Journal of Materials Chemistry A, 2020, 8, 422-432.	5.2	33
34320	MOF-derived conductive carbon nitrides for separator-modified Liâ€“S batteries and flexible supercapacitors. Journal of Materials Chemistry A, 2020, 8, 1757-1766.	5.2	107
34321	Charge-transfer descriptor for the cycle performance of Î²-Li₂MO₃ cathodes: role of oxygen dimers. Journal of Materials Chemistry A, 2020, 8, 2663-2671.	5.2	9
34322	Discovery of low-temperature GeTe-based thermoelectric alloys with high performance competing with Bi₂Te₃. Journal of Materials Chemistry A, 2020, 8, 1660-1667.	5.2	43

#	Article	IF	Citations
34323	Unveiling the pinning behavior of charged domain walls in BiFeO3 thin films via vacancy defects. Acta Materialia, 2020, 186, 68-76.	3.8	22
34324	Enhanced thermoelectric properties of p-type argyrodites Cu8GeS6 through Cu vacancy. Journal of Alloys and Compounds, 2020, 822, 153665.	2.8	27
34325	Room temperature ferromagnetic half metal in Mn doped cluster-assembled sodalite phase of III-N compounds. Journal of Magnetism and Magnetic Materials, 2020, 499, 166295.	1.0	4
34326	Understanding the role of Fe, Cr and Ni in Zircaloy-2 with special focus on the role of Ni on hydrogen pickup. Journal of Nuclear Materials, 2020, 530, 151956.	1.3	9
34327	Perfluorinated Self-Assembled Monolayers Enhance the Stability and Efficiency of Inverted Perovskite Solar Cells. ACS Nano, 2020, 14, 1445-1456.	7.3	115
34328	Toward enhanced CO2 adsorption on bimodal calcium-based materials with porous truncated architectures. Applied Surface Science, 2020, 505, 144512.	3.1	20
34329	Kinetic interactions between H2 and CO in catalytic oxidation over PdO. Combustion and Flame, 2020, 211, 270-280.	2.8	16
34330	Understanding hydrogen in perovskites from first principles. Computational Materials Science, 2020, 174, 109461.	1.4	14
34331	Effects of solute segregation on surface properties of dilute Al-X (XÂ=ÂLi, Sn) alloys from first-principles calculations. Computational Materials Science, 2020, 174, 109502.	1.4	12
34332	Three-in-One: Opened Charge-transfer channel, positively shifted oxidation potential, and enhanced visible light response of g-C3N4 photocatalyst through K and S Co-doping. International Journal of Hydrogen Energy, 2020, 45, 4534-4544.	3.8	46
34333	Phase equilibria and diffusion coefficients in the Fe-Zn binary system. Materials and Design, 2020, 188, 108437.	3.3	7
34334	SEHC: A high-throughput materials computing framework with automatic self-evaluation filtering. Materials Science and Engineering B: Solid-State Materials for Advanced Technology, 2020, 252, 114474.	1.7	7
34335	Influence of Sodium Iodide doped polypyrrole on green synthesized aluminum doped ZnO for the enhanced charge separation at the interface. Optical Materials, 2020, 99, 109568.	1.7	6
34336	Ab initio investigation of physical properties of LaT2B2C (T=ir, Rh) compounds: A density functional theory approach. Physica C: Superconductivity and Its Applications, 2020, 568, 1353585.	0.6	1
34337	Theoretical Prediction and Experimental Verification of the Chemically Ordered Atomic-Laminate i-MAX Phases (Cr_{2/3}Sc_{1/3})₂GaC and (Mn_{2/3}Sc_{1/3})₂GaC. Crystal Growth and Design, 2020, 20, 55-61.	1.4	16
34338	Theoretical Investigation of Monolayer RhTeCl Semiconductors as Photocatalysts for Water Splitting. Journal of Physical Chemistry C, 2020, 124, 639-646.	1.5	18
34339	Crystal Structure Analysis of Top Dross in a Molten Zinc Bath by First Principle Calculation and Synchrotron X-ray Diffraction. Tetsu-To-Hagane/Journal of the Iron and Steel Institute of Japan, 2020, 106, 205-213.	0.1	0
34340	Magnetic Properties of NiFe2O4 Compound: Ab Initio Calculation and Monte Carlo Simulation. Journal of Superconductivity and Novel Magnetism, 2020, 33, 1369-1375.	0.8	14

#	Article	IF	Citations
34341	Anisotropic Elastic, Electronic and Vibrational Properties of the Semiconductor AgScX (X = Ge, C) Compounds. Journal of Electronic Materials, 2020, 49, 1849-1856.	1.0	5
34342	Interstitial diffusion of a helium atom in bulk Li4SiO4 crystal from first-principles calculations. Ceramics International, 2020, 46, 8192-8199.	2.3	7
34343	New stable phases of glycine crystals. Chemical Physics, 2020, 530, 110645.	0.9	7
34344	Electronic structure and thermoelectric properties of PbTe1â^'xSex from first-principles calculations. Computational Materials Science, 2020, 173, 109404.	1.4	3
34345	Activity and selectivity of methanol-to-olefin conversion over Zr-modified H-SAPO-34/H-ZSM-5 zeolites - A theoretical study. Fuel Processing Technology, 2020, 199, 106302.	3.7	20
34346	The mechanism of magnetostructural transition in Heusler alloy Co2V1.5Ga0.5. Journal of Magnetism and Magnetic Materials, 2020, 498, 166252.	1.0	6
34347	Generalised stacking fault energy of Ni-Al and Co-Al-W superalloys: Density-functional theory calculations. Materialia, 2020, 9, 100555.	1.3	20
34348	Graphene-like BC6N single-layer: Tunable electronic and magnetic properties via thickness, gating, topological defects, and adatom/molecule. Physica E: Low-Dimensional Systems and Nanostructures, 2020, 118, 113850.	1.3	64
34349	Atomic structure of high Miller index Si(47 35 7) surface. Surface Science, 2020, 693, 121549.	0.8	4
34350	Passivating Detrimental DX Centers in CH₃NH₃PbI₃ for Reducing Nonradiative Recombination and Elongating Carrier Lifetime. Advanced Materials, 2020, 32, e1906115.	11.1	53
34351	Suppressing Metal Leaching in a Supported Co/SiO₂ Catalyst with Effective Protectants in the Hydroformylation Reaction. ACS Catalysis, 2020, 10, 914-920.	5.5	44
34352	Exchange bias and exchange spring effects in Fe/CrN bilayers. Journal Physics D: Applied Physics, 2020, 53, 125001.	1.3	13
34353	Structural, Electronic, and Magnetic Properties of Mn4N Perovskite: Density Functional Theory Calculations and Monte Carlo Study. Journal of Superconductivity and Novel Magnetism, 2020, 33, 1507-1512.	0.8	10
34354	Accelerating water dissociation kinetics on Ni3S2 nanosheets by P-induced electronic modulation. Journal of Catalysis, 2020, 381, 493-500.	3.1	37
34355	Fabrication of Hollow CoP/TiO_x Heterostructures for Enhanced Oxygen Evolution Reaction. Small, 2020, 16, e1905075.	5.2	117
34356	Reactive Element Effects in High-Temperature Alloys Disentangled. Oxidation of Metals, 2020, 93, 229-245.	1.0	19
34357	First-Principles Modeling of Oxygen Adsorption on Ag-Doped LaMnO3 (001) Surface. Journal of Electronic Materials, 2020, 49, 1421-1434.	1.0	4
34358	Hierarchical porous Rh nanosheets for methanol oxidation reaction. Applied Catalysis B: Environmental, 2020, 264, 118520.	10.8	92

#	Article	IF	Citations
34359	Bi2O2SO4, a new representative of the grandreefite structure type. Journal of Solid State Chemistry, 2020, 282, 121124.	1.4	9
34360	Atomistic building blocks of one-dimensional Guinierâ€“Prestonâ€“Bagaryatsky zones in Al-Cu-Mg alloys. Materials and Design, 2020, 187, 108393.	3.3	14
34361	Kinetics and Mechanism of the Hydrogen Peroxide Reduction Reaction on a Graphite Carbon Nitride Sensor. Journal of Physical Chemistry C, 2020, 124, 336-346.	1.5	8
34362	Cyanate and Cyanurate Adsorption at Silver Electrodes in Neutral Solutions: In Situ ATR-SEIRAS and DFT Studies. Journal of Physical Chemistry C, 2020, 124, 709-721.	1.5	4
34363	Highly Efficient B-Site Exsolution Assisted by Co Doping in Lanthanum Ferrite toward High-Performance Electrocatalysts for Oxygen Evolution and Oxygen Reduction. ACS Sustainable Chemistry and Engineering, 2020, 8, 302-310.	3.2	48
34364	Role of electronic correlation effect on charge ordering in Î²-V2OPO4. Computational Materials Science, 2020, 173, 109433.	1.4	0
34365	Zr-based nickel aluminides: Crystal structure and electronic properties. Journal of Alloys and Compounds, 2020, 821, 153326.	2.8	1
34366	Thermodynamics of the iron-nitrogen system with vacancies. From first principles to applications. Journal of Alloys and Compounds, 2020, 821, 153343.	2.8	3
34367	Unsaturated Single Atoms on Monolayer Transition Metal Dichalcogenides for Ultrafast Hydrogen Evolution. ACS Nano, 2020, 14, 767-776.	7.3	106
34368	First principles study on methane reforming over Ni/TiO2(110) surface in solid oxide fuel cells under dry and wet atmospheres. Science China Materials, 2020, 63, 364-374.	3.5	17
34369	Insights into KMnO4 etched N-rich carbon nanotubes as advanced electrocatalysts for Zn-air batteries. Applied Catalysis B: Environmental, 2020, 264, 118537.	10.8	81
34370	Structural, electronic, and magnetic properties of the CoGa (0â€¯0â€¯1) surface and the L10 MnGa/CoGa interface: A density functional theory study. Applied Surface Science, 2020, 504, 144332.	3.1	3
34371	Mechanistic evaluation of Li2O2 adsorption on carbon nanotube electrodes: A theoretical study. Applied Surface Science, 2020, 506, 145050.	3.1	9
34372	The growth pattern of Ptn (nâ€¯=â€¯1â€“6) clusters on pentagonal B2C monolayer support: A computational study. Applied Surface Science, 2020, 507, 145076.	3.1	20
34373	Examining the uniform strain effect on elastic, electronic and optical properties of CsPbCl3 through FP-LAPW calculations. Chemical Physics, 2020, 531, 110654.	0.9	8
34374	Promising zirconia-mixed Al-based nitrogen carriers for chemical looping of NH3: Reduced NH3 decomposition and improved NH3 yield. Fuel, 2020, 264, 116821.	3.4	24
34375	Optical response and magnetic moment of MoS2 material. Optik, 2020, 208, 164080.	1.4	18
34376	Unraveling the mechanism of the hydrodeoxygenation of propionic acid over a Pt (1Â1Â1) surface in vapor and liquid phases. Journal of Catalysis, 2020, 381, 547-560.	3.1	14

#	Article	IF	Citations
34377	Ab initio study of the magnetic, optical and electronic properties of spinel Co3O4 within DFT and GW approaches. Journal of Magnetism and Magnetic Materials, 2020, 499, 166306.	1.0	6
34378	Electronic, magnetism, and optical properties of transition metals adsorbed g-GaN. Physica E: Low-Dimensional Systems and Nanostructures, 2020, 118, 113871.	1.3	74
34379	Microstructure, mechanical and tribological properties of NiAl matrix composites with addition of BaO/TiO2 binary oxides. Tribology International, 2020, 144, 106108.	3.0	18
34380	Magnetic Polymer Chains of Iron and Zwitterionic Quinoidal Ligands on the Ag(111) Surface. Journal of Physical Chemistry C, 2020, 124, 1346-1351.	1.5	7
34381	Gas Molecules on Defective and Nonmetal-Doped MoS₂ Monolayers. Journal of Physical Chemistry C, 2020, 124, 1511-1522.	1.5	37
34382	Deep Phase Transition of MoS₂ for Excellent Hydrogen Evolution Reaction by a Facile C-Doping Strategy. ACS Applied Materials & Interfaces, 2020, 12, 877-885.	4.0	38
34383	Stacking-Dependent Interlayer Magnetic Coupling in 2D CrI₃/CrGeTe₃ Nanostructures for Spintronics. ACS Applied Nano Materials, 2020, 3, 1282-1288.	2.4	47
34384	Effect of Cu Preferential Orientation on the Microstructure and Properties of Anodized Cu_xO Films. European Journal of Inorganic Chemistry, 2020, 2020, 261-268.	1.0	10
34385	Band parameters for Zn1â^'xMoxTe studied by means of spin-polarized first-principles calculations. Journal of Computational Electronics, 2020, 19, 38-46.	1.3	5
34386	BOPcat software package for the construction and testing of tight-binding models and bond-order potentials. Computational Materials Science, 2020, 173, 109455.	1.4	6
34387	Design of a Z-scheme g-C3N4/CQDs/CdIn2S4 composite for efficient visible-light-driven photocatalytic degradation of ibuprofen. Environmental Pollution, 2020, 259, 113770.	3.7	50
34388	Green synthesis and characterization of nontoxic L-methionine capped silver and gold nanoparticles. Journal of Inorganic Biochemistry, 2020, 204, 110958.	1.5	30
34389	DFT computations and molecular dynamics investigations on conformers of some pyrazinamide derivatives as corrosion inhibitors for aluminum. Journal of Molecular Liquids, 2020, 300, 112309.	2.3	54
34390	Radiation-Induced Evolution of Tungsten Carbide in Fusion Reactors: Accommodation of Defect Clusters and Transmutation Elements. ACS Applied Energy Materials, 2020, 3, 868-878.	2.5	16
34391	Induced magnetism in oxygen-decorated N-doped graphene. Carbon, 2020, 159, 102-109.	5.4	7
34392	Evidence for bandwidth-control metal-insulator transition in Ti3O5. Computational Materials Science, 2020, 173, 109435.	1.4	7
34393	Firstâ€Principles Calculations of Phonons and Thermodynamic Properties of Zr(Hf)S₂â€Based Nanotubes. Journal of Computational Chemistry, 2020, 41, 759-768.	1.5	5
34394	Adsorption of toxic gas molecules on the pre-oxidized Cu2Si nanosheet â€“ A DFT study. Computational Materials Science, 2020, 173, 109414.	1.4	41

#	Article	IF	Citations
34395	Effects of gas flow on detailed microstructure inhomogeneities in LPCVD TiAlN nanolamella coatings. Materialia, 2020, 9, 100546.	1.3	15
34396	Hyperfine interaction of H-divacancy in diamond. Results in Physics, 2020, 16, 102860.	2.0	1
34397	Modified Generalized Stacking Fault Energy Surface of IIâ€“VI Ionic Crystals from Excess Electrons and Holes. ACS Applied Electronic Materials, 2020, 2, 56-65.	2.0	3
34398	Understanding the Extremely Poor Lattice Thermal Transport in Chalcogenide Perovskite BaZrS₃. ACS Applied Energy Materials, 2020, 3, 1139-1144.	2.5	23
34399	Size-Controlled Pd Nanoparticles Loaded on Co₃O₄ Nanoparticles by Calcination for Enhanced CO Oxidation. ACS Applied Nano Materials, 2020, 3, 486-495.	2.4	26
34400	Ab initio calculation of the evolution of [SiN_{4â€}_nO_n] tetrahedron during Î²â€Si₃N₄(0001) surface oxidation. Journal of the American Ceramic Society, 2020, 103, 2808-2816.	1.9	4
34401	Ab initio study of the magnetic properties of possible phases in binary Fe-Pd alloys. Journal of Magnetism and Magnetic Materials, 2020, 499, 166266.	1.0	12
34402	Sodium diffusion and redox properties of alluaudite Na2+2M2â€™(MoO4)3 (Mâ€¯=â€¯Fe, Co, Ni) from DFT+U study. Materials Today Communications, 2020, 22, 100825.	0.9	7
34403	Modulating Band Alignment in Mixed Dimensionality 3D/2D Perovskites by Surface Termination Ligand Engineering. Chemistry of Materials, 2020, 32, 105-113.	3.2	19
34404	Elucidating Interfacial Phenomena between Solid-State Electrolytes and the Sulfur-Cathode of Lithiumâ€“Sulfur Batteries. Chemistry of Materials, 2020, 32, 360-373.	3.2	38
34405	A nonlocal continuum model for the piezopotential of two-dimensional semiconductors. Journal Physics D: Applied Physics, 2020, 53, 045303.	1.3	2
34406	A Validation of Cluster Modeling in the Description of Matrix Isolation Spectroscopy. Journal of Computational Chemistry, 2020, 41, 751-758.	1.5	5
34407	Structural stability and magnetism in Cd0.875Mn0.125Z (Zâ€‰=â€‰S, Se). Applied Physics A: Materials Science and Processing, 2020, 126, 1.	1.1	1
34408	Prenucleation at the Interface Between MgO and Liquid Magnesium: An Ab Initio Molecular Dynamics Study. Metallurgical and Materials Transactions A: Physical Metallurgy and Materials Science, 2020, 51, 788-797.	1.1	25
34409	Structural dataset for Si(1 1 0) and Si(17 15 1) surface models and related calculated STM images. Data in Brief, 2020, 28, 104847.	0.5	4
34410	Density Functional Theory and Molecular Dynamics insights into the site-dependent adsorption of hydrogen fluoride on kaolinite. Journal of Molecular Liquids, 2020, 299, 112265.	2.3	16
34411	Study of Physicochemical and Explosive Properties of a 2,4,6-Trinitrotoluene/Aniline Cocrystal Solvate. Crystal Growth and Design, 2020, 20, 116-129.	1.4	10
34412	Periodic Electronic Structure Calculations with the Density Matrix Embedding Theory. Journal of Chemical Theory and Computation, 2020, 16, 130-140.	2.3	40

#	Article	IF	Citations
34413	Expedition on surface adsorption of N-nitrosodiethylamine from rubber fumes on blue phosphorene sheets â€“ a first-principles insight. Molecular Physics, 2020, 118, e1699184.	0.8	11
34414	Raman spectrum of layered jacutingaite (Pt 2 HgSe 3) crystalsâ€”Experimental and theoretical study. Journal of Raman Spectroscopy, 2020, 51, 357-365.	1.2	10
34415	Intrinsic Defect Limit to the Electrical Conductivity and a Twoâ€Step pâ€Type Doping Strategy for Overcoming the Efficiency Bottleneck of Sb₂S₃â€Based Solar Cells. Solar Rrl, 2020, 4, 1900503.	3.1	79
34416	Structural and elastic properties of CaCO3 hydrated phases: A dispersion-corrected density functional theory study. Journal of Physics and Chemistry of Solids, 2020, 138, 109295.	1.9	6
34417	The effects of dilute concentrations of substitutional Re or Os on the thermodynamics and kinetics of oxygen in tungsten. Physica B: Condensed Matter, 2020, 580, 411937.	1.3	1
34418	Lattice-Strain Control of Flexible Janus Indium Chalcogenide Monolayers for Photocatalytic Water Splitting. Journal of Physical Chemistry C, 2020, 124, 167-174.	1.5	30
34419	Mechanical, electronic and optical properties of SeZnO₃: a GGA+U study. Philosophical Magazine, 2020, 100, 601-618.	0.7	8
34420	Two-dimensional hydrogenated buckled gallium arsenide: an ab initio study. Journal of Physics Condensed Matter, 2020, 32, 145502.	0.7	2
34421	Synthesis of orthogonally assembled 3D cross-stacked metal oxide semiconducting nanowires. Nature Materials, 2020, 19, 203-211.	13.3	172
34422	Enhancement of photovoltaic efficiency in CdSe x Te1â^'x (where 0 â©½ x â©½ 1): insights from density functional theory. Journal of Physics Condensed Matter, 2020, 32, 125702.	0.7	15
34423	Deuterium addition to liquid Liâ€“Sn alloys: implications for plasma-facing applications. Nuclear Fusion, 2020, 60, 016025.	1.6	2
34424	Single-atom Sn-Zn pairs in CuO catalyst promote dimethyldichlorosilane synthesis. National Science Review, 2020, 7, 600-608.	4.6	42
34425	A reduced imidazolium cation layer serves as the active site for electrochemical carbon dioxide reduction. Applied Catalysis B: Environmental, 2020, 264, 118495.	10.8	26
34426	Phase stability, magnetic and elastic properties of Co2NiGa alloy: A first-principles calculation. Materials Today Communications, 2020, 22, 100810.	0.9	7
34427	Electronic property enhancement of zinc oxide by surface decoration with carbon nanotubes: experimental and theoretical studies. Applied Physics A: Materials Science and Processing, 2020, 126, 1.	1.1	3
34428	Tunable high workfunction contacts: Doped graphene. Applied Surface Science, 2020, 509, 144893.	3.1	10
34429	Development and application of EAM potentials for Ti, Al and Nb with enhanced planar fault energy of Ti. Computational Materials Science, 2020, 173, 109432.	1.4	7
34430	Giant tunability of interlayer friction in graphite via ion intercalation. Extreme Mechanics Letters, 2020, 35, 100616.	2.0	6

#	Article	IF	Citations
34431	Proton irradiation of Niâ€“Cr alloy: Understanding the evolution of the damage microstructure. Journal of Alloys and Compounds, 2020, 815, 152408.	2.8	4
34432	Effect of the bond polarity on interlayer interactions in Bâ€“Câ€“N layered materials: A dispersion-corrected density functional study. Materials Today Communications, 2020, 22, 100781.	0.9	1
34433	High-pressure, high-temperature phase stability of iron-poor dolomite and the structures of dolomite-IIIc and dolomite-V. Physics of the Earth and Planetary Interiors, 2020, 299, 106403.	0.7	16
34434	The role of magnetite/graphene oxide nano-composite as a high-efficiency adsorbent for removal of phenazopyridine residues from water samples, an experimental/theoretical investigation. Journal of Molecular Liquids, 2020, 298, 112040.	2.3	319
34435	Surface Nonlinear Optics on Centrosymmetric Dirac Nodalâ€Line Semimetal ZrSiS. Advanced Materials, 2020, 32, e1904498.	11.1	14
34436	High Curie temperature ferromagnetism in penta-MnN2 monolayer. Applied Surface Science, 2020, 505, 144620.	3.1	25
34437	Charge-modulated/electric-field controlled reversible CO2/H2 capture and storage on metal-free N-doped penta-graphene. Chemical Engineering Journal, 2020, 391, 123577.	6.6	35
34438	First principles study of the effects of doping with sp elements (As, Sb, Bi) and pressure on the properties of half-Heusler AuMnSn. Chemical Physics, 2020, 530, 110635.	0.9	8
34439	A general rule for transition metals doping on magnetic properties of Fe-based metallic glasses. Journal of Alloys and Compounds, 2020, 819, 153062.	2.8	10
34440	Theoretical prediction of 2D XI2 (X=Si, Ge, Sn, Pb) monolayers by density functional theory. Journal of Molecular Graphics and Modelling, 2020, 95, 107501.	1.3	19
34441	Non-Heisenberg magnetism in a quaternary spin-gapless semiconductor. Journal of Magnetism and Magnetic Materials, 2020, 497, 166058.	1.0	3
34442	Hybrid lead triiodide perovskites with unsaturated heterocyclic cations containing N, O, and S atoms: Ab initio study. Journal of Solid State Chemistry, 2020, 282, 121082.	1.4	4
34443	Structure and tensile properties of Mx(MnFeCoNi)100-x solid solution strengthened high entropy alloys. Materialia, 2020, 9, 100539.	1.3	10
34444	Fluorine-incorporated interface enhances cycling stability of lithium metal batteries with Ni-rich NCM cathodes. Nano Energy, 2020, 67, 104309.	8.2	101
34445	d-orbital-frustration-induced ferromagnetic monolayer Cu3O2. Physica B: Condensed Matter, 2020, 577, 411826.	1.3	3
34446	Strong Jahn-Teller effect at NiO4 tetrahedron in NiCo2O4 spinel. Physics Letters, Section A: General, Atomic and Solid State Physics, 2020, 384, 126114.	0.9	4
34447	Core effect of local atomic configuration and design principles in AlxCoCrFeNi high-entropy alloys. Scripta Materialia, 2020, 178, 181-186.	2.6	29
34448	Reversible lithium storage capacity on carbon nitride by electric field. Superlattices and Microstructures, 2020, 137, 106340.	1.4	3

#	Article	IF	Citations
34449	Mechanistic Insights into pH-Controlled Nitrite Reduction to Ammonia and Hydrazine over Rhodium. ACS Catalysis, 2020, 10, 494-509.	5.5	81
34450	Phase stability, elasticity, hardness and electronic structures for binary MnBm (Mâ€‰=â€‰Ni,) Tj ETQq1 1 0.784314 rgB Phase Transitions, 2020, 93, 158-174.	0.6	13
34451	Low thermal conductivity of peanut-shaped carbon nanotube and its insensitive response to uniaxial strain. Nanotechnology, 2020, 31, 115701.	1.3	4
34452	Non-chemical fluorination of hexagonal boron nitride by high-energy ion irradiation. Nanotechnology, 2020, 31, 125705.	1.3	5
34453	A decohesion pathway for hydrogen embrittlement in nickel: Mechanism and quantitative prediction. Acta Materialia, 2020, 185, 98-109.	3.8	55
34454	Ripples in isotropically compressed graphene. Computational Materials Science, 2020, 173, 109422.	1.4	6
34455	First-Principles Study of Structural, Elastic, and Thermodynamic Properties of PdSn4 with Ni Addition. Journal of Electronic Materials, 2020, 49, 1435-1444.	1.0	6
34456	ALD-assisted synthesis of V2O5 nanoislands on SnO2 nanowires for improving NO2 sensing performance. Applied Surface Science, 2020, 509, 144821.	3.1	18
34457	Haeckelite boron nitride as nano sensor for the detection of hazardous methyl mercury. Applied Surface Science, 2020, 506, 144860.	3.1	28
34458	Superconducting phases in a remarkable class of metallic ceramics. Journal of Physics and Chemistry of Solids, 2020, 138, 109275.	1.9	84
34459	Electric field effect in bilayered graphene nanomeshes. Nanotechnology, 2020, 31, 115203.	1.3	6
34460	PBCFâ€Graphene: A 2D Sp² Hybridized Honeycomb Carbon Allotrope with a Direct Band Gap. ChemNanoMat, 2020, 6, 139-147.	1.5	54
34461	First principles high pressure studies on group-14 element pernitrides. Journal of Alloys and Compounds, 2020, 819, 153193.	2.8	4
34462	Accuracy of Dispersion-Corrected Density Functional Theory Calculations of Elastic Tensors of Organic Molecular Structures. Crystal Growth and Design, 2020, 20, 206-213.	1.4	11
34463	Electrochemical CO₂ Reduction Reaction on M@Cu(211) Bimetallic Single-Atom Surface Alloys: Mechanism, Kinetics, and Catalyst Screening. ACS Sustainable Chemistry and Engineering, 2020, 8, 210-222.	3.2	86
34464	Effective modelling of the Seebeck coefficient of Fe₂VAl. Journal of Physics Condensed Matter, 2020, 32, 125401.	0.7	4
34465	Atomic Selfâ€reconstruction of Catalyst Dominated Growth Mechanism of Graphite Structures. ChemCatChem, 2020, 12, 1316-1324.	1.8	6
34466	Thickness effect on the structural, electronic and energetic properties of the cubic KMgF3 (0Â0Â1) surfaces: A first-principles study. Applied Surface Science, 2020, 506, 144678.	3.1	4

#	Article	IF	Citations
34467	Lattice vibration properties of MoS2/PtSe2 heterostructures. Journal of Alloys and Compounds, 2020, 820, 153192.	2.8	7
34468	First-principles study of sensing SO2 adsorption on IIIâ€“V nitride nanoribbons. Materials Chemistry and Physics, 2020, 242, 122437.	2.0	16
34469	Theoretical study on structural, mechanical and electronic properties of ternary mononitride Ti0.5W0.5N from first-principles calculations. Materials Chemistry and Physics, 2020, 242, 122476.	2.0	9
34470	Structural and mechanical properties of ternary MgCaSi phase: A study by density functional theory. Journal of Chemical Research, 2020, 44, 50-59.	0.6	2
34471	Erosion and cathodic arc plasma of Nbâ€“Al cathodes: composite versus intermetallic. Plasma Sources Science and Technology, 2020, 29, 025022.	1.3	10
34472	Role of phonons on phase stabilization of RE2Si2O7 over wide temperature range (RE = Yb, Gd). Journal of the European Ceramic Society, 2020, 40, 780-788.	2.8	8
34473	Construction of Hierarchical Nanotubes Assembled from Ultrathin V₃S₄@C Nanosheets towards Alkaliâ€Ion Batteries with Ionâ€Dependent Electrochemical Mechanisms. Angewandte Chemie, 2020, 132, 2494-2503.	1.6	18
34474	Construction of Hierarchical Nanotubes Assembled from Ultrathin V₃S₄@C Nanosheets towards Alkaliâ€Ion Batteries with Ionâ€Dependent Electrochemical Mechanisms. Angewandte Chemie - International Edition, 2020, 59, 2473-2482.	7.2	199
34475	Microscopic Properties of Na and Liâ€”A First Principle Study of Metal Battery Anode Materials. ChemSusChem, 2020, 13, 771-783.	3.6	18
34476	The Ci(Sil)n defect in neutron-irradiated silicon. Journal of Materials Science: Materials in Electronics, 2020, 31, 930-934.	1.1	1
34477	Hybrid Nanocomposites of Multi-walled Carbon Nanotubes (MWCNTs) and CuO as Electrode Materials for Energy Storage Devices. Journal of Electronic Materials, 2020, 49, 1096-1103.	1.0	7
34478	Density functional studies of the adsorption of OCN and coadsorption of O and CN on Ag(001) surface. Computational Condensed Matter, 2020, 22, e00446.	0.9	7
34479	Generalized regular <mml:math xmlns:mml="http://www.w3.org/1998/Math/MathML" altimg="si36.svg"><mml:mrow><mml:mi mathvariant="bold">k</mml:mi></mml:mrow></mml:math>-point grid generation on the fly. Computational Materials Science, 2020, 173, 109340.	1.4	8
34480	On preconditioning the self-consistent field iteration in real-space Density Functional Theory. Chemical Physics Letters, 2020, 739, 136983.	1.2	14
34481	A new intermediate phase in compressed nitinol. Journal of Alloys and Compounds, 2020, 817, 153234.	2.8	1
34482	In-situ topochemical nitridation derivative MoO2â€“Mo2N binary nanobelts as multifunctional interlayer for fast-kinetic Li-Sulfur batteries. Nano Energy, 2020, 68, 104356.	8.2	116
34483	Insights on electronic structures, elastic features and optical properties of mixed-valence double perovskites Cs2Au2X6 (X=F, Cl, Br, I). Physics Letters, Section A: General, Atomic and Solid State Physics, 2020, 384, 126169.	0.9	32
34484	Structural and electrical properties of CeO2 monolayers using first-principles calculations. Solid State Communications, 2020, 307, 113801.	0.9	12

#	Article	IF	Citations
34485	Experimental and DFT studies of the role of H2S in Hg0 removal from syngas over CuMn2O4 sorbent. Chemical Engineering Journal, 2020, 391, 123616.	6.6	39
34486	AICON: A program for calculating thermal conductivity quickly and accurately. Computer Physics Communications, 2020, 251, 107074.	3.0	20
34487	Diffusion coefficient and electrochemical performance of NaVO3 anode in Li/Na batteries. Electrochimica Acta, 2020, 331, 135293.	2.6	48
34488	Iron-rich carbonates stabilized by magnetic entropy at lower mantle conditions. Earth and Planetary Science Letters, 2020, 531, 115959.	1.8	12
34489	Rational synthesis of Cr0.5Nb24.5O62 microspheres as high-rate electrodes for lithium ion batteries. Journal of Colloid and Interface Science, 2020, 562, 511-517.	5.0	25
34490	Strain-controllable ferromagnetism in Mn-doped AlP semiconductor with constant visible light absorption. Journal of Physics and Chemistry of Solids, 2020, 138, 109274.	1.9	1
34491	Low temperature study of the structural stability, electronic and optical properties of the acanthite Î±-Ag2S: Spin-orbit coupling effects and new important ultra-refraction property. Materials Science in Semiconductor Processing, 2020, 107, 104801.	1.9	11
34492	Oxygen/sulfur decorated 2D MXene V2C for promising lithium ion battery anodes. Materials Today Communications, 2020, 22, 100713.	0.9	27
34493	Electronic structure theory of unusually matched BAs1-xPx alloys using high-throughput ab-initio computation. Physica B: Condensed Matter, 2020, 579, 411901.	1.3	1
34494	Coverage-Dependent Adsorption of Phenol on Pt(111) from First Principles. Journal of Physical Chemistry C, 2020, 124, 356-362.	1.5	12
34495	Phase transitions in Fe₃Al-based alloys: ab initio study. Phase Transitions, 2020, 93, 43-53.	0.6	1
34496	Single Fe atoms confined in two-dimensional MoS2 for sulfite activation: A biomimetic approach towards efficient radical generation. Applied Catalysis B: Environmental, 2020, 268, 118459.	10.8	86
34497	Solar-driven efficient methane catalytic oxidation over epitaxial ZnO/La0.8Sr0.2CoO3 heterojunctions. Applied Catalysis B: Environmental, 2020, 265, 118469.	10.8	44
34498	Tuning the electronic and optical properties of Type-I PbI2/Î±-tellurene van der Waals heterostructure via biaxial strain and external electric field. Applied Surface Science, 2020, 508, 144824.	3.1	49
34499	C568: A new two-dimensional sp2-sp3 hybridized allotrope of carbon. Carbon, 2020, 158, 827-835.	5.4	62
34500	Hydrogen on graphene with low amplitude ripples: First-principles calculations. Chemical Physics, 2020, 530, 110608.	0.9	9
34501	PyProcar: A Python library for electronic structure pre/post-processing. Computer Physics Communications, 2020, 251, 107080.	3.0	180
34502	Exploring adsorption behavior of ethylene dichloride and dibromide vapors on blue phosphorene nanosheets: A first-principles acumens. Journal of Molecular Graphics and Modelling, 2020, 95, 107505.	1.3	22

#	Article	IF	Citations
34503	Electronic and optical properties of Tl4GeX3 (X = S, Se and Te) compounds for optoelectronics applications: insights from DFT-computations. Journal of Materials Research and Technology, 2020, 9, 413-420.	2.6	6
34504	Adsorption of Bi adatom on InAs (001) â€“ Î²2 (2 Ã— 4) and Î±2 (2 Ã— 4) surface: A first principles study. Materials Science in Semiconductor Processing, 2020, 107, 104856.	1.9	3
34505	Zero-point vibration of the adsorbed hydrogen on the Pt(110) surface. Adsorption, 2020, 26, 453-459.	1.4	6
34506	NaV6O15: A promising cathode material for insertion/extraction of Mg2+ with excellent cycling performance. Nano Research, 2020, 13, 335-343.	5.8	28
34507	HCOOH dissociation over the core-shell M@Pd bimetallic catalysts: Probe into the effect of the core metal type on the catalytic performance. Applied Surface Science, 2020, 506, 144938.	3.1	13
34508	Non-covalently self-assembled organic molecules graphene aerogels to enhance supercapacitive performance. Applied Surface Science, 2020, 508, 145192.	3.1	24
34509	Ferromagnetic property of copper doped ZnO: A first-principles study. Computational Condensed Matter, 2020, 23, e00455.	0.9	6
34510	Relative Stability of Near-Surface Oxygen Vacancies at the CeO₂(111) Surface upon Zirconium Doping. Journal of Physical Chemistry C, 2020, 124, 625-638.	1.5	16
34511	Facile Combined Experimental and Computational Study: g-C₃N₄@PDMS-Assisted Knoevenagel Condensation Reaction under Phase Transfer Conditions. ACS Sustainable Chemistry and Engineering, 2020, 8, 2350-2360.	3.2	12
34512	The intrinsic magnetism, quantum anomalous Hall effect and Curie temperature in 2D transition metal trihalides. Physical Chemistry Chemical Physics, 2020, 22, 2429-2436.	1.3	42
34513	Anomalous lattice thermal conductivity in layered MNCl (M = Zr, Hf) materials driven by lanthanide contraction. Journal of Materials Chemistry A, 2020, 8, 3128-3134.	5.2	14
34514	Two-dimensional graphitic carbon nitride (g-C4N3) for superior selectivity of multiple toxic gases (CO, NO2, and NH3). Nanotechnology, 2020, 31, 145501.	1.3	19
34515	Coherently coupled quantum-well states in bimetallic Pb/Ag thin films. Physical Review B, 2020, 102, .	1.1	1
34516	Localized dimers drive strong anharmonicity and low lattice thermal conductivity in <mml:math xmlns:mml="http://www.w3.org/1998/Math/MathML"><mml:mrow><mml:mi>Zn</mml:mi><mml:msub><mml:mi>Sn</mml:mi></mml:msub><mml:mn></mml:mn></mml:mrow></mml:math> Physical Review B, 2020, 102, .	1.1	11
34517	Theoretical studies on electronic properties of a new carbon allotrope with paring of pentagonal and heptagonal rings. European Physical Journal Plus, 2020, 135, 1.	1.2	3
34518	Elastic, Mechanical, and Phonon Behavior of Orpiment Arsenic Trisulfide under Pressure. International Journal of Photoenergy, 2020, 2020, 1-6.	1.4	0
34519	First Principles Density Functional Theory Prediction of the Crystal Structure and the Elastic Properties of Mo2ZrB2 and Mo2HfB2. Crystals, 2020, 10, 865.	1.0	4
34520	Calculating Study on Properties of Al (111)/6H-SiC (0001) Interfaces. Metals, 2020, 10, 1197.	1.0	8

#	Article	IF	Citations
34521	Atomic Structure, Electronic and Mechanical Properties of Pyrophyllite under Pressure: A First-Principles Study. Minerals (Basel, Switzerland), 2020, 10, 778.	0.8	9
34522	Highâ€Throughput Computational Characterization of 2D Compositionally Complex Transitionâ€Metal Chalcogenide Alloys. Advanced Theory and Simulations, 2020, 3, 2000195.	1.3	11
34523	Density Functional Theory and Thermodynamics Modeling of Inner-Sphere Oxyanion Adsorption on the Hydroxylated Î±-Al₂O₃(001) Surface. Langmuir, 2020, 36, 13166-13180.	1.6	19
34524	Pnictogens Allotropy and Phase Transformation during van der Waals Growth. Nano Letters, 2020, 20, 8258-8266.	4.5	7
34525	Design of iso-material heterostructures of TiO₂via seed mediated growth and arrested phase transitions. Physical Chemistry Chemical Physics, 2020, 22, 25366-25379.	1.3	4
34526	Theoretical study of Sn and Te adsorption over graphene from ab initio calculations. AIP Advances, 2020, 10, 105313.	0.6	0
34527	Electrical resistivity of atomically smooth single-crystal Cu films. Physical Review B, 2020, 102, .	1.1	4
34528	Multiple robust Dirac states in hexagonal lattice induced by <mml:math xmlns:mml="http://www.w3.org/1998/Math/MathML"><mml:mi>p</mml:mi><mml:mo>â^'</mml:mo><mml:mi>d</mml:mi></mml:ma electron-counting rule and bilayer stacking. Physical Review B, 2020, 102, .	1.1	4
34529	Mayenite Electrides and Their Doped Forms for Oxygen Reduction Reaction in Solid Oxide Fuel Cells. Energies, 2020, 13, 4978.	1.6	0
34530	Insights of the anionic redox in P2â€“Na0.67Ni0.33Mn0.67O2. Nano Energy, 2020, 78, 105285.	8.2	49
34531	Tuning Sn3O4 for CO2 reduction to formate with ultra-high current density. Nano Energy, 2020, 77, 105296.	8.2	65
34532	Application of Nuclear Inelastic Scattering Spectroscopy to the Frequency Scale Calibration of Ab Initio Calculated Phonon Density of States of Quasi-One-Dimensional Ternary Iron Chalcogenide RbFeSe2. Applied Sciences (Switzerland), 2020, 10, 7212.	1.3	2
34533	The Mobile and Pinned Grain Boundaries in 2D Monoclinic Rhenium Disulfide. Advanced Science, 2020, 7, 2001742.	5.6	15
34534	Structural and spin state transition in the polar NiO(1 1 1) surface. Applied Surface Science, 2020, 532, 147427.	3.1	11
34535	A type-II GaSe/HfS2 van der Waals heterostructure as promising photocatalyst with high carrier mobility. Applied Surface Science, 2020, 534, 147607.	3.1	97
34536	First-principles study of FeNi1-xCrx (0â‰xâ‰1) disordered alloys from special quasirandom structures. Calphad: Computer Coupling of Phase Diagrams and Thermochemistry, 2020, 71, 102007.	0.7	7
34537	First-principles-only CALPHAD phase diagram of the solid aluminium-nickel (Al-Ni) system. Calphad: Computer Coupling of Phase Diagrams and Thermochemistry, 2020, 71, 102008.	0.7	10
34538	Density functional investigation of boron incorporation in silicon-vacancy complexes. Diamond and Related Materials, 2020, 109, 108016.	1.8	1

#	Article	IF	Citations
34539	Theoretical and experimental study of reversible intercalation of Li ions in the Jarosite NaFe3(SO4)2(OH)6 structure. Electrochimica Acta, 2020, 359, 136950.	2.6	6
34540	Platinum doped iron carbide for the hydrogen evolution reaction: The effects of charge transfer and magnetic moment by first-principles approach. International Journal of Hydrogen Energy, 2020, 45, 31825-31840.	3.8	16
34541	Mechanism study on CO2 reforming of methane over platinum cluster doped graphene: A DFT calculation. Molecular Catalysis, 2020, 497, 111205.	1.0	8
34542	Elastic behaviour and radiation tolerance in Nb-based 211 MAX phases. Materials Today Communications, 2020, 25, 101499.	0.9	10
34543	Harvesting vibration energy to piezo-catalytically generate hydrogen through Bi2WO6 layered-perovskite. Nano Energy, 2020, 78, 105351.	8.2	99
34544	Poly-p-phenylenes as Novel Bulk-type Anode Materials for Potassium-Ion Batteries: A First-Principles Study. Journal of Physical Chemistry C, 2020, 124, 23045-23051.	1.5	6
34545	Edge Influence on Charge Carrier Localization and Lifetime in CH₃NH₃PbBr₃ Perovskite: Ab Initio Quantum Dynamics Simulation. Journal of Physical Chemistry Letters, 2020, 11, 9100-9109.	2.1	39
34546	Identifying Native Point Defects in the Topological Insulator Bi₂Te₃. ACS Nano, 2020, 14, 13172-13179.	7.3	31
34547	The role of adsorbed hydroxide in hydrogen evolution reaction kinetics on modified platinum. Nature Energy, 2020, 5, 891-899.	19.8	400
34548	2D van der Waals heterostructures of graphitic BCN as direct Z-scheme photocatalysts for overall water splitting: the role of polar Ï€-conjugated moieties. Physical Chemistry Chemical Physics, 2020, 22, 23735-23742.	1.3	16
34549	Modulation of band alignment with water redox potentials by biaxial strain on orthorhombic NaTaO₃ thin films. Physical Chemistry Chemical Physics, 2020, 22, 23810-23815.	1.3	5
34550	Waterâ€“gas shift reaction co-catalyzed by polyoxometalate (POM)â€“gold composites: the â€œmagicâ€•role of POMs. Catalysis Science and Technology, 2020, 10, 8219-8229.	2.1	8
34551	Justification of crystal stability and origin of transport properties in ternary half-Heusler ScPtBi. RSC Advances, 2020, 10, 37482-37488.	1.7	10
34552	Prediction of improved thermoelectric performance by ordering in double half-Heusler materials. Journal of Materials Chemistry A, 2020, 8, 23590-23598.	5.2	29
34553	Design principles for self-forming interfaces enabling stable lithium-metal anodes. Proceedings of the National Academy of Sciences of the United States of America, 2020, 117, 27195-27203.	3.3	44
34554	Toughening a superstrong carbon crystal: Sequential bond-breaking mechanisms. Physical Review B, 2020, 102, .	1.1	8
34555	Charge density wave instability and pressure-induced superconductivity in bulk <mml:math xmlns:mml="http://www.w3.org/1998/Math/MathML"><mml:mrow><mml:mn>1</mml:mn><mml:mi>T</mml:mi><mml:mo>â^’</mml:mo><mml:mathvariant="normal">S</mml:mi><mml:mn>2</mml:mn></mml:msub></mml:mrow></mml:math>. Physical Review B, 2020, 102, .	1.1	27
34556	Three-dimensional Weyl hourglass networks in the nonsymmorphic half-metal <mml:math xmlns:mml="http://www.w3.org/1998/Math/MathML"><mml:mrow><mml:msub><mml:mi>Mg</mml:mi><mml:mn>2</mml:mn></mml:msub></mml:mrow></mml:math>. Physical Review B, 2020, 102, .	1.1	31

#	Article	IF	Citations
34557	Raman spectroscopy polarization dependence analysis in two-dimensional gallium sulfide. Physical Review B, 2020, 102, .	1.1	16
34558	Elastic properties and electronic structure of tetragonal KDP crystal under polishing pressures from first principles. International Journal of Modern Physics B, 2020, 34, 2050286.	1.0	5
34559	Poissonâ€™s ratio in the all-inorganic perovskite monolayers. Modern Physics Letters B, 2020, 34, 2150002.	1.0	0
34560	Substitutional impurities in monolayer hexagonal boron nitride as single-photon emitters. Nanomaterials and Nanotechnology, 2020, 10, 184798042094934.	1.2	1
34561	Quasi-smectic liquid crystal phase of octane in contact with 2D MoS2. Applied Surface Science, 2020, 533, 147386.	3.1	5
34562	First principles study of the effect of hydrogen in austenitic stainless steels and high entropy alloys. Acta Materialia, 2020, 200, 932-942.	3.8	38
34563	Electrolyte-mediated nanograin intermetallic formation enables superionic conduction and electrode stability in rechargeable batteries. Energy Storage Materials, 2020, 33, 164-172.	9.5	17
34564	AgGaTe2 â€“ The thermoelectric and solar cell material: Structure, electronic, optical, elastic and vibrational features. Infrared Physics and Technology, 2020, 111, 103476.	1.3	14
34565	Methane dry reforming on supported cobalt nanoparticles promoted by boron. Journal of Catalysis, 2020, 392, 126-134.	3.1	32
34566	Novel two-dimensional Ga(In)S1-Se as high-efficiency OER catalysts for photocatalytic water splitting. Journal of Solid State Chemistry, 2020, 292, 121730.	1.4	4
34567	Amino-functionalized MIL-101(Cr) photodegradation enhancement by sulfur-enriched copper sulfide nanoparticles: An experimental and DFT study. Journal of Molecular Liquids, 2020, 319, 114341.	2.3	22
34568	Approaching the theoretical capacity limit of Na2FeSiO4-based cathodes with fully reversible two-electron redox reaction for sodium-ion battery. Materials Today Nano, 2020, 12, 100098.	2.3	8
34569	Boosting nitrogen-doping and controlling interlayer spacing in pre-reduced graphene oxides. Nano Energy, 2020, 78, 105286.	8.2	24
34570	Direct and quasi-direct band gap silicon allotropes with low energy and strong absorption in the visible for photovoltaic applications. Results in Physics, 2020, 18, 103271.	2.0	12
34571	Intra- and Interchain Interactions in (Cu_{1/2}Au_{1/2})CN, (Ag_{1/2}Au_{1/2})CN, and (Cu_{1/3}Ag_{1/3}Au_{1/3})CN and Their Effect on One-, Two-, and Three-Dimensional Order. Inorganic Chemistry, 2020, 59, 11704-11714.	1.9	1
34572	Structural and Optical Properties of Struvite. Elucidating Structure of Infrared Spectrum in High Frequency Range. Journal of Physical Chemistry A, 2020, 124, 8668-8678.	1.1	18
34573	Bi-Doped Zirconium Alloys with Enhanced Water Oxidation Resistance. Journal of Physical Chemistry C, 2020, 124, 23116-23125.	1.5	2
34574	Experimental and theoretical determination of physical properties of Sm2Bi2Fe4O12ferromagnetic semiconductors. Journal of Materials Chemistry C, 2020, 8, 14925-14938.	2.7	9

#	Article	IF	Citations
34575	The Structure and proton conduction of inorganic acid Cs2(HSO4)(H2PO4) in molten and glass states: a molecular dynamics study. Molecular Simulation, 2020, 46, 1327-1333.	0.9	2
34576	Phonon hydrodynamics in crystalline GeTe at low temperature. Physical Review B, 2020, 102, .	1.1	8
34577	Continuous crossover from two-dimensional to one-dimensional electronic properties for metallic silicide nanowires. Physical Review B, 2020, 102, .	1.1	4
34578	Piezoelectric Electron-Phonon Interaction from AbÂInitio Dynamical Quadrupoles: Impact on Charge Transport in Wurtzite GaN. Physical Review Letters, 2020, 125, 136602.	2.9	52
34579	Properties of Bilayer Graphene Quantum Dots for Integrated Optics: An Ab Initio Study. Photonics, 2020, 7, 78.	0.9	8
34580	A₃BBi(P₂O₇)₂ (A = Rb, Cs; B = Pb, Ba): Isovalent Cation Substitution to Sustain Large Second-Harmonic Generation Responses. Chemistry of Materials, 2020, 32, 8713-8723.	3.2	73
34581	Development and application of interatomic potentials to study the stability and shear strength of Ti/TiN and Cu/TiN interfaces. Materials and Design, 2020, 196, 109123.	3.3	14
34582	Cation diffusion in polycrystalline thin films of monoclinic HfO2 deposited by atomic layer deposition. APL Materials, 2020, 8, .	2.2	7
34583	PyVibMS: a PyMOL plugin for visualizing vibrations in molecules and solids. Journal of Molecular Modeling, 2020, 26, 290.	0.8	14
34584	Theory-Guided Machine Learning Finds Geometric Structure-Property Relationships for Chemisorption on Subsurface Alloys. CheM, 2020, 6, 3100-3117.	5.8	65
34585	Ab initio molecular dynamics study of wet H2S adsorption and dissociation on Fe(100) surface. Journal of Molecular Liquids, 2020, 319, 114135.	2.3	11
34586	Role of higher-order exchange interactions for skyrmion stability. Nature Communications, 2020, 11, 4756.	5.8	59
34587	Strain-induced electronic structures, mechanical anisotropy, and piezoelectricity of transition-metal dichalcogenide monolayer CrS2. Journal of Applied Physics, 2020, 128, .	1.1	26
34588	Polarity-field driven conductivity in <mml:math xmlns:mml="http://www.w3.org/1998/Math/MathML"><mml:mrow><mml:msub><mml:mi>SrTiO</mml:mi><mml:mn>3</mml:mn></mml:msub></mml:mrow></mml:math>: A hybrid functional study. Physical Review B, 2020, 102, .	1.1	3
34589	Energy landscapes of graphene under general deformations: DFT-to-hyperelasticity upscaling. International Journal of Engineering Science, 2020, 154, 103342.	2.7	9
34590	Re-examining the silicon self-interstitial charge states and defect levels: A density functional theory and bounds analysis study. AIP Advances, 2020, 10, .	0.6	3
34591	Documenting capacity and cyclic stability enhancements in synthetic graphite potassium-ion battery anode material modified by low-energy liquid phase ball milling. Journal of Power Sources, 2020, 476, 228733.	4.0	25
34592	A highly efficient photocatalytic methanol fuel cell based on non-noble metal photoelectrodes: Study on its energy band engineering via experimental and density functional theory method. Journal of Power Sources, 2020, 478, 228756.	4.0	19

#	Article	IF	Citations
34593	Ab initio study of oxygen evolution reaction and hydrogen evolution reaction via water splitting on pure and nitrogen-doped graphene surface. Materials Today Communications, 2020, 25, 101602.	0.9	6
34594	Enabling Aqueous NiO Photocathodes by Passivating Surface Sites That Facilitate Proton-Coupled Charge Transfer. ACS Applied Energy Materials, 2020, 3, 10702-10713.	2.5	10
34595	GeSn optical gain and lasing characteristics modelling. Physical Review B, 2020, 102, .	1.1	8
34596	Interlayer energy of pyrophyllite: Implications for macroscopic friction. American Mineralogist, 2020, 105, 1204-1211.	0.9	5
34597	Investigation on elastic and thermodynamic properties of Fe25Cr20NiMnNb austenitic stainless steel at high temperatures from first principles. Computational Materials Science, 2020, 185, 109973.	1.4	6
34598	Atomic-scale studies of garnet-type Mg3Fe2Si3O12: Defect chemistry, diffusion and dopant properties. Journal of Power Sources Advances, 2020, 3, 100016.	2.6	2
34599	Insights into Copper Sulfide Formation from Cu and S K edge XAS and DFT studies. Inorganic Chemistry, 2020, 59, 15276-15288.	1.9	8
34600	Ethanol Conversion over La_{0.7}Sr_{0.3}MnO_{3â€“x}(100): Autocatalysis, Adjacent O-Vacancies, Disproportionation, and Dehydrogenation. ACS Catalysis, 2020, 10, 12920-12931.	5.5	6
34601	Electronic, vibrational, and electronâ€“phonon coupling properties in SnSe₂ and SnS₂ under pressure. Journal of Materials Chemistry C, 2020, 8, 16404-16417.	2.7	12
34602	Spinâ€“phonon coupling in NiO nanoparticle. Journal of Applied Physics, 2020, 128, .	1.1	19
34603	Correlations between first-principles calculations and electric properties of HfO2:Al2O3 alloys for metalâ€“insulatorâ€“metal (MIM) capacitor applications. Journal of Applied Physics, 2020, 128, 134101.	1.1	8
34604	Correlating structural, electronic, and magnetic properties of epitaxial VSe2 thin films. Physical Review B, 2020, 102, .	1.1	25
34605	Comparison of Sulfur Incorporation into CuInSe₂ and CuGaSe₂ Thinâ€Film Solar Absorbers. Physica Status Solidi (A) Applications and Materials Science, 2020, 217, 2000415.	0.8	5
34606	First principle calculation of mechanical stability, opto-electronic and thermo-electric properties of TaIrGeSn (0Ââ‰ÂxÂâ‰Â1) Half-Heusler alloy. Computational Condensed Matter, 2020, 25, e00511.	0.9	9
34607	Optical response functions and thermodynamic stability of BSb1-xNx ternary alloys in zinc blende structure. Optik, 2020, 222, 165472.	1.4	3
34608	Prediction of Highly Selective Electrocatalytic Nitrogen Reduction at Low Overpotential on a Mo-Doped g-GaN Monolayer. ACS Catalysis, 2020, 10, 12841-12857.	5.5	92
34609	A two-dimensional conductive Mo-based covalent organic framework as an efficient electrocatalyst for nitrogen fixation. Journal of Materials Chemistry A, 2020, 8, 23599-23606.	5.2	54
34610	Chemical short-range order in derivative Crâ€“Taâ€“Tiâ€“Vâ€“W high entropy alloys from the first-principles thermodynamic study. Physical Chemistry Chemical Physics, 2020, 22, 23929-23951.	1.3	45

#	Article	IF	Citations
34611	Ag5-induced stabilization of multiple surface polarons on perfect and reduced TiO2 rutile (110). Journal of Chemical Physics, 2020, 153, 164702.	1.2	14
34612	Insights into negative differential resistance in <mml:math xmlns:mml="http://www.w3.org/1998/Math/MathML"><mml:msub><mml:mi>MoS</mml:mi><mml:mn>2</mml:mn></mml:msub></mml Esaki diodes: A first-principles perspective. Physical Review B, 2020, 102, .	1.1	9
34613	Role of Câ€Defective Sites in CO Adsorption over Ïµâ€Fe 2 C and Î·â€Fe 2 C Fischerâ€Tropsch Catalysts. Chemistry - an Asian Journal, 2020, 15, 4014-4022.	1.7	9
34614	Structural, electronic, magnetic and half-metallic properties of cubic perovskites NaBeO3 and KBeO3 using PBE-GGA and TB-mBJ approach: A DFT perspective. Applied Physics A: Materials Science and Processing, 2020, 126, 1.	1.1	16
34615	Identifying Trends in the Field Ionization of Diatomic Molecules over Adsorbate Covered Pd(331) Surfaces. Topics in Catalysis, 2020, 63, 1510-1521.	1.3	0
34616	Why it is S-rich around Mo atom in the nitrogenase: A DFT investigation. Applied Surface Science, 2020, 534, 147595.	3.1	16
34617	Ba(MoO₂F)₂(XO₃)₂ (X = Se and Te): First Cases of Noncentrosymmetric Fluorinated Molybdenum Oxide Selenite/Tellurite Through Unary Substitution for Enlarging Band Gaps and Second Harmonic Generation. ACS Applied Materials & Interfaces, 2020, 12, 49812-49821.	4.0	25
34618	Long-Range Spin-Selective Transport in Chiral Metalâ€“Organic Crystals with Temperature-Activated Magnetization. ACS Nano, 2020, 14, 16624-16633.	7.3	51
34619	The structure of metallic melts in binary homogenous alloys: a thermodynamical understanding from the Wulff cluster model. Physical Chemistry Chemical Physics, 2020, 22, 23237-23245.	1.3	9
34620	Novel benzothiazole half-squaraines: model chromophores to study dyeâ€“TiO₂interactions in dye-sensitized solar cells. Journal of Materials Chemistry A, 2020, 8, 22191-22205.	5.2	4
34621	Perovskite Termination-Dependent Charge Transport Behaviors of the CsPbI₃/Black Phosphorus van der Waals Heterostructure*. Chinese Physics Letters, 2020, 37, 107301.	1.3	8
34622	Novel sulfur hydrides synthesized at extreme conditions. Physical Review B, 2020, 102, .	1.1	26
34623	Asymmetric modification of the magnetic proximity effect in Pt/Co/Pt trilayers by the insertion of a Ta buffer layer. Physical Review B, 2020, 102, .	1.1	17
34624	Tunable charge density wave in a lateral black/blue phosphorene heterostructure: A first-principles calculation. Physical Review B, 2020, 102, .	1.1	5
34625	First-principle study on ScAl₃C₃-type LaCd₃P₃ phases under high pressure. Modern Physics Letters B, 2020, 34, 2050347.	1.0	1
34626	Unraveling the Suppression of Oxygen Octahedra Rotations in <mml:math xmlns:mml="http://www.w3.org/1998/Math/MathML" display="inline"><mml:msub><mml:mi>A</mml:mi><mml:mn>3</mml:mn></mml:msub><mml:msub><mml:mi>B</mml:mi><mml:mi>2</mml:mi><mml:mn mathvariant="normal">O</mml:mi><mml:mn>7</mml:mn></mml:msub></mml:math> Ruddlesden-Popper Compounds: Engineering Multiferroicity and Beyond. Physical Review Letters, 2020, 125, 157601.	2.9	22
34627	First Principles Study of Bonding Mechanisms at the TiAl/TiO2 Interface. Metals, 2020, 10, 1298.	1.0	11
34628	Contribution of the Multiplicity Fluctuation in the Temperature Dependence of Phonon Spectra of Rare-Earth Cobaltites. Molecules, 2020, 25, 4316.	1.7	1

#	Article	IF	Citations
34629	Excitonic effects in the optoelectronic properties of graphene-like BC monolayer. Optical Materials, 2020, 110, 110476.	1.7	19
34630	Quantum size effect in conductive properties of silver nanofilms. Thin Solid Films, 2020, 710, 138263.	0.8	9
34631	Understanding the Structureâ€“Performance Relationship of Lithium-Rich Cathode Materials from an Oxygen-Vacancy Perspective. ACS Applied Materials & Interfaces, 2020, 12, 47655-47666.	4.0	44
34632	Monitoring the multiphasic evolution of bismuth telluride nanoplatelets. CrystEngComm, 2020, 22, 7918-7928.	1.3	5
34633	Two-dimensional stable Fe-based ferromagnetic semiconductors: FeI₃ and FeI_{1.5}Cl_{1.5} monolayers. Physical Chemistry Chemical Physics, 2020, 22, 24506-24515.	1.3	13
34634	First-principles investigations on the anisotropic elasticity and thermodynamic properties of U₃Si₂â€“Al. RSC Advances, 2020, 10, 35049-35056.	1.7	9
34635	Machine learning formation enthalpies of intermetallics. Journal of Applied Physics, 2020, 128, .	1.1	17
34636	Tuning the electronic properties and band gap engineering in stanene monolayers via codoping of Mn and Al/P/Ga/As atoms: A DFT study. Computational and Theoretical Chemistry, 2020, 1188, 112939.	1.1	4
34637	A novel layered birnessite-type sodium molybdate as dual-ion electrodes for high capacity battery. Electrochimica Acta, 2020, 363, 137229.	2.6	10
34638	Raman spectra of vacancy-containing LiF: Predictions from first principles. Nuclear Instruments & Methods in Physics Research B, 2020, 480, 33-37.	0.6	6
34639	First-principles study on sodium storage properties of beryllium and boron dual-doped graphyne. Surface Science, 2020, 702, 121721.	0.8	7
34640	Crystal structures and elastic properties of Ti(Cu,Pt)2 and Ti(Cu,Pt)3 phases. Transactions of Nonferrous Metals Society of China, 2020, 30, 1839-1848.	1.7	9
34641	Bromine Precursor Mediated Synthesis of Shape Controlled Cesium Bromide Nanoplatelets and Their Mechanism Study by DFT Calculation. Inorganic Chemistry, 2020, 59, 15717-15723.	1.9	1
34642	Theoretical and Experimental Studies of Ti₃C₂ MXene for Surface-Enhanced Raman Spectroscopy-Based Sensing. ACS Omega, 2020, 5, 26486-26496.	1.6	44
34643	Effects of the van der Waals Interactions on Structural and Electronic Properties of CH₃NH₃(Pb,Sn)(I,Br,Cl)₃ Halide Perovskites. ACS Omega, 2020, 5, 25723-25732.	1.6	21
34644	Influence of different ratios of Fe and N on the structural, mechanical, electronic properties of FexNy compounds: First-principles study. International Journal of Modern Physics B, 2020, 34, 2050256.	1.0	0
34645	2D Square Octagonal Molybdenum Disulfide: An Effective Anode Material for LIB/SIB Applications. Advanced Theory and Simulations, 2020, 3, 2000157.	1.3	8
34646	Vacancyâ€Induced Oxygen Reduction Activity in Janus Transition Metal Dichalcogenides. ChemElectroChem, 2020, 7, 4233-4238.	1.7	6

#	Article	IF	Citations
34647	Computational insights into the molecular mechanisms for chromium passivation of stainless-steel surfaces. Materials Today Chemistry, 2020, 17, 100298.	1.7	2
34648	Temperature dependence on dielectric properties of CdTe and ZnTe using first-principles method and experimental data. Procedia Computer Science, 2020, 174, 673-681.	1.2	2
34649	Electronic properties of the Sn1â^'xPbxO alloy and band alignment of the SnO/PbO system: a DFT study. Scientific Reports, 2020, 10, 16828.	1.6	9
34650	Thermoelectric properties of hydrogenated Sn2Bi monolayer under mechanical strain: a DFT approach. Physical Chemistry Chemical Physics, 2020, 22, 23246-23257.	1.3	10
34651	Tunable electronic properties of the dynamically stable layered mineral Pt2HgSe3 (Jacutingaite). Physical Chemistry Chemical Physics, 2020, 22, 24471-24479.	1.3	18
34652	Three-dimensional porous borocarbonitride BC₂N with negative Poisson's ratio. Journal of Materials Chemistry C, 2020, 8, 15771-15777.	2.7	5
34653	Tunable ferroelectricity and antiferromagnetism via ferroelastic switching in an FeOOH monolayer. Journal of Materials Chemistry C, 2020, 8, 13982-13989.	2.7	18
34654	ABX₃-type lead-free perovskites using superatom ions with tunable photovoltaic performances. Journal of Materials Chemistry A, 2020, 8, 21993-22000.	5.2	8
34655	Density fitting in periodic systems: Application to TDHF in diamond and oxides. Journal of Chemical Physics, 2020, 153, 064107.	1.2	8
34656	Theoretical investigation of cuprous oxide/silicon heterojunction solar cells. Optik, 2020, 223, 165534.	1.4	3
34657	Comparative study of chemically deposited CdS thin films and of the non-synthesized CdSO4 under pressure and temperature within first principles. Materials Today Communications, 2020, 25, 101518.	0.9	6
34658	Explorations of Second-Order Nonlinear Optical Materials in the Alkaline Earth Barbiturate System: Noncentrosymmetric Ca(H₃C₄N₂O₃)₂·H₂O and Centrosymmetric Sr(H₅C₈N₄O₅)₂·4H₂O. Inorganic Chemistry, 2020, 59, 15962-15968.	1.9	11
34659	High pressure chemical reactivity and structural study of the Naâ€“P and Liâ€“P systems. Journal of Materials Chemistry A, 2020, 8, 21797-21803.	5.2	5
34660	Remarkable High Thermoelectric Conversion Efficiency Materials of BeMF₃ (M = Al, Y). Advanced Theory and Simulations, 2020, 3, 2000171.	1.3	9
34661	Optical and Electronic Properties of Colloidal CdSe Quantum Rings. ACS Nano, 2020, 14, 14740-14760.	7.3	8
34662	Shaping the role of germanium vacancies in germanium telluride: metastable cubic structure stabilization, band structure modification, and stable N-type conduction. NPG Asia Materials, 2020, 12, .	3.8	32
34663	Cadmium-based ferroelectrics with the Ruddlesdenâ€“Popper and double perovskite structures: a theoretical study. Journal of Materials Chemistry C, 2020, 8, 14570-14578.	2.7	6
34664	Graphene-like boron nitride supported Irn, Pdn, and Ptn (nÂ=Â5, 6) clusters: A DFT study. Diamond and Related Materials, 2020, 110, 108110.	1.8	5

#	Article	IF	Citations
34665	Magnetic Heterostructures of Transition Metal Dichalcogenides: Antiparallel Magnetic Moments and Half-Metallic State. Journal of Physical Chemistry C, 2020, 124, 23352-23360.	1.5	3
34666	Surface coordination layer passivates oxidation of copper. Nature, 2020, 586, 390-394.	13.7	154
34667	Effects of native defects and cerium impurity on the monoclinic BiVO₄ photocatalyst obtained via PBE+U calculations. Physical Chemistry Chemical Physics, 2020, 22, 25297-25305.	1.3	17
34668	Origin of off-stoichiometry and electrical benignity at the grain boundaries in CuInSe2: A first-principles study. Journal of Applied Physics, 2020, 128, 145702.	1.1	0
34669	Lattice dynamics in improper ferroelectric YGaO₃. Ferroelectrics, 2020, 567, 28-36.	0.3	0
34670	Effect of Magnetic Field Annealing on Magnetic Properties of Ironâ€“Gallium Alloys. Physics of the Solid State, 2020, 62, 1746-1754.	0.2	5
34671	Optical and Magnetic Properties of Oxygen-Deficient Ba2MMoO6âˆ’Î¼ (M=Mn, Fe and Î¼=0, 0.5, 1.0) in a Monoclinic Phase: A First-Principles Study. Spin, 2020, 10, 2050023.	0.6	5
34672	Î²â€²CsCu₅Se₃: A Promising Thermoelectric Material going beyond Photovoltaic Application. Advanced Theory and Simulations, 2020, 3, 2000169.	1.3	8
34673	Hydrazine decomposition on nickel-embedded graphene. International Journal of Hydrogen Energy, 2020, 45, 33407-33418.	3.8	9
34674	Manipulating the electronic properties of CNT by doping metal. Materials Science and Engineering B: Solid-State Materials for Advanced Technology, 2020, 262, 114803.	1.7	4
34675	Electronic and optical properties of mercury-containing borate. Optical Materials, 2020, 108, 110192.	1.7	2
34676	Investigation on structural stability of as-cast Al0.5CrCuFeMnTi high entropy alloy. Vacuum, 2020, 182, 109686.	1.6	9
34677	Elucidating the Improved Electrolyte Stability with Novel Benzimidazole Salt on the Li Anode Surface: Insights into Interfacial Reactions. Journal of Physical Chemistry C, 2020, 124, 23523-23531.	1.5	8
34678	Theoretical Prediction and Synthesis of a Family of Atomic Laminate Metal Borides with In-Plane Chemical Ordering. Journal of the American Chemical Society, 2020, 142, 18583-18591.	6.6	55
34679	Light-induced irreversible structural phase transition in trilayer graphene. Light: Science and Applications, 2020, 9, 174.	7.7	40
34680	Quantum transport evidence of Weyl fermions in an epitaxial ferromagnetic oxide. Nature Communications, 2020, 11, 4969.	5.8	71
34681	Single crystalline quaternary sulfide nanobelts for efficient solar-to-hydrogen conversion. Nature Communications, 2020, 11, 5194.	5.8	64
34682	Dimethyl and ethyl methyl ether adsorption studies on Î²-antimonene nanosheets â€“ a first-principles study. Molecular Simulation, 2020, 46, 1354-1361.	0.9	17

#	Article	IF	Citations
34683	First-principles calculations of structural, elastic and electronic properties of (TaNb)0.67(HfZrTi)0.33 high-entropy alloy under high pressure. International Journal of Minerals, Metallurgy and Materials, 2020, 27, 1405-1414.	2.4	12
34684	The structural phase transition of ammonia borane under high pressure. International Journal of Hydrogen Energy, 2020, 45, 33047-33058.	3.8	6
34685	DFT+U study of CO2 reduction and CO oxidation on a reconstructed CeO2â˜(110) facet. Materials Today Advances, 2020, 8, 100111.	2.5	8
34686	Elucidating Stressâ€“Strain Relations of ZrB₁₂ from First-Principles Studies. Journal of Physical Chemistry Letters, 2020, 11, 9165-9170.	2.1	97
34687	The heterogeneous nucleation of threading dislocations on partial dislocations in III-nitride epilayers. Scientific Reports, 2020, 10, 17371.	1.6	12
34688	Oxygen vacancies induced photoluminescence in $$hbox {SrZnO}_2$$ nanophosphors probed by theoretical and experimental analysis. Scientific Reports, 2020, 10, 17364.	1.6	8
34689	Half-filled intermediate bands in doped inorganic perovskites for solar cells. Physical Chemistry Chemical Physics, 2020, 22, 23804-23809.	1.3	9
34690	Highly qualified InP based QDs through a temperature controlled ZnSe shell coating process and their DFT calculations. Nanoscale Advances, 2020, 2, 5615-5622.	2.2	6
34691	A structure and activity relationship for single-walled carbon nanotube growth confirmed by in situ observations and modeling. Nanoscale, 2020, 12, 21923-21931.	2.8	9
34692	What is the better choice for Pd cocatalysts for photocatalytic reduction of CO₂ to renewable fuels: high-crystallinity or amorphous?. Journal of Materials Chemistry A, 2020, 8, 21208-21218.	5.2	23
34693	Explainable and trustworthy artificial intelligence for correctable modeling in chemical sciences. Science Advances, 2020, 6, .	4.7	26
34694	Octahedral Coordinated Trivalent Cobalt Enriched Multimetal Oxygenâ€Evolution Catalysts. Advanced Energy Materials, 2020, 10, 2002593.	10.2	47
34695	Thermoelectric and Plasmonic Properties of Metal Nanoparticles Linked by Conductive Molecular Bridges. Physica Status Solidi (B): Basic Research, 2020, 257, 2000249.	0.7	6
34696	Electrical and Optical Properties of Beryllium Deep Acceptors in GaN. Journal of Electronic Materials, 2020, 49, 7472-7478.	1.0	1
34697	Effect of stress on vacancy formation and diffusion in fcc systems: Comparison between DFT calculations and elasticity theory. Acta Materialia, 2020, 200, 869-882.	3.8	18
34698	Theoretical study of the adsorption behaviors of gas molecules on the Au-functionalized MoS2 nanosheets: A search for highly efficient gas sensors. Computational and Theoretical Chemistry, 2020, 1188, 112935.	1.1	9
34699	Insights into solid-state properties of dopamine and L-Dopa hydrochloride crystals through DFT calculations. Chemical Physics Letters, 2020, 761, 138033.	1.2	7
34700	First-principles studies in Mg-based hydrogen storage Materials: A review. Energy, 2020, 211, 118959.	4.5	60

#	Article	IF	Citations
34701	Dual redox-active copper hexacyanoferrate nanosheets as cathode materials for advanced sodium-ion batteries. Energy Storage Materials, 2020, 33, 432-441.	9.5	43
34702	Exploring the initial oxidation of Pt, Pt3Ni, Pt3Au (111) surfaces: a genetic algorithm based global optimization with density functional theory. Green Chemical Engineering, 2020, 1, 56-62.	3.3	10
34703	DFT study of the hydrogen adsorption and storage on Ni4 cluster embedded in multivacancy graphene. International Journal of Hydrogen Energy, 2020, 45, 30805-30817.	3.8	21
34704	Effect of active site and charge transfer on methane dehydrogenation over different Co doped Ni surfaces by density functional theory. International Journal of Hydrogen Energy, 2020, 45, 31849-31862.	3.8	22
34705	Structural parameters and optical spectra of Zn1-xCoxO ternary alloys with zinc-blende, rocksalt and wurtzite phases. Optik, 2020, 224, 165732.	1.4	3
34706	A DFT-D2 study on the adsorption of phosgene derivatives and chloromethyl chloroformate on pristine and Fe4-decorated graphene. Journal of Molecular Graphics and Modelling, 2020, 101, 107754.	1.3	12
34707	Potential of porous nodal-line semi-metallic carbon for sodium-ion battery anode. Journal of Power Sources, 2020, 478, 228746.	4.0	14
34708	Enhanced solar light driven hydrogen generation and environment remediation through Nd incorporated ZnIn2S4. Renewable Energy, 2020, 162, 2031-2040.	4.3	16
34709	DFT coupled with NEGF study of structural, electronic and transport properties of two-dimensional InOBr. Vacuum, 2020, 182, 109745.	1.6	1
34710	First-Principles Calculation Study of Na⁺ Superionic Conduction Mechanism in W- and Mo-Doped Na₃SbS₄ Solid Electrolytes. Chemistry of Materials, 2020, 32, 8373-8381.	3.2	33
34711	Lattice Thermal Transport in Monolayer Group 13 Monochalcogenides MX (M = Ga, In; X = S, Se, Te): Interplay of Atomic Mass, Harmonicity, and Lone-Pair-Induced Anharmonicity. Inorganic Chemistry, 2020, 59, 14899-14909.	1.9	21
34712	Dinitrogen as a Universal Electron Acceptor in Solid-State Chemistry: An Example of Uncommon Metallic Compounds Na₃(N₂)₄ and NaN₂. Inorganic Chemistry, 2020, 59, 14819-14826.	1.9	20
34713	Design and Precursor-based Solid-State Synthesis of Mixed-Linker Zr-MIL-140A. Inorganic Chemistry, 2020, 59, 15250-15261.	1.9	4
34714	Solvation Free Energies and Adsorption Energies at the Metal/Water Interface from Hybrid Quantum-Mechanical/Molecular Mechanics Simulations. Journal of Chemical Theory and Computation, 2020, 16, 6539-6549.	2.3	34
34715	DFT Study on the Hydrogenation of CO₂ to Methanol on Ho-Doped Cu(211) Surface. Journal of Physical Chemistry C, 2020, 124, 22426-22434.	1.5	13
34716	Understanding and Improving the Kinetics of Bulk Carbonation on Sodium Carbonate. Journal of Physical Chemistry C, 2020, 124, 23106-23115.	1.5	5
34717	Tailoring the Electronic and Magnetic Properties of Hematene by Surface Passivation: Insights from First-Principles Calculations. Journal of Physical Chemistry C, 2020, 124, 22784-22792.	1.5	12
34718	How Do the Coadsorbates Affect the Oxygen Reduction Reaction Activity of Undoped and N-Doped Graphene Nanoribbon Edges? A Density Functional Theory Study. Journal of Physical Chemistry C, 2020, 124, 23177-23189.	1.5	6

#	Article	IF	Citations
34719	Can Single Metal Atoms Trapped in Defective h-BN/Cu(111) Improve Electrocatalysis of the H₂ Evolution Reaction?. Journal of Physical Chemistry C, 2020, 124, 23690-23698.	1.5	6
34720	Dynamics of H₂O Adsorption on Pt(110)-(1 Ã— 2) Based on a Neural Network Potential Energy Surface. Journal of Physical Chemistry C, 2020, 124, 23190-23199.	1.5	16
34721	Electrochemical N₂ Reduction to Ammonia Using Single Au/Fe Atoms Supported on Nitrogen-Doped Porous Carbon. ACS Applied Energy Materials, 2020, 3, 10061-10069.	2.5	40
34722	How PM2.5 Affects Pt-Catalyzed Oxygen Reduction Reaction. ACS Sustainable Chemistry and Engineering, 2020, 8, 9385-9392.	3.2	5
34723	Inhibition of oxygen dimerization by local symmetry tuning in Li-rich layered oxides for improved stability. Nature Communications, 2020, 11, 4973.	5.8	66
34724	High-power lithiumâ€“selenium batteries enabled by atomic cobalt electrocatalyst in hollow carbon cathode. Nature Communications, 2020, 11, 5025.	5.8	187
34725	Charge transport mechanisms in potassium superoxide. Physical Chemistry Chemical Physics, 2020, 22, 24480-24489.	1.3	6
34726	First-principles study of structural, elastic and electronic properties of naphyne and naphdiyne. RSC Advances, 2020, 10, 35349-35355.	1.7	4
34727	Two-dimensional van der Waals heterostructure CdO/PtSe₂: promising visible light photocatalyst for overall water splitting. Physical Chemistry Chemical Physics, 2020, 22, 24662-24668.	1.3	10
34728	Structural dynamics in Niâ€“Fe catalysts during CO₂ methanation â€“ role of iron oxide clusters. Catalysis Science and Technology, 2020, 10, 7542-7554.	2.1	48
34729	Tailoring nanoscale polarization patterns and transport properties in ferroelectric tunnel junctions by octahedral tilts in electrodes. RSC Advances, 2020, 10, 35367-35373.	1.7	0
34730	Coordinately unsaturated metalâ€“organic framework as an unpyrolyzed bifunctional electrocatalyst for oxygen reduction and evolution reactions. Journal of Materials Chemistry A, 2020, 8, 22111-22123.	5.2	40
34731	Cmme-SnS: a two-dimensional tin sulfide nanosheet. Journal of Materials Chemistry A, 2020, 8, 21219-21226.	5.2	4
34732	Visible/infrared light-driven high-efficiency CO₂ conversion into ethane based on a Bâ€“Co synergistic catalyst. Journal of Materials Chemistry A, 2020, 8, 22327-22334.	5.2	24
34733	Phase-controlled synthesis of Ni nanocrystals with high catalytic activity in 4-nitrophenol reduction. Journal of Materials Chemistry A, 2020, 8, 22143-22154.	5.2	22
34734	Metallization of diamond. Proceedings of the National Academy of Sciences of the United States of America, 2020, 117, 24634-24639.	3.3	29
34735	Atomic modelling of carbon atom diffusion in monoclinic zirconia volume, subsurface and surface. Journal of Nuclear Materials, 2020, 537, 152193.	1.3	0
34736	Adsorption and diffusion mechanisms of silver ad-atoms on Ag and Cu (110) surfaces: A first principles study. Materials Today Communications, 2020, 25, 101461.	0.9	4

#	Article	IF	Citations
34737	Phosphorous incorporation in Pd2Sn alloys for electrocatalytic ethanol oxidation. Nano Energy, 2020, 77, 105116.	8.2	48
34738	Electric Field-Tunable Structural Phase Transitions in Monolayer Tellurium. ACS Omega, 2020, 5, 18213-18217.	1.6	11
34739	Eliminating dissolution of platinum-based electrocatalysts at the atomic scale. Nature Materials, 2020, 19, 1207-1214.	13.3	127
34740	Adsorption energy scaling relation on bimetallic magnetic surfaces: role of surface magnetic moments. Physical Chemistry Chemical Physics, 2020, 22, 17960-17968.	1.3	8
34741	Perpendicular magnetocrystalline anisotropy energy (MAE) of 111-surface slab of Fe₂CoAl. Materials Research Express, 2020, 7, 064003.	0.8	7
34742	Electronic structure beyond the generalized gradient approximation for <mml:math xmlns:mml="http://www.w3.org/1998/Math/MathML"><mml:mrow><mml:msub><mml:mi>Ni</mml:mi><mml:mn>2</mml:mn></mml:msub></mml:mrow></mml:math>. Physical Review B, 2020, 102, .	1.1	13
34743	Towards Accurate Predictions of Proton NMR Spectroscopic Parameters in Molecular Solids. ChemPhysChem, 2020, 21, 2075-2083.	1.0	14
34744	On the coordination of Mg2+ in aragonite: Ab-initio absorption spectroscopy and isotope fractionation study. Geochimica Et Cosmochimica Acta, 2020, 286, 324-335.	1.6	11
34745	Study the optical properties of XC (X = Si, Ge and Sn) nanosheets using TB-mBJ exchange-correlation potential. Optik, 2020, 206, 164351.	1.4	1
34746	Partial Electrooxidation of Glycerol on Close-Packed Transition Metal Surfaces: Insights from First-Principles Calculations. Journal of Physical Chemistry C, 2020, 124, 17907-17915.	1.5	13
34747	Stable Multifunctional Single-Atom Catalysts Resulting from the Synergistic Effect of Anchored Transition-Metal Atoms and Host Covalentâ€“Organic Frameworks. Journal of Physical Chemistry C, 2020, 124, 17675-17683.	1.5	46
34748	Tuning the Bandgap in Silver Bismuth Iodide Materials by Partly Substituting Bismuth with Antimony for Improved Solar Cell Performance. ACS Applied Energy Materials, 2020, 3, 7372-7382.	2.5	30
34749	Steaming Drived Chemical Interactions of ZnCl_x with Y Zeolite Framework, Its Regulation to Dealumination/Silicon-Healing as well as Enhanced Availability of BrÃ¸nsted Acidity. ACS Catalysis, 2020, 10, 9197-9214.	5.5	20
34750	Niobium Carbide MXenes with Broad-Band Nonlinear Optical Response and Ultrafast Carrier Dynamics. ACS Nano, 2020, 14, 10492-10502.	7.3	96
34751	Highly durable fuel cell catalysts using crosslinkable block copolymer-based carbon supports with ultralow Pt loadings. Energy and Environmental Science, 2020, 13, 4921-4929.	15.6	61
34752	Oxygen reduction reaction on Pt-skin Pt₃V(111) fuel cell cathode: a density functional theory study. RSC Advances, 2020, 10, 27346-27356.	1.7	21
34753	Structural, elastic, vibrational, thermophysical properties and pressure-induced phase transitions of ThN2, Th2N3, and Th3N4: An ab initio investigation. Journal of Applied Physics, 2020, 128, .	1.1	6
34754	Dynamic spin fluctuations in the frustrated <mml:math xmlns:mml="http://www.w3.org/1998/Math/MathML"><mml:mrow><mml:mi>A</mml:mi></mml:mrow></mml:math>-site spinel <mml:math xmlns:mml="http://www.w3.org/1998/Math/MathML"><mml:mrow><mml:mi>Cu</mml:mi><mml:msub><mml:mi>Al</mml:mi><mml:mi mathvariant="normal">O</mml:mi><mml:mn>4</mml:mn></mml:msub></mml:mrow></mml:math>. Physical Review B, 2020, 102, .	1.1	8

#	Article	IF	Citations
34755	Zinc Tin Oxide Synaptic Device for Neuromorphic Engineering. IEEE Access, 2020, 8, 130678-130686.	2.6	41
34756	First-Principles Study on PdMnSn and PtMnSn Compounds in C1b Structure. Journal of Experimental and Theoretical Physics, 2020, 130, 673-680.	0.2	2
34757	Pressure-induced structural stability of alkali trihydrides and H2-desorption occurrence: Ab initio study for hydrogen storage improvement. International Journal of Hydrogen Energy, 2020, 45, 25065-25074.	3.8	17
34758	Diiron in extended carbon networks: Magnetic properties of model Fe2C6 and Fe2C12 from first principles. Journal of Magnetism and Magnetic Materials, 2020, 514, 167213.	1.0	2
34759	Electronic and vibrational properties of TcS2 and TcS2/Stanene heterobilayer using density functional theory. Physica E: Low-Dimensional Systems and Nanostructures, 2020, 124, 114380.	1.3	2
34760	Exploring the sub-stoichiometric behavior of plutonium mononitride. RSC Advances, 2020, 10, 24877-24881.	1.7	3
34761	First-principles study of luminescence properties of the Eu-doped defect pyrochlore oxide <mml:math xmlns:mml="http://www.w3.org/1998/Math/MathML"><mml:mrow><mml:msub><mml:mi>KNbWO</mml:mi><mml:mn>6</mml:mn><mml:mathvariant="normal">H</mml:mi><mml:mn>2</mml:mn></mml:msub><mml:mi mathvariant="normal">O</mml:mi><mml:mo>:</mml:mo><mml:mn>0.125</mml:mn><mml:msup><mml:mrow><mml:mi>Eu</mml:mi> Physical Review B, 2020, 102, .	1.1	3
34762	Low-temperature insulating phase of the <mml:math xmlns:mml="http://www.w3.org/1998/Math/MathML"><mml:mi>Si</mml:mi><mml:mo>(</mml:mo><mml:mn>111</mml:mn> surface. Physical Review B, 2020, 102, .	1.1	11
34763	Intrinsic axion insulating behavior in antiferromagnetic <mml:math xmlns:mml="http://www.w3.org/1998/Math/MathML"><mml:mrow><mml:msub><mml:mi>MnBi</mml:mi><mml:mn>6</mml:mn> Physical Review B, 2020, 102, .	1.1	63
34764	Gate-Tuned Interlayer Coupling in van der Waals Ferromagnet <mml:math xmlns:mml="http://www.w3.org/1998/Math/MathML" display="inline"><mml:mrow><mml:msub><mml:mrow><mml:mi>Fe</mml:mi></mml:mrow><mml:mrow><mml:mn>3</mml:mn> Nanoflakes. Physical Review Letters, 2020, 125, 047202.	2.9	87
34765	Spatial defects nanoengineering for bipolar conductivity in MoS2. Nature Communications, 2020, 11, 3463.	5.8	41
34766	Impact of strain, pressure, and electron correlation on magnetism and crystal structure of Mn2GaC from first-principles. Scientific Reports, 2020, 10, 11384.	1.6	13
34767	Alkali ions secure hydrides for catalytic hydrogenation. Nature Catalysis, 2020, 3, 703-709.	16.1	123
34768	PtSe₂/SiH van der Waals type-II heterostructure: a high efficiency photocatalyst for water splitting. Physical Chemistry Chemical Physics, 2020, 22, 17145-17151.	1.3	36
34769	Experimental and theoretical investigation of the chemical exfoliation of Cr-based MAX phase particles. Dalton Transactions, 2020, 49, 12215-12221.	1.6	10
34770	Uncovering the origin of enhanced field emission properties of rGOâ€“MnO₂heterostructures: a synergistic experimental and computational investigation. RSC Advances, 2020, 10, 25988-25998.	1.7	9
34771	Electrically precise control of the spin polarization of electronic transport at the single-molecule level. Physical Chemistry Chemical Physics, 2020, 22, 17229-17235.	1.3	11
34772	The optimal co-doping of SrFe_{1â^'x}Co_xO_{3â^'Î´} oxygen carriers in redox applications. Physical Chemistry Chemical Physics, 2020, 22, 16721-16726.	1.3	17

#	Article	IF	Citations
34773	Cobalt vacancies assisted ion diffusion in Co₂AlO₄ carbon nanofibers for enhancing lithium battery performance. Dalton Transactions, 2020, 49, 10127-10137.	1.6	2
34774	Thermoelectric properties of n-type half-Heusler NbCoSn with heavy-element Pt substitution. Journal of Materials Chemistry A, 2020, 8, 14822-14828.	5.2	44
34775	Theoretical study of structural, electronic and lattice dynamical properties of novel AlNiP half-Heusler alloy. Philosophical Magazine, 2020, 100, 2785-2801.	0.7	15
34776	Hydrogen Transport in Tungsten for Nuclear Energy Application: Temperature Dependence and Compensation Effect. Fusion Science and Technology, 2020, 76, 616-631.	0.6	3
34777	Dependence of mechanical properties on the site occupancy of ternary alloying elements in Î³â€²-Ni3Al: Ab initio description for shear and tensile deformation. Chinese Physics B, 2020, 29, 078103.	0.7	4
34778	Biomass hydrodeoxygenation catalysts innovation from atomistic activity predictors. Philosophical Transactions Series A, Mathematical, Physical, and Engineering Sciences, 2020, 378, 20200056.	1.6	8
34779	<mml:math xmlns:mml="http://www.w3.org/1998/Math/MathML"><mml:mrow><mml:msub><mml:mi mathvariant="normal">K</mml:mi><mml:mn>2</mml:mn></mml:msub><mml:msub><mml:mi>CoS</mml:mi><mml:mn>2</mml:mn></mml:msub></mml:mrow></mml:math> : A two-dimensional in-plane antiferromagnetic insulator. Physical Review B, 2020, 102, .	1.1	3
34780	Crystal fields of lithium rare-earth tetrafluorides and multiplet splitting of the <mml:math xmlns:mml="http://www.w3.org/1998/Math/MathML"><mml:mo>+</mml:mo><mml:mn>3</mml:mn></mml:math> rare-earth ions. Physical Review B, 2020, 102, .	1.1	5
34781	Anomalous Auger Recombination in PbSe. Physical Review Letters, 2020, 125, 037401.	2.9	16
34782	Detection of N2O gas using 2D MoSe2 Monolayer: A DFT Theory. , 2020, , .		2
34783	First-principles study of the structure, elastic constants, electronic and thermodynamic properties of C15 laves phase ZrMo₂. International Journal of Modern Physics B, 2020, 34, 2050170.	1.0	0
34784	A theoretical study of the structural and electronic properties of poly(9-vinylcarbazole) interacting with small-diameter single-walled carbon nanotubes. International Journal of Computational Materials Science and Engineering, 2020, 09, 2050009.	0.5	0
34785	A Combined Experimental and First-Principle Calculation (DFT Study) for In Situ Polymer Inclusion Membrane-Assisted Growth of Metal-Organic Frameworks (MOFs). International Journal of Polymer Science, 2020, 2020, 1-12.	1.2	6
34786	Atomic-scale insights on the plate-shaped Î³â€³ phase in Mgâ€“Gdâ€“Yâ€“Agâ€“Zr alloy. Journal of Materials Research, 2020, 35, 1837-1845.	1.2	2
34787	Fast optical absorption spectra calculations for periodic solid state systems. Communications in Applied Mathematics and Computational Science, 2020, 15, 89-113.	0.7	10
34788	Highâ€Efficiency Nonfullerene Organic Solar Cells Enabled by Atomic Layer Deposited Zirconiumâ€Doped Zinc Oxide. Solar Rrl, 2020, 4, 2000241.	3.1	18
34789	Strain-induced energetic and electronic properties of stanene nanomeshes. Journal of Computational Electronics, 2020, 19, 1357-1364.	1.3	2
34790	Structural Evolution and Optical Property Tunability by Halogen Substitution in [N(CH₃)₄]MX₂ (M = Ga⁺, In⁺, X = Cl, Br): A Family of Organically Templated Metal Halides. Inorganic Chemistry, 2020, 59, 10736-10745.	1.9	6

#	Article	IF	Citations
34791	Understanding the Ionic Diffusivity in the (Meta)Stable (Un)doped Solid-State Electrolyte from First-Principles: A Case Study of LISICON. Journal of Physical Chemistry C, 2020, 124, 17485-17493.	1.5	6
34792	The stability of P2-layered sodium transition metal oxides in ambient atmospheres. Nature Communications, 2020, 11, 3544.	5.8	204
34793	Enhancing power factor of SnSe sheet with grain boundary by doping germanium or silicon. Npj Computational Materials, 2020, 6, .	3.5	9
34794	Topologically protected spin diffusion and spin generator using chalcogenide superlattices. Npj 2D Materials and Applications, 2020, 4, .	3.9	8
34795	Molybdenum defect complexes in bismuth vanadate. Physical Chemistry Chemical Physics, 2020, 22, 16277-16285.	1.3	2
34796	Unexpected bowing band evolution in an all-inorganic CsSn_{1âˆ'x}Pb_xBr₃perovskite. RSC Advances, 2020, 10, 26407-26413.	1.7	4
34797	Transferability of neural network potentials for varying stoichiometry: Phonons and thermal conductivity of MnxGey compounds. Journal of Applied Physics, 2020, 127, .	1.1	27
34798	Atomistic simulation for the interaction between dislocation and solute atoms, clusters, and associated physical insights. Journal of Applied Physics, 2020, 128, 024301.	1.1	1
34799	Giant momentum-dependent spin splitting in centrosymmetric low- <mml:math xmlns:mml="http://www.w3.org/1998/Math/MathML"><mml:mi>Z</mml:mi></mml:math> antiferromagnets. Physical Review B, 2020, 102, .	1.1	101
34800	Regulation of oxygen reduction reaction by the magnetic effect of L10-PtFe alloy. Applied Catalysis B: Environmental, 2020, 278, 119332.	10.8	34
34801	Oxygen intercalation in PVD graphene grown on copper substrates: A decoupling approach. Applied Surface Science, 2020, 529, 147100.	3.1	10
34802	Electro-optical properties of monolayer and bilayer boron-doped <mml:math xmlns:mml="http://www.w3.org/1998/Math/MathML" altimg="si1.svg"><mml:mrow><mml:msub><mml:mtext>C</mml:mtext><mml:mn>3</mml:mn></mml:msub></mml:mrow></mml:ma Tunable electronic structure via strain engineering and electric field. Carbon, 2020, 168, 220-229.	5.4	66
34803	Influence of interfacial configuration on bonding strength and wettability between CuNiTi active filler metal and AlN ceramic. Ceramics International, 2020, 46, 25705-25718.	2.3	9
34804	Transition metal (TMÂ=ÂCr, Mn, Fe, Co, Ni) doped phosphorene as anode material for lithium-ion batteries predicted from first-principle calculations. Computational Materials Science, 2020, 183, 109877.	1.4	11
34805	Bulk and monolayer As2S3 as promising thermoelectric material with high conversion performance. Computational Materials Science, 2020, 183, 109913.	1.4	24
34806	Radionuclide incorporation in negative thermal expansion <mml:math xmlns:mml="http://www.w3.org/1998/Math/MathML" altimg="si9.svg"><mml:mrow><mml:mi>Î±</mml:mi></mml:mrow></mml:math>-Zr(WO4)2: A density functional theory study. Chemical Physics Letters, 2020, 744, 137172.	1.2	1
34807	Raman, DRIFT and ATR-IR spectra, corrosion inhibition, DFT and solid-state calculations of 4-amino-3-choloro-2,5,6-trifluoropyridine. Journal of Molecular Structure, 2020, 1207, 127837.	1.8	3
34808	Atomistic simulations of the interaction of basal dislocations with Mg2Zn <mml:math xmlns:mml="http://www.w3.org/1998/Math/MathML" display="inline" id="d1e2198" altimg="si40.svg"><mml:msub><mml:mrow /><mml:mrow><mml:mn>2</mml:mn></mml:mrow></mml:msub></mml:math> precipitates in Mg alloys. Materials Science & Engineering A: Structural Materials: Properties, Microstructure and Processing, 2020, 788, 139555.	2.6	19

#	Article	IF	Citations
34809	Comprehensive first-principles calculations on physical properties of ScV2Ga4 and ZrV2Ga4 in comparison with superconducting HfV2Ga4. Materials Today Communications, 2020, 24, 100935.	0.9	23
34810	Theoretical investigations on the structural stability, structural and physical properties, and bonding feature for RuX (X = Si, Ge, Sn) with B20 and B2 phases. Materials Today Communications, 2020, 24, 101116.	0.9	2
34811	The electronic and magnetic properties of the Mo doped ZnTe alloys with different configurations. Materials Today Communications, 2020, 24, 101258.	0.9	1
34812	Half-metallicity and enhanced Curie temperature of Ti-embedded CrI3 monolayer. Materials Today Communications, 2020, 25, 101438.	0.9	5
34813	Anion-cation replacement effect in lead free tin based variant perovskites. Physica B: Condensed Matter, 2020, 595, 412345.	1.3	14
34814	New direction's piezoelectricity and new applications of two-dimensional group V-IV-III-VI films: A theoretical study. Physica E: Low-Dimensional Systems and Nanostructures, 2020, 124, 114214.	1.3	9
34815	Electronic and structural properties of novel monolayer molybdenum disulfide and boron phosphide heterostructures. Physica E: Low-Dimensional Systems and Nanostructures, 2020, 124, 114347.	1.3	1
34816	First-principles exploration of the stabilization mechanism of long-period stacking ordered structures in high performance Al alloys. Progress in Natural Science: Materials International, 2020, 30, 424-431.	1.8	9
34817	Importance of Au nanostructures in CO2 electrochemical reduction reaction. Science Bulletin, 2020, 65, 796-802.	4.3	44
34818	Efficient Conversion of CO₂to Formate Using Inexpensive and Easily Prepared Post-Transition Metal Alloy Catalysts. Energy & Fuels, 2020, 34, 3467-3476.	2.5	23
34819	Density Functional Theory Study of Elemental Mercury Immobilization on CuSe(001) Surface: Reaction Pathway and Effect of Typical Flue Gas Components. Industrial & Engineering Chemistry Research, 2020, 59, 13603-13612.	1.8	20
34820	Probing Mg Intercalation in the Tetragonal Tungsten Bronze Framework V₄Nb₁₈O₅₅. Inorganic Chemistry, 2020, 59, 9783-9797.	1.9	7
34821	Hydrogen Evolution Reaction over Single-Atom Catalysts Based on Metal Adatoms at Defected Graphene and h-BN. Journal of Physical Chemistry C, 2020, 124, 16860-16867.	1.5	32
34822	DFT-Based Cu(111)||Cu₂O(111) Model for Copper Metal Covered by Ultrathin Copper Oxide: Structure, Electronic Properties, and Reactivity. Journal of Physical Chemistry C, 2020, 124, 17048-17057.	1.5	27
34823	Thermally Induced Diffusion and Restructuring of Iron Triade (Fe, Co, Ni) Nanoparticles Passivated by Several Layers of Gold. Journal of Physical Chemistry C, 2020, 124, 16680-16688.	1.5	14
34824	Rational Design of 2D h-BAs Monolayer as Advanced Sulfur Host for High Energy Density Liâ€“S Batteries. ACS Applied Energy Materials, 2020, 3, 7306-7317.	2.5	23
34825	Expediting Hydrogen Evolution through Topological Surface States on Bi₂Te₃. ACS Catalysis, 2020, 10, 2656-2666.	5.5	48
34826	Transforming Photocatalytic gâ€C₃N₄/MoSe₂ into a Direct Zâ€Scheme System via Boronâ€Doping: A Hybrid DFT Study. ChemSusChem, 2020, 13, 4985-4993.	3.6	33

#	Article	IF	Citations
34827	Diffusion of noble gases in subduction zone hydrous minerals. Geochimica Et Cosmochimica Acta, 2020, 291, 50-61.	1.6	4
34828	Electronic Structure Modeling of Metalâ€“Organic Frameworks. Chemical Reviews, 2020, 120, 8641-8715.	23.0	149
34829	Pressureâ€“Temperature Phase Diagram of Lithium, Predicted by Embedded Atom Model Potentials. Journal of Physical Chemistry B, 2020, 124, 6015-6023.	1.2	11
34830	A polarization propagation mechanism of Fe and Cu atoms co-doped in two-dimensional-Si₃N₄. New Journal of Chemistry, 2020, 44, 14082-14086.	1.4	0
34831	A structural modeling approach to solid solutions based on the similar atomic environment. Journal of Chemical Physics, 2020, 153, 034101.	1.2	18
34832	Machine learning substitutional defect formation energies in ABO3 perovskites. Journal of Applied Physics, 2020, 128, .	1.1	21
34833	Study of a New Type of Crimped-Shape Nanotubes Cut from Bilayer Graphene with the MoirÃ© Angle Î˜ = 27.8Â°. JETP Letters, 2020, 111, 397-402.	0.4	0
34834	Effect of chemical disorder on the electronic stopping of solid solution alloys. Acta Materialia, 2020, 196, 576-583.	3.8	11
34835	Computational screening of vdWs heterostructures of BSe with MoSe2 and WSe2 as sustainable hydrogen production materials. Current Applied Physics, 2020, , .	1.1	1
34836	Optical spectra of carbon-substituted silicene: A first principle study. Optik, 2020, 218, 165247.	1.4	3
34837	Ultra-low thermal conductivity of orthorhombic CH3NH3SnI3: A first principles investigation. Journal of Solid State Chemistry, 2020, 290, 121541.	1.4	9
34838	Fluorinated co-solvent promises Li-S batteries under lean-electrolyte conditions. Materials Today, 2020, 40, 63-71.	8.3	61
34839	Ab initio study of strain and electric field dependent variation in electronic and thermoelectric properties of PdS2. Materials Today Communications, 2020, 24, 100976.	0.9	12
34840	Methane Activation on Metal-Doped (111) and (100) Ceria Surfaces with Charge-Compensating Oxygen Vacancies. Journal of Physical Chemistry C, 2020, 124, 17578-17585.	1.5	13
34841	Self-Assembled SnO₂/SnSe₂ Heterostructures: A Suitable Platform for Ultrasensitive NO₂ and H₂ Sensing. ACS Applied Materials & Interfaces, 2020, 12, 34362-34369.	4.0	44
34842	Superfine MnO₂ Nanowires with Rich Defects Toward Boosted Zinc Ion Storage Performance. ACS Applied Materials & Interfaces, 2020, 12, 34949-34958.	4.0	156
34843	Mechanistic Insights into the Solvent-Driven Adsorptive Hydrodeoxygenation of Biomass Derived Levulinate Acid/Ester to 2-Methyltetrahydrofuran over Bimetallic Cuâ€“Ni Catalysts. ACS Sustainable Chemistry and Engineering, 2020, 8, 11477-11490.	3.2	33
34844	Influence of surface hydrophilicity and hydration on the rotational relaxation of supercooled water on graphene oxide surfaces. Physical Chemistry Chemical Physics, 2020, 22, 16080-16095.	1.3	6

#	Article	IF	Citations
34845	2D BeP₂ monolayer: investigation of electronic and optical properties by driven modulated strain. RSC Advances, 2020, 10, 26804-26812.	1.7	13
34846	Intrinsic ultra-wide completely spin-polarized state realized in a new CrO₂ monolayer. Physical Chemistry Chemical Physics, 2020, 22, 17038-17041.	1.3	9
34847	Structural, elasto-mechanical and phonon-related properties of MnCrP: A DFT Study. International Journal of Modern Physics B, 2020, 34, 2050200.	1.0	2
34848	Ab-initio study of ordered IIIâ€“V antimony-based semiconductor alloys $$mathbf{GaP }_{1-x}{} mathbf{Sb} _{x} mathbf{and} AlP _{1-x}{} mathbf{Sb} _{x}$$. Pramana - Journal of Physics, 2020, 94, 1.	0.9	8
34849	Predicting the structures and properties of few-layer two-dimensional (1Â1Â0)-oriented BN nanosheets: First-principles calculations. Chemical Physics, 2020, 534, 110765.	0.9	1
34850	Systematic exploration of magnetic mechanism of La3Co29Si4B10 by first principles calculation. Computational Materials Science, 2020, 184, 109853.	1.4	1
34851	Ab initio molecular dynamics studies on the transport mechanisms of oxygen atoms in the adiabatic reaction of Al/CuO nanothermite. Chemical Physics Letters, 2020, 745, 137278.	1.2	9
34852	Tritium species diffusion on and desorption from Î³-LiAlO2 (100) surface: A first-principles investigation. Journal of Nuclear Materials, 2020, 540, 152394.	1.3	4
34853	Thermodynamic Full Landscape Searching Scheme for Identifying the Mechanism of Electrochemical Reaction: A Case Study of Oxygen Evolution on Fe- and Co-Doped Grapheneâ€“Nitrogen Sites. Journal of Physical Chemistry A, 2020, 124, 5444-5455.	1.1	1
34854	Tuning the electronic and magnetic properties of pentagraphene through the C1 vacancy. 2D Materials, 2020, 7, 045024.	2.0	6
34855	Universal description of potential energy surface of interlayer interaction in two-dimensional materials by first spatial Fourier harmonics. Physical Review B, 2020, 102, .	1.1	9
34856	Dirac materials for sub-MeV dark matter detection: New targets and improved formalism. Physical Review D, 2020, 101, .	1.6	58
34857	First-principles study of the tritium reaction and diffusion on the Î³-LiAlO2 (1Â0Â0) surface with carbon impurity. Computational Materials Science, 2020, 181, 109748.	1.4	3
34858	Pyridinic-to-graphitic conformational change of nitrogen in graphitic carbon nitride by lithium coordination during lithium plating. Energy Storage Materials, 2020, 31, 505-514.	9.5	20
34859	Nanoalloys of Metals Which Do Not Form Bulk Alloys: The Case of Agâ€“Co. Journal of Physical Chemistry A, 2020, 124, 6468-6477.	1.1	12
34860	Compressive behavior and electronic properties of ammonia ice: a first-principles study. RSC Advances, 2020, 10, 26579-26587.	1.7	4
34861	Quantum Dots of [Na₄Cs₆PbBr₄]⁸⁺, Water Stable in Zeolite X, Luminesce Sharply in the Green. Advanced Materials, 2020, 32, e2001868.	11.1	14
34862	Structural, Electronic, Magnetic, and Optical Properties of Ir2ScZ (Zâ€‰=â€‰Si, Ge, Sn) Full-Heusler Compounds: A First-Principles Study. Journal of Electronic Materials, 2020, 49, 5947-5956.	1.0	7

#	Article	IF	Citations
34863	Adsorption structure of adenine on cerium oxide. Applied Surface Science, 2020, 530, 147257.	3.1	8
34864	Adsorption of CO, NH3, NO, and NO2 on pristine and defective g-GaN: Improved gas sensing and functionalization. Applied Surface Science, 2020, 530, 147275.	3.1	94
34865	Demonstration of X-ray Thomson scattering as diagnostics for miscibility in warm dense matter. Nature Communications, 2020, 11, 2620.	5.8	27
34866	Bias-controlled plasmon switching in lithium-doped graphene on dielectric model Al2O3 substrate. Npj 2D Materials and Applications, 2020, 4, .	3.9	6
34867	High performance photocatalytic and thermoelectric two-dimensional asymmetrically ordered Janus-like MXene alloys. Materials Advances, 2020, 1, 1176-1185.	2.6	14
34868	Synergistic effects of heteroatom-decorated MXene catalysts for CO reduction reactions. Nanoscale, 2020, 12, 15880-15887.	2.8	32
34869	Chemical Sensing with Atomically Thin Platinum Templated by a 2D Insulator. Advanced Materials Interfaces, 2020, 7, 1902104.	1.9	5
34870	Rb₂[U(NH₂)₆], a Rubidium Hexaamidouranate(IV) obtained from the Reaction of UI₃ with RbNH₂ in Anhydrous Ammonia. Zeitschrift Fur Anorganische Und Allgemeine Chemie, 2020, 646, 1023-1029.	0.6	3
34871	All-Nitrogen Cages and Molecular Crystals: Topological Rules, Stability, and Pyrolysis Paths. Computation, 2020, 8, 91.	1.0	7
34872	Structure-Property Relationships of 2D Ga/In Chalcogenides. Nanomaterials, 2020, 10, 2188.	1.9	2
34873	Boosting Activity and Selectivity of CO₂ Electroreduction by Preâ€Hydridizing Pd Nanocubes. Small, 2020, 16, e2005305.	5.2	32
34874	Spectroscopic Probe Molecule Selection Using Quantum Theory, First-Principles Calculations, and Machine Learning. ACS Nano, 2020, 14, 17295-17307.	7.3	12
34875	Phononic Thermal Transport in Yttrium Hydrides Allotropes. Frontiers in Materials, 2020, 7, .	1.2	4
34876	A Proposal for a Composite with Temperature-Independent Thermophysical Properties: HfV2â€“HfV2O7. Materials, 2020, 13, 5021.	1.3	4
34877	Structural Stability, Electronic, Mechanical, Phonon, and Thermodynamic Properties of the M2GaC (M) Tj ETQq0 0 0 rgBT /Overlock 10 T	1.3	20
34878	Electron Density and Its Relation with Electronic and Optical Properties in 2D Mo/W Dichalcogenides. Nanomaterials, 2020, 10, 2221.	1.9	11
34879	A new cubic superhard large-cell carbon allotrope: c-C200. Results in Physics, 2020, 19, 103457.	2.0	8
34880	Strain tunable ferroelectricity of SnSe/SnTe van der Waals heterostructures. Superlattices and Microstructures, 2020, 148, 106728.	1.4	6

#	Article	IF	Citations
34881	Oxophilicity Drives Oxygen Transfer at a Palladiumâ€“Silver Interface for Increased CO Oxidation Activity. ACS Catalysis, 2020, 10, 13878-13889.	5.5	7
34883	An Ab-initio competitive study of adsorption mechanism of lightest alkali and halide elements towards the AlC - Monolayer. AIP Conference Proceedings, 2020, , .	0.3	2
34884	Exploring alloying effect on phase stability and mechanical properties ofÎ³â€³-Ni3Nb precipitates with first-principles calculations. Materials and Design, 2020, 196, 109174.	3.3	22
34885	Structural Study of MgyAl(8+xâ€“2y)/3O4â€“xNx (0 < x < 0.5, 0 < y < 1) Spinel Probed by X-ray Diffraction, 27Al MAS NMR, and First-Principles Calculations. Inorganic Chemistry, 2020, 59, 17009-17017.	1.9	9
34886	High-pressure phase transition, elastic properties and lattice vibration modes in Rb2S compound material. Computational Condensed Matter, 2020, 25, e00508.	0.9	2
34887	Boron interaction with D03 phase in Fe-(27â€“29)Ga alloys. Intermetallics, 2020, 126, 106938.	1.8	0
34888	Defects and light elements (Li, Be, B, C, O and F) driven d0 magnetism in InN monolayer. Vacuum, 2020, 181, 109720.	1.6	3
34889	Theoretical Screening of Single Atoms Supported on Two-Dimensional Nb₂CN₂ for Nitrogen Fixation. ACS Applied Nano Materials, 2020, 3, 11274-11281.	2.4	34
34890	First-principles exploration of oxygen vacancy impact on electronic and optical properties of ABO_{3â^'Î´} (A = La, Sr; B = Cr, Mn) perovskites. Physical Chemistry Chemical Physics, 2020, 22, 27163-27172.	1.3	28
34891	Unraveling atomic-scale lithiation mechanisms in a NiO thin film electrode. Journal of Materials Chemistry A, 2020, 8, 25198-25207.	5.2	7
34892	First principles calculations on theoretical band gap improvement of IIIA-VA zinc-blende semiconductor InAs. International Journal of Modern Physics C, 2020, 31, 2050178.	0.8	1
34893	A₂BBi₂(PO₄)₂(P₂O₇) (A = K,) Tj ETQq1 1 0.784314 rg Chemistry, 2020, 2020, 4007-4014.	1.0	6
34894	A systematic study on the electronic structure of 3d, 4d, and 5d transition metal-doped WSe2 monolayer. Superlattices and Microstructures, 2020, 148, 106746.	1.4	12
34895	Electronic Excitations in Copper Oxides: Time-Dependent Density Functional Theory Calculations with a Self-Consistent Hybrid Kernel. Journal of Physical Chemistry C, 2020, 124, 24995-25003.	1.5	10
34896	Isotopic Exchange Extends Charge Carrier Lifetime in Metal Lead Perovskites by Quantum Dynamics Simulations. Journal of Physical Chemistry Letters, 2020, 11, 10298-10305.	2.1	11
34897	Towards understanding the catalytic properties of lead-based ballistic modifiers in double base propellants. Physical Chemistry Chemical Physics, 2020, 22, 25502-25513.	1.3	8
34898	Electron Structure of Beâ€“IVâ€“P2 Crystals with a Chalcopyrite Lattice. Physics of the Solid State, 2020, 62, 2016-2023.	0.2	6
34899	Study on the mechanism of helium platelets formation at low temperatures in SiC from the perspective of atomic diffusion. Journal of Nuclear Materials, 2020, 542, 152507.	1.3	9

#	Article	IF	Citations
34900	A comparative first principles study of quantum well states in MgO barrier MTJs for STT-RAMs. Microelectronics Journal, 2020, 105, 104909.	1.1	5
34901	Reaction mechanism of Ca2Fe2O5 oxygen carrier with CO in chemical looping hydrogen production. Applied Surface Science, 2020, 534, 147583.	3.1	18
34902	Thermal conductivity of hexagonal BC₂P â€“ a first-principles study. RSC Advances, 2020, 10, 42628-42632.	1.7	7
34903	Modelling Hydrogen Embrittlement using Density Functional Theory: A theoretical approach to understanding environmentally assisted cracking in 7xxx series aluminium alloys. MATEC Web of Conferences, 2020, 326, 04006.	0.1	0
34904	Crystal Structure and Atomic Vacancy Optimized Thermoelectric Properties in Gadolinium Selenides. Chemistry of Materials, 2020, 32, 10130-10139.	3.2	36
34905	Electronic Structure and High-Temperature Thermochemistry of Oxygen-Deficient BaMO3 (M = Ti â€“ Cu) Perovskites. Journal of Physical Chemistry C, 2020, 124, 27055-27063.	1.5	4
34906	Metalated Graphyne-Based Networks as Two-Dimensional Materials: Crystallization, Topological Defects, Delocalized Electronic States, and Site-Specific Doping. ACS Nano, 2020, 14, 16887-16896.	7.3	17
34907	Oxygen Chemisorption on the Surface of an In2O3 (011) Nanocrystal. Inorganic Materials, 2020, 56, 1138-1146.	0.2	3
34908	First-principles study of binary and ternary alloys based on PdCu as oxygen reduction catalysts. Chemical Physics Letters, 2020, 758, 137932.	1.2	0
34909	2D MgF2 nanosheet as a promising candidate for thermoelectric material. Materials Today: Proceedings, 2020, , .	0.9	1
34910	Negative thermal expansion driven by acoustic phonon modes in rhombohedral Zn2GeO4. Results in Physics, 2020, 19, 103531.	2.0	11
34911	Nanopyramidal Reconstruction of Cu2O(111): A Long-Standing Surface Puzzle Solved by STM and DFT. Journal of Physical Chemistry C, 2020, 124, 26937-26943.	1.5	17
34912	First-Principles Study on the Potential of Monolayer Ti₂N as an Adsorbent for Dissolved H₂ and C₂H₂ Gases in Oil. ACS Applied Nano Materials, 2020, 3, 12346-12354.	2.4	6
34913	Hybrid Density Functional Theory Study of Native Defects and Nonmetal (C, N, S, and P) Doping in a Bi₂WO₆Photocatalyst. ACS Omega, 2020, 5, 29081-29091.	1.6	33
34914	Synthesis and characterization of a strong ferromagnetic and high hardness intermetallic compound Fe₂B. Physical Chemistry Chemical Physics, 2020, 22, 27425-27432.	1.3	15
34915	Critical assessment of Co-Cu phase diagram from first-principles calculations. Physical Review B, 2020, 102, .	1.1	2
34916	High frequency atomic tunneling yields ultralow and glass-like thermal conductivity in chalcogenide single crystals. Nature Communications, 2020, 11, 6039.	5.8	36
34917	Nuclear quadrupole resonance supported by periodic quantum calculations: a sensitive tool for precise structural characterization of short hydrogen bonds. Physical Chemistry Chemical Physics, 2020, 22, 27681-27689.	1.3	3

#	Article	IF	Citations
34918	Adsorption and sensing of CO and NH₃ on chemically modified graphene surfaces. RSC Advances, 2020, 10, 42318-42326.	1.7	17
34919	Tuning the mechanical and electronic properties and carrier mobility of phosphorene via family atom doping: a first-principles study. Journal of Materials Chemistry C, 2020, 8, 14902-14909.	2.7	14
34920	Resistive switching in Al2O3 based trilayer structure with varying parameters via experimentation and computation. AIP Advances, 2020, 10, .	0.6	2
34921	The effect of the impurities on the magnetic, electronic and optical properties of Mn5Ge3. Chinese Journal of Physics, 2020, 68, 9-18.	2.0	4
34922	Density Functional Theory Modeling of Photo-electrochemical Reactions on Semiconductors: H₂ Evolution on 3C-SiC. Journal of Physical Chemistry C, 2020, 124, 26625-26639.	1.5	9
34923	Unraveling the effect of Al doping on CO adsorption at ZnO(101Ì„0). RSC Advances, 2020, 10, 40663-40672.	1.7	10
34924	First principles study on copper and iridium co-doped SrTiO3 for shifting the optical absorption into visible region. SN Applied Sciences, 2020, 2, 1.	1.5	3
34925	Unraveling the quantum dynamics origin of high photocatalytic activity in nitrogen-doped anatase TiO₂: time-domain ab initio analysis. Journal of Materials Chemistry A, 2020, 8, 25235-25244.	5.2	19
34926	Tailoring the thermoelectric and structural properties of Cuâ€“Sn based thiospinel compounds [CuM_{1+x}Sn_{1â^'x}S₄ (M = Ti, V, Cr, Co)]. Journal of Materials Chemistry C, 2020, 8, 16368-16383.	2.7	21
34927	Impact of stacking on the optoelectronic properties of 2D ZrS2/GaS heterostructure. Materials Today: Proceedings, 2021, 47, 526-528.	0.9	9
34928	Electronic, elastic, vibrational and superconducting properties of a ternary superconductors LaIrP (P) Tj ETQq0 0 0 rgBT /Overlock 10 Tf 5	0.9	16
34929	Topological Analysis of Hydroxyquinoline Derivatives Interacting with Aluminum Cations or with an Al(111) Surface. Inorganic Chemistry, 2020, 59, 17916-17928.	1.9	2
34930	Crystal Facet-Dependent CO₂ Photoreduction over Porous ZnO Nanocatalysts. ACS Applied Materials & Interfaces, 2020, 12, 56039-56048.	4.0	52
34931	Computational Study of Janus Transition Metal Dichalcogenide Monolayers for Acetone Gas Sensing. ACS Omega, 2020, 5, 31398-31406.	1.6	29
34932	Quantifying reversible nitrogenous ligand binding to Co(<scp>ii</scp>) porphyrin receptors at the solution/solid interface and in solution. Physical Chemistry Chemical Physics, 2020, 22, 24226-24235.	1.3	6
34933	Structures and optoelectronic properties of two-dimensional MC6 (Mâ€¯=â€¯Ti and Hf) predicted by computational approaches. Materials Today Communications, 2020, 25, 101606.	0.9	0
34934	Flux Growth of Uranyl Titanates: Rare Examples of TiO₄ Tetrahedra and TiO₅ Square Bipyramids. Journal of Physical Chemistry A, 2020, 124, 9487-9495.	1.1	7
34935	Heteroatom-Doped Transition Metal Nitrides for CO Electrochemical Reduction: A Density Functional Theory Screening Study. Journal of Physical Chemistry C, 2020, 124, 26344-26351.	1.5	8

#	Article	IF	Citations
34936	Inelastic Neutron Scattering Investigation of MgCl₂ Nanoparticle-Based Zieglerâ€“Natta Catalysts for Olefin Polymerization. ACS Applied Nano Materials, 2020, 3, 11118-11128.	2.4	5
34937	Tunable Superconductivity in 2H-NbSe₂ via in situ Li Intercalation. Chinese Physics Letters, 2020, 37, 097402.	1.3	8
34938	Filling-enforced Dirac nodal loops in nonmagnetic systems and their evolutions under various perturbations. Physical Review B, 2020, 102, .	1.1	4
34939	Stabilities, mechanical and thermodynamic properties of Alâ€“RE intermetallics: A first-principles study. Journal of Rare Earths, 2022, 40, 345-352.	2.5	15
34940	Coverage-Dependent Water Dissociative Adsorption Properties on Nickel Surfaces. Journal of Physical Chemistry C, 2020, 124, 25835-25845.	1.5	6
34941	Area-selective atomic layer deposition enabled by competitive adsorption. Journal of Vacuum Science and Technology A: Vacuum, Surfaces and Films, 2020, 38, 062411.	0.9	8
34942	Comprehensive Density Functional Theory Studies of Vibrational Spectra of Carbonates. Nanomaterials, 2020, 10, 2275.	1.9	29
34943	Anisotropic Strain in Rare-Earth Substituted Ceria Thin Films Probed by Polarized Raman Spectroscopy and First-Principles Calculations. ACS Applied Materials & Interfaces, 2020, 12, 56251-56259.	4.0	7
34944	Structural, electronic and optical properties of hexagonal boron-nitride (h-BN) monolayer: An Ab-initio study. Materials Today: Proceedings, 2021, 47, 529-532.	0.9	13
34945	Structural and electrical properties of TiO2 monolayers using first-principle calculations. Materials Today: Proceedings, 2021, 47, 563-566.	0.9	3
34946	An ab-initio study of blue phosphorene monolayer: Electronic, vibrational and optical properties. Materials Today: Proceedings, 2021, 47, 576-579.	0.9	2
34947	Precise Identification of the Active Phase of Cobalt Catalyst for Carbon Nanotube Growth by In Situ Transmission Electron Microscopy. ACS Nano, 2020, 14, 16823-16831.	7.3	51
34948	Tunable two dimensional ferromagnetic topological half-metal CrO2 by electronic correction and spin direction. Applied Physics Letters, 2020, 117, .	1.5	21
34949	Dynamical stability of two-dimensional metals in the periodic table. Physical Review B, 2020, 102, .	1.1	26
34950	Spontaneous chemical functionalization via coordination of Au single atoms on monolayer MoS ₂. Science Advances, 2020, 6, .	4.7	56
34951	Structural and Dynamical Properties of Short-Period GaN/AlN Superlattices: Experiment and Theory. Semiconductors, 2020, 54, 1706-1709.	0.2	0
34952	Elastic, electronic, bonding, and optical properties of WTe2 Weyl semimetal: A comparative investigation with MoTe2 from first principles. Results in Physics, 2020, 19, 103639.	2.0	27
34953	First-Principles Modeling of Sodium Ion and Water Intercalation into Titanium Disulfide Interlayers for Water Desalination. Chemistry of Materials, 2020, 32, 10678-10687.	3.2	7

#	Article	IF	Citations
34954	Na3FeH7 and Na3CoH6: Hydrogen-Rich First-Row Transition Metal Hydrides from High Pressure Synthesis. Inorganic Chemistry, 2020, 59, 16467-16473.	1.9	12
34955	Beyond the Reverse Horiutiâ€“Polanyi Mechanism in Propane Dehydrogenation over Pt Catalysts. ACS Catalysis, 2020, 10, 14887-14902.	5.5	44
34956	First-Principle Insight into the Ru-Doped PtSe₂ Monolayer for Detection of H₂ and C₂H₂ in Transformer Oil. ACS Omega, 2020, 5, 31872-31879.	1.6	19
34957	Effect of rare earth on physical properties of Na0.5Bi0.5TiO3 system: A density functional theory investigation. Journal of Rare Earths, 2022, 40, 473-481.	2.5	16
34958	Impact of Small Adsorbates in the Vibrational Spectra of Mg- and Zn-MOF-74 Revealed by First-Principles Calculations. ACS Applied Materials & Interfaces, 2020, 12, 54980-54990.	4.0	14
34959	Active learning for the power factor prediction in diamond-like thermoelectric materials. Npj Computational Materials, 2020, 6, .	3.5	43
34960	Influence of Alkali Metal Cations on the Photodimerization of Bromo Cinnamates Studied by Solid-State NMR. Journal of Physical Chemistry C, 2020, 124, 27614-27620.	1.5	1
34961	Atomistic Mechanisms for Contrasting Stressâ€“Strain Relations of B₁₃CN and B₁₃C₂. Journal of Physical Chemistry Letters, 2020, 11, 10454-10462.	2.1	9
34962	The effect of the elements Cr, Os, Ir, and Y additions on the mechanical and electronic properties of L12 Ni3Co alloys. Journal of Applied Physics, 2020, 128, .	1.1	4
34963	The theoretical study of Cs/O absorption on Ga0.9375Mg0.0625N (0001) surface: A first principle calculation. Journal of Physics: Conference Series, 2020, 1593, 012044.	0.3	0
34964	Oxygen-Mediated Superexchange Interactions and Their Impact on the Structural Stability, Magnetic Order, and Magnetocrystalline Anisotropy of One-Dimensional Co-Oxide Chains on Rh(553) Step-Surfaces. Journal of Physical Chemistry C, 2020, 124, 26026-26036.	1.5	4
34965	Facile Synthesis of Defect-Modified Thin-Layered and Porous g-C₃N₄ with Synergetic Improvement for Photocatalytic H₂ Production. ACS Applied Materials & Interfaces, 2020, 12, 52603-52614.	4.0	65
34966	Computational Study on Strain-Engineered Graphene Nanopores for Selective Gas Separation. ACS Applied Nano Materials, 2020, 3, 11474-11480.	2.4	6
34967	Structural, electronic and optical properties of pristine and functionalized MgO monolayers: a first principles study. RSC Advances, 2020, 10, 40411-40420.	1.7	22
34968	A first-principles investigation of topological phase transition in half-Heusler LiMgSb driven by volume expansive pressure. AIP Conference Proceedings, 2020, , .	0.3	6
34969	High-throughput calculations screening for new direct band gap superhard carbon allotropes. Chinese Journal of Physics, 2020, 68, 778-787.	2.0	3
34970	Direct sunlight-active Na-doped ZnO photocatalyst for the mineralization of organic pollutants at different pH mediums. Journal of the Taiwan Institute of Chemical Engineers, 2020, 115, 187-197.	2.7	27
34971	Modeling Exsolution of Pt from ATiO₃ Perovskites (A = Ca/Sr/Ba) Using First-Principles Methods. Chemistry of Materials, 2020, 32, 9642-9649.	3.2	11

#	Article	IF	Citations
34972	Hydroxide-Enhanced Superexchange Magnetic Couplings in Ionic Clathrate Hydrates. Journal of Physical Chemistry C, 2020, 124, 25455-25464.	1.5	0
34973	Vertically Aligned 2D MoS₂ Layers with Strain-Engineered Serpentine Patterns for High-Performance Stretchable Gas Sensors: Experimental and Theoretical Demonstration. ACS Applied Materials & Interfaces, 2020, 12, 53174-53183.	4.0	35
34974	First-principles calculations of physical properties and superconductivity of orthorhombic ScRuSi and ZrRhSi. Physical Review B, 2020, 102, .	1.1	0
34975	Diffusion, permeation and solubility of hydrogen, deuterium and tritium in crystalline tungsten: First principles DFT simulations. International Journal of Hydrogen Energy, 2020, 45, 29095-29109.	3.8	27
34976	Structural evolution, mechanical, electronic and vibrational properties of high capacity hydrogen storage TiH4. International Journal of Hydrogen Energy, 2020, 45, 30783-30791.	3.8	21
34977	Mechanical and thermodynamic properties study of Al-based binary and ternary solid solutions using the pseudoatomic potential method. Intermetallics, 2020, 126, 106931.	1.8	0
34978	Orbital Chemistry That Leads to High Valley Degeneracy in PbTe. Chemistry of Materials, 2020, 32, 9771-9779.	3.2	30
34979	Morphology Evolution of FCC and HCP Cobalt Induced by a CO Atmosphere from Ab Initio Thermodynamics. Journal of Physical Chemistry C, 2020, 124, 23200-23209.	1.5	10
34980	Pressure-Induced Phase Transitions in Danburite-Type Borosilicates. Journal of Physical Chemistry C, 2020, 124, 26048-26061.	1.5	6
34981	Embedded atom method potential for hydrogen on palladium surfaces. Journal of Molecular Modeling, 2020, 26, 336.	0.8	4
34982	Exploring Caâ€“Ceâ€“Mâ€“O (M = 3d Transition Metal) Oxide Perovskites for Solar Thermochemical Applications. Chemistry of Materials, 2020, 32, 9964-9982.	3.2	49
34983	Predicted Confinement-Enhanced Stability and Extraordinary Mechanical Properties for Carbon Nanotube Wrapped Chains of Linear Carbon. ACS Nano, 2020, 14, 17071-17079.	7.3	29
34984	Structural and Optical Properties of ZnO:Al Thin Films Produced by Magnetron Sputtering with Different Oxygen Flow: An Experimental and Ab Initio Study. Physica Status Solidi (A) Applications and Materials Science, 2020, 217, 2000167.	0.8	4
34985	Multidirectional Intrinsic Piezoelectricity of 2D Metal Chalcogenâ€“Diphosphate ABP 2 X 6 Monolayers. Physica Status Solidi - Rapid Research Letters, 2020, 14, 2000321.	1.2	14
34986	Oxygen octahedral coupling mediated ferroelectric-antiferroelectric phase transition based on domain wall engineering. Acta Materialia, 2020, 198, 145-152.	3.8	16
34987	Hydrogen adsorption on Li decorated graphyne-like carbon nanosheet: A density functional theory study. International Journal of Hydrogen Energy, 2020, 45, 24938-24946.	3.8	23
34988	Mechanochemical Metathesis between AgNO₃ and NaX (X = Cl, Br, I) and Ag₂XNO₃ Double-Salt Formation. Inorganic Chemistry, 2020, 59, 12200-12208.	1.9	7
34989	Intrinsic Isotropic Near-Zero Thermal Expansion in Zn₄B₆O₁₂X (X) Tj ETQq1 1 0.784314 rgBT	4.0	16

#	Article	IF	Citations
34990	A revised mechanistic model for sodium insertion in hard carbons. Energy and Environmental Science, 2020, 13, 3469-3479.	15.6	195
34991	Brillouin zone center phonon modes in ZnGa2O4. Applied Physics Letters, 2020, 117, .	1.5	5
34992	Sub-5-nm Monolayer Silicane Transistor: A First-Principles Quantum Transport Simulation. Physical Review Applied, 2020, 14, .	1.5	38
34993	Effect of Cr on the generalized stacking fault energy of impure doped Ni (111) surface: a first-principles study. European Physical Journal B, 2020, 93, 1.	0.6	3
34994	Probing the Microstructure in Pure Al & Cu Melts: Theory Meets Experiment. Frontiers in Chemistry, 2020, 8, 607.	1.8	13
34995	Kinetics and Mechanism of Turanite Reduction by Hydrogen. Journal of Physical Chemistry C, 2020, 124, 18356-18365.	1.5	3
34996	Theoretically designed two-dimensional Î³-C₄O as an effective gas separation membrane for hydrogen purification. Physical Chemistry Chemical Physics, 2020, 22, 19492-19501.	1.3	8
34997	Superhard sp²â€“sp³ hybridized B₂C₃N₂ with 2D metallicity. Physical Chemistry Chemical Physics, 2020, 22, 22918-22922.	1.3	5
34998	Stable Lithium Sulfur Battery Based on In Situ Electrocatalytically Formed Li₂S on Metallic MoS₂â€“Carbon Cloth Support. Small Methods, 2020, 4, 2000353.	4.6	49
34999	Effects of molecular vacancy and ethylenediamine on structural and electronic properties of CH3NO2 surfaces. Journal of Molecular Modeling, 2020, 26, 209.	0.8	0
35000	Surface alloying of chromium/tungsten/stannum on pure nickel and theoretical analysis of strengthening mechanism. Applied Surface Science, 2020, 532, 147477.	3.1	14
35001	Optoelectronic properties of pristine antimonene, phosphorene and their binary compound. Computational Condensed Matter, 2020, 24, e00488.	0.9	5
35002	Fe-doped Na0.47Bi0.47Ba0.06Ti0.98-xV0.02FexO3: Structure correlated vibrational, optical and electrical properties. Journal of Alloys and Compounds, 2020, 848, 156503.	2.8	9
35003	Gadolinium ion bonding on the surface of carboxylated detonation nanodiamond in terms of magnetochemistry and density functional theory. Mendeleev Communications, 2020, 30, 436-438.	0.6	6
35004	SrTiO3-based thermoelectrics: Progress and challenges. Nano Energy, 2020, 78, 105195.	8.2	127
35005	The first-principles calculation study on the magnetic properties of Mo doped GaSb. Physica B: Condensed Matter, 2020, 596, 412399.	1.3	1
35006	First-principles study of the topological surface states of Î±-Sn(111). Physics Letters, Section A: General, Atomic and Solid State Physics, 2020, 384, 126782.	0.9	5
35007	Effects of triaxial strain on carrier activity, carrier lifetime, and absorption spectrum of (S, Se, Te) and 2ÂN Co-doped ZnO. Vacuum, 2020, 182, 109684.	1.6	14

#	Article	IF	Citations
35008	Synergistic Catalytic Mechanism between Ni and Carbon Aerogel for Dehydrogenation of Mg-Based Hydrides. Energy & Fuels, 2020, 34, 10232-10240.	2.5	9
35009	KMC Study on Byproduct Formation in the Process of Acetylene to Vinyl Acetate. Industrial & Engineering Chemistry Research, 2020, 59, 13502-13515.	1.8	3
35010	Surprising Lateral Interactions between Negatively Charged Adatoms on Metal Surfaces. Journal of Physical Chemistry Letters, 2020, 11, 7122-7126.	2.1	9
35011	Rational Tuning of a Li₄SiO₄-Based Hybrid Interface with Unique Stepwise Prelithiation for Dendrite-Proof and High-Rate Lithium Anodes. ACS Applied Materials & Interfaces, 2020, 12, 39362-39371.	4.0	23
35012	Atomic-scale phase separation induced clustering of solute atoms. Nature Communications, 2020, 11, 3934.	5.8	11
35013	Length scales of interfacial coupling between metal and insulator phases in oxides. Nature Materials, 2020, 19, 1182-1187.	13.3	42
35014	Electron density modulation of a metallic GeSb monolayer by pnictogen doping for excellent hydrogen evolution. Physical Chemistry Chemical Physics, 2020, 22, 19823-19836.	1.3	9
35015	Superoxide formation in Li₂VO₂F cathode material â€“ a combined computational and experimental investigation of anionic redox activity. Journal of Materials Chemistry A, 2020, 8, 16551-16559.	5.2	18
35016	Theoretical study on the anomalies of the magnetic susceptibility in the honeycomb lattice compound <mml:math xmlns:mml="http://www.w3.org/1998/Math/MathML"><mml:mrow><mml:msub><mml:mi>Na</mml:mi><mml:mn>2</mml:mn></mml:msub><mml:msub><mml:mi mathvariant="normal">O</mml:mi><mml:mn>6</mml:mn></mml:msub></mml:mrow></mml:math>. Physical Review B, 2020, 102, .	1.1	7
35017	Defect topology and annihilation by cooperative movement of atoms in neutron-irradiated graphite. Physical Review B, 2020, 102, .	1.1	7
35018	Roles of nitrogen substitution and surface reconstruction in stabilizing nonpassivated single-layer diamond. Physical Review B, 2020, 102, .	1.1	12
35019	First Principle Analysis of Li-Doped Armchair Graphene Nanoribbons for Nanoscale Metal Interconnect Applications. , 2020, , .		1
35020	Adsorption of alkali metals on graphitic carbon nitride: A first-principles study. Modern Physics Letters B, 2020, 34, 2050361.	1.0	4
35021	A novel high-pressure polymorph of TaSi2. Results in Physics, 2020, 18, 103310.	2.0	2
35022	Surface segregation in Cr-Mn-Fe-Co-Ni high entropy alloys. Applied Surface Science, 2020, 533, 147471.	3.1	46
35023	Nanoscale oligopeptide adsorption behaviour on chlorite as revealed by scanning probe microscopy and density functional simulations. Applied Clay Science, 2020, 197, 105777.	2.6	5
35024	Probing physical properties and superconductivity of noncentrosymmetric superconductors LaPtGe and LaPtGe3: A first-principles study. Computational Materials Science, 2020, 185, 109949.	1.4	7
35025	Exploring the A₂BX₃ Family for New Functional Materials Using Crystallographic Database Mining and First-Principles Calculations. Journal of Physical Chemistry C, 2020, 124, 19413-19425.	1.5	2

#	Article	IF	Citations
35026	Directly linked metalloporphyrins: a quest for bio-inspired materials. Materials Advances, 2020, 1, 1895-1908.	2.6	4
35027	Computational prediction of muon stopping sites: A novel take on the unperturbed electrostatic potential method. Journal of Chemical Physics, 2020, 153, 044111.	1.2	7
35028	An ultra-incompressible Mn3N compound predicted by first-principles genetic algorithm. Journal of Applied Physics, 2020, 128, 055112.	1.1	2
35029	First-principles calculations of finite temperature electronic structures and transport properties of Heusler alloy Co2MnSi. Applied Physics Letters, 2020, 117, 042402.	1.5	15
35030	First-principles Study of the Impact of Hydrogen Passivation on the Charge State Transition Levels of the CiOi(Sii)n Defect Complexes in Silicon. Silicon, 2020, 12, 2699-2704.	1.8	1
35031	Superhard high-pressure structures of beryllium diborocarbides. Vacuum, 2020, 180, 109617.	1.6	1
35032	Structural, electronic and magnetic properties of Sc³⁺ doped CoCr₂O₄ nanoparticles. New Journal of Chemistry, 2020, 44, 14246-14255.	1.4	31
35033	Câ€“H activation of light alkanes on MXenes predicted by hydrogen affinity. Physical Chemistry Chemical Physics, 2020, 22, 18622-18630.	1.3	10
35034	Effects of Strain and Film Thickness on the Stability of the Rhombohedral Phase of <mml:math xmlns:mml="http://www.w3.org/1998/Math/MathML" display="inline" overflow="scroll"><mml:msub><mml:mrow><mml:mi>Hf</mml:mi><mml:mi mathvariant="normal">O</mml:mi></mml:mrow><mml:mn>2</mml:mn></mml:msub></mml:math>. Physical Review Applied, 2020, 14.	1.5	43
35035	Novel vacancy-dependence in the adsorption of M-TPP molecules (M=AC0, Ni, Zn) on Fe(001)-<mml:math xmlns:mml="http://www.w3.org/1998/Math/MathML" altimg="si108.svg"><mml:mrow><mml:mi>p</mml:mi><mml:mo stretchy="false">(</mml:mo><mml:mn>1</mml:mn><mml:mo>Ã—</mml:mo><mml:mn>1</mml:mn><mml:mo) Tj ETQq1 1 0.78431	3.1	17
35036	Effective interaction model for coupled magnetism and phase stability in bcc Fe-Co systems. Computational Materials Science, 2020, 183, 109906.	1.4	8
35037	Electronic, optical and thermoelectric properties of CaO mono- and bi-layers: Theoretical comparative investigation. Optik, 2020, 218, 165115.	1.4	3
35038	Interaction of irradiation-induced point defects with transmutants (H, He, Li, Be, B, Mg, Al and P) in 3C-SiC ceramics. Journal of the European Ceramic Society, 2020, 40, 5196-5204.	2.8	12
35039	Electronic, elastic, vibrational and dielectric properties of InPS4 by first principles. Materials Chemistry and Physics, 2020, 255, 123548.	2.0	1
35040	Hydrogen-enhanced intergranular failure of sulfur-doped nickel grain boundary: In situ electrochemical micro-cantilever bending vs.ÂDFT. Materials Science & Engineering A: Structural Materials: Properties, Microstructure and Processing, 2020, 794, 139967.	2.6	27
35041	Two-dimensional B3P monolayer as a superior anode material for Li and Na ion batteries: a first-principles study. Materials Today Energy, 2020, 17, 100486.	2.5	15
35042	First principles investigations of structural, elastic, mechanical, electronic and optical properties of triple perovskite Ba2K2Te2O9. Physica B: Condensed Matter, 2020, 596, 412404.	1.3	10
35043	Potassium Nickel Iron Hexacyanoferrate as Ultra-Long-Life Cathode Material for Potassium-Ion Batteries with High Energy Density. ACS Nano, 2020, 14, 9807-9818.	7.3	116

#	Article	IF	Citations
35044	Enhanced Thermoelectric Performances Driven by High-Pressure Phase Transition of Mg2Sn Compound. International Journal of Thermophysics, 2020, 41, 1.	1.0	3
35045	First-principles insights on the stability, linear and nonlinear optical properties of new potential thioborates AgBS2, CuBS2. Optical and Quantum Electronics, 2020, 52, 1.	1.5	1
35046	Al doped MoS2 for adsorption-based water collection. Applied Surface Science, 2020, 529, 147083.	3.1	15
35047	A DFT study of two-dimensional CdS/TiS2 on isotropic chalcogenide AgSbTe2 thermoelectric material: Electronic charge transfer and optical properties. Current Applied Physics, 2022, 40, 50-61.	1.1	2
35048	A density functional theory study of the thermoelectric properties of K3AuO. Computational Condensed Matter, 2020, 24, e00484.	0.9	4
35049	Dual-ion battery with MoS2 cathode. Energy Storage Materials, 2020, 32, 159-166.	9.5	18
35051	EQCM analysis of intercalation species into graphite positive electrodes for Al batteries. Journal of Alloys and Compounds, 2020, 846, 156469.	2.8	13
35052	Phase Distribution, Composition, and Disorder in Y₂(Hf,Sn)₂O₇ Ceramics: Insights from Solid-State NMR Spectroscopy and First-Principles Calculations. Journal of Physical Chemistry C, 2020, 124, 17073-17084.	1.5	7
35053	First-Principles Calculations of Graphene-Coated CH₃NH₃PbI₃ toward Stable Perovskite Solar Cells in Humid Environments. ACS Applied Nano Materials, 2020, 3, 7704-7712.	2.4	11
35054	Heterostructures of Îµ-Fe₂O₃ and Î±-Fe₂O₃: insights from density functional theory. RSC Advances, 2020, 10, 27474-27480.	1.7	8
35055	Synthesis and high-pressure studies of strontium diazenide by synchrotron X-ray diffraction and DFT calculations. RSC Advances, 2020, 10, 26308-26312.	1.7	0
35056	An accurate and transferable machine learning potential for carbon. Journal of Chemical Physics, 2020, 153, 034702.	1.2	137
35057	Conspicuous interatomic bonding in chalcogenide crystals and implications on electronic, optical, and elastic properties. AIP Advances, 2020, 10, .	0.6	11
35058	Nonlinear optical properties of tellurium oxide nanoclusters. Journal of Physics: Conference Series, 2020, 1461, 012137.	0.3	0
35059	CO oxidation through the formation of carboxyl intermediate on Pt(111) surface: A first principles study. Journal of Physics: Conference Series, 2020, 1494, 012040.	0.3	0
35060	Electrically controlled magnetism in iron thin film. Journal of Physics: Conference Series, 2020, 1506, 012009.	0.3	1
35061	Effects of Boron Nitride on the optical properties of Silicene: density functional theory calculations. Journal of Physics: Conference Series, 2020, 1568, 012005.	0.3	0
35062	Effects of Surface in the IR and Raman Spectrum of Porous Silicon Carbide. IOP Conference Series: Materials Science and Engineering, 2020, 840, 012009.	0.3	1

#	Article	IF	Citations
35063	Composition-balanced trimetallic MOFs as ultra-efficient electrocatalysts for oxygen evolution reaction at high current densities. Applied Catalysis B: Environmental, 2020, 279, 119375.	10.8	102
35064	Electronic transport through CNT-fluorographene-Au junction: First-principles study. Europhysics Letters, 2020, 131, 17001.	0.7	7
35065	C-2p Spin-Polarizations along with Two Mechanisms in Extended Carbon Multilayers: Insight from First Principles. Condensed Matter, 2020, 5, 48.	0.8	0
35066	A new concept: Volume photocatalysis for efficient H2 generation __ Using low polymeric carbon nitride as an example. Applied Catalysis B: Environmental, 2020, 279, 119379.	10.8	104
35067	VO2@Carbon foam as a freestanding anode material for potassium-ion batteries: First principles and experimental study. Journal of Alloys and Compounds, 2020, 845, 156232.	2.8	14
35068	Theory-Guided Design of Anode Catalysts for Hydrogenous Liquid Fuels. Journal of Physical Chemistry C, 2020, 124, 17494-17502.	1.5	1
35069	Ab initio modeling of the energy landscape for screw dislocations in body-centered cubic high-entropy alloys. Npj Computational Materials, 2020, 6, .	3.5	58
35070	Structural distortion and collinear-to-helical magnetism transition in rutile-type <mml:math xmlns:mml="http://www.w3.org/1998/Math/MathML"><mml:mrow><mml:mi>Fe</mml:mi><mml:msub><mml:mi mathvariant="normal">O</mml:mi><mml:mn>2</mml:mn></mml:msub></mml:mrow></mml:math>. Physical Review B, 2020, 102, .	1.1	1
35071	Symmetry breaking in the double moirÃ© superlattices of relaxed twisted bilayer graphene on hexagonal boron nitride. Physical Review B, 2020, 102, .	1.1	17
35072	Computational Studies, NMR and Ir Spectral Analysis, Normal Coordinate Analysis, and Thermodynamic Properties of 2-Fluoro-4-Pyridineboronic Acid. Journal of Structural Chemistry, 2020, 61, 400-418.	0.3	1
35073	Polar-discontinuity-induced stability of spontaneous polarization in ultrathin perovskite films. Ceramics International, 2020, 46, 26698-26704.	2.3	0
35074	Strain-Induced Band Modulation, Work Function, and QTAIM Analysis of Surface O-Functionalized Ti₂C MXene. ACS Omega, 2020, 5, 18403-18410.	1.6	9
35075	Two-dimensional square lattice polonium stabilized by the spinâ€“orbit coupling. Scientific Reports, 2020, 10, 11810.	1.6	13
35076	Janus two-dimensional materials based on group IV monochalcogenides. Journal of Applied Physics, 2020, 128, .	1.1	29
35077	Quantum dynamics origin of high photocatalytic activity of mixed-phase anatase/rutile TiO2. Journal of Chemical Physics, 2020, 153, 044706.	1.2	26
35078	Universal Approach to Magnetic Second-Order Topological Insulator. Physical Review Letters, 2020, 125, 056402.	2.9	91
35079	Exceptional plasticity in the bulk single-crystalline van der Waals semiconductor InSe. Science, 2020, 369, 542-545.	6.0	163
35080	Extraordinary Response of H-Charged and H-Free Coherent Grain Boundaries in Nickel to Multiaxial Loading. Crystals, 2020, 10, 590.	1.0	4

#	Article	IF	Citations
35081	A novel two-dimensional sp-sp2-sp3 hybridized carbon nanostructure with a negative in-plane Poisson ratio and high electron mobility. Computational Materials Science, 2020, 185, 109904.	1.4	20
35082	Reaction coordinate mapping of hydrogen evolution mechanism on Mg3N2 monolayer. International Journal of Hydrogen Energy, 2020, 45, 22848-22854.	3.8	7
35083	Theoretical study of enhanced ferromagnetism and tunable magnetic anisotropy of monolayer CrI3 by surface adsorption. Physics Letters, Section A: General, Atomic and Solid State Physics, 2020, 384, 126754.	0.9	16
35084	Pressure-induced the formation of Mg(CH3)2 and Ca(CH3)2 studied by the first principles. Solid State Communications, 2020, 320, 114027.	0.9	0
35085	Oxygen Affinity: The Missing Link Enabling Prediction of Proton Conductivities in Doped Barium Zirconates. Chemistry of Materials, 2020, 32, 7292-7300.	3.2	25
35086	Nanoporous V-Doped Ni₅P₄ Microsphere: A Highly Efficient Electrocatalyst for Hydrogen Evolution Reaction at All pH. ACS Applied Materials & Interfaces, 2020, 12, 37092-37099.	4.0	40
35087	Why Oxygen Increases Carrier Lifetimes but Accelerates Degradation of CH₃NH₃PbI₃ under Light Irradiation: Time-Domain Ab Initio Analysis. Journal of the American Chemical Society, 2020, 142, 14664-14673.	6.6	64
35088	A first-principle perspective on electronic nematicity in FeSe. Npj Quantum Materials, 2020, 5, .	1.8	15
35089	Thermomechanical properties of zero thermal expansion materials from theory and experiments. Physical Chemistry Chemical Physics, 2020, 22, 18518-18525.	1.3	3
35090	Computational design of (100) alloy surfaces for the hydrogen evolution reaction. Journal of Materials Chemistry A, 2020, 8, 17987-17997.	5.2	47
35091	Metallic antiferromagnets. Journal of Applied Physics, 2020, 128, .	1.1	57
35092	Pâ€doped <scp>gâ€C₃N₄</scp> as an efficient photocatalyst for <scp>CO₂</scp> conversion into valueâ€added materials: a joint experimental and theoretical study. International Journal of Quantum Chemistry, 2020, 120, e26388.	1.0	10
35093	Ni3B as a highly efficient and selective catalyst for the electrosynthesis of hydrogen peroxide. Applied Catalysis B: Environmental, 2020, 279, 119371.	10.8	48
35094	Orientation-dependent electric transport and band filling in hole co-doped epitaxial diamond films. Applied Surface Science, 2020, 528, 146795.	3.1	9
35095	Surface transformation and interactions of iron oxide in glassy lubricant: An ab initio study. Chemical Physics, 2020, 538, 110919.	0.9	4
35096	Engineering of new graphene-based materials as potential materials to assist near-infrared photothermal therapy cancer treatment. Heliyon, 2020, 6, e04131.	1.4	9
35097	Theoretical modelling of porous silicon decorated with metal atoms for hydrogen storage. International Journal of Hydrogen Energy, 2020, 45, 26321-26333.	3.8	14
35098	First-principles study of hydrogen trapping behavior in face centered cubic metals (M=Ni, Cu and Al) with monovacancy. International Journal of Hydrogen Energy, 2020, 45, 25555-25566.	3.8	8

#	Article	IF	Citations
35099	Probing into the global structural prediction, physical and electronic properties of A-X (AÂ= Ca, Sr, Ba;) Tj ETQq0 0 0 rgBT /Overlock 10 T	2.8	5
35100	Structural stability, mechanical, electronic and optical behaviour of RbXS2 (XÂ= Y and La) under high pressure: A first-principle study. Journal of Alloys and Compounds, 2020, 848, 156401.	2.8	6
35101	Formation, evolution and characteristics of copper sulfide nanoparticles in the reactions of aqueous cupric and sulfide ions. Materials Chemistry and Physics, 2020, 255, 123600.	2.0	14
35102	Electronic and elastic properties of rhombohedral GeTe: Exfoliation energy of a monolayer from (111) surface. Materials Today: Proceedings, 2020, 28, 1771-1775.	0.9	2
35103	Improving the oxidation resistance of WSi2 by boron doping: A DFT study. Materials Today Communications, 2020, 25, 101312.	0.9	3
35104	Ytterbium doping effects into the Ba and Ti sites of perovskite barium titanate: Electronic structures and optical properties. Results in Physics, 2020, 18, 103257.	2.0	8
35105	Effect of iodic acid concentration in preparation of zinc iodate: Experimental characterization of Zn(IO3)2, and its physical properties from density functional theory. Vacuum, 2020, 181, 109660.	1.6	14
35106	Local Strain and Polarization Mapping in Ferrielectric Materials. ACS Applied Materials & Interfaces, 2020, 12, 38546-38553.	4.0	14
35107	Highly Efficient Deoxydehydration and Hydrodeoxygenation on MoS₂-Supported Transition-Metal Atoms through a Câ€“H Activation Mechanism. ACS Catalysis, 2020, 10, 11346-11355.	5.5	10
35108	Effects of the methylammonium ion substitution by 5-ammoniumvaleric acid in lead trihalide perovskite solar cells: a combined experimental and theoretical investigation. New Journal of Chemistry, 2020, 44, 14642-14649.	1.4	4
35109	Probing the structural and electronic response of Magnus green salt compounds [Pt(NH2R)4][PtCl4] (R = H, CH3) to pressure. Physical Chemistry Chemical Physics, 2020, 22, 17668-17676.	1.3	3
35110	Effects of Oxygen Adsorption on Morphological Evolution of Epitaxial Ag Island Films Grown on Si. Journal of the Korean Physical Society, 2020, 76, 1071-1075.	0.3	2
35111	Investigation of optoelectronic properties of triphenylamine-based dyes featuring heterocyclic anchoring groups for DSSCsâ€™ applications: a theoretical study. Structural Chemistry, 2020, 31, 2451-2461.	1.0	13
35112	Oxygen Evolution and Reduction on Fe-doped NiOOH: Influence of Solvent, Dopant Position and Reaction Mechanism. Topics in Catalysis, 2020, 63, 833-845.	1.3	19
35113	Electronic, Band Offset, and Thermoelectric Properties of ZnO/GaN Heterostructure from First-Principles Study. Journal of Electronic Materials, 2020, 49, 5773-5781.	1.0	8
35114	From electricity to fuels: Descriptors for C1 selectivity in electrochemical CO2 reduction. Applied Catalysis B: Environmental, 2020, 279, 119384.	10.8	81
35115	Computational investigation of two-dimensional LDHs and the modification of their electronic structure induced by defects. Applied Surface Science, 2020, 532, 147159.	3.1	8
35116	A study on the adsorptions of SO2 on pristine and phosphorus-doped silicon carbide nanotubes as potential gas sensors. Ceramics International, 2020, 46, 25171-25188.	2.3	18

#	Article	IF	Citations
35117	Effect of Cu concentration and dopant site on the band gap of MoS2: A DFT study. Computational Condensed Matter, 2020, 24, e00494.	0.9	21
35118	Tetragonal and uniaxial strains in pristine and doped half-Heusler AuMnSn alloy. Journal of Alloys and Compounds, 2020, 848, 156186.	2.8	5
35119	Design and characterization of Eu2+-doped Ba4Si6O16 photostimulated phosphor for optical information storage. Journal of Luminescence, 2020, 227, 117556.	1.5	10
35120	Functionalization of monolayer-CdS by metal and non-metal elemental substitution: First-principle understanding. Journal of Magnetism and Magnetic Materials, 2020, 515, 167212.	1.0	8
35121	Magnetic behavior of transition metal solutes in<mml:math xmlns:mml="http://www.w3.org/1998/Math/MathML" altimg="si3.svg"><mml:mrow><mml:mi>Î±</mml:mi></mml:mrow></mml:math>-iron: A classification. Journal of Magnetism and Magnetic Materials, 2020, 513, 167223.	1.0	3
35122	First principle investigation of H2Se, H2Te and PH3 sensing based on graphene oxide. Physics Letters, Section A: General, Atomic and Solid State Physics, 2020, 384, 126775.	0.9	24
35123	Multiferroic properties of three-layer Aurivillius compound Bi4TiFeNbO12: A first-principles and experimental study. Solid State Communications, 2020, 320, 114028.	0.9	3
35124	Electronic properties, anisotropic elasticity, theoretical strengths, and lattice vibrational mode of orthorhombic YSi. Solid State Communications, 2020, 321, 114029.	0.9	4
35125	Chemical Trends in the Lattice Thermal Conductivity of Li(Ni, Mn, Co)O₂ (NMC) Battery Cathodes. Chemistry of Materials, 2020, 32, 7542-7550.	3.2	28
35126	Calculation of the Thermal Neutron Scattering Cross-Section of Solids Using OCLIMAX. Journal of Chemical Theory and Computation, 2020, 16, 5212-5217.	2.3	14
35127	Flexible Cation Distribution for Stabilizing a Spinel Surface. Journal of Physical Chemistry C, 2020, 124, 16431-16438.	1.5	10
35128	Prediction of Optimal Synthesis Conditions for the Formation of Ordered Double-Transition-Metal MXenes (o-MXenes). Journal of Physical Chemistry C, 2020, 124, 18797-18804.	1.5	11
35129	Understanding Disorder in 2D Materials: The Case of Carbon Doping of Silicene. Nano Letters, 2020, 20, 6336-6343.	4.5	8
35130	First-Principles Calculations on the Adsorption Behavior of Amino Acids on a Titanium Carbide MXene. ACS Applied Bio Materials, 2020, 3, 5913-5921.	2.3	39
35131	Intra-Crystalline Mesoporous Zeolite [Al,Zr]-Y for Catalytic Cracking. ACS Applied Nano Materials, 2020, 3, 9293-9302.	2.4	12
35132	Electronic Structure and Oxidation Mechanism of Nickelâ€“Copper Converter Matte from First-Principles Calculations. ACS Omega, 2020, 5, 20090-20099.	1.6	11
35133	A new class of lightweight, stainless steels with ultra-high strength and large ductility. Scientific Reports, 2020, 10, 12140.	1.6	46
35134	Transition metalâ€“N₄ embedded black phosphorus carbide as a high-performance bifunctional electrocatalyst for ORR/OER. Nanoscale, 2020, 12, 18721-18732.	2.8	39

#	Article	IF	Citations
35135	Modulation in structural and electronic properties of 2D Ga2O3 by chemical passivation. Journal of Materials Chemistry C, 2020, 8, 12551-12559.	2.7	13
35136	Compositional dependence of linear and nonlinear optical response in crystalline hafnium zirconium oxide thin films. Journal of Applied Physics, 2020, 128, .	1.1	19
35137	Defect, transport, and dopant properties of andradite garnet Ca3Fe2Si3O12. AIP Advances, 2020, 10, .	0.6	6
35138	Elastic anisotropy, electronic and magnetic behaviours of ferromagnetic Europium Niobate EuNbO₃ in orthorhombic structure: DFTâ€‰+â€‰U, MFA and QTAIM studies. Philosophical Magazine, 2020, 100, 2889-2911.	0.7	2
35139	First-principles calculations of the electronic structure and magnetism of nanostructured <mml:math xmlns:mml="http://www.w3.org/1998/Math/MathML"><mml:mrow><mml:mi>Co</mml:mi><mml:msub><mml:mi>Fe</mml:mi><mml:m mathvariant="normal">O</mml:mi><mml:mn>4</mml:mn></mml:msub></mml:mrow></mml:math> microgranules and nanoparticles. Physical Review B, 2020, 102, .	1.1	11
35140	Strain Dependence of Energetics and Kinetics of Vacancy in Tungsten. Materials, 2020, 13, 3375.	1.3	11
35141	Catalytic Activity of Tiâ€based MXenes for the Hydrogenation of Furfural. ChemCatChem, 2020, 12, 5733-5742.	1.8	20
35142	qvasp: A flexible toolkit for VASP users in materials simulations. Computer Physics Communications, 2020, 257, 107535.	3.0	88
35143	The impact of anion elements on the engineering of the electronic and optical characteristics of the two dimensional monolayer janus MoSSe for nanoelectronic device applications. Results in Physics, 2020, 18, 103284.	2.0	7
35144	Enhanced Visible Light-Driven Photocatalytic Activities and Photoluminescence Characteristics of BiOF Nanoparticles Determined via Doping Engineering. Inorganic Chemistry, 2020, 59, 11801-11813.	1.9	37
35145	Layered Perovskite (CH₃NH₃)₂Pb(SCN)₂I₂ Single Crystals: Phase Transition and Moisture Stability. ACS Applied Materials & Interfaces, 2020, 12, 37713-37721.	4.0	20
35146	Noncollinear frustrated antiferromagnetic Mn3P monolayer and its tunability via a spin degree of freedom. Journal of Materials Chemistry C, 2020, 8, 11369-11375.	2.7	3
35147	Structural, electronic, optical and magnetic properties of EuO and DyO compounds: ab initio study. Phase Transitions, 2020, 93, 865-876.	0.6	3
35148	Electronic and thermoelectric properties of the layered Zintl phase CaIn₂P₂: first-principles calculations. Philosophical Magazine, 2020, 100, 3023-3039.	0.7	105
35149	Thermodynamic and thermoelastic properties of wurtzite-ZnS by density functional theory. American Mineralogist, 2020, 105, 1212-1222.	0.9	7
35150	3D Ordering at the Liquidâ€“Solid Polar Interface of Nanowires. Advanced Materials, 2020, 32, e2001030.	11.1	10
35151	First principles study on optoelectronic properties of energetically stable Si/InS van der Waals heterobilayers. Journal of Materials Science, 2020, 55, 15199-15212.	1.7	17
35152	Electronic transport properties of graphene with Stone-Wales defects and multiple vacancy chains: a theoretical study. Applied Surface Science, 2020, 531, 147347.	3.1	17

#	Article	IF	Citations
35153	Quantum anomalous Hall insulator phases in Fe-doped GaBi honeycomb. Chinese Journal of Physics, 2020, 67, 246-252.	2.0	9
35154	Infrared and Raman spectroscopic features of clinochlore Mg6Si4O10(OH)8: A density functional theory contribution. Applied Clay Science, 2020, 197, 105779.	2.6	13
35155	Cu2Zn(Si,Ge)Se4 quaternary semiconductors as potential photovoltaic materials. Chemical Physics Letters, 2020, 756, 137820.	1.2	3
35156	Two-dimensional porphyrin sheet-supported single-atom manganese catalyst for CO oxidation: A DFT-D study. Materials Today Communications, 2020, 24, 101322.	0.9	12
35157	Tailoring electronic structure of bifunctional Cu/Ag layered electrocatalysts for selective CO2 reduction to CO and CH4. Nano Energy, 2020, 78, 105168.	8.2	45
35158	DFT study of the adsorption behavior of NO gas molecule on the Ga and As pair doped stanene nanosheets. Physica E: Low-Dimensional Systems and Nanostructures, 2020, 124, 114348.	1.3	8
35159	Flat-band splitting induced tunable magnetism in defective CrI3 monolayer. Solid State Communications, 2020, 321, 114037.	0.9	9
35160	Identification of the Active Sites in the Dehydrogenation of Methanol on Pt/Al₂O₃ Catalysts. Journal of Physical Chemistry C, 2020, 124, 19015-19023.	1.5	15
35161	Mechanical Properties of a 2D Lead-Halide Perovskite, (C₆H₅CH₂NH₃)₂PbCl₄, by Nanoindentation and First-Principles Calculations. Journal of Physical Chemistry C, 2020, 124, 19204-19211.	1.5	25
35162	Deciphering the Growth Mechanism of Self-Assembled Nanowires on Pt-Deposited Ge(001) via Scanning Tunneling Microscopy and Density Functional Theory Calculations. Journal of Physical Chemistry C, 2020, 124, 18165-18172.	1.5	2
35163	Revealing the Charge Storage Mechanism of Nickel Oxide Electrochromic Supercapacitors. ACS Applied Materials & Interfaces, 2020, 12, 39098-39107.	4.0	82
35164	Ab initio studies of propane dehydrogenation to propene with graphene. Molecular Physics, 2020, 118, .	0.8	6
35165	Electronic properties, optical spectra and magnetisation of MnAs material under compression. Philosophical Magazine, 2020, 100, 2972-2985.	0.7	0
35166	Quantum Simulations of Preferable H₂O Dissociation Pathway on the Ru-Alloyed Pt(111) Surface Based on Density Functional Theory. Key Engineering Materials, 0, 840, 495-500.	0.4	3
35167	Enhancement of the quantum capacitances of group-14 elemental two-dimensional materials by Ti-doping: A first principles study. Applied Surface Science, 2020, 530, 147301.	3.1	8
35168	Atomic surface structure of MOVPE-prepared GaP(1 1 1)B. Applied Surface Science, 2020, 534, 147346.	3.1	1
35169	CO2 Hydrogenation to Ethanol over Cu@Na-Beta. CheM, 2020, 6, 2673-2689.	5.8	130
35170	Zn0.1Ca0.1Sr0.4Ba0.4ZrO3: A non-equimolar multicomponent perovskite ceramic with low thermal conductivity. Journal of the European Ceramic Society, 2020, 40, 6272-6277.	2.8	46

#	Article	IF	Citations
35171	Photocatalytic mineralization of disperse red 167.1 by cubic Cu2O nanoparticles: Experimental and theoretical approach. Journal of Photochemistry and Photobiology A: Chemistry, 2020, 392, 112425.	2.0	6
35172	Properties and potential applications of two-dimensional AlN. Vacuum, 2020, 176, 109231.	1.6	30
35173	Investigation of strain and doping on the electronic properties of single layers of C₆N₆ and C₆N₈: a first principles study. RSC Advances, 2020, 10, 27743-27751.	1.7	35
35174	Suppressed Jahnâ€“Teller Distortion in MnCo₂O₄@Ni₂P Heterostructures to Promote the Overall Water Splitting. Small, 2020, 16, e2001856.	5.2	59
35175	Nonsymmorphic nodal-line metals in the two-dimensional rare earth monochalcogenides MX (Mâ€‰=â€‰Sc, Y;) Tj ETQq0 0 0 rgBT /Ov	1.7	7
35176	Hydrogen Adsorption on Ordered and Disordered Pt-Ni Alloys. Topics in Catalysis, 2020, 63, 714-727.	1.3	4
35177	Ab-initio study of structural, electronic, elastic, phonon properties, and phase transition path of sodium selenite. Chemical Physics, 2020, 539, 110934.	0.9	3
35178	Adsorption mechanism insights into CPAM structural units on kaolinite surfaces: A DFT simulation. Applied Clay Science, 2020, 197, 105719.	2.6	20
35179	Dimensionality effects in crystal plasticity, from 3D silicon to 2D silicene. Extreme Mechanics Letters, 2020, 40, 100892.	2.0	1
35180	Effect of titanium on the precipitation behaviors of transmutation elements in tungsten-titanium alloys from first-principles calculations. Fusion Engineering and Design, 2020, 158, 111673.	1.0	4
35181	Stabilization of complex orthorhombic o-Cr3C2 thin films under high energetic growth conditions: Experiments and calculations. Journal of Alloys and Compounds, 2020, 848, 156373.	2.8	3
35182	Ab initio study of Pr1-xSrxCrO3-Î´ cubic perovskites: Solid oxide fuel cells applications. Journal of Solid State Chemistry, 2020, 290, 121581.	1.4	5
35183	Adsorption of NO₂ and NO₃ on Cobalt Spinel Nanocubes and Interfacial Dynamics of the Resultant NO_x Adspecies (x = 1, 2, and 3): DFT, Atomistic Thermodynamic, IR, and Isotopic Exchange Study. Journal of Physical Chemistry C, 2020, 124, 19681-19697.	1.5	9
35184	Adsorption of Aspartic Acid on Ni{100}: A Combined Experimental and Theoretical Study. Langmuir, 2020, 36, 9399-9411.	1.6	5
35185	Performance of the Pentagonal PdSe₂ Sheet as a Channel Material in Contact with Metal Surfaces and Graphene. ACS Applied Electronic Materials, 2020, 2, 2535-2542.	2.0	14
35186	The Vital Role of Step-Edge Sites for Both CO Activation and Chain Growth on Cobalt Fischerâ€“Tropsch Catalysts Revealed through First-Principles-Based Microkinetic Modeling Including Lateral Interactions. ACS Catalysis, 2020, 10, 9376-9400.	5.5	37
35187	Origin of photocatalytic activity enhancement in Pd/Pt-deposited anatase N-TiO₂ â€“ experimental insights and DFT study of the (001) surface. Physical Chemistry Chemical Physics, 2020, 22, 18536-18547.	1.3	6
35188	A machine learning scheme for the catalytic activity of alloys with intrinsic descriptors. Journal of Materials Chemistry A, 2020, 8, 17507-17515.	5.2	60

#	Article	IF	Citations
35189	Two-dimensional chromium pnictides <mml:math xmlns:mml="http://www.w3.org/1998/Math/MathML"><mml:mi>Cr</mml:mi><mml:mi>X</mml:mi><mml:mo>Â</mml:mo><mml:mo>(</mml:mo> : Half-metallic ferromagnets with high Curie temperature. Physical Review B, 2020, 102, .	1.1	44
35190	Understanding the Effect of Mn Doping in CsPbBr₃ Using Ab-Initio Method With Experimental Validation. IEEE Journal of Photovoltaics, 2020, 10, 1359-1364.	1.5	5
35191	A First-Principles Simulation of Electronic Structure of MCN2 Crystals (M = Be, Mg, Ca, Zn, Cd, Hg). Journal of Structural Chemistry, 2020, 61, 337-343.	0.3	9
35192	Magnetic properties of the multiferroic double perovskite lead iron niobate: Role of disorder. Journal of Magnetism and Magnetic Materials, 2020, 515, 167309.	1.0	4
35193	Electronic and optical properties of Wâ€“Sn-Z and Wâ€²-Sn-Wâ€² monolayers using density functional theory. Solid State Communications, 2020, 321, 114016.	0.9	5
35194	Particle Size Effects in Stoichiometric Methane Combustion: Structureâ€“Activity Relationship of Pd Catalyst Supported on Gamma-Alumina. ACS Catalysis, 2020, 10, 10339-10349.	5.5	84
35195	Graphitic phosphorus coordinated single Fe atoms for hydrogenative transformations. Nature Communications, 2020, 11, 4074.	5.8	122
35196	Stability of ferroelectric and antiferroelectric hafniumâ€“zirconium oxide thin films. Journal of Applied Physics, 2020, 128, .	1.1	19
35197	Investigation of structural and magnetoelectronic properties of new halfâ€metallic Heusler alloys <scp>Ru₂VGe_xSb₁</scp>_{â^’x} (x =â€‰0,) Tj ETQq0 0 0 rgBT /O e26413.	1.0	7
35198	ATiO3/TiO (A=Pb, Sn) superlattice: Bridging ferroelectricity and conductivity. Computational Condensed Matter, 2020, 25, e00491.	0.9	2
35199	Room-temperature ferromagnetism on ZnO nanoparticles doped with Cr: An experimental and theoretical analysis. Journal of Alloys and Compounds, 2020, 849, 156587.	2.8	33
35200	Ferromagnetism and controllable half-metallicity of two-dimensional hexagonal CrOX (XÂ=ÂF, Cl, Br) monolayers. Journal of Magnetism and Magnetic Materials, 2020, 515, 167310.	1.0	11
35201	Tight-binding method for the electronic and optical properties of C and BN nanotubes. Materials Science and Engineering B: Solid-State Materials for Advanced Technology, 2020, 261, 114671.	1.7	1
35202	Structural stability, tunable electronic and optical properties of two-dimensional WS2 and GaN heterostructure: First-principles calculations. Materials Science and Engineering B: Solid-State Materials for Advanced Technology, 2020, 261, 114672.	1.7	46
35203	Superb Hydrogen Evolution by a Pt Nanoparticle-Decorated Ni₃S₂ Microrod Array. ACS Applied Materials & Interfaces, 2020, 12, 39163-39169.	4.0	41
35204	Sulfur-Doped Titanium Carbide MXenes for Room-Temperature Gas Sensing. ACS Sensors, 2020, 5, 2915-2924.	4.0	92
35205	Ultrafast photoinduced band splitting and carrier dynamics in chiral tellurium nanosheets. Nature Communications, 2020, 11, 3991.	5.8	39
35206	Using statistical learning to predict interactions between single metal atoms and modified MgO(100) supports. Npj Computational Materials, 2020, 6, .	3.5	16

#	Article	IF	Citations
35207	Electric field induced band tuning, optical and thermoelectric responses in tetragonal germanene: a theoretical approach. Physical Chemistry Chemical Physics, 2020, 22, 19957-19968.	1.3	31
35208	Stable and selective electrosynthesis of hydrogen peroxide and the electro-Fenton process on CoSe₂ polymorph catalysts. Energy and Environmental Science, 2020, 13, 4189-4203.	15.6	134
35209	Encapsulation of volatile fission products in a two-dimensional dicalcium nitride electride. Journal of Applied Physics, 2020, 128, 045112.	1.1	3
35210	Electronic and optical properties of biphenylene under pressure: first-principles calculations. Molecular Simulation, 2020, 46, 987-993.	0.9	2
35211	DFT study of electronic and optical properties of CH3NH3SnI3 perovskite. Energy Sources, Part A: Recovery, Utilization and Environmental Effects, 0, , 1-13.	1.2	12
35212	Large-gap topological insulators in functionalized ordered double transition metal carbide MXenes. Physical Review B, 2020, 102, .	1.1	24
35213	Origin of the monoclinic distortion and its impact on the electronic properties in <mml:math xmlns:mml="http://www.w3.org/1998/Math/MathML"><mml:msub><mml:mi>KO</mml:mi><mml:mn>2</mml:mn></mml:msub></mml Physical Review B, 2020, 102, .	1.1	2
35214	Dissolved gas analysis in transformer oil using Sb-doped graphene: A DFT study. Applied Surface Science, 2020, 533, 147509.	3.1	36
35215	Surface dangling bonds dependent magnetic properties in Mn-doped GaAs nanowires. Physics Letters, Section A: General, Atomic and Solid State Physics, 2020, 384, 126815.	0.9	1
35216	Unveiling the Active Site of Metal-Free Nitrogen-doped Carbon for Electrocatalytic Carbon Dioxide Reduction. Cell Reports Physical Science, 2020, 1, 100145.	2.8	53
35217	High mechanical strength and broad optical absorption in underexplored group IV nitride chalcogenides. Chemical Communications, 2020, 56, 10962-10965.	2.2	5
35218	Acceptor Decoration of Threading Dislocations in <mml:math xmlns:mml="http://www.w3.org/1998/Math/MathML" display="inline" overflow="scroll"><mml:mrow><mml:mrow><mml:mo stretchy="false">(</mml:mo><mml:mi>Al</mml:mi><mml:mo>,</mml:mo><mml:mi>Ga</mml:mi><mml:mo) Tj ETQq1 1 0.784314 rgBT mathvariant="normal">N</mml:mi><mml:mo>/</mml:mo></mml:mrow><mml:mi>Ga</mml:mi><mml:mi m	1.5	15
35219	Signatures of possible surface states in TaAs. Physical Review B, 2020, 102, .	1.1	9
35220	Extensive investigation of structural, electronic, optical, and thermoelectric properties of hybrid perovskite (<scp> CH ₃ NH ₃ PbBr ₃ </scp>) with mechanical stability constants. International Journal of Energy Research, 2020, 44, 11614-11628.	2.2	20
35221	Theoretical Study of the Local Vibrational Modes at Shock Wave Front for Energetic Material. Propellants, Explosives, Pyrotechnics, 2020, 45, 1523-1532.	1.0	0
35222	Metastable Al-Fe intermetallic stabilised by epitaxial relationship. Applied Surface Science, 2020, 533, 147492.	3.1	5
35223	Enhancing the electronic and phonon transport properties of two-dimensional hexagonal boron nitride through oxygenation: A first principles study. Applied Surface Science, 2020, 533, 147513.	3.1	18
35224	Interface characterization and mechanical properties of Mo-added chromium carbide-nickel composite. Ceramics International, 2020, 46, 27071-27079.	2.3	10

#	Article	IF	Citations
35225	Effects of nitrilotriacetic acid and corrosion inhibitor on cobalt barrier chemicalâ€“mechanical polishing: Experimental and density functional theory analysis. Colloids and Surfaces A: Physicochemical and Engineering Aspects, 2020, 605, 125392.	2.3	41
35226	Carbon clustering and effect on hydrogen trapping in tungsten: A first-principles study. Computational Materials Science, 2020, 184, 109932.	1.4	9
35227	An interconnected silver coated carbon cloth framework as a host to reduce lithium nucleation over-potential for dendrite-free lithium metal anodes. Journal of Electroanalytical Chemistry, 2020, 878, 114569.	1.9	21
35228	Novel green phosphorene sheets to detect tear gas molecules - A DFT insight. Journal of Molecular Graphics and Modelling, 2020, 100, 107706.	1.3	23
35229	A DFT study of the structural, elastic, electronic and magnetic properties of new quaternary compounds TiHfOsX(Al,Ga,In). Physics Letters, Section A: General, Atomic and Solid State Physics, 2020, 384, 126793.	0.9	11
35230	Optimal arrangement of Ï€-conjugated anionic groups in hydro-isocyanurates leads to large optical anisotropy and second-harmonic generation effect. Inorganic Chemistry Frontiers, 2020, 7, 3674-3686.	3.0	24
35231	A Symmetry-Breaking Phase in Two-Dimensional FeTe₂ with Ferromagnetism above Room Temperature. Journal of Physical Chemistry Letters, 2020, 11, 7893-7900.	2.1	59
35232	Magnetism, half-metallicity, and topological signatures in Fe_{2â^'x}V_xPO₅ (x = 0, 0.5, 1, 1.5, 2) materials: a potential class of advanced spintronic materials. Physical Chemistry Chemical Physics, 2020, 22, 20027-20036.	1.3	0
35233	Computational studies on triphenyldiyne as a two-dimensional visible-light-driven photocatalyst for overall water splitting. Physical Chemistry Chemical Physics, 2020, 22, 20061-20068.	1.3	4
35234	The mechanical, electronic, optical and thermoelectric properties of two-dimensional honeycomb-like of XSb (X = Si, Ge, Sn) monolayers: a first-principles calculations. RSC Advances, 2020, 10, 30398-30405.	1.7	26
35235	Double Atom Catalysts: Heteronuclear Transition Metal Dimer Anchored on Nitrogenâ€Doped Graphene as Superior Electrocatalyst for Nitrogen Reduction Reaction. Advanced Theory and Simulations, 2020, 3, 2000190.	1.3	26
35236	An experimental and theoretical insights into the dielectric properties of (Li, Nd) co-doped ZnO ceramics. Journal of Materials Science: Materials in Electronics, 2020, 31, 20113-20128.	1.1	6
35237	A DFT-D2 study on Mo4-xCox (x = 0â€“3) cluster-decorated graphene and the adsorption of SO2F2 and SOF2 on Mo4-decorated graphene. Journal of Nanoparticle Research, 2020, 22, 1.	0.8	2
35238	Pressure-dependent Raman scattering of polycrystalline KNb1â^'xTaxO3 solid solutions. SN Applied Sciences, 2020, 2, 1.	1.5	2
35239	Configurations of V4+ centers in the MoVO catalyst material. A systematic stability analysis of DFT results. SN Applied Sciences, 2020, 2, 1.	1.5	0
35240	Molecularly Engineered Strong Metal Oxideâ€“Support Interaction Enables Highly Efficient and Stable CO₂ Electroreduction. ACS Catalysis, 2020, 10, 13227-13235.	5.5	94
35241	Mechanistic insight into H2-mediated Ni surface diffusion and deposition to form branched Ni nanocrystals: a theoretical study. Physical Chemistry Chemical Physics, 2020, 22, 23869-23877.	1.3	1
35242	S-Vacancy induced indirect-to-direct band gap transition in multilayer MoS₂. Physical Chemistry Chemical Physics, 2020, 22, 26005-26014.	1.3	18

#	Article	IF	Citations
35243	Investigating the journal impact along the columns and rows of the publication-citation matrix. Scientometrics, 2020, 125, 2265-2282.	1.6	3
35244	Optical spectra of monolayer MoS2 from spin-polarized all electrons density-functional calculations. Optik, 2020, 222, 165477.	1.4	4
35245	Validation of defect association energy on modulating oxygen ionic conductivity in low temperature solid oxide fuel cell. Journal of Power Sources, 2020, 480, 229106.	4.0	10
35246	Herzbergâ€“Teller Effect on the Vibrationally Resolved Absorption Spectra of Single-Crystalline Pentacene at Finite Temperatures. Journal of Physical Chemistry A, 2020, 124, 9156-9165.	1.1	14
35247	Two-Dimensional Gold Halides: Novel Semiconductors with Giant Spinâ€“Orbit Splitting and Tunable Optoelectronic Properties. Journal of Physical Chemistry Letters, 2020, 11, 9759-9765.	2.1	3
35248	Theoretical Insights into the Favorable Functionalized Ti₂C-Based MXenes for Lithiumâ€“Sulfur Batteries. ACS Omega, 2020, 5, 29272-29283.	1.6	28
35249	Scalable colloidal synthesis of Bi₂Te_{2.7}Se_{0.3} plate-like particles give access to a high-performing n-type thermoelectric material for low temperature application. Nanoscale Advances, 2020, 2, 5699-5709.	2.2	13
35250	Structural, electronic, and magnetic properties of Ni nanoparticles supported on the TiC(001) surface. Physical Chemistry Chemical Physics, 2020, 22, 26145-26154.	1.3	8
35251	Cu and Sb in tetragonal ZrO2 on fuel cladding. Journal of Applied Physics, 2020, 128, 135101.	1.1	0
35252	Plasma modification of vanadium oxynitride surfaces: Characterization by in situ XPS experiments and DFT calculations. Journal of Chemical Physics, 2020, 153, 144709.	1.2	14
35253	The search for the new superconductors in the Ni-N system. Journal of Physics: Conference Series, 2020, 1590, 012010.	0.3	1
35254	Study of the energy band structure of xBa (Sc1/2Nb1/2)O3-(1-x)(K1/2Na1/2)NbO3 perovskite solid solution. Journal of Physics: Conference Series, 2020, 1629, 012068.	0.3	0
35255	First-principles theoretical analysis and electron energy loss spectroscopy of vacancy defects in bulk and nonpolar (101Â¯) surface of GaN. Journal of Vacuum Science and Technology A: Vacuum, Surfaces and Films, 2020, 38, .	0.9	4
35256	Au_xPd_(300â€“x) Alloy Nanoparticles for the Oxygen Reduction Reaction in Alkaline Media. ChemElectroChem, 2020, 7, 3824-3831.	1.7	9
35257	Tuning the electronic properties of C12A7 via Sn doping and encapsulation. Journal of Materials Science: Materials in Electronics, 2020, 31, 21203-21213.	1.1	1
35258	Electrical and thermal transport properties of medium-entropy Si Ge Sn alloys. Acta Materialia, 2020, 199, 443-452.	3.8	13
35259	Theoretical investigation of the AlN (0 0 0 1)-(2ÂÃ—Â2) surface doped with nickel: Structural, electronic and magnetic properties. Journal of Crystal Growth, 2020, 551, 125907.	0.7	3
35260	A density functional theory study of the vibrational spectra of aluminate sodalite, |M8X2|[Al12O24]-SOD (M=Ca, Cd, Sr; X=CrO4, MoO4, S, SO4, Se, SeO3, Te, TeO3). Microporous and Mesoporous Materials, 2020, 309, 110466.	2.2	4

#	Article	IF	Citations
35261	Structural and Electromechanical Properties of Sr-Substituted Barium Titanate (BST) as Potential Material for High Performance Electroacoustic Devices. Materials Today Communications, 2020, 25, 101643.	0.9	8
35262	Silicene oxide: a potential Battery500 cathode for sealed non-aqueous lithiumâ€“oxygen batteries. Materials Today Energy, 2020, 18, 100503.	2.5	6
35263	Enhanced the physical properties through the oxygen vacancy in (Eu1-xScx)2Zr2O7 Zirconate pyrochlore. Optical Materials, 2020, 110, 110499.	1.7	1
35264	Energetic Stability of Free-standing and Metal-Supported Borophenes: Quantum Monte Carlo and Density Functional Theory Calculations. Journal of Physical Chemistry C, 2020, 124, 24420-24428.	1.5	5
35265	Electrical control of spin polarization of transmission in pure-carbon systems of helical graphene nanoribbons. Journal of Applied Physics, 2020, 128, .	1.1	11
35266	Hierarchical bifunctional catalysts with tailored catalytic activity for high-energy rechargeable Zn-air batteries. Applied Energy, 2020, 279, 115876.	5.1	20
35267	Electronic properties of fluorine/hydrogen adsorbed two-dimensional tetrahex-carbon: A first-principles study. Applied Surface Science, 2020, 529, 147150.	3.1	2
35268	Insights into the predicted Hf2SN in comparison with the synthesized MAX phase Hf2SC: A comprehensive study. Computational Condensed Matter, 2020, 24, e00485.	0.9	17
35269	First-principles evaluation of the potential of using Mg2SiO4, Mg2VO4, and Mg2GeO4 for CO2 capture. Journal of CO2 Utilization, 2020, 42, 101293.	3.3	8
35270	On the formation and structure of Mn-Ni-Si Î“2 precipitates in steels. Journal of Nuclear Materials, 2020, 542, 152429.	1.3	6
35271	A thorough study on the F-decoration of Ï‡3 borophene and enhancement of anodic performance of Lithium-ion batteries. Journal of Molecular Liquids, 2020, 319, 114343.	2.3	11
35272	Probing the physical and superconducting properties of hexagonal ZrRuAs: A first-principles calculation. Physica C: Superconductivity and Its Applications, 2020, 577, 1353715.	0.6	2
35273	Role of Methane as a Second Guest Component in Thermodynamic Stability and Isomer Selectivity of Butane Clathrate Hydrates. Journal of Physical Chemistry C, 2020, 124, 18474-18481.	1.5	17
35274	Electronic Structure and Magnetic Properties of OsCrMnSb and IrCrMnSb from Ab Initio Calculations. Spin, 2020, 10, .	0.6	1
35275	First-Principles Study on the Magnetoelectric and Optical Properties of Novel Magnetic Semiconductor Li(Mg, Cr)P With Decoupled Spin and Charge Doping. Frontiers in Chemistry, 2020, 8, 594411.	1.8	2
35276	First-principles simulation of h interacting with transition elements in molybdenum for nuclear material application. Journal of Nuclear Materials, 2020, 541, 152437.	1.3	4
35277	Nickel â€“ p-block metal mixed chalcogenides based on AuCu₃-type fragments: iodine-assisted synthesis as a way of obtaining new structures. Dalton Transactions, 2020, 49, 15081-15094.	1.6	5
35278	Induced spin polarization in graphene via interactions with halogen doped MoS₂ and MoSe₂ monolayers by DFT calculations. Nanoscale, 2020, 12, 23248-23258.	2.8	13

#	Article	IF	Citations
35279	Investigation Insights into Electronic Structures, Exchange Splittings, Induced Ferromagnetism, and Half-Metallic Feature in New Ti-Doped BaS. JETP Letters, 2020, 112, 568-576.	0.4	1
35280	Hexagonal and Monoclinic Phases of La2O2CO3 Nanoparticles and Their Phase-Related CO2 Behavior. Nanomaterials, 2020, 10, 2061.	1.9	8
35281	Theoretical investigation of the interaction of gas molecules with Pt-adsorbed arsenene monolayers. Computational and Theoretical Chemistry, 2020, 1190, 112977.	1.1	7
35282	Hardness and Young's modulus of Al3Yb single crystal studied by nano indentation. Intermetallics, 2020, 127, 106980.	1.8	5
35283	First-principle investigations of martensitic transformation and magnetic properties in Ni24Mn17â^'In7Cu (xÂ=Â0â€“5) alloys. Journal of Magnetism and Magnetic Materials, 2020, 516, 167363.	1.0	4
35284	Understanding the influences of Mg doping on the physical properties of SrMoO3 perovskite. Results in Physics, 2020, 19, 103337.	2.0	56
35285	Doping Modulation of the Charge Injection Barrier between a Covalent Organic Framework Monolayer and Graphene. Chemistry of Materials, 2020, 32, 9228-9237.	3.2	18
35286	Theoretical Description, Synthesis, and Structural Characterization of Î²-Na_{0.33}V₂O₅ and Its Fluorinated Derivative Î²-Na_{0.33}V₂O_{4.67}F_{0.33}: Influence of Oxygen Substitution by Fluorine on the Electrochemical Properties. Inorganic Chemistry, 2020, 59, 16361-16374.	1.9	5
35287	Robust Active Site Design of Single-Atom Catalysts for Electrochemical Ammonia Synthesis. Journal of Physical Chemistry C, 2020, 124, 23164-23176.	1.5	8
35288	Effect of Ligand Adsorption on the Electronic Properties of the PbS(100) Surface. Langmuir, 2020, 36, 13312-13319.	1.6	3
35289	Understanding reactivity of a triazole derivative and its interaction with graphene and doped/undoped-coroneneâ€"a DFT study. Journal of Biomolecular Structure and Dynamics, 2022, 40, 2316-2326.	2.0	10
35290	Electronic, magnetic and optical properties of monolayer (ML) hexagonal ZnSe on vacancy defects at Zn sites from DFT-1/2 approach. Vacuum, 2020, 182, 109597.	1.6	17
35291	Intense d-p Hybridization Induced a Vast SHG Response Disparity between Tetrahedral Vanadates and Arsenates. Journal of Physical Chemistry C, 2020, 124, 24949-24956.	1.5	8
35292	Phononic and electronic features of diamond nanowires. Diamond and Related Materials, 2020, 109, 108051.	1.8	2
35293	Fe effect on hydrogen interactions with intrinsic point defects and hydrogen migration in Î±-Al2O3 based tritium permeation barriers. Journal of Nuclear Materials, 2020, 542, 152494.	1.3	5
35294	Magnetic Interactions in ZnMnO₃: Active Role of Zn 3d¹⁰ Orbitals, in Comparison with MgMnO₃. Inorganic Chemistry, 2020, 59, 16205-16214.	1.9	8
35295	Rationally Designed Semiconducting 2D Surface-Confined Metalâ€"Organic Network. ACS Applied Materials & Interfaces, 2020, 12, 51122-51132.	4.0	3
35296	Ab Initio Study of Polytetrafluoroethylene Defluorination for Tribocharging Applications. ACS Applied Polymer Materials, 2020, 2, 5129-5134.	2.0	5

#	Article	IF	Citations
35297	Strain effects in coreâ€“shell PtCo nanoparticles: a comparison of experimental observations and computational modelling. Physical Chemistry Chemical Physics, 2020, 22, 24784-24795.	1.3	15
35298	LaTiO₂N crystallographic orientation control significantly increases visible-light induced charge extraction. Journal of Materials Chemistry A, 2020, 8, 22867-22873.	5.2	5
35299	Pressure effects on magnetism in <mml:math xmlns:mml="http://www.w3.org/1998/Math/MathML"><mml:mrow><mml:msub><mml:mi>Ca</mml:mi><mml:mn>2</mml:mn></mml: mathvariant="normal">O</mml:mi><mml:mn>5</mml:mn></mml:msub></mml:mrow></mml:math> -type ferrites and manganites. Physical Review B, 2020, 102, .	1.1	2
35300	Blue phosphorus nanoscrolls. Physical Review B, 2020, 102, .	1.1	5
35301	CO2 and H2O Coadsorption and Reaction on the Low-Index Surfaces of Tantalum Nitride: A First-Principles DFT-D3 Investigation. Catalysts, 2020, 10, 1217.	1.6	7
35302	Structures and Properties of the Self-Assembling Diphenylalanine Peptide Nanotubes Containing Water Molecules: Modeling and Data Analysis. Nanomaterials, 2020, 10, 1999.	1.9	21
35303	Investigation of the reaction mechanism of the hydrodeoxygenation of propionic acid over a Rh(1 1 1) surface: A first principles study. Journal of Catalysis, 2020, 391, 98-110.	3.1	8
35304	Experimental and theoretical Raman study on the HTSC PrxY1â^'xBa2Cu3O7 family for different Pr concentrations and synthesis methods. Materials Chemistry and Physics, 2020, 256, 123737.	2.0	5
35305	Experimental and Computational Determination of Optimal Boron Content in Layered Superconductor Sc₂₀C_{8â€“x}B_xC₂₀. Inorganic Chemistry, 2020, 59, 14290-14295.	1.9	1
35306	Magnetism and Heterogeneous Catalysis: In Depth on the Quantum Spin-Exchange Interactions in Pt₃M (M = V, Cr, Mn, Fe, Co, Ni, and Y)(111) Alloys. ACS Applied Materials & Interfaces, 2020, 12, 50484-50494.	4.0	22
35307	Electronic properties of Janus MXY/graphene (M = Mo, W; X â‰ Y = S, Se) van der Waals structures: a first-principles study. Physical Chemistry Chemical Physics, 2020, 22, 25675-25684.	1.3	16
35308	Nanoleite: a new semiconducting carbon allotrope predicted by density functional theory. RSC Advances, 2020, 10, 38782-38787.	1.7	2
35309	Assessment of PBE+U and HSE06 methods and determination of optimal parameter U for the structural and energetic properties of rare earth oxides. Journal of Chemical Physics, 2020, 153, 164710.	1.2	13
35310	First-principles calculations of vibrational and optical properties of half-Heusler NaScSi. Indian Journal of Physics, 2021, 95, 2303-2312.	0.9	16
35311	Quantitative prediction of Suzuki segregation at stacking faults of the Î³â€™ phase in Ni-base superalloys. Acta Materialia, 2020, 200, 223-235.	3.8	24
35312	Microstructural study of Ti 45Nb alloy before and after HPT processing using experimental and ab initio data mining approach. Materials Characterization, 2020, 169, 110635.	1.9	11
35313	Evidence of an ordered ternary phase in the section Niâ€“Ti5Sn3 of the ternary Tiâ€“Niâ€“Sn: Crystal structure and phase stability. Solid State Sciences, 2020, 109, 106349.	1.5	2
35314	Huge Piezoelectric Response of LaN-based Superlattices. ACS Applied Materials & Interfaces, 2020, 12, 49805-49811.	4.0	12

#	Article	IF	Citations
35315	Theoretical Characterization of the High Pressure Nonclathrate CO₂ Hydrate. ACS Earth and Space Chemistry, 2020, 4, 2121-2128.	1.2	1
35316	Xenon iron oxides predicted as potential Xe hosts in Earthâ€™s lower mantle. Nature Communications, 2020, 11, 5227.	5.8	27
35317	Dynamic disorder phonon scattering mediated by Cu atomic hopping and diffusion in Cu3SbSe3. Npj Computational Materials, 2020, 6, .	3.5	7
35318	From magnetic order to quantum disorder in the Zn-barlowite series of Sâ€‰=â€‰1/2 kagomÃ© antiferromagnets. Npj Quantum Materials, 2020, 5, .	1.8	21
35319	Theoretical insights of codoping to modulate electronic structure of $$hbox {TiO}_2$$ and $$hbox {SrTiO}_3$$ for enhanced photocatalytic efficiency. Scientific Reports, 2020, 10, 15372.	1.6	8
35320	Ab initio study for molecular-scale adsorption, decomposition and desorption on AlN surfaces during MOCVD growth. Scientific Reports, 2020, 10, 17840.	1.6	2
35321	Tuning magnetic properties of penta-graphene bilayers through doping with boron, nitrogen, and oxygen. Scientific Reports, 2020, 10, 16748.	1.6	7
35322	Room temperature deformation of single crystals of Ti5Si3 with the hexagonal D88 structure investigated by micropillar compression tests. Scientific Reports, 2020, 10, 17983.	1.6	11
35323	Route to high-$$T_{c}$$ superconductivity of $$hbox {BC}_{{7}}$$ via strong bonding of boronâ€“carbon compound at high pressure. Scientific Reports, 2020, 10, 18090.	1.6	11
35324	An in-silico layer-by-layer adsorption study of the interaction between Rebaudioside A and the T1R2 human sweet taste receptor: modelling and biosensing perspectives. Scientific Reports, 2020, 10, 18391.	1.6	9
35325	Electronic and geometrical parametrization of the role of organic/inorganic cations on the photovoltaic perovskite band gap. Physical Chemistry Chemical Physics, 2020, 22, 27757-27769.	1.3	7
35326	Predicted 2D ferromagnetic Janus VSeTe monolayer with high Curie temperature, large valley polarization and magnetic crystal anisotropy. Nanoscale, 2020, 12, 22735-22742.	2.8	64
35327	Calcium-stannous oxide solid solutions for solar devices. Applied Physics Letters, 2020, 117, .	1.5	2
35328	Topological nodal line in <mml:math xmlns:mml="http://www.w3.org/1998/Math/MathML"><mml:msub><mml:mi>ZrTe</mml:mi><mml:mn>2</mml:mn></mml:msub></mml:math> demonstrated by nuclear magnetic resonance. Physical Review B, 2020, 102, .	1.1	12
35329	A First-Principles Study of TiX2 (X = S, Se, and Te) Compounds Optical Properties under the Effect of Externally Applied Electric Field and Strain. Physics of the Solid State, 2020, 62, 1905-1915.	0.2	6
35330	First-principles investigation on the adsorption and dissociation of O2 and H2O molecules on the Ni-rich TiNi alloy surface. Applied Surface Science, 2020, 534, 147570.	3.1	19
35331	First-principles calculations on adsorption-diffusion behavior of Boron atom with tungsten surface. Computational Materials Science, 2020, 183, 109908.	1.4	10
35332	Interaction of H2S with perfect and S-covered Ni(110) surface: A first-principles study. International Journal of Hydrogen Energy, 2020, 45, 30622-30633.	3.8	13

#	Article	IF	Citations
35333	Unveiling the energetic and structural properties of Pu doped zircon through electrochemical equilibrium diagram from DFT+U calculations. Journal of Nuclear Materials, 2020, 539, 152234.	1.3	0
35334	Insights into the zinc effect on radio-cobalt deposition on stainless steel piping surfaces under BWR conditions from experiment guided 1st principles modelling. Journal of Nuclear Materials, 2020, 540, 152361.	1.3	3
35335	Equilibrium concentration of hydrogen at tungsten surface. Journal of Nuclear Materials, 2020, 541, 152377.	1.3	0
35336	Impact of polytypism on the ground state properties of zinc oxide: A first-principles study. Results in Physics, 2020, 18, 103316.	2.0	8
35337	Electronic structure and sodium-ion diffusion in glaserite-type A3â˜Na1+(MoO4)2 (AÂ=ÂCs, K) studied with first-principles calculations. Solid State Ionics, 2020, 357, 115484.	1.3	2
35338	At the Limits of Isolobal Bonding: Ï€-Based Covalent Magnetism in Mn2Hg5. Inorganic Chemistry, 2020, 59, 12304-12313.	1.9	7
35339	Bulk and Surface Chemistry of the Niobium MAX and MXene Phases from Multinuclear Solid-State NMR Spectroscopy. Journal of the American Chemical Society, 2020, 142, 18924-18935.	6.6	35
35340	Marcusâ€“Hushâ€“Chidsey kinetics at electrodeâ€“electrolyte interfaces. Journal of Chemical Physics, 2020, 153, 134706.	1.2	22
35341	Electronic properties of substitutional impurities in graphenelike <mml:math xmlns:mml="http://www.w3.org/1998/Math/MathML"><mml:mrow><mml:msub><mml:mi mathvariant="normal">C</mml:mi><mml:mn>2</mml:mn></mml:msub><mml:mi mathvariant="normal">N</mml:mi></mml:mrow></mml:math> , <mml:math xmlns:mml="http://www.w3.org/1998/Math/MathML"><mml:mrow><mml:mi>t</mml:mi><mml:mi>g</mml:mi><mml:mtext>â˜</mml:mtext></mml:mrow></mml:math> , and <mml:math xmlns:mml="http://www.w3.org/1998/Math/MathML"><mml:mrow><mml:msub><mml:mi mathvariant="normal">C</mml:mi><mml:mn>3</mml:mn></mml:msub><mml:msub><mml:mi mathvariant	1.1	11
35342	Resolving Anharmonic Lattice Dynamics in Molecular Crystals with X-Ray Diffraction and Terahertz Spectroscopy. Physical Review Letters, 2020, 125, 103001.	2.9	14
35343	Enhancing Methanol Oxidation Reaction with Platinumâ€based Catalysts using a Nâ€Ðoped Threeâ€dimensional Graphitic Carbon Support. ChemCatChem, 2020, 12, 6000-6012.	1.8	11
35344	Zn₄B₆O₁₃: Efficient Borate Photocatalyst with Fast Carrier Separation for Photodegradation of Tetracycline. Inorganic Chemistry, 2020, 59, 13136-13143.	1.9	29
35345	Application of NMR Crystallography to Highly Disordered Templated Materials: Extensive Local Structural Disorder in the Gallophosphate GaPO-34A. Inorganic Chemistry, 2020, 59, 11616-11626.	1.9	9
35346	Mussel Inspired Highly Aligned Ti₃C₂T_x MXene Film with Synergistic Enhancement of Mechanical Strength and Ambient Stability. ACS Nano, 2020, 14, 11722-11732.	7.3	212
35347	Structural properties and thermal stability of multi-walled black phosphorene nanotubes and their operation as temperature driven nanorotors. Nanoscale, 2020, 12, 18313-18321.	2.8	6
35348	First-Principles Study of the Interaction of H2O2 with the SnO2 (110) Surface. Journal of Contemporary Physics, 2020, 55, 235-239.	0.1	3
35349	Hydrogen-Mediated Noncovalent Interactions in Solids: What Can NMR Crystallography Tell About?. Molecules, 2020, 25, 3757.	1.7	7
35350	Room temperature ferromagnetism in ultra-thin van der Waals crystals of 1T-CrTe2. Nano Research, 2020, 13, 3358-3363.	5.8	175

#	Article	IF	Citations
35351	Efficient Ambient Electrocatalytic Ammonia Synthesis by Nanogold Triggered via Boron Clusters Combined with Carbon Nanotubes. ACS Applied Materials & Interfaces, 2020, 12, 42821-42831.	4.0	27
35352	Determination of Structural, Electronic, Optical and Mechanical Properties of Brookite TiO₂Using Various Exchange-Correlation. , 2020, , .		4
35353	Predicting short-range order and correlated phenomena in disordered crystalline materials. Science Advances, 2020, 6, eabc2758.	4.7	28
35354	Electronic, Structural, and Optical Properties of Zinc Blende and Wurtzite Cadmium Sulfide (CdS) Using Density Functional Theory. Advances in Condensed Matter Physics, 2020, 2020, 1-8.	0.4	6
35355	Decoding of Oxygen Network Distortion in a Layered High-Rate Anode by In Situ Investigation of a Single Microelectrode. ACS Nano, 2020, 14, 11753-11764.	7.3	10
35356	The InSe/SiH type-II van der Waals heterostructure as a promising water splitting photocatalyst: a first-principles study. Physical Chemistry Chemical Physics, 2020, 22, 21436-21444.	1.3	30
35357	Enhanced electrocatalytic nitrogen reduction activity by incorporation of a carbon layer on SnS microflowers. Journal of Materials Chemistry A, 2020, 8, 20677-20686.	5.2	18
35358	Insight into Structural, Electronic, Magnetic, and Elastic Properties of Full-Heusler Alloys Co2YPb (Y) Tj ETQq1 1 0.784314 rgBT /Overl	0.4	9
35359	The Concept of Negative Capacitance in Ionically Conductive Van der Waals Ferroelectrics. Advanced Energy Materials, 2020, 10, 2001726.	10.2	30
35360	Firstâ€principle investigation of <scp>XSrH₃</scp> (X = K and Rb) perovskiteâ€type hydrides for hydrogen storage. International Journal of Quantum Chemistry, 2020, 120, e26419.	1.0	36
35361	First-Principles Study on the Stability of Weberite-Type, Pyrochlore, and Defect-Fluorite Structures of A₂³⁺B₂⁴⁺O₇ (A =) Tj ETQq0 0 0 rgBT /Overlock	1.5	10
35362	Potential Energy Landscape of CO Adsorbates on NaCl(100) and Implications in Isomerization of Vibrationally Excited CO. Journal of Physical Chemistry C, 2020, 124, 19146-19156.	1.5	12
35363	Ferroresistive Diode Currents in Nanometer-Thick Cobalt-Doped BiFeO₃ Films for Memory Applications. ACS Applied Nano Materials, 2020, 3, 8888-8896.	2.4	14
35364	Bifunctional water-electrolysis-catalysts meeting band-diagram analysis: case study of â€œFePâ€• electrodes. Journal of Materials Chemistry A, 2020, 8, 20021-20029.	5.2	25
35365	SIMULATION OF ELECTRONIC STRUCTURES OF Hgâ€“IVâ€“V2 COMPOUNDS. Journal of Structural Chemistry, 2020, 61, 1007-1016.	0.3	8
35366	Structural Insight of the Frailty of 2D Janus NbSeTe as an Active Photocatalyst. ChemCatChem, 2020, 12, 6013-6023.	1.8	20
35367	Oxygen Vacancies in the Single Layer of Ti₂CO₂ MXene: Effects of Gating Voltage, Mechanical Strain, and Atomic Impurities. Physica Status Solidi (B): Basic Research, 2020, 257, 2000343.	0.7	29
35368	Oxygen Redox Activity in Cathodes: A Common Phenomenon Calling for Density-Based Descriptors. Journal of Physical Chemistry C, 2020, 124, 19962-19968.	1.5	2

#	Article	IF	Citations
35369	Thermal Water Splitting on the WO₃ Surface: Experimental Proof. ACS Applied Electronic Materials, 2020, 2, 3254-3262.	2.0	12
35370	Spin-orbit quantum impurity in a topological magnet. Nature Communications, 2020, 11, 4415.	5.8	34
35371	Disclosing the behavior under hydrostatic pressure of rhombohedral MgIn₂Se₄ by means of first-principles calculations. Physical Chemistry Chemical Physics, 2020, 22, 21909-21918.	1.3	7
35372	Unveiling the origin of room-temperature ferromagnetism in monolayer VSe2: the role of extrinsic effects. Nanoscale, 2020, 12, 20875-20882.	2.8	26
35373	Reststrahlen band studies in cubic perovskite materials SmXO₃ (X = Al,Co) by computational investigations. International Journal of Modern Physics B, 2020, 34, 2050206.	1.0	0
35374	Elucidating energy scaling between atomic and molecular adsorbates in the presence of solvent. AICHE Journal, 2020, 66, e17036.	1.8	8
35375	The study of bending properties of monolayer MoS₂ in non-collinear electrodes using first principles theory. Physical Chemistry Chemical Physics, 2020, 22, 21888-21892.	1.3	2
35376	Theoretical Study of the Electronic and Optical Properties of a Heterostructure Based on PTCDA Organic Semiconductor and MoSe2. JETP Letters, 2020, 111, 627-632.	0.4	3
35377	Spontaneous Growth of CaBi4Ti4O15 Piezoelectric Crystal Using Mixed Flux Agents. Crystals, 2020, 10, 698.	1.0	2
35378	Tracking the formation, fate and consequence for catalytic activity of Pt single sites on CeO2. Nature Catalysis, 2020, 3, 824-833.	16.1	209
35379	The mechanism for CO2 reduction over Fe-modified Cu(100) surfaces with thermodynamics and kinetics: a DFT study. RSC Advances, 2020, 10, 32569-32580.	1.7	7
35380	Density functional study of CoFeCrZ (Z=Al, Si, Ga, Ge) quaternary Heusler alloys for phonon spectra. International Journal of Modern Physics B, 2020, 34, 2050215.	1.0	2
35381	Methane Conversion over C2N-Supported Fe2 Dimers. Catalysts, 2020, 10, 973.	1.6	1
35382	Hydrogen Adsorption on Ru-Encapsulated, -Doped and -Supported Surfaces of C60. Surfaces, 2020, 3, 408-422.	1.0	5
35383	Carrier and Transition Metals (M = Nb, Cr and Fe) Doping Effects on Structure and Electronic Structure in Spinel Li₄Ti₅O₁₂ Compounds. Solid State Phenomena, 0, 310, 88-95.	0.3	2
35384	Origin of the Distinct Thermoelectric Transport Properties of Chalcopyrite ABTe₂ (A) Tj ETQq1 1 0.784314 rgBT /Overloc	7.8	50
35385	Strong Electronâ€“Phonon Interaction in 2D Vertical Homovalent IIIâ€“V Singularities. ACS Nano, 2020, 14, 13127-13136.	7.3	8
35386	First-principles surface energies for monoclinic Ga2O3 and Al2O3 and consequences for cracking of (AlxGa1â^'x)2O3. APL Materials, 2020, 8, .	2.2	53

#	Article	IF	Citations
35387	Dynamical stability, vibrational, and optical properties of anti-perovskite A3BX (Ti3TlN,) Tj ETQq0 0 0 rgBT /Overlock 10 Tf	0.6	11
35388	Achieving room-temperature brittle-to-ductile transition in ultrafine layered Fe-Al alloys. Science Advances, 2020, 6, .	4.7	26
35389	Effects of lithium on the electronic properties of porous Ge as anode material for batteries. Journal of Computational Chemistry, 2020, 41, 2653-2662.	1.5	2
35390	Large Impact of Approximate Exchange-Correlation Functionals on Modeling the Water Gas Shift Reaction on Copper. Journal of Physical Chemistry C, 2020, 124, 22506-22520.	1.5	5
35391	Modulating the Electronic, Optical, and Transport Properties of CdTe and ZnTe Nanostructures with Organic Molecules: A Theoretical Investigation. ACS Omega, 2020, 5, 21922-21928.	1.6	2
35392	Co(NO3)2 as an inverted umbrella-type chiral noncoplanar ferrimagnet. Physical Review B, 2020, 102, .	1.1	5
35393	A theoretical approach to the structural, elastic and electronic properties of Ti8â^'xV4â^'yMox+y+zAl4â^'z lightweight shape memory alloys for biomaterial implant applications. Physica B: Condensed Matter, 2020, 598, 412416.	1.3	5
35394	Surface Charge and Electrostatic Spin Crossover Effects in CoN₄ Electrocatalysts. ACS Catalysis, 2020, 10, 12148-12155.	5.5	69
35395	Spectroscopic and first principle <mml:math xmlns:mml="http://www.w3.org/1998/Math/MathML"><mml:mrow><mml:mi>DFT</mml:mi><mml:mo>+</mml:mo><mml:mo>eDMFT< study of complex structural, electronic, and vibrational properties of <mml:math xmlns:mml="http://www.w3.org/1998/Math/MathML"><mml:mrow><mml:msub><mml:mi>M</mml:mi><mml:mn>2</mml:mn></mml:n mathvariant="normal">O</mml:mi><mml:mn>8</mml:mn></mml. Physical Review B, 2020, 102, .	1.1	15
35396	An experimentally validated neural-network potential energy surface for H-atom on free-standing graphene in full dimensionality. Physical Chemistry Chemical Physics, 2020, 22, 26113-26120.	1.3	14
35397	New possible candidate structure for phase IV of solid hydrogen. RSC Advances, 2020, 10, 26443-26450.	1.7	1
35398	How does the Li-distribution in the 16d sites determine the stability of A₃(Li,Ti₅)O₁₂ (A = Li and Na)?. RSC Advances, 2020, 10, 33509-33516.	1.7	6
35399	Exploring the potential of MnX (S, Sb) monolayers for antiferromagnetic spintronics: A theoretical investigation. Journal of Applied Physics, 2020, 128, .	1.1	15
35400	Lithium Polysulfide Interaction with Group III Atoms-Doped Graphene: A Computational Insight. Batteries, 2020, 6, 46.	2.1	9
35401	Charge Density Depinning in Defective MoTe₂ Transistor by Oxygen Intercalation. Advanced Functional Materials, 2020, 30, 2004880.	7.8	20
35402	Triple Interface Passivation Strategyâ€Enabled Efficient and Stable Inverted Perovskite Solar Cells. Small Methods, 2020, 4, 2000478.	4.6	44
35403	Key Experiments and Thermodynamic Description of the Co-Nb-Ni System. Metallurgical and Materials Transactions A: Physical Metallurgy and Materials Science, 2020, 51, 5892-5911.	1.1	11
35404	Structural characterization and property modification for two-dimensional (001) SrTiO3 nanosheets. Applied Nanoscience (Switzerland), 2020, 10, 4273-4279.	1.6	8

#	Article	IF	Citations
35409	Periodic Solids and Electron Bands. , 2020, , 81-108.		0
35410	Uniform Electron Gas and sp-Bonded Metals. , 2020, , 109-128.		0
35411	Density Functional Theory: Foundations. , 2020, , 129-144.		0
35412	The Kohnâ€“Sham Auxiliary System. , 2020, , 145-170.		0
35413	Functionals for Exchange and Correlation I. , 2020, , 171-187.		0
35414	Functionals for Exchange and Correlation II. , 2020, , 188-214.		0
35415	Electronic Structure of Atoms. , 2020, , 215-229.		0
35416	Pseudopotentials. , 2020, , 230-258.		0
35418	Plane Waves and Grids: Basics. , 2020, , 262-282.		0
35419	Plane Waves and Real-Space Methods: Full Calculations. , 2020, , 283-294.		0
35420	Localized Orbitals: Tight-Binding. , 2020, , 295-319.		0
35421	Localized Orbitals: Full Calculations. , 2020, , 320-331.		0
35422	Augmented Functions: APW, KKR, MTO. , 2020, , 332-364.		0
35423	Augmented Functions: Linear Methods. , 2020, , 365-385.		0
35424	Locality and Linear-Scaling O(N) Methods. , 2020, , 386-410.		0
35425	Quantum Molecular Dynamics (QMD). , 2020, , 411-426.		0
35426	Response Functions: Phonons and Magnons. , 2020, , 427-445.		0
35427	Excitation Spectra and Optical Properties. , 2020, , 446-464.		0

#	Article	IF	Citations
35428	Surfaces, Interfaces, and Lower-Dimensional Systems. , 2020, , 465-480.		0
35429	Wannier Functions. , 2020, , 481-498.		0
35430	Polarization, Localization, and Berry Phases. , 2020, , 499-516.		0
35431	Topology of the Electronic Structure of a Crystal: Introduction. , 2020, , 517-530.		0
35432	Two-Band Models: Berry Phase, Winding, and Topology. , 2020, , 531-546.		0
35433	Topological Insulators I: Two Dimensions. , 2020, , 547-568.		0
35434	Topological Insulators II: Three Dimensions. , 2020, , 569-580.		0
35453	Nanosized Znâ€“In Spinel-Type Sorbents for Elemental Mercury Removal from Flue Gas. Energy & Fuels, 2020, 34, 12853-12859.	2.5	16
35454	Sodium Storage Mechanism Investigations through Structural Changes in Hard Carbons. ACS Applied Energy Materials, 2020, 3, 9918-9927.	2.5	56
35455	Engineering the Electronic, Thermoelectric, and Excitonic Properties of Two-Dimensional Group-III Nitrides through Alloying for Optoelectronic Devices (B_{1â€“x}Al_xN, Al_{1â€“x}Ga_xN, and) Tj ETQq1 1 0.784314 rgBT /Overlock 10 Tf 50 46416 46428.	4.6	20
35456	Enhancing the Rapid Na⁺-Storage Performance via Electron/Ion Bridges through GeS₂/Graphene Heterojunction. ACS Nano, 2020, 14, 13952-13963.	7.3	55
35457	Fifth-degree elastic energy for predictive continuum stressâ€“strain relations and elastic instabilities under large strain and complex loading in silicon. Npj Computational Materials, 2020, 6, .	3.5	15
35458	Broken symmetries and the related interface-induced effects at Weyl-system TaAs in proximity of noble metals. Scientific Reports, 2020, 10, 14438.	1.6	0
35459	Antiferroelectricity in a family of pyroxene-like oxides with rich polymorphism. Communications Materials, 2020, 1, .	2.9	2
35460	P-doped nickel sulfide nanosheet arrays for alkaline overall water splitting. Catalysis Science and Technology, 2020, 10, 7581-7590.	2.1	18
35461	Straintronic effect for superconductivity enhancement in Li-intercalated bilayer MoS₂. Nanoscale Advances, 2020, 2, 3150-3155.	2.2	4
35462	AlN₄-Graphene as an efficient catalyst for CO oxidation: a DFT study. New Journal of Chemistry, 2020, 44, 17222-17228.	1.4	6
35463	Revealing the origin of dislocations in Pb_{1â^'x}Sb_{2x/3}Se (0 < x â‰¤ 0.07). Nanoscale, 2020, 12, 19165-19169.	2.8	3

#	Article	IF	Citations
35464	Hut-shaped lead nanowires with one-dimensional electronic properties. Physical Review B, 2020, 102, .	1.1	3
35465	New insights into the structural properties of Î²-(BEDT-TTF)₂Ag₂(CN)₃spin liquid. Acta Crystallographica Section B: Structural Science, Crystal Engineering and Materials, 2020, 76, 581-590.	0.5	1
35466	Band engineering of borophene superlattice based on zigzag nanoribbons: A DFT study. Modern Physics Letters B, 2020, 34, 2050359.	1.0	3
35467	Fe3 Cluster Anchored on the C2N Monolayer for Efficient Electrochemical Nitrogen Fixation. Catalysts, 2020, 10, 974.	1.6	15
35468	Mechanistic Insights for Dry Reforming of Methane on Cu/Ni Bimetallic Catalysts: DFT-Assisted Microkinetic Analysis for Coke Resistance. Catalysts, 2020, 10, 1043.	1.6	30
35469	Interlayer Bound Wannier Excitons in Germanium Sulfide. Materials, 2020, 13, 3568.	1.3	3
35470	Superhard Boron-Rich Boron Carbide with Controlled Degree of Crystallinity. Materials, 2020, 13, 3622.	1.3	19
35471	Novel III-V Nitride Polymorphs in the P42/mnm and Pbca Phases. Materials, 2020, 13, 3743.	1.3	11
35472	DFT-CEF Approach for the Thermodynamic Properties and Volume of Stable and Metastable Alâ€“Ni Compounds. Metals, 2020, 10, 1142.	1.0	4
35473	Cation and Anion Co-doped Perovskite Nanofibers for Highly Efficient Electrocatalytic Oxygen Evolution. ACS Applied Materials & Interfaces, 2020, 12, 41259-41268.	4.0	39
35474	Design of two-dimensional carbon-nitride structures by tuning the nitrogen concentration. Npj Computational Materials, 2020, 6, .	3.5	31
35475	Phase segregation reversibility in mixed-metal hydroxide water oxidation catalysts. Nature Catalysis, 2020, 3, 743-753.	16.1	199
35476	First-Principles Study of the Elastic Properties of Nickel Sulfide Minerals under High Pressure. Minerals (Basel, Switzerland), 2020, 10, 737.	0.8	5
35477	Formic Acid: A Hydrogen-Bonding Cocatalyst for Formate Decomposition. ACS Catalysis, 2020, 10, 10812-10825.	5.5	36
35478	Suitability of Cu-substituted Î²-Mn2V2O7 and Mn-substituted Î²-Cu2V2O7 for photocatalytic water-splitting. Journal of Chemical Physics, 2020, 153, 084704.	1.2	11
35479	Radiative capture rates at deep defects from electronic structure calculations. Physical Review B, 2020, 102, .	1.1	14
35480	Highly active dry methane reforming catalysts with boosted in situ grown Ni-Fe nanoparticles on perovskite via atomic layer deposition. Science Advances, 2020, 6, eabb1573.	4.7	79
35481	Ab Initio and Experimental Study of Electronic, Optical, and Vibrational Properties of CdGa2Te4. Physics of the Solid State, 2020, 62, 1426-1433.	0.2	3

#	Article	IF	Citations
35482	Crystal Facet Induced Singleâ€Atom Pd/Co_xO_y on a Tunable Metalâ€“Support Interface for Low Temperature Catalytic Oxidation. Small, 2020, 16, e2002071.	5.2	22
35483	Intrinsic ferromagnetism in 4H-SiC single crystal induced by Al-doping. Applied Physics A: Materials Science and Processing, 2020, 126, 1.	1.1	2
35484	Stable Surface Terminations of a Perovskite Oxyhydride from First-Principles. Journal of Physical Chemistry C, 2020, 124, 18557-18563.	1.5	5
35485	Antiferromagnetic and Electric Polarized States in Two-Dimensional Janus Semiconductor Fe2Cl3I3. Journal of Physical Chemistry C, 2020, 124, 19219-19227.	1.5	15
35486	Quantum Accurate Prediction of Plutoniumâ€“Plutonium Dihydride Phase Equilibrium Using a Lattice Gas Model. Journal of Physical Chemistry C, 2020, 124, 20881-20888.	1.5	4
35487	Hydrogen Evolution Reaction Activity of Heterogeneous Materials: A Theoretical Model. Journal of Physical Chemistry C, 2020, 124, 20911-20921.	1.5	48
35488	Understanding the Specific Heat Enhancement in Metal-Containing Nanofluids for Thermal Energy Storage: Experimental and Ab Initio Evidence for a Strong Interfacial Layering Effect. ACS Applied Energy Materials, 2020, 3, 9246-9256.	2.5	20
35489	Modulating oxygen coverage of Ti3C2Tx MXenes to boost catalytic activity for HCOOH dehydrogenation. Nature Communications, 2020, 11, 4251.	5.8	81
35490	Yang-Mills structure for electronâ€“phonon interactions in vanadium dioxide. Scientific Reports, 2020, 10, 12547.	1.6	0
35491	Facile synthesis of cesium trithiocyanurate with high ionic conductivity and large birefringence properties. CrystEngComm, 2020, 22, 6495-6501.	1.3	8
35492	Selenite bromide nonlinear optical materials Pb₂GaF₂(SeO₃)₂Br and Pb₂NbO₂(SeO₃)₂Br: synthesis and characterization. Dalton Transactions, 2020, 49, 14046-14051.	1.6	12
35493	New quaternary chalcogenide Ba4HgAs2S10 originating from the combination of linear [HgS2]2â^' and tetrahedral [AsS4]3â^' modules. Dalton Transactions, 2020, 49, 13060-13065.	1.6	4
35494	Charge carrier dynamics in two-dimensional hybrid perovskites: Dionâ€“Jacobson vs. Ruddlesdenâ€“Popper phases. Journal of Materials Chemistry A, 2020, 8, 22009-22022.	5.2	72
35495	Prediction of single-layer TiVI₆ as a promising two-dimensional valleytronic semiconductor with spontaneous valley polarization. Journal of Materials Chemistry C, 2020, 8, 13220-13225.	2.7	39
35496	Strain tuned high thermal conductivity in boron phosphide at nanometer length scales â€“ a first-principles study. Physical Chemistry Chemical Physics, 2020, 22, 20914-20921.	1.3	18
35497	Formation and crystallographic orientation of NiSi2â€“Si interfaces. Journal of Applied Physics, 2020, 128, 085301.	1.1	7
35498	Orbital selectivity of layer-resolved tunneling in the iron-based superconductor <mml:math xmlns:mml="http://www.w3.org/1998/Math/MathML"><mml:mrow><mml:msub><mml:mi>Ba</mml:mi><mml:mrow><mml:mn>0.6</mml:m mathvariant="normal">K</mml:mi><mml:mrow><mml:mn>0.4</mml:mn></mml:mrow></mml:msub><mml:msub><mml:mi>Fe</mml:m Physical Review B, 2020, 102, .	1.1	9
35499	A computational examination of the zeta and eta phases in the hafnium nitrides. Journal of the American Ceramic Society, 2020, 103, 7202-7212.	1.9	2

#	Article	IF	Citations
35500	Electrical Conduction Characteristic of a 2D MXene Device with Cu/Cr2C/TiN Structure Based on Density Functional Theory. Materials, 2020, 13, 3671.	1.3	7
35501	Atomistic Perspective on the Intrinsic White-Light Photoluminescence of Rare-Earth Free MgMoO₄ Nanoparticles. Crystal Growth and Design, 2020, 20, 6592-6603.	1.4	13
35502	Phase Behavior in Rhombohedral NaSiCON Electrolytes and Electrodes. Chemistry of Materials, 2020, 32, 7908-7920.	3.2	58
35503	Electron-Precise Semiconducting ReGa₂Ge: Extending the IrIn₃ Structure Type to Group 7 of the Periodic Table. Inorganic Chemistry, 2020, 59, 12748-12757.	1.9	9
35504	Understanding colossal barocaloric effects in plastic crystals. Nature Communications, 2020, 11, 4190.	5.8	30
35505	First-Principles Method to Study Near-Field Radiative Heat Transfer. Physical Review Applied, 2020, 14, .	1.5	8
35506	Strongly Enhanced Dielectric Response and Structural Investigation of (Sr²⁺,) Tj ETQq0 0 0 rgBT /Overlock 10 Tf 50 502 Td	1.5	43
35507	Thermodynamic feasibility of the four-stage chloride-induced depassivation mechanism of iron. Npj Materials Degradation, 2020, 4, .	2.6	11
35508	Regulating the phase transition of monoclinic Bi4O5Br2 through the synergistic effect of â€œdrag forceâ€•and facet recognition by branched polyethyleneimine. CrystEngComm, 2020, 22, 5871-5881.	1.3	5
35509	Assessing the defect tolerance of kesterite-inspired solar absorbers. Energy and Environmental Science, 2020, 13, 3489-3503.	15.6	28
35510	Recently synthesized (Ti_{1â^'x}Mo_x)₂AlC (0 â‰¤ x â‰¤ 0.20) solid solutions: deciphering the structural, electronic, mechanical and thermodynamic properties via ab initio simulations. RSC Advances, 2020, 10, 31535-31546.	1.7	41
35511	Computational Design of Copper doped Indium for electrocatalytic Reduction of CO₂ to Formic Acid. ChemCatChem, 2020, 12, 5632-5636.	1.8	13
35512	Density Functional Theory Studies of Si₂BN Nanosheets as Anode Materials for Magnesium-Ion Batteries. ACS Applied Nano Materials, 2020, 3, 9055-9063.	2.4	40
35513	Enhanced ion diffusion induced by structural transition of Li-modified borophosphene. Physical Chemistry Chemical Physics, 2020, 22, 21326-21333.	1.3	6
35514	8-Hydroxyquinoline complexes (Alq3) on Al(111): atomic scale structure, energetics and charge distribution. New Journal of Chemistry, 2020, 44, 15209-15222.	1.4	5
35515	Theoretical investigation on catalytic mechanisms of oxygen reduction and carbon monoxide oxidation on the MnN_x system. New Journal of Chemistry, 2020, 44, 15724-15732.	1.4	9
35516	Experimental and Theoretical Investigation of the Energy-Storage Behavior of a Polyaniline-Linked Reduced-Graphene-Oxideâ€“ <mml:math xmlns:mml="http://www.w3.org/1998/Math/MathML" display="inline" overflow="scroll"><mml:msub><mml:mrow><mml:mi>Sn</mml:mi><mml:mi mathvariant="normal">O</mml:mi></mml:mrow><mml:mn>2</mml:mn></mml:msub></mml:math> Ternary Nanohybrid Electrode. Physical Review Applied, 2020, 14, .	1.5	18
35517	The Obstruction Effect of Ni Layer on the Interdiffusion of Cu Substrate and Sn Solder: A Theoretical Investigation. Journal of Electronic Materials, 2020, 49, 6559-6571.	1.0	7

#	Article	IF	Citations
35518	Physical Properties and Characterization of the Binary Clathrate Hydrate with Methane + 1,1,1,3,3-Pentafluoropropane (HFC-245fa) + Water. Journal of Physical Chemistry C, 2020, 124, 20736-20745.	1.5	7
35519	Ultralow Thermal Conductivity and High Thermoelectric Figure of Merit in Two-Dimensional Thallium Selenide. ACS Applied Energy Materials, 2020, 3, 9315-9325.	2.5	24
35520	Site-dependent reactivity of MoS2 nanoparticles in hydrodesulfurization of thiophene. Nature Communications, 2020, 11, 4369.	5.8	44
35521	Uncertainty quantification in molecular simulations with dropout neural network potentials. Npj Computational Materials, 2020, 6, .	3.5	42
35522	Adsorption and dehydrogenation of C₂â€“C₆n-alkanes over a Pt catalyst: a theoretical study on the size effects of alkane molecules and Pt substrates. Physical Chemistry Chemical Physics, 2020, 22, 21835-21843.	1.3	18
35523	Electronic and photocatalytic properties of two-dimensional boron phosphide/SiC van der Waals heterostructure with direct type-II band alignment: a first principles study. RSC Advances, 2020, 10, 32027-32033.	1.7	18
35525	Interstitial defects in diamond: A quantum mechanical simulation of their EPR constants and vibrational spectra. Journal of Chemical Physics, 2020, 153, 024119.	1.2	6
35526	SnCN₂: A Carbodiimide with an Innovative Approach for Energy Storage Systems and Phosphors in Modern LED Technology. ChemElectroChem, 2020, 7, 4550-4561.	1.7	13
35527	Generalized gradient approximation adjusted to transition metals properties: Key roles of exchange and local spin density. Journal of Computational Chemistry, 2020, 41, 2598-2603.	1.5	25
35528	Sr₆(BO₃)₃BN₂: An Oxidoâ€“Nitridoâ€“Borate Phosphor Featuring BN₂ Dumbbells. Chemistry of Materials, 2020, 32, 8587-8594.	3.2	7
35529	On the importance of hexagonal phases in TM (TMâ€‰=â€‰Ti, Zr, and Hf) mono-nitrides. Journal of Applied Physics, 2020, 128, .	1.1	1
35530	Prediction of an Extended Ferroelectric Clathrate. Physical Review Letters, 2020, 125, 127601.	2.9	12
35531	Soft X-Ray and Cathodoluminescence Examination of a Tanzanian Graphite Deposit. Microscopy and Microanalysis, 2020, 26, 814-820.	0.2	2
35532	Revisiting Competing Paths in Electrochemical CO₂ Reduction on Copper via Embedded Correlated Wavefunction Theory. Journal of Chemical Theory and Computation, 2020, 16, 6528-6538.	2.3	21
35533	Radiation-Induced Interfacial Hydroxyl Transformation on Boehmite and Gibbsite Basal Surfaces. Journal of Physical Chemistry C, 2020, 124, 22185-22191.	1.5	8
35534	Structural, electronic, and optical properties of cubic formamidinium lead iodide perovskite: a first-principles investigation. RSC Advances, 2020, 10, 32364-32369.	1.7	24
35535	First-Principles Study of Effects of Combined Ti Supervalent Cations and Lithium Ion Vacancies Doping on Crystal and Electronic Structures and Conductivity in LiFePO₄. Key Engineering Materials, 0, 861, 277-283.	0.4	5
35536	Morphology-Persistent Carbonization of Self-Assembled Block Copolymers for Multifunctional Coupled Two-Dimensional Porous Carbon Hybrids. Chemistry of Materials, 2020, 32, 8971-8980.	3.2	11

#	Article	IF	Citations
35537	A Machine Learning Model on Simple Features for CO₂ Reduction Electrocatalysts. Journal of Physical Chemistry C, 2020, 124, 22471-22478.	1.5	125
35538	High Thermoelectric Performance in Two-Dimensional Janus Monolayer Material WS-X (X = Se) Tj ETQq1 1 0.784314 rgBT /Ove	4.0	130
35539	Two-Dimensional Boronâ€“Phosphorus Monolayer for Reversible NO₂ Gas Sensing. ACS Applied Nano Materials, 2020, 3, 10073-10081.	2.4	40
35540	Bulk vs Intrinsic Activity of NiFeO_x Electrocatalysts in the Oxygen Evolution Reaction: The Influence of Catalyst Loading, Morphology, and Support Material. ACS Catalysis, 2020, 10, 11768-11778.	5.5	23
35541	Toward lateral heterostructures with two-dimensional MoX₂H₂ (X = As, Sb). Physical Chemistry Chemical Physics, 2020, 22, 22584-22590.	1.3	1
35542	Simulations of X-ray absorption spectroscopy and energetic conformation of N-heterocyclic carbenes on Au(111). Physical Chemistry Chemical Physics, 2020, 22, 21504-21511.	1.3	6
35543	Magnetic Damping in Epitaxial <mml:math xmlns:mml="http://www.w3.org/1998/Math/MathML" display="inline" overflow="scroll"><mml:mi>Iron</mml:mi></mml:math> Alloyed with Vanadium and Aluminum. Physical Review Applied, 2020, 14, .	1.5	13
35544	Lattice dynamics effects on the magnetocrystalline anisotropy energy: Application to MnBi. Physical Review B, 2020, 102, .	1.1	6
35545	Pressure effect on the mechanical and electronic properties of the tungsten triboride doped with iron: a first-principles study. European Physical Journal B, 2020, 93, 1.	0.6	2
35546	Effects of masking titanium with a one-atom-thick carbon layer on the adsorption of nitrogen monoxide, nitrogen dioxide, ozone, and formaldehyde. Journal of Materials Science, 2020, 55, 17000-17018.	1.7	2
35547	Temperature-dependent optical constants of monolayer $${ext {MoS}}_2$$, $${ext {MoSe}}_2$$, $${ext {WS}}_2$$, and $${ext {WSe}}_2$$: spectroscopic ellipsometry and first-principles calculations. Scientific Reports, 2020, 10, 15282.	1.6	52
35548	Electric field tuned anisotropic to isotropic thermal transport transition in monolayer borophene without altering its atomic structure. Nanoscale, 2020, 12, 19178-19190.	2.8	15
35549	Vacancy-induced anion and cation redox chemistry in cation-deficient F-doped anatase TiO2. Journal of Materials Chemistry A, 2020, 8, 20393-20401.	5.2	8
35550	Computational screening of homo and hetero transition metal dimer catalysts for reduction of CO₂ to C₂ products with high activity and low limiting potential. Journal of Materials Chemistry A, 2020, 8, 21241-21254.	5.2	51
35551	Thermal effects on the electronic properties of sodium electride under high pressures. Physical Review B, 2020, 102, .	1.1	10
35552	Hybrid Pd38 nanocluster/Ni(OH)2-graphene catalyst for enhanced HCOOH dehydrogenation: First principles approach. Korean Journal of Chemical Engineering, 2020, 37, 1411-1418.	1.2	5
35553	Crystalline Structures and Energetic Properties of Lithium Pentazolate under Ambient Conditions. ACS Omega, 2020, 5, 24946-24953.	1.6	7
35554	Magnetism arising from Mexican-hat-like band dispersion in the WSe2/SnS2 heterostructure via interlayer strain. Physical Chemistry Chemical Physics, 2020, 22, 21961-21967.	1.3	1

#	Article	IF	Citations
35555	Atomic structures of high Miller index surfaces of NiO. Journal of Materials Chemistry C, 2020, 8, 14164-14171.	2.7	7
35556	Physiological silicon incorporation into bone mineral requires orthosilicic acid metabolism to SiO ₄ ^{4â^'}. Journal of the Royal Society Interface, 2020, 17, 20200145.	1.5	16
35557	RRuB2 (R=Y,ÂLu) , topological superconductor candidates with hourglass-type Dirac ring. Physical Review B, 2020, 102, .	1.1	6
35558	The External Electric Field-Induced Tunability of the Schottky Barrier Height in Graphene/AlN Interface: A Study by First-Principles. Nanomaterials, 2020, 10, 1794.	1.9	8
35559	An Emerging Leadâ€Free Doubleâ€Perovskite Cs₂AgFeCl₆:In Single Crystal. Advanced Functional Materials, 2020, 30, 2002225.	7.8	48
35560	Application of kÂ$$cdot $$Âp method on band structure of GaAs obtained through joint density-functional theory. Bulletin of Materials Science, 2020, 43, 1.	0.8	1
35561	Why choosing the right partner is important: stabilization of ternary CsyGUAxFA(1â^'yâ^'x)PbI3 perovskites. Physical Chemistry Chemical Physics, 2020, 22, 20880-20890.	1.3	2
35562	Influence of Nb, Ti and Mo on Microstructure and Mechanical Properties of Vanadium Solid Solutions. IOP Conference Series: Materials Science and Engineering, 2020, 882, 012012.	0.3	0
35563	Integrating Conductivity, Captivity, and Immobility Ability into N/O Dualâ€Doped Porous Carbon Nanocage Anchored with CNT as an Effective Se Host for Advanced Kâ€Se Battery. Advanced Functional Materials, 2020, 30, 2003871.	7.8	45
35564	Dirac and Weyl Semimetals in Sn_{1â^'x}In_xTe. Physica Status Solidi - Rapid Research Letters, 2020, 14, 2000362.	1.2	2
35565	Modeling and simulation of the adsorption and storage of hydrogen in calcite rock oil fields. Journal of Molecular Modeling, 2020, 26, 248.	0.8	15
35566	Predicted strong spin-phonon interactions in Li-doped diamond. Physical Chemistry Chemical Physics, 2020, 22, 20612-20617.	1.3	5
35567	Strong band-filling-dependence of the scattering lifetime in gated MoS 2 nanolayers induced by the opening of intervalley scattering channels. Journal of Applied Physics, 2020, 128, 063907.	1.1	5
35568	Magnetically driven loss of centrosymmetry in metallic <mml:math xmlns:mml="http://www.w3.org/1998/Math/MathML"><mml:mrow><mml:msub><mml:mi>Pb</mml:mi><mml:mn>12</mml:mn></mml:msub></mml:mrow></mml:math>. Physical Review B, 2020, 102, .	1.1	9
35569	First-principles study of the vacancy and layer defects in Ti3SiC2. International Journal of Modern Physics B, 2020, 34, 2050198.	1.0	3
35570	Microscopic Mechanism Study of 4f Electronsâ€™ Positive Effect on the Enhanced Proton Conduction in a Pr-Doped BaCeO₃ Electrolyte. Journal of Physical Chemistry C, 2020, 124, 21232-21241.	1.5	10
35571	From BiF₃to BiF₃Â·H₂O: diverse Bi(<scp>iii</scp>) coordination for structural transformation and birefringence regulation. CrystEngComm, 2020, 22, 6838-6846.	1.3	7
35572	Electronic, optical and thermoelectric properties of boron-doped nitrogenated holey graphene. Physical Chemistry Chemical Physics, 2020, 22, 21147-21157.	1.3	15

#	Article	IF	Citations
35573	A new planar BCN lateral heterostructure with outstanding strength and defect-mediated superior semiconducting to metallic properties. Physical Chemistry Chemical Physics, 2020, 22, 22066-22077.	1.3	30
35574	Integrated Plasmonics: Broadband Dirac Plasmons in Borophene. Physical Review Letters, 2020, 125, 116802.	2.9	67
35575	Topological analysis of chemical bonding in the layered <scp>FePSe₃</scp> upon pressureâ€induced phase transitions. Journal of Computational Chemistry, 2020, 41, 2610-2623.	1.5	4
35576	Amine-functionalized microporous covalent organic polymers for adsorptive removal of a gaseous aliphatic aldehyde mixture. Environmental Science: Nano, 2020, 7, 3447-3468.	2.2	18
35577	Insights into lithium ion deposition on lithium metal surfaces. Physical Chemistry Chemical Physics, 2020, 22, 21369-21382.	1.3	16
35578	Unraveling the mechanisms of S-doped carbon nitride for photocatalytic oxygen reduction to H₂O₂. Physical Chemistry Chemical Physics, 2020, 22, 21099-21107.	1.3	29
35579	First-principles study of two dimensional C₃N and its derivatives. RSC Advances, 2020, 10, 33469-33474.	1.7	15
35580	Singleâ€Atom Inâ€Doped Subnanometer Pt Nanowires for Simultaneous Hydrogen Generation and Biomass Upgrading. Advanced Functional Materials, 2020, 30, 2004310.	7.8	77
35581	Polar Morphologies from First Principles: PbTiO₃ Films on SrTiO₃ Substrates and the p(2Ã—1) Surface Reconstruction. Advanced Theory and Simulations, 2020, 3, 2000154.	1.3	11
35582	Effect of Heteroaromaticity on Adsorption of Pyrazine on the Ge(100)-2Ã—1 Surface. Journal of Physical Chemistry C, 2020, 124, 22055-22068.	1.5	3
35583	Tunable Electronic Structure of Two-Dimensional MoX₂ (X = S, Se)/SnS₂ van der Waals Heterostructures. Journal of Physical Chemistry C, 2020, 124, 21357-21365.	1.5	16
35584	Two-dimensional silicon bismotide (SiBi) monolayer with a honeycomb-like lattice: first-principles study of tuning the electronic properties. RSC Advances, 2020, 10, 31894-31900.	1.7	23
35585	Phonon Spectroscopy in Antimony and Tellurium Oxides. Journal of Physical Chemistry A, 2020, 124, 7869-7880.	1.1	6
35586	Two-Dimensional CdX/C₂N (X = S, Se) Heterostructures as Potential Photocatalysts for Water Splitting: A DFT Study. ACS Omega, 2020, 5, 23762-23768.	1.6	45
35587	Low dimensional nanostructures of fast ion conducting lithium nitride. Nature Communications, 2020, 11, 4492.	5.8	19
35588	An approach to calculate the free energy changes of surface reactions using free energy decomposition on ab initio brute-force molecular dynamics trajectories. Physical Chemistry Chemical Physics, 2020, 22, 21340-21349.	1.3	10
35589	Enhanced Electrocatalytic Activity in GaSe and InSe Nanosheets: The Role of Surface Oxides. Advanced Functional Materials, 2020, 30, 2005466.	7.8	35
35590	Large Magnetic Anisotropy Energy and Robust Halfâ€Metallic Ferromagnetism in 2D MnXSe₄ (X = As, Sb). Annalen Der Physik, 2020, 532, 2000365.	0.9	4

#	Article	IF	Citations
35591	Tuning Electronic and Magnetic Properties of Two-Dimensional Ferromagnetic Semiconductor CrI₃ through Adsorption of Benzene. Journal of Physical Chemistry C, 2020, 124, 22143-22149.	1.5	20
35592	Co₃O₄ Nanocrystals with an Oxygen Vacancy-Rich and Highly Reactive (222) Facet on Carbon Nitride Scaffolds for Efficient Photocatalytic Oxygen Evolution. ACS Applied Materials & Interfaces, 2020, 12, 44608-44616.	4.0	43
35593	Atomic Insights into Robust Ptâ€“PdO Interfacial Site-Boosted Hydrogen Generation. ACS Catalysis, 2020, 10, 11417-11429.	5.5	19
35594	Semiconducting to metallic transition with outstanding optoelectronic properties of CsSnCl3 perovskite under pressure. Scientific Reports, 2020, 10, 14391.	1.6	78
35595	Electron-beam irradiation of photopolymerized C60 film studied using in situ scanning tunneling microscope, in situ Fourier-transform infrared spectroscopy, and first-principles calculations. AIP Advances, 2020, 10, .	0.6	3
35596	Cooperative Binding of 1-Phenylimidazole to Cobalt(II) Octaethylporphyrin on Graphite: A Quantitative Imaging and Computational Study at Molecular Resolution. Journal of Physical Chemistry C, 2020, 124, 18639-18649.	1.5	8
35597	Unravelling the role of oxophilic metal in promoting the deoxygenation of catechol on Ni-based alloy catalysts. Catalysis Science and Technology, 2020, 10, 6849-6859.	2.1	25
35598	Understanding the enhanced catalytic activity of bimetallic AuCu/TiO₂ in CO₂ adsorption and activation: a density functional theory study. New Journal of Chemistry, 2020, 44, 14662-14669.	1.4	7
35599	Modulating the electro-optical properties of doped C₃N monolayers and graphene bilayers via mechanical strain and pressure. New Journal of Chemistry, 2020, 44, 15785-15792.	1.4	28
35600	Strain forces tuned the electronic and optical properties in GaTe/MoS₂ van der Waals heterostructures. RSC Advances, 2020, 10, 25136-25142.	1.7	5
35601	To investigate electronic properties of AlHO2 doped with trivalent impurities (Ga, In, Tl) by using density functional theory. AIP Conference Proceedings, 2020, , .	0.3	3
35602	Magnetocrystalline anisotropy of the easy-plane metallic antiferromagnet <mml:math xmlns:mml="http://www.w3.org/1998/Math/MathML"><mml:mrow><mml:mi mathvariant="normal">F</mml:mi><mml:msub><mml:mi mathvariant="normal">e</mml:mi><mml:mn>2</mml:mn></mml:msub><mml:mi>As</mml:mi></mml:mrow></mml:math>. Physical Review B, 2020, 102, .	1.1	7
35603	New investigation of nanosized co-doped Gd-Sm anatase TiO2 structural, magnetic, optical, and first-principles study. Applied Physics A: Materials Science and Processing, 2020, 126, 1.	1.1	10
35604	Superselective Removal of Lead from Water by Two-Dimensional MoS₂ Nanosheets and Layer-Stacked Membranes. Environmental Science & Technology, 2020, 54, 12602-12611.	4.6	87
35605	Evaluation of a V₈C₇ Anode for Oxygen Evolution in Alkaline Media: Unusual Morphological Behavior. ACS Sustainable Chemistry and Engineering, 2020, 8, 14101-14108.	3.2	6
35606	Design rules for strong electro-optic materials. Npj Computational Materials, 2020, 6, .	3.5	27
35607	A₂Bi₂(SeO₃)₃F₂ (A = K and Rb): Excellent Mid-Infrared Nonlinear Optical Materials with Both Strong SHG Responses and Large Band Gaps. Chemistry of Materials, 2020, 32, 7958-7964.	3.2	42
35608	Hydride-Reduced Eu2SrFe2O6: A T-to-Tâ€² Conversion Enabling Fe2+ in Square-Planar Coordination. Inorganic Chemistry, 2020, 59, 12913-12919.	1.9	2

#	Article	IF	Citations
35609	Spatial Confinement as an Effective Strategy for Improving the Catalytic Selectivity in Acetylene Hydrogenation. ACS Applied Materials & Interfaces, 2020, 12, 39352-39361.	4.0	11
35610	Identifying materials with chargeâ€“spin physics using chargeâ€“spin susceptibility computed from first principles. Journal of Chemical Physics, 2020, 153, 074105.	1.2	2
35611	Raman studies of hydrogen trapped in As4O6Â·2H2 at high pressure and low temperature. Journal of Chemical Physics, 2020, 153, 054501.	1.2	3
35612	Strain modulation using defects in two-dimensional <mml:math xmlns:mml="http://www.w3.org/1998/Math/MathML"><mml:mrow><mml:mi>Mo</mml:mi><mml:msub><mml:mi mathvariant="normal">S</mml:mi><mml:mn>2</mml:mn></mml:msub></mml:mrow></mml:math>. Physical Review B, 2020, 102, .	1.1	8
35613	The Adsorption of NH₃ on the FeS₂ (100) Surface: A First-Principles Investigation. Materials Science Forum, 2020, 1001, 22-27.	0.3	0
35614	Fundamental Understanding of the Formation Mechanism for Graphene Quantum Dots Fabricated by Pulsed Laser Fragmentation in Liquid: Experimental and Theoretical Insight. Small, 2020, 16, 2003538.	5.2	13
35615	Computer Simulation of the Structural Properties of Energetic Materials Using High Performance Computing. Advances in Intelligent Systems and Computing, 2020, , 623-632.	0.5	0
35616	A DFT investigation of electronic, elastic, and thermal properties of 3d transition metal carbides â€“TMC (TMA= Scâ€“Zn). Computational Condensed Matter, 2020, 25, e00500.	0.9	1
35617	Detachment of human mesenchymal stem cells from a gold substrate using electric current. Materialia, 2020, 13, 100866.	1.3	0
35618	Crystal and Electronic Structures of A₂NaIO₆ Periodate Double Perovskites (A = Sr, Ca, Ba): Candidate Wasteforms for I-129 Immobilization. Inorganic Chemistry, 2020, 59, 18407-18419.	1.9	13
35619	Anisotropic optical properties of single Si2Te3 nanoplates. Scientific Reports, 2020, 10, 19205.	1.6	9
35620	Phonon mode potential and its contribution to anharmonism. Scientific Reports, 2020, 10, 19783.	1.6	5
35621	Preferred oriented cation configurations in high pressure phases IV and V of methylammonium lead iodide perovskite. Scientific Reports, 2020, 10, 21138.	1.6	5
35622	First-principles study of the ternary effects on the plasticity of $$upgamma $$-TiAl crystals. Scientific Reports, 2020, 10, 21614.	1.6	7
35623	Theoretical investigation on $$hbox {BeN}_{{2}}$$ monolayer for an efficient bifunctional water splitting catalyst. Scientific Reports, 2020, 10, 21411.	1.6	6
35624	The impact of Fe atom on the spin-filter and spin thermoelectric properties of Au-Fe@C20-Au monomer and dimer systems. Scientific Reports, 2020, 10, 21134.	1.6	2
35625	Unveiling giant hidden Rashba effects in two-dimensional Si2Bi2. Npj 2D Materials and Applications, 2020, 4, .	3.9	14
35626	Dependency of solvation effects on metal identity in surface reactions. Communications Chemistry, 2020, 3, .	2.0	15

#	Article	IF	Citations
35627	Aliovalent-doped sodium chromium oxide (Na0.9Cr0.9Sn0.1O2 and Na0.8Cr0.9Sb0.1O2) for sodium-ion battery cathodes with high-voltage characteristics. RSC Advances, 2020, 10, 43273-43281.	1.7	9
35628	A predictive model for high-frequency operation of two-dimensional transistors from first-principles. Journal of Applied Physics, 2020, 128, .	1.1	8
35629	Response of the mode GrÃ¼neisen parameters with anisotropic compression: A pressure and temperature dependent Raman study of <mml:math xmlns:mml="http://www.w3.org/1998/Math/MathML"><mml:mi>Î²</mml:mi></mml:math> -Sn. Physical Review B, 2020, 102, .	1.1	4
35630	Mott localization in the van der Waals crystal <mml:math xmlns:mml="http://www.w3.org/1998/Math/MathML"><mml:msub><mml:mi mathvariant="normal">CrI</mml:mi><mml:mn>3</mml:mn></mml:msub></mml:math> : A <mml:math xmlns:mml="http://www.w3.org/1998/Math/MathML"><mml:mi>GGA</mml:mi><mml:mo>+</mml:mo><mml:mi>DMFT</mml:mi></ study. Physical Review B, 2020, 102, .	1.1	7
35631	Evaluations of nonlocal electron-phonon couplings in tetracene, rubrene, and C10â^'DNBDTâ^'NW based on density functional theory. Physical Review B, 2020, 102, .	1.1	11
35632	Effective Static Approximation: A Fast and Reliable Tool for Warm-Dense Matter Theory. Physical Review Letters, 2020, 125, 235001.	2.9	46
35633	Boosting Li-S battery performance by an efficient polysulfide double-blocking strategy. FlatChem, 2020, 24, 100209.	2.8	2
35634	Characteristics of K2Ca2(SO4)3:Eu TLD nanophosphor for its applications in electron and gamma rays dosimetry. Optical Materials, 2020, 109, 110272.	1.7	7
35635	CO-Induced Surface Reconstruction of the Co(11â€“20) Surfaceâ€”A Combined Theoretical and Experimental Investigation. Journal of Physical Chemistry C, 2020, 124, 28488-28499.	1.5	3
35636	Modeling Hydrogen Evolution Reaction Kinetics through Explicit Waterâ€“Metal Interfaces. Journal of Physical Chemistry C, 2020, 124, 28083-28092.	1.5	58
35637	Subsurface Nitrogen Dissociation Kinetics in Lithium Metal from Metadynamics. Journal of Physical Chemistry C, 2020, 124, 26368-26378.	1.5	14
35638	Strain and stress relationships for optical phonon modes in monoclinic crystals with <mml:math xmlns:mml="http://www.w3.org/1998/Math/MathML"><mml:mrow><mml:mi>Î²</mml:mi><mml:mtext>â^'</mml:mtext><mml:msub mathvariant="normal">O</mml:mi><mml:mn>3</mml:mn></mml:msub></mml:mrow></mml:math> as an example. Physical Review B, 2020, 102, .	1.1	13
35639	Na-functionalized <mml:math xmlns:mml="http://www.w3.org/1998/Math/MathML"><mml:mrow><mml:mi>Ir</mml:mi><mml:msub><mml:mi>Te</mml:mi><mml:mn monolayer: Suppressed charge ordering and electric field tuned topological phase transition. Physical Review B, 2020, 102, .	1.1	11
35640	Schottky barrier formation at the <mml:math xmlns:mml="http://www.w3.org/1998/Math/MathML"><mml:mrow><mml:mi>Fe</mml:mi><mml:mo>/</mml:mo><mml:msub><mml:mi (001) interface: Influence of oxygen vacancies and layer oxidation. Physical Review B, 2020, 102, .	1.1	6
35641	Origin of weak Fermi level pinning at the graphene/silicon interface. Physical Review B, 2020, 102, .	1.1	6
35642	Benchmarking boron carbide equation of state using computation and experiment. Physical Review E, 2020, 102, 053203.	0.8	6
35643	Stabilization of Competing Ferroelectric Phases of <mml:math xmlns:mml="http://www.w3.org/1998/Math/MathML" display="inline"><mml:mrow><mml:msub><mml:mrow><mml:mi>HfO</mml:mi></mml:mrow><mml:mrow><mml:mn>2</mml:mn></ Epitaxial Strain. Physical Review Letters, 2020, 125, 257603.	2.9	46
35644	A Comparison of the Structural, Electronic, Mechanical and Phonon Properties of Silicene and Carbon-Substituted Silicene from First Principles. Journal of the Korean Physical Society, 2020, 77, 1183-1187.	0.3	1

#	Article	IF	Citations
35645	Proton dynamics in high-pressure ice-VII from density functional theory. Physical Review B, 2020, 102, .	1.1	12
35646	Orthorhombic <mml:math xmlns:mml="http://www.w3.org/1998/Math/MathML"><mml:mrow><mml:mi>BiFe</mml:mi><mml:msub><mml:mi mathvariant="normal">O</mml:mi><mml:mn>3</mml:mn></mml:msub></mml:mrow></mml:math> : Theoretical studies on magnetoelectric effects of the multiferroic phase. Physical Review B, 2020, 102, .	1.1	2
35647	Calculation of Hole Concentrations in Zn Doped GaAs Nanowires. Nanomaterials, 2020, 10, 2524.	1.9	2
35648	Inverse Perovskite Oxysilicides and Oxygermanides as Candidates for Nontoxic Infrared Semiconductor and Their Chemical Bonding Nature. Inorganic Chemistry, 2020, 59, 18305-18313.	1.9	4
35649	First-principles study of solid hydrogen: Comparison among four exchange-correlation functionals. Physical Review B, 2020, 102, .	1.1	4
35650	Band Engineering of Large-Twist-Angle <mml:math xmlns:mml="http://www.w3.org/1998/Math/MathML" display="inline"><mml:mrow><mml:mtext>Graphene</mml:mtext><mml:mo>/</mml:mo><mml:mrow><mml:mi>h</mml:mi></mml:mrow></mml:mrow></mml:math> MoirÃ© Superlattices with Pressure. Physical Review Letters, 2020, 125, 226403.	2.9	17
35651	Pentamers with interstitial atoms as the building blocks of the Ge(3 3 1)-5ÂÃ—Â1 surface. Applied Surface Science, 2020, 533, 147507.	3.1	3
35652	Spin-polarized electrical transport in transition metal encapsulated C20 fullerenes: A theoretical account. Chemical Physics Impact, 2020, 1, 100002.	1.7	2
35653	Reaction Pathways for Î±-Ga2O3 and Î²-Ga2O3 Phase Transition under Pressure up to 40 GPa: A First-Principles Study. Journal of Physical Chemistry C, 2020, 124, 23280-23286.	1.5	6
35654	Linker Substituents Control the Thermodynamic Stability in Metalâ€“Organic Frameworks. Journal of the American Chemical Society, 2020, 142, 21720-21729.	6.6	36
35655	Structural, electronic and thermoelectric properties of SrTiO3 ceramic doped by lanthanum using first principles. IOP Conference Series: Materials Science and Engineering, 2020, 957, 012008.	0.3	0
35656	Electronic Structure and Surface Properties of Copper Thiocyanate: A Promising Hole Transport Material for Organic Photovoltaic Cells. Materials, 2020, 13, 5765.	1.3	8
35657	Highly Sensitive Gas Sensing Material for Environmentally Toxic Gases Based on Janus NbSeTe Monolayer. Nanomaterials, 2020, 10, 2554.	1.9	17
35658	Poisonous Vapor Adsorption on Pure and Modified Aluminum Nitride Nanosheet for Environmental Safety: A DFT Exploration. Sustainability, 2020, 12, 10097.	1.6	3
35659	Chemically stable new MAX phase V₂SnC: a damage and radiation tolerant TBC material. RSC Advances, 2020, 10, 43783-43798.	1.7	34
35660	Atomic structure and electronic properties of hydrogenated X (=C, Si, Ge, and Sn) doped TiO2: A theoretical perspective. AIP Advances, 2020, 10, .	0.6	3
35661	First-Principles Study on the Oxidation of Supported Î²12-Borophene. Journal of Physical Chemistry C, 2020, 124, 28145-28151.	1.5	13
35662	First-Principles Study on the Ferromagnetism of Mn-Doped LiZnAs Half-Heusler Compound. Physics of the Solid State, 2020, 62, 2077-2083.	0.2	1

#	Article	IF	Citations
35663	Enhanced hydrogen evolution reactivity on $${mathrm{Mo}}_2{mathrm{C}}$$â€“$${mathrm{Mo}}_2{mathrm{N}}$$ composites. Bulletin of Materials Science, 2020, 43, 1.	0.8	4
35664	Mechanistic aspects of facet-dependent CH4/C2+ selectivity over a Ï‡-Fe5C2 Fischerâ€“Tropsch catalyst. Green Energy and Environment, 2022, 7, 449-456.	4.7	8
35665	Efficient photoelectrochemical conversion of CO2 to syngas by photocathode engineering. Green Energy and Environment, 2022, 7, 545-553.	4.7	13
35666	Designing a sp3 nanoporous structure of carbon: A comprehensive study on the physical properties. Results in Physics, 2020, 19, 103473.	2.0	17
35667	Influence of the Fe-Si-O framework in crystal structure on the phase stability and electrochemical performance of Li2FeSiO4 cathode. Solid State Ionics, 2020, 356, 115436.	1.3	5
35668	Fundamental Mechanisms of Mercury Removal by FeCl₃- and CuCl₂-Impregnated Activated Carbons: Experimental and First-Principles Study. Energy & Fuels, 2020, 34, 16401-16410.	2.5	13
35669	A computational search for wurtzite-structured ferroelectrics with low coercive voltages. APL Materials, 2020, 8, .	2.2	19
35670	Micropillar compression deformation of single crystals of Î±-Nb₅Si₃ with the tetragonal D8_l structure. Science and Technology of Advanced Materials, 2020, 21, 805-816.	2.8	7
35671	Largely Enhanced Photogalvanic Effects in a Phosphorene Photodetector by Strain-Increased Device Asymmetry. Physical Review Applied, 2020, 14, .	1.5	26
35672	Role of Si Doping in Reducing Coercive Fields for Ferroelectric Switching in <mml:math xmlns:mml="http://www.w3.org/1998/Math/MathML" display="inline" overflow="scroll"><mml:msub><mml:mrow><mml:mi>Hf</mml:mi><mml:mi mathvariant="normal">O</mml:mi></mml:mrow><mml:mn>2</mml:mn></mml:msub></mml:math>. Physical Review Applied, 2020, 14, .	1.5	15
35673	Phase transitions and equation of state of zirconium under high pressure. Physical Review B, 2020, 102, .	1.1	16
35674	Shock compression of vanadium at extremes: Theory and experiment. Physical Review B, 2020, 102, .	1.1	13
35675	Manipulation of giant negative Poisson's ratios in three-dimensional graphene networks. Physical Review B, 2020, 102, .	1.1	5
35676	Experimental and theoretical study of the correlated compound YbCdSn: Evidence for large magnetoresistance and mass enhancement. Physical Review B, 2020, 102, .	1.1	11
35677	Collisional ionization and recombination in degenerate plasmas beyond the free-electron-gas approximation. Physical Review E, 2020, 102, 063204.	0.8	3
35678	Selective Toluene Detection with Mo₂CT_x MXene at Room Temperature. ACS Applied Materials & Interfaces, 2020, 12, 57218-57227.	4.0	83
35679	Self-Optimized Ligand Effect in L1₂-PtPdFe Intermetallic for Efficient and Stable Alkaline Hydrogen Oxidation Reaction. ACS Catalysis, 2020, 10, 15207-15216.	5.5	64
35680	Computational and Experimental Mechanistic Insights into the Ethanol-to-Butanol Upgrading Reaction over MgO. ACS Catalysis, 2020, 10, 15162-15177.	5.5	16

#	Article	IF	Citations
35681	Defect-Inducedin SituAtomic Doping in Transition Metal Dichalcogenides via Liquid-Phase Synthesis toward Efficient Electrochemical Activity. ACS Nano, 2020, 14, 17114-17124.	7.3	26
35682	Proton-Induced Disproportionation of Jahnâ€“Teller-Active Transition-Metal Ions in Oxides Due to Electronically Driven Lattice Instability. Journal of the American Chemical Society, 2020, 142, 21122-21130.	6.6	35
35683	Prediction of structure and cation ordering in an ordered normal-inverse double spinel. Communications Materials, 2020, 1, .	2.9	46
35684	Proton mobility in metallic copper hydride from high-pressure nuclear magnetic resonance. Physical Review B, 2020, 102, .	1.1	14
35685	Band-gap control of graphenelike borocarbonitride <mml:math xmlns:mml="http://www.w3.org/1998/Math/MathML"><mml:mrow><mml:mi>g</mml:mi><mml:mtext>â^'</mml:mtext><mml:msub><r mathvariant="normal">N</mml:mi></mml:mrow></mml:math> bilayers by electrical gating. Physical Review B, 2020, 102, .	1.1	40
35686	First-Principle Insight Into the Effects of Oxygen Vacancies on the Electronic, Photocatalytic, and Optical Properties of Monoclinic BiVO4(001). Frontiers in Chemistry, 2020, 8, 601983.	1.8	13
35687	First-principles prediction of a room-temperature ferromagnetic and ferroelastic 2D multiferroic MnNX (X = F, Cl, Br, and I). Nanoscale, 2020, 12, 24237-24243.	2.8	19
35688	Multiple striking negative differential resistance in a polyyne wire doped with an organometallic fragment. Journal of Applied Physics, 2020, 128, .	1.1	3
35689	Photoinduced Floquet mixed-Weyl semimetallic phase in a carbon allotrope. Physical Review B, 2020, 102, .	1.1	12
35690	Nitrogen Enables the Intensity Modulation of Charge Transfer and Spin Paramagnetism in Graphdiyne. Chemistry of Materials, 2020, 32, 9001-9007.	3.2	18
35691	Generating Cocrystal Polymorphs with Information Entropy Driven by Molecular Dynamics-Based Enhanced Sampling. Journal of Physical Chemistry Letters, 2020, 11, 9751-9758.	2.1	10
35692	Acetonitrile Transition Metal Interfaces from First Principles. Journal of Physical Chemistry Letters, 2020, 11, 9802-9811.	2.1	13
35693	Beyond Volume Variation: Anisotropic and Protrusive Lithiation in Bismuth Nanowire. ACS Nano, 2020, 14, 15669-15677.	7.3	18
35694	Anomalous mechanical materials squeezing three-dimensional volume compressibility into one dimension. Nature Communications, 2020, 11, 5593.	5.8	19
35695	Influence of tungsten doping on nonradiative electronâ€“hole recombination in monolayer MoSe2 with Se vacancies. Journal of Chemical Physics, 2020, 153, 154701.	1.2	8
35696	First principles density functional theory calculations on the elastic properties of Mo-Si based solid solutions. IOP Conference Series: Materials Science and Engineering, 2020, 882, 012024.	0.3	1
35697	Experimental and Theoretical Investigation of the Elastic Properties of HfV2O7. Crystals, 2020, 10, 172.	1.0	1
35698	Phase Stability of Chloroform and Dichloromethane at High Pressure. Crystals, 2020, 10, 920.	1.0	7

#	Article	IF	Citations
35699	Bismuth Polycations Revisited: Alternative Synthesis and Electronic Structure of Bi6Br7, and Bonding in Main-Group Polyatomic Ions from a Direct Space Perspective. Crystals, 2020, 10, 940.	1.0	4
35700	Cu-Doped KCl Unfolded Band Structure and Optical Properties Studied by DFT Calculations. Materials, 2020, 13, 4300.	1.3	0
35701	The Interstitial Carbonâ€“Dioxygen Center in Irradiated Silicon. Crystals, 2020, 10, 1005.	1.0	3
35702	Structural Insight in the Interfacial Effect in Ferroelectric Polymer Nanocomposites. Advanced Materials, 2020, 32, e2005431.	11.1	84
35703	Molecular modeling and computational study of the chiral-dependent structures and properties of the self-assembling diphenylalanine peptide nanotubes, containing water molecules. Journal of Molecular Modeling, 2020, 26, 326.	0.8	7
35704	Infrared emitting material using infrared wavelength manipulation. Applied Materials Today, 2020, 21, 100811.	2.3	4
35705	Thermophysical systematics of Ni3In and Ni3Sn compounds: Ab initio database and interrelations. Calphad: Computer Coupling of Phase Diagrams and Thermochemistry, 2020, 71, 102205.	0.7	3
35706	Mn5Ge3 ultra-thin films on GaAs (111)B substrates: Influence of initial growth conditions. Superlattices and Microstructures, 2020, 148, 106745.	1.4	3
35707	Effect of High Pressure on the Crystal Structures of Polymorphs of <scp>l</scp>-Histidine. Crystal Growth and Design, 2020, 20, 7788-7804.	1.4	15
35708	Lowering the Schottky barrier height of G/WSSe van der Waals heterostructures by changing the interlayer coupling and applying external biaxial strain. Physical Chemistry Chemical Physics, 2020, 22, 26231-26240.	1.3	43
35709	Thermoelectric response of anti-fluoride Sr2Ge semiconducting material: A first-principles study. AIP Conference Proceedings, 2020, , .	0.3	1
35710	Exploring the high carrier mobility of newly predicted SiSe2 monolayer. , 2020, , .		1
35711	Spatial decomposition of magnetic anisotropy in magnets: Application to doped Fe16N2. Physical Review B, 2020, 102, .	1.1	8
35712	A Linear Relationship between the Charge Transfer Amount and Level Alignment in Molecule/Two-Dimensional Adsorption Systems. ACS Omega, 2020, 5, 26748-26754.	1.6	11
35713	Nonlinear Optical Interactions and Relaxation in 2D Layered Transition Metal Dichalcogenides Probed by Optical and Photoacoustic Z-Scan Methods. ACS Photonics, 2020, 7, 3440-3447.	3.2	34
35714	Pentadiamond-like Metallic Hard Carbon Nitride. Journal of Physical Chemistry C, 2020, 124, 24978-24983.	1.5	12
35715	Boron Concentration Induced Co-Ta-B Composite Formation Observed in the Transition from Metallic to Covalent Glasses. Condensed Matter, 2020, 5, 18.	0.8	1
35716	Deposition of Tetracoordinate Co(II) Complex with Chalcone Ligands on Graphene. Molecules, 2020, 25, 5021.	1.7	15

#	Article	IF	Citations
35717	Electronic Structure and Optical Properties of a Mn-Doped InSe/WSe2 van der Walls Heterostructure: First Principles Calculations. Journal of the Korean Physical Society, 2020, 77, 587-591.	0.3	2
35718	2D Sandwiched Nano Heterostructures Endow MoSe₂/TiO_{2â"}_x/Graphene with High Rate and Durability for Sodium Ion Capacitor and Its Solid Electrolyte Interphase Dependent Sodiation/Desodiation Mechanism. Small, 2020, 16, e2004457.	5.2	38
35719	Crafting carbon sphere-titania coreâ€"shell interfacial structure to achieve enhanced visible light photocatalysis. Applied Surface Science, 2020, 534, 147566.	3.1	16
35721	Highly Enhanced Gas Sensing Performance Using a 1T/2H Heterophase MoS₂ Field-Effect Transistor at Room Temperature. ACS Applied Materials & Interfaces, 2020, 12, 50610-50618.	4.0	64
35722	Performance controlled via surface oxygen-vacancy in Ti-based oxide catalyst during methyl oleate epoxidation. Scientific Reports, 2020, 10, 18952.	1.6	27
35723	Computational investigation of Zn-doped and undoped SrEu₂Fe₂O₇ as potential mixed electron and proton conductors. RSC Advances, 2020, 10, 39988-39994.	1.7	1
35724	A comparative spin dependent first principle study of monolayer (2D), armchair and zigzag nanoribbon (1D) of chromium disulfide (CrS2). AIP Conference Proceedings, 2020, , .	0.3	8
35725	Structural, electronic and mechanical properties of rare-earth ErTl3 intermetallic compound. AIP Conference Proceedings, 2020, , .	0.3	0
35726	Structural stability, electronic and elastic properties of cubic RbTaO3 perovskite oxide. AIP Conference Proceedings, 2020, , .	0.3	2
35727	Probing the Electronic Structure of Warm Dense Nickel via Resonant Inelastic X-Ray Scattering. Physical Review Letters, 2020, 125, 195001.	2.9	10
35728	Adsorption of arsenic trihydride (<mml:math xmlns:mml="http://www.w3.org/1998/Math/MathML") Tj ETQq0 0 0 rgBT /Overlock 10 Tf 5 on palladium oxide (PdO) surface (001): ab initio study. Computational Condensed Matter, 2020, 25, e00515.	0.9	1
35729	Si solution in Î¸-Al13Fe4 from first-principles. Intermetallics, 2020, 126, 106939.	1.8	12
35730	Adsorption, diffusion and aggregation of Ir atoms on graphdiyne: a first-principles investigation. Physical Chemistry Chemical Physics, 2020, 22, 25841-25847.	1.3	7
35731	Revealing the veil of the stability of monolayer boron sulfide upon air and humidity exposure. AIP Conference Proceedings, 2020, , .	0.3	0
35732	Theoretical Investigation of the thermodynamic stability and Density of States in Î±-(Co, Cu)Sn3. , 2020, , .		0
35733	Equibiaxial Strained Oxygen Adsorption on Pristine Graphene, Nitrogen/Boron Doped Graphene, and Defected Graphene. Materials, 2020, 13, 4945.	1.3	5
35734	Electronic Properties of Calcium and Zirconium Co-Doped BaTiO₃. Materials Science Forum, 0, 1010, 308-313.	0.3	4
35735	Thermoelectric Properties of Sm Doped CaMnO₃ Using Density Functional Theory Method. Materials Science Forum, 0, 1010, 334-338.	0.3	1

#	Article	IF	Citations
35736	Magnetic Volume Effect of Hydrogen Diffusion in Palladium. Solid State Phenomena, 2020, 310, 29-33.	0.3	0
35737	Scalable Substitutional Reâ€Doping and its Impact on the Optical and Electronic Properties of Tungsten Diselenide. Advanced Materials, 2020, 32, e2005159.	11.1	32
35738	Multiscale Modeling of Defect Phenomena in Platinum Using Machine Learning of Force Fields. Jom, 2020, 72, 4346-4358.	0.9	5
35739	Cyclic oxidation behavior of NiCoCrAlY/YSZ@Ni composite coatings fabricated by laser cladding. Journal of Iron and Steel Research International, 2020, 27, 1226-1235.	1.4	4
35740	An Efficient Deep Learning Scheme To Predict the Electronic Structure of Materials and Molecules: The Example of Graphene-Derived Allotropes. Journal of Physical Chemistry A, 2020, 124, 9496-9502.	1.1	12
35741	Atomistic Insight into Cation Effects on Binding Energies in Cu-Catalyzed Carbon Dioxide Reduction. Journal of Physical Chemistry C, 2020, 124, 24765-24775.	1.5	25
35742	Influence of 4f filling on electronic and magnetic properties of rare earth-Au surface compounds. Nanoscale, 2020, 12, 22258-22267.	2.8	11
35743	Origin of band inversion in topological Bi2Se3. AIP Advances, 2020, 10, .	0.6	14
35744	Ag and Agâ€“Cu interactions in Si. Journal of Applied Physics, 2020, 128, .	1.1	1
35745	On the Impact of Substrate Uniform Mechanical Tension on the Graphene Electronic Structure. Materials, 2020, 13, 4683.	1.3	5
35746	Effect of the Free Volume on the Electronic Structure of Cu70Zr30 Metallic Glasses. Materials, 2020, 13, 4911.	1.3	2
35747	Spontaneously Splitting Copper Nanowires into Quantum Dots on Graphdiyne for Suppressing Lithium Dendrites. Advanced Materials, 2020, 32, e2004379.	11.1	74
35748	The structural, electronic, magnetic, and optical properties of the Cr-, Mo-, and W-doped ZnTe alloys. Applied Physics A: Materials Science and Processing, 2020, 126, 1.	1.1	2
35749	Atomic Ordering at the Liquid-Al/MgAl2O4 Interfaces from Ab Initio Molecular Dynamics Simulations. Metallurgical and Materials Transactions A: Physical Metallurgy and Materials Science, 2020, 51, 6318-6326.	1.1	13
35750	Evidence of superoxide-like CsO2 formation on a cesiated model surface. Applied Surface Science, 2020, 534, 147579.	3.1	5
35751	Strain and electric field tuning of semi-metallic character WCrCO₂ MXenes with dual narrow band gap. Journal of Physics Condensed Matter, 2020, 32, 355504.	0.7	33
35752	Weak localization competes with the quantum oscillations in a natural electronic superlattice: The case of <mml:math		

#	Article	IF	Citations
35754	2D-layered Ti3C2 MXenes for promoted synthesis of NH3 on P25 photocatalysts. Applied Catalysis B: Environmental, 2020, 273, 119054.	10.8	111
35755	Investigation of alkali-ion (Li, Na and K) intercalation in manganese hexacyanoferrate KxMnFe(CN)6 as cathode material. Chemical Engineering Journal, 2020, 396, 125269.	6.6	44
35756	Lattice dynamics of novel Heusler alloys MnY2Z (Z=Al and Si). Physica B: Condensed Matter, 2020, 590, 412222.	1.3	15
35757	The Potential of Overlayers on Tin-based Perovskites for Water Splitting. Journal of Physical Chemistry Letters, 2020, 11, 4124-4130.	2.1	4
35758	Pressure induced phase transitions in BaZr(PO4)2 studied using x-ray diffraction, Raman spectroscopy, and first principles calculations. Journal of Applied Physics, 2020, 127, .	1.1	2
35759	Inorganic gas sensing of green phosphorene nanosheet: insights from density functional theory. Journal of Physics Condensed Matter, 2020, 32, 355002.	0.7	2
35760	Nature of Novel 2D van der Waals Heterostructures for Superior Potassium Ion Batteries. Advanced Energy Materials, 2020, 10, 2000884.	10.2	85
35761	Dendritic Ag/Pd Alloy Nanostructure Arrays for Electrochemical CO 2 Reduction. ChemElectroChem, 2020, 7, 2608-2613.	1.7	12
35762	The Crystal Structure of MnF₃ Revisited. Zeitschrift Fur Anorganische Und Allgemeine Chemie, 2020, 646, 882-888.	0.6	4
35763	Selectivity switch in transformation of CO2 from ethanol to methanol on Cu embedded in the defect carbon. Science China Chemistry, 2020, 63, 722-730.	4.2	10
35764	Electronic, optical and magnetic properties of low concentration Ni-doped CdSe by first principle method. Bulletin of Materials Science, 2020, 43, 1.	0.8	16
35765	PLD-fabricated perovskite oxide nanofilm as efficient electrocatalyst with highly enhanced water oxidation performance. Applied Catalysis B: Environmental, 2020, 272, 119046.	10.8	29
35767	Unraveling the effects of the coordination number of Mn over Î±-MnO2 catalysts for toluene oxidation. Chemical Engineering Journal, 2020, 396, 125192.	6.6	110
35768	Strain tunable electronic and optical properties of 2D orthorhombic lithium sulfur monolayer. Chemical Physics, 2020, 535, 110762.	0.9	1
35769	Elucidation of photodegradation of p-chlorophenol in a biophotoelectric reductive degradation system by density functional theory calculations. International Biodeterioration and Biodegradation, 2020, 151, 104969.	1.9	10
35770	A new mixed-anion phosphate Cs2Bi2Sr(P2O7)(PO4)2: Synthesis, characterization, structure and its Eu3+-activated luminescence. Journal of Solid State Chemistry, 2020, 288, 121411.	1.4	9
35771	Photogenerated-Carrier Separation and Transfer in Two-Dimensional Janus Transition Metal Dichalcogenides and Graphene van der Waals Sandwich Heterojunction Photovoltaic Cells. Journal of Physical Chemistry Letters, 2020, 11, 4070-4079.	2.1	44
35772	Critical Hydrogen Coverage Effect on the Hydrogenation of Ethylene Catalyzed by Î´-MoC(001): An Ab Initio Thermodynamic and Kinetic Study. ACS Catalysis, 2020, 10, 6213-6222.	5.5	21

#	Article	IF	Citations
35773	Tuning lithium-peroxide formation and decomposition routes with single-atom catalysts for lithiumâ€“oxygen batteries. Nature Communications, 2020, 11, 2191.	5.8	181
35774	Mechanism of collective interstitial ordering in Feâ€“C alloys. Nature Materials, 2020, 19, 849-854.	13.3	32
35775	Cuâ€“Ag alloy for engineering properties and applications based on the LSPR of metal nanoparticles. RSC Advances, 2020, 10, 13277-13285.	1.7	31
35776	Effect of chemical composition, defect structure, and stress state on the elastic properties of (V_{1â^'x}Al_x)_{1â^'yâ€Š}N_{yâ€Š}. Journal of Physics Condensed Matter, 2020, 32, 025901.	2.7	7
35777	Ferromagnetic half-metallicity in half-Heusler AuMnSn:Te Alloy. Materials Research Express, 2020, 7, 076519.	0.8	5
35778	Density functional theory and machine learning guided search for RE₂Si₂O₇ with targeted coefficient of thermal expansion. Journal of the American Ceramic Society, 2020, 103, 4489-4497.	1.9	16
35779	Study on the Effect of Doping on Lattice Constant and Electronic Structure of Bulk AuCu by the Density Functional Theory. Journal of Multiscale Modeling, 2020, 11, 2030001.	1.0	21
35780	Tunable optical absorption of WS₂monolayer via alkali metal modulation. Modern Physics Letters B, 2020, 34, 2050089.	1.0	5
35781	Optical, Electronic Properties and Anisotropy in Mechanical Properties of â€œXâ€•Type Carbon Allotropes. Materials, 2020, 13, 2079.	1.3	26
35782	Electrochemical Li Intercalation in Black Phosphorus: In Situ and Ex Situ Studies. Journal of Physical Chemistry C, 2020, 124, 10710-10718.	1.5	18
35783	Origin of Confined Catalysis in Nanoscale Reactors between Two-Dimensional Covers and Metal Substrates: Mechanical or Electronic?. Journal of Physical Chemistry C, 2020, 124, 11564-11573.	1.5	14
35784	Pd-Functionalized ZnO:Eu Columnar Films for Room-Temperature Hydrogen Gas Sensing: A Combined Experimental and Computational Approach. ACS Applied Materials & Interfaces, 2020, 12, 24951-24964.	4.0	34
35785	Predicting Spinel Disorder and Its Effect on Oxygen Transport Kinetics in Hercynite. ACS Applied Materials & Interfaces, 2020, 12, 23831-23843.	4.0	11
35786	Density Functional Theory Study of Oxygen Adsorption on Polymer Surfaces for Atomic-Layer Etching: Implications for Semiconductor Device Fabrication. ACS Applied Nano Materials, 2020, 3, 5189-5202.	2.4	20
35787	Electronegativity and doping in Si1-xGex alloys. Scientific Reports, 2020, 10, 7459.	1.6	13
35788	Semiconducting two-dimensional group VAâ€“VA haeckelite compounds with superior carrier mobility. Physical Chemistry Chemical Physics, 2020, 22, 12260-12266.	1.3	7
35789	Pressure-induced first order phase transition in bulk GeSe. Journal of Applied Physics, 2020, 127, .	1.1	12
35790	Energetic, structural and electronic features of Sn-, Ga-, O-based defect complexes in cubic In₂O₃. Journal of Physics Condensed Matter, 2020, 32, 225703.	0.7	3

#	Article	IF	Citations
35791	Hydrogen coverage dependent C C hydrogenation activity on Rh(1Â1Â1). Chemical Physics Letters, 2020, 746, 137287.	1.2	3
35792	Crystal Site Feature Embedding Enables Exploration of Large Chemical Spaces. Matter, 2020, 3, 433-448.	5.0	33
35793	Theoretical Investigation of the Energies, Structures, and Growth Properties of Hydromagnesite Surfaces. Crystal Growth and Design, 2020, 20, 3722-3731.	1.4	11
35794	Ten Facets, One Force Field: The GAL19 Force Field for Waterâ€“Noble Metal Interfaces. Journal of Chemical Theory and Computation, 2020, 16, 4565-4578.	2.3	26
35795	Molecular Dynamics Study of sp-Defect Migration in Odd Fullerene: Possible Role in Synthesis of Abundant Isomers of Fullerenes. Journal of Physical Chemistry C, 2020, 124, 11652-11661.	1.5	9
35796	Identification of Active Sites of Pure and Nitrogen-Doped Carbon Materials for Oxygen Reduction Reaction Using Constant-Potential Calculations. Journal of Physical Chemistry C, 2020, 124, 12016-12023.	1.5	73
35797	Tuneable quantum spin Hall states in confined 1T' transition metal dichalcogenides. Scientific Reports, 2020, 10, 6670.	1.6	12
35798	The Volumetric Source Function: Looking Inside van der Waals Interactions. Scientific Reports, 2020, 10, 7816.	1.6	10
35799	Mutual dependence of oxygen and vacancy diffusion in bcc Fe and dilute iron alloys. Physical Review B, 2020, 101, .	1.1	3
35800	Two-dimensional <mml:math xmlns:mml="http://www.w3.org/1998/Math/MathML"><mml:msub><mml:mi mathvariant="normal">CP</mml:mi><mml:mn>3</mml:mn></mml:msub></mml:math> monolayer and its fluorinated derivative with promising electronic and optical properties: A theoretical study. Physical Review B, 2020, 101, .	1.1	27
35801	Pressure Effects on the Magnetic Phase Diagram of the CeNMSb2 (NM: Au and Ag): A DFT Study. Materials, 2020, 13, 2237.	1.3	4
35802	Synthesis, Structural Characterization and Chemical Bonding of Sr₇Li₆Sn₁₂ and its Quaternary Derivatives with Eu and Alkaline Earth Metal (Mg, Ca, Ba) Substitutions. A Tale of Seven Liâ€Containing Stannides and Two Complex Electronic and topological properties of <mml:math xmlns:mml="http://www.w3.org/1998/Math/MathML" altimg="si43.svg"><mml:mrow><mml:msub><mml:mrow><mml:mtext>Sn</mml:mtext></mml:mrow><mml:mrow><mml:mn>1</mml:mn> Electronic and topological properties of <mml:math xmlns:mml="http://www.w3.org/1998/Math/MathML" altimg="si44.svg"><mml:mrow><mml:msub><mml:mrow><mml:mtext>In</mml:mtext></mml:mrow><mml:mrow><mml:mi>x</mml:mi>	1.0	0
35803	Structural and Topological Properties of Zintl Phase Sr3Ga4Sn4. Chemistry, 2020, 2020, 1979-1988. Computational Materials Science, 2020, 182, 109777.	1.4	5
35804	Studies on covalent functionalization of single layer black phosphorus from GW calculations based on the many body perturbation theory. Electronic Structure, 2020, 2, 025005.	1.0	5
35805	Atomistic-Level Description of GaN/Water Interface by a Combined Spectroscopic and First-Principles Computational Approach. Journal of Physical Chemistry C, 2020, 124, 12466-12475.	1.5	6
35806	Controlling the Oxidation State of Fe-Based Catalysts through Nitrogen Doping toward the Hydrodeoxygenation of m-Cresol. ACS Catalysis, 2020, 10, 7884-7893.	5.5	32
35807	Catalytic oxidation mechanisms of carbon monoxide over single- and double-vacancy Mn-embedded graphene. New Journal of Chemistry, 2020, 44, 9402-9410.	1.4	22
35808	Structural, electronic, and magnetic properties of point defects in polyaniline (C3N) and graphene monolayers: A comparative study. Journal of Applied Physics, 2020, 127, 195102.	1.1	8

#	Article	IF	Citations
35809	Interaction studies of volatiles from jackfruit on Î±-phosphorene nanosheetâ€"a DFT outlook. Structural Chemistry, 2020, 31, 1851-1860.	1.0	15
35810	Electron density modulation of GaN nanowires by manganese incorporation for highly high-rate Lithium-ion storage. Electrochimica Acta, 2020, 350, 136380.	2.6	28
35811	Molecular Layer Deposition of â€œMagnesiconeâ€, a Magnesium-based Hybrid Material. Chemistry of Materials, 2020, 32, 4451-4466.	3.2	17
35812	Cooperative Catalysis by Multiple Active Centers in Nonoxidative Conversion of Methane. Journal of Physical Chemistry C, 2020, 124, 13656-13663.	1.5	18
35813	MAI Termination Favors Efficient Hole Extraction and Slow Charge Recombination at the MAPbI₃/CuSCN Heterojunction. Journal of Physical Chemistry Letters, 2020, 11, 4481-4489.	2.1	22
35814	Efficient Sensing Properties of Aluminum Nitride Nanosheets toward Toxic Pollutants under Gated Electric Field. ACS Applied Electronic Materials, 2020, 2, 1645-1652.	2.0	15
35815	Band engineering of mesoporous TiO2 with tunable defects for visible-light hydrogen generation. CrystEngComm, 2020, 22, 4030-4038.	1.3	6
35816	Promoting effect of tungsten carbide on the catalytic activity of Cu for CO₂ reduction. Physical Chemistry Chemical Physics, 2020, 22, 13666-13679.	1.3	16
35817	Effects of cation size and concentration of cationic chlorides on the properties of formamidinium lead iodide based perovskite solar cells. Sustainable Energy and Fuels, 2020, 4, 3753-3763.	2.5	17
35818	Ferroelectrically tunable magnetism in BiFeO3/BaTiO3 heterostructure revealed by the first-principles calculations. Journal of Advanced Research, 2020, 24, 371-377.	4.4	7
35819	Accuracy of Hybrid Functionals with Non-Self-Consistent Kohnâ€"Sham Orbitals for Predicting the Properties of Semiconductors. Journal of Chemical Theory and Computation, 2020, 16, 3543-3557.	2.3	17
35820	Porous-Carbon Aerogels with Tailored Sub-Nanopores for High Cycling Stability and Rate Capability Potassium-Ion Battery Anodes. ACS Applied Materials & Interfaces, 2020, 12, 27045-27054.	4.0	16
35821	Insights into Spectator-Directed Catalysis: CO Adsorption on Amine-Capped Platinum Nanoparticles on Oxide Supports. ACS Applied Materials & Interfaces, 2020, 12, 27765-27776.	4.0	14
35822	Naâ€"Niâ€"H Phase Formation at High Pressures and High Temperatures: Hydrido Complexes [NiH5]3â€" Versus the Perovskite NaNiH3. ACS Omega, 2020, 5, 8730-8743.	1.6	7
35823	Yield strength and misfit volumes of NiCoCr and implications for short-range-order. Nature Communications, 2020, 11, 2507.	5.8	162
35824	High-pressure characterization of multifunctional CrVO₄. Journal of Physics Condensed Matter, 2020, 32, 385403.	0.7	12
35825	Ab Initio Studies of Phase Transformations in Fe100Ââ€"ÂxSix. Physics of the Solid State, 2020, 62, 739-743.	0.2	2
35826	Hydrogen Trapping in bcc Iron. Materials, 2020, 13, 2288.	1.3	42

#	Article	IF	Citations
35827	Kinetically Limited Phase Formation of Pt-Ir Based Compositionally Complex Thin Films. Materials, 2020, 13, 2298.	1.3	2
35828	Effects of B on the Segregation Behavior of Mo at the Feâ€“Cr(111)/Cr2O3(0001) Interface: A First-Principles Study. Metals, 2020, 10, 577.	1.0	6
35829	Influence of gold on the reactivity behaviour of ceria nanorods in CO oxidation: combining operando spectroscopies and DFT calculations. Catalysis Science and Technology, 2020, 10, 3720-3730.	2.1	19
35830	Emergent atomistic Kondo resonances in strained carbon-benzene single chains. Physical Review B, 2020, 101, .	1.1	2
35831	LiIn₂SbO₆: A New Rutile-Related Structure Type with Unique Ion Channels. Chemistry of Materials, 2020, 32, 4785-4794.	3.2	10
35832	High pressure and elastic properties of a guanidinium-formate hybrid perovskite. Dalton Transactions, 2020, 49, 7228-7233.	1.6	11
35833	Topological Dirac nodal loops in nonsymmorphic hydrogenated monolayer boron. Physical Review B, 2020, 101, .	1.1	19
35834	Semimetal States of Crystalline Molecular Hydrogen at High Pressures. JETP Letters, 2020, 111, 162-166.	0.4	5
35835	Ab Initio Study of the Relation between the Structural, Magnetic, and Optical Properties of Normal and Inverse MnGa2O4 Spinels. Journal of Experimental and Theoretical Physics, 2020, 130, 418-422.	0.2	1
35836	An ultrathin two-dimensional vertical ferroelectric tunneling junction based on CuInP₂S₆ monolayer. Nanoscale, 2020, 12, 12522-12530.	2.8	40
35837	Galliumâ€“Boronâ€“Phosphide ($$hbox {GaBP}_{2}$$): a new IIIâ€“V semiconductor for photovoltaics. Journal of Materials Science, 2020, 55, 9448-9460.	1.7	5
35838	On the Dopability of Semiconductors and Governing Material Properties. Chemistry of Materials, 2020, 32, 4467-4480.	3.2	34
35839	A first-principles study of the substitutional doping of the MgCl₂ monolayer for spintronics applications. New Journal of Chemistry, 2020, 44, 8833-8839.	1.4	18
35840	Methylation Detection and DNA Sequencing Based on Adsorption of Nucleobases on Silicene Nanoribbon. Journal of Physical Chemistry C, 2020, 124, 10823-10831.	1.5	12
35841	Hybrid density functional theoretical study of NASICON-type Na_xTi₂(PO₄)₃ (x = 1â€“4). Physical Chemistry Chemical Physics, 2020, 22, 11861-11870.	1.3	6
35842	Band Structure of Strained $mathrm{Ge}_{1-x}~mathrm{Sn}_{x}$ Alloy: A Full-Zone 30-Band ${k}cdot{p}$ Model. IEEE Journal of Quantum Electronics, 2020, 56, 1-8.	1.0	4
35843	Highâ€Performance Overall CO₂ Splitting on Hierarchical Structured Cobalt Disulfide with Partially Removed Sulfur Edges. Advanced Functional Materials, 2020, 30, 2000154.	7.8	26
35844	Vibrational Entropy Stabilizes Distorted Half-Heusler Structures. Chemistry of Materials, 2020, 32, 4767-4773.	3.2	13

#	Article	IF	Citations
35845	Trends in the Adsorption of Oxygen and Li₂O₂ on Transition-Metal Carbide Surfaces: A Theoretical Study. Journal of Physical Chemistry C, 2020, 124, 7716-7724.	1.5	9
35846	Alkali Doping Leads to Charge-Transfer Salt Formation in a Two-Dimensional Metalâ€“Organic Framework. ACS Nano, 2020, 14, 7475-7483.	7.3	15
35847	Strain modulation of TaO4 planarity in tantalates ultrathin films: surface states engineering. Scientific Reports, 2020, 10, 7828.	1.6	5
35848	Operando identification of site-dependent water oxidation activity on ruthenium dioxide single-crystal surfaces. Nature Catalysis, 2020, 3, 516-525.	16.1	166
35849	A quantum chemical study of substituent effects on CN bonds in aryl isocyanide molecules adsorbed on the Pt surface. Physical Chemistry Chemical Physics, 2020, 22, 12200-12208.	1.3	4
35850	Density functional theory study of superoxide ions as impurities in alkali halides. Physical Chemistry Chemical Physics, 2020, 22, 13378-13389.	1.3	1
35851	The mechanism and ligand effects of single atom rhodium supported on ZSM-5 for the selective oxidation of methane to methanol. Physical Chemistry Chemical Physics, 2020, 22, 11686-11694.	1.3	22
35852	Surface functionalization of ZnO:Ag columnar thin films with AgAu and AgPt bimetallic alloy nanoparticles as an efficient pathway for highly sensitive gas discrimination and early hazard detection in batteries. Journal of Materials Chemistry A, 2020, 8, 16246-16264.	5.2	38
35853	A physics-based machine learning study of the behavior of interstitial helium in single crystal Wâ€“Mo binary alloys. Journal of Applied Physics, 2020, 127, .	1.1	10
35854	Superconducting boron allotropes. Physical Review B, 2020, 101, .	1.1	18
35855	Proximity-induced spin-orbit splitting in graphene nanoribbons on transition-metal dichalcogenides. Physical Review B, 2020, 101, .	1.1	9
35856	Experimental and Theoretical Study of the Atomic Structure Evolution of High-Entropy Alloys Based on Fe, Cr, Ni, Mn, and Co upon Thermal and Radiation Aging. Physics of the Solid State, 2020, 62, 389-400.	0.2	6
35857	Combining Theory and Experiment to Characterize the Voltammetric Behavior of Nickel Anodes in the Simons Process. Chemistry - A European Journal, 2020, 26, 10781-10786.	1.7	7
35858	A HfC nanowire point electron source with oxycarbide surface of lower work function for high-brightness and stable field-emission. Nano Research, 2020, 13, 1620-1626.	5.8	17
35859	High yield production of ultrathin fibroid semiconducting nanowire of Ta2Pd3Se8. Nano Research, 2020, 13, 1627-1635.	5.8	16
35860	A New Modification of TeI₄ Possessing the Crystal Structure Proposed for WI₄. Crystal Growth and Design, 2020, 20, 3780-3784.	1.4	1
35861	Development of a Reactive Force Field for Simulations on the Catalytic Conversion of C/H/O Molecules on Cu-Metal and Cu-Oxide Surfaces and Application to Cu/CuO-Based Chemical Looping. Journal of Physical Chemistry C, 2020, 124, 12512-12520.	1.5	25
35862	OER Performances of Cationic Substituted (100)-Oriented IrO₂ Thin Films: A Joint Experimental and Theoretical Study. ACS Applied Energy Materials, 2020, 3, 5229-5237.	2.5	14

#	Article	IF	Citations
35863	Density Functional Theory Study of Single-Atom V, Nb, and Ta Catalysts on Graphene and Carbon Nitride for Selective Nitrogen Reduction. ACS Applied Nano Materials, 2020, 3, 5149-5159.	2.4	51
35864	Solvent-mediated assembly of atom-precise goldâ€“silver nanoclusters to semiconducting one-dimensional materials. Nature Communications, 2020, 11, 2229.	5.8	91
35865	Negative Poissonâ€™s ratio in two-dimensional honeycomb structures. Npj Computational Materials, 2020, 6, .	3.5	56
35866	Computational characterization of N-type characteristics and optoelectronic properties in air-stable pyromellitic diimide derivatives. New Journal of Chemistry, 2020, 44, 8412-8421.	1.4	5
35867	Dependence on co-adsorbed water in the reforming reaction of ethanol on a Rh(111) surface. RSC Advances, 2020, 10, 17787-17794.	1.7	0
35868	Engineering the electronic structure of 1Tâ€²-ReS₂ through nitrogen implantation for enhanced alkaline hydrogen evolution. Journal of Materials Chemistry A, 2020, 8, 11607-11616.	5.2	39
35869	Theoretical study on NO_x adsorption properties over the Î±-MnO₂(110) surface. RSC Advances, 2020, 10, 9539-9548.	1.7	9
35870	Two-dimensional Dirac spin-gapless semiconductors with tunable perpendicular magnetic anisotropy and a robust quantum anomalous Hall effect. Materials Horizons, 2020, 7, 2071-2077.	6.4	45
35871	Ab initio simulation of warm dense matter. Physics of Plasmas, 2020, 27, .	0.7	114
35872	First-principles studies of Tin+1SiNn (nâ€‰=â€‰1, 2, 3) MAX phase. Philosophical Magazine, 2020, 100, 2183-2204.	0.4	4
35873	Transition Mechanism from Semimetallic to Semiconductor Behavior in a Graphene Film at the Formation of a Multiply Connected Structure. JETP Letters, 2020, 111, 235-238.	0.4	1
35874	Dimerization of Acetic Acid in the Gas Phaseâ€”NMR Experiments and Quantum-Chemical Calculations. Molecules, 2020, 25, 2150.	1.7	15
35875	Electronic and magnetic properties of the multiferroic TbMn2O5. Applied Physics A: Materials Science and Processing, 2020, 126, 1.	1.1	1
35876	Hydrogen-Bond-Assisted Reinforcement of Interlayer Connections in Zn₂BO₃XÂ·H₂O (X = Cl, Br): Two UV Nonlinear Optical Crystals with KBBF-Type Structure. Inorganic Chemistry, 2020, 59, 7789-7794.	1.9	6
35877	Significant Reduction in the Interfacial Resistance of Garnet-Type Solid Electrolyte and Lithium Metal by a Thick Amorphous Lithium Silicate Layer. ACS Applied Energy Materials, 2020, 3, 5533-5541.	2.5	25
35878	Comparison of CH₄ and CO₂ Adsorptions onto Calcite(10.4), Aragonite(011)Ca, and Vaterite(010)CO₃ Surfaces: An MD and DFT Investigation. ACS Omega, 2020, 5, 11369-11377.	1.6	20
35879	Engineering covalently bonded 2D layered materials by self-intercalation. Nature, 2020, 581, 171-177.	13.7	185
35880	The mechanism of Mg²⁺ conduction in ammine magnesium borohydride promoted by a neutral molecule. Physical Chemistry Chemical Physics, 2020, 22, 9204-9209.	1.3	70

#	Article	IF	Citations
35881	Charge doping induced reversible multistep structural phase transitions and electromechanical actuation in two-dimensional 1Tâ€²-MoS₂. Nanoscale, 2020, 12, 12541-12550.	2.8	19
35882	Unconventional stable stoichiometry of vanadium peroxide. Physical Chemistry Chemical Physics, 2020, 22, 11460-11466.	1.3	4
35883	Ab initio investigation of pressure-induced structural transitions and electronic evolution of Th3N4. High Pressure Research, 2020, 40, 267-282.	0.4	3
35884	Phase stability and magnetic properties in fcc Fe-Cr-Mn-Ni alloys from first-principles modeling. Physical Review B, 2020, 101, .	1.1	30
35885	Effect of strain on electronic structure of AA stacked GeSe bilayer. Materials Today: Proceedings, 2020, 28, 1853-1857.	0.9	0
35886	Alkali metals inside bi-layer graphene and MoS2: Insights from first-principles calculations. Nano Energy, 2020, 75, 104927.	8.2	30
35887	Ab initio study of the mechanical properties and thermal conductivity of Bi2O2X (X = Se, Te) under pressure. Solid State Sciences, 2020, 106, 106299.	1.5	4
35888	Amorphization of Indirect Band Gap Semiconductors To Tune Their Optoelectronic Properties. Journal of Physical Chemistry C, 2020, 124, 14432-14438.	1.5	7
35889	Do HOMOâ€“LUMO Energy Levels and Band Gaps Provide Sufficient Understanding of Dye-Sensitizer Activity Trends for Water Purification?. ACS Omega, 2020, 5, 15052-15062.	1.6	18
35890	The Effect of Surface Defects on Chloride-Induced Depassivation of Ironâ€”A Density Functional Theory Study. Corrosion, 2020, 76, 690-697.	0.5	14
35891	Electronic properties of sulfide minerals and floatability. , 2020, , 13-81.		5
35892	Exploring anchoring performance of InP3 monolayer for lithium-sulfur batteries: A first-principles study. Applied Surface Science, 2020, 526, 146717.	3.1	31
35893	Adhesion, bonding and mechanical properties of Mo doped diamond/Al (Cu) interfaces: A first principles study. Applied Surface Science, 2020, 527, 146817.	3.1	41
35894	Chalcopyrite based carbon composite electrodes for high performance symmetric supercapacitor. Chemical Engineering Journal, 2020, 399, 125711.	6.6	29
35895	Electronic, optical, and thermoelectric properties of sodium pnictogen chalcogenides: A first principles study. Computational Materials Science, 2020, 183, 109818.	1.4	21
35896	Novel 3D photoactive direct bandgap perovskites CsBiPbX6: Ab initio structure and electronic properties. Computational Materials Science, 2020, 183, 109819.	1.4	1
35897	Density Functional Theory investigation of rhombohedral multiferroic oxides for photocatalytic water splitting and organic photodegradation. Journal of Photochemistry and Photobiology A: Chemistry, 2020, 400, 112656.	2.0	16
35898	Physical properties of a novel phase of boron nitride and its potential applications. Materials Chemistry and Physics, 2020, 252, 123245.	2.0	22

#	Article	IF	Citations
35899	Theoretical study of oxygen adsorption energy on supported metal cluster using d-band center theory and HSAB concept. Surface Science, 2020, 696, 121601.	0.8	11
35900	Unusual Atmospheric Water Trapping and Water Induced Reversible Restacking of 2D Gallium Sulfide Layers in NaGaS₂ Formed by Supertetrahedral Building Unit. Chemistry of Materials, 2020, 32, 5589-5603.	3.2	21
35901	Chemistry with F Centers: Reduction of Organic Molecules on the Defective Potassium Chloride(100) Surface. Journal of Physical Chemistry C, 2020, 124, 12606-12616.	1.5	6
35902	Effect of Sn-self diffusion via H2 treatment on low temperature activation of hematite photoanodes. Catalysis Science and Technology, 2020, 10, 4245-4255.	2.1	3
35903	Catalytic activity atlas of ternary Coâ€“Feâ€“V metal oxides for the oxygen evolution reaction. Journal of Materials Chemistry A, 2020, 8, 15951-15961.	5.2	43
35904	Infrared-active phonon modes in single-crystal thorium dioxide and uranium dioxide. Journal of Applied Physics, 2020, 127, .	1.1	7
35905	Ferrotoroidic polarons in antiferrodistortive <mml:math xmlns:mml="http://www.w3.org/1998/Math/MathML"><mml:mrow><mml:mi>SrTi</mml:mi><mml:msub><mml:mi mathvariant="normal">O</mml:mi><mml:mn>3</mml:mn></mml:msub></mml:mrow></mml:math>. Physical Review B, 2020, 101, .	1.1	6
35906	Nanoâ€atomic scale hydrophobic/philic confinement of peptides on mineral surfaces by crossâ€correlated SPM and quantum mechanical DFT analysis. Journal of Microscopy, 2020, 280, 204-221.	0.8	7
35907	Diffusion Properties of Oxygen in the Î³-TiAl Alloy. Journal of Experimental and Theoretical Physics, 2020, 130, 579-590.	0.2	17
35908	Hydrogen/deuterium adsorption and absorption properties on and in palladium using a combined plane wave and localized basis set method. International Journal of Quantum Chemistry, 2020, 120, e26275.	1.0	4
35909	Role of surface frustrated Lewis pairs on reduced CeO2(110) in direct conversion of syngas. Chinese Journal of Catalysis, 2020, 41, 1906-1915.	6.9	23
35910	Critical evidence for direct interspecies electron transfer with tungsten-based accelerants: An experimental and theoretical investigation. Bioresource Technology, 2020, 311, 123519.	4.8	42
35911	Competitive adsorption between phosphate and arsenic in soil containing iron sulfide: XAS experiment and DFT calculation approaches. Chemical Engineering Journal, 2020, 397, 125426.	6.6	31
35912	Novel Si-C compounds with semiconducting and metallic properties: A DFT study. Computational Materials Science, 2020, 183, 109800.	1.4	4
35913	Novel gamma arsenene nanosheets as sensing medium for vomiting agents: A first-principles research. Computational and Theoretical Chemistry, 2020, 1185, 112876.	1.1	24
35914	Compressive behavior and elastic properties of Ni-based Î³/Î³â€™ ternary model superalloys: First-principles calculations and rule of mixtures predications. Journal of Alloys and Compounds, 2020, 839, 155661.	2.8	7
35915	Direct observations of Pdâ€“Te compound formation within noble metal inclusions in spent nuclear fuel. Journal of Nuclear Materials, 2020, 538, 152249.	1.3	2
35916	Enhanced stability and ferromagnetic property in transition metals co-doped rutile TiO2. Journal of Physics and Chemistry of Solids, 2020, 146, 109582.	1.9	3

#	Article	IF	Citations
35917	Structure-dependent sodium ion storage mechanism of cellulose nanocrystal-based carbon anodes for highly efficient and stable batteries. Journal of Power Sources, 2020, 468, 228371.	4.0	24
35918	Enhanced near-ultraviolet and visible light absorption of organic-inorganic halide perovskites by co-doping with cesium and barium: Insight from first-principles calculations. Journal of Solid State Chemistry, 2020, 289, 121477.	1.4	4
35920	SrNbO3 as a transparent conductor in the visible and ultraviolet spectra. Communications Physics, 2020, 3, .	2.0	48
35921	Intrinsic ferromagnetic semiconductivity realized in a new MoS₂ monolayer. Physical Chemistry Chemical Physics, 2020, 22, 13363-13367.	1.3	2
35922	Substrate strain engineering: an efficient strategy to enhance the catalytic activity of SACs on waved graphene for e-NRR. Sustainable Energy and Fuels, 2020, 4, 3773-3779.	2.5	13
35923	Control of transition metalâ€“oxygen bond strength boosts the redox ex-solution in a perovskite oxide surface. Energy and Environmental Science, 2020, 13, 3404-3411.	15.6	36
35924	Study on the properties of perovskite materials under light and different temperatures and electric fields based on DFT. RSC Advances, 2020, 10, 20960-20971.	1.7	8
35925	Electron-lattice interplay in <mml:math xmlns:mml="http://www.w3.org/1998/Math/MathML"><mml:msub><mml:mi>LaMnO</mml:mi><mml:mn>3</mml:mn></mml:msub> from canonical Jahn-Teller distortion notations. Physical Review B, 2020, 101, .	1.1	9
35926	First-order magnetic phase transition in <mml:math xmlns:mml="http://www.w3.org/1998/Math/MathML"><mml:mrow><mml:mi mathvariant="normal">P</mml:mi><mml:msub><mml:mi mathvariant="normal">r</mml:mi><mml:mn>2</mml:mn></mml:msub><mml:mi>In</mml:mi></mml:mrow></mml:math> with negligible thermomagnetic hysteresis. Physical Review B, 2020, 101, .	1.1	28
35927	Theoretical investigation of the thermoelectric properties of ACuO2(A = K, Rb and Cs). European Physical Journal B, 2020, 93, 1.	0.6	5
35928	Design of an Accurate Machine Learning Algorithm to Predict the Binding Energies of Several Adsorbates on Multiple Sites of Metal Surfaces. ChemCatChem, 2020, 12, 4611-4617.	1.8	24
35929	Zn-doping enhances the photoluminescence and stability of PbS quantum dots for in vivo high-resolution imaging in the NIR-II window. Nano Research, 2020, 13, 2239-2245.	5.8	33
35930	Ultrafast processes in photochromic material YHxOy studied by excited-state density functional theory simulation. Science China Materials, 2020, 63, 1579-1587.	3.5	14
35931	IrO2 nanoparticle-decorated single-layer NiFe LDHs nanosheets with oxygen vacancies for the oxygen evolution reaction. Chemical Engineering Journal, 2020, 399, 125738.	6.6	60
35932	High selective and efficient Fe2â€“N6 sites for CO2 electroreduction: A theoretical investigation. International Journal of Hydrogen Energy, 2020, 45, 14311-14319.	3.8	26
35933	Frank-Read source operation in six body-centered cubic refractory metals. Journal of the Mechanics and Physics of Solids, 2020, 141, 104017.	2.3	43
35934	Materials selection for nuclear applications in view of divacancy energies by comprehensive first-principles calculations. Journal of Nuclear Materials, 2020, 538, 152253.	1.3	5
35935	Three-Dimensional Topotactic Host Structure-Secured Ultrastable VP-CNO Composite Anodes for Long Lifespan Lithium- and Sodium-Ion Capacitors. ACS Applied Materials & Interfaces, 2020, 12, 29218-29227.	4.0	3

#	Article	IF	Citations
35936	Electrode interface optimization advances conversion efficiency and stability of thermoelectric devices. Nature Communications, 2020, 11, 2723.	5.8	101
35937	Stabilizing the crystal structures of NaFePO₄ with Li substitutions. Physical Chemistry Chemical Physics, 2020, 22, 13975-13980.	1.3	8
35938	Bimetallenes for selective electrocatalytic conversion of CO₂: a first-principles study. Journal of Materials Chemistry A, 2020, 8, 12457-12462.	5.2	14
35939	First-principles calculations of phonon transport in two-dimensional penta-X2C family. Journal of Applied Physics, 2020, 127, 205106.	1.1	13
35940	Superior and tunable gas sensing properties of Janus PtSSe monolayer. Nano Express, 2020, 1, 010042.	1.2	18
35941	Janus <mml:math xmlns:mml="http://www.w3.org/1998/Math/MathML" display="inline" overflow="scroll"><mml:mi>Pt</mml:mi></mml:math> <mml:math xmlns:mml="http://www.w3.org/1998/Math/MathML" display="inline" overflow="scroll"><mml:msub><mml:mi>X</mml:mi><mml:mi>n</mml:mi></mml:msub><mml:msub><mml:mi>Y</mml:mi><mml:mi><mml:mr		

#	Article	IF	Citations
35954	Strain engineering the behaviors of small molecules over defective MoS2 monolayers in the 2H and 1Tâ€² phases. Journal of Materials Science, 2020, 55, 10643-10655.	1.7	6
35955	Investigating potential hard materials: the case of tetragonal TaMoN. Chinese Journal of Physics, 2020, 66, 758-764.	2.0	2
35956	Insight into the energy conversion and structural evolution of magnesium hydride during high-energy ball milling for its controllable synthesis. Journal of Alloys and Compounds, 2020, 836, 155312.	2.8	7
35957	Influence of metalloid antimony on the physical properties of palladium-based half-Heusler compared to the metallic bismuth: A first-principle study. Journal of Alloys and Compounds, 2020, 836, 155395.	2.8	30
35958	Structural, elastic, electronic, and magnetic properties of Si-doped Co2MnGe full-Heusler type compounds. Journal of Alloys and Compounds, 2020, 845, 155499.	2.8	17
35959	Atomistic determination on stability, cluster and microstructures in terms of crystallographic and thermo-kinetic integration of Alâ^'Mgâ^'Si alloys. Materials Today Communications, 2020, 24, 101220.	0.9	5
35960	First-principles determination of pressure-induced structure, anisotropic elasticity and ideal strengths of CuInS2 and CuInSe2. Solid State Communications, 2020, 316-317, 113952.	0.9	2
35961	Conductivity models for electron energy loss spectroscopy of graphene in a scanning transmission electron microscope with high energy resolution. Ultramicroscopy, 2020, 214, 113012.	0.8	6
35962	Anion Charge and Lattice Volume Maps for Searching Lithium Superionic Conductors. Chemistry of Materials, 2020, 32, 4618-4626.	3.2	16
35963	Microwave-Driven Hexagonal-to-Monoclinic Transition in BiPO₄: An In-Depth Experimental Investigation and First-Principles Study. Inorganic Chemistry, 2020, 59, 7453-7468.	1.9	24
35964	Functional Chalcogenide Na2HgSn2Se6 and K2MnGe2Se6 Exhibiting Flexible Chain Structure and Intriguing Birefringence Tunability. Inorganic Chemistry, 2020, 59, 7614-7621.	1.9	13
35965	Molecules versus Nanoparticles: Identifying a Reactive Molecular Intermediate in the Synthesis of Ternary Coinage Metal Chalcogenides. Inorganic Chemistry, 2020, 59, 7727-7738.	1.9	10
35966	Electronic and Magnetic Properties of a Two-Dimensional Transition Metal Phosphorous Chalcogenide TMPS₄. Journal of Physical Chemistry C, 2020, 124, 12075-12080.	1.5	22
35967	First-Principles Investigation of the 1T-HfTe₂ Nanosheet for Selective Gas Sensing. ACS Applied Nano Materials, 2020, 3, 5160-5171.	2.4	27
35968	Synthesis, electronic structure and physical properties of two new layered compounds, EuFAgSe and EuFAg_{1â^'Î´}Te, featuring the active redox pair Eu²⁺/Ag⁺. Dalton Transactions, 2020, 49, 7426-7435.	1.6	2
35969	Metal-functionalized 2D boron sulfide monolayer material enhancing hydrogen storage capacities. Journal of Applied Physics, 2020, 127, .	1.1	19
35970	On thermal conductivity of amorphous niobium monoxide. Journal Physics D: Applied Physics, 2020, 53, 285303.	1.3	10
35971	Pressure dependence of room-temperature structural properties of CaAl2Si2. Journal of Physics Condensed Matter, 2020, 32, 365403.	0.7	3

#	Article	IF	Citations
35972	Possible role of grain-boundary and dislocation structure for the magnetic-flux trapping behavior of niobium: A first-principles study. Physical Review B, 2020, 101, .	1.1	7
35973	Effects of Lanthanum/Gadolinium Doping on Crystal Structures, Electronic Properties and Optical Characteristics of Bismuth Tungstate Photocatalyst: DFT Approach. Journal of the Physical Society of Japan, 2020, 89, 044707.	0.7	2
35974	Study of structural, elastic, electronic, and vibrational properties of MRh2O4 (M = Cd and Zn) spinels: DFT-based calculations. Journal of Molecular Modeling, 2020, 26, 140.	0.8	2
35975	Exploring phononic properties of two-dimensional materials using machine learning interatomic potentials. Applied Materials Today, 2020, 20, 100685.	2.3	96
35976	Syngas conversion catalyzed by copper-embedded graphene. Applied Surface Science, 2020, 525, 146500.	3.1	8
35977	Adsorptive removal of an eight-component volatile organic compound mixture by Cu-, Co-, and Zr-metal-organic frameworks: Experimental and theoretical studies. Chemical Engineering Journal, 2020, 397, 125391.	6.6	72
35978	Understanding the effect of Mo2C support on the activity of Cu for the hydrodeoxygenation of glycerol. Journal of Catalysis, 2020, 388, 141-153.	3.1	12
35979	Diamond(001)â€“Si(001) and Si(001)â€“Ti(0001) interfaces: A density functional theory study. Journal of Physics and Chemistry of Solids, 2020, 145, 109563.	1.9	5
35980	Enhanced hardness in tungstenâ€“substituted molybdenum diboride solid solutions by local symmetry reduction. Materials Chemistry and Physics, 2020, 251, 123188.	2.0	6
35981	First-principles study of elastic and thermal properties of scheelite-type molybdates and tungstates. Materials Today Communications, 2020, 24, 101089.	0.9	11
35982	Super-hygroscopic film for wearables with dual functions of expediting sweat evaporation and energy harvesting. Nano Energy, 2020, 75, 104873.	8.2	52
35983	Exploring the electronic and magnetic properties of noble metal (Pd, Pt, Au) adsorbed MoSe2 monolayers and their performance towards sensing gas molecules. Physica E: Low-Dimensional Systems and Nanostructures, 2020, 122, 114167.	1.3	16
35984	Strain-induced work function in h-BN and BCN monolayers. Physica E: Low-Dimensional Systems and Nanostructures, 2020, 123, 114180.	1.3	42
35985	Ab initio study of pressureâ€“induced metallization and superconductivity in orthorhombic LiBH2 phase under ultra-high pressure. Physics Letters, Section A: General, Atomic and Solid State Physics, 2020, 384, 126525.	0.9	5
35986	A first-principles investigation of physical properties and superconductivity of NbPS. Solid State Sciences, 2020, 103, 106183.	1.5	0
35987	Strain tunable electrical and optical properties of two dimensional tetragonal MgX (X=S, Se) monolayer semiconductors. Superlattices and Microstructures, 2020, 144, 106570.	1.4	7
35988	A first-principles study of hydrogen adsorption on Ni-decorated defective GaN monolayer. Solid State Communications, 2020, 316-317, 113951.	0.9	0
35989	What Rules the Relative Stability of Î±-, Î²-, and Î³-Glycine Polymorphs?. Crystal Growth and Design, 2020, 20, 4695-4706.	1.4	9

#	Article	IF	Citations
35990	Isomers Matter: Physicochemical Properties Dictated by the Position of S and Se in Single Layer MoSSe. Journal of Physical Chemistry C, 2020, 124, 11669-11680.	1.5	5
35991	Interdependence of Oxygenation and Hydration in Mixed-Conducting (Ba,Sr)FeO_{3â˜Î´} Perovskites Studied by Density Functional Theory. Journal of Physical Chemistry C, 2020, 124, 11780-11789.	1.5	24
35992	Selective Cl-Decoration on Nanocrystal Facets of Hematite for High-Efficiency Catalytic Oxidation of Cyclohexane: Identification of the Newly Formed Clâ€“O as Active Sites. ACS Applied Materials & Interfaces, 2020, 12, 26733-26745.	4.0	34
35993	Modeling Morphology and Catalytic Activity of Nanoparticle Ensembles Under Reaction Conditions. ACS Catalysis, 2020, 10, 6149-6158.	5.5	38
35994	Anion charge and lattice volume dependent lithium ion migration in compounds with fcc anion sublattices. Npj Computational Materials, 2020, 6, .	3.5	27
35995	Coverage-dependent electronic and optical properties of H- or F-passivated Si/Ag(111) from first principles. Physical Review B, 2020, 101, .	1.1	1
35996	First-principles study of hydrogen incorporation into the Ti3SiC2/Zr heterojunction. Modern Physics Letters B, 2020, 34, 2050014.	1.0	0
35997	Comparison of band -fitting and Wannier-based model construction for WSe2. MRS Advances, 2020, 5, 2281-2290.	0.5	0
35998	A molecular dynamics study of Fe50-XMXAl50 ternary alloy (M=Ag, Pt, Pd). MRS Advances, 2020, 5, 1185-1193.	0.5	1
35999	CNTâ€Assembled Octahedron Carbonâ€Encapsulated Cu₃P/Cu Heterostructure by In Situ MOFâ€Derived Engineering for Superior Lithium Storage: Investigations by Experimental Implementation and Firstâ€Principles Calculation. Advanced Science, 2020, 7, 2000736.	5.6	66
36000	Firstâ€principle calculation of distorted Tâ€carbon as a promising anode for Liâ€ion batteries with enhanced capacity, reversibility, and ion migration properties. , 2020, 2, 614-623.		9
36001	Enhancing Interfacial Properties of Mg₂Siâ€Based Thermoelectric Joint with Mg₂SiNi₃ Compound as Electrodes. Physica Status Solidi (A) Applications and Materials Science, 2020, 217, 1901035.	0.8	7
36002	Tuning the Electronic and Optical Properties of Sc2CF2 MXene Monolayer Using Biaxial Strain. Journal of Electronic Materials, 2020, 49, 4892-4902.	1.0	16
36003	Computational Prediction of Structural, Electronic, Elastic, and Thermoelectric Properties of FeVX (Xâ€‰=â€‰As, P) Half-Heusler Compounds. Journal of Electronic Materials, 2020, 49, 4916-4922.	1.0	28
36004	<mml:math xmlns:mml="http://www.w3.org/1998/Math/MathML" altimg="si105.svg"><mml:mrow><mml:mi mathvariant="italic">DFT</mml:mi><mml:mo linebreak="badbreak">+</mml:mo><mml:mi>U</mml:mi></mml:mrow></mml:math> approach on the electronic and thermal properties of hypostoichiometric <mml:math xmlns:mml="http://www.w3.org/1998/Math/MathML" altimg="si106.svg"><mml:mrow><mml:msub><mml:mrow><mml:mi mathvariant="normal">UO</mml:mi>	0.9	8
36006	Doping effect of small Rhn (nA=A1â€“4) clusters on the geometric and electronic behaviors of MoS2 monolayer: A first-principles study. Applied Surface Science, 2020, 526, 146659.	3.1	27
36007	Ground state structure and physical properties of silicon monoxide sheet. Applied Surface Science, 2020, 527, 146759.	3.1	1
36008	A review on phase transition and structure-performance relationship of second-order nonlinear optical polymorphs. Coordination Chemistry Reviews, 2020, 418, 213380.	9.5	67

#	Article	IF	Citations
36009	Theoretical study of structural, electronic, dynamic and thermodynamic properties of Ni2FeAl and Ni2CoAl alloys. Computational Condensed Matter, 2020, 24, e00480.	0.9	2
36010	CO2-mediated sulfur evolution chemistry of pyrite oxidation during oxy-fuel combustion. Combustion and Flame, 2020, 218, 75-83.	2.8	8
36011	Strong red emission with excellent thermal stability in double-perovskite type Ba2GdSbO6:Eu3+ phosphors for potential field-emission displays. Journal of Alloys and Compounds, 2020, 835, 155389.	2.8	52
36012	Atomic cooperation in enhancing magnetism: (Fe, Cu)-doped CeCo5. Journal of Alloys and Compounds, 2020, 839, 155549.	2.8	6
36013	Electronic structure of yttrium-doped zinc ferrite â€“ Insights from experiment and theory. Journal of Alloys and Compounds, 2020, 842, 155704.	2.8	15
36014	Structure stability and magnetic properties of Fe-doped Co2VGa Heusler alloys: Insights from first-principles calculations. Journal of Magnetism and Magnetic Materials, 2020, 513, 167059.	1.0	4
36015	Experimental and first-principles study of defect-induced electronic and magnetic properties of ZnO nanocrystals. Journal of Physics and Chemistry of Solids, 2020, 146, 109580.	1.9	10
36016	Electronic and optical properties of mono and co-doped anatase TiO2: First principles calculations. Materials Chemistry and Physics, 2020, 252, 123285.	2.0	19
36017	Electronic properties and Hirshfeld surface analysis of dihydroxylammonium 5,5â€²-bistetrazole-1,1â€²-diolate under pressure. Materials Today: Proceedings, 2020, 24, 683-689.	0.9	3
36018	Thermal expansion and vibrational properties of Î±-Se and Î±-TeSe2 based on first-principles calculations. Solid State Communications, 2020, 314-315, 113912.	0.9	1
36019	Toward Establishing Electronic and Phononic Signatures of Reversible Lattice Oxygen Oxidation in Lithium Transition Metal Oxides For Li-Ion Batteries. Chemistry of Materials, 2020, 32, 5502-5514.	3.2	17
36020	Effect of Composition on the Optical and Photocatalytic Properties of Visible Light Responsive Materials Bi_{26â€“x}Mg_xO₄₀. Inorganic Chemistry, 2020, 59, 8173-8183.	1.9	9
36021	Toward Atomic-Scale Inorganic Double Helices via Carbon Nanotube Matricesâ€”Induction of Chirality to Carbon Nanotubes. Journal of Physical Chemistry C, 2020, 124, 13338-13347.	1.5	7
36022	Crystal Structure, Lattice Dynamics, and Thermodynamic Properties of a Thermoelectric Orthorhombic BaCu₂Se₂ Compound. Journal of Physical Chemistry C, 2020, 124, 13627-13638.	1.5	6
36023	Mechanism and Effects of Coverage and Particle Morphology on Rh-Catalyzed NOâ€“H₂ Reactions. Journal of Physical Chemistry C, 2020, 124, 13291-13303.	1.5	10
36024	CoP/RGO-Pd Hybrids with Heterointerfaces as Highly Active Catalysts for Ethanol Electrooxidation. ACS Applied Materials & Interfaces, 2020, 12, 28903-28914.	4.0	16
36025	Colossal flexoresistance in dielectrics. Nature Communications, 2020, 11, 2586.	5.8	21
36026	Tellurium as a successor of silicon for extremely scaled nanowires: a first-principles study. Npj 2D Materials and Applications, 2020, 4, .	3.9	39

#	Article	IF	Citations
36027	Tuning the ORR activity of Pt-based Ti₂CO₂ MXenes by varying the atomic cluster size and doping with metals. Nanoscale, 2020, 12, 12497-12507.	2.8	31
36028	Crystal structure and properties of iodine monofluoride compounds at high pressure. Journal of Physics Condensed Matter, 2020, 32, 385404.	0.7	3
36029	Structural and electronic properties of chromium carbides and Fe-substituted chromium carbides. Materials Research Express, 2020, 7, 056508.	0.8	11
36030	Phase stability and mechanical response of tantalum nitrides to electronic excitation effect. Materials Research Express, 2020, 7, 066508.	0.8	2
36031	Role of quantum confinement and interlayer coupling in <mml:math xmlns:mml="http://www.w3.org/1998/Math/MathML"><mml:msub><mml:mi mathvariant="normal">CrI</mml:mi><mml:mn>3</mml:mn></mml:msub></mml:math> -graphene magnetic tunnel junctions. Physical Review B, 2020, 101, .	1.1	29
36032	Ab initio-based investigation of phase transition path and magnetism of Niâ€“Mnâ€“In alloys with excess Ni or Mn. Acta Materialia, 2020, 195, 109-122.	3.8	20
36033	Electronic properties and superior CO2 capture selectivity of metal nitride (XN) and phosphide (XP) (XÂ=ÂAl, Ga and In) sheets. Applied Surface Science, 2020, 527, 146445.	3.1	7
36034	Adsorption and gas-sensing properties of Pt2â€“GaNNTs for SF6 decomposition products. Applied Surface Science, 2020, 524, 146570.	3.1	56
36035	Probing pristine and defective NiB6 monolayer as promising anode materials for Li/Na/K ion batteries. Applied Surface Science, 2020, 527, 146580.	3.1	33
36036	First principles investigations of structure, stability and electronic properties of polar Ca2Fe2O5(0 1) Tj ETQq1 1 0.784314 rgBT /Over	3.1	6
36037	Non-lanthanide activated red emission in CdAl2O4 phosphors with nanotube type crystal structure. Journal of Alloys and Compounds, 2020, 842, 155787.	2.8	7
36038	Explicit Multielement Extension of the Spectral Neighbor Analysis Potential for Chemically Complex Systems. Journal of Physical Chemistry A, 2020, 124, 5456-5464.	1.1	36
36039	Emerging investigator series: first-principles and thermodynamics comparison of compositionally-tuned delafossites: cation release from the (001) surface of complex metal oxides. Environmental Science: Nano, 2020, 7, 1642-1651.	2.2	11
36040	Insights into the regularity of the formation of 2D 3d transition metal monocarbides. Nanoscale, 2020, 12, 13407-13413.	2.8	9
36041	Magnetoelastic interaction in the two-dimensional magnetic material MnPS₃ studied by first principles calculations and Raman experiments. 2D Materials, 2020, 7, 035030.	2.0	32
36042	Tailoring the Band Gap in Codoped GaN Nanosheet From First Principle Calculations. Frontiers in Materials, 2020, 7, .	1.2	8
36043	Theoretical Study of the Direct Conversion of Methane to Methanol Using H₂O₂ as an Oxidant on Pd and Au/Pd Surfaces. Journal of Physical Chemistry C, 2020, 124, 13231-13239.	1.5	17
36044	Recent Insights Into Electronic Performance, Magnetism and Exchange Splittings in the Cr-substituted CaO. Frontiers in Chemistry, 2020, 8, 526.	1.8	6

#	Article	IF	Citations
36045	Spatial Charge Separation as the Origin of Anomalous Stark Effect in Fluorous 2D Hybrid Perovskites. Advanced Functional Materials, 2020, 30, 2000228.	7.8	12
36046	Tuning Interfacial Thermal and Electrical Conductance across a Metal/MoS₂ Monolayer through Nâ€Methylâ€2â€pyrrolidone Wet Cleaning. Advanced Materials Interfaces, 2020, 7, 2000364.	1.9	7
36047	Structure and vibrational spectra of ReSe 2 nanoplates. Journal of Raman Spectroscopy, 2020, 51, 1305-1314.	1.2	6
36048	The ï£¿NH x Group Induced Formation of 3D Î±â€Co(OH) 2 Curly Nanosheet Aggregates as Efficient Oxygen Evolution Electrocatalysts. Small, 2020, 16, 2001973.	5.2	22
36049	Dispersibility and Photochemical Stability of Delaminated MXene Flakes in Water. Small, 2020, 16, e2002433.	5.2	55
36050	Rareâ€earth Metal Borosilicides R 9 Si 15â€“ x B 3 (R = Tb, Yb): New Ordered Structures Derived from the AlB 2 Structure Type. Zeitschrift Fur Anorganische Und Allgemeine Chemie, 2020, 646, 1168-1175.	0.6	2
36051	Experimental and computational investigation of PVDFâ€“$$hbox {BaTiO}_{{3}}$$ interface for impact sensing and energy harvesting applications. SN Applied Sciences, 2020, 2, 1.	1.5	3
36052	Interaction of water and oxygen with sulfide mineral surface. , 2020, , 113-179.		0
36053	Electronic structures and surface adsorption of impurity-bearing sulfide minerals. , 2020, , 307-359.		0
36054	Oxygen intercalated graphene on SiC(0001): Multiphase SiOx layer formation and its influence on graphene electronic properties. Carbon, 2020, 167, 746-759.	5.4	9
36055	Magnetic properties of 3C-SiC nanowires doped by transition metal and vacancy. Chemical Physics Letters, 2020, 754, 137643.	1.2	3
36056	Modeling hydrogen adsorption in the metal organic framework (MOF-5, connector): <mml:math xmlns:mml="http://www.w3.org/1998/Math/MathML" altimg="si1.svg"><mml:mrow><mml:mi mathvariant="bold">Z</mml:mi><mml:msub><mml:mi mathvariant="bold">n</mml:mi><mml:mn>4</mml:mn></mml:msub><mml:mi mathvariant="bold">O</mml:mi><mml:msub><mml:mrow><mml:mo		

#	Article	IF	Citations
36063	Structural Stability of Physisorbed Air-Oxidized Decanethiols on Au(111). Journal of Physical Chemistry C, 2020, 124, 11977-11984.	1.5	9
36064	Dislocations as Single Photon Sources in Two-Dimensional Semiconductors. Nano Letters, 2020, 20, 4136-4143.	4.5	16
36065	Tailoring the Electronic Structure of Transition Metals by the V₂C MXene Support: Excellent Oxygen Reduction Performance Triggered by Metalâ€“Support Interactions. ACS Applied Materials & Interfaces, 2020, 12, 28206-28216.	4.0	39
36066	Visualizing Orbital Content of Electronic Bands in Anisotropic 2D Semiconducting ReSe₂. ACS Nano, 2020, 14, 7880-7891.	7.3	19
36067	High-throughput screening platform for solid electrolytes combining hierarchical ion-transport prediction algorithms. Scientific Data, 2020, 7, 151.	2.4	90
36068	Fibrous red phosphorene: a promising two-dimensional optoelectronic and photocatalytic material with a desirable band gap and high carrier mobility. Physical Chemistry Chemical Physics, 2020, 22, 13713-13720.	1.3	27
36069	Transition from Schottky to Ohmic contacts in Janus MoSSe/germanene heterostructures. Nanoscale, 2020, 12, 11448-11454.	2.8	37
36070	Tiny amounts of fluorinated carbon nanotubes remove sodium dendrites for high-performance sodiumâ€“oxygen batteries. Sustainable Energy and Fuels, 2020, 4, 4108-4116.	2.5	3
36071	Graphene hetero-multilayer on layered platinum mineral jacutingaite (Pt₂HgSe₃): van der Waals heterostructures with novel optoelectronic and thermoelectric performances. Journal of Materials Chemistry A, 2020, 8, 13248-13260.	5.2	57
36072	Abnormal bandgap enlargement resulted in a promising mid-infrared nonlinear optical material Rb₂CdBrI₃with an ultrahigh laser damage threshold. Journal of Materials Chemistry C, 2020, 8, 9005-9011.	2.7	5
36073	First-principles study of two-dimensional electron and hole gases at the head-to-head and tail-to-tail <mml:math xmlns:mml="http://www.w3.org/1998/Math/MathML"><mml:msup><mml:mn>180</mml:mn><mml:mo>â˜</mml:mo></mml:msup></r domain walls in <mml:math xmlns:mml="http://www.w3.org/1998/Math/MathML"><mml:msub><mml:mi>PbTiO</mml:mi><mml:mn>3</mml:mn></mml:msub></m ferroelectric thin films. Physical Review B, 2020, 101.	1.1	14
36074	Atomic Diffusion in <mml:math xmlns:mml="http://www.w3.org/1998/Math/MathML" display="inline"><mml:mi>Î±</mml:mi></mml:math> -iron across the Curie Point: An Efficient and Transferable AbÂInitio â€“Based Modeling Approach. Physical Review Letters, 2020, 124, 215901.	2.9	23
36075	High-Pressure Polymeric Nitrogen Allotrope with the Black Phosphorus Structure. Physical Review Letters, 2020, 124, 216001.	2.9	119
36076	A broad theoretical investigation of Râ€3, R3c, and Râ€3c polymorphs of FeCrO₃. Journal of the American Ceramic Society, 2020, 103, 5688-5699.	1.9	7
36077	DFT insights into the adsorption properties of toxic gas molecules on pure and transition metal embedded stanene monolayers: Towards gas sensor devices. Synthetic Metals, 2020, 266, 116441.	2.1	23
36078	Electric Field Effects in Oxygen Reduction Kinetics: Rationalizing pH Dependence at the Pt(111), Au(111), and Au(100) Electrodes. Journal of Physical Chemistry C, 2020, 124, 14581-14591.	1.5	102
36079	Structural Transition in Oxidized Ca2N Electrenes: CaO/CaN 2D Heterostructures. Journal of Physical Chemistry C, 2020, 124, 14706-14712.	1.5	4
36080	Symmetric Sodium-Ion Battery Based on Dual-Electron Reactions of NASICON-Structured Na₃MnTi(PO₄)₃ Material. ACS Applied Materials & Interfaces, 2020, 12, 30328-30335.	4.0	65

#	Article	IF	Citations
36081	Identify Zr Promotion Effects in Atomic Scale for Co-Based Catalysts in Fischerâ€“Tropsch Synthesis. ACS Catalysis, 2020, 10, 7894-7906.	5.5	57
36082	Sulfate-Modified NiAl Mixed Oxides as Effective Câ€“H Bond-Breaking Agents for the Sole Production of Ethylene from Ethane. ACS Catalysis, 2020, 10, 7619-7629.	5.5	26
36083	3D Flexible, Conductive, and Recyclable Ti₃C₂T_x MXene-Melamine Foam for High-Areal-Capacity and Long-Lifetime Alkali-Metal Anode. ACS Nano, 2020, 14, 8678-8688.	7.3	164
36084	First-principles study on the selective hydrogenation of the Cî€O and Cî€C bonds of acrolein on Ptâ€“Mâ€“Pt (M = Pt, Cu, Ni, Co) surfaces. Physical Chemistry Chemical Physics, 2020, 22, 14645-14650.	1.3	4
36085	Flatband in a three-dimensional tungsten nitride compound. Journal of Chemical Physics, 2020, 152, 224503.	1.2	3
36086	Phonon thermodynamics and elastic behavior of GaAs at high temperatures and pressures. Physical Review B, 2020, 101, .	1.1	3
36087	Superconducting properties of <mml:math xmlns:mml="http://www.w3.org/1998/Math/MathML"><mml:msub><mml:mi>MoTe</mml:mi><mml:mn>2</mml:mn></mml:msub></m from ab initio anisotropic Migdal-Eliashberg theory. Physical Review B, 2020, 101, .	1.1	10
36088	Sodium-potassium system at high pressure. Physical Review B, 2020, 101, .	1.1	6
36089	Phase Transitions in Tungsten Monoborides. JETP Letters, 2020, 111, 343-349.	0.4	3
36090	Enhanced diffusion and permeation of hydrogen species on the partially carbon covered iron surfaces. Applied Surface Science, 2020, 515, 145899.	3.1	8
36091	Structural stability, mechanical, electronic and thermal behaviour of Ru2CrZ (Z=Sb, Si, Pb, Ge) Heusler alloys. Chinese Journal of Physics, 2020, 66, 124-134.	2.0	6
36092	Impact of nitrogen species and content on the catalytic activity to Câ€“O bond cleavage of lignin over N-doped carbon supported Ru-based catalyst. Fuel, 2020, 278, 118324.	3.4	26
36093	Calcium orthocarbonate, Ca2CO4-Pnma: A potential host for subducting carbon in the transition zone and lower mantle. Lithos, 2020, 370-371, 105637.	0.6	23
36094	Band gap engineering of monolayer ZrGeTe4 via strain: A first-principles study. Materials Chemistry and Physics, 2020, 253, 123308.	2.0	10
36095	Phase transformations in novel hot-deformed Alâ€“Znâ€“Mgâ€“Cuâ€“Siâ€“Mnâ€“Fe(â€“Scâ€“Zr) alloys. Materials and Design, 2020, 193, 108821.	3.3	21
36096	Exploring the performance of pristine and defective silicene and silicene-like XSi3 (X= Al, B, C, N, P) sheets as supercapacitor electrodes: A density functional theory calculation of quantum capacitance. Physica E: Low-Dimensional Systems and Nanostructures, 2020, 124, 114290.	1.3	15
36097	Reliable Computational Prediction of the Supramolecular Ordering of Complex Molecules under Electrochemical Conditions. Journal of Chemical Theory and Computation, 2020, 16, 5227-5243.	2.3	5
36098	Effect of Adsorbed Oxygen on the Dissociation of Water over Gadolinium Oxide Surfaces: Density Functional Theory Calculations and Experimental Results. Journal of Physical Chemistry C, 2020, 124, 14613-14621.	1.5	8

#	Article	IF	Citations
36099	Multimodal Structure Solution with 19F NMR Crystallography of Spin Singlet Molybdenum Oxyfluorides. Journal of the American Chemical Society, 2020, 142, 12288-12298.	6.6	11
36100	Vertically stacked SnSe homojunctions and negative capacitance for fast low-power tunneling transistors. RSC Advances, 2020, 10, 20801-20808.	1.7	9
36101	A new family of two-dimensional ferroelastic semiconductors with negative Poisson's ratios. Nanoscale, 2020, 12, 14150-14159.	2.8	21
36102	Rocksalt ZnMgO alloys for ultraviolet applications: Origin of band-gap fluctuations and direct-indirect transitions. Physical Review B, 2020, 101, .	1.1	16
36103	Prediction of Half-Metallic Ferromagnetism in Cu- and K-Doped MgS: A Comparative Study. Journal of Superconductivity and Novel Magnetism, 2020, 33, 3107-3112.	0.8	1
36104	Novel configurations of VN4 and VN4H defects in diamond platelets: Structure, energetics and vibrational properties. Diamond and Related Materials, 2020, 108, 107957.	1.8	5
36105	Stability and energetics of HenVm complexes in Feâ€“Cr alloys: Ab initio study. Materials Chemistry and Physics, 2020, 253, 123314.	2.0	4
36106	Application of the training of density functional theory potentials within machine learning to adsorptions and reactionÂpaths on Platinum surfaces. Materials Chemistry and Physics, 2020, 253, 123407.	2.0	5
36107	Mechanically Robust Tapioca Starch Composite Binder with Improved Ionic Conductivity for Sustainable Lithium-Ion Batteries. ACS Sustainable Chemistry and Engineering, 2020, 8, 9857-9865.	3.2	42
36108	Covalency competition dominates the water oxidation structureâ€“activity relationship on spinel oxides. Nature Catalysis, 2020, 3, 554-563.	16.1	284
36109	Potassium ions promote electrochemical nitrogen reduction on nano-Au catalysts triggered by bifunctional boron supramolecular assembly. Journal of Materials Chemistry A, 2020, 8, 13086-13094.	5.2	44
36110	Solution enthalpy calculation for impurity in liquid metal by first-principles calculations: A benchmark test for oxygen impurity in liquid sodium. Journal of Chemical Physics, 2020, 152, 154503.	1.2	4
36111	Predicting the dynamic behavior of the mechanical properties of platinum with machine learning. Journal of Chemical Physics, 2020, 152, 224709.	1.2	4
36112	Intrinsic role of â†‘â†‘â†“â†“-type magnetic structure on magnetoelectric coupling in Y2NiMnO6. Applied Physics Letters, 2020, 116, 242901.	1.5	3
36113	Thermodynamic stability of borophene, B₂O₃ and other B_{1â^'x}O_x sheets. Journal of Physics Communications, 2020, 4, 031001.	0.5	14
36114	Electronic Structure and Nonlinear Dielectric Susceptibility of Î³-Phase of Tellurium Oxide. Physics of the Solid State, 2020, 62, 621-627.	0.2	0
36115	Performance and mechanism study of LaFeO3 for biomass chemical looping gasification. Journal of Materials Science, 2020, 55, 11151-11166.	1.7	14
36116	An investigation on the stability of the structural and electronic properties of ErX$$_{3}$$ ($$hbox) Tj ETQq1 1 0.784314 rgBT /Ove	0.9	1

#	Article	IF	Citations
36117	Hydrogen induced vacancy clustering and void formation mechanisms at grain boundaries in palladium. Acta Materialia, 2020, 195, 708-719.	3.8	25
36118	Adsorption behaviour of Si anchored on g-C3N4/graphene van der Waals heterostructure for selective sensing of toxic gases: Insights from a first-principles study. Applied Surface Science, 2020, 525, 146590.	3.1	24
36119	Synthesis of the porous spinel Co-Al2O4 powder produced by ball milling and annealing. Advanced Powder Technology, 2020, 31, 2742-2748.	2.0	0
36120	Low-temperature growth of carbon shells on gold and copper nanoparticles in transmission electron microscope. Carbon, 2020, 167, 541-547.	5.4	2
36121	Revisiting galvanic replacement between silver nanoparticles and mercury(II) ions in a cellulose membrane intended for optical assay application: Some new insights into silver-mercury interaction. Colloids and Surfaces A: Physicochemical and Engineering Aspects, 2020, 602, 125140.	2.3	6
36122	Boron-based metallocene-like molecules and nanowires: A computational study. Chemical Physics Letters, 2020, 747, 137336.	1.2	2
36123	Probing the structural, electronic, mechanical strength and optical properties of tantalum-based oxide perovskites ATaO3 (A = Rb, Fr) for optoelectronic applications: First-principles investigations. Optik, 2020, 219, 165027.	1.4	16
36124	Experimental and theoretical study of deactivated HDT catalysts by Si species deposited on their surfaces: Models proposition, structural and thermodynamic analysis. Journal of Catalysis, 2020, 389, 578-591.	3.1	12
36125	Discovery of ABO4 scheelites with the extra low thermal conductivity through high-throughput calculations. Journal of Materiomics, 2020, 6, 702-711.	2.8	25
36126	Computational determination of the physical-thermoelectric parameters of tin-based organomatallic halide perovskites (CH3NH3SnX3, X = Br and I): Emerging materials for optoelectronic devices. Materials Chemistry and Physics, 2020, 253, 123389.	2.0	16
36127	Ensemble effect of heterogeneous Cu atoms promoting water-gas shift reaction. Molecular Catalysis, 2020, 493, 111046.	1.0	4
36128	The influence of exposed surface on trap state of PbS quantum dots. Superlattices and Microstructures, 2020, 145, 106616.	1.4	4
36129	Comparing the performance of density functionals in describing the adsorption of atoms and small molecules on Ni(111). Surface Science, 2020, 700, 121675.	0.8	8
36130	Oxygen Ion Migration and Conductivity in LaSrGa₃O₇ Melilites from First Principles. Chemistry of Materials, 2020, 32, 4442-4450.	3.2	18
36131	Unprecedented generation of 3D heterostructures by mechanochemical disassembly and re-ordering of incommensurate metal chalcogenides. Nature Communications, 2020, 11, 3005.	5.8	7
36132	Harnessing strong metalâ€“support interactions via a reverse route. Nature Communications, 2020, 11, 3042.	5.8	84
36133	First-principles investigation of nonmetal doped single-layer BiOBr as a potential photocatalyst with a low recombination rate. Physical Chemistry Chemical Physics, 2020, 22, 15354-15364.	1.3	74
36134	First-principles investigation of ScX₂ (X = Cl, Br, or I) monolayers for flexible spintronic and electronic applications. Physical Chemistry Chemical Physics, 2020, 22, 14781-14786.	1.3	7

#	Article	IF	Citations
36135	Transition of wide-band gap semiconductor h-BN(BN)/P heterostructure via single-atom-embedding. Journal of Materials Chemistry C, 2020, 8, 9755-9762.	2.7	7
36136	Superconductivity of alkali-metal intercalated BC2. AIP Advances, 2020, 10, 065213.	0.6	2
36137	Colloidal Quantum Dot Bulk Heterojunction Solids with Nearâ€Unity Charge Extraction Efficiency. Advanced Science, 2020, 7, 2000894.	5.6	22
36138	Terahertz Optical Constants of Solid CO2. Journal of Infrared, Millimeter, and Terahertz Waves, 2020, 41, 871-879.	1.2	2
36139	Thin film solar cells based on Ag-substituted CuSbS2 absorber. Chemical Engineering Journal, 2020, 400, 125906.	6.6	22
36140	Effect of biaxial strain on the p-type of conductive properties of (S, Se, Te) and 2â€N co-doped ZnO. Materials Today Communications, 2020, 24, 101063.	0.9	5
36141	Strain engineering induced indirect-direct band gap transition of difluorphosphorane. Solid State Communications, 2020, 311, 113873.	0.9	0
36142	Enhanced Oxygen Evolution Reaction Activity by Encapsulating NiFe Alloy Nanoparticles in Nitrogen-Doped Carbon Nanofibers. ACS Applied Materials & Interfaces, 2020, 12, 31503-31513.	4.0	78
36143	PdAg Alloy Nanocatalysts: Toward Economically Viable Nitrite Reduction in Drinking Water. ACS Catalysis, 2020, 10, 7979-7989.	5.5	64
36144	Visualization of moirÃ© superlattices. Nature Nanotechnology, 2020, 15, 580-584.	15.6	187
36145	An asymmetric Ti₂CO/WS₂ heterostructure as a promising anchoring material for lithiumâ€“sulfur batteries. Journal of Materials Chemistry A, 2020, 8, 13770-13775.	5.2	32
36146	High-temperature 2D ferromagnetism in conjugated microporous porphyrin-type polymers. Physical Chemistry Chemical Physics, 2020, 22, 14480-14488.	1.3	1
36147	Temperature effect on the phase stability of hydrogen C2/c phase from first-principles molecular dynamics calculations. Journal of Physics Condensed Matter, 2020, 32, 405404.	0.7	3
36148	Towards temperature-induced topological phase transition in SnTe: A first-principles study. Physical Review B, 2020, 101, .	1.1	9
36149	Crossover from weakly indirect to direct excitons in atomically thin films of InSe. Physical Review B, 2020, 101, .	1.1	6
36150	Theoretical Prediction of Enhanced Thermopower in n-Doped Si/Ge Superlattices Using Effective Mass Approximation. Journal of Electronic Materials, 2020, 49, 4431-4442.	1.0	6
36151	The deactivation mechanism of toluene on MnOx-CeO2 SCR catalyst. Applied Catalysis B: Environmental, 2020, 277, 119257.	10.8	86
36152	Atomistic modeling of energy band alignment in CdTe(1 0 0) and CdTe(1 1 1) surfaces. Applied Surface Science, 2020, 528, 146832.	3.1	10

#	Article	IF	Citations
36153	First-principles study on strain-modulated negative differential resistance effect of in-plane device based on heterostructure tellurene. Applied Surface Science, 2020, 528, 146957.	3.1	6
36154	Understanding reaction kinetics, deprotonation and solvation of brÃ¸nsted acidic protons in heteropolyacid catalyzed synthesis of biorenewable alkyl levulinates. Chemical Engineering Journal, 2020, 400, 125916.	6.6	41
36155	Magnetic and topological properties in hydrogenated transition metal dichalcogenide monolayers. Chinese Journal of Physics, 2020, 66, 15-23.	2.0	25
36156	A DFT study on production of hydrogen from biomass-derived formic acid catalyzed by Ptâ€“TiO2. International Journal of Hydrogen Energy, 2020, 45, 20993-21003.	3.8	19
36157	Crystal growth, structural characteristics and electronic structure of Ba1-xPbxFe12O19 (xÂ=) Tj ETQq0 0 0 rgBT /Overlock 10 Tf 50 582	2.8	21
36158	Computational and experimental investigation of refractory high entropy alloy Mo15Nb20Re15Ta30W20. Journal of Materials Research and Technology, 2020, 9, 8929-8936.	2.6	39
36159	First principles calculations of thermodynamic properties of RuB2. Materials Today: Proceedings, 2020, 26, 1054-1059.	0.9	0
36160	Density functional theory studies of structural distortion in lone pair substituted LuMnO3. Materials Today Communications, 2020, 24, 101079.	0.9	3
36161	Optical identification of point defects in monolayer beryllium oxide by ab initio calculations. Materials Today Communications, 2020, 24, 101344.	0.9	4
36162	Enhancement of the tensile strength by introducing alloy element Fe for Ti based alloy. Solid State Communications, 2020, 318, 113982.	0.9	16
36163	AGa₃F₆(SeO₃)₂ (A = Rb, Cs): A New Type of Phase-Matchable Hexagonal Tungsten Oxide Material with Strong Second-Harmonic Generation Responses. Chemistry of Materials, 2020, 32, 6906-6915.	3.2	46
36164	Molecular Understanding of Heterogeneous Mercury Adsorption and Oxidation Mechanisms over the CuCl₂/TiO₂ Sorbent. Industrial & Engineering Chemistry Research, 2020, 59, 12610-12616.	1.8	7
36165	BCN-Encapsulated Nano-nickel Synergistically Promotes Ambient Electrochemical Dinitrogen Reduction. ACS Applied Materials & Interfaces, 2020, 12, 31419-31430.	4.0	33
36166	Cluster expansion Monte Carlo study of indiumâ€“aluminum segregation and homogenization in CuInSe2â€“CuAlSe2 pseudobinary alloys. Physical Chemistry Chemical Physics, 2020, 22, 14694-14703.	1.3	0
36167	DFT and hybrid-DFT calculations on the electronic properties of vanadate materials: theory meets experiments. New Journal of Chemistry, 2020, 44, 11602-11607.	1.4	21
36168	Hydrogen storage characteristics of Li and Na decorated 2D boron phosphide. Sustainable Energy and Fuels, 2020, 4, 4538-4546.	2.5	49
36169	Intriguing electronic and optical prospects of FCC bimetallic two-dimensional heterostructures: epsilon near-zero behavior in UV-Vis range. Physical Chemistry Chemical Physics, 2020, 22, 16314-16324.	1.3	2
36170	Unraveling the enhancement mechanisms of H2S sensing on a SnO2 surface: an ab initio perspective. Physical Chemistry Chemical Physics, 2020, 22, 15006-15012.	1.3	1

#	Article	IF	Citations
36171	Understanding the role of Sn substitution and Pb-â–¡ in enhancing the optical properties and solar cell efficiency of CH(NH₂)₂Pb_{1â^'xâ^'y}Sn_xâ–¡_yBr₃. Journal of Materials Chemistry C, 2020, 8, 10362-10368.	2.7	13
36172	Dependence of NiTi hydride stability by co-substitution by (Zr,Mg) onto Ti and (Cr,Cu) onto Ni: first-principles study. Philosophical Magazine, 2020, 100, 2458-2476.	0.7	0
36173	Role of anions on electrochemical exfoliation of graphite into graphene in aqueous acids. Carbon, 2020, 167, 816-825.	5.4	54
36174	AMP2: A fully automated program for ab initio calculations of crystalline materials. Computer Physics Communications, 2020, 256, 107450.	3.0	8
36175	First-principles study on a new type of quaternary carbonitride VWCN with outstanding mechanical properties. International Journal of Refractory Metals and Hard Materials, 2020, 92, 105319.	1.7	8
36176	Structural, elastic, electronic and hardness properties of osmium diboride predicted from first principles calculations. Journal of Alloys and Compounds, 2020, 844, 156098.	2.8	12
36177	Phase stability, mechanical, electronic, magnetic and optical properties of tetragonal and cubic M3V (M: Pd, Pt) structures. Journal of Molecular Graphics and Modelling, 2020, 100, 107651.	1.3	0
36178	Magneto-optical coupling and Kerr effect in PbNiO3, PbCrO3, and PbMnO3 multiferroics: An excited-states approach. Journal of Magnetism and Magnetic Materials, 2020, 514, 167176.	1.0	7
36179	Ferromagnetism induced by calcium vacancies in Ca3BiP anti-perovskite: An ab-initio calculation. Journal of Solid State Chemistry, 2020, 289, 121520.	1.4	3
36180	Modeling competitive precipitations among iron carbides during low-temperature tempering of martensitic carbon steel. Materialia, 2020, 12, 100800.	1.3	10
36181	Self-integrated effects of 2D ZnIn2S4 and amorphous Mo2C nanoparticles composite for promoting solar hydrogen generation. Nano Energy, 2020, 76, 105031.	8.2	106
36182	Direct Observation of One-Dimensional Peierls-type Charge Density Wave in Twin Boundaries of Monolayer MoTe₂. ACS Nano, 2020, 14, 8299-8306.	7.3	23
36183	Formation of ammoniaâ€“helium compounds at high pressure. Nature Communications, 2020, 11, 3164.	5.8	39
36184	Structural, elastic, vibrational and optical properties of energetic material octanitrocubane studied from first-principles theory. Journal of Physics Condensed Matter, 2020, 32, 425502.	0.7	4
36185	Thermoelasticity of tremolite amphibole: Geophysical implications. American Mineralogist, 2020, 105, 904-916.	0.9	11
36186	Molecular and dissociative adsorption of tetrachlorodibenzodioxin on M-doped graphenes (Mâ€‰=â€‰B, Al,) Tj ETQq1 1 0.784314	0.8	3
36187	Design of MXene contacts for high-performance WS2 transistors. Applied Surface Science, 2020, 527, 146701.	3.1	22
36188	Nitrogen-decorated borophene: An empowering contestant for hydrogen storage. Applied Surface Science, 2020, 527, 146852.	3.1	23

#	Article	IF	Citations
36189	Optoelectronic properties of three PbSe polymorphs. Ceramics International, 2020, 46, 22181-22188.	2.3	8
36190	A first-principle study on the formation and migration of AlH3 defect on (1Â1Â2) NaAlH4 surface. Chemical Physics, 2020, 538, 110871.	0.9	2
36191	Study of effect of hydrostatic pressure on structural, electronic and magnetic properties of In0.75Mn0.25P using density functional theory. Materials Today: Proceedings, 2020, 28, 1510-1513.	0.9	0
36192	Uncovering the Zr segregation behavior and its effect on the fracture strength of Al Î£5 (210) [100] symmetrical tilt grain boundary: Insight from first principles calculation. Materials Today Communications, 2020, 25, 101268.	0.9	2
36193	Influence of Lithium Vacancy Defects on Tritium Diffusion in Î²-Li₂TiO₃. Journal of Physical Chemistry C, 2020, 124, 12286-12294.	1.5	12
36194	A super stable assembled P nanowire with variant structural and magnetic/electronic properties via transition metal adsorption. Nanoscale, 2020, 12, 12454-12461.	2.8	8
36195	Structural evolution of BCN systems from graphene oxide towards electrocatalytically active atomic layers. Materials Chemistry Frontiers, 2020, 4, 2330-2338.	3.2	11
36196	First-principles prediction of structural, mechanical and thermal properties of perovskite BaZrS3. European Physical Journal B, 2020, 93, 1.	0.6	15
36197	Synthesis of cesium, sodium and nitrogen derived titanates using the Pechini sol-gel method. Chemical Physics, 2020, 537, 110816.	0.9	6
36198	Adsorption of metal ions at kaolinite surfaces: Ion-specific effects, and impacts of charge source and hydroxide formation. Applied Clay Science, 2020, 194, 105706.	2.6	13
36199	Strain and Low-Coordination Effects on Monolayer Nanoislands of Pd and Pt on Au(111): A Comparative Analysis Based on Density Functional Results. Journal of Physical Chemistry C, 2020, 124, 13225-13230.	1.5	9
36200	Instant Postsynthesis Aqueous Dispersion of Sb-Doped SnO₂ Nanocrystals: The Synergy between Small-Molecule Amine and Sb Dopant Ratio. ACS Applied Materials & Interfaces, 2020, 12, 29937-29945.	4.0	3
36201	Dipole-Field Interactions Determine the CO₂ Reduction Activity of 2D Feâ€“Nâ€“C Single-Atom Catalysts. ACS Catalysis, 2020, 10, 7826-7835.	5.5	94
36202	Single-atom Pt in intermetallics as an ultrastable and selective catalyst for propane dehydrogenation. Nature Communications, 2020, 11, 2838.	5.8	169
36203	Stability and gas sensing properties of Ta₂X₃M₈ (X = Pd, Pt; M = S,) Tj ETQq0 0 0 rgBT /Overlock 14651-14659.	1.3	6
36204	Dissociation of (Li2O2)0,+ on graphene and boron-doped graphene: insights from first-principles calculations. Physical Chemistry Chemical Physics, 2020, 22, 14216-14224.	1.3	11
36205	Dynamic strain aging in Fe-Mn-Al-C lightweight steel. Philosophical Magazine Letters, 2020, 100, 355-364.	0.5	4
36206	Anti-twinning in nanoscale tungsten. Science Advances, 2020, 6, eaay2792.	4.7	49

#	Article	IF	Citations
36207	Ohmic contacts of monolayer Tl2O field-effect transistors. Journal of Materials Science, 2020, 55, 11439-11450.	1.7	9
36208	The Challenge of CO Hydrogenation to Methanol: Fundamental Limitations Imposed by Linear Scaling Relations. Topics in Catalysis, 2020, 63, 635-648.	1.3	19
36209	First-principles study of the oxygen reduction reaction on the boron-doped C9N4 metal-free catalyst. Applied Surface Science, 2020, 527, 146828.	3.1	16
36210	Facet-dependent electrocatalysis in the HCOOH synthesis from CO2 reduction on Cu catalyst: a density functional theory study. Applied Surface Science, 2020, 527, 146857.	3.1	17
36211	Nanoporous C3N4, C3N5 and C3N6 nanosheets; novel strong semiconductors with low thermal conductivities and appealing optical/electronic properties. Carbon, 2020, 167, 40-50.	5.4	72
36212	High thermal conductivity in semiconducting Janus and non-Janus diamanes. Carbon, 2020, 167, 51-61.	5.4	39
36213	Prediction of mechanical properties of grafted kaolinite â€“ A DFT study. Applied Clay Science, 2020, 193, 105692.	2.6	19
36214	Lithium-ion insertion kinetics of Na-doped Li2TiSiO5 as anode materials for lithium-ion batteries. Journal of Materials Science and Technology, 2020, 57, 18-25.	5.6	11
36215	Elucidating the methanol conversion in H-SAPO-5 from first principles: Nature of hydrocarbon pool and scission style. Molecular Catalysis, 2020, 490, 110948.	1.0	4
36216	Electronic properties and effective masses of hexagonal Bi9O7.5S6: First-principles calculations. Materials Science in Semiconductor Processing, 2020, 114, 105081.	1.9	4
36217	Atomic insights into single-layer and bilayer germanene on Al(111) surface. Materials Today Physics, 2020, 14, 100241.	2.9	11
36218	First-principles study on electronic, magnetic properties and optical absorption of vanadium doped rutile TiO2. Physics Letters, Section A: General, Atomic and Solid State Physics, 2020, 384, 126637.	0.9	7
36219	Theoretical study on the effect of different surfaces on structure, excess energy, electronic structure and impact sensitivity in 1,3,5,7-tetranitro-1,3,5,7-tetraazacyclooctane. Surface Science, 2020, 700, 121650.	0.8	1
36220	Computational framework for a systematic investigation of anionic redox process in Li-rich compounds. Npj Computational Materials, 2020, 6, .	3.5	17
36221	Synthesis of two new copper-sandwiched polyoxotungstates and the influence of nuclear number on catalytic hydrogen evolution activity. New Journal of Chemistry, 2020, 44, 11035-11041.	1.4	6
36222	Mottness collapse in monolayer 1T-TaSe2 with persisting charge density wave order. Journal of Materials Chemistry C, 2020, 8, 9742-9747.	2.7	18
36223	Concepts from the linear magnetoelectric effect that might be useful for antiferromagnetic spintronics. Journal of Applied Physics, 2020, 127, .	1.1	29
36224	Spin-orbit splitting of quantum well states in <mml:math xmlns:mml="http://www.w3.org/1998/Math/MathML"><mml:mi>n</mml:mi></mml:math> -monolayer Ir/Au(111) heterostructures. Physical Review B, 2020, 101, .	1.1	0

#	Article	IF	Citations
36225	DFT Study on the Electronic Structure and the Magnetic Properties of SmFe₂ and HoCo₂Binary Cubic C15-Laves Phases. Spin, 2020, 10, .	0.6	2
36226	Interaction of graphene oxide with barium titanate in composite: XPS and DFT studies. Journal of Alloys and Compounds, 2020, 840, 155747.	2.8	15
36227	Defect induced ferromagnetism in NiO nanocrystals: Insight from experimental and DFT+U study. Physica B: Condensed Matter, 2020, 593, 412319.	1.3	9
36228	Synthesis and characterization of Pt(Cu0.67Sn0.33). Solid State Sciences, 2020, 105, 106282.	1.5	1
36229	Thermodynamic Adsorption States of TNT and DNAN on Corundum and Hematite. Journal of Physical Chemistry C, 2020, 124, 13837-13844.	1.5	6
36230	The effect of spinâ€“orbit interaction on superconductivity in the filled skutterudites MPt₄Ge₁₂ (M=Ba, Sr and Th). Philosophical Magazine, 2020, 100, 2735-2758.	0.7	0
36231	Theoretical studies on alloying of germanene supported on Al (111) substrate*. Chinese Physics B, 2020, 29, 108103.	0.7	3
36232	Structural investigation of caffeine monolayers on Au(111). Physical Review B, 2020, 101, .	1.1	3
36233	A Study of the Structure and Magnetic Properties of FeRh1Ââ€“ÂxIrx (x = 0.5â€“1) Alloys by First-Principles Methods. Physics of the Solid State, 2020, 62, 963-967.	0.2	2
36234	Exploring the Possibility of Î²â€Phase Arsenicâ€Phosphorus Polymorph Monolayer as Anode Materials for Sodiumâ€Ion Batteries. Advanced Theory and Simulations, 2020, 3, 2000023.	1.3	14
36235	Carbon Dots@rGO Paper as Freestanding and Flexible Potassiumâ€Ion Batteries Anode. Advanced Science, 2020, 7, 2000470.	5.6	95
36236	Scaling law for strain dependence of Raman spectra in transitionâ€metal dichalcogenides. Journal of Raman Spectroscopy, 2020, 51, 1353-1361.	1.2	13
36237	d0 Half-Metallic Ferromagnetism in GeNaZ (Z = Ca, Sr, and Ba) Ternary Half-Heusler Alloys: an Ab initio Investigation. Journal of Superconductivity and Novel Magnetism, 2020, 33, 3121-3132.	0.8	11
36238	Interfacial engineering of Ni/V2O3 for hydrogen evolution reaction. Nano Research, 2020, 13, 2407-2412.	5.8	41
36239	Investigating geometric structure, energies, electronic structure and impact sensitivity illustrated with surfaces of Îµ-CL-20. Applied Surface Science, 2020, 527, 146940.	3.1	4
36240	Phase equilibria and thermodynamic investigation of the Inâ€“Li system. Calphad: Computer Coupling of Phase Diagrams and Thermochemistry, 2020, 70, 101779.	0.7	4
36241	Surface Orientation and Structure of LaTiO₂N Nanoparticles. ACS Applied Energy Materials, 2020, 3, 5867-5873.	2.5	4
36242	Boosting the efficiency of water oxidation via surface states on hematite photoanodes by incorporating Bi³⁺ ions. Sustainable Energy and Fuels, 2020, 4, 4207-4218.	2.5	10

#	Article	IF	Citations
36243	Revealing the structure of a catalytic combustion active-site ensemble combining uniform nanocrystal catalysts and theory insights. Proceedings of the National Academy of Sciences of the United States of America, 2020, 117, 14721-14729.	3.3	16
36244	Comparative study on structural, electronic, optical and mechanical properties of normal and high pressure phases titanium dioxide using DFT. Materials Research Express, 2020, 7, 054004.	0.8	19
36245	Effect of H Defects on Li Transport during the Deposition Process on an Hâ€Diamond Surface: A Firstâ€Principles Calculation Analysis. Advanced Theory and Simulations, 2020, 3, 2000067.	1.3	3
36246	Experimental and Computational Investigation of the Role of P in Moderating Ethane Dehydrogenation Performance over Ni-Based Catalysts. Industrial & Engineering Chemistry Research, 2020, 59, 12666-12676.	1.8	14
36247	Accelerating Auxiliary-Field Quantum Monte Carlo Simulations of Solids with Graphical Processing Units. Journal of Chemical Theory and Computation, 2020, 16, 4286-4297.	2.3	18
36248	Multiscale Study of the Mechanism of Catalytic CO₂ Hydrogenation: Role of the Ni(111) Facets. ACS Catalysis, 2020, 10, 8077-8089.	5.5	43
36249	B5N5 monolayer: a room-temperature light element antiferromagnetic insulator. Nanoscale Advances, 2020, 2, 4421-4426.	2.2	3
36250	Phase Stability in U-6Nb Alloy Doped with Ti from the First Principles Theory. Applied Sciences (Switzerland), 2020, 10, 3417.	1.3	9
36251	Tuning the high-Î¹ oxide (HfO2, ZrO2)/4H-SiC interface properties with a SiO2 interlayer for power device applications. Applied Surface Science, 2020, 527, 146843.	3.1	13
36252	Isolating the Role of the Node-Linker Bond in the Compression of UiO-66 Metalâ€“Organic Frameworks. Chemistry of Materials, 2020, 32, 5864-5871.	3.2	24
36253	Insights into the Impact of Yttrium Doping at the Ba and Ti Sites of BaTiO₃ on the Electronic Structures and Optical Properties: A First-Principles Study. ACS Omega, 2020, 5, 15502-15509.	1.6	20
36254	Reversing abnormal hole localization in high-Al-content AlGaN quantum well to enhance deep ultraviolet emission by regulating the orbital state coupling. Light: Science and Applications, 2020, 9, 104.	7.7	25
36256	Synergistic effects of dopant (Ti or Sn) and oxygen vacancy on the electronic properties of hematite: a DFT investigation. RSC Advances, 2020, 10, 23263-23269.	1.7	14
36257	Why the activity of the hydrogen oxidation reaction on platinum decreases as pH increases. Electrochimica Acta, 2020, 354, 136620.	2.6	28
36258	Transforming nonisostructural wurtzite (ZnO) and rocksalt (MgO) II-VI compounds into stable alloy: The case of MgZnO. Superlattices and Microstructures, 2020, 145, 106623.	1.4	5
36259	Mechanical and thermodynamical properties of Î² â^' Cu â^' Al â^' Mn alloys along the Cu3Al â†' Cu2AlMn compositional line. Solid State Communications, 2020, 319, 113980.	0.9	7
36260	Anion order in oxysulfide perovskites: origins and implications. Npj Computational Materials, 2020, 6, .	3.5	22
36261	Understanding the role of ionic flux on the polarity of the exposed surfaces of ZnO. Physical Chemistry Chemical Physics, 2020, 22, 15427-15436.	1.3	4

#	Article	IF	Citations
36262	Synthesis of heteroepitaxial BP and related Al-B-Sb-As-P films via CVD of Al(BH4)3 and MH3 (M=P, As, Sb) at temperatures below 600 Â°C. Semiconductor Science and Technology, 2020, 35, 085034.	1.0	2
36263	Phase stability and impact of water on CsSnI₃ perovskite. Applied Physics Express, 2020, 13, 071003.	1.1	10
36264	Antiphase Boundaries as Faceted Metallic Wires in 2D Transition Metal Dichalcogenides. Advanced Science, 2020, 7, 2000788.	5.6	3
36265	Surface Reactivity of Ag-Modified Ceria to Hydrogen: A Combined Experimental and Theoretical Investigation. ACS Applied Materials & Interfaces, 2020, 12, 27682-27690.	4.0	6
36266	Coexistence of nontrivial topological properties and strong ferromagnetic fluctuations in quasi-one-dimensional A2Cr3As3. Npj Computational Materials, 2020, 6, .	3.5	19
36267	Plasmon-driven carbonâ€“fluorine (C(sp3)â€“F) bond activation with mechanistic insights into hot-carrier-mediated pathways. Nature Catalysis, 2020, 3, 564-573.	16.1	81
36268	[O₂Pb₃]₂(BO₃)I: a new lead borate iodide with 1âˆž[O₂Pb₃] double chains. Dalton Transactions, 2020, 49, 8985-8990.	1.6	3
36269	Modifying structural polymorphs and tuning electronic properties in pressure-stabilized binary Irâ€“Sb phases. RSC Advances, 2020, 10, 19185-19191.	1.7	0
36270	Interlayer coupling and electric field controllable Schottky barriers and contact types in graphene/<mml:math xmlns:mml="http://www.w3.org/1998/Math/MathML"><mml:msub><mml:mi>PbI</mml:mi><mml:mn>2</mml:mn></mml:msub></mml heterostructures. Physical Review B, 2020, 101, .	1.1	76
36271	Preparation and Characterization of Paramagnetic Bis (8-Hydroxyquinoline) Manganese Crystals. Materials, 2020, 13, 2379.	1.3	1
36272	First-principles predication of facet-dependent electronic and optical properties in InSe/GaAs heterostructure with potential in solar energy utilization. Journal of Alloys and Compounds, 2020, 842, 155901.	2.8	15
36273	Electronic structure and carrier mobilities of twisted graphene helix. Physica E: Low-Dimensional Systems and Nanostructures, 2020, 124, 114280.	1.3	1
36274	Nature of Terminating Hydroxyl Groups and Intercalating Water in Ti₃C₂T_x MXenes: A Study by ¹H Solid-State NMR and DFT Calculations. Journal of Physical Chemistry C, 2020, 124, 13649-13655.	1.5	35
36275	First-Principles Investigation of the Thermal Degradation Mechanisms of Methylammonium Lead Triiodide Perovskite. Journal of Physical Chemistry C, 2020, 124, 14521-14530.	1.5	5
36276	Discovery of new boron-rich chalcogenides: orthorhombic B6X (X=S, Se). Scientific Reports, 2020, 10, 9277.	1.6	15
36277	Machine-learning interatomic potentials enable first-principles multiscale modeling of lattice thermal conductivity in graphene/borophene heterostructures. Materials Horizons, 2020, 7, 2359-2367.	6.4	124
36278	AgPd nanoparticles for electrocatalytic CO₂ reduction: bimetallic composition-dependent ligand and ensemble effects. Nanoscale, 2020, 12, 14068-14075.	2.8	36
36279	Crystal Hall and crystal magneto-optical effect in thin films of SrRuO3. Journal of Applied Physics, 2020, 127, .	1.1	37

#	Article	IF	Citations
36280	Angular dependent interatomic potential for Tiâ€“V system for molecular dynamics simulations. Modelling and Simulation in Materials Science and Engineering, 2020, 28, 055010.	0.8	8
36281	Symmetry-guaranteed ideal Weyl semimetallic phase in face-centered orthogonal C6. Physical Review B, 2020, 101, .	1.1	7
36282	Enabling reversible phase transition on K5/9Mn7/9Ti2/9O2 for high-performance potassium-ion batteries cathodes. Energy Storage Materials, 2020, 31, 20-26.	9.5	35
36283	Hybridization versus sublattice symmetry breaking in the band gap opening in graphene on Ni(111): A first-principles study. Surface Science, 2020, 700, 121651.	0.8	3
36284	Li-triggered superior catalytic activity of V in Li₃VO₄: enabling fast and full hydrogenation of Mg at lower temperatures. Journal of Materials Chemistry A, 2020, 8, 14935-14943.	5.2	24
36285	Interaction of SO2 with the Platinum (001), (011), and (111) Surfaces: A DFT Study. Catalysts, 2020, 10, 558.	1.6	9
36286	Observation of Electrically Tunable van Hove Singularities in Twisted Bilayer Graphene from NanoARPES. Advanced Materials, 2020, 32, 2001656.	11.1	25
36287	Exciton effect in new generation of carbon nanotubes: graphdiyne nanotubes. Journal of Molecular Modeling, 2020, 26, 171.	0.8	2
36288	Structural and Magnetic Properties of CrN: Investigated by First-Principles Calculations, Monte Carlo Simulation, and High-Temperature Series Expansions. Journal of Superconductivity and Novel Magnetism, 2020, 33, 3113-3120.	0.8	10
36289	The hydration of periclase: Atomistic insights from quantum-chemical look. Chemical Physics, 2020, 532, 110694.	0.9	4
36290	Investigation on adsorption properties of HCN and ClCN blood agents on Î¸â€“phosphorene nanosheets â€“ A firstâ€“principles insight. Chemical Physics, 2020, 538, 110896.	0.9	34
36291	Electronic transport of CNT-encapsulated carbyne. Computational Materials Science, 2020, 183, 109809.	1.4	8
36292	A novel antiferromagnetic semiconductor hidden in pyrite. Computational Materials Science, 2020, 183, 109852.	1.4	7
36293	Theoretical study of CH4 adsorption and dissociation on W-Cu(1Â0Â0) surface. Computational and Theoretical Chemistry, 2020, 1186, 112890.	1.1	5
36294	Ab initio prediction of the elastic, electronic and optical properties of a new family of diamond-like semiconductors, Li2HgMS4 (MÂ= Si, Ge and Sn). Journal of Alloys and Compounds, 2020, 843, 155991.	2.8	21
36295	Revealing the effect of phosphorus doping on Co@carbon in boosting oxygen evolution catalytic activity. Journal of Alloys and Compounds, 2020, 843, 156001.	2.8	8
36296	First-principles investigation of Mg substitution for Ga on martensitic transformation, magnetism and electronic structures in Ni2MnGa. Journal of Alloys and Compounds, 2020, 843, 156049.	2.8	10
36297	Investigation of the electronic, magnetic, elastic, thermodynamic and thermoelectric properties of Mn2CoCr Heusler compound: A DFT-based simulation. Journal of Magnetism and Magnetic Materials, 2020, 513, 167107.	1.0	33

#	Article	IF	Citations
36298	Investigation of martensitic transformation behavior in Ni-Mn-In Heusler alloy from a first-principles study. Journal of Materials Science and Technology, 2020, 58, 100-106.	5.6	5
36299	Marcasite-FeS2@carbon nanodots anchored on 3D cell-like graphenic matrix for high-rate and ultrastable potassium ion storage. Journal of Power Sources, 2020, 469, 228429.	4.0	39
36300	External-strain induced transition from Schottky to ohmic contact in Graphene/InS and Graphene/Janus In2SSe heterostructures. Journal of Solid State Chemistry, 2020, 289, 121511.	1.4	24
36301	Bilayer B 54 , B 60 , and B 62 Clusters in a Universal Structural Pattern. European Journal of Inorganic Chemistry, 2020, 2020, 3296-3301.	1.0	15
36302	Tuning adsorption strength of CO2 and its intermediates on tin oxide-based electrocatalyst for efficient CO2 reduction towards carbonaceous products. Applied Catalysis B: Environmental, 2020, 277, 119252.	10.8	50
36303	Strain-induced effects in the electronic and optical properties of Na0.5Bi0.5TiO3: An ab-initio study. Materials Today Communications, 2020, 24, 101348.	0.9	11
36304	Multi-walled MoS2 nanotubes. First principles and molecular mechanics computer simulation. Physica E: Low-Dimensional Systems and Nanostructures, 2020, 124, 114183.	1.3	9
36305	Structural, mechanical and electronic properties and hardness of ionic vanadium dihydrides under pressure from first-principles computations. Scientific Reports, 2020, 10, 8868.	1.6	12
36306	Multiferroic decorated Fe₂O₃ monolayer predicted from first principles. Nanoscale, 2020, 12, 14847-14852.	2.8	24
36307	A first-principles study on the site occupancy behavior of transition metals in L1₂-Al₃Li phase. Materials Research Express, 2020, 7, 046519.	0.8	2
36308	First principles studies of oxygen adsorption on the Î³-U (1â€¯1â€¯0) surface and influences of Mo doping. Computational Materials Science, 2020, 179, 109633.	1.4	16
36309	Ab initio calculations of pure and Co+2-doped MgF2 crystals. Nuclear Instruments & Methods in Physics Research B, 2020, 470, 10-14.	0.6	5
36310	Enhancing CO₂ Electroreduction to Ethanol on Copperâ€“Silver Composites by Opening an Alternative Catalytic Pathway. ACS Catalysis, 2020, 10, 4059-4069.	5.5	145
36311	First-Principles Study of 3d Transition-Metal-Atom Adsorption onto Graphene Embedded with the Extended Line Defect. ACS Omega, 2020, 5, 5900-5910.	1.6	18
36312	Electronic transport properties of a lithium-decorated ZrTe5 thin film. Scientific Reports, 2020, 10, 3537.	1.6	1
36313	Study of the GaAs/SiH van der Waals type-II heterostructure: a high efficiency photocatalyst promoted by a built-in electric field. Physical Chemistry Chemical Physics, 2020, 22, 8565-8571.	1.3	27
36314	Ion migration in Br-doped MAPbI3 and its inhibition mechanisms investigated via quantum dynamics simulations. Physical Chemistry Chemical Physics, 2020, 22, 7778-7786.	1.3	10
36315	Polytypism in few-layer gallium selenide. Nanoscale, 2020, 12, 8563-8573.	2.8	26

#	Article	IF	Citations
36316	Phase relations in the Fe-P system at high pressures and temperatures from ab initio computations. High Pressure Research, 2020, 40, 235-244.	0.4	9
36317	High Spin Polarization and Thermoelectric Efficiency of Half-Metallic Ferromagnetic CrYSn (Y=Ca, Sr) of Half-Heusler Compounds. Spin, 2020, 10, .	0.6	18
36318	Enhancement of hydrogen storage capacity on co-functionalized GaS monolayer under external electric field. International Journal of Hydrogen Energy, 2020, 45, 12384-12393.	3.8	24
36319	Two-dimensional Siâ€“Ge monolayers: Stabilities, structures, and electronic properties. Journal of Applied Physics, 2020, 127, .	1.1	6
36320	Temperature dependence of the Kohn anomaly in bcc Nb from first-principles self-consistent phonon calculations. Physical Review B, 2020, 101, .	1.1	11
36321	Selective Electroreduction of Carbon Dioxide over SnO₂â€Nanodot Catalysts. ChemSusChem, 2020, 13, 6353-6359.	3.6	16
36322	Stability, electronic, and optical properties of twoâ€dimensional phosphoborane. Journal of Computational Chemistry, 2020, 41, 1456-1463.	1.5	19
36323	Theoretical investigation on the surface and morphological properties of lead nickelate multiferroics: vacancy dependency. Journal of Materials Science, 2020, 55, 6875-6890.	1.7	8
36324	Ab initio study of the adsorption of 3d transition metals on Ni(100) surface. SN Applied Sciences, 2020, 2, 1.	1.5	2
36325	Computational Study of the Evolution of Ni-Based Catalysts during the Dry Reforming of Methane. Energy & Fuels, 2020, 34, 4855-4864.	2.5	22
36326	Stabilization of the High-Energy-Density CuN₅ Salts under Ambient Conditions by a Ligand Effect. ACS Omega, 2020, 5, 6221-6227.	1.6	15
36327	Structural and electronic properties of NaTaO₃cubic nanowires. Physical Chemistry Chemical Physics, 2020, 22, 7250-7258.	1.3	7
36328	The hydrothermal in situ construction of AgVO₃/LaVO₄ phase junctions for the efficient visible-light-driven disposal of pollutants and photoelectrocatalytic methanol oxidation. Sustainable Energy and Fuels, 2020, 4, 2569-2582.	2.5	9
36329	Nickel iron phosphide ultrathin nanosheets anchored on nitrogen-doped carbon nanoflake arrays as a bifunctional catalyst for efficient overall water splitting. Nanoscale, 2020, 12, 8443-8452.	2.8	55
36330	Mechanism and activity of the oxygen reduction reaction on WTe₂ transition metal dichalcogenide with Te vacancy. RSC Advances, 2020, 10, 8460-8469.	1.7	11
36331	The influence of oxygen vacancy and Ce3+ ion positions on the properties of small gold clusters supported on CeO2â^'x(111). Journal of Materials Chemistry A, 2020, 8, 15695-15705.	5.2	17
36332	N₂ positively charged defects in diamond. A quantum mechanical investigation of the structural, electronic, EPR and vibrational properties. Journal of Materials Chemistry C, 2020, 8, 5239-5247.	2.7	10
36333	Stochastic many-body perturbation theory for MoirÃ© states in twisted bilayer phosphorene. Journal of Physics Condensed Matter, 2020, 32, 234001.	0.7	20

#	Article	IF	Citations
36334	First-principles study of stability, electronic structure and quantum capacitance of B-, N- and O-doped graphynes as supercapacitor electrodes. Journal of Physics Condensed Matter, 2020, 32, 215501.	0.7	9
36335	Carbon dioxide gas sensing, capture, and storage potential of calcium oxide surface and single walled carbon nanotube: insights from ab initio simulation. Journal of Physics Condensed Matter, 2020, 32, 245901.	0.7	3
36336	Magnetic anisotropy and Curie temperature of two-dimensional VI₃ monolayer. Journal of Physics Condensed Matter, 2020, 32, 245803.	0.7	23
36337	Layer-dependent band engineering of Pd dichalcogenides: a first-principles study. New Journal of Physics, 2020, 22, 053010.	1.2	25
36338	Thermal conductivity measurements in nanosheets via bolometric effect. 2D Materials, 2020, 7, 035003.	2.0	9
36339	Electron-phonon interaction and zero-field charge carrier transport in the nodal-line semimetal ZrSiS. Physical Review B, 2020, 101, .	1.1	8
36340	First-principles calculations of the structural, elastic, mechanical, electronic and optical properties of monoclinic Hf₄CuSi₄. International Journal of Modern Physics B, 2020, 34, 2050035.	1.0	4
36341	Boosting Electrocatalytic N₂ Reduction to NH₃ over Two-Dimensional Gallium Selenide by Defect-Size Engineering. Inorganic Chemistry, 2020, 59, 4858-4867.	1.9	44
36342	Phase Behavior of TmVO₄ under Hydrostatic Compression: An Experimental and Theoretical Study. Inorganic Chemistry, 2020, 59, 4882-4894.	1.9	10
36343	Large Valley Splitting and Enhancement of Curie Temperature in a Two-Dimensional VI₃/CrI₃ Heterostructure. Journal of Physical Chemistry C, 2020, 124, 7156-7162.	1.5	18
36344	Novel microwave synthesis of near-metallic copper sulfide nanodiscs with size control: experimental and DFT studies of charge carrier density. Nanoscale Advances, 2020, 2, 1054-1058.	2.2	19
36345	First-Principles Mechanistic Insights into the Hydrogen Evolution Reaction on Ni2P Electrocatalyst in Alkaline Medium. Catalysts, 2020, 10, 307.	1.6	8
36346	DFT Study of Structural and Electronic Properties of MgZnO Alloy. Journal of Electronic Materials, 2020, 49, 4569-4576.	1.0	0
36347	The effect of (Si, Cr, Fe, Ni, Nb, Sn) and monovacancy on hydrogen incorporation into Zr (0001): Ab initio insights. Computational and Theoretical Chemistry, 2020, 1178, 112781.	1.1	7
36348	Effect of Oxygen and Fluorine Absorption on the Electronic Structure of the InSb(111) Surface. Semiconductors, 2020, 54, 1-10.	0.2	2
36349	Synthesis and Electrochemical Properties of Bi2MoO6/Carbon Anode for Lithium-Ion Battery Application. Materials, 2020, 13, 1132.	1.3	16
36350	Enhancing hydrogen storage by metal substitution in MIL-88A metal-organic framework. Adsorption, 2020, 26, 509-519.	1.4	15
36351	Elastic and thermodynamic properties of high entropy carbide (HfTaZrTi)C and (HfTaZrNb)C from ab initio investigation. Ceramics International, 2020, 46, 15104-15112.	2.3	58

#	Article	IF	Citations
36352	Half-metal effect on the MnAs/InP (0Â0Â1)-(2ÂÃ—Â4) interface. Computational Materials Science, 2020, 175, 109603.	1.4	5
36353	The effect of strain on the Li-storage performance of V2C and Nb2C: From first-principles study. Solid State Communications, 2020, 311, 113857.	0.9	7
36354	Effect of Extra-Framework Cations on Negative Linear Compressibility and High-Pressure Phase Transitions: A Study of KCd[Ag(CN)₂]₃. Journal of Physical Chemistry C, 2020, 124, 6896-6906.	1.5	5
36355	High-throughput and data-mining approach to predict new rare-earth free permanent magnets. Physical Review B, 2020, 101, .	1.1	34
36356	Symmetry-Protected Topological Triangular Weyl Complex. Physical Review Letters, 2020, 124, 105303.	2.9	78
36357	Theoretical study of structural, electronic, and optical properties of ternary metal sulfides MBiS2 (M) Tj ETQq1 1 0.784314 rgBT /Over	0.8	3
36358	Highly Effective Work Function Reduction of Î±â€Borophene via Caesium Decoration: A Firstâ€Principles Investigation. Advanced Theory and Simulations, 2020, 3, 1900249.	1.3	8
36359	Optical insights of indium-doped Î²â€“Ga2O3 nanoparticles and its luminescence mechanism. Journal of Materials Science: Materials in Electronics, 2020, 31, 6185-6191.	1.1	3
36360	Structural, electronic and magnetic properties of the ordered binary FePt, MnPt, and CrPt3 alloys. Heliyon, 2020, 6, e03545.	1.4	14
36361	Electronic structures and optical properties of two-dimensional (W2âˆ•3X1âˆ•3)2CO2 (X=SC,Y) iMXene by first-principles calculations. Materials Chemistry and Physics, 2020, 248, 122896.	2.0	3
36362	[n]Phenacenes: Promising Organic Anodes for Potassium-Ion Batteries. Journal of Physical Chemistry C, 2020, 124, 6964-6970.	1.5	13
36363	Computational Study of Plutoniumâ€“Americium Mixed Oxides (Pu0.92Am0.08O2â€“x); Water Adsorption on {111}, {110}, and {100} Surfaces. Journal of Physical Chemistry C, 2020, 124, 6646-6658.	1.5	10
36364	Structureâ€“Electronic Property Relationships of 2D Ruddlesdenâ€“Popper Tin- and Lead-based Iodide Perovskites. ACS Applied Materials & Interfaces, 2020, 12, 15328-15337.	4.0	56
36365	Contrasting Arene, Alkene, Diene, and Formaldehyde Hydrogenation in H-ZSM-5, H-SSZ-13, and H-SAPO-34 Frameworks during MTO. ACS Catalysis, 2020, 10, 4593-4607.	5.5	38
36366	Prospects of Heterogeneous Hydroformylation with Supported Single Atom Catalysts. Journal of the American Chemical Society, 2020, 142, 5087-5096.	6.6	98
36367	Limits on gas impermeability of graphene. Nature, 2020, 579, 229-232.	13.7	220
36368	Exfoliation of zirconium aminophosphonates: investigation into their electronic structures by ab initio calculations. New Journal of Chemistry, 2020, 44, 10111-10118.	1.4	5
36369	Catalytic activation of a non-noble intermetallic surface through nanostructuration under hydrogenation conditions revealed by atomistic thermodynamics. Journal of Materials Chemistry A, 2020, 8, 7422-7431.	5.2	10

#	Article	IF	Citations
36370	Ferroelectricity and multiferroicity in two-dimensional Sc₂P₂Se₆ and ScCrP₂Se₆ monolayers. Physical Chemistry Chemical Physics, 2020, 22, 7489-7496.	1.3	17
36371	Electronic properties of bare and functionalized two-dimensional (2D) tellurene structures. Physical Chemistry Chemical Physics, 2020, 22, 6727-6737.	1.3	28
36372	First-principles study of electronic structure and fermiology of covellite mineral and its B1, B3 phases. Journal of Physics Condensed Matter, 2020, 32, 295501.	0.7	5
36373	n -hourglass Weyl fermions in nonsymmorphic materials. Physical Review B, 2020, 101, .	1.1	6
36374	Monolayer diboron dinitride: Direct band-gap semiconductor with high absorption in the visible range. Physical Review B, 2020, 101, .	1.1	20
36375	Mechanical, electronic and stability properties of multi-walled beryllium oxide nanotubes and nanopeapods: a density functional theory study. Journal of Molecular Modeling, 2020, 26, 76.	0.8	18
36376	Structural Phase Transformation, Intermediate States and Electronic Properties of PbTe Under High Pressure. Journal of Electronic Materials, 2020, 49, 3089-3095.	1.0	4
36377	Activation of CO₂ on Copper Surfaces: The Synergy between Electric Field, Surface Morphology, and Excess Electrons. Journal of Physical Chemistry C, 2020, 124, 6747-6755.	1.5	33
36378	Development of Stable Boron Nitride Nanotube and Hexagonal Boron Nitride Dispersions for Electrophoretic Deposition. Langmuir, 2020, 36, 3425-3438.	1.6	13
36379	A Highly Efficient Coordination Polymer for Selective Trapping and Sensing of Perrhenate/Pertechnetate. ACS Applied Materials & Interfaces, 2020, 12, 15246-15254.	4.0	57
36380	First-Principles Predictions and Synthesis of B50C2 by Chemical Vapor Deposition. Scientific Reports, 2020, 10, 4454.	1.6	8
36381	First-principles prediction of incipient order in arbitrary high-entropy alloys: exemplified in Ti0.25CrFeNiAl. Acta Materialia, 2020, 189, 248-254.	3.8	52
36382	First-principles prediction of enhancing graphene/Al interface bonding strength by graphene doping strategy. Applied Surface Science, 2020, 517, 146040.	3.1	31
36383	Cd₄SiQ₆ (Q = S, Se): Ternary Infrared Nonlinear Optical Materials with Mixed Functional Building Motifs. Crystal Growth and Design, 2020, 20, 2489-2496.	1.4	15
36384	Specific Response of the Atomic and Electronic Structure of Ta₂Pd₃Se₈ and Ta₂Pt₃Se₈ Nanoribbons to the Uniaxial Strain. Journal of Physical Chemistry C, 2020, 124, 7539-7543.	1.5	17
36385	MassiveÂand massless charge carriers in an epitaxially strained alkali metal quantum well on graphene. Nature Communications, 2020, 11, 1340.	5.8	8
36386	Ab initio electron-defect interactions using Wannier functions. Npj Computational Materials, 2020, 6, .	3.5	8
36387	Effects of boron defects on mechanical strengths of TiB₂ at high temperature: ab initio molecular dynamics studies. Physical Chemistry Chemical Physics, 2020, 22, 6560-6571.	1.3	5

#	Article	IF	Citations
36388	Nickel induced electronic structural regulation of cobalt hydroxide for enhanced water oxidation. Journal of Materials Chemistry A, 2020, 8, 6699-6708.	5.2	29
36389	In situ construction of a MOF-derived carbon-encapsulated LiCoO₂ heterostructure as a superior cathode for elevated-voltage lithium storage: from experimental to theoretical study. Journal of Materials Chemistry A, 2020, 8, 6607-6618.	5.2	46
36390	Embedded carbon nanowire in black phosphorene and C-doping: the rule to control electronic properties. Nanotechnology, 2020, 31, 275201.	1.3	7
36391	Temperature dependence of electron-phonon interactions in vanadium. Physical Review B, 2020, 101, .	1.1	12
36392	Room-temperature ferromagnetism in boron-doped oxides: a combined first-principle and experimental study. Philosophical Magazine Letters, 2020, 100, 141-153.	0.5	12
36393	First Principles Study on Electronic Structure and Optical Properties of Ternary Semiconductor InxAl1 â€“xP Alloys. Semiconductors, 2020, 54, 58-66.	0.2	15
36394	Mechanical, electronic and optical properties of bulk and monolayer GeSe₂. International Journal of Modern Physics B, 2020, 34, 2050034.	1.0	6
36395	Data-driven design of B20 alloys with targeted magnetic properties guided by machine learning and density functional theory. Journal of Materials Research, 2020, 35, 890-897.	1.2	6
36396	Defective structures in FeCrAl alloys from first principles calculations. Japanese Journal of Applied Physics, 2020, 59, 046003.	0.8	6
36397	Crystal facet dependence of carbon chain growth mechanism over the Hcp and Fcc Co catalysts in the Fischer-Tropsch synthesis. Applied Catalysis B: Environmental, 2020, 269, 118847.	10.8	29
36398	2D CdOâ€Based Heterostructure as a Promising Visible Light Waterâ€Splitting Photocatalyst. Physica Status Solidi (A) Applications and Materials Science, 2020, 217, 1900859.	0.8	4
36399	Selective electrochemical CO2 reduction on Cu-Pd heterostructure. Applied Catalysis B: Environmental, 2020, 270, 118864.	10.8	66
36400	Sensing of volatile organic compounds on two-dimensional nitrogenated holey graphene, graphdiyne, and their heterostructure. Carbon, 2020, 163, 213-223.	5.4	77
36401	An effective combination reaction involved with sputtered and selenized Sb precursors for efficient Sb2Se3 thin film solar cells. Chemical Engineering Journal, 2020, 393, 124599.	6.6	95
36402	First principles calculations of the influence of nitrogen content on the mechanical properties of Î±-Ti. Materials Chemistry and Physics, 2020, 248, 122891.	2.0	8
36403	A comparative theoretical investigation of optoelectronic and mechanical properties of KYS2 and KLaS2. Materials Science in Semiconductor Processing, 2020, 113, 105048.	1.9	16
36404	The magnesium uranyl tricarbonate octadecahydrate mineral, bayleyite: Periodic DFT study of its crystal structure, hydrogen bonding, mechanical properties and infrared spectrum. Spectrochimica Acta - Part A: Molecular and Biomolecular Spectroscopy, 2020, 234, 118216.	2.0	6
36405	Physical properties and superconductivity of Heusler compound LiGa2Rh: A first-principles calculation. Solid State Communications, 2020, 311, 113859.	0.9	10

#	Article	IF	Citations
36406	Experimental and DFT Studies of Hybrid Silver/Cdots Nanoparticles. Journal of Physical Chemistry B, 2020, 124, 2425-2435.	1.2	10
36407	Sulfur Structures on Bare and Graphene-Covered Ir(111). Journal of Physical Chemistry C, 2020, 124, 6659-6668.	1.5	7
36408	Nanocrystal facet modulation to enhance transferrin binding and cellular delivery. Nature Communications, 2020, 11, 1262.	5.8	33
36409	Structural analysis of dehydrated gibbsite-based layered double hydroxides Liâ€“Alâ€“X (X = Fâ^', Clâ^', Brâ^',) Tj ETQq1 1 0.784314 rgBT	1.4	11
36410	Predicting metalâ€“metal interactions. II. Accelerating generalized schemes through physical insights. Journal of Chemical Physics, 2020, 152, 094702.	1.2	8
36411	Functionalisation of hexagonal boron phosphide (h-BP) monolayer via atomic adsorption. Philosophical Magazine Letters, 2020, 100, 116-127.	0.5	3
36412	Trace bismuth and iodine co-doping enhanced thermoelectric performance of PbTe alloys. Journal Physics D: Applied Physics, 2020, 53, 245501.	1.3	29
36413	Reducing lead toxicity in the methylammonium lead halide <mml:math xmlns:mml="http://www.w3.org/1998/Math/MathML"><mml:msub><mml:mi mathvariant="normal">MAPbI</mml:mi><mml:mn>3</mml:mn></mml:msub></mml:math> : Why Sn substitution should be preferred to Pb vacancy for optimum solar cell efficiency. Physical Review B, 2020, 101, .	1.1	25
36414	Ultrafast band-gap renormalization and build-up of optical gain in monolayer <mml:math xmlns:mml="http://www.w3.org/1998/Math/MathML"><mml:msub><mml:mi>MoTe</mml:mi><mml:mn>2</mml:mn></mml:msub></m Physical Review B, 2020, 101, .	1.1	22
36415	Consistency between ARPES and STM measurements on <mml:math xmlns:mml="http://www.w3.org/1998/Math/MathML"><mml:msub><mml:mi>SmB</mml:mi><mml:mn>6</mml:mn></mml:msub></mm Physical Review B, 2020, 101, .	1.1	16
36416	Strain Effect on the Hydrogen Evolution Reaction of V_{Mo}-SLMoS₂. IEEE Nanotechnology Magazine, 2020, 19, 192-196.	1.1	3
36417	Electronic and optical properties of non-hexagonal Dirac material S-graphene sheet and nanoribbons. Physica E: Low-Dimensional Systems and Nanostructures, 2020, 120, 114087.	1.3	26
36418	Metal-Coordination Network vs Charge Transfer Complex: The Importance of the Surface. Journal of Physical Chemistry C, 2020, 124, 7922-7929.	1.5	5
36419	Few-Layer Borophene Prepared by Mechanical Resonance and Its Application in Terahertz Shielding. ACS Applied Materials & Interfaces, 2020, 12, 19746-19754.	4.0	22
36420	Interaction Mediator Assisted Synthesis of Mesoporous Molybdenum Carbide: Mo-Valence State Adjustment for Optimizing Hydrogen Evolution. ACS Nano, 2020, 14, 4988-4999.	7.3	80
36421	Electronic structure, thermodynamic stability and high-temperature sensing properties of Er-Î±-SiAlON ceramics. Scientific Reports, 2020, 10, 4952.	1.6	17
36422	Exploration of the intrinsic factors limiting the photocurrent density in ferroelectric BiFeO₃ thin film. Journal of Materials Chemistry A, 2020, 8, 6863-6873.	5.2	30
36423	Enhancing the methane steam reforming catalytic performance of Ni monolithic catalysts via Niâ€“Re surface alloying. Catalysis Science and Technology, 2020, 10, 2004-2019.	2.1	20

#	Article	IF	Citations
36424	A novel C₆N₂monolayer as a potential material for charge-controlled CO₂capture. Journal of Materials Chemistry C, 2020, 8, 6542-6551.	2.7	23
36425	Stability and anion diffusion kinetics of Yttria-stabilized zirconia resolved from machine learning global potential energy surface exploration. Journal of Chemical Physics, 2020, 152, 094703.	1.2	15
36426	Mechanical, electronic and thermodynamic properties of TE-C36 under high pressure. Molecular Physics, 2020, 118, e1739769.	0.8	0
36427	2D honeycomb borophene oxide: a promising anode material offering super high capacity for Li/Na-ion batteries. Journal of Physics Condensed Matter, 2020, 32, 065001.	0.7	16
36428	Local structure investigations of accumulated damage in irradiated MgAl₂O₄. Journal of the American Ceramic Society, 2020, 103, 4654-4663.	1.9	6
36429	Polaron modulation mechanism of H2O and CO2 adsorption on PuO2(111) surface. Applied Surface Science, 2020, 516, 146164.	3.1	10
36430	Insight into electronic structure and optical properties of Nb and F co-doped SnO2 with hybrid functional theoretical method. Ceramics International, 2020, 46, 10341-10347.	2.3	11
36431	First-principles study of hydrogen behavior in Î±-Pu2O3. Computational Materials Science, 2020, 179, 109688.	1.4	7
36432	Novel Îµ-phosphorene nanosheet device for the detection of tear gas molecules â€“ A first-principles research. Chemical Physics Letters, 2020, 747, 137353.	1.2	40
36433	Observation of R-type ferrimagnetism in the intermetallic Mn1.25Sb. Journal of Magnetism and Magnetic Materials, 2020, 505, 166760.	1.0	3
36434	Crystal Structures, Electronic Structures, and Topological Signatures in Equiatomic TTâ€²X Compounds (T = Sc, Zr, Hf; Tâ€² = Co, Pt, Pd, Ir, Rh; X = Al, Ga, Sn). Journal of Physical Chemistry C, 2020, 124, 7378-7385.	1.5	16
36435	Infrared active phonons in monoclinic lutetium oxyorthosilicate. Journal of Applied Physics, 2020, 127, .	1.1	6
36436	Seeing Dirac electrons and heavy fermions in new boron nitride monolayers*. Chinese Physics B, 2020, 29, 057303.	0.7	4
36437	Effects of magnetic and structural phase transitions on the normal and anomalous Hall effects in Ni-Mn-In-B Heusler alloys. Physical Review B, 2020, 101, .	1.1	24
36438	InP/TiO2 heterojunction for photoelectrochemical water splitting under visible-light. International Journal of Hydrogen Energy, 2020, 45, 11615-11624.	3.8	18
36439	Double-centers of V,Ceâ€“Codoped LiNbO₃ from Hybrid Density Functional Theory Calculations: Electron Trapping and Excitation between the Defect Levels. Crystal Growth and Design, 2020, 20, 2774-2780.	1.4	2
36440	Molecular Packing-Dependent Thermal Expansion Behaviors in Metal Squarate Frameworks. Chemistry of Materials, 2020, 32, 2893-2898.	3.2	15
36441	Methanol Synthesis from CO₂Hydrogenation over a Potassium-Promoted Cu_xO/Cu(111) (xâ‰ˆ 2) Model Surface: Rationalizing the Potential of Potassium in Catalysis. ACS Catalysis, 2020, 10, 5723-5733.	5.5	36

#	Article	IF	Citations
36442	Metallic FeSe monolayer as an anode material for Li and non-Li ion batteries: a DFT study. Physical Chemistry Chemical Physics, 2020, 22, 8902-8912.	1.3	79
36443	Effect of doping Zn atom on the structural stability, mechanical and thermodynamic properties of AlLi phase in Mgâ€“Li alloys from first-principles calculations. Philosophical Magazine, 2020, 100, 1849-1867.	0.7	8
36444	Eu3+-activated Ca3Mo0.2W0.8O6 red-emitting phosphors: A near-ultraviolet and blue light excitable platform for solid-state lighting and thermometer. Journal of Luminescence, 2020, 223, 117212.	1.5	23
36445	Infrared spectroscopy data- and physics-driven machine learning for characterizing surface microstructure of complex materials. Nature Communications, 2020, 11, 1513.	5.8	77
36446	High-performance phosphorene electromechanical actuators. Npj Computational Materials, 2020, 6, .	3.5	13
36447	Structure of two-dimensional Fe3O4. Journal of Chemical Physics, 2020, 152, 114705.	1.2	10
36448	First principle study of the structural and electronic properties of Nihonium. MRS Advances, 2020, 5, 1175-1183.	0.5	1
36449	Impurity Effects on Habit Change and Polymorphic Transitions in the System: Aragoniteâ€“Calciteâ€“Vaterite. Crystal Growth and Design, 2020, 20, 2497-2507.	1.4	11
36450	Electronic Anisotropy and Superconductivity in One-Dimensional Electride Ca₃Si. Journal of Physical Chemistry C, 2020, 124, 7683-7690.	1.5	18
36451	Elasticity, piezoelectricity, and mobility in two-dimensional BiTeI from a first-principles study. Journal Physics D: Applied Physics, 2020, 53, 245301.	1.3	13
36452	Study of the mechanisms of contact electrification and charge transfer between polytetrafluoroethylene and metals. Journal Physics D: Applied Physics, 2020, 53, 285302.	1.3	7
36453	First-principles study the single-layer transition metal trihalide CrXSe₃ (Xâ€‰â€‰=â€‰â€‰Sn, Ge, Si) as monolayer ferromagnetic semiconductor. Journal of Physics Condensed Matter, 2020, 32, 085801.	0.7	5
36454	Effect of Sr substitution on the property and stability of CH₃NH₃SnI₃perovskite: A firstâ€principles investigation. International Journal of Energy Research, 2020, 44, 5765-5778.	2.2	19
36455	Core level photoemission line shape selection: Atomic adsorbates on iron. Surface and Interface Analysis, 2020, 52, 507-512.	0.8	6
36456	Adsorption of Water Molecule on Calcium Fluoride and Magnesium Fluoride Surfaces: A Combined Theoretical and Experimental Study. Journal of Physical Chemistry C, 2020, 124, 7853-7859.	1.5	8
36457	Optoelectronic Properties of Two-Dimensional Bromide Perovskites: Influences of Spacer Cations. Journal of Physical Chemistry Letters, 2020, 11, 2955-2964.	2.1	50
36458	Covalently Connected Nb₄N_{5â€“x}O_xâ€“MoS₂ Heterocatalysts with Desired Electron Density to Boost Hydrogen Evolution. ACS Nano, 2020, 14, 4925-4937.	7.3	50
36459	Nitrogen fixation on metal-free SiC(111) polar surfaces. Journal of Materials Chemistry A, 2020, 8, 7412-7421.	5.2	26

#	Article	IF	Citations
36460	2D CrCl₂(pyrazine)₂ monolayer: high-temperature ferromagnetism and half-metallicity. Journal of Physics Condensed Matter, 2020, 32, 135801.	0.7	6
36461	First principles study of electronic structure and thermoelectric transport in tin selenide and phase separated tin selenideâ€“copper selenide alloy. Journal of Physics Condensed Matter, 2020, 32, 265501.	0.7	8
36462	The Raman and IR vibration modes of metal pentazolate hydrates [Na(H2O)(N5)]Â·2H2O and [Mg(H2O)6(N5)2]Â·4H2O. Journal of Molecular Modeling, 2020, 26, 84.	0.8	3
36463	Dynamical properties of organo lead-halide perovskites and their interfaces to titania: insights from Density Functional Theory. Heliyon, 2020, 6, e03427.	1.4	4
36464	Ab-initio calculations of fission product diffusion on graphene. Journal of Nuclear Materials, 2020, 533, 152123.	1.3	8
36465	The influence of S vacancy on the adsorption of toxic gas molecules on SnS monolayer: A DFT study. Physica E: Low-Dimensional Systems and Nanostructures, 2020, 120, 114054.	1.3	18
36466	A Density Functional Theory Study of the Two-Dimensional Bis(iminothiolato)metal Monolayers as Efficient Electrocatalysts for Oxygen Reduction Reaction. Journal of Physical Chemistry C, 2020, 124, 7803-7811.	1.5	10
36467	Optimization of Ptâ€“Oxygen-Containing Species Anodes for Ethanol Oxidation Reaction: High Performance of Pt-AuSnO_x Electrocatalyst. Journal of Physical Chemistry Letters, 2020, 11, 2846-2853.	2.1	11
36468	Universal A-Cation Splitting in LiNbO₃-Type Structure Driven by Intrapositional Multivalent Coupling. Journal of the American Chemical Society, 2020, 142, 7168-7178.	6.6	7
36469	Mechanochemical Formation of Racemic Praziquantel Hemihydrate with Improved Biopharmaceutical Properties. Pharmaceutics, 2020, 12, 289.	2.0	21
36470	NMR crystallography of molecular organics. Progress in Nuclear Magnetic Resonance Spectroscopy, 2020, 118-119, 10-53.	3.9	95
36471	Adsorption of heavy-element monolayers of Tl, Pb, and Bi at silicene: A DFT study. Surface Science, 2020, 697, 121604.	0.8	3
36472	Engineering Metal-sp_{xy} Dirac Bands on the Oxidized SiC Surface. Nano Letters, 2020, 20, 3956-3962.	4.5	4
36473	Few-Layer Black Phosphorus Nanosheets: A Metal-Free Cocatalyst for Photocatalytic Nitrogen Fixation. ACS Applied Materials & Interfaces, 2020, 12, 17343-17352.	4.0	74
36474	Synthesis of a Smart Hybrid MXene with Switchable Conductivity for Temperature Sensing. ACS Applied Nano Materials, 2020, 3, 4069-4076.	2.4	26
36475	Electric field modulation in the auxetic effect of BP-analog monolayer As and Sb by first-principles calculations. Physical Chemistry Chemical Physics, 2020, 22, 8739-8744.	1.3	5
36476	Interaction between Mo and intrinsic or extrinsic defects of Mo doped LiNbO3 from first-principles calculations. Journal of Physics Condensed Matter, 2020, 32, 255701.	0.7	3
36477	Electronic structures and optoelectronic properties of ATiOPO₄ (AÂ=ÂH, Li, Na, K, Rb, Cs, Fr,) Tj ETQq1 1 0.784314 rgBT /O and photo-degradation. Materials Research Express, 2020, 7, 045901.	0.8	6

#	Article	IF	Citations
36478	Stacking-dependent topological phase in bilayer <mml:math xmlns:mml="http://www.w3.org/1998/Math/MathML"><mml:mrow><mml:mi>M</mml:mi><mml:mi mathvariant="normal">B</mml:mi><mml:msub><mml:mi mathvariant="normal">i</mml:mi><mml:mn>2</mml:mn></mml:msub><mml:mi mathvariant="normal">T</mml:mi><mml:msub><mml:mi		

#	Article	IF	Citations
36496	Extended 1D defect induced magnetism in 2D MoS₂ crystal. Journal of Physics Condensed Matter, 2020, 32, 215302.	0.7	2
36497	Pressure-induced gap modulation and topological transitions in twisted bilayer and twisted double bilayer graphene. Physical Review B, 2020, 101, .	1.1	19
36498	Synthesis of Highly-Oriented Black CsPbI₃ Microstructures for High-Performance Solar Cells. Chemistry of Materials, 2020, 32, 3235-3244.	3.2	23
36499	CO₂ Reduction on Metal- and Nitrogen-Codoped Graphene: Balancing Activity and Selectivity via Coordination Engineering. ACS Sustainable Chemistry and Engineering, 2020, 8, 6134-6141.	3.2	26
36500	Approaching the activity limit of CoSe2 for oxygen evolution via Fe doping and Co vacancy. Nature Communications, 2020, 11, 1664.	5.8	191
36501	Towards the understanding of the gold interaction with AIII-BV semiconductors at the atomic level. Nanoscale, 2020, 12, 9067-9081.	2.8	6
36502	A Ti₃C₂O₂ supported single atom, trifunctional catalyst for electrochemical reactions. Journal of Materials Chemistry A, 2020, 8, 7801-7807.	5.2	69
36503	Theoretical Studies of MoS₂ and Phosphorene Drug Delivery for Antituberculosis Drugs. Journal of Physical Chemistry C, 2020, 124, 8279-8287.	1.5	17
36504	Accurate Ab Initio Calculations on Various PV-Based Materials: Which Functional to Be Used?. Journal of Physical Chemistry C, 2020, 124, 8467-8478.	1.5	15
36505	Synergistic ultraviolet and visible light photo-activation enables intensified low-temperature methanol synthesis over copper/zinc oxide/alumina. Nature Communications, 2020, 11, 1615.	5.8	84
36506	Synthesis of a flower-like MoS₂/carbon nanocomposite with enhanced adsorption performance toward Eu(<scp>iii</scp>): the cooperative effects between S atoms and carboxyl groups. Environmental Science: Water Research and Technology, 2020, 6, 1482-1494.	1.2	12
36507	Atomic scale insight into the fundamental mechanism of Mn doped LiFePO₄. Sustainable Energy and Fuels, 2020, 4, 2741-2751.	2.5	17
36508	Engineering Sulfide-Phosphide Based Double Catalysts on 3D Nickel Phosphides Framework for Electrolytic Hydrogen Evolution: Activating Short-range Crystalline MoS₂ with Ni₅P₄-Ni₂P Template. Journal of the Electrochemical Society, 2020, 167, 026511.	1.3	8
36509	Syntheses, spectral characterization, single crystal X-ray diffraction and computational in gas and solid phases studies on chloro- acetic acid Nâ€²-(2- hydroxy-naphthalen- 1-ylmethylene)- N-[4-(3-methyl-3-phenyl-cyclobutyl)-thiazol-2-yl]-hydrazide. SN Applied Sciences, 2020, 2, 1.	1.5	1
36510	Altering the reactivity of pristine, N- and P-doped graphene by strain engineering: A DFT view on energy related aspects. Applied Surface Science, 2020, 514, 145937.	3.1	33
36511	Structure and electron affinity of (1 12Â¯0)â€“X 4Hâ€“SiC surface. Applied Surface Science, 2020, 518, 145986.	3.1	2
36512	The adsorption and migration behavior of divalent metals (Mg, Ca, and Zn) on pristine and defective graphene. Carbon, 2020, 163, 276-287.	5.4	36
36513	Electronic structure and related optical, thermoelectric and dynamical properties of Lilianite-type Pb7Bi4Se13: Ab-initio and Boltzmann transport theory. Materialia, 2020, 10, 100658.	1.3	11

#	Article	IF	Citations
36514	Unexpected band gap increase in the Fe2VAl Heusler compound. Materials Today Physics, 2020, 13, 100203.	2.9	20
36515	Double-layer hybrid chainmail catalyst for high-performance hydrogen evolution. Nano Energy, 2020, 72, 104700.	8.2	35
36516	Chemical instability of free-standing boron monolayers and properties of oxidized borophene sheets. Physica E: Low-Dimensional Systems and Nanostructures, 2020, 120, 114082.	1.3	6
36517	How to Avoid the Oxidation of Silicene/Ag(111)? Reaction Mechanisms of O2 with Chlorinated Silicene. Journal of Physical Chemistry C, 2020, 124, 7327-7333.	1.5	1
36518	Quantitative Resolution of Complex Stoichiometric Changes during Electrochemical Cycling by Density Functional Theory-Assisted Electrochemical Quartz Crystal Microbalance. ACS Applied Energy Materials, 2020, 3, 3347-3357.	2.5	14
36519	Active and Stable Ptâ€“Ni Alloy Octahedra Catalyst for Oxygen Reduction via Near-Surface Atomical Engineering. ACS Catalysis, 2020, 10, 4205-4214.	5.5	98
36520	The effect of organic cations on the electronic, optical and luminescence properties of 1D piperidinium, pyridinium, and 3-hydroxypyridinium lead trihalides. Dalton Transactions, 2020, 49, 4390-4403.	1.6	16
36521	Reversible gas capture using a ferroelectric switch and 2D molecule multiferroics on the In₂Se₃ monolayer. Journal of Materials Chemistry A, 2020, 8, 7331-7338.	5.2	59
36522	Hydrogen adsorption on two-dimensional germanene and its structural defects: an ab initio investigation. Physical Chemistry Chemical Physics, 2020, 22, 7210-7217.	1.3	12
36523	Surface adsorption studies of benzyl bromide and bromobenzyl cyanide vapours on black phosphorene nanosheets â€“ a first-principles perception. Molecular Physics, 2020, 118, .	0.8	15
36524	Vanadium doped polyoxometalate: induced active sites and increased hydrogen adsorption. Journal of Physics Condensed Matter, 2020, 32, 195001.	0.7	4
36525	Generation of low-symmetry perovskite structures for ab initio computation. Journal of Physics Condensed Matter, 2020, 32, 315901.	0.7	8
36526	High-performance monolayer MoS₂ photodetector enabled by oxide stress liner using scalable chemical vapor growth method. Nanophotonics, 2020, 9, 1981-1991.	2.9	21
36527	Defects and Dopants in CaFeSi2O6: Classical and DFT Simulations. Energies, 2020, 13, 1285.	1.6	11
36528	The Electronic Structure of Ga-Doped Hydrogen-Passivated Germanene: First Principle Study. Key Engineering Materials, 2020, 833, 157-161.	0.4	2
36529	Enhanced photoresponse of highly air-stable palladium diselenide by thickness engineering. Nanophotonics, 2020, 9, 2467-2474.	2.9	10
36530	Modifying the Surface Structure of Perovskite-Based Catalysts by Nanoparticle Exsolution. Catalysts, 2020, 10, 268.	1.6	32
36531	First Principles Investigation on Thermodynamic Properties and Stacking Fault Energy of Paramagnetic Nickel at High Temperatures. Metals, 2020, 10, 319.	1.0	6

#	Article	IF	Citations
36532	Thermoelectric Properties of NiCl3 Monolayer: A First-Principles-Based Transport Study. Nanomaterials, 2020, 10, 411.	1.9	7
36533	A First-Principles Study of Nonlinear Elastic Behavior and Anisotropic Electronic Properties of Two-Dimensional HfS2. Nanomaterials, 2020, 10, 446.	1.9	25
36534	Study on thermoelectric properties of CrI3 monolayer. Applied Physics Express, 2020, 13, 045001.	1.1	10
36535	First-principles studies of chalcopyrite-type (Cu, Li)GaS2 and (Cu, Li)InS2 systems. Japanese Journal of Applied Physics, 2020, 59, SCCB18.	0.8	0
36536	DFT and microkinetic comparison of Pt, Pd and Rh-catalyzed ammonia oxidation. Journal of Catalysis, 2020, 383, 322-330.	3.1	33
36537	Nonwetting Behavior of Alâ€“Co Quasicrystalline Approximants Owing to Their Unique Electronic Structures. ACS Applied Materials & Interfaces, 2020, 12, 15793-15801.	4.0	11
36538	Pt₅Se₄ Monolayer: A Highly Efficient Electrocatalyst toward Hydrogen and Oxygen Electrode Reactions. ACS Applied Materials & Interfaces, 2020, 12, 13896-13903.	4.0	26
36539	Anionic Redox Processes in Maricite- and Triphylite-NaFePO₄ of Sodium-Ion Batteries. ACS Omega, 2020, 5, 5192-5201.	1.6	16
36540	A tetranuclear cobalt(<scp>ii</scp>) phosphate possessing a D4R core: an efficient water oxidation catalyst. Dalton Transactions, 2020, 49, 4878-4886.	1.6	8
36541	A multifunctional separator based on scandium oxide nanocrystal decorated carbon nanotubes for high performance lithiumâ€“sulfur batteries. Nanoscale, 2020, 12, 6832-6843.	2.8	34
36542	Exploring the properties of Ag₅â€“TiO₂ interfaces: stable surface polaron formation, UV-Vis optical response, and CO₂ photoactivation. Journal of Materials Chemistry A, 2020, 8, 6842-6853.	5.2	26
36543	Optoelectronic Properties of MoS2/g-ZnO van der Waals Heterostructure Investigated by First-Principles Calculations. Journal of Electronic Materials, 2020, 49, 4557-4562.	1.0	8
36544	Implications of the fractional charge of hydroxide at the electrochemical interface. Physical Chemistry Chemical Physics, 2020, 22, 6964-6969.	1.3	6
36545	Efficient machine-learning based interatomic potentialsfor exploring thermal conductivity in two-dimensional materials. JPhys Materials, 2020, 3, 02LT02.	1.8	32
36546	Twoâ€Photon Absorption in Monolayer MXenes. Advanced Optical Materials, 2020, 8, 1902021.	3.6	50
36547	Metalâ€free Catalyst B 2 S Sheet for Effective CO 2 Electrochemical Reduction to CH 3 OH. ChemPhysChem, 2020, 21, 779-784.	1.0	6
36548	Syntheses, Crystal Structures, and Vibrational Properties of Two Lead Azide Halides PbN 3 X (X = Cl,) Tj ETQq0 0 0 rgBT /Overlock 10 Tf	0.6	3
36549	Excess enthalpy of mixing of mineral solid solutions derived from density-functional calculations. Physics and Chemistry of Minerals, 2020, 47, 15.	0.3	3

#	Article	IF	Citations
36550	Halomethane Adsorption Studies on Silicane Sheets: A First-Principles Perception. Journal of Inorganic and Organometallic Polymers and Materials, 2020, 30, 3263-3275.	1.9	16
36551	Theoretical study about alkali metal adsorption on pristine and defective (8,0) SWCNT: Geometrical, magnetic and electronic changes. Applied Surface Science, 2020, 513, 145769.	3.1	8
36552	First-principles investigation of interfacial stability, mechanical behavior and failure mechanism of Î²-SiC(1Â1Â1)/Al(1Â1Â1) interfaces. Computational Materials Science, 2020, 175, 109608.	1.4	17
36553	Structural, electronic and magnetic properties of Fe20Cr6Mn6 austenitic alloys with interstitial carbon and nitrogen atoms from density functional theory. Journal of Magnetism and Magnetic Materials, 2020, 504, 166663.	1.0	3
36554	Strain and electric field tuned electronic properties of BAs/MoSe2 van der Waals heterostructures for alternative electrodes and photovoltaic cell in photocatalysis. Physica E: Low-Dimensional Systems and Nanostructures, 2020, 120, 114055.	1.3	12
36555	Adsorption of gas molecules on group III atoms adsorbed g-C3N4: A first-principles study. Vacuum, 2020, 175, 109293.	1.6	43
36556	Rational Design of the Nonlinear Optical Response in a Tin Iodate Fluoride Sn(IO₃)₂F₂. Chemistry of Materials, 2020, 32, 2615-2620.	3.2	71
36557	Molecular Construction from AgGaS₂ to CuZnPS₄: Defect-Induced Second Harmonic Generation Enhancement and Cosubstitution-Driven Band Gap Enlargement. Chemistry of Materials, 2020, 32, 3288-3296.	3.2	63
36558	Surface Strain-Induced Collective Switching of Ensembles of Molecules on Metal Surfaces. Journal of Physical Chemistry Letters, 2020, 11, 2277-2283.	2.1	4
36559	How Size Matters: Electronic, Cooperative, and Geometric Effect in Perovskite-Supported Copper Catalysts for CO₂ Reduction. ACS Catalysis, 2020, 10, 4092-4102.	5.5	46
36560	Reaction Mechanism of Vapor-Phase Formic Acid Decomposition over Platinum Catalysts: DFT, Reaction Kinetics Experiments, and Microkinetic Modeling. ACS Catalysis, 2020, 10, 4112-4126.	5.5	51
36561	Nanoscale lightâ€“matter interactions in metalâ€“organic frameworks cladding optical fibers. Nanoscale, 2020, 12, 9991-10000.	2.8	25
36562	Surface reduction properties of ceriaâ€“zirconia solid solutions: a first-principles study. RSC Advances, 2020, 10, 4664-4671.	1.7	9
36563	Understanding the structural diversity of freestanding Al₂O₃ ultrathin films through a DFTB-aided genetic algorithm. Nanoscale, 2020, 12, 6153-6163.	2.8	10
36564	Tunable photoelectronic properties of hydrogenated-silicene/halogenated-silicene superlattices for water splitting. Journal of Applied Physics, 2020, 127, .	1.1	18
36565	Heteroatom doping effects on interaction of H2O and CeO2 (111) surfaces studied using density functional theory: Key roles of ionic radius and dispersion. Journal of Chemical Physics, 2020, 152, 014707.	1.2	13
36566	Plasmaâ€Assisted Catalytic Effects of TiO₂/Macroporous SiO₂ on the Synthesis of Light Hydrocarbons from Methane. ChemCatChem, 2020, 12, 5067-5075.	1.8	5
36567	CO2 thermoreduction to methanol on the MoS2 supported single Co atom catalyst: A DFT study. Applied Surface Science, 2020, 528, 147047.	3.1	46

#	Article	IF	Citations
36568	Alloying-element dependence of structural, elastic and electronic properties of nickel-based superalloys: Influence of Î³â€™ volume fraction. Journal of Alloys and Compounds, 2020, 838, 155141.	2.8	14
36569	Efficient capturing and oxidation of CO through bimetallic surface alloying on WC (0001). Journal of Alloys and Compounds, 2020, 844, 156125.	2.8	2
36570	Effects of N2-content on formation behavior in AlN thin films studied by NEXAFS: Theory and experiment. Journal of Alloys and Compounds, 2020, 844, 156128.	2.8	7
36571	A computational study of nanodiamond surface radicals and nitrogen-vacancy charge fluctuations. Journal of Physics and Chemistry of Solids, 2020, 146, 109637.	1.9	5
36572	Ab initio investigation of Î±- and Î¶-V2O5 for beyond lithium ion battery cathodes. Journal of Power Sources, 2020, 472, 228096.	4.0	17
36573	Anisotropic charge transport and optoelectronic properties of wide band gap organic semiconductors based on biphenyl derivatives: A computational study. Synthetic Metals, 2020, 267, 116474.	2.1	5
36574	A(H₃C₃N₃O₃)(NO₃) (A = K, Rb): Alkali-Metal Nitrate Isocyanurates with Strong Optical Anisotropy. Inorganic Chemistry, 2020, 59, 10361-10367.	1.9	30
36575	Semiconductor-to-conductor transition in 2D copper(<scp>ii</scp>) oxide nanosheets through surface sulfur-functionalization. Nanoscale, 2020, 12, 14549-14559.	2.8	6
36576	Electronic structure and thermoelectric properties of HfRhZ(Z = As, Sb and Bi) half-Heusler compounds. Applied Physics A: Materials Science and Processing, 2020, 126, 1.	1.1	9
36577	Effects of oxygen defects on electronic band structures and dopant migration in Sn-doped TiO2 by density functional studies. Chemical Physics Letters, 2020, 754, 137732.	1.2	11
36578	Tuning the magnetic and electronic properties of monolayer chromium tritelluride through strain engineering. Physics Letters, Section A: General, Atomic and Solid State Physics, 2020, 384, 126684.	0.9	10
36579	â€œStickierâ€•Surface Sb₂Te₃ Templates Enable Fast Memory Switching of Phase Change Material GeSb₂Te₄ with Growth-Dominated Crystallization. ACS Applied Materials & Interfaces, 2020, 12, 33397-33407.	4.0	53
36580	Molecular-level insights on the reactive facet of carbon nitride single crystals photocatalysing overall water splitting. Nature Catalysis, 2020, 3, 649-655.	16.1	427
36581	Two-dimensional IVâ€“VI materials with in-plane negative Poisson's ratio and anisotropic carrier mobility. Journal of Materials Chemistry C, 2020, 8, 10382-10389.	2.7	28
36582	Blocking of the martensitic transition at the nanoscale in a <mml:math xmlns:mml="http://www.w3.org/1998/Math/MathML"><mml:msub><mml:mrow><mml:mi>Ti</mml:mi></mml:mrow><mml:mn>2</mml:mn></mml:msub></mml:math> wedge. Physical Review B, 2020, 101, .	1.1	9
36583	Facetâ€dependent Chlorine and Oxygen Evolution Selectivity on RuO₂: An Ab initio Atomistic Thermodynamic Study. ChemCatChem, 2020, 12, 4922-4929.	1.8	19
36584	Prediction of the structural, electronic, and piezoelectric properties of narrow-bandgap compounds FeVX (Xâ€‰=â€‰P, As, Sb). Journal of Computational Electronics, 2020, 19, 1365-1372.	1.3	6
36585	Oxygen vacancyâ€“engineered Î´-MnO /activated carbon for room-temperature catalytic oxidation of formaldehyde. Applied Catalysis B: Environmental, 2020, 278, 119294.	10.8	87

#	Article	IF	Citations
36586	Evaluation of stabilities and thermophysical properties of Si-Sr intermetallics based on first-principles analysis. Results in Physics, 2020, 18, 103207.	2.0	2
36587	Femtosecond Nonlinear Optical Properties of 2D Metallic NbS₂ in the Near Infrared. Journal of Physical Chemistry C, 2020, 124, 15425-15433.	1.5	27
36588	Predicting the Effect of Dopants on CO₂ Adsorption in Transition Metal Carbides: Case Study on TiC (001). Journal of Physical Chemistry C, 2020, 124, 15969-15976.	1.5	10
36589	Hydrogen adsorption on In₂O₃(111) and In₂O₃(110). Physical Chemistry Chemical Physics, 2020, 22, 16193-16202.	1.3	21
36590	A first-principles study on the magnetoelectric coupling induced by Fe in a two-dimensional BaTiO₃(001) ultrathin film. Physical Chemistry Chemical Physics, 2020, 22, 18284-18293.	1.3	3
36591	Prediction of room-temperature ferromagnetism in a two-dimensional direct band gap semiconductor. Nanoscale, 2020, 12, 15670-15676.	2.8	38
36592	Enhanced carrier separation in ferroelectric In₂Se₃/MoS₂ van der Waals heterostructure. Journal of Materials Chemistry C, 2020, 8, 11160-11167.	2.7	44
36593	Hydrogen desorption from the surface and subsurface of cobalt. Physical Chemistry Chemical Physics, 2020, 22, 15281-15287.	1.3	7
36594	Computational modeling of piezochromism in molecular crystals. Journal of Chemical Physics, 2020, 152, 234106.	1.2	4
36595	Ultrafast Electron Correlations and Memory Effects at Work: Femtosecond Demagnetization in Ni. Physical Review Letters, 2020, 125, 017202.	2.9	35
36596	First-Principle Investigation of the (001) Surface Reconstructions of GaSb and InSb Semiconductors. Semiconductors, 2020, 54, 742-753.	0.2	2
36597	An adaptive design approach for defects distribution modeling in materials from first-principle calculations. Journal of Molecular Modeling, 2020, 26, 187.	0.8	11
36598	Effect of Tin in the Bulk of Platinumâ€“Tin Alloys for Ethane Dehydrogenation. Topics in Catalysis, 2020, 63, 700-713.	1.3	13
36599	High-pressure synthesis, crystal structure and physical properties of a new Cr-based arsenide La3CrAs5. Science China Materials, 2020, 63, 1750-1758.	3.5	7
36600	Triazine- and Keto-Functionalized Porous Covalent Organic Framework as a Promising Anode Material for Na-Ion Batteries: A First-Principles Study. Journal of Physical Chemistry C, 2020, 124, 15870-15878.	1.5	22
36601	Optical, Electronic, and Contact Properties of Janus-MoSO/MoS₂ Heterojunction. Journal of Physical Chemistry C, 2020, 124, 15988-15994.	1.5	8
36602	Local Distortions and Dynamics in Hydrated Y-Doped BaZrO₃. Journal of Physical Chemistry C, 2020, 124, 16689-16701.	1.5	12
36603	Reducing the charge overpotential of Liâ€“O₂ batteries through band-alignment cathode design. Energy and Environmental Science, 2020, 13, 2540-2548.	15.6	30

#	Article	IF	Citations
36604	Transport properties of hybrid biphenyl molecular junctions with zigzag graphene nanoribbon electrodes. AIP Conference Proceedings, 2020, , .	0.3	1
36605	Effects of gas adsorption on monolayer Si₂BN and implications for sensing applications. Journal of Physics Condensed Matter, 2020, 32, 355602.	0.7	8
36606	Distinguishing strain, charge and molecular orbital induced effects on the electronic structure: graphene/ammonia system. Journal of Physics Condensed Matter, 2020, 32, 455501.	0.7	1
36607	Vacancy trapping meachanism of multiple hydrogen/helium atoms in fcc-Fe: A first-principles study. IOP Conference Series: Earth and Environmental Science, 2020, 461, 012007.	0.2	1
36608	Indium doped phosphorene as a potential gas sensor: a study using density functional theory. Electronic Structure, 2020, 2, 035001.	1.0	3
36609	Unconventional spin-orbit torque in transition metal dichalcogenideâ€“ferromagnet bilayers from first-principles calculations. Physical Review B, 2020, 102, .	1.1	29
36610	Study on Heat Transfer Performance and Anti-Fouling Mechanism of Ternary Ni-W-P Coating. Applied Sciences (Switzerland), 2020, 10, 3905.	1.3	9
36611	First-Principles Study of the Stabilization and Mechanical Properties of Rare-Earth Ferritic Perovskites (RFeO3, R = La, Eu, Gd). Applied Sciences (Switzerland), 2020, 10, 4008.	1.3	4
36612	Mechanical Properties of DO3 Based on First Principles. Crystals, 2020, 10, 488.	1.0	5
36613	Electronic, mechanical and vibrational properties of a tubular tetragonal carbon. Chemical Physics Letters, 2020, 751, 137565.	1.2	0
36614	A DFT study of defects in SnO monolayer and their interaction with O2 molecule. Chemical Physics Letters, 2020, 754, 137717.	1.2	13
36615	Thermal transport across nanometre gaps: Phonon transmission vs. air conduction. International Journal of Heat and Mass Transfer, 2020, 158, 119963.	2.5	17
36616	Remarkably Stable Nickel Hydroxide Nanoparticles for Miniaturized Electrochemical Energy Storage. ACS Applied Energy Materials, 2020, 3, 7294-7305.	2.5	13
36617	Synaptic Characteristics of Amorphous Boron Nitride-Based Memristors on a Highly Doped Silicon Substrate for Neuromorphic Engineering. ACS Applied Materials & Interfaces, 2020, 12, 33908-33916.	4.0	52
36618	High-loaded single Cu atoms decorated on N-doped graphene for boosting Fenton-like catalysis under neutral pH. Journal of Materials Chemistry A, 2020, 8, 13685-13693.	5.2	104
36619	Dye-based covalent organic networks. JPhys Materials, 2020, 3, 025011.	1.8	3
36620	Scale-free ferroelectricity induced by flat phonon bands in HfO ₂. Science, 2020, 369, 1343-1347.	6.0	231
36621	First-Principles Study of the New Half-Metallic Ferromagnetic Quaternary-Heusler Alloys NaXNO (X=Ca, Sr, Ba). Spin, 2020, 10, .	0.6	7

#	Article	IF	Citations
36622	Role of Exchange-Correlation Functional in Bulk Bismuth. Materials Science Forum, 2020, 978, 446-453.	0.3	0
36623	First-Principles Study of the Adsorption of Carboxylic Acid on Cu(111). Materials Science Forum, 0, 985, 48-53.	0.3	0
36624	A comparative investigation of penta-graphene and Pt single atom@penta-graphene in H2 and O2 detection: DFT study with assessment of the van der Waals density functionals. Applied Surface Science, 2020, 528, 147043.	3.1	10
36625	Phase equilibria and thermodynamic assessment of the Moâ€“Nb-Re ternary system. Calphad: Computer Coupling of Phase Diagrams and Thermochemistry, 2020, 70, 101797.	0.7	4
36626	Effects of C/Si ratios on structures and behaviors of NbSiCN nanocomposite films synthesized by reactive magnetron sputtering. Materials Characterization, 2020, 167, 110466.	1.9	3
36627	Studies on magnetic and electronic properties of <mml:math xmlns:mml="http://www.w3.org/1998/Math/MathML" altimg="si1.svg"><mml:mi>Î´</mml:mi></mml:math>-Pu<mml:math xmlns:mml="http://www.w3.org/1998/Math/MathML" altimg="si2.svg"><mml:msub><mml:mi>X</mml:mi><mml:mn>3</mml:mn></mml:msub></mml:math>		

#	Article	IF	Citations
36640	Anisotropic in elasticity, sound velocity and minimum thermal conductivity of Alâ€“Cu intermetallic compounds. Intermetallics, 2020, 124, 106880.	1.8	24
36641	Emergence of ferrromagnetism in vanadium doped aluminium phosphide using density functional theory. Materials Today: Proceedings, 2020, 28, 1820-1824.	0.9	2
36642	Hybrid bromobismuthates: Synthesis, thermal stability and crystal structure of multicharged 3-ammoniopyridinium derivatives. Journal of Molecular Structure, 2020, 1221, 128807.	1.8	1
36643	Probing the interactions between interstitial hydrogen atoms in niobium through density functional theory calculations. Materials Today Communications, 2020, 25, 101415.	0.9	3
36644	Atomic-scale observation of the deformation and failure of diamonds by in-situ double-tilt mechanical testing transmission electron microscope holder. Science China Materials, 2020, 63, 2335-2343.	3.5	8
36645	Phenomenon of ultra-fast tracer diffusion of Co in HCP high entropy alloys. Acta Materialia, 2020, 196, 220-230.	3.8	27
36646	On the potential for superconductivity in ZrX (XÂ=ÂS and Te): a first-principles study. Physica C: Superconductivity and Its Applications, 2020, 577, 1353714.	0.6	12
36647	Localized High Concentration Electrolytes for High Voltage Lithiumâ€“Metal Batteries: Correlation between the Electrolyte Composition and Its Reductive/Oxidative Stability. Chemistry of Materials, 2020, 32, 5973-5984.	3.2	97
36648	Fundamental difference in the electronic reconstruction of infinite-layer versus perovskite neodymium nickelate films on <mml:math xmlns:mml="http://www.w3.org/1998/Math/MathML"><mml:msub><mml:mi>SrTiO</mml:mi><mml:mn>3</mml:mn></mml:msub></m (001). Physical Review B, 2020, 102, .	1.1	47
36649	Monitoring Hydrogen Evolution Reaction Intermediates of Transition Metal Dichalcogenides via Operando Raman Spectroscopy. Advanced Functional Materials, 2020, 30, 2003035.	7.8	64
36650	Electrochemical Performance of Bâ€Type Vanadium Dioxide as a Sodiumâ€Ion Battery Cathode: A Combined Experimental and Theoretical Study. ChemElectroChem, 2020, 7, 3151-3159.	1.7	4
36651	Investigation on electronic and mechanical properties of penta-graphene nanotubes. Journal of Materials Science, 2020, 55, 14336-14344.	1.7	8
36652	Mechanisms for As(OH)3 and H3AsO4 adsorption at anhydrous and hydrated surfaces of gibbsite and possibility for anionic As(III) and As(V) formation. Applied Surface Science, 2020, 525, 146494.	3.1	11
36653	Filamentary and interface switching of CMOS-compatible Ta2O5 memristor for non-volatile memory and synaptic devices. Applied Surface Science, 2020, 529, 147167.	3.1	44
36654	First-principles calculations of mechanical, electronic and optical properties of a new imidooxonitridophosphate. Chemical Physics, 2020, 538, 110917.	0.9	9
36655	Ordering and Structural Transformations in Layered K_xCrO₂ for K-Ion Batteries. Chemistry of Materials, 2020, 32, 6392-6400.	3.2	13
36656	Following the unusual breathing behaviour of¹⁷O-enriched mixed-metal (Al,Ga)-MIL-53 using NMR crystallography. Physical Chemistry Chemical Physics, 2020, 22, 14514-14526.	1.3	16
36657	An in-depth study of Sn substitution in Li-rich/Mn-rich NMC as a cathode material for Li-ion batteries. Dalton Transactions, 2020, 49, 10486-10497.	1.6	11

#	Article	IF	Citations
36658	Role of defects and dopants in zinc oxide nanotubes for gas sensing and energy storage applications. International Journal of Energy Research, 2020, 44, 10926-10936.	2.2	11
36659	Superconductivity of KFe2As2 Under Pressure: Ab Initio Study of Tetragonal and Collapsed Tetragonal Phases. Journal of Superconductivity and Novel Magnetism, 2020, 33, 2347-2354.	0.8	3
36660	Surface energetics of <mml:math xmlns:mml="http://www.w3.org/1998/Math/MathML" altimg="si35.svg"><mml:mrow><mml:msub><mml:mrow><mml:mi mathvariant="normal">Al</mml:mi></mml:mrow><mml:mrow><mml:mi>x</mml:mi></mml:mrow></mml:msub><mml:msub><mml:mrow><mml:mi mathvariant="normal">Ti</mml:mi></mml:mrow><mml:mrow><mml:mn>1</mml:mn><mml:mo>-</mml:mo><mml:mi>x</mml:mi></mml:mrow></mml:msub><mml:mi mathvariant="normal">N</mml:mi></mml:mrow></mml:math> alloys. Computational Materials Science, 2020, 183, 109813.	1.4	11
36661	Study of cation vacancies with localized hole states in MgAl2O4 crystals. Journal of Physics and Chemistry of Solids, 2020, 145, 109542.	1.9	12
36662	Computational study of protactinium incorporation effects in Th and Th compounds. Nuclear Engineering and Technology, 2020, 52, 2285-2289.	1.1	3
36663	Improving the magnetic, electronic and optical properties of the monolayer WSe2 via Mn-X (XÂ=ÂO, S, Se) Tj ETQq1 1 0.784314 rgBT /O	0.8	5
36664	On Hydrogenated Bilayer GaN: New Stable Structures along the c-Plane, m-Plane, or a-Plane. Journal of Physical Chemistry C, 2020, 124, 16888-16894.	1.5	4
36665	Promoting Z-to-E Thermal Isomerization of Azobenzene Derivatives by Noncovalent Interaction with Phosphorene: Theoretical Prediction and Experimental Study. Journal of Physical Chemistry C, 2020, 124, 15961-15968.	1.5	3
36666	An Ab Initio Perspective on the Key Defects of CsCu₅Se₃, a Possible Material for Optoelectronic Applications. Journal of Physical Chemistry C, 2020, 124, 4363-4368.	1.5	7
36667	Investigation of the effect of doped Zn atom to the hydroxyapatite based on experimental method and first-principles calculations. Journal of the Australian Ceramic Society, 2020, 56, 1413-1419.	1.1	1
36668	First-principles investigation of mechanical, electronic and optical properties of H-, F- and Cl-diamane. Applied Surface Science, 2020, 528, 147035.	3.1	47
36669	Facile renewable synthesis of nitrogen/oxygen co-doped graphene-like carbon nanocages as general lithium-ion and potassium-ion batteries anode. Carbon, 2020, 167, 685-695.	5.4	69
36670	Structural and electronic properties of defective AlN/GaN hybrid nanostructures. Computational Materials Science, 2020, 183, 109860.	1.4	4
36671	Understanding Reaction Pathways in High Dielectric Electrolytes Using Î²-Mo₂C as a Catalyst for Liâ€“CO₂ Batteries. ACS Applied Materials & Interfaces, 2020, 12, 32633-32641.	4.0	22
36672	Kinetics mechanism insights into the oxygen evolution reaction on the (110) and (022) crystal facets of Î²-Cu₂V₂O₇. Catalysis Science and Technology, 2020, 10, 5129-5135.	2.1	4
36673	2D monolayer boron sulfide as an efficient material for optical nanodevices. AIP Conference Proceedings, 2020, , .	0.3	2
36674	Ab initio molecular dynamics simulation of threshold displacement energies and defect formation energies in Y4Zr3O12. Journal of Applied Physics, 2020, 127, .	1.1	10
36675	Tuning structural and electronic properties of two dimensional Si and Ge based random alloys: an ab initio study. European Physical Journal B, 2020, 93, 1.	0.6	1

#	Article	IF	Citations
36676	Physisorption and Chemisorption of SF6 by Transition Metal-Porphyrin Structure Embedded on Graphene Surface with Different Hapticities. Journal of the Korean Physical Society, 2020, 76, 1001-1004.	0.3	1
36677	Large thermoelectric figure of merit in hexagonal phase of <scp>2D</scp> selenium and tellurium. International Journal of Quantum Chemistry, 2020, 120, e26267.	1.0	19
36678	Metalâ€Halide Perovskite Design for Nextâ€Generation Memories: Firstâ€Principles Screening and Experimental Verification. Advanced Science, 2020, 7, 2001367.	5.6	17
36679	Iron, Copper and Nitrogen Coâ€doped Carbon with Enhanced Electrocatalytic Activity towards Oxygen Reduction. ChemElectroChem, 2020, 7, 3116-3122.	1.7	3
36680	Firstâ€Principles Study of Chromium Defects in Î±â€Al₂O₃: The Origin of Red Color in Ruby. Physica Status Solidi (B): Basic Research, 2020, 257, 2000159.	0.7	4
36681	How Cobalt and Iron Doping Determine the Oxygen Evolution Electrocatalytic Activity of NiOOH. Cell Reports Physical Science, 2020, 1, 100077.	2.8	35
36682	Pressure-Induced Superconductivity in the Wide-Band-Gap Semiconductor Cu2Br2Se6 with a Robust Framework. Chemistry of Materials, 2020, 32, 6237-6246.	3.2	6
36683	Structural and Lattice-Dynamical Properties of Tb₂O₃ under Compression: A Comparative Study with Rare Earth and Related Sesquioxides. Inorganic Chemistry, 2020, 59, 9648-9666.	1.9	26
36684	Electronic and optical properties of a structural defect in 2D MgF2 monolayer. AIP Conference Proceedings, 2020, , .	0.3	4
36685	Structural, defect, transport and dopant properties of AgNbO 3. ChemNanoMat, 2020, 6, 1337-1345.	1.5	7
36686	Cu Atomic Chain Supported on Graphene Nanoribbon for Effective Conversion of CO 2 to Ethanol. ChemPhysChem, 2020, 21, 1768-1774.	1.0	9
36687	Insights on boosting oxygen evolution reaction performance via boron incorporation into nitrogen-doped carbon electrocatalysts. Applied Surface Science, 2020, 528, 146979.	3.1	18
36688	Experimental and theoretical study on the effect of different rare-earth oxides on the high-temperature stability of SiO2 glass at 1973K. Ceramics International, 2020, 46, 24371-24378.	2.3	19
36689	Enhanced nucleation and precipitation hardening in Alâ€“Mgâ€“Si(â€“Cu) alloys with minor Cd additions. Materials Science & Engineering A: Structural Materials: Properties, Microstructure and Processing, 2020, 792, 139698.	2.6	18
36690	Ultrasonically controlled growth of monodispersed octahedral BiVO4 microcrystals for improved photoelectrochemical water oxidation. Ultrasonics Sonochemistry, 2020, 68, 105233.	3.8	18
36691	A Density Functional Theory Study of the Hydrogen Absorption in High Entropy Alloy TiZrHfMoNb. Inorganic Chemistry, 2020, 59, 9774-9782.	1.9	31
36692	Calculating and Characterizing the Charge Distributions in Solids. Journal of Chemical Theory and Computation, 2020, 16, 5884-5892.	2.3	29
36693	Predicting Crystal Morphology Using a Geometric Descriptor: A Comparative Study of Elemental Crystals with High-Throughput DFT Calculations. Journal of Physical Chemistry C, 2020, 124, 15920-15927.	1.5	6

#	Article	IF	Citations
36694	Multicomponent gas separation and purification using advanced 2D carbonaceous nanomaterials. RSC Advances, 2020, 10, 24255-24264.	1.7	16
36695	On the structural stability and optical properties of germanium-based schwarzites: a density functional theory investigation. Physical Chemistry Chemical Physics, 2020, 22, 16286-16293.	1.3	1
36696	Exploring the role of vacancy defects in the optical properties of LiMgPO₄. Physical Chemistry Chemical Physics, 2020, 22, 16244-16257.	1.3	41
36697	First-principles study of the electronic properties of Pd1â^'x Ni x Te alloys. Materials Research Express, 2020, 7, 056516.	0.8	1
36698	Band-Structure Engineering of <mml:math xmlns:mml="http://www.w3.org/1998/Math/MathML" display="inline" overflow="scroll"><mml:msub><mml:mi>Zn</mml:mi><mml:mi>x</mml:mi></mml:msub><mml:msub><mml:mi>Cd</mml:mi><mml:mi><mml:mrow><mml:mi mathvariant="normal">S</mml:mi></mml:mrow><mml:mrow><mml:mi>y</mml:mi></mml:msub><mml:msub><mml:mi>Se</mml:mi>. Physical Review Applied, 2020, 13, .	4.6	31
36699	Discovery of a Quaternary Sulfide, Ba_{2â€“x}LiAlS₄:Eu²⁺, and Its Potential as a Fast-Decaying LED Phosphor. Chemistry of Materials, 2020, 32, 6697-6705.	3.2	27
36700	New refractory MAB phases and their 2D derivatives: insight into the effects of valence electron concentration and chemical composition. RSC Advances, 2020, 10, 25836-25847.	1.7	9
36701	Quasi-one-dimensional Sb2(S,Se)3 alloys as bandgap-tunable and defect-tolerant photocatalytic semiconductors. Journal of Chemical Physics, 2020, 153, 014703.	1.2	32
36702	Toggling Valley-Spin Locking and Nonlinear Optical Properties of Single-Element Multiferroic Monolayers via Light. Physical Review Applied, 2020, 14, .	1.5	17
36703	Intrinsic anomalous valley Hall effect in single-layer <mml:math xmlns:mml="http://www.w3.org/1998/Math/MathML"><mml:mrow><mml:mi mathvariant="normal">N</mml:mi><mml:msub><mml:mi mathvariant="normal">b</mml:mi><mml:mn>3</mml:mn></mml:msub><mml:msub><mml:mi mathvariant="normal">I</mml:mi><mml:mn>8</mml:mn></mml:msub></mml:mrow></mml:math>. Physical Review B, 2020, 102, .	1.1	108
36704	Defect behavior and radiation tolerance of MAB phases (MoAlB and Fe2AlB2) with comparison to MAX phases. Acta Materialia, 2020, 196, 505-515.	3.8	40
36705	First-principles study of the surface properties of uranium carbides. Journal of Nuclear Materials, 2020, 542, 152257.	1.3	8
36706	Site preference and atomic ordering in the structure of In3Pd5: AÂtheoretical study. Journal of Solid State Chemistry, 2020, 290, 121567.	1.4	2
36707	Tailoring single walled carbon nanotube for improved CO2 gas applications: Insights from ab initio simulations. Materialia, 2020, 11, 100694.	1.3	3
36708	Microstructure and mechanical properties of Cr doped WCoB based cermets by spark plasma sintering and first principle calculation. Progress in Natural Science: Materials International, 2020, 30, 417-423.	1.8	8
36709	Adsorption and diffusion of Au, Pt, and Co adatoms on SrTiO3(001) surfaces: A density functional theory study. Surface Science, 2020, 701, 121683.	0.8	9
36710	High Coordinate Metal Iodate Chlorides with Diverse Structural Motifs and Tunable Birefringence. Crystal Growth and Design, 2020, 20, 5473-5483.	1.4	8
36711	Local Structure Distortion Induced Broad Band Emission in the All-Inorganic BaScO₂F:Eu²⁺ Perovskite. Chemistry of Materials, 2020, 32, 6640-6649.	3.2	39

#	Article	IF	Citations
36712	Moltenâ€Saltâ€Assisted Chemical Vapor Deposition Process for Substitutional Doping of Monolayer MoS 2 and Effectively Altering the Electronic Structure and Phononic Properties. Advanced Science, 2020, 7, 2001080.	5.6	32
36713	Investigating greenhouse gas adsorption in MOFs SIFSIX-2-Cu, SIFSIX-2-Cu-i, and SIFSIX-3-Cu through computational studies. Journal of Molecular Modeling, 2020, 26, 188.	0.8	7
36714	Theoretical Study of Thermoelectric Properties of Covalent Organic Frameworks with Slipped Arrangement. Journal of Electronic Materials, 2020, 49, 5498-5507.	1.0	1
36715	Selective dissociation of benzoic acid on carbonate surfaces: A density functional theory perspective. Applied Surface Science, 2020, 529, 147103.	3.1	5
36716	Theoretical study on novel orthorhombic ternary monocarbides M0.5Re0.5C (M=V, Nb, Ta) from first-principles calculations. Ceramics International, 2020, 46, 24624-24634.	2.3	10
36717	First-principles study on strain-controllable magnetoelectric coupling behaviour of two-dimensional BaTiO3 (001) ultrathin film with surface Ba vacancy. Ceramics International, 2020, 46, 24682-24688.	2.3	2
36718	Electronic and optical properties of polar intermetallic compound BaSn3: First principles study. Optik, 2020, 219, 165028.	1.4	3
36719	Effects of charged interfaces on electrolyte decomposition at the lithium metal anode. Journal of Power Sources, 2020, 472, 228449.	4.0	41
36720	Hollow Mn3O4 nanospheres on graphene matrix for oxygen reduction reaction and supercapacitance applications: Experimental and theoretical insight. Journal of Power Sources, 2020, 471, 228465.	4.0	37
36721	Metal-free ferromagnetic semiconductor: Mechanical, electronic and magnetic properties of boron doped graphitic carbon nitride (<mml:math xmlns:mml="http://www.w3.org/1998/Math/MathML") Tj ETQq1 1 0.784314 rgBT /Overlo	2.0	16
36722	Dipotassium terephthalate as promising potassium storing anode with DFT calculations. Materials Today Energy, 2020, 17, 100454.	2.5	12
36723	Properties of RhP predicted by first-principles. Physics Letters, Section A: General, Atomic and Solid State Physics, 2020, 384, 126426.	0.9	0
36724	Orthorhombic carbon oC48: A new superhard carbon allotrope. Solid State Communications, 2020, 319, 113994.	0.9	10
36725	First-principles study of CO and NO adsorption on pristine and transition metal doped blue phosphorene. Vacuum, 2020, 179, 109503.	1.6	28
36726	Tailoring Electronic and Magnetic Properties of Graphene by Phosphorus Doping. ACS Applied Materials & Interfaces, 2020, 12, 34074-34085.	4.0	20
36727	Boosting hydrogen evolution on MoS2 via co-confining selenium in surface and cobalt in inner layer. Nature Communications, 2020, 11, 3315.	5.8	229
36728	Capacity enhancement of polylithiated functionalized boron nitride nanotubes: an efficient hydrogen storage medium. Physical Chemistry Chemical Physics, 2020, 22, 15675-15682.	1.3	18
36729	Oxidative dehydrogenation of propane on the oxygen adsorbed edges of boron nitride nanoribbons. Catalysis Science and Technology, 2020, 10, 5181-5195.	2.1	10

#	Article	IF	Citations
36730	Highly efficient light-driven methane coupling under ambient conditions based on an integrated design of a photocatalytic system. Green Chemistry, 2020, 22, 4669-4675.	4.6	54
36731	New nanosized Gdâ€“Hoâ€“Sm doped M-type strontium hexaferrite for water treatment application: experimental and theoretical investigations. RSC Advances, 2020, 10, 25239-25259.	1.7	44
36732	A first-principles study of damage induced by gaseous species He, Kr, and Xe on the structure of nuclear fuel, U3Si. Journal of Applied Physics, 2020, 127, .	1.1	5
36733	First-principles study of helium behavior in nickel with noble gas incorporation. Journal of Applied Physics, 2020, 127, 175903.	1.1	4
36734	High-pressure silica phase transitions: Implications for deep mantle dynamics and silica crystallization in the protocore. American Mineralogist, 2020, 105, 1014-1020.	0.9	7
36735	2D CoOOH Sheet-Encapsulated Ni2P into Tubular Arrays Realizing 1000ÂmAÂcmâ^'2-Level-Current-Density Hydrogen Evolution Over 100Âh in Neutral Water. Nano-Micro Letters, 2020, 12, 140.	14.4	83
36736	Effects of surface orientations of Cr2O3 on CO2 adsorption: A DFT approach. Applied Surface Science, 2020, 529, 147127.	3.1	27
36737	Study on the adsorption of OHâ^' and CaOH+ on Fe (100) surface and their effect on passivation of steel bar: Experiments and DFT modelling. Corrosion Science, 2020, 174, 108804.	3.0	20
36738	High thermal conductance across c-BN/diamond interface. Diamond and Related Materials, 2020, 108, 107979.	1.8	11
36739	Analysis of damage-tolerance of TRIP-assisted V10Cr10Fe45Co30Ni5 high-entropy alloy at room and cryogenic temperatures. Journal of Alloys and Compounds, 2020, 844, 156090.	2.8	41
36740	Effect of Al doping on the structural and optical properties of CuO nanoparticles prepared by solution combustion method: Experiment and DFT investigation. Journal of Physics and Chemistry of Solids, 2020, 147, 109646.	1.9	39
36741	First principles study of sarin nerve gas adsorption on graphene nanoribbon with single molecule resolution. Materials Today: Proceedings, 2020, 28, 1985-1989.	0.9	3
36742	Inherent Resistance of Seed-Mediated Grown MoSe₂ Monolayers to Defect Formation. ACS Applied Materials & Interfaces, 2020, 12, 34297-34305.	4.0	7
36743	First-principle based thermoelectric properties of Weyl semi-metal SrSi2. AIP Conference Proceedings, 2020, , .	0.3	1
36744	Adsorption and dissociation of H2O monomer on ceria(111): Density functional theory calculations. Modern Physics Letters B, 2020, 34, 2050254.	1.0	1
36745	Osmium Containing Double Perovskite Ba2XOsO6 (XÂ=ÂMg, Zn, Cd): Important Candidates for Half-Metallic Ferromagnetic and Spintronic Applications. , 2020, , .		1
36746	Phase Engineering of Transition Metal Dichalcogenides with Unprecedentedly High Phase Purity, Stability, and Scalability via Moltenâ€Metalâ€Assisted Intercalation. Advanced Materials, 2020, 32, e2001889.	11.1	63
36747	Quantum mechanical modeling of Znâ€based spinel oxides: Assessing the structural, vibrational, and electronic properties. International Journal of Quantum Chemistry, 2020, 120, e26368.	1.0	9

#	Article	IF	Citations
36748	High exothermic dissociation in van der Waals like hexagonal two dimensional nitrogene from firstâ€“principles molecular dynamics. Applied Surface Science, 2020, 529, 146552.	3.1	11
36749	2D anisotropic type-I SiS vdW heterostructures toward infrared polarized optoelectronics applications. Applied Surface Science, 2020, 529, 147026.	3.1	6
36750	Vacancy-driven variations in the phonon density of states of fast neutron irradiated nuclear graphite. Carbon, 2020, 168, 42-54.	5.4	13
36751	Lithium vacancy migration in Li2O2: From first principles studies. Computational Materials Science, 2020, 184, 109873.	1.4	6
36752	Interfacial chemical binding and improved kinetics assisting stable aqueous Znâ€“MnO2 batteries. Materials Today Energy, 2020, 17, 100475.	2.5	53
36753	First-principles investigations of intrinsic point defects and helium impurities in vanadium monocarbide. Nuclear Instruments & Methods in Physics Research B, 2020, 479, 163-170.	0.6	3
36754	A DFT study of the adsorption of noble metal adatoms (Pd, Pt, Ag, Au) on 2D tin disulfide monolayers: Potential towards nanoscale electronic devices. Physica E: Low-Dimensional Systems and Nanostructures, 2020, 120, 114080.	1.3	4
36755	First-principles study on Sb-doped SnS2 as a low cost and non-toxic absorber for intermediate band solar cell. Physics Letters, Section A: General, Atomic and Solid State Physics, 2020, 384, 126695.	0.9	13
36756	DFT+U study of the structural, electronic and optical properties of M1-xPrxF2+x (M= Ca, Ba, x=0.25). Solid State Communications, 2020, 319, 113995.	0.9	0
36757	Electronic and optical characteristics of GaS/g-C3N4 van der Waals heterostructures: Effects of biaxial strain and vertical electric field. Vacuum, 2020, 180, 109562.	1.6	35
36758	Theoretical study of two-dimensional bis(iminothiolato)metal monolayers as promising electrocatalysts for carbon dioxide reduction. New Journal of Chemistry, 2020, 44, 12299-12306.	1.4	11
36759	Two-dimensional aluminum phosphide semiconductor with tunable direct band gap for nanoelectric applications. RSC Advances, 2020, 10, 25170-25176.	1.7	9
36760	Comparative investigation of the thermal transport properties of Janus SnSSe and SnS₂ monolayers. Physical Chemistry Chemical Physics, 2020, 22, 16796-16803.	1.3	19
36761	First-principle investigations of Cl decorated armchair GaN nanoribbons. AIP Conference Proceedings, 2020, , .	0.3	1
36762	First principles prediction of structural, mechanical and thermodynamic stability in new 18-valence electron XVZ (X = Fe, Ni, Z = Ga, As) half-Heusler semiconductors. Semiconductor Science and Technology, 2020, 35, 105005.	1.0	3
36763	Anisotropic PC₆N Monolayer with Wide Band Gap and Ultrahigh Carrier Mobility. Journal of Physical Chemistry C, 2020, 124, 4330-4337.	1.5	14
36764	Large Second Harmonic Generation in Elemental Î±-Sb and Î±-Bi Monolayers. Journal of Physical Chemistry C, 2020, 124, 5506-5513.	1.5	14
36765	Rapid Decoherence Induced by Light Expansion Suppresses Charge Recombination in Mixed Cation Perovskites: Time-Domain ab Initio Analysis. Journal of Physical Chemistry Letters, 2020, 11, 1601-1608.	2.1	19

#	Article	IF	Citations
36766	Phase transition and mechanical properties of cesium bismuth silver halide double perovskites (Cs₂AgBiX₆, X = Cl, Br, I): a DFT approach. Physical Chemistry Chemical Physics, 2020, 22, 5959-5968.	1.3	30
36767	Structural stability, electronic and thermoelectric properties of ruthenium silicide. Journal of Alloys and Compounds, 2020, 826, 154164.	2.8	4
36768	Bimetallic Pd-Based surface alloys promote electrochemical oxidation of formic acid: Mechanism, kinetics and descriptor. Journal of Power Sources, 2020, 451, 227830.	4.0	27
36769	The effects of vanadium substitution on one-dimensional tunnel structures of cryptomelane: Combined TEM and DFT study. Nano Energy, 2020, 71, 104571.	8.2	11
36770	Two novel superhard structures: Monoclinic BC3N. Physica B: Condensed Matter, 2020, 584, 412061.	1.3	6
36771	Topochemical Reduction of La₂NiO₃F₂: The First Ni-Based Ruddlesdenâ€“Popper n = 1 Tâ€²-Type Structure and the Impact of Reduction on Magnetic Ordering. Chemistry of Materials, 2020, 32, 3160-3179.	3.2	19
36772	Spin Transition of Iron in Î´â€(Al,Fe)OOH Induces Thermal Anomalies in Earth's Lower Mantle. Geophysical Research Letters, 2020, 47, e2020GL087036.	1.5	22
36773	Superlubricity in phosphorene identified by means of ab initio calculations. 2D Materials, 2020, 7, 025033.	2.0	32
36774	Ferroelectric polarization switching induced from water adsorption in <mml:math xmlns:mml="http://www.w3.org/1998/Math/MathML"><mml:msub><mml:mi>BaTiO</mml:mi><mml:mn>3</mml:mn></mml:msub></m ultrathin films. Physical Review B, 2020, 101, .	1.1	5
36775	Nanoscale First-Principles Electronic Structure Simulations of Materials Relevant to Organic Electronics. , 2020, , 89-131.		1
36776	Carrier Dynamics in Ultrathin Gold Nanowires: Role of Auger Processes. Plasmonics, 2020, 15, 1151-1158.	1.8	2
36777	The Role of the Cu on OSL Emission in Gamma-LiAlO2:Cu Crystal. Journal of Electronic Materials, 2020, 49, 2521-2528.	1.0	1
36778	First-Principles Calculations for Stable Î²-Tiâ€“Mo Alloys Using Cluster-Plus-Glue-Atom Model. Acta Metallurgica Sinica (English Letters), 2020, 33, 968-974.	1.5	5
36779	Theoretical prediction of B/Al-doped black phosphorus as potential cathode material in lithium-sulfur batteries. Applied Surface Science, 2020, 512, 145639.	3.1	22
36780	Ultralow lattice thermal conductivity and anisotropic thermoelectric performance of AA stacked SnSe bilayer. Applied Surface Science, 2020, 512, 145640.	3.1	37
36781	Highly sensitive and selective sensing properties of modified green phosphorene monolayers towards SF6 decomposition gases. Applied Surface Science, 2020, 512, 145641.	3.1	28
36782	N-doped carbon/ultrathin 2D metallic cobalt selenide core/sheath flexible framework bridged by chemical bonds for high-performance potassium storage. Chemical Engineering Journal, 2020, 388, 124396.	6.6	94
36783	Effects of intrinsic defects on the photocatalytic water-splitting activities of PtSe2. International Journal of Hydrogen Energy, 2020, 45, 8549-8557.	3.8	19

#	Article	IF	Citations
36784	Unconventional magnetism of non-uniform distribution of Co in TiO2 nanoparticles. Journal of Alloys and Compounds, 2020, 826, 154194.	2.8	8
36785	Electronic and Phonon Instabilities in Bilayer Graphene under Applied External Bias. Materials Today: Proceedings, 2020, 20, 373-382.	0.9	4
36786	Coexistence of magnetism and ferroelectricity in (PbTiO3)mâ•(BaTiO3)n superlattices. Superlattices and Microstructures, 2020, 140, 106427.	1.4	4
36787	Density Functional Theory Study of the Gas Phase and Surface Reaction Kinetics for the MOVPE Growth of GaAs_{1â€“y}Bi_y. Journal of Physical Chemistry A, 2020, 124, 1682-1697.	1.1	0
36788	Tailoring the Mechanical Properties of Earth-Abundant Transition Metal Borides via Bonding Optimization. Journal of Physical Chemistry C, 2020, 124, 4430-4437.	1.5	5
36789	Time-Domain Terahertz Spectroscopy and Density Functional Theory Studies of Nitro/Nitrogen-Rich Aryl-Tetrazole Derivatives. ACS Omega, 2020, 5, 2541-2551.	1.6	14
36790	Materials synthesis, characterization and DFT calculations of the visible-light-active perovskite-like barium bismuthate Ba_{1.264(4)}Bi_{1.971(4)}O₄ photocatalyst. Journal of Materials Chemistry C, 2020, 8, 3509-3519.	2.7	12
36791	Aluminum Doped Germanene Nanoribbons: A First Principles Investigation. Integrated Ferroelectrics, 2020, 204, 58-62.	0.3	3
36792	First-Principles Calculations of the Electronic Structure and Optical Properties of Yttrium-Doped ZnO Monolayer with Vacancy. Materials, 2020, 13, 724.	1.3	13
36793	Controllable chemoselective hydrogenation of furfural by PdAg/C bimetallic catalysts under ambient operating conditions: an interesting Ag switch. Green Chemistry, 2020, 22, 1432-1442.	4.6	38
36794	Unraveling the dissolution mechanism of platinum and silver electrodes during composite electrodeposition in a deep eutectic solvent. Journal of Materials Chemistry A, 2020, 8, 4354-4361.	5.2	6
36795	Bi₂:Bi₂Te₃ stacking influence on the surface electronic response of the topological insulator Bi₄Te₃. Electronic Structure, 2020, 2, 015002.	1.0	8
36796	Searching the crystal structure of silicon using the generalized scaled hypersphere search method with the rapid nuclear motion approximation. Japanese Journal of Applied Physics, 2020, 59, 035503.	0.8	3
36797	Suppression of magnetism and Seebeck effect in Na0.875CoO2 induced by SbCo dopants. Materials for Renewable and Sustainable Energy, 2020, 9, 1.	1.5	4
36798	Strong electronic couple engineering of transition metal phosphides-oxides heterostructures as multifunctional electrocatalyst for hydrogen production. Applied Catalysis B: Environmental, 2020, 269, 118803.	10.8	94
36799	Ab-initio study of atomic structure and mechanical behaviour of <mml:math xmlns:mml="http://www.w3.org/1998/Math/MathML" altimg="si88.svg"><mml:mrow><mml:mi mathvariant="italic">Al</mml:mi><mml:mo>/</mml:mo><mml:mi mathvariant="italic">Fe</mml:mi></mml:mrow></mml:math> intermetallic interfaces. Computational Materials Science, 2020, 174, 109481.	1.4	18
36800	Nitrogen, sulfur Co-doped porous graphene boosting Li4Ti5O12 anode performance for high-rate and long-life lithium ion batteries. Energy Storage Materials, 2020, 27, 387-395.	9.5	87
36801	Understanding the interplay of bifunctional and electronic effects: Microkinetic modeling of the CO electro-oxidation reaction. Journal of Catalysis, 2020, 384, 1-13.	3.1	27

#	Article	IF	Citations
36802	Computational discovery of the novel half-metallic full-Heusler alloys Mn2LiAs and Mn2LiSb. Journal of Magnetism and Magnetic Materials, 2020, 503, 166642.	1.0	8
36803	Adsorption of gas molecules on penta-graphene nanoribbon and its implication for nanoscale gas sensor. Physics Open, 2020, 2, 100014.	0.7	23
36804	Electronic and optical properties of janus MoSSe and ZnO vdWs heterostructures. Superlattices and Microstructures, 2020, 140, 106445.	1.4	76
36805	Synthesis and Polymorphism of Mixed Aluminumâ€“Gallium Oxides. Inorganic Chemistry, 2020, 59, 3805-3816.	1.9	28
36806	Van der Waals induced molecular recognition of canonical DNA nucleobases on a 2D GaS monolayer. Physical Chemistry Chemical Physics, 2020, 22, 6706-6715.	1.3	5
36807	Half-metallicity in new Heusler alloys Mn₂ScZ (Z = Si, Ge, Sn). RSC Advances, 2020, 10, 7661-7670.	1.7	52
36808	A lattice-matched interface between in situ/artificial SEIs inhibiting SEI decomposition for enhanced lithium storage. Journal of Materials Chemistry A, 2020, 8, 11165-11176.	5.2	22
36809	Two-dimensional Ca4N2 as a one-dimensional electride [Ca4N2]2+Â·2eâ˜ with ultrahigh conductance. Nanoscale, 2020, 12, 5578-5586.	2.8	3
36810	First-principles perspectives on detection properties of sulphur mustard gas using novel electroresistive Ïµ-Arsenene nanosheet device. Molecular Physics, 2020, 118, e1725671.	0.8	12
36811	Facile diamond synthesis from lower diamondoids. Science Advances, 2020, 6, eaay9405.	4.7	26
36812	Synergistically Tuning Electronic Structure of Porous Î²â€Mo₂C Spheres by Co Doping and Moâ€Vacancies Defect Engineering for Optimizing Hydrogen Evolution Reaction Activity. Advanced Functional Materials, 2020, 30, 2000561.	7.8	141
36813	Origin of the structural diversity of the alkaline metal borohydride MBH4 (MÂ=ÂLi, Na, K, Rb and Cs): Insights from first-principles calculations. International Journal of Hydrogen Energy, 2020, 45, 9946-9958.	3.8	1
36814	Synergistic effect of antimony-triselenide on addition of conductive hybrid matrix for high-performance lithium-ion batteries. Journal of Alloys and Compounds, 2020, 828, 154410.	2.8	12
36815	Tuning of interactions between cathode and lithium polysulfide in Li-S battery by rational halogenation. Journal of Energy Chemistry, 2020, 49, 147-152.	7.1	19
36816	Band Alignment of the CuGaS2 Chalcopyrite Interfaces Studied by First-Principles Calculations. ACS Omega, 2020, 5, 3294-3301.	1.6	5
36817	Focus on the overlap density of wavefunctions inGWapproximations. Physical Chemistry Chemical Physics, 2020, 22, 5366-5376.	1.3	2
36818	Local geometry around B atoms in B/Si(1â€‰1â€‰1) from polarized x-ray absorption spectroscopy. Journal of Physics Condensed Matter, 2020, 32, 045901.	0.7	1
36819	Pyrene Coating Transition Metal Disulfides as Protection from Photooxidation and Environmental Aging. Nanomaterials, 2020, 10, 363.	1.9	13

#	Article	IF	Citations
36820	Porous Si Partially Filled with Water Moleculesâ€"Crystal Structure, Energy Bands and Optical Properties from First Principles. Nanomaterials, 2020, 10, 396.	1.9	5
36821	Strengthening the Interface between Flowerâ€Like VS₄ and Porous Carbon for Improving Its Lithium Storage Performance. Advanced Functional Materials, 2020, 30, 2000427.	7.8	47
36822	Halide Doubleâ€Perovskite Lightâ€Emitting Centers Embedded in Latticeâ€Matched and Coherent Crystalline Matrix. Advanced Functional Materials, 2020, 30, 2000653.	7.8	30
36823	Phase Modulation and Chemical Activation of MoSe₂ by Phosphorus for Electrocatalytic Hydrogen Evolution Reaction. Energy Technology, 2020, 8, 1901503.	1.8	16
36824	High gas-sensing selectivity of bilaterally edge-doped graphene nano-ribbons towards detecting NO2, O2 and SO3 gas molecules: Ab-initio investigation. Applied Surface Science, 2020, 514, 145866.	3.1	20
36825	Thermal and electrical decomposition products of C5F10O and their compatibility with Cu (1Â1Â1) and Al (1Â1Â1) surfaces. Applied Surface Science, 2020, 513, 145882.	3.1	17
36826	Hollow nanosheet array of phosphorus-anion-decorated cobalt disulfide as an efficient electrocatalyst for overall water splitting. Chemical Engineering Journal, 2020, 390, 124556.	6.6	84
36827	Design of Lead-Free and Stable Two-Dimensional Dionâ€"Jacobson-Type Chalcogenide Perovskite Aâ€²La2B3S10 (Aâ€² = Ba/Sr/Ca; B = Hf/Zr) with Optimal Band Gap, Strong Optical Absorption, and High Efficiency for Photovoltaics. Chemistry of Materials, 2020, 32, 2450-2460.	3.2	19
36828	Efficient Ab Initio Multiplet Calculations for Magnetic Adatoms on MgO. Journal of Physical Chemistry A, 2020, 124, 2318-2327.	1.1	11
36829	Identification of Efficient Active Sites in Nitrogen-Doped Carbon Nanotubes for Oxygen Reduction Reaction. Journal of Physical Chemistry C, 2020, 124, 8689-8696.	1.5	27
36830	Intermediate Adsorption States Switch to Selectively Catalyze Electrochemical CO₂ Reduction. ACS Catalysis, 2020, 10, 3871-3880.	5.5	89
36831	Bismuthene for highly efficient carbon dioxide electroreduction reaction. Nature Communications, 2020, 11, 1088.	5.8	278
36832	Elucidating the Effect of Planar Graphitic Layers and Cylindrical Pores on the Storage and Diffusion of Li, Na, and K in Carbon Materials. Advanced Functional Materials, 2020, 30, 1908209.	7.8	49
36833	Enhancement of chlorobenzene sensing by doping aluminum on nanotubes: A DFT study. Applied Surface Science, 2020, 514, 145897.	3.1	11
36834	The influence of point defects on Na diffusion in black phosphorene: First principles study. Journal of Physics and Chemistry of Solids, 2020, 143, 109432.	1.9	3
36835	Acepentalene Membrane Sheet: A Metallic Two-Dimensional Carbon Allotrope with High Carrier Mobility for Lithium Ion Battery Anodes. Journal of Physical Chemistry C, 2020, 124, 5999-6011.	1.5	14
36836	Robustness of Superatoms and Their Potential as Building Blocks of Materials: Al<sub>13</sup>^{â€"} vs B(CN)₄^{â€"}. Journal of Physical Chemistry C, 2020, 124, 6435-6440.	1.5	7
36837	1T-Phase Titanium Disulfide Nanosheets for Sensing H₂S and O₂. ACS Applied Nano Materials, 2020, 3, 3382-3394.	2.4	31

#	Article	IF	Citations
36838	Mechanistic Analysis-Guided Pd-Based Catalysts for Efficient Hydrogen Production from Formic Acid Dehydrogenation. ACS Catalysis, 2020, 10, 3921-3932.	5.5	82
36839	The Cu photoluminescence defect and the early stages of Cu precipitation in Si. Journal of Applied Physics, 2020, 127, .	1.1	5
36840	Nanoscale Scanning Electrochemical Cell Microscopy and Correlative Surface Structural Analysis to Map Anodic and Cathodic Reactions on Polycrystalline Zn in Acid Media. Journal of the Electrochemical Society, 2020, 167, 041507.	1.3	47
36841	S Vacancy Engineered Electronic and Optoelectronic Properties of Ni-Doped MoS2 Monolayer: A Hybrid Functional Study. Journal of Electronic Materials, 2020, 49, 3234-3241.	1.0	5
36842	Surface engineering in improving activity of Pt nanocubes for ammonia electrooxidation reaction. Applied Catalysis B: Environmental, 2020, 269, 118821.	10.8	58
36843	A comparative analysis of the phonon properties in UO2 using the Boltzmann transport equation coupled with DFTâ€¯+â€¯U and empirical potentials. Computational Materials Science, 2020, 177, 109594.	1.4	15
36844	Ab initio approach to the elastic, electronic, and optical properties of MoTe2 topological Weyl semimetal. Journal of Alloys and Compounds, 2020, 829, 154522.	2.8	39
36845	Tunable spin-polarized band gap in Si₂/NiI₂ vdW heterostructure. RSC Advances, 2020, 10, 8927-8935.	1.7	6
36846	Modulation of nearly free electron states in hydroxyl-functionalized MXenes: a first-principles study. Journal of Materials Chemistry C, 2020, 8, 5211-5221.	2.7	21
36847	CPMD investigation of Î±-RDX and Îµ-CL-20: the transition of deflagration to detonation depending on the self-produced radicals. Physical Chemistry Chemical Physics, 2020, 22, 7421-7429.	1.3	5
36848	0D/2D spatial structure of Cd_xZn_{1â^'x}S/Ni-MOF-74 for efficient photocatalytic hydrogen evolution. Dalton Transactions, 2020, 49, 5143-5156.	1.6	63
36849	Comparative electrochemical energy storage performance of cobalt sulfide and cobalt oxide nanosheets: experimental and theoretical insights from density functional theory simulations. Physical Chemistry Chemical Physics, 2020, 22, 7903-7911.	1.3	26
36850	Narrowing band gap and enhanced visible-light absorption of metal-doped non-toxic CsSnCl₃ metal halides for potential optoelectronic applications. RSC Advances, 2020, 10, 7817-7827.	1.7	54
36851	Two-dimensional boron monochalcogenide monolayer for thermoelectric material. Sustainable Energy and Fuels, 2020, 4, 2363-2369.	2.5	62
36852	Initial steps toward Auad island nucleation on a c(2 Ã— 2)-Cl Au(001) surface investigated by DFT. Journal of Chemical Physics, 2020, 152, 084701.	1.2	1
36853	Thermodynamics and structural properties of CaO: A molecular dynamics simulation study. Journal of Chemical Physics, 2020, 152, 084503.	1.2	16
36854	First-principles calculations of elastic constants for epsilon-carbide and the consequences. Materials Science and Technology, 2020, 36, 615-622.	0.8	3
36855	Relativistic effects in the interaction of fast charged particles with graphene. Radiation Effects and Defects in Solids, 2020, 175, 84-93.	0.4	0

#	Article	IF	Citations
36856	Nearly golden-ratio order in Ta metallic glass*. Chinese Physics B, 2020, 29, 046105.	0.7	4
36857	D-band Center Theory for the Case of Hydrogen Atom Adsorption on Fe(100) and Al(100) Surfaces: A Density Functional Study. Journal of Physics: Conference Series, 2020, 1445, 012011.	0.3	0
36858	Elastic properties of single crystal Bi₁₂SiO₂₀ as a function of pressure and temperature and acoustic attenuation effects in Bi₁₂MO₂₀ (MÂ=ÂSi, Ge and Ti). Materials Research Express, 2020, 7, 025701.	0.8	7
36859	First-principles study on the mechanical properties and thermodynamic properties of Moâ€“Ta alloys. Plasma Science and Technology, 2020, 22, 065601.	0.7	8
36860	Uncommon clustering in dilute Tiâ€“Fe alloys. JPhys Materials, 2020, 3, 025007.	1.8	0
36861	Lattice dynamics of Pnma Sn(S_{1â€“x}Se_x) solid solutions: energetics, phonon spectra and thermal transport. JPhys Energy, 2020, 2, 025006.	2.3	4
36862	Tuning the electronic properties of grapheneâ€“graphitic carbon nitride heterostructures and heterojunctions by using an electric field. Physical Review B, 2020, 101, .	1.1	54
36863	Coupled Sublattice Melting and Charge-Order Transition in Two Dimensions. Physical Review Letters, 2020, 124, 097602.	2.9	8
36864	A perspective on conventional high-temperature superconductors at high pressure: Methods and materials. Physics Reports, 2020, 856, 1-78.	10.3	304
36865	Disclosing the Structural, Electronic, Magnetic, and Morphological Properties of CuMnO₂: A Unified Experimental and Theoretical Approach. Journal of Physical Chemistry C, 2020, 124, 5378-5388.	1.5	22
36866	Enhanced Field Emission Properties of Au/SnSe Nano-heterostructure: A Combined Experimental and Theoretical Investigation. Scientific Reports, 2020, 10, 2358.	1.6	10
36867	Rectifying behavior in twisted bilayer black phosphorus nanojunctions mediated through intrinsic anisotropy. Nanoscale Advances, 2020, 2, 1493-1501.	2.2	13
36868	Switchable metal-to-half-metal transition at the semi-hydrogenated graphene/ferroelectric interface. Nanoscale, 2020, 12, 5067-5074.	2.8	6
36869	Encapsulation and substitution of Fe in C12A7 (12CaOâ‹…7Al2O3). AIP Advances, 2020, 10, 015242.	0.6	3
36870	Predictions on structural, electronic, optical and thermal properties of lithium niobate via first-principle computations. Philosophical Magazine, 2020, 100, 1150-1171.	0.7	13
36871	Tensor network strategies for calculating biexcitons and trions in monolayer two-dimensional materials beyond the ground state. Physical Review B, 2020, 101, .	1.1	9
36872	Highâ€Pressure Effect on Elastic Constants and Their Related Properties of MgCa Intermetallic Compound. Physica Status Solidi (B): Basic Research, 2020, 257, 1900537.	0.7	16
36873	Theoretical Study of Nonradiative Energy Transfer from Exciplex to Perovskites. Russian Physics Journal, 2020, 62, 1911-1916.	0.2	1

#	Article	IF	Citations
36874	Surface oxygen vacancies promoted photodegradation of benzene on TiO2 film. Applied Surface Science, 2020, 511, 145597.	3.1	60
36875	Mechanism of surface hydration of potassium carbonate: Insights from first-principles simulations. Applied Surface Science, 2020, 512, 145726.	3.1	7
36876	Electronic and vibrational properties of pure MnPS3 crystal: Theoretical and experimental investigation. Computational Materials Science, 2020, 177, 109592.	1.4	9
36877	Electronic and optical properties of halogen (H= F, Cl, Br)-doped Cu2O by hybrid density functional simulations. Optik, 2020, 207, 164440.	1.4	6
36878	Molecular Structure and Electronic Properties of para-Hexaphenyl Monolayer on Atomically Flat Rutile TiO₂(110). Journal of Physical Chemistry C, 2020, 124, 5681-5689.	1.5	3
36879	Facile and accelerated production of RuO2 monolayers via a dual-step intercalation process. Inorganic Chemistry Frontiers, 2020, 7, 1445-1450.	3.0	5
36880	Yolkâ€“shell or yolk-in-shell nanocatalysts? A proof-of-concept study. Journal of Materials Chemistry A, 2020, 8, 10217-10225.	5.2	14
36881	Anomalous solution softening by unique energy balance mediated by kink mechanism in tungsten-rhenium alloys. Journal of Applied Physics, 2020, 127, .	1.1	9
36882	An ab initio study on the effects of Na passivation on friction reduction of an iron oxide surface. Journal of Applied Physics, 2020, 127, 065305.	1.1	6
36883	Fundamental band gap and alignment of two-dimensional semiconductors explored by machine learning*. Chinese Physics B, 2020, 29, 046101.	0.7	17
36884	<mml:math xmlns:mml="http://www.w3.org/1998/Math/MathML"><mml:msub><mml:mrow><mml:mi>Ca</mml:mi></mml:mrow><mml:mn>3</mml:mn> mathvariant="normal">O</mml:mi></mml:mrow><mml:mn>7</mml:mn></mml:msub></mml:math> structural path unraveled by atomic-scale properties: A combined experimental and ab initio study. Physical Review B, 2020, 101, .	1.1	12
36885	A Heterostructure Coupling of Bioinspired, Adhesive Polydopamine, and Porous Prussian Blue Nanocubics as Cathode for Highâ€Performance Sodiumâ€Ion Battery. Small, 2020, 16, e1906946.	5.2	57
36886	A DFT study on the possibility of embedding a single Ti atom into the perfect stanene monolayer as a highly efficient gas sensor. Theoretical Chemistry Accounts, 2020, 139, 1.	0.5	10
36887	Phase-field study of IMC growth in Snâ€“Cu/Cu solder joints including elastoplastic effects. Acta Materialia, 2020, 188, 241-258.	3.8	27
36888	The mechanism of dynamic strain aging for type A serrations in tensile flow curves of Fe-18Mn-0.55C (wt.%) twinning-induced plasticity steel. Acta Materialia, 2020, 188, 366-375.	3.8	40
36889	Essential role of oxygen vacancies of Cu-Al and Co-Al spinel oxides in their catalytic activity for the reverse water gas shift reaction. Applied Catalysis B: Environmental, 2020, 266, 118669.	10.8	56
36890	Realizing synergistic effect of electronic modulation and nanostructure engineering over graphitic carbon nitride for highly efficient visible-light H2 production coupled with benzyl alcohol oxidation. Applied Catalysis B: Environmental, 2020, 269, 118772.	10.8	66
36891	Adsorption and sensing behaviors of SF6 decomposed species on Ni-doped C3N monolayer: A first-principles study. Applied Surface Science, 2020, 512, 145759.	3.1	236

#	Article	IF	Citations
36892	First-principles study of the ideal shear strengths and stacking fault energies of face-centered cubic Al3Ti. Computational Materials Science, 2020, 177, 109596.	1.4	13
36893	DP-GEN: A concurrent learning platform for the generation of reliable deep learning based potential energy models. Computer Physics Communications, 2020, 253, 107206.	3.0	271
36894	Fused pentagon carbon network: A new anode material for Li ion batteries. Chemical Physics Letters, 2020, 745, 137225.	1.2	6
36895	Synthesis of NdSc3(BO3)4 single crystals and study of its structure properties. Journal of Alloys and Compounds, 2020, 828, 154355.	2.8	6
36896	Corrugation Matters: Structure Models of Single Layer Heptazine-Based Graphitic Carbon Nitride from First-Principles Studies. Journal of Physical Chemistry C, 2020, 124, 4644-4651.	1.5	19
36897	Screening Promising Thermoelectric Materials in Binary Chalcogenides through High-Throughput Computations. ACS Applied Materials & Interfaces, 2020, 12, 11852-11864.	4.0	51
36898	The Mode of Incorporation of As(-I) and Se(-I) in Natural Pyrite Revisited. ACS Earth and Space Chemistry, 2020, 4, 379-390.	1.2	18
36899	Mechanistic studies on millerite chlorination with ammonium chloride. Physical Chemistry Chemical Physics, 2020, 22, 4832-4839.	1.3	5
36900	Local strain-driven migration of oxygen vacancies to apical sites in YBa₂Cu₃O_{7â”x}. Nanoscale, 2020, 12, 5922-5931.	2.8	14
36901	DFT prediction of structural, electronic and magnetic properties of Sr_{0.75}TM_{0.25}S (TM is 3d transition metals). Philosophical Magazine Letters, 2020, 100, 95-104.	0.5	4
36902	Regulating Lithium Nucleation and Deposition via MOFâ€Derived Co@Câ€Modified Carbon Cloth for Stable Li Metal Anode. Advanced Functional Materials, 2020, 30, 1909159.	7.8	170
36903	Asymmetric Lattice Disorder Induced at Oxide Interfaces. Advanced Materials Interfaces, 2020, 7, 1901944.	1.9	13
36904	Thermodynamic description of the Dyâ€“Siâ€“C system in silicon carbide ceramics. Calphad: Computer Coupling of Phase Diagrams and Thermochemistry, 2020, 68, 101738.	0.7	9
36905	Preparation of Niâ€“Siâ€“B nano-crystalline film and mechanism analysis using first-principle calculations. Journal of Alloys and Compounds, 2020, 828, 154407.	2.8	3
36906	Room-temperature conversion of Cu_{2â”x}Se to CuAgSe nanoparticles to enhance the photocatalytic performance of their composites with TiO₂. Dalton Transactions, 2020, 49, 3580-3591.	1.6	13
36907	Metal adsorbate interactions and the convergence of density functional calculations. Journal of Chemical Physics, 2020, 152, 061102.	1.2	0
36908	Oxygenation of monolayer gallium monochalcogenides: Design of two-dimensional ternary <mml:math xmlns:mml="http://www.w3.org/1998/Math/MathML"><mml:mrow><mml:msub><mml:mi>Ga</mml:mi><mml:mn>2</mml:mn></mml:		

#	Article	IF	Citations
36910	Widely Tunable Optical and Thermal Properties of Dirac Semimetal Cd₃As₂. Advanced Optical Materials, 2020, 8, 1901192.	3.6	27
36911	Structural, electronic, elastic and magnetic properties of heavier $$hbox {REIr}_{3}$$ (RE $$=$$ Gd,) Tj ETQq1 1 0.784314 rgBT /Ov	0.9	1
36912	Salt-assisted growth and ultrafast photocarrier dynamics of large-sized monolayer ReSe2. Nano Research, 2020, 13, 667-675.	5.8	19
36913	Thermoelectric and half-metallic behavior of the Co2TaAl: a DFT study. International Nano Letters, 2020, 10, 81-88.	2.3	2
36914	Catalytic decomposition of N2O on Pd Cu alloy catalysts: A density functional theory study. Applied Surface Science, 2020, 510, 145349.	3.1	20
36915	Graphdiyne nanosheets as a sensing medium for formaldehyde and formic acid â€“ A first-principles outlook. Computational and Theoretical Chemistry, 2020, 1176, 112751.	1.1	40
36916	First-principles study of the initial stage of aluminum oxidation. Chemical Physics Letters, 2020, 744, 137237.	1.2	1
36917	Effects of Fe doping on enhancing electrochemical properties of NiCo2S4 supercapacitor electrode. Electrochimica Acta, 2020, 340, 135939.	2.6	36
36918	Weakly nonlocal micromorphic elasticity for diamond structures vis-Ã-vis lattice dynamics. Mechanics of Materials, 2020, 147, 103365.	1.7	7
36919	ZnN and ZnP as novel graphene-like materials with high Li-ion storage capacities. Materials Today Energy, 2020, 16, 100392.	2.5	20
36920	Electromagnetic induction derived micro-electric potential in metal-semiconductor core-shell hybrid nanostructure enhancing charge separation for high performance photocatalysis. Nano Energy, 2020, 71, 104624.	8.2	56
36921	Phase transitions and superconductivity of iron-based superconductors from first-principles. Physics Letters, Section A: General, Atomic and Solid State Physics, 2020, 384, 126345.	0.9	5
36922	Effect of electric field on the electronic properties of functionalized germanane by organic molecular adsorption. Physics Letters, Section A: General, Atomic and Solid State Physics, 2020, 384, 126347.	0.9	1
36923	Enhancement of the piezoelectric effect in Fe-substituted GaAsO4: A combined XRD, Raman spectroscopy and first principles study. Solid State Sciences, 2020, 101, 106157.	1.5	2
36924	The characteristics of defective ZrS<mml:math xmlns:mml="http://www.w3.org/1998/Math/MathML" display="inline" id="d1e1160" altimg="si64.svg"><mml:msub><mml:mrow /><mml:mrow><mml:mn>2</mml:mn></mml:mrow></mml:msub></mml:math> monolayers adsorbed various gases on S-vacancies: A first-principles study. Superlattices and Microstructures, 2020, 140, 106454.	1.4	19
36925	Influence of Hydrogen/Fluorine Substitution on Structure, Thermal Phase Transitions, and Internal Molecular Motion of Aromatic Residues in the Crystal Lattice of Steroidal Rotors. Crystal Growth and Design, 2020, 20, 2202-2216.	1.4	8
36926	Atomistic Origins of the Limited Phase Stability of Cs⁺-Rich FA_xCs_(1â€“x)PbI₃ Mixtures. Chemistry of Materials, 2020, 32, 2605-2614.	3.2	24
36927	Molecular Oxygen-Induced Ferromagnetism and Half-Metallicity in Î±-BaNaO₄: A First-Principles Study. Journal of the American Chemical Society, 2020, 142, 5234-5240.	6.6	14

#	Article	IF	Citations
36928	Gas adsorption and light interaction mechanism in phosphorene-based field-effect transistors. Physical Chemistry Chemical Physics, 2020, 22, 5949-5958.	1.3	14
36929	Magnetic ground state in <mml:math xmlns:mml="http://www.w3.org/1998/Math/MathML"><mml:msub><mml:mi>FeTe</mml:mi><mml:mn>2</mml:mn></mml:msub><m , and <mml:math xmlns:mml="http://www.w3.org/1998/Math/MathML"><mml:msub><mml:mi>NiTe</mml:mi><mml:mn>2</mml:mn></mml:msub></ monolayers: Antiparallel magnetic moments at chalcogen atoms. Physical Review B, 2020, 101, .	1.1	31
36930	Effect of He on the Order-Disorder Transition in Ni3Al under Irradiation. Physical Review Letters, 2020, 124, 075901.	2.9	9
36931	Exploring the Adsorption Mechanism of Tetracene on Ag(110) by STM and Dispersion-Corrected DFT. Crystals, 2020, 10, 13.	1.0	2
36932	Molecular Modeling of Ammonia Gas Adsorption onto the Kaolinite Surface with DFT Study. Minerals (Basel, Switzerland), 2020, 10, 46.	0.8	10
36933	First Principles Calculation of the Stability of Iron Bearing Carbonates at High Pressure Conditions. Minerals (Basel, Switzerland), 2020, 10, 54.	0.8	5
36934	Superior stiffness and vibrational spectroscopic signature of two-dimensional diamond-like carbon nitrides. Physica E: Low-Dimensional Systems and Nanostructures, 2020, 119, 114007.	1.3	2
36935	Kinetic Monte Carlo Modeling for the NOâ€“CO Reaction Mechanism on Rh(100) and Rh(111). Langmuir, 2020, 36, 3127-3140.	1.6	7
36936	Evolutional carrier mobility and power factor of two-dimensional tin telluride due to quantum size effects. Journal of Materials Chemistry C, 2020, 8, 4181-4191.	2.7	11
36937	Insight into structural stability and helium diffusion behavior of Feâ€“Cr alloys from first-principles. RSC Advances, 2020, 10, 3277-3292.	1.7	12
36938	Spin-polarized quantum transport in Si dangling bond wires. Nanoscale, 2020, 12, 6079-6088.	2.8	4
36939	First-Principle Study of Cl Functionalized Zigzag AlN Nanoribbons. Integrated Ferroelectrics, 2020, 205, 114-121.	0.3	0
36940	Theoretical and Experimental Study on the Electrochemical Behavior of Beta-Sodium Vanadate in Rechargeable Magnesium Batteries Using Several Electrolyte Solutions. Journal of the Electrochemical Society, 2020, 167, 070512.	1.3	9
36941	Origin of pressureâ€induced insulatorâ€toâ€metal transition in the van der Waals compound FePS₃ from firstâ€principles calculations. Journal of Computational Chemistry, 2020, 41, 1337-1344.	1.5	23
36942	A DFT Investigation of the Dehydrogenation of Tetrahydropyrrole on Pt(111). Topics in Catalysis, 2020, 63, 688-699.	1.3	2
36943	Understanding the mechanism of CO2 reforming of methane to syngas on Ni@Pt surface compared with Ni(1Â1Â1) and Pt(1Â1Â1). Applied Surface Science, 2020, 513, 145840.	3.1	37
36945	A first principles investigation of W1-xMox (x=0â€“68.75Âat.%) alloys: Structural, electronic, mechanical and thermal properties. Journal of Alloys and Compounds, 2020, 829, 154480.	2.8	9
36946	Enhanced removal of vanadium(V) from groundwater by layered double hydroxide-supported nanoscale zerovalent iron. Journal of Hazardous Materials, 2020, 392, 122392.	6.5	62

#	Article	IF	Citations
36947	Separation principle of xylene isomers and ethylbenzene with hydrogen-bonded host frameworks via first-principles calculation. Journal of Industrial and Engineering Chemistry, 2020, 85, 276-281.	2.9	6
36948	DFT simulations of pyrite galvanic interactions with bulk, solid-solution and nanoparticle Au occurrences â€“ Insights into gold cyanidation. Minerals Engineering, 2020, 149, 106239.	1.8	22
36949	Synthesis, luminescence properties and theoretical calculations of La5BSi2O13:Dy3+ phosphor coatings for light-emitting diodes. Thin Solid Films, 2020, 698, 137865.	0.8	5
36950	Band Engineering and Thermoelectric Performance Optimization of p-Type GeTe-Based Alloys through Ti/Sb Co-Doping. Journal of Physical Chemistry C, 2020, 124, 5583-5590.	1.5	16
36951	Dynamics of RS-(Au-SR)_x Staple Motifs on Metal Surfaces: From Nanoclusters to 2D Surfaces. Journal of Physical Chemistry C, 2020, 124, 5452-5459.	1.5	6
36952	InTeI: a novel wide-bandgap 2D material with desirable stability and highly anisotropic carrier mobility. Nanoscale, 2020, 12, 5888-5897.	2.8	39
36953	Câ€“C coupling reactions promoted by CNT-supported bimetallic center in Fischerâ€“Tropsch synthesis. Sustainable Energy and Fuels, 2020, 4, 2638-2644.	2.5	2
36954	Atomic defects in monolayer ordered double transition metal carbide (Mo₂TiC₂T_x) MXene and CO₂ adsorption. Journal of Materials Chemistry C, 2020, 8, 4771-4779.	2.7	73
36955	Embedding of atoms into the nanopore sites of the C₆N₆and C₆N₈porous carbon nitride monolayers with tunable electronic properties. Physical Chemistry Chemical Physics, 2020, 22, 6418-6433.	1.3	38
36956	Heat Capacities of <scp>l</scp>-Alanine, <scp>l</scp>-Valine, <scp>l</scp>-Isoleucine, and <scp>l</scp>-Leucine: Experimental and Computational Study. Journal of Chemical & Engineering Data, 2020, 65, 1833-1849.	1.0	23
36957	Highly Selective and Sensitive Detection of Formaldehyde by Î²₁₂-Borophene/SnO₂ Heterostructures: The Role of an External Electric Field and In-Plain Biaxial Strain. Journal of Physical Chemistry A, 2020, 124, 2288-2300.	1.1	29
36958	Correctly Assessing Defect Tolerance in Halide Perovskites. Journal of Physical Chemistry C, 2020, 124, 6022-6027.	1.5	70
36959	Directionality in van der Waals Interactions: The Case of 4-Acetylbiphenyl Adsorbed on Au(111). Journal of Physical Chemistry C, 2020, 124, 4545-4551.	1.5	5
36960	In-Depth Study of ZnS Nanoparticle Surface Properties with a Combined Experimental and Theoretical Approach. Journal of Physical Chemistry C, 2020, 124, 7777-7789.	1.5	32
36961	Theoretical study of a pâ€“n homojunction SiGe field-effect transistor via covalent functionalization. RSC Advances, 2020, 10, 7682-7690.	1.7	2
36962	Na₃Sc₂(PO₄)₂F₃: rational design and synthesis of an alkali rare-earth phosphate fluoride as an ultraviolet nonlinear optical crystal with an enlarged birefringence. Journal of Materials Chemistry C, 2020, 8, 4965-4972.	2.7	34
36963	First-principles calculations of oxygen octahedral distortions in LaAlO3/SrTiO3(001) superlattices. Physical Chemistry Chemical Physics, 2020, 22, 5826-5831.	1.3	3
36964	Enhancement in electrical conductivity of a porous indium based metalâ€“organic framework upon I₂ uptake: combined experimental and theoretical investigations. Journal of Materials Chemistry C, 2020, 8, 4836-4842.	2.7	13

#	Article	IF	Citations
36965	Pressure Dependence of Structural, Electronic, and Optical Properties of Be0.25Zn0.75O Alloy. Physics of the Solid State, 2020, 62, 260-266.	0.2	3
36966	Accelerating CO₂ Electroreduction to CO Over Pd Singleâ€Atom Catalyst. Advanced Functional Materials, 2020, 30, 2000407.	7.8	173
36967	Explaining Cu@Pt Bimetallic Nanoparticles Activity Based on NO Adsorption. Chemistry - A European Journal, 2020, 26, 11478-11491.	1.7	5
36968	K + Intercalation of NH 4 HF 2 â€Exfoliated Ti 3 C 2 MXene as Binderâ€Free Electrodes with High Electrochemical Capacitance. Physica Status Solidi (A) Applications and Materials Science, 2020, 217, 1900806.	0.8	6
36969	An Effective Strategy for Photoelectric Performance Enhancement of 2D Perovskite via Halogenating Organic Cation: A Theoretical Prediction. Physica Status Solidi (B): Basic Research, 2020, 257, 1900599.	0.7	1
36970	Interaction of nitric oxide with the (1Â0Â0) surface of cobalt spinel nanocubes â€“ A comprehensive DFT, atomistic thermodynamic, IR and TPD account. Applied Surface Science, 2020, 513, 145835.	3.1	10
36971	DFT-based study of the bulk tin mixed-halide CsSnI3-Br perovskite. Computational Materials Science, 2020, 178, 109619.	1.4	19
36972	Influence of defects in graphene on electron transfer kinetics: The role of the surface electronic structure. Electrochimica Acta, 2020, 341, 136011.	2.6	42
36973	Coupling of bowl-like VS2 nanosheet arrays and carbon nanofiber enables ultrafast Na+-Storage and robust flexibility for sodium-ion hybrid capacitors. Energy Storage Materials, 2020, 28, 91-100.	9.5	82
36974	Interactions between hydrogen and the <mml:math xmlns:mml="http://www.w3.org/1998/Math/MathML" altimg="si1.svg"><mml:mrow><mml:mrow><mml:mo		

#	Article	IF	Citations
36983	Coexistence of type-I and type-II nodal lines in monolayer TiBF. Solid State Communications, 2020, 310, 113839.	0.9	6
36984	Structural Investigations of MA_{1â€“x}DMA_xPbI₃ Mixed-Cation Perovskites. Inorganic Chemistry, 2020, 59, 3730-3739.	1.9	21
36985	Large Enantiospecificity of Stepâ€“kink Metal Surfaces: Contributions from the Backbone and Side Chain of Î±-Amino Acids. Journal of Physical Chemistry C, 2020, 124, 742-748.	1.5	5
36986	A DFT Study and Microkinetic Simulation in Propylene Oxidation on the â€œ29â€• Cu_xO/Cu(111) Surface. Journal of Physical Chemistry C, 2020, 124, 6611-6623.	1.5	18
36987	Stoneâ€“Wales Defect Induced Performance Improvement of BC₃ Monolayer for High Capacity Lithium-Ion Rechargeable Battery Anode Applications. Journal of Physical Chemistry C, 2020, 124, 5910-5919.	1.5	52
36988	Predicting Core Level Photoelectron Spectra of Amino Acids Using Density Functional Theory. Journal of Physical Chemistry Letters, 2020, 11, 2256-2262.	2.1	11
36989	Universal Phase Transitions of AlB₂-Type Transition-Metal Diborides. ACS Omega, 2020, 5, 4620-4625.	1.6	9
36990	A First-Principles Study of the Adsorption of H2O on Ru- and Mo-Alloyed Pt(111) Surfaces. Journal of Electronic Materials, 2020, 49, 2642-2650.	1.0	6
36991	Electronic and magnetic properties of group-V TMDs monolayers with defects: A first-principles study. Computational Materials Science, 2020, 176, 109540.	1.4	20
36992	Structural, electronic, vibrational and magnetic properties of Zn2+ substituted MnCr2O4 nanoparticles. Journal of Magnetism and Magnetic Materials, 2020, 502, 166595.	1.0	48
36993	Oxygen trapping in defect clusters in Fe and FeCr alloy by ion channeling and ab-initio study. Journal of Nuclear Materials, 2020, 532, 152032.	1.3	1
36994	Metalâ€“Organic Frameworks for the Adsorptive Removal of Gaseous Aliphatic Ketones. ACS Applied Materials & Interfaces, 2020, 12, 10317-10331.	4.0	31
36995	Micro-kinetic model of electrochemical carbon dioxide reduction over platinum in non-aqueous solvents. Physical Chemistry Chemical Physics, 2020, 22, 9040-9045.	1.3	14
36996	Giant effect of spinâ€“lattice coupling on the thermal transport in two-dimensional ferromagnetic CrI₃. Journal of Materials Chemistry C, 2020, 8, 3520-3526.	2.7	31
36997	High performance supercapacitor electrodes based on spinel NiCo2O4@MWCNT composite with insights from density functional theory simulations. Journal of Chemical Physics, 2020, 152, 064706.	1.2	48
36998	Investigation of N2 adsorption on Fe3O4(001) using ambient pressure X-ray photoelectron spectroscopy and density functional theory. Journal of Chemical Physics, 2020, 152, 054717.	1.2	12
36999	Ferromagnetism, half-metallicity and spin-polarised electronic structures characterisation insights in Ca_{1â^'x}Ti_xO. Philosophical Magazine, 2020, 100, 1172-1190.	0.7	6
37000	Electronic properties and topological phases of a two-dimensional allotrope of nitrogenated carbon. Physical Review B, 2020, 101, .	1.1	4

#	Article	IF	Citations
37001	Preparation of Surface Modified Ceria Nanoparticles as Abrasives for the Application of Chemical Mechanical Polishing (CMP). ECS Journal of Solid State Science and Technology, 2020, 9, 024015.	0.9	18
37002	Defect-mediated intercalation of dysprosium on buffer layer graphene supported by SiC(0001) substrate. Chemical Physics Letters, 2020, 742, 137162.	1.2	3
37003	First-principles analysis of physical properties anisotropy for the Ag2SiS3 chalcogenide semiconductor. Journal of Alloys and Compounds, 2020, 826, 154232.	2.8	16
37004	Enhanced moisture stability of cesium lead iodide perovskite solar cells â€“ a first-principles molecular dynamics study. Physical Chemistry Chemical Physics, 2020, 22, 5693-5701.	1.3	29
37005	Suppressed phase transition of a Rb/K incorporated inorganic perovskite with a water-repelling surface. Nanoscale, 2020, 12, 6571-6581.	2.8	8
37006	Abnormally low thermal conductivity of 2D selenene: An ab initio study. Journal of Applied Physics, 2020, 127, .	1.1	26
37007	Structure of 2-(2-(anthracen-9-ylmethylene)hydrazinyl)-4-(3-methyl-3-phenylcyclobutyl)thiazole by combined X-Ray crystallographic and molecular modelling studies. Molecular Physics, 2020, 118, e1718224.	0.8	5
37008	Phonon linewidths in InAs/AlSb superlattices derived from first-principlesâ€”application towards quantum well hot carrier solar cells. Semiconductor Science and Technology, 2020, 35, 044001.	1.0	10
37009	Plastic flow between nanometer-spaced planar defects in nanostructured diamond and boron nitride. Physical Review B, 2020, 101, .	1.1	6
37010	Strain stiffening, high load-invariant hardness, and electronic anomalies of boron phosphide under pressure. Physical Review B, 2020, 101, .	1.1	24
37011	HfS2 and TiS2 Monolayers with Adsorbed C, N, P Atoms: A First Principles Study. Catalysts, 2020, 10, 94.	1.6	10
37012	A Fluorescence Probe for Metal Ions Based on Black Phosphorus Quantum Dots. Advanced Materials Interfaces, 2020, 7, 1902075.	1.9	17
37013	Two Covalent Ultraviolet Nonlinear Optical Crystals. Chemistry - an Asian Journal, 2020, 15, 775-779.	1.7	3
37014	Unusual mechanical and electronic behaviors of bulk layered hydrogen substituted graphdiyne under biaxial strain. Applied Surface Science, 2020, 513, 145694.	3.1	13
37015	Thermal dependence of the mechanical properties of NiTiSn using first-principles calculations and high-pressure X-ray diffraction. Journal of Alloys and Compounds, 2020, 823, 153611.	2.8	5
37016	The investigation of optoelectronic, magnetic and dynamical properties of Ce and Ti doped 2D blue phosphorene: A dispersion corrected DFT study. Journal of Alloys and Compounds, 2020, 827, 154255.	2.8	28
37017	First-principles study of structural and electronic properties of substitutionally doped arsenene. Physica E: Low-Dimensional Systems and Nanostructures, 2020, 119, 114018.	1.3	11
37018	Molecular Mechanistic Nature of Elemental Mercury Oxidation by Surface Oxygens over the Co₃O₄ Catalyst. Journal of Physical Chemistry C, 2020, 124, 4605-4612.	1.5	24

#	Article	IF	Citations
37019	Competitive Adsorption as a Route to Area-Selective Deposition. ACS Applied Materials & Interfaces, 2020, 12, 9989-9999.	4.0	14
37020	Modulating superexchange strength to achieve robust ferromagnetic couplings in two-dimensional semiconductors. Physical Review B, 2020, 101, .	1.1	17
37021	Electrical Control of Magnetic Phase Transition in a Type-I Multiferroic Double-Metal Trihalide Monolayer. Physical Review Letters, 2020, 124, 067602.	2.9	84
37022	Observation of a Charge-Neutral Muon-Polaron Complex in Antiferromagnetic <mml:math xmlns:mml="http://www.w3.org/1998/Math/MathML" display="inline"><mml:mrow><mml:msub><mml:mrow><mml:mi>Cr</mml:mi></mml:mrow><mml:mrow><mml:mn>2</mml:mn></mml:mrow></mml:msub><mml:msub><mml:mrow><mml:mi mathvariant="normal">O</mml:mi></mml:mrow><mml:mrow><mml:mn>3</mml:mn></mml:mrow></mml:msub></mml:mrow> Physical Review X, 2020, 10, .	2.8	12
37023	Dilute concentrations of Sb (Bi) dopants in Sn-site enhance the thermoelectric properties of TiNiSn half-Heusler alloys: a first-principles study. Japanese Journal of Applied Physics, 2020, 59, 035003.	0.8	2
37024	Superior high-temperature properties and deformation-induced planar faults in a novel L12-strengthened high-entropy alloy. Acta Materialia, 2020, 188, 517-527.	3.8	144
37025	Effect of Rh in Ni-based catalysts on sulfur impurities during methane reforming. Applied Catalysis B: Environmental, 2020, 267, 118691.	10.8	42
37026	CoSe2 modified Se-decorated CdS nanowire Schottky heterojunctions for highly efficient photocatalytic hydrogen evolution. Chemical Engineering Journal, 2020, 389, 124431.	6.6	57
37027	Out-of-plane ionicity versus in-plane covalency interplay and electronâ€“phonon coupling in MgB2 superconductor. Chinese Journal of Physics, 2020, 64, 287-294.	2.0	1
37028	Band-gap engineering of graphene by Al doping and adsorption of Be and Br on impurity: A computational study. Computational Condensed Matter, 2020, 23, e00463.	0.9	7
37029	Effect of oxygen deficiency on optical and magnetic properties of Ba2MMoO6 (M=Cr, Mn, Fe): A first-principles study. Computational Condensed Matter, 2020, 23, e00464.	0.9	15
37030	Self-supported MoSx/V2O3 heterostructures as efficient hybrid catalysts for hydrogen evolution reaction. Journal of Alloys and Compounds, 2020, 827, 154262.	2.8	7
37031	Theoretical Investigation of 6-Mercaptopurine Isomersâ€™ Adsorption on the Au(001) Surface: Revealing the Fate of Different Isomers. ACS Omega, 2020, 5, 610-618.	1.6	3
37032	Effect of interstitial carbon on the evolution of early-stage irradiation damage in equi-atomic FeMnNiCoCr high-entropy alloys. Journal of Applied Physics, 2020, 127, .	1.1	24
37033	First-principles study of structural, elastic, electronic and optical properties of RDX under pressure. Philosophical Magazine, 2020, 100, 1015-1031.	0.7	3
37034	Structural stability and optoelectronic properties of tetragonal MAPbI₃ under strain. Nanotechnology, 2020, 31, 225204.	1.3	19
37035	2D Hexagonal SnTe monolayer: a quasi direct band gap semiconductor with strain sensitive electronic and optical properties. European Physical Journal B, 2020, 93, 1.	0.6	12
37036	Chloroform Hydrodechlorination on Palladium Surfaces: A Comparative DFT Study on Pd(111), Pd(100), and Pd(211). Topics in Catalysis, 2020, 63, 762-776.	1.3	17

#	Article	IF	Citations
37037	Mechanistic insight into the role of N-doped carbon matrix in electrospun binder-free Si@C composite anode for lithium-ion batteries. Ionics, 2020, 26, 3297-3305.	1.2	14
37038	Solvent-free hydrodeoxygenation of bio-lipids into renewable alkanes over NiW bimetallic catalyst under mild conditions. Applied Catalysis B: Environmental, 2020, 269, 118718.	10.8	58
37039	Towards understanding the role of carbon atoms on transition metal surfaces: Implications for catalysis. Applied Surface Science, 2020, 513, 145765.	3.1	8
37040	High selective catalyst for ethylene epoxidation to ethylene oxide: A DFT investigation. Applied Surface Science, 2020, 513, 145799.	3.1	9
37041	First-principles study of phase stability and temperature-dependent mechanical properties of (Cr,) Tj ETQq0 0 0 rgBT /Overlock 10 Tf 50	2.8	17
37042	Topological analysis of electron density in half-Heusler ZrXBi (XÂ= Co, Rh) compounds: A density functional theory study accompanied by Baderâ€™s quantum theory of atoms in molecules. Journal of Alloys and Compounds, 2020, 828, 154287.	2.8	12
37043	Paper: In-situ high-pressure Raman scattering and ab-initio studies in Cu2Sb up to 45ÂGPa. Journal of Alloys and Compounds, 2020, 827, 154372.	2.8	2
37044	Tuning electronic correlations of ultra-small IrO2 nanoparticles with La and Pt for enhanced oxygen evolution performance and long-durable stability in acidic media. Applied Catalysis B: Environmental, 2020, 266, 118643.	10.8	57
37045	Encapsulated cobalt nanoparticles as a recoverable catalyst for the hydrolysis of sodium borohydride. Energy Storage Materials, 2020, 27, 187-197.	9.5	72
37046	CuN3 doped graphene as an active electrocatalyst for oxygen reduction reaction in fuel cells: A DFT study. Journal of Molecular Graphics and Modelling, 2020, 96, 107537.	1.3	13
37047	Influence of nitrogen vacancies on selective oxidation of aromatic alcohols on g-C3N4: A comparative DFT study. Molecular Catalysis, 2020, 482, 110747.	1.0	5
37048	Enthalpies and elastic properties of Ni-Co binary system by ab initio calculations and an energy comparison with the CALPHAD approach. Materials Today Communications, 2020, 23, 100905.	0.9	5
37049	Predicting the Most Suitable Surface Candidates of Ta₃N₅ Photocatalysts for Water-Splitting Reactions Using Screened Coulomb Hybrid DFT Computations. Journal of Physical Chemistry C, 2020, 124, 2472-2480.	1.5	21
37050	Basal Nanosuit of Graphite for High-Energy Hybrid Li Batteries. ACS Nano, 2020, 14, 1837-1845.	7.3	40
37051	Effects of Covalency on Anionic Redox Chemistry in Semiquinoid-Based Metalâ€“Organic Frameworks. Journal of the American Chemical Society, 2020, 142, 2653-2664.	6.6	75
37052	Atomic-level tuning of Coâ€“Nâ€“C catalyst for high-performance electrochemical H2O2 production. Nature Materials, 2020, 19, 436-442.	13.3	725
37053	Temperature tunability in Sr_{1â^'x}Ca_xFeO_{3â^'Î´} for reversible oxygen storage: a computational and experimental study. Journal of Materials Chemistry A, 2020, 8, 2602-2612.	5.2	26
37054	Re effects in model Ni-based superalloys investigated with first-principles calculations and atom probe tomography*. Chinese Physics B, 2020, 29, 043103.	0.7	4

#	Article	IF	Citations
37055	Universal Oriented van der Waals Epitaxy of 1D Cyanide Chains on Hexagonal 2D Crystals. Advanced Science, 2020, 7, 1900757.	5.6	13
37056	La₃B₆O₁₃(OH): The First Acentric Highâ€Pressure Borate Displaying Edgeâ€Sharing BO₄ Tetrahedra. Chemistry - A European Journal, 2020, 26, 6851-6861.	1.7	23
37057	Studying temperature effects on electronic and optical properties of cubic CH3NH3SnI3 perovskite. Journal of Computational Electronics, 2020, 19, 70-79.	1.3	51
37058	Atom vacancies induced electron-rich surface of ultrathin Bi nanosheet for efficient electrochemical CO2 reduction. Applied Catalysis B: Environmental, 2020, 266, 118625.	10.8	112
37059	Enhancing the partial oxidation of gasoline with Mo-doped Ni catalysts for SOFC applications: An integrated experimental and DFT study. Applied Catalysis B: Environmental, 2020, 266, 118626.	10.8	24
37060	Two-dimensional Janus-In2STe/InSe heterostructure with direct gap and staggered band alignment. Applied Surface Science, 2020, 509, 145317.	3.1	23
37061	Effect of external pressure on the structural stability, electronic structure, band gap engineering and optical properties of LiNbO3: An ab-initio calculation. Materials Today Communications, 2020, 23, 100919.	0.9	25
37062	Cooperative Effect of Multiple Active Sites and Hierarchical Chemical Bonds in Metalâ€“Organic Compounds for Improving Cathode Performance. ACS Energy Letters, 2020, 5, 477-485.	8.8	10
37063	Normal-to-topological insulator martensitic phase transition in group-IV monochalcogenides driven by light. NPG Asia Materials, 2020, 12, .	3.8	18
37064	Pdâ€“Cu alloy catalyst synthesized by citric acid-assisted galvanic displacement reaction for N2O reduction. Journal of Applied Electrochemistry, 2020, 50, 395-405.	1.5	6
37065	Hydrogen-dominated metal-free growth of graphitic-nitrogen doped graphene with n-type transport behaviors. Carbon, 2020, 161, 123-131.	5.4	16
37066	Ab initio studies of the structural, electronic and magnetic properties of stannite CuFe2-III-VI4 (IIIÂ= Al,) Tj ETQq1 1 0.784314 rgBT /O	0.9	3
37067	The charge transfer of intercalated Li atoms around islands on Li-halide (F, Br, Cl) surface of SEIs: A first principles calculation. Computational Materials Science, 2020, 176, 109535.	1.4	19
37068	Defect Engineering of MoS₂ for Room-Temperature Terahertz Photodetection. ACS Applied Materials & Interfaces, 2020, 12, 7351-7357.	4.0	52
37069	Catalysis Meets Spintronics; Spin Potentials Associated with Open-Shell Orbital Configurations Enhance the Activity of Pt₃Co Nanostructures for Oxygen Reduction: A Density Functional Theory Study. ACS Applied Nano Materials, 2020, 3, 506-515.	2.4	37
37070	Facet-Independent Oxygen Evolution Activity of Pure Î²-NiOOH: Different Chemistries Leading to Similar Overpotentials. Journal of the American Chemical Society, 2020, 142, 3600-3612.	6.6	114
37071	Unfolding the complexity of phonon quasi-particle physics in disordered materials. Npj Computational Materials, 2020, 6, .	3.5	22
37072	Flexible two-dimensional indium tin oxide fabricated using a liquid metal printing technique. Nature Electronics, 2020, 3, 51-58.	13.1	161

#	Article	IF	Citations
37073	Tuning the electronic structure of RhX₃ (X = Cl, Br, I) nonmagnetic monolayers: effects of charge-injection and external strain. Physical Chemistry Chemical Physics, 2020, 22, 4561-4573.	1.3	5
37074	Exploration of the strain and thermoelectric properties of hexagonal SiX (X = N, P, As, Sb, and Bi) monolayers. Physical Chemistry Chemical Physics, 2020, 22, 3990-3998.	1.3	39
37075	Temperature-dependent mechanical properties of Ti_{n+1}C_nO₂ (n = 1, 2) MXene monolayers: a first-principles study. Physical Chemistry Chemical Physics, 2020, 22, 3414-3424.	1.3	35
37076	Theoretical study of strain induced magnetic transition of single-layer CrTe3. Journal of Applied Physics, 2020, 127, .	1.1	11
37077	Doping induced charge density wave in monolayer TiS2 and phonon-mediated superconductivity. Journal of Applied Physics, 2020, 127, 044301.	1.1	9
37078	Electronic and elastic properties of brownmillerite. Materials Research Express, 2020, 7, 015516.	0.8	5
37079	Electron polarons and donor point defects in americium dioxide<mml:math xmlns:mml="http://www.w3.org/1998/Math/MathML"><mml:msub><mml:mi>AmO</mml:mi><mml:mn>2</mml:mn></mml:msub></mml:math> Physical Review B, 2020, 101, .	1.1	2
37080	Dimensionality-Mediated Semimetal-Semiconductor Transition in Ultrathin <mml:math xmlns:mml="http://www.w3.org/1998/Math/MathML" display="inline"><mml:mrow><mml:msub><mml:mrow><mml:mi>PtTe</mml:mi></mml:mrow><mml:mrow><mml:mn>2</mml:mn></mml:mrow> Films. Physical Review Letters, 2020, 124, 036402.	2.9	54
37081	Visualizing H ₂ O molecules reacting at TiO ₂ active sites with transmission electron microscopy. Science, 2020, 367, 428-430.	6.0	149
37082	Structural, Electronic and Vibrational Properties of YAl3(BO3)4. Materials, 2020, 13, 545.	1.3	17
37083	The mechanism of methanol dehydrogenation on the PdAu(1Â0Â0) surface: A DFT study. Applied Surface Science, 2020, 510, 145434.	3.1	9
37084	Constructing MoS2/g-C3N4 heterojunction with enhanced oxygen evolution reaction activity: A theoretical insight. Applied Surface Science, 2020, 510, 145489.	3.1	76
37085	Atomically thin titanium carbide used as high-efficient, low-cost and stable catalyst for oxygen reduction reaction. International Journal of Hydrogen Energy, 2020, 45, 6994-7004.	3.8	13
37086	Reassessing destructive quantum interference in azulene-based devices. Physical Chemistry Chemical Physics, 2020, 22, 3653-3660.	1.3	5
37087	Synthesis, Crystal and Electronic Structure of Layered AM Sb Compounds (A = Rb, Cs; M = Zn, Cd). Zeitschrift Fur Anorganische Und Allgemeine Chemie, 2020, 646, 1079-1085.	0.6	4
37088	Catalytic reaction mechanism of formaldehyde oxidation by oxygen species over Pt/TiO2 catalyst. Chemosphere, 2020, 248, 125980.	4.2	46
37089	Spin effect on electronic, magnetic and optical properties of spinel CoFe2O4: A DFT study. Materials Science and Engineering B: Solid-State Materials for Advanced Technology, 2020, 253, 114496.	1.7	31
37090	Intrinsic performance regulation in hierarchically porous Co3O4 microrods towards high-rate lithium ion battery anode. Materials Today Energy, 2020, 16, 100383.	2.5	10

#	Article	IF	Citations
37091	Structural and electronic descriptors for atmospheric instability of Li-thiophosphate using density functional theory. Solid State Ionics, 2020, 346, 115225.	1.3	13
37092	Enhancing Quantum Yield in Strained MoS₂ Bilayers by Morphology-Controlled Plasmonic Nanostructures toward Superior Photodetectors. Chemistry of Materials, 2020, 32, 2242-2252.	3.2	24
37093	Pyridinic-Nitrogen-Containing Carbon Cathode: Efficient Electrocatalyst for Seawater Batteries. ACS Applied Energy Materials, 2020, 3, 1602-1608.	2.5	21
37094	Catalysis on oxidized ferroelectric surfacesâ€"Epitaxially strained LaTiO2N and BaTiO3 for photocatalytic water splitting. Journal of Chemical Physics, 2020, 152, 024701.	1.2	9
37095	Pressureâ€induced anomalous behavior of thaumasite crystal. Journal of the American Ceramic Society, 2020, 103, 3763-3775.	1.9	3
37096	Structure and Quantification of Edge Sites of WS₂/Al₂O₃ Catalysts Coupling IR/CO Spectroscopy and DFT Calculations. ChemCatChem, 2020, 12, 2066-2076.	1.8	11
37097	Numerical quadrature in the Brillouin zone for periodic SchrÃ¶dinger operators. Numerische Mathematik, 2020, 144, 479-526.	0.9	15
37098	Adsorption of CH4 and SO2 on Unsupported Pd1â^'xMxO(101) Surface. Catalysis Letters, 2020, 150, 1870-1877.	1.4	3
37099	DFT study of adsorption of glyphosate pesticide on Pt-Cu decorated pyridine-like nitrogen-doped graphene. Journal of Nanoparticle Research, 2020, 22, 1.	0.8	17
37100	Simultaneous electrochemical ozone production and hydrogen evolution by using tantalum-based nanorods electrocatalysts. Applied Catalysis B: Environmental, 2020, 266, 118632.	10.8	42
37101	First-principles study on the structural, electronic, and Li-ion mobility properties of anti-perovskite superionic conductor Li3OCl (1Â0Â0) surface. Applied Surface Science, 2020, 510, 145394.	3.1	12
37102	Operando atomic-scale study of graphene CVD growth at steps of polycrystalline nickel. Carbon, 2020, 161, 528-534.	5.4	17
37103	Accelerating the development of multi-component Cu-Al-based shape memory alloys with high elastocaloric property by machine learning. Computational Materials Science, 2020, 176, 109521.	1.4	19
37104	First principles modelling of the N-doped Co0.5-terminated (0Â0Â1) Co3O4 surface. Nuclear Instruments & Methods in Physics Research B, 2020, 465, 11-14.	0.6	1
37105	Multisite-Occupancy-Driven Intense Narrow-Band Blue Emission from Sr₅SiO₄Cl₆:Eu²⁺ Phosphor with Excellent Stability and Color Performance. Inorganic Chemistry, 2020, 59, 1928-1939.	1.9	54
37106	Lavender-Like Ga-Doped Pt₃Co Nanowires for Highly Stable and Active Electrocatalysis. ACS Catalysis, 2020, 10, 3018-3026.	5.5	75
37107	Thermal transport properties of GaN with biaxial strain and electron-phonon coupling. Journal of Applied Physics, 2020, 127, .	1.1	59
37108	Intrinsic piezoelectricity of monolayer group IVâ€"V MX2: SiP2, SiAs2, GeP2, and GeAs2. Applied Physics Letters, 2020, 116, .	1.5	30

#	Article	IF	Citations
37109	A novel approach to the structural distortions of U/Th snub-disphenoids and their control on zirconâ€‰â€‰â†’â€‰â€‰reidite type phase transitions of U1â^'x Th x SiO4. Journal of Physics Condensed Matter, 2020, 32, 145401.	0.7	22
37110	On tuning the cytotoxicity of Ti₃C₂ (MXene) flakes to cancerous and benign cells by post-delamination surface modifications. 2D Materials, 2020, 7, 025018.	2.0	63
37111	Multifunctional electrocatalytic activity of coronene-based two-dimensional metal-organic frameworks: TM-PTC. Applied Surface Science, 2020, 511, 145393.	3.1	18
37112	A density functional theory study of CO2 hydrogenation to methanol over Pd/TiO2 catalyst: The role of interfacial site. International Journal of Hydrogen Energy, 2020, 45, 6328-6340.	3.8	35
37113	Vacancy mediated alloying strengthening effects on Al/Al3Zr interface and stabilization of L12-Al3Zr: A first-principles study. Journal of Alloys and Compounds, 2020, 825, 153825.	2.8	7
37114	Persulfate activation by two-dimensional MoS2 confining single Fe atoms: Performance, mechanism and DFT calculations. Journal of Hazardous Materials, 2020, 389, 122137.	6.5	72
37115	Al/Ga-Doped Li₇La₃Zr₂O₁₂ Garnets as Li-Ion Solid-State Battery Electrolytes: Atomistic Insights into Local Coordination Environments and Their Influence on ¹⁷O, ²⁷Al, and ⁷¹Ga NMR Spectra. Journal of the American Chemical Society, 2020, 142, 3132-3148.	6.6	51
37116	Dirac half-metallicity of Thin PdCl3 Nanosheets: Investigation of the Effects of External Fields, Surface Adsorption and Defect Engineering on the Electronic and Magnetic Properties. Scientific Reports, 2020, 10, 213.	1.6	33
37117	Perovskite-supported Pt single atoms for methane activation. Journal of Materials Chemistry A, 2020, 8, 4362-4368.	5.2	31
37118	Structural and electronic properties of two-dimensional hydrogenated Xenes. Journal of Physics Condensed Matter, 2020, 32, 205501.	0.7	15
37119	Tailoring electronic properties of two-dimensional antimonene with isoelectronic counterparts*. Chinese Physics B, 2020, 29, 037305.	0.7	6
37120	Tuning the electronic, mechanical, thermal, and optical properties of tetrahexcarbon via hydrogenation. Carbon, 2020, 161, 71-82.	5.4	31
37121	NiCo2S4 quantum dots with high redox reactivity for hybrid supercapacitors. Chemical Engineering Journal, 2020, 388, 124109.	6.6	58
37122	Thermoluminescence, photoluminescence and optically stimulated luminescence characteristics of CaSO4:Eu phosphor: Experimental and density functional theory (DFT) investigations. Journal of Luminescence, 2020, 221, 117051.	1.5	14
37123	First-principles study on the effects of doping and adsorption on the electronic and magnetic properties of diamond nanothreads. Physica E: Low-Dimensional Systems and Nanostructures, 2020, 118, 113949.	1.3	9
37124	General principles to high-throughput constructing two-dimensional carbon allotropes*. Chinese Physics B, 2020, 29, 037306.	0.7	8
37125	Mechanical and Electronic Properties of Tin Carbide Nanowires. Physica Status Solidi (A) Applications and Materials Science, 2020, 217, 1900590.	0.8	4
37126	Investigation of electronic, magnetic, elastic, mechanical, thermodynamic, and thermoelectronic properties of Mn2PtV Heusler alloy: ab initio study. Journal of Molecular Modeling, 2020, 26, 35.	0.8	11

#	Article	IF	Citations
37127	Strain-controlled magnetic ordering in 2D carbon metamaterials. Carbon, 2020, 161, 219-223.	5.4	5
37128	Ab initio study of pressure induced phase transition, structural and electronic structure properties of superconducting perovskite compound GdBa2Cu3O7-x. Computational Condensed Matter, 2020, 23, e00461.	0.9	3
37129	Magnetic anisotropy in Cr2GeC investigated by X-ray magnetic circular dichroism and ab initio calculations. Journal of Magnetism and Magnetic Materials, 2020, 501, 166470.	1.0	5
37130	How to get noWear? â€“ A new take on the design of in-situ formed high performing low-friction tribofilms. Materials and Design, 2020, 190, 108519.	3.3	25
37131	First principles calculations of thermodynamic properties of OsB2. Materials Today: Proceedings, 2020, 28, 23-27.	0.9	0
37132	Study of strain effects on electronic and optical properties of CH3NH3PbX3 (X= Cl, Br, I) perovskites. Physica B: Condensed Matter, 2020, 582, 412024.	1.3	11
37133	Synergy effects on Sn-Cu alloy catalyst for efficient CO2 electroreduction to formate with high mass activity. Science Bulletin, 2020, 65, 711-719.	4.3	142
37134	Steric Effects Control Dry Friction of H- and F-Terminated Carbon Surfaces. ACS Applied Materials & Interfaces, 2020, 12, 8805-8816.	4.0	15
37135	Dendrite-Free Lithium Anodes Enabled by a Commonly Used Copper Antirusting Agent. ACS Applied Materials & Interfaces, 2020, 12, 8168-8175.	4.0	35
37136	Determining Surface Terminations and Chirality of Noncentrosymmetric FeGe Thin Films via Scanning Tunneling Microscopy. ACS Applied Materials & Interfaces, 2020, 12, 9896-9901.	4.0	4
37137	Embedding tetrahedral 3d transition metal TM₄ clusters into the cavity of two-dimensional graphdiyne to construct highly efficient and nonprecious electrocatalysts for hydrogen evolution reaction. Physical Chemistry Chemical Physics, 2020, 22, 3254-3263.	1.3	20
37138	First-principles comparative study of perfect and defective CsPbX₃ (X = Br, I) crystals. Physical Chemistry Chemical Physics, 2020, 22, 3914-3920.	1.3	37
37139	Electronic and optical properties of monolayer MoS₂under the influence of polyethyleneimine adsorption and pressure. RSC Advances, 2020, 10, 4201-4210.	1.7	17
37140	Dimerization of pentacyclopentacorannulene C30H10 as a strategy to produce C60H20 as a precursor for C60. RSC Advances, 2020, 10, 3689-3693.	1.7	3
37141	Identification of the donor and acceptor states of the bond-centered hydrogenâ€“carbon pair in Si and diluted SiGe alloys. Journal of Applied Physics, 2020, 127, .	1.1	4
37142	First-principles investigation of the structural, dynamical, electronic, and elastic properties of WGe₂ and W₅Ge₃. Philosophical Magazine, 2020, 100, 1129-1149.	0.7	7
37143	Electronic Structure and Room Temperature of 2D Dilute Magnetic Semiconductors in Bilayer MoS₂-Doped Mn. Advances in Condensed Matter Physics, 2020, 2020, 1-8.	0.4	6
37144	Unusual Pressureâ€Driven Phase Transformation and Band Renormalization in 2D vdW Hybrid Lead Halide Perovskites. Advanced Materials, 2020, 32, e1907364.	11.1	23

#	Article	IF	Citations
37145	Wideâ€gap (Ag,Cu)(In,Ga)Se₂ solar cells with different buffer materialsâ€”A path to a better heterojunction. Progress in Photovoltaics: Research and Applications, 2020, 28, 237-250.	4.4	47
37146	Raman and Infrared Phonon Spectra of Novel Nonlinear Optical Materials PbGa₂GeS₆ and PbGa₂GeSe₆: Experiment and Theory. Physica Status Solidi (B): Basic Research, 2020, 257, 1900700.	0.7	3
37147	A high growth rate process of ALD CeOx with amidinato-cerium [(N-iPr-AMD)3Ce] and O3 as precursors. Journal of Materials Science, 2020, 55, 5378-5389.	1.7	7
37148	Structural, elastic, electronic and optical properties of lithium halides (LiF, LiCl, LiBr, and LiI): First-principle calculations. Materials Chemistry and Physics, 2020, 244, 122733.	2.0	22
37149	Theoretical design of SnTe/GeS lateral heterostructures: A first-principles study. Physica B: Condensed Matter, 2020, 583, 412047.	1.3	8
37150	First principles study of ferroelectric hexagonal compounds RInO3 (R = Dy, Er, and Ho): electronic structure, optical and dielectric properties. RSC Advances, 2020, 10, 4080-4086.	1.7	4
37151	High efficiency spin filtering in magnetic phosphorene. Physical Chemistry Chemical Physics, 2020, 22, 5893-5901.	1.3	28
37152	Structural electronic and dynamic properties of Li3Bi and Li2NaBi. Materials Research Express, 2020, 7, 015913.	0.8	6
37153	Large-scale synthesis of crystalline g-C ₃ N ₄ nanosheets and high-temperature H ₂ sieving from assembled films. Science Advances, 2020, 6, eaay9851.	4.7	105
37154	Tantalum disulfide quantum dots: preparation, structure, and properties. Nanoscale Research Letters, 2020, 15, 20.	3.1	15
37155	Lanthanide orthothiophosphates revisited: single-crystal X-ray, Raman, and DFT studies of TmPS₄ and YbPS₄. Zeitschrift Fur Naturforschung - Section B Journal of Chemical Sciences, 2020, 75, 225-231.	0.3	9
37156	First-Principles Study of the Electrochemical Sodiation of Rutile-Type Vanadium Dioxide. MRS Advances, 2020, 5, 1467-1474.	0.5	1
37157	Modified Density Functional Dispersion Correction for Inorganic Layered MFX Compounds (M = Ca, Sr,) Tj ETQq0 0 0 rgBT /Overlock 10	1.1	5
37158	Understanding the Inhibition of the Shuttle Effect of Sulfides (S â‰¥ 3) in Lithiumâ€“Sulfur Batteries by Heteroatom-Doped Graphene: First-Principles Study. Journal of Physical Chemistry C, 2020, 124, 3644-3649.	1.5	19
37159	Revisiting the anchoring behavior in lithium-sulfur batteries: many-body effect on the suppression of shuttle effect. Npj Computational Materials, 2020, 6, .	3.5	29
37160	Exsolution of Cu nanoparticles in (LaSr)0.9Fe0.9Cu0.1O4 Ruddlesden-Popper oxide as symmetrical electrode for solid oxide cells. Applied Surface Science, 2020, 511, 145525.	3.1	40
37161	Growth and characterization of PbI2-decorated ZnO nanowires for photodetection applications. Journal of Alloys and Compounds, 2020, 825, 154095.	2.8	9
37162	Evidence for flat zero-energy bands in bilayer graphene with a periodic defect lattice. Physica E: Low-Dimensional Systems and Nanostructures, 2020, 119, 113987.	1.3	4

#	Article	IF	Citations
37163	Identification of Efficient Single-Atom Catalysts Based on V₂CO₂ MXene by ab Initio Simulations. Journal of Physical Chemistry C, 2020, 124, 4090-4100.	1.5	31
37164	Effects of Oxygen Mobility in Laâ€“Fe-Based Perovskites on the Catalytic Activity and Selectivity of Methane Oxidation. ACS Catalysis, 2020, 10, 3707-3719.	5.5	132
37165	C3N monolayer with substitutional doping and strain modulation serving as anode material of lithium-ion batteries. Applied Surface Science, 2020, 510, 145324.	3.1	24
37166	The effect of hydrostatic pressure on melt-castable energetic materials bis-oxadiazole-bis-methylene dinitrate: A density functional theory study. Solid State Communications, 2020, 308, 113840.	0.9	4
37167	Large-area epitaxial growth of curvature-stabilized ABC trilayer graphene. Nature Communications, 2020, 11, 546.	5.8	47
37168	Tuning the photocatalytic water-splitting capability of two-dimensional Î±-In₂Se₃ by strain-driven band gap engineering. Physical Chemistry Chemical Physics, 2020, 22, 3520-3526.	1.3	21
37169	Electronic Structures and Thermoelectric Properties of ZnSb Doped with Cd and In from First Principles Calculations*. Chinese Physics Letters, 2020, 37, 017102.	1.3	4
37170	The H₂O Dissociation and Hydrogen Evolution Performance of Monolayer MoS₂ Containing Single Mo Vacancy: A Theoretical Study. IEEE Nanotechnology Magazine, 2020, 19, 163-167.	1.1	6
37171	Triple VTe2/graphene/VTe2 heterostructures as perspective magnetic tunnel junctions. Applied Surface Science, 2020, 510, 145315.	3.1	19
37172	Connecting the surface structure, morphology and photocatalytic activity of Ag2O: An in depth and unified theoretical investigation. Applied Surface Science, 2020, 509, 145321.	3.1	51
37173	Metallic VS2 monolayer as an anchoring material for lithium-sulfur batteries. Chemical Physics Letters, 2020, 741, 137121.	1.2	21
37174	Local Order and Rotational Dynamics in Mixed A-Cation Lead Iodide Perovskites. Journal of Physical Chemistry Letters, 2020, 11, 1068-1074.	2.1	31
37175	Exploring doped or vacancy-modified graphene-based electrodes for applications in asymmetric supercapacitors. Physical Chemistry Chemical Physics, 2020, 22, 3906-3913.	1.3	26
37176	Nickel nanograins anchored on a carbon framework for an efficient hydrogen evolution electrocatalyst and a flexible electrode. Journal of Materials Chemistry A, 2020, 8, 3499-3508.	5.2	18
37177	Theoretical prediction of T-graphene as a promising alkali-ion battery anode offering ultrahigh capacity. Physical Chemistry Chemical Physics, 2020, 22, 3281-3289.	1.3	51
37178	Periodic F-defects on the MgO surface as potential single-defect catalysts with non-linear optical properties. Chemical Physics, 2020, 532, 110680.	0.9	18
37179	Vibrational spectroscopy study and ab initio calculation on ZnMoO4 system. Journal of Molecular Structure, 2020, 1206, 127776.	1.8	7
37180	The effect of pre-deformation on the precipitation behavior of AlCuMg(Si) alloys with low Cu/Mg ratios. Journal of Alloys and Compounds, 2020, 823, 153831.	2.8	17

#	Article	IF	Citations
37181	Abnormal lattice occupation of Mo and related polarons in LiNbO3: Hybrid density functional theory investigation. Journal of Materiomics, 2020, 6, 183-191.	2.8	2
37182	First-Principles Insights into the Interface Chemistry between 4-Aminothiophenol and Zinc Phosphide (Zn₃P₂) Nanoparticles. ACS Omega, 2020, 5, 1025-1032.	1.6	10
37183	Fatigue of graphene. Nature Materials, 2020, 19, 405-411.	13.3	110
37184	First principles investigation of dissociative adsorption of H₂ during CO₂ hydrogenation over cubic and hexagonal In₂O₃ catalysts. Physical Chemistry Chemical Physics, 2020, 22, 3390-3399.	1.3	40
37185	EuNi₂P₄, the first magnetic unconventional clathrate preparedviaa mechanochemically assisted route. Inorganic Chemistry Frontiers, 2020, 7, 1115-1126.	3.0	8
37186	Computer modeling investigation of MgV2O4 for Mg-ion batteries. Journal of Applied Physics, 2020, 127, 035106.	1.1	10
37187	Thermodynamic descriptions of the light rareâ€earth elements in silicon carbide ceramics. Journal of the American Ceramic Society, 2020, 103, 3812-3825.	1.9	16
37188	Morphology Evolution of Hcp Cobalt Nanoparticles Induced by Ru Promoter. ChemCatChem, 2020, 12, 2083-2090.	1.8	7
37189	Highly efficient binary copperâ"iron catalyst for photoelectrochemical carbon dioxide reduction toward methane. Proceedings of the National Academy of Sciences of the United States of America, 2020, 117, 1330-1338.	3.3	93
37190	Phonon transport properties of NbCoSb compound. Materials Research Express, 2020, , .	0.8	4
37191	Controlling neutral and charged excitons in MoS₂ with defects. Journal of Materials Research, 2020, 35, 949-957.	1.2	12
37192	Nonlayered CdSe Flakes Homojunctions. Advanced Functional Materials, 2020, 30, 1908902.	7.8	28
37193	Hydrogen-rich syngas production with tar elimination via biomass chemical looping gasification (BCLG) using BaFe2O4/Al2O3 as oxygen carrier. Chemical Engineering Journal, 2020, 387, 124107.	6.6	74
37194	Ï‡3â€"borophene-based detection of hydrogen sulfide via gas nanosensors. Chemical Physics Letters, 2020, 741, 137066.	1.2	18
37195	Mechanics of carbon-coated silicon nanowire via second strain gradient theory. European Journal of Mechanics, A/Solids, 2020, 81, 103943.	2.1	5
37196	Magnetic semiconductor properties of RbLnSe2 (LnÂ=ÂCe, Pr, Nd, Gd): A density functional study. Journal of Magnetism and Magnetic Materials, 2020, 501, 166448.	1.0	11
37197	Probing martensitic transformation, kinetics, elastic and magnetic properties of Ni2-Mn1.5In0.5Co alloys. Journal of Materials Science and Technology, 2020, 44, 31-41.	5.6	21
37198	Quantum Transport beyond DC. , 2020, , 278-292.		0

#	Article	IF	Citations
37200	Mechanically Tunable Spontaneous Vertical Charge Redistribution in Few-Layer WTe₂. Journal of Physical Chemistry C, 2020, 124, 2008-2012.	1.5	8
37201	Filter function of graphene oxide: Trapping perfluorinated molecules. Journal of Chemical Physics, 2020, 152, 024704.	1.2	9
37202	Theoretical Investigation of Piezoelectric Properties of Graphene/Hexagonal Boron Nitride Hybrid Structures. Physica Status Solidi (B): Basic Research, 2020, 257, 1900733.	0.7	4
37203	Niobium pentoxide ultra-thin nanosheets: A photocatalytic degradation and recyclable surface-enhanced Raman scattering substrate. Applied Surface Science, 2020, 509, 145376.	3.1	21
37204	Characteristics of Sr1â^'xYxTi1â^'yRuyO3+/â^'Î´ and Ru-impregnated Sr1â^'xYxTiO3+/â^'Î´ perovskite catalysts as SOFC anode for methane dry reforming. Applied Surface Science, 2020, 510, 145450.	3.1	17
37205	Engineering oxygen vacancy on iron oxides/hollow carbon cloth electrode toward stable lithium-ion batteries. Chemical Engineering Journal, 2020, 388, 124229.	6.6	26
37206	Comparing study of picene thin films on SnSe and Au(1Â1Â1) surfaces. Chemical Physics, 2020, 532, 110689.	0.9	2
37207	Room temperature ferromagnetism in carbon doped MoO3 for spintronic applications: A DFT study. Journal of Magnetism and Magnetic Materials, 2020, 502, 166503.	1.0	19
37208	Density functional calculations of organic pollutants adsorbed on Hittorf's violet phosphorene. Physica E: Low-Dimensional Systems and Nanostructures, 2020, 120, 113963.	1.3	5
37209	New High Pressure Phases of the Znâ€“N System. Journal of Physical Chemistry C, 2020, 124, 4044-4049.	1.5	36
37210	2D Hybrid Superlattice-Based On-Chip Electrocatalytic Microdevice for in Situ Revealing Enhanced Catalytic Activity. ACS Nano, 2020, 14, 1635-1644.	7.3	36
37211	Prediction of superconductivity in pressure-induced new silicon boride phases. Physical Review B, 2020, 101, .	1.1	12
37212	Tunable Electronic Properties and Potential Applications of 2D GeP/Graphene van der Waals Heterostructure. Advanced Electronic Materials, 2020, 6, 1901024.	2.6	42
37213	Physicochemical properties of l- and dl-valine: first-principles calculations. Amino Acids, 2020, 52, 425-433.	1.2	5
37214	Critical effect of carbon vacancies on the reverse water gas shift reaction over vanadium carbide catalysts. Applied Catalysis B: Environmental, 2020, 267, 118719.	10.8	69
37215	Role of the surface density of states in understanding size-dependent surface band bending in GaN nanowires. Applied Surface Science, 2020, 510, 145502.	3.1	4
37216	Role of carbon nanotubes on growth of a nanostructured double-deck tribofilm yielding excellent self-lubrication performance. Carbon, 2020, 161, 445-455.	5.4	25
37217	Elastic moduli of high-density, sintered monoliths of yttrium dihydride. Journal of Alloys and Compounds, 2020, 826, 153955.	2.8	22

#	Article	IF	Citations
37218	Performance effects of doping engineering on graphene-like C3N as an anode material for alkali metal ion batteries. Materials Science in Semiconductor Processing, 2020, 109, 104946.	1.9	11
37219	Rational design of porous nitrogen-doped Ti3C2 MXene as a multifunctional electrocatalyst for Liâ€“S chemistry. Nano Energy, 2020, 70, 104555.	8.2	194
37220	Abnormally Low Activation Energy in Cubic Na₃SbS₄ Superionic Conductors. Chemistry of Materials, 2020, 32, 2264-2271.	3.2	35
37221	High-performance optoelectronic memory based on bilayer MoS₂ grown by Au catalyst. Journal of Materials Chemistry C, 2020, 8, 2664-2668.	2.7	9
37222	Few-Layer <mml:math xmlns:mml="http://www.w3.org/1998/Math/MathML" display="inline" overflow="scroll"><mml:mi>Î²</mml:mi></mml:math> - <mml:math xmlns:mml="http://www.w3.org/1998/Math/MathML" display="inline" overflow="scroll"><mml:mrow><mml:mi>Sn</mml:mi><mml:mi>Se</mml:mi></mml:mrow></mml:math> with Strong Visible Light Absorbance and Ultrahigh Carrier Mobility. Physical Review Applied, 2020, 13, .	1.5	8
37223	Bimetallic Ruâ€Fe Nanoparticles Supported on Carbon Nanotubes for Ammonia Decomposition and Synthesis. Chemical Engineering and Technology, 2020, 43, 719-730.	0.9	26
37224	Highâ€throughput firstâ€principle calculations of the structural, mechanical, and electronic properties of cubic XTiO₃ (X = Ca, Sr, Ba, Pb) ceramics under high pressure. International Journal of Quantum Chemistry, 2020, 120, e26168.	1.0	4
37225	Mixing enthalpies of alloys with dynamical instability: bcc Ti-V system. Acta Materialia, 2020, 188, 145-154.	3.8	10
37226	First-principles study of the structural, electronic, magnetic properties of orthorhombic PrCuO3 perovskites. Chemical Physics Letters, 2020, 743, 137166.	1.2	2
37227	Regenerable CoxMn3â^'xO4 spinel sorbents for elemental mercury removal from syngas: Experimental and DFT studies. Fuel, 2020, 266, 117105.	3.4	28
37228	Antiferromagnetic Semimetal in Ti-Intercalated Borophene Heterobilayer. Journal of Physical Chemistry C, 2020, 124, 4709-4716.	1.5	5
37229	Superior Catalytic Performance of Atomically Dispersed Palladium on Graphene in CO Oxidation. ACS Catalysis, 2020, 10, 3084-3093.	5.5	44
37230	Metalâ€“2D multilayered semiconductor junctions: layer-number dependent Fermi-level pinning. Journal of Materials Chemistry C, 2020, 8, 3113-3119.	2.7	33
37231	Atomically Dispersed Single Ni Site Catalysts for Nitrogen Reduction toward Electrochemical Ammonia Synthesis Using N₂ and H₂O. Small Methods, 2020, 4, 1900821.	4.6	148
37232	Combining Chirality and Hydrogen Bonding in Methylated Ethylenedithio-Tetrathiafulvalene Primary Diamide Precursors and Radical Cation Salts. Crystal Growth and Design, 2020, 20, 2516-2526.	1.4	10
37233	DFT-Assisted Spectroscopic Studies on the Coordination of Small Ligands to Palladium: From Isolated Ions to Nanoparticles. Journal of Physical Chemistry C, 2020, 124, 4781-4790.	1.5	4
37234	Silicon and Phosphorus Co-doped Bipyridine-Linked Covalent Triazine Framework as a Promising Metal-Free Catalyst for Hydrogen Evolution Reaction: A Theoretical Investigation. Journal of Physical Chemistry Letters, 2020, 11, 1542-1549.	2.1	37
37235	Deciphering the Role of Key Defects in Sb₂Se₃, a Promising Candidate for Chalcogenide-Based Solar Cells. ACS Applied Energy Materials, 2020, 3, 2496-2509.	2.5	49

#	Article	IF	Citations
37236	Ab Initio Studies of Discharge Mechanism of MnO₂ in Deep-Cycled Rechargeable Zn/MnO₂ Batteries. Journal of the Electrochemical Society, 2020, 167, 020557.	1.3	23
37237	Relationship between the Behavior of Hydrogen and Hydrogen Bubble Nucleation in Vanadium. Materials, 2020, 13, 322.	1.3	4
37238	Study of the Structure, Electronic and Optical Properties of BiOI/Rutile-TiO2 Heterojunction by the First-Principle Calculation. Materials, 2020, 13, 323.	1.3	14
37239	First-Principles Study on Structural, Mechanical, Anisotropic, Electronic and Thermal Properties of III-Phosphides: XP (X = Al, Ga, or In) in the P6422 Phase. Materials, 2020, 13, 686.	1.3	11
37240	Synthesis of Coâ€Doped MoS₂ Monolayers with Enhanced Valley Splitting. Advanced Materials, 2020, 32, e1906536.	11.1	84
37241	Effects of halogen substitutions on the properties of CH3NH3Sn0.5Pb0.5I3 perovskites. Computational Materials Science, 2020, 177, 109576.	1.4	5
37242	Effect of partial substitution of iron by tungsten on the crystal structure and electronic properties of WB3. Physica B: Condensed Matter, 2020, 583, 412026.	1.3	4
37243	Copper-doped induced ferromagnetic half-metal zirconium diselenide single crystals. Nanotechnology, 2020, 31, 235704.	1.3	5
37244	Chiral Magnetism and High-Temperature Skyrmions in B20-Ordered Co-Si. Physical Review Letters, 2020, 124, 057201.	2.9	31
37245	Local Electronic Structure in AlN Studied by Single-Crystal 27Al and 14N NMR and DFT Calculations. Molecules, 2020, 25, 469.	1.7	10
37246	Sodiumâ€Mediated Epitaxial Growth of 2D Ultrathin Sb₂Se₃ Flakes for Broadband Photodetection. Advanced Functional Materials, 2020, 30, 1909849.	7.8	88
37247	Effect of chemical nature of atoms on the electronic, dielectric, and dynamical properties of ABX 3 halide perovskite. International Journal of Quantum Chemistry, 2020, 120, e26172.	1.0	11
37248	First principle studies of oxygen reduction reaction on N doped graphene: Impact of N concentration, position and co-adsorbate effect. Applied Surface Science, 2020, 510, 145470.	3.1	16
37249	Effect of Mn doping defect on 180Â° domain wall in ferroelectric PbTiO3. Physics Letters, Section A: General, Atomic and Solid State Physics, 2020, 384, 126279.	0.9	6
37250	Oxygen-Plasma-Assisted Enhanced Acetone-Sensing Properties of ZnO Nanofibers by Electrospinning. ACS Applied Materials & Interfaces, 2020, 12, 23084-23093.	4.0	66
37251	Prediction of new thermodynamically stable ZnN2O3 at high pressure. Physical Chemistry Chemical Physics, 2020, 22, 10941-10948.	1.3	1
37252	Characterisation of the temperature-dependent M1 to R phase transition in W-doped VO2 nanorod aggregates by Rietveld refinement and theoretical modelling. Physical Chemistry Chemical Physics, 2020, 22, 7984-7994.	1.3	9
37253	Mechanistic insights into the oxidation of copper(<scp>i</scp>) species during NH₃-SCR over Cu-CHA zeolites: a DFT study. Catalysis Science and Technology, 2020, 10, 3586-3593.	2.1	25

#	Article	IF	Citations
37254	Conductivity and mixed conductivity of a novel dense diffusion barrier and the sensing properties of limiting current oxygen sensors. Dalton Transactions, 2020, 49, 6682-6692.	1.6	59
37255	A systematic computational study of electronic, mechanical, and optical properties of Fe_{1â^'x}Co_x alloy. Journal of Physics Communications, 2020, 4, 045003.	0.5	6
37256	Defect Assisted Carrier Multiplication in Amorphous Silicon. IEEE Journal of Quantum Electronics, 2020, 56, 1-11.	1.0	4
37257	A Nobleâ€Transition Alloy Excels at Hotâ€Carrier Generation in the Near Infrared. Advanced Materials, 2020, 32, e1906478.	11.1	11
37258	Photocatalytic and Thermometric Characteristics of Er³⁺â€Activated Bi₅IO₇ Upconverting Microparticles. Advanced Materials Interfaces, 2020, 7, 1902208.	1.9	54
37259	Efficient dual-function catalysts for triiodide reduction reaction and hydrogen evolution reaction using unique 3D network aloe waste-derived carbon-supported molybdenum-based bimetallic oxide nanohybrids. Applied Catalysis B: Environmental, 2020, 273, 119004.	10.8	59
37260	Probing the surface structure via the adsorbed hydrogen atoms â€“ The case of Cu(4â€¯1â€¯0). Applied Surface Science, 2020, 528, 146433.	3.1	2
37261	Low-pressure chemical vapor deposition of Cu on Ru substrate using CuI:<mml:math xmlns:mml="http://www.w3.org/1998/Math/MathML" altimg="si12.svg"><mml:mrow><mml:mi mathvariant="italic">Ab</mml:mi><mml:mspace width="0.35em" /><mml:mi mathvariant="italic">initio</mml:mi></mml:mrow></mml:math>calculations. Chemical Physics Letters, 2020, 741, 137108.	1.2	5
37262	Li+ co-doping induced phase transition as an efficient strategy to enhance upconversion of La2Zr2O7:Er,Yb nanoparticles. Journal of Luminescence, 2020, 224, 117312.	1.5	24
37263	First principle study of the structural and optoelectronic properties of direct bandgap double perovskite Cs2AgInCl6. Materials Today: Proceedings, 2020, 33, 1252-1256.	0.9	17
37264	Comparative quantum chemistry study of the F-center in lanthanum trifluoride. Nuclear Instruments & Methods in Physics Research B, 2020, 474, 57-62.	0.6	9
37265	Carbon influence on hydrogen absorption and adsorption on Fe-C alloy surfaces. Surface Science, 2020, 697, 121606.	0.8	5
37266	Tuning the structural and electronic properties of single-layer stanene through doping 4d transition metals (Mo, Nb, Rh and Ru): A DFT study. Synthetic Metals, 2020, 264, 116399.	2.1	2
37267	Phase Transition and Liquid-like Superionic Conduction in Ag₂S. Journal of Physical Chemistry C, 2020, 124, 10150-10158.	1.5	9
37268	High Curie temperature and carrier mobility of novel Fe, Co and Ni carbide MXenes. Nanoscale, 2020, 12, 11627-11637.	2.8	26
37269	The formation and effect of O-vacancies in doped TiO₂. New Journal of Chemistry, 2020, 44, 8559-8571.	1.4	7
37270	Bi2W2O9 : A potentially antiferroelectric Aurivillius phase. Physical Review B, 2020, 101, .	1.1	8
37271	Heavy Water Additive in Formamidinium: A Novel Approach to Enhance Perovskite Solar Cell Efficiency. Advanced Materials, 2020, 32, e1907864.	11.1	51

#	Article	IF	Citations
37272	A first-principles study of the proton and oxygen migration behavior in the rare-earth perovskite SmNiO3. Journal of Computational Electronics, 2020, 19, 905-909.	1.3	12
37273	Effect of transition metal doping on Crâ€“Ru alloys using first principles approach. Bulletin of Materials Science, 2020, 43, 1.	0.8	5
37274	<mml:math xmlns:mml="http://www.w3.org/1998/Math/MathML" altimg="si22.svg"><mml:mrow><mml:mi mathvariant="italic">Ab</mml:mi><mml:mspace width="0.35em" /><mml:mi mathvariant="italic">initio</mml:mi></mml:mrow></mml:math> calculations of the optical and electronic properties of Bi2WO6 doped with Mo, Cr, Fe, and Zn on the Wâ€“lattice site. Applied Surface Science, 2020, 515, 146036.	3.1	13
37275	Structural, elastic, electronic and transport properties of CoVX (XÂ= Ge and Si) compounds: A DFT prediction. Computational Condensed Matter, 2020, 24, e00475.	0.9	6
37276	Wood cellulose as a hydrogen storage material. International Journal of Hydrogen Energy, 2020, 45, 14907-14914.	3.8	9
37277	Designing a high-performance nitrogen-doped titanium dioxide anode material for lithium-ion batteries by unravelling the nitrogen doping effect. Nano Energy, 2020, 74, 104829.	8.2	38
37278	The role of anions on the Helmholtz Plane for the solid-liquid interface in aqueous rechargeable lithium batteries. Nano Energy, 2020, 74, 104864.	8.2	27
37279	Intrinsic Defect-Rich Hierarchically Porous Carbon Architectures Enabling Enhanced Capture and Catalytic Conversion of Polysulfides. ACS Nano, 2020, 14, 6222-6231.	7.3	89
37280	Importance of the decoration in shaped cobalt nanoparticles in the acceptor-less secondary alcohol dehydrogenation. Catalysis Science and Technology, 2020, 10, 4923-4937.	2.1	14
37281	Intercalated Cu+ ion dynamics in the two-dimensional layered compound Cu0.33TiSe2. Physical Review B, 2020, 101, .	1.1	4
37282	Manipulatable Interface Electric Field and Charge Transfer in a 2D/2D Heterojunction Photocatalyst via Oxygen Intercalation. Catalysts, 2020, 10, 469.	1.6	5
37283	The Effects of Doping on the Electronic Characteristics and Adsorption Behavior of Silicon Polyprismanes. Computation, 2020, 8, 25.	1.0	0
37284	Lithium Storage in Nanoporous Complex Oxide 12CaOâ€¢7Al2O3 (C12A7). Energies, 2020, 13, 1547.	1.6	4
37285	A theoretical study of gas adsorption on Î±-quartz (0Â0Â1) for CO2 enhanced natural gas recovery. Applied Surface Science, 2020, 525, 146472.	3.1	10
37286	Mechanism investigations on CO oxidation catalyzed by Fe-doped graphene: A theoretical study. Applied Surface Science, 2020, 523, 146496.	3.1	18
37287	Revisiting the identity of Î´-MgCl2: Part II. Morphology and exposed surfaces studied by vibrational spectroscopies and DFT calculation. Journal of Catalysis, 2020, 387, 1-11.	3.1	25
37288	Helping Thy Neighbor: How Cobalt Doping Alters the Electrocatalytic Properties of Hematite. Journal of Physical Chemistry Letters, 2020, 11, 4402-4407.	2.1	6
37289	Automated Generation and Analysis of the Complex Catalytic Reaction Network of Ethanol Synthesis from Syngas on Rh(111). ACS Catalysis, 2020, 10, 6346-6355.	5.5	40

#	Article	IF	Citations
37290	ZnO/CuSCN Nano-Heterostructure as a Highly Efficient Field Emitter: a Combined Experimental and Theoretical Investigation. ACS Omega, 2020, 5, 6715-6724.	1.6	12
37291	Adsorption and Gas Sensing Properties of the Pt₃-MoSe₂ Monolayer to SOF₂ and SO₂F₂. ACS Omega, 2020, 5, 7722-7728.	1.6	24
37292	Lattice distortion induced internal electric field in TiO2 photoelectrode for efficient charge separation and transfer. Nature Communications, 2020, 11, 2129.	5.8	108
37293	Performance of the standard exchange-correlation functionals in predicting melting properties fully from first principles: Application to Al and magnetic Ni. Physical Review B, 2020, 101, .	1.1	15
37294	Hybrid-functional electronic structure of multilayer graphene. Physical Review B, 2020, 101, .	1.1	7
37295	Tuning electronic and magnetic properties of the graphone/Ni(111) interface by oxygen intercalation: A first-principles prediction. Physical Review B, 2020, 101, .	1.1	2
37296	Synthesis and Characterization of Manganese Tetrafluoride Î²â€MnF₄. Zeitschrift Fur Anorganische Und Allgemeine Chemie, 2020, 646, 1481-1489.	0.6	7
37297	Adsorption of carbonyl sulfide on Pt-doped vacancy-defected SWCNT: A DFT study. Applied Surface Science, 2020, 525, 146331.	3.1	7
37298	Adamsite and chloropicrin molecular adsorption studies on novel green phosphorene nanotube â€“ First-principles investigation. Chemical Physics, 2020, 535, 110782.	0.9	27
37299	A new thermodynamic modeling of the Tiâ€“V system including the metastable Ï‰ phase. Intermetallics, 2020, 122, 106791.	1.8	18
37300	First-principles studies of intrinsic stacking fault energies and elastic properties of Al-based alloys. Materials Today Communications, 2020, 24, 101085.	0.9	7
37301	Identifying Key Structural Subunits and Their Synergism in Low-Iridium Triple Perovskites for Oxygen Evolution in Acidic Media. Chemistry of Materials, 2020, 32, 3904-3910.	3.2	29
37302	Formation of Hexagonal PdSe₂ for Electronics and Catalysis. Journal of Physical Chemistry C, 2020, 124, 10935-10940.	1.5	16
37303	Dissociative Oxygen Reduction Reaction Mechanism on the Neighboring Active Sites of a Boron-Doped Pyrolyzed Feâ€“Nâ€“C Catalyst. Journal of Physical Chemistry C, 2020, 124, 11383-11391.	1.5	32
37304	Designing Efficient Dual-Metal Single-Atom Electrocatalyst TMZnN₆ (TM = Mn, Fe, Co, Ni,) Tj ETQq0 0 0 rgBT /Overlock 10	1.5	47
37305	Compensation between Surface Energy and hcp/fcc Phase Energy of Late Transition Metals from First-Principles Calculations. Journal of Physical Chemistry C, 2020, 124, 11005-11014.	1.5	37
37306	1Tâ€´ Transition-Metal Dichalcogenides: Strong Bulk Photovoltaic Effect for Enhanced Solar-Power Harvesting. Journal of Physical Chemistry C, 2020, 124, 11221-11228.	1.5	11
37307	Improved Performance of Thermally Evaporated Sb₂Se₃ Thin-Film Solar Cells via Substrate-Cooling-Speed Control and Hydrogen-Sulfide Treatment. ACS Applied Materials & Interfaces, 2020, 12, 24112-24124.	4.0	34

#	Article	IF	Citations
37308	Investigation of Boron-Doped Graphdiyne as a Promising Anode Material for Sodium-Ion Batteries: A Computational Study. ACS Omega, 2020, 5, 10034-10041.	1.6	20
37309	Fe₃O₄-Functionalized Boron Nitride Nanosheets as Novel Adsorbents for Removal of Arsenic(III) from Contaminated Water. ACS Omega, 2020, 5, 10301-10314.	1.6	27
37310	First Principles Calculations on Elastic, Thermodynamic and Electronic Properties of Co2Zr and Co2Ti at High Temperature and Pressure. Applied Sciences (Switzerland), 2020, 10, 2097.	1.3	3
37311	Correlating surface chemistry and hydrophobicity of sulfidized nanoscale zerovalent iron with its reactivity and selectivity for denitration and dechlorination. Chemical Engineering Journal, 2020, 394, 124876.	6.6	79
37312	Effects of Mn, Fe, and Ce doping on the adsorption property of gas molecules and oxidation of SO2 on the NiO (1Â0Â0) surface. Computational Materials Science, 2020, 180, 109717.	1.4	13
37313	A black Phosphorus/BiVO4(010) heterostructure for promising photocatalytic performance: First-principles study. Journal of Physics and Chemistry of Solids, 2020, 143, 109466.	1.9	18
37314	Cd12O12 cage cluster-assembled nanowires and band gap regulation: A first-principles investigation. Physics Letters, Section A: General, Atomic and Solid State Physics, 2020, 384, 126463.	0.9	4
37315	Effect of intrinsic defects on the thermal conductivity of PbTe from classical molecular dynamics simulations. Journal of Physics Condensed Matter, 2020, 32, 045701.	0.7	11
37316	Structural, bonding, and elastic properties of Si:X (X = B, Al, and Ga): a theoretical study. Semiconductor Science and Technology, 2020, 35, 065004.	1.0	1
37317	Insights on the Excitation Spectrum of Graphene Contacted with a Pt Skin. Nanomaterials, 2020, 10, 703.	1.9	4
37318	H₂â€Directing Strategy on In Situ Synthesis of Coâ€MoS₂ with Highly Expanded Interlayer for Elegant HER Activity and its Mechanism. Advanced Energy Materials, 2020, 10, 2000291.	10.2	82
37319	Bimetalâ€organic Frameworkâ€derived Co₉S₈/ZnS@NC Heterostructures for Superior Lithiumâ€ion Storage. Chemistry - an Asian Journal, 2020, 15, 1613-1620.	1.7	24
37320	Structural, mechanical, electronic, and thermodynamic properties of pure tungsten metal under different pressures: A firstâ€principles study. International Journal of Quantum Chemistry, 2020, 120, e26231.	1.0	14
37321	The Analyses of Luminescent Properties and Structure of the Tetragonal Phase of Y₂WO₆:Eu³⁺ doped Phosphor. Zeitschrift Fur Anorganische Und Allgemeine Chemie, 2020, 646, 1122-1129.	0.6	1
37322	Theoretical study of the adsorption of diphenylalanine on pristine graphene. Theoretical Chemistry Accounts, 2020, 139, 1.	0.5	7
37323	First-principles microkinetic analysis of dehydrogenation of cyclohexene on the Pt/Cu/Pt (111) surface. Journal of Molecular Modeling, 2020, 26, 89.	0.8	3
37324	Pd-doped h-BN monolayer: a promising gas scavenger for SF6 insulation devices. Adsorption, 2020, 26, 619-626.	1.4	24
37325	Hydrogen sorption capacity of crystal lattice defects and low Miller index surfaces of copper. Journal of Materials Science, 2020, 55, 6623-6636.	1.7	13

#	Article	IF	Citations
37326	Two-dimensional intrinsic ferromagnetic half-metals: monolayers Mn3X4 (Xâ€‰=â€‰Te, Se, S). Journal of Materials Science, 2020, 55, 7680-7690.	1.7	20
37327	Catalysis at Metal/Oxide Interfaces: Density Functional Theory and Microkinetic Modeling of Water Gas Shift at Pt/MgO Boundaries. Topics in Catalysis, 2020, 63, 673-687.	1.3	17
37328	Dissociated dislocation-mediated carbon transport and diffusion in austenitic iron. Acta Materialia, 2020, 191, 43-50.	3.8	36
37329	Highly efficient methane decomposition to H2 and CO2 reduction to CO via redox looping of Ca2FexAl2-xO5 supported NiyFe3-yO4 nanoparticles. Applied Catalysis B: Environmental, 2020, 271, 118938.	10.8	24
37330	CO2 hydrogenation to formic acid over platinum cluster doped defective graphene: A DFT study. Applied Surface Science, 2020, 517, 146200.	3.1	27
37331	Electron transport properties of 2D IV-V semiconductors and their improvement by graphene contact. Applied Surface Science, 2020, 519, 146203.	3.1	11
37332	Thermodynamic reassessment of the Moâ€“Hf and Moâ€“Zr systems supported by first-principles calculations. Calphad: Computer Coupling of Phase Diagrams and Thermochemistry, 2020, 69, 101766.	0.7	11
37333	Nickel (II) modified porous boron nitride: An effective adsorbent for tetracycline removal from aqueous solution. Chemical Engineering Journal, 2020, 394, 124985.	6.6	66
37334	Exploration of stable stoichiometries, ground-state structures, and mechanical properties of the Wâ€“Si system. Ceramics International, 2020, 46, 17034-17043.	2.3	43
37335	Band-gap tuning of graphene by Mg doping and adsorption of Br and Be on impurity: A DFT study. Computational Condensed Matter, 2020, 23, e00469.	0.9	13
37336	Computational study of Be-doped hexagonal boron nitride (h-BN): Structural and electronic properties. Computational Condensed Matter, 2020, 23, e00474.	0.9	13
37337	Ab initio thermodynamic properties of certain compounds in Nd-Fe-B system. Computational Materials Science, 2020, 180, 109696.	1.4	7
37338	Predicted crystal structures of titanium nitrides at high pressures. Computational Materials Science, 2020, 180, 109720.	1.4	9
37339	Co nanoparticles coupling induced high catalytic activity of nitrogen doped carbon towards hydrogen evolution reaction in acidic/alkaline solutions. Electrochimica Acta, 2020, 342, 136076.	2.6	14
37340	ATR-FTIR in Kretschmann configuration integrated with electrochemical cell as in situ interfacial sensitive tool to study corrosion inhibitors for magnesium substrates. Electrochimica Acta, 2020, 345, 136166.	2.6	37
37341	Multi-scale stabilization of high-voltage LiCoO2 enabled by nanoscale solid electrolyte coating. Energy Storage Materials, 2020, 29, 71-77.	9.5	49
37342	Identification of active sites in CO2 activation on MgO supported Ni cluster. International Journal of Hydrogen Energy, 2020, 45, 11108-11115.	3.8	24
37343	Enhanced C atom adsorption on Cu(111) substrate by doping rare earth element Y for Cuâ€“diamond composites: A first-principles study. Journal of Alloys and Compounds, 2020, 831, 154747.	2.8	11

#	Article	IF	Citations
37344	Atomic-scale investigation on the structural evolution and deformation behaviors of Cuâ€“Cr nanocrystalline alloys processed by high-pressure torsion. Journal of Alloys and Compounds, 2020, 832, 154994.	2.8	4
37345	Reaction dynamics of metal/oxide catalysts: Methanol oxidation at vanadium oxide films on Rh(1Â1Â1) from UHV to 10âˆ'2 mbar. Journal of Catalysis, 2020, 385, 255-264.	3.1	13
37346	Selective activation of methane C H bond in the presence of methanol. Journal of Catalysis, 2020, 386, 12-18.	3.1	6
37347	ZnxCd1-xS nanoparticles dispersed on CoAl-layered double hydroxide in 2D heterostructure for enhanced photocatalytic hydrogen evolution. Journal of Colloid and Interface Science, 2020, 572, 62-73.	5.0	56
37348	Thermal and mechanical properties of U3Si2: A combined ab-initio and molecular dynamics study. Journal of Nuclear Materials, 2020, 533, 152090.	1.3	15
37349	Atomic deformation mechanism and interface toughening in metastable high entropy alloy. Materials Today, 2020, 37, 64-73.	8.3	48
37350	Control of framework Al distribution in ZSM-5 zeolite via post-synthetic TiCl4 treatment. Microporous and Mesoporous Materials, 2020, 302, 110223.	2.2	6
37351	Theoretical investigation of the structural, elastic, electronic, and optical properties of the ternary tetragonal tellurides KBTe2 (B = Al, In). Materials Science in Semiconductor Processing, 2020, 114, 105085.	1.9	29
37352	Strain engineering of oxide thin films for photocatalytic applications. Nano Energy, 2020, 72, 104732.	8.2	26
37353	First-principles investigation of high pressure effect on structure, mechanical and electronic properties of Mo2ScAlC2. Physica B: Condensed Matter, 2020, 588, 412171.	1.3	1
37354	Structures, mobilities, electronic and optical properties of two-dimensional Î±-phase group-VI binary compounds: Î±-Se2Te and Î±-SeTe2. Physics Letters, Section A: General, Atomic and Solid State Physics, 2020, 384, 126431.	0.9	10
37355	Strain and electric field dependent variation in electronic and thermoelectric properties of PtS2. Results in Physics, 2020, 17, 103088.	2.0	14
37356	Thickness dependence of solar cell efficiency in transition metal dichalcogenides MX2 (M: Mo, W; X: S,) Tj ETQq0 0 0 rgBT /Overlock 10	3.0	19
37357	Structural, mechanical, electronic and thermodynamic properties of cubic TiC compounds under different pressures: A first-principles study. Solid State Communications, 2020, 311, 113856.	0.9	16
37358	First-principles study of electronic structures and ferromagnetism in (Cr, X) (X= Ga, In) co-doped 4Hâ€“SiC. Solid State Communications, 2020, 313, 113878.	0.9	0
37359	An ab-initio study of H2O adsorption on the calcite (104) surface with different coverages. Solid State Communications, 2020, 313, 113892.	0.9	16
37360	First-principles computation of magnesium doped CaZrO3 perovskite: A study of phase transformation, bandgap engineering and optical response for optoelectronic applications. Solid State Communications, 2020, 313, 113907.	0.9	29
37361	Reactivity of bimetallic nanostructured electrocatalysts for the hydrogen adsorption. An atomistic view. Surface Science, 2020, 697, 121605.	0.8	7

#	Article	IF	Citations
37362	Noncovalent Sulfoxideâ€“Nitrile Coupling Involving Four-Center Heteroleptic Dipoleâ€“Dipole Interactions between the Sulfinyl and Nitrile Groups. Crystal Growth and Design, 2020, 20, 3417-3428.	1.4	17
37363	Chemical Shift Tensors of Cimetidine Form A Modeled with Density Functional Theory Calculations: Implications for NMR Crystallography. Journal of Physical Chemistry A, 2020, 124, 3109-3119.	1.1	26
37364	Unraveling the Origin of Ceria Activity in Waterâ€“Gas Shift by First-Principles Microkinetic Modeling. Journal of Physical Chemistry C, 2020, 124, 7823-7834.	1.5	21
37365	Functionalized Two-Dimensional Nanoporous Graphene as Efficient Global Anode Materials for Li-, Na-, K-, Mg-, and Ca-Ion Batteries. Journal of Physical Chemistry C, 2020, 124, 9734-9745.	1.5	28
37366	Engineering Atomically Sharp Potential Steps and Band Alignment at Solid Interfaces using 2D Janus Layers. Journal of Physical Chemistry C, 2020, 124, 9572-9580.	1.5	14
37367	Density Functional Theory Investigation of Oxidation Intermediates on Gold and Goldâ€“Silver Surfaces. Journal of Physical Chemistry C, 2020, 124, 8843-8853.	1.5	9
37368	Atomic-Scale Rolling Friction and Charge-Transfer Mechanism: An Integrated Study of Physical Deductions and DFT Simulations. Journal of Physical Chemistry C, 2020, 124, 8431-8438.	1.5	9
37369	First-Order Isostructural Phase Transition Induced by High Pressure in Fe(IO₃)₃. Journal of Physical Chemistry C, 2020, 124, 8669-8679.	1.5	24
37370	Role of Defects in Photocatalytic Water Splitting: Monodoped vs Codoped SrTiO₃. Journal of Physical Chemistry C, 2020, 124, 10272-10279.	1.5	32
37371	Emerging One-/Two-Dimensional Heteronanostructure Integrating SiC Nanowires with MoS₂ Nanosheets for Efficient Electrocatalytic Hydrogen Evolution. ACS Applied Materials & Interfaces, 2020, 12, 19519-19529.	4.0	40
37372	Preferential Oxidation of CO in Hydrogen at Nonmetal Active Sites with High Activity and Selectivity. ACS Catalysis, 2020, 10, 5362-5370.	5.5	8
37373	Facile Heterogeneously Catalyzed Nitrogen Fixation by MXenes. ACS Catalysis, 2020, 10, 5049-5056.	5.5	67
37374	Sodiophilic Decoration of a Three-Dimensional Conductive Scaffold toward a Stable Na Metal Anode. ACS Sustainable Chemistry and Engineering, 2020, 8, 5452-5463.	3.2	31
37375	Microphotoelectrochemical Surface-Enhanced Raman Spectroscopy: Toward Bridging Hot-Electron Transfer with a Molecular Reaction. Journal of the American Chemical Society, 2020, 142, 8483-8489.	6.6	31
37376	Surface Composition Dependent Ligand Effect in Tuning the Activity of Nickelâ€“Copper Bimetallic Electrocatalysts toward Hydrogen Evolution in Alkaline. Journal of the American Chemical Society, 2020, 142, 7765-7775.	6.6	234
37377	Twin T-graphene: a new semiconducting 2D carbon allotrope. Physical Chemistry Chemical Physics, 2020, 22, 10286-10294.	1.3	39
37378	Two-dimensional C₃N based sub-10 nanometer biosensor. Physical Chemistry Chemical Physics, 2020, 22, 11452-11459.	1.3	20
37379	Structural stability of single-layer PdSe₂ with pentagonal puckered morphology and its nanotubes. Physical Chemistry Chemical Physics, 2020, 22, 8289-8295.	1.3	26

#	Article	IF	Citations
37380	Electron paramagnetic resonance study of ferroelectric phase transition and dynamic effects in a Mn²⁺doped [NH₄][Zn(HCOO)₃] hybrid formate framework. Physical Chemistry Chemical Physics, 2020, 22, 8513-8521.	1.3	3
37381	High electron mobility, controllable magnetism and anomalous light absorption in a monolayered tin mononitride semiconductor. Journal of Materials Chemistry C, 2020, 8, 6396-6402.	2.7	6
37382	High-efficiency helium separation through an inorganic graphenylene membrane: a theoretical study. Physical Chemistry Chemical Physics, 2020, 22, 9789-9795.	1.3	32
37383	A multiporous carbon family with superior stability, tunable electronic structures and amazing hydrogen storage capability. Physical Chemistry Chemical Physics, 2020, 22, 9734-9739.	1.3	4
37384	Unexpected electrochemical behavior of an anolyte redoxmer in flow battery electrolytes: solvating cations help to fight against the thermodynamicâ€“kinetic dilemma. Journal of Materials Chemistry A, 2020, 8, 13470-13479.	5.2	17
37385	Morphology and reactivity of size-selected titanium oxide nanoclusters on Au(111). Journal of Chemical Physics, 2020, 152, 054714.	1.2	12
37386	Atomic-level calculations and experimental study of dislocations in InSb. Journal of Applied Physics, 2020, 127, 135104.	1.1	8
37387	Influence of 3d, 4d, and 5d dopants on the oxygen evolution reaction at Î±-Fe2O3(0001) under dark and illumination conditions. Journal of Chemical Physics, 2020, 152, 124709.	1.2	9
37388	Solvation at metal/water interfaces: An ab initio molecular dynamics benchmark of common computational approaches. Journal of Chemical Physics, 2020, 152, 144703.	1.2	103
37389	Exploring electronic, optoelectronic, and thermoelectric properties of ternary compound MgSrSe2 from first-principles study. AIP Advances, 2020, 10, 045010.	0.6	3
37390	Van der Waals heterostructures of MoS₂and Janus MoSSe monolayers on graphitic boron-carbon-nitride (BC₃,C₃N,C₃N₄andC₄N₃</sub> nanosheets: a first-principles study. Journal Physics D: Applied Physics, 2020, 53, 355106.	1.3	64
37391	Electric field control of Rashba spin splitting in 2D N^{III}X^{VI} (Nâ€‰â€‰=â€‰â€‰Ga, In; Xâ€‰â€‰=â€‰â€‰	0.7	17
37392	Strain, electric-field and functionalization induced widely tunable electronic properties in MoS₂/BC ₃, /C ₃ N and /$C_{3}N_{4}$ van der Waals heterostructures. Nanotechnology, 2020, 31, 295202.	1.3	48
37393	First-principles calculations of soluteâ€“vacancy interactions in aluminum*. Chinese Physics B, 2020, 29, 066103.	0.7	1
37394	Electronic Structure and Polarization of NaMgF3/NaCaF3 Superlattices: Insight from First-Principles. IOP Conference Series: Materials Science and Engineering, 2020, 774, 012016.	0.3	0
37395	Role of spin-orbit coupling in the alloying behavior of multilayer Bi1âˆ’xSbx solid solutions revealed by a first-principles cluster expansion. Physical Review B, 2020, 101, .	1.1	10
37396	Electronic and magnetic properties of 3d transition-metal adatoms on Mn/W(110). Physical Review B, 2020, 101, .	1.1	1
37397	Route to high- <mml:math xmlns:mml="http://www.w3.org/1998/Math/MathML"><mml:msub><mml:mi>T</mml:mi><mml:mi>c</mml:mi></mml:msub></mml:m superconductivity via <mml:math xmlns:mml="http://www.w3.org/1998/Math/MathML"><mml:msub><mml:mi>CH</mml:mi><mml:mn>4</mml:mn></mml:msub></mml -intercalated <mml:math xmlns:mml="http://www.w3.org/1998/Math/MathML"><mml:mrow><mml:msub><mml:mi mathvariant="n	1.1	98

#	Article	IF	Citations
37398	Manipulating magnetism in the topological semimetal <mml:math xmlns:mml="http://www.w3.org/1998/Math/MathML"><mml:mrow><mml:msub><mml:mi>EuCd</mml:mi><mml:mn>2</mml:mn></mml:msub></mml:mrow></mml:math> with magnetic vanadium substitution. Physical Review B, 2020, 101, .	1.1	58
37399	Conductance of quantum spin Hall edge states from first principles: The critical role of magnetic impurities and inter-edge scattering. Physical Review B, 2020, 101, .	1.1	18
37400	Intrinsic quantum anomalous Hall phase induced by proximity in the van der Waals heterostructure germanene/ <mml:math xmlns:mml="http://www.w3.org/1998/Math/MathML"><mml:mrow><mml:msub><mml:mi>Cr</mml:mi><mml:mn>2</mml:mn></mml:msub></mml:mrow></mml:math> Physical Review B, 2020, 101, .	1.1	23
37401	Competition of defect ordering and site disproportionation in strained <mml:math xmlns:mml="http://www.w3.org/1998/Math/MathML"><mml:msub><mml:mi>LaCoO</mml:mi><mml:mn>3</mml:mn></mml:msub></mml:math> on <mml:math xmlns:mml="http://www.w3.org/1998/Math/MathML"><mml:msub><mml:mi>SrTiO</mml:mi><mml:mn>3</mml:mn></mml:msub></mml:math> (001). Physical Review B, 2020, 101, .	1.1	12
37402	Two-dimensional graphitic carbon nitrides: Strain-tunable ferromagnetic ordering. Physical Review B, 2020, 101, .	1.1	37
37403	Conductivitylike Gilbert Damping due to Intraband Scattering in Epitaxial Iron. Physical Review Letters, 2020, 124, 157201.	2.9	41
37404	The electronic thickness of graphene. Science Advances, 2020, 6, eaay8409.	4.7	35
37405	Aluminumâ€“Carbon Interaction at the Aluminumâ€“Graphene and Aluminumâ€“Graphite Interfaces. Journal of Experimental and Theoretical Physics, 2020, 130, 214-227.	0.2	9
37406	Exchange coupling and Mn valency in GaN doped with Mn and co-doped with Mg. European Physical Journal B, 2020, 93, 1.	0.6	1
37407	The Combined Influence of Dopant Species and Surface Termination on the Electronic Properties of Diamond Surfaces. Journal of Carbon Research, 2020, 6, 22.	1.4	11
37408	Improved Predictive Tools for Structural Properties of Metalâ€“Organic Frameworks. Molecules, 2020, 25, 1552.	1.7	7
37409	Ab Initio Study of Ferroelectric Critical Size of SnTe Low-Dimensional Nanostructures. Nanomaterials, 2020, 10, 732.	1.9	7
37410	Effects of Components Modulation on the Type of Band Alignments for PbI 2 /WS 2 van der Waals Heterostructure. Physica Status Solidi - Rapid Research Letters, 2020, 14, 2000016.	1.2	23
37411	Engineering of Charged Defects at Perovskite Oxide Surfaces for Exceptionally Stable Solid Oxide Fuel Cell Electrodes. ACS Applied Materials & Interfaces, 2020, 12, 21494-21504.	4.0	43
37412	Sculpting Artificial Edges in Monolayer MoS₂ for Controlled Formation of Surface-Enhanced Raman Hotspots. ACS Nano, 2020, 14, 6258-6268.	7.3	45
37413	First-Principles Study of the Hydrogen Resistance Mechanism of PuO₂. ACS Omega, 2020, 5, 7211-7218.	1.6	9
37414	Elastic and optical properties of sillenites: First principle calculations. Ferroelectrics, 2020, 557, 98-104.	0.3	8
37415	Tuning the Schottky barrier height in graphene/monolayer-GeI₂ van der Waals heterostructure. Journal of Physics Condensed Matter, 2020, 32, 355501.	0.7	7

#	Article	IF	Citations
37416	Experimental evidence of monolayer AlB2 with symmetry-protected Dirac cones. Physical Review B, 2020, 101, .	1.1	20
37417	Phase Diagrams of Iron Hydrides at Pressures of 100â€“400 GPa and Temperatures of 0â€“5000 K. JETP Letters, 2020, 111, 145-150.	0.4	10
37418	An Environmentally Stable and Leadâ€Free Chalcogenide Perovskite. Advanced Functional Materials, 2020, 30, 2001387.	7.8	52
37419	The Electronic, Optical, and Thermoelectric Properties of Monolayer PbTe and the Tunability of the Electronic Structure by External Fields and Defects. Physica Status Solidi (B): Basic Research, 2020, 257, 2000182.	0.7	38
37420	The Role of Metal Species on Aldehyde Hydrogenation over Co 13 and Ni 13 Supported on Î³â€Al 2 O 3 (110) Surfaces: A Theoretical Study. ChemistrySelect, 2020, 5, 4058-4068.	0.7	6
37421	DFT investigations on the electronic structure, magnetism, thermodynamic and elastic properties of newly predicted cobalt based antiperovskites: Co3XN (XÂ=ÂPd, Pt & Rh). Results in Physics, 2020, 17, 103112.	2.0	6
37422	Catalytic Dehydrogenation of Ethane over Doped Perovskite via the Marsâ€“van Krevelen Mechanism. Journal of Physical Chemistry C, 2020, 124, 10462-10469.	1.5	12
37423	Dynamics Studies of O₂ Collision on Pt(111) Using a Global Potential Energy Surface. Journal of Physical Chemistry C, 2020, 124, 10573-10583.	1.5	7
37424	Optical properties of a hexagonal C/BN framework with sp2 and sp3 hybridized bonds. Scientific Reports, 2020, 10, 6808.	1.6	3
37425	Half-occupation approach for the ab initio calculation of strained Ga(AsSb)/GaAs valence band offsets. AIP Advances, 2020, 10, 045207.	0.6	1
37426	A first-principles study on hydrogen distributions in the Î±-U/UO2 interface. Journal of Physics Condensed Matter, 2020, 32, 195002.	0.7	0
37427	Peculiarities of the Optical and Energy Properties of Thin CdSe Films. Optics and Spectroscopy (English Translation of Optika I Spektroskopiya), 2020, 128, 49-56.	0.2	12
37428	Mechanical and Thermal Properties of Low-Density Al20+xCr20-xMo20-yTi20V20+y Alloys. Crystals, 2020, 10, 278.	1.0	20
37429	Penta-C20: A Superhard Direct Band Gap Carbon Allotrope Composed of Carbon Pentagon. Materials, 2020, 13, 1926.	1.3	31
37430	First-Principles Study of Nitrogen Adsorption and Dissociation on PuH2 (111) Surface. Molecules, 2020, 25, 1891.	1.7	2
37431	Catalytic Polysulfide Conversion and Physiochemical Confinement for Lithiumâ€“Sulfur Batteries. Advanced Energy Materials, 2020, 10, 1904010.	10.2	165
37432	Achieving indirectâ€toâ€direct band gap transition and enhanced photocatalytic performance in blue phosphorene through doping and strain. International Journal of Quantum Chemistry, 2020, 120, e26230.	1.0	14
37433	Electronic and Optical Properties of Zigzag BN/AlN Nanoribbons with Misfit Dislocations: First-Principles Calculations. Journal of Electronic Materials, 2020, 49, 4100-4110.	1.0	2

#	Article	IF	Citations
37434	Computational Chemistry-Based Evaluation of Metal Salts and Metal Oxides for Application in Mercury-Capture Technologies. Industrial & Engineering Chemistry Research, 2020, 59, 9015-9022.	1.8	4
37435	Structural and Electronic Properties of Bulk ZnX (X = O, S, Se, Te), ZnF₂, and ZnO/ZnF₂: A DFT Investigation within PBE, PBE + U, and Hybrid HSE Functionals. Journal of Physical Chemistry A, 2020, 124, 3778-3785.	1.1	31
37436	Interface and polarization effects induced Schottky-barrier-free contacts in two-dimensional MXene/GaN heterojunctions. Journal of Materials Chemistry C, 2020, 8, 7350-7357.	2.7	34
37437	Stability, geometry and electronic properties of BHn(nâ€‰â€‰=â€‰â€‰0 to 3) radicals on the Si{0â€‰0â€‰1}3â€‰â€‰Ã—â€ from first-principles. Journal of Physics Condensed Matter, 2020, 32, 235201.	0.7	4
37438	Structural and electronic properties of c-BN (111) surface with hydrogen/fluorine functionalization and nitrogen-based small-molecule adsorption. Journal of Physics Condensed Matter, 2020, 32, 265002.	0.7	4
37439	Giantâ€Enhanced SnS₂ Photodetectors with Broadband Response through Oxygen Plasma Treatment. Advanced Functional Materials, 2020, 30, 2001650.	7.8	48
37440	Elucidating the mechanism of Hg0 oxidation by chlorine species over Co3O4 catalyst at molecular level. Applied Surface Science, 2020, 513, 145885.	3.1	22
37441	M2C-type MXenes: Promising catalysts for CO2 capture and reduction. Applied Surface Science, 2020, 521, 146436.	3.1	77
37442	Exploring the real ground-state structures of W3Si silicides from first-principles calculations. Computational Materials Science, 2020, 180, 109719.	1.4	16
37443	Helium behaviors at Mn6Ni16Si7 precipitate in Î±-Fe: Insights from ab initio modeling. Computational Materials Science, 2020, 181, 109735.	1.4	2
37444	Polymer decoration of carbon support to boost Pt-catalyzed hydrogen generation activity and durability. Journal of Catalysis, 2020, 385, 289-299.	3.1	7
37445	First-principles investigation of the structural, electronic, optical and elastic properties of <mml:math xmlns:mml="http://www.w3.org/1998/Math/MathML" altimg="si1.svg"><mml:mrow><mml:mi mathvariant="bold-italic">CsC</mml:mi><mml:msub><mml:mi mathvariant="bold-italic">d</mml:mi><mml:mi mathvariant="bold-italic">x</mml:mi></mml:msub><mml:mi mathvariant="bold-italic">P</mml:mi><mml:msub><mml:mi mathvariant="bold-italic">b</mml:mi>	1.9	2
37446	Understanding the effect of the carbon on the photovoltaic properties of the Cu2ZnSnS4. Materials Chemistry and Physics, 2020, 251, 123065.	2.0	21
37447	Strain-tunable photogalvanic effect in phosphorene. Materials Today Communications, 2020, 24, 101154.	0.9	4
37448	Surface analysis of the stress-induced, impurity driven face centered cubic titanium phase and the ranging lattice parameter sizes. Materials Today Communications, 2020, 24, 101168.	0.9	1
37449	Alkynyl Linkers as a Design Tool to Gain Control over the Self-Assembly of Meso-Substituted Porphyrins on HOPG. Langmuir, 2020, 36, 4897-4907.	1.6	4
37450	Tunable Room-Temperature Ferromagnetism in Two-Dimensional Cr₂Te₃. Nano Letters, 2020, 20, 3130-3139.	4.5	175
37451	Enabling room temperature ferromagnetism in monolayer MoS2 via in situ iron-doping. Nature Communications, 2020, 11, 2034.	5.8	112

#	Article	IF	Citations
37452	Universal chemomechanical design rules for solid-ion conductors to prevent dendrite formation in lithium metal batteries. Nature Materials, 2020, 19, 758-766.	13.3	110
37453	Theoretical study of oxygen insertion and diffusivity in theg-TiAlL1₀system. Journal of Physics Condensed Matter, 2020, 32, 175702.	0.7	8
37454	Platinum and Palladium Monolayer Electrocatalysts for Formic Acid Oxidation. Topics in Catalysis, 2020, 63, 742-749.	1.3	17
37455	MoirÃ© patterns arising from bilayer graphone/graphene superlattice. Nano Research, 2020, 13, 1060-1064.	5.8	11
37456	Development of a multi-active center catalyst in mediating the catalytic destruction of chloroaromatic pollutants: A combined experimental and theoretical study. Applied Catalysis B: Environmental, 2020, 272, 119015.	10.8	71
37457	Comparison of sensing and electronic properties of C2H2 on different transition metal oxide nanoparticles (Fe2O3, NiO, TiO2) modified BNNT (10, 0). Applied Surface Science, 2020, 521, 146463.	3.1	59
37458	Ab initio thermodynamics studies on the phase stability of PtO2 under ambient and high-pressure conditions. Computational Materials Science, 2020, 180, 109708.	1.4	5
37459	Theoretical investigation on the effect of doped Pd on the Cu(1â€¯1â€¯1) surface for formic acid oxidation: Competing formation of CO2 and CO. Chemical Physics Letters, 2020, 751, 137509.	1.2	9
37460	3d transitional-metal single atom catalysis toward hydrogen evolution reaction on MXenes supports. International Journal of Hydrogen Energy, 2020, 45, 14396-14406.	3.8	59
37461	NaPb2(CO3)2Fx(OH)1-x(0 < x â‰¤ 1): A new member of alkali-lead carbonate fluoride system with large birefringence. Journal of Solid State Chemistry, 2020, 288, 121407.	1.4	1
37462	Adsorption and sensing of CO and C2H2 by S-defected SnS2 monolayer for DGA in transformer oil: A DFT study. Materials Chemistry and Physics, 2020, 249, 123006.	2.0	87
37463	Tuning the structural and electronic properties of arsenene monolayers by germanene, silicene, and stanene domain doping. Physica E: Low-Dimensional Systems and Nanostructures, 2020, 122, 114152.	1.3	4
37464	Assembling Homometallic Sb₆ and Heterometallic Ti₄Sb₂ Oxo Clusters. Inorganic Chemistry, 2020, 59, 6689-6696.	1.9	5
37465	First-Principles Design and Investigation of Siligraphene as a Potential Anode Material for Na-Ion Batteries. Journal of Physical Chemistry C, 2020, 124, 11293-11300.	1.5	25
37466	Azo-Dimerization Mechanisms of p-Aminothiophenol and p-Nitrothiophenol Molecules on Plasmonic Metal Surfaces Revealed by Tip-/Surface-Enhanced Raman Spectroscopy. Journal of Physical Chemistry C, 2020, 124, 11586-11594.	1.5	16
37467	Fundamental Electrochemical Insights of Vertically Aligned Carbon Nanofiber Architecture as a Catalyst Support for ORR. Journal of the Electrochemical Society, 2020, 167, 066523.	1.3	15
37468	Improvement of Ti/TiN interfacial shear strength by doping â€“ A first principles density functional theory study. Applied Surface Science, 2020, 517, 146185.	3.1	12
37469	Investigating the ability of iron nitride particles to polish titanium plate. Powder Technology, 2020, 366, 653-660.	2.1	2

#	Article	IF	Citations
37470	A Series of Organicâ€“Inorganic Hybrid Compounds [(C₂H₅)₄N]InCl_{4â€“x}Br_x (x = 0, 2, 4): Synthesis, Crystal Structure, and Nonlinear Optical Properties. Inorganic Chemistry, 2020, 59, 5721-5727.	1.9	28
37471	Synthesis and Crystal Structure of Three Ga-rich Lithium Gallides, LiGa₆, Li₁₁Ga₂₄, and LiGa₂. Inorganic Chemistry, 2020, 59, 6566-6580.	1.9	2
37472	A cyclic electrochemical strategy to produce acetylene from CO₂, CH₄, or alternative carbon sources. Sustainable Energy and Fuels, 2020, 4, 2752-2759.	2.5	9
37473	Discovery of stable and intrinsic antiferromagnetic iron oxyhalide monolayers. Physical Chemistry Chemical Physics, 2020, 22, 11731-11739.	1.3	32
37474	Iodine interstitials as a cause of nonradiative recombination in hybrid perovskites. Physical Review B, 2020, 101, .	1.1	76
37475	DFT insights into electrocatalytic CO₂ reduction to methanol on Î±-Fe₂O₃(0001) surfaces. Physical Chemistry Chemical Physics, 2020, 22, 10819-10827.	1.3	19
37476	Measurement of the Low-Energy Electron Inelastic Mean Free Path in Monolayer Graphene. Physical Review Applied, 2020, 13, .	1.5	10
37477	Novel 2D Transitionâ€Metal Carbides: Ultrahigh Performance Electrocatalysts for Overall Water Splitting and Oxygen Reduction. Advanced Functional Materials, 2020, 30, 2000570.	7.8	186
37478	Nitrogenâ€Doped Ti₃C₂ MXene: Mechanism Investigation and Electrochemical Analysis. Advanced Functional Materials, 2020, 30, 2000852.	7.8	166
37479	(Ni,Cu)/hexagonal BN nanohybrids â€“ New efficient catalysts for methanol steam reforming and carbon monoxide oxidation. Chemical Engineering Journal, 2020, 395, 125109.	6.6	39
37480	Mechanical behaviors of MoS nanowires under tension from molecular dynamics simulations. Computational Materials Science, 2020, 179, 109691.	1.4	5
37481	Tautomerism of azo dyes in the solid state studied by 15N, 14N, 13C and 1H NMR spectroscopy, X-ray diffraction and quantum-chemical calculations. Dyes and Pigments, 2020, 178, 108342.	2.0	13
37482	Correlation of octahedral distortion with vibrational and electronic properties of LaFe1-Ti O3 nanoparticles. Journal of Alloys and Compounds, 2020, 830, 154594.	2.8	17
37483	Surface charging activated mechanism change: A computational study of O, CO, and CO2 interactions on Ag electrodes. Journal of Energy Chemistry, 2020, 50, 307-313.	7.1	8
37484	Ab-initio prediction of the mechanical, magnetic and thermoelectric behaviour of perovskite oxides XGaO3 (XÂ= Sc, Ti, Ag) using LDA+U functional: For optoelectronic devices. Journal of Molecular Graphics and Modelling, 2020, 99, 107621.	1.3	18
37485	Exploration of magnesium based MgX2O4 (Xâ€¯=â€¯Rh, Bi) spinels for thermoelectric applications using density functional theory (DFT). Journal of Materials Research and Technology, 2020, 9, 6135-6142.	2.6	38
37486	Ab initio study of He, Ne, Ar, Kr incorporation in zirconium carbide. Journal of Nuclear Materials, 2020, 534, 152154.	1.3	2
37487	Magneto-structural coupling in SrTcxRu1-xO3 (x = 0.25,0.5) perovskites. Journal of Solid State Chemistry, 2020, 287, 121378.	1.4	3

#	Article	IF	Citations
37488	First principles studied tunable electronic and optical properties of 2D honeycomb ZnO monolayer engineered by biaxial strain and intrinsic vacancy. Materials Science and Engineering B: Solid-State Materials for Advanced Technology, 2020, 254, 114517.	1.7	15
37489	A study of structural, electronic, elastic, phonon properties, and transition mechanism of wurtzite CdTe under high pressure. Solid State Sciences, 2020, 105, 106209.	1.5	6
37490	Hittorf's violet phosphorene as a promising candidate for NO2, O3 and SO2 sensor: A first-principles investigation. Solid State Communications, 2020, 314-315, 113928.	0.9	9
37491	Volume Modulation of Nonlinear Optical Properties by Cation Substitution. Journal of Physical Chemistry C, 2020, 124, 10679-10686.	1.5	1
37492	Substituent Effects on the Thermal Decomposition of Phosphate Esters on Ferrous Surfaces. Journal of Physical Chemistry C, 2020, 124, 9852-9865.	1.5	24
37493	Experimental and Theoretical Investigation on Phase Formation and Mechanical Properties in Crâ€“Coâ€“Ni Alloys Processed Using a Novel Thin-Film Quenching Technique. ACS Combinatorial Science, 2020, 22, 232-247.	3.8	3
37494	Investigation on the interconversion from DMF-solvated to unsolvated copper(ii) pyrazolate coordination polymers. CrystEngComm, 2020, 22, 3294-3308.	1.3	8
37495	Tunable electronic and magnetic properties of monolayer and bilayer Janus Cr₂Cl₃I₃: a first-principles study. Materials Advances, 2020, 1, 244-253.	2.6	22
37496	Strategies for designing two-dimensional nonlinear optical layers from KBBF and BBO crystals. Molecular Systems Design and Engineering, 2020, 5, 985-995.	1.7	10
37497	Structure reinforced birnessite with an extended potential window for supercapacitors. Journal of Materials Chemistry A, 2020, 8, 8969-8978.	5.2	42
37498	Six novel carbon and silicon allotropes with their potential application in photovoltaic field. Journal of Physics Condensed Matter, 2020, 32, 355701.	0.7	20
37499	Interactions between a H2 Molecule and Carbon Nanostructures: A DFT Study. Journal of Carbon Research, 2020, 6, 16.	1.4	8
37500	Revisiting the Role of Conductivity and Polarity of Host Materials for Longâ€Life Lithiumâ€“Sulfur Battery. Advanced Energy Materials, 2020, 10, 1903934.	10.2	52
37501	Twoâ€Đimensional Layered Metallic VSe₂/SWCNTs/rGO Based Ternary Hybrid Materials for High Performance Energy Storage Applications. Chemistry - A European Journal, 2020, 26, 6662-6669.	1.7	43
37502	Probing Gold-Doped Germanene Nanoribbons for Nanoscale Interconnects Under DFT-NEGF Framework. Journal of Electronic Materials, 2020, 49, 3938-3946.	1.0	7
37503	Prediction of a ternary two-dimensional pentagonal Zn2C2P2 monolayer for photocatalytic water splitting with high carriers mobility. Applied Surface Science, 2020, 518, 146197.	3.1	13
37504	Intrinsic-strain-induced curling of free-standing two-dimensional Janus MoSSe quantum dots. Applied Surface Science, 2020, 519, 146251.	3.1	10
37505	Quantum-mechanical study of interaction between polycarbonate and M0.5Al0.5N(0ÂÔÂ1) surfaces (MÂ=ÂTi,) Tj ETQq1 1 0.784314	3.1	0

#	Article	IF	Citations
37507	Flexible graphene-assisted van der Waals epitaxy growth of crack-free AlN epilayer on SiC by lattice engineering. Applied Surface Science, 2020, 520, 146358.	3.1	14
37508	Graphene as interface modifier in ITO and ITO-Cr electrodes. Current Applied Physics, 2020, 20, 846-852.	1.1	3
37509	First-principles study on the adsorption and diffusion properties of non-noble (Fe, Co, Ni and Cu) and noble (Ru, Rh, Pt and Pd) metal single atom on graphyne. Chemical Physics, 2020, 536, 110783.	0.9	12
37510	The H2S dimer revisited â€“ Insights from wave-function and density functional theory methods. Ab initio molecular dynamics simulations of liquid H2S. Computational and Theoretical Chemistry, 2020, 1180, 112821.	1.1	3
37511	a-TDEP: Temperature Dependent Effective Potential for Abinit â€“ Lattice dynamic properties including anharmonicity. Computer Physics Communications, 2020, 254, 107301.	3.0	18
37512	Theoretical study on the effect of Mn promoter for CO2 reforming of CH4 on the Ni(1Â1Â1) surface. Fuel, 2020, 274, 117849.	3.4	8
37513	Impact of Al2O3 stress liner on two-dimensional SnS2 nanosheet for photodetector application. Journal of Alloys and Compounds, 2020, 830, 154716.	2.8	12
37514	In situ spectroscopic and theoretical investigation of methane activation on IrO2 nanoparticles: Role of Ir oxidation state on C-H activation. Journal of Catalysis, 2020, 385, 265-273.	3.1	27
37515	Fluorination over Cr doped layered perovskite Sr2TiO4 for efficient photocatalytic hydrogen production under visible light illumination. Journal of Energy Chemistry, 2020, 51, 30-38.	7.1	14
37516	Rational design of MoS2 nanosheets decorated on mesoporous hollow carbon spheres as a dual-functional accelerator in sulfur cathode for advanced pouch-type Liâ€“S batteries. Journal of Energy Chemistry, 2020, 51, 262-271.	7.1	69
37517	Porous LaFeO3 nanofiber with oxygen vacancies as an efficient electrocatalyst for N2 conversion to NH3 under ambient conditions. Journal of Energy Chemistry, 2020, 50, 402-408.	7.1	87
37518	Tunable electronic and magnetic properties of <mml:math xmlns:mml="http://www.w3.org/1998/Math/MathML" altimg="si12.svg"><mml:mrow><mml:mn>3</mml:mn><mml:mi>d</mml:mi></mml:mrow></mml:math> transition metal doped Bi2Fe4O9. Journal of Magnetism and Magnetic Materials, 2020, 509, 166893.	1.0	13
37519	Direct bandgap silicon through strain engineering of type-VIII silicon clathrate Si46: A first-principles study. Materials Chemistry and Physics, 2020, 250, 123021.	2.0	0
37520	Realizing high thermoelectric performance in eco-friendly SnTe via synergistic resonance levels, band convergence and endotaxial nanostructuring with Cu2Te. Nano Energy, 2020, 73, 104832.	8.2	81
37521	The effect of strain on the zigzag and armchair phosphorene nanoribbon. Physica E: Low-Dimensional Systems and Nanostructures, 2020, 121, 114088.	1.3	3
37522	First-principles comprehensive study of electronic and mechanical properties of novel uranium hydrides at different pressures. Progress in Natural Science: Materials International, 2020, 30, 251-259.	1.8	8
37523	Predicting the stable Type-I phase of <mml:math xmlns:mml="http://www.w3.org/1998/Math/MathML" altimg="si1.svg"><mml:mrow><mml:mi>X</mml:mi><mml:mi>M</mml:mi><mml:mi>n</mml:mi><mml:mi>S</mml:mi><mml:mi>b</mml:mi> (X= Co, Fe, Os) compounds and its thermodynamic, electronic and magnetic properties from first-principles calculations. Solid State Sciences, 2020, 105, 106208.	1.5	6
37524	Electrosynthesis of high-purity TbMn2O5 nanoparticles and its nanocomposite with conjugated polymer: Surface, density of state and electrochemical investigation. Solid State Sciences, 2020, 105, 106227.	1.5	14

#	Article	IF	Citations
37525	Theoretical investigation of structural and mechanical stability of Mo2N. Solid State Communications, 2020, 314-315, 113919.	0.9	4
37526	Mechanical and electronic properties of graphitic carbon nitride (g-C3N4) under biaxial strain. Vacuum, 2020, 176, 109358.	1.6	15
37527	Glycine Residue Twists HOMOÂ·Â·Â·HOMO Interactions in a Molecular Conductor. Crystal Growth and Design, 2020, 20, 3546-3554.	1.4	1
37528	Theoretical Study on the Intrinsic Source of the Large Thermal Conductivity of Li-Based Chalcogenide Nonlinear Optical Crystals: From AgGaS₂ to LiGaS₂. Crystal Growth and Design, 2020, 20, 4150-4156.	1.4	9
37529	Thermodynamics of Multicomponent Perovskites: A Guide to Highly Efficient and Stable Solar Cell Materials. Chemistry of Materials, 2020, 32, 4265-4272.	3.2	26
37530	Tailoring the Ratio of A-Site Cations in Pr_{1â€“x}Nd_xBaCo_{1.6}Fe_{0.4}O_{5+Î´} to Promote the Higher Oxygen Reduction Reaction Activity for Low-Temperature Solid Oxide Fuel Cells. Chemistry of Materials, 2020, 32, 3841-3849.	3.2	17
37531	Precise Characterization of the Rich Structural Landscape Induced by Pressure in Multifunctional FeVO₄. Inorganic Chemistry, 2020, 59, 6623-6630.	1.9	19
37532	Photogenerated Charge Separation in a CdSe Nanocluster Encapsulated in a Metalâ€“Organic Framework for Improved Photocatalysis. Journal of Physical Chemistry C, 2020, 124, 8504-8513.	1.5	14
37533	FeRh and Nitrogen Codoped Graphene, a Highly Efficient Bifunctional Catalyst toward Oxygen Reduction and Oxygen Evolution Reactions. Journal of Physical Chemistry C, 2020, 124, 9142-9150.	1.5	8
37534	Substituent Effects on Electronic Structures and Peroxidase-Mimicking Activities of Graphyne and Palladium-Doped Graphyne: A Computational Study. Journal of Physical Chemistry C, 2020, 124, 9917-9923.	1.5	10
37535	Properties of Î±-Brass Nanoparticles. 1. Neural Network Potential Energy Surface. Journal of Physical Chemistry C, 2020, 124, 12682-12695.	1.5	27
37536	Eumelanin Adsorption on Silicon: Optical Properties of Si(001)-Adsorbed Eumelanin Tetrameric Protomolecules. Journal of Physical Chemistry C, 2020, 124, 9376-9384.	1.5	3
37537	Experimental and DFT Investigation into Chloride Poisoning Effects on Nitrogen-Coordinated Ironâ€“Carbon (FeNC) Catalysts for Oxygen Reduction Reaction. Journal of Physical Chemistry C, 2020, 124, 10324-10335.	1.5	23
37538	Effects of Copper Substitution by Alkali Metals on the Properties of Chalcopyrites for Tandem Applications: Insights from Theory. Journal of Physical Chemistry C, 2020, 124, 10353-10366.	1.5	5
37539	Magnetic Dioxygen Clathrate Hydrates: A Type of Promising Building Blocks for Icy Crystalline Materials. Journal of Physical Chemistry C, 2020, 124, 10669-10678.	1.5	4
37540	Tailoring the Dimension of Halide Perovskites Enables Quantum Wires with Enhanced Visible Light Absorption. Journal of Physical Chemistry C, 2020, 124, 11124-11131.	1.5	1
37541	Penta-BCN: A New Ternary Pentagonal Monolayer with Intrinsic Piezoelectricity. Journal of Physical Chemistry Letters, 2020, 11, 3501-3506.	2.1	80
37542	Performance Limit of Monolayer WSe₂ Transistors; Significantly Outperform Their MoS₂ Counterpart. ACS Applied Materials & Interfaces, 2020, 12, 20633-20644.	4.0	39

#	Article	IF	Citations
37543	Involvement of the Unoccupied Site Changes the Kinetic Trend Significantly: A Case Study on Formic Acid Decomposition. ACS Catalysis, 2020, 10, 5153-5162.	5.5	14
37544	Impact of Metal and Heteroatom Identities in the Hydrogenolysis of Câ€“X Bonds (X = C, N, O, S, and Cl). ACS Catalysis, 2020, 10, 5086-5100.	5.5	21
37545	Performance of Metal-Catalyzed Hydrodebromination of Dibromomethane Analyzed by Descriptors Derived from Statistical Learning. ACS Catalysis, 2020, 10, 6129-6143.	5.5	23
37546	Unconventional Magnetization Generated from Electron Beam and Femtosecond Irradiation on Î±-Ag₂WO₄: A Quantum Chemical Investigation. ACS Omega, 2020, 5, 10052-10067.	1.6	20
37547	Selective Oxidation of Propylene on Cu₂O(111) and Cu₂O(110) Surfaces: A Systematically DFT Study. ACS Omega, 2020, 5, 6260-6269.	1.6	18
37548	Vibrational Analysis of Manganese(II) Oxalates Hydrates: An In Silico Statistical Approach. ACS Omega, 2020, 5, 9071-9077.	1.6	3
37549	Manipulating dehydrogenation kinetics through dual-doping Co3N electrode enables highly efficient hydrazine oxidation assisting self-powered H2 production. Nature Communications, 2020, 11, 1853.	5.8	229
37550	Reactions of CO2 and ethane enable CO bond insertion for production of C3 oxygenates. Nature Communications, 2020, 11, 1887.	5.8	49
37551	Hydrogen-accelerated spontaneous microcracking in high-strength aluminium alloys. Scientific Reports, 2020, 10, 1998.	1.6	38
37552	Chemical manipulation of hydrogen induced high p-type and n-type conductivity in Ga2O3. Scientific Reports, 2020, 10, 6134.	1.6	65
37553	Thermodynamical stability of substoichiometric plutonium monocarbide from first-principles calculations. Physical Chemistry Chemical Physics, 2020, 22, 9009-9013.	1.3	6
37554	Ni₁₂P₅ nanoparticles bound on graphene sheets for advanced lithiumâ€“sulfur batteries. Nanoscale, 2020, 12, 10760-10770.	2.8	40
37555	Testing the predictive power of theory for Pd_xIr_(100â^'x) alloy nanoparticles for the oxygen reduction reaction. Journal of Materials Chemistry A, 2020, 8, 8421-8429.	5.2	9
37556	A tetragonal phase Mn₂B₂ sheet: a stable room temperature ferromagnet with sizable magnetic anisotropy. Physical Chemistry Chemical Physics, 2020, 22, 10893-10899.	1.3	28
37557	N-Promoted Ru₁/TiO₂ single-atom catalysts for photocatalytic water splitting for hydrogen production: a density functional theory study. Physical Chemistry Chemical Physics, 2020, 22, 11392-11399.	1.3	28
37558	Spin-dependent Schottky barriers and vacancy-induced spin-selective ohmic contacts in magnetic vdW heterostructures. Physical Chemistry Chemical Physics, 2020, 22, 9460-9466.	1.3	14
37559	Bi-stimuli assisted engineering and control of magnetic phase in monolayer CrOCl. Physical Chemistry Chemical Physics, 2020, 22, 12806-12813.	1.3	34
37560	Impact of edge structures on interfacial interactions and efficient visible-light photocatalytic activity of metalâ€“semiconductor hybrid 2D materials. Catalysis Science and Technology, 2020, 10, 3279-3289.	2.1	37

#	Article	IF	Citations
37561	CO activation and methanation mechanism on hexagonal close-packed Co catalysts: effect of functionals, carbon deposition and surface structure. Catalysis Science and Technology, 2020, 10, 3387-3398.	2.1	5
37562	Structure, stability and electronic properties of one-dimensional tetrathia- and tetraselena[8]circulene-based materials: a comparative DFT study. New Journal of Chemistry, 2020, 44, 6872-6882.	1.4	5
37563	Crystallographic facet selective HER catalysis: exemplified in FeP and NiP₂ single crystals. Chemical Science, 2020, 11, 5007-5016.	3.7	51
37564	Thermodynamic stability, phase separation and Ag grading in (Ag,Cu)(In,Ga)Se₂ solar absorbers. Journal of Materials Chemistry A, 2020, 8, 8740-8751.	5.2	29
37565	Dendrite-free and air-stable lithium metal batteries enabled by electroless plating with aluminum fluoride. Journal of Materials Chemistry A, 2020, 8, 9218-9227.	5.2	16
37566	Bottom-up fabrication of the multi-layer carbon metal nanosheets. RSC Advances, 2020, 10, 7987-7993.	1.7	6
37567	Theoretical and experimental investigations on the bulk photovoltaic effect in lead-free perovskites MASnI₃ and FASnI₃. RSC Advances, 2020, 10, 14679-14688.	1.7	60
37568	Mechanisms of carbon dioxide reduction on strontium titanate perovskites. Journal of Materials Chemistry A, 2020, 8, 9392-9398.	5.2	23
37569	Predicting metalâ€“metal interactions. I. The influence of strain on nanoparticle and metal adlayer stabilities. Journal of Chemical Physics, 2020, 152, 094701.	1.2	12
37570	Intercalation induced ferromagnetism in group-V transition metal dichalcogenide bilayer. AIP Advances, 2020, 10, .	0.6	7
37571	Possible monoclinic distortion of Mo2GaC under high pressure. Journal of Applied Physics, 2020, 127, 145103.	1.1	2
37572	Support work function as a descriptor and predictor for the charge and morphology of deposited Au nanoparticles. Journal of Chemical Physics, 2020, 152, 144704.	1.2	3
37573	Large H ₂ O solubility in dense silica and its implications for the interiors of water-rich planets. Proceedings of the National Academy of Sciences of the United States of America, 2020, 117, 9747-9754.	3.3	34
37574	Strain-tunable electronic, elastic, and optical properties of CaI₂monolayer: first-principles study. Philosophical Magazine, 2020, 100, 1982-2000.	0.7	8
37575	The effect of strain on the structural and dynamical stability of hydrogenated penta-C₂Ge: a density functional theory study. Journal Physics D: Applied Physics, 2020, 53, 335101.	1.3	1
37576	Kohn anomaly and van Hove singularity in IV^B and V^B group transition metals nitrides and carbides. Journal of Physics Condensed Matter, 2020, 32, 075401.	0.7	0
37577	Semi-classical electronic transport properties of ternary compound AlGaAs2: role of different scattering mechanisms. Journal of Physics Condensed Matter, 2020, 32, 135704.	0.7	2
37578	Graphenylene nanoribbons: electronic, optical and thermoelectric properties from first-principles calculations. Journal of Physics Condensed Matter, 2020, 32, 345301.	0.7	14

#	Article	IF	Citations
37579	Thermally stimulated relaxation and behaviors of oxygen vacancies in SrTiO₃ single crystals with (100), (110) and (111) orientations. Materials Research Express, 2020, 7, 046305.	0.8	3
37580	In-Plane Dual-Gated Spin-Valve Device Based on the Zigzag Graphene Nanoribbon. Physical Review Applied, 2020, 13, .	1.5	22
37581	Stability, magnetic order, and electronic properties of ultrathin <mml:math xmlns:mml="http://www.w3.org/1998/Math/MathML"><mml:mrow><mml:msub><mml:mi>Fe</mml:mi><mml:mn>3</mml:mn></mml:r mathvariant="normal">O</mml:mi><mml:mn>4</mml:mn></mml:msub></mml:mrow></mml:math> nanosheets. Physical Review B, 2020, 101, .	1.1	3
37582	Gapless Dirac surface states in the antiferromagnetic topological insulator <mml:math xmlns:mml="http://www.w3.org/1998/Math/MathML"><mml:mrow><mml:msub><mml:mi>MnBi</mml:mi><mml:mn>2</mml:mn></mml Physical Review B, 2020, 101, .	1.1	134
37583	Improved description of perovskite oxide crystal structure and electronic properties using self-consistent Hubbard <mml:math xmlns:mml="http://www.w3.org/1998/Math/MathML"><mml:mi>U</mml:mi></mml:math> corrections from ACBN0. Physical Review B, 2020, 101, .	1.1	17
37584	Reversible spin storage in metal oxideâ€"fullerene heterojunctions. Science Advances, 2020, 6, eaax1085.	4.7	10
37585	Phase Transformations in Ni(Co)â€"Mn(Cr,C)â€"(In,Sn) Alloys: An Ab Initio Study. Physics of Metals and Metallography, 2020, 121, 202-209.	0.3	4
37586	Monolayer Honeycomb Borophene: A Promising Anode Material with a Record Capacity for Lithium-Ion and Sodium-Ion Batteries. Journal of the Electrochemical Society, 2020, 167, 090527.	1.3	28
37587	Electronic Structure and Ferromagnetic Properties of Doped Calcium Sulfide Ca1â^'xTM_xS (TM = V, Cr and Co). Spin, 2020, 10, .	0.6	5
37588	Experimental and Computational Studies on Superhard Material Rhenium Diboride under Ultrahigh Pressures. Materials, 2020, 13, 1657.	1.3	15
37589	Firstâ€Principles Study on the Molecular Mechanism of Solarâ€Driven CO₂ Reduction on Hâ€Terminated Si. ChemSusChem, 2020, 13, 3524-3529.	3.6	3
37590	A timeâ€dependent density functional study on optical response in allâ€inorganic leadâ€halide perovskite nanostructures. International Journal of Quantum Chemistry, 2020, 120, e26232.	1.0	6
37591	Labile oxygen promotion of the catalytic oxidation of acetone over a robust ternary Mn-based mullite GdMn2O5. Applied Catalysis B: Environmental, 2020, 271, 118932.	10.8	50
37592	Five carbon allotropes from Squaroglitter structures. Computational Materials Science, 2020, 178, 109634.	1.4	49
37593	Quantitative Analysis of Cation Selectivity of the Electrodes in Multi-ion Electrolytes Based on 2H-Phase MoS2. Journal of Physical Chemistry C, 2020, 124, 9665-9672.	1.5	3
37594	Viscosity of hcp iron at Earthâ€™s inner core conditions from density functional theory. Scientific Reports, 2020, 10, 6311.	1.6	20
37595	Charge localization control of electronâ€"hole recombination in multilayer two-dimensional Dionâ€"Jacobson hybrid perovskites. Journal of Materials Chemistry A, 2020, 8, 9168-9176.	5.2	38
37596	Giant optical absorption and ferroelectric polarization of BiCoO₂S perovskite oxysulfide by first principles prediction. Physical Chemistry Chemical Physics, 2020, 22, 11382-11391.	1.3	4

#	Article	IF	Citations
37597	Pressure-induced structure, electronic, thermodynamic and mechanical properties of Ti2AlNb orthorhombic phase by first-principles calculations. Rare Metals, 2021, 40, 1-11.	3.6	20
37598	Effect of synthesis temperature on the phase formation of NiTiAlFeCr compositionally complex alloy thin films. Journal of Alloys and Compounds, 2021, 854, 155178.	2.8	4
37599	Exploring single atom catalysts of transition-metal doped phosphorus carbide monolayer for HER: A first-principles study. Journal of Energy Chemistry, 2021, 52, 155-162.	7.1	54
37600	Loading Fe3O4 nanoparticles on paper-derived carbon scaffold toward advanced lithiumâ€“sulfur batteries. Journal of Energy Chemistry, 2021, 52, 1-11.	7.1	42
37601	Study on the optical spectra of MgAl2O4 with oxygen vacancies. Materials Technology, 2021, 36, 279-285.	1.5	7
37602	Electronic, magnetic and optical properties of Fe-doped nano-BN sheet: DFT study. Indian Journal of Physics, 2021, 95, 823-831.	0.9	7
37603	Electrochemical syngas production from CO2 and water with CNT supported ZnO catalysts. Catalysis Today, 2021, 364, 172-181.	2.2	7
37604	Surface stability of perovskite oxides under OER operating conditions: a first principles approach. Faraday Discussions, 2021, 229, 75-88.	1.6	19
37605	Magnetite Fe₃O₄ surface as an effective drug delivery system for cancer treatment drugs: density functional theory study. Journal of Biomolecular Structure and Dynamics, 2021, 39, 2798-2805.	2.0	13
37606	Electronic and thermoelectric properties of chalcopyrite compounds Cu2(XY)S4 (Xâ€‰=â€‰Zn, Cd and Yâ€‰=â€‰Sn,) Tj ETQq1	0.9	12
37607	CO₂ reduction to acetic acid on the greigite Fe₃S₄{111} surface. Faraday Discussions, 2021, 229, 35-49.	1.6	12
37608	First-principles study of electronic structure and optical properties of Er:Lu2O3. Journal of Rare Earths, 2021, 39, 453-459.	2.5	13
37609	Hydrogen storage capacities of alkali and alkaline-earth metal atoms on SiC monolayer: A first-principles study. International Journal of Hydrogen Energy, 2021, 46, 20266-20279.	3.8	39
37610	Alkali and transition metal atom-functionalized germanene for hydrogen storage: A DFT investigation. International Journal of Hydrogen Energy, 2021, 46, 20245-20256.	3.8	57
37611	Cu-Al spinel-oxide catalysts for selective hydrogenation of furfural to furfuryl alcohol. Catalysis Today, 2021, 367, 177-188.	2.2	25
37612	The vibrational, thermodynamic and mechanical properties of four types HMX based on the first-principles study. Journal of Energetic Materials, 2021, 39, 125-169.	1.0	12
37613	Search for potential K ion battery cathodes by first principles. Journal of Energy Chemistry, 2021, 54, 377-385.	7.1	8
37614	The role of oxygenated species in the catalytic self-coupling of MeOH on O pre-covered Au(111). Faraday Discussions, 2021, 229, 251-266.	1.6	7

#	Article	IF	Citations
37615	Controllable preparation of ultrathin 2D BiOBr crystals for high-performance ultraviolet photodetector. Science China Materials, 2021, 64, 189-197.	3.5	20
37616	First-principles study on predicting the crystal structures, mechanical properties and electronic structures of HfCxN1-x. Journal of the European Ceramic Society, 2021, 41, 3037-3044.	2.8	7
37617	The effect of edge functionalization on the device performance of monolayer Si0.5Ge0.5 nanoribbon transistors. Journal of Computational Electronics, 2021, 20, 95-106.	1.3	2
37618	Theoretical screening of the transition metal heteronuclear dimer anchored graphdiyne for electrocatalytic nitrogen reduction. Journal of Energy Chemistry, 2021, 54, 501-509.	7.1	116
37619	Solid phase microwave-assisted fabrication of Fe-doped ZIF-8 for single-atom Fe-N-C electrocatalysts on oxygen reduction. Journal of Energy Chemistry, 2021, 54, 579-586.	7.1	52
37620	Surface modification of macroporous La0.8Sr0.2CoO3 perovskite oxides integrated monolithic catalysts for improved propane oxidation. Catalysis Today, 2021, 376, 168-176.	2.2	13
37621	High-Pressure Structural and Electronic Properties of Potassium-Based Green Primary Explosives. Journal of Electronic Materials, 2021, 50, 1581-1590.	1.0	3
37622	Novel green phosphorene as a superior chemical gas sensing material. Journal of Hazardous Materials, 2021, 401, 123340.	6.5	71
37623	High-precision regulation synthesis of Fe-doped Co2P nanorod bundles as efficient electrocatalysts for hydrogen evolution in all-pH range and seawater. Journal of Energy Chemistry, 2021, 55, 92-101.	7.1	89
37624	Effects of surface functionalization of mxene-based nanocatalysts on hydrogen evolution reaction performance. Catalysis Today, 2021, 368, 187-195.	2.2	51
37625	Combination of theoretical and in situ experimental investigations of the role of lithium dopant in manganese nitride: a two-stage reagent for ammonia synthesis. Faraday Discussions, 2021, 229, 281-296.	1.6	9
37626	The integrated DL_POLY/DL_FIELD/DL_ANALYSER software platform for molecular dynamics simulations for exploration of the synthonic interactions in saturated benzoic acid/hexane solutions. Molecular Simulation, 2021, 47, 257-272.	0.9	5
37627	Lattice Dynamics and Thermodynamic Properties of Bulk Phases and Monolayers of GaTe and InTe: A Comparison from Firstâ€Principles Calculations. European Journal of Inorganic Chemistry, 2021, 2021, 126-138.	1.0	9
37628	Ring-opening and hydrodenitrogenation of indole under hydrothermal conditions over Ni, Pt, Ru, and Ni-Ru bimetallic catalysts. Chemical Engineering Journal, 2021, 406, 126853.	6.6	32
37629	Clarifying the polyaniline effect on superior electrochemical performances of hydrogen storage alloys. Electrochimica Acta, 2021, 365, 137336.	2.6	8
37630	Theoretical study of NO2 adsorption on SiCNT and P-doped SiCNT. Physica E: Low-Dimensional Systems and Nanostructures, 2021, 127, 114519.	1.3	5
37631	Structural, mechanical, thermal, and optical properties of inverse-Heusler alloys Cr2CoZ (Z = Al, In): A first-principles investigation. Physics Letters, Section A: General, Atomic and Solid State Physics, 2021, 385, 126967.	0.9	39
37632	Misfit Layer Compounds: A Platform for Heavily Doped 2D Transition Metal Dichalcogenides. Advanced Functional Materials, 2021, 31, 2007706.	7.8	17

#	Article	IF	Citations
37633	Metric-driven search for structurally stable inorganic compounds. Acta Materialia, 2021, 202, 437-447.	3.8	6
37634	The compatibility between environmentally friendly insulation gas C4F7N and Î±-Al2O3 (0001) surface: Theoretical and experimental insights. Applied Surface Science, 2021, 536, 147839.	3.1	6
37635	Engineering of MoS2 nanoribbons as high-performance materials for biosensing applications. Applied Surface Science, 2021, 540, 148349.	3.1	5
37636	Crystal face-dependent methylmercury adsorption onto mackinawite (FeS) nanocrystals: A DFT-D3 study. Chemical Engineering Journal, 2021, 420, 127594.	6.6	16
37637	Insights into the gradient-characteristic precipitation behaviors of laves phase induced by Fe/W/Mo addition in Ti42Al5Mn alloy. Intermetallics, 2021, 128, 107022.	1.8	8
37638	18 and 12 â€“ Member carbon rings (cyclo[n]carbons) â€“ A density functional study. Materials Science and Engineering B: Solid-State Materials for Advanced Technology, 2021, 263, 114895.	1.7	6
37639	High-pressure structural, lattice dynamics, and electronic properties of beryllium aluminate studied from first-principles theory. Materials Today Communications, 2021, 26, 101801.	0.9	9
37640	Ab initio study of elastic properties of orthorhombic cadmium stannate as a substrate for the manufacture of MEMS devices. Materials Today Communications, 2021, 26, 101822.	0.9	5
37641	Tailoring the chemical bonding of GeTe-based alloys by MgB2 alloying to simultaneously enhance their mechanical and thermoelectric performance. Materials Today Physics, 2021, 16, 100308.	2.9	29
37642	A first-principles investigation of Janus MoSSe as a catalyst for photocatalytic water-splitting. Applied Surface Science, 2021, 537, 147919.	3.1	36
37643	The performance of nanoporous phosphorene as membranes for separating three typical C3F7CN insulating gas decomposition products. Applied Surface Science, 2021, 537, 147975.	3.1	3
37644	Insights into electrochemical nitrogen reduction reaction mechanisms: Combined effect of single transition-metal and boron atom. Journal of Energy Chemistry, 2021, 58, 577-585.	7.1	66
37645	Prediction of the Half Metallicity in Ferromagnetic Germanium Telluride (GeTe) Doped with Titanium. Spin, 2021, 11, .	0.6	1
37646	Highly Efficient Nb₂C MXene Cathode Catalyst with Uniform Oâ€Terminated Surface for Lithiumâ€“Oxygen Batteries. Advanced Energy Materials, 2021, 11, .	10.2	130
37647	Ultra-incompressibility and high energy density of ReN8 with infinite nitrogen chains. Journal of Materials Science, 2021, 56, 3814-3826.	1.7	9
37648	Microstructure and electronic property of pristine and thermal barrier layers TiN/AlN/ZrB2 buffered 4H-SiC/W interface from first principles study. Applied Surface Science, 2021, 536, 147820.	3.1	5
37649	Strain engineering for C2N/Janus monochalcogenides van der Waals heterostructures: Potential applications for photocatalytic water splitting. Applied Surface Science, 2021, 536, 147845.	3.1	17
37650	Rapid generation of optimal generalized Monkhorst-Pack grids. Computational Materials Science, 2021, 187, 110100.	1.4	25

#	Article	IF	Citations
37651	Enhancing thermoelectric properties of Janus WSSe monolayer by inducing strain mediated valley degeneracy. Journal of Alloys and Compounds, 2021, 855, 157304.	2.8	46
37652	First-principles studies on behaviors of He impurities in d-MAX phase Zr3Al3C5. Journal of Nuclear Materials, 2021, 544, 152653.	1.3	1
37653	Effects of chemical composition on the structural stability, elastic, vibrational, and electronic properties of Cs₂NaLnX₆ (LnÂ=ÂLaâ€¦Lu, XÂ=ÂF, Cl, Br, I) elpasolites. Journal of the American Ceramic Society, 2021, 104, 1489-1500.	1.9	7
37654	Interaction between dispersant and coal slime added in semi-coke water slurry: An experimental and DFT study. Applied Surface Science, 2021, 540, 148327.	3.1	21
37655	Interactive network of the dehydrogenation of alkanes, alkenes and alkynes â€“ surface carbon hydrogenative coupling on Ru(111). Catalysis Science and Technology, 2021, 11, 191-210.	2.1	4
37656	Exploring Janus MoSSe monolayer as a workable media for SOF6 decompositions sensing based on DFT calculations. Computational Materials Science, 2021, 186, 109976.	1.4	21
37657	Prediction of a new 2D B2CO monolayer from density functional theory. Computational Materials Science, 2021, 186, 109975.	1.4	4
37658	Thermophysical properties of high-density, sintered monoliths of yttrium dihydride in the range 373â€“773ÂK. Journal of Alloys and Compounds, 2021, 850, 156303.	2.8	12
37659	Synthesis and simulation of surfactant free chemically derived highly polycrystalline lead iodide. Materials Today: Proceedings, 2021, 42, 1624-1628.	0.9	0
37660	Lignin derived hierarchical porous carbon with extremely suppressed polyselenide shuttling for high-capacity and long-cycle-life lithiumâ€“selenium batteries. Journal of Energy Chemistry, 2021, 55, 476-483.	7.1	31
37661	DFT study of structural, electronic, elastic and magnetic properties of In0.75Cr0.25P. Materials Today: Proceedings, 2021, 46, 76-80.	0.9	0
37662	Adsorption behavior of barium ions onto ZnO surfaces: Experiments associated with DFT calculations. Journal of Molecular Structure, 2021, 1223, 128991.	1.8	27
37663	Towards thermoneutral hydrogen evolution reaction using noble metal free molybdenum ditelluride/graphene nanocomposites. Journal of Colloid and Interface Science, 2021, 581, 847-859.	5.0	16
37664	Free-standing nanoporous NiMnFeMo alloy: An efficient non-precious metal electrocatalyst for water splitting. Chemical Engineering Journal, 2021, 404, 126530.	6.6	88
37665	Electronic origin of the main-group element dependences of elastic moduli in the Ni2Mn-based magnetic shape memory alloys. Journal of Physics and Chemistry of Solids, 2021, 148, 109671.	1.9	8
37666	First-principles investigation of B2 partial disordered structure, martensitic transformation, elastic and magnetic properties of all-d-metal Ni-Mn-Ti Heusler alloys. Journal of Materials Science and Technology, 2021, 68, 103-111.	5.6	31
37667	A theoretical investigation of electronic and optical properties of (6,1) single-wall carbon nanotube (SWCNT). Carbon Letters, 2021, 31, 441-448.	3.3	15
37668	Identifying electrocatalytic activity and mechanism of Ce1/3NbO3 perovskite for nitrogen reduction to ammonia at ambient conditions. Applied Catalysis B: Environmental, 2021, 280, 119419.	10.8	60

#	Article	IF	Citations
37669	DNA and RNA detection using graphene and hexagonal boron nitride based nanosensor. Carbon, 2021, 173, 493-500.	5.4	25
37670	Adsorption of nitrogen based gas molecules on noble metal functionalized carbon nitride nanosheets: A theoretical investigation. Computational and Theoretical Chemistry, 2021, 1194, 112950.	1.1	8
37671	A multiphase sodium vanadium phosphate cathode material for high-rate sodium-ion batteries. Journal of Materials Science and Technology, 2021, 66, 121-127.	5.6	19
37672	CO adsorption on the calcite(10.4) surface: a combined experimental and theoretical study. Physical Chemistry Chemical Physics, 2021, 23, 7696-7702.	1.3	12
37673	Experimental and DFT study of BaLaCuS3: Direct band gap semiconductor. Journal of Physics and Chemistry of Solids, 2021, 148, 109670.	1.9	12
37674	First-principles calculations of stability of graphene-like BC3 monolayer and its high-performance potassium storage. Chinese Chemical Letters, 2021, 32, 900-905.	4.8	32
37675	A Pt/MnV2O6 nanocomposite for the borohydride oxidation reaction. Journal of Energy Chemistry, 2021, 55, 428-436.	7.1	8
37676	Orbital symmetry matching: Achieving superior nitrogen reduction reaction over single-atom catalysts anchored on Mxene substrates. Chinese Journal of Catalysis, 2021, 42, 288-296.	6.9	41
37677	Turning chemistry into information for heterogeneous catalysis. International Journal of Quantum Chemistry, 2021, 121, e26382.	1.0	9
37678	Identifying the Znâ€“Co binary as a robust bifunctional electrocatalyst in oxygen reduction and evolution reactions via shifting the apexes of the volcano plot. Journal of Energy Chemistry, 2021, 55, 162-168.	7.1	33
37679	TMN4 complex embedded graphene as bifunctional electrocatalysts for high efficiency OER/ORR. Journal of Energy Chemistry, 2021, 55, 437-443.	7.1	117
37680	Understanding the atomistic origin of the magnetic phases in Cobalt-TM (V, Nb, Ta, Zr, Hf, W) pair co-doped boron nitride monolayer and the hydrogenation effect. Physica E: Low-Dimensional Systems and Nanostructures, 2021, 125, 114359.	1.3	7
37681	Twin Boundary and Fivefold Twins in Nickel Oxide. Physica Status Solidi (B): Basic Research, 2021, 258, 2000377.	0.7	5
37682	Theoretical study of magnetoâ€electronic properties of <scp>TmCo₂</scp> and <scp>NdCo₂</scp> intermetallic compounds through density functional theory calculations. International Journal of Quantum Chemistry, 2021, 121, e26488.	1.0	4
37683	Theoretical study of the phase transitions and electronic structure of (Zr0.5, Mg0.5)N and (Hf0.5,) Tj ETQq0 0 0 rgBT /Overlock 10 Tf 50	1.7	11
37684	Water Adsorption and Dissociation Promoted by Co*-/N-C*-Biactive Sites of Metallic Co/N-Doped Carbon Hybrids for Efficient Hydrogen Evolution. Applied Catalysis B: Environmental, 2021, 282, 119463.	10.8	77
37685	Magnetization effect of Mn-embedded in C2N on hydrogen adsorption and gas-sensing properties: Ab-initio analysis. Applied Surface Science, 2021, 537, 147970.	3.1	15
37686	Ab initio study of molybdenum sulfo-selenides alloy as a flexible anode for sodium-ion batteries. Applied Surface Science, 2021, 536, 147973.	3.1	15

#	Article	IF	Citations
37687	Ab initio insights into the interaction mechanisms between boron, nitrogen and oxygen doped diamond surfaces and water molecules. Carbon, 2021, 171, 575-584.	5.4	9
37688	â€œInside outâ€•growth method for high-quality nitrogen-doped graphene. Carbon, 2021, 171, 704-710.	5.4	20
37689	Two-dimensional blue-phase CX (X = S, Se) monolayers with high carrier mobility and tunable photocatalytic water splitting capability. Chinese Chemical Letters, 2021, 32, 1977-1982.	4.8	31
37690	Synthesis of flower-liked twin crystal ternary Ni/NiS/Zn0.2Cd0.8S catalyst for highly efficient hydrogen production. Chemical Engineering Journal, 2021, 406, 126878.	6.6	57
37691	Charge-regulated, electric-field and combined effect controlled switchable CO2 capture and separation on penta-C2N nanosheet: A computational study. Chemical Engineering Journal, 2021, 407, 127194.	6.6	24
37692	Structure and electronic properties of Î´-Bi2O3 tuned by vacancy and doping: A first-principles study. Ceramics International, 2021, 47, 205-213.	2.3	8
37693	Anisotropic elastic, thermal properties and electronic structures of M2AlB2 (M=Fe, Cr, and Mn) layer structure ceramics. Ceramics International, 2021, 47, 1421-1428.	2.3	17
37694	Strain engineering of electronic structure, phonon, and thermoelectric properties of p-type half-Heusler semiconductor. Journal of Alloys and Compounds, 2021, 850, 156615.	2.8	51
37695	Ab-initio, Monte Carlo and experimental investigation on structural, electronic and magnetic properties of Zn1-Ni O nanoparticles prepared via sol-gel method. Journal of Alloys and Compounds, 2021, 854, 157142.	2.8	10
37696	Influence of pressure on phase transition, electronic and thermoelectric properties of SnSe. Journal of Alloys and Compounds, 2021, 853, 157362.	2.8	6
37697	Investigating and comparing structural, electronic and optical properties of Ï‡3-Borophene in monolayer, nanoribbon and nanotube modes as a transparent metal. Journal of Physics and Chemistry of Solids, 2021, 148, 109683.	1.9	8
37698	First-principle calculations of adsorption of Ga (Al, N) adatoms on the graphene for the van-der-Waals epitaxy. Materials Today Communications, 2021, 26, 101571.	0.9	5
37699	Germanene/2D-SiC van der Waals heterobilayer: Structural features and tunable electronic properties. Materials Today Communications, 2021, 26, 101718.	0.9	22
37700	An Ab Initio study of electronic, mechanical, thermoelectric and vibrational properties of Dirac Semimetals Ca3PbO and Ca3SnO. Materials Today Communications, 2021, 26, 101741.	0.9	2
37701	Light-activated polydopamine coatings for efficient metal recovery from electronic waste. Separation and Purification Technology, 2021, 254, 117674.	3.9	10
37702	First-Principles Simulation of Structural, Electronic and Optical Properties of Cerium Trisulfide (Ce2S3) Compound. Journal of Electronic Materials, 2021, 50, 1637-1643.	1.0	9
37703	Two-dimensional carbon allotropes with tunable direct band gaps and high carrier mobility. Applied Surface Science, 2021, 537, 147885.	3.1	39
37704	Catalytic activity for hydrogen evolution reaction in square phase Janus MoSSe monolayer: A first-principles study. Physica E: Low-Dimensional Systems and Nanostructures, 2021, 126, 114485.	1.3	4

#	Article	IF	Citations
37705	Structural, magnetic properties and phase stability of CrAs in the zinc-blende structure: Investigated by first principle calculations and Monte Carlo simulation. Solid State Communications, 2021, 323, 114101.	0.9	7
37706	Driving Towards Highly Selective and Cokingâ€Resistant Natural Gas Reforming Through a Hybrid Oxygen Carrier Design. ChemCatChem, 2021, 13, 617-626.	1.8	7
37707	Unveiling the pseudocapacitive effects of ultramesopores on nanoporous carbon. Applied Surface Science, 2021, 537, 148037.	3.1	9
37708	Experimental and theoretical study of dense YBO3 and the influence of non-hydrostaticity. Journal of Alloys and Compounds, 2021, 850, 156562.	2.8	5
37709	Density functional theory-based investigation of hydrogen adsorption on zinc oxide (<mml:math) Tj ETQq0 0 0 rgBT /Overlock 10 Tf 50 5 surface: Revisited. Surface Science, 2021, 703, 121726.	0.8	3
37710	Effect of flue gas on elemental mercury removal capacity of defective carbonaceous surface: A first-principles study. Journal of Hazardous Materials, 2021, 404, 124013.	6.5	23
37711	Study of Structural, Electronic, Magnetic, Elastic, and Thermodynamic Properties of Co₄N Antiperovskite by First Principles and Monte Carlo Simulation. Physica Status Solidi (B): Basic Research, 2021, 258, 2000339.	0.7	4
37712	Theoretical investigation of CoTa2O6/graphene heterojunctions for oxygen evolution reaction. Frontiers of Physics, 2021, 16, 1.	2.4	6
37713	Selective dehydration of glycerol on copper based catalysts. Catalysis Today, 2021, 367, 58-70.	2.2	14
37714	Anchoring silicon on the basal plane of graphite via a three-phase heterostructure for highly reversible lithium storage. Energy Storage Materials, 2021, 34, 311-319.	9.5	65
37715	Elastic, Half-Metallicity, Thermodynamic, and Transport Properties of Ru2VGe and Ru2VSb Full-Heusler Compounds: a First-Principle Study. Journal of Superconductivity and Novel Magnetism, 2021, 34, 157-167.	0.8	5
37716	Two-dimensional transition metal borides as highly efficient N2 fixation catalysts. Applied Surface Science, 2021, 536, 147742.	3.1	58
37717	Rh-doped h-BN monolayer as a high sensitivity SF6 decomposed gases sensor: A DFT study. Applied Surface Science, 2021, 536, 147965.	3.1	76
37718	Optical and thermoelectric properties of graphenylene and octagraphene nanotubes from first-principles calculations. Computational Materials Science, 2021, 186, 109999.	1.4	15
37719	Ground state spin structure of GdFeO3: A computational and experimental study. Journal of Magnetism and Magnetic Materials, 2021, 518, 167407.	1.0	3
37720	Computational study of lattice dynamics and thermodynamic properties of energetic solid cyanuric triazide. Journal of Physics and Chemistry of Solids, 2021, 148, 109782.	1.9	5
37721	Structural, electronic and optical properties of lead-free antimony-copper based hybrid double perovskites for photovoltaics and optoelectronics by first principles calculations. Computational Materials Science, 2021, 186, 110009.	1.4	30
37722	An automated cluster surface scanning method for exploring reaction paths on metal-cluster surfaces. Computational Materials Science, 2021, 186, 110010.	1.4	10

#	Article	IF	Citations
37723	Predicting Nitrogenâ€Based Families of Compounds: Transitionâ€Metal Guanidinates TCN₃ (T=V, Nb, Ta) and Orthoâ€Nitrido Carbonates Tâ€²₂CN₄ (Tâ€²=Ti, Zr, Hf). Angewandte Chemie - International Edition, 2021, 60, 486-492.	7.2	18
37724	Design of grain boundary enriched bimetallic borides for enhanced hydrogen evolution reaction. Chemical Engineering Journal, 2021, 405, 126977.	6.6	56
37725	Bio-synthesised black Î±-Cr2O3 nanoparticles; experimental analysis and density function theory calculations. Journal of Alloys and Compounds, 2021, 850, 156671.	2.8	24
37726	Noncovalent functionalization of graphene through physisorption of 1,1-diamino-2,2-dinitroethene: Impacts of and cooperativity between hydrogen bond and Ï€Â·Â·Â·Ï€ interaction. Journal of Physics and Chemistry of Solids, 2021, 148, 109736.	1.9	4
37727	Presence of excited electronic states on terbium incorporation in CaMoO4: Insights from experimental synthesis and first-principles calculations. Journal of Physics and Chemistry of Solids, 2021, 149, 109790.	1.9	8
37728	Rational defect and anion chemistries in Co3O4 for enhanced oxygen evolution reaction. Applied Catalysis B: Environmental, 2021, 281, 119535.	10.8	90
37729	Enhancing thermoelectric performance of Sn1-Sb2/3Te via synergistic charge balanced compensation doping. Chemical Engineering Journal, 2021, 404, 126925.	6.6	16
37730	Theoretical study of adsorption mechanism of heavy metals As and Pb on the calcite (104) surface. Materials Today Communications, 2021, 26, 101742.	0.9	3
37731	Two-dimensional WSe2/SnSe p-n junctions secure ultrahigh thermoelectric performance in n-type Pb/I Co-doped polycrystalline SnSe. Materials Today Physics, 2021, 16, 100306.	2.9	51
37732	The Strain and Electric Field Effects on the Electronic and Optical Properties of Armchair MoSSe/WSSe Superlattice Nanoribbon: A Firstâ€Principles Study. Physica Status Solidi (B): Basic Research, 2021, 258, 2000361.	0.7	5
37733	Large valley-polarized state in single-layer NbX2 (X = S, Se): Theoretical prediction. Nano Research, 2021, 14, 834-839.	5.8	49
37734	Twin nucleation from a single <c+a> dislocation in hexagonal close-packed crystals. Acta Materialia, 2021, 202, 35-41.	3.8	13
37735	Insights into the physical properties of a new 211 MAX phase Nb2CuC. Journal of Physics and Chemistry of Solids, 2021, 149, 109759.	1.9	26
37736	A new bifunctional C3N nanosheet of NO2, SO2 gas sensor and CO2 separation: A first-principles study. Physica E: Low-Dimensional Systems and Nanostructures, 2021, 126, 114463.	1.3	19
37737	Practical Band Interpolation with a Generalized Luttingerâ€“Kohn Method. Physica Status Solidi (B): Basic Research, 2021, 258, 2000260.	0.7	0
37738	New insights into the efficient charge transfer of ternary chalcogenides composites of TiO2. Applied Catalysis B: Environmental, 2021, 282, 119612.	10.8	33
37739	Theoretical investigation of Ti2B monolayer as powerful anode material for Li/Na batteries with high storage capacity. Applied Surface Science, 2021, 538, 148048.	3.1	14
37740	A robust calcium-based microporous metal-organic framework for efficient CH4/N2 separation. Chemical Engineering Journal, 2021, 408, 127294.	6.6	72

#	Article	IF	Citations
37741	On segregation in multicomponent alloys: Surface segregation in austenite and FeCrCoNiMn alloys. Computational Materials Science, 2021, 187, 110080.	1.4	10
37742	Adsorption of lead on the surfaces of pristine and B, Si and N-doped graphene. Physica B: Condensed Matter, 2021, 600, 412639.	1.3	21
37743	Hexagonal boron phosphide monolayer exfoliation induced by arsenic incorporation in the BP (1 1 1) surface: A DFT study. Applied Surface Science, 2021, 538, 148163.	3.1	8
37744	A hidden precipitation scenario of the Î¸â€²-phase in Al-Cu alloys. Journal of Materials Science and Technology, 2021, 75, 126-138.	5.6	22
37745	An investigation of half-metallic variant perovskites A2NbCl6 (A= K, Rb) for spintronic based applications. Journal of Solid State Chemistry, 2021, 293, 121823.	1.4	14
37746	<scp>DFT</scp> â€based insight into the magnetic and thermoelectric characteristics of <scp> XTaO ₃ </scp> (X = Rb, Fr) ternary perovskite oxides for optoelectronic applications. International Journal of Energy Research, 2021, 45, 2753-2765.	2.2	17
37747	Mechanical behavior of high entropy carbide (<scp>HfTaZrTi</scp>)C and (<scp>HfTaZrNb</scp>)C under high pressure: Ab initio study. International Journal of Quantum Chemistry, 2021, 121, e26509.	1.0	6
37748	An exploration of the optoelectronic nature of 4,4-difluoro-8-(C4H3X)-4-bora-3a,4a-diaza-s-indacene (Xâ€‰=â€‰O, S, Se) (BODIPY) systems. Journal of Computational Electronics, 2021, 20, 368-376.	1.3	1
37749	Highly active multivalent multielement catalysts derived from hierarchical porous TiNb2O7 nanospheres for the reversible hydrogen storage of MgH2. Nano Research, 2021, 14, 148-156.	5.8	68
37750	Surface engineering induced hierarchical porous Ni12P5-Ni2P polymorphs catalyst for efficient wide pH hydrogen production. Applied Catalysis B: Environmental, 2021, 282, 119609.	10.8	123
37751	Efficient electrocatalytic reduction of CO2 to HCOOH by bimetallic In-Cu nanoparticles with controlled growth facet. Applied Catalysis B: Environmental, 2021, 283, 119646.	10.8	102
37752	Adsorption and diffusion of alkali atoms on FeX2 (XÂ=ÂSe, S) surfaces for potassium-ion battery applications. Applied Surface Science, 2021, 536, 147774.	3.1	12
37753	Pd-doped C3N monolayer: A promising low-temperature and high-activity single-atom catalyst for CO oxidation. Applied Surface Science, 2021, 537, 147881.	3.1	42
37754	Catalytic activity of Ni3Mo surfaces for hydrogen evolution reaction: A density functional theory approach. Applied Surface Science, 2021, 537, 147894.	3.1	25
37755	Predictive screening and validation on chemical looping oxygen carrier activation by tuning electronic structures via transition metal dopants. Chemical Engineering Journal, 2021, 406, 126729.	6.6	20
37756	Effect of silicon doping on the electronic and optical properties of phosphorous nanotubes. Optik, 2021, 225, 165808.	1.4	8
37757	Effect of the negative chemical pressure on physical properties of doped perovskite molybdates in the framework of DFT method. Journal of Alloys and Compounds, 2021, 854, 157088.	2.8	26
37758	Structural, electronic, magnetic and thermoelectric properties of pseudobrookite-type Fe2-xTi1+xO5 (xÂ=ÂO, 0.5 and 1) compounds: DFTÂ+ÂU approaches. Journal of Physics and Chemistry of Solids, 2021, 149, 109802.	1.9	7

#	Article	IF	Citations
37759	Design and synthesis of PbBiVO5 electrode by polymorph engineering for rechargeable battery. Journal of Solid State Chemistry, 2021, 293, 121777.	1.4	1
37760	Hydrogen evolution/spillover effect of single cobalt atom on anatase TiO2 from first-principles calculations. Applied Surface Science, 2021, 536, 147831.	3.1	13
37761	First Principles Investigations of Structural, Electronic and Transport Properties of $$hbox {BiI}_3/hbox {ZrS}_2$$ van der Waals Heterostructure: A Thermoelectric Perspective. Journal of Electronic Materials, 2021, 50, 1644-1654.	1.0	8
37762	Impact of B alloying on ductility and phase transition in the Niâ€“Mn-based magnetic shape memory alloys: Insights from first-principles calculation. Journal of Materials Science and Technology, 2021, 74, 27-34.	5.6	25
37763	Structural, electronic, optical and thermodynamic properties of the cubic quadratic quaternary alloys GaxIn1-xAsyN1-y. Insight from DFT computations. Materials Today Communications, 2021, 26, 101752.	0.9	4
37764	DFT study of gas adsorption and sensing based on noble metal (Ag, Au and Pt) functionalized boron selenide nanosheets. Physica E: Low-Dimensional Systems and Nanostructures, 2021, 125, 114409.	1.3	22
37765	High capacity and mobility in germanium sulfide/graphene (GeS/Gr) van der Waals heterostructure as anode materials for sodiumâ€“ion batteries: A first-principles investigation. Applied Surface Science, 2021, 536, 147779.	3.1	15
37766	The sources of hydrogen affect the productivity and selectivity of CO2 photoreduction on SiC. Applied Surface Science, 2021, 538, 148010.	3.1	6
37767	Theoretical insights into the performance of single and double transition metal atoms doped on N-graphenes for N2 electroreduction. Applied Surface Science, 2021, 537, 148012.	3.1	27
37768	Modulation of 2D GaS/BTe vdW heterostructure as an efficient HER catalyst under external electric field influence. Catalysis Today, 2021, 370, 14-25.	2.2	20
37769	First-principles study of tensile and shear strength of Fe-Al and<mml:math xmlns:mml="http://www.w3.org/1998/Math/MathML" altimg="si48.svg"><mml:mrow><mml:mi>Î±</mml:mi></mml:mrow></mml:math>-AlFeSi intermetallic compound interfaces. Computational Materials Science, 2021, 187, 110058.	1.4	18
37770	Accelerating first-principles estimation of thermal conductivity by machine-learning interatomic potentials: A MTP/ShengBTE solution. Computer Physics Communications, 2021, 258, 107583.	3.0	108
37771	New Icosahedra-based B4N phases by particle swarm optimization. Journal of Alloys and Compounds, 2021, 854, 157255.	2.8	5
37772	2D Sb2C3 monolayer: A promising material for the recyclable gas sensor for environmentally toxic nitrogen-containing gases (NCGs). Journal of Hazardous Materials, 2021, 405, 124168.	6.5	35
37773	Chalcogenide Materials Engineering for Phaseâ€Change Memory and Future Electronics Applications: From Sbâ€“Te to Biâ€“Te. Physica Status Solidi - Rapid Research Letters, 2021, 15, 2000414.	1.2	7
37774	Two-dimensional transition metal phthalocyanine sheet as a promising electrocatalyst for nitric oxide reduction: a first principle study. Environmental Science and Pollution Research, 2021, 28, 7191-7199.	2.7	22
37775	Hyperfine field studies of the high-pressure phase of noncentrosymmetric superconductor RhGe (B20) doped with hafnium. Journal of Alloys and Compounds, 2021, 850, 156601.	2.8	11
37776	Surface structures and equilibrium shapes of layered 2D Ruddlesden-Popper perovskite crystals from density functional theory calculations. Materials Today Communications, 2021, 26, 101745.	0.9	5

#	Article	IF	Citations
37777	Ultrathin Pd and Pt nanowires for potential applications as hydrogen economy. Materials Today Communications, 2021, 26, 101761.	0.9	4
37778	Ab-initio investigation for the microscopic thermodynamics and kinetics of martensitic transformation. Progress in Natural Science: Materials International, 2021, 31, 121-128.	1.8	6
37779	Chemical bonding, thermodynamic stability and mechanical strength of Ni3Ti/Î±-Al2O3 interfaces by first-principles study. Scripta Materialia, 2021, 190, 57-62.	2.6	30
37780	Product-Specific Active Site Motifs of Cu for Electrochemical CO2 Reduction. CheM, 2021, 7, 406-420.	5.8	72
37781	The magnetic and electronic properties of REAgSb2 compounds. Journal of Magnetism and Magnetic Materials, 2021, 519, 167442.	1.0	4
37782	Band engineering of non-hexagonal 2D tetragonal-silicene sheet and nanoribbons: A theoretical approach. Journal of Physics and Chemistry of Solids, 2021, 150, 109801.	1.9	17
37783	A quasi two dimensional metallic state of CaHCl driven by La doping studied from first principles theory. Materials Today Communications, 2021, 26, 101830.	0.9	0
37784	Comparison of the effects of Sr2+ and Ca2+ substitution on the structural and electronic properties of the perovskites CH3NH3Pb1-Y I3 (Y Sr, Ca) by using the Density Functional Theory. Physica B: Condensed Matter, 2021, 600, 412579.	1.3	3
37785	Elucidating the role of lattice thermal conductivity in<scp>Ï€â€phases</scp>of<scp>IVâ€VI</scp>monochalcogenides for highly efficient thermoelectric performance. International Journal of Energy Research, 2021, 45, 6369-6382.	2.2	6
37786	Uniaxial compression of [001]-oriented CaFe2As2 single crystals: the effect of microstructure and temperature on superelasticity Part II: Modeling. Acta Materialia, 2021, 203, 116462.	3.8	1
37787	Anti-sintering non-stoichiometric nickel ferrite for highly efficient and thermal-stable thermochemical CO2 splitting. Chemical Engineering Journal, 2021, 404, 127067.	6.6	13
37788	Electronic and optical properties of graphene/molybdenite bilayer composite. Composite Structures, 2021, 255, 112978.	3.1	12
37789	Highâ€temperature persistent luminescence and visual dualâ€emitting optical temperature sensing in selfâ€activated CaNb₂O₆: Tb³⁺ phosphor. Journal of the American Ceramic Society, 2021, 104, 1750-1759.	1.9	106
37790	Conjugated nickel phthalocyanine polymer selectively catalyzes CO2-to-CO conversion in a wide operating potential window. Applied Catalysis B: Environmental, 2021, 284, 119739.	10.8	45
37791	W-N3 center supported on blue phosphorus as a promising efficient electrocatalyst with ultra-low limiting potential for nitrogen fixation. Applied Surface Science, 2021, 536, 147706.	3.1	13
37792	Unconventional bi-vacancies activating inert Prussian blue analogues nanocubes for efficient hydrogen evolution. Chemical Engineering Journal, 2021, 420, 127671.	6.6	42
37793	Reaction induced multifunctional TiO2 rod/particle nanostructured materials for screen printed dye sensitized solar cells. Ceramics International, 2021, 47, 8094-8104.	2.3	4
37794	Study of structural, elastic, electronics, optical and thermodynamic properties of Hf2PbC under pressure by ab-initio method. Computational Condensed Matter, 2021, 26, e00512.	0.9	7

#	Article	IF	Citations
37795	A DFT investigation of the electronic, optical, and thermoelectric properties of pentadiamond. Chemical Physics Letters, 2021, 763, 138210.	1.2	24
37796	Structural stability, electronic structures, mechanical properties and debye temperature of W-Re alloys: A first-principles study. Fusion Engineering and Design, 2021, 162, 112081.	1.0	24
37797	1D metal-dithiolene wires as a new class of bi-functional oxygen reduction and evolution single-atom electrocatalysts. Journal of Catalysis, 2021, 393, 140-148.	3.1	18
37798	Ab initio comparative study of the magnetic, electronic and optical properties of AB2O4 (A, B= Mn, Fe) spinels. Materials Chemistry and Physics, 2021, 259, 124065.	2.0	16
37799	Synthesis of metal-free nitrogen-enriched porous carbon and its electrochemical sensing behavior for the highly sensitive detection of dopamine: Both experimental and theoretical investigation. Materials Chemistry and Physics, 2021, 260, 124094.	2.0	14
37800	Roles of Enhancement of Câˆ'H Activation and Diminution of Câˆ'O Formation Within M1â€Phase Pores in Propane Selective Oxidation. ChemCatChem, 2021, 13, 882-899.	1.8	9
37801	Quantum chemical DFT study of molecular adsorption of H2S on clean and chemically modified Au(1 1) Tj ETQq0 0 0 rgBT /Overlock 10	3.1	8
37802	The mechanism on retention of hydrogen in three representative tungsten nitride compounds in nuclear fusion reactors. Journal of Nuclear Materials, 2021, 544, 152687.	1.3	5
37803	Reaction pathways and the role of the carbonates during CO2 hydrogenation over hexagonal In2O3 catalysts. Applied Surface Science, 2021, 542, 148591.	3.1	9
37804	Balance between strength and ductility of dilute Fe2B by high-throughput first-principles calculations. Ceramics International, 2021, 47, 4758-4768.	2.3	16
37805	Theoretical investigation of solvent effects on the selective hydrogenation of furfural over Pt(111). International Journal of Hydrogen Energy, 2021, 46, 1592-1604.	3.8	13
37806	Computational studies on the structural, electronic and optical properties of M2CT2 (M=Y, Sc and) Tj ETQq1 1 0.784314 rgBT /Overlo	2.8	28
37807	Polysulfide reduction and Li2S phase formation in the presence of lithium metal and solid electrolyte interphase layer. Journal of Power Sources, 2021, 485, 229289.	4.0	9
37808	Surface and morphology investigation of FeCrO3 material in ilmenite-, corundum- and lithium niobate-polymorphs. Surfaces and Interfaces, 2021, 22, 100837.	1.5	3
37809	Transformation of a graphene nanoribbon into a hybrid 1D nanoobject with alternating double chains and polycyclic regions. Physical Chemistry Chemical Physics, 2021, 23, 425-441.	1.3	4
37810	Entropy driven preference for alkene adsorption at the pore mouth as the origin of pore-mouth catalysis for alkane hydroisomerization in 1D zeolites. Catalysis Science and Technology, 2021, 11, 563-574.	2.1	5
37811	Insights into the catalytic activity of trimetallic Al/Zn/Cu surfaces for the water gas shift reaction. Applied Surface Science, 2021, 542, 148589.	3.1	12
37812	Carbon nanotube boosting electrocatalytic oxygen evolution of NiFe-polyphenol coordination catalyst through donor-acceptor modulation. Journal of Colloid and Interface Science, 2021, 582, 396-404.	5.0	13

#	Article	IF	Citations
37813	Anchoring Mo on C9N4 monolayers as an efficient single atom catalyst for nitrogen fixation. Journal of Energy Chemistry, 2021, 57, 443-450.	7.1	41
37814	Effect of target peak power density on the phase formation, microstructure evolution, and mechanical properties of Cr2AlC MAX-phase coatings. Journal of the European Ceramic Society, 2021, 41, 1841-1847.	2.8	13
37815	Cataloguing the Energetic Contributions to the Supramolecular Assembly of para-Substituted N,Nâ€²-Diphenylureas and Their Organometallic Derivatives in the Solid State: A Density Functional Theory Approach. Crystal Growth and Design, 2021, 21, 563-571.	1.4	0
37816	S vacancy enhanced ferromagnetism in Mn-doped monolayer MoS2: A hybrid functional study. Chemical Physics, 2021, 541, 111043.	0.9	8
37817	Hydrogen adsorption of O/N-rich hierarchical carbon scaffold decorated with Ni nanoparticles: Experimental and computational studies. International Journal of Hydrogen Energy, 2021, 46, 5427-5440.	3.8	12
37818	Peculiarities of the phase transformation dynamics in bulk FeRh based alloys from magnetic and structural measurements. Journal of Magnetism and Magnetic Materials, 2021, 522, 167560.	1.0	10
37819	Towards the Circular Economy: Converting Aromatic Plastic Waste Back to Arenes over a Ru/Nb₂O₅ Catalyst. Angewandte Chemie - International Edition, 2021, 60, 5527-5535.	7.2	169
37820	Hybridâ€Functional Study of Native Point Defects and Ti/Fe Impurities in Î±â€Al₂O₃. Physica Status Solidi (B): Basic Research, 2021, 258, 2000498.	0.7	1
37821	A theoretical (DFT) study of structural, mechanical and thermodynamic properties of manganese arsenides CsMn4As3 and RbMn4As3. Computational Condensed Matter, 2021, 26, e00526.	0.9	1
37822	First-principles investigation on the electronic, mechanical and lattice dynamical properties of novel AlNiX (Xâ€¯=â€¯As and Sb) half-Heusler alloys. Materials Today Communications, 2021, 26, 101885.	0.9	10
37823	Towards the Circular Economy: Converting Aromatic Plastic Waste Back to Arenes over a Ru/Nb 2 O 5 Catalyst. Angewandte Chemie, 2021, 133, 5587-5595.	1.6	42
37824	Investigation of Structural, Electronic, and Dynamic Properties of Halfâ€Heusler Alloys XCuB (X = Ti,) Tj ETQq1 1 0.784314 rgBT /Over	0.6	3
37825	Activity and stability descriptors of Ni based alloy catalysts for dry reforming of methane: A density functional theory study. International Journal of Quantum Chemistry, 2021, 121, e26580.	1.0	7
37826	The impact of partial H intercalation on the quasi-free-standing properties of graphene on SiC(0001). Applied Surface Science, 2021, 541, 148668.	3.1	10
37827	Intrinsic property and catalytic performance of single and double metal atoms incorporated g-C3N4 for O2 activation: A DFT insight. Applied Surface Science, 2021, 541, 148671.	3.1	21
37828	Al, Fe-codoped CoP nanoparticles anchored on reduced graphene oxide as bifunctional catalysts to enhance overall water splitting. Chemical Engineering Journal, 2021, 421, 127856.	6.6	44
37829	High-pressure study of the structural phase transition in Cu1.875Te. Computational Materials Science, 2021, 186, 110020.	1.4	1
37830	The structure, mechanical, electronic and thermodynamic properties of bcc Zr-Nb alloy: A first principles study. Journal of Alloys and Compounds, 2021, 862, 158029.	2.8	18

#	Article	IF	Citations
37831	Theoretical study of hydrogen impact on concentration of intrinsic point defects during Czochralski Si crystal growth. Journal of Crystal Growth, 2021, 555, 125971.	0.7	3
37832	Tuning electronic structure of ZnO nanowires via 3d transition metal dopants for improved photo-electrochemical water splitting: An ab initio study. Materials Today Communications, 2021, 26, 101929.	0.9	5
37833	High-performance eco-friendly MnTe thermoelectrics through introducing SnTe nanocrystals and manipulating band structure. Nano Energy, 2021, 81, 105649.	8.2	40
37834	Spin transition mechanism in a cooperatively assembled Al/Fe-doped 2D SiC based on electric field manipulation. Physica E: Low-Dimensional Systems and Nanostructures, 2021, 127, 114546.	1.3	0
37835	TPDH-graphene: A new two dimensional metallic carbon with NDR behaviour of its one dimensional derivatives. Physica E: Low-Dimensional Systems and Nanostructures, 2021, 127, 114569.	1.3	19
37836	First principles calculation of metal (Ni and Cu) contact on the electronic transport properties of 2D GeP semiconductor. Applied Surface Science, 2021, 542, 148596.	3.1	12
37837	A new perspective on the composition-structure-property relationships on Nb/Mo/Cr-doped O3-type layered oxide as cathode materials for sodium-ion batteries. Chemical Engineering Journal, 2021, 413, 127824.	6.6	21
37838	Synthesis, characterization, optoelectronic and photocatalytic properties of Sr2Bi2O5/SrCO3 and Sr3Bi2O6/SrCO3 heterostructures with varying SrCO3 content. Chemosphere, 2021, 267, 129229.	4.2	9
37839	Computational study of elastic, structural stability and dynamics properties of penta-graphene membrane. Chemical Physics, 2021, 542, 111052.	0.9	16
37840	The effect of non-centrosymmetricity on optical and electronic properties of BaHfO3 perovskite. Computational Condensed Matter, 2021, 26, e00524.	0.9	1
37841	Polarized nucleation and efficient decomposition of Li2O2 for Ti2C MXene cathode catalyst under a mixed surface condition in lithium-oxygen batteries. Energy Storage Materials, 2021, 35, 669-678.	9.5	65
37842	Temperature-induced wear transition in ceramic-metal composites. Acta Materialia, 2021, 205, 116545.	3.8	47
37843	Machine learning potentials for tobermorite minerals. Computational Materials Science, 2021, 188, 110173.	1.4	15
37844	Not all platinum surfaces are the same: Effect of the support on fundamental properties of platinum adlayer and its implications for the activity toward hydrogen evolution reaction. Electrochimica Acta, 2021, 368, 137598.	2.6	9
37845	Elastic, mechanical, optical and magnetic properties of Ru2MnX (XÂ=ÂNb, Ta, V) Heusler alloys. Journal of Magnetism and Magnetic Materials, 2021, 523, 167614.	1.0	24
37846	Alkali metal adsorption on metal surfaces: new insights from new tools. Physical Chemistry Chemical Physics, 2021, 23, 7822-7829.	1.3	5
37847	Synthesis, characterization and first principle modelling of the MAB phase solid solutions: (Mn1-xCrx)2AlB2 and (Mn1-xCrx)3AlB4. Materials Research Letters, 2021, 9, 112-118.	4.1	17
37848	Artificial neural network potential for pure zinc. Computational Materials Science, 2021, 188, 110207.	1.4	12

#	Article	IF	Citations
37849	Properties of BSi6N monolayers derived by first-principle computation. Physica E: Low-Dimensional Systems and Nanostructures, 2021, 127, 114556.	1.3	5
37850	Thermoelectric Properties of Novel Semimetals: A Case Study of YbMnSb₂. Advanced Materials, 2021, 33, e2003168.	11.1	34
37851	Fluxâ€Assisted Synthesis of Prismâ€like Octahedral Ta₃N₅ Singleâ€Crystals with Controllable Facets for Promoted Photocatalytic H₂ Evolution. Solar Rrl, 2021, 5, 2000574.	3.1	10
37852	Improving the gas sensing performance of MoS2 nanosheets through silver adsorption: A theoretical study. Computational and Theoretical Chemistry, 2021, 1195, 113087.	1.1	6
37853	Light metal functionalized two-dimensional siligene for high capacity hydrogen storage: DFT study. International Journal of Hydrogen Energy, 2021, 46, 29348-29360.	3.8	38
37854	Segregation behavior of alloying elements at Ni Î£5 [001](210) symmetrical tilt grain boundary in nickel-based superalloys and their stabilization and strengthening mechanisms for the grain boundary. Materials Chemistry and Physics, 2021, 258, 123977.	2.0	17
37855	Strain effect on the electronic and optical properties of Germanene/MoS2 heterobilayer. Materials Today Communications, 2021, 26, 101845.	0.9	3
37856	Exploring the structural and electronic properties of heterostructures composed of gallium nitride and boron selenide monolayers. Physica E: Low-Dimensional Systems and Nanostructures, 2021, 126, 114480.	1.3	2
37857	External uniaxial compressive strain induced built-in electric field in bilayer two-dimensional As2S3 for photocatalytic water splitting: A first-principles study. Applied Surface Science, 2021, 535, 147701.	3.1	7
37858	Active and stable Fe-based catalyst, mechanism, and key role of alkali promoters in ammonia synthesis. Journal of Catalysis, 2021, 394, 353-365.	3.1	16
37859	CO2 electroreduction by transition metal-embedded two-dimensional C3N: A theoretical study. Journal of CO2 Utilization, 2021, 43, 101367.	3.3	19
37860	Electronic structure, optical and vibrational properties of Ti2FeNiSb2 and Ti2Ni2InSb double half heusler alloys. Materials Science in Semiconductor Processing, 2021, 123, 105531.	1.9	18
37861	Comprehensive first-principles study of bulk, bilayer, and monolayer Î±-PtO2 properties. Physica E: Low-Dimensional Systems and Nanostructures, 2021, 127, 114514.	1.3	7
37862	Ethanol dimerization to Ethyl acetate and hydrogen on the multifaceted copper catalysts. Surface Science, 2021, 703, 121742.	0.8	14
37863	Ab initio studies of structural, electronic and magnetic properties of Al1-xMnxN in zinc blende structure. Computational Condensed Matter, 2021, 26, e00517.	0.9	1
37864	Interwoven scaffolded porous titanium oxide nanocubes/carbon nanotubes framework for high-performance sodium-ion battery. Journal of Energy Chemistry, 2021, 59, 38-46.	7.1	25
37865	First principles investigation of the structural, elastic, electronic and vibrational properties of vanadium-based V3X (X = Fe, Co, and Ni) compounds. Journal of Physics and Chemistry of Solids, 2021, 150, 109854.	1.9	4
37866	Electronic and magnetic properties of 3d transition metal atom adsorbed Zr2CO2 Mxene: First-principles study. Solid State Communications, 2021, 325, 114140.	0.9	9

#	Article	IF	Citations
37867	First-principles calculation of 11B solid-state NMR parameters of boron-rich compounds I: the rhombohedral boron modifications and B12X2 (X = P, As, O). Physical Chemistry Chemical Physics, 2021, 23, 470-486.	1.3	3
37868	Engineering the interface between LiCoO₂ and Li₁₀GeP₂S₁₂ solid electrolytes with an ultrathin Li₂CoTi₃O₈ interlayer to boost the performance of all-solid-state batteries. Energy and Environmental Science, 2021, 14, 437-450.	15.6	82
37869	Newly Synthesized Taâ€Based MAX Phase (Ta_{1â€“x}Hf_x)₄AlC₃ and (Ta_{1â€“x}Hf_x)₄Al_{0.5}Sn_{0.5}C₃ (0â€‰â‰¤â€‰xâ€‰â‰¤â€‰0.25) Solid Solutions: Unravelling the Mechanical, Electronic, and Thermodynamic Properties. Physica Status Solidi (B): Basic Research, 2021, 258, 2000307.	1.7	11
37870	Dopingâ€Driven Antiferromagnetic to Ferromagnetic Phase Transition in Tetragonal Cr2B2 Monolayer. Physica Status Solidi (B): Basic Research, 2021, 258, 2000396.	0.7	9
37871	Adsorption of Mg2+ and K+ on the kaolinite (0 0 1) surface in aqueous system: A combined DFT and AIMD study with an experimental verification. Applied Surface Science, 2021, 538, 148158.	3.1	33
37872	Ammonia electro-oxidation mechanism on the platinum (100) surface. Catalysis Today, 2021, 371, 50-57.	2.2	28
37873	Elastic, electronic, vibrational and optical properties of filled skutterudite compound SrRu4As12: Insights from DFT-based computer simulation. Computational Condensed Matter, 2021, 26, e00519.	0.9	2
37874	Second-nearest-neighbor modified embedded-atom method interatomic potential for V-M (MÂ=ÂCu, Mo,) Tj ETQq1 1 0.784314 rgBT	1.4	12
37875	Advance on adsorption of amino-functionalized silica nanocarrier for the delivery of therapeutic ampicillin as drug model. Inorganic Chemistry Communication, 2021, 123, 108346.	1.8	1
37876	DFT-Based Calculations of the Structural Stability, Electronic and Elastic Characteristics of BBi1-xSbx Ternary Ordered Alloys. Journal of Electronic Materials, 2021, 50, 598-612.	1.0	2
37877	Stability of oxygen-functionalized graphenic surfaces: Theoretical and experimental insights into electronic properties and wettability. Applied Surface Science, 2021, 539, 148190.	3.1	15
37878	First-Principles study of structural, elastic and electronic properties for the KI-GaBP<mml:math xmlns:mml="http://www.w3.org/1998/Math/MathML" display="inline" id="d1e1334" altimg="si26.svg"><mml:msub><mml:mrow /><mml:mrow><mml:mn>2</mml:mn></mml:mrow></mml:msub></mml:math> semiconductor under pressure. Materials Science in Semiconductor Processing, 2021, 123, 105585.	1.9	0
37879	Stability of Zener order in martensite: an atomistic evidence. Scripta Materialia, 2021, 194, 113632.	2.6	9
37880	Controllable synthesis of tunable aspect ratios novel h-BN nanorods with an enhanced wetting performance for water repellent applications. Vacuum, 2021, 184, 109927.	1.6	15
37881	Mechanism of formaldehyde and formic acid formation on (101)-TiO₂@Cu₄ systems through CO₂ hydrogenation. Sustainable Energy and Fuels, 2021, 5, 564-574.	2.5	4
37882	2â€•and 2,7â€Substituted paraâ€Nâ€Methylpyridinium Pyrenes: Syntheses, Molecular and Electronic Structures, Photophysical, Electrochemical, and Spectroelectrochemical Properties and Binding to Doubleâ€Stranded (ds) DNA. Chemistry - A European Journal, 2021, 27, 2837-2853.	1.7	13
37883	Inserting an intermediate band in Cu- and Ag-based Kesterite compounds by Sb doping: A first-principles study. Materials Science and Engineering B: Solid-State Materials for Advanced Technology, 2021, 264, 114937.	1.7	9
37884	Design of solute clustering during thermomechanical processing of AA6016 Alâ€“Mgâ€“Si alloy. Acta Materialia, 2021, 203, 116455.	3.8	71

#	Article	IF	Citations
37885	DFTÂ+ÂU study of U1-An O2- (AnÂ=ÂNp, Pu, Am and Cm) {1 1 1}, {1 1 0} and {1 0 0} surfaces. Applied Surface Science, 2021, 537, 147972.	3.1	4
37886	Effect of thermally excited lattice vibrations on the thermodynamic stability of tungsten ditellurides WTe2 under high pressure: A first-principles investigation. Computational Materials Science, 2021, 186, 110024.	1.4	6
37887	Electromagnetic wave absorption performance of Ti2O3 and vacancy enhancement effective bandwidth. Journal of Materials Science and Technology, 2021, 76, 166-173.	5.6	32
37888	Electronic, optical, and dielectric properties of OsP2 marcasite structure investigated by DFT calculations. Materials Science in Semiconductor Processing, 2021, 123, 105564.	1.9	1
37889	Superhierarchical Inorganic/Organic Nanocomposites Exhibiting Simultaneous Ultrahigh Dielectric Energy Density and High Efficiency. Advanced Functional Materials, 2021, 31, 2007994.	7.8	46
37890	First-principles DFT insights into the adsorption of hydrazine on bimetallic Î²1-NiZn catalyst: Implications for direct hydrazine fuel cells. Applied Surface Science, 2021, 536, 147648.	3.1	15
37891	Effects of negative chemical pressure on the structural, mechanical, and electronic properties of molybdenum-doped strontium ferrite. Materials Today Communications, 2021, 26, 101908.	0.9	14
37892	Structural and elastic properties of TlInSe2 at high pressure. Solid State Sciences, 2021, 111, 106343.	1.5	18
37893	Design of phosphorus-functionalized MXenes for highly efficient hydrogen evolution reaction. Journal of Materials Chemistry A, 2021, 9, 597-606.	5.2	20
37894	Ab initio study of oxygen segregation in silicon grain boundaries: The role of strain and vacancies. Acta Materialia, 2021, 204, 116477.	3.8	12
37895	Where is the unpaired transition metal in substoichiometric diboride line compounds?. Acta Materialia, 2021, 204, 116510.	3.8	21
37896	Ab Initio Study of Structural, Electronic, Magnetic and Magnetoelastic Properties of the Magnetoelectric h-YMnO3 Semiconductor. Journal of Electronic Materials, 2021, 50, 657-663.	1.0	3
37897	Gate controllable optical spin current generation in zigzag graphene nanoribbon. Carbon, 2021, 173, 565-571.	5.4	17
37898	Manipulation of band alignment in InSe/GaTe and InSe/InS van der Waals heterostructures. Computational Materials Science, 2021, 188, 110153.	1.4	3
37899	Investigation of native defects and impurities in X-N (XÂ=ÂAl, Ga, In). Computational Materials Science, 2021, 188, 110169.	1.4	4
37900	Enhancing bifunctional electrocatalysts of hollow Co3O4 nanorods with oxygen vacancies towards ORR and OER for Liâ€“O2 batteries. Electrochimica Acta, 2021, 367, 137490.	2.6	49
37901	Magnetic, optoelectronic and thermodynamic properties of the double perovskite Ba2NiWO6 in its stable antiferromagnetic phase. Optik, 2021, 227, 166032.	1.4	3
37902	Development and characterization of Alâ€“Al3Niâ€“Sn metal matrix composite. Materials Chemistry and Physics, 2021, 259, 124027.	2.0	15

#	Article	IF	Citations
37903	Induced ferromagnetism in bilayer hexagonal Boron Nitride (h-BN) on vacancy defects at B and N sites. Physica E: Low-Dimensional Systems and Nanostructures, 2021, 126, 114436.	1.3	17
37904	Strain-improved electronic and magnetic properties of V-, Cr-, Mn- and Fe-doped Î±- and Î²-tellurene. Applied Surface Science, 2021, 541, 148454.	3.1	6
37905	Systematic study on mechanical and electronic properties of ternary VAlN, TiAlN and WAlN systems by first-principles calculations. Ceramics International, 2021, 47, 7511-7520.	2.3	29
37906	Hydrogen solubility and diffusivity near surface of nickel single crystals: Some implications of elastic energy. Computational Materials Science, 2021, 188, 110136.	1.4	3
37907	Exploration of new phase structure of FePd crystalline alloy with a stoichiometric of 1:1. Computational Materials Science, 2021, 188, 110168.	1.4	3
37908	Mineralogical phase transformation of Fe containing sphalerite at acidic environments in the presence of Cu2+. Journal of Hazardous Materials, 2021, 403, 124058.	6.5	12
37909	First-principles study on the mechanical, thermal properties and hydrogen behavior of ternary V-Ni-M alloys. Journal of Materials Science and Technology, 2021, 70, 83-90.	5.6	16
37910	Resolving the cathode passivation of lithiumâ€“oxygen batteries with an amination SiO2/TiO2 functional separator. Journal of Power Sources, 2021, 483, 229180.	4.0	6
37911	First-principles studies of the electronic and magnetic structures and bonding properties of boron subnitride B13N2. Journal of Solid State Chemistry, 2021, 294, 121840.	1.4	3
37912	Modified Becke-Johnson calculations using norm-conserving pseudopotential plane-wave approach: Systematic analysis. Materials Today Communications, 2021, 26, 101748.	0.9	1
37913	Low-Index Stoichiometric Surfaces of CuBiW2O8. Surface Science, 2021, 705, 121762.	0.8	1
37914	CO2 capture and separation on the penta-BN2 monolayer with the assistance of charge/electric field. Journal of Materials Science, 2021, 56, 4341-4355.	1.7	12
37915	High performance H2O2 production achieved by sulfur-doped carbon on CdS photocatalyst via inhibiting reverse H2O2 decomposition. Applied Catalysis B: Environmental, 2021, 284, 119690.	10.8	69
37916	An efficient approximation of the supercell approach to the calculation of the full phonon spectrum. Calphad: Computer Coupling of Phase Diagrams and Thermochemistry, 2021, 72, 102215.	0.7	1
37917	Insights into the Bond Behavior and Mechanical Properties of Hafnium Carbide under High Pressure and High Temperature. Inorganic Chemistry, 2021, 60, 515-524.	1.9	20
37918	Insights into the shape effect of H2 self-selective Ni catalysts for efficient acetone hydrogenation. Applied Surface Science, 2021, 536, 147844.	3.1	8
37919	Relevance of metal (Ca versus Mn) embedded C2N for energy-storage applications: Atomic-scale study. International Journal of Hydrogen Energy, 2021, 46, 2445-2463.	3.8	12
37920	Body-centered-cubic martensite and the role on room-temperature tensile properties in Si-added SiVCrMnFeCo high-entropy alloys. Journal of Materials Science and Technology, 2021, 76, 222-230.	5.6	14

#	Article	IF	Citations
37921	Unveiling the role of atomic defects on the electronic, mechanical and elemental diffusion properties in CuS. Scripta Materialia, 2021, 192, 94-99.	2.6	12
37922	The adsorption mechanisms of Hg0 on marcasite-type metal selenides: The influences of metal-terminated site. Chemical Engineering Journal, 2021, 406, 126723.	6.6	27
37923	Construction of atomically dispersed Cu-N4 sites via engineered coordination environment for high-efficient CO2 electroreduction. Chemical Engineering Journal, 2021, 407, 126842.	6.6	91
37924	Thermal Transport in Graphene Nanomesh: Unraveling the Role of Brillouin Zone Folding, Phonon Localization and Phonon Confinement. International Journal of Heat and Mass Transfer, 2021, 165, 120685.	2.5	14
37925	Understanding the Selectivity of the Oxygen Reduction Reaction at the Atomistic Level on Nitrogenâ€Doped Graphitic Carbon Materials. Advanced Energy Materials, 2021, 11, 2002459.	10.2	63
37926	Inter-relationship of the Structural Properties of Quaternary Chalcogenides CuZn2Ga(S/Se)4: A First-Principles Study. Journal of Electronic Materials, 2021, 50, 1707-1712.	1.0	3
37927	Isotope study reveals atomic motion mechanism for the formation of metal whiskers in MAX phase. Acta Materialia, 2021, 203, 116475.	3.8	15
37928	Electro-optical and mechanical properties of Zinc antimonide (ZnSb) monolayer and bilayer: A first-principles study. Applied Surface Science, 2021, 540, 148289.	3.1	16
37929	Antifouling performance analysis of peptide-modified glass microstructural surfaces. Applied Surface Science, 2021, 541, 148384.	3.1	21
37930	The mechanical and thermal properties of (Th,U)Si compounds: A systematic density functional theory research. Computational Materials Science, 2021, 188, 110148.	1.4	7
37931	Ni-doped activated carbon nanofibers for storing hydrogen at ambient temperature: Experiments and computations. Fuel, 2021, 288, 119608.	3.4	21
37932	Predicting the band structure, transport properties, electronic fitness function and effective mass of PdTiSn indirect band-gap half-Heusler semiconductor. Materials Science in Semiconductor Processing, 2021, 123, 105548.	1.9	4
37933	First-principles calculations to investigate the structural, electronic, elastic, vibrational and thermodynamic properties of the full-Heusler alloys X2ScGa (Xâ€‰=â€‰Ir and Rh). Materials Today Communications, 2021, 26, 101855.	0.9	6
37934	Introducing and studying origin of deep electron traps in Ba1-xZrSi3O9:xEu for optical data storage. Optical Materials, 2021, 111, 110617.	1.7	1
37935	Anti-phase boundary energy of Î² series precipitates in Mg-Y-Nd system. Scripta Materialia, 2021, 193, 127-131.	2.6	119
37936	Argentophillic interactions in argentum chalcogenides: First principles calculations and topological analysis of electron density. Journal of Computational Chemistry, 2021, 42, 242-247.	1.5	7
37937	Enhanced Fe 3d delocalization and moderate spin polarization in Fe Ni atomic pairs for bifunctional ORR and OER electrocatalysis. Applied Catalysis B: Environmental, 2021, 285, 119778.	10.8	131
37938	Iron-modulated nickel cobalt phosphide embedded in carbon to boost power density of hybrid sodiumâ€“air battery. Applied Catalysis B: Environmental, 2021, 285, 119786.	10.8	32

#	Article	IF	Citations
37939	Rational surface modification of ZnO with siloxane polymers for room-temperature-operated thin-film transistor-based gas sensors. Applied Surface Science, 2021, 542, 148704.	3.1	17
37940	Tetrahex carbides: Two-dimensional group-IV materials for nanoelectronics and photocatalytic water splitting. Carbon, 2021, 174, 368-381.	5.4	39
37941	Effect of alloying elements on hydrogen enhanced decohesion in bcc iron. Computational Materials Science, 2021, 188, 110215.	1.4	25
37942	Novel structural phase and superconductivity of W-Te compounds under high pressures. Computational Materials Science, 2021, 188, 110222.	1.4	4
37943	Elastic3rd: A tool for calculating third-order elastic constants from first-principles calculations. Computer Physics Communications, 2021, 261, 107777.	3.0	22
37944	DMFTwDFT: An open-source code combining Dynamical Mean Field Theory with various density functional theory packages. Computer Physics Communications, 2021, 261, 107778.	3.0	16
37945	Performance-enhanced lithium metal batteries through ionic liquid based electrolytes and mechanism research derived by density functional theory calculations. Electrochimica Acta, 2021, 368, 137535.	2.6	14
37946	Morphology and seebeck coefficients of electrodeposited Bi2Se3 films grown onto Au(111)/Si substrates. Electrochimica Acta, 2021, 368, 137554.	2.6	12
37947	Ternary boride Hf3PB4: Insights into the physical properties of the hardest possible boride MAX phase. Journal of Alloys and Compounds, 2021, 857, 158264.	2.8	59
37948	Exploring UiO-66(Zr) frameworks as nanotraps for highly efficient removal of EDTA-complexed heavy metals from water. Journal of Environmental Chemical Engineering, 2021, 9, 104932.	3.3	21
37949	Insight into enhanced thermoluminescence property of (Mg, Cu, Ag)-Doped LiF:A DFT study. Journal of Luminescence, 2021, 231, 117779.	1.5	8
37950	Ab initio molecular dynamics investigation of point defects in <mml:math xmlns:mml="http://www.w3.org/1998/Math/MathML" altimg="si1.svg"><mml:mi>Î³</mml:mi></mml:math>-U. Journal of Nuclear Materials, 2021, 545, 152714.	1.3	10
37951	Band structure and absorption spectra of NH4XI3 (X = Pb, Mg) based hybrid Perovskite for UV ray protector and electrochromic materials applications. Journal of Physics and Chemistry of Solids, 2021, 151, 109860.	1.9	4
37952	Crystal and electronic structure, thermochemical and photophysical properties of europium-silver sulfate monohydrate AgEu(SO4)2Â·H2O. Journal of Solid State Chemistry, 2021, 294, 121898.	1.4	10
37953	A density functional calculations on electronic, magnetic, optical, mechanical and half-metallic properties in molybdenum based pnictogens in GGA and GGA+U approach. Materials Chemistry and Physics, 2021, 260, 124159.	2.0	8
37954	(E)-2-styryl-1H-benzo[d]imidazole as novel green corrosion inhibitor for carbon steel: Experimental and computational approach. Journal of Molecular Liquids, 2021, 324, 115010.	2.3	31
37955	Exploring the electronic fitness function, effective mass, elastic and transport properties of RhTiP Half-Heusler alloy. Materials Science and Engineering B: Solid-State Materials for Advanced Technology, 2021, 264, 114987.	1.7	7
37956	G0W0 plus BSE calculations of quasiparticle band structure and optical properties of nitrogen-doped antimony trisulfide for near infrared optoelectronic and solar cells application. Materials Science in Semiconductor Processing, 2021, 124, 105592.	1.9	6

#	Article	IF	Citations
37957	Superconductivity from buckled-honeycomb-vacancy ordering. Science Bulletin, 2021, 66, 327-331.	4.3	1
37958	Mechanical properties, electronic structure, and Raman spectra of o-LiB13C2 from first-principles calculations. Solid State Sciences, 2021, 111, 106499.	1.5	4
37959	A first principle study of structural, elastic, electronic and thermodynamic properties of Half-Heusler compounds; YNiPn (Pn=As, sb, and bi). Solid State Sciences, 2021, 112, 106507.	1.5	8
37960	Structural and electronic properties of ZnO: A first-principles density-functional theory study within LDA(GGA) and LDA(GGA)+U methods. Solid State Communications, 2021, 325, 114166.	0.9	37
37961	Atomistic analysis of Li migration in Li1+AlTi2â˜'(PO4)3 (LATP) solid electrolytes. Solid State Ionics, 2021, 359, 115521.	1.3	23
37962	Adsorption of greenhouse gases (methane and carbon dioxide) on the pure and Pd-adsorbed stanene nanosheets: A theoretical study. Surfaces and Interfaces, 2021, 22, 100878.	1.5	6
37963	A low cost and nontoxic absorber for intermediate band solar cell based on P-doped Cu2SiS3: A first-principles study. Thin Solid Films, 2021, 718, 138473.	0.8	3
37964	A dual-protection strategy using CMK-3 coated selenium and modified separators for high-energy Alâ€“Se batteries. Inorganic Chemistry Frontiers, 2021, 8, 1030-1038.	3.0	16
37965	High-pressure and low-temperature structural study of claudetite I, a monoclinic layered As₂O₃polymorph. CrystEngComm, 2021, 23, 638-644.	1.3	5
37966	Electric field-driven one-step formation of vertical pâ€“n junction TiO₂ nanotubes exhibiting strong photocatalytic hydrogen production. Journal of Materials Chemistry A, 2021, 9, 2239-2247.	5.2	8
37967	Construction of cobalt oxyhydroxide nanosheets with rich oxygen vacancies as high-performance lithium-ion battery anodes. Journal of Materials Chemistry A, 2021, 9, 453-462.	5.2	47
37968	Firstâ€principle calculations of CrN(200)/Ni(111) interface: Atomic structure, stability, and electronic properties. Surface and Interface Analysis, 2021, 53, 167-175.	0.8	5
37969	An analysis of structural phase transition and allied properties of cubic ReN and MoN compounds. Journal of Molecular Modeling, 2021, 27, 1.	0.8	56
37970	Defect-rich ZnS nanoparticles supported on reduced graphene oxide for high-efficiency ambient N2-to-NH3 conversion. Applied Catalysis B: Environmental, 2021, 284, 119746.	10.8	46
37971	Effects of helium on critical hydrogen concentration for bubble formation in molybdenum. Journal of Nuclear Materials, 2021, 545, 152735.	1.3	3
37972	A predicted non-layered phase of In2Se3 by first principles. Solid State Communications, 2021, 325, 114159.	0.9	4
37973	Metastable structures of CaCO₃ and their role in transformation of calcite to aragonite and postaragonite. Crystal Growth and Design, 2021, 21, 65-74.	1.4	16
37974	Half metallicity and ferromagnetism of vanadium nitride nanoribbons: a first-principles study. Physical Chemistry Chemical Physics, 2021, 23, 1127-1138.	1.3	14

#	Article	IF	Citations
37975	Photovoltaic modulation of ferromagnetism within a FM metal/Pâ€“N junction Si heterostructure. Nanoscale, 2021, 13, 272-279.	2.8	6
37976	Reactivity Screening of Single Atoms on Modified Graphene Surface: From Formation and Scaling Relations to Catalytic Activity. Advanced Materials Interfaces, 2021, 8, 2001814.	1.9	8
37977	Tuning the Conduction Band Potential of Biâ€based Semiconductors Using a Combination of Organic Ligands. ChemSusChem, 2021, 14, 892-897.	3.6	7
37978	A density functional theory study on the underwater adhesion of catechol onto a graphite surface. Physical Chemistry Chemical Physics, 2021, 23, 1031-1037.	1.3	8
37979	Sn₂B₅O₉Br as an Outstanding Bifunctional Material with Strong Secondâ€Harmonic Generation Effect and Large Birefringence. Advanced Optical Materials, 2021, 9, 2001734.	3.6	49
37980	Firstâ€principles investigations on the groundâ€state bulk properties and lattice constant dependent halfâ€metallic ferrimagnetism of Mn 2 NbSi fullâ€Heusler compound. International Journal of Quantum Chemistry, 2021, 121, e26566.	1.0	3
37981	Effect of strain on gas adsorption in tight gas carbonates: A DFT study. Computational Materials Science, 2021, 188, 110186.	1.4	5
37982	Mechanistic insights into efficient reversible hydrogen storage in ferrotitanium. International Journal of Hydrogen Energy, 2021, 46, 906-921.	3.8	11
37983	Insights on alkylidene formation on Mo2C: A potential overlap between direct deoxygenation and olefin metathesis. Journal of Catalysis, 2021, 393, 381-389.	3.1	3
37984	Prussian blue analogues as platform materials for understanding and developing oxygen evolution reaction electrocatalysts. Journal of Catalysis, 2021, 393, 390-398.	3.1	19
37985	Elastic anisotropies and thermodynamic properties of metal dodecborides under high pressure. Journal of Chemical Thermodynamics, 2021, 154, 106346.	1.0	4
37986	Thermodynamics and kinetics of 2D g-GeC monolayer as an anode materials for Li/Na-ion batteries. Journal of Power Sources, 2021, 485, 229318.	4.0	60
37987	Electronic properties of black phosphorus using monochromated low-loss EELS. Materials Science and Engineering B: Solid-State Materials for Advanced Technology, 2021, 265, 115002.	1.7	3
37988	Ultrafast H2 gas nanosensor for ppb-level H2 gas detection based on GaN honeycomb nanonetwork. Sensors and Actuators B: Chemical, 2021, 329, 129079.	4.0	12
37989	High thermoelectric performance by chemical potential tuning and lattice anharmonicity in GeTe_{1â^'x}I_x compounds. Inorganic Chemistry Frontiers, 2021, 8, 1205-1214.	3.0	4
37990	Stability, edge passivation effect, electronic and transport properties of POPGraphene nanoribbons. Physical Chemistry Chemical Physics, 2021, 23, 2483-2490.	1.3	8
37991	Tunnel Intergrowth Li_xMnO₂ Nanosheet Arrays as 3D Cathode for Highâ€Performance Allâ€Solidâ€State Thin Film Lithium Microbatteries. Advanced Materials, 2021, 33, e2003524.	11.1	53
37992	The optical and elastic properties of strained ZnO by first principle calculations. Computational Condensed Matter, 2021, 26, e00525.	0.9	7

#	Article	IF	Citations
37993	Selective decoration of nitrogenated holey graphene (C2N) with titanium clusters for enhanced hydrogen storage application. International Journal of Hydrogen Energy, 2021, 46, 7371-7380.	3.8	63
37994	Vorhersage stickstoffbasierter Verbindungsklassen: Guanidinate TCN₃ (T=V,) Tj ETQq1 1 0.784314 rgBT /O Ãœbergangsmetallen. Angewandte Chemie, 2021, 133, 490-497.	1.6	2
37995	Electronic Structure and Thermoelectric Performance of Narrowâ€Gap GdNiSb Half Heusler Compound: Density Functional Calculations. Physica Status Solidi (B): Basic Research, 2021, 258, 2000491.	0.7	3
37996	Defective Bi.333(Bi6S9)Br/Bi2S3 heterostructure nanorods: Boosting the activity for efficient visible-light photocatalytic Cr(VI) reduction. Applied Catalysis B: Environmental, 2021, 284, 119730.	10.8	54
37997	A DFT study on pressure dependency of TiC and ZrC properties: Interconnecting elastic constants, thermodynamic, and mechanical properties. Ceramics International, 2021, 47, 9990-10005.	2.3	18
37998	The effects of fluorination and hydrogenation on the physical properties of two-dimensional (111)-oriented cubic boron nitride nanosheets. Thin Solid Films, 2021, 718, 138484.	0.8	2
37999	Generation of the Thermal Scattering Law of Uranium Dioxide with Ab Initio Lattice Dynamics to Capture Crystal Binding Effects on Neutron Interactions. Nuclear Science and Engineering, 2021, 195, 227-238.	0.5	5
38000	Synthesis, Structure and Electronic Properties of Three Tin Oxide Halides. European Journal of Inorganic Chemistry, 2021, 2021, 283-288.	1.0	6
38001	Quantum transport in functionalized epitaxial graphene without electrostatic gating. Carbon, 2021, 175, 490-498.	5.4	5
38002	Coordination interaction boosts energy storage in rechargeable Al battery with a positive electrode material of CuSe. Chemical Engineering Journal, 2021, 421, 127792.	6.6	28
38003	Highly efficient H2 generation over Cu2Se decorated CdS0.95Se0.05 nanowires by photocatalytic water reduction. Chemical Engineering Journal, 2021, 409, 128157.	6.6	22
38004	Photoelectric properties of Sr2MgSi2O7: Eu2+ phosphors produced by co-precipitation method. Journal of Luminescence, 2021, 231, 117787.	1.5	13
38005	DFT study of the adsorption of C6H6 and C6H5OH molecules on stanene nanosheets: Applications to sensor devices. Physica E: Low-Dimensional Systems and Nanostructures, 2021, 127, 114533.	1.3	10
38006	Thermoelectric properties of strontium oxide under pressure: First-principles study. Physics Letters, Section A: General, Atomic and Solid State Physics, 2021, 390, 127083.	0.9	9
38007	First-principles study of electronic and optical properties of ternary compounds AuBX2 (X = S, Se, Te) and AuMTe2 (M = Al, In, Ga). Solid State Sciences, 2021, 111, 106508.	1.5	27
38008	Native Defect Engineering in CuInTe₂. Chemistry of Materials, 2021, 33, 359-369.	3.2	18
38009	Chiral Switchable Low-Dimensional Perovskite Ferroelectrics. ACS Applied Materials & Interfaces, 2021, 13, 2044-2051.	4.0	66
38010	Weak Distance Dependence of Hot-Electron-Transfer Rates at the Interface between Monolayer MoS₂ and Gold. ACS Nano, 2021, 15, 819-828.	7.3	27

#	Article	IF	Citations
38011	Atomic Wires of Transition Metal Chalcogenides: A Family of 1D Materials for Flexible Electronics and Spintronics. Jacs Au, 2021, 1, 147-155.	3.6	16
38012	Suppression of isotopic polymorphism. CrystEngComm, 2021, 23, 769-776.	1.3	4
38013	Mechanistic insights into the phase transition and metal ex-solution phenomena of Pr_{0.5}Ba_{0.5}Mn_{0.85}Co_{0.15}O_{3â˜Î´} from simple to layered perovskite under reducing conditions and enhanced catalytic activity. Energy and Environmental Science, 2021, 14, 873-882.	15.6	37
38014	Nonlinear optical effects in two mercury cyanamide/guanidinium chlorides Hg3(NCN)2Cl2 and Hg2(C(NH2)3)Cl5. Journal of Materials Chemistry C, 2021, 9, 967-974.	2.7	3
38015	Efficient charge separation and visible-light response of two-dimensional Janus group-III monochalcogenide multilayers. Catalysis Science and Technology, 2021, 11, 542-555.	2.1	20
38016	Vanadium oxide integrated on hierarchically nanoporous copper for efficient electroreduction of CO₂ to ethanol. Journal of Materials Chemistry A, 2021, 9, 3044-3051.	5.2	32
38017	Catalytic mechanism and selectivity prediction for syngas conversion over pure and K-promoted Mo2C catalysts. Applied Catalysis A: General, 2021, 610, 117945.	2.2	8
38018	Single Atom Catalysts (SAC) trapped in defective and nitrogen-doped graphene supported on metal substrates. Carbon, 2021, 174, 772-788.	5.4	50
38019	The mechanical properties of ice X with particular emphasis on its auxetic potential. Journal of Physics and Chemistry of Solids, 2021, 150, 109717.	1.9	8
38020	Aging of Self-Assembled Lead Halide Perovskite Nanocrystal Superlattices: Effects on Photoluminescence and Energy Transfer. ACS Nano, 2021, 15, 650-664.	7.3	46
38021	Modifying an ultrathin insulating layer to suppress lithium dendrite formation within garnet solid electrolytes. Journal of Materials Chemistry A, 2021, 9, 3576-3583.	5.2	36
38022	Enhanced photocatalytic activity of Ho3+ doped ZnO NPs synthesized by modified sol-gel method: An experimental and theoretical investigation. Journal of Alloys and Compounds, 2021, 856, 158217.	2.8	33
38023	Synchronous nesting of hollow FeP nanospheres into a three-dimensional porous carbon scaffold via a salt-template method for performance-enhanced potassium-ion storage. Sustainable Energy and Fuels, 2021, 5, 844-854.	2.5	12
38024	O₂ dissociative adsorption on the Cuâ€, Agâ€, and Wâ€doped Al(111) surfaces from DFT computation. Surface and Interface Analysis, 2021, 53, 46-52.	0.8	4
38025	The average and local structure of TiVCrNbD<mml:math xmlns:mml="http://www.w3.org/1998/Math/MathML" altimg="si47.svg"><mml:msub><mml:mrow /><mml:mi>x</mml:mi></mml:msub></mml:math> (<mml:math) Tj ETQq0 0 0 rgBT /Overlock 10 Tf 50 182 Td (xmlns:mml="http://www	3.8	33
38026	Effective Ca2+-doping in Sr1-xCaxFeO3-Î´ oxygen carriers for chemical looping air separation: A theoretical and experimental investigation. Applied Energy, 2021, 281, 116040.	5.1	24
38027	First-principles study of dehydration interfaces between diaspore and corundum, gibbsite and boehmite, and boehmite and Î³-Al2O3: Energetic stability, interface charge effects, and dehydration defects. Applied Surface Science, 2021, 541, 148501.	3.1	19
38028	Oxidative etching mechanism of the diamond (100) surface. Carbon, 2021, 174, 36-51.	5.4	15

#	Article	IF	Citations
38029	Atomistic investigation of functionalized polyethylene-alumina interfacial strength and tensile behaviour. Computational Materials Science, 2021, 187, 110075.	1.4	5
38030	Thermally-driven gold@poly(N-isopropylacrylamide) core-shell nanotransporters for molecular extraction. Journal of Colloid and Interface Science, 2021, 584, 789-794.	5.0	5
38031	Chemical stability of caesium iodide deposits in air/steam atmosphere. Journal of Hazardous Materials, 2021, 409, 124519.	6.5	3
38032	Chemisorption, diffusion and permeation of hydrogen isotopes in bcc bulk cr and cr(100) surface: First-principles dft simulations. Journal of Nuclear Materials, 2021, 543, 152538.	1.3	11
38033	Two dimensional B2CX (X=O, S, Se) monolayer semiconductors for water splitting application. Superlattices and Microstructures, 2021, 149, 106759.	1.4	2
38034	Effect of insulator thickness on the electronic transport through CNT-HfO2-Au junction for optical rectenna applications. Surfaces and Interfaces, 2021, 22, 100823.	1.5	3
38035	On the signatures of oxygen vacancies in O1s core level shifts. Surface Science, 2021, 705, 121761.	0.8	27
38036	Theoretical and experimental investigation of structural and vibrational properties of L-arginineÂ·HCl Br1- monohydrate crystals. Vibrational Spectroscopy, 2021, 112, 103187.	1.2	6
38037	Influence of applied electric field on atom diffusion behavior and mechanism for W/NiFe interface in diffusion bonding of Steel/NiFe interlayer/W by spark plasma sintering. Applied Surface Science, 2021, 541, 148516.	3.1	5
38038	The potential application of VS2 as an electrode material for Mg ion battery: A DFT study. Applied Surface Science, 2021, 544, 148775.	3.1	50
38039	First principles calculations of 3d-4d transition metal based LiMgPdSnâ€“type FeCrRuZ (ZÂ=ÂAl, Ga, In, Si) equiatomic quaternary Heusler alloys. Computational Materials Science, 2021, 188, 110116.	1.4	5
38040	Intriguing Dimensional Transition Inducing Variable Birefringence in K₂Na₂Sn₃S₈ and Rb₃NaSn₃Se₈. Inorganic Chemistry, 2021, 60, 1055-1061.	1.9	18
38041	First-Principles Calculations of the Effects of Edge Functionalization and Size on the Band Gap of Be₃N₂ Nanoribbons: Implications for Nanoelectronic Devices. ACS Applied Nano Materials, 2021, 4, 493-502.	2.4	6
38042	Quantum spin Hall insulators and topological Rashba-splitting edge states in two-dimensional CX₃ (X = Sb, Bi). Physical Chemistry Chemical Physics, 2021, 23, 2134-2140.	1.3	7
38043	Lattice Thermal Conductivity Prediction Using Symbolic Regression and Machine Learning. Journal of Physical Chemistry A, 2021, 125, 435-450.	1.1	32
38044	Study of the Elastic Properties of the Energetic Molecular Crystals Using Density Functionals with van der Waals Corrections. ACS Omega, 2021, 6, 642-648.	1.6	11
38045	Predicting the bulk modulus of single-layer covalent organic frameworks with square-lattice topology from molecular building-block properties. Nanoscale, 2021, 13, 1077-1085.	2.8	8
38046	Defects and Passivation Mechanism of the Suboxide Layers at SiOâ„‚/4H-SiC (0001) Interface: A First-Principles Calculation. IEEE Transactions on Electron Devices, 2021, 68, 288-293.	1.6	13

#	Article	IF	Citations
38047	Revisiting the Optical Dispersion of Aluminumâ€Doped Zinc Oxide: New Perspectives for Plasmonics and Metamaterials. Advanced Photonics Research, 2021, 2, 2000086.	1.7	16
38048	Confinement Aided Simultanous Water Cleaning and Energy Harvesting Using Atomically Thin Wurtzite (Wurtzene). Advanced Sustainable Systems, 2021, 5, 2000189.	2.7	4
38049	An Atomically Thin Airâ€Stable Narrowâ€Gap Semiconductor Cr₂S₃ for Broadband Photodetection with High Responsivity. Advanced Electronic Materials, 2021, 7, 2000962.	2.6	22
38050	The external electricâ€fieldâ€induced <scp>Schottkyâ€toâ€ohmic</scp> contact transition in graphene/ <scp>As ₂ S ₃ </scp> interface: A study by the first principles. International Journal of Energy Research, 2021, 45, 4727-4734.	2.2	4
38051	Evolution of Lowâ€Frequency Vibrational Modes in Ultrathin GeSbTe Films. Physica Status Solidi - Rapid Research Letters, 2021, 15, 2000434.	1.2	2
38052	Solar Photoelectroreduction of Nitrate Ions on PbI 2 /CuI Nanocomposite Electrodes. Solar Rrl, 2021, 5, 2000418.	3.1	4
38053	Structural, Electronic, and Magnetic Properties of 3d Transition Metalâ€“Doped BP Nanotubes by First Principle Calculations. Journal of Superconductivity and Novel Magnetism, 2021, 34, 749-761.	0.8	1
38054	Lateral epitaxial growth of two-dimensional heterostructure linked by gold adatoms. Nano Research, 2021, 14, 887-892.	5.8	3
38055	A highly sensitive and selective SnS2 monolayer sensor in detecting SF6 decomposition gas. Applied Surface Science, 2021, 541, 148494.	3.1	38
38056	Adsorption enhancement of a fatty acid on iron surface with Î£3(1 1 1) grain boundary. Applied Surface Science, 2021, 543, 148604.	3.1	4
38057	A closer look inside TiO2 (P25) photocatalytic CO2/HCO3â^' reduction with water. Methane rate and selectivity enhancements. Chemical Engineering Journal, 2021, 409, 128141.	6.6	17
38058	Origin of ultra-wide IR transmission and ultra-large birefringence of mercurous halide series with one dimensional chain-like structure: An ab initio study. Computational Materials Science, 2021, 188, 110139.	1.4	7
38059	Difference in the electron energy loss spectra between the spinel-type Na3LiTi5O12 and Li4Ti5O12 clarified by density functional theory calculations. Computational Materials Science, 2021, 188, 110240.	1.4	5
38060	Adsorption studies of nucleobases on Îµ-arsenene nanosheet based on first-principles research. Journal of Molecular Graphics and Modelling, 2021, 103, 107827.	1.3	16
38061	Conductance switching of a gold-covalent organic framework nanojunction via proton transfer. Physics Letters, Section A: General, Atomic and Solid State Physics, 2021, 389, 127100.	0.9	2
38062	Mesoscopic self-ordering in oxygen doped Ce films adsorbed on Mo(112). Surface Science, 2021, 705, 121766.	0.8	3
38063	Tailoring Binding Abilities by Incorporating Oxophilic Transition Metals on 3D Nanostructured Ni Arrays for Accelerated Alkaline Hydrogen Evolution Reaction. Journal of the American Chemical Society, 2021, 143, 1399-1408.	6.6	161
38064	First-principles theoretical study on dry reforming of methane over perfect and boron-vacancy-containing h-BN sheet-supported Ni catalysts. Physical Chemistry Chemical Physics, 2021, 23, 617-627.	1.3	10

#	Article	IF	Citations
38065	First-principles study of aziridinium tin iodide perovskites for photovoltaics. Journal of Materials Chemistry C, 2021, 9, 982-990.	2.7	7
38066	Highly anisotropic gas sensing of atom-thin borophene: a first-principles study. Journal of Materials Chemistry C, 2021, 9, 1069-1076.	2.7	28
38067	Impact of molecular and packing structure on the charge-transport properties of hetero[8]circulenes. Journal of Materials Chemistry C, 2021, 9, 1451-1466.	2.7	11
38068	Elastic, Electronic, Optical, Thermodynamic, and Superconducting Properties of CaMSi3 (M = Ir, Pt) and LaMSi3 (M = Ir, Rh) Superconductors: Insights from DFT-Based Computer Simulation. Journal of Superconductivity and Novel Magnetism, 2021, 34, 1775-1789.	0.8	1
38069	Theoretical study of the adsorption of gas molecules on Mg-embedded boron carbide (C3B) nanosheets: Implications for gas sensors. Computational and Theoretical Chemistry, 2021, 1194, 113055.	1.1	1
38070	Room temperature d ferromagnetism in nitrogen doped WO3 for spintronic applications: A first-principles study. Chemical Physics Letters, 2021, 762, 138075.	1.2	12
38071	Structural, magnetic and electronic properties of Fe-Ga-Tb (0 â‰¤ x â‰¤ 1.85) alloys: Density-functional theory study. Journal of Alloys and Compounds, 2021, 857, 157540.	2.8	6
38072	Band gaps of the solar perovskites photovoltaic CsXCl3 (X=Sn, Pb or Ge). Materials Science in Semiconductor Processing, 2021, 122, 105484.	1.9	67
38073	The adsorption thermodynamics of H2O and CO2 on PuO2(1 1 1) surface: A comparative study based on DFT+U-D3. Applied Surface Science, 2021, 537, 147882.	3.1	10
38074	Ru to W electron donation for boosted HER from acidic to alkaline on Ru/WNO sponges. Nano Energy, 2021, 80, 105531.	8.2	85
38075	High-temperature-pulse synthesis of ultrathin-graphene-coated metal nanoparticles. Nano Energy, 2021, 80, 105536.	8.2	9
38076	Structural, Vibrational, Electronic and Thermodynamical properties of B2â€“HgMg amalgam: A DFT study. Physica B: Condensed Matter, 2021, 601, 412605.	1.3	4
38077	Solution processed Ni2Co layered double hydroxides for high performance electrochemical sensors. Applied Surface Science, 2021, 541, 148270.	3.1	14
38078	Phase transitions and elastic anisotropies of SiC polymorphs under high pressure. Ceramics International, 2021, 47, 6187-6200.	2.3	11
38079	Ab initio investigation of Co/TaC interfaces. Journal of Alloys and Compounds, 2021, 853, 156944.	2.8	10
38080	Small-scale effects on the piezopotential properties of tapered gallium nitride nanowires: The synergy between surface and flexoelectric effects. Nano Energy, 2021, 79, 105489.	8.2	11
38081	A computational study of CO oxidation on IrO2 (1 1 0) surface. Applied Surface Science, 2021, 539, 148244.	3.1	10
38082	Raman resonance tuning of quaterthiophene in filled carbon nanotubes at high pressures. Carbon, 2021, 173, 163-173.	5.4	12

#	Article	IF	Citations
38083	Negative thermal expansion in one-dimension of a new double sulfate AgHo(SO4)2 with isolated SO4 tetrahedra. Journal of Materials Science and Technology, 2021, 76, 111-121.	5.6	34
38084	[Fe(CN)6] vacancy-boosting oxygen evolution activity of Co-based Prussian blue analogues for hybrid sodium-air battery. Materials Today Energy, 2021, 20, 100572.	2.5	17
38085	Layer Edge States Stabilized by Internal Electric Fields in Two-Dimensional Hybrid Perovskites. Nano Letters, 2021, 21, 182-188.	4.5	14
38086	DFT calculations and in situ DRIFTS study of CO oxidation on CeO2/Co3O4 catalyst. Structural Chemistry, 2021, 32, 799-804.	1.0	0
38087	Charge transfer driven interaction of CH4, CO2 and NH3 with TiS2 monolayer: Influence of vacancy defect. Catalysis Today, 2021, 370, 189-195.	2.2	5
38088	Half-metallic ferromagnetism in molybdenum doped methylammonium lead halides (MAPbX3, XÂ=ÂCl, Br, I) system: First-principles study. Journal of Magnetism and Magnetic Materials, 2021, 519, 167463.	1.0	11
38089	Insights into atomic scale structure and interfacial fracture behaviors of Ti(0001)/Ti3Sn(0001) interface. Vacuum, 2021, 183, 109791.	1.6	2
38090	Thermoelectric and Piezoelectric Properties in Half-Heusler Compounds TaXSn (Xâ€‰=â€‰Co, Rh and Ir) Based on Ab Initio Calculations. International Journal of Thermophysics, 2021, 42, 1.	1.0	15
38091	Atomistic simulation of martensitic transformations induced by deformation of Î±-Fe single crystal during the mode-I fracture. Journal of Materials Science, 2021, 56, 2275-2295.	1.7	4
38092	Uncertainty Quantification in Atomistic Modeling of Metals and Its Effect on Mesoscale and Continuum Modeling: A Review. Jom, 2021, 73, 149-163.	0.9	7
38093	A first principles investigation of the hydrogen-strain synergy on the formation and phase transition of hydrides in zirconium. Acta Materialia, 2021, 202, 222-231.	3.8	11
38094	Scavenging properties of yttrium nitride monolayer towards toxic sulfur gases. Applied Surface Science, 2021, 537, 147711.	3.1	8
38095	MoirÃ© diamanes based on the hydrogenated or fluorinated twisted bigraphene: The features of atomic and electronic structures, Raman and infrared spectra. Applied Surface Science, 2021, 537, 148011.	3.1	21
38096	Substitution of Fe in hydroxyapatite as an efficient single-atom catalyst for oxygen reduction reaction in biofuel cells: A first-principles study. Applied Surface Science, 2021, 539, 148233.	3.1	7
38097	Adsorption of Evans blue and Congo red on carbon nanotubes and its influence on the fracture parameters of defective and functionalized carbon nanotubes studied using computational methods. Applied Surface Science, 2021, 539, 148236.	3.1	16
38098	Enhanced direct interspecies electron transfer with transition metal oxide accelerants in anaerobic digestion. Bioresource Technology, 2021, 320, 124294.	4.8	52
38099	Morphogenesis of mesoscopic surface patterns formed in polarized two-photon etching of diamond. Carbon, 2021, 173, 271-285.	5.4	5
38100	Intrinsic defect migration in Be12Ti. Intermetallics, 2021, 128, 106937.	1.8	4

#	Article	IF	Citations
38101	Influence of Cr-substitution on the structural, magnetic, electron transport, and mechanical properties of Fe3â^'Cr Ge Heusler alloys. Journal of Magnetism and Magnetic Materials, 2021, 521, 167398.	1.0	17
38102	Realizing ferromagnetic insulators in electron doped double perovskites Sr2-xAxMnVO6; AÂ=ÂSn, Bi. Journal of Magnetism and Magnetic Materials, 2021, 519, 167492.	1.0	5
38103	Electronic structure, elastic, optical and thermal properties of chalcopyrite CuBY2 (B = In, Ga, In0.5) Tj ETQq0 0 0 rgBT /Overlock 10 Tf 5	0.9	2
38104	Tailoring M7C3 carbide via electron work function-guided modification. Scripta Materialia, 2021, 190, 168-173.	2.6	19
38105	The growth of anti-friction and wear-resistance TiO2 nanotube arrays driven by residual stress. Tribology International, 2021, 154, 106736.	3.0	11
38106	Theoretical analysis of an intermediate band in Sn-doped hematite with wide-spectrum solar response. Journal of Solid State Electrochemistry, 2021, 25, 731-742.	1.2	5
38107	The investigation of electronic nature and mechanical properties under spin effects for new half-metallic ferromagnetic chalcogenides Ag3CrX4 (XÂ=ÂS, Se, and Te). Journal of Magnetism and Magnetic Materials, 2021, 519, 167482.	1.0	5
38108	rh.-B12 as host of interstitial atoms: Review of a large family with illustrative study of B12{CN2} from first-principles. Progress in Solid State Chemistry, 2021, 61, 100296.	3.9	5
38109	Theoretical study on the two-dimensional bis(iminothiolato)rhodium as oxygen reduction reaction catalyst. Molecular Physics, 2021, 119, e1817593.	0.8	0
38110	Effects of Two Nearest V Substitution Doping on Magnetism of Monolayer CrSi2 via First-Principles Investigations. Journal of Superconductivity and Novel Magnetism, 2021, 34, 305-311.	0.8	2
38111	CO oxidation on Ni and Cu embedded graphdiyne as efficient noble metal-free catalysts: A first-principles density-functional theory investigation. Applied Surface Science, 2021, 539, 148287.	3.1	23
38112	Interlayer coupling effect in van der Waals heterostructures of transition metal dichalcogenides. Frontiers of Physics, 2021, 16, 1.	2.4	15
38113	Single-Atom Cobalt-Based Electrochemical Biomimetic Uric Acid Sensor with Wide Linear Range and Ultralow Detection Limit. Nano-Micro Letters, 2021, 13, 7.	14.4	76
38114	Electric field-induced band modulation of predicted ternary 2D MXC3 [M:XÂ= As:Ge, Sb:Sn and Bi:Pb] with strong stability and optical properties. Carbon, 2021, 172, 791-803.	5.4	21
38115	Role of geometry, charge and fluxionality of clusters in CO2 activation on supported sub-nanometer metal clusters: The case of Cu tetramers on pristine and O-terminated MXene. Catalysis Today, 2021, 370, 93-103.	2.2	8
38116	An experimental and theoretical exploration of the role of tri-element metal-nonmetal nanohybrids in photovoltaics. Chemical Engineering Journal, 2021, 413, 127491.	6.6	12
38117	Adsorption of NH3 and NO2 molecules on the carbon doped C3N monolayer: A first principles study. Computational and Theoretical Chemistry, 2021, 1195, 113075.	1.1	9
38118	One-step hydrothermal synthesis of S-defect-controlled ZnIn2S4 microflowers with improved kinetics process of charge-carriers for photocatalytic H2 evolution. Journal of Energy Chemistry, 2021, 58, 397-407.	7.1	100

#	Article	IF	Citations
38119	High-throughput identification of high activity and selectivity transition metal single-atom catalysts for nitrogen reduction. Nano Energy, 2021, 80, 105527.	8.2	66
38120	Structural, mechanical and phonons properties of binary intermetallic compound BaSn3 under pressure. Solid State Communications, 2021, 323, 114110.	0.9	7
38121	New Phase Transitions Driven by Soft Phonon Modes for CsPbBr 3 : Density Functional Theory Study. Physica Status Solidi (B): Basic Research, 2021, 258, 2000289.	0.7	7
38122	Applied biaxial strain induced tunable sensing performance of green phosphorene monolayer towards small molecules: A DFT study. Applied Surface Science, 2021, 536, 147759.	3.1	16
38123	DFT insights into hydrogen activation on the doping Ni2P surfaces under the hydrodesulfurization condition. Applied Surface Science, 2021, 538, 148160.	3.1	11
38124	Revisiting surface chemistry in TiO2: A critical role of ionic passivation for pH-independent and anti-corrosive photoelectrochemical water oxidation. Chemical Engineering Journal, 2021, 407, 126929.	6.6	11
38125	Single- and multi-layer arsenene as an anode material for Li, Na, and K-ion battery applications. Computational Materials Science, 2021, 186, 110000.	1.4	11
38126	An efficient Z-scheme (Cr, B) codoped g-C3N4/BiVO4 photocatalyst for water splitting: A hybrid DFT study. International Journal of Hydrogen Energy, 2021, 46, 247-261.	3.8	59
38127	Bimetallic Agâ€“Cu nanosheets assembled flower-like structure for oxygen reduction reaction. Journal of Alloys and Compounds, 2021, 856, 157379.	2.8	11
38128	Isocyanic acid (HNCO) dissociation on Rh(001) surface: A DFT study with and without dispersion correction. Surface Science, 2021, 709, 121744.	0.8	7
38129	The Electronic Properties of Chlorine in GaN: An Ab Initio Study. Physica Status Solidi (B): Basic Research, 2021, 258, 2000303.	0.7	0
38130	Remarkable Enhancement of Euâ€“TiO2â€“GO Composite for Photodegradation of Indigo Carmine: A Design Method Based on Computational and Experimental Perspectives. Catalysis Letters, 2021, 151, 1111-1126.	1.4	14
38131	Deposition of the Spin Crossover Fe II â€“Pyrazolylborate Complex on Au(111) Surface at the Molecular Level. Chemistry - A European Journal, 2021, 27, 712-723.	1.7	12
38132	Firstâ€Principles Study on the Crystalline Ga 4 Sb 6 Te 3 Phase Change Compound. Physica Status Solidi - Rapid Research Letters, 2021, 15, 2000382.	1.2	2
38133	Sensing Applications of Atomically Thin Group IV Carbon Siblings Xenes: Progress, Challenges, and Prospects. Advanced Functional Materials, 2021, 31, 2005957.	7.8	37
38134	DFT investigation of 2-mercaptobenzothiazole adsorption on model oxidized copper surfaces and relationship with corrosion inhibition. Applied Surface Science, 2021, 537, 147802.	3.1	47
38135	Pressure effects on the electronic, magnetic, thermoelectric, and thermodynamic properties of Mn 2 CoSi halfâ€metallic compound. International Journal of Quantum Chemistry, 2021, 121, e26445.	1.0	2
38136	Highâ€Pressure Characterization of the Cageâ€Structured Explosive TEX by Dispersionâ€Corrected DFT Calculations. Physica Status Solidi (B): Basic Research, 2021, 258, 2000329.	0.7	5

#	Article	IF	Citations
38137	Ab initio calculations of interaction between Ni and Si in Î±-Fe. Journal of Nuclear Science and Technology, 2021, 58, 201-206.	0.7	0
38138	A Carbocationic Triarylmethaneâ€Based Porous Covalent Organic Network. Chemistry - A European Journal, 2021, 27, 2342-2347.	1.7	10
38139	Structural, elastic, and electronic properties of MgB 2 C 2 under pressure from firstâ€principles calculations. International Journal of Quantum Chemistry, 2021, 121, e26442.	1.0	1
38140	Physical Properties and Electronic Structure of Cr 2 B Under Pressure. Physica Status Solidi (B): Basic Research, 2021, 258, 2000212.	0.7	1
38141	Comprehensive investigation of the adsorption of 2-carboxyethylphenylphosphinic acid on cassiterite. Separation Science and Technology, 2021, 56, 2194-2203.	1.3	1
38142	Formation and superconducting properties of predicted ternary hydride <scp>ScYH₆</scp> under pressures. International Journal of Quantum Chemistry, 2021, 121, e26459.	1.0	20
38143	Evidencing Interfacial Charge Transfer in 2D CdS/2D MXene Schottky Heterojunctions toward Highâ€Efficiency Photocatalytic Hydrogen Production. Solar Rrl, 2021, 5, 2000414.	3.1	83
38144	Computational Study of Transition-Metal Substitutions in Rutile TiO2 (110) for Photoelectrocatalytic Ammonia Synthesis. Catalysis Letters, 2021, 151, 1142-1154.	1.4	4
38145	Can doping of transition metal oxide cathode materials increase achievable voltages with multivalent metals?. International Journal of Quantum Chemistry, 2021, 121, e26439.	1.0	2
38146	Self-aldol condensation of aldehydes over Lewis acidic rare-earth cations stabilized by zeolites. Chinese Journal of Catalysis, 2021, 42, 595-605.	6.9	24
38147	Structural, vibrational, mechanical, and optoelectronic properties of <scp>LiBH₄</scp> for hydrogen storage and optoelectronic devices: Firstâ€principles study. International Journal of Quantum Chemistry, 2021, 121, e26444.	1.0	8
38148	Obtaining, structure and gas sensor properties of nanopowder metal oxides. Materials Today: Proceedings, 2021, 35, 588-594.	0.9	11
38149	Phase Stability and Thermo-Physical Properties of Nickel-Aluminum Binary Chemically Disordered Systems via First-Principles Study. Metals and Materials International, 2021, 27, 1469-1477.	1.8	1
38150	Hydrogenation of substituted nitroaromatics on non-noble metal catalysts: mechanistic insights to improve selectivity. Faraday Discussions, 2021, 229, 297-317.	1.6	7
38151	Electronic structure of ZnO thin films doped with group III elements. Materials Today: Proceedings, 2021, 35, 604-608.	0.9	3
38152	Theoretical Investigation of the CO2 Capture Properties of Î³-LiAlO2 and Î±-Li5AlO4. Micro and Nanosystems, 2021, 13, 32-41.	0.3	7
38153	Interactions among components of fluid inclusions in sulfide mineral, mineral surfaces, and collectors. , 2021, , 179-230.		2
38154	High-performance aqueous Znâ€“MnO₂ batteries enabled by the coupling engineering of K⁺ pre-intercalation and oxygen defects. Journal of Materials Chemistry A, 2021, 9, 15637-15647.	5.2	46

#	Article	IF	Citations
38155	Defect structures of the Cr₂O₃(112Ì„0) surface: effect of electron beam irradiation. Journal of Materials Chemistry C, 2021, 9, 6324-6331.	2.7	6
38156	Femtosecond nonlinear refraction of 2D semi-metallic redox exfoliated ZrTe2 at 800â€‰nm. Applied Physics Letters, 2021, 118, .	1.5	13
38157	A comparison study of MnO₂ and Mn₂O₃ as zinc-ion battery cathodes: an experimental and computational investigation. RSC Advances, 2021, 11, 14408-14414.	1.7	12
38158	Two-dimensional topological insulators exfoliated from Na3Bi-like Dirac semimetals. Physical Chemistry Chemical Physics, 2021, 23, 10545-10550.	1.3	1
38159	Optoelectronic properties and strain regulation of the 2D WS₂/ZnO van der Waals heterostructure. RSC Advances, 2021, 11, 14085-14092.	1.7	18
38160	Performance Analysis of Transition Metal Dichalcogenide Based Multichannel Cylindrical Shaped Gate All Around (GAA) MOSFET. , 2021, , .		0
38161	Oxidative etching of S-vacancy defective MoS₂ monolayer upon reaction with O₂. Physical Chemistry Chemical Physics, 2021, 23, 10225-10235.	1.3	4
38162	Electronic excitation in graphene under single-particle irradiation. Nanotechnology, 2021, 32, 165702.	1.3	3
38163	Computational insights into structural, electronic, and optical properties of Janus GeSO monolayer. RSC Advances, 2021, 11, 28381-28387.	1.7	10
38164	Probing Kinetics and Mechanism of Formation of Mixed Metallic Nanoparticles in a Polymer Membrane by Galvanic Replacement between Two Immiscible Metals: Case Study of Nickel/Silver Nanoparticle Synthesis. Langmuir, 2021, 37, 1637-1650.	1.6	4
38165	Out-of-Plane Deformations Determined Mechanics of Vanadium Disulfide (VS₂) Sheets. ACS Applied Materials & Interfaces, 2021, 13, 3040-3050.	4.0	21
38166	Pressure-Driven Structural Phase Transitions and Superconductivity of Ternary Hydride MgVH₆. Journal of Physical Chemistry C, 2021, 125, 3150-3156.	1.5	18
38167	Molecularly Smooth and Conformal Nanocoating by Amine-Mediated Redox Modulation of Catechol. Chemistry of Materials, 2021, 33, 952-965.	3.2	9
38168	Mechanistic insight into oxygen vacancy migration in SrFeO_{3â^'Î´}from DFT+Usimulations. Physical Chemistry Chemical Physics, 2021, 23, 18628-18639.	1.3	6
38169	Novel two-dimensional AlSb and InSb monolayers with a double-layer honeycomb structure: a first-principles study. Physical Chemistry Chemical Physics, 2021, 23, 18752-18759.	1.3	44
38170	Benchmarking dispersion-corrected DFT methods for the evaluation of materials with anisotropic properties: structural, electronic, dielectric, optical and vibrational analysis of calcite (CaCO₃, space group R3l„c). Physical Chemistry Chemical Physics, 2021, 23, 18899-18907.	1.3	16
38171	Examining the electron transport in chalcogenide perovskite BaZrS₃. Journal of Materials Chemistry C, 2021, 9, 3892-3900.	2.7	24
38172	Structural, elastic and electronic properties of atomically thin pyridyne: theoretical predictions. Physical Chemistry Chemical Physics, 2021, 23, 5385-5391.	1.3	0

#	Article	IF	Citations
38173	Combined Ab Initio and Experimental Study of Hydrogen Sorption in Dual-Phase Steels. Minerals, Metals and Materials Series, 2021, , 730-741.	0.3	0
38174	Thermodynamic Properties of Tungsten Disulfide from First Principles in Quasi-Harmonic Approximation. Powder Metallurgy and Metal Ceramics, 2021, 59, 576-584.	0.4	5
38175	Ab initio simulation of the effects of substitutional doping of oxygen in the semifullerene (C₃₀). Journal of Physics: Conference Series, 2021, 1723, 012054.	0.3	2
38176	Defects as catalytic sites for the oxygen evolution reaction in Earth-abundant MOF-74 revealed by DFT. Catalysis Science and Technology, 2021, 11, 1443-1450.	2.1	17
38177	Effect of transition metal element additions on the mechanical and electronic properties of L10 CoNi alloys. Extreme Mechanics Letters, 2021, 42, 101128.	2.0	4
38178	Two-dimensional aluminium, gallium, and indium metallic crystals by first-principles design. Journal of Physics Condensed Matter, 2021, 33, 125901.	0.7	12
38179	Temperature and pressure-induced strains in anhydrous iron trifluoride polymorphs. Physical Chemistry Chemical Physics, 2021, 23, 2825-2835.	1.3	1
38180	Influence of Co and Mn substitution on magnetic properties of novel Y₂FeSi Heusler alloy. Modern Physics Letters B, 2021, 35, 2150088.	1.0	2
38181	Dynamic stabilization and heat transport characteristics of monolayer SnSe at finite temperature: A study by phonon quasiparticle approach. Physical Review B, 2021, 103, .	1.1	3
38182	Impact of the vertical strain on the Schottky barrier height for graphene/AlN heterojunction: a study by the first-principles method. European Physical Journal B, 2021, 94, 1.	0.6	6
38183	Pressure effects on electronic, elastic, and vibration properties of metallic antiperovskite PbNCa3 by ab initio calculations. Journal of Molecular Modeling, 2021, 27, 7.	0.8	3
38184	Phonon Thermal Edelstein Effect. Springer Theses, 2021, , 29-48.	0.0	0
38185	Understanding composition-dependent catalytic performance of PdAg for the hydrogenation of 1,3-butadiene to 1-butene. Catalysis Communications, 2021, 149, 106255.	1.6	6
38186	The first principle study of magnetic, electronic, and optical properties of Co- and Mn-doped boron nitride nanosheets. Indian Journal of Physics, 2022, 96, 419-431.	0.9	3
38187	Preferential lattice expansion of polypropylene in a trilayer polypropylene/polyethylene/polypropylene microporous separator in Li-ion batteries. Scientific Reports, 2021, 11, 1929.	1.6	3
38188	Simulations of ZnS deposition on Ag2S surface and formation of Ag2S/ZnS heteronanostructure. IOP Conference Series: Materials Science and Engineering, 0, 1008, 012020.	0.3	0
38189	Remarkable class of materials: Band structures and optical properties of non-superconducting and superconducting MAX phases. Journal of Physics: Conference Series, 2021, 1718, 012002.	0.3	0
38190	Intrinsic spinâ€“valley-coupled Dirac state in Janus functionalized Î²-BiAs monolayer. Nanoscale Horizons, 2021, 6, 283-289.	4.1	9

#	Article	IF	Citations
38191	First-principles study of nickel reactivity under two-dimensional cover: <mml:math xmlns:mml="http://www.w3.org/1998/Math/MathML"><mml:mrow><mml:msub><mml:mi>Ni</mml:mi><mml:mn>2</mml:mn></mml:r mathvariant="normal">C</mml:mi></mml:mrow></mml:math> formation at rotated graphene/Ni(111) interface. Physical Review Materials, 2021, 5, .	0.9	0
38192	Robust transport of charge carriers in in-plane 1Tâ€²-2H MoTe2 homojunctions with ohmic contact. Nano Research, 2021, 14, 1311-1318.	5.8	16
38193	A combined theoretical/experimental study highlighting the formation of carbides on Ru nanoparticles during CO hydrogenation. Nanoscale, 2021, 13, 6902-6915.	2.8	9
38194	Highly tunable electronic structure and linear dichroism in 90Â° twisted Î±-phosphorus carbide bilayer: a first-principles calculation. Physical Chemistry Chemical Physics, 2021, 23, 7080-7087.	1.3	9
38195	Highly efficient ammonia synthesis at low temperature over a Ruâ€“Co catalyst with dual atomically dispersed active centers. Chemical Science, 2021, 12, 7125-7137.	3.7	35
38196	Enabling multifunctional electrocatalysts by modifying the basal plane of unifunctional 1Tâ€²-MoS₂ with anchored transition metal single atoms. Nanoscale, 2021, 13, 13390-13400.	2.8	69
38197	Sustainable existence of solid mercury (Hg) nanoparticles at room temperature and their applications. Chemical Science, 2021, 12, 3226-3238.	3.7	10
38198	Synthesis and supramolecular organization of the iodide and triiodides of a polycyclic adamantane-based diammonium cation: the effects of hydrogen bonds and weak Iâ‹¯I interactions. CrystEngComm, 2021, 23, 2384-2395.	1.3	11
38199	MC₂ (M = Y, Zr, Nb, and Mo) monolayers containing C₂ dimers: prediction of anode materials for high-performance sodium ion batteries. Nanoscale Advances, 2021, 3, 6617-6627.	2.2	8
38200	Computational discovery of PtS₂/GaSe van der Waals heterostructure for solar energy applications. Physical Chemistry Chemical Physics, 2021, 23, 20163-20173.	1.3	19
38201	Formation of oxygen vacancies in Li₂FeSiO₄: first-principles calculations. Physical Chemistry Chemical Physics, 2021, 23, 20444-20452.	1.3	3
38202	Exploring 2D structures of indium oxide of different stoichiometry. CrystEngComm, 2021, 23, 6661-6667.	1.3	34
38203	Tailoring long-range superlattice chirality in molecular self-assemblies via weak fluorine-mediated interactions. Physical Chemistry Chemical Physics, 2021, 23, 21489-21495.	1.3	2
38204	In situ formed lithium ionic conductor thin film on the surface of high-crystal-layered LiCoO₂ as a high-voltage cathode material. Materials Chemistry Frontiers, 2021, 5, 6171-6181.	3.2	8
38205	First-principles calculation of 11B solid-state NMR parameters of boron-rich compounds II: the orthorhombic phases MgB7 and MgB12C2 and the boron modification Î³-B28. Physical Chemistry Chemical Physics, 2021, 23, 3883-3897.	1.3	3
38206	Formic acid dehydrogenation over PdNi alloys supported on N-doped carbon: synergistic effect of Pdâ€“Ni alloying on hydrogen release. Physical Chemistry Chemical Physics, 2021, 23, 11515-11527.	1.3	16
38207	High-Performance Giant Dielectric Properties of Cr³⁺/Ta⁵⁺ Co-Doped TiO₂ Ceramics. ACS Omega, 2021, 6, 1901-1910.	1.6	31
38208	Ab initio design of a new family of 2D materials: transition metal carbon nitrogen compounds (MCNs). Journal of Materials Chemistry C, 2021, 9, 4748-4756.	2.7	8

#	Article	IF	Citations
38209	Lattice-distorted lithiation behavior of a square phase Janus MoSSe monolayer for electrode applications. Nanoscale Advances, 2021, 3, 2902-2910.	2.2	9
38210	Monolayered Hâ€“Siâ€“P semiconductors: structural stability, electronic structure, optical properties, and prospects for photocatalytic water splitting. Physical Chemistry Chemical Physics, 2021, 23, 13594-13602.	1.3	0
38211	Chalcopyrite bioleaching catalyzed by silver. , 2021, , 183-209.		0
38212	Tuning the structural skeleton of a phenanthroline-based covalent organic framework for better electrochemical performance as a cathode material for Zn-ion batteries: a theoretical exploration. Physical Chemistry Chemical Physics, 2021, 23, 12644-12653.	1.3	19
38213	A key step for preparing highly active Mgâ€“Co composite oxide catalysts for N₂O decomposition. Catalysis Science and Technology, 2021, 11, 3737-3745.	2.1	6
38214	Electronic properties of monolayer graphene doped with nitrogen and boron atoms. AIP Conference Proceedings, 2021, , .	0.3	4
38215	Ab initio characterization of N doped T-graphene and its application as an anode material for Na ion rechargeable batteries. Sustainable Energy and Fuels, 2021, 5, 4060-4068.	2.5	9
38216	The prediction of structural, electronic, optical and vibrational behavior of ThS2 for nuclear fuel applications: a DFT study. Optical and Quantum Electronics, 2021, 53, 1.	1.5	9
38217	Hydrothermal control of the lithium-rich Li₂MnO₃ phase in lithium manganese oxide nanocomposites and their application as precursors for lithium adsorbents. Dalton Transactions, 2021, 50, 10765-10778.	1.6	8
38218	White light emission from co-doped La₂Hf₂O₇nanoparticles with suppressed host â†' Eu³⁺energy transferviaa U⁶⁺co-dopant. Inorganic Chemistry Frontiers, 2021, 8, 3830-3842.	3.0	10
38219	Electronic transport through molecules containing pyrimidine units: First-principles calculations. Journal of Computational Science, 2021, 48, 101261.	1.5	12
38220	Defect Processes in Halogen Doped SnO2. Applied Sciences (Switzerland), 2021, 11, 551.	1.3	9
38221	First principles characterisation of bioâ€“nano interface. Physical Chemistry Chemical Physics, 2021, 23, 13473-13482.	1.3	24
38222	Pockels effect in low-temperature rhombohedral <mml:math xmlns:mml="http://www.w3.org/1998/Math/MathML"><mml:mrow><mml:mi>BaTi</mml:mi><mml:msub><mml:mi mathvariant="normal">O</mml:mi><mml:mn>3</mml:mn></mml:msub></mml:mrow></mml:math>. Physical Review B, 2021, 103, .	1.1	11
38223	Mechanical ductile detwinning in CH₃NH₃PbI₃ perovskite. Physical Chemistry Chemical Physics, 2021, 23, 21863-21873.	1.3	0
38224	Ultrasensitive broadband photodetectors based on two-dimensional Bi₂O₂Te films. Journal of Materials Chemistry C, 2021, 9, 13713-13721.	2.7	12
38225	Ab initio study on crystal structure and phase stability of ZrC2 under high pressure. Chinese Physics B, 2021, 30, 016101.	0.7	3
38226	Pore control of Al-based MIL-53 isomorphs for the preferential capture of ethane in an ethane/ethylene mixture. Journal of Materials Chemistry A, 2021, 9, 14593-14600.	5.2	29

#	Article	IF	Citations
38227	Spin-orbit effects in ferroelectric <mml:math xmlns:mml="http://www.w3.org/1998/Math/MathML"><mml:mrow><mml:mi>Pb</mml:mi><mml:mi>Ti</mml:mi><mml:msub><mml:mi mathvariant="normal">O</mml:mi><mml:mn>3</mml:mn></mml:msub></mml:mrow></mml:math> under tensile strain. Physical Review B, 2021, 103, .	1.1	8
38228	Electronic and thermal transport in novel carbon-based bilayer with tetragonal rings: a combined study using first-principles and machine learning approach. Physical Chemistry Chemical Physics, 2021, 23, 14608-14616.	1.3	19
38229	Two-dimensional C3N/blue phosphorene vdW heterostructure for Li, Na and K-ion batteries. New Journal of Chemistry, 2021, 45, 12647-12654.	1.4	7
38230	Novel two-dimensional ZnO₂, CdO₂ and HgO₂ monolayers: a first-principles-based prediction. New Journal of Chemistry, 2021, 45, 9368-9374.	1.4	6
38231	Theoretical study of the octahedral substitution effect in delaminated pyrophyllite: physicochemical properties and applications. Physical Chemistry Chemical Physics, 2021, 23, 14601-14607.	1.3	2
38232	Highly efficient transverse thermoelectric devices with Re₄Si₇ crystals. Energy and Environmental Science, 2021, 14, 4009-4017.	15.6	29
38233	Insights into the physical properties and anisotropic nature of ErPdBi with an appearance of low minimum thermal conductivity. Chinese Physics B, 2021, 30, 016203.	0.7	16
38234	The local atomic structure and thermoelectric properties of Ir-doped ZnO: hybrid DFT calculations and XAS experiments. Journal of Materials Chemistry C, 2021, 9, 4948-4960.	2.7	7
38235	Growth, crystal structure and theoretical studies of energy and optical properties of CdTe1â^'xSex thin films. Applied Nanoscience (Switzerland), 2022, 12, 335-342.	1.6	9
38236	First Principle Study on Mg2X (X = Si, Ge, Sn) Intermetallics by Bi Micro-Alloying. Crystals, 2021, 11, 142.	1.0	5
38237	Solvent Effects for Methanol Electrooxidation on Gold. Journal of Physical Chemistry C, 2021, 125, 1355-1360.	1.5	13
38238	Exfoliation Energy as a Descriptor of MXenes Synthesizability and Surface Chemical Activity. Nanomaterials, 2021, 11, 127.	1.9	22
38239	Electron deficiency but semiconductive diamond-like B₂CN originated from three-center bonds. Physical Chemistry Chemical Physics, 2021, 23, 3087-3092.	1.3	4
38240	Discovery of intrinsic two-dimensional antiferromagnets from transition-metal borides. Nanoscale, 2021, 13, 8254-8263.	2.8	31
38241	Titanium and fluorine synergetic modification improves the electrochemical performance of Li(Ni_{0.8}Co_{0.1}Mn_{0.1})O₂. Journal of Materials Chemistry A, 2021, 9, 9354-9363.	5.2	62
38242	Transition from perovskite to misfit-layered structure materials: a highly oxygen deficient and stable oxygen electrode catalyst. Energy and Environmental Science, 2021, 14, 2472-2484.	15.6	53
38243	2D auxetic material with intrinsic ferromagnetism: a copper halide (CuCl₂) monolayer. Physical Chemistry Chemical Physics, 2021, 23, 22078-22085.	1.3	7
38244	Multi-functional photocatalytic activity of transition-metal tetraaza[14]annulene frameworks. Journal of Materials Chemistry A, 2021, 9, 4221-4229.	5.2	12

#	Article	IF	Citations
38245	Ultralow lattice thermal conductivity and dramatically enhanced thermoelectric properties of monolayer InSe induced by an external electric field. Physical Chemistry Chemical Physics, 2021, 23, 13633-13646.	1.3	10
38246	Me-graphane: tailoring the structural and electronic properties of Me-grapheneviahydrogenation. Physical Chemistry Chemical Physics, 2021, 23, 9483-9491.	1.3	9
38247	Cooperative B-site octahedral tilting, distortion and A-site conformational change induced phase transitions of a 2D lead halide perovskite. Materials Chemistry Frontiers, 2021, 5, 7587-7594.	3.2	10
38248	Superhydrophilic Fe³⁺ Doped TiO₂ Films with Long-Lasting Antifogging Performance. ACS Applied Materials & Interfaces, 2021, 13, 3377-3386.	4.0	40
38249	The nonlinear optical transition bleaching in tellurene. Nanoscale, 2021, 13, 15882-15890.	2.8	10
38250	Combined Merits of High Dielectric Breakdown Strength and Low Sintering Temperature Acquired in Mgo-Baseddielectric Ceramics: From Theoretical Prediction to Experimental Validation. SSRN Electronic Journal, 0, , .	0.4	0
38251	Activating the FeS (001) Surface for CO2 Adsorption and Reduction through the Formation of Sulfur Vacancies: A DFT-D3 Study. Catalysts, 2021, 11, 127.	1.6	16
38252	Tunable valley polarization in Janus WSSe by magnetic proximity coupling to a CrI₃ layer. Physical Chemistry Chemical Physics, 2021, 23, 18182-18188.	1.3	7
38253	Density Functional Theory Studies of Doping and Curvature Effects on the Electrocatalytic Hydrogen Evolution Activity of Carbon Nanotubes. ACS Applied Nano Materials, 2021, 4, 600-611.	2.4	14
38254	Water Oxidation Catalysis on the Nitrogen-Deficient SrNbO2N(001) Surface. Journal of Physical Chemistry C, 2021, 125, 2424-2430.	1.5	3
38255	Spin valve effect in VN/GaN/VN van der Waals heterostructures. Physical Review B, 2021, 103, .	1.1	21
38256	First-principles study of strain effect on the thermoelectric properties of LaP and LaAs. Physical Chemistry Chemical Physics, 2021, 23, 18189-18196.	1.3	7
38257	Magnetic and Electronic Properties of Heavy Lanthanides (Gd, Tb, Dy, Er, Ho, Tm). Crystals, 2021, 11, 82.	1.0	15
38258	Exploring the Intrinsic Point Defects in Cesium Copper Halides. Journal of Physical Chemistry C, 2021, 125, 1592-1598.	1.5	15
38259	Temperature-Dependent Band Renormalization in CoSb₃ Skutterudites Due to Sb-Ring-Related Vibrations. Chemistry of Materials, 2021, 33, 1046-1052.	3.2	16
38260	Bilayer Tellurene: A Potential pâ€Type Channel Material for Subâ€10 nm Transistors. Advanced Theory and Simulations, 2021, 4, 2000252.	1.3	14
38261	Approximate models for the lattice thermal conductivity of alloy thermoelectrics. Journal of Materials Chemistry C, 2021, 9, 11772-11787.	2.7	12
38262	Phase stability of the tin monochalcogenides SnS and SnSe: a quasi-harmonic lattice-dynamics study. Physical Chemistry Chemical Physics, 2021, 23, 19219-19236.	1.3	14

#	Article	IF	Citations
38263	Surface structure sensitivity of hydrodeoxygenation of biomass-derived organic acids over palladium catalysts: a microkinetic modeling approach. Catalysis Science and Technology, 2021, 11, 6163-6181.	2.1	4
38264	Germanene/2D-AlP van der Waals heterostructure: Tunable structural and electronic properties. AIP Advances, 2021, 11, .	0.6	22
38265	Oxygen chemistry of halogen-doped CeO₂(111). Physical Chemistry Chemical Physics, 2021, 23, 19375-19385.	1.3	2
38266	Understanding the origin of structure sensitivity in hydrodechlorination of trichloroethylene on a palladium catalyst. Reaction Chemistry and Engineering, 2021, 6, 2270-2279.	1.9	3
38267	Z-Scheme versus type-II junction in g-C₃N₄/TiO₂ and g-C₃N₄/SrTiO₃/TiO₂ heterostructures. Catalysis Science and Technology, 2021, 11, 3589-3598.	2.1	25
38268	Role of surface termination and quantum size in Î±-CsPbX₃ (X = Cl, Br, I) 2D nanostructures for solar light harvesting. Physical Chemistry Chemical Physics, 2021, 23, 3031-3040.	1.3	20
38269	Auxetic, flexible, and strain-tunable two-dimensional th-AlN for photocatalytic visible light water splitting with anisotropic high carrier mobility. Journal of Materials Chemistry C, 2021, 9, 4971-4977.	2.7	29
38270	Transition-metal single atoms embedded into defective BC₃as efficient electrocatalysts for oxygen evolution and reduction reactions. Nanoscale, 2021, 13, 1331-1339.	2.8	27
38271	Drivers of zirconium isotope fractionation in Zr-bearing phases and melts: The roles of vibrational, nuclear field shift and diffusive effects. Geochimica Et Cosmochimica Acta, 2021, 292, 217-234.	1.6	38
38272	Interfacial acidity on the strontium titanate surface: a scaling paradigm and the role of the hydrogen bond. Physical Chemistry Chemical Physics, 2021, 23, 23478-23485.	1.3	2
38273	Electrocatalytic nitrogen reduction on the transition-metal dimer anchored N-doped graphene: performance prediction and synergetic effect. Physical Chemistry Chemical Physics, 2021, 23, 4018-4029.	1.3	90
38274	Mechanistic Framework and Effects of High Coverage in Vinyl Acetate Synthesis. ACS Catalysis, 2021, 11, 1841-1857.	5.5	6
38275	Coalescence and shape oscillation of Au nanoparticles in CO₂ hydrogenation to methanol. Nanoscale, 2021, 13, 18218-18225.	2.8	6
38276	Modelling of high-temperature orderâ€“disorder phase transitions of non-stoichiometric Mo₂C and Ti₂C from first principles. Physical Chemistry Chemical Physics, 2021, 23, 22305-22312.	1.3	1
38277	Calculation of the vibrational spectra of AgGaS₂ crystal with chalcopyrite structure. Journal of Physical Studies, 2021, 25, .	0.2	3
38278	Mechanosynthesis of a Coamorphous Formulation of Creatine with Citric Acid and Humidity-Mediated Transformation into a Cocrystal. Crystal Growth and Design, 2021, 21, 1297-1306.	1.4	14
38279	Redox, Magnetic, and Structural Properties of Î±-NaMnO2 Cathode Material Analyzed by Fitting-Free DFT+U Calculations, Parameterized by the Linear Response Approach. Journal of Physical Chemistry C, 2021, 125, 1531-1543.	1.5	4
38280	Effects of Nitrogen/Fluorine Codoping on Photocatalytic Rutile TiO₂ Crystal Studied by First-Principles Calculations. Inorganic Chemistry, 2021, 60, 2381-2389.	1.9	9

#	Article	IF	Citations
38281	Fermi surface and 2D-Electron momentum density of covellite mineral. Materials Today: Proceedings, 2021, 43, 3121-3124.	0.9	0
38282	Identification of vanadium dopant sites in the metalâ€“organic framework DUT-5(Al). Physical Chemistry Chemical Physics, 2021, 23, 7088-7100.	1.3	1
38283	Pressure-induced stability and polymeric nitrogen in alkaline earth metal N-rich nitrides (XN6, X = Ca,) Tj ETQq0 0 0 rgBT /Overlock 10 Tf	1.7	0
38284	Theoretical study of the H/D isotope effect of CH₄/CD₄ adsorption on a Rh(111) surface using a combined plane wave and localized basis sets method. RSC Advances, 2021, 11, 10253-10257.	1.7	4
38285	Facile synthesis of carbon nanofiber confined FeS₂/Fe₂O₃ heterostructures as superior anode materials for sodium-ion batteries. Journal of Materials Chemistry C, 2021, 9, 2933-2943.	2.7	27
38286	Density functional theory study of thiophene desulfurization and conversion of desulfurization products on the Ni(111) surface and Ni₅₅ cluster: implication for the mechanism of reactive adsorption desulfurization over Ni/ZnO catalysts. Catalysis Science and Technology, 2021, 11, 1615-1625.	2.1	12
38287	On the Cauchy-Born approximation at finite temperature for alloys. Discrete and Continuous Dynamical Systems - Series B, 2021, .	0.5	0
38288	Effects of the organic molecule adsorption and substrate on electronic structure of germanene. Wuli Xuebao/Acta Physica Sinica, 2021, .	0.2	3
38289	Phonon dispersion and electronic structure in quasi-one-dimensional layered Ta2NiSe7 single crystal. Journal of Materials Chemistry C, 2021, 9, 5162-5166.	2.7	4
38290	Effect of Hf doping on He behavior in tritium storage material ZrCo. Physical Chemistry Chemical Physics, 2021, 23, 18686-18693.	1.3	4
38291	Phase Transformation and Superstructure Formation in (Ti0.5, Mg0.5)N Thin Films through High-Temperature Annealing. Coatings, 2021, 11, 89.	1.2	2
38292	Orientation-Dependent Conversion of VLS-Grown Lead Iodide Nanowires into Organic-Inorganic Hybrid Perovskites. Nanomaterials, 2021, 11, 223.	1.9	1
38293	Effect of Alloying Elements on the Mechanical Properties of Mo3Si. Metals, 2021, 11, 129.	1.0	2
38294	Topological surface states in epitaxial <mml:math		

#	Article	IF	Citations
38299	Computational assessment of the crystallization tendency of 1-ethyl-3-methylimidazolium ionic liquids. Physical Chemistry Chemical Physics, 2021, 23, 4951-4962.	1.3	8
38300	Growth and characterization of lithium chloride doped KDP crystals: a DFT and experimental approach. Ferroelectrics, 2021, 571, 1-25.	0.3	8
38301	The high power conversion efficiency of a two-dimensional GeSe/AsP van der Waals heterostructure for solar energy cells. Physical Chemistry Chemical Physics, 2021, 23, 6042-6050.	1.3	22
38302	Charge carrier dynamics investigation of Cu₂Sâ€“In₂S₃ heterostructures for the conversion of dinitrogen to ammonia via photo-electrocatalytic reduction. Journal of Materials Chemistry A, 2021, 9, 10497-10507.	5.2	19
38303	Evolutionary structure prediction-assisted design of anode materials for Ca-ion battery based on phosphorene. Physical Chemistry Chemical Physics, 2021, 23, 9466-9475.	1.3	13
38304	Study of the M-doped Effect (M=Al, Ag, W) on the Dissociation of O2 on Cu Surface Using a First Principles Method. Materials Research, 2021, 24, .	0.6	0
38305	Structural, Electronic, Mechanical, and Optical Properties of LaIn3 under Pressure: A First Principle Investigation. Journal of Superhard Materials, 2021, 43, 31-44.	0.5	0
38306	Gaussian Basis Sets for Solid State Calculations. Lecture Notes in Quantum Chemistry II, 2021, , 157-181.	0.3	5
38307	A first-principles study on the properties of Sn-doped LiCoO₂ for Li-ion batteries. Dalton Transactions, 2021, 50, 4680-4685.	1.6	7
38308	Pressure-induced Naâ€“Au compounds with novel structural units and unique charge transfer. Physical Chemistry Chemical Physics, 2021, 23, 6455-6461.	1.3	8
38309	Emergence of Ferromagnetism in Nanoparticles of BeTiO3 Ceramic with the Perovskite Structure. Inorganic Materials: Applied Research, 2021, 12, 88-93.	0.1	0
38310	Effect of atomic configuration and spinâ€“orbit coupling on thermodynamic stability and electronic bandgap of monolayer 2H-Mo_{1â^'x}W_xS₂ solid solutions. Physical Chemistry Chemical Physics, 2021, 23, 13535-13543.	1.3	3
38311	Oxygen ion transport in doped ceria: effect of vacancy trapping. Journal of Materials Chemistry A, 2021, 9, 13883-13889.	5.2	18
38312	Selective hydrogenation of acetylene on Cuâ€“Pd intermetallic compounds and Pd atoms substituted Cu(111) surfaces. Physical Chemistry Chemical Physics, 2021, 23, 8653-8660.	1.3	9
38313	State of charge dependent ordered and disordered phases in a Li[Ni1/3Co1/3Mn1/3]O2 cathode material. Materials Advances, 2021, 2, 3965-3970.	2.6	2
38314	Structural and Electronic Properties of Various Useful Metal Oxides. , 2021, , 49-84.		0
38315	BaCoO3 monoclinic structure and chemical bonding analysis: hybrid DFT calculations. Physical Chemistry Chemical Physics, 2021, 23, 17493-17501.	1.3	4
38316	Magnetic surface reconstruction in the van der Waals antiferromagnet <mml:math xmlns:mml="http://www.w3.org/1998/Math/MathML"><mml:mrow><mml:msub><mml:mi>Fe</mml:mi><mml:mrow><mml:mn>1</mml:mn> Physical Review B, 2021, 103, .	1.1	16

#	Article	IF	Citations
38317	Rare-earth-free ferrimagnetic Mn4N sub-20Ânm thin films as potential high-temperature spintronic material. AIP Advances, 2021, 11, 015334.	0.6	11
38318	Influence of ligand composition on crystal structure formation â€“ isostructurality and morphotropism. CrystEngComm, 2021, 23, 317-323.	1.3	6
38319	Cobalt single atoms anchored on nitrogen-doped porous carbon as an efficient catalyst for oxidation of silanes. Green Chemistry, 2021, 23, 1026-1035.	4.6	21
38320	Atomic Resonant Tunneling in the Surface Diffusion of H Atoms on Pt(111). Journal of Physical Chemistry C, 2021, 125, 464-480.	1.5	8
38321	Unveiling the Origin of Alloy-Seeded and Nondendritic Growth of Zn for Rechargeable Aqueous Zn Batteries. ACS Energy Letters, 2021, 6, 404-412.	8.8	148
38322	A van der Waals heterostructure of MoS₂/MoSi₂N₄: a first-principles study. New Journal of Chemistry, 2021, 45, 8291-8296.	1.4	59
38323	Mechanical and optical behaviors: strain synergy effects in high temperature phase oxides of lead. New Journal of Chemistry, 2021, 45, 19714-19722.	1.4	2
38324	Van der Waals heterostructure of graphene and germanane: tuning the ohmic contact by electrostatic gating and mechanical strain. Physical Chemistry Chemical Physics, 2021, 23, 21196-21206.	1.3	21
38325	Electronic Transport and Corrosion Mechanisms of Graphite-Like Nanocrystalline Carbon Films Used on Metallic Bipolar Plates in Proton-Exchange Membrane Fuel Cells. ACS Applied Materials & Interfaces, 2021, 13, 3825-3835.	4.0	21
38326	Surface free energy of diamond nanocrystals â€“ a molecular dynamics study of its size dependence. Physical Chemistry Chemical Physics, 2021, 23, 11075-11081.	1.3	5
38327	Synthesis, Crystal and Electronic Structure of La 2 SiP 4. Zeitschrift Fur Anorganische Und Allgemeine Chemie, 2021, 647, 91-97.	0.6	8
38328	Micro-/nano-sized multifunctional heterochiral metalâ€“organic frameworks for high-performance visibleâ€“blind UV photodetectors. Journal of Materials Chemistry C, 2021, 9, 7310-7318.	2.7	14
38329	Electronic structure and elastic properties of Cd16Se15Te solid state solution: first principles study. Condensed Matter Physics, 2021, 24, 23702.	0.3	2
38330	Role of substrate strain to tune energy bandsâ€“Seebeck relationship in semiconductor heterostructures. Journal of Applied Physics, 2021, 129, 025301.	1.1	4
38331	In situ coating of a lithiophilic interphase on a biporous Cu scaffold with vertical microchannels for dendrite-free Li metal batteries. Journal of Materials Chemistry A, 2021, 9, 13642-13652.	5.2	9
38332	Electrochemical behavior of a Ni₃N OER precatalyst in Fe-purified alkaline media: the impact of self-oxidation and Fe incorporation. Materials Advances, 2021, 2, 2299-2309.	2.6	28
38333	First-principles study of effect of Mg doping on structural stability and electronic structure of LiCoO₂ cathode material. Wuli Xuebao/Acta Physica Sinica, 2021, 70, 138201-138201.	0.2	1
38334	Effects of AgTi3 intermetallic on suppression of Ag agglomeration: a theoretical study. Molecular Simulation, 2021, 47, 586-593.	0.9	3

#	Article	IF	Citations
38335	3D ordered macroporous copper nitrideâ€“titanium oxynitride as highly efficient electrocatalysts for universal-pH hydrogen evolution reaction. Journal of Materials Chemistry A, 2021, 9, 14392-14399.	5.2	15
38336	Investigating the innate selectivity issues of methane to methanol: consideration of an aqueous environment. Chemical Science, 2021, 12, 4443-4449.	3.7	17
38337	Conducting chiral nickel(ii) bis(dithiolene) complexes: structural and electron transport modulation with the charge and the number of stereogenic centres. Journal of Materials Chemistry C, 2021, 9, 4119-4140.	2.7	10
38338	Structural and optoelectronic behavior of the copper-doped <mml:math xmlns:mml="http://www.w3.org/1998/Math/MathML"><mml:msub><mml:mrow><mml:mi>Cs</mml:mi></mml:mrow><mml:mn>2</mml:mn> double perovskite: A density functional theory investigation. Physical Review B, 2021, 103, .	1.7	11
38339	Electro-catalytic amplified sensor for determination of N-acetylcysteine in the presence of theophylline confirmed by experimental coupled theoretical investigation. Scientific Reports, 2021, 11, 1006.	1.6	4
38340	Enhanced performance of Se-alloyed CdTe solar cells: The role of Se-segregation on the grain boundaries. Journal of Applied Physics, 2021, 129, .	1.1	8
38341	Directional Monte Carlo Lattice Search Algorithm for the Structure Search of Alumina Clusters (Al2O3)n (n=1~50). Acta Chimica Sinica, 2021, 79, 1154.	0.5	1
38342	The origins of charge separation in anisotropic facet photocatalysts investigated through first-principles calculations. RSC Advances, 2021, 11, 18500-18508.	1.7	5
38343	Theoretical prediction by DFT and experimental observation of heterocation-doping effects on hydrogen adsorption and migration over the CeO₂(111) surface. Physical Chemistry Chemical Physics, 2021, 23, 4509-4516.	1.3	7
38344	ZnS/CdX (X = S, Se, Te) core/shell nanowires: an attempt at tuning the electronic bandgaps and SQ efficiencies. Journal of Materials Chemistry C, 2021, 9, 6605-6617.	2.7	4
38345	Electronic and optical properties of halide double-perovskites under strain: a density functional study. Energy Sources, Part A: Recovery, Utilization and Environmental Effects, 0, , 1-13.	1.2	9
38346	First chiral fluorinated lead vanadate selenite Pb₂(V₂O₄F)(VO₂)(SeO₃)₃with five asymmetric motifs and large optical properties. Dalton Transactions, 2021, 50, 7238-7245.	1.6	8
38347	Structural and electronic properties of FeCl₃ and CrO₃ interacting with GaP nanotubes from DFT calculations. New Journal of Chemistry, 2021, 45, 9483-9490.	1.4	1
38348	First principles investigations on the controversy of structural phase transitions in thorium dialuminide under pressure. Physical Chemistry Chemical Physics, 2021, 23, 13977-13983.	1.3	0
38349	Facile syntheses of silver thioantimonates exhibiting second-harmonic generation responses and large birefringence. Dalton Transactions, 2021, 50, 3568-3576.	1.6	7
38350	An interplay of various damage channels in polyethylene exposed to ultra-short XUV/X-ray pulses. Physical Chemistry Chemical Physics, 2021, 23, 16193-16205.	1.3	7
38351	Catalytic decomposition of methane into hydrogen and high-value carbons: combined experimental and DFT computational study. Catalysis Science and Technology, 2021, 11, 4911-4921.	2.1	24
38352	Highly dispersed Pt atoms and clusters on hydroxylated indium tin oxide: a view from first-principles calculations. Journal of Materials Chemistry A, 2021, 9, 15724-15733.	5.2	8

#	Article	IF	Citations
38353	Structural, dynamical, and photochemical properties ofortho-tetrafluoroazobenzene inside a flexible MOF under visible light irradiation. RSC Advances, 2021, 11, 3917-3930.	1.7	20
38354	Effect of doped H, Br, Cu, Kr, Ge, As and Fe on structural features and bandgap of poly C13H8OS-X: a DFT calculation. Designed Monomers and Polymers, 2021, 24, 53-62.	0.7	7
38355	DFT study on some polythiophenes containing benzo[d]thiazole and benzo[d]oxazole: structure and band gap. Designed Monomers and Polymers, 2021, 24, 274-284.	0.7	5
38356	Machine learned features from density of states for accurate adsorption energy prediction. Nature Communications, 2021, 12, 88.	5.8	108
38357	Theoretical assessment of Raman spectra on MXene Ti₂C: from monolayer to bilayer. Physical Chemistry Chemical Physics, 2021, 23, 19884-19891.	1.3	9
38358	A computational investigation of the adsorption of small copper clusters on the CeO₂(110) surface. Physical Chemistry Chemical Physics, 2021, 23, 19329-19342.	1.3	7
38359	Performance limit of monolayer MoSi₂N₄ transistors. Journal of Materials Chemistry C, 2021, 9, 14683-14698.	2.7	32
38360	Experimental and theoretical evidence for oriented aggregate crystal growth of CoO in a polyol. CrystEngComm, 2021, 23, 1756-1764.	1.3	9
38361	Theoretical insights into non-oxidative propane dehydrogenation over Fe3C. Physical Chemistry Chemical Physics, 2021, 23, 1401-1413.	1.3	9
38362	The role of surface oxidation and Feâ€“Ni synergy in Feâ€“Niâ€“S catalysts for CO₂ hydrogenation. Faraday Discussions, 2021, 230, 30-51.	1.6	21
38363	Surface modification of titanium carbide MXene monolayers (Ti₂C and) Tj ETQq0 0 0 rgBT /Overlock 10 Tf 50 347 Td (Ti<su Chemical Physics, 2021, 23, 15319-15328.	1.3	51
38364	Structural, vibrational and electronic properties of D03 FeNi3. Materials Today: Proceedings, 2021, 47, 605-611.	0.9	0
38365	First-principles study of the optical and thermoelectric properties of tetragonal-silicene. Physical Chemistry Chemical Physics, 2021, 23, 11863-11875.	1.3	14
38366	K₂Pb(H₂C₃N₃O₃)₄(H₂O)₄: a potential UV nonlinear optical material with large birefringence. Inorganic Chemistry Frontiers, 2021, 8, 3547-3555.	3.0	27
38367	Novel graphitic carbon nitride g-C₉N₁₀ as a promising platform to design efficient photocatalysts for dinitrogen reduction to ammonia: the first-principles investigation. Journal of Materials Chemistry A, 2021, 9, 20615-20625.	5.2	21
38368	RbPb8O4Cl9: the first alkali metal lead oxyhalide with distorted [PbO3Cl3] and [PbOCl5] mixed-anion groups. Dalton Transactions, 2021, 50, 14038-14043.	1.6	4
38369	Penta-MS₂ (M = Mn, Ni, Cu/Ag and Zn/Cd) monolayers with negative Poisson's ratios and tunable bandgaps as water-splitting photocatalysts. Journal of Materials Chemistry A, 2021, 9, 6993-7004.	5.2	42
38370	NaInX2 (Xâ€‰=â€‰S, Se) layered materials for energy harvesting applications: first-principles insights into optoelectronic and thermoelectric properties. Journal of Materials Science: Materials in Electronics, 2021, 32, 3878-3893.	1.1	9

#	Article	IF	Citations
38371	Different Oxygen Desorption Durabilities of Lithium Titanium Oxides as Confirmed by Transmission Electron Energy-Loss Spectroscopy Analysis of Li₄Ti₅O₁₂ and Î²-Li₂TiO₃ Biphase Specimens. ACS Applied Energy Materials, 2021, 4, 1377-1386.	2.5	6
38372	Boosting magnesium storage in MoS₂ via a 1T phase introduction and interlayer expansion strategy: theoretical prediction and experimental verification. Sustainable Energy and Fuels, 2021, 5, 5471-5480.	2.5	4
38373	Layer- and gate-tunable spin-orbit coupling in a high-mobility few-layer semiconductor. Science Advances, 2021, 7, .	4.7	16
38374	Combining artificial intelligence and physics-based modeling to directly assess atomic site stabilities: from sub-nanometer clusters to extended surfaces. Physical Chemistry Chemical Physics, 2021, 23, 22022-22034.	1.3	13
38375	First-principles calculations on the deposition behavior of Li_xNa_y (x + y â‰¤ 5) clusters during the hybrid storage of Li and Na atoms on graphene. Physical Chemistry Chemical Physics, 2021, 23, 21817-21824.	1.3	2
38376	Defects of monolayer PbI₂: a computational study. Physical Chemistry Chemical Physics, 2021, 23, 20553-20559.	1.3	4
38377	Hierarchical superhydrophilic/superaerophobic CoMnP/Ni₂P nanosheet-based microplate arrays for enhanced overall water splitting. Journal of Materials Chemistry A, 2021, 9, 22129-22139.	5.2	45
38378	Combined electrochemical and DFT investigations of iron selenide: a mechanically bendable solid-state symmetric supercapacitor. Sustainable Energy and Fuels, 2021, 5, 5001-5012.	2.5	34
38379	A new 2D auxetic CN₂ nanostructure with high energy density and mechanical strength. Physical Chemistry Chemical Physics, 2021, 23, 4353-4364.	1.3	8
38380	Monitoring the active sites for the hydrogen evolution reaction at model carbon surfaces. Physical Chemistry Chemical Physics, 2021, 23, 10051-10058.	1.3	21
38381	Boosting electrochemical nitrogen reduction reaction performance of two-dimensional Mo porphyrin monolayers via turning the coordination environment. Physical Chemistry Chemical Physics, 2021, 23, 4178-4186.	1.3	6
38382	Enhanced performance of Mo₂P monolayer as lithium-ion battery anode materials by carbon and nitrogen doping: a first principles study. Physical Chemistry Chemical Physics, 2021, 23, 4030-4038.	1.3	26
38383	Discovery and engineering of low work function perovskite materials. Journal of Materials Chemistry C, 2021, 9, 12778-12790.	2.7	15
38384	First-principles study on the electronic and optical properties of Bi₂WO₆. RSC Advances, 2021, 11, 32330-32338.	1.7	9
38385	Silver Nanowire Network Hybridized with Silver Nanoparticle-Anchored Ruthenium Oxide Nanosheets for Foldable Transparent Conductive Electrodes. ACS Applied Materials & Interfaces, 2021, 13, 11396-11402.	4.0	10
38386	Alkaline-earth metal substitution stabilizes the anionic redox of Li-rich oxides. Journal of Materials Chemistry A, 2021, 9, 10364-10373.	5.2	10
38387	Flexible ferroelasticity in monolayer PdS₂: a DFT study. Physical Chemistry Chemical Physics, 2021, 23, 10551-10559.	1.3	7
38388	Ab initio study of optical properties of the [0001] Ti-surface with a carbon layer coverage and of graphene with an extensive Ti coverage. Journal of Physics: Conference Series, 2021, 1723, 012055.	0.3	0

#	Article	IF	Citations
38389	Interfacial interactions and structures of protic ionic liquids on a graphite surface: A first-principles study and comparison with aprotic ionic liquids. Physical Chemistry Chemical Physics, 2021, 23, 18338-18348.	1.3	8
38390	Ab initio based models for temperature-dependent magnetochemical interplay in bcc Fe-Mn alloys. Physical Review B, 2021, 103, .	1.1	12
38391	Intense Raman D Band without Disorder in Flattened Carbon Nanotubes. ACS Nano, 2021, 15, 596-603.	7.3	44
38392	A multiaxial electrical switching in a one-dimensional organicâ€“inorganic (pyrrolidinium)₂Cd₂I₆ferroelectric and photoluminescent crystal. Journal of Materials Chemistry C, 2021, 9, 7665-7676.	2.7	16
38393	Controlled over-growth for nail-like and urchin-like cobalt with enhanced CO hydrogenation activity. Applied Surface Science, 2021, 537, 147931.	3.1	1
38394	Theoretical study on water adsorption and dissociation on the nickel surfaces. Journal of Molecular Modeling, 2021, 27, 36.	0.8	1
38395	An Integrated Methodology for Screening Hydrogen Evolution Reaction Catalysts: Pt/Mo2C as an Example. Springer Series in Materials Science, 2021, , 719-731.	0.4	0
38396	Study of the Structural, Dynamic and Thermodynamic Properties of the III- Antimonides Semiconductors. Defect and Diffusion Forum, 0, 406, 250-255.	0.4	2
38397	Structural, Elastic and Electronic Properties of Nitride Ti₂CdN Phase in Comparison with the Carbide Ti₂CdC Phase from First-principles Study. Journal of Physics: Conference Series, 2021, 1718, 012019.	0.3	2
38398	Examination of permittivity for depolarization field of ferroelectric by ab initio calculation, suggesting hidden mechanisms. Scientific Reports, 2021, 11, 2155.	1.6	2
38399	Hydrogenation and oxidation enhances the thermoelectric performance of Si₂BN monolayer. New Journal of Chemistry, 2021, 45, 3892-3900.	1.4	8
38400	Structural and electronic properties of layered nanoporous organic nanocrystals. RSC Advances, 2021, 11, 5773-5784.	1.7	4
38401	Strain-controlled electronic and magnetic properties of tVS₂/hVS₂ van der Waals heterostructures. Physical Chemistry Chemical Physics, 2021, 23, 4669-4680.	1.3	5
38402	First principle studies of ammonium chloride under high pressure. RSC Advances, 2021, 11, 5149-5155.	1.7	0
38403	Activated Lone-Pair Electrons Lead to Low Lattice Thermal Conductivity: A Case Study of Boron Arsenide. SSRN Electronic Journal, 0, , .	0.4	0
38404	Curvature-induced bandgap reduction in TiO2 double-walled nanotubes. Journal of Applied Physics, 2021, 129, 024303.	1.1	0
38405	Engineering the ligand states by surface functionalization: a new way to enhance the ferromagnetism of CrI₃. Nanoscale, 2021, 13, 4821-4827.	2.8	3
38406	The electronic and optical properties of SiO2â€“Alâ€“SiO2 withÂdensityÂfunctional theory. Modern Physics Letters B, 2021, 35, 2150136.	1.0	0

#	Article	IF	Citations
38407	Ab initio molecular dynamics of hydrogen on tungsten surfaces. Physical Chemistry Chemical Physics, 2021, 23, 7919-7925.	1.3	1
38408	The effect of the stacking arrangement on the device behavior of bilayer MoS2 FETs. Journal of Computational Electronics, 2021, 20, 161-168.	1.3	6
38409	First-Principle Analysis of Transition Metal Edge-Passivated Armchair Graphene Nanoribbons for Nanoscale Interconnects. IEEE Nanotechnology Magazine, 2021, 20, 92-98.	1.1	16
38410	Impact of Topological Edge Defects on Spin Transport Properties of Zigzag Graphene Nanoribbons. Physica Status Solidi (B): Basic Research, 2021, 258, 2000538.	0.7	2
38411	Vacancy-mediated effects for simultaneously enhancing the Cu/graphene/Al interfacial bonding strength and thermal conductance: a first-principles study. Journal of Materials Science, 2021, 56, 5697-5707.	1.7	8
38412	Thermo physical properties and pressure induced phase transition in thorium and uranium sesquicarbide (Th2C3, U2C3). Journal of Applied Physics, 2021, 129, 015902.	1.1	1
38413	Optimal water concentration for aqueous Li+ intercalation in vanadyl phosphate. Chemical Science, 2021, 12, 4450-4454.	3.7	5
38414	Facile pyrolysis approach of folic acid-derived high graphite N-doped porous carbon materials for the oxygen reduction reaction. New Journal of Chemistry, 2021, 45, 5949-5957.	1.4	5
38415	Mechanistic aspects of ammonia synthesis on Ta₃N₅ surfaces in the presence of intrinsic nitrogen vacancies. Physical Chemistry Chemical Physics, 2021, 23, 6959-6963.	1.3	2
38416	An Ab-initio Study of Structural, Elastic, Electronic, Vibrational and Optical Properties of Semiconductor NaAlSi Compound for Optoelectronic Applications. Advances in Material Research and Technology, 2021, , 125-144.	0.3	0
38417	Electronâ€“phonon interaction in In-induced structures on Si(111) from first-principles. Physical Chemistry Chemical Physics, 2021, 23, 7955-7960.	1.3	3
38418	Surface phase structures responsible for the activity and deactivation of the fcc MoC (111)-Mo surface in steam reforming: a systematic kinetic and thermodynamic investigation. Catalysis Science and Technology, 2021, 11, 823-835.	2.1	2
38419	Hybrid Memory Device (Memory/Selector) with Scalable and Simple Structure for XNORâ€Based Neural Network Applications. Advanced Electronic Materials, 2021, 7, 2000881.	2.6	2
38420	First-Principles study of structural stability and lithium storage property of Si_n clusters (n â‰¤ 6) adsorbed on graphene. Wuli Xuebao/Acta Physica Sinica, 2021, 70, 198101-198101.	0.2	1
38421	Role of Surfaces in the Magnetic and Ozone Gas-Sensing Properties of ZnFe₂O₄ Nanoparticles: Theoretical and Experimental Insights. ACS Applied Materials & Interfaces, 2021, 13, 4605-4617.	4.0	49
38422	Spontaneous electric polarization and electric field gradient in hybrid improper ferroelectrics: insights and correlations. Journal of Materials Chemistry C, 2021, 9, 7005-7013.	2.7	6
38423	Imaging and identification of point defects in PtTe2. Npj 2D Materials and Applications, 2021, 5, .	3.9	29
38424	First-principles calculations for understanding microstructures and mechanical properties of co-sputtered Al alloys. Nanoscale, 2021, 13, 14987-15001.	2.8	11

#	Article	IF	Citations
38425	Metallic 2H-Tantalum Selenide Nanomaterials as Saturable Absorber for Dual-Wavelength Q-Switched Fiber Laser. Sensors, 2021, 21, 239.	2.1	3
38426	On the adsorption mechanism of caffeine on MAPbI₃ perovskite surfaces: a combined UMC-DFT study. Physical Chemistry Chemical Physics, 2021, 23, 10807-10813.	1.3	6
38427	Bandgap evolution in nanographene assemblies. Physical Chemistry Chemical Physics, 2021, 23, 11501-11506.	1.3	1
38428	Selective hydrogenation of acetylene to ethylene on anatase TiO₂ through first-principles studies. Journal of Materials Chemistry A, 2021, 9, 14064-14073.	5.2	23
38429	Quasi-2D lead-free halide perovskite using superalkali cations for red-light-emitting diodes. Nanoscale, 2021, 13, 13152-13157.	2.8	4
38430	First-principles study of formation and performance of diamond (111)/Al interface. Wuli Xuebao/Acta Physica Sinica, 2021, 70, 188101-188101.	0.2	1
38431	Pressure-induced novel nitrogen-rich aluminum nitrides: AlN6, Al2N7 and AlN7 with polymeric nitrogen chains and rings. Physical Chemistry Chemical Physics, 2021, 23, 12350-12359.	1.3	8
38432	Electrochemical epitaxial (200) PbSe submicron-plates on single-layer graphene for an ultrafast infrared response. Journal of Materials Chemistry C, 2021, 9, 6536-6543.	2.7	8
38433	First-principle investigation of hybrid improper ferroelectricity of n = 2 Ruddlesden-Popper Sr₃B₂Se₇ (B = Zr, Hf). Wuli Xuebao/Acta Physica Sinica, 2021, 70, 116302-116302.	0.2	0
38434	First principles study of electrical and magnetic properties of two-dimensional ferromagnetic semiconductors CrI₃ adsorbed by atoms. Wuli Xuebao/Acta Physica Sinica, 2021, 70, 117101.	0.2	2
38435	Synthesis and characterization of GaN/ReS2, ZnS/ReS2 and ZnO/ReS2 core/shell nanowire heterostructures. Applied Surface Science, 2021, 536, 147841.	3.1	13
38436	3D self-supported porous vanadium-doped nickel nitride nanosheet arrays as efficient bifunctional electrocatalysts for urea electrolysis. Journal of Materials Chemistry A, 2021, 9, 4159-4166.	5.2	89
38437	Effects of support and oxygen vacancies on the energetics of NiO reduction with H₂ for the chemical looping combustion (CLC) reaction; a DFT study. Physical Chemistry Chemical Physics, 2021, 23, 12795-12806.	1.3	7
38438	Phase-selective active sites on ordered/disordered titanium dioxide enable exceptional photocatalytic ammonia synthesis. Chemical Science, 2021, 12, 9619-9629.	3.7	25
38439	Electronic and magnetic states of Fe ions in Co2FeBO5. Dalton Transactions, 2021, 50, 9735-9745.	1.6	4
38440	A first-principles study of the stability, electronic structure, and optical properties of halide double perovskite Rb₂Sn_{1â^'x}Te_xI₆ for solar cell applications. Physical Chemistry Chemical Physics, 2021, 23, 4646-4657.	1.3	19
38441	Prediction of low-Z collinear and noncollinear antiferromagnetic compounds having momentum-dependent spin splitting even without spin-orbit coupling. Physical Review Materials, 2021, 5, .	0.9	64
38442	Graphene-based frustrated Lewis pairs as bifunctional catalysts for CO₂ reduction via the dissociative chemisorption of molecular H₂: a periodic density functional perspective. New Journal of Chemistry, 2021, 45, 9959-9966.	1.4	3

#	Article	IF	Citations
38443	Green CsSnX₃ (X = Cl, Br, I)-Derived Quantum Dots for Photovoltaic Applications: First-Principles Investigations. Journal of Physical Chemistry C, 2021, 125, 2592-2606.	1.5	19
38444	Novel structures and mechanical properties of Zr₂N: Ab initio description under high pressures*. Chinese Physics B, 2021, 30, 016403.	0.7	3
38445	Electronic phase-crossover and room temperature ferromagnetism in a two-dimensional (2D) spin lattice. RSC Advances, 2021, 11, 946-952.	1.7	16
38446	Phonons in Short-Period GaN/AlN Superlattices: Group-Theoretical Analysis, Ab initio Calculations, and Raman Spectra. Nanomaterials, 2021, 11, 286.	1.9	14
38447	High magnetoresistance and perfect spin filtering effect in silicane/germanene based magnetic Li_{0.5}CrI₃|Si/Ge|Li_{0.5}CrI₃ tunnel junctions. Journal of Materials Chemistry C, 2021, 9, 13799-13809.	2.7	3
38448	Synthesis, crystal chemistry, and optical properties of two methylammonium silver halides: CH3NH3AgBr2 and CH3NH3Ag2I3. Journal of Materials Chemistry C, 0, , .	2.7	2
38449	Machine learning method for tight-binding Hamiltonian parameterization from ab-initio band structure. Npj Computational Materials, 2021, 7, .	3.5	30
38450	First-principles study of a 2-dimensional C-silicyne monolayer as a promising anode in Na/K ion secondary batteries. Physical Chemistry Chemical Physics, 2021, 23, 11755-11763.	1.3	21
38451	Hafniumâ€“zirconium oxide interface models with a semiconductor and metal for ferroelectric devices. Nanoscale Advances, 2021, 3, 4750-4755.	2.2	3
38452	Insights into the structural variations in SmNb_{1âˆ’x}Ta_xO₄ and HoNb_{1âˆ’x}Ta_xO₄ combined experimental and computational studies. Dalton Transactions, 2021, 50, 9103-9117.	1.6	11
38453	Enrichment of the field emission properties of NiCo₂O₄ nanostructures by UV/ozone treatment. Materials Advances, 2021, 2, 2658-2666.	2.6	8
38454	Lead-free CsSnCl₃ perovskite nanocrystals: rapid synthesis, experimental characterization and DFT simulations. Physical Chemistry Chemical Physics, 2021, 23, 22184-22198.	1.3	35
38455	Computational study of the staircase molecular conductivity of polyoxovanadates adsorbed on Au(111). Dalton Transactions, 2021, 50, 5540-5551.	1.6	7
38456	Theoretical investigation of polymorph- and coformer-dependent photoluminescence in molecular crystals. CrystEngComm, 2021, 23, 4264-4271.	1.3	9
38457	Point defects in two-dimensional BeO monolayer: a first-principles study on electronic and magnetic properties. Physical Chemistry Chemical Physics, 2021, 23, 24301-24312.	1.3	19
38458	Highly efficient bilateral doping of single-walled carbon nanotubes. Journal of Materials Chemistry C, 2021, 9, 4514-4521.	2.7	17
38459	First-principles calculation of diamond/Al interface properties and study of interface reaction. Wuli Xuebao/Acta Physica Sinica, 2021, .	0.2	1
38460	The First Principle Study of <i>β</i>-CuAgSe Subcells. Journal of Applied Mathematics and Physics, 2021, 09, 1549-1559.	0.2	0

#	Article	IF	Citations
38461	Single-atom catalysts based on TiN for the electrocatalytic hydrogen evolution reaction: a theoretical study. Physical Chemistry Chemical Physics, 2021, 23, 15685-15692.	1.3	6
38462	Surface acidity of tin dioxide nanomaterials revealed with ³¹P solid-state NMR spectroscopy and DFT calculations. RSC Advances, 2021, 11, 25004-25009.	1.7	3
38463	Local structure and NO adsorption/desorption property of Pd²⁺ cations at different paired Al sites in CHA zeolite. Physical Chemistry Chemical Physics, 2021, 23, 22273-22282.	1.3	15
38464	A hierarchical Co₃O₄/CoS microbox heterostructure as a highly efficient bifunctional electrocatalyst for rechargeable Znâ€“air batteries. Journal of Materials Chemistry A, 2021, 9, 17344-17352.	5.2	40
38465	Influence of diluent concentration in localized high concentration electrolytes: elucidation of hidden diluent-Li⁺ interactions and Li⁺ transport mechanism. Journal of Materials Chemistry A, 2021, 9, 17459-17473.	5.2	28
38466	Co-crystal AXÂ·(H₃C₃N₃O₃) (A = Na, Rb, Cs; X = Br, I): a series of strongly anisotropic alkali halide cyanurates with a planar structural motif and large birefringence. Dalton Transactions, 2021, 50, 11555-11561.	1.6	7
38467	Lithium nickel borides: evolution of [NiB] layers driven by Li pressure. Inorganic Chemistry Frontiers, 2021, 8, 1675-1685.	3.0	7
38468	Surface Transformations of Lead Oxides and Carbonates Using First-Principles and Thermodynamics Calculations. Inorganic Chemistry, 2021, 60, 1228-1240.	1.9	10
38469	Microscopic mechanisms behind hyperferroelectricity. Physical Review B, 2021, 103, .	1.1	8
38470	Discrete Kernel Functions for fcc Crystals Within Eringenâ€™s Nonlocal Theory of Elasticity. Journal of Elasticity, 2021, 143, 1-30.	0.9	3
38471	Mechanism of electrochemical oxygen reduction reaction at two-dimensional Pt-doped MoSe₂ material: an efficient electrocatalyst. Journal of Materials Chemistry C, 2021, 9, 11331-11342.	2.7	27
38472	Direct evidence for distinct colour origins in ROY polymorphs. Chemical Science, 2021, 12, 12711-12718.	3.7	13
38473	One-way rotation of a chemically anchored single molecule-rotor. Nanoscale, 2021, 13, 16077-16083.	2.8	11
38474	Defect chemistry and doping of BiCuSeO. Journal of Materials Chemistry A, 2021, 9, 20685-20694.	5.2	23
38475	Ru/Mo₂C@NC Schottky junction-loaded hollow nanospheres as an efficient hydrogen evolution electrocatalyst. Journal of Materials Chemistry A, 2021, 9, 20518-20529.	5.2	30
38476	Ethanol steam reforming on Rh: microkinetic analyses on the complex reaction network. Catalysis Science and Technology, 2021, 11, 7009-7017.	2.1	5
38477	Doping of ultra-thin Si films: Combined first-principles calculations and experimental study. Journal of Applied Physics, 2021, 129, .	1.1	4
38478	CH₃NH₃Pb_{1â€“x}Co_xBr_{3â€“2x}Cl_{2x} Perovskite Quantum Dots for Wide-Color Backlighting. ACS Applied Nano Materials, 2021, 4, 717-728.	2.4	17

#	Article	IF	Citations
38479	Two-step MAPbI₃ deposition by low-vacuum proximity-space-effusion for high-efficiency inverted semitransparent perovskite solar cells. Journal of Materials Chemistry A, 2021, 9, 16456-16469.	5.2	25
38480	Real-space density functional theory adapted to cyclic and helical symmetry: Application to torsional deformation of carbon nanotubes. Physical Review B, 2021, 103, .	1.1	22
38481	Factors controlling oxophilicity and carbophilicity of transition metals and main group metals. Journal of Materials Chemistry A, 2021, 9, 22325-22333.	5.2	16
38482	Crystal growth and properties characterization of Nd³⁺:Na₅Lu(MoO₄)₄ for continuous multi-wavelength NIR laser emission. CrystEngComm, 2021, 23, 7289-7297.	1.3	2
38483	Identifying Heteroatomic and Defective Sites in Carbon with Dual-Ion Adsorption Capability for High Energy and Power Zinc Ion Capacitor. Nano-Micro Letters, 2021, 13, 59.	14.4	78
38484	Ruthenium-based half Heusler alloys RuTiX (X = Si, Ge, Sn): An FP-LAPW-based analytical study of structural, electronic, elastic, mechanical and transport properties. International Journal of Modern Physics B, 2021, 35, 2150046.	1.0	2
38485	Cancer Cell Detection on the Surface of Top-Gated Monolayer Graphene via Raman Spectroscopy. ACS Applied Bio Materials, 2021, 4, 1493-1498.	2.3	4
38486	Charge-Transfer Resonance and Electromagnetic Enhancement Synergistically Enabling MXenes with Excellent SERS Sensitivity for SARS-CoV-2 S Protein Detection. Nano-Micro Letters, 2021, 13, 52.	14.4	137
38487	Imidazole-graphyne: a new 2D carbon nitride with a direct bandgap and strong IR refraction. Physical Chemistry Chemical Physics, 2021, 23, 10274-10280.	1.3	4
38488	Molecular mechanisms of methane dry reforming on Co₃Mo₃N catalyst with dual sites. Catalysis Science and Technology, 2021, 11, 3724-3736.	2.1	11
38489	Oxidation and Degradation of WS₂ Monolayers Grown by NaCl-Assisted Chemical Vapor Deposition: Mechanism and Prevention. Nanoscale, 2021, 13, 16629-16640.	2.8	7
38490	Design of non-transition-metal-doped nanoribbon catalysis to achieve efficient nitrogen fixation. Materials Advances, 2021, 2, 7423-7430.	2.6	2
38491	Stepped M@Pt(211) (M = Co, Fe, Mo) single-atom alloys promote the deoxygenation of lignin-derived phenolics: mechanism, kinetics, and descriptors. Catalysis Science and Technology, 2021, 11, 7047-7059.	2.1	13
38492	Tuning electrochemically driven surface transformation in atomically flat LaNiO3 thin films for enhanced water electrolysis. Nature Materials, 2021, 20, 674-682.	13.3	105
38493	First-Principles Investigation of Pd-Doped Armchair Graphene Nanoribbons as a Potential Rectifier. Journal of Electronic Materials, 2021, 50, 1196-1206.	1.0	27
38494	Fast operando spectroscopy tracking in situ generation of rich defects in silver nanocrystals for highly selective electrochemical CO2 reduction. Nature Communications, 2021, 12, 660.	5.8	68
38495	Local Kondo scattering in 4d-electron RuO_x nanoclusters on atomically-resolved ultrathin SrRuO₃ films. Physical Chemistry Chemical Physics, 2021, 23, 22526-22531.	1.3	0
38496	Quantum and classical effects in DNA point mutations: Watsonâ€“Crick tautomerism in AT and GC base pairs. Physical Chemistry Chemical Physics, 2021, 23, 4141-4150.	1.3	35

#	Article	IF	Citations
38497	A theoretical study on the electronic, structural and optical properties of armchair, zigzag and chiral siliconâ€“germanium nanotubes. Physical Chemistry Chemical Physics, 2021, 23, 13075-13086.	1.3	2
38498	The uptake mechanism of palladium ions into Prussian-blue nanoparticles in a nitric acid solution toward application for the recycling of precious metals from electronic and nuclear wastes. RSC Advances, 2021, 11, 20701-20707.	1.7	4
38499	Preparing high purity Î»-Ti₃O₅ and Li/Î»-Ti₃O₅ as high-performance electromagnetic wave absorbers. Journal of Materials Chemistry C, 0, , .	2.7	6
38500	Electronic and optical properties of two-dimensional heterostructures and heterojunctions between doped-graphene and C- and N-containing materials. Physical Chemistry Chemical Physics, 2021, 23, 4865-4873.	1.3	21
38501	Theoretical evidence of the spinâ€“valley coupling and valley polarization in two-dimensional MoSi₂X₄ (X = N, P, and As). Physical Chemistry Chemical Physics, 2021, 23, 3144-3151.	1.3	53
38502	Spatial-confinement induced electroreduction of CO and CO₂ to diols on densely-arrayed Cu nanopyramids. Chemical Science, 2021, 12, 8079-8087.	3.7	22
38503	Hard and superconducting cubic boron phase via swarm-intelligence structural prediction driven by a machine-learning potential. Physical Review B, 2021, 103, .	1.1	16
38504	The exceptionally high thermal conductivity after â€˜alloyingâ€™ two-dimensional gallium nitride (GaN) and aluminum nitride (AlN). Nanotechnology, 2021, 32, 135401.	1.3	22
38505	A synergetic effect between a single Cu site and S vacancy on an MoS₂ basal plane for methanol synthesis from syngas. Catalysis Science and Technology, 2021, 11, 3261-3269.	2.1	7
38506	Relating X-ray photoelectron spectroscopy data to chemical bonding in MXenes. Nanoscale Advances, 2021, 3, 2793-2801.	2.2	11
38507	Thermoelectric transport properties of two-dimensional materials <i>X</i>Te₂ (<i>X</i> = Pd, Pt) via first-principles calculations. Wuli Xuebao/Acta Physica Sinica, 2021, 70, 116301.	0.2	2
38508	Effect of electronâ€“phonon coupling on the transport properties of monolayers of ZrS2, BiI3 and PbI2: a thermoelectric perspective. Physical Chemistry Chemical Physics, 2021, 23, 11663-11671.	1.3	6
38509	Surface and morphological studies of LiNbO₃: p-type semiconductivity on stoichiometric surfaces. New Journal of Chemistry, 2021, 45, 16594-16605.	1.4	6
38510	Bimetallic RuNi nanoparticles as catalysts for upgrading biomass: metal dilution and solvent effects on selectivity shifts. Green Chemistry, 2021, 23, 8480-8500.	4.6	9
38511	Elastic, mechanical, anisotropic, optical and magnetic properties of V₂NiSb Heusler alloy. Physica Scripta, 2021, 96, 035807.	1.2	9
38512	Solar-driven electrochemical synthesis of ammonia using nitrate with 11% solar-to-fuel efficiency at ambient conditions. Energy and Environmental Science, 2021, 14, 6349-6359.	15.6	70
38513	Zn(H2C3N3O3)2Â·3H2O: the first single-d10 transition metal based ultraviolet hydroisocyanurate crystal with large birefringence. Dalton Transactions, 2021, 50, 5617-5623.	1.6	6
38514	Pseudoelastic Deformation in Refractory (MoW) ₈₅ Zr _{7.5}(TaTi) _{7.5} High-Entropy Alloy. SSRN Electronic Journal, 0, , .	0.4	0

#	Article	IF	Citations
38515	Operando Leaching of Pre-Incorporated Al and Mechanism in Transition Metal Hybrids for Elaborately Enhanced Charge Storage. SSRN Electronic Journal, 0, , .	0.4	0
38516	Synthesis of sub-nanometric Cu₂O catalysts for Pd-free Câ€“C coupling reactions. Reaction Chemistry and Engineering, 2021, 6, 929-936.	1.9	3
38517	Effects of spinâ€“phonon coupling on two-dimensional ferromagnetic semiconductors: a case study of iron and ruthenium trihalides. Nanoscale, 2021, 13, 7714-7722.	2.8	13
38518	Effects of A-site composition of perovskite (Sr1â^'xBaxZrO3) oxides on H atom adsorption, migration, and reaction. RSC Advances, 2021, 11, 7621-7626.	1.7	2
38519	Influence of calcium and zirconium as codopant on electronic and optical properties of BaTiO3 using first principle calculation. AIP Conference Proceedings, 2021, , .	0.3	2
38520	Ultrasonic assisted exfoliation for efficient production of RuO2 monolayer nanosheets. Inorganic Chemistry Frontiers, 0, , .	3.0	5
38521	Mapping surface morphology and phase evolution of iron sulfide nanoparticles. CrystEngComm, 2021, 23, 5645-5654.	1.3	4
38522	Theoretical assessments on the interaction between amino acids and the g-Mg₃N₂monolayer: dispersion corrected DFT and DFT-MD simulations. Physical Chemistry Chemical Physics, 2021, 23, 17440-17452.	1.3	43
38523	Na₂GaS₂Cl: a new sodium-rich chalcohalide with two-dimensional [GaS₂]_{â^ž} layers and wide interlayer space. Dalton Transactions, 2021, 50, 11167-11172.	1.6	12
38524	Unoccupied 3d orbitals make Li-unalloyable transition metals usable as anode materials for lithium ion batteries. Journal of Materials Chemistry A, 2021, 9, 17353-17365.	5.2	4
38525	Surface characterization and methane activation on SnO_x/Cu₂O/Cu(111) inverse oxide/metal catalysts. Physical Chemistry Chemical Physics, 2021, 23, 17186-17196.	1.3	10
38526	Theoretical inspection of the spin-crossover [Fe(tzpy)2(NCS)2] complex on Au(100) surface. Journal of Chemical Physics, 2021, 154, 034701.	1.2	6
38527	Fluorinated porous silicon as sensor material for environmentally toxic gases: a first-principles study. Materials Advances, 2021, 2, 1072-1082.	2.6	2
38528	Microscopic theory of cavity-confined monolayer semiconductors: Polariton-induced valley relaxation and the prospect of enhancing and controlling valley pseudospin by chiral strong coupling. Physical Review B, 2021, 103, .	1.1	7
38529	Band structure regulation in Fe-doped MgZnO by initial magnetic moments. RSC Advances, 2021, 11, 3209-3215.	1.7	2
38530	Tailoring the magnetic ordering of the Cr₄O₅/Fe(001) surface via a controlled adsorption of C₆₀ organic molecules. Physical Chemistry Chemical Physics, 2021, 23, 7948-7954.	1.3	1
38531	Adsorption of HOOO. radical on pristine and doped grapheneâ€”a first-principles study. Structural Chemistry, 2021, 32, 1171-1179.	1.0	3
38532	Shifting the scaling relations of single-atom catalysts for facile methane activation by tuning the coordination number. Chemical Science, 2021, 12, 3551-3557.	3.7	14

#	Article	IF	Citations
38533	Anomalous electronic properties in layered, disordered ZnVSb. Physical Review Materials, 2021, 5, .	0.9	2
38534	Effect of metal and non metal doping of TiO2 on photocatalytic activities: ab initio calculations. Optical and Quantum Electronics, 2021, 53, 1.	1.5	7
38535	Reactions of ruthenium cyclopentadienyl precursor in the metal precursor pulse of Ru atomic layer deposition. Journal of Materials Chemistry C, 2021, 9, 2919-2932.	2.7	5
38536	Computational simulation of al-based alloy surface structure dislocation: the first-principles calculation and atomic pair-potential lattice dynamics calculation. Modern Physics Letters B, 2021, 35, 2150143.	1.0	2
38537	Facet stability of GaN during tri-halide vapor phase epitaxy: an ab initio-based approach. CrystEngComm, 2021, 23, 1423-1428.	1.3	0
38538	Mo single atoms in the Cu(111) surface as improved catalytic active centers for deoxygenation reactions. Catalysis Science and Technology, 2021, 11, 4969-4978.	2.1	2
38539	New atomic-scale insights into the I/Ni(100) system: phase transitions and growth of an atomically thin NiI₂ film. Physical Chemistry Chemical Physics, 2021, 23, 1896-1913.	1.3	2
38540	DFT study of carbaryl pesticide adsorption on vacancy and nitrogen-doped graphene decorated with platinum clusters. Structural Chemistry, 2021, 32, 1541-1551.	1.0	5
38541	Single-side functionalized graphene as promising cathode catalysts in nonaqueous lithiumâ€“oxygen batteries. Nanoscale, 2021, 13, 12727-12737.	2.8	4
38542	Sublattice mixing in Cs2AgInCl6 for enhanced optical properties from first-principles. Applied Physics Letters, 2021, 118, .	1.5	9
38543	Unravelling high volumetric capacity of Co₃O₄ nanograin-interconnected secondary particles for lithium-ion battery anodes. Journal of Materials Chemistry A, 2021, 9, 6242-6251.	5.2	18
38544	Quaternary Heusler compound LiYNiSn: A search of new thermoelectric material by DFT study. AIP Conference Proceedings, 2021, , .	0.3	5
38545	Graphene-Based Dual-Metal Sites for Oxygen Reduction Reaction: A Theoretical Study. Journal of Physical Chemistry C, 2021, 125, 2334-2344.	1.5	32
38546	A solid electrolyte interphase to protect the sulfurized polyacrylonitrile (SPAN) composite for Liâ€“S batteries: computational approach addressing the electrolyte/SPAN interfacial reactivity. Journal of Materials Chemistry A, 2021, 9, 7888-7902.	5.2	9
38547	Interaction of First Row Transition Metals with M₂C (M = Ti, Zr, Hf, V, Nb, Ta, Cr, Mo, and) Tj ETQq0 0 0 rgBT /Overlock 10 T	1.5	38
38548	Electronic structures and defect properties of lithium-rich manganese-based ternary material Li1.21Ni0.33Co0.04Mn0.42O2. Wuli Xuebao/Acta Physica Sinica, 2021, .	0.2	0
38549	Robust half-metallicity in CoZrMnZ (Zâ€‰=â€‰P, As and Sb) quaternary Heusler alloys. Philosophical Magazine, 2021, 101, 892-904.	0.7	4
38550	Reversed selectivity of photocatalytic CO₂ reduction over metallic Pt and Pt(<scp>ii</scp>) oxide cocatalysts. Physical Chemistry Chemical Physics, 2021, 23, 9407-9417.	1.3	8

#	Article	IF	Citations
38551	A GGA + U investigation into the effects of cations on the electromagnetic properties of transition metal spinels. RSC Advances, 2021, 11, 21851-21856.	1.7	8
38552	Diffusivity and band offset analysis of a graphene interlayer at the back contact of a copper zinc tin sulphide solar cell. Physical Chemistry Chemical Physics, 2021, 23, 3511-3518.	1.3	1
38553	Properties of lithium phosphorus oxynitride (LiPON) solid electrolyte - Li anode interfaces. Wuli Xuebao/Acta Physica Sinica, 2021, 70, 136801-136801.	0.2	1
38554	Significant Enhancement of Piezoelectric Response in AlN by Yb Addition. Materials, 2021, 14, 309.	1.3	13
38555	Pb_{2.28}Ba_{1.72}B₁₀O₁₉ featuring a three-dimensional Bâ€“O anionic network with edge-sharing [BO₄] obtained under ambient pressure. Inorganic Chemistry Frontiers, 2021, 8, 3716-3722.	3.0	4
38556	Tailoring the cationic and anionic sites of LaFeO₃-based perovskite generates multiple vacancies for efficient water oxidation. Journal of Materials Chemistry A, 2021, 9, 16906-16916.	5.2	29
38557	Fluorinated graphene nanoribbons from unzipped single-walled carbon nanotubes for ultrahigh energy density lithium-fluorinated carbon batteries. Science China Materials, 2021, 64, 1367-1377.	3.5	38
38558	First-principles-based kinetic Monte Carlo simulations of CO oxidation on catalytic Au(110) and Ag(110) surfaces. Physical Chemistry Chemical Physics, 2021, 23, 14037-14050.	1.3	7
38559	Lead-free perovskite compounds CsSn_{1â^'x}Ge_xI_{3â^'y}Br_y explored for superior visible-light absorption. Physical Chemistry Chemical Physics, 2021, 23, 14449-14456.	1.3	10
38560	Properties of diamane anchored with different groups. Physical Chemistry Chemical Physics, 2021, 23, 14195-14204.	1.3	8
38561	Hypercoordinate two-dimensional transition-metal borides for spintronics and catalyst applications. Journal of Materials Chemistry C, 0, , .	2.7	18
38562	First-principles study of a topological phase transition induced by image potential states in MXenes. Physical Review B, 2021, 103, .	1.1	6
38563	Evidence for a spin acoustic surface plasmon from inelastic atom scattering. Scientific Reports, 2021, 11, 1506.	1.6	7
38564	A first-principles study of the relationship between modulus and ideal strength of single-layer, transition metal dichalcogenides. Materials Advances, 2021, 2, 6631-6640.	2.6	17
38565	Designing new ferromagnetic double perovskites: the coexistence of polar distortion and half-metallicity. Physical Chemistry Chemical Physics, 2021, 23, 19571-19578.	1.3	2
38566	Alkaline earth atom doping-induced changes in the electronic and magnetic properties of graphene: a density functional theory study. RSC Advances, 2021, 11, 6268-6283.	1.7	10
38567	Hydrogen induced interface engineering in Fe₂O₃â€“TiO₂ heterostructures for efficient charge separation for solar-driven water oxidation in photoelectrochemical cells. RSC Advances, 2021, 11, 4297-4307.	1.7	16
38568	Tunable band gaps and high carrier mobilities in stanene by small organic molecule adsorption under external electric fields. Physical Chemistry Chemical Physics, 2021, 23, 16023-16032.	1.3	5

#	Article	IF	Citations
38569	Electrically tunable band gap in strained h-BN/silicene van der Waals heterostructures. Physical Chemistry Chemical Physics, 2021, 23, 17033-17040.	1.3	4
38570	First-Principles Calculations of Exciton Radiative Lifetimes in Monolayer Graphitic Carbon Nitride Nanosheets: Implications for Photocatalysis. ACS Applied Nano Materials, 2021, 4, 1985-1993.	2.4	20
38571	MGa₂B₂O₇:Bi³⁺,Al³⁺ (M = Sr, Ba) blue phosphors with a quantum yield of 99% and negative thermal quenching. Inorganic Chemistry Frontiers, 2021, 8, 4257-4266.	3.0	7
38572	Energy storage mechanisms in vacancy-ordered Wadsleyâ€“Roth layered niobates. Journal of Materials Chemistry A, 2021, 9, 20006-20023.	5.2	12
38573	Hydrogen Induced Dislocation Core Reconstruction in Bcc Metals. SSRN Electronic Journal, 0, , .	0.4	0
38574	Exploring CO₂@sI Clathrate Hydrates as CO₂ Storage Agents by Computational Density Functional Approaches. ChemPhysChem, 2021, 22, 359-369.	1.0	11
38575	BaZnBe₂(BO₃)₂F₂: a novel zinc-beryllium borate with SBBO-type structure overcoming the polymorphism problem. Dalton Transactions, 2021, 50, 2138-2142.	1.6	8
38576	Possibilities and Limits of Decreasing the Gap of Anatase TiO₂ by Alloying with Nitrogen. Journal of Physical Chemistry C, 2021, 125, 3192-3197.	1.5	3
38577	Electronic band structure of cubic solid-state CdTe_{1ï¿½x}Se_x solutions. Ukrainian Journal of Physical Optics, 2021, 22, 101-109.	9.7	5
38578	Mechanical Properties of Atomically Thin Tungsten Dichalcogenides: WS₂, WSe₂, and WTe₂. ACS Nano, 2021, 15, 2600-2610.	7.3	65
38579	Promises of Main-Group Metal Chalcogenide-Based Broken-Gap van der Waals Heterojunctions for Tunneling Field Effect Transistors. ACS Applied Electronic Materials, 2021, 3, 898-904.	2.0	9
38580	Doping-Induced Charge Localization Suppresses Electronâ€“Hole Recombination in Copper Zinc Tin Sulfide: Quantum Dynamics Combined with Deep Neural Networks Analysis. Journal of Physical Chemistry Letters, 2021, 12, 835-842.	2.1	15
38581	Synthesis of CaSnN₂ via a High-Pressure Metathesis Reaction and the Properties of II-Sn-N₂ (II = Ca, Mg, Zn) Semiconductors. Inorganic Chemistry, 2021, 60, 1773-1779.	1.9	18
38582	Structural Origin of the Optical Properties of Ag-Doped Fluorophosphate and Sulfophosphate Glasses. Journal of Physical Chemistry B, 2021, 125, 637-656.	1.2	5
38583	Computational design of a polymorph for 2D IIIâ€“V orthorhombic monolayers by first principles calculations: excellent anisotropic, electronic and optical properties. Physical Chemistry Chemical Physics, 2021, 23, 3771-3778.	1.3	20
38584	Crystal structures and superconductivity of lithium and fluorine implanted gold hydrides under high pressures. Physical Chemistry Chemical Physics, 2021, 23, 21544-21553.	1.3	3
38585	Synthesis, characterization and theoretical investigation of a new chalcohalide, Ba₄GaS₄F₃. Dalton Transactions, 2021, 50, 6315-6320.	1.6	9
38586	Synthesis and first-principles study of structural, electronic and optical properties of tetragonal hybrid halobismuthathes [Py₂(XK)]₂[Bi₂Br_{10â^'x}I_x]. New Journal of Chemistry, 2021, 45, 18349-18357.	1.4	4

#	Article	IF	Citations
38587	Copper confined in vesicle-like BCN cavities promotes electrochemical reduction of nitrate to ammonia in water. Journal of Materials Chemistry A, 2021, 9, 23675-23686.	5.2	42
38588	Absence of phonon gap driven ultralow lattice thermal conductivity in half-Heusler LuNiBi. Journal of Materials Chemistry C, 2021, 9, 12420-12425.	2.7	8
38589	Spot the difference: hydrogen adsorption and dissociation on unsupported platinum and platinum-coated transition metal carbides. Physical Chemistry Chemical Physics, 2021, 23, 20255-20267.	1.3	10
38590	Linking Solid-State Reduction Mechanisms to Size-Dependent Reactivity of Metal Oxide Oxygen Carriers for Chemical Looping Combustion. ACS Applied Energy Materials, 2021, 4, 1163-1172.	2.5	14
38591	Newly synthesized MAX phase Zr₂SeC: DFT insights into physical properties towards possible applications. RSC Advances, 2021, 11, 16892-16905.	1.7	25
38592	Pressure-induced boron clathrates with ambient-pressure superconductivity. Journal of Materials Chemistry C, 2021, 9, 13782-13788.	2.7	12
38593	Tuning Ionic and Electronic Conductivities in the â€œHollowâ€•Perovskite {en}MAPbI₃. Chemistry of Materials, 2021, 33, 719-726.	3.2	24
38594	Co-embedded sulfur vacant MoS₂ monolayer as a promising catalyst for formaldehyde oxidation: a theoretical evaluation. New Journal of Chemistry, 2021, 45, 17407-17417.	1.4	2
38595	Tuning the band gap of M-doped titanate nanotubes (M = Fe, Co, Ni, and Cu): an experimental and theoretical study. Nanoscale Advances, 2021, 3, 1382-1391.	2.2	36
38596	Critical behavior of the ferromagnets <mml:math xmlns:mml="http://www.w3.org/1998/Math/MathML"><mml:msub><mml:mi mathvariant="normal">CrI</mml:mi><mml:mn>3</mml:mn></mml:msub><mml:mo>,</mml:mo><mml:mo>Â</mml:mo><mml:msub><mml:mi mathvariant="normal">CrBr</mml:mi><mml:mn>3</mml:mn></mml:msub></mml:math> , and <mml:math xmlns:mml="http://www.w3.org/1998/Math/MathML"><mml:msub><mml:mi mathvariant="normal">CrGeTe</mml:mi><mml:mn>3</mml:mn></mml:msub></mml:math> and the antife	1.1	36
38597	Ge 4s² lone pairs and band alignments in GeS and GeSe for photovoltaics. Journal of Materials Chemistry A, 2021, 9, 22440-22452.	5.2	15
38598	Adsorption of a single Pt atom on graphene: spin crossing between physisorbed triplet and chemisorbed singlet states. Physical Chemistry Chemical Physics, 2021, 23, 22147-22154.	1.3	3
38599	On the electronic properties and performance of new nano thick solar material based on GeSe/SnS hetro-bilayer. Optical and Quantum Electronics, 2021, 53, 1.	1.5	10
38600	Three-dimensional metallic carbon allotropes with superhardness. Nanotechnology Reviews, 2021, 10, 1266-1276.	2.6	24
38601	Interfacial Oxide Formation Limits the Photovoltage of Î±â€SnWO₄/NiO_x Photoanodes Prepared by Pulsed Laser Deposition. Advanced Energy Materials, 2021, 11, 2003183.	10.2	23
38602	A rechargeable zinc-air battery based on zinc peroxide chemistry. Science, 2021, 371, 46-51.	6.0	551
38603	Theoretical insights into the diffusion mechanism of alkali ions in Ruddlesdenâ€“Popper antiperovskites. New Journal of Chemistry, 2021, 45, 4219-4226.	1.4	8
38604	Propane Dehydrogenation on Ga₂O₃-Based Catalysts: Contrasting Performance with Coordination Environment and Acidity of Surface Sites. ACS Catalysis, 2021, 11, 907-924.	5.5	55

#	Article	IF	Citations
38605	Controlling the aqueous growth of urea crystals with different growth inhibitors: a molecular-scale study. RSC Advances, 2021, 11, 12938-12950.	1.7	6
38606	Unveiling the role of carbon oxidation in irreversible degradation of atomically-dispersed FeN₄ moieties for proton exchange membrane fuel cells. Journal of Materials Chemistry A, 2021, 9, 8721-8729.	5.2	11
38607	The effects of substitutional doping on Cu vacancy formation in Cu₂O(111): a density functional theory study. Physical Chemistry Chemical Physics, 2021, 23, 8800-8808.	1.3	5
38608	Amorphous Si_{1â^'y}C_y composite anode materials: ab initio molecular dynamics for behaviors of Li and Na in the framework. Physical Chemistry Chemical Physics, 2021, 23, 5571-5577.	1.3	0
38609	PdRuIr ternary alloy as an effective NO reduction catalyst: insights from first-principles calculation. Physical Chemistry Chemical Physics, 2021, 23, 7153-7163.	1.3	2
38610	Strain-driven phase transition and spin polarization of Re-doped transition-metal dichalcogenides. Physical Chemistry Chemical Physics, 2021, 23, 9962-9970.	1.3	1
38611	Defect structures of sodium and chloride co-substituted hydroxyapatite and its osseointegration capacity. Journal of Materials Science, 2021, 56, 5493-5508.	1.7	4
38612	Elucidating the electronic structures of Î²-Ag₂MoO₄ and Ag₂O nanocrystals via theoretical and experimental approaches towards electrochemical water splitting and CO₂ reduction. Physical Chemistry Chemical Physics, 2021, 23, 9539-9552.	1.3	17
38613	First-principles calculations to investigate the effects of strain, electric field, and atom impurity on the electronic and magnetic properties of RuX₂ (X = S, Se) nanosheets. Physical Chemistry Chemical Physics, 2021, 23, 16316-16323.	1.3	7
38614	First-principles study of electronic structure and optical properties of monolayer defective tellurene. Wuli Xuebao/Acta Physica Sinica, 2021, 70, 166301.	0.2	2
38615	Electrical conductivity of germanium selenide nanosheets in oxygen and butane. Wuli Xuebao/Acta Physica Sinica, 2021, 70, 178502.	0.2	0
38616	Correlation between surface chemistry and magnetism in iron nanoparticles. Nanoscale Advances, 2021, 3, 4471-4481.	2.2	3
38617	Effect of Impurities on the Initiation of the Methanol-to-Olefins Process: Kinetic Modeling Based on Ab Initio Rate Constants. Catalysis Letters, 2021, 151, 2595-2602.	1.4	4
38618	Computational study of X-doped hexagonal boron nitride (h-BN): structural and electronic properties (X = P, S, O, F, Cl). Journal of Molecular Modeling, 2021, 27, 31.	0.8	10
38619	Pressure-Driven Metallization in Hafnium Diselenide. Inorganic Chemistry, 2021, 60, 1746-1754.	1.9	8
38620	Crown ethers in hydrogenated graphene. Physical Chemistry Chemical Physics, 2021, 23, 18983-18989.	1.3	11
38621	A first-principles study of the atomic layer deposition of ZnO on carboxyl functionalized carbon nanotubes: the role of water molecules. Physical Chemistry Chemical Physics, 2021, 23, 3467-3478.	1.3	5
38622	Catalytic activity of PtCu intermetallic compound for CO oxidation: A theoretical insight. Catalysis Today, 2022, 383, 339-344.	2.2	2

#	Article	IF	Citations
38623	Effect of surface steps on chemical ordering in the subsurface of Cu(Au) solid solutions. Physical Review B, 2021, 103, .	1.1	5
38624	Stable deep blue emission with unity quantum yield in organicâ€“inorganic halide perovskite 2D nanosheets doped with cerium and terbium at high concentrations. Journal of Materials Chemistry C, 2021, 9, 2437-2454.	2.7	15
38625	First-Principles Study of the Electronic Properties and Thermal Expansivity of a Hybrid 2D Carbon and Boron Nitride Material. Journal of Carbon Research, 2021, 7, 5.	1.4	1
38626	Tuning electronic properties of bilayer Î±2-graphyne by external electric field: a density functional theory study. Monatshefte FÃ¼r Chemie, 2021, 152, 61-66.	0.9	1
38627	Theoretical investigation of tetrahedral distortion of four-coordinate iron(<scp>ii</scp>) centres in FePd(CN)₄. Dalton Transactions, 2021, 50, 1990-1994.	1.6	2
38628	Defects and dopants in zinc-blende aluminum arsenide: a first-principles study. New Journal of Physics, 2021, 23, 013018.	1.2	1
38629	Insight into the chargingâ€“discharging of magnetite electrodes: in situ XAS and DFT study. Physical Chemistry Chemical Physics, 2021, 23, 6051-6061.	1.3	5
38630	Elucidation of the mechanism and structureâ€“reactivity relationship in zeolite catalyzed alkylation of benzene with propylene. Catalysis Science and Technology, 2021, 11, 2792-2804.	2.1	9
38631	3D/2D Bi₂S₃/SnS₂ heterostructures: superior charge separation and enhanced solar light-driven photocatalytic performance. CrystEngComm, 2021, 23, 2276-2288.	1.3	7
38632	Ferroic dislocations in paraelectric <mml:math xmlns:mml="http://www.w3.org/1998/Math/MathML"><mml:mi>Sr</mml:mi><mml:mi>Ti</mml:mi><mml:msub><mml:mrow><mml:mi mathvariant="normal">O</mml:mi></mml:mrow><mml:mn>3</mml:mn></mml:msub></mml:math>. Physical Review B, 2021, 103, .	1.1	4
38633	On the Reaction Mechanism of Direct H₂O₂ Formation over Pd Catalysts. ACS Catalysis, 2021, 11, 2735-2745.	5.5	50
38634	A Theoretical Investigation on the Physical Properties of SrPd2Sb2 Superconductor. Journal of Superconductivity and Novel Magnetism, 2021, 34, 1133-1139.	0.8	16
38635	Theoretical study of the oxygen adsorption energy for the supported Pt cluster, focused on the electronic metal-support interaction. Surface Science, 2021, 704, 121747.	0.8	3
38636	Interplay of electric field and disorder in Dirac liquid silicene. European Physical Journal B, 2021, 94, 1.	0.6	1
38637	Exciton effect on shift current in single-walled boron-nitride nanotubes. Physical Review B, 2021, 103, .	1.1	4
38638	Elucidating the Influence of Electric Fields toward CO2 Activation on YSZ (111). Catalysts, 2021, 11, 271.	1.6	5
38639	Theoretical investigations on HgTe chalcogenide materials under high pressure. Physica Scripta, 2021, 96, 045703.	1.2	3
38640	Ab initio atomistic description of temperature-induced phase changes: The cases of zirconia and Ti-Y-co-doped zirconia. Physical Review Materials, 2021, 5, .	0.9	2

#	Article	IF	Citations
38641	Transition-metal adatoms on 2D-GaAs: a route to chiral magnetic 2D materials by design. Journal of Physics Condensed Matter, 2021, 33, 145803.	0.7	0
38643	Compositional ordering in relaxor ferroelectric Pb(BBâ€²)O3 : Nearest neighbor approach. Physical Review B, 2021, 103, .	1.1	4
38644	Dielectric and vibrational properties of CdTe studied by first-principles and terahertz time-domain spectroscopy. Physica B: Condensed Matter, 2021, 602, 412543.	1.3	3
38645	The electronic properties and structural stability of LaFeO3 oxide by niobium doping: A density functional theory study. International Journal of Hydrogen Energy, 2021, 46, 9193-9198.	3.8	10
38646	Thermodynamic stability and electronic structure of pristine wurtzite <mml:math xmlns:mml="http://www.w3.org/1998/Math/MathML"><mml:mrow><mml:mi>ZnO</mml:mi><mml:mo>{</mml:mo><mml:mn>0001</mml:mn></mml:mrow></mml:math> inversion domain boundaries. Physical Review Materials, 2021, 5, .	0.9	2
38647	Stability and elastic anisotropy of diamond related C8-yBy materials. International Journal of Physical Sciences, 2021, 16, 16-28.	0.1	0
38648	Electrical conductivity of warm dense silica from double-shock experiments. Nature Communications, 2021, 12, 840.	5.8	9
38649	First-principles calculations of the electronic and optical properties of $$ext {WSe}_2/ext {Cd}_{0.9}ext {Zn}_{0.1}ext {Te}$$ van der Waals heterostructure. Journal of Computational Electronics, 2021, 20, 13-20.	1.3	2
38650	Direct insight into the structure-property relation of interfaces from constrained crystal structure prediction. Nature Communications, 2021, 12, 811.	5.8	10
38651	Heterostructures of MXenes and CoNx-Graphene as highly active electrocatalysts for hydrogen evolution reaction in alkaline media. Journal of Applied Electrochemistry, 2021, 51, 871-878.	1.5	6
38652	Oxidation and Storage Mechanisms for Nitrogen Oxides on Variously Terminated (001) Surfaces of SrFeO_{3â^Î´} and Sr₃Fe₂O_{7â^Î´} Perovskites. ACS Applied Materials & Interfaces, 2021, 13, 7216-7226.	4.0	14
38653	Crystal Orientation-Dependent Oxidation of Epitaxial TiN Films with Tunable Plasmonics. ACS Photonics, 2021, 8, 847-856.	3.2	23
38654	2DEG and 2DHG in NaTaO₃ polar thin films: thickness and strain dependency. Nano Express, 2021, 2, 010016.	1.2	6
38655	Design of a Series of Metallic BxNx+1 with Tunable Mechanical Properties. Journal of Physical Chemistry Letters, 2021, 12, 1979-1984.	2.1	3
38656	Emergence of Metallic Conductivity in Ordered One-Dimensional Coordination Polymer Thin Films upon Reductive Doping. ACS Applied Materials & Interfaces, 2021, 13, 10249-10256.	4.0	5
38657	Effects of Al substitution by Si in Ti3AlC2 nanolaminate. Scientific Reports, 2021, 11, 3410.	1.6	27
38658	Pressure dependence of structural, elastic, electronic, thermodynamic, and optical properties of van der Waals-type NaSn2P2 pnictide superconductor: Insights from DFT study. Results in Physics, 2021, 21, 103848.	2.0	48
38659	Calculation for High Pressure Behaviour of Potential Solar Cell Materials Cu2FeSnS4 and Cu2MnSnS4. Crystals, 2021, 11, 151.	1.0	1

#	Article	IF	Citations
38660	Enhanced optical absorption and photocatalytic water splitting of g-C3N4/TiO2 heterostructure through C&B codoping: A hybrid DFT study. International Journal of Hydrogen Energy, 2021, 46, 9417-9432.	3.8	26
38661	Heterointerface Effects on Lithium-Induced Phase Transitions in Intercalated MoS₂. ACS Applied Materials & Interfaces, 2021, 13, 10603-10611.	4.0	17
38662	Nitrosonium nitrate (NO⁺NO₃ ^{â¯}) structure solution using in situ single-crystal X-ray diffraction in a diamond anvil cell. IUCrJ, 2021, 8, 208-214.	1.0	5
38663	A Study on the Anti-thermal Dy³⁺/Eu³⁺ Co-doped BaLa₄Si₃O₁₃ Red Phosphors for White-Light-Emitting Diodes and Optical Thermometry Applications. Industrial & Engineering Chemistry Research, 2021, 60, 2931-2943.	1.8	21
38664	Effect of Fluoroethylene Carbonate Additives on the Initial Formation of the Solid Electrolyte Interphase on an Oxygen-Functionalized Graphitic Anode in Lithium-Ion Batteries. ACS Applied Materials & Interfaces, 2021, 13, 8169-8180.	4.0	23
38665	Near-Broken-Gap Alignment between FeWO₄ and Fe₂WO₆ for Ohmic Direct pâ€“n Junction Thermoelectrics. ACS Applied Materials & Interfaces, 2021, 13, 7416-7422.	4.0	11
38666	Energy Barrier of Proton Transfer in 3d Transition Metal-Doped Boehmite. Journal of Physical Chemistry C, 2021, 125, 3804-3810.	1.5	3
38667	Communicationâ€”Electrochemical Reduction of N₂ to Ammonia by Vanadium Oxide Thin Films at Neutral pH: Oxophilicity and the NRR Reaction. Journal of the Electrochemical Society, 2021, 168, 026504.	1.3	10
38668	Quantum Simulation of the Silicene and Germanene for Sensing and Sequencing of DNA/RNA Nucleobases. Biosensors, 2021, 11, 59.	2.3	7
38669	Data on atomic structures of precipitates in an Al-Mg-Cu alloy studied by high resolution transmission electron microscopy and first-principles calculations. Data in Brief, 2021, 34, 106748.	0.5	3
38670	A first-principles study of Li and Na co-decorated T4,4,4-graphyne for hydrogen storage. International Journal of Hydrogen Energy, 2021, 46, 8104-8112.	3.8	10
38671	Formation of Î¸-Fe₃C Cementite via Îµâ€²-Fe₃C (Ï‰-Fe₃C) in Feâ€“C Alloys. Crystal Growth and Design, 2021, 21, 1683-1688.	1.4	4
38672	Effect of Oxygen and Aluminum Incorporation on the Local Structure of GaN Nanowires: Insight from Extended X-ray Absorption Fine Structure Analysis. Journal of Physical Chemistry C, 2021, 125, 3225-3234.	1.5	1
38673	A DFT based first-principles investigation of optoelectronic and structural properties of Bi₂Te₂Se. Physica Scripta, 2021, 96, 045810.	1.2	18
38674	Defect Physics of Ternary Semiconductor <mml:math xmlns:mml="http://www.w3.org/1998/Math/MathML" display="inline" overflow="scroll"><mml:msub><mml:mrow><mml:mi>Zn</mml:mi><mml:mi>Ge</mml:mi><mml:mi mathvariant="normal">P</mml:mi></mml:mrow><mml:mn>2</mml:mn></mml:msub></mml:math> with a High Density of Anion-Cation Antisites: A First-Principles Study. Physical Review Applied, 2021, 15, .	1.5	15
38675	Electronic, structural and optical properties of cerium and zinc co-doped organic-inorganic halide perovskites for photovoltaic application. Physica B: Condensed Matter, 2021, 603, 412703.	1.3	4
38676	Hydrogen evolution on different facets of Î´1- MoN and Î´3-MoN: Considering the adsorbed oxygen and hydroxyl by Surface Pourbaix diagrams. International Journal of Hydrogen Energy, 2021, 46, 9077-9086.	3.8	10
38677	Electronic and magnetic properties of yttria-stabilized zirconia (6.7Âmol% in Y2O3) doped with Er3+ ions from first-principle computations. Journal of Materials Science, 2021, 56, 8014-8023.	1.7	0

#	Article	IF	Citations
38678	Crystallographic and superconducting properties of filled skutterudite <mml:math xmlns:mml="http://www.w3.org/1998/Math/MathML"><mml:mrow><mml:msub><mml:mi>SrOs</mml:mi><mml:mn>4</mml:mn></mml:msub><mml:mathvariant="normal">P</mml:mi><mml:mn>12</mml:mn></mml:msub></mml:mrow></mml:math>. Physical Review B, 2021, 103, .	1.1	2
38679	Studies of electrical and optical properties of cadmiumâ€doped zinc oxide for energy conversion devices. Fuel Cells, 2021, 21, 164-171.	1.5	3
38680	Atomistic Site Control of Pd in Crystalline MnO₂ Nanofiber for Enhanced Electrocatalysis. Advanced Materials Interfaces, 2021, 8, 2002060.	1.9	1
38681	Enhanced Ultraviolet Damage Resistance in Magnesium Doped Lithium Niobate Crystals through Zirconium Co-Doping. Materials, 2021, 14, 1017.	1.3	11
38682	Barium strontium titanate-based perovskite materials from DFT perspective: assessing the structural, electronic, vibrational, dielectric and energetic properties. Theoretical Chemistry Accounts, 2021, 140, 1.	0.5	9
38683	Emergent orbital-selective many-body effects upon doping strained graphene. Physical Review B, 2021, 103, .	1.1	0
38684	Electronic structure behavior of PbO2, IrO2, and SnO2 metal oxide surfaces (110) with dissociatively adsorbed water molecules as a function of the chemical potential. Journal of Chemical Physics, 2021, 154, 074704.	1.2	4
38685	Enhancing performance of NiCo2S4/Ni3S2 supercapacitor electrode by Mn doping. Electrochimica Acta, 2021, 368, 137634.	2.6	38
38686	The nuts and bolts of core-hole constrained ab initio simulation for K-shell x-ray photoemission and absorption spectra. Journal of Physics Condensed Matter, 2021, 33, 154005.	0.7	20
38687	Type-III Dirac fermions in HfxZr1â^'xTe2 topological semimetal candidate. Journal of Applied Physics, 2021, 129, .	1.1	9
38688	Electronic dispersions of a stable twisted bilayer phosphorene in 2O-tÎ±P phase. Journal of Applied Physics, 2021, 129, .	1.1	2
38689	Precipitation processes and structural evolutions of various GPB zones and two types of S phases in a cold-rolled Al-Mg-Cu alloy. Materials and Design, 2021, 199, 109425.	3.3	31
38690	First principles study of electronic, elastic, optical and magnetic properties of Rh 2 MnX (X = Ti, Hf, Sc,) Tj ETQq0 0 0 rgBT /Overlock 10 T	1.0	14
38691	One-Dimensional Organicâ€“Inorganic Material (C6H9N2)2BiCl5: From Synthesis to Structural, Spectroscopic, and Electronic Characterizations. International Journal of Molecular Sciences, 2021, 22, 2030.	1.8	8
38692	Structure, phase stability, half-metallicity, and fully spin-polarized Weyl states in compound NaV2O4 : An example for topological spintronic material. Physical Review Materials, 2021, 5, .	0.9	7
38693	Sulfur doping optimized intermediate energetics of FeCoOOH for enhanced oxygen evolution catalytic activity. Cell Reports Physical Science, 2021, 2, 100331.	2.8	7
38694	Anisotropic correlation between the piezoelectricity and anion-polarizability difference in 2D phosphorene-type ternary GaXY (Xâ€‰=â€‰Se, Te; Yâ€‰=â€‰F, Cl, Br, I) monolayers. Journal of Materials Scienc, 2021, 56, 8024-8036.	1.7	9
38695	8-16-4 graphyne: Square-lattice two-dimensional nodal line semimetal with a nontrivial topological Zak index. Physical Review B, 2021, 103, .	1.1	26

#	Article	IF	Citations
38696	Simple physical mixing of zeolite prevents sulfur deactivation of vanadia catalysts for NOx removal. Nature Communications, 2021, 12, 901.	5.8	49
38697	Selective Etching Quaternary MAX Phase toward Single Atom Copper Immobilized MXene (Ti₃C₂Cl_x) for Efficient CO₂ Electroreduction to Methanol. ACS Nano, 2021, 15, 4927-4936.	7.3	139
38698	CsPbBr₃, MAPbBr₃, and FAPbBr₃ Bromide Perovskite Single Crystals: Interband Critical Points under Dry N₂ and Optical Degradation under Humid Air. Journal of Physical Chemistry C, 2021, 125, 4938-4945.	1.5	26
38699	Exploring thermoelectric properties and stability of half-Heusler PtXSn (XÂ=ÂZr, Hf) semiconductors: A first principle investigation. Computational Materials Science, 2021, 188, 110232.	1.4	19
38700	First-principles study of an <mml:math xmlns:mml="http://www.w3.org/1998/Math/MathML"><mml:mrow><mml:mi>S</mml:mi><mml:mo>=</mml:mo><mml:mn>1 quasi one-dimensional quantum molecular magnetic material. Physical Review B, 2021, 103, .	1.1	2
38701	Elastic stiffness coefficients of thiourea from thermal diffuse scattering. Journal of Applied Crystallography, 2021, 54, 287-294.	1.9	3
38702	Die entscheidende Rolle von lokalen Ladungsfluktuationen beim Wachstum von Dendriten auf Lithiumâ€Elektroden. Angewandte Chemie, 2021, 133, 5940-5945.	1.6	6
38703	Exploring structural, electronic, and mechanical properties of 2D hexagonal MBenes. Journal of Physics Condensed Matter, 2021, 33, 155503.	0.7	20
38704	Influence of Transition Metal Doping on the Structural and Electronic Behaviour of Quaternary Double Perovskite, Cs₂AgInCl₆, using First-Principles Calculations. IOP Conference Series: Earth and Environmental Science, 2021, 655, 012046.	0.2	2
38705	First-Principles Density Functional Theory Characterisation of the Adsorption Complexes of H3AsO3 on Cobalt Ferrite (Fe2CoO4) Surfaces. Minerals (Basel, Switzerland), 2021, 11, 195.	0.8	5
38706	First-principles study of the anomalous Hall effect based on exact muffin-tin orbitals. Physical Review B, 2021, 103, .	1.1	5
38707	First-principles insights into the electronic structure, optical and band alignment properties of earth-abundant Cu2SrSnS4 solar absorber. Scientific Reports, 2021, 11, 4755.	1.6	18
38708	New Insight into Microstructure Engineering of Niâ€Rich Layered Oxide Cathode for High Performance Lithium Ion Batteries. Advanced Functional Materials, 2021, 31, 2010095.	7.8	113
38709	First-principles investigation of W V and W Mo alloys as potential plasma facing materials (PFMs) for nuclear application. International Journal of Refractory Metals and Hard Materials, 2021, 95, 105448.	1.7	6
38710	Comparison of coherent phonon generation by electronic and ionic Raman scattering in <mml:math xmlns:mml="http://www.w3.org/1998/Math/MathML"><mml:msub><mml:mi>LaAlO</mml:mi><mml:mn>3 Physical Review Research, 2021, 3, .	1.3	9
38711	Observation of Dihydrogen Bonds in High-Pressure Phases of Ammonia Borane by X-ray and Neutron Diffraction Measurements. Inorganic Chemistry, 2021, 60, 3065-3073.	1.9	11
38712	Stabilization and electronic topological transition of hydrogen-rich metal Li5MoH11 under high pressures from first-principles predictions. Scientific Reports, 2021, 11, 4079.	1.6	12
38713	Nucleation of Yâ€“Siâ€“O Nano-clusters in Multi-microalloyed Nano-structured Ferritic Alloys: a First-principles Study. Acta Metallurgica Sinica (English Letters), 2021, 34, 955-962.	1.5	7

#	Article	IF	Citations
38714	Insights into adsorption, diffusion, and reactions of atomic nitrogen on a highly oriented pyrolytic graphite surface. Journal of Chemical Physics, 2021, 154, 074708.	1.2	5
38715	Reemergence of superconductivity in pressurized quasi-one-dimensional superconductor K2Mo3As3. Physical Review Materials, 2021, 5, .	0.9	5
38716	Atomic-level-designed copper atoms on hierarchically porous gold architectures for high-efficiency electrochemical CO2 reduction. Science China Materials, 2021, 64, 1900-1909.	3.5	26
38717	Density Functional Theory Driven Analysis of the Interplay among Structure, Composition, and Oxidation State of Titanium in Hibonite, Spinel, and Perovskite. ACS Earth and Space Chemistry, 2021, 5, 544-552.	1.2	3
38718	Detailed Characterization of MoO_x-Modified Rh Metal Particles by Ambient-Pressure XPS and DFT Calculations. Journal of Physical Chemistry C, 2021, 125, 4540-4549.	1.5	21
38719	Role of Surface Paramagnetic Oxygen Species in the Desulfurization Reactions on Zinc Oxide. Journal of Physical Chemistry C, 2021, 125, 4559-4566.	1.5	1
38720	Correlation between Photocorrosion of ZnO and Lattice Relaxation Induced by Its Surface Vacancies. Journal of Physical Chemistry C, 2021, 125, 3242-3255.	1.5	19
38721	A Battery-Like Self-Selecting Biomemristor from Earth-Abundant Natural Biomaterials. ACS Applied Bio Materials, 2021, 4, 1976-1985.	2.3	30
38722	Nonâ€Rareâ€Earth UVC Persistent Phosphors Enabled by Bismuth Doping. Advanced Optical Materials, 2021, 9, 2002065.	3.6	27
38723	Phase transition and mechanical, vibrational, and electronic properties of NbC under pressure. Physica B: Condensed Matter, 2021, 602, 412594.	1.3	3
38724	Comparison of electrochemical response and electric field emission characteristics of pristine La2NiO4 and La2NiO4/CNT composites: Origin of multi-functionality with theoretical penetration by density functional theory. Electrochimica Acta, 2021, 369, 137676.	2.6	15
38725	Bias dependence and defect analysis of Bi on Si(111) <mml:math xmlns:mml="http://www.w3.org/1998/Math/MathML"><mml:mrow><mml:msqrt><mml:mn>3</mml:mn></mml:msqrt><mml:mo>Ã—</mml:mo><mml:msqrt><mml:mn>3</mml:mn></mml:msqrt><mml:mi mathvariant="normal">R</mml:mi><mml:mn>30</mml:mn><mml:mi mathvariant="normal">°</mml:mi></mml:mrow></mml:math> -phase. Physical Review B, 2021, 103, .		
38726	Robust S-doped TiO2@N,S-codoped carbon nanotube arrays as free-binder anodes for efficient sodium storage. Journal of Energy Chemistry, 2021, 53, 175-184.	7.1	37
38727	Li interaction-induced phase transition from black to blue phosphorene. Physical Review Materials, 2021, 5, .	0.9	11
38728	Design of a Class of New sp ² â€“ sp ³ Carbons Constructed by Graphite and Diamond Building Blocks. Chinese Physics Letters, 2021, 38, 028102.	1.3	15
38729	Scaling of Transition State Vibrational Frequencies and Application of d-Band Theory to the BrÃ¸nstedâ€“Evansâ€“Polanyi Relationship on Surfaces. Journal of Physical Chemistry C, 2021, 125, 7119-7129.	1.5	3
38730	Anisotropic dielectric functions, band-to-band transitions, and critical points in Î± -Ga2O3. Applied Physics Letters, 2021, 118, .	1.5	19
38731	Elucidating the origin of selective dehydrogenation of propane on Î³-alumina under H2S treatment and co-feed. Journal of Catalysis, 2021, 394, 142-156.	3.1	21

#	Article	IF	Citations
38732	Layer Shift Factor in Layered Hybrid Perovskites: Univocal Quantitative Descriptor of Compositionâ€“Structureâ€“Property Relationships. Chemistry of Materials, 2021, 33, 1213-1217.	3.2	24
38733	Photocatalytic Nitrogen Reduction by Ti₃C₂ MXene Derived Oxygen Vacancyâ€Rich C/TiO₂. Advanced Sustainable Systems, 2021, 5, 2000282.	2.7	37
38734	The Crucial Role of Local Excess Charges in Dendrite Growth on Lithium Electrodes. Angewandte Chemie - International Edition, 2021, 60, 5876-5881.	7.2	30
38735	Exploring the transport and optoelectronic properties of silicon diselenide monolayer. Superlattices and Microstructures, 2021, 150, 106813.	1.4	9
38736	Van der waals BP/InSe heterojunction for tunneling field-effect transistors. Journal of Materials Science, 2021, 56, 8563-8574.	1.7	13
38737	Interfaces between crystalline Si and amorphous B: Interfacial interactions and charge barriers. Physical Review B, 2021, 103, .	1.1	4
38738	Pentagonal transition-metal (group X) chalcogenide monolayers: Intrinsic semiconductors for photocatalysis. International Journal of Hydrogen Energy, 2021, 46, 9371-9379.	3.8	27
38739	Breaking of inversion symmetry in <mml:math xmlns:mml="http://www.w3.org/1998/Math/MathML"><mml:mrow><mml:mi>NdGa</mml:mi><mml:msub><mml:mi mathvariant="normal">O</mml:mi><mml:mn>3</mml:mn></mml:msub></mml:mrow></mml:math>. Physical Review B, 2021, 103, .	1.1	2
38740	Interface atom mobility and charge transfer effects on CuO and Cu2O formation on Cu3Pd(111) and Cu3Pt(111). Scientific Reports, 2021, 11, 3906.	1.6	4
38741	Effects of Vacancy and Hydrogen on the Growth and Morphology of N-Type Phosphorus-Doped Diamond Surfaces. Applied Sciences (Switzerland), 2021, 11, 1896.	1.3	2
38742	Stability of spin-gapless semiconducting behavior in <mml:math xmlns:mml="http://www.w3.org/1998/Math/MathML"><mml:mrow><mml:msub><mml:mi>Ti</mml:mi><mml:mn>2</mml:mn></mml:m , <mml:math xmlns:mml="http://www.w3.org/1998/Math/MathML"><mml:mrow><mml:msub><mml:mi>Ti</mml:mi><mml:mn>2</mml:mn></mml:m , and <mml:math xmlns:mml="http://www.w3.org/1998/Math/MathML"><mml:mrow><mml:msub. Physical Review Materials, 2021, 5, .	2.9	4
38743	Ab initio study of the structural response to magnetic disorder and van der Waals interactions in FeSe. Physical Review B, 2021, 103, .	1.1	3
38744	Rational Design of Two-Dimensional Magnetic Chromium Borides Based on First-Principles Calculation. Chinese Physics Letters, 2021, 38, 027501.	1.3	2
38745	Strong Elastic Anisotropy of Low-Dimensional Ternary Compounds: InXTe3 (X = Si, Ge). Journal of Electronic Materials, 2021, 50, 2779-2788.	1.0	10
38746	A family of ionic supersalts with covalent-like directionality and unconventional multiferroicity. Nature Communications, 2021, 12, 1331.	5.8	19
38747	Controlling the Selectivity of Supported Ru Nanoparticles During Glycerol Hydrogenolysis: Câˆ’O vs Câˆ’C Cleavage. ChemCatChem, 2021, 13, 1595-1606.	1.8	1
38748	Emergence of âˆ’s, âˆ’pâ€“d band inversion in zincblende gold iodide topological insulator and its thermoelectric properties. Journal of Physics Condensed Matter, 2021, 33, 155402.	0.7	5
38749	Density functional theory modeling of cation diffusion in tetragonal bulk ZrO2 : Effects of humidity and hydrogen defect complexes on cation transport. Physical Review Research, 2021, 3, .	1.3	3

#	Article	IF	Citations
38750	Thermoelectric Potential of OsAl2 Chimney LadderCompound: a Theoretical Investigation. Journal of Superconductivity and Novel Magnetism, 2021, 34, 1215-1223.	0.8	0
38751	Effect of vanadium substitution in LixFeF3 by first-principles calculations. AIP Advances, 2021, 11, 025218.	0.6	0
38752	First-principle study of structural, electronic, thermoelectric and vibrational properties of Co2-based Weyl semimetal VCo2Al. Bulletin of Materials Science, 2021, 44, 1.	0.8	1
38753	Effect of Pd alloying on structural, electronic and magnetic properties of L10 Feâ€“Ni. Journal of Physics Condensed Matter, 2021, 33, 154003.	0.7	0
38754	Electrochemically induced in-situ generated Co(OH)2 nanoplates to promote the Volmer process toward efficient alkaline hydrogen evolution reaction. International Journal of Hydrogen Energy, 2021, 46, 8497-8506.	3.8	11
38755	The Vanadium-doping effect on physical properties of the Zr2AlC MAX phase compound. Materials Chemistry and Physics, 2021, 260, 124189.	2.0	21
38756	Ab initio predictions of structure and physical properties of the Zr2GaC and Hf2GaC MAX phases under pressure. Scientific Reports, 2021, 11, 3260.	1.6	21
38757	Random Structure Searching with Orbital-Free Density Functional Theory. Journal of Physical Chemistry A, 2021, 125, 1650-1660.	1.1	8
38758	Behavior of Atomic Vacancy in Puckered Arsenene. Journal of Physical Chemistry C, 2021, 125, 4175-4182.	1.5	0
38759	First-principles investigation on the structures, energies and electronic properties of low-index surfaces of Mg2Pb. Materials Chemistry and Physics, 2021, 260, 124028.	2.0	9
38760	Accelerated Synthesis of Graphene Oxide from Graphene. Nanomaterials, 2021, 11, 551.	1.9	48
38761	Mitigating the Effect of Nanoscale Porosity on Thermoelectric Power Factor of Si. ACS Applied Energy Materials, 2021, 4, 1915-1923.	2.5	10
38762	Computational Insights into As(V) Removal from Water by the UiO-66 Metalâ€“Organic Framework. Journal of Physical Chemistry C, 2021, 125, 3157-3168.	1.5	17
38763	The Combined Role of Faceting and Heteroatom Doping for Hydrogen Evolution on a WC Electrocatalyst in Aqueous Solution: A Density Functional Theory Study. Journal of Physical Chemistry C, 2021, 125, 4602-4613.	1.5	13
38764	Data-Driven Discovery and Understanding of Ultrahigh-Modulus Crystals. Chemistry of Materials, 2021, 33, 1276-1284.	3.2	16
38765	Electron thermalization and relaxation in laser-heated nickel by few-femtosecond core-level transient absorption spectroscopy. Physical Review B, 2021, 103, .	1.1	21
38766	Transition of Cationic Local Structures in Mg1-xNixAl2O4. Journal of Physical Chemistry C, 2021, 125, 5269-5277.	1.5	3
38767	Development of a Multiphase Beryllium Equation of State and Physics-based Variations. Journal of Physical Chemistry A, 2021, 125, 1610-1636.	1.1	16

#	Article	IF	Citations
38768	CdS Induced Passivation toward High Efficiency and Stable Planar Perovskite Solar Cells. ACS Applied Materials & Interfaces, 2021, 13, 9771-9780.	4.0	17
38769	Redox Photochemistry on Van Der Waals Surfaces for Reversible Doping in 2D Materials. Advanced Functional Materials, 2021, 31, 2009166.	7.8	9
38770	Constructing Surface Plasmon Resonance on Bi₂WO₆ to Boost High-Selective CO₂ Reduction for Methane. ACS Nano, 2021, 15, 3529-3539.	7.3	113
38771	Influences of Vacancy Concentration and Al Substitution on Structural, Electronic, and Elastic Properties of Nb₅Si₃ from Firstâ€Principles Calculations. Physica Status Solidi (B): Basic Research, 2021, 258, 2000591.	0.7	1
38772	Predicting the impact sensitivities of energetic materials through zone-center phonon up-pumping. Journal of Chemical Physics, 2021, 154, 064105.	1.2	33
38773	Structural and Electrical Properties of Be_xZn_{1â€“x}O Alloys under High Pressure. Chinese Physics Letters, 2021, 38, 026101.	1.3	7
38774	Possibility of interstitial Na as electron donor in Yb14MgSb11. MRS Communications, 2021, 11, 226-232.	0.8	4
38775	Structural, elastic and mechanical properties of Tiâ€“15Nbâ€“xGe alloys: insight from DFT calculations. Bulletin of Materials Science, 2021, 44, 1.	0.8	6
38776	The Degree of Oxidation of Graphene Oxide. Nanomaterials, 2021, 11, 560.	1.9	35
38777	Operando Electrochemical Spectroscopy for CO on Cu(100) at pH 1 to 13: Validation of Grand Canonical Potential Predictions. ACS Catalysis, 2021, 11, 3173-3181.	5.5	6
38778	Comparative computational study of antiferromagnetic and mixed-valent diamagnetic phase of AgF2: Crystal, electronic and phonon structure and p-T phase diagram. Computational Materials Science, 2021, 188, 110250.	1.4	7
38779	Ultra-broad spectral photo-response in FePS3 air-stable devices. Npj 2D Materials and Applications, 2021, 5, .	3.9	35
38780	Carbon deposition enhanced selective catalytic reduction of nitric oxide by a new catalytic process as well as increasing reducibility of catalyst. Science of the Total Environment, 2021, 756, 143834.	3.9	2
38781	Direct band gap and strong Rashba effect in van der Waals heterostructures of InSe and Sb single layers. Journal of Physics Condensed Matter, 2021, 33, 155001.	0.7	4
38782	Metallic Ferromagnetic Property of Mn-Doped BP Semiconductors. Journal of Molecular and Engineering Materials, 0, , 2130001.	0.9	0
38783	Fermi liquid theory sheds light on hot electron-hole liquid in <mml:math xmlns:mml="http://www.w3.org/1998/Math/MathML"><mml:mn>1</mml:mn><mml:mi>L</mml:mi><mml:mo>â^’</mml:mo><mml:m mathvariant="normal">S</mml:mi><mml:mn>2</mml:mn></mml:msub></mml:math>. Physical Review B, 2021, 103, .	1.1	9
38784	Ab Initio Electronic Structure Investigation of Antimony-Doped SnO2 (110) Nanosheet. Iranian Journal of Science and Technology, Transaction A: Science, 2021, 45, 745-751.	0.7	0
38785	First principle studies on the structures, electronic propertiesÂandÂRaman spectrums of monolayer WX₂ (X = S, Se, Te) under strain condition. Modern Physics Letters B, 2021, 35, 2150135.	1.0	3

#	Article	IF	Citations
38786	Nitrogen-doped char as a catalyst for wet oxidation of phenol-contaminated water. Biomass Conversion and Biorefinery, 2024, 14, 5861-5875.	2.9	4
38787	Atomicâ€Scale Visualization and Quantification of Configurational Entropy in Relation to Thermal Conductivity: A Proofâ€ofâ€Principle Study in tâ€GeSb₂Te₄. Advanced Science, 2021, 8, 2002051.	5.6	16
38788	Coexistence of fully spin-polarized Weyl nodal loop, nodal surface, and Dirac point in a family of quasi-one-dimensional half-metals. Physical Review B, 2021, 103, .	1.1	16
38789	Electronic structure of monolayer Cu, Ag and Au structures. Applied Nanoscience (Switzerland), 2022, 12, 781-794.	1.6	0
38790	Electric-polarization-driven magnetic phase transition in a ferroelectricâ€“ferromagnetic heterostructure. Applied Physics Letters, 2021, 118, .	1.5	4
38791	First-principles Investigation of Structure and Electronic Properties of NiTe2 Fermi Crossing Type-II Dirac Semimetal. Asian Journal of Research and Reviews in Physics, 0, , 27-33.	0.0	0
38792	Thermodynamic, elastic, and vibrational (IR/Raman) behavior of mixed type-AB carbonated hydroxylapatite by density functional theory. American Mineralogist, 2021, 106, 1928-1939.	0.9	7
38793	Properties and electronic structure of Al/Mo2C interfaces: insights from first principle simulation. Philosophical Magazine, 2021, 101, 1061-1080.	0.7	2
38794	Pressure-Induced Modifications in the Optoelectronic and Thermoelectric Properties of MgHfO3 for Renewable Energy Applications. Arabian Journal for Science and Engineering, 0, , 1.	1.7	1
38795	Mercury exchange in zeolites Na-A and Na-Y studied by classical molecular dynamics simulations and ion exchange experiments. Microporous and Mesoporous Materials, 2021, 315, 110903.	2.2	15
38796	Study of structural, electronic, elastic and magnetic properties of Al0.75X0.25P (X=Cr, Mn, Fe) using Density Functional Theory. Solid State Communications, 2021, 325, 114172.	0.9	1
38797	Nanodomain structure of single crystalline nickel oxide. Scientific Reports, 2021, 11, 3496.	1.6	12
38798	DFT based first principles study of novel combinations of perovskite-type hydrides XGaH3 (X = Rb, Cs,) Tj ETQq0 0 0 rgBT /Overlock 10 T	0.6	28
38799	Exploring cation disorder in mixedâ€metal pyrochlore ceramics using ¹⁷O NMR spectroscopy and firstâ€principles calculations. Magnetic Resonance in Chemistry, 2021, 59, 961-974.	1.1	0
38800	Effect of oxidation on the thermal expansion of a refractory multicomponent alloy. Philosophical Magazine Letters, 2021, 101, 173-182.	0.5	4
38801	First principles study of structural, elastic, mechanical and electronic properties of nitrogen-doped cubic diamond. Bulletin of Materials Science, 2021, 44, 1.	0.8	29
38802	IrN4 and IrN7 as potential high-energy-density materials. Journal of Chemical Physics, 2021, 154, 054706.	1.2	11
38803	Direct Observation and Quantitative Analysis of Lithium Dendrite Growth by In Situ Transmission Electron Microscopy. Journal of the Electrochemical Society, 2021, 168, 020535.	1.3	11

#	Article	IF	Citations
38804	Low-frequency Raman signature of Ag-intercalated few-layer MoS₂. 2D Materials, 2021, 8, 025031.	2.0	9
38805	Investigation on the Stability, Elastic Properties, and Electronic Structure of Mg₂Si Doped with Different Concentrations of Cu: A Firstâ€Principles Calculation. Physica Status Solidi (B): Basic Research, 2021, 258, 2000597.	0.7	7
38806	Going beyond Pentacene: Photoemission Tomography of a Heptacene Monolayer on Ag(110). Journal of Physical Chemistry C, 2021, 125, 2918-2925.	1.5	7
38807	Correct Structural Phase Stability of FeS₂, TiO₂, and MnO₂ from a Semilocal Density Functional. Journal of Physical Chemistry C, 2021, 125, 4284-4291.	1.5	14
38808	PbSe Nanocrystals Produced by Facile Liquid Phase Exfoliation for Efficient UVâ€“Vis Photodetectors. Advanced Functional Materials, 2021, 31, 2010401.	7.8	35
38809	Thermoelectric Performance of Cr Doped and Crâ€“Fe Double-Doped Higher Manganese Silicides with Adjusted Carrier Concentration and Significant Electronâ€“Phonon Interaction. ACS Applied Materials & Interfaces, 2021, 13, 8574-8583.	4.0	18
38810	Longâ€Range Surfaceâ€Assisted Moleculeâ€Molecule Hybridization. Small, 2021, 17, e2005974.	5.2	3
38811	Structural and vibrational study of<mml:math xmlns:mml="http://www.w3.org/1998/Math/MathML"><mml:mrow><mml:mi>Zn</mml:mi><mml:msub><mml:mrow><mml:mo>(</m High-pressure experiments and density functional theory. Physical Review B, 2021, 103, .	1.1	19
38812	Preventing Superoxide Generation on Molecule-Protected CH₃NH₃PbI₃ Perovskite: A Time-Domain Ab Initio Study. Journal of Physical Chemistry Letters, 2021, 12, 1664-1670.	2.1	13
38813	Uncovering the influence of Cu on the thickening and strength of the Î´â€²/Î¸â€²/Î´â€² nano-composite precipitate in Alâ€“Cuâ€“Li alloys. Journal of Materials Science, 2021, 56, 10092-10107.	1.7	11
38814	First-principles study of co-adsorption behavior of O₂ and CO₂ molecules on Î´-Pu(100) surface. Chinese Physics B, 2021, 30, 026601.	0.7	5
38815	Comparison of Thermal Annealing versus Hydrothermal Treatment Effects on the Detection Performances of ZnO Nanowires. ACS Applied Materials & Interfaces, 2021, 13, 10537-10552.	4.0	14
38816	Expansive open Fermi arcs and connectivity changes induced by infrared phonons in <mml:math xmlns:mml="http://www.w3.org/1998/Math/MathML"><mml:mrow><mml:mi>Zr</mml:mi><mml:msub><mml:mi>Te</mml:mi><mml:m Physical Review B, 2021, 103, .	1.1	9
38817	The As-surface of an iron-based superconductor CaKFe4As4. Nano Research, 2021, 14, 3921-3925.	5.8	6
38818	Dipole-Induced Raman Enhancement Using Noncovalent Azobenzene-Functionalized Self-Assembled Monolayers on Graphene Terraces. ACS Applied Materials & Interfaces, 2021, 13, 10271-10278.	4.0	12
38819	Iron-Content-Dependent, Quasi-Static Dielectric Resonances and Oxidative Transitions in Bornite and Chalcopyrite Copper Iron Sulfide Nanocrystals. Chemistry of Materials, 2021, 33, 1821-1831.	3.2	17
38820	Firstâ€principles exploration of MgTi 2 O 5 and MgV 2 O 5 for CO 2 capture and conversion. International Journal of Quantum Chemistry, 2021, 121, e26637.	1.0	3
38821	Electronic charge transfer during metal/SiO2 contact: Insight from density functional theory. Journal of Applied Physics, 2021, 129, .	1.1	12

#	Article	IF	Citations
38822	Influence of Cr, Mn, Co and Ni Addition on Crystallization Behavior of Al13Fe4 Phase in Al-5Fe Alloys Based on ThermoDynamic Calculations. Materials, 2021, 14, 768.	1.3	5
38823	Electronic structures and impurity segregation around extended defects in pentacene films: first-principles study. Japanese Journal of Applied Physics, 2021, 60, SBBG05.	0.8	1
38824	First principles investigation of structural, electronic, and room temperature ferromagnetism in V doped hexagonal pristine graphene. AIP Advances, 2021, 11, 025217.	0.6	2
38825	Effect of chemical modification on electronic transport properties of carbyne. Journal of Computational Electronics, 2021, 20, 848-854.	1.3	4
38826	Structural, Electronic, and Optical Properties of Group 6 Doped Anatase TiO2: A Theoretical Approach. Applied Sciences (Switzerland), 2021, 11, 1657.	1.3	4
38827	Native point defects from stoichiometry-linked chemical potentials in cubic boron arsenide. Journal of Applied Physics, 2021, 129, 075703.	1.1	2
38828	Remote Mesoscopic Signatures of Induced Magnetic Texture in Graphene. Physical Review Letters, 2021, 126, 086802.	2.9	0
38829	Two-dimensional Dirac dispersion in the layered compound <mml:math xmlns:mml="http://www.w3.org/1998/Math/MathML"><mml:msub><mml:mrow><mml:mi>BaCdSb</mml:mi></mml:mrow> Physical Review B, 2021, 103, .	1.1	2
38830	Enantioselective Effects in the Electrical Excitation of Amine Single-Molecule Rotors. Journal of Physical Chemistry C, 2021, 125, 3584-3589.	1.5	3
38831	Influences on Subsurface Plutonium and Americium Migration. ACS Earth and Space Chemistry, 2021, 5, 279-294.	1.2	4
38832	Rectifying and spin filtering behavior of aluminum doped silicon carbide nanoribbons: the first principles study. Journal Physics D: Applied Physics, 2021, 54, 165304.	1.3	3
38833	Theoretical investigation on stability and electronic properties of Janus MoSSe nanotubes for optoelectronic applications. Optik, 2021, 227, 166105.	1.4	11
38834	Electronic and Transport Properties of Bilayer Phosphorene Nanojunction: Effect of Paired Substitution Doping. ACS Applied Electronic Materials, 2021, 3, 733-742.	2.0	13
38835	3D Bimodal Porous Amorphous Carbon with Self-Similar Porosity by Low-Temperature Sequential Chemical Dealloying. Chemistry of Materials, 2021, 33, 1013-1021.	3.2	11
38836	The First Positive Uniaxial Cyanurate Crystals Containing a Crown-like Anionic Group Arrangement and Strengthened Optical Anisotropy. Crystal Growth and Design, 2021, 21, 2348-2354.	1.4	7
38837	Regulating Guanidinium-Based Hybrid Materials for Ultraviolet Nonlinear Optical Applications by Hybrid Strength and Hybrid Pattern. Inorganic Chemistry, 2021, 60, 3834-3842.	1.9	16
38838	Hollow Molybdate Microspheres as Catalytic Hosts for Enhancing the Electrochemical Performance of Sulfur Cathode under High Sulfur Loading and Lean Electrolyte. Advanced Functional Materials, 2021, 31, 2010693.	7.8	57
38840	High-entropy-stabilized chalcogenides with high thermoelectric performance. Science, 2021, 371, 830-834.	6.0	546

#	Article	IF	Citations
38841	Unveiling the Role of Sulfur in Rapid Defluorination of Florfenicol by Sulfidized Nanoscale Zero-Valent Iron in Water under Ambient Conditions. Environmental Science & Technology, 2021, 55, 2628-2638.	4.6	98
38842	Band-filling semiconductor to metal transition in <mml:math xmlns:mml="http://www.w3.org/1998/Math/MathML"><mml:mrow><mml:mi>M</mml:mi><mml:msub><mml:mi>A</mml:mi><mml:mn		

#	Article	IF	Citations
38859	Population analysis with Wannier orbitals. Journal of Chemical Physics, 2021, 154, 104111.	1.2	3
38860	Tunable electronic properties and large optical anisotropy in the CsPbXnY3-n (X, YÂ=ÂCl, Br, I) perovskite. Solar Energy, 2021, 217, 165-172.	2.9	2
38861	Tailoring the anomalous Hall effect of SrRuO3 thin films by strain: A first principles study. Journal of Applied Physics, 2021, 129, 093904.	1.1	5
38862	Thermodynamic, mechanical stabilities and thermoelectric behavior of the XVSi (Xâ€‰=â€‰Co, Rh) half-Heuslers. Indian Journal of Physics, 2022, 96, 1045-1057.	0.9	1
38863	Crystal structures and mechanical properties of osmium diboride at high pressure. Scientific Reports, 2021, 11, 5754.	1.6	4
38864	Piezoelectric and electronic properties of hydrogenated penta-BCN: A computational study. Journal of Applied Physics, 2021, 129, 095101.	1.1	11
38865	Diamond(001)â€“Si(001) and Si(001)â€“Ti(0001) interfaces: A density functional theory study. Journal of Physics and Chemistry of Solids, 2021, 150, 109865.	1.9	4
38866	Microstructure â€“ electron work function relationship: A crucial step towards â€œelectronic metallurgyâ€• Materials Today Communications, 2021, 26, 101977.	0.9	2
38867	Calcium decoration of boron nitride nanotubes with vacancy defects as potential hydrogen storage materials: A first-principles investigation. Materials Today Communications, 2021, 26, 101985.	0.9	9
38868	Itinerant magnetism in the half-metallic Heusler compound <mml:math xmlns:mml="http://www.w3.org/1998/Math/MathML"><mml:msub><mml:mi mathvariant="normal">Co</mml:mi><mml:mn>2</mml:mn></mml:msub><mml:mi mathvariant="normal">HfSn</mml:mi></mml:math> : Evidence from critical behavior combined with first-principles calculations. Physical Review B, 2021, 103, .	1.1	11
38869	Influence of antimony on the structural, electronic, mechanical, and anisotropic properties of cubic barium stannate. Materials Today Communications, 2021, 26, 101868.	0.9	11
38870	Discovery of a weak topological insulating state and van Hove singularity in triclinic RhBi2. Nature Communications, 2021, 12, 1855.	5.8	15
38871	Density functional theory insight into metal ions and vacancies for improved performance in storage devices. International Journal of Energy Research, 2021, 45, 10882-10894.	2.2	12
38872	Topology conversion of 1T MoS2 to S-doped 2H-MoTe2 nanosheets with Te vacancies for enhanced electrocatalytic hydrogen evolution. Science China Materials, 2021, 64, 2202-2211.	3.5	19
38873	First principles study of small hole polaron formation in doped olivine LiFe1â”Co PO4: Effects of Li deficiency. Materials Today Communications, 2021, 26, 102043.	0.9	1
38874	Ab initio investigations of the interfacial bond of Fe(001)/Al(001). Materials Today Communications, 2021, 26, 102107.	0.9	3
38875	Dimensional engineering of a topological insulating phase in Half-Heusler LiMgAs. Scientific Reports, 2021, 11, 6432.	1.6	6
38876	Oxidation mechanism of MAX phases (Ti3AlC2 powders) with and without Sn doping. Corrosion Science, 2021, 180, 109197.	3.0	32

#	Article	IF	Citations
38877	Efficient Photoexcited Charge Separation at the Interface of a Novel 0D/2D Heterojunction: A Time-Dependent Ultrafast Dynamic Study. Journal of Physical Chemistry Letters, 2021, 12, 2312-2319.	2.1	23
38878	Pressure effect on band inversion in AECd2As2 (AE=Ca,ÂSr,ÂBa). Physical Review B, 2021, 103, .	1.1	6
38879	An Efficient Approach Based on Tuned Nanoionics to Maximize Memory Characteristics in Agâ€Based Devices. Advanced Electronic Materials, 2021, 7, 2100022.	2.6	28
38880	Promoting a Weak Coupling of Monolayer MoSe₂ Grown on (100)-Faceted Au Foil. ACS Nano, 2021, 15, 4481-4489.	7.3	16
38881	High-Throughput Screening of Nitrogen-Coordinated Bimetal Catalysts for Multielectron Reduction of CO₂ to CH₄ with High Selectivity and Low Limiting Potential. Journal of Physical Chemistry C, 2021, 125, 7155-7165.	1.5	36
38882	A comparison of the mixing thermodynamics of the antifluorite-structured Mg2Si1â^'xGex, Mg2Sn1â^'xGex and Mg2Si1â^'xSnx alloys from first principles. Vacuum, 2021, 185, 110018.	1.6	2
38883	Equilibrium Cu isotope fractionation in copper minerals: a first-principles study. Chemical Geology, 2021, 564, 120060.	1.4	17
38884	Tuning the Schottky Barrier Height at the Interfaces of Metals and Mixed Conductors. ACS Applied Materials & Interfaces, 2021, 13, 15746-15754.	4.0	10
38885	Structure Determination of Multicomponent Crystalline Phases of (S)-Ibuprofen and l-Proline from Powder X-ray Diffraction Data, Augmented by Complementary Experimental and Computational Techniques. Crystal Growth and Design, 2021, 21, 2498-2507.	1.4	8
38886	Effect of boron incorporation into the carbon-site in Nb2SC MAX phase: Insights from DFT. Journal of Materials Research and Technology, 2021, 11, 1969-1981.	2.6	36
38887	Comparative study of predicted MAX phase Hf2AlN with recently synthesized Hf2AlC: a first principle calculations. Indian Journal of Physics, 2022, 96, 1321-1333.	0.9	6
38888	Comparative study of half-metallic ferromagnetic behaviour in ZnO monolayer doped with boron and carbon atoms. International Nano Letters, 2021, 11, 113.	2.3	3
38889	The adsorption and migration behaviors of Fe atoms on the diamond (1 1 1) surface. Applied Surface Science, 2021, 543, 148766.	3.1	7
38890	Tuning topological phases and electronic properties of monolayer ternary transition metal chalcogenides (ABX4, A/B = Zr, Hf, or Ti; X = S, Se, or Te). Applied Physics Letters, 2021, 118, .	1.5	16
38891	Adsorption of ethylene oxide on doped monolayers of MoS2: A DFT study. Materials Science and Engineering B: Solid-State Materials for Advanced Technology, 2021, 265, 115009.	1.7	15
38892	Mesoporous Iron(III)-Doped Hydroxyapatite Nanopowders Obtained via Iron Oxalate. Nanomaterials, 2021, 11, 811.	1.9	25
38893	Discovery of NLO Semiorganic (C₅H₆ON)⁺(H₂PO₄)^{â^'}: Dipole Moment Modulation and Superior Synergy in Solar-Blind UV Region. Journal of the American Chemical Society, 2021, 143, 3647-3654.	6.6	99
38894	Multiâ€Phase Heterostructure of CoNiP/Co_xP for Enhanced Hydrogen Evolution Under Alkaline and Seawater Conditions by Promoting H₂O Dissociation. Small, 2021, 17, e2007557.	5.2	83

#	Article	IF	Citations
38895	DFT and TDDFT studies of the new inorganic perovskite CsPbI3 for solar cell applications. Chemical Physics Letters, 2021, 766, 138347.	1.2	68
38896	Density Functional Theory Studies on Sulfurâ€“Polyacrylonitrile as a Cathode Host Material for Lithiumâ€“Sulfur Batteries. ACS Omega, 2021, 6, 9700-9708.	1.6	11
38897	Thermoelectric and mechanical properties of XHfSn (X=Ni, Pd and Pt) semiconducting Half-heusler alloys: A first-principles study. Computational Condensed Matter, 2021, 26, e00539.	0.9	13
38898	Spin-lattice model for cubic crystals. Physical Review B, 2021, 103, .	1.1	15
38899	An ab-initio study on structural, elastic, electronic, bonding, thermal, and optical properties of topological Weyl semimetal TaX (Xâ€‰=â€‰P, As). Scientific Reports, 2021, 11, 5592.	1.6	84
38900	Localized electronic vacancy level and its effect on the properties of doped manganites. Scientific Reports, 2021, 11, 6706.	1.6	8
38901	Reaction pathways in the solid state and the Hubbard U correction. Journal of Chemical Physics, 2021, 154, 124121.	1.2	6
38902	Controlling the Formation of Sodium/Black Phosphorus IntercalationCompounds Towards High Sodium Content. Batteries and Supercaps, 2021, 4, 1304-1309.	2.4	3
38903	Kinetic Control of the Li_{0.9}Mn_{1.6}Ni_{0.4}O₄ Spinel Structure with Enhanced Electrochemical Performance. ACS Applied Materials & Interfaces, 2021, 13, 14056-14067.	4.0	4
38904	Seismic Anisotropy in Subduction Zones: Evaluating the Role of Chloritoid. Frontiers in Earth Science, 2021, 9, .	0.8	5
38905	The Effect of Degrees of Inversion on the Electronic Structure of Spinel NiCo₂O₄: A Density Functional Theory Study. ACS Omega, 2021, 6, 9692-9699.	1.6	32
38906	Effect of Monovalent Metal Iodide Additives on the Optoelectric Properties of Two-Dimensional Sn-Based Perovskite Films. Chemistry of Materials, 2021, 33, 2498-2505.	3.2	28
38907	Coexistence of Ferroelectricity and Ferromagnetism in One-Dimensional SbN and BiN Nanowires. ACS Applied Materials & Interfaces, 2021, 13, 13517-13523.	4.0	18
38908	Nanoporous Silver Telluride for Active Hydrogen Evolution. ACS Nano, 2021, 15, 6540-6550.	7.3	10
38909	Orientation-dependent mechanical response of graphene/BN hybrid nanostructures. Nanotechnology, 2021, 32, 235703.	1.3	8
38910	Hollow Co₉S₈/CdS Nanocages as Efficient Photocatalysts for Hydrogen Evolution. ACS Applied Nano Materials, 2021, 4, 2743-2751.	2.4	35
38911	Semiconductor-to-metal transition in bilayer MoSi2N4 and WSi2N4 with strain and electric field. Applied Physics Letters, 2021, 118, .	1.5	65
38912	Copper-doped beryllium and beryllium oxide interface: A first-principles study. Journal of Nuclear Materials, 2021, 545, 152733.	1.3	6

#	Article	IF	Citations
38913	Predictive physical study of two different crystalline forms of glucose. Biochemistry and Biophysics Reports, 2021, 25, 100923.	0.7	3
38914	Effects of surface spatial structures and electronic properties of chalcopyrite and pyrite on Z-200 selectivity. Minerals Engineering, 2021, 163, 106803.	1.8	28
38915	Investigation on the interface characteristic between ZrC (111) and diamond (111) surfaces by first-principles calculation. Diamond and Related Materials, 2021, 113, 108297.	1.8	14
38916	Effects of Fe doping on the visible light absorption and bandgap tuning of lead-free (CsSnCl3) and lead halide (CsPbCl3) perovskites for optoelectronic applications. AIP Advances, 2021, 11, .	0.6	20
38917	Topological properties of noncentrosymmetric superconductors <mml:math xmlns:mml="http://www.w3.org/1998/Math/MathML"><mml:mi>T</mml:mi><mml:msub><mml:mi mathvariant="normal">Ir</mml:mi><mml:mn>2</mml:mn></mml:msub><mml:msub><mml:mi mathvariant="normal">B</mml:mi><mml:mn>2</mml:mn></mml:msub></mml:math> (<mml:math) Tj ETQq0 0 0 rgBT /Overlock 10 Tf	1.1	3
38918	Magnetic, Electronic, and Optical Properties of the Tetraborates NiB4O7 and CoB4O7 in Three Structural Modifications. Physics of the Solid State, 2021, 63, 468-476.	0.2	2
38919	High Charge-Storage Performance of Morphologically Modified Anatase TiO 2 : Experimental and Theoretical Insight. Physical Review Applied, 2021, 15, .	1.5	6
38920	Computational Study of Solute Effects in Tungsten under Irradiation. Materials Science Forum, 0, 1024, 87-94.	0.3	1
38921	Ab initio and Monte Carlo studies of physical properties of semiconductor radiation detectors. Indian Journal of Physics, 0, , 1.	0.9	0
38922	Monolayer Fe₃GeX₂ (X = S, Se, and Te) as Highly Efficient Electrocatalysts for Lithiumâ€“Sulfur Batteries. ACS Applied Materials & Interfaces, 2021, 13, 11845-11851.	4.0	45
38923	Impact of noble-gas filler atoms on the lattice thermal conductivity of CoSb₃ skutterudites: first-principles modelling. Journal of Physics Condensed Matter, 2021, 33, 164002.	0.7	8
38924	Large Perpendicular Magnetic Anisotropy in Nanometer-Thick Epitaxial Graphene/Co/Heavy Metal Heterostructures for Spinâ€“Orbitronics Devices. ACS Applied Nano Materials, 2021, 4, 4398-4408.	2.4	13
38925	A First-Principles Investigation on the Electronic and Mechanical Properties of 1T TiSe₂ Multilayers for Energy Storage. Journal of the Electrochemical Society, 2021, 168, 030531.	1.3	9
38926	Solute segregation induced stabilizing and strengthening effects on Ni Î£3 [110](111) symmetrical tilt grain boundary in nickel-based superalloys. Journal of Materials Research and Technology, 2021, 11, 1281-1289.	2.6	18
38927	Pressure effect of the mechanical, electronics and thermodynamic properties of Mgâ€“B compounds A first-principles investigations. Scientific Reports, 2021, 11, 6096.	1.6	5
38928	LaSiP₃ and LaSi₂P₆: Two Excellent Rareâ€Earth Pnictides with Strong SHG Responses as Midâ€and Farâ€Infrared Nonlinear Optical Crystals. Advanced Optical Materials, 2021, 9, 2002176.	3.6	9
38929	A combined ab-initio and empirical model for thermal conductivity of concentrated metal alloys with the focus on binary uranium alloys. Materialia, 2021, 15, 100990.	1.3	3
38930	Exploring dynamical, mechanical and optoelectronic properties of cubic Mg3CdO4: First-principle study. Materials Today Communications, 2021, 26, 102106.	0.9	3

#	Article	IF	Citations
38931	Semiconductor Bloch-equations formalism: Derivation and application to high-harmonic generation from Dirac fermions. Physical Review B, 2021, 103, .	1.1	24
38932	Structural, mechanical, electronic and optical properties of half-metallic XFeSi2O6 (XÂ=ÂLi, Na, K) clinopyroxenes: A first-principles investigation. Materials Science and Engineering B: Solid-State Materials for Advanced Technology, 2021, 265, 115026.	1.7	11
38933	Experimental and Theoretical Study of the Effect of Functionalized Pyrene Polymerization on Carbon Electrode Surfaces for Electrochemical Storage. Batteries and Supercaps, 2021, 4, 1018-1031.	2.4	0
38934	Synthesis, Crystal Structure, Electronic Structure, and Catalytic Properties of Ni 3 GaSb. European Journal of Inorganic Chemistry, 2021, 2021, 1410-1418.	1.0	3
38935	Theoretical study on compositionâ€dependent properties of ZnOÂ· n Al 2 O 3 spinels. Part I: Optical and dielectric. Journal of the American Ceramic Society, 2021, 104, 5099-5109.	1.9	5
38936	Rapid Charge Separation Boosts Solar Hydrogen Generation at the Grapheneâ€“MoS₂ Junction: Time-Domain Ab Initio Analysis. Journal of Physical Chemistry Letters, 2021, 12, 2763-2769.	2.1	16
38937	<mml:math xmlns:mml="http://www.w3.org/1998/Math/MathML" display="inline" overflow="scroll"><mml:msub><mml:mi>M</mml:mi><mml:mn>2</mml:mn></mml:msub><mml:mi>X</mml:mi></mml:math> Monolayers as Anode Materials for <mml:math xmlns:mml="http://www.w3.org/1998/Math/MathML" display="inline" overflow="scroll"><mml:mi>Li</mml:mi></mml:math> Ion Batteries. Physical Review Applied, 2021, 15, .	1.5	13
38938	Increasing electrocatalytic nitrate reduction activity by controlling adsorption through PtRu alloying. Journal of Catalysis, 2021, 395, 143-154.	3.1	94
38939	Engineering Mesopores and Unsaturated Coordination in Metalâ€“Organic Frameworks for Enhanced Oxygen Reduction and Oxygen Evolution Activity and Liâ€“Air Battery Capacity. ACS Sustainable Chemistry and Engineering, 2021, 9, 4509-4519.	3.2	25
38940	Disclosure of charge storage mechanisms in molybdenum oxide nanobelts with enhanced supercapacitive performance induced by oxygen deficiency. Rare Metals, 2021, 40, 2447-2454.	3.6	36
38941	Physical properties of new MAX phase borides M2SB (M = Zr, Hf and Nb) in comparison with conventional MAX phase carbides M2SC (M = Zr, Hf and Nb): Comprehensive insights. Journal of Materials Research and Technology, 2021, 11, 1000-1018.	2.6	70
38942	Crystal Symmetry and Static Electron Correlation Greatly Accelerate Nonradiative Dynamics in Lead Halide Perovskites. Journal of Physical Chemistry Letters, 2021, 12, 2444-2453.	2.1	13
38943	Effective Doping of Square/Octagonâ€Phase Arsenene by Adsorption of Organic Molecules. Advanced Theory and Simulations, 2021, 4, 2000300.	1.3	1
38944	MoirÃ©-induced electronic structure modifications in monolayer <mml:math xmlns:mml="http://www.w3.org/1998/Math/MathML"><mml:mrow><mml:msub><mml:mi mathvariant="normal">V</mml:mi><mml:mn>2</mml:mn></mml:msub><mml:msub><mml:mi mathvariant="normal">S</mml:mi><mml:mn>3</mml:mn></mml:msub></mml:mrow></mml:math> on Au(111). Physical Review B, 2021, 103, .	1.1	3
38945	Two-dimensional bipolar ferromagnetic semiconductors from layered antiferromagnets. Physical Review Materials, 2021, 5, .	0.9	22
38946	Correlated interface electron gas in infinite-layer nickelate versus cuprate films on <mml:math xmlns:mml="http://www.w3.org/1998/Math/MathML"><mml:mrow><mml:msub><mml:mi>SrTiO</mml:mi><mml:mn>3</mml:mn></mml:msub></mml:mrow></mml:math> Physical Review Research, 2021, 3, .	1.3	20
38947	THE FIRST PRINCIPLE STUDY OF COMPARISON OF DIVALENT AND TRIVALENT IMPURITY IN RRAM DEVICES USING GGA+U. Surface Review and Letters, 2021, 28, 2150039.	0.5	1
38948	Lowâ€Temperature Growth of Highâ€Quality Ag₂HgS₂ Crystals for Setup of Weakâ€Light UVâ€“Visibleâ€“NIR Photodetectors. Advanced Optical Materials, 2021, 9, 2002080.	3.6	3

#	Article	IF	Citations
38949	First-principles study on the geometric, electronic and thermodynamic properties of the CsPbI3 (001) surfaces. IOP Conference Series: Earth and Environmental Science, 2021, 692, 022020.	0.2	2
38950	High temperature stability, metallic character and bonding of the Si2BN planar structure. Journal of Physics Condensed Matter, 2021, 33, 165001.	0.7	2
38951	Tuning the Morphological, Photophysical, and Electronic Properties of CsPb(Cl/Br)₃ by Impurity Doping for Optoelectronic Applications: A Theoretical and Experimental Study. IEEE Journal of Photovoltaics, 2021, 11, 379-385.	1.5	4
38952	Transition metal doped C3N monolayer as efficient electrocatalyst for carbon dioxide electroreduction: A computational study. Applied Surface Science, 2021, 542, 148568.	3.1	14
38953	Structural, mechanical, electronic properties, and Debye temperature of quaternary carbide Ti₃NiAl₂C ceramics under high pressure: A first-principles study*. Chinese Physics B, 2021, 30, 036202.	0.7	1
38954	Hierarchical thermal transport mechanisms in Yb2Si2O7 multifunctional thermal and environmental barrier coating (TEBC) material. Scripta Materialia, 2021, 194, 113704.	2.6	5
38955	GW band structure of monolayer <mml:math xmlns:mml="http://www.w3.org/1998/Math/MathML"><mml:msub><mml:mrow><mml:mi>MoS</mml:mi></mml:mrow><mml:mn>2</r using the SternheimerGW method and effect of dielectric environment. Physical Review B, 2021, 103, .	1.1	11
38956	Atomistic study on helium-to-vacancy ratio of neutron irradiation induced helium bubbles during nucleation and growth in Î±-Fe. Nuclear Materials and Energy, 2021, 26, 100940.	0.6	1
38957	Computational insights in predicting structural, mechanical, electronic, magnetic and optical properties of EuAlO3 cubic-perovskite using FP-LAPW method. Computational Condensed Matter, 2021, 26, e00537.	0.9	6
38958	Effect of vacancy defects on the electronic transport properties of anÂAgâ€“ZnOâ€“Pt sandwich structure. Journal of Computational Electronics, 2021, 20, 798-804.	1.3	0
38959	Frontispiz: Die entscheidende Rolle von lokalen Ladungsfluktuationen beim Wachstum von Dendriten auf Lithiumâ€Elektroden. Angewandte Chemie, 2021, 133, .	1.6	0
38960	Electron-Phonon Coupling and Superconductivity in YC2 Compound upon Compression. Journal of Superconductivity and Novel Magnetism, 2021, 34, 1311.	0.8	2
38961	Single-Atom High-Valent Fe(IV) for Promoted Photocatalytic Nitrogen Hydrogenation on Porous TiO₂-SiO₂. ACS Catalysis, 2021, 11, 4362-4371.	5.5	70
38962	Theoretical study of reduction mechanism of Fe2O3 by H2 during chemical looping combustion. Chinese Journal of Chemical Engineering, 2021, 37, 175-183.	1.7	12
38963	Ab-Initio Calculations of Oxygen Vacancy in Ga₂O₃ Crystals. Latvian Journal of Physics and Technical Sciences, 2021, 58, 3-10.	0.4	12
38964	Colossal Spin Splitting in the Monolayer of the Collinear Antiferromagnet MnF₂. Journal of Physical Chemistry Letters, 2021, 12, 2363-2369.	2.1	17
38965	Competitive adsorption geometries for the arsenate As(V) and phosphate P(V) oxyanions on magnetite surfaces: Experiments and theory. American Mineralogist, 2021, 106, 374-388.	0.9	24
38966	2Dâ€HARECXS analysis of dopant and oxygen vacancy sites in Alâ€doped yttrium titanate. Journal of the American Ceramic Society, 2021, 104, 3760-3769.	1.9	3

#	Article	IF	Citations
38967	First principle calculation of structural, electronic and optical properties of CdS and doped Cdx-1AxS (A=Co, Fe, Ni) compounds. Materials Today Communications, 2021, 26, 101882.	0.9	4
38968	Influence of Se doping on recently synthesized NaInS2-xSex solid solutions for potential thermo-mechanical applications studied via first-principles method. Materials Today Communications, 2021, 26, 101988.	0.9	9
38969	Adsorption of small pollutant molecules on monolayer blue phosphorus. Materials Today Communications, 2021, 26, 102123.	0.9	2
38970	Single-metal-atom site with high-spin state embedded in defective BN nanosheet promotes electrocatalytic nitrogen reduction. Nano Research, 2021, 14, 4211-4219.	5.8	55
38971	oI20-carbon: A new superhard carbon allotrope. Diamond and Related Materials, 2021, 113, 108284.	1.8	9
38972	Energetic Validation of Various Crystal Structures in Zr₂CoZ (Z = Al, Ga, In) Heusler Alloys. Crystal Growth and Design, 2021, 21, 2222-2232.	1.4	3
38973	First-principles calculations study the mechanical and thermal properties of Crâ€“Alâ€“B ternary borides. Solid State Communications, 2021, 326, 114182.	0.9	16
38974	Dynamical polarizability of graphene with spatial dispersion. Physical Review B, 2021, 103, .	1.1	23
38975	Indentation Strengths of Zirconium Diboride: Intrinsic versus Extrinsic Mechanisms. Journal of Physical Chemistry Letters, 2021, 12, 2848-2853.	2.1	54
38976	A Vacancy-Driven Intermetallic Phase: Rh₃Cd_{5â^Î´} (Î´ â‰¤ 0.56). Inorganic Chemistry, 2021, 60, 5488-5496.	1.9	7
38977	Titanium Iodates with a Second-Harmonic-Generation Response. Inorganic Chemistry, 2021, 60, 5821-5828.	1.9	6
38978	Lattice stability of ordered Au-Cu alloys in the warm dense matter regime. Physical Review B, 2021, 103, .	1.1	8
38979	Radiation damage behavior of amorphous SiOC polymer-derived ceramics: the role of in situ formed free carbon. Journal of Nuclear Materials, 2021, 545, 152652.	1.3	1
38980	Reactivity of Single Transition Metal Atoms on a Hydroxylated Amorphous Silica Surface: A Periodic Conceptual DFT Investigation. Chemistry - A European Journal, 2021, 27, 6050-6063.	1.7	11
38981	Theoretical Prediction of P-Triphenylene-Graphdiyne as an Excellent Anode Material for Li, Na, K, Mg, and Ca Batteries. Applied Sciences (Switzerland), 2021, 11, 2308.	1.3	7
38982	Two-dimensional carbon nitride C₆N nanosheet with egg-comb-like structure and electronic properties of a semimetal. Nanotechnology, 2021, 32, 215702.	1.3	50
38983	Theoretical Insights into Morphologies of Alkali-Promoted Cobalt Carbide Catalysts for Fischerâ€“Tropsch Synthesis. Journal of Physical Chemistry C, 2021, 125, 6061-6072.	1.5	12
38984	High-throughput first-principles search for ceramic superlattices with improved ductility and fracture resistance. Acta Materialia, 2021, 206, 116615.	3.8	19

#	Article	IF	Citations
38985	The open-framework structure of KSbGe3O9 flux-grown crystals investigated by X-ray diffraction, vibrational spectroscopy, and DFT calculations. Journal of Solid State Chemistry, 2021, 295, 121925.	1.4	4
38986	Localized Electron Density Engineering for Stabilized B-Î³ CsSnI₃-Based Perovskite Solar Cells with Efficiencies >10%. ACS Energy Letters, 0, , 1480-1489.	8.8	125
38987	Zeolitic imidazole framework-derived FeN5-doped carbon as superior CO2 electrocatalysts. Journal of Catalysis, 2021, 395, 63-69.	3.1	27
38988	Theoretical Investigation of Structural, Electronic Properties and Half-Metallic Ferromagnetism in Ca1â^'xTixS ternary alloys. Journal of Superconductivity and Novel Magnetism, 2021, 34, 1441-1452.	0.8	3
38989	Constructed Interfacial Oxygenâ€Bridge Chemical Bonding in Coreâ€Shell Transition Metal Phosphides/Carbon Hybrid Boosting Oxygen Evolution Reaction. ChemSusChem, 2021, 14, 2188-2197.	3.6	26
38990	A strategy of optimizing magnetism and hysteresis simultaneously in Niâ€“Mn-based metamagnetic shape memory alloys. Intermetallics, 2021, 130, 107063.	1.8	8
38991	Construction of Spatial Effect from Atomically Dispersed Co Anchoring on Subnanometer Ru Cluster for Enhanced N₂-to-NH₃ Conversion. ACS Catalysis, 2021, 11, 4430-4440.	5.5	28
38992	Ozone Decomposition by a Manganese-Organic Framework over the Entire Humidity Range. Journal of the American Chemical Society, 2021, 143, 5150-5157.	6.6	53
38993	Physical properties of ultrasonically spray deposited Yttrium-doped SnO2 nanostructured films: supported by DFT study. Applied Physics A: Materials Science and Processing, 2021, 127, 1.	1.1	4
38994	Re-evaluation of the electronic structure and thermoelectric properties of narrow-gap semiconducting Î±-SrSi2: A complementary experimental and first-principles hybrid-functional approach. Journal of Applied Physics, 2021, 129, .	1.1	6
38995	First-Principles Calculation of the Evaporation Field and Roll-up Effect of M (M = Fe, Cu, Si, and Mn) on the Fe (001) and Fe Step Structure. Microscopy and Microanalysis, 2022, 28, 1181-1187.	0.2	4
38996	First-principles calculations of structural, elastic, electronic, and optical properties of CaYP (Y = Cu,) Tj ETQq1 1 0.784314 rgBT /Overlock	3.2	28
38997	First principle study of electronic properties of ZnO nanoclusters with native point defects during gas adsorption. Applied Nanoscience (Switzerland), 2022, 12, 983-993.	1.6	1
38998	Tuning electronic properties of pentagonal PdSe2 monolayer by applying external strain. Indian Journal of Physics, 2022, 96, 1037-1043.	0.9	1
38999	Topological insulators in the NaCaBi family with large spin-orbit coupling gaps. Physical Review Research, 2021, 3, .	1.3	7
39000	Intervalence charge transfer of Ti and Fe defects in blue kyanite. Journal of the Korean Physical Society, 2021, 78, 671-678.	0.3	0
39001	Simulations of hydrogen outgassing and sticking coefficients at a copper electrode surface: Dependencies on temperature, incident angle and energy. Physical Review Research, 2021, 3, .	1.3	4
39002	A new activity model for Feâ€“Mgâ€“Al biotites: Iâ€”Derivation and calibration of mixing parameters. Contributions To Mineralogy and Petrology, 2021, 176, 1.	1.2	0

#	Article	IF	Citations
39003	Decoupling Lattice and Magnetic Instabilities in Frustrated CuMnO₂. Inorganic Chemistry, 2021, 60, 6004-6015.	1.9	7
39004	Corrosion mechanism of Ni deposits on magnets by pulse current electro-deposition. Surface and Coatings Technology, 2021, 409, 126833.	2.2	6
39005	Investigations of the stability and electronic structures of U3Si2-Al: A first-principles study. Chemical Physics, 2021, 543, 111088.	0.9	7
39006	and <mml:math xmlns:mml="http://www.w3.org/1998/Math/MathML" altimg="si2.svg"><mml:mrow><mml:mo>{</mml:mo><mml:mrow><mml:mn>10</mml:mn><mml:mover	1.3	4
39007	Buckling of boron nanotubes under axial compression: Insights from molecular mechanics and continuum mechanics. Physica E: Low-Dimensional Systems and Nanostructures, 2021, 127, 114520.	1.3	3
39008	On the atomic structure of Pt(1 1 1)/Î³-Al2O3(1 1 1) interfaces and the changes in their interfacial energy with temperature and oxygen pressure. Applied Surface Science, 2021, 542, 148594.	3.1	5
39009	Fast Correction of Errors in the DFTâ€Calculated Energies of Gaseous Nitrogenâ€Containing Species. ChemCatChem, 2021, 13, 2508-2516.	1.8	21
39010	Firstâ€principles study on structural, electronic, magnetic, elastic, mechanical and thermodynamic properties of <scp> Mn ₂ PtCo </scp> Heusler alloy. International Journal of Energy Research, 2021, 45, 11305-11319.	2.2	27
39011	3d Transitionâ€Metalâ€Mediated Columbite Nanocatalysts for Decentralized Electrosynthesis of Hydrogen Peroxide. Small, 2021, 17, e2007249.	5.2	35
39012	Origin of low thermal conductivity in monolayer PbI2. Solid State Communications, 2021, 327, 114223.	0.9	7
39013	Atomic Design and Fine-Tuning of Subnanometric Pt Catalysts to Tame Hydrogen Generation. ACS Catalysis, 2021, 11, 4146-4156.	5.5	52
39014	Sulfur vacancy-rich MoS2 as a catalyst for the hydrogenation of CO2 to methanol. Nature Catalysis, 2021, 4, 242-250.	16.1	308
39015	A first-principles study of reaction mechanism over carbon decorated oxygen-deficient TiO2 supported Pd catalyst in direct synthesis of H2O2. Chinese Journal of Chemical Engineering, 2021, 31, 126-134.	1.7	10
39016	From Monolayers to Nanotubes: Toward Catalytic Transition-Metal Dichalcogenides for Hydrogen Evolution Reaction. Energy & Fuels, 2021, 35, 6282-6288.	2.5	10
39017	High-throughput screening to modulate electronic and optical properties of alloyed Cs₂AgBiCl₆ for enhanced solar cell efficiency. JPhys Materials, 2021, 4, 025005.	1.8	14
39018	Dimensional transformation of chemical bonding during crystallization in a layered chalcogenide material. Scientific Reports, 2021, 11, 4782.	1.6	16
39019	First-principles study on the structural, elastic, piezoelectric and electronic properties of (BaTiO3,) Tj ETQq0 0 0 rgBT /Overlock 10 Tf 50	0.9	4
39020	Highly Enhanced Electro-acoustic Properties of YAlN/Sapphire Based Surface Acoustic Wave Devices for Next Generation of Microelectromechanical Systems. Materials Today Communications, 2021, 26, 102067.	0.9	6

#	Article	IF	Citations
39021	Strain engineering the topological type-II Dirac semimetal NiTe2. Physical Review B, 2021, 103, .	1.1	23
39022	High thermoelectric efficiency fluoride perovskite materials of AgMF3 (MÂ= Zn, Cd). Materials Today Energy, 2021, 19, 100611.	2.5	12
39023	Preparation of hydrogen, fluorine and chlorine doped and co-doped titanium dioxide photocatalysts: a theoretical and experimental approach. Scientific Reports, 2021, 11, 5700.	1.6	30
39024	Selectivity of the First Two Glycerol Dehydrogenation Steps Determined Using Scaling Relationships. ACS Catalysis, 2021, 11, 3487-3497.	5.5	19
39025	Unraveling the intrinsic atomic physics behind x-ray absorption line shifts in warm dense silicon plasmas. Physical Review E, 2021, 103, 033202.	0.8	10
39026	Redirecting dynamic surface restructuring of a layered transition metal oxide catalyst for superior water oxidation. Nature Catalysis, 2021, 4, 212-222.	16.1	266
39027	Novel 2D B₂S₃ as a metal-free photocatalyst for water splitting. Nanotechnology, 2021, 32, 225401.	1.3	11
39028	Investigation of Sr_{0.7}Ca_{0.3}FeO₃ Oxygen Carriers with Variable Cobalt Bâ€Site Substitution. ChemSusChem, 2021, 14, 1893-1901.	3.6	7
39029	A Computational and Spectroscopic Study of the Electronic Structure of V2O5-Based Cathode Materials. Journal of Physical Chemistry C, 2021, 125, 5848-5858.	1.5	7
39030	Optimizing Active Sites for High CO Selectivity during CO₂ Hydrogenation over Supported Nickel Catalysts. Journal of the American Chemical Society, 2021, 143, 4268-4280.	6.6	100
39031	Oxygen Evolution on Iron Oxide Nanoparticles: The Impact of Crystallinity and Size on the Overpotential. Journal of the Electrochemical Society, 2021, 168, 034518.	1.3	15
39032	Strain effect on the electronic and optical properties of 2D Tetrahexcarbon: a DFT-based study. Indian Journal of Physics, 2021, 95, 2365-2373.	0.9	39
39033	Zinc gallate spinel dielectric function, band-to-band transitions, and Î“-point effective mass parameters. Applied Physics Letters, 2021, 118, .	1.5	9
39034	Beyond templating: Electronic structure impacts of aromatic cations in organicâ€“inorganic antimony chlorides. Zeitschrift Fur Anorganische Und Allgemeine Chemie, 2021, 647, 857-866.	0.6	1
39035	Effects of magnetic impurity concentration and hole carriers on ferromagnetic stability of Li(ZnCr)As and Li(ZnCrCu)As. Results in Physics, 2021, 22, 103901.	2.0	0
39036	Synergistic Effect of Boron Nitride and Carbon Domains in Boron Carbide Nitride Nanotube Supported Singleâ€Atom Catalysts for Efficient Nitrogen Fixation. Chemistry - A European Journal, 2021, 27, 6945-6953.	1.7	17
39037	Electrolyte Interphase Built from Anionic Covalent Organic Frameworks for Lithium Dendrite Suppression. Advanced Functional Materials, 2021, 31, 2009718.	7.8	43
39038	Theoretical investigation of novel half Heusler compounds MRhSb (M = Nb & Ta): For optoelectronic and thermoelectric applications. International Journal of Quantum Chemistry, 2021, 121, e26656.	1.0	0

#	Article	IF	Citations
39039	Regioselective Construction of Chemically Transformed Phosphideâ€“Metal Nanoheterostructures for Enhanced Hydrogen Evolution Catalysis. Inorganic Chemistry, 2021, 60, 7269-7275.	1.9	4
39040	FeMoO4 Revisited: Crosslike 90Â° Noncollinear Antiferromagnetic Structure Caused by Dzyaloshinskiiâ€“Moriya Interaction. Journal of Physical Chemistry C, 2021, 125, 5947-5956.	1.5	4
39041	Indium(III) in the â€œPeriodic Tableâ€•of Di(2-pyridyl) Ketone: An Unprecedented Transformation of the Ligand and Solid-State 115In NMR Spectroscopy as a Valuable Structural Tool. Inorganic Chemistry, 2021, 60, 4829-4840.	1.9	4
39042	Dynamic and Intermediate-Specific Local Coverage Controls the Syngas Conversion on Rh(111) Surfaces: An Operando Theoretical Analysis. ACS Catalysis, 2021, 11, 3830-3841.	5.5	9
39043	Impact of ordering on the reactivity of mixed crystals of topological insulators with anion substitution: Bi2SeTe2 and Sb2SeTe2. Applied Surface Science, 2021, 541, 148490.	3.1	0
39044	Electronic properties and stability of 4â€“8 B C N monolayers. Solid State Communications, 2021, 326, 114174.	0.9	0
39045	Effect of lattice polarisability in optical properties of methylammonium lead iodide by modified Becke-Johnson functionals and Bethe-Salpeter equation. Computational Materials Science, 2021, 189, 110245.	1.4	0
39046	Electronic properties, high pressure phase stability and elastic anisotropy of BC5. Scientific African, 2021, 11, e00710.	0.7	1
39047	Occurrence of nonohmic trend in the ballistic transport mode of a modelled low dimensional device capable of performing electronic functions. Superlattices and Microstructures, 2021, 151, 106808.	1.4	3
39048	A first-principles and machine learning combined method to investigate the interfacial friction between corrugated graphene. Modelling and Simulation in Materials Science and Engineering, 2021, 29, 035011.	0.8	2
39049	Group Theory Analysis to Study Phase Transitions of Quasi-2D Sr3Hf2O7. Nanomaterials, 2021, 11, 897.	1.9	5
39050	Robust quantum anomalous Hall effect in a pentagonal MoS2 monolayer grown on CuI(001) substrates. Physical Review B, 2021, 103, .	1.1	2
39051	Surface localized phonon modes at the Si(553)-Au nanowire system. Physical Review B, 2021, 103, .	1.1	6
39052	Real-space observation of ferroelectrically induced magnetic spin crystal in SrRuO3. Nature Communications, 2021, 12, 2007.	5.8	21
39053	Shock-compressed silicon: Hugoniot and sound speed up to 2100 GPa. Physical Review B, 2021, 103, .	1.1	13
39054	An ab initio study of structural, elastic and electronic properties of hexagonal MAuGe (M = Lu, Sc) compounds. Condensed Matter Physics, 2021, 24, 13706.	0.3	3
39055	Evaluation of similarities and differences of LiTaO₃ and LiNbO₃ based on high-T-conductivity, nonlinear optical fs-spectroscopy and ab initio modeling of polaronic structures. New Journal of Physics, 2021, 23, 033016.	1.2	19
39056	High-throughput computational search for two-dimensional binary compounds: Energetic stability versus synthesizability of three-dimensional counterparts. Physical Review B, 2021, 103, .	1.1	9

#	Article	IF	Citations
39057	A Convenient Method for Synthesis of Fe₃O₄/FeS₂ as High-Performance Electrocatalysts for Oxygen Evolution Reaction and Zinc-Air Batteries. Journal of the Electrochemical Society, 2021, 168, 030517.	1.3	4
39058	Site preference, atomic ordering, electronic structure and chemical bonding of A3Pd5 (A= Mg, Al, Ga): First principles study. Solid State Sciences, 2021, 113, 106544.	1.5	3
39059	Synthesis of the scandium chloride hydrates ScCl₃Â·3H₂O and Sc₂Cl₄(OH)₂Â·12H₂O and their characterisation by X-ray diffraction, ⁴⁵Sc NMR spectroscopy and DFT calculations. Zeitschrift Fur Naturforschung - Section B Journal of Chemical Sciences, 2021, 76, 217-225.	0.3	3
39060	Electrochemical reduction of acetonitrile to ethylamine. Nature Communications, 2021, 12, 1949.	5.8	47
39061	Electric field induced topological phase transition and large enhancements of spin-orbit coupling and Curie temperature in two-dimensional ferromagnetic semiconductors. Physical Review B, 2021, 103, .	1.1	33
39062	Theoretical insight into two-dimensional M-Pc monolayer as an excellent material for formaldehyde and phosgene sensing. Applied Surface Science, 2021, 543, 148805.	3.1	31
39063	Effect of Ni doping on optical, structural, and morphological properties of ZnO thin films synthesized by MSILAR: Experimental and DFT study. Materialia, 2021, 15, 101015.	1.3	9
39064	Structure-Dependent (Non)Linear Optical Excitons in Primary Cyclic Ammonium (CnH2nâ€“1NH2; n =) Tj ETQq1 1 0.784314 rgBT /Ov 6821-6831.	1.5	4
39065	Electrical Switch of Poissonâ€™s Ratio in IVâ€“VI Monolayers via Pseudophase Transitions. Journal of Physical Chemistry Letters, 2021, 12, 3217-3223.	2.1	1
39066	Effects of High and Low Salt Concentrations in Electrolytes at Lithiumâ€“Metal Anode Surfaces Using DFT-ReaxFF Hybrid Molecular Dynamics Method. Journal of Physical Chemistry Letters, 2021, 12, 2922-2929.	2.1	32
39067	Surface modification by poly(ethylene glycol) with different end-grafted groups: Experimental and theoretical study. Biointerphases, 2021, 16, 021002.	0.6	1
39068	Hydrogen Adsorption on Au-Supported Pt and Pd Nanoislands: A Computational Study of Hydrogen Coverage Effects. Journal of Physical Chemistry C, 2021, 125, 5110-5115.	1.5	6
39069	Semiconducting Chalcogenide Alloys Based on the (Ge, Sn, Pb) (S, Se, Te) Formula with Outstanding Properties: A First-Principles Calculation Study. ACS Omega, 2021, 6, 9433-9441.	1.6	20
39070	2D constraint modifies packing behaviour: a halobenzene monolayer with X3 halogen-bonding motif. Molecular Physics, 2021, 119, e1900940.	0.8	2
39071	Nominal Effect of Mg Intercalation on the Superconducting Properties of 2Hâ€“NbSe₂. Inorganic Chemistry, 2021, 60, 4588-4598.	1.9	9
39072	Interface Engineering of Cu(In,Ga)Se₂ Solar Cells by Optimizing Cd- and Zn-Chalcogenide Alloys as the Buffer Layer. ACS Applied Materials & Interfaces, 2021, 13, 15237-15245.	4.0	13
39073	N-doping enabled defect-engineering of MoS2 for enhanced and selective adsorption of CO2: A DFT approach. Applied Surface Science, 2021, 542, 148556.	3.1	37
39074	Polyelemental Nanoparticles as Catalysts for a Liâ€“O₂ Battery. ACS Nano, 2021, 15, 4235-4244.	7.3	38

#	Article	IF	Citations
39075	First-Principles Study of Bi³⁺-Related Luminescence and Electron and Hole Traps in (Y/Lu/La)PO₄. Inorganic Chemistry, 2021, 60, 4434-4446.	1.9	34
39076	Effect of Wâ€'O bonding on gas sensitivity of nanocrystalline Bi2WO6 and WO3. Journal of Alloys and Compounds, 2021, 856, 158159.	2.8	12
39077	Impact of stoichiometry and strain on Ge1â^'x Sn x alloys from first principles calculations. Journal Physics D: Applied Physics, 2021, 54, 245103.	1.3	4
39078	Theoretical prediction of structural stability, elastic and magnetic properties for Mn₂NiGa alloy. Modern Physics Letters B, 2021, 35, 2150231.	1.0	2
39079	Stability, electronic structure, mechanical properties and lattice thermal conductivity of FeS and FeS₂ polymorphs. Modern Physics Letters B, 2021, 35, 2150225.	1.0	1
39080	Study of the chromium doping effect in boron phosphide semiconductors. International Journal of Computational Materials Science and Engineering, 2021, 10, 2150006.	0.5	2
39081	Polymerization of silanes through dehydrogenative Siâ€"Si bond formation on metal surfaces. Nature Chemistry, 2021, 13, 350-357.	6.6	11
39082	Effects of copper ion irradiation on $${mathbf{C}mathbf{u}}_{mathbf{y}}{mathbf{Z}mathbf{n}}_{1-2mathbf{y}-mathbf{x}}{mathbf{M}mathbf{n}}_{mathbf{x}}{mathbf{O}}_{mathbf{y}}$$ supercapacitive electrodes. Journal of Applied Electrochemistry, 2021, 51, 829-845.	1.5	1
39084	First principle study of structural, elastic, electronic and optical properties of Pb0.5Sn0.5TiO3 and Pb0.5Sn0.5Ti0.5(Zr0.5)O3. Condensed Matter Physics, 2021, 24, 13702.	0.3	0
39085	Origin of the band gap in Bi-intercalated graphene on Ir(111). 2D Materials, 2021, 8, 035007.	2.0	1
39086	Revealing the Absolute Direction of the Dzyaloshinskii-Moriya Interaction in Prototypical Weak Ferromagnets by Polarized Neutrons. Physical Review X, 2021, 11, .	2.8	5
39087	Accurate calculation of excitonic signatures in the absorption spectrum of BiSBr using semiconductor Bloch equations. Physical Review B, 2021, 103, .	1.1	3
39088	Phase stability of Au-Li binary systems studied using neural network potential. Physical Review B, 2021, 103, .	1.1	12
39089	AB-stacked nanosheet-based hexagonal boron nitride. Acta Crystallographica Section B: Structural Science, Crystal Engineering and Materials, 2021, 77, 260-265.	0.5	7
39090	Interaction of hydrogen with palladiumâ€"copper nanoalloys. Theoretical Chemistry Accounts, 2021, 140, 1.	0.5	7
39091	Modified embedded-atom method potentials for the plasticity and fracture behaviors of unary fcc metals. Physical Review B, 2021, 103, .	1.1	5
39092	Identification of earth-abundant materials for selective dehydrogenation of light alkanes to olefins. Proceedings of the National Academy of Sciences of the United States of America, 2021, 118, .	3.3	10
39093	Computational studies of the electronic structure of copper-doped ZnO quantum dots. Journal of Chemical Physics, 2021, 154, 124710.	1.2	3

#	Article	IF	Citations
	Antiferromagnetic semiconductor in porous boron nitride (<mml:math) Tj ETQq0 0 0 rgBT /Overlock 10 Tf 50 757 Td (xmlns:mml="http:		
39094	sheet: First-principles investigation. Computational and Theoretical Chemistry, 2021, 1197, 113155.	1.1	9
39095	Two-dimensional Janus Ti3C2F O2- MXene with tunable electronic and mechanical properties. Scripta Materialia, 2021, 194, 113688.	2.6	3
39096	A first-principles computation-driven mechanism study on the solders dilute doping effects to Î·â€™-Cu6Sn5 growth kinetics. Journal of Materials Science, 2021, 56, 9741-9753.	1.7	5
39097	ab initio study of oxygen vacancy effects on structural, electronic and thermoelectric behavior of AZr1-xMxO3 (AÂ= Ba, Ca, Sr; M= Al, Cu, xÂ= 0.25) for application of memory devices. Journal of Molecular Graphics and Modelling, 2021, 103, 107825.	1.3	14
39098	Understanding Methanol Synthesis on Inverse ZnO/CuO_x/Cu Catalysts: Stability of CH₃O Species and Dynamic Nature of the Surface. Journal of Physical Chemistry C, 2021, 125, 6673-6683.	1.5	21
39099	Thiazoleâ€Linked Covalent Organic Framework Promoting Fast Twoâ€Electron Transfer for Lithiumâ€Organic Batteries. Advanced Energy Materials, 2021, 11, 2003735.	10.2	78
39100	Quantum spin liquid and cluster Mott insulator phases in the Mo3O8 magnets. Npj Quantum Materials, 2021, 6, .	1.8	13
39101	Band Engineering and Van Hove Singularity on HfX₂ Thin Films (X = S, Se, or Te). ACS Applied Electronic Materials, 2021, 3, 1071-1079.	2.0	17
39102	Diverse structural and electronic properties of pentagonal SiC2 nanoribbons: A first-principles study. Materials Today Communications, 2021, 26, 102047.	0.9	3
39103	Study of Surface Stability and Electronic Structure of a Bi-terminated InAs (001) Surface Based on Ab Initio Calculations. Journal of Electronic Materials, 2021, 50, 3527-3536.	1.0	3
39104	Enforced Long-Range Order in 1D Wires by Coupling to Higher Dimensions. Physical Review Letters, 2021, 126, 106101.	2.9	14
39105	First-principles prediction of ideal type-II Weyl phonons in wurtzite ZnSe. Physical Review B, 2021, 103, .	1.1	21
39106	Insights into the physical properties of inverse-Heusler alloy Cr₂CoGa via density functional theory. Physica Scripta, 2021, 96, 055704.	1.2	8
39107	Flexoelectric-like radial polarization of single-walled nanotubes from first-principles. Electronic Structure, 2021, 3, 015001.	1.0	11
39108	Two-dimensional Janus monolayers of MoSSe as promising sensor towards selected adulterants compounds. Applied Surface Science, 2021, 542, 148590.	3.1	29
39109	Theoretical analysis of the adsorption of phosphoric acid and model phosphate monoesters on CeO2(111). Surface Science, 2021, 705, 121776.	0.8	6
39110	Phase Relations in the Niâ€“S System at High Pressures from ab Initio Computations. ACS Earth and Space Chemistry, 2021, 5, 596-603.	1.2	2
39111	Enhanced electrochemical CO2 reduction to ethylene over CuO by synergistically tuning oxygen vacancies and metal doping. Cell Reports Physical Science, 2021, 2, 100356.	2.8	39

#	Article	IF	Citations
39112	Graphene on Rh(111): A template for growing ordered arrays of metal nanoparticles with different periodicities. Carbon, 2021, 173, 1073-1081.	5.4	10
39113	A comparative study on the twinning boundaries of five-fold twinned copper and gold nanorods. Applied Surface Science, 2021, 543, 148764.	3.1	6
39114	Strong metalâ€“support interaction between palladium and gallium oxide within monodisperse nanoparticles: self-supported catalysts for propyne semi-hydrogenation. Journal of Catalysis, 2021, 395, 36-45.	3.1	21
39115	Experimental and Theoretical Investigation of the Structural and Optoâ€electronic Properties of Feâ€Doped Leadâ€Free Cs₂AgBiCl₆ Double Perovskite. Chemistry - A European Journal, 2021, 27, 7408-7417.	1.7	28
39116	Interaction of Aromatic Molecules with Forsterite: Accuracy of the Periodic DFT-D4 Method. Journal of Physical Chemistry A, 2021, 125, 2770-2781.	1.1	2
39117	Highâ€Throughput Oneâ€Photon Excitation Pathway in 0D/3D Heterojunctions for Visibleâ€Light Driven Hydrogen Evolution. Advanced Functional Materials, 2021, 31, 2100816.	7.8	92
39118	Switching polymorph stabilities with impurities provides a thermodynamic route to benzamide form III. Communications Chemistry, 2021, 4, .	2.0	25
39119	An investigation on CdS1-xTex interface compound in CdS/CdTe hetero-junction solar cells by density functional theory (DFT). Superlattices and Microstructures, 2021, 151, 106805.	1.4	14
39120	Breaking atomic-level ordering via biaxial strain in functional oxides: A DFT study. Journal of Applied Physics, 2021, 129, 095301.	1.1	8
39121	M₃B₆O₁₀NO₃ (Mâ€…=â€…K, Rb): Two New Alkali Metal Borateâ€Nitrates with Noncentrosymmetric Structures. European Journal of Inorganic Chemistry, 2021, 2021, 1297-1304.	1.0	12
39122	Atomic forces by quantum Monte Carlo: Application to phonon dispersion calculations. Physical Review B, 2021, 103, .	1.1	12
39123	Role of Hydrogen-bonded Bimolecular Formic Acidâ€“Formate Complexes for Formic Acid Decomposition on Copper: A Combined First-Principles and Microkinetic Modeling Study. ACS Catalysis, 2021, 11, 4349-4361.	5.5	19
39124	Carboxylated Graphene Nanoribbons for Highly-Selective Ammonia Gas Sensors: Ab Initio Study. Chemosensors, 2021, 9, 84.	1.8	7
39125	Manipulation of CO adsorption over Me1/CeO2 by heterocation doping: Key roles of single-atom adsorption energy. Journal of Chemical Physics, 2021, 154, 164705.	1.2	5
39126	Comparative study of single-atom gold and iridium on CeO2{111}. Journal of Chemical Physics, 2021, 154, 164703.	1.2	2
39127	Superior thermoelectric performance of Î±-Se₂Te monolayer. Materials Research Express, 2021, 8, 045507.	0.8	4
39128	Columnar antiferromagnetic order of a MBene monolayer. Physical Review B, 2021, 103, .	1.1	10
39129	The First Principles Calculation on the Raman Spectrum and Optical Properties of the Defect Monolayer MoS2. Brazilian Journal of Physics, 2021, 51, 493-498.	0.7	6

#	Article	IF	Citations
39130	Quantum transport observed in films of the magnetic topological semimetal EuSb2. Physical Review B, 2021, 103, .	1.1	1
39131	Investigation of optoelectronic properties of AgIn1â^'xGaxY2 (Yâ€‰=â€‰Se, Te) semiconductors. Indian Journal of Physics, 0, , 1.	0.9	0
39132	Investigation of the new half metallic ferromagnetic quaternary Heusler compounds LiX'NO (X'= Ba,) Tj ETQq0 0 0 rgBT /Overlock 10 Tf	0.6	0
39133	High-mobility p-type semiconducting two-dimensional Î²-TeO2. Nature Electronics, 2021, 4, 277-283.	13.1	75
39134	A lithium nucleation-diffusion-growth mechanism to govern the horizontal deposition of lithium metal anode. Science China Materials, 2021, 64, 2409-2420.	3.5	22
39135	Study of the structural phase transition in diamond (100) & (111) surfaces. Carbon Trends, 2021, 3, 100033.	1.4	7
39136	Insight into the adsorption mechanisms of CH4, CO2, and H2O molecules on illite (001) surfaces: A first-principles study. Surfaces and Interfaces, 2021, 23, 101039.	1.5	4
39137	Theoretical investigation of the reactivity of flat Ni (111) and stepped Ni (211) surfaces for acetic acid hydrogenation to ethanol. International Journal of Hydrogen Energy, 2021, 46, 15454-15470.	3.8	7
39138	Materials properties, lattice dynamics and polaron characteristics in InSbxP1-x ternary alloys. Materials Science in Semiconductor Processing, 2021, 125, 105640.	1.9	2
39139	The mechanical and electronic properties of o-Fe2C, h-Fe3C, t-Fe5C2, m-Fe5C2 and h-Fe7C3 compounds: First-principles calculations. Physica B: Condensed Matter, 2021, 606, 412825.	1.3	4
39140	Structural, elastic, thermodynamic, electronic, and optical properties of $$hbox {CaMg}_{2}hbox {AN}_{3}$$($$hbox {A}=hbox {Al}$$ and Ga): ab initio investigation. European Physical Journal B, 2021, 94, 1.	0.6	3
39141	Electronic properties and tunability of the hexagonal SiGe alloys. Applied Physics Letters, 2021, 118, .	1.5	10
39142	Optical and electronic properties of lead sulfide spherical nano particle. Optik, 2021, 231, 166503.	1.4	4
39143	A Metalâ€“Organic Framework Nanorodâ€Assembled Superstructure and Its Derivative: Unraveling the Fast Potassium Storage Mechanism in Nitrogenâ€Modified Micropores. Small, 2021, 17, e2100135.	5.2	19
39144	Structural and optical properties of ionic liquid-based hybrid perovskitoid: A combined experimental and theoretical investigation. Functional Materials Letters, 2021, 14, 2150008.	0.7	1
39145	Energetic stability and geometrical structure of variously terminated and N-doped diamond (111) surfaces â€“ A theoretical DFT study. Materials Chemistry and Physics, 2021, 262, 124283.	2.0	4
39147	MoirÃ© superlattice on the surface of a topological insulator. Physical Review B, 2021, 103, .	1.1	28
39148	Computational Exploration of Structural, Electronic, and Optical Properties of Novel Combinations of Inorganic Ruddlesdenâ€“Popper Layered Perovskites Bi₂XO₄(Xâ€‰=â€‰Be, Mg) using Tran and Blahaâ€Modified Beckeâ€“Johnson Approach for Optoelectronic Applications. Energy Technology, 2021, 9, 2001026.	1.8	23

#	Article	IF	Citations
39149	Carbon corrosion mechanism on nitrogen-doped carbon support â€" A density functional theory study. International Journal of Hydrogen Energy, 2021, 46, 13273-13282.	3.8	11
39150	Modulating Curie Temperature and Magnetic Anisotropy in Nanoscale-Layered Cr₂Te₃ Films: Implications for Room-Temperature Spintronics. ACS Applied Nano Materials, 2021, 4, 4810-4819.	2.4	25
39151	An Ab Initio Perspective on the Key Vacancy Defects of KMgF₃. Journal of Physical Chemistry C, 2021, 125, 8253-8267.	1.5	5
39152	FTIR Measurement of the Hydrogenated Si(100) Surface: The Structure-Vibrational Interpretation by Means of Periodic DFT Calculation. Journal of Physical Chemistry C, 2021, 125, 9219-9228.	1.5	2
39153	Achieving Highly Efficient Carbon Dioxide Electrolysis by In Situ Construction of the Heterostructure. ACS Applied Materials & Interfaces, 2021, 13, 20060-20069.	4.0	32
39154	Bonding behavior and passivation mechanism of organic ligands (-SH, -NH2, -COOH) on ZnS (<mml:math) Tj ETQq1 1 0.784314 rgBT /O surface from first-principles calculations. Applied Surface Science, 2021, 545, 148878.	3.1	9
39155	Prediction of Phonon-Mediated Superconductivity with High Critical Temperature in the Two-Dimensional Topological Semimetal W₂N₃. Nano Letters, 2021, 21, 3435-3442.	4.5	31
39156	First-principles study of hydrogen storage on Ca-decorated defective boron nitride nanosheets. Physica E: Low-Dimensional Systems and Nanostructures, 2021, 128, 114588.	1.3	29
39157	Revealing the Effect of Sodium on Iron-Based Catalysts for CO₂ Hydrogenation: Insights from Calculation and Experiment. Journal of Physical Chemistry C, 2021, 125, 7637-7646.	1.5	20
39158	Mulch-assisted ambient-air synthesis of oxygen-rich activated carbon for hydrogen storage: A combined experimental and theoretical case study. Applied Surface Science, 2021, 544, 148963.	3.1	18
39159	Unraveling electrochemical CO reduction of the single-atom transition metals supported on N-doped phosphorene. Applied Surface Science, 2021, 545, 148953.	3.1	11
39160	Gas Sensor Based on Semihydrogenated and Semifluorinated h-BN for SFâ‚† Decomposition Components Detection. IEEE Transactions on Electron Devices, 2021, 68, 1878-1885.	1.6	12
39161	Terahertz Driven Reversible Topological Phase Transition of Monolayer Transition Metal Dichalcogenides. Advanced Science, 2021, 8, e2003832.	5.6	25
39162	Superior Room-Temperature Ammonia Sensing Using a Hydrothermally Synthesized MoS₂/SnO₂ Composite. ACS Omega, 2021, 6, 11602-11613.	1.6	49
39163	A data fusion approach to optimize compositional stability of halide perovskites. Matter, 2021, 4, 1305-1322.	5.0	75
39164	A statistical approach for atomistic calculations of vacancy formation energy and chemical potentials in concentrated solid-solution alloys. Computational Materials Science, 2021, 190, 110308.	1.4	24
39165	Intrinsically low lattice thermal conductivity of monolayer hexagonal aluminum nitride (h-AlN) from first-principles: A comparative study with graphene. International Journal of Thermal Sciences, 2021, 162, 106772.	2.6	23
39166	Surface Sulfate Ion on CdS Catalyst Enhances Syngas Generation from Biopolyols. Journal of the American Chemical Society, 2021, 143, 6533-6541.	6.6	87

#	Article	IF	Citations
39167	Molecular Engineering toward an Enlarged Optical Band Gap in a Bismuth Sulfate via Homovalent Cation Substitution. Inorganic Chemistry, 2021, 60, 5851-5859.	1.9	12
39168	Selective Electrochemical Decarboxylation of n-Octanoic Acid to Hydrocarbons on Pt Nanocrystals. ACS Sustainable Chemistry and Engineering, 2021, 9, 5288-5297.	3.2	6
39169	Formic Acid Electrooxidation on Pt or Pd Monolayer on Transition-Metal Single Crystals: A First-Principles Structure Sensitivity Analysis. ACS Catalysis, 2021, 11, 5294-5309.	5.5	15
39170	CrI₃/Y₂CH₂ Heterointerface-Induced Stable Half-Metallicity of Two-Dimensional CrI₃ Monolayer Ferromagnets. ACS Applied Materials & Interfaces, 2021, 13, 16694-16703.	4.0	8
39171	Engineering the edge-terminations and defect-density to enhance the electrochemical capacitance performance of vertical graphene nanosheets. Applied Surface Science, 2021, 545, 149045.	3.1	17
39172	High-throughput screening for Weyl semimetals with <mml:math xmlns:mml="http://www.w3.org/1998/Math/MathML" altimg="si89.svg"><mml:mrow><mml:msub><mml:mrow><mml:mi mathvariant="normal">S</mml:mi></mml:mrow><mml:mrow><mml:mn>4</mml:mn></mml:mrow></mml:msub></mml:mrow></mml:m symmetry. Science Bulletin, 2021, 66, 667-675.	4.3	16
39173	Afterglow-Catalysis and Self-Reporting of Pollutant Degradation by Ethylenediaminetetraacetic Acid Disodium-Etched Cr:ZnGa2O4. Journal of Physical Chemistry C, 2021, 125, 9096-9106.	1.5	7
39174	Controlling potential difference between electrodes based on self-consistent-charge density functional tight binding. Journal of Chemical Physics, 2021, 154, 144107.	1.2	10
39175	First principles study of Ir3Ru, IrRu and IrRu3 catalysts for hydrogen oxidation reaction: Effect of surface modification and ruthenium content. Applied Surface Science, 2021, 545, 149002.	3.1	17
39176	First-principle investigations of zigzag III-V nitride nanoribbons as CS2 scavengers. Applied Surface Science, 2021, 545, 148969.	3.1	5
39177	Molecular alignment descriptor to search for the most stable adsorption sites of saturated cyclic compounds on metal surfaces. Applied Surface Science, 2021, 544, 148904.	3.1	4
39178	Tuning the magnetic properties of Fe3GeTe2 by doping with 3d transition-metals. Physics Letters, Section A: General, Atomic and Solid State Physics, 2021, 396, 127219.	0.9	7
39179	The Band-Gap Studies of Short-Period CdO/MgO Superlattices. Nanoscale Research Letters, 2021, 16, 59.	3.1	12
39180	First-Principles Study on Electronic, Magnetic, Optical, Mechanical, and Thermodynamic Properties of Semiconducting Gadolinium Phosphide in GGA, GGA+U, mBJ, GGA+SOC and GGA+SOC+U approaches. Journal of Superconductivity and Novel Magnetism, 2021, 34, 1523-1538.	0.8	6
39181	First-principles study of mechanical and thermodynamic properties of W-V alloys. Physica Scripta, 2021, 96, 065706.	1.2	2
39182	Kinetics and Thermodynamics of Fe-X (X= Al, Cr, Mn, Ti, B, and C) Melts under High Pressure. , 0, 29, 143-160.		0
39183	Design of Highly Stable and Efficient Bifunctional MX ene-Based Electrocatalysts for Oxygen Reduction and Evolution Reactions. Physical Review Applied, 2021, 15, .	1.5	11
39184	Ab initio modeling and experimental investigation of <mml:math xmlns:mml="http://www.w3.org/1998/Math/MathML"><mml:mrow><mml:msub><mml:mi>Fe</mml:mi><mml:mn>2</mml:mn></mml:m mathvariant="normal">P</mml:mi></mml:mrow></mml:math> by DFT and spin spectroscopies. Physical Review Materials, 2021, 5, .	0.9	1

#	Article	IF	Citations
39185	Vibrational Spectral Analysis of Natisite (Na2TiSiO5) and its Structure Evolution in Water and Sulfuric Acid Solutions. Materials, 2021, 14, 2259.	1.3	4
39186	Conversation from antiferromagnetic MnBr2 to ferromagnetic Mn3Br8 monolayer with large MAE. Nanoscale Research Letters, 2021, 16, 72.	3.1	1
39187	A comparison study of the structural electronic, elastic and lattice dynamic properties of ZrInAu and ZrSnPt. Zeitschrift Fur Naturforschung - Section A Journal of Physical Sciences, 2021, 76, 559-567.	0.7	3
39188	Built-in electric field control of magnetic coupling in van der Waals semiconductors. Physical Review B, 2021, 103, .	1.1	19
39189	Inactivating SARS-CoV-2 by electrochemical oxidation. Science Bulletin, 2021, 66, 720-726.	4.3	18
39190	Mechanistic Insights into Catalytic Reduction of N₂O by CO over Cu-Embedded Graphene: A Density Functional Theory Perspective. ECS Journal of Solid State Science and Technology, 2021, 10, 041003.	0.9	63
39191	Improvement of Photocatalytic Activity of Bi2WO6 by Doping Ag and Y: A DFT Study. Journal of Electronic Materials, 2021, 50, 4027-4033.	1.0	7
39192	First-principles study of multiple-site substitutions of alloying elements in Ni-based single crystal superalloys. Science China Technological Sciences, 2021, 64, 1276-1284.	2.0	6
39193	Finite-temperature materials modeling from the quantum nuclei to the hot electron regime. Physical Review Materials, 2021, 5, .	0.9	20
39194	Theoretical Calculations Meet Experiment to Explain the Luminescence Properties and the Presence of Defects in m-ZrO₂. Chemistry of Materials, 2021, 33, 2984-2992.	3.2	9
39195	New Cadmiumâ€“Nitrogen Compounds at High Pressures. Inorganic Chemistry, 2021, 60, 6772-6781.	1.9	31
39196	Two-dimensional MnN utilized as high-capacity anode for Li-ion batteries*. Chinese Physics B, 2021, 30, 046302.	0.7	4
39197	Magnetic localized states and tunable magnetism of single vacancies in generalized chiral graphene nanoribbons. Materials Research Express, 2021, 8, 045602.	0.8	1
39198	Composition Stability and Cr-Rich Phase Formation in W-Cr-Y and W-Cr-Ti Smart Alloys. Metals, 2021, 11, 743.	1.0	4
39199	Structural, Electronic, Magnetic, and Elastic Properties of CoXâ€²CrZ (Xâ€²=â€‰Sc, Ti; Zâ€‰=â€‰Al, Ga) Quaternary Heusler Alloys: Firstâ€Principles Study. Physica Status Solidi (B): Basic Research, 2021, 258, 2100004.	0.7	4
39200	Substitution of nickel in Mg2Ni and its hydride with elements from groups XIII and XIV: An ab initio study. International Journal of Hydrogen Energy, 2021, 46, 15691-15701.	3.8	9
39201	Reaction mechanism of methane conversion over Ca2Fe2O5 oxygen carrier in chemical looping hydrogen production. Fuel, 2021, 290, 120094.	3.4	16
39202	Comparing half-metallic, MOKE, and thermoelectric behavior of the CrTiZ (ZÂ=ÂAs, P) half-Heuslers: a DFT study. Materials Research Express, 2021, 8, 046302.	0.8	4

#	Article	IF	Citations
39203	First-principles predictions of the structural, electronic, optical and elastic properties of the zintl-phases AE3GaAs3 (AE = Sr, Ba). Solid State Sciences, 2021, 114, 106563.	1.5	118
39204	Crystal and electronic structure engineering of tin monoxide by external pressure. Journal of Advanced Ceramics, 2021, 10, 565-577.	8.9	11
39205	Phase Tailoring of Ruddlesdenâ€“Popper Perovskite at Fixed Large Spacer Cation Ratio. Small, 2021, 17, e2100560.	5.2	10
39206	Influence of Fe and Ni Doping on the OER Performance at the Co₃O₄(001) Surface: Insights from DFT+UCalculations. ACS Catalysis, 2021, 11, 5601-5613.	5.5	86
39207	Microbial methylation potential of mercury sulfide particles dictated by surface structure. Nature Geoscience, 2021, 14, 409-416.	5.4	36
39208	Induced magnetic states upon electronâ€“hole injection at B and N sites of hexagonal boron nitride bilayer: A <scp>density functional theory</scp> study. International Journal of Quantum Chemistry, 2021, 121, e26680.	1.0	27
39209	Origin of the Giant Enhanced Raman Scattering by Sulfur Chains Encapsulated inside Single-Wall Carbon Nanotubes. ACS Nano, 2021, 15, 8574-8582.	7.3	10
39210	A computational study of MoS₂ for band gap engineering by substitutional doping of TMN (T = transition metal (Cu), MÂ=Âmetalloid (B) and N = non-metal (C)). Materials Research Express, 2021, 8, 046301.	0.8	6
39211	Tuning local chemistry of P2 layered-oxide cathode for high energy and long cycles of sodium-ion battery. Nature Communications, 2021, 12, 2256.	5.8	183
39212	High-Throughput Screening of a Single-Atom Alloy for Electroreduction of Dinitrogen to Ammonia. ACS Applied Materials & Interfaces, 2021, 13, 16336-16344.	4.0	58
39213	Structure and electron affinity of the 4Hâ€“SiC (0001) surfaces: a methodological approach for polar systems. Journal of Physics Condensed Matter, 2021, 33, 165003.	0.7	4
39214	Electronic and vibrational properties of the high T _c superconductor Bi₂Sr₂CaCu₂O₈: an ab initio study. Journal of Physics Condensed Matter, 2021, 33, 185705.	0.7	7
39215	Theoretical insights into strong intrinsic piezoelectricity of blue-phosphorus-like group-IV monochalcogenides. Nano Research, 2022, 15, 209-216.	5.8	17
39216	Emergence of magnetic anisotropy by surface adsorption of transition metal dimers on Î³-graphyne framework. Journal of Physics Condensed Matter, 2021, 33, 205501.	0.7	6
39217	Pristine and Janus monolayers of vanadium dichalcogenides: potential materials for overall water splitting and solar energy conversion. Journal of Materials Science, 2021, 56, 12270-12284.	1.7	6
39218	Manipulating Berry curvature of SrRuO₃thin films via epitaxial strain. Proceedings of the National Academy of Sciences of the United States of America, 2021, 118, .	3.3	41
39219	First-Principles Study of Graphene-6H SiC Surface Interactions. Balkan Journal of Electrical and Computer Engineering, 2021, 9, 171-177.	0.4	0
39220	First-principles study of the structural, electronic, and elastic properties of Sc2SiX (X=C, N). Revista Mexicana De FÃsica, 2021, 67, 500.	0.2	1

#	Article	IF	Citations
39221	DFT exploration of sensor performances of two-dimensional WO3 to ten small gases in terms of work function and band gap changes and I-V responses. Applied Surface Science, 2021, 546, 149104.	3.1	89
39222	Large anomalous Hall effect in the kagome ferromagnet LiMn6Sn6. Physical Review B, 2021, 103, .	1.1	35
39223	Sc/Ti-decorated and B-substituted defective C60 as efficient materials for hydrogen storage. International Journal of Hydrogen Energy, 2021, 46, 14508-14519.	3.8	11
39224	Structural and electronic properties of AlY (Y B, N, O) dual-doped twin graphene: A density functional theory study. Physica E: Low-Dimensional Systems and Nanostructures, 2021, 128, 114619.	1.3	7
39225	Ab-initio investigations on dynamical and lattice thermal behaviours of ThC. Bulletin of Materials Science, 2021, 44, 1.	0.8	3
39226	Possibility of Doping <mml:math xmlns:mml="http://www.w3.org/1998/Math/MathML" display="inline" overflow="scroll"><mml:msub><mml:mrow><mml:mi>Cu</mml:mi><mml:mi>Ga</mml:mi><mml:mi>Se</mml:mi></mml:mrow><mml:mrow><mml:mi>n</mml:mi> -Type by Hydrogen. Physical Review Applied, 2021, 15, .	1.5	2
39227	The effect of 3d states on band structure feature, optical and magnetic properties of TM-doped CdS: a theoretical insights. Indian Journal of Physics, 2022, 96, 1381-1392.	0.9	3
39228	Theoretical investigations of structural, mechanical, electronic and optical properties of NaScSi alloy. Emergent Materials, 2021, 4, 1465-1477.	3.2	71
39229	Influence of anisotropic strain and temperature on hydrogen dissolution in tungsten. Modelling and Simulation in Materials Science and Engineering, 2021, 29, 055011.	0.8	0
39230	Inversion domain boundaries in wurtzite GaN. Physical Review B, 2021, 103, .	1.1	1
39231	Tailoring acoustoelastic, piezoelectric and thermal properties of Janus GeC sheets. Physica E: Low-Dimensional Systems and Nanostructures, 2021, 128, 114625.	1.3	7
39232	Experiment and theory for acetylene adsorption in transformer oil. Journal of Molecular Structure, 2021, 1230, 129860.	1.8	14
39233	Synthesis and characterization of polypyrrole@MCM-41 nanocomposites. Microporous and Mesoporous Materials, 2021, 317, 110954.	2.2	6
39234	Mechanical Vibrational Relaxation of NO Scattering from Metal and Insulator Surfaces: When and Why They Are Different. Physical Review Letters, 2021, 126, 156101.	2.9	16
39235	First-principles investigation of electronic, optical, mechanical and heat transport properties of pentadiamond: A comparison with diamond. Carbon Trends, 2021, 3, 100036.	1.4	16
39236	Synthesis of calcium orthocarbonate, Ca2CO4-Pnma at P-T conditions of Earthâ€™s transition zone and lower mantle. American Mineralogist, 2022, 107, 336-342.	0.9	23
39237	Thermal Atomic Layer Etching of Aluminum Oxide (Al₂O₃) Using Sequential Exposures of Niobium Pentafluoride (NbF₅) and Carbon Tetrachloride (CCl₄): A Combined Experimental and Density Functional Theory Study of the Etch Mechanism. Chemistry of Materials, 2021, 33, 2883-2893.	3.2	11
39238	Hydrogen Absorption Mechanism into Iron in Aqueous Solution Including Metal Cations by Laser Ablation Tests and First-principles Calculations. ISIJ International, 2021, 61, 1085-1090.	0.6	3

#	Article	IF	Citations
39239	Changes in CO2 Adsorption Affinity Related to Ni Doping in FeS Surfaces: A DFT-D3 Study. Catalysts, 2021, 11, 486.	1.6	6
39240	Hydrostatic pressure on XLiH3 (X = Ba, Sr, Ca) perovskite hydrides: An insight into structural, thermo-elastic and ultrasonic properties through first-principles investigation. Solid State Communications, 2021, 328, 114222.	0.9	13
39241	Dynamic and thermodynamic properties of antiperovskite compound BiNCa3. Bulletin of Materials Science, 2021, 44, 1.	0.8	3
39242	High-pressure monoclinicâ€“monoclinic transition in fergusonite-type HoNbO₄. Journal of Physics Condensed Matter, 2021, 33, 195401.	0.7	9
39243	Role of charge doping and strain in the stabilization of in-plane ferromagnetism in monolayer VSe2 at room temperature. 2D Materials, 2021, 8, 035022.	2.0	24
39244	Graphene nanoribbons with mixed cove-cape-zigzag edge structure. Carbon, 2021, 175, 50-59.	5.4	20
39245	Atomic-Scale Local Work Function Characterizations of Br Islands on Cu(111). Journal of Physical Chemistry C, 2021, 125, 7944-7949.	1.5	6
39246	Highly Anisotropic Thermoelectric Properties of Two-Dimensional As₂Te₃. ACS Applied Electronic Materials, 2021, 3, 1610-1620.	2.0	24
39247	Effects of Uniaxial Lattice Strain and Explicit Water Solvation on CO₂ Electroreduction over a Cu Electrode: A Density Functional Theory Perspective. Journal of Physical Chemistry C, 2021, 125, 9138-9149.	1.5	10
39248	Understanding the Role of Oxygen Vacancies in the Stability of ZnO(0001)-(1 Ã— 3) Surface Reconstructions. Journal of Physical Chemistry C, 2021, 125, 7980-7989.	1.5	8
39249	H2S adsorption on pristine and metal-decorated (8, 0) SWCNT: a first principle study. Journal of Molecular Modeling, 2021, 27, 143.	0.8	3
39250	Enhanced Stability and Epitaxial Growth Mechanism of the Honeycomb Borophene Monolayer on a Two-Dimensional Ti₂C Substrate. Journal of Physical Chemistry C, 2021, 125, 8589-8596.	1.5	6
39251	NaNbO₃/NaTaO₃ Superlattices: Cation-Ordering Improved Band-Edge Alignment for Water Splitting and CO₂ Photocatalysis. Langmuir, 2021, 37, 4493-4503.	1.6	10
39252	Unraveling the Causes of the Instability of Au_n(SR)_x Nanoclusters on Au(111). Chemistry of Materials, 2021, 33, 3428-3435.	3.2	3
39253	Lattice dynamics and electronic properties of Heusler alloys Li2AlX (X=Ga, In): A comparison study. Chinese Journal of Chemical Physics, 2021, 34, 173-178.	0.6	5
39254	Importance of the oxyl character on the IrO2 surface dependent catalytic activity for the oxygen evolution reaction. Journal of Catalysis, 2021, 396, 192-201.	3.1	18
39255	Magnetism and DFT calculations for understanding magnetic ground state of Fe doped Mn2O3. Journal of Alloys and Compounds, 2021, 861, 158567.	2.8	8
39256	Spinorial formulation of the <mml:math xmlns:mml="http://www.w3.org/1998/Math/MathML"><mml:mrow><mml:mi>G</mml:mi><mml:mi>W</mml:mi></mml:mrow></mml:m -BSE equations and spin properties of excitons in two-dimensional transition metal dichalcogenides. Physical Review B, 2021, 103, .	1.1	16

#	Article	IF	Citations
39257	Engineering the band gap of Hf2CO2 MXene semiconductor by C/O doping. Journal of Materials Research, 2021, 36, 1678-1685.	1.2	8
39258	Layerâ€Controlled Lowâ€Power Tunneling Transistors Based on SnS Homojunction. Advanced Theory and Simulations, 2021, 4, 2000290.	1.3	6
39259	Van der waals SiSe2 homo-bilayers for optoelectronics applications. Superlattices and Microstructures, 2021, 152, 106858.	1.4	18
39260	DFT insights into new B-containing 212 MAX phases: Hf2AB2 (A = In, Sn). Journal of Alloys and Compounds, 2021, 860, 158408.	2.8	45
39261	Potassium-activated anionic copper and covalent Cuâ€“Cu bonding in compressed Kâ€“Cu compounds. Journal of Chemical Physics, 2021, 154, 134708.	1.2	5
39262	Mechanically stable with highly absorptive formamidinium lead halide perovskites		

#	Article	IF	Citations
39275	Anisotropies in Elasticity, Sound Velocity, and Minimum Thermal Conductivity of Low Borides VxBy Compounds. Metals, 2021, 11, 577.	1.0	3
39276	Strengthen metal-oxygen covalency of CoFe-layered double hydroxide for efficient mild oxygen evolution. Nano Research, 2022, 15, 162-169.	5.8	29
39277	Ballistic thermoelectric transport properties of two-dimensional group III-VI monolayers. Physical Review B, 2021, 103, .	1.1	19
39278	Acentric Organicâ€“Inorganic Hybrid Halide [N(CH₃)₄]₂HgBr₂I₂ Featuring an Isolated [HgBr₂I₂]^{2â€“} Tetrahedron and Second-Order Nonlinearity. Inorganic Chemistry, 2021, 60, 6829-6835.	1.9	13
39279	Molecular beam epitaxy of PdO on MgO (001). Physical Review Materials, 2021, 5, .	0.9	1
39280	Electrocatalytic activity of doped graphene: Quantum-mechanical theory view. Carbon, 2021, 175, 202-214.	5.4	7
39281	Novel borophosphene as a high capacity anode material for Li-ion storage. Journal of Solid State Chemistry, 2021, 296, 121950.	1.4	8
39282	Theoretical insights into magnetization in graphene containing single and interacting nanoporous defects. Physica E: Low-Dimensional Systems and Nanostructures, 2021, 128, 114564.	1.3	2
39283	Enhanced ductility and optoelectronic properties of environment-friendly CsGeCl3 under pressure. AIP Advances, 2021, 11, .	0.6	50
39284	Role of High-Index Facet Cu(711) Surface in Controlling the C2 Selectivity for CO₂ Reduction Reactionâ€”A DFT Study. Journal of Physical Chemistry C, 2021, 125, 10919-10925.	1.5	17
39285	Gallium nitride catalyzed the direct hydrogenation of carbon dioxide to dimethyl ether as primary product. Nature Communications, 2021, 12, 2305.	5.8	45
39286	Study on the Electronic Structure and Optical Properties of Nd-Incorporated Mg2Si by First Principles. Journal of Electronic Materials, 2021, 50, 4083-4089.	1.0	3
39287	Origin of the Band Gap Reduction of In-Doped Î²-Ga2O3. Journal of Electronic Materials, 2021, 50, 3856-3861.	1.0	11
39288	Theoretical investigation of physical properties of the spinel ZnFe₂O₄ compound: Ab-initio calculation. Phase Transitions, 2021, 94, 134-146.	0.6	2
39289	First principles study of the structural, electronic, optical and thermodynamic properties of cubic quaternary Al_xIn_{1â^'x}P_yBi_{1â^'y} alloys. Zeitschrift Fur Naturforschung - Section A Journal of Physical Sciences, 2021, 76, 517-534.	0.7	1
39290	Tuning the electronic structure of nanoporous Ag via alloying effect from Cu to boost the ORR and Zn-air battery performance. Applied Surface Science, 2021, 545, 149042.	3.1	18
39291	Oxygen-Evolution Reaction by a Palladium Foil in the Presence of Iron. Inorganic Chemistry, 2021, 60, 5682-5693.	1.9	26
39292	Need for Rationally Designed SnWO₄ Photo(electro)catalysts to Overcome the Performance Limitations for O₂ and H₂ Evolution Reactions. Journal of Physical Chemistry C, 2021, 125, 8488-8496.	1.5	7

#	Article	IF	Citations
39293	Identification of Active Metal Carbide and Nitride Catalytic Facets for Hydrodeoxygenation Reactions. Journal of Physical Chemistry C, 2021, 125, 8630-8637.	1.5	13
39294	Activating PtSe2 monolayer for hydrogen evolution reaction by defect engineering and Pd doping. Applied Surface Science, 2021, 545, 149013.	3.1	23
39295	Modeling and physical properties of diphenylalanine peptide nanotubes containing water molecules. Ferroelectrics, 2021, 574, 78-91.	0.3	11
39296	Two-Dimensional Graphene/BlueP/MoS₂ van der Waals Multilayer Heterostructure as a High-Performance Anode Material for LIBs. Journal of Physical Chemistry C, 2021, 125, 8980-8992.	1.5	8
39297	Theoretical Study of an almost Barrier-Free Water Dissociation on a Platinum (111) Surface Alloyed with Ruthenium and Molybdenum. ACS Omega, 2021, 6, 10770-10775.	1.6	2
39298	Tunable Synthesis of Ethanol or Methyl Acetate via Dimethyl Oxalate Hydrogenation on Confined Iron Catalysts. ACS Catalysis, 2021, 11, 4908-4919.	5.5	15
39299	Disassembly of TEMPO-Oxidized Cellulose Fibers: Intersheet and Interchain Interactions in the Isolation of Nanofibers and Unitary Chains. Journal of Physical Chemistry B, 2021, 125, 3717-3724.	1.2	6
39300	Enhancement of Pseudocapacitive Behavior, Cyclic Performance, and Field Emission Characteristics of Reduced Graphene Oxide Reinforced NiGa₂O₄ Nanostructured Electrode: A First Principles Calculation to Correlate with Experimental Observation. Journal of Physical Chemistry C, 2021, 125, 7898-7912.	1.5	15
39301	Demonstrating the Impact of the Adsorbate Orientation on the Charge Transfer at Organicâ€“Metal Interfaces. Journal of Physical Chemistry C, 2021, 125, 9129-9137.	1.5	10
39302	Fast periodic Gaussian density fitting by range separation. Journal of Chemical Physics, 2021, 154, 131104.	1.2	17
39303	Deep-Learning Approach to First-Principles Transport Simulations. Physical Review Letters, 2021, 126, 177701.	2.9	18
39304	A Combined Experimental and First-Principles Based Assessment of Finite-Temperature Thermodynamic Properties of Intermetallic Al3Sc. Materials, 2021, 14, 1837.	1.3	5
39305	Modification of Catalytic Properties of Hollandite Manganese Oxide by Ag Intercalation for Oxidative Acetalization of Ethanol to Diethoxyethane. ACS Catalysis, 2021, 11, 5347-5357.	5.5	14
39306	Thermal Transport Evolution Due to Nanostructural Transformations in Ga-Doped Indium-Tin-Oxide Thin Films. Nanomaterials, 2021, 11, 1126.	1.9	3
39307	Theoretical Insight on Anion Ordering, Strain, and Doping Engineering of the Oxygen Evolution Reaction in BaTaO2N. Chemistry of Materials, 2021, 33, 3297-3303.	3.2	15
39308	Scalable Synthesis of Atomically Thin Gallium Telluride Nanosheets for Supercapacitor Applications. ACS Applied Nano Materials, 2021, 4, 4829-4838.	2.4	38
39309	First-principles calculations to investigate mechanical, optoelectronic and thermoelectric properties of half-Heusler p-type semiconductor BaAgP. Results in Physics, 2021, 23, 104068.	2.0	25
39310	Atomistic insight into hydrogen trapping at MC/BCC-Fe phase boundaries: The role of local atomic environment. Acta Materialia, 2021, 208, 116744.	3.8	36

#	Article	IF	Citations
39311	Electronic and magnetic properties of two-dimensional of FeX (X = S, Se, Te) monolayers crystallize in the orthorhombic structures. Applied Physics Letters, 2021, 118, .	1.5	39
39312	Synthesis of Y6-xCa1.5xSi11N20O:Ce3+ (x = 0 ~ 2.5) Oxynitride Phosphor with Broad Emission Wavelength for 1pc-LED. Korean Journal of Materials Research, 2021, 31, 188-194.	0.1	1
39313	Impact of N₂O Gas Adsorption Upon Electronic Properties of 2D MoSe₂ Monolayer: A DFT Approach. IEEE Sensors Journal, 2021, 21, 9756-9762.	2.4	24
39314	Ab Initio thermoelectric calculations of ring-shaped bands in two-dimensional <mml:math xmlns:mml="http://www.w3.org/1998/Math/MathML"><mml:mrow><mml:msub><mml:mi>Bi</mml:mi><mml:mn>2</mml:mn></mml:msub><mml:msub><mml:mi>Se</mml:mi><mml:mn>3</mml:mn></mml:msub></mml:mrow></mml:math> , and <mml:math xmlns:mml="http://www.w3.org/1998/Math/MathML" width="0.28em" /><mml:msub><mml:mi>Bi</mml:mi><mml:mn>2</mml:mn></mml:msub><mml:msub><mml:mi>Se</mml:mi><mml:mn>3</mml:mn></mml:msub> , and <mml:math xmlns:mml="http://www.w3.org/1998/Math/. Physical Review B, 2021, 103, .	1.1	12
39315	An Insight into the Efficient Dimethoate Adsorption on Graphene-Based Materialsâ€”A Combined Experimental and DFT Study. Applied Sciences (Switzerland), 2021, 11, 4014.	1.3	0
39316	Cobalt anchored CN sheet boosts the performance of electrochemical CO oxidation*. Chinese Physics B, 2021, 30, 067104.	0.7	0
39317	Theoretical Study on the Lewis Acidity of the Pristine AlF3 and Cl-Doped Î±-AlF3 Surfaces. Catalysts, 2021, 11, 565.	1.6	5
39318	Surface Chirality Influences Molecular Rotation upon Desorption. Physical Review Letters, 2021, 126, 166101.	2.9	3
39319	Single Cr atom supported on boron nitride nanotubes for the reaction of N2O reduction by CO: A density functional theory study. Applied Surface Science, 2021, 544, 148776.	3.1	12
39320	Edge-exposed WS2 on 1D nanostructures for highly selective NO2 sensor at room temperature. Sensors and Actuators B: Chemical, 2021, 333, 129566.	4.0	30
39321	Interplay between Valence Band Tuning and Redox Stability in SnTiO₃: Implications for Directed Design of Photocatalysts. Chemistry of Materials, 2021, 33, 2824-2836.	3.2	16
39322	A Good Prediction of the Overall Reaction Rate May Not Mean a Correct Description of the Reaction Kinetics: A Case Study for CO Oxidation on RuO₂(110) Surfaces. Journal of Physical Chemistry C, 2021, 125, 9169-9177.	1.5	7
39323	Formation Mechanism of Î²-Li₃PS₄ through Decomposition of Complexes. Inorganic Chemistry, 2021, 60, 6964-6970.	1.9	19
39324	Doping of MoS₂ by â€œCuâ€•and â€œVâ€: An Efficient Strategy for the Enhancement of Hydrogen Evolution Activity. Langmuir, 2021, 37, 4847-4858.	1.6	22
39325	Formation of Corrugated n = 1 2D Tin Iodide Perovskites and Their Use as Lead-Free Solar Absorbers. ACS Nano, 2021, 15, 6395-6409.	7.3	18
39326	AuPt Bimetal-Functionalized SnSe₂ Microflower-Based Sensors for Detecting Sub-ppm NO₂ at Low Temperatures. ACS Applied Materials & Interfaces, 2021, 13, 20336-20348.	4.0	60
39327	Unlocking the Optimal Aqueous Î´-Bi2O3 Anode via Unifying Octahedrally Liberated Bi-Atoms and Spilled Nano-Bi Exsolution. Energy Storage Materials, 2021, 36, 376-386.	9.5	37
39328	Mechanochemical modification of LiAlH4 with Fe2O3 - A combined DFT and experimental study. International Journal of Hydrogen Energy, 2021, 46, 13070-13081.	3.8	7

#	Article	IF	Citations
39329	Polymer interfaces with carbon nanostructures: First principles density functional theory and molecular dynamics study of polyetheretherketone adsorption on graphene and nanotubes. Computational Materials Science, 2021, 191, 110320.	1.4	5
39330	A simple method to calculate solution-phase free energies of charged species in computational electrocatalysis. Journal of Physics Condensed Matter, 2021, 33, 204001.	0.7	7
39331	Tuning the thickness of graphitic nanofilms for wurtzite materials by vertical weak electric field under a certain pressure. Nano Express, 2021, 2, 020004.	1.2	0
39332	Modulation of electronic and magnetic properties of monolayer chromium trihalides by alloy and strain engineering. Journal of Applied Physics, 2021, 129, 155104.	1.1	3
39333	Flat-band-induced itinerant ferromagnetism in <mml:math xmlns:mml="http://www.w3.org/1998/Math/MathML"><mml:msub><mml:mi mathvariant="normal">RbCo</mml:mi><mml:mn>2</mml:mn></mml:msub><mml:msub><mml:mi mathvariant="normal">Se</mml:mi><mml:mn>2</mml:mn></mml:msub></mml:math>. Physical Review B, 2021, 103, .	1.1	8
39334	Exploiting the synergic strengthening effects of stacking faults in carbon nanotubes reinforced aluminum matrix composites for enhanced mechanical properties. Composites Part B: Engineering, 2021, 211, 108646.	5.9	65
39335	Topological gimbal phonons in <mml:math xmlns:mml="http://www.w3.org/1998/Math/MathML"><mml:mi>T</mml:mi></mml:math> -carbon. Physical Review B, 2021, 103, .	1.1	31
39336	Molecular dynamics simulation study on the effect of perfluorosulfonic acid side chains on oxygen permeation in hydrated ionomers of PEMFCs. Scientific Reports, 2021, 11, 8702.	1.6	19
39337	Absolute Volume Deformation Potentials of Inorganic ABX₃ Halide Perovskites: The Chemical Trends. Advanced Theory and Simulations, 2021, 4, 2100060.	1.3	11
39338	Linear regulation of electrical characteristics of InSe/Antimonene heterojunction via external electric field and strain. Surfaces and Interfaces, 2021, 23, 101014.	1.5	6
39339	First-principles study of electronic structures and elasticity of Al2Fe3Si3. Journal of Physics Condensed Matter, 2021, 33, 195501.	0.7	10
39340	Phonon-Assisted Ballistic Current from First-Principles Calculations. Physical Review Letters, 2021, 126, 177403.	2.9	32
39341	Electronic band structures of NdFe3(BO3)4 and NdGa3(BO3)4 crystals: ab initio calculations. Ferroelectrics, 2021, 575, 11-17.	0.3	1
39342	High capacity reversible hydrogen storage in zirconium doped 2D-covalent triazine frameworks: Density Functional Theory investigations. International Journal of Hydrogen Energy, 2021, 46, 14520-14531.	3.8	41
39343	Location-dependent effect of nickel on hydrogen dissociation and diffusion on Mg (0001) surface: Insights into hydrogen storage material design. Journal of Magnesium and Alloys, 2022, 10, 1617-1630.	5.5	34
39344	Magnetoelastic coupling and effects of uniaxial strain in <mml:math xmlns:mml="http://www.w3.org/1998/Math/MathML"><mml:mi>Î±</mml:mi><mml:mo>â^'</mml:mo><mml:msub><mml:mi mathvariant="normal">RuCl</mml:mi><mml:mn>3</mml:mn></mml:msub></mml:math> from first principles. Physical Review B, 2021, 103, .	1.1	25
39345	Structure stability, half metallic ferromagnetism, magneto-electronic and thermoelectric properties of new zintl XCr2Bi2 (X=Ca, Sr) compounds for spintronic and renewable energy applications. Physica B: Condensed Matter, 2021, 607, 412866.	1.3	21
39346	Stable Hollowâ€Structured Silicon Suboxideâ€Based Anodes toward Highâ€Performance Lithiumâ€Ion Batteries. Advanced Functional Materials, 2021, 31, 2101796.	7.8	127

#	Article	IF	Citations
39347	Lattice Strain Leads to High Thermoelectric Performance in Polycrystalline SnSe. ACS Nano, 2021, 15, 8204-8215.	7.3	66
39348	Assessing the Effects of Temperature and Oxygen Vacancy on Band Gap Renormalization in LaCrO_{3â˜Î´}: First-Principles and Experimental Corroboration. ACS Applied Materials & Interfaces, 2021, 13, 17717-17725.	4.0	18
39349	Computational Investigation of MgH₂/NbOx for Hydrogen Storage. Journal of Physical Chemistry C, 2021, 125, 8862-8868.	1.5	9
39350	Thermal conductivity of<mml:math xmlns:mml="http://www.w3.org/1998/Math/MathML"><mml:mrow><mml:mi>Ca</mml:mi><mml:msub><mml:mi mathvariant="normal">F</mml:mi><mml:mn>2</mml:mn></mml:msub></mml:mrow></mml:math>at high pressure. Physical Review B, 2021, 103, .	1.1	7
39351	Impact of Water Coadsorption on the Electrode Potential of H-Pt(1 1 1)-Liquid Water Interfaces. Physical Review Letters, 2021, 126, 166802.	2.9	21
39352	Effect of electric field and vertical strain on the electro-optical properties of the MoSi2N4 bilayer: A first-principles calculation. Journal of Applied Physics, 2021, 129, .	1.1	48
39353	Formaldehyde Molecules Adsorption on Zn Doped Monolayer MoS2: A First-Principles Calculation. Frontiers in Chemistry, 2020, 8, 605311.	1.8	10
39354	Electronic structure and optical properties of SnO2/HC(NH2)2PbI3 interfaces from first-principles calculations. Surfaces and Interfaces, 2021, 23, 100913.	1.5	3
39355	Bilayer MoTe2/XS2 (XÂ=ÂHf,Sn,Zr) heterostructures with efficient carrier separation and light absorption for photocatalytic water splitting into hydrogen. Applied Surface Science, 2021, 544, 148842.	3.1	24
39356	Dimensional crossover and band topology evolution in ultrathin semimetallic NiTe2 films. Npj 2D Materials and Applications, 2021, 5, .	3.9	13
39359	Effects of Zn and Mg Segregations on the Grain Boundary Sliding and Cohesion in Al: Ab Initio Modeling. Metals, 2021, 11, 631.	1.0	8
39360	Thermodynamic properties of Îµ -Fe with thermal electronic excitation effects on vibrational spectra. Physical Review B, 2021, 103, .	1.1	11
39361	Formation of Interstellar Silicate Dust via Nanocluster Aggregation: Insights From Quantum Chemistry Simulations. Frontiers in Astronomy and Space Sciences, 2021, 8, .	1.1	2
39363	Evolution of Topological Surface States Following Sb Layer Adsorption on Bi2Se3. Materials, 2021, 14, 1763.	1.3	7
39364	Cooper Pairs Distribution function for bcc Niobium under pressure from first-principles. Scientific Reports, 2021, 11, 7646.	1.6	4
39365	In-situ self-assembled Cu2O/ZnO core-shell catalysts synergistically enhance the durability of methanol steam reforming. Applied Catalysis A: General, 2021, 616, 118072.	2.2	28
39366	Environmental-sulfur-controlled surface properties of pyrite: a first principles PBEâ€‰+â€‰U study. Physics and Chemistry of Minerals, 2021, 48, 1.	0.3	6
39367	Mechanical manipulation of electronic properties of SnO2 monolayer. Computational Materials Science, 2021, 190, 110268.	1.4	1

#	Article	IF	Citations
39368	BiSbWO6: Properties of a mixed 5s/6s lone-pair-electron system. Chemical Physics, 2021, 544, 111117.	0.9	4
39369	Modelling the primary damage in Fe and W: Influence of the short range interactions on the cascade properties: Part 1 â€“ Energy transfer. Journal of Nuclear Materials, 2021, 547, 152816.	1.3	10
39370	Volumetric Strain Dependence of Quantum Diffusion of Hydrogen in bcc Iron. ISIJ International, 2021, 61, 1294-1299.	0.6	2
39371	Theoretical study of tunable magnetism of two-dimensional MnSe₂ through strain, charge, and defect. Journal of Physics Condensed Matter, 2021, 33, 215803.	0.7	12
39372	Pressure-induced electrides and metallic phases in the Yâ€“Cl system. Journal of Physics Condensed Matter, 2021, 33, 215401.	0.7	2
39373	The Elusive Structure of Magadiite, Solved by 3D Electron Diffraction and Model Building. Chemistry of Materials, 2021, 33, 3207-3219.	3.2	24
39374	Carbon and Oxygen Coordinating Atoms Adjust Transition Metal Single-Atom Catalysts Based On Boron Nitride Monolayers for Highly Efficient CO₂ Electroreduction. ACS Applied Materials & Interfaces, 2021, 13, 18934-18943.	4.0	13
39375	Revisiting Understanding of Electrochemical CO₂ Reduction on Cu(111): Competing Proton-Coupled Electron Transfer Reaction Mechanisms Revealed by Embedded Correlated Wavefunction Theory. Journal of the American Chemical Society, 2021, 143, 6152-6164.	6.6	65
39376	Birefringence and Dichroism in Quasiâ€1D Transition Metal Trichalcogenides: Direct Experimental Investigation. Small, 2021, 17, e2100457.	5.2	17
39377	First-principles calculations of effects of pressure on paramagnetic, ferromagnetic, and antiferromagnetic spin-web Cu3TeO6. Journal of Molecular Modeling, 2021, 27, 129.	0.8	1
39378	(W_{1â€x},M_x)C carbides with desired combinations of compatible density and properties â€“ A firstâ€principles study. Journal of the American Ceramic Society, 2021, 104, 4239-4256.	1.9	7
39379	Intrinsic triferroicity in a two-dimensional lattice. Physical Review B, 2021, 103, .	1.1	22
39380	Superior catalytic performance of Pd-loaded oxygen-vacancy-rich TiO2 for formaldehyde oxidation at room temperature. Journal of Catalysis, 2021, 396, 122-135.	3.1	65
39381	Interfacial Engineering of Bifunctional Niobium (V)â€Based Heterostructure Nanosheet Toward High Efficiency Leanâ€Electrolyte Lithiumâ€“Sulfur Full Batteries. Advanced Functional Materials, 2021, 31, 2102314.	7.8	93
39382	Exceptional piezoelectricity, high thermal conductivity and stiffness and promising photocatalysis in two-dimensional MoSi2N4 family confirmed by first-principles. Nano Energy, 2021, 82, 105716.	8.2	303
39383	Investigation of structural, electronic, magnetic, elastic and thermodynamic properties of Mn3GaN antiperovskite by first principle and Monte Carlo simulations. Philosophical Magazine, 2021, 101, 1587-1601.	0.7	3
39384	R10-graphene: A predicted two-dimensional metallic carbon. Diamond and Related Materials, 2021, 114, 108315.	1.8	10
39385	Synthesis and Characterization of a Pure 2D Antimony Film on Au(111). Journal of Physical Chemistry C, 2021, 125, 9273-9280.	1.5	9

#	Article	IF	Citations
39386	Revealing the Potential Crystal Structures of Earth-Abundant Nontoxic Photovoltaic CuBiI₄. Crystal Growth and Design, 2021, 21, 2850-2855.	1.4	8
39387	Modeling the Î± - and Î² -resorcinol phase boundary via combination of density functional theory and density functional tight-binding. Journal of Chemical Physics, 2021, 154, 134109.	1.2	7
39388	A thermodynamics study of hydrogen interaction with (1 1 0) transition metal surfaces. Applied Surface Science, 2021, 545, 148961.	3.1	6
39389	Preparation, characterization and adsorption properties of tetraalkylphosphonium organobeidellites. Applied Clay Science, 2021, 204, 105989.	2.6	7
39390	Proton-assisted calcium-ion storage in aromatic organic molecular crystal with coplanar stacked structure. Nature Communications, 2021, 12, 2400.	5.8	107
39391	Boron Doping and LiBO₂ Coating Synergistically Enhance the High-Rate Performance of LiNi_{0.6}Co_{0.1}Mn_{0.3}O₂ Cathode Materials. ACS Sustainable Chemistry and Engineering, 2021, 9, 5322-5333.	3.2	25
39392	Mechanical strength and flexibility in $$alpha '$$-4H borophene. Scientific Reports, 2021, 11, 7547.	1.6	15
39393	A New Porous Metallic Carbon Allotrope with Interlocking Pentagons for Sodiumâ€ion Battery Anode Material. Advanced Theory and Simulations, 2021, 4, 2100025.	1.3	9
39394	Metal nano-drills directionally regulate pore structure in carbon. Carbon, 2021, 175, 60-68.	5.4	7
39395	Minimizing hydrogen vacancies to enable highly efficient hybrid perovskites. Nature Materials, 2021, 20, 971-976.	13.3	92
39396	NiMoO₄ Nanosheets Anchored on Nï£¿S Doped Carbon Clothes with Hierarchical Structure as a Bidirectional Catalyst toward Accelerating Polysulfides Conversion for Lïï£¿S Battery. Advanced Functional Materials, 2021, 31, 2101285.	7.8	119
39397	CO adsorption on MnO(100): Experimental benchmarks compared to DFT. Surface Science, 2021, 707, 121808.	0.8	8
39398	Solving quasiparticle band spectra of real solids using neural-network quantum states. Communications Physics, 2021, 4, .	2.0	19
39399	Antiphase boundary migration as a diffusion mechanism in a P3 sodium layered oxide. Physical Review Materials, 2021, 5, .	0.9	5
39400	Predicted half-metallicity and ferromagnetism in the Fe (III) doped BaZrO3 perovskite: A theoretical insight. AIP Advances, 2021, 11, 055104.	0.6	1
39401	Revisiting the thermal conductivity of Si, Ge and diamond from first principles: roles of atomic mass and interatomic potential. Journal of Physics Condensed Matter, 2021, 33, 285702.	0.7	6
39402	Diverse electronic and magnetic properties of CrS2 enabling strain-controlled 2D lateral heterostructure spintronic devices. Npj Computational Materials, 2021, 7, .	3.5	35
39403	Widespread Negative Longitudinal Piezoelectric Responses in Ferroelectric Crystals with Layered Structures. Physical Review Letters, 2021, 126, 217601.	2.9	42

#	Article	IF	Citations
39404	Plasmon Triggered, Enhanced Lightâ€“Matter Interactions in Auâ€“MoS₂ Coupled System with Superior Photosensitivity. Journal of Physical Chemistry C, 2021, 125, 11023-11034.	1.5	18
39405	Understanding the promoter effect of bifunctional (Pt, Ni, Cu)-MoO3-x/TiO2 catalysts for the hydrodeoxygenation of p-cresol: A combined DFT and experimental study. Applied Surface Science, 2021, 547, 149170.	3.1	15
39406	Nonplanar core structure of 1/2<111> screw dislocations: An anisotropic Peierls-Nabarro model. Mechanics of Materials, 2021, 156, 103794.	1.7	4
39407	A computational prediction of a novel quasi hexagonal Al2SSi semiconductor monolayer. Chemical Physics, 2021, 545, 111148.	0.9	0
39408	Torsional buckling analysis of MWCNTs considering quantum effects of fine scaling based on DFT and molecular mechanics method. Journal of Molecular Graphics and Modelling, 2021, 104, 107843.	1.3	17
39409	Theoretical insights into the mechanism of oxygen evolution reaction (OER) on pristine BiVO₄ (001) and BiVO₄ (110) surfaces in acidic medium both in the gas and solution (water) phases. Nanotechnology, 2021, 32, 335401.	1.3	3
39410	An ab-initio study of 2 dimensional metal (Cu, Ag) - 1Tâ€™ ReS2 van der Waals heterostructure. , 2021, , .		0
39411	Behavior of S, SO, and SO3 on Pt (001), (011), and (111) surfaces: A DFT study. Journal of Chemical Physics, 2021, 154, 194701.	1.2	4
39412	Pressure-dependent modifications in the <mml:math xmlns:mml="http://www.w3.org/1998/Math/MathML"><mml:mrow><mml:mi>LaAu</mml:mi><mml:msub><mml:mi>Sb</mml:mi><mml:mi><mm charge density wave system. Physical Review B, 2021, 103, .	1.1	6
39413	Perfect in-plane <mml:math xmlns:mml="http://www.w3.org/1998/Math/MathML"><mml:msub><mml:mi>CrI</mml:mi><mml:mn>3</mml:mn></mml:msub></m spin-valve driven by photogalvanic effect. Physical Review Materials, 2021, 5, .	3.1	12
39414	Ab initio study of hydrogen storage on metal-decorated GeC monolayers. International Journal of Hydrogen Energy, 2021, 46, 29261-29271.	3.8	35
39415	First-Principles DFT Study on Inverse Ruddlesdenâ€“Popper Tetragonal Compounds as Solid Electrolytes for All-Solid-State Li⁺-Ion Batteries. Chemistry of Materials, 2021, 33, 5859-5871.	3.2	13
39416	First-principles study of tensile and shear strength of an Fe2Al5//Fe interface. Computational Materials Science, 2021, 192, 110319.	1.4	20
39417	Rotation Tunable Typeâ€I/Typeâ€II Band Alignment and Photocatalytic Performance of gâ€C 3 N 4 /InSe van der Waals Heterostructure. Physica Status Solidi - Rapid Research Letters, 2021, 15, 2100171.	1.2	6
39418	Nanoporous <scp>Titaniumâ€Oxo</scp> Molecular Cluster for <scp>CO₂</scp> Selective Adsorption. Bulletin of the Korean Chemical Society, 2021, 42, 1014-1019.	1.0	2
39419	Lattice Dynamics and thermodynamic Responses of XNbSn Half-Heusler Semiconductors: A First-Principles Approach. Journal of the Nigerian Society of Physical Sciences, 0, , 121-130.	0.0	1
39420	Engineering Electronic Structure and Band Alignment of 2D Mg(OH)2 via Anion Doping for Photocatalytic Applications. Materials, 2021, 14, 2640.	1.3	3
39421	Machine learning for deep elastic strain engineering of semiconductor electronic band structure and effective mass. Npj Computational Materials, 2021, 7, .	3.5	17

#	Article	IF	Citations
39422	Identification of the Nitrogen Interstitial as Origin of the 3.1â€‰eV Photoluminescence Band in Hexagonal Boron Nitride. Physica Status Solidi (B): Basic Research, 2021, 258, 2100031.	0.7	3
39423	Formation of ordered precipitates in Al-Sc-Er-(Si/Zr) alloy from first-principles study. Journal of Rare Earths, 2021, 39, 609-620.	2.5	13
39424	Electronic structure and thermal conductivity of zirconium carbide with hafnium additions. Journal of the American Ceramic Society, 2021, 104, 4708-4717.	1.9	10
39425	Computational and experimental evidence of Pd supported P-doped porous graphitic carbon nitride as a highly efficient and exceptionally durable photocatalyst for boosted visible-light-driven benzyl alcohol oxidation. Journal of Physics and Chemistry of Solids, 2021, 152, 109985.	1.9	11
39426	Edge Engineering in 2D Molybdenum Disulfide: Simultaneous Regulation of Lithium and Polysulfides for Stable Lithiumâ€“Sulfur Batteries. Advanced Energy and Sustainability Research, 2021, 2, 2100053.	2.8	6
39427	The influences of selenium species on mercury removal over pyrite surface: A density functional theory study. Fuel, 2021, 292, 120284.	3.4	17
39428	Stability of Atrazineâ€“Smectite Intercalates: Density Functional Theory and Experimental Study. Minerals (Basel, Switzerland), 2021, 11, 554.	0.8	7
39429	Chalcogenide Dopant-Induced Lattice Expansion in Cobalt Vanadium Oxide Nanosheets for Enhanced Supercapacitor Performance. ACS Applied Energy Materials, 2021, 4, 4758-4771.	2.5	20
39430	Origin of high hardness and optoelectronic and thermo-physical properties of boron-rich compounds B6X (Xâ€‰=â€‰S, Se): A comprehensive study via DFT approach. Journal of Applied Physics, 2021, 129, .	1.1	28
39431	Structural motifs and bonding in two families of boron structures predicted at megabar pressures. Physical Review Materials, 2021, 5, .	0.9	8
39432	Structural Effectiveness of AgCl-decorated Ag Nanowires Enhancing Oxygen Reduction. ACS Sustainable Chemistry and Engineering, 2021, 9, 7519-7528.	3.2	14
39433	Dual-atom Pt heterogeneous catalyst with excellent catalytic performances for the selective hydrogenation and epoxidation. Nature Communications, 2021, 12, 3181.	5.8	156
39434	High-mass loading V3O7Â·H2O nanoarray for Zn-ion battery: New synthesis and two-stage ion intercalation chemistry. Nano Energy, 2021, 83, 105835.	8.2	100
39435	Spin-polarized oxygen evolution reaction under magnetic field. Nature Communications, 2021, 12, 2608.	5.8	242
39436	N/O double-doped biomass hard carbon material realizes fast and stable potassium ion storage. Carbon, 2021, 176, 71-82.	5.4	105
39437	A hierarchical Ti2Nb10O29 composite electrode for high-power lithium-ion batteries and capacitors. Materials Today, 2021, 45, 8-19.	8.3	61
39438	Synergistic role of electron-trapped oxygen vacancy and exposed TiO2 [0 0 1] facets toward electrochemical p-nitrophenol reduction: Characterization, performance and mechanism. Chemical Engineering Journal, 2021, 411, 128485.	6.6	48
39439	Insights of $$hbox {XPt}_2$$ ($$hbox {X}=hbox {Eu}$$ and Gd) intermetallic systems: An ab-initio approach. Pramana - Journal of Physics, 2021, 95, 1.	0.9	0

#	Article	IF	Citations
39440	Engineering new limits to magnetostriction through metastability in iron-gallium alloys. Nature Communications, 2021, 12, 2757.	5.8	14
39441	Uncertainty of exchangeâ€correlation functionals in density functional theory calculations for lithiumâ€based solid electrolytes on the case study of lithium phosphorus oxynitride. Journal of Computational Chemistry, 2021, 42, 1283-1295.	1.5	6
39442	Unveiling the dopant segregation effect at hematite interfaces. Applied Physics Letters, 2021, 118, .	1.5	13
39443	Theoretical insights into bimetallic atoms supported on PC6 as highly efficient electrocatalysts for N2 electroreduction to NH3. Applied Surface Science, 2021, 547, 149208.	3.1	25
39444	Formaldehyde Selectivity in Methanol Partial Oxidation on Silver: Effect of Reactive Oxygen Species, Surface Reconstruction, and Stability of Intermediates. ACS Catalysis, 2021, 11, 6200-6209.	5.5	14
39445	Reduction in Work Functions of Transition-Metal Carbides and Oxycarbides upon Oxidation. ACS Omega, 2021, 6, 14559-14565.	1.6	5
39446	Structure-activity correlation of Ti₂CT₂ MXenes for Câ€“H activation. Journal of Physics Condensed Matter, 2021, 33, 235201.	0.7	5
39447	<i>Ab Initio</i> Study on Structural Properties of NaFeSO₄OH Cathode Material for Rechargeable Sodium Ion Battery. Solid State Phenomena, 0, 317, 400-405.	0.3	1
39448	Designing a new Mg-Zn-Ca-Y wrought alloy with high strength and ductility synergy. Materialia, 2021, 16, 101073.	1.3	1
39449	An Ab Initio Study of Allâ€Heusler Heterostructures: The Case of Ultrathin Multilayers. Physica Status Solidi - Rapid Research Letters, 2021, 15, 2100139.	1.2	2
39450	Effect of Electron Doping on the Crystal Structure and Physical Properties of an n = 3 Ruddlesdenâ€“Popper Compound La₄Ni₃O₁₀. ACS Applied Electronic Materials, 2021, 3, 2671-2684.	2.0	1
39451	Carbon nanotubes functionalized with Zinc(II) phthalocyanines: Effect of the expanded aromatic system and aromatic substituents on the binding energy. Applied Surface Science, 2021, 547, 149172.	3.1	9
39452	Evidence for an electromagnon in <mml:math xmlns:mml="http://www.w3.org/1998/Math/MathML"><mml:msub><mml:mi>GdMn</mml:mi><mml:mn>2</mml:mn></mml:msub><m mathvariant="normal">O</mml:mi><mml:mn>5</mml:mn></mml:msub></mml:math> : A multiferroic with a large electric polarization. Physical Review B, 2021, 103, .	1.1	5
39453	The chiral Hall effect in canted ferromagnets and antiferromagnets. Communications Physics, 2021, 4, .	2.0	15
39454	Structural and physical properties of 99 complex bulk chalcogenides crystals using first-principles calculations. Scientific Reports, 2021, 11, 9921.	1.6	18
39455	Investigation of the structural, electronic, optical, elastic, and thermodynamic properties of the zinc blende Ga1-xAlxAs1-yPy quaternary alloys: A DFT-Based simulation. Materials Science in Semiconductor Processing, 2021, 126, 105642.	1.9	5
39456	Revealing the trend of structural, electronic, mechanical and vibrational properties in Co2VX (X= Si,) Tj ETQq0 0 0 rgBT /Overlock 10 Tf 5	1.4	5
39457	Tuning graphene doping by carbon monoxide intercalation at the Ni(111) interface. Carbon, 2021, 176, 253-261.	5.4	7

#	Article	IF	Citations
39458	Laves polyhedra in synthetic tennantite, <mml:math xmlns:mml="http://www.w3.org/1998/Math/MathML" altimg="si1.svg"><mml:mrow><mml:msub><mml:mtext>Cu</mml:mtext><mml:mn>12</mml:mn></mml:msub><mml:msub><mml:mt and its lattice dynamics. Journal of Solid State Chemistry, 2021, 297, 122061.	1.4	2
39459	Computational Study of Electronic and Thermoelectric Properties of ZnO/Graphene Heterostructures. International Journal of Thermophysics, 2021, 42, 1.	1.0	7
39460	B₅N₃ and B₇N₅ Monolayers with High Carrier Mobility and Excellent Optical Performance. Journal of Physical Chemistry Letters, 2021, 12, 4823-4832.	2.1	18
39461	Treatment of highly concentrated formaldehyde effluent using adsorption and ultrasonic dissociation on mesoporous copper iodide (CuI) nano-powder. Journal of Environmental Management, 2021, 285, 112085.	3.8	16
39462	Two-dimensional nanodomains as quantum dots models in an ultra-thin hydrogenated SiC layer. Journal of Applied Physics, 2021, 129, .	1.1	4
39463	DFT Simulation of the Water Molecule Interaction with the (00l) Surface of Montmorillonite. Minerals (Basel, Switzerland), 2021, 11, 501.	0.8	7
39464	First-principles investigations of geometrical and electronic structures of Mn4+ doped A2SiF6 (A= K,) Tj ETQq0 0 0 rgBT /Overlock 10 Tf	1.7	10
39465	Surface Structures of CaFe₂O₄ (001), (100), (110) and (111): A Density Functional Theory Study. ISIJ International, 2021, 61, 1370-1378.	0.6	2
39466	Understanding lanthanum oxide surface structure by DFT simulation of oxygen 1s calibrated binding energy in XPS after in situ treatment. Applied Surface Science, 2021, 548, 149214.	3.1	42
39467	Electronic Structures of Twisted Bilayer InSe/InSe and Heterobilayer Graphene/InSe. ACS Omega, 2021, 6, 13426-13432.	1.6	4
39468	Structure and Band Alignment of InP Photocatalysts Passivated by TiO₂ Thin Films. Journal of Physical Chemistry C, 2021, 125, 11620-11627.	1.5	7
39469	Layered heterostructure of planar and buckled phases of silicene. 2D Materials, 2021, 8, 035038.	2.0	14
39470	Ab initio study of structural and electronic properties of lithium fluoride nanotubes. Journal of Applied Physics, 2021, 129, .	1.1	2
39471	First Principles Calculation of Band Structure and Physical Properties of Ferroelectric (NH4)2BeF4 Crystal. , 2021, , .		0
39472	Density functional theory study of chemical pressure in multicaloric MTX compounds. Applied Physics Letters, 2021, 118, 212408.	1.5	7
39473	Na and Cr co-doped BaCd2As2: A hexagonal structured diluted magnetic semiconductor with decoupled charge and spin doping. Journal of Magnetism and Magnetic Materials, 2021, 526, 167754.	1.0	2
39474	Adsorption and sensing characteristics of air decomposed species onto pyridine-like PdN3-doped CNT: a first-principles study. Carbon Letters, 2022, 32, 109-117.	3.3	5
39475	Mn KatkÄ±lÄ± Grafen YÃ¼zey Ãœzerinde NH3 Olmadan NOâ€™nun Katalitik Ä°ndirgenmesi: Bir YoÄŸunluk Fonksiyonel Teorisi Ã‡alÄ±ÅŸmasÄ±. European Journal of Science and Technology, 0, , .	0.5	0

#	Article	IF	Citations
39476	Effect of biaxial strain on the electronic structure of Nb-doped WSe₂ monolayer: a theoretical study. , 2021, , .		2
39477	Ab initio screening of metallic MAX ceramics for advanced interconnect applications. Physical Review Materials, 2021, 5, .	0.9	13
39478	Experimental and theoretical studies of the adsorption of Cu and Ni ions from wastewater by hydroxyapatite derived from eggshells. Environmental Nanotechnology, Monitoring and Management, 2021, 15, 100439.	1.7	20
39479	A Selfâ€Supported Highâ€Entropy Metallic Glass with a Nanosponge Architecture for Efficient Hydrogen Evolution under Alkaline and Acidic Conditions. Advanced Functional Materials, 2021, 31, 2101586.	7.8	89
39480	First principle modeling of a silicene anode for lithium ion batteries. Electrochimica Acta, 2021, 378, 138143.	2.6	14
39481	Predicting the energetic stabilization of Janus-MoSSe/AlN heterostructures: A DFT study. Chemical Physics Letters, 2021, 771, 138465.	1.2	2
39482	Metal-N4@Graphene as Multifunctional Anchoring Materials for Na-S Batteries: First-Principles Study. Nanomaterials, 2021, 11, 1197.	1.9	12
39483	Role of chromium in Crâ€“Fe oxide catalysts for high temperature water-gas shift reaction â€“ A DFT study. International Journal of Hydrogen Energy, 2021, 46, 17154-17162.	3.8	9
39484	The Phase Stability of Al3Er Studied by the First-Principles Calculations and Experimental Analysis. Metals, 2021, 11, 759.	1.0	4
39485	Density Functional Theory Study of Edge-Induced Atomic-Scale Structural Phase Transitions of MoS2 Nanocrystals: Implications for a High-Performance Catalyst. ACS Applied Nano Materials, 2021, 4, 5496-5502.	2.4	2
39486	Chemical ordering as a precursor to formation of ordered Î´-UZr₂ phase: a theoretical and experimental study. Journal of Physics Condensed Matter, 2021, 33, 254003.	0.7	12
39487	Spontaneous formation of filled-shell CsI-Xenon solid solutions under high temperature and high pressure. Computational Materials Science, 2021, 192, 110355.	1.4	0
39488	Water in the crystal structure of CaSiO3 perovskite. American Mineralogist, 2022, 107, 631-641.	0.9	5
39489	Electronic and magnetic properties of X-doped (X=V, Cr, Mn, and Fe) tellurene for the 2D spintronic device: Insights from the first-principles calculations. Physica E: Low-Dimensional Systems and Nanostructures, 2021, 129, 114667.	1.3	4
39490	First-principles study for comparison of the electronic and optic bandgaps of the CH3NH3Pb1-Y I3 (Y=Bi,) Tj ETQq0 0 0 rgBT /Overlock 1 2021, 608, 412897.	1.3	1
39491	Ground state properties of fluorine from DFT-hybrid functional. Vacuum, 2021, 187, 110118.	1.6	3
39492	A heterostructure of C3N/h-BN with effectively regulated electronic properties by E-field and strain. Chemical Physics Letters, 2021, 770, 138461.	1.2	5
39493	Higher photocatalytic removal of organic pollutants using pangolin-like composites made of 3â€“4 atomic layers of MoS2 nanosheets deposited on tourmaline. Environmental Chemistry Letters, 2021, 19, 3573-3582.	8.3	37

#	Article	IF	Citations
39494	Theoretical study on residual infrared absorption of Ti:sapphire laser crystals. Photonics Research, 2021, 9, 909.	3.4	5
39495	Ab initio based interionic interactions in calcium aluminotitanate oxide melts: structure and diffusion. Journal of Physics Condensed Matter, 2021, 33, 285401.	0.7	2
39496	The effect of hydrostatic pressure on structural, piezoelectric and dielectric properties of wurtzite and zinc-blende BeO crystals with DFT-DFPT calculations. Physica B: Condensed Matter, 2021, 618, 413152.	1.3	2
39497	Ferromagnetism in two-dimensional black phosphorus induced by phthalocyanine cobalt. Journal of Materials Science, 2021, 56, 13568-13578.	1.7	5
39498	A first principle study: Effect of tin substitution on magnetic properties of bismuth ferrite nanoparticles prepared by sol-gel synthesis method. Inorganic Chemistry Communication, 2021, 127, 108483.	1.8	16
39499	Prediction of crystal structures and motifs in the Fe-Mg-O system at Earthâ€™s core pressures. New Journal of Physics, 0, , .	1.2	1
39500	Monte Carlo transport analysis to assess intensity dependent response of a carbon-doped GaN photoconductor. Journal of Applied Physics, 2021, 129, .	1.1	7
39501	Simple linear response model for predicting energy band alignment of two-dimensional vertical heterostructures. Physical Review B, 2021, 103, .	1.1	2
39502	First principles study on the lattice dynamics and electron-phonon interaction of HfOs and HfRu compounds. Physica C: Superconductivity and Its Applications, 2021, 584, 1353862.	0.6	0
39503	Uniform Strain-Dependent Thermal Conductivity of Pentagonal and Hexagonal Silicene. Frontiers in Materials, 2021, 8, .	1.2	1
39504	Cadmium(II) Removal by Mackinawite under Anoxic Conditions. ACS Earth and Space Chemistry, 2021, 5, 1306-1315.	1.2	9
39505	Tuning Exchange Coupling in NiO-Based Bimagnetic Heterostructured Nanocrystals. ACS Applied Materials & Interfaces, 2021, 13, 24013-24023.	4.0	8
39506	Effects of rare-earth elements on the oxidation behavior of Î³-Ni in Ni-based single crystal superalloys: A first-principles study from a perspective of surface adsorption. Applied Surface Science, 2021, 547, 149173.	3.1	10
39507	Motion of water monomers reveals a kinetic barrier to ice nucleation on graphene. Nature Communications, 2021, 12, 3120.	5.8	20
39508	Polarization of CO2 for improved CO2 adsorption by MgO and Mg(OH)2. Applied Surface Science, 2021, 562, 150187.	3.1	25
39509	First-Principle Studies of the Vibrational Properties of Carbonates under Pressure. Sensors, 2021, 21, 3644.	2.1	16
39510	B2 ordering in body-centered-cubic AlNbTiV refractory high-entropy alloys. Physical Review Materials, 2021, 5, .	0.9	14
39511	Synthesis of Copper Nitride Layers by the Pulsed Magnetron Sputtering Method Carried out under Various Operating Conditions. Materials, 2021, 14, 2694.	1.3	11

#	Article	IF	Citations
39512	Theoretical Investigation of the Prospect to Tailor ZnO Electronic Properties with VP Thin Films. Nanomaterials, 2021, 11, 1412.	1.9	1
39513	<scp>PtZn</scp> intermetallic nanoalloy encapsulated in silicaliteâ€1 for propane dehydrogenation. AIChE Journal, 2021, 67, e17295.	1.8	34
39514	Elastic Properties of the Pyriteâ€Type FeOOHâ€AlOOH System From Firstâ€Principles Calculations. Geochemistry, Geophysics, Geosystems, 2021, 22, e2021GC009703.	1.0	2
39515	Anomalous Stopping and Charge Transfer in Proton-Irradiated Graphene. Nano Letters, 2021, 21, 4816-4822.	4.5	23
39516	Catalytic Conversion of CO and H₂ into Hydrocarbons on the Cobalt Co(111) Surface: Implications for the Fischerâ€“Tropsch Process. Journal of Physical Chemistry C, 2021, 125, 11891-11903.	1.5	11
39517	Synergy of Solid-State NMR, Single-Crystal X-ray Diffraction, and Crystal Structure Prediction Methods: A Case Study of Teriflunomide (TFM). Crystal Growth and Design, 2021, 21, 3328-3343.	1.4	10
39518	Tailoring the surface oxygen engineering of a carbon-quantum-dot-sensitized ZnO@H-ZnO1-x multijunction toward efficient charge dynamics and photoactivity enhancement. Applied Catalysis B: Environmental, 2021, 285, 119846.	10.8	20
39519	3D-to-2D Transition of Anion Vacancy Mobility in CsPbBr₃ under Hydrostatic Pressure. Journal of Physical Chemistry Letters, 2021, 12, 5169-5177.	2.1	7
39520	Impact of A-Site Cations on Fluorescence Quenching in Organicâ€“Inorganic Hybrid Perovskite Materials. Journal of Physical Chemistry C, 2021, 125, 11524-11531.	1.5	3
39521	An origin of corrosion resistance changes of Zr alloys: effects of Sn and Nb on grain boundary strength of surface oxide. Acta Materialia, 2021, 209, 116804.	3.8	31
39522	Computational insights into promoting effects of alkali metals, Re, and Cl for silver catalysts of ethylene epoxidation. Molecular Catalysis, 2021, 507, 111574.	1.0	1
39523	A Universal Approach to Quantify Overpotential-Dependent Selectivity Trends for the Competing Oxygen Evolution and Peroxide Formation Reactions: A Case Study on Graphene Model Electrodes. Journal of Physical Chemistry C, 2021, 125, 10413-10421.	1.5	9
39524	Room temperature ferromagnetic stability of SrTi1â^’ x M xO3 (M = V,) Tj ETQq0 0 0 rgBT /Overlock	0.6	3
39525	Iron-Doped Mesoporous Powders of Hydroxyapatite as Molybdenum-Impregnated Catalysts for Deep Oxidative Desulfurization of Model Fuel: Synthesis and Experimental and Theoretical Studies. Journal of Physical Chemistry C, 2021, 125, 11604-11619.	1.5	19
39526	The interaction of two-dimensional P2SiS nanosheet with environmental toxic NCG molecules for sensor application: A DFT study. Sensors and Actuators A: Physical, 2021, 322, 112608.	2.0	25
39527	Ferromagnetic half-metal with high Curie temperature: Janus Mn2PAs monolayer. Journal of Materials Science, 2021, 56, 13215-13226.	1.7	18
39528	First-principles study on improvement of two-dimensional hole gas concentration and confinement in AlN/GaN superlattices. Chinese Physics B, 2022, 31, 017104.	0.7	2
39529	Theoretical study of structural and electronic properties of <mml:math xmlns:mml="http://www.w3.org/1998/Math/MathML"><mml:mrow><mml:mn>2</mml:mn><mml:mi>H</mml:mi></mml:mrow></mml:math> -phase transition metal dichalcogenides. Physical Review B, 2021, 103, .	1.7	17

#	Article	IF	Citations
39530	Prediction of Chalcogenâ€Doped VCl 3 Monolayers as 2D Ferromagnetic Semiconductors with Enhanced Optical Absorption. Annalen Der Physik, 2021, 533, 2100064.	0.9	3
39531	Defects, diffusion, dopants and encapsulation of Na in NaZr2(PO4)3. Materialia, 2021, 16, 101039.	1.3	5
39532	A tetragonal high-pressure phase of PtAs2. Results in Physics, 2021, 24, 104188.	2.0	2
39533	Efficient N2- and O2-Sensing Properties of PtSe2 With Proper Intrinsic Defects. Frontiers in Chemistry, 2021, 9, 676438.	1.8	2
39534	Lithiophilic NiO Nanoarrays-Modified Ni Skeletons with Vertical Channels for High-Loading Li Metal Batteries. Journal of the Electrochemical Society, 2021, 168, 050536.	1.3	1
39535	Unravelling the Role of Strong Metalâ€“Support Interactions in Boosting the Activity toward Hydrogen Evolution Reaction on Ir Nanoparticle/N-Doped Carbon Nanosheet Catalysts. ACS Applied Materials & Interfaces, 2021, 13, 22448-22456.	4.0	34
39536	Computational analysis of doped (10, 0) MoS2 ANR metal junction by Schottky Barrier height modulation. , 2021, , .		0
39537	Single- and co-sensitization of triphenylamine-based and asymmetrical squaraine dyes on the anatase (001) surface for DSSC applications: Periodic DFT calculations. Journal of Molecular Graphics and Modelling, 2021, 104, 107833.	1.3	14
39538	Density Functional Theory Study of Heptafluoroisobutyronitrile and its Decompositions Adsorption on Î³-Al2O3. , 2021, , .		0
39539	High pressure core electron spectroscopy in 111 Fe-based superconducting materials: A first principles study. Computational Materials Science, 2021, 192, 110316.	1.4	7
39540	Role of the Hydration Shell in the pH-Dependent Adsorption of Maleic Acid. Journal of Physical Chemistry C, 2021, 125, 12305-12315.	1.5	2
39541	Improved lithium-ion batteries and their communication with hydrogen power. International Journal of Hydrogen Energy, 2021, 46, 17019-17036.	3.8	14
39542	Graphene Oxide/Fe₂O₃ Nanocomposite as an Efficient Catalyst for Thermal Decomposition of Ammonium Perchlorate via the Vacuum-Freeze-Drying Method. Langmuir, 2021, 37, 6132-6138.	1.6	34
39543	Effects of transition metal (Fe, Co & Ni) doping on structural, electronic and optical properties of CuO: DFTÂ+ÂU study. Chemical Physics, 2021, 545, 111160.	0.9	21
39544	Functionalization of electronic, spin and optical properties of GeSe monolayer by substitutional doping: a first-principles study. Nanotechnology, 2021, 32, 305701.	1.3	6
39546	Theoretical investigation on the structural, mechanical, electronic and thermodynamic properties of cubic Ti3NiAl2C compound. Physica B: Condensed Matter, 2021, 609, 412917.	1.3	0
39547	OCELOT: An infrastructure for data-driven research to discover and design crystalline organic semiconductors. Journal of Chemical Physics, 2021, 154, 174705.	1.2	23
39548	On-Surface Synthesis of Thiophene-Containing Large-Sized Organometallic Macrocycles on the Ag(111) Surface. Journal of Physical Chemistry C, 2021, 125, 11454-11461.	1.5	8

#	Article	IF	Citations
39549	Stability and mobility of tungsten clusters on tungsten (110) surface: Ab initio and atomistic simulations. Surface Science, 2021, 707, 121806.	0.8	3
39550	Effects of structural characteristics of Cu grain boundaries on graphene growth. Carbon, 2021, 176, 262-270.	5.4	4
39551	Silicene/ZnI₂ van der Waals heterostructure: tunable structural and electronic properties. Nanotechnology, 2021, 32, 305707.	1.3	8
39552	Dirac Semimetal Protected by Nonsymmorphic Mirror Symmetries in TPHâ€Graphene. Physica Status Solidi - Rapid Research Letters, 2021, 15, 2100039.	1.2	7
39553	Pressure induced semiconductor to metal phase transition in cubic CsSnBr3 perovskite. AIP Advances, 2021, 11, .	0.6	29
39554	Twoâ€“dimensional PC3 as a promising anode material for potassium-ion batteries: Firstâ€“principles calculations*. Chinese Physics B, 2021, 30, 056801.	0.7	5
39555	Theoretical Insights into the Formation Mechanism of Methane, Ethylene and Methanol in Fischerâ€Tropsch Synthesis at Co₂C Surfaces. ChemCatChem, 2021, 13, 2674-2682.	1.8	14
39556	Spontaneous Enhanced Visible-Light-Driven Photocatalytic Water Splitting on Novel Type-II GaSe/CN and Ga₂SSe/CN vdW Heterostructures. Journal of Physical Chemistry Letters, 2021, 12, 5064-5075.	2.1	95
39557	Understanding the adsorption behavior of small molecule in MoS₂ device based on first-principles calculations. Materials Research Express, 2021, 8, 055010.	0.8	5
39558	Ab initio study including spinâ€“orbit coupling of the electronic band structure and magnetic properties of h-HoMnO3. Indian Journal of Physics, 2022, 96, 1731-1739.	0.9	2
39559	Exploring the AgSb1â^'xBixI4 phase diagram: Thermochromism in layered CdCl2-type semiconductors. Journal of Solid State Chemistry, 2021, 297, 121997.	1.4	8
39560	Molecular Disorder Induces an Unusual Phase Transition in a Potential 2D Chiral Ferroelectric Perovskite. Chemistry - A European Journal, 2021, 27, 9054-9059.	1.7	15
39561	Effect of metal dopant on structural and magnetic properties of ZnO nanoparticles. Journal of Materials Science: Materials in Electronics, 2021, 32, 16153-16165.	1.1	5
39562	First Principles Study on Properties of Monolayer MoS2 Under Different Strains. Brazilian Journal of Physics, 2021, 51, 1230-1236.	0.7	5
39564	Study of the Structural, Elastic, and Electronic Properties of ZnN1Ââ€“ÂxOx. Russian Journal of Physical Chemistry A, 2021, 95, 995-1002.	0.1	0
39565	Enhancement of piezoelectric property in MgTMAlN (TM = Cr, Mo, W): First-principles study. Journal of Physics and Chemistry of Solids, 2021, 152, 109913.	1.9	10
39566	Mechanistic insights into carbonâ€“carbon coupling on NiAu and PdAu single-atom alloys. Journal of Chemical Physics, 2021, 154, 204701.	1.2	10
39567	Ammonium fluorideâ€™s analogy to ice: Possibilities and limitations. Journal of Chemical Physics, 2021, 154, 204501.	1.2	4

#	Article	IF	Citations
39568	Structural, Electronic and Optical Properties of CsPbBr3 and CH3NH3PbBr3: First-Principles Modeling. , 2021, , .		0
39569	Formation of CsPbI₃ Î³â€Phase at 80â€‰Â°C by Europiumâ€Assisted Snowplow Effect. Advanced Energy and Sustainability Research, 2021, 2, 2100091.	2.8	8
39570	Structure sensitivity of ammonia electro-oxidation on transition metal surfaces: A first-principles study. Journal of Catalysis, 2021, 397, 137-147.	3.1	31
39571	New Insights into the Bulk and Surface Defect Structures of Ceria Nanocrystals from Neutron Scattering Study. Chemistry of Materials, 2021, 33, 3959-3970.	3.2	24
39572	A Universal Method for Enhancing the Structural Stability of Ni-Rich Cathodes Via the Synergistic Effect of Dual-Element Cosubstitution. ACS Applied Materials & Interfaces, 2021, 13, 24925-24936.	4.0	43
39573	Ab initio prediction of semiconductivity in a novel two-dimensional Sb2X3 (X= S, Se, Te) monolayers with orthorhombic structure. Scientific Reports, 2021, 11, 10366.	1.6	44
39574	Effects of Site and Magnetic Disorder on the Oxygen Vacancy Formation and Electronic and Optical Properties of LaxSr1â€“xCoO3â^'Î´ and SrFeyCo1â€“yO3â^'Î´. Journal of Physical Chemistry C, 2021, 125, 12374-12381.	1.5	3
39575	Janus two-dimensional transition metal dichalcogenide oxides: First-principles investigation of <mml:math xmlns:mml="http://www.w3.org/1998/Math/MathML"><mml:mrow><mml:mi mathvariant="normal">W</mml:mi><mml:mi>X</mml:mi><mml:mi mathvariant="normal">O</mml:mi></mml:mrow></mml:math> monolayers with <mml:math xmlns:mml="http://www.w3.org/1998/Math/MathML"><mml:mi>X</mml:mi><mml:mo>=</mml:mo><mml:mi mathvariant="normal">S</mml:mi></mml:math> , Se, and Te. Physical Review B, 2021, 103, .	1.1	73
39576	Benchmarking binding energy calculations for organic structure-directing agents in pure-silica zeolites. Journal of Chemical Physics, 2021, 154, 174109.	1.2	26
39577	Synthesis, characterization and visible light-responsive photocatalysis properties of Ce doped CuO nanoparticles: A combined experimental and DFT+U study. Colloids and Surfaces A: Physicochemical and Engineering Aspects, 2021, 617, 126386.	2.3	45
39578	MoS₂ Nanosheet/ZnS Composites for the Visible-Light-Assisted Photocatalytic Degradation of Oxytetracycline. ACS Applied Nano Materials, 2021, 4, 4721-4734.	2.4	61
39579	Theoretical study on water behavior on the copper surfaces. Journal of Molecular Modeling, 2021, 27, 149.	0.8	3
39580	Second-Order Nonlinear Optical Properties of Monolayer Transition-Metal Dichalcogenides by Computational Analysis. Journal of Physical Chemistry C, 2021, 125, 11075-11084.	1.5	16
39581	A Dirac-semimetal two-dimensional BeN4: Thickness-dependent electronic and optical properties. Applied Physics Letters, 2021, 118, .	1.5	64
39582	Structural, electronic, magnetic and optical properties of CaO induced by oxygen incorporation effects: A first-principles study. Physics Letters, Section A: General, Atomic and Solid State Physics, 2021, 397, 127241.	0.9	12
39583	Thermal properties of energetic materials from quasi-harmonic first-principles calculations. Journal of Physics Condensed Matter, 2021, 33, 275702.	0.7	3
39584	High Thermopower and Optical Properties of A 2 MoS 4 (Aâ€‰=â€‰K, Rb, Cs) and Cs 2 MoSe 4. Physica Status Solidi (B): Basic Research, 2021, 258, 2000587.	0.7	0
39585	Anisotropic Angstrom-Wide Conductive Channels in Black Phosphorus by Top-down Cu Intercalation. Nano Letters, 2021, 21, 6336-6342.	4.5	10

#	Article	IF	Citations
39586	Silicon nanowires as acetone-adsorptive media for diabetes diagnosis. Applied Surface Science, 2021, 547, 149175.	3.1	5
39587	Multiphase tin equation of state using density functional theory. Physical Review B, 2021, 103, .	1.1	14
39588	Efficient Direct Band Gap Photovoltaic Material Predicted Via Doping Double Perovskites Cs₂AgBiX₆ (X = Cl, Br). Journal of Physical Chemistry C, 2021, 125, 10868-10875.	1.5	37
39589	Designing Active Sites for Structure-Sensitive Reactions via the Generalized Coordination Number: Application to Alcohol Dehydrogenation. Journal of Physical Chemistry C, 2021, 125, 10370-10377.	1.5	6
39590	Density Functional Theory Study on Sensing and Dielectric Properties of Arsenic Trisulfide Nanosheets for Detecting Volatile Organic Compounds. ACS Applied Nano Materials, 2021, 4, 5444-5453.	2.4	9
39591	Stability and electronic properties of bilayer graphene spirals. Physica E: Low-Dimensional Systems and Nanostructures, 2021, 129, 114638.	1.3	5
39592	Electronic topological transitions and vibrational properties of A-15 type X3Y (X= V, Cr and Mo; Y= Os,) Tj ETQq0 0 0 rgBT /Overlock 10 T 109953.	1.9	0
39593	Synergistic effect of Cu and Cr on pitting behavior induced by MnS inclusions in low alloy steels. Journal of Alloys and Compounds, 2021, 864, 158133.	2.8	10
39594	Distribution characteristics of phosphoric acid and PTFE binder on Pt/C surfaces in high-temperature polymer electrolyte membrane fuel cells: Molecular dynamics simulation approach. International Journal of Hydrogen Energy, 2021, 46, 17295-17305.	3.8	9
39595	Light-matter interactions in high quality manganese-doped two-dimensional molybdenum diselenide. Science China Materials, 2021, 64, 2507-2518.	3.5	6
39596	Spin Contamination Errors in DFT+U/Plane-wave Calculations for Li_xFeF₃ Systems (x = 0â€“1). Chemistry Letters, 2021, 50, 1057-1061.	0.7	4
39597	MoS2 doping for enhanced H2S detection. Applied Surface Science, 2021, 547, 149026.	3.1	20
39598	A computational study of physical, electronic, thermal and transport properties of one-dimensional boron and boron nitride systems. Journal of Solid State Chemistry, 2021, 297, 122037.	1.4	4
39599	First-Principles Insight into Pd-Doped C3N Monolayer as a Promising Scavenger for NO, NO2 and SO2. Nanomaterials, 2021, 11, 1267.	1.9	17
39600	First principles study of the electronic, optical, elastic and thermoelectric properties of Nb2WNi alloy. Molecular Physics, 0, , e1928314.	0.8	8
39601	Accurate Deep Potential model for the Alâ€“Cuâ€“Mg alloy in the full concentration space*. Chinese Physics B, 2021, 30, 050706.	0.7	25
39602	Vibrational spectroscopy and phononâ€related properties of monoclinic GABA, a nonâ€proteinogenic inhibitory neurotransmitter amino acid. Journal of Raman Spectroscopy, 2021, 52, 1294-1307.	1.2	1
39603	Structural evolution, lattice dynamics, electronic and thermal properties of VH2 under high pressure. Solid State Communications, 2021, 330, 114287.	0.9	6

#	Article	IF	Citations
39604	Training sets based on uncertainty estimates in the cluster-expansion method. JPhys Energy, 2021, 3, 034012.	2.3	7
39605	Sn-Based Perovskite with a Wide Visible-Light Absorption Band Assisted by Hydride Doping. Chemistry of Materials, 2021, 33, 3631-3638.	3.2	12
39606	Solidâ€state quantum chemistry with ÎĨ¦ (ThetaPhi): Spinâ€liquids , superconductors, and magnetic superstructures made computationally available. Journal of Computational Chemistry, 2021, 42, 1498-1513.	1.5	1
39607	Real time imaging of photocatalytic active site formation during H2 evolution by in-situ TEM. Applied Catalysis B: Environmental, 2021, 284, 119743.	10.8	19
39608	Surface functionalization of the honeycomb structure of zinc antimonide (ZnSb) monolayer: A first-Principles study. Surface Science, 2021, 707, 121796.	0.8	17
39609	The crystal structures and magnetic properties of TiFeSi coexisting in hexagonal and orthorhombic symmetries. Journal of Alloys and Compounds, 2021, 864, 158617.	2.8	4
39610	Electrochemical Construction of Low-Crystalline CoOOH Nanosheets with Short-Range Ordered Grains to Improve Oxygen Evolution Activity. ACS Catalysis, 2021, 11, 6104-6112.	5.5	103
39611	Competitive Cr³⁺ occupation in persistent phosphors toward tunable traps distribution for dynamic antiâ€counterfeiting. Journal of the American Ceramic Society, 2021, 104, 5224-5234.	1.9	11
39612	Exceptional Radiation Absorption in a Pentagon-Based Si Allotrope. Nano Letters, 2021, 21, 4287-4291.	4.5	0
39613	Large-area uniform few-layer PtS2: Synthesis, structure and physical properties. Materials Today Physics, 2021, 18, 100376.	2.9	20
39614	Effects of Strain and Electric Field on Molecular Doping in MoSSe. ACS Omega, 2021, 6, 14639-14647.	1.6	6
39615	Effect of B and O doping on the electronic structure and quantum capacitance of carbon nitride monolayers using first-principles calculations. Journal of Applied Physics, 2021, 129, .	1.1	8
39616	Binding of Oxygen on Single-Atom Sites on Au/Pd(100) Alloys with High Gold Coverages. Journal of Physical Chemistry C, 2021, 125, 9715-9729.	1.5	3
39617	Formation of a Small Electron Polaron in Tantalum Oxynitride: Origin of Low Mobility. Journal of Physical Chemistry C, 2021, 125, 11548-11554.	1.5	16
39618	Mechanisms and Properties of Bismuthene and Graphene/Bismuthene Heterostructures as Anodes of Lithium-/Sodium-Ion Batteries by First-Principles Study. Journal of Physical Chemistry C, 2021, 125, 11391-11401.	1.5	11
39619	An Efficient and Reversible Battery Anode Electrode Derived from a Lead-Based Metalâ€“Organic Framework. Energy & Fuels, 2021, 35, 9669-9682.	2.5	13
39620	Design of earth-abundant ternary Fe1âˆ’xCoxS2 on RGO as efficient electrocatalysts for hydrogen evolution reaction. Journal of Alloys and Compounds, 2021, 862, 158610.	2.8	16
39621	Anomalous layer-dependent electronic and piezoelectric properties of 2D GaInS3 nanosheets. Applied Physics Letters, 2021, 118, .	1.5	29

#	Article	IF	Citations
39622	Grain and grain boundary contributions to AC conductivity in ferroelectric Ba0.75Pb0.25Ti1-Zr O3 ceramics. Ceramics International, 2021, 47, 13118-13128.	2.3	9
39623	High-pressure structural, mechanical, and vibrational properties of NAPTO: The first fused-ring energetic material with a 2D layered structure. Solid State Communications, 2021, 331, 114293.	0.9	1
39624	Generalizable Trends in Electrochemical Protonation Barriers. Journal of Physical Chemistry Letters, 2021, 12, 5193-5200.	2.1	19
39625	Interlayer excitonic states in <mml:math xmlns:mml="http://www.w3.org/1998/Math/MathML"><mml:mrow><mml:mi>Mo</mml:mi><mml:msub><mml:mi>Se</mml:mi><mml:mi mathvariant="normal">S</mml:mi><mml:mn>2</mml:mn></mml:msub></mml:mrow></mml:math> van der Waals heterostructures. Physical Review B, 2021, 103, .	1.1	5
39626	Strain modulated quantum spin Hall effect in monolayer NiB. Applied Physics Letters, 2021, 118, .	1.5	6
39627	Bulk and Surface Conformations in Solid-State Lovastatin: Spectroscopic and Molecular Dynamics Studies. Crystals, 2021, 11, 509.	1.0	1
39628	Crystal structure characterization and electronic structure of a rare-earth-containing Zintl phase in the Ybâ€“Alâ€“Sb family: Yb₃AlSb₃. Acta Crystallographica Section C, Structural Chemistry, 2021, 77, 281-285.	0.2	3
39629	Control of Stepwise Hg²⁺ Reduction on Gold to Selectively Tune its Peroxidase and Catalaseâ€Like Activities and the Mechanism. Advanced Materials Interfaces, 2021, 8, 2100086.	1.9	13
39630	Crystalline, ferromagnetic-semiconductor and electronic features of the terbium-based cobalt-ferrite Tb2FeCoO6. Ceramics International, 2021, 47, 14408-14417.	2.3	7
39631	Theoretical study on hydrogen storage of pristine bilayer hexagonal boron nitride. Theoretical Chemistry Accounts, 2021, 140, 1.	0.5	6
39632	First Principles Study of Optical and Tunable Electronic Properties of Crystalline Li2TeO3. Bulletin of the Lebedev Physics Institute, 2021, 48, 152-157.	0.1	1
39633	The role of M@Ni6 superstructure units in honeycomb-ordered layered oxides for Li/Na ion batteries. Nano Energy, 2021, 83, 105834.	8.2	15
39634	Adsorption of transition metal clusters on Boron-graphdiyne. Applied Surface Science, 2021, 548, 149270.	3.1	4
39635	The influence of Cr on He trapping behavior and the coupling effect of Cr/He on the mechanical behavior of the C14-Laves Fe2W phase: Firstâ€“principle and quasi-harmonic approximation studies. Computational Materials Science, 2021, 192, 110359.	1.4	2
39636	Controlling magnetostructural transition and magnetocaloric effect in multi-component transition-metal-based materials. Journal of Applied Physics, 2021, 129, 193901.	1.1	14
39637	Adsorption of CO2 and CH4 molecules on the Pd-decorated C3N based sensors: A first-principles study. Physica E: Low-Dimensional Systems and Nanostructures, 2021, 129, 114622.	1.3	13
39638	Ab initio simulations of the surface free energy of TiN(001). Physical Review B, 2021, 103, .	1.1	9
39639	Noble Metal-Free FeOOH/Li_{0.1}WO₃ Coreâ€“Shell Nanorods for Selective Oxidation of Methane to Methanol with Visibleâ€“NIR Light. Environmental Science & Technology, 2021, 55, 7711-7720.	4.6	32

#	Article	IF	Citations
39640	On aliovalent cations control of Î±-alumina growth on doped and undoped NiAl. Acta Materialia, 2021, 210, 116809.	3.8	4
39641	Room temperature weakly ferromagnetic energy band opened graphene quantum dot coupled solid sheets â€“ A possible carbon based dilute magnetic semiconductor. Applied Surface Science, 2021, 548, 149195.	3.1	4
39642	Two-dimensional Haeckelite GeS with high carrier mobility and exotic polarization orders. Physical Review Materials, 2021, 5, .	0.9	7
39643	Mechanical anomalies in mercury oxalate and the deformation of the mercury cube coordination environment under pressure. Applied Physics A: Materials Science and Processing, 2021, 127, 1.	1.1	1
39644	Ab-initio Calculations; Mechanical and Electronic Properties of New M4As3Co (M: Al, Ga) Compounds. SDU Journal of Science, 0, , 86-94.	0.1	0
39645	Interfacial charge transfer and interaction in the <mml:math xmlns:mml="http://www.w3.org/1998/Math/MathML"><mml:mrow><mml:mrow><mml:mi>MXene</mml:mi><mml:mo>/</mml:mo><mml:mathvariant="normal">O</mml:mi><mml:mn>2</mml:mn></mml:msub></mml:mrow></mml:math> heterostructures. Physical Review Materials, 2021, 5, .	0.9	14
39646	Lattice dynamics and topological surface phonon states in cuprous oxide <mml:math xmlns:mml="http://www.w3.org/1998/Math/MathML"><mml:mrow><mml:msub><mml:mi>Cu</mml:mi><mml:mn>2</mml:mn></mml:msub><mml:mathvariant="normal">O</mml:mi></mml:mrow></mml:math>. Physical Review B, 2021, 103, .	1.1	12
39647	First Principles Analysis of Crystal Structure, Electronic and Optical Properties of CsSnI3â€“xBrx Perovskite for Photoelectric Applications. Journal of Surface Investigation, 2021, 15, 532-536.	0.1	9
39648	Transitionâ€Metal Borides (MBenes) as New Highâ€Efficiency Catalysts for Nitric Oxide Electroreduction to Ammonia by a Highâ€Throughput Approach. Small, 2021, 17, e2100776.	5.2	67
39649	Twisted helical armchair graphene nanoribbons: mechanical and electronic properties. European Physical Journal B, 2021, 94, 1.	0.6	2
39650	Effects of pressure on the structural, mechanical, anisotropic, and electronic properties of $$hbox {MgTi}_{2}hbox {O}_{4}$$ via density functional theory. European Physical Journal B, 2021, 94, 1.	0.6	4
39651	Equations of state of poly- <mml:math xmlns:mml="http://www.w3.org/1998/Math/MathML"><mml:mi>Î±</mml:mi></mml:math> -methylstyrene and polystyrene: First-principles calculations versus precision measurements. Physical Review B, 2021, 103, .	1.1	8
39652	Site Mixing for Engineering Magnetic Topological Insulators. Physical Review X, 2021, 11, .	2.8	50
39653	Assessing the Activity of Ni Clusters Supported on TiC(001) toward CO₂ and H₂ Dissociation. Journal of Physical Chemistry C, 2021, 125, 12019-12027.	1.5	15
39654	CsZrF₄(IO₃): The First Polar Zirconium Iodate with cis-[ZrO₂F₆] Polyhedra Inducing Optimized Balance of Large Band Gap and Second Harmonic Generation. Chemistry of Materials, 2021, 33, 5555-5562.	3.2	29
39655	Highly dispersed Co/N-rich carbon nanosheets for the oxidative esterification of biomass-derived alcohols: Insights into the catalytic performance and mechanism. Journal of Catalysis, 2021, 397, 148-155.	3.1	28
39656	Effect of anchoring groups on the electronic transport properties of biphenyl and phenyl-pyridine molecules. Journal of Materials Research and Technology, 2021, 12, 193-201.	2.6	14
39657	Experimental and Ab Initio Investigation of the Formation of Phosphoran Olivine. ACS Earth and Space Chemistry, 2021, 5, 1373-1383.	1.2	0

#	Article	IF	Citations
39658	Ce-introduced effects on modification of acidity and Pt electronic states on Pt-Sn/Î³-Al2O3 catalysts for catalytic reforming. Applied Catalysis A: General, 2021, 617, 118116.	2.2	17
39659	First-principles investigation on the interfacial interaction and electronic structure of BiVO4/WO3 heterostructure semiconductor material. Applied Surface Science, 2021, 549, 149309.	3.1	28
39660	Engineering Ru atomic structures toward enhanced kinetics of hydrogen generation. Chemical Engineering Science, 2021, 235, 116507.	1.9	6
39661	Atomic mechanism of the distribution and diffusion of lithium in a cracked Si anode. Scripta Materialia, 2021, 197, 113807.	2.6	4
39662	Photoelectron spectroscopy reveals molecular diffusion through physisorbed template layers on Au(111). Electronic Structure, 2021, 3, 024002.	1.0	4
39663	Insights into the Role of Framework and Nonframework Aluminum in the Protolytic Reaction of Carbonâ€“Carbon and Tertiary Carbonâ€“Hydrogen Bonds of Isobutane. Journal of Physical Chemistry C, 2021, 125, 11636-11647.	1.5	9
39664	Degradation mechanism of hybrid tin-based perovskite solar cells and the critical role of tin (IV) iodide. Nature Communications, 2021, 12, 2853.	5.8	236
39665	Ru-Doped Single Walled Carbon Nanotubes as Sensors for SO2 and H2S Detection. Chemosensors, 2021, 9, 120.	1.8	12
39666	Ab-initio study of the structural, electronic, elastic and thermodynamic properties of Sc3XB (X=Sn, Al,) Tj ETQq0 0 0 rgBT /Overlock 10 T	0.9	8
39667	Î±-Ca₂CdP₂ and Î²-Ca₂CdP₂: Two Polymorphic Phosphide-Based Infrared Nonlinear Crystals with Distorted NLO-Active Tetrahedral Motifs Realizing Large Second Harmonic Generation Effects and Suitable Band Gaps. Inorganic Chemistry, 2021, 60, 7553-7560.	1.9	14
39668	Exploring the Structural Competition between the Black and the Yellow Phase of CsPbI3. Nanomaterials, 2021, 11, 1282.	1.9	12
39669	Pure bulk orbital and spin photocurrent in two-dimensional ferroelectric materials. Npj Computational Materials, 2021, 7, .	3.5	34
39670	Theoretical study of the synthesis, characterization and hydrogen storage properties of a high-density hydrogen storage material: (CH3NH3)BH4. International Journal of Hydrogen Energy, 2021, 46, 19498-19507.	3.8	2
39671	Theoretical characterization of induced ferromagnetism, half-metallic behavior, electronic properties in new Ti-doped BaO. Optical and Quantum Electronics, 2021, 53, 1.	1.5	7
39672	BxCyNz nanotubes decorated with tracks of fluorine: atomic structure, stability and electronic properties. Thin Solid Films, 2021, 727, 138675.	0.8	0
39673	A Molecular View of the Ionic Liquid Catalyst Interface of SCILLs: Coverage-Dependent Adsorption Motifs of [C₄C₁Pyr][NTf₂] on Pd Single Crystals and Nanoparticles. Journal of Physical Chemistry C, 2021, 125, 13264-13272.	1.5	9
39674	A₂MoO₂F₃(IO₂F₂) (A = Rb,) Tj ETQq0 0 0 rgBT /Overloc Chemistry of Materials, 2021, 33, 5700-5708.	3.2	30
39675	Competing HCOOH and CO Pathways in CO₂ Electroreduction at Copper Electrodes: Calculations of Voltage-Dependent Activation Energy. Journal of Physical Chemistry C, 2021, 125, 13802-13808.	1.5	7

#	Article	IF	Citations
39676	Elucidating the Mechanism of Ambient-Temperature Aldol Condensation of Acetaldehyde on Ceria. ACS Catalysis, 2021, 11, 8621-8634.	5.5	14
39677	First Principles calculations of structural, electronic, elastic, vibrational, and thermodynamic properties of TMPs compounds (TM= Cr, Mo). Computational Condensed Matter, 2021, 27, e00541.	0.9	2
39678	Nitrogen doping in non-magnetic yttrium oxide: Induction of room temperature ferromagnetism from first principles simulations. Journal of Magnetism and Magnetic Materials, 2021, 528, 167840.	1.0	5
39679	Microstructure and phase dependence of magnetic softness of FeSiGaB nanocrystalline alloys. Journal of Magnetism and Magnetic Materials, 2021, 528, 167802.	1.0	3
39680	Structural, electronic, and optical properties of two-dimensional hafnium monoxide nanosheets. Physica E: Low-Dimensional Systems and Nanostructures, 2021, 130, 114690.	1.3	3
39681	Optical properties of two-dimensional AlOCl, BaFCl, and BiOCl monolayers using the density functional theory. Optik, 2021, 236, 166678.	1.4	2
39682	Solid-state and solution-state self-association of dimethylarsinic acid: IR, NMR and theoretical study. Journal of Molecular Structure, 2021, 1234, 130176.	1.8	7
39683	Unraveling the formation mechanism of hydrogenated vacancy at Î³-Ni/Î³'-Ni3Al phase interface and its roles in interfacial stability and strength. Computational Materials Science, 2021, 194, 110449.	1.4	8
39684	Substitutional carbon-dioxygen center in irradiated silicon. Materials Science in Semiconductor Processing, 2021, 127, 105661.	1.9	1
39685	Unraveling the mechanism of hydrogen evolution reaction on cobalt compound electrocatalysts. Applied Surface Science, 2021, 550, 149355.	3.1	12
39686	Tuning structure, electronic, and catalytic properties of non-metal atom doped Janus transition metal dichalcogenides for hydrogen evolution. Applied Surface Science, 2021, 552, 149146.	3.1	33
39687	Effect of Doping on the Photoelectric Properties of Borophene. Advances in Condensed Matter Physics, 2021, 2021, 1-7.	0.4	4
39688	One-dimensional polyhedral chain of ThCl6 encapsulated within single-walled carbon nanotubes. AIP Advances, 2021, 11, 065117.	0.6	1
39689	Computational insight of ZrS2/graphene heterobilayer as an efficient anode material. Applied Surface Science, 2021, 551, 149304.	3.1	20
39690	Chlorobenzene and 1, 4-dichlorobenzene adsorption studies on Î¸-Arsenene nanosheet â€“ a first-principles analysis. Molecular Physics, 2021, 119, e1936248.	0.8	11
39691	Enhancing fatigue life by ductile-transformable multicomponent B2 precipitates in a high-entropy alloy. Nature Communications, 2021, 12, 3588.	5.8	102
39692	An estimation on the mechanical stabilities of SAMs by low energy Ar+ cluster ion collision. Scientific Reports, 2021, 11, 12772.	1.6	12
39693	Phase transitions of alkaline-earth metal sulfides under pressure. Materials Research Express, 2021, 8, 065902.	0.8	4

#	Article	IF	Citations
39694	Band structures of RE₂O₃:Eu (RE = Lu, Y, Sc) from perspective of spin-polarized quasi-particle approximation. Modelling and Simulation in Materials Science and Engineering, 2021, 29, 065002.	0.8	3
39695	WANNIER FUNCTIONS AND CHEMICAL BONDING IN COMPOUNDS Beâ€“IVâ€“P2 (IVÂ=ÂC, Si, Ge, Sn) WITH CHALCOPYRITE STRUCTURE. Journal of Structural Chemistry, 2021, 62, 817-823.	0.3	1
39696	Enzyme-like antibacterial activities of Cu9S5 nanoflowers with vacancy-type dependence. Cell Reports Physical Science, 2021, 2, 100456.	2.8	9
39697	Spin-dependent electronâ€“radiation interaction. Journal of Physics Condensed Matter, 2021, 33, 285501.	0.7	2
39698	Investigation on Atomic Structure and Mechanical Property of Na- and Mg-Montmorillonite under High Pressure by First-Principles Calculations. Minerals (Basel, Switzerland), 2021, 11, 613.	0.8	9
39699	Critical analysis of the response function in low-dimensional materials. Journal of Physics Condensed Matter, 2021, 33, 295701.	0.7	1
39700	A density functional theory and grand canonical Monte Carlo simulations study the hydrogen storage on the Li-decorated net-I„. International Journal of Hydrogen Energy, 2021, 46, 21965-21972.	3.8	3
39701	Revealing the Pressure-Induced Softening/Weakening Mechanism in Representative Covalent Materials. Chinese Physics Letters, 2021, 38, 056101.	1.3	1
39702	Electronic properties of single-layer CoO₂/Au(111). 2D Materials, 2021, 8, 035050.	2.0	7
39703	A novel titanium oxycarbide phase with metal-vacancy (Ti1-C O1-): Structural and thermodynamic basis. Ceramics International, 2021, 47, 16324-16332.	2.3	8
39704	Out-of-plane and in-plane ferroelectricity of atom-thick two-dimensional InSe. Nanotechnology, 2021, 32, 385202.	1.3	15
39705	First-principles computational exploration of ferromagnetism in monolayer GaS via substitutional doping. Journal of Physics Condensed Matter, 2021, 33, 314003.	0.7	10
39706	Adsorption of gas molecules on graphene, silicene, and germanene: A comparative first-principles study. Surfaces and Interfaces, 2021, 24, 101054.	1.5	20
39707	First-principles study of solid-state properties of adrenergic neurotransmitters, orthorhombic noradrenaline, and monoclinic adrenaline. Journal of Applied Physics, 2021, 129, 234702.	1.1	1
39708	Structural Features of Y2O2SO4 via DFT Calculations of Electronic and Vibrational Properties. Materials, 2021, 14, 3246.	1.3	4
39709	1D/2D van der Waals Heterojunctions Composed of Carbon Nanotubes and a GeSe Monolayer. Nanomaterials, 2021, 11, 1565.	1.9	5
39710	Strain engineering and thermal conductivity of a penta-BCN monolayer: a computational study. Journal Physics D: Applied Physics, 2021, 54, 355301.	1.3	13
39711	Theoretical study of novel Bâ€“Câ€“O compounds with non-diamond isoelectronic. Chinese Physics B, 2022, 31, 026201.	0.7	26

#	Article	IF	Citations
39712	Electron work function: an indicative parameter towards a novel material design methodology. Scientific Reports, 2021, 11, 11565.	1.6	17
39713	Ab initio calculation of the detailed balance limit to the photovoltaic efficiency of single p-n junction kesterite solar cells. Applied Physics Letters, 2021, 118, .	1.5	7
39714	Effect of Noninteracting Intercalants on Layer Exfoliation in Transition-Metal Dichalcogenides. Physical Review Applied, 2021, 15, .	1.5	3
39715	Entropic Control of HD Exchange Rates over Dilute Pd-in-Au Alloy Nanoparticle Catalysts. ACS Catalysis, 2021, 11, 6971-6981.	5.5	25
39716	Electrochemical adsorption of hydrogen on mixed Pd₂Pt nanostructures. Journal of Physics Condensed Matter, 2021, 33, 344001.	0.7	4
39717	Design of refractory compositionally complex alloys with optimal mechanical properties. Physical Review Materials, 2021, 5, .	0.9	7
39718	Two-Dimensional Chromium Bismuthate: A Room-Temperature Ising Ferromagnet with Tunable Magneto-Optical Response. Physical Review Applied, 2021, 15, .	1.5	14
39719	Nitrogen doping and oxygen vacancy effects on the fundamental properties of BeO monolayer: a DFT study. Journal of Physics Condensed Matter, 2021, 33, 325305.	0.7	9
39720	First-principles study of structural, electronic, and thermal conductivity properties of monolayer SrFBr. Journal of Physics and Chemistry of Solids, 2021, 153, 109956.	1.9	10
39721	Resolving Site-Specific Energy Levels of Small-Molecule Donor-Acceptor Heterostructures Close to Metal Contacts. Nanomaterials, 2021, 11, 1618.	1.9	0
39722	Unraveling the effect of thickness on the structural, morphological, opto-thermal and DFT calculation of hematite Fe2O3 thin films for photo-catalytic application. Journal of Materials Science: Materials in Electronics, 2021, 32, 17974-17989.	1.1	1
39723	A first-principles study of the structural, electronic, optical, and vibrational properties for paramagnetic half-Heusler compound TiIrBi by GGA and GGAâ€¯+â€¯mBJ functional. Materials Today Communications, 2021, 27, 102246.	0.9	7
39724	Structural, Thermal, and Vibrational Properties of N,N-Dimethylglycineâ€“Chloranilic Acidâ€”A New Co-Crystal Based on an Aliphatic Amino Acid. Materials, 2021, 14, 3292.	1.3	1
39725	Oxidized MWCNTs as an Oxidizing Agent and Dopant in MWCNT@Polypyrrole Composite Formation**. ChemElectroChem, 2021, 8, 3049-3063.	1.7	2
39726	Integration of nickel phosphide nanodot-enriched 3D graphene-like carbon with carbon fibers as self-supported sulfur hosts for advanced lithium sulfur batteries. Electrochimica Acta, 2021, 382, 138267.	2.6	17
39727	High-Entropy 2D Carbide MXenes: TiVNbMoC₃ and TiVCrMoC₃. ACS Nano, 2021, 15, 12815-12825.	7.3	162
39728	Density functional theory study on the structural, electronic, optical and photocatalytic properties of BaTa2O6, Ba2Ta15O32, Ba3Ta5O15 and Ba5Ta4O15. Journal of Solid State Chemistry, 2021, 298, 122127.	1.4	4
39729	First-principles study of the effect of mechanical strength on ion transport in La-doped LiF-SEI on the Li (001) surface. Materials Today Chemistry, 2021, 20, 100451.	1.7	9

#	Article	IF	Citations
39730	BaYOBO3: A deep-ultraviolet rare-earth oxy-borate with a large second harmonic generation response. Science China Chemistry, 2021, 64, 1184-1191.	4.2	22
39731	Optical phonon modes, static and high-frequency dielectric constants, and effective electron mass parameter in cubic In2O3. Journal of Applied Physics, 2021, 129, .	1.1	11
39732	Facile construction of nickel-doped hierarchical BiOCl architectures for enhanced visible-light-driven photocatalytic activities. Materials Research Bulletin, 2021, 138, 111208.	2.7	34
39733	Electronic and optical aspects of GeP2S 2D monolayer under biaxial stress and strain conditions. Bulletin of Materials Science, 2021, 44, 1.	0.8	4
39734	Dispersion energy effects on oxygen interaction with cesiated molybdenum surfaces. Chemical Physics Letters, 2021, 773, 138603.	1.2	2
39735	Lead halide perovskite for efficient optoacoustic conversion and application toward high-resolution ultrasound imaging. Nature Communications, 2021, 12, 3348.	5.8	85
39736	Loofah activated carbon with hierarchical structures for high-efficiency adsorption of multi-level antibiotic pollutants. Applied Surface Science, 2021, 550, 149313.	3.1	33
39737	Ethylene oxidation on unpromoted silver catalysts: Reaction pathway and selectivity analysis using DFT calculations. Surface Science, 2021, 708, 121834.	0.8	6
39738	Boron interstitials in ordered phases of Fe-Pd binary alloys: A first principle study. Journal of Magnetism and Magnetic Materials, 2021, 528, 167766.	1.0	3
39739	The Thermodynamic Stability, Electronic and Photocatalytic Properties of the ZnWO₄(100) Surface as Predicted by Screened Hybrid Density Functional Theory. ACS Omega, 2021, 6, 15057-15067.	1.6	10
39740	Structural, elastic, electronic, optical and thermoelectric properties of oxychalcogenides BiCuChO (ChÂ= S and Se): A computational study. Computational Condensed Matter, 2021, 27, e00529.	0.9	2
39741	Influence of thickness on current-induced magnetization switching in L1₀-FePt single layer*. Chinese Physics B, 2021, 30, 107101.	0.7	1
39742	Theoretical investigation of intrinsic point defects and the oxygen migration behavior in rare earth hafnates. Ceramics International, 2021, 47, 15023-15029.	2.3	2
39743	Stabilization of charged substitutional ions in tetragonal zirconia. Materials Today: Proceedings, 2022, 51, 488-495.	0.9	1
39744	Additivation of MoS2 nanosheets to synthetic poly-alpha-olefins base oils: A theoretical study of nanolubrication. Journal of Molecular Liquids, 2021, 332, 115881.	2.3	9
39745	Missing Piece in the Crystal Chemistry of Znâ€“Sb Secondary Phases in ZnOâ€“Sb₂O₃â€“Bi₂O₃ Varistor Ceramics: Orthorhombic Î²-Zn₇Sb₂O₁₂. An Experimental and Theoretical Study of the Crystal Structure and Its Thermal and Vibrational Spectroscopic Characterization. Inorganic Chemistry, 2021, 60, 8649-8659.	1.9	3
39746	Leveraging Polar Discontinuities to Tune the Binding of Methanol on BCN and Grapheneâ€“BN Lateral Heterostructures. Journal of Physical Chemistry C, 2021, 125, 15012-15024.	1.5	5
39747	Machine Learning Screening of Metal-Ion Battery Electrode Materials. ACS Applied Materials & Interfaces, 2021, 13, 53355-53362.	4.0	42

#	Article	IF	Citations
39748	Hidden Effects of Negative Stacking Fault Energies in Complex Concentrated Alloys. Physical Review Letters, 2021, 126, 255502.	2.9	18
39749	Predicting carbon diffusion in cementite from first principles. Physical Review Materials, 2021, 5, .	0.9	2
39750	Achieving junction stability in heavily doped epitaxial Si:P. Materials Science in Semiconductor Processing, 2021, 127, 105672.	1.9	6
39751	Electronic structures and optical properties of nanoporous complex oxide 12CaOÂ·7Al2O3 (C12A7) under high pressure. Computational Materials Science, 2021, 194, 110456.	1.4	3
39752	High temperature oxidation behavior of disordered (Ti0.5Zr0.5)2AlC MAX phase via a Machine Learning-Augmented DFT approach. Materials Letters: X, 2021, 10, 100062.	0.3	1
39753	First principles calculation of structural, electronic and optical properties of K-doped ZnO. Computational Condensed Matter, 2021, 27, e00558.	0.9	6
39754	Synthesis and magnetism of MoCo2O4 spinel thin films. Thin Solid Films, 2021, 728, 138696.	0.8	3
39755	Substantial Variations in the Optical Absorption and Reflectivity of Graphene When the Concentrations of Vacancies and Doping with Fluorine, Nitrogen, and Oxygen Change. International Journal of Molecular Sciences, 2021, 22, 6832.	1.8	4
39756	One-dimensional yttrium silicide electride (Y5Si3:eâ^') for encapsulation of volatile fission products. Journal of Applied Physics, 2021, 129, .	1.1	2
39757	Observation of the critical state to multiple-type Dirac semimetal phases in KMgBi. Journal of Applied Physics, 2021, 129, .	1.1	1
39758	Nickel-decorated single vacancy phosphorene â€“ A favourable candidate for hydrogen storage. International Journal of Hydrogen Energy, 2021, , .	3.8	5
39759	Theoretical study of thermo-dynamical and thermoelectric properties of novel half-Heusler alloys AlNiAs and AlNiSb. Materials Today Communications, 2021, 27, 102195.	0.9	8
39760	Magnetic effects on ordering and surface segregation in NiPt nanoalloys. Applied Physics A: Materials Science and Processing, 2021, 127, 1.	1.1	0
39761	Observation of large Rashba spinâ€“orbit coupling at room temperature in compositionally engineered perovskite single crystals and application in high performance photodetectors. Materials Today, 2021, 46, 18-27.	8.3	20
39762	Influence of vacancy on the mechanical behavior, thermodynamic properties and electronic structure of orthorhombic Ti3Sn from first-principles calculations. Vacuum, 2021, 188, 110178.	1.6	7
39763	Optoelectronic behavior of ZnS compound and its alloy: A first principle approach. Materials Today Communications, 2021, 27, 102077.	0.9	4
39764	Structural, optoelectronic and thermodynamic characteristic of orthorhombic SnZrCH3(CH=S, Se) compounds: Insights from DFT computations. Materials Today Communications, 2021, 27, 102427.	0.9	3
39765	On the electronic structure and magnetism of CaCrO3: A hybrid-exchange density-functional-theory study. Materials Today Communications, 2021, 27, 102179.	0.9	1

#	Article	IF	Citations
39766	First-principles prediction of electronic transport in fabricated semiconductor heterostructures via physics-aware machine learning. Npj Computational Materials, 2021, 7, .	3.5	16
39767	Fe on molecular-layer MoS2 as inorganic Fe-S2-Mo motifs for light-driven nitrogen fixation to ammonia at elevated temperatures. Chem Catalysis, 2021, 1, 162-182.	2.9	32
39768	Cobalt Metal ALD: Understanding the Mechanism and Role of Zinc Alkyl Precursors as Reductants for Low-Resistivity Co Thin Films. Chemistry of Materials, 2021, 33, 5045-5057.	3.2	16
39769	Structural Origins of Voltage Hysteresis in the Na-Ion Cathode P2â€“Na_{0.67}[Mg_{0.28}Mn_{0.72}]O₂: A Combined Spectroscopic and Density Functional Theory Study. Chemistry of Materials, 2021, 33, 4890-4906.	3.2	24
39770	Theoretical predictions of structural electronic and optical properties of vanadium ferrite. Modern Physics Letters B, 2021, 35, 2150387.	1.0	0
39771	Insights into the activity and selectivity trends in non-oxidative dehydrogenation of primary and secondary alcohols over the copper catalyst. Catalysis Today, 2021, 370, 151-160.	2.2	17
39772	High pressure lattice dynamics and stress-strain responses of LaIn3 and LaTl3. Solid State Communications, 2021, 332, 114319.	0.9	1
39773	Corrosion inhibition properties of small peptides: DFT and Monte Carlo simulation studies. Journal of Molecular Liquids, 2021, 331, 115782.	2.3	27
39774	Tailoring the Performance of ZnO for Oxygen Evolution by Effective Transition Metal Doping. ChemSusChem, 2021, 14, 3064-3073.	3.6	9
39775	Electronic and magnetic investigation of half-metallic ferrimagnetic full-Heusler Mn2IrGe. Emergent Materials, 2021, 4, 1745-1760.	3.2	16
39776	Predication of topological states in the allotropes of group-IV elements. Frontiers of Physics, 2021, 16, 1.	2.4	0
39777	Structural, elastic and thermal properties of Laves phase Fe2Mo from first principles. Journal of Physics: Conference Series, 2021, 1942, 012017.	0.3	1
39778	Site preference and atomic ordering in the ternary Rh₅Ga₂As: first-principles calculations. Zeitschrift Fur Kristallographie - Crystalline Materials, 2021, 236, 147-154.	0.4	2
39779	New Pentaoctite Phase of Groupâ€V Nanostructures. Physica Status Solidi (B): Basic Research, 2021, 258, 2100112.	0.7	1
39780	The Nature of Chemical Bonds in the Tetragonal Polymorph of InTe: Firstâ€Principlesâ€Based Topological Analysis. Physica Status Solidi (B): Basic Research, 2021, 258, 2100072.	0.7	2
39781	Dynamic recrystallization of Silver nanocubes during high-velocity impacts. Acta Materialia, 2021, 212, 116892.	3.8	11
39782	Two orthorhombic superhard carbon allotropes: C16 and C24. Diamond and Related Materials, 2021, 116, 108426.	1.8	35
39783	Polytypism of Compounds with the General Formula Cs{Al2[TP6O20]} (T = B, Al): OD (Order-Disorder) Description, Topological Features, and DFT-Calculations. Minerals (Basel, Switzerland), 2021, 11, 708.	0.8	6

#	Article	IF	Citations
39784	Bandgap engineering of two-dimensional C3N bilayers. Nature Electronics, 2021, 4, 486-494.	13.1	36
39785	NaOH-Intercalated Iron Chalcogenides (Na1â€“xOH)Fe1â€“yX (X = Se, S): Ion-Exchange Synthesis and Physical Properties. Inorganic Chemistry, 2021, 60, 8742-8753.	1.9	9
39786	La2SrB8O16: A new rare earth borate with [B8O20]16â^' groups exhibiting a deep ultraviolet cutoff edge. Journal of Solid State Chemistry, 2021, 298, 122126.	1.4	5
39787	The rise of Nb-, Ta-, and Bi-based oxides/chalcogenides for photocatalytic applications. International Journal of Hydrogen Energy, 2022, 47, 3358-3370.	3.8	6
39788	Enhancing ferroelectric photovoltaic effect of BaTiO 3 by the lateral interface. Surface and Interface Analysis, 2021, 53, 773-778.	0.8	6
39789	Analyzing Discrepancies in Chemical-Shift Predictions of Solid Pyridinium Fumarates. Molecules, 2021, 26, 3857.	1.7	3
39790	Investigation of the thermoelectric properties of Lithium-Aluminium-Silicide (LiAlSi) compound from first-principles calculations. Computational Condensed Matter, 2021, 27, e00551.	0.9	10
39791	Atomicâ€Orderingâ€Induced Modulated Properties of Zigzag ZnTe Nanotubes. Physica Status Solidi (B): Basic Research, 2021, 258, 2100115.	0.7	0
39792	Understanding the influence of rare earth yttrium on surface characterizations of orthorhombic Î±-Mo2C(023) surface: A first-principle calculation approach. Surface Science, 2021, 708, 121823.	0.8	3
39793	A type-II WSe2/HfSe2 van der Waals heterostructure with adjustable electronic and optical properties. Results in Physics, 2021, 25, 104250.	2.0	17
39794	Arrangement of polyhedral units for [0001]-symmetrical tilt grain boundaries in zinc oxide. Acta Materialia, 2021, 212, 116864.	3.8	3
39795	Designed Synthesis of STA-30: A Small-Pore Zeolite Catalyst with Topology Type SWY. Chemistry of Materials, 2021, 33, 5242-5256.	3.2	6
39796	Kinetics-Driven One-Dimensional Growth of van der Waals Layered SnSe. Journal of Physical Chemistry C, 2021, 125, 12730-12737.	1.5	8
39797	Defect Engineering in Graphene-Confined Single-Atom Iron Catalysts for Room-Temperature Methane Conversion. Journal of Physical Chemistry C, 2021, 125, 12628-12635.	1.5	22
39798	Ohmic-to-Schottky Conversion in Monolayer Tellureneâ€“Metal Interface via Graphene Insertion. Journal of Physical Chemistry C, 2021, 125, 12975-12982.	1.5	2
39799	Inclination of self-interstitial dumbbells in molybdenum and tungsten: A first-principles study. AIP Advances, 2021, 11, 065012.	0.6	3
39800	Stability and Thermodynamics Properties of CrFeNiCoMn/Pd High Entropy Alloys from First Principles. Journal of Phase Equilibria and Diffusion, 2021, 42, 606-616.	0.5	7
39801	DFT Study of Methylene Blue Adsorption on ZnTiO3 and TiO2 Surfaces (101). Molecules, 2021, 26, 3780.	1.7	21

#	Article	IF	Citations
39802	Dynamic transverse magnetic susceptibility in the projector augmented-wave method: Application to Fe, Ni, and Co. Physical Review B, 2021, 103, .	1.1	14
39803	Robust gapless superconductivity in <mml:math xmlns:mml="http://www.w3.org/1998/Math/MathML"><mml:mrow><mml:mn>4</mml:mn><mml:mi>H</mml:mi><mml:mi>b</mml:mi> Physical Review B, 2021, 103, .	1.1	5
39804	Oxygen Defects Engineering of VO₂Â·xH₂O Nanosheets via In Situ Polypyrrole Polymerization for Efficient Aqueous Zinc Ion Storage. Advanced Functional Materials, 2021, 31, 2103070.	7.8	153
39805	A new family of copper-based MXenes. Scientific Reports, 2021, 11, 12393.	1.6	3
39806	Impact of oxygen on gallium doped germanium. AIP Advances, 2021, 11, 065122.	0.6	3
39807	Refinement mechanism of (Ti, Nb)(C, N) carbonitride in hypereutectic Fe-Cr-C-Ti-Nb-N coating by CeO2: A first principles study. Materials Today Communications, 2021, 27, 102315.	0.9	0
39808	Electronic structure of rhombohedral CrX3 (X=Br,ÂCl,ÂI) van der Waals crystals. Physical Review B, 2021, 103, .	1.1	6
39809	Ab initio modelling of interfacial electrochemical properties: beyond implicit solvation limitations. Journal of Physics Condensed Matter, 2021, 33, 304001.	0.7	7
39810	Sensitivity of As K-edge absorption to rare earth (RE) doping in <mml:math xmlns:mml="http://www.w3.org/1998/Math/MathML" altimg="si1.svg"><mml:mrow><mml:msub><mml:mtext>Ca</mml:mtext><mml:mrow><mml:mn>1</mml:mn><mml:mo>â^ A first principles study. Journal of Physics and Chemistry of Solids, 2021, 153, 109993.	1.9	9
39811	Nb6Mn1â€“xIr6+xB8 (x = 0.25): A Ferrimagnetic Boride Containing Planar B6 Rings Interacting with Ferromagnetic Mn Chains. Journal of Physical Chemistry C, 2021, 125, 13635-13640.	1.5	1
39812	Probing the Limiting Mechanism of Sodium-Ion Extraction in the Na₅V(PO₄)₂F₂ Cathode. Journal of Physical Chemistry C, 2021, 125, 14583-14589.	1.5	3
39813	Stability of Ca₂CO₄-Pnma against the Main Mantle Minerals from Ab Initio Computations. ACS Earth and Space Chemistry, 2021, 5, 1709-1715.	1.2	14
39814	Lattice Dynamics and Structural Phase Transitions in Eu₂O₃. Inorganic Chemistry, 2021, 60, 9571-9579.	1.9	24
39815	Crown ether-induced supramolecular passivation and two-dimensional crystal interlayer formation in perovskite photovoltaics. Cell Reports Physical Science, 2021, 2, 100450.	2.8	6
39816	Cyclic Self-Limiting Etching of Organic Polymers. ACS Applied Polymer Materials, 2021, 3, 3636-3648.	2.0	0
39817	Highâ€Efficiency Anionâ€Exchange Membrane Water Electrolyzer Enabled by Ternary Layered Double Hydroxide Anode. Small, 2021, 17, e2100639.	5.2	49
39818	Structural, electronic, magnetic and mechanical properties of vanadium-doped boron nitride monolayer. European Physical Journal B, 2021, 94, 1.	0.6	7
39819	Magnetic correlations in single-layer NbSe₂. Journal of Physics Condensed Matter, 2021, 33, 295804.	0.7	10

#	Article	IF	Citations
39820	Reversible Multi-Electron Storage Enabled by Na5V(PO4)2F2 for Rechargeable Magnesium Batteries. Energy Storage Materials, 2021, 38, 462-472.	9.5	21
39821	Modulation of electronic structure properties in bilayer phosphorene nanoribbons by transition metal atoms. Physica E: Low-Dimensional Systems and Nanostructures, 2021, 130, 114530.	1.3	5
39822	On the role of oxidized graphene interfaces in lithium sulfur batteries: Thermodynamic and kinetic aspects using density functional theory. Applied Surface Science, 2021, 550, 149358.	3.1	8
39823	Machine-learning interatomic potential for Wâ€“Mo alloys. Journal of Physics Condensed Matter, 2021, 33, 315403.	0.7	11
39824	Iron, magnesium, and titanium isotopic fractionations between garnet, ilmenite, fayalite, biotite, and tourmaline: Results from NRIXS, ab initio, and study of mineral separates from the Moosilauke metapelite. Geochimica Et Cosmochimica Acta, 2021, 302, 18-45.	1.6	34
39825	Structure-activity relationship of VO /TiO2 catalysts for mercury oxidation: A DFT study. Applied Surface Science, 2021, 552, 149462.	3.1	17
39826	Ballistic transport and optical properties of a new half-metallic monolayer: Vanadium phosphide. Materials Science and Engineering B: Solid-State Materials for Advanced Technology, 2021, 268, 115111.	1.7	6
39827	Câ€“doped TiO2(B): A density functional theory characterization. Applied Surface Science, 2021, 551, 149479.	3.1	20
39829	In Search of the Active Sites for the Selective Catalytic Reduction on Tungsten-Doped Vanadia Monolayer Catalysts Supported by TiO₂. ACS Catalysis, 2021, 11, 7411-7421.	5.5	14
39830	Spin pinning effect to reconstructed oxyhydroxide layer on ferromagnetic oxides for enhanced water oxidation. Nature Communications, 2021, 12, 3634.	5.8	186
39831	Ambient ammonia production via electrocatalytic nitrite reduction catalyzed by a CoP nanoarray. Nano Research, 2022, 15, 972-977.	5.8	98
39832	Synergistic photocatalytic NO removal of oxygen vacancies and metallic bismuth on Bi12TiO20 nanofibers under visible light irradiation. Chemical Engineering Journal, 2021, 414, 128748.	6.6	30
39833	Optical and Dynamic Properties of ZnGa₂S₄. Physica Status Solidi (B): Basic Research, 2021, 258, 2100101.	0.7	31
39834	Determination of Thermal Expansion, Defect Formation Energy, and Defect-Induced Strain of Î±-U Via ab Initio Molecular Dynamics. Frontiers in Materials, 2021, 8, .	1.2	10
39835	Construction of Cr-embedded graphyne electrocatalyst for highly selective reduction of CO2 to CH4: A DFT study. Chemical Engineering Journal, 2021, 414, 128857.	6.6	150
39836	Electronic, magnetic, optical and transport properties of wurtzite-GaN doped with rare earth (RE= Pm,) Tj ETQq1 1 0.784314 rgBT /Ov	1.5	15
39837	Soybean roots-derived N, P Co-doped mesoporous hard carbon for boosting sodium and potassium-ion batteries. Carbon, 2021, 178, 233-242.	5.4	61
39838	Regulating the Catalytic Performance of a Dual-Atom Iron Species Deposited on Graphitic Carbon Nitride for Electrochemical Nitrogen Reduction. Journal of Physical Chemistry C, 2021, 125, 14253-14262.	1.5	18

#	Article	IF	Citations
39839	Effect of intrinsic point-defect complex on elastic properties of Î³â€²-Ni3Al phases. Materials Research Express, 2021, 8, 066517.	0.8	1
39840	Catalytic Effect of Ti or Pt in a Hexagonal Boron Nitride Surface for Capturing CO2. Crystals, 2021, 11, 662.	1.0	5
39841	Structural, electronic, elastic, thermodynamical and thermoelectric properties of TMN (TM = Co, Ni). Physica Scripta, 2021, 96, 095703.	1.2	6
39842	Nonradiative Carrier Recombination Enhanced by Vacancy Defects in Ionic II-VI Semiconductors. Physical Review Applied, 2021, 15, .	1.5	4
39843	Hydroxyl-terminated carbon dots for efficient conversion of cyclohexane to adipic acid. Journal of Colloid and Interface Science, 2021, 591, 281-289.	5.0	18
39844	Predicted Operando Polymerization at Lithium Anode via Boron Insertion. ACS Energy Letters, 2021, 6, 2320-2327.	8.8	24
39845	Evidence for Electronically Isolated Atomic Chains: Sbâ€“Pb Structures on the Si(553) Surface. Journal of Physical Chemistry C, 2021, 125, 15061-15068.	1.5	2
39846	Oxygen Groups Enhancing the Mechanism of Nitrogen Reduction Reaction Properties on Ru- or Fe-Supported Nb₂C MXene. Journal of Physical Chemistry C, 2021, 125, 14636-14645.	1.5	24
39847	Development and Application of a ReaxFF Reactive Force Field for Cerium Oxide/Water Interfaces. Journal of Physical Chemistry A, 2021, 125, 5693-5708.	1.1	8
39848	Solidâ€state nuclear magnetic resonance of spinâ€9/2 nuclei ¹¹⁵In and ²⁰⁹Bi in functional inorganic complex oxides. Magnetic Resonance in Chemistry, 2021, 59, 1077-1088.	1.1	4
39849	High pressure structural and vibrational properties of nitrogen-rich compound 1,5-Diamino-1H-1,2,3,4-tetrazole. Chemical Physics, 2021, 546, 111188.	0.9	1
39850	Impact of spin-orbit coupling on the physical properties and superconductivity of Ir-rich superconductor Mg2Ir3Si: A first-principles investigation. Journal of Physics and Chemistry of Solids, 2021, 153, 110030.	1.9	0
39851	Thermodynamic stability of defects in hybrid MoS2/InAs heterostructures. Computational Materials Science, 2021, 194, 110426.	1.4	1
39852	Exploring the elastic and electronic properties of chromium molybdenum diboride alloys. Journal of Alloys and Compounds, 2021, 866, 158885.	2.8	8
39853	Theoretical and experimental investigation of the electronic, optical, electric, and elastic properties of Zn-doped anatase TiO2 for photocatalytic applications. Applied Physics A: Materials Science and Processing, 2021, 127, 1.	1.1	8
39854	Multibounce and Subsurface Scattering of H Atoms Colliding with a van der Waals Solid. Journal of Physical Chemistry A, 2021, 125, 5745-5752.	1.1	8
39855	Structural, mechanical, magnetic, electronic, and thermal investigations of Ag2YB (Yâ€‰=â€‰Nd, Sm, Gd) full-Heusler alloys. Emergent Materials, 2021, 4, 1769-1783.	3.2	61
39856	CO ₂ reduction on pure Cu produces only H ₂ after subsurface O is depleted: Theory and experiment. Proceedings of the National Academy of Sciences of the United States of America, 2021, 118, .	3.3	41

#	Article	IF	Citations
39857	Flat-to-Flat Polymerization of Single-Walled Carbon Nanotubes under High Pressure Mediated by Carbon Chain Encapsulation. Journal of Physical Chemistry C, 2021, 125, 12857-12869.	1.5	2
39858	Insights into the Coadsorption and Reactivity of O and CO on Ru(0001) and Their Coverage Dependence. Journal of Physical Chemistry C, 2021, 125, 12614-12627.	1.5	9
39859	Sub-Nanometer Pt Clusters on Defective NiFe LDH Nanosheets as Trifunctional Electrocatalysts for Water Splitting and Rechargeable Hybrid Sodiumâ€“Air Batteries. ACS Applied Materials & Interfaces, 2021, 13, 26891-26903.	4.0	31
39860	Hydrogen-Bonded Cyclic Dimers at Large Compression: The Case of 1H-pyrrolo[3,2-h]quinoline and 2-(2â€²-pyridyl)pyrrole. Molecules, 2021, 26, 3802.	1.7	1
39861	First-principles study of structural and opto-electronic characteristics of ultra-thin amorphous carbon films. Chinese Physics B, 2022, 31, 016102.	0.7	1
39862	Catalytic Effect of Ni and Cu Embedded Graphene Surface on SO2 Decomposition Reaction. Sakarya University Journal of Science, 0, , .	0.3	1
39863	Intrinsic two-dimensional multiferroicity in CrNCl₂ monolayer*. Chinese Physics B, 2021, 30, 117503.	0.7	5
39864	Magnetic exchange interactions in bilayer <mml:math xmlns:mml="http://www.w3.org/1998/Math/MathML"><mml:mrow><mml:mi>Cr</mml:mi><mml:msub><mml:mi>X</mml:mi><mml:mn> assessment of the <mml:math xmlns:mml="http://www.w3.. Physical Review B, 2021, 103, .	1.1	10
39865	Electronic, mechanical, optical and photocatalytic properties of perovskite RbSr2Nb3O10 compound. Journal of Alloys and Compounds, 2021, 867, 159077.	2.8	31
39866	Mo-doped ZnV2O6/reduced graphene oxide photoanodes for solar hydrogen production. Electrochimica Acta, 2021, 382, 138333.	2.6	11
39867	Interplay of quantum capacitance with Van der Waals forces, intercalation, co-intercalation, and the number of MoS2 layers. Materials Today Energy, 2021, 20, 100677.	2.5	17
39868	Synthesis of ZIF-9(III)/Co LDH layered composite from ZIF-9(I) based on controllable phase transition for enhanced electrocatalytic oxygen evolution reaction. Chemical Engineering Journal, 2021, 414, 128784.	6.6	38
39869	Point Defect Engineering: Coâ€Doping Synergy Realizing Superior Performance in nâ€Type Bi₂Te₃ Thermoelectric Materials. Small, 2021, 17, e2101328.	5.2	45
39870	Elastic dipole tensors and relaxation volumes of point defects in concentrated random magnetic Fe-Cr alloys. Computational Materials Science, 2021, 194, 110435.	1.4	24
39871	Exceptionally high open circuit thermoelectric figure of merit in two-dimensional tin sulphide. Journal of Physics Condensed Matter, 2021, 33, 315705.	0.7	4
39872	The Influence of Pressure on Structural, Elastic, Piezoelectric and Dielectric Properties of R3câ€BiAlO 3 Based on Ab Initio Calculations. ChemistrySelect, 2021, 6, 5559-5566.	0.7	2
39873	A promising carbon-based nanosheet as a suitable Na-anode material. Materials Science and Engineering B: Solid-State Materials for Advanced Technology, 2021, 268, 115121.	1.7	9
39874	Tunable natural terahertz and mid-infrared hyperbolic plasmons in carbon phosphide. Carbon, 2021, 178, 625-631.	5.4	12

#	Article	IF	Citations
39875	Superconductivity in metal intercalated graphite-like boron-carbon-nitrogen. Physics Letters, Section A: General, Atomic and Solid State Physics, 2021, 402, 127348.	0.9	1
39876	Sc doped arsenene as adsorbent for the detection and removal of SF6 decomposition gases: A DFT study. Applied Surface Science, 2021, 552, 149449.	3.1	20
39877	First-principles calculations study of the configurations, structural, electronic and magnetic properties of graphene and h-BN monolayers and bilayers adsorbed on Co(0001) surface. Physica B: Condensed Matter, 2021, 611, 412755.	1.3	2
39878	Manganese Migration in Li1-xMn2O4 Cathode Materials. Ultramicroscopy, 2021, 225, 113285.	0.8	4
39879	Self-assembly of N-heterocyclic carbenes on Au(111). Nature Communications, 2021, 12, 4034.	5.8	47
39880	Theoretical Prediction and Experimentally Realizing Cathodic Doping of Sulfur in Li₄Ti₅O₁₂ for Superior Lithium Storage Performance. ACS Applied Energy Materials, 2021, 4, 5995-6004.	2.5	10
39881	First-Principles Study on Structural, Electronic, Elastic, Phonon, and Thermodynamic Properties of Tungsten Oxide-Based Perovskite NaWO3. Journal of Electronic Materials, 2021, 50, 5402-5411.	1.0	3
39882	First-Principles Study of Au-Doped InN Monolayer as Adsorbent and Gas Sensing Material for SF6 Decomposed Species. Nanomaterials, 2021, 11, 1708.	1.9	12
39883	Type-II Dirac point in <mml:math xmlns:mml="http://www.w3.org/1998/Math/MathML"><mml:mrow><mml:msub><mml:mi>RbAg</mml:mi><mml:mn>5</mml:mn></mml:msub></mml:mrow></mml:math> Physical Review B, 2021, 103, .	1.1	4
39884	The study of spectroscopy and vibrational assignments of high nitrogen material 1,1â€²-azobis-1,2,3-triazole. Journal of Molecular Modeling, 2021, 27, 205.	0.8	0
39885	Unusual Force Constants Guided Distortion-Triggered Loss of Long-Range Order in Phase Change Materials. Materials, 2021, 14, 3514.	1.3	4
39886	Crystalline chirality and interlocked double hourglass Weyl fermion in polyhedra-intercalated transition metal dichalcogenides. NPG Asia Materials, 2021, 13, .	3.8	12
39887	Long-range anisotropic Heisenberg ferromagnets and electrically tunable ordering. Physical Review B, 2021, 103, .	1.1	4
39888	New developments in the <scp>GDIS</scp> simulation package: Integration of <scp>VASP</scp> and <scp>USPEX</scp>. Journal of Computational Chemistry, 2021, 42, 1602-1626.	1.5	3
39889	Structural stability and thermoelectric properties of new discovered half-Heusler KLaX (XÂ=ÂC, Si, Ge,) Tj ETQq0 0 0 rgBT /Overlock 10 T	1.1	16
39890	Quantum Chemical Investigation of Photocatalytical Sulfoxidation of Hydrocarbons on TiO₂. Journal of Physical Chemistry C, 2021, 125, 13313-13323.	1.5	2
39891	Performance Analysis of Perovskite Solar Cells Using DFT-Extracted Parameters of Metal-Doped TiO₂ Electron Transport Layer. Journal of Physical Chemistry C, 2021, 125, 13158-13166.	1.5	20
39892	Electrocatalytic Nitrogen Reduction by Transition Metal Single-Atom Catalysts on Polymeric Carbon Nitride. Journal of Physical Chemistry C, 2021, 125, 13880-13888.	1.5	28

#	Article	IF	Citations
39893	Photocatalytic Water Splitting Reaction Catalyzed by Ion-Exchanged Salts of Potassium Poly(heptazine) Tj ETQq0 0 0 rgBT /Overlock 10	1.5	30
39894	Experimental and Theoretical Insights into the Active Sites on WO_x/Pt(111) Surfaces for Dehydrogenation and Dehydration Reactions. ACS Catalysis, 2021, 11, 8023-8032.	5.5	11
39895	Reaction Pathway for Coke-Free Methane Steam Reforming on a Ni/CeO₂ Catalyst: Active Sites and the Role of Metalâ€“Support Interactions. ACS Catalysis, 2021, 11, 8327-8337.	5.5	39
39896	Thermoelectric Characteristics of Two-Dimensional Structures for Three Different Lattice Compounds of Bâ€“Câ€“N and Graphene Counterpart BX (X = P, As, and Sb) Systems. Journal of Physical Chemistry C, 2021, 125, 14525-14537.	1.5	10
39897	Superconductive Sodium Carbides with Pentagon Carbon at High Pressures. Journal of Physical Chemistry Letters, 2021, 12, 5850-5856.	2.1	16
39898	Factors controlling segregation tendency of solute Ti, Ag and Ta into different symmetrical tilt grain boundaries of tungsten: First-principles and experimental study. Acta Materialia, 2021, 211, 116868.	3.8	22
39899	Blue phosphorene nanosheets with point defects: Electronic structure and hydrogen storage capability. Applied Surface Science, 2021, 551, 149363.	3.1	13
39900	Opening the germanene monolayer band gap using halogen atoms: An efficient approach studied by first-principles calculations. Applied Surface Science, 2021, 551, 149318.	3.1	30
39901	Investigating the effect of edge and basal plane surface functionalisation of carbonaceous anodes for alkali metal (Li/Na/K) ion batteries. Carbon, 2021, 177, 226-243.	5.4	19
39902	Adsorption of SF₆ Decomposed Species on Ti₃C₂O₂ and Ti₃C₂F₂ with Point Defects by DFT Study. Advanced Theory and Simulations, 2021, 4, 2100074.	1.3	16
39903	Neutron thermalization in nuclear graphite: A modern story of a classic moderator. Annals of Nuclear Energy, 2021, 161, 108437.	0.9	4
39904	Stability of X-IV-IV half Heusler semiconductor alloys: a DFT study. Molecular Physics, 2021, 119, e1936249.	0.8	2
39905	Atomistic insights into the nucleation and growth of platinum on palladium nanocrystals. Nature Communications, 2021, 12, 3215.	5.8	18
39906	Theoretical Predictions of the Structural and Mechanical Properties of Tungstenâ€“Rare Earth Element Alloys. Materials, 2021, 14, 3046.	1.3	5
39907	Designing zero-dimensional dimer-type all-inorganic perovskites for ultra-fast switching memory. Nature Communications, 2021, 12, 3527.	5.8	38
39908	New insights in the electronic structure of doped graphene on adsorption with oxides of nitrogen. Materials Today Communications, 2021, 27, 102417.	0.9	5
39909	Bandgap Engineering and Near-Infrared-II Optical Properties of Monolayer MoS2: A First-Principle Study. Frontiers in Chemistry, 2021, 9, 700250.	1.8	20
39910	Improving Thermodynamic Stability of SmFe12-Type Permanent Magnets from High Entropy Effect. Journal of Phase Equilibria and Diffusion, 2021, 42, 592-605.	0.5	7

#	Article	IF	Citations
39911	Multi-scale regulation in S, N co-incorporated carbon encapsulated Fe-doped Co9S8 achieving efficient water oxidation with low overpotential. Nano Research, 2022, 15, 872-880.	5.8	31
39912	Giant GrÃ¼neisen parameter in a superconducting quantum paraelectric. Physical Review B, 2021, 103, .	1.1	6
39913	Screen the half-metallic X2Y (Al/Si) full-Heusler alloys based on the first-principle calculations. Computational Materials Science, 2021, 193, 110391.	1.4	5
39914	Tunable electronic band structure, luminescence properties and thermostability of (Gd1â€“La)2Si2O7:Ce scintillator by adjusting La/Gd ratio. Journal of Rare Earths, 2021, 39, 657-665.	2.5	4
39915	Adsorption of DTC-CTS on sphalerite (1 1 0) and Cu-activated sphalerite (1 1 0) surfaces: A DFT study. Applied Surface Science, 2021, 551, 149466.	3.1	19
39916	Structural, electronic, magnetic, elastic and thermodynamic properties of Ni₄N anti-perovskite. Phase Transitions, 2021, 94, 454-473.	0.6	3
39917	Hexagonal boron nitride (<mml:math xmlns:mml="http://www.w3.org/1998/Math/MathML") Tj ETQq0 0 0 rgBT /Overlock 10 Tf 50 507 T material: A density functional theory (DFT) study. Surfaces and Interfaces, 2021, 24, 101043.	1.5	38
39918	Structural, electronic and thermoelectric performance of narrow gap LuNiSb half Heusler compound: Potential thermoelectric material. Physica B: Condensed Matter, 2021, 610, 412823.	1.3	9
39919	Structurally Driven Environmental Degradation of Friction in MoS2 Films. Tribology Letters, 2021, 69, 1.	1.2	13
39920	Theoretical design of all-carbon networks with intrinsic magnetism. Carbon, 2021, 177, 11-18.	5.4	8
39921	Structural, Electronic, and Magnetic Properties of the Rare Earth-Based Solar Perovskites: GdAlO3, DyAlO3, and HoAlO3. Journal of Superconductivity and Novel Magnetism, 2021, 34, 2371-2380.	0.8	25
39922	First-principles-assisted band gap predictions of methylammonium metal formates. Materials Research Bulletin, 2021, 138, 111239.	2.7	1
39923	Optoelectronic properties of van der Waals stacked homo- and hetero-bilayers of tin-monochalcogenides: A first-principles study. Surfaces and Interfaces, 2021, 24, 101083.	1.5	1
39924	Hydrodechlorination of 1,2-Dichloroethane on Platinum Catalysts: Insights from Reaction Kinetics Experiments, Density Functional Theory, and Microkinetic Modeling. ACS Catalysis, 2021, 11, 7890-7905.	5.5	12
39925	Highly selective metal-organic framework-based electrocatalyst for the electrochemical reduction of CO2 to CO. Materials Research Bulletin, 2021, 138, 111228.	2.7	12
39926	Development of Bimetallic PdNi Electrocatalysts toward Mitigation of Catalyst Poisoning in Direct Borohydride Fuel Cells. ACS Catalysis, 2021, 11, 8417-8430.	5.5	28
39927	Aliovalent substitution in phosphideâ€based materials â€“ Crystal structures of Na 10 AlTaP 6 and Na 3 GaP 2 featuring edgeâ€sharing E P 4 tetrahedra (E =Al/Ta and Ga). Zeitschrift Fur Anorganische Und Allgemeine Chemie, 2021, 647, 1804-1814.	0.6	1
39928	Centrosymmetric or Noncentrosymmetric? Transition Metals Talking in K₂TGe₃S₈(T = Co, Fe). Inorganic Chemistry, 2021, 60, 10603-10613.	1.9	16

#	Article	IF	Citations
39929	Investigations of mechanical and thermoelectric properties of â€˜AlNiPâ€™ novel half-Heusler alloy. Materials Chemistry and Physics, 2021, 265, 124518.	2.0	23
39930	Point Defects in a Two-Dimensional ZnSnN₂ Nanosheet: A First-Principles Study on the Electronic and Magnetic Properties. Journal of Physical Chemistry C, 2021, 125, 13067-13075.	1.5	26
39931	Permeation of chemisorbed hydrogen through graphene: A flipping mechanism elucidated. Carbon, 2021, 178, 718-727.	5.4	10
39932	Computational exploration of magnesium-decorated carbon nitride (g-C3N4) monolayer as advanced energy storage materials. International Journal of Hydrogen Energy, 2021, 46, 21739-21747.	3.8	33
39933	Epitaxial stabilisation of Ge1 â’ x Sn x alloys. Journal Physics D: Applied Physics, 2021, 54, 325302.	1.3	0
39934	Electron-Beam Irradiation Induced Regulation of Surface Defects in Lead Halide Perovskite Thin Films. Research, 2021, 2021, 9797058.	2.8	9
39935	Coexistence of superconductivity and antiferromagentic order in Er2O2Bi with anti-ThCr2Si2 structure. Frontiers of Physics, 2021, 16, 1.	2.4	4
39936	Four superhard sp3 hybrid cubic boron nitride polymorphs: A first principles calculations. Physics Letters, Section A: General, Atomic and Solid State Physics, 2021, 400, 127325.	0.9	3
39937	Effect of Ca2+, Mg2+, Ba2+ and Sr2+ cations on calcium carbonate scaling formation in oil-gas well: Based on density functional theory study and molecular dynamics simulation. Journal of Crystal Growth, 2021, 563, 126089.	0.7	14
39938	DFT study on the nucleation of He bubbles in Pd: Effect of H and self-interstitial atoms. Journal of Nuclear Materials, 2021, 549, 152888.	1.3	2
39939	Cation and anion topotactic transformations in cobaltite thin films leading to Ruddlesden-Popper phases. Physical Review Materials, 2021, 5, .	0.9	7
39940	Multiple control of few-layer Janus MoSSe systems. Physical Review Materials, 2021, 5, .	0.9	4
39941	Entropic broadening of the spin-crossover pressure in ferropericlase. Physical Review B, 2021, 103, .	1.1	4
39943	Semiconducting character of LaN: Magnitude of the bandgap and origin of the electrical conductivity. AIP Advances, 2021, 11, .	0.6	2
39944	Penta carbides: Two-dimensional group-IV semiconductors containing <mml:math xmlns:mml="http://www.w3.org/1998/Math/MathML"><mml:msub><mml:mi mathvariant="normal">C</mml:mi><mml:mn>2</mml:mn></mml:msub></mml:math> dimers for nanoelectronics and photocatalytic water splitting. Physical Review Materials, 2021, 5, .	0.9	15
39945	The Relationship between Natural Pyrite and Impurity Element Semiconductor Properties: A Case Study of Vein Pyrite from the Zaozigou Gold Deposit in China. Minerals (Basel, Switzerland), 2021, 11, 596.	0.8	4
39946	Intrinsic thermoelectric figure of merit of bulk compositional SiGe alloys: A first-principles study. Physical Review Materials, 2021, 5, .	0.9	9
39947	Using ferroelectric polarization to regulate and preserve the valley polarization in a <mml:math xmlns:mml="http://www.w3.org/1998/Math/MathML"><mml:mrow><mml:msub><mml:mi>HfN</mml:mi><mml:mn>2</mml:mn></mml:msub></mml:mrow></mml:math> heterotrilayer. Physical Review B, 2021, 103, .	1.1	16

#	Article	IF	Citations
39948	Physical properties of predicted MAX phase borides Hf2AB (Aâ€¯=â€¯Pb, Bi): A DFT insight. Materials Today Communications, 2021, 27, 102411.	0.9	9
39949	First-principles investigation of structural, elastic, electronic and thermodynamic properties of strongly correlated ternary system: The DFT+U approach. Materials Science in Semiconductor Processing, 2021, 127, 105741.	1.9	5
39950	Comparative DFT study of the oxy(hydr)oxides of iron and aluminum â€“ structural, electronic and surface properties.. Surface Science, 2021, 708, 121821.	0.8	3
39951	Study of structural, elastic, electronic, dynamical and optical properties of beryllium selenide (BeSe) semiconductor in zinc blend and NiAs phases. Physica B: Condensed Matter, 2021, 610, 412858.	1.3	1
39952	Anharmonic phonons and anomalous thermal expansion of graphite. Solid State Communications, 2021, 332, 114324.	0.9	1
39953	First-principles model for voids decorated by transmutation solutes: Short-range order effects and application to neutron irradiated tungsten. Physical Review Materials, 2021, 5, .	0.9	7
39954	Melting temperature prediction by thermoelastic instability: An ab initio modelling, for periclase (MgO). Calphad: Computer Coupling of Phase Diagrams and Thermochemistry, 2021, 73, 102259.	0.7	5
39955	A theoretical study of sulfur poisoning tolerance at the interface of Mo doped Ni/Yttria-Stabilized Zirconia. International Journal of Hydrogen Energy, 2021, 46, 21075-21081.	3.8	3
39956	A density functional theory (DFT) investigation of how small molecules and atmospheric pollutants relevant to art conservation adsorb on kaolinite. Applied Clay Science, 2021, 206, 106075.	2.6	11
39957	Combined ab-initio and empirical model for irradiated metal alloys with a focus on uranium alloy fuel thermal conductivity. Journal of Nuclear Materials, 2021, 549, 152891.	1.3	1
39958	Electronic structure of reduced CeO2(111) surfaces interacting with hydrogen as revealed through electron energy loss spectroscopy in comparison with theoretical investigations. Journal of Electron Spectroscopy and Related Phenomena, 2021, , 147088.	0.8	6
39959	The newly-assisted catalytic mechanism of surface hydroxyl species performed as the promoter in syngas-to-C2 species on the Cu-based bimetallic catalysts. Green Energy and Environment, 2023, 8, 487-498.	4.7	2
39960	Cs₂Zr_{1â^'}_xTe_xCl₆ Perovskite Microcrystals with Ultrahigh Photoluminescence Quantum Efficiency of 79.46% for High Light Efficiency White Light Emitting Diodes. Advanced Optical Materials, 2021, 9, 2100804.	3.6	36
39961	Two distinct non-Arrhenius behaviors of hydrogen diffusivities in fcc aluminum, silver, and copper determined by ab initio path integral simulations. Physical Review Materials, 2021, 5, .	0.9	8
39962	Structure Sensitivity of Pd Facets for Enhanced Electrochemical Nitrate Reduction to Ammonia. ACS Catalysis, 2021, 11, 7568-7577.	5.5	194
39963	First-principles study of electronic structure, sodium diffusion, and (de)intercalation in NASICON NaMR(MoO4)3 (Mâ€‰=â€‰Mg, Ni; Râ€‰=â€‰Cr, Fe). Ionics, 2021, 27, 3383.	1.2	5
39964	Study on a stress-magnetic relationship of DO3 based on first principles. Materials Today Communications, 2021, 27, 102196.	0.9	5
39965	Rh-Doped ZnO Monolayer as a Potential Gas Sensor for Air Decomposed Species in a Ring Main Unit: A First-Principles Study. ACS Omega, 2021, 6, 15878-15884.	1.6	8

#	Article	IF	Citations
39966	Single-Dislocation Schottky Diodes. Nano Letters, 2021, 21, 5586-5592.	4.5	5
39967	Optoelectronic Properties of Chalcogenide Perovskites by Many-Body Perturbation Theory. Journal of Physical Chemistry Letters, 2021, 12, 5301-5307.	2.1	25
39968	Efficient electroreduction of CO2 by single-atom catalysts two-dimensional metal hexahydroxybenzene frameworks: A theoretical study. Applied Surface Science, 2021, 550, 149389.	3.1	15
39969	Forging Inspired Processing of Sodiumâ€Fluorinated Graphene Composite as Dendriteâ€Free Anode for Longâ€Life Naâ€“CO₂ Cells. Energy and Environmental Materials, 2022, 5, 572-581.	7.3	8
39970	Coexistence of ferromagnetism, antiferromagnetism, and superconductivity in magnetically anisotropic (Eu,La)FeAs2. Npj Quantum Materials, 2021, 6, .	1.8	4
39971	A theoretical investigation of quantum spin Hall state in ordered Mâ€²2Mâ€³2C3 MXenes (Mâ€² = V, Nb, Ta and Mâ€³) Tj ETQq1 1 0.78	0.7	3
39972	A DFT study on the structural, elastic and phonons properties of YP1â^'xSbx alloys. Applied Physics A: Materials Science and Processing, 2021, 127, 1.	1.1	2
39973	Adsorption behavior of cisplatin anticancer drug on the pristine, Al- and Ga-doped BN nanosheets: A comparative DFT study. Computational and Theoretical Chemistry, 2021, 1200, 113241.	1.1	26
39974	Space-Filling Curves for Real-Space Electronic Structure Calculations. Journal of Chemical Theory and Computation, 2021, 17, 4039-4048.	2.3	11
39975	Tendency of Gap Opening in Semimetal 1Tâ€²â€MoTe₂ with Proximity to a 3D Topological Insulator. Advanced Functional Materials, 2021, 31, 2103384.	7.8	8
39976	Multifunctional Ca10(PO4)6F2 as a host for radioactive waste immobilization: Am3+/Eu3+ ions distribution, phosphor characteristics and radiation induced changes. Journal of Hazardous Materials, 2021, 411, 125025.	6.5	19
39977	Strain-tunable triple point Fermions in diamagnetic rare-earth half-Heusler alloys. Scientific Reports, 2021, 11, 12029.	1.6	4
39978	Polymer-wrapped reduced graphene oxide/nickel cobalt ferrite nanocomposites as tertiary hybrid supercapacitors: insights from experiment and simulation. Journal of Science: Advanced Materials and Devices, 2021, 6, 291-301.	1.5	7
39979	Elimination of Charge Recombination Centers in Metal Halide Perovskites by Strain. Journal of the American Chemical Society, 2021, 143, 9982-9990.	6.6	52
39980	Ferroelectric properties of BaTiO3-BiScO3 weakly coupled relaxor energy-storage ceramics from first-principles calculations. Journal of Alloys and Compounds, 2021, 866, 158933.	2.8	17
39981	Mechanical and dynamic properties of stable two-dimensional boron-substituted ThMoB4â€“type graphene: First-Principles Study. Materials Today Communications, 2021, 27, 102322.	0.9	3
39982	Experimental and theoretical insights into the mechanism of spinel CoFe2O4 reduction in CO chemical looping combustion. Fuel, 2021, 293, 120473.	3.4	14
39983	Low lattice thermal conductivity of pentadiamond. Journal of Applied Physics, 2021, 129, .	1.1	9

#	Article	IF	Citations
39984	Adsorptive-photocatalytic performance and mechanism of Me (Mn,Fe)-N co-doped TiO2/SiO2 in cyanide wastewater. Journal of Alloys and Compounds, 2021, 867, 159020.	2.8	32
39985	Bi4O5Br2 nanosheets with vertical aligned facets for efficient visible-light-driven photodegradation of BPA. Applied Catalysis B: Environmental, 2021, 286, 119937.	10.8	69
39986	Chemical stability of hydrogen boride nanosheets in water. Communications Materials, 2021, 2, .	2.9	15
39987	Strain-sensitive ferromagnetic two-dimensional Cr2Te3. Nano Research, 2022, 15, 1254-1259.	5.8	26
39988	Evolving Defect Chemistry of (Pu,Am)O_{2Â±x}. Journal of Physical Chemistry C, 2021, 125, 15560-15568.	1.5	4
39989	Locally symmetric oxygen vacancy around Cd impurities in <mml:math xmlns:mml="http://www.w3.org/1998/Math/MathML"><mml:msub><mml:mi>CeO</mml:mi><mml:mn>2</mml:mn></mml:msub></mml:math> Physical Review B, 2021, 104, .	1.1	4
39990	High-Throughput Screening of Atomic Defects in MXenes for CO₂ Capture, Activation, and Dissociation. ACS Applied Materials & Interfaces, 2021, 13, 35585-35594.	4.0	30
39991	Computationally Designed Crystal Structures of the Supertetrahedral Ga4C and Ga4Si Solids. Journal of Physical Chemistry A, 2021, 125, 6556-6561.	1.1	1
39992	Theoretical prediction of the PtOX (X = S and Se) monolayers as promising optoelectronic and thermoelectric 2D materials. Physica E: Low-Dimensional Systems and Nanostructures, 2021, 131, 114732.	1.3	8
39993	Modeling and computation of thermal and optical properties in silicene supported honeycomb bilayer and heterobilayer nanostructures. Materials Science in Semiconductor Processing, 2021, 129, 105776.	1.9	10
39994	Environmental impact of amino acids on the release of selenate immobilized in hydrotalcite: Integrated interpretation of experimental and density-functional theory study. Chemosphere, 2021, 274, 129927.	4.2	5
39995	Oxygen vacancy formation and their role in the CO2 activation on Ca doped ZrO2 surface: An ab-initio DFT study. Applied Surface Science, 2021, 553, 149589.	3.1	20
39996	New stable two dimensional silicon carbide nanosheets. Journal of Alloys and Compounds, 2021, 868, 159201.	2.8	8
39997	Insight into the roles of ammonia during direct alcohol amination over supported Ru catalysts. Journal of Catalysis, 2021, 399, 121-131.	3.1	30
39998	First principles investigation of oxygen vacancies filaments in polymorphic Titania and their role in memristor's applications. Chaos, Solitons and Fractals, 2021, 148, 111024.	2.5	7
39999	Nanostructured Glass Composite for Selfâ€Calibrated Radiation Dose Rate Detection. Advanced Optical Materials, 0, , 2100751.	3.6	6
40000	Flow of polar and nonpolar liquids through nanotubes: A computational study. Physical Review Materials, 2021, 5, .	0.9	2
40001	Adsorbate modification of electronic nonadiabaticity: H atom scattering from p(2 Ã— 2) O on Pt(111). Journal of Chemical Physics, 2021, 155, 034702.	1.2	6

#	Article	IF	Citations
40002	Understanding the structure-performance relationship of cubic In2O3 catalysts for CO2 hydrogenation. Journal of CO2 Utilization, 2021, 49, 101543.	3.3	10
40003	InSe/Te van der Waals Heterostructure as a High-Efficiency Solar Cell from Computational Screening. Materials, 2021, 14, 3768.	1.3	7
40004	Magnetic and electronic properties of Zn-Ni ferrites: First principle calculations, mean-field theory, high-temperature series expansions and Monte Carlo study. Chemical Physics, 2021, 547, 111195.	0.9	8
40005	First-principles calculation of the adhesion work, fracture toughness and tensile behavior of the Fe/MCs (MÂ=ÂNb and Ta) interfaces by two different optimization methods. Chemical Physics, 2021, 547, 111193.	0.9	10
40006	Using DFTB to Model Photocatalytic Anataseâ€“Rutile TiO2 Nanocrystalline Interfaces and Their Band Alignment. Journal of Chemical Theory and Computation, 2021, 17, 5239-5247.	2.3	3
40007	Highly CO selective Ca and Zn hybrid metal-organic framework electrocatalyst for the electrochemical reduction of CO2. Current Applied Physics, 2021, 27, 31-37.	1.1	11
40008	MAELAS: MAgneto-ELAStic properties calculation via computational high-throughput approach. Computer Physics Communications, 2021, 264, 107964.	3.0	10
40009	A strategy to improve the electrochemical performance of Ni-rich positive electrodes: Na/F-co-doped LiNi0.6Mn0.2Co0.2O2 *. Chinese Physics B, 2021, 30, 073101.	0.7	3
40010	Accelerating finite-temperature Kohn-Sham density functional theory with deep neural networks. Physical Review B, 2021, 104, .	1.1	31
40011	Plasma phase transition. Physics-Uspekhi, 2021, 64, 1094-1124.	0.8	6
40013	Investigation into water-induced surface oxidization of GaN lamella structure. Semiconductor Science and Technology, 2021, 36, 085009.	1.0	0
40014	Charge density wave in single-layer Pb/Ge(111) driven by Pb-substrate exchange interaction. Physical Review B, 2021, 104, .	1.1	3
40015	Diverse magnetism in stable and metastable structures of CrTe. Frontiers of Physics, 2021, 16, 1.	2.4	6
40016	Antiferromagnetism-Induced Spin Splitting in Systems Described by Magnetic Layer Groups. Journal of Physical Chemistry C, 2021, 125, 16147-16154.	1.5	11
40017	Substituted 2D Janus WSSe monolayers as efficient nanosensor toward toxic gases. Journal of Applied Physics, 2021, 130, .	1.1	16
40018	Shear-induced chemical segregation in a Fe-based bulk metallic glass at room temperature. Scientific Reports, 2021, 11, 13650.	1.6	8
40019	Effect of copper concentration and sulfur vacancies on electronic properties of MoS2 monolayer: a computational study. Journal of Molecular Modeling, 2021, 27, 213.	0.8	10
40020	Ozonation of Group-IV Elemental Monolayers: A First-Principles Study. ACS Omega, 2021, 6, 19546-19552.	1.6	3

#	Article	IF	Citations
40021	Electronic and optical properties of armchair silicon carbide nanotubes from first principles. Optik, 2021, 237, 166740.	1.4	9
40022	Light Harvesting from Oxygen Vacancies and A- and B-Site Dopants in CaSnO₃ Perovskite through Efficient Photon Utilization and Local Site Engineering. ACS Applied Electronic Materials, 2021, 3, 3256-3270.	2.0	11
40023	Elucidating the underlying mechanism of relatively high Tc value of the orthorhombic MoRuP: a first-principles study. Philosophical Magazine, 2021, 101, 2054-2076.	0.7	0
40024	Mg₂In₃Si₂P₇: A Quaternary Diamond-like Phosphide Infrared Nonlinear Optical Material Derived from ZnGeP₂. Journal of the American Chemical Society, 2021, 143, 10309-10316.	6.6	77
40025	Utilization of impurities and carbon defects in natural microcrystalline graphite to prepare silicon-graphite composite anode for high-performance lithium-ion batteries. Journal of Materials Science, 2021, 56, 17682-17693.	1.7	8
40026	Two Tellurium(IV)-Based Sulfates Exhibiting Strong Second Harmonic Generation and Moderate Birefringence as Promising Ultraviolet Nonlinear Optical Materials. Inorganic Chemistry, 2021, 60, 11412-11418.	1.9	20
40027	Potential antiferromagnetic Weyl nodal line state in <mml:math xmlns:mml="http://www.w3.org/1998/Math/MathML"><mml:msub><mml:mrow><mml:mi>LiTi</mml:mi></mml:mrow><mml:mn>2</m mathvariant="normal">O</mml:mi></mml:mrow><mml:mn>4</mml:mn></mml:msub></mml:math> material. Physical Review B, 2021, 104, .	1.1	14
40028	Understanding potential-dependent competition between electrocatalytic dinitrogen and proton reduction reactions. Nature Communications, 2021, 12, 4353.	5.8	78
40029	Hierarchical molecular design of high-performance infrared nonlinear Ag2HgI4 material by defect engineering strategy. Materials Today Physics, 2021, 19, 100432.	2.9	91
40030	Electrochemical Oxidative Fluorination of an Oxide Perovskite. Chemistry of Materials, 2021, 33, 5757-5768.	3.2	11
40031	Ensemble learning-iterative training machine learning for uncertainty quantification and automated experiment in atom-resolved microscopy. Npj Computational Materials, 2021, 7, .	3.5	26
40032	High-pressure phase diagram of beryllium from ab initio free-energy calculations. Physical Review B, 2021, 104, .	1.1	11
40033	2D Vâ€“VI Binary Nanosheets with Square Lattice: A Theoretical Investigation. Physica Status Solidi (B): Basic Research, 2021, 258, 2100178.	0.7	4
40034	Structure and Electronic Effects from Mn and Nb Co-doping for Low Band Gap BaTiO₃ Ferroelectrics. Journal of Physical Chemistry C, 2021, 125, 14910-14923.	1.5	28
40035	Density Functional Theory Studies of Heteroatom-Doped Graphene-like GaN Monolayers as Electrocatalysts for Oxygen Evolution and Reduction. ACS Applied Nano Materials, 2021, 4, 7125-7133.	2.4	9
40036	Atomic structure and electronic properties of the intercalated Pb atoms underneath a graphene layer. Carbon, 2021, 179, 151-158.	5.4	10
40037	Copper single-atoms embedded in 2D graphitic carbon nitride for the CO2 reduction. Npj 2D Materials and Applications, 2021, 5, .	3.9	54
40038	Investigation of Tetravalent Cation Doping with (M = Sn4+, Zr4+, and Ge4+) on the Electrochemical Properties of Monoclinic Li3V2(PO4)3 Using First-Principles Calculations. Journal of the Electrochemical Society, 2021, 168, 070518.	1.3	3

#	Article	IF	Citations
40039	Influence of Magnetic Moment on Single Atom Catalytic Activation Energy Barriers. Catalysis Letters, 2022, 152, 1347-1357.	1.4	6
40040	<mml:math xmlns:mml="http://www.w3.org/1998/Math/MathML"><mml:mrow><mml:mi>Î²</mml:mi><mml:mtext>â^'</mml:mtext><mml:msub><: Pressure-induced three-dimensional Dirac semimetal with ultralow room-pressure lattice thermal conductivity. Physical Review B, 2021, 104, .	1.1	7
40041	Shear induced deformation twinning evolution in thermoelectric InSb. Npj Computational Materials, 2021, 7, .	3.5	16
40042	Coexistence of large out-of-plane and in-plane piezoelectricity in 2D monolayer Li-based ternary chalcogenides LiMX2. Results in Physics, 2021, 26, 104398.	2.0	14
40043	On the deactivation mechanisms of MnO2 electrocatalyst during operation in rechargeable zinc-air batteries studied via density functional theory. Journal of Alloys and Compounds, 2021, 869, 159280.	2.8	17
40044	T2 phase site occupancies in the Crâ€“Siâ€“B system: a combined synchroton-XRD/first-principles study. Scripta Materialia, 2021, 199, 113854.	2.6	3
40045	Theoretical studies on the initial oxidation of metallic lithium anodes. Applied Surface Science, 2021, 555, 149447.	3.1	3
40046	Structural stability of belite sulfoaluminate clinkering polymorphs. Solid State Ionics, 2021, 365, 115641.	1.3	3
40047	Effect of carbon content on the microstructure and bonding properties of hot-rolling pure titanium clad carbon steel plates. Materials Science & Engineering A: Structural Materials: Properties, Microstructure and Processing, 2021, 820, 141572.	2.6	27
40048	Investigation of hydration of potassium carbonate via reactive force-field molecular dynamics simulations. Journal of Energy Storage, 2021, 39, 102601.	3.9	5
40049	A ductility criterion for bcc high entropy alloys. Journal of the Mechanics and Physics of Solids, 2021, 152, 104389.	2.3	44
40050	First-principles study of the effect of V, Co, Ca, Sr, Ga, As doping on the mechanical properties of Al2Cu. Applied Physics A: Materials Science and Processing, 2021, 127, 1.	1.1	5
40051	First-principles calculations to investigate the anisotropic elasticity and thermodynamic properties of FeAl3 under pressure effect. Results in Physics, 2021, 26, 104361.	2.0	12
40052	Toward a Mechanistic Understanding of Pellet Cladding Interaction Using Advanced 3D Characterization and Atomistic Simulation. , 2021, , 904-926.		0
40053	Octahedral rotations trigger electronic and magnetic transitions in strontium manganate under volume expansion. Journal of Physics Condensed Matter, 2021, 33, 365501.	0.7	0
40054	External uniaxial and biaxial strains modulated adsorption behaviors of volatile organic compounds on fibrous red phosphorene. Applied Surface Science, 2021, 553, 149460.	3.1	6
40055	How Surface Proximity to Copper Dopants Affects Photoluminescence of CdSe Colloidal Quantum Dots. Journal of Physical Chemistry C, 2021, 125, 16827-16836.	1.5	4
40056	Pressure-Induced Phase Transition Study on Brookite to Rutile TiO₂ Transformation. ECS Journal of Solid State Science and Technology, 2021, 10, 071021.	0.9	7

#	Article	IF	Citations
40057	Mechanistic Insights into Oxygen Dynamics in Soot Combustion over Cryptomelane Catalysts in Tight and Loose Contact Modes via ¹⁸O₂/¹⁶O₂ Isotopic Variable Composition Measurements â€“ A Hot Ring Model of the Catalyst Operation. ACS Catalysis, 2021, 11, 9530-9546.	5.5	15
40058	Strain-tunable electronic structure of two-dimensional monolayer SiP. Modern Physics Letters B, 2021, 35, 2150404.	1.0	0
40059	Strong Metalâ€“Support Interaction for 2D Materials: Application in Noble Metal/TiB₂ Heterointerfaces and their Enhanced Catalytic Performance for Formic Acid Dehydrogenation. Advanced Materials, 2021, 33, e2101536.	11.1	47
40060	Modulating the bonding properties of Li2MoO3 via non-equivalent cationic doping to enhance its stability and electrochemical performance for lithium-ion battery application. Ceramics International, 2021, 47, 18304-18313.	2.3	5
40061	Dynamics and Hysteresis of Hydrogen Intercalation and Deintercalation in Palladium Electrodes: A Multimodal In Situ X-ray Diffraction, Coulometry, and Computational Study. Chemistry of Materials, 2021, 33, 5872-5884.	3.2	11
40062	Accurate and Efficient Computation of Optical Absorption Spectra of Molecular Crystals: The Case of the Polymorphs of ROY. Journal of Chemical Theory and Computation, 2021, 17, 5214-5224.	2.3	4
40063	Atomically Dispersed Co to an End-Adsorbing Molecule for Excellent Biomimetically and Prime Sensitively Detecting O₂^{â€¢â€“} Released from Living Cells. Analytical Chemistry, 2021, 93, 10789-10797.	3.2	13
40064	Theoretical Approach toward Optimum Anion-Doping on MXene Catalysts for Hydrogen Evolution Reaction: an Ab Initio Thermodynamics Study. ACS Applied Materials & Interfaces, 2021, 13, 37035-37043.	4.0	17
40065	Engineering the Thermal Conductivity of Doped SiGe by Mass Variance: A First-Principles Proof of Concept. Frontiers in Mechanical Engineering, 2021, 7, .	0.8	2
40066	Mechanism of Electron-Beam Manipulation of Single-Dopant Atoms in Silicon. Journal of Physical Chemistry C, 2021, 125, 16041-16048.	1.5	10
40067	Defect-engineered room-temperature ferromagnetism in quasi-two-dimensional nitrided CoTa2O6. Physical Review B, 2021, 104, .	1.1	0
40069	Deep Learning Method to Accelerate Discovery of Hybrid Polymer-Graphene Composites. Scientific Reports, 2021, 11, 15111.	1.6	13
40070	Spectroscopic Analysis of Rare-Earth Silicide Structures on the Si(111) Surface. Materials, 2021, 14, 4104.	1.3	3
40071	Reconstructed edges of T phase transition metal dichalcogenides. Materials Today Physics, 2021, 19, 100411.	2.9	12
40072	Quantitative comparison of electrically induced spin and orbital polarizations in heavy-metal/ <mml:math xmlns:mml="http://www.w3.org/1998/Math/MathML"><mml:mrow><mml:mn>3</mml:mn><mml:mi>d</mml:mi></mml:mrow></mml:r -metal bilayers. Physical Review Materials, 2021, 5, .	0.9	14
40073	Design of a Giant Magnetoresistance Device with High Spin Filter Efficiency. Journal of Physical Chemistry C, 2021, 125, 15544-15550.	1.5	0
40074	Role of the solvent in the activation of Li₂S as cathode material: a DFT study. Journal of Physics Condensed Matter, 2021, 33, 344003.	0.7	6
40075	Mechanism of transition metal interaction with graphene sheet reflected in its plasmonic excitations: Effect of gas adsorption phenomena studied by a combination of solid state and molecular orbital approaches. Applied Surface Science, 2021, 554, 149585.	3.1	1

#	Article	IF	Citations
40076	Possible half-metallic behavior of <mml:math xmlns:mml="http://www.w3.org/1998/Math/MathML"><mml:mrow><mml:msub><mml:mi>Co</mml:mi><mml:mrow><mml:mn>2</mml:mn> Heusler alloys: Theory and experiment. Physical Review B, 2021, 104, .	1.1	21
40077	Adsorption and sensing for SF₆ decomposed gases by Pt-BN monolayer: a DFT study. Molecular Physics, 2021, 119, .	0.8	6
40078	Assessing the structural, electronic, elastic and thermoelectric properties of PtTiSn and PdLaBi transition metal alloys from the first-principles prospective. Materials Science in Semiconductor Processing, 2021, 129, 105796.	1.9	3
40079	First-principles calculation of the electronic and optical properties of Gd2FeCrO6 double perovskite: Effect of Hubbard U parameter. Journal of Materials Research and Technology, 2021, 13, 2408-2418.	2.6	14
40080	Effect of alloying elements on stacking fault energies and twinnabilities in highâ€entropy transitionâ€metal carbides. Journal of the American Ceramic Society, 2021, 104, 6521-6532.	1.9	2
40081	Quantum phases and spin liquid properties of 1T-TaS2. Npj Quantum Materials, 2021, 6, .	1.8	32
40082	Indium-doped ZnOas efficient photosensitive material for sunlight driven hydrogen generation and DSSC applications: integrated experimental and computational approach. Journal of Solid State Electrochemistry, 2021, 25, 2279-2292.	1.2	2
40083	Theoretical insight into two-dimensional g-C6N6/InSe van der Waals Heterostructure: A promising visible-light photocatalyst. Applied Surface Science, 2021, 554, 149465.	3.1	13
40084	The early growth process of helium blistering in tungsten and molybdenum: First-principles and statistical model calculations. Journal of Nuclear Materials, 2021, 550, 152938.	1.3	2
40085	Pd-decorated GaN monolayer as a promising scavenger for SO2 and SOF2 in SF6 insulation equipment: A first-principles study. Computational and Theoretical Chemistry, 2021, 1201, 113276.	1.1	10
40086	Electronic and optical properties of O-doped porous boron nitride: A first principle study. Journal of Solid State Chemistry, 2021, 299, 122139.	1.4	3
40087	Controlled syngas production by electrocatalytic CO2 reduction on formulated Au25(SR)18 and PtAu24(SR)18 nanoclusters. Journal of Chemical Physics, 2021, 155, 014305.	1.2	24
40088	Shock to detonation transition of pentaerythritol tetranitrate (PETN) initially pressed to 1.65â€‰g/cm3. Journal of Applied Physics, 2021, 130, .	1.1	7
40089	Effects of pyridine-like and pyrrolic-like nitrogen on the photoluminescence blue-shift of nitrogen-doped graphene oxide quantum dots. Journal of Luminescence, 2021, 235, 117983.	1.5	5
40091	Ab initio study of the structural, electronic, mechanical, dynamical, thermodynamic, linear and nonlinear optical properties of BeSiP2xAs2(1â^'x) quaternary alloys. Journal of Physics and Chemistry of Solids, 2021, 154, 110042.	1.9	1
40092	Mechanical properties of single-walled penta-graphene-based nanotubes: A DFT and Classical molecular dynamics study. Chemical Physics, 2021, 547, 111187.	0.9	6
40093	Tuning Damping and Magnetic Anisotropy in Ultrathin Boronâ€Engineered MgO/Coâ€“Feâ€“B/MgO Heterostructures. Advanced Electronic Materials, 2021, 7, 2100351.	2.6	7
40094	The accepting and stabilizing role played by the phase during the <mml:math xmlns:mml="http://www.w3.org/1998/Math/MathML" altimg="si8.svg"><mml:mtext>â€‰</mml:mtext><mml:mfenced close="}" open="{"><mml:mn>112</mml:mn></mml:mfenced><mml:msub><mml:mrow><mml:mfenced close="â€‰" open="â€˜"><mml:mn>111</mml:mn></mml:mfenced></mml:mrow><mml:mi>Î²</mml:mi></mml:msub></mml:math> twinning in Ti-Mo alloys: A first-principles insight. Journal of Materials Science and Technology, 2021,	5.6	9

#	Article	IF	Citations
40095	Inverse proximity effects at spin-triplet superconductor-ferromagnet interface. Physical Review Research, 2021, 3, .	1.3	4
40096	Effect of oxygen based functional groups on the nucleation of TiO2 by atomic layer deposition: A theoretical and experimental study. Materials Chemistry and Physics, 2021, 267, 124588.	2.0	5
40097	Multiple Electronic Transition-Induced Anomalous Broadband Absorption in a New Class of [Ni-Tpy₂]-Based Lead-Free Perovskite Single Crystals. Journal of Physical Chemistry C, 2021, 125, 15579-15589.	1.5	5
40098	Compression behavior of energetic Îµ â€CLâ€20 crystals from density functional theory calculations. Journal of Raman Spectroscopy, 2021, 52, 1764.	1.2	2
40099	Computational Screening of Single Atoms Anchored on Defective Mo₂CO₂ MXene Nanosheet as Efficient Electrocatalysts for the Synthesis of Ammonia. Advanced Engineering Materials, 2021, 23, 2100405.	1.6	13
40100	Mechanical, Structural and Electronic Properties of CO2 Adsorbed Graphitic Carbon Nitride (g-C3N4) under Biaxial Tensile Strain. Materials, 2021, 14, 4110.	1.3	3
40101	Activating low-temperature NH3-SCR catalyst by breaking the strong interface between acid and redox sites: A case of model Ce2(SO4)3-CeO2 study. Journal of Catalysis, 2021, 399, 212-223.	3.1	61
40102	Understanding the anisotropic phonon thermal transport through 2D Î²-siligraphene. Carbon, 2021, 179, 523-530.	5.4	1
40103	Effects of pressure on narrowing the band gap, visible light absorption, and semi-metallic transition of lead-free perovskite CsSnBr3 for optoelectronic applications. Journal of Physics and Chemistry of Solids, 2021, 154, 110083.	1.9	33
40104	Computational Prediction of Superlubric Layered Heterojunctions. ACS Applied Materials & Interfaces, 2021, 13, 33600-33608.	4.0	11
40105	Oxygen injection during fast vs slow passivation in aqueous solution. Acta Materialia, 2021, 213, 116898.	3.8	11
40106	Defect Properties and Lithium Incorporation in Li2ZrO3. Energies, 2021, 14, 3963.	1.6	6
40107	Introducing Crown Ether as a Functional Additive for High-Performance Dendrite-free Li Metal Batteries. ACS Applied Energy Materials, 2021, 4, 7829-7838.	2.5	11
40108	Thermoelectric CoGeTe with an Orthorhombic Crystal Symmetry and Balance of the Electrical and Thermal Properties. Inorganic Chemistry, 2021, 60, 12331-12338.	1.9	1
40109	Strontium Stannate as an Alternative Anode Material for Li-Ion Batteries. Journal of Physical Chemistry C, 2021, 125, 14947-14956.	1.5	9
40110	Large Perpendicular Magnetic Anisotropy in Ta/CoFeB/MgO on Full-Coverage Monolayer MoS₂ and First-Principles Study of Its Electronic Structure. ACS Applied Materials & Interfaces, 2021, 13, 32579-32589.	4.0	11
40111	Probing the Effects of Acid Electrolyte Anions on Electrocatalyst Activity and Selectivity for the Oxygen Reduction Reaction. ChemElectroChem, 2021, 8, 2467-2478.	1.7	25
40112	Effect of Se incorporation on thermoelectric properties of Bi₂(Se _x) Tj ETQq1 1 0.784314 rgBT /Overlock 10	0.8	1

#	Article	IF	Citations
40113	Interplay of crystal thickness and in-plane anisotropy and evolution of quasi-one-dimensional electronic character in ReSe2. Physical Review B, 2021, 104, .	1.1	5
40114	An In Situ Synchrotron Dilatometry and Atomistic Study of Martensite and Carbide Formation during Partitioning and Tempering. Materials, 2021, 14, 3849.	1.3	0
40115	Spin-polarized electronic states and atomic reconstructions at antiperovskite <mml:math xmlns:mml="http://www.w3.org/1998/Math/MathML"><mml:mrow><mml:msub><mml:mi>Sr</mml:mi><mml:mn>3</mml:mn></mml:r mathvariant="normal">O</mml:mi><mml:mrow><mml:mo>(</mml:mo><mml:mn>001</mml:mn><mml:mo>)</mml:mo></mml:mrow> polar surfaces. Physical Review B, 2021, 104, .	1.1	4
40116	Some properties of LiInSi half-Heusler alloy via density functional theory. Bulletin of Materials Science, 2021, 44, 1.	0.8	12
40117	In-situ growth of heterophase Ni nanocrystals on graphene for enhanced catalytic reduction of 4-nitrophenol. Nano Research, 2022, 15, 1230-1237.	5.8	21
40118	Effect of Alloying Elements on the Stacking Fault Energy and Ductility in Mg₂Si Intermetallic Compounds. ACS Omega, 2021, 6, 20254-20263.	1.6	1
40119	Theoretical studies of photocatalytic behaviors of isoelectronic Sn/Pb-doped TiO2: DFT+U. Applied Surface Science, 2021, 555, 149714.	3.1	10
40120	First principles investigation of intrinsic and Na defects in XTe (X=Ca, Sr, Ba) nanostructured PbTe. Materials Today Physics, 2021, 19, 100415.	2.9	6
40121	Ab initio study of helium in Li4SiO4 crystals: Electronic properties, migration, and vacancy capture mechanism. Ceramics International, 2021, 47, 20239-20247.	2.3	3
40122	Theoretical evaluation and experimental investigation of layered 2H/1T-phase MoS2 and its reduced graphene-oxide hybrids for hydrogen evolution reactions. Journal of Alloys and Compounds, 2021, 868, 159272.	2.8	22
40123	Interstitial lithium doping in SrTiO₃. AIP Advances, 2021, 11, 075029.	0.6	2
40124	A Pseudopotential Study of Structural, Mechanical, and Lattice Dynamics Behavior of the Binary Intermetallic Yttrium Tristannide YSn 3. Physica Status Solidi (B): Basic Research, 2021, 258, 2100219.	0.7	1
40125	High-Performance Single-Atom Catalysts for CO Oxidation: the Importance of Hydrogen Bonds and Adsorption Strength of the Reactant. Journal of Physical Chemistry C, 2021, 125, 15987-15993.	1.5	2
40126	Lattice dynamics and magnetic exchange interactions in <mml:math xmlns:mml="http://www.w3.org/1998/Math/MathML"><mml:mrow><mml:msub><mml:mi>GeCo</mml:mi><mml:mn>2</mml:mn></ mathvariant="normal">O</mml:mi><mml:mn>4</mml:mn></mml:msub></mml:mrow></mml:math> : A spinel with <mml:math xmlns:mml="http://www.w3.org/1998/Math/MathML"><mml:mrow><mml:mi>S</mml:mi><mml:mo>=</mml:mo><mml:mfrac><mml:mn pyrochlore lattice. Physical Review B, 2021, 104, .	1.1	7
40127	Nb-doped ZrxSn1â^'xO2: Experimental and first-principles study. Journal of Applied Physics, 2021, 130, .	1.1	2
40128	o-Si32: A new direct band gap silicon allotrope. Chinese Physics B, 0, , .	0.7	0
40129	Ab-initio investigation on the electronic and thermoelectric properties of new half-Heusler compounds KBiX (X = Ba and Sr). Journal of Physics Condensed Matter, 2021, 33, 395701.	0.7	13
40130	Copper Complexes with Carbonâ€Related Radiation Defects in Silicon. Physica Status Solidi (A) Applications and Materials Science, 0, , 2100141.	0.8	1

#	Article	IF	Citations
40131	Ab-initio and Monte Carlo study of Fe-based two-dimensional magnets at borophene supported by Ag(111) surface. Physical Review Materials, 2021, 5, .	0.9	0
40132	Molecular-Level Insights into Selective Transport of Mg²⁺ in Metalâ€“Organic Frameworks. ACS Applied Materials & Interfaces, 2021, 13, 51974-51987.	4.0	3
40133	First-principles characterization of the electronic properties of h-BN layers. Materials Today: Proceedings, 2022, 50, 301-306.	0.9	4
40134	Molybdenum disulfide monolayer electronic structure information as explored using density functional theory and quantum theory of atoms in molecules. Applied Surface Science, 2021, 555, 149545.	3.1	11
40135	Surface structures of magnetostrictive D03-Fe3Ga(0Â0Â1). Applied Surface Science, 2021, 553, 149488.	3.1	5
40136	High-pressure behavior of disodered kesterite-type Cu2ZnSnS4. Applied Physics A: Materials Science and Processing, 2021, 127, 1.	1.1	3
40137	First-principles molecular dynamics study of the behavior of tritium in molten LiF-BeF2 eutectic. Journal of Molecular Liquids, 2022, 345, 117027.	2.3	5
40138	Comprehensive Mechanism of CO₂ Electroreduction toward Ethylene and Ethanol: The Solvent Effect from Explicit Waterâ€“Cu(100) Interface Models. ACS Catalysis, 2021, 11, 9688-9701.	5.5	65
40139	Mechanisms and rates of pyrite formation from hydrothermal fluid revealed by iron isotopes. Geochimica Et Cosmochimica Acta, 2021, 304, 281-304.	1.6	7
40140	Theoretical study on compositionâ€dependent properties of ZnOÂ·nAl₂O₃ spinels. Part II: Mechanical and thermophysical. Journal of the American Ceramic Society, 2021, 104, 6455-6466.	1.9	10
40141	Ab initio studies of A2PtH6 (AÂ=ÂK,Rb) materials for hydrogen storage purposes and optoelectronic applications. Materials Science and Engineering B: Solid-State Materials for Advanced Technology, 2021, 269, 115154.	1.7	6
40142	Interaction of Water Molecule with Two-Dimensional Tin Dioxide. Journal of Contemporary Physics, 2021, 56, 265-268.	0.1	0
40143	Anomalous Anisotropy of the Piezoelectric Response in 2D Copperâ€Based Ternary Chalcogenides CuMX₂. Physica Status Solidi - Rapid Research Letters, 2021, 15, 2100304.	1.2	3
40144	Assessing the performances of different continuum solvation models for the calculation of hydration energies of molecules, polymers and surfaces: a comparison between the SMD, VASPsol and FDPB models. Theoretical Chemistry Accounts, 2021, 140, 1.	0.5	13
40145	Intrinsic Defect Limit to the Growth of Orthorhombic HfO₂ and (Hf,Zr)O₂ with Strong Ferroelectricity: Firstâ€Principles Insights. Advanced Functional Materials, 2021, 31, 2104913.	7.8	39
40146	A MoS₂ and Graphene Alternately Stacking van der Waals Heterostructure for Li⁺/Mg²⁺ Coâ€Intercalation. Advanced Functional Materials, 2021, 31, 2103214.	7.8	35
40147	First-principles studies on sensing properties of delta arsenene nanoribbons towards hexane and heptane molecules. Computational and Theoretical Chemistry, 2021, 1201, 113256.	1.1	14
40148	Unraveling the Intermediate Reaction Complexes and Critical Role of Support-Derived Oxygen Atoms in CO Oxidation on Single-Atom Pt/CeO₂. ACS Catalysis, 2021, 11, 8701-8715.	5.5	51

#	Article	IF	Citations
40149	Computational evaluation of superalkali-decorated graphene nanoribbon as advanced hydrogen storage materials. International Journal of Hydrogen Energy, 2021, 46, 24510-24516.	3.8	20
40150	Computational screening of bifunctional single atom electrocatalyst based on boron nitride nanoribbon for water splitting. Applied Catalysis A: General, 2021, 622, 118235.	2.2	18
40151	A First-Principles-Based Microkinetic Study of CO₂ Reduction to CH₃OH over In₂O₃(110). ACS Catalysis, 2021, 11, 9996-10006.	5.5	19
40152	Atomic level N-coordinated Fe dual-metal embedded in graphene: An efficient double atoms catalyst for CO oxidation. Colloids and Surfaces A: Physicochemical and Engineering Aspects, 2021, 621, 126575.	2.3	7
40153	Doping-controllable high temperature magnetic semiconductor. Physica E: Low-Dimensional Systems and Nanostructures, 2021, 131, 114731.	1.3	3
40154	Investigation of physical and superconducting properties of newly synthesized CaPd2P2 and SrPd2P2. Journal of Alloys and Compounds, 2021, 868, 159199.	2.8	18
40155	Ab initio study of effect of Se vacancies on the electronic and thermoelectric properties of the two-dimensional Mo$$Se_2$$ monolayer. Applied Physics A: Materials Science and Processing, 2021, 127, 1.	1.1	6
40157	Atomic Structure of the Cu₂O(111) Surface: A Transmission Electron Microscopy and DFTâ€‰+â€‰U Study. Physica Status Solidi (B): Basic Research, 2021, 258, 2100185.	0.7	3
40158	Soft-mode dynamics in the ferroelectric phase transition of GeTe. Npj Computational Materials, 2021, 7, .	3.5	11
40159	Giant Spin Splitting in Chiral Perovskites Based on Local Electrical Field Engineering. Journal of Physical Chemistry Letters, 2021, 12, 6492-6498.	2.1	12
40160	Electronic and optical properties of 3N-doped graphdiyne/MoS2 heterostructures tuned by biaxial strain and external electric field. Chinese Physics B, 0, , .	0.7	1
40161	Infra-Red Active Dirac Plasmon Serie in Potassium Doped-Graphene (KC8) Nanoribbons Array on Al2O3 Substrate. Materials, 2021, 14, 4256.	1.3	3
40162	Probing the Structural, elastic, electronic and Thermoelectric Properties of C15-type Laves phase LaCo2: A DFT based ab-initio investigation. Revista Mexicana De FÃsica, 2021, 67, .	0.2	0
40163	Structural, mechanical, electronic properties and Debye temperature of tungsten-technetium alloy: A first-principles study. Fusion Engineering and Design, 2021, 168, 112433.	1.0	10
40164	Arc Synthesis, Crystal Structure, and Photoelectrochemistry of Copper(I) Tungstate. ACS Applied Materials & Interfaces, 2021, 13, 32865-32875.	4.0	11
40165	Structural, Thermal, and Electronic Properties of TwoâEĐimensional Gallium Oxide (Î²â€Ga₂O₃) from FirstâEPrinciples Design. ChemPhysChem, 2021, 22, 2362-2370.	1.0	10
40166	Ultra-low lattice thermal conductivity and high thermoelectric efficiency of K3AuO. Journal of Applied Physics, 2021, 130, 045101.	1.1	2
40167	Ferromagnetism and giant magnetoresistance in zinc-blende FeAs monolayers embedded in semiconductor structures. Nature Communications, 2021, 12, 4201.	5.8	5

#	Article	IF	Citations
40168	Structure and magnetic properties of the S = 3/2 zigzag spin chain antiferromagnet BaCoTe2O7. Science China: Physics, Mechanics and Astronomy, 2021, 64, 1.	2.0	11
40169	Effect of characteristic size on the collective phonon transport in crystalline GeTe. Physical Review Materials, 2021, 5, .	0.9	3
40170	Fluorescent Carbon Nitride Macrostructures Derived from Triazineâ€Based Cocrystals. Advanced Optical Materials, 2021, 9, 2100683.	3.6	8
40171	First-Principles Study on the Elastic Constants and Structural and Mechanical Properties of 30Â° Partial Dislocation in GaAs. Advances in Materials Science and Engineering, 2021, 2021, 1-7.	1.0	0
40172	Oxygen-vacancy-mediated catalytic methanation of lignocellulose at temperatures below 200Â°C. Joule, 2021, 5, 3031-3044.	11.7	39
40173	Tuning Schottky Barrier and Contact Type of Metalâ€“Semiconductor in Ti₃C₂T₂/MoS₂ (T = F, O, OH) by Strain: A First-Principles Study. Journal of Physical Chemistry C, 2021, 125, 16200-16210.	1.5	29
40174	Energetic and electronic properties of NH3, NO2 and SO2 interacting with GaN nanotube: a DFT study. Journal of Molecular Modeling, 2021, 27, 234.	0.8	5
40175	First-Principles Density Functional Theory Calculations of Bilayer Membranes Heterostructures of Ti3C2T2 (MXene)/Graphene and AgNPs. Membranes, 2021, 11, 543.	1.4	10
40176	Pressure-induced phase transition in magnetoresistance perovskite La0.75Ca0.25MnO3: a GGA + U study. Journal of Physics Communications, 2021, 5, 075007.	0.5	1
40177	Engineering Anisotropic Klein Tunneling in Black Phosphorene through Elemental Substitution. Physica Status Solidi (B): Basic Research, 2021, 258, 2100071.	0.7	2
40178	High pressure structural evolution of cubic solid solution YbInO3. Journal of Applied Physics, 2021, 130, .	1.1	3
40179	Local and Bulk Probe of Vanadium-Substituted Î±-Manganese Oxide (Î±-K_xV_yMn_{8â€“y}O₁₆) Lithium Electrochemistry. Inorganic Chemistry, 2021, 60, 10398-10414.	1.9	3
40180	Novel Thermoelectric Character of Rhenium Carbonitride, ReCN. ACS Omega, 2021, 6, 18364-18369.	1.6	2
40181	Cobalt Telluride: A Highly Efficient Trifunctional Electrocatalyst for Water Splitting and Oxygen Reduction. ACS Applied Energy Materials, 2021, 4, 8158-8174.	2.5	36
40182	Piezoelectricity in monolayer B C N structures: A first principles study. Computational Materials Science, 2021, 195, 110505.	1.4	5
40183	V₂CT_x MXene Artificial Solid Electrolyte Interphases toward Dendrite-Free Lithium Metal Anodes. ACS Sustainable Chemistry and Engineering, 2021, 9, 9961-9969.	3.2	13
40184	High tensile strength and thermal conductivity in BeO monolayer: A first-principles study. FlatChem, 2021, 28, 100257.	2.8	24
40185	Unravelling the chemical heterogeneity of Î±-Pu2O3(111) surface with the site-selective adsorption of H2O and CO2. Journal of Alloys and Compounds, 2021, 870, 159371.	2.8	1

#	Article	IF	Citations
40186	Dominant role of M element on the stability and properties of Prussian blue analogues NaxMFe(CN)6 (MÂ=Â3d transition metal) as cathode material for the sodium-ion batteries. Journal of Alloys and Compounds, 2021, 870, 159533.	2.8	12
40187	Selective electrocatalytic synthesis of urea with nitrate and carbon dioxide. Nature Sustainability, 2021, 4, 868-876.	11.5	264
40188	ELECTRONIC AND VIBRATIONAL STRUCTURES OF BeCâ€“V2 PNICTIDES. Journal of Structural Chemistry, 2021, 62, 985-994.	0.3	0
40189	Computational identification of B substitutional doped C<mml:math xmlns:mml="http://www.w3.org/1998/Math/MathML" altimg="si2.svg"><mml:msub><mml:mrow /><mml:mn>9</mml:mn></mml:msub></mml:math>N<mml:math xmlns:mml="http://www.w3.org/1998/Math/MathML" altimg="si3.svg"><mml:msub><mml:mrow /><mml:mn>4</mml:mn></mml:msub></mml:math> monolayer for electrocatalytic N<mml:math xmlns:mml="http://www.w3.org/1998/Math/MathML" altimg="si10.svg"><mml:msub><mml:mrow />	1.0	8
40190	High-Throughput Computation of New Carbon Allotropes with Diverse Hybridization and Ultrahigh Hardness. Crystals, 2021, 11, 783.	1.0	23
40191	Compositional Patterning in Carbon Implanted Titania Nanotubes. Advanced Functional Materials, 2021, 31, 2104250.	7.8	7
40192	High-Throughput Screening of Alloy Catalysts for Dry Methane Reforming. ACS Catalysis, 2021, 11, 8881-8894.	5.5	47
40193	Adsorption of hydrated [Y(OH)2]+ on kaolinite (001) surface: Insight from DFT simulation. Powder Technology, 2021, 387, 80-87.	2.1	20
40194	Crystal chemistry and electronic structure of the Î²-AlFeSi phase from first-principles. Journal of Solid State Chemistry, 2021, 299, 122199.	1.4	13
40195	Design and theoretical study of novel multifunctional 3D-BC2N polymorphs. Chemical Physics Letters, 2021, 774, 138610.	1.2	3
40196	The miscibility of calcium silicate perovskite and bridgmanite: A single perovskite solid solution in hot, iron-rich regions. Earth and Planetary Science Letters, 2021, 566, 116973.	1.8	5
40197	On the structure sensitivity of and CO coverage effects on formic acid decomposition on Pd surfaces. Surface Science, 2021, 709, 121846.	0.8	11
40198	Photonic spin Hall effect in twisted bilayer graphene. Journal of the Optical Society of America A: Optics and Image Science, and Vision, 2021, 38, 1232.	0.8	10
40199	Theoretical Study of Abnormal Thermal Expansion of CuSCN and Effect on Electronic Structure. Frontiers in Materials, 2021, 8, .	1.2	5
40200	Atomic-scale regulation of anionic and cationic migration in alkali metal batteries. Nature Communications, 2021, 12, 4184.	5.8	57
40201	Mechanical properties of layered tilkerodeite (Pd2HgSe3) and jacutingaite (Pt2HgSe3) crystals: Insights on the interlayer, intralayer interactions, and phonons. Journal of Applied Physics, 2021, 130, 015105.	1.1	1
40202	Emergence of Nontrivial Spin Textures in Frustrated Van Der Waals Ferromagnets. Nanomaterials, 2021, 11, 1770.	1.9	9
40203	Metastability relationship between two- and three-dimensional crystal structures: a case study of the Cu-based compounds. Scientific Reports, 2021, 11, 14588.	1.6	6

#	Article	IF	Citations
40204	Excited states of a phosphorus pair in silicon: Combining valley-orbital interaction and electron-electron interactions. Physical Review B, 2021, 104, .	1.1	3
40205	Insights into the atomic structure of the interface of ferroelectric <mml:math xmlns:mml="http://www.w3.org/1998/Math/MathML"><mml:mrow><mml:msub><mml:mi>Hf</mml:mi><mml:mrow><mml:mn>0.5</mml:mn> mathvariant="normal">O</mml:mi><mml:mn>2</mml:mn></mml:msub></mml:mrow></mml:math> grown epitaxially on <mml:math xmlns:mml="http://www.w3.org/1998/Math/MathML"><mml:mrow><mml:msub><mml:mi>La</mml:mi>. Physical Review Materials, 2021, 5, .	0.9	15
40206	Complex pressure-temperature structural phase diagram of the honeycomb iridate Cu2IrO3. Physical Review B, 2021, 104, .	1.1	12
40207	Large out-of-plane piezoelectric response of wurtzite InN under biaxial strain. Modelling and Simulation in Materials Science and Engineering, 2021, 29, 065013.	0.8	3
40208	Charge-density-wave melted superconductivity in 1T-TiSe₂. Europhysics Letters, 2021, 135, 57003.	0.7	2
40209	Enhancing Catalytic Properties of Iron- and Nitrogen-Doped Carbon for Nitrogen Reduction through Structural Distortion: A Density Functional Theory Study. Journal of Physical Chemistry C, 2021, 125, 16004-16012.	1.5	14
40210	Surface Magnetism in Pristine Î± Rhombohedral Boron and Intersurface Exchange Coupling Mechanism of Boron Icosahedra. Journal of Physical Chemistry Letters, 2021, 12, 6812-6817.	2.1	5
40211	Benzylic C_{sp³}â€“H Bond Oxidation on the (111) Facets of Octahedral Cu₂O Nanocrystals. ACS Applied Nano Materials, 2021, 4, 7840-7855.	2.4	4
40212	First-Principles Study of the Half-Metallic Properties of (001), (110), and (111) Surfaces of RbSe in the CsCl Structure. Journal of Electronic Materials, 2021, 50, 5473-5482.	1.0	0
40213	Hybrid Organicâ€“Inorganic Halide Postâ€Perovskite 3â€Cyanopyridinium Lead Tribromide for Optoelectronic Applications. Advanced Functional Materials, 2021, 31, 2102338.	7.8	18
40214	Room temperature ferromagnetism in Zn-doped NiO nanoparticles: An experimental and DFT+U approach. Journal of Alloys and Compounds, 2021, 868, 159176.	2.8	19
40215	A novel approach for metal extraction from metal sulfide ores with NH4Cl: A combined DFT and experimental studies. Separation and Purification Technology, 2021, 267, 118626.	3.9	8
40216	Nanointerface engineering of cobalt sulfide/manganese sulfate hollow spheres for electromagnetic wave absorption. Applied Surface Science, 2021, 554, 149238.	3.1	17
40217	New honeycomb-like M-based (MÂ=ÂC, Si, Ge and Sn) monochalcogenides polymorphs: An extended family as isoelectronic photocatalysts of Group-VA for water splitting. Applied Surface Science, 2021, 554, 149644.	3.1	10
40218	Beyond the Limit of Goldschmidt Tolerance Factor: Crystal Surface Engineering to Boost the Î±â€Phase Stability of Formamidiniumâ€Only Hybrid Inorganicâ€“Organic Perovskites. Solar Rrl, 2021, 5, 2100188.	3.1	8
40219	Electronic and optical properties of two-dimensional As2GeTe and P2SiS monolayers: Density functional study. Chemical Physics, 2021, 547, 111215.	0.9	6
40220	Design the PdCu/TaN C electrocatalyst with core-shell structure having high efficiency for methanol and formic acid oxidation reactions. Electrochimica Acta, 2021, 383, 138365.	2.6	24
40221	Enhancement of hydrogen storage properties of metal-organic framework-5 by substitution (Zn, Cd) Tj ETQq1 1 0.784314 rgBT /Over 26426-26436.	3.8	17

#	Article	IF	Citations
40222	1,2,4-Azadiphosphole-based piezoelectric penta-CNP sheet with high spontaneous polarization. Applied Surface Science, 2021, 554, 149499.	3.1	21
40223	Atomistic origin of compositional pulling effect in wurtzite (B, Al, In)xGa1â^'xN: A first-principles study. Journal of Applied Physics, 2021, 130, 035704.	1.1	7
40224	Theoretical investigation of group-IV binary compounds in the P4/ncc phase. Results in Physics, 2021, 26, 104349.	2.0	5
40225	Improved charge carrier dynamics through a type II staggered Ce MOF/mc BiVO4 n-n heterojunction for enhanced visible light utilisation. Applied Surface Science, 2021, 553, 149556.	3.1	16
40226	Synthesis of Two New Ni 12 â€Cluster Substituted Sandwiched Phosphotungstates Organicâ€Cluster and their Magnetic Property. European Journal of Inorganic Chemistry, 2021, 2021, 2718-2723.	1.0	2
40227	A Crystallographic, Spectroscopic, and Computational Investigation of Carbonyl and Oxalyl Diisothiocyanate. Inorganic Chemistry, 2021, 60, 10722-10728.	1.9	2
40228	Effect of CeO2 dispersion on the oxidation behavior of Ni-Al/Ni-Re coating in dry and wet CO2 gas at 650 Â°C. Corrosion Science, 2021, 187, 109498.	3.0	0
40229	GaAs quantum dot/TiO2 heterojunction for visible-light photocatalytic hydrogen evolution: promotion of oxygen vacancy. Advanced Composites and Hybrid Materials, 2022, 5, 450-460.	9.9	28
40230	Graphite-supported single copper catalyst for electrochemical CO2 reduction: A first-principles approach. Computational and Theoretical Chemistry, 2021, 1201, 113277.	1.1	5
40231	Investigation on wetting behavior and mechanism of AgCu-Xwt.%Ti filler metal/AlN ceramic reactive wetting system: Experiments and first-principles calculations. Journal of Alloys and Compounds, 2021, 869, 159323.	2.8	16
40232	A comparative study of hydrostatic pressure treated environmentally friendly perovskites CsXBr3 (X =) Tj ETQq0 0 0 rgBT /Overlock 10 T	0.6	40
40233	Predicted hexagonal titanium nitride monolayer as an intrinsic ferromagnetic semiconductor. EPJ Applied Physics, 2021, 95, 10601.	0.3	1
40234	Electronic, Vibrational, Elastic, and Piezoelectric Properties of Hâ€, Fâ€Functionalized AlN Sheets. Physica Status Solidi (B): Basic Research, 2021, 258, 2100216.	0.7	3
40235	Crystal structure of copper perchlorophthalocyanine analysed by 3D electron diffraction. Acta Crystallographica Section B: Structural Science, Crystal Engineering and Materials, 2021, 77, 662-675.	0.5	9
40236	Extension of the Linear Response Function of Electron Density to a Plane-wave Basis and the First Application to Periodic Surface Systems. Chemistry Letters, 2021, 50, 1801-1805.	0.7	2
40237	Elucidating the influence of anchoring geometry on the electronic transport of carbon-atom chains. International Journal of Modern Physics B, 2021, 35, 2150216.	1.0	0
40238	Direct and quasi-direct band gap of novel Si-Ge alloys in P-3m1 phase. Journal of Physics Condensed Matter, 2021, 33, 385702.	0.7	6
40239	Acid-base properties of hydroxyapatite(0001) by the adsorption of probe molecules: An ab initio investigation. Physical Review Materials, 2021, 5, .	0.9	2

#	Article	IF	Citations
40240	Crystal and electronic facet analysis of ultrafine Ni2P particles by solid-state NMR nanocrystallography. Nature Communications, 2021, 12, 4334.	5.8	17
40241	Enhancing electrocatalytic N2-to-NH3 fixation by suppressing hydrogen evolution with alkylthiols modified Fe3P nanoarrays. Nano Research, 2022, 15, 1039-1046.	5.8	74
40242	Theoretical and Experimental Studies of LiBH₄â€“LiBr Phase Diagram. ACS Applied Energy Materials, 2021, 4, 7327-7337.	2.5	12
40243	Prediction of two-dimensional bismuth-based chalcogenides Bi₂X₃(X = S, Se,) Tj ETQq1 1 0.784314 rgBT /O Physics, 2021, 54, 395103.	1.3	42
40244	Cobalt-embedded hierarchically-porous hollow carbon microspheres as multifunctional confined reactors for high-loading Li-S batteries. Nano Energy, 2021, 85, 105981.	8.2	85
40245	Electronic and dynamical properties of <mml:math xmlns:mml="http://www.w3.org/1998/Math/MathML"><mml:mrow><mml:msub><mml:mi>CeRh</mml:mi><mml:mn>2</mml:mn></ : Role of <mml:math xmlns:mml="http://www.w3.org/1998/Math/MathML"><mml:mrow><mml:msub><mml:mi>Rh</mml:mi><mml:mn>2</mml:mn></ layers and expected orbital order. Physical Review B, 2021, 104 .	1.1	19
40246	Firstâ€Principles Multiscale Modeling of Mechanical Properties in Graphene/Borophene Heterostructures Empowered by Machineâ€Learning Interatomic Potentials. Advanced Materials, 2021, 33, e2102807.	11.1	171
40247	First-principles study of electronic structure and thermoelectric properties of p-type XIrSb(X = Ti, Zr) Tj ETQq1 1 0.784314 rgBT /Over	1.9	11
40248	How does the defect ZnO@Au surface activate the methane via the precursor-mediated mechanism?. Applied Surface Science, 2021, 555, 149728.	3.1	3
40249	Theoretical Analysis of Energy Efficiency of Plasma-Assisted Heterogeneous Activation of Nitrogen for Ammonia Synthesis. Plasma Chemistry and Plasma Processing, 2021, 41, 1279-1291.	1.1	3
40250	Comparative study of electronic structure, optical properties, lattice dynamics and thermal expansion behaviour of energetic ammonium and potassium dinitramide salts. Materials Chemistry and Physics, 2021, 267, 124645.	2.0	4
40251	Ab-Initio Spectroscopic Characterization of Melem-Based Graphitic Carbon Nitride Polymorphs. Nanomaterials, 2021, 11, 1863.	1.9	7
40252	Ab initio studies for characterization and identification of nanocrystalline copper pyrophosphate confined in mesoporous silica. Nanotechnology, 2021, 32, 415701.	1.3	6
40253	Systematic Study of the Thermal Properties of Zeolitic Frameworks. Journal of Physical Chemistry C, 2021, 125, 15647-15658.	1.5	7
40254	High-Throughput Screening of Element-Doped Carbon Nanotubes Toward an Optimal One-Dimensional Superconductor. Journal of Physical Chemistry Letters, 2021, 12, 6667-6675.	2.1	4
40255	Density functional theory calculations of copperâ€doped rutile crystals: Local structural, electronic, optical, and electron paramagnetic resonance properties. Magnetic Resonance in Chemistry, 2022, 60, 104-112.	1.1	1
40256	Transformation of CrSe Monolayers into Room-Temperature Half Metals via Chemical Edge Modification. Journal of Physical Chemistry C, 2021, 125, 15664-15669.	1.5	5
40257	Effect of Ni Content on Anionic Redox Activity in Ru-Containing Li-Rich Cathode Material. Journal of the Electrochemical Society, 2021, 168, 070552.	1.3	2

#	Article	IF	Citations
40258	Composition-Dependent of 6ÂM Martensite Structure and Magnetism in Cu-Alloyed Ni-Mn-In-Co by First-Principles Calculations. Acta Metallurgica Sinica (English Letters), 0, , 1.	1.5	0
40259	Coupling of lattice dynamics and configurational disorder in metal deficient Al1â˜ÎB2 from first-principles. Journal of Applied Physics, 2021, 130, 015110.	1.1	6
40260	Fragile symmetry-protected half metallicity in two-dimensional van der Waals magnets: A case study of monolayer <mml:math xmlns:mml="http://www.w3.org/1998/Math/MathML"><mml:mrow><mml:mi>Fe</mml:mi><mml:msub><mml:mi>Cl</mml:mi><mml:m Physical Review B, 2021, 104, .	1.1	11
40261	Optical Absorption and Reflectivity of Four 2D Materials: MoS2, MoP2, NbS2, and NbP2. Frontiers in Materials, 2021, 8, .	1.2	2
40262	Structural phase transformation, insulator to semiconductor transition by Be/Sr doping and impact on optical properties of KMgF₃ fluro-perovskite. Molecular Physics, 2021, 119, .	0.8	0
40263	Study of the Molecule Adsorption Process during the Molecular Doping. Nanomaterials, 2021, 11, 1899.	1.9	1
40264	A First-Principles Study of Structure, Elastic and Electronic Properties of GeTiO3 as Environmentally Innocuous Ferroelectric Perovskites. Ukrainian Journal of Physics, 2021, 66, 539.	0.1	0
40265	Controllable pâ€Type Doping of 2D WSe₂ via Vanadium Substitution. Advanced Functional Materials, 2021, 31, 2105252.	7.8	40
40266	Paraelectric KH2PO4 nanocrystals in monolithic mesoporous silica: Structure and lattice dynamics. Journal of Alloys and Compounds, 2021, 868, 159177.	2.8	6
40267	Undamped plasmon modes and enhanced superconductivity in metal diborides. New Journal of Physics, 2021, 23, 073036.	1.2	3
40268	Size and strain induced phase formation and ferromagnetism in reduced TiO2 powders. Journal of Physics and Chemistry of Solids, 2021, 154, 110058.	1.9	5
40269	Photothermal Catalysis for Selective CO₂ Reduction on the Modified Anatase TiO₂ (101) Surface. ACS Applied Energy Materials, 2021, 4, 7702-7709.	2.5	21
40270	Borophene via Micromechanical Exfoliation. Advanced Materials, 2021, 33, e2102039.	11.1	56
40271	First-principles calculation of iron and silicon isotope fractionation between Fe-bearing minerals at magmatic temperatures: The importance of second atomic neighbors. Geochimica Et Cosmochimica Acta, 2021, 304, 101-118.	1.6	17
40272	High-throughput screening of carbon-supported single metal atom catalysts for oxygen reduction reaction. Nano Research, 2022, 15, 1054-1060.	5.8	34
40273	First principles study of the electronic structure and optical properties of triphenylene under pressure. Molecular Physics, 2021, 119, .	0.8	1
40274	Mechanical and dynamic stability of ZnX chalcogenide (X=O, S, Se, Te) monolayers and their electronic, optical, and thermoelectric properties. Journal of Applied Physics, 2021, 130, .	1.1	4
40275	Exploring the Full Potential of Functional Si₂BN Nanoribbons As Highly Reversible Anode Materials for Mg-Ion Battery. Energy & Fuels, 2021, 35, 12688-12699.	2.5	3

#	Article	IF	Citations
40276	Room-Temperature Plasticity of a Nanosized GaN Crystal. Nano Letters, 2021, 21, 6425-6431.	4.5	5
40277	Using first-principles calculations to predict the mechanical properties of transmuting tungsten under first wall fusion power-plant conditions. Journal of Physics Condensed Matter, 2021, 33, 345901.	0.7	3
40278	Machine learning and evolutionary prediction of superhard B-C-N compounds. Npj Computational Materials, 2021, 7, .	3.5	34
40279	Spin-polarized relativistic calculations in linear augmented-Slater-type-orbital method. Electronic Structure, 2021, 3, 034003.	1.0	3
40280	Multiple Dirac cones and Lifshitz transition in a two-dimensional Cairo lattice as a Hawking evaporation analogue. Journal of Physics Condensed Matter, 2021, 33, 365001.	0.7	5
40281	Structural and electronic properties of Cu₄O₃ (paramelaconite): the role of native impurities. Pure and Applied Chemistry, 2021, 93, 1229-1244.	0.9	2
40282	Boron-rich boron nitride nanomaterials as efficient metal-free catalysts for converting CO2 into valuable fuel. Applied Surface Science, 2021, 555, 149652.	3.1	20
40283	Electronic structure and magnetization of Zn1-xCoxO ternary alloys with zinc-blende, rocksalt and wurtzite phases. Optical and Quantum Electronics, 2021, 53, 1.	1.5	0
40284	In Situ Coexsolution of Metal Nanoparticle-Decorated Double Perovskites As Anode Materials for Solid Oxide Fuel Cells. ACS Applied Energy Materials, 2021, 4, 7992-8002.	2.5	12
40285	MAX phase Zr2SeC and its thermal conduction behavior. Journal of the European Ceramic Society, 2021, 41, 4447-4451.	2.8	33
40286	Activation of N₂ on Manganese Nitride-Supported Ni₃ and Fe₃ Clusters and Relevance to Ammonia Formation. Journal of Physical Chemistry Letters, 2021, 12, 6535-6542.	2.1	19
40287	Deformation of the Interatomic Bonds in the Upper Layers of the Ge(111) Surface with c(2 Ã— 8), 7 Ã— 7, and 5 Ã— 5 Structures. Journal of Experimental and Theoretical Physics, 2021, 133, 44-48.	0.2	1
40288	Hydrogenated group IV-V monolayer HAB6: A new type of Dirac material constructed by isoelectronic rule. Applied Surface Science, 2021, 554, 149635.	3.1	7
40289	Understanding the electronic metal-support interactions of the supported Ni cluster for the catalytic hydrogenation of ethylene. Molecular Catalysis, 2021, 511, 111731.	1.0	4
40290	Pushing Cu uphill of the volcano curve: Impact of a WC support on the catalytic activity of copper toward the hydrogen evolution reaction. International Journal of Hydrogen Energy, 2021, 46, 25092-25102.	3.8	7
40291	Lone-pair engineering: Achieving ultralow lattice thermal conductivity and enhanced thermoelectric performance in Al-doped GeTe-based alloys. Materials Today Physics, 2021, 20, 100497.	2.9	15
40292	Synthesis, luminescent properties and ab initio study of yellow-emitting Sr8MgGa(PO4)7:Eu2+phosphors for white light-emitting diodes. Journal of Luminescence, 2021, 235, 117982.	1.5	12
40293	Chemistry of Oxygen Ionosorption on SnO₂ Surfaces. ACS Applied Materials & Interfaces, 2021, 13, 33664-33676.	4.0	35

#	Article	IF	Citations
40294	Computational observation of the strengthening of Cu/TiN metal/ceramic interfaces by sub-nanometer interlayers and dopants. Applied Surface Science, 2021, 554, 149562.	3.1	4
40295	Mechanical characteristics and electric field-influenced thermoelectric and optical responses of tetragonal germanene. Journal Physics D: Applied Physics, 2021, 54, 405303.	1.3	12
40296	A first-principles research of two-dimensional AlN/C2N van der Waals heterostructure as photocatalyst. Physica E: Low-Dimensional Systems and Nanostructures, 2021, 132, 114754.	1.3	15
40297	Electronic and optical properties of PTCDI adsorbed graphene heterostructure: A first principles study. Journal of Physics and Chemistry of Solids, 2021, 155, 110109.	1.9	3
40298	Force-constant model for the vibrational modes in black-phosphorene and phosphorene nanoribbons (PNRs). Physica E: Low-Dimensional Systems and Nanostructures, 2021, 132, 114757.	1.3	5
40299	Synthesis of polyaniline nanotubes decorated with graphene quantum dots: Structural & electrochemical studies. Electrochimica Acta, 2021, 388, 138614.	2.6	15
40300	Electrocatalytic Decomposition of Formic Acid Catalyzed by M-Embedded Graphene (Mâ€‰=â€‰Ni and Cu): A DFT Study. Topics in Catalysis, 2022, 65, 1-13.	1.3	8
40301	Vortex creation and control in the Kitaev spin liquid by local bond modulations. Physical Review B, 2021, 104, .	1.1	7
40302	Chiral phonons in the honeycomb sublattice of layered CoSn-like compounds. Physical Review B, 2021, 104, .	1.1	17
40303	A First-Principles Study on Na and O Adsorption Behaviors on Mo (110) Surface. Metals, 2021, 11, 1322.	1.0	3
40304	Effects of Co and Coâ€‰+â€‰Mo additions on tensile properties of tungsten heavy alloys: first-principles study and experimental investigations. Powder Metallurgy, 2022, 65, 151-158.	0.9	2
40305	Effect of multiple Ti doping on helium behavior in ZrCo. Journal of Nuclear Materials, 2021, 551, 152955.	1.3	11
40306	Diffusionlessâ€Like Transformation Unlocks Pseudocapacitance with Bulk Utilization: Reinventing Fe₂O₃ in Alkaline Electrolyte. Energy and Environmental Materials, 2023, 6, .	7.3	20
40307	Defect and Doping Engineered Penta-graphene for Catalysis of Hydrogen Evolution Reaction. Nanoscale Research Letters, 2021, 16, 130.	3.1	19
40308	Critical Evaluation of Various Spontaneous Polarization Models and Induced Electric Fields in III-Nitride Multi-Quantum Wells. Materials, 2021, 14, 4935.	1.3	6
40309	A first principle investigation of the non-synthesized cubic perovskite LiGeX3 (X=I, Br, and Cl). Materials Science in Semiconductor Processing, 2021, 131, 105858.	1.9	18
40310	Strain induced modification in electronic properties of monolayer InSb. Superlattices and Microstructures, 2021, 156, 106979.	1.4	6
40311	Electronic and mechanical properties of two-dimensional hybridized CuOâ€“FeO superlattice: A first principles study. Superlattices and Microstructures, 2021, 156, 106966.	1.4	2

#	Article	IF	Citations
40312	Electronic structures and physical properties of Mg, C, and S doped g-GaN. Superlattices and Microstructures, 2021, 156, 106930.	1.4	5
40313	First-principles calculations of thermodynamic properties of Ni sulfides in the upper mantle. Physics and Chemistry of Minerals, 2021, 48, 1.	0.3	1
40314	Structural, Physical, and Thermodynamic Properties of Aragonitic CaxSr1â€“xCO3 Solid Solutions. Journal of Physical Chemistry C, 2021, 125, 17474-17481.	1.5	4
40315	Can Metal Intermixing Cooperatively Improve Perovskites as Redox Materials for Thermochemical Ammonia Synthesis? A Case Study on (Sr,Y)(Ti,Ru)O₃. Journal of Physical Chemistry C, 2021, 125, 17019-17030.	1.5	2
40316	Negative Linear Compressibility in [NH₃NH₂]Co(HCOO)₃ and Its Structural Origin Revealed from First Principles. Journal of Physical Chemistry Letters, 2021, 12, 7560-7565.	2.1	8
40317	Ultrahigh stiffness and anisotropic Dirac cones in BeN4 and MgN4 monolayers: a first-principles study. Materials Today Nano, 2021, 15, 100125.	2.3	23
40318	Structural and Electronic Properties of Intertwined Defect in Ruddlesdenâ€“Popper 2D Perovskites Study Using Density Functional Theory Calculations. Multiscale Science and Engineering, 2021, 3, 205.	0.9	0
40319	Application of Density Functional Tight Binding and Machine Learning to Evaluate the Stability of Biomass Intermediates on the Rh(111) Surface. Journal of Physical Chemistry C, 2021, 125, 18210-18216.	1.5	7
40320	Uncertainty Quantification and Error Propagation in the Enthalpy and Entropy of Surface Reactions Arising from a Single DFT Functional. Journal of Physical Chemistry C, 2021, 125, 18187-18196.	1.5	8
40321	Thermoelectric and optical properties of 2D hexagonal Dirac material Be3X2 (Xâ€‰=â€‰C, Si, Ge, Sn): A density functional theory study. Journal of Applied Physics, 2021, 130, .	1.1	4
40322	Carbon complexes in highly C-doped GaN. Physical Review B, 2021, 104, .	1.1	18
40323	A combinatorial study of electrochemical anion intercalation into graphite. Materials Research Express, 2021, 8, 085502.	0.8	5
40324	N-type diamond semiconductor induced by co-doping selenium and boron. Computational Materials Science, 2021, 196, 110515.	1.4	9
40325	Effects of alloying elements on the stability and mechanical properties of Î²-Ti0.5X0.5 (X = V, Cr, Mn, Fe;) Tj ETQq1 1 0.784314 rgBT /Ov Communications, 2021, 334-335, 114395.	0.9	1
40326	Interactions between Reduced Graphene Oxide with Monomers of (Calcium) Silicate Hydrates: A First-Principles Study. Nanomaterials, 2021, 11, 2248.	1.9	23
40327	Ptâ€“Cu Interaction Induced Construction of Single Pt Sites for Synchronous Electron Capture and Transfer in Photocatalysis. Advanced Functional Materials, 2021, 31, 2104343.	7.8	50
40328	Computational identification of efficient 2D Aluminium chalcogenides monolayers for optoelectronics and photocatalysts applications. Applied Surface Science, 2021, 556, 149561.	3.1	31
40329	A theoretical investigation of topological phase modulation in carbide MXenes: Role of image potential states. Carbon, 2021, 181, 370-378.	5.4	6

#	Article	IF	Citations
40330	Ab Initio Studies of Bimetallic-Doped {0001} Hematite Surface for Enhanced Photoelectrochemical Water Splitting. Catalysts, 2021, 11, 940.	1.6	6
40331	Anisotropic to Isotropic Transition in Monolayer Group-IV Tellurides. Materials, 2021, 14, 4495.	1.3	4
40332	Atomically dispersed Pb ionic sites in PbCdSe quantum dot gels enhance room-temperature NO2 sensing. Nature Communications, 2021, 12, 4895.	5.8	40
40333	First-Principles Study of Carrier-Mediated and Vacancy-Induced Ferromagnetism in Molybdenum Disulfide Monolayer. Solid State Phenomena, 0, 323, 166-174.	0.3	0
40334	Feature Analysis: Revealing the Importance of Bulk Nearest-Neighbor Distance Feature for CO Adsorption Energy on Bimetallic Alloys. Journal of Physical Chemistry C, 2021, 125, 19268-19275.	1.5	2
40335	Electronic structure transition of cubic CsSnCl3 under pressure: effect of rPBE and PBEsol functionals and GW method. Heliyon, 2021, 7, e07796.	1.4	7
40336	Structural, electronic and optical properties of GeX (Xâ€‰=â€‰N, P and As) monolayer: under stress and strain conditions. Optical and Quantum Electronics, 2021, 53, 1.	1.5	8
40337	Substrateâ€Adatom Interface Engineering of Transition Metal Decorated Boronâ€Doped Graphene Sheet for Enhanced Adsorption of Xe and Kr â€“ A Systematic Ab initio Study. Advanced Theory and Simulations, 2021, 4, 2100187.	1.3	2
40338	Designing Allâ€Inorganic EuOâ€Sensitized TiO 2 Solar Cell from 4fâ€3d Composite Bandgap Structure. Advanced Theory and Simulations, 2021, 4, 2100235.	1.3	2
40339	Boson Subsidiary Solver (BoSS) v1.1. Computer Physics Communications, 2021, 265, 107991.	3.0	5
40340	Two-dimensional MoS₂2H, 1T, and 1T^{â€²}crystalline phases with incorporated adatoms: theoretical investigation of electronic and optical properties. Applied Optics, 2021, 60, G232.	0.9	8
40341	Pressure- and temperature-dependent physical metallurgy in a face-centered cubic NiCoFeCrMn high entropy alloy and its subsystems. Journal of Alloys and Compounds, 2021, 873, 159843.	2.8	8
40342	Theoretical Screening of Metal Borocarbide Sheets for High-Capacity and High-Rate <mml:math xmlns:mml="http://www.w3.org/1998/Math/MathML" display="inline" overflow="scroll"><mml:mi>Li</mml:mi></mml:math> - and <mml:math xmlns:mml="http://www.w3.org/1998/Math/MathML" display="inline" overflow="scroll"><mml:mi>Na</mml:mi></mml:math> -Ion Batteries. Physical Review Applied, 2021, 16, .	1.5	15
40343	Probing into the In-Situ Exsolution Mechanism of Metal Nanoparticles from Doped Ceria Host. Nanomaterials, 2021, 11, 2114.	1.9	3
40344	Vibrational and Thermodynamic Properties of Hydrous Iron-Bearing Lowermost Mantle Minerals. Minerals (Basel, Switzerland), 2021, 11, 885.	0.8	0
40345	Multiple Strategies toward Advanced P2-Type Layered Na_xMnO₂ for Low-Cost Sodium-Ion Batteries. ACS Applied Energy Materials, 2021, 4, 8183-8192.	2.5	11
40346	A study of single-/multi-layer structures of CH3NH3SnI3 by density functional theory. Optical and Quantum Electronics, 2021, 53, 1.	1.5	4
40347	Nickel/Molybdenum Bimetallic Alloy for Dry Reforming of Methane: A Coverage-Dependence Microkinetic Model Simulation Based on the First-Principles Calculation. Journal of Physical Chemistry C, 2021, 125, 18653-18664.	1.5	16

#	Article	IF	Citations
40348	Solid Solution Yb2â€“xCaxCdSb2: Structure, Thermoelectric Properties, and Quality Factor. Inorganic Chemistry, 2021, 60, 13596-13606.	1.9	11
40349	Facet-Dependent Mn Doping on Shaped Co₃O₄ Crystals for Catalytic Oxidation. ACS Catalysis, 2021, 11, 11066-11074.	5.5	69
40350	Strain-Induced Magnetic Transitions in SrMO_{2.5} (M = Mn, Fe) Thin Films with Ordered Oxygen Vacancies. Inorganic Chemistry, 2021, 60, 13161-13167.	1.9	1
40351	Mechanisms of Double-Bond Isomerization Reactions of n-Butene on Different Lewis Acids. ACS Catalysis, 2021, 11, 11293-11304.	5.5	13
40352	Effect of Co doping in tailoring the crystallite size, surface morphology and optical band gap of CuO thin films prepared via thermal spray pyrolysis. Surfaces and Interfaces, 2021, 25, 101269.	1.5	12
40353	Thermoelectric Properties of SrTi(1â€‰â^'â€‰x)Zr(x)O3 Alloys: a First-Principle Study. Journal of Superconductivity and Novel Magnetism, 2021, 34, 2479-2484.	0.8	1
40354	Efficient Ohmic contacts and built-in atomic sublayer protection in MoSi2N4 and WSi2N4 monolayers. Npj 2D Materials and Applications, 2021, 5, .	3.9	98
40355	Hg₃P₂S₈: A New Promising Infrared Nonlinear Optical Material with a Large Second-Harmonic Generation and a High Laser-Induced Damage Threshold. Chemistry of Materials, 2021, 33, 6514-6521.	3.2	74
40356	Adsorption of Si(OH)4 and Al(OH)4 onto arsenopyrite surface: Exploring the sealing feasibility of geopolymer to arsenopyrite. Minerals Engineering, 2021, 170, 107017.	1.8	12
40357	Pulverizationâ€Tolerant CuSe Nanoflakes with High (110) Planar Orientation for Highâ€Performance Magnesium Storage. Advanced Functional Materials, 2021, 31, 2104730.	7.8	52
40358	High Voltageâ€Stabilized Graphdiyne Cathode Interface. Small, 2021, 17, e2102066.	5.2	18
40359	Switching Behavior of a Heterostructure Based on Periodically Doped Graphene Nanoribbon. Physical Review Applied, 2021, 16, .	1.5	55
40360	Density Functional Theory Study of the Partial Oxidation of Methane to Methanol on Au and Pd Surfaces. Journal of Physical Chemistry C, 2021, 125, 18770-18785.	1.5	2
40361	Selective transfer hydrogenation of biomass derived furanic molecules using cyclohexanol as a hydrogen donor over nanostructured Cu/MgO catalyst. Molecular Catalysis, 2021, 513, 111812.	1.0	8
40362	Re-Co alloys and single-atom Re catalysts in ammonia synthesis: A DFT study. Molecular Catalysis, 2021, 513, 111801.	1.0	0
40363	DFT study of silicene on metal (Al, Ag, Au) substrates of various thicknesses. Physics Letters, Section A: General, Atomic and Solid State Physics, 2021, 408, 127487.	0.9	11
40364	Paraffin-Enabled Compressive Folding of Two-Dimensional Materials with Controllable Broadening of the Electronic Band Gap. ACS Applied Materials & Interfaces, 2021, 13, 40922-40931.	4.0	8
40365	Atomic-scale defects restricting structural superlubricity: Ab initio study on the example of the twisted graphene bilayer. Physical Review B, 2021, 104, .	1.1	9

#	Article	IF	Citations
40366	From thermal conductive to thermal insulating: Effect of carbon vacancy content on lattice thermal conductivity of ZrC. Journal of Materials Science and Technology, 2021, 82, 105-113.	5.6	22
40367	Surface microenvironment engineering of black V2O5 nanostructures for visible light photodegradation of methylene blue. Journal of Alloys and Compounds, 2021, 871, 159615.	2.8	26
40368	Low thermal conductivity and semimetallic behavior in some TiNiSi structure-type compounds. Physical Review Materials, 2021, 5, .	0.9	3
40369	Unraveling electrochemical oxygen reduction mechanism on singleâ€atom catalysts by a computational investigation. International Journal of Energy Research, 2022, 46, 1032-1042.	2.2	6
40370	New insights on CO and CO2 hydrogenation for methanol synthesis: The key role of adsorbate-adsorbate interactions on Cu and the highly active MgO-Cu interface. Journal of Catalysis, 2021, 400, 325-331.	3.1	32
40371	Observation of a molecular muonium polaron and its application to probing magnetic and electronic states. Physical Review B, 2021, 104, .	1.1	0
40372	Uniform Deposition and Effective Confinement of Lithium in Three-Dimensional Interconnected Microchannels for Stable Lithium Metal Anodes. ACS Applied Materials & Interfaces, 2021, 13, 39311-39321.	4.0	15
40373	Elucidating active sites and decomposition mechanisms for oxythiomolybdate clusters (Mo₂O₂S_x, xÂ=Â6;8) as catalyzers for hydrogen evolution reactions. Electrochemical Science Advances, 2022, 2, e2100088.	1.2	2
40374	A New Type of Largeâ€Gap Quantum Spin Hall Insulator Material ZrSe₅. Physica Status Solidi (B): Basic Research, 2021, 258, 2100256.	0.7	2
40375	Computational study of <mml:math xmlns:mml="http://www.w3.org/1998/Math/MathML"><mml:mrow><mml:msub><mml:mi>Li</mml:mi><mml:mn>3</mml:mn></mml:mr and <mml:math xmlns:mml="http://www.w3.org/1998/Math/MathML"><mml:mrow><mml:msub><mml:mi>Li</mml:mi><mml:mn>3</mml:mn></mml:mr II. Stability analysis of pure phases and of model interfaces with Li. Physical Review Materials, 2021, 5, .	0.9	4
40376	Phase Relations in CaSiO3 System up to 100 GPa and 2500 K. Geochemistry International, 2021, 59, 791-800.	0.2	2
40377	Anion-exchange-mediated internal electric field for boosting photogenerated carrier separation and utilization. Nature Communications, 2021, 12, 4952.	5.8	45
40378	Enhanced H₂ Storage Capacity of Bilayer Hexagonal Boron Nitride (h-BN) Incorporating van der Waals Interaction under an Applied External Electric Field. ACS Omega, 2021, 6, 22374-22382.	1.6	17
40379	Correlations of Ionic Migration and Deep-Level Traps Leads to Surface Defect Formation in Perovskite Solar Cells. Journal of Physical Chemistry C, 2021, 125, 19551-19559.	1.5	10
40380	Computational Investigation of the Catalytic Hydrodeoxygenation of Propanoic Acid over a Cu(111) Surface. Journal of Physical Chemistry C, 2021, 125, 19276-19293.	1.5	3
40381	Roles of Polymerized Anionic Clusters Stimulating for Hydrolysis Deterioration in Li₇P₃S₁₁. Journal of Physical Chemistry C, 2021, 125, 19509-19516.	1.5	10
40382	The application of the nonlocal exchange potential matrix method to the study of ferromagnetic 3d transition metals. Chinese Journal of Physics, 2021, 72, 345-350.	2.0	2
40383	Atomic Scale Investigation of the CuPcâ€“MAPbX₃ Interface and the Effect of Non-Stoichiometric Perovskite Films on Interfacial Structures. ACS Nano, 2021, 15, 14813-14821.	7.3	8

#	Article	IF	Citations
40384	Theoretical investigation of the surface orientation impact on the hydrogen vacancy formation of MgH2. Surface Science, 2021, 710, 121850.	0.8	5
40385	Conversion of methane to methanol on C-doped boron nitride: A DFT study. Computational and Theoretical Chemistry, 2021, 1202, 113291.	1.1	8
40386	Extremely thin interlayer of multi-element intermetallic compound between Sn-based solders and FeCoNiMn high-entropy alloy. Applied Surface Science, 2021, 558, 149945.	3.1	21
40387	Development of Mg/Al/Si/O ReaxFF Parameters for Magnesium Aluminosilicate Glass Using an Artificial Neural Network-Assisted Genetic Algorithm. Journal of Physical Chemistry C, 2021, 125, 18380-18394.	1.5	13
40388	First principles study on the alkylation of benzene with ethene over different zeolites: Insight into the intrinsic mechanism and structure-reactivity relationship. Molecular Catalysis, 2021, 512, 111762.	1.0	1
40389	Novel two-dimensional Group-IV carbides containing C2 dimers: Sizable direct band gap, high carrier mobility, and anisotropic properties for nanoelectronics. Carbon, 2021, 181, 421-432.	5.4	17
40390	Mechanism of adhesion failure during interrupted cutting with cemented carbide tools: Experimental and ab-initio perspective. International Journal of Refractory Metals and Hard Materials, 2021, 98, 105549.	1.7	6
40391	Combined Spectroscopic and Computational Study of Nitrobenzene Activation on Non-Noble Metals-Based Mono- and Bimetallic Catalysts. Nanomaterials, 2021, 11, 2037.	1.9	5
40392	Real-Time Exciton Dynamics with Time-Dependent Density-Functional Theory. Physical Review Letters, 2021, 127, 077401.	2.9	17
40393	Interfacial interactions and structures of imidazolium-based ionic liquids on black phosphorus surface from first-principles. Journal of Molecular Liquids, 2021, 335, 116562.	2.3	7
40394	Investigation of transport in edge passivated armchair silicene nanoribbon field effect transistor by ab-initio based Wannierised tight binding. Superlattices and Microstructures, 2021, 156, 106933.	1.4	2
40395	Theoretical prediction on the immiscible Pb-Sn alloy stabilized on metal surfaces. Chemical Physics Letters, 2021, 776, 138696.	1.2	3
40396	Carbon Capture and Usage by MXenes. ACS Catalysis, 2021, 11, 11248-11255.	5.5	40
40397	Revisiting the BaBiO3 semiconductor photocatalyst: synthesis, characterization, electronic structure, and photocatalytic activity. Photochemical and Photobiological Sciences, 2021, 20, 1147-1160.	1.6	13
40398	Tuning the electronic and optical properties of Ga2SSe janus monolayer by adsorption of metals. Optical and Quantum Electronics, 2021, 53, 1.	1.5	4
40399	Facet effect of In2O3 for methanol synthesis by CO2 hydrogenation: A mechanistic and kinetic study. Surfaces and Interfaces, 2021, 25, 101244.	1.5	9
40400	First-principles study of the effect of Al and Hf impurities on Co3W antiphase boundary energies. Acta Materialia, 2021, 215, 117075.	3.8	2
40401	Adsorption of single metallic atoms on self-assembled molecular domain of terephthalic acid. Surfaces and Interfaces, 2021, 25, 101170.	1.5	0

#	Article	IF	Citations
40402	Extraordinarily strong magneto-responsiveness in phase-separated LaFe2Si. Acta Materialia, 2021, 215, 117083.	3.8	2
40403	Understanding phase equilibria in high-entropy alloys: I. Chemical potentials in concentrated solid solutions â€“ Atomic-scale investigation of AlCrFeMnMo. Journal of Alloys and Compounds, 2021, 872, 159745.	2.8	6
40404	Optoelectronic properties of 2D heterojunction ZrO2â€“ MoS2 material using first-principles calculations. Solid State Communications, 2021, 334-335, 114358.	0.9	16
40405	Calculating the hyperfine tensors for group-IV impurity-vacancy centers in diamond using hybrid density functional theory. Physical Review B, 2021, 104, .	1.1	9
40406	Band offset in semiconductor heterojunctions. Journal of Physics Condensed Matter, 2021, 33, 415002.	0.7	19
40407	Photocatalytic and sonocatalytic dye degradation by sulfur vacancy rich ZnS nanopowder. Journal of Nanoparticle Research, 2021, 23, 1.	0.8	8
40408	Magnetic single atom catalyst in C2N to induce adsorption selectivity toward oxidizing gases. Scientific Reports, 2021, 11, 15848.	1.6	10
40409	Orthorhombic C36: a sp2â€“sp3 carbon with pressure-induced metallization and superconductivity. Journal of Materials Science, 2021, 56, 17665-17673.	1.7	7
40410	Enhancement of vacancy diffusion by C and N interstitials in the equiatomic FeMnNiCoCr high entropy alloy. Acta Materialia, 2021, 215, 117093.	3.8	20
40411	First principle research on Ga rich GaAs0.5P0.5(001) Î²2(4â€‰Ã—â€‰2) and As(P) rich Î²2(2â€‰Ã—â€‰4) reconstruction surfaces with and without Cs adsorption. Optical and Quantum Electronics, 2021, 53, 1.	1.5	1
40412	The effect of chemical composition on the properties of LTA zeolite: A theoretical study. Computational Materials Science, 2021, 196, 110557.	1.4	14
40413	Development of an interatomic potential for Fe-He by neural network. Computational Materials Science, 2021, 196, 110549.	1.4	3
40414	Experimental and theoretical realization of an advanced bifunctional 2D Î´-MnO2 electrode for supercapacitor and oxygen evolution reaction via defect engineering. International Journal of Hydrogen Energy, 2021, 46, 28028-28042.	3.8	20
40415	Unravelling the Znâ€Cu Interaction during Activation of a Znâ€promoted Cu/MgO Model Methanol Catalyst. ChemCatChem, 2021, 13, 4120-4132.	1.8	20
40416	As a single atom Pd outperforms Pt as the most active co-catalyst for photocatalytic H2 evolution. IScience, 2021, 24, 102938.	1.9	33
40417	Î±-Fe2O3 as a versatile and efficient oxygen atom transfer catalyst in combination with H2O as the oxygen source. Nature Catalysis, 2021, 4, 684-691.	16.1	112
40418	Synthesis of Single- and Few-Layer Nitrogen-doped Graphene and Layer-Dependent Surface-Enhanced Raman Scattering Properties. Journal of Physical Chemistry C, 2021, 125, 17831-17840.	1.5	7
40419	Single-atom catalysts with anionic metal centers: Promising electrocatalysts for the oxygen reduction reaction and beyond. Journal of Energy Chemistry, 2021, 63, 285-293.	7.1	15

#	Article	IF	Citations
40420	Self-Assembly and Magnetic Order of Bi-Molecular 2D Spin Lattices of M(II,III) Phthalocyanines on Au(111). Magnetochemistry, 2021, 7, 119.	1.0	4
40421	Changes in the physical properties of Mg2Ir3Si compared to Li2IrSi3 due to the substitution of Li by Mg and the exchange of positions between Ir and Si. Solid State Communications, 2021, 334-335, 114361.	0.9	0
40422	Adsorption of alkali metal atoms on predicted C3N2 sheet. Solid State Communications, 2021, 334-335, 114367.	0.9	2
40423	Strain tuned low thermal conductivity in Indium Antimonide (InSb) through increase in anharmonic phonon scattering - A first-principles study. Solid State Communications, 2021, 334-335, 114378.	0.9	3
40424	New isostructural halide double perovskites Cs2GeNiX6 (X= Cl, Br) for semiconductor spintronics and thermoelectric advancements. Journal of Solid State Chemistry, 2021, 300, 122196.	1.4	13
40425	Conformal coating of lithium-zinc alloy on 3D conducting scaffold for high areal capacity dendrite-free lithium metal batteries. Carbon, 2021, 181, 99-106.	5.4	19
40426	Pd atomic layer coating enhances CO2 hydrogenation to CH3OH fuel on Cu@Pd(111) core-shell structure catalyst. Journal of Environmental Chemical Engineering, 2021, 9, 105749.	3.3	3
40427	Anharmonic lattice dynamics of SnS across phase transition: A study using high-dimensional neural network potential. Applied Physics Letters, 2021, 119, .	1.5	5
40428	Work Function Trends and New Low-Work-Function Boride and Nitride Materials for Electron Emission Applications. Journal of Physical Chemistry C, 2021, 125, 17400-17410.	1.5	13
40429	CoAsS Kristalinin BazÄ± Fiziksel Ã–zelliklerinin BasÄ±nÃ§ AltÄ±nda Ä°ncelenmesi. YÃ¼zÃ¼ncÃ¼ YÄ±l Ã¼niversitesi Fen Bilimleri EnstitÃ¼sÃ¼ Dergisi, 0, , .	0.0	0
40430	Structural and Optoelectronic Properties of Two-Dimensional Ruddlesdenâ€“Popper Hybrid Perovskite CsSnBr3. Nanomaterials, 2021, 11, 2119.	1.9	7
40431	Differentiable sampling of molecular geometries with uncertainty-based adversarial attacks. Nature Communications, 2021, 12, 5104.	5.8	34
40432	Electronic structure of a borophene layer in rare-earth aluminum/chromium boride and its hydrogenated derivative borophane. Physical Review Materials, 2021, 5, .	0.9	13
40433	Emergence of Topological Edge States in Oxidized Î±-In₂Se₃ Nanosheets: Implications for Field-Effect Transistors. ACS Applied Nano Materials, 2021, 4, 8154-8161.	2.4	7
40434	Nonlinear optical property and application of yttrium oxide in erbium-doped fiber lasers. Optics Express, 2021, 29, 29402.	1.7	26
40435	Firstâ€Principles Investigation of the Effect of Vanadium Doping on Hydrogen Incorporation in Tungsten. Crystal Research and Technology, 2021, 56, 2100115.	0.6	2
40436	Biaxial Strain-Induced Electronic Structure and Optical Properties of SiP$$_{2}$$S Monolayer. Journal of Electronic Materials, 2021, 50, 6253-6260.	1.0	11
40437	First-principles Study of Monolayer - <mml:math xmlns:mml="http://www.w3.org/1998/Math/MathML" display="inline" overflow="scroll"><mml:mi>p</mml:mi><mml:mi>e</mml:mi><mml:mi>n</mml:mi><mml:mi>t</mml:mi><mml:mi>a</mml:mi></mml:math> - <mml:math xmlns:mml="http://www.w3.org/1998/Math/MathML" display="inline" overflow="scroll"><mml:msub><mml:mrow><mml:mi>Co</mml:mi><mml:mi mathvariant="normal">3</mml:mi></mml:mrow><mml:mrow><mml:mn>2</mml:mn></mml:mrow></mml:msub></mml:math> as a p	1.5	26

#	Article	IF	Citations
40438	Designing highly incompressible transition metal nitrides: A new class of W0.5Al0.5N phases. Journal of Applied Physics, 2021, 130, 065105.	1.1	1
40439	Nonmetalâ€toâ€metal transition in dense fluid helium. Contributions To Plasma Physics, 0, , e202100105.	0.5	2
40440	Fast and robust all-electron density functional theory calculations in solids using orthogonalized enriched finite elements. Physical Review B, 2021, 104, .	1.1	9
40441	Alloying Process at the Interface of Au-Li Studied Using Neural Network Potential. Vacuum and Surface Science, 2021, 64, 369-374.	0.0	0
40442	Simulation-Based Defect Engineering in â€œÎ±-Spodumeneâ€• ChemEngineering, 2021, 5, 57.	1.0	0
40443	Au³⁺ Species Boost the Catalytic Performance of Au/ZnO for the Semi-hydrogenation of Acetylene. ACS Applied Materials & Interfaces, 2021, 13, 40429-40440.	4.0	19
40444	Pressure-Induced Polymorphic Transformations of Ethylenediamine Bisborane. Journal of Physical Chemistry C, 2021, 125, 18614-18622.	1.5	6
40445	Clues from Ab Initio Calculations on Titanium Isotopic Fractionation in Tholeiitic and Calc-Alkaline Magma Series. ACS Earth and Space Chemistry, 2021, 5, 2466-2480.	1.2	19
40446	Theoretical Study of Oxygen Vacancy on Indium Oxide for Promoted Photothermal Catalytic Water Splitting. Journal of Physical Chemistry C, 2021, 125, 19294-19300.	1.5	4
40447	Accelerating the discovery of novel Î³/Î³' Co-based superalloys by probing temperature and alloying effects on the Î³' precipitates. Materialia, 2021, 18, 101171.	1.3	6
40448	Spinâ€Đependent Charge Transport in 1D Chiral Hybrid Leadâ€Bromide Perovskite with High Stability. Advanced Functional Materials, 2021, 31, 2104605.	7.8	44
40449	Direct Oxidative Amination of the Methyl Câ€“H Bond in N-Heterocycles over Metal-Free Mesoporous Carbon. ACS Catalysis, 2021, 11, 10902-10912.	5.5	11
40450	Strain induced structural phase transition in TM6X6 (TM = Mo, W; X = S, Se, Te) nanowires. Journal of Solid State Chemistry, 2021, 300, 122194.	1.4	3
40451	Different Effects of Mg and Si Doping on the Thermal Transport of Gallium Nitride. Frontiers in Materials, 2021, 8, .	1.2	9
40452	Strain-driven modulation of the electronic, optical and thermoelectric properties of <mml:math xmlns:mml="http://www.w3.org/1998/Math/MathML" display="inline" id="d1e158" altimg="si13.svg"><mml:mi>Î²</mml:mi></mml:math>-antimonene monolayer: A hybrid functional study. Materials Science in Semiconductor Processing, 2021, 131, 105878.	1.9	5
40453	Oxygen Evolution Reaction on the Fe₃O₄(001) Surface: Theoretical Insights into the Role of Terminal and Bridging Oxygen Atoms. Journal of Physical Chemistry C, 2021, 125, 18752-18761.	1.5	8
40454	Oriented hyperlens based on passivated porous graphene phases for sub-diffraction visible imaging. Optical Materials Express, 2021, 11, 2839.	1.6	0
40455	Prediction of a new zigzag shape Be2C monolayer as a photo-catalyst for water splitting: A first principles study. Superlattices and Microstructures, 2021, 156, 106947.	1.4	1

#	Article	IF	Citations
40456	Revealing pressure-driven structural transitions in the hybrid improper ferroelectric <mml:math xmlns:mml="http://www.w3.org/1998/Math/MathML"><mml:msub><mml:mi mathvariant="normal">Sr</mml:mi><mml:mn>3</mml:mn></mml:msub><mml:msub><mml:mi mathvariant="normal">Sn</mml:mi><mml:mn>2</mml:mn></mml:msub><mml:msub><mml:mi mathvariant="normal">O</mml:mi><mml:mn>7</mml:mn></mml:msub></mml:math>. Physical Review B, 2021, 104, .	1.1	8
40457	Comment on â€˜High- Tc superconductivity in H₃S: pressure effects on the superconducting critical temperature and Cooper pair distribution functionâ€™. Superconductor Science and Technology, 2021, 34, 098002.	1.8	2
40458	Angle-dependent electron confinement in graphene moirÃ© superlattices. Physical Review B, 2021, 104, .	1.1	5
40459	Atomically dispersed S-Fe-N4 for fast kinetics sodium-sulfur batteries via a dual function mechanism. Cell Reports Physical Science, 2021, 2, 100531.	2.8	31
40460	Pressure-Induced Transition from Spin to Superconducting States in Novel MnN₂. ACS Omega, 2021, 6, 21830-21836.	1.6	2
40461	Combined Effects of Carbon and Nitrogen in Fe20Cr6Mn6CN Alloys from First-Principles Calculation. Journal of Materials Engineering and Performance, 2021, 30, 8322.	1.2	1
40462	Dynamical Immiscibility of Aqueous Carbonate Fluid in the Shortiteâ€“Water System at High-Pressureâ€“Temperature Conditions. Journal of Physical Chemistry C, 2021, 125, 18501-18509.	1.5	5
40463	Near edge absorption studies of pure and impure $$hbox {NbSe}_{2}$$; theory and experiment. Journal of Materials Science, 2021, 56, 17062-17079.	1.7	2
40464	Arene and functionalized arene based two dimensional <scp>organicâ€“inorganic</scp> hybrid perovskites for photovoltaic applications. Journal of Computational Chemistry, 2021, 42, 1982-1990.	1.5	16
40465	Application of germanene monolayers as efficient anchoring material to immobilize lithium polysulfides in Li-S batteries. Applied Surface Science, 2021, 558, 149850.	3.1	8
40466	Enhanced SOx sensing performance of BC3 nanosheets functionalized with Na atoms: A first-principles study. Physica E: Low-Dimensional Systems and Nanostructures, 2021, 132, 114762.	1.3	6
40467	A gap opening in graphene covered by a conducting polymer: The role of many-body effects. Physica B: Condensed Matter, 2021, 614, 413036.	1.3	2
40468	Double activation of oxygen intermediates of oxygen reduction reaction by dual inorganic/organic hybrid electrocatalysts. Nano Energy, 2021, 86, 106048.	8.2	5
40469	Mechanistic insights into the CO oxidation reaction catalyzed by P-coordinated metal-doped graphene: The roles of phosphorus and metal atom. Applied Surface Science, 2021, 556, 149776.	3.1	8
40470	H- and T-Li2O monolayers: Latest addition to 2D flatlands. Applied Surface Science, 2021, 556, 149737.	3.1	5
40471	Properties of the Pt(111)/electrolyte electrochemical interface studied with a hybrid DFTâ€“solvation approach. Journal of Physics Condensed Matter, 2021, 33, 444004.	0.7	22
40472	In situ study on the compression deformation of MoNbTaVW high-entropy alloy. Journal of Alloys and Compounds, 2021, 871, 159557.	2.8	7
40473	Bimetallic effects on Zn-Cu electrocatalysts enhance activity and selectivity for the conversion of CO2 to CO. Chem Catalysis, 2021, 1, 663-680.	2.9	42

#	Article	IF	Citations
40474	Computational investigation of structural, magnetic, electronic and optical properties of the cluster Mn-X6 (X=P, S, Cl, Br or Te) doped monolayer WSe2. Thin Solid Films, 2021, 732, 138793.	0.8	2
40475	Fundamental properties of octalithium plumbate ceramic breeder material. Journal of Nuclear Materials, 2021, 552, 152982.	1.3	3
40476	Effect of B-doping on the mechanical properties, thermal stability and oxidation resistance of TiAlN coatings. International Journal of Refractory Metals and Hard Materials, 2021, 98, 105531.	1.7	20
40477	Uranium In Situ Electrolytic Deposition with a Reusable Functional Grapheneâ€Foam Electrode. Advanced Materials, 2021, 33, e2102633.	11.1	52
40478	Role of the rare-earth doping on the multiferroic properties of BaTiO3: First-principles calculation. Physica B: Condensed Matter, 2021, 615, 413107.	1.3	6
40479	Vanadium based zinc spinel oxides: Potential materials as photoanode for water oxidation and optoelectronic devices. International Journal of Hydrogen Energy, 2021, 46, 28110-28120.	3.8	1
40480	CoCrFeNi High-Entropy Alloy as an Enhanced Hydrogen Evolution Catalyst in an Acidic Solution. Journal of Physical Chemistry C, 2021, 125, 17008-17018.	1.5	25
40481	A First-Principles Study of the Mechanism and Site Requirements for CO₂ Methanation over CeO₂-Supported Ru Catalyst. Journal of Physical Chemistry C, 2021, 125, 18161-18169.	1.5	10
40482	Effect of metal doping on visible light absorption and optical properties of lithium niobate (LiNbO3) crystal: a first-principles calculation. Bulletin of Materials Science, 2021, 44, 1.	0.8	13
40483	Mechanical and thermodynamic stabilities, half-metallic and thermoelectric comparison between CoFeMnZ (Zâ€‰=â€‰Si, Ge) Heuslers by DFT. Applied Physics A: Materials Science and Processing, 2021, 127, 1.	1.1	2
40484	Understanding Znâ€Ion Insertion Chemistry through Nonaqueous Electrochemical Investigation of 2Hâ€NbSe 2. Advanced Materials Interfaces, 2021, 8, 2100878.	1.9	3
40485	Shear band-driven precipitate dispersion for ultrastrong ductile medium-entropy alloys. Nature Communications, 2021, 12, 4703.	5.8	70
40486	Catalytic Role of Adsorption of Electrolyte/Molecules as Functional Ligands on Two-Dimensional TM-N₄ Monolayer Catalysts for the Electrocatalytic Nitrogen Reduction Reaction. ACS Applied Materials & Interfaces, 2021, 13, 40590-40601.	4.0	11
40487	Electronic Mechanism of Martensitic Transformation in Nb-doped NiTi Alloys: A First-Principles Investigation. ACS Omega, 2021, 6, 22033-22038.	1.6	2
40488	Surface structure of mass-selected niobium oxide nanoclusters on Au(111). Nanotechnology, 2021, 32, 475601.	1.3	7
40489	Facile Realization of Boosted Nearâ€Infraredâ€Visible Light Driven Photocatalytic Activities of BiOF Nanoparticles through Simultaneously Exploiting Doping and Upconversion Strategy. Advanced Materials Interfaces, 2021, 8, 2100749.	1.9	25
40490	Oxygen-Defect Enhanced Anion Adsorption Energy Toward Super-Rate and Durable Cathode for Niâ€“Zn Batteries. Nano-Micro Letters, 2021, 13, 167.	14.4	52
40491	Beyond graphene: Clean, hydrogenated and halogenated silicene, germanene, stanene, and plumbene. Progress in Surface Science, 2021, 96, 100615.	3.8	42

#	Article	IF	Citations
40492	Electronic metal-support interactions and their promotional effect on CO2 methanation on Ru/ZrO2 catalysts. Journal of Catalysis, 2021, 400, 407-420.	3.1	44
40493	Single, double and triple cobalt atoms confined in 2D regular framework for oxygen electrocatalysis. Journal of Alloys and Compounds, 2021, 872, 159689.	2.8	1
40494	First- and second-order phase transitions in RE6Co2Ga (RE = Ho, Dy or Gd) cryogenic magnetocaloric materials. Science China Materials, 2021, 64, 2846-2857.	3.5	62
40495	Insights into the impact of metal tin substitution on methylammonium lead bromide perovskite performance for photovoltaic application. Solar Energy, 2021, 224, 76-81.	2.9	10
40496	Study of the Diffusion Properties of Oxygen in TiO2. Journal of Experimental and Theoretical Physics, 2021, 133, 169-174.	0.2	13
40497	Tunable local and global piezopotential properties of graded InGaN nanowires. Nano Energy, 2021, 86, 106125.	8.2	4
40498	Electronic, optical, and vibrational properties of B3N3H6 from first-principles calculations. Journal of Molecular Modeling, 2021, 27, 241.	0.8	0
40499	Indirect light absorption model for highly strained silicon infrared sensors. Journal of Applied Physics, 2021, 130, .	1.1	6
40500	Study of the solar perovskite CsMBr3 (M=Pb or Ge) photovoltaic materials: Band-gap engineering. Solid State Sciences, 2021, 118, 106679.	1.5	20
40501	First principles study on formation and migration energies of sodium and lithium in graphite. Physical Review Materials, 2021, 5, .	0.9	2
40502	Band Alignment in Monolayer Boron Phosphide with Janus <mml:math xmlns:mml="http://www.w3.org/1998/Math/MathML" display="inline" overflow="scroll"><mml:mrow><mml:mi>Mo</mml:mi><mml:mi mathvariant="normal">S</mml:mi><mml:mi>Se</mml:mi></mml:mrow></mml:math> Heterobilayers under Strain and Electric Field. Physical Review Applied, 2021, 16, .	1.5	31
40503	Demonstration of an x-ray Raman spectroscopy setup to study warm dense carbon at the high energy density instrument of European XFEL. Physics of Plasmas, 2021, 28, 082701.	0.7	11
40504	Reaction mechanism of dichloromethane oxidation on LaMnO3 perovskite. Chemosphere, 2021, 277, 130194.	4.2	8
40505	Strain-induced electronic, stability and enhancement of thermoelectric performance of 2D Si2C3 monolayer: An emerging material for renewable energy. Physica E: Low-Dimensional Systems and Nanostructures, 2021, 132, 114769.	1.3	3
40506	Coupling between bulk thermal defects and surface segregation dynamics. Physical Review B, 2021, 104, .	1.1	3
40507	Computational study of mechanical stability and phonon properties of MXenes Mo2ScC2T2 (Tâ€‰=â€‰O and) Tj ETQq1 1 0.78431	1.1	2
40508	Polymorph of LiAlP₂O₇: Combined Computational, Synthetic, Crystallographic, and Ionic Conductivity Study. Inorganic Chemistry, 2021, 60, 14083-14095.	1.9	7
40509	Evolution of Structural, Thermal, Optical, and Vibrational Properties of Sc₂S₃, ScCuS₂, and BaScCuS₃ Semiconductors. European Journal of Inorganic Chemistry, 2021, 2021, 3355-3366.	1.0	2

#	Article	IF	Citations
40510	Understanding creep of a single-crystalline Co-Al-W-Ta superalloy by studying the deformation mechanism, segregation tendency and stacking fault energy. Acta Materialia, 2021, 214, 117019.	3.8	23
40511	Band gap and emission wavelength tuning of Sr-doped BaTiO3 (BST) perovskites for high-efficiency visible-light emitters and solar cells. Materials Science in Semiconductor Processing, 2021, 130, 105837.	1.9	17
40512	Machine learning assisted screening of non-rare-earth elements for Mg alloys with low stacking fault energy. Computational Materials Science, 2021, 196, 110544.	1.4	9
40513	Impact of anionic system modification on the desired properties for CuGa(S1â^'Se)2 solid solutions. Computational Materials Science, 2021, 196, 110553.	1.4	5
40514	Strain tuned thermal conductivity reduction in Indium Arsenide (InAs) â€“ A first-principles study. Computational Materials Science, 2021, 196, 110531.	1.4	4
40515	Theoretical design of ruthenium single-atom catalysts with different substrates for acetylene hydrochlorination. Molecular Catalysis, 2021, 513, 111826.	1.0	3
40516	Collaborative motion of helium and self-interstitial atoms enhanced self-healing efficiency of irradiation-induced defects in tungsten. Nuclear Fusion, 2021, 61, 106017.	1.6	4
40517	Encapsulation and Adsorption of Halogens into Single-Walled Carbon Nanotubes. Micro, 2021, 1, 140-150.	0.9	2
40518	X-ray Spectroscopy Fingerprints of Pristine and Functionalized Graphene. Journal of Physical Chemistry C, 2021, 125, 18234-18246.	1.5	9
40519	Dissociation of water on atomic oxygen-covered Rh nanoclusters supported on graphene/Ru(0001). Journal of Chemical Physics, 2021, 155, 074701.	1.2	1
40520	Interfacial Bonding Controls Friction in Diamondâ€“Rock Contacts. Journal of Physical Chemistry C, 2021, 125, 18395-18408.	1.5	9
40521	Antiscaling Evaluation and Quantum Chemical Studies of Nitrogen-Free Organophosphorus Compounds for Oilfield Scale Management. Industrial & Engineering Chemistry Research, 2021, 60, 12175-12188.	1.8	12
40522	Electrolyte-Guided Design of Electroreductive CO Coupling on Copper Surfaces. ACS Applied Energy Materials, 2021, 4, 8201-8210.	2.5	6
40523	Factors Governing Oxygen Vacancy Formation in Oxide Perovskites. Journal of the American Chemical Society, 2021, 143, 13212-13227.	6.6	75
40524	Two-Phase Transition Induced Amorphous Metal Phosphides Enabling Rapid, Reversible Alkali-Metal Ion Storage. ACS Nano, 2021, 15, 13486-13494.	7.3	23
40525	Ni-Al mixed metal oxide with rich oxygen vacancies: CO methanation performance and density functional theory study. Chinese Journal of Chemical Engineering, 2022, 46, 73-83.	1.7	1
40526	Defects Engineering of Lightweight Metalâ€“Organic Frameworks-Based Electrocatalytic Membrane for High-Loading Lithiumâ€“Sulfur Batteries. ACS Nano, 2021, 15, 13803-13813.	7.3	62
40527	NO Electroreduction by Transition Metal Dichalcogenides with Chalcogen Vacancies. ChemElectroChem, 2021, 8, 3113-3122.	1.7	19

#	Article	IF	Citations
40528	First-principles investigation of CO2, CO, and O2 adsorptions on the (001)-reconstructed surfaces of CsPbX3 (X = Cl, Br, and I) perovskites. Surfaces and Interfaces, 2021, 25, 101264.	1.5	2
40529	Manipulating Intermediates at the Auâ€“TiO₂ Interface over InP Nanopillar Array for Photoelectrochemical CO₂ Reduction. ACS Catalysis, 2021, 11, 11416-11428.	5.5	48
40530	Carbon Deposition on Heterogeneous Pt Catalysts Promotes the Selective Hydrogenation of Halogenated Nitroaromatics. ACS Applied Materials & Interfaces, 2021, 13, 52193-52201.	4.0	16
40531	Ruddlesden-Popper-based lanthanum cuprate thin film cathodes for solid oxide fuel cells: Effects of doping and structural transformation on the oxygen reduction reaction. International Journal of Hydrogen Energy, 2021, 46, 27173-27182.	3.8	6
40532	The effect of Na addition on the first hydrogen absorption kinetics of cast hypoeutectic Mgâ€“La alloys. International Journal of Hydrogen Energy, 2021, 46, 27096-27106.	3.8	10
40533	Theoretical and experimental investigations on mechanical properties of (Fe,Ni)Sn2 intermetallic compounds formed in SnAgCu/Fe-Ni solder joints. Materials Characterization, 2021, 178, 111195.	1.9	5
40534	Multifunctionality in (K,Na)NbO3-based ceramic near polymorphic phase boundary. Journal of Applied Physics, 2021, 130, 064102.	1.1	2
40535	Band Gap Engineering and 14 Electron Superatoms in 2D Superoctahedral Boranes B₄X₂ (B, N, P, As, Sb). Journal of Physical Chemistry C, 2021, 125, 17280-17290.	1.5	6
40536	Defect and Impurity-Complex Depassivation During Electron-Beam Irradiation of GaAs. IEEE Transactions on Nuclear Science, 2021, 68, 1548-1555.	1.2	2
40537	Decoupling of the Electrical and Thermal Transports in Strongly Coupled Interlayer Materials. Journal of Physical Chemistry Letters, 2021, 12, 7832-7839.	2.1	8
40538	A systematic investigation on quaternary NbTiZr-based refractory high entropy alloys using empirical parameters and first principles calculations. Modelling and Simulation in Materials Science and Engineering, 2021, 29, 075002.	0.8	3
40539	Phase transition mechanism of hexagonal graphite to hexagonal and cubic diamond: ab initio simulation. Journal of Physics Condensed Matter, 2021, 33, 425403.	0.7	1
40540	Nitrogen-doped graphdiyne for effective metal deposition and heterogeneous Suzuki-Miyaura coupling catalysis. Applied Catalysis A: General, 2021, 623, 118244.	2.2	11
40541	Syntheses and Characterization of the Mixed-Valent Manganese(II/III) Fluorides Mn₂F₅ and Mn₃F₈. Inorganic Chemistry, 2021, 60, 12651-12663.	1.9	5
40542	An orthorhombic superhard carbon allotrope: Pmma C24. Journal of Solid State Chemistry, 2021, 300, 122260.	1.4	33
40543	Band Structure and Optical Spectra of Bulk, Tri-Layer, Bi-Layer and Monolayer CdS System: A Comparative Study. Transactions on Electrical and Electronic Materials, 2022, 23, 404-413.	1.0	4
40544	Formation and influence of surface hydroxyls on product selectivity during CO2 hydrogenation by Ni/SiO2 catalysts. Journal of Catalysis, 2021, 400, 228-233.	3.1	27
40545	Ingenious control of adsorbed oxygen species to construct dual reaction centers ZnO@FePc photo-Fenton catalyst with high-speed electron transmission channel for PPCPs degradation. Applied Catalysis B: Environmental, 2021, 291, 120064.	10.8	50

#	Article	IF	Citations
40546	Atomic insights on intermixing of nanoscale nitride multilayer triggered by nanoindentation. Acta Materialia, 2021, 214, 117004.	3.8	19
40547	Theoretical Evaluation of MBenes as Catalysts for the CO₂ Reduction Reaction. Journal of Physical Chemistry C, 2021, 125, 19183-19189.	1.5	17
40548	Ab initio four-band Wannier tight-binding model for generic twisted graphene systems. Physical Review B, 2021, 104, .	1.1	12
40549	Understanding the optical and bonding properties of hybrid metal-halide (C5H16NP) PbX4 (XÂ=ÂCl, Br, I) perovskite: A density-functional theory study. Inorganic Chemistry Communication, 2021, 130, 108721.	1.8	9
40550	First-principles calculations to investigate structural and elastic properties of Y2C3 under external pressure. Computational and Theoretical Chemistry, 2021, 1202, 113320.	1.1	0
40551	Effect of <scp>K</scp> on carbon adsorption and deposition on the <scp>Co(111)</scp> surface. International Journal of Quantum Chemistry, 2021, 121, e26812.	1.0	1
40553	Coexistence of Negative and Positive Photoconductivity in Fewâ€Layer PtSe₂ Fieldâ€Effect Transistors. Advanced Functional Materials, 2021, 31, 2105722.	7.8	53
40554	Facile Fabrication of Robust Hydrogen Evolution Electrodes under High Current Densities via Pt@Cu Interactions. Advanced Functional Materials, 2021, 31, 2105579.	7.8	45
40555	Electronic band structure, elastic, optical and thermodynamic characteristic of cubic YF3: An ab initio study. Optik, 2021, 239, 166680.	1.4	7
40556	Comparison of the electronic, optical and photocatalytic properties of MoSe2, InN, and MoSe2/InN heterostructure nanosheet-A first-principle study. Materials Science in Semiconductor Processing, 2021, 131, 105861.	1.9	18
40557	Interfacial optimization of PtNi octahedrons@Ti3C2MXene with enhanced alkaline hydrogen evolution activity and stability. Applied Catalysis B: Environmental, 2021, 291, 120100.	10.8	67
40558	Structural and Electronic Effects of X-ray Irradiation on Prototypical [M(COD)Cl]₂Catalysts. Journal of Physical Chemistry A, 2021, 125, 7473-7488.	1.1	11
40559	Rattling and Band-Filling Effects in Substituted Tetrahedrites: An NMR Study. Journal of Physical Chemistry C, 2021, 125, 18877-18886.	1.5	1
40560	Sulfur doping effect on the electronic properties of zirconium dioxide ZrO2. Materials Science and Engineering B: Solid-State Materials for Advanced Technology, 2021, 270, 115200.	1.7	28
40561	Tuning the electronic and optical properties of molybdenite (MoS2) by adsorption of alkali metals and halogens. Optical Materials, 2021, 118, 111248.	1.7	6
40562	Comparing alkene-mediated and formaldehyde-mediated diene formation routes in methanol-to-olefins catalysis in MFI and CHA. Journal of Catalysis, 2021, 400, 124-139.	3.1	12
40563	Coordinatively unsaturated aluminum anchored Ru cluster for catalytic hydrogenation of benzene. Journal of Catalysis, 2021, 400, 255-264.	3.1	11
40564	Improvement in photocatalytic stability of AgBr under visible light through melt processing. Journal of Catalysis, 2021, 400, 160-165.	3.1	9

#	Article	IF	Citations
40565	Exsolved metal-boosted active perovskite oxide catalyst for stable water gas shift reaction. Journal of Catalysis, 2021, 400, 148-159.	3.1	18
40566	Exploring oxidation behavior of Nb4AC3 MAX phases (A = Si and Ga): Ab initio calculations. AIP Advances, 2021, 11, 085325.	0.6	1
40567	Elucidating the effects of oxygen- and nitrogen-containing functional groups in graphene nanomaterials for applied electrochemistry by density functional theory. Journal of Applied Physics, 2021, 130, .	1.1	2
40568	Graphyne as a second-order and real Chern topological insulator in two dimensions. Physical Review B, 2021, 104, .	1.1	30
40569	Transition state and formation process of Stoneâ€“Wales defects in graphene. Chinese Physics B, 2022, 31, 036102.	0.7	1
40570	Revealing the role of site occupation in phase stability, magnetic and electronic properties of Ni-Mn-In alloys by ab initio approach. Journal of Materials Science and Technology, 2021, 83, 90-101.	5.6	8
40571	Surface modification of 2-D Ti3C2Tx for the effective capture and elimination of acetaldehyde as a co-catalyst: A theoretical and experimental study. Surfaces and Interfaces, 2021, 25, 101284.	1.5	0
40572	The effects of quaternary alloying additions on the Î³TiAl alloy: Preferential site occupancy, interfacial energetics to physical parameters. Surfaces and Interfaces, 2021, 25, 101173.	1.5	0
40573	The investigation of the half-metallic properties of half-Heusler KXP (X = Cr & Mo) compounds: A first-principles study. Journal of Physics and Chemistry of Solids, 2022, 160, 110294.	1.9	8
40574	An efficient Ti0.95Cu0.05O1.95 catalyst for ipso â€“ hydroxylation of arylboronic acid and reduction of 4-nitrophenol. Journal of Chemical Sciences, 2021, 133, 1.	0.7	0
40575	Comparative Study on the Machine Learning-Based Prediction of Adsorption Energies for Ring and Chain Species on Metal Catalyst Surfaces. Journal of Physical Chemistry C, 2021, 125, 17742-17748.	1.5	10
40576	High-Pressure Yttrium Nitride, Y₅N₁₄, Featuring Three Distinct Types of Nitrogen Dimers. Journal of Physical Chemistry C, 2021, 125, 18077-18084.	1.5	11
40577	Various Exchange-Correlation Effects on Structural, Electronic, and Optical Properties of Brookite TiO₂. ECS Journal of Solid State Science and Technology, 2021, 10, 083010.	0.9	8
40578	Bimetallic phthalocyanine heterostructure used for highly selective electrocatalytic CO2 reduction. Science China Materials, 2022, 65, 155-162.	3.5	32
40579	Direct Visualization of Nearly Free Electron States Formed by Superatom Molecular Orbitals in a Li@C₆₀ Monolayer. Journal of Physical Chemistry Letters, 2021, 12, 7812-7817.	2.1	9
40580	Boron and Phosphorus Dual-Doped Carbon Coating Improves Electrochemical Performances of LiFe_{0.8}Mn_{0.2}PO₄ Cathode Materials. ACS Applied Energy Materials, 2021, 4, 8003-8015.	2.5	14
40581	A mechanistic periodic DFT study of CH, CO, and OH dissociations in methanol: M-doped carbon nanotubes (M=Pt, B, Al, N, P) versus Pt(100), Pt(110) and Pt(111) surfaces. Molecular Catalysis, 2021, 512, 111781.	1.0	2
40582	Tuning magnetic and optical properties through strain in epitaxial LaCrO3 thin films. Applied Physics Letters, 2021, 119, .	1.5	4

#	Article	IF	Citations
40583	Theoretical investigations on correlations between elastic behavior of Al-based alloys and their electronic structures. International Journal of Materials Research, 2021, 112, 636-641.	0.1	0
40584	Halfâ€Metallic CoO 2 and Semiconducting NiO 2 at High Pressures. Physica Status Solidi (B): Basic Research, 0, , 2100233.	0.7	0
40585	Revisiting the Electronic Structures and Phonon Properties of Thermoelectric Antimonide-Tellurides: Spinâ€“Orbit Coupling Induced Gap Opening in ZrSbTe and HfSbTe. Crystals, 2021, 11, 917.	1.0	6
40586	Reducing the Energy Band Gap of Cobalt Hydroxide Nanosheets with Silver Atoms and Enhancing Their Electrical Conductivity with Silver Nanoparticles. ACS Omega, 2021, 6, 20804-20811.	1.6	22
40587	Accelerated Discovery of the Valley-Polarized Quantum Anomalous Hall Effect in MXenes. Chemistry of Materials, 2021, 33, 6311-6317.	3.2	18
40588	Insights into the effect of hydroxyl-, epoxy-, and carboxyl-pores on the desolvation of K+ with water as a solvent: a first-principles study. Journal of Physics Condensed Matter, 2021, 33, 445201.	0.7	4
40589	P Doping Promotes the Spontaneous Visible-Light-Driven Photocatalytic Water Splitting in Isomorphic Type II GaSe/InS Heterostructure. Journal of Physical Chemistry Letters, 2021, 12, 7892-7900.	2.1	26
40590	In-plane magnetic structure and exchange interactions in the high-temperature antiferromagnet Cr2Al. Physical Review Materials, 2021, 5, .	0.9	1
40591	Empowering hydrogen storage properties of haeckelite monolayers via metal atom functionalization. Applied Surface Science, 2021, 556, 149709.	3.1	20
40592	Electroassisted Propane Dehydrogenation at Low Temperatures: Far beyond the Equilibrium Limitation. Jacs Au, 2021, 1, 1688-1693.	3.6	9
40593	Adsorption Mechanisms of Alkali Metal, Alkaline Earth Metal, and Halogen Atoms on Van der Waals Materials. Journal of Physical Chemistry C, 2021, 125, 19259-19267.	1.5	4
40594	Surface Pourbaix diagram of AgPd nanoalloys and its application in formate oxidation reaction. Electrochimica Acta, 2021, 386, 138465.	2.6	9
40595	On-the-fly assessment of diffusion barriers of disordered transition metal oxyfluorides using local descriptors. Electrochimica Acta, 2021, 388, 138551.	2.6	14
40596	A subtle structure evolution of metal-adsorbed water bilayer and the effect of dispersion correction. Computational Materials Science, 2021, 196, 110533.	1.4	3
40597	Outâ€Ofâ€Plane Ordered Laminate Borides and Their 2D Tiâ€Based Derivative from Chemical Exfoliation. Advanced Materials, 2021, 33, e2008361.	11.1	14
40598	Proton-Dominated Reversible Aqueous Zinc Batteries with an Ultraflat Long Discharge Plateau. ACS Nano, 2021, 15, 14766-14775.	7.3	38
40599	Sintering behavior and mechanical properties of hydroxyapatite ceramics prepared from Nile Tilapia (Oreochromis niloticus) bone and commercial powder for biomedical applications. Ceramics International, 2021, 47, 34575-34584.	2.3	12
40600	Exploring the corrosion behavior of Mn-implanted biomedical Mg. Journal of Alloys and Compounds, 2021, 873, 159739.	2.8	27

#	Article	IF	Citations
40601	Crystal chemistry and ab initio prediction of ultrahard rhombohedral B2N2 and BC2N. Solid State Sciences, 2021, 118, 106667.	1.5	13
40602	Polyethylene Hydrogenolysis at Mild Conditions over Ruthenium on Tungstated Zirconia. Jacs Au, 2021, 1, 1422-1434.	3.6	95
40603	Robust silver nanowire membrane with high porosity to construct stable Li metal anodes. Materials Today Energy, 2021, 21, 100751.	2.5	9
40604	Disconnected N-doped zigzag ZnO nanoribbon for potential Negative Differential Resistance (NDR) applications. Microelectronics Journal, 2021, 115, 105204.	1.1	13
40605	Ab-initio study on physical properties of intermetallic LiPb compound. Journal of Computational Science, 2021, 54, 101428.	1.5	3
40606	Doped Nickel Oxide Carrier-Selective Contact for Silicon Solar Cells. IEEE Journal of Photovoltaics, 2021, 11, 1176-1187.	1.5	10
40607	A hierarchical high-throughput first principles investigation on the adhesion work, interfacial energy and tensile strength of NiTi2 (100)/Î±-Al2O3 (0001) interfaces. Journal of Materials Research and Technology, 2021, 14, 2932-2944.	2.6	10
40608	Electronic structure modification in two-dimensional pentagonal PdS₂ by external strain. Canadian Journal of Physics, 2021, 99, 788-794.	0.4	2
40609	Ultrahigh thermal conductivity and strength in direct-gap semiconducting graphene-like BC6N: A first-principles and classical investigation. Carbon, 2021, 182, 373-383.	5.4	38
40610	Trimetallic Metalâ€Organic Framework Nanoframe Superstructures: A Stressâ€Buffering Architecture Engineering of Anode Material toward Boosted Lithium Storage Performance. Energy and Environmental Materials, 2023, 6, .	7.3	7
40611	Room-Temperature Ferroelectricity in 2D Metalâ€“Telluriumâ€“Oxyhalide Cd₇Te₇Cl₈O₁₇ via Selenium-Induced Selective-Bonding Growth. ACS Nano, 2021, 15, 16525-16532.	7.3	12
40612	Understanding the Synergistic Oxidation in Dichalcogenides through Electrochemiluminescence Blinking at Millisecond Resolution. Advanced Materials, 2021, 33, e2105039.	11.1	12
40613	Projector augmented-wave pseudopotentials for the actinide elements (Acâ€“Bk). Journal of Nuclear Materials, 2021, 553, 153031.	1.3	3
40614	TiN inducing ferrite nucleation based on the bcc-Fe/TiN interfaces formation at atomic scale by first-principles calculation. Computational Materials Science, 2021, 197, 110570.	1.4	16
40615	Modeling refractory high-entropy alloys with efficient machine-learned interatomic potentials: Defects and segregation. Physical Review B, 2021, 104, .	1.1	46
40616	Capacitive charge storage of tetraphenylporphyrin sulfonate-CNT composite electrodes. Electrochimica Acta, 2021, 389, 138593.	2.6	22
40617	Bimetallic Mixed Clusters Highly Loaded on Porous 2D Graphdiyne for Hydrogen Energy Conversion. Advanced Science, 2021, 8, e2102777.	5.6	27
40618	Structural instability of transition metals upon ultrafast laser irradiation. Physical Review B, 2021, 104, .	1.1	10

#	Article	IF	Citations
40619	Element-resolved local lattice distortion in complex concentrated alloys: An observable signature of electronic effects. Acta Materialia, 2021, 216, 117135.	3.8	22
40620	Stability and stoichiometry of L12 Al3(Sc,Zr) dispersoids in Al-(Si)-Sc-Zr alloys. Acta Materialia, 2021, 216, 117117.	3.8	24
40621	The Diffusion and Clustering Formation of Gold Atoms on Alpha-Graphyne. Journal of the Institute of Science and Technology, 0, , 1948-1958.	0.3	0
40622	Tailoring the Structural and Electronic Properties of Graphene through Ion Implantation. Materials, 2021, 14, 5080.	1.3	3
40623	Operando leaching of pre-incorporated Al and mechanism in transition-metal hybrids on carbon substrates for enhanced charge storage. Matter, 2021, 4, 2902-2918.	5.0	22
40624	Quantum anomalous Hall effect of Dirac half-metal monolayer TiCl₃ with high Chern number. Europhysics Letters, 2021, 136, 27004.	0.7	3
40625	New stable 2D and 3D GeC2 crystal structures predicted by first-principles study. Materials Today Communications, 2021, 28, 102567.	0.9	0
40626	Structural, elastic and thermodynamic properties of YRh: DFT study. Materials Today Communications, 2021, 28, 102529.	0.9	7
40627	Research of cation dependences of structural and elastic properties of metal carbonates series by density functional theory calculations. Materials Today Communications, 2021, 28, 102509.	0.9	5
40628	First-principles modeling of solute effects on thermal properties of nickel alloys. Materials Today Communications, 2021, 28, 102551.	0.9	5
40629	Mechanism of methanol decomposition on the Cu-Embedded graphene: A DFT study. International Journal of Hydrogen Energy, 2023, 48, 6624-6637.	3.8	17
40630	Anisotropic transport and optical birefringence of triclinic bulk and monolayer NbX₂Y₂ (X = S, Se and Y = Cl, Br, I). Journal of Physics Condensed Matter, 2021, 33, 485501.	0.7	0
40631	Study of compressed sulfur based on reliable first-principles calculations. Physical Review B, 2021, 104, .	1.1	2
40632	Experimental and theoretical insights into the reaction mechanism of spinel CuMn2O4 with CO in chemical-looping combustion. Applied Surface Science, 2021, 561, 150065.	3.1	17
40633	Effects of p-type conductive properties of triaxial strain-regulated ZnO (S, Se, Te) system. Physica Scripta, 2021, 96, 125815.	1.2	3
40634	Pressure- and temperature-dependent diffusion from first-principles: A case study of V and Ti in a TiN matrix. Surface and Coatings Technology, 2021, 422, 127491.	2.2	2
40635	Relevance of Dispersion and the Electronic Spin in the DFT + U Approach for the Description of Pristine and Defective TiO₂ Anatase. ACS Omega, 2021, 6, 23170-23180.	1.6	4
40636	Ab initio investigation of non-metal-doped ZnS monolayer. Applied Physics A: Materials Science and Processing, 2021, 127, 1.	1.1	6

#	Article	IF	Citations
40637	Abnormal Phase Transition and Band Renormalization of Guanidinium-Based Organicâ€“Inorganic Hybrid Perovskite. ACS Applied Materials & Interfaces, 2021, 13, 44964-44971.	4.0	8
40638	Enhancement of optoelectronic properties of layered MgIn$$_{2}$$Se$$_{4}$$ compound under uniaxial strain, an ab initio study. European Physical Journal B, 2021, 94, 185.	0.6	1
40639	Study of optoelectronic and thermoelectric properties of double perovskites for renewable energy. Physica Scripta, 2021, 96, 125828.	1.2	12
40640	Development of a solute and defect concentration dependant Ising model for the study of transmutation induced segregation in neutron irradiated Wâ€“(Re, Os) systems. Journal of Physics Condensed Matter, 2021, 33, 475902.	0.7	5
40641	Molecular-Level Insight into the Interfacial Reactivity and Ionic Conductivity of a Li-Argyrodite Li₆PS₅Cl Solid Electrolyte at Bare and Coated Li-Metal Anodes. ACS Applied Materials & Interfaces, 2021, 13, 43734-43745.	4.0	15
40642	Synthesis, Crystal Structure, and Nonlinear Optical Property of an Anhydrous Sulfate KTb(SO₄)₂. Inorganic Chemistry, 2021, 60, 15041-15047.	1.9	10
40643	Highly selective and efficient electrocatalytic synthesis of glycolic acid in coupling with hydrogen evolution. Chem Catalysis, 2021, 1, 941-955.	2.9	73
40644	Uncovering electronic and geometric descriptors of chemical activity for metal alloys and oxides using unsupervised machine learning. Chem Catalysis, 2021, 1, 923-940.	2.9	22
40645	Regulation of Hole Concentration and Mobility and First-Principle Analysis of Mg-Doping in InGaN Grown by MOCVD. Materials, 2021, 14, 5339.	1.3	2
40646	Adhesion and electric structure at Fe3O4/FeCr2O4 interface: A first principles study. Journal of Alloys and Compounds, 2021, 875, 160065.	2.8	11
40647	Spread-balanced Wannier functions: Robust and automatable orbital localization. Physical Review B, 2021, 104, .	1.1	3
40648	Tuning the magnetic phase diagram of Ni-Mn-Ga by Cr and Co substitution. Journal Physics D: Applied Physics, 0, , .	1.3	1
40649	High thermopower and birefringence in layered mercury-based halides. Materials Today Communications, 2022, 32, 102824.	0.9	0
40650	First Principles Calculations of Atomic and Electronic Structure of TiAl3+- and TiAl2+-Doped YAlO3. Materials, 2021, 14, 5589.	1.3	2
40651	Design strong anomalous Hall effect via spin canting in antiferromagnetic nodal line materials. Physical Review B, 2021, 104, .	1.1	7
40652	Robust large-gap topological insulator phase in transition-metal chalcogenide ZrTe₄Se. New Journal of Physics, 2021, 23, 093046.	1.2	0
40653	A Study in Red: The Overlooked Role of Azoâ€Moieties in Polymeric Carbon Nitride Photocatalysts with Strongly Extended Optical Absorption. Chemistry - A European Journal, 2021, 27, 17188-17202.	1.7	4
40654	Mechanistic Similarities and Differences for Hydrogenation of Aromatic Heterocycles and Aliphatic Carbonyls on Sulfided Ru Nanoparticles. ACS Catalysis, 2021, 11, 12585-12608.	5.5	3

#	Article	IF	Citations
40655	Dramatic Change in the Step Edges of the Cu(100) Electrocatalyst upon Exposure to CO: Operando Observations by Electrochemical STM and Explanation Using Quantum Mechanical Calculations. ACS Catalysis, 2021, 11, 12068-12074.	5.5	9
40656	Catalyst Design for Selective Hydrogenation of Benzene to Cyclohexene through Density Functional Theory and Microkinetic Modeling. ACS Catalysis, 2021, 11, 11831-11842.	5.5	14
40657	2D-layered Mg(OH)2 material adsorbing cellobiose via interfacial chemical coupling and its applications in handling toxic Cd2+ and UO22+ ions. Chemosphere, 2021, 279, 130617.	4.2	8
40658	Structure and energy of the (101) twin boundary in hot-deformed Nd-Fe-B magnets. Materials Characterization, 2021, 179, 111380.	1.9	2
40659	Effects of magnetic excitations and transitions on vacancy formation: Cases of fcc Fe and Ni compared to bcc Fe. Physical Review B, 2021, 104, .	1.1	5
40660	Donorâ€“Acceptor Competition via Halide Vacancy Filling for Oxygen Detection of High Sensitivity and Stability by Allâ€inorganic Perovskite Films. Small, 2021, 17, 2102733.	5.2	3
40661	Adsorption and rotational barrier for a single azobenzene molecule on Au(111) surface*. Chinese Physics B, 2021, 30, 096805.	0.7	1
40662	Ab initio framework for systems with helical symmetry: Theory, numerical implementation and applications to torsional deformations in nanostructures. Journal of the Mechanics and Physics of Solids, 2021, 154, 104515.	2.3	7
40663	Oxidation behavior of medium-entropy (Y1/3Yb1/3Lu1/3)2O3 modified SiC ceramic at 1700 Â°C: Experimental and theoretical study. Journal of the European Ceramic Society, 2021, 41, 5825-5834.	2.8	8
40664	Achievement of strain-driven ultrahigh carrier mobility in Î²-TeO2. Materials Research Bulletin, 2021, 141, 111343.	2.7	5
40665	Ab-initio studies of electronic and magnetic properties of titanium doped methylammonium lead halides. Computational Condensed Matter, 2021, 28, e00570.	0.9	4
40666	Influence of hydrogen isotopes on vacancy formation and antisite defect diffusion in palladium and vanadium metals. Computational Materials Science, 2021, 197, 110641.	1.4	3
40667	Vibrational Analysis of Paraelectricâ€“Ferroelectric Transition of LiNbO3: An Ab-Initio Quantum Mechanical Treatment. Symmetry, 2021, 13, 1650.	1.1	2
40668	High thermoelectric performance in cubic inorganic halide perovskite material AgCdX3 (XÂ= F and Cl) from first principles. Materials Today Energy, 2021, 21, 100820.	2.5	7
40669	Third-generation CALPHAD description of pure GeO2 at 1Âatm. Calphad: Computer Coupling of Phase Diagrams and Thermochemistry, 2021, 74, 102299.	0.7	6
40670	Van der Waals heterostructure of Janus transition metal dichalcogenides monolayers (WSSe-WX2) Tj ETQq1 1 0.784314 rgBT /Overlo	0.9	7
40671	On the design of models for an accurate description of the water â€“ hematite interface. Applied Surface Science, 2021, 560, 149884.	3.1	1
40672	The interaction of flotation reagents with metal ions in mineral surfaces: A perspective from coordination chemistry. Minerals Engineering, 2021, 171, 107067.	1.8	101

#	Article	IF	Citations
40673	The Effect of Structural Phase Transitions on Electronic and Optical Properties of CsPbI3 Pure Inorganic Perovskites. Coatings, 2021, 11, 1173.	1.2	5
40674	Mitrofanovite Pt₃Te₄: A Topological Metal with Termination-Dependent Surface Band Structure and Strong Spin Polarization. ACS Nano, 2021, 15, 14786-14793.	7.3	13
40675	Mg₃Si₃(MoO₆)₂ as a High-Performance Cathode Active Material for Magnesium-Ion Batteries. ACS Applied Materials & Interfaces, 2021, 13, 47749-47755.	4.0	6
40676	Emergent electronic properties in Co-deposited superatomic clusters. Journal of Chemical Physics, 2021, 155, 124309.	1.2	1
40677	Anomalous heavy doping in chemical-vapor-deposited titanium trisulfide nanostructures. Physical Review Materials, 2021, 5, .	0.9	3
40678	Layers engineering optoelectronic properties of 2D hexagonal GeS materials. Physica E: Low-Dimensional Systems and Nanostructures, 2021, 133, 114791.	1.3	9
40679	High-temperature ferromagnetism in monolayers MnGaX3 (XÂ=ÂTe, Se). Journal of Magnetism and Magnetic Materials, 2021, 534, 168041.	1.0	2
40680	A saccharide-based binder for efficient polysulfide regulations in Li-S batteries. Nature Communications, 2021, 12, 5375.	5.8	65
40681	Electronic structures of vacancies in Co3Sn2S2 *. Chinese Physics B, 2021, 30, 077102.	0.7	1
40682	Ab initio study of electromagnetic modes in two-dimensional semiconductors: Application to doped phosphorene. Physical Review B, 2021, 104, .	1.1	12
40683	Improving the Room-Temperature Ferromagnetism in ZnO and Low-Doped ZnO:Ag Films Using GLAD Sputtering. Materials, 2021, 14, 5337.	1.3	1
40684	Device performance limit of monolayer SnSe2 MOSFET. Nano Research, 0, , 1.	5.8	9
40685	Structural, elastic, electronic, thermal, and phononic properties of yttrium carbide: First-principles calculations. Materials Chemistry and Physics, 2021, 270, 124744.	2.0	9
40686	Modification of Lu's (2005) high pressure model for improved high pressure/high temperature extrapolations. Part II: Modeling of osmiumâ€“platinum system at high pressure/high temperature. Calphad: Computer Coupling of Phase Diagrams and Thermochemistry, 2021, 74, 102311.	0.7	2
40687	Structure and electronic properties of tin monoxide (SnO) and lithiated SnO terminated diamond (1 0) Tj ETQq0 0 0 rgBT /Overlock 10 T 149962.	3.1	14
40688	DFT calculations on the ternary MScP, quaternary MSc2P (M = Cu, Zn), and Cu and Zn doped in semiconducting scandium phosphide by GGA and GGA+U approach. Vacuum, 2021, 191, 110328.	1.6	1
40689	A geometric-information-enhanced crystal graph network for predicting properties of materials. Communications Materials, 2021, 2, .	2.9	27
40690	Boosted Solar Light Absorbance in PdS₂/PtS₂ Vertical Heterostructures for Ultrathin Photovoltaic Devices. ACS Applied Materials & Interfaces, 2021, 13, 43615-43621.	4.0	14

#	Article	IF	Citations
40691	OPTICS: Operant Probability Theory in Crystal Solutions, Application of ssNMR, and Probability Theory in Polymorph Identification. Crystal Growth and Design, 2021, 21, 5904-5913.	1.4	1
40692	High-Pressure Synthesis of the Î²-Zn₃N₂ Nitride and the Î±-ZnN₄ and Î²-ZnN₄ Polynitrogen Compounds. Inorganic Chemistry, 2021, 60, 14594-14601.	1.9	15
40693	Density Functional Theory Study of the Highâ€Pressure Characterization of Nitrogenâ€Rich Energetic Materials: Bisâ€Triaminoguanidinium Azotetrazolate (TAGzT). Physica Status Solidi (B): Basic Research, 0, , 2100365.	0.7	1
40694	The origin of ultra-low thermal conductivity of the Bi2Te2S compound and boosting the thermoelectric performance via carrier engineering. Materials Today Physics, 2021, 20, 100472.	2.9	15
40695	A porous nanotube network structure of metallic carbon. Results in Physics, 2021, 28, 104579.	2.0	17
40696	A 3D Graphene/WO3 nanowire composite with enhanced capture and polysulfides conversion catalysis for high-performance Liâ€“S batteries. Carbon, 2021, 182, 335-347.	5.4	34
40698	Low-energy structures and electronic properties of small titanium nitride nanoclusters. Nanotechnology, 2021, 32, .	1.3	4
40699	Assessment of the Accuracy of Density Functionals for Calculating Oxygen Reduction Reaction on Nitrogen-Doped Graphene. Journal of Chemical Theory and Computation, 2021, 17, 6405-6415.	2.3	9
40700	Microstructure and electronic structure of Cr2C and Fe2Y in the Cr-coating prepared by pack-cementation on the surface of ODS steel. Materials Today Communications, 2021, 28, 102591.	0.9	2
40701	Cyclohexylammoniumâ€Based 2D/3D Perovskite Heterojunction with Funnelâ€Like Energy Band Alignment for Efficient Solar Cells (23.91%). Advanced Energy Materials, 2021, 11, 2102236.	10.2	77
40702	Unraveling the electronic properties of graphene with substitutional oxygen. 2D Materials, 2021, 8, 045035.	2.0	9
40703	Imparting Î±-Borophene with High Work Function by Fluorine Adsorption: A First-Principles Investigation. Langmuir, 2021, 37, 11027-11040.	1.6	10
40704	Theoretical investigation of metal oxides for SO 2 capture through firstâ€principles calculations. International Journal of Quantum Chemistry, 0, , e26822.	1.0	1
40705	Direct Atomicâ€Scale Structure and Electric Field Imaging of Triazineâ€Based Crystalline Carbon Nitride. Advanced Materials, 2021, 33, e2106359.	11.1	19
40706	Serosa-Mimetic Nanoarchitecture Membranes for Highly Efficient Osmotic Energy Generation. Journal of the American Chemical Society, 2021, 143, 16206-16216.	6.6	70
40707	Tuning reaction pathways of peroxymonosulfate-based advanced oxidation process via defect engineering. Cell Reports Physical Science, 2021, 2, 100550.	2.8	9
40708	High thermoelectric power factor of pure and vanadium-alloyed chromium nitride thin films. Materials Today Communications, 2021, 28, 102493.	0.9	9
40709	Correlation between reduced dielectric loss and charge migration kinetics in NdFeO3-modified Ba0.7Sr0.3TiO3 ceramics. Journal of Materials Science: Materials in Electronics, 2021, 32, 24910.	1.1	2

#	Article	IF	Citations
40710	Adsorption and Activation of CO₂ on Nitride MXenes: Composition, Temperature, and Pressure effects. ChemPhysChem, 2021, 22, 2456-2463.	1.0	11
40711	Nobleâ€Metalâ€Assisted Fast Interfacial Oxygen Migration with Topotactic Phase Transition in Perovskite Oxides. Advanced Functional Materials, 2021, 31, 2106765.	7.8	18
40712	Termination-dependent electronic structure and atomic-scale screening behavior of the Cu₂O(111) surface. Journal of Physics Condensed Matter, 2021, 33, 484001.	0.7	2
40713	Unveiling the multilevel structure of midgap states in Sb-doped <mml:math xmlns:mml="http://www.w3.org/1998/Math/MathML"><mml:mrow><mml:mi>Mo</mml:mi><mml:msub><mml:mi>X</mml:mi><mml:mi>n</mml:mi></mml:msub></mml:mrow><mml:mo>(</mml:mo><mml:mi>X</mml:mi><mml:mo>=</mml:mo><mml:mi>S</mml:mi>, Te) Tj Physical Review B, 2021, 104, .	1.1	6
40714	Biphenylene monolayer as a two-dimensional nonbenzenoid carbon allotrope: a first-principles study. Journal of Physics Condensed Matter, 2022, 34, 015001.	0.7	45
40715	Supercritical CO2â€assisted Fabrication of Twoâ€dimensional Graphdiyne Oxide Nanosheets for Enhanced Photothermal Conversion. ChemNanoMat, 2021, 7, 1309.	1.5	3
40716	Modification of graphenylene nanostructure with transition metals (Fe, Sc and Ti) to promote hydrogen storage ability: A DFT-D3 study. International Journal of Hydrogen Energy, 2021, 46, 38370-38380.	3.8	14
40717	Density functional theory study of structural, mechanical, electronic and optical properties of MoAlX (XÂ=ÂB, C, N and O) compounds. Materials Research Express, 2021, 8, 096533.	0.8	2
40718	Magnetism in Au-Supported Planar Silicene. Nanomaterials, 2021, 11, 2568.	1.9	3
40719	The first foreseen of structural, mechanical, electronic and optical properties of novel alkali metal tetrafluoridobromate ABrF4 (A=Na, K and Rb). Physica B: Condensed Matter, 2021, 624, 413450.	1.3	0
40720	Single germanene phase formed by segregation through Al(111) thin films on Ge(111). 2D Materials, 2021, 8, 045039.	2.0	7
40721	The Effect of Pristine and Hydroxylated Oxide Surfaces on the Guaiacol HDO Process: A DFT Study. ChemPhysChem, 2022, 23, .	1.0	6
40722	Hydroxylation of the Zn terminated ZnO(0ÂÂ0ÂÂ1) surface under vacuum conditions. Applied Surface Science, 2022, 572, 151271.	3.1	5
40723	Structural, electronic and optical properties of M-doped anatase TiO2 (M= Fe or Au): A first principle investigation. Computational Condensed Matter, 2021, 28, e00576.	0.9	10
40724	Electronic, optical, elastic, mechanical and vibrational properties of hexagonal h-ZnS with density functional theory. Computational Condensed Matter, 2021, 28, e00572.	0.9	6
40725	Silver hollandite (AgxMn8O16 , xâ‰2): A highly anisotropic half-metal for spintronics. Physical Review Materials, 2021, 5, .	0.9	1
40726	Searching for highly efficient multifunctional electrocatalysts based on the single metal doped graphitic carbon nitride. Molecular Physics, 2021, 119, .	0.8	3
40727	Few-layer antimonene electrical properties. Applied Materials Today, 2021, 24, 101132.	2.3	6

#	Article	IF	Citations
40728	Boronâ€Mediated Grain Boundary Engineering Enables Simultaneous Improvement of Thermoelectric and Mechanical Properties in Nâ€Type Bi₂Te₃. Small, 2021, 17, e2104067.	5.2	30
40729	Dithiocarbamate modified glucose as a novel eco-friendly corrosion inhibitor for copper in sodium chloride media. Sustainable Chemistry and Pharmacy, 2021, 22, 100488.	1.6	12
40730	Engineering Co3+-rich crystal planes on Co3O4 hexagonal nanosheets for CO and hydrocarbons oxidation with enhanced catalytic activity and water resistance. Chemical Engineering Journal, 2021, 420, 130448.	6.6	34
40731	Role of intercalated water in calcium hydroxide interlayers for carbonation reaction. Chemical Engineering Journal, 2021, 420, 130422.	6.6	8
40732	Novel magnetic nanomaterial Co0.7Zn0.3Fe2â^'xGdxO4 for nanotechnology applications: experimental and theoretical investigations. Journal of Materials Science: Materials in Electronics, 2021, 32, 24748-24765.	1.1	4
40733	Atomic-scale imaging of CH3NH3PbI3 structure and its decomposition pathway. Nature Communications, 2021, 12, 5516.	5.8	36
40734	A novel two-dimensional boronâ€“carbonâ€“nitride (BCN) monolayer: A first-principles insight. Journal of Applied Physics, 2021, 130, .	1.1	23
40735	Effect of facile nitrogen doping on catalytic performance of NaW/Mn/SiO2 for oxidative coupling of methane. Applied Catalysis B: Environmental, 2021, 292, 120161.	10.8	10
40736	Difference between stress and magnetism relationships of ferromagnetic materials under tensile and compressive stresses. Results in Physics, 2021, 28, 104572.	2.0	7
40737	A comprehensive study of the thermophysical and optoelectronic properties of Nb2P5 via ab-initio technique. Results in Physics, 2021, 28, 104623.	2.0	20
40738	First-principles calculation for displacive phase transition of atomic-scale precipitates in aluminum alloys. Physics Letters, Section A: General, Atomic and Solid State Physics, 2021, 411, 127569.	0.9	4
40739	Describing the Migdal effect with a bremsstrahlung-like process and many-body effects. Physical Review D, 2021, 104, .	1.6	20
40740	Effect of hydrostatic compression on physical properties of Li2TmSi3 (Tm = Ir, Pt, Rh, Os) with ground-state optical features. Journal of Physics and Chemistry of Solids, 2021, 156, 110124.	1.9	5
40741	Investigations on magnetic properties of p-type ferromagnetic (Ca, Na)(Zn, Mn)2As2. Materials Science and Engineering B: Solid-State Materials for Advanced Technology, 2021, 271, 115282.	1.7	2
40742	A member of p-type TCO family: Sn2TaxNb2-xO7 with a tunable band gap and controllable hole mobility. Materials Science and Engineering B: Solid-State Materials for Advanced Technology, 2021, 271, 115255.	1.7	0
40743	The formaldehyde adsorption on anatase TiO2 (2Â1Â1) surface. Chemical Physics Letters, 2021, 778, 138771.	1.2	3
40744	Phase equilibria in the ZrO₂â€“Ta₂O₅â€“Nb₂O₅ system: Experimental studies and thermodynamic modeling. Journal of the American Ceramic Society, 2022, 105, 668-686.	1.9	24
40745	High-Density Ruthenium Single Atoms Anchored on Oxygen-Vacancy-Rich g-C₃N₄-C-TiO₂ Heterostructural Nanosphere for Efficient Electrocatalytic Hydrogen Evolution Reaction. ACS Applied Materials & Interfaces, 2021, 13, 46608-46619.	4.0	20

#	Article	IF	Citations
40746	Investigation of physical properties and superdislocation characters of Ni3Al under uniaxial tension/compression normal to slip plane. Intermetallics, 2021, 136, 107258.	1.8	7
40747	High-performance aqueous polysulfide-iodide flow battery realized by an efficient bifunctional catalyst based on copper sulfide. Materials Today Energy, 2021, 21, 100746.	2.5	14
40748	Thermophysical properties of hot fluid iron in the protolunar disk. Physics of the Earth and Planetary Interiors, 2021, 321, 106806.	0.7	0
40749	Restructuring highly electron-deficient metal-metal oxides for boosting stability in acidic oxygen evolution reaction. Nature Communications, 2021, 12, 5676.	5.8	92
40750	Theoretical investigation of electronic and optical properties of the 2D-MoSe2/GaN heterostructure nanosheet. Physica E: Low-Dimensional Systems and Nanostructures, 2022, 135, 114994.	1.3	18
40751	Effects of Intra-Structural Interactions of Indium Hexacyanoferrate on the Li+ and K+ Intercalation Potential. Journal of the Electrochemical Society, 0, , .	1.3	1
40752	Architecture of NaFe(MoO4)2 as a novel anode material for rechargeable lithium and sodium ion batteries. Applied Surface Science, 2021, 559, 149903.	3.1	7
40753	Investigation of C60 fullerenes modified g-GaN monolayer based on DFT study. Vacuum, 2021, 191, 110356.	1.6	7
40754	Modeling twin boundary structures in body centered cubic transition metals. Computational Materials Science, 2021, 197, 110649.	1.4	10
40755	Compositional effects on stacking fault energies in Ni-based alloys using first-principles and atomistic simulations. Computational Materials Science, 2021, 197, 110618.	1.4	7
40756	Probing the enhanced methanol electrooxidation mechanism by promoted CO tolerance on the Pd catalyst modified with TaN: A combined experimental and theoretical study. International Journal of Hydrogen Energy, 2021, 46, 37321-37332.	3.8	5
40757	Near-room temperature ferromagnetic behavior of single-atom-thick 2D iron in nanolaminated ternary MAX phases. Applied Physics Reviews, 2021, 8, .	5.5	14
40758	Cation complexation by mucoid Pseudomonas aeruginosa extracellular polysaccharide. PLoS ONE, 2021, 16, e0257026.	1.1	6
40759	Engineering MoTe2 and Janus SeMoTe nanosheet structures: First-principles roadmap and practical uses in hydrogen evolution reactions and symmetric supercapacitors. Nano Energy, 2021, 87, 106161.	8.2	50
40760	Ultra-high capacity of physisorption of hydrogen molecule on AlC3 monolayer: First-principles calculations. FlatChem, 2021, 29, 100291.	2.8	4
40761	Cooperative Oxide-Ion Transport in Pyrochlore Y₂Ti₂O₇: A First-Principles Molecular Dynamics Study. Journal of Physical Chemistry C, 2021, 125, 20460-20467.	1.5	3
40762	Adsorption behavior of carbonic acid on Î³â€dicalcium silicate surface from molecular simulations. Journal of the American Ceramic Society, 0, , .	1.9	5
40763	Theoretical insight into adsorption and dissociation of water on NiCr binary alloy surfaces: Early-stage oxidation mechanism. Journal of Applied Physics, 2021, 130, .	1.1	1

#	Article	IF	Citations
40764	The formation and dissociation energy of vacancies in cementite: A first-principles study. Nuclear Instruments & Methods in Physics Research B, 2021, 502, 157-163.	0.6	1
40765	Study on the optical properties of CdWO4 crystal with oxygen vacancies. Nuclear Instruments & Methods in Physics Research B, 2021, 502, 183-188.	0.6	1
40766	Catalyzing Bondâ€Dissociation in Graphene via Alkaliâ€Iodide Molecules. Small, 2021, 17, e2102037.	5.2	1
40767	Ab initio calculations of structural, electronic, magnetic and thermoelectric properties of Cr_{1â^'x}Al_xP. Phase Transitions, 2021, 94, 815-825.	0.6	2
40768	Electronic, Magnetic, and Mechanical Properties of YXâ€²CrZ (Xâ€² = Fe, Co, Ni; Z = Si, Ge, Sn) Quaternary Heusler Alloys. Journal of Superconductivity and Novel Magnetism, 2021, 34, 3019-3036.	0.8	5
40769	Significant improvement in the piezoelectric properties and electromechanical coupling factors of wurtzite AlN compound under high pressures. Journal of Computational Electronics, 2021, 20, 2420-2430.	1.3	6
40770	Surface and subsurface damage in 14â€‰MeV Au ion-irradiated diamond. Journal of Applied Physics, 2021, 130, 105303.	1.1	0
40771	Excited-state potentials for modelling dense plasmas from first principles. Plasma Physics and Controlled Fusion, 2021, 63, 114006.	0.9	2
40772	Growth and Selective Etching of Twinned Graphene on Liquid Copper Surface. Small, 2021, 17, 2103484.	5.2	7
40773	Large contribution of quasi-acoustic shear phonon modes to thermal conductivity in novel monolayer Ga2O3. Journal of Applied Physics, 2021, 130, .	1.1	5
40774	A first-principles study of the effect of doping and vacancy defects on the magnetic properties of ZnSnAs2:V. Indian Journal of Physics, 0, , 1.	0.9	0
40775	Correlating point defects with mechanical properties in nanocrystalline TiN thin films. Materials and Design, 2021, 207, 109844.	3.3	18
40776	Adjustable electro-optical properties of novel graphene-like SiC2 via strain engineering. Applied Surface Science, 2021, 559, 149956.	3.1	51
40777	The crystal structure of LiSc2SbO6. Journal of Solid State Chemistry, 2021, 304, 122615.	1.4	2
40778	Understanding of C/Tiâ€Doped SnS₂ Photocatalytic Behaviors from Electronic Structures. Physica Status Solidi - Rapid Research Letters, 2021, 15, 2100340.	1.2	3
40779	Deprotonation and cation adsorption on the NiOOH/water interface: A grand-canonical first-principles investigation. Electrochimica Acta, 2021, 398, 139253.	2.6	3
40780	Phonon transport anomaly in metavalent bonded materials: contradictory to the conventional theory. Journal of Materials Science, 2021, 56, 18534-18549.	1.7	11
40781	Plasma-engineered organic dyes as efficient polysulfide-mediating layers for high performance lithium-sulfur batteries. Chemical Engineering Journal, 2022, 430, 132679.	6.6	5

#	Article	IF	Citations
40782	Density functional study of structural, electronic and optical properties of bromine-doped CsPbI3 with the tetragonal symmetry. Journal of Alloys and Compounds, 2022, 892, 162165.	2.8	18
40783	Self-hydrogen transfer hydrogenolysis of native lignin over Pd-PdO/TiO2. Applied Catalysis B: Environmental, 2022, 301, 120767.	10.8	33
40784	Tuning the interaction between Na and Co2C to promote selective CO2 hydrogenation to ethanol. Applied Catalysis B: Environmental, 2021, 293, 120207.	10.8	57
40785	Computational exploration of biomedical HfNbTaTiZr and Hf_{0.5}Nb_{0.5}Ta_{0.5}Ti_{1.5}Zr refractory high-entropy alloys. Materials Research Express, 2021, 8, 096534.	0.8	8
40786	Agent molecule modulated low-temperature activation of solid-state lithium-ion transport for polymer electrolytes. Journal of Power Sources, 2021, 505, 229917.	4.0	4
40787	First principles investigation of high thermal conductivity in hexagonal germanium carbide(2H-GeC). Carbon Trends, 2021, 5, 100113.	1.4	6
40788	Corrosion inhibition of locally de-passivated surfaces by DFT study of 2-mercaptobenzothiazole on copper. Npj Materials Degradation, 2021, 5, .	2.6	15
40789	In Situ Constructed Ionicâ€Electronic Dualâ€Conducting Scaffold with Reinforced Interface for Highâ€Performance Sodium Metal Anodes. Small, 2021, 17, e2104021.	5.2	17
40790	Lithiation and Sodiation of Hydrogenated Silicene: A Density Functional Theory Investigation. ChemSusChem, 2021, 14, 5460-5469.	3.6	14
40791	Spectroelectrochemical and DFT approaches to the study of croconic acid adsorption at gold electrodes in acidic solutions. Journal of Electroanalytical Chemistry, 2021, 896, 115396.	1.9	1
40792	A Computational Exploration of Ammonia Adsorption on the Kaolinite Clay Surface. Chemistry Africa, 2021, 4, 905-914.	1.2	3
40794	Construction of Pd-Zn dual sites to enhance the performance for ethanol electro-oxidation reaction. Nature Communications, 2021, 12, 5273.	5.8	94
40795	Pressure-Induced Variation of the Crystal Stacking Order in the Hydrogen-Bonded Quasi-Two-Dimensional Layered Material Cu(OH)Cl. Materials, 2021, 14, 5019.	1.3	0
40796	Direct H-He chemical association in superionic FeO2H2He at Deep-Earth conditions. National Science Review, 0, , .	4.6	18
40797	How to Look for Compounds: Predictive Screening and inâ€…situ Studies in Naâ^'Znâ^'Bi System. Chemistry - A European Journal, 2021, 27, 15954-15966.	1.7	4
40798	DFT study for the absorption spectra evolution of CdS magic-size clusters. Chemical Physics Letters, 2021, 779, 138870.	1.2	6
40799	Basic physical behavior of impurity carbon in molybdenum for nuclear material: A systematical first-principles simulation. Nuclear Materials and Energy, 2021, 28, 101053.	0.6	1
40800	The activation of B-H bonds in borohydride on Cu(1 0 0) and Cu(1 1 0) surfaces. Computational and Theoretical Chemistry, 2021, 1203, 113376.	1.1	3

#	Article	IF	Citations
40801	Role of Chemical Structure of Support in Enhancing the Catalytic Activity of a Single Atom Catalyst Toward NRR: A Computational Study. Frontiers in Chemistry, 2021, 9, 733422.	1.8	2
40802	A model to partition the constituent elementâ€™s atomic energy in TiC crystal and to characterize the interface properties of Î±-Ti(0001)/TiC(111). Materials Today Communications, 2021, 28, 102581.	0.9	0
40803	Ab Initio Study of the Influence of Alloying Elements on Stability and Mechanical Properties of Selected TixAly Intermetallic Compounds and Their TixAly/Al, TixAly/Ti Interfaces in Explosively Welded Metalâ€“Metal Composites. Metallurgical and Materials Transactions A: Physical Metallurgy and Materials Science, 2021, 52, 5032-5042.	1.1	2
40804	A permeable electrochemical reactive barrier for underground water remediation using TiO2/graphite composites as heterogeneous electrocatalysts without releasing of chemical substances. Journal of Hazardous Materials, 2021, 418, 126318.	6.5	10
40805	A systematic computational study to understand the effect of metals (Mg, Ca, Sr) doping and external isotropic static pressure on phase stability, electronic band structure and optical properties of KNbO3. Materials Science and Engineering B: Solid-State Materials for Advanced Technology, 2021, 271, 115261.	1.7	7
40806	Spin-filtering effects and negative differential resistance in N/B-doped zigzag silicon carbide nanoribbons with asymmetric edge hydrogenation. Materials Science and Engineering B: Solid-State Materials for Advanced Technology, 2021, 271, 115253.	1.7	5
40807	Evaluating the stability and activity of dilute Cu-based alloys for electrochemical CO2 reduction. Journal of Chemical Physics, 2021, 155, 114702.	1.2	11
40808	K doping as a rational method to enhance the sluggish air-electrode reaction kinetics for proton-conducting solid oxide cells. Electrochimica Acta, 2021, 389, 138453.	2.6	20
40809	A comparative density functional theory study of oxygen doping versus adsorption on graphene to tune its band gap. Journal of Molecular Graphics and Modelling, 2021, 107, 107982.	1.3	5
40810	Understanding phase equilibria in high-entropy alloys: II. Atomic-scale study of incorporation of metallic elements in Cr carbides â€“ Application to equilibrium with AlCrFeMnMo. Journal of Alloys and Compounds, 2021, 874, 159959.	2.8	4
40811	Stable two-dimensional pentagonal tellurene: A high ZT thermoelectric material with a negative Poissonâ€™s ratio. Applied Surface Science, 2021, 559, 149851.	3.1	8
40812	SiOx microparticles embedded into 3D wrinkled N, S co-doped multilayer graphene sheets as a high-performance anode for long-life full lithium-ion batteries. Electrochimica Acta, 2021, 390, 138841.	2.6	21
40813	Mechanistic study on the role of oxygen vacancy for methylene chloride oxidation over La-Mn perovskite. Applied Surface Science, 2021, 559, 149979.	3.1	5
40814	Barium chromium nitride-hydride for ammonia synthesis. Chem Catalysis, 2021, 1, 1042-1054.	2.9	19
40815	Phonon Transport and Thermoelectric Properties of Imidazole-Graphyne. Materials, 2021, 14, 5604.	1.3	3
40816	Relationships between Distortions of Inorganic Framework and Band Gap of Layered Hybrid Halide Perovskites. Chemistry of Materials, 2021, 33, 7518-7526.	3.2	22
40817	Persulfate activation by nanodiamond-derived carbon onions: Effect of phase transformation of the inner diamond core on reaction kinetics and mechanisms. Applied Catalysis B: Environmental, 2021, 293, 120205.	10.8	35
40818	Generalized first-principles method to study near-field heat transfer mediated by Coulomb interaction. Physical Review B, 2021, 104, .	1.1	4

#	Article	IF	Citations
40819	An ab-initio based semi-empirical thermal conductivity model for multiphase uranium-zirconium alloys. Journal of Nuclear Materials, 2021, 553, 153044.	1.3	3
40820	Interfacial defective Ti3+ on Ti/TiO2 as visible-light responsive sites with promoted charge transfer and photocatalytic performance. Journal of Materials Science and Technology, 2022, 106, 139-146.	5.6	26
40821	Towards the understanding of promoting effects of Re, Cs and Cl promoters for silver catalysts of ethylene epoxidation: A computational study. Catalysis Today, 2021, 375, 585-590.	2.2	11
40822	Structural stability, electronic and mechanical properties of transition metal nitrides TMN compounds (TM=Zn, Mn and Tc). Phase Transitions, 2021, 94, 754-766.	0.6	2
40823	Enhanced Performance of Perovskite Solar Cells via Reactive Postâ€treatment Process Utilizing Guanidine Acetate as Interface Modifier. Solar Rrl, 2021, 5, 2100547.	3.1	16
40824	Thermoelectric Cu₁₂Sb₄S₁₃â€Based Synthetic Minerals with a Sublimationâ€Derived Porous Network. Advanced Materials, 2021, 33, e2103633.	11.1	46
40825	Structural, electronic and optical properties of strontium and nickel co-doped BaTiO3: A DFT based study. Computational Condensed Matter, 2021, 28, e00578.	0.9	19
40826	Electronic band structure, mechanical and thermodynamic properties of Erbium chalcogenides ErX (X) Tj ETQq1 1 0.784314 rgBT /Ov	0.9	5
40827	Cavity exciton polaritons in two-dimensional semiconductors from first principles. Physical Review Research, 2021, 3, .	1.3	7
40828	Magnetic structure and exchange interactions in pyrrhotite end member minerals: hexagonal FeS and monoclinic Fe₇S₈. Journal of Physics Condensed Matter, 2021, 33, 465801.	0.7	6
40829	Metalâ€Nitrogenâ€Carbon Clusterâ€Decorated Titanium Carbide is a Durable and Inexpensive Oxygen Reduction Reaction Electrocatalyst. ChemSusChem, 2021, 14, 4680-4689.	3.6	2
40830	The effect of vacancy defects on the adsorption of methane on calcite 104 surface. Journal of Materials Research and Technology, 2021, 14, 3051-3058.	2.6	3
40831	Lithium/bismuth co-functionalized phosphotungstic acid catalyst for promoting dinitrogen electroreduction with high Faradaic efficiency. Cell Reports Physical Science, 2021, 2, 100557.	2.8	11
40832	Abnormal Hypsochromic Shifts of Surface Plasmon Scattering by Atomic Ordering in Goldâ€“Copper Intermetallic Nanoparticles. Journal of Physical Chemistry C, 2021, 125, 19936-19946.	1.5	7
40833	An atomistic view on Oxygen, antisites and vacancies in the <mml:math xmlns:mml="http://www.w3.org/1998/Math/MathML" altimg="si165.svg"><mml:mrow><mml:mi>Î³</mml:mi></mml:mrow></mml:math>-TiAl phase. Computational Materials Science, 2021, 197, 110655.	1.4	5
40834	First-Principle Study of Co-Adsorption Behavior of H2O and O2 on Î´-Pu (100) Surface. Coatings, 2021, 11, 1098.	1.2	3
40835	Anisotropic Disorder and Thermal Stability of Silicane. ACS Nano, 2021, 15, 14557-14569.	7.3	5
40836	Strategy to utilize amorphous phase of semiconductor toward excellent and reliable photochemical water splitting performance: Roles of interface dipole moment and reaction parallelization. International Journal of Energy Research, 2022, 46, 3674-3685.	2.2	5

#	Article	IF	Citations
40837	Unraveling the effects of potassium incorporation routes and positions on toluene oxidation over Î±-MnO2 nanorods: Based on experimental and density functional theory (DFT) studies. Journal of Colloid and Interface Science, 2021, 598, 324-338.	5.0	87
40838	Engineering microstructure of LiFe(MoO4)2 as an advanced anode material for rechargeable lithium-ion battery. Journal of Materials Science: Materials in Electronics, 2021, 32, 24273-24284.	1.1	7
40839	Visually resolving the direct Z-scheme heterojunction in CdS@ZnIn2S4 hollow cubes for photocatalytic evolution of H2 and H2O2 from pure water. Applied Catalysis B: Environmental, 2021, 293, 120213.	10.8	123
40840	High-pressure synthesis, crystal structure, and physical properties of NaAlB14 single crystals. Ceramics International, 2022, 48, 1771-1777.	2.3	2
40841	Electronâ€“phonon superconductivity in C-doped topological nodal-line semimetal Zr₅Pt₃: a muon spin rotation and relaxation (Î¼SR) study. Journal of Physics Condensed Matter, 2022, 34, 035602.	0.7	6
40842	Optimizing the Electronic Structure of ZnS via Cobalt Surface Doping for Promoted Photocatalytic Hydrogen Production. Inorganic Chemistry, 2021, 60, 15712-15723.	1.9	14
40843	Amelioration of sintering and multi-frequency dielectric properties of Mg3B2O6: A mechanism study of nickel substitution using DFT calculation. Journal of Advanced Ceramics, 2021, 10, 1398-1407.	8.9	27
40844	Transferable Gaussian Attractive Potentials for Organic/Oxide Interfaces. Journal of Physical Chemistry B, 2021, 125, 10843-10853.	1.2	8
40845	A Semiconductive Nature of Bis(dithiolato)nickelate Radical Salt Exhibiting Broadband Photoconduction. Inorganic Chemistry, 2021, 60, 15659-15666.	1.9	4
40846	Enabling highly efficient and broadband electromagnetic wave absorption by tuning impedance match in high-entropy transition metal diborides (HE TMB2). Journal of Advanced Ceramics, 2021, 10, 1299-1316.	8.9	46
40847	A theoretical study on elastic, electronic, transport, optical and thermoelectric properties of Janus SnSO monolayer. Journal Physics D: Applied Physics, 2021, 54, 475306.	1.3	7
40848	Metal-free tellurene cocatalyst with tunable bandgap for enhanced photocatalytic hydrogen production. Materials Today Energy, 2021, 21, 100720.	2.5	18
40849	Improved Dielectric Properties and Grain Boundary Effect of Phenanthrene Under High Pressure. Frontiers in Physics, 2021, 9, .	1.0	2
40850	Mechanism of Nitrogen-Doped Ti₃C₂ Quantum Dots for Free-Radical Scavenging and the Ultrasensitive H₂O₂ Detection Performance. ACS Applied Materials & Interfaces, 2021, 13, 42442-42450.	4.0	30
40851	Tunable band gap energy of single-walled zigzag ZnO nanotubes as a potential application in photodetection. Current Applied Physics, 2021, 29, 138-147.	1.1	8
40852	A single step synthesis by mechanical alloying and characterization of nanostructured Fe2B of high magnetic moment. Ceramics International, 2021, 47, 26119-26124.	2.3	8
40853	First principles investigation of the Structural, Mechanical, Electronic Properties and Debye temperature of W-Co alloys. Fusion Engineering and Design, 2021, 170, 112715.	1.0	5
40854	Insights and comparison of structureâ€“property relationships in propane and propene catalytic combustion on Pd- and Pt-based catalysts. Journal of Catalysis, 2021, 401, 89-101.	3.1	24

#	Article	IF	Citations
40855	Theoretical study of Au20/WS2 composite material as a potential candidate for the capture of XO (X=C, N, S) gases. Computational Condensed Matter, 2021, 28, e00580.	0.9	4
40856	Unified and ultimate high-pressure phase of several nanolaminate Mn+1AXn (nâ€¯=â€¯1, 2, 3, etc.) ceramics from first principles. Results in Physics, 2021, 28, 104681.	2.0	2
40857	Unveiling the Mechanisms Ruling the Efficient Hydrogen Evolution Reaction with Mitrofanovite Pt₃Te₄. Journal of Physical Chemistry Letters, 2021, 12, 8627-8636.	2.1	13
40858	The Thermal Properties of L12 Phases in Aluminum Enhanced by Alloying Elements. Metals, 2021, 11, 1420.	1.0	3
40859	Nonlocal hcp kernel functions based on ab initio calculations: Pertinent dislocation problems revisited. Mechanics of Materials, 2021, 160, 103904.	1.7	0
40860	Binder-free metal-organic frameworks-derived CoP/Mo-doped NiCoP nanoplates for high-performance quasi-solid-state supercapacitors. Electrochimica Acta, 2021, 390, 138840.	2.6	17
40861	Bandgap Tuned WS₂ Thinâ€Film Photodetector by Strain Gradient in van der Waals Effective Homojunctions. Advanced Optical Materials, 2021, 9, 2101310.	3.6	13
40862	Molecule Confined Isolated Metal Sites Enable the Electrocatalytic Synthesis of Hydrogen Peroxide. Advanced Materials, 2022, 34, e2104891.	11.1	42
40863	Trapping and recombination of tritium in lithium vacancy of the Î³-LiAlO2 (100) surface: A first-principles study. Applied Surface Science Advances, 2021, 5, 100114.	2.9	1
40864	Surface segregation of PdM (M=Cu, Ag, Au) alloys and its implication to acetylene hydrogenation, DFT-based Monte Carlo simulations. Materials Today Communications, 2021, 28, 102475.	0.9	5
40865	Modulation of band gap and optical response of layered MoX2 (XÂ=ÂS, Se, Te) for electronic and optoelectronic applications. Materials Today Communications, 2021, 28, 102614.	0.9	6
40866	Lead-free indium-silver based double perovskites for thermoelectric applications: Structural, electronic and thermoelectric properties using first-principles approach. Materials Today Communications, 2021, 28, 102609.	0.9	4
40867	The magnetic, electronic, optical, and structural properties of the AB2O4 (AÂ=ÂMn, Fe, co; BÂ=ÂAl, Ga, In) spinels: Ab initio study. Journal of Magnetism and Magnetic Materials, 2021, 533, 168015.	1.0	8
40868	Critical evaluation and thermodynamic modeling of the Ag-X (X=Mn, Y, Sr) binary systems. Intermetallics, 2021, 136, 107260.	1.8	4
40869	Superior tunable photocatalytic properties for water splitting in two dimensional GeC/SiC van der Waals heterobilayers. Scientific Reports, 2021, 11, 17739.	1.6	20
40870	Baltimore SCIART: A Fully Virtual Undergraduate Research Experience at the Interface of Computational Chemistry and Art. Journal of Chemical Education, 0, , .	1.1	1
40871	Sol-gel prepared Cu2ZnSnS4 (CZTS) semiconductor thin films: Role of solvent removal processing temperature. Materials Science in Semiconductor Processing, 2021, 132, 105874.	1.9	14
40872	Bridge sulfur vacancies in MoS2 catalyst for reverse water gas shift: A first-principles study. Applied Surface Science, 2021, 561, 149925.	3.1	12

#	Article	IF	Citations
40873	H/D isotope effect between adsorbed water (H2O, D2O, and HDO) and H2O- and D2O-ice Ih(0Â0Â0Â1) basal surfaces based on the combined plane wave and localized basis set method. Applied Surface Science, 2021, 561, 150100.	3.1	1
40874	Segregation of alloying elements to stabilize Î¸â€² phase interfaces in Al-Cu based alloys. Scripta Materialia, 2021, 202, 114006.	2.6	10
40875	Facet-dependent stability of near-surface oxygen vacancies and excess charge localization at CeO₂ surfaces. Journal of Physics Condensed Matter, 2021, 33, 504003.	0.7	14
40876	Enhancing thermoelectric performance of BaMg₂-based compounds by forming solid solutions and biaxial strain. Journal Physics D: Applied Physics, 2021, 54, 485301.	1.3	1
40877	Interactions of solute atoms with self-interstitial atoms/clusters in vanadium: A first-principles study. Journal of Nuclear Materials, 2021, 553, 153055.	1.3	9
40878	First-principles prediction of layered MoO₂ and MoOSe as promising cathode materials for magnesium ion batteries. Nanotechnology, 2021, 32, 495405.	1.3	5
40879	Does Explicit Polarizability Improve Simulations of Phase Behavior of Ionic Liquids?. Journal of Chemical Theory and Computation, 2021, 17, 6225-6239.	2.3	7
40880	Impact of applied biaxial stress on the piezoelectric, elastic, and dielectric properties of scandium aluminum nitride alloys determined by density functional perturbation theory. AIP Advances, 2021, 11, .	0.6	3
40881	Absence of spillover of hydrogen adsorbed on small palladium clusters anchored to graphene vacancies. Applied Surface Science, 2021, 559, 149835.	3.1	17
40882	Impact of three-body interactions in a ReaxFF force field for Ni and Cr transition metals and their alloys on the prediction of thermal and mechanical properties. Computational Materials Science, 2021, 197, 110602.	1.4	9
40883	Atomistic study of the structure and deformation behavior of symmetric tilt grain boundaries in <mml:math xmlns:mml="http://www.w3.org/1998/Math/MathML" altimg="si46.svg"><mml:mrow><mml:mi>l±</mml:mi></mml:mrow></mml:math>-zirconium. Computational Materials Science, 2021, 197, 110600.	1.4	4
40884	Rapid preparation of zirconia/zircon composites ceramics by microwave method: Experiment and first-principle investigation. Progress in Nuclear Energy, 2021, 139, 103839.	1.3	2
40885	Hydrogen adsorption on doped graphene investigated by a DFT-based tight-binding method. Journal of Physics Condensed Matter, 2021, 33, 504001.	0.7	5
40886	Unexpected and enhanced electrostatic adsorption capacity of oxygen vacancy-rich cobalt-doped In2O3 for high-sensitive MEMS toluene sensor. Sensors and Actuators B: Chemical, 2021, 342, 129949.	4.0	26
40887	Phase diagrams and superconductivity of ternary Na-Al-H compounds at high pressure. Physical Review B, 2021, 104, .	1.1	5
40888	Negative differential resistance in all-benzene molecule of trefoil knot. Physics Letters, Section A: General, Atomic and Solid State Physics, 2021, 410, 127539.	0.9	0
40889	Active oxygen center in oxidative coupling of methane on La2O3 catalyst. Journal of Energy Chemistry, 2021, 60, 649-659.	7.1	28
40890	Benign Effects of Twin Boundaries on Charge Carrier Lifetime in Metal Halide Perovskites by a Time-Domain Study. Journal of Physical Chemistry Letters, 2021, 12, 8575-8582.	2.1	13

#	Article	IF	Citations
40891	Atomic-scale study of Si-doped AlAs by cross-sectional scanning tunneling microscopy and density functional theory. Physical Review B, 2021, 104, .	1.1	4
40892	Probing metal-molecule contact at the atomic scale via conductance jumps. Physical Review B, 2021, 104, .	1.1	8
40893	Zirconium Nitride: Optical Properties of an Emerging Intermetallic for Plasmonic Applications. Advanced Photonics Research, 2021, 2, 2100178.	1.7	15
40894	Finite-momentum excitons in rubrene single crystals. Physical Review B, 2021, 104, .	1.1	6
40895	Study on electronic properties and charge transfer doping of organic molecules adsorbed g-GaN monolayer. Semiconductor Science and Technology, 2021, 36, 125020.	1.0	4
40896	Synthesis, crystal and electronic structure of CaNi₂Al₈. Zeitschrift Fur Naturforschung - Section B Journal of Chemical Sciences, 2021, 76, 659-668.	0.3	2
40897	Hybridization-Induced Inversion of Spin Polarization at Rubrene/Ferromagnetic Cobalt Interface. Journal of Physical Chemistry C, 2021, 125, 20697-20705.	1.5	1
40898	Structural and optical behaviors of 2D-layered molybdenum disulfide thin film: experimental and ab-initio insights. Journal of Materials Research and Technology, 2021, 14, 780-796.	2.6	4
40899	First-principles calculations to investigate structural, elastic, electronic, lattice dynamic and optical properties for scandium and yttrium nitrides in zinc blend structure. Journal of Materials Research and Technology, 2021, 14, 1958-1968.	2.6	6
40900	New insights of the interaction of H2S with mackinawite FeS in a wet environment: An ab initio molecular dynamics study. International Journal of Hydrogen Energy, 2021, , .	3.8	2
40901	Basic aspects of the charge density wave instability of transition metal trichalcogenides NbSe₃ and monoclinic-TaS₃. Journal of Physics Condensed Matter, 2021, 33, 485401.	0.7	2
40902	On the impact of zero-point vibrations in calcium carbonate. Phase Transitions, 0, , 1-15.	0.6	1
40903	Importance of Van der Waals Interactions in Hydrogen Adsorption on a Silicon-carbide Nanotube Revisited with vdW-DFT and Quantum Monte Carlo. ACS Omega, 2021, 6, 24630-24636.	1.6	12
40904	Ni-based catalysts derived from Ni-Zr-Al ternary hydrotalcites show outstanding catalytic properties for low-temperature CO2 methanation. Applied Catalysis B: Environmental, 2021, 293, 120218.	10.8	62
40905	Pd and Pt decorated GeSe monolayers as promising materials for SOF2 and SO2F2 sensing. Applied Surface Science, 2021, 560, 150028.	3.1	32
40906	DFT calculations on selectivity enhancement by Br addition on Pd catalysts in the direct synthesis of hydrogen peroxide. Catalysis Today, 2022, 397-399, 232-239.	2.2	4
40907	Nanoparticle-Assisted Niâ€“Co Binary Single-Atom Catalysts Supported on Carbon Nanotubes for Efficient Electroreduction of CO₂ to Syngas with Controllable CO/H₂ Ratios. ACS Applied Energy Materials, 2021, 4, 9572-9581.	2.5	19
40908	High uptake and fixation ability of BC monolayer for CO and NO toxic gases: a computational analysis. Journal of Materials Science, 2021, 56, 18566-18580.	1.7	0

#	Article	IF	Citations
40909	Density Functional Theory Study on Dependence of Stability of Fe, Cu, and Ni Atoms on Surface Orientation of Si Crystal. ECS Journal of Solid State Science and Technology, 2021, 10, 094002.	0.9	0
40910	Mapping Orbital-Resolved Magnetism in Single Lanthanide Atoms. ACS Nano, 2021, 15, 16162-16171.	7.3	7
40911	First-principles calculations of electronic, optical, phononic and thermodynamic properties of C40-type TMSi2 (TM = Cr, Mo, W) disilicides. Vacuum, 2021, 191, 110324.	1.6	21
40912	The adsorption performance of harmful gas on Cu doped WS2: A first-principle study. Materials Today Communications, 2021, 28, 102488.	0.9	36
40913	Na2SO4â€“NaCl binary eutectic salt roasting to enhance extraction of lithium from pyrometallurgical slag of spent lithium-ion batteries. Chinese Journal of Chemical Engineering, 2022, 41, 294-300.	1.7	10
40914	Thermodynamic modeling of the Alâ€“Nbâ€“V system. Calphad: Computer Coupling of Phase Diagrams and Thermochemistry, 2021, 74, 102321.	0.7	5
40915	Thermodynamic activity of solute in multicomponent alloy from first-principles: Excess Mg in Mg3(Sb1-Bi)2 as an example. Calphad: Computer Coupling of Phase Diagrams and Thermochemistry, 2021, 74, 102318.	0.7	2
40916	Al/SiC nanocomposites with enhanced thermomechanical properties obtained from microwave plasma-treated nanopowders. Materials Science & Engineering A: Structural Materials: Properties, Microstructure and Processing, 2021, 824, 141817.	2.6	9
40917	Mechanical properties of cubic Cu3N and Cu4N: A theoretical investigation. Vacuum, 2021, 191, 110366.	1.6	4
40918	Emergence of intrinsically isolated flat bands and their topology in fully relaxed twisted multilayer graphene. Physical Review B, 2021, 104, .	1.1	4
40919	First-principles study on the effects of V, Nb, Cd, Ag, Ge and Sb doped in Al₂CuMg phase of Alâ€“Znâ€“Mgâ€“Cu alloy. Modern Physics Letters B, 2021, 35, .	1.0	3
40920	Exploration of Dynamic Structureâ€“Activity Relationship of a Platinum Nanoparticle in the CO Oxidation Reaction. Journal of Physical Chemistry C, 2021, 125, 19756-19762.	1.5	9
40921	First principles investigation of physically conductive bridge filament formation of aluminum doped perovskite materials for neuromorphic memristive applications. Chaos, Solitons and Fractals, 2021, 150, 111111.	2.5	8
40922	Refined Structures of O-Phospho-l-serine and Its Calcium Salt by New Multinuclear Solid-State NMR Crystallography Methods. Journal of Physical Chemistry B, 2021, 125, 10985-11004.	1.2	2
40923	Multilevel Theoretical Screening of Novel Two-Dimensional MA₂Z₄ Family for Hydrogen Evolution. Journal of Physical Chemistry Letters, 2021, 12, 9149-9154.	2.1	32
40924	Tuning of the electronic and optical properties of AlN monolayer by fluorination: Study of many-body effects. Computational Condensed Matter, 2021, 28, e00564.	0.9	3
40925	Novel family of topological semimetals with butterflylike nodal lines. Physical Review B, 2021, 104, .	1.1	4
40926	Electron beam irradiation induced metastable phase in a Mgâ€“9.8 wt%Sn alloy. Journal of Materials Science and Technology, 2021, 84, 133-138.	5.6	9

#	Article	IF	Citations
40927	Strong tribo-piezoelectric effect in bilayer indium nitride (InN). Scientific Reports, 2021, 11, 18669.	1.6	15
40928	Can We Predict the Isosymmetric Phase Transition? Application of DFT Calculations to Study the Pressure Induced Transformation of Chlorothiazide. International Journal of Molecular Sciences, 2021, 22, 10100.	1.8	4
40930	Selective hydrogenation of benzonitrile and its homologues to primary amines over platinum. Journal of Industrial and Engineering Chemistry, 2021, 101, 279-292.	2.9	11
40931	Structural, electronic and magnetic properties of L10 ordered CoPt nanoparticles: An experimental and DFT study. Materials Chemistry and Physics, 2021, 269, 124727. Novel properties of transition metal dichalcogenides monolayers and nanoribbons (<mml:math) Tj ETQq0 0 0 rgBT /Overlock 10 Tf 50 60	2.0	8
40932	Solid-State Materials for Advanced Technology, 2021, 271, 115237.	1.7	14
40933	Atomic structure of a single step and dynamics of Sn adatoms on the Si <mml:math xmlns:mml="http://www.w3.org/1998/Math/MathML"><mml:mrow><mml:mrow><mml:mo>(</mml:mo><mml:mn>111</mml:mn><mml:mn><mml:mn> Sn surface. Physical Review B, 2021, 104, .	1.1	3
40934	Valence State Modulation of Chromium in Selective Hydrogen Peroxide Production Electrocatalysts. ACS Applied Energy Materials, 2021, 4, 10114-10123.	2.5	2
40935	Promoting exsolution of RuFe alloy nanoparticles on Sr2Fe1.4Ru0.1Mo0.5O6â^'Î´ via repeated redox manipulations for CO2 electrolysis. Nature Communications, 2021, 12, 5665.	5.8	102
40936	First-principles calculation of oxygen vacancy effects on the magnetic properties of the perovskite <mml:math xmlns:mml="http://www.w3.org/1998/Math/MathML"><mml:mrow><mml:msub><mml:mi>SrNiO</mml:mi><mml:mn>3</mml:mn></mml:m Physical Review Materials, 2021, 5, .	0.9	7
40937	The bonding characteristics of the Cu(111)/WC(0001) interface: An insight from first-principle calculations. Vacuum, 2021, 191, 110218.	1.6	48
40938	Molecular-Scale Insights into Electrochemical Reduction of CO₂ on Hydrophobically Modified Cu Surfaces. ACS Applied Materials & Interfaces, 2021, 13, 47619-47628.	4.0	24
40939	On-surface synthesis of 2D COFs via molecular assembly directed photocycloadditions: a first-principles investigation. Journal of Physics Condensed Matter, 2021, 33, 475201.	0.7	0
40940	Theoretical and Experimental Characterization of Adsorbed CO and NO on Î³-Al₂O₃-Supported Rh Nanoparticles. Journal of Physical Chemistry C, 2021, 125, 19733-19755.	1.5	9
40941	Prediction of Transition-State Scaling Relationships and Universal Transition-State Vibrational and Entropic Correlations for Dehydrogenations. Journal of Physical Chemistry C, 2021, 125, 19780-19790.	1.5	3
40942	Interlayer Interaction Induced Layer-Dependent Catalytic Activity toward a Hydrogen Evolution Reaction on Two-Dimensional PtSe2. Journal of Physical Chemistry C, 2021, 125, 19716-19723.	1.5	1
40943	Density functional study on formic acid decomposition on Pd(111) surface: a revisit and comparison with other density functional methods. Journal of Molecular Modeling, 2021, 27, 285.	0.8	0
40944	Adsorption and Reductive Defluorination of Perfluorooctanoic Acid over Palladium Nanoparticles. Environmental Science & Technology, 2021, 55, 14836-14843.	4.6	26
40945	Synergistic Effects of Co and Fe on the OER activity of LaCoxFe1â^'xO3. Chemistry - A European Journal, 2021, 27, 17145-17158.	1.7	14

#	Article	IF	Citations
40946	Mixedâ€Halide Double Perovskite Cs₂AgBiX₆ (X=Br, I) with Tunable Optical Properties via Anion Exchange. ChemSusChem, 2021, 14, 4507-4515.	3.6	24
40947	A comprehensive DFT based insights into the physical properties of tetragonal superconducting Mo5PB2. Results in Physics, 2021, 28, 104612.	2.0	24
40948	Interplay between polarization, strain, and defect pairs in Fe-doped <mml:math xmlns:mml="http://www.w3.org/1998/Math/MathML"><mml:msub><mml:mi>SrMnO</mml:mi><mml:mrow><mml:mn>3</mml:mn></mml:mrow></mml:msub></mml:math> Physical Review Research, 2021, 3, .	1.3	3
40949	Role of Pairwise Reactions on the Synthesis of Li_{0.3}La_{0.57}TiO₃ and the Resulting Structureâ€“Property Correlations. Inorganic Chemistry, 2021, 60, 14831-14843.	1.9	6
40950	Theoretical study on near UV and visible optical absorption characteristics of Ti-doped Î±-Al2O3 single crystals. Materials Today Communications, 2021, 28, 102506.	0.9	4
40951	Beryllium sulfur doped with N, Li and Na: Promising p-type transparent semiconductor. Materials Today Communications, 2021, 28, 102513.	0.9	5
40952	Density Functional Theory Study of the Immobilization and Hindered Surface Migration of Pd₃ and Pd₄ Nanoclusters over Defect-Ridden Graphene: Implications for Heterogeneous Catalysis. ACS Applied Nano Materials, 2021, 4, 9068-9079.	2.4	7
40953	High pressure induced decomposition of antimony trisulfide. Materials Today Communications, 2021, 29, 102828.	0.9	3
40954	Tunable electronic and magnetic properties of MoSi2N4 monolayer via vacancy defects, atomic adsorption and atomic doping. Applied Surface Science, 2021, 559, 149862.	3.1	81
40955	Absence of proton tunneling during the hydrogen-bond symmetrization in Î´â€²AlOOH. Physical Review B, 2021, 104, .	1.1	7
40956	Revisiting the Chemical Stability of Germanium Selenide (GeSe) and the Origin of its Photocatalytic Efficiency. Advanced Functional Materials, 2021, 31, 2106228.	7.8	11
40957	Comparative analysis of sensing characteristics of Rh-doped defect h-BN monolayer to C₄F₇N decomposition components under partial discharge. Molecular Physics, 2021, 119, .	0.8	4
40958	Steam-created grain boundaries for methane Câ€“H activation in palladium catalysts. Science, 2021, 373, 1518-1523.	6.0	105
40959	Coexisting commensurate and incommensurate charge ordered phases in CoO. Scientific Reports, 2021, 11, 19415.	1.6	0
40960	Equilibrium Distribution of Dissolved Carbon in PdCx: Density Functional Theory and Canonical Monte Carlo Simulations. Journal of Physical Chemistry C, 2021, 125, 20930-20939.	1.5	2
40961	Impact of carbonâ€“carbon defects at the SiO₂/4H-SiC (0001) interface: a first-principles calculation. Journal Physics D: Applied Physics, 2022, 55, 025109.	1.3	4
40962	High-Performance Binary Moâ€“Ni Catalysts for Efficient Carbon Removal during Carbon Dioxide Reforming of Methane. ACS Catalysis, 2021, 11, 12087-12095.	5.5	61
40963	Hierarchically assembling cobalt/nickel carbonate hydroxide on copper nitride nanowires for highly efficient water splitting. Applied Catalysis B: Environmental, 2021, 292, 120148.	10.8	62

#	Article	IF	Citations
40964	Grain boundary segregation in Ni-base alloys: A combined atom probe tomography and first principles study. Acta Materialia, 2021, 221, 117354.	3.8	37
40965	Benzohydroxamic acid on rutile TiO2(110)-(1Ã—1)â€“ a comparison of ultrahigh-vacuum evaporation with deposition from solution. Surface Science, 2022, 716, 121955.	0.8	4
40966	A comprehensive study of titanium-doped tin oxide rutile for structural and optical properties. Physica B: Condensed Matter, 2021, 619, 413210.	1.3	1
40967	Thermal conductivity of magnesium telluride (MgTe) - A first principles study. Solid State Communications, 2021, 337, 114414.	0.9	5
40968	Temperature-dependent elastic properties of high entropy ceramic (ZrTaNbTi)C from self-consistent quasi-harmonic approximation. Solid State Communications, 2021, 336, 114432.	0.9	3
40969	Structural, electronic, dynamic, optic and elastic properties of MgScGa via density functional theory. Solid State Communications, 2021, 337, 114437.	0.9	0
40970	Density functional theory study on concentration of intrinsic point defects in growing N-doped Czochralski Si crystal. Journal of Crystal Growth, 2021, 571, 126249.	0.7	2
40971	First principles study of the electronic, elastic and vibrational properties of BiOI. Solid State Communications, 2021, 336, 114419.	0.9	3
40972	Drastic reduction of thermal conductivity in hexagonal AX (AÂ=ÂGa, In & Tl, XÂ=ÂS, Se & Te) monolayers due to alternative atomic configuration. Nano Energy, 2021, 88, 106248.	8.2	19
40973	Structural, electronic, magnetic and mechanical properties of Fe2SiC. Physica B: Condensed Matter, 2021, 618, 413136.	1.3	2
40974	Vibrational properties of High Entropy Alloy based metal hydrides probed by inelastic neutron scattering. Journal of Alloys and Compounds, 2021, 877, 160320.	2.8	4
40975	Optimization of hydrogen evolution reaction catalytic activity of Ti2CO2 via surface engineering with an isolated fluorine effect: An ab-initio density functional theory study. Applied Surface Science, 2021, 562, 150149.	3.1	4
40976	Quantitative description of the role of Cr on the ordering characteristics of a single phase Ni-16 wt.% Mo- 7wt.% Cr alloy. Acta Materialia, 2021, 219, 117263.	3.8	4
40977	Superhardness induced by Grain Boundary Vertical Sliding in (001)-textured ZrB<mml:math xmlns:mml="http://www.w3.org/1998/Math/MathML" altimg="si3.svg"><mml:msub><mml:mrow /><mml:mn>2</mml:mn></mml:msub></mml:math> and TiB<mml:math xmlns:mml="http://www.w3.org/1998/Math/MathML" altimg="si3.svg"><mml:msub><mml:mrow /><mml:mn>2</mml:mn></mml:msub></mml:math> Nano Films. Acta Materialia, 2021, 219, 117212.	3.8	11
40978	First principle investigation of polaronic resistive switching behavior in titania based memristors with different charge states. Physica E: Low-Dimensional Systems and Nanostructures, 2021, 134, 114857.	1.3	3
40979	Factors affecting the vacancy formation energy in Fe70Ni10Cr20 random concentrated alloy. Computational Materials Science, 2021, 198, 110669.	1.4	10
40980	Theoretical study on two dimensional group IV-VI ternary compounds with large in-plane spontaneous polarization. Computational Materials Science, 2021, 198, 110688.	1.4	4
40981	A novel Hf2CO2/WS2 van der Waals heterostructure as a potential candidate for overall water splitting photocatalyst. Materials Science in Semiconductor Processing, 2021, 133, 105947.	1.9	17

#	Article	IF	Citations
40982	Adsorption mechanism of sulphide gas molecules on Î³-Fe(1Â1Â1) surface: A density functional theory study. Applied Surface Science, 2021, 563, 150376.	3.1	5
40983	Switchable electric polarization of phosphorene in mixed dimensional van der Waals heterostructure. Applied Surface Science, 2021, 563, 150276.	3.1	3
40984	Functionalization of two-dimensional PbTiO3 film by surface modification: A first-principles study. Applied Surface Science, 2021, 563, 150268.	3.1	5
40985	Theoretical prediction of topological insulators in two-dimensional ternary transition metal chalcogenides (MM'X4, MÂ=ÂTa, Nb, or V; M'= Ir, Rh, or Co; XÂ=ÂSe or Te). Chinese Journal of Physics, 2021, 73, 95-102.	2.0	11
40986	Thermal effect of epilayer on phonon transport of semiconducting heterostructure interfaces. International Journal of Heat and Mass Transfer, 2021, 178, 121613.	2.5	12
40987	On the role of surface oxygen during nascent single-walled carbon nanotube cap spreading and tube nucleation on iron catalysts. Carbon, 2021, 184, 470-478.	5.4	6
40988	Doping effect of Cu (II) in the adsorption of CrO42- by the Fe3O4 (1 1 1) surface: A theoretical study. Chemical Physics Letters, 2021, 781, 138984.	1.2	6
40989	Structural, optical and photocatalytic properties of silver-doped magnesia: computational and experimental study. Journal of Molecular Liquids, 2021, 339, 117176.	2.3	4
40990	Charge-compensated codoped pseudohexagonal zinc selenide nanosheets towards enhanced visible-light-driven photocatalytic water splitting for hydrogen production. International Journal of Hydrogen Energy, 2021, 46, 34305-34317.	3.8	13
40991	Double bond effects induced by iron selenide as immobilized homogenous catalyst for efficient polysulfides capture. Chemical Engineering Journal, 2021, 421, 129770.	6.6	18
40992	Quantum chemical exploration on the inhibition performance of indole and some of its derivatives against copper corrosion. Journal of Molecular Liquids, 2021, 340, 117136.	2.3	11
40993	Enhancing Oxygen Evolution Reaction Activity by Using Switchable Polarization in Ferroelectric InSnO₂N. ACS Catalysis, 2021, 11, 12692-12700.	5.5	9
40994	Structural, electronic, mechanical, thermal, and optical properties of UIr3 under pressure: A comprehensive DFT study. AIP Advances, 2021, 11, .	0.6	14
40995	Synthesis, structure, magnetocaloric effect and DFT calculations of a MnII cluster-based inorganic coordination polymer. Journal of Alloys and Compounds, 2021, 878, 160353.	2.8	5
40996	Theoretical study of stress impact on formation enthalpy and thermal equilibrium concentration of impurities and dopants in Si single crystal. Journal of Crystal Growth, 2021, 572, 126284.	0.7	1
40997	First-principles study of structural and electronic properties of antimonene doped with Ge, Sn, Se, Te. Journal of Solid State Chemistry, 2021, 302, 122355.	1.4	8
40998	First-principles calculations of structural, electronic, magnetic, thermoelectric, and thermodynamic properties of BaMn2P2 in the Anti and ferromagnetic phase. Journal of Solid State Chemistry, 2021, 302, 122388.	1.4	14
40999	Theoretical study on the synthesis of methane by CO2 hydrogenation on Ni3Fe(111) surface. Journal of Natural Gas Science and Engineering, 2021, 94, 104114.	2.1	11

#	Article	IF	Citations
41000	Adsorption of habitat and industry-relevant molecules on the MoSi2N4 monolayer. Applied Surface Science, 2021, 564, 150326.	3.1	50
41001	Achievement of a polymer-free KAc gel electrolyte for advanced aqueous K-Ion battery. Energy Storage Materials, 2021, 41, 133-140.	9.5	19
41002	Enhanced thermal stability of (Ti,Al)N coatings by oxygen incorporation. Acta Materialia, 2021, 218, 117204.	3.8	26
41003	Enhanced quantum capacitance in 3d-transition metal porphyrin functionalized graphene. Materials Science and Engineering B: Solid-State Materials for Advanced Technology, 2021, 272, 115384.	1.7	4
41004	Heterostructure-based devices with enhanced humidity stability for H2 gas sensing applications in breath tests and portable batteries. Sensors and Actuators A: Physical, 2021, 329, 112804.	2.0	17
41005	Investigation of the phosphorene nano-sheet as a sensor for detecting aspartic-acid, alanine and glycine amino acids: A first principle study. Physica B: Condensed Matter, 2021, 618, 412771.	1.3	8
41006	Effect of dopants on the structural, optoelectronic and magnetic properties of pristine AgGaO3 perovskite: A first principles study. Optik, 2021, 244, 167555.	1.4	7
41007	Superhard carbon-rich Câ€“N compounds hidden in compression of the mixture of carbon black and tetracyanoethylene. Carbon, 2021, 184, 846-854.	5.4	5
41008	CO and H2 adsorption on Au-Ni bimetallic surfaces: a combined experimental and DFT theoretical study. Surface Science, 2021, 712, 121892.	0.8	6
41009	La-doped TiO2 nanorods toward boosted electrocatalytic N2-to-NH3 conversion at ambient conditions. Chinese Journal of Catalysis, 2021, 42, 1755-1762.	6.9	35
41010	Magnetic, magnetocaloric and thermoelectric investigations of perovskite LaFeO3 compound: First principles and Monte Carlo calculations. Computational and Theoretical Chemistry, 2021, 1204, 113421.	1.1	22
41011	Use of local density approximation within range separated hybrid exchangeâ€“correlation functional to investigate Pb doped SnO<mml:math xmlns:mml="http://www.w3.org/1998/Math/MathML" display="inline" id="d1e1360" altimg="si94.svg"><mml:msub><mml:mrow /><mml:mrow><mml:mn>2</mml:mn></mml:mrow></mml:msub></mml:math>. Physica B: Condensed Matter, 2021, 619, 413236.	1.3	2
41012	Hematite rhombuses for chemiresitive ozone sensors: Experimental and theoretical approaches. Applied Surface Science, 2021, 563, 150209.	3.1	8
41013	AlAs/SiH van der Waals heterostructures: A promising photocatalyst for water splitting. Physica E: Low-Dimensional Systems and Nanostructures, 2021, 134, 114869.	1.3	20
41014	Large gap two-dimensional topological insulators with prominent Rashba effect in ethynyl functionalized â...¢-Bi Buckled-Honeycomb monolayers. Superlattices and Microstructures, 2021, 158, 107026.	1.4	1
41015	Modulation of the selectivity of CO2 to CO electroreduction in palladium rich Palladium-Indium nanoparticles. Journal of Catalysis, 2021, 402, 229-237.	3.1	13
41016	Stabilization of Orthorhombic CoSe₂ by 2D-rGO/MWCNT Heterostructures for Efficient Hydrogen Evolution Reaction and Flexible Energy Storage Device Applications. ACS Applied Energy Materials, 2021, 4, 11386-11399.	2.5	30
41017	Hydrogen diffusivity and solubility in stressed fcc crystals. Journal of Alloys and Compounds, 2021, 879, 160425.	2.8	5

#	Article	IF	Citations
41018	Trimetallic magnetite-Ti-Au nanoparticle formation: A theoretical approach. Materials Chemistry and Physics, 2021, 271, 124847.	2.0	0
41019	Adsorption study of 4-nitrophenol onto kaolinite (001) surface: A van der Waals density functional study. Materials Chemistry and Physics, 2021, 271, 124887.	2.0	7
41020	Catalytic activity and water stability of the MgO(111) surface for 2-pentanone condensation. Applied Catalysis B: Environmental, 2021, 294, 120234.	10.8	9
41021	The effect of Ni/Co-doping on electronic structures and optical properties of cubic Ca2Ge. Optik, 2021, 243, 167422.	1.4	1
41022	First-Principles investigation on the behavior of Pt single and triple atoms supported on monolayer CuO (1 1 0) in CO oxidation. Applied Surface Science, 2021, 564, 150435.	3.1	3
41023	Ab-initio study of nanoporous phosphorene as anode material in rechargeable Li/Na ion batteries. Applied Surface Science, 2021, 564, 150155.	3.1	9
41024	Quantitative analysis of rhenium in irradiated tungsten. Journal of Nuclear Materials, 2021, 554, 153014.	1.3	0
41025	First-principles investigation of the electronic and optical properties of As2GeTe nanotubes. Solid State Communications, 2021, 336, 114421.	0.9	0
41026	Investigation into thermoelectric properties of M (M=Hf, Zr) X2(X=S, Se, Te) nanotubes using first-principles calculation. Solid State Communications, 2021, 336, 114289.	0.9	9
41027	First-principles calculations to investigate electronic structure and transport properties of CrC monolayers: A new horizon for spintronic application. Materials Science and Engineering B: Solid-State Materials for Advanced Technology, 2021, 272, 115379.	1.7	17
41028	Partial Disproportionation Gallium-Oxygen Reaction Boosts Lithium-Oxygen Batteries. Energy Storage Materials, 2021, 41, 475-484.	9.5	12
41029	Electrochemical properties of biomass-derived carbon and its composite along with Na2Ti3O7 as potential high-performance anodes for Na-ion and Li-ion batteries. Electrochimica Acta, 2021, 392, 139026.	2.6	27
41030	Superior sensing performance of two-dimensional ruthenium carbide (2D-RuC) in detection of NO, NO2 and NH3 gas molecules. Applied Surface Science, 2021, 563, 150232.	3.1	22
41031	Ab initio investigation of physical properties of the graphene/As-F hetero-bilayer. Applied Surface Science, 2021, 563, 150339.	3.1	6
41032	Adsorption and dissociation of <mml:math xmlns:mml="http://www.w3.org/1998/Math/MathML" altimg="si3.svg"><mml:msub><mml:mrow><mml:mi mathvariant="normal">NO</mml:mi></mml:mrow><mml:mn>2</mml:mn></mml:msub></mml:math> on <mml:math xmlns:mml="http://www.w3.org/1998/Math/MathML" altimg="si1.svg"><mml:msub><mml:mrow><mml:mi mathvariant="normal">MoS</mml:mi></mml:mrow><mml:mn>2</mml:mn></mml:msub></mml:math> do	0.8	8
41033	Impact of the charge transfer process on the Fe2+/Fe3+distribution at Fe3O4 magnetic surface induced by deposited Pd clusters. Surface Science, 2021, 712, 121879.	0.8	3
41034	Ab-Initio Molecular Dynamics investigation of gas adsorption on Î±-quartz (001) for CO2 enhanced natural gas recovery. Journal of Petroleum Science and Engineering, 2021, 205, 108963.	2.1	2
41035	Photodynamic therapy: When van der Waals heterojunction meets tumor. Chemical Engineering Journal, 2021, 421, 129773.	6.6	9

#	Article	IF	Citations
41036	Prediction of the Rb-Si compounds under high pressure. Computational Materials Science, 2021, 198, 110704.	1.4	1
41037	Titanium carbide/zeolite imidazole framework-8/polylactic acid electrospun membrane for near-infrared regulated photothermal/photodynamic therapy of drug-resistant bacterial infections. Journal of Colloid and Interface Science, 2021, 599, 390-403.	5.0	48
41038	Screen the thermomechanical and optical properties of the new ductile 314 MAX phase boride Zr3CdB4: A DFT insight. Journal of Alloys and Compounds, 2021, 877, 160248.	2.8	25
41039	Reduction of NO on chemically doped, metal-free graphene. Carbon Trends, 2021, 5, 100111.	1.4	6
41040	The effect of hydrogen on the mechanical properties of high entropy alloy TiZrHfMoNb: First-principles investigation. Journal of Alloys and Compounds, 2021, 879, 160482.	2.8	15
41041	Thermodynamics of the Lu2O3 â€“ SiO2 system and comparison to other rare earth silicates. Journal of Chemical Thermodynamics, 2021, 161, 106483.	1.0	7
41042	From Î1- to ÎT _c-pinning in CaKFe₄As₄ single crystals obtained by adjusting their defect structures. Superconductor Science and Technology, 2021, 34, 115020.	1.8	12
41043	Structure, elastic, and electronic properties of the Nb2SnC1âˆ'xBx phases MAX: ab initio calculations. Materials Today Communications, 2021, , 102840.	0.9	0
41044	Mixing properties of Al₂O₃(0001)-supported M ₂O₃ and MMâ€²O₃ monolayers (M, Mâ€² = Ti, V, Cr, Fe). Journal of Physics Condensed Matter, 2022, 34, 034002.	0.7	2
41045	Electric field tunable bandgap and anisotropic high carrier mobility in SiAs2/GeAs2 lateral heterostructure. Computational Materials Science, 2021, 198, 110697.	1.4	6
41046	Can borophenes with Dirac cone be promising electrodes for supercapacitors. Applied Surface Science, 2021, 562, 150154.	3.1	7
41047	Deep Density: Circumventing the Kohn-Sham equations via symmetry preserving neural networks. Journal of Computational Physics, 2021, 443, 110523.	1.9	11
41048	Investigating the formation mechanism of void lattice in tungsten under neutron irradiation: from collision cascades to ordered nanovoids. Acta Materialia, 2021, 219, 117239.	3.8	23
41049	A potential full Heusler thermoelectric material CO2ZrZ (Z=Al, Si, Ga and Sn) in low temperature: An Ab-initio investigation. Solid State Communications, 2021, 336, 114422.	0.9	15
41050	Investigation of structural, electronic and elastic properties of matlockite-type SrFI under high pressure: An Ab-initio study. Solid State Communications, 2021, 336, 114399.	0.9	2
41051	Pressure and temperature dependence of second-order elastic constants from third-order elastic constants in TMC (TM=Nb, Ti, V, Zr). Ceramics International, 2021, 47, 27535-27544.	2.3	11
41052	Halide double perovskite Cs2AgInBr6 for photovoltaicâ€™s applications: Optical properties and stability. Optik, 2021, 243, 167198.	1.4	18
41053	Carbon dots structural characterization by solution-state NMR and UVâ€“visible spectroscopy and DFT modeling. Applied Surface Science, 2021, 564, 150195.	3.1	26

#	Article	IF	Citations
41054	Atomistic investigation of uranium oxycarbide (UCO) phase stability at finite temperatures: DFT+<mml:math xmlns:mml="http://www.w3.org/1998/Math/MathML" altimg="si2.svg"><mml:mi>U</mml:mi></mml:math> and AIMD+<mml:math xmlns:mml="http://www.w3.org/1998/Math/MathML" altimg="si2.svg"><mml:mi>U</mml:mi></mml:math> approaches. Journal of Nuclear Materials, 2021, 554, 153046.	1.3	3
41055	Boosting alkaline hydrogen electrooxidation on an unconventional fcc-Ru polycrystal. Journal of Energy Chemistry, 2021, 61, 15-22.	7.1	36
41056	Hierarchical flower-like TiO2 microspheres for high-selective NH3 detection: A density functional theory study. Sensors and Actuators B: Chemical, 2021, 345, 130303.	4.0	27
41057	Oxidation thermodynamics of Nb-Ti alloys studied via first-principles calculations. Journal of Alloys and Compounds, 2021, 879, 160455.	2.8	13
41058	Single transition metal atom modified MoSe2 as a promising electrocatalyst for nitrogen Fixation: A first-principles study. Chemical Physics Letters, 2021, 780, 138939.	1.2	5
41059	Study on the electronic properties of M6X6 (MÂ=ÂMo, W; X Â=ÂS, Se, Te) nanowire arrays. Chemical Physics Letters, 2021, 780, 138905.	1.2	0
41060	Mechanism and morphology evolution of the O phase transformation in Ti-22Al-25Nb alloy. Journal of Materials Science and Technology, 2021, 89, 97-106.	5.6	8
41061	Porous N, B co-doped carbon nanotubes as efficient metal-free electrocatalysts for ORR and Zn-air batteries. Chemical Engineering Journal, 2021, 422, 130134.	6.6	98
41062	Chemical transformation approach for high-performance ternary NiFeCo metal compound-based water splitting electrodes. Applied Catalysis B: Environmental, 2021, 294, 120246.	10.8	67
41063	Single-atom iron as a promising low-temperature catalyst for selective catalytic reduction of NO with NH3: A theoretical prediction. Fuel, 2021, 302, 121041.	3.4	36
41064	Thermal conductivity of magnesium selenide (MgSe)â€“A first principles study. Computational Materials Science, 2021, 198, 110679.	1.4	10
41065	Persistent radical pairs trigger nano-gold to highly efficiently and highly selectively drive the value-added conversion of nitroaromatics. Chem Catalysis, 2021, 1, 1118-1132.	2.9	10
41066	Computational evaluation of Mg-decorated g-CN as clean energy gas storage media. International Journal of Hydrogen Energy, 2021, 46, 35130-35136.	3.8	22
41067	Tunable Schottky Barrier and Interfacial Electronic Properties in Graphene/ZnSe Heterostructures. Frontiers in Chemistry, 2021, 9, 744977.	1.8	1
41068	Understanding electrochemical and structural properties of copper hexacyanoferrate: Application in hydrogen peroxide analysis. Electrochimica Acta, 2021, 394, 139147.	2.6	5
41069	Cu acting as Fe activity promoter in dual-atom Cu/Fe-NC catalyst in CO2RR to C1 products. Applied Surface Science, 2021, 564, 150423.	3.1	52
41070	Atomic study of hydrogen behavior in different vanadium carbides. Journal of Nuclear Materials, 2021, 554, 153096.	1.3	3
41071	Half-metallicity in Fe2MnSi and Mn2FeSi heusler compounds: A comparative ab initio study. Materials Chemistry and Physics, 2021, 271, 124897.	2.0	9

#	Article	IF	Citations
41072	Substantial role of charge transfer on the diffusion mechanism of interstitial elements in Î±-titanium: A First-principles study. Scripta Materialia, 2021, 203, 114065.	2.6	12
41073	The tuning on the magnetism and the electronic structures of monolayer Ti2N MXene by electric field. Physica B: Condensed Matter, 2021, 618, 413183.	1.3	8
41074	The effect of additional element dissolving on the solid solubility of Zn in Mg alloy: A first-principles prediction strategy. Journal of Alloys and Compounds, 2021, 877, 160312.	2.8	4
41075	Novel two-dimensional <mml:math xmlns:mml="http://www.w3.org/1998/Math/MathML" altimg="si1.svg"><mml:mrow><mml:mtext>C</mml:mtext><mml:mtext>r</mml:mtext><mml:mtext>X</mml:mtext><mml:msub><mml (X=Cr, Ru) metal for high NÃ©el temperature antiferromagnetic spintronics. Journal of Solid State Chemistry, 2021, 302, 122427.	1.4	3
41076	Influence of the Fe-doping on hydrogen behavior on the ZrCo surface. International Journal of Hydrogen Energy, 2021, 46, 33877-33888.	3.8	10
41077	Reversible hydrogenation and dehydrogenation of N-ethylcarbazole over bimetallic Pd-Rh catalyst for hydrogen storage. Chemical Engineering Journal, 2021, 421, 127781.	6.6	40
41078	TiO2/Carbon allotrope nanohybrids for supercapacitor application with theoretical insights from density functional theory. Applied Surface Science, 2021, 563, 150259.	3.1	14
41079	Electron reservoir enhances methane conversion on Zn dimer supported by N doped graphene: A DFT study. Applied Surface Science, 2021, 563, 150328.	3.1	4
41080	The new valence state [Ga]â^'5 in Li-Ga-Te system under high pressure. Solid State Communications, 2021, 336, 114402.	0.9	0
41081	Water adsorption behaviour on (001) pyrophyllite surface from ab initio Density Functional Theory simulations. Applied Clay Science, 2021, 212, 106221.	2.6	6
41082	The pressure effect on the structural, elastic, and mechanical properties of orthorhombic MgSiN2 from first-principles calculations. Solid State Communications, 2021, 336, 114318.	0.9	9
41083	ns2-containing vacancy-ordered double perovskites for optoelectronic applications: A first-principles investigation. Solid State Communications, 2021, 337, 114462.	0.9	1
41084	Interaction between hydrogen and solute atoms in bcc iron. Computational Materials Science, 2021, 198, 110652.	1.4	5
41085	Vacancy effect on the structure and diffusion of a Li adatom on the 2D Janus MoSSe monolayer. Computational Materials Science, 2021, 198, 110687.	1.4	2
41086	Influence of vacancy defects on the thermoelectric performance of SnSe sheet. Physica E: Low-Dimensional Systems and Nanostructures, 2021, 134, 114814.	1.3	10
41087	Fatigue resistance of atomically thin graphene oxide. Carbon, 2021, 183, 780-788.	5.4	14
41088	Hex-C558: A new porous metallic carbon allotrope for lithium-ion battery anode. Carbon, 2021, 183, 652-659.	5.4	10
41089	Atomic/molecular layer deposition of Ti-organic thin films from different aromatic alcohol and amine precursors. Thin Solid Films, 2021, 736, 138896.	0.8	5

#	Article	IF	Citations
41090	Tailoring the selectivity of ultralow-power heterojunction gas sensors by noble metal nanoparticle functionalization. Nano Energy, 2021, 88, 106241.	8.2	21
41091	Ultra-hard rhombohedral carbon by crystal chemistry and ab initio investigations. Journal of Solid State Chemistry, 2021, 302, 122354.	1.4	7
41092	Dual-atom active sites embedded in two-dimensional C2N for efficient CO2 electroreduction: A computational study. Journal of Energy Chemistry, 2021, 61, 507-516.	7.1	69
41093	Pt atomic clusters catalysts with local charge transfer towards selective oxidation of furfural. Applied Catalysis B: Environmental, 2021, 295, 120290.	10.8	52
41094	Endogenous NO-releasing Carbon Nanodots for Tumor-specific Gas Therapy. Acta Biomaterialia, 2021, 136, 485-494.	4.1	18
41095	Identifying the Critical Surface Descriptors for the Negative Slopes in the Adsorption Energy Scaling Relationships via Density Functional Theory and Compressed Sensing. Journal of Physical Chemistry Letters, 2021, 12, 9791-9799.	2.1	5
41096	Theoretically Predicted CO Adsorption and Dissociation on Ru-doped Co(100) Surfaces. Applied Surface Science, 2021, 572, 151476.	3.1	1
41097	Enhanced properties of covalently coupled borophene-graphene layers through fluorination and hydrogenation. Applied Surface Science, 2021, 562, 150150.	3.1	17
41098	Resistive switching characteristics and theoretical simulation of a Pt/a-Ta2O5/TiN synaptic device for neuromorphic applications. Journal of Alloys and Compounds, 2021, 877, 160204.	2.8	20
41099	Theory prediction of band structures, densities of states, mechanical and thermodynamic properties of solid solutions BaxK1-xBi0.92Mg0.08O3. Physica B: Condensed Matter, 2021, 618, 413163.	1.3	2
41100	Efficient electrochemical CO2 reduction on C2N monolayer supported transition metals trimer catalysts: A DFT study. Applied Surface Science, 2021, 564, 150331.	3.1	24
41101	Effect of metal atoms on the superconducting properties of decahydrides, MH10 (MÂ=ÂGa, Nb & Mo). Physica B: Condensed Matter, 2021, 619, 413217.	1.3	0
41102	New nanosized (Gd3+, Sm3+) co-doped zinc ferrite: Structural, magnetic and first-principles study. Physica B: Condensed Matter, 2021, 619, 413262.	1.3	16
41103	Functionalization of monolayer MoS2 with transition metal oxide nanoclusters. Physica B: Condensed Matter, 2021, 619, 413245.	1.3	2
41104	A DFT+U study about agglomeration of Au atoms on reduced surface of rutile TiO2 (110). Materials Chemistry and Physics, 2021, 271, 124944.	2.0	8
41105	Structural, electronic, magnetic, and optical properties of new TiXY (X = F and Cl; Y = S, Se and Te) Janus monolayers: A first-principles study. Optik, 2021, 244, 167438.	1.4	1
41106	Semiconductor-metal transition induced by combined electric field and external strain in bilayer phosphorene. Solid State Communications, 2021, 337, 114434.	0.9	3
41107	Ab initio predictions of magnetism and half-metallicity of (111)-surfaces of Co2CrSi full-Heusler alloy. Vacuum, 2021, 192, 110455.	1.6	1

#	Article	IF	Citations
41108	Tuning electronic structure of palladium from wheat flour-derived N-doped mesoporous carbon for efficient selective hydrogenation of acetylene. Applied Surface Science, 2021, 562, 150141.	3.1	11
41109	Unveiling the electronic structure nature of twisted hybrid perovskites for solar cell applications: A combined experimental and theoretical study. Solar Energy, 2021, 227, 151-161.	2.9	3
41110	Ni diffusion in ceria lattice: A combined experimental and theoretical study. Acta Materialia, 2021, 219, 117252.	3.8	9
41111	Density functional theory studies of structural, electronic and optical properties of cubic 3d-transition metal nitrides. Intermetallics, 2021, 137, 107272.	1.8	9
41112	Insight into the mechanism of nanoparticle induced suppression of interfacial tension. Journal of Molecular Liquids, 2021, 339, 117177.	2.3	3
41113	Highly selective and reversible 2D PtX2 (XÂ=ÂP, As) hazardous gas sensors: Ab-initio study. Applied Surface Science, 2021, 563, 150391.	3.1	11
41114	Elastic properties of heterodesmic composite structures: The case of calcite CaCO3 (space group) Tj ETQq0 0 0 rgBT /Overlock 10 Tf 50 Part C: Open Access, 2021, 6, 100184.	1.5	4
41115	The precipitation competition of Î-series precipitates and Î‘ precipitates in Li-containing Al-Zn-Mg-Cu alloys. Computational Materials Science, 2021, 198, 110707.	1.4	7
41116	A comparison study of the structural, electronic, elastic, dielectric and dynamical properties of Zr-based monolayer dioxides (ZrO2) and dichalcogenides (ZrX2; X = S, Se or Te) as well as their Janus structures (ZrXY; X, Y = O, S, Se or Te, <mml:math xmlns:mml="http://www.w3.org/1998/Math/MathML") Tj ETQq0 0 0 rgBT /Overlock 1 Low-Dimensional Systems and Nanostructures, 2021, 134, 114855.	1.3	11
41117	Structural, electronic and magnetic properties of CrmSn and CrmSen nanoflakes: An ab initio investigation. Physica E: Low-Dimensional Systems and Nanostructures, 2021, 134, 114825.	1.3	5
41118	Electrical contacts in monolayer Ga2O3 field-effect tansistors. Applied Surface Science, 2021, 564, 150386.	3.1	11
41119	A GrÃ¼neisen tensor for rutile and its application to host-inclusion systems. American Mineralogist, 2021, 106, 1586-1595.	0.9	6
41120	Structural and Thermo-Physical Properties of 3C-SiC: High-Temperature and High-Pressure Effects. Silicon, 2022, 14, 6299-6309.	1.8	8
41121	Layer effect on thermal expansion in blue phosphorene monolayer and few-layer. Physics Letters, Section A: General, Atomic and Solid State Physics, 2021, 419, 127726.	0.9	2
41122	DFT approaches unraveling the surface and morphological properties of MnMoO4. Applied Surface Science, 2021, 567, 150882.	3.1	13
41123	Low Ru loading RuO2/(Co,Mn)3O4 nanocomposite with modulated electronic structure for efficient oxygen evolution reaction in acid. Applied Catalysis B: Environmental, 2021, 297, 120442.	10.8	128
41124	Layered quaternary chalcogenides KMgCuSe2 and KMgCuTe2 with paramagnetic semiconducting behavior. Journal of Alloys and Compounds, 2021, 883, 160820.	2.8	4
41125	Iron molybdenum selenide supported on reduced graphene oxide as an efficient hydrogen electrocatalyst in acidic and alkaline media. Journal of Colloid and Interface Science, 2021, 602, 384-393.	5.0	12

#	Article	IF	Citations
41126	Interaction studies of tuberculosis biomarker vapours on novel beta arsenene sheets â€“ A DFT insight. Computational and Theoretical Chemistry, 2021, 1205, 113426.	1.1	15
41127	Archimedean polyhedron LiCoO2 for ultrafast rechargeable Li-ion batteries. Chemical Engineering Journal, 2021, 423, 130122.	6.6	4
41128	Doping the permanent magnet CeFe11Ti with Co and Ni using ab-initio density functional methods. Physica B: Condensed Matter, 2021, 620, 413241.	1.3	3
41129	Physical properties of MAX phase Zr2PbC under pressure: Investigation via DFT scheme. Physica B: Condensed Matter, 2021, 620, 413258.	1.3	8
41130	Synergistic effects in ordered Co oxides for boosting catalytic activity in advanced oxidation processes. Applied Catalysis B: Environmental, 2021, 297, 120463.	10.8	30
41131	First-Principles investigation of Pressure-Induced structural transformations of barium borates in the BaO-B2O3-BaF2 system in the range of 0â€“10 GPa. Computational Materials Science, 2021, 199, 110735.	1.4	5
41132	Single-atomic Pt sites anchored on defective TiO2 nanosheets as a superior photocatalyst for hydrogen evolution. Journal of Energy Chemistry, 2021, 62, 1-10.	7.1	70
41133	Influence of high pressure on structural, electronic and mechanical properties of tetragonal FeH5. Solid State Communications, 2021, 338, 114483.	0.9	1
41134	Helium migration in Zr-Nb multilayers under electric field. Journal of Nuclear Materials, 2021, 555, 153133.	1.3	3
41135	Ab initio study of local lattice distortion of hexagonal closed-packed high-entropy (Mo0.25Nb0.25Ta0.25V0.25) (Al0.5Si0.5)2 and the influence on thermodynamic property. Journal of Solid State Chemistry, 2021, 303, 122469.	1.4	3
41136	Pseudoelastic deformation in Mo-based refractory multi-principal element alloys. Acta Materialia, 2021, 220, 117299.	3.8	11
41137	A DFT-based method to determine the hydrophobicity change mechanism on sphalerite and pyrite surfaces caused by sodium dithionite. Colloids and Surfaces A: Physicochemical and Engineering Aspects, 2021, 628, 127339.	2.3	2
41138	Differential clustering of self-interstitials during Si crystal growth. Journal of Crystal Growth, 2021, 574, 126313.	0.7	1
41139	Experimental and first-principle computational exploration on biomass cellulose/magnesium hydroxide composite: Local structure, interfacial interaction and antibacterial property. International Journal of Biological Macromolecules, 2021, 191, 584-590.	3.6	2
41140	Unraveling surface functionalization of Cr2B2T2 (TÂ=ÂOH, O, Cl, H) MBene by first-principles calculations. Computational Materials Science, 2021, 199, 110810.	1.4	14
41141	Emergence of bulk photovoltaic effect in anion-ordered perovskite sulfur diiodide MASbSI2 with spontaneous out-of-plane ferroelectricity. Materials Today Physics, 2021, 21, 100459.	2.9	4
41142	Strain-induced structural phase transition in GeN monolayer. Applied Surface Science, 2021, 567, 150793.	3.1	9
41143	Stabilization of unstable and metastable InP native oxide thin films by interface effects. Applied Surface Science, 2021, 567, 150848.	3.1	2

#	Article	IF	Citations
41144	Hydrogen molecule capacity physisorption on BC3 monolayer: First-principles calculations. Diamond and Related Materials, 2021, 119, 108583.	1.8	15
41145	Adsorption and dissociation behavior of H2O on PuH2 (1 1 0) surface: A density functional theory study. Applied Surface Science, 2021, 566, 150733.	3.1	6
41146	Formation of ordered B structure on W(100). Surface Science, 2021, 713, 121906.	0.8	7
41147	Coverage-dependent adsorption of nitrous oxide (N2O) on perfect and defective Cu(0 0 1) surfaces: A DFT investigation with and without van der Walls forces. Computational and Theoretical Chemistry, 2021, 1205, 113428.	1.1	1
41148	First-principles study of the surface properties of LiAl5O8: Stability and tritiated water formation. Journal of Nuclear Materials, 2021, 555, 153111.	1.3	5
41149	Effect of Lu2O3 addition on the oxidation behavior of SiC-ZrB2 composite coating at 1500Âă„ƒ: Experimental and theoretical study. Corrosion Science, 2021, 192, 109803.	3.0	5
41150	Positron annihilation investigation of thermal cycling induced martensitic transformation in NiTi shape memory alloy. Acta Materialia, 2021, 220, 117298.	3.8	6
41151	Formation of 1D coordination polymers by reaction of a tetrazine ligand and PbX2 (X: Br, I) salts: Spectral, structural and theoretical studies. Polyhedron, 2021, 208, 115440.	1.0	3
41152	Advanced analysis of laser-driven pulsed magnetic diffusion based on quantum molecular dynamics simulation. Matter and Radiation at Extremes, 2021, 6, 065901.	1.5	1
41153	Spinel NiFe2O4 nanoparticles decorated 2D Ti3C2 MXene sheets for efficient water splitting: Experiments and theories. Journal of Colloid and Interface Science, 2021, 602, 232-241.	5.0	63
41154	Single tungsten atom steered band-gap engineering for graphitic carbon nitride ultrathin nanosheets boosts visible-light photocatalytic H2 evolution. Chemical Engineering Journal, 2021, 424, 130004.	6.6	39
41155	Nb-based double transition metal silicides MAX-phase: A first-principle study. Chemical Physics, 2021, 551, 111321.	0.9	3
41156	Regulate chemical environment to control the formation of defects on Ta3N5 (1 1 0) surface: From theoretical perspectives. Chemical Physics Letters, 2021, 782, 139026.	1.2	2
41157	The spintronic and optoelectronic applications of substitutional doped CoS2. Materials Chemistry and Physics, 2021, 272, 125052.	2.0	1
41158	Enhanced piezoresponse and surface electric potential of hybrid biodegradable polyhydroxybutyrate scaffolds functionalized with reduced graphene oxide for tissue engineering. Nano Energy, 2021, 89, 106473.	8.2	28
41159	Effects of external electric field on adsorption behavior of organic molecules on stanene: Highly sensitive sensor devices. Solid State Communications, 2021, 338, 114459.	0.9	8
41160	Dual-salt-additive electrolyte enables high-voltage lithium metal full batteries capable of fast-charging ability. Nano Energy, 2021, 89, 106353.	8.2	90
41161	Thermal and elastic properties of binary and ternary high borate glass networks from first-principles methods. Journal of Non-Crystalline Solids, 2021, 571, 121059.	1.5	5

#	Article	IF	Citations
41162	First-principles prediction of NO2 and SO2 adsorption on MgO/(Mg0.5Ni0.5)O/MgO(1 0 0). Applied Surface Science, 2021, 566, 150650.	3.1	7
41163	Mechanism insight into MnO for CO activation and O removal processes on Co(0001) surface: A DFT and kMC study. Applied Surface Science, 2021, 567, 150854.	3.1	13
41164	Structural change from Pbnm to R3Ì…c phase with varying Fe/Mn content in (1-x) LaFeO3.xLaMnO3 solid solution leading to modifications in octahedral tilt and valence states. Journal of Alloys and Compounds, 2021, 883, 160761.	2.8	7
41165	Adsorption and spin polarization of pyridine on Fe/W(1 1 0) interface: A DFT study. Computational Materials Science, 2021, 199, 110734.	1.4	3
41166	Cold and hot uranium in DFT calculations: Investigation by the GTH pseudopotential, PAW, and APWÂ+Âlo methods. Computational Materials Science, 2021, 199, 110665.	1.4	3
41167	First-principles analysis of desired inherent photovoltaic functionalities of tetragonal CuAlX2 (X=O,) Tj ETQq1 1 0.784314 rgBT /Overl	1.4	3
41168	The studies of electronic structure, mechanical properties and ideal fracture behavior of U3Si1.75Al0.25: first-principle investigations. Journal of Materials Research and Technology, 2021, 15, 1356-1369.	2.6	4
41169	One- and two-dimensional structures based on gallium nitride. Journal of Solid State Chemistry, 2021, 303, 122513.	1.4	8
41170	Understanding the improvement of thermo-mechanical and optical properties of 212 MAX phase borides Zr2AB2 (A = In, Tl). Journal of Materials Research and Technology, 2021, 15, 2227-2241.	2.6	12
41171	Nitrogen diffusion in vacancy-rich ferrite and austenite, from first principles to applications. Acta Materialia, 2021, 220, 117292.	3.8	2
41172	KPFM and DFT as tools to correlate the charge distribution and molecular orientation of dendritic adsorbates on different surfaces. Applied Surface Science, 2021, 565, 150552.	3.1	5
41173	Unveiling the morphology dependence of ceria nanocrystals for boosting lowâ^'temperature cyclohexane oxidative dehydrogenation. Applied Surface Science, 2021, 565, 150609.	3.1	9
41174	Electronic, mechanical and thermodynamic properties of ZrC, HfC and their solid solutions studied by first-principles calculation. Solid State Communications, 2021, 338, 114481.	0.9	9
41175	Vacancy-cluster and off-lattice metal-atom diffusion mechanisms in transition metal carbides. Computational Materials Science, 2021, 199, 110713.	1.4	3
41176	Magnetism and topological Hall effect in antiferromagnetic Ru2MnSn-based Heusler compounds. Journal of Magnetism and Magnetic Materials, 2021, 537, 168104.	1.0	5
41177	Electronic and magnetic properties of metalâ€“organic polymers with 4d and 5d-transition metal ions. Journal of Magnetism and Magnetic Materials, 2021, 537, 168183.	1.0	6
41178	Engineering the electronic and magnetic properties of nitrogene monolayer and bilayer by doping: A first-principles study. Applied Surface Science, 2021, 566, 150711.	3.1	10
41179	Dual-doped carbon hollow nanospheres achieve boosted pseudocapacitive energy storage for aqueous zinc ion hybrid capacitors. Energy Storage Materials, 2021, 42, 705-714.	9.5	96

#	Article	IF	Citations
41180	A first-principles study of thiadiazole and dimercapto-thiadiazole adsorption on copper and silver surfaces. Materials Chemistry and Physics, 2021, 273, 125057.	2.0	6
41181	Electronic and optical properties of ZnSe by theoretical simulation TB-mBJ (Tran-Blaha modified Becke) Tj ETQq1 1 0.784314 rgBT /Over Science, 2021, 566, 150690.	3.1	7
41182	DFT investigation of mechanical and vibrational properties of CuTe. Physica B: Condensed Matter, 2021, 620, 413214.	1.3	2
41183	Ab-initio electronic structure simulations of transition metal doped Bi2Se3 topological insulator. Superlattices and Microstructures, 2021, 159, 107033.	1.4	4
41184	Trifle Pt coupled with NiFe hydroxide synthesized via corrosion engineering to boost the cleavage of water molecule for alkaline water-splitting. Applied Catalysis B: Environmental, 2021, 297, 120395.	10.8	109
41185	Functional group tuning of two-dimensional carbon nanosheets for boosting oxygen reduction electrocatalysis. Carbon, 2021, 185, 395-403.	5.4	10
41186	A systematic analysis of phase stability in refractory high entropy alloys utilizing linear and non-linear cluster expansion models. Acta Materialia, 2021, 220, 117269.	3.8	10
41187	Combined density functional theory/kinetic Monte Carlo investigation of surface morphology during cycling of Li-Cu electrodes. Electrochimica Acta, 2021, 397, 139272.	2.6	3
41188	Selectively constructing nitrogen vacancy in carbon nitrides for efficient syngas production with visible light. Applied Catalysis B: Environmental, 2021, 297, 120496.	10.8	31
41189	Diaphite-structured nanodiamonds with six- and twelve-fold symmetries. Diamond and Related Materials, 2021, 119, 108573.	1.8	16
41190	Numerical and experimental determination of the thermal conductivity of pristine and substituted Fe2VAl. Journal of Alloys and Compounds, 2021, 883, 160828.	2.8	3
41191	Intrinsic point defects and charge carrier trapping in monolayer BiOX (X = I, Br, and Cl). Ceramics International, 2021, 47, 30523-30530.	2.3	5
41192	Insights into the oxidation mechanism of millerite exposed to O2 and H2O using DFT study. Computational and Theoretical Chemistry, 2021, 1205, 113435.	1.1	1
41193	Two-dimensional ferromagnetic semiconductors of rare-earth monolayer GdX2 (XÂ= Cl, Br, I) with large perpendicular magnetic anisotropy and high Curie temperature. Materials Today Physics, 2021, 21, 100514.	2.9	32
41194	In-situ exsolution of Ni nanoparticles to achieve an active and stable solid oxide fuel cell anode catalyst on A-site deficient La0.4Sr0.4Ti0.94Ni0.06O3-Î´. Journal of Industrial and Engineering Chemistry, 2021, 103, 264-274.	2.9	17
41195	Theoretical investigation of hydrated [Lu(OH)2]+ adsorption on kaolinite(0Â0Â1) surface with DFT calculations. Applied Surface Science, 2021, 565, 150473.	3.1	20
41196	Penta-graphene as a Metal-free catalyst for CO and NO reaction -Insights from First-principles calculations. Applied Surface Science, 2021, 565, 150515.	3.1	2
41197	Gas (CO and NO) adsorption and sensing based on transition metals functionalized Janus MoSSe. Applied Surface Science, 2021, 565, 150509.	3.1	13

#	Article	IF	Citations
41198	Effects of intrinsic defects and doping on SrFe12O19: A first-principles exploration of the structural, electronic and magnetic properties. Journal of Magnetism and Magnetic Materials, 2021, 538, 168257.	1.0	14
41199	Theoretical study of structural, electronic, optical and thermoelectric properties of XN (X = Sc, Y). Materials Science in Semiconductor Processing, 2021, 135, 106090.	1.9	8
41200	Novel BCN2 and CN compounds in C2/m phase: First-principle calculations. Journal of Physics and Chemistry of Solids, 2021, 158, 110231.	1.9	7
41201	Pressure-induced two magnetic collapses in the ferromagnetic L12-Fe3Pd alloy and related elasticity and lattice dynamics anomalies. Journal of Magnetism and Magnetic Materials, 2021, 538, 168322.	1.0	4
41202	Modulating electronic properties of pyridinium lead halide perovskites via fluorinated methyl substituents. Materials Chemistry and Physics, 2021, 273, 125139.	2.0	5
41203	DFT insights into the migration of effective electrons towards O2 for OH formation over electron-rich sites on BiOBr (0 0 1) surface. Applied Surface Science, 2021, 567, 150828.	3.1	8
41204	5M and 7M martensitic stability and associated physical properties in Ni50Mn35In15 alloy: first-principles calculations and experimental verification. Scripta Materialia, 2021, 204, 114140.	2.6	4
41205	Tellurium vacancy in two-dimensional Si2Te3 for resistive random-access memory. Journal of Solid State Chemistry, 2021, 303, 122448.	1.4	2
41206	First-principles-based high-throughput computation for high entropy alloys with short range order. Journal of Alloys and Compounds, 2021, 882, 160776.	2.8	17
41207	C-doped ZnS-ZnO/Rh nanosheets as multijunctioned photocatalysts for effective H2 generation from pure water under solar simulating light. Applied Catalysis B: Environmental, 2021, 297, 120473.	10.8	45
41208	Surface energy and surface stress of polar GaN(0001). Applied Surface Science, 2021, 566, 150627.	3.1	3
41209	A lattice defect-inspired leaching strategy toward simultaneous recovery and separation of value metals from spent cathode materials. Waste Management, 2021, 135, 40-46.	3.7	9
41210	Identifying active sites of boron, nitrogen co-doped carbon materials for the oxygen reduction reaction to hydrogen peroxide. Journal of Colloid and Interface Science, 2021, 602, 799-809.	5.0	32
41211	Effect of a ferromagnetic STM cobalt tip on a single Co-phthalocyanine molecule adsorbed on a ferromagnetic substrate. Physics Open, 2021, 9, 100088.	0.7	1
41212	Transition metal single-atom anchored g-CN monolayer for constructing high-activity multifunctional electrocatalyst. Applied Surface Science, 2021, 565, 150547.	3.1	28
41213	Insight into the overpotential and thermodynamic mechanism of hydroxyl radical formation on diamond anode. Applied Surface Science, 2021, 565, 150559.	3.1	14
41214	The effective mass, fitness function and enhanced thermoelectric properties in CuSbS2 for p-type thermoelectric material applications: Density functional theory approach. Materials Science and Engineering B: Solid-State Materials for Advanced Technology, 2021, 273, 115404.	1.7	4
41215	Two-dimensional SnTe/Sb van der Waals heterostructure for photovoltaic application. Solid State Sciences, 2021, 121, 106736.	1.5	7

#	Article	IF	Citations
41216	Anomalous Hall and Nernst Conductivities in Co2NbGa: A first principles study. Journal of Magnetism and Magnetic Materials, 2021, 538, 168303.	1.0	6
41217	A comparative study of Ag doping effects on the electronic, optical, carrier conversion, photocatalytic and electrical properties of MoS2. Materials Science and Engineering B: Solid-State Materials for Advanced Technology, 2021, 273, 115442.	1.7	7
41218	Unraveling the relationship between bulk structure and exposed surfaces and its effect on the electronic structure and photoluminescent properties of Ba0.5Sr0.5TiO3: A joint experimental and theoretical approach. Materials Research Bulletin, 2021, 143, 111442.	2.7	7
41219	The enhanced near-infrared photocatalytic and photothermal effects of MXene-based heterojunction for rapid bacteria-killing. Applied Catalysis B: Environmental, 2021, 297, 120500.	10.8	68
41220	First principles predictions of Na and K storage in layered SnSe2. Applied Surface Science, 2021, 566, 150522.	3.1	29
41221	Functionalized Mo2B2 MBenes: Promising anchoring and electrocatalysis materials for Lithium-Sulfur battery. Applied Surface Science, 2021, 566, 150634.	3.1	29
41222	Investigation on phase structure and magnetic properties of high-temperature Ni-Pt-Co-Mn-Sn magnetic shape memory alloys by first-principles calculations. Computational Materials Science, 2021, 199, 110748.	1.4	5
41223	Reduced interstitial mobility through multicomponent alloying in bcc W. Fusion Engineering and Design, 2021, 172, 112745.	1.0	0
41224	Iminodiacetonitrile induce-synthesis of two-dimensional PdNi/Ni@carbon nanosheets with uniform dispersion and strong interface bonding as an effective bifunctional eletrocatalyst in air-cathode. Energy Storage Materials, 2021, 42, 118-128.	9.5	64
41225	Phonon thermal transport properties of GaN with symmetry-breaking and lattice deformation induced by the electric field. International Journal of Heat and Mass Transfer, 2021, 179, 121659.	2.5	11
41226	Predicted structural, elastic, electronic and optical properties of inorganic complex chloride and bromide CsInCl3 and CsInBr3. Materials Science in Semiconductor Processing, 2021, 135, 106033.	1.9	2
41227	Methane adsorption on the surface of metal (Fe, Ni, Pd) decorated SWCNT: A density functional theory (DFT) study. Surface Science, 2021, 713, 121913.	0.8	5
41228	Modeling the half-metallicity of the CrN/GaN (1Â1Â1) heterostructure. Applied Surface Science, 2021, 566, 150637.	3.1	4
41229	Synthesize of 3D-conductive supramolecular gel and derived N-doped Feâ€“C as high-performance lithium-ion battery anodes. Vacuum, 2021, 193, 110532.	1.6	2
41230	Press dependent electronic structure and optical property of Ba2Mg(PO4)2:Eu2+. Journal of Alloys and Compounds, 2021, 883, 160870.	2.8	1
41231	Te2Br: A new one-dimensional semiconductor with direct-band gap, high carrier mobility, superior flexibility, and strong quantum confinement effect. Physics Letters, Section A: General, Atomic and Solid State Physics, 2021, 416, 127668.	0.9	2
41232	A new method for calculating the thermodynamic and physical properties of compounds: Application to Laves phase Fe2Mo. Physica B: Condensed Matter, 2021, 621, 413307.	1.3	4
41233	Elasticity of selected icy satellite candidate materials (CO2, C6H6, MgSO4Â·7H2O and CaSO4Â·2H2O) revisited by dispersion corrected density functional theory. Icarus, 2021, 368, 114611.	1.1	3

#	Article	IF	Citations
41234	Interfacial charge redistribution in interconnected network of Ni2Pâ€“Co2P boosting electrocatalytic hydrogen evolution in both acidic and alkaline conditions. Chemical Engineering Journal, 2021, 424, 130444.	6.6	76
41235	First-principles calculation of the electronic properties and external force modulation of a new tetragonal structure C3N2 crystal. Solid State Communications, 2021, 338, 114455.	0.9	3
41236	Jadeite and related species in shocked meteorites: Limitations on inference of shock conditions. American Mineralogist, 2022, 107, 1868-1877.	0.9	3
41237	Impact of metal/ceramic interactions on interfacial shear strength: Study of Cr/TiN using a new modified embedded-atom potential. Materials and Design, 2021, 210, 110120.	3.3	4
41238	V2C MXene synergistically coupling FeNi LDH nanosheets for boosting oxygen evolution reaction. Applied Catalysis B: Environmental, 2021, 297, 120474.	10.8	106
41239	The optoelectronic properties of Eu/F-codoped tin oxide, an experimental and DFT study. Ceramics International, 2021, 47, 31756-31764.	2.3	2
41240	First-principles study on the Cu-Au alloy monolayer supported on WC for hydrogen evolution. Applied Surface Science, 2021, 565, 150568.	3.1	9
41241	Gas sensing of fibrous red phosphorene towards inorganic air pollutants: Insights from first-principles calculations. Applied Surface Science, 2021, 565, 150546.	3.1	7
41242	Density functional theoryâ€“based design of a Pt-skinned PtNi catalyst for the oxygen reduction reaction in fuel cells. Applied Surface Science, 2021, 565, 150518.	3.1	13
41243	Ab-initio study of the electronic structure and magnetic properties of Ce2Fe17. Journal of Alloys and Compounds, 2021, 888, 161521.	2.8	6
41244	Ab initio thermochemistry study of polymorphism in the Si2N2(NH) analog of Si2N2O. Computational Materials Science, 2021, 200, 110772.	1.4	1
41245	Prediction of optoelectronic features and efficiency for CuMX2 (M=Ga, In; X=S, Se) semiconductors using mbj+U approximation. Current Applied Physics, 2021, 32, 11-23.	1.1	1
41246	Transformations of silicon clathrate Si136 under high hydrogen pressure up to 11ÂGPa. Solid State Communications, 2021, 340, 114492.	0.9	1
41247	Nitrogen-doped graphdiyne for efficient electrocatalytic <mml:math xmlns:mml="http://www.w3.org/1998/Math/MathML" display="inline" id="d1e292" altimg="si39.svg"><mml:msub><mml:mrow><mml:mi mathvariant="normal">N</mml:mi></mml:mrow><mml:mrow><mml:mn>2</mml:mn></mml:mrow></mml:msub></mml:math> reduction: A first-principles study. Applied Surface Science, 2021, 570, 151109.	3.1	14
41248	Analysis of electronic structure and properties of Ga2O3/CuAlO2 heterojunction. Applied Surface Science, 2021, 568, 150826.	3.1	16
41249	Ethane dehydrogenation over the single-atom alloy catalysts: Screening out the excellent catalyst with the dual descriptors. Fuel, 2021, 306, 121641.	3.4	11
41250	Electronic modulation of CoP nanoarrays by Cr-doping for efficient overall water splitting. Chemical Engineering Journal, 2021, 425, 130651.	6.6	72
41251	Electrochemical catalytic mechanism of single transition metal atom embedded BC3 monolayer for oxygen reduction and evolution reactions. Chemical Engineering Journal, 2021, 425, 130631.	6.6	18

#	Article	IF	Citations
41252	Study of lattice dynamic, electronic and mechanical properties of Half-Heusler RuCrP alloy. Materials Today Communications, 2021, 29, 102799.	0.9	4
41253	Fabrication of cellulose@Mg(OH)2 composite filter via interfacial bonding and its trapping effect for heavy metal ions. Chemical Engineering Journal, 2021, 426, 130812.	6.6	24
41254	First-principles calculations on the adhesion strength, fracture mechanism, interfacial bonding of the semi-coherent Al(1 1 1)/Al3BC(0001) interfaces. Applied Surface Science, 2021, 569, 150996.	3.1	28
41255	Nd2CaB10O19: A potential self-activated and self-frequency-doubling multifunctional crystal. Journal of Solid State Chemistry, 2021, 304, 122558.	1.4	4
41256	A highly efficient and durable air electrode for intermediate-temperature reversible solid oxide cells. Applied Catalysis B: Environmental, 2021, 299, 120631.	10.8	37
41257	Effect of heterostructure engineering on electronic structure and transport properties of two-dimensional halide perovskites. Computational Materials Science, 2021, 200, 110823.	1.4	10
41258	Suppressing toxic intermediates during photocatalytic degradation of glyphosate by controlling adsorption modes. Applied Catalysis B: Environmental, 2021, 299, 120671.	10.8	18
41259	Mechanism for enhanced oil recovery from carbonate reservoirs by adding copper ions to seawater. Fuel, 2021, 305, 121605.	3.4	3
41260	The formation energy and interaction energy of point defects in ZrC. Journal of Nuclear Materials, 2021, 557, 153235.	1.3	12
41261	Fast start-up structured CuFeMg/Al2O3 catalyst applied in microreactor for efficient hydrogen production in methanol steam reforming. Chemical Engineering Journal, 2021, 426, 130644.	6.6	13
41262	Weak ferromagnetic â€“ Antiferromagnetic transition in MnFe0.25Sb. Journal of Magnetism and Magnetic Materials, 2021, 539, 168380.	1.0	1
41263	Dissociation of air pollutants on the uniform surface of pentagonal BeP2. Applied Surface Science, 2021, 570, 151061.	3.1	3
41264	Hydrogen evolution reaction on transition metal nanoparticles from first-principles. Applied Surface Science, 2021, 570, 151211.	3.1	7
41265	Revealing the atomic-scale structure and the fracture mechanism of the Î±-Al2O3/Î³-Fe ceramic-metal interface. Journal of Alloys and Compounds, 2021, 885, 161163.	2.8	11
41266	An improved oxygen reduction reaction activity and CO2-tolerance of La0.6Sr0.4Co0.2Fe0.8O3-Î´ achieved by a surface modification with barium cobaltite coatings. Journal of Power Sources, 2021, 514, 230573.	4.0	24
41267	Theoretical study of the pressure effects on the electronic and magnetic properties of Sc3In. Journal of Magnetism and Magnetic Materials, 2021, 539, 168353.	1.0	0
41268	Charge localization to optimize reactant adsorption on KCu7S4/CuO interfacial structure toward selective CO2 electroreduction. Applied Catalysis B: Environmental, 2021, 298, 120531.	10.8	25
41269	Thermodynamic evidence of the ferroelectric Berry phase in europium-based ferrobismuthite Eu2Bi2Fe4O12. Journal of Alloys and Compounds, 2021, 884, 161114.	2.8	4

#	Article	IF	Citations
41270	Defect enriched hierarchical iron promoted Bi2MoO6 hollow spheres as efficient electrocatalyst for water oxidation. Chemical Engineering Journal, 2021, 426, 131884.	6.6	16
41271	Mechanistic understanding of support effect on the activity and selectivity of indium oxide catalysts for CO2 hydrogenation. Chemical Engineering Journal, 2021, 426, 131767.	6.6	19
41272	Ab initio investigations on metal ion pre-intercalation strategy of layered V2O5 cathode for magnesium-ion batteries. Applied Surface Science, 2021, 569, 150983.	3.1	11
41273	Segregation of Ni and Si to coherent bcc Fe-Cu interfaces from density functional theory. Journal of Nuclear Materials, 2021, 556, 153185.	1.3	7
41274	Synthesis and characterization of new indium gallium selenides of the InSe-GaSe system. Journal of Solid State Chemistry, 2021, 304, 122569.	1.4	1
41275	Single-step synthesis of oxygen-doped hollow porous graphitic carbon nitride for photocatalytic ciprofloxacin decomposition. Chemical Engineering Journal, 2021, 425, 130502.	6.6	41
41276	Rational design of intermetallic compound catalysts for propane dehydrogenation from a descriptor-based microkinetic analysis. Journal of Catalysis, 2021, 404, 32-45.	3.1	15
41277	Photocatalytic production of H2O2 from water and dioxygen only under visible light using organic polymers: Systematic study of the effects of heteroatoms. Applied Catalysis B: Environmental, 2021, 299, 120666.	10.8	22
41278	Density functional theory calculations of the thermodynamic and kinetic properties of point defects in <mml:math xmlns:mml="http://www.w3.org/1998/Math/MathML" altimg="si2.svg"><mml:mi>Î²</mml:mi></mml:math>-U. Journal of Nuclear Materials, 2021, 557, 153238.	1.3	1
41279	Supercapattery electrode materials by Design: Plasma-induced defect engineering of bimetallic oxyphosphides for energy storage. Journal of Colloid and Interface Science, 2021, 603, 478-490.	5.0	30
41280	Exploring reaction mechanism of CO oxidation over SrCoO3 catalyst: A DFT study. Applied Surface Science, 2021, 570, 151234.	3.1	11
41281	Exploring the structural, elastic, lattice dynamical stability and thermoelectric properties of semiconducting novel quaternary Heusler alloy LiScPdPb. Journal of Solid State Chemistry, 2021, 304, 122601.	1.4	16
41282	Sc2CO-MXene/h-BN heterostructure with synergetic effect as an anchoring and catalytic material for lithium-sulfur battery. Journal of Alloys and Compounds, 2021, 887, 161273.	2.8	15
41283	High-pressures study by Raman spectroscopy and DFT calculations of L-tyrosine hydrobromide crystal. Spectrochimica Acta - Part A: Molecular and Biomolecular Spectroscopy, 2021, 263, 120142.	2.0	2
41284	Role of water on ozonation of cinnamaldehyde to benzaldehyde under Ca(OH)2 catalysis: A combined in situ DRIFTS and DFT study. Applied Surface Science, 2021, 569, 151071.	3.1	11
41285	Hydrogen storage properties of hexagonal C14 Laves phase Cu2Cd: A DFT study. Journal of Solid State Chemistry, 2021, 304, 122560.	1.4	7
41286	Ultrahigh thermal conductivity in hexagonal BC6N- An efficient material for nanoscale thermal management- A first principles study. Computational Materials Science, 2021, 200, 110773.	1.4	8
41287	Bayesian automated weighting of aggregated DFT, MD, and experimental data for candidate thermodynamic models of aluminum with uncertainty quantification. Materialia, 2021, 20, 101216.	1.3	4

#	Article	IF	Citations
41288	Coadsorption of hydrazine and OH on the Ni(211) surface: A DFT study. Surface Science, 2021, 714, 121931.	0.8	2
41289	Effect of alloying elements on stacking fault energy and ductility of iron. Vacuum, 2021, 194, 110633.	1.6	9
41290	Structure, mechanical and phonon stability of the Th-Sn system from ab initio. Journal of Nuclear Materials, 2021, 556, 153187.	1.3	1
41291	Stability and electronic properties of the graphene-supported FeO nanostructures including clusters and monolayer. Applied Surface Science, 2021, 569, 150976.	3.1	4
41292	ABX6 Monolayers: A new Dirac material family containing high Fermi velocities and topological properties. Applied Surface Science, 2021, 570, 151237.	3.1	11
41293	Atomic-level mechanism of the effects of NOx species on Pb adsorption over the Al2O3 sorbent surface. Applied Surface Science, 2021, 570, 151217.	3.1	6
41294	ADAQ: Automatic workflows for magneto-optical properties of point defects in semiconductors. Computer Physics Communications, 2021, 269, 108091.	3.0	8
41295	Formation of TiAlSi intermetallics during heating Ti-A356 Al mixed powder compact at semisolid temperature. Journal of Materials Science and Technology, 2021, 94, 247-263.	5.6	13
41296	Single-atom platinum or ruthenium on C4N as 2D high-performance electrocatalysts for oxygen reduction reaction. Chemical Engineering Journal, 2021, 426, 131347.	6.6	55
41297	Anomalous elastic behavior of tantalum at high pressures: Experimental and theoretical studies. International Journal of Refractory Metals and Hard Materials, 2021, 101, 105691.	1.7	1
41298	Appealing perspectives of structural, electronic, mechanical, and thermoelectric properties of Tl2(Se,) Tj ETQq0 0 0 rgBT /Overlock 10 Tf 110258.	1.9	34
41299	Efficient photoreduction strategy for uranium immobilization based on graphite carbon nitride/perovskite oxide heterojunction nanocomposites. Applied Catalysis B: Environmental, 2021, 298, 120625.	10.8	51
41300	Constructing accelerated charge transfer channels along V-Co-Fe via introduction of V into CoFe-layered double hydroxides for overall water splitting. Applied Catalysis B: Environmental, 2021, 298, 120587.	10.8	52
41301	First-principles study of the structural, elastic, vibrational and thermal properties of perovskite halides <mml:math xmlns:mml="http://www.w3.org/1998/Math/MathML" altimg="si96.svg" display="inline" id="d1e2235"><mml:mrow><mml:msub><mml:mrow><mml:mi mathvariant="normal">Cs</mml:mi></mml:mrow><mml:mrow><mml:mn>2</mml:mn></mml:mrow></mml:msub><mml:msub><mml:mi mathvariant="normal">TiBr</mml:mi></mml:mrow><mml:mrow><mml:mn>6</mml:mn><mml:mo>â^’</mml:mo><mml:mi>x</mml:mi> Computational Condensed Matter, 2021, 29, e00587.	0.9	6
41302	Microstructures and mechanical properties of (MoNbTa)6TixVy (xÂ+ÂyÂ=Â4) multi-component alloys. International Journal of Refractory Metals and Hard Materials, 2021, 101, 105664.	1.7	2
41303	Ima2 C32: An orthorhombic carbon allotrope with direct band gap. Diamond and Related Materials, 2021, 120, 108602.	1.8	8
41304	Structural and thermal stability of B20-type high-pressure phases FeGe and MnGe. Journal of Alloys and Compounds, 2021, 888, 161565.	2.8	4
41305	Oxygen vacancy-enriched Co3O4 as lithiophilic medium for ultra-stable anode of lithium metal batteries. Journal of Alloys and Compounds, 2021, 888, 161553.	2.8	13

#	Article	IF	Citations
41306	LaN structural and topological transitions driven by temperature and pressure. Computational Materials Science, 2021, 200, 110779.	1.4	3
41307	Two dimension transition metal boride Y2B2 as a promising anode in Li-ion and Na-ion batteries. Computational Materials Science, 2021, 200, 110776.	1.4	22
41308	Twisted bilayer arsenene sheets as a chemical sensor for toluene and M-xylene vapours â€“ A DFT investigation. Journal of Molecular Graphics and Modelling, 2021, 109, 108034.	1.3	17
41309	DFT calculation of thermo-elastic properties and phonon dispersions for Terbium monopnictides TbN and TbP in rock salt structure. Computational Condensed Matter, 2021, 29, e00596.	0.9	1
41310	OH and O mediated interaction of CO2 with Ni(1Â1Â0) surface, and its implications on biomimetic CO2 hydration. Chemical Engineering Science, 2021, 246, 116872.	1.9	2
41311	Cubic to tetragonal structural phase transformation in NaNbO3 with peculiar Mg and Ca doping and its repercussions on optoelectronic properties. Optik, 2021, 247, 168017.	1.4	3
41312	Electronic and elastic properties of two new B-C-N superhard materials from first principles. Solid State Communications, 2021, 340, 114520.	0.9	2
41313	First-principles study of helium in austenitic Fe 6.3 at% Cr alloys: Structural, stability, energetics, and clustering with vacancies. Materials Today Communications, 2021, 29, 102837.	0.9	4
41314	Investigating the magnetic and atomic interface configuration for a model Fe/CrN bilayer system. Journal of Vacuum Science and Technology A: Vacuum, Surfaces and Films, 2021, 39, 063209.	0.9	3
41315	Investigation of (001), (010), and (100) surface termination and surface energies of the Zintl Ca5Ga2Sb6. Surface Science, 2021, 714, 121918.	0.8	1
41316	A new two-dimensional carbon system as a potential Li-adsorbent and its isostructural nitrides with Dirac fermions. Applied Surface Science, 2021, 568, 150892.	3.1	5
41317	Preparation and electrochemical properties of boron-doped polycrystalline diamond film with five-fold twin structure. Applied Surface Science, 2021, 568, 150977.	3.1	13
41318	Theoretical insights of catalytic oxidation of Hg0 on g-C3N4-supported Fe/Co/Ni-based bi-metallic catalysts using O2 in coal-fired flue gas as the oxidant. Fuel, 2021, 306, 121593.	3.4	13
41319	Mechanistic insights of hydrogen evolution reaction on quaternary earth-abundant chalcogenide Cu2BaSnS4 from first principles. Applied Surface Science, 2021, 570, 151049.	3.1	1
41320	Theoretical study of physical properties of Ba3B(Nb,Ta)2O9 (B = Mg, Ca, Sr, Cd, Hg, Zn, Fe, Mn, Ni, Co) perovskites. Computational Condensed Matter, 2021, 29, e00595.	0.9	31
41321	Impact of Ni alloying on Fe-C martensite ageing: an atomistic investigation. Scripta Materialia, 2021, 205, 114182.	2.6	6
41322	Synergistic decomposition of H2S into H2 by Ni3S2 over ZrO2 support via a sulfur looping scheme with CO2 enabled carrier regeneration. Chemical Engineering Journal, 2021, 426, 131815.	6.6	13
41323	The electronic, optical, elastic, and mechanical properties of triclinic Ga2O3 with density functional theory. Computational Condensed Matter, 2021, 29, e00593.	0.9	7

#	Article	IF	Citations
41324	Insights into structural and dynamical characteristics of III-V boron polytypes. Materials Science in Semiconductor Processing, 2021, 136, 106138.	1.9	6
41325	Defective C3N4 frameworks coordinated diatomic copper catalyst: Towards mild oxidation of methane to C1 oxygenates. Applied Catalysis B: Environmental, 2021, 299, 120682.	10.8	32
41326	Structural predictions of superconducting phase in tungsten ditellurides WTe2 from first-principles evolutionary techniques under high pressure. Computational Materials Science, 2021, 200, 110795.	1.4	0
41327	First-principles study of vacancy interaction with grain boundaries of tungsten under tensile strains. Computational Materials Science, 2021, 200, 110760.	1.4	3
41328	Strain-engineering of anisotropic behavior in the electrical and optical properties of graphene-like borophene hydride, a DFT calculation. Computational Materials Science, 2021, 200, 110778.	1.4	9
41329	First-principles study on the electronic properties and enhanced ferromagnetism of alkali metals adsorbed monolayer CrI3. Vacuum, 2021, 194, 110561.	1.6	10
41330	Direct ammonia synthesis from the air via gliding arc plasma integrated with single atom electrocatalysis. Applied Catalysis B: Environmental, 2021, 299, 120667.	10.8	55
41331	A robust metal-organic framework with guest molecules induced splint-like pore confinement to construct propane-trap for propylene purification. Separation and Purification Technology, 2021, 279, 119656.	3.9	22
41332	Structural and electrical characterisation of PtS from H2S-converted Pt. Applied Materials Today, 2021, 25, 101163.	2.3	7
41333	Outstandingly high thermal conductivity, elastic modulus, carrier mobility and piezoelectricity in two-dimensional semiconducting CrC2N4: a first-principles study. Materials Today Energy, 2021, 22, 100839.	2.5	19
41334	The effects of second-alloying-element on the formability of Mg-Sn alloys in respect of the stacking fault energies of slip systems. Materials Today Communications, 2021, 29, 102829.	0.9	9
41335	Crystal chemistry rationale and ab initio investigation of ultra-hard dense rhombohedral carbon and boron nitride. Diamond and Related Materials, 2021, 120, 108607.	1.8	6
41336	Understanding <mml:math xmlns:mml="http://www.w3.org/1998/Math/MathML" altimg="si22.svg"><mml:mrow><mml:msub><mml:mrow><mml:mi mathvariant="normal">CO</mml:mi></mml:mrow><mml:mrow><mml:mn>2</mml:mn></mml:mrow></mml:msub></mml:mrow></mm conversion into hydrocarbons via a photoreductive process supported on the <mml:math xmlns:mml="http://www.w3.org/1998/Math/MathML" altimg="si23.svg"><mml:mrow><mml:msub><mml:mrow><mml:mi mathvariant="normal">Cu</mml:mi><.	3.4	12
41337	Se and O co-insertion induce the transition of MoS2 from 2H to 1T phase for designing high-active electrocatalyst of hydrogen evolution reaction. Chemical Engineering Journal, 2021, 425, 130611.	6.6	25
41338	Van der Waal heterostructure based on BY(Y As, P) and MX<mml:math xmlns:mml="http://www.w3.org/1998/Math/MathML" display="inline" id="d1e981" altimg="si31.svg"><mml:msub><mml:mrow /><mml:mrow><mml:mn>2</mml:mn></mml:mrow></mml:msub></mml:math>(M Mo, W; X S, Se) monolayers. Applied Surface Science, 2021, 568, 150846.	3.1	24
41339	Highly lithiophilic ZnO nanosheets decorated Ni foam as a stable host for high-performance lithium metal anodes. Journal of Alloys and Compounds, 2021, 889, 161597.	2.8	6
41340	Fluorine-substituted cyclobutenes in the solid state: Crystal structures, vibrational spectra and mechanical and thermodynamic properties. Journal of Physics and Chemistry of Solids, 2022, 160, 110337.	1.9	1
41341	d-Band center modulating of CoOx/Co9S8 by oxygen vacancies for fast-kinetics pathway of water oxidation. Chemical Engineering Journal, 2022, 427, 130915.	6.6	28

#	Article	IF	Citations
41342	N-containing silane coupling agent-assisted synthesis of highly dispersed and stable PdC phase for semi-hydrogenation of acetylene. Chemical Engineering Science, 2022, 247, 116939.	1.9	5
41343	Breaking the linear scaling relations in MXene catalysts for efficient CO2 reduction. Chemical Engineering Journal, 2022, 429, 132171.	6.6	32
41344	Graphene-boron nitride composite aerogel: A high efficiency adsorbent for ciprofloxacin removal from water. Separation and Purification Technology, 2021, 278, 119605.	3.9	26
41345	New selection rule of resonant Raman scattering in MoS2 monolayer under circular polarization. Journal of Materials Science and Technology, 2022, 102, 132-136.	5.6	5
41346	Active Co@CoO core/shell nanowire arrays as efficient electrocatalysts for hydrogen evolution reaction. Chemical Engineering Journal, 2022, 429, 132226.	6.6	32
41347	Solution-processed Cd-substituted CZTS nanocrystals for sensitized liquid junction solar cells. Journal of Alloys and Compounds, 2022, 890, 161575.	2.8	9
41348	2D high temperature ferromagnetic Co2Ti2Sn2 monolayer with tunable magnetic anisotropy and superior mechanical flexibility: A first-principles and Monte Carlo study. Physica E: Low-Dimensional Systems and Nanostructures, 2022, 135, 114939.	1.3	3
41349	A comprehensive study of structure and properties of nanocrystalline zinc peroxide. Journal of Physics and Chemistry of Solids, 2022, 160, 110318.	1.9	6
41350	Sandwiched Li plating between Lithiophilic-Lithiophobic gradient Silver@Fullerene interphase layer for ultrastable lithium metal anodes. Chemical Engineering Journal, 2022, 429, 132156.	6.6	36
41351	Ga doping enables superior alkaline hydrogen evolution reaction performances of CoP. Chemical Engineering Journal, 2022, 429, 132012.	6.6	25
41352	Effect of spin-polarization on structural, electronic, and lattice dynamical properties of â€˜MnY2Gaâ€™ Full Heusler alloy. Physica B: Condensed Matter, 2022, 624, 413425.	1.3	3
41353	Sr5(CO3)2(BO3)2: A new family member of isostructural mixed borate and carbonate Ba4M(BO3)2(CO3)2 (MÂ=ÂBa, Sr) with isolated BO3 and CO3 groups. Journal of Molecular Structure, 2022, 1247, 131382.	1.8	3
41354	Facet-dependent photocatalytic H2O2 production of single phase Ag3PO4 and Z-scheme Ag/ZnFe2O4-Ag-Ag3PO4 composites. Chemical Engineering Journal, 2022, 429, 132373.	6.6	37
41355	Transition-metal-free boron doped SbN monolayer for N2 adsorption and reduction to NH3: A first-principles study. Journal of Colloid and Interface Science, 2022, 607, 1551-1561.	5.0	8
41356	Effect of deposition temperature and surface reactions in atomic layer deposition of silicon oxide using Bis(diethylamino)silane and ozone. Applied Surface Science, 2022, 571, 151231.	3.1	12
41357	Fluorine-doped graphene oxide prepared by direct plasma treatment for supercapacitor application. Chemical Engineering Journal, 2022, 428, 132086.	6.6	41
41358	Core electron spectroscopic studies on new structure type iron based superconductors CaKFe4As4 and KCa2Fe4As4F2: DFT predictions. Journal of Physics and Chemistry of Solids, 2022, 160, 110310.	1.9	3
41359	Pressure dependent phase transformations of energetic material 2,4â^'dinitroanisole using Raman spectroscopy, X-ray diffraction and first principles calculations. Journal of Molecular Structure, 2022, 1247, 131356.	1.8	3

#	Article	IF	Citations
41360	A new thermodynamically stable Nb2Ni intermetallic compound phase revealed by peritectoid transition within binary Nb-Ni alloy system. Journal of Materials Science and Technology, 2022, 100, 246-253.	5.6	28
41361	Correlating structure and orbital occupation with the stability and mechanical properties of 3d transition metal carbides. Journal of Alloys and Compounds, 2022, 891, 161866.	2.8	12
41362	Insights into the mechanism of fluoride adsorption over different crystal phase alumina surfaces. Journal of Hazardous Materials, 2022, 423, 127109.	6.5	20
41363	Role of surface engineering of hybrid structure for high performance quantum dots based photoelectrochemical hydrogen generation. Chemical Engineering Journal, 2022, 429, 132425.	6.6	14
41364	Small-scale analysis of brittle-to-ductile transition behavior in pure tungsten. Journal of Materials Science and Technology, 2022, 105, 242-258.	5.6	15
41365	Phase transformation of ZrO2 by Si incorporation and catalytic activity for isopropyl alcohol dehydration and dehydrogenation. Chemical Engineering Journal, 2022, 428, 131766.	6.6	16
41366	The crucial role of deoxygenation in syngas refinement and carbon dioxide utilization during chemical looping-based biomass gasification. Chemical Engineering Journal, 2022, 428, 132068.	6.6	40
41367	Raman and IR spectra of a 2D Thiophene-Tetrathia-Annulene monolayer calculated via density-functional theory. Materials Chemistry and Physics, 2022, 275, 125181.	2.0	1
41368	Experimental and theoretical investigation of the effect of milling time on the magnetic properties of mechanically alloyed FeAlNi (wt%) powders. Journal of Alloys and Compounds, 2022, 891, 161950.	2.8	1
41369	Infrared spectra of the Î² and Î³ phases of oleic acid under high pressure. Spectrochimica Acta - Part A: Molecular and Biomolecular Spectroscopy, 2022, 265, 120290.	2.0	5
41370	Unraveling U6+, Am3+&Eu3+ ionâ€™s distribution in Ca10(PO4)6F2for radioactive waste immobilization and the associated U6+â†' Eu3+energy transfer dynamics for tunable emission characteristics. Journal of Hazardous Materials, 2022, 423, 126980.	6.5	6
41371	Improved thermal stability and infrared emissivity of high-entropy REMgAl11O19 and LaMAl11O19 (RE=La,) Tj ETQq1 1 0.784314 rgB	5.6	25
41372	An integrated strategy based on Schiff base reactions to construct unique two-dimensional nanostructures for intrinsic pseudocapacitive sodium/lithium storage. Chemical Engineering Journal, 2022, 429, 132339.	6.6	12
41373	Revealing the Al/L12-Al3Zr inter-facial properties: Insights from first-principles calculations. Vacuum, 2022, 195, 110620.	1.6	15
41374	Tunable electronic and magnetic properties of single layer CdS via Li substitutional doping: A first-principle study. Journal of Physics and Chemistry of Solids, 2022, 161, 110380.	1.9	4
41375	Compression tuned crystalline and amorphous phases of Gd2Si2O7: Raman spectroscopic and first-principles studies. Journal of Alloys and Compounds, 2022, 890, 161864.	2.8	0
41376	Existence of spin-polarized Dirac cone in Sc<mml:math xmlns:mml="http://www.w3.org/1998/Math/MathML" display="inline" id="d1e736" altimg="si20.svg"><mml:msub><mml:mrow /><mml:mrow><mml:mn>2</mml:mn></mml:mrow></mml:msub></mml:math>CrB<mml:math xmlns:mml="http://www.w3.org/1998/Math/MathML" display="inline" id="d1e744" altimg="si21.svg"><mml:msub><mml:mrow /><mml:mrow><mml:mn>6</mml:mn></mml:mrow></mml:ms	1.3	4
41377	Monolayer PC3: A promising material for environmentally toxic nitrogen-containing multi gases. Journal of Hazardous Materials, 2022, 422, 126761.	6.5	25

#	Article	IF	Citations
41378	Theoretical insights into the adsorption mechanism of Cd(II) on the basal surfaces of kaolinite. Journal of Hazardous Materials, 2022, 422, 126795.	6.5	15
41379	A theoretical study of the twinned ZnO nanostructures. Applied Surface Science, 2022, 571, 151295.	3.1	0
41380	Adsorption mechanism of H2S and CH3SH on Fe(110) surface: A density functional theory study. Physica E: Low-Dimensional Systems and Nanostructures, 2022, 135, 114938.	1.3	6
41381	Segregation of solute atoms in ZrC grain boundaries and their effects on grain boundary strengths. Journal of Materials Science and Technology, 2022, 101, 234-241.	5.6	13
41382	The promotion of sulfuric vacancy in two-dimensional molybdenum disulfide on the sensing performance of SF6 decomposition components. Applied Surface Science, 2022, 571, 151377.	3.1	10
41383	Understanding delivery and adsorption of Flutamide drug with ZnONS based on: Dispersion-corrected DFT calculations and MD simulations. Physica E: Low-Dimensional Systems and Nanostructures, 2022, 135, 114937.	1.3	27
41384	Anisotropic magnetoresistance in room temperature ferromagnetic single crystal CrTe flake. Journal of Alloys and Compounds, 2022, 890, 161818.	2.8	8
41385	Molecular Dynamics and Statics. , 2022, , 510-520.		0
41386	Chelating effect between uranyl and pyridine N containing covalent organic frameworks: A combined experimental and DFT approach. Journal of Colloid and Interface Science, 2022, 606, 1617-1626.	5.0	18
41387	Application of hybrid MOF composite in extraction of f-block elements: Experimental and computational investigation. Chemosphere, 2022, 287, 132232.	4.2	12
41388	The formation of atomic and sub-nano scale pores under tensile strain in oxide films on Zr alloys: A first-principles study. Applied Surface Science, 2022, 571, 151316.	3.1	2
41389	Theoretical study on the formation of diamond germanium vacancy color center. Surface Science, 2022, 715, 121950.	0.8	2
41390	Taming the challenges of activity and selectivity in catalysts for electrochemical N2 fixation via single metal atom supported on WS2. Applied Surface Science, 2022, 571, 151357.	3.1	16
41391	Size effect of band gap in semiconductor nanocrystals and nanostructures from density functional theory within HSE06. Materials Science in Semiconductor Processing, 2022, 137, 106214.	1.9	25
41392	Molecular dynamics and DFT study of 38-atom coinage metal clusters. Computational Materials Science, 2022, 201, 110908.	1.4	9
41393	Polaron assisted electrical transport and fertile field emission response in polycrystalline LiNi0.33Co0.33Mn0.33O2 with theoretical insight by density functional theory. Journal of Alloys and Compounds, 2022, 891, 162056.	2.8	2
41394	Interlayer-expanded MoS2 nanoflowers anchored on the graphene: A high-performance Li+/Mg2+ co-intercalation cathode material. Chemical Engineering Journal, 2022, 428, 131214.	6.6	23
41395	Fabrication and mechanism exploration of oxygen-incorporated 1T-MoS2 with high adsorption performance on methylene blue. Chemical Engineering Journal, 2022, 428, 130954.	6.6	34

#	Article	IF	Citations
41396	Ni2P nanosheet array for high-efficiency electrohydrogenation of nitrite to ammonia at ambient conditions. Journal of Colloid and Interface Science, 2022, 606, 1055-1063.	5.0	62
41397	Intrinsic disorder of dangling OH-bonds in the first water layer on noble metal surfaces. Computational Materials Science, 2022, 201, 110863.	1.4	0
41398	Carbonaceous-assisted confinement synthesis of refractory high-entropy alloy nanocomposites and their application for seawater electrolysis. Journal of Colloid and Interface Science, 2022, 607, 1580-1588.	5.0	11
41399	Ab-initio modelling for gas sensor device: based on Y-doped SnS2 monolayer. Physica E: Low-Dimensional Systems and Nanostructures, 2022, 135, 114962.	1.3	17
41400	Mechanism study on the high-performance BaFe2O4 during chemical looping gasification. Fuel, 2022, 307, 121847.	3.4	13
41401	Experimental and density functional theory studies on Cu/Ba-coimpregnated Î³-Al2O3 for low-temperature NO storage and adsorbent regeneration. Chemical Engineering Journal, 2022, 429, 132112.	6.6	7
41402	Sulfur encapsulation into yolk-shell Fe2N@nitrogen doped carbon for ambient-temperature sodium-sulfur battery cathode. Chemical Engineering Journal, 2022, 429, 132389.	6.6	26
41403	Ab-Initio investigations of electronic and optical properties of Sn-hBN hetero-structure. Physica B: Condensed Matter, 2022, 624, 413390.	1.3	13
41404	Two dimensional h-BSb mono-layer as a promising anode material for lithium-ion batteries studied from ab initio simulations. Materials Chemistry and Physics, 2022, 275, 125191.	2.0	15
41405	Experimental investigation and thermodynamic modeling of the ternary Tiâ€“Feâ€“Mn system for hydrogen storage applications. Journal of Alloys and Compounds, 2022, 891, 161957.	2.8	11
41406	Identifying a Li-rich superionic conductor from chargeâ€“discharge structural evolution study: Li₂MnO₃. Physical Chemistry Chemical Physics, 2021, 23, 4829-4834.	1.3	2
41407	Probing thermoelectric properties of high potential Ca3PbO: An Ab Initio Study. IOP Conference Series: Materials Science and Engineering, 0, 1033, 012080.	0.3	1
41408	Deep Insights into the Twinning Mechanism in High-Performance Al Alloys: A Comprehensive First-Principles Study. Metallurgical and Materials Transactions A: Physical Metallurgy and Materials Science, 2021, 52, 955-963.	1.1	6
41409	First-principles study of pristine and metal decorated blue phosphorene for sensing toxic H2S, SO2 and NO2 molecules. Applied Physics A: Materials Science and Processing, 2021, 127, 1.	1.1	5
41410	Electron-phonon coupling in the magnetic Weyl semimetal <mml:math xmlns:mml="http://www.w3.org/1998/Math/MathML"><mml:mi>Zr</mml:mi><mml:msub><mml:mrow><mml:mi>Co</mml:mi></mml:mrow><mml:mi></mml:mi></mml:msub><mml:mi></mml:mi></mml:math>. Physical Review B, 2021, 103, .	1.1	4
41411	Free Energy of Metals from Quasi-Harmonic Models of Thermal Disorder. Metals, 2021, 11, 195.	1.0	1
41412	Understanding Cu incorporation in the <mml:math xmlns:mml="http://www.w3.org/1998/Math/MathML"><mml:mrow><mml:msub><mml:mi>Cu</mml:mi><mml:mrow></mml:mrow></mml:msub><mml:mi></mml:mi><mml:mn>2</mml:mn></mml:mrow></mml:math> structure using resonant x-ray diffraction. Physical Review Materials, 2021, 5, .	0.9	3
41413	Multi-hole bands and quasiâ€“two-dimensionality in Cr₂Ge₂Te₆ studied by angle-resolved photoemission spectroscopy. Europhysics Letters, 2021, 133, 27002.	0.7	5

#	Article	IF	Citations
41414	Modeling and Comparing Gas Sensing Properties of CNT and CNT Decorated With Zinc Oxide. IEEE Nanotechnology Magazine, 2021, 20, 292-302.	1.1	7
41415	Investigation of electronic and vibrational properties of dihydroxylammonium 5,5â€²-bistetrazole-1,1â€²-diolate under high-pressure conditions. Physical Chemistry Chemical Physics, 2021, 23, 7442-7448.	1.3	6
41416	Construction and Application of 3D Graphene Materials Based on Templated Polymerization. Springer Theses, 2021, , 57-88.	0.0	0
41417	Pressure induced topochemical polymerization of solid acrylamide facilitated by anisotropic response of the hydrogen bond network. Physical Chemistry Chemical Physics, 2021, 23, 9448-9456.	1.3	0
41418	Alkylation of poly-substituted aromatics to probe effects of mesopores in hierarchical zeolites with differing frameworks and crystal sizes. Molecular Systems Design and Engineering, 2021, 6, 903-917.	1.7	6
41419	Accelerating the activation of Li₂MnO₃ in Li-rich high-Mn cathodes to improve its electrochemical performance. Nanoscale, 2021, 13, 4921-4930.	2.8	17
41420	First-principles study of Mn₃ adsorbed on Au(111) and Cu(111) surfaces. RSC Advances, 2021, 11, 31073-31083.	1.7	3
41421	Novel two-dimensional tetrahexagonal boron nitride with a sizable band gap and a sign-tunable Poisson's ratio. Nanoscale, 2021, 13, 9303-9314.	2.8	22
41422	A novel two-dimensional beryllium diphosphide (BeP₂) with superconductivity: the first-principles exploration. Physical Chemistry Chemical Physics, 2021, 23, 12834-12841.	1.3	9
41423	Hydrogen-induced tunable electronic and optical properties of a two-dimensional penta-Pt₂N₄ monolayer. Physical Chemistry Chemical Physics, 2021, 23, 10409-10417.	1.3	24
41424	Effects of Transition Element Additions on the Interfacial Interaction and Electronic Structure of Al(111)/6H-SiC(0001) Interface: A First-Principles Study. Materials, 2021, 14, 630.	1.3	8
41425	Syntheses, structure and properties of a new series of organicâ€“inorganic Hg-based halides: adjusting halogens resulted in huge performance mutations. Dalton Transactions, 2021, 50, 7563-7570.	1.6	9
41426	On the energy transfer in LiMgPO₄ doped with rare-earth elements. Journal of Materials Chemistry C, 2021, 9, 11272-11283.	2.7	7
41427	Nb-Doped nickel nitride-derived catalysts for electrochemical water splitting. Catalysis Science and Technology, 2021, 11, 6455-6461.	2.1	6
41428	Assembling organicâ€“inorganic building blocks for high-capacity electrode design. Materials Horizons, 2021, 8, 1825-1834.	6.4	1
41429	Mechanism of methanol synthesis on Ni(110). Catalysis Science and Technology, 2021, 11, 3279-3294.	2.1	6
41430	Sb2Te3 an optically potent topological insulator: A density functional study. Materials Today: Proceedings, 2021, 45, 4819-4823.	0.9	3
41431	Ternary alkali ion thiogallates, A₅GaS₄ (A = Li and Na), with isolated tetrahedral building units and their ionic conductivities. Dalton Transactions, 2021, 50, 7372-7379.	1.6	9

#	Article	IF	Citations
41432	Unveiling the mechanisms behind the ferroelectric response in the Sr(Nb,Ta)O₂N oxynitrides. Physical Chemistry Chemical Physics, 2021, 23, 17142-17149.	1.3	6
41433	Predicting an optimal oxide/metal catalytic interface for hydrodeoxygenation chemistry of biomass derivatives. Catalysis Science and Technology, 2021, 11, 5606-5618.	2.1	2
41434	Structural diversity, large interlayer spacing and switchable electronic properties of graphitic systems. Journal of Materials Science, 2021, 56, 5509-5519.	1.7	3
41435	Probing the Positions of TeO Moieties in the Channels of the MoVNbTeO M1 Catalyst: A Density Functional Theory Model Study. Catalysis Letters, 2021, 151, 2884-2893.	1.4	4
41436	Double boron atom-doped graphdiynes as efficient metal-free electrocatalysts for nitrogen reduction into ammonia: a first-principles study. Physical Chemistry Chemical Physics, 2021, 23, 17683-17692.	1.3	19
41437	The mechanism behind the photochromism and photomagnetism of type II biindenylidenediones: multiconfigurational, perturbative and density functional theory studies. Physical Chemistry Chemical Physics, 2021, 23, 17453-17465.	1.3	0
41438	Penta-BCN monolayer with high specific capacity and mobility as a compelling anode material for rechargeable batteries. Physical Chemistry Chemical Physics, 2021, 23, 17693-17702.	1.3	24
41439	Interfacial interaction and prenucleation at liquid-Al/Î³-Al₂O₃{1 1 1} interfaces. Journal of Physics Communications, 2021, 5, 015007.	0.5	12
41440	On the origin of the electron accumulation layer at clean InAs(111) surfaces. Physical Chemistry Chemical Physics, 2021, 23, 4811-4817.	1.3	4
41441	Nonvolatile electrical control of 2D Cr₂Ge₂Te₆ and intrinsic half metallicity in multiferroic hetero-structures. Nanoscale, 2021, 13, 1069-1076.	2.8	13
41442	The induction of half-metallicity and enhanced ferromagnetism in a Cr₂Ge₂Te₆ monolayer via electron doping and alkali metal adsorption. Journal of Materials Chemistry C, 2021, 9, 5952-5960.	2.7	10
41443	Hydroxyl Influence on Adsorption and Lubrication of an Ultrathin Aqueous Triblock Copolymer Lubricant. Langmuir, 2021, 37, 1465-1479.	1.6	4
41444	Ultra-low friction and patterning on atomically thin MoS₂via electronic tight-binding. Nanoscale, 2021, 13, 16860-16871.	2.8	15
41445	Temperature-responsive emission and elastic properties of a new 2D lead halide perovskite. Dalton Transactions, 2021, 50, 2648-2653.	1.6	18
41446	Understanding the Oxidation Degradation Mechanism to Enable Preparation of Ambient Ultra Stable Ti ₃C ₂T _x-MXene. SSRN Electronic Journal, 0, , .	0.4	1
41447	Effect of Mn-doping on the optical and electronics characteristics of cadmium sulfide photocatalyst prepared under different conditions. Applied Physics A: Materials Science and Processing, 2021, 127, 1.	1.1	9
41448	Unconventional distortion induced two-dimensional multiferroicity in a CrO₃ monolayer. Nanoscale, 2021, 13, 13048-13056.	2.8	7
41449	Influence of vacancy and adatom defects on the optoelectronic properties of monolayer GeS. AIP Conference Proceedings, 2021, , .	0.3	0

#	Article	IF	Citations
41450	Assessing Nickel Titanium Binary Systems Using Structural Search Methods and Ab Initio Calculations. Journal of Physical Chemistry C, 2021, 125, 1578-1591.	1.5	3
41451	Modulation effects of S vacancy and Mo edge on the adsorption and dissociation behaviors of toxic gas (H₂S, SO₂) molecules on the MoS₂ monolayer. Physical Chemistry Chemical Physics, 2021, 23, 15364-15373.	1.3	7
41453	Inhibition of hydrogen evolution without debilitating electrochemical CO₂ reduction via the local suppression of proton concentration and blocking of step-edges by pyridine functionalization on Cu electrocatalysts. Catalysis Science and Technology, 2021, 11, 4857-4865.	2.1	8
41454	The formation and evolution of carbonate species in CO oxidation over mono-dispersed Fe on graphene. Physical Chemistry Chemical Physics, 2021, 23, 10509-10517.	1.3	8
41455	High-throughput screening of single metal atom anchored on N-doped boron phosphide for N₂ reduction. Nanoscale, 2021, 13, 13437-13450.	2.8	18
41456	Singlet oxygen vs. triplet oxygen: functions of 2D-MoO₃ catalysts in conquering catastrophic parasitic-reactions in lithiumâ€“ and sodiumâ€“oxygen batteries. Journal of Materials Chemistry A, 2021, 9, 10186-10198.	5.2	15
41457	Fast lithium-ion conductivity in the â€˜empty-perovskiteâ€™ n = 2 Ruddlesdenâ€“Popper-type oxysulphide Y₂Ti₂S₂O₅. Journal of Materials Chemistry A, 2021, 9, 7068-7084.	5.2	8
41458	Computational density-functional approaches on finite-size and guest-lattice effects in CO2@sII clathrate hydrate. Journal of Chemical Physics, 2021, 154, 044301.	1.2	10
41459	Synthesis, crystal structure and structureâ€“property relations of strontium orthocarbonate, Sr₂CO₄. Acta Crystallographica Section B: Structural Science, Crystal Engineering and Materials, 2021, 77, 131-137.	0.5	16
41460	Sliding ferroelectricity in two-dimensional MoA₂N₄ (A = Si or Ge) bilayers: high polarizations and MoirÃ© potentials. Journal of Materials Chemistry A, 2021, 9, 19659-19663.	5.2	32
41461	Experimental and Theoretical Investigation of the Synergy Effect of Zr and Ce on the Catalytic Efficiency of NiMoS Grafted on SBA-15 for Oil Hydrodesulfurization. Energy & Fuels, 2021, 35, 2579-2589.	2.5	12
41462	Crystal structure and two-band superconductivity in unconventional high- <mml:math xmlns:mml="http://www.w3.org/1998/Math/MathML"><mml:msub><mml:mi>T</mml:mi><mml:mi>c</mml:mi></mml:msub></mml:math> cuprates <mml:math xmlns:mml="http://www.w3.org/1998/Math/MathML"><mml:msub><mml:mi mathvariant="normal">Ba</mml:mi><mml:mn>2</mml:mn></mml:msub><mml:mo>Â</mml:mo><mml:msub><mml:mi mathvariant="normal">CuO</mml:mi><mml:mrow><mml:mn>3</mml:mn><mml:mo>+</mml:mo><mml:mi>Î´</mml:mi></mml:mrow></mml:msub></mml:math>. Physical Review B, 2021, 103, .	1.1	9
41463	Mechanical study of a copper dietary supplement, copper glycinate hydrate. CrystEngComm, 2021, 23, 1815-1820.	1.3	1
41464	Prediction of allotropes of tellurium with molecular, one- and two-dimensional covalent nets for photofunctional applications. RSC Advances, 2021, 11, 29965-29975.	1.7	4
41465	Structural, mechanical, electronic, and anisotropic properties of niobium-doped strontium ferrite: first-principle calculations. Applied Physics A: Materials Science and Processing, 2021, 127, 1.	1.1	22
41466	Coâ€“Feâ€“Cr (oxy)Hydroxides as Efficient Oxygen Evolution Reaction Catalysts. Advanced Energy Materials, 2021, 11, 2003412.	10.2	94
41467	Facilely synthesized nitrogen-doped reduced graphene oxide functionalized with copper ions as electrocatalyst for oxygen reduction. Npj 2D Materials and Applications, 2021, 5, .	3.9	22
41468	Ultraviolet nonlinear optical crystals A₃SrBi(P₂O₇)₂ (A = K, Rb) with large second harmonic generation responses. Inorganic Chemistry Frontiers, 2021, 8, 2061-2067.	3.0	9

#	Article	IF	Citations
41469	Towards shape-oriented Bi-doped CoCr₂O₄ nanoparticles from theoretical and experimental perspectives: structural, morphological, optical, electrical and magnetic properties. Journal of Materials Chemistry C, 2021, 9, 6452-6469.	2.7	29
41470	Highâ€Density Frenkel Defects as Origin of Nâ€Type Thermoelectric Performance and Low Thermal Conductivity in Mg₃Sb₂â€Based Materials. Advanced Functional Materials, 2021, 31, 2008469.	7.8	38
41471	Anharmonic Correction to Adsorption Free Energy from DFT-Based MD Using Thermodynamic Integration. Journal of Chemical Theory and Computation, 2021, 17, 1155-1169.	2.3	29
41472	Unraveling the site-specific energy transfer driven tunable emission characteristics of Eu³⁺ & Tb³⁺ co-doped Ca₁₀(PO₄)₆F₂ phosphors. RSC Advances, 2021, 11, 31421-31432.	1.7	8
41473	Experimental and computational investigation on underlying factors promoting high coke resistance in NiCo bimetallic catalysts during dry reforming of methane. Scientific Reports, 2021, 11, 519.	1.6	14
41474	Nanosystemâ€™s density functional theory study of the chlorine adsorption on the Fe(100) surface. Nanotechnology Reviews, 2021, 10, 719-727.	2.6	5
41475	Metal dichalcogenide nanomeshes: structural, electronic and magnetic properties. Physical Chemistry Chemical Physics, 2021, 23, 21183-21195.	1.3	10
41476	Quantum well states and sizable Rashba splitting on Pb induced Î±-phase Bi/Si(111) surface reconstruction. Nanoscale, 2021, 13, 16622-16628.	2.8	5
41477	Kust-I: a high-performance two-dimensional graphene-based material for seawater desalination. Journal of Materials Chemistry A, 2021, 9, 21158-21166.	5.2	18
41478	Polyoxoplatinates as covalently dynamic electron sponges and molecular electronics materials. Nanoscale Advances, 2021, 3, 5663-5675.	2.2	5
41479	Single-defect phonons imaged by electron microscopy. Nature, 2021, 589, 65-69.	13.7	108
41480	Characterisation of oxygen defects and nitrogen impurities in TiO2 photocatalysts using variable-temperature X-ray powder diffraction. Nature Communications, 2021, 12, 661.	5.8	97
41481	Low lattice thermal conductivity of a 5â€“8-peanut-shaped carbon nanotube. Physical Chemistry Chemical Physics, 2021, 23, 5460-5466.	1.3	5
41482	Mixed-valence gold bis(diselenolene) complex turning metallic under pressure. Journal of Materials Chemistry C, 2021, 9, 12291-12302.	2.7	4
41483	Thermoelectric properties of Weyl semi-metal ZrTe. AIP Conference Proceedings, 2021, , .	0.3	1
41484	Anionic Oxygen Redox in the High-Lithium Material Li₈SnO₆. Chemistry of Materials, 2021, 33, 834-844.	3.2	10
41485	Self-diffusion in garnet-type Li7La3Zr2O12 solid electrolytes. Scientific Reports, 2021, 11, 451.	1.6	19
41486	Catalytic separators with Coâ€“Nâ€“C nanoreactors for high-performance lithiumâ€“sulfur batteries. Inorganic Chemistry Frontiers, 2021, 8, 3066-3076.	3.0	29

#	Article	IF	Citations
41487	Phase diagram exploration of Tcâ€“Alâ€“B: from bulk Tc₂AlB₂ to two-dimensional Tc₂B₂. Physical Chemistry Chemical Physics, 2021, 23, 22086-22095.	1.3	3
41488	Lean NO_x Capture and Reduction by NH₃ via NO⁺ Intermediates over H-CHA at Room Temperature. Journal of Physical Chemistry C, 2021, 125, 1913-1922.	1.5	15
41489	Structural and Kinetics Understanding of Support Effects in Pd-Catalyzed Semi-Hydrogenation of Acetylene. Engineering, 2021, 7, 103-110.	3.2	36
41490	The design of Co3S4@MXene heterostructure as sulfur host to promote the electrochemical kinetics for reversible magnesium-sulfur batteries. Journal of Magnesium and Alloys, 2021, 9, 78-89.	5.5	46
41491	Boosting thermo-photocatalytic CO2 conversion activity by using photosynthesis-inspired electron-proton-transfer mediators. Nature Communications, 2021, 12, 123.	5.8	75
41492	DFT insight into the effect of Cu atoms on adsorption and dissociation of CO₂ over a Pd₈/ TiO₂(101) surface. RSC Advances, 2021, 11, 17391-17398.	1.7	4
41493	Transformation of Co₃O₄ nanoparticles to CoO monitored by in situ TEM and predicted ferromagnetism at the Co₃O₄/CoO interface from first principles. Journal of Materials Chemistry C, 2021, 9, 5662-5675.	2.7	31
41494	Optimizing accuracy and efficacy in data-driven materials discovery for the solar production of hydrogen. Energy and Environmental Science, 2021, 14, 2335-2348.	15.6	23
41495	Energetic and electronic properties of CsPbBr₃ surfaces: a first-principles study. Physical Chemistry Chemical Physics, 2021, 23, 7145-7152.	1.3	22
41496	First-Principles Modeling and Calculations of HfO2/Si Interface in Nano Devices. Lecture Notes in Electrical Engineering, 2021, , 581-593.	0.3	0
41497	Ba₃YB₃O₉based phosphor ceramic plates with excellent thermal stability for wLED applications. Dalton Transactions, 2021, 50, 5287-5300.	1.6	11
41498	Atomistic electronic structure in the single-chain limit of organic conductors. Europhysics Letters, 2021, 133, 27004.	0.7	0
41499	Efficient polysulfide trapping in lithiumâ€“sulfur batteries using ultrathin and flexible BaTiO₃/graphene oxide/carbon nanotube layers. Nanoscale, 2021, 13, 6863-6870.	2.8	3
41500	Explanation for the conductivity difference of half-Heusler transparent conductors via ionization energy. Physical Chemistry Chemical Physics, 2021, 23, 9285-9293.	1.3	5
41501	Host guest chemistry and supramolecular doping in triphenylamine-based covalent frameworks on Au(111). Nanoscale, 2021, 13, 9798-9807.	2.8	5
41502	Scintillation in (C₆H₅CH₂NH₃)₂SnBr₄: green-emitting lead-free perovskite halide materials. RSC Advances, 2021, 11, 20635-20640.	1.7	13
41503	First-principles study of properties of rare-earth-doped LiFePO₄. Wuli Xuebao/Acta Physica Sinica, 2021, 70, 158203.	0.2	4
41504	N-type and p-type molecular doping on monolayer MoS₂. RSC Advances, 2021, 11, 8033-8041.	1.7	15

#	Article	IF	Citations
41505	Potential SiX (X = N, P, As, Sb, Bi) homo-bilayers for visible-light photocatalyst applications. Catalysis Science and Technology, 2021, 11, 4996-5013.	2.1	18
41506	Coreâ€“shell PdAu nanocluster catalysts to suppress sulfur poisoning. Physical Chemistry Chemical Physics, 2021, 23, 15010-15019.	1.3	10
41507	Unraveling the strong coupling between graphene/nickel interface and atmospheric adsorbates for versatile realistic applications. Carbon Trends, 2021, 2, 100013.	1.4	7
41508	Ligand-bridged charge extraction and enhanced quantum efficiency enable efficient nâ€“iâ€“p perovskite/silicon tandem solar cells. Energy and Environmental Science, 2021, 14, 4377-4390.	15.6	79
41509	Defects in H/He neutral beam irradiated potassium doped tungsten alloy by positron annihilation technique. Wuli Xuebao/Acta Physica Sinica, 2021, 70, 167803.	0.2	3
41510	Electronic and Thermoelectric Properties of Lead Sulfide PbS: DFT Approach. Springer Proceedings in Energy, 2021, , 417-426.	0.2	0
41511	Kagome quantum anomalous Hall effect with high Chern number and large band gap. Physical Review B, 2021, 103, .	1.1	17
41512	What does graphitic carbon nitride really look like?. Physical Chemistry Chemical Physics, 2021, 23, 2853-2859.	1.3	12
41513	An efficient and robust lanthanum strontium cobalt ferrite catalyst as a bifunctional oxygen electrode for reversible solid oxide cells. Journal of Materials Chemistry A, 2021, 9, 5507-5521.	5.2	21
41514	Mechanism of Electronegativity Heterojunction of Nanometer Amorphous-Boron on Crystalline Silicon: An Overview. Crystals, 2021, 11, 108.	1.0	2
41515	First-Principles Study of Germagraphene as an Anode Material for Lithium-Ion Batteries. Applied Physics, 2021, 11, 44-52.	0.0	0
41516	Single-layer polymeric tetraoxa[8]circulene modified by s-block metals: toward stable spin qubits and novel superconductors. Nanoscale, 2021, 13, 4799-4811.	2.8	9
41517	Evolution of Water Layer Adsorption on the GaN(0001) Surface and Its Influence on Electronic Properties. Journal of Physical Chemistry C, 2021, 125, 667-674.	1.5	5
41518	Bain and Nishiyamaâ€“Wassermann transition path separation in the martensitic transitions of Fe. RSC Advances, 2021, 11, 3043-3048.	1.7	6
41519	Theoretical investigation of the electronic structure, elastic, dynamic properties of intermetallic compound NiBe under pressure. European Physical Journal B, 2021, 94, 1.	0.6	4
41520	Experimental and computational study on roles of WOx promoting strong metal support promoter interaction in Pt catalysts during glycerol hydrogenolysis. Scientific Reports, 2021, 11, 530.	1.6	8
41521	Substrate induced electronic phase transitions of CrI$$_{3}$$ based van der Waals heterostructures. Scientific Reports, 2021, 11, 198.	1.6	5
41522	First Principle Calculations of Effect of Hydrostatic Pressure on Ga0.75Cr0.25P. IOP Conference Series: Materials Science and Engineering, 0, 1033, 012062.	0.3	0

#	Article	IF	Citations
41523	Typeâ€Ⅱ AsP/As van der Waals Heterostructures: Tunable Anisotropic Electronic Structures and Optical Properties. Advanced Materials Interfaces, 2021, 8, 2001555.	1.9	11
41524	Formation of atomic fluorine anions in 12CaOÂ·7Al2O3. AIP Advances, 2021, 11, 015146.	0.6	0
41525	DFT studies of selective oxidation of propene on the MoO₃(010) surface. Physical Chemistry Chemical Physics, 2021, 23, 2792-2804.	1.3	6
41526	Doping effects on catechol functionalized anatase TiO2(101) surface for dye-sensitized solar cells. Materials Research Express, 2021, 8, 015906.	0.8	3
41527	First-Principles Calculation of Defect Properties on Copper Doped KTaO3 Crystal. ECS Journal of Solid State Science and Technology, 2021, 10, 014009.	0.9	0
41528	A first-principles study of a new ternary silicide superconductor Li2IrSi3â€. Journal of Physics: Conference Series, 2021, 1718, 012018.	0.3	0
41529	DFT Study of Effect of Hydrostatic Pressure on Structural, Electronic and Magnetic Properties of In0.875Cr0.125P. IOP Conference Series: Materials Science and Engineering, 0, 1033, 012017.	0.3	0
41530	Electronic structure, mechanical and thermoelectric properties of the full Heusler Ba2AgZ (Zâ€‰=â€‰Bi, Sb) alloys: insights from DFT study. Indian Journal of Physics, 2021, 95, 2675-2686.	0.9	3
41531	Halfâ€Metallic Devices from Armchair Graphene Nanoribbons with Transition Metal Guest Atoms. ChemistrySelect, 2021, 6, 347-358.	0.7	1
41532	Introduction to mechanical metamaterials and their effective properties. Comptes Rendus Physique, 2020, 21, 751-765.	0.3	2
41533	Data-driven analysis of the rotational energy landscapes of an organic cation in a substituted alloy perovskite. Materials Advances, 2021, 2, 2366-2372.	2.6	0
41534	O<mml:math xmlns:mml="http://www.w3.org/1998/Math/MathML" display="inline" id="d1e362" altimg="si73.svg"><mml:msub><mml:mrow /><mml:mrow><mml:mn>2</mml:mn></mml:mrow></mml:msub></mml:math>adsorption on defective Penta-Graphene lattices: A DFT study. Chemical Physics Letters, 2021, 763, 138229.	1.2	12
41535	Effects of atomic substitutional doping on electronic structure of monolayer Janus WSeTe. Wuli Xuebao/Acta Physica Sinica, 2021, 70, 096301.	0.2	0
41536	Phase transition and trigger mechanism of initial reaction under pressure for benzofuroxan energetic materials: Raman spectroscopy and firstâ€principle calculations. Journal of Raman Spectroscopy, 2021, 52, 865-876.	1.2	5
41537	A photo-induced spin crossover based molecular switch and spin filter operating at room temperature. Dalton Transactions, 2021, 50, 6578-6587.	1.6	4
41538	Manipulation of Spin Splitting in Two-Dimensional Lead Bromide Perovskite Rashba Piezoelectrics. ACS Applied Electronic Materials, 2021, 3, 285-291.	2.0	13
41539	Relative Rates of Krypton and Rubidium Release from Zeolite Getters. Journal of Physical Chemistry C, 2021, 125, 1323-1333.	1.5	0
41540	Nesting-like band gap in bismuth sulfide Bi₂S₃. Journal of Materials Chemistry C, 2021, 9, 13733-13738.	2.7	18

#	Article	IF	Citations
41541	Charge-storage mechanism of highly defective NiO nanostructures on carbon nanofibers in electrochemical supercapacitors. Nanoscale, 2021, 13, 9590-9605.	2.8	14
41542	Crystalline Sb 2 Te 3 : Side Surfaces and Disappearance of Dirac Cones. Physica Status Solidi - Rapid Research Letters, 2021, 15, 2000418.	1.2	2
41543	Terahertz optics-driven phase transition in two-dimensional multiferroics. Npj 2D Materials and Applications, 2021, 5, .	3.9	16
41544	Outstanding spin-transport properties of a flexible phosphorene photodetector driven by the photogalvanic effect under mechanical strains. Physical Chemistry Chemical Physics, 2021, 23, 11961-11967.	1.3	7
41545	Narrowing bandgap and enhanced mechanical and optoelectronic properties of perovskite halides: Effects of metal doping. AIP Advances, 2021, 11, .	0.6	37
41546	Covalent photofunctionalization and electronic repair of 2H-MoS₂via nitrogen incorporation. Physical Chemistry Chemical Physics, 2021, 23, 18517-18524.	1.3	3
41547	Tuning the mechanical flexibility of organic molecular crystals by polymorphism for flexible optical waveguides. CrystEngComm, 2021, 23, 5815-5825.	1.3	30
41548	A Model for Atomic Precision p-Type Doping with Diborane on Si(100)-2Ã—1. Journal of Physical Chemistry C, 2021, 125, 481-488.	1.5	8
41549	Influence of molybdenum and technetium doping on visible light absorption, optical and electronic properties of lead-free perovskite CsSnBr₃for optoelectronic applications. RSC Advances, 2021, 11, 2405-2414.	1.7	23
41550	Interlayer-decoupled BiOX (X=Cl, Br, and I) sheets for photocatalytic water splitting: a computational study. Optoelectronics Letters, 2021, 17, 32-35.	0.4	4
41551	Electrically controlled spin reversal and spin polarization of electronic transport in nanoporous graphene nanoribbons. Physical Chemistry Chemical Physics, 2021, 23, 20702-20708.	1.3	7
41552	Probing reaction processes and reversibility in Earth-abundant Na₃FeF₆ for Na-ion batteries. Physical Chemistry Chemical Physics, 2021, 23, 20052-20064.	1.3	5
41553	Janus PtXO (X = S, Se) monolayers: the visible light driven water splitting photocatalysts with high carrier mobilities. Physical Chemistry Chemical Physics, 2021, 23, 21825-21832.	1.3	18
41554	Type-II lateral SnSe/GeTe heterostructures for solar photovoltaic applications with high efficiency. Nanoscale Advances, 2021, 3, 3643-3649.	2.2	7
41555	Sintering Activated Atomic Palladium Catalysts with High-Temperature Tolerance of â‰¥1,000Â°C. Cell Reports Physical Science, 2021, 2, 100287.	2.8	7
41556	Magnetic and electronic structures of antiferromagnetic topological material candidate EuMg2Bi2. Journal of Applied Physics, 2021, 129, .	1.1	19
41557	Unprecedented copper(ii) coordination induced nucleophilic cleavage of a quinoxaline heterocycle: structural and computational studies. CrystEngComm, 2021, 23, 5078-5086.	1.3	3
41558	Energetics of hydrogen adsorption and diffusion for the main surface planes and all magnetic structures of Î³-iron using density functional theory. RSC Advances, 2021, 11, 28892-28897.	1.7	0

#	Article	IF	Citations
41559	New Insight into the Metal-Catalyst-Free Direct Chemical Vapor Deposition Growth of Graphene on Silicon Substrates. Journal of Physical Chemistry C, 2021, 125, 1774-1783.	1.5	23
41560	Electronic and thermodynamic properties of native point defects in V₂O₅: a first-principles study. Physical Chemistry Chemical Physics, 2021, 23, 11374-11387.	1.3	18
41561	Catalytic direct oxidation of methane to methanol by redox of copper mordenite. Catalysis Science and Technology, 2021, 11, 3437-3446.	2.1	15
41562	Accelerating computational modeling and design of high-entropy alloys. Nature Computational Science, 2021, 1, 54-61.	3.8	44
41563	Novel ferrimagnetic nanomaterial Sr_(1â^'x)La_xGd_ySm_zFe_{(12â^'(z+y))}O₁₉ for recording media applications: experimental and theoretical investigations. New Journal of Chemistry, 2021, 45, 10761-10776.	1.4	10
41564	MoirÃ© patterns of twisted bilayer antimonene and their structural and electronic transition. Nanoscale, 2021, 13, 13427-13436.	2.8	5
41565	The structural stability and defect-tolerance of ionic spinel semiconductors for high-efficiency solar cells. Journal of Materials Chemistry A, 2021, 9, 14566-14575.	5.2	6
41566	Infrared spectroscopic measurements of the structure of organic thin films; furfural on Pd(111) and Au(111) surfaces. CrystEngComm, 2021, 23, 4534-4548.	1.3	8
41567	Ionic liquid in situ functionalized carbon nanotubes as metal-free catalyst for efficient electrocatalytic hydrogen evolution reaction. Nanoscale, 2021, 13, 4444-4450.	2.8	22
41568	Vacancy engineering of WO_{3â^'x} nanosheets for electrocatalytic NRR process â€“ a first-principles study. Physical Chemistry Chemical Physics, 2021, 23, 16658-16663.	1.3	9
41569	Long range interactions and related carbonâ€“carbon bond reconstruction between interior and surface defects in nanodiamonds. Physical Chemistry Chemical Physics, 2021, 23, 14592-14600.	1.3	3
41570	Gating the conductance of extended metal atom chains: a computational analysis of Ru₃(dpa)₄(NCS)₂ and [Ru₃(npa)₄(NCS)₂]. Physical Chemistry Chemical Physics, 2021, 23, 14836-14844.	1.3	0
41571	Modulation of electrical properties in carbon nanotube field-effect transistors through AuCl3 doping. Wuli Xuebao/Acta Physica Sinica, 2021, .	0.2	0
41572	Synergetic Effect of NiO_x Decoration and Oxygen Plasma Treatment on Electrochemical Capacitor Performance of Vertical Graphene Nanosheets. ACS Applied Energy Materials, 2021, 4, 791-800.	2.5	19
41573	Structural and electronic transition in liquid rubidium. Physical Review B, 2021, 103, .	1.1	2
41574	Unveiling the effect of the crystalline phases of iron oxyhydroxide for highly sensitive and selective detection of dopamine. Dalton Transactions, 2021, 50, 13497-13504.	1.6	5
41575	Mixed dimensional 0D/3D perovskite heterostructure for efficient green light-emitting diodes. Journal of Materials Chemistry C, 2021, 9, 14318-14326.	2.7	8
41576	Core-corona Co/CoP clusters strung on carbon nanotubes as a Schottky catalyst for glucose oxidation assisted H₂ production. Journal of Materials Chemistry A, 2021, 9, 10893-10908.	5.2	56

#	Article	IF	Citations
41577	Computational Investigation of MgH₂/Graphene Heterojunctions for Hydrogen Storage. Journal of Physical Chemistry C, 2021, 125, 2357-2363.	1.5	33
41578	High-throughput reaction engineering to assess the oxidation stability of MAX phases. Npj Computational Materials, 2021, 7, .	3.5	13
41579	MXene binder stabilizes pseudocapacitance of conducting polymers. Journal of Materials Chemistry A, 2021, 9, 20356-20361.	5.2	15
41580	Synergistic Doping and Surface Decoration of Carbon Nitride Macrostructures by Single Crystal Design. ACS Applied Energy Materials, 2021, 4, 1868-1875.	2.5	12
41581	Two dimensional CrGa₂Se₄: a spin-gapless ferromagnetic semiconductor with inclined uniaxial anisotropy. Nanoscale, 2021, 13, 6024-6029.	2.8	17
41582	Ni nanoparticles/V₄C₃T_x MXene heterostructures for electrocatalytic nitrogen fixation. Materials Chemistry Frontiers, 2021, 5, 2338-2346.	3.2	38
41583	Strain-controlled single Cr-embedded nitrogen-doped graphene achieves efficient nitrogen reduction. Materials Advances, 2021, 2, 5704-5711.	2.6	9
41584	Magnetism manipulated by ferroelectric polarization and epitaxial strain in a La_{0.75}Sr_{0.25}MnO₃/BaTiO₃system. Physical Chemistry Chemical Physics, 2021, 23, 6154-6161.	1.3	10
41585	Theoretical investigation of defective MXenes as potential electrocatalysts for CO reduction toward C₂ products. Physical Chemistry Chemical Physics, 2021, 23, 12431-12438.	1.3	11
41586	Theoretical evaluation of the corrosion inhibition performance of aliphatic dipeptides. New Journal of Chemistry, 2021, 45, 3610-3629.	1.4	11
41587	The adsorption of halogen molecules on Ti (110) surface. Journal of Materials Research, 2021, 36, 592-601.	1.2	8
41588	Enhanced solar-to-hydrogen efficiency for photocatalytic water splitting based on a polarized heterostructure: the role of intrinsic dipoles in heterostructures. Journal of Materials Chemistry A, 2021, 9, 14515-14523.	5.2	32
41589	Rb₃In(SO₄)₃: a defluorinated mixed main-group metal sulfate for ultraviolet transparent nonlinear optical materials with a large optical band gap. Journal of Materials Chemistry C, 2021, 9, 5124-5131.	2.7	16
41590	Defect-rich N-doped CeO₂ supported by N-doped graphene as a metal-free plasmonic hydrogen evolution photocatalyst. Journal of Materials Chemistry A, 2021, 9, 10217-10230.	5.2	32
41591	Electrochemically synthesized SnO₂ with tunable oxygen vacancies for efficient electrocatalytic nitrogen fixation. Nanoscale, 2021, 13, 16307-16315.	2.8	13
41592	Ferromagnetic TM₂BC (TM = Cr, Mn) monolayers for spintronic devices with high Curie temperature. Physical Chemistry Chemical Physics, 2021, 23, 6107-6115.	1.3	29
41593	Finite-temperature density-functional-theory investigation on the nonequilibrium transient warm-dense-matter state created by laser excitation. Physical Review E, 2021, 103, 013210.	0.8	6
41594	Experimental ¹³C and ¹H Solid-State NMR Response in Weakly Tetrel-Bonded Methyl Groups. Journal of Physical Chemistry C, 2021, 125, 2111-2123.	1.5	10

#	Article	IF	Citations
41595	MOF-derived CoNi,CoO,NiO@Nâ€“C bifunctional oxygen electrocatalysts for liquid and all-solid-state Znâ€“air batteries. Nanoscale, 2021, 13, 17655-17662.	2.8	14
41596	Potential thermoelectric materials: first-principles prediction of low lattice thermal conductivity of two-dimensional (2D) orthogonal ScX₂ (X = C and N) compounds. Physical Chemistry Chemical Physics, 2021, 23, 23718-23729.	1.3	2
41597	Theoretical exploration of quaternary hexagonal MAB phases and two-dimensional derivatives. Nanoscale, 2021, 13, 13208-13214.	2.8	16
41598	A DFT-based microkinetic study on methanol synthesis from CO₂ hydrogenation over the In₂O₃ catalyst. Physical Chemistry Chemical Physics, 2021, 23, 1888-1895.	1.3	20
41599	The first-principles-based microkinetic simulation of the dry reforming of methane over Ru(0001). Catalysis Science and Technology, 2021, 11, 1395-1406.	2.1	25
41600	Tunability of the Electronic Properties of Covalent Organic Frameworks. ACS Applied Electronic Materials, 2021, 3, 720-732.	2.0	26
41601	Data-driven analysis of the electronic-structure factors controlling the work functions of perovskite oxides. Physical Chemistry Chemical Physics, 2021, 23, 6880-6887.	1.3	7
41602	Armchair Graphene Nanoribbon-Based Spin Caloritronics. SSRN Electronic Journal, 0, , .	0.4	0
41603	Influence of the PO_uN_{4â^’u} structural units on the formation energies and transport properties of lithium phosphorus oxynitride: a DFT study. Physical Chemistry Chemical Physics, 2021, 23, 22567-22588.	1.3	2
41604	Machine-learned interatomic potentials for alloys and alloy phase diagrams. Npj Computational Materials, 2021, 7, .	3.5	75
41605	Stable, high-performance, dendrite-free, seawater-based aqueous batteries. Nature Communications, 2021, 12, 237.	5.8	174
41606	Tuning the electronic structure of Ag-Pd alloys to enhance performance for alkaline oxygen reduction. Nature Communications, 2021, 12, 620.	5.8	107
41611	Combining Electronic Structure Calculations and Spectroscopy to Unravel the Structure of Grafted Organometallic Complexes. , 0, , 359-374.		1
41612	Nonlinear Work Function Tuning of Leadâ€Halide Perovskites by MXenes with Mixed Terminations. Advanced Functional Materials, 2020, 30, 1909028.	7.8	58
41613	Acid and Base Resistant Zirconium Polyphenolateâ€Metalloporphyrin Scaffolds for Efficient CO₂ Photoreduction. Advanced Materials, 2018, 30, 1704388.	11.1	184
41614	Quasiâ€Binary Transition Metal Dichalcogenide Alloys: Thermodynamic Stability Prediction, Scalable Synthesis, and Application. Advanced Materials, 2020, 32, e1907041.	11.1	46
41615	In Situ Polymerized Conjugated Poly(pyreneâ€4,5,9,10â€tetraone)/Carbon Nanotubes Composites for Highâ€Performance Cathode of Sodium Batteries. Advanced Energy Materials, 2021, 11, 2002917.	10.2	69
41616	Alloying of Alkali Metals with Tellurene. Advanced Energy Materials, 2021, 11, 2003248.	10.2	11

#	Article	IF	Citations
41617	Identifying promising metalâ€“organic frameworks for heterogeneous catalysis via highâ€throughput periodic density functional theory. Journal of Computational Chemistry, 2019, 40, 1305-1318.	1.5	87
41618	Optical and magnetic properties of some XMnSb and Co ₂ YZ Compounds: ab initio calculations. Physica Status Solidi C: Current Topics in Solid State Physics, 2017, 14, 1600182.	0.8	3
41619	XYO ₃ (X â€‰=â€‰K, Na; Y â€‰=â€‰Nb, Ta) based superlattices for photocatalysis. Physica Status Solidi C: Current Topics in Solid State Physics, 2017, 14, 1700026.	0.8	6
41620	Auâ€Polyoxometalates Aâ€Bâ€Aâ€B Type Copolymerâ€Analogue Subâ€1 nm Nanowires. Small, 2021, 17, e2006260.	5.2	22
41621	Antiblocking Heterostructure to Accelerate Kinetic Process for Naâ€Ion Storage. Small, 2021, 17, e2006374.	5.2	24
41622	Supercell Methods for Defect Calculations. Topics in Applied Physics, 0, , 29-68.	0.4	10
41623	Quasiparticle Calculations for Point Defects at Semiconductor Surfaces. Topics in Applied Physics, 0, , 165-192.	0.4	1
41624	Modern Correlation Theories for Extended, Periodic Systems. Topics in Current Chemistry, 1999, , 121-145.	4.0	10
41625	Applications of Computer Simulations and Statistical Mechanics in Surface Electrochemistry. Modern Aspects of Electrochemistry, 2009, , 131-149.	0.2	2
41626	Ab Initio Study of Ideal Shear Strength. Solid Mechanics and Its Applications, 2004, , 401-410.	0.1	4
41627	Defects and Impurities in Semiconductors. , 2005, , 1877-1888.		2
41628	Hydrogen Bonds And Solvent Effects In Soil Processes: A Theoretical View. Challenges and Advances in Computational Chemistry and Physics, 2008, , 321-347.	0.6	1
41629	Challenges in the Design of Active and Durable Alloy Nanocatalysts for Fuel Cells. Modern Aspects of Electrochemistry, 2010, , 351-396.	0.2	3
41630	AB Definitio Calculation of Structure And Lattice Dynamics of GaAs. , 1983, , 65-99.		14
41631	First-Principles Determination of Phonon Lifetimes, Mean Free Paths, and Thermal Conductivities in Crystalline Materials: Pure Silicon and Germanium. Topics in Applied Physics, 2014, , 115-136.	0.4	9
41632	Theory of Electron States at Surfaces and Interfaces. , 1992, , 175-203.		1
41633	Current Ideas and Methods for Calculation of Ground State Properties of Solids. , 1985, , 175-225.		5
41634	Recent Results in Semiconductor Dynamics by Ab Initio â€˜Directâ€™ Approach. , 1985, , 227-312.		15

#	Article	IF	Citations
41635	Stress: Concepts and Applications. , 1985, , 313-333.		6
41636	Large-Scale Electronic Structure Calculations in Solids. , 1995, , 67-86.		3
41637	Density-Functional Theory of Surface Diffusion and Epitaxial Growth of Metals. NATO ASI Series Series B: Physics, 1997, , 83-101.	0.2	7
41638	Adhesion of Chromium, Nickel, and Copper to Polymers Containing Basic Functional Groups. , 1989, , 247-263.		3
41639	Models of the Interfaces in Superhard TiN-Based Heterostructures and Nanocomposites from First-Principles. , 2014, , 45-91.		1
41640	Photovoltaic Materials Design by Computational Studies: Metal Sulfides. , 2020, , 123-138.		2
41641	Progress in Warm Dense Matter and Planetary Physics. Lecture Notes in Computational Science and Engineering, 2014, , 203-234.	0.1	7
41642	Interfacial Properties and Growth Dynamics of Semiconductor Interfaces. , 2016, , 199-213.		1
41643	Thermal Transport by First-Principles Anharmonic Lattice Dynamics. , 2020, , 735-765.		3
41644	Optical Properties Of Cd1-xZnxSe From Density Functional Theory. , 2014, , 1141-1148.		1
41645	Structure and Thermodynamical Properties of Zirconium Hydrides from First-Principle. , 2011, , 671-681.		4
41646	First-Principles Study of Ferromagnetic Heusler Alloys: An Overview. , 2008, , 129-141.		4
41647	Molecular Orientation Dependence of the Ionization Energy of Pentacene in Thin Films. Springer Proceedings in Physics, 2009, , 141-145.	0.1	5
41648	Metalâ€“Insulator Transition in Dense Hydrogen. Springer Series in Materials Science, 2010, , 63-84.	0.4	3
41649	Adsorption of Cysteine on the Au(110)-surface: A Density Functional Theory Study. , 2010, , 53-60.		1
41650	H2 Carrying Capacity by Considering Charging and Discharging Processes â€“ Case Studies on Small Carbon- and Boron Nitride Nanotubes. , 2010, , 85-109.		1
41652	Hydrogen in SiC. Advanced Texts in Physics, 2004, , 57-88.	0.5	5
41653	Non-adiabatic Effects at Surfaces Simulated with TDDFT Molecular Dynamics. Springer Series in Surface Sciences, 2013, , 299-321.	0.3	1

#	Article	IF	Citations
41654	Role of step sites on water dissociation on stoichiometric ceria surfaces. Highlights in Theoretical Chemistry, 2014, , 19-25.	0.0	1
41656	Reciprocal Space Integration and Special-Point Techniques. Lecture Notes in Quantum Chemistry II, 1996, , 77-89.	0.3	1
41657	Intercalation Compounds of Transition-Metal Dichalcogenides. Springer Series in Materials Science, 1994, , 106-138.	0.4	7
41658	First-Principles Molecular Dynamical Studies of Polymerized C60. Springer Series in Materials Science, 2000, , 185-227.	0.4	1
41659	Ab initio Tensile Testing Simulation of Al, AlN and Al/AlN Composite. Advances in Materials Research, 1998, , 176-184.	0.2	1
41661	Topological Versus Physical and Chemical Properties of Negatively Curved Carbon Surfaces. Carbon Materials, 2013, , 105-136.	0.2	2
41662	Electronic Spectra of Solids, Impurities and Superstructures with the Recursion and Renormalization Methods. Physics and Chemistry of Materials With Low-dimensional Structures, 1989, , 409-438.	1.0	3
41663	Molecular Dynamics Studies of High Pressure Transformations and Structures. , 1999, , 59-85.		1
41664	Gas Sensing Using Monolayer MoS2. NATO Science for Peace and Security Series A: Chemistry and Biology, 2019, , 71-95.	0.5	1
41665	Realization of Switching Mechanism of CO2 by Alkaline Adatoms on g-B4N3 Surface. Springer Proceedings in Physics, 2019, , 423-440.	0.1	3
41666	Non-regular hexagonal 2D carbon, an allotrope of graphene: a first-principles computational study. Journal of Molecular Modeling, 2020, 26, 150.	0.8	3
41667	Mechanically ductile 3D spâ€“sp 2 microporous carbon. Journal of Materials Science, 2018, 53, 4316-4322.	1.7	10
41668	Ionic liquid-induced graphitization of biochar: N/P dual-doped carbon nanosheets for high-performance lithium/sodium storage. Journal of Materials Science, 2021, 56, 8186-8201.	1.7	13
41669	Structural, Electronic and Adsorption Characteristics of Transition Metal doped TM@C70 Endohedral Fullerenes. Journal of Cluster Science, 2021, 32, 77-84.	1.7	4
41670	Adsorption of methyl isocyanate on M4 (M=Fe, Ni, and Cu) cluster-decorated graphene and vacancy graphene: a DFT-D2 study. Structural Chemistry, 2020, 31, 1983-1997.	1.0	16
41671	Design of Active Centers in Ammonia Synthesis on Mo-Based Catalysts: A Theoretical Study. Topics in Catalysis, 2020, 63, 12-23.	1.3	1
41672	The Investigation of Electronic, Elastic and Vibrational Properties of an Interlanthanide Perovskite: PrYbO3. Journal of Electronic Materials, 2017, 46, 5827-5836.	1.0	19
41673	Elastic Properties and Stacking Fault Energies of Borides, Carbides and Nitrides from First-Principles Calculations. Acta Metallurgica Sinica (English Letters), 2019, 32, 1099-1110.	1.5	18

#	Article	IF	Citations
41674	Strong and tough graphene papers constructed with pyrene-containing small molecules via Ï€-Ï€/H-bonding synergistic interactions. Science China Materials, 2021, 64, 1206-1218.	3.5	5
41675	Quantum Theory of Structure: Tight-Binding Systems. Cohesion and Structure, 1989, 2, 287-362.	0.0	10
41676	Cohesive strength of zirconia/molybdenum interfaces and grain boundaries in molybdenum: A comparative study. Acta Materialia, 2017, 135, 150-157.	3.8	19
41677	Diffusion, defects and understanding the growth of a multicomponent interdiffusion zone between Pt-modified B2 NiAl bond coat and single crystal superalloy. Acta Materialia, 2020, 195, 35-49.	3.8	31
41678	Highly dispersed CuFe-nitrogen active sites electrode for synergistic electrochemical CO2 reduction at low overpotential. Applied Energy, 2020, 269, 115029.	5.1	36
41679	A comparative experimental and theoretical investigation on energy storage performance of CoSe2, NiSe2 and MnSe2 nanostructures. Applied Materials Today, 2020, 19, 100568.	2.3	35
41680	Effect of vacancy defects on electronic properties and wettability of coal surface. Applied Surface Science, 2020, 511, 145546.	3.1	20
41681	First-principles study of mechanical, electronic and optical properties of Janus structure in transition metal dichalcogenides. Applied Surface Science, 2020, 526, 146730.	3.1	46
41682	Defect-rich Ni3Sn4 quantum dots anchored on graphene sheets exhibiting unexpected reversible conversion reactions with exceptional lithium and sodium storage performance. Applied Surface Science, 2020, 526, 146756.	3.1	12
41683	Multiple-interface relay catalysis: Enhancing alkaline hydrogen evolution through a combination of Volmer promoter and electrical-behavior regulation. Chemical Engineering Journal, 2020, 397, 125457.	6.6	32
41684	Ti-enhanced exfoliation of V2AlC into V2C MXene for lithium-ion battery anodes. Ceramics International, 2017, 43, 11450-11454.	2.3	85
41685	The photophysical anisotropy and electronic structure of new narrow band gap perovskites Ln2AlMnO6 (Ln = La, Pr, Nd): An experimental and DFT perspective. Ceramics International, 2020, 46, 21021-21032.	2.3	15
41686	Elastic and mechanical properties of hydroxyapatite under pressure: A first-principles investigation. Computational Condensed Matter, 2020, 24, e00481.	0.9	13
41687	First principle study of V-implantation in highly-doped silicon materials. Computational Materials Science, 2017, 136, 207-215.	1.4	6
41688	Migration behavior of tellurium in bcc iron against typical alloying elements: A first-principles study. Computational Materials Science, 2020, 181, 109571.	1.4	7
41689	Effect of transmutation elements Re and Ta on the vacancy formation and dissociation behaviors in W bulk. Computational Materials Science, 2020, 179, 109624.	1.4	9
41690	Simulation and experiment of adsorption behavior of calcite, aragonite and vaterite on alpha-Fe2O3 surface. Computational Materials Science, 2020, 182, 109762.	1.4	9
41691	The effect of Kaoliniteâ€™s structure on migration and release characteristics of sodium under oxy-fuel combustion condition. Fuel, 2020, 277, 118154.	3.4	11

#	Article	IF	Citations
41692	Towards understanding the strong trapping effects of noble gas elements on hydrogen in tungsten. International Journal of Hydrogen Energy, 2017, 42, 6902-6917.	3.8	31
41693	Formation and characterization of gray Ta2O5 and its enhanced photocatalytic hydrogen generation activity. International Journal of Hydrogen Energy, 2020, 45, 16560-16568.	3.8	29
41694	Understanding the influence of the composition of the Ag Pd catalysts on the selective formic acid decomposition and subsequent levulinic acid hydrogenation. International Journal of Hydrogen Energy, 2020, 45, 17339-17353.	3.8	29
41695	Copper induced phosphide for enhanced electrochemical hydrogen evolution reaction. International Journal of Hydrogen Energy, 2020, 45, 21422-21430.	3.8	15
41696	Atomistic calculations of the generalized stacking fault energies in two refractory multi-principal element alloys. Intermetallics, 2020, 124, 106844.	1.8	40
41697	Vacancy ordering in Pd11Bi2Se2 - Crystal structure and properties. Journal of Alloys and Compounds, 2018, 735, 1914-1920.	2.8	5
41698	Electronic and mechanical property of high electron mobility semiconductor Bi2O2Se. Journal of Alloys and Compounds, 2018, 764, 674-678.	2.8	32
41699	Crystal structure and cation ordering in novel perovskite type oxides PrBaCoTa(Nb)O6â€“Î´. Journal of Alloys and Compounds, 2020, 824, 153909.	2.8	6
41700	Energy transfer, structural and luminescent properties of the color tunable phosphor Y2WO6:Sm3+. Journal of Alloys and Compounds, 2020, 835, 155381.	2.8	9
41701	The investigation of electronic, anisotropic elastic and lattice dynamical properties of MAB phase nanolaminated ternary borides: <mml:math xmlns:mml="http://www.w3.org/1998/Math/MathML" altimg="si1.svg"><mml:mrow><mml:msub><mml:mi mathvariant="bold-italic">M</mml:mi><mml:mn>2</mml:mn></mml:msub><mml:mi mathvariant="bold-italic">Al</mml:mi><mml:msub><mml:mi mathvariant="bold-italic">B</mml:mi><mml:mn>2</mml:mn></mml:msub></mml:mrow></mml:math>		

#	Article	IF	Citations
41710	On the possibility of thermoelectricity in half Heusler XRuSb (XÂ=ÂV, Nb, Ta) materials: A first principles prospective. Journal of Physics and Chemistry of Solids, 2017, 110, 108-115.	1.9	18
41711	Theoretical investigation on the high-pressure physical properties of ZnN in cubic zinc blende, rock salt, and cesium chloride structures. Journal of Physics and Chemistry of Solids, 2017, 110, 70-75.	1.9	7
41712	Influence of edge termination on the electronic and transport properties of sawtooth penta-graphene nanoribbons. Journal of Physics and Chemistry of Solids, 2020, 146, 109528.	1.9	20
41713	Copperâ€“antimonyâ€“red phosphorus composites as promising anode materials for sodium-ion batteries. Journal of Power Sources, 2017, 362, 115-122.	4.0	21
41714	Electronic and magnetic properties of Zn 1â^'x Fe x Se alloys. Journal of Solid State Chemistry, 2017, 256, 116-123.	1.4	5
41715	Strain dependent tuning electronic properties of noble metal di chalcogenides PdX 2 (XÂ=ÂS, Se) mono-layer. Materials Chemistry and Physics, 2017, 198, 162-166.	2.0	32
41716	Band gap tuning in aluminum doped two-dimensional hexagonal boron nitride. Materials Chemistry and Physics, 2020, 250, 123176.	2.0	19
41717	Packing high-energy together: Binding the power of pentazolate and high-valence metals with strong bonds. Materials and Design, 2020, 193, 108820.	3.3	14
41718	Band gap engineering in halide cubic perovskites CsPbBr3â^'yIy (yÂ=Â0, 1, 2, 3) â€“ A DFT study. Materials Science and Engineering B: Solid-State Materials for Advanced Technology, 2020, 258, 114560.	1.7	32
41719	DFT â€“ GGA calculations of magnetic, elastic, thermodynamic and thermoelectric properties of Co2YAl (YÂ=ÂTi, V) full Heusler alloy systems. Materials Science and Engineering B: Solid-State Materials for Advanced Technology, 2020, 262, 114739.	1.7	11
41720	Low-temperature synthesis of PdO-CeO2/C toward efficient oxygen reduction reaction. Materials Today Energy, 2020, 18, 100557.	2.5	11
41721	Ab initio modelling of titanium impurities in Î±-Fe lattice. Nuclear Instruments & Methods in Physics Research B, 2020, 483, 50-54.	0.6	1
41722	Density functional theory calculation of the properties of carbon vacancy defects in silicon carbide. Nami Jishu Yu Jingmi Gongcheng/Nanotechnology and Precision Engineering, 2020, 3, 211-217.	1.7	9
41723	Exploring performances of hybrid perovskites tin-based photovoltaic solar cells: Non-equilibrium Green's functions and macroscopic approaches. Physica B: Condensed Matter, 2020, 591, 412247.	1.3	13
41724	Newly synthesized A-site ordered cubic-perovskite superconductor (Ba0.54K0.46)4Bi4O12: A DFT investigation. Physica C: Superconductivity and Its Applications, 2020, 574, 1353669.	0.6	23
41725	CrI3 magnetic nanotubes: A comparative DFT and DFT+U study, and strain effect. Physica E: Low-Dimensional Systems and Nanostructures, 2020, 123, 114205.	1.3	12
41726	Defect induced room temperature ferromagnetism in methylammonium lead iodide perovskite. Physics Letters, Section A: General, Atomic and Solid State Physics, 2020, 384, 126278.	0.9	18
41727	Arsenic pentafluoride surface adsorption studies on Kagome-phosphorene â€“ a DFT outlook. Physics Letters, Section A: General, Atomic and Solid State Physics, 2020, 384, 126552.	0.9	16

#	Article	IF	Citations
41728	Investigating the solution and diffusion properties of hydrogen in Î±-Uranium by first-principles calculations. Progress in Nuclear Energy, 2020, 122, 103268.	1.3	8
41729	Designing a sp3 structure of carbon T-C9: First-principles calculations. Results in Physics, 2020, 19, 103690.	2.0	16
41730	Structural, electronic, magnetic, elastic and thermodynamic properties of <mml:math xmlns:mml="http://www.w3.org/1998/Math/MathML" display="inline" id="d1e1063" altimg="si46.svg"><mml:mrow><mml:mi>C</mml:mi><mml:msub><mml:mrow><mml:mi>r</mml:mi></mml:mrow><mml:mrow><mml perovskite. Solid State Sciences, 2020, 105, 106260.	1.5	9
41731	Tunable electronic and magnetic properties in stanene by 3d transition metal atoms absorption. Superlattices and Microstructures, 2017, 103, 139-144.	1.4	22
41732	Sodium-ion diffusion in alluaudite Na5In(MoO4)4. Solid State Ionics, 2020, 351, 115328.	1.3	9
41733	Improvement in erosion-corrosion resistance of high-chromium cast irons by trace boron. Wear, 2017, 376-377, 578-586.	1.5	17
41734	Lanthanide-regulated oxygen evolution activity of face-sharing IrO6 dimers in 6H-perovskite electrocatalysts. Chinese Journal of Catalysis, 2020, 41, 1692-1697.	6.9	18
41737	Reviving Inert Oxides for Electrochemical Water Splitting by Subsurface Engineering. Chemistry of Materials, 2020, 32, 5569-5578.	3.2	11
41738	Durable Multimetal Oxychloride Intergrowths for Visible Light-Driven Water Splitting. Chemistry of Materials, 2021, 33, 347-358.	3.2	19
41739	Crystal Structures, Superconducting Properties, and the Coloring Problem in ReAlSi and ReGaSi. Inorganic Chemistry, 2020, 59, 17310-17319.	1.9	5
41740	PrVO₄ under High Pressure: Effects on Structural, Optical, and Electrical Properties. Inorganic Chemistry, 2020, 59, 18325-18337.	1.9	8
41741	Sn₃B₈O₁₅: A Ternary Tin(II) Borate with Flexible [B₈O₁₈]^{12â€“} Fundamental Building Block Formed by [B₇O₁₆]^{11â€“} and [BO₃]^{3â€“} Groups. Inorganic Chemistry, 2021, 60, 883-891.	1.9	8
41742	Understanding the Structural and Electronic Properties of Bismuth Trihalides and Related Compounds. Inorganic Chemistry, 2020, 59, 3377-3386.	1.9	9
41743	Synthesis of Two-Dimensional Metalâ€“Organic Frameworks via Dehydrogenation Reactions on a Cu(111) Surface. Journal of Physical Chemistry C, 2020, 124, 12390-12396.	1.5	15
41744	Initial Steps of Oxidative Etching of MoS₂ Basal Plane Induced by O₂. Journal of Physical Chemistry C, 2020, 124, 13177-13186.	1.5	13
41745	An Emerging All-Inorganic CsSn_xPb_{1â€“x}Br₃ (0 â‰¤ Tj ETQq1 1 0.784314 rgBT Properties. Journal of Physical Chemistry C, 2020, 124, 13434-13446.	1.5	16
41746	Reaction Mechanism of the Metal Precursor Pulse in Plasma-Enhanced Atomic Layer Deposition of Cobalt and the Role of Surface Facets. Journal of Physical Chemistry C, 2020, 124, 11990-12000.	1.5	4
41747	Structure and Stability of the (001) Surface of Co₃O₄. Journal of Physical Chemistry C, 2020, 124, 25790-25795.	1.5	13

#	Article	IF	Citations
41748	Pathway Alteration of Water Splitting via Oxygen Vacancy Formation on Anatase Titanium Dioxide in Photothermal Catalysis. Journal of Physical Chemistry C, 2020, 124, 26214-26221.	1.5	19
41749	Shedding Light on the Interfacial Structure of Low-Coverage Alkanethiol Lattices. Journal of Physical Chemistry C, 2020, 124, 26748-26758.	1.5	6
41750	Hydrogenolysis of Asymmetric C_{aryl}â€“Oâ€“C_{alkyl} Bonds in Bio-Oils over Alloyed Catalysts: A Theoretical Insight. Journal of Physical Chemistry C, 2020, 124, 28052-28060.	1.5	14
41751	Lead Free Two-Dimensional Mixed Tin and Germanium Halide Perovskites for Photovoltaic Applications. Journal of Physical Chemistry C, 2021, 125, 74-81.	1.5	29
41752	Organic Gas Sensing Performance of the Borophene van der Waals Heterostructure. Journal of Physical Chemistry C, 2021, 125, 427-435.	1.5	30
41753	How Do Surface Defects Change Local Wettability of the Hydrophilic ZnS Surface? Insights into Sphalerite Flotation from Density Functional Theory Calculations. Journal of Physical Chemistry C, 2021, 125, 998-1009.	1.5	11
41754	First-Principles Study of Interhalogen Interactions and Triangular Windmill Structures in Self-Assembly of Fully Halogenated Benzenes on a Silver Surface. Journal of Physical Chemistry C, 2021, 125, 526-535.	1.5	6
41755	Extraordinary Electromechanical Actuation of Ti2C MXene. Journal of Physical Chemistry C, 2021, 125, 1060-1068.	1.5	13
41756	Conductance Switching in Molecular Self-Assembled Monolayers for Application of Data Storage. Journal of Physical Chemistry C, 2021, 125, 1069-1074.	1.5	6
41757	In Situ Studies of Methanol Decomposition Over Cu(111) and Cu₂O/Cu(111): Effects of Reactant Pressure, Surface Morphology, and Hot Spots of Active Sites. Journal of Physical Chemistry C, 2021, 125, 558-571.	1.5	18
41758	Anchoring Bond between Ru and N Atoms of Ru/Ca₂NH Catalyst: Crucial for the High Ammonia Synthesis Activity. Journal of Physical Chemistry C, 2017, 121, 20900-20904.	1.5	33
41759	Lateral and Vertical Heterostructures of h-GaN/h-AlN: Electron Confinement, Band Lineup, and Quantum Structures. Journal of Physical Chemistry C, 2017, 121, 27098-27110.	1.5	22
41760	Nitrophosphorene: A 2D Semiconductor with Both Large Direct Gap and Superior Mobility. Journal of Physical Chemistry C, 2017, 121, 28520-28526.	1.5	34
41761	Properties of Metal-Supported Oxide Honeycomb Monolayers: M₂O₃ and MMâ€²O₃ on Me(111) (M, Mâ€² = Ti, V, Cr, Fe; Me = Ag, Au, Pt). Journal of Physical Chemistry C, 2020, 124, 8186-8197.	1.5	12
41762	Structural Characterization of a Novel Two-Dimensional Material: Cobalt Sulfide Sheets on Au(111). Journal of Physical Chemistry Letters, 2020, 11, 9038-9044.	2.1	8
41763	High-Performance Borophene/Graphene Heterostructure Anode of Lithium-Ion Batteries Achieved via Controlled Interlayer Spacing. ACS Applied Energy Materials, 2020, 3, 11699-11705.	2.5	33
41764	Mechanical Engineering Effect in Electronic and Optical Properties of Graphene Nanomeshes. ACS Applied Materials & Interfaces, 2020, 12, 55189-55194.	4.0	9
41765	Sulfurized Polyacrylonitrile for High-Performance Lithiumâ€“Sulfur Batteries: In-Depth Computational Approach Revealing Multiple Sulfurâ€™s Reduction Pathways and Hidden Li⁺ Storage Mechanisms for Extra Discharge Capacity. ACS Applied Materials & Interfaces, 2021, 13, 491-502.	4.0	16

#	Article	IF	Citations
41766	Constructing Efficient Single Rh Sites on Activated Carbon via Surface Carbonyl Groups for Methanol Carbonylation. ACS Catalysis, 2021, 11, 682-690.	5.5	19
41767	Spectral Instability of Layered Mixed Halide Perovskites Results from Anion Phase Redistribution and Selective Hole Injection. ACS Nano, 2021, 15, 1486-1496.	7.3	18
41768	Electrochemical and Computational Insights on the Application of Expired Metformin Drug as a Novel Inhibitor for the Sweet Corrosion of C1018 Steel. ACS Omega, 2021, 6, 65-76.	1.6	29
41769	Unraveling Catalytic Mechanisms for CO Oxidation on Boron-Doped Fullerene: A Computational Study. ACS Omega, 2020, 5, 28870-28876.	1.6	4
41770	Ab Initio Calculations on the Structural and Electronic Properties of AgAu Alloys. ACS Omega, 2020, 5, 31391-31397.	1.6	25
41771	Doping-Enhanced Current Rectification in Carbon Nanotubeâ€“Metal Junctions for Rectenna Applications. ACS Omega, 2020, 5, 189-196.	1.6	13
41772	Effect of chemistry on the physical properties of perovskite and post-perovskite. Geophysical Monograph Series, 2007, , 115-128.	0.1	12
41773	Van der Waals epitaxy between the highly lattice mismatched Cu-doped FeSe and Bi2Te3. NPG Asia Materials, 2017, 9, e402-e402.	3.8	21
41774	Switchable encapsulation of polysulfides in the transition between sulfur and lithium sulfide. Nature Communications, 2020, 11, 845.	5.8	92
41775	Vibrational hierarchy leads to dual-phonon transport in low thermal conductivity crystals. Nature Communications, 2020, 11, 2554.	5.8	79
41776	Tuning the interfacial spin-orbit coupling with ferroelectricity. Nature Communications, 2020, 11, 2627.	5.8	19
41777	Exploiting two-dimensional morphology of molybdenum oxycarbide to enable efficient catalytic dry reforming of methane. Nature Communications, 2020, 11, 4920.	5.8	78
41778	Tweaking the Electronic and Optical Properties of Î±-MoO3 by Sulphur and Selenium Doping â€“ a Density Functional Theory Study. Scientific Reports, 2018, 8, 10144.	1.6	25
41779	Tuning Penta-Graphene Electronic Properties Through Engineered Line Defects. Scientific Reports, 2020, 10, 8014.	1.6	15
41780	Design of Advanced Photocatalysis System by Adatom Decoration in 2D Nanosheets of Group-IV and IIIâ€“V Binary Compounds. Scientific Reports, 2016, 6, 23104.	1.6	37
41781	Exploring perovskites for methane activation from first principles. Catalysis Science and Technology, 2018, 8, 702-709.	2.1	35
41782	Tuning the structure of bifunctional Pt/SmMn₂O₅ interfaces for promoted low-temperature CO oxidation activity. Nanoscale, 2019, 11, 8150-8159.	2.8	13
41783	Volume expansive pressure (VEP) driven non-trivial topological phase transition in LiMgBi. Physical Chemistry Chemical Physics, 2020, 22, 4602-4609.	1.3	7

#	Article	IF	Citations
41784	Interfacial structure-governed SO₂ resistance of Cu/TiO₂ catalysts in the catalytic oxidation of CO. Catalysis Science and Technology, 2020, 10, 1661-1674.	2.1	20
41785	Carbon-phosphide monolayer with high carrier mobility and perceptibleIâ€“Vresponse for superior gas sensing. New Journal of Chemistry, 2020, 44, 3777-3785.	1.4	23
41786	Exploring half-metallic Co-based full Heusler alloys using a DFT+Umethod combined with linear response approach. RSC Advances, 2019, 9, 30462-30478.	1.7	28
41787	Investigation of ferrimagnetism and ferroelectricity in Al_xFe_{2â^'x}O₃ thin films. Journal of Materials Chemistry C, 2020, 8, 706-714.	2.7	8
41788	Si₂BN monolayers as promising candidates for hydrogen storage. Physical Chemistry Chemical Physics, 2020, 22, 13563-13568.	1.3	34
41789	Strong dependence of the vertical charge carrier mobility on the Ï€â€“Ï€ stacking distance in molecule/graphene heterojunctions. Physical Chemistry Chemical Physics, 2020, 22, 13802-13807.	1.3	10
41790	NO disproportionation over defective 1Tâ€²-MoS₂ monolayers. Physical Chemistry Chemical Physics, 2020, 22, 13154-13159.	1.3	3
41791	A boron-decorated melon-based carbon nitride as a metal-free photocatalyst for N₂ fixation: a DFT study. Physical Chemistry Chemical Physics, 2020, 22, 21872-21880.	1.3	18
41792	Computational prediction of a novel 1D InSeI nanochain with high stability and promising wide-bandgap properties. Physical Chemistry Chemical Physics, 2020, 22, 27441-27449.	1.3	17
41793	Recent progress and approaches on the synthesis of Mn-doped zinc oxide nanoparticles: a theoretical and experimental investigation on the photocatalytic performance. New Journal of Chemistry, 2020, 44, 8805-8812.	1.4	28
41794	Electronic structure and thermoelectric properties of Mo-based dichalcogenide monolayers locally and randomly modified by substitutional atoms. RSC Advances, 2020, 10, 43035-43044.	1.7	10
41795	Effects of Cr- and Mn-alloying on the band gap tuning, and optical and electronic properties of lead-free CsSnBr₃perovskites for optoelectronic applications. RSC Advances, 2020, 10, 43660-43669.	1.7	26
41796	Improved H₂ utilization by Pd doping in cobalt catalysts for reductive amination of polypropylene glycol. RSC Advances, 2020, 10, 45159-45169.	1.7	6
41797	A self-smoothing Li-metal anode enabled via a hybrid interface film. Journal of Materials Chemistry A, 2020, 8, 12045-12054.	5.2	24
41798	Band convergence and carrier-density fine-tuning as the electronic origin of high-average thermoelectric performance in Pb-doped GeTe-based alloys. Journal of Materials Chemistry A, 2020, 8, 11370-11380.	5.2	41
41799	Optimizing electron density of nickel sulfide electrocatalysts through sulfur vacancy engineering for alkaline hydrogen evolution. Journal of Materials Chemistry A, 2020, 8, 18207-18214.	5.2	31
41800	Proton dynamics and the phase diagram of dense water ice. Journal of Chemical Physics, 2018, 148, 214501.	1.2	48
41801	Extrinsic dopants in quasi-one-dimensional photovoltaic semiconductor Sb2S3: A first-principles study. Journal of Applied Physics, 2020, 127, 183101.	1.1	19

#	Article	IF	Citations
41802	Ab initio calculations of the electronic structure for Mn2+-doped YAlO3 crystals. Low Temperature Physics, 2020, 46, 1160-1164.	0.2	3
41803	Two-dimensional GaTe/Bi2Se3 heterostructure: A promising direct Z-scheme water splitting photocatalyst. Chinese Journal of Chemical Physics, 2020, 33, 427-433.	0.6	5
41804	Large scale and linear scaling DFT with the CONQUEST code. Journal of Chemical Physics, 2020, 152, 164112.	1.2	55
41805	Toward a systematic improvement of the fixed-node approximation in diffusion Monte Carlo for solidsâ€"A case study in diamond. Journal of Chemical Physics, 2020, 153, 184111.	1.2	16
41806	Warm dense matter simulation via electron temperature dependent deep potential molecular dynamics. Physics of Plasmas, 2020, 27, .	0.7	19
41807	Prediction of crystalline Ta4O9 phase using first principles-based cluster expansion calculations. APL Materials, 2020, 8, .	2.2	2
41808	The Hubbard-U correction and optical properties of d metal oxide photocatalysts. Journal of Chemical Physics, 2020, 153, 224116.	1.2	10
41809	Defect-related photoluminescence and photoluminescence excitation as a method to study the excitonic bandgap of AlN epitaxial layers: Experimental and ab initio analysis. Applied Physics Letters, 2020, 117, .	1.5	9
41810	Identifying alternative ferroelectric materials beyond Hf(Zr)O2. Applied Physics Letters, 2020, 117, 262903.	1.5	3
41811	A computational investigation of the interstitial oxidation thermodynamics of a Mo-Nb-Ta-W high entropy alloy beyond the dilute regime. Journal of Applied Physics, 2020, 128, .	1.1	10
41812	Theoretical investigation of mixing and clustering thermodynamics of Ti1â^'xAlxB2 alloys with potential for age-hardening. Journal of Applied Physics, 2020, 128, 235101.	1.1	7
41813	Band alignment of Î²-(AlxGa1â^'x)2O3 alloys via atomic solid-state energy scale approach. AIP Advances, 2020, 10, 125321.	0.6	9
41814	Structural and electronic properties of monodomain ultrathin PbTiO3/SrTiO3/PbTiO3/SrRuO3 heterostructures: A first-principles approach. Journal of Applied Physics, 2020, 128, .	1.1	6
41815	Adsorption of methane on single metal atoms supported on graphene: Role of electron back-donation in binding and activation. Journal of Chemical Physics, 2020, 153, 244701.	1.2	8
41816	Direct and continuous generation of pure acetic acid solutions via electrocatalytic carbon monoxide reduction. Proceedings of the National Academy of Sciences of the United States of America, 2021, 118, .	3.3	93
41818	Probing the electronâ€"phonon interaction in superconductivity for KSn2 using the Migdal-Eliashberg theory and linear-response theory. Philosophical Magazine Letters, 2020, 100, 33-54.	0.5	2
41819	A study of polybromide chain formation using carbon nanomaterials via density functional theory approach. Cogent Engineering, 2016, 3, 1261509.	1.1	5
41820	Pressure-Stabilized New Phase of CaN₄*. Chinese Physics Letters, 2020, 37, 047101.	1.3	10

#	Article	IF	Citations
41821	Superconducting properties of the ternary transition-metal silicide Zr₂Ru₃Si₄. Superconductor Science and Technology, 2014, 27, 025012.	1.8	4
41822	Ab initiomolecular dynamics study of hydrogen removal by ionâ€“surface interactions. Journal of Physics Condensed Matter, 2005, 17, L137-L142.	0.7	11
41823	A theoretical explanation of RbBH4â€™s fractionally occupied ground-state phase and the reorientational motion of the [BH4]â^' group. Journal Physics D: Applied Physics, 2017, 50, 455501.	1.3	3
41824	Electron-phonon scattering limited intrinsic electrical conductivity of metallic MXenes X₂C (X= Ti or Mo). Journal Physics D: Applied Physics, 2021, 54, 015301.	1.3	5
41825	Charge-induced high-performance actuation of borophene. Journal Physics D: Applied Physics, 2021, 54, 105504.	1.3	8
41826	Density functional study of carbon vacancies in titanium carbide. Journal of Physics Condensed Matter, 2018, 30, 015702.	0.7	8
41827	Oxygen vacancies and hydrogen doping in LaAlO3/SrTiO3 heterostructures: electronic properties and impact on surface and interface reconstruction. Journal of Physics Condensed Matter, 2019, 31, 295601.	0.7	14
41828	DFT calculation of ²²⁹thorium-doped magnesium fluoride for nuclear laser spectroscopy. Journal of Physics Condensed Matter, 2020, 32, 255503.	0.7	11
41829	Distinguishing between chemical bonding and physical binding using electron localization function (ELF). Journal of Physics Condensed Matter, 2020, 32, 315502.	0.7	137
41830	SAKE: first-principles electron transport calculation code. Journal of Physics Condensed Matter, 2020, 32, 325901.	0.7	3
41831	Oxygen vacancy in ZnO- w phase: pseudohybrid Hubbard density functional study. Journal of Physics Condensed Matter, 2020, 32, 315503.	0.7	3
41832	Fermi surface electronâ€“hole instability of the (TMTSF)₂PF₆ Bechgaard salt revealed by the first-principles Lindhard response function. Journal of Physics Condensed Matter, 2020, 32, 345701.	0.7	4
41833	Cluster size effects on the adsorption of CO, O, and CO₂ and the dissociation of CO₂ on two-dimensional Cu_x (x = 1, 3, and 7) clusters supported on Cu(111) surface: a density functional theory study. Journal of Physics Condensed Matter, 2020, 32, 405201.	0.7	3
41834	Theoretical polarization of zero phonon lines in point defects. Journal of Physics Condensed Matter, 2020, 32, 385502.	0.7	9
41835	Robust intrinsic half-metallic ferromagnetism in stable 2D single-layer MnAsS₄. Journal of Physics Condensed Matter, 2020, 32, 385803.	0.7	6
41836	LCAO-TDDFT-k- Ï‰ : spectroscopy in the optical limit. Journal of Physics Condensed Matter, 2020, 32, 415901.	0.7	3
41837	Electronic structure and anisotropic compression of Os₂B₃ to 358 GPa. Journal of Physics Condensed Matter, 2020, 32, 405703.	0.7	9
41838	Temperature-dependent band gaps in several semiconductors: from the role of electronâ€“phonon renormalization. Journal of Physics Condensed Matter, 2020, 32, 475503.	0.7	23

#	Article	IF	Citations
41839	Effect of bond on negative thermal expansion of Prussian blue analogues MCo(CN)₆ (M) Tj ETQq0 0 0 rgBT /Overlock 10 Tf	0.7	14
41840	Quasi-harmonic approximation of lattice dynamics and thermodynamic properties of half Heusler ScXSb (x = Ni, Pd, Pt) from first principles. Journal of Physics Condensed Matter, 2020, 32, 475504.	0.7	2
41841	Lattice distortion inducing local antiferromagnetic behaviors in FeAl alloys. Journal of Physics Condensed Matter, 2020, 32, 465805.	0.7	4
41842	Crystal structure and phase transition of TlReO₄: a combined experimental and theoretical study. Journal of Physics Condensed Matter, 2021, 33, 065403.	0.7	6
41843	Microscopic Coulomb interaction in transition-metal dichalcogenides. Journal of Physics Condensed Matter, 2021, 33, 035301.	0.7	3
41844	Electronic properties of Bi₂Se₃ dopped by 3d transition metal (Mn, Fe, Co, or) Tj ETQq1 1 0.784314 rgBT /Ov	0.7	16
41845	Role of surface termination in forming type-II photocatalyst heterojunctions: the case of TiO₂/BiVO₄. Journal of Physics Condensed Matter, 2021, 33, 075001.	0.7	18
41846	Raman spectrum of layered tilkerodeite (Pd₂HgSe₃) topological insulator: the palladium analogue of jacutingaite (Pt₂HgSe₃). Journal of Physics Condensed Matter, 2021, 33, 065401.	0.7	6
41847	Anion ordering transition and Fermi surface electronâ€“hole instabilities in the (TMTSF)₂ClO₄ and (TMTSF)₂NO₃ Bechgaard salts analyzed through the first-principles Lindhard response function. Journal of Physics Condensed Matter, 2020, 33, 085705.	0.7	4
41848	Anab initiobased approach to optical properties of semiconductor heterostructures. Modelling and Simulation in Materials Science and Engineering, 2017, 25, 065001.	0.8	7
41849	Investigating the naturally occurring forms of TiO₂ on electronic and optical properties using OLCAO-MGGA-TBO9: a hybrid DFT study. Modelling and Simulation in Materials Science and Engineering, 2021, 29, 025001.	0.8	11
41850	Electronic origin of grain boundary segregation of Al, Si, P, and S in bcc-Fe: combined analysis of ab initio local energy and crystal orbital Hamilton population. Modelling and Simulation in Materials Science and Engineering, 2021, 29, 015001.	0.8	18
41851	Thermoelectric properties of antimony films: roles of oxidation and topological quantum state. Nanotechnology, 2020, 31, 485704.	1.3	4
41852	Insight the process of hydrazine gas adsorption on layered WS₂: a first principle study. Nanotechnology, 2020, 31, 495703.	1.3	6
41853	Strain modulated carrier mobility and optical properties of graphene nanowiggles. Nanotechnology, 2020, 31, 505202.	1.3	5
41854	Structural, electronic and optical properties of two-dimensional (M_{2/3}Y_{1/3})₂CO₂ (M = Mo,W) iMXene. Nanotechnology, 2021, 32, 015703.	1.3	7
41855	Why thermal conductivity of CaO is lower than that of CaS: a study from the perspective of phonon splitting of optical mode. Nanotechnology, 2021, 32, 025709.	1.3	13
41856	Phase transformation and its effect on the piezopotential in a bent zinc oxide nanowire. Nanotechnology, 2021, 32, 075404.	1.3	1

#	Article	IF	Citations
41857	The effects of substitutional Fe-doping on magnetism in MoS₂ and WS₂ monolayers. Nanotechnology, 2021, 32, 095708.	1.3	18
41858	Estimation of the single-particle band gap and exciton binding energy in two dimensional insulators: a modified G₀W₀-BSE method approach. New Journal of Physics, 2020, 22, 063052.	1.2	6
41859	Weyl fermions in ferromagnetic high-temperature phase of K₂Cr₈O₁₆. New Journal of Physics, 2020, 22, 073062.	1.2	2
41860	Fluorinating the graphene-like BeO monolayer: A spin-polarized first principles study of the electronic, magnetic and optical properties. Physica Scripta, 2020, 95, 105806.	1.2	10
41861	Pressure dependent elastic, electronic, superconducting, and optical properties of ternary barium phosphides (BaM ₂P₂; M = Ni, Rh): DFT based insights. Physica Scripta, 2020, 95, 105809.	1.2	27
41862	Revisiting the magnetic and magnetocaloric properties of bulk gadolinium: A combined DFT and Monte Carlo simulations. Physica Scripta, 2021, 96, 015808.	1.2	9
41863	Common electronic band gaps and similar optical properties of ZnO nanotubes. Chinese Physics B, 2008, 17, 3433-3443.	0.7	23
41864	Dissociations of O 2 molecules on ultrathin Pb(111) films: first-principles plane wave calculations. Chinese Physics B, 2012, 21, 016801.	0.7	5
41865	Pressure-dependent physical properties of cubic SrBO3 (B = Cr, Fe) perovskites investigated by density functional theory. Chinese Physics B, 2020, 29, 123101.	0.7	17
41866	Electronic structure and optical properties of Ge- and F-doped Î±-Ga₂O₃: First-principles investigations*. Chinese Physics B, 2020, 29, 126301.	0.7	7
41867	Strain tunable band structure of a new 2D carbon allotrope C568. Journal of Semiconductors, 2020, 41, 082005.	2.0	7
41868	Strain control of the competition between metallic and semiconducting states in single-layers of TaSe₃. 2D Materials, 2020, 7, 025038.	2.0	7
41869	Topological magnons in CrI₃ monolayers: an itinerant fermion description. 2D Materials, 2020, 7, 045031.	2.0	45
41870	First-principles investigation of structural, elastic, lattice dynamical and thermodynamic properties of lithium sulfur under pressure. Materials Research Express, 2017, 4, 105901.	0.8	1
41871	Specific heat at constant pressure from first principles: contributions from fully anharmonic vibrations. Materials Research Express, 2019, 6, 125924.	0.8	2
41872	Structural electronic and vibrational properties analysis of Li₂CaX (XÂ=ÂSn, Pb) heusler alloys: a comparative study. Materials Research Express, 2020, 7, 056523.	0.8	7
41873	Enhanced H-H binding and consequent H-aggregation around dislocation in Î±-Fe lattice. Materials Research Express, 2020, 7, 066518.	0.8	2
41874	Lattice thermal conductivity of NaCoO₂ and LiCoO₂ intercalation materials studied by hybrid density functional theory. Materials Research Express, 2020, 7, 075502.	0.8	10

#	Article	IF	Citations
41875	Superconductivity of superhydride CeH₁₀ under high pressure. Materials Research Express, 2020, 7, 086001.	0.8	26
41876	Study of a new layered ternary chalcogenide CuZnTe₂ and its potassium intercalation effect. Materials Research Express, 2020, 7, 105904.	0.8	5
41877	Fluorination-enhanced photoconductive effect in a wide band gap Ca3Ti2O7-x F x thin films. Materials Research Express, 2020, 7, 126402.	0.8	2
41878	Hafnium and zirconium nitrides with rock-salt and Th₃P₄ structures: electronic and phonon band structure calculations to examine hot carrier solar cell and thermoelectric properties. Electronic Structure, 2020, 2, 025004.	1.0	3
41879	The pseudoatomic orbital basis: electronic accuracy and soft-mode distortions in ABO₃ perovskites. Electronic Structure, 2020, 2, 025002.	1.0	2
41880	A combined density functional theory and x-ray photoelectron spectroscopy study of the aromatic amino acids. Electronic Structure, 2020, 2, 044005.	1.0	11
41881	Testing an interatomic force model. , 2003, , 129-157.		1
41882	Hybrid Schemes. , 2003, , 253-262.		1
41883	Ab initio electronic stopping power for protons in Ga _{0.5} In _{0.5} P/GaAs/Ge triple-junction solar cells for space applications. Royal Society Open Science, 2020, 7, 200925.	1.1	9
41884	Electron heating and mechanical properties of graphene. Physical Review B, 2020, 101, .	1.1	2
41885	Thermodynamic stabilization of <mml:math xmlns:mml="http://www.w3.org/1998/Math/MathML"><mml:mrow><mml:mi>Î³</mml:mi><mml:mtext>â^'</mml:mtext><mml:mi mathvariant="normal">U</mml:mi><mml:mo>â^'</mml:mo><mml:mi>Mo</mml:mi></mml:mrow></mml:math> alloys: Effect of Mo content and temperature. Physical Review B, 2020, 101, .	1.1	18
41886	Pressure-induced decomposition of binary lanthanum intermetallic compounds. Physical Review B, 2020, 101, .	1.1	9
41887	Doubly charged silicon vacancy center, Si-N complexes, and photochromism in N and Si codoped diamond. Physical Review B, 2020, 101, .	1.1	13
41888	Partially embedded Pb chains on a vicinal Si(113) surface. Physical Review B, 2020, 101, .	1.1	4
41889	Intralayer ferromagnetism between S=52 ions in MnBi2Te4 : Role of empty Bi p states. Physical Review B, 2020, 101, .	1.1	14
41890	First-principles study of the nontrivial topological phase in chains of 3d transition metals. Physical Review B, 2020, 101, .	1.1	7
41891	Longitudinal spin fluctuations in bcc and liquid Fe at high temperature and pressure calculated with a supercell approach. Physical Review B, 2020, 102, .	1.1	14
41892	Revealing electromigration on dielectrics and metals through the step-bunching instability. Physical Review B, 2020, 102, .	1.1	5

#	Article	IF	Citations
41893	<mml:math xmlns:mml="http://www.w3.org/1998/Math/MathML"><mml:msub><mml:mi mathvariant="normal">Ca</mml:mi><mml:mn>2</mml:mn></mml:msub><mml:mi mathvariant="normal">Mn</mml:mi><mml:msub><mml:mi mathvariant="normal">O</mml:mi><mml:mn>4</mml:mn></mml:msub></mml:math> structural path: Following the negative thermal expansion at the local scale. Physical Review B, 2020, 102, .	1.1	7
41894	Phase competition in <mml:math xmlns:mml="http://www.w3.org/1998/Math/MathML"><mml:msub><mml:mi>HfO</mml:mi><mml:mn>2</mml:mn></mml:msub></mml:math> with applied electric field from first principles. Physical Review B, 2020, 102, .	1.1	25
41895	Effect of non-Heisenberg magnetic interactions on defects in ferromagnetic iron. Physical Review B, 2020, 102, .	1.1	7
41896	Metallization of dense fluid helium from ab initio simulations. Physical Review B, 2020, 102, .	1.1	10
41897	Position-dependent stability and lifetime of the skyrmion state in nickel-substituted <mml:math xmlns:mml="http://www.w3.org/1998/Math/MathML"><mml:mrow><mml:msub><mml:mi>Cu</mml:mi><mml:mn></mml:mn></mml:msub></mml:mrow></mml:math> Physical Review B, 2020, 102, .	1.1	4
41898	Ferri-chiral compounds with potentially switchable Dresselhaus spin splitting. Physical Review B, 2020, 102, .	1.1	4
41899	Fermiology and type-I superconductivity in the chiral superconductor <mml:math xmlns:mml="http://www.w3.org/1998/Math/MathML"><mml:mi>Nb</mml:mi><mml:msub><mml:mrow><mml:mi></mml:mi></mml:mrow></mml:msub></mml:math> with Kramers-Weyl fermions. Physical Review B, 2020, 102, .	1.1	9
41900	Jacutingaite-family: A class of topological materials. Physical Review B, 2020, 102, .	1.1	13
41901	Koopmans-compliant screened exchange potential with correct asymptotic behavior for semiconductors. Physical Review B, 2020, 102, .	1.1	9
41902	Site substitution in <mml:math xmlns:mml="http://www.w3.org/1998/Math/MathML"><mml:msub><mml:mi>GdMnO</mml:mi><mml:mn>3</mml:mn></mml:msub></mml:math> : Effects on structural, electronic, and magnetic properties. Physical Review B, 2020, 102, .	1.1	16
41903	Hybridization-induced gapped and gapless states on the surface of magnetic topological insulators. Physical Review B, 2020, 102, .	1.1	29
41904	Geometric ferroelectricity in rare-earth compounds<mml:math xmlns:mml="http://www.w3.org/1998/Math/MathML" display="inline"><mml:mrow><mml:mi>R</mml:mi><mml:msub><mml:mrow><mml:mtext>GaO</mml:mtext></mml:mrow></mml:math> xmlns:mml="http://www.w3.org/1998/Math/MathML" display="inline"><mml:mrow><mml:mi>R</mml:mi><mml:msub><mml:mrow><mml:mtext>InO</mml:mtext></mml:mrow></mml:math> Physical Review B, 2020, 79.	1.1	42
41905	Coupling of magnetic order and charge transport in the candidate Dirac semimetal <mml:math xmlns:mml="http://www.w3.org/1998/Math/MathML"><mml:mrow><mml:msub><mml:mi>EuCd</mml:mi><mml:mn>2</mml:mn></mml:msub></mml:mrow></mml:math> Physical Review B, 2018, 97, .	1.1	77
41906	Spin Jahn-Teller antiferromagnetism in <mml:math xmlns:mml="http://www.w3.org/1998/Math/MathML"><mml:mrow><mml:msub><mml:mi>CoTi</mml:mi><mml:mn>2</mml:mn></mml:msub><mml:mi mathvariant="normal">O</mml:mi><mml:mn>5</mml:mn></mml:mrow></mml:math>. Physical Review B, 2019, 99, .	1.1	10
41907	Stacking-Dependent Spin Interactions in <mml:math xmlns:mml="http://www.w3.org/1998/Math/MathML" display="inline"><mml:mi>Pd</mml:mi><mml:mo>/</mml:mo><mml:mi>Fe</mml:mi></mml:math> Bilayers on Re(0001). Physical Review Letters, 2020, 125, 227205.	2.9	9
41908	Vibrational Frequencies of Cerium-Oxide-Bound CO: A Challenge for Conventional DFT Methods. Physical Review Letters, 2020, 125, 256101.	2.9	13
41909	Mechanical properties and phase stability of monoborides using density functional theory calculations. Physical Review Materials, 2017, 1, .	0.9	4
41910	Magnetic behavior and spin-lattice coupling in cleavable van der Waals layered <mml:math xmlns:mml="http://www.w3.org/1998/Math/MathML"><mml:msub><mml:mi>CrCl</mml:mi><mml:mn>3</mml:mn></mml:msub></mml:math> crystals. Physical Review Materials, 2017, 1, .	0.9	210

#	Article	IF	Citations
41911	Synthesis of borophene nanoribbons on Ag(110) surface. Physical Review Materials, 2017, 1, .	0.9	113
41912	High-pressure phase diagram, structural transitions, and persistent nonmetallicity of <mml:math xmlns:mml="http://www.w3.org/1998/Math/MathML"><mml:msub><mml:mi>BaBiO</mml:mi><mml:mn>3</mml:mn></mml:msub></mml: : Theory and experiment. Physical Review Materials, 2017, 1, .	0.9	8
41913	Î£3(111) grain boundary of body-centered cubic Ti-Mo and Ti-V alloys: First-principles and model calculations. Physical Review Materials, 2017, 1, .	0.9	3
41914	Molybdenum-titanium phase diagram evaluated from ab initio calculations. Physical Review Materials, 2017, 1, .	0.9	11
41915	Using forces to accelerate first-principles anharmonic vibrational calculations. Physical Review Materials, 2017, 1, .	0.9	5
41916	One-hundred-three compound band-structure benchmark of post-self-consistent spin-orbit coupling treatments in density functional theory. Physical Review Materials, 2017, 1, .	0.9	92
41917	Optical properties of titanium-doped lithium niobate from time-dependent density-functional theory. Physical Review Materials, 2017, 1, .	0.9	10
41918	First-principles study of the liquid and amorphous phases of <mml:math xmlns:mml="http://www.w3.org/1998/Math/MathML"><mml:mrow><mml:msub><mml:mi>In</mml:mi><mml:mn>2</mml:mn></mml:msub></mml:mr Physical Review Materials, 2017, 1, .	0.9	7
41919	Structure of naturally hydrated ferrihydrite revealed through neutron diffraction and first-principles modeling. Physical Review Materials, 2017, 1, .	0.9	11
41920	High-pressure behavior of CaMoO4. Physical Review Materials, 2017, 1, .	0.9	15
41921	Graphene/ <mml:math xmlns:mml="http://www.w3.org/1998/Math/MathML"><mml:msub><mml:mi>MoS</mml:mi><mml:mn>2</mml:mn></mml:msub></mml heterostructures as templates for growing two-dimensional metals: Predictions from ab initio calculations. Physical Review Materials, 2017, 1, .	0.9	13
41922	Ternary wurtzite CaAgBi materials family: A playground for essential and accidental, type-I and type-II Dirac fermions. Physical Review Materials, 2017, 1, .	0.9	59
41923	Adsorbed or intercalated: Na on graphene/Ir(111). Physical Review Materials, 2017, 1, .	0.9	14
41924	Towards diluted magnetism in TaAs. Physical Review Materials, 2017, 1, .	0.9	3
41925	Controlling the magnetism of oxygen surface vacancies in <mml:math xmlns:mml="http://www.w3.org/1998/Math/MathML"><mml:msub><mml:mi mathvariant="normal">SrTiO</mml:mi><mml:mn>3</mml:mn></mml:msub></mml:math> through charging. Physical Review Materials, 2017, 1, .	0.9	15
41926	Defects at the <mml:math xmlns:mml="http://www.w3.org/1998/Math/MathML"><mml:mrow><mml:mtext>Si</mml:mtext><mml:mo>(</mml:mo><mml:mn>0 interface: Analysis of structures generated with classical force fields and density functional theory. Physical Review Materials, 2017, 1, .	0.9	6
41927	Hyperhoneycomb boron nitride with anisotropic mechanical, electronic, and optical properties. Physical Review Materials, 2017, 1, .	0.9	3
41928	Controlling defects and secondary phases of CZTS by surfactant potassium. Physical Review Materials, 2017, 1, .	0.9	19

#	Article	IF	Citations
41929	Ab initio piezoelectric properties of <mml:math xmlns:mml="http://www.w3.org/1998/Math/MathML"><mml:mrow><mml:msub><mml:mi>Al</mml:mi><mml:mrow><mml:mn>0.5</mml:mn></mml:mrow></mml:msub><mml:msub><mml:mi mathvariant="normal">N</mml:mi></mml:msub></mml:mrow></mml:math> : Impact of alloy configuration on the <mml:math xmlns:mml="http://www.w3.org/1998/Math/MathML"><mml:msub><mml:mi>d</mml:mi><mml:mrow><mml:mn>33</mml:mn></mml:mrow></mml:msub></mml:math> Physical Review Materials, 2017, 1, .	0.9	18
41930	Thermodynamic properties of paramagnetic Î± - and Î²â˜Mn from first principles: The effect of transverse spin fluctuations. Physical Review Materials, 2017, 1, .	0.9	4
41931	Achieving giant tunneling electroresistance and magnetoresistance by <mml:math xmlns:mml="http://www.w3.org/1998/Math/MathML"><mml:mrow><mml:msub><mml:mi>BaTiO</mml:mi><mml:mn>3</mml:mn></mml:msub></mml:mrow></mml:math> barrier and Heusler alloy electrode. Physical Review Materials, 2017, 1, .	0.9	8
41932	Twelve inequivalent Dirac cones in two-dimensional <mml:math xmlns:mml="http://www.w3.org/1998/Math/MathML"><mml:msub><mml:mi>ZrB</mml:mi><mml:mn>2</mml:mn></mml:msub></mml:math> Physical Review Materials, 2018, 2, .	0.9	32
41933	Postaragonite phases of <mml:math xmlns:mml="http://www.w3.org/1998/Math/MathML"><mml:msub><mml:mi>CaCO</mml:mi><mml:mn>3</mml:mn></mml:msub></mml:math> at lower mantle pressures. Physical Review Materials, 2018, 2, .	0.9	31
41934	Robust large-gap quantum spin Hall insulators in methyl-functionalized III-Bi buckled honeycombs. Physical Review Materials, 2018, 2, .	0.9	11
41935	Nitrogen-hydrogen-oxygen ternary phase diagram: New phases at high pressure from structural prediction. Physical Review Materials, 2018, 2, .	0.9	17
41936	Fracture of coherent interfaces between an fcc metal matrix and the <mml:math xmlns:mml="http://www.w3.org/1998/Math/MathML"><mml:mrow><mml:msub><mml:mi>Cr</mml:mi><mml:mn>23</mml:mn></mml:msub><mml:msub><mml:mi mathvariant="normal">C</mml:mi><mml:mn>6</mml:mn></mml:msub></mml:mrow></mml:math> carbide precipitate from first principles. Physical Review Materials, 2018, 2, .	0.9	9
41937	Pressure-stabilized binary compounds of magnesium and silicon. Physical Review Materials, 2018, 2, .	0.9	13
41938	Prediction of a two-dimensional S3N2 solid for optoelectronic applications. Physical Review Materials, 2018, 2, .	0.9	10
41939	Towards novel organic high- <mml:math xmlns:mml="http://www.w3.org/1998/Math/MathML"><mml:msub><mml:mi>T</mml:mi><mml:mi>c</mml:mi></mml:msub></mml:math> superconductors: Data mining using density of states similarity search. Physical Review Materials, 2018, 2, .	0.9	18
41940	High-pressure-assisted design of porous topological semimetal carbon for Li-ion battery anode with high-rate performance. Physical Review Materials, 2018, 2, .	0.9	32
41941	Solid solution decomposition and Guinier-Preston zone formation in Al-Cu alloys: A kinetic theory with anisotropic interactions. Physical Review Materials, 2018, 2, .	0.9	4
41942	High-temperature thermophysical properties of <mml:math xmlns:mml="http://www.w3.org/1998/Math/MathML"><mml:mi>Î³</mml:mi></mml:math> - and <mml:math xmlns:mml="http://www.w3.org/1998/Math/MathML"><mml:mi>Î´</mml:mi></mml:math> -Mn from first principles. Physical Review Materials, 2018, 2, .	0.9	2
41943	Prediction of new ground-state crystal structure of <mml:math xmlns:mml="http://www.w3.org/1998/Math/MathML"><mml:mrow><mml:mi mathvariant="normal">T</mml:mi><mml:msub><mml:mi mathvariant="normal">a</mml:mi><mml:mn>2</mml:mn></mml:msub><mml:msub><mml:mi mathvariant="normal">O</mml:mi><mml:mn>5</mml:mn></mml:msub></mml:mrow></mml:math>. Physical Review Materials, 2018, 2, .	0.9	19
41944	Structure and energetics of carbon, hexagonal boron nitride, and carbon/hexagonal boron nitride single-layer and bilayer nanoscrolls. Physical Review Materials, 2018, 2, .	0.9	23
41945	Electronic and structural properties of <mml:math xmlns:mml="http://www.w3.org/1998/Math/MathML"><mml:mrow><mml:mi mathvariant="normal">B</mml:mi><mml:msub><mml:mi mathvariant="normal">i</mml:mi><mml:mn>2</mml:mn></mml:msub><mml:mi mathvariant="normal">S</mml:mi><mml:msub><mml:mi mathvariant="normal">e</mml:mi><mml:mn>3</mml:mn></mml:msub><mml:mo>:</mml:mo><mml:mi>Cu</mml:mi></mml:mrow></mml:math>	0.9	4
41946	Deep vs shallow nature of oxygen vacancies and consequent <mml:math xmlns:mml="http://www.w3.org/1998/Math/MathML"><mml:mi>n</mml:mi></mml:math> -type carrier concentrations in transparent conducting oxides. Physical Review Materials, 2018, 2, .	0.9	73

#	Article	IF	Citations
41947	Confinement- and strain-induced enhancement of thermoelectric properties in <mml:math xmlns:mml="http://www.w3.org/1998/Math/MathML"><mml:mrow><mml:msub><mml:mi>LaNiO</mml:mi><mml:mn>3</mml:mn></m superlattices. Physical Review Materials, 2018, 2, .	0.9	26
41948	Vibrational and dielectric properties of the bulk transition metal dichalcogenides. Physical Review Materials, 2018, 2, .	0.9	25
41949	Performance of the strongly constrained and appropriately normed density functional for solid-state materials. Physical Review Materials, 2018, 2, .	0.9	155
41950	First-principles calculations of threading screw dislocations in AlN and InN. Physical Review Materials, 2018, 2, .	0.9	6
41951	Inducing spontaneous electric polarizations in double perovskite iodide superlattices for ferroelectric photovoltaic materials. Physical Review Materials, 2018, 2, .	0.9	7
41952	Plasmon spectroscopy: Robust metallicity of Au wires on Si(557) upon oxidation. Physical Review Materials, 2018, 2, .	0.9	10
41953	Directed growth of hydrogen lines on graphene: High-throughput simulations powered by evolutionary algorithm. Physical Review Materials, 2018, 2, .	0.9	1
41954	Effect of fluoropolymer composition on topochemical synthesis of <mml:math xmlns:mml="http://www.w3.org/1998/Math/MathML"><mml:mrow><mml:mi>SrMn</mml:mi><mml:msub><mml:mi mathvariant="normal">O</mml:mi><mml:mrow><mml:mn>3</mml:mn><mml:mtext>â^'</mml:mtext><mml:mi>Î´</mml:mi></mml:mro mathvariant="normal">F</mml:mi><mml:mi>Î´</mml:mi></mml:msub></mml:mrow></mml:math> oxyfluoride films. Physical Review Materials, 2018, 2, .	0.9	18
41955	Role of oxygen functional groups in the friction of water-lubricated low-index diamond surfaces. Physical Review Materials, 2018, 2, .	0.9	17
41956	Crystallography and substitution patterns in the <mml:math xmlns:mml="http://www.w3.org/1998/Math/MathML"><mml:mrow><mml:mi>Zr</mml:mi><mml:msub><mml:mi mathvariant="normal">O</mml:mi><mml:mn>2</mml:mn></mml:msub><mml:mtext>â^'</mml:mtext><mml:mi>Yb</mml:mi><mml:mi><mml:mn mathvariant="normal">O</mml:mi><mml:mn>4</mml:mn></mml:msub></mml:mrow></mml:math> system. Physical Review Materials, 2018, 2, .	0.9	8
41957	Unusual composition dependence of transformation temperatures in Ti-Ta-X shape memory alloys. Physical Review Materials, 2018, 2, .	0.9	11
41958	Precipitate-induced nonlinearities of diffusion along grain boundaries in Al-based alloys. Physical Review Materials, 2018, 2, .	0.9	13
41959	<mml:math xmlns:mml="http://www.w3.org/1998/Math/MathML"><mml:msub><mml:mi mathvariant="normal">Al</mml:mi><mml:mi>x</mml:mi></mml:msub><mml:msub><mml:mi mathvariant="normal">Ga</mml:mi><mml:mrow><mml:mn>1</mml:mn><mml:mo>â^'</mml:mo><mml:mi>x</mml:mi></mml:mrow><mml:mi></mml:mi></mml:msub></mml:math> crystals with direct 2 eV band gaps from computational alchemy. Physical Review Materials, 2018, 2, .	0.9	17
41960	Nonempirical dielectric-dependent hybrid functional with range separation for semiconductors and insulators. Physical Review Materials, 2018, 2, .	0.9	122
41961	Large phosphorene in-plane contraction induced by interlayer interactions in graphene-phosphorene heterostructures. Physical Review Materials, 2018, 2, .	0.9	11
41962	Electronic structures of iMAX phases and their two-dimensional derivatives: A family of piezoelectric materials. Physical Review Materials, 2018, 2, .	0.9	31
41963	Ab initioinvestigation of monoclinic phase stability and martensitic transformation in crystalline polyethylene. Physical Review Materials, 2018, 2, .	0.9	14
41964	Combined ab initio and empirical model of the thermal conductivity of uranium, uranium-zirconium, and uranium-molybdenum. Physical Review Materials, 2018, 2, .	0.9	9

#	Article	IF	Citations
41965	Interpenetrating silicene networks: A topological nodal-line semimetal with potential as an anode material for sodium ion batteries. Physical Review Materials, 2018, 2, .	0.9	21
41966	Magnetocrystalline anisotropy in <mml:math xmlns:mml="http://www.w3.org/1998/Math/MathML"><mml:msub><mml:mi>YCo</mml:mi><mml:mn>5</mml:mn></mml:msub></mml and <mml:math xmlns:mml="http://www.w3.org/1998/Math/MathML"><mml:msub><mml:mi>ZrCo</mml:mi><mml:mn>5</mml:mn></mml:msub></mml compounds from first-principles real-space pseudopotentials calculations. Physical Review Materials, 2018, 2, .	0.9	4
41967	Real-space pseudopotential method for calculating magnetocrystalline anisotropy. Physical Review Materials, 2018, 2, .	0.9	7
41968	Metastable rocksalt ZnO is <mml:math xmlns:mml="http://www.w3.org/1998/Math/MathML"><mml:mi>p</mml:mi></mml:math> -type dopable. Physical Review Materials, 2018, 2, .	0.9	15
41969	Properties of mixed transition metal oxides:<mml:math xmlns:mml="http://www.w3.org/1998/Math/MathML"><mml:mrow><mml:mi>M</mml:mi><mml:msup><mml:mi>M</mml:mi><mml:mo corundum-type structures<mml:math		

#	Article	IF	Citations
41983	Promising quaternary chalcogenides as high-band-gap semiconductors for tandem photoelectrochemical water splitting devices: A computational screening approach. Physical Review Materials, 2018, 2, .	0.9	16
41984	Geometries of edge and mixed dislocations in bcc Fe from first-principles calculations. Physical Review Materials, 2018, 2, .	0.9	18
41985	Autonomous efficient experiment design for materials discovery with Bayesian model averaging. Physical Review Materials, 2018, 2, .	0.9	58
41986	<mml:math xmlns:mml="http://www.w3.org/1998/Math/MathML"><mml:msub><mml:mi>PtP</mml:mi><mml:mn>2</mml:mn></mml:msub></mml : An example of exploring the hidden Cairo tessellation in the pyrite structure for discovering novel two-dimensional materials. Physical Review Materials, 2018, 2, .	0.9	14
41987	Refrigeration in 2D: Electrostaticaloric effect in monolayer materials. Physical Review Materials, 2018, 2, .	0.9	5
41988	Understanding trends in lithium binding at two-dimensional materials. Physical Review Materials, 2018, 2, .	0.9	5
41989	Universal superconductivity phase diagram for pressurized tetradymite topological insulators. Physical Review Materials, 2018, 2, .	0.9	8
41990	Design of a polar half-metallic ferromagnet with accessible and enhanced electric polarization. Physical Review Materials, 2018, 2, .	0.9	6
41991	Structural dynamics in hybrid halide perovskites: Bulk Rashba splitting, spin texture, and carrier localization. Physical Review Materials, 2018, 2, .	0.9	19
41992	First-principles study of the linear electro-optical response in strained<mml:math xmlns:mml="http://www.w3.org/1998/Math/MathML"><mml:mrow><mml:mi>SrTi</mml:mi><mml:msub><mml:mi mathvariant="normal">O</mml:mi><mml:mn>3</mml:mn></mml:msub></mml:mrow></mml:math>. Physical Review Materials, 2018, 2, .	0.9	14
41993	Quantum-mechanical process of carbonate complex formation and large-scale anisotropy in the adsorption energy of <mml:math xmlns:mml="http://www.w3.org/1998/Math/MathML"><mml:mrow><mml:mi mathvariant="normal">C</mml:mi><mml:msub><mml:mi mathvariant="normal">O</mml:mi><mml:mn>2</mml:mn></mml:msub></mml:mrow></mml:math> on anatase <mml:math	0.9	9
41994	Kinetic Monte Carlo simulations of vacancy diffusion in nondilute Ni-<mml:math xmlns:mml="http://www.w3.org/1998/Math/MathML"><mml:mrow><mml:mi>Ti</mml <mml:mi>X</mml:mi></mml:math>(<mml:math) Tj ETQq1 1 0.784314 rgBT /Ov alloys. Physical Review Materials, 2018, 2, .	0.9	11
41995	Robust high-fidelity DFT study of the lithium-graphite phase diagram. Physical Review Materials, 2018, 2, .	0.9	18
41996	Presence of water at elevated temperatures, structural transition, and thermal expansion behavior in <mml:math xmlns:mml="http://www.w3.org/1998/Math/MathML"><mml:mrow><mml:mi>LaP</mml:mi><mml:msub><mml:mi mathvariant="normal">O</mml:mi><mml:mn>4</mml:mn></mml:msub><mml:mo>:</mml:mo><mml:mi>Eu</mml:mi></mml:mrow></ Physical Review Materials, 2018, 2, .	0.9	4
41997	First-principles study on the grain boundary embrittlement of bcc-Fe by Mn segregation. Physical Review Materials, 2019, 3, .	0.9	23
41998	Hidden Mn magnetic-moment disorder and its influence on the physical properties of medium-entropy NiCoMn solid solution alloys. Physical Review Materials, 2019, 3, .	0.9	14
41999	<mml:math xmlns:mml="http://www.w3.org/1998/Math/MathML"><mml:mrow><mml:msub><mml:mi>Na</mml:mi><mml:mi>x</mml:mi></mml:m phase stability and hierarchical orderings in the O3/P3 structure family. Physical Review Materials, 2019, 3, .	0.9	38
42000	Structure and stability of NaTaO3(001) and KTaO3(001) surfaces. Physical Review Materials, 2019, 3, .	0.9	16

#	Article	IF	Citations
42001	Active learning of uniformly accurate interatomic potentials for materials simulation. Physical Review Materials, 2019, 3, .	0.9	299
42002	Phonons, magnons, and lattice thermal transport in antiferromagnetic semiconductor MnTe. Physical Review Materials, 2019, 3, .	0.9	25
42003	First-principles calculations of solute transport in zirconium: Vacancy-mediated diffusion with metastable states and interstitial diffusion. Physical Review Materials, 2019, 3, .	0.9	12
42004	Dislocation core structures in Ni-based superalloys computed using a density functional theory based flexible boundary condition approach. Physical Review Materials, 2019, 3, .	0.9	11
42005	Energetics and cathode voltages of <mml:math xmlns:mml="http://www.w3.org/1998/Math/MathML"><mml:mrow><mml:mi>Li</mml:mi><mml:mi>M</mml:mi><mml:msub><mml:mi olivines (<mml:math) Tj ETQq0 0 0 rgBT /Overlock 10 Tf 50 577 Td (xmlns:mml="http://www.w3.org/1998/Math/MathML"><mml:mrow	0.9	38
42006	Efficient ab initio calculations of electron-defect scattering and defect-limited carrier mobility. Physical Review Materials, 2019, 3, .	0.9	28
42007	Influence of strain and chemical substitution on the magnetic anisotropy of antiferromagnetic <mml:math xmlns:mml="http://www.w3.org/1998/Math/MathML"><mml:mrow><mml:msub><mml:mi>Cr</mml:mi><mml:mn>2</mml:mn></mml:msub><mml:mi mathvariant="normal">O</mml:mi><mml:mn>3</mml:mn></mml:msub></mml:mrow></mml:math> : An ab-initio study. Physical Review Materials, 2019, 3, .	0.9	18
42008	Reduced thermal conductivity of epitaxial GaAs on Si due to symmetry-breaking biaxial strain. Physical Review Materials, 2019, 3, .	0.9	20
42009	First-principles investigation of the bulk properties of americium dioxide and sesquioxides. Physical Review Materials, 2019, 3, .	0.9	14
42010	Giant power output in lead-free ferroelectrics by shock-induced phase transition. Physical Review Materials, 2019, 3, .	0.9	29
42011	Enabling QM-accurate simulation of dislocation motion in <mml:math xmlns:mml="http://www.w3.org/1998/Math/MathML"><mml:mrow><mml:mi>Î³</mml:mi><mml:mtext>â^'</mml:mtext><mml:mi>Ni</ and <mml:math xmlns:mml="http://www.w3.org/1998/Math/MathML"><mml:mrow><mml:mi>Î±</mml:mi><mml:mtext>â^'</mml:mtext><mml:mi>Fe</ using a hybrid multiscale approach. Physical Review Materials, 2019, 3, .	0.9	7
42012	Phonon dispersion relation, high-pressure phase stability, and thermal expansion in <mml:math xmlns:mml="http://www.w3.org/1998/Math/MathML"><mml:msub><mml:mi>YVO</mml:mi><mml:mn>4</mml:mn></mml:msub></ Physical Review Materials, 2019, 3, .	0.9	19
42013	Ab initio investigation of structural stability and exfoliation energies in transition metal dichalcogenides based on Ti-, V-, and Mo-group elements. Physical Review Materials, 2019, 3, .	0.9	44
42014	Hexagonal supertetrahedral boron: A topological metal with multiple spin-orbit-free emergent fermions. Physical Review Materials, 2019, 3, .	0.9	18
42015	Magnetic order effects on the electronic structure of <mml:math xmlns:mml="http://www.w3.org/1998/Math/MathML"><mml:mrow><mml:mi mathvariant="normal">K</mml:mi><mml:mi>M</mml:mi><mml:msub><mml:mi>MnS</mml:mi><mml:mn>2</mml:mn></mml:msub><mml: width="4pt" /><mml:mo>(</mml:mo><mml:mi>M</mml:mi><mml:mo>=</mml:mo><mml:mtext>Cu</mml:mtext><mml:mo>,</mml:mo><mml:mte with the <mml:math xmlns:mml="http://www.w3.org/1998/Math/MathML"><mml:mrow><mml:ms. Physic	0.9	5
42016	Electronic band structure and optical properties of boron arsenide. Physical Review Materials, 2019, 3, .	0.9	18
42017	First-principles study on the effects of twin boundaries on anodic dissolution of Mg. Physical Review Materials, 2019, 3, .	0.9	14
42018	Reversible out-of-plane spin texture in a two-dimensional ferroelectric material for persistent spin helix. Physical Review Materials, 2019, 3, .	0.9	39

#	Article	IF	Citations
42019	Superconductivity in Li-intercalated <mml:math xmlns:mml="http://www.w3.org/1998/Math/MathML"><mml:mrow><mml:mn>1</mml:mn><mml:mi>T</mml:mi><mml:mtext>-</mml:mtext><mml:msub><mml:mi>TaS</mml:mi><mml:mn>2</mml:mn></mml:msub></mml:mrow></mml:math> driven by electric field gating. Physical Review Materials, 2019, 3, .	0.9	25
42020	Evidence for the weak coupling scenario of the Peierls transition in the blue bronze. Physical Review Materials, 2019, 3, .	0.9	15
42021	Stochastic replica voting machine prediction of stable cubic and double perovskite materials and binary alloys. Physical Review Materials, 2019, 3, .	0.9	10
42022	Orbital magnetic moments of phonons. Physical Review Materials, 2019, 3, .	0.9	80
42023	Strain engineering of ZnO thermal conductivity. Physical Review Materials, 2019, 3, .	0.9	13
42024	Influence of surface restructuring on the activity of <mml:math xmlns:mml="http://www.w3.org/1998/Math/MathML"><mml:msub><mml:mi>SrTiO</mml:mi><mml:mn>3</mml:mn></mml:msub></mml:math> photoelectrodes for photocatalytic hydrogen reduction. Physical Review Materials, 2019, 3, .	0.9	5
42025	Electronic properties of tetragraphene nanoribbons. Physical Review Materials, 2019, 3, .	0.9	14
42026	First-principles study of mechanical and electronic properties of bent monolayer transition metal dichalcogenides. Physical Review Materials, 2019, 3, .	0.9	28
42027	Topologically protected states and half-metal behaviors: Defect-strain synergy effects in two-dimensional antimonene. Physical Review Materials, 2019, 3, .	0.9	7
42028	Vibrational and dielectric properties of monolayer transition metal dichalcogenides. Physical Review Materials, 2019, 3, .	0.9	10
42029	Tuning phase stability and short-range order through Al doping in (CoCrFeMn)100â^'xAlx high-entropy alloys. Physical Review Materials, 2019, 3, .	0.9	16
42030	Two-dimensional nodal-loop half-metal in monolayer MnN. Physical Review Materials, 2019, 3, .	0.9	55
42031	Superconducting phase diagram and nontrivial band topology of structurally modulated<mml:math xmlns:mml="http://www.w3.org/1998/Math/MathML"><mml:mrow><mml:msub><mml:mi>Sn</mml:mi><mml:mrow><mml:mn>1</mml:mn></mml:mrow></mml:msub></mml:mrow></mml:math> Physical Review Materials, 2019, 3, .	0.9	5
42032	Strain tuning of plasma frequency in vanadate, niobate, and molybdate perovskite oxides. Physical Review Materials, 2019, 3, .	0.9	18
42033	Anharmonic thermodynamics of vacancies using a neural network potential. Physical Review Materials, 2019, 3, .	0.9	14
42034	New kagome prototype materials: discovery of <mml:math xmlns:mml="http://www.w3.org/1998/Math/MathML"><mml:mrow><mml:msub><mml:mi>KV</mml:mi><mml:mn>3</mml:mn></mml:msub></mml:mrow></mml:math>, and <mml:math xmlns:mml="http://www.w3.org/1998/Math/MathML"><mml:mrow><mml:msub><mml:mi>CsV</mml:mi><mml:mn>3</mml:mn></mml:msub></mml:mrow></mml:math> Physical Review Materials, 2019, 3, .	0.9	398
42035	Multiple band crossings and Fermi surface topology: Role of double nonsymmorphic symmetries in MnP-type crystal structures. Physical Review Materials, 2019, 3, .	0.9	18
42036	Discovery of<mml:math xmlns:mml="http://www.w3.org/1998/Math/MathML"><mml:mi>Ï‰</mml:mi></mml:math>-free high-temperature Ti-Ta-<mml:math xmlns:mml="http://www.w3.org/1998/Math/MathML"><mml:mi>X</mml:mi></mml:math>shape memory alloys from first-principles calculations. Physical Review Materials, 2019, 3, .	0.9	7

#	Article	IF	Citations
42037	Topological band crossings in epitaxial strained SnTe. Physical Review Materials, 2019, 3, .	0.9	6
42038	Cation role in the thermal properties of layered materials <mml:math xmlns:mml="http://www.w3.org/1998/Math/MathML"><mml:mrow><mml:msup><mml:mrow><mml:mi>M</mml:mi></mml:mrow><mml:mr		

#	Article	IF	Citations
42055	Artificial quantum confinement in <mml:math xmlns:mml="http://www.w3.org/1998/Math/MathML"><mml:mrow><mml:mi>LaAl</mml:mi><mml:msub><mml:mi mathvariant="normal">O</mml:mi><mml:mn>3</mml:mn></mml:msub><mml:mo>/</mml:mo><mml:mi>SrTi</mml:mi><mml:msub><mml:mi mathvariant="normal">O</mml:mi><mml:mn>3</mml:mn></mml:msub></mml:mrow></mml:math> heterostructures. Physical Review Materials, 2020, 4, .	0.9	6
42056	Indentation-strain stiffening in tungsten nitrides: Mechanisms and implications. Physical Review Materials, 2020, 4, .	0.9	41
42057	Structure-strength relations of distinct MoN phases from first-principles calculations. Physical Review Materials, 2020, 4, .	0.9	41
42058	Evaluating optimal <mml:math xmlns:mml="http://www.w3.org/1998/Math/MathML"><mml:mi>U</mml:mi></mml:math> for <mml:math xmlns:mml="http://www.w3.org/1998/Math/MathML"><mml:mrow><mml:mn>3</mml:mn><mml:mi>d</mml:mi></mml:mrow></mml:m transition-metal oxides within the SCAN+ <mml:math	0.9	55
42059	Computational and experimental (re)investigation of the structural and electrolyte properties of <mml:math xmlns:mml="http://www.w3.org/1998/Math/MathML"><mml:mrow><mml:msub><mml:mi>Li</mml:mi><mml:mn>4</mml:mn></mml:m mathvariant="normal">P</mml:mi><mml:mn>2</mml:mn></mml:msub><mml:msub><mml:mi mathvariant="normal">S</mml:mi><mml:mn>6</mml:mn></mml:msub></mml:mrow><mml:mo>,</mml:mo><mml:mo>Â</mml:mo><n mathvariant="normal">N</mml:mi></mml:mrow></mml:math> Physical Review Materials, 2020, 4, .	0.9	4
42060	<mml:math xmlns:mml="http://www.w3.org/1998/Math/MathML"><mml:msub><mml:mi mathvariant="normal">a</mml:mi><mml:mn>2</mml:mn></mml:msub><mml:mi mathvariant="normal">S</mml:mi><mml:msub><mml:mi	0.9	10
42061	Ab initio piezoelectric properties of wurtzite ZnO-based alloys: Impact of the c/a cell ratio. Physical Review Materials, 2020, 4, .	0.9	4
42062	MXenes atomic layer stacking phase transitions and their chemical activity consequences. Physical Review Materials, 2020, 4, .	0.9	31
42063	Native point defects in mono and bilayer phosphorene. Physical Review Materials, 2020, 4, .	0.9	9
42064	Phase stabilities of <mml:math xmlns:mml="http://www.w3.org/1998/Math/MathML"><mml:msub><mml:mi>MgCO</mml:mi><mml:mn>3</mml:mn></mml:msub> xmlns:mml="http://www.w3.org/1998/Math/MathML"><mml:msub><mml:mi>MgCO</mml:mi><mml:mn>3</mml:mn></mml:msub> studied by Raman spectroscopy, x-ray diffraction, and density functional theory calculations. Physical Review Materials, 2020, 4, .	0.9	23
42065	Tuned and screened range-separated hybrid density functional theory for describing electronic and optical properties of defective gallium nitride. Physical Review Materials, 2020, 4, .	0.9	17
42066	Stability of charged sulfur vacancies in 2D and bulk <mml:math xmlns:mml="http://www.w3.org/1998/Math/MathML"><mml:msub><mml:mi>MoS</mml:mi><mml:mn>2</mml:mn></mml:msub> from plane-wave density functional theory with electrostatic corrections. Physical Review Materials, 2020, 4, .	0.9	24
42067	Machine learning study of magnetism in uranium-based compounds. Physical Review Materials, 2020, 4, .	0.9	10
42068	Boron phosphide as a <mml:math xmlns:mml="http://www.w3.org/1998/Math/MathML"><mml:mi>p</mml:mi></mml:math> -type transparent conductor: Optical absorption and transport through electron-phonon coupling. Physical Review Materials, 2020, 4, .	0.9	11
42069	Comprehensive analysis of the influence of dispersion on group-14 rutile-type solids. Physical Review Materials, 2020, 4, .	0.9	1
42070	Sn 5s2 lone pairs and the electronic structure of tin sulphides: A photoreflectance, high-energy photoemission, and theoretical investigation. Physical Review Materials, 2020, 4, .	0.9	11
42071	Exploring the formation of intrinsic <mml:math xmlns:mml="http://www.w3.org/1998/Math/MathML"><mml:mi>p</mml:mi></mml:math> -type and <mml:math xmlns:mml="http://www.w3.org/1998/Math/MathML"><mml:mi>n</mml:mi></mml:math> -type defects in CuO. Physical Review Materials, 2020, 4, .	0.9	20
42072	<mml:math xmlns:mml="http://www.w3.org/1998/Math/MathML"><mml:mrow><mml:msub><mml:mi mathvariant="normal">V</mml:mi><mml:mn>2</mml:mn></mml:msub><mml:mi>AlC</mml:mi></mml:mrow></mml:math> and <mml:math xmlns:mml="http://www.w3.org/1998/Math/MathML"><mml:mrow><mml:mi mathvariant="normal">C</mml:mi><mml:msub><mml:mi mathvariant="normal">r</mml:mi><mml:mn>2</mml:mn></mml:msub><mml:mi>AlC</mml:mi></mml:mrow></mml:math>	0.9	4

#	Article	IF	Citations
42073	Interplay of charge density wave and multiband superconductivity in layered quasi-two-dimensional materials: The case of <mml:math xmlns:mml="http://www.w3.org/1998/Math/MathML"><mml:mn>2</mml:mn><mml:mi mathvariant="normal">H</mml:mi><mml:mtext>â^'</mml:mtext><mml:mi>Nb</mml:mi><mml:msub><mml:mrow><mml:mi mathvariant="normal">S</mml:mi></mml:mrow><mml:mn>2</mml:mn></mml:msub></mml:math> and <mml:math xmlns:mml="http://www.w3.org/1998/Math/MathML"><mml:mn>2</mml:mn><mml:mi mathva	0.9	36
42074	<mml:math xmlns:mml="http://www.w3.org/1998/Math/MathML"><mml:mrow><mml:mi>Mo</mml:mi><mml:msub><mml:mi>Te</mml:mi><mml:mi as a natural hyperbolic material across the visible and the ultraviolet region. Physical Review Materials, 2020, 4, .	0.9	15
42075	Stacking fault formation created by plastic deformation at low temperature and small scales in silicon. Physical Review Materials, 2020, 4, .	0.9	1
42076	Gaussian approximation potentials for body-centered-cubic transition metals. Physical Review Materials, 2020, 4, .	0.9	24
42077	Machine learning for metallurgy II. A neural-network potential for magnesium. Physical Review Materials, 2020, 4, .	0.9	32
42078	Split-vacancy defect complexes of oxygen in hcp and fcc cobalt. Physical Review Materials, 2020, 4, .	0.9	1
42079	Electronic correlation, magnetic structure, and magnetotransport in few-layer <mml:math xmlns:mml="http://www.w3.org/1998/Math/MathML"><mml:mrow><mml:mi>Cr</mml:mi><mml:msub><mml:mi mathvariant="normal">I</mml:mi><mml:mn>3</mml:mn></mml:msub></mml:mrow></mml:math>. Physical Review Materials, 2020, 4.	0.9	5
42080	Ferroelectric and antiferroelectric response owing to competing polar and antipolar instabilities in tetragonal tungsten bronze <mml:math xmlns:mml="http://www.w3.org/1998/Math/MathML"><mml:msub><mml:mi mathvariant="normal">K</mml:mi><mml:mn>2</mml:mn></mml:msub><mml:msub><mml:mrow><mml:mi>R</mml:mi><mml:mi>N	0.9	8
42081	Computational design of <mml:math xmlns:mml="http://www.w3.org/1998/Math/MathML"><mml:mi>f</mml:mi></mml:math> -electron Kitaev magnets: Honeycomb and hyperhoneycomb compounds <mml:math xmlns:mml="http://www.w3.org/1998/Math/MathML"><mml:mrow><mml:msub><mml:mi>A</mml:mi><mml:mn>2</mml:mn></mml:m		

#	Article	IF	Citations
42091	Effective Hamiltonian for nickelate oxides <mml:math xmlns:mml="http://www.w3.org/1998/Math/MathML"><mml:mrow><mml:msub><mml:mi>Nd</mml:mi><mml:mrow><mml:mn>1</mml:mn> Physical Review Research, 2020, 2, .	1.3	76
42092	Fingerprinting quantum emitters in hexagonal boron nitride using strain. Physical Review Research, 2020, 2, .	1.3	15
42093	Noncontacting optostriction driven anisotropic and inhomogeneous strain in two-dimensional materials. Physical Review Research, 2020, 2, .	1.3	9
42094	Cooperative interactions govern the fermiology of the polar metal <mml:math xmlns:mml="http://www.w3.org/1998/Math/MathML"><mml:mrow><mml:msub><mml:mi>Ca</mml:mi><mml:mn>3</mml:mn></ mathvariant="normal">O</mml:mi><mml:mn>7</mml:mn></mml:msub></mml:mrow></mml:math>. Physical Review Research, 2020, 2, .	1.3	14
42095	Self-consistent <mml:math xmlns:mml="http://www.w3.org/1998/Math/MathML"><mml:mrow><mml:mi>DFT</mml:mi><mml:mo>+</mml:mo><mml:mi>U</mml:mi> study of oxygen vacancies in <mml:math xmlns:mml="http://www.w3.org/1998/Math/MathML"><mml:msub><mml:mi>SrTiO</mml:mi><mml:mn>3</mml:mn></mml:msub> Physical Review Research, 2020, 2, .	1.3	50
42096	Magnetism and NÃ©el skyrmion dynamics in <mml:math xmlns:mml="http://www.w3.org/1998/Math/MathML"><mml:mrow><mml:msub><mml:mi>GaV</mml:mi><mml:mn>4</mml:mn></ mathvariant="normal">S</mml:mi><mml:mrow><mml:mn>8</mml:mn><mml:mtext>â€™</mml:mtext><mml:mi>y</mml:mi></mml: Physical Review Research, 2020, 2, .	1.3	9
42097	Layer-dependent electronic and magnetic properties of <mml:math xmlns:mml="http://www.w3.org/1998/Math/MathML"><mml:msub><mml:mrow><mml:mi>Nb</mml:mi></mml:mrow><mml:mn>3</mml:mn> mathvariant="normal">I</mml:mi></mml:mrow><mml:mn>8</mml:mn></mml:msub></mml:math>. Physical Review Research, 2020, 2, .	1.3	17
42098	Signature of band inversion in the antiferromagnetic phase of axion insulator candidate <mml:math xmlns:mml="http://www.w3.org/1998/Math/MathML"><mml:msub><mml:mi>EuIn</mml:mi><mml:mn>2</mml:mn></mml:msub><mml:m Physical Review Research, 2020, 2, .	1.3	25
42099	Mixing periodic topographies and structural patterns on silicon surfaces mediated by ultrafast photoexcited charge carriers. Physical Review Research, 2020, 2, .	1.3	21
42100	<mml:math xmlns:mml="http://www.w3.org/1998/Math/MathML"><mml:mrow><mml:mi>G</mml:mi><mml:mi>W</mml:mi></mml:mrow></mml:m study of pressure-induced topological insulator transition in group-IV tellurides. Physical Review Research, 2020, 2, .	1.3	12
42101	Lattice dynamics in the double-helix antiferromagnet FeP. Physical Review Research, 2020, 2, .	1.3	4
42102	Pressure-stabilized unconventional stoichiometric yttrium sulfides. Physical Review Research, 2020, 2, .	1.3	8
42103	X-ray diffraction using focused-ion-beam-prepared single crystals. Journal of Applied Crystallography, 2020, 53, 614-622.	1.9	7
42104	Robust manipulation of magnetism in LaAO₃/BaTiO₃ (A = Fe, Mn) Tj ETQq1 1 0.784314 rgBT	1.0	10
42105	High-pressure polymorphism in pyridine. IUCrJ, 2020, 7, 58-70.	1.0	12
42106	The crystal structure and phase stability of the zeta phase in the group VB transition metal carbides: a computational investigation. Acta Crystallographica Section B: Structural Science, Crystal Engineering and Materials, 2019, 75, 870-879.	0.5	6
42107	Ca-doped rare earth perovskite materials for tailored exsolution of metal nanoparticles. Acta Crystallographica Section B: Structural Science, Crystal Engineering and Materials, 2020, 76, 1055-1070.	0.5	15
42108	Borates or phosphates? That is the question. Acta Crystallographica Section A: Foundations and Advances, 2020, 76, 197-205.	0.0	2

#	Article	IF	Citations
42109	Dielectric Constant and van der Waals Interlayer Interaction of MoS2-Graphene Heterostructures. , 2020, , .		5
42110	Multicomponent bulk metal nitride (Nb_{1/3}Ta_{1/3}Ti_{1/3})N_{1â^'}_{Î´} synthesis via reaction flash sintering and characterizations. Journal of the American Ceramic Society, 2020, 103, 4876-4893.	1.9	6
42111	Lowâ€temperature preparation of highâ€performance porous ceramics composed of anorthite platelets. Journal of the American Ceramic Society, 2020, 103, 5365-5373.	1.9	24
42112	Optical and electronic properties of niobium oxynitrides with various N/O ratios: insights from first-principles calculations. Journal of Photonics for Energy, 2018, 8, 1.	0.8	9
42113	First-principle calculations of crystal structures, electronic structures, and optical properties of RETaO4 (RE = Y, La, Sm, Eu, Dy, Er). Optical Engineering, 2018, 57, 1.	0.5	6
42114	First-principles calculations of crystal structure, electronic structure and optical properties of RETaO4(RE= Y, La, Sm, Eu, Dy, Er). , 2017, , .		1
42115	Calculation of density of states for modeling photoemission using method of moments. , 2017, , .		1
42116	Density of states of Cs3Sb calculated using density-functional theory for modeling photoemission. , 2017, , .		3
42117	Modeling warm dense matter formation within tight binding approximation. , 2019, , .		2
42118	The effect of growth temperature and metal-to-chalcogen on the growth of WSe2 by molecular beam epitaxy. , 2019, , .		5
42119	Dynamic fracture of tantalum under extreme tensile stress. Science Advances, 2017, 3, e1602705.	4.7	41
42120	Microstructural control of new intercalation layered titanoniobates with large and reversible d-spacing for easy Na ⁺ ion uptake. Science Advances, 2017, 3, e1700509.	4.7	42
42121	Giant polarization in super-tetragonal thin films through interphase strain. Science, 2018, 361, 494-497.	6.0	173
42122	Interaction between Functionalized Graphene with Ti/C and Histidine/Leucine: Effects of Charging. Physics of the Solid State, 2020, 62, 2474-2481.	0.2	2
42123	Pressure dependence of the electronic structure in kaolinite: A first-principles study. Modern Physics Letters B, 2017, 31, 1750194.	1.0	5
42124	First-Principles Modeling of the Repassivation of Corrosion Resistant Alloys: Part I. O and Cl Adsorption Energy. Journal of the Electrochemical Society, 2020, 167, 111502.	1.3	10
42125	DFT-Based Calculation of Dissolution Activation Energy and Kinetics of Niâ€“Cr Alloys. Journal of the Electrochemical Society, 2020, 167, 131508.	1.3	12
42126	Application of the Chloride Susceptibility Index to Study the Effects of Ni, Cr, Mn and Mo on the Repassivation of Stainless Steels. Journal of the Electrochemical Society, 2020, 167, 131510.	1.3	10

#	Article	IF	Citations
42127	Bond Synergy Model for Bond Energies in Alloy Oxides. Journal of the Electrochemical Society, 2020, 167, 141511.	1.3	11
42128	Relation between Surface Composition and Electronic Properties of Native Oxide Films on an Aluminium-Copper Alloy Studied by DFT. Journal of the Electrochemical Society, 2020, 167, 161501.	1.3	13
42129	Favorable Lithium Nucleation on Lithiophilic Framework Porphyrin for Dendrite-Free Lithium Metal Anodes. Research, 2019, 2019, 1-11.	2.8	33
42130	Investigation of Structural, Electronic and Optical Properties of KCdF3. American Journal of Modern Physics, 2013, 2, 77.	0.1	3
42131	Effect of Nanoribbon Width and Strain on the Electronic Properties of the WS2 Nanoribbon. Journal of Low Power Electronics, 2014, 10, 368-372.	0.6	2
42132	Ab initiotheory of phase transitions and thermoelasticity of minerals. , 0, , 83-170.		23
42133	Basics of first-principles simulation of matter under extreme conditions. , 0, , 117-138.		2
42134	Raman tensor of layered black phosphorus. PhotoniX, 2020, 1, .	5.5	29
42135	Fundamental Concepts in Molecular Simulation of NOx Catalysis. , 2005, , 233-268.		5
42136	Structural and Physical Properties of GexAsySe1â€“xâ€“y Glasses. , 2014, , 109-154.		2
42137	Magnetic competition in Fe-based germanide and silicide superconductors. Europhysics Letters, 2019, 128, 47004.	0.7	3
42139	Universality of the Empty-Lattice Approximation to Predict the Topology of Energy Spectra of High-Symmetry Crystals and Superlattices Based upon Them. Acta Physica Polonica A, 2006, 110, 369-378.	0.2	2
42140	Thermodynamics of Fcc Al Crystal from First Principles - Performance of Local Density and Generalized Gradient Approximations. Acta Physica Polonica A, 2007, 112, 513-521.	0.2	1
42141	An ab initio Study of a Model of Single Wall GaN Nanotubes with Oxygen and Zinc as Impurities: Structural and Electronic Properties. Acta Physica Polonica A, 2008, 113, 713-722.	0.2	7
42142	Behaviour of Di-Transition-Metal Nitride Ti_{1-x}Zr_xN Alloy at High Pressure. Acta Physica Polonica A, 2009, 116, 1085-1089.	0.2	5
42143	First-Principles Study of Cubic B_xIn_{1-x}N Ternary Alloys. Acta Physica Polonica A, 2010, 117, 921-927.	0.2	11
42144	Elastic and Thermodynamic Properties of Anti-Perovskite Type Superconductor MCNi3(M = Zn, Cd). Acta Physica Polonica A, 2010, 118, 652-658.	0.2	6
42145	A First Principle Study of Antifluorite Be₂X (X = C, Si) Polymorph. Acta Physica Polonica A, 2011, 119, 442-446.	0.2	4

#	Article	IF	Citations
42146	Vacancy-Fluorine Clusters in Silicon. Acta Physica Polonica A, 2011, 119, 774-777.	0.2	1
42147	Phonon Dispersion Analysis as an Indispensable Tool for Predictions of Solid State Polymorphism and Dynamic Metastability: Case of Compressed Silane. Acta Physica Polonica A, 2011, 119, 895-900.	0.2	8
42148	High-Pressure Phase Transitions and Thermodynamic Behaviors of Cadmium Sulfide. Acta Physica Polonica A, 2011, 120, 501-506.	0.2	36
42149	DFT Study of Octanuclear Molecular Chromium-Based Ring Using New Pseudopotential Parameters. Acta Physica Polonica A, 2012, 121, 1115-1117.	0.2	7
42150	Structural and Magnetic Properties of Co Thin Films on Au(111) Substrates. Acta Physica Polonica A, 2012, 121, 653-659.	0.2	7
42151	Experimental and Theoretical Study of Zircon and Scheelite Phases of DyVO4. Acta Physica Polonica A, 2012, 121, 920-927.	0.2	2
42152	Effect of Interstitial Iron Defect and Doping on Physical Properties and Stability of Iron Telluride. Acta Physica Polonica A, 2012, 121, 928-931.	0.2	1
42153	First-Principles Study of Structural, Elastic and Mechanical Properties of Zinc-Blende Boron Nitride (B3-BN). Acta Physica Polonica A, 2012, 122, 109-115.	0.2	16
42154	Free-Standing Si and Ge, and Ge/Si Core-Shell Semiconductor Nanowires. Acta Physica Polonica A, 2012, 122, 294-298.	0.2	3
42155	Band Gap Calculations of Ternary InN0.03125P0.96875Alloy. Acta Physica Polonica A, 2015, 128, B-135-B-138.	0.2	1
42156	Structural and Electronic Properties of Ternary Al_xIn_{1-x}P Alloys. Acta Physica Polonica A, 2015, 128, B-97-B-100.	0.2	6
42157	The Elastic Anisotropic and Thermodynamic Properties of I4mm-B₃C. Acta Physica Polonica A, 2016, 129, 103-107.	0.2	10
42158	Elastic Anisotropic and Thermodynamic Properties of I-4m2-BCN. Acta Physica Polonica A, 2016, 129, 1124-1130.	0.2	13
42159	First Principles Study of Mechanical Stability and Thermodynamic Properties of K₂S under Pressure and Temperature Effect. Acta Physica Polonica A, 2016, 129, 315-322.	0.2	4
42160	Influence of the Hydrogen Adsorption to the Optical Properties of Boron Nitride Nanotubes. Acta Physica Polonica A, 2016, 129, 348-351.	0.2	3
42161	Electronic and Magnetic Properties of Ca-Doped Mn-Ferrite. Acta Physica Polonica A, 2016, 130, 362-364.	0.2	9
42162	High Pressure Behaviour of Elastic and Mechanical Properties of NiGa Intermetallic Compound. Acta Physica Polonica A, 2016, 130, 471-474.	0.2	5
42163	A Comparison of the~Structural, Electronic, Optical and Elastic Properties of Wurtzite, Zinc-Blende and Rock Salt TlN: A DFT Study. Acta Physica Polonica A, 2016, 130, 758-768.	0.2	7

#	Article	IF	Citations
42164	The Optoelectronic Properties of Sb Doped BBi Compounds. Acta Physica Polonica A, 2016, 130, 98-100.	0.2	4
42165	Hot Compression Test of Heat Resistant Steel. Acta Physica Polonica A, 2017, 131, 1340-1344.	0.2	1
42166	First Principle Investigations on Electronic, Magnetic, Thermodynamic, and Transport Properties of TlGdX2 (X = S, Se, Te). Acta Physica Polonica A, 2017, 132, 1371-1378.	0.2	6
42167	Characterization of Defects in Titanium Created by Hydrogen Charging. Acta Physica Polonica A, 2017, 132, 1606-1611.	0.2	3
42168	Specific Features of Content Dependences for Energy Gap in In_xTl_{1-x}I Solid State Crystalline Alloys. Acta Physica Polonica A, 2018, 133, 68-75.	0.2	16
42169	The effect of strain on the electronic properties of MoS₂ monolayers. Multiscale and Multiphysics Mechanics, 2016, 1, 77-86.	0.3	2
42170	Filled skutterudites: from single to multiple filling. Scientia Sinica: Physica, Mechanica Et Astronomica, 2011, 41, 706-728.	0.2	7
42171	Excitons in hexagonal boron nitride single-layer: a new platform for polaritonics in the ultraviolet. Journal of the Optical Society of America B: Optical Physics, 2019, 36, 674.	0.9	58
42172	Control of the nonlinear response of bulk GaAs induced by long-wavelength infrared pulses. Optics Express, 2019, 27, 30462.	1.7	6
42173	Extrinsic photoluminescence properties of individual micro-particle of Cs₄PbBr₆ perovskite with â€œdefectâ€•structure. Optics Express, 2019, 27, 31207.	1.7	13
42174	Tunable broadband hyperbolic light dispersion in metal diborides. Optics Express, 2019, 27, 36911.	1.7	12
42175	Nanopatterned sapphire substrates in deep-UV LEDs: is there an optical benefit?. Optics Express, 2020, 28, 3619.	1.7	18
42176	High sensitivity and rapid response ultraviolet photodetector of a tetragonal CsPbCl₃ perovskite single crystal. Optical Materials Express, 2020, 10, 1374.	1.6	34
42177	Mo^6+ substitution induced band structure regulation and efficient near-UV-excited red emission in NaLaMg(W,Mo)O_6:Eu phosphor. Optical Materials Express, 2017, 7, 2660.	1.6	15
42178	Dielectric function and plasmonic behavior of Ga(II) and Ga(III). Optical Materials Express, 2019, 9, 4050.	1.6	10
42179	Raman spectroscopy regulation in van der Waals crystals. Photonics Research, 2018, 6, 991.	3.4	25
42180	â€œConjugate Channelingâ€•Effect in Dislocation Core Diffusion: Carbon Transport in Dislocated BCC Iron. PLoS ONE, 2013, 8, e60586.	1.1	26
42181	H2 Dissociative Adsorption at the Zigzag Edges of Graphite. E-Journal of Surface Science and Nanotechnology, 2004, 2, 77-80.	0.1	27

#	Article	IF	Citations
42182	Hydrogen atom quantum migration on platinum. E-Journal of Surface Science and Nanotechnology, 2006, 4, 619-623.	0.1	15
42183	First Principles Investigations on Fuel Cell Reactions: H2-Pt(111) Interactions. E-Journal of Surface Science and Nanotechnology, 2008, 6, 134-137.	0.1	3
42184	Ab Initio Study of GaSb(001)-c(2*10) and (2*10) Reconstructions. E-Journal of Surface Science and Nanotechnology, 2009, 7, 429-431.	0.1	2
42185	Energetics of Mg, B, Cu, and Ti Atoms Adsorbed on the ZnO Polar Surfaces from First Principles. E-Journal of Surface Science and Nanotechnology, 2011, 9, 199-205.	0.1	2
42186	First-principle Calculations of Dopant-Oxygen Vacancy Complexes in Transparent Conducting TiO2 Systems. Hyomen Kagaku, 2010, 31, 343-351.	0.0	3
42188	A study of Platinum metal as a component of fuel cells. International Journal of Scientific and Engineering Research, 2019, 10, 8-19.	0.1	5
42189	Hydrogen Concentration Estimation Based on Density Functional Theory in Aluminum and Alpha Iron under Gaseous Hydrogen Environments. Transactions of the Materials Research Society of Japan, 2012, 37, 1-6.	0.2	5
42190	First-principle calculations of effective mass of silicon crystal with vacancy defects. Materials Science-Poland, 2016, 34, 916-923.	0.4	9
42191	Extending the knowledge on the quaternary rare earth nickel aluminum germanides of the RENiAl4Ge2 series (RE=Y, Sm, Gdâ€“Tm, Lu) â€“ structural, magnetic and NMR-spectroscopic investigations. Zeitschrift Fur Naturforschung - Section B Journal of Chemical Sciences, 2020, 75, 149-162.	0.3	2
42192	Phase Relations of Iron Carbides Fe2C, Fe3C, and Fe7C3 at the Earthâ€™s Core Pressures and Temperatures. Russian Geology and Geophysics, 2020, 61, 1345-1353.	0.3	6
42193	Optical-Energy Properties of the Bulk and Thin-Film Cadmium Telluride (CdTe). Nanosistemi, Nanomateriali, Nanotehnologii, 2018, 16, .	0.2	4
42194	Electron structure of the equilibrium and metastable phases in superionic Li2SiS3. Semiconductor Physics, Quantum Electronics and Optoelectronics, 2013, 16, 48-54.	0.3	2
42195	Electronic structure of Ag8GeS6. Semiconductor Physics, Quantum Electronics and Optoelectronics, 2017, 20, 19-25.	0.3	10
42196	Electronic structure and optical properties of HgSe. Semiconductor Physics, Quantum Electronics and Optoelectronics, 2018, 21, 288-293.	0.3	4
42197	Electronic, structural and paramagnetic properties of magnesium telluride. Semiconductor Physics, Quantum Electronics and Optoelectronics, 2019, 22, 5-10.	0.3	1
42198	Elastic properties of CdTe1â€“xSex(x = 1/16) solid solution: First principles study. Semiconductor Physics, Quantum Electronics and Optoelectronics, 2020, 23, 355-360.	0.3	3
42199	Anosotropy and Pressure Effect on the Elastic and Mechanical Properties of (B3) BN. Ukrainian Journal of Physics, 2014, 59, 418-425.	0.1	3
42200	Tuning Electronic Transport Properties of Zigzag Graphene Nanoribbons with Stone-Wales Defect. Communications in Physics, 2018, 28, 201.	0.0	3

#	Article	IF	Citations
42201	DENSITY FUNCTIONAL THEORY STUDY ON THE ADSORPTION OF METHANE ON KEROGEN WITH DIFFERENT FUNCTIONAL GROUPS. Applied Ecology and Environmental Research, 2017, 15, 861-869.	0.2	6
42202	Hydrogenâ€“Grain Boundary Interaction in Fe, Feâ€“C, and Feâ€“N Systems. Progress in Nuclear Science and Technology, 2011, 2, 9-15.	0.3	38
42204	Effect of Mercapto and Methyl Groups on the Efficiency of Imidazole and Benzimidazole-based Inhibitors of Iron Corrosion. Acta Chimica Slovenica, 2016, 63, 544-559.	0.2	10
42205	First-principles investigation of the structural and electronic properties of Sr3Sb2 in hexagonal phase. Journal of Zankoy Sulaimani - Part A, 2013, 15, 169-174.	0.1	1
42206	The First Principles Approach to The Structural, Elastic, Electronic, Vibrational and Thermal Properties of CsCl type-ErAu Alloy. Cumhuriyet Science Journal, 2017, 38, 611-618.	0.1	2
42207	A FIRST-PRINCIPLES INVESTIGATIONS OF LITHIUM ADSORPTION AND DIFFUSION ON BN, AlN AND GaN MONOLAYERS. EskiÅŸehir Technical University Journal of Science and Technology A - Applied Sciences and Engineering, 0, , .	0.4	3
42208	First-Principles Study of Segregation Behavior of Cr/Ti/Y at Grain Boundary in Vanadium. International Journal of Materials Mechanics and Manufacturing, 2018, 6, 31-36.	0.2	2
42209	Thermal Stability of the Mg2Ni-Based Hydrogen Storage Alloy Doped Ti Element. International Journal of Heat and Technology, 2016, 34, 245-250.	0.3	2
42210	Classic Articles Published by American Scientists (1900-2014): A Bibliometric Analysis. Current Science, 2016, 111, 1156.	0.4	28
42211	Normal and inverse ringwoodite at high pressures. American Mineralogist, 1999, 84, 288-293.	0.9	23
42213	Water Molecular Adsorption on the Low-Index Pt Surface: A Density Functional Study. Indonesian Journal of Chemistry, 2018, 18, 195.	0.3	3
42214	Adsorption of RGD Tripeptide on Au (111) Surface. Materials Transactions, 2019, 60, 1711-1715.	0.4	2
42215	Prediction of Face-Centered Cubic Single-Phase Formation for Non-Equiatomic Crâ€“Mnâ€“Feâ€“Coâ€“Ni High-Entropy Alloys Using Valence Electron Concentration and Mean-Square Atomic Displacement. Materials Transactions, 2020, 61, 1874-1880.	0.4	13
42216	Hydrogen Trapping in Mg₂Si and Al₇FeCu₂ Intermetallic Compounds in Aluminum Alloy: First-Principles Calculations. Materials Transactions, 2020, 61, 1907-1911.	0.4	20
42217	Electro-Magnetic Behavior of Highly Correlated Fluorides KFeF3, KCoF3 and KNiF3: A Comparative Ab-initio Study of Cation Effect. Annals of West University of Timisoara: Physics, 2020, 62, 23-51.	0.2	2
42219	The First Principles Investigation of Structural, Electronic, Mechanical and Lattice Dynamical Properties of the B and N Doped M2AX Type MAX Phases Ti2AlB0.5C0.5 and Ti2AlN0.5C0.5 Compounds. Journal of Boron, 0, , .	0.0	7
42220	Theoretical study of B segregation in Mo(110). Journal of Boron, 0, , .	0.0	1
42221	DFT study of native point defects in (ZnO)n (n = 34, 60) nanoclusters. Journal of Physical Studies, 2019, 23, .	0.2	3

#	Article	IF	Citations
42222	Band energy structure of K2ZnCl4 crystals under uniaxial pressures. Ukrainian Journal of Physical Optics, 2011, 12, 36.	9.7	2
42223	Amino Acid Adsorption Effects on Nanotube Electronics. Shinku/Journal of the Vacuum Society of Japan, 2006, 49, 440-442.	0.2	1
42224	A Behavior of a Hydrogen Atom of Pd0.75Ag0.25(111). Shinku/Journal of the Vacuum Society of Japan, 2007, 50, 440-443.	0.2	2
42225	Theoretical Study of Magnetic Anisotropy in Co/Ni Multi-Layers on W(110). Journal of the Vacuum Society of Japan, 2013, 56, 139-141.	0.3	2
42226	New Insights into Carbon Distribution in Bainitic Ferrite*. HTM - Journal of Heat Treatment and Materials, 2018, 73, 68-79.	0.1	3
42227	The Naâ€“H system: from first-principles calculations to thermodynamic modeling. International Journal of Materials Research, 2006, 97, 845-853.	0.1	13
42228	Thermochemical stability of Liâ€“Cuâ€“O ternary compounds stable at room temperature analyzed by experimental and theoretical methods. International Journal of Materials Research, 2017, 108, 959-970.	0.1	1
42229	Synthesis of Iron-Carbide Nanoparticles: Identification of the Active Phase and Mechanism of Fe-Based Fischerâ€“Tropsch Synthesis. CCS Chemistry, 2021, 3, 2712-2724.	4.6	41
42231	Theoretical Investigations Into the Variability of the 15N Solid-State NMR Parameters Within an Antimicrobial Peptide Ampullosporin A. Physiological Research, 2018, 67, S349-S356.	0.4	2
42234	Structural and Thermodynamic Properties of the High-Entropy Alloy AlCoCrFeNi Based on First-Principles Calculations. Frontiers in Materials, 2020, 7, .	1.2	6
42235	In Situ TEM Study of Rh Particle Sintering for Three-Way Catalysts in High Temperatures. Catalysts, 2021, 11, 19.	1.6	6
42236	Comparative Computational Study of L-Amino Acids as Green Corrosion Inhibitors for Mild Steel. Computation, 2021, 9, 1.	1.0	21
42237	Optoelectronic Properties of Ultrathin Indium Tin Oxide Films: A First-Principle Study. Crystals, 2021, 11, 30.	1.0	3
42238	Zeolite-Catalyzed Hydrocarbon Formation from Methanol: Density Functional Simulations. International Journal of Molecular Sciences, 2002, 3, 423-434.	1.8	51
42239	Insights on Substitution Preference of Pb Ions in Sulfoaluminate Cement Clinker Phases. Materials, 2021, 14, 44.	1.3	10
42240	DFT Prediction of Factors Affecting the Structural Characteristics, the Transition Temperature and the Electronic Density of Some New Conjugated Polymers. Polymers, 2020, 12, 1207.	2.0	17
42241	Facilitating Lithium-Ion Diffusion in Layered Cathode Materials by Introducing Li ⁺ /Ni ²⁺ Antisite Defects for High-Rate Li-Ion Batteries. Research, 2019, 2019, 2198906.	2.8	36
42242	Favorable Lithium Nucleation on Lithiophilic Framework Porphyrin for Dendrite-Free Lithium Metal Anodes. Research, 2019, 2019, 4608940.	2.8	29

#	Article	IF	Citations
42243	Synergistic O ²⁻ /Li ⁺ Dual Ion Transportation at Atomic Scale. Research, 2019, 2019, 9087386.	2.8	3
42244	The Electronic Transport Channel Protection and Tuning in Real Space to Boost the Thermoelectric Performance of Mg _{3+ Î´} Sb _{2- y} Bi _y near Room Temperature. Research, 2020, 2020, 1672051.	2.8	29
42245	Constructing Stable and Potentially High-Performance Hybrid Organic-Inorganic Perovskites with â€œUnstableâ€•Cations. Research, 2020, 2020, 1986576.	2.8	4
42246	Machine Learning Chemical Guidelines for Engineering Electronic Structures in Half-Heusler Thermoelectric Materials. Research, 2020, 2020, 6375171.	2.8	32
42247	Theoretical and Experimental Investigations of the Effect of Co Addition on the Structural and Properties of AB_{3.5}-type Hydrogen Storage Alloys. Wuji Cailiao Xuebao/Journal of Inorganic Materials, 2012, 27, 568-574.	0.6	2
42248	Ab initio calculation of band alignment of epitaxial La₂O₃ on Si(111) substrate. AIMS Materials Science, 2015, 2, 279-293.	0.7	4
42249	Modified Becke-Johnson exchange potential: improved modeling of lead halides for solar cell applications. AIMS Materials Science, 2016, 3, 149-159.	0.7	19
42250	Thermodynamic properties of nanotubes: zone-folding approach. Lithuanian Journal of Physics, 2016, 56, 164-172.	0.1	7
42251	Filled Skutterudites: from Single to Multiple Filling. Journal of the Korean Ceramic Society, 2010, 47, 54-60.	1.1	7
42252	Effect of B-Cation Doping on Oxygen Vacancy Formation and Migration in LaBO₃: A Density Functional Theory Study. Journal of the Korean Ceramic Society, 2015, 52, 331-337.	1.1	9
42253	Proton Conduction in Nonstoichiometric â˜3 BaZrO3 (210)[001] Tilt Grain Boundary Using Density Functional Theory. Journal of the Korean Ceramic Society, 2016, 53, 301-305.	1.1	5
42254	Investigation of LiO2 Adsorption on LaB1â˜'xBâ€²xO3(001) for Li-Air Battery Applications: A Density Functional Theory Study. Journal of the Korean Ceramic Society, 2016, 53, 306-311.	1.1	2
42255	The Effect of Domain Wall on Defect Energetics in Ferroelectric LiNbO3 from Density Functional Theory Calculations. Journal of the Korean Ceramic Society, 2016, 53, 312-316.	1.1	4
42256	ab initio Thermodynamic Study of the CO2 Capture Properties of M2CO3 (M = Na, K)- and CaCO3-Promoted MgO Sorbents Towards Forming Double Salts. Aerosol and Air Quality Research, 2014, 14, 470-479.	0.9	50
42257	The Structures and Properties of Y-Substituted Mg₂Ni Alloys and Their Hydrides: A First-Principles Study. American Journal of Analytical Chemistry, 2016, 07, 67-74.	0.3	5
42258	First-Principles Study of Electronic Structure and Optical Properties of Silicon/Carbon Nanotube. Computational Chemistry, 2017, 05, 159-171.	0.2	6
42259	Theoretical Investigation of Structural, Electronic, and Mechanical Properties of Two Dimensional C, Si, Ge, Sn. Crystal Structure Theory and Applications, 2016, 05, 43-55.	0.3	23
42260	A Comparative Study of Electronic Properties of Bulk MoS2 and Its Monolayer Using DFT Technique: Application of Mechanical Strain on MoS2 Monolayer. Graphene, 2014, 03, 52-59.	0.3	130

#	Article	IF	Citations
42261	Efficient Theoretical Screening of Solid Sorbents for CO₂ Capture Applications. International Journal of Clean Coal and Energy, 2012, 01, 1-11.	0.2	58
42262	First Principle Study of the Structural and Piezoelectric Properties of Perovskite ZrTi(PbO₃)₂ Materials for Naval SONAR. Journal of Applied Mathematics and Physics, 2019, 07, 271-280.	0.2	2
42263	Structural and Electronic Properties of Impurities on Boron Nitride Nanotube. Journal of Modern Physics, 2011, 02, 857-863.	0.3	14
42264	The Bowing Parameters of Ca_{Ï‡}Mg_{1-Ï‡}O Ternary Alloys. Journal of Modern Physics, 2014, 05, 1546-1551.	0.3	10
42265	Enhancement of Ferromagnetic Ordering Curie Temperature in N-Doped MgO under Hydrostatic Pressure. Modeling and Numerical Simulation of Material Science, 2012, 02, 37-42.	0.5	2
42266	First Principles Study of the Structural and Electronic Properties of the ZnO/Cu₂O Heterojunction. Materials Sciences and Applications, 2015, 06, 661-675.	0.3	2
42267	First Principles DFT Study of Hydrogen Storage on Graphene with La Decoration. Journal of Materials Science and Chemical Engineering, 2015, 03, 87-94.	0.2	3
42268	Electronic Structures and Magnetic Properties of Co-Adsorbed Monolayer WS₂. Journal of Materials Science and Chemical Engineering, 2016, 04, 32-41.	0.2	2
42269	Ab Initio Calculations of Optical Properties of TlBr and TlCl Radiation Detectors. World Journal of Condensed Matter Physics, 2011, 01, 63-69.	1.1	10
42270	Electronic and Optical Properties of Rare Earth Oxides: <i>Ab Initio</i> Calculation. World Journal of Condensed Matter Physics, 2015, 05, 78-85.	1.1	8
42271	Physical Properties of CrSb/InP(001): Effect of Interface in Half-Metallic. World Journal of Nano Science and Engineering, 2013, 03, 79-86.	0.3	2
42272	A First-principles Study on Magnetic and Electronic Properties of Ni Impurity in bcc Fe. Journal of Magnetics, 2008, 13, 124-127.	0.2	10
42273	A Convergence Test of the Full-potential Linearized Augmented Plane Wave (FLAPW) Method: Ferromagnetic Bulk BCC Fe. Journal of Magnetics, 2009, 14, 137-143.	0.2	12
42274	Fundamental Mechanisms of Platinum Catalyst for Oxygen Reduction Reaction in Fuel Cell: Density Functional Theory Approach. Daehan Hwan'gyeong Gonghag Hoeji, 2016, 38, 242-248.	0.4	3
42275	Structure Related Photocatalytic Properties of TiO₂. Bulletin of the Korean Chemical Society, 2009, 30, 402-404.	1.0	37
42276	Theoretical Investigation of Edge-modified Zigzag Graphene Nanoribbons by Scandium Metal with Pyridine-like Defects: A Potential Hydrogen Storage Material. Bulletin of the Korean Chemical Society, 2014, 35, 253-256.	1.0	24
42277	Carbon Nanotubes Doped with Nitrogen, Pyridine-like Nitrogen Defects, and Transition Metal Atoms. Journal of the Korean Chemical Society, 2012, 56, 34-46.	0.2	23
42278	Stability and Electronic Properties of the Adsorption of Molecular Hydrogen on Metal-containing Single-walled Carbon Nanotubes. Journal of the Korean Chemical Society, 2015, 59, 429-433.	0.2	24

#	Article	IF	Citations
42279	Semiconducting single-walled carbon nanotubes synthesized by S-doping. Nano-Micro Letters, 2010, 1, 9.	14.4	4
42282	A Comparative Study of Optical Anisotropies of BC3 and B3C Systems by Density Functional Theory. ISRN Nanotechnology, 2011, 2011, 1-9.	1.3	3
42283	Structural and Electronic Properties of Pure Ta, TaNO, and TaZrNO with Ab Initio Calculations. ISRN Metallurgy, 2012, 2012, 1-7.	0.7	2
42284	First principles investigations of HgX (X=S, Se and Te). Archives of Materials Science and Engineering, 2016, 79, 5-11.	0.7	16
42285	Mechanisms of Na adsorption on graphene and graphene oxide: density functional theory approach. Carbon Letters, 2015, 16, 116-120.	3.3	84
42286	Influence of defective sites in Pt/C catalysts on the anode of direct methanol fuel cell and their role in CO poisoning: a first-principles study. Carbon Letters, 2015, 16, 198-202.	3.3	7
42287	Density functional theory study of CH₄and CO₂adsorption by fluorinated graphene. Carbon Letters, 2016, 20, 81-85.	3.3	26
42289	High pressure phase transition and phonon-dispersion relations of BeO calculated by first-principles method. Wuli Xuebao/Acta Physica Sinica, 2010, 59, 8755.	0.2	8
42290	Elastic and thermodynamic properties of CaPo under pressure via first-principles calculations. Wuli Xuebao/Acta Physica Sinica, 2011, 60, 076501.	0.2	15
42291	Effects of Mn and N codoping on microstructure and performance of anatase TiO2. Wuli Xuebao/Acta Physica Sinica, 2011, 60, 087103.	0.2	4
42292	Temperature dependent Raman spectra and micro-structure study of hexagonal MgTiO3 crystal. Wuli Xuebao/Acta Physica Sinica, 2011, 60, 104209.	0.2	1
42293	Study of electronic structure and optical propertise of -AlON crystal. Wuli Xuebao/Acta Physica Sinica, 2012, 61, 027101.	0.2	12
42294	First-principles study of the electronic structure and optical properties of GaN(0001) surface. Wuli Xuebao/Acta Physica Sinica, 2012, 61, 067101.	0.2	15
42295	Adsorption and diffusion of oxygen on Pt (111) surface and subsurface. Wuli Xuebao/Acta Physica Sinica, 2012, 61, 076802.	0.2	2
42296	First-principles study of p-type ZnO by Te-N codoping. Wuli Xuebao/Acta Physica Sinica, 2012, 61, 176105.	0.2	6
42297	The electronic theory study on high-temperature oxidation mechanism of TiAl alloy. Wuli Xuebao/Acta Physica Sinica, 2012, 61, 177101.	0.2	7
42298	First-principle calculations of elastic, electronic and thermodynamic properties of TiC under high pressure. Wuli Xuebao/Acta Physica Sinica, 2012, 61, 186501.	0.2	9
42299	First-principles study on the electronic structure and phase transition of Î±-, Î²- and Î³-Si3N4. Wuli Xuebao/Acta Physica Sinica, 2012, 61, 197102.	0.2	4

#	Article	IF	Citations
42300	First-principles study on the electronic structures of Cr- and W-doped single-layer MoS2. Wuli Xuebao/Acta Physica Sinica, 2013, 62, 037103.	0.2	13
42301	First principles calculation of adsorption for H2S on Fe(100) surface. Wuli Xuebao/Acta Physica Sinica, 2013, 62, 077101.	0.2	6
42302	Elastic and optical properties of IVB group transition-metal nitrides. Wuli Xuebao/Acta Physica Sinica, 2013, 62, 087102.	0.2	8
42303	A first-principle study on the interfacial properties of Cu/CeO2(110). Wuli Xuebao/Acta Physica Sinica, 2013, 62, 117301.	0.2	7
42304	Study on the atomic and electronic structures of BiOCl{001} surface using first principles. Wuli Xuebao/Acta Physica Sinica, 2013, 62, 127301.	0.2	8
42305	The magnetism study of N-doped diamond. Wuli Xuebao/Acta Physica Sinica, 2013, 62, 166102.	0.2	5
42306	Study of phase transition of HoVO4 under high pressure by Raman scattering and ab initio calculations. Wuli Xuebao/Acta Physica Sinica, 2013, 62, 246101.	0.2	3
42307	Phase transition, electronic and optical properties of Si3N4 new phases at high pressure with density functional theory. Wuli Xuebao/Acta Physica Sinica, 2014, 63, 047101.	0.2	2
42308	Effect on the electronic structures and optical bandgaps of Ga-doped wurtzite TM0.125Zn0.875O(TM=Be, Mg). Wuli Xuebao/Acta Physica Sinica, 2014, 63, 087101.	0.2	2
42309	Influence of edge reconstruction on the electron transport in zigzag graphene nanoribbon. Wuli Xuebao/Acta Physica Sinica, 2014, 63, 117102.	0.2	3
42310	Surface absorptions of H2S, HS and S on Fe(111) investigated by density functional theory. Wuli Xuebao/Acta Physica Sinica, 2014, 63, 127101.	0.2	3
42311	Properties of Cu1-xWx alloys at high pressure and high temperature from first-principles calculations. Wuli Xuebao/Acta Physica Sinica, 2014, 63, 206501.	0.2	3
42312	Effect of strain on Li adsorption on silicene. Wuli Xuebao/Acta Physica Sinica, 2014, 63, 217101.	0.2	1
42313	First-principles study on stability and electronic properties of MC and Mn+1ACn phases. Wuli Xuebao/Acta Physica Sinica, 2014, 63, 237301.	0.2	1
42314	First-principles study on saturated adsorption of alkali metal atoms on silicene. Wuli Xuebao/Acta Physica Sinica, 2015, 64, 013101.	0.2	7
42315	Geometric stability and nitrogen adsorption properties of small BaxOy cluster-modified Ru(0001) surface. Wuli Xuebao/Acta Physica Sinica, 2015, 64, 016802.	0.2	3
42316	Structural and electronic properties of hydrogenated bilayer silicene. Wuli Xuebao/Acta Physica Sinica, 2015, 64, 076801.	0.2	2
42317	First-principles study of electronic and optical properties of BiTiO3. Wuli Xuebao/Acta Physica Sinica, 2015, 64, 147102.	0.2	2

#	Article	IF	Citations
42318	Raman spectroscopic study on the micro-structure of NH4H2PO4 and ND4D2PO4 crystals. Wuli Xuebao/Acta Physica Sinica, 2015, 64, 197801.	0.2	2
42319	First principles study on the H2 diffusion and desorption at the Li-doped MgH2(001) surface. Wuli Xuebao/Acta Physica Sinica, 2016, 65, 056801.	0.2	2
42320	Defect stabilities and magnetic properties of Ni-X-In (X= Mn, Fe and Co) alloys: a first-principle study. Wuli Xuebao/Acta Physica Sinica, 2016, 65, 096103.	0.2	3
42321	First principles investigations of structural, electronic and elastic properties of ammonium perchlorate under high pressures. Wuli Xuebao/Acta Physica Sinica, 2016, 65, 126102.	0.2	8
42322	Density functional theory study of structure stability and electronic structures of graphyne derivatives. Wuli Xuebao/Acta Physica Sinica, 2016, 65, 133101.	0.2	2
42323	First-principles study on thermodynamic properties of CdxZn1-xO alloys. Wuli Xuebao/Acta Physica Sinica, 2016, 65, 157303.	0.2	1
42324	Ferroelectric phase transition of perovskite SnTiO3 based on the first principles. Wuli Xuebao/Acta Physica Sinica, 2016, 65, 237101.	0.2	4
42325	Ferromagnetism of undoped anatase TiO2 based on the first-principles calculations. Wuli Xuebao/Acta Physica Sinica, 2017, 66, 056101.	0.2	2
42326	Interfacial cohesive interaction and band modulation of two-dimensional MoS2/graphene heterostructure. Wuli Xuebao/Acta Physica Sinica, 2017, 66, 087101.	0.2	8
42327	First-principle study of structure stability and electronic structures of graphyne derivatives. Wuli Xuebao/Acta Physica Sinica, 2017, 66, 107102.	0.2	8
42328	Electron-theoretical study on the influences of torsional deformation on electrical and optical properties of O atom absorbed graphene. Wuli Xuebao/Acta Physica Sinica, 2017, 66, 246301.	0.2	3
42329	First-principle calculation on electronic structures and optical properties of hybrid graphene and BiOI nanosheets. Wuli Xuebao/Acta Physica Sinica, 2018, 67, 116301.	0.2	3
42330	Electronic structure calculation of Cr content effect on corrosion resistance of Ti-Nb-Cr alloy. Wuli Xuebao/Acta Physica Sinica, 2018, 67, 197101.	0.2	2
42331	Density functional theory calculation of structure and electronic properties in N-methane hydrate. Wuli Xuebao/Acta Physica Sinica, 2019, 68, 169101.	0.2	2
42332	Electronic structures and optical properties of Fe, Co, and Ni doped GaSb. Wuli Xuebao/Acta Physica Sinica, 2019, 68, 184202.	0.2	4
42333	First-Principles Study for High-Pressure Tellurium near a Transition from bcc to fcc. Journal of the Physical Society of Japan, 2020, 89, 124603.	0.7	3
42334	Ferromagnetism Induced by Vacancies in Bulk and the (1010) Surfaces of ZnO: Density Functional Theory Calculations. Japanese Journal of Applied Physics, 2011, 50, 01BE05.	0.8	6
42335	First Principles Calculations of Defect Formation in In-Free Photovoltaic Semiconductors Cu2ZnSnS4and Cu2ZnSnSe4. Japanese Journal of Applied Physics, 2011, 50, 04DP07.	0.8	50

#	Article	IF	Citations
42336	Effect of Lithium Absorption at Tetrahedral Site and Isomorphic Substitution on Montmorillonite Properties: A Density Functional Theory Study. Japanese Journal of Applied Physics, 2011, 50, 055701.	0.8	3
42337	Phase Stability and Electronic Structure of In-Free Photovoltaic Materials Cu₂IISnSe₄(II: Zn, Cd, Hg). Japanese Journal of Applied Physics, 2011, 50, 05FF01.	0.8	25
42338	Accurate Electronic Structures of Eu-Doped SiAlON Green Phosphor with a Semilocal Exchangeâ€“Correlation Potential. Japanese Journal of Applied Physics, 2011, 50, 06GH10.	0.8	2
42339	Controllability of Electrical Conductivity by Oxygen Vacancies and Charge Carrier Trapping at Interface between CoO and Electrodes. Japanese Journal of Applied Physics, 2011, 50, 071101.	0.8	5
42340	Density Functional Theory Study of Cu Adhesion on Rh, Ir, Pd, Ta, Mo, Ru, Co, and Os Surfaces. Japanese Journal of Applied Physics, 2011, 50, 105701.	0.8	4
42341	Theoretical Calculations for Magnetic Property of FeRh Inter-Metallic Compound with Site-Exchange Defects. Japanese Journal of Applied Physics, 2011, 50, 105803.	0.8	4
42342	Oxygen Vacancy Chain Formation in TiO₂under External Strain for Resistive Switching Memory. Japanese Journal of Applied Physics, 2012, 51, 06FG14.	0.8	2
42343	A First-Principles Study of the Ferroelectric Phase of AgNbO₃. Japanese Journal of Applied Physics, 2012, 51, 09LE02.	0.8	9
42344	Interaction Effect of Protons on Their Migration in Bulk Undoped Barium Zirconate Using Density Functional Theory. Japanese Journal of Applied Physics, 2012, 51, 09MA01.	0.8	7
42345	First-Principles Study on Cd Doping in Cu₂ZnSnS₄and Cu₂ZnSnSe₄. Japanese Journal of Applied Physics, 2012, 51, 10NC11.	0.8	31
42346	Energetic evaluation of possible interstitial compound formation of BaSi₂with 2p-, 3s-, and 3d-elements using first-principle calculations. Japanese Journal of Applied Physics, 2015, 54, 07JE03.	0.8	4
42347	ACs₅Bi₄(PO₄)₂(P₂O₇)₃ (A = K, Rb and Cs) with two kinds of isolated Pâ€“O groups designed by dimensional reduction theory. Inorganic Chemistry Frontiers, 2021, 8, 5270-5276.	3.0	3
42348	The role of halogen bonding in metal free phosphors. Physical Chemistry Chemical Physics, 2021, 23, 23351-23359.	1.3	2
42349	Effects of external electric field on the sensing property of volatile organic compounds over Janus MoSSe monolayer: a first-principles investigation. RSC Advances, 2021, 11, 33276-33287.	1.7	10
42350	Exploring the electronic band gap of Janus MoSeO and WSeO monolayers and their heterostructures. New Journal of Chemistry, 0, , .	1.4	9
42351	First Principle Study on the Structural, Electronic and Elastic Properties of Tetragonal tP16-Mn3Ru and Cr3Ru Under Pressure. SSRN Electronic Journal, 0, , .	0.4	0
42352	Anharmonic lattice dynamics of superionic lithium nitride. Journal of Materials Chemistry A, 2022, 10, 2295-2304.	5.2	9
42353	Computational modelling of ammonia addition on partially reduced graphene oxide flakes. Physical Chemistry Chemical Physics, 2021, 23, 24738-24749.	1.3	4

#	Article	IF	Citations
42354	Low-dimensional HfS₂as SO₂adsorbent and gas sensor: effect of water and sulfur vacancies. Physical Chemistry Chemical Physics, 2021, 23, 23655-23666.	1.3	7
42355	Quantum mechanical modelling of phosphorus qubits in silicene under constrained magnetization. RSC Advances, 2021, 11, 33890-33894.	1.7	1
42356	Enhanced Electronic and Magnetic Properties of N₂O Gas Adsorbed Mn-Doped MoSe₂ Monolayer. IEEE Transactions on Electron Devices, 2022, 69, 1634-1641.	1.6	14
42357	Steric effects in the hydrogen evolution reaction based on the TMX₄ active center: Feâ€“BHT as a case study. Physical Chemistry Chemical Physics, 2021, 23, 25239-25245.	1.3	4
42358	A comparison of methods for the estimation of the enthalpy of formation of rare earth compounds. Physical Chemistry Chemical Physics, 2021, 23, 24273-24281.	1.3	9
42359	Electronic structure and stability of two-dimensional bimetallic ferromagnetic semiconductor CrMoI₆. Wuli Xuebao/Acta Physica Sinica, 2021, 70, 207301.	0.2	2
42360	Structure prediction of CuBiI ternary compound and first-principles study of photoelectric properties. Wuli Xuebao/Acta Physica Sinica, 2021, 70, 207305.	0.2	0
42361	Prediction of an Al₄C₄ superatom organic framework (SOF) material based on the superatom network model. Physical Chemistry Chemical Physics, 2021, 23, 24294-24300.	1.3	3
42362	Phase-junction engineering boosts the performance of CoSe₂ for efficient sodium/potassium storage. Journal of Materials Chemistry A, 2021, 9, 25954-25963.	5.2	30
42363	A MnS/FeS₂ heterostructure with a high degree of lattice matching anchored into carbon skeleton for ultra-stable sodium-ion storage. Journal of Materials Chemistry A, 2021, 9, 24024-24035.	5.2	38
42364	Insight into the Fischerâ€“Tropsch mechanism on hcp-Fe7C3 (211) by density functional theory: the roles of surface carbon and vacancies. RSC Advances, 2021, 11, 34533-34543.	1.7	4
42365	Performance Investigation of p-FETs Based on Highly Air-Stable Monolayer Pentagonal PdSe₂. IEEE Transactions on Electron Devices, 2021, 68, 6551-6557.	1.6	6
42366	First-principles investigation of structural and electronic properties of Tl_xAl_{1â^'x}P ternary alloys. Journal of Taibah University for Science, 2021, 15, 486-492.	1.1	1
42367	Two-dimensional FeTe₂ and predicted Janus FeXS (X: Te and Se) monolayers with intrinsic half-metallic character: tunable electronic and magnetic properties via strain and electric field. Physical Chemistry Chemical Physics, 2021, 23, 24336-24343.	1.3	44
42368	Two-dimensional layered type-II MS₂/BiOCl (M = Zr, Hf) van der Waals heterostructures: promising photocatalysts for hydrogen generation. New Journal of Chemistry, 2021, 45, 20365-20373.	1.4	12
42369	Construction of frustrated Lewis pairs on carbon nitride nanosheets for catalytic hydrogenation of acetylene. Physical Chemistry Chemical Physics, 2021, 23, 24349-24356.	1.3	14
42370	Theoretical insight into the interaction on Ni and Cu surfaces for HMF hydrogenation: a density functional theory study. New Journal of Chemistry, 2021, 45, 21543-21552.	1.4	3
42371	Stabilizing electrodeâ€“electrolyte interfaces to realize high-voltage Li||LiCoO₂ batteries by a sulfonamide-based electrolyte. Energy and Environmental Science, 2021, 14, 6030-6040.	15.6	84

#	Article	IF	Citations
42372	Calculating the adsorption energy of a charged adsorbent in a periodic metallic system â€“ the case of BH₄^{â¯} hydrolysis on the Ag(111) surface. Physical Chemistry Chemical Physics, 2021, 23, 25667-25678.	1.3	12
42373	Direct MoB MBene domain formation in magnetron sputtered MoAlB thin films. Nanoscale, 2021, 13, 18077-18083.	2.8	18
42374	How to extract adsorption energies, adsorbateâ€“adsorbate interaction parameters and saturation coverages from temperature programmed desorption experiments. Physical Chemistry Chemical Physics, 2021, 23, 24396-24402.	1.3	1
42375	First principles simulations of microscopic mechanisms responsible for the drastic reduction of electrical deactivation defects in Se hyperdoped silicon. Physical Chemistry Chemical Physics, 2021, 23, 24699-24710.	1.3	2
42376	Tuning the Electronic Structure of Monolayer MgI2 by Biaxial Strain and External Electric Field. Modern Physics, 2021, 11, 99-108.	0.1	1
42377	Understanding stress-induced disorder and breakage in organic crystals: beyond crystal structure anisotropy. Chemical Science, 2021, 12, 14270-14280.	3.7	5
42378	Understanding the role of axial O in CO₂ electroreduction on NiN₄ single-atom catalysts via simulations in realistic electrochemical environment. Journal of Materials Chemistry A, 2021, 9, 23515-23521.	5.2	45
42379	First-Principles Study of Adsorption of Hazardous Atoms on the Silica Surface. , 0, , .		0
42380	Stability and structural properties of vacancy-ordered and -disordered ZrC_x. RSC Advances, 2021, 11, 32573-32589.	1.7	6
42381	Ferroelectricity in Novel One-Dimensional P42-Insel Nanowire. SSRN Electronic Journal, 0, , .	0.4	0
42382	Two-dimensional polarized MoTe₂/GeS heterojunction with an intrinsic electric field for photocatalytic water-splitting. RSC Advances, 2021, 11, 34048-34058.	1.7	11
42383	First-Principles Prediction of Pressure Dependent Mechanical, Electronic, Optical, and Superconducting State Properties of NaC6: A Potential High-Tc Superconductor. SSRN Electronic Journal, 0, , .	0.4	0
42384	Pressure-induced orderâ€“disorder transitions in Î²-In₂S₃: an experimental and theoretical study of structural and vibrational properties. Physical Chemistry Chemical Physics, 2021, 23, 23625-23642.	1.3	3
42385	Effect of adsorption and substitutional B doping at different concentrations on the electronic and magnetic properties of a BeO monolayer: a first-principles study. Physical Chemistry Chemical Physics, 2021, 23, 24922-24931.	1.3	26
42386	Assessing cathode property prediction via exchange-correlation functionals with and without long-range dispersion corrections. Physical Chemistry Chemical Physics, 2021, 23, 24726-24737.	1.3	8
42387	Facilitating room-temperature oxygen ion migration via Coâ€“O bond activation in cobaltite films. Nanoscale, 2021, 13, 18256-18266.	2.8	8
42388	Structural study and evaluation of thermoelectric properties of single-phase isocubanite (CuFe₂S₃) synthesized via an ultra-fast efficient microwave radiation technique. Sustainable Energy and Fuels, 2021, 5, 5804-5813.	2.5	6
42389	Predictions of attainable compositions of layered quaternary i-MAB phases and solid solution MAB phases. Nanoscale, 2021, 13, 18311-18321.	2.8	12

#	Article	IF	Citations
42390	Unidirectional Alignment of AgCN Microwires on Distorted Transition Metal Dichalcogenide Crystals. ACS Applied Materials & Interfaces, 2021, 13, 8727-8735.	4.0	3
42391	Electronic Structure of Anode Material Li₂TiSiO₅ and Its Structural Evolution during Lithiation. Journal of Physical Chemistry C, 2021, 125, 3733-3744.	1.5	3
42392	The compatibility between environmental-friendly insulation gas C₄F₇N with alumina and zinc oxide: A comparative study. , 2021, , .		1
42393	Selenium Doped Hafnium Disulfide Alloy for Visible Photodetection. , 2021, , .		0
42394	A DFT Investigation on the Electronic Structures and Au Adatom Assisted Hydrogenation of Graphene Nanoflake Array. Chemical Research in Chinese Universities, 2021, 37, 1110-1115.	1.3	2
42395	Application of Computational Chemistry for Contaminant Adsorption on the Components of Soil Surfaces. , 2022, , 171-213.		2
42396	Hybrid Metalâ€“Boron Diatomic Site Embedded in C₂N Monolayer Promotes Câ€“C Coupling in CO₂ Electroreduction. Small, 2021, 17, e2104445.	5.2	46
42397	Ferroelectric Controlled Spin Texture in Two-Dimensional NbOI2 Monolayer. Chinese Physics Letters, 2021, 38, 087702.	1.3	7
42398	Effective Screening Route for Highly Active and Selective Metalâ^'Nitrogenâ€Doped Carbon Catalysts in CO₂ Electrochemical Reduction. Small, 2021, 17, e2103705.	5.2	12
42399	Two-dimensional porous graphitic carbon nitride C6N7 monolayer: First-principles calculations. Applied Physics Letters, 2021, 119, .	1.5	57
42400	Adsorption and gas-sensing properties of Pdn-GaNNTs to C2H2 and H2 gases. Physica E: Low-Dimensional Systems and Nanostructures, 2022, 136, 115004.	1.3	9
42401	Structural Dynamics and Thermal Transport in Bismuth Chalcogenide Alloys. Chemistry of Materials, 2021, 33, 8404-8417.	3.2	10
42402	Enhanced dielectric stability and coercivity of band gap tuned Baâ€“Al Co-doped bismuth ferrite: An experimental and DFT+U investigation. Ceramics International, 2022, 48, 3404-3416.	2.3	12
42403	Activity Origins of Graphdiyne Based Bifunctional Atom Catalysts for Hydrogen Evolution and Water Oxidation. Chemical Research in Chinese Universities, 2021, 37, 1334-1340.	1.3	4
42404	Atomistic Insights into the Reformation of CH₄ with CO₂ on Metal-Free gC₃N₄: Unraveling the Reaction Mechanisms Using First-Principles DFT Calculations. Journal of Physical Chemistry C, 2021, 125, 23021-23028.	1.5	7
42405	Oxygen (O2) reduction reaction on Ba-doped LaMnO3 cathodes in solid oxide fuel cells: a density functional theory study. Materials for Renewable and Sustainable Energy, 2021, 10, 1.	1.5	0
42406	d- and s-orbital populations in the d block: unbound atoms in physical vacuum versus chemical elements in condensed matter. A Dronskowski-population analysis. Zeitschrift Fur Naturforschung - Section B Journal of Chemical Sciences, 2021, 76, 547-557.	0.3	0
42407	Role of organic cation orientation in formamidine based perovskite materials. Scientific Reports, 2021, 11, 20433.	1.6	11

#	Article	IF	Citations
42408	Neural network-based order parameter for phase transitions and its applications in high-entropy alloys. Nature Computational Science, 2021, 1, 686-693.	3.8	14
42409	Janus monolayer transition-metal dichalcogenides: Ferroelectric, piezoelectric, and electronic properties of the Janus <mml:math xmlns:mml="http://www.w3.org/1998/Math/MathML"><mml:mrow><mml:mi>Bi</mml:mi><mml:mi>X</mml:mi><mml:mi>Y</mml:mi><mml:m		

#	Article	IF	Citations
42426	Experimental studies and DFT calculations to predict atomic arrangements at twin boundaries and distribution behaviors of different solutes in complex intermetallics. Journal of Physics and Chemistry of Solids, 2022, 161, 110453.	1.9	4
42427	Refractive indexÂof graphene AA and AB stacked bilayers under the influence of relative planar twisting. Journal of Physics Condensed Matter, 2022, 34, 015302.	0.7	3
42428	Breaking the Linear Scaling Relationship by a Proton Donor for Improving Electrocatalytic Oxygen Reduction Kinetics. ACS Catalysis, 2021, 11, 12712-12720.	5.5	4
42429	Air-Stable and Layer-Dependent Ferromagnetism in Atomically Thin van der Waals CrPS₄. ACS Nano, 2021, 15, 16904-16912.	7.3	34
42430	Electronic, Optical, and Thermoelectric Properties of Bulk and Monolayer Germanium Tellurides. Crystals, 2021, 11, 1290.	1.0	5
42431	High-Pressure Behavior and Disorder for Ag₂ZnSnS₄ and Ag₂CdSnS₄. ACS Omega, 2021, 6, 27387-27395.	1.6	3
42432	Facile Synthesis of Palladiumâ€Based Nanocrystals with Different Crystal Phases and a Comparison of Their Catalytic Properties. Advanced Materials, 2021, 33, e2103801.	11.1	18
42433	Deprotonating Melamine to Gain Highly Interconnected Materials: Melaminate Salts of Potassium and Rubidium. Inorganic Chemistry, 2021, 60, 15069-15077.	1.9	3
42434	Layered Dionâ€“Jacobson-Type Chalcogenide Perovskite CsLaM₂X₇ (M = Ta/Nb; X) Tj ETQq0 0 0 rgBT /Overlo ACS Applied Materials & Interfaces, 2021, 13, 48971-48980.	4.0	3
42435	Structureâ€“Compositionâ€“Property Relationships in Antiperovskite Nitrides: Guiding a Rational Alloy Design. ACS Applied Materials & Interfaces, 2021, 13, 48516-48524.	4.0	14
42436	Coherence control of directional nonlinear photocurrent in spatially symmetric systems. Physical Review B, 2021, 104, .	1.1	11
42437	Toward Targeted Kinetic Trapping of Organicâ€“Inorganic Interfaces: A Computational Case Study. ACS Physical Chemistry Au, 2022, 2, 38-46.	1.9	4
42438	Microscopic theory for the incoherent resonant and coherent off-resonant optical response of tellurium. Physical Review B, 2021, 104, .	1.1	8
42439	Heteroanionic Ruddlesden-Popper ferroelectrics from anion order and octahedral tilts. Physical Review Materials, 2021, 5, .	0.9	0
42440	Elemental Topological Dirac Semimetal Î±â€Sn with High Quantum Mobility. Advanced Materials, 2021, 33, e2104645.	11.1	12
42441	Understanding the roles of carbon in carbon/g-C3N4 based photocatalysts for H2 evolution. Nano Research, 0, , 1.	5.8	9
42442	Electronic properties and quasiparticle model of monolayer <mml:math xmlns:mml="http://www.w3.org/1998/Math/MathML"><mml:msub><mml:mrow><mml:mi>MoSi</mml:mi></mml:mrow><mml:mn>2</ mathvariant="normal">N</mml:mi></mml:mrow><mml:mn>4</mml:mn></mml:msub></mml:math>. Physical Review B, 2021, 104, .	1.1	17
42443	Feâ€“N System at High Pressures and Its Relevance to the Earthâ€™s Core Composition. Crystal Growth and Design, 0, , .	1.4	2

#	Article	IF	Citations
42444	Competing magnetic interactions and magnetocaloric effect in Ho₅Sn₃. Journal of Physics Condensed Matter, 2022, 34, 025801.	0.7	2
42445	Magnetic structure of the topological semimetal <mml:math xmlns:mml="http://www.w3.org/1998/Math/MathML"><mml:msub><mml:mi>YbMnSb</mml:mi><mml:mn>2</mml:mn></mml:msub> Physical Review B, 2021, 104, .	1.1	8
42446	Design of a Stable Heusler Alloy with Switchable Metalâ€toâ€Halfâ€Metal Transition at Finite Temperature. Advanced Theory and Simulations, 2021, 4, 2100311.	1.3	6
42447	Octahedral rotations in Ruddlesden-Popper layered oxides under pressure from first principles. Physical Review B, 2021, 104, .	1.1	4
42448	Defect Configurations and Ionization Energies of Carbon Vacancies, Hydrogen, Boron and Their Complexes in Diamond. Journal of Electronic Materials, 2021, 50, 6888-6896.	1.0	2
42449	Quantifying Temperature Dependence of Electronic Band Gaps and Optical Properties in SnO₂ and SnO via First-Principles Simulations. Journal of Physical Chemistry C, 2021, 125, 22231-22238.	1.5	9
42450	First-principles modeling of conductivity at the (001), (110), and (111) <mml:math xmlns:mml="http://www.w3.org/1998/Math/MathML"><mml:mrow><mml:msub><mml:mi>SrTiO</mml:mi><mml:mn>3</mml:mn> heterointerfaces. Physical Review B, 2021, 104, .	1.1	0
42451	First-Principle Study of Rh-Doped Nitrogen Vacancy Boron Nitride Monolayer for Scavenging and Detecting SF6 Decomposition Products. Polymers, 2021, 13, 3507.	2.0	3
42452	Crystal engineering of supramolecular 1,4â€benzene bisamides by side chain modification â€towards tuneable anisotropic morphologies and surfaces. ChemPhysChem, 2021, 22, 2585.	1.0	2
42453	Discovering Low-Electron-Affinity Semiconductors for Junction Partners of Photovoltaic BaSi₂ by Database Screening and First Principles Calculations. Journal of Physical Chemistry C, 2021, 125, 24310-24317.	1.5	5
42454	2D Molybdenum Carbide MXenes for Enhanced Selective Detection of Humidity in Air. Advanced Materials, 2021, 33, e2104878.	11.1	46
42455	Phase stability, band gap engineering and optical response of Li-, Be- and Mg-doped SrZrO3 perovskite: Theoretical perspective with GGA-PBE. European Physical Journal Plus, 2021, 136, 1.	1.2	5
42456	Multiple spintronic functionalities into single zinc-ferrous ferrite thin films. Journal of Alloys and Compounds, 2022, 895, 162425.	2.8	4
42457	Experimental and Theoretical Investigations of Terahertz Spectra of the Structural Isomers: Mannose and Galactose. Journal of Spectroscopy, 2021, 2021, 1-9.	0.6	3
42458	Threshold voltage modulation in monolayer MoS2 field-effect transistors via selective gallium ion beam irradiation. Science China Materials, 2022, 65, 741-747.	3.5	5
42459	A firstâ€principles prediction of thermophysical and thermoelectric performances of <scp> SrCeO ₃ </scp> perovskite. International Journal of Energy Research, 2022, 46, 2934-2946.	2.2	17
42460	Lattice dynamics of photoexcited insulators from constrained density-functional perturbation theory. Physical Review B, 2021, 104, .	1.1	8
42461	Point defects in <mml:math xmlns:mml="http://www.w3.org/1998/Math/MathML"><mml:mrow><mml:mi>p</mml:mi></mml:mrow></mml:math> -type transparent conductive <mml:math xmlns:mml="http://www.w3.org/1998/Math/MathML"><mml:mrow><mml:mi>Cu</mml:mi><mml:mi>M</mml:mi></mml:mrow><mml:m	1.1	0

#	Article	IF	Citations
42462	Confined Monolayer Ice Between CaF2 (111) and Graphene: Structure and Stability. Frontiers in Physics, 2021, 9, .	1.0	0
42463	Predicting Li-Rich Layered Oxide Compounds as High-Conductivity and Stable Solid Electrolytes. ACS Energy Letters, 2021, 6, 3793-3800.	8.8	5
42465	Hybrid Metalâ€Halide Infrared Nonlinear Optical Crystals of (TMEDA)MI₅ (M = Sb, Bi) with High Stability. Advanced Optical Materials, 2021, 9, 2101333.	3.6	20
42466	Probing defects and their implications in pH-controlled ZnO QDs: a theory-aided experimental investigation. Journal of Materials Science: Materials in Electronics, 2021, 32, 27084-27096.	1.1	2
42467	Defect-mediated ferromagnetism in correlated two-dimensional transition metal phosphorus trisulfides. Science Advances, 2021, 7, eabj4086.	4.7	35
42468	Electronic structure of molecular hydrogen in MoS₂ nanopores. Journal of Physics Condensed Matter, 2022, 34, 044005.	0.7	1
42469	Quasi-layered Crystal Structure Coupled with Point Defects Leading to Ultralow Lattice Thermal Conductivity in n-Type Cu_{2.83}Bi₁₀Se₁₆. ACS Applied Energy Materials, 2021, 4, 11325-11335.	2.5	5
42470	Promising Properties of a Sub-5-nm Monolayer <mml:math xmlns:mml="http://www.w3.org/1998/Math/MathML" display="inline" overflow="scroll"><mml:msub><mml:mrow><mml:mi>Mo</mml:mi><mml:mi>Si</mml:mi></mml:mrow><mml:mrow><mml:mn>2</mml:mn></mml:mrow></mml:msub><mml:msub><mml:mrow><mml:mi mathvariant="normal">N</mml:mi></mml:mrow><mml:mrow><mml:mn>4</mml:mn></mml:mrow></mml:msub></mml:math> Transistor. Physical Review Applied, 2021, 16, .	4.6	39
42471	First-principles study of Suzuki segregation at stacking faults in disordered face-centered cubic Co-Ni alloys. Acta Materialia, 2021, 221, 117358.	3.8	9
42472	Incorporation of Iron(II) and (III) in Hydroxyapatiteâ€”A Theoretical Study. Crystals, 2021, 11, 1219.	1.0	10
42473	Silica-Confined Two-Atom Single-Cluster Catalyst for Direct Nonoxidative Conversion of Methane: A DFT Study. Journal of Physical Chemistry C, 2021, 125, 23212-23218.	1.5	3
42474	Electronic structure, magnetic and structural properties of binary cubic C15 Laves phases PrX2 (Xâ€‰=â€‰Co) Tj ETQq1 1 0.784314	1.1	7
42475	Origins of bandgap bowing character in the common-anion transition-metal-dichalcogenide ternary alloyed monolayer: ab initio investigation. New Journal of Physics, 2021, 23, 103027.	1.2	7
42476	Roomâ€Temperature Onâ€Spinâ€Switching and Tuning in a Porphyrinâ€Based Multifunctional Interface. Small, 2021, 17, e2104779.	5.2	19
42477	Mesoporous Nâ€“P Codoped Carbon Nanosheets as Superior Cathodic Catalysts of Neutral Metalâ€“Air Batteries. Langmuir, 2021, 37, 12616-12628.	1.6	11
42478	Structural, Mechanical, Electronic and Optical Properties of KNaY (Y = S, Se and Te) as Ferroelectric Compounds. ECS Journal of Solid State Science and Technology, 2021, 10, 103012.	0.9	1
42479	High-Pressure Synthesis of Bulk Cobalt Cementite, Co₃C. Chemistry of Materials, 2021, 33, 9601-9607.	3.2	2
42480	Zero valence iron nanocube decoration of graphitic nanoplatelets. Nanotechnology, 2022, 33, 025704.	1.3	0

#	Article	IF	Citations
42481	The interaction of hydrogen with heteroatoms (B, N)-doped porous graphene: A computational study. Chemical Papers, 2022, 76, 1009-1017.	1.0	0
42482	Determination of the Cohesive Properties and Sublimation Temperatures of Glycine Polymorphs. Crystal Growth and Design, 2021, 21, 6266-6275.	1.4	2
42483	Designing orderâ€“disorder transformation in high-entropy ferritic steels. Journal of Materials Research, 2022, 37, 136-144.	1.2	3
42484	Mechanism and Prediction of Hydrogen Embrittlement in fcc Stainless Steels and High Entropy Alloys. Physical Review Letters, 2021, 127, 175501.	2.9	20
42485	AA _h BN crystal, basic structure of boron nitride nanotubes. IUCrJ, 2021, 8, 1018-1023.	1.0	1
42486	Epitaxial strain effect on the band gap of a Ga2O3 wide bandgap material. Journal of the Korean Physical Society, 2021, 79, 946-952.	0.3	2
42487	Fabrication of a NiFe Alloy Oxide Catalyst via Surface Reconstruction for Selective Hydrodeoxygenation of Fatty Acid to Fatty Alcohol. ACS Sustainable Chemistry and Engineering, 2021, 9, 15027-15041.	3.2	12
42488	Understanding the efficacy of concentrated interstitial carbon in enhancing the pitting corrosion resistance of stainless steel. Acta Materialia, 2021, 221, 117433.	3.8	24
42489	Theoretical analysis of reversible phase evolution in Li-ion conductive halides. Applied Surface Science, 2022, 574, 151621.	3.1	2
42490	Artificial solid-electrolyte interface facilitating uniform Zn deposition by promoting chemical adsorption. Science China Materials, 2022, 65, 663-674.	3.5	14
42491	Platinum Deposited Nitrogen-Doped Vertically Aligned Carbon Nanofibers as Methanol Tolerant Catalyst for Oxygen Reduction Reaction with Improved Durability. Applied Nano, 2021, 2, 303-318.	0.9	3
42492	Two-dimensional monolayer B2P6 with anisotropic elastic properties and carrier mobility. Vacuum, 2022, 195, 110651.	1.6	9
42493	The Surface and Interface Effects on the CoS2-FeS2 Interfacial Films. Journal of Superconductivity and Novel Magnetism, 2021, 34, 2983-2998.	0.8	0
42494	Two-dimensional Dirac half-metal in porous carbon nitride C₆N₇ monolayer via atomic doping. Nanotechnology, 2022, 33, 075707.	1.3	18
42495	Microstructure and electronic properties of La2Ti2O7 thin films on SrTiO3 substrates. Applied Surface Science, 2021, , 151599.	3.1	0
42496	Constructing a new 2D Janus black phosphorus/SMoSe heterostructure for spontaneous wide-spectral-responsive photocatalytic overall water splitting. International Journal of Hydrogen Energy, 2021, 46, 39183-39194.	3.8	17
42497	Simulation and Computer Study of Structures and Physical Properties of Hydroxyapatite with Various Defects. Nanomaterials, 2021, 11, 2752.	1.9	23
42498	Cs adsorption characteristics on Î²-Ga_{1.9375}Mg_{0.0625}O₃ (100) surface: the first principles calculation investigation. Ferroelectrics, 2021, 582, 171-184.	0.3	0

#	Article	IF	Citations
42499	Grafting of organic molecular precursors onto ZrC(100)//t-ZrO2(001) surfaces: When experimental and theoretical studies meet. Applied Surface Science, 2022, 576, 151622.	3.1	3
42500	Band gap engineering of 2D biphenylene carbon sheets with hydrogenation. Journal of the Korean Physical Society, 2021, 79, 846-850.	0.3	11
42501	Critical Role of Interfacial Charge Transfer in Reducing Charge Potential of Liâ€“O2 Battery. Journal of Physical Chemistry C, 0, , .	1.5	1
42502	Promising 2D/2D MoTe₂/Ti₃C₂T_x Hybrid Materials for Boosted Hydrogen Evolution Reaction. ACS Applied Energy Materials, 2021, 4, 11886-11897.	2.5	29
42503	Strain induced electronic transition in 1Tâ€²â€‰MoTe₂: high pressure Raman, x-ray diffraction, resistivity measurements and first principles theoretical studies. Electronic Structure, 2021, 3, 045002.	1.0	3
42504	Boron adsorption and its effect on stability and CO activation of Ï‡-Fe5C2 catalyst: An ab initio DFT study. Applied Catalysis A: General, 2021, 627, 118382.	2.2	2
42505	Pressure-induced ferromagnetism in the topological semimetal <mml:math xmlns:mml="http://www.w3.org/1998/Math/MathML"><mml:mrow><mml:mi>Eu</mml:mi><mml:msub><mml:mi>Cd</mml:mi><mml:m Physical Review B, 2021, 104, .	3.7	21
42506	Enhanced Thermoelectric Performance of Polycrystalline Si0.8Ge0.2 Alloys through the Addition of Nanoscale Porosity. Nanomaterials, 2021, 11, 2591.	1.9	7
42507	Electronâ€“phonon interaction and superconductivity in hexagonal ternary carbides Nb₂AC (A: Al, S, Ge, As and Sn). Electronic Structure, 2021, 3, 045001.	1.0	5
42508	Study of dynamic and thermodynamic properties of zinc-blend and wurtzite cadmium sulfide (CdS) using density functional theory. Zeitschrift Fur Naturforschung - Section A Journal of Physical Sciences, 2022, 77, 171-179.	0.7	0
42509	Short-range order in SiSn alloy enriched by second-nearest-neighbor repulsion. Physical Review Materials, 2021, 5, .	0.9	3
42510	Ab initio Investigation of Impurity Ferromagnetism in the Pd1âˆ’xFex Alloys: Concentration and Position Dependences. Crystals, 2021, 11, 1257.	1.0	1
42511	Interface properties of CsPbBr<mml:math xmlns:mml="http://www.w3.org/1998/Math/MathML" display="inline" id="d1e253" altimg="si29.svg"><mml:msub><mml:mrow /><mml:mrow><mml:mn>3</mml:mn></mml:mrow></mml:msub></mml:math>/CsPbI<mml:math xmlns:mml="http://www.w3.org/1998/Math/MathML" display="inline" id="d1e261" altimg="si29.svg"><mml:msub><mml:mrow /><mml:mrow><mml:mn>3</mml:mn></mml:mrow></mml:msub></mml:math> perovskite heterostructu	1.3	5
42512	Two-dimensional conducting states in infinite-layer oxide/perovskite oxide hetero-structures. Journal of Physics Condensed Matter, 2022, 34, 035003.	0.7	0
42513	Enhanced Thermoelectric Performance Achieved in SnTe via the Synergy of Valence Band Regulation and Fermi Level Modulation. ACS Applied Materials & Interfaces, 2021, 13, 50037-50045.	4.0	18
42514	Nonaqueous Solvent Adsorption on Transition Metal Surfaces with Density Functional Theory: Interaction of N,N-Dimethylformamide (DMF), Tetrahydrofuran (THF), and Dimethyl Sulfoxide (DMSO) with Ag, Cu, Pt, Rh, and Re Surfaces. Journal of Physical Chemistry C, 2021, 125, 21943-21957.	1.5	5
42515	Ga-doped Pd/CeO<mml:math xmlns:mml="http://www.w3.org/1998/Math/MathML" display="inline" id="d1e727" altimg="si34.svg"><mml:msub><mml:mrow /><mml:mrow><mml:mn>2</mml:mn></mml:mrow></mml:msub></mml:math> model catalysts for CO oxidation reactivity: A density functional theory study. Applied Surface Science, 2022, 575, 151655.	3.1	23
42516	Effect of excess Mg to control corrosion in molten MgCl2 and KCl eutectic salt mixture. Corrosion Science, 2022, 194, 109914.	3.0	16

#	Article	IF	Citations
42517	The effect of shape and size in the stability of triangular Janus MoSSe quantum dots. Scientific Reports, 2021, 11, 21061.	1.6	7
42518	Dimension-Dependent Bandgap Narrowing and Metallization in Lead-Free Halide Perovskite Cs3Bi2X9 (X) Tj ETQq1 1 0.784314 rgBT	1.9	12
42519	Spin-Injection Enhancements in van der Waals Magnetic Tunnel Junctions through Barrier Engineering. Physical Review Applied, 2021, 16, .	1.5	0
42520	Structureâ€“Property Relationships in Transition Metal Dichalcogenide Bilayers under Biaxial Strains. Nanomaterials, 2021, 11, 2639.	1.9	4
42521	Impact of Disorder on Properties of Vacancies: A Case Study of B2 and A2 Polymorphs of Non-Stoichiometric Fe2CoAl. Crystals, 2021, 11, 1207.	1.0	3
42522	Strong interlayer interaction in two-dimensional layered PtTe2. Journal of Solid State Chemistry, 2022, 305, 122657.	1.4	3
42523	Capturing polysulfides by sulfurizedâ€polyacrylonitrile in lithiumâ€sulfur batteries and the sulfurâ€chain effects through Density Functional Theory. Electrochemical Science Advances, 2022, 2, .	1.2	2
42524	3D Porous Metallic Boron Carbide Crystal Structure with Excellent Ductility. Advanced Theory and Simulations, 2021, 4, 2100325.	1.3	3
42525	Adhesion strength, stability and electronic properties of TiB2 reinforced copper matrix composites: A first principles study. Physica B: Condensed Matter, 2021, , 413457.	1.3	1
42526	Computational study of electronic properties of X-doped hexagonal boron nitride (h-BN): Xâ€‰=â€‰(Li, Be, Al,) Tj ETQq1 1 0.784314	0.8	4
42527	Role of R-f states on electronic structure and thermoelectric performance of RNiSb (Râ€‰=â€‰Gd, Er and Lu) half Heusler compounds: narrow gap thermoelectric materials. Applied Physics A: Materials Science and Processing, 2021, 127, 1.	1.1	5
42528	Design of less than 1Ânm Scale Spaces on SnO₂ Nanoparticles for Highâ€Performance Electrochemical CO₂ Reduction. Advanced Functional Materials, 2022, 32, 2107349.	7.8	23
42529	InP₃ Monolayer as a Promising 2D Sensing Material in SF₆ Insulation Devices. ACS Omega, 2021, 6, 29752-29758.	1.6	3
42530	Pressure effects on structure, mechanical properties and thermal conductivity of V₂SnC: a first-principles study. Philosophical Magazine, 2022, 102, 228-243.	0.7	4
42531	Influence of anharmonicity and interlayer interaction on Raman spectra in mono- and few-layer MoS2: A computational study. Physica E: Low-Dimensional Systems and Nanostructures, 2022, 136, 114999.	1.3	9
42532	Ultrathin epitaxial Bi film growth on 2D HfTe2 template. Nanotechnology, 2021, 33, .	1.3	1
42533	Screening and Understanding Li Adsorption on Two-Dimensional Metallic Materials by Learning Physics and Physics-Simplified Learning. Jacs Au, 2021, 1, 1904-1914.	3.6	12
42534	Atomically Dispersed Tin-Modified Î³-alumina for Selective Propane Dehydrogenation under H₂S Co-feed. ACS Catalysis, 2021, 11, 13472-13482.	5.5	8

#	Article	IF	Citations
42535	Efficient Iron Phosphide Catalyst as a Counter Electrode in Dye-Sensitized Solar Cells. ACS Applied Energy Materials, 2021, 4, 10618-10626.	2.5	39
42536	Structural and electronic properties of zigzag single wall (8,0), (9,0), and (10,0) silicon carbide nanotubes. Materialia, 2021, 20, 101257.	1.3	4
42537	A density functional theory approach to the effects of C and N substitution at the B-site of the first boride MAX phase Nb2SB. Materials Today Communications, 2021, 29, 102910.	0.9	6
42538	Wake-up Free Ferroelectric Rhombohedral Phase in Epitaxially Strained ZrO₂ Thin Films. ACS Applied Materials & Interfaces, 2021, 13, 51383-51392.	4.0	23
42539	Operando visualization of the hydrogen evolution reaction with atomic-scale precision at different metalâ€“graphene interfaces. Nature Catalysis, 2021, 4, 850-859.	16.1	81
42540	Band gap engineering of amine functionalized Ag(I)-based coordination polymers and their plasmonic Ag0 coupled novel visible light driven photo-redox system for selective oxidation of benzyl alcohol. Applied Catalysis B: Environmental, 2022, 303, 120821.	10.8	6
42541	Syntheses, Structures and Properties of Alkali and Alkaline Earth Metal Diamond-Like Compounds Li2MgMSe4 (M = Ge, Sn). Materials, 2021, 14, 6166.	1.3	6
42542	Conversion of CO₂ into Formic Acid on Transition Metal-Porphyrin-like Graphene: First Principles Calculations. ACS Omega, 2021, 6, 27045-27051.	1.6	3
42543	Synthesis, Characterisation, and Density Functional Theory Study of Encapsulated Bioactive Components of Ginger. Pertanika Journal of Science and Technology, 2021, 29, .	0.3	0
42544	GaSeCl₅O: A Molecular Compound with Very Strong SHG Effect. Inorganic Chemistry, 2021, 60, 15653-15658.	1.9	11
42545	Computational Study of A15 Ru-Based Alloys for High-Temperature Structural Applications. , 0, , .		0
42546	Tendencies in ABO3 Perovskite and SrF2, BaF2 and CaF2 Bulk and Surface F-Center Ab Initio Computations at High Symmetry Cubic Structure. Symmetry, 2021, 13, 1920.	1.1	30
42547	Engineering Oxidation States of a Platinum Cocatalyst over Chemically Oxidized Graphitic Carbon Nitride Photocatalysts for Photocatalytic Hydrogen Evolution. ACS Sustainable Chemistry and Engineering, 2021, 9, 14537-14549.	3.2	30
42548	Engineering Oxidation States of a Platinum Cocatalyst over Chemically Oxidized Graphitic Carbon Nitride Photocatalysts for Photocatalytic Hydrogen Evolution. ACS Sustainable Chemistry and Engineering, 2021, 9, 14537-14549. <mml:math xmlns:mml="http://www.w3.org/1998/Math/MathML" altimg="si24.svg"><mml:mrow><mml:msup><mml:mrow><mml:mo stretchy="false">(</mml:mo><mml:mi>ï‡</mml:mi></mml:mrow><mml:mfenced open="(") Tj ETQq1 1 0.784314 rgBT /Overlock 10 T	3.2	30
42549	Schottky Heterojunction Nanosheet Array Achieving Highâ€Currentâ€Density Oxygen Evolution for Industrial Water Splitting Electrolyzers. Advanced Energy Materials, 2021, 11, 2102353.	10.2	177
42550	Approaching the basis set limit in Gaussian-orbital-based periodic calculations with transferability: Performance of pure density functionals for simple semiconductors. Journal of Chemical Physics, 2021, 155, 164102.	1.2	14
42551	PbTe(core)/PbS(shell) Nanowire: Electronic Structure, Thermodynamic Stability, and Mechanical and Optical Properties. Journal of Physical Chemistry C, 2021, 125, 22660-22667.	1.5	5
42552	Polarimetric Image Sensor and Fermi Level Shifting Induced Multichannel Transition Based on 2D PdPS. Advanced Materials, 2022, 34, e2107206.	11.1	29

#	Article	IF	Citations
42553	Static isotropic pressure induced ultra-wide band gap response of NaCaF₃ fluoro-perovskite and its repercussions on optical properties: ab initio calculation. Molecular Simulation, 2021, 47, 1549-1557.	0.9	6
42554	Anisotropically large anomalous and topological Hall effect in a kagome magnet. Physical Review B, 2021, 104, .	1.1	23
42555	DFT-Based Approach Enables Deliberate Tuning of Alloy Nanostructure Plasmonic Properties. Journal of Physical Chemistry C, 2021, 125, 24032-24042.	1.5	5
42556	Topological descendants of a multicritical Dirac semimetal with magnetism and strain. Physical Review B, 2021, 104, .	1.1	2
42557	A Novel BN Polymorph in P4/mbm Phase with a (4,4) Nanotube. Physica Status Solidi (B): Basic Research, 2022, 259, 2100333.	0.7	7
42558	Ab-initio study of the structural, optoelectronic, magnetic, hydrogen storage properties and mechanical behavior of novel combinations of hydride perovskites LiXH3 (Xâ€‰=â€‰Cr, Fe, Co, & Zn) for hydrogen storage applications. Journal of Computational Electronics, 2021, 20, 2284-2299.	1.3	18
42559	Relation Between the Local Structure and Solid Solubility of the Layered Material LiMO2 (Mâ€‰=â€‰Co, Ni,) Tj ETQq0 0 0 rgBT /Overl	1.6	2
42560	Investigation of Nonequilibrium Electronic Dynamics of Warm Dense Copper with Femtosecond X-Ray Absorption Spectroscopy. Physical Review Letters, 2021, 127, 175003.	2.9	8
42561	A first-principles study of $${mathrm{Ru}}_{2}mathrm{VGe}$$ full-Heusler alloyâ€”pseudopotential approach. European Physical Journal Plus, 2021, 136, 1.	1.2	3
42562	Pressure-induced superconductivity in Li-Te electrides. Physical Review B, 2021, 104, .	1.1	14
42563	Edge-hosted Fe-N3 sites on a multiscale porous carbon framework combining high intrinsic activity with efficient mass transport for oxygen reduction. Chem Catalysis, 2021, 1, 1291-1307.	2.9	86
42564	Utilizing local phase transformation strengthening for nickel-base superalloys. Communications Materials, 2021, 2, .	2.9	19
42565	Design Principles of Large Cation Incorporation in Halide Perovskites. Molecules, 2021, 26, 6184.	1.7	6
42566	Surface Plasmons in Silicon Nanowires. Advanced Photonics Research, 2021, 2, 2100130.	1.7	3
42567	First-principles calculations of physical properties and superconductivity of orthorhombic Mo2BC and Nb2BN. Journal of Applied Physics, 2021, 130, 153902.	1.1	3
42568	Tuning crystal structure of potassium dihydrogen phosphate at ambient conditions. Physical Review Materials, 2021, 5, .	0.9	1
42569	Probing Magnetic Exchange Interactions with Helium. Physical Review Letters, 2021, 127, 166803.	2.9	1
42570	Unveiling the Atomic and Electronic Structure of Stacked-Cup Carbon Nanofibers. Nanoscale Research Letters, 2021, 16, 153.	3.1	3

#	Article	IF	Citations
42571	Multiorbital model reveals a second-order topological insulator in <mml:math xmlns:mml="http://www.w3.org/1998/Math/MathML"><mml:mrow><mml:mn>1</mml:mn><mml:mi>H</mml:mi></mml:mrow></mml:m transition metal dichalcogenides. Physical Review B, 2021, 104, .	3.7	26
42572	Emerging Yttrium Phosphides with Tetrahedron Phosphorus and Superconductivity under High Pressures. Chemistry - A European Journal, 2021, 27, 17420-17427.	1.7	5
42573	Valence Band Structure Engineering in Graphene Derivatives. Small, 2021, 17, 2104316.	5.2	8
42574	Shear band mediated Ï‰ phase transformation in Nb single crystals deformed at 77â€‰K. Materials Research Letters, 2021, 9, 523-530.	4.1	10
42575	Hydrostatic pressure dependent structural, elastic, vibrational, electronic, and optoelectronic properties of superconducting BaCuO3: A DFT insight. Journal of Physics and Chemistry of Solids, 2022, 161, 110452.	1.9	7
42576	Interface structure characterization and elements doping on interface bonding strength and tensile failure mechanism of NiCo coating/Cu matrix. Results in Physics, 2021, 30, 104883.	2.0	3
42577	Smâ€“Ti binary thermodynamic database and phase diagram. Calphad: Computer Coupling of Phase Diagrams and Thermochemistry, 2021, 75, 102357.	0.7	3
42578	Supercapacitor properties of V10O14(OH)2 and reduced graphene oxide hybrids: Experimental and theoretical insights. Electrochimica Acta, 2021, 399, 139357.	2.6	12
42579	First principles investigation into the interwoven nature of voltage and mechanical properties of the Li<mml:math xmlns:mml="http://www.w3.org/1998/Math/MathML" display="inline" id="d1e95" altimg="si118.svg"><mml:msub><mml:mrow /><mml:mrow><mml:mi>x</mml:mi></mml:mrow></mml:msub></mml:math>NMC-811 cathode. Journal of Power Sources, 2021, 516, 230620.	4.0	10
42580	Detection of hydrogen sulfide using polyaniline incorporated with graphene oxide aerogel. Synthetic Metals, 2021, 282, 116934.	2.1	15
42581	Electronic and magnetic properties in nitrogen-doped 2D titanium carbides (MXenes): Insight from first-principles calculations. Solid State Communications, 2021, 340, 114549.	0.9	7
42582	A novel adsorption-based method for revealing the Si distribution in SAPO molecular sieves: The case of SAPO-11. Microporous and Mesoporous Materials, 2021, 328, 111503.	2.2	5
42583	Potential valorization of granitic waste material as microproppant for induced unpropped microfractures in shale. Journal of Natural Gas Science and Engineering, 2021, 96, 104281.	2.1	4
42584	In-situ quantification and density functional theory elucidation of phase transformation in carbon steel during quenching and partitioning. Acta Materialia, 2021, 221, 117361.	3.8	12
42585	Electronic and optical properties of adsorbed of Zr-atom on vacancy-defective graphene: First principles calculations. Computational and Theoretical Chemistry, 2021, 1206, 113468.	1.1	1
42586	Direct thermal annealing synthesis of FeO nanodots anchored on N-doped carbon nanosheet for long-term electrocatalytic oxygen reduction. Electrochimica Acta, 2021, 398, 139361.	2.6	15
42587	Structural, vibrational, electronic, elastic and thermoelectric properties of monolayer alkali halide compounds from first principles investigation. Materials Today Communications, 2021, 29, 102855.	0.9	4
42588	Phase stability, mechanical, thermal, electronic properties, anisotropy, lattice dynamics and APB -energies of Ti2AlX intermetallics in Î±2, B2, and O phases: A first principle study. Materials Today Communications, 2021, 29, 102864.	0.9	2

#	Article	IF	Citations
42589	AB-INITIO MOLECULAR DYNAMICS SIMULATION OF AMORPHOUS SILICA SURFACE. , 2000, , 371-390.		0
42591	Lattice Trapping of Cracks in Fe Using an Interatomic Potential Derived from Experimental Data and Ab Initio Calculations. Materials Research Society Symposia Proceedings, 2000, 653, 1.	0.1	2
42592	Ab-Initio Calculations on the Structural and Electronic Properties of BaO/BatiO3 And SrO/SrTiO3 Interfaces. , 2002, , 561-571.		0
42593	Modeling Heterogeneous Catalytic Reactions. Fundamental and Applied Catalysis, 2002, , 79-102.	0.9	0
42594	Ab Initio Molecular Dynamical Simulation on H2 Adsorption and Storage in Carbon-Based Materials. , 2002, , 367-384.		0
42596	Theoretical ab initio Calculations of Hyperfine Interactions. Springer Series in Materials Science, 2003, , 309-413.	0.4	0
42597	Quantum Mechanical Studies of Boron Clustering in Silicon. , 2003, , 381-392.		0
42598	Ionic Models. , 2003, , 263-274.		0
42599	Essential Quantum Mechanics. , 2003, , 3-63.		0
42600	Pairwise potentials in simple metals. , 2003, , 158-186.		0
42601	Essential Density Functional Theory. , 2003, , 64-78.		0
42602	Linear Response Theory. , 2003, , 96-126.		1
42603	Tight Binding. , 2003, , 187-252.		0
42604	Exploiting the Variational Principle. , 2003, , 79-95.		1
42605	ãƒ«ãƒêãƒ«ï¼ˆï½‰ï¼‰ï¼ˆï¼‰ï¼ˆï¼‰ï¼ˆï¼‰ï¼‰è¡¨é¢ã®ç”©ç©¶. Hyomen Kagaku, 2004, 25, 548-554.	0.0	2
42606	Optimum designs of additional elements from first-principles simulations. Keikinzoku/Journal of Japan Institute of Light Metals, 2004, 54, 82-89.	0.1	24
42607	The Semiempirical Method for Finding Thermal Characteristics of Simple Crystals. Acta Physica Polonica A, 2004, 106, 487-495.	0.2	1
42608	Phase Separation and Ordering in Cubic Ternary and Quaternary Nitride Alloys. , 2005, , 455-478.		1

#	Article	IF	Citations
42610	Evaluation of Structural and Mechanical Properties of Amorphous Silicon Surabaces by a Combination Approach of Ab-initio and Classical Molecular Dynamics. Zairyo/Journal of the Society of Materials Science, Japan, 2005, 54, 45-50.	0.1	1
42612	Development of a Bond-Order Potential that can Reproduce the Elastic Constants and Melting Point of Silicon. Zairyo/Journal of the Society of Materials Science, Japan, 2006, 55, 1-7.	0.1	1
42613	Conditions and Accuracy for the First-principles Calculation, Sampled k Points, Cutoff Energy, and Pseudopotentials. Hyomen Kagaku, 2007, 28, 135-143.	0.0	5
42614	Electronic Properties and Fragmentation Dynamics of Organic Species Deposited on Silicon Surfaces. Challenges and Advances in Computational Chemistry and Physics, 2007, , 505-532.	0.6	0
42615	First-Principles Atomic-Scale Study of Superlow Friction. Nanoscience and Technology, 2007, , 201-217.	1.5	0
42616	Electronic Band Structure of In_xGa_{1-x}N under Pressure. Acta Physica Polonica A, 2007, 112, 203-208.	0.2	1
42618	SO2 Reaction on Cu(100): SO3 Structure and Formation â€“Density Functional Theory Investigationâ€“. Journal of the Physical Society of Japan, 2008, 77, 084601.	0.7	0
42619	Selected High-Impact Journal Articles on Defects in Microelectronic Materials and Devices. , 2008, , .		2
42621	A First-principles Study on the Effects on Magnetism of Si Impurity in BCC Fe by Considering Spin-orbit Coupling. Journal of the Korean Magnetics Society, 2008, 18, 211-216.	0.0	1
42622	Theory of Defects in Si: Past, Present, and Challenges. Springer Series in Materials Science, 2009, , 61-78.	0.4	0
42623	Electromechanical and Chemical Sensing at the Nanoscale: DFT and Transport Modeling. , 2009, , 47-69.		0
42624	Magnetism of BN Nanotubes with Transition Metal Substitution. Journal of the Korean Magnetics Society, 2009, 19, 43-46.	0.0	0
42625	Design of Heterogeneous Catalysts and the Application to the Oxygen Reduction Reaction. , 2010, , 303-328.		0
42626	Electronic Structure Methods Based on Density Functional Theory. , 2009, , 478-488.		0
42627	First-principles calculations of ZnO polar surfaces and N adsorption mechanism. Wuli Xuebao/Acta Physica Sinica, 2010, 59, 4170.	0.2	6
42628	The mechanism of structure phase transition from Î± Fe to Îµ Fe under uniaxial strain: First-principles calculations. Wuli Xuebao/Acta Physica Sinica, 2010, 59, 4303.	0.2	2
42629	First-principles study of the thermal transport property of Y3Al5O12. Wuli Xuebao/Acta Physica Sinica, 2010, 59, 2697.	0.2	2
42630	Influence of surface effect to the performance of LiMn2O4 cathode material for lithium ion batteries. Wuli Xuebao/Acta Physica Sinica, 2010, 59, 5863.	0.2	3

#	Article	IF	Citations
42631	The study on the electronic structure and optical properties of OsSi2. Wuli Xuebao/Acta Physica Sinica, 2010, 59, 2016.	0.2	9
42632	First-principles study on electronic structure of In-doped wurtzite ZnO. Wuli Xuebao/Acta Physica Sinica, 2010, 59, 4925.	0.2	15
42633	A low coverage investigation on Al adsorption on the (111) surface of Pt, Ir and Au. Wuli Xuebao/Acta Physica Sinica, 2010, 59, 4143.	0.2	4
42634	First-principles study on the band structure and optical properties of strained Ru2Si3 semiconductor. Wuli Xuebao/Acta Physica Sinica, 2010, 59, 2027.	0.2	1
42635	Band structure of Si-based superlattices Si1-xSnx/Si. Wuli Xuebao/Acta Physica Sinica, 2010, 59, 4843.	0.2	1
42637	A First-Principle Study of Oxonium Ylide Mechanism over HSAPO-34 Zeolite. Chinese Journal of Catalysis, 2010, 31, 33-37.	6.9	0
42638	Quantum mechanical study of tungsten carbide nanoparticles. UÄenye Zapiski KomsomolÊ¹skogo-na-Amure Gosudarstvennogo TehniÄeskogo Universiteta, 2010, 1, 86-91.	0.1	0
42639	A Density Functional Theory Study of 2-Chlorothiophene Adsorption on Rh(111) Surface. Chinese Journal of Catalysis, 2010, 31, 49-55.	6.9	0
42641	First-principles calculations of magnetism of Fe atomic sheet. Wuli Xuebao/Acta Physica Sinica, 2011, 60, 047502.	0.2	3
42642	First principles study on structure and property of Si2 CN4(010) surface. Wuli Xuebao/Acta Physica Sinica, 2011, 60, 027302.	0.2	0
42643	Ab initio calculation of pressure-induced phase transition of TiN polytypes. Wuli Xuebao/Acta Physica Sinica, 2011, 60, 057102.	0.2	1
42644	First principles study on half-metallic ferromagnetismof ternary compounds ZnVSe. Wuli Xuebao/Acta Physica Sinica, 2011, 60, 046301.	0.2	0
42645	First principles study of structural, electronic and elastic properties of Mg2 Si polymorphs. Wuli Xuebao/Acta Physica Sinica, 2011, 60, 087105.	0.2	6
42646	Crystal Structure and Electron Density of Imma Perovskite-Type Oxynitride LaTiO2N: Structural Origin of Visible-Light Response. Nihon Kessho Gakkaishi, 2011, 53, 107-112.	0.0	0
42647	Evaluation of the Oxygen Diffusion Coefficient in Nickel-Base Alloys. , 2011, , 1463-1475.		0
42648	Atomic-Scale Investigation on the Ti/Fe(001) Interface Structure: Molecular Dynamics Simulations andAb initioCalculations. Japanese Journal of Applied Physics, 2011, 50, 01BE07.	0.8	0
42650	First-principles calculation and experimental study of Si-doped Î²-Ga2O3. Wuli Xuebao/Acta Physica Sinica, 2011, 60, 037103.	0.2	4
42651	First-principles calculations of electronic structure, optical and elastic properties of LiGaX2(X=S, Se,) Tj ETQq1 1 0.784314 rgBT /Over	0.2	3

#	Article	IF	Citations
42652	Energies, electronic structures and magnetic properties of Ni atomic chain encapsulated in carbon nanotubes: a first-principles calculation. Wuli Xuebao/Acta Physica Sinica, 2011, 60, 078801.	0.2	2
42653	Structure and Bonding of Nanolayered Ternary Phosphides. Materials Sciences and Applications, 2011, 02, 1383-1391.	0.3	2
42654	First principles study of interactions between Au and N atoms on SrTiO3(001) surface. Wuli Xuebao/Acta Physica Sinica, 2011, 60, 056801.	0.2	1
42655	Lattice dynamical, dielectric and thermodynamic properties of LiNH2 from first principles. Wuli Xuebao/Acta Physica Sinica, 2011, 60, 087104.	0.2	2
42656	First-principles study of ordered structures in Ba0.5Sr0.5TiO3. Wuli Xuebao/Acta Physica Sinica, 2011, 60, 097102.	0.2	3
42657	Electronic Structures and Magnetism of Al/Fe(001) Thin-Film Systems: First-Principles Calculations. Japanese Journal of Applied Physics, 2011, 50, 01BF03.	0.8	0
42658	Density-functional theory investigation of atomic geometryand oxygen adsorption of Au(110) surface. Wuli Xuebao/Acta Physica Sinica, 2011, 60, 047301.	0.2	3
42659	A first principles study of the lattice dynamics property of LiFePO4. Wuli Xuebao/Acta Physica Sinica, 2011, 60, 028201.	0.2	5
42660	Influence of natural impurity on electronic structure and catalytic activity of pyrite. Wuli Xuebao/Acta Physica Sinica, 2011, 60, 097801.	0.2	1
42661	The structural stability and electronic properties of monolayer BC2N. Wuli Xuebao/Acta Physica Sinica, 2011, 60, 127305.	0.2	0
42662	Theorectical study of the oxide-ion conductorLa2Mo2-xMxO9(M=Cr,W). Wuli Xuebao/Acta Physica Sinica, 2011, 60, 046603.	0.2	2
42663	Organic-Metal Interface: Adsorption of Cysteine on Au(110) from First Principles. , 2011, , 119-134.		0
42664	Effect of Copper Oxide on Migration and Interaction of Protons in Barium Zirconate. Journal of the Korean Ceramic Society, 2011, 48, 195-199.	1.1	0
42665	Density Functional Study on Correlation between Magnetism and Crystal Structure of Fe-Al Transition Metal Compounds. Journal of the Korean Magnetics Society, 2011, 21, 43-47.	0.0	0
42668	Ab initioPhonons in Magnetic Ni₂MnAl. Japanese Journal of Applied Physics, 2011, 50, 05FE07.	0.8	0
42669	A Study on the Atomic and Electronic Structures of DNA-nucleobases-adsorbed Graphene Through First-principles LCAO Method. Journal of the Korean Institute of Electrical and Electronic Material Engineers, 2011, 24, 510-514.	0.0	0
42670	An Introduction to Linear-Scaling Ab Initio Calculations. , 2012, , 1-35.		0
42671	Structures of Butylthiolate Self-Assembled Monolayers on Au(111) with Gold Adatoms. Bulletin of the Korean Chemical Society, 2011, 32, 3614-3617.	1.0	0

#	Article	IF	Citations
42672	Electron Accumulation in LaAlO3/SrTiO3Interfaces by the Broken Symmetry of Crystal Field. Japanese Journal of Applied Physics, 2011, 50, 10PF03.	0.8	0
42674	Effect of Aluminum on Nitrogen Solubility in Zinc Oxide: Density Functional Theory. Korean Journal of Materials Research, 2011, 21, 639-643.	0.1	0
42675	First principles investigation of interaction between interstitials H atom and Nb metal. Wuli Xuebao/Acta Physica Sinica, 2012, 61, 047105.	0.2	6
42676	Study on the electronic structures and energy band properties of Cd-doped wurtzite BeO. Wuli Xuebao/Acta Physica Sinica, 2012, 61, 177102.	0.2	2
42677	Mechanical Properties of Carbon Nanotubes with One-Dimensional Intramolecular Junction. Zairyo/Journal of the Society of Materials Science, Japan, 2012, 61, 149-154.	0.1	0
42678	First-principles study of nanoscale friction between graphenes. Wuli Xuebao/Acta Physica Sinica, 2012, 61, 106801.	0.2	5
42679	First principles study of the uniaxial compressive strength of bct-C4 carbon allotrope. Wuli Xuebao/Acta Physica Sinica, 2012, 61, 093104.	0.2	3
42680	First-principles study of N-doped and N-V co-doped anatase TiO2. Wuli Xuebao/Acta Physica Sinica, 2012, 61, 207103.	0.2	3
42681	Electronic structure and optical properties of 0.5NdAlO3-0.5CaTiO3 from first-principles calculation. Wuli Xuebao/Acta Physica Sinica, 2012, 61, 077702.	0.2	3
42682	Electronic structure and optical properties of Cs/GaN(0001) adsorption system. Wuli Xuebao/Acta Physica Sinica, 2012, 61, 057102.	0.2	5
42683	First principles study of the elastic, electronic and optical properties of MgS under pressure. Wuli Xuebao/Acta Physica Sinica, 2012, 61, 177104.	0.2	2
42684	First-principles investigations on the electronic, elastic and thermodynamic properties of Cr2MC(M=Al, Ga). Wuli Xuebao/Acta Physica Sinica, 2012, 61, 046301.	0.2	7
42685	Electronic structure and optical properties of (Î±, Î², Î³)-Nb5Si3. Wuli Xuebao/Acta Physica Sinica, 2012, 61, 217101.	0.2	1
42687	Palladium-vacancy pairs in p-type and n-type germanium. , 2012, , 159-166.		0
42688	Cysteine on Gold: An ab-initio Investigation. , 2012, , 105-117.		0
42689	LCAO Calculations of Perfect-Crystal Properties. Springer Series in Solid-state Sciences, 2012, , 357-488.	0.3	0
42690	Ab initio calculation of phase transitions, elastic, and thermodynamic properties of MnPd alloys. Wuli Xuebao/Acta Physica Sinica, 2012, 61, 246201.	0.2	1
42691	Geometric structures and nitrogen adsorption properties of BaO adlayer on Ru(0001) surface. Wuli Xuebao/Acta Physica Sinica, 2012, 61, 136802.	0.2	1

#	Article	IF	Citations
42692	First principles study on the structure and mechanical properties of hcp-C3 carbon bulk ring. Wuli Xuebao/Acta Physica Sinica, 2012, 61, 043103.	0.2	4
42693	First-principles study on the sensitization of small molecule adsorbed on ZnO nanowire. Wuli Xuebao/Acta Physica Sinica, 2012, 61, 063103.	0.2	2
42694	Study on the lattice constants and energy band properties of Be and Ca doped wurtzite ZnO. Wuli Xuebao/Acta Physica Sinica, 2012, 61, 227101.	0.2	4
42695	First principles investigations of the structural stability and thermal dynamical properties of metal Ba under high pressure. Wuli Xuebao/Acta Physica Sinica, 2012, 61, 146301.	0.2	4
42696	First-principles analysis of properties of Cu surfaces. Wuli Xuebao/Acta Physica Sinica, 2012, 61, 016108.	0.2	5
42697	Structural and electronic properties of Al-doped spinel LiMn2O4. Wuli Xuebao/Acta Physica Sinica, 2012, 61, 187306.	0.2	1
42698	Density functional theory study on transparent conductive oxide CuScO2. Wuli Xuebao/Acta Physica Sinica, 2012, 61, 227401.	0.2	2
42699	Stability of hydrogen in tungsten with carbon impurity: a first-principles study. Wuli Xuebao/Acta Physica Sinica, 2012, 61, 046104.	0.2	0
42700	First-principles study of lattice dynamic of IrTi alloy. Wuli Xuebao/Acta Physica Sinica, 2012, 61, 148105.	0.2	1
42701	First-principles study of (InAs)1/(GaSb)1 superlattice nanowires. Wuli Xuebao/Acta Physica Sinica, 2012, 61, 117103.	0.2	2
42702	First-principles study of (InAs)1/(GaSb)1 superlattice atomic chains. Wuli Xuebao/Acta Physica Sinica, 2012, 61, 117104.	0.2	1
42703	Water adsorption on the Be(0001) surface: from monomer to trimer adsorption. Chinese Physics B, 2012, 21, 016802.	0.7	0
42705	First Principles Calculations of Close-Packed and Doped Carbon Nanotubes. E-Journal of Surface Science and Nanotechnology, 2012, 10, 411-413.	0.1	0
42706	Doped with Ag and Zn effects on electronic structure and optical properties of CdS. Wuli Xuebao/Acta Physica Sinica, 2012, 61, 017202.	0.2	7
42707	Investigation of the doping failure induced by DB in the SiNWs using first principles method. Wuli Xuebao/Acta Physica Sinica, 2012, 61, 153102.	0.2	1
42708	Electronic structure and photoelectric properties of OsSi2 epitaxially grown on a Si(111) substrate. Wuli Xuebao/Acta Physica Sinica, 2012, 61, 217102.	0.2	4
42709	First principles investigation of dynamic performance in the process of lithium intercalation into black phosphorus. Wuli Xuebao/Acta Physica Sinica, 2012, 61, 247101.	0.2	6
42710	Application of Quantum Mechanics for Computing the Vibrational Spectra of Nitrogen Complexes in Silicon Nanomaterials. , 0, , .		1

#	Article	IF	Citations
42711	Tunable Magnetic Properties of Rhombohedral Graphite Thin Films: Effects of Insulating Substrate on Magnetic Properties. Japanese Journal of Applied Physics, 2012, 51, 02BN04.	0.8	0
42712	First-principles simulations of the 27Al and 17O solid-state NMR spectra of the CaAl2Si3O10 glass. Highlights in Theoretical Chemistry, 2013, , 87-97.	0.0	0
42713	Nonisovalent Alloys for Photovoltaics Applications: Modelling IV-Doped III-V Alloys. , 0, , .		0
42714	Comprehensive Study of the X-Ray Photoelectron Spectroscopy Peak Shift of La-Incorporated Hf Oxide for Gate Dielectrics. Japanese Journal of Applied Physics, 2012, 51, 048005.	0.8	0
42715	First-Principles Calculations of Physical Properties of Planetary Ices. Astrophysics and Space Science Library, 2013, , 149-169.	1.0	0
42716	Magnetic Properties of Iron on Strained Graphene: Density Functional Theory Study. Japanese Journal of Applied Physics, 2012, 51, 06FD13.	0.8	0
42717	Analysis of Charge Compensation Mechanisms in Pr_{1-x}A_xCoO_{3-Î´}(A = Ca, Sr) by X-ray Absorption Near-Edge Structure. Japanese Journal of Applied Physics, 2012, 51, 073201.	0.8	1
42719	- Gas Adsorption by Fullerenes and Polyhedral Multi-Walled Carbon Nanostructures. , 2012, , 177-202.		0
42720	- Gas Desorption from Detonation Nanodiamonds During Temperature-Programmed Pyrolysis. , 2012, , 235-268.		0
42721	Adsorption of Benzene on 4H-SiC (0001) Surface: First Principles Calculations. Acta Physica Polonica A, 2012, 122, 1049-1051.	0.2	0
42722	First-principles study of structure and stability in Siâ€“Câ€“O-based materials. Highlights in Theoretical Chemistry, 2014, , 197-201.	0.0	0
42723	First-principles calculations of structural thermodynamic and mechanical properties of 5d transitional metal diborides. Wuli Xuebao/Acta Physica Sinica, 2013, 62, 046201.	0.2	10
42724	Structural phase transition of Ru at high pressure and temperature. Wuli Xuebao/Acta Physica Sinica, 2013, 62, 176402.	0.2	2
42725	First-principles study on the electronic and optical properties of the (Eu,N)-codoped anatase TiO2 photocatalyst. Wuli Xuebao/Acta Physica Sinica, 2013, 62, 193103.	0.2	1
42726	Density-Functional Theory. Springer Theses, 2013, , 5-21.	0.0	0
42727	First-Principles Simulations of the Initial Corrosion-Process of Iron Surface. , 2013, , 2809-2814.		0
42728	Dynamics of H2 Interacting with Substitutional Bimetallic Surface Alloys. Springer Series in Surface Sciences, 2013, , 131-155.	0.3	0
42729	Influences of strain on electronic structure and magnetic properties of CoFe2O4 from first-principles study. Wuli Xuebao/Acta Physica Sinica, 2013, 62, 167502.	0.2	3

#	Article	IF	Citations
42731	First-principles study on the energy bandgap bowing parameter of wurtzite BexZn1-xO. Wuli Xuebao/Acta Physica Sinica, 2013, 62, 037102.	0.2	0
42732	Ab initio study of the bcc-to-hcp transition mechanism in Fe under pressure. Wuli Xuebao/Acta Physica Sinica, 2013, 62, 056401.	0.2	0
42733	Strain control of the leakage current of the ferroelectric thin films. Wuli Xuebao/Acta Physica Sinica, 2013, 62, 067701.	0.2	4
42734	First-priciples study on Mn-doped LiZnAs, a new diluted magnetic semiconductor. Wuli Xuebao/Acta Physica Sinica, 2013, 62, 137101.	0.2	5
42735	First-principles study on anatase TiO2 photocatalyst codoped with nitrogen and cobalt. Wuli Xuebao/Acta Physica Sinica, 2013, 62, 017102.	0.2	2
42736	First-principles studies of the structural and thermodynamic properties of TiAl3 under high pressure. Wuli Xuebao/Acta Physica Sinica, 2013, 62, 068105.	0.2	4
42737	Influence of Al doping on stability of Mg1-xTix and their hydrides. Wuli Xuebao/Acta Physica Sinica, 2013, 62, 138801.	0.2	1
42738	First-principles study on the electronic structure and optical properties of RDX. Wuli Xuebao/Acta Physica Sinica, 2013, 62, 163102.	0.2	4
42739	First-principles study on electronic structures of Al, N Co-doped ZnO nanotubes. Wuli Xuebao/Acta Physica Sinica, 2013, 62, 056105.	0.2	0
42741	Atomic Structure of 180? Ferroelectric Domain Walls in PbTiO3. , 2013, , .		0
42742	First-Principles Investigation of the Surface Properties of LiNiO₂as Cathode Material for Lithium-ion Batteries. Journal of the Korean Electrochemical Society, 2013, 16, 169-176.	0.1	1
42743	Î©-Phase Transformation in Ti3Al2Mo Alloy: A First-Principles Approach. , 0, , 429-433.		0
42744	The Investigation of the Adsorption of Thiophene on NiMoS Surface: A Density Functional Theory Study. Lecture Notes in Electrical Engineering, 2014, , 25-39.	0.3	0
42745	First-principles study of Ag2ZnSnS4 as a photocatalyst. Wuli Xuebao/Acta Physica Sinica, 2014, 63, 247101.	0.2	4
42746	First-principles calculations of the mechanical properties of IrB and IrB2. Wuli Xuebao/Acta Physica Sinica, 2014, 63, 153101.	0.2	1
42747	First principles study on the electronic structures and optical properties of Na2Ge2Se5. Wuli Xuebao/Acta Physica Sinica, 2014, 63, 184208.	0.2	2
42748	First-principles study of 3d transition metal Co doped core-shell silicon nanowires. Wuli Xuebao/Acta Physica Sinica, 2014, 63, 163101.	0.2	1
42749	First-principles study of the structural, elastic and electronic properties of RhB under high pressure. Wuli Xuebao/Acta Physica Sinica, 2014, 63, 186401.	0.2	5

#	Article	IF	Citations
42750	First-Principles Analysis of Thermal Expansion Behavior of Mg Based on the Quasi-Harmonic Approximation Considering Structural Anisotropy. Zairyo/Journal of the Society of Materials Science, Japan, 2014, 63, 188-193.	0.1	1
42751	First-principles study of electronic structure and optical properties of TiO2 nanotubes. Wuli Xuebao/Acta Physica Sinica, 2014, 63, 243102.	0.2	4
42752	Research of the synergistic effects in Cu/N co-doped TiO2 surfaceï¼šA DFT calculation. Wuli Xuebao/Acta Physica Sinica, 2014, 63, 157102.	0.2	5
42753	First principles investigation of interaction between interstitial hydrogen atom and Fe metal. Wuli Xuebao/Acta Physica Sinica, 2014, 63, 227101.	0.2	3
42754	First principles calculation of occupancy, bonding characteristics and alloying effect of Cr, Mo, Ni in bulk Î±-Fe?. Wuli Xuebao/Acta Physica Sinica, 2014, 63, 197101.	0.2	9
42755	A DFT sight of oxygen and carbon monoxide coadsorption on Pt-alloy surfaces. , 0, , .		0
42756	Magnetic and electronic properties of fluorographene sheet with foreign atom substitutions. Wuli Xuebao/Acta Physica Sinica, 2014, 63, 046102.	0.2	5
42757	Electronic structures and phase instabilities of cubic Na1/2Bi1/2TiO3 and K1/2Bi1/2TiO3ï¼š a first-principles comparative study. Wuli Xuebao/Acta Physica Sinica, 2014, 63, 167101.	0.2	0
42758	Effects of niobium on helium behaviors in tungstenï¼ša first-principles investigation. Wuli Xuebao/Acta Physica Sinica, 2014, 63, 046103.	0.2	4
42759	Chromium concentration effect on an alloy surface stability and oxidation initiation. , 2014, , .		0
42760	Theoretical Assessment of the Mechanical, Electronic, and Vibrational Properties of the Paramagnetic Insulating Cerium Dioxide and Investigation of Intrinsic Defects. Advances in Chemical and Materials Engineering Book Series, 2014, , 431-446.	0.2	0
42761	Role of the Surface Nâ€“H Molecular Layer in High Quality In-RICH InGaN Growth by MOVPE. Journal of Chemical Engineering of Japan, 2014, 47, 615-619.	0.3	0
42762	Structural and electronic properties of hydrogenated bilayer boron nitride. Wuli Xuebao/Acta Physica Sinica, 2014, 63, 016801.	0.2	1
42763	First-Principles Estimation of Hydrogen Embrittlement Properties at the Grain Boundary of an Al-Mg-Zn Series Alloy. Zairyo/Journal of the Society of Materials Science, Japan, 2014, 63, 174-181.	0.1	1
42764	First-Principles Study on Electronic Band Structure and Optical Constants of Synthesized Si3Al(AsxP1-x) Alloys. , 2014, , .		0
42765	Phase Competition in Bismuth Layered Structure Based on First Principles Thermodynamics. Wuji Cailiao Xuebao/Journal of Inorganic Materials, 2014, 29, 1156.	0.6	0
42766	Quantum confinement effect on electronic and optical properties of SnS. Wuli Xuebao/Acta Physica Sinica, 2014, 63, 067101.	0.2	1
42767	Surface Stresses at the Initial Steps of the GexSi1-x/Si(001) Surface Oxidation. Ukrainian Journal of Physics, 2014, 59, 148-154.	0.1	0

#	Article	IF	Citations
42768	Bulk Electronic Structure of Disordered Transition and Noble Metal Alloys. , 1979, , 223-238.		0
42769	Dimensionality Effects in trans-(CH) x. NATO ASI Series Series B: Physics, 1989, , 151-164.	0.2	0
42770	Band Offsets at Semiconductor Heterojunctions: Bulk or Interface Properties?. NATO ASI Series Series B: Physics, 1989, , 51-60.	0.2	0
42771	High-pressure structural phase transition and electronic properties of the group-III nitrides. , 1993, , 422-425.		0
42772	Doping limits in ZnSe. , 1993, , 118-127.		0
42773	Clustering and Correlations on GaAs â€" Metal Interface. , 1993, , 121-126.		0
42774	Semiconductor Interfaces. , 1993, , 59-85.		1
42775	Predicting New Hard Materials. Kluwer International Series in Engineering and Computer Science, 1996, , 531-543.	0.2	0
42776	Ab Initio Pseudopotential Methods for Oxides: Î±-Quartz Near the Amorphous Transition. Kluwer International Series in Engineering and Computer Science, 1996, , 387-410.	0.2	0
42777	Ab Initio Lattice Dynamics: Methods, Results, and Applications. , 1998, , 99-124.		0
42778	Computational Modelling of Atomic-Scale Defect Phenomena in Compound Semiconductors. , 1998, , 11-36.		0
42779	Metal Oxide Nanoribbons and Carbon Nanotubes: Modeling. , 0, , 2479-2490.		0
42780	Magnetic Properties of Strained L1₀-ordered FePt and CoPt: An ab initio Study. Applied Science and Convergence Technology, 2014, 23, 273-278.	0.3	0
42781	Surface Charge of Clean LiNbO3 Z-Cut Surfaces. , 2015, , 163-178.		0
42782	Modulation of Anisotropy on Phonon Transportation in MgS: Theoretical Studies. Journal of Materials Science Research, 2014, 4, .	0.1	0
42783	Electronic Structure of Sodium Thiogermanate. Open Journal of Inorganic Non-metallic Materials, 2015, 05, 31-39.	2.7	3
42784	Electronic structure and optical properties of C doped rutile TiO2: the first-principles calculations. Wuli Xuebao/Acta Physica Sinica, 2015, 64, 224218.	0.2	3
42785	Tuning the electronic property of monolayer MoS2 adsorbed on metal Au substrate: a first-principles study. Wuli Xuebao/Acta Physica Sinica, 2015, 64, 187101.	0.2	1

#	Article	IF	Citations
42786	Molecular Dynamics Simulation: From â€œAb Initioâ€•to â€œCoarse Grainedâ€• , 2015, , 1-61.		0
42787	Conductive Path Formation by Aggregated Oxygen Ions in Titanium Dioxide: First-Principles Analyses. , 0, , .		0
42788	First-principles study of effects of quantum confinement and strain on the electronic properties of GaSb nanowires. Wuli Xuebao/Acta Physica Sinica, 2015, 64, 227303.	0.2	3
42789	First-principles study on the hydrogenation of the O2 on TiN4 embedded graphene. Wuli Xuebao/Acta Physica Sinica, 2015, 64, 216101.	0.2	0
42790	First-Principles Simulations of Bulk Crystal and Nanolayer Properties. Nanoscience and Technology, 2015, , 113-214.	1.5	0
42791	First-principles calculations of the diffusion behaviors of C, N and O atoms in V metal. Wuli Xuebao/Acta Physica Sinica, 2015, 64, 026602.	0.2	2
42792	First-principles study of electronic structures and phase stabilities of ternary intermetallic compounds in the Mg-Y-Zn alloys. Wuli Xuebao/Acta Physica Sinica, 2015, 64, 187102.	0.2	2
42793	Multiscale Modeling of Discontinuous Precipitation in U-Nb. , 2015, , 481-490.		0
42794	Binary Oxides of Transition Metals. Nanoscience and Technology, 2015, , 429-543.	1.5	0
42795	First-Principles Calculations and Thermodynamic Assessment of the Li-Rh and Tl-Tm Systems. International Journal of Materials Mechanics and Manufacturing, 2015, 4, 135-139.	0.2	0
42796	Charge-Transfer Metal-Insulator Transitions and Electronic Properties in Vanadium Dioxide. Advances in Condensed Matter Physics, 2015, 04, 119-127.	0.1	0
42797	Effects of dopants on the growth of oxidation-induced stacking faults in heavily doped n-type Czochralaki silicon. Wuli Xuebao/Acta Physica Sinica, 2015, 64, 096105.	0.2	0
42798	Photoactive Semiconducting Oxides for Energy and Environment: Experimental and Theoretical Insights. , 2015, , 1-48.		0
42799	The CO Absorption on Pt Film Tuned by Ferroelectric Polarization. Advances in Condensed Matter Physics, 2015, 04, 55-61.	0.1	0
42800	First-principles study on the elastic and thermal properties of Ca0.5Sr0.5TiO3. Wuli Xuebao/Acta Physica Sinica, 2015, 64, 207102.	0.2	1
42801	First-principles study of stability and electronic structure of N2H4 adsorption on NiFe(111) alloy surface. Wuli Xuebao/Acta Physica Sinica, 2015, 64, 203101.	0.2	1
42802	Study on thermodynamics basic and alloy phase evolution of Mg-Sn-Si magnesium alloy. Wuli Xuebao/Acta Physica Sinica, 2015, 64, 066401.	0.2	0
42803	Theoretical study on the influence of rare earth doping on the electronic structure and magnetic properties of cobalt ferrite. Wuli Xuebao/Acta Physica Sinica, 2015, 64, 037501.	0.2	5

#	Article	IF	Citations
42804	Mechanical properties of BBi compound under pressure. International Journal of Scientific World, 2014, 3, 69-75.	3.0	0
42805	First principle structural and electronic properties of Sr3Sb2 compound of the cubic Phase. Journal of Zankoy Sulaimani - Part A, 2015, 17, 219-226.	0.1	0
42806	Band Gap Characterization of Ternary BBi1-xNxAlloys: A First-Principles Study. Acta Physica Polonica A, 2015, 128, B-46-B-49.	0.2	0
42807	Structural hierarchy of NH4V3O7 particles prepared under hydrothermal conditions. Nanosystems: Physics, Chemistry, Mathematics, 2015, , 583-592.	0.2	0
42808	Quasi free-standing one-dimensional nanocrystals of PbTe grown in 1.4 nm SWNTs. Nanosystems: Physics, Chemistry, Mathematics, 2015, , 850-856.	0.2	1
42810	Effects of surface regulation on monolayers SbAs and BiSb. Wuli Xuebao/Acta Physica Sinica, 2016, 65, 217101.	0.2	2
42811	Strain field tuning the electronic and magnetic properties of semihydrogenated two-bilayer GaN nanosheets. Wuli Xuebao/Acta Physica Sinica, 2016, 65, 023101.	0.2	0
42812	Density functional theory study of hydrogen spillover mechanism on Pd doped covalent organic frameworks COF-108. Wuli Xuebao/Acta Physica Sinica, 2016, 65, 157302.	0.2	1
42813	DETERMINING THE OPTIMAL MODELING PARAMETERS FOR MAXIMUM PRECISE CALCULATIONS OF ENERGY IN BCC-IRON. Bulletin of the South Ural State University Series Mathematics Mechanics Physics, 2016, 8, 63-69.	0.2	0
42814	Effects of point defect concentrations on elastic properties of off-stoichiometric L12-type A13Sc. Wuli Xuebao/Acta Physica Sinica, 2016, 65, 076101.	0.2	4
42815	Preparation and characterization of orthorhombic Fe2(MoO4)3 and first-principle study of its negative thermal expansion properties. Wuli Xuebao/Acta Physica Sinica, 2016, 65, 056501.	0.2	0
42816	First-principles studies of multiple trapped impurity C by Ni vacancy and temperature effects in NiAl intermetallics. Wuli Xuebao/Acta Physica Sinica, 2016, 65, 206101.	0.2	0
42817	The structural and electronic properties of cubic AgMO3 (M=Nb, Ta) by first principles calculations. AIP Conference Proceedings, 2016, , .	0.3	2
42818	Novel compounds in the hafnium nitride system: first principle study of their crystal structures and mechanical properties. Wuli Xuebao/Acta Physica Sinica, 2016, 65, 118102.	0.2	2
42819	First-principles study on multiphase property and phase transition of monolayer MoS2. Wuli Xuebao/Acta Physica Sinica, 2016, 65, 127101.	0.2	0
42820	Hydrogen-Induced Core Structures Change of Screw and Edge Dislocations in Tungsten. , 2016, , 253-259.		0
42821	Growth, Structural and Electronic Properties of Functional Semiconductors Studied by First Principles. , 2016, , 145-162.		0
42822	Anharmonic Properties of MgO. Springer Theses, 2016, , 135-163.	0.0	0

#	Article	IF	Citations
42823	First-Principles Local Stress Analyses on Semiconductor Hetero-Interfaces of GaAs/XAs (X=Al, In). Zairyo/Journal of the Society of Materials Science, Japan, 2016, 65, 113-118.	0.1	0
42824	Electronic structure and magnetic properties of MnTe from first-principles calculations. Wuli Xuebao/Acta Physica Sinica, 2016, 65, 066101.	0.2	1
42825	First-principles study of the electronic properties and magnetism of LaMnO3/SrTiO3 heterointerface with the different component thickness ratios. Wuli Xuebao/Acta Physica Sinica, 2016, 65, 077301.	0.2	2
42826	Approach of the Molten Salt Chemistry for Aluminium Production: High Temperature NMR Measurements, Molecular Dynamics and DFT Calculations. , 2016, , 799-805.		0
42827	FT-IR, XPS and Density Functional Theory Study of Adsorption Mechanism of Sodium Formate onto Goethite or Hematite. , 2016, , 29-35.		0
42828			

#	Article	IF	Citations
42841	Magnetocrystalline Anisotropy of Î±''-Fe16N2. Journal of the Korean Magnetics Society, 2016, 26, 115-118.	0.0	1
42842	Chapter 3 Fe-Based Composite Absorbers. , 2016, , 79-128.		0
42843	Precipitation Reactions in Nickelâ€"Hydrogen System: ab initio Study. Metallofizika I Noveishie Tekhnologii, 2016, 38, 737-750.	0.2	2
42844	Nanoscale Deformation of GaAs Affected by Silicon Doping. Acta Physica Polonica A, 2016, 130, 1127-1130.	0.2	0
42845	First Principle Studies on Magnetism and Electronic Structure of Perovskite Structured CoFeX3(X =) Tj ETQq0 0 0 rgBT /Overlock 10 Tf 5	0.0	0
42846	Structural and electronic properties of T-graphene and its derivatives. Wuli Xuebao/Acta Physica Sinica, 2017, 66, 166101.	0.2	0
42847	Theoretical study on the stability and photoelectric properties of APbI3 perovskite. Wuli Xuebao/Acta Physica Sinica, 2017, 66, 057103.	0.2	6
42848	First-principles study on adsorption mechanism of hydrogen on tungsten trioxide surface. Wuli Xuebao/Acta Physica Sinica, 2017, 66, 086801.	0.2	1
42849	The Properties of Elasticity, Thermology, and Anisotropy in Pd-Based Alloys. Journal of Materials Science and Chemical Engineering, 2017, 05, 17-34.	0.2	0
42850	Theoretical Modelling Methods. Springer Theses, 2017, , 37-66.	0.0	0
42851	Growth of Crystalline Silicon for Solar Cells: Czochralski Si. , 2017, , 1-45.		1
42852	Effects of the doping of Al and O interstitial atoms on thermodynamic properties of -Al2O3:first-principles calculations. Wuli Xuebao/Acta Physica Sinica, 2017, 66, 016103.	0.2	2
42853	Effect of graphene substrate on the spectroscopic properties of photovoltaic molecules: role of the in-plane and out-of-plane Ï€-bonds. AIMS Materials Science, 2017, 4, 89-101.	0.7	0
42855	First-principle study of initial irradiation damage in aluminum. Wuli Xuebao/Acta Physica Sinica, 2017, 66, 057104.	0.2	1
42856	Vertical-Strain Effect on the Band Structures of Sr(Ti_{0.875}Fe_{0.125})O₃ Epitaxial Thin Films. Applied Physics, 2017, 07, 77-83.	0.0	0
42857	Alloy Design and Mechanical Properties: First-principles Calculations of Dislocation Core. Materia Japan, 2017, 56, 5-13.	0.1	1
42858	Theoretical study of the equation of state for warm dense matter. Wuli Xuebao/Acta Physica Sinica, 2017, 66, 036401.	0.2	2
42859	First principles study of mechanical properties of FeMnP1-xTx (T=Si, Ga, Ge) compounds. Wuli Xuebao/Acta Physica Sinica, 2017, 66, 126301.	0.2	0

#	Article	IF	Citations
42860	Interface electronic structure and the Schottky barrier at Al-diamond interface: hybrid density functional theory HSE06 investigation. Wuli Xuebao/Acta Physica Sinica, 2017, 66, 088102.	0.2	3
42861	First principles study of the effect of Cu doping on the martensitic transformation of TiNi alloy. Wuli Xuebao/Acta Physica Sinica, 2017, 66, 130501.	0.2	2
42862	First-principles Calculations of Structures and Micro-cracks of the Al-Ni Crystal Materials. , 2017, , .		0
42863	First-principle simulation of solid nitrobenzene under uniaxial compression. Wuli Xuebao/Acta Physica Sinica, 2017, 66, 036101.	0.2	1
42864	First-principles study of absorption mechanism of hydrogen on W20O58 (010) surface. Wuli Xuebao/Acta Physica Sinica, 2017, 66, 246801.	0.2	2
42865	Effect of surface passivation on the electronic properties of GaAs nanowire:A first-principle study. Wuli Xuebao/Acta Physica Sinica, 2017, 66, 197302.	0.2	1
42866	The Thermodynamic Approach in Thermoelectric Materials. SpringerBriefs in Materials, 2017, , 17-33.	0.1	0
42867	The Most Probable Path of Î²-Si₃N₄Transforming to Î²-C₃N₄ and the Comparison of Their Elasticity and Hardness. Material Sciences, 2017, 07, 266-274.	0.0	0
42868	Modeling Pressure Dependent Elastic Parameters of GaAsSb Alloy. Research & Reviews Journal of Material Sciences, 2017, 05, .	0.1	0
42869	Modelling of Phase Transitions in Calciumâ€“Strontium Superstructures at Low Pressures.. Modelling and Simulation in Engineering, 2017, 39, 113-125.	0.0	0
42870	The SrLiAl3N4:Eu2+ Phosphor Synthesized by the Raw Material Model Obtained by DFT Calculations. Journal of the Korean Ceramic Society, 2017, 54, 217-221.	1.1	0
42871	Transiciones de Fase Inducidas por PresiÃ³n en los Compuestos GaN, InN y AlN. Ciencia En Desarrollo, 2017, 8, .	0.1	0
42872	ELECTRONIC STRUCTURE OF DIVALENT METAL AZIDES. Science Evolution, 2017, , 3-10.	0.1	0
42874	Reassignment of O-related infrared absorption peaks in CdSe. Ceramics International, 2017, 43, S359-S363.	2.3	0
42875	Nanotubular-structured porous silicon. Series in Materials Science and Engineering, 2017, , 591-598.	0.1	0
42876	Assessment on The Accuracy of Piezoelectric Property Calculations of Single Layer Two Dimensional Hexagonal Crystals. Anadolu University Journal of Sciences & Technology, 0, , 1-1.	0.2	1
42877	High pressure tuning the geometrical and electronic structures of perylene. Molecular Simulation, 2018, 44, 330-334.	0.9	1
42878	Elastic Anisotropic and Thermodynamic Properties of Two BC7 Phases. Acta Physica Polonica A, 2017, 132, 1340-1346.	0.2	1

#	Article	IF	Citations
42879	First-Principles Study of the Structural, Electronic, Magnetic and Thermal Properties of the Cr Doped Ge₆Mn₂Te₈ and Ge₆Fe₂Te₈ Systems. Acta Physica Polonica A, 2017, 132, 1242-1250.	0.2	2
42880	High pressure study of structural, electronic, elastic, and vibrational properties of NaNb3O8. Journal of Alloys and Compounds, 2017, 725, 773-782.	2.8	3
42881	A 'Fluid' Nickel-Based Ferrite as an Efficient Redox Material for Thermochemical Two-Step CO ₂ Splitting. SSRN Electronic Journal, 0, , .	0.4	0
42882	First Principles Calculations of Hydrogen Storage on Calcium-Decorated, Boron-Doped Bilayer Graphene. Journal of Materials Science and Chemical Engineering, 2018, 06, 1-12.	0.2	0
42884	First-principles study on Jahn-Teller effect in Cr monolayer film. Wuli Xuebao/Acta Physica Sinica, 2018, 67, 237301.	0.2	2
42885	Photoelectric properties of Ag and Cr co-doped LiZnP new diluted magnetic semiconductors. Wuli Xuebao/Acta Physica Sinica, 2018, 67, 187101.	0.2	1
42886	Pt Decorating Effect on CNT Surface Towards Adsorption of SF6 Decomposed Components. Minerals, Metals and Materials Series, 2018, , 921-928.	0.3	0
42888	Tuning the electronic and magnetic property of semihydrogenated graphene and monolayer boron nitride heterostructure. Wuli Xuebao/Acta Physica Sinica, 2018, 67, 167101.	0.2	2
42889	Computational calculation of energetic stability, electronic properties and magnetism in the alloys Nb1-xCrxN. Contemporary Engineering Sciences, 2018, 11, 4347-4355.	0.2	0
42890	The First-Principles Investigation on Adsorption Mechanism of Pb(II) on the Kaolinite (001) Surface. Material Sciences, 2018, 08, 45-52.	0.0	0
42891	The Investigation DO3-type Fe3M (M=Al, Ga, Si and Ge) Full-Heusler Alloys Within First Principles Study. Journal of Polytechnic, 0, , .	0.4	0
42893	GÃ¼neÅŸ pilleri iÃ§in ZnO'nun yapÄ±sal ve elektronik Ã¶zelliklerinin incelenmesi: Ab-initio Ã§alÄ±ÅŸmasÄ±. BalÄ±kesir Ãœniversitesi Fen Bilimleri EnstitÃ¼sÃ¼ Dergisi, 0, , 1-12.	0.2	1
42894	The Quasiparticle Electronic Energy Bands of the Cubic KMgF3 Perovskite under Pressure Effect. Acta Physica Polonica A, 2018, 133, 990-993.	0.2	3
42895	Zincblende yapÄ±daki TlxIn1-xAsâ€™Ä±n Ã¶rgÃ¼ sabitleri ve eÄŸilme parametrelerinin YoÄŸunluk Fonksiyoneli Teorisi ile incelenmesi. BalÄ±kesir Ãœniversitesi Fen Bilimleri EnstitÃ¼sÃ¼ Dergisi, 0, , 1-10.	0.2	0
42896	Hidrojen depolama malzemeleri iÃ§in MgH2'nin yapÄ±sal ve elektronik Ã¶zellikleri. Gazi Ãœniversitesi Fen Bilimleri Dergisi, 0, , 451-461.	0.2	1
42897	Computational plasmonics with applications to bulk and nanosized systems. , 2018, , .		0
42898	First-Principles Modelling of N-Doped Co₃O₄. Latvian Journal of Physics and Technical Sciences, 2018, 55, 36-42.	0.4	1
42899	Effects of Organic Linkers on Energy gaps of Covalent based Triazine Frameworks. Walailak Journal of Science and Technology, 2018, 15, 811-817.	0.5	6

#	Article	IF	Citations
42900	AB Initio Calculations of CU_N@Graphene (0001) Nanostructures for Electrocatalytic Applications. Latvian Journal of Physics and Technical Sciences, 2018, 55, 30-34.	0.4	1
42901	Electronic Structures and Li Migration in Cubic Nickel Nitrides Intercalation compounds : From First Principles Studies. International Journal of Electrochemical Science, 0, , 12062-12071.	0.5	0
42903	First-principles investigation of the effect of crystal structure on sulfur isotope fractionation in sulfide polymorphs. European Journal of Mineralogy, 2018, 30, 1047-1061.	0.4	2
42904	First principles study of structural, electric, and magnetic properties of fluoride perovskite NaFeF₃. Wuli Xuebao/Acta Physica Sinica, 2019, 68, 147101.	0.2	0
42905	Theoretical study of atomic relaxation, surface energy, electronic structure and properties of B2- and B19'-NiTi surfaces. Wuli Xuebao/Acta Physica Sinica, 2019, 68, 053101.	0.2	1
42906	First-principles study of graphyne/graphene heterostructure resonant tunneling nano-transistors. Wuli Xuebao/Acta Physica Sinica, 2019, 68, 187102.	0.2	1
42907	First-principles study of rare-earth-doped cathode materials Li₂MnO₃ in Li-ion batteries. Wuli Xuebao/Acta Physica Sinica, 2019, 68, 138201.	0.2	4
42908	SiO2 Electronic Structure in Gas Giantsâ€™ Planetary Cores: A Density Functional Theory Approach. Communications in Computer and Information Science, 2019, , 76-85.	0.4	0
42909	Strain-Induced Changes in Vibrational Properties of Arsenene and Antimonene. Springer Proceedings in Physics, 2019, , 379-387.	0.1	1
42911	First-principles study of lattice dynamical and thermodynamic properties of Li₂NH. Wuli Xuebao/Acta Physica Sinica, 2019, 68, 137102.	0.2	0
42912	The first-principle study on the formation energies of Be, Mg and Mn doped CuInO₂. Wuli Xuebao/Acta Physica Sinica, 2019, 68, 106102.	0.2	2
42913	First-principles study of five isomers of two-dimensional GeSe under in-plane strain. Wuli Xuebao/Acta Physica Sinica, 2019, 68, 113103.	0.2	5
42914	First-principles study of reduction mechanism of oxygen molecule using nitrogen doped graphene as cathode material for lithium air batteries. Wuli Xuebao/Acta Physica Sinica, 2019, 68, 128801.	0.2	3
42915	Ab Initio Calculation of Vacancy Formation Energy in Antiperovskite Mn3GaC. Bulletin of the South Ural State University Series Mathematics Mechanics Physics, 2019, 11, 58-64.	0.2	0
42916	FIRST-PRINCIPLES INVESTIGATIONS OF REFERENCE STATES OF Co2CrIn HEUSLER ALLOYS. Bulletin of the South Ural State University Series Mathematics Mechanics Physics, 2019, 11, 59-66.	0.2	0
42917	Synergistic O²⁻/Li⁺ Dual Ion Transportation at Atomic Scale. Research, 2019, 2019, 1-8.	2.8	3
42918	Growth of Crystalline Silicon for Solar Cells: Czochralski Si. , 2019, , 129-174.		1
42919	Electronic structure and optical properties of phosphate bis-guanidinoacetate crystal containing guanidine phosphate interaction. Wuli Xuebao/Acta Physica Sinica, 2019, 68, 064210.	0.2	0

#	Article	IF	Citations
42920	Interfacial interaction and Schottky contact of two-dimensional WS₂/graphene heterostructure. Wuli Xuebao/Acta Physica Sinica, 2019, 68, 097101.	0.2	9
42921	High-pressure structure prediction and high-temperature structural stability of periclase. Wuli Xuebao/Acta Physica Sinica, 2019, 68, 126201.	0.2	1
42922	First-principles investigation on elastic, electronic, and optical properties of Ti₃O₅. Wuli Xuebao/Acta Physica Sinica, 2019, 68, 207301.	0.2	3
42923	Effect of intrinsic defects and copper impurities co-existing on electromagnetic optical properties of ZnO: First principles study. Wuli Xuebao/Acta Physica Sinica, 2019, 68, 087101.	0.2	5
42925	Electronic Structure Properties of ATe and A2Te (A: Cu, Ag and Cd). Springer Proceedings in Physics, 2019, , 1151-1157.	0.1	0
42926	Multiscale Simulation of Precipitation in Copper-Alloyed Pipeline Steels and in Cu-Ni-Si Alloys. , 2019, , 241-281.		1
42927	Modelling of Rhombohedral Magnetostriction in Fe-Ga Alloys. Bulletin of the South Ural State University, Series: Mathematical Modelling, Programming and Computer Software, 2019, 12, 158-165.	0.1	1
42928	Electronic structures and Li diffusion in cathode material Li₂FeO₂ of Li-ion batteries. Wuli Xuebao/Acta Physica Sinica, 2019, 68, 157201.	0.2	2
42929	Characterizing modulated structures with first-principles calculations: a unified superspace scheme of ordering in mullite. Acta Crystallographica Section A: Foundations and Advances, 2019, 75, 260-272.	0.0	1
42930	Effect of Mn content in Fe(_{1â^'x})Mn_xB (x = 0, 0.25, 0.5, 0.75 and 1) on physical properties - ab initio calculations. Materials Science-Poland, 2019, 37, 71-82.	0.4	2
42931	Effect of mechanical deformations on absorption spectrum of metallic films of nanometer thickness. , 2019, , .		0
42933	Phase stability of two-dimensional monolayer <mml:math xmlns:mml="http://www.w3.org/1998/Math/MathML"><mml:mrow><mml:msub><mml:mi>As</mml:mi><mml:mrow><mml:mn>1</mml:mn> mathvariant="normal">P</mml:mi><mml:mi>x</mml:mi></mml:msub></mml:mrow></mml:math> solid solutions revealed by a first-principles cluster expansion. Physical Review Materials, 2019, 3, .	0.9	2
42935	Electronic and optical properties of Î²-HgS. Semiconductor Physics, Quantum Electronics and Optoelectronics, 2019, 22, 150-155.	0.3	3
42936	Investigation on tuning of WS2/SiC band gap with an external electric field. , 2019, , .		2
42938	Thermopower of the electron-doped manganese pnictide LaMnAsO. Physical Review Materials, 2019, 3, .	0.9	1
42939	BaRu2As2 Malzemesinin Fiziksel Ã–zelliklerinin YoÄŸunluk Fonksiyonel Teorisi KullanÄ±larak Ä°ncelenmesi. GÃ¼mÃ¼ÅŸhane Ãœniversitesi Fen Bilimleri EnstitÃ¼sÃ¼ Dergisi, 0, , .	0.0	0
42940	First-principles Study on Formation of LPSO Structures for Ternary Alloys Revisited from Short-range Order. Transactions of the Materials Research Society of Japan, 2019, 44, 149-152.	0.2	0
42941	Determining Ideal Strength and Electronic Properties of Ge/Si Core-Shell Nanowires. Journal of the Korean Society for Precision Engineering, 2019, 36, 699-704.	0.1	0

#	Article	IF	Citations
42942	Controlling factors for alignment of solute clusters in magnesium alloys: A first-principles analysis. Keikinzoku/Journal of Japan Institute of Light Metals, 2019, 69, 471-478.	0.1	0
42943	Stability of edge magnetism against disorder in zigzag MoS2 nanoribbons. Physical Review Materials, 2019, 3, .	0.9	4
42944	Strain-gated infrared photodetector based on helical graphene nanoribbon. Physical Review Materials, 2019, 3, .	0.9	0
42945	Ab initio GGA+U investigations of the structural, electronic, and magnetic properties of Cd1-xMnxTe alloy. , 2019, , .		4
42946	First-principles study of the single- and double-walled nanotubes of TiO2. , 2019, , .		0
42947	Investigation of Structural, Electronic, Optic and Elastic Properties of Perovskite RbGeCl3 Crystal: A First Principles Study. Gazi University Journal of Science, 2019, 32, 1008-1019.	0.6	4
42948	Energy convergency of the first principles calculations on aluminum boundary ï¼Reliable methods of the first principles calculations on boundary energyï¼: Keikinzoku/Journal of Japan Institute of Light Metals, 2019, 69, 518-524.	0.1	0
42949	Comparison of Characteristics of Structural Phase Transitions under Pressure in Barium and Radium. Metallofizika I Noveishie Tekhnologii, 2019, 41, 851-861.	0.2	0
42951	Density functional theory calculations of the radial breathing mode in graphene quantum dots. Journal of Nanophotonics, 2019, 13, 1.	0.4	2
42953	The effects of Ru, Cu, Zr and Hf on mechanical properties in Ti-Pt high temperature shape memory alloys. IOP Conference Series: Materials Science and Engineering, 0, 655, 012011.	0.3	0
42954	Many-Body Spin Excitations in Ferromagnets from First Principles. , 2020, , 1-39.		1
42955	Asymmetric valley polarization and photoluminescence in MoS₂/MoO₃ heterostructure. Optics Express, 2019, 27, 38451.	1.7	2
42956	First-principles calculations of Fluorine-doped Titanium dioxide: A prospective material for solar cells application. Journal of the Nigerian Society of Physical Sciences, 0, , 131-137.	0.0	1
42957	Enhanced Reaction of Renewable Hydrogen Energy Production Using Platinum-based Nanoclusters. Daehan Hwan'gyeong Gonghag Hoeji, 2019, 41, 686-694.	0.4	1
42958	YoÄŸunluk Fonksiyoneli Teorisi ile LiAlSiâ€™un BasÄ±nÃ§ AltÄ±nda Elektronik ve TitreÅŸim Ã–zellikleri. European Journal of Science and Technology, 0, , 1340-1346.	0.5	0
42959	Lattice vibrations and electronic properties of GaSe nanosheets from first principles. Physical Review Materials, 2019, 3, .	0.9	5
42960	Binary Oxides of Transition Metals: ZnO, TiO$$_2$$, ZrO$$_2$$, HfO$$_2$$. Nanoscience and Technology, 2020, , 255-451.	1.5	0
42962	Electronic, Optical, Elastic and Magnetic Properties of Co2VZ (Z= As, B, In, Sb) Full Heusler Compounds. East European Journal of Physics, 2020, , .	0.1	1

#	Article	IF	Citations
42964	Origin of the enhanced photocatalytic activity of (Ni, Se, and B) mono- and co-doped anatase TiO2 materials under visible light: a hybrid DFT study. RSC Advances, 2020, 10, 43092-43102.	1.7	7
42965	Vibrational Up-Pumping: Predicting Impact Sensitivity of Some Energetic Azide. Springer Theses, 2020, , 65-111.	0.0	0
42966	Neon diffusion in goethite, Î±-FeO(OH): a theoretical multi-scale study. Physics and Chemistry of Minerals, 2020, 47, 1.	0.3	9
42967	The Effect of Spin-Orbit Interaction On Structural and Electronic Properties of Sclr2. Sakarya University Journal of Science, 0, , 406-411.	0.3	0
42968	A brief visit to the BeCl2/ZnCl2 system and the prediction of a new polymorph of ZnCl2. Zeitschrift Fur Naturforschung - Section B Journal of Chemical Sciences, 2020, 75, 491-496.	0.3	0
42969	Intrinsic adsorption behaviour related to the structural and mechanical properties of flexible metal-organic frameworks Co(bdp). Computational Materials Science, 2020, 177, 109543.	1.4	3
42970	Phonons and oxygen diffusion in Bi2O3 and (Bi0.7Y0.3)2O3. Journal of Physics Condensed Matter, 2020, 32, 334002.	0.7	2
42971	Magnetic behavior of Fe-doped zirconia studied by synchrotron radiation measurements and first-principles simulations. Physical Review Materials, 2020, 4, .	0.9	1
42973	Investigation of phase transition in electronic structure and magnetic properties of Fe_{2-x}Co_xTiSn Heusler alloys. Phase Transitions, 2020, 93, 690-708.	0.6	5
42974	First principle insights of NO₂ detection via III-V nitride nanoribbons with armchair edges. Nano Express, 2020, 1, 010059.	1.2	3
42975	Phase transition of GeO2 crystal at high pressure: An ab initio molecular dynamics study. International Journal of Chemistry and Technology, 2020, 4, 90-96.	0.8	0
42976	A Density Functional Theory (DFT) Study on the Effect of Chlorine in the Magnesium Zinc Oxide (MZO) Front Interface for Cadmium Telluride (CdTe) Thin Film Solar Cells. , 2020, , .		1
42977	First-principles study of the ferroelectric properties of SrTaO2N/SrTiO3 interfaces. Journal of Physics Condensed Matter, 2020, 32, 355003.	0.7	1
42978	Oxygen-vacancy-induced atomic and electronic reconstructions in magnetic Sr(Ti_{0.875}Fe_{0.125})O_{3-Î´} thin films. Materials Research Express, 2020, 7, 076105.	0.8	1
42979	Thickness-dependent Youngâ€™s modulus of polycrystalline Î±-PbO nanosheets. Nanotechnology, 2020, 31, 395712.	1.3	3
42980	RSAVS superconductors: Materials with a superconducting state that is robust against large volume shrinkage. Physical Review Materials, 2020, 4, .	0.9	7
42981	Metastable B-doped FeNi compounds for permanent magnets without rare earths. Physical Review Materials, 2020, 4, .	0.9	1
42983	Raman and infrared phonons in tetragonal ZnP₂and CdP₂crystals: a density functional study. Journal of Physics Condensed Matter, 2020, 32, 445401.	0.7	2

#	Article	IF	Citations
42984	First-principles identification of ferroelectric metal-organic frameworks of [CH3NH3][B(HCOO)3] (B =) Tj ETQq0 0 0 rgBT /Overlock 10 T	1.4	1
42985	Quantum transport simulations of a monolayer all-inorganic perovskite transistor. Journal Physics D: Applied Physics, 2020, 53, 455104.	1.3	3
42986	Influences of hole/electron-lattice coupling on phase transition between Î»-Ti₃O₅ and Î²-Ti₃O₅. Journal of Physics Condensed Matter, 2020, 32, 46LT01.	0.7	1
42987	First-principles study of the order-disorder transition and its effects on the optoelectronic property of ABiS2 (A=Na , K). Physical Review Materials, 2020, 4, .	0.9	1
42988	Fe3Se4: a possible ferrimagnetic half-metal?. Journal of Physics Condensed Matter, 2020, 32, 455801.	0.7	3
42989	Atomic Models of the Si(110)-5 Ã— 8 and Ge(110)-c(10 Ã— 8) Surfaces. Journal of Experimental and Theoretical Physics, 2020, 131, 322-328.	0.2	0
42990	Investigation of SiO2-Vo/SiO2 interface induced rectification characteristics at HRS for RRAM devices. Journal of Alloys and Compounds, 2020, 835, 155197.	2.8	1
42991	Molecular dynamics investigation of the configuration and shape of helium clusters in tungsten. Nuclear Fusion, 2020, 60, 126015.	1.6	4
42992	Scalable Production of Freestanding Few-Layer Î²₁₂-Borophene Single Crystalline Sheets as Efficient Electrocatalysts for Lithiumâ€“Sulfur Batteries. ACS Nano, 2021, 15, 17327-17336.	7.3	40
42993	Turning Electronic and Optical Properties of Monolayer Janus Sn-Dichalcogenides By Biaxial Strain. Lecture Notes in Mechanical Engineering, 2022, , 981-989.	0.3	1
42995	Two-Dimensional Iron Oxide on Au(111): Growth Mechanism and Interfacial Properties. Journal of Physical Chemistry C, 2021, 125, 24755-24763.	1.5	4
42996	Large exciton binding energy, superior mechanical flexibility, and ultra-low lattice thermal conductivity in BiI₃ monolayer. Journal of Physics Condensed Matter, 2022, 34, 055302.	0.7	0
42997	Engineering of Fe-pnictide heterointerfaces by electrostatic principles. NPG Asia Materials, 2021, 13, .	3.8	2
42998	Oxygen Coverage Effect on the Magnetic Properties of the Cr₂NO_x (0 â‰¤) Tj ETQq1 1 0.784314 rgBT	2.0	6
42999	Trifluoromethylâ€Group Bearing, Hydrophobic Bulky Cations as Defect Passivators for Highly Efficient, Stable Perovskite Solar Cells. Solar Rrl, 2021, 5, 2100712.	3.1	11
43000	Computational determination of structural, electronic, magnetic and thermodynamic properties of Co2HfZ (ZÂ=ÂAl, Ga, Si and Sn) full Heusler compounds for spintronic applications. Journal of Alloys and Compounds, 2022, 894, 162503.	2.8	15
43001	Mg-Doped GaAs Nanowires with Enhanced Surface Alloying for Use as Ohmic Contacts in Nanoelectronic Devices. ACS Applied Nano Materials, 0, , .	2.4	0
43002	Cooperatively enhanced coking resistance via boron nitride coating over Ni-based catalysts for dry reforming of methane. Applied Catalysis B: Environmental, 2022, 302, 120859.	10.8	61

#	Article	IF	Citations
43003	Bonding Properties of Manganese Nitrides at High Pressure and the Discovery of MnN₄with Planar N₄Rings. Journal of Physical Chemistry C, 2021, 125, 24605-24612.	1.5	8
43004	Role of Interfacial Oxide in the Preferred Orientation of Ga₂O₃ on Si for Deep Ultraviolet Photodetectors. ACS Omega, 2021, 6, 29149-29156.	1.6	4
43005	Magnetically Induced Polarization in Centrosymmetric Bonds. Physical Review Letters, 2021, 127, 187601.	2.9	2
43006	Comprehensive search for buckled honeycomb binary compounds based on noble metals (Cu, Ag, and) Tj ETQq1 1 0.784314 rgBT /Ov	0.9	4
43007	Excess heat capacity and entropy of mixing along the hydroxyapatite-chlorapatite and hydroxyapatite-fluorapatite binaries. Physics and Chemistry of Minerals, 2021, 48, 44.	0.3	2
43008	Tunable vertical ferroelectricity and domain walls by interlayer sliding in Î²-ZrI2. Npj Computational Materials, 2021, 7, .	3.5	14
43009	How much does surface polymorphism influence the work function of organic/metal interfaces?. Applied Surface Science, 2022, 575, 151687.	3.1	3
43010	Point and complex defects in monolayer <mml:math xmlns:mml="http://www.w3.org/1998/Math/MathML"><mml:mrow><mml:mi>Pd</mml:mi><mml:msub><mml:mi>Se</mml:mi> : Evolution of electronic structure and emergence of magnetism. Physical Review B, 2021, 104, .	3.2	11
43011	Stable Structures and Superconductivity in a Yâ€“Si System under High Pressure. Journal of Physical Chemistry Letters, 2021, 12, 10388-10393.	2.1	10
43012	Band Structure Engineering and Optical Properties of Pristine and Doped Monoclinic Zirconia (m-ZrO₂): Density Functional Theory Theoretical Prospective. ACS Omega, 2021, 6, 30061-30068.	1.6	26
43013	Mechanism of ammonia oxidation to dinitrogen, nitrite, and nitrate on Î²â€Ni(OH)₂ from firstâ€principles simulations. Electrochemical Science Advances, 2022, 2, 2100142.	1.2	21
43014	Enhanced adsorption properties of ZnO/GaN heterojunction for CO and H2S under external electric field. Computational and Theoretical Chemistry, 2021, 1206, 113495.	1.1	9
43015	Parameterization of magnetic vector potentials and fields for efficient multislice calculations of elastic electron scattering. Acta Crystallographica Section A: Foundations and Advances, 2021, 77, 509-518.	0.0	3
43016	Triboelectrification based on NiO-Mg magnetic nanocomposite: Synthesis, device fabrication, and energy harvesting performance. Nano Energy, 2022, 91, 106662.	8.2	20
43017	Lithium Storage Performance Boosted via Delocalizing Charge in Zn_xCo_{1â^’}_xPS₃/CoS₂ of 2D/3D Heterostructure. Small, 2022, 18, e2104295.	5.2	13
43018	Developing new antiferroelectric and ferroelectric oxides and chalcogenides within the A2BX3 family. Journal of Materials Research, 2022, 37, 346-359.	1.2	2
43019	Al/Mn co-doping endows V2O5â€¢4VO2 cathode with enhanced lithium storage performance. Electrochimica Acta, 2022, 401, 139483.	2.6	11
43020	0D Bismuth(III)-Based Hybrid Ferroelectric: Tris(acetamidinium) Hexabromobismuthate(III). Chemistry of Materials, 2021, 33, 8591-8601.	3.2	22

#	Article	IF	Citations
43021	A Potassium Tungsten Oxyfluoride with Strong Second-Harmonic Generation Response Derived from Anion-Ordered Functional Motif. Inorganic Chemistry, 2021, 60, 17364-17370.	1.9	13
43022	Improved photodegradation efficiency in Fe3+-doped Bi3TiNbO9 nanosheets through oxygen vacancies introduction and ferroelectric polarization enhancement simultaneously. Applied Surface Science, 2022, 575, 151749.	3.1	13
43023	Improving robustness of kinetic models for steam reforming based on artificial neural networks and ab initio calculations. Chemical Engineering Journal, 2022, 433, 133201.	6.6	9
43024	Comprehensive Mechanism of CO₂ Electroreduction on Nonâ€Noble Metal Singleâ€Atom Catalysts of Mo₂CS₂â€MXene. Chemistry - A European Journal, 2021, 27, 17900-17909.	1.7	16
43025	Water Splitting on Multifaceted SrTiO3 Nanocrystals: Computational Study. Catalysts, 2021, 11, 1326.	1.6	7
43026	Phase transition impact on electronic and optical properties of Fe-doped MoSe2 monolayer via N2O adsorption. Superlattices and Microstructures, 2021, 160, 107083.	1.4	10
43027	Simultaneous anchoring of Ni nanoparticles and single-atom Ni on BCN matrix promotes efficient conversion of nitrate in water into high-value-added ammonia. Chemical Engineering Journal, 2022, 433, 133190.	6.6	46
43028	Dynamic evolution of nitrogen and oxygen dual-coordinated single atomic copper catalyst during partial oxidation of benzene to phenol. Nano Research, 2022, 15, 3017-3025.	5.8	29
43029	DFT studies on PbO2 and binary PbO2/SnO2 thin films. Physica E: Low-Dimensional Systems and Nanostructures, 2022, 136, 115037.	1.3	7
43030	Electrodynamics of Topologically Ordered Quantum Phases in Dirac Materials. Nanomaterials, 2021, 11, 2914.	1.9	4
43031	Comparative first-principles study of elastic constants of covalent and ionic materials with LDA, GGA, and meta-GGA functionals and the prediction of mechanical hardness. Science China Technological Sciences, 2021, 64, 2755-2761.	2.0	3
43032	Tricopper Melaminate, a Metalâ€“Organic Framework Containing Dehydrogenated Melamine and Cuâ€“Cu Bonding. Inorganic Chemistry, 2021, 60, 16303-16307.	1.9	3
43033	Passivating buried interface via self-assembled novel sulfonium salt toward stable and efficient perovskite solar cells. Chemical Engineering Journal, 2022, 431, 133209.	6.6	74
43034	Balancing Anchoring and Diffusion for Screening of Metal Oxide Cathode Materials in Lithiumâ€“Sulfur Batteries. Journal of Physical Chemistry C, 2021, 125, 24318-24327.	1.5	3
43035	Magnetic exchange interactions in yttrium iron garnet: A fully relativistic first-principles investigation. Physical Review B, 2021, 104, .	1.1	9
43036	Fe decorated CeO2 microsphere catalyst with surface oxygen defect for NO reduction by CO. Molecular Catalysis, 2021, 516, 111973.	1.0	3
43037	Large-gap quantum anomalous Hall effect in monolayer halide perovskite. Physical Review B, 2021, 104, .	1.1	3
43038	In-medium screening effects for the Galactic halo and solar-reflected dark matter detection in semiconductor targets. Physical Review D, 2021, 104, .	1.6	6

#	Article	IF	Citations
43039	Constructing Pd/ferroelectric Bi4Ti3O12 nanoflake interfaces for O2 activation and boosting NO photo-oxidation. Applied Catalysis B: Environmental, 2022, 302, 120876.	10.8	19
43040	Mo and Ta addition in NbTiZr medium entropy alloy to overcome tensile yield strength-ductility trade-off. Journal of Materials Science and Technology, 2022, 109, 176-185.	5.6	13
43041	Theoretical compton profile of fcc zinc (Zn). Materials Today: Proceedings, 2022, 61, 914-920.	0.9	1
43042	Electronic and magnetic properties of oneâ€dimensional sandwich transition metalâ€anthracene molecular wires. International Journal of Quantum Chemistry, 0, , .	1.0	0
43043	Characterization of Strontium Telluride (SrTe) Nanosheets in Different Directions: A Density-Functional Theory Approach. ECS Journal of Solid State Science and Technology, 2021, 10, 113003.	0.9	0
43044	Boosting visible light photocatalysis in an Au@TiO2 yolk-in-shell nanohybrid. Applied Catalysis B: Environmental, 2022, 303, 120869.	10.8	39
43045	Adsorption of La on kaolinite (0 0 1) surface in aqueous system: A combined simulation with an experimental verification. Journal of Molecular Liquids, 2022, 347, 117956.	2.3	12
43046	F2 adsorption on penta-graphene: A first-principles study. Surfaces and Interfaces, 2021, 27, 101569.	1.5	0
43047	Structural stability and mechanical properties of TiAl+Mo alloys: A comprehensive ab initio study. Acta Materialia, 2021, 221, 117427.	3.8	8
43048	Ferroelectricity in novel one-dimensional P42-InSeI nanowires. Results in Physics, 2021, 31, 104960.	2.0	8
43049	Influence of Oxygen Vacancies in Gas Sensors Based on Metal-Oxide Semiconductors: A First-Principles Study. Lecture Notes in Electrical Engineering, 2020, , 309-314.	0.3	3
43050	First-Principles Modeling of Interface Effects in Oxides. , 2020, , 1119-1149.		0
43051	First-Principles Simulations of Bulk Crystal and Nanolayer Properties. Nanoscience and Technology, 2020, , 123-219.	1.5	0
43052	Vibrational properties of substitutional hexagonal boron nitride sheets. AIP Conference Proceedings, 2020, , .	0.3	0
43053	Structural, electronic, magnetic and optical properties of polycrystalline FeAlB and Fe2AlB2: A first-principles study. AIP Conference Proceedings, 2020, , .	0.3	2
43054	Electronic properties of Ge/2D-GaP heterobilayer: A first-principles investigation. , 2020, , .		3
43055	Electronic structures and band alignment transition in double-wall MoS₂/WS₂ nanotubes for optoelectronic applications. Journal Physics D: Applied Physics, 2021, 54, 095105.	1.3	2
43056	QUANTUM MECHANICAL MODELING OF THE COBALT MONOLAYER BEHAVIOR ON A TIC SURFACE. , 2020, , .		0

#	Article	IF	Citations
43057	Structural and dynamic properties of short-period GaN/AlN superlattices grown by submonolayer digital epitaxy. Journal of Physics: Conference Series, 2020, 1697, 012155.	0.3	1
43058	First Principles Study of Structural Stability and Electronic Properties of CdTe Nanowires. Journal of Computational and Theoretical Nanoscience, 2020, 17, 5210-5214.	0.4	0
43059	Low energy dissipation readout of single-molecule ferroelectronic states by a spin-Seebeck signal. Physical Review Research, 2020, 2, .	1.3	5
43060	The Features of Phase Stability of GaN and AlN Films at Nanolevel. Nanomaterials, 2021, 11, 8.	1.9	4
43061	The nature of the hydrogen interaction on the unreconstructed platinum (110) surface: ab-initio study. Physica Scripta, 2021, 96, 025707.	1.2	2
43062	Structural, electronic, elastic, magnetic and thermodynamic properties of <scp>Mn₂LuZ</scp> (Z = B, Al, Ga and In) <scp>Heusler</scp> compounds: A firstâ€principle study. International Journal of Quantum Chemistry, 2021, 121, .	1.0	4
43064	Crystal Structure and Some Thermodynamic Properties of Ca7MgSi4O16-Bredigite. Crystals, 2021, 11, 14.	1.0	4
43065	Improvement of Selectivity in Acetylene Hydrogenation with Comparable Activity over Ordered PdCu Catalysts Induced by Post-treatment. ACS Applied Materials & Interfaces, 2021, 13, 706-716.	4.0	15
43066	M-Site Vacancy-Mediated Adsorption and Diffusion of Sodium on Ti₂CO₂ MXene. Journal of Physical Chemistry C, 2021, 125, 82-90.	1.5	10
43067	Changes in the geometric structure and hydrogen-termination modify the electronic and optical properties of porous silicon. Optik, 2020, 224, 165539.	1.4	4
43068	Structure of graphene and a surface carbide grown on the (0001) surface of rhenium. Physical Review Materials, 2020, 4, .	0.9	0
43069	CO Diffusion and Bond Weakening on Cu(410) â€"Probing Surface Structureâ€". E-Journal of Surface Science and Nanotechnology, 2020, 18, 307-311.	0.1	0
43070	Synthesis, XRD analysis and electronic structure of InGaTe2 chain semiconductor. International Journal of Modern Physics B, 2021, 35, 2150029.	1.0	1
43071	Electronic and Magnetic Structures of New Interstitial Boron Sub-Oxides B12O2:X (X = B, C, N, O). Molecules, 2021, 26, 123.	1.7	3
43072	The effect of isovalent doping on the electronic band structure of group IV semiconductors. Journal Physics D: Applied Physics, 2021, 54, 085102.	1.3	1
43073	Meissner to ferromagnetic phase transition in La-decorated functionalized Nb₂C MXene: an experimental and computational analysis. Nanotechnology, 2021, 32, 085711.	1.3	5
43074	Thermodynamic property of ternary compound MgCaSi: A study from ab initio Debye-GrÃ¼neisen model. Chinese Journal of Chemical Engineering, 2021, 40, 315-322.	1.7	1
43075	First-principles prediction of enhanced thermoelectric properties of double transition metal MXenes: <mml:math xmlns:mml="http://www.w3.org/1998/Math/MathML"><mml:mrow><mml:msub><mml:mi>Ti</mml:mi><mml:mrow><mml:mn>3</mml:mn></mml:mrow></mml:msub><mml:mi mathvariant="normal">C</mml:mi><mml:mn>2</mml:mn></mml:msub><mml:msub><mml:mi>T</mml:mi><mml:mn>2</mml:mn></mml:msub></mml:mrow></mml:math> Physical Review Materials, 2020, 4, .	0.9	7

#	Article	IF	Citations
43076	Cu(I)â€“I-2,4-diaminopyrimidine Coordination Polymers with Optoelectronic Properties as a Proof of Concept for Solar Cells. Inorganic Chemistry, 2021, 60, 1208-1219.	1.9	11
43077	Analysis of the effects of alloying with Si and Cr on the properties of manganese austenite based on AB INITIO modelling. Eastern-European Journal of Enterprise Technologies, 2020, 6, 28-36.	0.3	3
43078	Experimental and theoretical P-V-T equation of state for Os₂B₃. High Pressure Research, 2021, 41, 27-38.	0.4	1
43079	Supreme enhancement of ferromagnetism in a spontaneous-symmetry-broken 2D nanomagnet. Journal Physics D: Applied Physics, 2021, 54, 105001.	1.3	12
43080	Local electronic structure of stable monolayers of Î±-MoO_{3â^'} _x grown on graphite substrate. 2D Materials, 2021, 8, 025005.	2.0	10
43081	Defect engineering for nontrivial multiferroic orders inSrTiO3. Physical Review Materials, 2020, 4, .	0.9	8
43082	Lanthanide-doped metal-organic frameworks with multicolor mechanoluminescence. Science China Materials, 2021, 64, 931-941.	3.5	13
43083	Strong Boronâ€“Carbon Bonding Interaction Drives CO₂ Reduction to Ethanol over the Boron-Doped Cu(111) Surface: An Insight from the First-Principles Calculations. Journal of Physical Chemistry C, 2021, 125, 572-582.	1.5	12
43084	First principles study of the electronic, elastic, infrared and electrical properties of LiZnPS4. Solid State Communications, 2020, 322, 114057.	0.9	0
43085	Analysis of Thermodynamic and Volume Expansion Properties of Nacl Solid at High Temperatures and Pressures. International Journal of Advanced Research in Science, Communication and Technology, 0, , 178-181.	0.0	0
43086	Phonons splitting induces the second harmonic of tetragonal KH2PO4 by first-principles calculations. Optik, 2020, 223, 165645.	1.4	0
43087	Metallic ferroelectric-ferromagnetic multiferroics in strained EuTiO3â^'xHx. Physical Review B, 2020, 102, .	1.1	1
43088	Thermoelectric properties of MoC monolayers from first-principles calculations. AIP Advances, 2020, 10, .	0.6	3
43089	Metallic ground states of undoped Ti2O3 films induced by elongated c-axis lattice constant. Scientific Reports, 2020, 10, 22109.	1.6	12
43090	First-principles LCAO study of the low- and room-temperature phases of CdPS3. Low Temperature Physics, 2020, 46, 1217-1222.	0.2	2
43091	Investigations on pressure dependent physical properties of cubic AMoO₃ (A = Ca, Sr) perovskites: A DFT calculation. International Journal of Materials Research, 2020, 111, 1038-1046.	0.1	3
43092	First-principles study on the influence of biaxial strain on the electronic and magnetic properties of defective blue phosphorene. Physics Letters, Section A: General, Atomic and Solid State Physics, 2020, 384, 126853.	0.9	1
43093	Various polymorphs of group IIIâ€“VI (GaSe, InSe, GaTe) monolayers with quasi-degenerate energies: facile phase transformations, high-strain plastic deformation, and ferroelastic switching. Materials Today Physics, 2020, 15, 100229.	2.9	4

#	Article	IF	Citations
43094	Oxygen Evolution Reaction on a N-Doped Co_{0.5}-Terminated Co₃o₄ (001) Surface. Proceedings of the Latvian Academy of Sciences, 2020, 74, 396-403.	0.0	0
43095	ELECTRONIC STRUCTURE OF PNICTIDES HgCX2. Journal of Structural Chemistry, 2020, 61, 1839-1844.	0.3	3
43096	Firstâ€principles study of Cs 2 Ti 1â^' x M x Br 6 (M = Pb, Sn) and numerical simulation of the solar cells based on Cs 2 Ti 0.25 Sn 0.75 Br 6. International Journal of Energy Research, 2021, 45, 8049-8060.	2.2	5
43097	Improved band gaps and structural properties from Wannierâ€"Fermiâ€"LÃ¶wdin self-interaction corrections for periodic systems. Journal of Physics Condensed Matter, 2021, 33, 115501.	0.7	29
43099	Efficient approaches to solutions of partition function for condensed matters. Journal of Physics Condensed Matter, 2021, 33, 115901.	0.7	4
43100	Dense and Low Oxygen Permeability Bilayer Ceramic Interconnect for Tubular Anode-Support Solid Oxide Cells. ACS Applied Energy Materials, 2021, 4, 341-349.	2.5	1
43101	Optimizing Configurations for Determining the Electromagnetic Properties of CsFeF3, NaFeF3, and RbFeF3 Fluorides: GGA vs GGA+U and TB-mBj Approaches. Annals of West University of Timisoara: Physics, 2020, 62, 71-94.	0.2	0
43102	Kinetic Processes and Surfactant Design of Group I Elements on the CZTS (1Ì…1Ì…2Ì…) Surface. Journal of Physical Chemistry C, 2021, 125, 376-384.	1.5	3
43103	Structural Stability and Magnetic Ordering in BiFeO3 Perovskite Oxide: A Comparative Study GGA+U vs L(S)DA+U. Annals of West University of Timisoara: Physics, 2020, 62, 52-70.	0.2	1
43104	Graphene-Supported Fe/Ni, Î²-Mo2C Nanoparticles: Experimental and DFT Integrated Approach to Catalyst Development for Synergistic Hydrogen Production through Lignin-Rich Biomass Reforming and Reduced Shale Gas Flaring. ACS Catalysis, 2021, 11, 364-382.	5.5	9
43105	High-Pressure Neutron Powder Diffraction Study of Îµ-CL-20: A Gentler Way to Study Energetic Materials. Journal of Physical Chemistry C, 2020, 124, 27985-27995.	1.5	9
43106	Aggregation of retained helium and hydrogen in titanium beryllide Be₁₂Ti: a first-principles study. RSC Advances, 2021, 11, 34860-34869.	1.7	4
43107	Understanding the charge storage mechanism of supercapacitors:in situ/operandospectroscopic approaches and theoretical investigations. Journal of Materials Chemistry A, 2021, 9, 25852-25891.	5.2	48
43108	Prediction of bimetal embedded in two-dimensional materials for CO₂ reduction electrocatalysis with a new integrated descriptor. Physical Chemistry Chemical Physics, 2021, 23, 26241-26249.	1.3	3
43109	Spin-crossover complexes in nanoscale devices: main ingredients of the moleculeâ€"substrate interactions. Nanoscale, 2021, 13, 18702-18713.	2.8	13
43110	Unveiling the role of 2D monolayer Mn-doped MoS₂material: toward an efficient electrocatalyst for H₂evolution reaction. Physical Chemistry Chemical Physics, 2021, 24, 265-280.	1.3	21
43111	Electronic, optical and thermoelectric properties of a novel two-dimensional SbXY (X = Se, Te; Y = Br, I) family: ab initio perspective. Physical Chemistry Chemical Physics, 2021, 23, 25866-25876.	1.3	17
43112	First-principles studies of oxygen ion migration behavior for different valence B-site ion doped SrFeO_{3â^'Î´} ceramic membranes. Physical Chemistry Chemical Physics, 2021, 23, 27266-27272.	1.3	4

#	Article	IF	Citations
43113	Tunable phase stability of negative thermal expansion materials by theory and experiment. Physical Chemistry Chemical Physics, 2021, 23, 25533-25541.	1.3	1
43114	Insight into mechanical and thermodynamic properties of Al2Si2La and Al2Si2Pr from first-principles calculations. Journal of Solid State Chemistry, 2022, 305, 122662.	1.4	0
43115	Coexistence of two gold-induced one-dimensional structures on a single terrace of the Si(11 11 13). Applied Surface Science, 2022, 573, 151501.	3.1	0
43116	The synthesis mechanism of nitrogen to ammonia on the Fe, Co, Ni-doped Cu(1 0 0) Surface: A DFT study. Applied Surface Science, 2022, 573, 151477.	3.1	4
43117	Interactions of oxygen with intrinsic defects in L1<mml:math xmlns:mml="http://www.w3.org/1998/Math/MathML" display="inline" id="d1e1983" altimg="si96.svg"><mml:msub><mml:mrow /><mml:mrow><mml:mn>0</mml:mn></mml:mrow></mml:msub></mml:math> <mml:math xmlns:mml="http://www.w3.org/1998/Math/MathML" display="inline" id="d1e1991" altimg="si48.svg"><mml:mi>Î³</mml:mi></mml:math>-TiAl in presence of substitutional solutes: Influenc	1.4	3
43118	A superhard carbon allotrope with cage structure: oS44-carbon. Journal of Solid State Chemistry, 2022, 305, 122653.	1.4	5
43119	First-principles calculations of nickel, cadmium, and lead nanoclusters adsorption on single-wall (10,0) boron-nitride nanotube. Applied Surface Science, 2022, 573, 151547.	3.1	7
43120	Exploration of the icosahedral clusters in Niâ€“Nb binary metallic glasses via first-principles theory. Journal of Non-Crystalline Solids, 2022, 575, 121232.	1.5	1
43121	An investigation of vacancy defects on electronic and magnetic properties of TlN nanosheet: By density function calculation. Solid State Communications, 2022, 341, 114576.	0.9	1
43122	A DFT study of GaSe/AlN(ZnO) two-dimensional vdW heterostructure practiced as an encouraging photocatalyst for water splitting. Computational Materials Science, 2022, 201, 110912.	1.4	12
43123	Predicted double perovskite material Ca2ZrTiO6 with enhanced n-type thermoelectric performance. Journal of Solid State Chemistry, 2022, 305, 122661.	1.4	17
43124	Oxidation mechanism of the arsenopyrite surface by oxygen with and without water: Experimental and theoretical analysis. Applied Surface Science, 2022, 573, 151574.	3.1	14
43125	A diagnosis approach for semiconductor properties evaluation from ab initio calculations: Ag-based materials investigation. Journal of Solid State Chemistry, 2022, 305, 122670.	1.4	7
43126	Exploring thermal expansion of carbon-based nanosheets by machine-learning interatomic potentials. Carbon, 2022, 186, 501-508.	5.4	30
43127	Controllable fabrication of novel graphene quantum dots/fluorinated boron nitride ultralight composites for broadband and high-performance microwave absorption. Carbon, 2022, 186, 391-405.	5.4	18
43128	Antiferromagnetic coupling in the initial stages of the MnN epitaxial growth on the CrN (0 0 1) surface. Applied Surface Science, 2022, 573, 151451.	3.1	7
43129	Investigation of the structural and electronic properties and surface passivation influence on electronic properties of (001) SbNSr3 nano-surfaces: A hybrid DFT study. Journal of Physics and Chemistry of Solids, 2022, 161, 110407.	1.9	0
43130	First-principles calculations to investigate structural, elastic, electronic and magnetic properties of novel d half metallic half Heusler alloys XSrB (X=Be, Mg). Intermetallics, 2022, 140, 107392.	1.8	3

#	Article	IF	Citations
43131	Sheet doping for improved sensitivity of HCl on MoTe2. Surface Science, 2022, 716, 121964.	0.8	3
43132	Ordered structure and solute-suppressed atomic ordering in iron-cobalt alloys. Computational Materials Science, 2022, 202, 111005.	1.4	8
43133	NiO/NiFe2O4@N-doped reduced graphene oxide aerogel towards the wideband electromagnetic wave absorption: Experimental and theoretical study. Chemical Engineering Journal, 2022, 430, 132814.	6.6	19
43134	Zinc enhances catalytic performance of pyridine-adsorbed HMOR: Dimethyl ether carbonylation. Fuel, 2022, 310, 122225.	3.4	1
43135	A computational estimation on structural, electronic, elastic, optic and dynamic properties of Li2TlA (A=Sb and Bi): First-principles calculations. Materials Science in Semiconductor Processing, 2022, 138, 106302.	1.9	10
43136	Porous Carbon/Borocarbonitride hybrid with enhanced tap density as a polar host for ultralong life Lithium-Sulfur batteries. Chemical Engineering Journal, 2022, 430, 132987.	6.6	10
43137	High pressure phase stability, elastic anisotropy and electronic properties of GePd. Materials Science in Semiconductor Processing, 2022, 138, 106223.	1.9	0
43138	Machine-learning interatomic potential for radiation damage effects in bcc-iron. Computational Materials Science, 2022, 202, 110960.	1.4	9
43139	Effects of spin-orbit coupling on the electronic properties of the buckled IIIâ€“V monolayers. Journal of Magnetism and Magnetic Materials, 2022, 543, 168638.	1.0	9
43140	Atomic Structures of Single-Layer Nanoislands of Ni, Cu, Rh, Pd, Ag, Ir, Pt, Au Supported on Au(111) from Density Functional Theory Calculations. Surface Science, 2022, 716, 121960.	0.8	1
43141	Adsorption of benzene on defective Pt surfaces: A DFT study. Surface Science, 2022, 716, 121959.	0.8	3
43142	First-principles and Monte Carlo investigation of magnetic properties of two-dimensional transition metal alloyed boron-carbide<mml:math xmlns:mml="http://www.w3.org/1998/Math/MathML" altimg="si2.svg"><mml:mrow><mml:mi mathvariant="normal">C</mml:mi><mml:mi mathvariant="normal">r</mml:mi><mml:mi mathvariant="normal">F</mml:mi><mml:mi mathvariant="normal">e</mml:mi><mml:mi mathvariant="normal">B</mml:mi><mml:mi mathvariant="normal">C</mml:mi></mml:mrow></mml:math> monolayer. Computational Materials Science,	1.4	2
43143	Synergistic coupling between Fe7S8-MoS2 heterostructure and few layers MoS2-embeded N-/P-doping carbon nanocapsule enables superior Li-S battery performances. Applied Surface Science, 2022, 574, 151586.	3.1	25
43144	The effect of SrFeO25 native point defects on its electrical properties: First principles investigations. Computational Materials Science, 2022, 202, 110922.	1.4	0
43145	Towards predictive simulations of spinodal decomposition in Fe-Cr alloys. Computational Materials Science, 2022, 202, 110955.	1.4	4
43146	On the ensemble requirement of fully selective chemical looping methane partial oxidation over La-Fe-based perovskites. Applied Catalysis B: Environmental, 2022, 301, 120788.	10.8	34
43147	Anions influence on the electrochemical performance of Co3X4 (XÂ=ÂO, Se) for supercapacitor: Experiments and theoretical calculations. Applied Surface Science, 2022, 574, 151646.	3.1	12
43148	Defects assisted photosensing and dye degradation of Ni/Ga co-doped ZnO: A theory added experimental investigation. Journal of Alloys and Compounds, 2022, 893, 162229.	2.8	6

#	Article	IF	Citations
43149	Ligand effects on surface oxide at RhPd(100) alloy surfaces: A density functional theory calculation study. Surface Science, 2022, 716, 121958.	0.8	3
43150	Light emission of Lu2Sn2O7 pyrochlore driven by oxygen vacancy and local site engineering. Journal of Alloys and Compounds, 2022, 893, 162249.	2.8	5
43151	Theoretical prediction of layered boron-rich ZnB12O14(OH)10 with higher carrier separation and strong oxidation potential for photocatalysis. Journal of Physics and Chemistry of Solids, 2022, 161, 110431.	1.9	3
43152	Role of surface steps in activation of surface oxygen sites on Ir nanocrystals for oxygen evolution reaction in acidic media. Applied Catalysis B: Environmental, 2022, 302, 120834.	10.8	29
43153	On calculations of basic structural parameters in multi-principal element alloys using small atomistic models. Computational Materials Science, 2022, 202, 110942.	1.4	10
43154	Atomic origin of magnetic coupling of antiphase boundaries in magnetite thin films. Journal of Materials Science and Technology, 2022, 107, 92-99.	5.6	8
43155	Electronic structure investigation of intrinsic and extrinsic defects in LiF. Computational Materials Science, 2022, 202, 110977.	1.4	11
43156	Unveiling the shape-selective CoCr2-yScyO4 nanomagnetism. Applied Surface Science, 2022, 574, 151555.	3.1	15
43157	Achieving the robust immobilization of CoP nanoparticles in cellulose nanofiber network-derived carbon via chemical bonding for a stable potassium ion storage. RSC Advances, 2020, 10, 44611-44623.	1.7	6
43158	Effect of Nb Alloying Addition on Local Phase Transformation at Microtwin Boundaries in Nickel-Based Superalloys. Minerals, Metals and Materials Series, 2020, , 640-650.	0.3	6
43159	The thermoelectric properties of Î±-XP (X = Sb and Bi) monolayers from first-principles calculations. Physical Chemistry Chemical Physics, 2021, 23, 24598-24606.	1.3	8
43160	Factors affecting the electronâ€“phonon coupling in FeSe under pressure. Physical Chemistry Chemical Physics, 2021, 23, 25107-25113.	1.3	3
43161	Promising thermoelectric candidate based on a CaAs₃ monolayer: A first principles study. Physical Chemistry Chemical Physics, 2021, 23, 24039-24046.	1.3	2
43162	Effects of the Hubbard U correction on the electronic and magnetic properties of the tetragonal V₂P₂ sheet. RSC Advances, 2021, 11, 35061-35068.	1.7	2
43163	Optical properties and applications of SnS₂ SAs with different thickness. Opto-Electronic Advances, 2021, 4, 200029-200029.	6.4	35
43164	Rationalisation of the Micromechanisms Behind the High-Temperature Strength Limit in Single-Crystal Nickel-Based Superalloys. Minerals, Metals and Materials Series, 2020, , 260-272.	0.3	4
43165	Supersolvus Hot Workability and Dynamic Recrystallization in Wrought Coâ€“Alâ€“W-Base Alloys. Minerals, Metals and Materials Series, 2020, , 857-869.	0.3	0
43166	Dependence of Carbon Concentration and Alloying Elements on the Stability of Iron Carbides. Tetsu-To-Hagane/Journal of the Iron and Steel Institute of Japan, 2020, 106, 352-361.	0.1	1

#	Article	IF	Citations
43167	Ferroelectric critical size of SnTe nanoribbon and its mechanical strain engineering. Transactions of the JSME (in Japanese), 2020, 86, 19-00430-19-00430.	0.1	0
43168	Interaction of flotation reagents with mineral surface. , 2020, , 237-305.		0
43169	Ground State Structural, Elastic, Electronic Properties and Pressure-Induced Structural Phase Transition of XCoSb (X = Sc, Ti, V, Cr and Mn). Journal of Superconductivity and Novel Magnetism, 2020, 33, 1821-1829.	0.8	3
43170	Twinnability of Ti-V Binary Alloys: Simulation and Experiment. MATEC Web of Conferences, 2020, 321, 11092.	0.1	0
43171	Structural, electronic and thermoelectric properties of two-dimensional GeSe bilayer. AIP Conference Proceedings, 2020, , .	0.3	0
43172	Effect of biaxial strain on the gas-sensing of monolayer GeSe. Wuli Xuebao/Acta Physica Sinica, 2020, 69, 196801.	0.2	4
43173	Ab Initio Simulations of Semiconductor Surfaces and Interfaces. Springer Handbooks, 2020, , 119-153.	0.3	0
43174	Chemical and electronic structures of cobalt oxynitride films deposited by NH₃vs. N₂ plasma: theory vs. experiment. Physical Chemistry Chemical Physics, 2020, 22, 24640-24648.	1.3	6
43175	Group III monochalcogenide of single-layered haeckelites structure MX (M = Al, Ga, In;) Tj ETQq0 0 0 rgBT /Overlock 10 Tf	0.2	0
43176	Structural phase transition, electronic and thermoelectric properties of osmium silicide. AIP Conference Proceedings, 2020, , .	0.3	0
43177	A first-principles study of the switching mechanism in GeTe/InSbTe superlattices. Nanoscale Advances, 2020, 2, 5209-5218.	2.2	3
43178	First principles study of optical properties of 2D PtP2 and PtAs2 monolayers. AIP Conference Proceedings, 2020, , .	0.3	0
43179	Study of effect of hydrostatic pressure on structural, electronic and magnetic properties of In0.75Cr0.25P. AIP Conference Proceedings, 2020, , .	0.3	0
43180	Experimental and Computational Methods. Springer Theses, 2020, , 33-64.	0.0	0
43181	Ternary Oxides. Nanoscience and Technology, 2020, , 519-629.	1.5	0
43182	Binary Oxides of Transition Metals: V$$_2$$O$$_5$$. Nanoscience and Technology, 2020, , 453-518.	1.5	0
43183	Study of the Stoichiometry Effect on the Interaction of Hexagonal HgSe with Electromagnetic Radiation. Springer Proceedings in Energy, 2020, , 269-278.	0.2	0
43185	Structural and Elastic Properties of Fe-Ge Alloys: ab initio studies. Bulletin of the South Ural State University Series Mathematics Mechanics Physics, 2020, 12, 49-56.	0.2	0

#	Article	IF	Citations
43186	Study of surface effect in n-type SrTiO3/LaAlO3 heterostructure by first principle calculations. AIP Conference Proceedings, 2020, , .	0.3	0
43187	Spin-dimer ground state driven by consecutive charge and orbital ordering transitions in the anionic mixed-valence compound <mml:math xmlns:mml="http://www.w3.org/1998/Math/MathML"><mml:mrow><mml:msub><mml:mi>Rb</mml:mi><mml:mn>14</mml:mn><mml:mn></mml:mn></mml:msub><mml:msub><mml:mi mathvariant="normal">O</mml:mi><mml:mn>6</mml:mn></mml:msub></mml:mrow></mml:math>. Physical Review B, 2020, 101, .	1.1	3
43188	Thermodynamic/Electrochemical Description of High-Voltage Spinels for Lithium-Ion Batteries. Journal of the Electrochemical Society, 2020, 167, 130511.	1.3	3
43189	Chalcogenides. Nanoscience and Technology, 2020, , 631-833.	1.5	0
43190	Pd-P antibonding interactions in <mml:math xmlns:mml="http://www.w3.org/1998/Math/MathML"><mml:mrow><mml:mi>A</mml:mi><mml:msub><mml:mi>Pd</mml:mi><mml:mn></mml:mn></mml:msub><mml:msub><mml:mi mathvariant="normal">P</mml:mi><mml:mn>2</mml:mn></mml:msub></mml:mrow></mml:math> () Tj ETQq0 0 0 rgBT /Overlock 10 T	0.9	7
43191	First principles calculations for electronic, optical and magnetic properties of full heusler compounds. East European Journal of Physics, 2020, , .	0.1	1
43192	Iron- and Silicon-Intercalated Graphene on Silicon Carbide: from Hybridization to Quasi-Freestanding Bilayer Graphene. Reviews on Advanced Materials and Technologies, 2020, 2, 42-46.	0.1	0
43193	Giant piezoresistive gauge factor in vein-membrane/graphene sensors with a wide linear working range. Journal of Materials Chemistry C, 2020, 8, 16957-16966.	2.7	8
43194	Vibrational Up-Pumping in Polymorphic Materials. Springer Theses, 2020, , 157-178.	0.0	0
43195	First-principles study of stability, electronic and optical properties of two-dimensional Nb₂SiTe₄-based materials. Wuli Xuebao/Acta Physica Sinica, 2020, 69, 197102.	0.2	0
43196	First-principles study of atomic bond nature of one-dimensional carbyne chain under different strains. Wuli Xuebao/Acta Physica Sinica, 2020, 69, 246802.	0.2	1
43197	Numerical prediction of structural stability and thermodynamic properties for MgF₂ with fluorite- type structure under high pressure. Wuli Xuebao/Acta Physica Sinica, 2020, 69, 156202.	0.2	1
43198	First principles study of the atomic and electronic structure in graphene-fullerene hybrid systems. Letters on Materials, 2020, 10, 365-370.	0.2	3
43199	Compression-induced resistance of singlet oxygen dissociation on phosphorene. Physical Review Materials, 2020, 4, .	0.9	0
43200	Role of lone pair electrons in n-type thermoelectric properties of tin oxides ^{**}. Journal of Physics Condensed Matter, 2020, 33, 065504.	0.7	1
43201	Alloy design for improvement of ductility and toughness in magnesium alloy: First-principles-calculation approaches. Keikinzoku/Journal of Japan Institute of Light Metals, 2020, 70, 73-81.	0.1	0
43202	High-pressure crystal structure and properties of BrCl. Journal of Physics Condensed Matter, 2020, 33, 095401.	0.7	2
43203	HOT Graphene and HOT Graphene Nanotubes: New Low Dimensional Semimetals and Semiconductors. Nanoscale Research Letters, 2020, 15, 56.	3.1	4

#	Article	IF	Citations
43204	Tuning CuZn interfaces in metalâ€“organic framework-derived electrocatalysts for enhancement of CO₂ conversion to C₂ products. Catalysis Science and Technology, 2021, 11, 8065-8078.	2.1	17
43205	Zn(NH₃)CO₃: a â€œthree-in-oneâ€•UV nonlinear optical crystal built by a polar molecule bonding strategy. Journal of Materials Chemistry C, 2021, 9, 16477-16484.	2.7	8
43206	Intrinsic ferromagnetism in 2D h-CrC semiconductors with strong magnetic anisotropy and high Curie temperatures. Journal of Materials Chemistry C, 2021, 9, 16495-16505.	2.7	15
43207	Haeckelite phosphorus: an emerging 2D allotrope of phosphorus for potential use in LIBs/SIBs. Physical Chemistry Chemical Physics, 2021, 23, 26547-26560.	1.3	5
43208	Capturing excitonic and polaronic effects in lead iodide perovskites using many-body perturbation theory. Journal of Materials Chemistry C, 2021, 9, 17113-17123.	2.7	8
43209	Estabilidad estructural y electrÃ³nica para la adsorciÃ³n de Nb sobre la superficie polar del AlN. Revista Facultad De Ciencias BÃ¡sicas, 2020, 15, 21-30.	0.2	0
43210	First Principles Based Compact Model for 2D-Channel MOSFETs. , 2020, , .		1
43213	Electronic band profiles and magneto-electronic properties of ternary XCu₂P₂ (Xâ€,=â€,Ca, Sr) compounds: insight from ab initio calculations. Zeitschrift Fur Naturforschung - Section A Journal of Physical Sciences, 2020, 75, 543-549.	0.7	9
43214	Intrinsic defects of GaSe. Journal of Physics Condensed Matter, 2020, 32, 285503.	0.7	4
43215	Experimental and theoretical studies of spherical Î²-cyclodextrin modified titanium dioxide composites for uranium removal. Ecological Engineering, 2020, 149, 105835.	1.6	11
43216	First Principles Study of Structural, Elastic, Electronic and Optical Features of the Non-centrosymmetric Superconductors SrMGe3 (Where M= Ir, Pt, and Pd). International Journal of Material and Mathematical Sciences, 2020, , 16-28.	0.2	3
43217	Kinetic Monte Carlo for Process Simulation: First Principles Calibrated Parameters for BO2. , 2021, , .		0
43218	Theoretical considerations of superconducting HfBH2 and HfB2H under high pressure. Journal of Applied Physics, 2021, 130, 153904.	1.1	3
43219	Impacts of terminal molecules on metal-atom diffusion into alkane SAM films: first-principles study. Japanese Journal of Applied Physics, 0, , .	0.8	0
43220	In Situ Bulk Observations and Ab Initio Calculations Revealing the Temperature Dependence of Stacking Fault Energy in Feâ€“Crâ€“Ni Alloys. Metallurgical and Materials Transactions A: Physical Metallurgy and Materials Science, 2021, 52, 5357-5366.	1.1	7
43221	Probing into the crystal plane effect on the reduction of Î±-Fe2O3 in CO by Operando Raman spectroscopy. Journal of Fuel Chemistry and Technology, 2021, 49, 1558-1566.	0.9	9
43222	Energetic, Electronic, and Optical Properties of Intrinsic Charge Carrier-Trapping Defects in KTaO₃: Insights from a Hybrid DFT Study. Journal of Physical Chemistry C, 2021, 125, 24067-24078.	1.5	8
43223	Induced ferromagnetism on late transition metals adsorbed on Antimony Arsenide monolayer from First-Principles. Journal of Magnetism and Magnetic Materials, 2022, 545, 168658.	1.0	1

#	Article	IF	Citations
43224	First-Principles Studies on the Formation of Oxygen Vacancies in Li₂CoSiO₄. Journal of the Electrochemical Society, 2021, 168, 110527.	1.3	2
43225	Metalâ€“Support Interactions in Rhodium Catalysts Supported on Tetravalent Metal Pyrophosphates (MP2O7; M = Si, Ti, and Zr). Journal of Physical Chemistry C, 0, , .	1.5	2
43226	Analysis of Ionicity-Magnetism Competition in 2D-MX3 Halides towards a Low-Dimensional Materials Study Based on GPU-Enabled Computational Systems. Nanomaterials, 2021, 11, 2967.	1.9	2
43227	Defluorination and adsorption of tetrafluoroethylene (TFE) on TiO2(110) and Cr2O3(0001). Scientific Reports, 2021, 11, 21551.	1.6	0
43228	Modification of the Surface Structure and Electronic Properties of Diamond (100) with Tin as a Surface Termination: A Density Functional Theory Study. Journal of Physical Chemistry C, 2021, 125, 25165-25174.	1.5	3
43229	Dual optimization approach to Mo single atom dispersed g-C3N4 photocatalyst: Morphology and defect evolution. Applied Catalysis B: Environmental, 2022, 303, 120904.	10.8	203
43230	Quantum anharmonic enhancement of superconductivity in P63/mmc ScH6 at high pressures: A first-principles study. Journal of Applied Physics, 2021, 130, .	1.1	9
43231	Ultralow lattice thermal conductivity and high thermoelectric performance of penta-Sb2C monolayer: A first principles study. Journal of Applied Physics, 2021, 130, 185104.	1.1	7
43232	Janus Monolayers of Transition Metal Dichalcogenides: A DFT Study. Physica Status Solidi (B): Basic Research, 2022, 259, .	0.7	2
43233	Intrinsic magnetism in two-dimensional Cr₂X₂Se (XÂ=ÂI, Br, Cl) monolayers. Europhysics Letters, 2021, 135, 67005.	0.7	0
43234	Microwave Dielectric Materials with Defect-Dipole Clusters Induced Colossal Permittivity and Ultra-low Loss. ACS Applied Electronic Materials, 2021, 3, 5015-5022.	2.0	8
43235	Ca₃(TeO₃)₂(MO₄) (M = Mo, W): Mid-Infrared Nonlinear Optical Tellurates with Ultrawide Transparency Ranges and Superhigh Laser-Induced Damage Thresholds. Inorganic Chemistry, 2021, 60, 18512-18520.	1.9	16
43236	Effects of topological band structure on thermoelectric transport of bismuthene. Physical Review B, 2021, 104, .	1.1	5
43237	Reaction chemistry of PbSO4 formation over Al2O3 sorbent. Fuel, 2022, 310, 122407.	3.4	5
43238	Dynamic State and Active Structure of Niâ€“Co Catalyst in Carbon Nanofiber Growth Revealed by in Situ Transmission Electron Microscopy. ACS Nano, 2021, 15, 17895-17906.	7.3	25
43239	Evaluation of the structural, electronic, optical, elastic, mechanical, and vibrational properties of graphene-like g-GaN using density functional theory. AIP Advances, 2021, 11, .	0.6	5
43240	Designing high-entropy ceramics via incorporation of the bond-mechanical behavior correlation with the machine-learning methodology. Cell Reports Physical Science, 2021, 2, 100640.	2.8	10
43241	Selective Methane Oxidation to Methanol on ZnO/Cu₂O/Cu(111) Catalysts: Multiple Site-Dependent Behaviors. Journal of the American Chemical Society, 2021, 143, 19018-19032.	6.6	41

#	Article	IF	Citations
43242	Electromechanically Actuated MXene Nanotubes for Tunable Mass Transport. Journal of Physical Chemistry C, 2021, 125, 25275-25283.	1.5	1
43243	An Ab Initio Study of Lithization of Two-Dimensional Siliconâ€“Carbon Anode Material for Lithium-Ion Batteries. Materials, 2021, 14, 6649.	1.3	7
43244	A Lowâ€Power CuSCN Hydrogen Sensor Operating Reversibly at Room Temperature. Advanced Functional Materials, 2022, 32, 2102635.	7.8	8
43245	Photo-Sono Interfacial Engineering Exciting the Intrinsic Property of Herbal Nanomedicine for Rapid Broad-Spectrum Bacteria Killing. ACS Nano, 2021, 15, 18505-18519.	7.3	61
43246	Anisotropy in elasticity, sound velocity, thermal conductivity, and thermodynamics properties of dodecaboride Zr 0.5 Y 0.5 B 12. International Journal of Quantum Chemistry, 0, , e26836.	1.0	0
43247	Optimization of Nanostructured Copper Sulfide to Achieve Enhanced Enzyme-Mimic Activities for Improving Anti-Infection Performance. ACS Applied Materials & Interfaces, 2021, 13, 53659-53670.	4.0	11
43248	Charged domain boundaries stabilized by translational symmetry breaking in the hybrid improper ferroelectric Ca3â€“xSrxTi2O7. Communications Materials, 2021, 2, .	2.9	8
43249	Pressure and doping effects on the structural stability of thermoelectric BaAg₂Te₂. Journal of Physics Condensed Matter, 2022, 34, 065401.	0.7	0
43250	The effect of substitutional doping of Yb²⁺ on structural, electronic, and optical properties of CsCaX ₃ (X: Cl, Br, I) phosphors: a first-principles study. Journal of Physics Condensed Matter, 2022, 34, 065502.	0.7	4
43251	Strain and electric field tunable electronic and optical properties in antimonene/C3N van der Waals heterostructure. Solid State Sciences, 2021, 122, 106771.	1.5	9
43252	Ab initio calculations of the elastic, vibrational, electronic properties, and electron-phonon constant of superconducting YB₆ compound under low pressure. Physica Scripta, 2021, 96, 125850.	1.2	2
43253	Signatures of bosonic Landau levels in a finite-momentum superconductor. Nature, 2021, 599, 51-56.	13.7	5
43254	Robust Pipekâ€“Mezey Orbital Localization in Periodic Solids. Journal of Chemical Theory and Computation, 2021, 17, 7406-7415.	2.3	2
43255	First-Principles Studies of the Adsorption and Catalytic Properties for Gas Molecules on h-BN Monolayer Doped with Various Transition Metal Atoms. Catalysis Surveys From Asia, 2022, 26, 69-79.	1.0	6
43256	Understanding the oxygen-vacancy-related catalytic cycle for H2 oxidation on ceria-based SOFC anode and the promotion effect of lanthanide doping from theoretical perspectives. Applied Surface Science, 2022, 576, 151803.	3.1	6
43257	Site occupancy behavior of the binary Î¼ phase. Journal of Solid State Chemistry, 2022, 305, 122704.	1.4	8
43258	Magnetic and structural properties of Co-Ni-<mml:math xmlns:mml="http://www.w3.org/1998/Math/MathML" display="inline" id="d1e1016" altimg="si84.svg"><mml:mi>Z</mml:mi></mml:math>Â(<mml:math) Tj ETQq0 0 0 rgBT /Overlock 10 Tf 50 107 Td (xmlns:mml="http://w	1.0	2
43259	Effect of Point Defects on Electronic Structure of Monolayer GeS. Nanomaterials, 2021, 11, 2960.	1.9	2

#	Article	IF	Citations
43260	Prediction of an unusual trigonal phase of superconducting LaH10 stable at high pressures. Physical Review B, 2021, 104, .	1.1	2
43261	Perovskite-like K₃TiOF₅ Exhibits (3 + 1)-Dimensional Commensurate Structure Induced by Octahedrally Coordinated Potassium Ions. Journal of the American Chemical Society, 2021, 143, 18907-18916.	6.6	4
43262	Adsorption of acetic acid and benzoic acid on pristine and defect containing graphene: A DFT study. Computational and Theoretical Chemistry, 2022, 1207, 113504.	1.1	2
43263	Highly efficient electrochemical carbon dioxide reduction to syngas with tunable ratios over pyridinic- nitrogen rich ultrathin carbon nanosheets. Journal of Colloid and Interface Science, 2022, 608, 2650-2659.	5.0	11
43264	Azobenzene-Iron(III)porphyrin Hybrid Composite as a Light-Driven Molecular Spin Regulator: Some Promising Insights from DFT. Chemistry of Materials, 2021, 33, 8786-8799.	3.2	4
43265	Investigation of vacancy defects and substitutional doping in AlSb monolayer with double layer honeycomb structure: a first-principles calculation. Journal of Physics Condensed Matter, 2022, 34, 065701.	0.7	18
43266	The barrier free splitting of O-H bond in H2O and CH3OH due to the synergetic effects of single atom (Cu1/Fe1) coordination change and ZnO(1 1 0) surface oxygen activation. Applied Surface Science, 2022, 576, 151750.	3.1	3
43267	Computational Design of Pd Nanoclusters and Pd Single-Atom Catalysts Supported on O-Functionalized Graphene. ACS Applied Nano Materials, 2021, 4, 12235-12249.	2.4	9
43268	A <scp>Twoâ€Đimensional</scp> Semiconductive <scp>Metalâ€Organic</scp> Framework for Highly Efficient Microwave Absorption. Chinese Journal of Chemistry, 2022, 40, 467-474.	2.6	23
43269	Alkyne-Functionalized Cyclooctyne on Si(001): Reactivity Studies and Surface Bonding from an Energy Decomposition Analysis Perspective. Molecules, 2021, 26, 6653.	1.7	1
43270	Growth of Open Honeycomb-like Sn Structures on Ag(111) at Low Temperatures. Journal of Physical Chemistry C, 2021, 125, 25332-25338.	1.5	0
43271	First-principles study of hydrogen adsorption behavior in C15 Laves phase compound ZrV2. AIP Advances, 2021, 11, 115010.	0.6	3
43272	Hydrogen Storage in Bilayer Hexagonal Boron Nitride: A First-Principles Study. ACS Omega, 2021, 6, 30362-30370.	1.6	16
43273	New insight into the structural stability, ductility and melting point of Mo5SiB2 under high-pressure environment. Vacuum, 2022, 196, 110727.	1.6	64
43274	Extended first-principles molecular dynamics model for high temperature simulations in the Abinit code: Application to warm dense aluminum. Computer Physics Communications, 2022, 271, 108215.	3.0	11
43275	Doping limitation due to self-compensation by native defects in In-doped rocksalt Cd_xZn_{1â^'x}O. Journal of Physics Condensed Matter, 2022, 34, 065702.	0.7	1
43276	Theoretical and Experimental Studies of Charge Ordering in CaFeO₃ and SrFeO₃ Crystals. Physica Status Solidi (B): Basic Research, 2022, 259, 2100238.	0.7	6
43277	Cofactorâ€Assisted Artificial Enzyme with Multiple Liâ€Bond Networks for Sustainable Polysulfide Conversion in Lithiumâ€“Sulfur Batteries. Advanced Science, 2022, 9, e2104205.	5.6	20

#	Article	IF	Citations
43278	The effect of ionic liquid-based electrolytes for dendrite-inhibited and performance-boosted lithium metal batteries. Electrochimica Acta, 2022, 401, 139527.	2.6	9
43279	Metastable Metallic Phase of a Bilayer Blue Phosphorene Induced by Interlayer Bonding and Intralayer Charge Redistributions. Journal of Physical Chemistry Letters, 2021, 12, 10981-10986.	2.1	4
43280	Solution-Phase Growth of Cu Nanowires with Aspect Ratios Greater Than 1000: Multiscale Theory. ACS Nano, 2021, 15, 18279-18288.	7.3	15
43281	Calculation of xmlns:mml="http://www.w3.org/1998/Math/MathML"><mml:mi>Na</mml:mi><mml:mi>Zn</mml:mi><mml:msub><mml:mi mathvariant="normal">F</mml:mi><mml:mn>3</mml:mn></mml:msub></mml:math> as a low-pressure analog of <mml:math xmlns:mml="http://www.w3.org/1998/Math/MathML"><mml:mi>Mg</mml:mi><mml:mi>Si</mml:mi><mml:msub><mml:mi mathvariant="normal">O</mml:mi><mml:mn>3</mml:mn></mml:msub></mml:math>. Physical Review Ma	0.9	1
43282	Vacancy-Induced Magnetism in Fluorographene: The Effect of Midgap State. Molecules, 2021, 26, 6666.	1.7	1
43283	Pressure-induced structural and electronic phase transitions of uranium trioxide. Physical Review B, 2021, 104, .	1.1	6
43284	A Universal Force Field for Materials, Periodic GFN-FF: Implementation and Examination. Journal of Chemical Theory and Computation, 2021, 17, 7827-7849.	2.3	10
43285	Understanding Solid Electrolyte Interphase Nucleation and Growth on Lithium Metal Surfaces. Batteries, 2021, 7, 73.	2.1	3
43286	Dual-Silicon-Doped Graphitic Carbon Nitride Sheet: An Efficient Metal-Free Electrocatalyst for Urea Synthesis. Journal of Physical Chemistry Letters, 2021, 12, 10837-10844.	2.1	40
43287	Defect chemistry of Cr-B binary and Cr-Al-B MAB phases: Effects of covalently bonded B networks. Physical Review Materials, 2021, 5, .	0.9	5
43288	High active crystalline {1 1 0} facets with high surface energy in Tin monoxide photocatalyst. Inorganic Chemistry Communication, 2021, 134, 109043.	1.8	1
43289	High-pressure monoclinic phase of MoAlB. Results in Physics, 2021, 31, 104980.	2.0	4
43290	Low-loss hyperbolic dispersion and anisotropic plasmonic excitation in nodal-line semimetallic yttrium nitride. Optics Express, 2020, 28, 22076.	1.7	8
43291	Site-preferential copper substitution for silicon leads to Cu-chains in the new ternary silicide Ir_{4â¯x}CuSi₂. Zeitschrift Fur Kristallographie - Crystalline Materials, 2020, 235, 391-399.	0.4	0
43292	GÃ¼mÃ¼ÅŸ-TabanlÄ± SÃ¼lfÃ¼rÃ¼n Manyetik DoÄŸasÄ± ve Elektronik DavranÄ±ÅŸÄ± Ãœzerine Ä°lk-Ä°lkeler Ã‡alÄ±ÅŸmasÄ±: Ag3M Journal of Science, 0, , .	0.1	0
43294	Tension and compression effect on mechanical properties of Fe and B2. Materials Research Express, 2020, 7, 076509.	0.8	3
43295	Born effective charges and electric polarization in bulk Îµ-Fe2O3: An ab-initio approach. Chemical Physics, 2020, 535, 110789.	0.9	3
43296	Valance Band Maximum and Thermoelectric Properties of Bi(_2)O(_2)Se: First-Principles Calculations. Communications in Physics, 2020, 30, 267.	0.0	2

#	Article	IF	Citations
43297	Extreme incompressibility and hardness of Re-N system. Physica Scripta, 2020, 95, 095701.	1.2	2
43298	Structural, Electronic and Mechanical Properties of Few-Layer GaN Nanosheet: A First-Principle Study. Materials Transactions, 2020, 61, 1438-1444.	0.4	3
43299	Surface reducibility, reactivity, and stability induced by noble metal modifications on the Î³ -Fe₂O₃ maghemite (001) surfaces. Journal of Physics Condensed Matter, 2020, 32, 425004.	0.7	0
43300	Graphene-Based Sensors for Monitoring Strain. , 0, , 602-611.		0
43303	Reaction Processes on Catalytically Active Surfaces. , 2007, , 311-340.		0
43305	Large-Scale Ab initio Simulations for Embedded Nanodots. , 2007, , 153-160.		0
43306	The Basic Structure of Ti-Si-N Superhard Nanocomposite Coatings: Ab Initio Studies. , 2008, , 117-136.		0
43307	The Electronic, Optical and Lattice Dynamical Properties of YIr2X2 (X=Si, Ge) Polymorphs: A DFT Study. Aksaray University Journal of Science and Engineering, 0, , .	0.4	0
43308	Pressure induced nodal line semimetal in YH₃. Zeitschrift Fur Naturforschung - Section A Journal of Physical Sciences, 2020, 75, 971-979.	0.7	1
43309	Extension of the LDA-1/2 method to the material class of bismuth containing IIIâ€“V semiconductors. AIP Advances, 2020, 10, 115003.	0.6	1
43310	OH molecule-involved formation of point defects in monolayer graphene. Nanotechnology, 2021, 32, 025704.	1.3	0
43311	Negative thermal expansion of cubic silicon dicarbodiimide, Si(NCN)₂, studied by ab initio lattice dynamics. Journal of Physics Condensed Matter, 2020, 32, 465402.	0.7	5
43312	Electronâ€“electron correlations and structural, spectral and polarization properties of tetragonal BaTiO₃. Journal of Physics Condensed Matter, 2020, 32, 475601.	0.7	1
43313	Modeling the ternary chalcogenide Na₂MoSe₄ from first-principles. Journal of Physics Condensed Matter, 2021, 33, 025501.	0.7	1
43314	Electronic transport properties of hydrogenated and fluorinated graphene: a computational study. Journal of Physics Condensed Matter, 2020, 32, 495502.	0.7	7
43315	Spinâ€“phonon coupling and thermodynamic behaviour in YCrO₃ and LaCrO₃: inelastic neutron scattering and lattice dynamics. Journal of Physics Condensed Matter, 2020, 32, 505402.	0.7	3
43316	Density functional study of gallium clusters on graphene: electronic doping and diffusion. Journal of Physics Condensed Matter, 2021, 33, 025002.	0.7	0
43317	Mechanical anisotropy and electronic properties of X2N2(XH2): first-principles calculations. Communications in Theoretical Physics, 2020, 72, 115701.	1.1	1

#	Article	IF	Citations
43318	Structural characteristics and elasticities of coesite and coesite-II at high pressure. New Journal of Physics, 2020, 22, 093044.	1.2	1
43319	Theoretical study on the change of thermoelectric properties by substitution of group 4 elements in Fe₂TiSn. Modern Physics Letters B, 2021, 35, 2150047.	1.0	1
43320	Preferential Energetics of Mg-based Ternary Alloys Revisited by Short-Range Order in Disordered Phases through First Principles. Transactions of the Materials Research Society of Japan, 2020, 45, 167-172.	0.2	0
43321	Prediction System for Solid Solubility Limits of Ag-, Cu-, Al-, and Mg-Based Alloys Using Artificial Neural Networks and First-Principles Calculations. Materials Transactions, 2020, 61, 2083-2090.	0.4	3
43322	Ferromagnetism triggered by nitrogen defects in graphitic carbon nitride. Journal Physics D: Applied Physics, 2020, 53, 495002.	1.3	2
43323	Effect of N-type doping and vacancy formation on the thermodynamic, electrical, structural, and bonding properties of Si: X. (X = P, As, and Sb): a theoretical study. Semiconductor Science and Technology, 2020, 35, 125005.	1.0	1
43324	Stacking faults and alternate crystal structures for the shape-memory alloy NiTi. Physical Review Materials, 2020, 4, .	0.9	1
43325	Breakdown of ion-polarization-correspondence and born effective charges: Algebraic formulas of accurate polarization under field. Physical Review Materials, 2020, 4, .	0.9	1
43326	DFT investigation of electronic and elastic properties of Î± -CdP₂. Materials Research Express, 2020, 7, 095901.	0.8	1
43327	Toward controlled thermoelectric properties of Pb and Sb co-doped nanostructured Thallium Telluride for energy applications. Materials Research Express, 2020, 7, 105010.	0.8	5
43328	Mn3GaC inverse perovskite thin films by magnetron sputtering from elemental targets. Materials Research Express, 2020, 7, 106102.	0.8	3
43329	Generating robust two-dimensional hole gas at the interface between boron nitride and diamond. Japanese Journal of Applied Physics, 2020, 59, 090910.	0.8	3
43330	Physical properties investigation of Fe_{1â^'x}Al_x (x â‰ 50%-at) alloys using DFT and Wagner-Schottky model. Physica Scripta, 2020, 95, 115702.	1.2	2
43331	Preparation of Two Quantumâ€Chemically Predicted, Isomeric [Br₄F₁₃]^{â€“} Anions in the Solid State. European Journal of Inorganic Chemistry, 2020, 2020, 4568-4576.	1.0	2
43332	Charge localization induced by reorientation of FA cations greatly suppresses nonradiative electron-hole recombination in FAPbI₃ perovskites: A time-domain Ab Initio study. Chinese Journal of Chemical Physics, 2020, 33, 642-648.	0.6	1
43333	Electronic, phononic and superconducting properties of trigonal Li₂ MSi₂ (M) Tj ETQq1 1 0.784314 rgBT /Ov	0.7	2
43334	Interaction between impurity elements (C, N and O) and hydrogen in hcp-Zr: a first-principles study. Modelling and Simulation in Materials Science and Engineering, 2020, 28, 085007.	0.8	3
43335	Role of hydrogen co-doping on opto-electronic behaviors of Na-H co-doped zinc oxide: a first principle study. Journal of Physics Communications, 2020, 4, 115002.	0.5	2

#	Article	IF	Citations
43336	Staggered spin Hall conductivity. Physical Review B, 2020, 102, .	1.1	3
43337	Combining DFT and CALPHAD for the development of on-lattice interaction models: The case of Fe-Ni system. Physical Review Materials, 2020, 4, .	0.9	3
43338	First-principles investigation of charged dopants and dopant-vacancy defect complexes in monolayer <mml:math xmlns:mml="http://www.w3.org/1998/Math/MathML"><mml:mrow><mml:mi>Mo</mml:mi><mml:msub><mml:mi mathvariant="normal">S</mml:mi><mml:mn>2</mml:mn></mml:msub></mml:mrow></mml:math>. Physical Review Materials, 2020, 4, .	0.9	9
43339	Pressure-induced Pbâ€“Pb bonding and phase transition in Pb₂SnO₄. Acta Crystallographica Section B: Structural Science, Crystal Engineering and Materials, 2020, 76, 979-991.	0.5	8
43340	Atomistic insight into the significantly enhanced photovoltaic cells of monolayer GaTe₂ via two-dimensional van der Waals heterostructures engineering. ChemistrySelect, 2022, 7, 629-644.	0.7	0
43341	Crystal structure and temperature-dependent properties of Na2H4Ga2GeO8Ââ€“ a novel gallogermanate. Zeitschrift Fur Naturforschung - Section B Journal of Chemical Sciences, 2020, 75, 805-813.	0.3	0
43343	Ð†Ð¾Ð½Ð½Ð¸Ð¹ Ñ…Ð°Ñ€Ð°ÐºÑ‚ÐµÑ€, Ñ„Ð°Ð·Ð¾Ð²Ñ– Ð¿ÐµÑ€ÐµÑ…Ð¾Ð´Ð¸ Ñ‚Ð° Ð¼ÐµÑ…Ð°Ð½Ñ–Ñ‡Ð½Ñ– Ð²Ð»Ð°ÑÑ‚Ð¸Ð²Ð¾ÑÑ‚Ñ–		
43344	Negative differential resistance in oligomeric phenylene ethynylenes molecular device with C2N-h2D nanoribbon electrodes. Japanese Journal of Applied Physics, 2020, 59, 126001.	0.8	1
43345	Computer Simulation of Oxygen Vacancy Formation in YFeO₃ Perovskite. Solid State Phenomena, 0, 312, 355-360.	0.3	2
43347	The pressure effect on optoelectronic and mechanical properties of chalcopyrite BeSiN2. Materials Today Communications, 2020, 24, 101263.	0.9	2
43348	Accelerated modeling of interfacial phases in the Ni-Bi system with machine learning interatomic potential. Scripta Materialia, 2020, 186, 14-18.	2.6	5
43349	YÃ¼ksek BasÄ±nÃ§ AltÄ±nda SbSeI'nin Elektronik Ã–zelliklerin Ä°lk Ä°lk Hesaplamalar Ä°le Ä°ncelenmesi. International Journal of Advances in Engineering and Pure Sciences, 0, , .	0.2	1
43350	Synthesis of Silicates for High-Performance Oxide Semiconductors: Electronic Structure Analysis. ACS Applied Electronic Materials, 2021, 3, 299-308.	2.0	5
43351	Quantum transport: general concepts. , 0, , 91-117.		1
43353	Theoretical study on stability and ion transport property with halide doping of Na₃SbS₄ electrolyte for all-solid-state batteries. Journal of Materials Chemistry A, 2022, 10, 2235-2248.	5.2	17
43354	Halogen-driven bandgap opening in graphdiyne for overall photocatalytic water splitting. Chinese Journal of Chemical Physics, 2021, 34, 805-813.	0.6	7
43355	Theoretical prediction of structural, mechanical, and electronic properties of Janus GeSnX₂ (X = S, Se, Te) single-layers. RSC Advances, 2021, 11, 36682-36688.	1.7	2
43356	Negating Li ⁺ Transfer Barrier at Solid-Liquid Electrolyte Interface in Hybrid Batteries. SSRN Electronic Journal, 0, , .	0.4	0

#	Article	IF	Citations
43357	Fast Na diffusion and anharmonic phonon dynamics in superionic Na₃PS₄. Energy and Environmental Science, 2021, 14, 6554-6563.	15.6	36
43358	Theoretical insight into hydroxyl production via H₂O₂ decomposition over the Fe₃O₄(311) surface. RSC Advances, 2021, 11, 36257-36264.	1.7	12
43359	Metallic C₅N monolayer as an efficient catalyst for accelerating redox kinetics of sulfur in lithiumâ€“sulfur batteries. Physical Chemistry Chemical Physics, 2021, 24, 180-190.	1.3	9
43360	Tantalum based single, double, and triple atom catalysts supported on g-C₂N monolayer for effective nitrogen reduction reaction: a comparative DFT investigation. Catalysis Science and Technology, 2022, 12, 310-319.	2.1	20
43361	A DFT study on magnetic interfaces based on half-metallic Co₂FeGe_{1/2}Ga_{1/2} with h-BN and MoSe₂ monolayers. Physical Chemistry Chemical Physics, 2022, 24, 1023-1028.	1.3	5
43362	Ultra-violet to visible band gap engineering of cubic halide KCaCl₃ perovskite under pressure for optoelectronic applications: insights from DFT. RSC Advances, 2021, 11, 36367-36378.	1.7	27
43363	First Principles Calculation of Electrical and Optical Properties of Cu₃AsO₄: Promising Thin-Film Solar Cell Absorber from Nonferrous Metal Manufacturing By-Products. Materials Transactions, 2021, , .	0.4	0
43364	Correction methods for first-principles calculations of the solution enthalpy of gases and compounds in liquid metals. Physical Chemistry Chemical Physics, 2022, 24, 757-770.	1.3	3
43365	Strain-induced enhancement in the electronic and thermal transport properties of the tin sulphide bilayer. Physical Chemistry Chemical Physics, 2021, 24, 211-221.	1.3	2
43366	Vacancy Formation Energies and Migration Barriers in Multi-Principal Element Alloys. SSRN Electronic Journal, 0, , .	0.4	0
43367	RbMo2P3O14 with large birefringence mainly induced by highly distorted [MoO6] in uncommon [Mo2P3O14]â^ž layers. Dalton Transactions, 2021, 50, 17559-17565.	1.6	3
43368	Ammonium ionic liquid cation promotes electrochemical CO₂ reduction to ethylene over formate while inhibiting the hydrogen evolution on a copper electrode. Catalysis Science and Technology, 2022, 12, 519-529.	2.1	14
43369	Effects of pseudopotentials and exchange-correlation functionals on phase transition of LaH10. Solid State Communications, 2022, 341, 114583.	0.9	1
43370	Efficient CO2 reduction with H2O via photothermal chemical reaction based on Au-MgO dual catalytic site on TiO2. Journal of CO2 Utilization, 2022, 55, 101801.	3.3	9
43371	First-principles calculation to investigate the influence of shear deformation on the electronic structure and optical properties of hydrogenated silicene. Computational and Theoretical Chemistry, 2022, 1207, 113506.	1.1	0
43372	Effects of Zr addition on lattice strains and electronic structures of NbTaTiV high-entropy alloy. Materials Science & Engineering A: Structural Materials: Properties, Microstructure and Processing, 2022, 831, 142293.	2.6	12
43373	Asymmetric janus functionalities induced changes in structural, electronic, optical characteristics of MXenes Ta4C3Tx. Solid State Communications, 2022, 341, 114585.	0.9	3
43374	Gas processing with intrinsically porous 2D membranes. Materials Chemistry and Physics, 2022, 276, 125426.	2.0	2

#	Article	IF	Citations
43375	Crystal phase induced direct band-gap modifications in bulk GaP and GaAsP. Solid State Communications, 2022, 341, 114584.	0.9	1
43376	Separation of ethane/ethylene gas mixture by ethane-selective CAU-3-NDCA adsorbent. Microporous and Mesoporous Materials, 2022, 330, 111572.	2.2	9
43377	Local magnetic spin mismatch promoting photocatalytic overall water splitting with exceptional solar-to-hydrogen efficiency. Energy and Environmental Science, 2022, 15, 265-277.	15.6	37
43378	Unraveling the effects of metal incorporation in cubic perovskite SrCoO3 by partially replacing Co atoms. Chemical Physics Letters, 2022, 786, 139208.	1.2	4
43379	Effect of oxygen defects in tuning the half-metallic and optical nature of Sr2CoXO6 (X=Mo & W): A first-principles study. Materials Chemistry and Physics, 2022, 277, 125429.	2.0	8
43380	Highly-defective graphene as a metal-free catalyst for chemical vapor deposition growth of graphene glass. Carbon, 2022, 187, 272-279.	5.4	3
43381	Influence of supercell size on Gas-Surface Scattering: A case study of CO scattering from Au(1 1 1). Chemical Physics, 2022, 554, 111423.	0.9	11
43382	Dislocation core structure and motion in pure titanium and titanium alloys: A first-principles study. Computational Materials Science, 2022, 203, 111081.	1.4	13
43383	Defects, dopants and lithium incorporation in LiPON electrolyte. Computational Materials Science, 2022, 202, 111000.	1.4	5
43384	Unveiling the underlying mechanism of nitrogen fixation by a new class of electrocatalysts two-dimensional TM@g-C4N3 monosheets. Applied Surface Science, 2022, 576, 151839.	3.1	37
43385	Computational materials design: Composition optimization to develop novel Ni-based single crystal superalloys. Computational Materials Science, 2022, 202, 111021.	1.4	6
43386	Atomistic study of the effect of crystallographic orientation on the twinning and detwinning behavior of NiTi shape memory alloys. Computational Materials Science, 2022, 203, 111080.	1.4	6
43387	Tunable indirect to direct band gap transition of Fe<mml:math xmlns:mml="http://www.w3.org/1998/Math/MathML" display="inline" id="d1e1193" altimg="si40.svg"><mml:msub><mml:mrow /><mml:mrow><mml:mn>2</mml:mn></mml:mrow></mml:msub></mml:math>TaX (X=Al and Ga) Heusler alloy under hydrostatic pressure effect. Computational Materials Science, 2022, 203, 111049.	1.4	8
43388	Towards stacking fault energy engineering in FCC high entropy alloys. Acta Materialia, 2022, 224, 117472.	3.8	44
43389	Effect of pressure on structural and elastic properties of SnSe: First-principles calculations. Solid State Communications, 2022, 342, 114596.	0.9	0
43390	First-principle studies on the metal/semiconductor properties and strain-tuned electronic structures of SnP3 monolayer. Computational Materials Science, 2022, 203, 111047.	1.4	3
43391	Ab initio modeling of helically periodic nanostructures using CRYSTAL17: A general algorithm first applied to nanohelicenes. Computational Materials Science, 2022, 203, 111063.	1.4	8
43392	Thermodynamic stability and superconductivity of tantalum carbides from first-principles cluster expansion and isotropic Eliashberg theory. Computational Materials Science, 2022, 202, 111004.	1.4	6

#	Article	IF	Citations
43393	Electronic simulations of alanine and water coadsorption over Defect-free and Sulfur-depleted sphalerite surfaces. Applied Surface Science, 2022, 576, 151899.	3.1	6
43394	Ab initio study of the electronic, optical, and water-splitting properties of Fe-doped ZnO monolayer. Physica E: Low-Dimensional Systems and Nanostructures, 2022, 137, 115059.	1.3	5
43395	Mechanistic insights into the simultaneous removal of As(V) and Cr(VI) oxyanions by a novel hierarchical corolla-like MnO2-decorated porous magnetic biochar composite: A combined experimental and density functional theory study. Applied Surface Science, 2022, 578, 151991.	3.1	16
43396	Cumulative cationic and anionic redox reaction in Mg3V2(SiO4)3 and impact on the battery performance. Journal of Power Sources, 2022, 520, 230828.	4.0	3
43397	Temperature dependence of adsorption and desorption dynamics of NO2 molecule on boron-doped graphene. Physica E: Low-Dimensional Systems and Nanostructures, 2022, 137, 115083.	1.3	9
43398	Nano-phase transformation of composite precipitates in multicomponent Al-Mg-Si(-Sc) alloys. Journal of Materials Science and Technology, 2022, 110, 216-226.	5.6	20
43399	Assembling biphenylene into 3D porous metallic carbon allotrope for promising anode of lithium-ion batteries. Carbon, 2022, 188, 95-103.	5.4	31
43400	Pyro-polymerization of organic pigments for superior lithium storage. Carbon, 2022, 188, 187-196.	5.4	4
43401	Formation energy, mechanical and electronic properties of buckled heptazine (<mml:math) Tj ETQq0 0 0 rgBT /Overlock 10 Tf 50 437 Tc First-principles calculations. Computational Condensed Matter, 2022, 30, e00619.	0.9	7
43402	In-situ enhanced catalytic reforming behavior of cobalt-based materials with inherent zero-valent aluminum in spent lithium ion batteries. Applied Catalysis B: Environmental, 2022, 303, 120920.	10.8	19
43403	Theoretical estimation of surface magnetic anisotropy on <mml:math xmlns:mml="http://www.w3.org/1998/Math/MathML" altimg="si6.svg"><mml:mrow><mml:mi>L</mml:mi><mml:msub><mml:mn>1</mml:mn><mml:mn>0</mml:mn></mml:msub></mml:m thin films: Case of perfect and defect Surfaces.. Surface Science, 2022, 717, 121999.	0.8	3
43404	A Theoretical Study on Electronic Behavior and Mechanical Properties of Ferromagnetic Manganese Selenide: AgMn2Se4. SDU Journal of Science, 0, , .	0.1	0
43405	A comparative study of biaxial strain modulated electronic structure of MSe₂ (M = W,) Tj ETQq0 0 0 rgBT /Overlock 10 Tf 5		1
43406	First-principles and experimental investigations on ductility/brittleness of intermetallic compounds and joint properties in steel/aluminum laser welding. Transactions of Nonferrous Metals Society of China, 2021, 31, 2962-2977.	1.7	17
43407	Theoretical and Experimental Studies of Electronic and Optical Properties of Layered TlIn(S_{0.75}Se_{0.25})₂ Ferroelectric Crystal. Integrated Ferroelectrics, 2021, 220, 18-29.	0.3	4
43408	Electronic and magnetic properties of iridium ilmenites <mml:math xmlns:mml="http://www.w3.org/1998/Math/MathML"><mml:mrow><mml:mi>A</mml:mi><mml:msub><mml:mi>IrO</mml:mi><mml <mml:math		

#	Article	IF	Citations
43411	The Mechanical, Electronic and Optical Properties of Sn₂P₂S₆ Compound in Different Phases. Integrated Ferroelectrics, 2021, 220, 56-70.	0.3	1
43412	Layered GeP₂S₆, GeP₂Se₆, GeP₂Te₆, SnP₂S₆, SnP₂Se₆, and SnP₂Te₆ Polar Crystals with Semiconductorâ€“Metal Transitions Induced by Pressure or Chemical Composition. Integrated Ferroelectrics, 2021, 220, 90-99.	0.3	5
43413	Slater Insulator Phase of X₂ (Xâ€‰=â€‰Na, Li)IrO₃: First Principles Calculation. Integrated Ferroelectrics, 2021, 220, 80-89.	0.3	0
43414	Efficient Helium Separation with Two-Dimensional Metalâ€“Organic Framework Fe/Ni-PTC: A Theoretical Study. Membranes, 2021, 11, 927.	1.4	1
43415	Pressure Tuned Structural, Electronic and Elastic Properties of U3Si2C2: A First Principles Study. Crystals, 2021, 11, 1420.	1.0	0
43416	From CeF₂(SO₄)Â·H₂O to Ce(IO₃)₂(SO₄): Defluorinated Homovalent Substitution for Strong Second-Harmonic-Generation Effect and Sufficient Birefringence. Chemistry of Materials, 2021, 33, 9317-9325.	3.2	23
43417	Solid-State Structural Properties of Alloxazine Determined from Powder XRD Data in Conjunction with DFT-D Calculations and Solid-State NMR Spectroscopy: Unraveling the Tautomeric Identity and Pathways for Tautomeric Interconversion. Crystal Growth and Design, 2022, 22, 524-534.	1.4	8
43418	Finding the order in complexity: The electronic structure of 14-1-11 zintl compounds. Applied Physics Letters, 2021, 119, .	1.5	6
43419	Spin-valley coupling and valley splitting in the MoSi2N4/CrCl3 van der Waals heterostructure. Applied Physics Letters, 2021, 119, .	1.5	24
43420	Promoting ethylene production over a wide potential window on Cu crystallites induced and stabilized via current shock and charge delocalization. Nature Communications, 2021, 12, 6823.	5.8	61
43421	Synthesis and Characterization of New-Type Ionic Cocrystals with Cyanuric Acid and Alkali Halides: AXÂ·(H3C3N3O3)2 (A = Rb, Cs; X = Cl, Br). Crystal Growth and Design, 2021, 21, 7194-7200.	1.4	0
43422	Native Atomic Defects Manipulation for Enhancing the Electronic Transport Properties of Epitaxial SnTe Films. ACS Applied Materials & Interfaces, 2021, 13, 56446-56455.	4.0	2
43423	Can We Predict Interface Dipoles Based on Molecular Properties?. ACS Omega, 2021, 6, 32270-32276.	1.6	4
43424	Functionalized tellurene; a candidate large-gap 2D topological insulator. Journal of Physics Condensed Matter, 2022, 34, 08LT01.	0.7	1
43425	Growth and Temperature-Dependent Mechanical and Thermal Properties of One-Dimensional Chain Structure Hg2Br2 Crystals for Infrared Acousto-Optic Device Application. Crystal Growth and Design, 2021, 21, 7034-7042.	1.4	3
43426	Fabrication and characterization of high entropy pyrochlore ceramics. Boletin De La Sociedad Espanola De Ceramica Y Vidrio, 2023, 62, 66-76.	0.9	9
43427	Exploring DFT+U parameter space with a Bayesian calibration assisted by Markov chain Monte Carlo sampling. Npj Computational Materials, 2021, 7, .	3.5	8
43428	Superconductivity of <mml:math xmlns:mml="http://www.w3.org/1998/Math/MathML"><mml:msub><mml:mrow><mml:mi mathvariant="normal">H</mml:mi></mml:mrow><mml:mn>3</mml:mn></mml:msub><mml:mi mathvariant="normal">S</mml:mi></mml:math> doped with light elements. Physical Review Research, 2021, 3, .	1.3	12

#	Article	IF	Citations
43429	The stabilization potential of a standing molecule. Science Advances, 2021, 7, eabj9751.	4.7	5
43430	Firstâ€principles investigation of solution mechanism of C in TMâ€Siâ€C matrix as the potential highâ€temperature ceramics. Journal of the American Ceramic Society, 2022, 105, 2858-2868.	1.9	60
43431	DFT analysis of Thymine adsorption on Ti doped graphene for biosensor applications. Journal of Physics: Conference Series, 2021, 2070, 012012.	0.3	2
43432	Synergistic effect of Cu-doped NiO for enhancing urea electrooxidation: Comparative electrochemical and DFT studies. Journal of Alloys and Compounds, 2022, 896, 162857.	2.8	46
43433	Electron-phonon coupling of Fe-adatom electron states on MgO/Ag(100). Physical Review B, 2021, 104, .	1.1	2
43434	Strontium stannate as an alternative anode for Na- and K-Ion batteries: A theoretical study. Journal of Physics and Chemistry of Solids, 2022, 162, 110505.	1.9	6
43435	Accelerated prediction of Cu-based single-atom alloy catalysts for CO2 reduction by machine learning. Green Energy and Environment, 2023, 8, 820-830.	4.7	16
43436	In situ imaging of amorphous intermediates during brucite carbonation in supercritical CO2. Nature Materials, 2022, 21, 345-351.	13.3	18
43437	Aâ€™â€“B Intersite Cooperation-Enhanced Water Splitting in Quadruple Perovskite Oxide CaCu₃Ir₄O₁₂. Chemistry of Materials, 2021, 33, 9295-9305.	3.2	11
43438	TaCo₂Te₂: An Airâ€Stable, High Mobility Van der Waals Material with Probable Magnetic Order. Advanced Functional Materials, 2022, 32, .	7.8	10
43439	Quasi-Type II Coreâ€“Shell Perovskite Nanocrystals for Improved Structural Stability and Optical Gain. ACS Applied Materials & Interfaces, 2021, 13, 58170-58178.	4.0	15
43440	Revisited Electronic Structure Properties of GaN-ZnO Quaternary Alloys for High Solar Absorption. Journal of Electronic Materials, 2022, 51, 594-600.	1.0	1
43441	3D graphene-like semiconductor Ba2HfTe4 with electronic structure similar to graphene and bandgap close to silicon. Cell Reports Physical Science, 2021, 2, 100658.	2.8	4
43442	Electronic properties tuning of defective heterostructured CBN nanotubes by uniaxial pressure: a density functional study. Applied Physics A: Materials Science and Processing, 2021, 127, 1.	1.1	5
43443	Physical properties of chromium-doped barium titanate: Effects of chromium incorporation. Physica B: Condensed Matter, 2022, 626, 413494.	1.3	7
43444	Uncovering the coordination effect on the Ni single-atom catalysts for CO2 reduction including vacancy defect and non-vacancy defect structures. Fuel, 2022, 310, 122472.	3.4	17
43445	First-principles study on the surface oxidation behavior of ternary M6C6 (M6Â=ÂZr5Ti, Zr5Ta, Hf5Ti,) Tj ETQq0 0 0 rgBT /Overlock 10 Tf	1.4	1
43446	Stable polar oxynitrides through epitaxial strain. Physical Review Materials, 2021, 5, .	0.9	2

#	Article	IF	Citations
43447	Unified mechanistic understanding of CO2 reduction to CO on transition metal and single atom catalysts. Nature Catalysis, 2021, 4, 1024-1031.	16.1	154
43448	Structural effect of Nitrogen/Carbon on the stability of anchored Ru catalysts for CO2 hydrogenation to formate. Chemical Engineering Journal, 2022, 433, 133571.	6.6	23
43449	Investigation of the Antiscaling Performance of Phosphonated Chitosan for Upstream Petroleum Industry Application. ACS Sustainable Chemistry and Engineering, 2021, 9, 16494-16505.	3.2	12
43450	First-Principles Calculations of Magnetic Moment Modulation of 3d Transition Metal Atoms Encapsulated in C60/C70 Cages on Si(100) Surfaces: Implications for Spintronic Devices. ACS Applied Nano Materials, 2021, 4, 12356-12364.	2.4	2
43451	Metallization and Superconductivity in the van der Waals Compound CuP₂Se through Pressure-Tuning of the Interlayer Coupling. Journal of the American Chemical Society, 2021, 143, 20343-20355.	6.6	10
43452	Quantitatively regulating defects of 2D tungsten selenide to enhance catalytic ability for polysulfide conversion in a lithium sulfur battery. Energy Storage Materials, 2022, 45, 1229-1237.	9.5	81
43453	Atomistic discharge studies of sulfurized-polyacrylonitrile through ab initio molecular dynamics. Electrochimica Acta, 2022, 403, 139538.	2.6	4
43454	Light doping effects of rare-earth elements: Sc, Y, La and Lu in rockSalt AlNâ€”first-principles study. Applied Physics A: Materials Science and Processing, 2021, 127, 1.	1.1	8
43455	Tailoring Oxygen-Containing Groups on Graphene for Ratiometric Electrochemical Measurements of Ascorbic Acid in Living Subacute Parkinsonâ€™s Disease Mouse Brains. Analytical Chemistry, 2021, 93, 16598-16607.	3.2	13
43456	Atomically dispersed palladium catalyzes H/D exchange and isomerization of alkenes via reversible insertion and elimination. Chem Catalysis, 2021, 1, 1480-1492.	2.9	13
43457	Structural and electronic properties of ternary alloys of alkaline-earth oxides and chalcogenides. Phase Transitions, 0, , 1-21.	0.6	0
43458	RbCeX2 Crystal (X = S, Se, Te): Pressure-Induced Spin-Selective Gapless Transition and Response Properties. Journal of Alloys and Compounds, 2022, 898, 162760.	2.8	3
43459	In-situ release of phosphorus combined with rapid surface reconstruction for Coâ€“Ni bimetallic phosphides boosting efficient overall water splitting. Chemical Engineering Journal, 2022, 433, 133523.	6.6	60
43460	Effects of Bi and Mn codoping on the physical properties of barium titanate: investigation via DFT method. Applied Physics A: Materials Science and Processing, 2021, 127, 1.	1.1	24
43461	Cooper-pair distribution function $$D_{cp}(omega ,T_c)$$ for superconducting $$hbox {D}_3hbox {S}$$ and $$hbox {H}_3hbox {S}$$. Scientific Reports, 2021, 11, 22618.	1.6	1
43462	Understanding hydroxyl radicals addition to CO <mml:math xmlns:mml="http://www.w3.org/1998/Math/MathML" display="inline" id="d1e861" altimg="si167.svg"><mml:msub><mml:mrow /><mml:mrow><mml:mn>2</mml:mn></mml:mrow></mml:msub></mml:math> on <mml:math xmlns:mml="http://www.w3.org/1998/Math/MathML" display="inline" id="d1e869" altimg="si124.svg"><mml:mi>Fe</mml:mi></mml:math>-Fe2O3(1 1 0) surface photocatalyst for organic pollutants.	3.4	3
43463	Platinum-silicon doped graphitic carbon nitride: A first principle calculation. Physica B: Condensed Matter, 2022, 627, 413547.	1.3	4
43464	Rashba-split surface state and spin-dependent photon emission from Re(0001) at <mml:math xmlns:mml="http://www.w3.org/1998/Math/MathML"><mml:mover><mml:mi mathvariant="normal">Î“</mml:mi><mml:mo>Â¯</mml:mo></mml:mover></mml:math>. Physical Review B, 2021, 104, .	1.1	4

#	Article	IF	Citations
43465	The effect of Ti on Ca-pv and Mg-pv phase stability. Physics of the Earth and Planetary Interiors, 2022, 322, 106825.	0.7	1
43466	Electronic Origin of Non-Zone-Center Phonon Condensation: Octahedral Rotation as a Case Study. Physical Review Letters, 2021, 127, 215701.	2.9	7
43467	Hyper-coordinated iodine in HIO3 under pressure. Vibrational Spectroscopy, 2021, 117, 103318.	1.2	1
43468	The ferroelastic phase transition in hydrogen cyanide studied by density functional theory. Journal of Physics Condensed Matter, 2021, , .	0.7	1
43469	Vapor-phase self-assembly for generating thermally stable single-atom catalysts. CheM, 2022, 8, 731-748.	5.8	23
43470	Insight into the synergy effect on the improved reactivity of spinel NiMn2O4 oxygen carrier in chemical looping combustion. Fuel, 2022, 313, 122680.	3.4	5
43471	Characterization of nanostructures in a high pressure die cast Al-Si-Cu alloy. Acta Materialia, 2022, 224, 117500.	3.8	16
43472	Li migration, nucleation and growth behavior regulated by a lithiophilic cobalt phosphide-doped carbon nanofibers derived ion/electron conductive framework. Energy Storage Materials, 2022, 45, 1109-1119.	9.5	30
43473	Potential of Vanadium (V) doped CNT(10, 0) and Manganese (Mn) doped carbon nanocage (C60) as catalysts for oxygen reduction reaction in fuel cells. Inorganic Chemistry Communication, 2021, 135, 109095.	1.8	0
43474	Self-Assembled NbOPO₄ Nanosheet/Reduced Graphene Oxide Heterostructure for Capacitive Desalination. ACS Applied Nano Materials, 2021, 4, 12629-12639.	2.4	11
43475	Significant Effect of Rh on the h-BN-Supported Ni Catalyst for Dry Reformation of CH4: Insights from Density Functional Theory and Microkinetic Analysis. Journal of Physical Chemistry C, 0, , .	1.5	6
43476	Screening criteria for high-performance p-type transparent conducting materials and their applications. Materials Today Physics, 2022, 22, 100583.	2.9	17
43477	Robust evidence for the stabilization of the premartensite phase in Ni-Mn-In magnetic shape memory alloys by chemical pressure. Physical Review Materials, 2021, 5, .	0.9	3
43478	Silver Clusterâ€Porphyrinâ€Assembled Materials as Advanced Bioprotective Materials for Combating Superbacteria. Advanced Science, 2022, 9, e2103721.	5.6	32
43479	First-Principles Investigation of Structural, Electronic, and Room Temperature Ferromagnetism in Si-Doped Monolayer BN. Advances in Condensed Matter Physics, 2021, 2021, 1-8.	0.4	4
43480	CO2 to ethanol: A selective photoelectrochemical conversion using a ternary composite consisting of graphene oxide/copper oxide and a copper-based metal-organic framework. Electrochimica Acta, 2022, 404, 139612.	2.6	17
43481	Effect of Ga excess concentration on the structural, electronic, magnetic, elastic and thermoelectric properties of Fe2â^'xNiGa1+x Heusler alloys: results of FP-LAPW calculations. European Physical Journal Plus, 2021, 136, 1.	1.2	0
43482	Single-Crystal X-ray and Solid-State NMR Characterisation of AND-1184 and Its Hydrochloride Form. Materials, 2021, 14, 7175.	1.3	0

#	Article	IF	Citations
43483	Theoretical and experimental study of effects of Co2+ doping on structural and electronic properties of ZnO. Journal of Physics and Chemistry of Solids, 2021, , 110501.	1.9	5
43484	Physical Properties Investigations of Ternary-Layered Carbides M2PbC (M = Ti, Zr and Hf): First-Principles Calculations. Crystals, 2021, 11, 1445.	1.0	6
43485	Robust Hydrophobic Materials by Surface Modification in Transition-Metal Diborides. ACS Applied Materials & Interfaces, 2021, 13, 58162-58169.	4.0	6
43486	Hydrogen-incorporated vanadium dioxide nanosheets enable efficient uranium confinement and photoreduction. Nano Research, 2022, 15, 2943-2951.	5.8	14
43487	Promoting Electrochemical Performance of Ti₃C₂O₂ MXene-Based Electrodes of Alkali-Ion Batteries via S Doping: Theoretical Insight. ACS Applied Materials & Interfaces, 2021, 13, 57306-57316.	4.0	16
43488	Formation of a Polar Structure in the Metallic Niobium Sulfide Nb4S3. Inorganic Chemistry, 2021, 60, 17669-17676.	1.9	1
43489	Activating and modulating inert basal planes of BiOX (XÂ=ÂI, Br, and Cl) for hydrogen evolution reaction. International Journal of Hydrogen Energy, 2022, 47, 1683-1691.	3.8	3
43490	Transition Metal-Modified Co₄ Clusters Supported on Graphdiyne as an Effective Nitrogen Reduction Reaction Electrocatalyst. Inorganic Chemistry, 2021, 60, 18251-18259.	1.9	21
43491	Structural evolution and phase transition mechanism of $$hbox {MoSe}_2$$ under high pressure. Scientific Reports, 2021, 11, 22090.	1.6	3
43492	Exotic Spintronic Properties of Transitionâ€Metal Monolayers on Graphyne. Advanced Theory and Simulations, 2022, 5, 2100287.	1.3	1
43493	Comparative Study of H₂O and O₂ Adsorption on the GaN Surface. Journal of Physical Chemistry C, 2021, 125, 25807-25815.	1.5	5
43494	Modulation of magnetoelectric coupling through systematically engineered spin canting in nickelâ€“zinc ferrite. Journal of the American Ceramic Society, 2022, 105, 2655-2662.	1.9	7
43495	Effect of strain on interactions of Î£ 3{111} silicon grain boundary with oxygen impurities from firstâ€principles. Physica Status Solidi (B): Basic Research, 0, , 2100377.	0.7	3
43496	The effect of phase transition of crednerite/delafossite CuMn 1â^' x Cr x O 2 on optical, thermal, and power factor properties. Journal of the American Ceramic Society, 0, , .	1.9	0
43497	Giant anomalous Nernst signal in the antiferromagnet YbMnBi2. Nature Materials, 2022, 21, 203-209.	13.3	72
43498	Dirac-like band structure and strain-tunable electronic structure of Zr2CCl2 monolayer. Applied Surface Science, 2021, 577, 151931.	3.1	0
43499	Toward Rational Design of Polarity Probes by Noncovalent Functionalization of Phosphorene. Journal of Physical Chemistry C, 2021, 125, 26099-26107.	1.5	0
43500	Electronic reconstruction and charge transfer in strained <mml:math xmlns:mml="http://www.w3.org/1998/Math/MathML"><mml:mrow><mml:msub><mml:mi>Sr</mml:mi><mml:mn>2</mml:mn></mml:msub><mml:mn></mml:mn></mml:mrow></mml:math> double perovskite. Physical Review B, 2021, 104, .	1.1	1

#	Article	IF	Citations
43501	Targeted Regulation of the Electronic States of Nickel Toward the Efficient Electrosynthesis of Benzonitrile and Hydrogen Production. ACS Applied Materials & Interfaces, 2021, 13, 56140-56150.	4.0	21
43502	Preparation of copper-loaded porous carbons through hydrothermal carbonization and ZnCl2 activation and their application to selective CO adsorption: Experimental and DFT calculation studies. Journal of Hazardous Materials, 2022, 426, 127816.	6.5	15
43503	Interfacial electronic modulation of Ni3S2 nanosheet arrays decorated with Au nanoparticles boosts overall water splitting. Applied Catalysis B: Environmental, 2022, 304, 120935.	10.8	80
43504	Phase engineering of Mo-V oxides molecular sieves for zinc-ion batteries. Science China Materials, 2022, 65, 939-946.	3.5	4
43505	Intercalation-deintercalation design in MXenes for high-performance supercapacitors. Nano Research, 2022, 15, 3213-3221.	5.8	17
43506	Achieving synergistic performance through highly compacted microcrystalline rods induced in Mo doped GeTe based compounds. Materials Today Physics, 2022, 22, 100571.	2.9	3
43507	Aluminum distribution in mordenite-zeolite framework: A new outlook based on density functional theory calculations. Journal of Solid State Chemistry, 2022, 306, 122725.	1.4	7
43508	Prediction of three-dimensional stretchable boron nitride nanoribbons. Diamond and Related Materials, 2021, 121, 108740.	1.8	1
43509	Dimensionality reduction made high-performance mid-infrared nonlinear halide crystal. Materials Today Physics, 2021, 21, 100569.	2.9	44
43510	Unveiling the key factor for the phase reconstruction and exsolved metallic particle distribution in perovskites. Nature Communications, 2021, 12, 6814.	5.8	28
43511	Enhanced activity of a WOx-incorporated Pt/Al2O3 catalyst for the dehydrogenation of homocyclic LOHCs: Effects of impregnation sequence on Ptâ€“WOx interactions. Fuel, 2022, 313, 122654.	3.4	9
43512	Adsorption of small organic acids and polyphenols on hematite surfaces: Density Functional TheoryÂ+Âthermodynamics analysis. Journal of Colloid and Interface Science, 2022, 609, 469-481.	5.0	11
43513	Identifying the Atomic Layer Stacking of Mo₂C MXene by Probe Molecule Adsorption. Journal of Physical Chemistry C, 2021, 125, 26808-26813.	1.5	8
43514	Tunable magnetic skyrmions in ferrimagnetic Mn4N. Applied Physics Letters, 2021, 119, .	1.5	18
43515	Effect of alloying on the carrier dynamics in high-performance perovskite solar cells. Journal of Energy Chemistry, 2022, 68, 267-274.	7.1	2
43516	Maximal superconductivity in proximity to the charge density wave quantum critical point in <mml:math xmlns:mml="http://www.w3.org/1998/Math/MathML"><mml:msub><mml:mrow><mml:mi>Cu</mml:mi></mml:mrow><mml:mi>x</m Physical Review B, 2021, 104, .	1.1	2
43517	Surface energies and relaxation of NiCoCr and NiFeX (X = Cu, Co or Cr) equiatomic multiprincipal element alloys from first principles calculations. Modelling and Simulation in Materials Science and Engineering, 2022, 30, 025001.	0.8	2
43518	Enhanced Oxygen Evolution Reaction Electrocatalysis on Co(OH)₂@MnO₂Decorated Carbon Nanoarrays: Effect of Heterostructure, Conductivity and Charge Storgae Capability. Journal of the Electrochemical Society, 2021, 168, 114515.	1.3	1

#	Article	IF	Citations
43520	A selective Au-ZnO/TiO2 hybrid photocatalyst for oxidative coupling of methane to ethane with dioxygen. Nature Catalysis, 2021, 4, 1032-1042.	16.1	156
43521	Oxygen-controlled photo-reforming of biopolyols to CO over Z-scheme CdS@g-C3N4. CheM, 2022, 8, 465-479.	5.8	61
43522	Crystal structures and mechanical properties of tungsten monocarbide predicted by first-principles investigations. Journal of Applied Physics, 2021, 130, 195902.	1.1	0
43523	Intriguing features of Dirac cones in phagraphene with site specific doping. Applied Surface Science, 2021, 577, 151782.	3.1	10
43524	Absolute surface energies of wurtzite (10 1Â¯1) surfaces and the instability of the cation-adsorbed surfaces of IIâ€“VI semiconductors. Applied Physics Letters, 2021, 119, 201603.	1.5	0
43525	Strain engineering of electronic and optical properties of monolayer diboron dinitride. Physical Review B, 2021, 104, .	1.1	6
43526	Thickness-dependent enhanced optoelectronic performance of surface charge transfer-doped ReS2 photodetectors. Nano Research, 2022, 15, 3638-3646.	5.8	11
43527	Stretchable MoS₂ Artificial Photoreceptors for Eâ€Skin. Advanced Functional Materials, 2022, 32, 2107524.	7.8	24
43528	X-ray absorption spectroscopy of trivalent Eu, Gd, Tb, and Dy chlorides and oxychlorides. Journal of Alloys and Compounds, 2022, 897, 162629.	2.8	4
43529	Theoretical study of structure sensitivity on Au doped CeO2 surfaces for formaldehyde oxidation: The effect of crystal planes and Au doping. Chemical Engineering Journal, 2022, 433, 133599.	6.6	7
43530	Substitution effect on electronic and optical properties of Tetraphenyldipyranylidene; A theoretical study. Journal of Physics and Chemistry of Solids, 2022, 162, 110504.	1.9	3
43531	Preferential Growth Mode of Large-Sized Vacancy Clusters in Silicon: A Neural-Network Potential and First-Principles Study. Journal of Physical Chemistry C, 0, , .	1.5	3
43532	Effects of the orientation relationships between TCP phases and matrix on the morphologies of TCP phases in Ni-based single crystal superalloys. Materials Characterization, 2022, 183, 111609.	1.9	10
43533	Heterointerface Control over Lithium-Induced Phase Transitions in MoS₂ Nanosheets: Implications for Nanoscaled Energy Materials. ACS Applied Nano Materials, 2021, 4, 14105-14114.	2.4	7
43534	Theoretical Design of thermal spin molecular logic gates by using a combinational molecular junction. Chinese Physics B, 0, , .	0.7	3
43535	Band structure tuning of g-C₃N₄ via sulfur doping for broadband near-infrared ultrafast photonic applications. Nanophotonics, 2021, 11, 139-151.	2.9	11
43536	A Metastable p-Type Semiconductor as a Defect-Tolerant Photoelectrode. Molecules, 2021, 26, 6830.	1.7	2
43537	Temperature dependence of bismuth structures under high pressure. Chinese Physics B, 2022, 31, 056101.	0.7	1

#	Article	IF	Citations
43538	Electron beam analysis induces Cl vacancy defects in a NaCl thin film. Nanotechnology, 2021, 33, .	1.3	4
43539	First principles study of stability, electronic structure and fracture toughness of Ti3SiC2/TiC interface. Vacuum, 2022, 196, 110745.	1.6	17
43540	Strain Engineering to Release Trapped Hole Carriers in p-Type Haeckelite GaN. ACS Applied Electronic Materials, 2021, 3, 5257-5264.	2.0	1
43541	First principles prediction of the stable MgFCl Janus monolayer with tunable properties. Physica E: Low-Dimensional Systems and Nanostructures, 2022, 137, 115023.	1.3	5
43542	Electrolyte Modulators toward Polarizationâ€Mitigated Lithiumâ€Ion Batteries for Sustainable Electric Transportation. Advanced Materials, 2022, 34, e2107787.	11.1	15
43543	First-principles investigations of tricarbon: From the isolated C3 molecule to a novel ultra-hard anisotropic solid. Carbon Trends, 2022, 6, 100132.	1.4	5
43544	Radiation damage of MoAlB at elevated temperatures: Investigating MAB phases as potential neutron shielding materials. Journal of the European Ceramic Society, 2022, 42, 1311-1321.	2.8	8
43545	Spontaneous valley polarization in two-dimensional organometallic lattices. Physical Review B, 2021, 104, .	1.1	11
43546	In-plane quasi-single-domain BaTiO3 via interfacial symmetry engineering. Nature Communications, 2021, 12, 6784.	5.8	16
43547	First-principles analysis of the grain boundary segregation of transition metal alloying elements in Î³Fe. Computational Materials Science, 2022, 210, 111050.	1.4	20
43548	Inorganic gas sensing performance of Ï‡3-borophene and the van der Waals heterostructure. Applied Surface Science, 2022, 581, 151906.	3.1	18
43549	Pd(1 1 1)/SnO2(1 0 1) heterostructure on porous N-carbon material as enhanced catalyst for formic acid electrooxidation. Applied Surface Science, 2022, 577, 151922.	3.1	1
43550	Molecular-level insights into the electronic effects in platinum-catalyzed carbon monoxide oxidation. Nature Communications, 2021, 12, 6888.	5.8	18
43551	Prediction of spin-dependent electronic structures of 3d transition metals doped Hittorf's violet phosphorene towards spintronics. Physica E: Low-Dimensional Systems and Nanostructures, 2022, 138, 115068.	1.3	1
43552	Molybdenum Atom-Mediated Salphen-Based Covalent Organic Framework as a Promising Electrocatalyst for the Nitrogen Reduction Reaction: A First-Principles Study. Journal of Physical Chemistry C, 2021, 125, 26061-26072.	1.5	34
43553	Structural Insights into Multiâ€Metal Spinel Oxide Nanoparticles for Boosting Oxygen Reduction Electrocatalysis. Advanced Materials, 2022, 34, e2107868.	11.1	30
43554	Fully exposed cobalt nanoclusters anchored on nitrogen-doped carbon synthesized by a host-guest strategy for semi-hydrogenation of phenylacetylene. Journal of Catalysis, 2022, 405, 499-507.	3.1	16
43555	Sustainable oxidation catalysis supported by light: Fe-poly (heptazine imide) as a heterogeneous single-atom photocatalyst. Applied Catalysis B: Environmental, 2022, 304, 120965.	10.8	46

#	Article	IF	Citations
43556	Quantum Confinement in Aligned Zigzag â€œPseudoâ€Ribbonsâ€•Embedded in Graphene on Ni(100). Advanced Functional Materials, 2022, 32, 2105844.	7.8	5
43557	Pressure-Induced High-Energy-Density BeN4 Materials with Nitrogen Chains: First-Principles Study. Journal of Physical Chemistry C, 2021, 125, 25376-25382.	1.5	7
43558	Twist-Dependent Electron Charge Transfer and Transport in Phosphoreneâ€“Graphene Heterobilayers. Journal of Physical Chemistry C, 2021, 125, 25886-25897.	1.5	4
43559	Atomistic studies on waterâ€induced lithium corrosion. ChemSusChem, 2021, , .	3.6	2
43560	Atomic structures and electronic properties of different interface types at Al/c-SiO2 interfaces. Applied Surface Science, 2022, 578, 151932.	3.1	9
43561	Modeling Potential-Dependent Electrochemical Activation Barriers: Revisiting the Alkaline Hydrogen Evolution Reaction. Journal of the American Chemical Society, 2021, 143, 19341-19355.	6.6	25
43562	Theoretical Prediction of a Bi-Doped Î²-Antimonene Monolayer as a Highly Efficient Photocatalyst for Oxygen Reduction and Overall Water Splitting. ACS Applied Materials & Interfaces, 2021, 13, 56254-56264.	4.0	10
43563	Tuning electronic properties of MSb (M = C, Si, Ge and Sn) monolayers by strain engineering. Physica E: Low-Dimensional Systems and Nanostructures, 2022, 138, 115065.	1.3	7
43564	Stability and Anisotropic Elastic Properties of a Hexagonal Î´-WN Compound. Journal of Electronic Materials, 0, , 1.	1.0	0
43565	Cluster Assembled Silicon-Lithium Nanostructures: A Nanowire Confined Inside a Carbon Nanotube. Frontiers in Chemistry, 2021, 9, 767421.	1.8	1
43566	Impact of magnetic transition on Mn diffusion in<mml:math xmlns:mml="http://www.w3.org/1998/Math/MathML"><mml:mi>Î±</mml:mi></mml:math>-iron: Correlative state-of-the-art theoretical and experimental study. Physical Review B, 2021, 104, .	1.1	3
43567	Compression Behavior and Vibrational Properties of New Energetic Material LLM-105 Analyzed Using the Dispersion-Corrected Density Functional Theory. Molecules, 2021, 26, 6831.	1.7	3
43568	Bayesian probabilistic assignment of chemical shifts in organic solids. Science Advances, 2021, 7, eabk2341.	4.7	13
43569	Synthesis of bilayer borophene. Nature Chemistry, 2022, 14, 25-31.	6.6	105
43570	First-principles calculations of phase transition, elasticity, phonon spectra, and thermodynamic properties for CeO2 polymorphs. Journal of Solid State Chemistry, 2022, 307, 122761.	1.4	6
43571	The Lithium Iodostannate LiSn 3 I 7 : Synthesis, Properties and its Relationship to SnI 2. European Journal of Inorganic Chemistry, 2021, 2021, 4929.	1.0	0
43572	Study of the electronic and opto-electronic properties of the perovskite KPbBr3 by DFT and TDDFT methods. Computational Condensed Matter, 2022, 33, e00617.	0.9	15
43573	Resistivity size effect due to surface steps on ruthenium thin films computed with a realistic tight-binding model. Journal of Applied Physics, 2021, 130, 195108.	1.1	0

#	Article	IF	Citations
43574	Density Functional Theory Study on Anisotropic Arrangement of Interstitial Oxygen Atoms at (001) Interface of Oxide Precipitates in Si Crystal. ECS Journal of Solid State Science and Technology, 2021, 10, 123003.	0.9	1
43575	Impact of stresses and alloying elements on ferrous martensite nanodomains. Materials Letters, 2021, , 131248.	1.3	1
43576	Direct growth of wafer-scale highly oriented graphene on sapphire. Science Advances, 2021, 7, eabk0115.	4.7	43
43577	Temperature-dependent selective nucleation of single-walled carbon nanotubes from stabilized catalyst nanoparticles. Chemical Engineering Journal, 2022, 431, 133487.	6.6	13
43578	Investigation of room-temperature ferromagnetism in $$hbox {SrTiO}_3$$ perovskite structure via substitutional doping. European Physical Journal Plus, 2021, 136, 1.	1.2	2
43579	Modeling dark- and light-induced crystal structures and single-crystal optical absorption spectra of ruthenium-based complexes that undergo SO2-linkage photoisomerization. Journal of Chemical Physics, 2021, 155, 234111.	1.2	0
43580	Chemical short-range order in body-centered-cubic TiZrHfNb high-entropy alloys. Applied Physics Letters, 2021, 119, .	1.5	15
43581	Corrosion inhibitors: physisorbed or chemisorbed?. Corrosion Science, 2022, 196, 109939.	3.0	113
43582	Intrareticular charge transfer regulated electrochemiluminescence of donorâ€“acceptor covalent organic frameworks. Nature Communications, 2021, 12, 6808.	5.8	81
43583	Emergent magnetic states due to stacking and strain in the van der Waals magnetic trilayer CrI3. Physical Review B, 2021, 104, .	1.1	11
43584	Nitrogenâ€induced changes in the electronic and structural properties of 4Hâ€SiC (0001)/SiO 2 interfaces. Physica Status Solidi (B): Basic Research, 0, , 2100224.	0.7	3
43585	Fatigue and its effect on the piezopotential properties of gallium nitride nanowires. Nanotechnology, 2022, 33, 095401.	1.3	0
43586	Ultrahigh Capacity Retention of a Li₂ZrO₃-Coated Ni-Rich LiNi_{0.8}Co_{0.1}Mn_{0.1}O₂ Cathode Material through Covalent Interfacial Engineering. ACS Applied Energy Materials, 2021, 4, 13785-13795.	2.5	16
43587	Improving Pdâ€“Nâ€“C fuel cell electrocatalysts through fluorination-driven rearrangements of local coordination environment. Nature Energy, 2021, 6, 1144-1153.	19.8	108
43588	Y₂O₃:Eu and the MÃ¶ssbauer isomer shift coefficient of Eu compounds from ab-initio simulations. Journal of Physics Condensed Matter, 2022, 34, 075502.	0.7	1
43589	Reaction of Dichlorophenylborane with Hâ€“Si(100). ACS Omega, 2021, 6, 33645-33651.	1.6	0
43590	First-principles study of helium-vacancy complexes in Be12Ti. Physics Letters, Section A: General, Atomic and Solid State Physics, 2021, 424, 127841.	0.9	1
43591	High-pressure synthesis of boron-rich chalcogenides B12S and B12Se. Journal of Alloys and Compounds, 2021, 898, 162874.	2.8	1

#	Article	IF	Citations
43592	Theoretical Insights into Superior Nitrate Reduction to Ammonia Performance of Copper Catalysts. ACS Catalysis, 2021, 11, 14417-14427.	5.5	150
43593	Atomic-Scale Mechanisms of Electrochemical Pt Dissolution. ACS Catalysis, 2021, 11, 14439-14447.	5.5	19
43594	Intrinsically Honeycombâ€Patterned Hydrogenated Graphene. Small, 2022, 18, e2102687.	5.2	3
43595	Impressive Thermoelectric Figure of Merit in Two-Dimensional Tetragonal Pnictogens: a Combined First-Principles and Machine-Learning Approach. ACS Applied Materials & Interfaces, 2021, 13, 59092-59103.	4.0	24
43596	Thermoelectric properties of Janus AsSBr monolayer from first-principles study. Solid State Communications, 2022, 342, 114612.	0.9	4
43597	Competition of Superconductivity and Charge Density Wave in Selective Oxidized <mml:math xmlns:mml="http://www.w3.org/1998/Math/MathML" display="inline"><mml:mrow><mml:mrow><mml:msub><mml:mrow><mml:mi>CsV</mml:mi></mml:mrow><mml:mrow><mml:mn> Thin Flakes. Physical Review Letters, 2021, 127, 237001.	2.9	73
43598	A novel BN polymorph with ductile manner. Journal of Solid State Chemistry, 2022, 306, 122794.	1.4	13
43599	First-principles energy band calculation of Pr-doped ZrSiO₄. Journal of the Ceramic Society of Japan, 2021, 129, 764-769.	0.5	2
43600	Electron-phonon interaction in <mml:math xmlns:mml="http://www.w3.org/1998/Math/MathML"><mml:mrow><mml:msub><mml:mi>Ti</mml:mi><mml:mi>n</mml:mi></mml:ms mathvariant="normal">O</mml:mi><mml:mrow><mml:mn>2</mml:mn><mml:mi>n</mml:mi><mml:mo>â^'</mml:mo><mml:mn>1</m using first-principles calculations. Physical Review B, 2021, 104, .	1.1	6
43601	Enhanced electronic and optical responses of nitrogen- or boron-doped BeO monolayer: First principle computation. Superlattices and Microstructures, 2022, 162, 107102.	1.4	4
43602	Bandgap modulation in the two-dimensional core-shell-structured monolayers of WS2. IScience, 2022, 25, 103563.	1.9	4
43603	Effects of trace calcium and strontium on microstructure and properties of Cu-Cr alloys. Journal of Materials Science and Technology, 2022, 112, 11-23.	5.6	29
43604	First-Principles Investigation on Phase Stability, Elastic and Magnetic Properties of Boron Doping in Ni-Mn-Ti Alloy. Acta Metallurgica Sinica (English Letters), 2022, 35, 1175-1183.	1.5	4
43605	Van der Waals coherent epitaxy of GaN and InGaN/GaN multi-quantum-well via a graphene inserted layer. Optical Materials Express, 2021, 11, 4118.	1.6	4
43606	Dzyaloshinskii-Moriya anisotropy effect on field-induced magnon condensation in the kagome antiferromagnet <mml:math xmlns:mml="http://www.w3.org/1998/Math/MathML"><mml:mrow><mml:mi>Î±</mml:mi><mml:mtext>â^'</mml:mtext><mml:msub><mml: Physical Review B, 2021, 104, .	1.1	0
43607	Investigation of mechanical, thermodynamical, dynamical and electronic properties of RuYAs (Y = Cr) Tj ETQq1 1 0.784314 rgBT /Over	0.7	2
43608	Electronic and magnetic properties of <mml:math xmlns:mml="http://www.w3.org/1998/Math/MathML" altimg="si1.svg"><mml:mrow><mml:mi mathvariant="bold-italic">Ru</mml:mi><mml:msub><mml:mi mathvariant="bold-italic">O</mml:mi><mml:mn>2</mml:mn></mml:msub></mml:mrow></mml:math> monolayer: DFT+U investigation. Computational Condensed Matter, 2021, 29, e00614.	0.9	7
43609	Skutterudite materials; AlyFexCo4-x-ySb12 (x = y = 1; x = 2, y = 1) for spintronics and optoelectronics applications. Computational Condensed Matter, 2021, 29, e00613.	0.9	0

#	Article	IF	Citations
43610	Electric field and strain induced gap modifications in multilayered GaN. Applied Surface Science, 2022, 578, 151970.	3.1	4
43611	Experimental and theoretical investigation of crystal structure of formamidiniumâ€“copperâ€“iodide single crystals grown from aqueous solution. Journal of Solid State Chemistry, 2021, 306, 122778.	1.4	2
43612	Adsorption and migration of a single lithium on TPHâ€graphene nanoribbon: a DFT approach. Physica Status Solidi (B): Basic Research, 0, , 2100369.	0.7	0
43613	PbSe sensitized with iodine and oxygen: a combined computational and experimental study. Journal of Alloys and Compounds, 2021, , 163119.	2.8	8
43614	Solid-State Study of the Structure, Dynamics, and Thermal Processes of Safinamide Mesylateâ”€A New Generation Drug for the Treatment of Neurodegenerative Diseases. Molecular Pharmaceutics, 2021, , .	2.3	2
43615	Facile hydrothermal synthesis of V2O5 nanofibers as cathode material for aqueous zinc-ion batteries. Journal of Alloys and Compounds, 2022, 896, 163071.	2.8	12
43616	Blue and black phosphorene on metal substrates: a density functional theory study. Journal of Physics Condensed Matter, 2022, 34, 084001.	0.7	1
43617	Recruiting Perovskites to Degrade Toxic Trinitrotoluene. Materials, 2021, 14, 7387.	1.3	5
43618	Interface features and electronic structure of Bi2SiO5/Î²-Bi2O3 hetero-junction. , 2021, , .		0
43619	Exploring the alloying effects on generalized stacking fault energy and ideal strength of Ni and Ni3Al phases in Ni-based superalloys. Mechanics of Materials, 2022, 165, 104183.	1.7	11
43620	Multifunctional ZnCo₂O₄ Quantum Dots Encapsulated In Carbon Carrier for Anchoring/Catalyzing Polysulfides and Selfâ€Repairing Lithium Metal Anode in Lithiumâ€Sulfur Batteries. Advanced Functional Materials, 2022, 32, 2109462.	7.8	44
43621	Dual-Phase Nanocomposite TiB₂/MoS_{1.7}B_{0.3}: An Excellent Ultralow Friction and Ultralow Wear Self-Lubricating Material. ACS Applied Materials & Interfaces, 2021, 13, 59352-59363.	4.0	11
43622	O2 on Ag(110): A puzzle for exchange-correlation functionals. Chemical Physics, 2021, 554, 111424.	0.9	0
43623	Exploring failure mode and enhancement mechanism of doped rare-earth elements iron-based/alumina-ceramic interface. Ceramics International, 2022, 48, 7827-7835.	2.3	3
43624	Vapor-Phase Intercalation of Cesium into Black Phosphorous. Journal of Physical Chemistry C, 2021, 125, 27440-27448.	1.5	2
43625	Thermal excitation studies on the silica coating magnetite composite microspheres with MÃ¶ssbauer spectra and first principle calculations. Journal of Magnetism and Magnetic Materials, 2022, 546, 168909.	1.0	1
43626	Lattice dynamics and thermodynamic properties of Y3Al5O12 (YAG). Journal of Physics and Chemistry of Solids, 2021, 162, 110512.	1.9	6
43627	Phase transitions and potential ferroelectricity in noncentrosymmetric KNaNbOF5. Physical Review Materials, 2021, 5, .	0.9	1

#	Article	IF	Citations
43628	Intrinsic Nature of Spontaneous Magnetic Fields in Superconductors with Time-Reversal Symmetry Breaking. Physical Review Letters, 2021, 127, 237002.	2.9	13
43629	First-Principles Calculations to Investigate the Third-Order Elastic Constants and Mechanical Properties of Mg, Be, Ti, Zn, Zr, and Cd. Advances in Materials Science and Engineering, 2021, 2021, 1-12.	1.0	2
43630	Firstâ€Principles Calculations on the Elastic, Electronic, and Phononic Properties of Sc 2 Al 2 C 3. Physica Status Solidi (B): Basic Research, 0, , 2100336.	0.7	0
43631	Highly Efficient Hole Transport Layerâ€Free Low Bandgap Mixed Pbâ€“Sn Perovskite Solar Cells Enabled by a Binary Additive System. Advanced Functional Materials, 2022, 32, 2110069.	7.8	30
43632	Van der Waals Epitaxy of Bi₂Te₂Se/Bi₂O₂Se Vertical Heterojunction for High Performance Photodetector. Small, 2022, 18, e2105211.	5.2	21
43633	Experimental and Theoretical Insights into Transition-Metal (Mo, Fe) Codoping in a Bifunctional Nickel Phosphide Microsphere Catalyst for Enhanced Overall Water Splitting. ACS Applied Energy Materials, 2021, 4, 14169-14179.	2.5	39
43634	Gas sensing behavior and adsorption mechanism on Ï‡3 borophene surface. Chemical Engineering Journal, 2022, 431, 133947.	6.6	13
43635	Oxygen-rich tetrahedral surface phase on high-temperature rutile <mml:math xmlns:mml="http://www.w3.org/1998/Math/MathML"><mml:mrow><mml:mi mathvariant="normal">V</mml:mi><mml:msub><mml:mi mathvariant="normal">O</mml:mi><mml:mn>2</mml:mn></mml:msub><mml:msub><mml:mrow><mml:mo>(</mml:mo><mml:mn>1</mml:mn> mathvariant="normal">T</mml:mi></mml:msub></mml:mrow></mml:math> single crystals. Physical Review Materials, 2021, 5, .	0.9	3
43636	Vacancy Defects in Ga2O3: First-Principles Calculations of Electronic Structure. Materials, 2021, 14, 7384.	1.3	40
43637	First-principles calculations of the high-pressure behavior, electronic, magnetic, and elastic properties of praseodymium pnictides: PrX (XÂ=ÂP, As and Bi). Journal of Magnetism and Magnetic Materials, 2022, 546, 168919.	1.0	1
43638	Two-Dimensional MoS₂ Nanosheet-Functionalized Optical Microfiber for Room-Temperature Volatile Organic Compound Detection. ACS Applied Nano Materials, 2021, 4, 13440-13449.	2.4	10
43639	Cysteine Adsorption on Twisted-Bilayer Graphene. Journal of Physical Chemistry C, 2021, 125, 27314-27322.	1.5	6
43640	Two-step Brillouin zone sampling for eï¬ƒcient computation of electron dynamics in solids. Journal of Physics Condensed Matter, 2021, , .	0.7	1
43641	Alloy Engineering of 2D Van der Waals Chromium Mixed Trihalides as Ferromagnetic Semiconductors. Physica Status Solidi (B): Basic Research, 2022, 259, .	0.7	1
43642	Newly Synthesized Three-Dimensional Boron-Rich Chalcogenides B₁₂X (X = S and Se): Theoretical Characterization of the Physical Properties for Optoelectronic and Mechanical Applications. ACS Omega, 2021, 6, 33899-33913.	1.6	17
43643	1T-VS₂/MXene Hybrid as a Superior Electrode Material for Asymmetric Supercapacitors: Experimental and Theoretical Investigations. ACS Applied Energy Materials, 2021, 4, 14198-14209.	2.5	34
43644	The structural, mechanical and electronic properties of novel superhard carbon allotropes: ab initio study. Materials Today Communications, 2021, 29, 102980.	0.9	4
43645	Physical properties of rare earth perovskites CeMO3 (M = Co, Cu) in the context of density functional theory. Materials Today Communications, 2021, 29, 102973.	0.9	7

#	Article	IF	Citations
43646	Enhanced OER activity of FePc molecule by substrate effects: A first principles study. Surface Science, 2022, 717, 122000.	0.8	3
43647	Phase Stability of Nanolaminated Epitaxial (Cr_{1â€“x}Fe_x)₂AlC MAX Phase Thin Films on MgO(111) and Al₂O₃(0001) for Use as Conductive Coatings. ACS Applied Nano Materials, 2021, 4, 12761-12770.	2.4	6
43648	Role of rare earth sites and vacancies in the anomalous compression of modulated scheelite tungstates <mml:math xmlns:mml="http://www.w3.org/1998/Math/MathML"><mml:msub><mml:mrow><mml:mi>R</mml:mi><mml:mi>E</mml:mi></mml:mro (<mml:math) Tj ETQq0 0 0 rgBT /Overlock 10 Tf 50 652 Td (xmlns:mml="http://www.w3.org/1998/Math/MathML"><mml:mrow><mml:r	0.9	3
43649	Physical Review Materials, 2021, 5, . Modified band alignment method to obtain hybrid functional accuracy from standard DFT: Application to defects in highly mismatched III-V:Bi alloys. Physical Review Materials, 2021, 5, .	0.9	2
43650	Strain engineering in the oxygen reduction reaction and oxygen evolution reaction catalyzed by Pt-doped Ti₂CF₂. Journal of Materials Chemistry A, 2022, 10, 1390-1401.	5.2	27
43651	Electronic structure, optical dispersion and luminescence properties of terbium gallium garnet crystal. CrystEngComm, 2022, 24, 877-885.	1.3	6
43652	High-Pressure Synthesis and Ambient-Pressure Tem Investigation of Mg-Orthocarbonate. SSRN Electronic Journal, 0, , .	0.4	3
43653	Effect of point defects on acetylene hydrogenation reaction over Ni(111) surface: a density functional theory study. Physical Chemistry Chemical Physics, 2021, 23, 27340-27347.	1.3	1
43654	Two-dimensional layered MSi₂N₄ (M = Mo, W) as promising thermal management materials: a comparative study. Physical Chemistry Chemical Physics, 2022, 24, 3086-3093.	1.3	24
43655	A Novel Strategy for Enhancing Photoelectrochemical Performance of Ca ₂Fe ₂O ₅ Photocathodes: An Integrated Experimental and DFT-Based Approach. SSRN Electronic Journal, 0, , .	0.4	0
43656	Structural, elastic, electronic and optical properties of the half-Heusler ScPtSb and YPtSb compounds under pressure. Condensed Matter Physics, 2021, 24, 43702.	0.3	9
43657	The Carbonate-catalyzed Transesterification of Sunflower Oil for Biodiesel Production: in situ Monitoring and Density Functional Theory Calculations. South African Journal of Chemistry, 2021, 74, .	0.3	0
43658	A first principles study on aluminium-sulfur co-doped graphene as an electro-catalyst for oxygen reduction reaction in a PEM fuel cell. AIP Conference Proceedings, 2021, , .	0.3	0
43659	Role of topological surface states and mirror symmetry in topological crystalline insulator SnTe as an efficient electrocatalyst. Nanoscale, 2021, 13, 18160-18172.	2.8	14
43660	High-throughput computation of novel ternary Bâ€“Câ€“N structures and carbon allotropes with electronic-level insights into superhard materials from machine learning. Journal of Materials Chemistry A, 2021, 9, 27596-27614.	5.2	21
43661	Structure and electronic properties of CsPbBr3 perovskite: first principle calculations. Journal of Physical Studies, 2021, 25, .	0.2	1
43662	Elasticity, Mechanical and Thermal Properties of Polycrystalline Hafnium Carbide and Tantalum Carbide at High Pressure. SSRN Electronic Journal, 0, , .	0.4	0
43663	High Compositional Dependence of Activity of Platinumâ€“Dysprosium Alloys for Oxygen Reduction in Alkaline Media: Experimental and Theoretical Study. SSRN Electronic Journal, 0, , .	0.4	0

#	Article	IF	Citations
43664	The effect of the composition and pressure on the phase stability and electronic, magnetic, and elastic properties of M₂AX (M = Mn, Fe; A = Al, Ga, Si, Ge; X = C, N) phases. Physical Chemistry Chemical Physics, 2021, 23, 26376-26384.	1.3	5
43665	A flexible Mn_{0.5}Ti₂(PO₄)₃/C nanofiber film with superior cycling stability for potassium-ion batteries. Nanoscale, 2021, 13, 19956-19965.	2.8	9
43666	Coordination environment engineering on nickel single-atom catalysts for CO₂ electroreduction. Nanoscale, 2021, 13, 19133-19143.	2.8	27
43667	Mn-Dopant Induced Octahedral Configuration Strongly Stabilizes Ni ₁₂P ₅ Nanowires for Battery-Supercapacitor Hybrid Devices. SSRN Electronic Journal, 0, , .	0.4	0
43668	Piezoelectricity of Janus BiTeX (X = Cl, Br, I) Monolayer: A First-Principles Study. IEEE Transactions on Electron Devices, 2021, , 1-5.	1.6	1
43669	Surface Stability of Wn Ultrathin Films Under O ₂ and H ₂O Exposure: A First-Principles Study. SSRN Electronic Journal, 0, , .	0.4	0
43670	Modeling of the Cathodic and Anodic Polarization Curves of Metals and Alloys at an Electronic Level. SSRN Electronic Journal, 0, , .	0.4	0
43671	Influence of Doping with Selected Organic Molecules on Magnetic and Electronic Properties of Bare, Surface Terminated and Defect Patterned Ti2C MXene Monolayer. Physical Chemistry Chemical Physics, 2022, , .	1.3	5
43672	Halogenated Ti₃C₂ MXene as High Capacity Electrode Material for Li-ion Batteries. Wuji Cailiao Xuebao/Journal of Inorganic Materials, 2022, 37, 660.	0.6	4
43673	Half-Negative Poisson's Ratio in Graphene+ With Intrinsic Dirac Cone: A Competitor to Graphene?. SSRN Electronic Journal, 0, , .	0.4	0
43674	Electronic Properties and Defect Levels Induced by n/p-Type Defect-Complexes in Ge. SSRN Electronic Journal, 0, , .	0.4	0
43675	The Role of Zr in Co-Segregation Behavior of Zr- X Solutes and Their Effects on the Thermodynamic Stability and Fracture Strength of Ni Î£5 [001](210) Grain Boundary. SSRN Electronic Journal, 0, , .	0.4	0
43676	Revealing Effects of Common Nonmetallic Impurities on the Stability and Strength of Cu-Sn Solder Joints: A First-Principles Investigation. SSRN Electronic Journal, 0, , .	0.4	0
43677	Mechanical Strain and Electric Field Tunable Electronic Structure of Black/Violet Phosphorene Van Der Waals Heterostructure: From Type I to Z-Scheme System. SSRN Electronic Journal, 0, , .	0.4	0
43678	Adsorption of CO2 on Fe-montmorillonite: A density functional theory study. AIP Conference Proceedings, 2021, , .	0.3	0
43679	The Influence of Iodide on the Solution-Phase Growth of Cu Microplates: A Multi-Scale Theoretical Analysis from First Principles. Faraday Discussions, 2022, , .	1.6	4
43680	Designing sp3 networks of two novel carbon allotropes in the P4/mmm phase. Chinese Journal of Physics, 2022, 75, 90-103.	2.0	23
43681	Competing Superior Electronic Structure and Complex Defect Chemistry in Quasi-One-Dimensional Antimony Chalcogenide Photovoltaic Absorbers. ACS Applied Energy Materials, 2022, 5, 492-502.	2.5	14

#	Article	IF	Citations
43682	Fe Singleâ€Atom Catalyst for Efficient and Rapid Fentonâ€Like Degradation of Organics and Disinfection against Bacteria. Small, 2022, 18, e2104941.	5.2	53
43683	Intercalation of cobalt cations into Co₉S₈ interlayers for highly efficient and stable electrocatalytic hydrogen evolution. Journal of Materials Chemistry A, 2022, 10, 3522-3530.	5.2	21
43684	Improvement of electric insulation in dielectric layered perovskite nickelate films via fluorination. Journal of Materials Chemistry C, 2022, 10, 1711-1717.	2.7	2
43685	Superexchange Ferromagnetic Coupling and Thermodynamic Features of the La2FeCoO6 Semiconductor. Journal of Low Temperature Physics, 2022, 206, 269-280.	0.6	7
43686	Engineering the geometric and electronic structure of Ru via Ruâ€“TiO₂ interaction for enhanced selective hydrogenation. Catalysis Science and Technology, 2022, 12, 1005-1016.	2.1	12
43687	Gold boosts nitrate reduction and deactivation resistance to indium-promoted palladium catalysts. Applied Catalysis B: Environmental, 2022, 305, 121048.	10.8	29
43688	Palladium Nanoparticles-Decorated Î²-Cyclodextrinâ€“Cyanoguanidine Modified Graphene Oxide: A Heterogeneous Nanocatalyst for Suzukiâ€“Miyaura Coupling and Reduction of 4-Nitrophenol Reactions in Aqueous Media. Journal of Inorganic and Organometallic Polymers and Materials, 2022, 32, 791-802.	1.9	6
43689	Diffusion-enhanced preferential growth of <mml:math xmlns:mml="http://www.w3.org/1998/Math/MathML" display="inline" id="d1e570" altimg="si37.svg"><mml:mi>m</mml:mi></mml:math>-oriented GaN micro-domains on directly grown graphene with a large domain size on Ti/SiO2/Si(001). Materials Today Communications, 2022, 30, 103113.	0.9	3
43690	Electronic properties of TaAs₂ topological semimetal investigated by transport and ARPES. Journal of Physics Condensed Matter, 2022, 34, 125601.	0.7	16
43691	The Orbital Origins of Chemical Bonding in Geâ^'Sbâ^'Te Phaseâ€Change Materials**. Angewandte Chemie - International Edition, 2022, 61, .	7.2	19
43692	A high-performance and durable direct NH3 tubular protonic ceramic fuel cell integrated with an internal catalyst layer. Applied Catalysis B: Environmental, 2022, 306, 121071.	10.8	33
43693	Two-dimensional buckling structure induces the ultra-low thermal conductivity: a comparative study of the group GaX (X = N, P, As). Journal of Materials Chemistry C, 2022, 10, 1436-1444.	2.7	13
43694	Phase controlled synthesis of transition metal carbide nanocrystals by ultrafast flash Joule heating. Nature Communications, 2022, 13, 262.	5.8	52
43695	Reply to the â€˜Comment on â€œHigh-temperature superconductivity in transition metallic hydrides MH₁₁ (M = Mo, W, Nb, and Ta) under high pressureâ€â€™ by X. Zheng and J. Zheng, Phys. Chem. Chem. Phys., 2022, 24, DOI: 10.1039/D1CP01474A. Physical Chemistry Chemical Physics, 2022, 24, 1898-1899.	1.3	1
43696	Mechanical, thermal transport, electronic and photocatalytic properties of penta-PdPS, -PdPSe and -PdPTe monolayers explored by first-principles calculations. Journal of Materials Chemistry C, 2021, 10, 329-336.	2.7	14
43697	Effects of transition metal dopants on the electronic structure of potassium niobate. Journal of Applied Physics, 2022, 131, 023102.	1.1	0
43698	Theoretical investigations into the hydrogen evolution reaction of the carbon schwarzites: From electronics to structure-catalytic activity relationship. Carbon, 2022, 190, 136-141.	5.4	9
43699	A periodic DFT study of CO adsorption over Pdâ€“Cu alloy (111) surfaces. Research on Chemical Intermediates, 2022, 48, 853.	1.3	0

#	Article	IF	Citations
43700	Enhanced thermoelectric performance in Sbâ€“Br codoped Bi₂Se₃ with complex electronic structure and chemical bond softening. RSC Advances, 2022, 12, 1653-1662.	1.7	10
43701	Adsorption mechanisms and effects of thiocarbamate collectors in the separation of chalcopyrite from pyrite minerals: DFT and experimental studies. Minerals Engineering, 2022, 176, 107318.	1.8	28
43702	Hydrogen trapping and storage in the group IVB-VIB transition metal carbides. Materials and Design, 2022, 214, 110399.	3.3	20
43703	Synergetic effect of Si addition on mechanical properties in face-centered-cubic high entropy alloys: a first-principles study. Modelling and Simulation in Materials Science and Engineering, 2022, 30, 024003.	0.8	8
43704	HgSO4: An excellent mid-infrared sulfate nonlinear optical crystal with wide band gap and strong second harmonic generation response. Journal of Alloys and Compounds, 2022, 902, 163727.	2.8	6
43705	Improving sensing of formaldehyde using ZnO nanostructures with surface-adsorbed oxygen. Nanoscale Advances, 2022, 4, 546-561.	2.2	5
43706	In situ surface reconstruction of a Ni-based perovskite hydroxide catalyst for an efficient oxygen evolution reaction. Journal of Materials Chemistry A, 2022, 10, 1369-1379.	5.2	20
43707	First-principles study on the heterostructure of twisted graphene/hexagonal boron nitride/graphene sandwich structure. Journal of Physics Condensed Matter, 2022, 34, 125504.	0.7	5
43708	A Symmetric Fâ^'Hâ^'F Hydrogen Bond in Strontium Bifluoride, Sr[HF 2] 2. Zeitschrift Fur Anorganische Und Allgemeine Chemie, 0, , e202100374.	0.6	0
43709	First-principles investigation of the structural and dynamical stability, electronic and thermal properties of two-dimensional Yn+1Cn (nÂ=Â1, 2, and 3) MXenes. FlatChem, 2022, 31, 100328.	2.8	8
43710	Metastable FeCN₂@nitrogen-doped carbon with high pseudocapacitance as an anode material for sodium ion batteries. Nanoscale, 2022, 14, 780-789.	2.8	7
43711	Dopant precursor adsorption into single-dimer windows: Towards guided self-assembly of dopant arrays on Si(100). Chemical Physics Letters, 2022, 787, 139258.	1.2	2
43712	C₃ production from CO₂ reduction by concerted *CO trimerization on a single-atom alloy catalyst. Journal of Materials Chemistry A, 2022, 10, 5998-6006.	5.2	25
43713	DFTB investigations of the electronic and magnetic properties of fluorographene with vacancies and with adsorbed chemical groups. Physical Chemistry Chemical Physics, 2022, 24, 3312-3321.	1.3	4
43714	Spin-crossover Fe(<scp>ii</scp>) complexes on a surface: a mixture of low-spin and high-spin molecules at low temperature from quantum-chemistry calculations. Inorganic Chemistry Frontiers, 2022, 9, 753-760.	3.0	5
43715	CO2 capture and separation from H2/CH4/N2 gas mixtures by a novel ternary pentagonal monolayer â€œPenta-BCNâ€• First principles investigation. Journal of Molecular Liquids, 2022, 348, 118474.	2.3	4
43716	Magnetic Moment Evolution in FeGaGeB(Si) Alloys that Dominate the Saturation Magnetization. Journal of Superconductivity and Novel Magnetism, 0, , 1.	0.8	0
43717	Analysis of atomic structure, magnetic ordering, and oxygen diffusion in oxygen deficient Sr3Fe2O7â^'Î´ perovskite: Toward rational catalysts design. Physical Review Materials, 2022, 6, .	0.9	1

#	Article	IF	Citations
43718	The effect of ferromagnetism on the CO activation over FCC crystal phase transition metal catalysts: Insights from DFT calculations. Molecular Catalysis, 2022, 518, 112071.	1.0	3
43719	Modulating Thermal Transport in Porous Carbon Honeycomb by Cutting and Deformation Techniques. Physical Chemistry Chemical Physics, 2022, , .	1.3	1
43720	A Reentrant Phase Transition and a Novel Polymorph Revealed in High-Pressure Investigations of CF4 up to 46.5 GPa. Journal of Chemical Physics, 2022, 156, 044503.	1.2	2
43721	Assessing doping strategies for monolayer MoS₂ towards non-enzymatic detection of cortisol: a first-principles study. Physical Chemistry Chemical Physics, 2022, 24, 1048-1058.	1.3	2
43722	First principles studies on the electronic and contact properties of single layer 2H-MoS₂/1Tâ€²-MX₂ heterojunctions. Physical Chemistry Chemical Physics, 2022, 24, 3289-3295.	1.3	2
43723	Ab-initio-driven prediction of puckered penta-like PdPSeX (X O, S, Te) Janus monolayers: Study on the electronic, optical, mechanical and photocatalytic properties. Applied Surface Science, 2022, 582, 152356.	3.1	55
43724	Thermodynamics and Catalytic Properties of Two Novel Energetic Complexes Based on 3-Amino-1,2,4-triazole-5-carboxylic Acid. ACS Omega, 2022, 7, 3024-3029.	1.6	7
43725	Finite-size scaling effects of chemically induced transformations: From T12â€˘carbon to a composite carbon-cage structure. Diamond and Related Materials, 2022, 122, 108829.	1.8	2
43726	Carbon adsorption and incorporation on the (110)AlAs surface. Physica B: Condensed Matter, 2022, 627, 413583.	1.3	0
43727	Structural characterisation, Hirshfeld surfaces, DSC, periodic DFT modeling, vibrational and optical study of heptylenediammonium pentachlorobismuthate H3N(CH2)7NH3BiCl5. Journal of Solid State Chemistry, 2022, 306, 122805.	1.4	10
43728	A first-principles study on D022 precipitation phases of Ni-based superalloys with loading stress and high temperature. Solid State Communications, 2022, 342, 114632.	0.9	4
43729	First-principles studies of imidazolium chloroaluminate ionic liquids with different substitutions on the Pt(111) surface. Colloids and Surfaces A: Physicochemical and Engineering Aspects, 2022, 635, 128079.	2.3	1
43730	Armchair graphene nanoribbon-based spin caloritronics. Physics Letters, Section A: General, Atomic and Solid State Physics, 2022, 426, 127892.	0.9	5
43731	Sudoku-inspired high-Shannon-entropy alloys. Acta Materialia, 2022, 225, 117556.	3.8	5
43732	One-dimensional metallic grain boundary in transition metal dichalcogenides. Computational Materials Science, 2022, 203, 111115.	1.4	2
43733	Self-energy corrected band-gap tuning induced by strain in the hexagonal boron phosphide monolayer. Computational Materials Science, 2022, 203, 111144.	1.4	7
43734	First-principles studies of the concentration-dependent tritium diffusion in the zirconium hydrides with and without Sn impurity. Computational Materials Science, 2022, 203, 111158.	1.4	2
43735	Interatomic Feâ€“Cr potential for modeling kinetics on Fe surfaces. Computational Materials Science, 2022, 203, 110840.	1.4	1

#	Article	IF	Citations
43736	First examples of nickelâ€“Aluminum mixed chalcogenides based on the AuCu3-type fragments: Breaking a robust intermetallic bond system in Ni3Al. Journal of Solid State Chemistry, 2022, 306, 122815.	1.4	6
43737	Nonlinear elastic analysis of 2D materials of arbitrary symmetries with application to black phosphorus. Mechanics of Materials, 2022, 165, 104159.	1.7	2
43738	Metalloid substitution elevates simultaneously the strength and ductility of face-centered-cubic high-entropy alloys. Acta Materialia, 2022, 225, 117571.	3.8	64
43739	Structural and photodetector characteristics of Zn and Al incorporated ZnGa2O4 films via co-sputtering. Results in Physics, 2022, 33, 105206.	2.0	8
43740	First-principles calculations to investigate ultra-wide bandgap semiconductor behavior of NaMgF3 fluoro-perovskite with external static isotropic pressure and its impact on optical properties. Optik, 2022, 252, 168532.	1.4	24
43741	Ab initio investigation of phase stability, thermo-physical and mechanical properties of (Mo0.2Cr0.2Ta0.2Nb0.2X0.2)Si2 (XÂ=ÂW, V) high-entropy refractory metal silicides. Computational Materials Science, 2022, 203, 111116.	1.4	8
43742	Electronic, elastic, mechanical and anisotropic response of W3XC2 (X: Si, Ge and Al) alloys via first-principles. Solid State Communications, 2022, 343, 114648.	0.9	2
43743	The impact of anionic vacancies on the mechanical properties of NbC and NbN: An ab initio study. Computational Materials Science, 2022, 203, 111113.	1.4	2
43744	First-principles calculations to investigate electronic structure and optical properties of 2D MgCl2 monolayer. Superlattices and Microstructures, 2022, 162, 107132.	1.4	15
43745	Defect-rich engineering of Ni-incorporated tungsten oxides micro-flowers on carbon cloth: A binder-free electrode for highly efficient hydrogen evolution reaction. Journal of Power Sources, 2022, 520, 230862.	4.0	11
43746	Deprivation of unpaired electrons on graphitic carbon nitride-based carbocatalysts by peroxydisulfate driving a nonradical oxidation process. Journal of Cleaner Production, 2022, 334, 130220.	4.6	3
43747	Structure, mechanical stability, lattice dynamics and thermodynamic properties of C15-Laves phase Mg2Ce. Solid State Communications, 2022, 342, 114641.	0.9	1
43748	New high-pressure monoclinic phase of Sn. Solid State Communications, 2022, 342, 114635.	0.9	1
43749	Effect of substitutional doping and disorder on the phase stability, magnetism, and half-metallicity of Heusler alloys. Acta Materialia, 2022, 225, 117477.	3.8	12
43750	Multidimensional VO2 nanotubes/Ti3C2 MXene composite for efficient electrochemical lithium/sodium-ion storage. Journal of Power Sources, 2022, 521, 230946.	4.0	14
43751	Atomic structure of PbBr2 thin films on Ag (111). Solid State Communications, 2022, 343, 114651.	0.9	1
43752	First-principles prediction of pressure dependent mechanical, electronic, optical, and superconducting state properties of NaC6: A potential high-Tc superconductor. Results in Physics, 2022, 33, 105182.	2.0	11
43753	Evaluation of oxygen-vacancy concentration through simulated hydrogen diffusion in amorphous In-Ga-Zn-O. Computational Materials Science, 2022, 203, 111109.	1.4	4

#	Article	IF	Citations
43754	Monolayer penta-BCN: A promising candidate for harmful gases detection. Sensors and Actuators A: Physical, 2022, 334, 113326.	2.0	13
43755	Interlayer water structure of phyllomanganates: Insights from MD simulations of chalcophanite-group oxide dehydration. Geochimica Et Cosmochimica Acta, 2022, 318, 495-509.	1.6	3
43756	Enhance the interlayer coupling and modify the properties through Janus WSeTe. Computational Materials Science, 2022, 203, 111140.	1.4	3
43757	Adsorption of toxic gases on metal doped C3N monolayer: A theoretical study. Computational and Theoretical Chemistry, 2022, 1208, 113559.	1.1	1
43758	Photo-electrochemical enhanced mechanism enables a fast-charging and high-energy aqueous Al/MnO2 battery. Energy Storage Materials, 2022, 45, 586-594.	9.5	19
43759	Nickel B-site substitution in bulk Sr1â^'xCaxFeO3 perovskite oxygen carriers: Benefits and limitations. Journal of Alloys and Compounds, 2022, 896, 162783.	2.8	7
43760	Ab initio predictions of structures and physical properties of the KCuX (X = Se and Te) phases under pressure. Computational Condensed Matter, 2022, 30, e00616.	0.9	2
43761	Insight into adsorption mechanism of water on tricalcium silicate from first-principles calculations. Cement and Concrete Research, 2022, 152, 106684.	4.6	11
43762	Ta concentration effect on nucleation of defects in W-Ta alloy from first-principles model. Materials Today Communications, 2022, 30, 103071.	0.9	0
43763	Coexistence of a self-interstitial atom with light impurities in a tungsten grain boundary. Journal of Nuclear Materials, 2022, 560, 153481.	1.3	5
43764	Spin transport properties of boron nitride nanotubes: A DFT study. Computational Condensed Matter, 2022, 30, e00636.	0.9	2
43765	Deposition of Co islands on Cu(111) and Cuâ€“Al(111): A comparative study from DFT calculations. Vacuum, 2022, 197, 110812.	1.6	1
43766	A mechanistic periodic DFT study on the dissociation of tetrachlorodibenzofuran (TCDF) by M-doped carbon nanotube catalysts (MÂ=ÂAl, Fe, Mn). Applied Surface Science, 2022, 579, 152217.	3.1	3
43767	Compatibility of UN with refractory metals (V, Nb, Ta, Cr, Mo and W): An ab initio approach to interface reactions and diffusion behavior. Journal of Nuclear Materials, 2022, 560, 153482.	1.3	5
43768	Single Ni atom doped WS2 monolayer as sensing substrate for dissolved gases in transformer oil: A first-principles study. Applied Surface Science, 2022, 579, 152141.	3.1	40
43769	Encapsulation of atomic hydrogen and gaseous molecules in single-walled boronâ€“nitrogen nanotubes: A computational study. Applied Surface Science, 2022, 579, 152098.	3.1	0
43770	Insights into the mechanism of ethanol conversion into 1,3-butadiene on Zr-Î² zeolite. Applied Surface Science, 2022, 579, 152212.	3.1	9
43771	Identification of active sites available for hydrogen evolution of Single-Atom Ni1/TiO2 catalysts. Applied Surface Science, 2022, 579, 152139.	3.1	11

#	Article	IF	Citations
43772	The new stable phases of Fe2Pd crystal alloy and their properties. Computational Materials Science, 2022, 204, 111183.	1.4	1
43773	Exploring the exemplary electronic and optical nature in NaInX2 (X = S, Se and Te) ternary type chalcogenides materials: A GGA+U and hybrid functionals study. Journal of Solid State Chemistry, 2022, 307, 122853.	1.4	2
43774	Cationic variation for LnAl2Si2 (LnÂ=ÂY, Sm, Tb, Dy, Yb) compounds by density functional theory. Journal of Molecular Structure, 2022, 1252, 132136.	1.8	9
43775	Surface functionalization of Ta4C3 MXene for broadband ultrafast photonics in the near-infrared region. Applied Materials Today, 2022, 26, 101341.	2.3	17
43776	Experimental investigation and thermodynamic re-assessment of the Tiâ€“Zn system and atomic mobility of its bcc phase. Calphad: Computer Coupling of Phase Diagrams and Thermochemistry, 2022, 76, 102392.	0.7	4
43777	Reinforced upconversion and charge separation via mid-gap states in WO3 nanosheet with infrared light driven tetracycline degradation. Chemical Engineering Journal, 2022, 431, 134134.	6.6	12
43778	Electronic structure regulation of Na2FePO4F cathode toward superior high-rate and high-temperature sodium-ion batteries. Energy Storage Materials, 2022, 45, 851-860.	9.5	18
43779	Thermodynamic assessment of the Feâ€“Niâ€“Rhâ€“Ti system. Calphad: Computer Coupling of Phase Diagrams and Thermochemistry, 2022, 76, 102386.	0.7	0
43780	Designing Pt-based subsurface alloy catalysts for the dehydrogenation of perhydro-dibenzyltoluene: A first-principles study. Applied Surface Science, 2022, 579, 152142.	3.1	13
43781	Structural, electronic, elastic, phonon and thermoelectric properties of Heusler-structured intermetallic HfCu2In: Using density functional theory. Physica B: Condensed Matter, 2022, 629, 413633.	1.3	7
43782	Group three nitride clusters as promising components for nanoelectronics. Materials Today Chemistry, 2022, 23, 100751.	1.7	2
43783	First-principles screening in Cu-embedded PtSe2 monolayer as a potential gas sensor upon CO and HCHO in dry-type transformers. Computational and Theoretical Chemistry, 2022, 1209, 113586.	1.1	6
43784	First-principles studies of electronic structure, magnetic and optical properties of rare-earth (RE=) Tj ETQq0 0 0 rgBT /Overlock 10 Tf 50	0.9	6
43785	First-principles study of surface orientation dependent corrosion of BCC iron. Corrosion Science, 2022, 196, 110029.	3.0	23
43786	A multi-platform sensor for selective and sensitive H2S monitoring: Three-dimensional macroporous ZnO encapsulated by MOFs with small Pt nanoparticles. Journal of Hazardous Materials, 2022, 426, 128075.	6.5	41
43787	A first principles investigation on the structural, elastic, and mechanical properties of MAX phase M3AlC2 (M= Ta, Ti, V) as a function of pressure. Computational Condensed Matter, 2022, 30, e00638.	0.9	2
43788	Temperature-induced orbital polarizations and tunable charge dynamics in layered double perovskite thin films. Materials Today Energy, 2022, 24, 100921.	2.5	5
43789	Investigations on the electronic properties and effect of chitosan capping on the structural and optical properties of zinc aluminate quantum dots. Applied Surface Science, 2022, 579, 152162.	3.1	5

#	Article	IF	Citations
43790	Theoretical investigation of structural, electronic and optical properties of Sc-doped SnO2. Computational Condensed Matter, 2022, 30, e00642.	0.9	6
43791	Understanding flotation processes at the atomic scale using density functional theory â€“ A case study on adsorption of 2-Mercaptobenzothiazole on chalcopyrite and pyrite surfaces. Applied Surface Science, 2022, 579, 152112.	3.1	11
43792	Adjusting the catalytic activity of C2N/SiH heterojunction for water splitting: A first-principles study. Applied Surface Science, 2022, 579, 152233.	3.1	20
43793	Evaluation of structural, electronic, optical, elastic, and mechanical properties of triclinic Sn-doped Ga2O3 using density functional theory. Computational Condensed Matter, 2022, 30, e00641.	0.9	3
43794	Evaluation of the structural, electronic, optical, elastic, and mechanical properties of As2Se3. Computational Condensed Matter, 2022, 30, e00633.	0.9	1
43795	A machine-learning-based investigation on the mechanical/failure response and thermal conductivity of semiconducting BC2N monolayers. Carbon, 2022, 188, 431-441.	5.4	34
43796	Bifunctional water splitting enhancement by manipulating Mo-H bonding energy of transition Metal-Mo2C heterostructure catalysts. Chemical Engineering Journal, 2022, 431, 134126.	6.6	49
43797	Adsorption and decomposition of <mml:math xmlns:mml="http://www.w3.org/1998/Math/MathML" altimg="si14.svg"><mml:mrow><mml:msub><mml:mi mathvariant="bold">H</mml:mi><mml:mn>2</mml:mn></mml:msub><mml:mi mathvariant="bold">S</mml:mi></mml:mrow></mml:math> on <mml:math xmlns:mml="http://www.w3.org/1998/Math/MathML" altimg="si15.svg"><mml:mrow><mml:msub><mml:mi mathvariant="bold">C</mml:mi><mml:mn>2</mml:mn></mml:msub>	0.9	2
43798	Tuning the electronic and optical properties of two-dimensional hydrogenated c-BN nanosheets by Be and C dopants and vacancy defects. Chemical Physics, 2022, 555, 111441.	0.9	1
43799	Novel bipolar magnetic semiconductor materials formed by adsorption of methyl or halomethyles on the graphene: A spin-polarized density functional theory study. Applied Surface Science, 2022, 581, 152338.	3.1	7
43800	Effect of Fe on Bi2Te3: Structure, magnetic properties, and XPS valence band. Journal of Alloys and Compounds, 2022, 899, 163297.	2.8	27
43801	In situ nanopores enrichment of Mesh-like palladium nanoplates for bifunctional fuel cell reactions: A joint etching strategy. Journal of Colloid and Interface Science, 2022, 611, 523-532.	5.0	71
43802	Au adsorption on stepped Si(hhk)-Au surfaces. Surface Science, 2022, 718, 122010.	0.8	0
43803	Atomic insight into iron corrosion exposed to supercritical water environment with an improved Fe-H2O reactive force field. Applied Surface Science, 2022, 580, 152300.	3.1	14
43804	Crystal and electronic structure of the sub-stoichiometric photocatalyst Cu4Se6: DFT study. Journal of Physics and Chemistry of Solids, 2022, 162, 110529.	1.9	1
43805	DFT insights into competitive adsorption and reaction mechanism of benzothiophene and naphthalene on Fe-doped Ni2P catalyst. Fuel, 2022, 314, 123114.	3.4	3
43806	Copper-based thiospinel quantum dots as potential candidates for nonlinear optical applications. Optics and Laser Technology, 2022, 148, 107752.	2.2	8
43807	Investigation of the mechanical properties of MnSi via EBSD-nanoindentation coupling and ab-initio calculation. Journal of Alloys and Compounds, 2022, 900, 163458.	2.8	3

#	Article	IF	Citations
43808	An ab initio study of the interaction of graphene and silicene with one-, two-, and three-layer planar silicon carbide. Physica E: Low-Dimensional Systems and Nanostructures, 2022, 138, 115120.	1.3	3
43809	The microstructural, mechanical and thermal properties of TiAlVN, TiAlSiN monolithic and TiAlVN/TiAlSiN multilayered coatings. Journal of Alloys and Compounds, 2022, 899, 163332.	2.8	15
43810	H-passivated nanoporous graphene membranes for CO2/N2 separation: A reactive molecular dynamic simulation. Journal of Molecular Structure, 2022, 1253, 132255.	1.8	2
43811	Concunrent manipulation of anion and cation adsorption kinetics in pancake-like carbon achieves ultrastable potassium ion hybrid capacitors. Energy Storage Materials, 2022, 46, 10-19.	9.5	32
43812	Enhancing the interaction between Mn and Ce oxides supported on fly ash with organic acid ligands interface modification for effective VOC removal: A combined experimental and DFTÂ+ÂU study. Fuel, 2022, 313, 123043.	3.4	14
43813	Structural phase transition in cobalt oxyfluoride Co3Sb4O6F6 observed by high-resolution synchrotron and neutron diffraction. Journal of Physics and Chemistry of Solids, 2022, 163, 110568.	1.9	2
43814	Theory-guided design of Pd/C nanocomposite for H2 sensing at room-temperature. Applied Surface Science, 2022, 581, 152367.	3.1	6
43815	Effect of pressure on dynamical stability, electronic and thermoelectric properties of equiatomic quaternary Heusler alloy LaCoTiGe. Materials Science in Semiconductor Processing, 2022, 141, 106432.	1.9	8
43816	Smart construction of multifunctional Li1.5Al0.5Ge1.5(PO4)3 | Li intermediate interfaces for solid-state batteries. Energy Storage Materials, 2022, 46, 68-75.	9.5	34
43817	A simulated-TPD study of H2 desorption on metal surfaces. Surface Science, 2022, 718, 122015.	0.8	7
43818	Janus MoCrSSe monolayer: A strong two dimensional polar antiferromagnet. Applied Surface Science, 2022, 581, 152420.	3.1	4
43819	Modulating the blue and green luminescence in the Î²-Ga2O3 films. Journal of Alloys and Compounds, 2022, 900, 163431.	2.8	24
43820	Signature of half-metallicity in <mml:math xmlns:mml="http://www.w3.org/1998/Math/MathML" display="inline" id="d1e709" altimg="si6.svg"><mml:msub><mml:mrow><mml:mtext>BiFeO</mml:mtext></mml:mrow><mml:mrow><mml:mtext>3</mml:mtext></mml:mrow></mml:msub></mml:math> A DFT study. Computational Materials Science, 2022, 204, 111107.	1.4	5
43821	Defect stabilized Fe atom on porous BN sheet as a potential electrocatalyst for oxygen reduction reaction: A first-principles investigation. Applied Surface Science, 2022, 580, 152271.	3.1	6
43822	Adsorption of toxic H2S, CO and NO molecules on pristine and transition metal doped Î±-AsP monolayer by first-principles calculations. Physica E: Low-Dimensional Systems and Nanostructures, 2022, 138, 115109.	1.3	8
43823	Green self-derived templating preparation of nitrogen, sulfur co-doped porous carbon/tin composites with synergistic effect towards high-performance lithium-ion batteries. Applied Surface Science, 2022, 580, 152319.	3.1	5
43824	Abnormal enhancement of thermal conductivity by planar structure: A comparative study of graphene-like materials. International Journal of Thermal Sciences, 2022, 174, 107438.	2.6	14
43825	Building-block approach to the discovery of Na8Mn2(Ge2Se6)2: A polar chalcogenide exhibiting promising harmonic generation signals with a high laser-induced damage threshold. Journal of Alloys and Compounds, 2022, 900, 163392.	2.8	5

#	Article	IF	Citations
43826	Z-scheme WO3/PANI heterojunctions with enhanced photocatalytic activity under visible light: A depth experimental and DFT studies. Chemosphere, 2022, 292, 133468.	4.2	53
43827	Controlling the magnetic alignment at the MnGa/Co2MnSi interface: A DFT study. Journal of Magnetism and Magnetic Materials, 2022, 547, 168936.	1.0	3
43828	The role of Dy doping on cyclic oxidation behavior of Al-Si coating on new cobalt-based Î³/Î³â€² superalloy. Corrosion Science, 2022, 197, 110077.	3.0	1
43829	Restricted diffusion preparation of fully-exposed Fe single-atom catalyst on carbon nanospheres for efficient oxygen reduction reaction. Applied Catalysis B: Environmental, 2022, 305, 121058.	10.8	42
43830	Stabilization of the (1 1 1) surface of NiO and CoO by segregation of point defects. Applied Surface Science, 2022, 582, 152473.	3.1	3
43831	Boosting photocatalytic hydrogen evolution: Orbital redistribution of ultrathin ZnIn2S4 nanosheets via atomic defects. Applied Catalysis B: Environmental, 2022, 305, 121007.	10.8	61
43832	Computational insights into the structural, mechanical, optical, electronic and magnetic properties of EuTiO3 semiconductor in cubic-perovskite using FP-LAPW method. Materials Science in Semiconductor Processing, 2022, 142, 106455.	1.9	7
43833	Influence mechanism of boron segregation on the microstructure evolution and hot ductility of super austenitic stainless steel S32654. Journal of Materials Science and Technology, 2022, 112, 184-194.	5.6	23
43834	Atomic Pd-promoted ZnZrO solid solution catalyst for CO2 hydrogenation to methanol. Applied Catalysis B: Environmental, 2022, 304, 120994.	10.8	59
43835	Electric field-induced electronic-thermoelectric-optical properties of typical isoelectronic HNC6 monolayers: A theoretical study. Applied Surface Science, 2022, 581, 152094.	3.1	5
43836	Dry reforming of methane on Ni(1 1 1) surface with different Mo doping ratio: DFT-assisted microkinetic study. Applied Surface Science, 2022, 581, 152310.	3.1	20
43837	Optoelectronic and thermodynamic properties, infrared and Raman spectra of NbO2 and Nb2O5 from DFT formalism. Journal of Physics and Chemistry of Solids, 2022, 163, 110549.	1.9	11
43838	A promising ZnO/Graphene van der Waals heterojunction as solar cell devices: A first-principles study. Energy Reports, 2022, 8, 904-910.	2.5	19
43839	Metallic penta-Graphene/penta-BN2 heterostructure with high specific capacity: A novel application platform for Li/Na-ion batteries. Journal of Alloys and Compounds, 2022, 901, 163538.	2.8	8
43840	Two-dimensional graphdiyne analogue containing Mo-coordinated porphyrin covalent organic framework as a high-performance electrocatalyst for nitrogen fixation. Applied Surface Science, 2022, 580, 152359.	3.1	12
43841	ÐÑ‚Ð¾Ð¼Ð½Ð¾Ð»Ñ– Ð»Ð°Ð½Ñ†ÑŽÐ¶ÐºÐ¸ Ñ…Ð»Ð¾Ñ€Ñƒ Ð½Ð° Ð¿Ð¾Ð²ÐµÑ€Ñ…Ð½Ñ– Ag(111). Ukrainian Journal of Physics, 202	0.4	0
43842	Effect of Substrate on Structural and Electronic Properties of Au-Pd, Au-Pt and Au-Ag Atomic Chains. Asian Journal of Physical and Chemical Sciences, 0, , 7-18.	0.3	0
43843	The Adsorption of C5F10O on $alpha$-Alumina Surface under Electric Field: A DFT Study. , 2020, , .		1

#	Article	IF	Citations
43844	Effect of Electric Field on Adsorption Characteristics of Perfluorocarbonone Gas on Copper Surface by DFT Calculation. , 2020, , .		0
43847	Understanding the Effect of Dispersion Corrections on the Calculated Spectra of $alpha$-Lactose Monohydrate. , 2020, , .		0
43849	Thermodynamic Margin in Carbon Network Modulated Activity Control of Oxygen Reduction Reaction Iron Catalyst. Journal of Physical Chemistry C, 2020, 124, 26982-26989.	1.5	1
43851	Adsorption and Removal of Hazardous Metallic Elements Hg ⁰, Ni ⁰ and Pb ⁰: A DFT Study on g-C ₃N ₄ Monolayer Modified with Pt _n (n=1 - 7) Clusters. SSRN Electronic Journal, 0, , .	0.4	0
43852	Adsorption of Sorbitan Ester Surfactant on Copper and Copper Oxidized Surfaces: A Density Functional Theory Study. SSRN Electronic Journal, 0, , .	0.4	0
43853	Mo ₂CS ₂-Mxene Supported Single-Atom Catalysts for Efficient and Selective CO ₂ Electrochemical Reduction. SSRN Electronic Journal, 0, , .	0.4	0
43854	Infinite-layer/perovskite oxide heterostructure-induced high-spin states in SrCuO₂/SrRuO₃ bilayer films. Materials Horizons, 2021, 8, 3468-3476.	6.4	8
43855	Mechanism of Co ₂ Hydrogenation Over Zr ₁-Cu Singleâ€Atom Catalyst. SSRN Electronic Journal, 0, , .	0.4	0
43856	Atomic structures of twin boundaries in CoO. Physical Chemistry Chemical Physics, 2021, 23, 25590-25596.	1.3	6
43857	Probing the Band Gap of Xino3 (X = as, Sb) Compound for Solar Cell Applications by Dft. SSRN Electronic Journal, 0, , .	0.4	0
43858	Enhanced Photogenerated Hole Oxidation Capability in Photocatalysis Through Band Structure Modification. SSRN Electronic Journal, 0, , .	0.4	0
43859	2D MoS ₂-MoSe ₂and MoS ₂-NbS ₂ Lateral Hetero Structures as Anode Materials for LIBs/SIBs. SSRN Electronic Journal, 0, , .	0.4	1
43860	A Comprehensive First Principles Calculations On (Ba _{0.82}K) Tj ETQq0 0 0 rgBT /Overlock 10 Tf 50 26 ₃ Single-Cubic-Perovskite Superconductor. SSRN Electronic Journal, 0, , .	0.4	1
43861	A Key Role of Soft and Refractory Coke in the Deactivation of Î³-Al ₂O ₃ Catalysts During Low-Temperature Methyl Oleate Epoxidation. SSRN Electronic Journal, 0, , .	0.4	0
43862	High Throughput Investigation of an Emergent and Naturally Abundant 2D Material: Clinochlore. SSRN Electronic Journal, 0, , .	0.4	1
43863	High Compositional Dependence of Activity of Platinumâ€“Dysprosium Alloys for Oxygen Reduction in Alkaline Media: Experimental and Theoretical Study. SSRN Electronic Journal, 0, , .	0.4	0
43864	A DFT investigation on optical properties of Mg doped SrMoO₃ for optoelectronic applications. , 2021, , .		0
43865	Structural, Elastic and Electronic Properties of Transition Metal Hydrides TiH₂ and ZrH₂ from First Principles Calculations. , 2021, , .		1

#	Article	IF	Citations
43866	Interplay of Halogen and Weak Hydrogen Bonds in the Formation of Magic Nanoclusters on Surfaces. Journal of Physical Chemistry C, 2022, 126, 588-596.	1.5	7
43867	Understanding copper diffusion in CuInSe2 with first-principles based atomistic and continuum models. Journal of Applied Physics, 2021, 130, .	1.1	1
43868	Bandgap renormalization and indirect optical absorption in MgSiN2 at finite temperature. Journal of Applied Physics, 2021, 130, 225703.	1.1	1
43869	Catalytic and Sulfur-Tolerant Performance of Bimetallic Niâ€“Ru Catalysts on HI Decomposition in the Sulfur-Iodine Cycle for Hydrogen Production. Energies, 2021, 14, 8539.	1.6	0
43870	A First-Principles Study of the Cu-Containing Î²â€³ Precipitates in Al-Mg-Si-Cu Alloy. Materials, 2021, 14, 7879.	1.3	2
43871	Electronegativity Difference as a Descriptor for the Oxidation-Inhibiting Effect of the Alloying Element during the Early Stages of Titanium Oxidation. Langmuir, 2022, 38, 1448-1457.	1.6	3
43872	Layer parity dependent Raman-active modes and crystal symmetry in <mml:math xmlns:mml="http://www.w3.org/1998/Math/MathML"><mml:msub><mml:mi mathvariant="normal">ReS</mml:mi><mml:mn>2</mml:mn></mml:msub></mml:math>. Physical Review B, 2022, 105, .	1.1	5
43873	Controlled growth of ultrathin ferromagnetic Î²â€MnSe semiconductor. SmartMat, 2022, 3, 482-490.	6.4	7
43874	Ammonia Mono Hydrate IV: An Attempted Structure Solution. Crystals, 2022, 12, 135.	1.0	0
43875	Insight into the stacking and the species-ordering dependences of interlayer bonding in SiC/GeC polar heterostructures. Nanotechnology, 2022, 33, 155706.	1.3	5
43876	Ni²⁺-Doped Garnet Solid-Solution Phosphor-Converted Broadband Shortwave Infrared Light-Emitting Diodes toward Spectroscopy Application. ACS Applied Materials & Interfaces, 2022, 14, 4265-4275.	4.0	68
43877	Catalytic resonance of ammonia synthesis by simulated dynamic ruthenium crystal strain. Science Advances, 2022, 8, eabl6576.	4.7	24
43878	DFT study of structural, electronic, magnetic, elastic, vibrational, thermodynamic and thermoelectric properties of XCrP (X= Ni, Pd and Pt). Computational Condensed Matter, 2022, 31, e00645.	0.9	2
43879	New insights into the key bifunctional role of sulfur in Feâ€“Nâ€“C single-atom catalysts for ORR/OER. Nanoscale, 2022, 14, 3212-3223.	2.8	32
43880	Ba₆(Cu_xZ_y)Sn₄S₁₆ (Z = Mg,) Tj ETQq0 0 0 rgBT /Overlo Inorganic Chemistry, 2022, 61, 2640-2651.	1.9	7
43881	CO2 and CH2 Adsorption on Copper-Decorated Graphene: Predictions from First Principle Calculations. Crystals, 2022, 12, 194.	1.0	9
43882	Long Cycle Life and Highâ€Rate Sodium Metal Batteries Enabled by Regulating 3D Frameworks with Artificial Solidâ€State Interphases. Advanced Energy Materials, 2022, 12, .	10.2	29
43883	SrZnSnSe4: A quaternary selenide with large second harmonic generation and birefringence. Journal of Alloys and Compounds, 2022, 904, 163944.	2.8	24

#	Article	IF	Citations
43884	Electronic, Structural, Mechanical, and Thermodynamic Properties of CoYSb (Y = Cr, Mo, W) Half-Heusler Compounds as Potential Spintronic Materials. Solids, 2022, 3, 22-33.	1.1	10
43885	Pb₄SeBr₆: A Congruently Melting Midâ€Infrared Nonlinear Optical Material with Excellent Comprehensive Performance. Advanced Optical Materials, 2022, 10, .	3.6	21
43886	DFT study of crystal structure and electronic properties of metal-doped AlH3 polymorphs. International Journal of Hydrogen Energy, 2022, 47, 6142-6153.	3.8	6
43887	Role of Mn-substitution towards the enhanced hydrogen storage performance in FeTi. International Journal of Hydrogen Energy, 2022, 47, 9357-9371.	3.8	4
43888	Catalytic reduction of 4-nitrophenol using CuO@Na₂Ti(PO₄)₂â‹…H₂O. Journal of Environmental Science and Health - Part A Toxic/Hazardous Substances and Environmental Engineering, 2022, 57, 65-79.	0.9	3
43889	Applying Hydrogenation to Stabilize N-TiO2 and Enhance Its Visible Light Photocatalytic Activity. Catalysts, 2022, 12, 178.	1.6	2
43890	Compression-induced charge disproportionation in the orthorhombic NaTaO$$_{3}$$ (100) monolayer: Structural, electronic, and magnetic transitions. Journal of Materials Research, 2022, 37, 490-499.	1.2	2
43891	Biaxial stress and strain effects on optical and electronic aspects of B2C nanostructure: a first-principles calculation. Indian Journal of Physics, 0, , 1.	0.9	1
43892	Microscopic origins and stability of ferromagnetism in <mml:math xmlns:mml="http://www.w3.org/1998/Math/MathML"><mml:mrow><mml:msub><mml:mi>Co</mml:mi><mml:mn>3</mml:mn></mml:msub><mml:mathvariant="normal">S</mml:mi><mml:mn>2</mml:mn></mml:msub></mml:mrow></mml:math>. Physical Review B, 2022, 105, .	1.1	6
43893	The effect of oxygen impurities on the stability and structural properties of vacancy-ordered and -disordered ZrC_x. RSC Advances, 2022, 12, 3198-3215.	1.7	5
43894	Iridium boosts the selectivity and stability of cobalt catalysts for syngas to liquid fuels. CheM, 2022, 8, 1050-1066.	5.8	26
43895	Giant barocaloric effects in formamidinium iodide. APL Materials, 2022, 10, .	2.2	6
43896	A study on the evolution of Ï‰-phase in Zr-20Nb alloy under the influence of electron irradiation. Journal of Alloys and Compounds, 2022, 904, 163968.	2.8	3
43897	Prediction of semiconducting ferromagnetic CrVI(6) monolayer. Europhysics Letters, 0, , .	0.7	0
43898	Structure and Properties of Copper Pyrophosphate by First-Principle Calculations. Materials, 2022, 15, 842.	1.3	3
43899	First-Principles Prediction of Superconductivity in Hole Doping of MgCN2. Journal of Superconductivity and Novel Magnetism, 2022, 35, 339-343.	0.8	1
43900	Synergistic Electronic and Pore Structure Modulation in Open Carbon Nanocages Enabling Efficient Electrocatalytic Production of H₂O₂ in Acidic Medium. Advanced Functional Materials, 2022, 32, .	7.8	33
43901	Electronic properties of graphene oxide: nanoroads towards novel applications. Nanoscale, 2022, 14, 4131-4144.	2.8	3

#	Article	IF	Citations
43902	Orderâ€“Disorder Competitive Cooperation in EquiatomicÂ3dâ€“Transitionâ€“Metal Quaternary Alloys: Phase Stability and Electronic Structure. SSRN Electronic Journal, 0, , .	0.4	1
43903	First Principle Calculation of Magnetic Properties of Doped Mn:ZnGa2S4. Journal of Superconductivity and Novel Magnetism, 2022, 35, 1107-1111.	0.8	14
43904	Unveiling the layer-dependent electronic properties in transition-metal dichalcogenide heterostructures assisted by machine learning. Nanoscale, 2022, 14, 2511-2520.	2.8	6
43905	EquationÂof state and strength of diamond in high-pressure ramp loading. Physical Review B, 2022, 105, .	1.1	4
43906	Switching the Nonlinear Optical Absorption of Titanium Carbide MXene by Modulation of the Surface Terminations. ACS Nano, 2022, 16, 394-404.	7.3	32
43907	DFT Investigation of Ammonia Formation via a Langmuirâ€“Hinshelwood Mechanism on Mo-Terminated Î´-MoN(0001). ACS Omega, 2022, 7, 4277-4285.	1.6	3
43908	First-Principles Plane-Wave-Based Exploration of Cathode and Anode Materials for Li- and Na-Ion Batteries Involving Complex Nitrogen-Based Anions. Chemistry of Materials, 2022, 34, 652-668.	3.2	9
43909	Phase Evolution, Polymorphism, and Catalytic Activity of Nickel Dichalcogenide Nanocrystals. Chemistry of Materials, 2022, 34, 746-755.	3.2	6
43910	DFT study of NH3 adsorption on 2D monolayer MXenes (M2C, MÂ=ÂCr, Fe) via oxygen functionalization: Suitable materials for gas sensors. FlatChem, 2022, 31, 100329.	2.8	22
43911	Anisotropic charge transport in 1D and 2D BeN4 and MgN4 nanomaterials: A first-principles study. FlatChem, 2022, 31, 100327.	2.8	13
43912	Dynamic Jahn-Teller effect on the optical spectrum and EPR parameters of V4+ in Î±-Al2O3. Optical Materials, 2022, 123, 111836.	1.7	1
43913	Direct observation of hydrogen permeation through grain boundaries in tungsten. Emergent Materials, 2022, 5, 1075-1087.	3.2	6
43914	In situ neutron diffraction unravels deformation mechanisms of a strong and ductile FeCrNi medium entropy alloy. Journal of Materials Science and Technology, 2022, 116, 103-120.	5.6	16
43915	Porous carbon-doped g-C3N4 with tunable band structure for boosting photocatalytic H2O2 production with simultaneous pollutants removal. Journal of Environmental Chemical Engineering, 2022, 10, 107116.	3.3	7
43916	Density functional theory study of electronic and optical properties of ScN nitride in NaCl-B1, CsCl-B2, ZB-B3 and NiAs-B8 phases. Bulletin of Materials Science, 2022, 45, 1.	0.8	4
43917	Understanding the high performance of PdSnâ€“TaN(tantalum nitride)/C electrocatalysts for the methanol oxidation reaction: coupling nitrides and oxophilic elements. Journal of Materials Chemistry A, 2021, 10, 266-287.	5.2	18
43918	Ferromagnetic half-metallicity of the cubic NaMgO₃ perovskite: from bulk to (001) surfaces. Physical Chemistry Chemical Physics, 2022, 24, 2209-2218.	1.3	3
43919	Mechanistic Insight and Local Structure Evolution of NiPS₃ upon Electrochemical Lithiation. ACS Applied Materials & Interfaces, 2022, 14, 3980-3990.	4.0	9

#	Article	IF	Citations
43920	Structural dynamics of Schottky and Frenkel defects in ThO₂: a density-functional theory study. Journal of Materials Chemistry A, 2022, 10, 1861-1875.	5.2	9
43921	Enantiotropy of Simvastatin as a Result of Weakened Interactions in the Crystal Lattice: Entropy-Driven Double Transitions and the Transient Modulated Phase as Seen by Solid-State NMR Spectroscopy. Molecules, 2022, 27, 679.	1.7	2
43922	Electronic structure and physical properties of EuAuAs single crystal. Physical Review B, 2022, 105, .	1.1	10
43923	Effects of the incorporation amounts of CdS and Cd(SCN2H4)2Cl2 on the performance of perovskite solar cells. International Journal of Minerals, Metallurgy and Materials, 2022, 29, 283-291.	2.4	16
43924	Superhard metallic compound <mml:math xmlns:mml="http://www.w3.org/1998/Math/MathML"><mml:msub><mml:mi>TaB</mml:mi><mml:mn>2</mml:mn></mml:msub></mm via crystal orientation resolved strain stiffening. Physical Review B, 2022, 105, .	1.1	7
43925	Impact of Mn- and Fe-Doping on Electronic and Magnetic Properties of MoXâ„‚ (X = S, Se) Monolayer. IEEE Transactions on Electron Devices, 2022, 69, 1553-1560.	1.6	7
43926	DFT study on electronic and optical properties of graphene under an external electric field. E3S Web of Conferences, 2022, 336, 00006.	0.2	2
43927	Generalizing Performance Equations in Heterogeneous Catalysis from Hybrid Data and Statistical Learning. ACS Catalysis, 2022, 12, 1581-1594.	5.5	6
43928	Mechanistic effects of solvent systems on the Niâ€“Sn-catalyzed hydrodeoxygenation of lignin derivatives to none-oxygenates. Catalysis Science and Technology, 2022, 12, 154-166.	2.1	2
43929	Phase transitions in partial summation methods: Results from the three-dimensional Hubbard model. Physical Review B, 2022, 105, .	1.1	6
43930	Dynamic structural transformation induced by defects in nano-rod FeOOH during electrochemical water splitting. Journal of Materials Chemistry A, 2022, 10, 602-610.	5.2	18
43931	Adsorption and dissociation of diatomic molecules on monolayer <mml:math xmlns:mml="http://www.w3.org/1998/Math/MathML"><mml:mrow><mml:mn>1</mml:mn><mml:mi>H</mml:mi></mml:mrow><mml:mn Physical Review B, 2022, 105, .	1.1	3
43932	Orbital-selective behavior in cubanite <mml:math xmlns:mml="http://www.w3.org/1998/Math/MathML"><mml:msub><mml:mi mathvariant="normal">CuFe</mml:mi><mml:mn>2</mml:mn></mml:msub><mml:msub><mml:mi mathvariant="normal">S</mml:mi><mml:mn>3</mml:mn></mml:msub></mml:math>. Physical Review B, 2022, 105, .	1.1	1
43933	Investigation of structural, electronic and thermoelectric properties of two-dimensional graphdiyne/borophene monolayers and hetero-bilayers. Journal of Physics Condensed Matter, 2022, 34, 125501.	0.7	2
43934	Effect of lattice strain on magnetism in epitaxial YCrO₃ films. Materials Research Letters, 2022, 10, 29-35.	4.1	5
43935	Disorder-Induced Ordering in Gallium Oxide Polymorphs. Physical Review Letters, 2022, 128, 015704.	2.9	36
43936	First Principles Study of Regulation of Monolayer ZnO and Vacancy Defects Equibiaxial Strain. Journal of Superconductivity and Novel Magnetism, 2022, 35, 925-934.	0.8	2
43937	Insight into enhanced hydrogen evolution of single-atom Cu1/TiO2 catalysts from first principles. International Journal of Hydrogen Energy, 2022, 47, 4653-4661.	3.8	15

#	Article	IF	Citations
43938	Thermoelectric properties plus phonon and de Haasâ€“van Alphen frequencies of hole/electron-doped $$hbox {CeIn}_3$$. Scientific Reports, 2022, 12, 663.	1.6	4
43939	Novel trigonal BC11 as model structure of heavily-doped diamond: Crystal chemistry rationale and first principles characterizations. Diamond and Related Materials, 2022, 123, 108842.	1.8	2
43940	Influence of tetraethylammonium cation on electrochemical CO2 reduction over Cu, Ag, Ni, and Fe surfaces. Journal of Catalysis, 2022, 406, 213-221.	3.1	13
43941	Anti-Ferromagnetic RuO₂: A Stable and Robust OER Catalyst over a Large Range of Surface Terminations. Journal of Physical Chemistry C, 2022, 126, 1337-1345.	1.5	21
43942	Exploring Coupled Martensitic and Orderâ€“Disorder Phase Transitions in Fe₇Pd₃ Shape Memory Alloys Equilibrated Along the Bain Path: An Embedded Atom Method and Ab Initio Based Monte Carlo Study. Advanced Theory and Simulations, 2022, 5, .	1.3	1
43943	Interfacial Chemistry Triggers Ultrafast Radiative Recombination in Metal Halide Perovskites. Angewandte Chemie, 2022, 134, .	1.6	1
43944	Evaluation of Olivine LiFePO₄ Polyanionic Cathode Material Using Density Functional Theory. Key Engineering Materials, 0, 908, 293-298.	0.4	1
43945	Pressure-stabilized hexafluorides of first-row transition metals. Physical Chemistry Chemical Physics, 2022, 24, 1736-1742.	1.3	4
43946	Sulfur/Nitrogen Coâ€Doped Inâ€Plane Porous Carbon Nanosheets as Superior Anode of Potassiumâ€Ion Batteries. Batteries and Supercaps, 2022, 5, .	2.4	4
43947	Excitonic Effects in Fe/As K â€Edge Absorption for Iron Based Superconductors: A Combined DFT and BSE Analysis. Advanced Theory and Simulations, 0, , 2100525.	1.3	0
43948	Water-gas shift reaction over supported Au nanoparticles. Journal of Catalysis, 2022, 405, 475-488.	3.1	6
43949	Superconductivity in In₂Te₃ under Compression Induced by Electronic and Structural Phase Transitions. Journal of Physical Chemistry Letters, 2022, 13, 1226-1233.	2.1	7
43950	Proton sponge promotion of electrochemical CO2 reduction to multi-carbon products. Joule, 2022, 6, 205-220.	11.7	57
43951	Investigation of anisotropic mechanical, electronic, and charge carrier transport properties of germanium-pnictogen monolayers. Journal Physics D: Applied Physics, 2022, 55, 185302.	1.3	11
43952	Modulation of Water Dissociation Kinetics with a â€œBreathableâ€•Wooden Electrode for Efficient Hydrogen Evolution. ACS Applied Materials & Interfaces, 2022, 14, 6818-6827.	4.0	11
43953	The surface phase structure evolution of the fcc MoC (001) surface in a steam reforming atmosphere: systematic kinetic and thermodynamic investigations. Catalysis Science and Technology, 0, , .	2.1	1
43954	Study elastic properties of the leucine and isoleuicine from first principles calculations. Journal of Physics Condensed Matter, 2022, 34, 145702.	0.7	3
43955	Designing two-dimensional dodecagonal boron nitride. CrystEngComm, 2022, 24, 471-474.	1.3	7

#	Article	IF	Citations
43956	Biomass-assisted approach for large-scale construction of multi-functional isolated single-atom site catalysts. Nano Research, 2022, 15, 3980-3990.	5.8	20
43957	Unraveling the Structure and Properties of Layered and Mixed ReO₃â€“WO₃ Thin Films Deposited by Reactive DC Magnetron Sputtering. ACS Omega, 2022, 7, 1827-1837.	1.6	3
43958	Insight into the Adsorption Structure of TIPS-Pentacene on Noble Metal Surfaces. Journal of Physical Chemistry C, 2022, 126, 2689-2698.	1.5	0
43959	Direct Observation of Orbital Driven Strong Interlayer Coupling in Puckered Twoâ€Đimensional PdSe 2. Small, 2022, , 2106053.	5.2	6
43960	Quantum confinement and effective masses dependence in black phosphorus quantum dots and phosphorene. Journal of Industrial and Engineering Chemistry, 2022, 108, 429-437.	2.9	1
43961	Magnetism and perfect spin filtering in pristine MgCl₂ nanoribbons modulated by edge modification. Physical Chemistry Chemical Physics, 2022, 24, 3370-3378.	1.3	3
43962	In situ formation of circular and branched oligomers in a localized high concentration electrolyte at the lithium-metal solid electrolyte interphase: a hybrid ab initio and reactive molecular dynamics study. Journal of Materials Chemistry A, 2022, 10, 632-639.	5.2	15
43963	Theoretical study on the controllable preparation of superhard BC₂N under high pressure. Journal of Materials Chemistry C, 2022, 10, 1660-1665.	2.7	6
43964	Variable dimensionality of the anion framework in four new borophosphates and fluoroborophosphates with short cutoff edges. Dalton Transactions, 2022, 51, 2840-2845.	1.6	7
43965	Surprisingly Low Reactivity of Layered Manganese Oxide toward Water Oxidation in Fe/Ni-Free Electrolyte under Alkaline Conditions. Inorganic Chemistry, 2022, 61, 2292-2306.	1.9	21
43966	Î³-BaB₂O₄: High-Pressure High-Temperature Polymorph of Barium Borate with Edge-Sharing BO₄ Tetrahedra. Inorganic Chemistry, 2022, 61, 2340-2350.	1.9	7
43967	Novel Two-Dimensional Metal-Based Ï€-d Conjugated Nanosheets as Photocatalyst for Nitrogen Reduction Reaction: The First-Principle Investigation. ACS Applied Materials & Interfaces, 2022, 14, 5384-5394.	4.0	10
43968	Ab Initio Computational Details With Facile High-Temperature Synthesis of Pure and Alloyed CsPbI₃ With Inherent Stability Analysis for Optoelectronic Applications. IEEE Journal of Photovoltaics, 2022, 12, 625-633.	1.5	5
43969	Selective Detection of Carbon Monoxide on P-Block Doped Monolayers of MoTe₂. ACS Sensors, 2022, 7, 272-285.	4.0	20
43970	Ab-Initio Investigation of Finite Size Effects in Rutile Titania Nanoparticles with Semilocal and Nonlocal Density Functionals. Journal of Physical Chemistry C, 2022, 126, 2121-2130.	1.5	3
43971	Temperature- and vacancy-concentration-dependence of heat transport in Li3ClO from multi-method numerical simulations. Npj Computational Materials, 2022, 8, .	3.5	16
43972	Atomically-dispersed NiN₄â€“Cl active sites with axial Niâ€“Cl coordination for accelerating electrocatalytic hydrogen evolution. Journal of Materials Chemistry A, 2022, 10, 6007-6015.	5.2	22
43973	Benchmarking Plane Waves Quantum Mechanical Calculations of Iron(II) Tris(2,2â€²-bipyridine) Complex by X-ray Absorption Spectroscopy. Condensed Matter, 2022, 7, 16.	0.8	1

#	Article	IF	Citations
43974	Bimetallic Goldâ€“Silver Nanostructures Drive Low Overpotentials for Electrochemical Carbon Dioxide Reduction. ACS Applied Materials & Interfaces, 2022, 14, 6604-6614.	4.0	14
43975	Homogenizing the Li-ion flux by multi-element alloying modified for 3D dendrite-free lithium anode. Energy Storage Materials, 2022, 48, 114-122.	9.5	11
43976	Adsorption of H₂S on AgO(001) surface: A densityâ€functional theory investigation. Surface and Interface Analysis, 2022, 54, 1107-1120.	0.8	2
43977	Cobalt based new quaternary Heusler alloys for Spintronic and thermoelectric applications: an Ab-initio study. Materials Technology, 2022, 37, 1936-1946.	1.5	9
43978	Heterogeneity in a metalâ€“organic framework in situ guides engineering Co@CoO heterojunction for electrocatalytic H₂ production in tandem with glucose oxidation. Journal of Materials Chemistry A, 2022, 10, 4791-4799.	5.2	35
43979	The Defluorination of SiF4 on Si (1 1 1) Surfaces: a Density Functional Theory Study. Silicon, 0, , 1.	1.8	0
43980	Nickel cobaltite/multi-walled carbon nanotube flexible sensor for the electrochemical detection of dopamine released by human neural cells. Journal of Materials Chemistry C, 2022, 10, 3048-3060.	2.7	25
43981	Theoretical investigation of CH-bond activation by photocatalytic excited SO₂ and the effects of C-, N-, S-, and Se-doped TiO₂. Physical Chemistry Chemical Physics, 2022, 24, 2051-2069.	1.3	6
43982	Safeguarding the RuO₂ phase against lattice oxygen oxidation during acidic water electrooxidation. Energy and Environmental Science, 2022, 15, 1119-1130.	15.6	66
43983	Hexatetra-Carbon: A Novel Two-Dimensional Semiconductor Allotrope of Carbon. Computation, 2022, 10, 19.	1.0	5
43984	Can oxygen vacancies in ceria surfaces be measured by O1s photoemission spectroscopy?. Journal of Physics Condensed Matter, 2022, 34, 174004.	0.7	11
43985	Anomalous transverse optical phonons in SnTe and PbTe. Physical Review B, 2022, 105, .	1.1	7
43986	Direct Visualization of a Gold Nanoparticle Electron Trapping Effect. Journal of the American Chemical Society, 2022, 144, 1034-1044.	6.6	9
43987	Tuning valley degeneracy with band inversion. Journal of Materials Chemistry A, 2022, 10, 1588-1595.	5.2	6
43988	Convergence acceleration in machine learning potentials for atomistic simulations. , 2022, 1, 61-69.		18
43989	FeSi₂: a two-dimensional ferromagnet containing planar hexacoordinate Fe atoms. Nanoscale Advances, 2022, 4, 600-607.	2.2	8
43990	A wafer-scale two-dimensional platinum monosulfide ultrathin film via metal sulfurization for high performance photoelectronics. Materials Advances, 2022, 3, 1497-1505.	2.6	14
43991	Ferromagnetic and nonmagnetic <mml:math xmlns:mml="http://www.w3.org/1998/Math/MathML"><mml:mrow><mml:mn>1</mml:mn><mml:msup><mml:mi>T</mml:mi><mml:mi><mml:m charge density wave states in transition metal dichalcogenides: Physical mechanisms and charge doping induced reversible transition. Physical Review B, 2022, 105, .	1.1	4

#	Article	IF	Citations
43992	Resistance characteristics of CdZnTe films with structure of Cu/CdZnTe/ITO and Cu/CdZnTe/Cu. Applied Physics A: Materials Science and Processing, 2022, 128, 1.	1.1	0
43993	Conduction band engineering of half-Heusler thermoelectrics using orbital chemistry. Journal of Materials Chemistry A, 2022, 10, 3051-3057.	5.2	25
43994	Design, Synthesis, and Characterization of the Nonlinear Optical Material MnTeW_xMo_{1â€“x}O₆. Journal of Physical Chemistry C, 2022, 126, 815-822.	1.5	2
43995	Theoretical Investigation of Half-Metallic Ferrimagnetic Heusler Alloys: the Case of DO3-Type Cr3Z (Zâ€‰=â€‰P, As, Sb, S, Se, and Te). Journal of Superconductivity and Novel Magnetism, 2022, 35, 763.	0.8	1
43996	Simulating intergranular hydrogen enhanced decohesion in aluminium using density functional theory. Modelling and Simulation in Materials Science and Engineering, 2022, 30, 035009.	0.8	3
43997	Investigation of Oxygen Reduction Reaction on Ni Doped Silicon Nanotube (7, 0), Titanium (Ti) Doped Silicon Nanotube (9, 0) and Copper (Cu) Doped Silicon Nanocage (Si72) for Fuel Cells. Silicon, 2022, 14, 8173-8178.	1.8	2
43998	Stacking order and Coulomb correlation effect in the layered charge density wave phase of 1Tâ˜NbS2. Physical Review B, 2022, 105, .	1.1	13
43999	Analogous Atomic and Electronic Properties between V N and V N. Advances in Condensed Matter Physics, 2022, 2022, 1-6.	0.4	2
44000	Mechanistic Study of 1,2-Dichloroethane Hydrodechlorination on Cu-Rich Ptâ€“Cu Alloys: Combining Reaction Kinetics Experiments with DFT Calculations and Microkinetic Modeling. ACS Sustainable Chemistry and Engineering, 2022, 10, 1509-1523.	3.2	4
44001	Machine learned interatomic potentials using random features. Npj Computational Materials, 2022, 8, .	3.5	11
44002	Voltage plateau variation in a bismuth-potassium battery. Journal of Materials Chemistry A, 2022, 10, 2917-2923.	5.2	6
44003	Structural modification from centrosymmetric Rb₄Hg₂Ge₂S₈ to noncentrosymmetric (Na₃Rb)Hg₂Ge₂S₈: mixed alkali metals strategy for infrared nonlinear optical material design. Journal of Materials Chemistry C, 2022, 10, 3300-3306.	2.7	13
44004	Investigations of Structural, Electronic and Magnetic Properties of MnSe under High Pressure. Materials, 2022, 15, 1109.	1.3	0
44005	First-Principles Investigation of the Interfacial Stability, Precipitate Formation, and Mechanical Behavior of Al3Li/Al3Zr/Al Interfaces. Metallurgical and Materials Transactions A: Physical Metallurgy and Materials Science, 2022, 53, 1308-1321.	1.1	3
44006	Structural, optical, and magnetic properties of a new complex (1â˜x)Bi1/2Na1/2TiO3â€‰+â€‰xMgNiO3â˜Î´ solid solution system. Applied Physics A: Materials Science and Processing, 2022, 128, 1.	1.1	5
44007	Enhancing Electrocatalytic Methanol Oxidation on PtCuNi Coreâ€“Shell Alloy Structures in Acid Electrolytes. Inorganic Chemistry, 2022, 61, 2612-2618.	1.9	20
44008	Computational Studies of MoS₂ Nanotubes for Hydrodesulfurization. ACS Applied Nano Materials, 2022, 5, 2029-2037.	2.4	3
44009	Second-Order Real Nodal-Line Semimetal in Three-Dimensional Graphdiyne. Physical Review Letters, 2022, 128, 026405.	2.9	34

#	Article	IF	Citations
44010	A B₂N monolayer: a direct band gap semiconductor with high and highly anisotropic carrier mobility. Nanoscale, 2022, 14, 930-938.	2.8	11
44011	Manipulation of current rectification in van der Waals ferroionic CuInP2S6. Nature Communications, 2022, 13, 574.	5.8	60
44012	Clustering feature of metal atoms in pentacene molecular solids: a first-principles study. Japanese Journal of Applied Physics, 2022, 61, 021003.	0.8	2
44013	Carrier doping-induced strong magnetoelastic coupling in 2D lattice. Nanoscale, 2022, 14, 3261-3268.	2.8	5
44014	Route to a direct-gap silicon allotrope Si₃₂. Journal of Physics Condensed Matter, 2022, 34, 154006.	0.7	1
44015	Observation of dielectric dispersion and relaxation behavior in Ni²⁺-substituted cobalt ferrite nanoparticles. Journal of Materials Chemistry C, 2022, 10, 3418-3428.	2.7	18
44016	Realizing High Thermoelectric Performance in p-Type SnSe Crystals via Convergence of Multiple Electronic Valence Bands. ACS Applied Materials & Interfaces, 2022, 14, 4091-4099.	4.0	8
44017	Exceptional phonon point versus free phonon coupling in Zn1â^'xBexTe under pressure: an experimental and ab initio Raman study. Scientific Reports, 2022, 12, 753.	1.6	2
44018	Colloidal Platinumâ€“Copper Nanocrystal Alloy Catalysts Surpass Platinum in Low-Temperature Propene Combustion. Journal of the American Chemical Society, 2022, 144, 1612-1621.	6.6	24
44019	Determination of length scale parameters of strain gradient continuum theory for crystalline solids using a computational quantum mechanical model based on density functional theory. Current Applied Physics, 2022, 36, 97-104.	1.1	3
44020	Enhancing the photocatalytic hydrogen generation performance and strain regulation of the vertical GeI₂/C₂N van der Waals heterostructure: insights from first-principles study. Energy Advances, 2022, 1, 146-158.	1.4	15
44021	Worm-graphene: A two-dimensional orthorhombic carbon semimetal with massless Dirac fermion. Applied Surface Science, 2022, 585, 152457.	3.1	5
44022	Bandgap engineering of Î±-Ga2O3 by hydrostatic, uniaxial, and equibiaxial strain. Japanese Journal of Applied Physics, 2022, 61, 021005.	0.8	7
44023	Tin carbide monolayers decorated with alkali metal atoms for hydrogen storage. International Journal of Hydrogen Energy, 2022, 47, 41329-41335.	3.8	13
44024	Dopamine Adsorption on Rutile TiO₂(110): Geometry, Thermodynamics, and Core-Level Shifts from First Principles. ACS Omega, 2022, 7, 4185-4193.	1.6	3
44025	Relationship between the Crystal Structure and Tuberculostatic Activity of Some 2-Amidinothiosemicarbazone Derivatives of Pyridine. Materials, 2022, 15, 349.	1.3	1
44026	On electrically tunable stacking domains and ferroelectricity in moirÃ© superlattices. Npj 2D Materials and Applications, 2022, 6, .	3.9	22
44027	Zinc-Blende GeC Stabilized on GaN (001): An Ab Initio Study. Advances in Condensed Matter Physics, 2022, 2022, 1-8.	0.4	0

#	Article	IF	Citations
44028	Screening strain sensitive transition metals using oxygen adsorption. New Journal of Chemistry, 2022, 46, 2178-2188.	1.4	2
44029	Molecular beam epitaxial growth of Sb₂Te₃â€“Bi₂Te₃ lateral heterostructures. 2D Materials, 2022, 9, 025006.	2.0	6
44030	Synergistic effect of Ru-N4 sites and Cu-N3 sites in carbon nitride for highly selective photocatalytic reduction of CO2 to methane. Applied Catalysis B: Environmental, 2022, 307, 121154.	10.8	57
44031	Partitioning of noble gases (He, Ne, Ar, Kr, Xe) during Earthâ€™s core segregation: A possible core reservoir for primordial noble gases. Geochimica Et Cosmochimica Acta, 2022, 321, 329-342.	1.6	9
44032	Unraveling Unique Surface Chemistry of Transition Metal Nitrides in Controlling Selective Câ€“O Bond Scission Pathways of Glycerol. Jacs Au, 2022, 2, 367-379.	3.6	10
44033	Resolving atomic diffusion in <mml:math xmlns:mml="http://www.w3.org/1998/Math/MathML"><mml:mrow><mml:mi>Ru</mml:mi><mml:mrow><mml:mo>(</mml:mo><mml:mn mathvariant="normal">0</mml:mi><mml:mo>(</mml:mo><mml:mn>2</mml:mn><mml:mo>Ã—</mml:mo><mml:mn>2</mml:mn><mml:mn> with spiral high-speed scanning tunneling microscopy. Physical Review B, 2022, 105, .	1.1	4
44034	Photocatalytic Activity and Hole-Scavenging Behaviors on Rutile TiO₂(100) Surfaces: A Theoretical Study. Journal of Physical Chemistry C, 2022, 126, 974-985.	1.5	4
44035	Novel Calcium sp³ Carbonate CaC₂O₅-I4Ì…2d May Be a Carbon Host in Earthâ€™s Lower Mantle. ACS Earth and Space Chemistry, 2022, 6, 73-80.	1.2	13
44036	Providing Atomistic Insights into the Dissolution of Rutile Oxides in Electrocatalytic Water Splitting. Journal of Physical Chemistry C, 2022, 126, 922-932.	1.5	22
44037	Artificial Neural Network Potential for Encapsulated Platinum Clusters in MOF-808. Journal of Physical Chemistry C, 2022, 126, 1204-1214.	1.5	10
44038	Molecular dynamics simulations of radiation damage in YBa₂Cu₃O₇. Superconductor Science and Technology, 2022, 35, 035010.	1.8	6
44039	Adsorption of diatomic gas molecules on transition-metal-decorated GeC monolayers. Journal of Materials Science, 2022, 57, 8455-8463.	1.7	4
44040	Unveiling nonmonotonic chemical trends in the solubility of H in complex Fe-Cr-Mn carbides by means of ab initio based approaches. Physical Review Materials, 2022, 6, .	0.9	1
44041	Oxide-ion diffusion in brownmillerite-type Ca₂AlMnO_{5+Î´} from first-principles calculations. Physical Chemistry Chemical Physics, 2022, 24, 1503-1509.	1.3	4
44042	Comment on â€œHigh-temperature superconductivity in transition metallic hydrides MH11 (M = Mo, W,) Tj ETQq0 0 0 rgBT /Overlock 1 Phys. Chem. Chem. Phys., 2021, 23, 6717. Physical Chemistry Chemical Physics, 2022, 24, 1896-1897.	1.3	1
44043	Structure and properties of dislocations and the twin boundary on (101) in Î²-cyclotetramethylene tetranitramine. Philosophical Magazine, 2022, 102, 977-992.	0.7	5
44044	The enzymatic performance derived from the lattice planes of Ir nanoparticles. Catalysis Science and Technology, 2022, 12, 1017-1024.	2.1	3
44045	Critical assessment of machine-learned repulsive potentials for the density functional based tight-binding method: A case study for pure silicon. Journal of Chemical Physics, 2022, 156, 064101.	1.2	4

#	Article	IF	Citations
44046	Electronic properties and surface reactive sites of carbon and oxygen doped porous boron nitride: A DFT study. Diamond and Related Materials, 2022, 121, 108802.	1.8	1
44047	Sodium diffusion and dynamics in Na₂Ti₃O₇: neutron scattering and ab initio simulations. Materials Advances, 2022, 3, 2104-2116.	2.6	4
44048	An efficient strategy to enhance the photocatalytic activity of Ir-doped SrTiO₃: a hybrid DFT approach. New Journal of Chemistry, 2022, 46, 1507-1515.	1.4	4
44049	Cobalt metal organic framework (Co-MOF) derived CoSe₂/C hybrid nanostructures for the electrochemical hydrogen evolution reaction supported by DFT studies. New Journal of Chemistry, 2022, 46, 2730-2738.	1.4	15
44050	Interfacial engineering of lattice coherency at ZnO-ZnS photocatalytic heterojunctions. Chem Catalysis, 2022, 2, 125-139.	2.9	56
44051	Finding Key Factors for Efficient Water and Methanol Activation at Metals, Oxides, MXenes, and Metal/Oxide Interfaces. ACS Catalysis, 2022, 12, 1237-1246.	5.5	5
44052	Borazatruxenes as precursors for hybrid C-BN 2D molecular networks. Nanoscale, 2022, 14, 1929-1943.	2.8	2
44053	First-principles study of the structural, electronic, optical, and thermoelectric properties of the RhVZ (Z= Si, Ge, Sn). Superlattices and Microstructures, 2022, 164, 107162.	1.4	3
44054	Theoretical Study of Small Molecules Adsorption on Pristine and Transition Metal Doped GeSe Monolayer for Gas Sensing Application. Langmuir, 2022, 38, 1287-1295.	1.6	15
44056	Corrosion Protection Oxide Scale Formed on Surface of Fe-Ni-M (M = Al, Cr, Cu) Inert Anode for Molten Salt Electrolysis. Materials, 2022, 15, 719.	1.3	3
44058	Giant tunneling magnetoresistance in atomically thin VSi2N4/MoSi2N4/VSi2N4 magnetic tunnel junction. Applied Physics Letters, 2022, 120, .	1.5	17
44059	Thickness-dependent phase transition kinetics in lithium-intercalated MoS₂. 2D Materials, 2022, 9, 025009.	2.0	8
44060	Spatially Confined Synthesis of SnSe Spheres Encapsulated in N, Se Dual-Doped Carbon Networks toward Fast and Durable Sodium Storage. ACS Applied Materials & Interfaces, 2022, 14, 4230-4241.	4.0	43
44061	Orientational dependence of intrinsic orbital and spin Hall effects in hcp structure materials. Physical Review B, 2022, 105, .	1.1	2
44062	Interplay of lattice, spin, and dipolar properties in <mml:math xmlns:mml="http://www.w3.org/1998/Math/MathML"><mml:msub><mml:mi>CoTeMoO</mml:mi><mml:mn>6</mml:mn></mml:msub> : Emergence of Griffiths-like phase, metamagnetic transition, and magnetodielectric effect. Physical Review B, 2022, 105, .	1.1	5
44063	Air-grown hybrid copper(<scp>i</scp>) halide single crystals: structural transformations and ultraviolet-pumped photoluminescence applications. Materials Advances, 2022, 3, 2447-2455.	2.6	16
44064	Modulating hardness in Sc₂(Ru_{5â^'x}TM_x)B₄ through empirical considerations and computational analysis. Journal of Materials Chemistry C, 2022, 10, 1488-1497.	2.7	1
44065	Identification of the active site during CF₄ hydrolytic decomposition over Î³-Al₂O₃. Environmental Science: Nano, 2022, 9, 954-963.	2.2	6

#	Article	IF	Citations
44066	Simulating Segregation in a Ternary Cuâ€“Pdâ€“Au Alloy with Density Functional Theory, Machine Learning, and Monte Carlo Simulations. Journal of Physical Chemistry C, 2022, 126, 1800-1808.	1.5	7
44067	Unravelling the Impact of Ta Doping on the Electronic and Structural Properties of Titania: A Combined Theoretical and Experimental Approach. Journal of Physical Chemistry C, 2022, 126, 2285-2297.	1.5	2
44068	Promotion of the oxygen evolution reaction via the reconstructed active phase of perovskite oxide. Journal of Materials Chemistry A, 2022, 10, 2271-2279.	5.2	17
44069	First-principles investigation of oxidation mechanism of Al-doped Mo5Si3 silicide. Ceramics International, 2022, 48, 11518-11526.	2.3	68
44070	A Theoretical Study on Nonâ€Bridging Dimer Formation of a Cationic Platinum Complex with a Redoxâ€Active Ligand. ChemistrySelect, 2022, 7, .	0.7	0
44071	A self-regulated gradient interphase for dendrite-free solid-state Li batteries. Energy and Environmental Science, 2022, 15, 1325-1333.	15.6	98
44072	Defects in an orthorhombic MoAlB MAB phase thin film grown at moderate synthesis temperature. Nanoscale, 2022, 14, 2578-2585.	2.8	13
44073	Janus Ga₂SeTe/In₂SSe heterostructures: tunable electronic, optical, and photocatalytic properties. Physical Chemistry Chemical Physics, 2022, 24, 4425-4436.	1.3	8
44074	Controlling magnetic-semiconductor properties of the Si- and Al-doped blue phosphorene monolayer. Journal Physics D: Applied Physics, 2022, 55, 165302.	1.3	3
44075	Strain-induced bandgap engineering in CsGeX₃ (X = I, Br or Cl) perovskites: insights from first-principles calculations. Physical Chemistry Chemical Physics, 2022, 24, 5448-5454.	1.3	12
44076	Revealing the Competition between Defectâ€Trapped Exciton and Bandâ€Edge Exciton Photoluminescence in Monolayer Hexagonal WS₂. Advanced Optical Materials, 2022, 10, .	3.6	8
44077	First-principles investigations into the effect of oxygen vacancies on the enhanced reactivity of NiO via Bader charge and density of states analysis. Catalysis Today, 2023, 407, 172-181.	2.2	12
44078	N2O Hydrogenation on Silver Doped Gold Catalysts, a DFT Study. Nanomaterials, 2022, 12, 394.	1.9	0
44079	Electronic and optical properties of hydrogen-terminated biphenylene nanoribbons: a first-principles study. Physical Chemistry Chemical Physics, 2021, 24, 357-365.	1.3	23
44080	Quasiparticle, optical, and excitonic properties of layer dependent GaSe. Physica E: Low-Dimensional Systems and Nanostructures, 2022, 139, 115155.	1.3	3
44081	An ab-initio study on the thermodynamics of disulfide, sulfide, and bisulfide incorporation into apatite and the development of a more comprehensive temperature, pressure, pH, and composition-dependent model for ionic substitution in minerals. American Mineralogist, 2022, 107, 1995-2007.	0.9	1
44082	Stabilization of S3O4 at high pressure: implications for the sulfur-excess paradox. Science Bulletin, 2022, 67, 971-976.	4.3	6
44083	A low resistance and stable lithium-garnet electrolyte interface enabled by a multifunctional anode additive for solid-state lithium batteries. Journal of Materials Chemistry A, 2022, 10, 2519-2527.	5.2	22

#	Article	IF	Citations
44084	Computational Evaluation of Li-doped g-C2N Monolayer as Advanced Hydrogen Storage Media. International Journal of Hydrogen Energy, 2022, 47, 3625-3632.	3.8	25
44085	Effect of Cr doping on interface properties of DLC/CrN composite coatings: First-principles study. Diamond and Related Materials, 2022, 121, 108721.	1.8	8
44086	Î²-SnS/GaSe heterostructure: a promising solar-driven photocatalyst with low carrier recombination for overall water splitting. Journal of Materials Chemistry A, 2022, 10, 3443-3453.	5.2	28
44087	Interfacial-confined coordination to single-atom nanotherapeutics. Nature Communications, 2022, 13, 91.	5.8	49
44088	Influence of Isostatic Pressure on the Elastic and Electronic Properties of K2SiF6:Mn4+. Materials, 2022, 15, 613.	1.3	4
44089	Substitutional alkaline earth metals delay nonradiative charge recombination in CH3NH3PbI3 perovskite: A time-domain study. Journal of Chemical Physics, 2022, 156, 014702.	1.2	2
44090	Implementation of the relativistic effects on spin in first-principles electronic structure and magnetic property calculations. Chinese Journal of Physics, 2022, , .	2.0	2
44091	Highly polarized [GeOTe₃] motif-driven structural order promotion and an enhanced second harmonic generation response in the new nonlinear optical oxytelluride Ba₃Ge₂O₄Te₃. Journal of Materials Chemistry C, 2021, 10, 150-159.	2.7	21
44092	Understanding the role of spacer cation in 2D layered halide perovskites to achieve stable perovskite solar cells. Materials Advances, 2022, 3, 2464-2474.	2.6	7
44093	Ab initio surface free energies of tungsten with full account of thermal excitations. Physical Review B, 2022, 105, .	1.1	10
44094	Stability and electronic properties of monolayer and multilayer structures of group-IV elements and compounds of complementary groups in biphenylene network. Physical Review B, 2022, 105, .	1.1	22
44095	A superconducting boron allotrope featuring anticlinal pentapyramids. Journal of Materials Chemistry C, 2022, 10, 672-679.	2.7	10
44096	Efficient modulation of the catalytic performance of electrocatalytic nitrogen reduction with transition metals anchored on N/O-codoped graphene by coordination engineering. Journal of Materials Chemistry A, 2022, 10, 1481-1496.	5.2	43
44097	Reduction Mechanism of Solid Electrolyte Interphase Formation on Lithium Metal Anode: Fluorine-Rich Electrolyte. Journal of the Electrochemical Society, 2022, 169, 010503.	1.3	5
44098	Experimental and first-principles study on the effect of oxygen vacancy on infrared emissivity of CeO2. Ceramics International, 2022, 48, 11313-11319.	2.3	10
44099	First Principles Investigation of Binary Chromium Carbides Cr7C3, Cr3C2 and Cr23C6: Electronic Structures, Mechanical Properties and Thermodynamic Properties under Pressure. Materials, 2022, 15, 558.	1.3	18
44100	Bulk <mml:math xmlns:mml="http://www.w3.org/1998/Math/MathML"><mml:mrow><mml:mi>NdNi</mml:mi><mml:msub><mml:mi mathvariant="normal">O</mml:mi><mml:mn>2</mml:mn></mml:msub></mml:mrow></mml:math> is thermodynamically unstable with respect to decomposition while hydrogenation reduces the instability and transforms it from metal to insulator. Physical Review B, 2022, 105, .	1.1	33
44101	Atomic Edge-Guided Polyethylene Crystallization on Monolayer Two-Dimensional Materials. Macromolecules, 2022, 55, 559-567.	2.2	6

#	Article	IF	Citations
44102	Boronâ€Rich Boron Nitride Nanotubes as Highly Selective Adsorbents for Selected Diatomic Air Pollutants: A DFT Study. Advanced Theory and Simulations, 2022, 5, .	1.3	8
44103	Ab initio prediction of vacancy energetics in HCP Al-Hf-Sc-Ti-Zr high entropy alloys and the subsystems. Acta Materialia, 2022, 227, 117677.	3.8	22
44104	Ammonia synthesis on BaTiO_{2.5}H_{0.5}: computational insights into the role of hydrides. Physical Chemistry Chemical Physics, 2022, 24, 1496-1502.	1.3	4
44105	Benchmarking exchange-correlation functionals in the spin-polarized inhomogeneous electron gas under warm dense conditions. Physical Review B, 2022, 105, .	1.1	17
44106	Synergizing Surface Hydride Species and Ru Clusters on Sm₂O₃ for Efficient Ammonia Synthesis. ACS Catalysis, 2022, 12, 2178-2190.	5.5	23
44107	Deciphering the Exceptional Performance of NiFe Hydroxide for the Oxygen Evolution Reaction in an Anion Exchange Membrane Electrolyzer. ACS Applied Energy Materials, 2022, 5, 2221-2230.	2.5	22
44108	Pb0.8Sn0.2Se thin films: synthesis, sensitization, and properties evolution. Journal of Materials Science: Materials in Electronics, 2022, 33, 5564-5574.	1.1	2
44109	Oneâ€Step MOFâ€Templated Strategy to Fabrication of Ceâ€Doped ZnIn₂S₄ Tetrakaidecahedron Hollow Nanocages as an Efficient Photocatalyst for Hydrogen Evolution. Advanced Science, 2022, 9, e2104579.	5.6	90
44110	Linear strain and stress potential parameters for the three fundamental band to band transitions in Î² -Ga2O3. Applied Physics Letters, 2022, 120, .	1.5	3
44111	Structural, magnetic and ferroelectric properties of VOBr₂monolayer: A first-principles study. Wuli Xuebao/Acta Physica Sinica, 2022, 71, 037101.	0.2	2
44112	Electronic and Magnetic Properties of Eutectoid Growth Mn-rich Ge1-xMnx Dilute Magnetic Semiconductors. Current Chinese Science, 2022, 2, 101-108.	0.2	1
44113	A computational study of the interaction of oxygenates with the surface of rutile TiO2(110). Structural and electronic trends.. Journal of Physics Condensed Matter, 2022, , .	0.7	3
44114	Highly thermostable white-emitting Ca₉ZnK(PO₄)₇:Ce³⁺,Dy³⁺ single-phase phosphor with tunable photoluminescence and energy transfer. Dalton Transactions, 2022, 51, 2770-2781.	1.6	17
44115	Effect of the Oxygen Composition Control of HfO x Films on Threshold and Memory Switching Characteristics for Hybrid Memory Applications. Advanced Electronic Materials, 0, , 2101257.	2.6	2
44116	High-Pressure Synthesis of Light Lanthanide Dodecaborides (PrB₁₂ and CeB₁₂): Effects of Valence Fluctuation on Volume and Formation Pressure. Inorganic Chemistry, 2022, 61, 2568-2575.	1.9	3
44117	A one-dimensional perovskite with ferroelectric and switchable nonlinear optical properties: [azetidinium]CdCl₃. Journal of Materials Chemistry C, 2022, 10, 3036-3047.	2.7	17
44118	Theoretical insights into effective electron transfer and migration behavior for CO₂ reduction on the BiOBr(001) surfaces. Physical Chemistry Chemical Physics, 2022, 24, 2032-2039.	1.3	3
44119	Determination of acid structures on the surface of sulfated monoclinic and tetragonal zirconia through experimental and theoretical approaches. Catalysis Science and Technology, 2022, 12, 596-605.	2.1	7

#	Article	IF	Citations
44120	Escalating Ferromagnetic Order via Seâ€Vacancies Near Vanadium in WSe₂ Monolayers. Advanced Materials, 2022, 34, e2106551.	11.1	20
44121	Effects of potassium on propylene epoxidation by molecular oxygen on Cu₂O (111): a DFT study. Catalysis Science and Technology, 2022, 12, 1487-1498.	2.1	2
44122	Structural vacancies in (Ti,Al)N: An ab initio study. Physical Review Materials, 2022, 6, .	0.9	1
44123	Exploring the Compositional Space of High-Entropy Alloys for Cost-Effective High-Temperature Applications. Frontiers in Materials, 2022, 8, .	1.2	5
44124	Emergence of Magnetic Transition in Cobalt Oxide Nanowires on Vicinal Pt Substrate. IEEE Magnetics Letters, 2022, 13, 1-5.	0.6	1
44125	Hard and soft materials: putting consistent van der Waals density functionals to work. Electronic Structure, 2022, 4, 014001.	1.0	4
44126	Substitutional transition metal doping in MoSi₂N₄ monolayer: structural, electronic and magnetic properties. Physical Chemistry Chemical Physics, 2022, 24, 3035-3042.	1.3	10
44127	Formation of twelve-fold iodine coordination at high pressure. Nature Communications, 2022, 13, 412.	5.8	23
44128	Inverse Design of Ferroelectricâ€Order in Perovskite Crystal for Selfâ€Powered Ultraviolet Photodetection. Advanced Materials, 2021, , 2105108.	11.1	7
44129	From fundamental to CO₂ and COCl₂ gas sensing properties of pristine and defective Si₂BN monolayers. Physical Chemistry Chemical Physics, 2022, 24, 4394-4406.	1.3	10
44130	DFT study of electronic structure and mobility of pristine and fluorinated methylammonium lead halide perovskites (CH ₃ NH ₃ PbX ₃ , X = I, Br, Cl). International Journal of Energy Research, 2022, 46, 6889-6900.	2.2	5
44131	Adsorption of nitrogen oxides on modified BN nanosheets: improved gas sensing and functionalization. New Journal of Chemistry, 2022, 46, 4373-4384.	1.4	2
44132	Structural, electronic and magnetic properties of the Half-Heusler alloy CrZSi (ZÂ=ÂSc, Ti). Journal of Crystal Growth, 2022, 583, 126556.	0.7	12
44133	Effect of strain on magnetic and optical properties in (Ga,Mo)Sb by the first-principles*. Wuli Xuebao/Acta Physica Sinica, 2022, .	0.2	0
44134	Hydrothermal synthesis and crystal structure of a novel double-perovskite-type bismuth oxide with 3â€‰:â€‰1 ordering at the B-site. New Journal of Chemistry, 2022, 46, 3595-3601.	1.4	5
44135	Predicting diffusion barriers and diffusivities of C6â€“C12 methylbenzenes in MFI zeolites. Microporous and Mesoporous Materials, 2022, 333, 111705.	2.2	7
44136	Strain-Tunable Carrier Mobility of Fe-Doped GaN: A First-Principles Study. SSRN Electronic Journal, 0, , .	0.4	0
44137	Pb₂Al₂B₃O₈F₃: structure and properties of a new fluoroaluminoborate with non-traditional chain-like B₃O₈ groups. Dalton Transactions, 2022, 51, 3964-3969.	1.6	2

#	Article	IF	Citations
44138	Microkinetic Modeling of Propene Combustion on a Stepped, Metallic Palladium Surface and the Importance of Oxygen Coverage. ACS Catalysis, 2022, 12, 1742-1757.	5.5	13
44139	Surface and interface effects in oxygen-deficient SrMnO₃ thin films grown on SrTiO₃. Physical Chemistry Chemical Physics, 2022, 24, 3951-3957.	1.3	4
44140	Why ZnO is the Support for Cu in Methanol Synthesis? A Systematic Study of the Strong Metal Support Interactions. ACS Sustainable Chemistry and Engineering, 2022, 10, 1722-1730.	3.2	12
44141	Stable interphase chemistry of textured Zn anode for rechargeable aqueous batteries. Science Bulletin, 2022, 67, 716-724.	4.3	80
44142	Insight into the Roles of Metal Loading on CO2 Photocatalytic Reduction Behaviors of TiO2. Nanomaterials, 2022, 12, 474.	1.9	10
44143	SbCl₄: An Exceptional Superhalogen as the Building Block of a Mixed Valence Supercrystal with Unconventional Ferroelectricity. Journal of Physical Chemistry Letters, 2022, 13, 1049-1056.	2.1	6
44144	Toward Exotic Layered Materials: 2D Cuprous Iodide. Advanced Materials, 2022, 34, e2106922.	11.1	28
44145	Density functional theory method for twisted geometries with application to torsional deformations in group-IV nanotubes. Journal of Computational Physics, 2022, 456, 111023.	1.9	6
44146	Approaching theoretical specific capacity of iron-rich lithium iron silicate using graphene-incorporation and fluorine-doping. Journal of Materials Chemistry A, 2022, 10, 4006-4014.	5.2	10
44147	La₂MoO₆ as an Effective Catalyst for the Cathode Reactions of Lithiumâ€“Sulfur Batteries. ACS Applied Materials & Interfaces, 2022, 14, 5247-5256.	4.0	5
44148	Dealloying layered PdBi₂ nanoflakes to palladium hydride leads to enhanced electrocatalytic N₂ reduction. Journal of Materials Chemistry A, 2022, 10, 11904-11916.	5.2	6
44149	Influence of an electrified interface on the entropy and energy of solvation of methanol oxidation intermediates on platinum(111) under explicit solvation. Physical Chemistry Chemical Physics, 2022, 24, 4251-4261.	1.3	5
44150	Interfacial Chemistry Triggers Ultrafast Radiative Recombination in Metal Halide Perovskites. Angewandte Chemie - International Edition, 2022, 61, .	7.2	22
44151	Significant Improvement of Cleanliness and Macro/Microstructure of As-Cast AISI M42 High-Speed Steel by Mg Treatment. Metallurgical and Materials Transactions B: Process Metallurgy and Materials Processing Science, 2022, 53, 1196-1211.	1.0	21
44152	Two-dimensional antimony selenide (Sb2Se3) nanosheets prepared by hydrothermal method for visible-light photodetectors. Solar Energy, 2022, 233, 213-220.	2.9	13
44153	The Extent, Nature, and Origin of K and Rb Depletions and Isotopic Fractionations in Earth, the Moon, and Other Planetary Bodies. Planetary Science Journal, 2022, 3, 29.	1.5	16
44154	Isotropic spin polarization in Heusler Co2FeAl thin films. AIP Advances, 2022, 12, 025005.	0.6	4
44155	Density functional theory study of the selective oxidation of 5-Hydroxymethylfurfural (HMF) to 5-Hydroxymethyl-2-furancarboxylic acid (HMFCA) on the Silver oxide surface (001). Molecular Catalysis, 2022, 519, 112117.	1.0	5

#	Article	IF	Citations
44156	Supercapacitor performance and charge storage mechanism of brannerite type CuV2O6/PANI nanocomposites synthesis with their theoretical aspects. Electrochimica Acta, 2022, 410, 140015.	2.6	15
44157	High electrocatalytical performance of FeCoNiCuPd high-entropy alloy for nitrogen reduction reaction. Molecular Catalysis, 2022, 519, 112141.	1.0	13
44158	Photo-enhanced thermal catalytic CO2 methanation activity and stability over oxygen-deficient Ru/TiO2 with exposed TiO2 {001} facets: Adjusting photogenerated electron behaviors by metal-support interactions. Chinese Journal of Catalysis, 2022, 43, 391-402.	6.9	22
44159	Orbitale als Ausgangspunkt der Chemischen Bindung in Geâˆ'Sbâˆ'Teâ€Phasenwechselmaterialien**. Angewandte Chemie, 0, , e202115778.	1.6	0
44160	Role of the voltage window on the capacity retention of P2-Na2/3[Fe1/2Mn1/2]O2 cathode material for rechargeable sodium-ion batteries. Communications Chemistry, 2022, 5, .	2.0	12
44161	Metal organic frameworks derived Ni-doped hierarchical NiXCo1-XS@C bundled-like nanostructures for enhanced supercapacitors. Electrochimica Acta, 2022, 406, 139872.	2.6	23
44162	Surface Activation of the g-C₃N₄ Bilayer by Ï€-Conjugation and Interlayer Orbital Interaction to Promote OER and HER. Journal of Physical Chemistry C, 2022, 126, 2573-2586.	1.5	7
44163	Extrinsic magnetoelectric effect at the BaTiO3/Ni interface. Journal of Applied Physics, 2022, 131, 054101.	1.1	6
44164	The electronic structure and chemical bonding in MgPbP 2. Physica Status Solidi (B): Basic Research, 0, , .	0.7	1
44165	Charge Carrier Transport Mechanism in Ta₂O₅, TaON, and Ta₃N₅ Studied by Applying Polaron Hopping and Bandlike Models. ChemPhysChem, 2022, 23, e202100859.	1.0	1
44166	Selectively Growing a Highly Active Interface of Mixed Nbâ€"Rh Oxide/2D Carbon for Electrocatalytic Hydrogen Production. Advanced Science, 2022, 9, e2104706.	5.6	15
44167	DFT screening of adsorption of biodiesel molecules on aluminum and stainless steel surfaces. Results in Surfaces and Interfaces, 2022, 6, 100050.	1.0	2
44168	Tetrazine Based Covalent Organic Framework as a Promising Metal-Free Photo and Electro-Catalyst for HER. Catalysis Letters, 0, , 1.	1.4	5
44169	Enhancing the optical absorption of Ga2SeTe Janus monolayer by adsorption of transition metals. European Physical Journal D, 2022, 76, .	0.6	2
44170	Strain dependent electronic and optical responses of penta-BCN monolayer. Carbon Trends, 2022, 7, 100162.	1.4	6
44171	Promotion effects of Ni-doping on H2S removal and ZnO initial sulfuration over ZnO nanowire by first-principle study. Molecular Catalysis, 2022, 519, 112148.	1.0	3
44172	Two-Dimensional WO₃-Transition-Metal Dichalcogenide Vertical Heterostructures for Nitrogen Fixation: A Photo(Electro) Catalysis Theoretical Strategy. Journal of Physical Chemistry C, 2022, 126, 3043-3053.	1.5	8
44173	Electronegativityâ€Induced Charge Balancing to Boost Stability and Activity of Amorphous Electrocatalysts. Advanced Materials, 2022, 34, e2100537.	11.1	39

#	Article	IF	Citations
44174	The behavior of zeolites wairakite and phillipsite at high P-T parameters. Spectrochimica Acta - Part A: Molecular and Biomolecular Spectroscopy, 2022, 273, 120979.	2.0	3
44175	Ab-initio study of structural stability, electronic and optical properties of X2GeSe (X = P and Sb) monolayers. Solid State Communications, 2022, 343, 114673.	0.9	4
44176	GaN/Surface-modified graphitic carbon nitride heterojunction: Promising photocatalytic hydrogen evolution materials. International Journal of Hydrogen Energy, 2022, 47, 7202-7213.	3.8	18
44177	The joint effect of spinâ€“orbit coupling and atomistic disorder on bandgap evolution in inorganic CsSn1âˆ’xPbxI3 mixed perovskite. Journal of Applied Physics, 2022, 131, 055107.	1.1	1
44178	Electronic properties of MoS2/Be2C van der Waals heterostructure: Effect of Bi-axil strain and vertical electric field. Physica E: Low-Dimensional Systems and Nanostructures, 2022, 139, 115172.	1.3	1
44179	High Performance Space Lubrication of MoS₂ with Tantalum. Advanced Functional Materials, 2022, 32, .	7.8	18
44180	Tetragonal distortion in magnetron sputtered bcc-W films with supersaturated carbon. Materials and Design, 2022, 214, 110422.	3.3	1
44181	IIIâ€“VI and IVâ€“VI van der Waals Semiconductors InSe, GaSe and GeSe: A Suitable Platform for Efficient Electrochemical Water Splitting, Photocatalysis and Chemical Sensing. Israel Journal of Chemistry, 2022, 62, .	1.0	7
44182	Negative linear compressibility in Se at ultra-high pressure above 120 GPa. IUCrJ, 2022, 9, 253-260.	1.0	3
44183	Ultrasensitive N-Channel Graphene Gas Sensors by Nondestructive Molecular Doping. ACS Nano, 2022, 16, 2176-2187.	7.3	42
44184	Impact of oxygen content on the thermal stability of Ti-Al-O-N coatings based on computational and experimental studies. Acta Materialia, 2022, 227, 117706.	3.8	8
44185	A DFT+U study of site dependent Fe-doped TiO2 diluted magnetic semiconductor material: Room-temperature ferromagnetism and improved semiconducting properties. AIP Advances, 2022, 12, .	0.6	7
44186	The phase diagrams of beryllium and magnesium oxide at megabar pressures. Journal of Physics Condensed Matter, 2022, 34, 144003.	0.7	3
44187	First-Principles Study of Transition Metal Ti-Based MXenes (Ti₂MC₂T_x and) Tj ETQq1 1 0.784314 rgBT /Overlock 10 Tf 50 222 Td (M₂ ACS Applied Nano Materials, 2022, 5, 2358-2366.	2.4	8
44188	Unveiling the effect of interstitial dopants on CO2 activation over CsPbBr3 catalyst for efficient photothermal CO2 reduction. Chemical Engineering Journal, 2022, 435, 135071.	6.6	35
44189	Surface half metallicity and thermodynamic stability of 001-plane Ti2XSi (X=Mn, Co) Heusler alloys (HAs): A DFT approach. Surfaces and Interfaces, 2022, 28, 101602.	1.5	1
44190	Okra-like hollow Cu0.15-CoP/Co3O4@CC nanotube arrays catalyst for overall water splitting. International Journal of Hydrogen Energy, 2022, 47, 7168-7179.	3.8	3
44191	Experiments combined with theoretical research on the effect of hydrogen evolution by the nanosheet of NiSâ€“CdSâ€“CN catalyst. International Journal of Hydrogen Energy, 2022, 47, 7724-7737.	3.8	10

#	Article	IF	Citations
44192	Stability and Bandgap Engineering of In1âˆ'xGaxSe Monolayer. Nanomaterials, 2022, 12, 515.	1.9	0
44193	First-principles investigation of a symmetry incompatible adsorbate-substrate system: PF3 on Cu(001). Surface Science, 2022, 719, 122045.	0.8	0
44194	Three-dimensional tetrahexcarbon: Stability and properties. Materials Today Physics, 2022, 23, 100628.	2.9	8
44195	Adsorption dynamics and intrinsic mechanism of POPs on corrole-based COF: A computational study. Journal of Cleaner Production, 2022, 338, 130566.	4.6	11
44196	DFT modeling of unintentional oxygen incorporation enhanced by magnesium in GaN(0001) and AlN(0001) growth surfaces during metalorganic vapor phase epitaxy. Physica Status Solidi (B): Basic Research, 0, , .	0.7	0
44197	Pressure induced structural phase transition and piezochromism in photovoltaic sillen compounds PbBiO2X (XÂ=ÂCl, Br & I). Applied Materials Today, 2022, 26, 101372.	2.3	0
44198	Alkali ions pre-intercalation of Î´-MnO2 nanosheets for high-capacity and stable Zn-ion battery. Materials Today Energy, 2022, 24, 100934.	2.5	35
44199	First-principles study on the absorber for intermediate band solar cell from Si, Ge, and Sn-doped LiGaTe2. Optik, 2022, 254, 168657.	1.4	2
44200	Pd-decorated C3N monolayer as a potential toxic gas sensor in dry-type transformers: A first-principles study. Computational and Theoretical Chemistry, 2022, 1209, 113611.	1.1	1
44201	Pressure induced Lifshitz transition and anomalous crystal field splitting in AFeAs (A = Li/Na) Fe-based superconducting compounds: A first principles study. Computational Materials Science, 2022, 204, 111170.	1.4	5
44202	Visualizing crystal structure evolution of electrode materials upon doping and during charge/discharge cycles in lithium-ion batteries. STAR Protocols, 2022, 3, 101099.	0.5	1
44203	Vacancy formation energies and migration barriers in multi-principal element alloys. Acta Materialia, 2022, 226, 117611.	3.8	24
44204	Non-uniform He bubble formation in W/W2C composite: Experimental and ab-initio study. Acta Materialia, 2022, 226, 117608.	3.8	3
44205	Influence of Nitrogen and Boron on the magnetization of nanoporous graphene : A first-principle investigation. Computational Condensed Matter, 2022, 30, e00603.	0.9	2
44206	Photoelectric properties of 2D ZnO, graphene, silicene materials and their heterostructures. Composites Part B: Engineering, 2022, 233, 109645.	5.9	33
44207	Low-hysteresis manganese hexacyanoferrate (MnHCF) aqueous battery for low-grade thermal energy harvesting. Journal of Power Sources, 2022, 524, 231080.	4.0	3
44208	Helium impurities and interactions in lithium. Computational Materials Science, 2022, 204, 111176.	1.4	0
44209	Hydrogen induced dislocation core reconstruction in bcc tungsten. Acta Materialia, 2022, 226, 117622.	3.8	16

#	Article	IF	Citations
44210	Intermediate carbon phase. New experimental data and atomic model. Diamond and Related Materials, 2022, 123, 108825.	1.8	2
44211	NJOY+NCrystal: An open-source tool for creating thermal neutron scattering libraries with mixed elastic support. Nuclear Instruments and Methods in Physics Research, Section A: Accelerators, Spectrometers, Detectors and Associated Equipment, 2022, 1027, 166227.	0.7	14
44212	Effects of nanostructures on the hydrogen storage properties of MgH2 - A first principles study. Computational Condensed Matter, 2022, 30, e00643.	0.9	8
44213	Electronic and magnetic properties of <mml:math xmlns:mml="http://www.w3.org/1998/Math/MathML" altimg="si0044.svg"><mml:mrow><mml:mi mathvariant="italic">Ru</mml:mi><mml:msub><mml:mrow><mml:mi mathvariant="italic">Te</mml:mi></mml:mrow><mml:mrow><mml:mn>2</mml:mn></mml:mrow></mml:msub><mml:mrow></mml:m Janus <mml:math xmlns:mml="http://www.w3.org/1998/Math/MathML" altimg="si0045.svg"><mml:mi mathvariant="italic">RuSTe</mml:mi></mml:math> and <mml:math xmlns:mml="http://www.w3.org/1998	0.9	0
44214	Enhanced visible light photocatalytic activity of KTaO3 (Se,V): DFT investigation. Computational Condensed Matter, 2022, 30, e00648.	0.9	1
44215	Quantum spin Hall insulating phase and van Hove singularities in Zintl single-quintuple-layer AM2X2 (A = Ca, Sr, or Ba; M = Zn or Cd; X = Sb or Bi) family. Applied Physics Reviews, 2022, 9, .	5.5	17
44216	Boron carbide under torsional deformation: Evidence of the formation of chain vacancies in the plastic regime. Acta Materialia, 2022, 226, 117553.	3.8	5
44217	Rational design of microporous biochar based on ion exchange using carboxyl as an anchor for high-efficiency capture of gaseous p-xylene. Separation and Purification Technology, 2022, 286, 120402.	3.9	7
44218	An optimum thermoelectric figure of merit using Ge2Se2 monolayer: An ab-initio approach. Physica E: Low-Dimensional Systems and Nanostructures, 2022, 138, 115060.	1.3	5
44219	A first principles study of the adsorption and hydrogenation of formic acid on a Cu3Zn material: Implication for bulk alloying effect on CO2 hydrogenation reactivity of Cu/ZnO-based catalysts. Computational Materials Science, 2022, 205, 111222.	1.4	1
44220	Interfacial covalent bonding enables transition metal phosphide superior lithium storage performance. Applied Surface Science, 2022, 582, 152404.	3.1	22
44221	Adsorption of metal atoms on two-dimensional BC3 and AlC3 nanosheets: Computational studies. Chemical Physics Letters, 2022, 792, 139403.	1.2	5
44222	Effect of native point defects on the photocatalytic performance of ZnIn2S4. Physica B: Condensed Matter, 2022, 630, 413674.	1.3	2
44223	Effects of strain and electric field on electronic and optical properties of monolayer <mml:math xmlns:mml="http://www.w3.org/1998/Math/MathML" display="inline" id="d1e1140" altimg="si41.svg"><mml:mi>Î³</mml:mi></mml:math>-GeX (X <mml:math) Tj ETQq1 1 0.784314 rgBT /Overlock 10 Tf 50 222 Td (xml 152321.	3.1	17
44224	Evidence of strong correlation and magnetotransport scaling in YbFe2As2. Physica B: Condensed Matter, 2022, 630, 413696.	1.3	0
44225	Role of Ni on the helium diffusion, stability and energetics of vacancyâ€“type clusters in Feâ€"6.25Crâ€"3.13Ni (at.%) ternary alloys: From first-principles. Computational Materials Science, 2022, 205, 111213.	1.4	1
44226	Structureâ€“compressibility correlation among MoBx. Journal of Physics and Chemistry of Solids, 2022, 163, 110599.	1.9	4
44227	Improving performance of zinc-manganese battery via efficient deposition/dissolution chemistry. Energy Storage Materials, 2022, 46, 165-174.	9.5	32

#	Article	IF	Citations
44228	Theoretical investigation of the HgTe topological edge states with a Fe impurity. Physica B: Condensed Matter, 2022, 630, 413673.	1.3	0
44229	Ab initio molecular dynamics investigation of <mml:math xmlns:mml="http://www.w3.org/1998/Math/MathML" altimg="si2.svg"><mml:mi>Î³</mml:mi></mml:math>-(U,Zr) structural and thermal properties as a function of temperature and composition. Journal of Nuclear Materials, 2022, 561, 153523.	1.3	6
44230	Narrow gap electronic structure and thermoelectric performance of p-type ErMSb (M = Ni, Pd) half Heusler compounds. Physica B: Condensed Matter, 2022, 631, 413709.	1.3	4
44231	Mechanism of CO2 hydrogenation to methanol on the W-doped Rh(111) surface unveiled by first-principles calculation. Colloids and Surfaces A: Physicochemical and Engineering Aspects, 2022, 638, 128332.	2.3	10
44232	Stability and ordering of bcc and hcp TiAl+Mo phases: An ab initio study. Computational Materials Science, 2022, 205, 111163.	1.4	5
44233	Density functional theory analysis of structural and electronic properties of hexagonal hybrid perovskite (CH3NH3)3Bi2I9. Physica B: Condensed Matter, 2022, 630, 413695.	1.3	3
44234	Effects of the phase transition on the structural, mechanical, electronic and vibrational properties of the CaSnO3 perovskite: Study under hydrostatic pressure. Journal of Physics and Chemistry of Solids, 2022, 163, 110594.	1.9	5
44235	Element-dependent unique properties of Janus Cr2I3X3 (XÂ=ÂF, Cl, Br) monolayer: Insight from first-principles calculations. Materials Science and Engineering B: Solid-State Materials for Advanced Technology, 2022, 278, 115610.	1.7	7
44236	Electronic phase transition from semiconducting to metallic in cubic halide CsYbCl3 perovskite under hydrostatic pressure. Physica B: Condensed Matter, 2022, 630, 413650.	1.3	16
44237	Electronic and magnetic properties of polar magnets M2Mo3O8 (M = Mn, Fe, Co and Ni) from first principles studies. Journal of Solid State Chemistry, 2022, 308, 122910.	1.4	2
44238	Self-adaptive evolution of nickel silicide nanowires for the enhancement of bifunctional electrocatalytic activities. Chemical Engineering Journal, 2022, 434, 134668.	6.6	5
44239	Annihilation dynamics of a dislocation pair in graphene: Density-functional tight-binding molecular dynamics simulations and first principles study. Computational Materials Science, 2022, 205, 111224.	1.4	6
44240	Designing and optimizing Î²1-borophene organic gas sensor: A theoretical study. Surface Science, 2022, 719, 122030.	0.8	8
44241			

#	Article	IF	Citations
44246	Modeling the cobalt deposit on the AlN (0001)-(2ÂÃ—Â2) surface: Density functional theory studies. Journal of Magnetism and Magnetic Materials, 2022, 549, 169005.	1.0	3
44247	A freestanding nanoporous NiCoFeMoMn high-entropy alloy as an efficient electrocatalyst for rapid water splitting. Chemical Engineering Journal, 2022, 435, 134898.	6.6	60
44248	DFT insights into the adsorption mechanism of five-membered aromatic heterocycles containing N, O, or S on Fe(1 1 0) surface. Applied Surface Science, 2022, 583, 152524.	3.1	13
44249	A first-principles study of formic acid adsorption on CaO (001). Applied Surface Science, 2022, 583, 152296.	3.1	7
44250	Mn-dopant induced Octahedral Configuration Strongly Stabilizes Ni12P5 Nanowires for Battery-Supercapacitor Hybrid Devices. Journal of Alloys and Compounds, 2022, 903, 163897.	2.8	10
44251	Pd and octahedra do not get along: Square planar [PdS4] units in non-centrosymmetric La6PdSi2S14. Journal of Alloys and Compounds, 2022, 902, 163756.	2.8	8
44252	Influence of Cu/W interfacial structure on the resistance against harmful helium atoms: A mechanism analysis. Journal of Alloys and Compounds, 2022, 903, 163817.	2.8	6
44253	Design of hydrangea-type Co/Mo bimetal MOFs and MOF-derived Co/Mo2C embedded carbon composites for highly efficient oxygen evolution reaction. Chemical Engineering Journal, 2022, 435, 134815.	6.6	26
44254	High-performance electroreduction CO2 to formate at Bi/Nafion interface. Applied Catalysis B: Environmental, 2022, 306, 121135.	10.8	37
44255	Oxygen-mediated selection of Cu crystallographic orientation for growth of single-crystalline graphene. Applied Surface Science, 2022, 584, 152585.	3.1	1
44256	Improved oxygen balance and effective energy density by coligand and dehydration strategy: Synthesis and characterization of two new energetic coordination polymers. Chemical Thermodynamics and Thermal Analysis, 2022, 6, 100035.	0.7	1
44257	Hydrogen-bond-stabilized high density catechol monolayer on magnetite Fe3O4(111). Surface Science, 2022, 719, 122027.	0.8	1
44258	1T-MoS2 monolayer as a promising anode material for (Li/Na/Mg)-ion batteries. Applied Surface Science, 2022, 584, 152537.	3.1	66
44259	Possible ferromagnetism or antiferromagnetism in defective AlN via strain engineering: Hybrid versus GGA calculations. Journal of Magnetism and Magnetic Materials, 2022, 549, 168965.	1.0	0
44260	Unveiling the mechanism of yttrium significantly improving high-temperature oxidation resistance of super-austenitic stainless steel S32654. Journal of Materials Science and Technology, 2022, 115, 103-114.	5.6	16
44261	Low-temperature dielectric relaxation associated with NbO6 octahedron distortion in antimony modified potassium sodium niobate ceramics. Journal of Materials Science and Technology, 2022, 115, 189-198.	5.6	14
44262	In-situ construction of N-doped carbon nanosnakes encapsulated FeCoSe nanoparticles as efficient bifunctional electrocatalyst for overall water splitting. Journal of Energy Chemistry, 2022, 68, 699-708.	7.1	31
44263	DFT calculations of elastic, electronic and thermal properties of TiB2Mo. Oxford Open Materials Science, 2022, 2, .	0.5	1

#	Article	IF	Citations
44264	Simulation of the Physicochemical Properties of Anatase TiO2 with Oxygen Vacancies and Doping of Different Elements for Photocatalysis Processes. Lecture Notes in Networks and Systems, 2022, , 238-249.	0.5	0
44265	Manifestation of the Ferroelastoelectric Phase Transition in the Absorption Spectra of (NH) Tj ETQq1 1 0.784314 rgBT /Overlock 10 Tf 5 0, , .	0.4	0
44266	Heterogeneous Chemical State of Carbon in Feâ€“C Binary Alloys. ISIJ International, 2022, , .	0.6	0
44267	DFT-based study of the structural, optoelectronic, mechanical and magnetic properties of Ti₃AC₂ (A = P, As, Cd) for coating applications. RSC Advances, 2022, 12, 4395-4407.	1.7	11
44268	Mechanism of CO₂ hydrogenation over a Zr₁â€“Cu single-atom catalyst. New Journal of Chemistry, 2022, 46, 5043-5051.	1.4	8
44269	Two-dimensional semiconductor materials with high stability and electron mobility in group-11 chalcogenide compounds: MNX (M = Cu, Ag, Au; N = Cu, Ag, Au; X = S, Se, Te; M â‰ N). Nanoscale, 2022, 14, 4271-4280.	2.8	6
44270	Chemical order or disorder â€“ a theoretical stability expose for expanding the compositional space of quaternary metal borides. Materials Advances, 2022, 3, 2908-2917.	2.6	9
44271	A biphenylene nanoribbon-based 3D metallic and ductile carbon allotrope. Nanoscale, 2022, 14, 3801-3807.	2.8	9
44272	NiO nanobelts with exposed {110} crystal planes as an efficient electrocatalyst for the oxygen evolution reaction. Physical Chemistry Chemical Physics, 2022, 24, 6087-6092.	1.3	10
44273	First-Principles Calculations of Oxygen Solution and Segregation Effect on Mo/Cr Interface. SSRN Electronic Journal, 0, , .	0.4	0
44274	Highly active postspinel-structured catalysts for oxygen evolution reaction. RSC Advances, 2022, 12, 5094-5104.	1.7	3
44275	Size and structure effects on platinum nanocatalysts: theoretical insights from methanol dehydrogenation. Nanoscale, 2022, 14, 4145-4155.	2.8	3
44276	Layered TiCl₂ Monolayer as an Antiferromagnetic Semiconductor. Spin, 2022, 12, .	0.6	2
44277	Predicting magnetic anisotropy energies using site-specific spin-orbit coupling energies and machine learning: Application to iron-cobalt nitrides. Physical Review Materials, 2022, 6, .	0.9	3
44278	Nonvolatile Ferroelastic Strain from Flexoelectric Internal Bias Engineering. Physical Review Applied, 2022, 17, .	1.5	9
44279	Chemical-Mechanical Effects in Ni-Rich Cathode Materials. Chemistry of Materials, 2022, 34, 1509-1523.	3.2	34
44280	Surface Noble Metal Concentration on Ceria as a Key Descriptor for Efficient Catalytic CO Oxidation. ACS Catalysis, 2022, 12, 2473-2486.	5.5	19
44281	Survey of Tetragonal Transition Metal Chalcogenide Heteroâ€Bilayers for Promising Photocatalysts. Advanced Materials Interfaces, 2022, 9, .	1.9	4

#	Article	IF	Citations
44282	First-principles insights into mechanical, optoelectronic, and thermo-physical properties of transition metal dichalcogenides ZrX2 (X = S, Se, and Te). AIP Advances, 2022, 12, .	0.6	16
44283	Deep transfer learning correlation study of electronic and spin properties in buckled III-V monolayers. Physica E: Low-Dimensional Systems and Nanostructures, 2022, 140, 115130.	1.3	1
44284	Theoretical study of copper nitrides Cu_nN (n=1, 3 and 4): insight first-principles calculations. Phase Transitions, 2022, 95, 225-238.	0.6	0
44285	Formation of <mml:math xmlns:mml="http://www.w3.org/1998/Math/MathML" display="inline" overflow="scroll"><mml:mi>Bi</mml:mi><mml:mstyle displaystyle="false" scriptlevel="0"><mml:mtext>â^'</mml:mtext></mml:mstyle><mml:mi>Bi</mml:mi></mml:math> Dimers in Heavily <mml:math xmlns:mml="http://www.w3.org/1998/Math/MathML" display="inline" overflow="scroll"><mml:mi>Bi</mml:mi></mml:math> -Doped Lead Halide Perovskites: Origin of Carrier Density Saturation. Physical Review Applied, 2022, 17, .	1.5	1
44286	Robust valley polarization induced by super-exchange effects in HfNX (Xâ€‰=â€‰Cl, Br, I)/FeCl2 two-dimensional ferrovalley heterostructures. Applied Physics Letters, 2022, 120, .	1.5	18
44287	Rational Design of Cu-Doped ZnS Nanospheres for Photocatalytic Evolution of H₂ with Visible Light. ACS Applied Energy Materials, 2022, 5, 1849-1857.	2.5	8
44288	Design metal-free single-atom catalyst P@BN for CO oxidation: A DFT-D study. Journal of Physics and Chemistry of Solids, 2022, 164, 110615.	1.9	2
44289	Oxygen Exchange on Vanadium Pentoxide. Journal of Physical Chemistry C, 2022, 126, 3443-3456.	1.5	8
44290	First-Principles Calculations to Investigate the Influence of Irradiation Defects on the Swelling Behavior of Fe-13Cr Alloys. Materials, 2022, 15, 1267.	1.3	0
44291	Exotic magnetic and electronic properties of layered <mml:math xmlns:mml="http://www.w3.org/1998/Math/MathML"><mml:msub><mml:mi>CrI</mml:mi><mml:mn>3</mml:mn></mml:msub></mml:math> single crystals under high pressure. Physical Review B, 2022, 105, .	1.1	12
44292	Coâ€Đoping Strategies to Improve the Electrochemical Properties of Li_xMn₂O₄ Cathodes for Liâ€Ion Batteries. ChemElectroChem, 2022, 9, .	1.7	8
44293	Tuning electronic structures and optical properties of graphene/phosphorene heterostructure via electric field. Superlattices and Microstructures, 2022, 164, 107184.	1.4	0
44294	Theoretical investigation of nitrogen-vacancy defects in silicon. AIP Advances, 2022, 12, .	0.6	4
44295	Designing Electrophilic and Nucleophilic Dual Centers in the ReS₂ Plane toward Efficient Bifunctional Catalysts for Li-CO₂ Batteries. Journal of the American Chemical Society, 2022, 144, 3106-3116.	6.6	93
44296	A Strategy to Enhance the Catalytic Activity of Electrode Materials by Doping Bismuth for Symmetrical Solid Oxide Electrolysis Cells. ACS Applied Energy Materials, 2022, 5, 2339-2348.	2.5	11
44297	Enhancement Effect of Chemisorbed Sulfate toward Electrochemical Oxidation of Ethanol on Platinum Electrodes. Journal of Physical Chemistry C, 2022, 126, 3397-3403.	1.5	8
44298	Synthesis and characterization of Taâ€“Bâ€“C coatings prepared by DCMS and HiPIMS co-sputtering. Vacuum, 2022, 199, 110937.	1.6	4
44299	Photon energy dependent appearance and disappearance of magnetic dipole transition in Gd2Hf2O7:Sm3+ nanophosphors. Journal of Luminescence, 2022, 245, 118789.	1.5	3

#	Article	IF	Citations
44300	Atypical pathways for lamellar and twinning transformations in rapidly solidified TiAl alloy. Acta Materialia, 2022, 227, 117718.	3.8	20
44301	Nanoscale Control of Polar Surface Phases in Layered van der Waals CuInP₂S₆. ACS Nano, 2022, 16, 2452-2460.	7.3	12
44302	Giant interlayer magnetic exchange interaction and charge-spin coupling in a van der Waals magnetic interface driven by <mml:math xmlns:mml="http://www.w3.org/1998/Math/MathML"><mml:mi>p</mml:mi><mml:mo>â^'</mml:mo><mml:mi>d</mml:mi></mml:math coupling. Physical Review B, 2022, 105, .	1.1	3
44303	Identification of Copper as an Ideal Catalyst for Electrochemical Alkyne Semi-hydrogenation. Journal of Physical Chemistry C, 2022, 126, 3037-3042.	1.5	10
44304	Dynamic structural evolution of iron catalysts involving competitive oxidation and carburization during CO ₂ hydrogenation. Science Advances, 2022, 8, eabm3629.	4.7	92
44305	Size Effect of MgO on the Ionic Conduction Properties of a LiBH₄Â·1/2NH₃â€“MgO Nanocomposite. ACS Applied Materials & Interfaces, 2022, 14, 8947-8954.	4.0	5
44306	First-Principles Study of High-Pressure Phase Stability and Electron Properties of Be-P Compounds. Materials, 2022, 15, 1255.	1.3	0
44307	QUANTAS: a Python software for the analysis of thermodynamics and elastic behavior of solids fromab initioquantum mechanical simulations and experimental data. Journal of Applied Crystallography, 2022, 55, 386-396.	1.9	3
44308	First-principles insight into the structural and optoelectronic properties of Sn- and Pb-based hybrid halide perovskites for photovoltaic applications. Molecular Physics, 2022, 120, .	0.8	5
44309	Comparative study on the linear thermal expansion coefficient of laser host crystals by first principles calculations. Optical Materials Express, 0, , .	1.6	4
44310	Defects investigation of bipolar exfoliated phosphorene nanosheets. Surface Science, 2022, 720, 122052.	0.8	7
44311	Mechanisms for Graphene Growth on SiO₂ Using Plasma-Enhanced Chemical Vapor Deposition: A Density Functional Theory Study. ACS Applied Materials & Interfaces, 2022, 14, 9492-9503.	4.0	6
44312	Two novel carbon allotropes with tetragonal symmetry: First-principles calculations. Journal of Solid State Chemistry, 2022, 309, 122971.	1.4	21
44313	Tailoring the electronic, optical and mechanical properties of KMgH3 and RbCaH3 perovskite hydrides without and with Samarium. Journal of Solid State Chemistry, 2022, 309, 122952.	1.4	4
44314	Suppressing effect of tantalum on the radiation-induced clustering of rhenium in tungsten. Journal of Nuclear Materials, 2022, 562, 153588.	1.3	4
44315	Surface ion isolated platinum-thiocyanate catalysts for hydrogen peroxide production via 2-electron oxygen reduction in acidic media. Chemical Engineering Journal, 2022, 435, 135105.	6.6	6
44316	Structural, elastic, thermal and mechanical properties of LnTa2O6(Ln Ce-Tb) ceramics from first-principles calculations. Materials Today Communications, 2022, 31, 103251.	0.9	0
44317	Atomic control of active-site ensembles in ordered alloys to enhance hydrogenation selectivity. Nature Chemistry, 2022, 14, 523-529.	6.6	51

#	Article	IF	Citations
44318	Probing the onset of wurtzite phase formation in (V,Al)N thin films by transmission electron microscopy and atom probe tomography. Surface and Coatings Technology, 2022, 442, 128235.	2.2	7
44319	Cuâ€doped Ba_{0.5}Sr_{0.5}FeO_{3â€Î´} for electrochemical synthesis of hydrogen peroxide via a 2â€electron oxygen reduction reaction¹. Electrochemical Science Advances, 2023, 3, .	1.2	0
44320	Efficient electrosynthesis of n-propanol from carbon monoxide using a Agâ€“Ruâ€“Cu catalyst. Nature Energy, 2022, 7, 170-176.	19.8	96
44321	Herzbergâ€“Teller Effect in Single-Crystalline Hexacene at Finite Temperatures. Journal of Physical Chemistry C, 2022, 126, 3366-3374.	1.5	3
44322	Structural changes of hydrotalcite-based Co-containing mixed oxides with calcination temperature and their effects on NOx adsorption: A combined experimental and DFT study. Chemical Engineering Journal, 2022, 437, 135209.	6.6	6
44323	The Temperature Effect on the Physical Properties of CoMnSb Half-Heusler Ferromagnetic: Density Functional Theory and Monte Carlo Simulation. ECS Journal of Solid State Science and Technology, 2022, 11, 033002.	0.9	2
44324	Impact of Molybdenum Dichalcogenides on the Active and Holeâ€Transport Layers for Perovskite Solar Cells, Xâ€Ray Detectors, and Photodetectors. Small, 2022, 18, e2104216.	5.2	22
44325	Large magnetoresistance and unexpected low thermal conductivity in topological semimetal CrP4 single crystal. Applied Physics A: Materials Science and Processing, 2022, 128, 1.	1.1	3
44326	Non-oxidized bare copper nanoparticles with surface excess electrons in air. Nature Nanotechnology, 2022, 17, 285-291.	15.6	34
44327	Efficient Hydrogen Evolution Reaction with Bulk and Nanostructured Mitrofanovite Pt3Te4. Nanomaterials, 2022, 12, 558.	1.9	3
44328	Investigation of New 2D Half Metallic Ferromagnetic Materials. Spin, 2022, 12, .	0.6	2
44329	Unraveling the Synergistic Effect of Re and Cs Promoters on Ethylene Epoxidation over Silver Catalysts with Machine Learning-Accelerated First-Principles Simulations. ACS Catalysis, 2022, 12, 2540-2551.	5.5	13
44330	Monoclinicâ€“triclinic phase transition induced by pressure in fergusonite-type YbNbO₄. Journal of Physics Condensed Matter, 2022, 34, 174007.	0.7	7
44331	Ferroelectric incommensurate spin crystals. Nature, 2022, 602, 240-244.	13.7	30
44332	The effect of strain and pressure on the electron-phonon coupling and superconductivity in MgB2â€”Benchmark of theoretical methodologies and outlook for nanostructure design. Journal of Applied Physics, 2022, 131, 063902.	1.1	1
44333	The effect of Bi content on the photocatalytic performance of bismuth oxybromides. Journal of Fuel Chemistry and Technology, 2022, 50, 250-256.	0.9	0
44334	W 4f electron binding energies in amorphous W-B-C systems. Applied Surface Science, 2022, 586, 152824.	3.1	4
44335	The properties of typical Î²/Ï‰ and Î²/Î±â€³ heterophase interfaces in Î²-Ti alloys from a first-principles insight. Journal of Materials Science, 2022, 57, 4625-4642.	1.7	4

#	Article	IF	Citations
44336	Tuning the magnetic and electronic properties of MoI3 monolayer by 3d transition metal doping: A first-principles study. Journal of Magnetism and Magnetic Materials, 2022, 551, 169163.	1.0	7
44337	DFT Investigation of the Structual and Optoelectronic Properties of Alkali Metal Hydrides MH (M=Li,) Tj ETQq1 1 0.784314 rgBT /Over	0.8	0
44338	Surface steps dominate the water formation on Pd(111) surfaces. Journal of Chemical Physics, 2022, 156, 064701.	1.2	8
44339	Sulfur infiltration and allotrope formation in porous cathode hosts for lithiumâ€sulfur batteries. AICHE Journal, 2022, 68, .	1.8	5
44340	Interaction of Na with 2D WO₃ and MoO₃ Layers on Pd(100): From Doping to 2D Bronze Formation. Journal of Physical Chemistry C, 2022, 126, 3289-3300.	1.5	5
44341	A complete description of thermodynamic stabilities of molecular crystals. Proceedings of the National Academy of Sciences of the United States of America, 2022, 119, .	3.3	21
44342	Theoretical investigation of methane oxidation reaction over a novel metal-free catalyst biphenylene network. Diamond and Related Materials, 2022, 124, 108897.	1.8	10
44343	Pt-O4 moiety induced electron localization toward In2O-Triggered acetylene Semi-Hydrogenation. Journal of Catalysis, 2022, 407, 290-299.	3.1	9
44344	Interfacial Electronic Properties and Photocatalytic CO₂ Reduction of a Z-Scheme SnS/(CH₃NH₃)₂AgBiI₆ Double Perovskite Heterostructure. ACS Applied Energy Materials, 2022, 5, 1942-1952.	2.5	11
44345	Route to a novel tetragonal carbon allotrope via T-carbon. Diamond and Related Materials, 2022, , 108895.	1.8	0
44346	Electrical control of orbital and vibrational interlayer coupling in bi- and trilayer <mml:math xmlns:mml="http://www.w3.org/1998/Math/MathML"><mml:mrow><mml:mn>2</mml:mn><mml:mi mathvariant="normal">H</mml:mi><mml:mtext>â^'</mml:mtext><mml:msub><mml:mi>MoS</mml:mi><mml:mn>2</mml:mn></mml:r Physical Review Materials, 2022, 6, .	0.9	4
44347	Modification of electronic and thermoelectric properties of InSe/GaSe superlattices by strain engineering. Physical Review Materials, 2022, 6, .	0.9	6
44348	The Importance of Avoided Crossings in Understanding High Valley Degeneracy in Halfâ€Heusler Thermoelectric Semiconductors. Advanced Electronic Materials, 2022, 8, .	2.6	11
44349	Propane Dehydrogenation on Platinum Catalysts: Identifying the Active Sites through Bayesian Analysis. ACS Catalysis, 2022, 12, 2487-2498.	5.5	15
44350	Electronic properties and lattice dynamics of Li x CoO 2 and Na x CoO 2 (x =0, 0.5, 1) studied by hybrid density functional theory. Physica Status Solidi (B): Basic Research, 0, , .	0.7	2
44351	Electrochemical CO₂ Reduction On Two-Dimensional Metal 1,3,5-triamino-2,4,6-Benzenetriol Frameworks: A Density Functional Study. Journal of the Electrochemical Society, 2022, 169, 024513.	1.3	6
44352	Exploration of the Defect Passivation in Perovskite Materials Using Organic Spacer Cations. Advanced Materials Interfaces, 2022, 9, .	1.9	4
44353	Intrinsic Multiferroic in VNI Monolayer. ACS Applied Electronic Materials, 2022, 4, 3177-3182.	2.0	6

#	Article	IF	Citations
44354	The influence of temperature and composition on the crystal properties of Al$$_{1-x}$$B$$_{{x}}$$N semiconducting ternary alloys. Pramana - Journal of Physics, 2022, 96, 1.	0.9	0
44355	Adsorption and dissociation mechanism of toluene on Pd (111) and PdO (101) surface: First principle calculation. Surface Science, 2022, 720, 122051.	0.8	12
44356	First-principles calculations to investigate variation of cationic-ligand LmAl2Ge2 (Lmâ€‰=â€‰Ca, Y, La and Ce). Indian Journal of Physics, 2022, 96, 3151-3159.	0.9	5
44357	Synthesis of Uranium Single Atom from Radioactive Wastewater for Enhanced Water Dissociation and Hydrogen Evolution. Small, 2022, 18, e2107444.	5.2	17
44358	Tetraphenyl Tetrel Molecules and Molecular Crystals: From Structural Properties to Nonlinear Optics. Journal of Physical Chemistry C, 2022, 126, 3713-3726.	1.5	4
44359	First-Principles Calculations of the Hydrolysis Mechanism of Hexagonal Boron Nitride Nanosheets: Implications for Preventing Hydrolytic Degradation. ACS Applied Nano Materials, 0, , .	2.4	1
44360	Successful prediction of the elastic properties of multiphase high entropy alloys in the AlTiVCr-Si system through a novel computational approach. Materialia, 2022, 21, 101365.	1.3	1
44361	Phase transition and enhanced hardness of LaB4 under pressure. Journal of Physics and Chemistry of Solids, 2022, , 110622.	1.9	0
44362	Light-assisted ozone gas-sensing performance of SnO2 nanoparticles: Experimental and theoretical insights. Sensors and Actuators Reports, 2022, 4, 100081.	2.3	3
44363	Simulating and Predicting Adsorption of Organic Pollutants onto Black Phosphorus Nanomaterials. Nanomaterials, 2022, 12, 590.	1.9	4
44364	A theoretical perspective of the ultrafast transient absorption dynamics of <scp>CsPbBr₃</scp>. Journal of Computational Chemistry, 2022, 43, 577-582.	1.5	3
44365	High-capacity NCNT-encapsulated metal NP catalysts on carbonised loofah with dual-reaction centres over Câ€“M bond bridges for Fenton-like degradation of antibiotics. Applied Catalysis B: Environmental, 2022, 307, 121205.	10.8	37
44366	Hydroxylation and molecular adsorption behavior of SnO2 (110) crystal plane. Materials Research Bulletin, 2022, 150, 111787.	2.7	5
44367	A comparative study of the structural, electronic, vibrational, dielectric and elastic properties of the two phases CaAgBi through first-principles calculations. Chemical Physics, 2022, 555, 111449.	0.9	4
44368	Electric field induced Mott transition and bipolar resistive switching in La2Ti2O7-x thin film. Applied Materials Today, 2022, 26, 101395.	2.3	1
44369	Band offset and leakage current in fluorine doped Si/HfO2/SiO2 gate stack of metal oxide semiconductor field effect transistors: An ab initio investigation. Thin Solid Films, 2022, 746, 139116.	0.8	2
44370	Unusual crystal phases of noble metals Ir, Os, and hardness of Ir-Os systems from high throughput density functional calculations. Results in Physics, 2022, 34, 105325.	2.0	1
44371	Band gap shifting of halide perovskite CsCaBr3 from ultra-violet to visible region under pressure for photovoltaic applications. Materials Science and Engineering B: Solid-State Materials for Advanced Technology, 2022, 278, 115645.	1.7	24

#	Article	IF	Citations
44372	Doping-induced structural transformation in the spin-1/2 triangular-lattice antiferromagnet Na2Ba1-xSrxCo(PO4)2. Journal of Alloys and Compounds, 2022, 905, 164147.	2.8	2
44373	High-efficiency ammonia electrosynthesis on self-supported Co2AlO4 nanoarray in neutral media by selective reduction of nitrate. Chemical Engineering Journal, 2022, 435, 135104.	6.6	71
44374	Mechanical properties of tungsten-rhenium, lanthanum and copper doped tungsten-rhenium nanostructures â€“ A DFT study. Materials Science and Engineering B: Solid-State Materials for Advanced Technology, 2022, 278, 115626.	1.7	5
44375	Antiferromagnetism-induced spin splitting in monolayers of layered and non-layered crystals: Symmetry-based analysis and Density Functional Theory calculation. Physica E: Low-Dimensional Systems and Nanostructures, 2022, 139, 115118.	1.3	4
44376	Experimental and DFT investigations of the performance of ZrO2 catalysts modified with Ce, La, Y, Mg, and Ba oxides during methyl stearate ketonization. Applied Surface Science, 2022, 585, 152627.	3.1	5
44377	Effect of aluminum substitution on structural, electronic and dielectric properties of cubic CaCu3Ti4O12 ceramics: A first-principles study. Journal of Physics and Chemistry of Solids, 2022, 164, 110617.	1.9	0
44378	Retarded transport properties of graphene oxide based chiral separation membranes modified with dipeptide. Separation and Purification Technology, 2022, 288, 120642.	3.9	9
44379	Combination of Fe(II)-induced oxygen deficiency and metal doping strategy for construction of high efficiency water oxidation electrocatalysts under industrial-scale current density. Chemical Engineering Journal, 2022, 435, 135048.	6.6	6
44380	The influence of tungsten oxide concentration on a carbon surface for capacitance improvement in energy storage devices: A combined experimental and theoretical study. Journal of Physics and Chemistry of Solids, 2022, 164, 110610.	1.9	2
44381	Oxygen vacancy inducing phase transition during charge storage in MnOx@rGO supercapacitor electrode. Chemical Engineering Journal, 2022, 435, 135103.	6.6	42
44382	Nitrogen incorporated zinc oxide thin film for efficient ethanol detection. Sensors and Actuators B: Chemical, 2022, 358, 131544.	4.0	8
44383	Efficient photocatalytic hydrogen evolution through reverse hydrogen spillover on photoactivated copper-doped mesoporous titania spheres. Applied Materials Today, 2022, 27, 101417.	2.3	2
44384	Immobilisation of diuron herbicide employing smectites. Materials Today Communications, 2022, 31, 103252.	0.9	0
44385	Spherical vs. planar: Steering the electronic communication between Ru nanoparticle and single atom to boost the electrocatalytic hydrogen evolution activity both in acid and alkaline. Applied Catalysis B: Environmental, 2022, 307, 121193.	10.8	36
44386	Theoretical investigation of structural, energetic and magnetic properties of B2 type MnM alloys, DFT and data mining approach. Computational Condensed Matter, 2022, 31, e00656.	0.9	0
44387	The effects of active elements on adhesion strength of SiC/Cu interface in SiC reinforced Cu-based composite: A first-principles investigation. Materials Today Communications, 2022, 31, 103233.	0.9	4
44388	High thermal conductivity of carbon allotropes and its relationship with mechanical properties: A first-principles study. International Journal of Thermal Sciences, 2022, 176, 107481.	2.6	5
44389	Design and analysis of III-V two-dimensional van der Waals heterostructures for ultra-thin solar cells. Applied Surface Science, 2022, 586, 152799.	3.1	16

#	Article	IF	Citations
44390	Role of Pr-Vacancies and O-Interstitials on the Activity and Stability of (Pr_{1â^'x}Ln_x)₂NiO₄ (Ln = La, Nd, Pm, Sm, Gd, Tb, Dy, and) Tj ETQq0 0 0 rgBT /Overlo 168, 124508.	1.3	3
44391	Tunable giant nonlinear optical susceptibility in BaSnO3 quantum wells. Physical Review B, 2021, 104, .	1.1	2
44392	Role of Interfacial Cuâ€ Ions in Polycrystalline Cuâ€CeO 2 : Inâ€Situ Raman, Inâ€situ DRIFT and DFT Studies for Preferential Oxidation of CO in Presence of Excess H 2 **. ChemistrySelect, 2021, 6, 13051-13059.	0.7	7
44393	High Oxideâ€Ion Conductivity in a Hexagonal Perovskiteâ€Related Oxide Ba₇Ta_{3.7}Mo_{1.3}O_{20.15} with Cation Site Preference and Interstitial Oxide Ions. Small, 2022, 18, e2106785.	5.2	21
44394	In situ grown Fe3O4 particle on stainless steel: A highly efficient electrocatalyst for nitrate reduction to ammonia. Nano Research, 2022, 15, 3050-3055.	5.8	108
44395	First-principles investigation on stability and electronic structure of Sc-doped Î¸â€²/Al interface in Alâ^'Cu alloys. Transactions of Nonferrous Metals Society of China, 2021, 31, 3342-3355.	1.7	14
44396	Capturing Individual Hydrogen Bond Strengths in Ices via Periodic Local Vibrational Mode Theory: Beyond the Lattice Energy Picture. Journal of Chemical Theory and Computation, 2022, 18, 562-579.	2.3	17
44397	Edge Effect Promotes Graphene-Confining Single-Atom Coâ€“N₄ and Rhâ€“N₄ for Bifunctional Oxygen Electrocatalysis. Journal of Physical Chemistry C, 2022, 126, 30-39.	1.5	17
44398	Uncovering the Self-Organized Nanowires on Au-Modified Ge(001) Surfaces. Journal of Physical Chemistry C, 2021, 125, 27876-27883.	1.5	4
44399	NMR Response of the Tetrel Bond Donor. Journal of Physical Chemistry C, 2022, 126, 851-865.	1.5	10
44400	Insights into the Mechanism of Methanol Steam Reforming for Hydrogen Production over Niâ€“Cu-Based Catalysts. ACS Catalysis, 2022, 12, 512-526.	5.5	31
44401	Piezoelectricity in hafnia. Nature Communications, 2021, 12, 7301.	5.8	37
44402	Reversal of the magnetoelectric effect at a ferromagnetic metal/ferroelectric interface induced by metal oxidation. Npj Computational Materials, 2021, 7, .	3.5	7
44403	Assessing density functionals for describing methane dissociative chemisorption on Pt(110)-(2Ã—1) surface. Chinese Journal of Chemical Physics, 2021, 34, 883-895.	0.6	2
44404	First-principles calculations on the structural, electronic, magnetic, and elastic properties of (Fe,) Tj ETQq0 0 0 rgBT /Overlock 10 Tf 50 1	1.1	3
44405	Discovery of Two Families of Vsb-Based Compounds with V-Kagome Lattice. Chinese Physics Letters, 2021, 38, 127102.	1.3	14
44406	Intrinsic staggered spin-orbit torque for the electrical control of antiferromagnets: Application to CrI3. Physical Review B, 2021, 104, .	1.1	10
44407	Type-II nodal line fermions in the <mml:math xmlns:mml="http://www.w3.org/1998/Math/MathML"><mml:msub><mml:mi mathvariant="double-struck">Z</mml:mi><mml:mn>2</mml:mn></mml:msub></mml:math> topological semimetals <mml:math xmlns:mml="http://www.w3.org/1998/Math/MathML"><mml:mi>A</mml:mi><mml:msub><mml:mrow><mml:mi mathvariant="normal">V</mml:mi></mml:mrow><mml:mn>6</mml:mn></mml:msub><mml:msub><mml:mrow><mml:mi>Sb</mml:mi>	1.1	8

#	Article	IF	Citations
44408	Modeling of Ferroelectric Oxide Perovskites: From First to Second Principles. Annual Review of Condensed Matter Physics, 2022, 13, 325-364.	5.2	17
44409	Theoretical Investigations of a BN Polymorph with sp2 + sp3 Hybridizations. Crystals, 2021, 11, 1574.	1.0	6
44410	Interfacial Stabilities, Electronic Properties and Interfacial Fracture Mechanism of 6H-SiC Reinforced Copper Matrix Studied by the First Principles Method. Crystals, 2022, 12, 51.	1.0	2
44412	Structural, Elastic and Optoelectronic Properties of Inorganic Cubic Frbx3 (B = Ge, Sn; X = Cl, Br, I) Perovskite: The Density Functional Theory Approach. SSRN Electronic Journal, 0, , .	0.4	0
44413	Surface Spinel and Oxygen Vacancies Enhanced Lithium-Rich Layered Oxides with Excellent Electrochemical Performances. SSRN Electronic Journal, 0, , .	0.4	0
44414	High-Rate and Durable Sulfide-Based All-Solid-State Lithium Battery with <i>in situ</i> Li ₂O Buffering. SSRN Electronic Journal, 0, , .	0.4	0
44415	Study of the Thermal Stability of a Monolayer SnS2 Film on a Graphite Substrate. High Temperature, 2021, 59, 66-72.	0.1	1
44417	The Structural, Lattice Dynamic, Thermodynamic and Mechanical Characterization of Na ₂Mo ₂O ₇ Crystal by First-Principles Calculation. SSRN Electronic Journal, 0, , .	0.4	0
44418	Homologous Nicop@Nifep Heterojunction Array Achieving High-Current Hydrogen Evolution for Alkaline Anion Exchange Membrane Electrolyzers. SSRN Electronic Journal, 0, , .	0.4	0
44419	Electronic Structure of Graphene on Silicon Carbide Intercalated with Silicon and Cobalt Atoms. Physics of the Solid State, 2021, 63, 819-824.	0.2	0
44420	Ti4o7 Regulating Both Zn(Oh)42â€“ and Electrons for Improving Znâ€“Ni Batteries. SSRN Electronic Journal, 0, , .	0.4	0
44421	A Rational Design of Garnet-Type Li7la3zr2o12 with Ultrahigh Moisture Stability. SSRN Electronic Journal, 0, , .	0.4	0
44422	Elucidation of the reaction mechanism on dry reforming of methane in an electric field by in situ DRIFTs. RSC Advances, 2022, 12, 9036-9043.	1.7	15
44423	Accommodation of helium in PuO_{2Â±x} and the role of americium. Physical Chemistry Chemical Physics, 2022, 24, 8245-8250.	1.3	3
44424	Exploring mechanistic routes for light alkane oxidation with an ironâ€“triazolate metalâ€“organic framework. Physical Chemistry Chemical Physics, 2022, 24, 8129-8141.	1.3	6
44425	First Principales Calculation for Generating New Thermal Neutron Scattering Data for Zirconium Hydride. SSRN Electronic Journal, 0, , .	0.4	0
44426	Oxygen-vacancy-rich Fe₃O₄/carbon nanosheets enabling high-attenuation and broadband microwave absorption through the integration of interfacial polarization and charge-separation polarization. Journal of Materials Chemistry A, 2022, 10, 8479-8490.	5.2	26
44427	Promising application of a SiC₂/C₃B heterostructure as a new platform for lithium-ion batteries. Physical Chemistry Chemical Physics, 2022, 24, 6926-6934.	1.3	5

#	Article	IF	Citations
44428	Tunable Dirac states in doping B₂S₃ monolayer. Physical Chemistry Chemical Physics, 2022, , .	1.3	1
44429	Pressure-stabilized MnB₆ that exhibits high-temperature ferromagnetism and high ductility at ambient pressure. Journal of Materials Chemistry C, 2022, 10, 4365-4371.	2.7	3
44431	Cubic-Spinel Agin5s8-Based Thermoelectric Materials: Synthesis, Phonon Transport and Defect Chemistry. SSRN Electronic Journal, 0, , .	0.4	0
44432	Nain(C2o4)(Hpo4)(H2o)5: An Ultraviolet Transparent Nonlinear Optical Oxalate-Phosphate with Large Birefringence. SSRN Electronic Journal, 0, , .	0.4	0
44433	A first-principles study of electronic and optical properties of the tetragonal phase of monolayer ZnS modulated by biaxial strain. RSC Advances, 2022, 12, 6166-6173.	1.7	5
44434	Ultralow work function of the electride Sr₃CrN₃. Physical Chemistry Chemical Physics, 2022, 24, 8854-8858.	1.3	3
44435	Mechanistic insights for electrochemical reduction of CO₂ into hydrocarbon fuels over O-terminated MXenes. Catalysis Science and Technology, 2022, 12, 2223-2231.	2.1	22
44436	Benchmarks of the density functional tight-binding method for redox, protonation and electronic properties of quinones. Physical Chemistry Chemical Physics, 2022, 24, 6742-6756.	1.3	0
44437	Efficient electrocatalytic H₂ evolution mediated by 2D Janus MoSSe transition metal dichalcogenide. Sustainable Energy and Fuels, 2022, 6, 1733-1752.	2.5	14
44438	Tailoring Nanostructured Materials Based on Modified Î“â€“Graphyne Monolayers with AU Heteroatom for Application in Energy Storage Devices: A First Principle Study. SSRN Electronic Journal, 0, , .	0.4	0
44439	Hydride ion intercalation and conduction in the electride Sr₃CrN₃. Journal of Materials Chemistry C, 2022, 10, 6628-6633.	2.7	6
44440	Ab Initio Study of the Effects of Cr on Helium Behaviors in Feâ€“Ycr (Y = 9.38, 12.50 At.%) Austenitic Binary Alloys. SSRN Electronic Journal, 0, , .	0.4	0
44441	H2o2 Formation Mechanisms on the (112) and (310) Facets of Sno2 Via Water Oxidation Reaction with the Participation of Bicarbonate: Dft and Experimental Investigations. SSRN Electronic Journal, 0, , .	0.4	0
44442	Influence of pressure on the electronic energy structure of cadmium sulphide crystal with zincblende structure. Journal of Physical Studies, 2022, 26, .	0.2	0
44443	Characterization of Pertechnetates Atco4: A First-Principles Study. SSRN Electronic Journal, 0, , .	0.4	0
44444	An analysis of Schottky barrier in silicene/Ga₂SeS heterostructures by employing electric field and strain. Physical Chemistry Chemical Physics, 2022, 24, 10210-10221.	1.3	21
44445	Direct Z-scheme WTe₂/InSe van der Waals heterostructure for overall water splitting. Catalysis Science and Technology, 2022, 12, 3272-3280.	2.1	17
44446	In Situ FTIR Spectroscopy Study to Reveal Ga Modified ZSM-5 for Boosting Isobutene Amination. Reaction Chemistry and Engineering, 0, , .	1.9	2

#	Article	IF	Citations
44447	Functionalized few-layer silicene nanosheets: stability, elastic, structural, and electronic properties. Physical Chemistry Chemical Physics, 2022, 24, 8705-8715.	1.3	7
44448	Influence of Carbon on the Formation of Î“ÍÎ“â€² Microstructure and Îš-Phase in the Wc/Co-Ni-Al-W System: Ab Initio Calculations and Experimental Studies. SSRN Electronic Journal, 0, , .	0.4	0
44449	Atomic Structure and Electrical/Ionic Activity of Antiphase Boundary in CH ₃NH ₃PbI ₃. SSRN Electronic Journal, 0, , .	0.4	0
44450	Chemically Anchoring Molybdenum Atoms Onto Micropore-Rich Vn Nanosheet for Boosted Nitrogen Electro-Fixation Via Hydrogen Bonds. SSRN Electronic Journal, 0, , .	0.4	0
44451	The consistent behavior of negative Poisson's ratio with interlayer interactions. Materials Advances, 2022, 3, 4334-4341.	2.6	7
44452	Impact of alkaline-earth doping on electronic properties of the photovoltaic perovskite CsSnI₃: insights from a DFT perspective. Dalton Transactions, 2022, 51, 6607-6621.	1.6	7
44453	Synergistic effects of bithiophene ammonium salt for high-performance perovskite solar cells. Journal of Materials Chemistry A, 2022, 10, 9971-9980.	5.2	14
44454	Theoretical exploration of mechanical, electronic structure and optical properties of aluminium based double halide perovskite. RSC Advances, 2022, 12, 10209-10218.	1.7	11
44455	Exchange-Correlation and Spin-Orbit Coupling Effects in 18-Electrons Transparent Conductors Half-Heusler: Ab-Initio Study. SSRN Electronic Journal, 0, , .	0.4	0
44456	Cu Atoms Induce a New Reconstruction in the Mnga(001) Surface: An Ab-Initio Study. SSRN Electronic Journal, 0, , .	0.4	0
44457	Circumventing the scaling relationship on bimetallic monolayer electrocatalysts for selective CO₂ reduction. Chemical Science, 2022, 13, 3880-3887.	3.7	9
44458	A structure determination protocol based on combined analysis of 3D-ED data, powder XRD data, solid-state NMR data and DFT-D calculations reveals the structure of a new polymorph of<scp>l</scp>-tyrosine. Chemical Science, 2022, 13, 5277-5288.	3.7	15
44459	Unraveling the Phase Stability and Physical Nature of Modulated Martensite in Ni ₂Mn _{1.5}In _{0.5} Alloys by First-Principles Calculations. SSRN Electronic Journal, 0, , .	0.4	0
44460	Dft Insights into Hydrodesulfurization Mechanism of 2-Methylthiophene Catalyzed by Ni2p. SSRN Electronic Journal, 0, , .	0.4	0
44461	New functionalisation reactions of graphitic carbon nitrides: Computational and experimental studies. Journal of Chemical Research, 2022, 46, 174751982110738.	0.6	1
44462	Origin of the enhanced edge optical transition in transition metal dichalcogenide flakes. Journal of Materials Chemistry C, 2022, 10, 5303-5310.	2.7	1
44463	Cation substitution effects on the structural, electronic and sun-light absorption features of all-inorganic halide perovskites. Inorganic Chemistry Frontiers, 2022, 9, 1337-1353.	3.0	2
44464	Infrared nonlinear optical sulfide CsCd₄In₅S₁₂ exhibiting large second harmonic generation response. Journal of Materials Chemistry C, 2022, 10, 5183-5189.	2.7	10

#	Article	IF	Citations
44465	A pre-reaction suppressing strategy for Î±-Ga₂O₃ halide vapor pressure epitaxy using asymmetric precursor gas flow. CrystEngComm, 2022, 24, 3049-3056.	1.3	4
44466	Effective medium theory for bcc metals: electronically non-adiabatic H atom scattering in full dimensions. Physical Chemistry Chemical Physics, 2022, 24, 8738-8748.	1.3	5
44467	Towards a computational understanding of water oxidation at graphene-bound Mn_xO_y and Mn_xO_yM²⁺ particles. Sustainable Energy and Fuels, 0, , .	2.5	0
44468	Improving the performance of silicon monoxide anodes via tuning a multiple pre-doping system: a first-principles study. Physical Chemistry Chemical Physics, 2022, 24, 7405-7414.	1.3	1
44469	Mechanism of High Magnetic Field Effect on the D03-L12 Phase Transition in Fe-Ga Alloys. SSRN Electronic Journal, 0, , .	0.4	0
44470	Tuning the Activity and Selectivity of Nitrogen Reduction Reaction on Double-Atom Catalysts by B Doping: A Density Functional Theory Study. SSRN Electronic Journal, 0, , .	0.4	0
44471	Effects of vibrational and rotational excitations on dissociative chemisorption dynamics of N2 on Fe(111). Chinese Journal of Chemical Physics, 2022, 35, 443-450.	0.6	2
44472	Phase Transition and Electronic Properties of Co-As Binary Compounds at High Pressures. SSRN Electronic Journal, 0, , .	0.4	0
44473	Dft Combined with Xanes to Investigate the Sulfur Fixation Mechanisms of H2s on Different Cao Surfaces. SSRN Electronic Journal, 0, , .	0.4	0
44474	The effect of electronâ€“phonon and electron-impurity scattering on the electronic transport properties of silicon/germanium superlattices. Journal of Materials Chemistry C, 2022, 10, 7525-7542.	2.7	3
44475	Ultrahigh-stability SnOX (X = S, Se) nanotubes with a built-in electric field as a highly promising platform for sensing NH₃, NO and NO₂: a theoretical investigation. Journal of Materials Chemistry A, 2022, 10, 7948-7959.	5.2	4
44476	Role of Redox Reactions Involving Interfacial Oxygen Migration in Ignition of Nanolayered Al/A-Al2ox/Cuo Energetic Composite. SSRN Electronic Journal, 0, , .	0.4	0
44477	Design of 3D topological nodal-net porous carbon for sodium-ion battery anodes. Journal of Materials Chemistry A, 2022, 10, 7754-7763.	5.2	15
44478	Doped Metals IR and Pt on Tio2 in Improving Activity Toward Oxidative Coupling of Methane: Activation Oxygen Species and Reaction Network. SSRN Electronic Journal, 0, , .	0.4	0
44479	Rashba spin splitting and anomalous spin textures in the bulk ferroelectric oxide perovskite KIO₃. Materials Advances, 2022, 3, 4170-4178.	2.6	10
44480	Identification and manipulation of dynamic active site deficiency-induced competing reactions in electrocatalytic oxidation processes. Energy and Environmental Science, 2022, 15, 2386-2396.	15.6	71
44481	Fabricating Ga doped and MgO embedded nanomaterials for sorption-enhanced steam reforming of methanol. Journal of Materials Chemistry A, 2022, 10, 7300-7313.	5.2	14
44482	Prediction the Structural, Electronic, Elastic and Dynamical Properties of Lialge and Liinge Half-Heusler Crystals by Density Functional Theory. SSRN Electronic Journal, 0, , .	0.4	0

#	Article	IF	Citations
44483	Two-dimensional penta-like PdPSe with a puckered pentagonal structure: a first-principles study. Physical Chemistry Chemical Physics, 2022, 24, 9990-9997.	1.3	53
44484	Lead-free layered Aurivillius-type Sn-based halide perovskite Ba₂X₂[Cs_{nâ^'1}Sn_nX_{3n+1}] (X = I/Br/Cl) with an optimal band gap of â^¼1.26 eV and theoretical efficiency beyond 27% for photovoltaics. Journal of Materials Chemistry A, 2022, 10, 10682-10691.	5.2	1
44485	Enhanced Degradation of Phenol by Catalytic Wet Oxidation Over Novel Ceria Promoted Mesoporous Silica Supported Ru-Fe3o4 Catalyst: A Combined Experimental and Dft Study. SSRN Electronic Journal, 0, , .	0.4	0
44486	Ultrahigh mechanical flexibility induced superior piezoelectricity of InSeBr-type 2D Janus materials. Physical Chemistry Chemical Physics, 2022, 24, 8371-8377.	1.3	6
44487	The quantum size and spinâ€“orbit coupling effects in BiVO₄ with several atomic layers studied by density functional theory. Physical Chemistry Chemical Physics, 2022, 24, 10168-10174.	1.3	3
44488	Exploring a novel two-dimensional metallic Y₄C₃ sheet applied as an anode material for sodium-ion batteries. Physical Chemistry Chemical Physics, 2022, 24, 8859-8866.	1.3	7
44489	First-row transition metal embedded pyrazine-based graphynes as high-performance single atom catalysts for the CO₂reduction reaction. Journal of Materials Chemistry A, 2022, 10, 9048-9058.	5.2	21
44490	Single-Atom Metal Tuned Sulfur Vacancy for Efficient H2 Activation and Hydrogen Evolution Reaction on Mos2 Basal Plane. SSRN Electronic Journal, 0, , .	0.4	0
44491	Strain modulation of the exciton anisotropy and carrier lifetime in black phosphorene. Physical Chemistry Chemical Physics, 2022, , .	1.3	1
44492	Engineering metalâ€“metal oxide surfaces for high-performance oxygen reduction on Agâ€“Mn electrocatalysts. Energy and Environmental Science, 2022, 15, 1611-1629.	15.6	22
44493	A first-principles investigation of pressure induced topological phase transitions in half-Heusler AgSrBi. Materials Advances, 2022, 3, 3938-3944.	2.6	6
44494	Hydrogen evolution reaction mechanism on Ti₃C₂ MXene revealed by in situ/operando Raman spectroelectrochemistry. Nanoscale, 2022, 14, 5068-5078.	2.8	20
44495	Solar driven efficient direct conversion of methane to multicarbon oxygenates. Journal of Materials Chemistry A, 2022, 10, 7856-7868.	5.2	7
44496	Theoretical study of two-dimensional tetragonal transition metal chalcogenides and the potassium derivatives. Sustainable Energy and Fuels, 2022, 6, 1770-1779.	2.5	4
44497	A Perovskite-Based Sns/Cspbbr3ÂHeterostructure Used for SuperiorÂOptical Absorption. SSRN Electronic Journal, 0, , .	0.4	0
44498	Water-oxygen interaction on marcasite (1 0 1) surface: DFT calculation. International Journal of Mining Science and Technology, 2022, 32, 191-199.	4.6	18
44499	Controllable Fabrication of Atomic Dispersed Low-Coordination Nickel-Nitrogen Sites for Highly Efficient Electrocatalytic Co2 Reduction. SSRN Electronic Journal, 0, , .	0.4	0
44500	A new aggregation induced emission enhancement (AIEE) dye which self-assembles to panchromatic fluorescent flowers and has application in sensing dichromate ions. Soft Matter, 2022, 18, 3019-3030.	1.2	5

#	Article	IF	Citations
44501	First Principles and Experimental Study on the Atomic Formation of MnSâ€“Al₂SiO₅ Inclusions in Steel. ISIJ International, 2022, 62, 1126-1135.	0.6	7
44502	Microscopic Functionality of Fen4 Sites in Polymeric Carbon Nitride for Efficient H2s Oxidation. SSRN Electronic Journal, 0, , .	0.4	0
44503	Hybridized Heterostructure of Cos and Mos2 Nanoparticles for Highly-Efficient and Robust Bifunctional Water Electrolysis. SSRN Electronic Journal, 0, , .	0.4	0
44504	Bi catalysts supported on GaN nanowires toward efficient photoelectrochemical CO₂ reduction. Journal of Materials Chemistry A, 2022, 10, 7869-7877.	5.2	18
44505	RbSnX₃ (X = Cl, Br, I): promising lead-free metal halide perovskites for photovoltaics and optoelectronics. RSC Advances, 2022, 12, 7497-7505.	1.7	39
44507	Magnetic Properties of the Gas Molecules Adsorbed on the Fepc Sheet. SSRN Electronic Journal, 0, , .	0.4	0
44508	Effect of oxygen termination on the interaction of first row transition metals with M₂C MXenes and the feasibility of single-atom catalysts. Journal of Materials Chemistry A, 2022, 10, 8846-8855.	5.2	18
44509	Study on the Adsorption Behavior of Tin from Waste Liquid Crystal Display Using a Novel Macroporous Silica-Based Adsorbent in One-Step Separation. SSRN Electronic Journal, 0, , .	0.4	0
44510	Predicting the Optimal Chemical Composition of Functionalized Carbon Catalysts Towards Oxidative Dehydrogenation of Ethanol to Acetaldehyde. SSRN Electronic Journal, 0, , .	0.4	0
44511	Theoretical design and study of two-dimensional organic ferroelectric monolayer based on cyclobutene-1,2-dicarboxylic acid. Wuli Xuebao/Acta Physica Sinica, 2022, 71, 067302.	0.2	1
44512	Exploiting Weak Magnetic Anisotropy on the Stability Ofspin-Spirals and Skyrmions Lattice in Vx2(X=S,) Tj ETQq0 0 0 rgBT /Overlock 10	0.4	0
44513	Partial reduction of NO to N₂O on Cu{311}: role of intermediate N₂O₂. Catalysis Science and Technology, 2022, 12, 2793-2803.	2.1	2
44514	Ultrafast Photoenhanced Extraction of Uranium by Cu2o/Cuo Heterojunction from Seawater. SSRN Electronic Journal, 0, , .	0.4	0
44515	Defect-Mediated Work Function Regulation in Graphene Film for High-Performing Triboelectric Nanogenerators. SSRN Electronic Journal, 0, , .	0.4	0
44516	The Dynamical Stability, Electronic, Elastic Properties and Ideal Strength of Diamond-Like Cubic B2cn: A First-Principles Study. SSRN Electronic Journal, 0, , .	0.4	0
44517	Tuning the chemoselectivity of the Pd-catalysed hydrogenation of pyridinecarbonitriles: an efficient and simple method for preparing pyridyl- or piperidylmethylamines. Catalysis Science and Technology, 2022, 12, 2634-2648.	2.1	4
44518	Pressure-stabilized polymerization of nitrogen in manganese nitrides at ambient and high pressures. Physical Chemistry Chemical Physics, 2022, 24, 5738-5747.	1.3	8
44519	Metal dimers embedded vertically in defect-graphene as gas sensors: a first-principles study. Physical Chemistry Chemical Physics, 2022, 24, 9842-9847.	1.3	5

#	Article	IF	Citations
44520	Thgraphene: a novel two-dimensional carbon allotrope as a potential multifunctional material for electrochemical water splitting and potassium-ion batteries. Journal of Materials Chemistry A, 2022, 10, 9848-9857.	5.2	20
44521	Strain modulation in small molecule physisorption in two dimensions: LEED structure analysis and DFT modeling of the system. Physical Chemistry Chemical Physics, 2022, , .	1.3	0
44522	Directional Utilization Disorder Charge Via In-Plane Driving Force of Functionalized Graphite Carbon Nitride for the Robust Photocatalytic Degradation of Fluoroquinolone. SSRN Electronic Journal, 0, , .	0.4	0
44523	The doping effects on antibonding states and carriers of two-dimensional PC6. Physical Chemistry Chemical Physics, 2022, , .	1.3	2
44524	Dft Insights into Hydrodesulfurization Mechanism of 2-Methylthiophene Catalyzed by Ni2p. SSRN Electronic Journal, 0, , .	0.4	0
44525	Single-, double-, and triple-atom catalysts on graphene-like C₂N enable electrocatalytic nitrogen reduction: insight from first principles. Catalysis Science and Technology, 2022, 12, 2604-2617.	2.1	15
44526	The Density Functional Theory Study of Substitution Effect in Antiferromagnetic Usn0.5sb1.5. SSRN Electronic Journal, 0, , .	0.4	0
44527	Computational Screening of Single Transition Metal Atom Embedded in Nitrogen Doped Graphene for Ch4 Detection. SSRN Electronic Journal, 0, , .	0.4	0
44528	First principle investigation of Niobium (Nb) doped MgO. Materials Today: Proceedings, 2022, 51, 2091-2095.	0.9	1
44529	Design and Analysis of Iii-V Two-Dimensional Van Der Waals Heterostructures for Ultra-Thin Solar Cells. SSRN Electronic Journal, 0, , .	0.4	0
44530	Tailoring Nanostructured Materials Based on Modified Î“â€“Graphyne Monolayers with AU Heteroatom for Application in Energy Storage Devices: A First Principle Study. SSRN Electronic Journal, 0, , .	0.4	0
44531	Strain Induced Effects on the Electronic and Phononic Properties of 2h and 1t â€² Monolayer Mos 2. SSRN Electronic Journal, 0, , .	0.4	1
44532	Surface morphology evolution of cobalt nanoparticles induced by hydrogen adsorption: a theoretical study. New Journal of Chemistry, 2022, 46, 9272-9279.	1.4	2
44533	Controllable Repairing the Single Vacancies of Bc3 Monolayer Using Co and Bf Molecules: A First-Principles Study. SSRN Electronic Journal, 0, , .	0.4	0
44534	Multi-component crystals containing urea: mechanochemical synthesis and characterization by ³⁵Cl solid-state NMR spectroscopy and DFT calculations. CrystEngComm, 2022, 24, 2626-2641.	1.3	7
44535	First-principles calculations of bulk, surface and interfacial phases and properties of silicon graphite composites as anode materials for lithium ion batteries. Physical Chemistry Chemical Physics, 2022, , .	1.3	4
44536	Structural, Electronic, and Mechanical Properties of D0c Ru-Based Intermetallic Alloys: An Ab-Initio Study. SSRN Electronic Journal, 0, , .	0.4	0
44537	Experimental and Theoretical Insights on the O Ptical and Morphological Properties of Germanium Oxide Thin Films Deposited Via Rf Magnetron Sputtering. SSRN Electronic Journal, 0, , .	0.4	0

#	Article	IF	Citations
44538	Investigation of W/Mo Co-Doping with Multiple Concentrations in Photocatalyst Bivo4ÂBy First-Principles Calculations. SSRN Electronic Journal, 0, , .	0.4	0
44539	Homologous NiCoP@NiFeP heterojunction array achieving high-current hydrogen evolution for alkaline anion exchange membrane electrolyzers. Journal of Materials Chemistry A, 2022, 10, 10209-10218.	5.2	24
44540	Experimental and Theoretical Insight into Dsscs Mechanism Influenced by Different Doping Metal Ions. SSRN Electronic Journal, 0, , .	0.4	0
44541	Effects of adatom species on the structure, stability, and work function of adatom-Î±-borophene nanocomposites. Physical Chemistry Chemical Physics, 2022, 24, 8923-8939.	1.3	4
44542	Light-Matter Interaction in Tungsten Sulfide-Based Janus Monolayers: A First-Principles Study. SSRN Electronic Journal, 0, , .	0.4	0
44543	Theoretical insights into dual-atom catalysts for the oxygen reduction reaction: the crucial role of orbital polarization. Journal of Materials Chemistry A, 2022, 10, 9150-9160.	5.2	25
44544	Exploring a silicene monolayer as a promising sensor platform to detect and capture NO and CO gas. RSC Advances, 2022, 12, 9828-9835.	1.7	12
44545	A computational study of direct CO₂ hydrogenation to methanol on Pd surfaces. Physical Chemistry Chemical Physics, 2022, 24, 9360-9373.	1.3	7
44546	Pressure tuned incommensurability and guest structure transition in compressed scandium from machine learning atomic simulation. Physical Chemistry Chemical Physics, 2022, 24, 7007-7013.	1.3	3
44547	XMCD and ab initio study of interface-engineered ultrathin Ru/Co/W/Ru films with perpendicular magnetic anisotropy and strong Dzyaloshinskiiâ€“Moriya interaction. Physical Chemistry Chemical Physics, 2022, 24, 8225-8232.	1.3	3
44548	Hybrid density functional study on band structure engineering of ZnS(110) surface by anionâ€“cation codoping for overall water splitting. New Journal of Chemistry, 0, , .	1.4	2
44549	Research on Interface Bonding Properties of Tialsin/Wc-Co Doped with Graphene. SSRN Electronic Journal, 0, , .	0.4	0
44550	Carbide coating on nickel to enhance the stability of supported metal nanoclusters. Nanoscale, 2022, 14, 3589-3598.	2.8	2
44551	A Pt/SnO₂/rGO interface more capable of converting ethanol to CO₂ in ethanol electro-oxidation: a detailed experimental/DFT study. Journal of Materials Chemistry A, 2022, 10, 10150-10161.	5.2	11
44552	Effects of Alloying Elements on the Interfacial Segregation of Bismuth in Tin-Based Solders. SSRN Electronic Journal, 0, , .	0.4	0
44553	Favorable photocatalytic properties of a GeS/GeS heterostructure by combining parallel and vertical electric fields: a theoretical study. Journal of Materials Chemistry C, 0, , .	2.7	0
44554	Molecular Dopant Induced Growth of Black Phase Cs _xFA _(1-x)PbI ₃ for Highly Efficient and Stable Perovskite Solar Cells. SSRN Electronic Journal, 0, , .	0.4	0
44555	Radial and Axial Vibration Modes of Graphyne Nanotubes. SSRN Electronic Journal, 0, , .	0.4	0

#	Article	IF	Citations
44556	On the Nature of Planar Defects in Transition Metal Diboride Line Compounds. SSRN Electronic Journal, 0, , .	0.4	0
44557	Self-limiting nitrogen/hydrogen plasma radical chemistry in plasma-enhanced atomic layer deposition of cobalt. Nanoscale, 2022, 14, 4712-4725.	2.8	5
44558	Origin of multiple voltage plateaus in P2-type sodium layered oxides. Materials Horizons, 2022, 9, 1460-1467.	6.4	5
44559	Synthesis of Ultrathin Aupt Alloy Porous Nanowires with AbundantÂ Electrocatalytic Active Sites for Excellent Electrocatalysts. SSRN Electronic Journal, 0, , .	0.4	0
44560	Edge-sharing BO₄ tetrahedra and penta-coordinated silicon in the high-pressure modification of NaBSi₃O₈. Inorganic Chemistry Frontiers, 2022, 9, 1735-1742.	3.0	6
44561	Transition-Metal Single Atom Catalyst Embedded in C2n for Toxic-Gas Reduction Reaction and Selective Gas-Sensing Application: Atomic-Scale Study. SSRN Electronic Journal, 0, , .	0.4	1
44562	Correlated organicâ€“inorganic motion enhances stability and charge carrier lifetime in mixed halide perovskites. Nanoscale, 2022, 14, 4644-4653.	2.8	18
44563	The Role of Spin-Orbit Coupling on the Physical and Superconducting Properties of the Ir-Rich Cubic Laves Superconductors Air 2 (a= Y, Lu and T). SSRN Electronic Journal, 0, , .	0.4	0
44564	Structural Diversity and Unusual Valence States in Compressed Na-Hg System. SSRN Electronic Journal, 0, , .	0.4	0
44565	The Effect of Sr composition on the microstructure and mechanical properties of Al-Si-Zn filler for the brazing of AA6061. Materials Research Express, 2022, 9, 026529.	0.8	0
44566	The Stability and Electronic Structure of Cu(200)/AuCu(200) Interface: An Insight from First-Principle Calculation. Materials, 2022, 15, 1506.	1.3	4
44567	Unveiling the Bonding Nature of C3 Intermediates in the CO₂ Reduction Reaction through the Oxygen-Deficient Cu₂O(110) Surfaceâ€A DFT Study. Journal of Physical Chemistry C, 2022, 126, 5502-5512.	1.5	11
44568	High-Field Magnetoelectric and Spin-Phonon Coupling in Multiferroic (NH₄)₂[FeCl₅Â·(H₂O)]. Inorganic Chemistry, 2022, 61, 3434-3442.	1.9	3
44569	Modeling Electronic Response Properties with an Explicit-Electron Machine Learning Potential. Journal of Chemical Theory and Computation, 2022, 18, 1672-1691.	2.3	10
44570	Real-Time Modulation of Hydrogen Evolution Activity of Graphene Electrodes Using Mechanical Strain. ACS Applied Materials & Interfaces, 2022, 14, 10691-10700.	4.0	2
44571	Physical and Superconducting Properties of Chiral Noncentrosymmetric TaRh₂B₂ and NbRh₂B₂: A Comprehensive DFT Study. ACS Applied Electronic Materials, 2022, 4, 1143-1152.	2.0	8
44572	First-principles database for fitting a machine-learning silicon interatomic force field. MRS Advances, 2022, 7, 39-47.	0.5	0
44573	Computational Design of Gas Sensors Based on V3S4 Monolayer. Nanomaterials, 2022, 12, 774.	1.9	7

#	Article	IF	Citations
44574	Redox-mediated electrosynthesis of ethylene oxide from CO2 and water. Nature Catalysis, 2022, 5, 185-192.	16.1	40
44575	Electronic phase transition, spin filtering effect, and spin Seebeck effect in 2D high-spin-polarized VSi2X4 (X = N, P, As). Applied Physics Letters, 2022, 120, .	1.5	31
44576	A Study on the Properties of Transition Metal Nitride Coating Materials for the Recovery of Tungsten and Rare Metals. , 2022, 31, 46-55.		0
44577	Unified picture for the pressure-controlled band gap in inorganic halide perovskites: Role of strain-phonon and phonon-phonon couplings. Physical Review B, 2022, 105, .	1.1	1
44579	Effect of Nonequilibrium Transient Electronic Structures on Lattice Stability in Metals: Density Functional Theory Calculations. Frontiers in Physics, 2022, 10, .	1.0	1
44580	Thermodynamic Modeling of the Ge-X (X = As, Se, S, P) Systems. Journal of Electronic Materials, 2022, 51, 2114-2130.	1.0	3
44581	Engineering Steam Induced Surface Oxygen Vacancy onto Niâ€“Fe Bimetallic Nanocomposite for CO₂ Electroreduction. Small, 2022, 18, e2108034.	5.2	20
44582	Designing light-element materials with large effective spin-orbit coupling. Nature Communications, 2022, 13, 919.	5.8	26
44583	Optoelectronic properties of Ag2S/graphene and FeS2/graphene nanostructures and interfaces: A density functional study including dispersion forces. Journal of Materials Research, 2022, 37, 1047-1058.	1.2	2
44584	Giant magnetoresistance, Fermi-surface topology, Shoenberg effect, and vanishing quantum oscillations in the type-II Dirac semimetal candidates <mml:math xmlns:mml="http://www.w3.org/1998/Math/MathML"><mml:msub><mml:mi>MoSi</mml:mi><mml:mn>2</mml:mn></mml:msub></mml and <mml:math xmlns:mml="http://www.w3.org/1998/Math/MathML"><mml:msub><mml:mi>WSi</mml:mi><mml:mn>2</mml:mn></mml:msub></mml Physical Review B, 2022, 105, .	1.1	8
44585	Modelling of Electron and Thermal Transport in Quasi-Fractal Carbon Nitride Nanoribbons. Fractal and Fractional, 2022, 6, 115.	1.6	3
44586	Ferroelectric Properties of KNbO3 Doped with Na : First-Principles Calculations. Journal of Physics: Conference Series, 2022, 2209, 012003.	0.3	2
44587	Ground-state properties of the narrowest zigzag graphene nanoribbon from quantum Monte Carlo and comparison with density functional theory. Journal of Chemical Physics, 2022, 156, 084112.	1.2	4
44588	Strainâ€Plasmonic Coupled Broadband Photodetector Based on Monolayer MoS₂. Small, 2022, 18, e2107104.	5.2	25
44589	Niâ€“Zn Dual Sites Switch the CO₂ Hydrogenation Selectivity via Tuning of the d-Band Center. ACS Catalysis, 2022, 12, 3346-3356.	5.5	36
44590	Trends in Formic Acid Electro-Oxidation on Transition Metals Alloyed with Platinum and Palladium. Journal of Physical Chemistry C, 2022, 126, 4374-4390.	1.5	8
44591	Electrospun V₂O₃@Carbon Nanofibers as a Flexible and Binder-Free Cathode for Highly Stable Aqueous Zn-Ion Full Batteries. ACS Applied Energy Materials, 2022, 5, 3525-3535.	2.5	27
44592	Pressureâ€induced enhancement of mechanical performance in ZrC system. International Journal of Quantum Chemistry, 0, , .	1.0	0

#	Article	IF	Citations
44593	Outsideâ€in Nanostructure Fabricated on LiCoO₂ Surface for Highâ€Voltage Lithiumâ€Ion Batteries. Advanced Science, 2022, 9, e2104841.	5.6	51
44594	Anisotropic electrical properties of aligned PtSe2 nanoribbon arrays grown by a pre-patterned selective selenization process. Nano Research, 0, , 1.	5.8	1
44595	Pressure-induced phase transitions and mechanical properties of insensitive high explosive 1,1-diamino-2,2-dinitroethylene. Zeitschrift Fur Naturforschung - Section B Journal of Chemical Sciences, 2022, 77, 131-140.	0.3	2
44596	Acid anion electrolyte effects on platinum for oxygen and hydrogen electrocatalysis. Communications Chemistry, 2022, 5, .	2.0	48
44597	Ab-initio DFT Calculations on Elastic Coeï¬ƒcients, (001) Surface Energy, Stability Limit of Pure Metals and Separation Energy of Bimetal Interface. Zairyo/Journal of the Society of Materials Science, Japan, 2022, 71, 127-134.	0.1	2
44598	Ð¡Ñ‚ÑƒÐºÑƒÑ€Ð¸ Ð°Ð´ÑÐ¾Ñ€Ð±Ð¾Ð²Ð°Ð½Ð¸Ñ… Ñˆ Ð°Ñ€Ñ––Ð² Cl Ð½Ð° Ð¿Ð¾Ð²ÐµÑ…Ð½Ñ– Ag(111). Ukrainian Journa	0.1	0
44599	Synthesis of cobalt single atom catalyst by a solid-state transformation strategy for direct C-C cross-coupling of primary and secondary alcohols. Nano Research, 2022, 15, 4023-4031.	5.8	16
44600	Investigation of Atomic Layer Futuristic Memory Devices of Binary Chalcogenides WX₂ (X) Tj ETQq1 1 0.784314 rgBT /O		0
44601	High-pressure <mml:math xmlns:mml="http://www.w3.org/1998/Math/MathML"><mml:mrow><mml:msub><mml:mi>Na</mml:mi><mml:mn>3</mml:mn></mml: <mml:math		

#	Article	IF	Citations
44611	Curly-Packed Structure Polymers for High-Temperature Capacitive Energy Storage. Chemistry of Materials, 2022, 34, 2333-2341.	3.2	25
44612	Engineering Pore Walls of Mesoporous Tungsten Oxides via Ce Doping for the Development of High-Performance Smart Gas Sensors. Chemistry of Materials, 2022, 34, 2321-2332.	3.2	18
44613	The Important Role of Optical Absorption in Determining the Efficiency of Intermediate Band Solar Cells and a Design Principle for Perovskite Doping. Journal of Physical Chemistry Letters, 2022, 13, 2012-2018.	2.1	7
44614	Unusual Properties of Hydrogen-Bonded Ferroelectrics: The Case of Cobalt Formate. Physical Review Letters, 2022, 128, 077601.	2.9	6
44615	First-Principles Investigations of the Physical Properties of Experimentally Feasible Novel Aluminum Nitride Polytypes. Crystal Growth and Design, 2022, 22, 2342-2353.	1.4	3
44616	Metal-Coordinating Single-Boron Sites Confined in Antiperovskite Borides for N₂-to-NH₃ Catalytic Conversion. ACS Catalysis, 2022, 12, 2967-2978.	5.5	11
44617	Direct Growth of Magnetic Non-van der Waals Cr₂X₃(X = S, Se, and Te) on SiO₂/Si Substrates through the Promotion of KOH. Chemistry of Materials, 2022, 34, 2342-2351.	3.2	11
44618	Engineering Isolated S Vacancies over 2D MoS₂ Basal Planes for Catalytic Hydrogen Evolution. ACS Applied Nano Materials, 2022, 5, 3521-3530.	2.4	14
44619	Thermal conductivity of two stable bilayer phosphorene stackings: A computation study. Journal of Applied Physics, 2022, 131, 075101.	1.1	0
44620	Competition between Ta-Ta and Te-Te bonding leading to the commensurate charge density wave in <mml:math xmlns:mml="http://www.w3.org/1998/Math/MathML"><mml:mrow><mml:mi>Ta</mml:mi><mml:msub><mml:mi>Te</mml:mi><mml:mi>m</mml:mi> Physical Review B, 2022, 105, .	1.1	6
44621	Theoretical investigations on the evolution of ordering in Niâ€“Mo-based alloys. Transactions of the Indian Institute of Metals, 2022, 75, 949-957.	0.7	0
44622	Effect of Doped Metals Rh, Pd, and Cu over the IrO₂(110) Surface: Improving C₂ Selectivity during Oxidative Coupling of Methane. Journal of Physical Chemistry C, 2022, 126, 4306-4318.	1.5	7
44623	LModeA-nano: A PyMOL Plugin for Calculating Bond Strength in Solids, Surfaces, and Molecules via Local Vibrational Mode Analysis. Journal of Chemical Theory and Computation, 2022, 18, 1821-1837.	2.3	16
44624	A Stable Cu(I)-Based Ultramicroporous NKMOF-8-Br with High CH₄ Uptake for Efficient Separation of CH₄/N₂ Mixtures. Journal of Chemical & Engineering Data, 2022, 67, 1654-1662.	1.0	6
44625	Understanding Lithium Local Environments in LiMn_{0.5}Ni_{0.5}O₂ Cathodes: A DFT-Supported ⁶Li Solid-State NMR Study. Journal of Physical Chemistry C, 2022, 126, 4276-4285.	1.5	2
44626	Two-Dimensional Bismuthene Nanosheets for Selective Detection of Toxic Gases. ACS Applied Nano Materials, 2022, 5, 2984-2993.	2.4	29
44627	First-Principles Calculations to Investigate the Mechanical Structure and Optical Properties of Lead Halide Perovskite CH3NH3PbI3. Advances in Condensed Matter Physics, 2022, 2022, 1-9.	0.4	4
44628	N-doped MoS2 via assembly transfer on an elastomeric substrate for high-photoresponsivity, air-stable and stretchable photodetector. Nano Research, 2022, 15, 9866-9874.	5.8	8

#	Article	IF	Citations
44629	First-principles calculations of terahertz dielectric and thermal properties of 3C-SiC. , 2022, , .		0
44630	Highâ€Performance Monolayer SiMeâ€Graphene nâ€Type Fieldâ€Effect Transistors with Low Supply Voltage and High Onâ€State Current in Subâ€5 nm Gate Length. Advanced Electronic Materials, 0, , 2101359.	2.6	0
44631	Effects of local bonding between solute atoms and vacancy on formation of nanoclusters in Al-Mg-Si alloys. Keikinzoku/Journal of Japan Institute of Light Metals, 2022, 72, 47-53.	0.1	0
44632	Prospect of DFT Utilization in Polymer-Graphene Composites for Electromagnetic Interference Shielding Application: A Review. Polymers, 2022, 14, 704.	2.0	8
44633	Graph-based discovery and analysis of atomic-scale one-dimensional materials. National Science Review, 2022, 9, .	4.6	5
44634	Enhanced valley splitting of WSe2 in twisted van der Waals WSe2/CrI3 heterostructures. Npj Computational Materials, 2022, 8, .	3.5	13
44635	Pressure-induced phase transition and increase of oxygen-iodine coordination in magnesium iodate. Physical Review B, 2022, 105, .	1.1	9
44636	Energy-gap driven low-temperature magnetic and transport properties in<mml:math xmlns:mml="http://www.w3.org/1998/Math/MathML"><mml:mrow><mml:msub><mml:mi mathvariant="normal">Cr</mml:mi><mml:mrow><mml:mn>1</mml:mn><mml:mo>/</mml:mo><mml:mn>3</mml:mn></mml:mrow><mml:mi mathvariant="normal">S</mml:mi><mml:mn>2</mml:mn></mml:msub><mml:mspace width="4pt" /><mml:mi>M</mml:mi></mml:mrow></mml:math> (M = Nb, Ta). Physical Review B, 2022, 105, .	1.1	4
44637	Spinâ€“orbit coupling in buckled monolayer nitrogene. Scientific Reports, 2022, 12, 3201.	1.6	3
44638	Self-assembled monolayers direct a LiF-rich interphase toward long-life lithium metal batteries. Science, 2022, 375, 739-745.	6.0	368
44639	Heterostructured Metallic 1T-VSe₂/Ti₃C₂T_x MXene Nanosheets for Energy Storage. ACS Applied Nano Materials, 2022, 5, 4423-4436.	2.4	21
44640	High Energy Density Polymeric Nitrogen Nanotubes inside Carbon Nanotubes. Chinese Physics Letters, 2022, 39, 036101.	1.3	8
44641	Hirshfeld atom refinement based on projector augmented wave densities with periodic boundary conditions. IUCrJ, 2022, 9, 286-297.	1.0	9
44642	<mml:math xmlns:mml="http://www.w3.org/1998/Math/MathML"><mml:msup><mml:mrow><mml:mi>Fe</mml:mi></mml:mrow><mml:mrow><mml:mn>4</mml:mn></mml:mrow><mml:n -hosting carbon phases in the deep Earth. Physical Review B, 2022, 105, .	1.1	4
44643	Strong renormalization of Ba vibrations in thermoelectric type-IX clathrate <mml:math xmlns:mml="http://www.w3.org/1998/Math/MathML"><mml:mrow><mml:msub><mml:mi>Ba</mml:mi><mml:mn>24</mml:mn></mml:msub><mml:mn>2</mml:mn></mml:mrow></mml:math> Physical Review B, 2022, 105, .	1.1	2
44644	Origin of observed narrow bandgap of mica nanosheets. Scientific Reports, 2022, 12, 2868.	1.6	9
44645	The Effect of an External Electric Field on the Electronic Properties of Defective CBN Nanotubes: A Density Functional Theory Approach. Crystals, 2022, 12, 321.	1.0	7
44646	Strain-Driven Optical, Electronic, and Mechanical Properties of Inorganic Halide Perovskite CsGeBr₃. ECS Journal of Solid State Science and Technology, 2022, 11, 033001.	0.9	27

#	Article	IF	Citations
44647	Crystal Chemistry and Electronic Properties of the Al-Rich Compounds, Al2Cu, Ï‰-Al7Cu2Fe and Î¸-Al13Fe4 with Cu Solution. Metals, 2022, 12, 329.	1.0	7
44648	Reaction product-driven restructuring and assisted stabilization of a highly dispersed Rh-on-ceria catalyst. Nature Catalysis, 2022, 5, 119-127.	16.1	46
44649	Layered Perovskite-like Nitrate Cs₂Pb(NO₃)₂Br₂ as a Multifunctional Optical Material. Inorganic Chemistry, 2022, 61, 4184-4192.	1.9	14
44650	Formamidinium Perovskitizers and Aromatic Spacers Synergistically Building Bilayer Dionâ€“Jacobson Perovskite Photoelectric Bulk Crystals. ACS Applied Materials & Interfaces, 2022, 14, 11690-11698.	4.0	20
44651	Theoretical Investigation of the Active Sites in N-Doped Graphene Bilayer for the Oxygen Reduction Reaction in Alkaline Media in PEMFCs. Journal of Physical Chemistry C, 2022, 126, 5863-5872.	1.5	8
44652	Advancement of the Homogeneous Background Method for the Computational Simulation of Electrochemical Interfaces. Journal of Chemical Theory and Computation, 2022, 18, 1883-1893.	2.3	9
44653	Density Functional Theory Calculations of the Stability, Electronic Structure, and Magnetism of ReS₂ Nanoribbons: An Emerging Material for Electrocatalytic Reactions. ACS Applied Nano Materials, 2022, 5, 2385-2394.	2.4	4
44654	Electronic, Structural, and Mechanical Properties of <mml:math xmlns:mml="http://www.w3.org/1998/Math/MathML" display="inline"><mml:mrow><mml:msub><mml:mrow><mml:mi>SiO</mml:mi></mml:mrow><mml:mrow><mml:mn>2</mml:mn><m Glass at High Pressure Inferred from its Refractive Index. Physical Review Letters, 2022, 128, 077403.	2.9	4
44655	Flame Spray Pyrolysis as a Synthesis Platform to Assess Metal Promotion in In₂O₃â€Catalyzed CO₂ Hydrogenation. Advanced Energy Materials, 2022, 12, .	10.2	34
44656	MoirÃ© induced topology and flat bands in twisted bilayer <mml:math xmlns:mml="http://www.w3.org/1998/Math/MathML"><mml:msub><mml:mi mathvariant="normal">WSe</mml:mi><mml:mn>2</mml:mn></mml:msub></mml:math> : A	1.1	11
44657	Enhanced thermoelectric performance by lone-pair electrons and bond anharmonicity in the two-dimensional <mml:math xmlns:mml="http://www.w3.org/1998/Math/MathML"><mml:mrow><mml:msub><mml:mi mathvariant="normal">Ge</mml:mi><mml:mn>2</mml:mn></mml:msub><mml:msub><mml:mi>Y</mml:mi><mml:mn>2</mml:mn></ family of materials with <mml:math xmlns:mml="http://www.w3.org/1998/Math/MathML"><mml:mrow><mml:mi>Y</mml:mi><mml:mo>=</mml:mo><mml:mi	1.1	15
44658	Half-metallic Characteristics of the Novel Half Heusler Alloys XCrSb (X=Ti, Zr, Hf). Journal of the Nigerian Society of Physical Sciences, 0, , 138-145.	0.0	4
44659	Superconducting YAu₃Si and Antiferromagnetic GdAu₃Si with an Interpenetrating Framework Structure Built from 16-Atom Polyhedra. Inorganic Chemistry, 2022, 61, 4322-4334.	1.9	1
44660	Prediction of thermal conductivity of diamond film by neural network based on first principles. Scientia Sinica: Physica, Mechanica Et Astronomica, 2022, 52, 297306.	0.2	1
44661	Magnetic Properties of a (1â^'x)Bi0.5Na0.5TiO3+xCaNiO3-Î´ Solid Solution System Prepared by Solâ€“Gel Technique. Journal of Electronic Materials, 2022, 51, 1905-1921.	1.0	3
44662	Probing the electronic, elastic, mechanical and anisotropic features of ZrTiX(4) alloys via density functional theory. Europhysics Letters, 0, , .	0.7	0
44663	Anisotropic Growth of Copper Nanorods Mediated by Cl^{â€“} Ions. ACS Omega, 2022, 7, 7414-7420.	1.6	0
44664	Ab initio investigations of point and complex defect structures in B2-FeAl. Physical Review Materials, 2022, 6, .	0.9	3

#	Article	IF	Citations
44665	First principle study of Rh/Ru doped pentagonal PdSe2 for detection of SO2 and SO3 gas. Materials Today: Proceedings, 2022, 58, 696-701.	0.9	6
44666	Unraveling the Factors Affecting the Mechanical Properties of Halide Perovskites from First-Principles Calculations. Journal of Physical Chemistry C, 2022, 126, 4715-4725.	1.5	15
44667	Polarization-Enhanced Photovoltaic Effects in a High-Temperature Molecular Ferroelectric [C₆N₂H₁₈][SbI₅]-Based Solar Device. ACS Applied Energy Materials, 2022, 5, 2738-2746.	2.5	4
44668	Controllable Synthesis of Narrow-Gap van der Waals Semiconductor Nb₂GeTe₄ with Asymmetric Architecture for Ultrafast Photonics. ACS Nano, 2022, 16, 4239-4250.	7.3	15
44669	First-Principles Surface Characterization and Water Adsorption of Fe₃P Schreibersite. ACS Earth and Space Chemistry, 2022, 6, 512-520.	1.2	2
44670	Pressure-Induced Phase Transition and Compression Properties of HfO₂ Nanocrystals. Inorganic Chemistry, 2022, 61, 3498-3507.	1.9	4
44671	Revealing essence of magnetostructural coupling of Ni-Co-Mn-Ti alloys by first-principles calculations and experimental verification. Rare Metals, 2022, 41, 1933-1947.	3.6	18
44672	First-Principles Exploration into the Physical and Chemical Properties of Certain Newly Identified SnO₂ Polymorphs. ACS Omega, 2022, 7, 10382-10393.	1.6	13
44673	Ordered structure and mechanical properties of ternary Sc0.5TM0.5B2 (TM = Ti, V, Zr) alloys under high pressure. Ceramics International, 2022, 48, 16778-16791.	2.3	2
44674	Uncovering a Vital Band Gap Mechanism of Pnictides. Advanced Science, 2022, 9, e2105787.	5.6	15
44675	Theoretical study of decomposition of formic acid over <scp>Pd</scp> catalyst anchored on <scp>N</scp> â€doped graphene. International Journal of Quantum Chemistry, 0, , .	1.0	1
44676	First-Principles Study of Tritium Trapping in Î³-LiAlO₂ Nanovoids. Journal of Physical Chemistry C, 2022, 126, 5767-5776.	1.5	3
44677	Anisotropic mechanical response, high negative thermal expansion, and outstanding dynamical stability of biphenylene monolayer revealed by machine-learning interatomic potentials. FlatChem, 2022, 32, 100347.	2.8	24
44678	Insight into Subsurface Adsorption Derived from a Lattice-Gas Model and Monte Carlo Simulations. Journal of Physical Chemistry C, 2022, 126, 5343-5353.	1.5	2
44679	Interplay between Charge-Density-Wave, Superconductivity, and Ferromagnetism in CuIr_{2â€“x}Cr_xTe₄ Chalcogenides. Journal of Physical Chemistry Letters, 2022, 13, 2442-2451.	2.1	12
44680	Silicene/Silicene Oxide Nanosheets for Broadband Photodetectors. ACS Applied Nano Materials, 2022, 5, 4325-4335.	2.4	10
44681	Europium (II) Sulfate EuSO₄: Synthesis Methods, Crystal and Electronic Structure, Luminescence Properties. European Journal of Inorganic Chemistry, 2022, 2022, .	1.0	5
44682	A density-functional benchmark of vibrational free-energy corrections for molecular crystal polymorphism. Journal of Chemical Physics, 2022, 156, 114108.	1.2	7

#	Article	IF	Citations
44683	In situ study of Calcite-III dimorphism using dynamic diamond anvil cell. Chinese Physics B, 0, , .	0.7	1
44684	First-Principles Study of Electronic Properties of Substitutionally Doped Monolayer SnP3. Materials, 2022, 15, 2462.	1.3	1
44685	Hybrid nodal-ring phonons with hourglass dispersion in <mml:math xmlns:mml="http://www.w3.org/1998/Math/MathML"><mml:msub><mml:mi>AgAlO</mml:mi><mml:mn>2</mml:mn></mml:msub></m Physical Review Materials, 2022, 6, .	0.9	17
44686	DFT reveals the support effects in Pd nanoclusters over defect-ridden graphene for the oxidative addition of bromobenzene. Molecular Catalysis, 2022, 521, 112205.	1.0	1
44687	Enhanced photo-fenton and photoelectrochemical activities in nitrogen doped brownmillerite KBiFe2O5. Scientific Reports, 2022, 12, 5111.	1.6	7
44688	Macroscale Robust Superlubricity on Metallic NbB₂. Advanced Science, 2022, 9, e2103815.	5.6	8
44689	Preferred Spin Excitations in the Bilayer Iron-Based Superconductor <mml:math xmlns:mml="http://www.w3.org/1998/Math/MathML" display="inline"><mml:mrow><mml:mi>CaK</mml:mi><mml:msub><mml:mrow><mml:mo stretchy="false">(</mml:mo><mml:msub><mml:mrow><mml:mi>Fe</mml:mi></mml:mrow><mml:mrow><mml:mn>0.96</mml:mn></</m Letters, 2022, 128, 137003.	2.9	7
44690	Screening transition metal-based polar pentagonal monolayers with large piezoelectricity and shift current. Npj Computational Materials, 2022, 8, .	3.5	13
44691	Heterogeneous manganese-oxide-catalyzed successive cleavage and functionalization of alcohols to access amides and nitriles. CheM, 2022, 8, 1906-1927.	5.8	18
44692	A First-Principles Study on Electronic and Magnetic Properties of Intrinsic Point Defects in SrO Crystals. Journal of Electronic Materials, 0, , 1.	1.0	0
44693	Nanocrystalline TaCN coated titanium bipolar plate dedicated to proton exchange membrane fuel cell. Ceramics International, 2022, 48, 19217-19231.	2.3	10
44694	Insights into the Prediction Structural Electronic Optic Elastic and Phonon Features of Half-Heusler Compound LiAgSe via Density Functional Theory. YÃ¼zÃ¼ncÃ¼ YÄ±l Ã¼niversitesi Fen Bilimleri EnstitÃ¼sÃ¼ Dergisi, 0, , .	0.0	0
44695	Solid-State Photo-NMR Study on Light-Induced Nitrosyl Linkage Isomers Uncovers Their Structural, Electronic, and Diamagnetic Nature. Analytical Chemistry, 2022, 94, 4474-4483.	3.2	10
44696	Controllable Growth of Î±- and Î²-Antimonene by Interfacial Strain. Journal of Physical Chemistry C, 2022, 126, 5022-5027.	1.5	5
44697	Adverse effect of K-Mesh shifting in several crystal Systems: An analytical study. Materials Today: Proceedings, 2022, 57, 275-278.	0.9	4
44698	Charged Lithium adsorption on pristine and defective silicene: A theoretical study. Journal of Physics Condensed Matter, 2022, , .	0.7	1
44699	Two-Dimensional Janus GePAs Monolayer: A Direct-Band-Gap Semiconductor with High and Anisotropic Mobility for Efficient Photocatalytic Water Splitting. Physical Review Applied, 2022, 17, .	1.5	10
44700	Density functional theory study of nitrogen-doped black phosphorene doped with monatomic transition metals as high performance electrocatalysts for N₂ reduction reaction. Nanotechnology, 2022, 33, 245401.	1.3	9

#	Article	IF	Citations
44701	Neutron irradiation induced magnetization and persistent defects at high temperatures in graphite. Physical Review B, 2022, 105, .	1.1	1
44702	Structural phase transition of monochalcogenides investigated with machine learning. Physical Review B, 2022, 105, .	1.1	7
44703	Crystal structure, ion transport and optical properties of new high-conductivity Ag7(Si1â€‰â^'â€‰xGex)S5I solid solutions. Journal of Materials Science, 2022, 57, 6706-6722.	1.7	11
44704	Atomic Model of Gold Adsorption onto the Pyrite Surface with DFT Study. Minerals (Basel,) Tj ETQq1 1 0.784314 rgBT /Overlock 10 T	0.8	4
44705	Selfâ€Coâ€Electrolysis for Coâ€Production of Phosphate and Hydrogen in Neutral Phosphate Buffer Electrolyte. Advanced Materials, 2022, 34, e2200058.	11.1	17
44706	Quantum oscillatory interaction between isovalent centers in semiconductors. Europhysics Letters, 0, , .	0.7	0
44707	FeAl/MgO/FeAl MTJ with enhanced TMR and low resistance area product for MRAM: A first principle study. , 2022, 165, 207192.		2
44708	Theoretical Predictions on the Effective Piezoelectric Coefficients of Wurtzite LaN Compound from DFT and DFPT Calculations. Journal of Electronic Materials, 2022, 51, 3162-3172.	1.0	1
44709	Elucidating Active COâ€“Au Species on Au/CeO2(111): A Combined Modulation Excitation DRIFTS and Density Functional Theory Study. Topics in Catalysis, 2022, 65, 779-787.	1.3	5
44710	Ab initio study on the possible magnetic topological semimetallic state in MnMg₂O₄. AIP Advances, 2022, 12, 035331.	0.6	0
44711	Cluster- and energy-separated extreme states in a synthesized superatomic solid. Physical Review B, 2022, 105, .	1.1	1
44712	Synthesis and Theoreticalâ€“Experimental Characterization of BiOBr: The Role of Oxygen and Halide Vacancies on the Optoelectric Properties of this Bismuth Oxyhalide. Topics in Catalysis, 2022, 65, 824-838.	1.3	4
44713	The uptake characteristics of Prussian-blue nanoparticles for rare metal ions for recycling of precious metals from nuclear and electronic wastes. Scientific Reports, 2022, 12, 5135.	1.6	6
44714	Revealing the interplay between â€œintelligent behaviorâ€•and surface reconstruction of non-precious metal doped SrTiO3 catalysts during methane combustion. Catalysis Today, 2022, , .	2.2	5
44715	Half-negative Poissonâ€™s ratio in graphene+ with intrinsic Dirac nodal loop. Cell Reports Physical Science, 2022, 3, 100790.	2.8	14
44716	Phase transitions and pâ€“T phase diagram of the multiferroic TbFe ₃ (BO ₃) ₄ crystal. Journal of Raman Spectroscopy, 0, , .	1.2	2
44717	Photo-magnetization in two-dimensional sliding ferroelectrics. Npj 2D Materials and Applications, 2022, 6, .	3.9	8
44718	Enhancing Oxygen Reduction Reaction Activity Using Single Atom Catalyst Supported on Tantalum Pentoxide. ChemCatChem, 0, , .	1.8	1

#	Article	IF	Citations
44719	Insights into Interaction of CO(_2) with N and B-doped Graphenes. Communications in Physics, 2022, 32, .	0.0	0
44720	Cs₂Bi₂OSi₂O₇: A Promising Bismuth Silicate Nonlinear Optical Crystal with Face-Sharing BiO₅ Polyhedra Exhibiting Strengthened Second Harmonic Generation Response and Birefringence. Chemistry of Materials, 2022, 34, 3365-3372.	3.2	19
44721	Thermoelectric Performance of n-Type Magnetic Element Doped Bi₂S₃. ACS Applied Energy Materials, 2022, 5, 3845-3853.	2.5	19
44722	Synergistic Effects of V and Ni Catalysts on Hydrogen Sorption Kinetics of Mg-Based Hydrogen Storage Materials: A Computational Study. Journal of Physical Chemistry C, 2022, 126, 5483-5492.	1.5	5
44723	Clarâ€™s Goblet on Graphene: Field-Modulated Charge Transfer in a Hydrocarbon Heterostructure. Journal of Physical Chemistry C, 2022, 126, 5640-5648.	1.5	2
44724	First-Principles Study on Tuning of Contact Electrification and Adhesion of Bio-inspired Adhesive Carbon-Based Materials via an External Electric Field. Journal of Physical Chemistry C, 2022, 126, 5354-5361.	1.5	1
44725	Density Functional Theory (DFT) as a Nondestructive Probe in the Field of Art Conservation: Small-Molecule Adsorption on Aragonite Surfaces. ACS Applied Materials & Interfaces, 2022, 14, 13858-13871.	4.0	1
44726	Topological properties of Sb(111) surface: A first-principles study. Chinese Physics B, 2022, 31, 047105.	0.7	0
44727	Explaining the structure sensitivity of Pt and Rh for aqueous-phase hydrogenation of phenol. Journal of Chemical Physics, 2022, 156, 104703.	1.2	7
44728	Chiral phonons in lattices with <mml:math xmlns:mml="http://www.w3.org/1998/Math/MathML"><mml:msub><mml:mi>C</mml:mi><mml:mn>4</mml:mn></mml:msub></mm symmetry. Physical Review B, 2022, 105, .	1.1	7
44729	Two-dimensional weak topological insulators in inversion-symmetric crystals. Physical Review B, 2022, 105, .	1.1	7
44730	Toward accurate and efficient dynamic computational strategy for heterogeneous catalysis: Temperature-dependent thermodynamics and kinetics for the chemisorbed on-surface CO. Chinese Chemical Letters, 2022, 33, 4936-4942.	4.8	7
44731	Effect of Sc, V, Zr, and Hf doping on the mechanical properties of TiB3 under high pressure. Applied Physics A: Materials Science and Processing, 2022, 128, 1.	1.1	1
44732	Highly anisotropic mechanical and optical properties of 2D NbOX2 (XÂ=ÂCl, Br, I) revealed by first-principle. Nanotechnology, 2022, 33, 275701.	1.3	7
44733	Fe binuclear sites convert methane to acetic acid with ultrahigh selectivity. CheM, 2022, 8, 1658-1672.	5.8	40
44734	Firstâ€Principles Investigation About Different Sequence of Stereochemical Activity and Birefringence in Antimony Halides. Physica Status Solidi (B): Basic Research, 0, , 2100576.	0.7	1
44735	Dynamical tuning of the thermal conductivity via magnetophononic effects. Physical Review B, 2022, 105, .	1.1	7
44736	Novel Boron Nitride Polymorphs with Graphite-Diamond Hybrid Structure. Chinese Physics Letters, 2022, 39, 036301.	1.3	5

#	Article	IF	Citations
44737	Resistive switching properties for fluorine doped titania fabricated using atomic layer deposition. APL Materials, 2022, 10, .	2.2	9
44738	Multiscale manipulating induced flexible heterogeneous V-NiFe2O4@Ni2P electrocatalyst for efficient and durable oxygen evolution reaction. Nano Research, 2022, 15, 4942-4949.	5.8	26
44739	Investigating Electronic, Optical, and Phononic Properties of Bulk Î³-M₂ON₂ and Î²-M₇O₈N₄ (M = Hf and Zr) Insulators Using Density Functional Theory. ACS Omega, 2022, 7, 9196-9205.	1.6	2
44740	Polymorphism, Structure, and Nucleation of CholesterolÂ·H₂O at Aqueous Interfaces and in Pathological Media: Revisited from a Computational Perspective. Journal of the American Chemical Society, 2022, 144, 5304-5314.	6.6	8
44741	Electronic properties of germanene on pristine and defective <mml:math xmlns:mml="http://www.w3.org/1998/Math/MathML"><mml:msub><mml:mrow><mml:mi>MoS</mml:mi></mml:mrow><mml:mn>2</mml:mn></mml:msub></mml:math> : A first-principles study. Physical Review B, 2022, 105, .	1.1	1
44742	Migration Barrier Estimation of Carbon in Lead for Leadâ€“Acid Battery Applications: A Density Functional Theory Approach. Solids, 2022, 3, 177-187.	1.1	2
44743	Tetrahedral W₄ cluster confined in graphene-like C₂N enables electrocatalytic nitrogen reduction from theoretical perspective. Nanotechnology, 2022, 33, 245706.	1.3	8
44744	Orthorhombic <mml:math xmlns:mml="http://www.w3.org/1998/Math/MathML"><mml:msub><mml:mi>ScB</mml:mi><mml:mn>3</mml:mn></mml:msub></mml:math> and hexagonal <mml:math xmlns:mml="http://www.w3.org/1998/Math/MathML"><mml:msub><mml:mi>ScB</mml:mi><mml:mn>6</mml:mn></mml:msub></mml:math> with High Hardness. Physical Review B, 2022, 105, .	1.1	10
44745	Mode-locked erbium-doped fiber laser based on a mechanically exfoliated ReS₂ saturable absorber onto D-shaped optical fiber. Optical Materials Express, 2022, 12, 1657.	1.6	11
44746	Tunable electronic properties and band alignments of MoSi2N4/GaN and MoSi2N4/ZnO van der Waals heterostructures. Applied Physics Letters, 2022, 120, .	1.5	33
44747	Dynamics of Hydrogen in Silicon at Finite Temperatures from First Principles. Physica Status Solidi (B): Basic Research, 2022, 259, .	0.7	7
44748	Adsorption of Oxygen to High Entropy Alloy Surfaces for up to 2 ML Coverage Using Density Functional Theory and Monte Carlo Calculations. Langmuir, 2022, 38, 3158-3169.	1.6	9
44749	Computational Mechanism of Methyl Levulinate Conversion to Î³-Valerolactone on UiO-66 Metal Organic Frameworks. ACS Sustainable Chemistry and Engineering, 2022, 10, 3567-3573.	3.2	8
44750	Realization of Coexisting Charge Density Wave and Quantum Spin/Anomalous Hall State in Monolayer NbTe₂. Advanced Functional Materials, 2022, 32, .	7.8	11
44751	A First-Principles Investigation on Electronic Structure and Optical Properties of Tetragonal Iron Antimonide FeSb2. Journal of Superconductivity and Novel Magnetism, 2022, 35, 1507-1516.	0.8	1
44752	Molecular Inclusion of Small Aging Products into the Hexanitrohexaazaisowurtzitane (CLâ€20) Lattice: Part I, Infrared Spectra. Propellants, Explosives, Pyrotechnics, 2022, 47, .	1.0	2
44753	Remarkable decrease in lattice thermal conductivity of transition metals borides TiB₂ by dimensional reduction. Nanotechnology, 2022, 33, 235706.	1.3	3
44754	Hexacene on Cu(110) and Ag(110): Influence of the Substrate on Molecular Orientation and Interfacial Charge Transfer. Journal of Physical Chemistry C, 2022, 126, 5036-5045.	1.5	7

#	Article	IF	Citations
44755	First-Principles Study of Methanol Adsorption and Dissociation Reactivity on the Anatase TiO2(101) Surface: The Effect of Co doping and Oxygen Vacancy. Catalysis Letters, 0, , 1.	1.4	5
44756	Van der Waals force-induced intralayer ferroelectric-to-antiferroelectric transition via interlayer sliding in bilayer group-IV monochalcogenides. Npj Computational Materials, 2022, 8, .	3.5	20
44757	Pattern of covalent and nonâ€covalent interactions within the pentaiodide anion in the structure of (3â€HOC ₅ H ₉ NH ₂)I ₅. Zeitschrift Fur Anorganische Und Allgemeine Chemie, 0, , .	0.6	3
44758	Electronic, Thermal, and Thermoelectric Transport Properties of Îµ-Ga₂O₃ from First Principles. ACS Omega, 2022, 7, 11643-11653.	1.6	9
44759	Pressure Dependence of Structural and Elastic Properties of Na₂O: First-Principles Calculations. Integrated Ferroelectrics, 2022, 224, 256-263.	0.3	3
44760	Kinetics study of catalytic wet oxidation of phenol over novel ceria promoted mesoporous silica supported Ru-Fe3O4 catalyst. Chemical Engineering Research and Design, 2022, 182, 120-132.	2.7	4
44761	Hydrogen-Evolution Reaction in Two-Dimensional <mml:math xmlns:mml="http://www.w3.org/1998/Math/MathML" display="inline" overflow="scroll"><mml:msub><mml:mrow><mml:mi>Pd</mml:mi><mml:mi mathvariant="normal">S</mml:mi></mml:mrow><mml:mn>2</mml:mn></mml:msub></mml:math> by Phase and Defect Engineering. Physical Review Applied, 2022, 17, .	1.5	3
44762	Computational analysis of the optical response of ZnSe with d-orbital defects. Journal of Physics Condensed Matter, 2022, 34, 205402.	0.7	3
44763	Vibrational fingerprints of ferroelectric HfO2. Npj Quantum Materials, 2022, 7, .	1.8	24
44764	Two-Dimensional Oxide Alloys Probed at the Atomic Level: (V,Fe)₂O₃ Honeycomb Monolayers on Pt(111). Journal of Physical Chemistry C, 2022, 126, 5070-5078.	1.5	2
44765	Structures and Electromagnetic Properties of Boron Nitride Nanoribbons Doped with Transition Metals. ChemPhysChem, 2022, , .	1.0	1
44766	Stepwise Dopant Selection Process for Highâ€Nickel Layered Oxide Cathodes. Advanced Energy Materials, 2022, 12, .	10.2	35
44767	Improved chloride binding stability for hydration products of calcium aluminates by phosphorus modification. Journal of the American Ceramic Society, 2022, 105, 4870-4882.	1.9	1
44768	Electronic and Near-Infrared-II Optical Properties of I-Doped Monolayer MoTe₂: A First-Principles Study. ACS Omega, 2022, 7, 11956-11963.	1.6	7
44769	Ferroelectric control of band structures in the two-dimensional Janus WSSe/In2Se3 van der Waals heterostructures. Physica E: Low-Dimensional Systems and Nanostructures, 2022, 142, 115256.	1.3	6
44770	Effect of Transition Metal and Nitrogen Co-Doping on Quantum Capacitance of Silicene-Based Electrode Materials. Journal of Physical Chemistry C, 2022, 126, 5682-5690.	1.5	3
44771	Alâ€“Au Thin Films for Thermally Stable and Highly Sensitive Plasmonic Sensors. Journal of Physical Chemistry C, 2022, 126, 5628-5639.	1.5	2
44772	Multiscale Simulation of Irregular Shape Evolution during the Initial Stage of Zn Electrodeposition on a Negative Electrode Surface. Journal of Physical Chemistry C, 2022, 126, 5224-5232.	1.5	2

#	Article	IF	Citations
44773	Spin-polarized topological phases in a ferromagnetic <mml:math xmlns:mml="http://www.w3.org/1998/Math/MathML"><mml:mrow><mml:msub><mml:mi>Bi</mml:mi><mml:mn>2</mml:mn></mml:msub></mml:mrow></mml:math> bilayer tuned by electric and magnetic fields. Physical Review B, 2022, 105, .	2.1	2
44774	Ab Initio Study of Chiral Phonons in Ternary YAlSi Compound. Crystals, 2022, 12, 436.	1.0	4
44775	SrAl₅Pt₃ and Sr₂Al₁₆Pt₉ â€“ two new strontium aluminum platinides. Zeitschrift Fur Naturforschung - Section B Journal of Chemical Sciences, 2022, 77, 367-379.	0.3	2
44776	Ternary pentagonal BNSi monolayer: Two-dimensional structure with potentially high carrier mobility and strong excitonic effects for photocatalytic applications. Physical Review Materials, 2022, 6, .	0.9	15
44777	Predicting the stability and electronic structure of alkali metal aurides. Journal of Physics Condensed Matter, 2022, , .	0.7	0
44778	Ruthenium Icosahedra and Ultrathin Platelets: The Role of Surface Chemistry on the Nanoparticle Structure. Chemistry of Materials, 2022, 34, 2931-2944.	3.2	5
44779	Collective Motion Improves the Stability and Charge Carrier Lifetime of Metal Halide Perovskites: A Phonon-Resolved Nonadiabatic Molecular Dynamics Study. Journal of Physical Chemistry Letters, 2022, 13, 3016-3022.	2.1	12
44780	Highly Efficient Supramolecular Nucleating Agents for Poly(3-hexylthiophene). Macromolecules, 2022, 55, 2861-2871.	2.2	4
44781	Metalâ€“Metal Bonding as an Electrode Design Principle in the Low-Strain Cluster Compound LiScMo₃O₈. Journal of the American Chemical Society, 2022, 144, 5841-5854.	6.6	11
44782	Strain and electric field tuning the electronic properties of two-dimensional MoS2/ScCl3 van der Waals heterostructure. Journal of Materials Science: Materials in Electronics, 2022, 33, 10461-10470.	1.1	1
44783	First-principles calculations of high-pressure physical properties anisotropy for magnesite. Scientific Reports, 2022, 12, 3691.	1.6	3
44784	Activation of CO2 on the Surfaces of Bare, Ti-Adsorbed and Ti-Doped C60. Fuels, 2022, 3, 176-183.	1.3	1
44785	Computational Insight into TMâ€“N_x Embedded Graphene Bifunctional Electrocatalysts for Oxygen Evolution and Reduction Reactions. ACS Physical Chemistry Au, 2022, 2, 305-315.	1.9	10
44786	Structural, Electronic, and Magnetic Properties of Sr(_{1-x})Mn(_{x})F(_{2}) Alloys Studied by First-principles Calculations. Communications in Physics, 2022, 32, 157.	0.0	0
44787	Free and open source software for computational chemistry education. Wiley Interdisciplinary Reviews: Computational Molecular Science, 2022, 12, .	6.2	19
44788	First-principles study of the elastic, thermal and optical properties of Î±-PbO2 and Î²-PbO2. Indian Journal of Physics, 2022, 96, 3449-3460.	0.9	1
44789	Uncovering the crystal defects within aragonite CaCO ₃. Proceedings of the National Academy of Sciences of the United States of America, 2022, 119, e2122218119.	3.3	10
44790	A DFT-Based Descriptor to Predict the Water Vapor Corrosion Resistance of Rare-Earth Monosilicates. Materials, 2022, 15, 2414.	1.3	0

#	Article	IF	Citations
44791	Observation of multiple nodal lines in SmSbTe. Physical Review Materials, 2022, 6, .	0.9	14
44792	Combination of optical properties acquired by first principles calculations with the empirical Tauc method for determining the band gap energy of alkaline-earth metal oxides: MO (M = Be, Mg, Ca, Sr, Ba). Journal of Computational Methods in Sciences and Engineering, 2022, , 1-10.	0.1	0
44793	Cadmium selenium nanocrystal: first-principles insight into the structural, electronic, and optical properties. Journal of the Korean Physical Society, 0, , 1.	0.3	0
44794	The Theoretical Study of Unexpected Magnetism in 2D Si-Doped AlN. Frontiers in Physics, 2022, 10, .	1.0	1
44795	Mercury goes Solid at room temperature at nanoscale and a potential Hg waste storage. Scientific Reports, 2022, 12, 3494.	1.6	2
44796	Pressure-induced emission enhancement and bandgap narrowing: Experimental investigations and first-principles theoretical simulations on the model halide perovskite <mml:math xmlns:mml="http://www.w3.org/1998/Math/MathML"><mml:msub><mml:mrow><mml:mi>Cs</mml:mi></mml:mrow><mml:mn>3</mml:mn> Physical Review B, 2022, 105, .	1.1	8
44797	Electrocatalytic Reduction of N₂ to NH₃ Over Defective 1Tâ€²â€WX₂ (X=S, Se, Te) Monolayers. ChemSusChem, 2022, 15, .	3.6	6
44798	Effect of spin orbit coupling on antiperovskites: Sr₃BO (B = Pb, Sn). Physica Scripta, 2022, 97, 045701.	1.2	1
44799	Synthesis and Characterization of (1â^'x)Bi1/2Na1/2TiO3+xSrNiO3-Î´ Solid Solution System. Journal of Electronic Materials, 2022, 51, 2716-2731.	1.0	1
44800	Niobium-doped cobalt phosphide nanowires realizing enhanced electrocatalytic activity for overall water splitting. International Journal of Hydrogen Energy, 2022, 47, 13251-13260.	3.8	17
44801	Thermoelectric Properties of Pnma and Rocksalt SnS and SnSe. Solids, 2022, 3, 155-176.	1.1	7
44802	Effects of sulfur phase transition on moisture-induced damages in bitumen colloidal structure. Journal of Industrial and Engineering Chemistry, 2022, 107, 109-117.	2.9	4
44803	Combined first-principles-Monte Carlo analysis to evaluate the effect of surface hydrogen on the secondary electron yield of nickel. Journal of Applied Physics, 2022, 131, .	1.1	6
44804	Band Structure of Organic-Ion-Intercalated (EMIM)xFeSe Superconductor. Materials, 2022, 15, 1856.	1.3	0
44805	Synthesis of a magnetic Ï€-extended carbon nanosolenoid with Riemann surfaces. Nature Communications, 2022, 13, 1239.	5.8	20
44806	The equation of state and shock-driven decomposition of polymethylmethacrylate (PMMA). Journal of Applied Physics, 2022, 131, .	1.1	5
44807	X-ray Absorption Near-Edge Structure (XANES) at the O K-Edge of Bulk Co3O4: Experimental and Theoretical Studies. Nanomaterials, 2022, 12, 921.	1.9	7
44808	Role of Oxygen and Fluorine in Passivation of the GaSb(111) Surface Depending on Its Termination. Crystals, 2022, 12, 477.	1.0	3

#	Article	IF	Citations
44809	Disproportionation of <mml:math xmlns:mml="http://www.w3.org/1998/Math/MathML" display="inline"><mml:mrow><mml:msub><mml:mrow><mml:mi>SO</mml:mi></mml:mrow><mml:mrow><mml:mn>2</mml:mn></mml:mrow></mml:msub></mml:mrow></mml:math> at High Pressure and Temperature. Physical Review Letters, 2022, 128, 106001.	2.9	18
44810	Anomalous Hall effect in a compensated ferrimagnet: Symmetry analysis for <mml:math xmlns:mml="http://www.w3.org/1998/Math/MathML"><mml:msub><mml:mrow><mml:mi>Mn</mml:mi></mml:mrow><mml:mrow><mml:mn>3</mml:mn></mml:mrow></mml:msub></mml:math> Physical Review Research, 2022, 4, .	1.8	8
44811	Deep ultra-violet plasmonics: exploiting momentum-resolved electron energy loss spectroscopy to probe germanium. Optics Express, 2022, 30, 12630.	1.7	2
44812	<mml:math xmlns:mml="http://www.w3.org/1998/Math/MathML" display="inline" overflow="scroll"><mml:msub><mml:mrow><mml:mrow><mml:mi mathvariant="normal">C</mml:mi></mml:mrow><mml:mrow><mml:mn>5</mml:mn></mml:mrow></mml:msub><mml:mrow><mml:mrow><mml:mi mathvariant="normal">N</mml:mi></mml:mrow></mml:mrow></mml:math> : A Promising Building Block for the Anode of <mml:math xmlns:mml="http://www.w3.org/1998/Math/MathML"	1.5	5
44813	High pressure enhanced magnetic ordering and magnetostructural coupling in the geometrically frustrated spinel <mml:math xmlns:mml="http://www.w3.org/1998/Math/MathML"><mml:mrow><mml:msub><mml:mi>Mn</mml:mi><mml:mrow><mml:mn>3</mml:mn></mml:mrow></mml:msub><mml:msub><mml:mrow><mml:mi mathvariant="normal">O</mml:mi></mml:mrow><mml:mrow><mml:mn>4</mml:mn></mml:mrow></mml:msub></mml:mrow></mml:math>. Physical Review B, 2022, 105, .	1.3	4
44814	Electronic and optical properties of fully fluorinated Janus MoSSe monolayer. , 2022, , 207199.		0
44815	A Local Atomic Mechanism for Monoclinic-Tetragonal Phase Boundary Creation in Li-Doped Na_{0.5}K_{0.5}NbO₃ Ferroelectric Solid Solution. Inorganic Chemistry, 2022, 61, 4335-4349.	1.9	9
44816	Ultra-low lattice thermal conductivity and high figure of merit for Janus MoSeTe monolayer: a peerless material for high temperature regime thermoelectric devices. Journal of Materials Science, 2022, 57, 7012-7022.	1.7	5
44817	The Influence of Surface Chemistry on Critical Current Density for Garnet Electrolyte. Advanced Functional Materials, 2022, 32, .	7.8	22
44818	Coexistence of Ferroelectriclike Polarization and Dirac-like Surface State in <mml:math xmlns:mml="http://www.w3.org/1998/Math/MathML" display="inline"><mml:mrow><mml:msub><mml:mrow><mml:mi>TaNiTe</mml:mi></mml:mrow><mml:mrow><mml:mn>5</mml:mn></mml:mrow></mml:msub></mml:mrow></mml:math> Physical Review Letters, 2022, 128, 106802.	2.9	7
44819	Alkali ion-promoted palladium subnanoclusters stabilized on porous alumina nanosheets with enhanced catalytic activity for benzene oxidation. Nano Research, 2022, 15, 5912-5921.	5.8	13
44820	Potassium hydride-intercalated graphite as an efficient heterogeneous catalyst for ammonia synthesis. Nature Catalysis, 2022, 5, 222-230.	16.1	37
44821	Firstâ€principles design of Naâ€ion superionic conductors: Interstitialâ€based Na diffusion in NaCuZrS3. Chemistry - A European Journal, 2022, , .	1.7	0
44822	Firstâ€Principles Studies on the Atomistic Properties of Metallic Magnesium as Anode Material in Magnesiumâ€ion Batteries. ChemSusChem, 2022, 15, .	3.6	9
44823	Different Bonding Defects on Dualâ€Metal Singleâ€Atom Electrocatalyst CoZnN ₆ (OH) for Oxygen Reduction Reaction. ChemPhysChem, 2022, , .	1.0	1
44824	Preparation, electronic structure and optical properties of Na2GeSe3 crystals. Semiconductor Physics, Quantum Electronics and Optoelectronics, 2022, 25, 19-29.	0.3	0
44825	Molecular Inclusion of Small Aging Products into the Hexanitrohexaazaisowurtzitane (CLâ€20) Lattice: Part II, Polymorph Dependence. Propellants, Explosives, Pyrotechnics, 0, , .	1.0	1
44826	Effects of LiCl template amount on structure, morphology, and electrochemical performance of porous Si@C anodes. Ionics, 0, , 1.	1.2	0

#	Article	IF	Citations
44827	A direct approach to calculate the temperature dependence of the electronic relaxation time in 2D semiconductors from Boltzmann transport theory. Journal of Applied Physics, 2022, 131, .	1.1	4
44828	Fluorinated Zigzag ZnO Nanoribbons for Negative Differential Resistance-Based Nanoelectronic Devices: First-Principles Investigation. Journal of Electronic Materials, 2022, 51, 3288-3298.	1.0	10
44829	Structural stability, electronic, mechanical, and thermodynamic properties of the new MAX phases Mn2SiC1, Mn3SiC2 and Mn4SiC3: ab-initio calculations. Indian Journal of Physics, 0, , 1.	0.9	5
44830	Interplay between Thermal Stress and Interface Binding on Fracture of WS₂ Monolayer with Triangular Voids. ACS Applied Materials & Interfaces, 2022, 14, 16876-16884.	4.0	10
44831	Selective CO-to-acetate electroreduction via intermediate adsorption tuning on ordered Cuâ€“Pd sites. Nature Catalysis, 2022, 5, 251-258.	16.1	118
44832	First principles study of 2D half-metallic ferromagnetism in Janus Mn2XSb (X = As, P) monolayers. Applied Physics Letters, 2022, 120, .	1.5	10
44833	Chemical environment dependent Stabilities, electronic properties and diffusions behaviors of intrinsic point defects in novel Two-Dimensional MoSi2N4 monolayer. Applied Surface Science, 2022, 592, 153214.	3.1	6
44834	Atomic Ordering at the Interfaces Between Liquid Aluminum and Polar AlN{0 0 0 1} Substrates. Metallurgical and Materials Transactions A: Physical Metallurgy and Materials Science, 2022, 53, 2040-2047.	1.1	1
44835	Exploring far-from-equilibrium ultrafast polarization control in ferroelectric oxides with excited-state neural network quantum molecular dynamics. Science Advances, 2022, 8, eabk2625.	4.7	8
44836	Excitonic response of <mml:math xmlns:mml="http://www.w3.org/1998/Math/MathML"><mml:msup><mml:mrow><mml:mi>AA</mml:mi></mml:mrow><mml:mo>â€²	1.1	6
44837	Atomic reconfiguration among tri-state transition at ferroelectric/antiferroelectric phase boundaries in Pb(Zr,Ti)O3. Nature Communications, 2022, 13, 1390.	5.8	17
44838	Insights into Pathway Selectivity during Anodic Formic Acid Oxidation over La_{1â€“x}Sr_xCoO₃. Industrial & Engineering Chemistry Research, 2022, 61, 4784-4793.	1.8	0
44839	Threshold potentials for fast kinetics during mediated redox catalysis of insulators in Liâ€“O2 and Liâ€“S batteries. Nature Catalysis, 2022, 5, 193-201.	16.1	51
44840	Ethanol adsorption on Ni doped Mo2C(001): a theoretical study. Topics in Catalysis, 2022, 65, 839-847.	1.3	3
44841	Spatially controlled graphene- <mml:math xmlns:mml="http://www.w3.org/1998/Math/MathML"><mml:msub><mml:mrow><mml:mi>MoSe</mml:mi></mml:mrow><mml:mn>2< lateral heterostructure for sensing applications: Insights from first-principles calculations. Physical Review B, 2022, 105, .	1.1	2
44842	Structural, elastic, electronic and optical properties of the newly synthesized selenides Tl2CdXSe4 (Xâ€‰=â€‰Ge, Sn). European Physical Journal B, 2022, 95, 1.	0.6	6
44843	Existence of BeCN₂ and Its First-Principles Phase Diagram: Be and C Introducing Structural Diversity. Journal of the American Chemical Society, 2022, 144, 5155-5162.	6.6	12
44844	Ab Initio Study of the Thermodynamics of Intrinsic Point Defects in Thermoelectric Oxychalcogenide BiCuSeO. Journal of Physical Chemistry C, 2022, 126, 5960-5969.	1.5	0

#	Article	IF	Citations
44845	Negative Linear Compressibility in Organicâ€“Inorganic Hybrid Perovskite [NH₂NH₃]X(HCOO)₃ (X = Mn, Fe, Co). Journal of Physical Chemistry Letters, 2022, 13, 3143-3149.	2.1	9
44846	Computational Investigation of Hydriding and Strain Effects on the Binding Energies of Electrochemical CO2RR and HER Intermediates. Journal of Physical Chemistry C, 2022, 126, 5513-5520.	1.5	5
44847	Improving Lattice Rigidity and Charge Carrier Lifetime by Engineering Spacer Cation of Ruddlesdenâ€“Popper Perovskites: A Time-Domain Ab Initio Study. Journal of Physical Chemistry Letters, 2022, 13, 2718-2724.	2.1	11
44848	Spin Splitting in Systems Described by Magnetic Rod Groups. Journal of Physical Chemistry C, 2022, 126, 5362-5367.	1.5	3
44849	First-principles study on electronic and optical properties of single-walled carbon nanotube under an external electric field. Journal of Molecular Modeling, 2022, 28, 97.	0.8	5
44850	A comparison of waterâ€“gas shift reaction on ZnO $$left(10overline{1 }0ight)$$ surface and 6Cu cluster deposited over ZnO $$left(10overline{1 }0ight)$$ surface using density functional theory studies. Journal of Molecular Modeling, 2022, 28, 84.	0.8	4
44851	Suppressing Oxygen-Induced Deterioration of Metal Halide Perovskites by Alkaline Earth Metal Doping: A Quantum Dynamics Study. Journal of the American Chemical Society, 2022, 144, 5543-5551.	6.6	29
44852	Structural and Theoretical Investigations on the Unique Coloring Scheme of the Î³â€Brass Type Phase: Cu _{5+Î´} Cd _{8â€Î´} (â^'1.0â‰¤Î´â‰¤0.1). Zeitschrift Fur Anorganische Und Allgemeine Chemie, 0, , .	0.6	0
44853	Investigation of Topological and Catalytic Properties of Gold Iodide Monolayer: A Density Functional Theory Study. Physica Status Solidi - Rapid Research Letters, 2022, 16, .	1.2	2
44854	Interaction of Oxygen with the Stable Ti5Si3 Surface. Metals, 2022, 12, 492.	1.0	7
44855	Isotopic responses of magnesium to two types of dissolution-reprecipitation processes for the growth of the double-carbonate mineral norsethite. American Mineralogist, 2023, 108, 326-337.	0.9	1
44856	First-principles study on the atomic structure of two-dimensional molybdenum boride. Materials Research Express, 2022, 9, 035002.	0.8	1
44857	Strong interlayer interactions in bilayer and trilayer moirÃ© superlattices. Science Advances, 2022, 8, eabk1911.	4.7	9
44858	Longitudinal piezoelectric, elastic, and dielectric properties of rare-earth aluminum nitride alloys determined by density-functional perturbation theory. Physical Review Materials, 2022, 6, .	0.9	2
44859	Structure Factors and Charge Density Description of Aluminum: A Quantum Crystallographic Study. Journal of Physical Chemistry A, 2022, 126, 2042-2049.	1.1	1
44860	Engineering Electronic Transfer Dynamics and Ion Adsorption Capability in Dual-Doped Carbon for High-Energy Potassium Ion Hybrid Capacitors. ACS Nano, 2022, 16, 6255-6265.	7.3	65
44861	Ternary Cu(OH)₂/P(g-C₃N₄)/MoS₂ Nanostructures for Photocatalytic Hydrogen Production. ACS Applied Nano Materials, 2022, 5, 4848-4859.	2.4	20
44862	First-Principles Investigation of Graphene and Fe₂O₃ Catalytic Activity for Decomposition of Ammonium Perchlorate. Langmuir, 2022, 38, 3844-3851.	1.6	17

#	Article	IF	Citations
44863	Metal Halide Double Perovskite Fast Lithium Ion Conductors with a Unique Octahedral B-Site Vacancy Migration Mechanism. ACS Applied Energy Materials, 2022, 5, 4926-4933.	2.5	1
44864	Electronic Tuning in WSe₂/Au via van der Waals Interface Twisting and Intercalation. ACS Nano, 2022, 16, 6541-6551.	7.3	17
44865	Elucidating the Correlation between ORR Polarization Curves and Kinetics at Metalâ€“Electrolyte Interfaces. ACS Applied Materials & Interfaces, 2022, 14, 13891-13903.	4.0	18
44866	Effects of carbon impurities on the performance of silicon as an anode material for lithium ion batteries: An ab initio study. AIP Advances, 2022, 12, 035315.	0.6	5
44867	Ultrathin (In, Mg) films on Si(111): A nearly freestanding double-layer metal. Physical Review B, 2022, 105, .	1.1	3
44868	Electronic and magnetic properties of honeycomb arsenicâ€“phosphorus nanoribbons via a first-principles study. Canadian Journal of Physics, 2022, 100, 277-283.	0.4	2
44869	Toward Addressing the Challenge to Predict the Heat Capacities of RDX and HMX Energetic Materials. Propellants, Explosives, Pyrotechnics, 0, , .	1.0	1
44870	Multiscale simulation approach to investigate the binder distribution in catalyst layers of high-temperature polymer electrolyte membrane fuel cells. Scientific Reports, 2022, 12, 3810.	1.6	3
44871	Adsorbateâ€induced modifications in the optical response of Si(553)â€Au nanowires. Physica Status Solidi - Rapid Research Letters, 0, , .	1.2	0
44872	First Principle Study on Electronic and Transport Properties of Finite-Length Nanoribbons and Nanodiscs for Selected Two-Dimensional Materials. Molecules, 2022, 27, 2228.	1.7	2
44873	First-principles investigation of CZTS Raman spectra. Physical Review Materials, 2022, 6, .	0.9	4
44874	Tailoring 2-electron oxygen reduction reaction selectivity on h-BN-based single-atom catalysts from superoxide dismutase: A DFT investigation. Applied Surface Science, 2022, 592, 153233.	3.1	18
44875	Compositional phase stability in medium-entropy and high-entropy Cantor-Wu alloys from an ab initio all-electron Landau-type theory and atomistic modeling. Physical Review B, 2022, 105, .	1.1	8
44876	Flat-surface-assisted and self-regulated oxidation resistance of Cu(111). Nature, 2022, 603, 434-438.	13.7	59
44877	Pressure-dependent phase diagrams and elastic properties of TixCo1â^'x: first-principle and Monte-Carlo calculations. European Physical Journal B, 2022, 95, 1.	0.6	0
44878	Self-healing Growth of LaNiO₃ on a Mixed-Terminated Perovskite Surface. ACS Applied Materials & Interfaces, 2022, 14, 16928-16938.	4.0	4
44879	Spectroscopic evidence of multigap superconductivity in noncentrosymmetric AuBe. Physical Review B, 2022, 105, .	1.1	2
44880	Dielectric response of rock-salt crystals at finite temperatures from first principles. Physical Review Materials, 2022, 6, .	0.9	5

#	Article	IF	Citations
44881	Two-Dimensional Electron Gas with High Mobility Forming at BaO/SrTiO₃ Interface. Chinese Physics Letters, 2022, 39, 047301.	1.3	8
44882	A Theoretical Study of Fe Adsorbed on Pure and Nonmetal (N, F, P, S, Cl)-Doped Ti3C2O2 for Electrocatalytic Nitrogen Reduction. Nanomaterials, 2022, 12, 1081.	1.9	6
44883	Trends in oxygenate/hydrocarbon selectivity for electrochemical CO(2) reduction to C2 products. Nature Communications, 2022, 13, 1399.	5.8	56
44884	Thermoelectric, structural, electronic, magnetic, and thermodynamic properties of CaZn2Ge2 compound. European Physical Journal Plus, 2022, 137, 1.	1.2	10
44885	Experimental and first-principles simulation study on oxidation behavior at 1700ÂÂ°C of Lu2O3â€“SiC-HfB2 ternary coating for SiC coated carbon/carbon composites. Ceramics International, 2022, 48, 8088-8096.	2.3	5
44886	Nonlocal pseudopotential energy density functional for orbital-free density functional theory. Nature Communications, 2022, 13, 1385.	5.8	10
44887	Prediction of structural, electronic, mechanical, thermal, and thermoelectric properties in PbMO3 (Mâ€‰=â€‰Sb, Bi) perovskite compounds: a DFT study. European Physical Journal Plus, 2022, 137, 1.	1.2	12
44888	Amorphization of Pseudocapacitive Tâ^'Nb ₂ O ₅ Accelerates Lithium Diffusivity as Revealed Using Tunable Isomorphic Architectures. Batteries and Supercaps, 0, , .	2.4	3
44889	Pressure-driven symmetry transitions in dense <mml:math xmlns:mml="http://www.w3.org/1998/Math/MathML"><mml:msub><mml:mi mathvariant="normal">H</mml:mi><mml:mn>2</mml:mn></mml:msub><mml:mi mathvariant="normal">O</mml:mi></mml:math> ice. Physical Review B, 2022, 105, .	1.1	9
44890	Chlorine-Decorated Ceria Nanocubes for Facilitating Low-Temperature Cyclohexane Oxidative Dehydrogenation: Unveiling the Decisive Role of Surface Species and Acid Properties. ACS Catalysis, 2022, 12, 4501-4516.	5.5	10
44891	Unravelling the functional complexity of oxygen-containing groups on carbon for the reduction of NO with NH3. Journal of the Taiwan Institute of Chemical Engineers, 2022, 133, 104261.	2.7	4
44892	Computational Screening of Single-Metal-Atom Embedded Graphene-Based Electrocatalysts Stabilized by Heteroatoms. Frontiers in Chemistry, 2022, 10, 873609.	1.8	6
44893	A₂BeS₂O₈ (A = NH₄, K, Rb, Cs) Deep Ultraviolet Nonlinear Optical Crystals. Chemistry of Materials, 2022, 34, 3781-3788.	3.2	18
44894	Molecular Simulation Study on Electronic Property and Thermal Conductivity of Graphyne/Polypyrrole Composite. Macromolecular Theory and Simulations, 2022, 31, .	0.6	1
44895	Enhanced optoelectronic and elastic responses in fluorinated penta-BCN. Applied Surface Science, 2022, 593, 153239.	3.1	4
44896	Crystal growth engineering and origin of the weak ferromagnetism in antiferromagnetic matrix of orthochromates from t-e orbital hybridization. IScience, 2022, 25, 104111.	1.9	10
44897	Photothermal Catalytic Water Splitting at Diverse Two-Phase Interfaces Based on Cuâ€“TiO₂. ACS Applied Energy Materials, 2022, 5, 4564-4576.	2.5	12
44898	First-Principles Investigation of Graphenylene as a Long-Life Cathode Material in Aluminum Ion Batteries. ACS Applied Energy Materials, 2022, 5, 4970-4975.	2.5	4

#	Article	IF	Citations
44899	Theoretical and experimental study of the effects of cobalt and nickel doping within IrO2 on the acidic oxygen evolution reaction. Journal of Catalysis, 2022, 408, 64-80.	3.1	10
44900	An Experimental and Theoretical Study of the Optical Properties of (C2H7N4O)2BiCl5 for an Optoelectronic Application. Inorganics, 2022, 10, 48.	1.2	5
44901	First principle calculations on pristine and Mn-doped iron fluorophosphates as sodium-ion battery cathode materials. Computational Materials Science, 2022, 206, 111292.	1.4	7
44902	Formation energies, electronic properties and elemental diffusion of Cuâ€“Crâ€“Nb (GRCop) alloys. Physica B: Condensed Matter, 2022, 637, 413909.	1.3	5
44903	Structural Modularization of Cu₂Te Leading to High Thermoelectric Performance near the Mottâ€“Ioffeâ€“Regel Limit. Advanced Materials, 2022, 34, e2108573.	11.1	20
44904	Inducing a deep impurity level in Li2SnO3 by ionic Biâ€“O bonding to enhance light absorption in photocatalysis. International Journal of Hydrogen Energy, 2022, 47, 13683-13692.	3.8	5
44905	First-principles calculations of transition elements interaction with hydrogen in vanadium. Journal of Nuclear Materials, 2022, 564, 153710.	1.3	4
44906	Strongly Tunable Raman Resonance in InSe under Pressure. Journal of Physical Chemistry C, 2022, 126, 6344-6350.	1.5	6
44907	Tunable electronic properties of the GeC/MoS2 heterostructures: A first-principles study. Solid State Communications, 2022, 345, 114703.	0.9	4
44908	An Endotenon Sheath-Inspired Double-Network Binder Enables Superior Cycling Performance of Silicon Electrodes. Nano-Micro Letters, 2022, 14, 87.	14.4	31
44909	Mo2CS2-MXene supported single-atom catalysts for efficient and selective CO2 electrochemical reduction. Applied Surface Science, 2022, 592, 153339.	3.1	20
44910	Octahedral rotation induced spin state and metalâ€“insulator transition in LaCoO<mml:math xmlns:mml="http://www.w3.org/1998/Math/MathML" display="inline" id="d1e389" altimg="si83.svg"><mml:msub><mml:mrow /><mml:mrow><mml:mn>3</mml:mn></mml:mrow></mml:msub></mml:math> films. Journal of Magnetism and Magnetic Materials, 2022, 555, 169318.	1.0	1
44911	First-principle studies of the pressure effect on metal carbonates elastic properties. Solid State Communications, 2022, 346, 114706.	0.9	4
44912	Znâ€“Sn alloy anode with repressible dendrite grown and meliorative corrosion resistance for Zn-air battery. Journal of Power Sources, 2022, 526, 231173.	4.0	28
44913	Symmetry-protected Dirac nodal lines and large spin Hall effect in a <mml:math xmlns:mml="http://www.w3.org/1998/Math/MathML"><mml:mrow><mml:msub><mml:mi mathvariant="normal">V</mml:mi><mml:mn>6</mml:mn></mml:msub><mml:msub><mml:mi>Sb</mml:mi><mml:mn>4</mml:mn></ kagome bilayer. Physical Review B, 2022, 105, .	1.1	3
44914	Electronic structure and thermoelectric properties of biaxial strained SnSe from first principles calculations. Physica Scripta, 0, , .	1.2	1
44915	Conversion of Catalytically Inert 2D Bismuth Oxide Nanosheets for Effective Electrochemical Hydrogen Evolution Reaction Catalysis via Oxygen Vacancy Concentration Modulation. Nano-Micro Letters, 2022, 14, 90.	14.4	51
44916	Unraveling the Synergetic Effect of the FeO_xâ€“Cu Model System in Catalyzing the Waterâ€“Gas Shift Reaction. Journal of Physical Chemistry C, 2022, 126, 6241-6248.	1.5	1

#	Article	IF	Citations
44917	Probing the elastic, mechanical and thermodynamic properties of Weyl semimetals ZrX (X=S and Te). Pramana - Journal of Physics, 2022, 96, 1.	0.6	1
44918	Comment on â€˜Biphenylene monolayer as a two-dimensional nonbenzenoid carbon allotrope: a first-principles studyâ€™. Journal of Physics Condensed Matter, 2022, 34, 248001.	0.7	0
44919	Collective plasmonic modes in the chiral multifold fermionic material CoSi. Physical Review B, 2022, 105, .	1.1	9
44920	A Fully Integrated Flexible Tunable Chemical Sensor Based on Gold-Modified Indium Selenide Nanosheets. ACS Sensors, 2022, 7, 1183-1193.	4.0	29
44921	Tunable Nonlinearity in 2D Graphdiyne Oxide for Highâ€Performance Allâ€Optical Modulation. Advanced Optical Materials, 2022, 10, .	3.6	3
44922	Catalytic cycloaddition of CO2 to epoxides by the synergistic effect of acidity and alkalinity in a functionalized biochar. Chemical Engineering Journal, 2022, 442, 136265.	6.6	27
44923	Effects of oxygen concentration and irradiation defects on the oxidation corrosion of body-centered-cubic iron surfaces: A first-principles study. Chinese Physics B, 0, , .	0.7	2
44924	A new transition metal diphosphide Î±-MoP₂ synthesized by a high-temperature and high-pressure technique. Chinese Physics B, 2023, 32, 018102.	0.7	3
44925	Theoretical investigation of the hydrogen production by adsorption of methanol on bimetallic Pd-Ge (1 1 0) surface as future green combustible using DFT-D method: Energetic and structural aspect of interaction pathways of metal with methanol. Computational and Theoretical Chemistry, 2022, 1210, 113635.	1.1	2
44926	Enhanced linear dichroism of flattened-edge black phosphorus nanoribbons. Journal of Physics Condensed Matter, 2022, 34, 225701.	0.7	1
44927	First principles approach to solar energy conversion efficiency of semiconductor heterojunctions. Solar Energy, 2022, 236, 445-454.	2.9	6
44928	Robust Î±-Fe2O3@TiO2 Coreâ€“Shell Structures With Tunable Buffer Chambers for High-Performance Lithium Storage. Frontiers in Chemistry, 2022, 10, 866369.	1.8	2
44929	Enhancement in magnetization of two-dimensional cobalt telluride and its magnetic field-assisted photocatalytic activity. Applied Physics A: Materials Science and Processing, 2022, 128, 1.	1.1	8
44930	First-principles calculations of carboxylic acid adsorption on carbonate surfaces: Chain size and aqueous interface effects. Applied Surface Science, 2022, , 153216.	3.1	1
44931	Two-Dimensional Heterostructure of MoS₂/BA₂PbI₄ 2D Ruddlesdenâ€“Popper Perovskite with an S Scheme Alignment for Solar Cells: A First-Principles Study. ACS Applied Electronic Materials, 2022, 4, 1939-1948.	2.0	11
44932	Adsorption of molecular iodine on the Ag(111) surface: Phase transitions, silver reconstruction, and iodide growth. Journal of Chemical Physics, 2022, 156, 164702.	1.2	4
44933	The strongest and toughest predicted materials: Linear atomic chains without a Peierls instability. Matter, 2022, 5, 1192-1203.	5.0	11
44934	Photoelectron-induced quantitative regulation of ferromagnetism in Permalloy at room temperature for photovoltaic flexible spintronics. Journal of Alloys and Compounds, 2022, 910, 164903.	2.8	4

#	Article	IF	Citations
44935	Theoretical insights into the diverse and tunable charge transport behavior of stilbene-based single-molecule junctions. Chemical Physics, 2022, 556, 111478.	0.9	2
44936	A Firstâ€Principles Study of the Structural, Magnetic, Optical Properties and Doping Effect in Chromium Arsenide. Physica Status Solidi (B): Basic Research, 0, , 2200062.	0.7	0
44937	Multiscale Characterization of the Influence of the Organicâ€“Inorganic Interface on the Dielectric Breakdown of Nanocomposites. ACS Nano, 2022, 16, 6744-6754.	7.3	15
44938	Oxygen Vacancy Formation and Migration within the Antiphase Boundaries in Lanthanum Scandate-Based Oxides: Computational Study. Materials, 2022, 15, 2695.	1.3	0
44939	Sampling lattices in semi-grand canonical ensemble with autoregressive machine learning. Npj Computational Materials, 2022, 8, .	3.5	3
44940	Metalâ€Doped PdH(111) Catalysts for CO₂ Reduction. ChemSusChem, 2022, 15, .	3.6	7
44941	Adsorption Behavior of Pd-Doped PtSâ„ Monolayer Upon SFâ„† Decomposed Species and the Effect of Applied Electric Field. IEEE Sensors Journal, 2022, 22, 6764-6771.	2.4	22
44942	Unsupervised machine learning to classify crystal structures according to their structural distortion: A case study on Li-argyrodite solid-state electrolytes. Energy and AI, 2022, 9, 100159.	5.8	3
44943	Theoretical insight on dopamine, ascorbic acid and uric acid adsorption on graphene as material for biosensors. Computational and Theoretical Chemistry, 2022, 1212, 113705.	1.1	1
44944	Bonding character of intermediates in onâ€surface Ullmann reactions revealed with energy decomposition analysis. Journal of Computational Chemistry, 2023, 44, 179-189.	1.5	2
44945	First-Principles Computational Exploration of Thermoelectric Properties of Bulk-GaN and Monolayer-GaN. Journal of Electronic Materials, 2022, 51, 3317-3328.	1.0	6
44946	Identification of potential metal oxides for NO₂ capture: A density functional theory study. Journal of the American Ceramic Society, 2022, 105, 5299-5308.	1.9	3
44947	First principles study of Li adsorption properties of a Borophene based hybrid 2D material B5Se. Applied Surface Science Advances, 2022, 8, 100218.	2.9	1
44948	First principles design of 2 dimensional Nickel dichalcogenide Janus materials NiXY (X,YÂ=ÂS,Se,Te). Computational Materials Science, 2022, 206, 111278.	1.4	7
44949	Hydrogen adsorption behavior on AXenes Na₂N and K₂N: a first-principles study. Materials Research Express, 2022, 9, 045501.	0.8	4
44950	Ab-initio method to investigate perovskites BiXO3(X = Be, Ca, Mg, Na, K, Li) for spintronics applications. Solid State Sciences, 2022, 126, 106839.	1.5	9
44951	Spontaneous Magnetic Skyrmions in Single-Layer CrInX₃ (X = Te, Se). Nano Letters, 2022, 22, 3440-3446.	4.5	34
44952	Chalcogen Atom-Doped Graphene and Its Performance in N2 Activation. Surfaces, 2022, 5, 228-237.	1.0	0

#	Article	IF	Citations
44953	Thermodynamic and thermoelectric properties of titanium oxycarbide with metal vacancy. International Journal of Minerals, Metallurgy and Materials, 2022, 29, 787-795.	2.4	5
44954	Design Principles for Metastable Standing Molecules. Journal of Physical Chemistry C, 2022, 126, 6880-6891.	1.5	2
44955	First-Principles Calculations on Lateral Heterostructures of Armchair Graphene Antidot Nanoribbons for Band Alignment. ACS Applied Nano Materials, 2022, 5, 5699-5708.	2.4	1
44956	First-principles investigation of equilibrium phase, mechanical and thermodynamic properties of the Nowotny TM5Si3C ternary phase. Ceramics International, 2022, 48, 20438-20445.	2.3	49
44957	A Defect Engineered Electrocatalyst that Promotes High-Efficiency Urea Synthesis under Ambient Conditions. ACS Nano, 2022, 16, 8213-8222.	7.3	109
44958	Controllable repairing the single vacancies of BC3 monolayer using CO and BF molecules: A first-principles study. Results in Physics, 2022, 35, 105365.	2.0	5
44959	Cobalt-regulation-induced dual active sites in Ni2P for hydrazine electrooxidation. Chinese Journal of Catalysis, 2022, 43, 1131-1138.	6.9	9
44960	Ultrahard BC5 â€“ An efficient nanoscale heat conductor through dominant contribution of optical phonons. Computational Materials Science, 2022, 206, 111276.	1.4	1
44961	Lead-Free Alloyed Double Perovskites: An Emerging Class of Materials for Optoelectronic Applications. Journal of Physical Chemistry C, 2022, 126, 6753-6760.	1.5	5
44962	Fast and Simple Ag/Cu Ion Exchange on Cu Foil for Anode-Free Lithium-Metal Batteries. ACS Applied Materials & Interfaces, 2022, 14, 17454-17460.	4.0	21
44963	Enhanced reversible hydrogen storage performance of light metal-decorated boron-doped siligene: A DFT study. International Journal of Hydrogen Energy, 2022, 47, 41310-41319.	3.8	26
44964	Predicted superior hydrogen evolution activities of MoC via surface dopant. International Journal of Hydrogen Energy, 2022, 47, 13664-13673.	3.8	7
44965	Calculation of the vibrational spectra of CdSe and CdS crystals with zinc blende structure. Materials Today: Proceedings, 2022, 62, 5812-5818.	0.9	2
44966	Accurate and efficient approximate quasiparticle DFTâ€1/2 band structure calculations of transition metal oxide perovskites. Physica Status Solidi (B): Basic Research, 0, , .	0.7	0
44967	Enhancement of the lattice thermal conductivity of two-dimensional functionalized MXenes by inversion symmetry breaking. Physical Review B, 2022, 105, .	1.1	14
44968	Novel polymerization of nitrogen in zinc nitrides at high pressures. Journal of Physics Condensed Matter, 2022, 34, 235702.	0.7	3
44969	Ferroelectricity coexisted with p-orbital ferromagnetism and metallicity in two-dimensional metal oxynitrides. Npj Computational Materials, 2022, 8, .	3.5	20
44970	Equilibrium phase diagrams of isostructural and heterostructural two-dimensional alloys from first principles. IScience, 2022, 25, 104161.	1.9	1

#	Article	IF	Citations
44971	Adsorption of Cr (III) and Cr (VI) ions on muscovite mica: Experimental and molecular modeling studies. Journal of Molecular Liquids, 2022, 357, 119116.	2.3	20
44972	Effects of Mono-Vacancies of Oxigen and Manganese on the Properties of the MnO2/Graphene Heterostructure. Materials, 2022, 15, 2731.	1.3	2
44973	Effect of Magnetic Tuning and Induced Charge Transfer Isotropy in a CrI₃-Based 2D Trilayer Heterostructure. Journal of Physical Chemistry C, 2022, 126, 6394-6404.	1.5	2
44974	Overlapping electron density and the global delocalization of Ï€â€aromatic fragments as the reason of conductivity of the biphenylene network. Journal of Computational Chemistry, 2023, 44, 168-178.	1.5	8
44975	Simulation of thermodynamic properties of magnetic transition metals from an efficient tight-binding model: The case of cobalt and beyond. Physical Review B, 2022, 105, .	1.1	1
44976	Nitrogen-vacancy defects in germanium. AIP Advances, 2022, 12, 045110.	0.6	2
44977	Theoretical study on the influence of Cr, Mo, and W alloying additions on the helium behavior in nickel. Journal of Nuclear Materials, 2022, 565, 153720.	1.3	5
44978	Correlation between d-orbital bandwidth and local coordination environment in RE₂SiO₅ compounds with implications in minimizing the coefficient of thermal expansion anisotropy (RE = Sc, Y, La). AIP Advances, 2022, 12, 045012.	0.6	1
44979	Orbital selective switching of ferromagnetism in an oxide quasi two-dimensional electron gas. Npj Quantum Materials, 2022, 7, .	1.8	11
44980	An experimental and theoretical study of the structural, optical, electrical, and dielectric properties of PrAsO4. Journal of Alloys and Compounds, 2022, 910, 164894.	2.8	6
44981	Possibility of Chemisorption for Benzene on Stepped Surface of Coinage Metals. Surface Science, 2022, , 122084.	0.8	0
44982	Theoretical investigation on un-doped and doped TiO₂ for solar cell application. Physica Scripta, 2022, 97, 055806.	1.2	4
44983	Electronic and optical properties of lead halide perovskite (MAPbX₃) (XÂ=ÂI, Br, and Cl) by first principles calculations. Physica Scripta, 2022, 97, 055818.	1.2	3
44984	A hybrid density functional design of intermediate band semiconductor for photovoltaic application based on group IV elements (Si, Ge, Sn, and Pb)-doped CdIn2S4. Journal of Applied Physics, 2022, 131, .	1.1	2
44985	Redox-active Hexaazatriphenylene@MXene composite for high-performance flexible proton batteries. Composites Part B: Engineering, 2022, 235, 109750.	5.9	21
44986	A DFT insight into the mechanical, electronic and thermodynamic properties of (TiZrHf)C medium-entropy carbide ceramic. Results in Physics, 2022, 35, 105341.	2.0	19
44987	Exploring a high-carrier-mobility black phosphorus/MoSe2 heterostructure for high-efficiency thin film solar cells. Solar Energy, 2022, 236, 576-585.	2.9	13
44988	Unveiling Zn substitution and carbon nanotubes enwrapping in Na3V2(PO4)3 with high performance for sodium ion batteries: Experimental and theoretical study. Electrochimica Acta, 2022, 411, 140073.	2.6	32

#	Article	IF	Citations
44989	Recyclable regeneration of NiO/NaF catalyst: Hydrogen evolution via steam reforming of oxygen-containing volatile organic compounds. Energy Conversion and Management, 2022, 258, 115456.	4.4	12
44990	Superassembly of Surface-Enriched Ru Nanoclusters from Trappingâ€“Bonding Strategy for Efficient Hydrogen Evolution. ACS Nano, 2022, 16, 7993-8004.	7.3	54
44991	Comprehensive Modulation of Conductance Anisotropy in Low-Symmetry <mml:math xmlns:mml="http://www.w3.org/1998/Math/MathML" display="inline" overflow="scroll"><mml:msub><mml:mrow><mml:mi>Re</mml:mi><mml:mi mathvariant="normal">S</mml:mi></mml:mrow><mml:mn>2</mml:mn></mml:msub></mml:math> Transistors. Physical Review Applied, 2022, 17, .	1.5	2
44992	Promoting Water Activation by Photogenerated Holes in Monolayer C₂N. Journal of Physical Chemistry Letters, 2022, 13, 3332-3337.	2.1	7
44993	Enhanced dissociation activation of CO2 on the Bi/Cu(1 1 1) interface by the synergistic effect. Journal of Catalysis, 2022, 410, 1-9.	3.1	8
44994	Hydrogen diffusion on and into the hydrogen-covered Pd(1 0 0) surfaces from first-principles. Chemical Physics Letters, 2022, 794, 139509.	1.2	2
44995	Machine-learning enabled thermodynamic model for the design of new rare-earth compounds. Acta Materialia, 2022, 229, 117759.	3.8	13
44996	Lattice inversion potential with neural network corrections for metallic systems. Computational Materials Science, 2022, 207, 111311.	1.4	1
44997	Structures of boundaries and corners of fully-closed hexagonal domains in HVPE-AlN film. Acta Materialia, 2022, 229, 117838.	3.8	0
44998	L12-strengthened multicomponent Co-Al-Nb-based alloys with high strength and matrix-confined stacking-fault-mediated plasticity. Acta Materialia, 2022, 229, 117763.	3.8	36
44999	Unveiling the effect of vacancy defects on structural, mechanical, electronic and diffusion properties of copper (I) iodide. Scripta Materialia, 2022, 213, 114634.	2.6	4
45000	Optical response, lithiation and charge transfer in Sn-based 211 MAX phases with electron localization function. Journal of Materials Research and Technology, 2022, 18, 2470-2479.	2.6	13
45001	Pd-doped PtSe2 monolayer with strain-modulated effect for sensing SF6 decomposed species: a first-principles study. Journal of Materials Research and Technology, 2022, 18, 629-636.	2.6	28
45002	Orientation relationships and interface structure between Al11Ce3 and Al in Alâ€“Ce eutectic. Journal of Materials Research and Technology, 2022, 18, 693-704.	2.6	11
45003	Influence of titanium on the clustering of vacancy, rhenium and osmium in tungsten-titanium alloys: First-principles study. Fusion Engineering and Design, 2022, 178, 113098.	1.0	1
45004	Ohmic contact in graphene and hexagonal III-V monolayer (GaP, GaAs, InP, and InAs) van der Waals heterostructures: Role of electric field. Physics Letters, Section A: General, Atomic and Solid State Physics, 2022, 433, 128029.	0.9	4
45005	Correlation-assisted Peierls gap in divalent metal ion (Zn+2, Cd+2, Mg+2, Ca+2, Sr+2 and Ba+2) doped M-VO2: First principle analysis. Solid State Communications, 2022, 347, 114710.	0.9	2
45006	Oddâ€“even effect and bandgap modulation by C-H doping in armchair nanoribbons of monolayer WS<mml:math xmlns:mml="http://www.w3.org/1998/Math/MathML" display="inline" id="d1e710" altimg="si2.svg"><mml:msub><mml:mrow /><mml:mrow><mml:mn>2</mml:mn></mml:mrow></mml:msub></mml:math>. Solid State Communications, 2022, 347, 114719.	0.9	0

#	Article	IF	Citations
45007	Assessing Mgâ€“Scâ€“(rare earth) ternary phase stability via constituent binary cluster expansions. Computational Materials Science, 2022, 207, 111240.	1.4	1
45008	Carbon driven oxygen retention in uranium oxycarbide (UCO) fluorite phase. Journal of Nuclear Materials, 2022, 563, 153662.	1.3	0
45009	First-principles calculations to investigate Structural, electronic, and optical properties of MgF2 monolayer in 1T-phase and 2H-phase using hybrid functional. Chemical Physics, 2022, 557, 111473.	0.9	1
45010	Operando electrochemical TEM, ex-situ SEM and atomistic modeling studies of MnS dissolution and its role in triggering pitting corrosion in 304L stainless steel. Corrosion Science, 2022, 199, 110184.	3.0	22
45011	Unusual structure and properties of germanium under pressure. Computational Materials Science, 2022, 207, 111310.	1.4	2
45012	Lithiation MAX derivative electrodes with low overpotential and long-term cyclability in a wide-temperature range. Energy Storage Materials, 2022, 47, 611-619.	9.5	3
45013	Ferromagnetism in V and Cr doped ScN diluted magnetic semiconductor in B3 phase: A DFT study. Solid State Communications, 2022, 347, 114724.	0.9	3
45014	High-throughput generation of potential energy surfaces for solid interfaces. Computational Materials Science, 2022, 207, 111302.	1.4	4
45015	The effect mechanism of Zn, Ni and Mn solute elements on the WC/Cu-based filler metal interfacial properties: first-principles calculations and experiments. Journal of Materials Research and Technology, 2022, 18, 2354-2362.	2.6	12
45016	Ab initio investigations of electronic structure, mechanical properties, phonon stability, and thermodynamics of the Mgâ€“Er system. Vacuum, 2022, 199, 110968.	1.6	8
45017	NiCo-layered double hydroxide with cation vacancy defects for high-performance supercapacitors. Electrochimica Acta, 2022, 413, 140143.	2.6	18
45018	Interfacial characterization and its influence on the corrosion behavior of Mg-SiO2 nanocomposites. Acta Materialia, 2022, 230, 117840.	3.8	13
45019	Transport behavior and thermoelectric properties of SnSe/SnS heterostructure modulated with asymmetric strain engineering. Computational Materials Science, 2022, 207, 111271.	1.4	5
45020	Study on the structural properties of refining slags by molecular dynamics with deep learning potential. Journal of Molecular Liquids, 2022, 353, 118787.	2.3	7
45021	Passivation effect of NTCDA nanofilm on black phosphorus. Results in Physics, 2022, 36, 105466.	2.0	0
45022	Effect of linkage mode on the spin-polarized transport of a TPV radical-based molecular device. Chemical Physics Letters, 2022, 794, 139515.	1.2	4
45023	Effect of the local chemical environment on oxidation resistance mechanisms in AlNbTiZr refractory high entropy alloys: A first-principles study. Scripta Materialia, 2022, 213, 114624.	2.6	4
45024	A coupled electrochemomechanical model for the cycling of a Cu15Si<mml:math xmlns:mml="http://www.w3.org/1998/Math/MathML" display="inline" id="d1e1095" altimg="si3.svg"><mml:msub><mml:mrow /><mml:mrow><mml:mn>4</mml:mn></mml:mrow></mml:msub></mml:math>-hosted silicon nanowire. Journal of Power Sources, 2022, 529, 231197.	4.0	2

#	Article	IF	Citations
45025	An ab-initio probe to predict the stability of SrLa, Sr2La and Sr3La intermetallic alloys with the aid of high pressures. Computational and Theoretical Chemistry, 2022, 1211, 113660.	1.1	1
45026	The spin effects on electronic, optical and mechanical properties of new ferromagnetic chalcopyrite: YMnS2. Materials Chemistry and Physics, 2022, 284, 126030.	2.0	1
45027	Fundamental invariant-neural network potential energy surface and dissociative chemisorption dynamics of N2 on rigid Ni(1 1 1). Computational and Theoretical Chemistry, 2022, 1211, 113679.	1.1	1
45028	A Simplified Continuum Particle Model Bridging Interatomic Potentials and Elasticity of Solids. Journal of Engineering Mechanics - ASCE, 2022, 148, .	1.6	8
45029	Enhanced electrochemical properties of W-doped Na3V2(PO4)2F3@C as cathode material in sodium ion batteries. Electrochimica Acta, 2022, 415, 140256.	2.6	12
45030	Raman spectra characterization of boron carbide using first-principles calculations. Physica B: Condensed Matter, 2022, 633, 413738.	1.3	8
45031	Re-entrant ferromagnetism at ultrahigh temperatures in epsilonâ€“iron as possible origin of the geomagnetic field. Physics of the Earth and Planetary Interiors, 2022, 326, 106856.	0.7	0
45032	Prediction the photocatalytic water splitting of bismuth vanady1 oxyhalide BiVO3F based on density functional theory. Molecular Catalysis, 2022, 524, 112244.	1.0	0
45033	Theoretical study about adsorbed oxygen reduction over Ï‡-Fe5C2: formation of H2O and CO2. Molecular Catalysis, 2022, 524, 112236.	1.0	3
45034	Structural, electronic and optical properties of the anhydrous orthorhombic 2C14H12Br2S3Bis (2-Bromobenzyl) trisulfide crystals. Journal of Materials Research and Technology, 2022, 18, 396-404.	2.6	2
45035	First principles study of the structural, optoelectronic and mechanical properties of XLaS2 (X Cu, Zn) for optoelectronic applications. Optik, 2022, 258, 168940.	1.4	1
45036	Pairwise dilatational strain as a parametric model describing potential secondary phase formation and high-angle grain misorientation in as-cast high-entropy alloys. Intermetallics, 2022, 144, 107462.	1.8	0
45037	Ab initio study of mechanical properties of hexagonal high-entropy ceramic (Mo0.25Nb0.25Ta0.25V0.25)(Al0.5Si0.5)2 with dual mixing of cation and anion sublattice. Journal of Physics and Chemistry of Solids, 2022, 165, 110701.	1.9	3
45038	Monoclinic mC28 carbon: A sp2-sp3 hybridized carbon allotrope with superhard and metallic properties. Chemical Physics, 2022, 558, 111503.	0.9	0
45039	Study of vacancy, voids, atom adsorption and domain substitution in hexagonal gallium nitride monolayer. Surfaces and Interfaces, 2022, 30, 101898.	1.5	1
45040	Anchoring of phthalic acid on MgO(100). Surface Science, 2022, 720, 122007.	0.8	1
45041	High performance Li-ion capacitor based on novel carbon-coated chalcogenide anode. Journal of Energy Storage, 2022, 50, 104251.	3.9	12
45042	Correlation between redox active sites and sodium storage behavior in dye/graphene nanohybrids. Applied Surface Science, 2022, 587, 152859.	3.1	2

#	Article	IF	Citations
45043	Determination of thermodynamic growth conditions for a high-efficiency Cu<mml:math xmlns:mml="http://www.w3.org/1998/Math/MathML" display="inline" id="d1e1705" altimg="si10.svg"><mml:msub><mml:mrow		

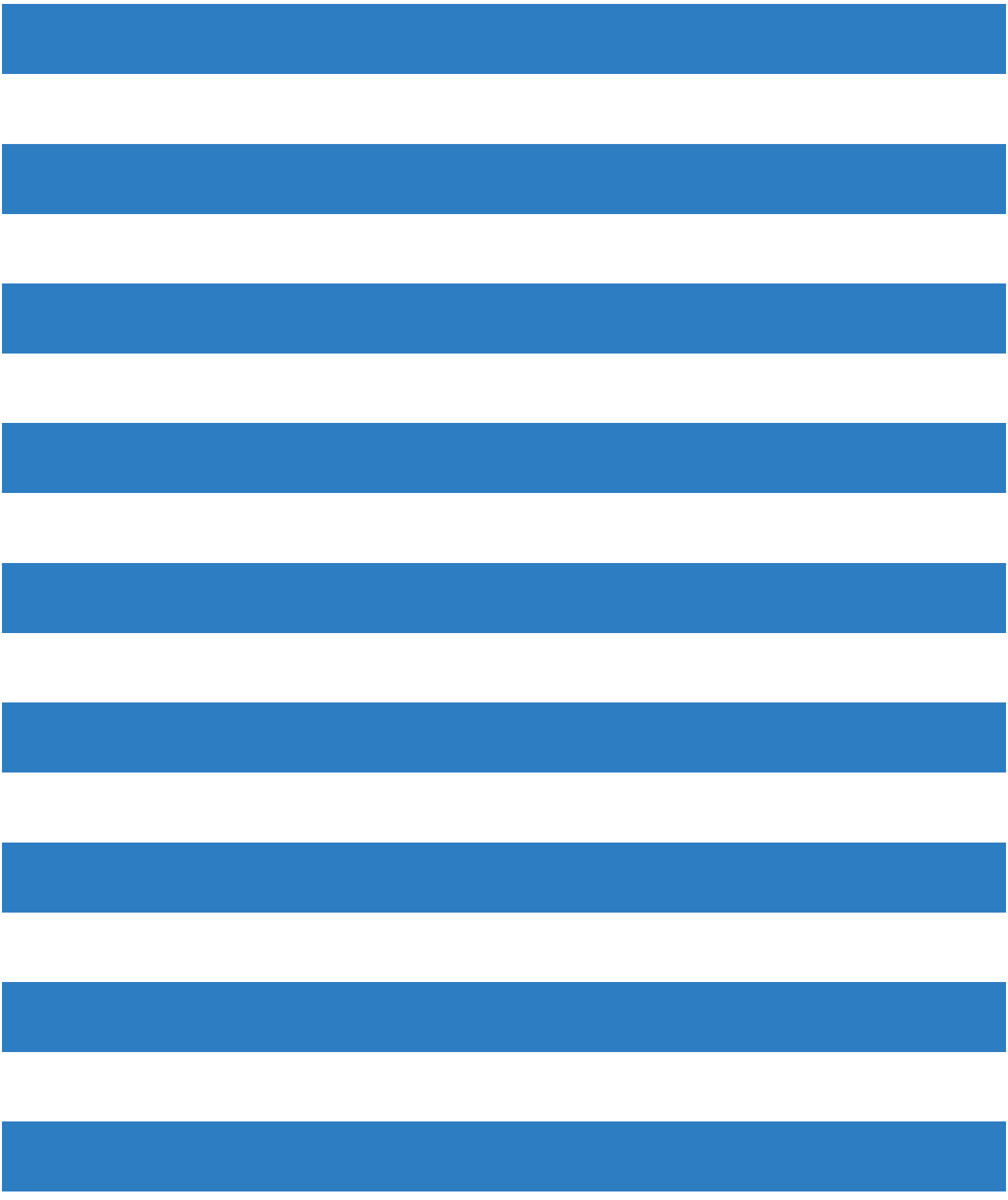

#	Article	IF	Citations
45061	Cu vacancy engineering of cage-compound BaCu2Se2: Realization of temperature-dependent hole concentration for high average thermoelectric figure-of-merit. Chemical Engineering Journal, 2022, 437, 135302.	6.6	6
45062	Property changes in two-dimensional electride bilayers through compression, sliding, and twisting. Applied Surface Science, 2022, 586, 152596.	3.1	4
45063	A first-principles study of optoelectronic properties of Y2MS4 (M=Zn, Mg and Be): Direct bandgap ternary sulfides. Optik, 2022, 259, 168944.	1.4	1
45064	Atomic structures and stability of finite-size extended interstitial defects in silicon: Large-scale molecular simulations with a neural-network potential. Scripta Materialia, 2022, 214, 114650.	2.6	2
45065	First principles study on the structures and properties of SnOâ€“ZnO alloys under high pressure. Materials Science in Semiconductor Processing, 2022, 144, 106566.	1.9	3
45066	Construction of organic-inorganic â€œchelateâ€•adsorption sites on metal oxide semiconductor for room temperature NO2 sensing. Journal of Hazardous Materials, 2022, 432, 128623.	6.5	15
45067	Mechanism insight into MnO for CHx(xÂ=Â1 to 3) hydrogenation and C1-C1 coupling processes on Co(0001) surface: A DFT and kMC study. Applied Surface Science, 2022, 586, 152840.	3.1	2
45068	Nitrogen and sulfur co-doped graphene nanoribbons with well-ordered stepped edges for high-performance potassium-ion battery anodes. Energy Storage Materials, 2022, 48, 325-334.	9.5	16
45069	Self-templating construction of flower-like mesoporous magnesium silicate composites from sepiolite for high-efficiency adsorption of aflatoxin B1. Separation and Purification Technology, 2022, 291, 120953.	3.9	19
45070	Structure and electronic properties of LnScO3 compounds: A GGAÂ+ÂU calculation. Computational Materials Science, 2022, 208, 111350.	1.4	1
45071	Computational screening of single transition metal atom embedded in nitrogen doped graphene for CH4 detection. Materials Today Communications, 2022, 31, 103383.	0.9	0
45072	Engineering of graphene nanoribbon as a promising platform for detection of carbon-based molecules. Chinese Journal of Physics, 2022, 77, 534-543.	2.0	1
45073	Towards pure: The single-phase bulk omega titanium and modulation on its elastic properties under biaxial strains. Journal of Alloys and Compounds, 2022, 906, 164312.	2.8	2
45074	2D Janus and non-Janus diamanes with an in-plane negative Poisson's ratio for energy applications. Materials Today Advances, 2022, 14, 100225.	2.5	10
45075	Revealing effects of common nonmetallic impurities on the stability and strength of Cuâ€“Sn solder joints: A first-principles investigation. Vacuum, 2022, 200, 110997.	1.6	15
45076	Crystal plasticity including a phase-field deformation twinning model for the high-rate deformation of cyclotetramethylene tetranitramine. Journal of the Mechanics and Physics of Solids, 2022, 163, 104872.	2.3	8
45077	Electronic structure properties of boronâ€“doped and carbonâ€“boronâ€“codoped TiO2(B) for photocatalytic applications. Journal of Physics and Chemistry of Solids, 2022, 165, 110685.	1.9	3
45078	First-principles study of optoelectronic and thermoelectric properties of LiCaX (X=N, P and As) half-Heusler semiconductors. Journal of Solid State Chemistry, 2022, 310, 123020.	1.4	17

#	Article	IF	Citations
45079	Performance of the modified Beckeâ€“Johnson potential employing the pseudopotential plane-wave approach for band structure calculations. Computational Materials Science, 2022, 208, 111324.	1.4	6
45080	Interface bonding and failure mechanism of Ti(001)/Si(001) and TiO2(001)/Si(001) interfaces: A firstâ€“principles study. Surfaces and Interfaces, 2022, 30, 101833.	1.5	3
45081	Tunable electronic and magnetic properties of two-dimensional magnetic semiconductor VIBr<mml:math xmlns:mml="http://www.w3.org/1998/Math/MathML" display="inline" id="d1e368" altimg="si32.svg"><mml:msub><mml:mrow /><mml:mrow><mml:mn>2</mml:mn></mml:mrow></mml:msub></mml:math>. Computational Materials Science, 2022, 209, 111319.	1.4	5
45082	First-principles analysis of aluminium interaction with nitrogen-doped graphene nanoribbons â€“ from adatom bonding to various potential applications. Materials Today Communications, 2022, 31, 103388.	0.9	0
45083	Study on the most effective pressure application method to increase the critical temperature of MgB2. Materials Today Communications, 2022, 31, 103432.	0.9	0
45084	Highly selective formaldehyde sensor using silicon doped graphene: A theoretical study. Materials Today Communications, 2022, 31, 103452.	0.9	2
45085	Outstanding thermal conductivity and mechanical properties in the direct gap semiconducting penta-NiN2 monolayer confirmed by first-principles. Physica E: Low-Dimensional Systems and Nanostructures, 2022, 140, 115221.	1.3	10
45086	Surface stability of WN ultrathin films under O2 and H2O exposure: A first-principles study. Applied Surface Science, 2022, 588, 152940.	3.1	5
45087	Rational nanopositioning of homogeneous amorphous phase on crystalline tungsten oxide for boosting solar water oxidation. Chemical Engineering Journal, 2022, 438, 135532.	6.6	14
45088	Investigation of electronic stabilities and properties of Mn-doped Janus WSSe monolayer. Computational Condensed Matter, 2022, 31, e00677.	0.9	2
45089	Exploring the elastic, mechanical and anisotropic response of Ti-5Al-XSn alloys through DFT calculations. Chinese Journal of Physics, 2022, 77, 151-160.	2.0	7
45090	Tuning the magnetic properties of FeTe2 monolayer doped by (TM: V, Mn, and Co). Journal of Magnetism and Magnetic Materials, 2022, 552, 169204.	1.0	6
45091	The spin-state transition in ACo2O4 spinels (AÂ=ÂBe, Mg, Ca, Cd, Zn). Journal of Magnetism and Magnetic Materials, 2022, 552, 169206.	1.0	1
45092	Nitrogen-doped carbon black supported synergistic palladium single atoms and nanoparticles for electrocatalytic oxidation of methanol. Chemical Engineering Journal, 2022, 438, 135585.	6.6	19
45093	Adsorption of hydrated Al3+ on the kaolinite (001) surface: A density functional theory study. Applied Clay Science, 2022, 223, 106498.	2.6	16
45094	Mechanistic insights into benzene oxidation over CuMn2O4 catalyst. Journal of Hazardous Materials, 2022, 431, 128640.	6.5	16
45095	Predicted crystal structures of AlN4 at high pressure. Solid State Communications, 2022, 348-349, 114745.	0.9	0
45096	Solid supported ruthenium catalyst for growing single-walled carbon nanotubes with narrow chirality distribution. Carbon, 2022, 193, 35-41.	5.4	7

#	Article	IF	Citations
45097	First-principles study of CO gas adsorption on pristine and Fe-doped H<mml:math xmlns:mml="http://www.w3.org/1998/Math/MathML" display="inline" id="d1e1723" altimg="si98.svg"><mml:msub><mml:mrow /><mml:mrow><mml:mn>4</mml:mn><mml:mo>,</mml:mo><mml:mn>4</mml:mn><mml:mo>,</mml:mo><mml:mn>4</mml:mn></mml:mrow></mml:msub></mml:math>N monolayer. Applied Surface Science, 2022, 586, 152749.	3.1	5
45098	Quantitative calculations of thermal-expansion coefficient in Feâ€“Ni alloys: First-principles approach. Current Applied Physics, 2022, 38, 76-80.	1.1	3
45099	Controllable electrochemical activation of Mn3O4: Anion effect on phase transition, morphology and capacitive performance. Electrochimica Acta, 2022, 416, 140281.	2.6	1
45100	Transition metal-decorated germanene for NO, N2 and O2 sensing: A DFT study. Surfaces and Interfaces, 2022, 30, 101886.	1.5	12
45101	Vapor pressure-controllable molecular inorganic precursors for growth of monolayer WS2: Influence of precursor-substrate interaction on growth thermodynamics. Applied Surface Science, 2022, 587, 152829.	3.1	4
45102	Investigation of protonation and deprotonation processes of kaolinite and its effect on the adsorption stability of rare earth elements. Colloids and Surfaces A: Physicochemical and Engineering Aspects, 2022, 642, 128596.	2.3	7
45103	Boosting capacitive performance of nitrogen-doped carbon by atomically dispersed iron. Journal of Power Sources, 2022, 532, 231335.	4.0	15
45104	First principles study of the structural, electronic, magnetic and optical properties of the Fe doped CoS2 thin films. Thin Solid Films, 2022, 751, 139228.	0.8	1
45105	First-principles study of the effect of aluminum content on the elastic properties of Cu-Al alloys. Materials Today Communications, 2022, 31, 103399.	0.9	5
45106	Study of the structural stability and electronic properties of the C-doped boron nanomaterials. Solid State Communications, 2022, 350, 114773.	0.9	0
45107	Energetic MOF-derived hollow carbon tubes with interconnected channels and encapsulated nickel-cobalt alloy sites as bifunctional catalysts for Znâ€“air batteries with stable cycling over 600 cycles. Applied Surface Science, 2022, 591, 153070.	3.1	10
45108	The flexible Janus X2PAs (XÂ=ÂSi, Ge and Sn) monolayers with in-plane and out-of-plane piezoelectricity. Applied Surface Science, 2022, 589, 152999.	3.1	23
45109	Layered Pt-Co alloys: Bulk, surface and nanoparticle analysis, based on DFT. Surface Science, 2022, 721, 122082.	0.8	1
45110	Titania crystal-plane-determined activity of copper cluster in water-gas shift reaction. Applied Surface Science, 2022, 591, 153145.	3.1	6
45111	Piezocatalytic oxidation of 5-hydroxymethylfurfural to 5-formyl-2-furancarboxylic acid over Pt decorated hydroxyapatite. Applied Catalysis B: Environmental, 2022, 309, 121281.	10.8	23
45112	Surface functionalization of penta-siligraphene monolayer for nanoelectronic, optoelectronic and photocatalytic water-splitting: A first-principles study. Applied Surface Science, 2022, 590, 152972.	3.1	14
45113	A computational study of strained MoS2 as catalysts for the electrocatalytic nitrogen reduction reaction. Journal of Molecular Structure, 2022, 1259, 132746.	1.8	10
45114	Surface effect of the MgCl2 support in Zieglerâ€“Natta catalyst for ethylene polymerization: A computational study. Applied Surface Science, 2022, 589, 153002.	3.1	38

#	Article	IF	Citations
45115	Controllable fabrication of atomic dispersed low-coordination nickel-nitrogen sites for highly efficient electrocatalytic CO2 reduction. Chemical Engineering Journal, 2022, 440, 135956.	6.6	23
45116	Graphene on SiC as a promising platform for magnetic field detection under neutron irradiation. Applied Surface Science, 2022, 590, 152992.	3.1	13
45117	Two-dimensional XY monolayers (X = Al, Ga, In; Y = N, P, As) with a double layer hexagonal structure: A first-principles perspective. Applied Surface Science, 2022, 590, 152998.	3.1	53
45118	Different strategies for GaN-MoS2 and GaN-WS2 coreâ€“shell nanowire growth. Applied Surface Science, 2022, 590, 153106.	3.1	2
45119	A novel strategy for enhancing photoelectrochemical performance of Ca2Fe2O5 photocathodes: An integrated experimental and DFT-based approach. Applied Surface Science, 2022, 589, 153012.	3.1	2
45120	DFT+ U analysis of the stability of Pd<mml:math xmlns:mml="http://www.w3.org/1998/Math/MathML" display="inline" id="d1e2091" altimg="si147.svg"><mml:msub><mml:mrow /><mml:mrow><mml:mi>n</mml:mi></mml:mrow></mml:msub></mml:math>/CeO<mml:math xmlns:mml="http://www.w3.org/1998/Math/MathML" display="inline" id="d1e2099" altimg="si326.svg"><mml:msub><mml:mrow /><mml:mrow><mml:mn>2</mml:mn><mml:mo>â^’</mml:mo><mml:mi>δ</mml:mi></mml:mrow></mml:msub></mml:math>	3.1	2
45121	A combined first-principles and machine-learning investigation on the stability, electronic, optical, and mechanical properties of novel C6N7-based nanoporous carbon nitrides. Carbon, 2022, 194, 230-239.	5.4	24
45122	Evaluating the properties of the intermetallic compound HoN for magnetic refrigerator application: Combined DFT and Monte Carlo simulation. Solid State Communications, 2022, 350, 114737.	0.9	4
45123	Oneâ€“pot synthesis of boron and nitrogen coâ€“doped nanocarbons for efficient catalytic reduction of nitrophenols. Chemical Engineering Journal, 2022, 439, 135733.	6.6	25
45124	Optimal surface/diffusion-controlled kinetics of bimetallic selenide nanotubes for hybrid supercapacitors. Journal of Colloid and Interface Science, 2022, 617, 304-314.	5.0	18
45125	Density functional theory study of CH4 dissociation and C C coupling on W-terminated WC(0001) surface. Applied Surface Science, 2022, 591, 153128.	3.1	5
45126	Anomalous elasticity of talc at high pressures: Implications for subduction systems. Geoscience Frontiers, 2022, 13, 101381.	4.3	4
45127	2D-Mo3S4 phase as promising contact for MoS2. Applied Surface Science, 2022, 589, 152971.	3.1	6
45128	Tuning of n-type doping by intercalation of group V and VII atoms in SnS2 bilayer. Materials Science in Semiconductor Processing, 2022, 145, 106649.	1.9	1
45129	Tuning the electronic transport properties in few-layers GeP<mml:math xmlns:mml="http://www.w3.org/1998/Math/MathML" display="inline" id="d1e899" altimg="si9.svg"><mml:msub><mml:mrow /><mml:mrow><mml:mn>3</mml:mn></mml:mrow></mml:msub></mml:math> intercalated by Cr-atoms. Physica E: Low-Dimensional Systems and Nanostructures, 2022, 141, 115242.	1.3	0
45130	Titanium and fluorine co-modification strengthens high-voltage electrochemical performance of LiCoO2. Journal of Alloys and Compounds, 2022, 909, 164787.	2.8	5
45131	Asymmetric surfaces endow Janus bismuth oxyhalides with enhanced electronic and catalytic properties for the hydrogen evolution reaction. Journal of Colloid and Interface Science, 2022, 617, 204-213.	5.0	12
45132	A biocompatible bismuth based metal-organic framework as efficient light-sensitive drug carrier. Journal of Colloid and Interface Science, 2022, 617, 578-584.	5.0	12

#	Article	IF	Citations
45133	Adsorption of sorbitan ester surfactant on copper and Cuprous oxide surfaces: A density functional theory study. Applied Surface Science, 2022, 589, 153061.	3.1	2
45134	Janus Aluminum Oxysulfide Al2OS: A promising 2D direct semiconductor photocatalyst with strong visible light harvesting. Applied Surface Science, 2022, 589, 152997.	3.1	21
45135	The catalytic mechanism of CO2 electrochemical reduction over transition metal-modified 1T'-MoS2 monolayers. Applied Surface Science, 2022, 590, 153001.	3.1	16
45136	Strain adjustment Pt-doped Ti2CO2 as an efficient bifunctional catalyst for oxygen reduction reactions and oxygen evolution reactions by first-principles calculations. Applied Surface Science, 2022, 590, 153149.	3.1	16
45137	Nonlinear optical and detonation properties of semiorganic nitrate crystal C6H14N2(NO3)3Â·H3O. Journal of Alloys and Compounds, 2022, 908, 164632.	2.8	1
45138	Formation of carbonate and oxalate species on a Cobalt-modified Fe3O4(111) surface: Comparison of DFT+U, hybrid functionals, and the random phase approximation. Surface Science, 2022, 721, 122068.	0.8	2
45139	Nitrogen-stabilized oxygen vacancies in TiO2 for site-selective loading of Pt and CoOx cocatalysts toward enhanced photoreduction of CO2 to CH4. Chemical Engineering Journal, 2022, 439, 135744.	6.6	24
45140	N-doped carbon nanosheets supported-single Fe atom for p-nitrophenol degradation via peroxymonosulfate activation. Applied Surface Science, 2022, 591, 153124.	3.1	21
45141	Crystal chemistry, DFT calculation and optical properties of the double perovskite stannate Sr2Sn0.8In0.8W0.4O6. Journal of Molecular Structure, 2022, 1259, 132716.	1.8	2
45142	Effect of Fe2+/3+ doping on the new magnetic mechanism and itinerant electronic characteristics of ZnO. Journal of Magnetism and Magnetic Materials, 2022, 554, 169305.	1.0	2
45143	Water structures on Pb(100) and (111) surface studied with the Interface force field. Applied Surface Science, 2022, 589, 152838.	3.1	7
45144	On the issue of textured crystallization of Ba(NO3)2 in mesoporous SiO2: Raman spectroscopy and lattice dynamics analysis. Spectrochimica Acta - Part A: Molecular and Biomolecular Spectroscopy, 2022, 275, 121157.	2.0	4
45145	Effect of edge groups on the electronic transport properties of tetrapodal diazatriptycene molecule. Physica E: Low-Dimensional Systems and Nanostructures, 2022, 141, 115212.	1.3	2
45146	Room temperature NO2 sensing performance of a-C-decorated TeO2 nanowires. Sensors and Actuators B: Chemical, 2022, 363, 131853.	4.0	12
45147	A key role of soft and refractory coke in the deactivation of Î³â€“Al2O3 catalysts during low-temperature methyl oleate epoxidation: An experiment and DFT study. Fuel, 2022, 321, 124064.	3.4	2
45148	MOF etching-induced Co-doped hollow carbon nitride catalyst for efficient removal of antibiotic contaminants by enhanced perxymonosulfate activation. Chemical Engineering Journal, 2022, 441, 136074.	6.6	45
45149	Photocatalytic applications of 2D surface decorated boron phosphides: A density functional theory investigation. Applied Surface Science, 2022, 592, 153236.	3.1	3
45150	Hydrogen storage by spillover on Ni4 cluster embedded in three vacancy graphene. A DFT and dynamics study. Journal of Physics and Chemistry of Solids, 2022, 167, 110706.	1.9	6

#	Article	IF	Citations
45151	Experimental and density functional theory study of the Li+ desorption in spinel/layered lithium manganese oxide nanocomposites using HCl. Chemical Engineering Journal, 2022, 441, 136019.	6.6	18
45152	Directional utilization disorder charge via In-plane driving force of functionalized graphite carbon nitride for the robust photocatalytic degradation of fluoroquinolone. Chemical Engineering Journal, 2022, 442, 135943.	6.6	14
45153	Multianion induced out-of-plane proper polarization in oxyfluoride Aurivillius Bi2TiO4F2. Journal of Physics and Chemistry of Solids, 2022, 167, 110720.	1.9	4
45154	Stable electrolysis of ammonia on platinum enhanced by methanol in non-aqueous electrolyte for an in-situ hydrogen production. Chemical Engineering Journal, 2022, 442, 136167.	6.6	2
45155	The in-depth description of phonon transport mechanisms for XC (X=Si, Ge) under hydrostatic pressure: Considering pressure-induced phase transitions. International Journal of Heat and Mass Transfer, 2022, 191, 122851.	2.5	4
45156	Unraveling the active sites of Cs-promoted Ru/Î³-Al2O3 catalysts for ammonia synthesis. Applied Catalysis B: Environmental, 2022, 310, 121269.	10.8	12
45157	Electric resonance-induced hydrate dissociation acceleration to extract methane gas. Fuel, 2022, 321, 124014.	3.4	4
45158	Hybridized heterostructure of CoS and MoS2 nanoparticles for highly-efficient and robust bifunctional water electrolysis. Applied Surface Science, 2022, 592, 153196.	3.1	17
45159	Design, crystal structures, electronic structures and absorption spectra of MnSe Te1â^'MoO6: A first principles exploration. AEJ - Alexandria Engineering Journal, 2022, 61, 9235-9241.	3.4	0
45160	Diameter Dependence of Band Gap of Single-Walled Boron Nitride Nanotubes. Physics of the Solid State, 2021, 63, 1126-1130.	0.2	1
45161	Why the Magnetiteâ€“Gold Coreâ€“Shell Nanoparticles Are Not Quite Good and How to Improve Them. Physics of the Solid State, 2021, 63, 1536-1540.	0.2	5
45162	First-principles DFT Investigation of the Photocatalytic Capability of Cl Doped Rutile TiO₂ as a Self-Cleaning Coating for Photovoltaic Panels. , 2021, , .		1
45163	High pressure phase stability, elastic anisotropy and electronic properties of BC2N. International Journal of Physical Sciences, 2021, 16, 146-157.	0.1	0
45164	Elastic and mechanical properties of Y1 â€“ xScxN alloying system as a function of Sc content: First principles study. Mechanics of Solids, 2021, 56, 1028-1038.	0.3	1
45165	Effect of a Silicon Oxide Substrate on the Electronic Properties and the Electrical Conductivity of Mono- and Bilayer Films of Armchair Single-Wall Carbon Nanotubes: a Quantum-Mechanical Study. Physics of the Solid State, 2021, 63, 1655-1661.	0.2	0
45167	The Doping Effect on the Electronic Properties of the Titanium Dioxide TiO₂: A DFT Study. Integrated Ferroelectrics, 2021, 221, 199-214.	0.3	3
45168	Strain tunable intrinsic ferromagnetic in 2D square CrBr₂. AIP Advances, 2021, 11, 115220.	0.6	4
45169	Synthesis, characterization, and structure computational calculations of the oxycalcogenide LaCuOSe for thermoelectric applications. , 2021, , .		0

#	Article	IF	Citations
45170	Ab Initio and Experimental Study of Vibrational Properties of TlFeS2 and TlFeSe2 Crystals. Physics of the Solid State, 2021, 63, 1643-1649.	0.2	1
45171	First Principal Simulation of Palladium Nanocatalysts Surfaces. Journal of Surface Investigation, 2021, 15, 1270-1277.	0.1	0
45172	Ionic Rectification across Ionic and Mixed Conductor Interfaces. Nano Letters, 2021, 21, 10086-10091.	4.5	1
45173	Coupled Current Jumps and Domain Wall Creeps in a Defectâ€Engineered Ferroelectric Resistive Memory. Advanced Electronic Materials, 0, , 2101059.	2.6	5
45174	The Deep Eutectic Solvent Precipitation Synthesis of Metastable Zn₄V₂O₉. Inorganic Chemistry, 2022, 61, 154-169.	1.9	9
45175	Orientation-Dependent Electronic and Mechanical Properties of Tungsten Nitride Nanosheets: Implications for Flexible Devices. ACS Applied Nano Materials, 2021, 4, 13771-13777.	2.4	7
45176	Enhanced Photovoltaic Performance via a Bifunctional Additive in Tin-Based Perovskite Solar Cells. ACS Applied Energy Materials, 2022, 5, 108-115.	2.5	12
45177	Electronic Structure and Diffusion of Sodium in Na4Ââ€“ÂxKxMg(MoO4)3. Physics of the Solid State, 2021, 63, 1833-1839.	0.2	0
45178	Can Chargeâ€Modulated Metalâ€Organic Frameworks Achieve Highâ€Performance CO ₂ Capture and Separation over H ₂ , N ₂ , and CH ₄ ?. ChemSusChem, 2022, 15, .	3.6	8
45179	Chemical passivation of methylammonium fragments eliminates traps, extends charge lifetimes, and restores structural stability of CH3NH3PbI3 perovskite. Nano Research, 2022, 15, 4765-4772.	5.8	12
45180	Toward an Understanding of the Reversible Li-CO₂ Batteries over Metalâ€“N₄-Functionalized Graphene Electrocatalysts. ACS Nano, 2022, 16, 1523-1532.	7.3	52
45181	A Low-Temperature Structural Transition in Canfieldite, Ag₈SnS₆, Single Crystals. Inorganic Chemistry, 2021, 60, 19345-19355.	1.9	3
45182	Computational prediction of Mo2@g-C6N6 monolayer as an efficient electrocatalyst for N2 reduction. Chinese Chemical Letters, 2022, 33, 4623-4627.	4.8	24
45183	First-Principles Calculations of Structural, Thermodynamic, and Elastic Properties of Lead Chalcogenides PbX (X = S, Se, and Te) in NaCl (B1) Phase. Russian Journal of Inorganic Chemistry, 2021, 66, 2084-2090.	0.3	4
45184	First-principles characterisation and comparison of clean, hydrated, and defect Î±-Al₂O₃ and Î±-Fe₂O₃ (110) surfaces. Molecular Simulation, 2022, 48, 247-263.	0.9	4
45185	Effects of oxygenated groups on the adsorption removal of dibenzofuran by activated coke: Experimental and DFT studies. Journal of Environmental Chemical Engineering, 2021, 9, 106775.	3.3	10
45186	Effect of vacancy defects on electronic and magnetic properties of zigzag silicon nanoribbons. , 2021, , .		0
45187	Extending Absorption of Cs₂AgBiBr₆ to Nearâ€Infrared Region (â‰ˆ1350Ânm) with Intermediate Band. Advanced Functional Materials, 2022, 32, .	7.8	30

#	Article	IF	Citations
45188	Armchair Janus MoSSe Nanoribbon with Spontaneous Curling: A First-Principles Study. Nanomaterials, 2021, 11, 3442.	1.9	3
45189	First-Principles Study on Adsorption and Decomposition of NOx on Mo (110) Surface. Advances in Condensed Matter Physics, 2021, 2021, 1-10.	0.4	0
45190	Advanced Design Methods From Materials and Devices to Circuits for Brain-Inspired Oscillatory Neural Networks for Edge Computing. IEEE Journal on Emerging and Selected Topics in Circuits and Systems, 2021, 11, 586-596.	2.7	9
45191	Inverse design of two-dimensional materials with invertible neural networks. Npj Computational Materials, 2021, 7, .	3.5	15
45192	Anomalous suppressed thermal conductivity in CuInTe2 under pressure. Applied Physics Letters, 2021, 119, .	1.5	11
45193	Structure, Electronic Properties, and Stability of Carbon Double Layers Composed of Atoms in the sp3-Hybridized State. Journal of Experimental and Theoretical Physics, 2021, 133, 744-753.	0.2	5
45194	Epitaxial Growth of Ultraflat Bismuthene with Large Topological Band Inversion Enabled by Substrate-Orbital-Filtering Effect. ACS Nano, 2022, 16, 1436-1443.	7.3	16
45195	Discharging Behavior of Hollandite Î±-MnO₂ in a Hydrated Zinc-Ion Battery. ACS Applied Materials & Interfaces, 2021, 13, 59937-59949.	4.0	28
45196	Improvement of Thermoelectric Properties via Texturation Using a Magnetic Slip Casting Processâ€“The Illustrative Case of CrSi₂. Chemistry of Materials, 2022, 34, 1143-1156.	3.2	3
45197	Probing Photoexcited Charge Carrier Trapping and Defect Formation in Synergistic Doping of SrTiO₃. ACS Applied Energy Materials, 2022, 5, 1159-1168.	2.5	9
45198	Accelerating Anode Reaction with Electro-oxidation of Alcohols over Ru Nanoparticles to Reduce the Potential for Water Splitting. ACS Applied Materials & Interfaces, 2022, 14, 1452-1459.	4.0	13
45199	A comparison of CO oxidation on cleaned ZnO $$(10overline{1 }0)$$ surface and defective ZnO $$(10overline{1 }0)$$ surface using density functional theory studies. Journal of Molecular Modeling, 2022, 28, 12.	0.8	0
45200	Effect of off-stoichiometry on the thermal conductivity of amorphous GeTe. Physica Scripta, 2021, 96, 125730.	1.2	0
45201	Unintended consequence of topochemical reduction of <mml:math xmlns:mml="http://www.w3.org/1998/Math/MathML"><mml:mrow><mml:mi>SrFe</mml:mi><mml:msub><mml:mi mathvariant="normal">O</mml:mi><mml:mn>3</mml:mn></mml:msub></mml:mrow></mml:math> to <mml:math xmlns:mml="http://www.w3.org/1998/Math/MathML"><mml:mrow><mml:mi>SrFe</mml:mi><mml:msub><mml:mi mathvariant="normal">O</mml:mi><mml:mn>2</mml:mn></mml:msub></mml:mrow></mml:math>:	0.9	2
45202	Alleviation of Ï€â€“Ï€* Transition Enabling Enhanced Luminescence in Emerging TpyInCl_x (xÂ= 3, 5) Perovskite Single Crystals. Advanced Optical Materials, 2022, 10, .	3.6	19
45203	Carbon doping effect on the optoelectronic properties of the KNO₃material. Ferroelectrics, 2021, 585, 240-254.	0.3	2
45204	Pressure-induced isostructural clustering and semiconductor-to-semimetal transition in <mml:math xmlns:mml="http://www.w3.org/1998/Math/MathML"><mml:mrow><mml:mn>2</mml:mn><mml:mi>H</mml:mi></mml:mrow><mml:m mathvariant="normal">W</mml:mi><mml:msub><mml:mrow><mml:mo>(</mml:mo><mml:msub><mml:mi>Se</mml:mi><mml:mrow> Physical Review B, 2021, 104, .	1.1	2
45205	Probing Electron-Phonon Interactions Away from the Fermi Level with Resonant Inelastic X-Ray Scattering. Physical Review X, 2021, 11, .	2.8	6

#	Article	IF	Citations
45206	Local structure analysis of Sb, Bi, and Ag dopant atoms in Mg₂Si semiconductor by x-ray absorption spectroscopy and first-principles calculation. Journal of Applied Physics, 2021, 130, 245105.	1.1	1
45207	Research on the Electronic Properties of Tyrosine Dipeptide Molecule: Evaluation of the First-principles Theory. Russian Journal of Physical Chemistry B, 2021, 15, S181-S188.	0.2	0
45208	Superconductivity in the Layered Cage Compound Ba₃Rh₄Ge₁₆. Chinese Physics Letters, 2021, 38, 127402.	1.3	2
45209	Large magnetic anisotropy in Coâ€“Feâ€“Niâ€“N ordered structures: a first-principles study. Journal of Physics Condensed Matter, 2022, 34, 095503.	0.7	2
45210	Surface functionalization of phosphorene via P-H bond for ambient protection and robust photocatalytic H2 evolution. Science China Materials, 2022, 65, 1245-1251.	3.5	2
45211	Light-Tunable Charge Density Wave Orders in <mml:math xmlns:mml="http://www.w3.org/1998/Math/MathML" display="inline"><mml:mrow><mml:msub><mml:mrow><mml:mi>MoTe</mml:mi></mml:mrow><mml:mrow><mml:mn>2</mml:mn></ and <mml:math xmlns:mml="http://www.w3.org/1998/Math/MathML" display="inline"><mml:mrow><mml:msub><mml:mrow><mml:mi>WTe</mml:mi></mml:mrow><mml:mrow><mml:mn>2</mml:mn> Single Layers. Physical Review Letters, 2021, 127, 257401.	2.9	10
45212	Effect of Concrete Composition on the Thermodynamic Binding of Dopamine: A DFT Study. Langmuir, 2022, 38, 472-481.	1.6	6
45213	Ab Initio Modeling of the ZnO-Cu(111) Interface. Journal of Physical Chemistry C, 2022, 126, 764-771.	1.5	7
45214	Study on the relationship between uniaxial strain and critical transition temperature of MgB₂ based on first-principles. Journal of Physics Condensed Matter, 2022, 34, 105601.	0.7	1
45215	First-Principles Study of All Thermoelectric Properties of <mml:math xmlns:mml="http://www.w3.org/1998/Math/MathML" display="inline" overflow="scroll"><mml:mi>Si</mml:mi></mml:math> - <mml:math xmlns:mml="http://www.w3.org/1998/Math/MathML" display="inline" overflow="scroll"><mml:mi>Ge</mml:mi></mml:math> Alloys Showing Large Phonon Drag from 150 to 1100AK. Physical Review Applied, 2021, 16, .	1.5	8
45216	Surface Roughening Strategy for Highly Efficient Bifunctional Electrocatalyst: Combination of Atomic Layer Deposition and Anion Exchange Reaction. Small Methods, 2022, 6, e2101308.	4.6	15
45217	Visualizing band structure hybridization and superlattice effects in twisted MoS₂/WS₂ heterobilayers. 2D Materials, 2022, 9, 015032.	2.0	9
45218	Charged vacancy defects in monolayer phosphorene. Physical Review Materials, 2021, 5, .	0.9	5
45219	Atomic Scale Insight into Corrosion Inhibition: DFT Study of 2-Mercaptobenzimidazole on Locally De-Passivated Copper Surfaces. Journal of the Electrochemical Society, 2021, 168, 121507.	1.3	7
45220	DyOCl: A rare-earth based two-dimensional van der Waals material with strong magnetic anisotropy. Physical Review B, 2021, 104, .	1.1	13
45221	Frustrated network of indirect exchange paths between tetrahedrally coordinated Co in <mml:math xmlns:mml="http://www.w3.org/1998/Math/MathML"><mml:msub><mml:mi mathvariant="normal">Ba</mml:mi><mml:mn>2</mml:mn></mml:msub><mml:msub><mml:mi mathvariant="normal">CoO</mml:mi><mml:mn>4</mml:mn></mml:msub></mml:math>. Physical Review Materials, 2021, 5, .	0.9	0
45222	Contact Electrification and Adhesion Between Carbon Nanotube and Graphene on Metal Surfaces: Insights from First-principles Study. Journal of Bionic Engineering, 2022, 19, 103-112.	2.7	2
45223	Type-II Dirac cones and electron-phonon interaction in monolayer biphenylene from first-principles calculations. Physical Review B, 2021, 104, .	1.1	33

#	Article	IF	Citations
45224	Identifying an Alternative Hydride Transfer Pathway for CO ₂ Reduction on CdTe(111) and CuInS ₂ (112) Surfaces. Advanced Theory and Simulations, 2022, 5, 2100413.	1.3	5
45225	On the possibility that PbZrO3 not be antiferroelectric. Npj Computational Materials, 2021, 7, .	3.5	20
45226	Unexpected Electron Transport Suppression in a Heterostructured Grapheneâ€“MoS₂Multiple Field-Effect Transistor Architecture. ACS Nano, 2022, 16, 1291-1300.	7.3	9
45227	Spin Polarization-Assisted Dopant Segregation at a Coherent Phase Boundary. ACS Nano, 2021, 15, 19938-19944.	7.3	6
45228	Band Engineering SnTe via Trivalent Substitutions for Enhanced Thermoelectric Performance. Chemistry of Materials, 2021, 33, 9624-9637.	3.2	17
45229	Nitrogen and Oxygen Coâ€Doped Porous Hard Carbon Nanospheres with Coreâ€Shell Architecture as Anode Materials for Superior Potassiumâ€Ion Storage. Small, 2022, 18, e2104296.	5.2	33
45230	Effective Breaking of the Fluorocarbon Chain by the Interface Bi₂O₂XÂ·Â·Â·PFOA Complex Strategy via Coordinated Se on Construction of the Internal Photogenerated Carrier Pathway. ACS Applied Materials & Interfaces, 2022, 14, 654-667.	4.0	13
45231	Thermodynamic and Electronic Properties of Two-Dimensional SrTiO₃. Journal of Physical Chemistry C, 2022, 126, 517-524.	1.5	9
45232	First-Principles Study of the Structural, Electronic, and Enhanced Optical Properties of SnS/TaS₂ Heterojunction. ACS Applied Materials & Interfaces, 2022, 14, 2177-2184.	4.0	5
45233	Biphasic Î±/Î²-Type NaMn_{0.89}Fe_{0.11}O₂ as a Cathode for Sodium-Ion Batteries: Structural Insight and High-Performance Relation. ACS Applied Energy Materials, 2022, 5, 116-125.	2.5	5
45234	Sublayer Stable Fe Dopant in Porous Pd Metallene Boosts Oxygen Reduction Reaction. ACS Nano, 2022, 16, 522-532.	7.3	52
45235	Atomistic Observation of Temperature-Dependent Defect Evolution within Sub-stoichiometric WO_{3â€“x} Catalysts. ACS Applied Materials & Interfaces, 2022, 14, 2194-2201.	4.0	14
45236	Electrocatalytic Reduction of Nitrogen to Ammonia: the Roles of Lattice O and N in Reduction at Vanadium Oxynitride Surfaces. ACS Applied Materials & Interfaces, 2022, 14, 531-542.	4.0	14
45237	First principles study on the structures and properties of aluminum under high pressures. , 2021, , .		0
45238	Bandgap Correction and Spin-Orbit Coupling Induced Absorption Spectra of Dimethylammonium Lead Iodide for Solar Cell Absorber. Frontiers in Energy Research, 2021, 9, .	1.2	1
45239	Identifying the fingerprints of topological states by tuning magnetoresistance in a semimetal: The case of topological half-Heusler <mml:math xmlns:mml="http://www.w3.org/1998/Math/MathML"><mml:mrow><mml:msub><mml:mi>Pt</mml:mi><mml:mrow><mml:mn>1</mml:m Physical Review Materials, 2021, 5, .	0.9	1
45240	Adsorption of NO and NO₂ on Rhâ€Doped Hexagonal Boron Nitride Monolayers: A Firstâ€Principles Study. ChemistrySelect, 2021, 6, 13609-13615.	0.7	3
45241	Enhanced out-of-plane piezoelectricity of group-III(A) Janus hydrofluoride monolayers. Physical Review B, 2021, 104, .	1.1	17

#	Article	IF	Citations
45242	Effect of Fullerene Encapsulation on Optical and Thermoelectrical Properties of Carbon Nanotubes. Semiconductors, 2021, 55, 1024-1028.	0.2	0
45243	Investigation of hydrogen diffusion behavior in 12Cr2Mo1R(H) steel by electrochemical tests and first-principles calculation. Anti-Corrosion Methods and Materials, 2022, 69, 17-28.	0.6	1
45244	Navigating the Ti-C-O and Al-C-O ternary systems through theory-driven discovery. Physical Review Materials, 2021, 5, .	0.9	2
45245	Puffing Up Hollow Carbon Nanofibers with Highâ€Energy Metalâ€Organic Frameworks for Capacitiveâ€Dominated Potassiumâ€Ion Storage. Small, 2022, 18, e2105767.	5.2	13
45246	Semiconductor nanochannels in metallic carbon nanotubes by thermomechanical chirality alteration. Science, 2021, 374, 1616-1620.	6.0	32
45247	Magnetically Collected Platinum/Nickel Alloy Nanoparticles as Catalysts for Hydrogen Evolution. ACS Applied Nano Materials, 2021, 4, 12957-12965.	2.4	9
45248	First-principles study of electronic transport in germanane and hexagonal boron nitride. Physical Review B, 2021, 104, .	1.1	14
45249	Visualizing band selective enhancement of quasiparticle lifetime in a metallic ferromagnet. Nature Communications, 2021, 12, 7169.	5.8	4
45250	Insight into the Anchoring Effect of Two-Dimensional TiX₂ (X = S, Se, Te) Materials for Lithium-Sulfur Batteries: A DFT Study. Journal of the Electrochemical Society, 2021, 168, 120516.	1.3	7
45251	Seamlessly Merging the Capacity of P into Sb at Same Voltage with Maintained Superior Cycle Stability and Lowâ€temperature Performance for Liâ€ion Batteries. Energy and Environmental Materials, 2023, 6, .	7.3	3
45252	High-performance thermoelectric properties of strained two-dimensional tellurium. Physical Review Materials, 2021, 5, .	0.9	5
45253	Magnetization of silicene via coverage with gadolinium: Effects of thickness, symmetry, strain, and coverage. Physical Review B, 2021, 104, .	1.1	5
45254	First-principles study of excitons in optical spectra of silver chloride. Physical Review B, 2021, 104, .	1.1	3
45255	Ð•Ð»ÐµÐºÑ‚Ñ€Ð¾ÑÑ‚Ð°Ñ‚Ð¸Ñ‡ÐµÑÐºÐ¸Ðµ Ñ‚Ñ€Ð°Ð½Ð·Ð¸ÑÑ‚Ð¾Ñ€Ñ‹ Ð½Ð° Ð¾ÑÐ½Ð¾Ð²Ðµ GaInN Ð· Ð´Ð¾Ð¿Ð¾Ð²Ð°Ð½Ð¸Ð¼ ÐºÐ°Ð½Ð°Ð»Ð¾Ð¼ Ñ.		
45256	Design of nanoscale capacitors based on metallic borophene and insulating boron nitride layers. Physical Review Materials, 2021, 5, .	0.9	1
45257	Band tuning in WS2 monolayer via substitutional doping. Superlattices and Microstructures, 2022, 164, 107120.	1.4	3
45258	Pressure dependent structural, elastic and mechanical properties with ground state electronic and optical properties of half-metallic Heusler compounds Cr2YAl (Y=Mn, Co): first-principles study. Heliyon, 2021, 7, e08585.	1.4	9
45259	Covalent Functionalization of Nickel Phosphide Nanocrystals with Aryl-Diazonium Salts. Chemistry of Materials, 2021, 33, 9652-9665.	3.2	9

#	Article	IF	Citations
45260	Computational Screening of Bimetallic Catalysts: Application to Ammonia Decomposition. Journal of Physical Chemistry C, 2022, 126, 192-202.	1.5	1
45261	Self-Etherification of 5-Hydroxymethylfurfural to 5,5â€²(Oxy-bis(methylene))bis-2-furfural over Hierarchically Micromesoporous ZSM-5: The Role of BrÃ¸nsted- and Lewis-Acid Sites. Industrial & Engineering Chemistry Research, 2022, 61, 987-994.	1.8	3
45262	A first-principles study of hydrogen surface coverage on Î´-Pu (100), (111), and (110) surfaces. Journal of Chemical Physics, 2021, 155, 234702.	1.2	2
45263	Investigating the theoretical performance of<scp>Cs₂TiBr₆</scp>â€based perovskite solar cell with Laâ€doped<scp>BaSnO₃</scp>and<scp>CuSbS₂</scp>as the charge transport layers. International Journal of Energy Research, 2022, 46, 6045-6064.	2.2	29
45264	CO2 coordination-driven top-down synthesis of a 2D non-layered metalâ€“organic framework. Fundamental Research, 2022, 2, 674-681.	1.6	11
45265	Tuning the near room temperature oxidation behavior of high-entropy alloy nanoparticles. Nano Research, 2022, 15, 3569-3574.	5.8	6
45266	The Interaction of the 2D MoP2 and NbP2 Surfaces with Carbon Dioxide and Carbon Monoxide and Changes in Their Optical Properties. Crystals, 2022, 12, 45.	1.0	1
45267	Complex Oxides under Simulated Electric Field: Determinants of Defect Polarization in ABO₃ Perovskites. Advanced Science, 2022, 9, e2104476.	5.6	7
45268	Absence of long-range magnetic order in <mml:math xmlns:mml="http://www.w3.org/1998/Math/MathML"><mml:msub><mml:mi mathvariant="normal">Fe</mml:mi><mml:mrow><mml:mn>1</mml:mn><mml:mo>â^’</mml:mo><mml:mi>Î´</mml:mi></mml:mrow></ mathvariant="normal">Te</mml:mi><mml:mn>2</mml:mn></mml:msub></mml:math> (<mml:math) Tj ETQq0 0 0 rgBT /Overlock 10 Tf	1.1	3
45269	Structural, electronic and dielectric properties of Tellurium 1-D nanostructures : a DFT study. Applied Physics A: Materials Science and Processing, 2022, 128, 1.	1.1	1
45270	First-principles calculation of ballistic current from electron-hole interaction. Physical Review B, 2021, 104, .	1.1	8
45271	Anomalous magnetic exchange in a dimerized quantum magnet composed of unlike spin species. Physical Review B, 2021, 104, .	1.1	2
45272	Specialising neural network potentials for accurate properties and application to the mechanical response of titanium. Npj Computational Materials, 2021, 7, .	3.5	26
45273	Firstâ€principles investigation of the (HfSe ₂) _{4â^’ n} â€“(HfSSe) _n (n Â=Â0, 1, 2, 3, 4) lateral heterostructures. International Journal of Quantum Chemistry, 2022, 122, .	1.0	2
45274	<mml:math xmlns:mml="http://www.w3.org/1998/Math/MathML"><mml:msub><mml:mi>CrSbSe</mml:mi><mml:mn>3</mml:mn></mml:msub></ : A pseudo one-dimensional ferromagnetic semiconductor. Physical Review Materials, 2021, 5, .	0.9	1
45275	Relationship between ferroelectric polarization and stoichiometry of <mml:math xmlns:mml="http://www.w3.org/1998/Math/MathML"><mml:msub><mml:mi>HfO</mml:mi><mml:mn>2</mml:mn></mml:msub></ surfaces. Physical Review Materials, 2021, 5, .	0.9	4
45276	New van der Waals Heterostructures Based on Borophene and Rhenium Sulfide/Selenide for Photovoltaics: An Ab Initio Study. Applied Sciences (Switzerland), 2021, 11, 11636.	1.3	1
45277	Lattice siteâ€dependent metal leaching in perovskites toward a honeycomb-like water oxidation catalyst. Science Advances, 2021, 7, eabk1788.	4.7	41

#	Article	IF	Citations
45278	Posttreatment Effects on the Crystal Structure and Superconductivity of Ca-Free Double-Layered Cuprate Sr₂SrCu₂O_{4+y}F_{2â€“y}. Chemistry of Materials, 2021, 33, 9690-9697.	3.2	1
45279	Ironâ€“Cobalt-Based Materials: An Efficient Bimetallic Catalyst for Ammonia Synthesis at Low Temperatures. ACS Catalysis, 2022, 12, 587-599.	5.5	17
45280	Investigations on the Synthesis, Crystal Structure, Linear- and Nonlinear-Optical Properties of the Zinc Germanate Rb₂ZnGe₂O₆. Inorganic Chemistry, 2022, 61, 706-712.	1.9	15
45281	Highly Stable Germanium Microparticle Anodes with a Hybrid Conductive Shell for High Volumetric and Fast Lithium Storage. ACS Applied Materials & Interfaces, 2022, 14, 750-760.	4.0	2
45282	Predicted Structural, Elastic, Electronic, Lattice Dynamic, Thermodynamic and Optical Properties of Cubic SN̄F3 from First-Principles Calculations. Russian Journal of Physical Chemistry A, 2021, 95, S296-S306.	0.1	1
45283	Crystal structure of phenanthrenide salts stabilized by 15-crown-5 and 18-crown-6. Zeitschrift Fur Naturforschung - Section B Journal of Chemical Sciences, 2022, 77, 197-201.	0.3	1
45284	A generalizable machine learning potential of Agâ€“Au nanoalloys and its application to surface reconstruction, segregation and diffusion. Modelling and Simulation in Materials Science and Engineering, 2022, 30, 025003.	0.8	8
45285	Decoupling between Shockley partials and stacking faults strengthens multiprincipal element alloys. Proceedings of the National Academy of Sciences of the United States of America, 2021, 118, .	3.3	11
45286	Assessing the effect of H on the electronic properties of 4H-SiC. Chinese Physics B, 0, , .	0.7	2
45287	Proton dynamics in water confined at the interface of the grapheneâ€“MXene heterostructure. Journal of Chemical Physics, 2021, 155, 234707.	1.2	5
45288	Making Yb₂Hf₂O₇ Defect Fluorite Uncompressible by Particle Size Reduction. Journal of Physical Chemistry C, 2021, 125, 27354-27362.	1.5	12
45289	Structural, mechanical, thermodynamic, electronic and optical characteristics of LaPtBi half-Heusler compound from first principles analyses. Ferroelectrics, 2021, 585, 118-127.	0.3	4
45290	Spin qubit based on the nitrogen-vacancy center analog in a diamond-like compound C3BN. Journal of Applied Physics, 2021, 130, .	1.1	2
45291	Oxygen Diffusion in Platinum Electrodes: A Molecular Dynamics Study of the Role of Extended Defects. Advanced Materials Interfaces, 2022, 9, .	1.9	7
45292	Growth mechanisms of vermicular graphite in cast iron. Materials Today Communications, 2021, 29, 102993.	0.9	3
45293	Effect of Ni Doping on the Embrittlement of Liquid Zinc at Î£5 Fe Austenite Grain Boundary. Metals, 2022, 12, 27.	1.0	1
45294	Volume Increments for Crystalline Borates. European Journal of Inorganic Chemistry, 2022, 2022, .	1.0	0
45295	The Third-Order Elastic Constants and Mechanical Properties of 30Â° Partial Dislocation in Germanium: A Study from the First-Principles Calculations and the Improved Peierlsâ€“Nabarro Model. Crystals, 2022, 12, 4.	1.0	0

#	Article	IF	Citations
45296	Quantum transport simulation of the two-dimensional GaSb transistors. Journal of Semiconductors, 2021, 42, 122001.	2.0	3
45297	Tuning the magnetic anisotropy of ferromagnetic <mml:math xmlns:mml="http://www.w3.org/1998/Math/MathML"><mml:msub><mml:mi>MnS</mml:mi><mml:mn>2</mml:mn></mml:msub></mml monolayers via electron occupation of Mn <mml:math xmlns:mml="http://www.w3.org/1998/Math/MathML"><mml:mi>d</mml:mi></mml:math> orbitals. Physical Review B, 2021, 104, .	1.1	6
45298	Processing Agricultural Cornstalks toward Highâ€Efficient Stable Bifunctional ORR/OER Electrocatalysts. Advanced Sustainable Systems, 2022, 6, .	2.7	10
45299	Structural, Electronic and Magnetic Properties of CaSe Doped with 3d (V, Cr and Mn). Spin, 2021, 11, .	0.6	1
45300	Experimental and Theoretical Study on the Substitution Patterns in Lithium Germanides: The Case of Li₁₅Ge₄vs Li₁₄ZnGe₄. European Journal of Inorganic Chemistry, 2022, 2022, .	1.0	2
45301	Point defect induced incommensurate dipole moments in the <mml:math xmlns:mml="http://www.w3.org/1998/Math/MathML"><mml:mrow><mml:mi mathvariant="normal">K</mml:mi><mml:msub><mml:mi>Ca</mml:mi><mml:mn>2</mml:mn></mml:msub><mml:msub><mml:mi>Nb <mml:mi mathvariant="normal">O</mml:mi><mml:mn>10</mml:mn></mml:msub></mml:mrow></mml:math> Dion-Jacobson layered perovskite. Physical Review B, 2021, 104, .	1.1	1
45302	Monoelemental two-dimensional iodinene nanosheets: a first-principles study of the electronic and optical properties. Journal Physics D: Applied Physics, 2022, 55, 135104.	1.3	5
45303	Boron-Functionalized Organic Framework as a High-Performance Metal-Free Catalyst for N₂ Fixation. Journal of Physical Chemistry Letters, 2021, 12, 12142-12149.	2.1	9
45304	N/P-Doped MoS₂ Monolayers as Promising Materials for Controllable CO₂ Capture and Separation under Reduced Electric Fields: A Theoretical Modeling. Journal of Physical Chemistry C, 2022, 126, 203-211.	1.5	6
45305	Electron structure and thermodynamics of solid solutions in Niâ€“H system. Material Science & Engineering International Journal, 2018, 2, 101-109.	0.0	4
45306	Self-powered perovskite CH3NH3PbBr3 field effect transistor with fast response and high sensitivity in sensing. Materials Today Advances, 2021, 12, 100185.	2.5	2
45307	First principle insight into co-doped MoS2 for sensing NH3 and CH4. Facta Universitatis - Series Electronics and Energetics, 2022, 35, 43-59.	0.6	7
45308	Mechanistic insight into the selective catalytic reduction of NOx with propene on the Ce0.875Zr0.125O2 (110) surface. Catalysis Science and Technology, 0, , .	2.1	3
45309	Anchoring boron on a covalent organic framework as an efficient single atom metal-free photo-electrocatalyst for nitrogen fixation: a first-principles analysis. Physical Chemistry Chemical Physics, 2022, 24, 10765-10774.	1.3	12
45310	A critical evaluation of the catalytic role of CO₂ in propane dehydrogenation catalyzed by chromium oxide from a DFT-based microkinetic simulation. Physical Chemistry Chemical Physics, 2022, 24, 11030-11038.	1.3	3
45311	Extremely Sensitive and Selective No2 Detection at Relative Humidity 90% in 2-Dimensional Tin Sulfides/Sno2 Nanorod Heterostructure. SSRN Electronic Journal, 0, , .	0.4	0
45312	Cooperative coupling of anisotropic phonon modes intensifies visible thermochromism in layered Î±-MoO₃. Materials Horizons, 2022, 9, 1631-1640.	6.4	7
45313	Metavalent bonding in chalcogenides: DFT-chemical pressure approach. Physical Chemistry Chemical Physics, 2022, 24, 9936-9942.	1.3	3

#	Article	IF	Citations
45314	Hydrovoltaic energy harvesting from moisture flow using an ionic polymerâ€“hydrogelâ€“carbon composite. Energy and Environmental Science, 2022, 15, 2489-2498.	15.6	35
45315	Biphenylene monolayer: a novel nonbenzenoid carbon allotrope with potential application as an anode material for high-performance sodium-ion batteries. Physical Chemistry Chemical Physics, 2022, 24, 10712-10716.	1.3	22
45316	The crystal structures, phase stabilities, electronic structures and bonding features of iridium borides from first-principles calculations. RSC Advances, 2022, 12, 11722-11731.	1.7	7
45317	Uncovering the multifaceted roles of nitrogen defects in graphitic carbon nitride for selective photocatalytic carbon dioxide reduction: a density functional theory study. Physical Chemistry Chemical Physics, 2022, 24, 11124-11130.	1.3	4
45318	Modification of Mgf(2-X)B(X) (X=0.0 and 1.0) and Mgf1 (F-Defected) for Anti-Reflective Material Commonly Used in Opticianry Lenses and Coatings with Boron Dopant: The First-Principles Study. SSRN Electronic Journal, 0, , .	0.4	0
45319	Electronâ€“phonon coupling and superconductivity in a 2D Tlâ€“Pb compound on Si(111). Physical Chemistry Chemical Physics, 2022, 24, 10140-10146.	1.3	2
45320	NiOâ€“Ti nanocomposites for contact electrification and energy harvesting: experimental and DFT+U studies. Sustainable Energy and Fuels, 2022, 6, 2439-2448.	2.5	3
45321	Effect of stress regulation on electronic structure and optical properties of TiOCl₂ monolayer. Wuli Xuebao/Acta Physica Sinica, 2022, 71, 077101.	0.2	2
45322	A Synergistic effect on the atomic cluster M₄ supported on MN₄-graphene (M) Tj ETQq0 0 0 rgBT /Overlock 1 11704-11712.	1.3	11
45323	Ion Mobility in Triple Sodium Molybdates and Tungstates with a NASICON Structure. Journal of Experimental and Theoretical Physics, 2022, 134, 42-50.	0.2	5
45324	Exoergic pathways triggered by O/H radicals in different metallic carbohydrazide perchlorates (M²⁺= Mn²⁺, Fe²⁺, Co²⁺, Ni²⁺,) Tj ETQq0 0 0 rgBT /Overlock 10 Tf 5		7
45325	Modulation of the coordination environment enhances the electrocatalytic efficiency of Mo single atoms toward water splitting. Journal of Materials Chemistry A, 2022, 10, 8784-8797.	5.2	17
45326	Interatomic Interaction at the Aluminumâ€“Fullerene C60 Interface. Journal of Experimental and Theoretical Physics, 2022, 134, 69-84.	0.2	2
45327	Self-Assembled Molecular Nanowires on Prepatterned Ge(001) Surfaces. Chemical Science, 0, , .	3.7	0
45328	Theoretical predictions of phase stability for orthorhombic and hexagonal ternary MAB phases. Physical Chemistry Chemical Physics, 2022, 24, 11249-11258.	1.3	18
45329	Theoretical investigation of the olefin cycle in H-SSZ-13 for the ethanol-to-olefins process using ab initio calculations and kinetic modeling. Catalysis Science and Technology, 2022, 12, 3311-3321.	2.1	2
45330	INVESTIGATION OF STRUCTURAL, ELECTRONIC, ELASTIC AND OPTICAL PROPERTIES OF Cd1-x-yZnxHgyTe ALLOYS. World Science, 2022, , .	0.0	0
45331	Diamond-Like Films from Twisted Few-Layer Graphene. JETP Letters, 2022, 115, 161-166.	0.4	4

#	Article	IF	Citations
45332	CrI3 monolayer: magnetic and electronic behaviors under biaxial strain and external electric fieldâ€”a first principle study. European Physical Journal B, 2022, 95, .	0.6	8
45333	Defect-Induced Different Band Alignment and Transport of All-Phosphorene Devices from First Principles. ACS Applied Electronic Materials, 2022, 4, 2070-2076.	2.0	4
45334	Effect of pressure on anisotropy in elasticity, sound velocity, and thermal conductivity of vanadium borides. Advanced Composites and Hybrid Materials, 2022, 5, 2297-2305.	9.9	23
45335	Electron-Level Mechanistic Insights into Ce Doping for Enhanced Efficiency Degradation of Bisphenol A under Visible Light Irradiation. Nanomaterials, 2022, 12, 1382.	1.9	6
45336	Elastic and phonon-mode anomalies with temperature in the energetic material <mml:math xmlns:mml="http://www.w3.org/1998/Math/MathML"><mml:mrow><mml:msub><mml:mi mathvariant="normal">C</mml:mi><mml:mn>6</mml:mn></mml:msub><mml:msub><mml:mi mathvariant="normal">H</mml:mi><mml:mn>6</mml:mn></mml:msub><mml:msub><mml:mi mathvariant="normal">N</mml:mi><mml:mn>4</mml:mn></mml:msub><mml:msub><mml:mi mathvariant="normal">O</mml:mi><mml:mn>8</mml:mn></mml:msub></mml:mrow></mml:math>. Physi	1.1	1
45337	Enriched dâ€Band Holes Enabling Fast Oxygen Evolution Kinetics on Atomicâ€Layered Defectâ€Rich Lithium Cobalt Oxide Nanosheets. Advanced Functional Materials, 2022, 32, .	7.8	24
45338	Efficient machine-learning model for fast assessment of elastic properties of high-entropy alloys. Acta Materialia, 2022, 232, 117924.	3.8	39
45339	Structure and energetics of ZrC(100)||c-ZrO2(001) interface: A combination of experiments, finite temperature molecular dynamics, periodic DFT and atomistic thermodynamic modeling. Ceramics International, 2022, 48, 21327-21343.	2.3	1
45340	High-T_C Two-Dimensional Ferroelectric CuCrS₂ Grown via Chemical Vapor Deposition. ACS Nano, 2022, 16, 8141-8149.	7.3	23
45341	Interstitial doping of K and Mn induced structural distortion and electronic properties changes in allâ€inorganic CsPbI₂Br perovskite. Materials Research Express, 2022, 9, 046304.	0.8	3
45342	Lightâ€Induced Synthesis of Oxygenâ€Vacancyâ€Functionalized Ni(OH)₂ Nanosheets for Highly Selective CO₂ Reduction. ChemSusChem, 2022, 15, .	3.6	13
45343	Structures, stabilities, optoelectronic and photocatalytic properties of Janus aluminium mono-chalcogenides Al(Ga, In)STe monolayers. Physica E: Low-Dimensional Systems and Nanostructures, 2022, 142, 115229.	1.3	2
45344	NaClO-induced sodium-doped cyano-rich graphitic carbon nitride nanosheets with nitrogen vacancies to boost photocatalytic hydrogen peroxide production. Chemical Engineering Journal, 2022, 443, 136501.	6.6	22
45345	Unconventional spin Hall effects in nonmagnetic solids. Physical Review Materials, 2022, 6, .	0.9	28
45346	Electronic phase transition and enhanced optoelectronic performance of lead-free halide perovskites AGeI3 (A = Rb, K) under pressure. Materials Today Communications, 2022, 31, 103532.	0.9	13
45347	A rational design of garnet-type Li7La3Zr2O12 with ultrahigh moisture stability. Energy Storage Materials, 2022, 49, 278-290.	9.5	21
45348	Effect of MnO₂ Polymorphsâ€™ Structure on Low-Temperature Catalytic Oxidation: Crystalline Controlled Oxygen Vacancy Formation. ACS Applied Materials & Interfaces, 2022, 14, 18525-18538.	4.0	27
45349	Influence of hydrogen and helium nucleation on the mechanical properties of beryllium by first-principles calculations. Nuclear Materials and Energy, 2022, 31, 101181.	0.6	2

#	Article	IF	Citations
45350	Electronic and Optical Properties of Twin T-Graphene Co-Doped with Boron and Phosphorus. Materials, 2022, 15, 2876.	1.3	5
45351	Layer-by-Layer Assembly of CeO_{2â€“x}@C-rGO Nanocomposites and CNTs as a Multifunctional Separator Coating for Highly Stable Lithiumâ€“Sulfur Batteries. ACS Applied Materials & Interfaces, 2022, 14, 18634-18645.	4.0	24
45352	Experimental and DFT study of Al doped ZnO nanoparticles with enhanced antibacterial activity. Ceramics International, 2022, 48, 20838-20847.	2.3	12
45353	A density functional theory study on the adsorption reaction mechanism of double CO2 on the surface of graphene defects. Journal of Molecular Modeling, 2022, 28, 118.	0.8	5
45354	Augmented hydrogen adsorption on metal (Mg, Mn) doped Î±-phase TeO2: A DFT investigation. International Journal of Hydrogen Energy, 2022, , .	3.8	2
45355	Structural Design and Physical Properties of Gallium Nitrides under High Pressures. Journal of Physical Chemistry C, 2022, 126, 7773-7777.	1.5	2
45356	Precise control of surface oxygen vacancies in ZnO nanoparticles for extremely high acetone sensing response. Journal of Advanced Ceramics, 2022, 11, 769-783.	8.9	33
45357	Two-Dimensional Negative Thermal Expansion in a Crystal of LiBO₂. Chemistry of Materials, 2022, 34, 4195-4201.	3.2	7
45358	Pressure-induced structural transformations on linear carbon chains encapsulated in carbon nanotubes: A potential route for obtaining longer chains and ultra-hard composites. Carbon, 2022, 196, 20-28.	5.4	4
45359	Penta-SiCN: A Highly Auxetic Monolayer. ACS Applied Electronic Materials, 2022, 4, 2561-2569.	2.0	12
45360	Pressure dependent magnetic properties on bulk CrBr3 single crystals. Journal of Alloys and Compounds, 2022, 911, 165034.	2.8	5
45361	Probing the role of grain boundaries in single Cu nanoparticle oxidation by in situ plasmonic scattering. Physical Review Materials, 2022, 6, .	0.9	4
45362	A DFT study to determine the structure and composition of Îµ-W2B5â^'x. Journal of Alloys and Compounds, 2022, 911, 164962.	2.8	5
45363	Exploring the sensing ability of <scp>B</scp> â€•and <scp>Si</scp> â€doped <scp> WS ₂ </scp> monolayer toward <scp>CO</scp> and <scp>NO</scp> gas. International Journal of Quantum Chemistry, 0, , .	1.0	2
45364	The binding of atomic hydrogen on graphene from density functional theory and diffusion Monte Carlo calculations. Journal of Chemical Physics, 2022, 156, 144702.	1.2	3
45365	Photocatalytic Degradation of Rhodamine B Dye and Hydrogen Evolution by Hydrothermally Synthesized NaBH4â€”Spiked ZnS Nanostructures. Frontiers in Chemistry, 2022, 10, 835832.	1.8	10
45366	Dissociative adsorption of H2 on metal cluster and (1 1 1) surface of Ag, Co, Cu and Ru. Chemical Physics, 2022, 559, 111546.	0.9	2
45367	Surface spinel and interface oxygen vacancies enhanced lithium-rich layered oxides with excellent electrochemical performances. Chemical Engineering Journal, 2022, 443, 136434.	6.6	29

#	Article	IF	Citations
45368	Observation of mid-gap states emerging in the O-terminated interface of Cr2O3/graphene: A combined study of ab initio prediction and photoemission analysis. Applied Surface Science, 2022, , 153416.	3.1	1
45369	Intrinsic ferromagnetic and antiferromagnetic axion insulators in van der Waals materials <mml:math xmlns:mml="http://www.w3.org/1998/Math/MathML"><mml:mrow><mml:mi>Mn</mml:mi><mml:msub><mml:mi>X</mml:mi><mml:mn family. Physical Review Research, 2022, 4, .	1.3	2
45370	DFT Study of the BH₄^{â^'} Hydrolysis on Au(111) Surface. ChemPhysChem, 2022, 23, .	1.0	3
45371	Hybrid <scp>Ni₂P</scp>/<scp>CoP</scp> Nanosheets as Efficient and Robust Electrocatalysts for Domestic Wastewater Splitting. Energy and Environmental Materials, 2023, 6, .	7.3	10
45372	High-Pressure Synthesis, Electronic Properties, and Raman Spectroscopy of Barium Tetraborate BaB₄O₇ Polymorphs. Crystal Growth and Design, 2022, 22, 3405-3412.	1.4	2
45373	Giant Stokes shift for charged vacancies in monolayer SnS. Physical Review Materials, 2022, 6, .	0.9	2
45374	Electronic and optical properties of TMDs/Hg0.33Cd0.66Te. Journal of Materials Science: Materials in Electronics, 2022, 33, 11542.	1.1	0
45375	Eu₂Mg₃Bi₄: Competing Magnetic Orders on a Buckled Honeycomb Lattice. Chemistry of Materials, 2022, 34, 3902-3909.	3.2	0
45376	Tuning Spin Texture and Spectroscopic Limited Maximum Efficiency through Chemical Composition Space in Double Halide Perovskites. ACS Applied Energy Materials, 2022, 5, 5579-5588.	2.5	5
45377	First-principles study of interface stability and behaviors of He at the W/Y2O3 interface. Materials Today Communications, 2022, , 103520.	0.9	0
45378	NiX₂ (X = S, Se, and Te) Monolayers: Promising Anodes in Li/Na-Ion Batteries and Superconductors. Journal of Physical Chemistry C, 2022, 126, 6925-6933.	1.5	13
45379	NiS/MoS2 Mott-Schottky heterojunction-induced local charge redistribution for high-efficiency urea-assisted energy-saving hydrogen production. Chemical Engineering Journal, 2022, 443, 136321.	6.6	58
45380	Experimental and theoretical investigations of a multiwalled carbon nanotubes/SnO2/polyaniline ternary nanohybrid electrode for energy storage. Surfaces and Interfaces, 2022, 30, 101978.	1.5	5
45381	Quantum-metric-enabled exciton condensate in double twisted bilayer graphene. Physical Review B, 2022, 105, .	1.1	10
45382	Plasmonic Carbon Nitride Polymers to Boost Hydrogen Generation. Advanced Sustainable Systems, 2022, 6, .	2.7	6
45383	Abnormal Evolution of a Layered Structure and Band Gap in AgInP₂S₆ under Compression. Journal of Physical Chemistry C, 0, , .	1.5	1
45384	Electronic structure and magnetism of the triple-layered ruthenate <mml:math xmlns:mml="http://www.w3.org/1998/Math/MathML"><mml:msub><mml:mi mathvariant="normal">Sr</mml:mi><mml:mn>4</mml:mn></mml:msub><mml:msub><mml:mi mathvariant="normal">Ru</mml:mi><mml:mn>3</mml:mn></mml:msub><mml:msub><mml:mi mathvariant="normal">O</mml:mi><mml:mn>10</mml:mn></mml:msub></mml:math>. Physical Review B, 2022, 105, .	1.1	4
45385	CO₂ Reduction to C₁ and C₂ Compounds on Sulfur-Deficient Mackinawite (FeS): A Density Functional Theory Study. Journal of Physical Chemistry C, 2022, 126, 7012-7021.	1.5	7

#	Article	IF	Citations
45386	Boron Nitrideâ€Based Release Agent Coating Stabilizes Li_{1.3}Al_{0.3}Ti_{1.7}(PO₄)₃/Li Interface with Superior Leanâ€Lithium Electrochemical Performance and Thermal Stability. Advanced Functional Materials, 2022, 32, .	7.8	27
45387	Mechanistic Insights into the Effect of Sulfur on the Selectivity of Cobalt-Catalyzed Fischerâ€“Tropsch Synthesis: A DFT Study. Catalysts, 2022, 12, 425.	1.6	4
45388	Electronic transport properties of a single biphenyl molecule anchored on Au(111)with sulfur, selenium, and tellurium atoms. Journal of Chemical Physics, 2022, 156, 174701.	1.2	1
45389	Temperatureâ€and Pressureâ€Dependent Phonon Dynamics Properties of Gallium Selenide Telluride. Journal of Raman Spectroscopy, 0, , .	1.2	3
45390	Novel ultra-hard hexacarbon allotropes from first principles. Solid State Sciences, 2022, 129, 106884.	1.5	2
45391	Structural reconstruction and anisotropic conductance in 4f-ferromagnetic monolayer. Materials Today Physics, 2022, 24, 100693.	2.9	4
45392	Dopant-sheet interaction and its role in the enhanced chemical activity of doped MoTe2. Surface Science, 2022, 723, 122093.	0.8	4
45393	Insight into the Effect of Iodine Doping Soft Carbon and Iodine Functional Separator for Lithiumâ€Sulfur Batteries. Batteries and Supercaps, 2022, 5, .	2.4	6
45394	Advanced Ru/Ni/WC@NPC Multiâ€Interfacial Electrocatalyst for Efficient Sustainable Hydrogen and Chlorâ€Alkali Coâ€Production. Advanced Energy Materials, 2022, 12, .	10.2	52
45395	Manifestation of the ferroelastoelectric phase transition in the absorption spectra of (NH4)2CuCl4Ã—2Đ²Đž crystals. Physica B: Condensed Matter, 2022, , 413929.	1.3	1
45396	Adhesion of thin metallic layers on Au surfaces. Journal of Physics Condensed Matter, 2022, , .	0.7	0
45397	Structural modification enhances the optoelectronic properties of defect blue phosphorene thin films. Journal of Physics Condensed Matter, 2022, 34, 285702.	0.7	2
45398	Observation on Volatile and Nonvolatile Magnetic Reversions Mediated by Electric Current in Highly Conductive Gd₃Fe₅O₁₂. Journal of Physical Chemistry C, 2022, 126, 7660-7666.	1.5	1
45399	Heavy 2D VSi2N4: High capacity and full battery open-circuit voltage as Li/Na-ion batteries anode. Applied Surface Science, 2022, 593, 153354.	3.1	12
45400	Enhanced Catalytic Performance of N-Doped Carbon Sphere-Supported Pd Nanoparticles by Secondary Nitrogen Source Regulation for Formic Acid Dehydrogenation. ACS Applied Materials & Interfaces, 2022, 14, 18550-18560.	4.0	16
45401	First-principles study of magnetic properties of the cobalt doped silver copper sulfides. Computational Condensed Matter, 2022, , e00680.	0.9	1
45402	Direct Experimental Evidence for Substrate Adatom Incorporation into a Molecular Overlayer. Journal of Physical Chemistry C, 2022, 126, 7346-7355.	1.5	6
45403	Machine learning approach for longitudinal spin fluctuation effects in bcc Fe at<mml:math xmlns:mml="http://www.w3.org/1998/Math/MathML"><mml:msub><mml:mi>T</mml:mi><mml:mi>c</mml:mi></mml:msub></mml:ma under Earth-core conditions. Physical Review B, 2022, 105, .	1.1	4

#	Article	IF	Citations
45404	Mechanical and opto-electronic properties of Î±-MoSi2: a DFT scheme with hydrostatic pressure. Indian Journal of Physics, 2022, 96, 4155-4172.	0.9	5
45405	Effects of Nb concentration on Nb-doped anatase TiO₂: DFTÂ+ÂU calculations. Physica Scripta, 2022, 97, 055819.	1.2	2
45406	First-principles calculations of AlAs/CdS heterostructure with tunable electronic properties. Scientia Sinica: Physica, Mechanica Et Astronomica, 2022, 52, 297303.	0.2	3
45407	Insight into the Active Sites of N,P-Codoped Carbon Materials for Electrocatalytic CO₂ Reduction. Inorganic Chemistry, 2022, 61, 6073-6082.	1.9	13
45408	Î²-Al4.5FeSi: Hierarchical crystal and defect structure: Reconciling experimental and theoretical evidence including the influence of Al vs. Si ordering on the crystal structure. Journal of Alloys and Compounds, 2022, 911, 165015.	2.8	7
45409	Bridging microscopy with molecular dynamics and quantum simulations: an atomAI based pipeline. Npj Computational Materials, 2022, 8, .	3.5	10
45410	Taming Electrons in Pt/C Catalysts to Boost the Mesokinetics of Hydrogen Production. Engineering, 2022, 14, 124-133.	3.2	1
45411	Multimodal Gas Sensor Detecting Hydroxyl Groups with Phase Transition Based on Ecoâ€Friendly Leadâ€Free Metal Halides. Advanced Functional Materials, 2022, 32, .	7.8	8
45412	Symmetry Engineering Induced Inâ€Plane Polarization in MoS₂ through Van der Waals Interlayer Coupling. Advanced Functional Materials, 2022, 32, .	7.8	31
45413	Elementary mechanism for the electrocatalytic reduction of nitrobenzene on late-transition-metal surfaces from density functional theory. Chem Catalysis, 2022, 2, 1362-1379.	2.9	7
45414	Exploring the Stability of Single-Atom Catalysts Using the Density Functional Theory-Based Global Optimization Method: H₂ Formation on VO_x/Î³-Al₂O₃(100). Journal of Physical Chemistry C, 2022, 126, 6973-6981.	1.5	7
45415	Assessing the role of surface carbon on the surface stability and reactivity of Î²-Mo2C catalysts. Applied Surface Science, 2022, , 153415.	3.1	3
45416	Sensing properties of nonmetal doped blue phosphorene toward <scp>NO</scp> and <scp>NO₂</scp> molecules: A firstâ€principles study. International Journal of Quantum Chemistry, 2022, 122, .	1.0	4
45417	Synthesis of Hydride-Doped Perovskite Stannate with Visible Light Absorption Capability. Inorganic Chemistry, 2022, , .	1.9	2
45418	Oxygen Evolution Reaction Activity of Sr₂Ta₂O₇ and Sr₂Nb₂O₇ Surfaces. Journal of Physical Chemistry C, 2022, 126, 6556-6563.	1.5	6
45419	Stabilizing p-type conductivity in CuYO2 by co-doping: A first-principles study. Materials Chemistry and Physics, 2022, , 126101.	2.0	0
45420	Possible applications of Mo2C in the orthorhombic and hexagonal phases explored via ab-initio investigations of elastic, bonding, optoelectronic and thermophysical properties. Results in Physics, 2022, 37, 105505.	2.0	30
45421	Optical absorption and stability enhancement in mixed lead, tin, and germanium hybrid halide perovskites for photovoltaic applications. Vacuum, 2022, 201, 111106.	1.6	8

#	Article	IF	Citations
45422	Theoretical probing the anchoring properties of BNP2 monolayer for lithium-sulfur batteries. Applied Surface Science, 2022, 594, 153393.	3.1	7
45423	Configurational entropy-induced phase transition in spinel LiMn₂O₄. Chinese Physics B, 2022, 31, 098202.	0.7	3
45424	First-principles calculations and experimental study of Al-doped Fe1-xAlxF3Â·0.33H2O/C cathodes for Li-ion batteries. Ionics, 0, , 1.	1.2	2
45425	The physical properties of a semi-hard magnetic Fe3Pd alloy with negative enthalpy of formation. Journal of Magnetism and Magnetic Materials, 2022, , 169395.	1.0	0
45426	A Generic Sacrificial Layer for Wideâ€Range Freestanding Oxides with Modulated Magnetic Anisotropy. Advanced Functional Materials, 2022, 32, .	7.8	24
45427	Density Functional Theory Approach to the Vibrational Properties and Magnetic Specific Heat of the Covalent Chain Antiferromagnet KFeS2. Molecules, 2022, 27, 2663.	1.7	3
45428	Ab initio study on electronic and optical properties of Cu2NiGeS4 for photovoltaic applications. Solar Energy, 2022, 237, 333-339.	2.9	5
45429	Complexions and stoichiometry of the 60.8Â°//[100](011) symmetrical tilt grain boundary in Mg2SiO4 forsterite: A combined empirical potential and first-principles study. American Mineralogist, 2022, 107, 2034-2043.	0.9	3
45430	Si-containing 3D cage-functionalized graphene oxide grafted with Ferrocene for high-performance supercapacitor application: An experimental and theoretical study. Journal of Energy Storage, 2022, 50, 104635.	3.9	9
45431	Study of band alignment type in Janus HfSe2/Ga2SeS and HfSeS/GaSe heterostructures. Computational Materials Science, 2022, 209, 111432.	1.4	2
45432	First-principles insights into the mechanical, optoelectronic, thermophysical, and lattice dynamical properties of binary topological semimetal BaGa2. Results in Physics, 2022, 37, 105507.	2.0	14
45433	Study on the adsorption behavior of tin from waste liquid crystal display using a novel macroporous silica-based adsorbent in one-step separation. Separation and Purification Technology, 2022, 292, 121006.	3.9	13
45434	Effects of the cation ordering in Mg:Al and Zn:Al layered double hydroxides on crystallographic and spectroscopical properties by means of first principles calculations. Applied Clay Science, 2022, 223, 106496.	2.6	6
45435	First principle design of new thermoelectrics from TiNiSn based pentanary alloys based on 18 valence electron rule. Computational Materials Science, 2022, 209, 111396.	1.4	4
45436	Molecular insight into iron corrosion induced by chloride and sulphate. Computational Materials Science, 2022, 209, 111429.	1.4	16
45437	Theoretical investigation on electrocatalytic reduction of CO2 to methanol and methane by bimetallic atoms TM1/TM2-N@Gra (TMÂ=ÂFe, Co, Ni, Cu). Applied Surface Science, 2022, 593, 153377.	3.1	27
45438	Metal-organic framework-derived three-dimensional CoSe2/Cd0.8Zn0.2S Schottky junction for highly efficient photocatalytic H2 evolution. Applied Surface Science, 2022, 593, 153420.	3.1	14
45439	Investigation of structural, magnetic and electronic properties of CoMnSb superstructure: A DFT study. Computational Materials Science, 2022, 210, 111441.	1.4	3

#	Article	IF	Citations
45440	Quasi-two-dimensional topological Co3Sn2S2 composite toward high rate sodium ion storage. Chemical Engineering Journal, 2022, 443, 136420.	6.6	4
45441	Electronic and magnetic properties of sub-unit cell Î±-Fe2O3 films on the Î±-Al2O3 (0001) substrate. Computational Materials Science, 2022, 210, 111442.	1.4	2
45442	Selective transfer hydrogenation coupling of nitroaromatics to azoxy/azo compounds by electron-enriched single Ni-N4 sites on mesoporous N-doped carbon. Chemical Engineering Journal, 2022, 443, 136416.	6.6	10
45443	Rational design of highly efficient electrocatalytic single-atom catalysts for nitrogen reduction on nitrogen-doped graphene and g-C2N supports. Journal of Power Sources, 2022, 535, 231449.	4.0	12
45444	High performance of non-enzymatic glucose biosensors based on the design of microstructure of Ni2P/Cu3P nanocomposites. Applied Surface Science, 2022, 593, 153395.	3.1	10
45445	Ti4O7 regulating both Zn(OH)42â€“ and electrons for improving Znâ€“Ni batteries. Chemical Engineering Journal, 2022, 443, 136342.	6.6	10
45446	Temperature- and pressure-dependent phonon transport properties of SnS across phase transition from machine-learning interatomic potential. International Journal of Heat and Mass Transfer, 2022, 192, 122859.	2.5	9
45447	DFT insights into the new Hf-based chalcogenide MAX phase Hf2SeC. Vacuum, 2022, 201, 111072.	1.6	20
45448	Active site switching of Fe-N-C as a chloride-poisoning resistant catalyst for efficient oxygen reduction in seawater-based electrolyte. Chemical Engineering Journal, 2022, 443, 136456.	6.6	11
45449	Effect of Ti addition on interfacial properties of Al (111)/B4C (0001): A combined experimental and theoretical methods. Materials Science in Semiconductor Processing, 2022, 147, 106707.	1.9	2
45450	Klein tunneling and ballistic transport in graphene and related materials. , 0, , 118-142.		0
45451	Quantum transport in disordered graphene-based materials. , 0, , 143-218.		0
45452	Ab initio and multiscale quantum transport in graphene-based materials. , 0, , 232-299.		0
45453	Electronic structure calculations: the density functional theory (DFT). , 0, , 314-331.		0
45454	Electronic structure calculations: the many-body perturbation theory (MBPT). , 0, , 332-337.		0
45455	Green's functions and ab initio quantum transport in the Landauerâ€“BÃ¼ttiker formalism. , 0, , 338-357.		0
45456	Ab Initio Study of Mechanical Deformation. , 2005, , 439-448.		0
45470	Defect formation in Yb-doped <mml:math xmlns:mml="http://www.w3.org/1998/Math/MathML"><mml:msub><mml:mi>CsPbCl</mml:mi><mml:mn>3</mml:mn></mml:msub> from first principles with implications for quantum cutting. Physical Review Materials, 2022, 6, .		

#	Article	IF	Citations
45471	Realâ€Space Crystal Structure Analysis by Lowâ€Dose Focalâ€Series TEM Imaging of Organic Materials with Nearâ€Atomic Resolution. Advanced Materials, 2022, 34, e2202088.	11.1	4
45472	Deciphering the Role of Substitution in Transitionâ€Metal Phosphorous Trisulfide (100) Surface: A Highly Efficient and Durable Ptâ€free ORR Electrocatalyst. ChemPhysChem, 2022, 23, .	1.0	1
45473	Charge Modulation at Atomicâ€Level through Substitutional Sulfur Doping into Atomically Thin Bi₂WO₆ toward Promoting Photocatalytic CO₂ Reduction. ChemSusChem, 2022, 15, .	3.6	18
45474	Electronic structure, sodium diffusion and redox potentials of <scp>lowâ€symmetry Na</scp> M <scp>Fe</scp> (<scp> MoO ₄ </scp>) ₃ (M Â=ÂMg, Ni). Journal of Computational Chemistry, 2022, 43, 953-960.	1.5	2
45475	Interactions between glucosides of the tip of the S1 subunit of SARS-CoV-2 spike protein and dry and wet surfaces of CuO and Cuâ€”A model for the surfaces of coinage metals. Colloids and Surfaces B: Biointerfaces, 2022, 214, 112465.	2.5	2
45476	Two-Dimensional Quaternary Transition Metal Sulfide CrMoA₂S₆ (A = C, Si, or) Tj ETQq1 1 0.784314 rgBT /Ov Chemistry Letters, 2022, 13, 3850-3856.	2.1	6
45477	Puckered Penta-like PdPX (X = O, S, Te) Semiconducting Nanosheets: First-Principles Study of the Mechanical, Electro-Optical, and Photocatalytic Properties. ACS Applied Materials & Interfaces, 2022, 14, 21577-21584.	4.0	19
45478	Syngas Conversion to C₂ Species over WC and M/WC (M = Cu or Rh) Catalysts: Identifying the Function of Surface Termination and Supported Metal Type. ACS Applied Materials & Interfaces, 2022, 14, 19491-19504.	4.0	2
45479	Ultrafast Carbothermal Shock Constructing Ni₃Fe_{1â€“x}Cr_x Intermetallic Integrated Electrodes for Efficient and Durable Overall Water Splitting. ACS Applied Materials & Interfaces, 2022, 14, 19524-19533.	4.0	10
45480	Engineering Magnetic Anisotropy and Emergent Multidirectional Soft Ferromagnetism in Ultrathin Freestanding LaMnO₃ Films. ACS Nano, 2022, 16, 7580-7588.	7.3	14
45481	Unveiling the charge transfer dynamics steered by built-in electric fields in BiOBr photocatalysts. Nature Communications, 2022, 13, 2230.	5.8	117
45482	Surface restructuring of a perovskite-type air electrode for reversible protonic ceramic electrochemical cells. Nature Communications, 2022, 13, 2207.	5.8	65
45483	Stabilization of hexazine rings in potassium polynitride at high pressure. Nature Chemistry, 2022, 14, 794-800.	6.6	22
45484	Enhancing ionic conductivity in solid electrolyte by relocating diffusion ions to under-coordination sites. Science Advances, 2022, 8, eabj7698.	4.7	37
45485	Cooperative Catalytic Mo-S-Co Heterojunctions with Sulfur Vacancies for Kinetically Boosted Lithium-Sulfur Battery. SSRN Electronic Journal, 0, , .	0.4	0
45486	Dissociation of ammonia borane and its subsequent nucleation on the Ru(0001) surface revealed by density functional theoretical simulations. Physical Chemistry Chemical Physics, 2022, 24, 12226-12235.	1.3	21
45487	Enhancement of Gas Sensing by Doping of Transition Metal in Two-Dimensional As2c3 Nanosheet. SSRN Electronic Journal, 0, , .	0.4	0
45488	Enhancing Electrochemical Nitrogen Fixation by Mimicking Î Back-Donation on Laser-Tuned Lewis Acid Sites in Noble-Metal-Molybdenum Carbide. SSRN Electronic Journal, 0, , .	0.4	0

#	Article	IF	Citations
45489	Theoretical and experimental study of the microstructure of a metallic melt in an In₅₀Bi₅₀ alloy based on the Wulff cluster model. Physical Chemistry Chemical Physics, 2022, 24, 10798-10806.	1.3	1
45490	Towards an atomistic understanding of polymorphism in molecular solids. Physical Chemistry Chemical Physics, 2022, 24, 11278-11294.	1.3	4
45491	Epitaxially Grown Porous Heterostructure of Hexagonal Boron Nitride/Graphene as Efficient Electrocatalyst for H2o2ÂGeneration. SSRN Electronic Journal, 0, , .	0.4	0
45492	Predicted stable electrides in Mgâ€“Al systems under high pressure. Physical Chemistry Chemical Physics, 2022, , .	1.3	0
45493	Superconducting properties in doped 2M-WS₂ from first principles. Journal of Materials Chemistry C, 2022, 10, 7917-7924.	2.7	2
45494	2D GeP₃ and blue P: promising thermoelectric materials for room- and high-temperature applications. Materials Advances, 0, , .	2.6	2
45495	Exploring the similarity of single-layer covalent organic frameworks using electronic structure calculations. RSC Advances, 2022, 12, 12283-12291.	1.7	6
45496	Quantum spin Hall effect in tilted penta silicene and its isoelectronic substitutions. Physical Chemistry Chemical Physics, 2022, 24, 15201-15207.	1.3	6
45497	Water on porous, nitrogen-containing layered carbon materials: the performance of computational model chemistries. Physical Chemistry Chemical Physics, 2022, , .	1.3	0
45498	Quantum Anomalous Hall Effect in Monolayer Ferromagnetic Crc with Extremly High Curie Temperature. SSRN Electronic Journal, 0, , .	0.4	0
45499	Two Dimensional Pts2/Bn Heterostructure as an S-Scheme Photocatalyst with Enhanced Activity for Overall Water Decomposition. SSRN Electronic Journal, 0, , .	0.4	0
45500	Toward graphene-based devices for nanospintronics. Theoretical and Computational Chemistry, 2022, , 249-274.	0.2	0
45502	Micro-AlloyingÂModulated Strength-Ductility Trade-Offs in 6111 Al Alloys. SSRN Electronic Journal, 0, , .	0.4	0
45503	Out-of-plane dipole-modulated photogenerated carrier separation and recombination at Janus-MoSSe/MoS₂ van der Waals heterostructure interfaces: an ab initio time-domain study. Physical Chemistry Chemical Physics, 2022, 24, 11743-11757.	1.3	2
45504	A theoretical study on CO₂ at Li₄SiO₄ and Li₃NaSiO₄ surfaces. Physical Chemistry Chemical Physics, 2022, 24, 13678-13689.	1.3	5
45505	Direct Evidence for the Decisive Role of OH* Activation in CO Electro-Oxidation Reaction. SSRN Electronic Journal, 0, , .	0.4	0
45506	First principles study on structural, electronic and optical properties of HfS_{2(1â^'x)}Se_{2x} and ZrS_{2(1â^'x)}Se_{2x} ternary alloys. RSC Advances, 2022, 12, 14061-14068.	1.7	6
45507	FeP2 monolayer: Isoelectronic analogue of MoS2 with excellent electronic and optical properties. Physical Chemistry Chemical Physics, 0, , .	1.3	1

#	Article	IF	Citations
45508	Mechanical Strain and Electric Field Tunable Electronic Structure of Black/Violet Phosphorene Van Der Waals Heterostructure: From Type I to Z-Scheme System. SSRN Electronic Journal, 0, , .	0.4	0
45509	The steps of thermal treatment of Na-magadiite: a computational study using ab initio DFT calculations. Physical Chemistry Chemical Physics, 2022, 24, 14416-14423.	1.3	3
45510	Reaction surfaces and interfaces of metal sulfides: cryo-XPS meets HAXPES and DFT. Faraday Discussions, 2022, , .	1.6	3
45511	First-Principles Study of Electronic Properties of Amine Ligand-Capped Cspbbr3 Surface with Organo-Metallic Alumina Precursor Treatment. SSRN Electronic Journal, 0, , .	0.4	0
45512	Single Atom Supported on Mos2 as Efficient Electrocatalysts for the Co2 Reduction Reaction: A Dft Study. SSRN Electronic Journal, 0, , .	0.4	0
45513	First Principle Study of Van Der Waals Heterostructure Based on Ms2 (M= Mo, W) and Janus Crsse Monolayers. SSRN Electronic Journal, 0, , .	0.4	0
45514	Engineering the photocatalytic efficiency of nanoscale TiO₂ anatase with doped (Nd/Y) and co-doped (Ndâ€“Y/Ndâ€“Sm) lanthanides to decompose the azo dye orange G under UV-VIS irradiation. New Journal of Chemistry, 2022, 46, 10162-10183.	1.4	4
45515	Polarization Induced Self-Doping Effects and P-N Junctions in Heterostructures Based on F-Gan-H Stacking. SSRN Electronic Journal, 0, , .	0.4	0
45516	Electrocatalytic CO₂ reduction reaction on dual-metal- and nitrogen-doped graphene: coordination environment effect of active sites. Materials Advances, 2022, 3, 4566-4577.	2.6	10
45517	Incorporating Au₁₁ nanoclusters on MoS₂ nanosheet edges for promoting the hydrogen evolution reaction at the interface. Nanoscale, 2022, 14, 7919-7926.	2.8	9
45519	Mechanism Elaboration of the Thermal Decomposition for Ether Electrolyte in Sodium-Ion Battery. SSRN Electronic Journal, 0, , .	0.4	0
45520	Effect of van der Waals stacking in CdS monolayer on enhancing the hydrogen production efficiency of SiH monolayer. Materials Advances, 2022, 3, 4629-4640.	2.6	8
45521	Structural Stabilization of Cation Disordered Rock-Salt Cathode Materials: Coupling between High-Ratio Inactive Ti4+ Cation and Mn2+/Mn4+ Two-Electron Redox Pair. SSRN Electronic Journal, 0, , .	0.4	0
45522	Towards a new packing pattern of Li adsorption in two-dimensional pentagonal BCN. Physical Chemistry Chemical Physics, 2022, 24, 13194-13200.	1.3	8
45523	In situ Raman spectroscopy reveals the structure evolution and lattice oxygen reaction pathway induced by the crystallineâ€“amorphous heterojunction for water oxidation. Chemical Science, 2022, 13, 5639-5649.	3.7	14
45524	Theoretical Exploration of Site Selective PerovskitesÂ for the Application of Flexible Optoresponsive MemoryÂ Devices. SSRN Electronic Journal, 0, , .	0.4	0
45525	Tailoring Î± ₂/Î³ And Î³/Î³ Interfaces in TiAl Alloys Via Segregation: A Multiscale QM/MM Study. SSRN Electronic Journal, 0, , .	0.4	0
45526	Doping-Induced Modulation of Electronic, Optical and Wetting Properties of Ceo2. SSRN Electronic Journal, 0, , .	0.4	0

#	Article	IF	Citations
45527	Two-Dimensional Cds/Sii2ÂHeterostructure with Low Carrier Recombination as a Promising Photocatalyst for Water Splitting. SSRN Electronic Journal, 0, , .	0.4	0
45528	Superior energy storage properties in NaNbO₃-based ceramics via synergistically optimizing domain and band structures. Journal of Materials Chemistry A, 2022, 10, 11613-11624.	5.2	40
45529	Robust route to photocatalytic nitrogen fixation mediated by capitalizing on defect-tailored InVO₄ nanosheets. Environmental Science: Nano, 2022, 9, 1996-2005.	2.2	13
45530	Rational design of Mâ€“N₄â€“Gr/V₂C heterostructures as highly active ORR catalysts: a density functional theory study. RSC Advances, 2022, 12, 14368-14376.	1.7	6
45531	Role of metal and anions in organo-metal halide perovskites CH₃NH₃MX₃ (M: Cu, Zn, Ga, Ge, Sn, Pb; X: Cl, Br, I) on structural and optoelectronic properties for photovoltaic applications. RSC Advances, 2022, 12, 13281-13294.	1.7	15
45532	Synergetic effect between Pd²⁺ and Ir⁴⁺ species promoting direct ethane dehydrogenation into ethylene over bimetallic PdIr/AC catalysts. Catalysis Science and Technology, 0, , .	2.1	1
45533	An Ab Initio Approach to Understand the Structural, Thermophysical, Electronic, and Optical Properties of Binary Silicide Srsi2: A Double Weyl Semimetal. SSRN Electronic Journal, 0, , .	0.4	0
45534	Metallic-semiconducting transition and spin polarized-unpolarized transition in a single molecule with negative Poisson's ratio. Physical Chemistry Chemical Physics, 2022, , .	1.3	0
45535	Investigation of Sensing Properties of NOx Adsorbed Gas Molecules on Fe-Doped MoSeâ,, Monolayer. IEEE Sensors Journal, 2022, 22, 11665-11672.	2.4	7
45536	Electronic and Optical Properties of Mg3xn (X=P, as, Sb, Bi) Antiperovskites: The Gw/Bse Approach. SSRN Electronic Journal, 0, , .	0.4	0
45537	Influence of Intercalated Gd Atoms on Graphene-4h-Sic(0001) Properties. SSRN Electronic Journal, 0, , .	0.4	0
45538	Electronic, mechanical, optical and piezoelectric properties of glass-like sodium silicate (Na₂SiO₃) under compressive pressure. RSC Advances, 2022, 12, 12453-12462.	1.7	9
45539	First-principles study of polymer-passivated silicon nanowire outer-shell defects. Physical Chemistry Chemical Physics, 2022, 24, 11169-11174.	1.3	1
45540	Enhanced Microstructural and Magneto-Optical Properties of Fe2co1-Xnixo4 Ferrites Nanoparticles for Hyperthermia Applications. SSRN Electronic Journal, 0, , .	0.4	0
45541	Solubility and segregation of B in paramagnetic fcc Fe. Physical Review Materials, 2022, 6, .	0.9	4
45542	Vibrational properties of <mml:math xmlns:mml="http://www.w3.org/1998/Math/MathML"><mml:mrow><mml:msub><mml:mi>SrVO</mml:mi><mml:mn>2</mml:mn></ mathvariant="normal">H</mml:mi></mml:mrow></mml:math> with large spin-phonon coupling. Physical Review Materials, 2022, 6, .	0.9	0
45543	Vibrational properties of <mml:math xmlns:mml="http://www.w3.org/1998/Math/MathML"><mml:mrow><mml:msub><mml:mi>CuInP</mml:mi><mml:mn>2</mml:mn></m mathvariant="normal">S</mml:mi><mml:mn>6</mml:mn></mml:msub></mml:mrow></mml:math> across the ferroelectric transition. Physical Review B, 2022, 105, .	1.1	14
45544	Engineering Low-Coordination Single-Atom Cobalt on Graphitic Carbon Nitride Catalyst for Hydrogen Evolution. ACS Catalysis, 2022, 12, 5517-5526.	5.5	67

#	Article	IF	Citations
45545	FIRST-PRINCIPLE STUDY OF THE BUCKLING COMPRESSIVE STRAIN INDUCED ON OPTOELECTRONIC ASPECTS OF TWO-DIMENSIONAL B₂C NANOSTRUCTURE. Surface Review and Letters, 2022, 29, .	0.5	3
45546	Assessment of the Heat Capacity by Thermodynamic Approach Based on Density Functional Theory Calculations. , 0, , .		0
45547	Modeling antiphase boundary energies of Ni3Al-based alloys using automated density functional theory and machine learning. Npj Computational Materials, 2022, 8, .	3.5	15
45548	New Insights into Phase Separation of Cerium Hydrides under Pressure. ACS Omega, 2022, 7, 15681-15687.	1.6	0
45549	Understanding the CH4 Conversion over Metal Dimers from First Principles. Nanomaterials, 2022, 12, 1518.	1.9	2
45550	Cu(C3H3N3S3)3 Adsorption onto ZnTiO3/TiO2 for Coordination-Complex Sensitized Photochemical Applications. Materials, 2022, 15, 3252.	1.3	6
45551	Prediction of nature of band gap of perovskite oxides (ABO3) using a machine learning approach. Journal of Materiomics, 2022, 8, 937-948.	2.8	11
45552	Understanding the Effect of the Valence State of Perovskite Bâ€Site Ions on Its Oxygen Electrocatalytic Performance. Advanced Materials Interfaces, 2022, 9, .	1.9	7
45553	NdAlSi: A magnetic Weyl semimetal candidate with rich magnetic phases and atypical transport properties. Physical Review B, 2022, 105, .	1.1	17
45554	First-principles studies on electronic structure and optical properties of two-dimensional ZrO₂. Modern Physics Letters B, 0, , .	1.0	0
45555	Comment on â€œAb-initio-driven prediction of puckered penta-like PdPSeX (X=O, S, Te) Janus monolayers: Study on the electronic, optical, mechanical and photocatalytic properties [Applied Surface Science 582 (2022) 152356]â€. Applied Surface Science, 2022, , 153515.	3.1	1
45556	Cellulose nanofiberâ€derived carbon aerogel for advanced roomâ€temperature sodiumâ€“sulfur batteries. , 2023, 5, .		15
45557	SnS₂ Monolayer-Supported Transition Metal Atoms as Efficient Bifunctional Oxygen Electrocatalysts: A Theoretical Investigation. Energy & Fuels, 2022, 36, 4992-4998.	2.5	9
45558	Dependency of sliding friction for two-dimensional systems on electronegativity. Physical Review B, 2022, 105, .	1.1	3
45559	Automated exploitation of the big configuration space of large adsorbates on transition metals reveals chemistry feasibility. Nature Communications, 2022, 13, 2087.	5.8	8
45560	Four Carbon Allotropes Form COT Structures. ACS Applied Electronic Materials, 2022, 4, 2353-2363.	2.0	9
45561	Density Functional Theory Perspective on the Nonlinear Response of Correlated Electrons across Temperature Regimes. Journal of Chemical Theory and Computation, 2022, 18, 2900-2912.	2.3	17
45562	<mml:math xmlns:mml="http://www.w3.org/1998/Math/MathML"><mml:mrow><mml:mi>B</mml:mi><mml:mn>1</mml:mn><mml:mtext>â€“</mml:mtext>â€“</mml:mrow></mml:math> phase transition of ferropericlase at planetary interior conditions. Physical Review B, 2022, 105, .	1.1	2

#	Article	IF	Citations
45563	Pressure-induced structural transformation of clathrate <mml:math xmlns:mml="http://www.w3.org/1998/Math/MathML"><mml:msub><mml:mi>Ge</mml:mi><mml:mn>136</mml:mn></mml:msub></mml:math> via ultrafast recrystallization of an amorphous intermediate. Physical Review B, 2022, 105, .	1.1	1
45564	Electronic and optical properties of layered Van der Waals heterostructures based on blue phosphorus and zinc oxide. , 2022, , .		0
45565	Structural Stability, Thermodynamic and Elastic Properties of Cubic Zr0.5Nb0.5 Alloy under High Pressure and High Temperature. Crystals, 2022, 12, 631.	1.0	2
45566	Strain effects on the behavior of intrinsic point defects within the GaN/AlN interface. International Journal of Modern Physics C, 0, , .	0.8	0
45567	Generalized universal equation of states for magnetic materials: A novel formulation for an interatomic potential in Fe. Physical Review Materials, 2022, 6, .	0.9	0
45568	Maximizing the linear and nonlinear optical responses of alkaline tricyanomelaminate. Fundamental Research, 2022, , .	1.6	5
45569	KrÃ¶hnkite-type K2Mn(SO4)2(H2O)2 double salt: synthesis, structure, and properties. Journal of Materials Science, 2022, 57, 8195-8210.	1.7	3
45570	Resolving the Mechanism of Acoustic Plasmon Instability in Graphene Doped by Alkali Metals. International Journal of Molecular Sciences, 2022, 23, 4770.	1.8	5
45571	Van der Waals Heterostructures Based on Porous Graphene for Photocatalytic Water Splitting. Journal of Physical Chemistry C, 2022, 126, 7849-7858.	1.5	7
45572	Electronic and Magnetic Properties of Iron Doped Graphene Nanoribbons. Russian Journal of Physical Chemistry A, 2022, 96, S132-S138.	0.1	0
45573	Ab initio simulations of Î±- and Î²-ammonium carbamate (NH₄Â·NH₂CO₂), and the thermal expansivity of deuterated Î±-ammonium carbamate from 4.2 to 180â€…K by neutron powder diffraction. Acta Crystallographica Section B: Structural Science, Crystal Engineering and Materials, 2022, 78, 459-475.	0.5	2
45574	Supported Bimetallic Trimers Fe₂M@NG: Triple-Atom Catalysts for CO₂ Electroreduction. ACS Omega, 2022, 7, 16080-16086.	1.6	5
45575	Lattice Dynamics in the NASICON NaZr₂(PO₄)₃ Solid Electrolyte from Temperature-Dependent Neutron Diffraction, NMR, and Ab Initio Computational Studies. Chemistry of Materials, 2022, 34, 4029-4038.	3.2	6
45576	Reversely trapping atoms from a perovskite surface for high-performance and durable fuel cell cathodes. Nature Catalysis, 2022, 5, 300-310.	16.1	175
45577	Layered double hydroxide nanosheets activate CsPbBr3 nanocrystals for enhanced photocatalytic CO2 reduction. Nano Research, 2022, 15, 5953-5961.	5.8	22
45578	Signature of a randomness-driven spin-liquid state in a frustrated magnet. Communications Physics, 2022, 5, .	2.0	7
45579	First-principles study on the superconductivity of doped zirconium diborides. Physical Review Materials, 2022, 6, .	0.9	2
45580	Structureâ^'Reactivity Relationship of $$hbox {Pt}_n$$ (nÂ=Â1,3,7) Nanoparticles Supported on (5,5) CNT: An Ab Initio Study. Topics in Catalysis, 0, , 1.	1.3	0

#	Article	IF	Citations
45581	Unraveling Molecular Fingerprints of Catalytic Sulfur Poisoning at the Nanometer Scale with Near-Field Infrared Spectroscopy. Journal of the American Chemical Society, 2022, 144, 8848-8860.	6.6	8
45582	Hydrogen Activation and Spillover on Anatase TiO₂-Supported Ag Single-Atom Catalysts. Journal of Physical Chemistry C, 2022, 126, 7482-7491.	1.5	13
45583	Formation and stability of Rh₂Cd₅ and its strucural correlation with RhCd and Rh₃Cd_{5â^'Î´} (Î´ â^¼ 0.56). Zeitschrift Fur Kristallographie - Crystalline Materials, 2021, .	0.4	1
45584	Fully exposed palladium cluster catalysts enable hydrogen production from nitrogen heterocycles. Nature Catalysis, 2022, 5, 485-493.	16.1	118
45585	Modulation Doping Enables Ultrahigh Power Factor and Thermoelectric ZT in nâ€Type Bi₂Te_{2.7}Se_{0.3}. Advanced Science, 2022, 9, e2201353.	5.6	19
45586	DFT Investigations of Aun Nano-Clusters Supported on TiO2 Nanotubes: Structures and Electronic Properties. Molecules, 2022, 27, 2756.	1.7	0
45587	Intermediate spin state and the <mml:math xmlns:mml="http://www.w3.org/1998/Math/MathML"><mml:mrow><mml:mi>B</mml:mi><mml:mn>1</mml:mn><mml:mtext>â^'</mml transition in ferropericlase. Physical Review Research, 2022, 4, .	1.3	8
45588	A first-principles study of structural, electronic and optical properties of Î±-Te tubular nanostructures modulated by uniaxial strain. New Journal of Physics, 2022, 24, 053037.	1.2	2
45589	First Principle Calculations and Monte Carlo Simulations Investigation of Structural, Electronic, Magnetic, Elastic and Thermoelectric Properties of Antiperovskites $$Mn_3ZnX (mathrm{X}=) Tj ETQq0 0 0 rgBT /Overlock 10 Tf 50 41	0.8	11
45590	Unlocking New Redox Activity in Alluaudite Cathodes through Compositional Design. Chemistry of Materials, 2022, 34, 4088-4103.	3.2	5
45591	Peroxymonosulfate Activation on Synergistically Enhanced Single-Atom Co/Co@C for Boosted Chemiluminescence of Tris(bipyridine) Ruthenium(II) Derivative. Analytical Chemistry, 2022, 94, 6866-6873.	3.2	21
45592	optical, and thermoelectric properties of semiconducting <mml:math xmlns:mml="http://www.w3.org/1998/Math/MathML"><mml:mrow><mml:msub><mml:mi>ZnIn</mml:mi><mml:mn>2</mml:mn></ <mml:math		

#	Article	IF	Citations
45599	Robust Tunable Large-Gap Quantum Spin Hall States in Monolayer Cu₂S on Insulating Substrates. ACS Omega, 2022, 7, 15760-15768.	1.6	4
45600	Ab Initio Study of the Interaction of a Graphene Surface Decorated with a Metal-Doped C30 with Carbon Monoxide, Carbon Dioxide, Methane, and Ozone. International Journal of Molecular Sciences, 2022, 23, 4933.	1.8	4
45601	Tetravalent doping in hafnium-zirconium oxides to lower polarization switching voltage. , 2022, , .		0
45602	Origin of the discrepancy between the fundamental and optical gaps and native defects in two dimensional ultra-wide bandgap semiconductor: Gallium thiophosphate. Applied Physics Letters, 2022, 120, 172108.	1.5	1
45603	Ab Initio Computer Simulations on Interfacial Properties of Single-Layer MoS₂ and Au Contacts for Two-Dimensional Nanodevices. ACS Applied Nano Materials, 2022, 5, 10192-10202.	2.4	1
45604	Exploring Stability of Transition-Metal Single Atoms on Cu₂O Surfaces. Journal of Physical Chemistry C, 2022, 126, 8065-8078.	1.5	5
45605	Enabling high energy lithium metal batteries via single-crystal Ni-rich cathode material co-doping strategy. Nature Communications, 2022, 13, 2319.	5.8	143
45606	Freeâ€Energy Parameterization and Thermodynamics in Siâ€Geâ€Sn Alloys. Physica Status Solidi (B): Basic Research, 0, , .	0.7	0
45607	Theoretical Insights on the Two-Dimensional Transitional Metal Trihydroxytriaminophenalenyl for Highly Efficient Carbon Dioxide Electroreduction. Journal of the Electrochemical Society, 2022, 169, 056512.	1.3	0
45608	Anisotropic terahertz optostriction in group-IV monochalcogenide compounds. Physical Review B, 2022, 105, .	1.1	1
45609	Slipâ€Lineâ€Guided Growth of Graphene. Advanced Materials, 2022, 34, e2201188.	11.1	7
45610	Ultra-low turn-off current 2D material heterojunction selectors: first-principle calculations. Semiconductor Science and Technology, 2022, 37, 065024.	1.0	0
45611	Single-atom metal tuned sulfur vacancy for efficient H2 activation and hydrogen evolution reaction on MoS2 basal plane. Applied Surface Science, 2022, 597, 153614.	3.1	9
45612	Atomic Stress State Inside fcc and bcc Random Alloys: A First-Principles Approach. Frontiers in Materials, 2022, 9, .	1.2	4
45613	Ultralow diffusion barrier of double transition metal MoWC monolayer as Li-ion battery anode. Journal of Materials Science, 2022, 57, 10702-10713.	1.7	8
45614	Cu atoms induce a new reconstruction in the MnGa(001) surface: An ab-initio study. Applied Surface Science, 2022, 597, 153514.	3.1	3
45615	Interlaboratory study on Sb2S3 interplay between structure, dielectric function, and amorphous-to-crystalline phase change for photonics. IScience, 2022, 25, 104377.	1.9	29
45616	Manifestation of interface-induced effects of two-dimensional MSi2/Si(111) quantum heterostructures: A first principles study. Physica E: Low-Dimensional Systems and Nanostructures, 2022, , 115291.	1.3	0

#	Article	IF	Citations
45617	Low-frequency lattice vibrations from atomic displacement parameters of Î±-FOX-7, a high energy density material. Acta Crystallographica Section B: Structural Science, Crystal Engineering and Materials, 2022, 78, 376-384.	0.5	2
45618	Synergistic Effect, Structural and Morphology Evolution, and Doping Mechanism of Spherical Brâ€Doped Na₃V₂(PO₄)₂F₃/C toward Enhanced Sodium Storage. Small, 2022, 18, e2201719.	5.2	24
45619	Nitrogen Decoration of Basal-Plane Dislocations in <mml:math xmlns:mml="http://www.w3.org/1998/Math/MathML" display="inline" overflow="scroll"><mml:mn>4</mml:mn><mml:mrow><mml:mrow><mml:mi mathvariant="normal">H</mml:mi></mml:mrow></mml:mrow></mml:math> - <mml:math xmlns:mml="http://www.w3.org/1998/Math/MathML" display="inline" overflow="scroll"><mml:mi>SiC</mml:mi></mml:math>. Physical Review Applied, 2022, 17, .	1.5	5
45620	First-Principles Study on the Interaction of H2O and Interface Defects in A-SiO2/Si(100). Frontiers in Materials, 2022, 9, .	1.2	0
45621	Heteroanionic Melilite Oxysulfide: A Promising Infrared Nonlinear Optical Candidate with a Strong Second-Harmonic Generation Response, Sufficient Birefringence, and Wide Bandgap. ACS Applied Materials & Interfaces, 2022, 14, 23645-23652.	4.0	33
45622	An Ab Initio Study of Clusters as Building Blocks for Crystals: From Prussian Blue Analogs to Hybrid Perovskites. Physica Status Solidi (B): Basic Research, 2022, 259, .	0.7	1
45623	Regression Machine Learning Models Used to Predict DFT-Computed NMR Parameters of Zeolites. Computation, 2022, 10, 74.	1.0	6
45624	First-principles study of the adsorption and dissociation of NO on the Be(0001) surface. European Physical Journal B, 2022, 95, .	0.6	0
45625	Improved performances of Cr2N monolayer as electrode of lithium ion battery through surface termination: A first-principles calculation. Journal of Physics and Chemistry of Solids, 2022, 168, 110794.	1.9	5
45626	Giant magneto optical Kerr effect in antiferromagnetic <mml:math xmlns:mml="http://www.w3.org/1998/Math/MathML"><mml:msub><mml:mi>M</mml:mi><mml:mn>2</mml:mn></mml:msub><mml:mi mathvariant="normal">As</mml:mi><mml:mo>Â</mml:mo><mml:mrow><mml:mo>(</mml:mo><mml:mi>M</mml:mi><mml:mo>=	1.1	2
45627	Electronâ€“Phonon Coupling Constant of Uranium and Lutetium. Journal of Superconductivity and Novel Magnetism, 0, , .	0.8	0
45628	The Structural, Lattice Dynamic, Thermodynamic, and Mechanical Characterization of Na ₂ Mo ₂ O ₇ Crystal by Firstâ€Principles. Physica Status Solidi (B): Basic Research, 0, , 2200036.	0.7	0
45629	Atomic mechanisms of hexagonal close-packed Ni nanocrystallization revealed by in situ liquid cell transmission electron microscopy. Nano Research, 2022, 15, 6772-6778.	5.8	2
45630	Pt-based intermetallic compounds with tunable activity and selectivity toward hydrogen production from formic acid. Applied Surface Science, 2022, 597, 153530.	3.1	7
45631	A spin promotion effect in catalytic ammonia synthesis. Nature Communications, 2022, 13, 2382.	5.8	38
45632	Characterizing the ZrC(111)/c-ZrO2(111) Hetero-Ceramic Interface: First Principles DFT and Atomistic Thermodynamic Modeling. Molecules, 2022, 27, 2954.	1.7	0
45633	New quaternary sulfide LiGaSiS4: Synthesis, structure and optical properties. Journal of Solid State Chemistry, 2022, , 123230.	1.4	0
45634	Establishing a theoretical insight for penta-coordinated iron-nitrogen-carbon catalysts toward oxygen reaction. Nano Research, 2022, 15, 6067-6075.	5.8	28

#	Article	IF	Citations
45635	Titanium Monoxide with in Situ Grown Rutile TiO₂ Nanothorns as a Heterostructured Job-Sharing Anode Material for Lithium-Ion Storage. ACS Applied Energy Materials, 2022, 5, 5691-5703.	2.5	5
45636	First-principles study of bilayer polymeric manganese phthalocyanine. Physical Review B, 2022, 105, .	1.1	1
45637	Catalytic activity of Coâ€“Ag nanoalloys to dissociate molecular hydrogen. New insights on the chemical environment. International Journal of Hydrogen Energy, 2022, 47, 19038-19050.	3.8	3
45638	xmlns:mml="http://www.w3.org/1998/Math/MathML" display="inline" id="d1e1248" altimg="si35.svg"><mml:msub><mml:mrow /><mml:mrow><mml:mi mathvariant="normal">x</mml:mi></mml:mrow></mml:msub></mml:math>@Pd<mml:math xmlns:mml="http://www.w3.org/1998/Math/MathML" display="inline" id="d1e1256"	1.0	1
45639	Phonon contribution to nuclear spin diffusion in ruby crystal estimated by lattice dynamics calculations. European Physical Journal Plus, 2022, 137, .	1.2	0
45640	First-principles Prediction of Structural, Electronic, Magnetic and Optical Properties of ErN and TmN in the Hexagonal Structure. Optik, 2022, , 169226.	1.4	3
45641	Integrated Highâ€Throughput and Machine Learning Methods to Accelerate Discovery of Molten Salt Corrosionâ€Resistant Alloys. Advanced Science, 2022, 9, e2200370.	5.6	15
45642	Magnetization in CNT induced by nitrogen doping and enhanced by transversal electric field application. Journal of Materials Science, 2022, 57, 9277-9298.	1.7	4
45643	Atomic-scale interactions between quorum sensing autoinducer molecules and the mucoid P. aeruginosa exopolysaccharide matrix. Scientific Reports, 2022, 12, 7724.	1.6	4
45644	Importance of vibrational anharmonicity for electron-phonon coupling in molecular crystals. Physical Review B, 2022, 105, .	1.1	8
45645	Tuning Molecular Inhibitors and Aluminum Precursors for the Area-Selective Atomic Layer Deposition of Al₂O₃. Chemistry of Materials, 2022, 34, 4646-4659.	3.2	15
45646	Patchwork-Structured Heterointerface of 1T-WS₂/a-WO₃ with Sustained Hydrogen Spillover as a Highly Efficient Hydrogen Evolution Reaction Electrocatalyst. ACS Applied Materials & Interfaces, 2022, 14, 24008-24019.	4.0	21
45647	A Gapped Phase in Semimetallic T_dâ€WTe₂ Induced by Lithium Intercalation. Advanced Materials, 2022, 34, e2200861.	11.1	7
45648	A DFT Study on the Activity Origin of Feâ€Nâ€C Sites for Oxygen Reduction Reaction. ChemPhysChem, 2022, 23, .	1.0	7
45649	Design of a two-dimensional interplanar heterojunction for catalytic cancer therapy. Nature Communications, 2022, 13, 2425.	5.8	65
45650	Exploring the exemplary structural, electronic, optical, and elastic nature of inorganic ternary cubic XBaF₃ (X = Al and Tl) employing the accurate TB-mBJ approach. Semiconductor Science and Technology, 2022, 37, 075004.	1.0	20
45651	Site-Dependent Properties of Quantum Emitters in Nanostructured Silicon Carbide. PRX Quantum, 2022, 3, .	3.5	1
45652	Nonequilibrium electron and lattice dynamics of <mml:math xmlns:mml="http://www.w3.org/1998/Math/MathML"><mml:mrow><mml:msub><mml:mi>Sb</mml:mi><mml:mn>12</mml:mn></mml:msub></mml:mrow></mml:math> under pressure. Physical Review B, 2022, 105, .	1.1	3

#	Article	IF	Citations
45653	Robust structure symmetry and electronic band structure of the chiral topological semimetal CoSi against high pressure. Materials Today Communications, 2022, , 103667.	0.9	0
45654	Buckled Honeycomb Lattice Compound Sr₃CaOs₂O₉ Exhibiting Antiferromagnetism above Room Temperature. Chemistry of Materials, 2022, 34, 4741-4750.	3.2	3
45655	Quantitative Analysis of Nanorough Hydrogenated Si(111) Surfaces through Vibrational Spectral Assignment by Periodic DFT Calculations. Journal of Physical Chemistry C, 2022, 126, 8278-8286.	1.5	0
45656	Ethanol electro-oxidation on the PdSn-TaN/C catalyst in alkaline media: Making TaN capable of splitting C C bond. Applied Catalysis B: Environmental, 2022, 314, 121473.	10.8	14
45657	Computational Design of Î±-AsP/Î³-AsP Vertical Two-Dimensional Homojunction for Photovoltaic Applications. Nanomaterials, 2022, 12, 1662.	1.9	1
45658	The density functional theory study of substitution effect in antiferromagnetic USn05Sb15. Journal of Solid State Chemistry, 2022, , 123174.	1.4	0
45659	Negative thermal expansion of group III-Nitride monolayers. Journal Physics D: Applied Physics, 2022, 55, 315303.	1.3	5
45660	Defective NiO as a Stabilizer for Au Single-Atom Catalysts. ACS Catalysis, 2022, 12, 6149-6158.	5.5	30
45661	First-principles computational tensile test of Î³-Fe grain boundaries considering the effect of magnetism: Electronic origin of grain boundary embrittlement due to Zn segregation. Physical Review Materials, 2022, 6, .	0.9	4
45662	Spin Polarization of Mn Could Enhance Grain Boundary Sliding in Mg. Materials, 2022, 15, 3483.	1.3	0
45663	Allowable stretching bond force constants on carbon nanomaterials: A DFT study. Diamond and Related Materials, 2022, 126, 109083.	1.8	2
45664	A new high-pressure structure of SiO₂ directly converted from Î±-quartz under nonhydrostatic compression. Journal of Physics Condensed Matter, 2022, 34, 304003.	0.7	3
45665	3dâ€Transition metal doped two-dimensional SnTe: Modulation of thermoelectric properties. Materials Today Communications, 2022, 31, 103656.	0.9	2
45666	Effects of Fluorination and Molybdenum Codoping on Monoclinic BiVO₄ Photocatalyst by HSE Calculations. ACS Omega, 0, , .	1.6	2
45667	Revealing the Origin of Lowâ€Temperature Activity of Niâ€“Rh Nanostructures during CO Oxidation Reaction with Operando TEM. Advanced Science, 2022, 9, e2105599.	5.6	6
45668	Two-dimensional germanene-based Janus material Ge8HnX8â^'n (nâ€¯=â€¯0â€“8, Xâ€¯=â€¯F, Cl, Br, I) for photovoltaic and photocatalytic applications. Applied Surface Science, 2022, 598, 153633.	6.1	6
45669	Bifunctional catalytic activity of 2D boron monochalcogenides BX (XÂ=ÂS, Se, Te). Materials Today Energy, 2022, 27, 101026.	2.5	7
45670	Superconducting Li10Se electride under pressure. Journal of Chemical Physics, 2022, 156, .	1.2	8

#	Article	IF	Citations
45671	Anionic and Cationic Co-Substitutions of S into Vertically Aligned WTe₂ Nanosheets as Catalysis for Hydrogen Evolution under Alkaline Conditions. ACS Applied Nano Materials, 2022, 5, 7123-7131.	2.4	3
45672	Electron count dictates phase separation in Heusler alloys. Physical Review Materials, 2022, 6, .	0.9	2
45673	Role of Defects and Radiation Damage on He Diffusion in Magnetite: Implication for (U-Th)/He Thermochronology. Minerals (Basel, Switzerland), 2022, 12, 590.	0.8	6
45674	Maximizing intrinsic anomalous Hall effect by controlling the Fermi level in simple Weyl semimetal films. Physical Review B, 2022, 105, .	1.1	4
45675	Low-temperature magnetic crossover in the topological kagome magnet TbMn6Sn6. Communications Physics, 2022, 5, .	2.0	12
45676	First-principles calculations to investigate elasto-mechanical and opto-electronic properties of pyrochlore oxides X2Zr2O7 (X=La, Nd). Journal of Materials Research and Technology, 2022, 18, 5005-5018.	2.6	3
45677	First-principle study of the effects of Ni doping and point vacancy on the magnetic and absorption spectrum and itinerant electron properties of ZnO. Solid State Communications, 2022, , 114813.	0.9	1
45678	Unravelling the Nature of the Intrinsic Complex Structure of Binaryâ€Phase Naâ€Layered Oxides. Advanced Materials, 2022, 34, e2202137.	11.1	21
45679	Experimental and theoretical insight into DSSCs mechanism influenced by different doping metal ions. Applied Surface Science, 2022, 597, 153607.	3.1	4
45680	Enhanced catalytic performance of transition metal-doped Cr2O3 catalysts for propane dehydrogenation: A microkinetic modeling study. Chemical Engineering Journal, 2022, 446, 136913.	6.6	4
45681	Single-Atom Catalysts Supported by Graphene and Hexagonal Boron Nitride: Structural Stability in the Oxygen Environment. Journal of Physical Chemistry C, 2022, 126, 8637-8644.	1.5	2
45682	High Dielectric Permittivity of Î±-NaFeO₂-Type Layered Nitrides. Chemistry of Materials, 2022, 34, 4505-4513.	3.2	4
45683	Nitriding behavior and mechanical properties of AerMet100 steel and first-principles calculations of phase interfaces. Journal of Materials Research and Technology, 2022, 19, 46-60.	2.6	3
45684	Nitrite reduction over Ag nanoarray electrocatalyst for ammonia synthesis. Journal of Colloid and Interface Science, 2022, 623, 513-519.	5.0	71
45685	Alternative Cu3Zn catalysts for enhanced reduction of CO2 to CH4: A density functional theory-based approach. Surfaces and Interfaces, 2022, 31, 102030.	1.5	2
45686	Atomic structure of an FeCrMoCBY metallic glass revealed by high energy x-ray diffraction. Journal of Physics Condensed Matter, 2022, 34, 285301.	0.7	2
45687	Tunability of the bandgap of SnS by variation of the cell volume by alloying with A.E. elements. Scientific Reports, 2022, 12, 7434.	1.6	9
45688	Gate-Tuned Gas Molecule Sensitivity of a Two-Dimensional Semiconductor. ACS Applied Materials & Interfaces, 2022, 14, 23617-23623.	4.0	7

#	Article	IF	Citations
45689	Thermodynamics and Magnetism of SmFe12 Compound Doped with Co and Ni: An Ab Initio Study. Applied Sciences (Switzerland), 2022, 12, 4860.	1.3	7
45690	Triangular Arrangement of Ferromagnetic Iron Chains in the Highâ€‹T_C Ferromagnet TiFe_{1â^'x}Os_{2+x}B₂. Chemistry - A European Journal, 2022, 28, .	1.7	2
45691	The interaction between H and CH3 of adsorption on the diamond (100)-2â€‰Ã—â€‰1 surface based on DFT Calculations. Journal of Molecular Modeling, 2022, 28, 147.	0.8	0
45692	Analysis of the behavior of Zn atoms with a Pb additive on the surface during Zn electrodeposition. Electrochemistry Communications, 2022, 138, 107291.	2.3	2
45693	Synthesis of distorted octahedral C-doped nickel nanocrystals encapsulated in CNTs: A highly active and stable catalyst for water pollutions treatment. Chemical Engineering Journal, 2022, 446, 136805.	6.6	4
45694	Cycling stability and adsorption mechanism at room temperature of the upscaled Ni-doped hierarchical carbon scaffold. International Journal of Hydrogen Energy, 2022, , .	3.8	0
45695	H2O2 formation mechanisms on the (1 1 2) and (3 1 0) facets of SnO2 via water oxidation reaction with the participation of Bicarbonate: DFT and experimental Investigations. Applied Surface Science, 2022, 596, 153634.	3.1	4
45696	Highly efficient two-dimensional Ag2Te cathode catalyst featuring a layer structure derived catalytic anisotropy in lithium-oxygen batteries. Energy Storage Materials, 2022, 50, 96-104.	9.5	27
45697	Unveiling the Valence State of Interstitial Bromine on Charge Carrier Lifetime in CH₃NH₃PbBr₃ by Quantum Dynamics Simulation. Journal of Physical Chemistry Letters, 2022, 13, 4193-4199.	2.1	2
45698	Cubic-spinel AgIn5S8-based thermoelectric materials: synthesis, phonon transport and defect chemistry. Materials Today Energy, 2022, 27, 101029.	2.5	4
45699	Atomistic mechanism of phase transformation between topologically close-packed complex intermetallics. Nature Communications, 2022, 13, 2487.	5.8	15
45700	Effects of Conjugated Structure on Electronic and Transport Properties in Organic-inorganic Hybrid Superlattices Cd₂Se₂(C₂H₄N₂)_{1/2}. Journal of Physics Condensed Matter, 2022, 34, .	0.7	2
45701	Strongly Quantum-Confined Perovskite Nanowire Arrays for Color-Tunable Blue-Light-Emitting Diodes. ACS Nano, 2022, 16, 8388-8398.	7.3	19
45702	Mixed Halide Ordering as a Tool for the Stabilization of Ruddlesdenâ€“Popper Structures. Chemistry of Materials, 2022, 34, 4286-4297.	3.2	7
45703	Transformation of Thermal Expansion from Large Volume Contraction to Nonlinear Strong Negative Thermal Expansion in PbTiO₃â€“Bi(Co_{1â€“x}Fe_x)O₃ Perovskites. ACS Applied Materials & Interfaces, 2022, 14, 23610-23616.	4.0	5
45704	Strategic design and fabrication of MXenes-Ti3CNCl2@CoS2 core-shell nanostructure for high-efficiency hydrogen evolution. Nano Research, 2022, 15, 5977-5986.	5.8	61
45705	Effect of the charge injection and N and S co-doping on the structural and electronic properties, and hydrogen storage capacity of graphdiyne 2D structure. Surfaces and Interfaces, 2022, 31, 102031.	1.5	3
45706	BAND INVERSION IN Bi2Se3 FROM FAT BAND ANALYSIS. Journal of Crystal Growth, 2022, , 126719.	0.7	0

#	Article	IF	Citations
45707	Strain-tunable self-passivated porous phosphorene for high-efficiency helium separation. Journal Physics D: Applied Physics, 2022, 55, 315501.	1.3	1
45708	The Origin of the Thermochromic Property Changes in Doped Vanadium Dioxide. ACS Applied Materials & Interfaces, 2022, 14, 23928-23943.	4.0	11
45709	Multiscale machine-learning interatomic potentials for ferromagnetic and liquid iron. Journal of Physics Condensed Matter, 2022, 34, 305402.	0.7	5
45710	Role of the M point phonons for the dynamical stability of B2 compounds. Scientific Reports, 2022, 12, 7258.	1.6	1
45711	Understanding the complementarities of surface-enhanced infrared and Raman spectroscopies in CO adsorption and electrochemical reduction. Nature Communications, 2022, 13, 2656.	5.8	53
45712	Exploration of structural, electronic, optical, mechanical, thermoelectric, and thermodynamic properties of <scp> XInO ₃ </scp> (XÂ=ÂAs, Sb) compounds for energy harvesting applications. International Journal of Energy Research, 2022, 46, 13409-13423.	2.2	1
45713	Realization of Enlarged Birefringence from BaCdBe₂(BO₃)₂F₂ to NaMgBe₂(BO₃)₂F via the Cation Size Effect as a Potential Deep-Ultraviolet Birefringent Material. Inorganic Chemistry, 2022, 61, 7624-7630.	1.9	8
45714	Organic Cation Diffusion-Induced Heterogeneous Viscoelasticity in Organicâ€“Inorganic Hybrid Perovskite Polycrystalline Films. ACS Applied Materials & Interfaces, 2022, 14, 22582-22592.	4.0	1
45715	Design of novel dilute magnetic semiconductors by exhaustive first-principles calculations and scale-bridging simulations. Materials Today Communications, 2022, 31, 103604.	0.9	3
45716	<mml:math xmlns:mml="http://www.w3.org/1998/Math/MathML"><mml:mrow><mml:msub><mml:mi>Cr</mml:mi><mml:mn>2</mml:mn></mml:msub><mml:mi mathvariant="normal">S</mml:mi><mml:mn>3</mml:mn></mml:mrow></mml:math> a bipolar semiconducting fully compensated ferrimagnet. Physical Review Materials, 2022, 6, .	0.9	1
45717	Tailoring Photoinduced Nonequilibrium Magnetizations in In₂Se₃ Bilayers. Advanced Optical Materials, 2022, 10, .	3.6	5
45718	Two novel large-cell boron nitride polymorphs. Diamond and Related Materials, 2022, 126, 109046.	1.8	7
45719	The stable behavior of low thermal conductivity in 1T-sandwich structure with different components. Journal of Applied Physics, 2022, 131, .	1.1	2
45720	First-principle study of new insights on the magnetic mechanism of ZnO through rare-earth Nd doping and Zn vacancies. Materials Today Communications, 2022, 31, 103608.	0.9	0
45721	First-principles calculations to investigate structural, electronic and phonon properties of sodium bromide (NaBr) and sodium iodide (NaI) crystals. Computational Condensed Matter, 2022, 31, e00682.	0.9	1
45722	Pressure effect on the electronic spectra of CdSe and CdS. Molecular Crystals and Liquid Crystals, 0, , 1-7.	0.4	0
45723	DFT study of the occurrence state of In and the correlation of In and Fe in sphalerite. Minerals Engineering, 2022, 183, 107596.	1.8	13
45724	Elastic, electronic, optical and thermoelectric properties of the novel Zintl-phase Ba2ZnP2. Solid State Sciences, 2022, 128, 106893.	1.5	75

#	Article	IF	Citations
45725	Sn-assisted nickel synergistically catalyzes the direct cleavage of CArO bond in lignin-derived m-cresol: Theoretical and experimental analysis. Journal of Catalysis, 2022, 410, 180-193.	3.1	5
45726	Significant improvement of the Seebeck coefficient of Fe2VAlÂwith antisite defects. Materials Today Communications, 2022, 31, 103510.	0.9	2
45727	To what extent do bond length and angle govern the 13C and 1H NMR response to weak CHâ‹¯O hydrogen bonds? A case study of caffeine and theophylline cocrystals. Solid State Nuclear Magnetic Resonance, 2022, 119, 101795.	1.5	2
45728	Zn stable isotope fractionation during adsorption onto todorokite: A molecular perspective from X-ray absorption spectroscopy and density functional theory. Geochimica Et Cosmochimica Acta, 2022, 327, 116-136.	1.6	12
45729	Electronic structure of chabazite zeolites H-SSZ-13 and H-SAPO-34. Microporous and Mesoporous Materials, 2022, 338, 111957.	2.2	3
45730	Experimental study and thermodynamic modeling of the Tiâ€“Cuâ€“B system. Calphad: Computer Coupling of Phase Diagrams and Thermochemistry, 2022, 77, 102431.	0.7	0
45731	Interaction between helium and transition metals in vanadium: A first-principles investigation. Nuclear Materials and Energy, 2022, 31, 101189.	0.6	2
45732	Structural, electronic, mechanical and thermodynamic properties of Uâ€“Si intermetallic compounds: A comprehensive first principles calculations. Progress in Nuclear Energy, 2022, 148, 104229.	1.3	5
45733	Two orthorhombic superhard carbon allotropes: Hcc-C14 and DHcc-C20. Diamond and Related Materials, 2022, 126, 109065.	1.8	9
45734	Interface robust magnetoelectric coupling effect in ferromagnetic/ferroelectric BiFeO3/KNbO3 heterostructure: First-principles calculations. Results in Physics, 2022, 37, 105538.	2.0	4
45735	First-principles calculations of (0 0 1)-Al//(0 0 1) interface in Al-Cu alloys: Atomic structure, bonding strength, stability and electronic properties. Computational Materials Science, 2022, 210, 111485.	1.4	4
45736	Influence of heavy Hf doping in CeO2: Prediction on various physical properties. Results in Physics, 2022, 37, 105569.	2.0	5
45737	Pt accelerated coarsening of A15 precipitates in Cr-Si alloys. Materials and Design, 2022, 218, 110655.	3.3	0
45738	Achieving enhanced high-temperature mechanical properties in Mg-Nd-Sm-Zn-Ca-Zr alloy by Ag addition. Materials Today Communications, 2022, 31, 103666.	0.9	5
45739	Cyclic and tensile deformations of Goldâ€“Silver core shell systems using newly parameterized MEAM potential. Mechanics of Materials, 2022, 169, 104304.	1.7	2
45740	Hydrogen assisted intergranular cracking of alloy 725: The effect of boron and copper alloying. Corrosion Science, 2022, 203, 110331.	3.0	8
45741	Radial and axial vibration modes of graphyne nanotubes. Materials Today Communications, 2022, 31, 103610.	0.9	1
45742	Screening of the mechanical stability of M2AX phases for nuclear applications. Computational Materials Science, 2022, 210, 111443.	1.4	1

#	Article	IF	Citations
45743	First-principle studies of electronic, elastic and vibrational properties of barytocalcite and paralstonite. Materials Today Communications, 2022, 31, 103644.	0.9	0
45744	First principles study of the lattice thermal conductivity of alkaline earth oxides. Computational Materials Science, 2022, 210, 111446.	1.4	4
45745	Revisiting the mechanism of highly efficient CO oxidation by single iron atom catalysis on Pt(100). Materials Today Communications, 2022, 31, 103609.	0.9	0
45746	Gilbert damping, electronic and magnetic properties for quaternary Heusler alloys CrYCoZ: First-principles and Monte Carlo studies. Computational Materials Science, 2022, 210, 111453.	1.4	11
45747	Exploring original properties of GaN-BN alloys using high-throughput ab initio computation. Optik, 2022, 261, 169166.	1.4	0
45748	Insight to Se-doping effects on Fe7S8/carbon nanotubes composite as anode for sodium-ion batteries. Journal of Power Sources, 2022, 536, 231458.	4.0	23
45749	Carbon diffusion in bcc- and bct-Fe: Influence of short-range Câ€“C pair interactions studied from first-principles calculations. Materials Chemistry and Physics, 2022, 286, 126159.	2.0	3
45750	CoSe2 nanodots confined in multidimensional porous nanoarchitecture towards efficient sodium ion storage. Nano Energy, 2022, 98, 107326.	8.2	46
45751	Synthesis, crystal structure and optical properties of the first bromine-containing iodate: Pb2IO3Br3. Solid State Sciences, 2022, 129, 106898.	1.5	0
45752	A DFT study of the electronic and optical properties of four 2D thin films. Materials Chemistry and Physics, 2022, 286, 126158.	2.0	5
45753	Investigations on electronic properties and optical properties of Zn9-xAgxO/G based on first-principles. Materials Science in Semiconductor Processing, 2022, 147, 106748.	1.9	2
45754	First principles electronic structure, molecular dynamics, and optical properties of GaOF monolayer without and with defects. Materials Science and Engineering B: Solid-State Materials for Advanced Technology, 2022, 281, 115736.	1.7	4
45755	Flexible 3D porous boron nitride interconnected network as a high-performance Li-and Na-ion battery electrodes. Electrochimica Acta, 2022, 421, 140491.	2.6	9
45756	Investigation of W/Mo co-doping with multiple concentrations in photocatalyst BiVO4 by first-principles calculations. Solid State Communications, 2022, 351, 114794.	0.9	2
45757	Low coverage disordered decanethiol monolayers on Au(001): A conjecture regarding the formation of Au-adatom-molecule complexes. Applied Surface Science, 2022, 594, 153364.	3.1	2
45758	Mechanical properties of the novel L12-Ir3Z ultra-high temperature alloys (Z =Ti, V, Zr, Nb, Hf and Ta). Journal of Alloys and Compounds, 2022, 912, 165244.	2.8	6
45759	Spin polarized study of alkaline earth-cubic lead perovskites (PbXO3, XÂ=ÂMg, Ca & Sr) for emerging spintronic technology. Journal of Crystal Growth, 2022, 590, 126699.	0.7	13
45760	Oxidation mechanism of arsenopyrite under alkaline conditions: Experimental and theoretical analyses. Journal of Cleaner Production, 2022, 358, 131987.	4.6	9

#	Article	IF	Citations
45761	Charge compensation and solid-state lighting application for dysprosium-activated Ba2TeP2O9 phosphor. Journal of Alloys and Compounds, 2022, 912, 165188.	2.8	11
45762	First-principles calculations of the structural, mechanical, electronic, and optical properties of BaX2 (X=O, S, Se and Te) compounds. Materials Science in Semiconductor Processing, 2022, 147, 106755.	1.9	3
45763	Characterization of two dimensional ferromagnetic binary and Janus manganese dichalcogenides. Journal of Magnetism and Magnetic Materials, 2022, 556, 169412.	1.0	7
45764	Novel atomic-scale graphene metamaterials with broadband electromagnetic wave absorption and ultra-high elastic modulus. Carbon, 2022, 196, 146-153.	5.4	9
45765	A new insight into heterogeneous nucleation mechanism of Al by non-stoichiometric TiCx. Acta Materialia, 2022, 233, 117977.	3.8	23
45766	Ab initio study of negative electron affinity on the scandium-terminated diamond (100) surface for electron emission devices. Carbon, 2022, 196, 176-185.	5.4	6
45767	Ground-state structure, orbital ordering and metal-insulator transition in double-perovskite PrBaMn2O6. Journal of Alloys and Compounds, 2022, 912, 165150.	2.8	5
45768	The influence of nitrogen proportion on the mechanical property of Feâ€“Ni alloy at extreme pressure. Solid State Communications, 2022, 351, 114798.	0.9	0
45769	Atomic structure and electrical/ionic activity of antiphase boundary in CH3NH3PbI3. Acta Materialia, 2022, 234, 118010.	3.8	6
45770	Antiperovskite materials as promising candidates for efficient tandem photovoltaics: First-principles investigation. Materials Science in Semiconductor Processing, 2022, 147, 106727.	1.9	6
45771	Changes in electronic structure of graphene by adsorption of low melamine coverages. Surface Science, 2022, 723, 122120.	0.8	2
45772	The trapping effects of silicon and phosphorus on point defects in Î³-Fe. Computational Materials Science, 2022, 210, 111488.	1.4	1
45773	Ba3(ZnB5O10)PO4:Tb3+ green phosphor: Microwave-assisted sintering synthesis and thermally stable photoluminescence. Journal of Alloys and Compounds, 2022, 911, 165087.	2.8	15
45774	In-situ phase transformation and corrosion behavior of TiNi via LPBF. Corrosion Science, 2022, 203, 110348.	3.0	11
45775	First principles study on optical and thermal properties of BaTiS3. Optik, 2022, 261, 169196.	1.4	4
45776	Tuning the HOMO and LUMO energy levels of dye sensitizers with electron-accepting capability and electron-drawing capability of substituents to optimize the efficiency of dye-sensitized solar cells: Approach of theoretical. Inorganic Chemistry Communication, 2022, 141, 109522.	1.8	0
45777	First-principles study of pyroxene structure LiVO3. Journal of Solid State Chemistry, 2022, 312, 123177.	1.4	3
45778	Locating the rate-limiting step of hydrogen conversion on Sr2Fe1.5Mo0.5O6 (0 0 1) surface: Implications for efficient SOFC anode design. Applied Surface Science, 2022, 595, 153513.	3.1	6

#	Article	IF	Citations
45779	Nonmetallic surface plasmon resonance coupling with pyroelectric effect for enhanced near-infrared-driven CO2 reduction. Chemical Engineering Journal, 2022, 445, 136739.	6.6	14
45780	Chemically anchoring molybdenum atoms onto micropore-rich VN nanosheet for boosted nitrogen electro-fixation via hydrogen bonds. Chemical Engineering Journal, 2022, 446, 136915.	6.6	4
45781	First-principles screening of Pt doped Ti2CNL (Nâ€¯=â€¯O, S and Se, Lâ€¯=â€¯F, Cl, Br and I) as high-performance catalysts for ORR/OER. Applied Surface Science, 2022, 596, 153574.	3.1	31
45782	Study of Î³-valerolactone production from hydrogenation of levulinic acid over nanostructured Pt-hydrotalcite catalysts at low temperature. Fuel, 2022, 323, 124272.	3.4	12
45783	Investigation on the WC/Cu interfacial bonding properties: First-principles prediction and experimental verification. International Journal of Refractory Metals and Hard Materials, 2022, 106, 105872.	1.7	13
45784	Electronic and catalytic properties of Ti single atoms@SnO2 and its implications on sensing mechanism for CO. Applied Surface Science, 2022, 594, 153500.	3.1	5
45785	Tuning the activity and selectivity of nitrogen reduction reaction on double-atom catalysts by B doping: A density functional theory study. Nano Energy, 2022, 99, 107363.	8.2	21
45786	Direct Z-scheme MoSe2/TiO2 heterostructure with improved piezoelectric and piezo-photocatalytic performance. Journal of Colloid and Interface Science, 2022, 622, 637-651.	5.0	15
45787	The dynamical stability, electronic, elastic properties and ideal strength of diamond-like cubic B2CN: A first-principles study. Solid State Communications, 2022, 352, 114805.	0.9	3
45788	Triptycene incorporated carbon nitride based donor-acceptor conjugated polymers with superior visible-light photocatalytic activities. Journal of Colloid and Interface Science, 2022, 622, 675-689.	5.0	8
45789	The type-II PtSe2/WS2 van der Waals heterostructure: A high efficiency water-splitting photocatalyst. Surface Science, 2022, 723, 122103.	0.8	18
45790	A dual-site doping strategy for developing efficient perovskite oxide electrocatalysts towards oxygen evolution reaction. Nano Energy, 2022, 99, 107344.	8.2	34
45791	Helium interaction with solutes and impurities in neutron-irradiated nanostructured ferritic alloys: A first principles study. Journal of Nuclear Materials, 2022, 566, 153771.	1.3	2
45792	Adsorption and dissociation of water molecules on the <mml:math xmlns:mml="http://www.w3.org/1998/Math/MathML" altimg="si2.svg"><mml:mi>Î±</mml:mi></mml:math>-Pu<mml:math xmlns:mml="http://www.w3.org/1998/Math/MathML" altimg="si3.svg"><mml:msub><mml:mrow /><mml:mn>2</mml:mn></mml:msub></mml:math>O<mml:math xmlns:mml="http://www.w3.org/1998/Math/MathML" altimg="si4.svg"><mml:msub><mml:mrow	1.3	1
45793	Boosting the Fischer-Tropsch synthesis performances of cobalt-based catalysts via geometric and electronic engineering: Construction of hollow structures. Applied Catalysis B: Environmental, 2022, 313, 121469.	10.8	9
45794	2D MoS2-MoSe2 and MoS2-NbS2 lateral heterostructures as anode materials for LIBs/SIBs. Applied Surface Science, 2022, 596, 153529.	3.1	9
45795	Magnetic Properties of PrFe11Ti Alloys by Co and Zr Doping. Studia Universitatis BabeÈ™-Bolyai Physica, 2021, 66, 9-17.	0.0	0
45796	Study on the Electronic Structure and Optical Properties of Two-dimensional Monolayer MoSi₂X₄ (X=N, P, As). Acta Chimica Sinica, 2022, 80, 510.	0.5	3

#	Article	IF	Citations
45797	Formation of oxygen vacancies in the Li-rich Mn-based cathode material Li_{1.167}Ni_{0.167}Co_{0.167}Mn_{0.5}O<sub&g calculations. Wuli Xuebao/Acta Physica Sinica, 2022, .	0.3	0
45798	Delving into guest-free and He-filled sI and sII clathrate hydrates: a first-principles computational study. Physical Chemistry Chemical Physics, 2022, 24, 13119-13129.	1.3	4
45799	Structural diversity and hydrogen storage properties in the system Kâ€“Siâ€“H. Physical Chemistry Chemical Physics, 2022, 24, 13033-13039.	1.3	3
45800	Map of Two-Dimensional Tungsten Chalcogenide Compounds (Wâ€“S, Wâ€“Se, Wâ€“Te) Based on USPEX Evolutionary Search. JETP Letters, 2022, 115, 292-296.	0.4	3
45801	Oxygenate Reactions over PdCu and PdAg Catalysts: Distinguishing Electronic and Geometric Effects on Reactivity and Selectivity. ACS Catalysis, 2022, 12, 5766-5775.	5.5	4
45802	Investigation of the W/Y₂O₃ heterogeneous interface properties and its effect on hydrogen behavior using first-principles calculations. Nuclear Fusion, 2022, 62, 086015.	1.6	2
45803	Magnetically tunable Dirac and Weyl fermions in the Zintl materials family. Physical Review Materials, 2022, 6, .	0.9	9
45804	Electronic and interfacial properties of graphene/HfS2 van der Waals heterostructure. Electronic Structure, 0, , .	1.0	0
45805	SnP₂S₆: A Promising Infrared Nonlinear Optical Crystal with Strong Nonresonant Second Harmonic Generation and Phase-Matchability. ACS Photonics, 2022, 9, 1724-1732.	3.2	11
45806	Highly Efficient Invisible TaO_x/ZTO Bilayer Memristor for Neuromorphic Computing and Image Sensing. ACS Applied Electronic Materials, 2022, 4, 2180-2190.	2.0	20
45807	High Open-Circuit Voltage in Double Perovskite Oxide A2NdSbO6 (A = Ba, Sr) Photoanode-Based Dye-Sensitized Solar Cells. Journal of Electronic Materials, 2022, 51, 4281-4287.	1.0	3
45808	Plastic deformation of bulk and micropillar single crystals of Mo5Si3 with the tetragonal D8 structure. International Journal of Plasticity, 2022, , 103339.	4.1	1
45809	Effect of Structural Disorder on the Physical Properties of the Pd Based Heusler Alloys: PdCoMnAl, Pd2CoAl and Pd2MnAl. Integrated Ferroelectrics, 2022, 225, 334-350.	0.3	8
45810	Energy band gaps and novel thermoelectric properties of two-dimensional functionalized Yttrium carbides (MXenes). Physica B: Condensed Matter, 2022, 639, 413922.	1.3	9
45811	Capacity development of Pd doped Si2BN nanotube for hydrogen storage. International Journal of Hydrogen Energy, 2022, 47, 19132-19145.	3.8	6
45812	Concurrent promotion of phase transition and bimetallic nanocatalyst exsolution in perovskite oxides driven by Pd doping to achieve highly active bifunctional fuel electrodes for reversible solid oxide electrochemical cells. Applied Catalysis B: Environmental, 2022, 314, 121517.	10.8	16
45813	Modeling Fission Spikes in Nuclear Fuel using a Multigroup Model of Electronic Energy Transport. Journal of Nuclear Materials, 2022, , 153797.	1.3	0
45814	Adsorption and sensing behaviors of SF6 decomposed species on pristine and Ru/Ti-modified stanene monolayer: A first-principles study. Physica E: Low-Dimensional Systems and Nanostructures, 2022, 142, 115307.	1.3	8

#	Article	IF	Citations
45815	Catalytic Growth of Ultralong Graphene Nanoribbons on Insulating Substrates. Advanced Materials, 2022, 34, e2200956.	11.1	12
45816	Investigation of structural, magneto-electronic, elastic, mechanical and thermoelectric properties of novel lead-free halide double perovskite Cs2AgFeCl6: First-principles calcuations. Journal of Physics and Chemistry of Solids, 2022, 167, 110795.	1.9	108
45817	Enhancing effect of Sn doping for the optical absorption of BaO/BaTiO ₃ interphase by first principles calculations. Surface and Interface Analysis, 0, , .	0.8	0
45818	Manganese promotion of a cobalt Fischer-Tropsch catalyst to improve operation at high conversion. Journal of Catalysis, 2022, 411, 97-108.	3.1	12
45819	Elastic strain modulation of energy bandgap in Î²-Ga2O3 sheet: experimental and computational investigations. Materials Today Physics, 2022, , 100697.	2.9	0
45820	Molecular simulation investigations on the coating of Al-alloy surface by nano-SiO2-epoxy composite. Current Applied Physics, 2022, 39, 263-271.	1.1	1
45821	Structural analysis and magnetic properties of cobalt-doped nanotitania. Materials Science and Engineering B: Solid-State Materials for Advanced Technology, 2022, 282, 115761.	1.7	3
45822	Site preference, thermodynamic, and magnetic properties of the ternary Laves phase Ti(Fe<sub>1 â€“) Tj ETQq1 1 0.784314 rgBT /Ov MgZn₂-type. International Journal of Materials Research, 2022, 97, 450-460.	0.1	0
45823	The Naâ€“H system: from first-principles calculations to thermodynamic modeling. International Journal of Materials Research, 2022, 97, 845-853.	0.1	5
45824	Ab initio study of electronic structure and magnetic properties of CoMnTaZ (Zâ€‰=â€‰Si, Ge) quaternary Heusler compounds. Physica Status Solidi C: Current Topics in Solid State Physics, 2017, 14, 1700127.	0.8	3
45825	Revisiting Stabilities of Cubic Zincblende IVâ€“IV Materials From Density Functional Theory. Physica Status Solidi C: Current Topics in Solid State Physics, 2017, 14, 1700226.	0.8	1
45826	Direct correlation between void formation and lithium dendrite growth in solid-state electrolytes with interlayers. Nature Materials, 2022, 21, 1050-1056.	13.3	84
45827	Thermodynamic modeling of the sodium alanates and the Naâ€“Alâ€“H system. International Journal of Materials Research, 2022, 97, 1484-1494.	0.1	4
45828	The non-centrosymmetric layered compounds IrTe₂I and RhTe₂I. Dalton Transactions, 2022, 51, 8688-8694.	1.6	1
45829	Enhanced Câ€“H bond activation by tuning the local environment of surface lattice oxygen of MoO₃. Chemical Science, 2022, 13, 7468-7474.	3.7	3
45830	Superior mechanical flexibility, lattice thermal conductivity and electron mobility of the hexagonal honeycomb carbon nitride monolayer. Physical Chemistry Chemical Physics, 2022, 24, 13951-13964.	1.3	2
45831	2D phosphorus carbide as promising anode materials for Na/K-ion batteries from first-principles study. Journal of Molecular Modeling, 2022, 28, 152.	0.8	2
45832	Revealing superstructure ordering in <mml:math xmlns:mml="http://www.w3.org/1998/Math/MathML"><mml:mrow><mml:msub><mml:mi>Co</mml:mi><mml:mrow><mml:mn>1</mml:mn> Heusler alloys and its effect on structural, magnetic, and electronic properties. Physical Review B, 2022, 105, .	1.1	2

#	Article	IF	Citations
45833	Spin splitting in monoperiodic systems described by magnetic line groups. Journal of Physics Condensed Matter, 2022, 34, 315803.	0.7	2
45834	Dependence of cuprous oxide conductivity on metal doping: a hybrid density functional simulation. European Physical Journal B, 2022, 95, .	0.6	0
45835	Mid-Infrared Nonlinear Optical Halides with Diamond-like Structures: A Theoretical and Experimental Study. Chemistry of Materials, 2022, 34, 5301-5310.	3.2	9
45836	Effects of rare earth element Ce on structural, electronic, magnetic and optical properties of CeYFeO (xÂâ€‹=Ââ€‹0.0625, 0.125): ab initio study. Journal of Solid State Chemistry, 2022, 312, 123226.	1.4	1
45837	Analysis of the Metallic Intermediate Band in Cr-doped AgGaS₂ Semiconductor for the Photovoltaic Application. Key Engineering Materials, 0, 920, 172-178.	0.4	0
45838	Atomically chemically graded Ti/TiN interface. Applied Surface Science, 2022, 597, 153637.	3.1	6
45839	Work function of the oxygen functionalized graphenic surfaces â€“ integral experimental and theoretical approach. Applied Surface Science, 2022, , 153671.	3.1	3
45840	Mechanism and Dynamics of CO‹sub›2‹/sub› Formation in Formic Acid Decomposition on Pt Surfaces. ACS Catalysis, 2022, 12, 6486-6494.	5.5	2
45841	Two-Dimensional V‹sub›2‹/sub›N MXene Monolayer as a High-Capacity Anode Material for Lithium-Ion Batteries and Beyond: First-Principles Calculations. ACS Omega, 2022, 7, 17756-17764.	1.6	18
45842	Friction in clay-bearing faults increases with the ionic radius of interlayer cations. Communications Earth & Environment, 2022, 3, .	2.6	8
45843	Study on the Catalytic Decomposition Reaction of N2O on MgO (100) in SO2 and CO Environments. Applied Sciences (Switzerland), 2022, 12, 5034.	1.3	1
45844	Simulated carbon K edge spectral database of organic molecules. Scientific Data, 2022, 9, 214.	2.4	6
45845	Improving the HCHO Sensing Selectivity on Ag-Doped Graphene by Oxygen Functionalization: A First-Principles Study. ACS Omega, 0, , .	1.6	1
45846	Multiple optimization strategies for improving photocatalytic performance of the h-BN/flower-ring g-C3N4 heterostructures: Morphology engineering and internal electric field effect. Chemical Engineering Journal, 2022, 446, 137027.	6.6	51
45847	Itinerant magnetism, electronic properties and half-metallicity of Co2ZrSn and Co2HfSn Heusler alloys. Journal of Alloys and Compounds, 2022, 918, 165464.	2.8	3
45848	Structural, elastic and mechanical properties of Hf-doped TiAl2 and Î±-TiAl3 intermetallic compounds: first-principle calculations. European Physical Journal B, 2022, 95, .	0.6	5
45849	Atomically dispersed transition metal-N4 doped graphene as a Li O nucleation site in nonaqueous lithium-oxygen batteries. Electrochimica Acta, 2022, 422, 140554.	2.6	5
45850	Role of redox reactions involving interfacial oxygen migration in ignition of nanolayered Al/a-Al2O /CuO energetic composite. Chemical Engineering Journal Advances, 2022, 11, 100322.	2.4	1

#	Article	IF	Citations
45851	Morphology-controllable ZnO catalysts enriched with oxygen-vacancies for boosting CO2 electroreduction to CO. Journal of CO2 Utilization, 2022, 61, 102051.	3.3	19
45852	Exploring the CO <mml:math xmlns:mml="http://www.w3.org/1998/Math/MathML" display="inline" id="d1e329" altimg="si184.svg"><mml:msub><mml:mrow /><mml:mrow><mml:mn>2</mml:mn></mml:mrow></mml:msub></mml:math> conversion into hydrocarbons <mml:math xmlns:mml="http://www.w3.org/1998/Math/MathML" display="inline" id="d1e337" altimg="si12.svg"><mml:mrow><mml:mi>v</mml:mi><mml:mi>i</mml:mi><mml:mi>a</mml:mi></mml:mrow></mml:math>	3.4	5
45853	Vanadiumâ€Doped Molybdenum Diselenide Atomic Layers with Roomâ€Temperature Ferromagnetism. ChemPhysChem, 2022, 23, .	1.0	5
45854	Nitrogen Disturbance Awakening the Intrinsic Activity of Nickel Phosphide for Boosted Hydrogen Evolution Reaction. ChemSusChem, 2022, 15, .	3.6	3
45855	High CO-Tolerant Ru-Based Catalysts by Constructing an Oxide Blocking Layer. Journal of the American Chemical Society, 2022, 144, 9292-9301.	6.6	29
45856	A new class of bilayer kagome lattice compounds with Dirac nodal lines and pressure-induced superconductivity. Nature Communications, 2022, 13, 2773.	5.8	19
45857	Breaking scaling relationships in alkynol semi-hydrogenation by manipulating interstitial atoms in Pd with d-electron gain. Nature Communications, 2022, 13, 2754.	5.8	36
45858	Atomic-scale understanding of the Na and Cl trapping on the Mo1.33C(OH)2-MXene. Scientific Reports, 2022, 12, 8340.	1.6	4
45859	Ab-initio Study of structural, elastic, electronic and optical properties of hexahalometallate single crystals K2XBr6(Xâ€‰=â€‰Se, Pt). Scientific Reports, 2022, 12, 8345.	1.6	2
45860	The quantum confinement effects on the electronic properties of monolayer GeS nanoribbon with tube-edged reconstruction. Nanotechnology, 2022, 33, 345202.	1.3	2
45861	BA₂XBr₄ (X = Pb, Cu, Sn): from lead to lead-free halide perovskite scintillators. Materials Advances, 2022, 3, 5087-5095.	2.6	16
45862	Electron paramagnetic resonance spectroscopy and first-principles calculations of Cr³⁺ doped KDP crystals. CrystEngComm, 2022, 24, 4948-4954.	1.3	7
45863	Theoretical study on the effect of Ge-S/F co-doping on the crystal structure and properties of Li₂MSiO₄(M=Mn,Fe). Wuli Xuebao/Acta Physica Sinica, 2022, .	0.2	0
45864	Pd speciation on black phosphorene in a CO and C₂H₄ atmosphere: a first-principles investigation. Physical Chemistry Chemical Physics, 2022, 24, 14284-14293.	1.3	1
45865	Sodium tungsten bronze-supported Pt electrocatalysts for the high-performance hydrogen evolution reaction. Catalysis Science and Technology, 2022, 12, 4498-4510.	2.1	11
45866	Metal ions impact on the isostructurality and properties of 2D coordination polymers. CrystEngComm, 2022, 24, 4430-4439.	1.3	5
45867	Theoretical insight into the anion vacancy healing process during the oxygen evolution reaction on TaON and Ta₃N₅. Physical Chemistry Chemical Physics, 2022, 24, 13999-14006.	1.3	4
45868	Optical generation and electric control of pure spin photocurrent in ferroelectric Ruddlesden-Popper perovskite (MA)₂Pb(SCN)₂I₂ monolayer. Journal of Materials Chemistry C, 0, , .	2.7	2

#	Article	IF	Citations
45869	Compression-induced crimping of boron nanotubes from borophenes: a DFT study. Physical Chemistry Chemical Physics, 2022, 24, 14566-14572.	1.3	2
45870	Tuning the metal-insulator transition and magnetic properties of (SrVO₃)₅/(SrTiO₃)₁ (111) heterostructures. Wuli Xuebao/Acta Physica Sinica, 2022, .	0.2	0
45871	Indirect to direct band gap transition through order to disorder transformation of Cs₂AgBiBr₆via creating antisite defects for optoelectronic and photovoltaic applications. RSC Advances, 2022, 12, 15461-15469.	1.7	21
45872	Enhancing the catalytic activity of CdX and ZnX (X = S, Se and Te) nanostructures for the hydrogen evolution reaction via transition metal doping. Materials Advances, 2022, 3, 5772-5777.	2.6	2
45873	Heterointerfaces of nickel sulphides and selenides on Ni-foam as efficient bifunctional electrocatalysts in acidic environments. Journal of Materials Chemistry A, 2022, 10, 12733-12746.	5.2	26
45874	A flexible functional module to regulate ultraviolet optical nonlinearity for achieving a balance between a second-harmonic generation response and birefringence. Chemical Science, 2022, 13, 6990-6997.	3.7	14
45875	Machine learning accelerated search for new double perovskite oxide photocatalysis. Wuli Xuebao/Acta Physica Sinica, 2022, 71, 177101.	0.2	2
45876	Insight into the inclusion of heteroatom impurities in Silicon structures. Physical Chemistry Chemical Physics, 0, , .	1.3	0
45877	Effect of strain on the formation of Guinierâ€"Preston zone in Alâ€"Cu alloys from first-principles. Materials Express, 2022, 12, 369-372.	0.2	0
45878	A Nonempirical Study of Oxygen Adsorption on the (011) In2O3 Surface. Inorganic Materials, 2022, 58, 278-283.	0.2	0
45879	Role of hydrogen in stability and mobility of vacancy clusters in tungsten. Tungsten, 2022, 4, 219-230.	2.0	7
45880	Influence of Th, Zr, and Ti Dopants on Solution Property of Xe in Uranium Dioxide with Defects: A DFT + U Study. Metals, 2022, 12, 879.	1.0	3
45881	ÐÐ´ÑÐ¾Ñ€Ð±Ñ†Ð¸Ñ•Ð¿ÐµÑ€Ð¾ÐºÑ•Ð¸Ð´Ð° Ð²Ð¾Ð´Ð¾Ñ€Ð¾Ð´Ð° Ð½Ð° Ð´Ð²ÑƒÑ…Ñ‰ÐµÐ»Ñ‹Ñ… Ñ…Ð»ÐŒÐ¾Ð¾Ð¾ÐµÐ½Ð¸Ð		
45882	Inelastic scattering of electrons in water from first principles: cross sections and inelastic mean free path for use in Monte Carlo track-structure simulations of biological damage. Royal Society Open Science, 2022, 9, .	1.1	4
45883	A comprehensive analysis on elastic, mechanical, thermodynamic and thermoelectric properties of <scp> PbSnO ₃ </scp> : A density functional theory study. International Journal of Energy Research, 2022, 46, 13377-13392.	2.2	7
45884	Using in-plane anisotropy to engineer Janus monolayers of rhenium dichalcogenides. Physical Review Materials, 2022, 6, .	0.9	0
45885	Effective decoupling of ferromagnetic sublattices by frustration in Heusler alloys. Physical Review B, 2022, 105, .	1.1	9
45886	Characterization of imperfections in scintillator crystals using gamma-ray induced positron annihilation lifetime spectroscopy. Optical Materials: X, 2022, 14, 100156.	0.3	3

#	Article	IF	Citations
45887	Mitigating the Jahn-Teller distortion driven by the spin-orbit coupling of lithium manganate cathode. Journal of Energy Chemistry, 2022, 72, 379-387.	7.1	11
45888	Doping-induced modulation of electronic, optical and wetting properties of CeO2. Journal of Physics and Chemistry of Solids, 2022, 168, 110820.	1.9	6
45889	Lattice Dynamics of Bi1.9Dy0.1Te3 Topological Insulator. Physica B: Condensed Matter, 2022, 640, 414050.	1.3	2
45890	Pressure-induced electronic transitions in samarium monochalcogenides. Physical Review B, 2022, 105, .	1.1	2
45891	Theoretical Investigation of Effects of Transition Elements on Phase Stabilities and Elastic Properties of the Î³â€² Phase in Coâ€“Vâ€“Ta Superalloys. Frontiers in Materials, 2022, 9, .	1.2	0
45892	Optimal model of semi-infinite graphene for ab initio calculations of reactions at graphene edges by the example of zigzag edge reconstruction. Computational and Theoretical Chemistry, 2022, 1214, 113755.	1.1	3
45893	Helical spin ordering in room-temperature metallic antiferromagnet Fe3Ga4. Journal of Alloys and Compounds, 2022, 917, 165532.	2.8	2
45894	Unraveling the effect of sulfur doping into electronic and optical performance of monoclinic hafnium dioxide (m-HfO2: S): an (DFTâ€‰+â€‰U) insights report. Applied Physics A: Materials Science and Processing, 2022, 128, .	1.1	3
45895	Phonon-mediated superconductivity near the lattice instability in hole-doped hydrogenated monolayer hexagonal boron nitride. Physical Review Materials, 2022, 6, .	0.9	3
45896	Amorphous and Crystalline Vanadium Orthophosphate and Oxidized Multiwalled Carbon Nanotube Composites as Anode Materials in Sodiumâ€ion Batteries. ChemElectroChem, 2022, 9, .	1.7	1
45897	Optoelectronic and mechanical properties of the orthogonal and tetragonal Cu2CdGe(SxSe1â^'x)4 semiconducting system via first principles methods. Journal of Applied Physics, 2022, 131, .	1.1	7
45898	Effect of urea on arrangement of novel Mg(II) perrhenate crystal structures and their optical properties: Experimental and theoretical insight. Journal of Solid State Chemistry, 2022, 312, 123263.	1.4	2
45899	Effect of Mg(II), Mn(II), and Fe(II) doping on the mechanical properties and electronic structure of calcite. Materials Today Communications, 2022, , 103725.	0.9	2
45900	The Electronic Behavior and Mechanical Characteristics of CuGa5S8. SDU Journal of Science, 2022, 17, 72-81.	0.1	0
45901	A Nonstoichiometric Niobium Oxide/Graphite Composite for Fastâ€Charge Lithiumâ€ion Batteries. Small, 2022, 18, .	5.2	13
45902	Effect of off-stoichiometric composition on half-metallic character of Co₂Fe(Ga,Ge) investigated using saturation magnetization and giant magnetoresistance effect. Journal Physics D: Applied Physics, 2022, 55, 345003.	1.3	1
45903	Crystallographic Insights into the Crystal Structure and Intrinsic Properties of Ca₁₂Al₁₄O₃₃-Type Rb₃LiZn₂(MoO₄)₄ Single Crystals. Inorganic Chemistry, 0, , .	1.9	1
45904	Local Structure Investigation of Cu Precipitates in Modified 18CrNiMo7-6 Steels by Synchrotron X-ray Absorption Spectroscopy. ISIJ International, 2022, 62, 977-983.	0.6	0

#	Article	IF	Citations
45905	Ab Initio Study of the Mechanism of Proton Migration in Perovskite LaScO3. Applied Sciences (Switzerland), 2022, 12, 5302.	1.3	3
45906	Effect of hydrostatic pressure on the structural, mechanical, vibrational and electronic properties of the solid solution W1â^'xTaxB3. European Physical Journal B, 2022, 95, .	0.6	1
45907	Study of structural, electronic, elastic, optical and thermoelectric properties of half-Heusler compound RbScSn: A TB-mBJ DFT study. Optical and Quantum Electronics, 2022, 54, .	1.5	3
45908	The effect of grinding condition on superconducting properties for iron chalcogenide Fe(SeTe) crystals. Journal of Materials Science, 2022, 57, 9323-9333.	1.7	2
45909	Diamond (111) surface reconstruction and epitaxial graphene interface. Physical Review B, 2022, 105, .	1.1	3
45910	Ab Initio Computations of O and AO as well as ReO2, WO2 and BO2-Terminated ReO3, WO3, BaTiO3, SrTiO3 and BaZrO3 (001) Surfaces. Symmetry, 2022, 14, 1050.	1.1	23
45911	Investigation of novel quaternary Heusler alloys XRuCrZ (X = Co, Ni, Rh, and Pd; Z = Si and Ge) via first-principles calculation for spintronics and thermoelectric applications. AIP Advances, 2022, 12, .	0.6	5
45912	Extremely Stable, Highly Conductive Boronâ€Hydrogen Complexes in Forsterite and Olivine. Journal of Geophysical Research: Solid Earth, 2022, 127, .	1.4	1
45913	Novel Self-assembly Pd(II)-Schiff Base Complex Modified Glassy Carbon Electrode for Electrochemical Detection of Paracetamol. Electrocatalysis, 2022, 13, 598-610.	1.5	19
45914	Surface Resonant Raman Scattering from Cu(110). Physical Review Letters, 2022, 128, .	2.9	1
45915	Bioleaching of sphalerite mineralized with discrepant iron incorporations: experiment and DFT calculation. Journal of Materials Research and Technology, 2022, 19, 794-808.	2.6	2
45916	Unconventional Highly Active and Stable Oxygen Reduction Catalysts Informed by Computational Design Strategies. Advanced Energy Materials, 2022, 12, .	10.2	4
45917	Solidlike to liquidlike behavior of Cu diffusion in superionic <mml:math xmlns:mml="http://www.w3.org/1998/Math/MathML"><mml:mrow><mml:msub><mml:mi>Cu</mml:mi><mml:mn>2</mml:mn></mml: mathvariant="normal">X</mml:mi></mml:mrow></mml:math> <mml:math xmlns:mml="http://www.w3.org/1998/Math/MathML"><mml:mrow><mml:mo>(</mml:mo><mml:mi>X</mml:mi><mml:mo>=</mml:mo	0.9	7
45918	: A. Physical Review Materials, 2022, 6, . A Class of Magnetic Topological Material Candidates with Hypervalent Bi Chains. Journal of the American Chemical Society, 2022, 144, 9785-9796.	6.6	9
45919	Surface Chemistry of the Molecular Solar Thermal Energy Storage System 2,3â€Dicyanoâ€Norbornadiene/Quadricyclane on Ni(111). ChemPhysChem, 2022, 23, .	1.0	7
45920	Cl-induced passivity breakdown in Î±-Fe2O3 (0001), Î±-Cr2O3 (0001), and their interface: A DFT study. Journal of Materials Science and Technology, 2022, 129, 70-78.	5.6	13
45921	Volumes and spin states of FeHx: Implication for the density and temperature of the Earthâ€™s core. American Mineralogist, 2023, 108, 667-674.	0.9	2
45922	Surface defects engineered Bi4Ti3O12 nanosheets for photocatalytic degradation of antibiotic levofloxacin. Applied Catalysis A: General, 2022, 640, 118675.	2.2	11

#	Article	IF	Citations
45923	Computational screening of O-functional MXenes for electrocatalytic ammonia synthesis. Chinese Journal of Catalysis, 2022, 43, 1860-1869.	6.9	9
45924	CdS/SiI2: A promising two-dimensional materials for photocatalytic water splitting. Results in Physics, 2022, 38, 105636.	2.0	3
45925	Density functional theory study of quaternary InPBiN alloys lattice matched to InP substrate: Structural, electronic and optical properties. Optik, 2022, 262, 169344.	1.4	2
45926	Exploring the structural, phononic, electronic, magnetic, optical, and thermoelectric properties of Pb-free vanadium-based double perovskites using the first-principles approach for optoelectronic and thermoelectric applications. Solar Energy, 2022, 240, 27-37.	2.9	7
45927	Impact of pauli-blocking effect on optical limiting properties of WSe2 thin films. Optical Materials, 2022, 129, 112479.	1.7	3
45928	Influence of nitrogen interstitials in Î±-titanium and nitrogen vacancies in Î´-titanium nitride on lattice parameters and bulk modulus - computational study. Computational Materials Science, 2022, 211, 111509.	1.4	3
45929	Coordination Li diffusion chemistry in NASICON Li1.5Al0.5Ge1.5(PO4)3 solid electrolyte. Solid State Ionics, 2022, 381, 115947.	1.3	3
45930	The effects of solutes on precipitated phase/matrix interface stability and their distribution tendencies between the two phases in Co-based superalloys. Computational Materials Science, 2022, 211, 111547.	1.4	3
45931	Optical absorption measurements and optoelectronic DFT calculations for ethanol solvated quercetin and anhydrous/hydrated quercetin crystals. Journal of Solid State Chemistry, 2022, 312, 123242.	1.4	3
45932	Chlorine in NiO promotes electroreduction of CO2 to formate. Applied Materials Today, 2022, 28, 101528.	2.3	4
45933	Adsorption mechanism of aliphatic amino acids on kaolinite surfaces. Applied Clay Science, 2022, 226, 106566.	2.6	11
45934	Atomically dispersed non-noble Cu dimer anchored on a novel graphitic carbon nitride as a promising catalyst for the conversion of CO to CH2CH2. Applied Surface Science, 2022, 597, 153761.	3.1	3
45935	Electronic structure, optical and elastic properties of AgAlS2 crystal under hydrostatic pressure. Materials Science in Semiconductor Processing, 2022, 148, 106814.	1.9	6
45936	Two-dimensional semiconducting Ag2X (XÂ=ÂS, Se) with Janus-induced built-in electric fields and moderate band edges for overall water splitting. Applied Surface Science, 2022, 597, 153707.	3.1	9
45937	Elucidating the effect of sodium on the carburization behaviors of Î±-Fe under CO or C2H4. Applied Catalysis B: Environmental, 2022, 315, 121527.	10.8	3
45938	Theoretical Study on the Stability Mechanism of a High Energy System Composed of Molecules Containing C-O-C or -N3 Groups and Aluminum Hydride. SSRN Electronic Journal, 0, , .	0.4	0
45940	Selective and sensitive toxic gas-sensing mechanism in a 2D Janus MoSSe monolayer. Physical Chemistry Chemical Physics, 2022, 24, 15292-15304.	1.3	13
45941	Unusual Ordering Behavior of Co3al-Based Î“â€² Phase with L12 Structure Predicted by the Thermodynamic Model with Support of First-Principles Calculations. SSRN Electronic Journal, 0, , .	0.4	0

#	Article	IF	Citations
45942	Understanding the effect of lattice polarisability on the electrochemical properties of lithium tetrahaloaluminates, LiAlX₄ (X = Cl, Br, I). Journal of Materials Chemistry A, 0, , .	5.2	3
45943	Modeling Ni Redistribution in the Fuel Electrode of Solid Oxide Cells Through Ni(Oh)2 Diffusion and Ni-Ysz Wettability Change. SSRN Electronic Journal, 0, , .	0.4	0
45944	Integration of negative, zero and positive linear thermal expansion makes borate optical crystals light transmission temperature-independent. Materials Horizons, 2022, 9, 2207-2214.	6.4	3
45945	Predicting Mechanical Properties of High Entropy Alloys with Face Centered Cubic Structure from First Principles Calculations. SSRN Electronic Journal, 0, , .	0.4	0
45946	Contact Analysis of Elemental Transition Metal Electrodes for Complementary 2D-FET Applications Using MoS₂ and WSe₂. IEEE Electron Device Letters, 2022, 43, 1137-1140.	2.2	0
45947	Off-stoichiometry in Iâ€“IIIâ€“VI₂ chalcopyrite absorbers: a comparative analysis of structures and stabilities. Faraday Discussions, 0, 239, 357-374.	1.6	2
45948	Dissociative Adsorption of Azoles on Cu(111) Promoted by Chemisorbed O and Oh. SSRN Electronic Journal, 0, , .	0.4	0
45949	Data-Driven Design of a High-Performance, Two-Dimensional Graphene-Based Seawater Desalination Membrane. SSRN Electronic Journal, 0, , .	0.4	0
45950	Efficient Extraction of Resonant States in Systems with Defects. SSRN Electronic Journal, 0, , .	0.4	0
45951	A Type-Ii Gan/Ins Van Der Waals Heterostructure with High Solar-to-Hydrogen Efficiency of Photocatalyst for Water Splitting. SSRN Electronic Journal, 0, , .	0.4	0
45952	Hydrogen Atoms in Tungsten Nitride Compounds Promoting the Formation of Atomic Vacancies in Nuclear Fusion Reactors. SSRN Electronic Journal, 0, , .	0.4	0
45953	Experimental and theoretical investigation on the ORR activity of AgVO₃. Materials Chemistry Frontiers, 2022, 6, 2042-2050.	3.2	2
45954	Co-crystallization of red emitting (NH₄)₃Sc(SO₄)₃:Eu³⁺ microfibers: structureâ€“luminescence relationship for promising application in optical thermometry. CrystEngComm, 2022, 24, 4819-4830.	1.3	4
45955	Pressure-Driven Ferroelectric Phase Transition for the Pnma-Cspbbr3: Mechanical and Dynamical Stability Study. SSRN Electronic Journal, 0, , .	0.4	0
45956	High-performance potassium poly(heptazine imide) films for photoelectrochemical water splitting. Chemical Science, 2022, 13, 7541-7551.	3.7	24
45957	Insights into the Ultra-High Temperature Solid Solutions Hf-Ta-C-N Quaternary System Using High-Throughput Calculation. SSRN Electronic Journal, 0, , .	0.4	0
45958	Single-Site Co-Anchored Î‘- In2se3 with Enhanced and Polarization-Dependent Hydrogen and Oxygen Evolution Activity. SSRN Electronic Journal, 0, , .	0.4	0
45959	Insights into the Removal Paths of Adsorbed Oxygen in the Synthesis of Light Olefins from Syngas on Îš-Fe5c2(510) Surface. SSRN Electronic Journal, 0, , .	0.4	0

#	Article	IF	Citations
45960	Molecular Adsorption Behavior of Zn2sno4 (111) Crystal Surface. SSRN Electronic Journal, 0, , .	0.4	0
45961	Construction of Cos-Encapsulated in Ultrahigh Nitrogen Doped Carbon Nanofibers from Energetic Metal-Organic Frameworks for Superior Sodium Storage. SSRN Electronic Journal, 0, , .	0.4	0
45962	Understanding the interaction of N-doped graphene and sulfur compounds in a lithium-sulfur battery â€“ a density functional theory investigation. New Journal of Chemistry, 0, , .	1.4	4
45963	Quantum theory of electronic excitation and sputtering by transmission electron microscopy. Nanoscale, 2023, 15, 1053-1067.	2.8	5
45964	Construction of multidimensional CdS@MoS2 heterojunction for enhancing the activity and transfer efficiency of photogenerated carriers. New Journal of Chemistry, 0, , .	1.4	0
45965	Infrared and Raman Vibrational Modelling of Î²-C2s and C3s Compounds. SSRN Electronic Journal, 0, , .	0.4	0
45966	First-principles design of hetero CoM (M = 3d, 4d, 5d block metals) double-atom catalysts for oxygen evolution reaction under alkaline conditions. Nanoscale Advances, 2022, 4, 2913-2921.	2.2	3
45967	Multi-interfacial engineering of a coil-like NiSâ€“Ni₂P/Ni hybrid to efficiently boost electrocatalytic hydrogen generation in alkaline and neutral electrolyte. Journal of Materials Chemistry A, 2022, 10, 13410-13417.	5.2	16
45968	Surface Functionalization of Two-Dimensional Boridene Family: Enhanced Stability, Tunable Electronic Property, and High Catalytic Activity. SSRN Electronic Journal, 0, , .	0.4	0
45969	Insights into the Electronic Structure and Vibrational Dynamics of Li7mnn4 Anode Material for Li-Ion Battery: A Combined Experimental and Computational Study. SSRN Electronic Journal, 0, , .	0.4	0
45970	A family of superconducting boron crystals made of stacked bilayer borophenes. Nanoscale, 2022, 14, 9754-9761.	2.8	5
45971	Boosting the Interfacial Hydrogen Migration for Efficient Alkaline Hydrogen Evolution on Pt-Based Nanowires. SSRN Electronic Journal, 0, , .	0.4	0
45972	Intrinsic Magnetic Properties of the Rfe11ti (R = Y and Gd) Alloys by Co, Zr and C Doping. SSRN Electronic Journal, 0, , .	0.4	0
45973	Ab Initio Study of Electronic and Magnetic Properties of Zigzag and Armchair Aln Nanosheets. SSRN Electronic Journal, 0, , .	0.4	0
45974	Theoretical Study on Defective g-GaN for CO₂ Adsorption. Journal of Nanoelectronics and Optoelectronics, 2022, 17, 218-226.	0.1	3
45975	Adsorption of Hydrogen Peroxide on Two-Dimensional Transition Metal Chalcogenides. Journal of Contemporary Physics, 2022, 57, 170-173.	0.1	1
45976	Bismides ternary alloys GaSb1â^'xBix: Structural, optoelectronic, and thermodynamic properties under pressure. Journal of Materials Research, 2022, 37, 1877-1891.	1.2	1
45977	Quantum Phase Transition in the Spin Transport Properties of Ferromagnetic Metal-Insulator-Metal Hybrid Materials. Nanomaterials, 2022, 12, 1836.	1.9	4

#	Article	IF	Citations
45978	Surface facet dependence of Ru and Ru-based alloy oxidation resistance using ab initio thermodynamics calculation. Surface Science, 2022, 724, 122129.	0.8	1
45979	Symmetry-enforced nodal cage phonons in <mml:math xmlns:mml="http://www.w3.org/1998/Math/MathML"><mml:mrow><mml:msub><mml:mi>Th</mml:mi><mml:mn>12</mml:mn></mml:msub></mml:mrow></mml:math> Physical Review B, 2022, 105, .	1.1	16
45980	Electronic and Band Structure calculation of Wurtzite CdS Using GGA and GGA+U functionals. Journal of Physics: Conference Series, 2022, 2267, 012155.	0.3	5
45981	Nearâ€Direct Band Alignment of MoTe₂/ReSe₂ Typeâ€II pâ€n Heterojunction for Efficient VNIR Photodetection. Advanced Materials Technologies, 2022, 7, .	3.0	9
45982	Crystal structure, electronic structure and phase stability of the Cu2-xMxCd (M=Zn, Ga, Ge, Sn) pseudo-binary Laves phases: effect of valence electron concentration. Journal of Solid State Chemistry, 2022, 313, 123283.	1.4	3
45983	Effect of Manganese Catalysts on the Performance of Anodes in Direct Carbon Fuel Cells. ACS Applied Energy Materials, 0, , .	2.5	0
45984	The Role of Local DFT+U Minima in the First-Principles Modeling of the Metalâ€“Insulator Transition in Vanadium Dioxide. Journal of Physical Chemistry A, 2022, 126, 3604-3611.	1.1	3
45985	Comparative Study of Cold Electron Emission from 2D Ti₃C₂T_X MXene Nanosheets with Respect to Its Precursor Ti₃SiC₂ MAX Phase. ACS Applied Electronic Materials, 2022, 4, 2656-2666.	2.0	32
45986	Theoretical study on S/Fe-doped hexagonal boron nitride (h-BN) sheet: Electronic and optical properties. Applied Surface Science, 2022, 598, 153719.	3.1	7
45987	Physically Informed Machine Learning Prediction of Electronic Density of States. Chemistry of Materials, 2022, 34, 4848-4855.	3.2	23
45988	Optimization and inference of bin widths for histogramming inelastic neutron scattering spectra. Journal of Applied Crystallography, 2022, 55, 533-543.	1.9	0
45989	Electronic Properties and Structure of Silicene on Cu and Ni Substrates. Materials, 2022, 15, 3863.	1.3	6
45990	Single-crystalline transition metal phosphide superconductor WP studied by Raman spectroscopy and first-principles calculations. Physical Review B, 2022, 105, .	1.1	1
45991	Bandgap engineering of PbO/PbTiO₃ for ferroelectric photovoltaics by interface effect. Surface Review and Letters, 0, , .	0.5	0
45992	Ab Initio Calculations of Structural, Electronic, Elastic, Optical, and Dynamical Properties of Half-Heusler LiSiB Compound. Journal of Superconductivity and Novel Magnetism, 0, , .	0.8	0
45993	Intrinsic defects and the influences on electrical transport properties in quaternary diamond-like compounds: Cd2Cu3In3Te8 as an example. Journal of Materiomics, 2022, 8, 1222-1229.	2.8	4
45994	Revisiting Activity Tuning Using Lattice Strain: CO Decomposition in Terrace Ru(0001) and Stepped Ru(1015) Surfaces. Journal of Physical Chemistry C, 0, , .	1.5	1
45995	Magnetic Order, Electrical Doping, and Charge-State Coupling at Amphoteric Defect Sites in Mn-Doped 2D Semiconductors. ACS Nano, 2022, 16, 9452-9460.	7.3	7

#	Article	IF	Citations
45996	Band gap engineering to stimulate the optoelectronic performance of lead-free halide perovskites RbGeX3 (Xâ€‰=â€‰Cl, Br) under pressure. Journal of Materials Science: Materials in Electronics, 2022, 33, 13860-13875.	1.1	13
45997	Microstructure Evolution and Its Correlation with Performance in Nitrogen-Containing Porous Carbon Prepared by Polypyrrole Carbonization: Insights from Hybrid Calculations. Materials, 2022, 15, 3705.	1.3	1
45998	Computational Analysis of Structural, Electronic, Magnetic and Optical Properties of MgTM2O4 (TM =) Tj ETQq0 0 0 rgBT /Overlock 10	1.0	1
45999	Unraveling the MnMoO4 polymorphism: a comprehensive DFT investigation of Î±, Î², and Ï‰ phases. Journal of Materials Science, 2022, 57, 10179-10196.	1.7	4
46000	Toluene Adsorption on CeO2 (111) Studied by FTIR and DFT. Topics in Catalysis, 2022, 65, 934-943.	1.3	3
46001	Investigation of Carbon Dioxide Interaction with Transition Metal Dichalcogenides by First Principles. Journal of Contemporary Physics, 2022, 57, 166-169.	0.1	3
46002	Ð˜ÑÑ»ÐµÐ´Ð¾Ð²Ð°Ð½Ð¸Ðµ Ð²Ð·Ð°Ð¸Ð¼Ð¾Ð´ÐµÐ¹ÑÑ‚Ð²Ð¸Ñ Ð´Ð¸Ð¾Ð¼ÐµÑ‚Ð¸Ð´Ð° Ñƒ Ð³Ð»ÐµÐ¾Ð´Ð° Ñ•Ð²Ñƒ Ñ¼ÐµÑ€ÐºÐ½		
46003	Which Is Better for Hydrogen Evolution on Metal@MoS₂ Heterostructures from a Theoretical Perspective: Single Atom or Monolayer?. ACS Applied Materials & Interfaces, 2022, 14, 25592-25600.	4.0	2
46004	Orbital and electronic responses in the GaN/AlN quantum structures constructed on different crystal planes. Applied Physics Express, 2022, 15, 071002.	1.1	1
46005	Two-dimensional magnetoelectric multiferroics in a <mml:math xmlns:mml="http://www.w3.org/1998/Math/MathML"><mml:mrow><mml:mi>MnSTe</mml:mi><mml:mo>/</mml:mo><mml:msub> heterobilayer with ferroelectrically controllable skyrmions. Physical Review B, 2022, 105, .	1.1	21
46006	Accelerated Deep Learning Dynamics for Atomic Layer Deposition of Al(Me)₃ and Water on OH/Si(111). ACS Applied Materials & Interfaces, 2022, 14, 26116-26127.	4.0	5
46007	Atomic Layer Deposition of Intermetallic Fe₄Zn₉ Thin Films from Diethyl Zinc. Chemistry of Materials, 2022, 34, 5241-5248.	3.2	2
46008	The study of optical and thermoelectric behaviour of thalium based flouropervoskite (TlSiF3) for photovoltaic and renewable energy applications by DFT. Journal of Solid State Chemistry, 2022, 313, 123266.	1.4	10
46009	Hubbard <mml:math xmlns:mml="http://www.w3.org/1998/Math/MathML"><mml:mi>U</mml:mi></mml:math> parameters for transition metals from first principles. Physical Review B, 2022, 105, .	1.1	23
46010	Enhanced DFT insights of doped phosphorene: Structural and electronic considerations. Computational and Theoretical Chemistry, 2022, 1214, 113754.	1.1	0
46011	Blueâ€“violet emitting K2CuCl3 compound: facile synthesis, photoluminescence and radioluminescence properties. Journal of Materials Science, 2022, 57, 10260-10270.	1.7	3
46012	Mechanism in chlorineâ€enhanced Pd catalyst for H₂O₂in situ synthesis in electroâ€Fenton system. AICHE Journal, 2022, 68, .	1.8	3
46013	Lattice dynamics and elastic properties of black phosphorus. Physical Review B, 2022, 105, .	1.1	8

#	Article	IF	Citations
46014	Structural, Electronic, Elastic, Mechanical, Optical and Thermoelectric Properties of the Chalcogenide Double Perovskites A₂GaNbS₆ (A = Ca, Sr and Ba): Insights From Density Functional Theory Calculations. Annals of West Univesity of TimiÅŸoara Physics Series, 2022, 64, 37-54.	0.0	4
46015	Nucleation and growth of L12-Al3RE particles in aluminum alloys: A first-principles study. Journal of Rare Earths, 2023, 41, 1116-1126.	2.5	5
46016	Silicon in intericosahedra chains of boron carbide. Journal of the European Ceramic Society, 2022, 42, 5515-5521.	2.8	5
46017	Investigation of the oxygen coverage of propylene epoxidation on Ag(1 1 1) surfaces from DFT. Computational and Theoretical Chemistry, 2022, 1214, 113739.	1.1	5
46018	New structure and insight on the phase transition within the Cu-Pd-Sn system with 25 at. % Sn. Materialia, 2022, 24, 101461.	1.3	0
46019	The Impact of Nanoscale Percolation in Yttriumâ€Doped BaZrO₃ on the Oxygen Ion and Proton Conductivities: A Density Functional Theory and Kinetic Monte Carlo Study. Advanced Energy and Sustainability Research, 2022, 3, .	2.8	5
46020	Surface conversion derived core-shell nanostructures of Co particles@RuCo alloy for superior hydrogen evolution in alkali and seawater. Applied Catalysis B: Environmental, 2022, 315, 121554.	10.8	29
46021	Strong Hydrogen Bonds in Acetylenedicarboxylic Acid Dihydrate. International Journal of Molecular Sciences, 2022, 23, 6164.	1.8	0
46022	Constructing two-dimensional holey graphyne with unusual annulative Ï€-extension. Matter, 2022, 5, 2306-2318.	5.0	34
46023	Shear strain alters the structure and migration mechanism of self-interstitial atoms in copper. Physical Review Materials, 2022, 6, .	0.9	1
46024	Insights into the influence of functional groups on the properties of graphene from firstâ€principles calculations. Journal of Physical Organic Chemistry, 2022, 35, .	0.9	2
46025	Interfacially Enhanced Stability and Electrochemical Properties of C/SiO_x Nanocomposite Lithiumâ€Ion Battery Anodes. Advanced Materials Interfaces, 2022, 9, .	1.9	12
46026	Atomic study of hydrogen behaviors at â˜3(111) grain boundary in equiatomic CoCrNi and CoCrNiFe alloys. Tungsten, 2022, 4, 239-247.	2.0	4
46027	Tuning band gap and enhancing optical functions of AGeF3 (Aâ€‰=â€‰K, Rb) under pressure for improved optoelectronic applications. Scientific Reports, 2022, 12, .	1.6	33
46028	Enhanced Photogenerated Hole Oxidation Capability of Li2SnO3 by Sb Incorporation in Photocatalysis Through Band Structure Modification. Catalysis Letters, 2023, 153, 1109-1119.	1.4	1
46029	Ab-initio study for the elastic stability, mechanical, electronic and optical properties of RuCrX (X = Si,) Tj ETQq1 1 0.784314 rgBT /Ove	1.2	3
46030	Space group determination and first-principles structure optimization of the <mml:math xmlns:mml="http://www.w3.org/1998/Math/MathML"><mml:mi>A</mml:mi></mml:math> -site ordered perovskite-type manganite <mml:math xmlns:mml="http://www.w3.org/1998/Math/MathML"><mml:mrow><mml:msub><mml:mi>NdBaMn</mml:mi><mml:mn>2</mml:mn><mml:mathvariant="normal">O</mml:mi><mml:mn>6</mml:mn></mml:msub></mml:mrow></mml:math>. Physical Review B, 2022, 105, .	1.1	1
46031	First-Principles Estimation of Core Level Shifts for Hf, Ta, W, and Re. Journal of Physical Chemistry C, 2022, 126, 9135-9142.	1.5	2

#	Article	IF	Citations
46032	Correlating the crystal structure and facet of indium oxides with their activities for CO2 electroreduction. Fundamental Research, 2022, , .	1.6	1
46033	Facile Dissolutionâ€“Crystallization Strategy to Achieve Rapid and Uniform Distribution of Sulfur on Porous Carbon for Lithiumâ€“Sulfur Batteries. ACS Omega, 0, , .	1.6	1
46034	Investigation of the preferred orientation relationships between the in-situ synthesized TiC and titanium matrix. Materials Today Communications, 2022, , 103756.	0.9	1
46035	Modeling Interfacial Evolutions at Atomistic Scale in the Process of Titanium Oxide Inducing Ferrite Nucleation in Steels. Crystal Growth and Design, 2022, 22, 4059-4071.	1.4	5
46036	Unraveling the role of Ni13 catalyst supported on ZrO2 for CH4 dehydrogenation: The d-band electron reservoir. Journal of Fuel Chemistry and Technology, 2022, 50, 601-609.	0.9	0
46037	Fabrication of FeO3 sites in FeO /ZnO for efficient and selective photo-catalytic oxidation of methane to liquid oxygenates. Cell Reports Physical Science, 2022, 3, 100909.	2.8	2
46038	Visualizing the Anomalous Catalysis in Two-Dimensional Confined Space. Nano Letters, 2022, 22, 4661-4668.	4.5	3
46039	High-density/efficient surface active sites on modified separators to boost Li-S batteries via atomic Co3+-Se termination. Nano Research, 2022, 15, 7199-7208.	5.8	18
46040	Repurposing N-Doped Grape Marc for the Fabrication of Supercapacitors with Theoretical and Machine Learning Models. Nanomaterials, 2022, 12, 1847.	1.9	20
46041	Ab-initio study on the hydrogen storage in h-BN monolayers doped with Mn and Fe transition metals. Materials Today: Proceedings, 2022, 67, 81-84.	0.9	2
46042	First-principles calculations to explore the metallic behavior of semiconducting lead-free halide perovskites RbSnX3 (Xâ€‰=â€‰Cl, Br) under pressure. European Physical Journal Plus, 2022, 137, .	1.2	13
46043	Dynamics of Proton Transfer on Boehmite (010) Surface in Anhydrous and Hydrous Environments. Physica Status Solidi (B): Basic Research, 0, , 2200058.	0.7	0
46044	Oxidation of two-dimensional electrides: Structural transition and the formation of half-metallic channels protected by oxide layers. Physical Review B, 2022, 105, .	1.1	1
46045	Cationâ€Alloyingâ€Induced Blueâ€Shifted and Wideâ€Spectrum Polarizationâ€Sensitive Photodetection in Quasiâ€1D SbBiS₃. Small Structures, 2022, 3, .	6.9	10
46046	Phase equilibria in the Y2O3-Nb2O5 system up to 2500Ââ„ƒ: New high-temperature experiments and thermodynamic modeling. Journal of Alloys and Compounds, 2022, 918, 165714.	2.8	3
46047	Rational design of copper-based single-atom alloy catalysts for electrochemical CO2 reduction. Nano Research, 2022, 15, 7116-7123.	5.8	43
46048	Investigation of <mml:math xmlns:mml="http://www.w3.org/1998/Math/MathML" altimg="si2.svg"><mml:mi>Î³</mml:mi></mml:math>-<mml:math xmlns:mml="http://www.w3.org/1998/Math/MathML" altimg="si12.svg"><mml:mrow><mml:mo>(</mml:mo><mml:mi>U</mml:mi><mml:mo>,</mml:mo><mml:mi>Z</mml:mi><mml:mi>r</ structural properties and its interfacial properties with liquid sodium using ab initio molecular dynamics. Journal of Nuclear Materials, 2022, 567, 153835.	1.3	0
46049	Allotropes selection apropos of photocatalytic CO2 reduction from first principles studies. Materials Today Physics, 2022, , 100751.	2.9	3

#	Article	IF	Citations
46050	Exploring the correlation between the spin-state configuration and the magnetic order in Co-substituted <mml:math xmlns:mml="http://www.w3.org/1998/Math/MathML"><mml:msub><mml:mi>BiFeO</mml:mi><mml:mn>3</mml:mn></mml:msub></m Physical Review Materials, 2022, 6, .	0.9	1
46051	Phase diagrams and critical temperatures for coherent and incoherent mixtures of InAs_{1â^'x}Sb_x alloys using first-principles calculations. Journal of Applied Physics, 2022, 131, 215102.	1.1	1
46052	Highly active Ni/Co-metal organic framework bifunctional electrocatalyst for water splitting reaction. International Journal of Hydrogen Energy, 2022, 47, 22787-22795.	3.8	20
46053	DFT and TDDFT studies of structural, electronic and optical properties of the inorganic solar perovskites XPbBr₃ (Xâ€‰=â€‰Li or Na). Phase Transitions, 2022, 95, 501-514.	0.6	17
46054	A first-principles investigation of nitrogen reduction to ammonia on zirconium nitride and oxynitride surfaces. Journal of Materials Science, 2022, 57, 10213-10224.	1.7	8
46055	Atomically dispersed Pt and Fe sites and Ptâ€“Fe nanoparticles for durable proton exchange membrane fuel cells. Nature Catalysis, 2022, 5, 503-512.	16.1	155
46056	Unfolding the structural stability of nanoalloys via symmetry-constrained genetic algorithm and neural network potential. Npj Computational Materials, 2022, 8, .	3.5	9
46057	Synthesis and Characterization of Biotene: A New 2DÂNatural Oxide From Biotite. Small, 2022, 18, .	5.2	7
46058	Controlled growth of two-dimensional InAs single crystals via van der Waals epitaxy. Nano Research, 0, , .	5.8	4
46059	Competing dynamical and lattice instabilities in <mml:math xmlns:mml="http://www.w3.org/1998/Math/MathML"><mml:mrow><mml:msub><mml:mrow><mml:mi>R</mml:mi><mml:mi mathvariant="normal">VO</mml:mi></mml:mrow><mml:mn>4</mml:mn></mml:msub></mml:mrow></mml:math> rare-earth vanadium oxides under high pressure. Physical Review Materials, 2022, 6, .	0.9	2
46060	Electronic, Magnetic, Electric and Magnetocaloric Properties of the Multiferroic Orthorhombic YMnO3. Journal of Superconductivity and Novel Magnetism, 2022, 35, 2493-2503.	0.8	3
46061	Stimuli assisted electronic, magnetic and optical phase control in CrOBr monolayer. Physica E: Low-Dimensional Systems and Nanostructures, 2022, 143, 115332.	1.3	9
46062	Predicting the optimal chemical composition of functionalized carbon catalysts towards oxidative dehydrogenation of ethanol to acetaldehyde. Nano Today, 2022, 44, 101508.	6.2	4
46063	2,5<scp>â€Dimercapto</scp>â€1,3,4â€Thiadiazole (<scp>DMCT</scp>)â€Based Polymers for Rechargeable Metalâ€“Sulfur Batteries. Energy and Environmental Materials, 2023, 6, .	7.3	2
46064	Comment on â€œA novel two-dimensional boron-carbon-nitride (BCN) monolayer: A first-principles insightâ€•[J. Appl. Phys. 130, 114301 (2021)]. Journal of Applied Physics, 2022, 131, 216101.	1.1	0
46065	Thermoelectric properties of monolayer and bilayer buckled XTe (XÂ=ÂGe, Sn, and Pb). Advances in Natural Sciences: Nanoscience and Nanotechnology, 2022, 13, 025008.	0.7	2
46066	Physical properties and superconductivity in the cubic A15-type Ta<mml:math xmlns:mml="http://www.w3.org/1998/Math/MathML" display="inline" id="d1e553" altimg="si66.svg"><mml:msub><mml:mrow /><mml:mrow><mml:mn>3</mml:mn></mml:mrow></mml:msub></mml:math>Ge compound: A first principles study. Solid State Communications, 2022, 353, 114838.	0.9	1
46067	First-Principles Study of Electronic and Optical Properties of Tri-Layered van der Waals Heterostructures Based on Blue Phosphorus and Zinc Oxide. Journal of Composites Science, 2022, 6, 163.	1.4	0

#	Article	IF	Citations
46068	First-principles prediction of anomalously strong phase dependence of transport and mechanical properties of lithium fluoride. Acta Materialia, 2022, 235, 118077.	3.8	10
46069	Tin (Sn) at high pressure: Review, X-ray diffraction, DFT calculations, and Gibbs energy modeling. Journal of Alloys and Compounds, 2022, 919, 165675.	2.8	7
46070	Enhancing thermoelectric properties in TiNiSi structure-type semimetal ZrNiSi by doping. Physical Review Materials, 2022, 6, .	0.9	3
46071	Dual-Metal Active Sites Mediated by p-Block Elements: Knowledge-Driven Design of Oxygen Reduction Reaction Catalysts. ACS Omega, 2022, 7, 19676-19686.	1.6	2
46072	Strain-tunable carrier mobility of Fe-doped GaN: A first-principles study. , 2022, 168, 207300.		2
46073	Exploring the Interfacial Reaction of Nano Al/CuO Energetic Films through Thermal Analysis and Ab Initio Molecular Dynamics Simulation. Molecules, 2022, 27, 3586.	1.7	4
46074	Hydrogen interaction with Mn-doped Zr2Fe (101) surface: A DFT study. International Journal of Hydrogen Energy, 2022, 47, 20932-20941.	3.8	4
46075	Intercalation-driven ferroelectric-to-ferroelastic conversion in a layered hybrid perovskite crystal. Nature Communications, 2022, 13, .	5.8	27
46076	Influence of orderâ€“disorder effects on the optical parameters of Ag7(Si1â^'xGex)S5I-mixed crystals. Journal of Materials Science: Materials in Electronics, 2022, 33, 15054-15066.	1.1	4
46077	Spinâ€Transport through Van der Waals Heterojunctions Based on 2Dâ€Ferromagnet and Transition Metal Dichalcogenides: A Study from Firstâ€Principles Calculations. Advanced Theory and Simulations, 2022, 5, .	1.3	2
46078	Role of Titanium replacement with Pd atom on band gap reduction in the anatase Titanium Dioxide: First-Principles calculation approach. Results in Physics, 2022, 38, 105688.	2.0	8
46079	First-Principles Dynamics of Fluorine Adsorption on Clean and Monohydrogenated Si{001}. Langmuir, 2022, 38, 7256-7271.	1.6	1
46080	Hydrogenation/Hydrodeoxygenation Selectivity Modulation by Cometal Addition to Palladium on Carbon-Coated Supports. ACS Sustainable Chemistry and Engineering, 2022, 10, 7759-7771.	3.2	4
46081	Design of Fe2B-based ductile high temperature ceramics: First-principles calculations and experimental validation. Ceramics International, 2022, 48, 27163-27173.	2.3	11
46082	Janus transition-metal dichalcogenides heterostructures for highly efficient excitonic solar cells. Applied Surface Science, 2022, 598, 153835.	3.1	11
46083	Band gap modulation of penta-BCN through different ways. Diamond and Related Materials, 2022, 126, 109114.	1.8	1
46084	Atomic Interactions and Orderâ€“Disorder Transition in FCC-Type FeCoNiAl1-xTix High-Entropy Alloys. Materials, 2022, 15, 3992.	1.3	2
46085	First-principles calculations of double resonance Raman spectra for monolayer <mml:math xmlns:mml="http://www.w3.org/1998/Math/MathML"><mml:msub><mml:mrow><mml:mi>MoTe</mml:mi></mml:mrow><mml:mn> Physical Review B, 2022, 105, .	3.7	11

#	Article	IF	Citations
46086	Decomposition Kinetics of H₂O₂ on Pd Nanocrystals with Different Shapes and Surface Strains. ChemCatChem, 2022, 14, .	1.8	5
46087	Theoretical design of BAs/WX2 (XÂ=ÂS, Se) heterostructures for high-performance photovoltaic applications from DFT calculations. Applied Surface Science, 2022, 599, 153865.	3.1	5
46088	High-throughput first-principles study of physical properties of L12-Al3M particles. Materials Today Communications, 2022, , 103748.	0.9	0
46089	Ab initio Study of New Fen+1CdCn (nâ€‰=â€‰1â€“3) MAX Material in Its Stable Magnetic Configuration. Journal of Superconductivity and Novel Magnetism, 2022, 35, 1995-2014.	0.8	4
46090	Coadsorption Interfered CO Oxidation over Atomically Dispersed Au on h-BN. Molecules, 2022, 27, 3627.	1.7	4
46091	Oxygen vacancy suppress room temperature ferromagnetism of p-type Cu doped ZnO: Synthesis and density functional theory. , 2022, 167, 207291.		5
46092	First-Principles Study on the Elastic Mechanical Properties and Anisotropies of Goldâ€“Copper Intermetallic Compounds. Metals, 2022, 12, 959.	1.0	9
46093	Simultaneously Enhancing Catalytic Performance and Increasing Density of Bifunctional CuN₃ Active Sites in Dopant-Free 2D C₃N₃Cu for Oxygen Reduction/Evolution Reactions. ACS Omega, 2022, 7, 19794-19803.	1.6	4
46094	Electronic properties of hydrogen/fluorine adsorbed two-dimensional C568: A first-principles study. Surfaces and Interfaces, 2022, 31, 102067.	1.5	1
46095	Diffusion behavior of gas molecules in the one-dimensional channel of AlPO4-5 molecular sieves. Microporous and Mesoporous Materials, 2022, 340, 112024.	2.2	4
46096	Effect of solute elements (Ni, Sn, P) on the adhesion electronic properties of Î³-Fe/Cu heterogeneous interface: A first-principles study. Results in Physics, 2022, 38, 105659.	2.0	3
46097	Methoxy-substituted naphthothiophenes â€“ Single molecules' vs. condensed phase properties and prospects for organic electronics applications. Synthetic Metals, 2022, 287, 117094.	2.1	2
46098	Detection of carcinogenic heavy metals using ZnO nanoribbons (ZnONRs): Ab-initio analysis. Physica E: Low-Dimensional Systems and Nanostructures, 2022, 142, 115289.	1.3	7
46099	2D lead free Ruddlesden-Popper phase perovskites as efficient photovoltaic materials: A first-principles investigation. Computational Materials Science, 2022, 211, 111545.	1.4	6
46100	Ultra-high efficiency, stability and low-cost perovskite solar cell materials <mml:math xmlns:mml="http://www.w3.org/1998/Math/MathML" altimg="si59.svg"><mml:mrow><mml:msub><mml:mtext>Cs</mml:mtext><mml:mtext>2</mml:mtext></mml:msub><mml:msub><mm Materials Science and Engineering B: Solid-State Materials for Advanced Technology, 2022, 282, 115794.	1.7	2
46101	Layered iron dichalcogenides with high ion mobility and capacity as promising anode materials for alkali metal-ion batteries: A first-principles study. Computational Materials Science, 2022, 211, 111523.	1.4	0
46102	Understanding the p-doping of spiroOMeTAD by tris(pentafluorophenyl)borane. Electrochimica Acta, 2022, 424, 140602.	2.6	9
46103	Thermodynamics of point defect disorder and off-stoichiometry in ThO2 and Th1-U O2. Journal of Nuclear Materials, 2022, 567, 153804.	1.3	4

#	Article	IF	Citations
46104	Influence of annealing process on structural, optical and electronic properties of nano-structured ZnO films synthesized by hydrothermal technique: Supported by DFT study. Materials Science and Engineering B: Solid-State Materials for Advanced Technology, 2022, 282, 115793.	1.7	7
46105	Defect-mediated work function regulation in graphene film for high-performing triboelectric nanogenerators. Nano Energy, 2022, 99, 107411.	8.2	10
46106	First-principles calculations to investigate variation in the bandgap of NaSrF3 Fluoro-Perovskite with external static isotropic pressure and its Impact on optical properties. Computational and Theoretical Chemistry, 2022, 1214, 113766.	1.1	21
46107	Highly transparent Pb8O7I2, a novel lead oxyiodide. Journal of Solid State Chemistry, 2022, 312, 123277.	1.4	1
46108	Modifying electronic and magnetic properties of the <mml:math xmlns:mml="http://www.w3.org/1998/Math/MathML" display="inline" id="d1e536" altimg="si31.svg"><mml:mi>Î²</mml:mi></mml:math>-Sb monolayer by doping with III-, IV-, and V-group atoms. Physica E: Low-Dimensional Systems and Nanostructures, 2022, 142, 115315.	1.3	3
46109	First principle calculations of the structural, elastic, electronic and transport properties of XRuAs (X = Ta and V). Materials Science in Semiconductor Processing, 2022, 148, 106837.	1.9	4
46110	Surface plasmon resonance and oxygen vacancy on Bi/BiO1â˜'y ClxBr1â˜'x synergistically boost high-efficiently photodegradation acetaminophen in waste water. Colloids and Surfaces A: Physicochemical and Engineering Aspects, 2022, 648, 129310.	2.3	3
46111	Blue-emitting 0D Cs3ZnX5 (X = Cl, Br) perovskite nanocrystals based on self-trapped excitons. Journal of Luminescence, 2022, 249, 119048.	1.5	6
46112	Ab-initio calculations of transport, optical and dielectric properties of substituted Lizardite. Applied Clay Science, 2022, 226, 106578.	2.6	1
46113	Quantum spin Hall effect in two-dimensional transition-metal chalcogenides MX<mml:math xmlns:mml="http://www.w3.org/1998/Math/MathML" display="inline" id="d1e813" altimg="si33.svg"><mml:msub><mml:mrow /><mml:mrow><mml:mn>5</mml:mn></mml:mrow></mml:msub></mml:math> (M = Zr, Hf and X = S, Se,) Tj ETQq1 1 0.784314 rgBT	1.3	2
46114	Ab initio phase stabilities of rare-earth lean Nd-based hard magnets. Journal of Magnetism and Magnetic Materials, 2022, 559, 169529.	1.0	3
46115	The structural, magnetic, electronic, and mechanical properties of orthogonal/hexagonal MC (M = Fe) Tj ETQq1 1 0.784314 rgBT /Ove	1.6	5
46116	In-situ engineered heterostructured nickel tellur-selenide nanosheets for robust overall water splitting. Chemical Engineering Journal, 2022, 446, 137297.	6.6	22
46117	Mechanistic exploring the catalytic activity of single-atom catalysts anchored in graphitic carbon nitride toward electroreduction of nitrate-to-ammonia. Applied Surface Science, 2022, 598, 153829.	3.1	18
46118	Tailoring nanostructured materials based on <mml:math xmlns:mml="http://www.w3.org/1998/Math/MathML" display="inline" id="d1e974" altimg="si104.svg"><mml:mi>Î³</mml:mi></mml:math>-graphyne monolayers modified with Au heteroatoms for application in energy storage devices: A first principle study. Applied Surface Science, 2022, 598, 153771.	3.1	4
46119	Ab initio investigations of Fe(110)/graphene interfaces. Applied Surface Science, 2022, 598, 153714.	3.1	4
46120	Photocatalysis/enzymolysis-based biomimetic Schottky junction reduces tumor interstitial solid and fluid phases for deep-penetrating tumor therapy. Chemical Engineering Journal, 2022, 446, 137196.	6.6	3
46121	The homojunction formed by h-In2O3(1 1 0) and c-In2O3(4 4 0) promotes carbon dioxide hydrogenation to methanol on graphene oxide modified In2O3. Journal of Colloid and Interface Science, 2022, 623, 1048-1062.	5.0	12

#	Article	IF	Citations
46126	A Systematic Theoretical Study the Active Sites of Potassium Promoter on the Activity of Water Gas Shift Reaction Over Pt(111). SSRN Electronic Journal, 0, , .	0.4	0
46127	Single boron modulated graphdiyne nanosheets for efficient electrochemical nitrogen fixation: a first-principles study. Physical Chemistry Chemical Physics, 2022, 24, 19817-19826.	1.3	2
46128	Vacancy assisted growth of copper tantalum sulfide nanocrystals. Journal of Materials Chemistry A, 2022, 10, 19925-19934.	5.2	2
46129	Sonochemical synthesis of ZnCo₂O₄/Ag₃PO₄ heterojunction photocatalysts for the degradation of organic pollutants and pathogens: a combined experimental and computational study. New Journal of Chemistry, 2022, 46, 14030-14042.	1.4	6
46130	New Approach to the Compound Energy Formalism (Nacef)Part Ii. Thermodynamic Modelling of the Alâ€“Nb System Supported by First-Principles Calculations. SSRN Electronic Journal, 0, , .	0.4	0
46131	Computational Investigation of Magnetic Properties of (Fe)-Doped-MoSe₂ Monolayer Through Spin Angle Rotation. IEEE Transactions on Magnetics, 2022, 58, 1-8.	1.2	0
46132	Antiferromagnetic ordering in the TM-adsorbed AlN monolayer (TM = V and Cr). RSC Advances, 2022, 12, 16677-16683.	1.7	2
46133	Grazing incidence fast atom and molecule diffraction: theoretical challenges. Physical Chemistry Chemical Physics, 2022, 24, 15628-15656.	1.3	3
46134	Improving oxygen evolution activity by constructing a perylene imide based Z-scheme heterojunction. Journal of Materials Chemistry A, 2022, 10, 14513-14528.	5.2	17
46135	Comparison Among Various Physical Properties of Perovskite Oxides Bamo3 (M = Ru, Os) for Predicting Potential Applications. SSRN Electronic Journal, 0, , .	0.4	0
46136	Pressure induced phase diagram of double-layer ice under confinement: A first-principles study. Physical Chemistry Chemical Physics, 0, , .	1.3	2
46137	Efficient Synthesis of the Liquid Fuel 2,5-Dimethylfuran from Biomass Derived 5-(Chloromethyl)Furfural at Room Temperature. SSRN Electronic Journal, 0, , .	0.4	0
46138	Unraveling the Effects of P and S Doping Over G-C3n4 in Strengthening Lewis Basicity for Co2/Glycerol Conversion: A Theoretical and Experimental Study. SSRN Electronic Journal, 0, , .	0.4	0
46139	Piezoelectricity and related properties in orthorhombic cadmium diiodate. Journal of Materials Chemistry C, 2022, 10, 9499-9511.	2.7	2
46140	Dynamics in the O(2 Ã— 1) adlayer on Ru(0001): bridging timescales from milliseconds to minutes by scanning tunneling microscopy. Physical Chemistry Chemical Physics, 2022, 24, 15265-15270.	1.3	3
46141	Photocatalytic hydrogen production and storage in carbon nanotubes: a first-principles study. RSC Advances, 2022, 12, 17029-17035.	1.7	6
46142	AAg₃Ga₈Se₁₄ (A = Rb, Cs): second-harmonic generation responses realized through the parallel arrangement of AgSe₄ and GaSe₄ tetrahedrons. Dalton Transactions, 2022, 51, 11048-11053.	1.6	2
46143	Ab initio high-throughput screening of transition metal double chalcogenide monolayers as highly efficient bifunctional catalysts for photochemical and photoelectrochemical water splitting. Journal of Materials Chemistry A, 2022, 10, 14060-14069.	5.2	7

#	Article	IF	Citations
46144	Tuning the electronic and magnetic properties of lizardite clay by chemical substitution. Molecular Systems Design and Engineering, 2022, 7, 1154-1161.	1.7	1
46145	High Ampacity On-Chip Wires Implemented by Aligned Carbon Nanotube-Cu Composite. SSRN Electronic Journal, 0, , .	0.4	0
46146	The Raman scattering of linear-chained carbon on platinum substrate: DFT simulation. AIP Conference Proceedings, 2022, , .	0.3	0
46147	Angle-resolved photoemission spectroscopy of electronic structure of 1<i>T</i>-NbSeTe. Wuli Xuebao/Acta Physica Sinica, 2022, 71, 127901.	0.2	1
46148	A new concept of atomically thin pâ€“n junction based on Ca₂N/Na₂N donorâ€“acceptor heterostructure: a first-principles study. Nanoscale, 0, , .	2.8	4
46149	Facile synthesis and phase stability of Cu-based Na₂Cu(SO₄)₂Â·xH₂O (x = 0â€“2) sulfate minerals as conversion type battery electrodes. Dalton Transactions, 2022, 51, 11169-11179.	1.6	2
46150	Delamination of MoS₂/SiO₂ interfaces under nanoindentation. Physical Chemistry Chemical Physics, 2022, 24, 15991-16002.	1.3	7
46151	Pressure and temperature stability boundaries of cubic SiC polymorphs: a first-principles investigation. Physical Chemistry Chemical Physics, 2022, 24, 16228-16236.	1.3	3
46152	Exploration of Stable Novel Al2o3 by High-Throughput Calculation Screening and Density Functional Theory. SSRN Electronic Journal, 0, , .	0.4	0
46153	A caveat of the charge-extrapolation scheme for modeling electrochemical reactions on semiconductor surfaces: an issue induced by a discontinuous Fermi level change. Physical Chemistry Chemical Physics, 0, , .	1.3	1
46154	Desulfurization Mechanism of Thioether Compounds in Heavy Oil on the (111) Surface of Inverse Spinel Fe3O4. Physical Chemistry Chemical Physics, 0, , .	1.3	0
46155	Theoretical and experimental investigations of enhanced uranium(VI) adsorption by nitrogen doping strategy. Physical Chemistry Chemical Physics, 0, , .	1.3	1
46156	Computational mechanistic insights on Ag₂O as a host for Li in lithium-ion batteries. Physical Chemistry Chemical Physics, 0, , .	1.3	2
46157	Computational Screening on Two-Dimensional Metal-Embedded Poly-Phthalocyanine as Cathode Catalysts in Lithium-Nitrogen Batteries. SSRN Electronic Journal, 0, , .	0.4	0
46158	Electronic and Optical Properties of C₁₆S₈ and C₁₆S₄Se₄ Molecules and Crystals. New Journal of Chemistry, 0, , .	1.4	1
46159	Engineering the Photocatalytic Performance of B-C3n4@Bi2s3 Hybrid Heterostructures for Fullâ€Spectrumâ€Driven Cr(Vi) Reduction and In-Situ H2o2 Generation: Experimental and Dft Studies. SSRN Electronic Journal, 0, , .	0.4	0
46160	Combined Density Functional Theory Calculation and Non-Equilibrium Green's Function Approach to Predict the Sensitivity of Nitrogen-Containing Gases Over Pttens2-N Monolayers (N =0 - 2). SSRN Electronic Journal, 0, , .	0.4	0
46161	Thermal Properties and Pressure-Dependent Elastic Constants of Cadmium Stannate as a Substrate for Mems: An Ab Initio Study. SSRN Electronic Journal, 0, , .	0.4	0

#	Article	IF	Citations
46162	Prediction of novel boronâ€“carbon based clathrates. Physical Chemistry Chemical Physics, 2022, 24, 16884-16890.	1.3	7
46163	Phase transition and electronic properties of Coâ€“As binary compounds at high pressure. RSC Advances, 2022, 12, 18102-18106.	1.7	0
46164	Enhanced promotion of Ru-based ammonia catalysts by in situ dosing of Cs. Energy and Environmental Science, 0, , .	15.6	12
46165	A transferable prediction model of molecular adsorption on metals based on adsorbate and substrate properties. Physical Chemistry Chemical Physics, 2022, 24, 16545-16555.	1.3	3
46166	Transport signatures of few-atom carbon rings. Physical Chemistry Chemical Physics, 0, , .	1.3	1
46167	A penta-BCP sheet with strong piezoelectricity and a record high positive Poisson's ratio. Journal of Materials Chemistry C, 2022, 10, 10302-10309.	2.7	6
46168	BAND STRUCTURE OF BePbâ€“V2 PNICTIDES: AB INITIO CALCULATIONS. Journal of Structural Chemistry, 2022, 63, 588-592.	0.3	0
46169	Ab initio investigation of structural and electronic properties of BaTiO₃/Si heterostructure. Ferroelectrics, 2022, 590, 66-72.	0.3	0
46170	Toward Room-Temperature Electrical Control of Magnetic Order in Multiferroic van der Waals Materials. Nano Letters, 2022, 22, 5191-5197.	4.5	25
46171	Adhesion strength, stability and electronic properties of Î±-Mg/Mg2Pb interface from first-principles calculation. Journal of Materials Research, 2022, 37, 1859-1867.	1.2	4
46172	Dielectric-dependent hybrid functional calculations on the electronic band gap of <mml:math xmlns:mml="http://www.w3.org/1998/Math/MathML"><mml:mn>3</mml:mn><mml:mi>d</mml:mi></mml:math> transition metal doped <mml:math xmlns:mml="http://www.w3.org/1998/Math/MathML"><mml:msub><mml:mi>SnS</mml:mi><mml:mn>2</mml:mn></mml:msub></mm and their optical properties. Physical Review B, 2022, 105, .	1.1	5
46173	Electronic structure of intrinsic defects in <mml:math xmlns:mml="http://www.w3.org/1998/Math/MathML"><mml:mi>c</mml:mi></mml:math> -gallium nitride: Density functional theory study without the jellium approximation. Physical Review B, 2022, 105, .	1.1	2
46174	Reversible switching of anomalous valley Hall effect in ferrovalley Janus <mml:math xmlns:mml="http://www.w3.org/1998/Math/MathML"><mml:mrow><mml:mn>1</mml:mn><mml:mi>T</mml:mi><mml:mo>â^'</mml:m	1.1	23
46175	Manipulation of Spin Polarization in Boron-Substituted Graphene Nanoribbons. ACS Nano, 2022, 16, 11244-11250.	7.3	12
46176	Surface Reactivity of Lithium (Poly)sulfides in a Polarizable Environment from First Principles. Topics in Catalysis, 2022, 65, 966-978.	1.3	1
46177	How adsorbed H, O, OH, and Cl affect plain adsorption of imidazole on copper. Corrosion Science, 2022, 205, 110443.	3.0	13
46178	Twisted nodal wires and three-dimensional quantum spin Hall effect in distorted square-net compounds. Physical Review B, 2022, 105, .	1.1	7
46179	Predicting Material Properties by Deep Graph Networks. Crystal Research and Technology, 2022, 57, .	0.6	2

#	Article	IF	Citations
46180	On the nature of planar defects in transition metal diboride line compounds. Materialia, 2022, 24, 101478.	1.3	4
46181	Enhanced mechanical, electronic, magnetic, and optical properties of penta-BCN by Ni-doping. Applied Surface Science, 2022, 599, 153997.	3.1	3
46182	Intrinsic Valley Splitting and Direct-to-Indirect Band Gap Transition in Monolayer HfZrSiCO₂. Journal of Physical Chemistry Letters, 2022, 13, 5204-5212.	2.1	11
46183	First-principles insights into thermoelectric properties of topological nontrivial semimetal LiAuTe material. Physica Scripta, 2022, 97, 075703.	1.2	1
46184	Optical and electronic anisotropy of a 2D semiconductor SiP. Nano Research, 2022, 15, 8579-8586.	5.8	8
46185	First-principles predictions of qubits in defective MgS. Physical Review B, 2022, 105, .	1.1	1
46186	Electronic Structure, Optical, and Elastic Properties of AgGaS ₂ Crystal: Theoretical Study. Advanced Theory and Simulations, 0, , 2200247.	1.3	1
46187	Dual-metal atoms embedded into two-dimensional covalent organic framework as efficient electrocatalysts for oxygen evolution reaction: A DFT study. Nano Research, 2022, 15, 7994-8000.	5.8	25
46188	First-Principles Calculations of the Exchange Interaction of the CrGeTe3/NiO Interface. Frontiers in Materials, 0, 9, .	1.2	0
46189	Surface Structure Engineering of PtPd Nanoparticles for Boosting Ammonia Oxidation Electrocatalysis. ACS Applied Materials & Interfaces, 2022, 14, 28816-28825.	4.0	20
46190	Effect of MgO on the structure of SiO₂â€poor/rich MgOâ€CaOâ€SiO₂ melts by in situ high temperature timeâ€gated Raman spectroscopy and theoretical calculation. Journal of Raman Spectroscopy, 2022, 53, 1635-1646.	1.2	2
46191	Accelerated Mining of 2D Van der Waals Heterojunctions by Integrating Supervised and Unsupervised Learning. Chemistry of Materials, 2022, 34, 5571-5583.	3.2	7
46192	Key Role of aâ€Top CO on Terrace Sites of Metallic Pd Clusters for CO Oxidation. Chemistry - A European Journal, 2022, 28, .	1.7	5
46193	Influence of Hexagonal Boron Nitride on Electronic Structure of Graphene. Molecules, 2022, 27, 3740.	1.7	2
46194	Pressure-induced superconductivity and nontrivial band topology in compressed Î³-InSe. Physical Review B, 2022, 105, .	1.1	7
46195	Electronic transport coefficients from density functional theory across the plasma plane. Physical Review E, 2022, 105, .	0.8	7
46196	Theoretical Study on the Structural, Elastic, Electronic and Thermodynamic Properties of Long-Period Superstructures h- and r-Al2Ti under High Pressure. Materials, 2022, 15, 4236.	1.3	1
46197	Effect of hydrogen on magnetic properties in MgO studied by first-principles calculations and experiments. Scientific Reports, 2022, 12, .	1.6	2

#	Article	IF	Citations
46198	Designing doping strategy in arsenene monolayer for spintronic and optoelectronic applications: a case study of germanium and nitrogen as dopants. Journal of Physics Condensed Matter, 2022, 34, 355301.	0.7	2
46199	First-principles calculations to investigate pressure effect on structural, elastic and thermodynamic properties of AlCu, Al2Cu and Al4Cu9. Vacuum, 2022, 203, 111279.	1.6	15
46200	Experimental and Theoretical Study of Stable and Metastable Phases in Sputtered CuInS₂. Advanced Science, 2022, 9, .	5.6	8
46201	Alkaline-Earth Metal Effects on Physical Properties of Ferromagnetic AVO₃ (A = Ba, Sr, Ca,) Tj ETQq1 1 0.784314 rgBT /Ov	1.6	16
46202	Elucidation of Structureâ€“Activity Relations in Proton Electroreduction at Pd Surfaces: Theoretical and Experimental Study. Small, 2022, 18, .	5.2	7
46203	Elasticity, mechanical and thermal properties of polycrystalline hafnium carbide and tantalum carbide at high pressure. Journal of the European Ceramic Society, 2022, 42, 5220-5228.	2.8	6
46204	Physically driven enhancement of the stability of Bi2O3-based ionic conductors via grain boundary engineering. NPG Asia Materials, 2022, 14, .	3.8	7
46205	Preparation and characteristic analysis of carbon coated nanoscale SnO₂ system: an integrated experimental and first principles approach. Physica Scripta, 2022, 97, 075818.	1.2	0
46206	Boron nanostructure formation on Mo(112) surface. Surface Science, 2022, 724, 122145.	0.8	5
46207	Structural and Electronic Properties of Î²-MnO2 Compound Under High Pressure for Energy Storage Devices. Karadeniz Fen Bilimleri Dergisi, 2022, 12, 155-167.	0.1	0
46208	Multi-Level Resistive Switching in SnSe/SrTiO3 Heterostructure Based Memristor Device. Nanomaterials, 2022, 12, 2128.	1.9	8
46209	Mechanistic Differences between Electrochemical Hydrogenation and Hydrogenolysis of 5â€Hydroxymethylfurfural and Their pH Dependence. ChemSusChem, 2022, 15, .	3.6	18
46210	Mechanistic and Experimental Study of the CuxO@C Nanocomposite Derived from Cu3(BTC)2 for SO2 Removal. Catalysts, 2022, 12, 689.	1.6	0
46211	Band Alignment Engineering by Twist Angle and Composition Modulation for Heterobilayer. Small, 2022, 18, .	5.2	2
46212	An analysis of point defects in ZnTe using density functional theory calculations. Journal of Alloys and Compounds, 2022, 921, 166017.	2.8	2
46213	Spin-Resolved Visible Optical Spectra and Electronic Characteristics of Defect-Mediated Hexagonal Boron Nitride Monolayer. Crystals, 2022, 12, 906.	1.0	2
46214	Dynamical study of the origin of the charge density wave in <mml:math xmlns:mml="http://www.w3.org/1998/Math/MathML"><mml:mrow><mml:mi>A</mml:mi><mml:msub><mml:mi mathvariant="normal">V</mml:mi><mml:mn>3</mml:mn></mml:msub><mml:msub><mml:mi>Sb</mml:mi><mml:mn>5</mml:mn></ (<mml:math) Tj ETQq0 0 0 rgBT /Overlock 10 Tf 50 97 Td (xmlns:mml="http://www.w3.org/1998/Math/MathML"><mml:mrow><mml:m	1.1	17
46215	2 Effect of Pressure on the Superconducting Transition Temperature and Physical Properties of CaPd₂P₂: A DFT Investigation. ACS Omega, 2022, 7, 21528-21536.	1.6	5

#	Article	IF	Citations
46216	First-principles DFT investigation of the electronic and optical properties of Br doped rutile TiO2 for application in photovoltaic Panelsâ€™ coatings and Self-Cleaning. Materials Today: Proceedings, 2022, 66, 353-358.	0.9	1
46217	Theoretical Study on the Selective 1,2â€Reduction of Î±,Î²â€Unsaturated Ketones by Hydrogen Transfer Reaction on MgO(100). ChemPhysChem, 2022, 23, .	1.0	1
46218	First-principles prediction of outstanding mechanical and thermodynamic properties of YX2Si2 (XÂ=ÂPd) Tj ETQq0 0 0 rgBT /Overlock 10	0.9	5
46219	Active Sites on Zn_xZr_{1â€“x}O_{2â€“x} Solid Solution Catalysts for CO₂-to-Methanol Hydrogenation. ACS Catalysis, 2022, 12, 7748-7759.	5.5	37
46220	Microscopic functionality of FeN4 sites in polymeric carbon nitride for efficient H2S oxidation. Applied Surface Science, 2022, 600, 154011.	3.1	6
46221	Emergent and Tunable Topological Surface States in Complementary Sb/Bi₂Te₃ and Bi₂Te₃/Sb Thin-Film Heterostructures. ACS Nano, 2022, 16, 9953-9959.	7.3	2
46222	Importance of the Hubbard U parameter to explore accurate electronic and optical behaviour of BiFeO₃. Journal Physics D: Applied Physics, 2022, 55, 375303.	1.3	4
46223	Two-dimensional polymers made of carbonyl-bridged heterotriangulenes are promising anode materials for Li-ion batteries. 2D Materials, 2022, 9, 034003.	2.0	6
46224	Chemical Interpretation of Charged Point Defects in Semiconductors: A Case Study of Mg₂Si. ChemNanoMat, 2022, 8, .	1.5	2
46225	Stability of high-temperature salty ice suggests electrolyte permeability in water-rich exoplanet icy mantles. Nature Communications, 2022, 13, .	5.8	13
46226	Investigation of the bulk and point defect properties in uraniumâ€“plutonium mixed oxides (U,Pu)O₂ using DFT+U: Effect of a low americium content. Journal of Applied Physics, 2022, 131, 225106.	1.1	1
46227	Modeling of two-dimensional MoxW_{1â^'x}S_{2y}Se_{2(1â^'y)} alloy band structure. Russian Technological Journal, 2022, 10, 56-63.	0.6	1
46228	Transition-metal single atom catalyst embedded in C2N for toxic-gas reduction reaction and selective gas-sensing application: Atomic-scale study. Applied Surface Science, 2022, 599, 154037.	3.1	13
46229	Firstâ€principles calculation of mechanical properties and electronic structures of W ₄ Co _{4â^'} _n X _n B ₄ (XÂ=ÂV, Mn, Fe, Ni; n) Tj ETQq1 1 0.784314	1.1	1
46230	Mechanical and electronic properties of <mml:math xmlns:mml="http://www.w3.org/1998/Math/MathML"><mml:mi>Î±</mml:mi><mml:mtext>â^'</mml:mtext><mml:mrow><mml:msub>< (<mml:math xmlns:mml="http://www.w3.org/1998/Math/MathML"><mml:mi>M</mml:mi></mml:math>) Tj ETQq0 0 0 rgBT /Overlock 1	1.1	17
46231	monolayers. Physical Review B, 2022, 105, . A first principle study of electronic structure and magnetic properties of TlFe2Se2. Materials Today: Proceedings, 2022, , .	0.9	0
46232	Platinum equationÂof state to greater than two terapascals: Experimental data and analytical models. Physical Review B, 2022, 105, .	1.1	8
46233	Thickness-Dependent Magnetism and Topological Properties of EuSn₂As₂. ACS Applied Electronic Materials, 2022, 4, 3212-3219.	2.0	5

#	Article	IF	Citations
46234	Strained Cs₂AgInCl₆ double perovskite material: band structure, optical spectra and mechanical stability. Physica Scripta, 2022, 97, 085801.	1.2	3
46235	Phonon Analysis of 2D Organicâ€Halide Perovskites in the Lowâ€and Midâ€IR Region. Advanced Optical Materials, 0, , 2100439.	3.6	2
46236	Pd-GaSe and Pd3-GaSe Monolayers: Two Promising Candidates for Detecting Dissolved Gases in Transformer Oil. Chemosensors, 2022, 10, 236.	1.8	2
46237	Multi-defects engineering of NiCo2O4 for catalytic propane oxidation. Applied Surface Science, 2022, 600, 154040.	3.1	45
46238	Revealing the interface characteristic of the semi-coherent Co(111)/WC(0001) interface: a first principles investigation. Philosophical Magazine, 2022, 102, 2031-2055.	0.7	5
46239	Insights into the Interfacial Contact and Charge Transport of Gas-Sensing Liquid Metal Marbles. ACS Applied Materials & Interfaces, 2022, 14, 30112-30123.	4.0	9
46240	Novel design of single transition metal atoms anchored on C6N6 nanosheet for electrochemical and photochemical N2 reduction to Ammonia. Catalysis Today, 2023, 424, 113804.	2.2	6
46241	Efficient CO₂ Capture and Activation on Novel Two-Dimensional Transition Metal Borides. ACS Applied Materials & Interfaces, 2022, 14, 29703-29710.	4.0	15
46242	Gallium-Doped Zinc Oxide Nanostructures for Tunable Transparent Thermoelectric Films. ACS Applied Nano Materials, 2022, 5, 8631-8639.	2.4	13
46243	Machine learning for metallurgy V: A neural-network potential for zirconium. Physical Review Materials, 2022, 6, .	0.9	9
46244	Electronic â€œBridgeâ€•Construction via Ag Intercalation to Diminish Catalytic Anisotropy for 2D Tin Diselenide Cathode Catalyst in Lithiumâ€“Oxygen Batteries. Advanced Energy Materials, 2022, 12, .	10.2	33
46245	A density functional theory study of methane activation on MgO supported Ni9M1 cluster: role of M on C-H activation. Frontiers of Chemical Science and Engineering, 2022, 16, 1485-1492.	2.3	10
46246	MnTa₂N₄: A Ternary Nitride Spinel with a Strong Magnetic Frustration. Chemistry of Materials, 2022, 34, 6098-6107.	3.2	2
46247	First-principles calculations of Raman and infrared spectroscopy for phase identification and strain calibration of hafnia. Applied Physics Letters, 2022, 120, 242903.	1.5	6
46248	Quantum confinement effect on defect level of hydrogen doped rutile VO2 nanowires. Journal of Applied Physics, 2022, 131, .	1.1	4
46249	Electronic phase transitions in quasi-one-dimensional atomic chains: Au wires on Si(553). Physical Review B, 2022, 105, .	1.1	0
46250	Molecular modulating of cobalt phthalocyanines on amino-functionalized carbon nanotubes for enhanced electrocatalytic CO2 conversion. Nano Research, 2023, 16, 3649-3657.	5.8	14
46251	High-pressure study of hydrogen storage material ethylenediamine bisborane from first-principle calculations. Journal of Materials Research and Technology, 2022, , .	2.6	2

#	Article	IF	Citations
46252	Novel Van Der Waals Heterostructures Based on Borophene, Graphene-like GaN and ZnO for Nanoelectronics: A First Principles Study. Materials, 2022, 15, 4084.	1.3	9
46253	Ion motion and charge transfer through a solid-electrolyte interphase: an atomistic view. Journal of Solid State Electrochemistry, 0, , .	1.2	1
46254	On native point defects in ZnSe. Applied Physics Letters, 2022, 120, .	1.5	3
46255	Layered gallium sulfide optical properties from monolayer to CVD crystalline thin films. Optics Express, 2022, 30, 27609.	1.7	8
46256	Crucial role of vibrational entropy in the <mml:math xmlns:mml="http://www.w3.org/1998/Math/MathML"><mml:mrow><mml:mi>Si</mml:mi><mml:mo>(</mml:mo><mml:mn>111</mml:mn><mml:mo>)</mml:mo><mml:mo>-</mml:mo><mml:mrow><mml:mo>(</mml:mo><mml:mn>1</mml:mn><mml:mo>×</mml:mo><mml:mn>1</mml:mn></mml:mrow></mml:mrow></mml:math> surface structure stability. Physical Review B, 2022, 105, .	1.1	1
46257	Homogeneous nitrogen-doped (111)-type layered Sr5Nb4O15â^'xNx as a visible-light-responsive photocatalyst for water oxidation. Nano Research, 2022, 15, 9976-9984.	5.8	8
46258	Electronic and topological band evolution of VB-group transitionmetal monocarbides M2C (M=V, Nb,) Tj ETQq0 0 0 rgBT /Overlock 10 Tf	0.9	4
46259	Screening and Design of Bipolar Magnetic-Semiconducting Monolayers and Heterostructures. ACS Applied Electronic Materials, 0, , .	2.0	3
46260	Surfaceâ€toâ€Bulk Synergistic Modification of Single Crystal Cathode Enables Stable Cycling of Sulfideâ€Based Allâ€Solidâ€State Batteries at 4.4 V. Advanced Energy Materials, 2022, 12, .	10.2	30
46261	Oxidation behaviour of sperrylite and platarsite (100) surfaces: A DFT study. Materials Today Communications, 2022, 32, 103868.	0.9	1
46262	Compressing the Channels in the Crystal Structure of Copper Squarate Metal-Organic Framework. Solids, 2022, 3, 374-384.	1.1	2
46263	Prominent Electrode Material for Na-, K-, and Mg-ion Batteries: 2D Î²-Sb Monolayer. Energy & Fuels, 2022, 36, 7087-7095.	2.5	16
46264	First-Principles Calculation of the Bonding Strength of the Al2O3-Fe Interface Enhanced by Amorphous Na2SiO3. Materials, 2022, 15, 4415.	1.3	2
46265	Prediction of the pressure-induced phase transition, mechanical properties, and electronic structures for ScB4 via first principle calculations. Applied Physics A: Materials Science and Processing, 2022, 128, .	1.1	0
46266	Simple Chemical Rules for Predicting Band Structures of Kagome Materials. Journal of the American Chemical Society, 2022, 144, 10978-10991.	6.6	20
46267	The Fe₂O₃ (0001) Surface Under Electroreduction Conditions: A DFT Study of L-Cysteine Adsorption. Journal of the Electrochemical Society, 2022, 169, 064513.	1.3	1
46268	Pushing Down the Limit of NH₃ Detection of Graphene-Based Chemiresistive Sensors through Functionalization by Thermally Activated Tetrazoles Dimerization. ACS Nano, 2022, 16, 10456-10469.	7.3	8
46269	Unravelling the adsorption performance of BN, AlN, GaN and InN 2D nanosheets towards the ciclopirox, 5-fluorouracil and nitrosourea for anticancer drug delivery motive: A DFT-D with QTAIM, PCM and COSMO investigations. Computational and Theoretical Chemistry, 2022, 1214, 113797.	1.1	13

#	Article	IF	Citations
46270	Density functional theory: The structural, electronic, optical, mechanical, and vibrational properties of bulk and Te-doped SnSe₂. International Journal of Modern Physics B, 2022, 36, .	1.0	2
46271	Atomic and Electronic Manipulation of Robust Ferroelectric Polymorphs. Advanced Materials, 2022, 34, .	11.1	4
46272	Ion migration suppression mechanism via 4-sulfobenzoic acid monopotassium salt for 22.7% stable perovskite solar cells. Science China Materials, 2022, 65, 3368-3381.	3.5	19
46273	Nonlinear optical response of ferroelectric oxides: First-principles calculations within the time and frequency domains. Physical Review Materials, 2022, 6, .	0.9	5
46274	Two-dimensional tetragonal and hexagonal lattices of transition metal carbides MC (M = Ti, Zr, Hf): Observation of two nodal loops and strong light-harvesting ability. Applied Physics Letters, 2022, 120, .	1.5	2
46275	Electronic and Magnetic properties of nitrogen substituted cubic perovskites of RbNbO3 and CsNbO3 using PBE-GGA and TB-mBJ methods. Materials Research Innovations, 0, , 1-12.	1.0	2
46276	Metal-Rich Phosphides Obtained from the Lead Flux: Synthesis, Crystal, and Electronic Structure of Sr₅Pt₁₂P₉ and BaPt₃P₂. Inorganic Chemistry, 2022, 61, 9173-9183.	1.9	3
46277	Enhanced reversible hydrogen storage efficiency of zirconiumâ€decorated biphenylene monolayer: A computational study. Energy Storage, 2022, 4, .	2.3	13
46278	Metal-Decorated Phthalocyanine Monolayer as a Potential Gas Sensing Material for Phosgene: A First-Principles Study. ACS Omega, 2022, 7, 21994-22002.	1.6	8
46279	Design of New Borates with Deep Ultraviolet Transparency Inspired by the Flexibility of Unusual Triple-Layered Frameworks. Crystal Growth and Design, 0, , .	1.4	1
46280	Dynamical properties of the magnetic topological insulator <mml:math xmlns:mml="http://www.w3.org/1998/Math/MathML"><mml:mrow><mml:mi>T</mml:mi><mml:msub><mml:mi>Bi</mml:mi><mml:mn>1</mml:mn></mml:msub><mml:msub><mml:mi>Te</mml:mi><mml:mn> : Phonons dispersion, Raman active modes, and chiral phonons study. Physical Review B, 2022, 105, .	1.4	7
46281	Calibration of Fermi Velocity to Explore the Plasmonic Character of Graphene Nanoribbon Arrays by a Semi-Analytical Model. Nanomaterials, 2022, 12, 2028.	1.9	9
46282	Strain-Enhanced Thermoelectric Performance in GeS2 Monolayer. Materials, 2022, 15, 4016.	1.3	4
46283	Lithiating magneto-ionics in a rechargeable battery. Proceedings of the National Academy of Sciences of the United States of America, 2022, 119, .	3.3	5
46284	Theoretical study of potential n-type and p-type dopants in GaN from data mining and first-principles calculation. Semiconductor Science and Technology, 2022, 37, 085004.	1.0	1
46285	Band Edge Engineering of 2D Perovskite Structures through Spacer Cation Engineering for Solar Cell Applications. Journal of Physical Chemistry C, 2022, 126, 9937-9947.	1.5	6
46286	Cobalt Anti-MXenes as Promising Anode Materials for Sodium-Ion Batteries. Journal of Physical Chemistry C, 2022, 126, 10298-10308.	1.5	8
46287	Graphyne Nanotubes as Promising Sodium-Ion Battery Anodes. Catalysts, 2022, 12, 670.	1.6	4

#	Article	IF	Citations
46288	Effects of order-disorder transition on phase relationship, elastic strength, and mechanical anisotropy of Al-Li alloys. Materialia, 2022, 24, 101483.	1.3	0
46289	Ab-Initio Investigations on Hydrogen Dissociation and Cross-Linking of Hydrocarbon Chains of Self-Assembled Monolayers of Alkanes. Applied Sciences (Switzerland), 2022, 12, 6020.	1.3	1
46290	Band filling effects on the emergence of magnetic skyrmions: Pd/Fe and Pd/Co bilayers on Ir(111). Physical Review B, 2022, 105, .	1.1	5
46291	Regulating iron species compositions by Fe-Al interaction in CO2 hydrogenation. Journal of Catalysis, 2022, 413, 331-341.	3.1	17
46292	Formation of cesium carbonate in ion-implanted graphite, examined with dual-source x-ray photoelectron spectroscopy, density functional theory calculations and thermodynamic modelling. Carbon, 2022, 197, 226-237.	5.4	4
46293	Probing the states around the charge neutrality point of reduced graphene oxide with time-resolved gated Kelvin Probe Force Microscopy. , 2022, , .		0
46294	Li₈MnO₆: A Novel Cathode Material with Only Anionic Redox. ACS Applied Materials & Interfaces, 2022, 14, 29832-29843.	4.0	2
46295	High carbon utilization in CO2 reduction to multi-carbon products in acidic media. Nature Catalysis, 2022, 5, 564-570.	16.1	197
46296	Long-chain hydrocarbons by CO2 electroreduction using polarized nickel catalysts. Nature Catalysis, 2022, 5, 545-554.	16.1	107
46297	Thermodynamic modeling of Cr and Crâ€“H systems up to high temperatures and high pressures. International Journal of Hydrogen Energy, 2022, , .	3.8	2
46298	Composition of Oxygen Functional Groups on Graphite Surfaces. Journal of Physical Chemistry C, 2022, 126, 10653-10667.	1.5	6
46299	Applicability of Allenâ€“Heineâ€“Cardona Theory on MO_x Metal Oxides and ABO₃ Perovskites: Toward High-Temperature Optoelectronic Applications. Chemistry of Materials, 2022, 34, 6108-6115.	3.2	7
46300	Phase Stability, Elastic and Electronic Properties of Ni₃Ti Intermetallic Doped with Mn and Fe: Firstâ€Principles Calculations. Physica Status Solidi (B): Basic Research, 2022, 259, .	0.7	2
46301	SrAgAsS₄: A Noncentrosymmetric Sulfide with Good Infrared Nonlinear Optical Performance Induced by Aliovalent Substitution from Centrosymmetric SrGa₂S₄. Inorganic Chemistry, 2022, 61, 9205-9212.	1.9	6
46302	A novel 2D sulfide gallium heterojunction as a high-performance electrocatalyst for overall water splitting. Journal of Solid State Chemistry, 2022, , 123365.	1.4	11
46303	Photodegradation under UV Light Irradiation of Various Types and Systems of Organic Pollutants in the Presence of a Performant BiPO4 Photocatalyst. Catalysts, 2022, 12, 691.	1.6	17
46304	First-principle study of highly controllable boron-doped graphene (BC₂₀) as a high-capacity anode for potassium-ion batteries. Materials Research Express, 2022, 9, 065604.	0.8	2
46305	Selective Hydroxylation of In₂O₃ as A Route to Site-Selective Atomic Layer Deposition. Journal of Physical Chemistry C, 0, , .	1.5	6

#	Article	IF	Citations
46306	Reversible Al Metal Anodes Enabled by Amorphization for Aqueous Aluminum Batteries. Journal of the American Chemical Society, 2022, 144, 11444-11455.	6.6	63
46307	Tetravalent Doping in Fluorite-Based Ferroelectric Oxides for Reduced Voltage Operations. ACS Applied Materials & Interfaces, 0, , .	4.0	3
46308	Magnetic octupole tensor decomposition and second-order magnetoelectric effect. Annals of Physics, 2022, 447, 168964.	1.0	6
46309	Spin-thermoelectric properties and giant tunneling magnetoresistance of boron-substituted graphene nanoribbon: a first principle study. Journal of Physics Condensed Matter, 2022, 34, 345802.	0.7	2
46310	Theoretical approach to the phonon modes of GaSb nanowires. Physica E: Low-Dimensional Systems and Nanostructures, 2022, 143, 115372.	1.3	1
46311	Not a Mere Decoration: Impact of Submonolayer Coverages of Nickel on Fundamental Properties of Platinum. Journal of Physical Chemistry C, 2022, 126, 10167-10180.	1.5	3
46312	Unraveling Synergistic Redox Interactions in Tetraphenylporphyrinâ€“Polyluminolâ€“Carbon Nanotube Composite for Capacitive Charge Storage. ACS Applied Materials & Interfaces, 2022, 14, 28359-28369.	4.0	17
46313	Theoretical validation of inhibition mechanisms of benzotriazole with copper and cobalt for CMP and post-CMP cleaning applications. Microelectronic Engineering, 2022, 262, 111833.	1.1	7
46314	Energy Harvesting Using Cotton Fabric Embedded with 2D Hexagonal Boron Nitride. ACS Applied Materials & Interfaces, 2022, 14, 30343-30351.	4.0	6
46315	Elastic Constants of Tetragonal Cu₂ZnSnS₄ Semiconductor: AB-Initio Calculation. Annals of West Univesity of TimiÅŸoara Physics Series, 2022, 64, 55-67.	0.0	5
46316	Thermodynamics and phase stability of Li₈XO₆ octalithium ceramic breeder materials (X = Pb, Ce, Ge, Zr, Sn). Journal of Physics Condensed Matter, 0, , .	0.7	1
46317	Structural And Electronic Properties of PtSe2/GaP Heterostructure. Materials Today: Proceedings, 2022, 67, 161-164.	0.9	13
46318	Developing a force field for the <mml:math xmlns:mml="http://www.w3.org/1998/Math/MathML"><mml:mrow><mml:msub><mml:mi>Ba</mml:mi><mml:mrow><mml:mn>1</mml:mn></mml:mrow></mml:msub><mml:mi>Ti</mml:mi><mml:msub><mml:mi>O</mml:mi><mml:mn>3</mml:mn></mml:msub></mml:mrow></mml:math> ferroelectric alloy: Prediction of a ferroelectric superlattice structure. Physical Review B, 2022, 105, .	1.1	3
46319	Al₂O₃/ZnO Heterostructure-Based Sensors for Volatile Organic Compounds in Safety Applications. ACS Applied Materials & Interfaces, 2022, 14, 29331-29344.	4.0	15
46320	Impact of passivation on the Dirac cones of 2D topological insulators. Journal of Applied Physics, 2022, 131, .	1.1	2
46321	Low Thermal Conductivity of Hydrous Phase D Leads to a Selfâ€Preservation Effect Within a Subducting Slab. Journal of Geophysical Research: Solid Earth, 2022, 127, .	1.4	5
46322	Magnetic and Structural Properties of Novel-Coated Ni0.5Co0.5Fe1.6Gd0.2Mo0.1Sm0.1O4 Spinel Ferrite Nanomaterial: Experimental and Theoretical Investigations. Journal of Superconductivity and Novel Magnetism, 2022, 35, 2799-2820.	0.8	6
46323	Insights into the electronic structure and vibrational dynamics of Li7MnN4 anode material for Li-ion battery: a combined experimental and computational study. Journal of Alloys and Compounds, 2022, , 166004.	2.8	2

#	Article	IF	Citations
46324	The Structural, Mechanical, Lattice Dynamical, and Thermal Properties of 3D Dirac Semimetals BaXBi (X=Cu, Ag, Au) from Firstâ€Principles Calculations. Physica Status Solidi (B): Basic Research, 0, , 2200132.	0.7	1
46325	Unraveling the Phase Stability and Physical Property of Modulated Martensite in Ni2Mn1.5In0.5 Alloys by First-Principles Calculations. Materials, 2022, 15, 4032.	1.3	1
46326	Optimizing thermoelectric performance of CoSbS0.85Se0.15 by doping 3d transition metal ions M (M =) Tj ETQq0 0 0 rgBT /Overlock 10	1.4	2
46327	Structural defects in compounds <mml:math xmlns:mml="http://www.w3.org/1998/Math/MathML"><mml:mrow><mml:mi>Zn</mml:mi><mml:mi>X</mml:mi><mml:mi>Sb</mml:mi> <mml:math xmlns:mml="http://www.w3.org/1998/Math/MathML"><mml:mo>(</mml:mo><mml:mi>X</mml:mi><mml:mo>=</mml:mo><mml:mi>C . Origin of disorder and its relationship with electronic pro. Physical Review Materials, 2022, 6, .	0.9	2
46328	CO2 chemisorption and dissociation on flat and stepped transition metal surfaces. Applied Surface Science, 2022, 599, 154024.	3.1	11
46329	Tuning magnetic anisotropy and Dzyaloshinskii-Moriya interaction via interface engineering in nonisostructural <mml:math xmlns:mml="http://www.w3.org/1998/Math/MathML"><mml:mrow><mml:msub><mml:mi>SrCuO</mml:mi><mml:mn>2</mml:mn></ heterostructures. Physical Review B, 2022, 105, .	1.1	2
46330	Strong bulk-surface interaction dominated in-plane anisotropy of electronic structure in GaTe. Communications Physics, 2022, 5, .	2.0	10
46331	Ag implanted TiO2 nanoparticle/nanofibers composites for dye sensitized solar cells applications. Solar Energy, 2022, 241, 109-119.	2.9	14
46333	Superconductivity in compressed ternary alkaline boron hydrides. Physical Review B, 2022, 105, .	1.1	24
46334	Adsorption mechanism of hydrated Lu(OH)2+ and Al(OH)2+ ions on the surface of kaolinite. Powder Technology, 2022, 407, 117611.	2.1	4
46335	Multi-scale Design and Synthesis Strategy of Ni-doped SnO2 Hollow Spheres as Anode Material for Lithium-ion Batteries. International Journal of Electrochemical Science, 0, , ArticleID:220737.	0.5	1
46336	Novel Two-Dimensional MC2N4 (MÂ=ÂCr, Mo, W) Monolayers for Overall Water Splitting with High Visible-Light Absorption. Solar Energy, 2022, 241, 416-427.	2.9	6
46337	Water oxidation sites located at the interface of Pt/SrTiO3 for photocatalytic overall water splitting. Chinese Journal of Catalysis, 2022, 43, 2223-2230.	6.9	18
46338	Reversible transformation between terrace and step sites of Pt nanoparticles on titanium under CO and O2 environments. Chinese Journal of Catalysis, 2022, 43, 2026-2033.	6.9	2
46339	Efficient NO2 removal induced by transition-metal doped and co-doped graphene: An ab-initio study. Computational and Theoretical Chemistry, 2022, 1214, 113782.	1.1	3
46340	Structural diversity and unusual valence states in compressed Na-Hg system. Computational Materials Science, 2022, 211, 111561.	1.4	0
46341	Electronic and magnetic properties of the WSO Janus monolayer engineered by intrinsic defects. Surfaces and Interfaces, 2022, 32, 102114.	1.5	2
46342	Structural properties, electronic band structure, magnetic and mechanical characteristic of XFeGe (XÂ=ÂCo, Cr, Ni) half Heusler compounds: Insights from DFT calculation. Inorganic Chemistry Communication, 2022, 142, 109675.	1.8	1

#	Article	IF	Citations
46343	Magnetic properties of FePc sheet modified by the adsorption of gas molecules. Computational and Theoretical Chemistry, 2022, 1214, 113793.	1.1	0
46344	Physical insights on the ultralow thermal conductivity of Ag8XSe6 (XÂ=ÂSi, Ge, and Sn). Inorganic Chemistry Communication, 2022, 142, 109689.	1.8	3
46345	Iron promoted MOF-derived carbon encapsulated NiFe alloy nanoparticles core-shell catalyst for CO2 methanation. Journal of CO2 Utilization, 2022, 62, 102093.	3.3	17
46346	Prediction of a series of superhard BC4N structures. Diamond and Related Materials, 2022, 127, 109192.	1.8	3
46347	AbstAb-initio insights into the elastic, bonding, phonon, optoelectronic and thermophysical properties of SnTaS2. Solid State Sciences, 2022, 131, 106947.	1.5	12
46348	Three new C N compounds in orthorhombic symmetry: Theoretical investigations. Diamond and Related Materials, 2022, 127, 109181.	1.8	4
46349	Six novel silicon carbide with direct bandgaps: A comprehensive study. Chemical Physics, 2022, 561, 111603.	0.9	0
46350	First principles calculation for generating new thermal neutron scattering data for Zirconium hydride. Applied Radiation and Isotopes, 2022, 187, 110313.	0.7	0
46351	Structural, Electronic, and Optical Properties of Ga-Based Lead-Free Mixed-Halide Perovskites Cs3GaI6-xBrx (0 â‰¤ x â‰¤ 6) for Solar Cell Applications: A DFT Study. Physica B: Condensed Matter, 2022, 640, 414085.	1.3	1
46352	Ab initio study of the pressure dependence of mechanical and thermodynamic properties of GeB2O4 (B) Tj ETQq1 1 0.784314 rgBT /Ov	0.9	54
46353	Adsorption and dissociation of mercury species on the surface of 1T-MnO2/graphene. Computational Condensed Matter, 2022, 32, e00704.	0.9	0
46354	First-principles investigation of V2CSe2 MXene as a potential anode material for non-lithium metal ion batteries. Current Applied Physics, 2022, 41, 7-13.	1.1	7
46355	Preferential growth of HT-LiCo1-xAlxO2 cathode micro-bricks via an intermediate-facilitated solid-solid-gas reaction. Journal of Power Sources, 2022, 542, 231700.	4.0	2
46356	Numerical study of defects in protactinium carbide. Computational Condensed Matter, 2022, 32, e00703.	0.9	0
46357	First-principles study of surface segregation in bimetallic Cu3M(1 1 1) (MÂ=ÂAu, Ag, and Zn) alloys in presence of adsorbed CO. Computational Materials Science, 2022, 212, 111550.	1.4	2
46358	New method of atomistic modeling of <mml:math xmlns:mml="http://www.w3.org/1998/Math/MathML" display="inline" id="d1e340" altimg="si168.svg"><mml:mrow><mml:mi>Î±</mml:mi><mml:mo linebreak="goodbreak" linebreakstyle="after">â^'</mml:mo><mml:mi>Î±</mml:mi><mml:mo>â€²</mml:mo></mml:mrow></mml:math> phase transition in Feâ€“Cr alloy with effective accounting for vibrational entropy. Computational Materials Science, 2022, 212, 111563.	1.4	1
46359	Nb-doped PtS2 monolayer for detection of C2H2 and C2H4 in on-load tap-changer of the oil-immersed transformers: A first-principles study. Chemical Physics Letters, 2022, 802, 139755.	1.2	14
46360	First-principles calculations to investigate structural, electronic, thermoelectric, and optical properties of heavy thallium perovskite TlPbX3 (X = Cl, Br, I). Materials Science and Engineering B: Solid-State Materials for Advanced Technology, 2022, 283, 115781.	1.7	12

#	Article	IF	Citations
46361	Theoretical study on the hydrogen capture and damage mechanisms of PuO2 nanograin boundary. Journal of Solid State Chemistry, 2022, 313, 123314.	1.4	2
46362	Band structure calculation and crystal field induced electronic properties illustration for spinel CuGa2O4*. Computational Materials Science, 2022, 212, 111579.	1.4	1
46363	A first principles study of zirconium grain boundaries. Journal of Nuclear Materials, 2022, 568, 153853.	1.3	1
46364	Evolution of the structure and properties of (Zr1-xHfx)B2 solid solution ceramics from first-principle theory. Vacuum, 2022, 203, 111283.	1.6	4
46365	Exploring two-dimensional carbides as highly active catalysts for the oxygen reduction reaction: A density functional theory approach. Applied Surface Science, 2022, 599, 153907.	3.1	1
46366	Probing the chemical reactivity of the B2O3 -I (1 0 1) Surface: Interaction with H2O and H2S. Applied Surface Science, 2022, 599, 153999.	3.1	0
46367	Gap switching in metal-organic coordination chains. Journal of Magnetism and Magnetic Materials, 2022, 560, 169561.	1.0	1
46368	Defective and doped MgO monolayer as promising 2D materials for optoelectronic and spintronic applications. Materials Science in Semiconductor Processing, 2022, 149, 106876.	1.9	10
46369	Tuning the selectivity of cerium oxide for ethanol dehydration to ethylene. Applied Surface Science, 2022, 599, 153963.	3.1	7
46370	Mechanism of high magnetic field effect on the D03-L12 phase transition in Fe-Ga alloys. Journal of Alloys and Compounds, 2022, 919, 165818.	2.8	2
46371	Single-atom transition metals supported on defective graphene for electrochemical reduction of acetonitrile to ethylamine. Applied Surface Science, 2022, 599, 153948.	3.1	4
46372	Understanding the mechanism of carbon deposition of Ni3Co catalysts for methane dry reforming. Applied Surface Science, 2022, 599, 154002.	3.1	14
46373	High throughput investigation of an emergent and naturally abundant 2D material: Clinochlore. Applied Surface Science, 2022, 599, 153959.	3.1	8
46374	Lanthanum Oxyfluoride modifications boost the electrochemical performance of Nickel-rich cathode. Applied Surface Science, 2022, 599, 153928.	3.1	4
46375	Stabilities, electronic and piezoelectric properties of blue-phosphorene-phase MXs (MÂ=ÂGe, Sn; XÂ=ÂS, Se,) Tj ETQq0 0 0 rgBT /Overloc	3.1	2
46376	Enhancement of gas sensing by doping of transition metal in two-dimensional As2C3 nanosheet: A density functional theory investigation. Applied Surface Science, 2022, 599, 153941.	3.1	1
46377	Multistage charge redistribution constructing heterostructured WO3@RuSe2 on Si for enhanced photoelectrochemical hydrogen evolution. Chemical Engineering Journal, 2022, 446, 137462.	6.6	12
46378	Light-matter interaction in tungsten Sulfide-based Janus monolayers: A First-Principles study. Applied Surface Science, 2022, 599, 153967.	3.1	5

#	Article	IF	Citations
46379	First principles modeling of CO2 adsorption on (100), (010), and (001) surfaces of wollastonite for applications in enhanced rock weathering. Surface Science, 2022, 724, 122143.	0.8	2
46380	Characterization of structural orientation and optical properties of Al and Cr in rubies. Radiation Physics and Chemistry, 2022, 199, 110315.	1.4	0
46381	Electron transfer accelerated polymer-TiO2 coatings for enhanced photocatalytic activity in photocathodic protection. Applied Surface Science, 2022, 599, 153984.	3.1	6
46382	Mn3O4 nanoparticles in situ embedded in TiO2 for High-Performance Na-ion capacitor: Balance between 3D ordered hierarchically porous structure and heterostructured interfaces. Chemical Engineering Journal, 2022, 447, 137450.	6.6	15
46383	CO conversion over LaFeO3 perovskite during chemical looping processes: Influences of Ca-doping and oxygen species. Applied Catalysis B: Environmental, 2022, 316, 121598.	10.8	20
46384	First principles on the structure and electronic properties of vertically regulated two-dimensional cubic boron nitride and diamond like carbon sandwich heterostructures. Surface Science, 2022, 724, 122146.	0.8	2
46385	Unveiling the nanoalloying modulation on hydrogen evolution activity of ruthenium-based electrocatalysts encapsulated by B/N co-doped graphitic nanotubes. Applied Catalysis B: Environmental, 2022, 316, 121626.	10.8	13
46386	Exploiting the trade-offs of electron transfer in MOF-derived single Zn/Co atomic couples for performance-enhanced zinc-air battery. Applied Catalysis B: Environmental, 2022, 316, 121591.	10.8	51
46387	Fluorine induced surface reconstruction of perovskite ferrite oxide as cathode catalyst for prolong-life Li-O2 battery. Chemical Engineering Journal, 2022, 448, 137684.	6.6	13
46388	Metal organic framework derived perovskite/spinel heterojunction as efficient bifunctional oxygen electrocatalyst for rechargeable and flexible Zn-air batteries. Journal of Colloid and Interface Science, 2022, 625, 502-511.	5.0	21
46389	Multiscale modeling of hydrogenolysis of ethane and propane on Ru(0001): Implications for plastics recycling. Applied Catalysis B: Environmental, 2022, 316, 121597.	10.8	14
46390	Improvement in interfacial stability of high-rate Ni-rich oxide cathode by multifunctional LiTi0.5Zr1.5(PO4)3 conductive buffer layer. Chemical Engineering Journal, 2022, 448, 137663.	6.6	7
46391	Blue Luminescence of Lead-Free Cs2cucl4ÂGlass Ceramics with Long-Term Water-Resistance Stability. SSRN Electronic Journal, 0, , .	0.4	0
46392	Tunable Band Gap of Diamond Twin Boundaries by Strain Engineering. SSRN Electronic Journal, 0, , .	0.4	0
46393	Ion mobility and solvation complexes at liquidâ€“solid interfaces in dilute, high concentration, and localized high concentration electrolytes. Materials Advances, 2022, 3, 6352-6363.	2.6	6
46394	Graphene-encapsulated selenium@polyaniline nanowires with three-dimensional hierarchical architecture for high-capacity aluminumâ€“selenium batteries. Journal of Materials Chemistry A, 2022, 10, 15146-15154.	5.2	9
46395	Experimental and Computational Insights into the Anomalous Thermal Expansion of (Nh4)Reo4,. SSRN Electronic Journal, 0, , .	0.4	0
46396	High-throughput computational evaluation of lattice thermal conductivity using an optimized Slack model. Materials Advances, 2022, 3, 6826-6830.	2.6	17

#	Article	IF	Citations
46397	Strain tunable nanoporous r-N-GDY membrane for efficient seawater desalination. Journal of Materials Chemistry A, 2022, 10, 16533-16540.	5.2	7
46398	Improved Photovoltaic Properties of Cubic Snzro3 and Snhfo3 Under Pressure: An Insight Dft Study. SSRN Electronic Journal, 0, , .	0.4	0
46399	Lattice Dynamics and Spin-Phonon Coupling in the Noncollinear Antiferromagnetic Antiperovskite Mn3nin. SSRN Electronic Journal, 0, , .	0.4	0
46400	The rise of MAX phase alloys â€“ large-scale theoretical screening for the prediction of chemical order and disorder. Nanoscale, 2022, 14, 10958-10971.	2.8	15
46401	Ordered assembly of non-planar vanadyl-tetraphenylporphyrins on ultra-thin iron oxide. Physical Chemistry Chemical Physics, 2022, 24, 17077-17087.	1.3	3
46402	Green chemistry and first-principles theory enhance catalysis: synthesis and 6-fold catalytic activity increase of sub-5 nm Pd and Pt@Pd nanocubes. Nanoscale, 2022, 14, 10155-10168.	2.8	4
46403	Effects of Tungsten on Vacancy Aggregation Behavior and its Induction for Interstitial and Vacancy Migration in Tantalumâ€“Tungsten Alloys: A First-Principles Study. SSRN Electronic Journal, 0, , .	0.4	0
46404	Electronic, Mechanical and Piezoelectric Properties of Glass Like Complex Na2si1â˜’ X Ge X O3(X) Tj ETQq1 1 0.784314 rgBT /Overloc	0.4	0
46405	XSnS₃ (X = Ga, In) monolayer semiconductors as photo-catalysts for water splitting: a first principles study. Journal of Materials Chemistry C, 2022, 10, 11412-11423.	2.7	6
46406	First-Principles Kinetic Monte Carlo Modeling of Propylene Epoxidation on the Ti2cuo6/Cu(111) and Cu2o(111) Surfaces. SSRN Electronic Journal, 0, , .	0.4	0
46407	A combined experimental and computational study of the effect of electron irradiation on the transport properties of aromatic and aliphatic molecular self-assemblies. Nanoscale Advances, 2022, 4, 3745-3755.	2.2	3
46408	Computational Simulation Study on Adsorption and Separation of Ch4/H2 in Five Higher-Valency Covalent Organic Frameworks. SSRN Electronic Journal, 0, , .	0.4	0
46409	In Silico Study of Adsorption of Oxide Gases by Mn4 (M = Be, Mg) Monolayers. SSRN Electronic Journal, 0, , .	0.4	0
46410	Periodically nanoporous hydrogen-bonded organic frameworks for high performance photocatalysis. Nanoscale, 2022, 14, 9762-9770.	2.8	4
46411	A Novel Mechanism for Visible-Light Degradation of Phenol by Oxygen Vacancy Bi2moo6 Homojunction. SSRN Electronic Journal, 0, , .	0.4	0
46412	High-Pressure Study of the Aurophilic Topological Dirac Material Aui. SSRN Electronic Journal, 0, , .	0.4	0
46413	Methane plasma-mediated phase engineering of Ni nanosheets for alkaline hydrogen evolution. Nanoscale, 2022, 14, 12275-12280.	2.8	2
46414	A first principles study of a van der Waals heterostructure based on MS₂ (M = Mo, W) and Janus CrSSe monolayers. Nanoscale Advances, 2022, 4, 3557-3565.	2.2	5

#	Article	IF	Citations
46415	Insights into the Performance and Mechanism of Electrocatalytic Hydrodechlorination on a Pdco Bimetallic Catalyst Loaded on Rgo-Ppy/Ni. SSRN Electronic Journal, 0, , .	0.4	0
46416	Effective regulation of the electronic properties of a biphenylene network by hydrogenation and halogenation. RSC Advances, 2022, 12, 20088-20095.	1.7	7
46417	Nitric Oxide (No) on Vo2(010) Surface: A Density Functional Theory Study with Thestandard Gga Functional and Effect of Van Der Waals Dispersion. SSRN Electronic Journal, 0, , .	0.4	0
46418	Remarkably enhanced dynamic oxygen migration on graphene oxide supported by copper substrate. Nanoscale Horizons, 2022, 7, 1082-1086.	4.1	5
46419	Modulation of intrinsic defect in vertically grown ZnO nanorods by ion implantation. Physical Chemistry Chemical Physics, 0, , .	1.3	1
46420	Dual Experimental and Computational Approach to Elucidate the Effect of Ga on Cu/Ceo2â€“Zro2 Catalyst for Co2 Hydrogenation. SSRN Electronic Journal, 0, , .	0.4	0
46421	Construction of a fast Li-ion path in a MOF-derived Fe₃O₄@NC sulfur host enables high-rate lithiumâ€“sulfur batteries. Dalton Transactions, 0, , .	1.6	2
46422	Computational Investigation of Li Anchored Graphene as a Catalyst for Nitrogen Fixation. SSRN Electronic Journal, 0, , .	0.4	0
46423	Co-doping studies to enhance the life and electro-chemo-mechanical properties of the LiMn₂O₄cathode using multi-scale modeling and neuro-computing techniques. Physical Chemistry Chemical Physics, 2022, 24, 18645-18666.	1.3	3
46424	Photodetection and scintillation characterizations of novel lead-bismuth double perovskite halides. Journal of Materials Chemistry C, 2022, 10, 11266-11275.	2.7	7
46425	Exploring the air stability of all-inorganic halide perovskites in the presence of photogenerated electrons by DFT and AIMD studies. Sustainable Energy and Fuels, 2022, 6, 3778-3787.	2.5	3
46426	Correlating O-Vacancy and Hydrogen Spillover in Ru/TiO2-SiO2 Catalysts with Their Activity and Selectivity Towards Furfural Hydrogenation. SSRN Electronic Journal, 0, , .	0.4	0
46427	An All-Heusler Alloy Magnetic Tunneling Junction with Low Resistance Area Product and High Magnetocrystalline Anisotropy: A Dft Study. SSRN Electronic Journal, 0, , .	0.4	0
46428	Density Functional Theory Study of Ni Segregation in Cuni(111) Alloy with Chemisorbed Co, O, or H. SSRN Electronic Journal, 0, , .	0.4	0
46429	First principles study of magnetic transition of strain induced monolayer NbSi₂N₄. Wuli Xuebao/Acta Physica Sinica, 2022, 71, 206303.	0.2	2
46430	The flexoelectric effect of perovskite superlattice based on first principles. Wuli Xuebao/Acta Physica Sinica, 2022, .	0.2	0
46431	Synergistic Effects of Oxygen Vacancies and Heterostructures for Visible-Light-Driven Photoreduction of Uranium. SSRN Electronic Journal, 0, , .	0.4	0
46432	Composition Stability of Single Fcc Phase in Cr-Fe-Mn-Ni Alloys: First-Principles Prediction and Experimental Validation. SSRN Electronic Journal, 0, , .	0.4	0

#	Article	IF	Citations
46433	Triple-Doping (Cu, P, N) for the Activation of Catalytic Sites in Co0.4mn0.6o2 Nanosheets for Zn-Air Battery Applications. SSRN Electronic Journal, 0, , .	0.4	0
46434	Precursor Chemistry-Mediated Defect Regulation of Asphalt-Derived Carbonaceous Materials for Slope-Dominated Sodium Storage. SSRN Electronic Journal, 0, , .	0.4	0
46435	Monolayer GaOCl: a novel wide-bandgap 2D material with hole-doping-induced ferromagnetism and multidirectional piezoelectricity. Nanoscale, 2022, 14, 11369-11377.	2.8	3
46436	Re-examining the giant magnetization density in Î±â€²â€²-Fe₁₆N₂ with the SCAN+U method. Physical Chemistry Chemical Physics, 2022, 24, 17879-17884.	1.3	3
46437	Experimental and computational approaches to study the chlorination mechanism of pentlandite with ammonium chloride. RSC Advances, 2022, 12, 19232-19239.	1.7	0
46438	Modulating Intermediate Reactants Adsorption Via In-Sn Interface for Selective Co2 Electroreduction. SSRN Electronic Journal, 0, , .	0.4	0
46439	A vapochromic dye/graphene coated long-period fiber grating for benzene vapor sensing. Materials Chemistry Frontiers, 2022, 6, 2438-2446.	3.2	3
46440	Tunable mono- and di-methylation of amines with methanol over bimetallic CuCo nanoparticle catalysts. Green Chemistry, 2022, 24, 5965-5977.	4.6	7
46441	Strain- and electric field-enhanced optical properties of the penta-siligraphene monolayer. New Journal of Chemistry, 2022, 46, 13905-13917.	1.4	6
46442	Topological Defect and Sp3/Sp2 Carbon Interface Derived from Zif-8 with Linker Vacancies for Oxygen Reduction Reaction. SSRN Electronic Journal, 0, , .	0.4	0
46443	Amine Functionalization Derived Lattice Engineered and Electron Deficient Palladium CatalystÂFor Selective Production of Hydrogen Peroxide. SSRN Electronic Journal, 0, , .	0.4	0
46444	Enhancing Electrocatalytic Nitrogen Fixation Beyond Coherent Heterointerfacial Boundaries. SSRN Electronic Journal, 0, , .	0.4	0
46445	Nanoconfining red phosphorus within MOF-derived hierarchically porous carbon networks for high performance potassium storage. Materials Chemistry Frontiers, 2022, 6, 2184-2189.	3.2	2
46446	Strain-tunable charge carrier transport properties and optical properties of CrI₃> monolayer using first-principles. Wuli Xuebao/Acta Physica Sinica, 2022, .	0.2	0
46447	FIRST-PRINCIPLES CALCULATIONS FOR Ni-Al-Cr ALLOYS USING CLUSTER-PLUS-GLUE-ATOM MODEL. Wuli Xuebao/Acta Physica Sinica, 2022, .	0.2	0
46448	A Bimetallic Strategy to Tailoring the D-Band Center and Surface Formation Energy of Ni-Based Catalyst by Cu for Efficient and Stable Catalytic Hydrogenation of Dioctyl Phthalate. SSRN Electronic Journal, 0, , .	0.4	0
46449	Role of Î±-MoC(100) in Methanol Steam Reforming: A Mechanistic Study of DFT. Chinese Journal of Chemical Physics, 0, , .	0.6	1
46450	Screening binary alloys for electrochemical CO₂ reduction towards multi-carbon products. Journal of Materials Chemistry A, 2022, 10, 16171-16181.	5.2	11

#	Article	IF	Citations
46451	The origins of segregation behaviors of solute atoms and their effect on the strength of Î±-Al//Î¸â€²-Al₂Cu interfaces in Alâ€“Cu alloys. Physical Chemistry Chemical Physics, 2022, 24, 18370-18392.	1.3	6
46452	Structural engineering brings new electronic properties to Janus ZrSSe and HfSSe monolayers. Physical Chemistry Chemical Physics, 2022, 24, 17824-17831.	1.3	1
46453	Solidification Paths and Thermodynamic Assessment of the Alâ€“Agâ€“Sc System. SSRN Electronic Journal, 0, , .	0.4	0
46454	Well-Ordered Surface Metal Atoms Complexation by Deposition of Pd Cyclometallated Compounds on Ag (110). SSRN Electronic Journal, 0, , .	0.4	0
46455	Increasing the Adhesion of W to Si Substrates Using Cr/Ti Interlayers. SSRN Electronic Journal, 0, , .	0.4	0
46456	Electrically-driven robust tuning of lattice thermal conductivity. Physical Chemistry Chemical Physics, 2022, 24, 17479-17484.	1.3	5
46457	Computational discovery of In₂XY₂ (X, Y = S, Se, and Te; X â‰ Y) monolayers as multifunctional energy conversion materials. Journal of Materials Chemistry C, 0, , .	2.7	4
46458	First-principles prediction on antimony-doping effects on the cyclic stability of tin anodes for lithium-ion batteries. Physical Chemistry Chemical Physics, 2022, 24, 17542-17546.	1.3	1
46459	Study on cation-tuned performance of halide solid electrolyte. Wuli Xuebao/Acta Physica Sinica, 2022, .	0.2	0
46460	Studies on Structural, Electronic and Optical Properties of Nonlinear Optical Material Li-in-Se and Li-in-Te Under High Pressure. SSRN Electronic Journal, 0, , .	0.4	0
46461	Study of Adsorption Behaviour of Nucleobases on Si and P doped WSe₂: DFT Approach. , 2022, , .		1
46462	Contribution to the Calculation of Physical Properties of BeSe Semiconductor. , 0, , .		0
46463	Parallelized Ab Initio Quantum Transport Simulation of Nanoscale Bismuthene Devices. , 2022, , .		3
46464	Cationic-potential tuned biphasic layered cathodes for stable desodiation/sodiation. Science Bulletin, 2022, 67, 1589-1602.	4.3	31
46465	Atomic-scale operando observation of oxygen diffusion during topotactic phase transition of a perovskite oxide. Matter, 2022, 5, 3009-3022.	5.0	6
46466	Pentacene-Based Single Electron Transistor for a Low Concentration Gas Sensor. Chemistry Africa, 0, , .	1.2	0
46467	Nanopatterning by Length-Dependent Self-Assembly from Fluorene-Terpyridine Derivatives. Journal of Physical Chemistry C, 2022, 126, 10833-10841.	1.5	2
46468	Focusing on the Structural, Electronic, Optic and Elastic Behaviours of RhBiSe Compound by Ab-initio Calculations. International Scientific and Vocational Studies Journal, 2022, 6, 13-21.	0.2	1

#	Article	IF	Citations
46469	Li2TlIn'in BazÄ± Fiziksel Ã–zelliklerine Odaklanmak: Bir Temel Ä°lkeler Ã‡alÄ±ÅŸmasÄ±. YÃ¼zÃ¼ncÃ¼ YÄ±l Ã¼niversitesi Fen Bilimleri EnstitÃ¼sÃ¼ Dergisi, 0, , .	0.0	0
46470	Structural Characterization and Influence of Defects on the Optical Properties of the Oxygen-Deficient Perovskite Ba₃LiNb₂O_{8.5}â–¡_{0.5}. Inorganic Chemistry, 2022, 61, 10272-10282.	1.9	0
46471	Graph representation-based machine learning framework for predicting electronic band structures of quantum-confined nanostructures. Science China Materials, 2022, 65, 3157-3170.	3.5	5
46472	Phase evolution and thermal stability of novel high-entropy (Mo0.2Nb0.2Ta0.2V0.2W0.2)Si2 ceramics. Journal of the European Ceramic Society, 2022, 42, 5314-5322.	2.8	12
46473	Elucidating CO Oxidation Pathways on Rh Atoms and Clusters on the â€œ29â€•Cu₂O/Cu(111) Surface. Journal of Physical Chemistry C, 2022, 126, 11091-11102.	1.5	1
46474	Electrochemical Stability of ZnMn₂O₄: Understanding Zn-Ion Rechargeable Battery Capacity and Degradation. Journal of Physical Chemistry C, 2022, 126, 10957-10967.	1.5	4
46475	Effect of Multiple Oxygen Vacancies on the Optical and Thermodynamic Properties of La_{0.75}Sr_{0.25}Co_{0.25}Fe_{0.75}O_{3â˜Î´} Perovskite. Journal of Physical Chemistry C, 2022, 126, 11421-11425.	1.5	1
46476	Energetics of Phase Transformation Mechanisms in Li-CF_x Batteries. Chemistry of Materials, 2022, 34, 5799-5807.	3.2	3
46477	Magneto-optical Kerr effect in surface engineered 2D hexagonal boron nitride. Scientific Reports, 2022, 12, .	1.6	0
46478	Understanding the <mml:math xmlns:mml="http://www.w3.org/1998/Math/MathML"><mml:mrow><mml:mi>s</mml:mi><mml:mi>p</mml:mi></mml:mrow></mml:ma magnetism in substitutional doped graphene. Physical Review B, 2022, 105, .	1.1	3
46479	DFT Study on the CO2 Reduction to C2 Chemicals Catalyzed by Fe and Co Clusters Supported on N-Doped Carbon. Nanomaterials, 2022, 12, 2239.	1.9	5
46480	Single-molecule DNA sequencing using two-dimensional Ti2C(OH)2 MXene nanopores: A first-principles investigation. Nano Research, 2022, 15, 9843-9849.	5.8	7
46481	Substrate-Selective Intermolecular Interaction and the Molecular Self-Assemblies: 1,3,5-Tris(4-bromophenyl)benzene Molecules on the Ag(111) and Si(111) (âˆš3 Ã— âˆš3)-Ag Surfaces. Langmuir, 2022, 38, 8881-8889.	1.6	2
46482	Magnetic structure of oxygen-deficient perovskite nickelates with ordered vacancies. Physical Review Research, 2022, 4, .	1.3	6
46483	Thorough Descriptor Search to Machine Learn the Lattice Thermal Conductivity of Half-Heusler Compounds. ACS Applied Energy Materials, 0, , .	2.5	3
46484	Extraordinary Mechanical Performance in Charged Carbyne. Chinese Physics B, 0, , .	0.7	0
46485	Theory of polar domains in moirÃ© heterostructures. Physical Review B, 2022, 105, .	1.1	7
46486	Computational Study of Zn Single-Atom Catalysts on In₂O₃ Nanomaterials for Direct Synthesis of Acetic Acid from CH₄ and CO₂. ACS Applied Nano Materials, 0, , .	2.4	5

#	Article	IF	Citations
46487	CO₂ gas sensor based on Pt, Ag, Au and Pd doped InSe monolayer: the first-principles study. Semiconductor Science and Technology, 0, , .	1.0	0
46488	First-Principles Investigation of the Structural, Elastic and Thermodynamic Properties of CaRu2X2 (Xâ€‰=â€‰P, As) under Pressure. Journal of Superconductivity and Novel Magnetism, 0, , .	0.8	0
46489	Synthesis and Characterization of (FA)₃(HEA)₂Pb₃I₁₁: A Rare Example of <1 1 0>-Oriented Multilayered Halide Perovskites. Chemistry of Materials, 2022, 34, 5780-5790.	3.2	2
46490	Theoretical prediction on structure evolution and optimal properties of silicon modified hexagonal boron nitride as interphase in SiCf/SiC composite. Journal of the European Ceramic Society, 2022, 42, 5323-5333.	2.8	4
46491	A Newly Developed Dispersive Interaction Approach, DFT-D3, to the Three-Dimensional Topological Host Material Sb₂Te₃. Materials Science Forum, 0, 1065, 195-202.	0.3	0
46492	Effect of mixing the low-valence transition metal atoms <mml:math xmlns:mml="http://www.w3.org/1998/Math/MathML"><mml:mi>Y</mml:mi></mml:math> = Co, Fe, Mn, Cr, V, Ti, or Sc on the properties of quaternary Heusler compounds <mml:math xmlns:mml="http://www.w3.org/1998/Math/MathML"><mml:mrow><mml:msub><mml:mi mathvariant="normal">Co</mml:mi><mml:mrow><mml:mn>2</mml:mn><mml:mo>â€“</mml:mo><mml:mi>x</mml:mi></mml:mrow><mml:mi mathvariant="normal">Norm. Physical Review Materials, 2022, 6, .	0.9	4
46493	Maximizing the mechanical performance of Ti3AlC2-based MAX phases with aid of machine learning. Journal of Advanced Ceramics, 2022, 11, 1307-1318.	8.9	43
46494	Anisotropic Elastic and Thermal Properties of M2InX (M = Ti, Zr and X = C, N) Phases: A First-Principles Calculation. Metals, 2022, 12, 1111.	1.0	28
46495	Metal-Organic Frameworks Offering Tunable Binary Active Sites toward Highly Efficient Urea Oxidation Electrolysis. Research, 2022, 2022, .	2.8	18
46496	Phonon-Assisted Nonradiative Recombination Tuned by Organic Cations in Ruddlesden-Popper Hybrid Perovskites. Physical Review Applied, 2022, 17, .	1.5	4
46497	Giant bipolar unidirectional photomagnetoresistance. Proceedings of the National Academy of Sciences of the United States of America, 2022, 119, .	3.3	4
46498	Prediction of stable Li-Sn compounds: boosting ab initio searches with neural network potentials. Npj Computational Materials, 2022, 8, .	3.5	7
46499	Metal-Decoration-Free Li₃C₂ Monolayer with Heptacoordinate Carbons as a Promising Hydrogen Storage Medium. , 2022, 4, 1402-1410.		8
46500	High-Performance and Low-Power Transistors Based on Anisotropic Monolayer I - <mml:math xmlns:mml="http://www.w3.org/1998/Math/MathML" display="inline" overflow="scroll"><mml:msub><mml:mrow><mml:mi>Te</mml:mi><mml:mi mathvariant="normal">O</mml:mi></mml:mrow><mml:mn>2</mml:mn></mml:msub></mml:math>. Physical Review Applied, 2022, 17, .	1.5	15
46501	Giant second-harmonic generation in ferroelectric NbOI2. Nature Photonics, 2022, 16, 644-650.	15.6	57
46502	First-principles study of optical properties of monolayer h-BN and its defect structures under equibiaxial strain. Applied Physics A: Materials Science and Processing, 2022, 128, .	1.1	9
46503	Electronic band structure of <mml:math xmlns:mml="http://www.w3.org/1998/Math/MathML"><mml:mrow><mml:msub><mml:mi>Ti</mml:mi><mml:mn>2</mml:mn></mml:m mathvariant="normal">O</mml:mi><mml:mn>3</mml:mn></mml:msub></mml:mrow></mml:math> thin films studied by angle-resolved photoemission spectroscopy. Physical Review B, 2022, 105, .	1.1	4
46504	Superconducting density of states and band structure at the surface of the candidate topological superconductor <mml:math xmlns:mml="http://www.w3.org/1998/Math/MathML"><mml:msub><mml:mi mathvariant="normal">Au</mml:mi><mml:mn>2</mml:mn></mml:msub><mml:mi mathvariant="normal">Pb</mml:mi></mml:math>. Physical Review Research, 2022, 4, .	1.3	6

#	Article	IF	Citations
46505	Theory of ultrafast magnetization of nonmagnetic semiconductors with localized conduction bands. Physical Review B, 2022, 105, .	1.1	1
46506	Investigation of thermoelectric properties of galena using density functional theory. Materials Today: Proceedings, 2022, 67, 137-140.	0.9	2
46507	Experimental and firstâ€principles investigations on gâ€C ₃ N ₄ /ZnS heterostructures with enhanced photocatalyst capability. Micro and Nano Letters, 2022, 17, 259-271.	0.6	3
46508	Two-dimensional Ruddlesden-Popper halide perovskite solar absorbers with short-chain interlayer spacers. Physical Review Materials, 2022, 6, .	0.9	5
46509	Magnetic Collapse in Fe3Se4 under High Pressure. Materials, 2022, 15, 4583.	1.3	1
46510	Two-gap superconductivity in a Janus MoSH monolayer. Physical Review B, 2022, 105, .	1.1	24
46511	The factors affecting the diffusion properties of hydrogen in palladium copper alloys: Ab initio study. International Journal of Hydrogen Energy, 2022, 47, 27579-27589.	3.8	6
46512	Deep-Level Defects Induced Degradation of Negative Differential Resistance in GaN-Based Resonant Tunneling Diodes. ACS Applied Electronic Materials, 2022, 4, 3535-3542.	2.0	2
46513	Fate of Water Molecules on (11-20) and (1-102) Î±-Alumina Surfaces: 2D Periodic Self-Consistent Charge-Density Functional Tight-Binding/Molecular Mechanics Molecular Dynamics Study. Journal of Physical Chemistry C, 2022, 126, 11148-11157.	1.5	0
46514	Carrier Doping Modulates 2D Intrinsic Ferromagnetic Mn₂Ge₂Te₆ Monolayer, High Curie Temperature, Large Magnetic Crystal Anisotropy. Journal of Physical Chemistry C, 2022, 126, 11330-11340.	1.5	9
46515	Covalent and van der Waals interactions in a vertical heterostructure composed of boron and carbon. Physical Review B, 2022, 105, .	1.1	14
46516	Computational Studies on Holey TMC6 (TM = Mo and W) Membranes for H2 Purification. Membranes, 2022, 12, 709.	1.4	0
46517	Bloch's theorem in orbital-density-dependent functionals: Band structures from Koopmans spectral functionals. Physical Review B, 2022, 106, .	1.1	5
46518	Evaluation of the electronic, optical, elastic, mechanical, and vibrational properties of B₂O₃ using hybrid functional. Modern Physics Letters B, 2022, 36, .	1.0	2
46519	Anti-dissolution Pt single site with Pt(OH)(O3)/Co(P) coordination for efficient alkaline water splitting electrolyzer. Nature Communications, 2022, 13, .	5.8	73
46520	Phase-Transition Mechanism and the Atomic Interface Structure of Brookite to Rutile: Resolving from Machine-Learning Global Pathway Sampling. Journal of Physical Chemistry C, 2022, 126, 11846-11854.	1.5	1
46521	Thermoelectric properties of a high entropy half-Heusler alloy processed by a fast powder metallurgy route. Journal of Alloys and Compounds, 2022, 924, 166108.	2.8	8
46522	First-principles study of electronic structure of Calvertite and effect of substitution by Si and Sn. Computational Condensed Matter, 2022, 32, e00715.	0.9	7

#	Article	IF	Citations
46523	A first-principles-based high fidelity, high throughput approach for the design of high entropy alloys. Scientific Reports, 2022, 12, .	1.6	12
46524	First-principles calculations to investigate new ferromagnetic quaternary Heusler alloys FeZrTiZ(Z=Si, Sn, Pb): Compatible for spin polarized device and waste heat recovery applications. Solid State Sciences, 2022, 132, 106964.	1.5	4
46525	Effect of pressure on structural, elastic and mechanical properties of cubic perovskites XCoO3 (X =) Tj ETQq0 0 0 rgBT /Overlock 10 Tf 5 4233-4241.	2.6	17
46526	DFT + U Study of Uranium Dioxide and Plutonium Dioxide with Occupation Matrix Control. Journal of Physical Chemistry C, 2022, 126, 11426-11435.	1.5	13
46527	Surface Redox Pseudocapacitance Boosting Vanadium Nitride for Highâ€Power and Ultraâ€Stable Potassiumâ€Ion Capacitors. Advanced Functional Materials, 2022, 32, .	7.8	15
46528	Optical and Thermoelectric Behavior of Phagraphene with Siteâ€Specific Bâ€N Coâ€Doping. Advanced Theory and Simulations, 2022, 5, .	1.3	3
46529	Chalcogenide Perovskites (ABS₃; A = Ba, Ca, Sr; B = Hf, Sn): An Emerging Class of Semiconductors for Optoelectronics. Journal of Physical Chemistry Letters, 2022, 13, 6439-6446.	2.1	9
46530	First-principles predictions of tunable half metallicity in zigzag GaN nanoribbons with possible applications in CO detection and spintronics. Journal Physics D: Applied Physics, 2022, 55, 405002.	1.3	4
46531	Magnetic phase transition of monolayer chromium trihalides investigated with machine learning: toward a universal magnetic Hamiltonian. Journal of Physics Condensed Matter, 2022, 34, 395901.	0.7	1
46532	AgGaGeSe4: An Infrared Nonlinear Quaternary Selenide with Good Performance. Symmetry, 2022, 14, 1426.	1.1	1
46533	Engineering Electronic Platinumâ€“Carbon Support Interaction to Tame Carbon Monoxide Activation. Fundamental Research, 2022, , .	1.6	2
46534	Optoelectronic properties of 2D van der Waals heterostructure As/PtS2 by first-principles calculations. Materials Today: Proceedings, 2022, 67, 250-253.	0.9	1
46535	Synthesis of Nano-Oxide Precipitates by Implantation of Ti, Y and O Ions in Fe-10%Cr: Towards an Understanding of Precipitation in Oxide Dispersion-Strengthened (ODS) Steels. Materials, 2022, 15, 4857.	1.3	1
46536	Ultimate mechanical properties of enstatite. Physics and Chemistry of Minerals, 2022, 49, .	0.3	1
46537	Precise Tuning of Skyrmion Density in a Controllable Manner by Ion Irradiation. ACS Applied Materials & Interfaces, 2022, 14, 34011-34019.	4.0	8
46538	Thermodynamic investigation of phase transformation in Sn anode for magnesium batteries. APL Materials, 2022, 10, .	2.2	3
46539	Novel permeable material â€œyttrium decorated zeolite templated carbonâ€•for hydrogen storage: Perspectives from density functional theory. International Journal of Hydrogen Energy, 2022, 47, 28573-28584.	3.8	13
46540	Soft-mode-phonon-mediated insulatorâ€“superconductor transition in doped two-dimensional topological insulator RuC. Applied Physics Letters, 2022, 121, 013102.	1.5	0

#	Article	IF	Citations
46541	Tower carbon: a new large-cell carbon allotrope. Journal of Physics Condensed Matter, 2022, 34, 365702.	0.7	5
46542	Crystallization of A₃Ln(BO₃)₂ (A = Na, K; Ln = Lanthanide) from a Boric Acid Containing Hydroxide Melt: Synthesis and Investigation of Lanthanide Borates as Potential Nuclear Waste Forms. Inorganic Chemistry, 2022, 61, 11232-11242.	1.9	7
46543	Interatomic Potential for InP. Materials, 2022, 15, 4960.	1.3	0
46544	The New High-Pressure Phases of Nitrogen-Rich Agâ€“N Compounds. Materials, 2022, 15, 4986.	1.3	5
46545	Construction of CoS-encapsulated in ultrahigh nitrogen doped carbon nanofibers from energetic metal-organic frameworks for superior sodium storage. Carbon, 2022, 198, 353-363.	5.4	19
46546	Intrinsic valley-related multiple Hall effect in the two-dimensional organometallic lattice of NbTa-benzene. Physical Review B, 2022, 106, .	1.1	3
46547	NiFe Layered Double Hydroxide Electrocatalysts for an Efficient Oxygen Evolution Reaction. ACS Applied Energy Materials, 2022, 5, 8592-8600.	2.5	23
46548	Nanopore-Patterned CuSe Drives the Realization of the PbSeâ€“CuSe Lateral Heterostructure. ACS Applied Materials & Interfaces, 2022, 14, 32738-32746.	4.0	6
46549	Influence of ion irradiation-induced defects on phase formation and thermal stability of Ti0.27Al0.21N0.52 coatings. Acta Materialia, 2022, 237, 118160.	3.8	7
46550	Catalytic dissociation of a water molecule on the (1 1 1) surfaces of Pt0.5Ni0.5 bimetal: Density functional theory (DFT) study. Applied Surface Science, 2022, 602, 154238.	3.1	2
46551	Tunable electronic properties of silicon nanowires as sodiumâ€battery anodes. International Journal of Energy Research, 2022, 46, 17151-17162.	2.2	1
46552	Understanding Cd2+ Adsorption Mechanism on Montmorillonite Surfaces by Combining DFT and MD. Processes, 2022, 10, 1381.	1.3	3
46553	Manipulating alloying reaction to achieve the stable and dendrite-free zinc metal anodes. Chemical Engineering Journal, 2022, 450, 138048.	6.6	26
46554	<scp>Ultralowâ€Energyâ€Barrier H₂O₂</scp> Dissociation on Coordinatively Unsaturated Metal Centers in Binary <scp>Ceâ€Fe</scp> Prussian Blue Analogue for Efficient and Stable <scp>Photoâ€Fenton</scp> Catalysis. Energy and Environmental Materials, 2023, 6, .	7.3	3
46555	First-principles calculation of gate-tunable ferromagnetism in magic-angle twisted bilayer graphene under pressure. Journal of Physics Condensed Matter, 2022, 34, 385501.	0.7	2
46556	Anisotropic Chalcogenide Perovskite CaZrS₃: A Promising Thermoelectric Material. Journal of Physical Chemistry C, 2022, 126, 11751-11760.	1.5	13
46557	Artificial neural network-based path integral simulations of hydrogen isotope diffusion in palladium. JPhys Energy, 2022, 4, 034004.	2.3	10
46558	Surface Transformation Enables a Dendriteâ€Free Zincâ€Metal Anode in Nonaqueous Electrolyte. Advanced Materials, 2022, 34, .	11.1	34

#	Article	IF	Citations
46559	Design of Infrared Nonlinear Optical Compounds with Diamond-like Structures and Balanced Optical Performance. Inorganic Chemistry, 2022, 61, 11454-11462.	1.9	5
46560	Controlled photoinduced electron transfer from g-C3N4 to CuCdCe-LDH for efficient visible light hydrogen evolution reaction. International Journal of Hydrogen Energy, 2022, 47, 40227-40241.	3.8	13
46561	Angstrom-confined catalytic water purification within Co-TiOx laminar membrane nanochannels. Nature Communications, 2022, 13, .	5.8	97
46562	Phosphonated Lower-Molecular-Weight Polyethyleneimines as Oilfield Scale Inhibitors: An Experimental and Theoretical Study. Industrial & Engineering Chemistry Research, 2022, 61, 9586-9599.	1.8	2
46563	Ultralow Lattice Thermal Conductivity in Metastable Ag₂GeS₃ Revealed by a Combined Experimental and Theoretical Study. Chemistry of Materials, 2022, 34, 6420-6430.	3.2	1
46564	Magnetoâ€Optical Properties of Oxidized Co Nanowires on Pt Substrate. Physica Status Solidi (B): Basic Research, 2022, 259, .	0.7	4
46565	Adhesion and Electron Properties of Quasi-2D Mo2C, Ti2C, and V2C MXene Flakes after Van Der Waals Adsorption of Alcohol Molecules: Influence of Humidity. Lubricants, 2022, 10, 159.	1.2	3
46566	Tunnel cation and water structures of todorokite: Insights into metal partitioning and isotopic fractionation. Geochimica Et Cosmochimica Acta, 2022, 333, 153-165.	1.6	3
46567	Directional Construction of New Nonlinear Optical Bifunctional Units through Molecular Engineering Design Inspired by the B₃O₇-Typed Configuration. ACS Applied Materials & Interfaces, 2022, 14, 32270-32278.	4.0	6
46568	In-situ oxidized tungsten disulfide nanosheets achieve ultrafast photocatalytic extraction of uranium through hydroxyl-mediated binding and reduction. Nano Research, 2022, 15, 8810-8818.	5.8	11
46569	Platinumâ€“Dysprosium Alloys as Oxygen Electrodes in Alkaline Media: An Experimental and Theoretical Study. Nanomaterials, 2022, 12, 2318.	1.9	1
46570	Magnetochemical effects on phase stability and vacancy formation in fcc Fe-Ni alloys. Physical Review B, 2022, 106, .	1.1	7
46571	Controlled Synthesis of Transition Metal Phosphide Nanoparticles to Establish Composition-Dependent Trends in Electrocatalytic Activity. Chemistry of Materials, 2022, 34, 6255-6267.	3.2	17
46572	Charting the Atomic C Interaction with Transition Metal Surfaces. ACS Catalysis, 2022, 12, 9256-9269.	5.5	6
46573	Calcium poisoning mechanism on the selective catalytic reduction of NOx by ammonia over the Î³-Fe2O3 (001) surface. Environmental Science and Pollution Research, 2022, 29, 88256-88268.	2.7	4
46574	Controlling Spinâ€“Orbit Coupling to Tailor Type-II Dirac Bands. ACS Nano, 2022, 16, 11227-11233.	7.3	6
46575	First-Principles Prediction of Structural, Elastic, Mechanical, and Electronic Properties of Cu2ZnSnS4 under Pressure. ECS Journal of Solid State Science and Technology, 0, , .	0.9	1
46576	Multiscale modeling of semimetal contact to two-dimensional transition metal dichalcogenide semiconductor. Applied Physics Letters, 2022, 121, .	1.5	6

#	Article	IF	Citations
46577	Metal-insulator transition and robust thermoelectricity via strain-tuned interplay between structural and electronic properties in <mml:math xmlns:mml="http://www.w3.org/1998/Math/MathML"><mml:mrow><mml:msub><mml:mrow><mml:mo>(</mml:mo><mml:msub><mml:mm Physical Review Research, 2022, 4, .	1.3	3
46578	Electronic and optical properties of a hexagonal boron nitride monolayer in its pristine form and with point defects from first principles. Physical Review B, 2022, 106, .	1.1	12
46579	Exploration of a Ce_{0.65}Zr_{0.25}Pr_{0.1}O_{2â¯Î´}-Based Electrocatalyst That Exhibits Rapid Performance Deterioration Despite Its High Oxygen Storage Capability. ACS Applied Energy Materials, 0, , .	2.5	1
46580	Tailoring the Emission Wavelength of Color Centers in Hexagonal Boron Nitride for Quantum Applications. Nanomaterials, 2022, 12, 2427.	1.9	13
46581	Rational Design of Synergistic Structure Between Single-Atoms and Nanoparticles for CO2 Hydrogenation to Formate Under Ambient Conditions. Frontiers in Chemistry, 0, 10, .	1.8	3
46582	Electronic, magnetic and thermoelectric properties of Nb-substituted Fe2TiO5 pseudobrookite compound: Ab initio study. Journal of Computational Electronics, 2022, 21, 1070-1078.	1.3	2
46583	Experimental and DFT studies of flower-like Ni-doped Mo2C on carbon fiber paper: A highly efficient and robust HER electrocatalyst modulated by Ni(NO3)2 concentration. Journal of Advanced Ceramics, 2022, 11, 1294-1306.	8.9	75
46584	Atomic cerium modulated palladium nanoclusters exsolved ferrite catalysts for lean methane conversion. Exploration, 2022, 2, .	5.4	5
46585	Identification of the phosphorus-doping defect in MgS as a potential qubit. Chinese Physics B, 0, , .	0.7	0
46586	A first-principles investigation of electronic structure and ferromagnetic properties in alkali metal-doped ZnS/Se semiconductors. Journal of Computational Electronics, 2022, 21, 1061-1069.	1.3	1
46587	Lattice deformation and phase transition of aluminum nitride studied by density functional theory calculations. Journal of the Ceramic Society of Japan, 2022, 130, 452-457.	0.5	2
46588	Rational design of selenium inserted 1T/2H mixed-phase molybdenum disulfide for energy storage and pollutant degradation applications. Nanotechnology, 2022, 33, 445703.	1.3	7
46589	Shedding Light on the Structure and Characterization of K₂ZnGe₂O₆: A Phase-Matchable Nonlinear Optical Crystal. Inorganic Chemistry, 2022, 61, 11471-11477.	1.9	10
46590	First principles study of structural, elastic, and thermodynamic properties of LiAl2X (Xâ€‰=â€‰Rh, Pd, Ir and) Tj ETQq1 1 0.784314	0.6	7
46591	Ab Initio Study of Electronic Properties on WS₂ Monolayer and Transition Metal Doped WS₂. ECS Journal of Solid State Science and Technology, 2022, 11, 073003.	0.9	6
46592	Single Atom Catalysts: What Matters Most, the Active Site or The Surrounding?. ChemCatChem, 2022, 14, .	1.8	18
46593	Translational Covariance of Flexoelectricity at Ferroelectric Domain Walls. Physical Review X, 2022, 12, .	2.8	4
46594	Enhanced thermoelectric ZT in the tails of the Fermi distribution via electron filtering by nanoinclusions: Model electron transport in nanocomposites. Physical Review Materials, 2022, 6, .	0.9	1

#	Article	IF	Citations
46595	Prediction study of the structural, elastic, electronic, dynamic, optical and thermodynamic properties of cubic perovskite BiGaO3. Bulletin of Materials Science, 2022, 45, .	0.8	5
46596	Floating Particles in the Melt during the Growth of Î²-Ga2O3 Single Crystals Using the Czochralski Method. Metals, 2022, 12, 1171.	1.0	2
46597	Growth, characterization, and photovoltaic application of copper oxide thin films. Thin Solid Films, 2022, 757, 139381.	0.8	6
46598	First-principles calculations on the electronic structure and thermoelectric properties of quaternary Heusler compounds: LiScPtSi and LiScPdGe. Materials Today Communications, 2022, 32, 103961.	0.9	3
46599	Synthesis of the Two-Dimensional Robust Kagome Lattice on Au(111) via the Introduction of Fe Atoms. Journal of Physical Chemistry C, 2022, 126, 12009-12014.	1.5	3
46600	Revisiting the Iodine Vacancy Surface Defects to Rationalize Passivation Strategies in Perovskite Solar Cells. Journal of Physical Chemistry Letters, 2022, 13, 6694-6700.	2.1	15
46601	Spaceâ€Confined Oneâ€Step Growth of 2D MoO₂/MoS₂ Vertical Heterostructures for Superior Hydrogen Evolution in Alkaline Electrolytes. Small, 2022, 18, .	5.2	20
46602	Photocatalytic Câ€“H Bond Activation of Toluene on Rutile TiO₂(110). Journal of Physical Chemistry C, 2022, 126, 11963-11970.	1.5	9
46603	Transition of the generation mechanism of high-order harmonics in an extended neon system. Matter and Radiation at Extremes, 2022, 7, 044403.	1.5	1
46604	Uncovering strong Ï€-metal interactions on Ag and Au nanosurfaces under ambient conditions via in-situ surface-enhanced Raman spectroscopy. CheM, 2022, 8, 2514-2528.	5.8	13
46605	Mechanism of local lattice distortion effects on vacancy migration barriers in fcc alloys. Physical Review Materials, 2022, 6, .	0.9	0
46606	Enhanced acidic gas adsorption performance of arsenene by Pt mediation. AIP Advances, 2022, 12, 075108.	0.6	0
46607	Robust route to H2O2 and H2 via intermediate water splitting enabled by capitalizing on minimum vanadium-doped piezocatalysts. Nano Research, 2022, 15, 7986-7993.	5.8	24
46608	Computational analysis of the enhancement of photoelectrolysis using transition metal dichalcogenide heterostructures. Journal of Physics Condensed Matter, 2022, 34, 375001.	0.7	3
46609	Ferroelectricity induced by the absorption of water molecules on double helix SnIP. Chinese Physics B, 2023, 32, 037701.	0.7	2
46610	Design of Three-Dimensional Metallic Biphenylene Networks for Na-Ion Battery Anodes with a Record High Capacity. ACS Applied Materials & Interfaces, 2022, 14, 32043-32055.	4.0	7
46611	Identifying Substrate-Dependent Chemical Bonding Nature at Molecule/Metal Interfaces Using Vibrational Sum Frequency Generation Spectroscopy and Theoretical Calculations. Journal of Physical Chemistry C, 2022, 126, 11298-11309.	1.5	3
46612	First principle study of the electronic and structural properties of NaFeAs superconductor. Materials Today: Proceedings, 2022, 66, 3349-3354.	0.9	0

#	Article	IF	Citations
46613	First-principles study of the Ti(0001)/TiAl3(110) interfacial properties. Materials Today Communications, 2022, 32, 104049.	0.9	2
46614	Effect of defect types in monolayer MoS2 on SO2 adsorption. Journal of the Korean Physical Society, 2022, 81, 409-418.	0.3	3
46615	Benzenehexol-based 2D MOF as high-performance electrocatalyst for oxygen reduction reaction. Applied Surface Science, 2022, 601, 154187.	3.1	10
46616	Photoluminescence Enhancement by Band Alignment Engineering in MoS₂/FePS₃ van der Waals Heterostructures. ACS Applied Materials & Interfaces, 2022, 14, 33482-33490.	4.0	8
46617	Effects of intrinsic point defects on antiphase boundary energy of Î³'-Ni3Al from first-principles calculations. Journal of Materials Science, 2022, 57, 12916-12928.	1.7	4
46618	Size-effect on Ni electrocatalyst: The case of electrochemical benzyl alcohol oxidation. Nano Research, 2023, 16, 202-208.	5.8	7
46619	Surface-Based Post-synthesis Manipulation of Point Defects in Metal Oxides Using Liquid Water. ACS Applied Materials & Interfaces, 2022, 14, 34059-34068.	4.0	3
46620	Chern Number Tunable Quantum Anomalous Hall Effect in Monolayer Transitional Metal Oxides via Manipulating Magnetization Orientation. Physical Review Letters, 2022, 129, .	2.9	36
46621	<mml:math xmlns:mml="http://www.w3.org/1998/Math/MathML"><mml:msub><mml:mi>Ïƒ</mml:mi><mml:mi>h</mml:mi></mml:msub></mml:ma symmetry and electron-phonon interaction in two-dimensional crystalline systems. Physical Review B, 2022, 106, .	1.1	4
46622	Bixbyite-type Ln2O3 as promoters of metallic Ni for alkaline electrocatalytic hydrogen evolution. Nature Communications, 2022, 13, .	5.8	62
46623	Tailoring Nitrogen Species in Diskâ€Like Carbon Anode Towards Superior Potassium Ion Storage. Small, 2022, 18, .	5.2	11
46624	A theoretical investigation of glide dislocations in BN/AlN heterojunctions. Chinese Physics B, 0, , .	0.7	0
46625	Unveiling Electronic Structure and Spin-Resolve of Bulk Bi₂O₂X (X = S, Se, and Te) Materials: A Computational Study Based-On Density Functional Theory. Materials Science Forum, 0, 1066, 150-155.	0.3	0
46626	Activating lattice oxygen of two-dimensional MnXnâ''1O2 MXenes via zero-dimensional graphene quantum dots for water oxidation. Science China Materials, 2022, 65, 3053-3061.	3.5	12
46627	Investigation of electronic structure, magnetic stability, spin coupling, and thermodynamic properties of novel antiferromagnets XMn2Y2 (XÂ=ÂCa, Sr; YÂ=ÂP, As). Journal of Molecular Structure, 2022, 1268, 133698.	1.8	9
46628	Structural, thermal, elastic, and magnetoelectronic properties of FeNiMnZ (Zâ€‰=â€‰Al, Si) quaternary Heuslers under hydrostatic pressure. European Physical Journal B, 2022, 95, .	0.6	3
46629	Oxygen Vacancy Formation and Interface Charge Transfer at Misfit Dislocations in Gd-Doped CeO₂/MgO Heterostructures. Journal of Physical Chemistry C, 2022, 126, 11735-11750.	1.5	2
46630	Higher-indexed MoirÃ© patterns and surface states of MoTe2/graphene heterostructure grown by molecular beam epitaxy. Npj 2D Materials and Applications, 2022, 6, .	3.9	6

#	Article	IF	Citations
46631	Computational investigation of Ba2ZrTiO6 double perovskite for optoelectronic and thermoelectric applications. Journal of Solid State Chemistry, 2022, 314, 123385.	1.4	6
46632	Selective decorating of BC3 and C3N nanosheets with single metal atom for hydrogen storage. International Journal of Hydrogen Energy, 2022, 47, 24004-24013.	3.8	8
46633	Understanding and Modifying the Scaling Relations for Ammonia Synthesis on Dilute Metal Alloys: From Single-Atom Alloys to Dimer Alloys. ACS Catalysis, 2022, 12, 9201-9212.	5.5	18
46634	The simplest dense carbon allotrope: Ultra-hard body-centered tetragonal C4. Journal of Solid State Chemistry, 2022, 314, 123424.	1.4	5
46635	Polarization Electric Field in 2D Polar Monolayer Silicon Monochalcogenides SiX (Xâ€‰=â€‰S, Se) as Potential Photocatalysts for Water Splitting. Physica Status Solidi - Rapid Research Letters, 2023, 17, .	1.2	1
46636	Exploiting weak magnetic anisotropy on the stability of spin-spirals and skyrmions lattice in VX2 (X=S,) Tj ETQq1 1 0.784314 rgBT /Over	0.9	3
46637	Trapping Capability of Small Vacancy Clusters in the Î±-Zr Doped with Alloying Elements: A First-Principles Study. Crystals, 2022, 12, 997.	1.0	0
46638	Engineering width and directness of the band gap in diamond-based materials: An ab initio investigation towards electron-structure features control. Diamond and Related Materials, 2022, , 109237.	1.8	0
46639	A First-Principles Study of Enhanced Ferromagnetism in a Two-Dimensional Cr-Doped InS Monolayer. Journal of Electronic Materials, 2022, 51, 6252-6263.	1.0	1
46640	Computational Screening and Synthesis of M (M = Mo and Cu)-Doped CeO₂/silicalite-1 for Medium-/Low-Temperature NH₃â€“SCR. Industrial & Engineering Chemistry Research, 2022, 61, 10091-10105.	1.8	8
46641	Enhanced Photocatalytic Hydrogen Evolution from Water Splitting on Ta₂O₅/SrZrO₃ Heterostructures Decorated with Cu_xO/RuO₂ Cocatalysts. ACS Applied Materials & Interfaces, 2022, 14, 31767-31781.	4.0	15
46642	Influence of carbon on the formation of Î³/Î³â€² microstructure and Îº-phase in the WC/Coâ€“Niâ€“Alâ€“W system: ab initio calculations and experimental studies. Journal of Materials Science, 0, , .	1.7	0
46643	Atomically dispersed iron sites with a nitrogenâ€“carbon coating as highly active and durable oxygen reduction catalysts for fuel cells. Nature Energy, 2022, 7, 652-663.	19.8	258
46644	Investigation of structural properties of Mg-doped twisted bilayer graphene for phosphine gas detection. Molecular Simulation, 0, , 1-9.	0.9	0
46645	Highly Efficient and Ultraâ€Broadband Yellow Emission of Leadâ€Free Antimony Halide toward White Lightâ€Emitting Diodes and Visible Light Communication. Laser and Photonics Reviews, 2022, 16, .	4.4	36
46646	Electrochemical reduction of CO2 on single-atom catalysts anchored on N-terminated TiN (1 1 1): Low overpotential and high selectivity. Applied Surface Science, 2022, 602, 154239.	3.1	5
46647	Ni Substitution Effect on the Structural, Magnetic, Electronic, Elastic, Thermodynamic, Vibrational and Thermoelectric Properties of $$Co_{2-x}Ni_xMnSb$$ ($$x=0,1,2$$) Ferromagnetic Heusler Alloys. Journal of Superconductivity and Novel Magnetism, 2022, 35, 2943-2954.	0.8	2
46648	Clusterâ€Glass for Lowâ€Cost Whiteâ€Light Emission. Advanced Materials, 2022, 34, .	11.1	8

#	Article	IF	Citations
46649	Insights into the substitutional chemistry of La1â^'xSrxCo1â^'yMyO3 (M = Pd, Ru, Rh, and Pt) probed by in situ DRIFTS and DFT analysis of CO oxidation. Applied Catalysis A: General, 2022, 643, 118768.	2.2	4
46650	Understanding the role of Ga on the activation mechanism of CO2 over modified Cu surface by DFT calculation. Molecular Catalysis, 2022, 528, 112477.	1.0	3
46651	Insight into the graphitization mechanism of the interface between iron and diamond: A DFT study. Diamond and Related Materials, 2022, 127, 109213.	1.8	8
46652	A comparison study of the structural, electronic and electronic transport properties of nanoribbons based on Penta-graphene, Penta-P2C and Penta-SiC2. Materials Today Communications, 2022, 32, 103912.	0.9	1
46653	Differentiating the {100} surfaces of Cu2O nanocrystals from {111} and {110} for benzylic Csp3-H bond oxidation: Oxidations of diphenyl methane to benzophenone and cumene to cumene hydroperoxide under mild conditions. Molecular Catalysis, 2022, 528, 112490.	1.0	1
46654	Microstructure and properties of Cuâ€"Niâ€"Coâ€"Siâ€"Crâ€"Mg alloys with different Si contents after multi-step thermo-mechanical treatment. Materials Science & Engineering A: Structural Materials: Properties, Microstructure and Processing, 2022, 850, 143532.	2.6	15
46655	Understanding the optoelectronic properties of interface between Cs2TiBr6 and TiO2 for solar cell applications. Materials Today Communications, 2022, 32, 103963.	0.9	0
46656	Kinetics investigation of the oxygen evolution reaction on the characteristic facets of Î³-Cu3V2O8. Molecular Catalysis, 2022, 528, 112493.	1.0	1
46657	Selective CO2 reduction to methane catalyzed by mesoporous Ru-Fe3O4/CeOx-SiO2 in a fixed bed flow reactor. Molecular Catalysis, 2022, 528, 112486.	1.0	5
46658	Synergetic effects of Sn and Ti incorporated in MWW zeolites on promoting the oxidative hydration of ethylene with H2O2 to ethylene glycol. Journal of Catalysis, 2022, 413, 554-564.	3.1	7
46659	Experimental and theoretical investigations of electronic structure and optical in Ln3+-doped In2S3 nanoparticles. Solid State Communications, 2022, 353, 114882.	0.9	4
46660	The electronic structure, elastic properties, dynamical stability and thermoelectric properties of rock-salt and orthorhombic phases of CdS: First-principles calculations. Solid State Communications, 2022, 353, 114878.	0.9	4
46661	Key roles of formyl insertion mechanism and C-O scission of oxygenates on cobalt carbide in syngas Conversion: A detailed reaction network analysis. Journal of Catalysis, 2022, 413, 455-466.	3.1	6
46662	Interface chemistry effects in nanofluids: Experimental and computational study of oil-based nanofluids with gold nanoplates. Journal of Molecular Liquids, 2022, 362, 119762.	2.3	3
46663	Precipitation-based grain boundary design alters Inter- to Trans-granular Fracture in AlCrN Thin Films. Acta Materialia, 2022, 237, 118156.	3.8	10
46664	Multi-objective materials bayesian optimization with active learning of design constraints: Design of ductile refractory multi-principal-element alloys. Acta Materialia, 2022, 236, 118133.	3.8	22
46665	Theoretical investigation of some fundamental physical properties of the ternary nitrides Ca4SiN4 and Ca4GeN4 under pressure and temperature effect. Computational Condensed Matter, 2022, 32, e00711.	0.9	5
46666	The improved textural properties, thermal stability, and cytocompatibility of mesoporous hydroxyapatite by Mg2+ doping. Materials Chemistry and Physics, 2022, 289, 126461.	2.0	10

#	Article	IF	Citations
46667	Exchange-correlation and spin-orbit coupling effects in 18-electrons transparent conductors half-Heusler: Ab-initio study. Computational Condensed Matter, 2022, 32, e00690.	0.9	3
46668	Structural and elastic behaviour of aragonite at high-pressure: A contribution from first-principle simulations. Computational Materials Science, 2022, 212, 111600.	1.4	3
46669	Nonthermal effects in H-doped tungsten at high electronic temperatures. Journal of Nuclear Materials, 2022, 568, 153896.	1.3	1
46670	Designing a type of material with a vacancy-independent lattice volume: A case study on Ti0.19Zr0.81N1-. Chemical Physics Letters, 2022, 803, 139827.	1.2	0
46671	Accurate Ab-initio calculation of elastic constants of anisotropic binary alloys: A case of Feâ€“Al. Solid State Communications, 2022, 353, 114879.	0.9	4
46672	Opto-electro-mechanical properties of lead-free hybrid double perovskites Cs2AgSbX6 (X = Cl, Br, I) for solar cells: A first-principles study. Journal of Physics and Chemistry of Solids, 2022, 169, 110880.	1.9	16
46673	A potential absorber for PHz electronics using Sn/h-BN Van der Waals structure: A hybrid DFT and macroscopic investigations. Physica E: Low-Dimensional Systems and Nanostructures, 2022, 144, 115423.	1.3	0
46674	Analyzing the electronic and optical properties of bulk, unstrained, and strained monolayers of SrS2 by DFT. Physica E: Low-Dimensional Systems and Nanostructures, 2022, 143, 115403.	1.3	4
46675	Thermal properties of single crystals of the low-positive thermal expansion material Al2W3O12. Solid State Communications, 2022, 353, 114873.	0.9	4
46676	Predicting impact sensitivity of energetic materials: insights from energy transfer of carriers. Acta Materialia, 2022, 236, 118137.	3.8	36
46677	A first-principles based microkinetic study of ZnMn1.5TM0.5O4 (TMÂ=Â3d transition metal) for NO oxidation. Applied Surface Science, 2022, 600, 154069.	3.1	1
46678	Tuning the adsorption and diffusion capabilities of titanium disulfide monolayers by doping and strain engineering: Implications for lithium-ion batteries. Applied Surface Science, 2022, 600, 154164.	3.1	6
46679	Adsorption and sensing performances of Rh-embedded PtSe2 monolayer upon CO and HCHO in dry-type reactors: A first-principles study. Chemical Physics, 2022, 562, 111652.	0.9	4
46680	Effect of chemical composition and atomic configuration on thermodynamic stability and elastic properties of AlB<mml:math xmlns:mml="http://www.w3.org/1998/Math/MathML" display="inline" id="d1e2304" altimg="si41.svg"><mml:msub><mml:mrow /><mml:mrow><mml:mn>2</mml:mn></mml:mrow></mml:msub></mml:math>-type Sc<mml:math xmlns:mml="http://www.w3.org/1998/Math/MathML" display="inline" id="d1e2312" altimg="si158.svg"><mml:msub><mml:mrow />	1.4	2
46681	First-principles calculations to investigate band gap of cubic BaThO3 with systematic isotropic external static pressure and its impact on structural, elastic, mechanical, anisotropic, electronic and optical properties. Journal of Physics and Chemistry of Solids, 2022, 169, 110878.	1.9	14
46682	Insight into the origin of magnetism in 3d transition-metal atoms doped PC6: A first-principles study. Physica E: Low-Dimensional Systems and Nanostructures, 2022, 144, 115363.	1.3	0
46683	Lattice dynamics of LiH<mml:math xmlns:mml="http://www.w3.org/1998/Math/MathML" altimg="si407.svg" display="inline" id="d1e1832"><mml:msub><mml:mrow /><mml:mrow><mml:mn>2</mml:mn></mml:mrow></mml:msub></mml:math>PO<mml:math xmlns:mml="http://www.w3.org/1998/Math/MathML" altimg="si409.svg" display="inline" id="d1e1840"><mml:msub><mml:mrow /><mml:mrow><mml:mn>4</mml:mn></mml:mrow></mml:msub></mml:math> crystal. Physica B: Conden	1.3	1
46684	Ab initio modeling of helical polyacetylenes: Peierls and Mott-Hubbard metalâ€“insulator transitions. Computational Materials Science, 2022, 213, 111642.	1.4	5

#	Article	IF	Citations
46685	Tuning bandgap and energy stability of Organic-Inorganic halide perovskites through surface engineering. Computational Materials Science, 2022, 213, 111649.	1.4	1
46686	Extremely Sensitive and Selective NO2 Detection at Relative Humidity 90% in 2-Dimensional Tin Sulfides/SnO2 Nanorod Heterostructure. Sensors and Actuators B: Chemical, 2022, 369, 132319.	4.0	7
46687	Double layer in ionic liquids: Temperature effect and bilayer model. Journal of Molecular Liquids, 2022, 363, 119747.	2.3	10
46688	Three-dimensional nitrogen-doped MXene as support to form high-performance platinum catalysts for water-electrolysis to produce hydrogen. Chemical Engineering Journal, 2022, 446, 137443.	6.6	18
46689	Mechanical characterisation of V-4Cr-4Ti alloy: Tensile tests under high energy synchrotron diffraction. Journal of Nuclear Materials, 2022, 569, 153911.	1.3	3
46690	Evolution of in-plane heat transport in tellurium from 2D to 3D. Materials Today Physics, 2022, 27, 100776.	2.9	1
46691	Adsorption mechanism of yttrium ions onto ion-adsorption type rare earths ore. Separation and Purification Technology, 2022, 299, 121641.	3.9	13
46692	The <mml:math xmlns:mml="http://www.w3.org/1998/Math/MathML" altimg="si1.svg" display="inline"		

#	Article	IF	Citations
46703	Theoretical insight into the effect of impurity on the acetoxylation of ethylene to form vinyl acetate: A DFT study of acetylene coversion on PdAu(1 0 0) surface. Fuel, 2022, 326, 125047.	3.4	5
46704	Three non-metallic carbon materials with comparable electrical conductivity to metals. Diamond and Related Materials, 2022, 128, 109230.	1.8	4
46705	Mechanical strain and electric field tunable electronic structure of black/violet phosphorene van der Waals heterostructure: From type I to Z-scheme system. Journal of Physics and Chemistry of Solids, 2022, 169, 110863.	1.9	3
46706	First principles study of the structural stability, lattice dynamics, optical and thermoelectric properties of NaSrX(X = As, Sb and Bi). Materials Science in Semiconductor Processing, 2022, 149, 106840.	1.9	6
46707	Metallic Penta-BN2 monolayer: A novel platform for non-lithium-ion batteries with high capacity and splendid cyclicity. Materials Science in Semiconductor Processing, 2022, 149, 106849.	1.9	9
46708	Two-dimensional conductive Ï€-conjugated metal-organic frameworks as promising electrocatalysts for highly efficient hydrogen evolution reaction. Applied Surface Science, 2022, 601, 154241.	3.1	7
46709	Defected NiFe layered double hydroxides on N-doped carbon nanotubes as efficient bifunctional electrocatalyst for rechargeable zincâ€“air batteries. Applied Surface Science, 2022, 601, 154253.	3.1	17
46710	First principles study of Co and Ni based half Heusler alloys. Materials Science in Semiconductor Processing, 2022, 150, 106908.	1.9	6
46711	DFT combined with XANES to investigate the sulfur fixation mechanisms of H2S on different CaO surfaces. Fuel, 2022, 327, 125204.	3.4	3
46712	Multifunctional two-dimensional graphene-like boron nitride allotrope of g-B3N5: A competitor to g-BN?. Journal of Alloys and Compounds, 2022, 921, 165913.	2.8	3
46713	Multiphase nanosheet-nanowire cerium oxide and nickel-cobalt phosphide for highly-efficient electrocatalytic overall water splitting. Applied Catalysis B: Environmental, 2022, 316, 121678.	10.8	67
46714	Do two-dimensional group IV-VI M4X9 monolayers have photocatalytic activity toward overall water splitting? A comprehensive theoretical investigation. Applied Surface Science, 2022, 601, 154225.	3.1	1
46715	Bi/BiFe(oxy)hydroxide for sustainable lattice oxygen-boosted electrocatalysis at a practical high current density. Applied Catalysis B: Environmental, 2022, 317, 121685.	10.8	7
46716	Systematic investigation of the piezocatalysisâ€“adsorption duality of polymorphic MoS2 nanoflowers. Applied Catalysis B: Environmental, 2022, 317, 121717.	10.8	35
46717	Effect of aliovalent substituted highly disordered GeTe compound's thermoelectric performance. Journal of Alloys and Compounds, 2022, 922, 166221.	2.8	1
46718	Y2CF2 and Lu2CF2 MXenes under applied strain: Electronic, optical, and photocatalytic properties. Journal of Alloys and Compounds, 2022, 922, 166198.	2.8	5
46719	Atomistic investigation on the impact of substitutional Al and Si atoms on the carbon kinetics in ferrite. Journal of Alloys and Compounds, 2022, 921, 166031.	2.8	2
46720	Influence of Al doping on crystal structure, optical, and photoluminescence characteristics of ZnGa2O4 films. Materials Science in Semiconductor Processing, 2022, 150, 106962.	1.9	7

#	Article	IF	Citations
46721	First-principles study on the electric control of ferromagnetic behaviour of two-dimensional BaTiO3 (0Â0Â1) ultrathin film doped with Cr. Applied Surface Science, 2022, 601, 154240.	3.1	0
46722	Chemical functionalization of low-buckled SiGe monolayer: Effects on the electronic and magnetic properties. Materials Science in Semiconductor Processing, 2022, 150, 106949.	1.9	1
46723	Electronic properties and defect levels induced by <mml:math xmlns:mml="http://www.w3.org/1998/Math/MathML" display="inline" id="d1e1065" altimg="si112.svg"><mml:mrow><mml:mi>n</mml:mi><mml:mo>/</mml:mo><mml:mi>p</mml:mi></mml:mrow></mml:math>-type defect-complexes in Ge. Materials Science in Semiconductor Processing, 2022, 150, 106906.	1.9	4
46724	Two-dimensional V-shaped PdI2: Auxetic semiconductor with ultralow lattice thermal conductivity and ultrafast alkali ion mobility. Applied Surface Science, 2022, 601, 154176.	3.1	10
46725	Bamboo-shaped Co@NCNTs as superior sulfur host for Li-S batteries. Applied Surface Science, 2022, 601, 154245.	3.1	14
46726	Bilayer armchair graphene nanoribbon photodetector with Stone-Wales defect: A computational study. Materials Science in Semiconductor Processing, 2022, 150, 106918.	1.9	9
46727	Mn-doped FeS with larger lattice spacing as advance anode for sodium ion half/full battery. Chemical Engineering Journal, 2022, 450, 137960.	6.6	15
46728	Enhanced electrocatalytic full water-splitting reaction by interfacial electric field in 2D/2D heterojunction. Chemical Engineering Journal, 2022, 450, 137789.	6.6	27
46729	Carbide-directed enhancement of electrochemical hydrogen evolution reaction on tungsten carbideâ€“oxide heterostructure. Chemical Engineering Journal, 2022, 450, 137915.	6.6	12
46730	Cooperative catalytic Mo-S-Co heterojunctions with sulfur vacancies for kinetically boosted lithium-sulfur battery. Chemical Engineering Journal, 2022, 450, 138115.	6.6	23
46731	Insight into the elemental mercury immobilization mechanism with carbon and sulfur over the mackinawite (FeS) surface via density functional theory. Chemical Engineering Journal, 2022, 450, 137934.	6.6	6
46733	Identifying the crystal structure of T1 precipitates in Al-Li-Cu alloys by ab initio calculations and HAADF-STEM imaging. Journal of Materials Science and Technology, 2023, 133, 41-57.	5.6	17
46734	Synthesis, formation mechanism, and intrinsic physical properties of several As/P-containing MAX phases. Journal of Materials Science and Technology, 2023, 133, 23-31.	5.6	1
46735	Graphene and hexagonal boron nitride based nano-electronic biosensor. , 2020, , .		0
46736	Tuning and control of the magnetic properties of a 2D nanomagnet. , 2020, , .		0
46737	Electronic and magnetic phase transition in monolayer Cr₂Ge₂Se₆. , 2020, , .		0
46738	High-capacity, high-rate, and dendrite-free lithium metal anodes based on a 3D mixed electronic-ionic conductive and lithiophilic scaffold. Science China Materials, 2022, 65, 2989-2996.	3.5	1
46739	The determining role of T species in the catalytic potential of MXenes: Water adsorption and dissociation on Mo2CT. Catalysis Today, 2023, 424, 113848.	2.2	8

#	Article	IF	Citations
46740	Interaction of graphene with Au _n clusters: a first-principles study. Journal of Physics Condensed Matter, 2022, 34, 405701.	0.7	2
46741	Study on Stability and Elastic Properties of Î²-TiX (X=Nb, Ta) Alloys From First-Principles Calculations. Frontiers in Materials, 0, 9, .	1.2	0
46742	Strain-tunable pure Hâ^' conduction in one-atom-thick hexagonal boron nitride for high-energyâ€“density fuel cells. Chemical Engineering Journal, 2022, 450, 138223.	6.6	3
46743	First-Principles Study on the Adsorption Behavior of O2 on the Surface of Plutonium Gallium System. Materials, 2022, 15, 5035.	1.3	2
46744	Dark matter direct detection in materials with spin-orbit coupling. Physical Review D, 2022, 106, .	1.6	8
46745	Density functional theory screening of some fundamental physical properties of Cs2InSbCl6 and Cs2InBiCl6 double perovskites. European Physical Journal B, 2022, 95, .	0.6	34
46746	Theoretical and experimental insights into CO2 formation on Co2C catalysts in syngas conversion to Value-Added chemicals. Applied Surface Science, 2022, 602, 154379.	3.1	3
46747	Microscopic identification of stepped SiC(0001) and the reaction site of hydrogen-rich epitaxial growth. Physical Review B, 2022, 106, .	1.1	0
46748	Probing the local structure of LaFe11.4Si1.6 by pair distribution function analysis. Journal of Magnetism and Magnetic Materials, 2022, 562, 169750.	1.0	0
46749	First-Principles Study on the Adsorption and Dissociation Behavior of H2 on the Surface of a Plutoniumâ€“Gallium System. Coatings, 2022, 12, 1019.	1.2	1
46750	Effect of halogenation on the electronic transport properties of aromatic and alkanethiolate molecules. Physica E: Low-Dimensional Systems and Nanostructures, 2022, , 115428.	1.3	1
46751	Evolution of geometric and electronic structures of oxygen-induced superstructures on Mo(110) surface: A LEED, ARPES, and DFT study. Physical Review B, 2022, 106, .	1.1	0
46752	Elucidating the Initial Steps in Î±-Uranium Hydriding Using First-Principles Calculations. Langmuir, 2022, 38, 9335-9346.	1.6	2
46753	Single atom supported on MoS2 as efficient electrocatalysts for the CO2 reduction reaction: A DFT study. Applied Surface Science, 2022, 602, 154211.	3.1	21
46754	Probing Copper and Copperâ€“Gold Alloy Surfaces with Space-Quantized Oxygen Molecular Beam. Jacs Au, 0, , .	3.6	2
46755	Effect of disorder on thermodynamic instability of binary Rare-earth â€“ Nickel â€“ Palladium compounds. Acta Materialia, 2022, 238, 118205.	3.8	1
46756	Photoprotection in metal halide perovskites by ionic defect formation. Joule, 2022, 6, 2152-2174.	11.7	16
46757	First-Principles Calculations of the Spin-Dependent Electronic Structure and Strain Tunability in 2D Non-van der Waals Chromium Chalcogenides Cr₂X₃ (X = S, Se, Te): Implications for Spintronics Applications. ACS Applied Nano Materials, 0, , .	2.4	5

#	Article	IF	Citations
46758	Effects of transition metal doping on CsGeBr3 perovskite: First-principles study. AIP Advances, 2022, 12, .	0.6	1
46759	Structural, electronic, mechanical and thermodynamic properties of antiperovskites Ti3InX (X=C and) Tj ETQq1 1 0.784314 rgBT /Ove	1.6	5
46760	Towards targeted electronic properties of two-dimensional BaTiO3 films by tailoring surface structures: A first-principles study. Applied Surface Science, 2022, 602, 154377.	3.1	2
46761	Dynamic strain and switchable polarization: A pathway to enhance the oxygen evolution reaction on InSnO2N. Journal of Catalysis, 2022, 413, 720-727.	3.1	3
46762	Thickness and defect dependent electronic, optical and thermoelectric features of $$hbox {WTe}_2$$. Scientific Reports, 2022, 12, .	1.6	6
46763	DFTâ€“Assisted Structure Determination from Powder X-ray Diffraction Data of a New Zonisamide/Ĩµ-Caprolactam Cocrystal. Crystals, 2022, 12, 1020.	1.0	1
46764	First-principle studies of twisted bilayer black phosphorus. Journal of the Korean Physical Society, 0, , .	0.3	1
46765	First-principles study of elastic, electronic and optical properties of Rb1-xCsxMgH3 and Cs1-yRbyMgH3 perovskite hybrides. Journal of Physics and Chemistry of Solids, 2022, 170, 110902.	1.9	0
46766	Ab-initio calculations of substitutional co-segregation interactions at coherent bcc Fe-Cu interfaces. Journal of Nuclear Materials, 2022, , 153923.	1.3	0
46767	Ru Single-Atom Decorated Black TiO₂ Nanosheets for Efficient Solar-Driven Hydrogen Production. ACS Sustainable Chemistry and Engineering, 2022, 10, 10311-10317.	3.2	11
46768	Calculated Elasticity of Al-Bearing Phase D. Minerals (Basel, Switzerland), 2022, 12, 922.	0.8	2
46769	Impact of surface-active site heterogeneity and surface hydroxylation in Ni doped ceria catalysts on oxidative dehydrogenation of propane. Journal of Catalysis, 2022, 413, 681-691.	3.1	6
46770	Prediction the structural, electronic, elastic and dynamical properties of LiAlGe and LiInGe half-Heusler crystals by density functional theory. Materials Today Communications, 2022, 32, 104082.	0.9	2
46771	MXenes Ã la Carte: Tailoring the Epitaxial Growth Alternating Nitrogen and Transition Metal Layers. ACS Nano, 2022, 16, 12541-12552.	7.3	6
46772	Cooperative Catalysis of Vibrationally Excited CO₂ and Alloy Catalyst Breaks the Thermodynamic Equilibrium Limitation. Journal of the American Chemical Society, 2022, 144, 14140-14149.	6.6	24
46773	High-density Fe single atoms anchored on 2D-Fe2C12 monolayer materials for N2 reduction to NH3 with high activity and selectivity. Applied Surface Science, 2022, 602, 154380.	3.1	4
46774	Insight into stepwise dealumination in acid-treatment of IM-5 for catalytic cracking of n-heptane and Fischer-Tropsch naphtha. Microporous and Mesoporous Materials, 2022, 342, 112117.	2.2	2
46775	Structure, magnetic and adsorption properties of novel FePt/h-BN heteromaterials. Nano Research, 0, , .	5.8	2

#	Article	IF	Citations
46776	Enhanced tunneling magnetoresistance and spin filtering in perovskite magnetic tunnel junctions via oxygen octahedral tilting. Physical Review B, 2022, 106, .	1.1	0
46777	Free Energy and Solvation Structure Analysis for Adsorption of Aromatic Molecules at Pt(111)/Water Interface by 3D-RISM Theory. Chemistry Letters, 2022, 51, 791-795.	0.7	1
46778	Polyguluronate simulations shed light onto the therapeutic action of OligoG CF-5/20. Bioorganic and Medicinal Chemistry, 2022, 72, 116945.	1.4	4
46779	Effective Mass for Holes in Paramagnetic, Plasmonic Cu₅FeS₄ Semiconductor Nanocrystals. Journal of Physical Chemistry C, 0, , .	1.5	2
46780	Room-temperature deposited fluorine-doped tantalum pentoxide for stable organic solar cells. Organic Electronics, 2022, , 106607.	1.4	0
46781	Prediction of dynamical, thermodynamic and mechanical properties of RuMnAs compound under hydrostatic pressure. Bulletin of Materials Science, 2022, 45, .	0.8	1
46782	Coherent interfaces govern direct transformation from graphite to diamond. Nature, 2022, 607, 486-491.	13.7	60
46783	Energy and mechanical properties predictions in Fe-Ni binary system by ab initio calculations. Materials Today Communications, 2022, 33, 104118.	0.9	1
46784	Machine Learning for Designing Mixed Metal Halides for Efficient Ammonia Separation and Storage. Journal of Physical Chemistry C, 2022, 126, 12184-12196.	1.5	5
46785	A-type antiferromagnetic order in semiconducting <mml:math xmlns:mml="http://www.w3.org/1998/Math/MathML"><mml:msub><mml:mi mathvariant="normal">EuMg</mml:mi><mml:mn>2</mml:mn></mml:msub><mml:msub><mml:mi mathvariant="normal">Sb</mml:mi><mml:mn>2</mml:mn></mml:msub></mml:math> single crystals. Physical Review B, 2022, 106, .	1.1	12
46786	Exploring the Bounds on the Youngâ€™s Modulus and Gravimetric Youngâ€™s Modulus. Physical Review Applied, 2022, 18, .	1.5	6
46787	A first-principle assisted framework for designing high elastocaloric Niâ€“Mn-based magnetic shape memory alloy. Journal of Materials Science and Technology, 2023, 134, 151-162.	5.6	10
46788	Collective mode excitations and simulated <mml:math xmlns:mml="http://www.w3.org/1998/Math/MathML"><mml:mi>L</mml:mi></mml:math> -edge resonant inelastic x-ray scattering spectra in antiferromagnetic <mml:math xmlns:mml="http://www.w3.org/1998/Math/MathML"><mml:msub><mml:mi mathvariant="normal">Ca</mml:mi><mml:mn>2</mml:mn></mml:msub><mml:msub><mml:mi mathvariant="normal">RuO</mml:mi><mml:mn>4</mml:mn></mml:msub></mml:math>. Physical Review	1.1	1
46789	Exploration of electrical contact type in two-dimensional WS2/Nb2CX2 (XÂ=ÂH, F, Cl) heterostructures. Applied Surface Science, 2022, 602, 154390.	3.1	6
46790	Electron delocalization triggers nonradical Fenton-like catalysis over spinel oxides. Proceedings of the National Academy of Sciences of the United States of America, 2022, 119, .	3.3	99
46791	Tri-MX: New group-IV monochalcogenide monolayers with excellent piezoelectricity and special optical properties. Applied Surface Science, 2022, 602, 154391.	3.1	4
46792	Adsorption-Mediated n-Type ZnO Surface Reconstruction for Optically Enhanced Volatile Organic Compound Sensing. ACS Applied Electronic Materials, 2022, 4, 3825-3833.	2.0	3
46793	From an atomistic study of olivine under pressure to the understanding of the macroscopic energy release in earthquakes. Geosystems and Geoenvironment, 2023, 2, 100108.	1.7	1

#	Article	IF	Citations
46794	Ab-initio calculation of structural and electronic properties of ZnO and ZnSe compounds with wurtzite structure. International Journal of Modern Physics B, 2022, 36, .	1.0	3
46795	Defect structure in quantum-cutting <mml:math xmlns:mml="http://www.w3.org/1998/Math/MathML"><mml:msup><mml:mrow><mml:mi>Yb</mml:mi></mml:mrow><mml:mrow><m -doped <mml:math xmlns:mml="http://www.w3.org/1998/Math/MathML"><mml:mrow><mml:mi>CsPb</mml:mi><mml:msub><mml:mi>Cl</mml:mi><mml perovskites probed by x-ray absorption and atomic pair distribution function analysis. Physical Review Materials, 2022, 6, .	0.9	4
46796	Predicting mechanical properties of high entropy alloys with face centered cubic structure from first principles calculations. Materials Today Communications, 2022, 32, 104059.	0.9	1
46797	Descriptor of catalytic activity nanoparticles surface: Atomic and molecular hydrogen on gold. Molecular Catalysis, 2022, 529, 112534.	1.0	2
46798	Effects of Excess Cu Atoms on Hydrogen Permeability, Solubility, and Diffusivity in Pd-Cu Alloys with B2-Type Crystal Structures. Nippon Kinzoku Gakkaishi/Journal of the Japan Institute of Metals, 2022, 86, 140-148.	0.2	1
46799	Planar carbon allotrope B-graphyne as lithium-ion battery anode materials. Chemical Physics Letters, 2022, 804, 139897.	1.2	1
46800	Constructing Cu-CuO heterostructured skin on Cu cubes to promote electrocatalytic ammonia production from nitrate wastewater. Journal of Hazardous Materials, 2022, 439, 129653.	6.5	32
46801	Fabrication of CoS/CdS heterojunctions for enhanced photocatalytic hydrogen production. Inorganica Chimica Acta, 2022, 541, 121085.	1.2	5
46802	Enhanced charge storage performance of MXene based all-solid-state supercapacitor with vertical graphene arrays as the current collector. Journal of Energy Storage, 2022, 54, 105355.	3.9	19
46803	First-principles calculations to investigate the Electronic and Optical Properties of Hexagonal, Triclinic, and Monoclinic Structures of <mml:math xmlns:mml="http://www.w3.org/1998/Math/MathML" altimg="si22.svg" display="inline" id="d1e768"><mml:mi>Î±</mml:mi></mml:math>-BiFeO<mml:math xmlns:mml="http://www.w3.org/1998/Math/MathML" altimg="si23.svg" display="inline"	1.7	4
46804	Computational investigation of half-metallicity in <mml:math xmlns:mml="http://www.w3.org/1998/Math/MathML" altimg="si4.svg" display="inline" id="d1e958"><mml:msup><mml:mrow><mml:mi>d</mml:mi></mml:mrow><mml:mrow><mml:mn>0</mml:mn></mml:mrow></mml:m half-Heusler alloys GeKZ (Z = Ca, Sr) using first-principles calculations. Computational Materials Science, 2022, 213, 111665.	1.4	1
46805	Group IV element allotropes in the Fmmm phase: First-principles calculations. Computational Materials Science, 2022, 213, 111666.	1.4	5
46806	Electronic properties of rutile and anatase TiO2 and their effect on CO2 adsorption: A comparison of first principle approaches. Fuel, 2022, 328, 125322.	3.4	6
46810	Fundamental Physical Properties of LiInS2 and LiInSe2 Chalcopyrite Structured Solids. East European Journal of Physics, 2021, , 62-69.	0.1	5
46811	Investigations of Lead Free Halides in Sodium Based Double Perovskites Cs2NaBiX6(X=Cl, Br, I): an Ab Intio Study. East European Journal of Physics, 2021, , 74-80.	0.1	8
46812	Stretched three-dimensional white graphene with a tremendous lattice thermal conductivity increase rate. RSC Advances, 2022, 12, 22581-22589.	1.7	2
46813	First-Principles Exploration of the Interface Characteristic between Cnt and Inorganic Lead-Free Perovskites Cssnx3 (X = Cl, Br, I). SSRN Electronic Journal, 0, , .	0.4	0
46814	High-Efficiency ResistiveÂSwitchÂAnd Artificial Synaptic Simulation InÂAntimony-Based Perovskite Devices. SSRN Electronic Journal, 0, , .	0.4	0

#	Article	IF	Citations
46815	First-principles high-throughput screening of bulk piezo-photocatalytic materials for sunlight-driven hydrogen production. Journal of Materials Chemistry A, 2022, 10, 18132-18146.	5.2	14
46816	Unveiling concentration effects on the structural and optoelectronic characteristics of Zn_{1â^'x}Cd_xS (x = 0, 0.25, 0.50, 0.75, 1) cubic semiconductors: a theoretical study. RSC Advances, 2022, 12, 22783-22791.	1.7	7
46817	Selectivity of volatile organic compounds on the surface of zinc oxide nanosheets for gas sensors. Physical Chemistry Chemical Physics, 2022, 24, 20491-20505.	1.3	2
46818	Interactions of Xanthates of Increasing Chain Length with Pyrite Surfaces: A Dft-D and Microcalorimetry Studies. SSRN Electronic Journal, 0, , .	0.4	0
46819	Ab-Initio Study of Structural, Mechanical, and Dynamical Stability, Electronic, Thermal, and Optical Properties of Silver Halide Agx (X = F, Cl, Br, and I) Semiconductors. SSRN Electronic Journal, 0, , .	0.4	0
46820	Mechanical, Electronic and Thermodynamic Properties of (Nbzrhfti)C High-Entropy Ceramics from First-Principles. SSRN Electronic Journal, 0, , .	0.4	0
46821	Noble-Metal-Free Chalcogenide Nanotwins for Efficient and Stable Photocatalytic Pure Water Splitting by Surface Phosphorization and Cocatalyst Modification. SSRN Electronic Journal, 0, , .	0.4	0
46822	A Novel Mechanism for Visible-Light Degradation of Phenol by Oxygen Vacancy Bi2moo6 Homojunction. SSRN Electronic Journal, 0, , .	0.4	0
46823	First Principles Investigation of Photoelectric Properties of Ga2o3 Doped with Group IV Elements (Si,Ge,Sn). SSRN Electronic Journal, 0, , .	0.4	0
46824	Role of Oxygen Vacancies on Surface Reaction of Water Oxidation in Wo3 Studied by Density Functional Theory (Dft) and Experiment. SSRN Electronic Journal, 0, , .	0.4	0
46825	Layered Topological Semimetal Gagete: New Polytype with Non-Centrosymmetric Structure. SSRN Electronic Journal, 0, , .	0.4	0
46826	Nitric oxide electrochemical reduction reaction on transition metal-doped MoSi₂N₄ monolayers. Physical Chemistry Chemical Physics, 2022, 24, 18943-18951.	1.3	10
46827	High electron mobility and wide-bandgap properties in a novel 1D PdGeS₃ nanochain. Physical Chemistry Chemical Physics, 2022, 24, 18868-18876.	1.3	3
46828	Enhanced photoluminescence stability and internal defect evolution of the all-inorganic lead-free CsEuCl₃ perovskite nanocrystals. Physical Chemistry Chemical Physics, 2022, 24, 18860-18867.	1.3	2
46829	Strengthening and High-Temperature Softening Resistance of Low Si-Added Cu-Cr-Zr Alloy for Fusion Reactor Application. SSRN Electronic Journal, 0, , .	0.4	0
46830	Spray Coated Few-Layer Graphene as Aluminium Battery Cathode. Sustainable Energy and Fuels, 0, , .	2.5	1
46831	The Co-Adsorption Potential of Metal-Organic Framework/Activated Carbon Composites Against Both Polar and Non-Polar Volatile Organic Compounds in Air. SSRN Electronic Journal, 0, , .	0.4	0
46832	Competition between reverse water gas shift reaction and methanol synthesis from CO₂: influence of copper particle size. Nanoscale, 2022, 14, 13551-13560.	2.8	11

#	Article	IF	Citations
46833	Physical insights into the Au growth on the surface of a LaAlO₃/SrTiO₃ heterointerface. RSC Advances, 2022, 12, 24146-24155.	1.7	1
46834	Macroporous perovskite nanocrystal composites for ultrasensitive copper ion detection. Nanoscale, 2022, 14, 11953-11962.	2.8	5
46835	On-purpose design of dual active sites in single V atom anchored C₂N nanosheets for propane dehydrogenation catalysis. Inorganic Chemistry Frontiers, 2022, 9, 5517-5526.	3.0	2
46836	Axial ligand engineering for highly efficient oxygen reduction catalysts in transition metalâ€“N₄ doped graphene. New Journal of Chemistry, 2022, 46, 16138-16150.	1.4	9
46837	The mechanochemical excitation of crystalline LiN₃. Faraday Discussions, 0, 241, 230-249.	1.6	3
46838	Functionalization of Quasi-Two-Dimensional Materials: Chemical and Strain-Induced Modifications. Progress in Physics of Metals, 2022, 23, 147-238.	0.5	20
46839	A giant thermoelectric figure of merit and ultra-low lattice thermal conductivity using Janus $$Ge_{2}SeTe$$ monolayer: a first principle investigation. European Physical Journal Plus, 2022, 137, .	1.2	1
46840	Topological Phases in AB-Stacked <mml:math xmlns:mml="http://www.w3.org/1998/Math/MathML" display="inline"><mml:mrow><mml:msub><mml:mrow><mml:mi>MoTe</mml:mi></mml:mrow><mml:mrow><mml:mn>2</mml:mn></ : <mml:math xmlns:mml="http://www.w3.org/1998/Math/MathML" display="inline"><mml:mrow><mml:msub><mml:mrow><mml:mi mathvariant="double-struck">Z</mml:. Physical Review Letters, 2022, 129, .	2.9	32
46841	Compositional Glass: A State with Inherent Chemical Disorder, Exemplified by Ti-rich Ni3(Al,Ti)1 D024 Phase. Crystals, 2022, 12, 1049.	1.0	3
46842	Dynamic Response of Oxygen Vacancies in the Deacon Reaction over Reduced Single Crystalline CeO_{2â€“x}(111) Surfaces. Journal of Physical Chemistry C, 2022, 126, 13202-13212.	1.5	4
46843	A theoretical investigation of the effect of Ga alloying on thermodynamic stability, electronic-structure, and oxidation resistance of Ti2AlC MAX phase. Scientific Reports, 2022, 12, .	1.6	2
46844	Localized orbital scaling correction for periodic systems. Physical Review B, 2022, 106, .	1.1	3
46845	Electronic Structure of Conventional Slater Type Antiferromagnetic Insulators: AIrO₃ (A=Sr, Ba) Perovskites. Journal of Physics: Conference Series, 2022, 2315, 012033.	0.3	0
46846	Unraveling the Key Atomic Interactions in Determining the Varying Li/Na/K Storage Mechanism of Hard Carbon Anodes. Advanced Energy Materials, 2022, 12, .	10.2	18
46847	New QSPR model for prediction of corrosion inhibition using conceptual density functional theory. Journal of Molecular Modeling, 2022, 28, .	0.8	8
46848	Computational Evaluation of Al-Decorated g-CN Nanostructures as High-Performance Hydrogen-Storage Media. Nanomaterials, 2022, 12, 2580.	1.9	2
46849	Fully auxetic and multifunctional of two-dimensional <mml:math xmlns:mml="http://www.w3.org/1998/Math/MathML"><mml:mi>Î´</mml:mi></mml:math> -GeS and <mml:math xmlns:mml="http://www.w3.org/1998/Math/MathML"><mml:mi>Î´</mml:mi></mml:math> -GeSe. Physical Review B, 2022, 106, .	1.1	5
46850	Effects of uniaxial/biaxial/triaxial strain on carrier lifetime and photocatalytic performance of ZnO: Sâ€“Se system. Journal of Materials Science, 2022, 57, 14918-14935.	1.7	0

#	Article	IF	Citations
46851	Adsorption of Polycyclic Aromatic Hydrocarbons and C₆₀ onto Forsterite: Câ€“H Bond Activation by the Schottky Vacancy. ACS Earth and Space Chemistry, 2022, 6, 2009-2023.	1.2	3
46852	Room temperature spin-orbit torque efficiency in sputtered low-temperature superconductor Î´ -TaN. Physical Review Materials, 2022, 6, .	0.9	1
46853	Molecular simulation on hydrogen storage properties of five novel covalent organic frameworks with the higher valency. International Journal of Hydrogen Energy, 2022, 47, 29390-29398.	3.8	4
46854	Equivariant analytical mapping of first principles Hamiltonians to accurate and transferable materials models. Npj Computational Materials, 2022, 8, .	3.5	15
46855	Elucidating the effect of oxides on the zeolite catalyzed alkylation of benzene with 1-dodecene. Chinese Journal of Chemical Engineering, 2023, 56, 126-135.	1.7	4
46856	Pressure Induced Disorder-Order Phase Transitions in the Al4Cr Phases. Crystals, 2022, 12, 1008.	1.0	1
46857	Soft-phonon anharmonicity, floppy modes, and Na diffusion in <mml:math xmlns:mml="http://www.w3.org/1998/Math/MathML"><mml:mrow><mml:msub><mml:mi>Na</mml:mi><mml:mn>3</mml:mn></mml: mathvariant="normal">F</mml:mi><mml:mi>Y</mml:mi></mml:mrow><mml:mo>Â</mml:mo><mml:mrow><mml:mo>(</mml:mo><mr : Ab initio. Physical Review B, 2022, 106, .	1.1	9
46858	Molecular-level insight into photocatalytic CO2 reduction with H2O over Au nanoparticles by interband transitions. Nature Communications, 2022, 13, .	5.8	100
46859	A Theoretical Investigation on the Physical Properties of Zirconium Trichalcogenides, ZrS3, ZrSe3 and ZrTe3 Monolayers. Energies, 2022, 15, 5479.	1.6	4
46860	Unexpected Chemical Activity of a Mineral Surface: The Role of Crystal Water in Tobermorite. Journal of Physical Chemistry C, 2022, 126, 12405-12412.	1.5	13
46861	The Orbital Nature of Electron Holes in BaFeO₃ and Implications for Defect Chemistry. Journal of Physical Chemistry C, 2022, 126, 12809-12819.	1.5	4
46862	Theoretical Study of Ba₂X₆ (X = S, Se, Te) for Thermoelectric Applications Based on First-Principles Calculations and Machine Learning. Journal of Physical Chemistry C, 2022, 126, 12735-12741.	1.5	1
46863	First principles DFT analysis on the diffusion kinetics of hydrogen isotopes through bcc iron (Fe): Role of temperature and surface coverage. International Journal of Hydrogen Energy, 2022, 47, 31481-31498.	3.8	6
46864	First-principles study of magnetic properties of the transition metal ion-doped methylamonium lead bromide. International Journal of Modern Physics B, 0, , .	1.0	1
46865	Atomicâ€Scale Homogeneous Ruï¿¿Cu Alloy Nanoparticles for Highly Efficient Electrocatalytic Nitrogen Reduction. Advanced Materials, 2022, 34, .	11.1	34
46866	Dry reforming of methane on doped Ni nanoparticles: Feature-assisted optimizations and ranking of doping metals for direct activations of CH4 and CO2. Nano Research, 2022, 15, 9670-9682.	5.8	6
46867	Quantifying temperature-induced magnetic disorder effects on the anisotropy of MnBi. Physical Review B, 2022, 106, .	1.1	1
46868	Sodium diffusion in scheelite-type Na2Zr(MoO4)3 and Na4Zr(MoO4)4. Ceramics International, 2022, 48, 32338-32347.	2.3	2

#	Article	IF	Citations
46869	The BS Nanotubes with High Carrier Mobility for Potential Photocatalytic Hydrolysis Applications: First-Principles Study. Journal of Electronic Materials, 2022, 51, 6002-6010.	1.0	1
46870	A Nonaqueous Mgâ€CO₂ Battery with Low Overpotential. Advanced Energy Materials, 2022, 12, .	10.2	15
46871	Nuclear magnetic resonance of <mml:math xmlns:mml="http://www.w3.org/1998/Math/MathML"><mml:mmultiscripts><mml:mi>Li</mml:mi><mml:mprescripts /><mml:none /><mml:mn>8</mml:mn></mml:mmultiscripts></mml:math> ions implanted in ZnO. Physical Review B, 2022, 106, .	1.1	2
46872	Extraction of lithium from the simulated pyrometallurgical slag of spent lithium-ion batteries by binary eutectic molten carbonates. International Journal of Minerals, Metallurgy and Materials, 2022, 29, 1715-1721.	2.4	9
46873	Evidence for electronic signature of a magnetic transition in the topological magnet HoSbTe. Physical Review B, 2022, 106, .	1.1	2
46874	On the choice of shape and size for truncated cluster-based x-ray spectral simulations of 2D materials. Journal of Chemical Physics, 2022, 157, .	1.2	3
46875	Nanotube Matrices for Flexible SnIP Nanowires. Journal of Physical Chemistry C, 2022, 126, 12603-12614.	1.5	1
46876	Quantum effects in thermal reaction rates at metal surfaces. Science, 2022, 377, 394-398.	6.0	11
46877	Na₃H(ZnH₄) Antiperovskite: A Large Octahedral Distortion with an Off-Centering Hydride Anion Coupled to Molecular Hydride. Chemistry of Materials, 2022, 34, 6815-6823.	3.2	8
46878	Interaction between solute atoms and vacancies in Al-Mg-X (Xï¼Si, Ge) alloys. Keikinzoku/Journal of Japan Institute of Light Metals, 2022, 72, 427-429.	0.1	1
46879	Inactive (PbI ₂) ₂ RbCl stabilizes perovskite films for efficient solar cells. Science, 2022, 377, 531-534.	6.0	623
46880	Hierarchical Thiospinel NiCo₂S₄/Polyaniline Hybrid Nanostructures as a Bifunctional Electrocatalyst for Highly Efficient and Durable Overall Water Splitting. Advanced Materials Interfaces, 2022, 9, .	1.9	6
46881	A computational study on the mechanical properties of Pentahexoctite single-layer: Combining DFT and classical molecular dynamics simulations. Chemical Physics, 2022, 563, 111686.	0.9	2
46882	Unveiling the interplay of deformation mechanism in wrought Mgâ€“Sc alloy with different content of manganese. Journal of Materials Research and Technology, 2022, 20, 3522-3536.	2.6	7
46883	Dynamic Evolution of Methane Oxidation on Pd-Based Catalysts: A Reactive Force Field Molecular Dynamics Study. Journal of Physical Chemistry C, 2022, 126, 14201-14210.	1.5	5
46884	Thermoelectric properties of the Janus PtSTe monolayer compared with its parent structures. Physical Review Materials, 2022, 6, .	0.9	3
46885	Nanoscale MXene Interlayer and Substrate Adhesion for Lubrication: A Density Functional Theory Study. ACS Applied Nano Materials, 2022, 5, 10516-10527.	2.4	28
46886	Modulation of Redox Chemistry of Na₂Mn₃O₇ by Selective Boron Doping Prompted by Na Vacancies. ACS Applied Materials & Interfaces, 2022, 14, 38769-38777.	4.0	7

#	Article	IF	Citations
46887	turboMagnon â€“ A code for the simulation of spin-wave spectra using the Liouville-Lanczos approach to time-dependent density-functional perturbation theory. Computer Physics Communications, 2022, 280, 108500.	3.0	8
46888	Temperature-dependent Raman spectra of KTaO3 crystal and melt along with its phonon and electronic properties. Journal of Molecular Liquids, 2022, , 120098.	2.3	1
46889	Local Epitaxial Templating Effects in Ferroelectric and Antiferroelectric ZrO₂. ACS Applied Materials & Interfaces, 2022, 14, 36771-36780.	4.0	7
46890	Bandgap engineering and modulation of thermodynamic, and optical properties of III-N monolayers XN (X = In, Ga & Al) by mutual alloying. Physica Scripta, 2022, 97, 095806.	1.2	0
46891	Physics-Guided Descriptors for Prediction of Structural Polymorphs. Journal of Physical Chemistry Letters, 2022, 13, 7342-7349.	2.1	4
46892	Amplified Local Strain Signal in Strain-Plasmonic Coupled van der Waals Heterostructures. Physical Review Applied, 2022, 18, .	1.5	1
46893	Kinetic Origins of High Selectivity of Metal Phosphides for Ethane Dehydrogenation. Industrial & Engineering Chemistry Research, 2022, 61, 12083-12091.	1.8	3
46894	Defect Engineered Ternary Spinel: An Efficient Cathode for an Aqueous Rechargeable Zinc-Ion Battery of Long-Term Cyclability. ACS Applied Materials & Interfaces, 2022, 14, 37577-37586.	4.0	12
46895	Graphene frameworks-confined synthesis of 2D-layered NiCoP for the electrochemical sensing of H2O2 at lower overpotential. Mikrochimica Acta, 2022, 189, .	2.5	5
46896	Exploiting Nanoscale Complexion in LATP Solid-State Electrolyte via Interfacial Mg2+ Doping. Nanomaterials, 2022, 12, 2912.	1.9	3
46897	Multilevel Computational Studies Reveal the Importance of Axial Ligand for Oxygen Reduction Reaction on Feâ€“Nâ€“C Materials. Journal of the American Chemical Society, 2022, 144, 16524-16534.	6.6	44
46898	Atomic-Scale Etching Mechanism of Aluminum with Fluorine-Based Plasma. Journal of Physical Chemistry C, 2022, 126, 14180-14186.	1.5	4
46899	Atomic transistors based on seamless lateral metal-semiconductor junctions with a sub-1-nm transfer length. Nature Communications, 2022, 13, .	5.8	22
46900	Pressure-stabilized structures of water-neon system under high pressure. Physical Review B, 2022, 106, .	1.1	1
46901	Comment on â€œComputational study of H$$_{2}$$S adsorption on the pristine and transitional metal-doped phosphoreneâ€. Journal of Molecular Modeling, 2022, 28, .	0.8	0
46902	Broadband BiOCl Nonlinear Saturable Absorber for Wattâ€Level Passively Qâ€Switched Yb:LuAG Single Crystal Fiber Laser. Advanced Optical Materials, 2022, 10, .	3.6	14
46903	Theoretical prediction of Curie temperature in two-dimensional ferromagnetic monolayer. Journal of Applied Physics, 2022, 132, .	1.1	8
46904	First-Principles Study of Two-Dimensional B-Doped Carbon Nanostructures for Toxic Phosgene Gas Detection. ACS Applied Nano Materials, 2022, 5, 12737-12745.	2.4	11

#	Article	IF	Citations
46905	Pressure-induced structural phase transition of vanadium: a revisit from the perspective of ensemble theory. Journal of Physics Condensed Matter, 2022, 34, 425404.	0.7	4
46906	Detection of Weyl fermions and the metal to Weyl-semimetal phase transition in <mml:math xmlns:mml="http://www.w3.org/1998/Math/MathML"><mml:msub><mml:mrow><mml:mi>WTe</mml:mi></mml:mrow><mml:mn>2</mml:mn> via broadband high resolution NMR. Physical Review Research, 2022, 4, .	1.3	0
46907	Firstâ€Principles Investigation of Phase Stability in Substoichiometric Zirconium Carbide under High Pressure. Advanced Theory and Simulations, 2022, 5, .	1.3	1
46908	Activity Trends of Methane Oxidation Catalysts under Emission Conditions. ACS Catalysis, 2022, 12, 10255-10263.	5.5	3
46909	Linear paired electrochemical valorization of glycerol enabled by the electro-Fenton process using a stable NiSe2 cathode. Nature Catalysis, 2022, 5, 716-725.	16.1	48
46910	Mechanism of improved crystallinity by defect-modification in proton-irradiated GaAsPN photovoltaics: Experimental and first-principle calculations approach. Journal of Applied Physics, 2022, 132, .	1.1	1
46911	The Role of Carbon in the Formation of Intrinsic Point Defects and Hydrogen Migration in Î±â€Al₂O₃â€Based Tritium Permeation Barriers. Physica Status Solidi (B): Basic Research, 2022, 259, .	0.7	1
46912	Hydrolysis of Acetamide on Low-Index CeO₂ Surfaces: Ceria as a Deamidation and General De-esterification Catalyst. ACS Catalysis, 2022, 12, 10222-10234.	5.5	5
46913	Structural transformations and thermal stability of RhGe synthesized under high temperature and pressure. Journal of Physics Condensed Matter, 2022, 34, 424001.	0.7	0
46914	Frustration and 120Â° Magnetic Ordering in the Layered Triangular Antiferromagnets AFe(PO₃F)₂ (A = K, (NH₄)₂Cl,) Tj ETQq1 1 0.784314 rgBT /Overlock	3.2	3
46915	Niâ€“Cuâ€“Co Grid-like Hydroxyl Oxide Ammonia Oxidation Reaction Catalyst Supported on Carbon Nanotubes. Energy & Fuels, 2022, 36, 10339-10345.	2.5	2
46917	Selective Chemical Substitution of Cu in the Structure of TiAl₃ Type InPd₃: Experimental and Theoretical Studies. European Journal of Inorganic Chemistry, 2022, 2022, .	1.0	3
46918	First-principles calculations to investigate switching from semiconducting to metallic with enhanced mechanical and optoelectronic properties of CsPbCl₃ under pressure. International Journal of Materials Research, 2022, 113, 833-846.	0.1	2
46919	Synthesis, structural, and DFT studies of Cu(II) dithiocarbamate complexes. Journal of Molecular Structure, 2023, 1271, 133988.	1.8	5
46920	Structural and electronic effects boosting Ni-doped Mo2C catalyst toward high-efficiency C O/C C bonds cleavage. Journal of Energy Chemistry, 2022, 75, 109-116.	7.1	10
46921	From highâ€pressure Î²â€V₂O₅ to Î³â€Na_xV₂O₅ (xâ€‰=â€‰0.4â€‰â^¼â€‰0.55): A structural, chemical and kinetic insight into a sodiated phase with a large interlayer space. , 2023, 2, .	0	0
46922	Coexistence of the Piezoelectricity and Intrinsic Quantum-Spin Hall Effect in GaTeS and InTeS Monolayers: Implications for Spintronic Devices. ACS Applied Nano Materials, 2022, 5, 11037-11044.	2.4	2
46923	High-surface-area corundum nanoparticles by resistive hotspot-induced phase transformation. Nature Communications, 2022, 13, .	5.8	16

#	Article	IF	Citations
46924	Single-site Co-anchored Î±- In2Se3 with enhanced and polarization-dependent hydrogen and oxygen evolution activity. Journal of Alloys and Compounds, 2022, 927, 166877.	2.8	1
46925	Firstâ€Principles Calculations of the Thermal Expansion Path of the Co₇Mo₆ Î¼â€Phase. Physica Status Solidi (B): Basic Research, 2023, 260, .	0.7	2
46926	High Pressure Rapid Synthesis of LiCrTiO₄ with Oxygen Vacancy for High Rate Lithiumâ€Ion Battery Anodes. Small, 2022, 18, .	5.2	10
46927	Thermal topological phase transition in SnTe from ab initio calculations. Physical Review B, 2022, 106, .	1.1	2
46928	Design of Cuâ€“Cr Alloys with High Strength and High Ductility Based on First-Principles Calculations. Metals, 2022, 12, 1406.	1.0	3
46929	The electronic, structural, ferroelectric and optical properties of strontium and zirconium co-doped BaTiO<mml:math xmlns:mml="http://www.w3.org/1998/Math/MathML" altimg="si54.svg" display="inline" id="d1e364"><mml:msub><mml:mrow /><mml:mrow><mml:mn>3</mml:mn></mml:mrow></mml:msub></mml:math>: First-principles calculations. Solid State Communications, 2022, 355, 114939.	0.9	9
46930	Theoretical and Experimental Research on the Preparation of Ordered Diamond Nanoarrays by the Al Mask Method. Crystal Research and Technology, 0, , 2200101.	0.6	0
46931	Substitutional Tungsten doping in Silicon Carbide introducing magnetic properties: A Computational DFT Approach. Nanoscience and Nanotechnology - Asia, 2022, 12, .	0.3	0
46932	Photoinduced Small Hole Polarons Formation and Recombination in All-Inorganic Perovskite from Quantum Dynamics Simulation. Journal of Physical Chemistry Letters, 2022, 13, 7532-7540.	2.1	8
46933	Experimental and theoretical study on the complete phase separation of ceria-zirconia solid solution into two end members, ceria and zirconia. JPhys Energy, 0, , .	2.3	0
46934	Optimization of configurations of atomic species on two-dimensional hexagonal lattices for copper-based systems. AIP Advances, 2022, 12, 085313.	0.6	0
46935	Enabling Ab Initio Material Design of <mml:math xmlns:mml="http://www.w3.org/1998/Math/MathML" display="inline" overflow="scroll"><mml:mrow><mml:mi>In</mml:mi><mml:mi>As</mml:mi></mml:mrow><mml:mo>/</mml:mo><mml:mrow><mml:mm Superlattices for Infrared Detection. Physical Review Applied, 2022, 18, .	1.5	1
46936	Static Electronic Density Response of Warm Dense Hydrogen: AbÂInitio Path Integral MonteÂCarlo Simulations. Physical Review Letters, 2022, 129, .	2.9	21
46937	Nature of interfacial Dzyaloshinskii-Moriya interactions in graphene/Co/Pt(111) multilayer heterostructures. Physical Review B, 2022, 106, .	1.1	2
46938	First-principles calculations of Schottky barrier height at barium titanate/metal interface. Japanese Journal of Applied Physics, 2022, 61, SN1029.	0.8	0
46941	Anisotropic Thermal Expansion and Electronic Structure of LiInSe2. Molecules, 2022, 27, 5078.	1.7	10
46942	Lithium decorated <scp>C₃N</scp> as high capacity reversible hydrogen storage material: Insights from density functional theory. International Journal of Quantum Chemistry, 2022, 122, .	1.0	8
46943	Demonstration of Low Work Function Perovskite SrVO₃ Using Thermionic Electron Emission. Advanced Functional Materials, 2022, 32, .	7.8	11

#	Article	IF	Citations
46944	Ionic forces and stress tensor in all-electron density functional theory calculations using an enriched finite-element basis. Physical Review B, 2022, 106, .	1.1	3
46945	Novel Ternary Nitride Thin Filmâ€Based Selfâ€Powered, Broad Spectral Responsive Photodetector with a High Detectivity for Weak Light. Advanced Materials Technologies, 2023, 8, .	3.0	3
46946	<mml:math xmlns:mml="http://www.w3.org/1998/Math/MathML"><mml:msub><mml:mi>MN</mml:mi><mml:mn>4</mml:mn></mml:msub></mm embedded graphene layers: Tunable decay rate of the RKKY interaction. Physical Review B, 2022, 106, .	1.1	2
46947	Phase transitions and compressibility of alkali-bearing double carbonates at high pressures: a first-principles calculations study. Physics and Chemistry of Minerals, 2022, 49, .	0.3	1
46948	Graphene/Nanotube Quasi-1D-Structures in Strong Electric Fields. Physics of the Solid State, 2022, 64, 185-192.	0.2	1
46949	Strain-induced collapse of Landau levels in real Weyl semimetals. Physical Review B, 2022, 106, .	1.1	1
46950	Strontium Nitridoborate Hydride Sr₂BN₂H Verified by Single-Crystal X-ray and Neutron Powder Diffraction. Inorganic Chemistry, 2022, 61, 12685-12691.	1.9	5
46951	Distribution of multiple Al substitution in HY zeolite and BrÃ¸nsted acid strength - A periodic DFT study. Microporous and Mesoporous Materials, 2022, 344, 112184.	2.2	3
46952	DFT Insight to Ag2O Modified InN as SF6-N2 Mixture Decomposition Components Detector. Applied Sciences (Switzerland), 2022, 12, 7873.	1.3	0
46953	Phase Engineering of a Ruthenium Nanostructure toward High-Performance Bifunctional Hydrogen Catalysis. ACS Nano, 2022, 16, 14885-14894.	7.3	36
46954	First-principles study on electronic and optical properties of van der Waals heterostructures stacked by g-ZnO and Janus-WSSe monolayers. Applied Surface Science, 2022, 604, 154620.	3.1	10
46955	The structural, elastic, electronic, magnetic and optical properties of SrNiO3 perovskite: A DFT and DFT+U study. Results in Physics, 2022, 41, 105920.	2.0	4
46956	Topological properties of CsCl type superconducting materials. Physics Letters, Section A: General, Atomic and Solid State Physics, 2022, , 128385.	0.9	1
46957	Transition metal atoms anchored on nitrogen-doped Î±-arsenene as efficient electrocatalysts for nitrogen electroreduction reaction. International Journal of Hydrogen Energy, 2022, 47, 29781-29793.	3.8	7
46958	Electronic Structure-Based Modeling of Dislocation Motion and Its Application to Nanoscale Mechanics. Zairyo/Journal of the Society of Materials Science, Japan, 2022, 71, 660-665.	0.1	0
46959	Sticking coefficient and Si/C ratio of silicon carbide growth spaces on reconstructed <mml:math xmlns:mml="http://www.w3.org/1998/Math/MathML" altimg="si1.svg"><mml:mrow><mml:mn>4</mml:mn><mml:mi mathvariant="bold">H</mml:mi><mml:mo linebreak="goodbreak" linebreakstyle="after">â^’</mml:mo><mml:mi mathvariant="bold">S</mml:mi><mml:mi mathvariant="bold">i</mml:mi><mml:mi mathvariant="bold">C</mml:mi></mml:mrow><mml:mo		

#	Article	IF	Citations
46962	Effective Hydrogenation Strategies to Boost Efficiency over 20% for Crystalline Silicon Solar Cell with Al₂O₃/Cu₂O Passivating Contact. Advanced Functional Materials, 2022, 32, .	7.8	8
46963	CO₂ Hydrogenation to Methanol over Inverse ZrO₂/Cu(111) Catalysts: The Fate of Methoxy under Dry and Wet Conditions. Journal of Physical Chemistry C, 2022, 126, 14479-14486.	1.5	8
46964	Mg2+ doping into Li sites to improve anionic redox reversibility and thermal stability of lithium-rich manganese-based oxides cathode. Materials Today Energy, 2022, 29, 101116.	2.5	12
46965	Electronâ€“phonon coupling of the Ti₃Sb compound. Journal of Applied Physics, 2022, 132, 075103.	1.1	2
46966	Crystal structure, electronic structure, and optical properties of the novel Li₄CdGe₂S₇, a wide-bandgap quaternary sulfide with a polar structure derived from lonsdaleite. Acta Crystallographica Section C, Structural Chemistry, 2022, 78, 470-480.	0.2	3
46967	Probing the Spin Dimensionality in Singleâ€Layer CrSBr Van Der Waals Heterostructures by Magnetoâ€Transport Measurements. Advanced Materials, 2022, 34, .	11.1	26
46968	Laser damage mechanism and threshold improvement of nonlinear optical La₃Ga_{5.5}Nb_{0.5}O₁₄ crystal for a mid-infrared high-intensity laser. Optical Materials Express, 2022, 12, 3449.	1.6	3
46969	Hole doping in a negative charge transfer insulator. Communications Physics, 2022, 5, .	2.0	3
46970	High-capacity hydrogen storage in yttrium-decorated Î¨-graphene: Acumen from density functional theory. Journal of Applied Physics, 2022, 132, .	1.1	7
46971	Anisotropic dielectric function, direction dependent bandgap energy, band order, and indirect to direct gap crossover in Î±-(Al_xGa_{1â€“x})₂O₃ (0â‰¤xâ‰¤1). Applied Physics Letters, 2022, 121, 052101.	1.5	7
46972	DFT calculations of 2D graphene like ZnS:Mn sheet for RESOLFT microscopic applications. Journal of Computational Electronics, 2022, 21, 1191-1201.	1.3	1
46973	Computational Investigation of the Stability of Di-p-Tolyl Disulfide â€œHiddenâ€•and â€œConventionalâ€• Polymorphs at High Pressures. Crystals, 2022, 12, 1157.	1.0	3
46974	A superhard orthorhombic carbon allotrope. Chinese Journal of Physics, 2022, 79, 409-419.	2.0	10
46975	Introducing BrÃ¸nsted acid sites to accelerate the bridging-oxygen-assisted deprotonation in acidic water oxidation. Nature Communications, 2022, 13, .	5.8	42
46976	Hybrid Density Functional Investigation of Cu Doping Impact on the Electronic Structures and Optical Characteristics of TiO2 for Improved Visible Light Absorption. Materials, 2022, 15, 5645.	1.3	7
46977	Theoretical investigation of charged vacancies and clusters in UXO2 (X = La, Ce, Pu, Am). Journal of Applied Physics, 2022, 132, .	1.1	1
46978	Ground-State Properties of Metallic Solids from Ab Initio Coupled-Cluster Theory. Journal of Physical Chemistry Letters, 2022, 13, 7497-7503.	2.1	11
46979	Role of exact exchange in the structural and electronic properties of the Î± and Î³ phases of cerium: a density functional theory study. New Journal of Physics, 2022, 24, 093032.	1.2	2

#	Article	IF	Citations
46980	CeO2 nanoparticles with oxygen vacancies decorated N-doped carbon nanorods: A highly efficient catalyst for nitrate electroreduction to ammonia. Nano Research, 2022, 15, 8914-8921.	5.8	41
46981	Improving Material Property Prediction by Leveraging the Large-Scale Computational Database and Deep Learning. Journal of Physical Chemistry C, 2022, 126, 16297-16305.	1.5	4
46982	The stability and properties of the PtFe2 Laves phases. Physica B: Condensed Matter, 2022, , 414268.	1.3	0
46983	Non-Dyson Algebraic Diagrammatic Construction Theory for Charged Excitations in Solids. Journal of Chemical Theory and Computation, 2022, 18, 5337-5348.	2.3	5
46984	Density Functional Theory Plus Dynamical Mean Field Theory within the Framework of Linear Combination of Numerical Atomic Orbitals: Formulation and Benchmarks. Journal of Chemical Theory and Computation, 2022, 18, 5589-5606.	2.3	2
46985	On the energetics of the cubicâ€toâ€hexagonal transformations in TiAl+Mo alloys. Acta Materialia, 2022, 240, 118268.	3.8	1
46986	Selective electronic excitations in nearly half-metallic Heusler alloy NiFeMnSnâ€”A Raman spectroscopic study. Applied Physics Letters, 2022, 121, .	1.5	2
46987	Theoretical Analysis on the Stability of 1-Pyrenebutanoic Acid Succinimidyl Ester Adsorbed on Graphene. ACS Omega, 0, , .	1.6	2
46988	First principles calculations to investigate Li-based quaternary Heusler compounds LiHfCoX (XÂ=ÂGe, Sn) for thermoelectric applications. Physica Scripta, 2022, 97, 105706.	1.2	5
46989	Structural Stabilization of Cation-Disordered Rock-Salt Cathode Materials: Coupling between a High-Ratio Inactive Ti⁴⁺ Cation and a Mn²⁺/Mn⁴⁺ Two-Electron Redox Pair. ACS Applied Materials & Interfaces, 2022, 14, 38865-38874.	4.0	7
46990	Enhancing electrochemical nitrogen fixation by mimicking Ï€ back-donation on laser-tuned Lewis acid sites in noble-metal-molybdenum carbide. Applied Catalysis B: Environmental, 2023, 320, 121777.	10.8	9
46991	Suppression of Pressure-Induced Phase Transitions in a Monoclinically Distorted LiNbO₃-Type CuNbO₃ by Preference for a CuO₃ Triangular Coordination Environment. Inorganic Chemistry, 2022, 61, 12719-12725.	1.9	0
46992	Anomalous bond softening mediated by strain-induced Friedel-like oscillations in a <mml:math xmlns:mml="http://www.w3.org/1998/Math/MathML"><mml:mrow><mml:msub><mml:mi>BC</mml:mi><mml:mn>2</mml:mn></mml:msub><mml:mi mathvariant="normal">N</mml:mi></mml:mrow></mml:math> superlattice. Physical Review B, 2022, 106, .	1.1	2
46993	Ab Initio Study of NaMFe(MoO4)3 (M = Mn, Fe, Co, Ni, Zn): Electron Structure, Sodium Diffusion and Potentials. Physics of the Solid State, 0, , .	0.2	0
46994	Mixed-Functionalized <mml:math xmlns:mml="http://www.w3.org/1998/Math/MathML" display="inline" overflow="scroll"><mml:msub><mml:mi>Sc</mml:mi><mml:mn>2</mml:mn></mml:msub><mml:mi mathvariant="normal">C</mml:mi><mml:msub><mml:mi>T</mml:mi><mml:mi>x</mml:mi></mml:msub></mml:math> (<mml:math xmlns:mml="http://www.w3.org/1998/Math/MathML" display="inline") Tj ETQq0 0 0 rgBT /Overlock 10 Tf 50 177 Td (overf	10.3	7
46995	Improving the Efficiency of Gallium Telluride for Photocatalysis, Electrocatalysis, and Chemical Sensing through Defects Engineering and Interfacing with its Native Oxide. Advanced Functional Materials, 2022, 32, .	7.8	10
46996	Multiscale Strategy for Predicting Radiation Chemistry in Polymers. Journal of Chemical Theory and Computation, 2022, 18, 5117-5124.	2.3	1
46997	Modulation of electronic and magnetic properties of MoX₂ (XÂ=ÂS and Se) monolayer via mono- and co-transition metal dopants: Spin density functional theory. Physica Scripta, 2022, 97, 095805.	1.2	1

#	Article	IF	Citations
46998	High capacity hydrogen storage on zirconium decorated Î³-graphyne: A systematic first-principles study. International Journal of Hydrogen Energy, 2023, 48, 37834-37846.	3.8	6
46999	Electronic and structural properties of crystalline and amorphous (TaNbHfTiZr)C from first principles. Journal of Physics Condensed Matter, 2022, 34, 425403.	0.7	1
47000	Understanding the Photoelectrochemical Properties of Theoretically Predicted Waterâ€Splitting Catalysts for Effective Materials Discovery. Advanced Energy Materials, 2022, 12, .	10.2	7
47001	Suppressing Polysulfides Shuttling and Promoting Sulfur Utilization via Transition Metal and Nitrogen Co-Doping on Graphdiyne Cathodes of Lithium-Sulfur Batteries: A First-Principles Modeling. ACS Applied Energy Materials, 2022, 5, 9722-9732.	2.5	3
47002	Effect of Li⁺ Addition during Initial Stage of Electrodeposition Process on Nucleation and Growth of Zn. Journal of the Electrochemical Society, 0, , .	1.3	1
47003	Insight into Atomic-Scale Adhesion at the Câ€“Cu Interface During the Initial Stage of Nanoindentation. Nanomanufacturing and Metrology, 2022, 5, 250-258.	1.5	2
47004	Structural and photocatalytic properties and X-ray absorption spectroscopic study of BiVO4 nanoparticles incorporated with Fe synthesized by sonochemical method. Radiation Physics and Chemistry, 2022, 201, 110480.	1.4	1
47005	DFT study of structural, mechanical, and opto-electronic properties of scadium-based halide double perovskite Cs2ScInBr6 for optoelectronic applications. , 2022, 170, 207370.		3
47006	Constructing synergy of sufficient hydroxyl and oxygen in <scp>PtNi</scp>/<scp>Al₂O₃</scp> enables roomâ€temperature catalytic <scp>HCHO</scp> oxidation. AIChE Journal, 2023, 69, .	1.8	1
47007	Electronic structure factors and the importance of adsorbate effects in chemisorption on surface alloys. Npj Computational Materials, 2022, 8, .	3.5	15
47008	Ab initio study of hypothetical <scp> Ti ₃ AlB ₂ </scp> and two new designed layered ordered doubleâ€transition metals <scp>MAX</scp> compound <scp> Ti ₂ ZrAlB ₂ </scp>. International Journal of Quantum Chemistry, 0, , .	1.0	1
47009	A DFT study of the adsorption of O2 and [Fe(H2O)2(OH)3] on the (001) and (112) surfaces of chalcopyrite. Journal of Molecular Modeling, 2022, 28, .	0.8	1
47010	Heteroepitaxial Growth of B₅â€Siteâ€Rich Ru Nanoparticles Guided by Hexagonal Boron Nitride for Lowâ€Temperature Ammonia Dehydrogenation. Advanced Materials, 2023, 35, .	11.1	4
47011	Kinetics of Ordering and Decomposition in Ti-Al-X (X = Si, Zr) Alloys: Monte Carlo Modeling. Materials, 2022, 15, 5722.	1.3	1
47012	Ultrafast metal oxide reduction at Pd/PdO2 interface enables one-second hydrogen gas detection under ambient conditions. Nano Research, 2023, 16, 1149-1157.	5.8	3
47013	Mechanistic Insights and Rational Design of Ca-Doped CeO₂ Catalyst for Acetic Acid Ketonization. ACS Sustainable Chemistry and Engineering, 2022, 10, 11068-11077.	3.2	3
47014	Direct Determination of Band Gap of Defects in a Wide Band Gap Semiconductor. ACS Applied Materials & Interfaces, 2022, 14, 36875-36881.	4.0	7
47015	Prediction of the ferroelastic and negative Poissonâ€™s ratio of a two-dimensional Î±-CaX (Xâ€‰=â€‰S, Se) monolayer. European Physical Journal Plus, 2022, 137, .	1.2	1

#	Article	IF	Citations
47016	Room-temperature ferromagnetism in two-dimensional <mml:math xmlns:mml="http://www.w3.org/1998/Math/MathML"><mml:msub><mml:mi>CrBr</mml:mi><mml:mn>3</mml:mn></mml:msub></mml Physical Review Materials, 2022, 6, .	0.9	1
47017	Tackling Disorder in Î³â€Ga₂O₃. Advanced Materials, 2022, 34, .	11.1	10
47018	Electrically tunable two-dimensional heterojunctions for miniaturized near-infrared spectrometers. Nature Communications, 2022, 13, .	5.8	36
47019	Liquid-Phase Effects on Adsorption Processes in Heterogeneous Catalysis. Jacs Au, 2022, 2, 2119-2134.	3.6	10
47020	Quantum confinement in chalcogenides 2D nanostructures from first principles. Journal of Physics Condensed Matter, 2022, 34, 405301.	0.7	1
47021	Structure of Zinc and Nickel Histidine Complexes in Solution Revealed by Molecular Dynamics and Raman Optical Activity. Chemistry - A European Journal, 2022, 28, .	1.7	3
47022	Effective hamiltonian of crystal field method for periodic systems containing transition metals. Molecular Physics, 0, , .	0.8	2
47023	Active Surface Structure of SnO₂ Catalysts for CO₂ Reduction Revealed by Ab Initio Simulations. Journal of Physical Chemistry C, 2022, 126, 14441-14447.	1.5	7
47024	Dimensional Transformation of Molecular Magnetic Materials. ACS Nano, 2022, 16, 13232-13240.	7.3	0
47025	Electron-Injection and Atomic-Interface Engineering toward Stabilized Defected 1T-Rich MoS₂ as High Rate Anode for Sodium Storage. ACS Nano, 2022, 16, 12425-12436.	7.3	34
47026	Conversion of n-type to p-type conductivity in ZnO by incorporation of Ag and Ag-Li. Materials Today Communications, 2022, 33, 104278.	0.9	1
47027	Theoretical Insights on the Comparison of Li-Ion Conductivity in Halide Superionic Conductors Li₃MCl₆, Li₂M_{2/3}Cl₄, and LiMCl₄ (M = Y, Sc, Al, and Sm). Journal of Physical Chemistry C, 2022, 126, 13105-13113.	1.5	10
47028	Spin resolved-Electronic, Magnetic and Thermodynamic properties of perovskites XTiO₃ (X= Rb, Cs) using GGA, TB-mBJ and GGA+U Potentials -A DFT approach. Canadian Journal of Physics, 0, , .	0.4	0
47029	Heusler alloy catalysts for electrochemical CO2 reduction. Journal of Chemical Physics, 2022, 157, .	1.2	6
47030	Evidence of lattice deformation induced metal-insulator transition in <mml:math xmlns:mml="http://www.w3.org/1998/Math/MathML"><mml:mrow><mml:msub><mml:mi>Ti</mml:mi><mml:mn>2</mml:mn></mml:m mathvariant="normal">O</mml:mi><mml:mn>3</mml:mn></mml:msub></mml:mrow></mml:math>. Physical Review B, 2022, 106, .	1.1	3
47031	Effect of ReÂand Ta on self-trapping of helium in tungsten: a first-principles calculation. Nuclear Fusion, 2022, 62, 096017.	1.6	1
47032	Changes in electronic and optical characteristics of halogenâ€“alkali adsorbed WSe2 monolayer. Journal of Materials Science: Materials in Electronics, 0, , .	1.1	0
47033	Interaction of molecular nitrogen with vanadium oxide in the absence and presence of water vapor at room temperature: Near-ambient pressure XPS. Journal of Chemical Physics, 2022, 157, .	1.2	4

#	Article	IF	Citations
47034	Boosting the stability of perovskites with exsolved nanoparticles by B-site supplement mechanism. Nature Communications, 2022, 13, .	5.8	27
47035	A comprehensive DFT analysis on structural, electronic, optical, thermoelectric, SLME properties of new Double Perovskite Oxide Pb2ScBiO6. Chemical Physics Letters, 2022, 806, 139987.	1.2	19
47036	The Piezoelectricity and Dopingâ€Induced Ferromagnetism of Janus XYP ₂ (X/Y = Si, Ge, Sn,) Tj ETQq0 0 0 rgBT /Overlock 1	0.7	0
47037	A Theoretical Study of the In Situ Structural Reconstruction of Pdn (n = 6, 19, 44) Clusters for Catalytic Hydrogen Evolution. Symmetry, 2022, 14, 1753.	1.1	0
47038	Tunable electronic and magnetic properties of thin <mml:math xmlns:mml="http://www.w3.org/1998/Math/MathML"><mml:mrow><mml:msub><mml:mi>Nb</mml:mi><mml:mn>3</mml:mn></mml: mathvariant="normal">I</mml:mi><mml:mn>8</mml:mn></mml:msub></mml:mrow></mml:math> nanofilms: Interplay between strain and thickness. Physical Review B, 2022, 106, .	1.1	9
47039	Controlled growth of 2D structured Cu2WS4 nanoflakes for high-performance all-solid-state supercapacitors. Journal of Electroanalytical Chemistry, 2022, 922, 116718.	1.9	9
47040	Surface and Trapping Energies as Predictors for the Photocatalytic Degradation of Aromatic Organic Pollutants. Journal of Physical Chemistry C, 2022, 126, 14859-14877.	1.5	6
47041	Tuning the electronic and optical properties of SrTiO3 for optoelectronic and photocatalytic applications by plasmonic-metal doping: a DFT-computation. Optical and Quantum Electronics, 2022, 54, .	1.5	4
47042	The effect of functional groups (O, F, or OH) on reversible hydrogen storage properties of Ti2X (X=C) Tj ETQq0 0 0 rgBT /Overlock 10 Tf	3.8	7
47043	Pressure effects on structural, electronic and anisotopic elastic properties of Si doped RuGe compound with different concentrations by first-principles calculations. Materials Chemistry and Physics, 2022, , 126695.	2.0	3
47044	Ab initio inspection of thermophysical experiments for zirconium near melting. Journal of Applied Physics, 2022, 132, .	1.1	6
47045	Ab initio study of shock-compressed copper. Physical Review B, 2022, 106, .	1.1	9
47046	Mechanical and thermodynamic properties of layered ThB₂C. International Journal of Modern Physics C, 0, , .	0.8	0
47047	Synergistic Lubrication Effect between Oxidized Black Phosphorus and Oil Molecules Triggers Superlubricity. Journal of Physical Chemistry Letters, 0, , 8245-8253.	2.1	4
47048	Modeling of Structure H Carbon Dioxide Clathrate Hydrates: Guestâ€“Lattice Energies, Crystal Structure, and Pressure Dependencies. Journal of Physical Chemistry C, 2022, 126, 14832-14842.	1.5	4
47049	Hydrogen Activation by C ₂ H ₂ Acting as a Substrate Molecule on Atomically Dispersed Catalysts for the Semiâ€hydrogenation of C ₂ H ₂. ChemistrySelect, 2022, 7, .	0.7	0
47050	First-Principles Calculations of the Structural, Electronic, Optical, and Mechanical Properties of 21 Pyrophosphate Crystals. Crystals, 2022, 12, 1139.	1.0	3
47051	Identification of a Unique Pyridinic FeN₄C_x Electrocatalyst for N₂ Reduction: Tailoring the Coordination and Carbon Topologies. Journal of Physical Chemistry C, 2022, 126, 14460-14469.	1.5	1

#	Article	IF	Citations
47052	Structural, electronic, and magnetic properties of <mml:math xmlns:mml="http://www.w3.org/1998/Math/MathML"><mml:msub><mml:mi>CrTe</mml:mi><mml:mn>2</mml:mn></mml:msub></mml:math> Physical Review Materials, 2022, 6, .	0.9	4
47053	Effect of O-Vacancy Concentration and Proximity on Electronic Metalâ€“Support Interactions: Ru/ZrO₂ Catalysts. ACS Catalysis, 2022, 12, 10065-10079.	5.5	5
47054	Biphenylene: A Twoâ^'Dimensional Grapheneâ^'Based Coating with Superior Antiâ^'Corrosion Performance. Materials, 2022, 15, 5675.	1.3	4
47055	Interactions of Water with Pristine and Defective MoS₂. Langmuir, 2022, 38, 10419-10429.	1.6	4
47056	Revealing the role of Î£3{112} Si grain boundary local structures in impurity segregation. Journal of Applied Physics, 2022, 132, 085102.	1.1	0
47057	Experimental and Theoretical Validation of Room Temperature Intrinsic Ferromagnetism in Cr ₃ C ₂ Due to Interstitial Carbon Atoms. Physica Status Solidi - Rapid Research Letters, 0, , 2200192.	1.2	0
47058	Single transition metal atom stabilized on double metal carbide MXenes for hydrogen evolution reaction: a density functional theory study. Journal Physics D: Applied Physics, 0, , .	1.3	2
47059	Siliceneâ€™s pervasive surface alloy on Ag(111): a scaffold for two-dimensional growth. 2D Materials, 2022, 9, 045021.	2.0	6
47060	Buckling variation effects on optical and electronic properties of GeP2S nanostructure: a first-principles calculation. Optical and Quantum Electronics, 2022, 54, .	1.5	1
47061	Entropy and heterogeneous interface engineering promote the low thermal conductivity in SnTe-based thermoelectric materials. Applied Physics A: Materials Science and Processing, 2022, 128, .	1.1	2
47062	First-principles investigation of effects of defects on the physical properties of 3C-SiC under high temperatures and pressures. Journal of Materials Research and Technology, 2022, 20, 3633-3645.	2.6	3
47063	New insights into the interaction between monomers from acrylamide-based polymeric flocculants and montmorillonite: A DFT study. Journal of Molecular Liquids, 2022, 365, 120171.	2.3	6
47064	Effect of oxidation on mechanical properties of Ni/Cu interface: A density functional theory study. Materials Today Communications, 2022, 33, 104307.	0.9	3
47065	Heterostructure nanoarchitectonics with ZnO/SnO2 for ultrafast and selective detection of CO gas at low ppm levels. Ceramics International, 2022, 48, 36556-36569.	2.3	6
47066	Effects of charging, strain, and doping on the interaction between H2 and nitrogen-rich Penta-CN2 sheet. International Journal of Hydrogen Energy, 2022, 47, 34183-34194.	3.8	5
47067	Broad Elastic Softening of (Mg,Fe)O Ferropericlase Across the Iron Spin Crossover and a Mixedâ€Spin Lower Mantle. Journal of Geophysical Research: Solid Earth, 2022, 127, .	1.4	3
47068	Band-gap engineering of rutile-structured <mml:math xmlns:mml="http://www.w3.org/1998/Math/MathML"><mml:mrow><mml:msub><mml:mi>SnO</mml:mi><mml:mn>2</mml:mn></mml:msub></mml:mrow></mml:math> alloy system. Physical Review Materials, 2022, 6, .	0.9	3
47069	Efficient Control of the Shuttle Effect in Sodiumâ€“Sulfur Batteries with Functionalized Nanoporous Graphenes. ACS Applied Nano Materials, 0, , .	2.4	5

#	Article	IF	Citations
47070	Noble-Nanoparticle-Decorated Ti₃C₂T_x MXenes for Highly Sensitive Volatile Organic Compound Detection. ACS Omega, 2022, 7, 29195-29203.	1.6	13
47071	Boosting Electrochemical CO₂ Reduction to Methane via Tuning Oxygen Vacancy Concentration and Surface Termination on a Copper/Ceria Catalyst. ACS Catalysis, 2022, 12, 10973-10983.	5.5	34
47072	Dynamical Study of Adsorbate-Induced Restructuring Kinetics in Bimetallic Catalysts Using the PdAu(111) Model System. Journal of the American Chemical Society, 2022, 144, 15132-15142.	6.6	13
47073	Stress-driven structural and bond reconstruction in 2D ferromagnetic semiconductor VSe₂. Nanotechnology, 2022, 33, 455706.	1.3	3
47074	Phase Transformations and Phase Segregation during Potassiation of Sn_xP_y Anodes. Chemistry of Materials, 2022, 34, 7460-7467.	3.2	4
47075	Self-Assembled Decanethiolate Monolayers on Au(001): Expanding the Family of Known Phases. Langmuir, 2022, 38, 10202-10215.	1.6	1
47076	Revealing Phosphorus Nitrides up to the Megabar Regime: Synthesis of Î±â€²â€²P₃N_{5,} Î´â€²P₃N₅ and PN₂. Chemistry - A European Journal, 2022, 28, .	1.7	6
47077	Superconcentrated Electrolytes for Aqueous Batteries Based on Alkali Metal Formates and Propionates. Journal of Physical Chemistry C, 0, , .	1.5	0
47078	Trinuclear Magnesium Imidazolate Borohydride Complex. Inorganic Chemistry, 2022, 61, 12708-12718.	1.9	0
47079	Modeling stepped Pt/water interfaces at potential of zero charge with ab initio molecular dynamics. Journal of Chemical Physics, 2022, 157, .	1.2	5
47080	Ab initio study of Li-Mg-B superconductors. Physical Review Materials, 2022, 6, .	0.9	6
47081	Functional Pyromellitic Diimide as a Corrosion Inhibitor for Galvanized Steel: An Atomic-Scale Engineering. ACS Omega, 2022, 7, 27116-27125.	1.6	1
47082	Bromo- and iodo-bridged building units in metal-organic frameworks for enhanced carrier transport and CO2 photoreduction by water vapor. Nature Communications, 2022, 13, .	5.8	42
47083	Hydrothermally decorated robust bimetallic sulfides with heterojunction interfaces for efficient hydrogen generation. International Journal of Hydrogen Energy, 2022, 47, 40254-40263.	3.8	3
47084	First-principles study of the structural, electronic and optical properties of two-dimensional PC6X and PX6 (X=N, As). Vacuum, 2022, 205, 111429.	1.6	5
47085	Temperature- and Field-Induced Transformation of the Magnetic State in Co_{2.5}Ge_{0.5}BO₅. Inorganic Chemistry, 2022, 61, 13034-13046.	1.9	0
47086	Vanadium Carbide (V4C3) MXene as an Efficient Anode for Li-Ion and Na-Ion Batteries. Nanomaterials, 2022, 12, 2825.	1.9	27
47087	Suppressing Charged Cation Antisites via Se Vapor Annealing Enables pâ€Type Dopability in AgBiSe₂â€“SnSe Thermoelectrics. Advanced Materials, 2022, 34, .	11.1	7

#	Article	IF	Citations
47088	Phase transitions and suppression of magnetoresistance in WTe_{2-x}Se_x system. Journal of Physics Condensed Matter, 0, , .	0.7	0
47089	Using neural network potentials to study defect formation and phonon properties of nitrogen vacancies with multiple charge states in GaN. Physical Review B, 2022, 106, .	1.1	2
47090	Interfacial charge transfer and Schottky barriers at c-Si/a-In heterojunctions. Journal of Physics Communications, 2022, 6, 085010.	0.5	0
47091	Large nonsaturating magnetoresistance, weak anti-localization, and non-trivial topological states in <mml:math xmlns:mml="http://www.w3.org/1998/Math/MathML"><mml:mrow><mml:msub><mml:mi>SrAl</mml:mi><mml:mn>2</mml:mn></m Physical Review B, 2022, 106, .	1.1	0
47092	Prediction of phonon-mediated superconductivity in new Ti-based M$$_2$$AX phases. Scientific Reports, 2022, 12, .	1.6	9
47093	Yttrium doped covalent triazine frameworks as promising reversible hydrogen storage material: DFT investigations. International Journal of Hydrogen Energy, 2022, 47, 30567-30579.	3.8	17
47094	High curie temperature, large magnetocrystalline anisotropy energy and piezoelectricity in 2D tetrahedral VXCl (X = Te, Se, S) & VMSe₂ (M = Al, Ga, In). Semiconductor Science and Technology, 2022, 37, 095028.	1.0	2
47095	Ab initio investigation of the magnetic and ferroelectric properties of <mml:math xmlns:mml="http://www.w3.org/1998/Math/MathML"><mml:msub><mml:mi>BaCuF</mml:mi><mml:mn>4</mml:mn></mml:msub><m under hydrostatic pressure. Physical Review B, 2022, 106, .	1.1	0
47096	Magnetic and Electronic Properties of <mml:math xmlns:mml="http://www.w3.org/1998/Math/MathML" display="inline" overflow="scroll"><mml:mrow><mml:mi>Al</mml:mi><mml:mi mathvariant="normal">N</mml:mi></mml:mrow><mml:mo>/</mml:mo><mml:msub><mml:mi>VSe</mml:mi><mml:mn>2</mml:mn></ van der Waals Heterostructures from Combined First-Principles and SchrÃ¶dinger-Poisson Simulations. Physical Review Applied, 2022, 18, .	1.5	5
47097	Topological alloy engineering and locally linearized gap dependence on concentration. Physical Review B, 2022, 106, .	1.1	2
47098	First-principles study on persistent luminescence mechanism of LiYGeO4:Eu3+. Journal of Rare Earths, 2023, 41, 1519-1524.	2.5	5
47099	Accurate and Efficient Calculation of the Solution Enthalpy and Diffusivity of Solutes in Liquid Metals Using Machine Learning Potential. Journal of Chemical Theory and Computation, 2022, 18, 5568-5576.	2.3	2
47100	Critical Evaluation and Thermodynamic Modeling of the Li-Se and Na-Se Binary Systems Using Combined CALPHAD and First-Principles Calculations Method. Metals, 2022, 12, 1349.	1.0	1
47101	Evidence for Topological Features in the Electronic and Phononic Bands of ZGeSb (Z = Hf, Zr, Ti) Class of Compounds. Journal of Physics Condensed Matter, 0, , .	0.7	0
47102	Understanding the Effect of Ni-Substitution on the Oxygen Evolution Reaction of (100) IrO₂ Surfaces. ACS Catalysis, 2022, 12, 10961-10972.	5.5	3
47103	DFT insights into the electronic structure, mechanical behaviour, lattice dynamics and defect processes in the first Sc-based MAX phase Sc2SnC. Scientific Reports, 2022, 12, .	1.6	14
47104	Intrinsic magnetic properties of the RFe11Ti (R = Y and Gd) alloys by Co, Zr and C doping. Solid State Communications, 2022, 355, 114922.	0.9	3
47105	Phase Stability and Electronic Properties of Hybrid Organicâ€“Inorganic Perovskite Solid Solution (CH(NH₂)₂)_x(CH₃NH₃)_{1â€“x}Pb(Br<sub as a Function of Composition. Journal of Physical Chemistry C, 2022, 126, 13640-13648.	1.5	4

#	Article	IF	Citations
47106	Charge Transfer in Metallocene Intercalated Transition Metal Dichalcogenides. Journal of Physical Chemistry C, 2022, 126, 13994-14002.	1.5	4
47107	Deep Insights into Complicated Superdislocation Dissociation and Core Properties of Dislocation in L1 ₂ â€Al ₃ RE Compounds: A Comprehensive Firstâ€Principles Study. Physica Status Solidi (B): Basic Research, 0, , 2200211.	0.7	0
47108	Theoretical study of the interaction of lactose with collagen, the electronic and mechanical properties of crystalline lactose. Materialia, 2022, 25, 101537.	1.3	1
47109	Pressure-induced phase transitions and mechanical properties of ternary nanolaminated carbide Mo2Ga2C from first-principles calculations. Journal of Materials Research and Technology, 2022, 20, 1699-1707.	2.6	0
47110	First-principles study on the electronic structure transition of Î²-UH3 under high pressure. Matter and Radiation at Extremes, 2022, 7, .	1.5	4
47111	Computational screening of TMN4 based graphene-like BC6N for CO2 electroreduction to C1 hydrocarbon products. Molecular Catalysis, 2022, 530, 112571.	1.0	2
47112	Interstitial hydrogen atoms in W-nitride compounds promoting the formation of atomic vacancies in nuclear fusion reactors. Nuclear Materials and Energy, 2022, 32, 101229.	0.6	3
47113	Surface functionalization effect on physical properties and quantum capacitance of Ca2C MXenes. FlatChem, 2022, 35, 100414.	2.8	9
47114	Revealing the effects of Nb micro-alloying on microstructure and mechanical properties of FeCrAl thin films: Experimental and computational investigations. Surface and Coatings Technology, 2022, 446, 128774.	2.2	4
47115	First Principle Study of Spin Tunneling Current Under Field Effect in Magnetic Tunnel Junction for Possible Application in STT-RAM. IEEE Transactions on Electron Devices, 2022, 69, 4894-4899.	1.6	3
47116	Combined density functional theory calculation and non-equilibrium Green's function approach to predict the sensitivity of nitrogen-containing gases over PtTenS2-n monolayers (nÂ=Â0â€“2). FlatChem, 2022, 35, 100418.	2.8	5
47117	First-principles investigation on narrow bandgap InSb1â^'Bi dilute bismide alloys for highly efficient long-wavelength infrared optoelectronics. Infrared Physics and Technology, 2022, 125, 104319.	1.3	4
47118	Modeling Ni redistribution in the hydrogen electrode of solid oxide cells through Ni(OH)2 diffusion and Ni-YSZ wettability change. Journal of Power Sources, 2022, 545, 231924.	4.0	4
47119	Insights into strain dependent lattice thermal conductivity of tin oxide. Acta Materialia, 2022, 239, 118289.	3.8	1
47120	First-principles studies on electronic and optical properties of formate-doped organic-inorganic perovskites MAPbI3. Solar Energy Materials and Solar Cells, 2022, 246, 111941.	3.0	5
47121	Critical issues on coherent interface energy calculations revisited: The case of Al/TiB<mml:math xmlns:mml="http://www.w3.org/1998/Math/MathML" altimg="si5.svg" display="inline" id="d1e6011"><mml:msub><mml:mrow /><mml:mrow><mml:mn>2</mml:mn></mml:mrow></mml:msub></mml:math>. Surfaces and Interfaces, 2022, 33, 102272.	1.5	0
47122	Band gap engineering of the top layer of mica by organized defect formation. Surfaces and Interfaces, 2022, 33, 102283.	1.5	3
47123	Pressure-driven ferroelectric phase transition for the Pnma-CsPbBr3: Mechanical and dynamical stability study. Journal of Solid State Chemistry, 2022, 314, 123402.	1.4	1

#	Article	IF	Citations
47124	The structural, elastic, electronic, and optical properties of Janus Zr2COT (T = S, Se, and Te) MXenes. Solid State Communications, 2022, 354, 114893.	0.9	5
47125	Semi-hydrogenated SiB: A promising anode material for lithium-ion and sodium-ion batteries. Acta Materialia, 2022, 239, 118292.	3.8	2
47126	Capacitance of edge-free three-dimensional graphene: New perspectives on the design of carbon structures for supercapacitor applications. Electrochimica Acta, 2022, 429, 141009.	2.6	6
47127	Modified embedded-atom method interatomic potentials for Al-Ti, Al-Ta, Al-Zr, Al-Nb and Al-Hf binary intermetallic systems. Computational Materials Science, 2022, 213, 111685.	1.4	8
47128	ZW-21: A novel two-dimensional graphene-based anode material for the lithium-ion battery. Diamond and Related Materials, 2022, 128, 109298.	1.8	4
47129	Graphdiyne supported single-atom cobalt catalyst for oxygen reduction reaction: The role of the co-adsorbates. Chemical Physics Letters, 2022, 804, 139805.	1.2	2
47130	Adsorption behavior of molecules on Zn2SnO4(1 1 1) crystal plane and its effect on electrical conductivity. Inorganic Chemistry Communication, 2022, 144, 109770.	1.8	3
47131	Interactions between irradiation defects and nitrogen in <mml:math xmlns:mml="http://www.w3.org/1998/Math/MathML" altimg="si72.svg"><mml:mi>Î±</mml:mi></mml:math>â€Fe: an integrated experimental and theoretical study. Acta Materialia, 2022, 239, 118227.	3.8	3
47132	Tunning magnetism and anisotropy by ferroelectric polarization in 2D van der Waals multiferroic heterostructures. Materials Today Physics, 2022, 27, 100803.	2.9	6
47133	Ion implanted substitutionally dispersed Au in TiO2 nanostructures for efficient and stable dye sensitized solar cells. Optical Materials, 2022, 132, 112800.	1.7	8
47134	Interaction of CO2 with TiO2/reduced graphene oxide as superior catalysts: Dispersion-corrected density functional theory simulation. Diamond and Related Materials, 2022, 128, 109279.	1.8	1
47135	Local Phase Transformation Strengthening at Microtwin Boundaries in Nickel-Based Superalloys. Acta Materialia, 2022, 238, 118206.	3.8	10
47136	N-based single and double transition metal V2N/CrVN monolayers as high capacity anode materials for Li-ion batteries. Materials Chemistry and Physics, 2022, 290, 126531.	2.0	4
47137	Thermodynamic, mechanical, and electronic properties of ettringite and AFm phases from first-principles calculations. Construction and Building Materials, 2022, 350, 128777.	3.2	8
47138	Improved photoresponse of graphitic carbon nitride films via pressure engineering. Carbon, 2022, 199, 453-461.	5.4	5
47139	Flexible quasi-solid-state supercapacitors based on Ti3C2-Polypyrrole nanocomposites. Electrochimica Acta, 2022, 429, 141051.	2.6	10
47140	DFT study of the structural, electronic, and optical properties of bulk, monolayer, and bilayer Sn-monochalcogenides. Applied Surface Science Advances, 2022, 11, 100275.	2.9	5
47141	Numerical investigation on optical properties of SnO2 by co-doping with Al and N. Solid State Communications, 2022, 354, 114921.	0.9	1

#	Article	IF	Citations
47142	N-doped graphene nanoribbons intertwined on 3D graphene skeleton as superior metal-free electrocatalyst for oxygen reduction. Colloids and Surfaces A: Physicochemical and Engineering Aspects, 2022, 652, 129832.	2.3	4
47143	Shell DFT-1/2 method towards engineering accuracy for semiconductors: GGA versus LDA. Computational Materials Science, 2022, 213, 111669.	1.4	5
47144	Molecular insights into the effects of N-doping on synthesis of vinyl acetate over carbon-supported zinc acetate. Catalysis Communications, 2022, 170, 106490.	1.6	1
47145	Superconductivity in clathrate LiLaB8 with nontrivial band topology. Materials Today Physics, 2022, 27, 100817.	2.9	1
47146	CO2-ZrO2 interaction in CDRM: A combined experimental and theoretical study. Surface Science, 2022, 725, 122164.	0.8	2
47147	Charge-dependent deposition/dissolution of Cu on different faces in a non-corrosive electrolyte: An insight from multiscale calculations. Surface Science, 2022, 725, 122160.	0.8	1
47148	Janus penta-PdSeTe: A two-dimensional candidate with high thermoelectric performance. Journal of Alloys and Compounds, 2022, 924, 166581.	2.8	9
47149	Thermoelectric properties of A2BCl6: A first principles study. Journal of Physics and Chemistry of Solids, 2022, 170, 110940.	1.9	27
47150	Lattice dynamics and spinâ€“phonon coupling in the noncollinear antiferromagnetic antiperovskite Mn<mml:math xmlns:mml="http://www.w3.org/1998/Math/MathML" altimg="si49.svg" display="inline" id="d1e1524"><mml:msub><mml:mrow /><mml:mrow><mml:mn>3</mml:mn></mml:mrow></mml:msub></mml:math>NiN. Journal of Magnetism and Magnetic Materials, 2022, 562, 169813.	1.0	8
47151	Anomalous transverse thermoelectric in antiferromagnetic compounds Co<mml:math xmlns:mml="http://www.w3.org/1998/Math/MathML" altimg="si84.svg" display="inline" id="d1e1114"><mml:msub><mml:mrow /><mml:mrow><mml:mn>2</mml:mn></mml:mrow></mml:msub></mml:math>TaX (X = Al, Ga). Journal of Magnetism and Magnetic Materials, 2022, 562, 169766.	1.0	1
47152	First-principles study on the electronic properties of layered Ga2O3/TeO2 heterolayers for high-performance electronic devices. Applied Surface Science, 2022, 602, 154382.	3.1	4
47153	A comprehensive DFT study of CO2 methanation on the Ru-doped Ni(111) surface. Colloids and Surfaces A: Physicochemical and Engineering Aspects, 2022, 652, 129858.	2.3	7
47154	Crystal and magnetic structures of the Ir(V) JeffIr = 0 double perovskite LaSrNiIrO6. Journal of Solid State Chemistry, 2022, 315, 123477.	1.4	1
47155	Thermoelectric properties of monolayer MoSi2N4 and MoGe2N4 with large Seebeck coefficient and high carrier mobility: A first principles study. Journal of Solid State Chemistry, 2022, 315, 123447.	1.4	13
47156	Effect of Eu3+ on the Structural, Magnetic and MÃ¶ssbauer Spectroscopy Studies of Copper Ferrite. Journal of Magnetism and Magnetic Materials, 2022, 562, 169789.	1.0	11
47157	Vacancy-based diffusion mechanisms in B2-FeAl: DFT study. Computational Materials Science, 2022, 214, 111712.	1.4	2
47158	Interfacial electronic structure modulation of CoP nanowires with FeP nanosheets for enhanced hydrogen evolution under alkaline water/seawater electrolytes. Applied Catalysis B: Environmental, 2022, 317, 121799.	10.8	40
47159	Effect of 3.7Âat% F doping on the atomic structure and reducibility of CeO2(111) surface: A first principles calculation. Current Applied Physics, 2022, 43, 9-14.	1.1	3

#	Article	IF	Citations
47160	Mechanism elaboration on the thermal decomposition of ether electrolyte in sodium-ion battery. Energy Storage Materials, 2022, 52, 238-249.	9.5	2
47161	Dimethyl fumarate molecule, crystal, and plane: Optical absorption measurement and structural/optoelectronic properties by density functional theory calculations. Journal of Physics and Chemistry of Solids, 2022, 170, 110958.	1.9	0
47162	Surface functionalization of two-dimensional boridene family: Enhanced stability, tunable electronic property, and high catalytic activity. Applied Surface Science, 2022, 602, 154374.	3.1	3
47163	Electronic structure and magnetic properties of bulk and (001) surfaces of <mml:math xmlns:mml="http://www.w3.org/1998/Math/MathML" altimg="si52.svg" display="inline" id="d1e889"><mml:msup><mml:mrow><mml:mi>Î³</mml:mi></mml:mrow><mml:mrow><mml:mo>â€²</mml:mo></mml:mrow></mml:msup></mml:math> from first principles. Journal of Magnetism and Magnetic Materials, 2022, 562, 169741.	1.9	3
47164	Guidelines for the synthesis of molybdenum nitride: Understanding the mechanism and the control of crystallographic phase and nitrogen content. Journal of Alloys and Compounds, 2022, 924, 166576.	2.8	3
47165	Investigations on ion irradiation induced modifications in Th 5f occupancy in thoria. Journal of Nuclear Materials, 2022, 570, 153961.	1.3	1
47166	Vacancy defect assisted enhanced nitrogen fixation in boron nitride nanomaterials. Applied Surface Science, 2022, 602, 154406.	3.1	3
47167	Investigation on luminescence behavior of Mg4Ta2O9 through experimental and first-principles calculation methods. Journal of Luminescence, 2022, 251, 119221.	1.5	0
47168	Pyridazine doped g-C3N4 with nitrogen defects and spongy structure for efficient tetracycline photodegradation and photocatalytic H2 evolution. Chemosphere, 2022, 307, 136087.	4.2	14
47169	First-principles and machine-learning study of electronic and phonon transport in carbon-based AA-stacked bilayer biphenylene nanosheets. Journal of Physics and Chemistry of Solids, 2022, 170, 110909.	1.9	7
47170	Improved the stability and enhanced luminescence of Er doped CsPbBr3 perovskite. Materials Science in Semiconductor Processing, 2022, 151, 107021.	1.9	5
47171	Bayesian calibration of interatomic potentials for binary alloys. Computational Materials Science, 2022, 214, 111660.	1.4	2
47172	Dion-Jacobson phase lead-free halide (PDA)MX4 (M=Sn/Ge; X=I/Br/Cl) perovskites: A first-principles theory. Journal of Solid State Chemistry, 2022, 315, 123449.	1.4	2
47173	Evolution of ferromagnetic stability with magnetic impurity and vacancies in Cr-doped CaZn2As2 system. Materials Science and Engineering B: Solid-State Materials for Advanced Technology, 2022, 285, 115955.	1.7	0
47174	Effect of alloying elements on the interface of fcc-Fe/Ni3Al by first principle calculations. Computational Materials Science, 2022, 214, 111673.	1.4	6
47175	Synergistic effects of oxygen vacancies and heterostructures for visible-light-driven photoreduction of uranium. Separation and Purification Technology, 2022, 301, 121966.	3.9	10
47176	High temperature non-harmonic evaluation and bonding in CaO. Physica B: Condensed Matter, 2022, 645, 414250.	1.3	2
47177	High-throughput screening of protective layers to stabilize the electrolyte-anode interface in solid-state Li-metal batteries. Nano Energy, 2022, 102, 107640.	8.2	12

#	Article	IF	Citations
47178	MEAM interatomic potential for thermodynamic and mechanical properties of lithium allotropes. Computational Materials Science, 2022, 214, 111706.	1.4	3
47179	The effect of Ru-Ru coordination numbers on CO2 methanation over Ru supported catalyst. Applied Surface Science, 2022, 603, 154398.	3.1	6
47180	Measurements of high phase transition temperatures and construction of Ni-Si-Zr phase diagram. Journal of Alloys and Compounds, 2022, 926, 166838.	2.8	3
47181	Stacking surface derived catalytic capability and by-product prevention for high efficient two dimensional Bi2Te3 cathode catalyst in Li-oxygen batteries. Applied Catalysis B: Environmental, 2022, 318, 121844.	10.8	11
47182	Transition metal decorated ZnO monolayer for CO and NO sensing: A DFTÂ+ÂU study with vdW correction. Applied Surface Science, 2022, 604, 154570.	3.1	6
47183	Tuning the selective sensing properties of transition metal dichalcogenides (MoX2: X= Se, Te) toward sulfurrich gases. Materials Today Chemistry, 2022, 26, 101069.	1.7	7
47184	An ab-initio investigation of novel double halide perovskite Cs2InCoX6(X=F, Cl, Br) materials with direct band structure and broadband light absorption. Materials Science in Semiconductor Processing, 2022, 152, 107047.	1.9	6
47185	A type-II GaN/InS van der Waals heterostructure with high solar-to-hydrogen efficiency of photocatalyst for water splitting. Applied Surface Science, 2022, 604, 154602.	3.1	23
47186	Computational screening on two-dimensional metal-embedded poly-phthalocyanine as cathode catalysts in lithium-nitrogen batteries. Applied Surface Science, 2022, 604, 154507.	3.1	9
47187	Theoretical study on the stability mechanism of a high energy system composed of molecules containing C O C or â€“N3 groups and aluminum hydride. Applied Surface Science, 2022, 604, 154509.	3.1	1
47188	Ab initio study of the effects of Cr on helium behaviors in Feâ€“YCr (Y = 9.38, 12.50Âat%) austenitic binary alloys. Materials Today Communications, 2022, 33, 104207.	0.9	0
47189	Amine functionalization derived lattice engineered and electron deficient palladium catalyst for selective production of hydrogen peroxide. Applied Surface Science, 2022, 604, 154464.	3.1	2
47190	The extended Ising model Hamiltonian for order-disorder phase transition on the clean Si (001) surface. Surface Science, 2022, 726, 122163.	0.8	0
47191	First-principles study of Co21W18 with pressure effect: The structural, mechanical, electronic properties and Debye temperature. Materials Today Communications, 2022, 33, 104276.	0.9	2
47192	Structural, optoelectronic and thermoelectric properties of Cs-based fluoroperovskites CsMF3 (M=) Tj ETQq0 0 0 rgBT /Overlock 10 Tf 5	1.9	36
47193	Quasi-Planar tetracoordiante carbon Networks with tunable electronic properties combined with Ultra-High carrier mobility and optical absorption Coefficient: Two-dimensional Be2C. Applied Surface Science, 2022, 604, 154644.	3.1	5
47194	Tuning electronic behaviors of WS2 by molecular doping. Materials Today Communications, 2022, 33, 104226.	0.9	2
47195	Synchrotron EXAFS spectroscopy and density functional theory studies of Pd/MoS2 Schottky-type nano/hetero-junctions. Applied Surface Science, 2022, 604, 154557.	3.1	2

#	Article	IF	Citations
47196	Surface transformation thermodynamics of alkaline earth carbonates using first-principles calculations. Surface Science, 2022, 726, 122165.	0.8	5
47197	Experimental and theoretical studies on the adsorption performance of lead by thermal pre-activation and phosphate modified kaolin sorbent. Chemical Engineering Journal, 2023, 451, 138762.	6.6	16
47198	Boosting elementary steps kinetics towards energetic alkaline hydrogen evolution via dual sites on phase-separated Niâ€“Cuâ€“Mn/hydroxide. Chemical Engineering Journal, 2023, 451, 138540.	6.6	11
47199	Local chemical inhomogeneities in TiZrNb-based refractory high-entropy alloys. Journal of Materials Science and Technology, 2023, 135, 221-230.	5.6	22
47201	Gold Decorated Hydroxyapatiteâ€“CeO₂ Enabled Surface Frustrated Lewis Pairs for CO Oxidation. Advanced Energy and Sustainability Research, 2022, 3, .	2.8	3
47202	Investigation of the structural properties and the magneto-electronic performances in new Ba1â^'xCrxS materials. Optical and Quantum Electronics, 2022, 54, .	1.5	2
47203	Tailored Ordered Structures with Functional Units of Distorted [NbO₆] and Antiparallel [GeO₄] for Enhanced Birefringence in Germanate Crystal. Advanced Optical Materials, 2022, 10, .	3.6	7
47204	Pt2MnGa (001) surface stability and its effect on the magnetic and electronic properties: A DFT study. Materials Today Communications, 2022, 33, 104467.	0.9	3
47205	Modeling Hydrogen and Oxygen Evolution Reactions on Single Atom Catalysts with Density Functional Theory: Role of the Functional. Advanced Theory and Simulations, 2023, 6, .	1.3	20
47206	Surface Film Formation from Sodium Polysulfide Decomposition on Sodium-Metal Anode Surface. Journal of Physical Chemistry C, 2022, 126, 16615-16626.	1.5	5
47207	Cobalt-Molybdenum Oxides for Effective Coupling of Ethane Activation and Carbon Dioxide Reduction Catalysis. ACS Catalysis, 2022, 12, 12227-12245.	5.5	4
47208	Two-Dimensional Ionic Crystals: The Cases of IA-VII Alkali Halides and IA-IB CsAu. Journal of the Physical Society of Japan, 2022, 91, .	0.7	2
47209	Computational Investigation of a NASICON-Type Solid Electrolyte Material LiGe2(PO4)3. Sustainable Chemistry, 2022, 3, 404-414.	2.2	1
47210	DFT-1/2 method applied to 3D topological insulators. Journal of Physics Condensed Matter, 2022, 34, 465501.	0.7	2
47211	Freestanding and Flexible Interfacial Layer Enables Bottom-Up Zn Deposition Toward Dendrite-Free Aqueous Zn-Ion Batteries. Nano-Micro Letters, 2022, 14, .	14.4	32
47212	Superoxo and Peroxo Complexes on Single-Atom Catalysts: Impact on the Oxygen Evolution Reaction. ACS Catalysis, 2022, 12, 11682-11691.	5.5	33
47213	The effect of the electric field intensity on the hydrogen storage of B/N-co-doped graphdiyne nanosheet. International Journal of Hydrogen Energy, 2022, 47, 36886-36897.	3.8	8
47214	Fabrication of Lithium Indolide and Derivates for Ion Conduction. ACS Applied Materials & Interfaces, 2022, 14, 41095-41102.	4.0	3

#	Article	IF	Citations
47215	Effects of Gas Impurities on the Surface Interactions between Hydrogen and Gadolinium Oxides: DFT Calculations and Experimental Study. Journal of Physical Chemistry C, 2022, 126, 16140-16147.	1.5	0
47216	First principles calculations to investigate electronic, magnetic anisotropy energy and optical properties of MnCrP half-Heusler alloy. Journal of Materials Research and Technology, 2022, 20, 4220-4230.	2.6	11
47217	Interactions of xanthates of increasing chain length with pyrite surfaces: A DFT-D and microcalorimetry study. Applied Surface Science, 2023, 607, 154910.	3.1	11
47218	Effects of high-order anharmonicity on anomalous lattice dynamics and thermal transport in fully filled skutterudite <mml:math xmlns:mml="http://www.w3.org/1998/Math/MathML"><mml:mrow><mml:msub><mml:mi>YbFe</mml:mi><mml:mn>4</mml:mn></ Physical Review Materials, 2022, 6, .	0.9	8
47219	High-resolution diffraction reveals magnetoelastic coupling and coherent phase separation in tetragonal CuMnAs. Physical Review Materials, 2022, 6, .	0.9	0
47220	First-principles exploration of the interface characteristic between CNT and inorganic lead-free perovskites CsSnX3 (XÂ=ÂCl, Br, I). Materials Today Communications, 2022, 33, 104524.	0.9	1
47221	Fe@Ï‡3-borophene as a promising catalyst for CO oxidation reaction: A first-principles study. Frontiers in Chemistry, 0, 10, .	1.8	2
47222	The Role of Cobalt Clusters (Co_n, n = 1â€“5) Supported on Defective Î³â€“Graphyne for Efficient Hydrogen Adsorption: A First Principles Study. Advanced Theory and Simulations, 2022, 5, .	1.3	2
47223	Towards Ge-based electronic devices: Increased longevity of alkanethiol-passivated Ge(100) in low humidity environments. Thin Solid Films, 2022, 759, 139466.	0.8	3
47224	Pronounced inhibitory mechanism of Cr on vacancy-like defects in Fe9Cr alloy irradiation with helium ions. Nuclear Materials and Energy, 2022, 33, 101235.	0.6	0
47225	Enhancement of polypyrrole electrochemical performance with graphene quantum dots in polypyrrole nanoparticle/graphene quantum dot composites. Journal of Electroanalytical Chemistry, 2022, 923, 116767.	1.9	11
47226	Fast proton and water transport in ceramic membrane-based magic-angle graphene. Water Research, 2022, 225, 119076.	5.3	1
47227	Piezoelectricity and optical properties of janus MXY (M = Sb, As; X = Te, Se; Y = Br, I) monolayers. , 2022, 170, 207396.		4
47229	Extraordinary thermoelectric performance, thermal stability and mechanical properties of n-type Mg3Sb1.5Bi0.5 through multi-dopants at interstitial site. Materials Today Physics, 2022, 27, 100835.	2.9	8
47230	Designing limiting-efficiency BaSi<mml:math xmlns:mml="http://www.w3.org/1998/Math/MathML" altimg="si184.svg" display="inline" id="d1e1122"><mml:msub><mml:mrow /><mml:mrow><mml:mn>2</mml:mn></mml:mrow></mml:msub></mml:math> solar cells by device simulation and computational material screening. Solar Energy, 2022, 245, 136-145.	2.9	8
47231	Pitting resistance of reduced graphene oxide-layered double hydroxide reinforced aluminum composite coating deposited by cold spraying. Surface and Coatings Technology, 2022, 448, 128878.	2.2	1
47232	Theoretical analysis of Polyethylene terephthalate (PET) adsorption on Co and Mn-doped ZnO (000-1). Molecular Catalysis, 2022, 531, 112688.	1.0	3
47233	Sensing performance of CdPc monolayer toward the SF6 decomposition gases: A DFT study. Chemical Physics Letters, 2022, 806, 140030.	1.2	10

#	Article	IF	Citations
47234	Adsorption of CO, NO, and SO2 gases on pristine and single Ni3 cluster doped arsenene monolayer for its potential application as sensor or adsorbent by density functional theory study. Computational and Theoretical Chemistry, 2022, 1217, 113871.	1.1	8
47235	Interfacial structures and decomposition reactions of hybrid anion-based ionic liquids at lithium metal surface from first-principles and ab initio molecular dynamics. Journal of Molecular Liquids, 2022, 366, 120232.	2.3	2
47236	Two-dimensional penta-siligraphene with high performance for nonâ€'lithium metal ions batteries anode materials. Solid State Ionics, 2022, 385, 116020.	1.3	3
47237	Equilibrium fractionation of S, Fe, and Ni isotopes in Fe-Ni sulfides: A first-principles investigation. Chemical Geology, 2022, 610, 121100.	1.4	0
47238	Hazardous gas adsorption of Janus HfSeTe monolayer adjusted by surface vacancy defect: A DFT study. Surfaces and Interfaces, 2022, 34, 102316.	1.5	5
47239	Ab initio quantum transport simulations of monolayer GeS nanoribbons. Solid-State Electronics, 2022, 197, 108460.	0.8	7
47240	A comprehensive investigation on electronic and thermal transport properties at the Cu/diamond interface. Diamond and Related Materials, 2022, 129, 109390.	1.8	1
47241	Electronic, elastic and thermodynamic properties of LaMgRe4 (Re= Co, Ni, Cu): A first-principles study. Vacuum, 2022, 205, 111473.	1.6	7
47242	Anisotropic and outstanding mechanical, thermal conduction, optical, and piezoelectric responses in a novel semiconducting BCN monolayer confirmed by first-principles and machine learning. Carbon, 2022, 200, 500-509.	5.4	16
47243	Revealing the electronic, optical, phonon and thermoelectrical characteristics of bulk and monolayered RbLiS and RbLiSe compounds by DFT. Journal of Physics and Chemistry of Solids, 2022, 170, 110972.	1.9	1
47244	Determination of the equilibrium magnesium isotope fractionation factors between brucite and aqueous inorganic and organic species. Geochimica Et Cosmochimica Acta, 2022, 336, 33-49.	1.6	2
47245	An ab initio approach to understand the structural, thermophysical, electronic, and optical properties of binary silicide SrSi: A double Weyl semimetal. Results in Physics, 2022, 42, 105973.	2.0	3
47246	Experimental and computational insights into the anomalous thermal expansion of (NH4)ReO4. Journal of Solid State Chemistry, 2022, 315, 123531.	1.4	0
47247	Optoelectronic properties and ion diffusion mechanism in 2D perovskites Cs3BX5 (BÂ=ÂGe, Sn, and Pb; X) Tj ETQq1 1 0.784314 rgBT	1.2	1
47248	First-principles calculations to investigate structural, elastic, electronic, thermodynamic, and thermoelectric properties of CaPd3B4O12 (BÂ=ÂTi, V) perovskites. Results in Physics, 2022, 42, 105977.	2.0	54
47249	Design of a new ultraviolet nonlinear optical material KNO3SO3NH3 exhibiting an unexpected strong second harmonic generation response. Materials Today Physics, 2022, 28, 100849.	2.9	19
47250	Equilibrium mass-dependent isotope fractionation of antimony between stibnite and Sb secondary minerals: A first-principles study. Chemical Geology, 2022, 611, 121115.	1.4	12
47251	Sandwich-like GaN/MoSe2/GaN heterostructure nanosheet: A First-principle study of the structure, electronic, optical, and thermodynamical properties. Surfaces and Interfaces, 2022, 34, 102298.	1.5	2

#	Article	IF	Citations
47252	The site preference and doping effect on mechanical properties of Ni3Al-based Î³â€² phase in superalloys by combing first-principles calculations and thermodynamic model. Arabian Journal of Chemistry, 2022, 15, 104278.	2.3	9
47253	Ab-initio-based interface modeling and statistical analysis for estimate of the water contact angle on a metallic Cu(111) surface. Surfaces and Interfaces, 2022, 34, 102342.	1.5	2
47254	Tunable band gap of diamond twin boundaries by strain engineering. Carbon, 2022, 200, 483-490.	5.4	2
47255	Influence of impurity configuration on electronic and optical properties of Ce-doped YVO4: Semi-local & hybrid functionals. Computational Materials Science, 2022, 214, 111741.	1.4	1
47256	Structural superlubricity in graphene/GaSe van der Waals heterostructure. Physics Letters, Section A: General, Atomic and Solid State Physics, 2022, 452, 128435.	0.9	5
47257	Liquid phase exfoliated ReS2 nanocrystals on paper based electrodes for hydrogen evolution and supercapacitor applications. Surfaces and Interfaces, 2022, 34, 102318.	1.5	13
47258	Ultrahigh yield strength and large uniform elongation achieved in ultrafine-grained titanium containing nitrogen. Acta Materialia, 2022, 240, 118356.	3.8	18
47259	Ionic covalent organic frameworks triggered efficient synergy: Li+ de-solvation and the formation of LiF-rich interphase. Journal of Power Sources, 2022, 548, 232001.	4.0	3
47260	Analysis of structural stability and optoelectronic properties of new direct band gap halide double perovskites <mml:math xmlns:mml="http://www.w3.org/1998/Math/MathML" altimg="si12.svg" display="inline" id="d1e946"><mml:mrow><mml:mi>C</mml:mi><mml:msub><mml:mrow><mml:mi>s</mml:mi></mml:mrow><mml:mrow><mml:mn> Solid State Communications, 2022, 355, 114928.	0.9	1
47261	Optical and electronic parameters of Rb2SO4 crystals. Optik, 2022, 269, 169875.	1.4	2
47262	Electronic and optical properties of Mg3XN (X = P, As, Sb, Bi) antiperovskites: The GW/BSE approach. Solid State Communications, 2022, 355, 114927.	0.9	8
47263	Effects of rare-earth elements on twinning deformation of Al alloys from first-principles calculations. Solid State Communications, 2022, 356, 114946.	0.9	2
47264	First-principles calculations to investigate the structural, electronic, optical anisotropy, and bonding properties of a newly synthesized ThRhGe equiatomic ternary intermetallic superconductor. Results in Physics, 2022, 42, 106004.	2.0	6
47265	Exploring structural evolution and graphitization of the interface between tungsten and diamond (1 1) Tj ETQq1 1 0.784314 rgBT /Ov	3.1	3
47266	Electronic modulation of fiber-shaped-CoFe2O4 via Mg doping for improved PMS activation and sustainable degradation of organic pollutants. Applied Surface Science, 2022, 605, 154732.	3.1	12
47267	Variation of magnetism in two-dimensional MnS2 thin films. Journal of Magnetism and Magnetic Materials, 2022, 563, 169966.	1.0	2
47268	Formation and migration behavior of vacancy in multi-component alloys. Intermetallics, 2022, 151, 107724.	1.8	2
47269	Superior lithium storage in Fe2O3 nanoporous arrays endowed by surface phosphorylation and bulk phosphorous doping. Applied Surface Science, 2022, 604, 154668.	3.1	5

#	Article	IF	Citations
47270	Study on lattice discreteness effect on superdislocation core properties of Ni3Al by improved semi-discrete variational Peierls-Nabarro model. Intermetallics, 2022, 151, 107695.	1.8	1
47271	Two-Dimensional metal-free compounds of BC4N and BC6N2 with boron atoms as highly efficient catalytic centers toward sulfur redox in lithium-sulfur batteries. Applied Surface Science, 2022, 606, 154773.	3.1	3
47272	Strategy to weaken the oxygen adsorption on single-atom catalysts towards oxygen-involved reactions. Materials Today Advances, 2022, 16, 100280.	2.5	3
47273	First-principles kinetic Monte Carlo modeling of propylene epoxidation on the Ti2CuO6/Cu(111) and Cu2O(111) surfaces. Applied Surface Science, 2022, 605, 154683.	3.1	1
47274	Effect of substitution of Mn and Ga atoms by Fe atom in the Mn2GaC MAX phase. Journal of Magnetism and Magnetic Materials, 2022, 563, 169860.	1.0	1
47275	Effects of vacancies on the electronic structures and photocatalytic properties of g-C3N4. Vacuum, 2022, 206, 111483.	1.6	4
47276	Computational simulation study on adsorption and separation of CH4/H2 in five higher-valency covalent organic frameworks. Materials Today Communications, 2022, 33, 104374.	0.9	3
47277	Enhanced d0 ferromagnetism via carbon doping in rare-earth sesquioxides: DFT prediction. Journal of Magnetism and Magnetic Materials, 2022, 563, 169910.	1.0	1
47278	Realization of transition metal selenide active facets via synergistic sulfur doping for bifunctional alkaline water splitting applications: A comparative study. Applied Surface Science, 2022, 605, 154804.	3.1	9
47279	An embedded-atom method potential for studying the properties of Fe-Pb solid-liquid interface. Journal of Nuclear Materials, 2022, 572, 154041.	1.3	1
47280	Electrochemical formic acid oxidation catalyzed by graphene supported bimetallic Pd-Ni clusters: The role of Ni content and the hydrogen coverage effect. Applied Surface Science, 2022, 606, 154944.	3.1	4
47281	Effect of oxygen vacancy defects on electronic and optical properties of MgO monolayers: First principles study. Materials Science and Engineering B: Solid-State Materials for Advanced Technology, 2022, 286, 116074.	1.7	10
47282	First principles study of adsorption and simulation of desorption properties of <mml:math xmlns:mml="http://www.w3.org/1998/Math/MathML" altimg="si8.svg" display="inline" id="d1e1251"><mml:mrow><mml:msub><mml:mrow><mml:mi mathvariant="normal">Pd</mml:mi></mml:mrow><mml:mrow><mml:mn>1</mml:mn><mml:mo>â^’</mml:mo><mml:mi mathvariant="normal">x</mml:mi></mml:mrow></mml:msub><mml:msub><mml:mrow><mml:mi mathvariant="normal">Ag</mml:mi></mml:mrow><mml:mrow><mml:mi mathvariant="normal">x</mml	0.0	4
47283	Theoretical exploration on mechanical properties for Ni-RE intermetallic compounds in nickel alloy. Materials Today Communications, 2022, 33, 104521.	0.9	0
47284	High-pressure study of the aurophilic topological Dirac material AuI. Journal of Alloys and Compounds, 2022, 928, 167178.	2.8	12
47285	An ab initio insight into the structural, physical, thermodynamic and optoelectronic properties of superconducting Heusler-like LiGa2Rh. Physica C: Superconductivity and Its Applications, 2022, 603, 1354142.	0.6	6
47286	First-principles calculations to investigate physical properties of single-cubic (Ba0.82K0.18)(Bi0.53Pb0.47)O3 novel perovskite superconductor. Materials Today Communications, 2022, 33, 104302.	0.9	22
47287	The ordering behavior of Co3Al-based Î³â€² phase with L12 structure predicted by the thermodynamic model with support of first-principles calculations. Materials Today Communications, 2022, 33, 104447.	0.9	1

#	Article	IF	Citations
47288	New superhard tetragonal BCN from crystal chemistry and first principles. Materialia, 2022, 26, 101581.	1.3	8
47289	A in-plane biaxial strain tunable electronic structures and magnetic properties of Fe2C monolayer. Journal of Magnetism and Magnetic Materials, 2022, 563, 169959.	1.0	5
47290	In silico investigation on the twisting of gold nanowires. Materials Today Communications, 2022, 33, 104319.	0.9	1
47291	Theoretical investigation of compressed hexagonal and rock-salt structures of molybdenum and chromium carbides. Materials Today Communications, 2022, 33, 104334.	0.9	1
47292	Investigating the electrochemical properties of SnO monolayer in sodium-ion batteries. Journal of Physics and Chemistry of Solids, 2022, 171, 110975.	1.9	6
47293	In silico study of adsorption of oxide gases by MN4 (MÂ=ÂBe, Mg) monolayers. Applied Surface Science, 2022, 605, 154711.	3.1	5
47294	The mechanical, dynamical, thermodynamical properties and elastic anisotropies of cubic YbAu compound under pressure. Materials Today Communications, 2022, 33, 104456.	0.9	2
47295	Hydrogen delaying the formation of Guinier-Preston zones in aluminium alloys. Acta Materialia, 2022, 241, 118373.	3.8	5
47296	Tandem Coâ€“O dual sites on halloysite with promoted reaction kinetics for sulfur reduction. Journal of Energy Chemistry, 2022, 75, 486-493.	7.1	8
47297	Elucidation of formation and transformation mechanisms of Ca-rich Laves phase in Mg-Al-Ca-Mn alloys. Journal of Alloys and Compounds, 2022, 928, 167177.	2.8	2
47298	Heterogeneous nucleation interface between LaAlO3 and niobium carbide: First-principles calculation. Applied Surface Science, 2022, 606, 154731.	3.1	4
47299	Exploring the effect of partial RE (Nd, Eu, Tm) substitution on Sn sites on the electronic and physical properties of BaSnO3. Physica B: Condensed Matter, 2022, 646, 414306.	1.3	1
47300	Blue luminescence of Cs2CuCl4 glass ceramics with long-term water-resistance stability. Journal of Non-Crystalline Solids, 2022, 597, 121867.	1.5	5
47301	Rational design of the first and second coordination spheres for copper single-atom catalyst to boost highly efficient oxygen reduction. Applied Surface Science, 2022, 605, 154832.	3.1	6
47302	Precursor chemistry-mediated defect regulation of asphalt-derived carbonaceous materials for slope-dominated sodium storage. Journal of Alloys and Compounds, 2022, 928, 167103.	2.8	4
47303	A novel mechanism for visible-light degradation of phenol by oxygen vacancy Bi2MoO6 homojunction. Applied Surface Science, 2022, 605, 154671.	3.1	12
47304	First-principles calculation on effects of oxygen vacancy on Î±-MnO2 and Î²-MnO2 during oxygen reduction reaction for rechargeable metal-air batteries. Journal of Alloys and Compounds, 2022, 926, 166929.	2.8	9
47305	V8SiB4 â€" A new ternary phase in the Vâ€“Siâ€“B system. Intermetallics, 2022, 151, 107691.	1.8	0

#	Article	IF	Citations
47306	Theoretical insights into multi-metal atoms embedded nitrogen-doped graphene as efficient bifunctional catalysts for oxygen reduction and evolution reactions. Applied Surface Science, 2022, 605, 154714.	3.1	10
47307	A first principle comparison of arsenic-based double halide perovskite materials for photovoltaic and optoelectronic application. Journal of Solid State Chemistry, 2022, 316, 123557.	1.4	3
47308	First-principles study of electronic states, optical properties, water adsorption and dissociation properties of Pt-doped two-dimensional ZnO. Materials Science and Engineering B: Solid-State Materials for Advanced Technology, 2022, 286, 116019.	1.7	1
47309	Sensing applications of GeBi nanosheet for environmentally toxic/non-toxic gases: Insights from density functional theory calculations. Applied Surface Science, 2022, 606, 154741.	3.1	5
47310	New salts of teriflunomide (TFM) â€“ Single crystal X-ray and solid state NMR investigation. Solid State Nuclear Magnetic Resonance, 2022, 122, 101820.	1.5	1
47311	Hydrogen passivated <mml:math xmlns:mml="http://www.w3.org/1998/Math/MathML" altimg="si11.svg" display="inline" id="d1e548"><mml:msub><mml:mrow><mml:mi>Î²</mml:mi></mml:mrow><mml:mrow><mml:mn>12</mml:mn></mml:mrow></mml:msub></mml:mrow></mml:mrow> nanoribbon: A propitious one-dimensional metallic anode for sodium-ion rechargeable batteries.	3.1	7
47312	Shortening the screening process towards high-performance 2D-MOF NRR electrocatalysts with <mml:math xmlns:mml="http://www.w3.org/1998/Math/MathML" altimg="si7.svg"><mml:mrow><mml:mi mathvariant="normal">Î”</mml:mi><mml:mfenced open="(" close=")"><mml:mrow><mml:mi width="0.333333em" /><mml:msub><mml:mi>Î¼</mml:mi><mml:mrow><mml:mtext>B</mml:mtext><mml:mi>_<. Applied Surface	3.1	11
47313	Porous silicon particles embedded in N-doped graphene and carbon nanotube framework for high-performance lithium-ion batteries. Journal of Alloys and Compounds, 2022, 927, 167055.	2.8	8
47314	MoirÃ© and non-twisted sp-hybridized structures based on hexagonal boron nitride bilayers: Ab initio insight into infrared and Raman spectra, bands structures and mechanical properties. Applied Surface Science, 2022, 606, 154909.	3.1	7
47315	Well-ordered surface metal atoms complexation by deposition of Pd cyclometallated compounds on Ag (1 1 0). Applied Surface Science, 2022, 606, 154960.	3.1	1
47316	Nitrogenated Holey Graphene (C2N-h2D): An excellent sensor for neurotransmitter amino acids. Applied Surface Science, 2022, 606, 154740.	3.1	1
47317	Exploration of new direct gap semiconductor Na2X (X = S and Se) monolayers. Applied Surface Science, 2022, 606, 154809.	3.1	4
47318	Perforated nitrogen-rich graphene-like carbon nanolayers supported Cu-In catalyst for boosting CO2 electroreduction to CO. Journal of Energy Chemistry, 2022, 75, 383-390.	7.1	16
47319	Direct band gap double perovskite halide Cs2ScInCl6 for optoelectronic applicationsâ€”A first principle study. Computational Condensed Matter, 2022, 33, e00736.	0.9	1
47320	Two-dimensional HfTe2 monolayer treated by dispersed single Pt atom for hazardous gas Detection: A First-principles study. Applied Surface Science, 2022, 605, 154572.	3.1	7
47321	A general strategy and a consolidated mechanism for low-methane hydrogenolysis of polyethylene over ruthenium. Applied Catalysis B: Environmental, 2022, 319, 121899.	10.8	25
47322	High-throughput informed machine learning models for ultrastrong B-N solids. Computational Materials Science, 2022, 215, 111789.	1.4	3
47323	Optical properties and simulated x-ray near edge spectra for Y2O2S and Er doped Y2O2S. Materials Today Communications, 2022, 33, 104328.	0.9	1

#	Article	IF	Citations
47324	First-principles study of <mml:math xmlns:mml="http://www.w3.org/1998/Math/MathML" altimg="si71.svg" display="inline" id="d1e3448"><mml:mi>A</mml:mi></mml:math>TcO<mml:math xmlns:mml="http://www.w3.org/1998/Math/MathML" altimg="si72.svg" display="inline" id="d1e3453"><mml:msub><mml:mrow /><mml:mrow><mml:mn>4</mml:mn></mml:mrow></mml:msub></mml:math> pertechnetates. Journal of Physics and Chemistry of Solids, 2022, 171, 110979.	1.9	4
47325	Strain tailored electronic structure and magnetic properties of Fe-doped Zr8C4T8 (TÂ=ÂF, O) monolayers. Physica E: Low-Dimensional Systems and Nanostructures, 2023, 145, 115488.	1.3	2
47326	Relationship between resistive switching and Mott transition in atomic layer deposition prepared La2Ti2O7-x thin film. Scripta Materialia, 2023, 222, 115050.	2.6	3
47327	Towards an ultra-long lifespan Li-CO2: electron structure and charge transfer pathway regulation on hierarchical architecture. Chemical Engineering Journal, 2023, 451, 138953.	6.6	2
47328	Construction of Co/Ni-Free P2-layered metal oxide cathode with high reversible oxygen redox for sodium ion batteries. Chemical Engineering Journal, 2023, 452, 138912.	6.6	13
47329	Iron nitride nanoparticles for rapid dechlorination of mixed chlorinated ethene contamination. Journal of Hazardous Materials, 2023, 442, 129988.	6.5	10
47330	Theoretical investigations of Sc2C based functionalized MXenes for applications in nanoelectromechanical systems. Physica E: Low-Dimensional Systems and Nanostructures, 2023, 145, 115491.	1.3	5
47331	On the structure of rare-earth sesquioxide Sm2O3 in Sm2Co17-type magnets. Scripta Materialia, 2023, 222, 115018.	2.6	3
47332	Achieving high-energy and long-cycling aqueous zinc-metal batteries by highly reversible insertion mechanisms in Ti-substituted Na0.44MnO2 cathode. Chemical Engineering Journal, 2023, 451, 139059.	6.6	13
47333	Magnetic and optoelectronic modification of graphene-like ZnO monolayer by doping of Ag, Au and Pt atoms. Physica E: Low-Dimensional Systems and Nanostructures, 2023, 145, 115506.	1.3	5
47334	N-bridged Ni and Mn single-atom pair sites: A highly efficient electrocatalyst for CO2 conversion to CO. Applied Catalysis B: Environmental, 2023, 320, 121953.	10.8	13
47335	Insights into highly efficient piezocatalytic molecule oxygen activation over Bi2Fe4O9: Active sites and mechanism. Chemical Engineering Journal, 2023, 452, 139300.	6.6	19
47336	Strain engineered thermodynamic stability, electronic and thermoelectric characteristics of TiB2 and ZrB2 monolayers. Physica E: Low-Dimensional Systems and Nanostructures, 2023, 145, 115477.	1.3	0
47337	Theoretical evaluation of charge transport properties and mobility of tetraphenyldipyranylidene derivatives in organic field-effect transistors. Journal of Photochemistry and Photobiology A: Chemistry, 2023, 435, 114283.	2.0	1
47338	Atomic-structure and charge redistribution modified by intrinsic strain in Î±-fe/TMN (TM=Ti/Zr/Hf/V/Nb/Ta) interfaces. Physica E: Low-Dimensional Systems and Nanostructures, 2023, 145, 115495.	1.3	3
47339	Analysis of interaction between dislocation and interface of aluminum matrix/second phase from electronic behavior. Journal of Materials Science and Technology, 2023, 136, 78-90.	5.6	6
47340	Identification of Hydrogen Trapping in Aluminum Alloys Via Muon Spin Relaxation Method and First-Principles Calculations. SSRN Electronic Journal, 0, , .	0.4	0
47341	The structure and electronic properties of the MoSe₂/PtS₂ van der Waals heterostructure. Physical Chemistry Chemical Physics, 2022, 24, 19853-19864.	1.3	2

#	Article	IF	Citations
47342	First-principles study of CO₂ hydrogenation to formic acid on single-atom catalysts supported on SiO₂. Physical Chemistry Chemical Physics, 2022, 24, 19938-19947.	1.3	2
47343	Photoelectrochemical alcohols oxidation over polymeric carbon nitride photoanodes with simultaneous H₂ production. Journal of Materials Chemistry A, 2022, 10, 16585-16594.	5.2	13
47344	Geometry of tellurene adsorbed on the Si(111)-R30Â°-Sb surface from first principles calculations. Physical Chemistry Chemical Physics, 2022, 24, 18608-18614.	1.3	0
47345	Co2ÂActivation and Dissociation Over Ag(111) Surfaces in the Presence of Surface Charge Density: A Static Gas Phase Dft Study. SSRN Electronic Journal, 0, , .	0.4	0
47346	Computational screen of M₂P metal phosphides for catalytic ethane dehydrogenation. Catalysis Science and Technology, 2022, 12, 5629-5639.	2.1	1
47347	In Situ Synthesis and Stabilization of Co2c for Co2 Hydrogenation to Valuable Hydrocarbon. SSRN Electronic Journal, 0, , .	0.4	0
47348	Defective Lithium Titanate Oxide with Stable Cycling Over a Wide Voltage Window. SSRN Electronic Journal, 0, , .	0.4	0
47349	Potassium-Enriched Graphite for Use as Stable Hybrid Anodes in High-Efficiency Potassium Batteries. SSRN Electronic Journal, 0, , .	0.4	0
47350	Probing the Low Friction Mechanism of Hydrogen-Free Dlc Film in Oxygen and Nitrogen Environments by First-Principles Calculations and Molecular Dynamics Simulation. SSRN Electronic Journal, 0, , .	0.4	0
47351	Molecular Adsorption of the Nco, Cno and Con Isomers on the Rh(001) Surface: A Density Functional Theory Study. SSRN Electronic Journal, 0, , .	0.4	0
47352	Molecular Adsorption of the Nco, Cno and Con Isomers on the Rh(001) Surface: A Density Functional Theory Study. SSRN Electronic Journal, 0, , .	0.4	0
47353	Phosphorus Doping and Phosphate Coating Enhance the Performance OfÂÂLini0.8co0.1mn0.1o2. SSRN Electronic Journal, 0, , .	0.4	0
47354	Metal-Organic Framework-Induced Edge-Riched Growth of Layered Bi2se3 Towards Ultrafast Na-Ion Storage. SSRN Electronic Journal, 0, , .	0.4	0
47355	Pressure-Induced Enhancement of Thermoelectric Performance of CoP ₃ By the Structural Phase Transition. SSRN Electronic Journal, 0, , .	0.4	0
47356	A Bimetallic Strategy to Tailoring the Surface Formation Energy and D-Band Center of Ni-Based Catalyst for Efficient and Stable Catalytic Hydrogenation of Dioctyl Phthalate. SSRN Electronic Journal, 0, , .	0.4	0
47357	High-Pressure Stabilisation of R = Y Member of R2cutio6 Double Perovskite Series. SSRN Electronic Journal, 0, , .	0.4	0
47358	Modulating the Schottky barrier of MXenes/2D SiC contacts via functional groups and biaxial strain: a first-principles study. Physical Chemistry Chemical Physics, 2022, 24, 20837-20847.	1.3	7
47359	First-principles study of lead-free Ge-based 2D Ruddlesdenâ€“Popper hybrid perovskites for solar cell applications. Physical Chemistry Chemical Physics, 2022, 24, 21052-21060.	1.3	2

#	Article	IF	Citations
47360	H atom scattering from W(110): A benchmark for molecular dynamics with electronic friction.. Physical Chemistry Chemical Physics, 2022, 24, 20813-20819.	1.3	2
47361	Lattice distortion derived catalytic degradation in multi-oxide cathode catalyst for Liâ€“oxygen batteries. Journal of Materials Chemistry A, 2022, 10, 18078-18086.	5.2	2
47362	Tailoring the optoelectronic properties and dielectric profiles of few-layer S-doped MoO₃ and O-doped MoS₂ nanosheets: a first-principles study. Physical Chemistry Chemical Physics, 2022, 24, 25440-25451.	1.3	6
47363	First-principles determination of the crystallography of the low-temperature phase for NbRu and TaRu shape memory alloys. Physical Chemistry Chemical Physics, 2022, 24, 22599-22604.	1.3	0
47364	Twist-stacked 2D bilayer Fe₃GeTe₂ with tunable magnetism. Journal of Materials Chemistry C, 2022, 10, 12741-12750.	2.7	8
47365	Lower thermal conductivity of body centered cubic carbon (C14): a comparative study with diamond. Physical Chemistry Chemical Physics, 2022, 24, 23817-23824.	1.3	2
47366	Anisotropy, segmental dynamics and polymorphism of crystalline biogenic carboxylic acids. Physical Chemistry Chemical Physics, 2022, 24, 25904-25917.	1.3	2
47367	Unexpected NMR shieldings of sp- and sp²-hybridized carbon atoms in graphyne systems. Physical Chemistry Chemical Physics, 2022, 24, 25513-25521.	1.3	2
47368	Formation of Diphenyl-Bipyridine Units by Surface Assisted Cross Coupling in Pd-Cyclometalled Complexes. SSRN Electronic Journal, 0, , .	0.4	1
47369	High throughput exploration of the oxidation landscape in high entropy alloys. Materials Horizons, 2022, 9, 2644-2663.	6.4	5
47370	Tuning photoelectron dynamic behavior of thiolate-protected MAu₂₄ nanoclusters via heteroatom substitution. Nanoscale Horizons, 2022, 7, 1192-1200.	4.1	17
47371	Influence of Alloying Elements on Various Properties of Face-Centered-Cubic Iron. SSRN Electronic Journal, 0, , .	0.4	0
47372	Polymorphs and solid solutions: materials with new luminescent properties obtained through mechanochemical transformation of dicyanoaurate(I) salts. Faraday Discussions, 0, , .	1.6	3
47373	Ba₂HgTe₅: a Hg-based telluride with giant birefringence induced by linear [HgTe₂] units. Inorganic Chemistry Frontiers, 2022, 9, 5024-5031.	3.0	6
47374	Perovskite-structure TlBO₃ (B = Cr, Mn) for thermomechanical and optoelectronic applications: an investigation via a DFT scheme. RSC Advances, 2022, 12, 27492-27507.	1.7	6
47375	Catalytic formation of oxalic acid on the partially oxidised greigite Fe₃S₄(001) surface. Physical Chemistry Chemical Physics, 2022, 24, 20104-20124.	1.3	2
47376	The magnetic anisotropy and spin filtering effect in ferromagnetic phosphorene. Materials Today: Proceedings, 2022, 67, 931-934.	0.9	0
47377	A sustainable approach to synthesize phosphonated chitosan using ball milling and its application for oilfield scale management. Green Chemistry, 2022, 24, 7171-7183.	4.6	7

#	Article	IF	Citations
47378	Theoretical prediction of alkali oxide M₂O (M = Na and K) monolayers and formation of their Janus structure. New Journal of Chemistry, 2022, 46, 17386-17393.	1.4	1
47379	Crystal habit analysis of LiFePO₄ microparticles by AFM and first-principles calculations. CrystEngComm, 2022, 24, 6891-6901.	1.3	4
47380	Theoretical investigation of a tetrazine based covalent organic framework as a promising anode material for sodium/calcium ion batteries. Physical Chemistry Chemical Physics, 2022, 24, 21729-21739.	1.3	19
47381	Homonuclear Transition-Metal Dimers Embedded Monolayer C2n as Promising Anchoring and Electrocatalytic Materials for Lithium-Sulfur Battery: First-Principles Calculations. SSRN Electronic Journal, 0, , .	0.4	0
47382	A coordination environment effect of single-atom catalysts on their nitrogen reduction reaction performance. Physical Chemistry Chemical Physics, 2022, 24, 18854-18859.	1.3	6
47383	A large-gap quantum spin Hall state in exfoliated Na₃Bi-like two-dimensional materials. Journal of Materials Chemistry C, 2022, 10, 11329-11337.	2.7	2
47384	Vapor-phase hydrothermal construction of defective MoS₂ for highly selective electrocatalytic hydrogenation of cinnamaldehyde. Materials Advances, 2022, 3, 8250-8259.	2.6	0
47385	First-principles calculation of the electronic structure, elastic and optical properties of LiSn2N3 nitrogen base stable perovskite semiconductor material. Materials Today: Proceedings, 2022, 67, 943-947.	0.9	2
47386	An ab initio investigation of the temperature-dependent energetic barriers towards CrAlB and (Mo,Cr)AlB formation in a metastable synthesis scenario. Nanoscale, 2022, 14, 12866-12874.	2.8	3
47387	Lithium stabilizes square-two-dimensional metal sheets: a computational exploration. Nanoscale, 2022, 14, 11770-11778.	2.8	0
47388	Anomalous Behavior of Strain Modulated Lattice Thermal Transport in Piezoelectric Crystals and the Effect of Polarization. SSRN Electronic Journal, 0, , .	0.4	0
47389	Effect of Torsional Deformation on the Electrical and Optical Properties of Be Adsorbed Stanene. SSRN Electronic Journal, 0, , .	0.4	0
47391	A Density Functional Theory Study of the Co Oxidation on Pt1 Supported on Ptx2 (X = S, Se, Te). SSRN Electronic Journal, 0, , .	0.4	0
47392	Effect of 4d Transition Metals on the Electronic and Magnetic Properties of Twin Graphene. SSRN Electronic Journal, 0, , .	0.4	0
47393	Hybrid Density Functional Theory Study of Substitutional Gd in ÃŸ-Ga2O3. SSRN Electronic Journal, 0, , .	0.4	0
47394	Lead-free double perovskites: how divalent cations tune the electronic structure for photovoltaic applications. Journal of Materials Chemistry C, 2022, 10, 12276-12285.	2.7	6
47395	Intrinsic type-II van der Waals heterostructures based on graphdiyne and XSSe (X = Mo, W): a first-principles study. Physical Chemistry Chemical Physics, 2022, 24, 21331-21336.	1.3	1
47396	Electronic, mechanical and piezoelectric properties of glass-like complex Na₂Si_{1â"'x}Ge_xO₃ (x = 0.0, 0.25, 0.50,) Tj ET Qq 1 1 0.78431	1.7	0

#	Article	IF	Citations
47397	Effects of pâ€“d orbital mixings on magnetocrystalline anisotropy for D_{3d}-symmetric ferromagnetic semiconducting monolayers. Physical Chemistry Chemical Physics, 2022, 24, 24553-24561.	1.3	1
47398	Edges in bilayered h-BN: insights into the atomic structure. Nanoscale, 2022, 14, 14155-14160.	2.8	1
47399	Improving the DFT Computational Accuracy for CO Activation on Fe Surfaces by Bayesian Error Estimation Functional With Van der Waals Correlation. SSRN Electronic Journal, 0, , .	0.4	0
47400	Experimental Study of Covalent Cr ₃C ₂ with High Ionicity: Sound Velocities, Elasticity and Mechanical Properties Under High Pressure. SSRN Electronic Journal, 0, , .	0.4	0
47401	Detection of cadaverine and putrescine on (10,0) carbon, boron nitride and gallium nitride nanotubes: a density functional theory study. New Journal of Chemistry, 0, , .	1.4	0
47402	Modulation of electronic bandgaps and subsequent implications on SQ efficiencies via strain engineering in ultrathin SnX (X = S, Se) nanowires. Journal of Materials Chemistry C, 0, , .	2.7	0
47403	Rational design of mixed Snâ€“Ge based hybrid halide perovskites for optoelectronic applications: a first principles study. RSC Advances, 2022, 12, 25511-25519.	1.7	6
47404	Thermoelectric, spin-dependent optical and quantum transport properties of 2D half-metallic Co₂Se₃. Physical Chemistry Chemical Physics, 2022, 24, 22016-22027.	1.3	2
47405	A theoretical roadmap for the best oxygen reduction activity in two-dimensional transition metal tellurides. Chemical Science, 2022, 13, 11048-11057.	3.7	2
47406	Demonstration of 10+ hour energy storage with Ï•1â€²â€² laboratory size solid oxide ironâ€“air batteries. Energy and Environmental Science, 2022, 15, 4659-4671.	15.6	2
47407	Inhibiting the decomposition of methylammonium using cations with low deprotonation energy. Journal of Materials Chemistry A, 2022, 10, 22742-22749.	5.2	3
47408	2d Titanium Carbonitride Ti3cntx Mxene with Attractive Microwave Absorption Properties in X and Ku Bands. SSRN Electronic Journal, 0, , .	0.4	0
47409	Dehydrogenation of ammonia on free-standing and epitaxial hexagonal boron nitride. Physical Chemistry Chemical Physics, 2022, 24, 20426-20436.	1.3	1
47410	Ab initio determination of a simultaneous dual-ion charging mechanism for Ni_{0.25}Mn_{0.75}O₂ through redox reactions of Ni²⁺/Ni⁴⁺ and O^{2â^’}/O^{â^’}. Journal of Materials Chemistry A, 2022, 10, 18916-18927.	5.2	1
47411	Electrocatalytic selectivity for nitrogen reduction vs. hydrogen evolution: a comparison of vanadium and cobalt oxynitrides at different pH values. Journal of Materials Chemistry A, 2022, 10, 21401-21415.	5.2	7
47412	Strain Regulating Mechanical Stability and Photoelectric Properties of Ch3nh3pbi3 Containing the Asymmetric Ch3nh3 Cations. SSRN Electronic Journal, 0, , .	0.4	0
47413	Supplementary Data of â€˜Discovering Novel Low Young's Modulus Nbâ€“Tiâ€“Zr Biomedical Alloys Via Combined Machine Learning and First Principles Approachâ€™. SSRN Electronic Journal, 0, , .	0.4	0
47414	Few-layered V₂C MXene derived 3D V₃S₄nanocrystal functionalized carbon flakes boosting polysulfide adsorption and catalytic conversion towards Liâ€“S batteries. Journal of Materials Chemistry A, 2022, 10, 18679-18689.	5.2	17

#	Article	IF	Citations
47415	Anomalous thermal transport behavior in graphene-like carbon nitride (C₃N). Journal of Materials Chemistry C, 2022, 10, 12080-12090.	2.7	2
47416	Modeling of the cathodic and anodic polarization curves of metals and alloys at an electronic level. Journal of Materials Chemistry A, 2022, 10, 17652-17658.	5.2	0
47417	Vibrational, Electronic and Structural Study of Sprayed ZnO Thin Film Based on the IR-Raman Spectra and DFT Calculations. Crystal Structure Theory and Applications, 2022, 11, 23-38.	0.3	1
47418	Novel Janus MoSiGeN₄ nanosheet: adsorption behaviour and sensing performance for NO and NO₂ gas molecules. RSC Advances, 2022, 12, 24743-24751.	1.7	4
47419	Unfolding the terahertz spectrum of soft porous crystals: rigid unit modes and their impact on phase transitions. Journal of Materials Chemistry A, 2022, 10, 17254-17266.	5.2	10
47420	First-Principles Approach to Physical Properties of Scga3and Luga3 Superconductors with and Without the Spin-Orbit Coupling. SSRN Electronic Journal, 0, , .	0.4	0
47421	A predicted orthogonal semimetallic carbon with negative thermal expansion and compressibility. Physical Chemistry Chemical Physics, 2022, 24, 23497-23506.	1.3	2
47422	High-throughput screening of transition metal doping and defect engineering on single layer SnS₂ for the water splitting hydrogen evolution reaction. Journal of Materials Chemistry A, 2022, 10, 21315-21326.	5.2	9
47423	Elemental (im-)miscibility determines phase formation of multinary nanoparticles co-sputtered in ionic liquids. Nanoscale Advances, 2022, 4, 3855-3869.	2.2	3
47424	Significantly suppressed thermal transport by doping In and Al atoms in gallium nitride. Physical Chemistry Chemical Physics, 2022, 24, 21085-21093.	1.3	2
47425	The surface reconstruction induced enhancement of the oxygen evolution reaction on Î±-SnWO₄ (010) based on a density functional theory study. Physical Chemistry Chemical Physics, 2022, 24, 19382-19392.	1.3	1
47426	The effect of Sr substitution on the structural and physical properties of manganite perovskites Ca_{1â^'x}Sr_xMnO_{3â^'Î´} (0 â‰¤ x â‰¤ 1). Physical Chemistry Chemical Physics, 2022, 24, 19414-19431.	1.3	7
47427	Hybrid Dense Carbon Allotropes from Crystal Chemistry and First Principles: 'Glitter' C6, 'Isoglitter' C8 and 'Metaglitter' C8. SSRN Electronic Journal, 0, , .	0.4	0
47428	Intriguing Two-Dimensional Transition Metal Oxide for Tracing Hazardous Organic Mercury. SSRN Electronic Journal, 0, , .	0.4	0
47429	Construction of Group Iii Nitride Van Der Waals Heterostructures for Highly Efficient Photocatalyst. SSRN Electronic Journal, 0, , .	0.4	0
47430	2D NbIrTe₄ and TaRhTe₄ monolayers: two fascinating topological insulators as electrocatalysts for oxygen reduction. Inorganic Chemistry Frontiers, 2022, 9, 6133-6146.	3.0	2
47431	Mo₃(C₆O₆)₂ monolayers as promising electrocatalysts for the CO₂ reduction reaction: a first-principles study. Physical Chemistry Chemical Physics, 0, , .	1.3	1
47432	First principles investigation of anionic redox in bisulfate lithium battery cathodes. Physical Chemistry Chemical Physics, 2022, 24, 22756-22767.	1.3	1

#	Article	IF	Citations
47433	Integrating ferromagnetism and ferroelectricity in an iron chalcogenide monolayer: a first-principles study. Nanoscale, 2022, 14, 14231-14239.	2.8	2
47434	Extreme structural stability of Ti_{0.5}Sn_{0.5}O₂ nanoparticles: synergistic effect in the cationic sublattice. Nanoscale, 2022, 14, 14286-14296.	2.8	0
47435	[ASr₄Cl][Ge₃S₁₀] (A = Na, K) and [KBa₄Cl][Ge₃S₁₀]: new salt-inclusion infrared nonlinear optical crystals with zero-dimensional [Ge₃S₉] clusters. Inorganic Chemistry Frontiers, 2022, 9, 5932-5940.	3.0	16
47436	Improvement of No2 Gas Sensing Characteristics of Graphene-Sno2 Hybrid Nanocomposites by Proton Irradiation: Experimental and Dft Studies. SSRN Electronic Journal, 0, , .	0.4	0
47437	Sc₂F₂(B₂O₅): a deep ultraviolet scandium borate fluoride exhibiting large birefringence induced by the synergistic effect of B₂O₅and ScO_nF₂groups. Inorganic Chemistry Frontiers, 2022, 9, 5153-5160.	3.0	23
47438	An interactive design for sustainable oxygen capacity in alkali-ion batteries. Energy and Environmental Science, 2022, 15, 4554-4560.	15.6	4
47439	Selective oxidation of CH₄ to valuable HCHO over a defective rTiO₂/GO metal-free photocatalyst. Catalysis Science and Technology, 2022, 12, 5869-5878.	2.1	0
47440	Tracking the solid-state incorporation of Sn into the framework of dealuminated zeolite beta, and consequences for catalyst design. Journal of Materials Chemistry A, 2022, 10, 22025-22041.	5.2	5
47441	â€œBreathingâ€•organic cation to stabilize multiple structures in low-dimensional Ge-, Sn-, and Pb-based hybrid iodide perovskites. Inorganic Chemistry Frontiers, 2022, 9, 4892-4898.	3.0	3
47442	Isotopic evidence for the tangled mechanism of the CO-PROX reaction over mixed and bare cobalt spinel catalysts. Catalysis Science and Technology, 2022, 12, 5723-5741.	2.1	6
47443	Capillary-force-driven self-assembly of carbon nanotubes: from ab initio calculations to modeling of self-assembly. Nanoscale Advances, 2022, 4, 4131-4137.	2.2	3
47444	Axial coordination modification of Mâ€“N₄single-atom catalysts to regulate the electrocatalytic CO₂reduction reaction. Journal of Materials Chemistry C, 2022, 10, 15948-15956.	2.7	14
47445	STUDY OF ELECTRONIC PROPERTIES FOR PURE AND DOPED A-TIO2 USING MGGA: AN AB-INITIO APPROACH. Composites: Mechanics, Computations, Applications, 2022, 13, 133-145.	0.2	0
47446	Neural network-based pseudopotential: development of a transferable local pseudopotential. Physical Chemistry Chemical Physics, 2022, 24, 20094-20103.	1.3	5
47447	Reaction-intermediate-induced atomic mobility in heterogeneous metal catalysts for electrochemical reduction of CO₂. Physical Chemistry Chemical Physics, 2022, 24, 19432-19442.	1.3	3
47448	Emergent superconductivity in K₂ReH₉ under pressure. Journal of Materials Chemistry C, 2022, 10, 14626-14632.	2.7	2
47449	A new family of NaTMGe (TM = 3d transition metals) half-Heusler compounds: the role of TM modification. RSC Advances, 2022, 12, 26418-26427.	1.7	2
47450	Unexpected low thermal expansion coefficients of pentadiamond. Physical Chemistry Chemical Physics, 2022, 24, 23561-23569.	1.3	3

#	Article	IF	Citations
47451	Exploring room-temperature ferromagnetism in WXBC (X = W, Mn, Fe) monolayers. RSC Advances, 2022, 12, 28433-28440.	1.7	6
47452	Ï€-Orbital mediated charge transfer channels in a monolayer Grâ€“NiPc heterointerface unveiled by soft X-ray electron spectroscopies and DFT calculations. Nanoscale, 2022, 14, 13166-13177.	2.8	2
47453	Spin and valence variation in cobalt doped barium strontium titanate ceramics. Physical Chemistry Chemical Physics, 2022, 24, 19865-19881.	1.3	2
47454	Diverse Electronic Structures Governed by N-Substitution in Stable Two-Dimensional Dumbbell Carbonitrides. SSRN Electronic Journal, 0, , .	0.4	0
47455	The origin of high Na⁺ ion conductivity in Na_{1+x}Zr₂Si_xP_{3â^'x}O₁₂ NASICON materials. Physical Chemistry Chemical Physics, 2022, 24, 22154-22167.	1.3	6
47456	A theoretical study of thePnmaandR3Ì„mphases of Sb₂S₃, Bi₂S₃, and Sb₂Se₃. Journal of Materials Chemistry C, 2022, 10, 15061-15074.	2.7	6
47457	The exploration of new infrared nonlinear optical crystals based on the polymorphism of BaGa₄S₇. Inorganic Chemistry Frontiers, 2022, 9, 4632-4641.	3.0	14
47458	An Ab Initio Approach to Understand the Structural, Thermophysical, Electronic, and Optical Properties of Binary Silicide Srsi2: A Double Weyl Semimetal. SSRN Electronic Journal, 0, , .	0.4	0
47459	DFT calculations of thermo-mechanical properties of Be-chalcogenides. AIP Conference Proceedings, 2022, , .	0.3	0
47460	Theoretical Insights into the Removal Pathways of Adsorbed Oxygen on the Surface of Îš-Fe5c2(510). SSRN Electronic Journal, 0, , .	0.4	0
47461	Non-equilibrium spin-transport properties of Co/phosphorene/Co MTJ with non-collinear electrodes under mechanical bending. Physical Chemistry Chemical Physics, 0, , .	1.3	0
47462	Mitigating Coke Formations for Dry Reforming of Methane on Dual-Site Catalysts: A Microkinetic Modeling Study. SSRN Electronic Journal, 0, , .	0.4	0
47463	Improved Interfacial Thermal Conductance by Enhancing the Coupling Strength at Metal/Semiconductor Interfaces. SSRN Electronic Journal, 0, , .	0.4	0
47464	Transition Metal Dualâ€“Atom Ni2/Tio2 Catalysts for Photoelectrocatalytic Hydrogen Evolution: A Density Functional Theory Study. SSRN Electronic Journal, 0, , .	0.4	0
47465	The synergetic effect of Pd, In and Zr on the mechanism of Pd/In₂O₃â€“ZrO₂ for CO₂ hydrogenation to methanol. Reaction Chemistry and Engineering, 0, , .	1.9	0
47466	Heterointerface and Oxygen Vacancy of Co(Oh)2/Con to Synergistically Boost Alkaline Water Splitting. SSRN Electronic Journal, 0, , .	0.4	0
47467	A tight-binding model for the electronic structure of MXene monolayers. Nanoscale, 2022, 14, 11760-11769.	2.8	2
47468	From symmetry breaking in the bulk to phase transitions at the surface: a quantum-mechanical exploration of Li₆PS₅Cl argyrodite superionic conductor. Physical Chemistry Chemical Physics, 2022, 24, 22978-22986.	1.3	6

#	Article	IF	Citations
47469	Band Structures and Transport Properties of Broken-Gap Heteostructures: 2d C3n/Mx Case. SSRN Electronic Journal, 0, , .	0.4	0
47470	Tailoring spin waves in 2D transition metal phosphorus trichalcogenides via atomic-layer substitution. Dalton Transactions, 2022, 51, 16816-16823.	1.6	3
47471	DFT exchange: sharing perspectives on the workhorse of quantum chemistry and materials science. Physical Chemistry Chemical Physics, 2022, 24, 28700-28781.	1.3	91
47472	Electronic structure, defect properties, and optimization of the band gap of the earth-abundant and low-toxicity photovoltaic absorber Cu₃SbS₄. Physical Chemistry Chemical Physics, 2022, 24, 25258-25269.	1.3	3
47473	The role of Mo species in Niâ€“Mo catalysts for dry reforming of methane. Physical Chemistry Chemical Physics, 2022, 24, 21461-21469.	1.3	4
47474	Intrinsic ferromagnetism and the quantum anomalous Hall effect in two-dimensional MnOCl₂ monolayers. Physical Chemistry Chemical Physics, 2022, 24, 20530-20537.	1.3	1
47475	Computational investigation of van der Waals corrections in the adsorption properties of molecules on the Cu(111) surface. Physical Chemistry Chemical Physics, 2022, 24, 20294-20302.	1.3	3
47476	Lattice dynamics across the ferroelastic phase transition in Ba₂ZnTeO₆: a Raman and first-principles study. Physical Chemistry Chemical Physics, 2022, 24, 20152-20163.	1.3	2
47477	Tunable magnetocrystalline anisotropy of two-dimensional Fe₃GeTe₂ with adsorbed 5d-transition metal. Physical Chemistry Chemical Physics, 2022, 24, 21470-21476.	1.3	5
47478	Two-dimensional carbon materials with an anisotropic Dirac cone: high stability and tunable Fermi velocity. Physical Chemistry Chemical Physics, 2022, 24, 19263-19268.	1.3	2
47479	Revealing the pH-dependent mechanism of nitrate electrochemical reduction to ammonia on single-atom catalysts. Nanoscale, 2022, 14, 15422-15431.	2.8	5
47480	First principles study of hydrogen adsorption and dissociation behavior on Î³-U (100)/Mo surface. Wuli Xuebao/Acta Physica Sinica, 2022, 71, 226601.	0.2	1
47481	Single atom functionalization in vanadium dichalcogenide monolayers: towards enhanced electrocatalytic activity. Sustainable Energy and Fuels, 2022, 6, 5337-5344.	2.5	3
47482	Mechanistic insight into electrocatalytic glyoxal reduction on copper and its relation to CO₂ reduction. Chemical Science, 2022, 13, 11205-11214.	3.7	3
47483	Nanostructured Pt-doped 2D MoSe₂: an efficient bifunctional electrocatalyst for both hydrogen evolution and oxygen reduction reactions. Physical Chemistry Chemical Physics, 2022, 24, 22823-22844.	1.3	7
47484	Combining in Situ Electrochemistry, Operando Xrd & Raman and Density Functional Theory to Investigate the Fundamentals of Li2co3 Formation in Supercapacitor. SSRN Electronic Journal, 0, , .	0.4	0
47485	Structural, Electronic and Mechanical Properties of Mo2gec Under Strain Engineering. SSRN Electronic Journal, 0, , .	0.4	0
47486	Insights into the Ultra-High Temperature Solid Solutions Hf-Ta-C-N Quaternary System Using High-Throughput Calculation. SSRN Electronic Journal, 0, , .	0.4	0

#	Article	IF	Citations
47487	Influence of Interfacial Configuration on Bonding Properties and Thermal Conductivity of Heterogeneous Interface in Al/Graphite Composite Used for Electronic Packaging. SSRN Electronic Journal, 0, , .	0.4	0
47488	Spintronic Properties in Complex Perovskites: A Concordance Between Experiments and Ab-Initio Calculations. Engineering Materials, 2022, , 183-207.	0.3	1
47489	Confinement catalysis of a single atomic vacancy assisted by aliovalent ion doping enabled efficient NO electroreduction to NH₃. Journal of Materials Chemistry A, 2022, 10, 18690-18700.	5.2	42
47490	Quantum anomalous Hall effect in germanene by proximity coupling to a semiconducting ferromagnetic substrate NiI₂. Physical Chemistry Chemical Physics, 2022, 24, 21631-21637.	1.3	5
47491	Systematics of vibrational properties of Au nanoparticles: a molecular dynamics approach. Physical Chemistry Chemical Physics, 2022, 24, 21833-21840.	1.3	2
47492	LiSrSbS₃: parallel configurations of lone pair electrons inducing a large birefringence. Dalton Transactions, 2022, 51, 14545-14550.	1.6	2
47493	A high-rate capability and energy density sodium ion full cell enabled by F-doped Na₂Ti₃O₇ hollow spheres. Journal of Materials Chemistry A, 2022, 10, 23232-23243.	5.2	5
47494	Electronic, magnetic, optical and thermoelectric properties of co-doped Sn_{1â^'2x}Mn_xA_xO₂ (A = Mo, Tc): a first principles insight. RSC Advances, 2022, 12, 28451-28462.	1.7	2
47495	Magnetic and Transport Properties of Two-Dimensional Ferromagnet Vse2 with Se Vacancies. SSRN Electronic Journal, 0, , .	0.4	0
47496	Theoretical investigation of the optoelectronic response of highly correlated Cu₃P photocatalyst. RSC Advances, 2022, 12, 20721-20726.	1.7	1
47497	The Inhibitory Effect of Magnetism on the Thermal Transport in Nd2fe14b. SSRN Electronic Journal, 0, , .	0.4	0
47498	The Electronic Structures and Optical Properties of Cu-Doped Anatase Tio2 from Calculations of Density Functional Theory. SSRN Electronic Journal, 0, , .	0.4	0
47499	Anchoring Highly Distributed Pt Species with a Strong Metal-Support Interaction Over Chemically Oxidized Graphitic Carbon Nitride for Photocatalytic Hydrogen Evolution: The Effect of Reducing Agents on Photocatalytic Properties. SSRN Electronic Journal, 0, , .	0.4	0
47500	Transition metal Dualâ€“Atom Ni2/TiO2 catalysts for photoelectrocatalytic hydrogen Evolution: A density functional theory study. Applied Surface Science, 2023, 608, 155132.	3.1	7
47501	Fabrication of wide-spectra-responsive NA/NH2-MIL-125(Ti) with boosted activity for Cr(VI) reduction and antibacterial effects. Chemical Engineering Journal, 2023, 452, 139417.	6.6	82
47502	Improved oxygen evolution reaction performance in Co0.4Mn0.6O2 nanosheets through Triple-doping (Cu, P, N) strategy and its application to Zn-air battery. Applied Catalysis B: Environmental, 2023, 320, 122023.	10.8	15
47503	Tuning oxygen vacancy in SnO2 inhibits Pt migration and agglomeration towards high-performing fuel cells. Applied Catalysis B: Environmental, 2023, 320, 122017.	10.8	19
47504	Engineering the photocatalytic performance of B-C3N4@Bi2S3 hybrid heterostructures for fullâ€spectrumâ€driven Cr(VI) reduction and in-situ H2O2 generation: Experimental and DFT studies. Chemical Engineering Journal, 2023, 452, 139435.	6.6	27

#	Article	IF	Citations
47505	Theoretical expolartion of site selective Perovskites for the application of electronic and optoresponsive memory devices. Physica E: Low-Dimensional Systems and Nanostructures, 2023, 145, 115514.	1.3	2
47506	Valence engineering at the interface of MoS2/Mo2C heterostructure for bionic nitrogen reduction. Chemical Engineering Journal, 2023, 452, 139515.	6.6	9
47507	Systematic DFT studies of CO-Tolerance and CO oxidation on Cu-doped Ni surfaces. Journal of Molecular Graphics and Modelling, 2023, 118, 108343.	1.3	16
47508	Electronic changes at the platinum interface induced by bismuth and tellurium adatom adsorption. Applied Surface Science, 2023, 608, 155137.	3.1	2
47509	Using first-principles modeling to investigate dehydrogenation of perhydro-dibenzyltoluene on Pt/M surface alloys (MÂ=ÂFe, Ni, and Cu). Fuel, 2023, 331, 125779.	3.4	7
47510	Unraveling the effects of P and S doping over g-C3N4 in strengthening Lewis basicity for CO2/glycerol conversion: A theoretical and experimental study. Carbon, 2023, 201, 129-140.	5.4	18
47511	Effect of Substitution on Magnetic Moments of Iron and Chromium Atoms in MAX Phases of Type (Cr4) Tj ETQq0 0 0 rgBT /Overlock 10	0.3	1
47512	Investigation of Ag(Ga,In)Se2 as thin-film solar cell absorbers: A first-principles study. Science China: Physics, Mechanics and Astronomy, 2022, 65, .	2.0	5
47513	Theoretical realization of fully spin-polarized nodal box with traversing Brillouin zone surface state. Physical Review B, 2022, 106, .	1.1	5
47514	Magneto-optical Kerr effect and magnetoelasticity in a weakly ferromagnetic <mml:math xmlns:mml="http://www.w3.org/1998/Math/MathML"><mml:msub><mml:mrow><mml:mi>RuF</mml:mi></mml:mrow><mml:mn>4</mml:mn> monolayer. Physical Review B, 2022, 106, .	1.1	1
47515	Strong Influence of the Anion Radius on the Passivation of Selenium Vacancy in Monolayer InSe: Insights from Time-Domain Ab Initio Analysis. Journal of Physical Chemistry C, 2022, 126, 15072-15079.	1.5	0
47516	Selective Reduction of CO₂ on Ti₂C(OH)₂ MXene through Spontaneous Crossing of Transition States. ACS Applied Materials & Interfaces, 2022, 14, 40913-40920.	4.0	8
47517	Electrocatalytic CO2 reduction to alcohols by modulating the molecular geometry and Cu coordination in bicentric copper complexes. Nature Communications, 2022, 13, .	5.8	52
47518	Yeni Ferromanyetik GÃ¼mÃ¼ÅŸ BazlÄ± Sulfo-spinelin (AgV2S4) Elektronik DavranÄ±ÅŸÄ± ve Optik Ã–zellikleri. DÃ¶MF MÃ¼hendislik Dergisi, 0, , .	0.2	0
47519	Li2TiO3 Dopant and Phosphate Coating Improve the Electrochemical Performance of LiCoO2 at 3.0â€“4.6ÂV. Transactions of Tianjin University, 2023, 29, 46-61.	3.3	4
47521	First-principles insights into the electronic, optical, mechanical, and thermodynamic properties of lead-free cubic ABO3 [A = Ba, Ca, Sr; B = Ce, Ti, Zr] perovskites. AIP Advances, 2022, 12, .	0.6	29
47522	What Happens at Surfaces and Grain Boundaries of Halide Perovskites: Insights from Reactive Molecular Dynamics Simulations of CsPbI₃. ACS Applied Materials & Interfaces, 2022, 14, 40841-40850.	4.0	19
47523	Metal Embedded Phthalocyanine Monolayers as Promising Materials for Toxic Formaldehyde Gas Detection: Insights from DFT Calculations. Metals, 2022, 12, 1442.	1.0	5

#	Article	IF	Citations
47524	Study of optoelectronic and thermoelectric properties of double perovskites Rb2AgBiX6 (Xâ€‰=â€‰Br, I): by DFT approach. European Physical Journal Plus, 2022, 137, .	1.2	20
47525	Large Exotic Spin Torques in Antiferromagnetic Iron Rhodium. Physical Review Applied, 2022, 18, .	1.5	4
47526	Trends in the Behavior of Point Defects in MB and MAB Phases. Chemistry of Materials, 2022, 34, 7807-7816.	3.2	1
47527	A brief review of reconstructions and electronic structures of MoS₂ zigzag edges. Journal of Applied Physics, 2022, 132, 080702.	1.1	1
47528	Exceptional strain strengthening and tuning of mechanical properties of TiN. Physical Review B, 2022, 106, .	1.1	3
47529	Hydrogenated Carbon Monolayer in Biphenylene Network Offers a Potential Paradigm for Nanoelectronic Devices. Journal of Physical Chemistry C, 2022, 126, 15491-15500.	1.5	8
47530	Humble planar defects in SiGe nanopillars. Physical Review B, 2022, 106, .	1.1	1
47531	Prediction and Characterization of Graphitic Structures at Diamond Grain Boundaries. Journal of Physical Chemistry C, 2022, 126, 15019-15029.	1.5	2
47532	Pressure-stabilized superconducting electride <mml:math xmlns:mml="http://www.w3.org/1998/Math/MathML"><mml:msub><mml:mrow><mml:mi>Li</mml:mi></mml:mrow><mml:mn>5</mml:mn></mml:msub><mml:mi mathvariant="normal">C</mml:mi></mml:math>. Physical Review B, 2022, 106, .	1.1	10
47533	Heterostrain-enabled ultrahigh electrostrain in lead-free piezoelectric. Nature Communications, 2022, 13, .	5.8	39
47534	Enhancement of Photoactivity of TiO₂ for Potential Applications in CO₂ Conversion and Water Splitting: A Hybrid Density Functional Theory Study. Journal of Physical Chemistry C, 2022, 126, 15080-15093.	1.5	3
47535	Thermoelectric Performance of XXYIn (Xâ€‰=â€‰Fe, Ru; Yâ€‰=â€‰Nb, V) Heusler Alloys: A DFT Study. Journal of Superconductivity and Novel Magnetism, 0, , .	0.8	0
47536	Ab-initio molecular dynamics simulations of the reactivity of MoS2 towards F2 molecules: Implications for etching processes. Applied Surface Science, 2023, 607, 154637.	3.1	4
47537	First-Principles Study on the Nanofriction Properties of Diamane: The Thinnest Diamond Film. Nanomaterials, 2022, 12, 2939.	1.9	5
47538	Above-room-temperature strong intrinsic ferromagnetism in 2D van der Waals Fe3GaTe2 with large perpendicular magnetic anisotropy. Nature Communications, 2022, 13, .	5.8	87
47540	Acetate formation on metals via CH4 carboxylation by CO2: A DFT study. Catalysis Today, 2022, , .	2.2	0
47541	In Silico Band-Gap Engineering of Cr₂C MXenes as Efficient Photocatalysts for Water-Splitting Reactions. Journal of Physical Chemistry C, 2022, 126, 14886-14896.	1.5	7
47542	Revealing the topological phase diagram of ZrTe5 using the complex strain fields of microbubbles. Npj Computational Materials, 2022, 8, .	3.5	3

#	Article	IF	Citations
47543	Efficient Sensing of Selected Amino Acids as Biomarker by Green Phosphorene Monolayers: Smart Diagnosis of Viruses. Advanced Theory and Simulations, 2022, 5, .	1.3	6
47544	Lattice strain modulation toward efficient blue perovskite light-emitting diodes. Science Advances, 2022, 8, .	4.7	23
47545	Urea Production on Metalâ€Free Dual Silicon Doped C9N4 Nanosheet Under Ambient Conditions by Electrocatalysis: A First Principles Study. ChemPhysChem, 0, , .	1.0	3
47546	Impact of Carcinogenic Benzene on Electronic Properties of Mn- and Fe-Doped MoSe2 Monolayer. Lecture Notes in Electrical Engineering, 2023, , 111-118.	0.3	0
47547	Quantitative determination of interlayer electronic coupling at various critical points in bilayer <mml:math xmlns:mml="http://www.w3.org/1998/Math/MathML"><mml:mrow><mml:mi>Mo</mml:mi><mml:msub><mml:mi mathvariant="normal">S</mml:mi><mml:mn>2</mml:mn></mml:msub></mml:mrow></mml:math>. Physical Review B, 2022, 106, .	1.1	4
47548	Ab initio calculation of mechanical, electronic and optical characteristics of chalcogenide perovskite BaZrS₃ at high pressures. Acta Crystallographica Section C, Structural Chemistry, 2022, 78, 570-577.	0.2	2
47549	High Pressure Study of New Type of MAX Phases: Hf ₂ AB ₂ (Aâ€‰=â€‰In, Sn). Physica Status Solidi (B): Basic Research, 0, , 2200102.	0.7	1
47550	Electric Field Guided Fast and Oriented Assembly of MXene into Scalable Pristine Hydrogels for Customized Energy Storage and Water Evaporation Applications. Advanced Functional Materials, 2022, 32, .	7.8	14
47551	Broken-symmetry self-consistent GW approach: Degree of spin contamination and evaluation of effective exchange couplings in solid antiferromagnets. Journal of Chemical Physics, 2022, 157, .	1.2	6
47552	Experimental and Theoretical Study of Sorption Capacity of Hexagonal Boron Nitride Nanoparticles: Implication for Wastewater Purification from Antibiotics. Nanomaterials, 2022, 12, 3157.	1.9	5
47553	Plane-wave-based stochastic-deterministic density functional theory for extended systems. Physical Review B, 2022, 106, .	1.1	2
47554	Magnetic and optical properties of 2H VSe2 and VSSe monolayer. Journal of the Korean Physical Society, 0, , .	0.3	0
47555	Phonon Structure, Infra-Red and Raman Spectra of Li2MnO3 by First-Principles Calculations. Materials, 2022, 15, 6237.	1.3	3
47556	Insights into the high-pressure behavior of solid bromine from hybrid density functional theory calculations. Physical Review B, 2022, 106, .	1.1	1
47557	Enhancing the Photoinduced Interlayer Charge Transfer and Spatial Separation in Type-II Heterostructure of WS₂ and Asymmetric Janus-MoSSe with Intrinsic Self-Build Electric Field. Journal of Physical Chemistry Letters, 2022, 13, 8484-8494.	2.1	13
47558	Effects of Mono-Vacancies and Co-Vacancies of Nitrogen and Boron on the Energetics and Electronic Properties of Heterobilayer h-BN/graphene. Materials, 2022, 15, 6369.	1.3	1
47559	Edge-Driven Phase Transitions in 2D Ice. Journal of Physical Chemistry C, 2022, 126, 16006-16015.	1.5	5
47560	CO2-free high-purity ethylene from electroreduction of CO2 with 4% solar-to-ethylene and 10% solar-to-carbon efficiencies. Cell Reports Physical Science, 2022, 3, 101053.	2.8	8

#	Article	IF	Citations
47561	Unraveling the Effect of A-Site Sr-Doping in Double Perovskites Ca_{2â€“x}Sr_xScRuO₆ (x = 0 and 1): Structural Interpretation and Mechanistic Investigations of Trifunctional Electrocatalytic Effects. ACS Applied Energy Materials, 2022, 5, 11632-11645.	2.5	7
47562	Synergetic storage of ammonia over Al quantum dots embedded graphene sheets: A first principles perspective. International Journal of Hydrogen Energy, 2022, 47, 36873-36885.	3.8	1
47563	3D nano-micro structured NiCoP/CC as high-performance cathode for hybrid supercapacitor. Journal of Alloys and Compounds, 2023, 930, 167316.	2.8	6
47564	Microstructure, mechanical properties and wear resistance of rare earth doped WC/steel matrix composites:Experimental and calculations. Ceramics International, 2023, 49, 2638-2647.	2.3	9
47565	High-capacity hydrogen storage in zirconium decorated zeolite templated carbon: Predictions from DFT simulations. International Journal of Hydrogen Energy, 2022, 47, 38671-38681.	3.8	7
47566	Angular Dependence of the Second-Order Nonlinear Optical Response in Janus Transition Metal Dichalcogenide Monolayers. Journal of Physical Chemistry C, 2022, 126, 16243-16252.	1.5	9
47567	Anharmonicity-induced strong temperature-dependent thermal conductivity in <mml:math xmlns:mml="http://www.w3.org/1998/Math/MathML"><mml:mi>CuIn</mml:mi><mml:msub><mml:mi>X</mml:mi><mml:mn>2</mml:mn></mml:msub></mml:math> (<mml:math) Tj ETQq0 0 0 rgBT /Overlock 10 Tf 50 497 Td (xmlns:mml="http://www.w3.org/1998/Math/MathML"><mml:mrow><mml:	1.1	0
47568	Molecular adsorption behavior and photoelectric properties of SnO2 (221) crystal plane. Sensors and Actuators B: Chemical, 2023, 374, 132753.	4.0	4
47569	First-Principles Insight into a B4C3 Monolayer as a Promising Biosensor for Exhaled Breath Analysis. Journal of Electronic Materials, 2022, 51, 6568-6578.	1.0	6
47570	Ultrathin Niobate Nanosheet Assembly with Au NPs and CdS QDs as a Highly Efficient Photocatalyst. Chemistry - A European Journal, 0, , .	1.7	0
47571	Strong Dzyaloshinskii-Moriya interaction in monolayer <mml:math xmlns:mml="http://www.w3.org/1998/Math/MathML"><mml:msub><mml:mi>CrI</mml:mi><mml:mn>3</mml:mn></mml:msub></mml: on metal substrates. Physical Review B, 2022, 106, .	1.1	6
47572	Thorium dicarbide under high pressure and high temperature: Ab initio investigation. Journal of Applied Physics, 2022, 132, 125904.	1.1	0
47573	Pressure Tuning Resonance Raman Scattering in Monolayer, Trilayer, and Many-Layer Molybdenum Disulfide. ACS Applied Nano Materials, 2022, 5, 14464-14469.	2.4	3
47574	Novel Class of Rhenium Borides Based on Hexagonal Boron Networks Interconnected by Short B₂ Dumbbells. Chemistry of Materials, 2022, 34, 8138-8152.	3.2	2
47575	Density Functional Theory Study of Two-Dimensional Post-Transition Metal Chalcogenides and Halides for Interfacial Charge Transport in Perovskite Solar Cells. ACS Applied Nano Materials, 2022, 5, 14456-14463.	2.4	2
47576	Performance investigation of Ti _x N_{xâ^'1}O₂ MXene (x = 2, 3, 4) as anode materials for Na-ion batteries by first-principles calculation. Nanotechnology, 2022, 33, 495403.	1.3	1
47577	Could one non-noble metal surface with non-noble substrate be a good hydrogen evolution catalyst: Performance of transition metal A monolayer on B substrate in theory frame. International Journal of Hydrogen Energy, 2022, 47, 36149-36162.	3.8	1
47578	First-principles study of O-functionalized two-dimensional AsP monolayers: electronic structure, mechanical, piezoelectric, and optical properties. Nanotechnology, 2023, 34, 015201.	1.3	3

#	Article	IF	Citations
47579	Dissociative adsorption of azoles on Cu(111) promoted by chemisorbed O and OH. Corrosion Science, 2022, 209, 110680.	3.0	8
47580	Hydrogen adsorption and diffusion on doped Zr(0001) surfaces: A first-principles study. International Journal of Hydrogen Energy, 2022, 47, 38644-38654.	3.8	2
47581	Magnetic properties of transition metal ion-doped AgCuS: an ab-initio calculation. Philosophical Magazine, 0, , 1-13.	0.7	0
47582	Oxidative Addition of Methane and Reductive Elimination of Ethane and Hydrogen on Surfaces: From Pure Metals to Single Atom Alloys. Journal of the American Chemical Society, 2022, 144, 18650-18671.	6.6	5
47583	Force-based gradient descent method for ab initio atomic structure relaxation. Physical Review B, 2022, 106, .	1.1	0
47584	Interface Capture Effect Printing Atomicâ€Thick 2D Semiconductor Thin Films. Advanced Materials, 2022, 34, .	11.1	9
47585	Optical and thermoelectric properties of non-Janus CuI and AgI, and Janus <mml:math xmlns:mml="http://www.w3.org/1998/Math/MathML"><mml:msub><mml:mi>Cu</mml:mi><mml:mn>2</mml:mn></mml:msub><mml:m and <mml:math xmlns:mml="http://www.w3.org/1998/Math/MathML"><mml:mrow><mml:msub><mml:mi>Ag</mml:mi><mml:mn>2</mml:mn></mml:m monolayers by many-body perturbation theory. Physical Review B, 2022, 106, .	1.1	5
47586	Unraveling 1-Hexene Hydrogenation over Dilute Pd-in-Au Alloys. Journal of Physical Chemistry C, 2022, 126, 15710-15723.	1.5	6
47587	Single- and Multilayers of Alkali Metal Atoms inside Graphene/MoS₂ Heterostructures: A Systematic First-Principles Study. Journal of Physical Chemistry C, 2022, 126, 15558-15564.	1.5	4
47588	Atomistic simulations of <scp>â^3</scp> [110](111) grain boundary in diamond: Structure, stability, and properties. International Journal of Quantum Chemistry, 2023, 123, .	1.0	2
47589	Stopping and image forces acting on a charged particle moving near a graphene- <mml:math xmlns:mml="http://www.w3.org/1998/Math/MathML"><mml:mrow><mml:msub><mml:mi>Al</mml:mi><mml:mn>2</mml:mn></mml:m mathvariant="normal">O</mml:mi><mml:mn>3</mml:mn></mml:msub></mml:mrow></mml:math> -graphene heterostructure. Physical Review B, 2022, 106, .	1.1	0
47590	Dissociative Chemisorption Dynamics of Ammonia on Ni(111). Journal of Physical Chemistry C, 2022, 126, 15694-15702.	1.5	4
47591	Superatom Molecular Orbitals of Li@C₆₀: Effects of the Li Position and the Substrate. Journal of Physical Chemistry C, 2022, 126, 15891-15898.	1.5	4
47592	Accelerating syngas-to-aromatic conversion via spontaneously monodispersed Fe in ZnCr2O4 spinel. Nature Communications, 2022, 13, .	5.8	15
47593	The Crystal Structure of Carbonic Acid. Inorganics, 2022, 10, 132.	1.2	1
47594	Modified HSE06 functional applied to anatase TiO₂: influence of exchange fraction on the quasiparticle electronic structure and optical response. Electronic Structure, 2022, 4, 045001.	1.0	4
47595	CoSe₂ Subnanometer Belts with Se Vacancies and Ni Substitutions for the Efficient Electrosynthesis of High-Value-Added Nitriles Coupled with Hydrogen Generation. ACS Catalysis, 2022, 12, 11391-11401.	5.5	19
47596	Effects of thin metal contacts on few-layer van der Waals ferrielectric CuInP2S6. Journal of Applied Physics, 2022, 132, .	1.1	1

#	Article	IF	Citations
47597	A Universal Machine Learning Framework for Electrocatalyst Innovation: A Case Study of Discovering Alloys for Hydrogen Evolution Reaction. Advanced Functional Materials, 2022, 32, .	7.8	30
47598	High-Throughput Predictions of the Stabilities of Multi-Type Long-Period Stacking Ordered Structures in High-Performance Mg Alloys. Nanomaterials, 2022, 12, 3240.	1.9	1
47599	Predicting phase preferences of two-dimensional transition metal dichalcogenides using machine learning. Physical Review Materials, 2022, 6, .	0.9	3
47600	BaCO3 Nanoparticles-Modified Composite Cathode with Improved Electrochemical Oxygen Reduction Kinetics for High-Performing Ceramic Fuel Cells. Catalysts, 2022, 12, 1046.	1.6	4
47601	Reconfigurable band alignment of <mml:math xmlns:mml="http://www.w3.org/1998/Math/MathML"><mml:mrow><mml:mi>m</mml:mi><mml:mtext>â^'</mml:mtext><mml:mi>GaS (<mml:math) Tj ETQq0 0 0 rgBT /Overlock 10 Tf 50 577 Td (xmlns:mml="http://www.w3.org/1998/Math/MathML"><mml:mrow><mml:r	1.1	8
47602	Structural and charge transfer properties of ion intercalated 2D and bulk ice. Journal of Chemical Physics, 0, , .	1.2	0
47603	Memristive Switching and Density-Functional Theory Calculations in Double Nitride Insulating Layers. Micromachines, 2022, 13, 1498.	1.4	0
47604	Sr Doping and Oxygen Vacancy Formation in La1â^'xSrxScO3â^'Î´ Solid Solutions: Computational Modelling. Crystals, 2022, 12, 1300.	1.0	2
47605	Softened <mml:math xmlns:mml="http://www.w3.org/1998/Math/MathML"><mml:mrow><mml:mi>s</mml:mi><mml:msup><mml:mrow></mml:mrow><mml:mi>p</mml:mi><mml:r bonding network leads to strong anharmonicity and weak hydrodynamics in graphene+. Physical Review B, 2022, 106, .	1.1	12
47606	First-principles prediction of the lattice thermal conductivity of two-dimensional (2D) h-BX (Xâ€‰=â€‰P, As,) Tj ETQq1 1 0.784314 gf 132, .	1.1	10
47607	Revisiting the Role of Physical Confinement and Chemical Regulation of 3D Hosts for Dendrite-Free Li Metal Anode. Nano-Micro Letters, 2022, 14, .	14.4	23
47608	Tunable magnetocrystalline anisotropy and valley polarization in an intrinsic ferromagnetic Janus <mml:math xmlns:mml="http://www.w3.org/1998/Math/MathML"><mml:mn>2</mml:mn><mml:mi>H</mml:mi></mml:math> -VTeSe monolayer. Physical Review B, 2022, 106, .	1.1	8
47609	Atomic-scale study of type-II Dirac semimetal PtTe₂ surface. JPhys Materials, 2022, 5, 044003.	1.8	4
47610	Construction of novel PG/GeP2 and PG/SiP2 vdW heterostructures for high-efficiency photocatalytic water splitting. Applied Surface Science, 2023, 608, 155106.	3.1	34
47611	Exploration of the structural, optoelectronic and vibrational behavior of Sb2S3 through the first principles approach for phenomenal applications in solar cells. Optical and Quantum Electronics, 2022, 54, .	1.5	4
47612	Ultrasmall SnS₂ quantum dotâ^'based photodetectors with high responsivity and detectivity. Nanophotonics, 2022, 11, 4781-4792.	2.9	5
47613	Effect of Segregation of Sc, Y and La Atoms on Prenucleation at the Liquid-Al/Î³-Al2O3{1 1 1} Interfaces. Metals, 2022, 12, 1550.	1.0	2
47614	Single atom precise, ultrafast, and universal emulation of biological synapses using atomically thin vertical heterostructures. Journal of Applied Physics, 2022, 132, 124306.	1.1	0

#	Article	IF	Citations
47615	Defective g-C3N4 supported Ru3 single-cluster catalyst for ammonia synthesis through parallel reaction pathways. Nano Research, 2023, 16, 3580-3587.	5.8	8
47616	Spontaneous Polarization and Polarization-Induced Electron Sheet Charge of YbAlN on GaN: A First-Principles Study. ACS Applied Electronic Materials, 2022, 4, 4772-4780.	2.0	1
47617	Diffusion Studies of H of Different Charge States and Their Interplay with Co Spin States in SrCoO_{2.5}. Journal of Physical Chemistry C, 2022, 126, 16315-16331.	1.5	2
47618	Activating basal plane of Janus VSSe for efficient hydrogen evolution reaction by non-noble metal element doping: A first-principal study. International Journal of Hydrogen Energy, 2022, 47, 34924-34931.	3.8	5
47619	Coexistence of two types of short-range order in Siâ€“Geâ€“Sn medium-entropy alloys. Communications Materials, 2022, 3, .	2.9	3
47620	Atomicâ€Scale Oxygenâ€Mediated Etching of 2D MoS₂ and MoTe₂. Advanced Materials Interfaces, 2022, 9, .	1.9	3
47621	Tuning exciton complexes in twisted bilayer <mml:math xmlns:mml="http://www.w3.org/1998/Math/MathML"><mml:msub><mml:mi>WSe</mml:mi><mml:mn>2</mml:mn></mml:msub></mml:math> at intermediate misorientation. Physical Review B, 2022, 106, .	1.1	2
47622	Highly tunable band inversion in <mml:math xmlns:mml="http://www.w3.org/1998/Math/MathML"><mml:mrow><mml:mi>A</mml:mi><mml:msub><mml:mi>B</mml:mi><mml:mn>		

#	Article	IF	Citations
47635	Bonding Inhomogeneity and Strong Anharmonicity Induce Ultralow Lattice Thermal Conductivity in Calcium Pyrovanadate. Journal of Physical Chemistry C, 2022, 126, 16492-16498.	1.5	2
47636	The electronic and mechanical properties of Fe₁₆N₂ up to 150â€‰GPa: First-principles calculation. Journal of Applied Physics, 2022, 132, 095904.	1.1	1
47637	Pressure Effects on the Structural, Elastic Properties and Mechanical Parameters of Al-Doped GaAs. Advanced Materials Research, 0, 1174, 113-122.	0.3	0
47638	Pressure-induced decomposition of cadmium iodide. Europhysics Letters, 2022, 140, 16003.	0.7	4
47639	Facilitating Hydrogen Dissociation over Dilute Nanoporous Tiâ€“Cu Catalysts. Journal of the American Chemical Society, 2022, 144, 16778-16791.	6.6	10
47640	Mechanism of Efficient Adsorption of <mml:math xmlns:mml="http://www.w3.org/1998/Math/MathML" display="inline" overflow="scroll"><mml:mi>Na</mml:mi></mml:math> Atoms on Electron-Deficient Doped <mml:math xmlns:mml="http://www.w3.org/1998/Math/MathML" display="inline" overflow="scroll"><mml:msub><mml:mrow><mml:mi>Mo</mml:mi><mml:mi mathvariant="normal">S</mml:mi></mml:mrow><mml:mn>2</mml:mn></mml:msub></mml:math> for Battery Electrodes. Physical Review Applied, 2022, 18, .	1.5	3
47641	Surface Organometallic Chemistry on Zeolites: Synthesis of Group IV Metal Alkyls and Metal Hydrides on Hierarchical Mesoporous H-ZSM-5. Chemistry of Materials, 2022, 34, 8777-8789.	3.2	1
47642	Prediction of stability and lifetime of carbyne, carbyneâ€“graphene and similar low-dimensional nanostructures. Applied Nanoscience (Switzerland), 0, , .	1.6	1
47643	Understanding the surface segregation of solute atoms in Sn-Biâ€“based solder from first principles. Europhysics Letters, 2022, 139, 66002.	0.7	0
47644	Adsorption Energy in Oxygen Electrocatalysis. Chemical Reviews, 2022, 122, 17028-17072.	23.0	45
47645	Structure, Stability, and Electronic Properties of Boron Suboxide: A Density Functional Theory Study. Journal of Physical Chemistry C, 2022, 126, 16050-16060.	1.5	2
47646	Machine Learning-Aided Exploration of Ultrahard Materials. Journal of Physical Chemistry C, 2022, 126, 15952-15961.	1.5	3
47647	A quest to high-capacity hydrogen storage in zirconium decorated pentagraphene: DFT perspectives. International Journal of Hydrogen Energy, 2022, 47, 36190-36203.	3.8	15
47648	Investigation on the Reaction Mechanism of Methane Oxidation over MgAl2O4â€supported Singleâ€Atom Catalyst Prepared at High Temperature. ChemCatChem, 0, , .	1.8	2
47649	What is the Real Origin of the Activity of Feâ€“Nâ€“C Electrocatalysts in the O₂ Reduction Reaction? Critical Roles of Coordinating Pyrrolic N and Axially Adsorbing Species. Journal of the American Chemical Society, 2022, 144, 18144-18152.	6.6	105
47650	The electron transfer mechanism between metal and silicon oxide composites for triboelectric nanogenerators. Advanced Composites and Hybrid Materials, 2022, 5, 3223-3231.	9.9	5
47651	Ultrasensitive Formaldehyde Sensor Based on SnO₂ with Rich Adsorbed Oxygen Derived from a Metal Organic Framework. ACS Sensors, 2022, 7, 2577-2588.	4.0	17
47652	Carbon-oxygen surface formation enhances secondary electron yield in Cu, Ag and Au. Scientific Reports, 2022, 12, .	1.6	5

#	Article	IF	Citations
47653	Adhesion strength, interfacial bonding, and fracture mechanism of the Mg/Ti2AlC interface from first-principles calculation. Journal of Materials Research and Technology, 2022, 20, 3195-3207.	2.6	22
47654	Structural Dynamics, Phonon Spectra and Thermal Transport in the Silicon Clathrates. Molecules, 2022, 27, 6431.	1.7	2
47655	Manipulating Nucleation Potency of Substrates by Interfacial Segregation: An Overview. Metals, 2022, 12, 1636.	1.0	5
47656	PbBi(SeO₃)₂F and Pb₂Bi(SeO₃)₂Cl₃: Coexistence of Three Kinds of Stereochemically Active Lone-Pair Cations Exhibiting Excellent Nonlinear Optical Properties. Inorganic Chemistry, 2022, 61, 15368-15376.	1.9	19
47657	A Machine Learning Model of Chemical Shifts for Chemically and Structurally Diverse Molecular Solids. Journal of Physical Chemistry C, 2022, 126, 16710-16720.	1.5	15
47658	CH₄ Activation over Perovskite Catalysts: True Density and Reactivity of Active Sites. ACS Catalysis, 2022, 12, 11845-11853.	5.5	7
47659	Two-dimensional Janus like scandium-based MXenes as photocatalysts for overall water splitting: A first-principles study. Sustainable Materials and Technologies, 2022, 34, e00502.	1.7	3
47660	Lecture Notes on First-Principles Methods Using a Plane-Wave Basis Set (Part 1). Materia Japan, 2022, 61, 588-594.	0.1	0
47661	Edge states of topological acoustic phonons in graphene zigzag nanoribbons. Physical Review B, 2022, 106, .	1.1	25
47662	Confinement of volatile fission products in the crystalline organic electride Cs+(15C5)2â€¢eâ˜. Journal of Applied Physics, 2022, 132, .	1.1	2
47663	Highâ€Throughput Dataâ€Driven Prediction of Stable Highâ€Performance Naâ€Ion Sulfide Solid Electrolytes. Advanced Functional Materials, 2022, 32, .	7.8	4
47664	Structural and electronic properties of ZnSnAs2: A first-principles study by MGGA method. Pramana - Journal of Physics, 2022, 96, .	0.6	1
47665	Tunable Weyl half-semimetals in two-dimensional iron-based materials <mml:math xmlns:mml="http://www.w3.org/1998/Math/MathML"><mml:mrow><mml:mi>M</mml:mi><mml:mi>FeSe</mml:mi></mml:mrow><mm Physical Review B, 2022, 106, .	1.1	6
47666	High switching ratio and inorganic gas sensing performance in BeN₄ based nanodevice: a first-principles study. Journal of Physics Condensed Matter, 2022, 34, 465302.	0.7	6
47667	DFT Modelling of Li6SiO4Cl2 Electrolyte Material for Li-Ion Batteries. Batteries, 2022, 8, 137.	2.1	1
47668	Rhodium nanocrystals on porous graphdiyne for electrocatalytic hydrogen evolution from saline water. Nature Communications, 2022, 13, .	5.8	101
47669	Mott transition and superexchange mechanism in magnetically doped <mml:math xmlns:mml="http://www.w3.org/1998/Math/MathML"><mml:mrow><mml:mi>X</mml:mi><mml:msub><mml:mi>Si</mml:mi><mml:mn mathvariant="normal">N</mml:mi><mml:mn>4</mml:mn></mml:msub></mml:mrow></mml:math> caused by large <mml:math xmlns:mml="http://www.w3.org/1998/Math/MathML"><mml:mrow><mml:mn>3</mml:mn><mml:mi>d</mml:mi></mml:mrow></mml:r orbital onsite Coulomb interaction. Physical Review B, 2022, 106, .	1.1	3
47670	High-Temperature Ferromagnetism in a Two-Dimensional Semiconductor with a Rectangular Spin Lattice. Journal of Physical Chemistry C, 2022, 126, 16034-16041.	1.5	6

#	Article	IF	Citations
47671	Electron-lattice coupling effects in nonadiabatic polarization switching of charge-order-induced ferroelectrics. Physical Review B, 2022, 106, .	1.1	1
47672	Boosting Electrocatalytic Reduction of CO₂ to HCOOH on Ni Single Atom Anchored WTe₂ Monolayer. Small, 2022, 18, .	5.2	37
47673	Functional-Unit-Based Material Design: Ultralow Thermal Conductivity in Thermoelectrics with Linear Triatomic Resonant Bonds. Journal of the American Chemical Society, 2022, 144, 18552-18561.	6.6	14
47674	Emergence of cubic ordered full-plane persistent spin textures in lead-free materials. Physical Review Materials, 2022, 6, .	0.9	10
47675	High Quantum Efficiency of Stable Sbâ€Based Perovskiteâ€Like Halides toward White Light Emission and Flexible Xâ€Ray Imaging. Advanced Optical Materials, 2022, 10, .	3.6	31
47676	Concentration dependences of electronic band structure of CdSe1â€“xSx thin films. Applied Nanoscience (Switzerland), 0, , .	1.6	1
47677	Ion slippage through Li ⁺ -centered G-quadruplex. Science Advances, 2022, 8, .	4.7	1
47678	Bromine Pentafluoride BrF₅, the Formation of [BrF₆]^{â^'} Salts, and the Stereochemical (In)activity of the Bromine Lone Pairs. Chemistry - A European Journal, 2022, 28, .	1.7	7
47679	Effects of the pH Value on the Electrodeposition of Feâ€“P Alloy as a Magnetic Film Material. Journal of Physical Chemistry C, 2022, 126, 15472-15484.	1.5	6
47680	High-temperature nodal ring semimetal in two-dimensional honeycomb-kagome Mn₂N₃ lattice. Chinese Physics B, 2022, 31, 127203.	0.7	1
47681	The Magnetic Properties of Fe4BO7 and Mn4BO7 Tetraborates in Three Structural Types. JETP Letters, 0, , .	0.4	0
47682	Investigation of spatially localized defects in synthetic <mml:math xmlns:mml="http://www.w3.org/1998/Math/MathML"><mml:msub><mml:mi>WS</mml:mi><mml:mn>2</mml:mn></mml:msub></m monolayers. Physical Review B, 2022, 106, .	1.1	2
47683	Thermodynamic Properties of Crystalline Cellulose Allomorphs Studied with Dispersion-Corrected Density Functional Methods. Molecules, 2022, 27, 6240.	1.7	2
47684	Searching for Circular Photo Galvanic Effect in Oxyhalide Perovskite Bi₄NbO₈Cl. Advanced Functional Materials, 2022, 32, .	7.8	5
47685	Graphdiyne oxide nanosheets display selective anti-leukemia efficacy against DNMT3A-mutant AML cells. Nature Communications, 2022, 13, .	5.8	20
47686	Circumventing the stability problems of graphene nanoribbon zigzag edges. Nature Chemistry, 2022, 14, 1451-1458.	6.6	15
47687	Electronic and Magnetic Properties of Spinâ€“Orbit-Entangled Honeycomb Lattice Iridates MIrO₃ (M = Cd, Zn, and Mg). Inorganic Chemistry, 2022, 61, 15007-15015.	1.9	2
47689	Ambient-Pressure Recoverable Polynitrogen Solids Assembled by Pentazolate Rings with High Energy Density. Inorganic Chemistry, 2022, 61, 15532-15539.	1.9	1

#	Article	IF	Citations
47690	Ultrathin ferrite nanosheets for room-temperature two-dimensional magnetic semiconductors. Nature Communications, 2022, 13, .	5.8	39
47691	Oxychalcogenides as Promising Ultraviolet Nonlinear Optical Candidates: Experimental and Theoretical Studies of AEGeOS₂(AE = Sr and Ba). Inorganic Chemistry, 2022, 61, 15711-15720.	1.9	13
47692	Filamentary and Interface-Type Memristors Based on Tantalum Oxide for Energy-Efficient Neuromorphic Hardware. ACS Applied Materials & Interfaces, 2022, 14, 44561-44571.	4.0	24
47693	Topological and quantum stability of low-dimensional crystalline lattices with multiple nonequivalent sublattices*. New Journal of Physics, 2022, 24, 103015.	1.2	8
47694	Large-gap quantum anomalous Hall states induced by functionalizing buckled Bi-III monolayer/ <mml:math xmlns:mml="http://www.w3.org/1998/Math/MathML"><mml:mrow><mml:msub><mml:mi>Al</mml:mi><mml:mn>2</mml:mn><mml:mathvariant="normal">O</mml:mi><mml:mn>3</mml:mn></mml:msub></mml:mrow></mml:math>. Physical Review B, 2022, 106, .	3.7	2
47695	Distortion of SiC lattice induced by carbon-coating on (100) and (111) surfaces - ab-initio and molecular dynamics study. Surface Science, 2023, 728, 122179.	0.8	2
47696	Single-Crystal Diffraction, Raman Spectroscopy, and Density Functional Theory of DTO [N-(1,7-Dinitro-1,2,6,7-tetrahydro-[1,3,5]triazino[1,2-c][1,3,5]oxadiazin-8(4H)-ylidene)nitramide]. Journal of Physical Chemistry A, 2022, 126, 6648-6656.	1.1	0
47697	Efficient Catalytic Upgrading of Ethanol to Higher Alcohols via Inhibiting Câ€“C Cleavage and Promoting Câ€“C Coupling over Biomass-Derived NiZn@NC Catalysts. ACS Catalysis, 2022, 12, 11573-11585.	5.5	37
47698	Effect of Pt Decoration on the Optical Properties of Pristine and Defective MoS2: An Ab-Initio Study. International Journal of Molecular Sciences, 2022, 23, 11199.	1.8	1
47699	Assessing the Drawbacks and Benefits of Ion Migration in Lead Halide Perovskites. ACS Energy Letters, 2022, 7, 3401-3414.	8.8	46
47700	First Principles Calculations of the Optical Response of LiNiO2. Condensed Matter, 2022, 7, 54.	0.8	3
47701	Observation of competing, correlated ground states in the flat band of rhombohedral graphite. Science Advances, 2022, 8, .	4.7	9
47702	Firstâ€principles study on structural, electronic, elastic, mechanical, thermodynamic, and thermoelectric properties of <scp> RbSnX ₃ </scp> (XÂ=ÂF, Cl, and Br) perovskites. International Journal of Energy Research, 2022, 46, 23893-23907.	2.2	13
47703	Comprehensive study of band structure driven thermoelectric response of <mml:math xmlns:mml="http://www.w3.org/1998/Math/MathML"><mml:msub><mml:mi>ZrTe</mml:mi><mml:mn>5</mml:mn></mml:msub></mml:math> Physical Review B, 2022, 106, .	3.7	4
47704	Biased self-diffusion on Cu surface due to electric field gradients. Journal Physics D: Applied Physics, 2022, 55, 465302.	1.3	3
47705	Efficient microwave absorption with Vn+1CnT MXenes. Cell Reports Physical Science, 2022, 3, 101073.	2.8	29
47706	Theoretical Investigation of the Oxygen Reduction Reaction over Platinum Catalysts Supported by Multiâ€Edged Vertically Aligned Carbon Nanofiber for Electrocatalyst Preparation. ChemElectroChem, 0, , .	1.7	2
47707	The Effect of La3+ on the Methylene Blue Dye Removal Capacity of the La/ZnTiO3 Photocatalyst, a DFT Study. Nanomaterials, 2022, 12, 3137.	1.9	11

#	Article	IF	Citations
47708	Hydrogen Separation with a Graphenylene Monolayer: Diffusion Monte Carlo Study. Journal of Chemical Physics, 0, , .	1.2	0
47709	Ab Initio Molecular Dynamics Investigation of Prenucleation at Liquidâ€“Metal/Oxide Interfaces: An Overview. Metals, 2022, 12, 1618.	1.0	4
47710	A first-principles study on the physical properties of two-dimensional Nb3Cl8, Nb3Br8 and Nb3I8. Applied Physics A: Materials Science and Processing, 2022, 128, .	1.1	4
47711	Prediction of Ground State Structures and Robust Weyl Fermionic States in MnRhP. Journal of Physical Chemistry C, 2022, 126, 17328-17337.	1.5	0
47712	Symmetry-enforced electronic nodal straight lines in CsNb₃SBr₇. New Journal of Physics, 2022, 24, 093033.	1.2	0
47713	Layer-Dependent Nonlinear Absorption and Refraction of <mml:math xmlns:mml="http://www.w3.org/1998/Math/MathML" display="inline" overflow="scroll"><mml:mi>Re</mml:mi></mml:math> <mml:math xmlns:mml="http://www.w3.org/1998/Math/MathML" display="inline" overflow="scroll"><mml:msub><mml:mi>X</mml:mi><mml:mn>2</mml:mn></mml:msub><mml:mo		

#	Article	IF	Citations
47726	Pressure-induced novel structure with graphene-like boron-layer in titanium monoboride. Chinese Physics B, 0, , .	0.7	3
47727	Crystal Structure of Î³â€Ca2P2O7. Zeitschrift Fur Anorganische Und Allgemeine Chemie, 0, , .	0.6	2
47728	First-Principles Calculations to Investigate the Effect of Van der Waals Interactions on the Crystal and Electronic Structures of Tin-Based 0D Hybrid Perovskites. Inorganics, 2022, 10, 155.	1.2	25
47729	Chemical interaction, self-ordering and corrosion inhibition properties of 2-mercaptobenzothiazole monolayers: DFT atomistic modeling on metallic copper. Corrosion Science, 2022, 209, 110658.	3.0	8
47730	Remote Oxygen Scavenging of the Interfacial Oxide Layer in Ferroelectric Hafniumâ€“Zirconium Oxide-Based Metalâ€“Oxideâ€“Semiconductor Structures. ACS Applied Materials & Interfaces, 2022, 14, 43897-43906.	4.0	4
47731	Adsorption of imidazolium-based ionic liquids on the Fe(1 0 0) surface for corrosion inhibition: Physisorption or chemisorption?. Journal of Molecular Liquids, 2022, 367, 120489.	2.3	12
47732	Graphene grown on transition metal substrates: Versatile templates for organic molecules with new properties and structures. Surface Science Reports, 2022, , 100575.	3.8	1
47733	Iron decorated defective phosphorene as a viable hydrogen storage medium â€“ A DFT study. International Journal of Hydrogen Energy, 2022, 47, 34976-34993.	3.8	6
47734	OH spectator at IrMo intermetallic narrowing activity gap between alkaline and acidic hydrogen evolution reaction. Nature Communications, 2022, 13, .	5.8	48
47735	Magnon Straintronics in the 2D van der Waals Ferromagnet CrSBr from First-Principles. Nano Letters, 2022, 22, 8771-8778.	4.5	20
47736	New CrOX (XÂ=ÂCl, Br, I) monolayer with ultra-wide single spin states. Europhysics Letters, 2022, 140, 16002.	0.7	0
47737	Strain Effects on the Two-Dimensional Cr₂N MXene: An Ab Initio Study. ACS Omega, 2022, 7, 33884-33894.	1.6	6
47738	First Experimental Synthesis of Mg Orthocarbonate by the MgCO3 + MgO = Mg2CO4 Reaction at Pressures of the Earthâ€™s Lower Mantle. JETP Letters, 2022, 116, 477-484.	0.4	7
47739	Engineering Atomic Single Metalâ€“FeN₄Cl Sites with Enhanced Oxygen-Reduction Activity for High-Performance Proton Exchange Membrane Fuel Cells. ACS Nano, 2022, 16, 15165-15174.	7.3	60
47740	Vacancy dynamics in niobium and its native oxides and their potential implications for quantum computing and superconducting accelerators. Physical Review B, 2022, 106, .	1.1	7
47741	Emergent topological states via digital (001) oxide superlattices. Npj Computational Materials, 2022, 8, .	3.5	1
47742	Fe₂C- and Mn₂(W/Mo)B₄-based rare-earth-free permanent magnets as a result of the high-throughput and data-mining search. Materials Research Letters, 2023, 11, 76-83.	4.1	4
47743	Basal Surface Hybridization of Group V Layered Transition Metal Dichalcogenides. ACS Materials Au, 0, , .	2.6	1

#	Article	IF	Citations
47744	Bonding Strength and Fracture Properties of Al (021)/Al₂CuMg (001) Interface and Agâ€Doped Modification: A Firstâ€Principles Study. Advanced Engineering Materials, 2023, 25, .	1.6	1
47745	Two-dimensional intrinsic ferrovalley Janus 2H-VSeS monolayer with high Curie temperature and robust valley polarization. Physical Review Materials, 2022, 6, .	0.9	2
47746	Controllable synthesis and crystal facet, composition and temperature dependent gas sensing properties of Sn1â^'xS-CdS superlattice nanowires with ultrafast response. Sensors and Actuators B: Chemical, 2023, 377, 132762.	4.0	2
47747	Coupling between tilts and charge carriers at polar-nonpolar perovskite interfaces. Physical Review B, 2022, 106, .	1.1	0
47748	First-Principles Study of Enhanced Absorption in Van der Waals Heterostructure of MoS2/Cd0.90Zn0.10Te0.93Se0.07 in the Visible Region. Journal of Electronic Materials, 2022, 51, 6595-6602.	1.0	1
47749	The first-principle study on structural, mechanical, electronic and optical properties of half-metallic CaMSi2O6 (M= Co, Fe, Mn) clinopyroxenes. Computational Condensed Matter, 2022, 33, e00749.	0.9	3
47750	Phase Stability, Magnetic Properties, and Martensitic Transformation of Ni2â^'xMn1+x+ySn1â^'y Heusler Alloy with Excess Mn by First-Principles Calculations. Acta Metallurgica Sinica (English Letters), 2023, 36, 513-528.	1.5	1
47751	A first-principles study of Janus monolayer MXY (Mâ€‰=â€‰Mo, W; X, Yâ€‰=â€‰S, Se, Te)/SiO2 van der Waals heterojunctions for integrated optical fibers. Advanced Composites and Hybrid Materials, 2022, 5, 3232-3244.	9.9	10
47752	Novel two-dimensional PdSe phase: A puckered material with excellent electronic and optical properties. Frontiers of Physics, 2022, 17, .	2.4	4
47753	Lattice dynamics, elastic, magnetic, thermodynamic and thermoelectric properties of the two-dimensional semiconductors MPSe₃ (M = Cd, Fe and NI): a first-principles study. Materials Research Express, 2022, 9, 106302.	0.8	1
47754	Beyond the ionic radii: A multifaceted approach to understand differences between the structures of LnNbO4 and LnTaO4 fergusonites. Journal of Alloys and Compounds, 2023, 930, 167399.	2.8	1
47755	Strategy to consider element distribution when constructing training datasets for developing machine learning potentials of alloys based on a Monte-Carlo-like method. Physical Review B, 2022, 106, .	1.1	0
47757	Building efficient interfacial property with graphene heterogeneous interface. International Journal of Mechanical Sciences, 2023, 237, 107782.	3.6	10
47758	Tuning the Coordination Microenvironment to Boost the Electrocatalytic HER Activity of M₃(C₆O₃S₃)₂. Journal of Physical Chemistry C, 2022, 126, 16606-16614.	1.5	1
47759	Emergent Negative Differential Resistance with an Undisturbed Topological Surface State. Journal of Physical Chemistry C, 2022, 126, 16744-16750.	1.5	1
47760	Probing Intermolecular H-Bonding Interactions in Cyanuric Acid Networks: Quenching of the N K-Edge Sigma Resonances. Journal of Physical Chemistry A, 2022, 126, 6870-6881.	1.1	2
47761	Trends of earthâ€abundant transition metalâ€doped in <scp> CoSe ₂ </scp> microstructures towards improved water splitting and supercapacitor applications. International Journal of Energy Research, 2022, 46, 24588-24601.	2.2	6
47762	A DFT study of gas molecules adsorption on intrinsic and Cu-doped graphene gas nanosensors. Physica Scripta, 2022, 97, 105807.	1.2	1

#	Article	IF	Citations
47763	Superconducting properties of doped blue phosphorene: effects of non-adiabatic approach. 2D Materials, 2022, 9, 045029.	2.0	6
47764	Time-reversal symmetry broken quantum spin Hall phase in the van der Waals heterostructure ZrTe₅/Cr₂Ge₂Te₆. New Journal of Physics, 2022, 24, 093029.	1.2	1
47765	Atomic Simulations of Primary Irradiation Damage in U-Mo-Xe system. Chinese Physics B, 0, , .	0.7	1
47766	Capturing the ground state of uranium dioxide from first principles: Crystal distortion, magnetic structure, and phonons. Physical Review B, 2022, 106, .	1.1	7
47767	First-principles study on remote van der Waals epitaxy through graphene monolayer on semiconductor substrates. Chinese Physics B, 0, , .	0.7	0
47768	Scaleability of dielectric susceptibility <mml:math xmlns:mml="http://www.w3.org/1998/Math/MathML"><mml:msub><mml:mi>Îµ</mml:mi><mml:mrow><mml:mi>z</mml:mi><mml:mi> with the number of layers and additivity of ferroelectric polarization in van der Waals semiconductors. Physical Review B, 2022, 106, .	1.1	3
47769	Density functional theory: The evaluation of structural, electronic, optical, and mechanical properties of WO3. Computational Condensed Matter, 2022, 33, e00752.	0.9	4
47770	Robust spin glass state with exceptional thermal stability in a chemically complex alloy. Physical Review Materials, 2022, 6, .	0.9	1
47771	Heisenbergâ€™s uncertainty principle in the PTOLEMY project: A theory update. Physical Review D, 2022, 106, .	1.6	14
47772	Large Negative Poissonâ€™s Ratio and Anisotropic Mechanics in New Penta-PBN Monolayer. ACS Omega, 2022, 7, 36235-36243.	1.6	5
47773	Strain-Modulated Interlayer Charge and Energy Transfers in MoS₂/WS₂ Heterobilayer. ACS Applied Materials & Interfaces, 2022, 14, 46841-46849.	4.0	4
47774	Catalytic mechanism and activity of N₂ reduction on boron-decorated crystalline carbon nitride. 2D Materials, 2022, 9, 045035.	2.0	2
47775	Two-dimensional FePc and MnPc monolayers as promising materials for SF6 decomposition gases detection: Insights from DFT calculations. Applied Surface Science, 2023, 608, 155119.	3.1	22
47776	Novel two-dimensional SiC2 monolayer with potential as a superior anode for sodium-ion batteries. Journal of Materials Science, 2022, 57, 18406-18416.	1.7	1
47777	2D Dumbbell Silicene as a High Storage Capacity and Fast Ion Diffusion Anode for Li-Ion Batteries. ACS Applied Materials & Interfaces, 2022, 14, 47262-47271.	4.0	23
47778	Theoretical Study and Application of Doped 2D PbSe for Toxic Gases. Physica Status Solidi (B): Basic Research, 0, , 2200250.	0.7	1
47779	Catalytic Reduction of 4-Nitrophenol to 4-Aminophenol Using Ag@Ĩ±-Ti(HPO₄)₂Â·H₂O: Experimental and Computational Studies. Industrial & Engineering Chemistry Research, 2022, 61, 15181-15194.	1.8	1
47780	Improving optical properties of wurtzite GaN with C and Fe co-doping: A DFT+U study. Journal of Physics Communications, 0, , .	0.5	0

#	Article	IF	Citations
47781	First-principles investigation of a-line Shockley partial dislocations in wurtzite GaN: core reconstruction and electronic structure. Modelling and Simulation in Materials Science and Engineering, 2022, 30, 085004.	0.8	1
47782	Stable Isotope Fractionations Involving Caâ€“Mg Carbonates: Evaluation of the Î²-Factors by the â€œFrozen Phononâ€•Method. Geochemistry International, 2022, 60, 947-964.	0.2	1
47783	A first-principles study of magnetic switching and hysteresis effect in the ferromagnetic Fe metal. Chinese Journal of Physics, 2022, , .	2.0	0
47784	Nonuniform grids for Brillouin zone integration and interpolation. Physical Review B, 2022, 106, .	1.1	4
47785	Revealing photovoltaic behavior in 2D hybrid perovskite ferroelectric single-crystalline microwire arrays for self-powered photodetectors. Materials Today Physics, 2022, 28, 100867.	2.9	5
47786	Firstâ€Principles Calculations of Physical Properties and Stability of Orthorhombic FeN₂ under High Pressure. Physica Status Solidi (B): Basic Research, 2023, 260, .	0.7	0
47787	Negative Longitudinal Piezoelectricity Coexisting with both Negative and Positive Transverse Piezoelectricity in a Hybrid Formate Perovskite. ACS Applied Materials & Interfaces, 2022, 14, 46449-46456.	4.0	3
47788	Efficient electrochemical CO2 reduction reaction on a robust perovskite type cathode with in-situ exsolved Fe-Ru alloy nanocatalysts. Separation and Purification Technology, 2023, 304, 122287.	3.9	17
47789	Defective hBN-Supported Fe₂N Single Cluster Catalyst for Active and Selective Electro-Reduction of Multiple CO to Propane: Theoretical Elucidation of Metalâ€“Nonmetal Synergic Effects. ACS Applied Materials & Interfaces, 2022, 14, 46657-46664.	4.0	2
47790	Theoretical study of the line defect in Ï‡3-borophene: structures, electronic properties, direct-current and alternating-current transport properties. Applied Surface Science, 2023, 608, 155033.	3.1	3
47791	Origin of the herringbone reconstruction of Au(111) surface at the atomic scale. Science Advances, 2022, 8, .	4.7	12
47792	First-principles study on structural, mechanical, and electronic properties of REAuBi₂ (RE) Tj ETQq1 1 0.784314 rgBT /Over	0.6	0
47793	First principles study of Mo, W doped CrBr3 alloy compounds. Materials Today Communications, 2022, 33, 104592.	0.9	0
47794	The role of the surface passivation in the mechanical properties of wurtzite InAs and InP nanowires: first-principles calculations. European Physical Journal Plus, 2022, 137, .	1.2	0
47795	Electronic structure of Humble defects in Ge and <mml:math xmlns:mml="http://www.w3.org/1998/Math/MathML"><mml:mrow><mml:msub><mml:mi>Ge</mml:mi><mml:mrow	1.1	0
	Physical Review B, 2022, 106, .		
47796	First Principles Study of Structural Phase Transition in Ag₂S under High Pressure. Integrated Ferroelectrics, 2022, 230, 23-28.	0.3	2
47797	Pressure-induced phase transitions of CsSnBr₃ perovskite from first-principles calculations. Physica Scripta, 2022, 97, 115811.	1.2	1
47798	Pressure-dependence of mechanical properties and thermodynamic behavior of hexagonal and orthorhombic Ti3Sn: A first-principles investigation. Vacuum, 2023, 207, 111575.	1.6	9

#	Article	IF	Citations
47799	Ab initio computations of BaZrO₃, CaTiO₃, SrTiO₃ perovskite as well as WO₃ and ReO₃ (001) surfaces. Low Temperature Physics, 2022, 48, 811-818.	0.2	0
47800	Composition-dependent phase transformation path involving 4O martensite in Niâ€“Mnâ€“Sn magnetic shape memory alloys. Journal of Applied Physics, 2022, 132, 135110.	1.1	0
47801	High performance LiFePO4 nanomaterial obtained by a tavorite-to-olivine phase transition at low-temperature. Chemical Engineering Journal, 2023, 453, 139611.	6.6	11
47802	Emergent properties from CuPd alloy films under near-infrared excitation. Journal of Chemical Physics, 2022, 157, .	1.2	1
47803	Prediction of Room-Temperature Ferromagnetic Semiconductors in CrMoA₂B₂ (A = Se and Te; B = Br and I) Monolayers. Journal of Physical Chemistry C, 2022, 126, 17390-17397.	1.5	6
47804	Aluminum-Doped Mesoporous Copper Oxide Nanofibers Enabling High-Efficiency CO₂ Electroreduction to Multicarbon Products. Chemistry of Materials, 2022, 34, 9023-9030.	3.2	8
47805	Unraveling the electrocatalytic reduction mechanism of enols on copper in aqueous media. Nature Communications, 2022, 13, .	5.8	3
47806	Band Structure and Phonon Transport Engineering Realizing Remarkable Improvement in Thermoelectric Performance of Cu₂SnSe₄ Incorporated with In₂Te₃. ACS Applied Materials & Interfaces, 2022, 14, 45628-45635.	4.0	3
47807	Ab Initio to Activity: Machine Learning-Assisted Optimization of High-Entropy Alloy Catalytic Activity. , 2023, 1, 120-133.		10
47809	A first-principles investigation of point defect structure and energetics in ThO2. Journal of Applied Physics, 2022, 132, .	1.1	3
47810	From Heterostructures to Solidâ€Solutions: Structural Tunability in Mixed Halide Perovskites. Advanced Materials, 2023, 35, .	11.1	5
47811	Transition-Metal-Doped SiP₂ Monolayer for Effective CO₂ Capture: A Density Functional Theory Study. ACS Omega, 2022, 7, 36848-36855.	1.6	5
47812	Modelling hydrogen mobility in forsterite as diffusion coupled to inter-site reaction. Contributions To Mineralogy and Petrology, 2022, 177, .	1.2	4
47813	Computational study of structural, electronic, elastic and vibrational properties of LiAlSi, NaAlSi, and KAlSi Half-Heusler alloys. Indian Journal of Physics, 2023, 97, 1389-1395.	0.9	2
47814	Periodically Poled Monolayer Lithium Niobate for Photonic Chips of Quantum Devices. , 2023, 1, 115-122.		1
47815	Band alignment and interlayer hybridisation in transition metal dichalcogenide/hexagonal boron nitride heterostructures. 2D Materials, 2022, 9, 045036.	2.0	2
47816	Unifying the Nitrogen Reduction Activity of Anatase and Rutile TiO₂ Surfaces. ChemPhysChem, 2023, 24, .	1.0	3
47817	<scp>Kineticsâ€Assisted</scp> Identification and Regulation of Active Sites for <scp>Pdâ€Catalyzed</scp> Propyne Selective Hydrogenation. AICHE Journal, 0, , .	1.8	1

#	Article	IF	Citations
47818	Template Driven Self-Assembly of the Pentacene Structure on the Si(553)-Pb Surface. Journal of Physical Chemistry C, 0, , .	1.5	0
47819	A green and sustainable strategy toward lithium resources recycling from spent batteries. Science Advances, 2022, 8, .	4.7	26
47820	Ab Initio Study of Electronic and Lattice Dynamical Properties of Monolayer ZnO Under Strain. Journal of Electronic Materials, 0, , .	1.0	1
47821	Electron-doping induced tunable magnetisms in 2D Janus TiXO (X = S, Se). Physica E: Low-Dimensional Systems and Nanostructures, 2023, 145, 115518.	1.3	3
47822	Structural, Electronic, and Optical Properties of Cs₂SnX₄ (Xâ€‰=â€‰Cl, Br, and I) Multilayers: A Density Functional Theory Study. Physica Status Solidi (B): Basic Research, 2023, 260, .	0.7	2
47823	High-mobility two-dimensional carriers from surface Fermi arcs in magnetic Weyl semimetal films. Npj Quantum Materials, 2022, 7, .	1.8	12
47824	Identification of B33 and Cm martensitic products in CuZr-based alloys: A DFT study. Materials Today Communications, 2022, 33, 104635.	0.9	0
47825	High-Efficiency Electrochemical Nitrate Reduction to Ammonia on a Co₃O₄ Nanoarray Catalyst with Cobalt Vacancies. ACS Applied Materials & Interfaces, 2022, 14, 46595-46602.	4.0	62
47826	Role of the Magnetic Anisotropy in Atomic-Spin Sensing of 1D Molecular Chains. ACS Nano, 2022, 16, 16402-16413.	7.3	13
47827	Unconventional Ferroelectricity with Quantized Polarizations in Ionic Conductors: High-Throughput Screening. Journal of Physical Chemistry Letters, 2022, 13, 9552-9557.	2.1	7
47828	Plasmonic Photocatalysis with Chemically and Spatially Specific Antennaâ€“Dual Reactor Complexes. ACS Nano, 2022, 16, 17365-17375.	7.3	18
47829	Systematic Mapping of Electrocatalytic Descriptors for Hybrid and Non-Hybrid Molybdenum Dichalcogenides with Graphene Support for Cathodic Hydrogen Generation. Journal of Physical Chemistry C, 2022, 126, 17011-17024.	1.5	6
47830	The kagomÃ© metals RbTi₃Bi₅ and CsTi₃Bi₅. Zeitschrift Fur Naturforschung - Section B Journal of Chemical Sciences, 2022, 77, 757-764.	0.3	14
47831	First principle study of the electronic and catalytic properties of palladium-silver (PdAg) alloys catalyst for direct liquid fuel cells. Chemical Physics, 2023, 564, 111711.	0.9	4
47832	Explorations on properties of Îµâ€² phase and new crystalline phase of Fe3Ge alloy under high pressures. Physics Letters, Section A: General, Atomic and Solid State Physics, 2022, 452, 128450.	0.9	0
47833	A first-principles study on the potential of MAB2 (M=Nb, ta; A=Co, Ni) ternary borides as friction-resistance cermet. Solid State Communications, 2022, 356, 114971.	0.9	4
47834	Selective incorporation of Fe and Co into the Ni2MnGa (001) surfaces: a DFT analysis. Surfaces and Interfaces, 2022, 34, 102367.	1.5	4
47835	Operando Raman spectroelectrochemical study of polyaniline degradation: A joint experimental and theoretical analysis. Journal of Energy Storage, 2022, 55, 105770.	3.9	3

#	Article	IF	Citations
47836	Dual experimental and computational approach to elucidate the effect of Ga on Cu/CeO2â€“ZrO2 catalyst for CO2 hydrogenation. Journal of CO2 Utilization, 2022, 65, 102251.	3.3	3
47837	Theoretical SERS study of the strength and suitability of Cu12 nanostar for SERS: Complete theoretical studies, coinage metal SM12 comparisons, benzothiazole (BTH) adsorbent. Computational and Theoretical Chemistry, 2022, 1217, 113889.	1.1	8
47838	Effects of titanium and carbon on cohesion property and brittleness of grain boundary of molybdenum. Solid State Communications, 2022, 356, 114963.	0.9	0
47839	Impact of a dopant vis-a-vis site and concentration on the photovoltaic effect of BiFeO3. Physica B: Condensed Matter, 2022, 647, 414366.	1.3	0
47840	Two new BN polymorphs with wide-bandgap. Diamond and Related Materials, 2022, 130, 109410.	1.8	3
47841	Comparative characteristics of various solvents of the Na, Ba, B//O, F system for the growth of Î²-BaB2O4 crystals and PT-diagram of BaB2O4 polymorphs. Journal of Crystal Growth, 2022, 599, 126895.	0.7	0
47842	Strain regulating mechanical stability and photoelectric properties of CH3NH3PbI3 containing the asymmetric CH3NH3 cations. Materials Today Communications, 2022, 33, 104527.	0.9	1
47843	Density functional theory study of Ni segregation in CuNi(111) alloy with chemisorbed CO, O, or H. Journal of Physics and Chemistry of Solids, 2022, 171, 111021.	1.9	2
47844	Fabrication of antifouling two-dimensional MoS2 layered PVDF membrane: Experimental and density functional theory calculation. Separation and Purification Technology, 2022, 303, 122226.	3.9	5
47845	Enhanced polymerization interface of Ni12P5 nanowires toward high-rate and durable cathode for alkaline Niâ€“Zn batteries. Journal of Power Sources, 2022, 550, 232170.	4.0	11
47846	Insights on the proton mechanism in carbonyl-based organic electrode of neutral aqueous battery. Journal of Power Sources, 2022, 550, 232110.	4.0	4
47847	Electronic properties of van der Waals heterostructures based on F-GaN-H stacking and TMDs single layer. Vacuum, 2022, 206, 111546.	1.6	2
47848	Charge analysis in (RE)CrO4 scheelites by combined Raman spectroscopy and computer simulations. Journal of Solid State Chemistry, 2022, 316, 123624.	1.4	3
47849	A comparative DFT exploration on M- and A-site double transition metal MAX phase, Ti3ZnC2. Open Ceramics, 2022, 12, 100308.	1.0	13
47850	Microstructure changes and enhanced properties of an automotive AlMgSi alloy improved by micro-alloying La-addition. Materials Characterization, 2022, 194, 112331.	1.9	4
47851	Adhesion, tensile and shear properties of a-C/TiC interface: A first-principles study. Diamond and Related Materials, 2022, 130, 109416.	1.8	5
47852	Correlation of the antibacterial activity and local structure in Zn- and Mn-doped hydroxyapatites by Rietveld refinement and the first-principles method. Materialia, 2022, 26, 101586.	1.3	2
47853	In-situ surface patch-passivation via phosphorus oxygen bond for efficient PbS colloidal quantum dot infrared solar cells. Solar Energy Materials and Solar Cells, 2022, 248, 112040.	3.0	2

#	Article	IF	Citations
47854	Anomalous behavior of strain modulated lattice thermal transport in piezoelectric crystals and the effect of polarization. Acta Materialia, 2022, 241, 118406.	3.8	0
47856	One-pot construction of CoSe nanoparticles anchored on single-atomic-Co doped carbon for pH-universal hydrogen evolution. Materials Chemistry Frontiers, 2022, 6, 3577-3588.	3.2	6
47857	2D Be₂C as multi-time reversible environmental oxygen and nitrogen containing gases sensor material under first principle investigations. IEEE Sensors Journal, 2022, , 1-1.	2.4	1
47858	Electronic structure evolution induced by the charge redistribution during the construction of two-dimensional polymer networks from monomers to crystal frameworks. Physical Chemistry Chemical Physics, 2022, 24, 28003-28011.	1.3	1
47859	Structure optimization and electronic properties of full Heusler Fe2NbIn and half Heusler fenbin. AIP Conference Proceedings, 2022, , .	0.3	0
47860	A trade-off between ligand and strain effects optimizes the oxygen reduction activity of Pt alloys. Energy and Environmental Science, 2022, 15, 5181-5191.	15.6	21
47861	Insights into the alkylation of benzene with olefins: effect of chain length of the olefins. Catalysis Science and Technology, 0, , .	2.1	0
47862	Formulating electronic descriptors to rationally design graphene-supported single-atom catalysts for oxygen electrocatalysis. Journal of Materials Chemistry A, 2022, 10, 25098-25105.	5.2	1
47863	Co-doping of tellurium with bismuth enhances stability and photoluminescence quantum yield of Cs₂AgInCl₆ double perovskite nanocrystals. Nanoscale, 2022, 14, 15691-15700.	2.8	7
47864	Ru/Rh catalyzed selective hydrogenation of CO₂ to formic acid: a first principles microkinetics analysis. Catalysis Science and Technology, 2022, 12, 7219-7232.	2.1	7
47865	Lithium Selenometallates of Triel Elements, Li5MSe4 (M = Al and Ga), Aliovalent Doping and Their Ionic Conductivity. Dalton Transactions, 0, , .	1.6	0
47866	Ultrahigh thermoelectric performance of Janus Î±-STe₂ and Î±-SeTe₂ monolayers. Physical Chemistry Chemical Physics, 0, , .	1.3	0
47867	Length dependence thermal conductivity of zinc selenide (ZnSe) and zinc telluride (ZnTe) â€“ a combined first principles and frequency domain thermoreflectance (FDTR) study. Physical Chemistry Chemical Physics, 2022, 24, 28814-28824.	1.3	2
47868	DFT Calculations for Structural, Electronic, and Magnetic Properties of ZnFe2O4 Spinel Oxide: The Role of Exchange-Correlation Functional. Materials Research, 0, 25, .	0.6	4
47869	The effect of composition on phonon softening in ABO₃-type perovskites: DFT modelling. Physical Chemistry Chemical Physics, 2022, 24, 27064-27074.	1.3	4
47870	Si₅-pentagonal rings and Y-shaped Si₄ building blocks in Li₃₂Si₁₈ system: similarities with the crystalline Zintl phase Li₁₂Si₇. Molecular Systems Design and Engineering, 0, , .	1.7	0
47871	First principles crystal structure prediction. , 2022, , .		0
47872	Novel two-dimensional ferromagnetic materials CrX₂ (X = O, S, Se) with high Curie temperature. Journal of Materials Chemistry C, 2022, 10, 17665-17674.	2.7	13

#	Article	IF	Citations
47873	K₂(BeS)O₄F₂: a novel fluorosulfate with unprecedented 1D [(BeO₃F)â€“(SO₃F)]_{â^ž}chains exhibiting large birefringence. Inorganic Chemistry Frontiers, 2022, 9, 6490-6497.	3.0	4
47874	Understanding the tunable sodium storage performance in pillared MXenes: a first-principles study. Physical Chemistry Chemical Physics, 2022, 24, 27184-27194.	1.3	2
47875	Two-Dimensional Nanomaterials Based Biosensors. Topics in Applied Physics, 2022, , 767-778.	0.4	1
47876	Transition-metal decorated graphdiyne monolayer as an efficient sensor toward phosphide (PH₃) and arsine (AsH₃). Physical Chemistry Chemical Physics, 2022, 24, 26622-26630.	1.3	3
47877	Easy-axis rotation in ferromagnetic monolayer CrN induced by fluorine and chlorine functionalization. Physical Chemistry Chemical Physics, 2022, 24, 25426-25433.	1.3	7
47878	Modulation of the kinetics of outer-sphere electron transfer at graphene by a metal substrate. Physical Chemistry Chemical Physics, 2022, 24, 25203-25213.	1.3	1
47879	Structure-related bandgap of hybrid lead halide perovskites and close-packed APbX₃ family of phases. Journal of Materials Chemistry C, 2022, 10, 16838-16846.	2.7	4
47880	Breaking scaling relations in nitric oxide reduction by surface functionalization of MXenes. Journal of Materials Chemistry A, 2022, 10, 25201-25211.	5.2	8
47881	TiO₂nanotubular arrays decorated with ultrafine Ag nanoseeds enabling a stable and dendrite-free lithium metal anode. Nanoscale Advances, 2022, 4, 4639-4647.	2.2	1
47882	Study of spacer-layer-tunable ferromagnetic half-metalâ€"ferromagnetic insulator transition in SrVO₃/SrTiO₃ superlattice<. Wuli Xuebao/Acta Physica Sinica, 2022, .	0.2	0
47883	Spin filtering and magnetoresistance effects in a dithiane ultra-short single-molecule insulator. Physical Chemistry Chemical Physics, 2022, 24, 27804-27811.	1.3	2
47884	Insights into the multifunctional applications of strategically Co doped MoS₂ nanoflakes. Materials Advances, 2022, 3, 8740-8759.	2.6	1
47885	Critical stresses in mechanochemical reactions. Chemical Science, 2022, 13, 12651-12658.	3.7	7
47886	Effects of low work-function lanthanum oxides on stable electron field emissions from nanoscale emitters. Nanoscale Advances, 2022, 4, 4669-4676.	2.2	0
47887	Structural principles of cation ordering and octahedral tilting in A-site ordered double perovskites: ferroelectric CaMnTi₂O₆ as a model system. Dalton Transactions, 2022, 51, 16508-16516.	1.6	4
47888	Introducing the 1H-Na₂S monolayer as a new direct gap semiconductor with feature-rich electronic and magnetic properties. Physical Chemistry Chemical Physics, 2022, 24, 27505-27514.	1.3	2
47889	KMnCuTe₂: a layered antiferromagnetic semiconductor with long metalâ€"metal distance. RSC Advances, 2022, 12, 29003-29009.	1.7	0
47890	One-dimensional metal thiophosphate nanowires by cluster assembly. Nanoscale, 0, , .	2.8	0

#	Article	IF	Citations
47891	NghiÃªn cá»©u cáº¥u trÃºc vÃ tÃnh cháº¥t Ä'iá»‡n tá»-cá»§a dÃ£y nano P2C dáº¡ng ngÅ© giÃ¡c biÃªn rÄƒng cÆ°a báº±ng phÆ°Æ¡ng ph hÃm máº·t Ä'á»™. Tap Chi Khoa Hoc = Journal of Science, 2022, 58, 23-28.	0.1	0
47892	In situ self-nucleophilic synthesis of nano-Li4Ti5O12/reduced graphite oxide composite with mesopore-oriented porous structure for high-rate lithium ion batteries. Journal of Central South University, 2022, 29, 2911-2929.	1.2	3
47893	Stress-Tuned Optical Transitions in Layered 1T-MX2 (M=Hf, Zr, Sn; X=S, Se) Crystals. Nanomaterials, 2022, 12, 3433.	1.9	4
47894	Adsorption of NO and NO₂ on a M-doped graphene+ semifullerene (C₃₀) surface (M= Ti, Pt, Li): a DFT study. Journal of Physics: Conference Series, 2022, 2307, 012048.	0.3	0
47895	On the Possible Magnetic Properties of Ultrathin Mn2GaC Films on Al2O3 Substrates. JETP Letters, 2022, 116, 323-328.	0.4	2
47896	Gap opening at the Dirac point of graphene on Cu(111): Hybridization versus sublattice symmetry breaking. Surface Science, 2022, , 122196.	0.8	0
47897	Optimal data generation for machine learned interatomic potentials. Machine Learning: Science and Technology, 2022, 3, 045031.	2.4	3
47898	Pressure-induced structural phase transitions of zirconium: an ab initio study based on statistical ensemble theory. Journal of Physics Condensed Matter, 2022, 34, 505402.	0.7	1
47899	Computational study of CO2 methanation over two-dimensional molybdenum carbide catalysts. International Journal of Hydrogen Energy, 2023, 48, 24826-24832.	3.8	1
47900	First principle study for the influence of alkali metals (Li, Na, K) on the adsorption of O and CO on Ir(100) surface. European Physical Journal B, 2022, 95, .	0.6	1
47901	An ab initio study on phase stability, elastic and mechanical properties of Zr-doped TiAl₂ and Î±-TiAl₃ intermetallics. Europhysics Letters, 2022, 140, 36004.	0.7	2
47902	Theoretical Study of ZnS Monolayer Adsorption Behavior for CO and HF Gas Molecules. ACS Omega, 2022, 7, 40176-40183.	1.6	2
47904	Reciprocal space study of Heisenberg exchange interactions in ferromagnetic metals. Physical Review B, 2022, 106, .	1.1	1
47905	Delicate superconductivity in nodal-line NaAlGe single crystal. Journal of Physics Condensed Matter, 2022, 34, 495702.	0.7	2
47906	Determination and comparison of the electrical and thermal transport properties of BCC and FCC Feâ€"Ni based ternary alloys in the Earthâ€™s inner core. Journal of Earth System Science, 2022, 131, .	0.6	1
47907	Sulfur-induced dynamic reconstruction of iron-nitrogen species for highly active neutral oxygen reduction reactions. Science China Chemistry, 2022, 65, 2476-2486.	4.2	3
47908	Achieving Low Lattice Thermal Conductivity in Halfâ€Heusler Compound LiCdSb via Zintl Chemistry. Small Science, 0, , 2200065.	5.8	4
47909	Stability of Pt₁₀Sn₃ Clusters Supported on Î³â€Al₂O₃ in Oxidizing Environment: a DFT Comparison of Alloying and Size Effects. ChemCatChem, 2022, 14, .	1.8	2

#	Article	IF	Citations
47910	Prediction of ferroelectric superconductors with reversible superconducting diode effect. Physical Review B, 2022, 106, .	1.1	15
47911	Strain-driven tunability of the optical, electronic, and mechanical properties of lead-free inorganic CsGeCl₃ perovskites. Physica Scripta, 2022, 97, 125817.	1.2	5
47912	Multifunctional Histidine Cross-Linked Interface toward Efficient Planar Perovskite Solar Cells. ACS Applied Materials & Interfaces, 2022, 14, 47872-47881.	4.0	13
47913	In operandoâ€formed interface between silver and perovskite oxide for efficient electroreduction of carbon dioxide to carbon monoxide. , 2023, 5, .		2
47914	Electronic Band Structure and Surface States in Dirac Semimetal LaAgSb2. Materials, 2022, 15, 7168.	1.3	4
47915	Dissociative adsorption of hydrogen and methane molecules at high-angle grain boundaries of pipeline steel studied by density functional theory modeling. International Journal of Hydrogen Energy, 2022, 47, 41069-41086.	3.8	13
47916	Zn-doping and oxygen vacancy effects on the reactivity and properties of monoclinic and tetragonal ZrO2: a DFT study. Journal of Molecular Modeling, 2022, 28, .	0.8	2
47917	Electronic Band Gap Tuning and Calculations of Mechanical Strength and Deformation Potential by Applying Uniaxial Strain on MX₂ (M = Cr, Mo, W and X = S, Se) Monolayers and Nanoribbons. ACS Omega, 2022, 7, 40054-40066.	1.6	7
47918	How are Hydroxyl Groups Localized on a Graphene Sheet?. ACS Omega, 2022, 7, 37221-37228.	1.6	3
47919	Layered Pd oxide on PdSn nanowires for boosting direct H2O2 synthesis. Nature Communications, 2022, 13, .	5.8	17
47920	The SWSe-BP vdW Heterostructure as a Promising Photocatalyst for Water Splitting with Power Conversion Efficiency of 19.4%. ACS Omega, 2022, 7, 37061-37069.	1.6	4
47921	Practical Error Bounds for Properties in Plane-Wave Electronic Structure Calculations. SIAM Journal of Scientific Computing, 2022, 44, B1312-B1340.	1.3	2
47922	Abnormal trapping of hydrogen in the elastic stress field of dislocations in body-centered cubic iron. International Journal of Hydrogen Energy, 2022, 47, 39255-39264.	3.8	5
47923	Constructing hierarchical nanosheet-on-microwire FeCo LDH@Co3O4 arrays for high-rate water oxidation. Nano Research, 2022, 15, 10021-10028.	5.8	11
47924	Emerging negative Poisson's ratio driven by strong intralayer interaction response in rectangular transition metal chalcogenides. Applied Surface Science, 2023, 610, 155478.	3.1	5
47925	Br Vacancy Defects Healed Perovskite Indoor Photovoltaic Modules with Certified Power Conversion Efficiency Exceeding 36%. Advanced Science, 2022, 9, .	5.6	18
47926	A DFT Characterization of Structural, Mechanical, and Thermodynamic Properties of Ag9In4 Binary Intermetallic Compound. Metals, 2022, 12, 1852.	1.0	0
47927	Firstâ€Principles Study on the Electronic Properties and Mechanical Stabilities of Anionâ€Cation Multipleâ€Doped LiFePO₄. ChemistrySelect, 2022, 7, .	0.7	3

#	Article	IF	Citations
47928	Electronic and Optical Properties of $$V-Doped$$ ÂAlN Rock-salt Structure: A First-principles Study Within GGA and $$GGA+U$$ Method. Journal of Superconductivity and Novel Magnetism, 2022, 35, 3661-3669.	0.8	1
47929	Electronic Properties and Chemical Bonding in V2FeSi and Fe2VSi Heusler Alloys. Crystals, 2022, 12, 1546.	1.0	3
47930	Photocatalytic Oxidative Dehydrogenation of Propane for Selective Propene Production with TiO₂. Jacs Au, 2022, 2, 2607-2616.	3.6	3
47931	The effects of point defect type, location, and density on the Schottky barrier height of Au/MoS2 heterojunction: a first-principles study. Scientific Reports, 2022, 12, .	1.6	6
47932	A novel two-dimensional C36 fullerene network; an isotropic, auxetic semiconductor with low thermal conductivity and remarkable stiffness. Materials Today Nano, 2023, 21, 100280.	2.3	11
47933	A study of anisotropic thermoelectric properties of bulk Germanium Sulfide in its Pnma phase: a combined first-principles and machine-learning approach. Physica Scripta, 2022, 97, 125804.	1.2	6
47934	Tuning the Nonradiative Electronâ€“Hole Recombination with Defects in Monolayer Black Phosphorus. Journal of Physical Chemistry Letters, 2022, 13, 10162-10168.	2.1	7
47935	Electro-Acoustic Properties of Scandium-Doped Aluminum Nitride (ScxAl1-xN) Material and its Application to Phononic Crystal-Coupled SAW Devices. Crystals, 2022, 12, 1431.	1.0	4
47936	Graphene/Cs₂PbI₂Cl₂ van der Waals heterostructure with tunable Schottky barriers and contact types. Journal of Applied Physics, 2022, 132, 165101.	1.1	0
47937	Directing the Surface Atomic Geometry on Copper Sulfide for Enhanced Electrochemical Nitrogen Reduction. ACS Catalysis, 2022, 12, 13638-13648.	5.5	5
47938	Computational Insights into Ru, Pd and Pt fcc Nano-Catalysts from Density Functional Theory Calculations: The Influence of Long-Range Dispersion Corrections. Catalysts, 2022, 12, 1287.	1.6	2
47939	Dynamic Polarization Behaviors of Equimolar CoCrFeNi High-Entropy Alloy Compared with 304 Stainless Steel in 0.5 M H2SO4 Aerated Aqueous Solution. Materials, 2022, 15, 6976.	1.3	1
47940	ZIF-75 under Pressure: Negative Linear Compressibility and Pressure-Induced Instability. Applied Sciences (Switzerland), 2022, 12, 10413.	1.3	5
47941	Realizing ultra-low thermal conductivity by strong synergy of asymmetric geometry and electronic structure in boron nitride and arsenide. Rare Metals, 2023, 42, 210-221.	3.6	3
47942	Anharmonic Cationâ€“Anion Coupling Dynamics Assisted Lithiumâ€Ion Diffusion in Sulfide Solid Electrolytes. Advanced Materials, 2022, 34, .	11.1	12
47943	Intrinsic Valley-Polarized Quantum Anomalous Hall Effect and Controllable Topological Phase Transition in Janus Fe₂SSe. Journal of Physical Chemistry Letters, 2022, 13, 10297-10304.	2.1	7
47944	First-Principles Study on the Structural, Electronic, and Lithium Storage Properties of Ti₃C₂T₂ (T = O, F, H, OH) MXene. ACS Omega, 2022, 7, 40578-40585.	1.6	5
47945	Engineering the insulator-to-metal transition by tuning the population of dopant defects: first principles simulations of Se hyperdoped Si. Semiconductor Science and Technology, 2023, 38, 014002.	1.0	3

#	Article	IF	Citations
47946	Pair vacancy defects in Î²-Ga2O3 crystal: Ab initio study. Optical Materials: X, 2022, 16, 100200.	0.3	2
47947	Tunable magnetic anisotropy in two-dimensional <mml:math xmlns:mml="http://www.w3.org/1998/Math/MathML"><mml:mrow><mml:mi>Cr</mml:mi><mml:msub><mml:mi>X</mml:mi><mml:mn> heterostructures. Physical Review B, 2022, 106, .	1.1	5
47948	Electron and configuration engineering of atomic Cu and multi-oxidated Cu2+1O centers via gasifiable reductant strategy for efficient oxygen reduction toward Zn-air battery. Nano Research, 2023, 16, 2383-2391.	5.8	2
47949	Transition metal atom adsorption on the titanium carbide MXene: Trends across the periodic table for the bare and O-terminated surfaces. Physical Review Materials, 2022, 6, .	0.9	2
47950	Revealing the Magnetic Structure and Properties of Mn(Co,Ge)₂. Inorganic Chemistry, 0, , .	1.9	1
47951	Structural and Elastic Behaviour of Sodalite Na8(Al6Si6O24)Cl2 at High-Pressure by First-Principle Simulations. Minerals (Basel, Switzerland), 2022, 12, 1323.	0.8	2
47952	Theoretical calculation and experimental research for structural stability and electronic properties induced by certain cluster defects in ADP crystal. Optical Materials Express, 2022, 12, 4422.	1.6	1
47953	Oxygen vacancy formation and electronic reconstruction in strained <mml:math xmlns:mml="http://www.w3.org/1998/Math/MathML"><mml:msub><mml:mi>LaNiO</mml:mi><mml:mn>3</mml:mn></mml:msub><m and <mml:math xmlns:mml="http://www.w3.org/1998/Math/MathML"><mml:msub><mml:mi>LaNiO</mml:mi><mml:mn>3</mml:mn></mml:msub><m superlattices. Physical Review B, 2022, 106, .	1.1	3
47954	Two-Dimensional Nanosheets of Titanium Carbonitride Ti₃CNT_x MXene for Microwave Absorption in the X and Ku Bands. ACS Applied Nano Materials, 2022, 5, 17133-17141.	2.4	4
47955	Theoretical study on photocatalytic performance of ZnO/C2N heterostructure towards high efficiency water splitting. Frontiers in Chemistry, 0, 10, .	1.8	0
47956	Chemical Bonding Effects and Physical Properties of Noncentrosymmetric Hexagonal Fluorocarbonates ABCO3F (A: K, Rb, Cs; B: Mg, Ca, Sr, Zn, Cd). Molecules, 2022, 27, 6840.	1.7	3
47957	NO Degradation on the Anatase TiO₂ (001) Surface in the Presence of Water. Journal of Physical Chemistry C, 2022, 126, 17544-17553.	1.5	2
47958	Waterâ€“Gas Shift Reaction over Au(111): The Effect of Potassium from a First-Principles-Based Microkinetic Model Analysis. Journal of Physical Chemistry C, 2022, 126, 17579-17588.	1.5	6
47959	The fracture mechanical behavior simulation of calcium-deficient hydroxyapatite crystals by molecular dynamics and first-principles calculation. Journal of the Mechanical Behavior of Biomedical Materials, 2023, 137, 105526.	1.5	7
47960	Hydrogen Dissociation Controls 1-Hexyne Selective Hydrogenation on Dilute Pd-in-Au Catalysts. ACS Catalysis, 2022, 12, 13321-13333.	5.5	6
47961	Carrier trapping centers in a two-dimensional silica bilayer: Strongly localized shallow gap states and resonances induced by oxygen vacancies. Physical Review B, 2022, 106, .	1.1	0
47962	Two-dimensional Janus monolayers with tunable electronic and magnetic properties. Journal of Materials Research, 0, , .	1.2	6
47963	Temperatureâ€dependent elastic and thermodynamic properties of ZrC, HfC, and their solid solutions (Zr_{0.5}Hf_{0.5})C. Journal of the American Ceramic Society, 2023, 106, 2024-2036.	1.9	2

#	Article	IF	Citations
47964	Li_xAg_{1â€“}_xGaSe₂: Interplay Between Lithium and Silver in Midâ€Infrared Nonlinear Optical Chalcogenides. Advanced Optical Materials, 2022, 10, .	3.6	14
47965	Strain-induced enhancement of carrier mobility and optoelectronic properties in antimonene/germanane vdW heterostructure. Applied Physics A: Materials Science and Processing, 2022, 128, .	1.1	1
47966	Nanostructured AlGaAsSb Materials for Thermophotovoltaic Solar Cells Applications. Nanomaterials, 2022, 12, 3486.	1.9	0
47967	In-Plane Strain Tuned Electronic and Optical Properties in Germanene-MoSSe Heterostructures. Nanomaterials, 2022, 12, 3498.	1.9	11
47968	New Ion Substitution Method to Enhance Electrochemical Reversibility of Coâ€Rich Layered Materials for Liâ€Ion Batteries. Advanced Energy Materials, 2023, 13, .	10.2	11
47969	CO2 adsorption and activation on Ag(1 1 1) surfaces in the presence of surface charge density: A static gas phase DFT study. Applied Surface Science, 2023, 610, 155498.	3.1	5
47970	Revealing the electronic, optical, elastic, mechanical, anisotropic, and thermoelectric responses of <scp> Sc ₂ NiZ </scp> (<scp>Z</scp> Â=Â <scp>Si</scp> , <scp>Ge</scp> , and <scp>Sn</scp>) <scp>Heusler</scp> alloys via <scp>DFT</scp> calculations. International Journal of Quantum Chemistry, 0, .	1.0	1
47971	Multigap superconductivity in the filled-skutterudite compound <mml:math xmlns:mml="http://www.w3.org/1998/Math/MathML"><mml:msub><mml:mi mathvariant="normal">LaRu</mml:mi><mml:mn>4</mml:mn></mml:msub><mml:msub><mml:mi mathvariant="normal">As</mml:mi><mml:mn>12</mml:mn></mml:msub></mml:math> probed by muon spin rotation. Physical Review B, 2022, 106, .	1.1	2
47972	Inhibiting dendrites on Zn anode by ZIF-8 as solid electrolyte additive for aqueous zinc ion battery. Colloids and Surfaces A: Physicochemical and Engineering Aspects, 2023, 656, 130255.	2.3	9
47973	In Situ Growth of Fe₂O₃ Nanorod Arrays on Carbon Cloth with Rapid Charge Transfer for Efficient Nitrate Electroreduction to Ammonia. ACS Applied Materials & Interfaces, 2022, 14, 49765-49773.	4.0	21
47974	Effect of hydrostatic pressure on the mechanical, thermodynamic, and optical properties of orthorhombic WAlB. Journal of Materials Research, 0, , .	1.2	0
47975	A Mechanistic Study of Methanol Steam Reforming on Ni2P Catalyst. Catalysts, 2022, 12, 1174.	1.6	7
47976	Effects of ferromagnetism in ab initio calculations of basic structural parameters of Fe-A (A = Mo, Nb,) Tj ETQq0 0 0 rgBT /Overlock 10 Tf	0.8	3
47977	Carrier-driven magnetic and topological phase transitions in two-dimensional IIIâ€“V semiconductors. Nano Research, 0, , .	5.8	2
47978	Quinary, Senary, and Septenary High Entropy Alloy Nanoparticle Catalysts from Core@Shell Nanoparticles and the Significance of Intraparticle Heterogeneity. ACS Nano, 2022, 16, 18873-18885.	7.3	32
47979	Chemically coupling SnO ₂ quantum dots and MXene for efficient CO ₂ electroreduction to formate and Znâ€“CO ₂ battery. Proceedings of the National Academy of Sciences of the United States of America, 2022, 119, .	3.3	27
47980	Topological defect and sp3/sp2 carbon interface derived from ZIF-8 with linker vacancies for oxygen reduction reaction. Carbon, 2023, 203, 76-87.	5.4	10
47981	An unconstrained approach to systematic structural and energetic screening of materials interfaces. Nature Communications, 2022, 13, .	5.8	8

#	Article	IF	Citations
47982	A first principle study of <scp>pressureâ€induced</scp> properties of <scp> MoS ₂ </scp> â€“graphene heterostructures. International Journal of Quantum Chemistry, 0, , .	1.0	0
47983	Machine learning interatomic potentials for aluminium: application to solidification phenomena. Journal of Physics Condensed Matter, 2023, 35, 035402.	0.7	3
47984	Superatomic-Charge-Density-Wave in Cluster-Assembled Au₆Te₁₂Se₈ Superconductors. Journal of the American Chemical Society, 2022, 144, 20915-20922.	6.6	6
47985	In Situ Derived Co₂B Nanosheet Array: A High-Efficiency Electrocatalyst for Ambient Ammonia Synthesis via Nitrate Reduction. ACS Applied Materials & Interfaces, 2022, 14, 49650-49657.	4.0	19
47986	Polarization sensitive photodetector based on quasi-1D ZrSe₃. Journal of Semiconductors, 2022, 43, 102001.	2.0	3
47988	Regulating nitrogen vacancies within graphitic carbon nitride to boost photocatalytic hydrogen peroxide production. SusMat, 2022, 2, 617-629.	7.8	17
47989	Temperature-dependent structural, mechanical, and thermodynamic properties of B2-phase Ti2AlNb for aerospace applications. Journal of Materials Science, 2022, 57, 19553-19570.	1.7	4
47990	Zigzag direction nanoarchitectonics of monolayer GeSe for SO2 gas sensors with high sensitivity and selectivity: a first-principles study. Applied Physics A: Materials Science and Processing, 2022, 128, .	1.1	2
47991	Computational Design of a Strain-Induced 2D/2D g-C₃N₄/ZnO S-Scheme Heterostructured Photocatalyst for Water Splitting. ACS Applied Energy Materials, 2022, 5, 13997-14007.	2.5	16
47992	Designing TiO2/Au/Prussian blue heterostructures nanorod arrays for ultra-stable cycle and ultra-fast response electrochromism. Nano Research, 2023, 16, 3294-3303.	5.8	7
47993	Prediction for high superconducting ternary hydrides below megabar pressure. Journal of Physics Condensed Matter, 2022, 34, 505404.	0.7	7
47994	Two-dimensional mineral hydrogel-derived single atoms-anchored heterostructures for ultrastable hydrogen evolution. Nature Communications, 2022, 13, .	5.8	25
47995	Modulating the optical and electrical properties of MoSe2 (Molybdenum diselenide) and WS2 (Tungsten disulfide) monolayer by the adsorption of halogen (F, Cl, Br, I and At) atoms. Optical and Quantum Electronics, 2022, 54, .	1.5	1
47996	Comprehensive Study of Electronic, Optical, and Thermophysical Properties of Metavanadates CaV₂O₆ and MgV₂O₆. Inorganic Chemistry, 2022, 61, 17623-17633.	1.9	1
47997	Partial Discharge Elimination in Transformer Oils by Nanofluids: From Theory to Practice. Arabian Journal for Science and Engineering, 2023, 48, 6253-6270.	1.7	8
47998	The crystallographic structure and properties of novel quaternary nanolaminated rare-earth-Cr-based i-MAX phases. Acta Materialia, 2023, 242, 118479.	3.8	8
47999	Enhanced Oxide Reduction by Hydrogen at Cuprous Oxideâ€“Copper Interfaces near Ascending Step Edges. Journal of Physical Chemistry C, 2022, 126, 18645-18651.	1.5	1
48000	Correlation between the activity of Fe@ (N, S, and P) doped graphene catalysts and the coordination environment: A density functional theory study. International Journal of Hydrogen Energy, 2023, 48, 171-179.	3.8	5

#	Article	IF	Citations
48001	Computational insights into the energy storage of ultraporous MOFs NU-1501-M (M = Al or Fe): Protonization revealing and performance improving by decoration of superalkali clusters. International Journal of Hydrogen Energy, 2022, 47, 41034-41045.	3.8	5
48002	Self-organized quantum dots in marginally twisted MoSe2/WSe2 and MoS2/WS2 bilayers. Npj 2D Materials and Applications, 2022, 6, .	3.9	6
48003	Photo-controllable Ion-Gated Metalâ€“Organic Framework MIL-53 Sub-nanochannels for Efficient Osmotic Energy Generation. ACS Nano, 2022, 16, 16343-16352.	7.3	12
48004	Insight into the Stability and Properties of Znâ€Ðoped KH ₂ PO ₄ Crystal by Hybrid Density Functional Theory. Crystal Research and Technology, 0, , 2200107.	0.6	0
48005	Functionalized boronâ€“nitride nanotubes: First-principles calculations. Applied Surface Science, 2023, 611, 155358.	3.1	3
48006	Emergent Behavior in Oxidation Catalysis over Single-Atom Pd on a Reducible CeO₂ Support via Mixed Redox Cycles. ACS Catalysis, 2022, 12, 12927-12941.	5.5	12
48007	Studies on the local structure of the Fâ€‰â‹•â€‰OH site in topaz by magic angle spinning nuclear magnetic resonance and Raman spectroscopy. European Journal of Mineralogy, 2022, 34, 507-521.	0.4	0
48008	Photocatalytic CO ₂ â€“toâ€“Ethylene Conversion over Bi ₂ S ₃ /CdS Heterostructures Constructed via Facile Cation Exchange. Research, 2022, 2022, .	2.8	4
48009	Passivating {100} Facets of PbS Colloidal Quantum Dots via Perovskite Bridges for Sensitive and Stable Infrared Photodiodes. Advanced Functional Materials, 2023, 33, .	7.8	15
48010	High- versus Low-Spin Ni²⁺ in Elongated Octahedral Environments: Sr₂NiO₂Cu₂Se₂, Sr₂NiO₂Cu₂S₂, and Sr₂NiO₂Cu₂(Se_{1â€“x}S_x)₂. Chemistry of Materials, 2022, 34, 9503-9516.	3.2	1
48011	Strong Metalâ€“Sulfur Hybridization in the Conduction Band of the Quasi-One-Dimensional Transition-Metal Trichalcogenides: TiS₃ and ZrS₃. Journal of Physical Chemistry C, 2022, 126, 17647-17655.	1.5	4
48012	Stable configurations and electronic properties of hydrogenated 10-18-6 graphyne. Applied Physics A: Materials Science and Processing, 2022, 128, .	1.1	0
48013	Unusual electric polarization behavior in elemental quasi-two-dimensional allotropes of selenium. Physical Review Materials, 2022, 6, .	0.9	1
48014	First-principles calculations for the effect of energetic point defect formation on electronic properties of the Weyl MX family (Mâ€²=â€²Nb, Ta; Xâ€²=â€²P, As). Chinese Journal of Physics, 2023, 82, 15-30.	2.0	2
48015	Iron Hydride in the Earth's Inner Core and Its Geophysical Implications. Geochemistry, Geophysics, Geosystems, 2022, 23, .	1.0	4
48016	Screening and design of 2D metalâ€“organic frameworks for hydrogen evolution reaction through controlling transition metals and heteroligands. Materials Today Nano, 2022, 20, 100278.	2.3	2
48017	Sulfur/Polyacrylonitrile-Based N-Terminated Graphene Nanoribbon Cathodes for Li-S Batteries. Physical Review Applied, 2022, 18, .	1.5	1
48018	V (Nb) Single Atoms Anchored by the Edge of a Graphene Armchair Nanoribbon for Efficient Electrocatalytic Nitrogen Reduction: A Theoretical Study. Inorganic Chemistry, 2022, 61, 17864-17872.	1.9	9

#	Article	IF	Citations
48019	Investigating the elastic, mechanical, and thermal properties of polycrystalline Mo2C under high pressure and high temperature. Ceramics International, 2023, 49, 7341-7349.	2.3	3
48020	Prediction of electronic and optical properties of monoclinic 1Tâ€™-phase OsSe2 monolayer using DFT principles. Materials Today Communications, 2022, 33, 104764.	0.9	5
48021	Experimental Study of Diamond-like Carbon Film on Aermet100 Steel and First-Principles Calculation of Interfacial Adhesion. ACS Applied Materials & Interfaces, 2022, 14, 48262-48275.	4.0	4
48022	Niâ€“O₄ as Active Sites for Efficient Oxygen Evolution Reaction with Electronic Metalâ€“Support Interactions. ACS Applied Materials & Interfaces, 2022, 14, 47542-47548.	4.0	3
48023	Tunable Photocatalytic Water Splitting Performance of Armchair MoSSe Nanotubes Realized by Polarization Engineering. Inorganic Chemistry, 2022, 61, 17353-17361.	1.9	7
48024	A Codoping Strategy for Efficient Planar Heterojunction Sb₂S₃ Solar Cells. Advanced Energy Materials, 2022, 12, .	10.2	22
48025	Effect of strain on quantum transport in fully-hydrogenated silicene based field effect transistor. , 2022, 172, 207432.		2
48026	Gold-catalyzed reduction of metal ions for core-shell structures with subnanometer shells. Cell Reports Physical Science, 2022, 3, 101105.	2.8	3
48027	Cu-Doping-Modified Order State, Ferroelectric Property, Multiscale Inhomogeneities, and Local Structure in the Relaxor KTa_{1â€“x}Nb_xO₃ Crystal. Crystal Growth and Design, 2022, 22, 6766-6774.	1.4	1
48028	Bilayer Heterostructure of Boron Nitride and Graphene for Hydrogen Storage: A First-Principles Study. Energy & Fuels, 2022, 36, 13307-13316.	2.5	6
48029	Theoretical Prediction of Two-Dimensional Metal Boride Mg₄B₆ as a High-Capacity Electrode Material for Lithium-Ion Batteries. Journal of Physical Chemistry C, 2022, 126, 17474-17481.	1.5	3
48030	Non-iridium-based electrocatalyst for durable acidic oxygen evolution reaction in proton exchange membrane water electrolysis. Nature Materials, 2023, 22, 100-108.	13.3	195
48031	Intrinsic oxygen defects in UO2 (1 1 1) and PuO2 (1 1 1) surfaces. Applied Surface Science, 2023, 610, 155511.	3.1	5
48033	AB INITIO STUDY OF THE COMPRESSIBILITY AND ELECTRONIC PROPERTIES OF CRYSTALLINE PURINE. Journal of Structural Chemistry, 2022, 63, 1670-1677.	0.3	2
48034	DFT Investigation of Single Metal Atom-Doped 2D MA₂Z₄ Materials for NO Electrocatalytic Reduction to NH₃. Journal of Physical Chemistry C, 2022, 126, 17598-17607.	1.5	7
48035	Efficient Quasi-2D Perovskite Light-Emitting Diodes Enabled by Regulating Phase Distribution with a Fluorinated Organic Cation. Nanomaterials, 2022, 12, 3495.	1.9	5
48036	Switchable single-molecule electronic and thermoelectric device induced by light in a designed diarylethene molecule. Physical Review B, 2022, 106, .	1.1	4
48037	Schottkyâ€“Mott limit in graphene inserted 2D semiconductorâ€“metal interfaces. Journal of Applied Physics, 2022, 132, 145301.	1.1	1

#	Article	IF	Citations
48038	Tunable Energy-Level Alignment in Multilayers of Carboxylic Acids on Silver. Physical Review Applied, 2022, 18, .	1.5	1
48039	Adsorption of NH3 and NO2 Molecules on Sn-Doped and Undoped ZnO (101) Surfaces Using Density Functional Theory. Processes, 2022, 10, 2027.	1.3	2
48040	Density functional description of spin, lattice, and spin-lattice dynamics in antiferromagnetic and paramagnetic phases at finite temperatures. Physical Review B, 2022, 106, .	1.1	10
48041	First-principle calculations of the structural, vibrational, mechanical, electronic, and optical properties of Îµ-O8 under pressure. Journal of Molecular Modeling, 2022, 28, .	0.8	1
48042	Nucleation of Single-Wall Carbon Nanotubes from Faceted Pt Catalyst Particles Revealed by in Situ Transmission Electron Microscopy. ACS Nano, 2022, 16, 16574-16583.	7.3	5
48043	Single Transition Metal Atoms Anchored on Defective MoS₂ Monolayers for the Electrocatalytic Reduction of Nitric Oxide into Ammonia and Hydroxylamine. Inorganic Chemistry, 2022, 61, 17448-17458.	1.9	9
48044	Highâ€Performance Organic Solar Cells by Adding Twoâ€Dimensional GeSe. Advanced Functional Materials, 2022, 32, .	7.8	10
48045	Vibration Spectra of Double Kâ€“Ca, Kâ€“Mg, and Naâ€“Mg Carbonates under Pressure. Geochemistry International, 2022, 60, 1103-1113.	0.2	1
48046	Structure Sensitivity of CO₂ Conversion over Nickel Metal Nanoparticles Explained by Micro-Kinetics Simulations. Jacs Au, 2022, 2, 2714-2730.	3.6	28
48047	Elasticity of Mg3Bi2-xSbx. Materials, 2022, 15, 7161.	1.3	4
48048	Planar MN₄ (Mâ€‰=â€‰Zn, Cd) Monolayers: 2D Anisotropic Dirac Semimetals of Ultrahigh Fermi Velocities. Physica Status Solidi - Rapid Research Letters, 2023, 17, .	1.2	1
48049	Strong Metalâ€“Support Interaction Mechanisms of Rh Supports in the COâ€“NO Reaction: Rh/Rh₂O₃ Interconversion in Promoting NO Dissociation and CO₂ Generation. Journal of Physical Chemistry C, 2022, 126, 17904-17912.	1.5	1
48050	Tuning optical bandgap of crystalline MgO by MeV Co ion beam induced defects. Applied Physics A: Materials Science and Processing, 2022, 128, .	1.1	5
48051	A High-Rate, Durable Cathode for Sodium-Ion Batteries: Sb-Doped O3-Type Ni/Mn-Based Layered Oxides. ACS Nano, 2022, 16, 18058-18070.	7.3	38
48052	Spherical hydroxyapatite nanoparticle scaffolds for reduced lead release from damaged perovskite solar cells. Communications Materials, 2022, 3, .	2.9	3
48053	Structural Dimensionality Dependence of the Band Gap in A_{n+1}B_nX_{3n+1} Ruddlesdenâ€“Popper Perovskites: A Global Picture. Journal of Physical Chemistry Letters, 2022, 13, 9632-9641.	2.1	2
48054	Favorable Electrocatalytic Ammonia Oxidation Reaction Thermodynamics on the Î²-NiOOH(0001) Surface Computed by Density Functional Theory. Journal of Physical Chemistry C, 2022, 126, 17952-17965.	1.5	6
48055	Electronic, Optical, Mechanical and Li-Ion Storage Properties of Novel Benzotrithiophene-Based Graphdiyne Monolayers Explored by First Principles and Machine Learning. Batteries, 2022, 8, 194.	2.1	3

#	Article	IF	Citations
48056	Defect Thermodynamics and Transport Properties of Proton Conducting Oxide BaZr1â^'xYxO3â^'Î´ (xâ€‰â‰‰â€‰0.1) Guided by Density Functional Theory Modeling. Jom, 2022, 74, 4506-4526.	0.9	5
48057	Synthetic Engineering in Na₂MSn₂(NCN)₆ (M = Mn, Fe, Co, and Ni) Based on Electronic Structure Theory. Inorganic Chemistry, 2022, 61, 18221-18228.	1.9	3
48058	Charting Câ€“C coupling pathways in electrochemical CO ₂ reduction on Cu(111) using embedded correlated wavefunction theory. Proceedings of the National Academy of Sciences of the United States of America, 2022, 119, .	3.3	21
48059	First-principles study of vacancy defects in TiVTa and TiVTaNb concentrated solid-solution alloys. Journal of Nuclear Materials, 2023, 573, 154096.	1.3	4
48060	Intrinsic bitunable magnetism/polarity behavior in 2D Janus Cr2I3Y3 (Yâ€‰=â€‰F, Cl, or Br) systems. Npj 2D Materials and Applications, 2022, 6, .	3.9	4
48061	Defectâ€Induced Dense Amorphous/Crystalline Heterophase Enables Highâ€Rate and Ultrastable Sodium Storage. Advanced Science, 2022, 9, .	5.6	21
48062	Estimates of Quantum Tunneling Effects for Hydrogen Diffusion in PuO2. Applied Sciences (Switzerland), 2022, 12, 11005.	1.3	1
48063	Ab initio qui- guided minimal model for the â€œkitaevâ€material <mml:math xmlns:mml="http://www.w3.org/1998/Math/MathML"><mml:msub><mml:mi mathvariant="normal">BaCo</mml:mi><mml:mn>2</mml:mn></mml:msub></mml:math> (<mml:math) Tj ETQq1 1 0.784314 rgBT /	1.1	17
48064	Importance of direct hopping, third-neighbor. Physical Review B, 2022, 106 Reconstruction of Zigzag Graphene Edges: Energetics, Kinetics, and Residual Defects. Journal of Physical Chemistry Letters, 2022, 13, 10326-10330.	2.1	1
48065	Reconstruction of Thiospinel to Active Sites and Spin Channels for Water Oxidation. Advanced Materials, 2023, 35, .	11.1	27
48066	Molecular Assembled Electrocatalyst for Highly Selective CO₂ Fixation to C₂₊ Products. ACS Nano, 2022, 16, 17021-17032.	7.3	10
48067	Synthesis and Characterization of Catalytically Active Au Coreâ”€Pd Shell Nanoparticles Supported on Alumina. Langmuir, 2022, 38, 12859-12870.	1.6	2
48068	Toward Understanding the Effect of Fluoride Ions on the Solvation Structure in Lithium Metal Batteries: Insights from First-Principles Simulations. ACS Applied Materials & Interfaces, 2022, 14, 48762-48769.	4.0	3
48069	Ab-initio investigation on the phase stabilities of Au-M Alloys (M= Na, K, Rb and Cs). Physica Scripta, 0, , .	1.2	0
48070	Aluminum Frenkel defects cause hysteresis in Al₂O₃/AlGaN capacitors. Journal of Applied Physics, 2022, 132, 165105.	1.1	0
48071	The solvent-driven impurity migration over graphene in the presence of electric field. Applied Surface Science, 2023, 611, 155512.	3.1	1
48072	Experimental and theoretical studies of native deep-level defects in transition metal dichalcogenides. Npj 2D Materials and Applications, 2022, 6, .	3.9	10
48073	Adsorption of croconic acid anions at silver electrodes in sodium fluoride solutions. Interplay of DFT calculations and in situ ATR-SEIRAS measurements for the interpretation of experimental spectra of adsorbed species. Microchemical Journal, 2022, 183, 108109.	2.3	0

#	Article	IF	Citations
48074	Exploring Hydrogen Incorporation into the Nb4AlC3 MAX Phases: Ab Initio Calculations. Materials, 2022, 15, 7576.	1.3	5
48075	Thermoelectric Efficiency of Two-Dimensional Pentagonal-PdSe₂ at High Temperatures and the Role of Strain. ACS Applied Energy Materials, 2022, 5, 14522-14530.	2.5	6
48076	Theoretical Study of the Effect of Pressure on the Structure and Electronic Properties of Metal Carbonates. Bulletin of the Russian Academy of Sciences: Physics, 2022, 86, 1230-1241.	0.1	0
48077	Extremely Suppressed Energetic Disorder in a Chemically Doped Conjugated Polymer. Advanced Materials, 2023, 35, .	11.1	5
48078	Understanding Activity Trends in Furfural Hydrogenation on Transition Metal Surfaces. ACS Catalysis, 2022, 12, 12902-12910.	5.5	21
48079	Plasmaâ€induced Moâ€doped Co₃O₄ with enriched oxygen vacancies for electrocatalytic oxygen evolution in water splitting. , 2023, 5, .		79
48080	Mechanical Amorphization of Chitosan with Different Molecular Weights. Polymers, 2022, 14, 4438.	2.0	12
48081	Plasma Functionalization of Silica Bilayer Polymorphs. ACS Applied Materials & Interfaces, 2022, 14, 48609-48618.	4.0	0
48082	Synergistic electronic and geometric effects of Au/<scp>CeO₂</scp> catalyst for oxidative esterification of methacrolein. AICHE Journal, 2023, 69, .	1.8	3
48083	Computational screening of nonmetal dopants to active MoS2 basal-plane for hydrogen evolution reaction via structural descriptor. Journal of Catalysis, 2022, 416, 47-57.	3.1	7
48084	Insight into the Effect of Oxygen Vacancies on Ion Intercalation and Polaron Conduction in LiV₃O₈ Cathodes of Li-Ion Batteries. Journal of Physical Chemistry C, 2022, 126, 18216-18228.	1.5	1
48085	Theoretical investigation of vibrational and electronic properties of HMX crystal under uniaxial compression. Journal of Physics Condensed Matter, 2022, 34, 505405.	0.7	4
48086	First-principle study of the basal-plane stacking fault energies of ternary Mg alloys. Journal of Materials Science, 2022, 57, 18417-18436.	1.7	5
48087	Physical Insights on the Thermoelectric Performance of Cs₂SnBr₆ with Ultralow Lattice Thermal Conductivity. Journal of Physical Chemistry Letters, 2022, 13, 9736-9744.	2.1	2
48088	Nucleation and Growth of Dendritic Islands during Platinum Oxidation-Reduction Cycling. Journal of the Electrochemical Society, 2022, 169, 112506.	1.3	3
48089	Surface Chemistry of Ketones and Diketones on Lewis Acidic Î³-Al₂O₃ Probed by Infrared Spectroscopy. Journal of Physical Chemistry C, 2022, 126, 17554-17568.	1.5	1
48090	Enhancement of Electrocatalytic Activity for both Hydrogen and Oxygen Evolution Reactions of a Perovskite Oxide. Journal of Physical Chemistry C, 0, , .	1.5	3
48091	Superhalogen-based Li-rich double antiperovskite Li6OS(BH4)2 as solid electrolyte. MRS Communications, 2022, 12, 1140-1146.	0.8	2

#	Article	IF	Citations
48092	Valence-Band Electronic Structure of ZnO and ZnO:N: Experimental and Theoretical Evidence of Defect Complexes. Physical Review Applied, 2022, 18, .	1.5	5
48093	Tunable goniopolarity of graphenelike boron layers in metal diborides. Physical Review B, 2022, 106, .	1.1	4
48094	Is the Carbon Nanotubeâ€Catalyst Interface Clean during Growth?. Small, 2022, 18, .	5.2	3
48095	Enhanced Charge-Modulated Switchable CO₂ Capture on Graphene-like BeN₄ with Beryllium Vacancy. Journal of Physical Chemistry C, 2022, 126, 18189-18197.	1.5	4
48096	High-Throughput Screening of Strong Electronâ€“Phonon Couplings in Ternary Metal Diborides. Inorganic Chemistry, 2022, 61, 18154-18161.	1.9	5
48097	High Cationic Dispersity Boosted Oxygen Reduction Reactivity in Multiâ€Element Doped Perovskites. Advanced Functional Materials, 2023, 33, .	7.8	4
48098	Vacancy clustering behaviors and stable configurations in vanadium metal: First-principles investigations. Nuclear Materials and Energy, 2022, 33, 101296.	0.6	1
48099	Indium-doped Î²-MnO2 catalyst for activation of peroxymonosulfate to generate singlet oxygen with complete selectivity. Journal of Cleaner Production, 2022, 380, 134953.	4.6	8
48100	Bifunctional zeolitic imidazolate framework-67 coupling with CoNiSe electrocatalyst for efficient hydrazine-assisted water splitting. Journal of Colloid and Interface Science, 2023, 630, 888-899.	5.0	32
48101	Chemical-Potential-Dependent Thermodynamic Study of Electrochemical Nitric Oxide Reduction to Ammonia on Single-Cluster Catalysts. Journal of Physical Chemistry C, 2022, 126, 19209-19218.	1.5	2
48102	First-principles study of two-dimensional half-metallic ferromagnetism in NiXCl (X = S and Se) monolayer. AIP Advances, 2022, 12, 115105.	0.6	1
48103	Constructing 1ÂT-2ÂH TaS2 nanosheets with architecture and defect engineering for enhance hydrogen evolution reaction. Journal of Alloys and Compounds, 2023, 935, 167877.	2.8	3
48104	Ultralow Lattice Thermal Conductivity in the Aikinite Structure Family, Cu_xPb_xBi_{2â€“x}S₃, and Thermoelectric Properties of Cu_{0.14}Pb_{0.14}Bi_{1.86}S₃. ACS Applied Energy Materials, 2022, 5, 14222-14230.	2.5	4
48105	Accurate and Efficient Prediction of Highly Disordered Bi₂O₃ with Optimum Structure Pool: Combined Approach of the Special Quasirandom Structure Method and Structure Sampling. Journal of Physical Chemistry C, 2022, 126, 18885-18892.	1.5	3
48106	Hydrates of active pharmaceutical ingredients: A 35Cl and 2H solid-state NMR and DFT study. Solid State Nuclear Magnetic Resonance, 2022, 122, 101837.	1.5	6
48107	DFT study on decomposition of hydrazine nitrate on Ir(1 0 0) surface. Computational and Theoretical Chemistry, 2022, 1217, 113917.	1.1	4
48108	Why mercury is a superconductor. Physical Review B, 2022, 106, .	1.1	4
48109	The negative thermal expansion behavior in Prussian blue analogue Zn3[Fe(CN)6]2: A first-principles study. Physics Letters, Section A: General, Atomic and Solid State Physics, 2022, 453, 128493.	0.9	1

#	Article	IF	Citations
48110	Two dimensional Zr₂CO₂/H-FeCl₂ van der Waals heterostructures with tunable band gap, potential difference and magnetic anisotropy. Journal of Physics Condensed Matter, 2023, 35, 024001.	0.7	1
48111	Macroscale superdurable superlubricity achieved in lubricant oil via operando tribochemical formation of fullerene-like carbon. Cell Reports Physical Science, 2022, 3, 101130.	2.8	3
48112	Stable nitrogen-rich yttrium nitrides under high pressure. Solid State Communications, 2022, 358, 115001.	0.9	3
48113	First-principles study on the mechanical, electronic and optical properties of double halide perovskite Cs₂TlSbX₆ (X = Cl, Br, I). Physica Scripta, 2022, 97, 125821.	1.2	3
48114	Lifshitz transitions and hybrid Weyl points in RbAg5Se3. New Journal of Physics, 0, , .	1.2	0
48115	Physical properties and electronic structure of chalcogenide perovskite BaZrS3 under pressure. , 2022, 19, 743-751.		0
48116	RE(OH)₂NO₃ (RE = Tb, Dy, Ho, and Er): Synthesis and Nonlinear Optical Properties of Water-Resistant Lanthanide Hydroxide Nitrates. Inorganic Chemistry, 2022, 61, 18162-18169.	1.9	5
48117	Role of alloying in the phonon and thermal transport of SnSâ€“SnSe across the phase transition. Materials Today Physics, 2022, 28, 100890.	2.9	1
48118	Chiral Dirac-like fermion in spin-orbit-free antiferromagnetic semimetals. Innovation(China), 2022, 3, 100343.	5.2	4
48119	CO2 capture and separation with metalloporphyrin nanosheets in an electric field: A DFT study. Applied Surface Science, 2022, , 155340.	3.1	1
48120	Massive and massless plasmons in germanene nanosheets. Scientific Reports, 2022, 12, .	1.6	6
48121	Effect of the number of graphene layers on the electron transfer kinetics at metal/graphene heterostructures. Journal of Electroanalytical Chemistry, 2022, 925, 116895.	1.9	2
48122	Mid-infrared nonlinear optical heptachlorodigallate AGa2Cl7 (A = Ga+, In+) with a unique second harmonic generation mechanism induced by monovalent cations. Materials Today Physics, 2022, 28, 100894.	2.9	4
48123	Molecular interaction with defected h-BN. Computational and Theoretical Chemistry, 2022, 1217, 113911.	1.1	1
48124	Strain-induced tunable electronic properties in graphite-diamond hybrids. Materials Today Physics, 2022, 28, 100879.	2.9	1
48125	Enhancement of tunneling currents by isoelectronic nitrogen-atom doping at semiconductor pn junctions; comparison of indirect and direct band-gap systems. Japanese Journal of Applied Physics, 2022, 61, 124002.	0.8	1
48126	MNBr (M = Mo, Cr, V) monolayer: two-dimensional ferromagnetic half-metallic materials with high Curie temperature. Journal Physics D: Applied Physics, 2022, 55, 505002.	1.3	3
48127	Investigation of mechanical properties of KCaH3 and KSrH3 orthorhombic perovskite hydrides under high pressure for hydrogen storage applications. European Physical Journal B, 2022, 95, .	0.6	4

#	Article	IF	Citations
48128	Electronic and magnetic properties of pure and Cu doped non-polar ZnO (10 1Â¯0) surfaces. Journal of Applied Physics, 2022, 132, 173903.	1.1	0
48129	Sn₃B₁₀O₁₇Cl₂ Achieving Birefringence Enhancement by Stereochemical Activity Lone Pair. Inorganic Chemistry, 2022, 61, 18238-18244.	1.9	7
48130	Beyond single-crystal surfaces: The GAL21 water/metal force field. Journal of Chemical Physics, 2022, 157, .	1.2	2
48131	Computational Investigation of Metal Oxides as Candidate Hydrogen Storage Materials. Journal of Physical Chemistry C, 2022, 126, 18661-18669.	1.5	3
48132	Transparency and p-Type Conductivity of BeSe Doped with Group VA Atoms: A Hybrid Functional Study. Journal of Physical Chemistry C, 2022, 126, 19446-19454.	1.5	4
48133	Homonuclear transition-metal dimers embedded monolayer C2N as promising anchoring and electrocatalytic materials for lithium-sulfur battery: First-principles calculations. Applied Surface Science, 2023, 610, 155507.	3.1	2
48134	First principle studies of TiO₂-ZnO alloys under high pressure. Journal of Physics Condensed Matter, 2023, 35, 024003.	0.7	1
48135	Lithium and potassium decorated naphthylene for high capacity hydrogen storage by DFT and GCMC study. Surfaces and Interfaces, 2022, 34, 102395.	1.5	2
48136	Metal-decorated siligene as work function type sensor for NH3 detection: A DFT approach. Applied Surface Science, 2023, 610, 155541.	3.1	8
48137	Toward Coarse-Grained Elasticity of Single-Layer Covalent Organic Frameworks. Journal of Physical Chemistry C, 2022, 126, 18943-18951.	1.5	6
48138	Polaronic optical transitions in hematite (Î±-Fe2O3) revealed by first-principles electronâ€“phonon coupling. Journal of Chemical Physics, 2022, 157, .	1.2	5
48139	First-principles investigation of phase stability in layered <mml:math xmlns:mml="http://www.w3.org/1998/Math/MathML"><mml:mrow><mml:msub><mml:mi>Na</mml:mi><mml:mi>x</mml:mi> Physical Review Materials, 2022, 6, .	3.1	1
48140	Synthesis and characterization of the ceramic refractory metal high entropy nitride thin films from Cr-Hf-Mo-Ta-W system. Surface and Coatings Technology, 2022, 449, 128987.	2.2	6
48141	Quantum Chemical Simulation of Double-Walled Nanotubes Based on Gallium and Indium Chalcogenides. Russian Journal of Inorganic Chemistry, 2022, 67, 2009-2017.	0.3	2
48142	Probing the activity origin of the enhanced methanol electrooxidation on Ni-induced PdNix(OH)y-TaN/C catalyst with nitrogen vacancies. Applied Catalysis B: Environmental, 2023, 322, 122142.	10.8	7
48143	The Limits of Proxy-Guided Superhard Materials Screening. Chemistry of Materials, 2022, 34, 10003-10010.	3.2	3
48144	Tuning the half-metallicity in reconstructed CrN (111) surfaces. Surfaces and Interfaces, 2022, 35, 102420.	1.5	4
48145	Exploring high pressure structural transformations, electronic properties and superconducting properties of MH2 (MÂ=ÂNb, Ta). Arabian Journal of Chemistry, 2022, 15, 104347.	2.3	1

#	Article	IF	Citations
48146	Tunable oxygen-vacancy mediated NiCo2O4 microspheres coupled by holey graphene framework with superior lithium-ion storage properties. Materials Chemistry and Physics, 2022, 292, 126876.	2.0	2
48147	Theoretical study on site preference of Mn in B-containing Ni3Al alloys and elastic properties. Materials Today Communications, 2022, 33, 104816.	0.9	0
48148	Effect of 4d transition metals on the electronic and magnetic properties of twin graphene. Journal of Magnetism and Magnetic Materials, 2022, 564, 170127.	1.0	4
48149	Cu-Nx active sites derived from copper phthalocyanine in porous carbon promoting oxygen reduction reaction. Synthetic Metals, 2022, 291, 117204.	2.1	2
48150	Designing two sp3 hybridization polymorphs of BN: A comprehensive study. Diamond and Related Materials, 2022, 130, 109468.	1.8	3
48151	Non-metal doping in triple perovskite Ba2K2Te2O9 for enhanced photovoltaic properties: A first-principles study. Optik, 2022, 271, 170098.	1.4	0
48152	Regulating on photocatalytic overall water splitting performance of gallium thiophosphate based on transition metal doping: A first-principles study. Molecular Catalysis, 2022, 533, 112765.	1.0	0
48153	Sulfur nano-confinement in hierarchically porous jute derived activated carbon towards high-performance supercapacitor: Experimental and theoretical insights. Journal of Energy Storage, 2022, 56, 105944.	3.9	44
48154	Transition Metalâ^'N/Graphene for advanced Lithiumâ€“Sulfur Batteries: A first principles study. Chemical Physics Letters, 2022, 808, 140118.	1.2	2
48155	Carbon nanomaterials with ThymolÂ+ÂMenthol Type V natural deep eutectic solvent: From surface properties to nano-Venturi effect through nanopores. Journal of Molecular Liquids, 2022, 368, 120637.	2.3	1
48156	PO-C32: A two-dimensional graphene-based membrane for efficient seawater desalination. Diamond and Related Materials, 2022, 130, 109497.	1.8	3
48157	Layered topological semimetal GaGeTe: New polytype with non-centrosymmetric structure. Materials Today Advances, 2022, 16, 100309.	2.5	7
48158	Martensitic transformation, mechanical and magnetic properties of Ni-Cu-Mn-Ti-(B) Heusler alloys by first-principles investigations. Materials Today Communications, 2022, 33, 104725.	0.9	1
48159	Thermodynamic stability reversal of iron sulfides at the nanoscale: Insights into the iron sulfide formation in low-temperature aqueous solution. Geochimica Et Cosmochimica Acta, 2022, 338, 220-228.	1.6	6
48160	Electronic-level deciphering of the desalination mechanism of high-performance graphenylene membranes. Journal of Membrane Science, 2022, 664, 121068.	4.1	9
48161	Electronic and optical properties of TM-doped (8,0) SiC SWNT and the prospect of hydrogen storage. Optical Materials, 2022, 134, 113094.	1.7	0
48162	Electronic properties and magnetism of CrCl3 nanoribbons. Journal of Magnetism and Magnetic Materials, 2022, 564, 170105.	1.0	4
48163	Structural, electronic and mechanical properties of Mo2GeC under strain engineering. Materials Today Communications, 2022, 33, 104721.	0.9	0

#	Article	IF	Citations
48164	First principles calculations of the inorganic halide perovskite RbSnBr3: Optical and thermoelectric properties of its three phases. Computational Condensed Matter, 2022, 33, e00761.	0.9	1
48165	Single Pd atom embedded Janus HfSeTe as promising sensor for dissolved gas detection in transformer oil: A density functional theory study. Surfaces and Interfaces, 2022, 35, 102398.	1.5	2
48166	Aniline and chlorobenzene interaction studies on Î¸-arsenene nanosheet - a first-principles study. Inorganic Chemistry Communication, 2022, 146, 110081.	1.8	11
48167	Atomically thin bismuthene nanosheets for sensitive electrochemical determination of heavy metal ions. Analytica Chimica Acta, 2022, 1235, 340510.	2.6	12
48168	CoFe2O4-APTES nanocomposite for the selective determination of tacrolimus in dosage forms: Perspectives from computational studies. Surfaces and Interfaces, 2022, 35, 102406.	1.5	1
48169	Structural, vibrational, electronic, thermodynamic and thermoelectric properties of CaCdSi Half Heusler compound: A first-principles study. Materials Today Communications, 2022, 33, 104668.	0.9	2
48170	Experimental and density functional theory studies of laminar double-oxidized graphene oxide nanofiltration membranes. Chemical Engineering Research and Design, 2022, 188, 590-606.	2.7	5
48171	First-principles calculations on structural, electronic, elastic, optical and thermoelectric properties of thallium based chloroperovskites TlMCl3 (M = Zn and Cd). Computational Condensed Matter, 2022, 33, e00756.	0.9	11
48172	Synthesis, crystal structure, electronic structure, and intensive zero-phonon-line emission of Mn4+ in K5Nb3OF18 lattice. Optical Materials, 2022, 134, 113175.	1.7	1
48173	Effect of hydrogen content on superconductivity in Laâ€“H compounds. Results in Physics, 2022, 43, 106060.	2.0	0
48174	SEI formation mechanisms and Li+ dissolution in lithium metal anodes: Impact of the electrolyte composition and the electrolyte-to-anode ratio. Journal of Power Sources, 2022, 551, 232203.	4.0	9
48175	First-principles study on selenium-doped Li10GeP2S12 solid electrolyte: Effects of doping on moisture stability and Li-ion transport properties. Materials Today Chemistry, 2022, 26, 101223.	1.7	3
48176	Impact of electron-phonon interactions on phonon transport in diamond and c-BN. Diamond and Related Materials, 2022, 130, 109485.	1.8	0
48177	Tuning the magnetic and electronic properties of monolayer SnS2 by 3d transition metal doping: A DFT study. Materials Today Communications, 2022, 33, 104626.	0.9	3
48178	Application of graphdiyne oxide in photoelectrochemical-type photodetectors and ultrafast fiber lasers. Nano Today, 2022, 47, 101653.	6.2	10
48179	Thermodynamic properties and hydration behavior of ye'elimite. Cement and Concrete Research, 2022, 162, 106995.	4.6	10
48180	The effect of heavy and light electronic bands on thermoelectric properties of Mg2Si1-xSnx alloys: Insights from an ab-initio study. Chemical Physics, 2023, 564, 111729.	0.9	2
48181	First principle studies on electronic and thermoelectric properties of Fe2TiSn based multinary Heusler alloys. Computational Materials Science, 2023, 216, 111856.	1.4	3

#	Article	IF	Citations
48182	Theoretical study of transition metal atom pairs anchored in g-CN monolayers for ammonia decomposition. Applied Surface Science, 2023, 609, 155280.	3.1	8
48183	First-principles calculations of phosphorus-doped SnO2 transparent conducting oxide: Structural, electronic, and electrical properties. Computational Materials Science, 2023, 216, 111877.	1.4	2
48184	Î¸â€²â€²â€² precipitate phase, GP zone clusters and their origin in Al-Cu alloys. Journal of Alloys and Compounds, 2023, 930, 167396.	2.8	1
48185	Deciphering the electronic-level mechanism of Na+ transport in a graphdiyne desalination membrane with periodic nanopores. Desalination, 2023, 546, 116183.	4.0	6
48186	Effects of Li contents on the stability, electronic and Li-ion diffusion properties of Li_{3x}La_{(2/3)-x}<teshuzifu>Â†_{(1/3)-2x}TiO₃ surface. Wuli Xuebao/Acta Physica Sinica, 2023, .	0.8	0
48187	First-principles calculations to investigate structural, electronic, and thermodynamic properties of ammonia monochloroborane (NH3BH2Cl) as a promising hydrogen storage candidate. Physica B: Condensed Matter, 2023, 648, 414412.	1.3	1
48188	Microscopic poisoning mechanism of heavy metals on the deNOx over the Î²-MnO2 catalyst. Applied Surface Science, 2023, 609, 155342.	3.1	4
48189	Potassium-enriched graphite for use as stable hybrid anodes in high-efficiency potassium batteries. Carbon, 2023, 201, 1030-1037.	5.4	10
48190	Influence of intercalated Gd atoms on graphene-4H-SiC(0001) properties. Applied Surface Science, 2023, 609, 155365.	3.1	1
48191	Seeking widely applicable dispersion-corrected GGA functionals: The performances of TCA+D3 and RevTCA+D3 on solid-state systems. Computational Materials Science, 2023, 216, 111826.	1.4	1
48192	Unraveling the substitution and strain-induced hydrogen diffusion performance of ZrCo-based intermetallics. Computational Materials Science, 2023, 216, 111849.	1.4	2
48193	Multiatom activation of single-atom electrocatalysts via remote coordination for ultrahigh-rate two-electron oxygen reduction. Journal of Energy Chemistry, 2023, 76, 622-630.	7.1	14
48194	Nickel-iron layered silicate nanomembrane as efficient electrocatalyst for oxygen evolution reaction in alkaline media. Fuel, 2023, 332, 126209.	3.4	5
48195	Effects of strain and Al doping on monolayer h-BN: First-principles calculations. Physica E: Low-Dimensional Systems and Nanostructures, 2023, 146, 115546.	1.3	4
48196	Formation of diphenyl-bipyridine units by surface assisted cross coupling in Pd-cyclometalled complexes. Applied Surface Science, 2023, 609, 155307.	3.1	0
48197	Band structures and transport properties of broken-gap heterostructures: 2D C3N/MX case. Carbon, 2023, 202, 119-127.	5.4	7
48198	Structural deformation and mechanical response of CrS<mml:math xmlns:mml="http://www.w3.org/1998/Math/MathML" altimg="si116.svg" display="inline" id="d1e1038"><mml:msub><mml:mrow /><mml:mrow><mml:mn>2</mml:mn></mml:mrow></mml:msub></mml:math>, CrSe<mml:math xmlns:mml="http://www.w3.org/1998/Math/MathML" altimg="si116.svg" display="inline" id="d1e1046"><mml:msub><mml:mrow /><mml:mrow><mml:mn>2</mml:mn></mml:mrow></mml:msub><	1.3	7
48199	Diverse electronic structures governed by N-substitution in stable two-dimensional dumbbell carbonitrides. Applied Surface Science, 2023, 609, 155463.	3.1	0

#	Article	IF	Citations
48200	Cu-doped MoSi2N4 monolayer as a highly efficient catalyst for CO reduction toward C2+ products. Applied Surface Science, 2023, 609, 155332.	3.1	6
48201	Innovative strategy to optimize the temperature-dependent lattice misfit and coherency of iridium-based Î³/Î³â€™ interfaces. Applied Surface Science, 2023, 609, 155369.	3.1	0
48202	Hybrid materials based on pyrene-substituted metallo phthalocyanines as sensing layers for ammonia detection: Effect of the number of pyrene substituents. Sensors and Actuators B: Chemical, 2023, 375, 132843.	4.0	9
48203	First principles calculations to investigate electronic and optical properties of Tl<mml:math xmlns:mml="http://www.w3.org/1998/Math/MathML" altimg="si62.svg" display="inline" id="d1e591"><mml:msub><mml:mrow /><mml:mrow><mml:mn>4</mml:mn></mml:mrow></mml:msub></mml:math>GaPbX<mml:math xmlns:mml="http://www.w3.org/1998/Math/MathML" altimg="si63.svg" display="inline" id="d1e599"><mml:msub><mml:mrow />	0.9	7
48204	Spatial segregation of substitutional B atoms in graphene patterned by the moirÃ© superlattice on Ir(111). Carbon, 2023, 201, 881-890.	5.4	4
48205	Theoretical studies of optoelectronic properties of AlP1xBix ternaries: Promising light sources for fiber optic communications. Radiation Physics and Chemistry, 2023, 202, 110591.	1.4	1
48206	A comprehensive DFT evaluation of catalytic and optoelectronic properties of BaTiO3 polymorphs. Physica B: Condensed Matter, 2023, 648, 414418.	1.3	16
48207	TM-N4C (TMÂ=ÂCo, Pd, Pt and Ru) as OER electrocatalysts in lithium-oxygen batteries: First-principles study. Applied Surface Science, 2023, 609, 155331.	3.1	4
48208	Anchoring highly distributed Pt species over oxidized graphitic carbon nitride for photocatalytic hydrogen evolution: The effect of reducing agents. Applied Surface Science, 2023, 609, 155305.	3.1	6
48209	Discovery of high-pressure post-perovskite phase in HoCrO3. Journal of Physics and Chemistry of Solids, 2023, 172, 111078.	1.9	4
48210	A density functional theory study of the CO oxidation on Pt1 supported on PtX2 (XÂ=ÂS, Se, Te). Applied Surface Science, 2023, 609, 155341.	3.1	0
48211	Easily exfoliable monolayer of GdTe<mml:math xmlns:mml="http://www.w3.org/1998/Math/MathML" altimg="si40.svg" display="inline" id="d1e691"><mml:msub><mml:mrow /><mml:mrow><mml:mn>3</mml:mn></mml:mrow></mml:msub></mml:math>: ab initio study. Computational Materials Science, 2023, 216, 111869.	1.4	0
48212	Electronic and transport properties of Heusler alloy based magnetic tunneling junctions: A first principles study. Computational Materials Science, 2023, 216, 111852.	1.4	3
48213	High-pressure stabilisation of R = Y member of R2CuTiO6 double perovskite series. Journal of Solid State Chemistry, 2023, 317, 123646.	1.4	2
48214	Impact of substitutional doping of Tl<mml:math xmlns:mml="http://www.w3.org/1998/Math/MathML" altimg="si50.svg" display="inline" id="d1e641"><mml:msup><mml:mrow /><mml:mrow><mml:mo>+</mml:mo></mml:mrow></mml:msup></mml:math> on optoelectronic and thermoelectric properties of NaF phosphor material. Journal of Physics and Chemistry of Solids, 2023, 172, 111023.	1.9	1
48215	Defects study in zinc blende ZnS utilizing optimized hybrid functional. Computational Materials Science, 2023, 216, 111827.	1.4	4
48216	Efficient polyselenides anchoring and conversion by functionalized Mo2B2 MBene for advanced Li-Se battery. Journal of Alloys and Compounds, 2023, 932, 167722.	2.8	6
48217	High-pressure induced structural changes of energetic ionic salts: Dihydroxylammonium 3,3â€²-dinitro-5,5â€²-bis-1,2,4-triazole-1,1â€²-diolate (MAD-X1). Chemical Physics, 2023, 564, 111727.	0.9	0

#	Article	IF	Citations
48218	Seebeck coefficient variations of Î±-MgAgSb in crystalline Mg-Ag-Sb thin films. Journal of Alloys and Compounds, 2023, 932, 167692.	2.8	2
48219	Fermi surface of LaSb2 and direct observation of a CDW transition. Applied Surface Science, 2023, 610, 155477.	3.1	2
48220	Influence of oxygen addition on the oxidation resistance of TiAlN. Scripta Materialia, 2023, 224, 115148.	2.6	3
48221	Experimental study of covalent Cr3C2 with high ionicity: Sound velocities, elasticity, and mechanical properties under high pressure. Scripta Materialia, 2023, 224, 115146.	2.6	2
48222	PHP-graphene nanoribbon-assembled porous metallic carbon for sodium-ion battery anode with high specific capacity. Carbon, 2023, 202, 112-118.	5.4	5
48223	Deep eutectic solvent induced ultrathin Co4N/N-doped carbon nanosheets self-supporting electrode for boosting hydrogen evolution integrated with biomass electrooxidation. Applied Surface Science, 2023, 608, 155283.	3.1	8
48224	Intermetallic niobium boride toward efficient adsorption and catalysis of polysulfides in Lithium-Sulfur batteries. Chemical Engineering Journal, 2023, 453, 139566.	6.6	5
48225	A bimetallic strategy to tailoring the surface formation energy and d-band center of Ni-based catalyst for efficient and stable catalytic hydrogenation of dioctyl phthalate. Chemical Engineering Journal, 2023, 453, 139779.	6.6	5
48226	Photocatalytic degradation of organic pollutants over MoS2/Ag-ZnFe2O4 Z-scheme heterojunction: Revealing the synergistic effects of exposed crystal facets, defect engineering, and Z-scheme mechanism. Chemical Engineering Journal, 2023, 453, 139775.	6.6	47
48227	Hydrogen trapping potential of a few novel molecular clusters and ions. , 2023, , 297-312.		0
48228	Tuning the catalytic activity of Ag7Au6 cluster for oxygen reduction reaction via support interactions. Journal of Molecular Graphics and Modelling, 2023, 118, 108355.	1.3	0
48229	Selective hydrogenation of acetylene to ethylene: Performance of a Pt monolayer over an Î±-WC(0001) surface for binding and hydroconversion of acetylene. Surface Science, 2023, 728, 122197.	0.8	1
48230	ZnO/Ti3C2 composite with oxygen vacancies and Schottky barrier for effective detection of ppb-level NO2 at room temperature. Applied Surface Science, 2023, 610, 155440.	3.1	14
48231	Insights into the removal of chloramphenicol by electrochemical reduction on Pd/NiFe-MOF/foam-Ni electrode: Performance and mechanism. Applied Catalysis B: Environmental, 2023, 322, 122076.	10.8	24
48232	Efficient catalytic ozonation over Co-ZFO@Mn-CN for oxalic acid degradation: Synergistic effect of oxygen vacancies and HOO-Mn-NX bonds. Applied Catalysis B: Environmental, 2023, 322, 122085.	10.8	14
48233	A DFT study on the stability and optoelectronic properties of Pb/Sn/Ge-based MA₂B(SCN)₂I₂ perovskites. New Journal of Chemistry, 0, , .	1.4	0
48234	Cu-ZnO Heterojunction Catalytic SF₆/H₂ Gas Conversion Mechanism and Reaction Network Construction. IEEE Transactions on Dielectrics and Electrical Insulation, 2023, 30, 667-673.	1.8	0
48235	Exploration of the physical properties of the newly synthesized kagome superconductor LaIr₃Ga₂ using different exchangeâ€“correlation functionals. Physical Chemistry Chemical Physics, 2022, 24, 29640-29654.	1.3	5

#	Article	IF	Citations
48236	Crystal structure of formamidiniumâ€“leadâ€“chlorideâ€“dimethyl sulfoxide and phase relationship of related crystalline systems. CrystEngComm, 0, , .	1.3	0
48237	Spin evolution and flip in the oxygen reduction reaction: a theoretical study of Cu(Ni)XP₂S₆(X = In, Bi and Cr). Journal of Materials Chemistry A, 2022, 10, 25262-25271.	5.2	3
48238	¹H chemical shift anisotropy: a high sensitivity solid-state NMR dynamics probe for surface studies?. Physical Chemistry Chemical Physics, 2023, 25, 5348-5360.	1.3	4
48239	Study on the electronic and optical properties of van der Waals heterostructures of blue phosphorene and Janus-WSeS monolayers for photocatalytic water splitting. Materials Advances, 2022, 3, 9063-9070.	2.6	4
48240	The record low thermal conductivity of monolayer cuprous iodide (CuI) with a direct wide bandgap. Nanoscale, 2022, 14, 17401-17408.	2.8	3
48241	Water interaction with B-site (B = Al, Zr, Nb, and W) doped SrFeO_{3â^'Î´}-based perovskite surfaces for thermochemical water splitting applications. Physical Chemistry Chemical Physics, 2022, 24, 28975-28983.	1.3	2
48242	Charge transfer modulated heterointerfaces for hydrogen production at all pH values. Journal of Materials Chemistry A, 2022, 10, 24927-24937.	5.2	6
48243	Catalytic Activity of 1D Chains of Gold Oxide on a Stepped Gold Surface from Density Functional Theory. Physical Chemistry Chemical Physics, 0, , .	1.3	0
48244	Synergistic effect of p-type and n-type dopants in semiconductors for efficient electrocatalytic water splitting. Chemical Science, 2022, 13, 13879-13892.	3.7	2
48245	Construction of dual active sites for efficient alkaline hydrogen evolution: single-metal-atoms supported on BC₂N monolayers. Physical Chemistry Chemical Physics, 2022, 24, 29141-29150.	1.3	3
48246	Effect of oxygen coordination on the electrocatalytic nitrogen fixation of a vanadium single-atom catalyst embedded in graphene. New Journal of Chemistry, 2022, 46, 22936-22943.	1.4	5
48247	Enhanced photoelectric performance of MoSSe/MoS₂ van der Waals heterostructures with tunable multiple band alignment. Physical Chemistry Chemical Physics, 2022, 24, 29882-29890.	1.3	4
48248	The phase stability of predicted pentazole derivate compounds under high pressure. Physical Chemistry Chemical Physics, 0, , .	1.3	0
48249	Defect engineering in the MA₂Z₄ monolayer family for enhancing the hydrogen evolution reaction: first-principles calculations. Sustainable Energy and Fuels, 2022, 7, 164-171.	2.5	7
48250	Janus zirconium halide ZrXY (X, Y = Br, Cl and F) monolayers with high lattice thermal conductivity and strong visible-light absorption. Physical Chemistry Chemical Physics, 2023, 25, 4690-4700.	1.3	3
48251	Modulating the water gas shift reaction via strong interfacial interaction between a defective oxide matrix and exsolved metal nanoparticles. Journal of Materials Chemistry A, 2022, 10, 24995-25008.	5.2	1
48252	A glutamate anion boosted zinc anode for deep cycling aqueous zinc ion batteries. Journal of Materials Chemistry A, 2022, 10, 25029-25038.	5.2	19
48253	Investigating the Infrared Absorption and Optoelectronic Properties of Mn-Doped MoSe₂ ML by Adsorption of NO_x Gas Molecules. IEEE Sensors Journal, 2022, 22, 22564-22570.	2.4	3

#	Article	IF	Citations
48254	Structure andÂElectronic Properties ofÂUltrathin (In, Mg) Films onÂSi(111). Springer Theses, 2022, , 53-69.	0.0	0
48255	The role of hydration water in inorganic M+n -magadiites (M+nÂ=ÂK+, Ca+2, Mg+2): Advances in structural and electronic analysis by DFT calculations.. Applied Clay Science, 2023, 231, 106749.	2.6	1
48256	First-principles study of chalcogen-bonded self-assembly structures on silicene: Some insight into the fabrication of molecular architectures on surfaces through chalcogen bonding. Chemical Physics, 2023, 565, 111763.	0.9	0
48257	Effect of biaxial [110] strain on monolayer MoS2 and its vacancy defect system: A first-principles study. Journal of Solid State Chemistry, 2023, 317, 123711.	1.4	2
48258	Local lattice distortions, phase stability, and mechanical properties of NbMoTaWHfx alloys: A combined theoretical and experimental study. Computational Materials Science, 2023, 217, 111891.	1.4	3
48259	Insight into the electronic structure, magnetic, and thermoelectric properties of transition metal pnictides KCr2L2 (K= Ca, Sr; L = P, As): As substitute source for renewing energy. Physica B: Condensed Matter, 2023, 649, 414470.	1.3	3
48260	The effects of solutes like ruthenium on precipitation of Ïƒ phase and Ïƒ/Î³ interface stability in Ni-based superalloys. Intermetallics, 2023, 152, 107768.	1.8	4
48261	A comprehensive study of Indole adsorption on highly oriented pyrolytic graphite. Carbon, 2023, 202, 475-486.	5.4	1
48262	Adsorption of NO gas molecule on the vacancy defected and transition metal doped antimonene: A first-principles study. Vacuum, 2023, 207, 111654.	1.6	7
48263	Structural behavior of CoB under extreme conditions and its high incompressibility. Journal of Solid State Chemistry, 2023, 317, 123702.	1.4	1
48264	Metal-organic framework-induced edge-riched growth of layered Bi2Se3 towards ultrafast Na-ion storage. Journal of Power Sources, 2023, 555, 232387.	4.0	18
48265	Achieving fast ion diffusion in aqueous zinc-ion batteries by cathode reconstruction design. Chemical Engineering Journal, 2023, 454, 140260.	6.6	8
48266	Insight of the role of F-impurity on the structural, electro-optical properties of ZnO: DFT and experiment. Materials Science in Semiconductor Processing, 2023, 154, 107223.	1.9	7
48267	The co-adsorption potential of metalâ€“organic framework/activated carbon composites against both polar and non-polar volatile organic compounds in air. Separation and Purification Technology, 2023, 306, 122594.	3.9	11
48268	Stabilization of high-voltage layered oxide cathode by multi-electron rare earth oxide. Chemical Engineering Journal, 2023, 454, 140249.	6.6	13
48269	Contributions of bonding heterogeneity to mechanical and thermal properties of rare earth molybdates for thermal barrier coatings. Journal of Physics and Chemistry of Solids, 2023, 173, 111087.	1.9	4
48270	A systematic theoretical study the active sites of potassium promoter on the activity of water-gas shift reaction over Pt(1 1 1). Applied Surface Science, 2023, 611, 155638.	3.1	5
48271	DFT crystal and electronic structure of the direct bandgap Cu(1-x)NaxPF6: (x = 0.125n, n = 1â€“7). Journal of Physics and Chemistry of Solids, 2023, 173, 111116.	1.9	0

#	Article	IF	Citations
48272	Influence of uncoordinated N content on Ni N C electrocatalyst for CO2 reduction: Combining first principle with machine learning. Fuel, 2023, 333, 126563.	3.4	3
48273	Effects of alloying elementsÂXÂ(Cr, Fe and Mo) on the interfacial properties of Î³-Ni(110)/TiC(110) in TiC-particles reinforced NMCs: First-principles study. Optics and Laser Technology, 2023, 158, 108870.	2.2	0
48274	Formation mechanism of stacking faults within Î±â€²â€² martensite in Ti-7Âwt%Mo alloy. Journal of Alloys and Compounds, 2023, 934, 168039.	2.8	3
48275	Core-shell heterojunction engineering of Ni0.85Se-O/CN electrocatalyst for efficient OER. Chemical Engineering Journal, 2023, 454, 140291.	6.6	32
48276	The adsorption and diffusion behaviors of nitrogen impurities in <mml:math xmlns:mml="http://www.w3.org/1998/Math/MathML" altimg="si80.svg" display="inline" id="d1e548"><mml:mi>h</mml:mi></mml:math>-BN by first-principles study. Materials Science in Semiconductor Processing, 2023, 154, 107175.	1.9	1
48277	Inverse spinel cobalt manganese oxide nanosphere materials as an electrode for high-performance asymmetric supercapacitor. Journal of Alloys and Compounds, 2023, 933, 167645.	2.8	6
48278	Coordination engineering of single-atom copper embedded graphene-like borocarbonitrides for hydrogen production. Applied Surface Science, 2023, 610, 155506.	3.1	5
48279	Evolutional solid phase and solid-liquid interface uranium immobilization mechanisms by nanoscale zero-valent iron and enhanced uranium stability control strategy. Chemical Engineering Journal, 2023, 453, 139924.	6.6	15
48280	Electrocatalysis in Liâ€“O2 battery over single-atom catalyst based on g-C3N4 substrate. Applied Surface Science, 2023, 610, 155481.	3.1	5
48281	Comparative analysis of NOx reduction on Pt, Pd, and Rh catalysts by DFT calculation and microkinetic modeling. Applied Surface Science, 2023, 611, 155572.	3.1	4
48282	Experimental investigation and thermodynamic assessment of the Alâ€“Agâ€“Sc system. Journal of Alloys and Compounds, 2023, 934, 167980.	2.8	8
48283	Effect of Pressure on Electronic, Mechanical and Dynamic Properties for Orthorhombic WP. Gazi University Journal of Science, 2023, 36, 1759-1773.	0.6	1
48284	Janus V₂AsP monolayer : a ferromagnetic semiconductor with a narrow band gap, a high Curie temperature and controllable magnetic anisotropy. Journal of Physics Condensed Matter, 0, , .	0.7	0
48285	Structure and Stoichiometry Self-Organization in a Mixed Vanadiumâ€“Iron Oxide Honeycomb Film on Ru(0001). Journal of Physical Chemistry C, 2022, 126, 19947-19955.	1.5	1
48286	Cr₃GeN: A Nitride with Orthorhombic Antiperovskite Structure. Chemistry of Materials, 2022, 34, 10304-10310.	3.2	4
48287	Accelerating NADH oxidation and hydrogen production with mid-gap states of nitrogen-rich carbon nitride photocatalyst. IScience, 2022, 25, 105567.	1.9	7
48288	Unraveling charge transfer pathways and mechanisms in CdS@CoWO4 Z-scheme heterojunction photocatalysts for high-efficiency environmental remediation. Separation and Purification Technology, 2023, 306, 122664.	3.9	4
48289	Revealing the dynamics of the alloying and segregation of Pt-Co nanoparticles via in-situ environmental transmission electron microscopy. Nano Research, 2023, 16, 3055-3062.	5.8	4

#	Article	IF	Citations
48290	On the mechanical properties of CO ₂ â€‖ with particular emphasis on its auxetic potential. Physica Status Solidi (B): Basic Research, 0, , .	0.7	1
48291	Synergistic effect of diatomic Moâ€“B site confined in graphene-like C2N enables electrocatalytic nitrogen reduction via novel mechanism. Journal of Chemical Physics, 2022, 157, .	1.2	6
48292	Mechanical Properties of a New Hybrid Inorganicâ€“Organic Framework: A Nanoindentation, High-Pressure X-ray Diffraction, and Computational Study. Crystal Growth and Design, 2022, 22, 6984-6994.	1.4	0
48293	Effects of Site Geometry and Local Composition on Hydrogenation of Surface Carbon to Methane on Ni, Co, and NiCo Catalysts. Catalysts, 2022, 12, 1380.	1.6	0
48294	Origin of the distinction in hardness of lower tungsten carbides: An experimental and ab initio theoretical study. Journal of the American Ceramic Society, 2023, 106, 2184-2195.	1.9	2
48295	Pinpointing the axial ligand effect on platinum single-atom-catalyst towards efficient alkaline hydrogen evolution reaction. Nature Communications, 2022, 13, .	5.8	77
48296	The hydrogen bond continuum in solid isonicotinic acid. Journal of Magnetic Resonance, 2022, , 107334.	1.2	0
48297	Formation Mechanism of Monocyclic Aromatic Hydrocarbons during Pyrolysis of Styrene Butadiene Rubber in Waste Passenger Car Tires. ACS Omega, 0, , .	1.6	2
48298	Effect of dopants and microstructure on the electrochemical cyclic stability of layered P2-type Na0.67MnO2 prepared by different chemical routes: An experimental and theoretical study. Ceramics International, 2023, 49, 6654-6665.	2.3	3
48299	A theoretical study of the atomic layer deposition of HfO2 on Si(100) surfaces using tetrakis(ethylmethylamino) hafnium and water. Applied Surface Science, 2022, , 155702.	3.1	3
48300	Blue TiO2 with tunable oxygen-vacancy defects for enhanced photocatalytic diesel oil degradation. Applied Surface Science, 2023, 611, 155716.	3.1	5
48301	Exploring the effect of layer spacing of graphene for lithium single-atom diffusion using first principles calculations. Computational and Theoretical Chemistry, 2022, 1217, 113937.	1.1	0
48302	Insights into thin film blistering of gold coating on metal substrate. Applied Surface Science, 2023, 611, 155700.	3.1	4
48303	Plastic bending in a semiconducting coordination polymer crystal enabled by delamination. Nature Communications, 2022, 13, .	5.8	14
48304	Heat-conserving three-temperature model for ultrafast demagnetization in nickel. Physical Review B, 2022, 106, .	1.1	5
48305	Computational evaluation of 2D metal-organic frameworks with TMX4-centers (X = O, S and Se) for CO2 electroreduction. International Journal of Hydrogen Energy, 2023, 48, 3486-3494.	3.8	10
48306	Vibrational instabilities in multilayer graphene and graphite: Effects of strain and number of layers. Physical Review B, 2022, 106, .	1.1	0
48307	Anisotropic mechanical response of a 2D covalently bound fullerene lattice. Carbon, 2023, 202, 118-124.	5.4	12

#	Article	IF	Citations
48308	Chloride-Promoted High-Rate Ambient Electrooxidation of Methane to Methanol on Patterned Cuâ€“Ti Bimetallic Oxides. ACS Catalysis, 2022, 12, 14321-14329.	5.5	7
48309	K₃C₆N₇O₃Â·2H₂O: A Multifunctional Nonlinear Optical Cyamelurate Crystal with Colossal Ï€-Conjugated Orbitals. ACS Applied Materials & Interfaces, 2022, 14, 53074-53080.	4.0	14
48310	Few-Layer Graphene as an Efficient Buffer for GaN/AlN Epitaxy on a SiO2/Si Substrate: A Joint Experimental and Theoret-ical Study. Applied Sciences (Switzerland), 2022, 12, 11516.	1.3	1
48311	Electronic structure, vibrational properties, and optical spectra of two- and three-dimensional hexagonal InSe: Layer-dependent ab initio calculations. Physical Review Materials, 2022, 6, .	0.9	1
48312	Electronic properties of defects induced by hydrogen and helium radiation on semimetal <mml:math xmlns:mml="http://www.w3.org/1998/Math/MathML" display="inline" id="d1e607" altimg="si6.svg"><mml:msub><mml:mrow><mml:mi>M</mml:mi><mml:mi>o</mml:mi><mml:mi>T</mml:mi><mml:mi>e</mml:mi></m Chemical Physics, 2022, , 111764.	0.9	0
48313	The first-principles study of structural and electronic properties of two-dimensional SiC/GeC lateral polar heterostructures. Journal of Applied Physics, 2022, 132, 184301.	1.1	0
48314	Porosity Engineering towards Nitrogen-Rich Carbon Host Enables Ultrahigh Capacity Sulfur Cathode for Room Temperature Potassiumâ€“Sulfur Batteries. Nanomaterials, 2022, 12, 3968.	1.9	2
48315	Growth of fiberform nanostructures on metal surfaces by helium plasma irradiation. Journal of Applied Physics, 2022, 132, .	1.1	12
48316	NCNT grafted perovskite oxide as an active bifunctional electrocatalyst for rechargeable zinc-air battery. Materials Today Nano, 2023, 21, 100287.	2.3	15
48317	Three-phase interface induced charge modulation on MoO2/Mo2C-carbon tube for enhanced hydrogen evolution. Nano Research, 2023, 16, 4706-4714.	5.8	9
48318	Single-Atom Low-Valent Alkaline-Earth-Metal Catalysts for Electrochemical Nitrogen Reduction with an Acceptanceâ€“Backdonation Mechanism. ACS Applied Materials & Interfaces, 2022, 14, 52079-52086.	4.0	8
48319	Fortnet, a software package for training Behler-Parrinello neural networks. Computer Physics Communications, 2023, 284, 108580.	3.0	2
48320	Machine learning prediction of the mechanical properties of refractory multicomponent alloys based on a dataset of phase and first principles simulation. , 0, 1, .		0
48321	Ultrathin Feâ€“ReS₂ Nanosheets as Electrocatalysts for Accelerating Sulfur Reduction in Liâ€“S Batteries. ACS Applied Materials & Interfaces, 2022, 14, 50870-50879.	4.0	6
48322	Development of a ReaxFF potential for Auâ€“Pd. Journal of Physics Condensed Matter, 2023, 35, 065901.	0.7	1
48323	Diffusion-Mediated Morphological Transformation in Bifunctional Mn₂O₃/CuOâ€“(VO)₃(PO₄)₂Â·6H₂O for Enhanced Electrochemical Water Splitting. ACS Applied Materials & Interfaces, 2022, 14, 52204-52215.	4.0	6
48324	Theoretical analysis of the thermoelectric properties of penta-PdX2 (X = Se, Te) monolayer. Frontiers in Chemistry, 0, 10, .	1.8	1
48325	Iron-rich Feâ€“O compounds at Earthâ€™s core pressures. Innovation(China), 2023, 4, 100354.	5.2	4

#	Article	IF	Citations
48326	Structural and electronic properties of hydrogenated gallium nitride with vacancy and doping defects. Applied Physics A: Materials Science and Processing, 2022, 128, .	1.1	2
48327	Simultaneously improving Rashba-type and Zeeman effects in two-dimensional multiferroics. Physical Review B, 2022, 106, .	1.1	0
48328	Tailoring the Properties of Ni(111)/Graphone Interfaces by Intercalation of Al and Na: A DFT Study. Journal of Carbon Research, 2022, 8, 62.	1.4	1
48329	Excitons and light-emission in semiconducting MoSi2X4 two-dimensional materials. Npj 2D Materials and Applications, 2022, 6, .	3.9	37
48330	Photoinduced Rippling of Two-Dimensional Hexagonal Nitride Monolayers. Nano Letters, 2022, 22, 9006-9012.	4.5	5
48331	Electrochemical Reduction of Carbon Dioxide at TiO₂/Au Nanocomposites. ACS Applied Materials & Interfaces, 2022, 14, 51889-51899.	4.0	9
48332	Molecular and periodic DFT calculations of the corrosion protection of Fe(1 1 0) by individual components of Aerva lanata flower as a green corrosion inhibitor. Journal of Saudi Chemical Society, 2022, 26, 101566.	2.4	6
48333	MAX phase forming mechanism of Mâ€“Alâ€“C (MÂ=ÂTi, V, Cr) coatings: In-situ X-ray diffraction and first-principle calculations. Journal of Materials Science and Technology, 2023, 143, 140-152.	5.6	8
48334	Role of Cuâ€doping in <scp>CdTe</scp> thin films: Experiments and simulations. Surface and Interface Analysis, 2023, 55, 151-161.	0.8	1
48335	Atomically dispersed bimetallic Feâ€“Co electrocatalysts for green production of ammonia. Nature Sustainability, 2023, 6, 169-179.	11.5	30
48336	Two-Dimensional Transition Metal-Hexaaminobenzene Monolayer Single-Atom Catalyst for Electrocatalytic Carbon Dioxide Reduction. Nanomaterials, 2022, 12, 4005.	1.9	6
48337	Plasmon resonances in silicon nanowires: geometry effects on the trade-off between dielectric and metallic behaviour. Optical Materials Express, 2023, 13, 598.	1.6	1
48338	Correlating the perovskite/polymer multi-mode reactions with deep-level traps in perovskite solar cells. Joule, 2022, 6, 2849-2868.	11.7	29
48339	Structural, electronic and optical properties of monolayer InGeX₃ (Xâ€‰=â€‰S, Se, Te) by first-principles calculations. Journal of Physics Condensed Matter, 2023, 35, 064002.	0.7	0
48340	Effects of Carboxyl Functionalized CNT on Electrochemical Behaviour of Polyluminol-CNT Composites. Chemistry, 2022, 4, 1561-1575.	0.9	5
48341	Cathodoluminescence and optical absorption spectroscopy of plasmonic modes in chromium micro-rods. Nanotechnology, 2023, 34, 075707.	1.3	1
48342	Phthalocyanine-Carbon Nanotube Hybrid Materials: Mechanism of Sensor Response to Ammonia from Quantum-Chemical Point of View. Chemosensors, 2022, 10, 479.	1.8	2
48343	The Structural, Electronic, Magnetic and Elastic Properties of Full-Heusler Co2CrAl and Cr2MnSb: An Ab Initio Study. Crystals, 2022, 12, 1580.	1.0	2

#	Article	IF	Citations
48344	Ultrahigh strength and negative thermal expansion and low thermal conductivity in graphyne nanosheets confirmed by machine-learning interatomic potentials. FlatChem, 2022, 36, 100446.	2.8	11
48345	Tuning the electron transport behavior at Li/LATP interface for enhanced cyclability of solid-state Li batteries. Nano Research, 2023, 16, 1634-1641.	5.8	12
48346	Evaluation of phase relationship in W-Fe-C ternary system through symmetry principles and first-principles calculation. Materials and Design, 2022, 224, 111376.	3.3	2
48347	A theoretical study of the effect of exchange cations in surface of ZSM-5 lamellar zeolites. Journal of Solid State Chemistry, 2023, 317, 123725.	1.4	1
48348	Low thermal conductivity in bournonite <mml:math xmlns:mml="http://www.w3.org/1998/Math/MathML"><mml:msub><mml:mi>PbCuSbS</mml:mi><mml:mn>3</mml:mn></mml:msub> : A comprehensive study. Physical Review B, 2022, 106, .	1.1	4
48349	Nature of support plays vital roles in H2O promoted CO oxidation over Pt catalysts. Journal of Catalysis, 2022, 416, 364-374.	3.1	4
48350	Pressure-induced ferroelectric transition in LiBC. Physical Review B, 2022, 106, .	1.1	0
48351	Effect of Sn addition on the mechanical properties and high-temperature oxidation resistance of intermetallic TiAl alloys by first principles study and experimental investigation. Journal of Materials Research and Technology, 2022, 21, 3666-3677.	2.6	8
48352	Planar defectâ€“free pure red perovskite light-emitting diodes via metastable phase crystallization. Science Advances, 2022, 8, .	4.7	23
48353	Prediction of a superhard high-pressure phase for CN: First-principles. Modern Physics Letters B, 2022, 36, .	1.0	1
48354	Photovoltaic and related properties of Sn-doped disordered CsPbxSn1â^'xBr3 perovskite: a first-principles calculation. Journal of Materials Science, 2022, 57, 19846-19856.	1.7	0
48355	Cloning the Dirac cones of bilayer graphene to the zone center by selenium adsorption. Npj 2D Materials and Applications, 2022, 6, .	3.9	2
48356	Ab Initio Investigation of the Adsorption and Dissociation of O2 on Cu-Skin Cu3Au(111) Surface. Catalysts, 2022, 12, 1407.	1.6	2
48357	2-Imidazoline Nitroxide Derivatives of Cymantrene. Molecules, 2022, 27, 7545.	1.7	0
48358	A crystal glassâ€“nanostructured Al-based electrocatalyst for hydrogen evolution reaction. Science Advances, 2022, 8, .	4.7	20
48359	First-Principles Insights into the Thermocatalytic Cracking of Ammonia-Hydrogen Blends on Fe(110): 1. Thermodynamics. Journal of Physical Chemistry C, 2022, 126, 19733-19744.	1.5	2
48360	Sensitivity of structural and electronic properties of Li-ion battery cathode materials to Hubbard U correction: an efficient first-principle approach. Physica Scripta, 2022, 97, 125819.	1.2	5
48361	Effect of (NH4)2SO4 on the co-electrodeposition of Fe-Co alloys. Applied Surface Science, 2023, 612, 155567.	3.1	4

#	Article	IF	Citations
48362	Influence of Impurity Atoms on Hydrogen Diffusion into Ruthenium. Journal of Physical Chemistry C, 2022, 126, 19895-19903.	1.5	1
48363	Xâ€ray excited luminescence of highâ€quality doped GaN single crystals. Physica Status Solidi (A) Applications and Materials Science, 0, , .	0.8	1
48364	Decrease in Tumor Interstitial Pressure for Enhanced Drug Intratumoral Delivery and Synergistic Tumor Therapy. ACS Nano, 2022, 16, 18376-18389.	7.3	17
48365	Effect of Various Electron and Hole Transport Layers on the Performance of CsPbI₃-Based Perovskite Solar Cells: A Numerical Investigation in DFT, SCAPS-1D, and wxAMPS Frameworks. ACS Omega, 2022, 7, 43210-43230.	1.6	118
48366	First-principle investigation of LiSrX (X=P and As) half-Heusler semiconductor compounds. Indian Journal of Physics, 2023, 97, 1727-1737.	0.9	5
48367	Electronically Nonadiabatic H Atom Scattering from Low Miller Index Surfaces of Silver. Langmuir, 2022, 38, 14162-14171.	1.6	0
48368	Theoretical investigation of CO oxidation by single cobalt atom within two-dimensional porphyrin sheet. Functional Materials Letters, 2022, 15, .	0.7	1
48369	Effect of Sr-Doping on the Photocatalytic Performance of LaNiO3â^Ïƒ. Catalysts, 2022, 12, 1434.	1.6	3
48370	Topological hinge modes in Dirac semimetals. Frontiers of Physics, 2023, 18, .	2.4	8
48371	Atomically Precise Incorporation of BN-Doped Rubicene into Graphene Nanoribbons. Journal of Physical Chemistry C, 2022, 126, 19726-19732.	1.5	4
48372	Epitaxial Growth of Single-Layer Kagome Nanoflakes with Topological Band Inversion. ACS Nano, 2022, 16, 21079-21086.	7.3	2
48373	Rational Design of Metal-Alkoxide-Functionalized Metalâ€“Organic Frameworks for Synergistic Dual Activation of CH₄ and CO₂ toward Acetic Acid Synthesis. ACS Applied Materials & Interfaces, 2022, 14, 52979-52992.	4.0	2
48374	Surfacial proton conducting CeO2 nanosheets. Ceramics International, 2023, 49, 9138-9146.	2.3	4
48375	Dynamic Response of Single Crystal Al, Cu & Ni Upon Impact : MD and Ab-Initio Calculations. Journal of Dynamic Behavior of Materials, 2023, 9, 24-35.	1.1	5
48376	Exploration of NaSICON Frameworks as Calcium-Ion Battery Electrodes. Chemistry of Materials, 2022, 34, 10133-10143.	3.2	5
48377	Charge Recombination Dynamics in a Metal Halide Perovskite Simulated by Nonadiabatic Molecular Dynamics Combined with Machine Learning. Journal of Physical Chemistry Letters, 2022, 13, 10734-10740.	2.1	7
48378	A density functional based tight binding (DFTB+) study on the sulfidization-xanthate flotation mechanism of cerussite. Applied Surface Science, 2023, 612, 155677.	3.1	11
48379	Stacked Si2BN monolayers as ultra-high-capacity anode material for divalent Mg-ion batteries. FlatChem, 2022, 36, 100444.	2.8	2

#	Article	IF	Citations
48380	Pressure-induced first-order antiferromagnetic to ferromagnetic transition in MnN. Journal of Alloys and Compounds, 2022, , 168120.	2.8	0
48381	A Novel Membrane-like 2D Aâ€™-MoS2 as Anode for Lithium- and Sodium-Ion Batteries. Membranes, 2022, 12, 1156.	1.4	4
48382	Realization of high-quality Sr4Fe6O13 epitaxial film and its phase competition with SrFeO2.5. Ceramics International, 2022, , .	2.3	1
48383	Electronic effects on the radiation damage in high-entropy alloys. Acta Materialia, 2023, 244, 118511.	3.8	7
48384	Origin of Enhanced Photocatalytic Activity in Direct Band Gap g-C₃N₄ Nanoribbons with Tunable Electronic Properties for Water-Splitting Reaction: A First-Principles Study. Journal of Physical Chemistry C, 2022, 126, 19627-19636.	1.5	6
48385	Strain-Tuneable Magnetism and Spintronics of Distorted Monovacancies in Graphene. Journal of Physical Chemistry C, 2022, 126, 19435-19445.	1.5	1
48386	Construction of group III nitride van der Waals heterostructures for highly efficient photocatalyst. Applied Surface Science, 2022, , 155679.	3.1	2
48387	Thermal expansion of plasma-exposed tungsten. Journal of Applied Physics, 2022, 132, .	1.1	1
48388	Interaction between peptides and an MoS2 monolayer containing a nanopore: First-principles calculations. Chinese Journal of Physics, 2023, 84, 486-499.	2.0	0
48389	Comparative study on high-pressure physical properties of monoclinic MgCO3 and Mg2CO4. Scientific Reports, 2022, 12, .	1.6	1
48390	TaIrTe₄ Monolayer with Topological Insulator Characteristic: A New and Highly Efficient Electrocatalyst toward Oxygen Reduction Reaction. Journal of Physical Chemistry C, 2022, 126, 19685-19692.	1.5	2
48391	Understanding the impact of Y2+ (Y Mn, Fe, and co) cations on physical properties of SrYGe2O6 clinopyroxene: A DFT insight. Journal of Physics and Chemistry of Solids, 2022, , 111112.	1.9	0
48392	First-principles study of the interaction between H/He impurities and vacancy in tetragonal Be$$_{12}$$Ti. Journal of Materials Science, 2022, 57, 20631-20640.	1.7	1
48393	Phonon mediated superconductivity in field-effect doped molybdenum dichalcogenides. 2D Materials, 2023, 10, 015013.	2.0	2
48394	Stabilization of Dinuclear Rhodium and Iridium Clusters on Layered Titanate and Niobate Supports. Inorganic Chemistry, 2023, 62, 1113-1121.	1.9	0
48395	Two-dimensional titanium carbide (MXene)-supported Pt3Ti intermetallic compound catalysts for efficient room-temperature oxidative removal of gaseous formaldehyde. Materials Today Nano, 2023, 21, 100283.	2.3	1
48396	Effect of Composition and Local Environment on CO₂ Adsorption on Nickel and Magnesium Oxide Solid Solutions. Journal of Physical Chemistry C, 2022, 126, 19705-19714.	1.5	0
48397	Transport characteristics and lattice dynamics with phonon topology accentuation in layered CuTlX (X: S, Se). Physica Scripta, 2022, 97, 125820.	1.2	1

#	Article	IF	Citations
48399	Hydrogenation of CO₂ to Methane over a Ru/RuTiO₂ Surface: A DFT Investigation into the Significant Role of the RuO₂ Overlayer. ACS Catalysis, 2022, 12, 14654-14666.	5.5	3
48400	Fully-exposed Pt-Fe cluster for efficient preferential oxidation of CO towards hydrogen purification. Nature Communications, 2022, 13, .	5.8	34
48401	The structural, electronic, magnetic, optical and vibrational properties of the delafossite CuAlO2: DFT calculations and experimental study. Journal of Materials Science: Materials in Electronics, 2022, 33, 26474-26483.	1.1	2
48402	Halide-sodalites: thermal behavior at low temperatures and local deviations from the average structure. Zeitschrift Fur Kristallographie - Crystalline Materials, 2023, 238, 27-38.	0.4	0
48403	Nitric oxide (NO) on VO2(010) surface: A density functional theory study with the standard GGA functional and effect of van der Waals dispersion. Computational Condensed Matter, 2022, 33, e00766.	0.9	1
48404	Meta-stable initial condition for improving the switching probability in azobenzene derivatives on surface. Applied Surface Science, 2023, 612, 155747.	3.1	1
48405	Anomalous Hall conductivity control in <mml:math xmlns:mml="http://www.w3.org/1998/Math/MathML"><mml:msub><mml:mrow><mml:mi>Mn</mml:mi></mml:mrow><mml:mn>3</mml:mn></mml:msub></mml:math> antiperovskite by epitaxial strain along the kagome plane. Physical Review B, 2022, 106, .	1.1	7
48406	Influence of Group-IVA Doping on Electronic and Optical Properties of ZnS Monolayer: A First-Principles Study. Nanomaterials, 2022, 12, 3898.	1.9	3
48407	Study of Structural, Elastic and Thermodynamic Properties of Metal Carbides MC (M = Ir, Rh and Ru) Using First-Principles Calculations. Physics of Metals and Metallography, 2022, 123, 1376-1386.	0.3	1
48408	Anti-phase boundary accelerated exsolution of nanoparticles in non-stoichiometric perovskite thin films. Nature Communications, 2022, 13, .	5.8	12
48409	Electric Resonance-Based Depressurization and Augmented Injection in Low-Permeability Reservoirs. Energy & Fuels, 0, , .	2.5	1
48410	Two-Dimensional Penta-NiPS Sheets: Two Stable Polymorphs. Journal of Physical Chemistry C, 2022, 126, 19455-19461.	1.5	3
48411	Adsorption Mechanism and Optical Behaviors of Typical Volatile Organic Compounds on Pristine and Cu/Niâ€Modified C₃N Monolayer: A Firstâ€Principles Study. Advanced Theory and Simulations, 2023, 6, .	1.3	2
48412	Zn₃GaB₆O₁₂As and Zn₄P₆N₁₂S: Isotropic Zero Thermal Expansion Materials Based on the â€œCage-Restrictingâ€•Model. Chemistry of Materials, 2022, 34, 9915-9922.	3.2	4
48413	Structure, electronic, optical and elastic properties of (NH4)2BeF4 crystal in paraelectric phase. Current Applied Physics, 2023, 45, 76-85.	1.1	3
48414	Amorphous iron fluorosulfate as a high-capacity cathode utilizing combined intercalation and conversion reactions with unexpectedly high reversibility. Nature Energy, 2023, 8, 30-39.	19.8	18
48415	High-pressure synthesis of seven lanthanum hydrides with a significant variability of hydrogen content. Nature Communications, 2022, 13, .	5.8	14
48416	Experimental and theoretical insights on the structural and optical properties of GeOx thin films deposited via RF magnetron sputtering under varying oxygen percentage. Physica B: Condensed Matter, 2022, , 414494.	1.3	0

#	Article	IF	Citations
48417	Theoretical Prediction of Spinel Na₂In_xSc_{0.666â˜'}_xCl₄ and Rockâ€Salt Na₃In_{1â˜'}_xSc_xCl₆ Superionic Conductors for Allâ€Solidâ€State Sodiumâ€Ion Batteries. Advanced Theory and Simulations, 2023, 6, .	1.3	3
48418	Li₂NiSe₂: a new type intrinsic two dimensional ferromagnetic semiconductor above 200 K. Chinese Physics B, 0, , .	0.7	0
48419	Realizing high thermoelectric performance of Cu and Ce co-doped p-type polycrystalline SnSe via inducing nanoprecipitation arrays. Journal of Advanced Ceramics, 2022, 11, 1671-1686.	8.9	11
48420	Electronic, Thermodynamic Stability ,and Band Alignment Behavior of the CoVSi/NaCl Heterojunction. ECS Journal of Solid State Science and Technology, 0, , .	0.9	0
48421	Vanadium Dioxide-Based Miniaturized Thermal Sensors: Humidity Effects on Phase Change and Sensitivity. ACS Applied Electronic Materials, 2022, 4, 5456-5467.	2.0	2
48422	Large Gap Topological Insulating Phase and Anisotropic Rashba and Chiral Spin Textures in Monolayer Zintl A₂MX₂. ACS Applied Electronic Materials, 2022, 4, 5308-5316.	2.0	1
48423	Facet-Dependent Electron Transfer Regulates Photocatalytic Valorization of Biopolyols. Journal of the American Chemical Society, 2022, 144, 21224-21231.	6.6	16
48424	Bis(Vinylenedithio)â€Tetrathiafulvaleneâ€Based Coordination Networks. Chemistry - A European Journal, 2023, 29, .	1.7	4
48425	Ab initio study of RaWO4: Comparison with isoelectronic tungstates. Journal of Solid State Chemistry, 2023, 317, 123709.	1.4	2
48426	Pressure stabilized polymeric nitrogen in N2F and N10F compounds. Results in Physics, 2022, 43, 106093.	2.0	1
48427	Controlled dislocation density as enhancer of the magnetic response in multiferroic oxide nanoparticles. Applied Materials Today, 2022, 29, 101680.	2.3	2
48428	Experimental and DFT study of structural and optical properties of Ni-doped ZnO nanofiber thin films for optoelectronic applications. Optical Materials, 2022, 134, 113188.	1.7	9
48429	Strengthening and high-temperature softening resistance of low Si-added Cuâ€“Crâ€“Zr alloy for fusion reactor application. Materials Science & Engineering A: Structural Materials: Properties, Microstructure and Processing, 2022, 861, 144328.	2.6	4
48430	Tunable magnetoresistance in Li2BaSi. Physics Letters, Section A: General, Atomic and Solid State Physics, 2022, 456, 128541.	0.9	0
48431	Thermodynamic modeling of the Ni-Ti-Cr system and the B2/B19â€² martensitic transformation. Calphad: Computer Coupling of Phase Diagrams and Thermochemistry, 2022, 79, 102505.	0.7	2
48432	Enhanced electronic and thermoelectric properties of Zr<mml:math xmlns:mml="http://www.w3.org/1998/Math/MathML" altimg="si90.svg" display="inline" id="d1e1048"><mml:msub><mml:mrow /><mml:mrow><mml:mn>2</mml:mn></mml:mrow></mml:msub></mml:math>CO<mml:math xmlns:mml="http://www.w3.org/1998/Math/MathML" altimg="si90.svg" display="inline" id="d1e1056"><mml:msub><mml:mrow /><mml:mrow><mml:mn>2</mml:mn></mml:mrow></mml:msub></mml:math>	1.5	2
48433	Solute clustering governed elastic properties in aluminum. Calphad: Computer Coupling of Phase Diagrams and Thermochemistry, 2022, 79, 102494.	0.7	1
48434	Density functional theory study of active sites and reaction mechanism of ORR on Pt surfaces under anhydrous conditions. Chinese Journal of Catalysis, 2022, 43, 3126-3133.	6.9	4

#	Article	IF	Citations
48435	Ni-doped boron nitride nanotubes as promising gas sensing material for dissolved gases in transformer oil. Materials Today Communications, 2022, 33, 104845.	0.9	2
48436	Influence of interfacial configuration on bonding properties and thermal conductivity of heterogeneous interface in Al/Graphite composite used for electronic packaging. Surfaces and Interfaces, 2022, 35, 102452.	1.5	2
48437	Packing of inhibitor molecules during area-selective atomic layer deposition studied using random sequential adsorption simulations. Journal of Vacuum Science and Technology A: Vacuum, Surfaces and Films, 2022, 40, .	0.9	8
48438	Investigation of the Structure of Atomically Dispersed NiN_x Sites in Ni and N-Doped Carbon Electrocatalysts by ⁶¹Ni MÃ¶ssbauer Spectroscopy and Simulations. Journal of the American Chemical Society, 2022, 144, 21741-21750.	6.6	2
48439	BinPo: An open-source code to compute the band structure of two-dimensional electron systems. Computer Physics Communications, 2023, 284, 108595.	3.0	1
48440	Two-Dimensional (2D) TM-Tetrahydroxyquinone Metalâ€“Organic Framework for Selective CO2 Electrocatalysis: A DFT Investigation. Nanomaterials, 2022, 12, 4049.	1.9	4
48441	Ferroelectric and antiferroelectric distortions coupling of nitride perovskite LaWN₃ under epitaxial strain using first-principles calculations. Europhysics Letters, 2022, 140, 56001.	0.7	1
48442	Anomalous thermal response of bulk diamond to uniaxial (100) strain: A first-principles prediction. Physical Review B, 2022, 106, .	1.1	4
48443	First-principles study of He retention and clustering in Al-Ga alloy. International Journal of Modern Physics C, 0, , .	0.8	0
48444	Structural investigation of flat overlayer and surface alloy of Sn on Mo(110). Surface Science, 2023, 729, 122224.	0.8	2
48445	Sulfur Vacancy-Rich Carbonaceous Co₉S₈-ZnS Nanotubes for the Oxygen Evolution Reaction. ACS Applied Energy Materials, 2022, 5, 14869-14880.	2.5	1
48446	A comparative study of interfacial thermal conductance between metal and semiconductor. Scientific Reports, 2022, 12, .	1.6	2
48447	Investigation of the Optoelectronic and Photovoltaic Properties of Y_xIN_{1-x}P Alloys using First Principles Calculations. Annals of West Univesity of TimiÅŸoara Physics Series, 2022, 64, 126-147.	0.0	0
48448	Understanding the Reactivity of Supported Late Transition Metals on a Bare Anatase (101) Surface: A Periodic Conceptual DFT Investigation. ChemPhysChem, 2023, 24, .	1.0	4
48449	Composition-dependent photocatalytic activity and high-mobility carrier gas in NaTaO3/BaBiO3 heterojunctions. Surfaces and Interfaces, 2023, 36, 102486.	1.5	2
48450	Discovery of Salt Hydrates for Thermal Energy Storage. Journal of the American Chemical Society, 2022, 144, 21617-21627.	6.6	6
48451	2D transitional-metal nickel compounds monolayer: Highly efficient multifunctional electrocatalysts for the HER, OER and ORR. International Journal of Hydrogen Energy, 2023, 48, 4242-4252.	3.8	17
48452	Lattice dynamics of <mml:math xmlns:mml="http://www.w3.org/1998/Math/MathML"><mml:mi>Î²</mml:mi><mml:mo>â^'</mml:mo><mml:msub><mml:mi mathvariant="normal">FeSi</mml:mi><mml:mn>2</mml:mn></mml:msub></mml:math> nanorods. Physical Review B, 2022, 106, .	1.1	0

#	Article	IF	Citations
48453	Group 14 elements in the Cmcm phase with a direct band structure for photoelectric application. Physica Scripta, 2023, 98, 015701.	1.2	11
48454	Thermal properties of the metallic delafossite <mml:math xmlns:mml="http://www.w3.org/1998/Math/MathML"><mml:mrow><mml:mi>PdCo</mml:mi><mml:msub><mml:mi mathvariant="normal">O</mml:mi><mml:mn>2</mml:mn></mml:msub></mml:mrow></mml:math> : A combined experimental and first-principles study. Physical Review Materials, 2022, 6, .	0.9	2
48455	A DFT Based Approach to Sense the SF₆ÂDecomposed Gases Using Ni-doped WS₂ Monolayer. IETE Technical Review (Institution of Electronics and Telecommunication Engineers, India), 2023, 40, 621-631.	2.1	2
48456	Study of structural and electronic properties of graphene and some graphene derivatives based on orthorhombic unit cell by density functional theory. Science and Technology, 2022, 60, 794-802.	0.1	0
48457	DFT study of the effect of impurity defects on the inner-layer adsorption of hydrated Al(OH)2+ on the kaolinite (0 0 1) surface. Journal of Molecular Liquids, 2022, 368, 120819.	2.3	3
48458	Effects of Alloying Elements on Hydrogen Adsorption Properties on Zirconium Surface. Metallurgical and Materials Transactions A: Physical Metallurgy and Materials Science, 2023, 54, 286-292.	1.1	0
48459	Influence of carbon on hydrogen retention in molybdenum for nuclear material application: A first-principles investigation. Nuclear Materials and Energy, 2022, 33, 101311.	0.6	0
48460	Controllable ferroelectricity and bulk photovoltaic effect in elemental group-V monolayers through strain engineering. Physical Review B, 2022, 106, .	1.1	4
48461	Controllable synthesis of nano-spherical and spinel structure hausmannite for asymmetric supercapacitor electrode application with long-term cyclic stability and its photocatalytic activity. Materials Chemistry and Physics, 2023, 296, 127028.	2.0	2
48462	Revealing the Origin of Heterogeneous Phase Transition and Deformation Behavior in Au-Ag-Cu-Based Multicomponent Alloys. Metals, 2022, 12, 1966.	1.0	1
48463	Interactions of alloying Cr/Ti with substitutional solutes and self-interstitial atoms in vanadium. Journal of Nuclear Materials, 2023, 574, 154160.	1.3	3
48464	Vacancy-Mediated Anomalous Emission Characteristics of Size-Confined Semiconducting CoTe₂. ACS Applied Materials & Interfaces, 2022, 14, 53139-53149.	4.0	1
48465	Impact of vacancies on structure, stability and properties of hexagonal transition metal diborides, MB2 (MÂ=ÂSc, Y, Ti, Zr, Hf, V, Nb, Ta, Cr, Mo, W, Mn, and Fe). Materialia, 2022, 26, 101629.	1.3	6
48466	Self-layering of (Ti,Al)N by interface-directed spinodal decomposition of (Ti,Al)N/TiN multilayers: First-principles and experimental investigations. Materials and Design, 2022, 224, 111392.	3.3	5
48467	First principles prediction of the Al-Li phase diagram including configurational and vibrational entropic contributions. Computational Materials Science, 2023, 217, 111898.	1.4	3
48468	Large in-plane and out-of-plane piezoelectricity in 2D Î³-LiMX2 (M=Al, Ga and In; X=S, Se and Te) monolayers. Materials Science in Semiconductor Processing, 2023, 154, 107222.	1.9	5
48469	Fe isotope fractionation caused by phase transition of FeS and implications for Fe isotope signatures of the mantle and core. Geochimica Et Cosmochimica Acta, 2023, 340, 38-50.	1.6	1
48470	Density Functional Evaluation of Catechol Adsorption on Pristine and Reduced TiO₂(B)(100) Ultrathin Sheets for Dye-Sensitized Solar Cell Applications. Inorganic Chemistry, 0, , .	1.9	1

#	Article	IF	Citations
48471	Effect of point defect-induced surface active sites of MoSi2N4 on performance of photocatalytic CO2 reduction. Applied Catalysis A: General, 2023, 650, 118975.	2.2	3
48472	Role of solute atoms and vacancy in hydrogen embrittlement mechanism of aluminum: A first-principles study. International Journal of Hydrogen Energy, 2023, 48, 4516-4528.	3.8	4
48473	Spin Selectivity in Chiral Hybrid Cobalt Halide Films with Ultrasmooth Surface. Small Methods, 2022, 6, .	4.6	5
48474	Towards In Silico Mining for Superconductors â€“ Cutting the Gordian Knot. Physica C: Superconductivity and Its Applications, 2022, , 1354187.	0.6	0
48475	Hydrogenated V2O5 with fast Zn-ion migration kinetics as high-performance cathode material for aqueous zinc-ion batteries. Electrochimica Acta, 2023, 439, 141717.	2.6	11
48476	First-principles study of room-temperature ferromagnetism in transition-metal doped H-SiNWs. Physical Chemistry Chemical Physics, 2023, 25, 2999-3010.	1.3	1
48477	Density functional theory analysis of the adsorption behaviors of H₂O and CO₂ on the CaCl₂(110) surface. New Journal of Chemistry, 2023, 47, 2264-2272.	1.4	1
48478	A density functional theory study of a water gas shift reaction on Ag(111): potassium effect. Physical Chemistry Chemical Physics, 2022, 25, 768-777.	1.3	1
48479	Pressure-induced phase transition and band-gap decrease in semiconducting Na3Bi(IO3)6. Results in Physics, 2023, 44, 106156.	2.0	4
48480	High-pressure equation of state of cesium fluoride to 120â€…GPa. , 2017, 6, 011101-011101.		0
48481	First-principles study of phosphorus under high pressure: Crystal structure, superconductivity, and anharmonicity. , 2017, 6, 011104-011104.		1
48482	Defect related room temperature ferromagnetism in N-implanted ZnO film. , 2018, 7, 011104-011104.		0
48483	Combined DFT, SCAPS-1D, and wxAMPS frameworks for design optimization of efficient Cs₂BiAgI₆-based perovskite solar cells with different charge transport layers. RSC Advances, 2022, 12, 34850-34873.	1.7	92
48484	Condensability sieving porous coordination polymer membranes for preferential permeation of C1â€“C4 alkanes over H2. , 2022, 2, 100044.		0
48485	Role of inorganic cations in the excitonic properties of lead halide perovskites. Physical Chemistry Chemical Physics, 2023, 25, 2468-2476.	1.3	2
48486	Structure and registry of the silica bilayer film on Ru(0001) as viewed by LEED and DFT. Physical Chemistry Chemical Physics, 2022, 24, 29721-29730.	1.3	1
48487	Electronic and transport properties of new carbon nanoribbons with 5â€“8â€“5 carbon rings: tuning stability by the edge shape effect. Physical Chemistry Chemical Physics, 2022, 24, 29966-29976.	1.3	2
48488	Exploring the direction-dependency of conductive filament formation and oxygen vacancy migration behaviors in HfO₂-based RRAM. Physical Chemistry Chemical Physics, 2023, 25, 3521-3534.	1.3	2

#	Article	IF	Citations
48489	Highly sensitive work function type room temperature gas sensor based on Ti doped hBN monolayer for sensing CO₂, CO, H₂S, HF and NO. A DFT study. RSC Advances, 2022, 12, 34185-34199.	1.7	12
48490	Pressure effects on the anomalous thermal transport and anharmonic lattice dynamics of CsX (X = Cl,) Tj ETQq1 1 0.784314 rgBT /Overl	1.3	0
48491	Transition Metal Doped Bismuthene and Mn-Bi/CrI₃ Heterostructure for High Anisotropy Energy and Half-Metallicity. IEEE Open Journal of Nanotechnology, 2023, 4, 1-9.	0.9	2
48492	Identification of distinctive structural and optoelectronic properties of Bi₂O₃ polymorphs controlled by tantalum addition. Journal of Materials Chemistry C, 2022, 10, 17925-17935.	2.7	1
48493	A theoretical study of new polar and magnetic double perovskites for photovoltaic applications. RSC Advances, 2022, 12, 34503-34511.	1.7	0
48494	Charge and adsorption height dependence of the self-metalation of porphyrins on ultrathin MgO(001) films. Physical Chemistry Chemical Physics, 2022, 24, 28540-28547.	1.3	0
48495	Why copper catalyzes electrochemical reduction of nitrate to ammonia. Faraday Discussions, 0, 243, 502-519.	1.6	9
48496	First-principles study of structural, electronic, elastic and optical properties of alkali lead iodides MPbI3 (M = Li, Na, K). Ukrainian Journal of Physical Optics, 2023, 24, 1-21.	9.7	1
48497	Does the Oxygen Evolution Reaction follow the classical OH*, O*, OOH* path on single atom catalysts?. Journal of Catalysis, 2023, 417, 351-359.	3.1	27
48498	Substrate temperature effects on the structural, morphological and optical properties of Bi2S3 thin films deposited by spray pyrolysis: An experimental and first-principles study. Optical Materials, 2023, 135, 113215.	1.7	5
48499	Fast electrochemical redox kinetics of two-dimensional TiO2/Ti3C2T (MXene) heterostructure for high-performance lithium-ion capacitor. Journal of Electroanalytical Chemistry, 2023, 928, 117034.	1.9	5
48500	Effect of alkali metal adsorption over pristine Ga2STe janus monolayer in enhancing the visible region absorption. , 2023, 173, 207463.		0
48501	Effects of Cl/Br substitution of antimony octahedra on photoluminescence and a new engineering strategy for performance optimization. Materials Today Chemistry, 2023, 27, 101275.	1.7	0
48502	Large second harmonic generation in a penta-CdO₂ sheet exfoliated from its bulk phase. Journal of Materials Chemistry A, 2022, 11, 167-177.	5.2	3
48503	A first-principles study of the adsorption mechanism of NO₂ on monolayer antimonide phosphide: a highly sensitive and selective gas sensor. New Journal of Chemistry, 2023, 47, 1413-1421.	1.4	1
48504	Scalable production of reduced graphene oxide via biowaste valorisation: an efficient oxygen reduction reaction towards metal-free electrocatalysis. New Journal of Chemistry, 2023, 47, 1360-1370.	1.4	3
48505	Theoretical design of two-dimensional AMInP₂X₃Y₃ (AM = Li, Na,) Tj ETQq0 0 0 rgBT /Overlock 1 570-577.	2.6	2
48506	Effective defect passivation with a designer ionic molecule for high-efficiency vapour-deposited inorganic phase-pure CsPbBr₃ perovskite solar cells. Journal of Materials Chemistry A, 2022, 11, 408-418.	5.2	10

#	Article	IF	Citations
48507	Catalytic active centers beyond transition metals: atomically dispersed alkaline-earth metals for the electroreduction of nitrate to ammonia. Journal of Materials Chemistry A, 2023, 11, 1817-1828.	5.2	51
48508	Photocatalytic reductive carboxylation of terminal alkynes with CO2 using heterostructured ZIF-7/BiOBr under visible-light illumination. Journal of CO2 Utilization, 2023, 67, 102334.	3.3	5
48509	Aluminum functionalized few-layer silicene as anode material for alkali metal ion batteries. Molecular Systems Design and Engineering, 2023, 8, 379-387.	1.7	5
48510	Transport properties of As-F-based molecular magnetic tunnel junctions. Physics Letters, Section A: General, Atomic and Solid State Physics, 2023, 457, 128570.	0.9	1
48511	Boriding of tungsten by the powder-pack process: Phase formation, growth kinetics and enhanced neutron shielding. International Journal of Refractory Metals and Hard Materials, 2023, 110, 106049.	1.7	4
48512	New lead-iodide formates with a strong second-harmonic generation response and suitable birefringence obtained by the substitution strategy. Chemical Science, 2022, 14, 136-142.	3.7	3
48513	Influence of Co doping concentrations and strains on the electronic structure and absorption spectrum of graphene-like ZnO monolayer. Results in Physics, 2023, 44, 106161.	2.0	1
48514	DFT study of hydrogen interaction with transition metal doped graphene for efficient hydrogen storage: effect of d-orbital occupancy and Kubas interaction. Physical Chemistry Chemical Physics, 2022, 25, 262-273.	1.3	13
48515	Exploring a novel class of Janus MXenes by first principles calculations: structural, electronic and magnetic properties of Sc₂CXT, X = O, F, OH; T = C, S, N. Physical Chemistry Chemical Physics, 2023, 25, 1881-1888.	1.3	5
48516	Stabilization of Eu²⁺ in Li₂B₄O₇ with the BO₃ network through U⁶⁺ co-doping and defect engineering. Physical Chemistry Chemical Physics, 2023, 25, 1889-1902.	1.3	3
48517	Constructing asymmetrical dual catalytic sites in manganese oxides enables fast and stable lithiumâ€“oxygen catalysis. Journal of Materials Chemistry A, 2023, 11, 1188-1198.	5.2	3
48518	Vacancy-fused multiple layers of copper sulfoselenide superstructures: a propitious HER electrocatalyst in acidic medium. Catalysis Science and Technology, 2023, 13, 694-704.	2.1	2
48519	Effect of different oxygen species on the oxidative coupling of methane over TiO2 catalysts. Applied Catalysis A: General, 2023, 650, 118998.	2.2	4
48520	An orthorhombic carbon allotrope with a quasi-direct band gap and superhard. Diamond and Related Materials, 2023, 131, 109592.	1.8	15
48521	Enhancing the stability of the polymeric Lewis-base-assisted dual-phase 3D CsPbBr₃â€“Cs₄PbBr₆ perovskite by molecular engineering and self-passivation. Journal of Materials Chemistry C, 2022, 11, 307-320.	2.7	2
48522	First-principles calculations to investigate magnetic, electronic, mechanical and dynamical properties of the bimetallic M-Pt (M: Mn Co and Ni) alloys. Journal of Magnetism and Magnetic Materials, 2023, 565, 170298.	1.0	2
48523	Enhanced photocatalytic reduction of CO2 into CH4 over N, Eu co-doped TiO2: Insight into the synergistic effect of N and Eu. Applied Catalysis A: General, 2023, 650, 118977.	2.2	4
48524	Physical properties of BaRu2X2 (XÂ=ÂP, As) superconducting compound sunder pressure effects: Ab initio study. Physica C: Superconductivity and Its Applications, 2023, 604, 1354176.	0.6	1

#	Article	IF	Citations
48525	Improving the DFT computational accuracy for CO activation on Fe surfaces by Bayesian error estimation functional with van der Waals correlation. Computational and Theoretical Chemistry, 2023, 1219, 113968.	1.1	0
48526	Nanoscale structural and electronic properties of cellulose/graphene interfaces. Physical Chemistry Chemical Physics, 0, , .	1.3	1
48527	High capacity and stability induced by sandwich-like structure and metalâ€“O configuration for CoNi2S4/Ti3C2Tx heterostructure electrode. Electrochimica Acta, 2023, 439, 141643.	2.6	2
48528	Volcano relationships and a new activity descriptor of 2D transition metalâ€“Fe layered double hydroxides for efficient oxygen evolution reaction. Materials Horizons, 0, , .	6.4	8
48529	Deoxydehydration of glycerol to allyl alcohol catalysed by ceria-supported rhenium oxide. Molecular Catalysis, 2023, 535, 112856.	1.0	2
48530	Axially coordinated Coâ€“N₄ sites for the electroreduction of nitrobenzene. Journal of Materials Chemistry A, 2023, 11, 5095-5103.	5.2	4
48531	Adsorption and sensing of formaldehyde on pristine and noble metal doped tellurene: A first-principles investigation. Chemical Physics Letters, 2023, 811, 140244.	1.2	4
48532	Computational insight into electro-catalytic reduction of carbon monoxide by two-dimensional metal-embedded poly-phthalocyanine. Catalysis Communications, 2023, 174, 106573.	1.6	2
48533	Structural stability and lithium storage property of Sn clusters (xÂâ‰Â6) deposited on graphene based on first-principles calculation. Diamond and Related Materials, 2023, 131, 109567.	1.8	0
48534	Adsorption of aromatic molecules on a black phosphorene surface: a first-principles study. New Journal of Chemistry, 2023, 47, 1842-1851.	1.4	1
48535	Accelerating the evaluation of crucial descriptors for catalyst screening via message passing neural network. , 2023, 2, 59-68.		1
48536	A new high capacity cathode material for Li/Na-ion batteries: dihafnium sulfide (Hf₂S). Physical Chemistry Chemical Physics, 2023, 25, 1114-1122.	1.3	1
48537	Effects of oxygen pressure on the morphology and surface energetics of Î²-PbO₂: insight from DFT calculations. Physical Chemistry Chemical Physics, 2023, 25, 2793-2802.	1.3	3
48538	First-principles calculations to investigate elastic, electronic, optical and thermodynamic properties of Pt3X (Xâ€¯=â€¯Ti, Cu). Results in Physics, 2023, 44, 106141.	2.0	7
48539	Strain engineering the electronic properties of the type-II CdO/MoS2 van der Waals heterostructure. Thin Solid Films, 2023, 764, 139626.	0.8	7
48540	Exploring coverage-dependent chain-growth mechanisms on Ru(111) for Fischerâ€“Tropsch synthesis. Catalysis Science and Technology, 2023, 13, 437-456.	2.1	2
48541	NiO and CrO_x interaction promoting in situ generation of the coordinatively unsaturated Crâ€“O acidâ€“base for oxygen-lean propane dehydrogenation. Catalysis Science and Technology, 0, , .	2.1	3
48542	Effect of pressure on structural, electronic dispersion relations, optical and thermoelectric properties of CsNbO3 perovskite for photovoltaic and energy applications. Polyhedron, 2023, 230, 116217.	1.0	2

#	Article	IF	Citations
48543	The behavior of aluminum sites in H-[Al]-RUB-18 catalysts: A theoretical-experimental investigation. Molecular Catalysis, 2023, 535, 112870.	1.0	0
48544	Nanoporous cyanuric acid nanosheets for semiconductors: Insights from chemical bonding. Chemical Physics Letters, 2023, 811, 140236.	1.2	0
48545	Thermophysical properties in the Al-Cu-Ag system: A combined CALPHAD and first-principles study. Journal of Molecular Liquids, 2023, 370, 121001.	2.3	1
48546	Biaxial strain induced tunable electronic properties study of ZnO nanoparticles via first-principles density functional theory. Materials Science and Engineering B: Solid-State Materials for Advanced Technology, 2023, 288, 116186.	1.7	5
48547	A computational study on CO₂ electrochemical reduction on two dimensional metal-1,2,3,4,5,6,7,8,9,10,11,12-perthiolated coronene frameworks. New Journal of Chemistry, 0, , .	1.4	0
48548	Advanced materials based on montmorillonite modified with poly(ethylenimine) and poly(2-methyl-2-oxazoline): Experimental and DFT study. Colloids and Surfaces A: Physicochemical and Engineering Aspects, 2023, 659, 130784.	2.3	3
48549	Designing Mg alloys with high strength and ductility by reducing the strength difference between the basal and non-basal slips. Materials and Design, 2023, 225, 111476.	3.3	12
48550	Interstitial diffusion of hydrogen in M<mml:math xmlns:mml="http://www.w3.org/1998/Math/MathML" altimg="si91.svg" display="inline" id="d1e831"><mml:msub><mml:mrow /><mml:mrow><mml:mn>7</mml:mn></mml:mrow></mml:msub></mml:math>C<mml:math xmlns:mml="http://www.w3.org/1998/Math/MathML" altimg="si92.svg" display="inline" id="d1e839"><mml:msub><mml:mrow /><mml:mrow><mml:mn>3</mml:mn></mml:mrow></mml:msub></mml:math> (M=Cr,Mn,Fe): A computation	1.4	1
48551	Î³-P₄S₃I₂: a new metal-free infrared second-order nonlinear optical crystal designed by polymorphism strategy. Inorganic Chemistry Frontiers, 2023, 10, 1119-1126.	3.0	9
48552	Heterostructured Ti-MOF/g-C3N4 driven light assisted reductive carboxylation of aryl aldehydes with CO2 under ambient conditions. Journal of Catalysis, 2023, 417, 116-128.	3.1	5
48553	Mechanical properties of AlMgB14-related boron carbide structures. A first principle study. Physica B: Condensed Matter, 2023, 651, 414601.	1.3	0
48554	Ab initio atomic displacement simulation of <mml:math xmlns:mml="http://www.w3.org/1998/Math/MathML" altimg="si39.svg" display="inline" id="d1e1073"><mml:mi>I</mml:mi></mml:math>-MH<mml:math xmlns:mml="http://www.w3.org/1998/Math/MathML" altimg="si7.svg" display="inline" id="d1e1078"><mml:msub><mml:mrow		

#	Article	IF	Citations
48561	Small atoms fall into bulk from non-close-packed metal surfaces?. Computational Materials Science, 2023, 218, 111959.	1.4	0
48562	Thermal properties and pressure-dependent elastic constants of cadmium stannate as a substrate for MEMS: An ab initio study. Physica B: Condensed Matter, 2023, 651, 414599.	1.3	1
48563	Computational screening of single-atom catalysts for direct electrochemical NH3 synthesis from NO on defective boron phosphide monolayer. Applied Surface Science, 2023, 611, 155764.	3.1	10
48564	An atomic scale study on self-interstitial formation and diffusion behaviors in TiVTa and TiVTaNb concentrated solid-solution alloys. Computational Materials Science, 2023, 218, 111943.	1.4	6
48565	First-principles study on optoelectronic properties of nonmetal-doped PtS2. Solid State Communications, 2023, 360, 115045.	0.9	0
48566	Ab-initio based modeling of precipitation in Alâ€“(Sc,Zr) alloy. Formation and stability of a coreâ€“shell structure. Computational Materials Science, 2023, 218, 111912.	1.4	1
48567	An ab initio study of structural phase transitions of crystalline aluminium under ultrahigh pressures based on ensemble theory. Computational Materials Science, 2023, 218, 111960.	1.4	1
48568	Effect of Mo addition on hydrogen segregation at Î±-Fe grain boundaries: A first-principles investigation of the mechanism by which Mo addition improves hydrogen embrittlement resistance in high-strength steels. Computational Materials Science, 2023, 218, 111951.	1.4	10
48569	Hybrid density functional theory study of substitutional Gd in <mml:math xmlns:mml="http://www.w3.org/1998/Math/MathML" altimg="si1.svg"><mml:mrow><mml:mi>Î²</mml:mi></mml:mrow></mml:math>-Ga2O3. Physica B: Condensed Matter, 2023, 651, 414558.	1.3	4
48570	Topological properties and strain effects of binary monoclinic superconductors RhX2 (X=Sb,Bi). Physica B: Condensed Matter, 2023, 650, 414569.	1.3	2
48571	The structure and mechanical properties of NbHfTaW refractory high-entropy alloy: A combined theoretical and experimental study. International Journal of Refractory Metals and Hard Materials, 2023, 111, 106067.	1.7	3
48572	Structural, electronic, magnetic, and optical properties of Fe-doped Na2ZnP2O7 host: ab-initio calculation. Physica B: Condensed Matter, 2023, 650, 414554.	1.3	4
48573	Exploring the relationship between the accelerated austenite reversion and two-steps solution treatment in a Cr-Ni-Mo cryogenic maraging stainless steel. Materials Characterization, 2023, 196, 112581.	1.9	3
48574	First-principles DFT study of structural, electronic and optical properties of Cu-doped TiO<mml:math xmlns:mml="http://www.w3.org/1998/Math/MathML" altimg="si113.svg" display="inline" id="d1e719"><mml:msub><mml:mrow /><mml:mrow><mml:mn>2</mml:mn></mml:mrow></mml:msub></mml:math> (112) surface for enhanced visible-light photocatalysis. Computational Materials Science, 2023, 218, 111952.	1.4	5
48575	Enhancing the thermal stability of n-type Mg3+xSb1.5Bi0.49Te0.01 by defect manipulation. Nano Energy, 2023, 106, 108036.	8.2	7
48576	Thermoelectric performance and optoelectronic properties of Janus monolayer of ZrXY(XÂ=ÂO, S) (YÂ=ÂS,) Tj ETQq1 1 0.784314 rgB	1.4	5
48577	Density functional theory study of formation and diffusion of hydrogen, deuterium, and tritium in Pd-V intermetallic compounds. Computational Materials Science, 2023, 218, 111976.	1.4	2
48578	First-principles study on the role of anion in the physical properties of lead-free halide double perovskites. Computational Materials Science, 2023, 218, 111975.	1.4	2

#	Article	IF	Citations
48579	Selective sensing of DNA/RNA nucleobases by metal-functionalized silicon nanowires: A DFT approach. Surfaces and Interfaces, 2023, 36, 102529.	1.5	3
48580	Accurate Feâ€“He machine learning potential for studying He effects in BCC-Fe. Journal of Nuclear Materials, 2023, 574, 154183.	1.3	1
48581	Pressure-induced dynamically stable HeK2S under moderate conditions. Solid State Communications, 2023, 360, 115054.	0.9	0
48582	Effects of Ti, Zr, Ta, and W on elastic properties, stacking fault energy, and ductility of HfC. International Journal of Refractory Metals and Hard Materials, 2023, 111, 106056.	1.7	4
48583	An investigation of dynamical stability, electronic, and optical properties of sodium metaborate (NaBO2): A many-body G0W0+BSE approach. Solid State Communications, 2023, 360, 115055.	0.9	1
48584	Evolution of microstructure, mechanical and thermal properties with varied oxygen contents in TiAlON coatings. International Journal of Refractory Metals and Hard Materials, 2023, 111, 106074.	1.7	1
48585	Molecular adsorption of the NCO, CNO and CON isomers on the Rh(001) surface : A standard DFT and DFT+<mml:math xmlns:mml="http://www.w3.org/1998/Math/MathML" altimg="si77.svg" display="inline" id="d1e2504"><mml:mi>U</mml:mi></mml:math> calculations. Computational and Theoretical Chemistry, 2023, 1220, 113971.	1.1	3
48586	Structural, electrical, magnetic & optical properties of Nickel, cobalt doped and Co-doped wurtzite GaN: A first-principle investigation. , 2023, 174, 207470.		1
48587	First-principles study on interfacial performance of Cl, Br and O-doped Li3PS4 against lithium for all-solid-state batteries. Journal of Solid State Chemistry, 2023, 318, 123771.	1.4	1
48588	Screening of single transition metal substitution in two-dimensional Mo2CT MXene electrocatalyst with ultrahigh activity for oxygen reduction reaction. Surfaces and Interfaces, 2023, 36, 102585.	1.5	6
48589	Photoelectrocatalytic degradation of sulfamethoxazole over Sâ€“Scheme Co3Se4/BiVO4 heterojunction photoanode: An experimental and density functional theory investigations. Surfaces and Interfaces, 2023, 36, 102534.	1.5	1
48590	Ab-initio study of vacancy-defective aluminium nitride nanosheets as trifluoroacetonitrile gas sensor. Applied Surface Science, 2023, 612, 155803.	3.1	2
48591	Surface modification of hemimorphite via double-complexation by ammonium fluoride and copper ion to promote sulfidation. Applied Surface Science, 2023, 612, 155797.	3.1	4
48592	Determination of the mechanical, thermal, electronic and optoelectronics properties of BaMoO4 with oxygen vacancy by ab-initio calculations. Materials Today Communications, 2023, 34, 105074.	0.9	1
48593	Theoretical study on the photocatalytic behavior of isoelectronic S/Se-doped BiVO4: DFT+U approach. Physica B: Condensed Matter, 2023, 650, 414535.	1.3	4
48594	High pressure mediated physical properties of Hf2AB (A = Pb, Bi) via DFT calculations. Materials Today Communications, 2023, 34, 105147.	0.9	2
48595	Study on microstructure, mechanical properties and thermal performance of single-phase (Ti,Zr,Hf)B2 solid solution. Materials Today Communications, 2023, 34, 105228.	0.9	0
48596	Single-wall pristine and Janus nanotubes based on post-transition metal chalcogenides. First-principles study. Physica E: Low-Dimensional Systems and Nanostructures, 2023, 147, 115611.	1.3	2

#	Article	IF	Citations
48597	Martensitic transformation during electrochemical polishing of metastable austenitic stainless steel. Acta Materialia, 2023, 245, 118612.	3.8	10
48598	Longer cycle life and higher discharge voltage of a small molecular indanthrone resulting from the extended conjugated framework. Journal of Power Sources, 2023, 556, 232518.	4.0	8
48599	A combined experimental and computational approach on La0.6Sr0.4MnO3 perovskite. Materials Chemistry and Physics, 2023, 295, 127163.	2.0	1
48600	A DFT study on the size and defect induced properties of 2H-Au nano surface by small molecules adsorption. Surface Science, 2023, 729, 122228.	0.8	0
48601	Catalytic performance and mechanism of bismuth molybdate nanosheets decorated with platinum nanoparticles for formaldehyde decomposition at room temperature. Journal of Colloid and Interface Science, 2023, 633, 453-467.	5.0	8
48602	Adsorption and infrared spectra simulations of acrylic acid over (001) surface of molybdenum carbide. Chemical Physics, 2023, 566, 111798.	0.9	0
48603	Structural and thermal-mechanical properties of Ln3Ta5O15 (LnÂ=ÂCe, Pr, Nd, Sm, Eu, Gd, Tb) for thermal barrier coatings. Computational Materials Science, 2023, 218, 111938.	1.4	4
48604	Integration of amorphous CoSnO3 onto wrinkled MXene nanosheets as efficient electrocatalysts for alkaline hydrogen evolution. Separation and Purification Technology, 2023, 308, 122947.	3.9	14
48605	Computational studies of Ag5 atomic quantum clusters deposited on anatase and rutile TiO2 surfaces. Applied Surface Science, 2023, 613, 156054.	3.1	4
48606	Effect of strain on the band structure and optical properties of Na2Bi2(SeO3)3F2. Computational Materials Science, 2023, 218, 111962.	1.4	0
48607	Large-scale atomistic simulation of dislocation core structure in face-centered cubic metal with Deep Potential method. Computational Materials Science, 2023, 218, 111941.	1.4	0
48608	Synergy between nitrogen, phosphorus co-doped carbon quantum dots and ZnO nanorods for enhanced hydrogen production. Journal of Alloys and Compounds, 2023, 937, 168397.	2.8	12
48609	Interfacial hydrogen-related species in low-vacuum-deposited coatings on extrinsic substrates: Insights from experimental and theoretical studies. Materials Today Communications, 2023, 34, 105050.	0.9	0
48610	Mixed occupation, double valence and tunable emission of Eu in BaIn2(P2O7)2. Journal of Luminescence, 2023, 255, 119603.	1.5	6
48611	Adsorption behavior of small molecule on monolayered SiAs and sensing application for NO2 toxic gas. Applied Surface Science, 2023, 613, 156010.	3.1	7
48612	DFT study of cubic, tetragonal and trigonal structures of KGeCl3 perovskites for photovoltaic applications. Computational Condensed Matter, 2023, 34, e00772.	0.9	7
48613	Strain engineering of electronic and spin properties in SnX (X = P, As, Sb, Bi) monolayers. Journal of Physics and Chemistry of Solids, 2023, 174, 111131.	1.9	6
48614	Uncovering the effect of surface basicity on the carbon deposition of Ni/CeO2 catalyst modified by oxides in DRM. Fuel, 2023, 335, 126994.	3.4	14

#	Article	IF	Citations
48615	Structure and reaction condition dependent mechanism for ammonia synthesis on Ru-based catalyst. Applied Surface Science, 2023, 613, 156060.	3.1	3
48616	Synthesis, structural characterization, Hirshfeld surface and DFT calculations of 2-ethyl-2,4,5-trimethyl-2H-1,3-thiazine-6(3H)-thione. Journal of Molecular Structure, 2023, 1275, 134640.	1.8	1
48617	Crystal plane-orientation dependent phase evolution from precursor to porous intermediate phase in the vapor phase dealloying of a Co-Zn alloy. Acta Materialia, 2023, 245, 118617.	3.8	4
48618	Theoretical calculation of cesium deposition and co-deposition with electronegative elements on the plasma grid in negative ion sources. Nuclear Materials and Energy, 2023, 34, 101334.	0.6	0
48619	First-principles investigation of the structural, mechanical, electronic and thermoelectric properties of ZnFeNbAl Heusler compound. Materials Today Communications, 2023, 34, 105046.	0.9	0
48620	Computational prediction of stable semiconducting Zn-C binary compounds. Materials Science in Semiconductor Processing, 2023, 155, 107237.	1.9	1
48621	Odd-even alternating exchange coupling and optical properties of 2D 2Hâ€“VSe2 film. Physica E: Low-Dimensional Systems and Nanostructures, 2023, 147, 115583.	1.3	2
48622	Nanocrystalline vanadium carbides as highly active catalysts on vanadium foils for high temperature hydrogen separation. Separation and Purification Technology, 2023, 307, 122778.	3.9	3
48623	The effect of spinâ€“orbit coupling on the physical and superconducting properties of the Ir-rich cubic Laves superconductors AIr<mml:math xmlns:mml="http://www.w3.org/1998/Math/MathML" altimg="si91.svg" display="inline" id="d1e1439"><mml:msub><mml:mrow /><mml:mrow><mml:mn>2</mml:mn></mml:mrow></mml:msub></mml:math> (A = Y, Lu, and Th). Journal of Physics and Chemistry of Solids, 2023, 174, 111178.	1.9	2
48624	Oxygen dissociation on the C3N monolayer: A first-principles study. Applied Surface Science, 2023, 613, 155912.	3.1	3
48625	Hydrogen sorption kinetics and mechanism of Mg2Fe(1â^'x)NixH6. Journal of Alloys and Compounds, 2023, 937, 168212.	2.8	2
48626	The structural, mechanical and electronic properties of BaxNy compounds. Materials Science in Semiconductor Processing, 2023, 156, 107268.	1.9	0
48627	Two novel phases of germa-graphene: Prediction, electronic and transport applications. Applied Surface Science, 2023, 614, 156107.	3.1	5
48628	Optical and thermoelectric properties of square lattice phases of alkali halide compounds. Journal of Physics and Chemistry of Solids, 2023, 174, 111142.	1.9	1
48629	Firstâ€“principles study of Î²â€² phase in Mgâ€“RE alloys. International Journal of Mechanical Sciences, 2023, 243, 108045.	3.6	15
48630	First principles study on the influence of multi-element doping on the mechanical properties of Î¸/Al interface in Al-Cu alloy. Materials Today Communications, 2023, 34, 105114.	0.9	0
48631	Mechanical and thermodynamic behaviors of AlSi2Sc2 under uniaxial tensile loading: A first-principles study. Journal of Physics and Chemistry of Solids, 2023, 174, 111160.	1.9	3
48632	Defective lithium titanate oxide with stable cycling over a wide voltage window. Applied Surface Science, 2023, 614, 156134.	3.1	2

#	Article	IF	Citations
48633	Insights into crystal structure, elasticity, lattice dynamics, and thermodynamics of ternary magnesium alloy MgZn2Ce. Vacuum, 2023, 209, 111755.	1.6	1
48634	A comparative analysis of different van der Waals treatments for molecular adsorption on the basal plane of 2H-MoS2. Surface Science, 2023, 729, 122226.	0.8	5
48635	Strengthening the Ti/TiN interface against shear failure with Al dopants: A molecular dynamics study. Applied Surface Science, 2023, 613, 156024.	3.1	1
48636	First-principles investigation of photocatalytic properties of Ga<mml:math xmlns:mml="http://www.w3.org/1998/Math/MathML" altimg="si188.svg" display="inline" id="d1e1006"><mml:msub><mml:mrow /><mml:mn>2</mml:mn></mml:msub></mml:math>O<mml:math xmlns:mml="http://www.w3.org/1998/Math/MathML" altimg="si189.svg" display="inline" id="d1e1014"><mml:msub><mml:mrow />	0.9	0
48637	Piezo-photocatalysts based on a ferroelectric high-entropy oxide. Applied Catalysis B: Environmental, 2023, 324, 122204.	10.8	16
48638	Predicting the adsorption and reduction of NO2 on Sr-doped CeO2(1 1 1) using first-principles calculations. Applied Surface Science, 2023, 612, 155896.	3.1	0
48639	Refilling strategy of crosslinked aromatic SAMs for enhancing the molecular packing density. Applied Surface Science, 2023, 612, 155867.	3.1	2
48640	The low symmetry 1Tâ€²-MoS2 enabling the lithium directional diffusion through ferroelastic domain switching. Applied Surface Science, 2023, 612, 155761.	3.1	2
48641	First-principles study of the microstructure evolution of the diamond (110) surface with the adsorption of Fe atoms. Applied Surface Science, 2023, 613, 156053.	3.1	3
48642	Heterogeneous nucleation of T1 precipitates in solid solution of Al-Cu-Li alloys from Ag-rich structures: An ab initio study. Scripta Materialia, 2023, 225, 115191.	2.6	11
48643	SPIN: [S]imple [P]ython [I]pywidgets [N]otebook interface to obtain the optoelectronic properties of materials employing DFT. Computer Physics Communications, 2023, 284, 108614.	3.0	0
48644	Density functional investigation of the interaction of H2O with spinel Li1-xMn2O4 surfaces: Implications for aqueous Li-ion batteries. Applied Surface Science, 2023, 612, 155822.	3.1	3
48645	Experimental determination of the Hâ€“Hf phase diagram using in situ neutron diffraction. Journal of Alloys and Compounds, 2023, 937, 168353.	2.8	3
48646	Metallic boro-carbides of A₂BC (A = Ti, Zr, Hf and W): a comprehensive theoretical study for thermo-mechanical and optoelectronic applications. RSC Advances, 2022, 12, 32994-33007.	1.7	6
48647	Experimental and theoretical investigations on the anti-perovskite nitrides Co₃CuN, Ni₃CuN and Co₃MoN for ammonia synthesis. Faraday Discussions, 0, 243, 97-125.	1.6	2
48648	Carbon dioxide hydrogenation over the carbon-terminated niobium carbide (111) surface: a density functional theory study. Physical Chemistry Chemical Physics, 2023, 25, 2498-2509.	1.3	1
48649	Spatial charge separation on the (110)/(102) facets of cocatalyst-free ZnIn₂S₄for the selective conversion of 5-hydroxymethylfurfural to 2,5-diformylfuran. Green Chemistry, 2023, 25, 692-699.	4.6	13
48650	Mechanism of Ammonia Synthesis on Fe₃Mo₃N. Faraday Discussions, 0, , .	1.6	1

#	Article	IF	Citations
48651	Intermetallic studies on the mechanical and dynamical properties of Fe_{1-x}Y_xAl (Y = Pt and Ru) Alloys. MATEC Web of Conferences, 2022, 370, 09006.	0.1	1
48652	Realization of a piezoelectric quantum spin Hall phase with a large band gap in MBiH (M = Ga and In) monolayers. Journal of Materials Chemistry A, 2022, 10, 25683-25691.	5.2	1
48653	Tuning low-temperature CO oxidation activities via N-doping on graphene-supported three-coordinated nickle single-atom catalysts. Physical Chemistry Chemical Physics, 2022, 24, 29586-29593.	1.3	1
48654	A mechanism for aragonite to post-aragonite transition in MCO₃ (M = Ca, Sr and Ba) carbonates: evidence of a hidden metastable polymorph. Physical Chemistry Chemical Physics, 2022, 24, 29205-29213.	1.3	2
48655	Computational studies of structural, mechanical and magnetic properties of the B2-phase Fe₅₀Co_{50-x}Cr_x magnetic alloys. MATEC Web of Conferences, 2022, 370, 09007.	0.1	0
48656	Surface Properties of Ti₂AlV (100) and (110) Surfaces Using First-Principle Calculations. MATEC Web of Conferences, 2022, 370, 09005.	0.1	2
48657	Experimental and Computational Studies of Sulfided NiMo Supported on Pillared Clay: Catalyst Activation and Guaiacol Adsorption Sites. Physical Chemistry Chemical Physics, 0, , .	1.3	0
48658	Room temperature plasticity of zirconia-yttria-titania ceramics: Experimental indications and structural modelling. Processing and Application of Ceramics, 2022, 16, 367-373.	0.4	0
48659	Multielectron reaction of AlCl _n in borophene for rechargeable aluminum batteries. Energy Material Advances, 2022, 2022, .	4.7	10
48660	Tuning reactivity in trimetallic dual-atom alloys: molecular-like electronic states and ensemble effects. Chemical Science, 2022, 13, 14070-14079.	3.7	6
48661	Polarization-resolved and helicity-resolved Raman spectra of monolayer XP3 (X=Ge and In). Physical Chemistry Chemical Physics, 0, , .	1.3	0
48662	Effect of Gadolinium rare-earth element on Nd₂Fe₁₄B permanent magnet. MATEC Web of Conferences, 2022, 370, 09001.	0.1	0
48663	Ab Initio Studies of the Influence of Pressure on the Structure and Electronic and Elastic Properties of Carbonates of Alkaline and Alkaline-Earth Metals. Physics of the Solid State, 2022, 64, 405-415.	0.2	1
48664	Magnezyum BazlÄ± Mg3Bi Biyo-Emilebilir AlaÅŸÄ±mlarÄ±n Elastik Ã–zelliklerinin Ab Ä°nitio Ã‡alÄ±ÅŸmasÄ±. Osmaniye Korkut Ata Ãœniversitesi Fen Bilimleri EnstitÃ¼sÃ¼ Dergisi, 0, , .	0.2	0
48665	Intrinsic Ferroelectric Quantum Spin Hall Insulator in Monolayer Na₃Bi with Surface Trimerization. Journal of Physical Chemistry Letters, 2022, 13, 11059-11064.	2.1	3
48666	Strengthening Analysis of Ni-Sn Alloy Layer by Double Alloying Method Combined with First-Principles Calculation. Nanomaterials, 2022, 12, 4127.	1.9	0
48668	Nanometer-Thick Oxide Semiconductor Transistor with Ultra-High Drain Current. ACS Nano, 2022, 16, 21536-21545.	7.3	8
48669	First-principles study of quantum defect candidates in beryllium oxide. Physical Review B, 2022, 106, .	1.1	1

#	Article	IF	Citations
48670	Reconstruction of Cooperite (PtS) Surfaces: A DFT-D+U Study. ACS Omega, 2022, 7, 43390-43410.	1.6	4
48671	Study on Corrosion and Wear Behavior Mechanism of Reactor Material in Metastannic Acid Synthesis. Metals, 2022, 12, 2045.	1.0	2
48672	Simulation of BCC dissolution in Feâ€“Crâ€“Ni system by ICME. Journal of Iron and Steel Research International, 2023, 30, 660-676.	1.4	4
48673	Rational Design of Fe/Co-based Diatomic Catalysts for Li-S Batteries by First-principles Calculations. Chinese Physics B, 0, , .	0.7	0
48674	Improving the interfacial stability, conductivity, and electrochemical performance of Li2MoO3@g-C3N4 composite as a promising cathode for lithium-ion battery. Journal of Industrial and Engineering Chemistry, 2022, , .	2.9	0
48675	mm-band surface acoustic wave devices utilizing two-dimensional boron nitride. Scientific Reports, 2022, 12, .	1.6	0
48676	Investigation of the hexagonal boron nitride (h-BN) electronic and structural parameters and its dependency on the known semi-local functionals. Journal of Physics: Conference Series, 2022, 2376, 012009.	0.3	0
48677	The role of adsorbed oxygen for the ethane oxidative dehydrogenation on NiO(110) and (100) surface: A DFT theoretical study. Catalysis Communications, 2023, 174, 106575.	1.6	1
48678	First-principle calculations of sulfur dioxide adsorption on the Ca-montmorillonite. Scientific Reports, 2022, 12, .	1.6	2
48679	Tunable bulk photovoltaic effect in strained <mml:math xmlns:mml="http://www.w3.org/1998/Math/MathML"><mml:mi>Î³</mml:mi></mml:math> -GeSe. Physical Review B, 2022, 106, .	1.1	0
48680	Dualâ€Site Functionalization on Supported Metal Monolayer Electrocatalysts for Selective CO₂ Reduction. Advanced Energy Materials, 2023, 13, .	10.2	17
48681	Grain Boundary Complexions Enable a Simultaneous Optimization of Electron and Phonon Transport Leading to Highâ€Performance GeTe Thermoelectric Devices. Advanced Energy Materials, 2023, 13, .	10.2	22
48682	DFT study on the removal of polyacrylamide by titanium dioxide nanoparticles/polyacrylonitrile (rTiO2@PAC) composite in aqueous solutions. Journal of Molecular Modeling, 2022, 28, .	0.8	1
48683	Synergistic Hybridization of Twin-Induced Red/Black Phosphorus and Tungsten Oxide as Homoâ€“Hetero Dynamic Dual Junctions for Z-Scheme CO₂ Photoreduction. ACS Applied Energy Materials, 2022, 5, 15257-15268.	2.5	4
48684	Pressure-induced ferroelectric and anti-ferroelectric phase transitions in LaN. Science China: Physics, Mechanics and Astronomy, 2023, 66, .	2.0	3
48685	Unconventional Superconductivity at LaVO₃/SrTiO₃ Interfaces. ACS Applied Electronic Materials, 2022, 4, 5859-5866.	2.0	4
48686	Triggering the Phase Conversion of GeP from Monoclinic to Cubic by Zn Substitution toward a Highâ€Rate Ge_{1â^'x}Zn_xP Solid Solution Anode for Liâ€Ion Batteries. Advanced Energy Materials, 2023, 13, .	10.2	2
48687	Classical and machine learning interatomic potentials for BCC vanadium. Physical Review Materials, 2022, 6, .	0.9	3

#	Article	IF	Citations
48688	The Effect of Yttrium on the Solution and Diffusion Behaviors of Helium in Tungsten: First-Principles Simulations. Materials, 2022, 15, 8468.	1.3	0
48689	Fast light-switchable polymeric carbon nitride membranes for tunable gas separation. Nature Communications, 2022, 13, .	5.8	12
48690	Earth-abundant photocatalyst for H ₂ generation from NH ₃ with light-emitting diode illumination. Science, 2022, 378, 889-893.	6.0	62
48691	The First-Principles Study On The Investigation of Magnetic and Electronic Properties of Ga4X3Mn (X =) Tj ETQq1 1 0.784314 rgBT /O	0.1	0
48692			0
48693	Influence Mechanism of O2/H2O Adsorption on Cu(111) Surface on SF6 Overheating Failure Decomposition. Plasma Chemistry and Plasma Processing, 0, , .	1.1	0
48694	DFT insights into the origin of d0 ferromagnetism, mechanical stability, elastic, and acoustic anisotropy in AZrO3 (A= K, rb, Cs) cubic perovskites. Physica B: Condensed Matter, 2023, 654, 414521.	1.3	3
48695	Ground-State Surface of All-Inorganic Halide Perovskites. Journal of Physical Chemistry C, 2022, 126, 21155-21161.	1.5	4
48696	Bimetallic NiM/C (M = Cu and Mo) Catalysts for the Hydrogen Oxidation Reaction: Deciphering the Role of Unintentional Surface Oxides in the Activity Enhancement. ACS Catalysis, 2022, 12, 15341-15351.	5.5	6
48697	A peroxidase-like single-atom Fe-N5 active site for effective killing human lung adenocarcinoma cells. Nano Research, 2023, 16, 5216-5225.	5.8	3
48698	Two-dimensional SiC/AlN based type-II van der Waals heterobilayer as a promising photocatalyst for overall water disassociation. Scientific Reports, 2022, 12, .	1.6	7
48699	AeMg₆Ga₆S₁₆ (Ae = Ca, Sr, Ba): The First Double Alkalineâ€Earth Metal Chalcogenides with Excellent Performances. Advanced Optical Materials, 2023, 11, .	3.6	8
48700	First-principles study on the preferential sites of Cr in Co₇W₆. Materials Research Express, 0, , .	0.8	1
48701	Structural and electronic properties of the Te-Si(111) surface from first principles. Physical Review B, 2022, 106, .	1.1	1
48702	Nitrogen-Doped Bismuth Nanosheet as an Efficient Electrocatalyst to CO2 Reduction for Production of Formate. International Journal of Molecular Sciences, 2022, 23, 14485.	1.8	5
48703	Spin-Polarized Resonant Tunneling in Antiferromagnetic Heterojunctions of Graphene Nanoribbons with <mml:math xmlns:mml="http://www.w3.org/1998/Math/MathML" display="inline" overflow="scroll"><mml:mn>3</mml:mn><mml:mi>d</mml:mi></mml:math> Adatoms. Physical Review Applied, 2022, 18, .	1.5	1
48704	Room-temperature antiferromagnetic order in monolayer <mml:math xmlns:mml="http://www.w3.org/1998/Math/MathML"><mml:mrow><mml:msub><mml:mi>Fe</mml:mi><mml:mn>2</mml:mn></mml:msub><mml:msub><mml:mi>X</mml:mi><mml:mn></mml:mn></mml:msub><mml:mathvariant="normal">C</mml:mi></mml:mrow></mml:math>. Physical Review B, 2022, 106, .	1.1	3
48705	Understanding the Highly Electrocatalytic Active Mixed Triple Conducting Na_xCa_{3â€“}_xCo₄O_{9â€“Î´} Oxygen Electrode Materials. Advanced Energy Materials, 2023, 13, .	10.2	11

#	Article	IF	Citations
48706	Low Lattice Thermal Conductivity in a Wider Temperature Range for Biphasic-Quaternary (Ti,V)CoSb Half-Heusler Alloys. ACS Applied Materials & Interfaces, 2022, 14, 54736-54747.	4.0	9
48707	Tunable intrinsic spin Hall conductivity in BiTeI by applying hydrostatic pressure. Journal of Applied Physics, 2022, 132, 203903.	1.1	0
48708	NaHSO₄Â·H₂O: A Promising Deep-Ultraviolet Nonlinear-Optical Bisulfate with Large Birefringence and a Second-Harmonic-Generation Effect. Inorganic Chemistry, 2022, 61, 19673-19677.	1.9	4
48709	Lattice Distortions and Multiple Valence Band Convergence Contributing to High Thermoelectric Performance in MnTe. Small, 2023, 19, .	5.2	8
48710	Pressure-dependent electronic properties in the rocksalt structure of lithium fluoride: A DFT Study. Journal of Physics: Conference Series, 2022, 2376, 012010.	0.3	0
48711	First-principle calculation of silicon carbide (SiC) for the superhard material applications. Journal of Physics: Conference Series, 2022, 2376, 012011.	0.3	0
48712	Low-crystalline Ni(OH)2 ultrathin nanosheets upcycled from solid wastes for efficient photoconversion of low-concentration CO2. Chemical Engineering Journal, 2022, , 140507.	6.6	1
48713	Effect of Different Heteroatoms Anchoring a Cu Single-Atom Catalyst on Acetylene Hydrochlorination. Journal of Physical Chemistry C, 2022, 126, 20401-20410.	1.5	13
48714	Contact Electrification of Biological and Bio-Inspired Adhesive Materials on SiO2 Surfaces: Perspectives from DFT Calculations. Biomimetics, 2022, 7, 216.	1.5	0
48715	Exploring the Optimal Alloy for Nitrogen Activation by Combining Bayesian Optimization with Density Functional Theory Calculations. ACS Omega, 2022, 7, 45403-45408.	1.6	4
48716	Discovery of LaAlO3 as an efficient catalyst for two-electron water electrolysis towards hydrogen peroxide. Nature Communications, 2022, 13, .	5.8	21
48718	High-refractive index and mechanically cleavable non-van der Waals InGaS3. Npj 2D Materials and Applications, 2022, 6, .	3.9	9
48719	The structural, mechanical, electronic, and optical properties of Janus Hf2CXY (X, Y = O, S, Se or Te, X â‰) Tj ETQq0 0 0 rgBT /Overlock	2	
48720	2D Oxides Realized via Confinement Heteroepitaxy. Advanced Functional Materials, 2023, 33, .	7.8	4
48721	The thermoelectric properties of XTe (X = Ge, Sn and Pb) monolayers from first-principles calculations. Physica Scripta, 2022, 97, 125709.	1.2	1
48722	Bonding Heterogeneity Leads to Hierarchical and Ultralow Lattice Thermal Conductivity in Sodium Metavanadate. Journal of Physical Chemistry Letters, 2022, 13, 11160-11168.	2.1	2
48723	Sulfur-Vacancy Passivation via Selenium Doping in Sb₂S₃ Solar Cells: Density Functional Theory Analysis. Journal of Physical Chemistry C, 2022, 126, 20786-20792.	1.5	4
48724	Controlled Synthesis of Palladium Phosphides with Tunable Crystal Phases and Their Sulfur-Tolerant Performance. ACS Catalysis, 2022, 12, 15193-15206.	5.5	13

#	Article	IF	Citations
48725	Rational Design of Dynamic Bimetallic NiCoSe₂/2D Ti₃C₂T_x MXene Hybrids for a High-Performance Flexible Supercapacitor and Hydrogen Evolution Reaction. Energy & Fuels, 2022, 36, 15066-15079.	2.5	8
48726	Designing Reactive Bridging O^{2â€“} at the Atomic Cuâ€“Oâ€“Fe Site for Selective NH₃ Oxidation. ACS Catalysis, 2022, 12, 15207-15217.	5.5	3
48727	2D/1D MoS₂/TiO₂ Heterostructure Photocatalyst with a Switchable CO₂ Reduction Product. Small Methods, 2023, 7, .	4.6	18
48728	Understanding Structural Incorporation of Oxygen Vacancies in Perovskite Cobaltite Films and Potential Consequences for Electrocatalysis. Chemistry of Materials, 2022, 34, 10373-10381.	3.2	4
48729	Atomistic Insights into the Oxidation of Flat and Stepped Platinum Surfaces Using Large-Scale Machine Learning Potential-Based Grand-Canonical Monte Carlo. ACS Catalysis, 2022, 12, 14812-14824.	5.5	7
48730	Electronic, Tensile, and Sliding Characteristics of the C/Ti Interface: A First-Principles Study. Langmuir, 2022, 38, 15113-15120.	1.6	2
48731	First-Principles Prediction of New 2D p-SiPN: A Wide Bandgap Semiconductor. Nanomaterials, 2022, 12, 4068.	1.9	4
48732	Origin of Near-Zero Thermal Expansion in A₂O(PO₄)₂ Oxides over an Ultrawide Temperature Range. Journal of Physical Chemistry C, 2022, 126, 21871-21881.	1.5	1
48733	Twist-engineered tunability in vertical MoS2/MoSe2 heterostructure. Applied Physics A: Materials Science and Processing, 2023, 129, .	1.1	8
48734	Antibacterial, UV-Protective, Hydrophobic, Washable, and Heat-Resistant BN-Based Nanoparticle-Coated Textile Fabrics: Experimental and Theoretical Insight. ACS Applied Bio Materials, 2022, 5, 5595-5607.	2.3	2
48735	Tuning the electronic properties of molybdenum di-sulphide monolayers via doping using first-principles calculations. Physica Scripta, 2023, 98, 025807.	1.2	6
48736	Effect of M-doping (M = Al, Y, La) on the electronic structure of V-doped ZrO₂: A first-principles study. Journal of the Ceramic Society of Japan, 2022, 130, 925-932.	0.5	0
48737	Investigation on electronic properties modulation of vdW GaN/WSe₂ heterostructure by electric field. Modern Physics Letters B, 0, , .	1.0	0
48738	Selective and rapid extraction of trace amount of gold from complex liquids with silver(I)-organic frameworks. Nature Communications, 2022, 13, .	5.8	31
48739	Explorations of Second-Order Nonlinear Optical Materials in the Monovalent Trithiocyanurate System. Crystal Growth and Design, 2023, 23, 362-368.	1.4	2
48740	Exploring the Ti₂CO₂â€“WSe₂ Heterostructure as a Direct Z-Scheme Photocatalyst for Water Splitting: A Non-Adiabatic Study. Journal of Physical Chemistry C, 2022, 126, 20852-20863.	1.5	14
48741	N-doped LaPO4: An effective Pt-free catalyst for electrocatalytic oxygen reduction. Chem Catalysis, 2022, 2, 3590-3606.	2.9	40
48742	Interlayer Registry Dictates Interfacial 2D Material Ferroelectricity. ACS Applied Materials & Interfaces, 2022, 14, 57492-57499.	4.0	2

#	Article	IF	Citations
48743	Investigating the Î²-Mg17Al12 Alloy under Pressure Using First-Principles Methods: Structure, Elastic Properties, and Mechanical Properties. Crystals, 2022, 12, 1741.	1.0	0
48744	Theoretical Approach for Electron Dynamics and Ultrafast Spectroscopy (EDUS). Journal of Chemical Theory and Computation, 2023, 19, 333-348.	2.3	2
48745	Predicting the Stability and Loading for Electrochemical Preparation of Single-Atom Catalysts. ACS Catalysis, 2023, 13, 79-86.	5.5	5
48746	Effects of structural ordering on infrared active vibrations within <mml:math xmlns:mml="http://www.w3.org/1998/Math/MathML"><mml:mrow><mml:msub><mml:mi>Bi</mml:mi><mml:mn>21</mml:mn></mml:msub></mml:mrow></mml:math> Physical Review B, 2022, 106, .	3.7	3
48747	Strain-induced ultrahigh power conversion efficiency in BP-MoSe₂ vdW heterostructure. Nanotechnology, 2023, 34, 085403.	1.3	1
48748	Tuning the Magnetic Properties of Cr2TiC2Tx through Surface Terminations: A Theoretical Study. Nanomaterials, 2022, 12, 4364.	1.9	1
48749	Ab initio study of pressure dependence of the structural, elastic and thermodynamic properties of AlXY₃ (Xâ€‰=â€‰B, C). Phase Transitions, 2023, 96, 1-15.	0.6	3
48750	Unraveling the roles of single transition metal atom anchored on equivalent stoichiometry graphitic carbon nitride (gC₆N₆) for carbon dioxide reduction: a density functional theory study. Journal Physics D: Applied Physics, 2022, 56, 024004.	1.3	0
48751	Density Functional Calculations of the Sequential Adsorption of Hydrogen on Single Atom and Small Clusters of Pd and Pt Supported on Au(111). Electrocatalysis, 0, , .	1.5	0
48752	Strong interlayer transition in a staggered gap <scp>GeSe</scp>/<scp>MoTe₂</scp> heterojunction diode for highly efficient visible and nearâ€infrared photodetection and logic inverter. EcoMat, 2023, 5, .	6.8	4
48753	Exploring the Zr X O (X â€‰=â€‰S and Se) Janus Monolayers for Optoelectronic and Spintronic Applications. Physica Status Solidi - Rapid Research Letters, 0, , 2200427.	1.2	0
48754	Anisotropic Optical, Mechanical, and Thermoelectric Properties of Two-Dimensional Fullerene Networks. Journal of Physical Chemistry Letters, 2022, 13, 11622-11629.	2.1	14
48755	Quantum dynamics reveal different ligand effects by vibrational excitation in the dissociative chemisorption of HCl on the Au/Ag(111) surface. Journal of Chemical Physics, 2022, 157, .	1.2	3
48756	First-principles prediction of 1H-Na₂Se monolayer: effects of external strain and point defects associated with constituent atoms. Physica Scripta, 2023, 98, 025805.	1.2	1
48757	Bilayer MN4-O-MN4 by bridge-bonded oxygen ligands: Machine learning to accelerate the design of bifunctional electrocatalysts. Renewable Energy, 2023, 203, 445-454.	4.3	8
48758	Isomerism effects in relaxation dynamics of Au₂₄(SR)₁₆ thiolate-protected gold nanoclusters. Nanotechnology, 2023, 34, 105701.	1.3	3
48759	Origin of the nucleation preference of coherent and semicoherent nanoprecipitates in Al–Cu alloys based on atomistically informed classical nucleation theory. Journal of Alloys and Compounds, 2022, , 168559.	2.8	0
48760	Effects of Multiple Local Environments on Electron Energy Loss Spectra of Epitaxial Perovskite Interfaces. Journal of Physical Chemistry C, 2022, 126, 21453-21466.	1.5	0

#	Article	IF	Citations
48761	Tailoring the Optical and Electronic Properties of 2D Hybrid Dionâ€“Jacobson Copper Chloride Perovskites. Journal of Physical Chemistry C, 2022, 126, 21297-21307.	1.5	2
48762	Boosting Electrocatalytic Ammonia Synthesis of Bio-Inspired Porous Mo-Doped Hematite via Nitrogen Activation. ACS Applied Materials & Interfaces, 2022, 14, 55559-55567.	4.0	11
48763	On synthesis, stability and superconductivity of ThNb2H12under pressure: ab-inito calculations. Journal of Physics and Chemistry of Solids, 2022, , 111193.	1.9	0
48764	Peripheral-nitrogen effects on the Ru1 centre for highly efficient propane dehydrogenation. Nature Catalysis, 2022, 5, 1145-1156.	16.1	42
48765	New Insights into the Crystal Chemistry of FeB-Type Compounds: The Case of CeGe. Materials, 2022, 15, 9089.	1.3	0
48766	Yttrium incorporation in Cr₂AlC: On the metastable phase formation and decomposition of (Cr,Y)₂AlC MAX phase thin films. Journal of the American Ceramic Society, 2023, 106, 2652-2665.	1.9	1
48767	Quenchingâ€Induced Defects Liberate the Latent Reversible Capacity of Lithium Titanate Anode. Advanced Materials, 2023, 35, .	11.1	7
48768	Implementation of realâ€time <scp>TDDFT</scp> for periodic systems in the openâ€source <scp>PySCF</scp> software package. Journal of Computational Chemistry, 2023, 44, 980-987.	1.5	4
48769	Strain Engineering of Two-Dimensional Piezophotocatalytic Materials for Improved Hydrogen Evolution Reaction. ACS Sustainable Chemistry and Engineering, 2022, 10, 16924-16934.	3.2	7
48770	Anion Exchange Reaction of CsPbBr₃ Perovskite Nanocrystals: Affinity of Halide Ion Matters. ChemistrySelect, 2022, 7, .	0.7	4
48771	Study of physical adsorption of aromatic molecules on hydroxylated Î±-SiO2 (001) surface using dispersion-corrected density functional theory. Computational and Theoretical Chemistry, 2022, , 113991.	1.1	1
48772	Designing a functionalized 2D-TMD (MoX2, XÂ=ÂS, Se) hosting half-metallicity for selective gas-sensing applications: Atomic-scale study. Acta Materialia, 2023, 246, 118655.	3.8	14
48773	Insights into the surface catalysis of CeO<mml:math xmlns:mml="http://www.w3.org/1998/Math/MathML" altimg="si84.svg" display="inline" id="d1e394"><mml:msub><mml:mrow /><mml:mrow><mml:mn>2</mml:mn><mml:mo>â^’</mml:mo><mml:mi>Î´</mml:mi></mml:mrow></mml:msub></mml:math> supported Pd<mml:math xmlns:mml="http://www.w3.org/1998/Math/MathML" altimg="si83.svg" display="inline" id="d1e406"><mml:msub><mml:mrow />	3.1	0
48774	Developing Waste Forms for Transuranic Elements: Quaternary Neptunium Fluorides of the Type Na_xMNp₆F₃₀ (M = Ti, V, Cr, Mn, Fe, Co, Ni, Al, Ga). Journal of the American Chemical Society, 2023, 145, 465-475.	6.6	1
48775	Alkali Metal Cations as Chargeâ€Transfer Bridge for Polarization Promoted Solarâ€toâ€H₂ Conversion. Advanced Functional Materials, 2023, 33, .	7.8	9
48776	Metal Anodes with Ultrahigh Reversibility Enabled by the Closest Packing Crystallography for Sustainable Batteries. Advanced Materials, 2023, 35, .	11.1	22
48777	Half-Metallic Heusler Alloy/MoS₂ Based Magnetic Tunnel Junction. ACS Applied Materials & Interfaces, 2022, 14, 55167-55173.	4.0	1
48778	Element-wise representations with ECNet for material property prediction and applications in high-entropy alloys. Npj Computational Materials, 2022, 8, .	3.5	3

#	Article	IF	Citations
48779	Physical origin of the endurance improvement for HfO2-ZrO2 superlattice ferroelectric film. Applied Physics Letters, 2022, 121, .	1.5	6
48780	Sulfurâ€Doped rGO Aerogel Enables the Anchoring of 1T/2H MoS₂ for Durable Oxygen Reduction Reaction Catalyst Support. ChemSusChem, 2023, 16, .	3.6	2
48781	The Local Coordination Effects on the Reactivity and Speciation of Active Sites in Graphene-Embedded Single-Atom Catalysts over Wide pH and Potential Range. Nanomaterials, 2022, 12, 4309.	1.9	3
48782	First-Principles Investigations of Thermoelectric Behavior of RuCrX (X = Si, Ge, Sn). ACS Omega, 2022, 7, 45353-45360.	1.6	2
48783	Theoretical Investigation of Origin of Quantized Conduction in 2D Layered Ruddlesonâ€“Popper Perovskite Heterostructure for the RRAM Applications. Energies, 2022, 15, 9410.	1.6	3
48784	Interaction-driven topological phase transition in monolayer <mml:math xmlns:mml="http://www.w3.org/1998/Math/MathML"><mml:msub><mml:mi mathvariant="normal">CrCl</mml:mi><mml:mn>2</mml:mn></mml:msub></mml:math> (pyrazine) <mml:math xmlns:mml="http://www.w3.org/1998/Math/MathML"><mml:msub><mml:mrow /><mml:mn>2</mml:mn></mml:msub></mml:math>. Physical Review B, 2022, 106, .	1.1	1
48785	First-principles-based screening method for resistivity scaling of anisotropic metals. Physical Review Materials, 2022, 6, .	0.9	1
48786	On the mechanism of dehalogenation of methyl halides (Br and Cl) on Ag(111) and Au(111) surfaces: A DFT study. Applied Surface Science, 2023, 615, 156059.	3.1	3
48787	The role of coverage effects on the structureâ€“sensitivity of formic acid electrooxidation on Pd surfaces. Journal of Catalysis, 2023, 417, 408-420.	3.1	1
48788	Modeling of Gold Adsorption by the Surface of Defect Graphene. Russian Microelectronics, 2022, 51, 413-425.	0.1	1
48789	Sustainable removal of fluorine ions using ZrO2-MgO@C composite. Separation and Purification Technology, 2023, 310, 122933.	3.9	3
48790	Density Functional Theory Analysis Identifying the Mechanism for Ignition Sensitivity of Ammonium Periodate Compared with Ammonium Perchlorate. Journal of Physical Chemistry C, 2022, 126, 21723-21733.	1.5	1
48791	Controlling optical properties of small SWCNT using new N-doping chains method: A first-principles study. Physica E: Low-Dimensional Systems and Nanostructures, 2023, 148, 115627.	1.3	1
48792	Theoretical analysis of structural stability and allied properties of new brittle perovskites: RbTaO3 and RbNbO3. Indian Journal of Physics, 2023, 97, 2061-2076.	0.9	1
48793	Highly efficient photocatalytic water splitting in direct Z-scheme <mml:math xmlns:mml="http://www.w3.org/1998/Math/MathML" altimg="si70.svg" display="inline" id="d1e839"><mml:mi>Î±</mml:mi></mml:math>-In2Se3/Are van der Waals heterostructures. Surfaces and Interfaces, 2023, 36, 102608.	1.5	4
48794	Density functional theory study of reversible hydrogen storage in monolayer beryllium hydride by decoration with boron and lithium. International Journal of Hydrogen Energy, 2023, 48, 7400-7418.	3.8	7
48795	Strain and Composition Dependencies of the Near-Band-Gap Optical Transitions in Monoclinic <mml:math xmlns:mml="http://www.w3.org/1998/Math/MathML" display="inline" overflow="scroll"><mml:mo stretchy="false">(</mml:mo><mml:msub><mml:mi>Al</mml:mi><mml:mi>x</mml:mi></mml:msub><mml:msub><mml:mi>Ga</mml:m	1.5	3
48796	mathvariant="normal">O</mml:. Physical Review Applied, 2022, 18, . Electric-controlled tunable thermal switch based on Janus monolayer MoSSe. Npj Computational Materials, 2022, 8, .	3.5	3

#	Article	IF	Citations
48797	Band valley flattening and exciton appearance/disappearance under isotropic strain in monolayer WS2. European Physical Journal Plus, 2022, 137, .	1.2	0
48798	Theoretical Prediction of Structural, Mechanical, and Thermophysical Properties of the Precipitates in 2xxx Series Aluminum Alloy. Metals, 2022, 12, 2178.	1.0	2
48799	Hexagonal boron nitride nanoribbon as a novel metal-free catalyst for high-efficiency NO reduction to NH3. Fuel, 2023, 339, 126943.	3.4	7
48800	Pressure dependent structural, dynamical, mechanical and electronic properties of magnesium dicarbide. Philosophical Magazine, 0, , 1-22.	0.7	0
48801	Exchange-mediated magnon-phonon scattering in monolayer <mml:math xmlns:mml="http://www.w3.org/1998/Math/MathML"><mml:msub><mml:mi mathvariant="normal">CrI</mml:mi><mml:mn>3</mml:mn></mml:msub></mml:math>. Physical Review B, 2022, 106, .	1.1	8
48802	Effect of h-BN Support on Photoluminescence of ZnO Nanoparticles: Experimental and Theoretical Insight. Materials, 2022, 15, 8759.	1.3	1
48803	Impact of defects on the Ї‡(3) optical nonlinearity of sputtered WSe2 thin films in the optical communication band. Journal of Applied Physics, 2022, 132, .	1.1	2
48805	First-Principles Calculations of the Phonon, Mechanical and Thermoelectric Properties of Half-Heusler Alloy VIrSi Alloys. Crystals, 2022, 12, 1838.	1.0	4
48806	Bifunctional synergistic CoP/Coral-like g-C3N4 catalyst: Boosting the photocatalytic water splitting hydrogen evolution and appreciation of anisalcohol at same time. Applied Surface Science, 2023, 614, 156187.	3.1	4
48807	Diamane Oxide. Two-Dimensional Film with Mixed Coverage and a Variety of Electronic Properties. Journal of Physical Chemistry Letters, 2022, 13, 11383-11390.	2.1	3
48808	WanTiBEXOS: A Wannier based Tight Binding code for electronic band structure, excitonic and optoelectronic properties of solids. Computer Physics Communications, 2023, 285, 108636.	3.0	4
48809	TM₂â˜B₂ Quadruple Active Sites Supported on a Defective C₃N Monolayer as Catalyst for the Electrochemical CO₂ Reduction: A Theoretical Perspective. ChemSusChem, 2023, 16, .	3.6	3
48810	Theoretical Modeling of Oxide Ion Conductivity in Doped LaSrGa₃O₇ Melilites. Journal of Physical Chemistry C, 2022, 126, 21375-21380.	1.5	0
48811	A Universal Perovskite Nanocrystal Ink for Highâ€Performance Optoelectronic Devices. Advanced Materials, 2023, 35, .	11.1	14
48812	Photoluminescence studies of non-toxic monoclinic yttrium oxide quantum dots synthesized at low temperature for live cell imaging applications. Ceramics International, 2023, 49, 13200-13207.	2.3	3
48813	Modeling the structural, electronic, optoelectronic, thermodynamic, and core-level spectroscopy of Xâ€“SnO3 (X=Ag, Cs, Hf) perovskites. Computational and Theoretical Chemistry, 2023, 1220, 114003.	1.1	7
48814	Ab Initio Microkinetics of H₂S Interactions with Clean and Sulfided Au(110) at Low Temperature: A Strong Assistance in Partial Dissociation from Single Sulfur Atoms. Journal of Physical Chemistry C, 2022, 126, 21585-21595.	1.5	0
48815	Schwarz <scp>P</scp>â€surface via isolated <scp>sp²</scp> carbon heptagons: Design and properties. Journal of Computational Chemistry, 2023, 44, 954-961.	1.5	1

#	Article	IF	Citations
48816	Firstâ€Principles Investigation of Charged GermaGraphene as a Novel Cathode Material for Dualâ€Carbon Batteries. ChemSusChem, 0, , .	3.6	0
48817	Low-frequency anharmonic couplings in crystalline bromoform: Theory. Journal of Chemical Physics, 2023, 158, .	1.2	2
48818	In Quest of Lowâ€Leakage Dynamic Random Access Memory Enabled by Doped TiO₂ Dielectrics. Advanced Theory and Simulations, 2023, 6, .	1.3	1
48819	Analyzing the physical properties of perovskite oxides BaMO3 (M = Ru, Os) for predicting potential applications. Computational Condensed Matter, 2023, 34, e00782.	0.9	5
48820	Single- and two-particle finite size effects in interacting lattice systems. Physical Review B, 2022, 106, .	1.1	0
48821	Rational design of nitrogenâ€'doped carbon nanotubes by defect engineering for Znâ€'air batteries with high performance. Carbon, 2023, 204, 411-426.	5.4	11
48822	Electronic level modelling of graphene-borophene lateral heterostructures as anodes in Li-ion batteries. Applied Surface Science, 2023, 614, 156227.	3.1	2
48823	Full-potential KKR within the removed-sphere method: A practical and accurate solution to the Poisson equation. Physical Review B, 2022, 106, .	1.1	0
48824	DFT study of methanethiol (CH3SH) adsorptions on the Fe(110) surface. Pramana - Journal of Physics, 2023, 97, .	0.6	1
48825	Coexistence of trihexagonal and star-of-David pattern in the charge density wave of the kagome superconductor <mml:math xmlns:mml="http://www.w3.org/1998/Math/MathML"><mml:mrow><mml:mi>A</mml:mi><mml:msub><mml:mi mathvariant="normal">V</mml:mi><mml:mn>3</mml:mn></mml:msub><mml:msub><mml:mi>Sb</mml:mi><mml:mn>5</mml:mn> Physical Review B, 2022, 106, .	1.1	31
48826	The Rise of 212 MAX Phase Borides: DFT Insights into the Physical Properties of Ti₂PB₂, Zr₂PbB₂, and Nb₂AB₂ [A = P, S] for Thermomechanical Applications. ACS Omega, 2023, 8, 954-968.	1.6	9
48827	Stability of FeVO4-II under Pressure: A First-Principles Study. Crystals, 2022, 12, 1835.	1.0	4
48828	Phase stability of double perovskite in Pr[Ba1Ââ˜'ÂxSrx][Co1 â˜' yFey]2O5.5 using genetic algorithm and density functional theory. Journal of the Korean Ceramic Society, 2023, 60, 434-439.	1.1	1
48829	Axial Coordination Effect on the Oxygen Reduction Reaction of FeN₄ Electrocatalysts Based on Grand Canonical Density Functional Theory. Journal of Physical Chemistry C, 2022, 126, 21606-21615.	1.5	12
48830	Anchoring Ru active sites on Nâ€CNTs for an improved oneâ€pot cellobiose conversion. ChemNanoMat, 0, , .	1.5	0
48831	Efficient and Reusable Sorbents Based on Nanostructured BN Coatings for Water Treatment from Antibiotics. International Journal of Molecular Sciences, 2022, 23, 16097.	1.8	1
48832	A tailored direct-to-indirect band structure transition in double perovskite oxides influences its photocatalysis efficiency. Ceramics International, 2023, 49, 8634-8645.	2.3	2
48833	Tuning the Electronic and Mechanical Properties of Kagome Graphene via Hydrogenation. Journal of Physical Chemistry C, 2022, 126, 21426-21437.	1.5	1

#	Article	IF	Citations
48834	Study on the hydrogen barrier performance of the SiOC coating. International Journal of Hydrogen Energy, 2023, 48, 8286-8295.	3.8	3
48835	A Crystalline Dimeric Steroidal Diboronate with Electronically Impeded Rotation. Journal of Organic Chemistry, 0, , .	1.7	2
48836	First-principles calculations to investigate structural, elastic, electronic and thermodynamic properties of NbCoSn and VRhSn Half-Heusler compounds. Results in Physics, 2022, 43, 106132.	2.0	5
48837	Elasticity and Viscosity of hcp Iron at Earth's Inner Core Conditions From Machine Learningâ€Based Largeâ€Scale Atomistic Simulations. Geophysical Research Letters, 2022, 49, .	1.5	2
48838	Partial Sulphidation to Regulate Coordination Structure of Single Nickel Atoms on Graphitic Carbon Nitride for Efficient Solar H₂ Evolution. Small, 2023, 19, .	5.2	6
48839	Synergetic effects of combining TM single- and double-atom catalysts embedded in C₂N on inducing half-metallicity: DFT study. 2D Materials, 2023, 10, 015016.	2.0	0
48840	Anion Doping Delays Nonradiative Electronâ€“Hole Recombination in Cs-Based All-Inorganic Perovskites: Time Domain ab Initio Analysis. Journal of Physical Chemistry Letters, 2022, 13, 11375-11382.	2.1	10
48841	Revealing carbon capture chemistry with 17-oxygen NMR spectroscopy. Nature Communications, 2022, 13, .	5.8	4
48842	Influence of pressure-induced formation of dihydrogen bonds on lattice parameters, volume, and vibrational modes of ammonia borane. Journal of Chemical Physics, 2022, 157, .	1.2	2
48843	Machine learning guided discovery of ternary compounds involving La and immiscible Co and Pb elements. Npj Computational Materials, 2022, 8, .	3.5	4
48844	Effects of alloying elements on diamond/Cu interface properties based on first-principles calculations. Journal of Physics Condensed Matter, 2023, 35, 115001.	0.7	4
48845	Pd single atom supported on N-doped egg tray graphene as formic acid dehydrogenation catalysts. 2D Materials, 0, , .	2.0	1
48846	Formation of Diamane Nanostructures in Bilayer Graphene on Langasite under Irradiation with a Focused Electron Beam. Nanomaterials, 2022, 12, 4408.	1.9	5
48847	Insight into the Effect of Anionicâ€“Anionic Co-Doping on BaTiO3 for Visible Light Photocatalytic Water Splitting: A First-Principles Hybrid Computational Study. Catalysts, 2022, 12, 1672.	1.6	6
48848	High-throughput theoretical optimization of the selective reduction reaction of NO with NH3 on metal-organic frameworks. Surface Science, 2022, , 122238.	0.8	0
48849	The rare earth doped Mg2Ni (0 1 0) surface enhances hydrogen storage. Applied Surface Science, 2023, 614, 156243.	3.1	4
48850	Are Janus MoSSe/Ti3C2-MXene heterostructures excellent anode materials for Na-ion batteries? A computational insight combined experiment. Applied Surface Science, 2023, 614, 156196.	3.1	4
48851	Blocking Directional Lithium Diffusion in Solid-State Electrolytes at the Interface: First-Principles Insights into the Impact of the Space Charge Layer. ACS Applied Materials & Interfaces, 2022, 14, 55471-55479.	4.0	0

#	Article	IF	Citations
48852	Artificial heterointerfaces of defect-rich Ni and amorphous/crystalline MoN enable efficient hydrogen evolution reaction. Chemical Engineering Journal, 2023, 457, 141173.	6.6	16
48853	Evolution of Graphene Supported Ru_N (N=1â€“4) Clusters in CO Atmosphere: A Firstâ€Principles Investigation. European Journal of Inorganic Chemistry, 2023, 26, .	1.0	0
48854	The Mutual Incorporation of Mg2+ and CO32â^' into Hydroxyapatite: A DFT Study. Materials, 2022, 15, 9046.	1.3	8
48855	First principles-based study of the influence of pressure on the gas adsorption performance of coal. Materials Today Communications, 2023, 34, 105269.	0.9	0
48856	Influence of the cation distribution, atomic substitution, and atomic vacancies on the physical properties of <mml:math xmlns:mml="http://www.w3.org/1998/Math/MathML"><mml:mrow><mml:msub><mml:mrow><mml:mi>C</mml:mi><mml:mi>o</mml:m and <mml:math xmlns:mml="http://www.w3.org/1998/Math/MathML"><mml:mrow><mml:msub><mml:mrow><mml:mi>N</mml:mi><mml:mi>i</. Physical Review Materials, 2022, 6, .	0.9	3
48857	Atomic-Level Structure of Zinc-Modified Cementitious Calcium Silicate Hydrate. Journal of the American Chemical Society, 2022, 144, 22915-22924.	6.6	9
48858	Topological phase transitions without symmetry indication in NaZnSb$$_{1-x}$$Bi$$_x$$. Scientific Reports, 2022, 12, .	1.6	1
48859	Chiral magnetism, lattice dynamics, and anomalous Hall conductivity in <mml:math xmlns:mml="http://www.w3.org/1998/Math/MathML"><mml:mrow><mml:msub><mml:mi mathvariant="normal">V</mml:mi><mml:mn>3</mml:mn></mml:msub><mml:mi>AuN</mml:mi></mml:mrow></mml:math> antiferromagnetic antiperovskite. Physical Review Materials, 2022, 6, .	0.9	2
48860	Superconductivity in Thâ€“H and Puâ€“H Compounds under Highâ€Pressure Conditions: A Firstâ€Principles Study. Physica Status Solidi (B): Basic Research, 2023, 260, .	0.7	1
48861	Effects of Aâ€site replacement (Sm, Y, and Pr) on catalytic performances of mullite catalysts for NO oxidation. Fuel, 2023, 337, 126838.	3.4	2
48863	Compositional texture engineering for highly stable wide-bandgap perovskite solar cells. Science, 2022, 378, 1295-1300.	6.0	103
48864	Crystal Chemistry and Physical Properties of A Quaternary Intermetallic Compound, Î¸-(Al0.8718Cu0.0256Si0.1026)13Fe4. Metals, 2022, 12, 2112.	1.0	0
48865	Influence of High Pressure on the Pedal-like Motion and Photoreactivity in the Cocrystals of 1,2-Di(4-pyridyl)ethylene with trans-2-(4-Fluorophenyl)vinylboronic Acid. Crystal Growth and Design, 2023, 23, 246-255.	1.4	0
48866	Mean-field approach for Anderson-type off-diagonal disorder. Physical Review B, 2022, 106, .	1.1	2
48867	Effective Method for the Determination of the Unit Cell Parameters of New MXenes. Materials, 2022, 15, 8798.	1.3	4
48868	Impacts of Microalloying Elements on the Hardening Î²"-Phase in Automotive AlMgSi Alloys. Acta Metallurgica Sinica (English Letters), 2023, 36, 495-506.	1.5	2
48869	Computational investigation to explore the effects of metals (Mg, Ca, Sr) doping on phase transition, electronic band structure and their repercussions on optical, elastic and mechanical properties of BaThO₃. Physica Scripta, 2023, 98, 015814.	1.2	0
48870	Computational description of surface hydride phases on Pt(111) electrodes. Journal of Chemical Physics, 2023, 158, .	1.2	8

#	Article	IF	Citations
48871	Insights into the ultra-high temperature solid solutions Hf-Ta-C-N quaternary system using high-throughput calculation. Journal of Materials Research and Technology, 2023, 22, 2239-2250.	2.6	0
48872	Electronic and optical properties of the buckled and puckered phases of phosphorene and arsenene. Scientific Reports, 2022, 12, .	1.6	4
48873	Ab initio study of magnetic structure transitions of <mml:math xmlns:mml="http://www.w3.org/1998/Math/MathML"><mml:msub><mml:mi>FePS</mml:mi><mml:mn>3</mml:mn></mml:msub></mml under high pressure. Physical Review B, 2022, 106, .	1.1	1
48874	WI3 Monolayer: Electronic Band Structure and Magnetic Anisotropy Under an External Electric Field. Journal of Electronic Materials, 0, , .	1.0	0
48875	Effects of lattice strain on hydrogen diffusion, trapping and escape in bcc iron from ab-initio calculations. International Journal of Hydrogen Energy, 2023, 48, 8198-8215.	3.8	6
48876	Achieving highly selective electrochemical CO2 reduction to C2H4 on Cu nanosheets. Journal of Energy Chemistry, 2023, 79, 312-320.	7.1	11
48877	Changes in the Optical Properties of an M-Doped (M = Pt, Ti) hBN Sheet and CO2 Capturing. Crystals, 2022, 12, 1773.	1.0	1
48878	Room Temperature Ferromagnetism in Hydrogenated Janus CrSSe Monolayer Using Quantum Monte Carlo Simulation. Crystal Growth and Design, 2023, 23, 511-523.	1.4	2
48879	The analysis of structural, elastic, and electronic properties of Na3N compound under high hydrostatic pressure with the first principles method. Indian Journal of Physics, 0, , .	0.9	0
48880	Ultra-strong Mg alloy with nano-grain structures produced by a high-throughput magnetron co-sputtering method for the full chemistry spectra. Journal of Materials Science, 2022, 57, 21813-21827.	1.7	1
48881	Single atom catalysts supported on metallic C5N monolayers for oxygen reduction/evolution reactions with more active sites than loaded metal atoms. Applied Surface Science, 2023, 614, 156048.	3.1	4
48882	Insights into molecular cluster materials with adamantaneâ€like core structures by considering dimer interactions. Journal of Computational Chemistry, 2023, 44, 843-856.	1.5	1
48883	First-Principles Calculations of Crystallographic and Electronic Structural Properties of Au-Cu Alloys. Journal of Composites Science, 2022, 6, 383.	1.4	3
48884	A Theoretical Study of Structural, Electronic, and Vibration Properties of Acetylcholine Chloride and Bromide. Food Processing: Techniques and Technology, 2022, 52, 718-728.	0.3	0
48885	Orderâ€“disorder competition in equiatomic 3dâ€“transitionâ€“metal quaternary alloys: phase stability and electronic structure. Science and Technology of Advanced Materials Methods, 2023, 3, .	0.4	0
48886	Efficient Ti₃C₂T_x MXene/TiO₂ Hybrid Photoanodes for Dye-Sensitized Solar Cells. ACS Applied Energy Materials, 2022, 5, 15928-15938.	2.5	11
48887	Dense Structure of Yttrium Nitride as a Post-Rock-Salt Phase: High-Pressure Experiments and Computations. Inorganic Chemistry, 2022, 61, 20906-20912.	1.9	1
48888	Unraveling the Electrocatalytic Activity of Platinum Doped Zirconium Disulfide toward the Oxygen Reduction Reaction. Energy & Fuels, 2023, 37, 567-579.	2.5	3

#	Article	IF	Citations
48889	Pd/Co Catalyst with High Pd Atom Utilization Efficiency for Nitrobenzene Hydrogenation at Room Temperature: Experimental and DFT Studies. Chemistry - A European Journal, 2023, 29, .	1.7	1
48890	LiNaB₆O₉F₂: A Promising UV NLO Crystal Having Fluorineâ€Directed Optimal Performances and Double Interpenetrating ³[B₆O₉F₂]_{â^ž} Networks. Advanced Optical Materials, 2023, 11, .	3.6	11
48891	Formation of Monolayer Charge Density Waves and Anomalous Edge Doping in Na Doped Bulk VSe₂. Advanced Materials Interfaces, 2023, 10, .	1.9	1
48892	Strain Induces Ferromagnetism in a Janus Transition Metal Dichalcogenides: CrSTe-1H Monolayer. Journal of Electronic Materials, 2023, 52, 1036-1049.	1.0	3
48893	Thruâ€Hole Epitaxy: A Highway for Controllable and Transferable Epitaxial Growth. Advanced Materials Interfaces, 2023, 10, .	1.9	5
48894	Phenylâ€Free Polynorbornenes for Potential Anion Exchange Ionomers for Fuel Cells and Electrolyzers. Advanced Energy Materials, 2023, 13, .	10.2	16
48895	Large magnetostriction of heavy-metal-element doped Fe-based alloys. Journal of Applied Physics, 2022, 132, 215105.	1.1	0
48896	Advantageous Role of N-doping on K@Al in COS/CS2 Hydrolysis: Diminished Oxygen Mobility and Rich basic sites. Fuel, 2023, 337, 126882.	3.4	7
48897	Hydrogen storage in gas reservoirs: A molecular modeling and experimental investigation. International Journal of Hydrogen Energy, 2023, 48, 7419-7430.	3.8	10
48898	Ethane dehydrogenation over the g-C3N4 supported metal single-atom catalysts to enhance reactivity and coking-resistance ability. Nano Research, 2023, 16, 6142-6152.	5.8	4
48899	First-principles investigation of TiC(001)/TiAl(100) interface: atomic structure, stability and electronic property. Journal of Materials Science, 2022, 57, 21339-21351.	1.7	3
48900	Hydrogen storage in Li decorated and defective pentaoctite phosphorene: A density functional theory study. International Journal of Hydrogen Energy, 2023, 48, 7794-7806.	3.8	6
48901	Efficient electrocatalytic valorization of chlorinated organic water pollutant to ethylene. Nature Nanotechnology, 2023, 18, 160-167.	15.6	31
48902	Grain Refinement via Changing the Shuffling Motion of the Grain Boundary by Traces of Ce and Lu in Gold Alloys. Journal of Physical Chemistry C, 2022, 126, 21864-21870.	1.5	0
48903	A new family of rare earth â€“ strontium tellurite chlorides, SrLn4(TeO3)4Cl6 (Ln = Ce, Nd, Sm): Synthesis, crystal structures, possible polytypism, and crystal-chemical relationships. Journal of Solid State Chemistry, 2023, 320, 123822.	1.4	1
48904	PdCu Electrocatalysts for Selective Nitrate and Nitrite Reduction to Nitrogen. ACS Catalysis, 2023, 13, 87-98.	5.5	15
48905	Density Functional Theory Study of the Point Defects on KDP (100) and (101) Surfaces. Molecules, 2022, 27, 9014.	1.7	2
48906	Periodic Density Functional Theory Calculations of Uranyl Tetrachloride Compounds Engaged in Uranylâ€“Cation and Uranylâ€“Hydrogen Interactions: Electronic Structure, Vibrational, and Thermodynamic Analyses. Inorganic Chemistry, 2023, 62, 372-380.	1.9	11

#	Article	IF	Citations
48907	Theoretical and Experimental Study of the Crystal Orientation Effect of the Anode on the Aluminum-Air Battery Performance. Journal of the Electrochemical Society, 2022, 169, 120541.	1.3	3
48908	A Multifunctional â€œHalideâ€Equivalentâ€•Anion Enabling Efficient CsPb(Br/I)₃ Nanocrystals Pureâ€Red Lightâ€Emitting Diodes with External Quantum Efficiency Exceeding 23%. Advanced Materials, 2023, 35, .	11.1	38
48909	Band Structure and Quantum Conductance of Surface-unsaturated and Hydrogenated Sb and Bi Monolayer Nanoribbons. ECS Journal of Solid State Science and Technology, 2022, 11, 121006.	0.9	0
48910	Realizing Metastable Cobaltite Perovskite via Proton-Induced Filling of Oxygen Vacancy Channels. ACS Applied Materials & Interfaces, 2023, 15, 1574-1582.	4.0	5
48911	Theoretical prediction of two-dimensional BC2X (XÂ=ÂN, P, As) monolayers: ab initio investigations. Scientific Reports, 2022, 12, .	1.6	40
48912	Visualizing the atomic defects by scanning tunneling microscopy in the type-II Dirac semimetal NiTe₂. Physica Scripta, 2023, 98, 015020.	1.2	1
48913	Selectivity of Electrochemical Ion Insertion into Manganese Dioxide Polymorphs. ACS Applied Materials & Interfaces, 2023, 15, 1513-1524.	4.0	1
48914	Defect Chemistry in Zn3V4(PO4)6. Batteries, 2023, 9, 5.	2.1	0
48915	Suppressed Internal Intrinsic Stress Engineering in Highâ€Performance Niâ€Rich Cathode Via Multilayered In Situ Coating Structure. Energy and Environmental Materials, 0, , .	7.3	1
48916	The Ti0.2V1.8C MXene Ink-Prepared Chemiresistor: From Theory to Tests with Humidity versus VOCs. Chemosensors, 2023, 11, 7.	1.8	13
48917	Modulating spintronic properties of transition metals doped <scp>GaN</scp> nanotubes with high Curie temperature. International Journal of Quantum Chemistry, 2023, 123, .	1.0	5
48918	Theoretical Study of Dynamical and Electronic Properties of Noncentrosymmetric Superconductor NbReSi. Materials, 2023, 16, 78.	1.3	2
48919	High-Pressure Synthesized Perovskite CdMnO₃ with C-Type Antiferromagnetic Spin Configuration. Inorganic Chemistry, 2022, 61, 21011-21015.	1.9	0
48920	Lithium Intercalation in Covalent Organic Frameworks: A Porous Electrode Material for Lithium-Ion Batteries. ACS Applied Electronic Materials, 2022, 4, 6237-6252.	2.0	2
48921	Formation Mechanism and Bandgap Reduction of GaNâ€“ZnO Solidâ€Solution Thin Films Fabricated by Nanolamination of Atomic Layer Deposition. Advanced Materials, 2023, 35, .	11.1	5
48922	Efficient Visibleâ€Lightâ€Initiated Dehydrogenative Coupling of Amines for Coproduction of Imines and Hydrogen over NiS/ZnIn₂S₄. Solar Rrl, 2023, 7, .	3.1	2
48923	Engineering the Near-Surface Structure of WO₃ by an Amorphous Layer with Trivalent Ni and Self-Adapting Oxygen Vacancies for Efficient Photocatalytic and Photoelectrochemical Acidic Oxygen Evolution Reaction. ACS Applied Materials & Interfaces, 2022, 14, 54769-54780.	4.0	6
48924	Lithium-Ion Transport through Complex Interphases in Lithium Metal Batteries. ACS Applied Materials & Interfaces, 2022, 14, 56758-56766.	4.0	1

#	Article	IF	Citations
48925	Atomically dispersed golds on degradable zero-valent copper nanocubes augment oxygen driven Fenton-like reaction for effective orthotopic tumor therapy. Nature Communications, 2022, 13, .	5.8	11
48926	Highly sensitive amphetamine drug detection based on silicon nanowires: Theoretical investigation. Surfaces and Interfaces, 2023, 36, 102584.	1.5	3
48927	Unveiling the dehydrogenation mechanism of 1,1,6,6-tetracyclohexylhexane: A first-principles study. International Journal of Hydrogen Energy, 2023, 48, 37811-37818.	3.8	2
48928	Surface ferromagnetism of complex defects leadâ€free ferroelectric Bi _{0.5} Na _{0.5} TiO ₃ materials. Surface and Interface Analysis, 0, , .	0.8	1
48929	Correlated Rattling of Sodiumâ€Chains Suppressing Thermal Conduction in Thermoelectric Stannides. Advanced Materials, 0, , 2207646.	11.1	0
48930	Fast monitoring of organic dye degradation coupled with a colorimetric approach in a Ag-modified TiO2 nanotube photocatalytic system. Ceramics International, 2022, , .	2.3	6
48931	First-principles calculations to investigate the physical properties of silicate perovskites ASiO3 (Aâ€‰=â€‰Al,) Tj ETQq0 0 0 rgBT /Over	0.9	2
48932	K-modified MnOÎ´ catalysts with tunnel structure and layered structure: Facile preparation and catalytic performance for soot combustion. Nano Research, 2023, 16, 6187-6199.	5.8	3
48933	Mechanisms and Kinetics of the Dehydrogenation of C₆â€“C₈ Cycloalkanes, Cycloalkenes, and Cyclodienes to Aromatics in H-MFI Zeolite Framework. ACS Catalysis, 2023, 13, 99-112.	5.5	5
48934	Atomic-Scale Insights into the Interfacial Polarization Effect in the InGaN/GaN Heterostructure for Solar Cells. ACS Applied Materials & Interfaces, 2022, 14, 55762-55769.	4.0	5
48935	Temperature-dependent mechanical properties of TaC and HfC. Journal of Materials Science, 2023, 58, 157-169.	1.7	4
48936	Phase Relations of Ni2In-Type and CaC2-Type Structures Relative to Fe2P-Type Structure of Titania at High Pressure: A Comparative Study. Crystals, 2023, 13, 9.	1.0	0
48937	High-Throughput Computational Screening of Two-Dimensional Semiconductors. Journal of Physical Chemistry Letters, 2022, 13, 11581-11594.	2.1	51
48938	Manifesting Epoxide and Hydroxyl Groups in XPS Spectra and Valence Band of Graphene Derivatives. Nanomaterials, 2023, 13, 23.	1.9	3
48939	Degradation of bisphenol A in an oxidation system constructed from Mo2C MXene and peroxymonosulfate. Npj Clean Water, 2022, 5, .	3.1	9
48940	Structural characteristics of mixed nidoâ€[Si_{9â^’x}Ge_x]^{4â^’} (x=1, 2) Zintl clusters in solution and within solvent crystals. Zeitschrift Fur Anorganische Und Allgemeine Chemie, 2023, 649, .	0.6	1
48941	Broadened photocatalytic capability to near-infrared for CdS hybrids and positioning hydrogen evolution sites. Applied Catalysis B: Environmental, 2023, 325, 122327.	10.8	7
48942	Formation mechanism of Î²â€²Mg5Si6 and its PFZ in an Al-Mg-Si-Mn alloy: Experiment and first-principles calculations. Materials Characterization, 2023, 197, 112617.	1.9	3

#	Article	IF	Citations
48943	Low-energy properties of electrons and holes in <mml:math xmlns:mml="http://www.w3.org/1998/Math/MathML"><mml:msub><mml:mi>CuFeS</mml:mi><mml:mn>2</mml:mn></mml:msub></m Physical Review B, 2022, 106, .	3.7	3
48944	Electronic and magnetic structure of ultrathin Co₉Se₈ nanosheets and Co₉Se₈ bulk from density functional theory calculations. Journal of Applied Physics, 2022, 132, 234303.	1.1	1
48945	Phonon-limited mobility and quantum transport in fluorinated diamane MOSFETs from the first-principles calculations. Carbon, 2023, 204, 295-304.	5.4	1
48946	First Principles Investigation of the Effects of Chemical Short-Range Ordering Clusters on the Ideal Tensile Strength and Ductility of Aluminum Alloys. Metals, 2022, 12, 2143.	1.0	1
48947	Band Gap Opening in Borophene/GaN and Borophene/ZnO Van der Waals Heterostructures Using Axial Deformation: First-Principles Study. Materials, 2022, 15, 8921.	1.3	2
48949	Preferential Decomposition of the Major Anion in a Dual-Salt Electrolyte Facilitates the Formation of Organic-Inorganic Composite Solid Electrolyte Interphase. Journal of Chemical Physics, 0, , .	1.2	1
48950	Coupled ferroelectricity and superconductivity in bilayer Td-MoTe2. Nature, 2023, 613, 48-52.	13.7	50
48951	TCAD Modeling of High-Field Electron Transport in Bulk Wurtzite GaN: The Full-Band SHE-BTE. IEEE Access, 2023, 11, 6293-6298.	2.6	0
48952	Delafossite as hole transport layer a new pathway for efficient perovskite-based solar sells: Insight from experimental, DFT and numerical analysis. Solar Energy, 2023, 250, 18-32.	2.9	29
48953	Tunable electronic and photodiode characteristics of Janus WSeTe: A first-principles study. Surfaces and Interfaces, 2023, 37, 102572.	1.5	6
48954	Strain data augmentation enables machine learning of inorganic crystal geometry optimization. Patterns, 2023, 4, 100663.	3.1	0
48955	Metallic to half-metallic transition driven by pressure and anion composition in niobium oxyfluoride. Journal of Materials Chemistry C, 2023, 11, 1791-1797.	2.7	1
48956	Novel Janus 2D structures of XMoY (X, Y = O, S, Se, Te) composition for solar hydrogen production. International Journal of Hydrogen Energy, 2023, 48, 14226-14237.	3.8	5
48957	First-Principles Calculations with Six Structures of Alkaline Earth Metal Cyanide A(CN)₂ (A = Be, Mg, Ca, Sr, and Ba): Structural, Electrical, and Phonon Properties. ACS Omega, 0, , .	1.6	1
48958	Defect Engineering of Green Phosphorene Nanosheets for Detecting Volatile Organic Compounds: A Computational Approach. ACS Applied Nano Materials, 2023, 6, 1496-1506.	2.4	5
48959	Pt nanoclusters on GaN nanowires for solar-asssisted seawater hydrogen evolution. Nature Communications, 2023, 14, .	5.8	23
48960	Electronic and optical properties of Janus-like hexagonal monolayer materials of group IV-VI. Physical Review Materials, 2023, 7, .	0.9	2
48961	Single-metal atom sandwiched by graphdiyne and BN-doped graphdiyne sheets as an electrocatalyst for nitrogen reduction: a first-principles study. Physical Chemistry Chemical Physics, 2023, 25, 4803-4809.	1.3	4

#	Article	IF	Citations
48962	Mechanism of Li-Ion Migration in the Superionic Conducting Open-Framework Structure Li₆B₁₈(Li₃N)_{1â€“x}(Li₂O)_x (0 â‰¤ x â‰¤ 1). Journal of Physical Chemistry C, 2023, 127, 1622-1632.	3.3	0
48963	Hydrogen protection using CrN coatings: Experimental and theoretical study. Surfaces and Interfaces, 2023, 37, 102629.	1.5	2
48964	The role of single-atom Rh-dopants in the adsorption properties of OH and CO on stepped Ag(211) surfaces. Physical Chemistry Chemical Physics, 2023, 25, 4939-4949.	1.3	1
48965	The Physical Properties of a Novel Carbon Allotrope in Tetragonal Symmetry. Journal of Electronic Materials, 2023, 52, 2071-2079.	1.0	11
48966	Breathing Behaviour Modification of Gallium MILâ€53 Metalâ€“Organic Frameworks Induced by the Bridging Framework Inorganic Anion. Chemistry - A European Journal, 2023, 29, .	1.7	1
48967	Machine learning-driven synthesis of TiZrNbHfTaC5 high-entropy carbide. Npj Computational Materials, 2023, 9, .	3.5	8
48968	The pressure and temperature evolution of the Ca₃V₂O₈ crystal structure using powder X-ray diffraction. CrystEngComm, 2023, 25, 1240-1251.	1.3	5
48969	Synergistic Catalytic Effect of Ag and MgO Nanoparticles Supported on Defective BN Surface in CO Oxidation Reaction. Materials, 2023, 16, 470.	1.3	0
48970	Prediction of monolayer <mml:math xmlns:mml="http://www.w3.org/1998/Math/MathML"><mml:mrow><mml:mi>Fe</mml:mi><mml:msub><mml:mi mathvariant="normal">P</mml:mi><mml:mn>4</mml:mn></mml:msub></mml:mrow></mml:math> with intrinsic half-metal ferrimagnetism above room temperature. Physical Review B, 2023, 107, .	1.1	10
48971	Computational and experimental studies of the wide bandgap semiconductors NH₄TiOF₃ and (NH₄)₂TiOF₄. Physical Chemistry Chemical Physics, 2023, 25, 4701-4709.	1.3	2
48972	Equilibrium Shapes of Ag, Ni, and Ir Nanoparticles under CO Conditions. Catalysts, 2023, 13, 146.	1.6	0
48973	First principles study on stability of base and precious metals pentlandite-like compounds. Theoretical Chemistry Accounts, 2023, 142, .	0.5	0
48974	First-principles investigations for the electronic and transport properties of zigzag SiC nanoribbons with Fluorine passivation/adsorption. Journal of Molecular Graphics and Modelling, 2023, 120, 108416.	1.3	0
48975	Two-dimensional metal-phase layered molybdenum disulfide for electrocatalytic hydrogen evolution reaction. Nanoscale, 2023, 15, 4429-4437.	2.8	4
48976	Ab Initio Theoretical Study of DyScO3 at High Pressure. Crystals, 2023, 13, 165.	1.0	0
48977	Unexpected Enhanced Thermal Conductivity of Ga_xIn_{1â€“x}Sb Ternary Alloys. Journal of Physical Chemistry C, 2023, 127, 3246-3255.	1.5	2
48978	Bonding iron chalcogenides in a hierarchical structure for high-stability sodium storage. Journal of Colloid and Interface Science, 2023, 637, 251-261.	5.0	5
48979	Passivation of Large <mml:math xmlns:mml="http://www.w3.org/1998/Math/MathML" display="inline" overflow="scroll"><mml:mrow><mml:mi>Pb</mml:mi><mml:mi mathvariant="normal">S</mml:mi></mml:mrow></mml:math> Colloidal Quantum Dots to Reduce Dark-Current Density for Near-Infrared Detection. Physical Review Applied, 2023, 19, .	1.5	7

#	Article	IF	Citations
48980	Firstâ€principles Density Functional Theory Elucidation of the Hydrogen Evolution Reaction on TMâ€promoted TiC₂ (TM=Fe, Co, Ni, Cu, Ru, Rh, Pd, Ag, Os, Ir, Pt, and Au). ChemPhysChem, 2023, 24, .	1.0	2
48981	Structural and Luminescence Properties of Cu(I)X-Quinoxaline under High Pressure (X = Br, I). Crystals, 2023, 13, 100.	1.0	0
48982	Strain dependence of the thermoelectric properties of perovskite MgSiO₃: A first principles study. Journal of Applied Physics, 2023, 133, 025101.	1.1	0
48983	Dodecagonal Zinc Oxide (<mml:math xmlns:mml="http://www.w3.org/1998/Math/MathML"> Tj ETQq1 1 0.784314 rgBT /Overlock 10 Tf Detection of Toxic Gases. Physical Review Applied, 2023, 19, .	1.5	5
48984	High-temperature oxidation mechanism of ZrCoSb-based half-Heusler thermoelectric compounds. Journal of Materials Science and Technology, 2023, 148, 242-249.	5.6	4
48985	Impact of single Pt atom adsorption on fundamental properties of blue phosphorene and its activity toward hydrogen evolution reaction. International Journal of Hydrogen Energy, 2023, 48, 12321-12332.	3.8	5
48986	Prediction of Novel Ultrahard Phases in the Bâ€“Câ€“N System from First Principles: Progress and Problems. Materials, 2023, 16, 886.	1.3	11
48987	Halogen-Doped Chevrel Phase Janus Monolayers for Photocatalytic Water Splitting. Nanomaterials, 2023, 13, 368.	1.9	1
48988	Synthesis of metal cation doped nanoparticles for single atom alloy catalysts using spontaneous cation exchange. Journal of Materials Chemistry A, 0, , .	5.2	1
48989	Band gap anomaly in single-layer Nb₂SiTe₄-based compounds. Wuli Xuebao/Acta Physica Sinica, 2023, .	0.2	0
48990	First-principles investigation of phase stability and elastic properties of Laves phase TaCr₂ by ruthenium alloying. High Temperature Materials and Processes, 2023, 42, .	0.6	1
48991	Long distance bimetallic site in crystal with relay metal-N-N-metal mechanism and new descriptors for electrocatalytic nitrogen reduction reaction. Applied Catalysis A: General, 2023, 652, 119030.	2.2	5
48992	Unraveling the Surface State Evolution of IrO₂ in Ethane Chemical Looping Oxidative Dehydrogenation. ACS Catalysis, 2023, 13, 1381-1399.	5.5	8
48993	3D-strain-induced multiple semiconductorâ€“metallic phase transition in monolayer SrTiO3. Applied Physics Letters, 2023, 122, .	1.5	3
48994	Efficient Ohmic Contact in Monolayer CrX₂N₄ (X = C, Si) Based Fieldâ€Effect Transistors. Advanced Electronic Materials, 2023, 9, .	2.6	11
48995	Low-Dimensional Metalâ€“Organic Magnets as a Route toward the S = 2 Haldane Phase. Journal of the American Chemical Society, 2023, 145, 1783-1792.	6.6	2
48996	Pressure-induced reentrant Dirac semimetallic phases in twisted bilayer graphene. Physical Review B, 2023, 107, .	1.1	1
48997	O-doping effects on the adsorption and detection of acetaldehyde and ethylene oxide on phosphorene monolayer: A DFT investigation. Chemical Physics Letters, 2023, 813, 140315.	1.2	1

#	Article	IF	Citations
48998	Energy- and carbon-efficient CO2/CO electrolysis to multicarbon products via asymmetric ion migrationâ€“adsorption. Nature Energy, 2023, 8, 179-190.	19.8	41
48999	Screening rareâ€earth aluminates as promising thermal barrier coatings by highâ€throughput firstâ€principles calculations. Journal of the American Ceramic Society, 2023, 106, 3089-3102.	1.9	1
49000	Optoelectronic properties of monolayer and bilayer AgI: role of many-body interactions. Journal of Computational Electronics, 0, , .	1.3	0
49001	Mechanism of Selective Chlorination of Fe from Fe2SiO4 and FeV2O4 Based on Density Functional Theory. Metals, 2023, 13, 139.	1.0	1
49002	A semiconductor Sc₂S₃ monolayer with ultrahigh carrier mobility for UV blocking filter application. Physical Chemistry Chemical Physics, 2023, 25, 5550-5558.	1.3	1
49003	Giant Electrostriction Enabled by Defect-Induced Critical Phenomena in Relaxor Ferroelectric Polymers. Macromolecules, 2023, 56, 690-696.	2.2	8
49004	Widely Tunable Berry Curvature in the Magnetic Semimetal Cr₁₊_{Î´}Te₂. Advanced Materials, 2023, 35, .	11.1	11
49005	ZIF-derived non-bonding Co/Zn coordinated hollow carbon nitride for enhanced removal of antibiotic contaminants by peroxymonosulfate activation: Performance and mechanism. Applied Catalysis B: Environmental, 2023, 325, 122401.	10.8	29
49006	Efficient Electrochemical Reduction of CO₂ on gâ€C₃N₄ Monolayerâ€supported Metal Trimer Catalysts: A DFT Study. Chemistry - an Asian Journal, 2023, 18, .	1.7	3
49007	Band gap opening in graphene by hybridization with Au (001) reconstructed surfaces. Physical Review Materials, 2023, 7, .	0.9	4
49008	Adsorption of water and organic solvents on the calcite <mml:math xmlns:mml="http://www.w3.org/1998/Math/MathML" altimg="si1.svg"><mml:mrow><mml:mo stretchy="false">[</mml:mo><mml:mn>10</mml:mn><mml:mover accent="true"><mml:mrow><mml:mn>1</mml:mn></mml:mrow><mml:mrow><mml:mo stretchy="false">Â¯</mml:mo></mml:mrow></mml:mover><mml:mn>4</mml:mn><mml:mo stretchy="false">]</mml:mo></mml:mrow></mml:math> surface: Implications for marble conservation	3.1	2
49009	Energetics and Kinetics of Hydrogen Electrosorption on a Graphene-Covered Pt(111) Electrode. Jacs Au, 2023, 3, 526-535.	3.6	5
49010	Differences in solvation thermodynamics of oxygenates at Pt/Al2O3 perimeter versus Pt(111) terrace sites. IScience, 2023, 26, 105980.	1.9	1
49011	Octahedral rotations and defect-driven metallicity at the (001) surface of <mml:math xmlns:mml="http://www.w3.org/1998/Math/MathML"><mml:msub><mml:mrow><mml:mi>CaTiO</mml:mi></mml:mrow><mml:mn> Physical Review B, 2023, 107, .	1.1	1
49012	A first-principles study of the electronic, mechanical, vibrational, and optical properties of the zirconium carbide under high pressure. Physica Scripta, 2023, 98, 025817.	1.2	4
49013	Narrowing the band gap and suppressing electronâ€“hole recombination in Î²-Fe₂O₃ by chlorine doping. Physical Chemistry Chemical Physics, 2023, 25, 3695-3701.	1.3	3
49014	<mml:math xmlns:mml="http://www.w3.org/1998/Math/MathML"><mml:mi>Î¼</mml:mi><mml:mi mathvariant="normal">SR</mml:mi></mml:math> investigation of magnetism in <mml:math xmlns:mml="http://www.w3.org/1998/Math/MathML"><mml:mi>Î¹</mml:mi><mml:mtext>â€™</mml:mtext><mml:mrow><mml:msub><mml:m : Antiferromagnetism. Physical Review Research, 2023, 5, .	1.3	1
49015	Novel electronic and magnetic features in XC (X = Si and Ge) monolayers induced by doping with group-VA atoms. New Journal of Chemistry, 2023, 47, 2787-2796.	1.4	3

#	Article	IF	Citations
49016	Corrosive Influence of Carbon Dioxide on Crack Initiation in Quartz: Comparison with Liquid Water and Vacuum Environments. Journal of Geophysical Research: Solid Earth, 0, , .	1.4	1
49017	Highly efficient hydrogen storage of a Sc decorated biphenylene monolayer near ambient temperature: ab initio simulations. Sustainable Energy and Fuels, 2023, 7, 996-1010.	2.5	7
49018	Effect of osmium substitution on structural, electronic, mechanical, and thermodynamic properties of Wâ€“Os alloys: A first-principles study. Journal of Materials Research, 2023, 38, 883-893.	1.2	1
49019	Optoelectronic and magnetic properties of transition metals-adsorbed GeC monolayer. Modern Physics Letters B, 0, , .	1.0	0
49020	Toward the design of ultrahigh-entropy alloys via mining six million texts. Nature Communications, 2023, 14, .	5.8	18
49021	On the atomistic origin of the polymorphism and the dielectric physical properties of beryllium oxide. Journal of Computational Chemistry, 0, , .	1.5	2
49022	Improved Defect Tolerance and Charge Carrier Lifetime in Tinâ€“Lead Mixed Perovskites: Ab Initio Quantum Dynamics. Journal of Physical Chemistry Letters, 2023, 14, 499-507.	2.1	6
49023	Mechanistic Understanding of the Electrocatalytic Nitrate Reduction Activity of Double-Atom Catalysts. Journal of Physical Chemistry C, 2023, 127, 994-1005.	1.5	7
49024	A First-principles investigation of the structural and electronic properties of Two-dimensional Hf2CSe2. Materials Today: Proceedings, 2023, , .	0.9	0
49025	First principles computation of insulatorâ€“semiconductorâ€“metal transition and its impact on structural, elastic, mechanical, anisotropic and optical properties of CsSrF₃ under systematic static isotropic pressure. Molecular Simulation, 2023, 49, 453-471.	0.9	2
49026	DFT computations combined with semiempirical modeling of variations with temperature of spectroscopic and magnetic properties of Gd³⁺-doped PbTiO₃. Physical Chemistry Chemical Physics, 0, , .	1.3	0
49027	Doping-induced magnetism and magnetoelectric coupling in one-dimensional NbOCl₃ and NbOBr₃. Physical Chemistry Chemical Physics, 0, , .	1.3	4
49028	High-throughput identification of materials for silicon tandem solar cells. Sustainable Energy and Fuels, 0, , .	2.5	0
49029	Study of the solar perovskites: XZnF3 (Xâ€‰=â€‰Ag, Li or Na) by DFT and TDDFT methods. Journal of the Korean Ceramic Society, 2023, 60, 424-433.	1.1	6
49030	Monolayer group-V binary compounds <mml:math xmlns:mml="http://www.w3.org/1998/Math/MathML"><mml:mi>Ï</mml:mi></mml:math> -BiP and <mml:math xmlns:mml="http://www.w3.org/1998/Math/MathML"><mml:mi>Ï</mml:mi></mml:math> -SbP with ultrahigh piezoelectricity and stability. Physical Review Materials, 2023, 7, .	0.9	4
49031	Enhancement in photocatalytic water splitting using van der Waals heterostructure materials based on penta-layers. Physical Chemistry Chemical Physics, 2023, 25, 3401-3412.	1.3	3
49032	A comparative study of the structural, elastic, thermophysical, and optoelectronic properties of CaZn2X2 (XÂ=ÂN, P, As) semiconductors via ab-initio approach. Results in Physics, 2023, 44, 106214.	2.0	5
49033	First-principles study of H2 adsorption mechanism on defective MoSe2/graphene heterostructures. MRS Advances, 2023, 8, 365-370.	0.5	0

#	Article	IF	Citations
49034	Tuning the electronic and magnetic properties of MgO monolayer by nonmetal doping: A first-principles investigation. Materials Today Communications, 2023, 34, 105422.	0.9	1
49035	Theab initiopotential energy curves of atom pairs and transport properties of high-temperature vapors of Cu and Si and their mixtures with He, Ar, and Xe gases. Physical Chemistry Chemical Physics, 2023, 25, 4872-4898.	1.3	2
49036	Anisotropic Rashba coupling to polar modes in KTaO₃. JPhys Materials, 2023, 6, 014007.	1.8	4
49037	Superconductivity of graphenelike hydrogen in <mml:math xmlns:mml="http://www.w3.org/1998/Math/MathML"><mml:mrow><mml:msub><mml:mi mathvariant="normal">H</mml:mi><mml:mn>2</mml:mn></mml:msub><mml:mi>He</mml:mi></mml:mrow></mml:math> at high pressure. Physical Review B, 2023, 107, .	1.1	1
49038	Switchable Giant Bulk Photocurrents and Photo-spin-currents in Monolayer PT-Symmetric Antiferromagnet MnPSe₃. Journal of Physical Chemistry Letters, 2023, 14, 370-378.	2.1	4
49039	A BC₂N/blue phosphorene heterostructure as an anode material for high-performance sodium-ion batteries: first principles insights. Physical Chemistry Chemical Physics, 2023, 25, 3160-3174.	1.3	5
49040	The effect of chemical disorder on magnetic properties of FeNi and Fe2Ni2N alloys. Journal of Magnetism and Magnetic Materials, 2023, 568, 170362.	1.0	2
49041	Nanoprecipitates to Enhance Radiation Tolerance in High-Entropy Alloys. ACS Applied Materials & Interfaces, 2023, 15, 3912-3924.	4.0	3
49042	Tunable anomalous valley Hall effect and magnetic phase transition in MHfN2Cl2 (M = V, Cr) bimetallic nitrogen halide monolayers. Applied Physics Letters, 2023, 122, .	1.5	5
49043	Ab initio study on structural, magnetic phase and helium migration behaviour of FCC Fe 6.25 at.% Cr binary alloys. Philosophical Magazine, 0, , 1-24.	0.7	0
49044	Kondo resonance effects in emergent flat band materials. Frontiers in Physics, 0, 10, .	1.0	1
49045	Computational study on the impact of Nb doping on electronic structure, magnetic and optical properties of hexagonal bilayer BN. Materials Research Express, 0, , .	0.8	0
49046	Insights into the physical properties of newly synthesized AMn2P2 (A= Ca, Sr) via density functional theory. Physica B: Condensed Matter, 2023, 653, 414651.	1.3	1
49047	Temperature dependence of (111) and (110) ceria surface energy. Physical Review B, 2023, 107, .	1.1	2
49048	Redrawing HER Volcano with Interfacial Processesâ€”The Role of Hydrogen Spillover in Boosting H2 Evolution in Alkaline Media. Catalysts, 2023, 13, 89.	1.6	3
49049	Magnetic proximity enabled bulk photovoltaic effects in van der Waals heterostructures. Physical Review Research, 2023, 5, .	1.3	3
49050	Doping Limits of Phosphorus, Arsenic, and Antimony in CdTe. Journal of Physical Chemistry Letters, 2023, 14, 273-278.	2.1	7
49051	Refined DFT¼<mml:math xmlns:mml="http://www.w3.org/1998/Math/MathML" altimg="si81.svg" display="inline" id="d1e1616"><mml:mi>U</mml:mi></mml:math> method for computation of layered oxide cathode materials. Electrochimica Acta, 2023, 443, 141912.	2.6	3

#	Article	IF	Citations
49052	Tuned electronic and magnetic properties in 3d transition metal doped VCl₃ monolayer: a first-principles study. Physica Scripta, 2023, 98, 025814.	1.2	1
49053	Journeys in crystal energy landscapes: actual and virtual structures in polymorphic 5-nitrobenzo[c][1,2,5]thiadiazole. CrystEngComm, 0, , .	1.3	2
49054	Enhanced Blue Emission in Rb₂HfCl₆ Double Perovskite via Bi³⁺ Doping and Cs⁺ Alloying. Chemistry of Materials, 2023, 35, 948-953.	3.2	6
49055	Colloidally Engineered Pd and Pt Catalysts Distinguish Surface- and Vapor-Mediated Deactivation Mechanisms. ACS Catalysis, 2023, 13, 1812-1822.	5.5	4
49056	Corrosion inhibition at emergent grain boundaries studied by DFT for 2-mercaptobenzothiazole on bi-crystalline copper. Npj Materials Degradation, 2023, 7, .	2.6	4
49057	S-functionalized 2D V₂B as a promising anode material for rechargeable lithium ion batteries. Physical Chemistry Chemical Physics, 0, , .	1.3	0
49058	Electronic Structure and Minimal Models for Flat and Corrugated CuO Monolayers: An Ab Initio Study. Materials, 2023, 16, 658.	1.3	0
49059	Predicting the work function of 2D MXenes using machine-learning methods. JPhys Energy, 2023, 5, 034005.	2.3	6
49060	Monolayer and bilayer lanthanide compound Gd2C with large magnetic anisotropy energy and high Curie temperature. Journal of Materials Science, 2023, 58, 268-280.	1.7	1
49061	Structural stabilities and half-metallicity properties of the OsTiVIn and OsZrVIn quaternary Heusler alloys under high pressure. Journal of Magnetism and Magnetic Materials, 2023, 566, 170316.	1.0	2
49062	Strain engineering of hyperbolic plasmons in monolayer carbon phosphide: a first-principles study. Nanoscale, 0, , .	2.8	1
49063	Revisiting two thiophosphate compounds constituting d⁰transition metal HfP₂S₆and d¹⁰transition metal Î±-Ag₄P₂S₆as multifunctional materials for combining second harmonic generation response and photocurrent response. CrystEngComm, 2023, 25, 1175-1185.	1.3	4
49064	Ab-initio investigation of mechanical and fracture-related properties of W-Re Ïƒ and Ï‡ precipitates. Journal of Nuclear Materials, 2023, 577, 154261.	1.3	0
49065	Enhanced reversibility of fluorine substituted bis-BN cyclohexane for hydrogen storage: A first-principles approach. International Journal of Hydrogen Energy, 2023, 48, 13503-13515.	3.8	3
49066	Kirigami-Inspired Thermal Regulator. Physical Review Applied, 2023, 19, .	1.5	2
49067	Two-Dimensional Î´-Be₂C with Hepta-Coordinated Carbons: A Highly Stable Direct-Band-Gap Semiconductor Predicted by First-Principles Calculations. Journal of Physical Chemistry C, 2023, 127, 1687-1696.	1.5	5
49068	CO₂ hydrogenation to formic acid on Pdâ€“Cu nanoclusters: a DFT study. Physical Chemistry Chemical Physics, 2023, 25, 2584-2594.	1.3	4
49069	Clathrateâ€Like Alkali and Alkalineâ€Earth Metal Borides: A New Family of Superconductors with Superior Hardness. Advanced Functional Materials, 0, , 2213377.	7.8	2

#	Article	IF	Citations
49070	Roomâ€Temperatureâ€Processable Highly Reliable Resistive Switching Memory with Reconfigurability for Neuromorphic Computing and Ultrasonic Tissue Classification. Advanced Functional Materials, 2023, 33, .	7.8	9
49071	Large Surface Gap Solitons and Their Stabilities in Quasi-1D BEC with Three-body Interactions. Wuli Xuebao/Acta Physica Sinica, 2023, .	0.2	0
49072	First principle comparative study of transitional elements Co, Rh, Ir(III)-based double halide perovskites. Materials Today Communications, 2023, 34, 105431.	0.9	4
49073	A new high voltage alluaudite sodium battery insertion material. Materials Today Chemistry, 2023, 27, 101316.	1.7	1
49074	The Transfer Hydrogenation of Cinnamaldehyde Using Homogeneous Cobalt(II) and Nickel(II) (E)-1-(Pyridin-2-yl)-N-(3-(triethoxysilyl)propyl)methanimine and the Complexes Anchored on Fe3O4 Support as Pre-Catalysts: An Experimental and In Silico Approach. Molecules, 2023, 28, 659.	1.7	1
49075	An iron-base oxygen-evolution electrode for high-temperature electrolyzers. Nature Communications, 2023, 14, .	5.8	15
49076	Fundamentals of energy storage from first principles simulations: Challenges and opportunities. Frontiers in Energy Research, 0, 10, .	1.2	2
49077	Improved Thermoelectric Performance of NbCoSb with Intrinsic Nb Vacancies and Ni-Doping-Induced Band Degeneracy. ACS Applied Energy Materials, 0, , .	2.5	1
49078	First principles study of layered scandium disulfide for use as Li-ion and beyond-Li-ion batteries. Physical Chemistry Chemical Physics, 2023, 25, 2167-2178.	1.3	7
49079	Piezoelectricity of strain-induced overall water splitting of Ni(OH)₂/MoS₂ heterostructure. Journal of Materials Chemistry A, 2023, 11, 3481-3492.	5.2	11
49080	Superconductivity in <mml:math xmlns:mml="http://www.w3.org/1998/Math/MathML"><mml:mrow><mml:msub><mml:mi>SrB</mml:mi><mml:mn>3</mml:mn></mml mathvariant="normal">C</mml:mi><mml:mn>3</mml:mn></mml:msub></mml:mrow></mml:math> clathrate. Physical Review Research, 2023, 5, .	1.3	10
49081	Phonon dispersion curves in the type-I crystalline and moltenclathrate compound Eu₈Ga₁₆Ge₃₀. Journal of Physics Condensed Matter, 0, , .	0.7	0
49082	Importance of accurately measuring LDOS maps using scanning tunneling spectroscopy in materials presenting atom-dependent charge order: The case of the correlated Pb/Si(111) single atomic layer. Physical Review B, 2023, 107, .	1.1	1
49083	Investigation of the phonon dispersion associated with superlattice reflections in the <mml:math xmlns:mml="http://www.w3.org/1998/Math/MathML"><mml:msub><mml:mi>BiS</mml:mi><mml:mn>2</mml:mn></mml:msub></m -based superconductor <mml:math xmlns:mml="http://www.w3.org/1998/Math/MathML"><mml:mrow><mml:msub><mml:mi>LaBiS</mml:mi><mml:mn>2</mml:mn></ mathvariant="normal">O</mml:mi><mml:mrow><mml:mn>0.5</mml:mn></mml:mrow></mml:msub><mml:msub><mml:mi mathvariant="normal">F</mml. Physical Review B, 2023, 107, .	1.1	1
49084	A theoretical study of the improved CO oxidation on WC supported Au monolayer by Cu doping. Physica Scripta, 2023, 98, 035809.	1.2	1
49085	Effects of excess electrons/holes on fracture toughness of single-crystal Si. Journal of Applied Physics, 2023, 133, .	1.1	4
49086	Galvanic displacement of Co with Rh boosts hydrogen and oxygen evolution reactions in alkaline media. Journal of Solid State Electrochemistry, 2023, 27, 1877-1887.	1.2	0
49087	Mechanochemistry and the Evolution of Ionic Bonds in Dense Silver Iodide. Jacs Au, 2023, 3, 402-408.	3.6	4

#	Article	IF	Citations
49088	First-principles calculations to investigate pressure-driven electronic phase transition of lead-free halide perovskites KMCl3 (MÂ=ÂGe, Sn) for superior optoelectronic performance. Results in Physics, 2023, 44, 106212.	2.0	10
49089	Synthesis, characterization, computational studies, and photocatalytic properties of Cu doped Bi2S3 nanorods. Materials Today Communications, 2023, 34, 105418.	0.9	0
49090	Insight at the atomic scale of corrosion inhibition: DFT study of 8-hydroxyquinoline on oxidized aluminum surfaces. Physical Chemistry Chemical Physics, 2023, 25, 4284-4296.	1.3	4
49091	Effective strategies toward imine-linked cationic covalent organic frameworks for rapid and selective removal of ⁹⁹TcO₄^{â^'} from water: insights from DFT and MD calculations. Environmental Science: Nano, 2023, 10, 611-624.	2.2	2
49092	The Screening of Homoâ€•and Heteroâ€Đual Atoms Anchored Graphdiyne for Boosting Electrochemical CO₂ Reduction. Advanced Materials Interfaces, 2023, 10, .	1.9	3
49093	Machine learning-based discovery of vibrationally stable materials. Npj Computational Materials, 2023, 9, .	3.5	3
49094	Giant electron-phonon interaction for a prototypical semiconductor interface: <mml:math xmlns:mml="http://www.w3.org/1998/Math/MathML"><mml:mi mathvariant="normal">Sn</mml:mi><mml:mo>/</mml:mo><mml:mi mathvariant="normal">Ge</mml:mi><mml:mo>(</mml:mo><mml:mn>111</mml:mn><mml:mo>)</mml:mo><mml:mtext>â^'</mml:mte Physical Review B, 2023, 107, .	1.1	2
49095	Excellent photocatalytic properties in 2D ZnO/SiC van der Waals hetero-bilayers: water-splitting H₂-fuel production. RSC Advances, 2023, 13, 1943-1954.	1.7	4
49096	Tuning Discharge Behavior of Hollandite Î±-MnO₂ in Hydrated Zinc Ion Battery by Transition Metal Substitution. Journal of Physical Chemistry C, 2023, 127, 907-918.	1.5	2
49097	First-principles investigation of defective graphene anchored with small silicon clusters as a potential anode material for lithium-ion batteries. Surface Science, 2023, , 122250.	0.8	2
49098	Fullerene Latticeâ€Confined Ru Nanoparticles and Single Atoms Synergistically Boost Electrocatalytic Hydrogen Evolution Reaction. Advanced Functional Materials, 2023, 33, .	7.8	40
49099	One-pot synthesized nano-heterostructure with dual-modal catalytic ROS generation ability for high-metastatic orthotopic osteosarcoma therapy. Carbon, 2023, 204, 196-210.	5.4	5
49100	Role of charged oxygen vacancies and substrate lattice constraint on structural stability of Ga₂O₃ polymorphs. Applied Physics Express, 2023, 16, 015508.	1.1	1
49101	Li/Na atoms' substitution effects on the structural, electronic, and mechanical properties of the CaSnO3 perovskite for battery applications. Computational Materials Science, 2023, 219, 112006.	1.4	4
49102	Dynamics of the fcc-to-bcc phase transition in single-crystalline PdCu alloy nanoparticles. Nature Communications, 2023, 14, .	5.8	11
49103	Metal halide HgI2 monolayer with auxetic property and photocatalysis application. Computational Materials Science, 2023, 219, 112007.	1.4	1
49104	The promotion effect of uniaxial strain on hydrogen aggregation in tungsten. Frontiers in Materials, 0, 9, .	1.2	0
49105	High-performance monoclinic WO3 nanospheres with the novel NH4+ diffusion behaviors for aqueous ammonium-ion batteries. Chemical Engineering Journal, 2023, 458, 141381.	6.6	137

#	Article	IF	Citations
49106	Effect of doping concentration on the antiferromagnetic transition temperature of multiferroic YMnO3: A first-principles study. Computational Materials Science, 2023, 218, 111999.	1.4	0
49107	First-principles study on stability, electronic and mechanical properties of 4^3T175 carbon allotrope. Computational Materials Science, 2023, 219, 111956.	1.4	1
49108	Phononic crystalsâ€™ band gap manipulation via displacement modes. Solid State Communications, 2023, 361, 115061.	0.9	3
49109	Atomistic investigation of the impact of phosphorus impurities on the tungsten grain boundary decohesion. Computational Materials Science, 2023, 219, 112017.	1.4	3
49110	Ground state and phase stability of GaP-ZnS and GaP-ZnSe quaternary systems from first-principles. Solid State Communications, 2023, 361, 115075.	0.9	0
49111	Strain engineering for tuning the electronic and optical properties of lithium niobate for optoelectronic applications. Solid State Communications, 2023, 361, 115074.	0.9	1
49112	Lattice dynamical and thermodynamic properties study of ceria using density functional theory and Hubbard correction. Physica B: Condensed Matter, 2023, 651, 414600.	1.3	0
49113	Determining anisotropic reactive facet of ilmenite photocatalyst with Hubbard U assisted density functional theory. Computational Materials Science, 2023, 219, 112024.	1.4	2
49114	A universal multifunctional rare earth oxide coating to stabilize high-voltage lithium layered oxide cathodes. Energy Storage Materials, 2023, 56, 155-164.	9.5	21
49115	Facile fabrication of atomically dispersed Ru-P-Ru ensembles for efficient hydrogenations beyond isolated single atoms. Chinese Journal of Catalysis, 2023, 45, 107-119.	6.9	3
49116	The Importance of Mgâ€“Sb Interactions in Achieving High Conduction Band Degeneracy in Mg3Sb2 for High n-Type Thermoelectric Performance. Materials Today Physics, 2023, 31, 100959.	2.9	4
49117	Highly sensitive and selective sensing-performance of 2D Co-decorated phthalocyanine toward NH3, SO2, H2S and CO molecules. Surfaces and Interfaces, 2023, 36, 102641.	1.5	9
49118	Electronic, magnetic and optical properties of transition metal doped Nd2O3: A DFT insight. Computational and Theoretical Chemistry, 2023, 1220, 114016.	1.1	0
49119	Enhancing the radiation tolerance of high-entropy alloys via solute-promoted chemical heterogeneities. Acta Materialia, 2023, 245, 118662.	3.8	30
49120	Novel PEO-based composite electrolyte for low-temperature all-solid-state lithium metal batteries enabled by interfacial cation-assistance. Energy Storage Materials, 2023, 56, 121-131.	9.5	30
49121	Microstructural and magneto-optical properties of Co1-xNix Fe2O4 nanocomposites for hyperthermia applications. Solid State Sciences, 2023, 136, 107107.	1.5	9
49122	Calculation of tunable electronic and optical properties of AlSb/CdSe heterojunction based on first principles. Applied Surface Science, 2023, 614, 156261.	3.1	4
49123	Structural, optical, electronic, elastic properties and population inversion of novel 2D carbides and nitrides MXene: A DFT study. Materials Science and Engineering B: Solid-State Materials for Advanced Technology, 2023, 289, 116230.	1.7	5

#	Article	IF	Citations
49124	Anaerobic environment-induced efficient degradation of chloroquine phosphate: Insights into the role of metal-free C3N4 nanotube in visible light-driven peroxymonosulfate activation. Chemical Engineering Journal, 2023, 457, 141219.	6.6	13
49125	Band alignment study at the SrTaO2N / H2O interface varying lattice constants and surface termination from first-principles calculations. Computational Condensed Matter, 2023, 34, e00784.	0.9	0
49126	An unexpectedly stable Y2B5 compound with the fractional stoichiometry under ambient pressure. Arabian Journal of Chemistry, 2023, 16, 104546.	2.3	5
49127	Theoretical study on the organic acid promoted dissolution mechanism of forsterite mineral. Applied Surface Science, 2023, 614, 156063.	3.1	8
49128	Manipulating the electronic, magnetic, and optical properties of single-walled armchair phosphorus nanotubes by encapsulating transition metal nanowires. Materials Today Communications, 2023, 34, 105253.	0.9	1
49129	Strong binding of heavy metals in fayalite of copper smelting slags: Lattice site substitution. Science of the Total Environment, 2023, 866, 161351.	3.9	2
49130	Bulk and monolayer thermoelectric and optical properties of anisotropic NbS<mml:math xmlns:mml="http://www.w3.org/1998/Math/MathML" altimg="si61.svg" display="inline" id="d1e859"><mml:msub><mml:mrow /><mml:mrow><mml:mn>2</mml:mn></mml:mrow></mml:msub></mml:math>Cl<mml:math xmlns:mml="http://www.w3.org/1998/Math/MathML" altimg="si61.svg" display="inline" id="d1e867"><mml:msub><mml:mrow /><mml:mrow><mml:mn>2</mml:mn></mml:mrow></mml:msub></	0.9	0
49131	Theoretical study for exploring the adsorption behavior of aniline and phenol on pristine and Cu-doped phosphorene surface. Applied Surface Science, 2023, 614, 156194.	3.1	4
49132	Multihyperuniform long-range order in medium-entropy alloys. Acta Materialia, 2023, 246, 118678.	3.8	9
49133	Band gap tuning of non-toxic Sr-based perovskites CsSrX3 (XÂ=ÂCl, Br) under pressure for improved optoelectronic applications. Materials Today Communications, 2023, 34, 105188.	0.9	10
49134	Computational design of two-dimensional GeP based flexible strain sensor: Distinct J-V response. Sensors and Actuators A: Physical, 2023, 351, 114155.	2.0	4
49135	Eu3+-activated SrY2O4:Ce4+/3+ red-phosphor for WLEDs: Structural and luminescent insights from experimental and theoretical approaches. Journal of Alloys and Compounds, 2023, 938, 168595.	2.8	5
49136	Thermodynamic reassessment of Feâ€“Nbâ€“V system. Calphad: Computer Coupling of Phase Diagrams and Thermochemistry, 2023, 80, 102529.	0.7	1
49137	New approach to the compound energy formalism (NACEF) Part II. Thermodynamic modelling of the Alâ€“Nb system supported by first-principles calculations. Calphad: Computer Coupling of Phase Diagrams and Thermochemistry, 2023, 80, 102522.	0.7	0
49138	Investigation on the electronic structures, elastic and thermodynamic properties of TiNi, Ti2Ni and TiNi3 intermetallic compound. Materials Today Communications, 2023, 34, 105273.	0.9	5
49139	Improved mechanical properties of Co-free high-entropy Cantor alloy: A first-principles study. Results in Materials, 2023, 17, 100364.	0.9	2
49140	Dopant-based modulation of structural, electronic, and electrochemical properties of Li-excessive Li2NiO2 cathodes. Current Applied Physics, 2023, 48, 1-10.	1.1	0
49141	Excellent high temperature elasticity and thermodynamic properties of W-Cr alloys: A first-principles study. Nuclear Materials and Energy, 2023, 34, 101367.	0.6	1

#	Article	IF	Citations
49142	Interaction effects in a two-dimensional AlSi<mml:math xmlns:mml="http://www.w3.org/1998/Math/MathML" altimg="si11.svg" display="inline" id="d1e513"><mml:msub><mml:mrow /><mml:mrow><mml:mn>6</mml:mn></mml:mrow></mml:msub></mml:math>P nanosheet: A first-principles study on the electronic, mechanical, thermal, and optical properties. Physica B: Condensed Matter, 2023, 652, 414627.	1.3	1
49143	Nonlinear elastic behavior of 2D materials using molecular statics and comparisons with first principles calculations. Physica E: Low-Dimensional Systems and Nanostructures, 2023, 148, 115633.	1.3	2
49144	A first-principles study of the heterogeneous nucleation of Mg on AlN reinforcement particles. Materials Today Communications, 2023, 34, 105277.	0.9	0
49145	Green synthesis of NiO nanoparticle using Punica granatum peel extract and its characterization for methyl orange degradation. Materials Today Communications, 2023, 34, 105302.	0.9	5
49146	Two-dimensional valleytronic semiconductor with spontaneous spin and huge valley polarization in monolayer MnCoO6Bi2. Physica E: Low-Dimensional Systems and Nanostructures, 2023, 148, 115654.	1.3	1
49147	Curvature effect on graphene-based Co/Ni single-atom catalysts. Applied Surface Science, 2023, 615, 156357.	3.1	17
49148	Enhanced secondary electron emission properties of Zn doped MgO thin films prepared by aerosol assisted chemical vapor deposition. Materials Science in Semiconductor Processing, 2023, 157, 107323.	1.9	1
49149	SnS2/AuNPs surface-enhanced Raman scattering sensor for rapid and selective quantification of methimazole in serum and meat samples. Sensors and Actuators B: Chemical, 2023, 380, 133325.	4.0	8
49150	Incorporation of volatile fission products in UN and PuN and comparison to oxides. Journal of Nuclear Materials, 2023, 576, 154267.	1.3	3
49151	â€œSniffâ€•lung cancer biomarkers in breath using N-doped monolayer WS2: A theoretical feasibility. Applied Surface Science, 2023, 614, 156257.	3.1	4
49152	Tuning pyridinic-N and graphitic-N doping with 4,4â€²-bipyridine in honeycomb-like porous carbon and distinct electrochemical roles in aqueous and ionic liquid gel electrolytes for symmetric supercapacitors. Journal of Colloid and Interface Science, 2023, 635, 254-264.	5.0	13
49153	The role of vacancy in alloyed (001)-Al//(001) interface. Materials Today Communications, 2023, 34, 105260.	0.9	0
49154	Functionalized Mo<mml:math xmlns:mml="http://www.w3.org/1998/Math/MathML" altimg="si141.svg" display="inline" id="d1e1015"><mml:msub><mml:mrow /><mml:mrow><mml:mn>2</mml:mn></mml:mrow></mml:msub></mml:math>BX<mml:math xmlns:mml="http://www.w3.org/1998/Math/MathML" altimg="si141.svg" display="inline" id="d1e1023"><mml:msub><mml:mrow /><mml:mrow><mml:mn>2</mml:mn></mml:mrow></mml:msub></mml:math> (X = H, OH, O) MBenes as a	3.1	7
49155	Unifying stability and plasmonic properties in hybrid nanoislands: Auâ€“Ag synergistic effects and application in SERS. Sensors and Actuators B: Chemical, 2023, 380, 133326.	4.0	4
49156	DFT and ab-initio molecular dynamics of pyrochlore surface dissolution in aqueous media â€“ Effect of cleavage plane and surface atomic vacancies. Applied Surface Science, 2023, 615, 156425.	3.1	3
49157	Tuning the electronic properties of WS2 monolayer by doping transition metals: DFT Approach. Materials Science in Semiconductor Processing, 2023, 157, 107339.	1.9	6
49158	Nickel-doped tungsten oxide promotes stable and efficient hydrogen evolution in seawater. Applied Catalysis B: Environmental, 2023, 325, 122397.	10.8	16
49159	MXene V2CO2 monolayerï¼ša promising adsorbent to capture toxic NH3 gas. Physica E: Low-Dimensional Systems and Nanostructures, 2023, 148, 115651.	1.3	4

#	Article	IF	Citations
49160	Investigation of the crystal structure, electronic and optical properties of Cr-doped BaTiO3 on the Ti site using first principles calculations. Journal of Physics and Chemistry of Solids, 2023, 175, 111209.	1.9	10
49161	Effects of tungsten on vacancy aggregation behavior and its induction for interstitial and vacancy migration in tantalumâ€“tungsten alloys: A first-principles study. Annals of Nuclear Energy, 2023, 183, 109618.	0.9	0
49162	Giant band gap bowing in two dimensional Pb<mml:math xmlns:mml="http://www.w3.org/1998/Math/MathML" altimg="si65.svg" display="inline" id="d1e531"><mml:msub><mml:mrow /><mml:mrow><mml:mn>1</mml:mn><mml:mo>â^’</mml:mo><mml:mi>x</mml:mi></mml:mrow></mml:msub></mml:math>Sn<mml:math xmlns:mml="http://www.w3.org/1998/Math/MathML" altimg="si66.svg" display="inline" id="d1e543"><mml:msub><mml:mrow /><mml:mrow><mml:mi>x</mml:mi></mml:mrow></mml:msub></m	1.9	6
49163	A structural study of size selected WSe2 nanoflakes prepared via liquid phase exfoliation: X-ray absorption to electrochemical application. Radiation Physics and Chemistry, 2023, 206, 110788.	1.4	3
49164	Designing a thermodynamically stable and intrinsically ductile refractory alloy. Journal of Alloys and Compounds, 2023, 939, 168597.	2.8	5
49165	Boosting ethanol oxidation by NiOOH-CuO nano-heterostructure for energy-saving hydrogen production and biomass upgrading. Applied Catalysis B: Environmental, 2023, 325, 122388.	10.8	49
49166	Combined experimental and computational 1H NMR study of water adsorption onto graphenic materials. Journal of Magnetic Resonance Open, 2023, 14-15, 100091.	0.5	1
49167	Density Functional Theory Study on the Adsorption of Fe(OH)2+ on Kaolinite Surface in Water Environment. Processes, 2023, 11, 38.	1.3	0
49168	Direction-Based Graph Representation to Accelerate Stable Catalyst Discovery. Chemistry of Materials, 2023, 35, 63-70.	3.2	3
49169	Activated Lone-Pair Electrons Lead to Low Lattice Thermal Conductivity: A Case Study of Boron Arsenide. Journal of Physical Chemistry Letters, 2023, 14, 139-147.	2.1	2
49170	DFT Simulations of Zn_xMg_{1â€“X}O Solid Solutions for Solar-Blind UV Sensors: Evaluation of Electronic Structure and Phase Stability. Latvian Journal of Physics and Technical Sciences, 2022, 59, 3-11.	0.4	0
49171	Vickers hardness prediction from machine learning methods. Scientific Reports, 2022, 12, .	1.6	1
49172	Theoretical Investigations on the Structure, Elastic and Thermal Conductivities of Li₂MO₃ (Mâ€‰=â€‰Sn, Zr and Ti) Ceramics. Integrated Ferroelectrics, 2023, 231, 153-162.	0.3	5
49173	Discriminating and understanding molecular crystal polymorphism. Journal of Computational Chemistry, 0, , .	1.5	0
49174	Embedding Group VIII Elements into a 2D Rigid pc-C3N2 Monolayer to Achieve Single-Atom Catalysts with Excellent OER Activity: A DFT Theoretical Study. Molecules, 2023, 28, 254.	1.7	6
49175	Electronic, Elastic, and Thermoelectric Properties of Half-Heusler Topological Semi-Metal HfIrAs from First-Principles Calculations. Crystals, 2023, 13, 37.	1.0	2
49176	Theory of shallow and deep boron defects in <mml:math xmlns:mml="http://www.w3.org/1998/Math/MathML"><mml:mrow><mml:mn>4</mml:mn><mml:mi mathvariant="normal">H</mml:mi></mml:mrow></mml:math> -SiC. Physical Review B, 2022, 106, .	1.1	4
49177	High-Pressure X-ray Diffraction and DFT Studies on Spinel FeV2O4. Crystals, 2023, 13, 53.	1.0	0

#	Article	IF	Citations
49178	KÃ¼bik Perovskit LaZnO3 BileÅŸiÄŸinin YapÄ±sal, Elektronik, Elastik ve Termodinamik Ã–zelliklerini AraÅŸtÄ±rmak iÃ§in Ab Initio HesaplamalarÄ±. , 2022, 4, 113-124.		2
49179	Electronic Structures of Monolayer Binary and Ternary 2D Materials: MoS2, WS2, Mo1â^'xCrxS2, and W1â^'xCrxS2 Using Density Functional Theory Calculations. Nanomaterials, 2023, 13, 68.	1.9	1
49180	Anisotropic Carrier Mobility and Spectral Fingerprints of Two-Dimensional Î³-Phosphorus Carbide with Antisite Defects. Journal of Physical Chemistry Letters, 2023, 14, 214-220.	2.1	3
49181	Facile Synthesis of Gram-Scale Mesoporous Ag/TiO₂ Photocatalysts for Pharmaceutical Water Pollutant Removal and Green Hydrogen Generation. ACS Omega, 2023, 8, 1249-1261.	1.6	5
49182	First-Principles Calculations to Investigate Direct-Band Novel Cobalt-Based Double Perovskite Materials for Optoelectronic Applications. Energy & Fuels, 2023, 37, 1266-1274.	2.5	3
49183	Designing orbital and charge ordering multiferroics by superlattice strategy and strain engineering. Physical Review B, 2022, 106, .	1.1	2
49184	The Ultrahigh Adsorption Capacity and Excellent Photocatalytic Degradation Activity of Mesoporous CuO with Novel Architecture. Nanomaterials, 2023, 13, 142.	1.9	3
49185	Optimizing density-functional simulations for two-dimensional metals. Physical Review Materials, 2022, 6, .	0.9	1
49186	4H-SiC Ohmic contacts formation by MoS2 layer intercalation: A first-principles study. Journal of Applied Physics, 2022, 132, .	1.1	1
49187	Photocatalytic property of two dimensional heterostructure MoS2/WS2 for hydrogen evolution via water splitting; a first principles calculation. International Journal of Hydrogen Energy, 2023, 48, 9371-9376.	3.8	6
49188	Binding Energy and Diffusion Barrier of Formic Acid on Pd(111). Journal of Physical Chemistry A, 2023, 127, 142-152.	1.1	0
49189	Photoelectric Properties of Single Layer TiS2 Modified by Non-Metal Doping. Russian Journal of Physical Chemistry A, 2022, 96, 3031-3037.	0.1	3
49190	Systematic Theoretical Study of CO Activation over Clean and Potassium-Modified Transition Metals. Journal of Physical Chemistry C, 2023, 127, 265-278.	1.5	1
49191	Electrical characteristics and conductive mechanisms of AlN-based memristive devices. , 2022, 18, 815-825.		0
49192	First-Principle Study of Ca3Y2Ge3O12 Garnet: Dynamical, Elastic Properties and Stability under Pressure. Crystals, 2023, 13, 29.	1.0	0
49193	A first principles study on H-atom interaction with bcc metals. International Journal of Hydrogen Energy, 2023, 48, 9911-9920.	3.8	6
49194	First Ultrathin Pure Polyoxometalate 2D Material as a Peroxidase-Mimicking Catalyst for Detecting Oxidative Stress Biomarkers. ACS Applied Materials & Interfaces, 2023, 15, 1486-1494.	4.0	14
49195	Hybrid-Density Functional Calculations of Structural, Electronic, Magnetic, and Thermodynamic Properties of Î±-Cu2P2O7. Applied Sciences (Switzerland), 2023, 13, 498.	1.3	2

#	Article	IF	Citations
49196	Photocatalytic NO_x Oxidation of BiOCl Nanostructure-Based Films Grown Using Aerosol-Assisted Chemical Vapor Deposition. ACS Applied Nano Materials, 2023, 6, 738-749.	2.4	2
49197	Synergism between B and Nb Improves Fire Resistance in Microalloyed Steels. Metals, 2023, 13, 84.	1.0	2
49198	Ab-initio optimization of CoHfSi Half-Heusler alloy. Materials Today: Proceedings, 2022, , .	0.9	1
49199	Semiconductor Characteristic and Ferromagnetism in Rare Earth (Eu, Er)-Doped AlGaN Alloy: LSDAâ€‰+â€‰U Approach. Brazilian Journal of Physics, 2023, 53, .	0.7	1
49200	Theoretical prediction of thermal properties of $$hbox {YP}_{1-x}hbox {Sb}_{x}$$ alloys. Indian Journal of Physics, 0, , .	0.9	0
49201	Stability of Subnanometer MoS Wires under a Realistic Environment. Journal of Physical Chemistry Letters, 2023, 14, 183-189.	2.1	0
49202	High-efficiency hydrogen evolution reaction photocatalyst for water splitting of Type-II Î²-AsP/g-C3N4 van der Waals heterostructure. International Journal of Hydrogen Energy, 2023, 48, 10051-10061.	3.8	10
49203	Enhanced Intrinsic Anomalous Valley Hall Effect Induced by Spinâ€“Orbit Coupling in MXene Monolayer M₃N₂O₂ (M = Y, La). Journal of Physical Chemistry Letters, 2023, 14, 132-138.	2.1	9
49204	Evaluating the Effect of 18O Incorporation on the Vibrational Spectra of Vaterite and Calcite. Crystals, 2023, 13, 48.	1.0	0
49205	Enhanced Proton Conduction with Low Oxygen Vacancy Concentration and Favorable Hydration for Protonic Ceramic Fuel Cells Cathode. ACS Applied Materials & Interfaces, 2023, 15, 1339-1347.	4.0	16
49206	Thermal and electrical transport conductivities of novel ordered double two-dimensional MXenes via density functional theory. Canadian Journal of Chemistry, 0, , .	0.6	0
49207	Atomistic simulations of diffusion in <mml:math xmlns:mml="http://www.w3.org/1998/Math/MathML"><mml:msup><mml:mi>Î³</mml:mi><mml:mo>â€²</mml:mo></mml:msup></m -strengthened Co-based superalloys and its connection to selective alumina formation in early-stage oxidation. Physical Review Materials, 2023, 7, .	0.9	1
49208	Enhanced Catalytic Activity of Bimetallic Ordered Catalysts for Nitrogen Reduction Reaction by Perturbation of Scaling Relations. ACS Catalysis, 2023, 13, 2190-2201.	5.5	15
49209	Supported Metal Nanohydrides for Hydrogen Storage. Chemistry of Materials, 2023, 35, 1134-1147.	3.2	4
49210	First-Principles Calculations Study of Small Polarons Around Oxygen Vacancies in SrMoO4. Journal of Electronic Materials, 0, , .	1.0	0
49211	Ensemble Effects in Adsorbateâ€“Adsorbate Interactions in Microkinetic Modeling. Journal of Chemical Theory and Computation, 0, , .	2.3	1
49212	High-Pressure X-ray Diffraction Study of Orthorhombic Ca₂Zr₅Ti₂O₁₆. Journal of Physical Chemistry C, 2023, 127, 2069-2077.	1.5	0
49213	Collective Variables for Conformational Polymorphism in Molecular Crystals. Journal of Physical Chemistry Letters, 2023, 14, 971-976.	2.1	5

#	Article	IF	Citations
49214	Graphene Formation through Spontaneous Exfoliation of Graphite by Chlorosulfonic Acid: A DFT Study. Micro, 2023, 3, 143-155.	0.9	1
49215	Nb₂C MXenes with surface chalcogenation and halogenation as high capacity electrode materials for lithium-ion batteries. Modern Physics Letters B, 2023, 37, .	1.0	1
49216	Increasing the Efficiency of Photocatalytic Water Splitting via Introducing Intermediate Bands. Journal of Physical Chemistry Letters, 2023, 14, 779-784.	2.1	5
49217	Donorâ€“Acceptor Co-Adsorption Ratio Controls the Structure and Electronic Properties of Two-Dimensional Alkaliâ€“Organic Networks on Ag(100). Journal of Physical Chemistry C, 2023, 127, 2716-2727.	1.5	2
49218	Segregation and Oxidation Behavior in Be {101Ì…1} Grain Boundary by First-Principles Calculations. Journal of Physical Chemistry C, 2023, 127, 2648-2656.	1.5	1
49219	Elucidating the rate-determining step of ammonia decomposition on Ru-based catalysts using ab initio-grounded microkinetic modeling. Catalysis Science and Technology, 2023, 13, 2026-2037.	2.1	5
49220	Surface charge as activity descriptors for electrochemical CO2 reduction to multi-carbon products on organic-functionalised Cu. Nature Communications, 2023, 14, .	5.8	30
49221	Large spontaneous valley polarization and high magnetic transition temperature in stable two-dimensional ferrovalley <mml:math xmlns:mml="http://www.w3.org/1998/Math/MathML"><mml:mrow><mml:mi		

#	Article	IF	Citations
49234	First-Principles Calculations of 2D Janus WSSiN₂Monolayer for Photocatalytic Water Splitting. ACS Applied Nano Materials, 2023, 6, 1956-1964.	2.4	18
49235	Ultrafast relaxation of lattice distortion in two-dimensional perovskites. Nature Physics, 2023, 19, 545-550.	6.5	19
49236	Ultrabroadband Emission from CsCu₂I₃/Cs₃Cu₂I₅ Dual-Phase Glass-Ceramics with Long-Term Stability. , 2023, 1, 481-490.		4
49237	Spin-selective contact type and strong Fermi level pinning at a CrI3/metal interface. Materials Today Nano, 2023, 22, 100309.	2.3	3
49238	Ab initio studies of the gas adsorption on the surface CdSe1â€“xSx ultra-thin films. Applied Nanoscience (Switzerland), 0, , .	1.6	0
49239	Geometrical and magnetic properties of small titanium and chromium clusters on monolayer hexagonal boron nitride. Physical Chemistry Chemical Physics, 0, , .	1.3	0
49240	Exploring the Dirac nature of <mml:math xmlns:mml="http://www.w3.org/1998/Math/MathML"><mml:msub><mml:mi>RbBi</mml:mi><mml:mn>2</mml:mn></mml:msub></mml:math> Physical Review B, 2023, 107, .	1.1	1
49241	First-principles calculations of Ni-(Co)-Mn-Cu-Ti all-d-metal Heusler alloy on martensitic transformation, mechanical and magnetic properties. International Journal of Minerals, Metallurgy and Materials, 2023, 30, 930-938.	2.4	0
49242	Formation of oxygen vacancy clusters in Li-rich Mn-based cathode Materials of lithium-ion batteries: First-principles calculations. Wuli Xuebao/Acta Physica Sinica, 2023, 72, 078201.	0.2	0
49243	Heat transport properties of novel carbon monolayer (net-Y): a comparative study with graphene. Physical Chemistry Chemical Physics, 2023, 25, 4915-4922.	1.3	1
49244	High Pressureâ€Driven Magnetic Disorder and Structural Transformation in Fe₃GeTe₂: Emergence of a Magnetic Quantum Critical Point. Advanced Science, 2023, 10, .	5.6	8
49245	Tuning the elastic variant switching to tune ferromagnetic properties of <mml:math xmlns:mml="http://www.w3.org/1998/Math/MathML"><mml:mrow><mml:mn>1</mml:mn><mml:mi mathvariant="normal">T</mml:mi></mml:mrow><mml:mo>â€²</mml:mo></mml:math> <mml:math xmlns:mml="http://www.w3.org/1998/Math/MathML"><mml:mi>Cr</mml:mi><mml:msub><mml:mi>X</mml:mi><mml:mn>2</mml:mn></mml:msub></mml:math> <mml:math		

#	Article	IF	Citations
49252	First Theoretical Realization of a Stable Two-Dimensional Boron Fullerene Network. Applied Sciences (Switzerland), 2023, 13, 1672.	1.3	1
49253	Proton transfer in layered hydrogen-bonded system Î³-MOOH (M = Al, Sc): Robust bi-mode ferroelectricity and 1D superionic conductivity. Applied Physics Letters, 2023, 122, 042901.	1.5	2
49254	Density Functional Theory Combined with Thermodynamics Exploration of Novel 2D Materials Created Using Aqueous Exfoliation. Journal of Physical Chemistry C, 2023, 127, 2314-2325.	1.5	1
49255	Short-range order and compositional phase stability in refractory high-entropy alloys via first-principles theory and atomistic modeling: NbMoTa, NbMoTaW, and VNbMoTaW. Physical Review Materials, 2023, 7, .	0.9	3
49256	Effect of External Pressure and Quantum State on the Local Magnetization of Germanium Layers: Ab Initio Calculation. Advanced Theory and Simulations, 2023, 6, .	1.3	1
49257	Multiple Chelation-Assisted Lithiation Improves the Performance of Phosphate-Modified LiNi_{0.8}Co_{0.1}Mn_{0.1}O₂. Journal of the Electrochemical Society, 2023, 170, 010525.	1.3	1
49258	Phase stability of Fe from first principles: Atomistic spin dynamics coupled with ab initio molecular dynamics simulations and thermodynamic integration. Physical Review B, 2023, 107, .	1.1	3
49259	Ab Initio Investigation of the Adsorption of CO2 Molecules on Defect Sites of Graphene Surfaces: Role of Local Vacancy Structures. Materials, 2023, 16, 981.	1.3	5
49260	Effect of Nickel on the Hydroxide Ion Adsorption of Copper Sulfide: A viewpoint from a first-principle calculation. Journal of Physics: Conference Series, 2023, 2421, 012011.	0.3	0
49261	Shape-Dependent CO₂ Hydrogenation to Methanol over Cu₂O Nanocubes Supported on ZnO. Journal of the American Chemical Society, 2023, 145, 3016-3030.	6.6	19
49262	Dynamic rhenium dopant boosts ruthenium oxide for durable oxygen evolution. Nature Communications, 2023, 14, .	5.8	77
49263	Electron-Transfer Mechanism in P2â€“Na_{0.67}MnO₂/Graphene Electrodes: Experimental and First-Principles Investigations. ACS Applied Energy Materials, 2023, 6, 1723-1730.	2.5	3
49264	Ferro-piezoelectricity in emerging Janus monolayer BMX₂ (M = Ga, In and X = S, Se): ab initio investigations. Nanoscale Advances, 2023, 5, 1425-1432.	2.2	5
49265	Crystallographic Insight of Reduced Lattice Volume Expansion in Mesoporous Cu²⁺â€Doped TiNb₂O₇ Microspheres during Li⁺ Insertion. Advanced Functional Materials, 2023, 33, .	7.8	11
49266	Phase Transformation of Colloidal Cs₃Cu₂Cl₅ Nanocrystals to CsMCl (M = Zn, Bi, Cd) by Cation Exchange and Their Thermodynamic Study by Density Functional Theory Calculations. Chemistry of Materials, 2023, 35, 1301-1309.	3.2	3
49267	First-principles calculations of plasmon excitations in graphene, silicene, and germanene. Physical Review B, 2023, 107, .	1.1	6
49268	Compression of gaseous hydrogen into warm dense states up to 95ÂGPa using multishock compression technique. Physical Review B, 2023, 107, .	1.1	1
49269	Evidence for chiral superconductivity on a silicon surface. Nature Physics, 2023, 19, 500-506.	6.5	10

#	Article	IF	Citations
49270	Tracking and Understanding Dynamics of Atoms and Clusters of Late Transition Metals with In-Situ DRIFT and XAS Spectroscopy Assisted by DFT. Journal of Physical Chemistry C, 2023, 127, 3032-3046.	1.5	6
49271	Effect of uniaxial strain on the excitonic properties of monolayer <mml:math xmlns:mml="http://www.w3.org/1998/Math/MathML"><mml:mrow><mml:msub><mml:mi mathvariant="normal">C</mml:mi><mml:mn>3</mml:mn></mml:msub><mml:mi mathvariant="normal">N</mml:mi></mml:mrow></mml:math> : A symmetry-based analysis. Physical Review B, 2023, 107, .	1.1	1
49272	How Adsorbed Oxygen Atoms Inhibit Hydrogen Dissociation on Tungsten Surfaces. Journal of Physical Chemistry Letters, 2023, 14, 1246-1252.	2.1	3
49273	Mitigating Coke Formations for Dry Reforming of Methane on Dual-Site Catalysts: A Microkinetic Modeling Study. Journal of Physical Chemistry C, 2023, 127, 2274-2284.	1.5	2
49274	pâ€d Orbital Hybridization Engineered Singleâ€Atom Catalyst for Electrocatalytic Ammonia Synthesis. Energy and Environmental Materials, 0, , .	7.3	7
49275	Effect of Varying Stiffness and Functionalization on the Interfacial Failure Behavior of Isotactic Polypropylene on Hydroxylated Î³-Al₂O₃ by MD Simulation. ACS Applied Materials & Interfaces, 2023, 15, 6133-6141.	4.0	0
49276	Ab initio study of changing the oxygen reduction activity of Coâ€“Fe-based perovskites by tuning the B-site composition. Physical Chemistry Chemical Physics, 2023, 25, 4236-4242.	1.3	0
49277	Phonon Dominated Thermal Transport in Metallic Niobium Diselenide from First Principles Calculations. Nanomaterials, 2023, 13, 315.	1.9	0
49278	Ethanol Solvent Used in Constructing Ultra-Low-Temperature Zinc-Ion Capacitors with a Long Cycling Life. ACS Applied Materials & Interfaces, 2023, 15, 5180-5190.	4.0	7
49279	Effect of Defects in Graphene/Cu Composites on the Density of States. Materials, 2023, 16, 962.	1.3	0
49280	Ab-initio probe into the elastic, mechanical and thermo-mechanical properties of CsSe binary compound. International Journal of Modern Physics B, 0, , .	1.0	0
49281	Interfacial bonding between iron and Mo- and Cr-doped tungsten carbides. Journal of Applied Physics, 2023, 133, .	1.1	8
49282	Insight into the Anchoring Effect of Twoâ€Dimensional TiX₂ (X = S, Se) Materials for Sodiumâ€“Sulfur Batteries: A Firstâ€Principles Study. Advanced Theory and Simulations, 2023, 6, .	1.3	1
49283	First-principles calculations of Mg2FeH6 under high pressures and hydrogen storage properties. Journal of Molecular Modeling, 2023, 29, .	0.8	3
49284	Topological Impact of Delocalization on the Stability and Band Gap of Partially Oxidized Graphene. ACS Omega, 2023, 8, 5124-5135.	1.6	5
49285	Adsorption of Cyclic (Alkyl) (Amino) Carbenes on Monohydride Si(001) Surfaces: Interface Bonding and Electronic Properties. Journal of Physical Chemistry C, 2023, 127, 1973-1980.	1.5	1
49286	First-principles screening of transition metal doped anatase TiO₂(101) surfaces for the electrocatalytic nitrogen reduction. Physical Chemistry Chemical Physics, 2023, 25, 5827-5835.	1.3	2
49287	Stability and Physical Properties of the L12-Î³â€² Phase in the CoNiAlTi-System. Metallurgical and Materials Transactions A: Physical Metallurgy and Materials Science, 0, , .	1.1	0

#	Article	IF	Citations
49288	Phonon transport in Janus monolayer siblings: a comparison of 1T and 2H-ISbTe. RSC Advances, 2023, 13, 4202-4210.	1.7	1
49289	Ground-State Structure of Quaternary Alloys (SiC)1â^'x (AlN)x and (SiC)1â^'x (GaN)x. Micromachines, 2023, 14, 250.	1.4	0
49290	Combined ab initio and experimental screening of phase stabilities in the Ce-Fe-Ti- <mml:math		

#	Article	IF	Citations
49308	Unexpected giant negative area compressibility in palladium diselenide. National Science Review, 2023, 10, .	4.6	3
49309	Experimental and theoretical investigation of the effect of alkali (Li, Na and K) doping on the properties of nickel oxide thin films: Comparative study. Main Group Chemistry, 2024, 23, 73-88.	0.4	0
49310	Molecular-Dynamics Analysis of the Mechanical Behavior of Plasma-Facing Tungsten. ACS Applied Materials & Interfaces, 2023, 15, 8709-8722.	4.0	2
49311	DFT calculations of structural, magnetic, and stability of FeNiCo-based and FeNiCr-based quaternary alloys. Journal of Applied Physics, 2023, 133, .	1.1	3
49312	Investigation of the anchoring and electrocatalytic properties of pristine and doped borophosphene for Naâ€“S batteries. Physical Chemistry Chemical Physics, 2023, 25, 5443-5452.	1.3	3
49313	First-Principles Investigation on the High-Temperature Mechanical Properties and Thermal Properties of Pt-40Rh. Transactions of the Indian Institute of Metals, 2023, 76, 1545-1552.	0.7	1
49314	Unconventional Anisotropy in Excitonic Properties and Carrier Mobility in Iodine-Based XTeI (X = Ga,) Tj ETQq0 0 0 rgBT /Overlock 10 Tf 5 127, 1992-2002.	1.5	10
49315	Raman Spectroscopy Signatures of Boron-Rich Superhard Materials from Density Functional Theory. Journal of Physical Chemistry C, 2023, 127, 2104-2115.	1.5	6
49316	Influence of Element Doping and Surface Oxidation on CoP for Overall Water Splitting: A First-Principles Study. Journal of Physical Chemistry C, 2023, 127, 1808-1821.	1.5	4
49317	Ordered vacancy compounds: the case of the MangÃ©li phases of TiO2. , 2023, , 533-565.		0
49318	Electronic structure and density functional theory. , 2023, , 3-35.		0
49319	Theoretical design of porous dodecagonal germanium carbide (d-GeC) monolayer. RSC Advances, 2023, 13, 3290-3294.	1.7	7
49320	Sc2CX (X=N2, ON, O2) MXenes as a promising anode material: A first-principles study. Journal of Applied Physics, 2023, 133, .	1.1	5
49321	First-principles study of thermoelasticity and structural phase diagram of CaO. Physical Review B, 2023, 107, .	1.1	1
49322	Structure and Characterization of K₂Na₃B₂P₃O₁₃, a New Nonlinear Optical Borophosphate with One-Dimensional Chain Structure and Short Ultraviolet Cutoff Edge. Inorganic Chemistry, 2023, 62, 2480-2488.	1.9	2
49323	Gas Sensors Based on Borophene Nanoribbon Edge-Terminated by Fluorine. Journal of Electronic Materials, 2023, 52, 2359-2371.	1.0	3
49324	Automated Graph Neural Networks Accelerate the Screening of Optoelectronic Properties of Metalâ€“Organic Frameworks. Journal of Physical Chemistry Letters, 2023, 14, 1239-1245.	2.1	2
49325	Chlorine Adsorption on the Ag(110) Surface: STM and DFT Study. Journal of Physical Chemistry C, 2023, 127, 2266-2273.	1.5	1

#	Article	IF	Citations
49326	First-principles study of the ferrielectric of X-doped KNbO₃ (Xâ€‰=â€‰Na, Rb, and Cs). Ferroelectrics, 2023, 603, 267-275.	0.3	1
49327	Evaluation of the structural, electronic, optical, and mechanical properties of Sb₂Se₃ using density functional theory. International Journal of Modern Physics B, 0, , .	1.0	0
49330	Raman strainâ€“shift measurements and prediction from first-principles in highly strained silicon. Journal of Materials Science: Materials in Electronics, 2023, 34, .	1.1	2
49331	Ab Initio Study of the Electronic Properties of a Silicene Anode Subjected to Transmutation Doping. International Journal of Molecular Sciences, 2023, 24, 2864.	1.8	0
49332	Interstitial Zinc Boosted Light Tunability, Afterglow, and Ultrabright White Emission in Zinc Germanate (Zn₂GeO₄). ACS Applied Electronic Materials, 2023, 5, 1286-1294.	2.0	10
49333	Dipolar effects on the work function of an alkali-iodide overlayer (XI, X= Li, Na, K, Rb, and Cs) on tungsten surfaces. Physica Scripta, 0, , .	1.2	1
49334	Multicomponent solid solution with pyrochlore structure. Boletin De La Sociedad Espanola De Ceramica Y Vidrio, 2023, 62, 515-526.	0.9	1
49335	Bismuth and oxygen vacancies induce (2ÂÃ—Â1) reconstructions in bismuth oxyhalide (BiOX, XÂ=ÂCl, Br, I) (0) Tj ETQq1 1 0.784314	3.1	7
49336	Structural, mechanical, electronic, vibrational and thermoelectric properties of novel double perovskites Ba2MgPdO6 and Ba2MgPtO6 within DFT framework. Materials Science in Semiconductor Processing, 2023, 158, 107381.	1.9	9
49337	DFT approach for predicting the pH-potential-dependent durabilities of Pt-skinned Pt-M (MÂ=ÂNi, Co, and) Tj ETQq1 1 0.784314 rgBT	3.1	1
49338	Shifting the plasmonic resonance to infrared region for AlP by inducing high S concentration: Indirect to direct band gap. Physica B: Condensed Matter, 2023, 654, 414718.	1.3	1
49339	Facile synthesis of flexible and scalable Cu/Cu2O/CuO nanoleaves photoelectrodes with oxidation-induced self-initiated charge-transporting platform for photoelectrochemical water splitting enhancement. Journal of Alloys and Compounds, 2023, 942, 169094.	2.8	11
49340	Competition between Li2Se2Sx conversion and Li Ion transport on graphene surface coordination doped with transition metal and N. Chemical Engineering Journal Advances, 2023, 14, 100468.	2.4	0
49341	Band gap tailoring in a low toxicity and low-cost solar cell absorber Cu3SbS4 through Na alloying: a first-principles study. Journal of Crystal Growth, 2023, , 127132.	0.7	1
49342	Feature-rich electronic and magnetic properties in silicene monolayer induced by nitrogenation: A first-principles study. Chemical Physics, 2023, 568, 111844.	0.9	0
49343	Novel coexistence of resistive switching and ferromagnetism modulation in Ta/La2/3Sr1/3MnO3/Nb:SrTiO3/Ag device. Materials Letters, 2023, 338, 134031.	1.3	0
49344	Tuning electronic properties and contact type in van der Waals heterostructures of bilayer SnS and graphene. Applied Surface Science, 2023, 616, 156489.	3.1	5
49345	Theoretical investigation of the structural, electronic, elastic and optical properties of the new layered ternary chalcogenide tetragonal compounds Cu2MX4 (M = W and Mo; X=S and Se). Journal of Solid State Chemistry, 2023, 321, 123880.	1.4	3

#	Article	IF	Citations
49346	Ta2C MXene: Nonlinear optical properties and application in femtosecond fiber laser. Optics and Laser Technology, 2023, 161, 109178.	2.2	3
49347	First-principles approach to the structural, physical, electronic, magnetic and optical properties of honeycomb ordered antimonates Na3Fe2SbO6. Journal of Physics and Chemistry of Solids, 2023, 176, 111258.	1.9	1
49348	First-principles insights into structural stability, elastic anisotropies, mechanical and thermodynamic properties of the Hf<mml:math xmlns:mml="http://www.w3.org/1998/Math/MathML" altimg="si98.svg" display="inline" id="d1e2137"><mml:msub><mml:mrow /><mml:mrow><mml:mn>2</mml:mn></mml:mrow></mml:msub></mml:math>Ge<mml:math xmlns:mml="http://www.w3.org/1998/Math/MathML" altimg="si99.svg" display="inline"		

#	Article	IF	Citations
49364	Role of defect engineering in revealing the electronic and sensing applications of Janus WSSe monolayer. Journal of Materials Chemistry C, 2023, 11, 4219-4234.	2.7	2
49365	Searching for d⁰ spintronic materials: bismuthene monolayer doped with IVA-group atoms. RSC Advances, 2023, 13, 5885-5892.	1.7	7
49366	Systematic investigation of the mechanical, electronic, and interfacial properties of high mobility monolayer InAs from first-principles calculations. Physical Chemistry Chemical Physics, 2023, 25, 10769-10777.	1.3	2
49367	Janus Î²-PdXY (X/Y = S, Se, Te) materials with high anisotropic thermoelectric performance. Nanoscale, 2023, 15, 5964-5975.	2.8	5
49368	Discovery of a metastable van der Waals semiconductor via polymorphic crystallization of an amorphous film. Materials Horizons, 2023, 10, 2254-2261.	6.4	2
49369	Ternary pentagonal BXN (X = C, Si, Ge, and Sn) sheets with high piezoelectricity. RSC Advances, 2023, 13, 9636-9641.	1.7	3
49370	One-Dimensional TeSe Nano-Heterojunction: Formation, Calculations, Carrier Dynamics, and Application in Broad-Spectrum Photodetectors. Nanoscale, 0, , .	2.8	0
49371	SENSITIVE ELEMENTS OF TEMPERATURE CONVERTERS BASED ON HfNi1-xCuxSn THERMOMETRICAL MATERIAL. Measuring Equipment and Metrology, 2023, 84, 11-17.	0.1	0
49372	Optoelectronic performance of perovskite Cs₂KMI₆ (M = Ga, In) based on high-throughput screening and first-principles calculations. Physical Chemistry Chemical Physics, 2023, 25, 11484-11492.	1.3	4
49373	Pressure-induced second-order phase transition in fluorine. Physical Chemistry Chemical Physics, 2023, 25, 9935-9943.	1.3	1
49374	Enabling triferroics coupling in breathing kagome lattice Nb₃X₈ (X = Cl, Br, I) monolayers. Journal of Materials Chemistry C, 2023, 11, 5762-5769.	2.7	4
49375	Rational design of 2D/2D CS/SiC van der Waals type-II heterojunctions: a visible-light-driven photocatalyst for hydrogen production. Materials Advances, 2023, 4, 1949-1963.	2.6	4
49376	Understanding green-hydrocarbon production through the strategy of biomass ketalization reaction. Sustainable Energy and Fuels, 2023, 7, 2244-2258.	2.5	1
49377	AlO3Â·H6TeO6 (A = NH4+, Rb+): Two telluric acid and iodate Co-crystalline compounds with second harmonic generation response. , 2023, 42, 100025.		2
49378	A novel lithium decorated N-doped 4,6,8-biphenylene for reversible hydrogen storage: Insights from density functional theory. International Journal of Hydrogen Energy, 2023, 48, 17216-17229.	3.8	15
49379	Large intrinsic spin Hall conductivity in orthorhombic tungsten. Physical Review Materials, 2023, 7, .	0.9	0
49380	Customized reaction route for ruthenium oxide towards stabilized water oxidation in high-performance PEM electrolyzers. Nature Communications, 2023, 14, .	5.8	66
49381	Band structure, superconductivity, and polytypism in <mml:math xmlns:mml="http://www.w3.org/1998/Math/MathML"><mml:msub><mml:mi>AuSn</mml:mi><mml:mn>4</mml:mn></mml:msub></ Physical Review Materials, 2023, 7, .	0.9	3

#	Article	IF	Citations
49382	Nonharmonic contributions to the high-temperature phonon thermodynamics of Cr. Physical Review B, 2023, 107, .	1.1	0
49383	Internal and External Coâ€Engineering of Stable Cathode Interface Improves Cycle Performance of Polymer Sodium Batteries. Advanced Functional Materials, 2024, 34, .	7.8	2
49384	Carbon nanotubes and nanobelts as potential materials for biosensor. Scientific Reports, 2023, 13, .	1.6	6
49385	Optical and electronic properties of defect chalcopyrite ZnGa₂S₄. International Journal of Modern Physics B, 2024, 38, .	1.0	0
49386	Phase stability, mechanical properties and thermal conductivity of technetium diborides in different crystal structures. Applied Physics A: Materials Science and Processing, 2023, 129, .	1.1	1
49387	Structure and Optical Properties of Polymeric Carbon Nitrides from Atomistic Simulations. Chemistry of Materials, 2023, 35, 1547-1559.	3.2	9
49388	Structural, Electronic, and Optical Properties of SnBr2 Monolayer by Density Functional Approach. Materials Today: Proceedings, 2023, , .	0.9	4
49389	Microstructural Manipulation for Enhanced Average Thermoelectric Performance: A Case Study of Tin Telluride. ACS Applied Materials & Interfaces, 2023, 15, 9656-9664.	4.0	8
49390	Defect-Engineering of 2D Dichalcogenide VSe2 to Enhance Ammonia Sensing: Acumens from DFT Calculations. Biosensors, 2023, 13, 257.	2.3	6
49391	Theoretical prediction of novel two-dimensional MA₂Z₄ family for Li/Na battery anodes. 2D Materials, 2023, 10, 025020.	2.0	2
49392	Simulation studies of secondary electron yield with electron transport from Cu (110) surfaces containing C2, N2, CO2, or NO2 adsorbates. Frontiers in Materials, 0, 10, .	1.2	0
49393	Tunable Schottky barrier in a graphene/AlP van der Waals heterostructure. Semiconductor Science and Technology, 2023, 38, 045009.	1.0	4
49394	First-principles theory of the pressure-induced invar effect in FeNi alloys. Physical Review B, 2023, 107, .	1.1	2
49395	Efficient extraction of resonant states in systems with defects. Journal of Computational Physics, 2023, 477, 111928.	1.9	2
49396	Ductility reduction upon cobalt substitution in B2 NiTi. Computational Materials Science, 2023, 220, 112049.	1.4	1
49397	A highly-stable bifunctional NiCo2S4 nanoarray@carbon paper electrode for aqueous polysulfide/iodide redox flow battery. Journal of Power Sources, 2023, 561, 232607.	4.0	5
49398	Nano FeSb₂S₄ Anchored on Exfoliated Graphite for Sodium-Ion Battery Anode via a Two-Step Fabrication. Energy & Fuels, 2023, 37, 5577-5585.	2.5	2
49399	Molecular Locking with Allâ€Organic Surface Modifiers Enables Stable and Efficient Slotâ€Dieâ€Coated Methylâ€Ammoniumâ€Free Perovskite Solar Modules. Advanced Materials, 2023, 35, .	11.1	9

#	Article	IF	Citations
49400	Understanding the poisoning mechanisms of Si and Zr atoms on L12 Al3Ti (111) surface: A first-principles investigation. Vacuum, 2023, 210, 111891.	1.6	0
49401	Ultraefficient Heterogeneous Electroâ€“Fenton Process Integrated a Natural Dual-Interface Air-Diffusion Cathode for Water Decontamination. ACS ES&T Engineering, 2023, 3, 762-772.	3.7	2
49402	Hydrogen adsorption on Au (111), U (110), and nAu/U (110) alloy surfaces: A first-principles study. Journal of Nuclear Materials, 2023, 577, 154331.	1.3	3
49403	First-principles prediction of superconductivity in <mml:math xmlns:mml="http://www.w3.org/1998/Math/MathML"><mml:mrow><mml:msub><mml:mi>MgB</mml:mi><mml:mn>3</mml:mn></mml:msub><mml:mi mathvariant="normal">C</mml:mi><mml:mn>3</mml:mn></mml:mrow></mml:math>. Physical Review B, 2023, 107, .	1.1	2
49404	Ultraâ€fast Piezocatalysts Enabled By Interfacial Interaction of Reduced Graphene Oxide/MoS₂ Heterostructures. Advanced Materials, 2023, 35, .	11.1	26
49405	Double resonant tunable second harmonic generation in two-dimensional layered materials through band nesting. Physical Review B, 2023, 107, .	1.1	1
49406	Modeling laser interactions with aluminum and tantalum targets using a hybrid atomistic-continuum model. Journal of Applied Physics, 2023, 133, .	1.1	1
49407	An ab initio study of novel quaternary Heusler alloys for spin polarized and waste heat recycling systems. Journal of Magnetism and Magnetic Materials, 2023, 571, 170541.	1.0	5
49408	Adsorption and sensing properties of SF6 decomposed gases on Mg-MOF-74. Solid State Communications, 2023, 363, 115120.	0.9	7
49409	Crystallinity engineering for overcoming the activityâ€“stability tradeoff of spinel oxide in Fenton-like catalysis. Proceedings of the National Academy of Sciences of the United States of America, 2023, 120, .	3.3	23
49410	Theoretical investigation on CO oxidation by single nickel atom within two-dimensional porphyrin sheet. Journal of Molecular Structure, 2023, 1286, 135580.	1.8	7
49411	Thermal behaviour and microstructure evolution of new ternary eutectic alloy in Al-Cu-Si-Ni system. Journal of Alloys and Compounds, 2023, 941, 168942.	2.8	3
49412	Active and durable R2MnRuO7 pyrochlores with low Ru content for acidic oxygen evolution. Nature Communications, 2023, 14, .	5.8	9
49413	Synergy of VN and Fe₂O₃ Enables High Performance Anodes for Asymmetric Supercapacitors. ACS Applied Materials & Interfaces, 2023, 15, 18819-18827.	4.0	13
49414	The effect mechanism of HCl on chromium removal by CaO sorbent. Journal of Cleaner Production, 2023, 397, 136559.	4.6	5
49415	Effects of native and H related defects on magnetic properties of SrCoO_{2.5} and HSrCoO_{2.5}. Journal of Applied Physics, 2023, 133, 135702.	1.1	1
49416	Plasma-catalytic reforming of biogas into syngas over Ni-based bimetallic catalysts. Chemical Engineering Journal, 2023, 462, 142044.	6.6	4
49417	High symmetry structure and large strain field fluctuation lead enhancement of thermoelectric performance of quaternary alloys by tuning configurational entropy. Chemical Engineering Journal, 2023, 462, 142185.	6.6	2

#	Article	IF	Citations
49418	Assessing factors that determine adatom migration and clustering on a thin film oxide; Pt1 and Rh1 on the â€œ29â€•CuxO/Cu(1 1 1) surface. Applied Surface Science, 2023, 628, 157145.	3.1	2
49419	Effect of doping IVB, VB and VIB elements on structure, stability, elastic and electronic properties of the O and B2 of Ti2AlNb intermetallic: A first principles study. Journal of Physics and Chemistry of Solids, 2023, 179, 111362.	1.9	1
49420	Efficient atomistic simulations of radiation damage in W and Wâ€“Mo using machine-learning potentials. Journal of Nuclear Materials, 2023, 577, 154325.	1.3	5
49421	Ag@Pt core-shell icosahedral nanocrystals with solid solution interface improve pH-Universal hydrogen evolution at large current densities. Composites Part B: Engineering, 2023, 254, 110600.	5.9	5
49422	Pressure-induced enhancement of thermoelectric performance of CoP3 by the structural phase transition. Acta Materialia, 2023, 248, 118773.	3.8	4
49423	Monovacancy-hydrogen interaction in pure aluminum: Experimental and ab-initio theoretical positron annihilation study. Acta Materialia, 2023, 248, 118770.	3.8	6
49424	Discovery of novel low modulus Nbâ€“Tiâ€“Zr biomedical alloys via combined machine learning and first principles approach. Materials Chemistry and Physics, 2023, 299, 127537.	2.0	5
49425	Efficient Synthesis of 2D Mica Nanosheets by Solvothermal and Microwave-Assisted Techniques for CO2 Capture Applications. Materials, 2023, 16, 2921.	1.3	2
49426	Computational Insights into Alloying and Confinement Effects on Promoted Activity and Selectivity of C₂ Oxygenate over Rh-Based Catalysts. Journal of Physical Chemistry C, 0, , .	1.5	0
49427	First-principles study of the bandgap renormalization and optical property of Î²-LiGaO₂. Chinese Physics B, 2023, 32, 047101.	0.7	0
49428	Highly active cobalt-free perovskites with Bi doping as bifunctional oxygen electrodes for solid oxide cells. Chemical Engineering Journal, 2023, 461, 142051.	6.6	8
49429	Understanding formation of the InPd₃polymorphs: a DFT study. Zeitschrift Fur Naturforschung - Section B Journal of Chemical Sciences, 2023, 78, 355-361.	0.3	1
49430	Two-Dimensional Ultrahigh Unconventional Piezoelectricity Driven by Charge Screening. Journal of Physical Chemistry Letters, 2023, 14, 3430-3435.	2.1	0
49431	Gate switchable spin-orbit splitting in a <mml:math xmlns:mml="http://www.w3.org/1998/Math/MathML"><mml:mrow><mml:msub><mml:mi>MoTe</mml:mi><mml:mn>2</mml:mn></mml:msub></mml:mrow></mml:math> heterostructure from first-principles calculations. Physical Review B, 2023, 107, .	3.7	0
49432	Investigation of the electronic, optical, elastic, mechanical and vibrational properties of CuI using HSE03. Modern Physics Letters B, 0, , .	1.0	0
49433	Enhanced Durability of Automotive Fuel Cells via Selectivity Implementation by Hydrogen Spillover on the Electrocatalyst Surface. ACS Energy Letters, 2023, 8, 2201-2213.	8.8	7
49434	Chemistry of the Interaction and Retention of Tc^{VII} and Tc^{IV} Species at the Fe₃O₄(001) Surface. Journal of Physical Chemistry C, 0, , .	1.5	0
49435	Influence of Mo Doping on Electronic and Magnetic Properties of Monolayer CrX₃: A First-Principles Study. ECS Journal of Solid State Science and Technology, 2023, 12, 043001.	0.9	0

#	Article	IF	Citations
49436	Magnetic Heating Amorphous NiFe Hydroxide Nanosheets Encapsulated Ni Nanoparticles@Wood Carbon to Boost Oxygen Evolution Reaction Activity. Small, 2023, 19, .	5.2	5
49437	Enhancing the accuracy of density functional tight binding models through ChIMES many-body interaction potentials. Journal of Chemical Physics, 2023, 158, .	1.2	3
49438	DFT Study of CO2 Reduction Reaction to CH3OH on Low-Index Cu Surfaces. Catalysts, 2023, 13, 722.	1.6	3
49439	Predicted the structural diversity and electronic properties of Ptâ¯N compounds under high pressure. Journal of Physics Condensed Matter, 2023, 35, 285501.	0.7	0
49440	Regulating the Anion Redox and Suppressing the Structural Distortion of Cation-Disordered Rock-Salt Cathode Materials to Improve Cycling Durability through Chlorine Substitution. ACS Applied Materials & Interfaces, 2023, 15, 17938-17946.	4.0	3
49441	Nanostructured conversion-type anode materials of metal-organic framework-derived spinel XMn2O4 (XÂ=ÂZn, Co, Cu, Ni) to boost lithium storage. Journal of Colloid and Interface Science, 2023, 643, 502-515.	5.0	1
49442	Deforming lanthanum trihydride for superionic conduction. Nature, 2023, 616, 73-76.	13.7	12
49443	Can NbO Keep nbo Topology under Electrons? â€“Unveiling Novel Aspects of Niobium Monoxide at Atomic Scale. Chemistry - A European Journal, 0, , .	1.7	1
49444	Stability and Thermoelectric Properties of FeZrTe Alloy. Journal of Electronic Materials, 0, , .	1.0	0
49445	High-throughput exploration of the WMoVTaNbAl refractory multi-principal-element alloys under multiple-property constraints. Acta Materialia, 2023, 248, 118784.	3.8	13
49446	In-situ construction of hierarchical 2D MoS2/1D Te hybrid for supercapacitor applications. Journal of Energy Storage, 2023, 60, 106703.	3.9	9
49447	Role of spinâ€“orbit coupling on the physical properties of APb<mml:math xmlns:mml="http://www.w3.org/1998/Math/MathML" altimg="si61.svg" display="inline" id="d1e1640"><mml:msub><mml:mrow /><mml:mrow><mml:mn>3</mml:mn></mml:mrow></mml:msub></mml:math> (A = Na, Ca, Y, and Th) superconductors. Physica C: Superconductivity and Its Applications, 2023, 608, 1354250.	0.6	1
49448	Unconstrained Machine Learning Screening for New Liâ€ion Cathode Materials Enhanced by Class Balancing. Advanced Theory and Simulations, 0, , .	1.3	1
49449	The effect of alkyl chain length on imidazole chloroaluminate ionic liquid/Pt(1 1 1) interface and aluminum deposition: A DFT-D3 study. Chemical Physics, 2023, 568, 111842.	0.9	1
49450	Investigation of Structural, Mechanical, DynamicStability and Electronic Properties of Anti-perovskiteNitrides ANLa3 (A=Al, Ga): A DFT and DFPT Studies. Physica Scripta, 0, , .	1.2	0
49451	Energetic and configurational mechanisms to facilitate mica nanosheets synthesis by organo-ammonium cation intercalation. Computational Materials Science, 2023, 224, 112162.	1.4	1
49452	Cluster structure of doped atoms and elastic properties in Î³-Ni by first-principles calculations. Computational Materials Science, 2023, 224, 112183.	1.4	0
49453	Promising high temperature thermoelectric performance of layered oxypnictide YZnAsO. Physica B: Condensed Matter, 2023, 657, 414811.	1.3	0

#	Article	IF	Citations
49454	Magnetic and transport properties of two-dimensional ferromagnet VSe2 with Se vacancies. Journal of Magnetism and Magnetic Materials, 2023, 574, 170683.	1.0	2
49455	Strain induced effects on the electronic and phononic properties of 2H and 1T<mml:math xmlns:mml="http://www.w3.org/1998/Math/MathML" altimg="si11.svg" display="inline" id="d1e274"><mml:msup><mml:mrow /><mml:mrow><mml:mo>â€²</mml:mo></mml:mrow></mml:msup></mml:math> monolayer MoS2. Physica B: Condensed Matter, 2023, 655, 414701.	1.3	3
49456	Vacancy defects in nitrogen doped diamond. Physica B: Condensed Matter, 2023, 655, 414769.	1.3	0
49457	Hierarchical 2D MnO2@1D mesoporous NiTiO3 core-shell hybrid structures for high-performance supercapattery electrodes: Theoretical and experimental investigations. Journal of Electroanalytical Chemistry, 2023, 936, 117359.	1.9	10
49458	Optimizing CO2RR selectivity on single atom catalysts using graphical construction and identification of energy descriptor. Carbon, 2023, 208, 330-337.	5.4	9
49459	Evaluating residual stresses in compositionally graded TiN films via ab initio and Rietveld simulation. Materialia, 2023, 28, 101715.	1.3	0
49460	Ion kinetic energy- and ion flux-dependent mechanical properties and thermal stability of (Ti,Al)N thin films. Acta Materialia, 2023, 250, 118864.	3.8	9
49461	Magnetic, optoelectronic, and rietveld refined structural properties of Al3+ substituted nanocrystalline Ni-Cu spinel ferrites: An experimental and DFT based study. Journal of Magnetism and Magnetic Materials, 2023, 573, 170675.	1.0	7
49462	First principles insights on the structural, mechanical, dynamical, thermoelectric and thermodynamics properties of novel topological (ScSb) semi-metal. Materials Science and Engineering B: Solid-State Materials for Advanced Technology, 2023, 291, 116372.	1.7	9
49463	Mechanism of sulfur poisoning to Ru-based catalysts in supercritical water gasification of glycerol: From experiment to combined DFT and kinetics studies. Chemical Engineering Journal, 2023, 464, 142622.	6.6	4
49464	Room-temperature deformation of single crystals of the sigma-phase compound FeCr with the tetragonal D8b structure investigated by micropillar compression. Acta Materialia, 2023, 249, 118829.	3.8	5
49465	Influence of Indium addition on microstructural and mechanical behavior of Sn solder alloys: Experiments and first principles calculations. Acta Materialia, 2023, 249, 118853.	3.8	11
49466	The interplay between solute atoms and vacancy clusters in magnesium alloys. Acta Materialia, 2023, 249, 118805.	3.8	4
49467	Phosphoric acid resistance PtCu/C oxygen reduction reaction electrocatalyst for HT-PEMFCs: A theoretical and experimental study. Applied Surface Science, 2023, 619, 156663.	3.1	7
49468	Transfer learning aided high-throughput computational design of oxygen evolution reaction catalysts in acid conditions. Journal of Energy Chemistry, 2023, 80, 744-757.	7.1	7
49469	First-principles calculation and experimental study of mixed crystal Tm:(LuxY1-x)3AG. Infrared Physics and Technology, 2023, 130, 104588.	1.3	2
49470	First-principles study of the native defects with charge states in ZrSe<mml:math xmlns:mml="http://www.w3.org/1998/Math/MathML" altimg="si10.svg" display="inline" id="d1e937"><mml:msub><mml:mrow /><mml:mrow><mml:mn>2</mml:mn></mml:mrow></mml:msub></mml:math>. Solid State Communications, 2023, 365, 115138.	0.9	2
49471	Efficient catalytic oxidation of chlorinated volatile organic compounds over RuO2-WOx/Sn0.2Ti0.8O2 catalysts: Insight into the Cl poisoning mechanism of acid sites. Chemical Engineering Journal, 2023, 464, 142471.	6.6	5

#	Article	IF	Citations
49472	Four superhard tetragonal carbon allotropes: First-principles calculations. Diamond and Related Materials, 2023, 135, 109854.	1.8	7
49473	Adjacent diatomic Cu1N3/Mo1S2 entities decorated carbon nitride for markedly enhanced photocatalytic hydrogen generation. Chemical Engineering Journal, 2023, 463, 142470.	6.6	2
49474	Pressure dependent electronic, spintronic, optical and mechanical properties of equiatomic quaternary Heusler alloys NbMnVAl and NbFeCrAl. Physica B: Condensed Matter, 2023, 657, 414787.	1.3	3
49475	Chemically modified graphene sheets as potential sensors for organophosphate compounds(pesticide): A DFT study. Applied Surface Science, 2023, 619, 156745.	3.1	4
49476	Prediction of mechanical properties of AlTiCrVNb high entropy alloys with B2 ordered structure. Journal of Materials Research and Technology, 2023, 24, 440-448.	2.6	2
49477	One-dimensional 3d-TMâ€“solophene polymers as high-activity singleâ€atom catalysts for CO oxidation. Applied Surface Science, 2023, 618, 156680.	3.1	1
49478	Oxygen Reduction and Hydrogen Evolution Reactions on Zigzag ReS2 Nanoribbons. Applied Surface Science, 2023, 618, 156677.	3.1	1
49479	Monolayer black phosphorus: Tunable band gap and optical properties. Physica B: Condensed Matter, 2023, 657, 414780.	1.3	4
49480	Synergistic effects of Ta and Mo on the hydrogen embrittlement resistance in ultra-high strength hot stamping steel. Materials Science & Engineering A: Structural Materials: Properties, Microstructure and Processing, 2023, 872, 144956.	2.6	5
49481	Al2O3/ZnO composite-based sensors for battery safety applications: An experimental and theoretical investigation. Nano Energy, 2023, 109, 108301.	8.2	8
49482	Understanding electron transport on hybrid perovskite/carbon allotropes for energy conversion and storage applications: A first principles study. Solar Energy, 2023, 255, 180-190.	2.9	0
49483	Theoretical studies of sliding ferroelectricity, magnetoelectric couplings, and piezo-multiferroicity in two-dimensional magnetic materials. Chemical Physics Letters, 2023, 818, 140430.	1.2	8
49484	Prediction of new stable crystal structures for ternary ErAgTe2 and YAgTe2 semiconductors: Ab initio study. Solid State Sciences, 2023, 139, 107160.	1.5	1
49485	Water-induced synthesis of Pd nanotetrahedrons on g-C3N4 for highly efficient hydrogenation of nitroaromatic. Colloids and Surfaces A: Physicochemical and Engineering Aspects, 2023, 665, 131201.	2.3	2
49486	Compatibility of DFT+U with non-collinear magnetism and spin-orbit coupling within a framework of numerical atomic orbitals. Computer Physics Communications, 2023, 286, 108684.	3.0	1
49487	Two-dimensional BAs/GeC van der waals heterostructures: A widely tunable photocatalyst for water splitting and hydrogen production. Journal of Physics and Chemistry of Solids, 2023, 176, 111263.	1.9	11
49488	Syngas-to-C2 oxygenates over the inverse Mo6C4/Cu catalyst: Identifying the role of synergistic effect. Applied Surface Science, 2023, 619, 156746.	3.1	0
49489	Dynamics of palladium single-atoms on graphitic carbon nitride during ethylene hydrogenation. Journal of Catalysis, 2023, 421, 134-144.	3.1	0

#	Article	IF	Citations
49490	Theoretical insights into the removal pathways of adsorbed oxygen on the surface of Ï‡-Fe5C2(5 1 0). Chemical Engineering Science, 2023, 271, 118576.	1.9	4
49491	An exceptionally strong, ductile and impurity-tolerant austenitic stainless steel prepared by laser additive manufacturing. Acta Materialia, 2023, 250, 118868.	3.8	4
49492	Efficient discovery of room temperature magnetic transition metal monolayers assisted by artificial neural network. Computational Materials Science, 2023, 224, 112166.	1.4	3
49493	Density functional theory studies of Pt2Ga and Pd2Ga monolayers as multifunctional electrocatalytic materials. Computational Materials Science, 2023, 224, 112164.	1.4	0
49494	Stability, mechanical and electronic properties of Occ carbon allotropes: Four new tetragonal 3D superhard carbon crystals. Diamond and Related Materials, 2023, 135, 109838.	1.8	5
49495	Equilibrium fractionation of REE isotopes in nature: Insights from NRIXS and DFT+U studies of Eu and Dy phonon density of states. Geochimica Et Cosmochimica Acta, 2023, 348, 323-339.	1.6	5
49496	Tuning the UV absorbing ability of CeO2 nanoparticles with Fâ˜' doping. FlatChem, 2023, 39, 100494.	2.8	6
49497	Surface alloy with sulfur leading piezoelectricity from non-piezoelectricity of pentagonal-PdPSe. Journal of Alloys and Compounds, 2023, 947, 169640.	2.8	3
49498	CO oxidation mechanism on surfaces of B-site doped SrFeO3--based perovskite materials for thermochemical water splitting. Computational and Theoretical Chemistry, 2023, 1224, 114109.	1.1	0
49499	Indirect interactions between the ionic liquid and Cu surface in 0.5ÂM HCl: a novel mechanism explaining cathodic corrosion inhibition. Corrosion Science, 2023, 216, 111100.	3.0	12
49500	Dual MOF-derived Fe/N/P-tridoped carbon nanotube as high-performance oxygen reduction catalysts for zinc-air batteries. Applied Catalysis B: Environmental, 2023, 327, 122469.	10.8	58
49501	On the enhanced performance of Pt-based high-entropy alloys catalyst during waterâ€“gas shift reaction: A density functional theory study. Applied Surface Science, 2023, 623, 157023.	3.1	3
49502	Impact of aminosilane and silanol precursor structure on atomic layer deposition process. Applied Surface Science, 2023, 621, 156869.	3.1	1
49503	Half metallic Heusler alloys XMnGe (X = Ti, Zr, Hf) for spin flip and thermoelectric device application â€“ Material computations. Materials Science in Semiconductor Processing, 2023, 159, 107367.	1.9	7
49504	Defective 1TËŠ-MoX2 (XÂ=ÂS, Se, Te) monolayers for electrocatalytic ammonia synthesis: Steric and electronic effects on the catalytic activity. Fuel, 2023, 342, 127779.	3.4	1
49505	Phase transformation induced transitional twin boundary in body-centered cubic metals. Acta Materialia, 2023, 249, 118815.	3.8	10
49506	Structural and electrochemical analysis of Ni/NiO supercapacitor materials: A theoretical and experimental study. Solid State Ionics, 2023, 394, 116194.	1.3	1
49507	Predicting formation of chemically graded metal/ceramic interfaces. Computational Materials Science, 2023, 224, 112155.	1.4	0

#	Article	IF	Citations
49508	Theoretical insight on the electronic band structure, mechanical, vibrational and thermodynamic characteristic of antiperovskitesÂRE3InN (RE=Y and La). Materials Today Communications, 2023, 35, 105618.	0.9	12
49509	Structural and mechanical properties of Al/TiC interface with vacancies: First-principles study. Physics Letters, Section A: General, Atomic and Solid State Physics, 2023, 471, 128786.	0.9	1
49510	Interfacial properties of In-plane monolayer 2H-MoTe2/1T'-WTe2 heterostructures. Applied Surface Science, 2023, 623, 157022.	3.1	1
49511	Unraveling the role of defect types in Fe3O4 for efficient NIR-driven photocatalytic inactivation. Applied Surface Science, 2023, 622, 156860.	3.1	4
49512	Dehydroxylation of smectites from Nudged Elastic Band and Born-Oppenheimer Molecular Dynamics simulations. Applied Clay Science, 2023, 238, 106880.	2.6	0
49513	Stable single iron atom within two-dimensional porphyrin sheet catalysis for CO oxidation: A computational investigation. Fuel, 2023, 342, 127890.	3.4	17
49514	Through the Self-Optimization process to achieve high OER activity of SAC catalysts within the framework of TMO3@G and TMO4@G: A High-Throughput theoretical study. Journal of Colloid and Interface Science, 2023, 640, 405-414.	5.0	2
49515	A comparative study of cubic methylammonium lead iodide (CH3NH3PbI3) perovskite by using density functional theory. Materials Today Communications, 2023, 35, 105814.	0.9	1
49516	Effect of molybdenum disulfide doping with substitutional nitrogen and sulfur vacancies on lithium intercalation. Journal of Alloys and Compounds, 2023, 947, 169689.	2.8	5
49517	Efficient electrocatalysts of single metal atom supported on defective graphene for oxygen reduction reaction (ORR): A first principles study. Chemical Physics, 2023, 570, 111888.	0.9	2
49518	Synthesis of large-size bulk hierarchically graphene-structured porous carbon and its versatile applications as hosts of sulfur and lithium for Li-S full cells and electrocatalyst for water splitting. Journal of Alloys and Compounds, 2023, 947, 169587.	2.8	0
49519	Insight into the interfacial interactions of CO2 with PuH2 (100), (110), and (111) surfaces from first-principles calculations. Vacuum, 2023, 212, 112026.	1.6	0
49520	Construction of strong built-in electric field in binary metal sulfide heterojunction to propel high-loading lithium-sulfur batteries. Journal of Energy Chemistry, 2023, 81, 492-501.	7.1	10
49521	DFT based investigations for the structural and electronic properties of coved zigzag BP nanoribbons. Journal of Molecular Graphics and Modelling, 2023, 121, 108453.	1.3	0
49522	Calculation of tunable electronic and optical properties of AlP/InSe heterostructure based on first principles. Materials Science in Semiconductor Processing, 2023, 160, 107443.	1.9	0
49523	Red anatase TiO2 microspheres with exposed major {0 0 1} facets and boron-stabilized hydrogen-occupied oxygen vacancies for visible-light-responsive water oxidation. Journal of Colloid and Interface Science, 2023, 640, 211-219.	5.0	2
49524	Sb-doped Î²-SrZrS3 as a low-toxic and low-priced absorber for intermediate band solar cells: A first-principles investigation. Physica B: Condensed Matter, 2023, 658, 414839.	1.3	1
49525	The thermal and mechanical properties of Li-based Half Heusler alloys LiAlZ(Z = Si, Ge) using Quasi-Harmonic Approach. Computational Condensed Matter, 2023, 35, e00794.	0.9	5

#	Article	IF	Citations
49526	First-principles calculations to investigate electronic structure and optical spectra of CdxZn1-xS ternary semiconductor alloys. Chemical Physics Impact, 2023, 6, 100177.	1.7	0
49527	Effects of alloying elements on the interfacial segregation of bismuth in tin-based solders. Materials Today Communications, 2023, 35, 105713.	0.9	1
49528	Theoretical study on mechanical and electronic properties of ternary diborides Sc0.5V0.5B2, Sc0.5Nb0.5B2 and Sc0.5Ta0.5B2. Materials Today Communications, 2023, 35, 105760.	0.9	1
49529	The effects of mixing non-metal atoms in the B1 structured transition metal carbo-nitrides on their structure and mechanical properties: HfC1-N. Open Ceramics, 2023, 14, 100356.	1.0	0
49530	Cubic to pseudo-cubic tetragonal phase transformation with Mg, Ca, and Be doping and its impact on optoelectronic, elastic and mechanical properties of SrHfO3. Journal of Physics and Chemistry of Solids, 2023, 177, 111279.	1.9	0
49531	K2(H2O)WO3F2: A new nonlinear optical material with remarkable second-harmonic generation response and enhanced laser damage threshold. Journal of Alloys and Compounds, 2023, 945, 169288.	2.8	2
49532	TC++: First-principles calculation code for solids using the transcorrelated method. Computer Physics Communications, 2023, 287, 108687.	3.0	4
49533	Exploring the electronic and mechanical properties of lithium-decorated silicon carbide nanowires for energy storage. Journal of Energy Storage, 2023, 62, 106840.	3.9	5
49534	Ab initio study of electronic and magnetic properties of zigzag and armchair AlN nanosheets. Physica E: Low-Dimensional Systems and Nanostructures, 2023, 150, 115670.	1.3	2
49535	First-principles prediction of room-temperature half-metallicity in strain- and carrier-tunable monolayer Mn2Sn2Te6. Physica E: Low-Dimensional Systems and Nanostructures, 2023, 150, 115704.	1.3	1
49536	Probing temperature effects on the stacking fault energy of GH3536 superalloy using first-principles theory. Intermetallics, 2023, 157, 107882.	1.8	3
49537	First-principles studies the optical properties of defective-GQDs and -fullerene. Computational Condensed Matter, 2023, 35, e00793.	0.9	0
49538	A novel smart framework for sustainable nanocomposite electrolytes based on ionic liquids of dye-sensitized solar cells by a covalently multifunctional graphene oxide-vinyl imidazole/4-tert-butylpyridine cobalt complex. Journal of Alloys and Compounds, 2023, 945, 169241.	2.8	2
49539	Full-scale simulation and experimental verification of the phase-transition temperature of a VO2 nanofilm as smart window materials. Materials Today Communications, 2023, 35, 105758.	0.9	0
49540	Investigating the electronic, elastic, mechanical, anisotropic, and optical aspects of Sc2RuZ (Z: Al, Ga,) Tj ETQq0 0 0 rgBT /Overlock 10 T	1.3	2
49541	Computational screening of Ï‡3 borophene based single-atom catalysts for N2 reduction. Catalysis Today, 2023, 418, 114079.	2.2	4
49542	Visible light response in 2D QBi (Q=Si, Ge and Sn) monolayer semiconductors: A DFT based study. Materials Today Communications, 2023, 35, 105886.	0.9	0
49543	DFT and DFPT calculations of the structural, electronic, optical, vibrational and thermodynamic properties of silicon tetraborate. Computational Condensed Matter, 2023, 35, e00796.	0.9	4

#	Article	IF	Citations
49544	Surface Li effects on the electronic properties of GaAs nanowires: A first principles approach. Surfaces and Interfaces, 2023, 38, 102745.	1.5	1
49545	A theoretical benchmark for the electronic, optical, and thermoelectrical characteristics of bulk and monolayer BiS2. , 2023, 178, 207568.		2
49546	Manipulation of contact type in MoSSe/Ti3C2 heterostructures via the functionalization of chalcogens and halogens. Surfaces and Interfaces, 2023, 38, 102855.	1.5	0
49547	Synthesize, construction and enhanced performance of Bi2WO6/ZnS heterojunction under visible light: Experimental and DFT study. Arabian Journal of Chemistry, 2023, 16, 104760.	2.3	3
49548	On ionic transport through pores in a boropheneâ€“graphene membrane. Materials Today Chemistry, 2023, 30, 101512.	1.7	2
49549	Electronic structure and carrier mobility of BC6N/BN van der Waals heterostructure induced by in-plane strains. Applied Surface Science, 2023, 623, 157007.	3.1	11
49550	1D/2D CdS/WS2 heterojunction photocatalyst: First-principles insights for hydrogen production. Materials Today Communications, 2023, 35, 105991.	0.9	2
49551	Copper decorated graphyne as a promising nanocarrier for cisplatin anti-cancer drug: A DFT study. Applied Surface Science, 2023, 622, 156885.	3.1	4
49552	Thermodynamic assessment of the ternary Niâ€“Ti-Hf system. Calphad: Computer Coupling of Phase Diagrams and Thermochemistry, 2023, 81, 102546.	0.7	0
49553	Biaxial strain tunable electronic properties, photocatalytic properties and quantum capacitance of Sc2CO2 MXenes. Vacuum, 2023, 212, 112016.	1.6	7
49554	Metal-free single atom catalysts towards efficient acetonitrile reduction to ethylamine. Applied Surface Science, 2023, 622, 156891.	3.1	1
49555	Theoretical investigation of the V2BX2 (XÂ=ÂS, Se, and Te) monolayers as anode materials for Na-ion batteries. Materials Today Communications, 2023, 35, 105923.	0.9	0
49556	Anchored Coâ€“oxo generated by cobalt single atoms outperformed aqueous species from the counterparts in peroxymonosulfate treatment. Applied Catalysis B: Environmental, 2023, 328, 122483.	10.8	6
49557	Computational evaluation of sensing properties of a novel 2D diboron dinitride for detecting toxic gas molecules. Materials Science in Semiconductor Processing, 2023, 161, 107446.	1.9	2
49558	Cubic and tetragonal phases competition of magnetic RuVZ(Si;Ge) Heusler compounds: ab initio investigation. Solid State Communications, 2023, 366-367, 115161.	0.9	1
49559	Structural, mechanical and electronic properties of orthorhombic Nb2X4Si5 (X=V, Nb, Ta, Cr, Mo, W) compounds from first-principles calculations. Computational Condensed Matter, 2023, 35, e00792.	0.9	1
49560	Crystal structure modulation of SnSe thermoelectric material by AgBiSe2 solid solution. Journal of the European Ceramic Society, 2023, 43, 3383-3389.	2.8	6
49561	Theoretical and mechanistic insights into control factor-assisted CO2 mineralization with olivine. Journal of Industrial and Engineering Chemistry, 2023, 122, 241-250.	2.9	0

#	Article	IF	Citations
49562	Anharmonic phonons in binary compounds <mml:math xmlns:mml="http://www.w3.org/1998/Math/MathML" altimg="si17.svg" display="inline" id="d1e1274"><mml:mi>A</mml:mi></mml:math>Bi (<mml:math xmlns:mml="http://www.w3.org/1998/Math/MathML" altimg="si12.svg" display="inline" id="d1e1285"><mml:msub><mml:mrow /><mml:mrow><mml:mn>1</mml:mn></mml:mrow></mml:msub></	0.9	3
49563	Unraveling the role of Fe5C2 in CH4 formation during CO2 hydrogenation over hydrophobic iron catalysts. Applied Catalysis B: Environmental, 2023, 327, 122449.	10.8	7
49564	Ti-decorated nitrogen-rich BeN4 monolayer for reversible hydrogen storage: DFT investigations. Applied Surface Science, 2023, 622, 156806.	3.1	6
49565	New insights into the co-adsorption behavior of H2O and H2 on defective PuH2 (100), (110), and (111) surfaces from first-principles study. Vacuum, 2023, 212, 112044.	1.6	1
49566	Zn-doped nickel iron (oxy)hydroxide nanocubes passivated by polyanions with high catalytic activity and corrosion resistance for seawater oxidation. Journal of Energy Chemistry, 2023, 81, 82-92.	7.1	6
49567	Prediction of novel final phases in aged uranium-niobium alloys. Journal of Nuclear Materials, 2023, 579, 154394.	1.3	2
49568	Investigating the effect of Al, Mo or Mn addition to CoCrFeNi entropy alloys on the interface binding properties of WC/HEA cemented carbides. Materials Today Communications, 2023, 35, 105891.	0.9	3
49569	Theoretical study on structural transformation and mechanical properties of Ni3Ti1-xNbx. Results in Materials, 2023, 18, 100387.	0.9	0
49570	First-principles study of Xe behavior in Î´-UZr2. Journal of Nuclear Materials, 2023, 579, 154387.	1.3	1
49571	First-principles study on electronic and optical properties of Cu<mml:math xmlns:mml="http://www.w3.org/1998/Math/MathML" altimg="si1.svg"><mml:msub><mml:mrow /><mml:mn>2</mml:mn></mml:msub></mml:math>CoGeS<mml:math xmlns:mml="http://www.w3.org/1998/Math/MathML" altimg="si33.svg"><mml:msub><mml:mrow /><mml:mn>4</mml:mn></mml:msub></mml:math> for photovoltaic conversion and photocatalytic applications. Materials Research Bulletin, 2023, 164, 112235.	2.7	4
49572	First-principles calculations to investigate structural, electronics, optical, and mechanical properties of Bi-based novel fluoroperovskites TBiF3 (T = Hg, Xe) for optoelectronic applications. Materials Science in Semiconductor Processing, 2023, 160, 107399.	1.9	13
49573	Probing the structural, electronic and optical properties of Cs2Ag1-xNaxInCl6 lead-free double perovskite from first principles. Journal of Solid State Chemistry, 2023, 322, 123913.	1.4	4
49574	CALPHAD aided mechanical properties screening in full composition space of NbC-TiC-VC-ZrC ultra-high temperature ceramics. International Journal of Refractory Metals and Hard Materials, 2023, 113, 106191.	1.7	3
49575	Two-dimensional van der Waals layered VSi2N4 as anode materials for alkali metal (Li, Na and K) ion batteries. Journal of Physics and Chemistry of Solids, 2023, 178, 111339.	1.9	3
49576	Elucidating the dissociative and associative mechanisms on the surface-anchored Fe3 cluster under the effect of external electric field. Applied Surface Science, 2023, 623, 157021.	3.1	1
49577	Atomistic mechanism of Î·â€™-to-Î· transformation in Al-Zn-Mg-Cu alloys. Scripta Materialia, 2023, 231, 115474.	2.6	6
49578	Significance of different dopamine species as reducing agents of graphene oxide: Fundamental aspects. Surface Science, 2023, 732, 122285.	0.8	1
49579	Defect engineered Janus MoSiGeN4 as highly efficient electrocatalyst for hydrogen evolution reaction. Applied Surface Science, 2023, 622, 156894.	3.1	9

#	Article	IF	Citations
49580	Study of the brittleness mechanism of aluminum/steel laser welded joints with copper and vanadium interlayers. Optics and Laser Technology, 2023, 163, 109319.	2.2	3
49581	Efficient biobased carboxylic acids synthesis by synergistic electrocatalysis of multi-active sites on bimetallic Cu-Co oxide/oxyhydroxide. Applied Catalysis B: Environmental, 2023, 331, 122709.	10.8	8
49582	Dual functional effect of oxygen vacancies and depolarity shield embedded NiCo2O4 cathode in lithium sulfur battery. Applied Surface Science, 2023, 622, 156939.	3.1	3
49583	T-BN nanosheets as High-capacity anode for Li- and Na-Ion Batteries: An ab initio study. Computational and Theoretical Chemistry, 2023, 1224, 114105.	1.1	1
49584	Data-driven design of Ni-based turbine disc superalloys to improve yield strength. Journal of Materials Science and Technology, 2023, 155, 175-191.	5.6	4
49585	Influence of Pt or Au doping on improving the detection of CO by ZnO: A first-principles calculations study. Chemical Physics, 2023, 570, 111908.	0.9	0
49586	Atomic-scale engineering of cation vacancies in two-dimensional unilamellar metal oxide nanosheets for electricity generation from water evaporation. Nano Energy, 2023, 110, 108348.	8.2	8
49587	Multi-functional lead-free Ba2XSbO6 (XÂ=ÂAl, Ga) double perovskites with direct bandgaps for photocatalytic and thermoelectric applications: A first principles study. Materials Today Communications, 2023, 35, 105617.	0.9	6
49588	Unexpectedly spontaneous water dissociation on graphene oxide supported by copper substrate. Journal of Colloid and Interface Science, 2023, 642, 112-119.	5.0	3
49589	A revisit to the role of Mo in an MP35N superalloy: An experimental and theoretical study. Journal of Materials Science and Technology, 2023, 157, 60-70.	5.6	2
49590	Length-dependent high-frequency response of aromatic and aliphatic molecules: predictions from first-principles calculations. Journal of Physics and Chemistry of Solids, 2023, 178, 111343.	1.9	3
49591	Computational investigation on CO2 capturing capacity of N-doped and Na-decorated Graphdiyne. Fuel, 2023, 345, 128169.	3.4	3
49592	Unravelling the role of metal-metal oxide interfaces of Cu/ZnO/ZrO2/Al2O3 catalyst for methanol synthesis from CO2: Insights from experiments and DFT-based microkinetic modeling. Applied Catalysis B: Environmental, 2023, 332, 122743.	10.8	8
49593	New Janus structure photocatalyst having widely tunable electronic and optical properties with strain engineering. Journal of Materials Science and Technology, 2023, 155, 142-147.	5.6	4
49594	Evaluating the potential of planar h-BSb monolayer as anode materials for sodium-ion batteries from first principles methods. Journal of Energy Storage, 2023, 64, 107260.	3.9	4
49595	Unusual mechanical properties of CO2â€“V: Auxetic potential in a high-pressure polymorph of carbon dioxide. Journal of Physics and Chemistry of Solids, 2023, 178, 111349.	1.9	0
49596	Nonlinear optical crystals KPb3(3-C5H4NCOO)2Br5 and KPb3(3-C5H4NCOO)2Cl3Br2 with new Pb-centered nitrogen-halide polyhedrons obtained by the halide anionic substitution. Journal of Alloys and Compounds, 2023, 951, 169945.	2.8	0
49597	Observation of low thermal expansion behavior and weak thermal anisotropy in M3A2C phases. Journal of Materials Science and Technology, 2023, 154, 210-216.	5.6	2

#	Article	IF	Citations
49598	Electronic structure and oxygen vacancy tuning of Co & Ni co-doped W18O49 nanourchins for efficient TEA gas sensing. Chemical Engineering Journal, 2023, 465, 142815.	6.6	16
49599	Cu4@C2N for effective electrochemical CO2 reduction and intermediates dependent adsorption behaviours: A computational study. Applied Surface Science, 2023, 626, 157126.	3.1	4
49600	Experimental and computational study on the C15 phase structure stability of Y Ni2-Mn system. Journal of Alloys and Compounds, 2023, 952, 169632.	2.8	1
49601	Design, synthesis and investigating the interaction of novel s-triazine collector with pyrite surface: A DFT-D3+U and experimental studies. Surfaces and Interfaces, 2023, 38, 102820.	1.5	1
49602	Introducing dual metal centers in high purity pyrrolic-N for superior oxygen reduction reaction. Carbon, 2023, 209, 118031.	5.4	5
49603	Low-temperature phase transitions and reorientational dynamics studied by 11B NMR in glassy crystal ortho-carborane. Journal of Non-Crystalline Solids: X, 2023, 18, 100180.	0.5	0
49604	Infrared and Raman vibrational modelling of Î²-C2S and C3S compounds. Cement and Concrete Research, 2023, 169, 107162.	4.6	7
49605	Understanding ZnO surface defects from first-principles simulation. Surface Science, 2023, 732, 122272.	0.8	1
49606	Comparative study of the structural, mechanical, electronic, optical and thermodynamic properties of superconducting disilicide YT2Si2 (T=Co, Ni, Ru, Rh, Pd, Ir) by DFT simulation. Journal of Physics and Chemistry of Solids, 2023, 178, 111342.	1.9	4
49607	Electronic excitation induced non-thermal phase transition of tungsten. Journal of Alloys and Compounds, 2023, 952, 170087.	2.8	1
49608	The electronic, optical, and vibrational properties of Ag₃X (X = S, Se) with density functional theory. Modern Physics Letters B, 0, , .	1.0	0
49609	Structural and electronic properties of hexagonal MXH (M = C, Si, Ge and Sn; X = N, P, As and Sb) monolayers: A first-principles prediction. Physica E: Low-Dimensional Systems and Nanostructures, 2023, 151, 115710.	1.3	3
49610	First-principles prediction of electronic, optical, and thermodynamic properties of c-TiAl3 with M doping (Mâ€‰=â€‰V, Nb, Ta). Indian Journal of Physics, 0, , .	0.9	0
49611	Rational design of heterogenized molecular phthalocyanine hybrid single-atom electrocatalyst towards two-electron oxygen reduction. Nature Communications, 2023, 14, .	5.8	36
49612	Influence of phosphorus-doped bilayer graphene configuration on the oxygen reduction reaction in acidic solution. Carbon, 2023, 210, 118012.	5.4	0
49613	Structural arrangement and improved thermoelectric figure of merit in hexagonal SiX(X=N,P,As,Sb,Bi) monolayers: understanding from first-principles calculations. Journal Physics D: Applied Physics, 0, , .	1.3	0
49614	Adsorption effects and mechanisms of phosphorus by nanosized laponite. Chemosphere, 2023, 331, 138684.	4.2	7
49615	Hydrogen Absorption Performance and O2 Poisoning Resistance of Pd/ZrCo Composite Film. Materials, 2023, 16, 3159.	1.3	0

#	Article	IF	Citations
49616	Ab-Initio Calculation of the Electrical Conductivity, Optical Absorption, and Reflectivity of the 2D Materials SnC and NbC. Crystals, 2023, 13, 682.	1.0	1
49617	[illegible] monolayer X<mml:math xmlns:mml="http://www.w3.org/1998/Math/MathML" altimg="si86.svg" display="inline" id="d1e657"><mml:msub><mml:mrow /><mml:mrow><mml:mn>3</mml:mn></mml:mrow></mml:msub></mml:math>YZ<mml:math xmlns:mml="http://www.w3.org/1998/Math/MathML" altimg="si87.svg" display="inline" id="d1e665"><mml:msub><mml:mrow />	1.3	0
49618	Combining Theoretical and Experimental Methods to Probe Confinement within Microporous Solid Acid Catalysts for Alcohol Dehydration. ACS Catalysis, 2023, 13, 5955-5968.	5.5	4
49619	Removal of Pb ions using green Co3O4 nanoparticles: Simulation, modeling, adsorption, and biological studies. Environmental Research, 2023, 222, 115335.	3.7	12
49620	Comparison of adsorption capacity of water and hydroxide with collector reagents on geversite (PtSb2) mineral surface: A DFT-D insights. Computational Materials Science, 2023, 224, 112174.	1.4	3
49621	A theoretical study of the functionalized carbon dots surfaces binding with silver nanostructures. Computational and Theoretical Chemistry, 2023, 1223, 114087.	1.1	1
49622	Density Functional Theory Studies of the Direct Conversion of Methane to Methanol Using O₂ on Graphitic MN₄G-BN (M = Fe, Co, Cu) and CuN₄G-PN Single-Atom Catalysts. ACS Applied Nano Materials, 0, , .	2.4	3
49623	Synergistic double-atom catalysts of metal-boron anchored on g-C2N for electrochemical nitrogen reduction: Mechanistic insight and catalyst screening. Journal of Energy Chemistry, 2023, 80, 350-360.	7.1	13
49624	Structural parameters, electronic structure and linear optical functions of LuXCo2Sb2 (X = V, Nb and) Tj ETQq0 0 0 rgBT /Overlock 10 Tf	1.3	12
49625	Unveiling load carriers between nanoparticles capable of passing through a glassy disordered phase: A theoretical multiscale analysis. Acta Materialia, 2023, 252, 118950.	3.8	2
49626	Understanding the hydrogen evolution reaction activity of doped single-atom catalysts on two-dimensional GaPS4 by DFT and machine learning. Journal of Energy Chemistry, 2023, 81, 93-100.	7.1	17
49627	Electronic structure, phonon stability, mechanical and high-temperature thermoelectric properties of Li-based quaternary Heusler alloys. Current Applied Physics, 2023, 50, 161-167.	1.1	2
49628	Computational design of one FeCoNiCuZn high-entropy alloy for high-performance electrocatalytic nitrate reduction. Applied Surface Science, 2023, 626, 157246.	3.1	2
49629	Confined MoS2 nanosheets grown on 3D interconnected N, S co-doped carbon nanofibers as a free-standing anode for sodium-ion batteries. Journal of Solid State Chemistry, 2023, 323, 124046.	1.4	0
49630	When carbon impurities trigger the synthesis of alpha boron at high pressure and high temperature. Acta Materialia, 2023, 249, 118820.	3.8	1
49631	Strain driven anomalous anisotropic enhancement in the thermoelectric performance of monolayer MoS2. Applied Surface Science, 2023, 626, 157139.	3.1	12
49632	First principles analysis on void-reduction mechanism and impact of oxygen in nitrogen-doped CZ-Si crystal. Journal of Crystal Growth, 2023, 610, 127176.	0.7	2
49633	A computational study of adsorption of H2S and SO2 on the activated carbon surfaces. Journal of Molecular Graphics and Modelling, 2023, 122, 108463.	1.3	2

#	Article	IF	Citations
49634	Chemical and interfacial design in the visible-light-absorbing ferroelectric thin films. Journal of the European Ceramic Society, 2023, 43, 3275-3288.	2.8	1
49635	Coordination-number-determined activity of copper catalyst in water-gas shift reaction. Fuel, 2023, 343, 127850.	3.4	3
49636	Investigation on the photocatalytic property of direct Z-type van der Waals g-C3N4/AlN heterojunction and its mechanism. Chemical Physics, 2023, 571, 111913.	0.9	5
49637	Revealing the effects of transition metal doping on CoSe cocatalyst for enhancing photocatalytic H2 production. Applied Catalysis B: Environmental, 2023, 328, 122503.	10.8	24
49638	Preventing H2S poisoning of dense Pd membranes for H2 purification using an electric-field: An Ab initio study. Surface Science, 2023, 733, 122303.	0.8	2
49639	Reactivity of diamanes against oxidation: A DFT study. Chemical Physics, 2023, 571, 111916.	0.9	1
49640	Atomistic insight into impact of solute segregation on Î±-Mg/FCC-Al2Ca interface stability. Journal of Alloys and Compounds, 2023, 948, 169766.	2.8	0
49641	A new carbon allotrope: Biphenylene as promising anode materials for Li-ion and Li O2 batteries. Solid State Ionics, 2023, 395, 116214.	1.3	3
49642	Probing structural, optical and magnetic properties of Sm-doped ZnO nanomaterials via experimental and DFT approach: Enhanced photocatalytic degradation and antibacterial performance. Colloids and Surfaces A: Physicochemical and Engineering Aspects, 2023, 668, 131470.	2.3	8
49643	Electronic structure and magnetic properties of YXâ€²CrZ (Xâ€²â€‰=â€‰Fe, Co, Ni; Zâ€‰=â€‰Al,Ga, In) quaternary Heusler alloys. Indian Journal of Physics, 2023, 97, 733-749.	0.9	4
49645	Fabrication and characterization of PEG-In2O3 modified PbO2 anode for electrochemical degradation of metronidazole. Electrochimica Acta, 2023, 442, 141919.	2.6	1
49646	Revealing the bifunction mechanism of LaCoO3 as electrocatalyst: Oxygen vacancies effect and synergistic reaction process. Journal of Alloys and Compounds, 2023, 941, 168918.	2.8	3
49647	Optoelectronic properties of Portulacaxanthin III (PXIII), GQD/Os-GQD-PXIII nanocomposites, and their coupling with photoanode in dye-sensitized solar cells: Molecular and periodic DFT calculations. Optik, 2023, 274, 170591.	1.4	1
49648	First-principles calculations to investigate mechanical, electronic, optical, and thermodynamic properties of Zr-based ternary compounds. Journal of Materials Research and Technology, 2023, 23, 1417-1434.	2.6	0
49649	Unveiling the synergistic effects of Re-Mo alloying on diffusion behaviors in Î³-Ni: From a theoretical perspective. Journal of Materials Research and Technology, 2023, 23, 1214-1224.	2.6	3
49650	First-principles assessment of chemical lithiation of sulfide solid electrolytes and its impact on their transport, electronic and mechanical properties. Journal of Power Sources, 2023, 560, 232689.	4.0	4
49651	Saturation magnetisation as an indicator of the disintegration of barium hexaferrite nanoplatelets during the surface functionalisation. Scientific Reports, 2023, 13, .	1.6	2
49652	Dynamic investigations on hydrogenâ€“helium interaction around the vacancy in BCC iron from ab-initio calculations. Nuclear Fusion, 2023, 63, 046005.	1.6	2

#	Article	IF	Citations
49653	Possible Raman signature of broken symmetry states near the quantum critical point in P doped BaFe<mml:math xmlns:mml="http://www.w3.org/1998/Math/MathML" altimg="si121.svg" display="inline" id="d1e426"><mml:msub><mml:mrow /><mml:mrow><mml:mn>2</mml:mn></mml:mrow></mml:msub></mml:math>As<mml:math xmlns:mml="http://www.w3.org/1998/Math/MathML" altimg="si121.svg" display="inline" id="d1e434"><mml:msub><mml:mrow /><mml:mrow><mml:mn>2</mml:mn></mml:mrow></mml:msub></	0.6	2
49654	Theoretical study on the influence of the extra N in transition metal-N4 embedded graphene as efficient CO2 reduction catalysts. Applied Surface Science, 2023, 616, 156494.	3.1	1
49655	Electronic properties and photon scattering of buckled and planar few-layer 2D GaN. Vacuum, 2023, 210, 111861.	1.6	10
49656	The interaction of oxygen with the Î³-U (001) and (110) surfaces: An ab initio study. Computational Materials Science, 2023, 219, 112025.	1.4	2
49657	Computational studies for boosting nitrate electroreduction activity of Fe-N4-C Single-Atom catalyst via axial fifth ligand. Applied Surface Science, 2023, 616, 156440.	3.1	6
49658	Tunable local piezopotential properties of zinc oxide nanowires grown by remote epitaxy. Materials Science in Semiconductor Processing, 2023, 157, 107345.	1.9	0
49659	Thickness-dependent oxygen chemisorption behaviors on (1 1 1) surfaces of two-dimensional FCC metals Al and Cu: First-principles study. Computational Materials Science, 2023, 219, 112022.	1.4	1
49660	First principle calculation of structural, electronic, magnetic, and elastic properties of ferromagnetic Cu2MnZ (Z = Pb, P, As, Bi, S, Se, and Te) Heusler alloys. Physica B: Condensed Matter, 2023, 653, 414673.	1.3	3
49661	Enhancement of the magnetic and mechanical properties by introducing element carbon for Ti-based alloy. Journal of Magnetism and Magnetic Materials, 2023, 568, 170438.	1.0	2
49662	Enhanced free-exciton luminescence in Cs2SnBr6â^'I : A first-principles study. Chemical Engineering Journal, 2023, 458, 141533.	6.6	3
49663	Structural features, thermal stability and catalytic implication of Feâ€“Ni nanoparticles. Journal of Solid State Chemistry, 2023, 320, 123863.	1.4	1
49664	Atomistic mechanism of high ionic conductivity in lithium ytterbium-based halide solid electrolytes: A first-principles study. Journal of Rare Earths, 2024, 42, 155-162.	2.5	1
49665	First-principles insights into sulfur oxides (SO2 and SO3) adsorption and dissociation on layered iron sulfide (FeS) catalyst. Materials Today Communications, 2023, 34, 105452.	0.9	0
49666	The effect of the spin-orbit coupling on the physical properties of SrGa<mml:math xmlns:mml="http://www.w3.org/1998/Math/MathML" altimg="si84.svg" display="inline" id="d1e1413"><mml:msub><mml:mrow /><mml:mrow><mml:mn>3</mml:mn></mml:mrow></mml:msub></mml:math> and LuGa<mml:math xmlns:mml="http://www.w3.org/1998/Math/MathML" altimg="si84.svg" display="inline" id="d1e1421"><mml:msub><mml:mrow	1.6	1
49667	Synthesis, Crystal, and Electronic Structure of (HpipeH2)2[Sb2I10](I2), with I2 Molecules Linking Sb2X10 Dimers into a Polymeric Anion: A Strategy for Optimizing a Hybrid Compoundâ€™s Band Gap. International Journal of Molecular Sciences, 2023, 24, 2201.	1.8	3
49668	Efficient Hydrogenation of Methyl Palmitate to Hexadecanol over Cu/m-ZrO₂ Catalysts: Synergistic Effect of Cu Species and Oxygen Vacancies. ACS Catalysis, 2023, 13, 2047-2060.	5.5	18
49669	As <mml:math xmlns:mml="http://www.w3.org/1998/Math/MathML" altimg="si31.svg" display="inline" id="d1e1295"><mml:mi>K</mml:mi></mml:math>-edge absorption at high pressures in AFeAs (A=Na/Li): First principles results. Journal of Electron Spectroscopy and Related Phenomena, 2023, 263, 147286.	0.8	1
49670	Anisotropic elastic properties of triclinic 2D materials using density functional theory with application to rhenium disulfide. Computational Condensed Matter, 2023, 34, e00790.	0.9	1

#	Article	IF	Citations
49671	Coexistence of Bulk-Nodal and Surface-Nodeless Cooper Pairings in a Superconducting Dirac Semimetal. Physical Review Letters, 2023, 130, .	2.9	6
49672	Wave-layered dendrite-free lithium deposition with unprecedented long-term cyclability. Journal of Power Sources, 2023, 560, 232697.	4.0	0
49673	Pressure-dependent semiconductorâ€“metal transition and elastic, electronic, optical, and thermophysical properties of orthorhombic SnS binary chalcogenide. Results in Physics, 2023, 45, 106236.	2.0	2
49674	Realizing spontaneous valley polarization and topological phase transitions in monolayer ScX2 (XÂ=ÂCl,) Tj ETQq1 1 0.784314 rgBT /Ov	3.8	17
49675	Red shift of lead-free halide perovskite RbCaCl₃ under pressure for enhancing optoelectronic performance. Physica Scripta, 2023, 98, 035806.	1.2	0
49676	First-Principles Microkinetic Modeling Unravelling the Performance of Edge-Decorated Nanocarbons for Hydrogen Production from Methane. ACS Applied Materials & Interfaces, 2023, 15, 6951-6962.	4.0	9
49677	Adsorption of 3d transition-metal atoms on two-dimensional penta-graphene: A first-principles study. Journal of Saudi Chemical Society, 2023, 27, 101611.	2.4	3
49678	Ab-initio investigation of the structural stability, electronic and optical properties of the LiBO2 compound by using the G0W0+BSE approach. Computational Condensed Matter, 2023, 34, e00789.	0.9	1
49679	A theoretical prediction of novel Janus NiSX (XÂ=ÂO, Se, Te) Monolayers: Electronic, optical, and thermoelectric properties. Applied Surface Science, 2023, 616, 156560.	3.1	6
49680	Strong phonon mode induced by carbon vacancy accelerating hole transfer in SiC/MoS2 heterostructure. Applied Surface Science, 2023, 617, 156554.	3.1	5
49681	Outstanding High Fieldâ€Effect Mobility of 299Âcm²ÂV^{â^'1}Âs^{â^'1} by Nitrogenâ€Doped SnO₂ Nanosheet Thinâ€Film Transistor. Advanced Materials Technologies, 2023, 8, .	3.0	3
49682	Electrocatalytic nitrogen fixation performance of two-dimensional Metal-Organic Frameworks Cu3(C6O6) and TM/Cu3(C6O6) from first-principle study. Chemical Physics, 2023, 568, 111837.	0.9	1
49683	First principles study on structural, vibrational, electronic and elastic properties of 2D alkaline-earth carbides as a metallic material. Synthetic Metals, 2023, 293, 117281.	2.1	0
49684	Reaction pathways of oxidative coupling of methane on lithiated lanthanum oxide. Molecular Catalysis, 2023, 538, 112974.	1.0	2
49685	Band offsets at the interfaces between <mml:math xmlns:mml="http://www.w3.org/1998/Math/MathML"><mml:mi>Î²</mml:mi><mml:mo>â^'</mml:mo><mml:msub><mml:mi mathvariant="normal">Ga</mml:mi><mml:mn>2</mml:mn></mml:msub><mml:msub><mml:mi mathvariant="normal">O</mml:mi><mml:mn>3</mml:mn></mml:msub></mml:math> and <mml:math xmlns:mml="http://www.w3.org/1998/Math/MathML"><mml:msub><mml:mi mathvariant="normal">Al</mml:mi><mml:mn>2</mml:mn></mml:msub><mml:msub><mml:mi mathvarian	0.9	1
49686	High Ampacity On-Chip Wires Implemented by Aligned Carbon Nanotube-Cu Composite. Materials, 2023, 16, 1131.	1.3	0
49687	Atomic structure and large magnetic anisotropy in air-sensitive layered ferromagnetic VI₃. Nanoscale, 2023, 15, 4628-4635.	2.8	1
49688	First-principles prediction of two-dimensional MnOX (X = Cl, Br) monolayers: the half-metallic multiferroics with magnetoelastic coupling. Nanoscale, 2023, 15, 4546-4552.	2.8	4

#	Article	IF	Citations
49689	Room temperature d ⁰ ferromagnetism in carbon doped LaH₃: insights from density functional theory simulations. Journal Physics D: Applied Physics, 2023, 56, 095001.	1.3	0
49690	Variations in the elastic properties and lattice parameters of Moâ€“Ti and Moâ€“Cr BCC solid solutions, as estimated by DFT calculations. Computational Materials Science, 2023, 220, 112026.	1.4	2
49691	How does CO co-adsorption affect glycerol electro-oxidation on polycrystalline platinum? in situ FTIR and DFT approaches. Electrochimica Acta, 2023, 443, 141978.	2.6	0
49692	Structural, elastic, and electronic properties of BC12 carbon under pressure. Chemical Physics, 2023, 568, 111838.	0.9	3
49693	Improved interfacial bonding of c-BN with Ni-based binder alloys: Fast searching of alloying elements based on first principles. Diamond and Related Materials, 2023, 133, 109739.	1.8	2
49694	Superconducting state of the van der Waals layered PdH2 structure at high pressure. International Journal of Hydrogen Energy, 2023, 48, 16769-16778.	3.8	3
49695	Bandgap Change in Shortâ€Period InN/AlN Superlattices Induced by Lattice Strain. Physica Status Solidi (B): Basic Research, 2023, 260, .	0.7	0
49696	Novel ultrahard sp2/sp3 hybrid carbon allotrope from crystal chemistry and first principles: Body-centered tetragonal C6 (â€˜neoglitterâ€™). Diamond and Related Materials, 2023, 133, 109747.	1.8	3
49697	Ni Ingress and Egress in SrTiO₃ Single Crystals of Different Facets. Journal of Physical Chemistry C, 2023, 127, 2875-2884.	1.5	2
49698	Grain refinement in titanium prevents low temperature oxygen embrittlement. Nature Communications, 2023, 14, .	5.8	8
49700	Conjugated dual size effect of core-shell particles synergizes bimetallic catalysis. Nature Communications, 2023, 14, .	5.8	18
49701	Influences of point defects on electron transport of two-dimensional gep semiconductor device. Nanotechnology, 2023, 34, 185204.	1.3	3
49702	Effects of chemical complexity on the initial oxidation resistance of HfC1â^’N ceramics. Computational Materials Science, 2023, 220, 112037.	1.4	2
49703	Fast ion-conductive electrolyte based on a doped LaAlO3 with an amorphous surface layer for low-temperature solid oxide fuel cells. Journal of Power Sources, 2023, 561, 232723.	4.0	6
49704	Direct observation of cation diffusion driven surface reconstruction at van der Waals gaps. Nature Communications, 2023, 14, .	5.8	3
49705	Emerging dâ^’d orbital coupling between non-d-block main-group elements Mg and I at high pressure. IScience, 2023, 26, 106113.	1.9	1
49706	A room temperature rechargeable Li ₂ O-based lithium-air battery enabled by a solid electrolyte. Science, 2023, 379, 499-505.	6.0	70
49707	3D/2D Core/Shell Perovskite Nanocrystals for Highâ€Performance Solar Cells. Small, 2023, 19, .	5.2	5

#	Article	IF	Citations
49708	Ni-Decorated PtS₂ Monolayer as a Strain-Modulated and Outstanding Sensor upon Dissolved Gases in Transformer Oil: A First-Principles Study. ACS Omega, 2023, 8, 6090-6098.	1.6	1
49709	Ab Initio Static Exchangeâ€“Correlation Kernel across Jacobâ€™s Ladder without Functional Derivatives. Journal of Chemical Theory and Computation, 2023, 19, 1286-1299.	2.3	14
49710	Designing sub-5 nm monolayer AlP MOSFETs. , 2023, 176, 207524.		1
49711	Electronic properties and surface states of RbNi<mml:math xmlns:mml="http://www.w3.org/1998/Math/MathML" altimg="si2.svg" display="inline" id="d1e205"><mml:msub><mml:mrow /><mml:mrow><mml:mn>2</mml:mn></mml:mrow></mml:msub></mml:math>Se<mml:math xmlns:mml="http://www.w3.org/1998/Math/MathML" altimg="si2.svg" display="inline" id="d1e213"><mml:msub><mml:mrow />	1.3	2
49713	Thermodynamics modeling of ZrCo-H systems with biaxial compressive strain during desorption. Journal of Nuclear Materials, 2023, 577, 154301.	1.3	1
49715	DFT exploration of the electronic, optical, phonon and thermoelectrical performances of bulk and monolayered AuCN. Theoretical Chemistry Accounts, 2023, 142, .	0.5	2
49716	Accurate description of hydrogen diffusivity in bcc metals using machine-learning moment tensor potentials and path-integral methods. Acta Materialia, 2023, 247, 118739.	3.8	6
49717	Tunable sliding ferroelectricity and magnetoelectric coupling in two-dimensional multiferroic MnSe materials. Npj Computational Materials, 2023, 9, .	3.5	24
49718	Atomically Unveiling an Atlas of Polytypes in Transition-Metal Trihalides. Journal of the American Chemical Society, 2023, 145, 3624-3635.	6.6	6
49720	Quasi-in-situ analysis of adhesion failure at reduced iron/substrate interface of advanced high strength steel. Materials Characterization, 2023, 197, 112712.	1.9	2
49721	Intrinsic thermal stability enhancement in n-type Mg3Sb2 thermoelectrics toward practical applications. Acta Materialia, 2023, 247, 118752.	3.8	6
49722	Halogenated and chalcogenated Ti2C MXenes: High capacity electrode materials for lithium-ion batteries. Chemical Physics Letters, 2023, 814, 140356.	1.2	3
49723	Coupled Spin-Valley, Rashba Effect, and Hidden Spin Polarization in WSi₂N₄ Family. Journal of Physical Chemistry Letters, 2023, 14, 1494-1503.	2.1	17
49724	Giant Rashba effect and nonlinear anomalous Hall conductivity in a two-dimensional molybdenum-based Janus structure. Physical Review B, 2023, 107, .	1.1	1
49725	First-principles calculations of the high pressure and temperature properties of Fe₇C₃. Chinese Physics B, 0, , .	0.7	0
49726	Thermochromic composite film of VO2 nanoparticles and [(C2H5)2NH2]2NiBr4@SiO2 nanospheres for smart window applications. Chemical Engineering Journal, 2023, 460, 141715.	6.6	3
49727	Terminal Atomâ€Controlled Etching of 2Dâ€TMDs. Advanced Materials, 2023, 35, .	11.1	9
49728	Electronic structure analysis of light-element-doped anatase TiO<mml:math xmlns:mml="http://www.w3.org/1998/Math/MathML" altimg="si154.svg" display="inline" id="d1e1646"><mml:msub><mml:mrow /><mml:mrow><mml:mn>2</mml:mn></mml:mrow></mml:msub></mml:math>using all-electron GW approach. Computational Materials Science, 2023, 220, 112059.	1.4	2

#	Article	IF	Citations
49729	Magnetic and structural properties of novel-coated multi-doped Niâ€“Co ferrite nanomaterial: Experimental and theoretical investigations. Journal of Materials Research, 2023, 38, 1669-1682.	1.2	2
49730	Enhanced reversible hydrogen storage performance of Mg-decorated g-C2N: First principles calculations. Computational Materials Science, 2023, 220, 112046.	1.4	4
49731	Development and Validation of a ReaxFF Reactive Force Field for Modeling Siliconâ€“Carbon Composite Anode Materials in Lithium-Ion Batteries. Journal of Physical Chemistry C, 2023, 127, 2818-2834.	1.5	6
49732	Theoretical study of thermal and magnetoâ€electronic properties of <scp> YbX ₂ </scp> (XÂ=ÂCo and Fe) intermetallic compounds. Energy Storage, 0, , .	2.3	1
49733	Interplay between H-bonding proton dynamics and Fe valence fluctuations in <mml:math xmlns:mml="http://www.w3.org/1998/Math/MathML"><mml:mrow><mml:msub><mml:mi>Fe</mml:mi><mml:mn>3</mml:mn></mml:r Physical Review B, 2023, 107, .	1.1	0
49734	Ab-initio and Monte Carlo studies of the structural, electronic and magnetic properties of V-doped ZnO compound. Physica B: Condensed Matter, 2023, 654, 414717.	1.3	0
49735	Vibrational, thermodynamic and acoustic properties of AgAlS2 crystal. Physica B: Condensed Matter, 2023, 654, 414731.	1.3	0
49736	Adsorption and diffusion of potassium on layered SnO: a DFT analysis. Journal of Materials Science, 2023, 58, 3208-3218.	1.7	5
49737	First principles characterization of C-doped magnetically-enhanced D022-Mn<mml:math xmlns:mml="http://www.w3.org/1998/Math/MathML" altimg="si19.svg" display="inline" id="d1e226"><mml:msub><mml:mrow /><mml:mrow><mml:mn>3</mml:mn></mml:mrow></mml:msub></mml:math>Ga surfaces. Computational Materials Science, 2023, 220, 112027.	1.4	1
49738	Strain Engineering of Sc2CBr2 MXene Monolayer by First Principle Approach. Materials Today: Proceedings, 2023, , .	0.9	10
49739	Electronic, mechanical, optical and thermodynamic properties of the quaternary semiconductors Sr3GeMgN4 and Ba3GeMgN4. Materials Science and Engineering B: Solid-State Materials for Advanced Technology, 2023, 290, 116292.	1.7	0
49740	Interfacial interaction of monolayer MX2 (M=Mo, W; X=S, Se, Te)/SiO2 interfaces for composite optical fibers. Surfaces and Interfaces, 2023, 37, 102739.	1.5	1
49741	Computational mining of GeH-based Janus IIIâ€“VI van der Waals heterostructures for solar cell applications. Physical Chemistry Chemical Physics, 2023, 25, 6674-6683.	1.3	0
49742	Comparative study of first-principles approaches for effective Coulomb interaction strength Ueff between localized f-electrons: Lanthanide metals as an example. Journal of Chemical Physics, 2023, 158, .	1.2	3
49743	Reversible Hydrogen Storage Media by g-CN Monolayer Decorated with NLi4: A First-Principles Study. Nanomaterials, 2023, 13, 647.	1.9	2
49744	Single atom solutions for carbon dioxide capture. Journal of Chemical Physics, 2023, 158, .	1.2	3
49745	Hierarchical compositional ordering in lead-based perovskite relaxors. Physical Review B, 2023, 107, .	1.1	5
49746	Coherent consolidation of trillions of nucleations for mono-atom step-level flat surfaces. Nature Communications, 2023, 14, .	5.8	1

#	Article	IF	Citations
49747	Delocalized Bi-tetrahedral cluster induced ultralow lattice thermal conductivity in Bi3Ir3O11. Materials Today Physics, 2023, 32, 101005.	2.9	2
49748	[2,1,3]-Benzothiadiazole-Spaced Co-Porphyrin-Based Covalent Organic Frameworks for O₂ Reduction. ACS Nano, 2023, 17, 3492-3505.	7.3	13
49749	Singleâ€atomic tungstenâ€doped Co₃O₄ nanosheets for enhanced electrochemical kinetics in lithiumâ€“sulfur batteries. , 2023, 5, .		15
49750	Raman study of Cd_{1â^'x}Zn_xTe phonons and phononâ€“polaritonsâ€”Experiment and ab initio calculations. Journal of Applied Physics, 2023, 133, 065701.	1.1	1
49751	Monolayer Iron Oxychloride with a Resonant Band Structure for Ultrasensitive Molecular Sensing. ACS Applied Materials & Interfaces, 2023, 15, 10166-10174.	4.0	2
49752	Influence of chirp and carrier-envelope phase on noninteger high-harmonic generation. Physical Review B, 2023, 107, .	1.1	1
49753	Ferroelectric-Tunable Photoresponse in Î±- <mml:math xmlns:mml="http://www.w3.org/1998/Math/MathML" display="inline" overflow="scroll"><mml:msub><mml:mi>In</mml:mi><mml:mn>2</mml:mn></mml:msub><mml:msub><mml:mi>Se</mml:mi><mml:m Photovoltaic Photodetectors: An Ab Initio Quantum Transport Study. Physical Review Applied, 2023, 19, .	4.6	3
49754	Molecular Î³-amino butyric acid and its crystals: Structural, electronic and optical properties. Journal of Solid State Chemistry, 2023, 321, 123900.	1.4	0
49755	Structural, Spectroscopic, Electric and Magnetic Properties of New Trigonal K5FeHf(MoO4)6 Orthomolybdate. Molecules, 2023, 28, 1629.	1.7	6
49756	Influence of f Electrons on the Electronic Band Structure of Rare-Earth Nickelates. Condensed Matter, 2023, 8, 19.	0.8	3
49757	Predicting lattice thermal conductivity from fundamental material properties using machine learning techniques. Journal of Materials Chemistry A, 2023, 11, 5801-5810.	5.2	9
49758	First-Principles-Based Insight into Electrochemical Reactivity in a Cobalt-Carbonate-Hydroxide Pseudocapacitor. ACS Omega, 2023, 8, 6743-6752.	1.6	0
49759	A simple Pb-doping to achieve bonding evolution, VSn and resonant level shifting for regulating thermoelectric transport behavior of SnTe. Journal of Materials Science and Technology, 2023, 151, 66-72.	5.6	6
49761	Reconstructed Cd(0001) Surface Induced by Adsorption of Triphenyl Bismuth. Coatings, 2023, 13, 394.	1.2	0
49762	On the self-consistency of DFT-1/2. Journal of Chemical Physics, 2023, 158, .	1.2	0
49763	Observation of highly anisotropic bulk dispersion and spin-polarized topological surface states in <mml:math xmlns:mml="http://www.w3.org/1998/Math/MathML"><mml:msub><mml:mi>CoTe</mml:mi><mml:mn>2</mml:mn></mml:msub></ Physical Review B, 2023, 107, .	1.1	5
49764	Two-Dimensional Octuple-Atomic-Layer M2Si2N4 (M = Al, Ga and In) with Long Carrier Lifetime. Micromachines, 2023, 14, 405.	1.4	0
49765	Propane Dehydrogenation on Pt_xSn_y (x, y â‰ 4) Clusters on Al₂O₃(110). ACS Catalysis, 2023, 13, 2802-2812.	5.5	13

#	Article	IF	Citations
49766	Comparative study of neutronic, mechanical and thermodynamic properties of accident tolerant cladding materials: SiC, TiC and ZrC. Materials Science and Engineering B: Solid-State Materials for Advanced Technology, 2023, 290, 116352.	1.7	3
49767	Atomistic simulations for investigation of substrate effects on lipid in-source fragmentation in secondary ion mass spectrometry. Biointerphases, 2023, 18, .	0.6	2
49768	First-Principle Investigation of AlSi2P and GaGe2As Crystals. Russian Physics Journal, 2023, 65, 1738-1745.	0.2	0
49769	NO2 Physical-to-Chemical Adsorption Transition on Janus WSSe Monolayers Realized by Defect Introduction. Molecules, 2023, 28, 1644.	1.7	9
49770	Potential rules for stable transition metal hexafluorides with high oxidation states under high pressures. Physical Chemistry Chemical Physics, 2023, 25, 6726-6732.	1.3	0
49771	Monolayer group IV monochalcogenides T-MX (M = Sn, Ge; X = S, Se) with fine piezoelectric performance and stability. Applied Physics Letters, 2023, 122, .	1.5	5
49772	Coherent description of the magnetic properties of <mml:math xmlns:mml="http://www.w3.org/1998/Math/MathML"><mml:msub><mml:mi mathvariant="normal">SeCuO</mml:mi><mml:mn>3</mml:mn></mml:msub></mml:math> versus temperature and magnetic field. Physical Review B, 2023, 107, .	1.1	0
49773	Adsorption and decomposition steps on Cu(111) of liquid aromatic hydrocarbon precursors for low-temperature CVD of graphene: A DFT study. Carbon, 2023, 206, 142-149.	5.4	2
49774	Effect of strain and electric field on electronic structure and optical properties of Ga₂SeTe/In₂Se₃ heterojunction. Wuli Xuebao/Acta Physica Sinica, 2023, 72, 076301.	0.2	0
49775	Effective band gap engineering in multi-principal oxides (CeGdLa-Zr/Hf)Ox by temperature-induced oxygen vacancies. Scientific Reports, 2023, 13, .	1.6	3
49776	Intrinsic layer-polarized anomalous Hall effect in bilayer <mml:math xmlns:mml="http://www.w3.org/1998/Math/MathML"><mml:mrow><mml:mi>Mn</mml:mi><mml:msub><mml:mi>Bi</mml:mi><mml:m Physical Review B, 2023, 107, .	1.1	11
49777	X-ray Absorption Spectroscopy Studies of a Molecular CO₂-Reduction Catalyst Deposited on Graphitic Carbon Nitride. Journal of Physical Chemistry C, 2023, 127, 3626-3633.	1.5	1
49778	Electronic structure and photoconductivity properties of GaP under high pressure. Journal of Materials Science, 2023, 58, 3657-3669.	1.7	3
49779	First-principles study of the effect of the local coordination environment on the electrochemical activity of Pd1-CxNy single atom catalysts. Chemical Engineering Science, 2023, 270, 118551.	1.9	2
49780	Structural dynamics of Schottky and Frenkel defects in CeO₂: a density-functional theory study. JPhys Energy, 2023, 5, 025004.	2.3	1
49781	Dopant-enhanced sodium and potassium-ion adsorption and diffusion in two-dimensional titanium disulfide. Journal of Applied Physics, 2023, 133, .	1.1	6
49782	CO₂ Reduction Mechanism on the Cu₂O(110) Surface: A Firstâ€Principles Study. ChemPhysChem, 2023, 24, .	1.0	2
49783	Phonon, electron, and magnon excitations in antiferromagnetic <mml:math xmlns:mml="http://www.w3.org/1998/Math/MathML"><mml:mrow><mml:mi>L</mml:mi><mml:msub><mml:mn>1</mml:mn> -type MnPt. Physical Review B, 2023, 107, .	1.1	2

#	Article	IF	Citations
49784	Microscopic nature of the charge-density wave in the kagome superconductor<mml:math xmlns:mml="http://www.w3.org/1998/Math/MathML"><mml:msub><mml:mi mathvariant="normal">RbV</mml:mi><mml:mn>3</mml:mn></mml:msub><mml:msub><mml:mi mathvariant="normal">Sb</mml:mi><mml:mn>5</mml:mn></mml:msub></mml:math>. Physical Review Research, 2023, 5, .	1.3	10
49785	Combined experimental and DFT investigation of temozolomide sensing properties of 2Dâ^Â2D interface of rich oxygen vacancies of WO3â^'x and sulfur-doped g-C3N4 nanosheets hybrids composites. Journal of Environmental Chemical Engineering, 2023, 11, 109459.	3.3	0
49786	First-principles study of the structural and electronic properties of tetragonal ZrOX (X = S, Se, and) Tj ETQq0 0 0 rgBT /Overlock 10 Tf 50 photocatalysis. Journal of Chemical Physics, 2023, 158, 094708.	1.2	2
49787	Thoriumâ€Doped Lithium Fluoride Single Crystal: A Potential Promising Candidate for Solid State Nuclear Optical Clock Materials. Advanced Optical Materials, 2023, 11, .	3.6	4
49788	Effect of strain on the thermoelectric properties of threeâ€dimensional <scp>PtS₂</scp>: A firstâ€principles study. International Journal of Quantum Chemistry, 2023, 123, .	1.0	1
49789	Exploration and investigation of stable novel Al2O3 by high-throughput screening and density functional theory. Journal of Materials Research and Technology, 2023, 23, 4244-4257.	2.6	8
49790	Unlocking the potential of hexagonal boron sheets: Giant improvements in thermal conductivity and mechanics through molybdenum intercalation. Materials Today Physics, 2023, 32, 101012.	2.9	2
49791	Vibrational and electronic properties of Na₂Ti₆O₁₃. Journal of Raman Spectroscopy, 2023, 54, 551-561.	1.2	1
49792	Band Engineering of the Second Phase to Reach High Thermoelectric Performance in Cu₂Seâ€Based Composite Material. Advanced Materials, 2023, 35, .	11.1	11
49793	Two-Dimensional Ferroelectricity in a Single-Atom Adsorbed BiI₃ Monolayer. Journal of Physical Chemistry C, 2023, 127, 3898-3903.	1.5	1
49794	Enhanced Magnetization in CoFe₂O₄ Through Hydrogen Doping. Advanced Functional Materials, 2023, 33, .	7.8	7
49795	High pseudocapacitive lithium-storage behaviors of amorphous titanium oxides with titanium vacancies and open channels. Electrochimica Acta, 2023, 444, 142021.	2.6	4
49796	Preserving Bond Ionicity under Illumination to Achieve Photostable Halide Perovskites. Journal of Physical Chemistry C, 2023, 127, 3750-3759.	1.5	2
49797	Tuning charge carrier dynamics through spacer cation functionalization in layered halide perovskites: an ab initio quantum dynamics study. Journal of Materials Chemistry C, 2023, 11, 3521-3532.	2.7	0
49798	Tuning Catalytic Performance of C₂N/GaN Heterostructure for Hydrogen Evolution Reaction by Doping. Advanced Theory and Simulations, 2023, 6, .	1.3	2
49799	Research on Interface Bonding Properties of TiAlSiN/WC-Co Doped with Graphene. Micromachines, 2023, 14, 431.	1.4	0
49800	First-principles study on the thermoelectric properties of Sr2Si and Sr2Ge. Materials Today Physics, 2023, 32, 101015.	2.9	5
49801	Assessing the Surface Chemistry of 2D Transition Metal Carbides (MXenes): A Combined Experimental/Theoretical ¹³C Solid State NMR Approach. Journal of the American Chemical Society, 2023, 145, 4003-4014.	6.6	6

#	Article	IF	Citations
49802	First-principles study of the strain effect with half-metallic ferromagnetism in Cd _{1â^'x} V _x Te alloys: supercell approaches. Physica Scripta, 2023, 98, 035828.	1.2	0
49803	An extensive study on multiple ETL and HTL layers to design and simulation of high-performance lead-free CsSnCl3-based perovskite solar cells. Scientific Reports, 2023, 13, .	1.6	102
49804	Atomic scale understanding the periodic modulation in ferroelastic alloy Ni-Mn-Ti. Acta Materialia, 2023, 248, 118768.	3.8	4
49805	Impact of Hydrogen Coverage Trend on Methyl Formate Adsorption on MoS₂ Surface: A First Principles Study. ACS Omega, 2023, 8, 6523-6529.	1.6	0
49806	Structural, mechanical, electronic, and thermoelectric properties of TiZrCo2Bi2, TiHfCo2Bi2, and ZrHfCo2Bi2 double half Heusler semiconductors. Emergent Materials, 2023, 6, 681-690.	3.2	4
49807	Heteroepitaxy of 2D CuCr₂Te₄ with Robust Roomâ€temperature Ferromagnetism. Advanced Materials, 2023, 35, .	11.1	12
49808	High Curie temperature Chern insulator and spin-gapless semiconducting ferromagnetic h-CrC monolayer: A first-principles study. Computational Materials Science, 2023, 220, 112070.	1.4	2
49809	Layer Dependence of Thermally Induced Quantum Confinement and Higher Order Phonon Scattering for Thermal Transport in CVD-Grown Triangular MoS₂. Journal of Physical Chemistry C, 2023, 127, 3787-3799.	1.5	9
49810	Ultra-high thermal conductivity of two-dimensional C₂₃. Nanotechnology, 2023, 34, 175704.	1.3	1
49811	Optical method for quantifying the potential of zero charge at the platinumâ€“water electrochemical interface. Nature Materials, 2023, 22, 503-510.	13.3	18
49812	Firstâ€Principles Density Functional Theory and Machine Learning Technique for the Prediction of Water Adsorption Site on PtPdâ€Based Highâ€Entropyâ€Alloy Catalysts. Advanced Theory and Simulations, 2023, 6, .	1.3	3
49813	First-principles study on tuning electronic and optical properties in graphene rotation on h-BN. Chemical Physics Letters, 2023, 815, 140366.	1.2	0
49814	Study on low hydrostatic pressure-dependent optoelectronic, mechanical, and anisotropic properties of heavy thallium perovskites TlPbX3 (Xâ€‰=â€‰Cl, Br). Journal of Materials Research, 2023, 38, 2007-2017.	1.2	4
49815	Regulating Na Occupation in P2â€Type Layered Oxide Cathode for Allâ€Climate Sodiumâ€Ion Batteries. Advanced Energy Materials, 2023, 13, .	10.2	18
49816	The effects of cation and halide anion on the stability, electronic and optical properties of double perovskite Cs2NaMX6 (MÂ=ÂIn, Tl, Sb, bi; X Â=ÂCl, Br, I). Computational Materials Science, 2023, 220, 112058.	1.4	13
49817	First-Principles Study of the Doping Effect in Half Delithiated LiNiO₂ Cathodes. ACS Applied Energy Materials, 2023, 6, 2134-2139.	2.5	1
49818	DFT insights into Nb-based 211 MAX phase carbides: Nb₂AC (A = Ga, Ge, Tl, Zn, P, In, and Cd). RSC Advances, 2023, 13, 5538-5556.	1.7	4
49819	Fermi-Level Instability as a Way to Tailor the Properties of La₃Te₄. Journal of Physical Chemistry Letters, 2023, 14, 1962-1967.	2.1	3

#	Article	IF	Citations
49820	CO₂ coverage on Pd catalysts accelerates oxygen removal in oxy-combustion systems. Physical Chemistry Chemical Physics, 2023, 25, 6527-6536.	1.3	0
49821	Modeling 2D Arrangements of Graphene Nanoribbons. Crystals, 2023, 13, 311.	1.0	0
49822	Proton migration barriers in BaFeO_{3â^'Î´} â€“ insights from DFT calculations. Journal of Materials Chemistry A, 2023, 11, 6336-6348.	5.2	4
49823	An improved meta-heuristic algorithm for developing high-quality ReaxFF force fields of Fe/Ni transition metals and alloys. Computational Materials Science, 2023, 221, 112083.	1.4	2
49825	pH- and Facet-Dependent Surface Chemistry of TiO₂ in Aqueous Environment from First Principles. ACS Applied Materials & Interfaces, 2023, 15, 11216-11224.	4.0	13
49826	High-Pressure Pulsing of Ammonia Results in Carbamate as Strongly Inhibiting Adsorbate of Methanol Synthesis over Cu/ZnO/Al₂O₃. Journal of Physical Chemistry C, 2023, 127, 3497-3505.	1.5	0
49827	Increasing the Strain Resistance of Si/SiO₂ Interfaces for Flexible Electronics. ACS Omega, 2023, 8, 7555-7565.	1.6	1
49828	Spinâ€Resolved Imaging of Antiferromagnetic Order in Fe₄Se₅ Ultrathin Films on SrTiO₃. Advanced Materials, 2023, 35, .	11.1	3
49829	Elastic, electronic, optical, and thermodynamic properties of M₂SeC (M = Hf, Zr) under high pressure. AIP Advances, 2023, 13, 025154.	0.6	0
49830	First-principles study on structural, electronic, and elastic properties of SrFCl. Indian Journal of Physics, 0, , .	0.9	0
49831	Double-perovskite van der Waals heterostructure Cs2NaInCl6-XS2 (X=Cr, Mo, W) as great potential material in photovoltaic devices. Surfaces and Interfaces, 2023, 37, 102734.	1.5	0
49832	Alloying engineering for thermoelectric performance enhancement in p-type skutterudites with synergistic carrier concentration optimization and thermal conductivity reduction. Journal of Advanced Ceramics, 2023, 12, 539-552.	8.9	1
49833	Unraveling different influences of the fraction of the tetragonal phase in oxide films on the corrosion resistance of Zr alloys from the phase transition mechanism. Physical Chemistry Chemical Physics, 2023, 25, 8934-8947.	1.3	0
49834	The effect of long-range interactions on the infrared and Raman spectra of aragonite (CaCO3, Pmcn) up to 25 GPa. Scientific Reports, 2023, 13, .	1.6	2
49835	First-principles study for discovery of novel synthesizable 2D high-entropy transition metal carbides (MXenes). Journal of Materials Chemistry A, 2023, 11, 5681-5695.	5.2	6
49836	An ab initio investigation of electronic, elastic, mechanical and vibrational properties of Co2VX (XÂ=ÂAl,) Tj ETQq1 1 0.784314 rgBT /O	0.9	0
49837	Ultraâ€low singleâ€atom Pt on gâ€C₃N₄ for electrochemical hydrogen peroxide production. , 2023, 5, .		8
49838	Numerical stability and efficiency of response property calculations in density functional theory. Letters in Mathematical Physics, 2023, 113, .	0.5	1

#	Article	IF	Citations
49839	Dual Metal Site Fe Single Atom Catalyst with Improved Stability in Acidic Conditions. Catalysts, 2023, 13, 418.	1.6	0
49840	Ethane Dehydrogenation over the Coreâ€“Shell Pt-Based Alloy Catalysts: Driven by Engineering the Shell Composition and Thickness. ACS Applied Materials & Interfaces, 2023, 15, 10679-10695.	4.0	4
49841	Sulfide (H₂S) Corrosion Modeling of Cr-Doped Iron (Fe) Using a Molecular Modeling Approach. ACS Omega, 2023, 8, 7395-7406.	1.6	1
49842	Ultrahigh Nitrogen Content Carbon Nanosheets for High Stable Sodium Metal Anodes. Advanced Science, 2023, 10, .	5.6	11
49843	Tailoring alloy compositions by glucose towards superior Niâ€“Cuâ€“C electrocatalysts for hydrogen evolution reaction. International Journal of Hydrogen Energy, 2024, 52, 334-342.	3.8	2
49844	Composition Engineering Opens an Avenue Toward Efficient and Sustainable Nitrogen Fixation. Energy and Environmental Materials, 2024, 7, .	7.3	5
49845	Hysteresis and training effect in the electric control of spin current in <mml:math xmlns:mml="http://www.w3.org/1998/Math/MathML"><mml:mi>Pt</mml:mi><mml:mo>/</mml:mo><mml:msub><mml:mrow><mml:mi mathvariant="normal">Y</mml:mi></mml:mrow><mml:mn>3</mml:mn></mml:msub><mml:msub><mml:mrow><mml:mi>Fe</mml:mi><mml:mi mathvariant="normal">O</mml:mi></mml:mrow><mml:mn>12</mml:mn></mml:msub></mml:math> heterostructures. Physical Review B, 2023, 107, .	1.1	2
49846	Continuous-flow electrosynthesis of ammonia by nitrogen reduction and hydrogen oxidation. Science, 2023, 379, 707-712.	6.0	107
49847	Design of Flameâ€Made ZnZrO_x Catalysts for Sustainable Methanol Synthesis from CO₂. Advanced Energy Materials, 2023, 13, .	10.2	7
49848	Atypical stability of exsolved Ni-Fe alloy nanoparticles on double layered perovskite for CO2 dry reforming of methane. Applied Catalysis B: Environmental, 2023, 328, 122479.	10.8	11
49849	Theoretical study of hydrogen adsorption kinetics: Mg17Al12 vs pure Mg. International Journal of Hydrogen Energy, 2023, , .	3.8	0
49850	Delocalized electron holes on oxygen in a battery cathode. Nature Energy, 2023, 8, 351-360.	19.8	25
49851	Exploring structural, electronic, phonon, mechanical, elastic, thermodynamic, and thermoelectric properties of the Li based quaternary Heusler LiTaCoAl by DFT: A multifunctional smart material. Materials Today: Proceedings, 2023, , .	0.9	2
49852	The highest melting point material: Searched by Bayesian global optimization with deep potential molecular dynamics. Journal of Advanced Ceramics, 2023, 12, 803-814.	8.9	3
49853	Nanoscale-mixed ZnNiCu hydroxide composite catalyst for improved photocatalytic hydrogen evolution. International Journal of Hydrogen Energy, 2023, 48, 18657-18669.	3.8	0
49854	Bottom-up building of two-dimensional magnetic materials with self-assembly of superatom TM@Sn₁₂ (TM = Sc, Ti, V, Cr, Mn, Fe) clusters. Journal Physics D: Applied Physics, 2023, 56, 144001.	1.3	1
49855	Computational screening of chemically active metal center in coordinated dipyridyl tetrazine network. Journal of Physics Condensed Matter, 2023, 35, 154001.	0.7	0
49856	Substrate-Induced Modulation of Quantum Emitter Properties in 2D Hexagonal Boron Nitride: Implications for Defect-Based Single Photon Sources in 2D Layers. ACS Applied Nano Materials, 2023, 6, 3446-3452.	2.4	2

#	Article	IF	Citations
49857	Thermal batteries based on inverse barocaloric effects. Science Advances, 2023, 9, .	4.7	7
49858	First principles approach for promising oxide ion conducting ABGa₃O₇ melilite structures. Physical Chemistry Chemical Physics, 2023, 25, 7028-7031.	1.3	0
49859	Site occupancy of Ru in Î¼ phases: A density functional theory study. International Journal of Modern Physics B, 0, , .	1.0	0
49860	Role of oxygen vacancies on surface reaction of water oxidation in WO3 studied by density functional theory (DFT) and experiment. Molecular Catalysis, 2023, 539, 113005.	1.0	3
49861	Controlling interfacial composition and improvement in bonding strength of compound casted Al/steel bimetal via Cr interlayer. Journal of Materials Research and Technology, 2023, 23, 4385-4395.	2.6	5
49862	Impact of spinâ€“orbit coupling on physical properties and superconductivity in noncentrosymmetric superconductors Ru<mml:math xmlns:mml="http://www.w3.org/1998/Math/MathML" altimg="si180.svg" display="inline" id="d1e2111"><mml:msub><mml:mrow /><mml:mrow><mml:mn>7</mml:mn></mml:mrow></mml:msub></mml:math>B<mml:math xmlns:mml="http://www.w3.org/1998/Math/MathML" altimg="si181.svg" display="inline" id="d1e2119"><mml:msub><mml:mrow /><mml:mrow><mml:mn>3</mml:mn></mml:mrow></mml:msub></	1.3	0
49863	Formation of ibrutinib solvates: so similar, yet so different. IUCrJ, 2023, 10, 210-219.	1.0	1
49864	Effect of intrinsic point defects on the catalytic and electronic properties of <mml:math xmlns:mml="http://www.w3.org/1998/Math/MathML"><mml:msub><mml:mrow><mml:mi>Cu</mml:mi></mml:mrow><mml:mn>2</mml:mn> single layer: Ab initio calculations. Physical Review Materials, 2023, 7, .	2.9	12
49865	Two new barium phosphides predicted by first-principles evolutionary algorithm. International Journal of Modern Physics C, 0, , .	0.8	0
49866	Facile synthesis of MgAl2O4 spinel matrix nanocomposite with TiC, AlTi3, and Al2O3 reinforcements by mechanical alloying. Journal of the Australian Ceramic Society, 2023, 59, 269-280.	1.1	1
49867	Accurate descriptions of molecule-surface interactions in electrocatalytic CO2 reduction on the copper surfaces. Nature Communications, 2023, 14, .	5.8	12
49868	Phase Evolution on the Hydrogen Adsorption Kinetics of NiFeâ€Based Heterogeneous Catalysts for Efficient Water Electrolysis. Small Methods, 2023, 7, .	4.6	55
49869	Composition-dependent structural characteristics and mechanical properties of amorphous SiBCN ceramics by ab-initio calculations. Journal of Advanced Ceramics, 2023, 12, 984-1000.	8.9	2
49870	Dualâ€Atomâ€Site Snâ€Cu/C₃N₄ Photocatalyst Selectively Produces Formaldehyde from CO₂ Reduction. Advanced Functional Materials, 2023, 33, .	7.8	11
49871	Topography of high-speed steel substrates sputter cleaned by an Ar/Ti cathodic arc plasma. Surface and Coatings Technology, 2023, 458, 129344.	2.2	1
49872	Understanding of Active Sites and Interconversion of Pd and PdO during CH4 Oxidation. Molecules, 2023, 28, 1957.	1.7	2
49873	Dynamic crystallography reveals spontaneous anisotropy in cubic GeTe. Nature Materials, 2023, 22, 311-315.	13.3	9
49874	NaGaSe₂: A Water-Loving Multifunctional Non-van der Waals Layered Selenogallate. Inorganic Chemistry, 2023, 62, 3886-3895.	1.9	2

#	Article	IF	Citations
49875	Structural ordering governs stiffness and ductile-to-brittle transition in Alâ€“Li alloys. Journal of Chemical Physics, 2023, 158, .	1.2	2
49876	Ullmann-Like Covalent Bond Coupling without Participation of Metal Atoms. ACS Nano, 2023, 17, 4387-4395.	7.3	0
49877	First-Principles Study of the Structural, Mechanical and Thermodynamic Properties of Al11RE3 in Aluminum Alloys. Crystals, 2023, 13, 347.	1.0	3
49878	Structural and Spectroscopic Effects of Li+ Substitution for Na+ in LixNa1â^'xCaLa0.5Er0.05Yb0.45(MoO4)3 Upconversion Scheelite-Type Phosphors. Crystals, 2023, 13, 362.	1.0	7
49879	Van der Waals Epitaxy Growth of 2D Singleâ€Element Roomâ€Temperature Ferromagnet. Advanced Materials, 2023, 35, .	11.1	3
49880	Voltage-controlled magnetic anisotropy in heterostructures with a two-dimensional magnetic material. Physical Review B, 2023, 107, .	1.1	3
49881	Rh-doped ultrathin NiFeLDH nanosheets drive efficient photocatalytic water splitting. International Journal of Hydrogen Energy, 2024, 52, 371-384.	3.8	4
49882	Understanding the piezocatalytic properties of the BaTiO₃(001) surfaceviadensity functional theory. Physical Chemistry Chemical Physics, 2023, 25, 8631-8640.	1.3	2
49883	Magnetic phase transition in a machine trained spin model: A study of hexagonal CrN monolayer. Physica A: Statistical Mechanics and Its Applications, 2023, 615, 128589.	1.2	0
49884	Study of Structural, optoelectronic and elastic properties of MAX phase of Ti2BrX (XÂ=ÂB, C and N) by density functional theory. Inorganic Chemistry Communication, 2023, 150, 110515.	1.8	1
49885	Multiple Quantum States Induced in 1Tâ€TaSe₂ by Controlling the Stacking Order of Charge Density Waves. Advanced Functional Materials, 2023, 33, .	7.8	3
49886	A general thermodynamics-triggered competitive growth model to guide the synthesis of two-dimensional nonlayered materials. Nature Communications, 2023, 14, .	5.8	10
49887	Mixed Germaniaâ€Silica Films on Ru(0001): A combined experimental and theoretical study. Israel Journal of Chemistry, 0, , .	1.0	0
49888	Two-dimensional XY ferromagnetism above room temperature in Janus monolayer V₂XN (X) Tj ETQq1 1 0.784314 rgBT /Ov	1.3	7
49889	High-temperature ferromagnetism in <mml:math xmlns:mml="http://www.w3.org/1998/Math/MathML"><mml:msub><mml:mrow><mml:mi>Cr</mml:mi></mml:mrow><mml:mrow><mml:mathvariant="normal">P</mml:mi></mml:math>. Physical Review Materials, 2023, 7, .	0.9	2
49890	Electronic structure and physical properties of the candidate topological material GdAgGe. Physical Review B, 2023, 107, .	1.1	2
49891	Modulation of Local Charge Distribution Stabilized the Anionic Redox Process in Mn-Based P2-Type Layered Oxides. ACS Applied Materials & Interfaces, 2023, 15, 11691-11702.	4.0	9
49892	Phase stability and physical properties of lanthanum dicarbide under pressure. Philosophical Magazine, 2023, 103, 969-986.	0.7	0

#	Article	IF	Citations
49893	Cooperative Pseudo Jahn Teller distortion derives phase transitions in bismuth oxide. Materials Chemistry and Physics, 2023, 299, 127534.	2.0	0
49894	Structure and magnetism of rhodium particles as a size effect. Europhysics Letters, 2023, 141, 66002.	0.7	0
49895	Effects of Temperature Induced Phase Transition in Bulk CdS Structures. , 2022, , .		0
49896	Ion Irradiation Effects on Two-Dimensional MXene Ti₂C for Applications in Extreme Conditions: Combined Ab Initio and Monte Carlo Simulations. ACS Applied Nano Materials, 2023, 6, 3463-3471.	2.4	2
49897	Controllable p-type doping of 2D MoS₂via Sodium intercalation for optoelectronics. Journal of Materials Chemistry C, 2023, 11, 3386-3394.	2.7	0
49898	Comprehensive study on electronic structures of SiGe/Ga$$_{2}$$SeTe vdW heterobilayer. Journal of Materials Science, 2023, 58, 4020-4030.	1.7	4
49899	Doping Engineering for Optimizing Piezoelectric and Elastic Performance of AlN. Materials, 2023, 16, 1778.	1.3	0
49900	Two-dimensional Janus MGeSiP₄ (M = Ti, Zr, and Hf) with an indirect band gap and high carrier mobilities: first-principles calculations. Physical Chemistry Chemical Physics, 2023, 25, 8779-8788.	1.3	5
49901	One dimensional wormhole corrosion in metals. Nature Communications, 2023, 14, .	5.8	14
49902	Effective Hubbard Parametrization for Optimizing Electronic Bandgap of monolayer CrI₃. , 2022, , .		0
49903	Effects of an external electric field on the electronic properties and optical excitations of germanane and silicane monolayers. Journal of Physics Condensed Matter, 2023, 35, 175502.	0.7	0
49904	Boron vacancy-driven thermodynamic stabilization and improved mechanical properties of AlB₂-type tantalum diborides as revealed by first-principles calculations. JPhys Materials, 2023, 6, 025002.	1.8	3
49905	The First-Principles Investigation of Structural Stability, Mechanical, Vibrational, Thermodynamic, and Optical Properties of CaHfS3 for Optoelectronic Application. Advances in Condensed Matter Physics, 2023, 2023, 1-13.	0.4	0
49906	Density Functional Theory-Based Study of Ag/ZnO Schottky Diode. Journal of Electronic Materials, 2023, 52, 3228-3241.	1.0	1
49907	Ab initio study of the adsorption of SO2 on single-atom Cu-decorated ZnO(0001) surface. Journal of Molecular Modeling, 2023, 29, .	0.8	1
49908	2D carbon nitride as a support with single Cu, Ag, and Au atoms for carbon dioxide reduction reaction. Physical Chemistry Chemical Physics, 2023, 25, 8574-8582.	1.3	11
49909	Expanding the low-dimensional interface engineering toolbox for efficient perovskite solar cells. Nature Energy, 2023, 8, 284-293.	19.8	23
49910	Lithium adsorption on the interface of graphene/boron nitride nanoribbons. Journal of Materials Science, 2023, 58, 4513-4524.	1.7	1

#	Article	IF	Citations
49911	Phonon-Induced Localization of Excitons in Molecular Crystals from First Principles. Physical Review Letters, 2023, 130, .	2.9	9
49912	The strengthening effects and mechanisms of alloying elements on interfaces for multiphase Ni-based superalloys: A first-principles study. Journal of Materials Research and Technology, 2023, 23, 4802-4813.	2.6	5
49913	Tunable magnetic interactions in mono-transition metal spinels <mml:math xmlns:mml="http://www.w3.org/1998/Math/MathML"><mml:mrow><mml:msub><mml:mi mathvariant="normal">MgCr</mml:mi><mml:mn>2</mml:mn></mml:msub><mml:mi>X</mml:mi></mml:mrow><mml:msub><mml:mr /><mml:mn>4</mml:mn></mml:msub><mml:mo>Â</mml:mo><mml:mo>(</mml:mo><mml:mi>X</mml:mi><mml:mo>=</mml:mo><m	0.9	0
49914	Physic Rattling-induced suppression of thermal transport in cubic In₂O₃ with Sn-Ga diatomic defect. Journal of Physics Condensed Matter, 2023, 35, 195701.	0.7	0
49915	Grain-boundary segregation and superior mechanical properties in a multicomponent L12 Ni46.5Co24Fe8Al12.5Ti9 superlattice alloy. Frontiers in Materials, 0, 10, .	1.2	0
49916	Double-Heterostructure Resonant Tunneling Transistors of Surface-Functionalized Sb and Bi Monolayer Nanoribbons. Crystals, 2023, 13, 379.	1.0	0
49917	Theoretical Study on the Role of Solvents in Lithium Polysulfide Anchoring on Vanadium Disulfide Facets for Lithiumâ€“Sulfur Batteries. Journal of Physical Chemistry C, 2023, 127, 4416-4424.	1.5	3
49918	Prediction of LiCrTe$_2$ monolayer as a half-metallic ferromagnet with a high Curie temperature. Chinese Physics B, 0, , .	0.7	0
49919	Thermodynamic stability of Liâ€“Bâ€“C compounds from first principles. Physical Chemistry Chemical Physics, 2023, 25, 7344-7353.	1.3	2
49920	Rapid Interlayer Charge Separation and Extended Carrier Lifetimes due to Spontaneous Symmetry Breaking in Organic and Mixed Organicâ€“Inorganic Dionâ€“Jacobson Perovskites. Journal of the American Chemical Society, 2023, 145, 5297-5309.	6.6	24
49921	Optical, electronic, and structural properties of <mml:math xmlns:mml="http://www.w3.org/1998/Math/MathML"><mml:mrow><mml:mi>ScAlMg</mml:mi><mml:msub><mml:mi mathvariant="normal">O</mml:mi><mml:mn>4</mml:mn></mml:msub></mml:mrow></mml:math>. Physical Review B, 2023, 107, .	1.1	2
49922	Modulating Trinaryâ€Heterostructure of MoS₂ via Controllably Carbon Doping for Enhanced Electrocatalytic Hydrogen Evolution Reaction. Advanced Functional Materials, 2023, 33, .	7.8	14
49923	A DFT+U Based Study of Fullâ€Heusler Alloy Ru ₂ VSi. Macromolecular Symposia, 2023, 407, .	0.4	0
49924	Theoretical investigation of the structural, electronic, elastic and optical properties of the ternary monoclinic compounds KGaQ2 (Q = S, Se and Te). Bulletin of Materials Science, 2023, 46, .	0.8	2
49925	Mixed-Valence Conductors from Ni Bis(diselenolene) Complexes with a Thiazoline Backbone. Inorganic Chemistry, 2023, 62, 4197-4209.	1.9	2
49926	High thermoelectric performance of layered <mml:math xmlns:mml="http://www.w3.org/1998/Math/MathML"><mml:mi>LaAg</mml:mi><mml:mi>X</mml:mi><mml:mi mathvariant="normal">O</mml:mi><mml:mo>Â</mml:mo><mml:mo>(</mml:mo><mml:mi>X</mml:mi><mml:mo>=</mml:mo><mml:mo><mml from electrical and thermal transport calculations. Physical Review Materials, 2023, 7, .	0.9	3
49927	Chloride Adsorbates Enhance the Photocarrier Separation and Promote the Bioâ€Syngas Evolution. Small, 2023, 19, .	5.2	3
49928	Carbon nanowires made by the insertion-and-fusion method toward carbonâ€“hydrogen nanoelectronics. Nanoscale, 2023, 15, 6143-6155.	2.8	1

#	Article	IF	Citations
49929	Pd encapsulated core-shell ZIF-8/ZIF-67 for efficient oxygen evolution reaction. Electrochimica Acta, 2023, 447, 142100.	2.6	9
49930	Theoretical investigation of the MXene precursors MoxV4-xAlC3 (0â€‰â‰â€‰xâ€‰â‰â€‰4). Scientific Reports, 2023, 13, .	1.6	1
49931	Anomalous doping effects on stabilizing unusual phases of lithium fluoride for enhanced rechargeable battery interfaces. Acta Materialia, 2023, 248, 118813.	3.8	4
49932	First-principles calculations to investigate electronic, magnetic and half-metallic ferromagnetic properties of full-Heusler Mn ₂ OsSn. Philosophical Magazine, 2023, 103, 1090-1114.	0.7	1
49933	Unraveling the effects of Ni particle size and facet on CH4 activation: From cluster to nanoparticle. International Journal of Hydrogen Energy, 2023, 48, 19486-19493.	3.8	12
49934	Revealing the band structure of <mml:math xmlns:mml="http://www.w3.org/1998/Math/MathML"><mml:msub><mml:mi>ZrTe</mml:mi><mml:mn>5</mml:mn></mml:msub></mml:math> using multicarrier transport. Physical Review B, 2023, 107, .	1.1	2
49935	Theoretical and Experimental Assessments of Elementary Steps and Bound Intermediates in Catalytic H₂â€“O₂ Reactions on Dispersed Pt Nanoparticles. Journal of Physical Chemistry C, 2023, 127, 4553-4569.	1.5	1
49936	Highly Active Interfacial Sites in <scp>SFTâ€“SnO₂</scp> Heterojunction Electrolyte for Enhanced Fuel Cell Performance via Engineered Energy Bands: Envisioned Theoretically and Experimentally. Energy and Environmental Materials, 0, , .	7.3	9
49937	Analytical Forces for the Optimized Effective Potential Calculations. Journal of Chemical Theory and Computation, 2023, 19, 1744-1752.	2.3	0
49938	Using ternary steric hindrance synergy of a defective MoS₂ monolayer to manipulate the electrocatalytic mechanism toward nitric oxide reduction: a first-principles and machine learning study. Journal of Materials Chemistry A, 2023, 11, 7159-7169.	5.2	6
49939	Effect of terminations on the hydrogen evolution reaction mechanism on Ti₃C₂ MXene. Journal of Materials Chemistry A, 2023, 11, 6886-6900.	5.2	15
49940	Achieving Ultra-High Selectivity to Hydrogen Production from Formic Acid on Pdâ€“Ag Alloys. Journal of the American Chemical Society, 2023, 145, 5114-5124.	6.6	22
49941	A Comprehensive First-Principles Investigation of SnTiO3 Perovskite for Optoelectronic and Thermoelectric Applications. Crystals, 2023, 13, 408.	1.0	12
49942	Evidence of linear and cubic Rashba effect in non-magnetic heterostructure. Journal of Physics Condensed Matter, 2023, 35, 205501.	0.7	2
49943	The Atomistic Understanding of the Ice Recrystallization Inhibition Activity of Antifreeze Glycoproteins. Crystals, 2023, 13, 405.	1.0	1
49944	Electrical and thermal conductivity of fcc and hcp iron under conditions of the Earth's core from ab initio simulations. Physical Review B, 2023, 107, .	1.1	4
49945	Templated Synthesis of Exfoliated Porous Carbon with Dominant Graphitic Nitrogen. ACS Materials Au, 2023, 3, 231-241.	2.6	3
49946	Interface Calculation of In Situ Micro-Nano TaC/NbC Ceramic Particle Composites. Materials, 2023, 16, 1887.	1.3	1

#	Article	IF	Citations
49947	Theoretical analysis of electrochromism of Ni-deficient nickel oxide â€“ from bulk to surfaces. Physical Chemistry Chemical Physics, 2023, 25, 7974-7985.	1.3	1
49948	Robust half-metallicity and tunable ferromagnetism in two-dimensional VCl2. Journal of Applied Physics, 2023, 133, .	1.1	5
49949	Strain effect on the high T _c superconductor YBa₂Cu₃O₇: an ab initio study comparing bulk and monolayer models. Electronic Structure, 2023, 5, 015002.	1.0	0
49950	Comprehensive Mechanism for CO Electroreduction on Dualâ€Atomâ€Catalystâ€Anchored Nâ€Doped Graphene. ChemPhysChem, 0, , .	1.0	0
49951	Geometric Tuning of Singleâ€Atom FeN₄ Sites via Edgeâ€Generation Enhances Multiâ€Enzymatic Properties. Advanced Materials, 2023, 35, .	11.1	14
49952	New C_{2h} phase of group III monochalcogenide monolayers AlX (X = S, Se, and Te) with anisotropic crystal structure: first-principles study. RSC Advances, 2023, 13, 6838-6846.	1.7	1
49953	The first-principle study on certain structural, band-structural, elastic, optical and piezoelectric properties of the Ca, Zr and Ca/Zr-doped BaTiO3. Modern Physics Letters B, 2023, 37, .	1.0	4
49954	An Efficient Way to Model Complex Iron Carbides: A Benchmark Study of DFTB2 against DFT. Journal of Physical Chemistry A, 2023, 127, 2071-2080.	1.1	3
49955	Amorphous As2S3 Doped with Transition Metals: An Ab Initio Study of Electronic Structure and Magnetic Properties. Nanomaterials, 2023, 13, 896.	1.9	1
49956	Pressure-Induced Reversible Local Structural Disorder in Superconducting AuAgTe4. Inorganics, 2023, 11, 99.	1.2	1
49957	Ferromagnetic GdX (X = Cl, Br) Monolayers with Large Perpendicular Magnetic Anisotropy and High Curie Temperature. Journal of Physical Chemistry C, 2023, 127, 4643-4650.	1.5	3
49958	Tantalum half-Heusler alloys RbTaSi and RbTaGe: potential candidates for desirable thermoelectric and spintronic applications. RSC Advances, 2023, 13, 7087-7101.	1.7	2
49959	Rb₄Li₂TiOGe₄O₁₂: a novel high-performance titanyl germanate anode for Li-ion batteries. Journal of Materials Chemistry A, 2023, 11, 7170-7178.	5.2	0
49960	Topological Nodal Surface and Quadratic Dirac Semimetal States and van Hove Singularities in ScH₃ and LuH₃ Superconductors. ACS Omega, 2023, 8, 9607-9613.	1.6	4
49961	Catalysis of surface dispersed Cu²⁺ species on t-ZrO₂: square-planar Cu catalyzed cross-coupling of arylboronic acid and imidazole. Catalysis Science and Technology, 2023, 13, 2247-2254.	2.1	4
49962	Mechanism of CO₂ photoreduction by selenium-doped carbon nitride with cobalt clusters as cocatalysts. Physical Chemistry Chemical Physics, 2023, 25, 8705-8713.	1.3	1
49963	Regioselective Reduction of NAD⁺ to 1,4â€NADH with a Bioinspired Metal Sulfide Electrocatalyst. ChemCatChem, 2023, 15, .	1.8	0
49964	Ti-6Al-4V to over 1.2 TPa: Shock Hugoniot experiments, <mml:math xmlns:mml="http://www.w3.org/1998/Math/MathML"><mml:mrow><mml:mi>a</mml:mi><mml:mi>b</mml:mi></mml:mrow><mml:mo calculations, and a broad-range multiphase equation of state. Physical Review B, 2023, 107, .	1.1	1

#	Article	IF	Citations
49965	Realization of quasi-1D topological magnetism at the V-alloyed MoS₂ zigzag edge. Physical Chemistry Chemical Physics, 2023, 25, 8843-8852.	1.3	0
49966	Influence of Nitrogen Substitution on the Electronic Structure of Ti₂O₃: Insights into the Dopingâ€Induced Insulatorâ€toâ€Metal Transition. Physica Status Solidi (B): Basic Research, 2023, 260, .	0.7	0
49967	Density functional theory study of Zn(1â^'x)FexSe: Electronic structure, phonon, and magnetic properties. AIP Advances, 2023, 13, .	0.6	1
49968	Stoichiometryâ€Directed Twoâ€Level Hierarchical Growth of Lanthanideâ€Based Supramolecular Nanoarchitectures. Chemistry - A European Journal, 2023, 29, .	1.7	2
49969	New stable ultrawide bandgap As₂O₃ semiconductor materials. JPhys Materials, 2023, 6, 025003.	1.8	7
49970	Theoretical and experimental investigation of structural, thermal, and vibrational properties of Bis-glycine hydrochlorobromide crystal. Journal of Materials Science: Materials in Electronics, 2023, 34, .	1.1	0
49971	Preparation, photoluminescence and excited state properties of the homoleptic cluster cation [(W₆I₈)(CH₃CN)₆]⁴⁺. Dalton Transactions, 2023, 52, 3777-3785.	1.6	1
49972	Polysulfide cluster formation, surface reaction, and role of fluorinated additive on solid electrolyte interphase formation at sodium-metal anode for sodiumâ€“sulfur batteries. Journal of Chemical Physics, 2023, 158, .	1.2	3
49973	Strain induced metal-semiconductor transition in two-dimensional topological half metals. IScience, 2023, 26, 106312.	1.9	4
49974	Iron-Based Active Sites Encapsulated in Carbon Nanotubes for an Efficient Hydride Process. ACS Applied Nano Materials, 2023, 6, 3218-3225.	2.4	3
49975	Estimation of electron temperature dynamics in warm dense gold using measured and DFT-calculated plasma frequency. Physica Scripta, 2023, 98, 045813.	1.2	0
49976	The Relationship between Photoluminescence Emissions and Photocatalytic Activity of CeO₂ Nanocrystals. Inorganic Chemistry, 2023, 62, 4291-4303.	1.9	4
49977	Structural, electronic, and Li-ion mobility properties of garnet-type Li₇La₃Zr₂O₁₂ surface: An insight from first-principles calculations. Chinese Physics B, 2023, 32, 068201.	0.7	1
49978	Effect of Magnetic Coupling on the Optical Properties of Oxide Co Nanowires on Vicinal Pt Surfaces. Magnetochemistry, 2023, 9, 72.	1.0	0
49979	Atomic reconstruction and oxygen adsorption behavior of the pyrite (100) surface: a DFT study. Physical Chemistry Chemical Physics, 2023, 25, 8826-8835.	1.3	0
49980	Extremely promising monolayer materials with robust ferroelectricity and extraordinary piezoelectricity: Î´-AsN, Î´-SbN, and Î´-BiN. Nanoscale, 2023, 15, 6363-6370.	2.8	7
49981	A comprehensive investigation of the plasmonic-photocatalytic properties of gold nanoparticles for CO₂ conversion to chemicals. Nanoscale, 2023, 15, 7051-7067.	2.8	2
49982	Polarityâ€Driven Atomic Displacements at the 2D Mg₂TiO₄â€MgO (001) Oxide Interface for Hosting Potential Interlayer Excitons. Advanced Materials Interfaces, 2023, 10, .	1.9	0

#	Article	IF	Citations
49983	Onâ€line Optimization of Integrated Carbon Capture and Conversion Process via the Ratings Concept: A Combined DFT and Microkinetic Modeling Approach. ChemCatChem, 0, , .	1.8	0
49984	[illegible] xmlns:mml="http://www.w3.org/1998/Math/MathML"><mml:mrow><mml:mi>T</mml:mi><mml:mtext>a</mml:mtext><mml:mi>x</mml:mi> phase diagrams of Na- and Ag-substituted <mml:math xmlns:mml="http://www.w3.org/1998/Math/MathML"><mml:msub><mml:mi mathvariant="normal">EuCd</mml:mi><mml:mn>2</mml:mn></mml:msub><mml:msub><mml:mi	0.9	2
49985	Use of <mml:math xmlns:mml="http://www.w3.org/1998/Math/MathML"><mml:mrow><mml:mi>DFT</mml:mi><mml:mo>+</mml:mo><mml:mi mathvariant="normal">U</mml:mi><mml:mo>+</mml:mo><mml:mi mathvariant="normal">J</mml:mi></mml:mrow></mml:math> with linear response parameters to predict non-magnetic oxide band gaps with hybrid-functional accuracy. Physical Review Research, 2023, , .	1.3	6
49986	Prediction of topological phases in metastable ferromagnetic <mml:math xmlns:mml="http://www.w3.org/1998/Math/MathML"><mml:mrow><mml:mi>M</mml:mi><mml:mi mathvariant="normal">P</mml:mi><mml:msub><mml:mi>X</mml:mi><mml:mn>3</mml:mn></mml:msub></mml:mrow></mml:math> monolayers. Physical Review B, 2023, 107, .	1.1	3
49987	Atmospheric chemical behaviors of (<scp> CF ₃ </scp>) <scp> ₂ CFCN </scp> by densityâ€functional theory method: The relationship between electronic structure and atmosphere lifetime. International Journal of Quantum Chemistry, 0, , .	1.0	1
49988	Surfaceâ€Dependent Electrocatalytic Activity of CoSe₂ for Lithium Sulfur Battery. Advanced Materials Interfaces, 2023, 10, .	1.9	2
49989	The electronic and mechanical properties of (U, Th)O₂ compounds: a first-principles study. RSC Advances, 2023, 13, 7206-7211.	1.7	0
49990	Structure Determination and Analysis of the Ceramic Material La0.987Ti1.627Nb3.307O13 by Synchrotron and Neutron Powder Diffraction and DFT Calculations. Crystals, 2023, 13, 439.	1.0	0
49991	Electronic structural and lattice thermodynamic properties of MAlO2 and M5AlO4 (Mâ€‰=â€‰Li, Na, K) sorbents for CO2 capture applications. Discover Chemical Engineering, 2023, 3, .	1.1	3
49992	Ab Initio Melting Temperatures of Bcc and Hcp Iron Under the Earthâ€™s Inner Core Condition. Geophysical Research Letters, 2023, 50, .	1.5	10
49993	Atomicâ€Scale Revealing the Structure Distribution between LiMO₂ and Li₂MnO₃ in Liâ€Rich and Mnâ€Based Oxide Cathode Materials. Advanced Energy Materials, 2023, 13, .	10.2	19
49994	Achieving Ferroelectricity in a Centrosymmetric Highâ€Performance Semiconductor by Strain Engineering. Advanced Materials, 2023, 35, .	11.1	4
49995	Iridium oxide nanoribbons with metastable monoclinic phase for highly efficient electrocatalytic oxygen evolution. Nature Communications, 2023, 14, .	5.8	31
49996	Innate dynamics and identity crisis of a metal surface unveiled by machine learning of atomic environments. Journal of Chemical Physics, 2023, 158, .	1.2	6
49997	Crotonaldehyde Adsorption on Cu-Pt Surface Alloys: A Quantum Mechanics Study. Chemistry, 2023, 5, 463-478.	0.9	2
49998	Interaction Modification of Transition Metal Dichalcogenide Layers by Halogenation. Journal of Physical Chemistry C, 2023, 127, 5134-5144.	1.5	1
49999	Thermal Stability and Vibrational Properties of the 6,6,12-Graphyne-Based Isolated Molecules and Two-Dimensional Crystal. Materials, 2023, 16, 1964.	1.3	2
50000	Crystal and electronic structure of thiazolium pentaiodide: an experimental and theoretical study of covalent and non-covalent bonds. Structural Chemistry, 0, , .	1.0	0

#	Article	IF	Citations
50001	In Situ Neutron Scattering Study of the Structure Dynamics of the Ru/Ca₂N:e^{â€“} Catalyst in Ammonia Synthesis. Chemistry of Materials, 2023, 35, 2456-2462.	3.2	3
50002	First Principles Calculation of Adsorption of Water on MgO (100) Plane. Materials, 2023, 16, 2100.	1.3	0
50003	Selective binding and periodic arrangement of magic boron clusters on monolayer borophene. Proceedings of the National Academy of Sciences of the United States of America, 2023, 120, .	3.3	2
50004	Methane Activation and Coupling Pathways on Ni2P Catalyst. Catalysts, 2023, 13, 531.	1.6	3
50005	Prediction of electronic structural properties of semi-Heusler CoHfZ (Z: Sb, Sn). Materials Today: Proceedings, 2023, , .	0.9	0
50006	Ambipolar Electrochemistry of Preâ€Intercalated Ti₃C₂T_x MXene in Ionic Liquid Electrolyte. Batteries and Supercaps, 2023, 6, .	2.4	2
50007	Effect of the surface termination on the adsorption of flue gas by the titanium carbide MXene. Materials Today Chemistry, 2023, 29, 101441.	1.7	5
50008	Aromatic hexazine [N6]4â^' anion featured in the complex structure of the high-pressure potassium nitrogen compound K9N56. Nature Chemistry, 2023, 15, 641-646.	6.6	9
50009	The enhanced photocatalytic and photothermal effects of Ti3C2 Mxene quantum dot/macroscopic porous graphitic carbon nitride heterojunction for Hydrogen Production. Journal of Colloid and Interface Science, 2023, 641, 309-318.	5.0	11
50010	Study on the Half-Auxetic Behavior of Layered Nitrogen-Doped Graphdiyne. Advances in Condensed Matter Physics, 2023, 12, 1-8.	0.1	0
50011	Enhancement of Polarization Properties of Bulk PbTiO₃ by Engineering Strain. Integrated Ferroelectrics, 2023, 232, 186-196.	0.3	1
50012	Vacancy at stacking fault-assisted nucleation of transition-metal carbides and nitrides in Fcc-Fe. Applied Physics A: Materials Science and Processing, 2023, 129, .	1.1	0
50013	Anomalous Photoluminescence Enhancement and Resonant Charge Transfer in Type-II 2D Lateral Heterostructures. Chinese Physics B, 0, , .	0.7	0
50014	Electrically tunable Gilbert damping in van der Waals heterostructures of two-dimensional ferromagnetic metals and ferroelectrics. Applied Physics Letters, 2023, 122, .	1.5	3
50017	An interlinked prediction-experiment paradigm discovering deep-ultraviolet fluorooxoborates with desired optical nonlinearity and birefringence. Matter, 2023, 6, 1188-1202.	5.0	24
50018	Superconductivity in Te-Deficient ZrTe₂. Journal of Physical Chemistry C, 2023, 127, 5162-5168.	1.5	2
50019	Universal Solid-Phase Seed-Mediated Synthesis of Monodisperse and Ultrasmall L1₀-PtM Intermetallic Nanocrystals. Chemistry of Materials, 2023, 35, 2559-2568.	3.2	6
50020	(n, m) Distribution of Single-Walled Carbon Nanotubes Grown from a Non-Magnetic Palladium Catalyst. Molecules, 2023, 28, 2453.	1.7	1

#	Article	IF	Citations
50021	Phase formation capability and compositional design of Î²-phase multiple rare-earth principal component disilicates. Nature Communications, 2023, 14, .	5.8	3
50022	Tungsten Oxide Mediated Quasi-van der Waals Epitaxy of WS₂ on Sapphire. ACS Nano, 2023, 17, 5399-5411.	7.3	8
50023	An automated reaction route mapping for the reaction of NO and active species on Ag₄ clusters in zeolites. Physical Chemistry Chemical Physics, 2023, 25, 8524-8531.	1.3	1
50024	Eu₄Al₁₃Pt₉ â€“ a coloring variant of the Ho₄Ir₁₃Ge₉ type structure. Zeitschrift Fur Naturforschung - Section B Journal of Chemical Sciences, 2023, 78, 147-156.	0.3	0
50025	Theoretical study of the properties of Nb-doped Li3YbCl6 solid-state electrolytes. , 2023, , .		0
50026	Water Oxidation-Induced Surface Reconstruction and Dissolution at the RuO₂(110) Surface Revealed by First-Principles Simulation. Journal of Physical Chemistry C, 2023, 127, 5334-5342.	1.5	7
50027	First-Principles Study of the Effects of Ti Content on Mechanical Properties and Microscopic Mechanism in Cu2AlMn1â€“xTix Alloys. Crystals, 2023, 13, 466.	1.0	0
50028	Templateâ€Free Synthesis of Phosphorusâ€Doped gâ€C₃N₄ Microâ€Tubes with Hierarchical Coreâ€“Shell Structure for Highâ€Efficient Visible Light Responsive Catalysis. Small, 2023, 19, .	5.2	13
50029	Hybrid Functional-Based Scissors Operator for Perovskite Oxide Nanostructures: A NaTaO₃ Case Study. Journal of Physical Chemistry C, 2023, 127, 5604-5612.	1.5	0
50030	Coexistence and coupling of ferroelectricity and magnetism in an oxide two-dimensional electron gas. Nature Physics, 2023, 19, 823-829.	6.5	4
50031	SiCO Ceramics as Storage Materials for Alkali Metals/Ions: Insights on Structure Moieties from Solidâ€State NMR and DFT Calculations. ChemSusChem, 2023, 16, .	3.6	0
50032	Synthesis, Structure, and Non-Covalent Interactions of 5-Methyl-2,3-dihydrothiazolo[2,3-b]thiazolium Halides. Russian Journal of General Chemistry, 2023, 93, 22-30.	0.3	1
50033	Asymmetric Janus functionalization induced magnetization and switchable out-of-plane polarization in 2D MXene Mo₂CXXâ€². Physical Chemistry Chemical Physics, 2023, 25, 8676-8683.	1.3	3
50034	Comment on â€œTwo-dimensional penta-like PdPSe with a puckered pentagonal structure: a first-principles studyâ€• by A. Bafekry, M. M. Fadlallah, M. Faraji, A. Shafique, H. R. Jappor, I. Abdolhoseini Sarsari, Y. S. Ang and M. Ghergherehchii, Phys. Chem. Chem. Phys., 2022, 24, 9990. Physical Chemistry Chemical Physics, 2023, 25, 8961-8965.	1.3	0
50035	Pentagonal C_mX_nY_{6â€“mâ€“n} (m =) Tj ETQq0 0 0 rgBT /Over Poisson Ratios with Giant Piezoelectric Effects. Journal of Physical Chemistry Letters, 2023, 14, 2692-2701.	2.1	2
50036	AB INITIO STUDY OF L4-, L3-6-, AND L3-4-6-DIAMOND-LIKE TUBULAR NANOSTRUCTURES. Journal of Structural Chemistry, 2023, 64, 324-334.	0.3	1
50037	Theoretical exploration on the activity of copper single-atom catalysts for electrocatalytic reduction of CO₂. Journal of Materials Chemistry A, 2023, 11, 7735-7745.	5.2	8
50038	Boosting Pseudocapacitive Behavior of Supercapattery Electrodes by Incorporating a Schottky Junction for Ultrahigh Energy Density. Nano-Micro Letters, 2023, 15, .	14.4	21

#	Article	IF	Citations
50039	Ab initio studies on graphyne (GY) for the detection of rare bases in DNA. Physical Chemistry Chemical Physics, 2023, 25, 10472-10480.	1.3	1
50040	A DFT study of structural and electronic properties of some B₁₂-based compounds under hydrostatic pressure. Physica Scripta, 2023, 98, 045907.	1.2	0
50041	Dualâ€Channel Dielectric Tunability in Highly Textured BaTi_{0.99}Fe_{0.01}O_{3â^'}_{Î´} Ceramics With Microâ€Twin Boundary. Advanced Electronic Materials, 2023, 9, .	2.6	1
50042	Anomalous transient blueshift in the internal stretch mode of CO/Pd(111). Physical Review B, 2023, 107, .	1.1	1
50043	Strain tunability of the properties of Fe- doped lithium niobate for optoelectronic applications: Theoretical insights. Main Group Chemistry, 2023, , 1-10.	0.4	1
50044	Insights into plastic deformation mechanisms of austenitic steels by coupling generalized stacking fault energy and semi-discrete variational Peierls-Nabarro model. Progress in Natural Science: Materials International, 2023, 33, 83-91.	1.8	2
50045	Ab-initio study of electronic, mechanical and thermodynamic properties of Î²-Tiâ€“15Nbâ€“xSi alloys for biomaterials applications. International Journal of Modern Physics B, 2024, 38, .	1.0	0
50046	Electrochemical Reduction of Nitrates on CoO Nanoclustersâ€Functionalized Graphene with Highest Mass Activity and Nearly 100% Selectivity to Ammonia. Advanced Energy Materials, 2023, 13, .	10.2	22
50047	Interface synergism and engineering of Pd/Co@N-C for direct ethanol fuel cells. Nature Communications, 2023, 14, .	5.8	33
50048	Controlled synthesis of monodispersed ZnSe microspheres for enhanced photo-catalytic application and its corroboration using density functional theory. Physical Chemistry Chemical Physics, 2023, 25, 10567-10582.	1.3	1
50049	From high-entropy alloys to high-entropy ceramics: The radiation-resistant highly concentrated refractory carbide (CrNbTaTiW)C. Acta Materialia, 2023, 250, 118856.	3.8	16
50050	Ensemble Effect of Ruthenium Single-Atom and Nanoparticle Catalysts for Efficient Hydrogen Evolution in Neutral Media. ACS Applied Materials & Interfaces, 0, , .	4.0	0
50051	Thermoelectric Performance of an n-Doped CaSbK Half-Heusler Compound. Journal of Electronic Materials, 2023, 52, 3499-3507.	1.0	0
50052	Neural network potentials for accelerated metadynamics of oxygen reduction kinetics at Auâ€“water interfaces. Chemical Science, 2023, 14, 3913-3922.	3.7	8
50053	Unraveling the Detailed Interactions between the Surface Species and Nanoparticle Catalyst by a Temperature-Programed Desorption Spectrum at the Molecular Level via a Multi-Scale Simulation and Modeling Experiment. Journal of Physical Chemistry C, 2023, 127, 5299-5307.	1.5	0
50054	Constructing imine groups on the surface of Cu₁/Pd(111) as a novel strategy for CO₂ hydrogenation to methanol. Nanoscale, 2023, 15, 6999-7005.	2.8	2
50055	Visibleâ€lightâ€responsive Photocatalyst Based on Nitrogenâ€doped Bulk Oxide YTaO_{4â^'x}N_y for Zâ€scheme Overall Water Splitting. Chemistry - an Asian Journal, 2023, 18, .	1.7	4
50056	Strain-Induced Electronic Structure and Bandgap Transition in Bilayer $ext{MoSe}_{2}$ of AB and AA Stacking Order. , 2022, , .		0

#	Article	IF	Citations
50057	PEA2PbI4: fast two-dimensional lead iodide perovskite scintillator with green and red emission. Materials Today Chemistry, 2023, 29, 101455.	1.7	6
50058	Remarkable Electrical Conductivity Increase and Pure Metallic Properties from Semiconducting Colloidal Nanocrystals by Cation Exchange for Solutionâ€Processable Optoelectronic Applications. Small, 0, , 2207511.	5.2	0
50059	Quantum Catalytic Performance for the Hydrogen Evolution Reaction and the Ethanol Oxidation Reaction in Topological Edge States of SrPd and BaPd Semimetal Monolayers: A Theoretical Study. Journal of Physical Chemistry C, 2023, 127, 5271-5280.	1.5	2
50060	Fluence dependent dynamics of excitons in monolayer MoSi₂Z₄ (Z =) Tj ETQq1 1 0.784314 rgBT /Overlock	0.7	4
50061	Quantum Chemical Investigation of Snowâ€“Mercury Interactions and Their Implication of Mercury Deposition in the Arctic. Journal of Physical Chemistry A, 2023, 127, 2554-2563.	1.1	0
50062	The Temperature Dependence of the Hexagonal Boron Nitride Oxidation Resistance, Insights from Firstâ€Principle Computations. Nanomaterials, 2023, 13, 1041.	1.9	1
50063	Theoretical Assessment of the Mechanism and Active Sites in Alkene Dimerization on Ni Monomers Grafted onto Aluminosilicates: (Niâ€“OH)⁺ Centers and Câ€“C Coupling Mediated by Lewis Acidâ€“Base Pairs. Journal of the American Chemical Society, 2023, 145, 6349-6361.	6.6	8
50064	A DFT study on how vanadium affects hydrogen storage kinetics in magnesium nickel hydride. International Journal of Hydrogen Energy, 2023, 48, 20378-20387.	3.8	2
50065	Characterizing the Impact of Mg-Doped Li Metal Anode and Excess Electrons on High Concentration Electrolyte Interfacial Stability: A Theoretical Study. ACS Applied Energy Materials, 2023, 6, 3291-3300.	2.5	0
50066	Mechanistic Insights into Nonoxidative Ethanol Dehydrogenation on NiCu Single-Atom Alloys. ACS Catalysis, 2023, 13, 4290-4303.	5.5	10
50067	Structural and thermodynamic properties of quasi-2D Mo_(1â€“x)W_x(S, Se,) Tj ETQq0 0 0 rgBT /Overlock 10	1.3	1
50068	Effects of functional groups in iron porphyrin on the mechanism and activity of oxygen reduction reaction. RSC Advances, 2023, 13, 8523-8534.	1.7	2
50069	Catalytic Reduction of N2O by CO on Single-Atom Catalysts Au/C2N and Cu/C2N: A First-Principles Study. Catalysts, 2023, 13, 578.	1.6	1
50070	Theoretical Study of Pressure-Induced Phase Transitions in Sb2S3, Bi2S3, and Sb2Se3. Crystals, 2023, 13, 498.	1.0	3
50071	Computational Investigation of Precursor Blocking during Area-Selective Atomic Layer Deposition Using Aniline as a Small-Molecule Inhibitor. Langmuir, 2023, 39, 4265-4273.	1.6	2
50072	Isotopic Constraints on the Nature of Primary Precipitates in Archeanâ€“Early Paleoproterozoic Iron Formations from Determinations of the Iron Phonon Density of States of Greenalite and 2L- and 6L-Ferrihydrite. ACS Earth and Space Chemistry, 2023, 7, 712-727.	1.2	4
50073	Voltage-Dependent First-Principles Simulation of Insertion of Chloride Ions into Al/Al₂O₃ Interfaces Using the Quantum Continuum Approximation. Journal of the Electrochemical Society, 2023, 170, 031506.	1.3	2
50074	An effective strategy for CO₂ reduction to C1 products using Cu-embedded MoS₂ electrocatalyst: DFT study. New Journal of Chemistry, 2023, 47, 6932-6942.	1.4	2

#	Article	IF	Citations
50075	Healing double vacancy defects on graphene: reconstruction by C₂ adsorption. Physical Chemistry Chemical Physics, 2023, 25, 10759-10768.	1.3	0
50076	A {Cu₂I₃^{â^'}}_{âˆž} chain hybrid with two-step phase transition, switchable dielectrics, thermochromism and piezochromism. Dalton Transactions, 0, , .	1.6	1
50077	Bulk Modulus, Elastic Constants, and Force Constants of Interatomic Bonds of IIâ€“III₂â€“VI₄ Compounds. Physica Status Solidi (B): Basic Research, 2023, 260, .	0.7	0
50078	Single atom modified two-dimensional bismuthenes for toxic gas detection. Physical Chemistry Chemical Physics, 2023, 25, 9249-9255.	1.3	4
50079	Study of pnictides for photovoltaic applications. Physical Chemistry Chemical Physics, 2023, 25, 9626-9635.	1.3	1
50080	Chemically induced ferromagnetism near room temperature in single crystal (Zn_{1â^'x}Cr_x)Te half-metal. RSC Advances, 2023, 13, 8551-8556.	1.7	0
50081	Polytypism of Ln(SeO₃)(HSeO₃)Â·2H₂O compounds: synthesis and crystal structure of the first monoclinic modification of Nd(SeO₃)(HSeO₃)Â·2H₂O, DFT calculations and order/disorder description. Acta Crystallographica Section B: Structural Science, Crystal Engineering and Materials, 2023, 79, 176-183.	0.5	2
50082	Ab initio investigation of Bi/BaTiO₃ and Bi/PbTiO₃ heterostructures for spintronic applications. Ferroelectrics, 2023, 605, 27-35.	0.3	1
50083	Investigating the role of phonons in the phase stability of uranium-based Laves phases. RSC Advances, 2023, 13, 8646-8656.	1.7	2
50084	Tunable growth of one-dimensional graphitic materials: graphene nanoribbons, carbon nanotubes, and nanoribbon/nanotube junctions. Scientific Reports, 2023, 13, .	1.6	3
50085	Cd implantation in <mml:math xmlns:mml="http://www.w3.org/1998/Math/MathML"><mml:mrow><mml:mi>Î±</mml:mi><mml:mtext>â^'</mml:mtext><mml:msub><: An atomic scale study. Physical Review Materials, 2023, 7, .	0.0	0
50086	Theoretical exploration of Rh1/CeO2 catalysts with high performance using CO oxidation as a probe reaction. Molecular Catalysis, 2023, 541, 113077.	1.0	0
50087	Intercalation of p-Aminopyridine and p-Ethylenediamine Molecules into Orthorhombic In1.2Ga0.8S3 Single Crystals. Materials, 2023, 16, 2368.	1.3	1
50088	Novel tungsten nitride crystal providing nanochannels for hydrogen removal and recycling in PFMs. Journal of Chemical Physics, 2023, 158, 124125.	1.2	0
50089	Highly active hydrogen evolution facilitated by topological surface states on a Pd/SnTe heterostructure. Cell Reports Physical Science, 2023, 4, 101332.	2.8	2
50090	Facile Tailoring of Surface Terminations of MXenes by Doping Nb Element: Toward Extraordinary Pseudocapacitance Performance. ACS Applied Materials & Interfaces, 2023, 15, 15367-15376.	4.0	6
50091	Selective Pb2+ removal and electrochemical regeneration of fresh and recycled FeOOH. Nano Research, 2023, 16, 9352-9363.	5.8	3
50092	Matrix transformation of lunar regolith and its use as a feedstock for additive manufacturing. IScience, 2023, 26, 106382.	1.9	2

#	Article	IF	Citations
50093	Effect of Adsorbed Sulfate on the Product Selectivity of Ethanol Oxidation on Pt Nanoparticles in Acidic Solution. Journal of Physical Chemistry C, 2023, 127, 5743-5753.	1.5	3
50094	Van der Waals Stacked 2D-Layered Co₂Ge₂Te₆ with High Curie Temperature and Large Magnetic Crystal Anisotropy. Journal of Physical Chemistry C, 2023, 127, 5991-6001.	1.5	0
50095	Quantitative Evaluation of the Carrier Separation Performance of Heterojunction Photocatalysts: The Case of g-C₃N₄/SrTiO₃. Journal of Physical Chemistry Letters, 2023, 14, 2927-2932.	2.1	1
50096	Frequency Splitting of Chiral Phonons from Broken Time-Reversal Symmetry in <mml:math xmlns:mml="http://www.w3.org/1998/Math/MathML" display="inline"><mml:mrow><mml:msub><mml:mrow><mml:mi>CrI</mml:mi></mml:mrow><mml:mrow><mml:mn>3</mml:mn></ Physical Review Letters, 2023, 130, .	2.9	7
50097	Temperature phase transitions in silver niobate and lithium tantalate-modified silver niobate ceramics. Physical Chemistry Chemical Physics, 2023, 25, 11410-11417.	1.3	1
50098	Early melting of tantalum carbide under anisotropic stresses: An <mml:math xmlns:mml="http://www.w3.org/1998/Math/MathML"><mml:mrow><mml:mi>a</mml:mi><mml:mi>b</mml:mi></mml:mrow></mml: <mml:math xmlns:mml="http://www.w3.org/1998/Math/MathML"><mml:mrow><mml:mi>i</mml:mi><mml:mi>n</mml:mi><mml:mi>i</mml:mi> molecular dynamics study. Physical Review B, 2023, 107, .	1.1	4
50099	Unique features of the structural phase transition in acetylene showing simultaneous characteristics of reconstructive, displacive and orderâ€“disorder. Physical Chemistry Chemical Physics, 2023, 25, 9909-9924.	1.3	0
50100	Investigation of the Interaction Between Au and Brookite TiO2 Using Transmission Electron Microscopy and Density Functional Theory. Bulletin of the Chemical Society of Japan, 2023, 96, 373-380.	2.0	3
50101	Improving the adsorption capacity of amino-modified Mg-Al LDH using a combined DFT and experiment. Journal of CO2 Utilization, 2023, 71, 102454.	3.3	0
50102	Nitrogen and sulfur co-doped Ti₃C₂T_x MXenes for high-rate lithium-ion batteries. Physical Chemistry Chemical Physics, 2023, 25, 10635-10646.	1.3	2
50103	The charge effects on the hydrogen evolution reaction activity of the defected monolayer MoS₂. Physical Chemistry Chemical Physics, 2023, 25, 10956-10965.	1.3	5
50104	Tunable Electronic Properties of Substitutionally Doped CSb Monolayer. Physica Status Solidi - Rapid Research Letters, 0, , .	1.2	0
50105	Prediction of elastic properties of face-centered cubic high-entropy alloys by machine learning. Transactions of Nonferrous Metals Society of China, 2023, 33, 518-530.	1.7	6
50106	First-Principles Density Functional Theory Calculations on the Potential of Sc₂CO₂ MXene Nanosheets as a Dual-Mode Sensor for Detection of Volatile Organic Compounds in Exhaled Human Breath. ACS Applied Nano Materials, 2023, 6, 5345-5356.	2.4	12
50107	Influence of Capping Ligands, Solvent, and Thermal Effects on CdSe Quantum Dot Optical Properties by DFT Calculations. ACS Omega, 2023, 8, 11467-11478.	1.6	3
50108	Identification of Hydrogen Trapping in Aluminum Alloys Via Muon Spin Relaxation Method and First-Principles Calculations. Metallurgical and Materials Transactions A: Physical Metallurgy and Materials Science, 2023, 54, 2374-2383.	1.1	1
50109	Ab initio investigation of charge density wave and superconductivity in two-dimensional Janus <mml:math xmlns:mml="http://www.w3.org/1998/Math/MathML"><mml:mrow><mml:mn>2</mml:mn><mml:mi>H</mml:mi></mml:mrow><mml:m -MoSH monolayers. Physical Review B, 2023, 107, .	1.1	6
50110	A systematic computational investigation of lithiation-induced structural phase transitions of O-functionalized MXenes. Physical Chemistry Chemical Physics, 2023, 25, 9428-9436.	1.3	2

#	Article	IF	Citations
50111	Origin of the variation in lattice thermal conductivities in pyrite-type dichalcogenides. Physical Review B, 2023, 107, .	1.1	2
50113	Mesoporous Pt@Pt-skin Pt3Ni core-shell framework nanowire electrocatalyst for efficient oxygen reduction. Nature Communications, 2023, 14, .	5.8	38
50114	DFT characterization of a new possible two-dimensional BN allotrope with a biphenylene network structure. Physical Chemistry Chemical Physics, 2023, 25, 11613-11619.	1.3	4
50115	The role of interstitial Cu on thermoelectric properties of ZrNiSn half-Heusler compounds. Materials Today Physics, 2023, 33, 101049.	2.9	3
50116	Regulating the Coordination Environment of Single-Atom Catalysts Anchored on Thiophene Linked Porphyrin for an Efficient Nitrogen Reduction Reaction. ACS Applied Materials & Interfaces, 2023, 15, 15545-15560.	4.0	15
50117	Surface energy and surface stability of cesium tin halide perovskites: a theoretical investigation. Physical Chemistry Chemical Physics, 2023, 25, 10583-10590.	1.3	4
50118	The Study of Nickel Impurity Segregation on LSNT Perovskite Open Surfaces by Ab Initio Molecular Dynamics. Russian Microelectronics, 2022, 51, 654-658.	0.1	0
50119	Theoretical study on structural and mechanical properties of Si-containing ternary transition metal nitrides M_{0.5}Si_{0.5}N (M = Ti, Zr, Hf). RSC Advances, 2023, 13, 9109-9118.	1.7	0
50120	Observation of ferromagnetism in CeCr₂Si₂C single crystals. Journal of Materials Chemistry A, 2023, 11, 8817-8825.	5.2	1
50121	Aromatic Clusters and Hydrogen Storage. Energies, 2023, 16, 2833.	1.6	0
50122	Near-Field Radiative Heat Transfer between $eta-$GeSe monolayers: An ab initio study. Nanoscale and Microscale Thermophysical Engineering, 2023, 27, 95-109.	1.4	1
50123	An effective strategy of indium half-doping to stabilize the structure and improve optoelectronic characteristics of Tl-Co based double perovskite: First principles study. Results in Physics, 2023, 47, 106375.	2.0	4
50124	Interface of Ni-MgCr₂O₄ Spinel Promotes the Autothermal Reforming of Acetic Acid through Accelerated Oxidation of Carbon-Containing Intermediate Species. ACS Catalysis, 2023, 13, 4560-4574.	5.5	9
50125	Strong Magnetocaloric Coupling in Oxyorthosilicate with Dense Gd³⁺ Spins. Inorganic Chemistry, 2023, 62, 5282-5291.	1.9	6
50126	A DFT Study of Ruthenium fcc Nano-Dots: Size-Dependent Induced Magnetic Moments. Nanomaterials, 2023, 13, 1118.	1.9	2
50127	Highly Oxidized Oxide Surface toward Optimum Oxygen Evolution Reaction by Termination Engineering. ACS Nano, 2023, 17, 6811-6821.	7.3	8
50128	2D carbon nitrides: Regulating non-metal boron-doped C3N5 for elucidating the mechanism of wide pH range photocatalytic hydrogen evolution reaction. Chinese Journal of Catalysis, 2023, 47, 150-160.	6.9	15
50129	Electronic signatures of successive itinerant, antiferromagnetic transitions in hexagonal La₂Ni₇. Journal of Physics Condensed Matter, 2023, 35, 245501.	0.7	1

#	Article	IF	Citations
50130	First-principles structure prediction of two-dimensional HCN polymorphs obtained via formal molecular polymerization. Nanoscale, 0, , .	2.8	0
50131	First-principles study of square chalcogen bond interactions and its adsorption behavior on silver surface. Physical Chemistry Chemical Physics, 2023, 25, 10836-10844.	1.3	0
50132	Computational Study of the Adsorption of Small Gas Molecules on Pillar[5]arenes. ChemistrySelect, 2023, 8, .	0.7	1
50133	Ab Initio Study of the Electronic Structure and Lattice Dynamics of Scheelite Type AgTcO₄. Physica Status Solidi (B): Basic Research, 2023, 260, .	0.7	0
50134	Rediscovering the intrinsic mechanical properties of bulk nanocrystalline indium arsenide. Nanoscale, 0, , .	2.8	0
50135	Water Splitting on a Pt1/C3N4 Single Atom Catalyst: A Modeling Approach. Topics in Catalysis, 0, , .	1.3	3
50136	Prominent Size Effects without a Depolarization Field Observed in Ultrathin Ferroelectric Oxide Membranes. Physical Review Letters, 2023, 130, .	2.9	11
50137	Phosphorous/Fluorine Coâ€doped Biomassâ€derived Carbon for Enhanced Sodiumâ€ion and Lithiumâ€ion Storage. ChemNanoMat, 2023, 9, .	1.5	3
50138	Accelerating ammonia synthesis in a membraneless flow electrolyzer through coupling ambient dinitrogen oxidation and water splitting. IScience, 2023, 26, 106407.	1.9	1
50139	Ni nanoparticle coupled surface oxygen vacancies for efficient synergistic conversion of palmitic acid into alkanes. Chinese Journal of Catalysis, 2023, 47, 229-242.	6.9	7
50140	Evidence of half-metallicity at the BiFeO₃(001) surface. New Journal of Chemistry, 2023, 47, 6983-6992.	1.4	0
50141	CrPS4 Nanoflakes as Stable Direct-Band-Gap 2D Materials for Ultrafast Pulse Laser Applications. Nanomaterials, 2023, 13, 1128.	1.9	2
50142	Strong Scattering from Low-Frequency Rattling Modes Results in Low Thermal Conductivity in Antimonide Clathrate Compounds. Chemistry of Materials, 2023, 35, 2918-2935.	3.2	3
50143	An Isothiazolanthroneâ€Based Selfâ€Assembling Anticancer Colorâ€Changing Dye for Concurrent Imaging and Monitoring of Cell Viability. Chemistry - an Asian Journal, 2023, 18, .	1.7	1
50144	Transport in electron-photon systems. Frontiers of Physics, 2023, 18, .	2.4	7
50145	Fine electron and phonon transports manipulation by Mn compensation for high thermoelectric performance of Sb2Te3(SnTe)n materials. Materials Today Physics, 2023, 33, 101055.	2.9	2
50146	Geometrical and Electronic Structure Analysis of Mnâ€Doped CaMO₃ (Mâ€‰=â€‰Ti, Zr, and Sn). Physica Status Solidi (B): Basic Research, 2023, 260, .	0.7	2
50147	Ruâ€Catalyzed Hydrogenolysis of Methanol: A Computational and Kinetics Study. ChemCatChem, 2023, 15, .	1.8	1

#	Article	IF	Citations
50148	A new two-dimensional MgICl Janus monolayer for optoelectronic applications. European Physical Journal B, 2023, 96, .	0.6	0
50149	PtTe₂/Sb₂S₃ Nanoscale Heterostructures for the Photocatalytic Direct Z-Scheme with High Solar-to-Hydrogen Efficiency: A Theoretical Investigation. ACS Applied Nano Materials, 2023, 6, 5591-5601.	2.4	11
50150	Effect of Oxygen Reduction Reaction on Pt/Pd3Fe (111) Alloy Electrocatalyst: A DFT Study. Russian Journal of Physical Chemistry A, 2022, 96, 3170-3178.	0.1	0
50151	Electronic, Optical, Thermoelectric and Elastic Properties of RbxCs1â^'xPbBr3 Perovskite. Molecules, 2023, 28, 2880.	1.7	5
50152	Data-Driven Design of High-Performance Graphene-Based Seawater Desalination Membranes. ACS Applied Nano Materials, 2023, 6, 5889-5900.	2.4	8
50153	Structural, mechanical, and electronic properties of Niâ€“Co-based layered transition metal oxide LiNixCo1â^'xO2 for Li-ion batteries from first principles. Journal of Chemical Physics, 2023, 158, .	1.2	1
50154	Structure engineering of CeO₂for boosting the Au/CeO₂nanocatalyst in the green and selective hydrogenation of nitrobenzene. Nanoscale Horizons, 2023, 8, 812-826.	4.1	5
50155	Polymorphism mediated by electric fields: a first principles study on organic/inorganic interfaces. Nanoscale Advances, 2023, 5, 2288-2298.	2.2	0
50156	Dynamics of Dissociative Chemisorption of NH₃ on Fe(111) on a Twelve-Dimensional Potential Energy Surface. Journal of Physical Chemistry C, 2023, 127, 6328-6336.	1.5	2
50157	Activation of NO₂ by Modifying the Porphyrin Unit with Oxygen in a MnN₄ Graphene Layer. ChemistrySelect, 2023, 8, .	0.7	0
50158	Li self-diffusion and ion conductivity in congruent <mml:math xmlns:mml="http://www.w3.org/1998/Math/MathML"><mml:msub><mml:mi>LiNbO</mml:mi><mml:mn>3</mml:mn></mml:msub></m and <mml:math xmlns:mml="http://www.w3.org/1998/Math/MathML"><mml:msub><mml:mi>LiTaO</mml:mi><mml:mn>3</mml:mn></mml:msub></m single crystals. Physical Review Materials, 2023, 7, .	0.9	6
50159	Automatic differentiation for orbital-free density functional theory. Journal of Chemical Physics, 2023, 158, .	1.2	2
50160	DFT-based study of the buckling variation effects on optical and electronic aspects of TH-carbon monolayer. International Journal of Modern Physics B, 2024, 38, .	1.0	0
50161	Dynamics of photoinduced ferromagnetism in oxides with orbital degeneracy. Physical Review Research, 2023, 5, .	1.3	0
50162	Highâ€rate electrochemical H₂O₂ production over multimetallic atom catalysts under acidicâ€“neutral conditions. , 2024, 6, .		2
50163	Size Limiting Elemental Ferroelectricity in Bi Nanoribbons: Observation, Mechanism, and Opportunity. Journal of Physical Chemistry Letters, 2023, 14, 3160-3167.	2.1	6
50164	Improving the Oxygen Evolution Reaction on Fe₃O₄(001) with Single-Atom Catalysts. ACS Catalysis, 2023, 13, 4811-4823.	5.5	7
50165	Stable self-trapped broadband emission from an organolead halide coordination polymer with strong layer corrugation and high chemical robustness. Inorganic Chemistry Frontiers, 2023, 10, 2645-2652.	3.0	2

#	Article	IF	Citations
50166	Oxygen nonstoichiometry as a source of ferromagnetism in GdCoO₃: first-principle investigation. Spin, 0, , .	0.6	0
50167	Atomic-scale study clarifying the role of space-charge layers in a Li-ion-conducting solid electrolyte. Nature Communications, 2023, 14, .	5.8	16
50168	Development of an equation of state to characterize an electron beam interacting with an aluminum target. Journal of Applied Physics, 2023, 133, 125901.	1.1	0
50169	Substrate-Induced Changes on the Optical Properties of Single-Layer WS2. Materials, 2023, 16, 2591.	1.3	0
50170	High-efficiency resistive switch and artificial synaptic simulation in antimony-based perovskite devices. Science China Technological Sciences, 2023, 66, 1141-1151.	2.0	4
50171	Polar meron-antimeron networks in strained and twisted bilayers. Nature Communications, 2023, 14, .	5.8	9
50172	First-Principles Studies in Pd-Based $${varvec{R}}{{varvec{P}}{varvec{d}}}_{2}{{varvec{P}}}_{2}$$ÂÂ(Râ€‰=â€‰Pr and Nd) Superconductors Under Pressure. Journal of Superconductivity and Novel Magnetism, 2023, 36, 885-902.	0.8	3
50173	Structural, elastic, electronic, and optical properties of NaAlSi3O8 and Al4[Si4O10](OH)8 from first-principles calculations. Journal of Molecular Modeling, 2023, 29, .	0.8	1
50174	The contribution of phonons to the thermal expansion of some simple cubic hexaboride structures: SmB₆, CaB₆, SrB₆ and BaB₆. Physical Chemistry Chemical Physics, 2023, 25, 10749-10758.	1.3	1
50175	Ti3CNT MXene/rGO scaffolds directing the formation of a robust, layered SEI toward high-rate and long-cycle lithium metal batteries. Energy Storage Materials, 2023, 58, 322-331.	9.5	10
50176	DFT-Based Investigation of the Structural Stability, Elastic, Electronic, and Magnetic in Pd2CrGe Heusler Alloy. Journal of Superconductivity and Novel Magnetism, 2023, 36, 1061-1074.	0.8	3
50177	Two-dimensional dichalcogenides of type XY$$_2$$ (X=Mo,W; Y=S,Se): A DFT study of the structural, optoelectronic, thermodynamic properties, infrared, and Raman spectra. Journal of Materials Research, 2023, 38, 2072-2083.	1.2	2
50178	Single Selenium Atomic Vacancy Enabled Efficient Visible-Light-Response Photocatalytic NO Reduction to NH3 on Janus WSSe Monolayer. Molecules, 2023, 28, 2959.	1.7	5
50179	Highâ€Activity Fe₃C as pHâ€Universal Electrocatalyst for Boosting Oxygen Reduction Reaction and Zincâ€Air Battery. Small, 2023, 19, .	5.2	15
50180	Interface-vacancy synergy of Co(OH)2/CoN to boost alkaline water splitting. Science China Materials, 2023, 66, 2246-2256.	3.5	4
50181	Defect-Engineered 3D Nanostructured MoS₂ for Detection of Ammonia Gas at Room Temperature. ACS Applied Nano Materials, 2023, 6, 5284-5297.	2.4	6
50182	Structural, mechanical and thermal properties of cubic bixbyite-structured high-entropy oxides. Chemical Engineering Journal, 2023, 464, 142649.	6.6	6
50183	Enhanced Photocatalytic Activity of Two-Dimensional Polar Monolayer SiTe for Water-Splitting via Strain Engineering. Molecules, 2023, 28, 2971.	1.7	0

#	Article	IF	Citations
50184	Resolving the polar interface of infinite-layer nickelate thin films. Nature Materials, 2023, 22, 466-473.	13.3	13
50185	Hollow sphere of heterojunction (NiCu)S/NC as advanced anode for sodium-ion battery. Journal of Energy Chemistry, 2023, 82, 248-258.	7.1	9
50186	Deterministic Magnetic Switching in Perpendicular Magnetic Trilayers Through Sunlightâ€Induced Photoelectron Injection. Small, 2023, 19, .	5.2	5
50187	Electronic band structure, mechanical and optical characteristics of new lead-free halide perovskites for solar cell applications based on DFT computation. Bulletin of Materials Science, 2023, 46, .	0.8	5
50188	The interfacial twin boundary phases tailored by Î²-stabilizers in Î²-Ti alloys: A first-principles study. Scripta Materialia, 2023, 231, 115455.	2.6	1
50189	Efficient GW calculations in two dimensional materials through a stochastic integration of the screened potential. Npj Computational Materials, 2023, 9, .	3.5	7
50190	Prediction of two stable freestanding <mml:math xmlns:mml="http://www.w3.org/1998/Math/MathML"><mml:msub><mml:mi>Î²</mml:mi><mml:mn>12</mml:mn></mml:msub></mml borophanes: Structure, electronic properties, and superconductivity. Physical Review Materials, 2023, 7, .	0.9	5
50191	Exploring Spin-Phonon Coupling in Magnetic 2D Metal-Organic Frameworks. Nanomaterials, 2023, 13, 1172.	1.9	0
50192	Role of Oxygen in Vacancy-Induced Phase Formation and Crystallization of Al₂TiO₅-Based Chemical Vapor-Deposited Coatings. Journal of Physical Chemistry C, 2023, 127, 6456-6465.	1.5	1
50193	Evaluating the harmonic approximation for the prediction of thermodynamic formation properties of solids. Computational Materials Science, 2023, 223, 112152.	1.4	2
50194	First-Principles Study of the Magnetic and Electronic Structure of NdB4. Materials, 2023, 16, 2627.	1.3	1
50195	Predicting the Na⁺ ion transport properties of NaSICON materials using density functional theory and Kinetic Monte Carlo. Journal of Materials Chemistry A, 2023, 11, 9160-9177.	5.2	2
50196	Stripe helical magnetism and two regimes of anomalous Hall effect in NdAlGe. Physical Review Materials, 2023, 7, .	0.9	4
50197	Optimized 2D nanostructures for catalysis of hydrogen evolution reactions. MRS Advances, 2023, 8, 307-310.	0.5	1
50198	Prediction of a Reentrant Phase Transition Behavior of Cotunnite in Zirconia and Hafnia at High Pressures. Journal of Superhard Materials, 2023, 45, 10-19.	0.5	2
50199	Radial-tangential mode of single-wall carbon nanotubes manifested by Landau regulation: reinterpretation of low- and intermediate-frequency Raman signals. Scientific Reports, 2023, 13, .	1.6	4
50200	Surface modification with lithium-ion conductor Li3PO4 to enhance the electrochemical performance of lithium-rich layered Li1.2Ni0.2Mn0.6O2. Ionics, 2023, 29, 2141-2152.	1.2	5
50201	Two-component density functional theory study of quantized muons in solids. Physical Review B, 2023, 107, .	1.1	4

#	Article	IF	Citations
50202	Electrochemical partial reduction of Ni(OH)2 to Ni(OH)2/Ni via coupled oxidation of an interfacing NiAl intermetallic compound for robust hydrogen evolution. Journal of Energy Chemistry, 2023, 82, 560-571.	7.1	7
50203	Unique (100) Surface Configuration Enables Promising Oxygen Reduction Performance for Pt₃Co Nanodendrite Catalysts. ACS Applied Materials & Interfaces, 2023, 15, 18217-18228.	4.0	3
50204	Machine Learning for Halide Perovskite Materials ABX3 (B = Pb, X = I, Br, Cl) Assessment of Structural Properties and Band Gap Engineering for Solar Energy. Materials, 2023, 16, 2657.	1.3	4
50205	Supported Pt Nanoclusters on Single-Layer MoS₂ for the Detection of Cortisol: From Atomistic Scale to Device Modeling. ACS Applied Electronic Materials, 2023, 5, 2977-2987.	2.0	1
50206	Electronic structure and optical properties of Br- and Cl-doped rutile TiO2 for application in self-cleaning and photovoltaic panelâ€™s coatings: first-principle calculations. Environmental Science and Pollution Research, 2023, 30, 81697-81706.	2.7	2
50207	Silicate Dissolution Mechanism from Metakaolinite Using Density Functional Theory. Nanomaterials, 2023, 13, 1196.	1.9	8
50208	A first principles study of structural and optoelectronic properties and photocatalytic performance of GeCâ€“MX₂ (M = Mo and W; X = S and Se) van der Waals heterostructures. Physical Chemistry Chemical Physics, 2023, 25, 11169-11175.	1.3	3
50209	Dopability and Magnetic Properties of 3d Transition Metals in an Atomic-Thick SnTe (001) Monolayer. Journal of Physical Chemistry C, 2023, 127, 6389-6395.	1.5	0
50210	Thermomechanical analysis of the new ferromagnetic MAX-phase compound Mn2VSnC2: Insights from DFT calculations. Pramana - Journal of Physics, 2023, 97, .	0.6	1
50211	Band Modification and Localized Lattice Engineering Leads to High Thermoelectric Performance in Ge and Bi Codoped SnTeâ€“AgBiTe₂ Alloys. Small, 2023, 19, .	5.2	4
50212	Tuning magnetocrystalline anisotropy by controlling the orbital electronic configuration of two-dimensional magnetic materials. Nanoscale Advances, 0, , .	2.2	0
50213	Ammonia free catalytic reduction of nitric oxide on Ni-embedded graphene nanostructure: A density functional theory investigation. Molecular Catalysis, 2023, 541, 113119.	1.0	1
50214	Nanoscale fluctuation of stacking fault energy strengthens multi-principal element alloys. Journal of Materials Science and Technology, 2023, 158, 218-225.	5.6	0
50215	Can Li Atoms Anchored on Boronâ€•and Nitrogenâ€Doped Graphene Catalyze Dinitrogen Molecules to Ammonia? A DFT Study. ChemPhysChem, 2023, 24, .	1.0	1
50216	Intraband and interband transitions in X$$_2$$MnSi(X=Fe,Co,Ni), Fe$$_2$$YSi(Y=V,Cr,Mn) and Fe$$_2$$MnZ(Z=Si,Ge,Sn) full-Heusler alloys: first principles calculations. European Physical Journal Plus, 2023, 138, .	1.2	0
50217	Experimental and Theoretical Analysis for Hypoeutectic Cast Iron Oxidation Behaviors. Journal of the Electrochemical Society, 2023, 170, 041507.	1.3	0
50218	Magnetic iron-cobalt silicides discovered using machine-learning. Physical Review Materials, 2023, 7, .	0.9	3
50219	Thousands of conductance levels in memristors integrated on CMOS. Nature, 2023, 615, 823-829.	13.7	66

#	Article	IF	Citations
50220	Two-dimensional rare-earth Janus <mml:math		

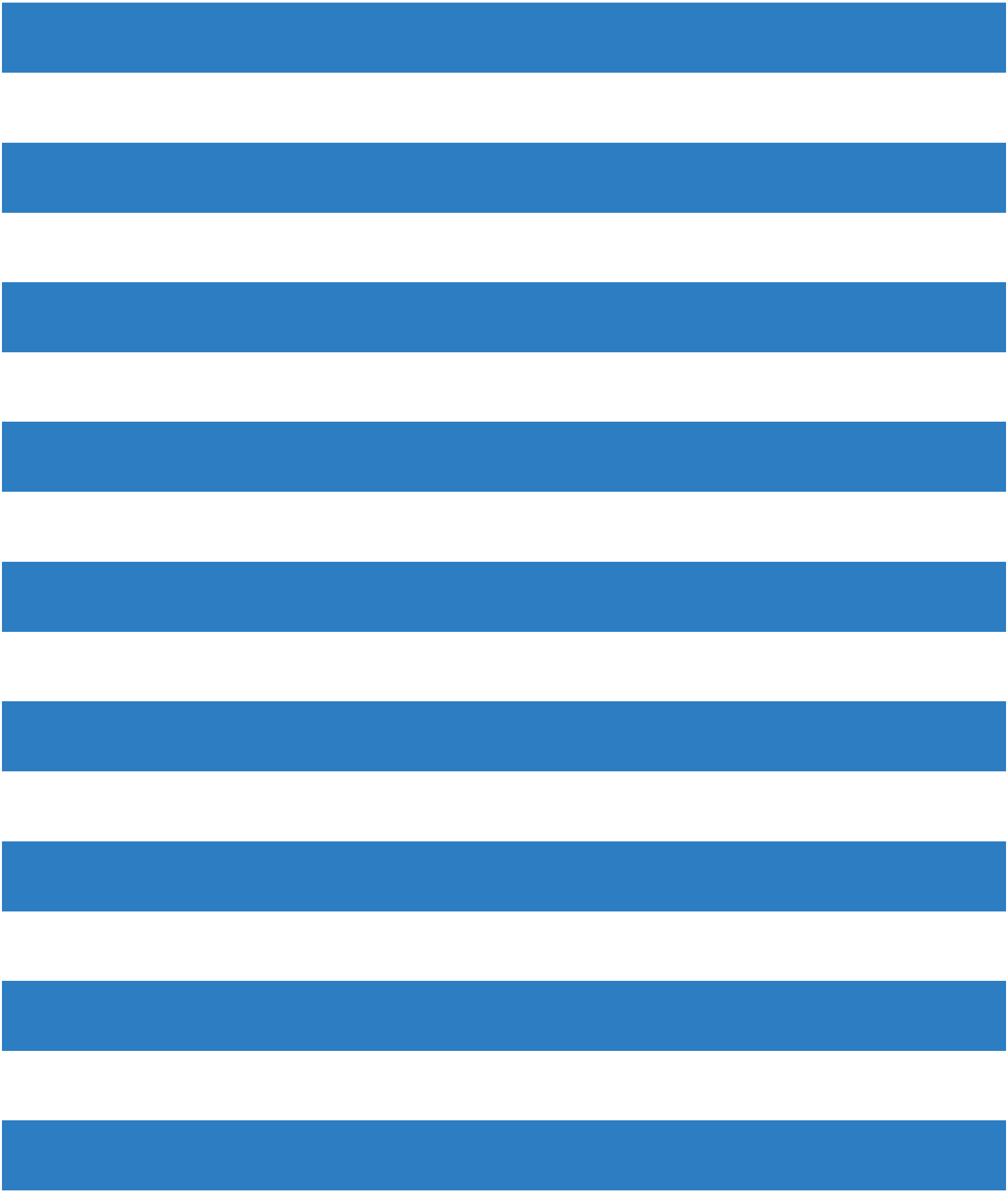

#	Article	IF	Citations
50238	Theory of sigma bond resonance in flat boron materials. Nature Communications, 2023, 14, .	5.8	1
50239	DFTç”ç©¶ä¸‰å•åŽŸå,¬åŒ–å‰‚ç”¨äºŽä¸€æ¥Nâ€“Câ€“Nå¶è•”åˆæˆ•å°¿ç´. Science China Materials, 2023, 66, 2346-2353.	8.1	3
50240	Experimental and computational investigation on the charge storage performance of a novel Al2O3-reduced graphene oxide hybrid electrode. Scientific Reports, 2023, 13, .	1.6	10
50241	Exceptional alkaline hydrogen evolution by molybdenum-oxide-nitride-based electrocatalysts with fast water-dissociation and hydrogen-adsorption kinetics. Materials Chemistry Frontiers, 2023, 7, 2683-2692.	3.2	6
50242	Second-harmonic-generation of [(Se,Te)Cl₃]⁺[GaCl₄]^{â^'} with aligned ionic tetrahedra. Inorganic Chemistry Frontiers, 2023, 10, 2636-2644.	3.0	3
50243	Lu doping nickel oxide thin films using sol-gel spin coated and density functional theory: optoelectronic and magnetic properties. Heliyon, 2023, 9, e14874.	1.4	2
50244	Insights into the Oxygen Evolution Reaction on Graphene-Based Single-Atom Catalysts from First-Principles-Informed Microkinetic Modeling. ACS Catalysis, 2023, 13, 5225-5235.	5.5	8
50245	Quasi-2D FCC lithium crystals inside defective bi-layer graphene: insights from first-principles calculations. Materials Today Energy, 2023, 34, 101293.	2.5	2
50246	Theoretical design of defects as a driving force for ion transport in <scp> Li ₃ OBr </scp> solid electrolyte. Energy and Environmental Materials, 0, , .	7.3	0
50247	Singleâ€Orientation Epitaxy of Quasiâ€1D Tellurium Nanowires on Mâ€Plane Sapphire for Highly Uniform Polarization Sensitive Shortâ€Wave Infrared Photodetection. Advanced Functional Materials, 2023, 33, .	7.8	12
50248	Ab initio study of tungsten-based alloys under fusion power-plant conditions. Journal of Nuclear Materials, 2023, 581, 154422.	1.3	0
50249	Large electrical strain in lead-free K0.5Na0.5NbO3-based ceramics by heterovalent doping. Journal of Materiomics, 2023, 9, 959-970.	2.8	2
50250	Effect of vacancies and edges in promoting water chemisorption on titanium-based MXenes. Nano Convergence, 2023, 10, .	6.3	4
50251	Solubility and diffusivity of hydrogen and its isotopes in the BeO system. Journal of the American Ceramic Society, 0, , .	1.9	0
50252	Bayesian optimization with active learning of design constraints using an entropy-based approach. Npj Computational Materials, 2023, 9, .	3.5	15
50253	Valley-Polarized Interlayer Excitons in 2D Chalcogenideâ€“Halide Perovskiteâ€“van der Waals Heterostructures. ACS Nano, 2023, 17, 7487-7497.	7.3	6
50254	Hybrid interatomic potential for Sn. Physical Review Materials, 2023, 7, .	0.9	2
50255	Aluminum Phosphide van der Waals Bilayers with Tunable Optoelectronic Properties under Biaxial Strain. Crystals, 2023, 13, 597.	1.0	0

#	Article	IF	Citations
50256	Experimental Investigation and Thermodynamic Assessment of the Ternary Alâ€“Niâ€“Er System. Processes, 2023, 11, 1061.	1.3	1
50257	Superhard <mml:math xmlns:mml="http://www.w3.org/1998/Math/MathML"><mml:msub><mml:mi mathvariant="normal">BC</mml:mi><mml:mn>2</mml:mn></mml:msub><mml:mi mathvariant="normal">N</mml:mi></mml:math> in cubic diamondlike structure. Physical Review B, 2023, 107, .	1.1	5
50258	Improved Hydrogen Storage Properties and Air Stability of Metal Hydrides by Constructing Heterophase Composites. Chemistry of Materials, 0, , .	3.2	0
50259	Energy level alignments between organic and inorganic layers in 2D layered perovskites: conjugation vs. substituent. Nanoscale, 0, , .	2.8	0
50260	DFT assessment on stabilities, electronic and thermal transport properties of CoZrSb1â˜'xBix half-Heusler alloys and their superlattices. European Physical Journal Plus, 2023, 138, .	1.2	22
50261	Elastic stability criteria of seven crystal systems and their application under pressure: Taking carbon as an example. Journal of Applied Physics, 2023, 133, .	1.1	4
50262	CO ₂ Capture and Separation by Monoâ€Vacancy Doped Graphene in Electric Field: A DFT study. ChemistrySelect, 2023, 8, .	0.7	2
50263	Spontaneous spin and valley polarizations in a two-dimensional Cr2S3 monolayer. Journal of Applied Physics, 2023, 133, .	1.1	2
50264	Elastic Properties of Binary d-Metal Oxides Studied by Hybrid Density Functional Methods. Crystal Growth and Design, 2023, 23, 3427-3436.	1.4	1
50265	<mml:math xmlns:mml="http://www.w3.org/1998/Math/MathML" altimg="si34.svg" display="inline" id="d1e1137"><mml:msub><mml:mrow /><mml:mrow><mml:mn>4</mml:mn></mml:mrow></mml:msub></mml:math>N<mml:math xmlns:mml="http://www.w3.org/1998/Math/MathML" altimg="si34.svg" display="inline" id="d1e1145"><mml:msub><mml:mrow /><mml:mrow><mml:mn>4</mml:mn></mml:mrow></mml:msub></mml:math>: A symmetry-protected 2D	1.4	1
50266	Relative Stability of Pyrazinamide Polymorphs Revisited: A Computational Study of Bending and Brittle Forms Phase Transitions in a Broad Temperature Range. Crystals, 2023, 13, 617.	1.0	2
50267	Structural and theoretical investigations on the â€œcoloringâ€•scheme of Î³-brass type phase Ag5Cd8. Journal of Solid State Chemistry, 2023, 323, 124019.	1.4	1
50268	Promotion Effect of Well-Defined Deposited Water Layer on Carbon Monoxide Oxidation Catalyzed by Single-Atom Alloys. Journal of Physical Chemistry Letters, 2023, 14, 3498-3505.	2.1	1
50269	Multiple surface states, nontrivial band topology, and antiferromagnetism in GdAuAl₄Ge₂. Chinese Physics B, 2023, 32, 077401.	0.7	2
50270	Simulation of Supercell Defect Structure and Transfer Phenomena in TlInTe2. Russian Microelectronics, 2023, 52, 21-31.	0.1	0
50271	Two-dimensional TiCl₂: a high-performance anode material for Na-ion batteries with high capacity and fast diffusion. Physical Chemistry Chemical Physics, 2023, 25, 11513-11521.	1.3	3
50272	A pyrolysis-free Ni/Fe bimetallic electrocatalyst for overall water splitting. Nature Communications, 2023, 14, .	5.8	56
50273	Superior mechanical properties of multilayer covalent-organic frameworks enabled by rationally tuning molecular interlayer interactions. Proceedings of the National Academy of Sciences of the United States of America, 2023, 120, .	3.3	7

#	Article	IF	Citations
50274	Tuning 2D Magnetism in Cobalt Monoxide Nanosheets Via In Situ Nickelâ€Doping. Advanced Materials, 2023, 35, .	11.1	9
50275	Self-Limited Embedding Alternating 585-Ringed Divacancies and Metal Atoms into Graphene Nanoribbons. Journal of the American Chemical Society, 0, , .	6.6	4
50276	Helium-induced damage in MAB phase MoAlB and Fe₂AlB₂: first-principles simulation. Materials Research Express, 2023, 10, 045503.	0.8	0
50277	Detailed Mechanical Characterization of LiCoO₂ and LiNi_{0.33}Co_{0.33}Mn_{0.33}O₂ Cathode Materials Using DFT Calculations. Chemistry Letters, 2023, 52, 317-321.	0.7	0
50279	Synthesis, Characterization, and Modeling of a Chemically Ordered Quaternary Boride, Mo₄MnSiB₂. Crystal Growth and Design, 0, , .	1.4	0
50280	Biphenylene Nanotube: A Promising Anode Material for Sodiumâ€Ion Batteries. Advanced Materials Interfaces, 2023, 10, .	1.9	3
50281	Bulk and surface electronic structure of <mml:math xmlns:mml="http://www.w3.org/1998/Math/MathML"><mml:msub><mml:mrow><mml:mi>NiBi</mml:mi></mml:mrow><mml:mn>3</m Physical Review B, 2023, 107, .	1.1	
50282	WhereWulff: A Semiautonomous Workflow for Systematic Catalyst Surface Reactivity under Reaction Conditions. Journal of Chemical Information and Modeling, 2023, 63, 2427-2437.	2.5	1
50283	Two-dimensional ferroelectricity in a single-element bismuth monolayer. Nature, 2023, 617, 67-72.	13.7	40
50284	Chirality Effects and Semiconductor versus Metallic Nature in Halide Nanotubes. Journal of Physical Chemistry C, 2023, 127, 7162-7171.	1.5	0
50285	Large tunneling magnetoresistance in spin-filtering 1T-MnSe₂/h-BN van der Waals magnetic tunnel junction. Nanoscale, 2023, 15, 8447-8455.	2.8	2
50287	Control the electronic and optical properties of AlN nanosheet by the electric field. Results in Optics, 2023, 11, 100423.	0.9	1
50288	Electronic and structural properties of Y₆Pt₁₃X₄, site occupancy variants of the Ba₆Na₁₆N subnitride (X = Al, Ga). Dalton Transactions, 0, , .	1.6	0
50289	Efficient all-thermally evaporated perovskite light-emitting diodes for active-matrix displays. Nature Photonics, 2023, 17, 435-441.	15.6	25
50290	Effect of magnon-magnon interaction on ferromagnetism in hexagonal manganese pnictide monolayers. Physical Review B, 2023, 107, .	1.1	2
50291	Crystal structure and electronic properties of low-dimensional hexamethylenediaminium lead halide perovskites. Dalton Transactions, 0, , .	1.6	1
50292	Insights to the fracture toughness, damage tolerance, electronic structure, and magnetic properties of carbides M₂C (M = Fe, Cr). Materials Research Express, 2023, 10, 046515.	0.8	0
50293	Symmetryâ€Mismatchâ€Induced Ferromagnetism in the Interfacial Layers of CaRuO₃/SrTiO₃ Superlattices. Advanced Functional Materials, 2023, 33, .	7.8	6

#	Article	IF	Citations
50294	From Layered Antiferromagnet to 3D Ferromagnet: LiMnBi-to-MnBi Magneto-Structural Transformation. Chemistry of Materials, 0, , .	3.2	0
50295	CO₂ Activation on Cu/TiO₂ Nanostructures: Importance of Dual Binding Site. Chemistry - A European Journal, 2023, 29, .	1.7	2
50296	Acrossâ€Layer Sliding Ferroelectricity in 2D Heterolayers. Advanced Functional Materials, 2023, 33, .	7.8	14
50297	An ab-initio study of hydrogen storage performance of Si2BN nanotubes decorated with group 8B transition metals. International Journal of Hydrogen Energy, 2023, 48, 25438-25449.	3.8	2
50298	Insight into the effects of S-vacancy and O-doping in monolayer VS2 as lithium-ion battery anodes from first-principles calculations. Surfaces and Interfaces, 2023, 38, 102851.	1.5	2
50299	Oxidation State Dependent Conjugation Controls Electrocatalytic Activity in a Two-Dimensional Di-Copper Metalâ€“Organic Framework. Journal of Physical Chemistry C, 2023, 127, 7299-7307.	1.5	1
50300	Numerical Analysis in DFT and SCAPS-1D on the Influence of Different Charge Transport Layers of CsPbBr₃ Perovskite Solar Cells. Energy & Fuels, 2023, 37, 6078-6098.	2.5	61
50301	Role of Non-covalent Interaction toward Conductivity in a One-Dimensional Tube-like Silver-Thiolate Structure. Crystal Growth and Design, 2023, 23, 3164-3170.	1.4	1
50302	Formation of active sites on transition metals through reaction-driven migration of surface atoms. Science, 2023, 380, 70-76.	6.0	33
50303	Two-dimensional half-metallicity in transition metal atoms decorated Cr2Ge2Te6. Frontiers in Physics, 0, 11, .	1.0	3
50304	First principles analysis on the nucleation interface of La2O3<mml:math xmlns:mml="http://www.w3.org/1998/Math/MathML" altimg="si0032.svg"><mml:mrow><mml:mo stretchy="false">(</mml:mo><mml:mn>1</mml:mn><mml:mover) Tj ETQq0 0 0 rgBT /Overlock 10 Tf 50 347 Td (accent="true"><mml:m xmlns:mml="http://www.w3.org/1998/Math/MathML" altimg="si0033.svg"><mml:mrow><mml:mo stretch	0.9	0
50305	Rapid and Scalable Transfer of Largeâ€Area Graphene Wafers. Advanced Materials, 2023, 35, .	11.1	8
50306	Tailoring the Angular Mismatch in MoS₂ Homobilayers through Deformation Fields. Small, 2023, 19, .	5.2	2
50307	High-mobility transport symmetry and effect of strain on electronic and optical properties in few-layer blue phosphorus. Computational Materials Science, 2023, 224, 112177.	1.4	2
50308	Structural, vibrational, electronic, and elastic properties of 2D alkali carbide as a metallic material. Computational Condensed Matter, 2023, , e00805.	0.9	0
50309	Unconventional Self-Reconstructed Trimer-like Metal Zigzag Edge of 1T-Phase Transition Metal Dichalcogenides. Journal of Physical Chemistry Letters, 2023, 14, 3651-3657.	2.1	0
50310	Insight into the structural, electronic, optical, and elastic properties of niobium carbide. Phase Transitions, 0, , 1-13.	0.6	0
50311	Metastable Polymorphic Phases in Monolayer TaTe₂. Small, 2023, 19, .	5.2	7

#	Article	IF	Citations
50312	Bi2S3/rGO nanocomposites with covalent heterojunctions as a high-performance aqueous zinc ion battery material. Ceramics International, 2023, 49, 22160-22169.	2.3	3
50313	Carbon-driven coherent nanoprecipitates enable ultrahigh yield strength in a high-entropy alloy. Materials Today Nano, 2023, 22, 100331.	2.3	0
50314	Positive correlation of Nb/Cr doping with dehydrogenation performance of ZrCo-based hydrides. International Journal of Hydrogen Energy, 2023, , .	3.8	0
50315	Elucidating the Role of Noncovalent Interactions in Favipiravir, a Drug Active against Various Human RNA Viruses; a 1H-14N NQDR/Periodic DFT/QTAIM/RDS/3D Hirshfeld Surfaces Combined Study. Molecules, 2023, 28, 3308.	1.7	4
50316	A Ï€â€Bridge Spacer Embedded Electron Donorâ€“Acceptor Polymer for Flexible Electrochromic Znâ€ion Batteries. Advanced Materials, 2023, 35, .	11.1	7
50317	On the faulting and twinning mediated strengthening and plasticity in a Î³Ê¹ strengthened CoNi-based superalloy at room temperature. Acta Materialia, 2023, 252, 118928.	3.8	6
50318	Nanoclayâ€Modulated Interfacial Chemical Bond and Internal Electric Field at the Co₃O₄/TiO₂ pâ€n Junction for Efficient Charge Separation. Small, 2023, 19, .	5.2	7
50319	Adaptive Exploration and Optimization of Materials Crystal Structures. INFORMS Journal on Data Science, 0, , .	0.7	3
50320	Tailoring planar slip to achieve pure metal-like ductility in body-centred-cubic multi-principal element alloys. Nature Materials, 2023, 22, 950-957.	13.3	27
50321	Machine learning-assisted exploration of the intrinsic factors affecting the catalytic activity of ORR/OER bifunctional catalysts. Applied Surface Science, 2023, 628, 157225.	3.1	8
50322	Magnetic bond-order potential for iron-cobalt alloys. Physical Review Materials, 2023, 7, .	0.9	1
50323	Reversible hydrogen storage tendency of light-metal (Li/Na/K) decorated carbon nitride (C9N4) monolayer. International Journal of Hydrogen Energy, 2023, 48, 26301-26313.	3.8	11
50324	Magnetic excitations in infinite-layer LaNiO₂. Applied Physics Letters, 2023, 122, 152401.	1.5	1
50325	Calculated Outstanding Energy-Storage Media by Aluminum-Decorated Carbon Nitride (g-C3N4): Elucidating the Synergistic Effects of Electronic Structure Tuning and Localized Electron Redistribution. Crystals, 2023, 13, 655.	1.0	1
50326	Modelling of the structural, electronic, magnetic properties and magnetocaloric effect of Cr₂Ge₂Te₆ and Cr₂Si₂Te₆ compounds: DFT combined with the Monte Carlo method. Molecular Physics, 0, , .	0.8	0
50327	Elucidating the Role of Contact-Induced Gap States and Passivation Molecules at Perovskite/Metal Contacts. ACS Applied Energy Materials, 2023, 6, 4111-4118.	2.5	2
50328	Enhanced Activity and Selectivity for Electrochemical CO₂ Reduction through Water Activation by Oxophilic Metal Deposited on Ag. ACS Applied Energy Materials, 0, , .	2.5	1
50329	Spinâ€“Orbit-Coupling-Induced Topological Transition and Anomalously Strong Intervalley Scattering in Two-Dimensional Bismuth Allotropes with Enhanced Thermoelectric Performances. ACS Applied Materials & Interfaces, 2023, 15, 19545-19559.	4.0	1

#	Article	IF	Citations
50331	Structure and Reactivity of the Ionic Liquid [C1C1Im][Tf2N] on Cu(111). Topics in Catalysis, 0, , .	1.3	3
50332	Computational screening of two-dimensional metal-benzenehexathial for the oxygen reduction reaction. Catalysis Science and Technology, 0, , .	2.1	0
50333	Density functional theory study of energetics, local chemical environment and magnetic properties in a high-entropic MnNiSi_{0.2}Ge_{0.2}Sn_{0.2}Al_{0.2}Ga_{0.2} intermetallic magnet. JPhys Energy, 2023, 5, 024019.	2.3	0
50334	Synthesis and physical properties of a new layered ferromagnet <mml:math xmlns:mml="http://www.w3.org/1998/Math/MathML"><mml:mrow><mml:msub><mml:mi>Cr</mml:mi><mml:mrow><mml:mn>1.21</mml:mn></mml:mrow> Physical Review Materials, 2023, 7, .	2.9	0
50335	Cation disorder dominates the defect chemistry of high-voltage LiMn_{1.5}Ni_{0.5}O₄ (LMNO) spinel cathodes. Journal of Materials Chemistry A, 2023, 11, 13353-13370.	5.2	7
50336	B2 to ordered omega transformation during isothermal annealing of refractory high entropy alloys: Implications for high temperature phase stability. Journal of Alloys and Compounds, 2023, 953, 170065.	2.8	4
50337	Investigation of electronic and magnetic properties in vacancy incorporated monolayer magnesium bromide for spintronics application: an ab-initio study. Physica Scripta, 2023, 98, 055937.	1.2	1
50338	Coverage-dependent adsorption and dissociation of H2O on Al surfaces. Physical Chemistry Chemical Physics, 0, , .	1.3	1
50339	Anharmonic Correction to Free Energy Barriers from DFT-Based Molecular Dynamics Using Constrained Thermodynamic Integration. Journal of Chemical Theory and Computation, 2023, 19, 2455-2468.	2.3	2
50340	Lattice constants and magnetism of L10-ordered FePt under high pressure. Applied Physics Letters, 2023, 122, .	1.5	3
50341	Density functional theory study of the VmN2On (m,n = 1,2) complexes in silicon. Modern Physics Letters B, 2023, 37, .	1.0	1
50342	First-principles calculations of structural, electronic, elastic, and thermal properties of phase M2CdC (Mâ€‰=â€‰Sc, V, and Nb). Indian Journal of Physics, 2023, 97, 2991-3002.	0.9	2
50343	Morphology-dependent adsorption energetics of Ru nanoparticles on hcp-boron nitride (001) surface â€“ a first-principles study. Nanoscale Advances, 2023, 5, 2422-2426.	2.2	1
50344	Boron-Pnictogen Monolayers with Negative Poissonâ€™s ratio and Excellent Band Edge Positions for Photocatalytic Water Splitting. Physical Chemistry Chemical Physics, 0, , .	1.3	0
50345	Tetra-penta-deca-hexagonal-graphene (TPDH-graphene) hydrogenation patterns: dynamics and electronic structure. Physical Chemistry Chemical Physics, 2023, 25, 13088-13093.	1.3	0
50346	A machine learning methodology to investigate the lattice thermal conductivity of defected PbTe. Journal of Materials Chemistry A, 2023, 11, 10612-10627.	5.2	3
50347	Morphological modification of Mg2Si phase and strengthening mechanism in Mg2Si/Al composites by Eu addition and T6 heat treatment. Journal of Materials Science and Technology, 2023, 159, 151-162.	5.6	2
50348	Stacks of Equidistant 5,6-Dichloro-2,3-dicyanosemiquinone (DDQ) Radicals under Variable-Temperature and High-Pressure Conditions. Crystal Growth and Design, 0, , .	1.4	1

#	Article	IF	Citations
50349	An atomistic modeling study of high-throughput RVO3(R=La, Nd) perovskites for efficient solar energy conversion materials. Physica B: Condensed Matter, 2023, 660, 414879.	1.3	4
50350	Exploration of spatial confinement and ligand effects for oxygen reduction reaction on Fe-Nx embedded hole-graphene. Physical Chemistry Chemical Physics, 0, , .	1.3	0
50351	Exploration of reaction mechanism of LaFeO3 oxygen carrier for chemical-looping steam methane reforming: A DFT study. Physical Chemistry Chemical Physics, 0, , .	1.3	0
50352	Theoretical investigation on NO reduction electro-catalyzed by transition-metal-anchored SnOSe nanotubes. Nano Research, 2023, 16, 8533-8541.	5.8	3
50353	Electrochemistry-assisted selective butadiene hydrogenation with water. Nature Communications, 2023, 14, .	5.8	8
50354	Diffusion behavior determined by the new n-body potential in highly immiscible W/Cu system through molecular dynamics simulations. Journal of Materials Research and Technology, 2023, 24, 3731-3745.	2.6	5
50355	Pressure-Controlled Layer-by-Layer to Continuous Oxidation of ZrS₂(001) Surface. ACS Nano, 0, , .	7.3	0
50356	Lone Pair Rotation and Bond Heterogeneity Leading to Ultralow Thermal Conductivity in Aikinite. Journal of the American Chemical Society, 2023, 145, 9313-9325.	6.6	10
50357	A chemically inspired convolutional neural network using electronic structure representation. Journal of Materials Chemistry A, 2023, 11, 10184-10194.	5.2	1
50358	Size of electron polarons in anatase <mml:math xmlns:mml="http://www.w3.org/1998/Math/MathML"><mml:msub><mml:mi>TiO</mml:mi><mml:mn>2</mml:mn></mml:msub></m and their role in photocatalysis. Physical Review B, 2023, 107, .	3.7	3
50359	Bend-Induced Ferroelectric Domain Walls in Î±-In₂Se₃. ACS Nano, 2023, 17, 7881-7888.	7.3	5
50360	Electrosynthesis of polymer-grade ethylene via acetylene semihydrogenation over undercoordinated Cu nanodots. Nature Communications, 2023, 14, .	5.8	11
50361	Theoretical Comparison Study of Iodine and Astatine Adsorption on Au(111) Surface. E-Journal of Surface Science and Nanotechnology, 2023, 21, 318-323.	0.1	2
50362	Theoretical insight into the generation mechanism of vinyl acrylate in the production of vinyl acetate on PdAu(100). New Journal of Chemistry, 2023, 47, 9323-9334.	1.4	1
50363	Localized Surface Plasmon Resonance in Metamaterials Composed of As1â^'zSbz Semimetal Nanoparticles in AlxGa1â^'xAs1â^'ySby Semiconductor Matrix. Nanomaterials, 2023, 13, 1355.	1.9	2
50364	Segregation of Alkaline Earth Atoms Affects Prenucleation at L-Al/Î³-Alumina Interfaces. Metals, 2023, 13, 761.	1.0	0
50365	Theoretical insights into the stability of buckled tetragonal graphene and the prediction of novel carbon allotropes. Physical Chemistry Chemical Physics, 0, , .	1.3	0
50366	A quasi-one-dimensional bulk thermoelectrics with high performance near room temperature. Science Bulletin, 2023, 68, 920-927.	4.3	4

#	Article	IF	Citations
50367	Computational simulation of self-cleaning carbon-based membranes with zeolite porous structure for desalination. Diamond and Related Materials, 2023, 136, 109925.	1.8	1
50368	Intrinsic point defects and the <mml:math xmlns:mml="http://www.w3.org/1998/Math/MathML"><mml:mi>n</mml:mi></mml:math> -type dopability of <mml:math xmlns:mml="http://www.w3.org/1998/Math/MathML"><mml:mrow><mml:msub><mml:mi>Bi</mml:mi><mml:mn>2</mml:mn></mml:msub><mml:msub><mml:mi mathvariant="normal">O</mml:mi><mml:mn>6</mml:mn></mml:msub></mml:mrow></mml:math> with higher photocatalytic performance: A hybrid functional study. Physical Review Materials, 2023, 7, .	2.9	2
50369	Structural, Elastic, and Mechanical Properties of Orthorhombic Goethite (Î±-FeOOH) under Pressure from First-Principles Calculations. Russian Journal of Physical Chemistry A, 2023, 97, 50-56.	0.1	0
50370	MIL-101(Fe) Metalâ€“Organic Framework Nanoparticles Functionalized with Amino Groups for Cr(VI) Capture. ACS Applied Nano Materials, 2023, 6, 6820-6830.	2.4	7
50371	Ï‰â€Graphene: A Graphene Allotrope with Desirable Auxeticity and Dirac Cone. Advanced Theory and Simulations, 0, , .	1.3	0
50372	On the coexistence of ferroelectric and antiferroelectric polymorphs in NaNbO₃ fibers at room temperature. Journal of Materials Chemistry C, 0, , .	2.7	0
50373	Enhanced quantum capacitance in Ti, V, Cr, Fe, Ga, Ge, Se, and Br doped arsenene: A first principles investigation. Chemical Physics Letters, 2023, 823, 140500.	1.2	1
50374	Designing dithiolene and bis(iminothiolato)-based 1D metal-organic-frameworks for electrocatalytic hydrogen evolution reaction. Theoretical Chemistry Accounts, 2023, 142, .	0.5	2
50375	Structural, electronic and thermoelectric properties of SnTe with dilute co-doping of Ag and Cu. Journal of Alloys and Compounds, 2023, 954, 170182.	2.8	3
50376	Mechanistic Insights into the High Selectivity and Photocatalytic Activity of Brookite TiO₂ toward NO_X Abatement. Journal of Physical Chemistry C, 0, , .	1.5	0
50377	Electronic Structure, Magnetism and Magnetocrystalline Anisotropy of Antiferromagnetic Semiconducting Chalcopyrite. Defect and Diffusion Forum, 0, 423, 23-31.	0.4	0
50378	Adjustment of the Single Atom/Nanoparticle Ratio in Pd/CNT Catalysts for Phenylacetylene Selective Hydrogenation. ChemCatChem, 2023, 15, .	1.8	2
50379	Stacking effect on the electronic structures of hexagonal GaTe. Journal Physics D: Applied Physics, 0, , .	1.3	1
50380	Cation Distribution Effect on Structural and Electronic Properties of Oxygen Vacancy and Niobium Substituted Spinel Lithium Titanium Oxide Anode Material in Lithium-ion Batteries. Defect and Diffusion Forum, 0, 423, 57-66.	0.4	0
50381	Ab-initio study of <mml:math xmlns:mml="http://www.w3.org/1998/Math/MathML" display="inline" id="d1e527" altimg="si79.svg"><mml:msub><mml:mrow><mml:mi mathvariant="normal">SiF</mml:mi></mml:mrow><mml:mrow><mml:mn>2</mml:mn></mml:mrow></mml:msub></mml:math> molecule adsorption on Si(001)-p(2ÂÃ—Â2) reconstructed surface. Solid State Communications, 2023, , 115176.	2.1	1
50382	Chalcogen bonding and variable charge transfer degree in two polymorphs of 1â€‰:â€‰1 conducting salts with segregated stacks. CrystEngComm, 2023, 25, 3189-3197.	1.3	1
50383	Unveiling deformation twin nucleation and growth mechanisms in BCC transition metals and alloys. Materials Today, 2023, 65, 90-99.	8.3	6
50384	Spinâ€Lattice Coupled Metamagnetism in Frustrated van der Waals Magnet CrOCl. Small, 0, , .	5.2	3

#	Article	IF	Citations
50385	Enhanced Photoassisted Liâ€O₂ Battery with Ceâ€UiOâ€66 Metalâ€Organic Framework Based Photocathodes. Advanced Materials Interfaces, 2023, 10, .	1.9	1
50386	Single silicon-doped CNT as a metal-free electrode for robust nitric oxide reduction utilizing a Lewis base site: an ingenious electronic â€œReflux-Feedbackâ€•mechanism. Physical Chemistry Chemical Physics, 2023, 25, 13072-13079.	1.3	4
50387	Highly Selective Electrochemical Reduction of CO₂ into Methane on Nanotwinned Cu. Journal of the American Chemical Society, 2023, 145, 9136-9143.	6.6	19
50388	Unraveling the structural and mechanical stability, electronic, and optical properties of (LaxSr1-xVO3)n (n =1, 2; x = 0, 0.5, 1). Solid State Communications, 2023, , 115173.	0.9	0
50389	Superior hydrogen storage capacity of Vanadium decorated biphenylene (Bi+V): A DFT study. International Journal of Hydrogen Energy, 2023, 48, 28076-28090.	3.8	10
50390	First-principles study on silicon emission from interface into oxide during silicon thermal oxidation. Materials Science in Semiconductor Processing, 2023, 162, 107527.	1.9	0
50391	Ab initio lattice thermal conductivity of (Mg,Fe)O ferropericlase at the Earthâ€™s lower mantle pressure and temperature. Journal of Physics Condensed Matter, 2023, 35, 305402.	0.7	1
50392	First-principles study of structural, electronic and vibrational properties of bulk and monolayer TiS2. Journal of Physics and Chemistry of Solids, 2023, 179, 111382.	1.9	1
50393	Effect of strontium (Sr) doping on the structural, electronic and optical properties of ZnO, by first-principles calculations. Physica B: Condensed Matter, 2023, 660, 414903.	1.3	4
50394	Machine learning and DFT investigation of CO, CO₂ and CH₄ adsorption on pristine and defective two-dimensional magnesene. Physical Chemistry Chemical Physics, 2023, 25, 13170-13182.	1.3	3
50395	A systematic first-principles exploration of the impact of metal doping on the electronic properties of MOF MIP-177(Ti). Microporous and Mesoporous Materials, 2023, , 112607.	2.2	0
50396	The Remarkably Robust, Photoactive Tungsten Iodide Cluster [W6I12(NCC6H5)2]. European Journal of Inorganic Chemistry, 0, , .	1.0	0
50397	Atomic-scale structural characterization and twin formation mechanisms of Î¼ phase within refractory Nb Ni alloy. Materials Characterization, 2023, 201, 112921.	1.9	0
50398	Cs₂Ln₃CuS₈ (Ln = Laâ€“Nd, Smâ€“Tb): Synthesis, Crystal Structure, and Magnetic and Optical Properties. Inorganic Chemistry, 0, , .	1.9	2
50399	Ionâ€Charged Dielectric Nanolayers for Enhanced Surface Passivation in High Efficiency Photovoltaic Devices. Advanced Materials Interfaces, 0, , .	1.9	0
50400	Atomic structure and peculiarities of the electronic properties of Br layers on Ag(111) at different coverages. Surface Science, 2023, 734, 122304.	0.8	1
50401	Using a computationally driven screening to enhance magnetocaloric effect of metal monoborides. JPhys Energy, 0, , .	2.3	1
50402	NOVEL BORIDES OF THE BORON FILLED Î²-Mn-TYPE STRUCTURE. Journal of Alloys and Compounds, 2023, , 170214.	2.8	0

#	Article	IF	Citations
50403	Carbon dioxide reduction processes on a samarium doped ceria electrocatalyst with exsolved Fe particles. Journal of Materials Chemistry A, 2023, 11, 10646-10658.	5.2	4
50404	Weak electron-phonon renormalization effect caused by the counteraction of the different phonon vibration modes in FeS₂. Physica Scripta, 2023, 98, 065902.	1.2	1
50405	Gaussian approximation potentials for accurate thermal properties of two-dimensional materials. Nanoscale, 2023, 15, 8772-8780.	2.8	1
50406	The structural, electronic, and mechanical properties of FeH under extreme pressures: First-principles calculation. Solid State Communications, 2023, 368, 115180.	0.9	1
50407	AgIn₅Se₈: a defect diamond-like non-linear optical selenide. Inorganic Chemistry Frontiers, 2023, 10, 3248-3254.	3.0	4
50408	On correlations between local chemistry, distortions and kinetics in high entropy nitrides: An ab initio study. Acta Materialia, 2023, 255, 118951.	3.8	3
50409	Universal Maximum Strength of Solid Metals and Alloys. Physical Review Letters, 2023, 130, .	2.9	6
50410	Interaction of Water and Oxygen Molecules with Phosphorene: An Ab Initio Study. Molecules, 2023, 28, 3570.	1.7	0
50411	A 3D printable alloy designed for extreme environments. Nature, 2023, 617, 513-518.	13.7	29
50412	Atomic level mechanisms of graphene healing by methane-based plasma radicals. FlatChem, 2023, , 100506.	2.8	0
50413	Unusual transport and impact of nonparabolic electronic band structure on the thermoelectric performance in nâ€ type In ₄ Se ₃ based thermoelectric materials. Physica Status Solidi (B): Basic Research, 0, , .	0.7	2
50414	Highly efficient hydrogen production from methanol by single nickel atoms anchored on defective boron nitride nanosheet. Nano Research, 0, , .	5.8	0
50415	Role of surface terminations in the chemical stability of CH3NH3PbI3 perovskite in combined light, H2O, and O2 environments: DFT/AIMD calculations and experimental validation. Materials Today Advances, 2023, 18, 100370.	2.5	1
50416	Unconventional surface state pairs in a high-symmetry lattice with anti-ferromagnetic band-folding. Communications Physics, 2023, 6, .	2.0	3
50417	Sign-tunable exchange bias effect in proton-intercalated <mml:math xmlns:mml="http://www.w3.org/1998/Math/MathML"><mml:mrow><mml:msub><mml:mi>Fe</mml:mi><mml:mn>x</mml:mn></mml:r nanoflakes. Physical Review B, 2023, 107, .	3.7	1
50418	Defect Origin of the Light-Soaking Effects in Hybrid Perovskite Solar Cells. , 2023, , 239-263.		1
50419	Distinct ferrovalley characteristics of the Janus RuClX (X = F, Br) monolayer. Nanoscale, 2023, 15, 8278-8288.	2.8	13
50420	Band Structure of Bilayer Graphene Intercalated by Potassium Atoms. Ab Initio Calculations. JETP Letters, 2023, 117, 357-362.	0.4	0

#	Article	IF	Citations
50421	Magnetic Properties of the Fe2B Alloy Doped with Transition Metal Elements. Magnetochemistry, 2023, 9, 109.	1.0	2
50422	Beyond single tetrahedron physics of the breathing pyrochlore compound <mml:math xmlns:mml="http://www.w3.org/1998/Math/MathML"><mml:msub><mml:mi>Ba</mml:mi><mml:mn>3</mml:mn></mml:msub><mml:mi mathvariant="normal">O</mml:mi></mml:mrow><mml:mn>11</mml:mn></mml:msub></mml:math>. Physical Review B, 2023, 107, .	1.1	2
50423	Strong ferromagnetism of g-C3N4 achieved by atomic manipulation. Nature Communications, 2023, 14, .	5.8	20
50424	Density functional theoretical assessment of titanium metal for adsorption of hydrogen, deuterium and tritium isotopes. Theoretical Chemistry Accounts, 2023, 142, .	0.5	0
50425	DFT Insights into Noble Gold-Based Compound Li₅AuP₂: Effect of Pressure on Physical Properties. ACS Omega, 2023, 8, 15673-15683.	1.6	3
50426	Prediction of 2D IV-V semiconductors: Flexible monolayers with tunable bandgap and strong optical absorption as water-splitting photocatalysts. Nanoscale, 0, , .	2.8	1
50427	Density functional theory investigation on the structural, mechanical, lattice dynamical and thermal properties of nodal-line semimetals CaAgX (X: P, As). Bulletin of Materials Science, 2023, 46, .	0.8	0
50428	Identification of Cu/Sc and Cu/Ti subsurface alloys for highly efficient CO electroreduction to C2 products. Applied Surface Science, 2023, , 157314.	3.1	1
50429	Quantum size effects in stacked multilayer graphene. Physica Scripta, 0, , .	1.2	0
50430	Electronic structure and optical properties of tin (IV) doped transparent perovskite crystal BaTiO3 for efficient visible optoelectronic devices and solar cells. Materials Today Communications, 2023, 35, 106035.	0.9	1
50431	Improved Mechanical Characterization of LiCoO2 Cathode Material by Ab-Initio Calculations Using Density Functional Theory. Bulletin of the Chemical Society of Japan, 2023, 96, 475-483.	2.0	0
50432	Observation of gapless nodal-line states in NdSbTe. Physical Review Materials, 2023, 7, .	0.9	2
50433	Effect of an electric field on ferroelectric and piezoelectric properties of brownmillerite <mml:math xmlns:mml="http://www.w3.org/1998/Math/MathML"><mml:mrow><mml:msub><mml:mi>Ca</mml:mi><mml:mn>2</mml:mn></mml:mi mathvariant="normal">O</mml:mi><mml:mn>5</mml:mn></mml:msub></mml:mrow></mml:math>. Physical Review B, 2023, 107, .	1.1	2
50434	Covalent bonding strategy to enable non-volatile organic cation perovskite for highly stable and efficient solar cells. Joule, 2023, 7, 1033-1050.	11.7	13
50435	Impact of charge-compensated Fe and Nb co-substitution on BaTiO3: Bandgap and grain size reduction and enhanced bulk photovoltaic power of Al/BFNT/Ag solar cell. Solar Energy, 2023, 257, 34-44.	2.9	4
50436	Theoretical predication of two-dimensional ferroelectric metal X2Y3 monolayer and Van der Waals heterostructures. Physica E: Low-Dimensional Systems and Nanostructures, 2023, , 115739.	1.3	0
50437	Spontaneous topological Hall effect induced by non-coplanar antiferromagnetic order in intercalated van der Waals materials. Nature Physics, 2023, 19, 961-968.	6.5	13
50439	Equation of state, phase transitions, and band-gap closure in <mml:math xmlns:mml="http://www.w3.org/1998/Math/MathML"><mml:mrow><mml:mi>Pb</mml:mi><mml:msub><mml:mi>Cl</mml:mi><mml:mi and <mml:math xmlns:mml="http://www.w3.org/1998/Math/MathML"><mml:mrow><mml:mi>Sn</mml:mi><mml:msub><mml:mi>Cl</mml:mi><mml:mi> Physical Review B, 2023, 107, .	1.1	0

#	Article	IF	Citations
50440	Structural-disorder-driven critical quantum fluctuation and localization in two-dimensional semiconductors. Nature Communications, 2023, 14, .	5.8	3
50441	Cr$$_2$$AlN and the search for the highest temperature superconductor in the M$$_2$$AX family. Scientific Reports, 2023, 13, .	1.6	0
50442	Synthesis and Characterization of Xylazine Hydrochloride Polymorphs, Hydrates, and Cocrystals: A ³⁵Cl Solid-State NMR and DFT Study. Crystal Growth and Design, 2023, 23, 3412-3426.	1.4	3
50443	On the use of Monkhorstâ€“Pack scheme to evaluate superconductivity and the issue of umklapp electronâ€“phonon interactions. Physical Chemistry Chemical Physics, 2023, 25, 13049-13060.	1.3	1
50444	Stacking and layer dependence of magnetic properties in Ti₂C and Fe₂C. Journal Physics D: Applied Physics, 2023, 56, 345002.	1.3	2
50445	Ultralow Lattice Thermal Conductivity and High Thermoelectric Performance in Ge_{1â€“xâ€“y}Bi_xCa_yTe with Ultrafine Ferroelectric Domain Structure. ACS Applied Materials & Interfaces, 2023, 15, 21187-21197.	4.0	1
50446	Electronic signatures of Lorentzian dynamics and charge fluctuations in lithiated graphite structures. Nature Communications, 2023, 14, .	5.8	1
50447	Protection of titanium alloys against high temperature oxidation during closed-die forging: Structural analysis of the boro-silicate glass coating/Ti-6Al-4V alloy interfacial region by correlative imaging. Corrosion Science, 2023, 220, 111198.	3.0	2
50448	High throughput calculations for a dataset of bilayer materials. Scientific Data, 2023, 10, .	2.4	2
50449	Enabling enhanced lithium storage capacity of two-dimensional pentagonal BN₂ by aluminum doping. Journal of Materials Chemistry C, 0, , .	2.7	0
50450	Water Purification by 2â€Dimensional Dodecagonal Nitride and Graphenylene via First Principles Calculations. ChemPhysChem, 2023, 24, .	1.0	1
50451	<mml:math xmlns:mml="http://www.w3.org/1998/Math/MathML"><mml:mrow><mml:mi>Mn</mml:mi><mml:msub><mml:mrow><mml:mo>(</mml:mo><mml:mi mathvariant="normal">P</mml:mi></mml:mrow></mml:math> : Isovalent tuning of Mn-sublattice magnetic order. Physical Review B, 2023, 107, .	1.1	1
50452	A first-principles study on the early-stage corrosion of a NiWNb alloy in a chloride salt environment. Journal of Nuclear Materials, 2023, 582, 154457.	1.3	0
50453	Tribo-catalysis triggered the in-situ formation of amphiphilic molecules to reduce friction and wear. Tribology International, 2023, 185, 108541.	3.0	2
50454	Predicting the Lithium-Vacancy Arrangements of Layered Cathode Materials by a Voronoi Finite Element Method. Journal of the Electrochemical Society, 0, , .	1.3	0
50455	Magnetic properties of defect induced Î²-Ga2O3: A first principles study. Computational Condensed Matter, 2023, 35, e00810.	0.9	1
50456	Atomic, electronic, and superconducting properties of Zr<mml:math xmlns:mml="http://www.w3.org/1998/Math/MathML" altimg="si13.svg" display="inline" id="d1e1096"><mml:msub><mml:mrow /><mml:mrow><mml:mn>2</mml:mn></mml:mrow></mml:msub></mml:math>Ir compound. Physica B: Condensed Matter, 2023, 661, 414904.	1.3	1
50457	Graphdiyne supported single-cluster catalysts catalyzed electrochemical nitrogen reduction reaction: A first-principles investigation. FlatChem, 2023, 39, 100507.	2.8	1

#	Article	IF	Citations
50458	Thickness-dependent piezoelecticity of black arsenic from few-layer to monolayer. Solid State Communications, 2023, 368, 115175.	0.9	1
50459	Extreme flexibility and unusual piezomechanical properties of zinc-alkyl-based metal-organic frameworks: A first principles study. Materials Today Communications, 2023, 35, 106054.	0.9	4
50460	Irradiation damage reduces alloy corrosion rate via oxide space charge compensation effects. Acta Materialia, 2023, 253, 118956.	3.8	2
50461	Surface Ligand Engineering Ruthenium Nanozyme Superior to Horseradish Peroxidase for Enhanced Immunoassay. Advanced Materials, 2024, 36, .	11.1	29
50462	New detail insight into Halloysite structure: Mechanism behind nanotubular morphology described by density functional theory and molecular dynamics supported by experiments. Journal of Molecular Structure, 2023, 1287, 135639.	1.8	2
50463	Ab initio predictions of the structural, electronic, optical, elastic, and thermoelectric properties of quasi-two-dimensional BaFZnP. Computational Condensed Matter, 2023, 35, e00809.	0.9	7
50464	Electronic, Optical, piezoelectric properties and photocatalytic water splitting performance of Two-dimensional group IV-V compounds. Applied Surface Science, 2023, 627, 157317.	3.1	4
50465	Enhanced Cycling Stability of 4.6ÂV LiCoO₂ Cathodes by Inhibiting Catalytic Activity of its Interface Via MXene Modification. Advanced Functional Materials, 2023, 33, .	7.8	9
50466	Site selective behaviour of B, C and N doping in MgO monolayers towards spintronic and optoelectronic applications. Materials Science in Semiconductor Processing, 2023, 162, 107514.	1.9	2
50472	Structural andÂElectronic Properties ofÂSmall-Diameter Carbon NanoTubes: A DFT Study. Lecture Notes in Computer Science, 2023, , 392-402.	1.0	0
50516	Charge transfer and quantum emitters in two-dimensional heterostructures: An Ab initio study. AIP Conference Proceedings, 2023, , .	0.3	0
50574	Unique Chiro-optical Properties of the Weakly-2D (R-/S-MBA)₂CuBr₄ Hybrid Material. , 2023, 5, 1556-1564.		8
50643	Hydrogen adsorption and diffusion through a two dimensional sheet of lithium: a first principles study. Physical Chemistry Chemical Physics, 2023, 25, 15104-15109.	1.3	0
50734	DFT Modeling of a MoS₂ Monolayer for C₆H₁₂ and C₄H₈O Detection in Lung Cancer. , 2023, , .		0
50738	RE-T-silicon/-germanium intermetallic materials. , 2023, , 389-400.		0
50769	Ab Initio Study of the Electronic and Energy Properties of Diamond Carbon. , 0, , .		1
50866	Elucidating solid electrolyte interphase formation in sodium-based batteries: key reductive reactions and inorganic composition. Journal of Materials Chemistry A, 0, , .	5.2	1
50896	Quantum Mechanically Informed Kinetic Monte Carlo Models for Hydrogen Diffusion in BCC-Iron. RILEM Bookseries, 2023, , 88-95.	0.2	0

#	Article	IF	Citations
51009	Strain-Dependent Electronic and Optical Properties of Dirac-Semimetal Monolayer BeN₄. , 2022, , .		0
51025	Water Adsorption on Pt(111) Surfaces. , 2023, , 135-159.		0
51061	Electronic and optical properties of different concentrations of Ga doped ZnO: CASTEP study. , 2023, , .		0
51104	Tunneling Attenuation and Leakage Current in MoS₂ Nanoribbon MOSFETs. , 2023, , .		0
51117	Transport Properties and Device Performance of Quasi-One-Dimensional MoS2 FETs. , 2023, , .		0
51186	Investigation of structural and electronic properties of boron carbide based on SCAN meta-GGA functional. AIP Conference Proceedings, 2023, , .	0.3	0
51241	Large Ï€-conjugated indium-based metal-organic frameworks for high-performance electrochemical conversion of CO2. Nano Research, 2023, 16, 8743-8750.	5.8	1
51245	Investigation of structural, electronic and transport properties of Silicene on Graphene heterostructure by ab-initio calculations. , 2022, , .		0
51246	Hydrogen Adsorption on Two Dimensional Aluminene. , 2022, , .		0
51319	A first principle study of adsorption and dissociation of H2 molecule on MoS2 and Ni-promoted MoS2 surfaces. AIP Conference Proceedings, 2023, , .	0.3	0
51387	Gas Sensor device based on SnSe₂ Monolayer: Ab-initio Modelling. , 2023, , .		0
51430	Adsorption and Thermal Stability of Hydrogen Terminationá¹‡ on Diamond Surface: A First-Principles Study. Lecture Notes in Computer Science, 2023, , 406-412.	1.0	0
51639	Thermodynamic Limits of Electronic Systems. , 2023, , 307-331.		0
51646	Pt single atoms meet metalâ€“organic frameworks to enhance electrocatalytic hydrogen evolution activity. Nanoscale Horizons, 0, , .	4.1	0
51830	Study on strain effects on the electronic and optical properties of hexagonal boron phosphide monolayer. , 2023, , .		0
52048	LaOMS₂ (M = Ti, V, and Cr): novel crystal spin valves without contact. Materials Horizons, 0, , .	6.4	0
52095	Exploitation of mixed-valency chemistry for designing a monolayer with double ferroelectricity and triferroic couplings. Nanoscale, 2023, 15, 13567-13573.	2.8	0
52310	DFT predictions of the electronic, phonon, optical, and thermoelectric characteristics of CaCu2S2. MRS Communications, 0, , .	0.8	0

#	Article	IF	Citations
52543	DFT calculations on heat capacity and Debye temperature of Cs2GeF6 perovskite under high temperature and pressure. AIP Conference Proceedings, 2023, , .	0.3	0
52544	Abinitio calculations of structural, electronic, and thermodynamic performance of Cs2GeF6 perovskite. AIP Conference Proceedings, 2023, , .	0.3	0
52545	Investigation on structural stability and electronic properties of RuN. AIP Conference Proceedings, 2023, , .	0.3	0
52546	Structural and electronic properties of TcSi in B20 structure. AIP Conference Proceedings, 2023, , .	0.3	0
52661	Short communication: Effect of Sn on the formation of <c>-component dislocation loops in Zr alloys: In situ ion irradiation studies and atomistic simulations. Journal of Nuclear Materials, 2023, 587, 154756.	1.3	1
52663	Investigation ofÂtheÂBulk andÂElectronic Properties ofÂBoron/Nitrogen/Indium Doped Armchair Graphene Nanoribbon forÂSensing Plant VOC: A DFT Study. Communications in Computer and Information Science, 2023, , 239-251.	0.4	0
52684	First principles study of Bi2Fe4O9 in the hybrid HSE06 approach. AIP Conference Proceedings, 2023, , .	0.3	0
52711	Near-IR response of highly-strained Si photodetector linking first principles and TCAD. , 2023, , .		0
52732	Exploring dynamics, disorder, and anharmonicity in THz spectra of crystalline materials. , 2023, , .		0
52734	Theoretical study of structural, electronic, electric and optical properties of PbTiO3 using DFT-LDA approach. AIP Conference Proceedings, 2023, , .	0.3	0
52741	DFT based investigation of the structural and electronic properties of ferroelectric phase of lithium niobate. AIP Conference Proceedings, 2023, , .	0.3	0
52863	Fe-doped Co3O4 nanowire strutted 3D pinewood-derived carbon: A highly selective electrocatalyst for ammonia production via nitrate reduction. Nano Research, 2024, 17, 2276-2282.	5.8	2
52885	The Use of DFT-Based ab-initio Technique to Determine the Stability Difference in B2 Ti-PGM Compounds. , 0, , .		0
52952	The role of oxygen defects in the electronic, optical and phonon dispersion of the LAGO perovskite: a density functional theory investigation. Dalton Transactions, 2023, 52, 16128-16139.	1.6	0
53111	Surface termination and strain-induced modulation of the structure and electronic properties in 2D perovskites (Cs₂BCl₄ & CsB₂Cl₅, B = Pb, Sn): a first-principles study. Physical Chemistry Chemical Physics, 2023, 25, 32330-32335.	1.3	0
53133	The regulation effect of coordination number on the conductance of single-molecule junctions. Journal of Materials Chemistry C, 0, , .	2.7	0
53295	Excitonic Features in the Optical Response of Layered Gallium Sulphide. , 2023, , .		0
53301	Thermoelectric properties of graphane, silicane, germanane, and stanane: Hydrogenation effects. AIP Conference Proceedings, 2023, , .	0.3	0

#	Article	IF	Citations
53376	Catalytic Performance of Doped Ni2P Surfaces for Ammonia Synthesis â€. , 0, , .		0
53526	Mica nanosheets synthesized via liquid Ga embrittlement: demonstrating enhanced CO₂ capture. Materials Advances, 0, , .	2.6	0
53660	First Principles Characterization of $P_{n}V_{m}$ Clusters in Crystalline Silicon. , 2023, , .		0
53709	Tunable electronic structure and optical characteristics of two - Dimensional black P/CrI3 vDw heterostructure. AIP Conference Proceedings, 2023, , .	0.3	0
53993	Precipitation Engineering. Topics in Mining, Metallurgy and Materials Engineering, 2024, , 89-117.	1.4	0
54112	First-principles investigation of A-X [A: Mg, Ca, Sr, Ba; X: La, Nd, Sm] compounds: Their crystal structures prediction, electronic and mechanical properties. AIP Conference Proceedings, 2024, , .	0.3	0
54114	Unravelling abnormal in-plane stretchability of two-dimensional metalâ€“organic frameworks by machine learning potential molecular dynamics. Nanoscale, 2024, 16, 3438-3447.	2.8	0
54117	First-principles investigation of the solid-solid interface energy of bcc Ti/hcp Ti. AIP Conference Proceedings, 2024, , .	0.3	0
54119	Thermoelectric properties of K2SnBr6: A DFT insight. AIP Conference Proceedings, 2024, , .	0.3	0
54120	Transformation of GaAs nanoclusters from nanoflakes: A first principle study. AIP Conference Proceedings, 2024, , .	0.3	0
54121	Structural, electronic and thermal properties of NbSe2 monolayer: First principle study. AIP Conference Proceedings, 2024, , .	0.3	0
54122	Ab-initio simulations of Ni and Ni0.5Cu0.5 generalized stacking fault energies. AIP Conference Proceedings, 2024, , .	0.3	0
54126	Impact of biaxial strain on optoelectronic properties of Janus monolayer PtSeTe. AIP Conference Proceedings, 2024, , .	0.3	1
54129	First principle study of structural and electronic properties of copper Thiocyanate (CuSCN) monolayers. AIP Conference Proceedings, 2024, , .	0.3	0
54192	On the application of Marcusâ€“Hush theory to small polaron chemical dynamics in oxides: its relationship to the Holstein model and the importance of latticeâ€“orbital symmetries. Physical Chemistry Chemical Physics, 2024, 26, 4812-4827.	1.3	0
54251	Unraveling the role of varying composition on electronic and optical properties of bilayer MoxW(1â^'x)S2 for photovoltaic applications. , 2024, , .		0
54271	DFT and TDDFT Calculations of Ground and Excited States of Photoelectron Emission. , 0, , .		0
54289	Investigation of Bulk,ÂElectronicÂand Transport Properties of Armchair Silicene Nanoribbon as Liquefied Petroleum Gas Combustion Indicator: A DFT Study. Lecture Notes in Electrical Engineering, 2024, , 273-287.	0.3	0

#	Article	IF	Citations
54415	Superalkali halide perovskites with suitable direct band gaps for photovoltaic applications. Nanoscale, 2024, 16, 5130-5136.	2.8	0
54417	Electrodeposition Preparation and Performance Enhancement Mechanisms for Niâ€“Coâ€“Fe Coatings. Minerals, Metals and Materials Series, 2024, , 706-716.	0.3	0
54441	Density functional theory methods applied to homogeneous and heterogeneous catalysis: a short review and a practical user guide. Physical Chemistry Chemical Physics, 2024, 26, 7950-7970.	1.3	0
54581	Freestanding Large-Scale Lead Iodide Hydroxide Microwire Crystal for X-Ray Detector Application. , 2023, , .		0
54836	Electronic and Electrochemical Properties of Novel Cathode Material NaFeSO4OH by First-Principle Calculations. Lecture Notes in Mechanical Engineering, 2024, , 285-298.	0.3	0
55040	Oxygen-induced SO2 formation and desorption on NiMoS (1Â¯010) edge surface on NiMoS2 catalyst. AIP Conference Proceedings, 2024, , .	0.3	0